The chemistry of
organic silicon compounds
Volume 2

THE CHEMISTRY OF FUNCTIONAL GROUPS

A series of advanced treatises under the general editorship of
Professors Saul Patai and Zvi Rappoport

The chemistry of alkenes (2 volumes)
The chemistry of the carbonyl group (2 volumes)
The chemistry of the ether linkage
The chemistry of the amino group
The chemistry of the nitro and nitroso groups (2 parts)
The chemistry of carboxylic acids and esters
The chemistry of the carbon–nitrogen double bond
The chemistry of amides
The chemistry of the cyano group
The chemistry of the hydroxyl group (2 parts)
The chemistry of the azido group
The chemistry of acyl halides
The chemistry of the carbon–halogen bond (2 parts)
The chemistry of the quinonoid compounds (2 volumes, 4 parts)
The chemistry of the thiol group (2 parts)
The chemistry of the hydrazo, azo and azoxy groups (2 volumes, 3 parts)
The chemistry of amidines and imidates (2 volumes)
The chemistry of cyanates and their thio derivatives (2 parts)
The chemistry of diazonium and diazo groups (2 parts)
The chemistry of the carbon–carbon triple bond (2 parts)
The chemistry of ketenes, allenes and related compounds (2 parts)
The chemistry of the sulphonium group (2 parts)
Supplement A: The chemistry of double-bonded functional groups (3 volumes, 6 parts)
Supplement B: The chemistry of acid derivatives (2 volumes, 4 parts)
Supplement C: The chemistry of triple-bonded functional groups (2 volumes, 3 parts)
Supplement D: The chemistry of halides, pseudo-halides and azides (2 volumes, 4 parts)
Supplement E: The chemistry of ethers, crown ethers, hydroxyl groups
and their sulphur analogues (2 volumes, 3 parts)
Supplement F: The chemistry of amino, nitroso and nitro compounds and their derivatives
(2 volumes, 4 parts)
The chemistry of the metal–carbon bond (5 volumes)
The chemistry of peroxides
The chemistry of organic selenium and tellurium compounds (2 volumes)
The chemistry of the cyclopropyl group (2 volumes, 3 parts)
The chemistry of sulphones and sulphoxides
The chemistry of organic silicon compounds (2 volumes, 5 parts)
The chemistry of enones (2 parts)
The chemistry of sulphinic acids, esters and their derivatives
The chemistry of sulphenic acids and their derivatives
The chemistry of enols
The chemistry of organophosphorus compounds (4 volumes)
The chemistry of sulphonic acids, esters and their derivatives
The chemistry of alkanes and cycloalkanes
Supplement S: The chemistry of sulphur-containing functional groups
The chemistry of organic arsenic, antimony and bismuth compounds
The chemistry of enamines (2 parts)
The chemistry of organic germanium, tin and lead compounds

UPDATES

The chemistry of α-haloketones, α-haloaldehydes and α-haloimines
Nitrones, nitronates and nitroxides
Crown ethers and analogs
Cyclopropane derived reactive intermediates
Synthesis of carboxylic acids, esters and their derivatives
The silicon–heteroatom bond
Synthesis of lactones and lactams
Syntheses of sulphones, sulphoxides and cyclic sulphides
Patai's 1992 guide to the chemistry of functional groups — *Saul Patai*

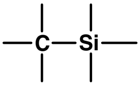

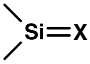

The chemistry of
organic silicon compounds

Volume 2

Edited by
ZVI RAPPOPORT
The Hebrew University, Jerusalem
and
YITZHAK APELOIG
Technion–Israel Institute of Technology, Haifa

1998

JOHN WILEY & SONS
CHICHESTER–NEW YORK–WEINHEIM–BRISBANE–SINGAPORE–TORONTO
An Interscience® Publication

Baffins Lane, Chichester,
West Sussex PO19 1UD, England

National 01243 779777
International (+44) 1243 779777
e-mail (for orders and customer service enquiries): cs-books@wiley.co.uk
Visit our Home Page on http://www.wiley.co.uk
or http://www.wiley.com

Other Wiley Editorial Offices

John Wiley & Sons, Inc., 605 Third Avenue,
New York, NY 10158-0012, USA

WILEY-VCH Verlag GmbH, Pappelallee 3,
D-69469 Weinheim, Germany

Jacaranda Wiley Ltd, 33 Park Road, Milton,
Queensland 4064, Australia

John Wiley & Sons (Asia) Pte Ltd, Clementi Loop #02-01,
Jin Xing Distripark, Singapore 129809

John Wiley & Sons (Canada) Ltd, 22 Worcester Road,
Rexdale, Ontario M9W 1L1, Canada

British Library Cataloguing in Publication Data

A catalogue record for this book is available from the British Library

ISBN 0 471 96757 2

Typeset in 9/10pt Times by Laser Words, Madras, India
Printed and bound in Great Britain by Biddles Ltd, Guildford, Surrey
This book is printed on acid-free paper responsibly manufactured from sustainable forestry,
in which at least two trees are planted for each one used for paper production.

To

Sara and Zippi

Dedicated to

Robert West
a pioneer in silicon chemistry
and a dear friend

Dedicated to

Saul Patai

teacher, editor and friend

Contributing authors

Wataru Ando	Department of Chemistry, University of Tsukuba, Tsukuba, Ibaraki 305, Japan
Yitzhak Apeloig	Department of Chemistry and the Lise-Meitner Minerva Center for Computational Quantum Chemistry, Technion–Israel Institute of Technology, Haifa 32000, Israel
D. A. ('Fred') Armitage	Department of Chemistry, King's College London, Strand, London, WC2R 2LS, UK
Norbert Auner	Fachinstitut für Anorganische und Allgemeine Chemie, Humboldt-Universität zu Berlin, Hessische Str. 1–2, D-10115 Berlin, Germany
David Avnir	Institute of Chemistry, The Hebrew University of Jerusalem, Jerusalem 91904, Israel
Alan R. Bassindale	Department of Chemistry, The Open University, Milton Keynes, MK7 6AA, UK
Rosa Becerra	Instituto de Quimica Fisica 'Rocasolano', C/Serrano 119, 28006 Madrid, Spain
Johannes Belzner	Institut für Organische Chemie der Georg-August-Universität Göttingen, Tammannstrasse 2, D-37077 Göttingen, Germany
M. B. Boisen Jr	Department of Materials Science and Engineering,Virginia Tech, Blacksburg, VA 24061, USA
Mark Botoshansky	Department of Chemistry, Technion–Israel Institute of Technology, Haifa 32000, Israel
A. G. Brook	Lash Miller Chemical Laboratories, University of Toronto, Toronto, Ontario M5S 3H6, Canada
C. Chatgilialoglu	I. Co. C. E. A., Consiglio Nazionale delle Ricerche, Via P. Gobetti 101, 40129 Bologna, Italy
Buh-Luen Cheng	Department of Chemistry, Tsing Hua University, Hsinchu, Taiwan 30043, Republic of China
Nami Choi	Department of Chemistry, University of Tsukuba, Tsukuba, Ibaraki 305, Japan
Ernest W. Colvin	Department of Chemistry, University of Glasgow, Glasgow, G12 8QQ, UK

Uwe Dehnert	Institut für Organische Chemie der Georg-August-Universität Göttingen, Tammannstrasse 2, D-37077 Göttingen, Germany
Robert Drake	Dow Corning Ltd, Cardiff Road, Barry, South Glamorgan, CF63 2YL, UK
Jacques Dubac	Hétérochimie Fondamentale et Appliqué, ESA-CNRS 5069, Université Paul-Sabatier, 118 route de Narbonne, 31062 Toulouse Cedex, France
Moris S. Eisen	Department of Chemistry, Technion–Israel Institute of Technology, Kiryat Hatechnion, Haifa 32000, Israel
C. Ferreri	Departimento di Chimica Organica e Biologica, Università di Napoli 'Federico II', Via Mezzocannone 16, 80134 Napoli, Italy
Toshio Fuchigami	Department of Electrochemistry, Tokyo Institute of Technology, 4259 Nagatsuta, Midori-ku, Yokohama 226, Japan
Peter P. Gaspar	Department of Chemistry, Washington University, St Louis, Missouri 63130-4899, USA
Christian Guérin	Chimie Moléculaire et Organisation du Solide, UMR-CNRS 5637, Université Montpellier II, Place E. Bataillon, 34095 Montpellier Cedex 5, France
G. V. Gibbs	Department of Materials Science and Engineering,Virginia Tech, Blacksburg, VA 24061, USA
T. Gimisis	I. Co. C. E. A., Consiglio Nazionale delle Ricerche, Via P. Gobetti 101, 40129 Bologna, Italy
Simon J. Glynn	Department of Chemistry, The Open University, Milton Keynes, MK7 6AA, UK
Norman Goldberg	Technische Universität Braunschweig, Institut für Organische Chemie, Hagenring 30, D-38106 Braunschweig, Germany
Edwin Hengge	(Deceased)
Reuben Jih-Ru Hwu	Department of Chemistry, Tsing Hua University, Hsinchu, Taiwan 30043, Republic of China
Jörg Jung	Institut für Organische Chemie der Justus-Liebig Universität Giessen, Heinrich-Buff-Ring 58, D-35392 Giessen, Germany
Peter Jutzi	Faculty of Chemistry, University of Bielefeld, Universitätsstr. 25, D-33615 Bielefeld, Germany
Yoshio Kabe	Department of Chemistry, University of Tsukuba, Tsukuba, Ibaraki 305, Japan
Menahem Kaftory	Department of Chemistry, Technion–Israel Institute of Technology, Haifa 32000, Israel
Inna Kalikhman	Department of Chemistry, Ben-Gurion University of the Negev, Beer Sheva 84105, Israel
Moshe Kapon	Department of Chemistry, Technion-Israel Institute of Technology, Haifa 32000, Israel

Miriam Karni	Department of Chemistry and the Lise-Meitner Minerva Center for Computational Quantum Chemistry, Technion–Israel Institute of Technology, Haifa 32000, Israel
Mitsuo Kira	Department of Chemistry, Graduate School of Science, Tohoku University, Aoba-ku, Sendai 980-77, Japan
Sukhbinder S. Klair	Department of Chemistry, Loughborough University, Loughborough, Leicestershire, LE11 3TU, UK
Lisa C. Klein	Ceramics Department, Rutgers–The State University of New Jersey, Piscataway, New Jersey 08855-0909, USA
Daniel Kost	Department of Chemistry, Ben-Gurion University of the Negev, Beer Sheva 84105, Israel
Takahiro Kusukawa	Department of Chemistry, University of Tsukuba, Tsukuba, Ibaraki 305, Japan
R. M. Laine	Department of Chemistry, University of Michigan, Ann Arbor, Michigan 48109-2136, USA
David Levy	Instituto de Ciencia de Materiales de Madrid, C.S.I.C., Cantoblanco, 28049 Madrid, Spain
Larry N. Lewis	GE Corporate Research and Development Center, Schenectady, NY 12309, USA
Zhaoyang Li	Department of Chemistry, State University of New York at Stony Brook, Stony Brook, New York 11794-3400, USA
Paul D. Lickiss	Department of Chemistry, Imperial College of Science, Technology and Medicine, London, SW7 2AY, UK
Shiuh-Tzung Liu	Department of Chemistry, National Taiwan University, Taipei, Taiwan 106
Tien-Yau Luh	Department of Chemistry, National Taiwan University, Taipei, Taiwan 106
Gerhard Maas	Abteilung Organische Chemie I, Universität Ulm, Albert-Einstein-Allee 11, D-89081 Ulm, Germany
Iain MacKinnon	Dow Corning Ltd, Cardiff Road, Barry, South Glamorgan, CF63 2YL, UK
Svetlana Kirpichenko	Irkutsk Institute of Chemistry, Siberian Branch of the Russian Academy of Sciences, 1 Favorsky St, 664033 Irkutsk, Russia
Christoph Maerker	Laboratoire de Chimie Biophysique, Institut Le Bel, Université Louis Pasteur, 4 rue Blaise Pascal, F-67000 Strasbourg, France
Günther Maier	Institut für Organische Chemie der Justus-Liebig Universität Giessen, Heinrich-Buff-Ring 58, D-35392 Giessen, Germany
Michael J. McKenzie	Department of Chemistry, Loughborough University, Loughborough, Leicestershire, LE11 3TU, UK
Andreas Meudt	Institut für Organische Chemie der Justus-Liebig Universität Giessen, Heinrich-Buff-Ring 58, D-35392 Giessen, Germany

Philippe Meunier	Synthèse et Electrosynthèse Organométalliques, UMR-CNRS 5632, Universitë de Bourgogne, 6 Boulevard Gabriel, 21004 Dijon Cedex, France
Takashi Miyazawa	Photodynamics Research Center, The Institute of Physical and Chemical Research, 19-1399, Koeji, Nagamachi, Aoba-ku, Sendai 980, Japan
Thomas Müller	Fachinstitut für Anorganische und Allgemeine Chemie, Humboldt-Universität zu Berlin, Hessische Str. 1–2, D-10115 Berlin, Germany
Shigeru Nagase	Department of Chemistry, Faculty of Science, Tokyo Metropolitan University, Hachioji, Tokyo 192-03, Japan
Iwao Ojima	Department of Chemistry, State University of New York at Stony Brook, Stony Brook, New York 11794-3400, USA
Renji Okazaki	Department of Chemistry, School of Science, The University of Tokyo, Bunkyo-ku, Tokyo 113, Japan
Harald Pacl	Institut für Organische Chemie der Justus-Liebig Universität Giessen, Heinrich-Buff-Ring 58, D-35392 Giessen, Germany
Philip C. Bulman Page	Department of Chemistry, Loughborough University, Loughborough, Leicestershire, LE11 3TU, UK
Vadim Pestunovich	Irkutsk Institute of Chemistry, Siberian Branch of the Russian Academy of Sciences, 1 Favorsky St, 664033 Irkutsk, Russia
Stephen Rosenthal	Department of Chemistry, Loughborough University, Loughborough, Leicestershire, LE11 3TU, UK
Hideki Sakurai	Department of Industrial Chemistry, Faculty of Science and Technology, Science University of Tokyo, Yamazaki 2641, Noda, Chiba 278, Japan
Paul von Ragué Schleyer	Center for Computational Quantum Chemistry, The University of Georgia, Athens, Georgia 30602, USA
Ulrich Schubert	Institute for Inorganic Chemistry, The Technical University of Vienna, A-1060 Vienna, Austria
Helmut Schwarz	Institut für Organische Chemie der Technischen Universität Berlin, Straße des 17 Juni 135, D-10623 Berlin, Germany
Akira Sekiguchi	Department of Chemistry, Graduate School of Science, University of Tsukuba, Tsukuba, Ibaraki 305, Japan
A. Sellinger	Sandia National Laboratory, Advanced Materials Laboratory, 1001 University Blvd, University of New Mexico, Albuquerque, New Mexico 87106, USA
Hans-Ullrich Siehl	Abteilung für Organische Chemie I der Universität Ulm, D-86069 Ulm, Germany
Harald Stüger	Institut für Anorganische Chemie, Erzherzog-Johann-Universität Graz, Stremayrgasse 16, A-8010 Graz, Austria
Reinhold Tacke	Institut für Anorganische Chemie, Universität Würzburg, Am Hubland, D-97074 Würzburg, Germany

Toshio Takayama	Department of Applied Chemistry, Faculty of Engineering, Kanagawa University, 3-27-1 Rokkakubashi, Yokohama, Japan 221
Yoshito Takeuchi	Department of Chemistry, Faculty of Science, Kanagawa University, 2946 Tsuchiya, Hiratsuka, Japan 259-12
Peter G. Taylor	Department of Chemistry, The Open University, Milton Keynes, MK7 6AA, UK
Richard Taylor	Dow Corning Ltd, Cardiff Road, Barry, South Glamorgan, CF63 2YL, UK
Norihiro Tokitoh	Department of Chemistry, School of Science, The University of Tokyo, Bunkyo-ku, Tokyo 113, Japan
Shwu-Chen Tsay	Department of Chemistry, Tsing Hua University, Hsinchu, Taiwan 30043, Republic of China
Mikhail Voronkov	Irkutsk Institute of Chemistry, Siberian Branch of the Russian Academy of Sciences, 1 Favorsky St, 664033 Irkutsk, Russia
Stephan A. Wagner	Institut für Anorganische Chemie, Universität Würzburg, Am Hubland, D-97074 Würzburg, Germany
Robin Walsh	The Department of Chemistry, The University of Reading, P O Box 224, Whiteknights, Reading, RG6 6AD, UK
Robert West	Department of Chemistry, University of Wisconsin at Madison, Madison, Wisconsin 53706, USA
Anna B. Wojcik	Ceramics Department, Rutgers−The State University of New Jersey, Piscataway, New Jersey 08855-0909, USA
Jiawang Zhu	Department of Chemistry, State University of New York at Stony Brook, Stony Brook, New York 11794-3400, USA
Wolfgang Ziche	Fachinstitut für Anorganische und Allgemeine Chemie, Humboldt-Universität zu Berlin, Hessische Str. 1−2, D-10115 Berlin, Germany

Foreword

The preceding volume in 'The Chemistry of Functional Groups' series, *The chemistry of organic silicon compounds* (S. Patai and Z. Rappoport, Eds), appeared a decade ago and was followed in 1991 by an update volume, *The silicon–heteroatom bond.* Since then the chemistry of organic silicon compounds has continued its rapid growth, with many important contributions in the synthesis of new and novel types of compounds, in industrial applications, in theory and in understanding the chemical bonds of silicon, as well as in many other directions. The extremely rapid growth of the field and the continued fascination with the chemistry of this unique element, a higher congener of carbon — yet so dramatically different in its chemistry — convinced us that a new authoritative book in the field is highly desired.

Many of the recent developments, as well as topics not covered in the previous volume are reviewed in the present volume, which is the largest in 'The Chemistry of Functional Groups' series. The 43 chapters, written by leading silicon chemists from 12 countries, deal with a wide variety of topics in organosilicon chemistry, including theoretical aspects of several classes of compounds, their structural and spectral properties, their thermochemistry, photochemistry and electrochemistry and the effect of silicon as a substituent. Several chapters review the chemistry of various classes of reactive intermediates, such as silicenium ions, silyl anions, silylenes, and of hypervalent silicon compounds. Multiple-bonded silicon compounds, which have attracted much interest and activity over the last decade, are reviewed in three chapters: one on silicon–carbon and silicon–nitrogen multiple bonds, one on silicon–silicon multiple bonds and one on silicon–hereroatom multiple bonds. Other chapters review the synthesis of several classes of organosilicon compounds and their applications as synthons in organic synthesis. Several chapters deal with practical and industrial aspects of silicon chemistry in which important advances have recently been made, such as silicon polymers, silicon-containing ceramic precursors and the rapidly growing field of organosilica sol–gel chemistry.

The literature covered in the book is mostly up to mid-1997.

Several of the originally planned chapters, on comparison of silicon compounds with their higher group 14 congeners, interplay between theory and experiment in organisilicon chemistry, silyl radicals, recent advances in the chemistry of silicon–phosphorous,–arsenic,–antimony and –bismuth compounds, and the chemistry of polysilanes, regrettably did not materialize. We hope to include these important chapters in a future complementary volume. The current pace of research in silicon chemistry will certainly soon require the publication of an additional updated volume.

We are grateful to the authors for the immense effort they have invested in the 43 chapters and we hope that this book will serve as a major reference in the field of silicon chemistry for years to come.

We will be grateful to readers who will draw our attention to mistakes and who will point out to us topics which should be included in a future volume of this series.

Jerusalem and Haifa
March, 1998

ZVI RAPPOPORT
YITZHAK APELOIG

The Chemistry of Functional Groups
Preface to the series

The series 'The Chemistry of Functional Groups' was originally planned to cover in each volume all aspects of the chemistry of one of the important functional groups in organic chemistry. The emphasis is laid on the preparation, properties and reactions of the functional group treated and on the effects which it exerts both in the immediate vicinity of the group in question and in the whole molecule.

A voluntary restriction on the treatment of the various functional groups in these volumes is that material included in easily and generally available secondary or tertiary sources, such as Chemical Reviews, Quarterly Reviews, Organic Reactions, various 'Advances' and 'Progress' series and in textbooks (i.e. in books which are usually found in the chemical libraries of most universities and research institutes), should not, as a rule, be repeated in detail, unless it is necessary for the balanced treatment of the topic. Therefore each of the authors is asked not to give an encyclopaedic coverage of his subject, but to concentrate on the most important recent developments and mainly on material that has not been adequately covered by reviews or other secondary sources by the time of writing of the chapter, and to address himself to a reader who is assumed to be at a fairly advanced postgraduate level.

It is realized that no plan can be devised for a volume that would give a complete coverage of the field with no overlap between chapters, while at the same time preserving the readability of the text. The Editors set themselves the goal of attaining reasonable coverage with moderate overlap, with a minimum of cross-references between the chapters. In this manner, sufficient freedom is given to the authors to produce readable quasi-monographic chapters.

The general plan of each volume includes the following main sections:

(a) An introductory chapter deals with the general and theoretical aspects of the group.

(b) Chapters discuss the characterization and characteristics of the functional groups, i.e. qualitative and quantitative methods of determination including chemical and physical methods, MS, UV, IR, NMR, ESR and PES — as well as activating and directive effects exerted by the group, and its basicity, acidity and complex-forming ability.

(c) One or more chapters deal with the formation of the functional group in question, either from other groups already present in the molecule or by introducing the new group directly or indirectly. This is usually followed by a description of the synthetic uses of the group, including its reactions, transformations and rearrangements.

(d) Additional chapters deal with special topics such as electrochemistry, photochemistry, radiation chemistry, thermochemistry, syntheses and uses of isotopically labelled compounds, as well as with biochemistry, pharmacology and toxicology. Whenever applicable, unique chapters relevant only to single functional groups are also included (e.g. 'Polyethers', 'Tetraaminoethylenes' or 'Siloxanes').

This plan entails that the breadth, depth and thought-provoking nature of each chapter will differ with the views and inclinations of the authors and the presentation will necessarily be somewhat uneven. Moreover, a serious problem is caused by authors who deliver their manuscript late or not at all. In order to overcome this problem at least to some extent, some volumes may be published without giving consideration to the originally planned logical order of the chapters.

Since the beginning of the Series in 1964, two main developments have occurred. The first of these is the publication of supplementary volumes which contain material relating to several kindred functional groups (Supplements A, B, C, D, E, F and S). The second ramification is the publication of a series of 'Updates', which contain in each volume selected and related chapters, reprinted in the original form in which they were published, together with an extensive updating of the subjects, if possible, by the authors of the original chapters. A complete list of all above mentioned volumes published to date will be found on the page opposite the inner title page of this book. Unfortunately, the publication of the 'Updates' has been discontinued for economic reasons.

Advice or criticism regarding the plan and execution of this series will be welcomed by the Editors.

The publication of this series would never have been started, let alone continued, without the support of many persons in Israel and overseas, including colleagues, friends and family. The efficient and patient co-operation of staff-members of the publisher also rendered us invaluable aid. Our sincere thanks are due to all of them.

The Hebrew University SAUL PATAI
Jerusalem, Israel ZVI RAPPOPORT

Contents

List of abbreviations used

Ac	acetyl (MeCO)
acac	acetylacetone
Ad	adamantyl
AIBN	azoisobutyronitrile
Alk	alkyl
All	allyl
An	anisyl
Ar	aryl
Bn	benzyl
Bz	benzoyl (C_6H_5CO)
Bu	butyl (also *t*-Bu or Bu^t)
CD	circular dichroism
CI	chemical ionization
CIDNP	chemically induced dynamic nuclear polarization
CNDO	complete neglect of differential overlap
Cp	η^5-cyclopentadienyl
Cp*	η^5-pentamethylcyclopentadienyl
DABCO	1,4-diazabicyclo[2.2.2]octane
DBN	1,5-diazabicyclo[4.3.0]non-5-ene
DBU	1,8-diazabicyclo[5.4.0]undec-7-ene
DIBAH	diisobutylaluminium hydride
DME	1,2-dimethoxyethane
DMF	*N*,*N*-dimethylformamide
DMSO	dimethyl sulphoxide
ee	enantiomeric excess
EI	electron impact
ESCA	electron spectroscopy for chemical analysis
ESR	electron spin resonance
Et	ethyl
eV	electron volt

Fc	ferrocenyl
FD	field desorption
FI	field ionization
FT	Fourier transform
Fu	furyl(OC_4H_3)
GLC	gas liquid chromatography
Hex	hexyl(C_6H_{13})
c-Hex	cyclohexyl(C_6H_{11})
HMPA	hexamethylphosphortriamide
HOMO	highest occupied molecular orbital
HPLC	high performance liquid chromatography
i-	iso
Ip	ionization potential
IR	infrared
ICR	ion cyclotron resonance
LAH	lithium aluminium hydride
LCAO	linear combination of atomic orbitals
LDA	lithium diisopropylamide
LUMO	lowest unoccupied molecular orbital
M	metal
M	parent molecule
MCPBA	*m*-chloroperbenzoic acid
Me	methyl
MNDO	modified neglect of diatomic overlap
MS	mass spectrum
n	normal
Naph	naphthyl
NBS	*N*-bromosuccinimide
NCS	*N*-chlorosuccinimide
NMR	nuclear magnetic resonance
Pc	phthalocyanine
Pen	pentyl(C_5H_{11})
Pip	piperidyl($C_5H_{10}N$)
Ph	phenyl
ppm	parts per million
Pr	propyl (also *i*-Pr or Pr^i)
PTC	phase transfer catalysis or phase transfer conditions
Pyr	pyridyl (C_5H_4N)

R	any radical
RT	room temperature
s-	secondary
SET	single electron transfer
SOMO	singly occupied molecular orbital
t-	tertiary
TCNE	tetracyanoethylene
TFA	trifluoroacetic acid
THF	tetrahydrofuran
Thi	thienyl(SC_4H_3)
TLC	thin layer chromatography
TMEDA	tetramethylethylene diamine
TMS	trimethylsilyl or tetramethylsilane
Tol	tolyl(MeC_6H_4)
Tos or Ts	tosyl(*p*-toluenesulphonyl)
Trityl	triphenylmethyl(Ph_3C)
Xyl	xylyl($Me_2C_6H_3$)

In addition, entries in the 'List of Radical Names' in *IUPAC Nomenclature of Organic Chemistry*, 1979 Edition, Pergamon Press, Oxford, 1979, p. 305–322, will also be used in their unabbreviated forms, both in the text and in formulae instead of explicitly drawn structures.

CHAPTER 1

Theoretical aspects and quantum mechanical calculations of silaaromatic compounds

YITZHAK APELOIG and MIRIAM KARNI

Department of Chemistry and the Lise Meitner-Minerva Center for Computational Quantum Chemistry, Technion — Israel Institute of Technology, Haifa 32000, Israel

---

I. INTRODUCTION

The last two decades have witnessed increasing interest in the synthesis and chemistry of doubly-bonded silicon compounds[1−3]. The successful synthesis and isolation in 1981 of the first stable silene[4] and disilene[5] stimulated efforts to synthesize other stable doubly-bonded silicon compounds. These efforts led to the synthesis of new stable silenes[1a,2a,3a,b] and disilenes[1a,2b,3c], to a stable 1-sillaallene[6], as well as to stable compounds containing a variety of other double bonds to silicon, i.e. Si=N[2a,3d], Si=P[3e], Si=As[3e], Si=S[2c] and Si=Se[2c,2f]. Stable silanones (i.e. compounds containing a Si=O bond) are still elusive, but there is strong evidence for their existence in a matrix at low temperature[1a,2c,d] and in the gas phase[7].

Aromatic compounds are common in carbon chemistry and in the chemistry of other first-row elements, such as nitrogen and oxygen. In contrast, the first stable benzenoid silaaromatic compound **1**, protected by the large Tbt group **(2)**, was isolated by Okazaki and coworkers only in 1997[8]. A marginally stable silaaromatic compound is 1,4-di-*tert*-butyl-2,6-bis(trimethylsilyl)silabenzene **(3)** which is stable in solution below −100 °C[9]. All other attempts to produce silaaromatic compounds resulted only in their observation in a matrix or in the gas phase[2d]. The synthesis and characterization of stable benzenoid silaaromatic compounds remains a major challenge in contemporary organosilicon chemistry.

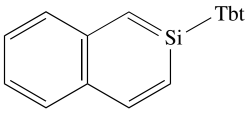

(1)

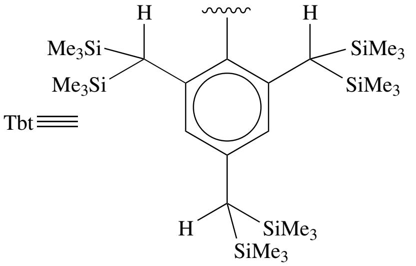

(2)

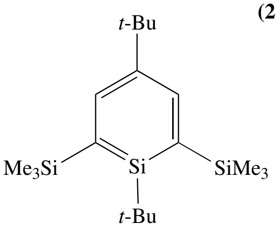

(3)

In addition to silaaromatic benzenoid compounds, new exciting families of silaaromatic non-benzenoid compounds, possessing various degrees of aromaticity, have recently attracted much attention. Some examples are: (a) the recently isolated stable silylenes **(4)**[2e]; (b) alkali metal complexes of silole anions **(5a)** and dianions **(5b)**[10]; (c) transition metal complexes of silole (e.g. **6a** and **6b**)[10d]; (d) silafullerenes.

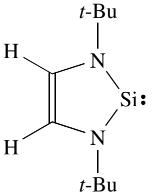

(4)

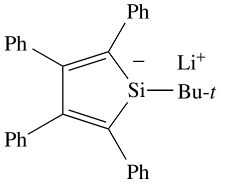

(5a)

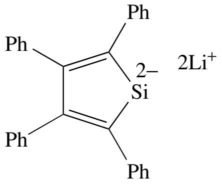

(5b)

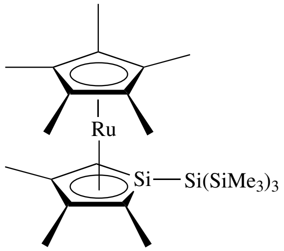

(6a)

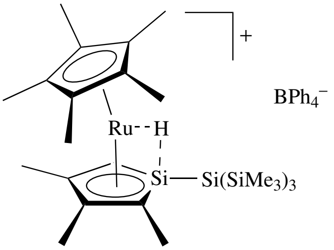

(6b)

The experimental knowledge on silaaromatic compounds is still very limited, leaving theory as one of the main sources of reliable information about the basic properties of these compounds[1b]. Computational methods have proved to be unusually helpful in the study of organosilicon compounds and in particular of transients and other unstable silicon compounds, for which experimental data are scarce[1b].

In this chapter we will review the available computational studies on silaaromatic and silaantiaromatic compounds. The compounds that are reviewed belong mainly to the categories obeying the Hückel rule[11], and we will refer to compounds having $4n + 2$ π-electrons as being 'aromatic' and to compounds with $4n$ π-electrons as being 'antiaromatic'. However, we stress that by using the 'aromatic–antiaromatic' notation we do not imply that the compound thus referred to actually has the characteristics of an 'aromatic' or of an 'antiaromatic' compound. As discussed in detail in Section II below, the degree of 'aromaticity' of a particular compound is difficult to define and is highly controversial even for simple organic molecules, and the issue is even more problematic for organosilicon compounds. The reader is therefore advised to regard the notation 'aromatic' or 'antiaromatic' only as a guideline and he should consult the specific discussion regarding the 'degree of aromaticity' for each particular compound of interest.

We have made an effort to review all the important theoretical studies on silaaromatic compounds, emphasizing those published in the period January 1990–May 1997, and we include also unpublished data that was brought to our attention. Although we did our best to cover all studies, we might have missed some, and if so we apologize to their authors. Earlier studies theoretical and experimental have been reviewed by Apeloig in the preceding volume of *The Chemistry of Organic Silicon Compounds*[1b]. However, for the sake of completeness we will also discuss older studies which are of importance. We do not review or explain the theoretical methods which were used by the various researchers and the interested reader is referred to the original papers or to the recent extensive encyclopedia of computational chemistry[12]. We use the generally accepted notation to give the level of theory at which the calculations were carried out; e.g. MP2/6-31G*//RHF/6-31G* denotes a single point MP2/6-31G* calculation at the RHF/6-31G* optimized geometry. Relevant experimental studies are mentioned, but no attempt was made to fully review all the experimental studies related to silaaromatic compounds. In some cases we also discuss the analogous compounds of the higher congeners of Si in group 14 of the Periodic Table, i.e. Ge, Sn and Pb. As the reader will realize, this chapter points to many open questions which still require up-to-date calculations to provide reliable data on the still elusive family of silaaromatic compounds.

The list of abbreviations used in this chapter, including those of the theoretical methods, are given in Section XI.

II. COMPUTATIONAL CRITERIA FOR ESTIMATING THE DEGREE OF AROMATICITY

What is aromaticity? This fundamental and widely used chemical concept is nevertheless one of the most controversial concepts in modern chemistry[13–16]. Many definitions and criteria for characterizing and estimating the degree of aromaticity have been considered, and they are discussed extensively and critically in a recently published comprehensive book by Minkin and coworkers[13a]. Schleyer and Jiao have recently emphasized the importance of magnetic properties for estimating aromaticity[16]. We will summarize here briefly the most widely used *computational criteria* for estimating the degree of aromaticity whilst the reader is referred to References 13, 14 and 16 and the papers cited therein for a more comprehensive discussion.

Aromaticity is associated with cyclic arrays of ‘mobile electrons’ with favourable symmetries. The ‘mobile electron’ arrays may be π, σ or mixed in character[16]. The $4n+2/4n$ Hückel rule provides a quantum mechanical framework which allows one to relate the stability and structure of π-systems to their π-electron count, and is widely utilized for classifying π-cyclic systems as aromatic or antiaromatic[13].

The main computational criteria used for determining aromaticity are: (a) the geometric criterion, (b) the energetic criterion, (c) the magnetic criterion. These criteria are discussed below.

A. The Geometric Criterion

This widely used criterion is manifested in: (a) bond length equalization due to cyclic delocalization and (b) planarity of the cyclic systems[13–16]. The planarity of cyclic conjugated systems is regarded as a manifestation of aromaticity, while the non-planarity of cyclic conjugated systems is often taken as an indication of antiaromaticity.

The most widely used method for quantifying the equalization of bond lengths is by calculating Julg’s parameter A, using equation 1[17]. This parameter defines the degree of aromaticity in terms of the deviation of n individual CC bond lengths (r_i) from the mean CC bond length (r); $A = 1$ for benzene (D_{6h}) and $A = 0$ for a ‘Kékule benzene’ (D_{3h}).

$$A = 1 - [(225/n)\sum(1 - r_i/r)^2] \tag{1}$$

Both geometric criteria (i.e. bond equalization and planarity) do not provide definite answers. Thus, bond equalization is found in borazine ($B_3N_3H_6$) and boroxine ($B_3O_3H_3$) which have 6 π-electrons, but these molecules were shown to be non-aromatic according to the magnetic criterion[16,18,19]. Similarly, bond equalization was found in acyclic conjugated non-aromatic compounds, such as $H_2NCH{=}CH{-}CH{=}CHNH_2$[16]. On the other hand, substantial bond-length alternation can be found in compounds which are believed to be highly aromatic such as naphthalene, anthracene, phenanthrene etc.[13a,15a,16]. Cyclic π-electron delocalization stabilizes planar structures, but other effects such as σ-skeleton strain may cause deviation from planarity, diminishing the degree of aromaticity[14]. Deviation from planarity is found in many silicon compounds such as hexasilabenzene and silole anions which, according to other criteria, are believed to be aromatic (see below).

Shaik and coworkers, have argued recently that the bond length equalization in aromatic molecules is *not* due to π-electron delocalization but is forced by the preference of the σ-framework for symmetric structures[15]. According to Shaik and coworkers, the tendency to adopt a symmetric or a distorted geometry results from competition between two opposite driving forces: that of the σ-skeleton which is always symmetrizing, and that of the π-electrons which, in all cases studied, favours localized non-symmetric structures. Thus, according to Shaik bond-length equalization does *not* indicate a high degree of aromaticity[15]. Shaik and coworkers have criticized in particular the use of the $4n + 2/4n$ Hückel rule for predicting the geometries of molecules other than hydrocarbons, and this criticism is therefore particularly relevant to silaaromatic compounds.

B. The Energetic Criterion

This criterion is a measure of the stabilization/(destabilization) of the aromatic/(antiaromatic) compounds due to cyclic electron delocalization, relative to suitable reference systems such as olefins or conjugated polyenes[13,14,16,20,21]. This is demonstrated for benzene in equations 2–5. The resonance stabilization energy (RE) may be estimated by isodesmic equations[21a] (e.g. equation 2 or 3) and the aromatic stabilization energy (ASE) by homodesmotic equations[21b,c] (e.g. equation 4 or 5) or hyperhomodesmotic equations[21d]. The homodesmotic and hyperhomodesmotic equations, and thus the ASEs, are considered to be the more reliable as there is a better match of the number of single and double bonds on both sides of the equation. The major problem with the energetic criterion is that the estimation of the extra stability resulting from aromaticity is dependent on the reference compound chosen, as demonstrated for benzene by equations 2–5[16] (the RE and ASE values reported for equations 2–5 use experimental data[22]). In addition to aromatic stabilization, these equations reflect also the contribution of strain energy and other factors. It is therefore difficult to apply the energy criterion to strained systems, but even for regular systems its use is controversial

$$\mathrm{C_6H_6 + 6CH_4 \longrightarrow 3C_2H_4 + 3C_2H_6} \qquad \mathrm{RE} = 64.2\ \mathrm{kcal\,mol^{-1}} \tag{2}$$

$$\mathrm{C_6H_6 + 3C_2H_6 \longrightarrow 3C_2H_4} + \text{cyclohexane} \qquad \mathrm{RE} = 48.9\ \mathrm{kcal\,mol^{-1}} \tag{3}$$

$$\mathrm{C_6H_6 + 3C_2H_4} \longrightarrow 3(\textit{trans}\text{-1, 3-butadiene}) \qquad \mathrm{ASE} = 21.7\ \mathrm{kcal\,mol^{-1}} \tag{4}$$

$$\mathrm{C_6H_6} + 3(\text{cyclohexane}) \longrightarrow 3(\text{1, 3-cyclohexadiene}) \qquad \mathrm{ASE} = 35.2\ \mathrm{kcal\,mol^{-1}} \tag{5}$$

C. The Magnetic Criterion

A special magnetic behaviour of aromatic compounds is believed to result from the occurrence of aromatic ring currents. The following magnetic criteria can be used to determine if a molecule is aromatic.

1. Magnetic susceptibility anisotropy and susceptibility exaltation

Magnetic susceptibility anisotropy, $\Delta\chi$, is a characteristic attribute of aromaticity[16,23]. The magnetic tensor which is normal to the aromatic ring is much larger than the average of the other tensors. For aromatic systems $\Delta\chi$ is highly negative, while highly antiaromatic compounds exhibit positive $\Delta\chi$ values. Unfortunately, the absolute $\Delta\chi$ values cannot serve as an aromaticity index because, in addition to ring currents, local π- and σ-bonds as well as local paramagnetic ring currents also contribute to the anisotropy[13a]. These additional effects have to be subtracted from the total anisotropy in order to find the net contribution of the aromaticity to $\Delta\chi$, e.g. by comparing $\Delta\chi$ of benzene with the sum of the $\Delta\chi$ of three ethylenes.

Another characteristic manifestation of aromaticity is the exaltation of the diamagnetic susceptibility, Λ, which is defined as the difference between the diamagnetic susceptibility of a conjugated cyclic system (χ_M) and the diamagnetic susceptibility of a hypothetical reference system without cyclic electron delocalization (χ'_M)[24]. A molecule is considered to be aromatic when $\Lambda < 0$, antiaromatic when $\Lambda > 0$ and non-aromatic when $\Lambda \sim 0$. Thus, the determination of aromaticity from Λ is dependent on the reference system, as is the calculation of RE or ASE. The magnetic susceptibility associated with the ring current (London susceptibility[25]) is dependent on the ring area, and so are the magnetic susceptibility exaltations. This fact must be taken into consideration when systems of different ring sizes are compared, for example, by defining a ring-size-adjusted aromaticity index ρ which is calculated by equation 6, where n is the number of electrons, S is the ring area and k is a scaling factor[13a,19].

$$\rho = k[n\Lambda/S^2] \tag{6}$$

2. Anomalous ^{1}H chemical shifts

Anomalous ^{1}H chemical shifts manifest the deshielding of protons of aromatic cyclic molecules, caused by ring currents induced by an external magnetic field. For aromatic compounds, the protons located inside the ring are shifted upfield and those outside the ring are shifted downfield; for antiaromatic compounds the direction is opposite[13,16,26]. Although this criterion is widely used[13a], it is not general and many exceptions are known[16].

3. Other magnetic probes of aromaticity (e.g. NICS)

(i) For aromatic compounds that do not include protons, such as C_{60}, the chemical shift of an encapsulated ^{3}He is used, both experimentally and computationally, as a probe for aromaticity[27].

(ii) The chemical shift value of a Li^+ ion which complexes the π-face of aromatic systems is shifted upfield due to ring current effects, and thus can serve as an inner-ring current probe.

(iii) An efficient computational probe for diatropic and paratropic ring currents associated with aromaticity and antiaromaticity, respectively, is the recently developed Nucleus-Independent Chemical Shifts (NICS) method, which computes the absolute magnetic shieldings at ring centres[26]. The total NICS values can be divided into the diamagnetic contributions from the π-bonds, NICS(π), the paramagnetic contributions from the ring σ-bonds, NICS(σ), and the contributions of other electrons (i.e. bonds to hydrogens, in-plane lone pairs and core orbitals)[19]. In aromatic delocalized systems the negative NICS(π) values are larger than the positive NICS(σ) values and thus they have significantly negative total NICS values. Positive total NICS values indicate antiaromaticity, and in the absence of significant delocalization the NICS(π) and NICS(σ) values tend to cancel, resulting in total NICS values that are near zero[19]. The total NICS values show only modest dependence on the ring size and they can therefore be used also to evaluate the aromaticity and antiaromaticity contributions of individual rings in polycyclic systems[26].

D. Interrelations between the Geometric, Energetic and Magnetic Criteria

The extensive literature on aromaticity reveals a significant degree of confusion and controversy regarding the assessment of aromaticity using the above-mentioned criteria and regarding the correlation between them. The examples below demonstrate the current state of the issue:

(i) According to Minkin and coworkers, the best way to evaluate aromaticity is by the energetic criterion which is based on the determination of aromatic stabilization by ‘making use of various schemes for calculating resonance energy’[13a].

(ii) Haddon proposed the existence of an analytic relationship between ring currents and the resonance energy[28].

(iii) Katritzky and coworkers concluded from a comparison of a variety of heterocycles with different ring sizes that the geometric and energetic criteria of aromaticity on the one hand, and the magnetic criterion on the other, are almost completely orthogonal[29].

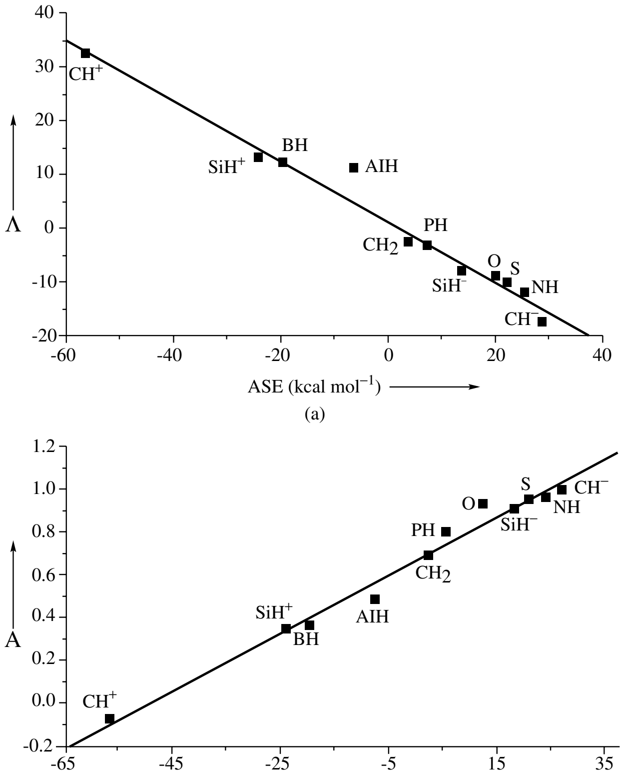

(a)

(b)

FIGURE 1. Correlation between various criteria for aromaticity for cyclic-C_4H_4X molecules: (a) Magnetic susceptibility exaltations $\Lambda(10^{-6}\ \mathrm{cm^3\,mol^{-1}})$ vs ASE ($\mathrm{kcal\,mol^{-1}}$); (b) Julg’s paprameter A vs ASE ($\mathrm{kcal\,mol^{-1}}$); (c) Julg’s parameter A vs magnetic susceptibility exaltations Λ; (d) NICS (ppm) vs ASE ($\mathrm{kcal\,mol^{-1}}$). Plots (a)–(c) are reproduced by permission of WILEY-VCH, D-69451 Weinheim, 1995 from Reference 31a. Plot (d) is reprinted with permission from Reference 26. Copyright (1996). American Chemical Society

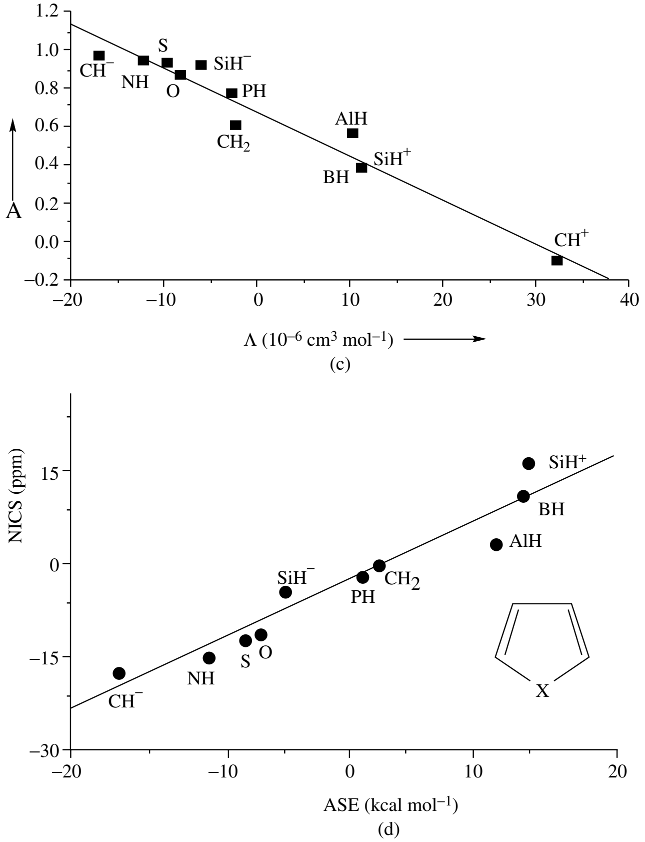

FIGURE 1. *(continued)*

(iv) Jug and Köster concluded that the geometric and energetic criteria are orthogonal to each other while the magnetic criterion correlates with the energetic criteria[30].

(v) Schleyer and coworkers found for a set of cyclic C_4H_4X 5-membered ring systems with 4π- and 6π-electrons[26,31a] that linear relationships exist between the energetic, geometric and magnetic criteria of aromaticity. Diagrams showing the linear correlation between ASEs, Julg's parameter A, the magnetic susceptibility exaltation Λ and the NICS values are shown in Figure 1. Houk and Mendel suggested[31b] that the contradiction between the conclusions of Katritzky[29] and Schleyer[31a] may result from a combination of experimental uncertainties in the magnetic Λ values that Katritzky used, as well as from a comparison of systems with different ring sizes. In a recent study of nearly 50 aromatic and heteroaromatic ring systems, Bird[31c] confirms the conclusions of Schleyer and coworkers[31a] and reports the existence of a good linear relationship between experimental diamagnetic susceptibility enhancements and the corresponding resonance energies as well as other aromaticity indices[31c].

(vi) According to Schleyer and coworkers exaltation of the diamagnetic susceptibility Λ is 'the only uniquely applicable' criterion for aromaticity; other criteria serve only as useful supplementary tools for characterizing aromaticity[16,26]. Schleyer and Jiao recently proposed the following definition of aromaticity: ‘Compounds which exhibit significantly exalted diamagnetic susceptibility are aromatic. Cyclic electron delocalization may also result in bond length equalization, abnormal chemical shifts and magnetic anisotropies, as well as chemical and physical properties which reflect energetic stabilization’[16].

In view of the above-mentioned controversy about the definition of aromaticity, it is obvious that there is no unique way to quantify the ‘degree of aromaticity’ of a particular compound and that any quantification of aromaticity is likely to be highly controversial. Keeping in mind the above discussion on the nature and definition of aromaticity we now examine the available theoretical studies of silaaromatic and silaantiaromatic compounds.

III. SILABENZENOIDS

A. Experimental Background

Barton and Banasink were the first in 1977 to generate and trap a silaaromatic compound, the silatoluene, **7**[32a]. This discovery was soon followed by a matrix isolation and IR, UV and PE spectral characterization of both **7**[32b,c] and silabenzene **(8)**[33]. In 1988 Märkel and Schlosser reported the synthesis of the substituted silabenzene **3** which was stable in solution up to 170 K[9]. Kinetic stabilization by bulky substituents led to the isolation in an argon matrix of **9,** R = Me_3Si or *i*-$PrMe_2Si$ by Jutzi, Maier and coworkers[34]; **9**, R = *i*-$PrMe_2Si$ was stable up to 90 K even without an argon cage[34]. In 1991 Maier and coworkers isolated and characterized spectroscopically in the gas phase and in an argon matrix at 12 K the 9-silaanthracenes, **10**, R = H, Ph[35]. Most recently, Okazaki and coworkers reported the synthesis and isolation of 2-silanaphthalene **(1)**, the first silabenzenoid compound which is a stable crystalline material even at room temperature[8].

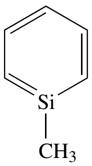

(7)

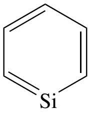

(8)

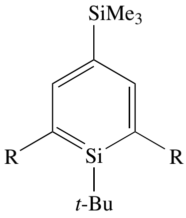

(9) R = Me_3Si, *i*-$PrMe_2Si$

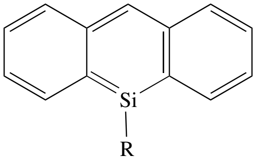

(10) R = H, Ph

Several studies reported on silabenzenes in which more than one carbon was substituted by silicon. Maier and coworkers observed 1,4-disilabenzene **(11)** in a matrix and identified it by its IR absorbtion at 1273 cm^{-1} and its electronic absorptions at 408, 340 and 275 nm[36]. Evidence for the formation in the gas phase of 1,3,5-trisilabenzene **(12)** as a ligand in the dehydrogenation reaction of 1,3,5-trisilacyclohexane with $[Cp,Fe]^+$, $[Cp,Co]^+$ and $[Cp,Ni]^+$ was recently reported by Bjarnason and Arnason[37]. The structure of **12** was assigned on the basis of the collision-induced dissociation spectrum and from deuterium-labelling experiments[37].

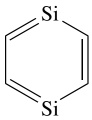

(11)

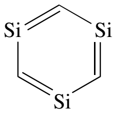

(12)

B. Monosilabenzenes

1. Silabenzene

Theory preceded experiment in predicting that silabenzene should be stable with respect to other isomers and to possible decomposition products. Many calculations are available for silabenzene, but most of them are relatively old and thus have used low levels of theory. The available calculations include the following levels of theory: MINDO/3^{38}, floating spherical Gaussian orbitals^{39}, MNDO^{40}, HF/STO-2G^{41}, HF/STO-3G^{40,42}, HF/3-21G^{*43a} and HF/6-31G^{*43b}. The best available calculations are the recent B3LYP/6-311+G** calculations^{8}, but this study which concentrates on 2-silanaphthalene does not discuss silabenzene in detail.

Is silabenzene aromatic? **8** is calculated to be a planar molecule with a Si−C bond length of 1.771 Å at B3LYP/6-311+G^{**8} (1.760 Å at 3-21G^{*43a}, see Figure 2a for a

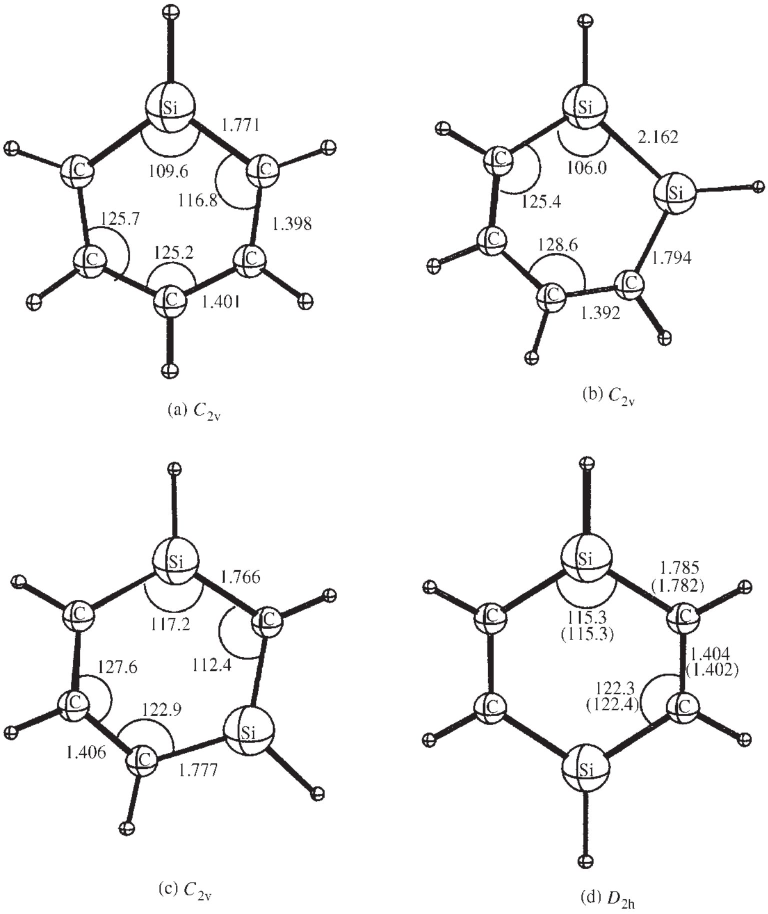

FIGURE 2. (a) B3LYP/6-311+G** optimized structure of silabenzene (**8**); (b–d) B3LYP/3-21G* optimized geometries of *ortho*-, *meta*- and *para*- disilabenzenes, respectively; values in parentheses are at MP2/6-31G**. All data are from Y. Apeloig, M. Bendikov and S. Sklenak, unpublished results

detailed structure). This distance is intermediate between that of a single and a double C−Si bond, displaying almost the same relative shortening relative to a Si−C single bond as found for the C−C bond in benzene. Thus, the calculated structure exhibits the expected partial double-bond character which is indicative of a delocalized system, and all researchers have therefore concluded that silabenzene possesses some degree of aromaticity. Further support for the aromatic character of **8** is provided by the molecular orbital coefficients, which indicate that the π-electrons are delocalized over the entire heavy-atom framework and by the nearly uniform π-electron distribution. The silicon atom has a somewhat smaller electron density than the carbons, i.e. 0.82 electrons on Si vs 1.09, 0.96 and 1.09 electrons on the *ortho*-, *meta*- and *para*-carbons, respectively, exhibiting the charge build-up on the *ortho*- and *para*-carbons, typical of a benzenoid π-system[42]. The σ-electrons are polarized away from the electropositive silicon towards the neighbouring carbon atoms[39,42].

The photoelectron spectra of silabenzene was measured and assigned on the basis of a double-zeta *ab initio* SCF calculation[44]. The lowest ionization energy of **8** is 8.11 eV ($^2B_1$ state, calculated to be 7.8 eV at HF/DZ[44]), by *ca* 1 eV lower than in benzene. The authors conclude that silabenzene is best considered as a symmetry-distorted (due to the presence of the Si atom) cyclic 6π-electron system.

Several energetic comparisons indicate that the degree of aromaticity of **8** is *ca* 70–85% of that of benzene[42,43] (depending on the reference compound and the level of calculation). For example, the calculated (at HF/3-21G*) resonance energy (RE) of **8** (equation 7) of 47.0 kcal mol^{-1} is *ca* 77% of the RE of benzene (equation 2) of 61.0 kcal mol^{-1} (64.2 kcal mol^{-1}, experimental)[43]. Similar results were obtained by using the more reliable homodesmotic equation 8 and hyperhomodesmotic equation 9, according to which the aromatic stabilization energy (ASE) of silabenzene is 70–85% (HF/6-31G*) of that of benzene[43b].

$$\mathbf{8} + 5CH_4 + SiH_4 \longrightarrow 2C_2H_6 + 2C_2H_4 + CH_3SiH_3 + CH_2{=}SiH_2 \qquad (7)$$

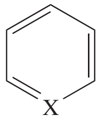

$$+ 3H_2C{=}CH_2 \longrightarrow$$

$$2\ \textit{trans}\text{-}H_2C{=}CH{-}CH{=}CH_2 + \textit{trans}\text{-}H_2C{=}XH{-}CH{=}CH_2 \qquad (8)$$

ASE (HF/6-31G*, kcal mol^{-1}): X = Si, 17.2[43b]; X = C, 24.8[45]

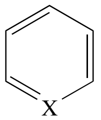

$$+ 3\ \textit{trans}\text{-}H_2C{=}CH{-}CH{=}CH_2 \longrightarrow$$

$$2\ \textit{trans}\text{-}H_2C{=}CH{-}CH{=}CH{-}CH{=}CH_2\ + \qquad (9)$$

$$\textit{trans}\text{-}H_2C{=}CH{-}XH{=}CH{-}CH{=}CH_2$$

ASE (HF/6-31G*, kcal mol^{-1}): X = Si, 17.6[43b]; X = C, 23.5[45]

The high degree of aromaticity of silabenzene suggested by the geometric and energetic criteria was supported in a recent paper by its high NICS value of −9.1 (GIAO-HF/6-31+G*//B3LYP/6-311+G**), which is almost as high as that of benzene (−9.7)[8].

Schleyer and coworkers[40] studied in detail the energetic relationships between silabenzene **8** and four of its isomers, **13–16**. However, as this study is quite old, the calculated relative energies of **8** and **13–16**, which have been calculated only at HF/3-21G(*)//HF/STO-3G, are probably only approximate and higher level calculations are required for a more reliable estimate of these relative energies.

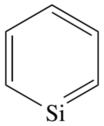

(8)

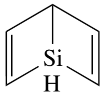

(13)

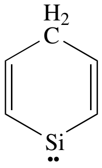

(14)

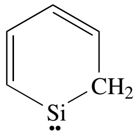

(15)

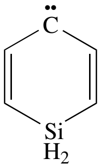

(16)

According to the HF/3-21G(*)//HF/STO-3G calculations the silylene isomers of silabenzene, **14** and **15**, are 20–25 kcal mol^{-1} higher in energy than **8**. The carbene isomer, **16**, which is a ground-state triplet, lies about 60 kcal mol^{-1} above silabenzene. The **8–14** (or **8–15**) energy difference is much smaller than that between the analogous isomers of benzene, reflecting the preference of silicon to adopt divalent structures instead of forming multiple bonds (e.g. $H_3C\ddot{Si}H$ and $H_2C{=}SiH_2$ have almost the same energy[46a] while ethylene is by *ca* 80 kcal mol^{-1} more stable than $CH_3\ddot{C}H$[46b]). The 20–25 kcal mol^{-1} energy difference between **8** and **14** can be taken as yet another measure of the degree of aromaticity of silabenzene. Dewar silabenzene **13** is by 38 kcal mol^{-1} less stable than silabenzene. This value is expected to be reduced at higher levels of theory[40] but even this value is much smaller than the corresponding energy difference of 60 kcal mol^{-1} (experimental) between benzene and Dewar benzene.

In summary, all the calculations find silabenzene to be highly aromatic. However, in view of the relatively basic level of theory which was used in most of the available studies, it is highly desirable to repeat the calculations for this fundamentally important molecule using more reliable levels of theory.

2. Substituted silabenzenes

An extensive systematic study of 48 substituted silabenzenes was carried out by Baldridge and Gordon[41b]. Twelve substituents, namely F, Cl, OH, SH, OCH_3, NH_2, PH_2, CH_3, SiH_3, CN, NO_2 and COOH, were attached to the four unique positions of silabenzene, i.e. at the silicon, and at the *ortho*, *meta* and *para* positions (cf **17**). The analogous substituted benzenes were studied for comparison[41b]. The questions studied included the relative energies of the isomers, the degree of aromaticity, the electron density distributions and the dipole moments. Although the calculations used a relatively simple level of theory (in general HF/3-21G//HF/STO-2G, and in some cases HF/3-21G(*)//HF/STO-2G), the qualitative conclusions will probably hold also when better calculations become available (which is highly desirable). A summary of the major findings is given below.

Of the four possible isomers, substitution at silicon produces the most stable isomer (except for COOH), as shown in Table 1. The authors concluded that 'the degree of stability

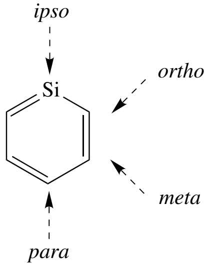

(17)

appears to be a reflection of the electronegativity of the substituent; i.e. the more electronegative the substituent, the more stable the silicon-substituted species relative to the other isomers'[41b]. However, examination of Table 1 seems not to support this conclusion, e.g. for the highly electronegative NO_2 or CN substituents the energy difference between the *ipso* and the other isomers is much smaller than for the significantly less electronegative SH or NH_2 substituents (Table 1). Apparently π-effects also play an important role. A full analysis as well as better calculations of the energy differences between the isomers are still lacking. The relation between the stability of Si- and C-substituted silenes and the electronegativity of the substituent was discussed earlier by Apeloig and Karni[47]. According to Baldridge and Gordon[41b] the relative stability of the *ortho*-, *meta*- and *para*-isomers appears to be controlled by the effect of the substituent on the charge density at silicon, favouring positions in which the substituent directs electron density away from the silicon. Thus, the *meta*-substituted isomer is the most stable (after the *ipso*-substituted isomer) when the substituents are *ortho* and *para* directing (i.e. directing electron density away from the Si). Similarly, the *ortho*-substituted species is the most stable for *meta*-directing substituents (except for NO_2 and SH) (Table 1).

TABLE 1. Relative energies (HF/3-21G//HF/STO-2G, kcal mol^{-1}) of the four isomers of several substituted silabenzenes (see **17**) and the directing effects of the substituents[a]

Substituent	Relative energies position of substitution				Directing effect[b]
	ipso	*ortho*	*meta*	*para*	
F	0.0	45.2	35.2	38.1	*o*, *p*
Cl	0.0	33.8	31.9	32.6	*o*, *p*
OH	0.0	38.8	29.1	33.6	*o*, *p*
SH	0.0	24.0	22.3	24.3	*m*
NH_2	0.0	31.7	27.3	28.6	*o*, *p*
PH_2	0.0	11.7	13.3	12.9	*m*
CN	0.0	8.6	12.9	10.2	*m*
NO_2	0.0	6.9	10.7	6.4	*m*
CH_3	0.0	14.0	13.0	14.2	*o*, *p*
SiH_4	0.0	2.3	6.2	5.6	*m*
OCH_3	0.0	35.2	29.4	32.7	*o*, *p*
COOH	0.0	−7.0	−2.3	−6.4	*m*

[a] From Reference 41b.

[b] As predicted by electron density difference plots (see text). *o*,*p* = *ortho*- and *para*-directing (relative to silicon); *m* = *meta*-directing (relative to silicon).

The π-directing effects of the substituents were determined from density difference plots, constructed by subtracting the electron density of silabenzene (or benzene) from that of the substituted silabenzene (or benzene). From such density difference plots Baldridge and Gordon concluded that all the substituents studied have the same qualitative directing effects in silabenzene and in benzene (see Table 1)[41b]. It should be pointed out, however, that charge distributions are not always a reliable guide for predicting the substitution site in electrophilic reactions. In principle, the relative energies of the appropriate intermediates should be used for such predictions and such calculations are not yet available. A general feature of all the electron density difference plots is the lack of any negative charge build-up on silicon, regardless of whether the particular substituent is *ortho*-, *para*- or *meta*-directing. Silicon, which is the least electronegative atom in the molecules considered, prefers to remain positive.

The effect of *ipso*-substitution on the stability of the silabenzene was evaluated by equation 10,[41b] which compares the effects of the substituent X in the aromatic system with that in H_3SiX (we think that a comparison with $H_2C{=}SiHX$ would have been a better choice). The results presented in Table 2[41b] show that F, Cl, SH, NO_2 and CN

TABLE 2. Calculated substituent effects on the thermodynamic stability, ΔE (in kcal mol^{-1}), of *ipso*-substituted silabenzenes and of substituted benzenes (HF/3-21G)[a]

Substituent X	Conformation	$\Delta E^{b,c}$ silabenzenes	$\Delta E^{c,d}$ benzenes
F		−1.2	12.9
Cl		−2.3	3.5
OH	planar[e]	−1.5	12.3
	orthogonal[f]	1.9	10.1
OCH_3	planar[e]	−0.8	12.5
	orthogonal[f]	1.4	11.0
SH	planar[e]	−1.0	2.7
	orthogonal[f]	−0.1	4.4
NH_2	pyramidal (1)[g]	3.0	5.8
	pyramidal (2)[h]	1.3	9.2
	planar[e]	10.4	—
PH_2	pyramidal (1)[g]	1.9	3.3
	pyramidal (2)[h]	3.5	4.0
	planar[e]	−18.5	—
CN		−1.2	1.9
NO_2	planar	−4.6	7.4
CH_3		1.1	2.1
SiH_3		3.4	1.4
COOH	planar	13.1	11.3

[a] From Reference 41b.
[b] Calculated by equation 10.
[c] Positive values indicate stabilization.
[d] Calculated by the equation: $XC_6H_5 + CH_4 \rightarrow C_6H_6 + H_3CX$.
[e] $\angle$ HYSiC (or $\angle$ HYCC in benzene)[i] = 0°.
[f] $\angle$ HYSiC (or $\angle$HYCC in benzene)[i] = 90°.
[g] $\angle$ HYSiC (or $\angle$ HYCC in benzene)[i] = 60°.
[h] $\angle$ HYSiC (or $\angle$ HYCC in benzene)[i] = 150°.
[i] Y is the atom in group X directly bonded to the ring.

destabilize the silabenzene (or alternatively, stabilize H_3SiX more than the ring) while the other substituents slightly stabilize the ring. Relatively large stabilizing effects are found for X=COOH and planar NH_2. In general, the energies of equation 10 are similar to those calculated for the analogous substitutions in $H_2C{=}SiHX$[47]. The same substituents in benzene are always stabilizing but their effects are generally much larger than for the silabenzenes. This reflects the smaller conjugating ability of silabenzene relative to benzene[41b].

$$ipso\text{-}XSiC_5H_5 + SiH_4 \longrightarrow C_5H_6Si\ (\mathbf{8}) + H_3SiX \qquad (10)$$

C. Silanaphthalenes

The recent synthesis and spectroscopic characterization of the crystalline, stable 2-silanaphthalene **1**, was accompanied by density-functional calculations of the geometries, the NICS values and the NMR chemical shifts of three isomeric silanaphthalenes **18**, **19a** and **20**[8] and two substituted 2-silanaphthalenes **19b** and **19c** (Table 3), of which **19c** is the closest model for **1**. The reliability of the calculations is demonstrated by their ability to reproduce the experimental Raman and NMR spectra of **1**. Thus, the strongest observed Raman shifts for **1** (at 1368 cm^{-1}) and for naphthalene (1382 cm^{-1}) are in good agreement with the calculated (B3LYP/6-31G*, scaled by 0.98) vibrational frequencies for **19a** (1377 cm^{-1}), for **19c** (1378 cm^{-1}) and for naphthalene (1389 cm^{-1}).

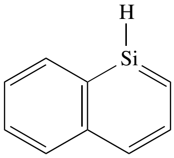

(18)

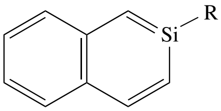

(19a) R = H
(19b) R = Me
(19c) R = Ph

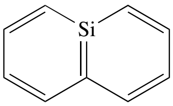

(20)

The computational results point to an aromatic character of the silanaphthalenes **18–20**. The chemical shifts which were observed for **1** are similar to those calculated for **19a–c** (Table 3). The observed (in **1**) and calculated (for **19a–c**) $\delta(^{29}Si)$ and $\delta(^{13}C)$ chemical shifts are similar to those previously reported for other sp^2-hybridized Si and C atoms[3a,8]. All the ^1H NMR signals are, as expected, in the aromatic region (Table 3). The highly negative NICS values calculated for **18**, **19a** and **20** (Figure 3), which are very similar to those of benzene, also indicate that all the calculated silanaphthalenes (**18–20**) are aromatic.

TABLE 3. Calculated ^1H, ^{13}C and ^{29}Si NMR chemical shifts[a] for **19a**, **19b** and **19c** and the experimental values measured for **1**

	$\delta(^1H)$			$\delta(^{13}C)$			$\delta(^{29}Si)$
	$H_{(1)}$	$H_{(3)}$	$H_{(4)}$	$C_{(1)}$	$C_{(3)}$	$C_{(4)}$	$Si_{(2)}$
19a	7.74	7.27	8.64	128.45	125.13	153.38	67.80
19b	6.97	7.03	8.50	120.43	122.68	153.26	100.97
19c	7.32	7.08	8.55	121.63	123.56	152.45	94.32
1	7.40	7.24	8.48	116.01	122.56	148.95	87.35

[a] In ppm, calculated with GIAO-B3LYP/6-311G(3d) for Si and GIAO-B3LYP/6-311G* for C and H, at the B3LYP/6-31G* optimized geometries, the atom numbering is defined in Figure 3; from Reference 8.

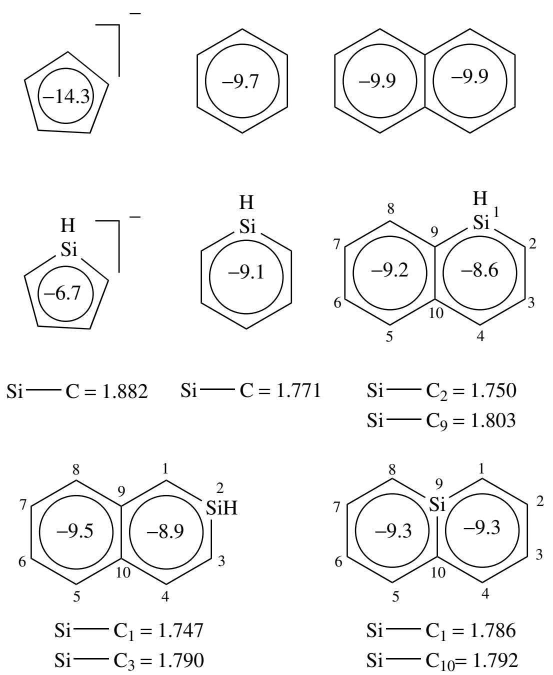

FIGURE 3. Calculated NICS values (ppm) at the ring centres for silanaphthalenes **18**, **19a**, **20** and related aromatic systems, at GIAO-SCF/6-31+G*. The optimized Si−C bond lengths (Å) are at B3LYP/6-311+G**. Reprinted with permission from Reference 8. Copyright (1997). American Chemical Society

The calculated Si−C bond lengths (B3LYP/6-311+G*, Figure 3) also suggest the occurrence of a π-electron delocalization in the three isomeric silanaphthalenes[8]. Thus, for **18**: $r(\text{Si}-\text{C}_{(2)}) = 1.750$ Å and $r(\text{Si}-\text{C}_{(9)}) = 1.803$ Å; for **19a**: $r(\text{Si}-\text{C}_{(1)}) = 1.747$ Å (exp. in **1**: 1.704 Å); and $r(\text{Si}-\text{C}_{(3)}) = 1.790$ Å (exp. in **1**: 1.765 Å); for **20**: $r(\text{Si}-\text{C}_{(1)}) = 1.786$ Å and $r(\text{Si}-\text{C}_{(10)}) = 1.792$ Å, compared to 1.771 Å in silabenzene, 1.708 Å in $H_2Si{=}CH_2$ and 1.885 Å in H_3SiCH_3. (Note that the reported experimental Si−C bond lengths in **1** are considerably shorter that the calculated values for **19a**. However, the authors comment that the reported structure of **1** is preliminary, as the naphthalene ring in **1** is severely disordered.) The calculated vibrational modes of **19a** and **19c** are similar to those of naphthalene, also suggesting that the 2-silanaphthalene **(1)** possesses a significant aromatic character[8].

Unfortunately, the relative energies of the 3 isomeric silanaphthalenes **18**, **19a** and **20** were not reported[8].

D. Disilabenzenes

1. Geometry and the degree of aromatic stabilization

Of the three possible disilabenzene isomers, *ortho*-**21**, *meta*-**22** and *para*-**11**, only **11** is known experimentally and was observed in a matrix[36]. The published calculations on disilabenzenes are all at relatively low levels of theory (i.e. they used a relatively small basis set and electron correlation was not included), except for unpublished density functional, B3LYP/3-21G*, calculations by Apeloig and coworkers which are reported below[48]. Schaefer and coworkers found, in a study of 1,3,5-trisilabenzene, that upon the addition of a set of d-orbitals to the basis set (especially important for Si) the Si−C bond lengths are contracted dramatically[49] (see Section III.E). This shows that results of calculations which use small basis sets (e.g. HF/STO-2G or HF/STO-3G) should be treated with caution. Unfortunately, there is very little experimental data[36] that can be compared with the calculations for **11**. Experimental UV and IR absorptions of **11** were reported, but unfortunately related computational results which might help to assess the reliability of the computational studies were not reported.

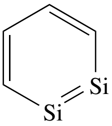

(21)

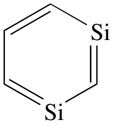

(22)

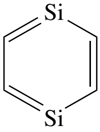

(11)

Density functional B3LYP/3-21G*[48] (as well as HF/STO-2G[50a]) calculations show that the three disilabenzene isomers have planar geometries. The fact that *ortho*-disilabenzene is planar whereas disilene is slightly non-planar may indicate some electron delocalization in **21** which stabilizes the planar Si=Si moiety. The calculated geometries of the disilabenzenes at B3LYP/3-21G* (shown in Figure 2b–d) reveal that the bond lengths, including the bonds to silicon, are intermediate between single and double bond lengths, reflecting electron delocalization and aromaticity[48].

meta-Disilabenzene **(22)** is the most stable disilabenzene. The other isomers **21** and **11** are by 6.1 kcal mol^{-1} and 11.1 kcal mol^{-1}, respectively (at B3LYP/3-21G*//B3LYP/3-21G*), less stable. At HF/3-21G//HF/STO-2G the relative energies are: **22** (0.0) $>$ **21** (2.0) $>$ **11** (10.8)[50a]. Baldridge and Gordon suggested that the relative stabilities of the disilabenzenes may be rationalized by considering the contributing ionic Kekulé structures in the three isomers. Thus, only for the *meta*-isomer **22** do all contributing structures (e.g. **22a**) have a formal positive charge on silicon, while for **11** and **21** the undesirable resonance structures with negative charge on silicon are also possible (e.g. **11a** and **21a**)[50a]. We believe that other factors, such as the relative energies of C=Si vs Si=Si bonds, might be more important than these charge effects, and a high-level computational study of these interesting molecules is highly desirable.

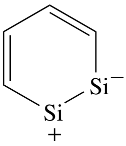

(21a)

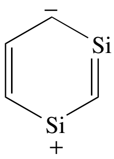

(22a)

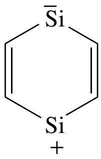

(11a)

Using the appropriate bond-separation reactions, the HF/3-21G aromatic stabilization energies are calculated to be 47.2, 36.4 and 22.5 kcal mol^{-1} for **22**, **11** and **21**, respectively, compared to 59.0 kcal mol^{-1} for benzene[50a]; thus the *meta*-, *para*- and *ortho*-isomers have 80, 62 and 38% of the aromaticity of benzene. The different orders of the thermodynamic stability of the three isomeric disilabenzene and of their aromatic stabilization energies result from the different reference compounds in the bond separation equations for **21**, **22** and **11**. Thus, the aromatic stabilization of **21** is calculated relative to disilene + ethylene, while the aromatic stabilizations of **22** and **11** are calculated relative to two molecules of silaethylene[50a].

The molecular orbitals (MOs) of the disilabenezenes shown in Figure 4 are also of interest. In all three isomers, the highest lying MO (HOMO) has the largest silicon contribution. In **21** and **11** this orbital is strongly polarized toward the silicons, while in **22** the HOMO is more delocalized[50a].

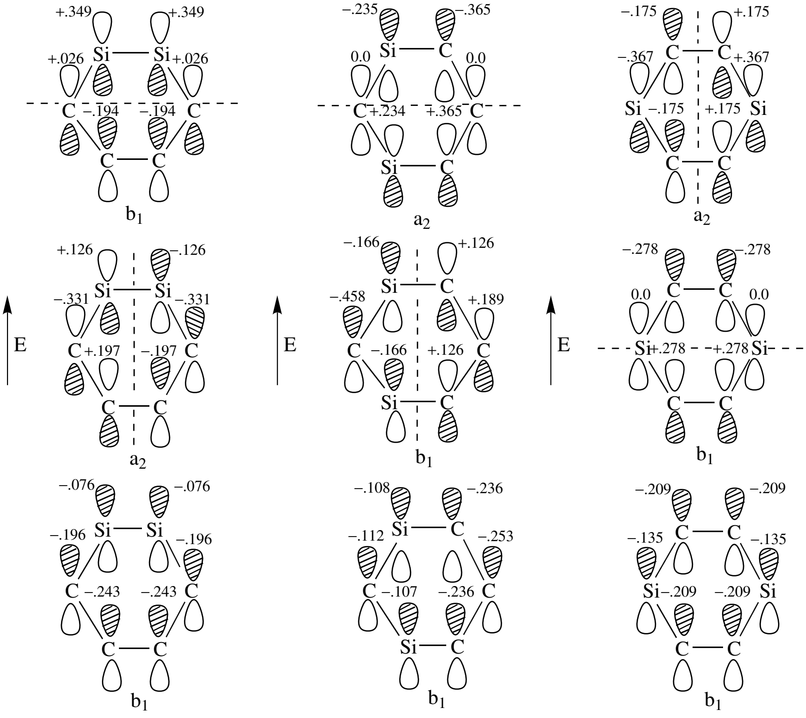

FIGURE 4. The π-molecular orbitals of disilabenzenes: (a) 1,2-disilabenzene (**21**); (b) 1,3-disilabenzene (**22**); (c) 1,4-disilabenzene (**11**). The orbital coefficients given are of the outer valence π-atomic orbitals (at HF/3-21G). Reproduced by permission of Elsevier Sequoia S.A., from Reference 50a

2. Relation to isomers

Comparison of the energy of *para*-disilabenzene **(11)** with that of the isomeric Dewar disilabenzene **(23)** and the silylenes **24** and **25** follows the trends discussed above for the isomers of silabenzene. At HF/3-21G(*)//HF/STO-3G the most stable isomer is the silylene **24**, which is more stable than **11** by 10 kcal mol^{-1}[50b]. The remarkable stability of the silylene **24** relative to **11** results mainly from the fact that C=C bonds are by at least 25 kcal mol^{-1} stronger than C=Si bonds, thus compensating for the loss of aromaticity in **24**, which is estimated to stabilize **11** by only 23 kcal mol^{-1}[50b]. The Dewar isomer **23** is by only 6 kcal mol^{-1} higher in energy than **11**[50b] (2.3 kcal mol^{-1} at HF/6-31G*[51a]). **25** is the highest in energy being by 21 kcal mol^{-1} (at HF/STO-3G, a HF/3-21G* value was not reported) less stable than **11**. When a larger basis set is used and the contribution of electron correlation is taken into account, ΔE **(23–11)** increases to 10.0 kcal mol^{-1} at CCSD(T)/6-31G**//MP2/6-31G** +ZPE (13.3 kcal mol^{-1} at MP2/6-31G**//MP2/6-31G** +ZPE and 14.4 kcal mol^{-1} at B3LYP/6-31G**//B3LYP/6-31G** +ZPE)[48]. The **23–11** energy difference is considerably smaller than the energy difference between Dewar silabenzene **(13)** and silabenzene (38 kcal mol^{-1} at HF/3-21G*//HF/STO-3G) and dramatically smaller than the calculated Dewar benzene–benzene energy difference of 81.1 kcal mol^{-1} (at MP2/6-31G**//MP2/6-31G**[52]). Two major factors are responsible for the observed energy differences: (1) Ring strain decreases in the order: Dewar benzene > Dewar silabenzene > Dewar disilabenzene, because silicon accommodates better than carbon smaller valence angles. (2) Successive replacement of unsaturated carbon centres by silicon destabilizes the planar 'aromatic' structure. Experimentally, it was observed that irradiation at $\lambda = 405$ nm of the matrix-isolated 1,4-disilabenzene caused its disappearance, probably yielding Dewar disilabenzene[36]. Most recently Ando has isolated and characterized spectroscopically a substituted Dewar benzene (having Me groups at Si and $SiMe_3$ groups at the carbon atoms)[51b].

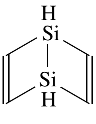

(23)

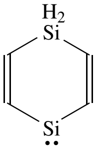

(24)

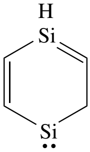

(25)

Ando and coworkers have very recently isolated a bis(silacyclopropene) **26a**, a valence isomer of a substituted *para*-disilabenzene, and have shown that its thermolysis in benzene afforded the corresponding stable crystalline disilabenzvalene **27a**, yet another substituted valence isomer of *para*-disilabenzene[51a]. It was suggested that the isomerization of **26a** to **27a** could proceed via the initial formation of the corresponding Dewar disilabenzene, or *para*-disilabenzene, or the silylenic isomer **28a**. At HF/6-31G* the calculated relative thermodynamic stabilities (kcal mol^{-1}) of the valence isomers of **11** considered here are: **11** (0) > **23** (2.3) > **27b** (8.5) > **26b** (32.7) > **28b** (36.3)[51a]. It was suggested that since large basis sets and inclusion of electron correlation tend to favour tricyclic over bicyclic or monocyclic structures, **27b**, **23** and **11** may actually have similar energies (and even the stability order may be reversed)[51a]. The possible reaction paths connecting these isomers were not studied, and concrete conclusions about the mechanism of the rearrangement of **26a** to **27a** were not given.

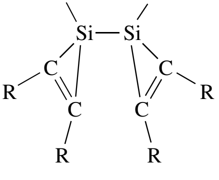

(26a) R = $SiMe_3$; R′ = Ph
(26b) R = R′ = H

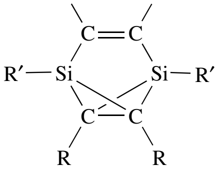

(27a) R = $SiMe_3$; R′ = Ph
(27b) R = R′ = H

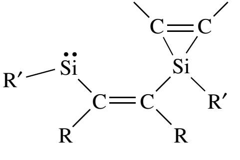

(28a) R = $SiMe_3$; R′ = Ph
(28b) R = R′ = H

E. Trisilabenzenes

1. Geometry and the degree of aromaticity

The D_{3h} 1,3,5-trisilabenzene **12** (TSB) was studied by Gordon and coworkers[53], who used effective core potentials[54] and a polarized basis set for geometry optimizations, and more recently by Schaefer and coworkers at HF/TZ2P and at CCSD(T)/DZP//CISD/DZP[49] and by Apeloig and Hrusàk at MP2/6-31G**[55]. The planar D_{3h} geometry is a minimum on the PES at all these levels of theory. The optimized C=Si bond length of 1.754–1.759 Å (1.755 Å at HF/DZP; 1.754 Å at CISD/DZP[49]; 1.759 Å at MP2/6-31G**[55]), which is intermediate between those of typical C=Si (1.70 Å) and C−Si (1.87 Å) bond lengths, and the CSiC and SiCSi bond angles of 120.5° and 119.5° (CISD/DZP[49]), respectively, are indicative of an aromatic system. It was found that the inclusion of polarization functions in the basis set is crucial for obtaining a reliable geometry[49]. The calculated r(C=Si) is shortened significantly when going from a DZ basis set (1.778 Å) to a DZP basis set (1.755 Å), while the change on going to the larger TZ2P basis set is relatively small (1.750 Å). The HF/DZP Si=C bond length remains almost unchanged upon inclusion of electron correlation (i.e. 1.754 Å at CISD/DZP). From these calculations one can conclude that earlier calculations of various silabenzenes[40,41b,50] which used small non-polarized basis sets (e.g. HF/STO-3G, HF/3-21G) produced unreliable geometries. The DZ basis set also seriously underestimates the spatial extent of electron delocalization in **12**; upon the addition of a set of d-orbitals (especially on Si) the orbital overlap and electron delocalization increase dramatically, contracting the Si−C bond length[49].

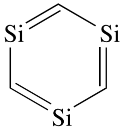

(12)

The calculated resonance energies (RE) of **12** (equation 11) and of benzene (equation 2) are 53.1 kcal mol^{-1} and 63.8 kcal mol^{-1}, respectively (at CCSD(T)/DZP//CISD/DZP), indicating that **12** has 83% of the aromaticity of benzene[49]. Similar results were obtained with lower levels of theory[53a], but this is probably fortuitous. The addition of polarization functions changes the **12**/benzene RE ratio from 84% at DZ to 99% at DZP, while electron correlation acts in the opposite direction, decreasing the above ratio to 83%[49]. The existence of aromatic stabilization in **12** can also be concluded from the large difference of 27 kcal mol^{-1} (MP2/6-31G**//MP2/6-31G**) in the stability of the Si=C double bonds in the aromatic 1,3,5-trisilabenzene and the non-aromatic 1,3,5-silacyclohexadiene; i.e. $\Delta E = -35.3$ and 8.5 kcal mol^{-1} for equations 12 and 13, respectively[55]. The calculated π-atomic populations and π-bond-orders point to a similar degree of aromaticity in C_6H_6, $C_3Si_3H_6$ and Si_6H_6[53a].

$$\mathbf{12} + 3CH_4 + 3SiH_4 \longrightarrow 3H_3SiCH_3 + 3H_2C{=}SiH_2 \tag{11}$$

$$\mathbf{12} + H_3CSiH_3 \longrightarrow H_2C{=}SiH_2 + c\text{-}C_3Si_3H_8 \tag{12}$$

$$c\text{-}C_3Si_3H_8 + H_3CSiH_3 \longrightarrow H_2C{=}SiH_2 + c\text{-}C_3Si_3H_{10} \tag{13}$$

2. Relation to isomers

Schaefer and coworkers[49] have also studied the relative stability of 1,3,5-trisilabenzene **(12)** and its isomeric 1,3,5-trisilylene **29**. Both isomers are possible products of the triple dehydrogenation reaction of 1,3,5-trisilacyclohexane[37]. Two minima were located for **29**: one having a chair conformation **(29a)** and one having a boat conformation **(29b)**, the latter being by 1.5 kcal mol^{-1} higher in energy. The trisilylene **29a**, is by 35.0 kcal mol^{-1} less stable than the aromatic **12** [CCSD(T)/DZP//CISD/DZP][49]. A third isomer, the trisilaprismane **30**, is by 35.3 kcal mol^{-1} higher in energy than **12** (MP2/6-311G**//HF/effective core potentials)[53b]. These computational results may be taken as partial support for the claim by Bjarnason and Arnason that 1,3,5-trisilabenzene is formed in the triple dehydrogenation reaction of 1,3,5-trisilacyclohexane in the gas phase[37], but additional experimental and theoretical studies are required to support more firmly the intermediacy of **12** in this reaction.

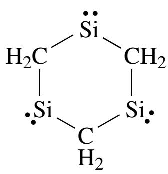

(29)

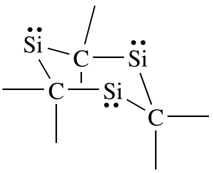

(29a)

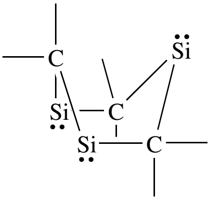

(29b)

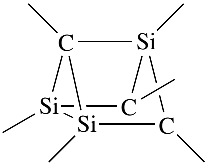

(30)

F. Hexasilabenzenes

1. The parent hexasilabenzene

a. Geometry and the degree of aromaticity. Hexasilabenzene **(31)**, being a complete silicon analogue of benzene, has attracted considerable theoretical interest and as a result our knowledge about this fascinating molecule is quite extensive, although it has not yet been observed experimentally.

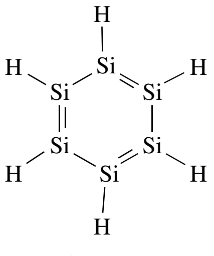

(31) D_{6h}

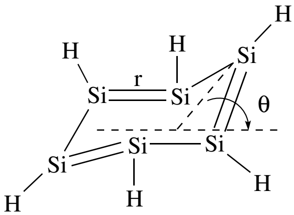

(32) D_{3d}

Is Si_6H_6 a planar D_{6h} molecule analogous to benzene? The answer varies between the D_{6h} structure **(31)** and the D_{3d} structure **(32)**, depending on the theoretical method used[19,52,56–61]. The calculated optimized geometries of the D_{6h} and D_{3d} structures of Si_6H_6 at various theoretical levels are shown in Figure 5. While early HF/3-21G calculations found Si_6H_6 to have D_{6h} symmetry with r(Si–Si) equal to 2.220 Å[56], this is not the case at higher levels of theory[19,52,58–61]. Thus when d-functions are added to

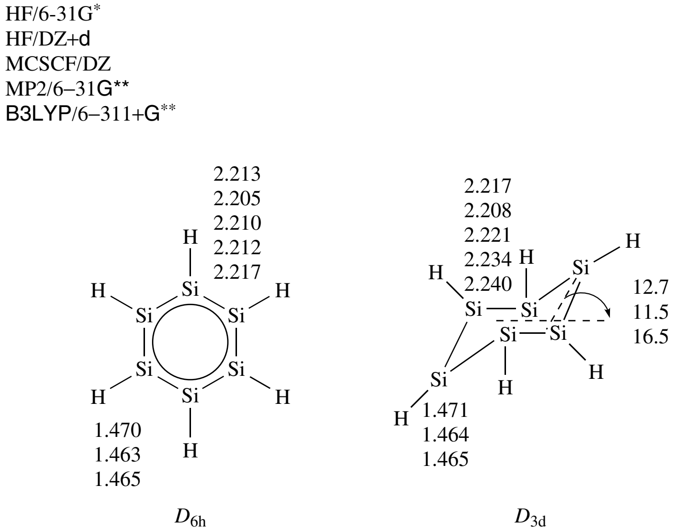

FIGURE 5. Optimized structures of D_{6h} and D_{3d} Si_6H_6 at (from top to bottom): HF/6-31G*, HF/DZ+d, MCSCF/DZ, MP2/6-31G** and B3LYP/6-311+G**. The D_{6h} values and the D_{3d} MCSCF/DZ values are from Reference 60, the D_{3d} HF values are from Reference 59. The MP2/6-31G** and B3LYP/6-311+G** Si−Si bond lengths for both structures are from References 52 and 19, respectively

the basis set the planar D_{6h} structure becomes a maximum on the Si_6H_6 potential energy surface[59]. Full geometry optimization at HF/6-31G* (or at HF/6-31G** or at HF/DZ+d) leads to a minimum which is a chair-like puckered structure of D_{3d} symmetry **(32)** with equal Si−Si (2.218 Å at HF/6-31G**) and Si−H (1.471 Å) bond lengths[59]. The deviation from planarity is, however, relatively small ($\theta = 13.5°$ at HF/6-31G**[59]), as is the gain in energy (0.6 kcal mol^{-1}[59] at HF/6-31G**). However, the use of more extended basis sets [including double sets of d-functions (HF/6-31++G(2d,p)] or a set of f-functions on Si [HF/6-31G(df,p)] reverses the relative stability of the two structures and the D_{3d} minimum disappears, leaving the D_{6h} structure as a minimum[59]. On the other hand, the addition of electron correlation makes the Si_6H_6 potential energy surface less flat, and leads again to a greater preference of the D_{3d} puckered structure over the D_{6h} planar structure [$\Delta E = 2.3$ kcal mol^{-1} at B3LYP/6-311+G**//B3LYP/6-311+G**[19]; 4.3 kcal mol^{-1} at MP2/6-31G**//MP2/6-31G**[52]; 4.8 kcal mol^{-1} at MCSCF/DZ[60]; 3.0 kcal mol^{-1} at MP2/6-31G**//HF/ECP(d)[53b]; 7.05 kcal mol^{-1} at MP2/6-31G*//6-31G*[59]] whilst the deviation from planarity increases [$\theta = 16.5°$ and 19.0° at MCSCF/ZD[60] and MP2/6-31G**//HF/ECP(d)[53b], respectively]. The most reliable results available to date[19,53b,59–61] conclude that *hexasilabenzene adopts a chair-like puckered structure of* D_{3d} *symmetry* (with equal Si−Si and Si−H bonds). The preference of the D_{3d} structure over the D_{6h} structure was explained by Nagase in terms of atom localization of the π-electrons onto each Si, generating a radical character at each silicon atom, and as silyl radicals (in contrast to methyl radicals) have strongly pyramidal structures Si_6H_6 prefers the puckered structure[61a]. On the other hand, a detailed analysis by Janoschek and coworkers shows that the propensity to puckering is due solely to contributions of electron correlation from the σ-framework while correlation of the π-electrons is of little relevance[60]. It is interesting to note that at all computational levels the Si−Si bond distances in the D_{6h}

and D_{3d} structures are quite similar being always intermediate in length between regular Si=Si (2.15 Å) and Si−Si (2.35 Å) bond lengths, indicating the existence of electron delocalization.

Another important question is the degree of aromatic stabilization in the planar hexasilabenzene. Using the appropriate bond-separation reactions, hexasilabenzene, **31** is calculated to possess *ca* 50–80% of the aromatic stabilization energy of benzene[19,53a,56,58,62] depending on the theoretical method or the equations used. The aromatic stabilization energies calculated according to equations 14a and 14b for benzene and Si_6H_6 **(31)**, predict that **31** has 50–60% of the aromaticity of benzene; i.e. the ASE of **31** and benzene are 15.1 and 24.7 kcal mol^{-1}, respectively (at MP2/6-31G**//MP2/6-31G**[52]), according to equation 14a and 15.6 kcal mol^{-1} and 34.1 kcal mol^{-1}, respectively, according to equation 14b (at B3LYP/6-311+G**//B3LYP/6-311+G**)[19]. The ASE of the D_{3d} non-planar structure **(32)** is by 2.3 kcal mol^{-1} larger than for **31** because of the reduced strain in **32** relative to **31**[19]. The resonance energies (RE) calculated for C_6H_6 and Si_6H_6 (according to equation 15) predict that Si_6H_6 possesses 77% of the aromaticity of benzene, i.e. RE = 57.8 and 74.7 kcal mol^{-1}, respectively [at MP2/6-31G**//HF/ECP(d)][53a]. The significant degree of aromaticity of hexasilabenzene suggested by the structural and energetic criteria is supported also by the magnetic criteria. Thus, the calculated (CSGT-B3LYP/6-311+G**//B3LYP/6-311+G**) π-contributions to the chemical shifts [based on NICS(π) values] decrease from −16.8 ppm for benzene to −14.1 ppm for **31**, a result consistent with a relatively large π-electron delocalization in Si_6H_6 **(31)**[19]. The computed magnetic susceptibility exaltations (Λ) are larger for **31** (and **32**) than for benzene. However, Λ depends on the ring size, which is larger in Si_6H_6 than in benzene. Using the ring-size-adjusted aromaticity index ρ (see equation 6 in Section II.C.1), it was deduced that **31** possesses 37% of the aromaticity of benzene[19]. A similar degree of aromaticity was deduced for Ge_6H_6 according to its ASE and magnetic criteria[19].

$$X_6H_6 + 3H_2X{=}XH_2 \longrightarrow 3\ \textit{trans}\text{-}H_2X{=}XH{-}XH{=}XH_2 \qquad X = C; Si \qquad (14a)$$

$$X_6H_6 + 3H_2X{=}XH_2 \longrightarrow 3\ \textit{cis}\text{-}H_2X{=}XH{-}XH{=}XH_2 \qquad X = C; Si \qquad (14b)$$

$$X_6H_6 + 6XH_4 \longrightarrow 3H_2X{=}XH_2 + 3H_3X{-}XH_3 \qquad X = C; Si \qquad (15)$$

In the context of the question of the aromaticity of Si_6H_6, special attention should be paid to the recent studies by Shaik and coworkers[15]. Using VB crossing diagrams and MO calculations that separate the energetic effects of the σ- and π-electrons on the distortion (localization) of a conjugated system from a fully symmetric delocalized structure (i.e. ΔE_σ and ΔE_π, respectively), they reached the following conclusions:

(a) The geometry is *not* a proper measure of aromaticity. The tendency to adopt a symmetric or a distorted geometry is the result of the balance between two opposite driving forces: that of the σ-skeleton which by nature is always symmetrizing, and that of the π-electrons which favour localized structures; i.e. if $\Delta E_\pi + \Delta E_\sigma > 0$, the structure is dictated by the symmetric σ-skeleton and it is delocalized. The localizing propensity of the π-electrons is dependent on the singlet–triplet energy gap of the π-bond and consequently on its strength. For second-row elements both the π-distortion propensity and the σ-resistance to distortion are weaker than for first-row elements, but the former is weakened proportionally more. Thus, for Si_6H_6, ΔE_σ = 5.3 kcal mol^{-1} (16.3 kcal mol^{-1} for C_6H_6) and ΔE_π = −2.4 kcal mol^{-1} (−9.7 kcal mol^{-1} for benzene), resulting in a net positive $\Delta E_\pi + \Delta E_\sigma$. Consequently, second-row atoms generate less distortive π-systems than first-row atoms, and therefore Si_6H_6 would tend to maintain its D_{6h} symmetry more than benzene. However, the high stability of σ-bonds relative to π-bonds in second-row elements drives Si_6H_6 towards non-planar structures, e.g. the more stable hexasilaprismane (see below)[15c].

(b) The Quantum Molecular Resonance Energy (QMRE), that is the resonance interaction between the Kékule forms at the symmetric geometry, is an energetic measure of the degree of aromaticity of a cyclic π-system. QMRE is related to measured thermochemical properties, e.g. resonance energy (RE). The calculated QMRE of planar Si_6H_6 is about half of that of C_6H_6 (41.6 kcal mol^{-1} vs 85.2 kcal mol^{-1}, respectively, at HF/6-31G)[15b,c] reflecting the difference in the aromaticity between hexasilabenzene and benzene. Hence the degree of aromaticity of Si_6H_6, which according to VB theory is *ca* 50% of that of benzene, is similar to that deduced on the basis of MO theory.

The HOMO of hexasilabenzene is by *ca* 2 eV higher than in benzene, while the HOMO–LUMO gap is much smaller in **31** than in benzene[60]. This suggest that hexasilabenzene should be more reactive than benzene towards both electrophiles and nucleophiles.

b. Relation to isomers. In addition to the structural isomers of hexasilabenzene itself (i.e. **31** and **32**) discussed above, 5 additional Si_6H_6 isomers, **33** –**37**, were located on the PES at various theoretical levels[52,56,58,60]. Of these isomers the D_{6h} hexasilabenzene **(31)**, the Dewar hexasilabenzene **(34a)** and the hexasilabenzvalene **(35a)** are not minima on the MP2/6-31G** PES[52] (the highest available level of calculation for this problem); **34a**[52,60] and **35a**[52] are, however, minima on the HF PES. The calculated relative energies of these isomers and of the analogous C_6H_6 isomers are given in Table 4 and are also shown graphically in Figure 6a.

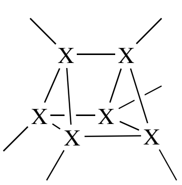

(33a) X = Si
(33b) X = C

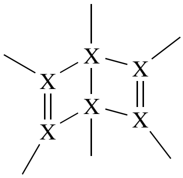

(34a) X = Si
(34b) X = C

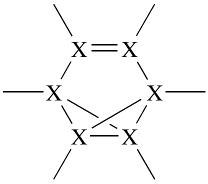

(35a) X = Si
(35b) X = C

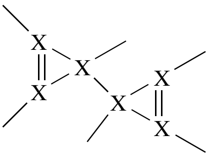

(36a) X = Si
(36b) X = C

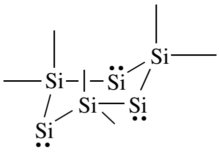

(37)

The most interesting conclusion from Table 4 and Figure 6a is that, contrary to the $(CH)_6$ series where benzene is by far the most stable isomer, hexasilabenzene is not the most stable isomer on the PES. The most stable Si_6H_6 isomer is the hexasilaprismane, **33a**. In general, the energy spacing between the X_6H_6 isomers is much larger for X = C (ranging over *ca* 120 kcal mol^{-1}) than for X = Si where it ranges over *ca* 55 kcal mol^{-1} and five Si_6H_6 isomers have energies within 15 kcal mol^{-1} (Table 4, Figure 6a).

TABLE 4. Relative energies and strain energies ($kcal\,mol^{-1}$) of Si_6H_6 and the analogous C_6H_6 isomers[a]

Compound	Relative energies		Strain energies	
	Si_6H_6	C_6H_6	Si_6H_6	C_6H_6
31	11.9[b]	0.0[c]	−15.1[d]	−24.7[c,e]
32	7.6	*f*	*f*	*f*
33	0.0	117.5 (127.6[g])	110.0	148.9[h]
34	10.5[i]	81.0 (88.1[g])	26.2	63.6[h]
35	5.9[i]	74.8 (84.5[g])	68.7	81.3[h]
36	56.8	126.4	72.5	107.2[h]
37	43.4[j]	*f*	*f*	*f*

[a] From Reference 52 at MP2/6-31G**//MP2/6-31G**, unless stated otherwise.

[b] Not a minimum at the HF and the MP2 levels of theory.

[c] For benzene.

[d] ASE energies according to equation 14a, X = Si.

[e] ASE energies according to equation 14a, X = C.

[f] Not available.

[g] At HF/6-31G*//HF/3-21G, from Reference 58.

[h] At MP2/6-31G*//6-31G*, from Reference 63.

[i] Not a minimum at the MP2/6-31G** level, a minimum at HF.

[j] At CISDQ/TZP from Reference 60.

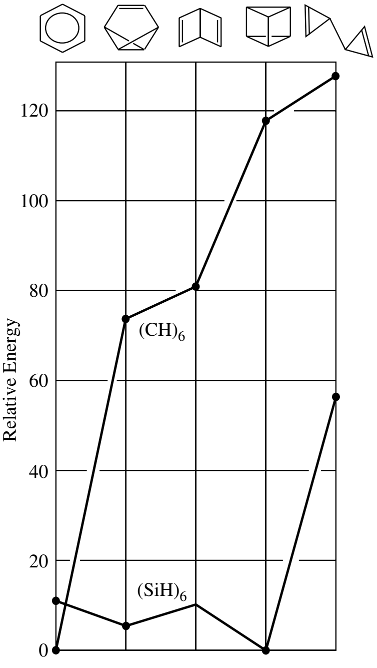

(a)

FIGURE 6. (a) Relative energies of $(XH)_6$ (X = Si, C) isomers; (b) relative energies of $(XH)_6$, X = Si, C, isomers, based on the bond additivity model (centre) and as stabilized by resonance or destabilized by strain (edges). All energies are in $kcal\,mol^{-1}$ calculated at MP2/6-31G**//MP2/6-31G**. Reprinted with permission from Reference 52. Copyright (1996) American Chemical Society

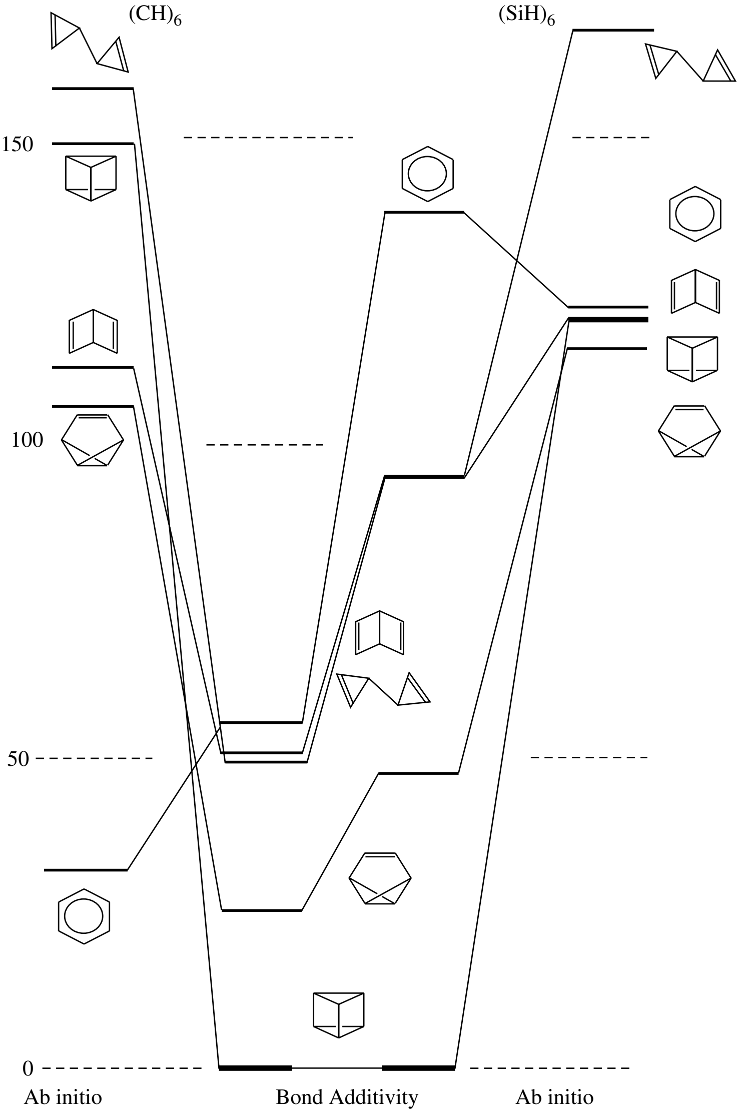

FIGURE 6. *(continued)*

D_{3d} hexasilabenzene **32** (which is by 4.3 kcal mol^{-1} more stable than D_{6h} **31**[52]) is by 7.6 kcal mol^{-1} *less stable* than hexasilaprismane **(33a)**[52]. In contrast, benzene is *more stable* than prismane **(33b)** by 117.5 kcal mol^{-1} (all values are at MP2/6-31G**//MP2/6-31G**)[52]. The aromatic **31** (and **32**) have a similar energy to that of hexasilabenzvalene **(35a).**

The reasons for the dramatic differences between the Si_6H_6 and C_6H_6 systems are already familiar to the reader (see the discussion above regarding silabenzene, and di- and tri-silabenzenes) and they are repeated and extended here. The energy of a Si=X (or C=X) bond is lower than twice the energy of the corresponding Si−X (or C−X) bond. However, these differences are much larger in silicon than in carbon compounds; e.g. the C−C and Si−Si dissociation energies in $H_3X{-}XH_3$ and $H_2X{=}XH_2$ are 86.8 and 176.8 kcal mol^{-1}, respectively, for X = C, and 70.1 and 59.8 kcal mol^{-1}, respectively, for X = Si[64]. This explains the higher preference of Si to be involved in σ-bonds rather than in π-bonds, and it is manifested in the order of stability of the Si_6H_6 isomers (Table 4): **33a** (most stable) > **35a** > **34a** (note that at MP2/6-31G** **34a** and **35a** are not minima on the PES), where the stability increases as the number of Si=Si double bonds decreases. The difference in ring strain between the C_6H_6 and Si_6H_6 isomers also contributes, but to a much smaller degree, i.e. hexasilaprismane **(33a)** is less strained than prismane **(33b)** by 39 kcal mol^{-1} (see Table 4). An interesting insight is provided when the effects of ring strain and resonance energy are subtracted from the relative energies of the Si_6H_6 and C_6H_6 isomers, leaving only the 'inherent differences' in their average single and double bond energies (i.e 'bond additivity model'[52]). The relative energies of the isomers calculated by this procedure are interpreted as given by the value of $m\bullet\Delta$ for a particular system, where m is the number of double bonds in the particular isomer and $\Delta = 2D(X{-}X) - D(X{=}X)$, i.e. the energy difference between two X−X single bonds and one X=X double bond. Using this procedure (the reader is referred to the original paper for a more detailed description) the following relative energies of the X_6H_6 isomers (X = C, Si) were calculated (kcal mol^{-1}, in descending stability order): **33** (0, X = C; Si) > **35** [24.9 (X = C); 47.1 (X = Si)] > **34** [48.8 (X = C); 94.3 (X = Si)] > **37** [(50.6 (X = C); 94.3 (X = Si)] > **31** [56.1 (X = C); 137.0 (X = Si)][52]. Figure 6b shows a schematic description of these relative 'inherent' energies and how they are changed when X_6H_6, X = C, Si, are stabilized by resonance or destabilized by strain. These results indicate that when the resonance stabilization, on the one hand, and the destabilization caused by strain, on the other, are removed from the total energies, the relative energies of the various X_6H_6 (X = Si, C) structures increase with the number of double bonds that they possess. The bond energy difference Δ for silicon is almost twice that for carbon, and as a result, according to the 'bond additivity model'[52] the relative energies of the $(SiH)_6$ isomers are spread out compared to the corresponding $(CH)_6$ isomers and hexasilaprismane becomes dramatically more stable than hexasilabenzene.

2. Substituted hexasilabenzenes

The effect of several substituents, i.e. R = F, CH_3, SiH_3 and BH_2, on the structure and the aromatic stabilization energies of R_6Si_6 (**31a** or **32a**) was studied by Nagase and the main results are summarized in Table 5[61a].

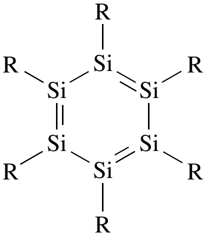

(31a)

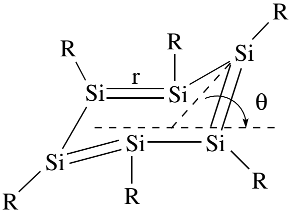

(32a)

TABLE 5. Substituent effects on the structure and aromatic stabilization energy (ASE) of Si_6R_6 (**31a** or **32a**)[a]

R	r(Si=Si) (Å)	$\theta^{\circ b}$	$\Delta E^{c,d}$	$\Delta E_{pyr}{}^{c,e}$	$\mathrm{ASE}^{c,f}$
H	2.231	12.7	−0.4	−2.6	11.8[g]
F	2.278	50.3	−14.4	−7.7	−8.7
CH_3	2.222	10.8	−0.2	−3.6	8.5
SiH_3	2.226	0.0	*h*	−1.0	21.7
BH_2	2.239	0.0	*h*	*i*	15.5

[a] At HF/6-31G*, from Reference 61a.

[b] Defined in **32a**.

[c] In kcal mol^{-1}.

[d] $\Delta E = E$ (non-planar) $-E$ (planar); a minus sign indicates that the non-planar structure (**32a**) is more stable.

[e] $\Delta E_{pyr} = E$ (pyramidal) $-E$ (planar) for the $(H_3Si)_2SiR$ radical. A minus sign indicates that the pyramidal structure is more stable.

[f] For the planar **31a**.

[g] 15.6 and 15.1 kcal mol^{-1} at B3LYP/6-311+G**//B3LYP/6-311+G**[19] and MP2/6-31G**//MP2/6-31G**[52], respectively.

[h] Only the planar structure was identified as a minimum.

[i] A minimum for the pyramidal radical could not be located.

Fluorine imposes a very large deviation from planarity ($\theta = 50.3°$) which results also in a long Si−Si bond of 2.278 Å; this is in agreement with the strong preference of the $(H_3Si)_2SiF$ radical to adopt a pyramidal structure [ΔE_{pyr}(pyramidalization) = 7.7 kcal mol^{-1}]. On the other hand, the σ-donor SiH_3 and the π-acceptor BH_2 substituents increase the aromatic stability of the R_6Si_6 skeleton and prevent pyramidalization. Thus, $Si_6(BH_2)_6$ and $Si_6(SiH_3)_6$ are both planar having aromatic stabilization energies (ASEs) of 15.5 and 21.7 kcal mol^{-1}, respectively, compared with 11.8 kcal mol^{-1} for Si_6H_6 and 24.7 kcal mol^{-1} for benzene (HF/6-31G*)[61a]. The substituent effects described above are very similar to the effects that these substituents have on the geometry and stability of disilenes; i.e. F causes a very strong *trans*-bending and elongation of the Si=Si bond, while $(H_3Si)_2Si{=}Si(SiH_3)_2$ is planar[1c,65]. Based on these results we believe that $Si_6(SiR_3)_6$ with bulky R groups, which are required for kinetic stabilization, may be good candidates for the synthesis and isolation of the first planar hexasilabenzene.

G. Higher Congeners of Hexasilabenzene

Substitution of the Si atoms in Si_6H_6 by heavier group 14 atoms results in an increased deviation from planarity (the planar structures are not minima on the PES) and an increased stabilization upon ring puckering measured by ΔE(**38**−**39**). For $Si_3Ge_3H_6$, $\theta = 36.8°$ and ΔE(**38**−**39**) = 4.8 kcal mol^{-1} [MP2/6-31G**//HF/ECP(d)][53b]; for Ge_6H_6, $\theta = 38.0°$ and ΔE(**38**−**39**) = 9.1 kcal mol^{-1}; for Sn_6H_6, $\theta = 50.8°$ and ΔE(**38**−**39**) = 23.1 kcal mol^{-1}; and for Pb_6H_6, $\theta = 58.0°$ and ΔE((**38**−**39**) = 63.3 kcal mol^{-1} [MP2/DZ(d)//HF/DZ(d)][61b]. The increased deviation from planarity and the larger energy differences between the D_{6h} and D_{3d} structures on moving down along group 14 of the Periodic Table is explained by the increased tendency of the π-electrons to localize, and is consistent with the progressively favoured pyramidal structure on going along the radical series: germyl, stannyl and plumbyl[61]. Similar behaviour was observed for the $H_2X{=}XH_2$ series, where X = Si[65,66], Ge, Sn and Pb[66,62].

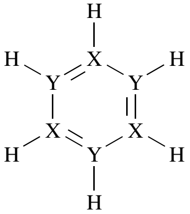

(38)

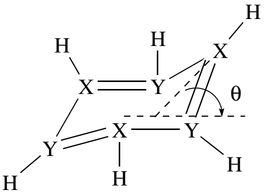

(39)

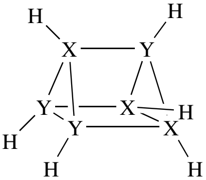

(40)

Substitution of the Si atoms in Si_6H_6 by its higher congeners has a small effect on their aromatic stabilization energies; i.e. the ASEs calculated according to equation 14a for X_6H_6 (X = Si, Ge, Sn and Pb) are all in the range of 9–12 kcal mol^{-1}[62]. The calculated resonance stabilization energy of **39** (X = Si; Y = Ge) according to equation 15 is 60.2 kcal mol^{-1}, identical to that of 1,3,5-trisilabenzene **(12)** and very similar to that of Si_6H_6 [57.8 kcal mol^{-1} at MP2/ECP(d)//HF/ECP(d)][53a], indicating the small effect of substituting three Si atoms in Si_6H_6 by C or Ge.

The stability of the prismane isomers **(40)** in the $X_3Y_3H_6$ (X, Y = C, Si, Ge, Sn, Pb) series, relative to the corresponding aromatic **38** isomers, decreases in the following order [ΔE, kcal mol^{-1} at MP2/6-311G**//HF/ECP(d)[53b], unless stated otherwise; a negative ΔE indicates that the prismane isomer is more stable]: X = Y = Sn (−31.3, MP2/DZ+d//HF/DZ+d[67]) > X = Y = Pb (−67.0, MP2/DZ+d//HF/DZ+d[67]) > X = Y = Si (−13.6) > X = Y = Ge (−11.1) > X = Si; Y = Ge (−6.4) > X = C; Y = Ge (27.2) > X = C; Y = Si (35.5) > X = Y = C (113.9). The stability of the Dewar benzene **(34)** and the benzvalene **(35)** isomers relative to the corresponding aromatic D_{6h} X_6H_6 isomer also increases along the series X = C → X = Pb, though to a smaller degree than the increase in the stability of the corresponding prismane isomers[67].

H. Silabenzenoids Containing Heteroatoms

The potentially aromatic silabenzenoids, *s*-1,3,5-trisilatriazine **(41)**[68] and 2-, 3- and 4-silapyridines **(42–44)**[69], were studied by Veszprémi and coworkers. The MP2/6-31G* calculated geometries of **41–44** are given in Figure 7 (almost identical geometries were calculated for **41** also at MP2/6-311G** and CCSD/6-31G*[68]). **41** has D_{3h} symmetry

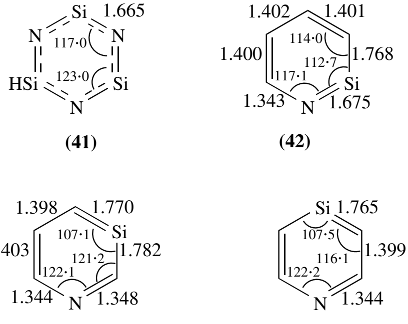

(41) **(42)** **(43)** **(44)**

FIGURE 7. MP2/6-31G* optimized geometries of **41–44**. Drawn from data in References 68 and 69

and thus the Si−N bond lengths (1.665 Å) show no alternation, indicating a delocalized aromatic system. The geometries of **42**–**44** also suggest an aromatic character; the C−C bonds in **42**–**44** show almost no bond alternation, with bond lengths around 1.40 Å, very similar to those in benzene. The Si−C bond lengths in **42**–**44** of *ca* 1.77 Å are intermediate between typical Si−C and Si=C bond lengths, also indicating the existence of electron delocalization.

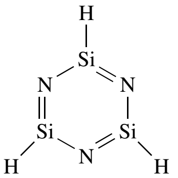

(41)

(42)

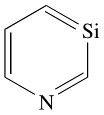

(43)

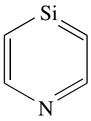

(44)

The calculated aromatic stabilization energy of **41** is 19.6 kcal mol^{-1} (at MP2/6-31G*//MP2/6-31G* using the homodesmotic equation 16)[68]. A very similar ASE of 19.4 kcal mol^{-1} was calculated for **42** using equation 17 (ASEs for **43** and **44** were not reported)[69]. The ASE calculated for benzene and pyridine (at the same level of theory) are 28.2 and 28.0 kcal mol^{-1}, respectively, indicating a high degree of aromaticity (*ca* 70% of that of benzene) for both **41** and **42**[69]. This is very similar to the carbon analogue of **41**, *s*-triazine (*c*-$C_3N_3H_3$), which was estimated to have 76% of the aromaticity of benzene according to the calculated relative magnetic susceptibility anisotropies[18] and the relatively high NICS(π) value[19].

$$\mathbf{41} + 3H_2Si{=}NH \longrightarrow 3H_2Si{=}N{-}SiH{=}NH \tag{16}$$

$$\mathbf{42} + H_2Si{=}NH + 2CH_2{=}CH_2 \longrightarrow \tag{17}$$

$$CH_2{=}CH{-}SiH{=}NH + CH_2{=}CH{-}N{=}SiH_2 + CH_2{=}CH{-}CH{=}CH_2$$

The relative stability of the three silapyridines **42**–**44** follows the order (kcal mol^{-1}): **42** (0.0, most stable) > **44** (11.0) > **43** (37.8), but no explanation was given for this stability order[68]. The thermodynamic stability of *s*-1,3,5-trisilatriazine, **41**, and of the silapyridines **42**–**44** relative to their isomeric silylenes is discussed in Section V.B.I.

I. Concluding Comments

The silabenzenoids are an exciting family of molecules and much remains to be learned about their properties and chemistry. Table 6 summarizes the degree of aromaticity as calculated from the ASE and NICS values (when available) of the various silabenzenoids that were discussed in this section. Their degree of aromaticity is in the range of *ca* 40–90% of that of benzene. Unfortunately, as pointed out during the discussion, much of the current data are based on quite old calculations which used relatively simple and therefore unreliable computational methods. Hence a reliable comparison of the aromaticity of the various silabenzenoids is not yet possible. New theoretical studies of these intriguing molecules using higher levels of theory and more sophisticated criteria for evaluating aromaticity (such as the magnetic criteria) are needed for a better understanding of these molecules.

TABLE 6. 'Degree of aromaticity' of silabenzenoids relative to benzene (R) as estimated from their ASEs calculated by various homodesmotic equations

Silabenzenoid	ASE (kcal mol^{-1})	R[a]	Equation[b]	Method	References
Monosilabenzene **(8)**	17.2	0.69[c]	8	HF/6-31G*//HF/6-31G*	43b,45
meta-Disilabenzene **(22)**	47.2	0.80	*d*	HF/3-21G//HF/STO-3G	50a
para-Disilabenzene **(11)**	36.4	0.62	*d*	HF/3-21G//HF/STO-3G	50a
ortho-Disilabenzene **(21)**	22.5	0.38	*e*	HF/3-21G//HF/STO-3G	50a
Trisilabenzene **(12)**	53.1[f]	0.83	11[g]	CCSD(T)/DZP//CISD/DZP	49
Hexasilabenzene **(31)**	15.1	0.61	14a	MP2/6-31G**//MP2/6-31G**	52
	15.6	0.46[h]	14b	B3LYP/6-311G**//B3LYP/6-311G**	19
2-Silapyridine **(42)**	19.4	0.69	17	MP2/6-31G*//MP2/6-31G*	69
s-Trisilatriazine **(41)**	19.1	0.68	16	MP2/6-31G*//MP2/6-31G*	68

[a] ASE(silabenzenoid)/ASE(benzene).

[b] The number in the text of the homodesmotic equation used to evaluate ASE.

[c] NICS values are −9.1 ppm and −9.7 ppm for **8** and benzene, respectively[8].

[d] According to the equation: **22** (or **11**) + $2SiH_4 + 4CH_4 \rightarrow 2H_2Si{=}CH_2 + C_2H_4 + C_2H_6 + 2H_3CSiH_3$.

[e] According to the equation: **21** + $2SiH_4 + 4CH_4 \rightarrow H_2Si{=}SiH_2 + C_2H_4 + C_2H_6 + 2H_3CSiH_3$.

[f] Resonance energy (RE); ASE is not reported.

[g] The RE of benzene was calculated from equation 2.

[h] NICS(π) values are −14.1 ppm and −16.8 ppm for **31** and benzene, respectively[19].

IV. CHARGED SILAAROMATIC SYSTEMS

In this section we will discuss charged silaaromatic systems which formally possess $4n+2$ π-electrons, such as **45–49**. These species are isoelectronic with the cyclopropenium cation, tropylium cation and cyclopentadienyl anions, respectively, which are all well established aromatic systems[13a,18].

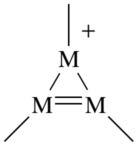

(45)

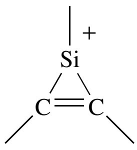

(46)

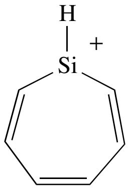

(47)

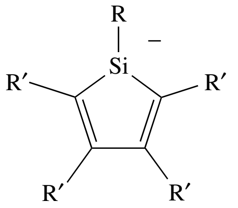

(48)
(48a) R = R′ = H

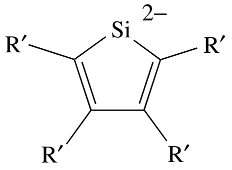

(49)
(49a) R′ = H

A. Systems with Two π-Electrons

1. The monosilacyclopropenium cation

The cyclopropenium cation (**45,** M = C) is a well established aromatic system with a high aromatic stabilization energy of 58.7 kcal mol^{-1} [equation 18, M = C, at B3LYP/6-311++G(2d,2p)]^{70}. What happens when one carbon atom is substituted by silicon? At HF/STO-2G the monosilacyclopropenium cation, **46**, has a rather delocalized structure with r(C−C) = 1.393 Å, r(C−Si) = 1.722 Å and with CSiC and SiCC bond angles of 46.3° and 66.9°, respectively^{41a}. However, according to equation 19 which measures the effect of delocalization, **46** is destabilized by 11 kcal mol^{-1} (HF/3-21G//HF/STO-2G) while **45**, M = C is stabilized by 36 kcal mol^{-1}. Unfortunately, this study used a very low computational level and should be repeated using more reliable methods.

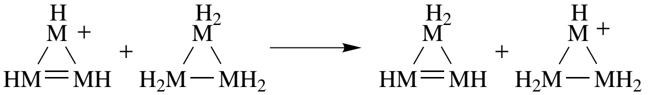

(18)

M = Si, C

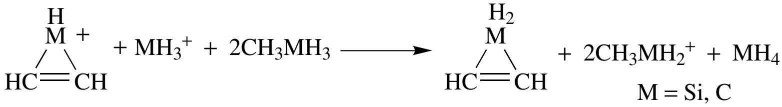

(19)

M = Si, C

2. The trisilacyclopropenium cation and its higher congeners

The trisilacyclopropenium cation (**45**, M = Si), the full silicon analogue of the cyclopropenium cation, was calculated to be the global minimum on the $Si_3H_3{}^+$ PES. The aromatic stabilization energy of **45**, M = Si according to equation 18 is 35.6 kcal mol^{-1} [B3LYP/6-311++G(2d,2p)]^{70}, about 60% of the aromatic stabilization energy of the cyclopropenium cation. The silacyclopropenium cation has D_{3h} symmetry with a Si−Si bond length of 2.203 Å [B3LYP/6-311++G(2d,2p)^{70}; 2.199 Å at MP2/6-31G*^{71}], intermediate between typical Si−Si and Si=Si bond lengths. Based on these facts it can be concluded that **45**, M = Si has a considerable degree of aromaticity. On going down group 14 the π-stabilization of **45** decreases, i.e. ΔE(equation 18) = 58.7, 35.6, 31.9, 26.4 and 24.1 kcal mol^{-1} for M = C, Si, Ge, Sn and Pb^{70}.

Three non-classical hydrogen-bridged isomers, **50a**, **50b** and **51** (M = Si), which are by about 20 kcal mol^{-1} less stable than **45** (M = Si), were also located as minima on the $Si_3H_3{}^+$ PES^{70,71}. On going down group 14 the preference for the hydrogen-bridged isomer **51** increases and for M = Ge, Sn and Pb it becomes the global minimum on the $M_3H_3{}^+$ PES, i.e. ΔE(**51**−**45**) = 23.7, −17.4, −32.4 and −63.3 kcal mol^{-1} for M = Si, Ge, Sn and Pb, respectively^{70}. This trend was attributed to the increased stability of divalent arrangements when moving down group 14 of the Periodic Table.^{70}

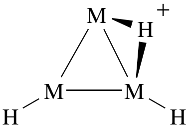

(50a) C_1

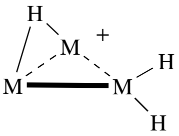

(50b) C_1

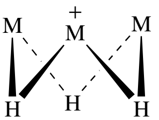

(51) C_{3v}

3. The tetrasilacyclobutadiene dication

The most stable isomer on the $Si_4H_4^{2+}$ PES is the slightly puckered (D_{2d} symmetry) potentially 2π-aromatic tetrasilacyclobutadiene dication, **52a**, having a SiSiSiSi dihedral angle of 9° (the planar D_{4h} isomer is not a minimum on the PES). The analogous D_{2d} cyclobutadiene dication **52b** is considerably more puckered ($\angle$CCCC = 32.5°)[71]. This is a unique example of a silicon system which is less folded than the carbon analogue. The identical Si−Si bond lengths of 2.268 Å indicate electron delocalization and thus aromaticity. The calculated ASE of **52a** and **52b** according to equation 20 are 32.4 kcal mol^{-1} and 26.8 kcal mol^{-1}, respectively [at MP2(full)/6-31G*]. The unusual higher ASE of **52a** relative to **52b** is attributed, however, to the destabilization of the corresponding reference compounds in equation 20 for M = Si and not to its higher aromatic character[71].

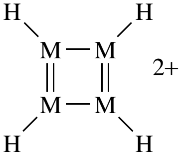

(52a) M = Si
(52b) M = C

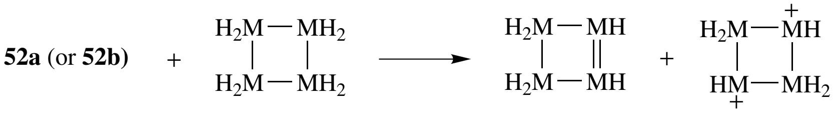

(20)

B. The Silatropylium Cation and its Isomers

Gas-phase experiments by Beauchamp and coworkers[72] point to the existence of two distinct $C_6SiH_7^+$ isomers, which are formed by loss of a hydrogen from a silatoluene cation-radical. Based on the observed gas-phase chemistry, the authors proposed that these isomers are the silabenzyl cation **53** and the silatropylium cation **47**. They have also concluded from indirect evidence that the silatropylium ion is thermodynamically more stable than the silabenzyl cation, similar to the stability order in the analogous carbon systems[72]. Based on the reluctance of **47** to react with cycloheptatriene, it was concluded that the hydride affinity of **47** is even lower than that of the tropylium cation, which has one of the lowest hydride affinities known for organic cations[72]. In order to shed more light on these conclusions Nicolaides and Radom studied computationally the $C_6SiH_7^+$ surface[73], using very high computational levels, up to G2 and G2(MP2)[74]. The calculations reveal a fascinating complex $C_6SiH_7^+$ PES with 9 minima, i.e. **47**, **53**–**59**, several of which have 'non-classical'. The most surprising result of the calculations is that *the global minimum on the PES is the pyramidal 'non-classical' structure* **59**, which is by 20–26 kcal mol^{-1} lower in energy than the silabenzyl cation **53** and 29–35 kcal mol^{-1} below the silatropylium cation **47**. The remarkable stability of **59** is also exhibited in its high dissociation energy to Si plus $CH_3C_5H_4^+$ of 145.2 kcal mol^{-1} [at G2(MP2)][73a]. The other $C_6SiH_7^+$ isomers, **47** and **53**–**58**, are clustered in a rather narrow energy range of 14 kcal mol^{-1}, arranged in the following stability order [in kcal mol^{-1} at QCISD(T)/6-311G**//MP2/6-31G*]: **59** (0.0) < **53** (26.3) < **58** (31.8) < **54** (34.0) < **47** (35.4) < **57a** (37.5) < **57b** (38.3) < **55** (39.0) < **56** (40.2)[73].

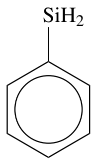

(53)

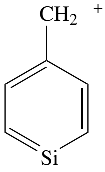

(54)

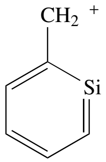

(55)

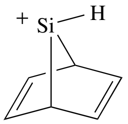

(56)

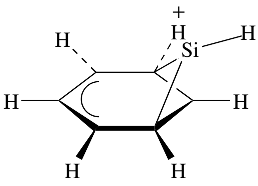

(57a)

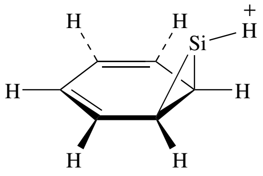

(57b)

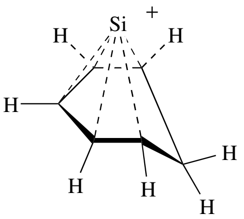

(58)

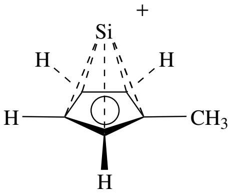

(59)

In contrast to the conclusions of Beauchamp and coworkers[72], the computational results predict that the silatropylium cation **(47)** is *less stable* than the silabenzyl cation, this being the case at all *ab initio* levels, e.g. by 9.1 kcal mol^{-1} at QCISD(T)/6-311G(d,p)//MP2/6-31G(d)+ZPE (in the $C_7H_7^+$ analogue the tropylium cation is by 7.6 kcal mol^{-1} more stable than the benzyl cation)[73]. Moreover, the calculated hydride affinity of **47** is by 11.0 kcal mol^{-1} higher than that of the tropylium cation, in contrast to the experimental suggestion[72]. Based on the calculations it was concluded that, in addition to the silabenzyl cation, the other $C_6SiH_7^+$ isomer that was observed in the gas-phase experiments is most likely the (η^5-methylcyclopentadienyl)silanium cation, **59**. This cation has a calculated hydride affinity 33 kcal mol^{-1} lower than that of the tropylium cation[73a], in agreement with the experimental observation that the hydride affinity of the 'second isomer' is smaller than that of the tropylium cation. However, in a later study by Jarek and Shin[73c] low-energy collision-induced dissociation (CID) of the unreactive $C_6SiH_7^+$ isomer yielded SiH^+ and C_6H_6. The authors concluded that the unreactive $C_6SiH_7^+$ isomer is a η^4-$C_6H_6{\cdot}SiH^+$ adduct and not **59** as predicted earlier[73a,b] (e.g. **59** is also expected to yield Si^+ as a fragment, and this is not observed experimentally)[73c]. *Ab initio* calculations find that the hydride affinity of η^4-$C_6H_6{\cdot}SiH^+$ is by 11.9 kcal mol^{-1} at MP2/6-311G** lower than that of a tropylium ion, in agreement with the experimental relative value of −7.0 kcal mol^{-1}. Further experimental and theoretical studies are needed to clarify the identity of the observed $C_6SiH_7^+$ species.

Nicolaides and Radom emphasize the crucial importance of the inclusion of electron correlation, especially for the 'non-classical' isomers, for a reliable calculation of the relative energies, heats of formation and hydride affinities of the various $C_6SiH_7^+$ isomers. For the 'non-classical' structures, even the MP2 computational level does not always describe correctly their relative energies. For cases where the relative stabilities of the isomers oscillate at the MPn levels, the authors recommend using the QCISD(T) method[73b].

The structure of the planar C_{2v} silatropylium cation **47** is quite sensitive to the computational level; whereas at HF/6-31G* the C−C bonds are alternating, being 1.360 Å, 1.440 Å and 1.355 Å; the inclusion of electron correlation tends to narrow their range and at MP2/6-31G* they are 1.387 Å, 1.416 Å and 1.393 Å, consistent with a more delocalized structure. The calculated Si−C bonds are 1.781 Å and 1.782 Å at HF/6-31G* and MP2/6-31G*, respectively. The degree of electron delocalization or aromaticity in the silatropylium ring (and its isomers) was not discussed[73].

The most stable $C_6SiH_7^+$ isomer **59** may be viewed as an η^5-ion-molecule complex involving a Si^{2+} cation and a methylcyclopentadienyl anion. In **59**, the five-membered ring is flat and the distances of the apical Si from the ring carbons are 2.143 Å, 2.147 Å and 2.178 Å at MP2/6-31G*. The cyclopentadienyl C−C bond lengths are almost identical: 1.429 Å, 1.426 Å and 1.422 Å (MP2/6-31G*), indicating a delocalized system.

In this context, it is interesting to note the related $C_6SiH_6^{+\bullet}$ isomers, which are obtained by a gas-phase reaction of $Si^{+\bullet}$ and C_6H_6[75]. MP2/6-31G**//UHF/3-21G* calculations identified 3 minima on the $C_6SiH_6^{+\bullet}$ PES, the π-complex **60**, the C−H insertion isomer **61** and the ionized seven-membered ring structure **62**[75] (these are formally hydrogen abstraction products of **57a**, **53** and **47**, respectively). Their calculated relative energies ($kcal\,mol^{-1}$) are: **60** (0.0) > **61** (5.5) > **62** (30.8), the π-complex **60** being the most stable. The potentially aromatic **62** is planar and has C_{2v} symmetry. The C−C bond lengths are alternating (i.e. 1.375 Å, 1.422 Å and 1.382 Å), indicating small π-delocalization. The calculated Si−C bond length is 1.788 Å, i.e. it is slightly shorter than a single Si−C bond. The structure of **62** is very similar to the structure calculated at HF/6-31G* for **47**. However, inclusion of electron correlation in the geometry optimization may result in a more delocalized structure also for **62** as was found for **47** (see above).

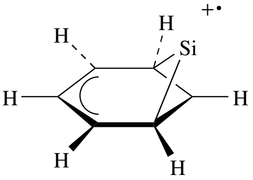

(60)

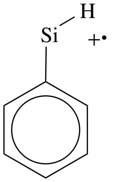

(61)

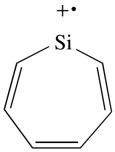

(62)

C. $C_5H_5Si^+$ Isomers

The pyramidal silicon capped cation **63a** is a potential 'three-dimensional' 6π-electron aromatic system[76a], where the formal coordination number of the silicon is five (as in **59**). The interest in **63a** results from the detection of a $C_5SiH_5^+$ fragment in the gas phase[76b]. The crucial question is the stability of the pyramidal ion **63a** relative to other possible $C_5SiH_5^+$ isomers, such as **64a** and **65a**. A comparison with the analogous $C_6H_5^+$ isomers is of interest.

The available, rather low level calculations (HF/STO-3G, HF/STO-3G* and HF/3-21G, all at the HF/STO-3G optimized geometries) show that the pyramidal aromatic structure **63a** is more stable than the two planar structures. In the analogous carbon cations, on the other hand, the planar cations **64b** and **65b** are considerably lower in energy than the

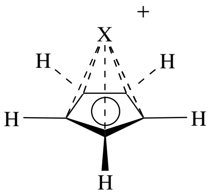

(63a) X = Si
(63b) X = C

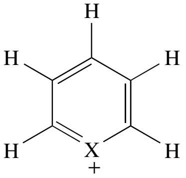

(64a) X = Si
(64b) X = C

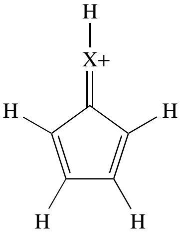

(65a) X = Si
(65b) X = C

pyramidal structure **63b**. Obviously, the reluctance of silicon to participate in multiple bonding destabilizes the planar structures relative to the pyramidal one, while in the all-carbon compounds the situation is reversed. The calculated Si−C distances in **63a** of 1.745 Å are very short, considerably shorter than the value of 2.189 Å (HF/6-31G*, 2.178 Å at MP2/6-31G*)[73a] in the very closely related **59**, and is by only *ca* 0.04 Å longer than that of a Si=C double bond. This short Si−C bond length is probably an artifact of the small STO-3G basis set used in the geometry optimization. In view of the relatively low level of calculations used so far, we recommend that this interesting system should be reinvestigated.

D. Silacyclopentadienyl Anions and Dianions

1. Experimental background

The search in recent years for silicon compounds with multiple bonds or cyclic π-systems has renewed interest in siloles **(66)**[77] and their mono- and di-anions (**48** and **49**), and led to the successful isolation of stable silole anions coordinated to various metal counter ions (Li^+, Na^+, K^+)[10a–c,78–86] and as complexes with ruthenium (e.g. **6a** and **6b**)[10d].

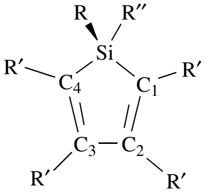

(66)
(66a) R = R′ = R″ = H

The conclusions regarding the aromaticity of silole anions and dianions as gathered from the experimental studies of their structural and magnetic properties are summarized in Table 7, which reveals some controversy regarding the degree of aromaticity of silole anions. Hong and Boudjouk[79] found that the chemical shift of the ring Si atom in Li[*c*-$Ph_4C_4Si(Bu$-*t*)] (in THF) is shifted downfield relative to that of the parent silole, and this was interpreted as indicating charge delocalization in the anion. On the other hand, Tilley and coworkers[10a] find that in Li[*c*-$Me_4C_4Si(SiMe_3)$] (in THF) and K(18-crown-6)[*c*-$Me_4C_4Si(SiMe_3)$], $\delta(^{29}Si)$ of the ring silicon is shifted considerably upfield with respect to the analogous neutral silole compounds (Table 7). This result was interpreted as indicative of a localized structure[10a]. The latter interpretation is strongly supported

TABLE 7. Experimental structural and magnetic properties of silole anions and dianions and conclusions regarding their degree of aromaticity

Silole anion	Bond length (Å)			$\delta(^{29}Si)$ (ppm)	$\delta(^{13}C)$ (ppm)		Aromaticity	Ref.
	$Si-C_{(1)}$	$C_{(1)}-C_{(2)}$	$C_{(2)}-C_{(3)}$		$C_{(1)}$	$C_{(3)}$		
a. Monoanions								
$Li[c\text{-}Ph_4C_4Si(Bu\text{-}t)]$ (in THF)	—	—	—	25.1^a	139.5^b	155.8^b	Magnetic properties indicate charge delocalization	79
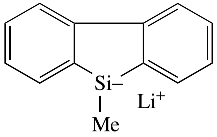 (in THF)	—	—	—	-22.1^c	$\Delta T^d = 9.65$		No π-delocalization (NMR)	80
$Li[c\text{-}Me_4C_4Si(SiMe_3)]$ (in THF)	—	—	—	-45.4^e	138.7^f	146.4^f	MNR shifts and bond-length	10a
$[K(18\text{-crown-}6)][c\text{-}Me_4C_4Si(SiMe_3)]$	1.880^g	1.360	1.450	-41.5^e	135.8^f	149.6^f	alternation suggest non-aromatic character	10a
Ruthenium complexes, **6b** **(6a)**	$1.830^{h,i}$	1.391	1.462	−27.1(−7.35)	74.4(73.1)	108.8(88.5)	Magnetic and structural properties indicate charge delocalization	10d 10d
b. Dianions								
$Li^+{}_2[c\text{-}Me_4C_4Si]^{2-}$ (in THF)	—	—	—	29.8^j	139.0^k	120.0^k	NMR shifts indicate some aromatic character	84

$Li^+{}_2[c\text{-}Ph_4C_4Si]^{2-}$: (a) Solid[l]	1.850	1.448	1.430	87.3			NMR shifts and the structure are consistent with significant charge delocalization	10b
(b) in THF				68.5[m]	129.7[n]	151.22[n]		10c
$[K(18\text{-crown-6})^+]_2[c\text{-}Me_4C_4Si^{2-}]$	1.851[o]	1.400	1.440	—	—	—	The structure indicates significant charge delocalization	82

---

[a] Considerably downfield shifted relative to **66,** $R = t$-Bu; $R' = Ph$; $R'' = [(PhC)_4SiBu\text{-}t]$ where $\delta(^{29}Si) = 3.6$ ppm and relative to the relevant silyl anions (e.g. Ph_3SiLi: −30 ppm; Me_3SiK: −34.4 ppm).

[b] Shifted upfield relative to the corresponding precursor, **66** (i.e. $C_{(1)} = 144.8$ ppm; $C_{(2)} = 158.0$ ppm).

[c] Shifted upfield relative to $\delta(^{29}Si)$ of −18.7 ppm of the corresponding precursor, **66**.

[d] ΔT = the total chemical shift change of the phenyl ring carbons relative to the neutral precursor. This small downfield shift relative to the neutral parent was interpreted as indicating that additional π-electron density is not accumulated in the phenyl ring of the anion.

[e] Considerable upfield shift with respect to analogous neutral siloles, e.g. $\delta(^{29}Si) = -8.9$ ppm in **66** ($R = Me$, $R' = H$, $R'' = SiMe_3$).

[f] For **66** ($R = Me$, $R' = H$, $R'' = SiMe_3$) $\delta(^{13}C_{(1)}) = 129.5$ ppm and $\delta(^{13}C_{(2)}) = 150.9$ ppm.

[g] The silicon is pyramidal.

[h] The ring Si centre is planar.

[i] Crystallographic data are for **6b; 6a** could not be crystallized.

[j] Downfield shifted relative to $\delta(^{29}Si) = 8.1$ ppm in the neutral precursor.

[k] Upfield shifted relative to $\delta(^{13}C_{(1)}) = 152.3$ ppm and $\delta(^{13}C_{(2)}) = 124.1$ ppm of its neutral precursor.

[l] The Li atoms have η^1,η^5-coordination to the five-membered ring; the ring is almost planar, with the Si deviating by only 11 ppm from the plane of the four carbon atoms.

[m] Shifted downfield relative to the neutral silole precursor [$\delta(^{29}Si) = 6.8$ ppm].

[n] $\delta(^{13}C_{(1)}) = 132.3$ ppm and $\delta(^{13}C_{(2)}) = 154.7$ ppm in the relevant silole precursor.

[o] The $K(18\text{-crown-6})^+$ ions have η^5,η^5-coordination to the silacyclopentadienyl ring.

by the X-ray structure of K(18-crown-6)[*c*-$Me_4C_4Si(SiMe_3)$], which shows a difference of *ca* 0.1 Å between the $C_{(1)}-C_{(2)}$ and $C_{(2)}-C_{(3)}$ bond lengths (see **66** for the atom notation) and a high degree of pyramidalization at silicon, the angle between the C_4Si plane and the Si−Si bond being 99.6° (see Figure 8a for the ORTEP diagram). The long Si···K distance of 3.60 Å suggests a weak Si···K interaction, indicating that the inherent electronic properties of the anion were preserved. This might not be the case for the Li-coordinated silolyl ion in THF, studied by Hong and Boudjouk and whose structure is unknown[79]. A localized structure was also suggested for the analogous germolyl anion, e.g. Li(12-crown-4)$_2$[*c*-$Me_4C_4Ge(Si(SiMe_3)_3)$], which also does not show any indication for a strong interaction with the counter ion, and which was therefore considered to be a free ion[10a]. The different NMR behaviour of Li[*c*-Ph_4C_4Si(Bu-*t*)][79] and the closely related Li[*c*-$Me_4C_4Si(SiMe_3)$][10a] (both in THF) may be attributed to the phenyl vs Me substitution or to the different degrees of interaction between the alkali metal ions and the silolyl ring in the two systems[82], but these points were not further evaluated. Complexation to ruthenium as in **6a** and **6b** reduces the pyramidality at the ring Si (Figure 8b), thus enhancing the electron delocalization within the ring[10d].

The known silole dianions are coordinated to the metallic counter ions either by η^5,η^5-bonding[10a,82] or by η^1,η^5-bonding[10b] (Figures 8c and 8d). Pyramidality at Si is, of course, not a problem for the silole dianions where the Si is dicoordinated, and the known dianions are all planar (Figures 8c and 8d). The structural and magnetic properties of the silole dianions are consistent with charge delocalization and aromatic character of these species, as shown by the data collected in Table 7.

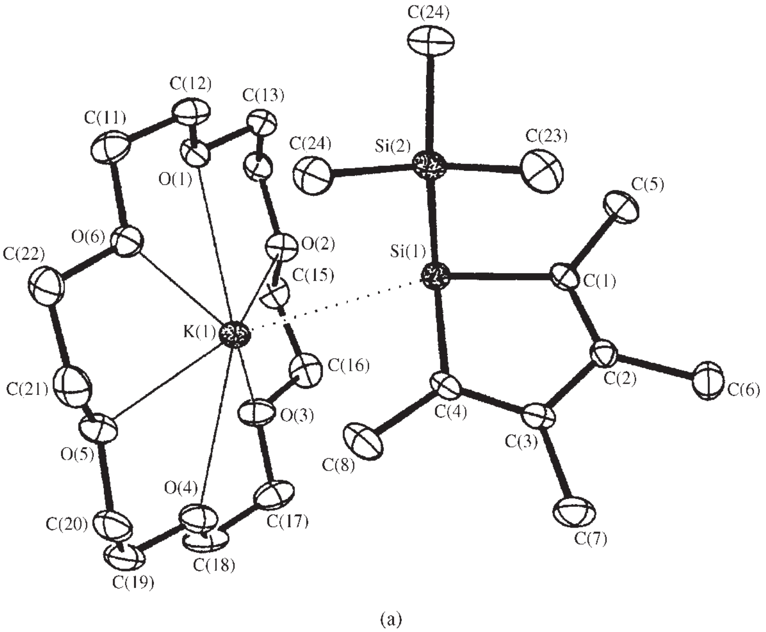

FIGURE 8. ORTEP drawings of several silolyl anion complexes: (a) K(18-crown-6)[*c*-$Me_4C_4Si(SiMe_3)$][10a]; (b) silolyl anion–ruthenium complex **6b**[10d]; (c) η^5,η^5-2[K(18-crown-6)$^+$][*c*-$C_4Me_4Si^{2-}$][10a]; (d) η^1,η^5-2Li^+[*c*-$Ph_4C_4Si^{2-}$]•(5THF)[10b]. Reprinted with permission from References 10a, 10b and 10d. Copyright (1994, 1995, 1996) American Chemical Society

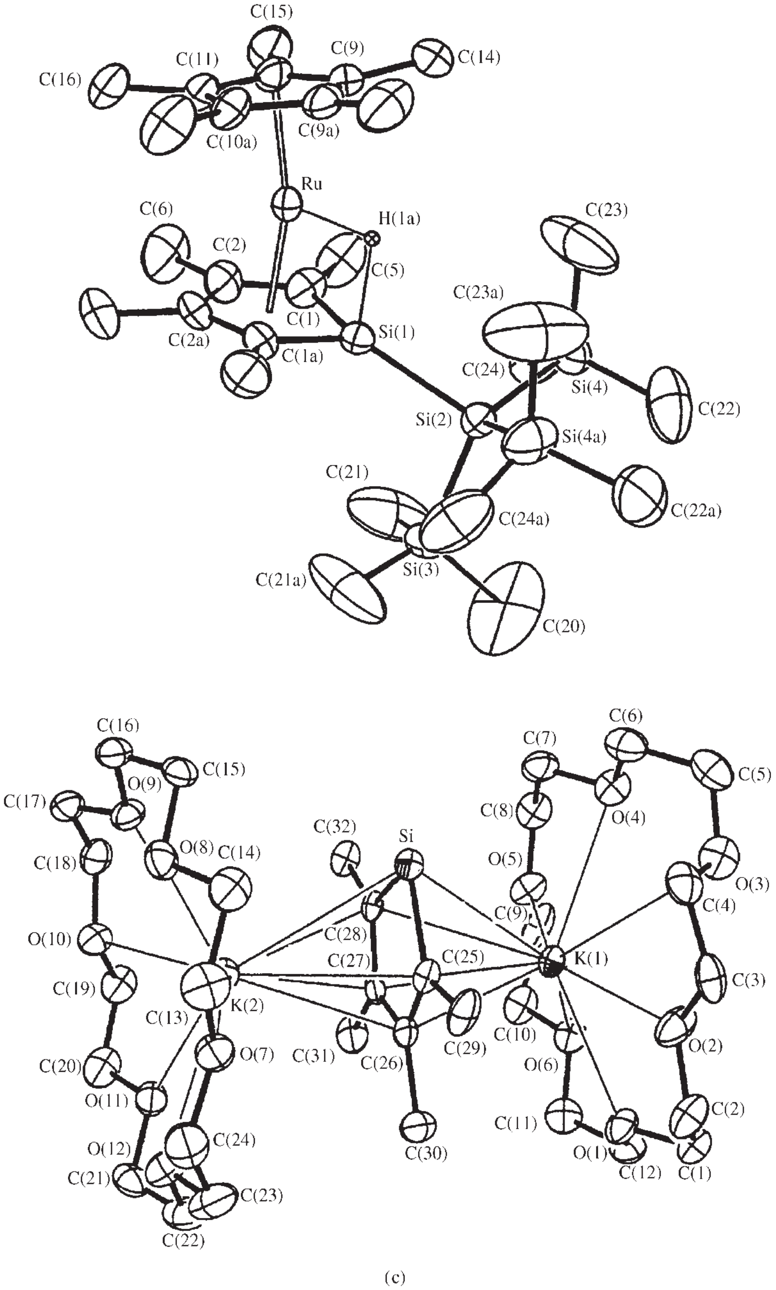

FIGURE 8. *(continued)*

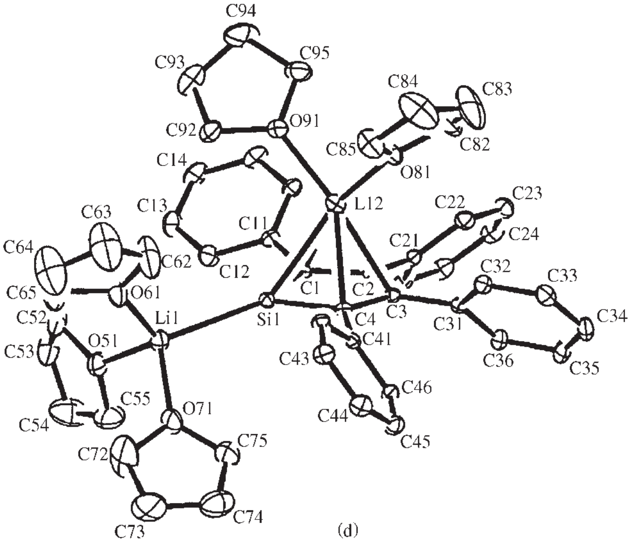

FIGURE 8. *(continued)*

2. *c*-$C_4H_4SiR^-$ *silolyl anions*

a. The parent ion c-$C_4H_4SiH^-$ *and its lithiated complexes.* The cyclopentadienyl anion ($C_5H_5^-$) is a well characterized aromatic system calculated to have, according to π-ring currents and magnetic susceptibility, about 80–90% of the aromaticity of benzene[18]. In contrast, the analogous silacyclopentadienyl anion, **48a**, is still unknown. Low-level early computational studies of the geometry and thermodynamic stability of **48a** were in conflict regarding the degree of its aromaticity[41a,87]. According to HF/3-21G//HF/STO-2G calculations, **48a** is planar and possesses *ca* 25% of the aromaticity of $C_5H_5^-$[41a]. On the other hand, according to HF/6-31G*//HF/6-31G* calculations, the silacyclopentadienyl anion has a C_s pyramidal structure, **67a**, and the planar C_{2v} structure **48a** is the transition state for pyramidal inversion at silicon[87]. The degree of the aromaticity of **67a** as estimated from its ASE is negligible[87]. Recent high-level computational studies[26,31a,86,88,89] that were stimulated by the experimental progress in this field showed clearly that the silacyclopentadienyl anion indeed has a C_s symmetry but that it has a significant degree of aromaticity. The calculated structural, energetic and magnetic properties of silolyl anions (and of silole dianions) and their lithium silolides, together with a comparison to their carbon analogues and the conclusions regarding their degree of aromaticity, are presented in Table 8.

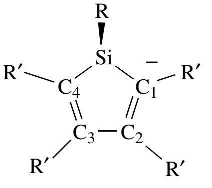

(67) Cs
(67a) R = R′ = H

TABLE 8. Calculated structural and magnetic properties of c-$C_4H_4SiH^-$ (**48a** and **67a**) and c-$C_4H_4Si^{2-}$ **(49a)** and their lithium complexes and conclusions regarding the degree of their aromaticity

Compound	ASE or RE[a]	Bond lengths (Å)				Magnetic properties[b]					Degree of aromaticity	Ref.
		$Si-C_{(1)}$	$C_{(1)}-C_{(2)}$	$C_{(2)}-C_{(3)}$	A[c]	$\delta(^{29}Si)$	$\delta(^{13}C_{(1)})$	$\delta(^{13}C_{(2)})$	Λ	NICS		
a. Monoanions												
$C_5H_5^-$ (D_{5h})	28.8[d]; 23.6[e]	—	1.413[f]	1.413[f]	1.0	—	109.2[g]	109.2[g]	−17.3	−14.3[h]	high	31a
C_5H_5Li (C_{5h})	40.2[e]	—	1.423[i]	1.423[i]	1.0	—	112.9[g]	112.9[g]	−14.5	−17.2[j]	high	88,89, 93a
c-$C_4H_4SiH^-$ (**48a**, C_{2v})	23.0[k]	1.821	1.377	1.433	—	—	—	—	—	—	*ca* 25% of that in $C_5H_5^-$	41a
c-$C_4H_4SiH^-$ (**67a**, C_s)	2.2[l]	1.924	1.341[m]	1.472[m]	—	—	—	—	—	—	negligible	87
c-$C_4H_4SiH^-$ (**48a**, C_{2v})	—	1.794[n]	1.422[n]	1.414[n]	0.998[n]	−6.6[o]	100.5[o]	121.1[o]	−18.5	—	high	88
c-$C_4H_4SiH^-$ (**67a**, C_s)	12.9[e]	1.847[n]	1.399[n]	1.433[n]	0.971[n]	−50.6[o]	153.4[o]	134.6[o]	−10.4	−6.7[h]	*ca* 50% of that in $C_5H_5^-$	88
η^5-Li[c-C_4H_4SiH] **(68)**	32.0[e]	1.823[n]	1.420[n]	1.424[n]	0.999[n]	−22.4[o]	123.6[o]	130.0[o]	−14.1	—	significant	88
b. Dianions												
c-$C_4H_4Si^{2-}$ **(49a)**	17.9[p]	1.869[n]	1.421[n]	1.419[n]	1.0	51.9[o] (18.5)[q]	145.1[o]	119.2[o]	−30.0	−12.8[r]	high	93a
η^5-Li^+[c-$C_4H_4Si^{2-}$] **(69)**	40.4[d]; 36.4[s]	1.884[t]	1.429[t]	1.425[t]	1.0	83.7[q]	—	—	−20.7	−17.1[r]	high	93a

(*continued overleaf*)

TABLE 8. (*continued*)

Compound	ASE or RE[a]	Bond lengths (Å)				Magnetic properties[b]					Degree of aromaticity	Ref.
		Si−$C_{(1)}$	$C_{(1)}$−$C_{(2)}$	$C_{(2)}$−$C_{(3)}$	A^c	$\delta(^{29}Si)$	$\delta(^{13}C_{(1)})$	$\delta(^{13}C_{(2)})$	Λ	NICS		
η^5,η^5-$2Li^+[c$-$C_4H_4Si^{2-}]$ **(70)**	—	1.901^n	1.437^n	1.433^n	1.0	77.7^o $(55.7)^q$	$153.3^{o,u}$	$125.8^{o,u}$	−23.5	-17.6^r	high[v]	93a
η^1,η^5-$2Li^+[c$-$C_4H_4Si^{2-}]$ **(72)**	—	1.855^w	1.420^w	1.426^w	0.999	—	—	—	—	-18.4^r	high	10b

[a] In kcal mol^{-1}, ASE according to equation 21.

[b] δ in ppm; Λ in 10^{-6}cm^3 mol^{-1}; NICS in ppm.

[c] Julg's parameter[17].

[d] At MP2(fc)/6-31G*//MP2(fc)/6-31G*+ZPE.

[e] At MP2(fc)/6-31+G*//MP2(fc)/6-31+G*+ZPE, from Reference 88.

[f] At MP2(fc)/6-31G*.

[g] From Reference 88, calculated by IGLO (basis II) using MP2(fc)6-31+G* geometries.

[h] At GIAO-HF/6-31+G*, from Reference 26.

[i] From Reference 89 at B3LYP/6-31+G*.

[j] From Reference 89 at GIAO-SCF/6-31+G*//B3LYP/6-31G*.

[k] RE at 3-21G, according to the following isodesmic reaction: **48a** (C_{2v}) + SiH_3^- + $4CH_4$ → C_2H_6 + $2C_2H_4$ + $2CH_3SiH_2^-$; the RE for $C_5H_5^-$ (according to an analogous equation) is 87.0 kcal mol^{-1}.

[l] According to the following equation: **48a** + SiH_4 → **66a** + SiH_3^-, at 6-31G*; the ASE for the carbon analogue is 73.4 kcal mol^{-1}.

[m] At HF/6-31G*; for **67**, R = SiH_3, R′ = H, $r(C_{(1)}-C_{(2)})$ = 1.367 Å and $r(C_{(2)}-C_{(3)})$ = 1.477 Å, indicating a localized ring; the Si−Si bond is strongly bent out of the ring plane[86].

[n] At MP2(fc)/6-31+G**.

[o] δ at IGLO (basis II).

[p] at MP2(fc)/6-31+G*, from Reference 93b.

[q] At GIAO/MP2/tz2p(Si),tzp(C,Li),dz(H)//MP2/6-31+G*, from Reference 93b.

[r] At GIAO/HF/6-31G*//MP2/6-31+G*, from Reference 93b.

[s] At MP2/6-31+G**//MP2/6-31+G**.

[t] At MP2(fc)/6-31+G*.

[u] Better agreement between the experimental $C_{(1)}/C_{(2)}$ chemical shifts of $2Li^+[c$-$C_4Ph_4Si^{2-}]$ (in THF) and the calculated values for η^5,η^5-$Li_2[c$-$C_4H_4Si^{2-}]$ is achieved if the experimental $C_{(1)}(\alpha)$ and $C_{(2)}(\beta)$ signal assignments are interchanged[93a].

[v] Similar conclusions were drawn when the coordinating metal was Na or K.

[w] At MP2/6-31+G* from Reference 10b.

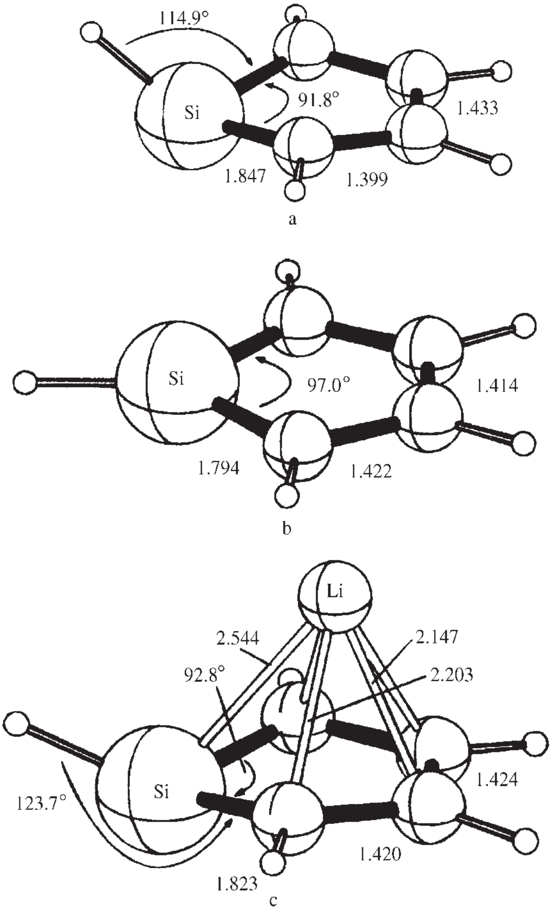

FIGURE 9. Optimized structures of the silolyl anion and its lithium silolide. Bond lengths in Å, bond angles in degrees. (a) The C_s structure of **67a** at MP2/6-31+G**; (b) the C_{2v} structure of **48a** at MP2/6-31+G**; (c) the structure of the lithium silolide **68** at MP2/6-31G**. Reprinted with permission from Reference 88. Copyright (1995) American Chemical Society

Calculations at MP2/6-31+G**[88] find that the parent silolyl anion **67a** has a C_s nonplanar structure (Figure 9a), possessing a pyramidal Si centre with an angle sum at the silicon of 321.6°. Yet, the Si atom in **67a** is less pyramidal than in SiH_3^- (angle sum = 289.3°). The difference between $r(C_{(1)}-C_{(2)})$ and $r(C_{(2)}-C_{(3)})$ is relatively small, 0.043 Å compared to 0.124 Å in the neutral **66a**, indicating some degree of electron delocalization in **67a**. The structural evidence for electron delocalization in **67a** is supported by its calculated ASE of 12.9 kcal mol^{-1} compared to 23.6 kcal mol^{-1} for $C_5H_5^-$ (equation 21, X = SiH^- and CH^-, respectively) and also by its magnetic properties; **67a** has a negative magnetic susceptibility exaltation (-10.4×10^{-6} cm^3 mol^{-1})[88] and a negative NICS value (−6.7 ppm; Table 8)[26]. Based on these structural, energetic and magnetic properties it was concluded that the silolyl anion, **67a**, has *ca* 50% of the aromaticity of

$C_5H_5{}^-$, contrary to the earlier conclusions of Damewood[87] which were based on a significantly lower level of theory. This emphasizes again the need for high level calculations for silicon-containing molecules.

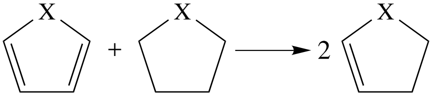

X = SiH$^-$, SiHLi, CH$^-$, CHLi, Si^{2-}, SiLi$^-$ (21)

The calculated ^{29}Si NMR chemical shift of **67a** (−50.6 ppm) is shifted upfield by 8.6 ppm relative to **66a**, indicating that in the parent silolyl anion the effect of the negative charge (causing an upfield shift) is larger than the effect of electron delocalization (causing a downfield shift). Upfield shifts of $\delta(^{29}\text{Si})$ were reported when neutral silanes are converted to silyl anions, as in going from $Me_3SiSiMe_3$ (−19.7 ppm) to Me_3SiK [−34.4 ppm, $\Delta\delta(^{29}\text{Si}) = 14.7$ ppm][90] where no electron delocalization takes place. A significant upfield shift of 36.5 ppm was measured for the ring silicon in Li[*c*-$Me_4C_4Si(SiMe_3)$] [$\delta(^{29}\text{Si}) = -45.4$ ppm] relative to its neutral precursor (**66**, R = Me, R′ = H, R″ = $SiMe_3$). According to Tilley and coworkers, these NMR data as well as the structural data are consistent with a significant localization of the charge on the silicon and with a non-aromatic bond-localized structure[10a] (see above and Table 7). However, this interpretation contradicts the conclusions of Goldfuss and Schleyer (who have also calculated an upfield shift for **67a** relative to **66a**) that **67a** possesses a significant degree of aromaticity[88,89]. This conclusion was based on other evidence, namely ASE, NICS values and the susceptibility exaltation of **67a**. The different conclusions by Tilley and coworkers[10a] on the one hand, and by Goldfuss and Schleyer on the other[88,89], may be due to the different substituents or to interactions with the Li^+ counter ion in Li[*c*-$Me_4C_4Si(SiMe_3)$]. We believe that Tilley's conclusion should be revised, because chemical shifts and geometry are not the most indicative criteria for aromaticity and, as suggested by Schleyer and Jiao[16], we prefer to rely on magnetic criteria such as Λ and NICS. Interestingly, Hong and Boudjouk found a downfield shift in the ^{29}Si NMR chemical shift in Li[*c*-$Ph_4C_4Si(Bu$-*t*)] in line with electron delocalization of the negative charge of the silicon into the hydrocarbon moiety[79] (see Section IV.D.1).

The C_{2v} parent silolyl anion **48a**, in which the Si atom is forced to be planar (Figure 9b), is a transition state for the inversion at Si, but the inversion barrier is only 3.8 kcal mol^{-1} (MP2/6-31+G**//MP2/6-31+G**), much smaller than that computed previously at HF/6-31G* (16.2 kcal mol^{-1})[87]. The bond length equalization in **48a** (Figure 9b), its large negative magnetic susceptibility exaltation of -18.4×10^{-6} cm^3 mol^{-1} which is even more negative than that of $C_5H_5{}^-$ (-17.3×10^{-6} cm^3 mol^{-1}, Table 8) and the downfield shift of its $\delta(^{29}\text{Si})$ relative to **66a** [$\delta(^{29}\text{Si}) = -6.6$ and −42 ppm, respectively] are all strong indications of a highly aromatic system[88].

The lower degree of aromaticity of **67a** relative to $C_5H_5{}^-$ is due mostly to the pyramidal geometry around the silicon. A similar reduction in aromaticity is observed for phosphole *c*-C_4H_4PH relative to pyrrole[31a]. This implies that reduction or elimination of the pyramidality problem should result in increased charge delocalization. Computationally, this could be demonstrated by η^5-coordination of Li^+ to the silolyl anions, i.e. as in **68**. Such coordination reduces the pyramidality at the Si (sum of angles around the Si is 340.2) and enhances its CC bond equalization (Figure 9c). Furthermore, η^5-Li^+ coordination to **67** increases its ASE to −32 kcal mol^{-1} (equation 21) which is about 80% of the ASE of η^5-C_5H_5Li, causes a considerable downfield shift in $\delta(^{29}\text{Si})$ to −22.4 ppm and increases the diamagnetic susceptibility exaltation to -14.1×10^{-6} cm^3 mol^{-1}, which is nearly as large as that of η^5-C_5H_5Li (Table 8). All these facts together are best interpreted as indicating that Li^+ coordination to **67** results in a strong 'three-dimensional aromaticity'[91] and in stabilization of the π-electrons[92]. Thus, the structural, energetic and magnetic criteria all agree that **68** is highly delocalized and shows a significant aromatic character[88,89,93a]. The recent experimental conclusions regarding the aromaticity of Li[*c*-Ph_4C_4Si(Bu-*t*)][79] are in agreement with this computational conclusion. Similar 'three-dimensional aromaticity' was achieved in **6a** and **6b** by complexation of the silolyl anion to a η^5-$Me_5C_5Ru^+$ fragment (Figure 8b, Table 7)[10d].

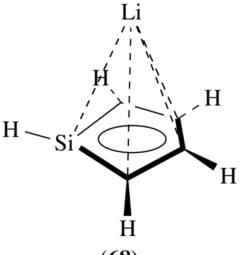

(68)

b. The silyl substituted silolyl anion, c-$C_4H_4Si(SiH_3)^-$. The structure and charge distribution of the silyl substituted metalolyl anions, *c*-$C_4H_4E(SiH_3)^-$, E = C, Si, Ge and Sn, were studied at HF/6-31G* by Tilley and coworkers[86]. The calculated structure of *c*-$C_4H_4Si(SiH_3)^-$ exhibits a strong pyramidality at the ring silicon. The angle α between the Si−Si bond and the plane of the ring is 104.5°. This strong pyramidality is accompanied by a localized π-system with $C_{(1)}-C_{(2)}$ and $C_{(2)}-C_{(3)}$ bond lengths of 1.367 Å and 1.477 Å, respectively[86]. Note, however, that a very similar localized structure was calculated at the same level of theory for **67a**[87], which indicates that the effect of the silyl group is small. Going down along group 14, the pyramidality at E as well as the degree of bond localization increases[86] (similar conclusions were reached by Goldfuss and Schleyer[89] for *c*-$C_4H_4EH^-$; see Section IV.D.4)

3. The parent silole dianion c-$C_4H_4Si^{2-}$ and its lithiated complexes

The parent silole dianion, **49a**, where the pyramidality at the silicon is removed, shows a high degree of aromaticity as concluded from its structure (equalized bond lengths of 1.42 Å; $A = 1$[93a], see Figure 10a) and its magnetic properties, i.e. $\Lambda = -30 \times 10^{-6}$ cm^3 mol^{-1}[93a], NICS = −12.8 ppm[93b], relative to $\Lambda = -17.3 \times 10^{-6}$ cm^3 mol^{-1}[31a] and a NICS value of −14.3 ppm[26] for $C_5H_5^-$ (Table 8). The η^5-Li^+ coordinated **69** and the η^5,η^5-$2Li^+$ coordinated inverse sandwich structure **70** are also highly aromatic molecules. The optimized structures of **69** and **70** are shown in Figures 10b and 10c, respectively. Their $C_{(1)}-C_{(2)}$ and $C_{(2)}-C_{(3)}$ bond lengths are nearly equal with a Julg parameter of 1.0, indicating a strong delocalization. Analysis of the nature of the $Si-C_{(1)}$ σ-bonds shows a large p-character on Si, and this may be responsible for the particularly long $Si-C_{(1)}$ bond distances, i.e. 1.884 Å and 1.901 Å in **69** and **70**, respectively[93a]. The diamagnetic susceptibility exaltation calculated for **69** and **70** are highly negative, i.e. -20.7×10^{-6} and -23.5×10^{-6} cm^3 mol^{-1}, respectively (relative to -17.3×10^{-6} cm^3 mol^{-1} for $C_5H_5^-$). The NICS values for **69** and **70** of −17.1 ppm

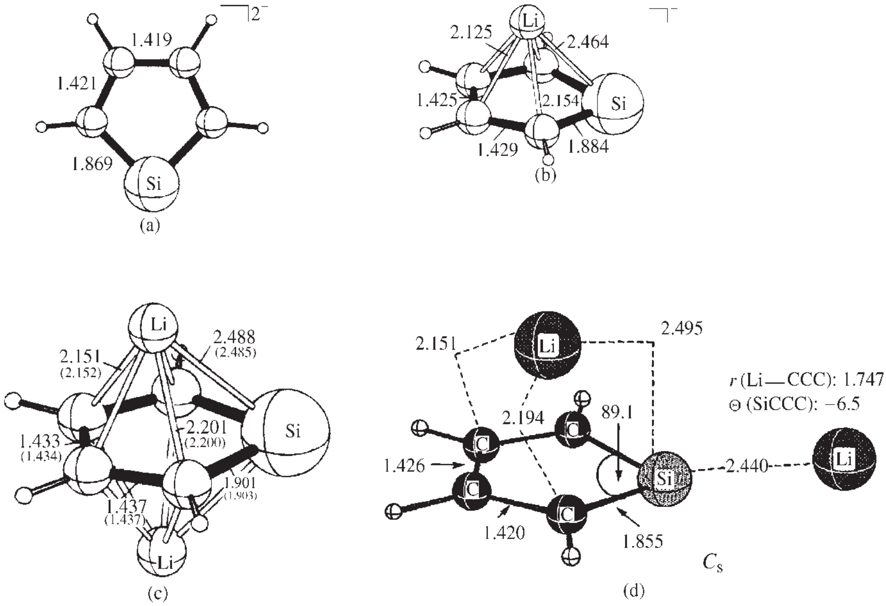

FIGURE 10. Optimized structures of the silole dianion **49a** and its mono- (**69**) and dilithium (**70** and **72**) salts. Bond lengths in Å, bond angles in degrees: (a) **49a** at MP2/6-31+G**[93a]; (b) **69** at MP2/6-31+G*[93a]; (c) η^5,η^5-dilithium silole **70** at MP2/6-31+G** (in parentheses at MP2/6-31G*)[93a]; (d) η^1,η^5-dilithium silole **72** at MP2/6-31+G*[10b]. Reprinted with permission from References 10b and 93a. Copyright (1995, 1996) American Chemical Society

and −17.6 ppm, respectively, are almost identical to that of C_5H_5Li (−17.7 ppm[89]), pointing to large aromatic ring currents in all these molecules. The NICS values for **69** and **70** are considerably more negative than for **49**, and this might point to a remarkable aromaticity of the lithiated complexes or might be caused by diamagnetic contributions from the bonds between Li and the ring atoms[93b]. This point should be further investigated computationally. Note, however, that the diamagnetic susceptibility exaltations of **69** and **70** are less negative than those of the free dianion **49**, which may point to a smaller degree of aromaticity in the lithiated complexes. The aromatic ring currents in **70** are responsible for the strong magnetic shielding of the Li^+ ions [$\delta(^7Li) = -7.7$ ppm[93a]; −6.2 ppm in **68** and −9.1 ppm in C_5H_5Li[88]]. The Na^+ and K^+ analogues of **69** and **70** show similar characteristics and are therefore also highly aromatic[93a].

West, Apeloig and coworkers reported recently an X-ray structure of an η^1,η^5-dilithium silole (**71**). One Li atom (with its associated two THF solvation molecules) is η^5-bonded to the silole ring and the second Li is η^1-bonded to the Si as well as to three THF molecules (Figure 8d)[10b]. Considering the fact that the solvating THF molecules were not included in the calculations, the MP2/6-31+G* optimized structure of the model system **72** (Figure 10d) is in reasonable agreement with the experimental structure of **71**. The calculated $C_{(1)}-C_{(2)}$ and $C_{(2)}-C_{(3)}$ bond lengths are 1.420 Å and 1.426 Å, respectively, compared to the measured bond lengths of 1.448 Å and 1.430 Å, respectively[10b]. The experimental distances involving the Li atoms are longer in **71** than those calculated for

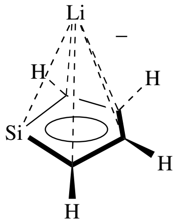

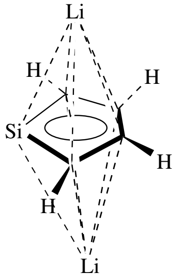

(69) **(70)**

72, as expected, because the THF solvation is not present in the calculations. According to the calculations **70** is by 21 kcal mol^{-1} more stable than **72** (MP2/6-31+G*//MP2/6-31+G*), but the authors suggest that solvation by THF may reverse this order. The effect of solvation on the **70**–**72** energy difference is currently being investigated computationally by Apeloig and coworkers. The structure of $2Li^+[c\text{-}Ph_4C_4Si^{2-}]$ in solution is still uncertain, although some NMR evidence [i.e. an upfield shift of $\delta(^{29}Si)$ to 68.5 ppm in solution, from 87.3 ppm in the solid state, and a single signal in the ^{7}Li NMR (at 0.23 ppm) even at −100 °C] might point to a single environment for the two Li atoms as in the thermodynamically more stable isomer **70**. The nearly equal, calculated C−C bond lengths in **72** and its NICS value (−18.4 ppm)[93b] point to the highly aromatic character of **72**, similar to that of **69** and **70**. More recently, the analogous germoles **73a** and **73b** were crystallized from dioxane in two distinct structures: one with η^1,η^5-coordination of the two Li$^+$ cations **(73a)** and the other having a η^5,η^5-coordination **(73b).** As in the silicon case, also for germanium the calculations (MP2/LANL2DZ) find the $\eta^5,\eta^5\text{-}2Li^+[c\text{-}H_4C_4Ge^{2-}]$ isomer to be by 25 kcal mol^{-1} more stable than the $\eta^1,\eta^5\text{-}2Li^+[c\text{-}H_4C_4Ge^{2-}]$ isomer[85].

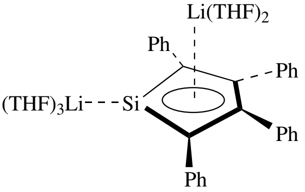

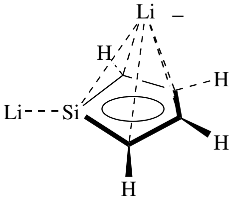

(71) **(72)**

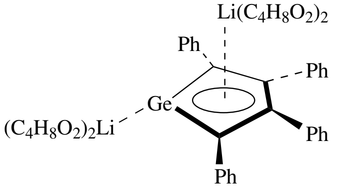

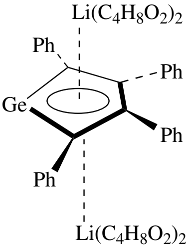

(73a) **(73b)**

4. Higher congeners of the silolyl anion and silole dianion

How is the aromaticity of the silolyl anion and dianion affected by substitution of the Si atom by its higher congeners Ge, Sn and Pb? In a comprehensive study Goldfuss and Schleyer[89] evaluated the degree of the aromaticity of mono- and dianions of group 14 metalloles: $c\text{-}C_4H_4EH^-$ and $c\text{-}C_4H_4E^{2-}$ ($E = C$, Si, Ge, Sn and Pb) by using a variety of criteria: structural, energetic (ASE) and magnetic (diamagnetic susceptibility exaltations and NICS). Their main conclusions are summarized briefly below.

(a) The aromaticity of the metallolyl monoanions $c\text{-}C_4H_4EH^-$ decreases in the order: C (most aromatic) > Si > Ge > Sn > Pb (least aromatic). This is exhibited in an increased bond alternation, stronger pyramidality at E, higher inversion barriers and decreased ASE along the C→Pb series. Similarly, the Λ and NICS values become less negative in going down along group 14, also indicating a decrease in aromaticity.

(b) The aromaticity of the lithium metallolides $Li[c\text{-}C_4H_4EH]$ decreases along the C→Pb series similarly to the $c\text{-}C_4H_4EH^-$ series. However, $Li\cdots H$ interactions between the η^5-coordinated Li atoms and the E−H hydrogen stabilize significantly the heavier metalloles with $E = Sn$ and Pb relative to their lower congeners.

(c) In contrast to the $c\text{-}C_4H_4EH^-$ and $Li[c\text{-}C_4H_4EH]$ systems, the degree of aromaticity of the metallole dianions $c\text{-}C_4H_4E^{2-}$ and of their dilithium $2Li^+[c\text{-}C_4H_4E^{2-}]$ complexes is remarkably constant for all group 14 elements.

5. The pentasilacyclopentadienyl anion

$c\text{-}Si_5H_5^-$ **(74)** has [at MP2(full)/6-31G*] two non-planar minima of C_s and C_2 symmetry which have identical energies[71]. The planar, formally 'fully aromatic' D_{5h} structure **(74)** is not a minimum on the MP2(full)/6-31G* $Si_5H_5^-$ PES and it is by 8.3 kcal mol^{-1} higher in energy than the C_s or C_2 structures. The calculated geometries of the C_s, C_2 and D_{5h} $Si_5H_5^-$ structures are shown in Figure 11. The aromatic stabilization energy of C_s $Si_5H_5^-$ according to equation 22 is 52.8 kcal mol^{-1}, much smaller than for its all-carbon analogue $C_5H_5^-$ (84.7 kcal mol^{-1})[71], pointing to a significantly lower degree of aromaticity in $Si_5H_5^-$. Yet, this ASE is much higher than the ASE of only 2.2 kcal mol^{-1} (HF/6-31G*) calculated for the monosilacyclopentadienyl anion **(67a)** according to an analogous isodesmic equation[87].

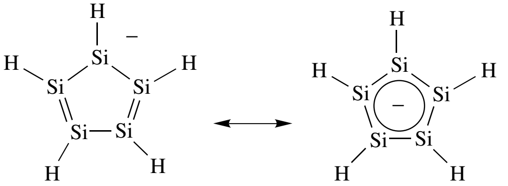

(74)

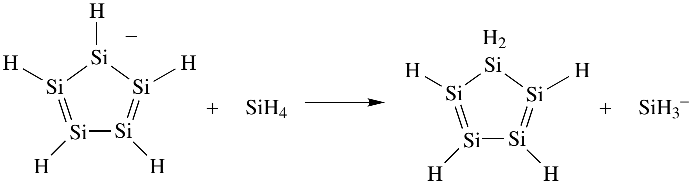

(22)

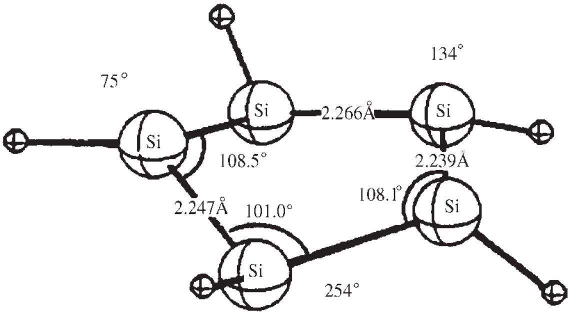

C_s' 0.0 kcal mol^{-1}

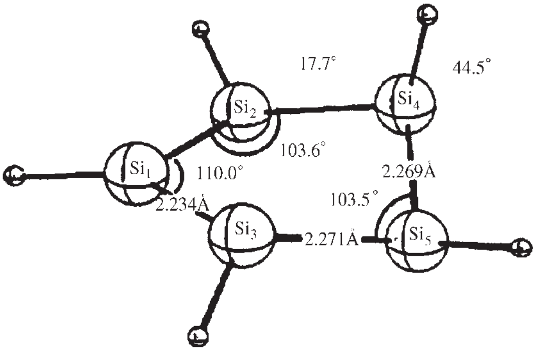

C_2' 0.00 kcal mol^{-1}

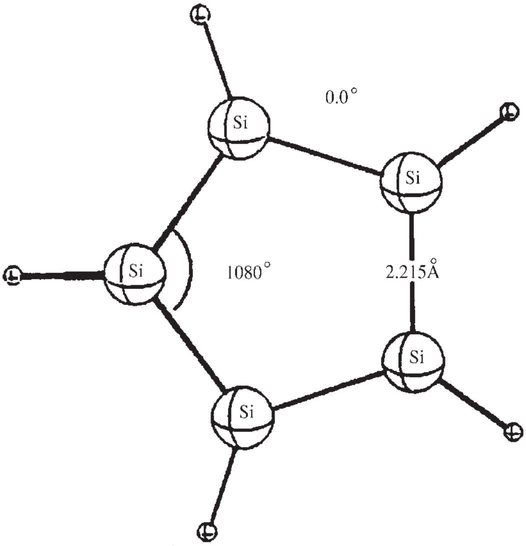

D_{5h}' 8.31 kcal mol^{-1}

FIGURE 11. Calculated structures and relative energies at MP2(full)/6-31G* of C_s, C_2 and D_{5h} *c*-$Si_5H_5^-$ (**74**). Bond lengths in Å, bond angles in degrees. The angles given outside the ring are dihedral angles. Reproduced by permission of John Wiley & Sons from Reference 71

V. SILYLENES WITH AROMATIC CHARACTER

A. Stable 'Arduengo-type' Silylenes

1. Experimental background

Divalent group 14 compounds (carbenes, silylenes and germylenes) are generally highly reactive intermediates which, until recently, were directly observed only in matrices at low temperatures[2e,94]. In 1991 Arduengo and coworkers reported the synthesis of the first stable carbenes **75a**[95a,b] and **76a**[95c]. This remarkable achievement stimulated numerous studies which reported physico-chemical measurements[95d–g] and theoretical studies[95d–h,96] of these stable carbenes. Consequently, the isostructural germylenes **75b** and **76b**[97] and silylenes **75c**[98a,c,d] and **76c**[98b,c,d] were synthesized and characterized. The silylene **75c** exhibits remarkable thermal and kinetic stability[98a,c,d]. Thus, it does not dimerize or react with various bases and other known silylene scavengers under conditions in which simple silylenes react instantaneously[98a]. The saturated analogue **76c** is also highly stable, but it slowly dimerizes with a half-life of *ca* 5 days[98b,c,d]. These studies were supplemented by theoretical calculations of the corresponding parent silylenes **75d** and **76d** and the related silanes **77a** and **78**[98].

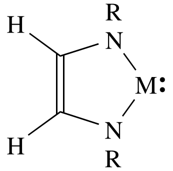

(75a) M = C, R = H, *t*-Bu, 1-Ad, Ar
(75b) M = Ge, R = *t*-Bu
(75c) M = Si, R = *t*-Bu
(75d) M = Si, R = H

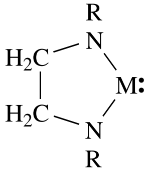

(76a) M = C, R = Ar
(76b) M = Ge, R = *t*-Bu
(76c) M = Si, R = *t*-Bu
(76d) M = Si, R = H

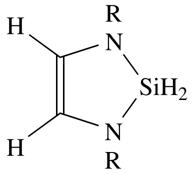

(77a) R = H
(77b) R = *t*-Bu

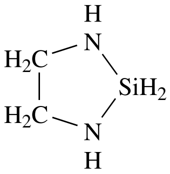

(78)

Most recently, stable crystalline 1,3-di(*neo*-pentyl)-2-silabenzimidazol-2-ylidene, **79a**, and its related saturated 2,2-dihydro-1,3-di(*neo*-pentyl)-2-silabenzodiaminosilole, **80a**, were synthesized[99]. **79a** can be stored under nitrogen for more than a year at ambient conditions and it can be distilled or sublimed without significant decomposition[99]. **79a** was characterized by its X-ray and by the UV photoelectron spectrum which was assigned with the help of MP2/6-31G*//MP2/6-31G* calculations for **79b**[99c].

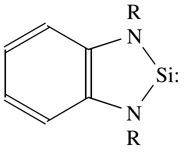

(79a) R = CH_2Bu-*t*
(79b) R = H

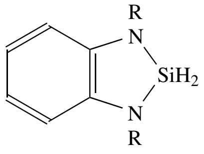

(80a) R = CH_2Bu-*t*
(80b) R = H

2. Aromaticity

Why are silylenes **75c** or **79a** so highly stable? Is the stabilization due to the presence of the two α-amino groups? Are these silylenes aromatic? The calculations show that $(H_2N)_2Si\colon$ is by 37.2 kcal mol^{-1} more stable than $H_2Si\colon$ (CCSD/6-31G*//MP2/6-31G*)[68], 30.0 kcal mol^{-1} at MP4/6-31G*//6-31G*+ZPE[100]. If this is the only factor contributing to the stability of **75c**, why then is the analogous four-membered ring diamidosilylene **(81)** stable only below 77 K[101]?

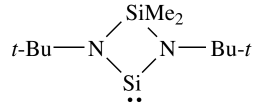

(81)

The high kinetic stability of **75c** and **76c** towards dimerization was explained by Denk and coworkers in terms of their high singlet-triplet energy difference, ΔE_{ST}[98b]. Thus, ΔE_{ST} **(75d)** of 69 kcal mol^{-1} and ΔE_{ST} **(76d)** of 74 kcal mol^{-1} (MP4/6-31G*//6-31G*) are larger than 60 kcal mol^{-1} — a value which was predicted[65] to be the limit above which the resulting dimers (i.e. the disilenes) dissociate spontaneously to the corresponding silylenes. It is therefore expected that **75c** and **76c** would dimerize very slowly, if at all[98b]. However, the lower reactivity of **75c** relative to **76c** towards dimerization and hydrogenation at silicon and its higher thermodynamic stability (see below) point to an additional stabilizing effect which is present in **75c** but not in **76c**[98b]. The additional stabilizing effect in **75c** was attributed to the contribution of the 6π-electron delocalization, i.e. to aromaticity, as shown in resonance structure **82**[96,98,100,102,103].

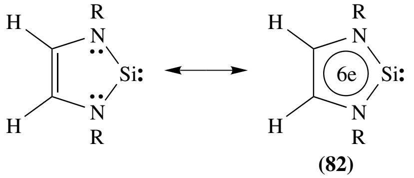

(82)

The occurrence of cyclic 6π-electron delocalization in imidazol-2-ylidene-type systems **(75)** is supported by a variety of structural, energetic, and magnetic criteria, as well as by the charge distributions and low-energy ionization processes which have been carefully analysed theoretically[96,98,100,102,103]. A summery of the conclusions of the theoretical studies regarding the degree of aromaticity in imidazol-2-ylidene-type systems is presented in Table 9.

TABLE 9. Experimental and theoretical studies on imidazol-2-ylidenes **(75a)** and their silicon analogues **(75c, 75d** and **79a, 79b)**[a]

Property studied	Method	Conclusions	Ref.
Carbenes			
Electronic structure of imidazol-2-ylidene in the lowest singlet and triplet states; proton affinity	Correlated *ab initio* calculations	Bonding character is carbenic rather than ylidic; π-delocalization is important in the imidazolium cation but not in the carbene	95h
Electronic structure of imidazol-2-ylidene: Bond orders, atomic charges, localized orbitals	Correlated *ab initio* calculations	Stabilization of singlet ground state by σ-back-donation along C-N bonds; π-delocalization plays only a minor role in imidazol-2-ylidene, but a major role in imidazolium cation	95d
Electronic structure of aminocarbenes: Singlet–triplet splittings, Mulliken populations, barriers for 1,2-rearrangements to imines	Correlated *ab initio* calculations	Singlet–triplet splitting in imidazol-2-ylidene is 15 kcal mol^{-1} higher than in imidazolin-2-ylidene, **76a,** R=H; consequently, there is a smaller propensity of the former towards dimerization; imidazol-2-ylidene is kinetically stable towards rearrangement to imidazole	95g
Chemical shielding tensor of a substituted imidazol-2-ylidene	Solid-state NMR; Correlated *ab initio* and density-functional calculations	Dominance in **75a** of carbenic over ylidic resonance structures	95e
Photoelectron spectra of **75a**, R = H and **75d**	Photoelectron spectroscopy; density-functional calculations	Degree of interaction between the π-electrons of the five-membered ring and the divalent group 14 atom is higher in silylenes **75c** and **75d** as compared to carbene **75a**	96
Electron distribution in a substituted imidazol-2-ylidene	X-ray and neutron diffraction; density-functional calculations	π-Delocalization not dominant in imidazol-2-ylidenes; stability of **75a** is kinetic in origin	95f
Electronic structure of stable carbenes, silylenes and germylenes	Correlated *ab initio* calculations	**75a**, R = H has partial aromatic character. π-Delocalization is more extensive in **75a**, R = H than in **76a**, R = H. Similar conclusions were reached for the corresponding silylenes and germylenes	103
Silylenes			
Gas-phase structure and solution-phase NMR of **75c;** theoretical heats of hydrogenation for **75d** and **76d**	Electron diffraction; correlated *ab initio* calculations	**75c** and **75d** benefit from aromatic stabilization	98a

TABLE 9. (*continued*)

Property studied	Method	Conclusions	Ref.
Photoelectron spectra of **75c** and **76c**; rotational barriers in $Si(NH_2)_2$ and $C(NH_2)_2$	Photoelectron spectroscopy; correlated *ab initio* calculations	Significant $p_\pi - p_\pi$ interaction between divalent group 14 centres and amino substituents; aromatic resonance structures contribute significantly in **75c** and **75d**	98b
Chemical shifts and anisotropies in aminosilylenes	Correlated *ab initio* calculations	Significant degree of 6π-aromaticity in **75d**	102
Thermodynamic stabilization, structure, chemical shift anisotropies and charge distribution	Correlated *ab initio* calculations, 'atoms-in-molecules' charge distribution analysis	Significant conjugation in **75d** relative to **76d** according to the thermodynamic and magnetic criteria. Small cyclic delocalization according to the topological analysis of charge density. More extensive π-resonance is found in the carbene **75a**	100
Photoelectron spectra, structure and thermodynamic stability of **79a** and **79b**	Photoelectron spectroscopy and correlated *ab initio* calculations	Cyclic delocalization plays an important role in the stability of **79a** and **79b**	99c
Nucleus independent chemical shifts	Correlated *ab initio* calculations	**75c, 75d, 79a** and **79b** possess a discernible ring current, which however is *ca* half as large as that in benzene. The ring current in **76c** and **76d** is negligible	107

[a] Based on Reference 100.

The structural, energetic, magnetic and charge distribution data that support the occurrence of 6π-electron delocalization in imidazol-2-ylidene-type silylenes and carbenes are discussed below:

a. Structural criteria. The experimental X-ray and calculated structures of **75c** (at ECP/6-31G*[104]) and **75d** (at 6-31G*[98a,b] and MP2/6-31G*[98a,100,103]) are in very good agreement. The calculated structures of **75c**[104] and **75d**[98a,b,100,103] are very similar. There is also good agreement between the experimental structure of **79a** and the MP2/6-31G*//MP2/6-31G* calculated structure of **79b**[99c]. The MP2/6-31G* optimized structures of **75d, 76d, 77a, 78** and **79b** are shown in Figure 12. There is no significant difference between the experimental structures of **75c** and of the corresponding benzo-derivatives **79a**, or between the calculated structures of the corresponding hydrogen-substituted **75d** and **79b**.

The calculated Si−N bond length in **75d** is 1.774 Å, by 0.034 Å longer than in **76d** (exp. 1.753 Å and 1.719 Å in **75c** and **76c**, respectively)[98b]. The shorter Si−N bonds in **76c** (or **76d**) were interpreted as resulting from the fact that in these molecules the lone-pairs on the nitrogen atoms can conjugate only with the empty 3p(Si) orbital, whereas in **75c** (or **75d**) the N lone-pair electrons are cyclically delocalized as shown in **82**, resulting in a longer Si−N bond in **75** relative to **76**[98b]. The assumption of cyclic delocalization in **75c** (or **75d**) is reinforced by the 0.011 Å longer calculated $r(C{=}C)$ in **75d** (1.333 Å, MP2/6-31G*) than in the corresponding silane **77a** (where cyclic electron delocalization

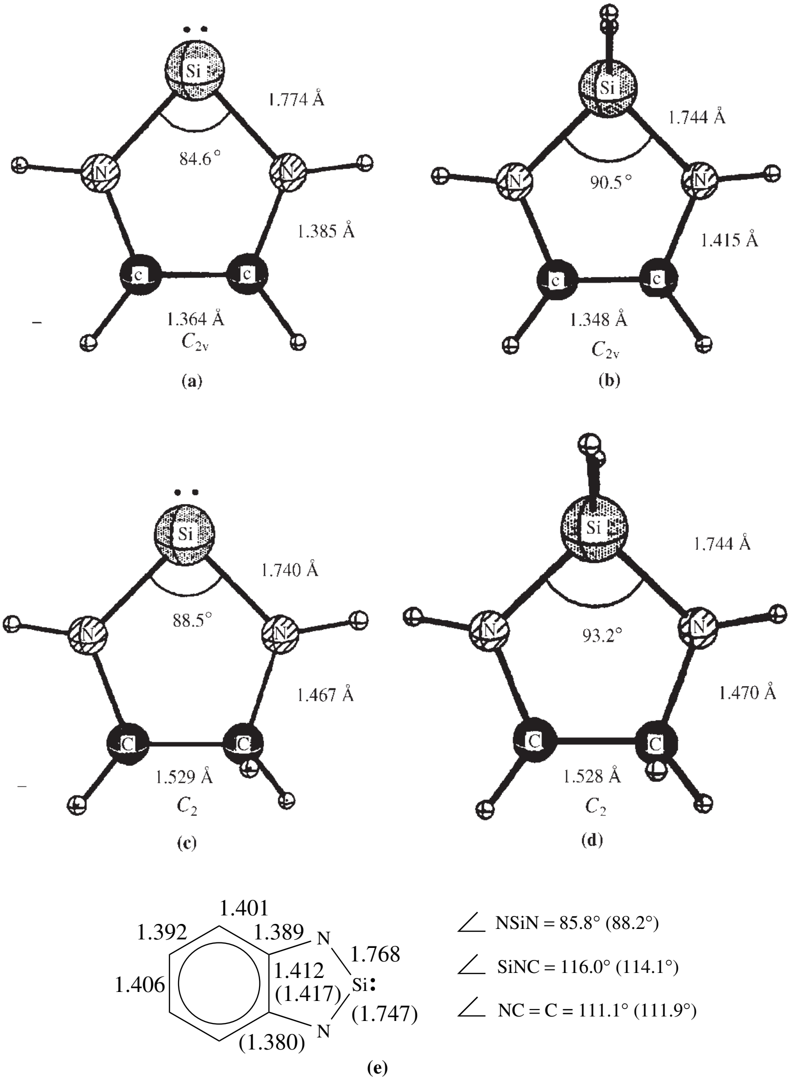

FIGURE 12. MP2/6-31G* optimized geometries of **75d** (a), **76d** (b) and of their corresponding silanes **77a** (c), **78** (d) and of 2-silabenzimidazol-2-ylidene **79b** (e); the experimental structure of **79a** is given in parentheses. Reprinted with permission from References 100 and 99c. Copyright (1996) American Chemical Society

is not possible)[98b,100]. The structures of the 2-silabenzimidazol-2-ylidenes **79a** and **79b** are indicative of a small but significant double-bond character in its Si—N bonds[99c]. Comparison of the cyclosilylenes **75c** and **75d** with the corresponding cyclic carbenes (**75a,** R = *t*-Bu or H) shows that the structural effects in the two types of species are similar, but they are somewhat smaller in the cyclosilylenes, indicating a smaller degree of electron delocalization in the silylenes[100].

b. Energetic criteria. According to the energies of equations 23a, 23b and 23c, the unsaturated cyclic silylene **75d** is by 20.5 and 11.8 kcal mol^{-1} (MP4/6-31G*//6-31G*+ZPE) more stable than $(H_2N)_2Si\colon$ and **76d**, respectively[100]. Similarly, **75d** is by 25-27 kcal mol^{-1} more stable than **76d** relative to ethane and ethene, respectively (equation 24)[100,103]. Thus, the results of equations 23 and 24 indicate an additional stabilization in **75d** due to the endocyclic C=C double bond. This additional stabilization is not due to a localized conjugative interaction within the HN−CH=CH−NH 'backbone', since 1,2-diaminoethene (in the planar C_{2v} geometry) is stabilized by only 1.4 kcal mol^{-1} (MP4/6-31G*//6-31G*+ZPE) relative to 1,2-diaminoethane[100]. The extra stabilization of **75d** over **76d** was interpreted to indicate cyclic electron delocalization in **75d**, which is absent in the C−C saturated silylene **76d**. However, Heinemann and coworkers pointed out that this interpretation relies on the *a priori* assumption that the π-electrons do in fact undergo cyclic delocalization and that such electron delocalization indeed results in a thermodynamic stabilization[100]. The occurrence of cyclic conjugation in **75d** was consequently studied directly by analysis of the charge distribution in **75d** and **76d** (see below).

$$R_2Si\colon + SiH_4 \longrightarrow R_2SiH_2 + H_2Si\colon \qquad (23)$$

$$R = NH_2 \qquad \Delta E = 30.0\ \text{kcal mol}^{-1}\ {}^{100} \qquad (23a)$$

$$R_2Si\colon = \mathbf{75d} \qquad \Delta E = 50.5\ \text{kcal mol}^{-1}\ {}^{100} \qquad (23b)$$

$$R_2Si\colon = \mathbf{76d} \qquad \Delta E = 38.7\ \text{kcal mol}^{-1}\ {}^{100} \qquad (23c)$$

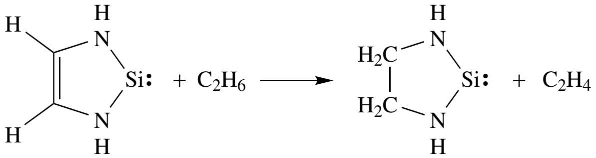

(24)

(75d) **(76d)**

ΔE = 25.0 kcal mol^{-1} (MP4/6-31G*//HF/6-31G*[100]);
27.4 kcal mol^{-1} (MP2/6-31G*//MP2/6-31G*[103])

The higher exothermicity, by 13 kcal mol^{-1}, of the hydrogenation energy of the silicon atom in **76d** (equation 25) compared to that of **75d** (equation 26)[98a] and also in the hydrogenation energy of the C=C double bond in **77a** (equation 27) compared to that of **75d** (equation 28)[98b] are also believed to be manifestations of the cyclic 6π-electron delocalization in **75d**[98a,b].

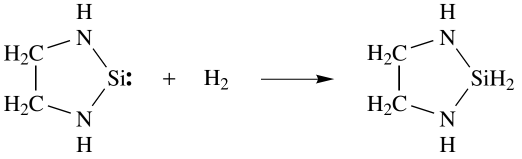

(25)

(76d) **(78)**

ΔE = 15.1 kcal mol^{-1} (MP2/6-31G*//HF/6-31G*[98a])

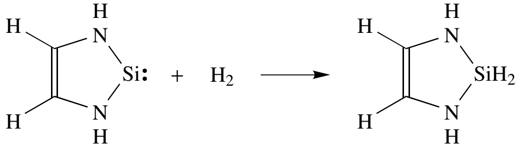

(75d) **(77a)**

(26)

$\Delta E = -1.7$ kcal mol^{-1} (MP2/6-31G*//HF/6-31G*[98a]);
-9.8 kcal mol^{-1} (MP4/6-311G**//MP2/6-31G*[103])

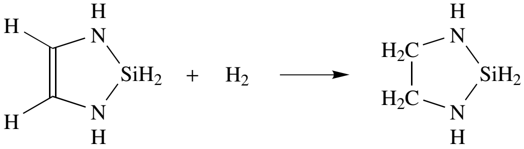

(77a) **(78)**

(27)

$\Delta E = -19.7$ kcal mol^{-1} (MP4/6-31G*//HF/6-31G*[98b]);

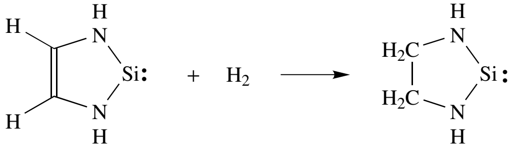

(75d) **(76d)**

(28)

$\Delta E = -6.7$ kcal mol^{-1} (MP4/6-31G*//HF/6-31G*[98b]);

Cyclic delocalization plays an important role also in the stabilization of the benzimidazol-2-ylidenes, **79**[99c], as concluded from the calculated ring fragmentation energies (equations 29 and 30), i.e. $\Delta E = 40.9$ and 22.9 kcal mol^{-1}, respectively (MP2/6-31G*//MP2/6-31G*). The effect of the five-membered ring is taken into account by keeping the geometry of the N−Si−N units in H_2NSiNH_2 in the same geometry as that in **79** or in **80**. A significant delocalization stabilization of 31.6 kcal mol^{-1} was suggested also for the isomeric silaimine **83** (equation 31)[99c].

$$\mathbf{79b} + 2NH_3 + 2CH_4 \longrightarrow H_2N{-}Si{-}NH_2 + 2H_2NCH_3 + C_6H_6 \tag{29}$$

$$\mathbf{80b} + 2NH_3 + 2CH_4 \longrightarrow H_2N{-}SiH_2{-}NH_2 + 2H_2NCH_3 + C_6H_6 \tag{30}$$

$$\mathbf{83} + 2NH_3 + 2CH_4 \longrightarrow H_2N{-}SiH{=}NH + 2H_2NCH_3 + C_6H_6 \tag{31}$$

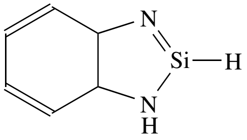

(83)

c. Magnetic criteria. The isolation of **75c** allowed to record the first NMR spectra of a silylene, and the measured chemical shifts[98a] are given in Figure 13.

GIAO[105] [MP2/TZ2P(Si),TZP(C,N),DZ(H)] calculations for the hydrogen substituted silylene **75d** predict chemical shifts which are in very good agreement with the experimental values measured for the substituted **75c** (Figure 13)[102]. In particular, the ^{29}Si chemical shift of **75d** is calculated to be 64 ppm[102], compared with the experimental value for **75c** of 78 ppm[98a]. The experimental–theoretical agreement for the carbon and nitrogen chemical shifts is also good[102]. Similar calculations for the saturated silylene **76d** predict a ^{29}Si chemical shift of 117 ppm[102], again in very good agreement with the experimental value for **76c** of 119 ppm[98d]. This success suggests that GIAO calculations can be used to elucidate the NMR spectra of transient silylenes which cannot yet be studied experimentally. Such studies can provide important fundamental information on the electronic structure of silylenes.

Further insight into the NMR spectrum of **75c** and **76c** was provided by additional GIAO calculations for H_2Si**:** and for several diaminosilylenes, carried out by Apeloig, Karni and Müller (Table 10)[102]. The calculated ^{29}Si chemical shift for the parent H_2Si**:** is 817 ppm (relative to TMS), and it shows a very large ^{29}Si chemical shift anisotropy (CSA), $\Delta\sigma$, of 1516 ppm (Table 10)[102]. This very high CSA indicates a strong charge anisotropy around the silicon, as is required by its electronic structure having perpendicular empty and filled orbitals, as shown by the magnetic axes of silylenes **75** and **79** drawn in Figure 14. Both the ^{29}Si chemical shift and the CSA of H_2Si**:** decrease strongly upon substitution of the hydrogens by two amino groups. In the planar $(H_2N)_2Si$**:** $\delta(^{29}Si) =$ 108 ppm and $\Delta\sigma(^{29}Si) = 214$ ppm. This large substituent effect can be attributed to the conjugation between the lone pairs on N and the empty 3p(Si) orbital. This interpretation is supported by the much higher $\delta(^{29}Si)$ and CSA in the perpendicular $(H_2N)_2Si$**:**, where such 2p(N)–3p(Si) conjugation is not possible (Table 10). The endocyclic C=C π-bond in **75d** causes an additional 53 ppm upfield shift in $\delta(^{29}Si)$ relative to **76d**, and to a significant increase in the CSA (from 73 ppm in **76d** to 165 ppm in **75d**)[102]. These trends, in both the ^{29}Si chemical shifts and in the CSAs, seem to support the hypothesis that the 'aromatic' resonance structure **82** contributes significantly to the total wave function of

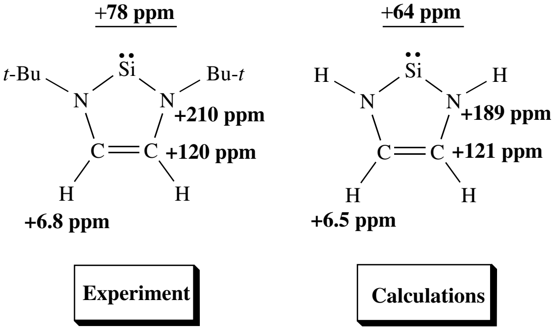

FIGURE 13. Experimental and calculated [GIAO/(MP2/TZ2P(Si)TZP(C)DZ(H))] chemical shifts of **75c** and **75d**, respectively. ^{15}N chemical shifts are relative to NH_3. The reported experimental ^{15}N chemical shift (relative to CH_3NO_2[98a]) was corrected using the experimental difference of 380 ppm between the ^{15}N chemical shifts of CH_3NO_2 and NH_3. Reproduced by permission of VCH Verlagsgesellschaft from Reference 102

75d[102]. The large anisotropies of the magnetic susceptibility, $\Delta\chi$ (calculated using the IGLO method[106]), support the occurrence of ring currents in **75d** ($\Delta\chi = 6.46$ au), as well as in the corresponding potentially aromatic silicenium cation **84** ($\Delta\chi = 5.64$ au), but not in **76d** or **78**—the correspondingly saturated analogues ($\Delta\chi = 1.41$ and 1.96 au, respectively)[100]. The smaller calculated $\Delta\chi$ for the silylene **75d**, relative to that of the analogous carbene **75a**, R = H ($\Delta\chi = 8.17$ au), also indicates a smaller ring current and thus a reduced 'aromaticity' in **75d** relative to that in **75a**, R = H[100].

The NICS values of the silylenes **75c** and **79a**, calculated at a distance of 2.0 Å above the ring centre, are −2.7 ppm and −2.6 ppm, respectively[107]. These values are significantly lower than for benzene (−5.3 ppm) or thiophene (−4.7 ppm), but still indicate that these silylenes possess a discernible diamagnetic ring current of about half of that in benzene. In contrast, the NICS value of the saturated silylene **76c** is negligible (−0.6 ppm), indicating the absence of a significant ring current[107].

TABLE 10. Calculated ^{29}Si chemical shifts [$\delta(^{29}\text{Si})$] and chemical shift anisotropies [CSA, $\Delta\sigma(^{29}\text{Si})$] for several silylenes (in ppm)[a]

Silylene	$\delta(^{29}\text{Si})$[b]	$\Delta\sigma(^{29}\text{Si})$[c]
H_2Si	817	1516
$(H_2N)_2Si$, per[d]	421	558
$(H_2N)_2Si$, pl[e]	108	214
76d	117[f]	73[g]
75d	64[h]	165

[a] From Reference 102 at GIAO[MP2/TZ2P(Si), TZP(C,N), DZ(H)],

[b] Relative to $(CH_3)_4Si$,

[c] Calculated from absolute chemical shielding values,

[d] Perpendicular conformation, i.e. ∠HNSiN = 90°C.

[e] Planar conformation, i.e. ∠HNSiN = 0°.

[f] 131.9 ppm at GIAO[B3LYP/6-311+G(2df,p)(Si), HF/6-31G*(C,N,H)//B3LYP/6-31G*[107]], Experimental values for **76c:** 117.0 ppm[98d] and 119.0 ppm[107] in solution and in the solid, respectively.

[g] The CSA values (calculated from chemical shifts) are 447.7 and 363.1 ppm for **76d** and **75d**, respectively [at GIAO(B3LYP/6-311+G(2df,p)(Si), HF/6-31G*(C,N,H)//B3LYP/6-31G*[107]]; the corresponding experimental values for **76c** and **75c** are 354.0 and 314.6 ppm, respectively[107].

[h] 84.8 ppm at GIAO[B3LYP/6-311+G(2df,p)(Si), HF/6-31G*(C,N,H)//B3LYP/6-31G*[107]] Experimental values for **75c**: 78 ppm in solution[98d] and 75.2 ppm in the solid[107].

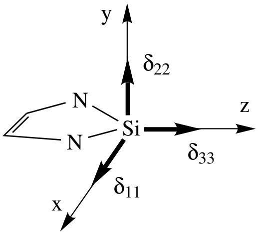

FIGURE 14. Molecular and magnetic axes for silylene **75**. The same axes also apply for **79**. Reprinted with permission from Reference 107. Copyright (1998) American Chemical Society

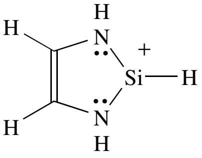

(84)

d. Charge distribution and ionization potentials. The degree of π-delocalization in **75**, from the −NCH=CHN− backbone into the formally empty p atomic orbital of M, can be evaluated by several theoretical approaches. NBO analysis[108] of the charge distribution in **75d** and **76d** (at MP2/6-31G*) shows significant electron occupancy of the 3p(Si) orbital in both silylenes. However, as expected if **75d** is aromatic, the electron occupancy of the 3p(Si) in orbital in **75d** (0.54e) is higher than in the saturated silylene **76d** (0.33e)[103]. The 3p(Si) electron occupation in **75d** is smaller than in the corresponding carbene **75a**, R = H (0.67e) and germylene **75**, M = Ge, R = H (0.63e), as expected from their electronegativites (Ge is more electronegative than Si)[103]. This result contrasts with that of DFT calculations, which predicted that the degree of π-electron delocalization in divalent **75** will decrease in the order M = Ge > Si > C, i.e. delocalization is most efficient for **75**, M = Ge[96]. Arduengo and coworkers suggested a 'chelated-atom' model to account for this trend[96]. Boehme and Frenking pointed out that this model and the DFT trend of the occupation of the 3p-orbital would suggest that the oxidation strength increases in the order Ge > Si > C, which is difficult to understand[103]. Analysis using the 'Atoms in Molecules' theory[109] also provides evidence for some degree of cyclic electron delocalization in the unsaturated Arduengo-type cyclic carbene **75a**, R = H (although to a smaller degree than calculated by other methods) and to an even smaller extent of delocalization in the analogous silylene **75d**[100].

Another argument in favour of the aromaticity of unsaturated cyclic silylenes such as **75c** (or **75d**) comes from the analysis of their ionization potentials. Denk and coworkers argued[98b] that the energy lowering by 0.5 eV (HF/6-31G*) of the HOMO of **75d** shown in **85a** (E = −7.62 eV) as compared to the HOMO of the silane **77a** shown in **85b** (E = −7.1 eV)[98b], is consistent with a contribution of the 3p(Si) orbital to the stability of the HOMO orbital in **75d** but not in **77a**. The calculated difference in the orbital energies of 0.5 eV is in excellent agreement with the measured vertical ionization potentials of 6.96 eV and 6.56 eV for **75c** and **77b**, respectively[96,98b]. A similar stabilization of the HOMO of **79b**, by 0.33 eV (0.41 eV, experimental), relative to that of the corresponding silane **80b**, was also attributed to the contribution of the empty 3p(Si) orbital to the delocalization of the π-electrons[99c].

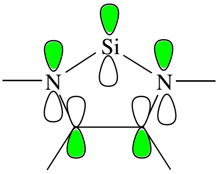

(85a)

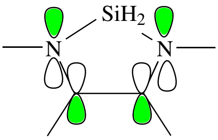

(85b)

In conclusion, all the criteria discussed above point to the existence of π-electron delocalization and thus to some degree of aromaticity in the unsaturated carbenes, silylenes and germylenes of type **75**. However, the degree of conjugation and aromaticity depends on the criteria that are used to evaluate these effects. The degree of aromaticity in **75** is quite small according to the 'Atoms in Molecules' topological charge analysis[100], but is more significant according to NBO charge analysis[103] or according to the structural, energetic and magnetic properties[100,103]. However, regardless of the criteria used, π-electron delocalization is generally found to be less extensive in the unsaturated silylenes (and germylenes) compared to their carbene analogues, and it is much smaller than in prototypic aromatic systems such as imidazolium cations or benzene[100,103].

3. Reactions

As mentioned above, the cyclic silylenes **75c** and also **76c** (or **79a** and **79b**) are dramatically less reactive than other known silylenes which are all transients. Thus, **75c** has such a low Lewis acidity that, unlike other silylenes, it does not react as an electrophile. However, **75c** reacts as a Lewis base, i.e. as a nucleophilic reagent[98c]. The known reactions of 'Arduengo-type' silylenes are summarized in References 2e, 98c, 98d and 99b and the references cited therein. The theoretical study of the possible reactions of 'Arduengo-type' silylenes is quite limited and awaits the attention of computational chemists.

a. 1,2-H rearrangements. An important factor which contributes to the kinetic stability of silylene **75c** is the fact that 1,2-H rearrangements to give the corresponding tetravalent silaimines do not occur. CCSD(T)/DZP calculations carried out by Heinemann and coworkers[104] showed that the rearrangement of simple aminosilylenes via a 1,2-H shift to produce the corresponding silaimines (equations 32–34) are endothermic, i.e. the silylenes are more stable than the isomeric silaimines. The isomerization energy, ΔE_r, of the cyclic silylene **75d** to the corresponding silaimine, of 31.8 kcal mol^{-1}, is significantly higher than for the rearrangements of the parent aminosilylene **86** to **87** or of the diaminosilylene **88** to **89**. A similar isomerization energy of 33.3 kcal mol^{-1} (MP2/6-31G*//MP2/6-31G*) was calculated for the rearrangement of **79b** to **83**. The high isomerization energy was attributed to the high strain of the five-membered ring in **83**[99c]. Furthermore, the energy barriers for these rearrangements, E_a, are very high, larger than 50 kcal mol^{-1} (above the silylenes). The high barrier of 54.4 kcal mol^{-1} calculated for the **75d**→**90** rearrangement explains why for **75c** such rearrangements were not observed experimentally[2e]. The relatively low barrier of 22.6 kcal mol^{-1} for the reverse **90**→**75d** rearrangement suggests that this type of reaction might be used to synthesize novel cyclic aminosilylenes[104]. The barrier for the analogous isomerization of the carbene **75a**, R = H to the corresponding imidazole of 44.1 kcal mol^{-1} is somewhat lower than for **75d**, but the barrier for the reverse reaction is significantly higher for the carbene (71.1 kcal mol^{-1} at MP4/6-311G**//MP2/6-31G*)[103].

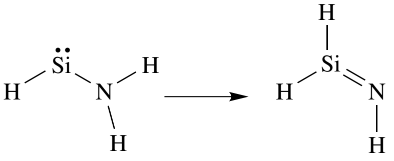

(32)

(86) **(87)**

$\Delta E_r = 14.2$ kcal mol^{-1}

$E_a = 68.8$ kcal mol^{-1}

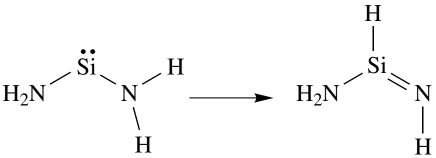

(88) **(89)**

$\Delta E_r = 19.2\ \text{kcal mol}^{-1}$

$E_a = 70.0\ \text{kcal mol}^{-1}$

(33)

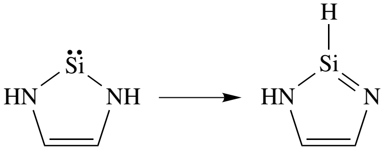

(75d) **(90)**

$\Delta E_r = 31.8\ \text{kcal mol}^{-1}$

$E_a = 54.4\ \text{kcal mol}^{-1}$

(34)

b. Dimerization. The report that the saturated silylene **76c** dimerizes slowly to give an unidentified product[98b] stimulated a theoretical study of the structure of this dimer[110]. Silylenes usually dimerize to give disilenes **(91)** as shown schematically in equation 35 for M = Si, and this is the main experimental route for the synthesis of disilenes[1a]. However, Apeloig and coworkers[102,110,111] and Trinquier and coworkers[66d,112] pointed out that the dimerization of two silylenes can in principle lead also to the bridged **92** (equation 36, both *trans* and *cis* arrangements of the R groups are possible). **92** was indeed found to be a minimum on the M_2H_4 surfaces for M = Si and Ge, but not for M = C, and it is even the global minimum for M = Sn and Pb[66d,112]. **92**, M = Si, R = H is by 21.3 kcal mol^{-1} less stable than $H_2Si{=}SiH_2$ at the G2 level of theory[102,110].

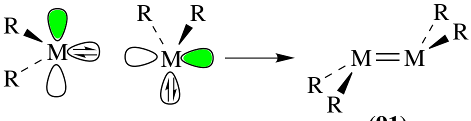

(91)

(35)

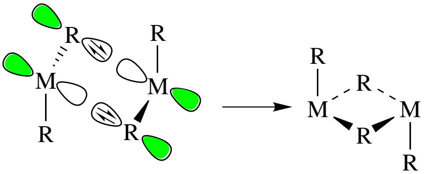

(92)

(36)

Apeloig and Müller found that electronegative substituents having lone-pairs(e.g. R = F, OH and NH_2) stabilize considerably the bridged isomer **(92)** relative to the corresponding isomeric disilene **(91)**. For example, when the bridging R groups are NH_2 and the exocyclic R groups are H, **92** is more stable than **91** by 10 kcal mol^{-1} at MP4/6-311G**//6-31G**[102,110]. Furthermore, disilenes substituted with four NH_2, F or OH substituents are no longer minima on the Si_2R_4 PES (at HF/6-31G**). On the other hand, the corresponding bridged isomers **92**, R = NH_2, OH and F are local minima on the PES; e.g. **92**, R = NH_2, is by 15.3 kcal mol^{-1} more stable than two isolated diaminosilylenes at MP2(fc)/6-31G*//MP2(fc)/6-31G*[110]. Calculations at HF/6-31G** show that, in analogy to $(H_2N)_2Si{=}Si(NH_2)_2$, also the disilene **93**, R = H, the formal dimer of **76d**, is not a minimum on the PES. In contrast, the corresponding bridged dimer **94**, R = H is a minimum on the PES, lying 7.8 kcal mol^{-1} below the energy level of two isolated **76d** silylenes. Apeloig and Müller therefore proposed that **76c** does not dimerize to the corresponding disilene **93**, R = *t*-Bu, but to the bridged cage-like structure **94**, R = *t*-Bu[110]. This prediction awaits experimental testing.

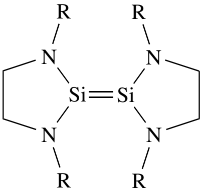

(93)

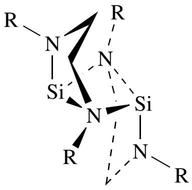

(94)

B. Miscellaneous Potentially Aromatic Silylenes

1. Cyclic aminosilylenes

Veszprèmi and coworkers[68,69] suggested that silylenes such as **95** and **96** are also potentially aromatic and that therefore they should be good candidates for synthesis. The formal trisilylene **95** is calculated to be by 30.5 kcal mol^{-1} (CCSD/6-31G*//MP2/6-31G*; 16.5 kcal mol^{-1} at MP2/6-31G*//MP2/6-31G*) more stable than the isomeric aromatic **41**[68] (see Section III.H. for a discussion on **41** and **42**). Similarly, the silylene **96a** is by 8.9 kcal mol^{-1} more stable than 2-silapyridine **42** (MP2/6-311G**//MP2/6-311G**[69]). **96a** and **42** are separated by a high barrier of 56 kcal mol^{-1}, similar to the barrier of 54 kcal mol^{-1} that separates **75d** from **90** (see Section V.A.2.a). The **96**–**42** stability order is reversed upon methyl substitution; **96b** is by 5.6 kcal mol^{-1} less stable than the methyl-substituted (on Si) **42**.

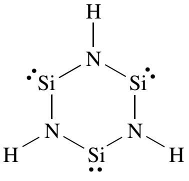

(95)

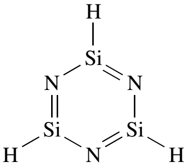

(41)

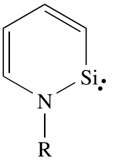

(96a) R = H
(96b) R = Me

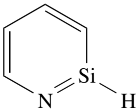

(42)

The higher stability of **95** and **96a** relative to their silaimine isomers is consistent with the relative energies of other silylimine–aminosilylene pairs (e.g. compare the relative energies of **86** vs **87**, **88** vs **89** and **75d** vs **90**). It is also in harmony with the relative bond energies of Si–H and N–H bonds, N–H being by about 16 kcal mol^{-1} stronger than Si–H[104] (based on the dissociation energies of SiH$_4$[113a] and NH$_3$[113b]). This stability order is in sharp contrast to that for the related phosphinine-2-ylidene **(97)**–phosphinine **(98)** pair, for which the carbene isomer is by 75 kcal mol^{-1} less stable than the phosphinine[114].

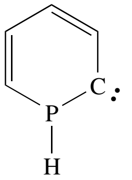

(97)

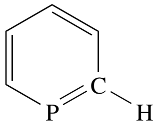

(98)

Veszprémi and coworkers concluded, on the basis of geometric and energetic criteria, that the silylenes **95** and **96a**, as well as the isomeric silaimines **41** and **42**, exhibit some degree of aromaticity. The geometries of the silaimine isomers, **41** and **42**, were discussed already in Section III.H and they are shown in Figure 7. We will compare here their geometries to those of the silylidene isomers **95** and **96a**. The Si–N bond lengths of 1.756 Å in **95** and 1.665 Å in **41** (MP2/6-31G*) show no bond alternation. The SiNSi and NSiN bond angles in **95** are 129.6° and 110.4°, respectively, while in **41** they are more similar, i.e. 117.0° and 123.0°, respectively. The three C–C bonds in the *cis*-butadiene unit in **42** are almost identical and are similar to those in benzene (i.e. 1.40 Å, Figure 7) while in **96a** these bonds (i.e. 1.382 Å, 1.413 Å and 1.373 Å at MP2/6-31G*[69] show some bond length alternation, similar to that in pyrrole, but smaller than that in *cis*-1,3-butadiene[69]. Based on the C–C bond length alternations, the authors concluded that the delocalization in **42** is somewhat larger than in **96a**[69].

The aromatic stabilization energies (at MP2/6-31G*//MP2/6-31G*) of **95** and **41**, according to the homodesmotic equations 37 and 16, are 6.0 and 19.6 kcal mol^{-1}, respectively, and those of **96a** and **42** (equations 38 and 17) are 14.7 and 19.4 kcal mol^{-1}, respectively. These aromatic stabilization energies, although significant, are considerably smaller than the aromatic stabilization energies of benzene, phosphabenzene, pyridine and silabenzene of 28.2, 27.1, 28.0 and 23.5 kcal mol^{-1}, respectively[69]. Note that these homodesmotic reactions do not provide a pure measure of the aromatic stabilization as they also include the ring strain of 10.0, 5.5 and 14.1 kcal mol^{-1} for **41**, **96a** and **42**, respectively[69] (the ring strain of **95** was not reported), which is released upon ring cleavage.

$$\mathbf{95} + 3\mathrm{HSiNH_2} \longrightarrow 3\mathrm{HSiNHSiNH_2} \tag{37}$$

$$\mathbf{96a} + \mathrm{HSiNH_2} + 2\mathrm{CH_2{=}CH_2} \longrightarrow \mathrm{CH_2{=}CHSiNH_2} + \mathrm{CH_2{=}CHNHSiH} + \mathrm{CH_2{=}CH{-}CH{=}CH_2} \tag{38}$$

Thus, according to the geometric and energetic criteria the silylenes **95** and **96a** possess some degree of aromaticity, although smaller than that of the corresponding silaimine isomers **41** and **42**. Magnetic properties, which might help in evaluating reliably the degree of aromaticity of these compounds, were not yet reported.

To evaluate the kinetic stability of **96a** its dimerization reaction was studied[69]. The authors find, in analogy to the previous findings of Apeloig and Müller for **76c** (Section V.A.3.b)[102,110], that the head-to-head dimerization of **96a** to give the corresponding disilene **99** (equation 39) is not feasible as **99** is not a minimum on the HF/6-31G* PES. On the other hand, the head-to-tail bridged dimer **100** (equation 40) is a minimum on the PES. However, **100** is by 18.4 kcal mol^{-1} less stable than the two isolated silylenes (**96a**). This contrasts the situation with the bridged dimer **94**, which is by 7.8 kcal mol^{-1} more stable than the corresponding two isolated silylenes **76d**[110]. Thus, **96a** and its substituted derivatives are expected to be highly stable towards dimerization, making silylene **96a** (and especially its sterically protected derivatives) a promising target for synthesis.

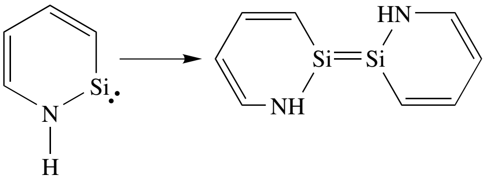

(96a) **(99)**

(39)

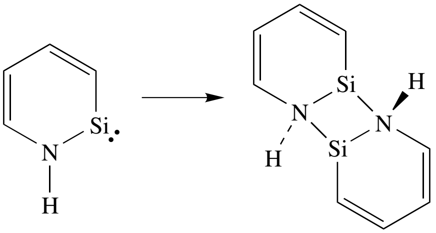

(96a) **(100)**

(40)

2. Silacyclopropenylidene and silacyclopropynylidene

Kinetic studies of the reaction of Si(^{3}P) with acetylene suggested the formation of stable complexes[115]. The potentially 2π-aromatic silylene, 1-silacyclopropenylidene **101**, was suggested as a possible intermediate, but at that time spectroscopic evidence which supports this suggestion was not available[115]. **101** and its cation-radical were later identified in the gas phase by a neutralization–reionization experiment[116]. Most recently in a beautiful study, Maier and coworkers have generated **101** in a matrix by pulsed flash pyrolysis of $HC\equiv CSiH_2Si(CH_3)_3$. Irradiation of **101** produced the non-cyclic isomers **102** and **103** and, surprisingly, due to their high strain, also silacyclopropyne (**104**) and silacyclopropynylidene (**105**)[117a,b]. **104** and **105** are calculated to have strain energies of *ca* 100 kcal mol^{-1}[117a,b] and are the most strained cycloalkynes ever identified. Isomers **101**–**105** were identified spectroscopically by comparison of their experimental and calculated (MP2/6-31G**[117b]) IR spectra. The structure of 1-silacyclopropenylidene, **101**, was determined by microwave spectroscopy[117c].

Extensive computational studies of **101**[117b,118,119] and also of other singlet[118,119] and triplet[119,120] C_2H_2Si isomers followed the first prediction of the existence of **101**[115]. The optimized geometries of singlet **101** at various theoretical levels are shown in Figure 15.

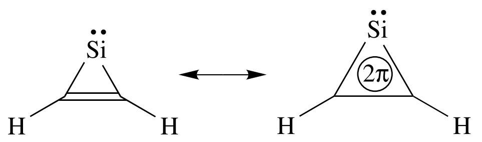

(101a) **(101b)**

$:Si{=}C{=}CH_2$

(102)

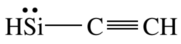

$H\ddot{S}i{-}C{\equiv}CH$

(103)

(104)

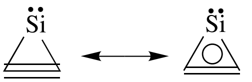

(105a) **(105b)**

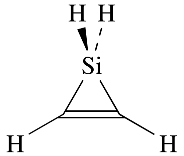

(106)

$:C{=}C{=}SiH_2$

(107)

$:C{=}Si{=}CH_2$

(108)

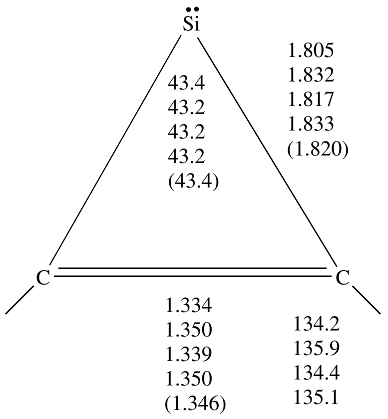

FIGURE 15. Optimized structures of singlet ($^1A_1$) **101**, at (from top to bottom): SCF/TZ2P[118b], MP2/6-311G**[117b], CISD/TZ2P[118b] and CCSD(T)/TZ(2df,2pd)[119]. Experimental values[117c] are given in parentheses, bond lengths in Å, bond angles in degrees

Is **101** aromatic? The C−C and Si−C bond distances in **101** [at CCSD(T)/TZ(2df,2pd), the best available level of theory for this system], of 1.350 Å and 1.833 Å respectively[119], are in good agreement with the experimental values of 1.346 Å and 1.820 Å, respectively[117c]. The C−C bond is somewhat longer than in the analogous cyclopropenylidene (1.328 Å[119]) and the C−Si bond distance is somewhat shorter than a regular single C−Si bond. These structural data and the results of Mulliken[118a,b] and NBO[117b] population analyses indicate some degree of 2π-aromatic delocalization of the C=C π-electrons into the formally empty 3p-orbital of the silicon, as described by resonance structure **101b**. The stabilization energy resulting from π-delocalization in **101**, as calculated according to equation 41a, is very high, 38.1 kcal mol^{-1} (MP2/6-31G**//MP2/6-311G**)[117b]. The authors attributed this large effect to the 'differences in the silanediyl structure'[117b]. A more detailed analysis of this large ASE was not given[117b], but it certainly supports the aromatic character of **101**. The ring strain energy of **101** is estimated to be *ca* 50 kcal mol^{-1} according to equation 41b and assuming that **101** and **106** have similar ring strain energies[117b].

$$\mathbf{101} + \mathrm{H_2Si(CH_3)_2} \longrightarrow \mathbf{106} + \mathrm{(CH_3)_2Si\colon} \qquad (41a)$$

$$\mathbf{106} + \mathrm{C_2H_6} + \mathrm{Si_2H_6} \longrightarrow \mathrm{H_2Si(CH_3)_2} + (Z)\text{-}\mathrm{H_3SiHC{=}CHSiH_3} \qquad (41b)$$

101 is the global minimum, on both the singlet[117a,118a] and triplet[120] C_2H_2Si PES. The vinylidenesilanediyl **102** and the ethynylsilylene **103** are by 17 and 22 kcal mol^{-1}, respectively, higher in energy than **101** (at CI/DZP+Davidson's correction[118a]; the relative energies at MP2/6-31G** are similar[117a]). The isomeric carbenes **107** and **108** are by 55.8 and 116.7 kcal mol^{-1}, respectively, higher in energy than **101** (at HF/DZ)[118a]. The interesting cyclic silane **104** was calculated to be by 47.4 kcal mol^{-1} higher in energy than **101** at CCSD(T)/TZ(2df,2pd)[119] (54.4 kcal mol^{-1} at MP2/6-31G**[17a,b]; 86.7 kcal mol^{-1} at SCF/DZ[118a]).

Calculations at UMP4/6-31G**//UHF/6-31G* show that the $^2A_1$ cation-radical of **101**, that was detected in the gas phase[116] and which formally is also 2π-aromatic, is by 43.7 kcal mol^{-1} more stable than its $\mathrm{Si}^{+\cdot}$ and C_2H_2 fragments, and that it is by only 0.5 and 8.5 kcal mol^{-1} more stable than the isomeric $\mathbf{102}^{+\cdot}$ and $\mathbf{103}^{+\cdot}$, respectively[121].

105, one of the irradiation products of **101**, is also a potentially 2π-aromatic silylene (see **105b**). **105** was identified earlier in gas-phase experiments by IR and electronic spectra[122a]. According to an NBO analysis, **105** is best described by a Lewis structure that has a delocalized 3-centre aromatic-type π-orbital and an in-plane CC π-orbital that has essentially a non-bonding character[117b]. The calculated C≡C and C−Si bond lengths in **105** are 1.285 and 1.838 Å, respectively (MP2/6-311G**[117b], 1.294 and 1.838 Å at MBPT(2)/DZ+d[122b]). The C≡C bond length is intermediate between that of a C=C bond in ethylene and a C≡C bond in acetylene, and it was therefore described as a 'weak triple bond'[122c], a description which is supported by NBO analysis[117b]. The calculated delocalization stabilization energy of **105** is very high, 42.0 kcal mol^{-1} (equation 42a), and it is calculated to have an incredibly high ring strain energy of *ca* 100 kcal mol^{-1} (equation 42b)

$$\mathbf{105} + \mathrm{H_2Si(CH_3)_2} \longrightarrow \mathbf{104} + \mathrm{(CH_3)_2Si\colon} \qquad (42a)$$

$$\mathbf{105} + \mathrm{C_2H_6} + \mathrm{Si_2H_6} \longrightarrow \mathrm{H_2Si(CH_3)_2} + \mathrm{H_3SiC{\equiv}CSiH_3} \qquad (42b)$$

3. *Trisilapropenylidene and other Si_3H_2 isomers*

The Si_3H_2 PES was studied at CISD/TZP//HF/DZP[123]. The global minimum is the potentially 2π-aromatic trisilapropenylidene **(109)**. The degree of aromaticity of **109** was not discussed. The Si=Si bond length is 2.11 Å, typical of a Si=Si double bond, and the Si−Si: bond distances are 2.28 Å (HF/DZP), very close to that of a typical Si−Si: single bond of *ca* 2.24 Å. **109** can isomerize with relatively low barriers of 12.5 and 13.6 kcal mol^{-1}, respectively, to the planar hydrogen-bridged structures **110a** and **110b**, which are by only 1.4 and 1.7 kcal mol^{-1}, respectively, less stable than **109**[123]. Another interesting Si_3H_2 isomer is the planar **111a** (C_s symmetry) which is by only

6.6 kcal mol^{-1} less stable than **109**. The conventional 'perpendicular' C_{2v} isomer **111b** is by 47.8 kcal mol^{-1} less stable than **111a**. The remarkable high stability of planar **111a** was rationalized as due to a 3-centre π-interaction in the cyclic Si_3 skeleton[123]. Higher level calculations are required to substantiate this interesting PES.

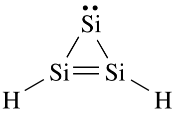
(109)

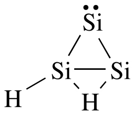
(110a)

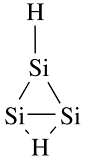
(110b)

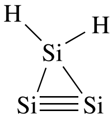
(111a)

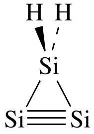
(111b)

VI. SILAFULLERENES

A. Are Fullerenes and Silafullerenes Aromatic?

The remarkable series of experiments by Kroto and coworkers[124] leading to the discovery of the spheroidal C_{60} Buckminsterfullerene and of larger carbon clusters, followed by the development by Kräschmer and coworkers[125] of methods which enabled the synthesis of macroscopic amounts of C_{60}, have stimulated an outburst of interest, both experimental and theoretical, in this class of compounds[126]. The silicon analogues of C_{60} and of larger carbon clusters have not been yet synthesized, but silicon clusters are currently of growing experimental and theoretical interest.

Are fullerenes and silafullerenes, e.g. C_{60}, Si_{60}, C_{70} and Si_{70}, aromatic? The suggestion by Kroto and coworkers[124a] that C_{60} and related molecules are aromatic raised considerable controversy and inspired analysis of this question by a variety of criteria, such as structure, energy, reactivity and magnetic properties[13a,127–133]. Studies of the magnetic properties included the chemical shifts of encapsulated He atoms[128,129] as well as NICS calculations[26,132]. These studies lead to the conclusion that C_{60} is aromatic, but only to a modest extent[127–130]. The degree of aromaticity of C_{70}, $C_{60}{}^{-6}$ and $C_{70}{}^{-6}$ is considerably larger[129,131,132]. Larger spheroidal carbon clusters such as C_{76}, C_{78}, C_{82} and C_{84} have a higher degree of aromaticity than C_{60}, but smaller than that of C_{70}[133]. The interested reader is referred to the above-mentioned references for a full discussion of this interesting topic.

The studies reported to date on silafullerenes have not assessed explicitly their aromatic character. We will assume here that as C_{60} and C_{70} are aromatic, so are their silicon analogues Si_{60} and Si_{70}, although they probably possess a smaller degree of aromaticity than their carbon analogues. Consequently, we include a discussion on Si_{60} and Si_{70}.

Due to their large size, most theoretical studies on silafullerenes were carried out using relatively simple computational levels. The theoretical studies on Si_{60} conducted up to the end of 1991 were reviewed by Nagase[61], and here we will summarize briefly only the most important conclusions of the earlier studies and add the few new studies which appeared after 1991.

The dramatic developments in computer technology and, in particular, the development of density functional methods will enable one in the near future to repeat and extend the studies discussed below, using more accurate and reliable computational methods. The study of the magnetic properties of silafullerenes and the evaluation of the degree of their aromaticity is also a worthwhile field of exploration for the future.

B. Si_{60}

1. Structure

As mentioned above, Si_{60} is still unknown and theory therefore remains the main tool for establishing its structure. Does Si_{60} possess the buckyball icosohedral structure **112** (Figure 16) that is constructed form 12 five-membered rings (5-MRs) and 20 6-MRs, as in C_{60}? Does Si_{60} adopt an isomeric structure? Several possible Si_{60} isomers **112–116** are shown in Figure 16. In view of the observation that in the gas phase silicon cluster ions lose mainly Si_6 and Si_{10} units[134], it was suggested[135,136] that these clusters are built either as stacked plates of silanaphthalenes **(113)** or as a cylinder of stacked benzenes **(114)**, both structures being stabilized by electron conjugation within the silicon plates. However, Nagase and Kobayashi found, using the semiempirical AM1 method[61,137], that the most stable structure of Si_{60} is the icosohedral silafullerene **112**, while the planar stacked **113** and **114** are by 158 and 228 kcal mol^{-1} less stable, respectively. Single-point HF/DZ calculations at the AM1 geometries predict that **113** is by as much as 606 kcal mol^{-1} less stable than **112**, indicating that AM1 strongly underestimates strain energies. This stability order is not surprising in view of the high strain in structures **113** and **114**, which contain many bond angles that deviate significantly from the tetrahedral value of 109.5°. The preference of **112** over **113** and **114** suggests that the gas-phase fragmentation data do not reflect in a simple way the structure of Si_{60}[61,37].

Si_{60} with I_h symmetry **(112)** is by 16.3 and 21.1 kcal mol^{-1} at AM1 and HF/DZ//AM1, respectively, more stable than the C_{2v} isomer of Si_{60} **(115)**. The higher stability of **112** ensures its higher population up to 2080 K. Above this temperature the less symmetric **115** is computed to dominate the Si_{60} equilibrium mixture[138]. The finding that the C_{2v} structure is destabilized relative to the I_h structure is consistent with the 'isolated pentagon rule'[139] which states that the fusion of pentagons is energetically unfavourable as a result of increased strain and the resulting induced antiaromatic character[139]. C_{2v} Si_{60} **(115)** has two paris of edge-sharing pentagons, causing its destabilization relative to I_h Si_{60}, which has no edge-sharing pentagons. The number of adjacent pentagons increases as the cluster becomes smaller, causing its destabilization. Thus, at HF/DZ//HF/DZ the smaller spheroidal clusters, Si_{50} (D_{5h}), Si_{30} (C_{2v}) and Si_{24} (D_3), are by 2.0, 5.8 and 9.3 kcal mol^{-1}, respectively, less stable per atom than Si_{60}[137]. This effect is much larger in the analogous carbon clusters, which suffer higher strain and antiaromaticity due to the presence of adjacent pentagons[137]. Larger silicon clusters such as Si_{70}, Si_{78} and Si_{84}, with a larger number of hexagons, are thermodynamically slightly more stable (per Si atom) than Si_{60}[61,137]. The full hydrogenation of Si_{60} leads to the saturated $Si_{60}H_{60}$. The strain energy in $Si_{60}H_{60}$ of 114 kcal mol^{-1} (at AM1, 207 kcal mol^{-1} at HF/DZ//HF/DZ) is considerably smaller than the strain energy in $C_{60}H_{60}$ of 530 kcal mol^{-1} (at AM1). This may also reflect the fact that Si_{60} is significantly less strained than C_{60}[61,137].

Optimization of the structure of Si_{60} without any symmetry restrictions, using a tight binding molecular dynamic technique, resulted in a C_{2h} structure **(116)**. This relaxed geometry is probably preferred over the I_h structure because it allows increased

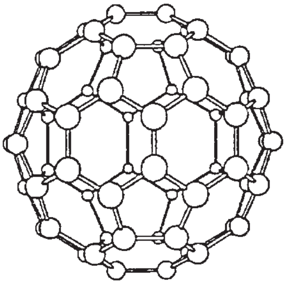

(112)

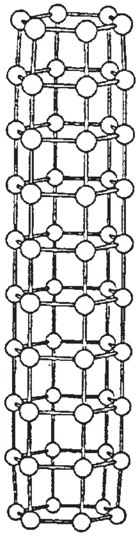

(114)

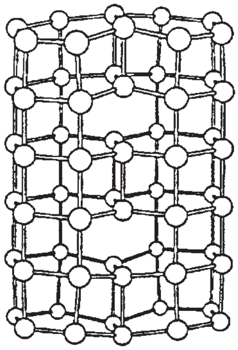

(113)

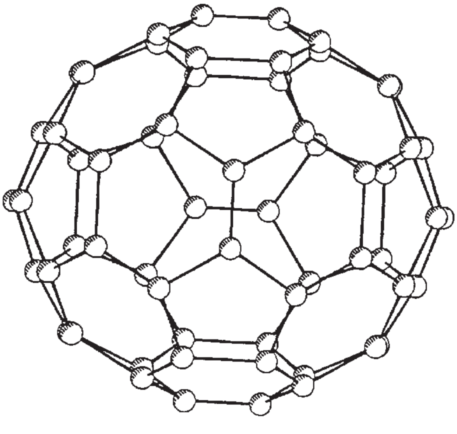

(115)

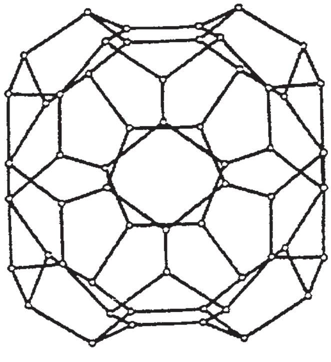

(116)

FIGURE 16. Various structures of Si_{60}: fullerene (**112**, I_h)[137]; stacked naphthalene (**113**, D_{2h})[137], stacked benzene (**114**, C_{2v})[137], fullerenes (**115**, C_{2v})[138] and (**166**, C_{2h})[140]. Reproduced from Reference 137, Copyright (1993) by courtesy of Marcel Dekker Inc. and from References 138 and 140, Copyright (1994) with kind permission of Elsevier Science–NL, Sara Burgehartstraat 25, 1055 KV Amsterdam, The Netherlands

tetrahedrality of the atoms, so that out of the 60 vertices, 10 have the ideal tetrahedral angle[140]. Higher level calculations are required to establish whether Si_{60} has I_h or a lower symmetry structure.

I_h Si_{60} has two distinct Si−Si bond lengths, one which fuses two adjacent 6-MRs [designated as r(6−6)], and the second which is longer and fuses a 5-MR and a 6-MR [designated as r(5−6)]. The calculated bond lengths at various levels of theory are given in Table 11, which also lists the corresponding bond lengths in C_{60}.

The r(5−6) − r(6−6) bond length difference, Δ, is quite large when using the AM1 and PM3 semiempirical levels but is reduced significantly to 0.077−0.088 Å at *ab initio* levels (Table 11). The size of the basis set has a small effect on Δ but, based on the experience with C_{60} (Table 11), it is expected that inclusion of electron correlation will decrease Δ considerably also in Si_{60}. A small Δ may be considered as an indication of aromaticity.

I_h Si_{60} has a five-fold-degenerate HOMO and a three-fold-degenerate LUMO[143,148]. At HF/3-21G the HOMO and LUMO energies are −6.39 and −1.95 eV, respectively[148] (−6.5 and −2.1 eV at HF/DZ+ECP[61,143]), resulting in a small HOMO−LUMO gap of only 5.0 eV, indicating its high polarizability. This HOMO−LUMO gap is only about 65% of that in C_{60} (Table 12). A similar reduction of the HOMO−LUMO gap was calculated also for the hexasilabenzene/benzene pair[59]. The HOMO−LUMO gap is further reduced to 4.3 eV in Ge_{60}[148].

TABLE 11. Optimized X−X bond lengths in I_h X_{60} (X = Si and C) at various levels of calculation

r(6−6)[a]	r(5−6)[a]	Δ[b]	Method	Reference
		Si_{60}		
2.092	2.297	0.205	AM1	141
1.879	2.247	0.368	PM3	147
2.088	2.169	0.081	STO-3G	142
2.067	2.152	0.085	STO-3G*	142
2.213	2.301	0.088	3-21G	142
2.229	2.307	0.078	6-31G	142
2.189	2.266	0.077	ECP/DZ	143
		C_{60}		
1.385	1.464	0.079	AM1	141
1.400	1.474	0.074	MNDO	144
1.384	1.457	0.073	PM3	147
1.367	1.453	0.086	3-21G	129
1.406	1.446	0.040	MP2/TZP	145
1.401	1.458	0.057	exp.[c]	146

[a] In Å.
[b] Bond length difference, in Å.
[c] Gas-phase electron diffraction.

2. Endohedral complexes of Si_{60}

One of the most remarkable properties of fullerenes is their ability to encapsulate atoms, ions and small molecules, to form the so-called endohedral fullerene complexes, denoted

TABLE 12. Encaged ion population (N_{ion}), HOMO and LUMO energies (eV) and stabilization energies (ΔE, kcal mol^{-1}) of endohedral complexes of Y_{60} (Y = C, Si and Ge) with various ions[a,b,c]

Ion	N_{ion}	E(HOMO)	E(LUMO)	Δ[d]	ΔE[e]
			C_{60}		
none	—	−8.3 (−8.0)[f]	−0.69 (−0.3)[f]	7.61 (7.3)	—
Ne	—	(−8.0)	(−0.3)	(7.7)	(0.4)
Li^+	2.004	−11.78	−4.16	7.62	−9.37
Na^+	10.0	−11.79 (−11.4)	−4.17 (−3.8)	7.62 (7.6)	−8.66 (−6.7)
K^+	18.05	−11.82	−4.19	7.63	−2.21
Rb^+	36.05	−11.83	−4.20	7.63	3.90
F^-	9.92	−4.79 (−4.5)	2.81 (3.1)	7.59 (7.6)	−22.54 (−39.8)
Cl^-	17.86	−4.82	2.78	7.60	−5.29
Br^-	35.78	−4.84	2.74	7.58	7.73
I^-	53.72	−4.93	2.67	7.60	39.27
			Si_{60}		
none	—	−6.39 (−6.5)[g]	−1.95 (−2.1)[g]	4.98 (4.4)	—
Ne	—	(−6.5)	(−2.1)	(4.40)	(0.0)
Li^+	2.002	−8.60	−4.14	4.46	−30.27
Na^+	9.996	−8.59 (−8.8)	−4.14 (−4.4)	4.45 (4.4)	−30.30 (−20.3)
K^+	18.00	−8.58	−4.13	4.45	−30.36
Rb^+	36.02	−8.54	−4.13	4.41	−30.09
F^-	9.98	−4.16 (−4.2)	0.26 (0.2)	4.42 (4.4)	6.69 (2.2)
Cl^-	17.98	−4.18	0.25	4.43	5.49
Br^-	35.93	−4.18	0.25	4.43	4.45
I^-	53.93	−4.19	0.24	4.43	5.02
			Ge_{60}		
none	—	−5.99	−1.73	4.26	—
Ne	—	−6.1[f]	−2.1[f]	4.1[f]	0.0
Li^+	2.002	−8.08	−3.81	4.27	−23.37
Na^+	9.997	−8.08	−3.80	4.28	−29.86
K^+	18.00	−8.07	−3.80	4.27	−29.83
Rb^+	36.01	−8.07	−3.80	4.27	−22.34
F^-	9.99	−3.89	0.35	4.24	6.73
Cl^-	17.98	−3.90	0.35	4.25	5.97
Br^-	35.94	−3.90	0.35	4.25	5.24
I^-	53.94	−3.91	0.35	4.26	5.55

[a] Based on data from Reference 148 unless stated otherwise.

[b] At HF/3-21G (3-21+G for the halide ions), the fullerene cages have I_h symmetry with bond distances of 1.370 and 1.450 Å for C_{60}[150], 2.189 and 2.266 Å for Si_{60}[143] and 2.315 and 2.398 Å for Ge_{60}[61] and the ion is placed at the centre of the cage.

[c] Values in parentheses are from Reference 149 for X@C_{60}, at HF/4-31G for the carbons and HF/DZP for the guest atom; from Reference 143 and for X@Si_{60} at HF/DZ+ECP.

[d] HOMO–LUMO energy difference, in eV.

[e] According to equation 43, corrected for basis-set superposition error. Negative values indicate stabilization by the ion.

[f] At AM1 the HOMO and LUMO energies are −9.64 eV and −2.95 eV, respectively[141].

[g] At AM1 the HOMO and LUMO energies are −8.0 eV and −3.38 eV, respectively[141].

as, e.g., X@C_{60}, where X is the encapsulated atom. The diameter of the hollow spherical cage of I_h Si_{60} of 11.1 Å[143] is much larger than that of I_h C_{60} (7.1 Å)[146]. In addition, Si_{60} is also more polarizable than C_{60} and, as a result, it is expected to form endohedral complexes even with larger guest atoms and ions than C_{60}. Nagase and Kobayashi[61,143] have studied the properties of X@Y_{60} complexes where Y = Si, Ge and X = Ne, Na^+ and F^-; Cioslowsky and Fleischmann[149] studied X@C_{60} complexes with the same guests and Geerlings and coworkers[148] studied X@Y_{60} complexes with X = Li^+, Na^+, K^+, Rb^+, F^-, Cl^-, Br^- and I^- and Y = C, Si and Ge. Their main conclusions are summarized below and in Table 12.

(1) Charge transfer from the ion or neutral atom to the Y_{60} cage, or in the opposite direction, is negligible. The interactions in the complexes are electrostatic in origin and are due mainly to polarization[61,143,148].

(2) The ionic radii of the encaged ions are strongly expanded within the fullerene cage, compared to that of the isolated ions, especially in the larger Si_{60} and Ge_{60} cages[148].

(3) Encapsulation of a cation in C_{60}, Si_{60} and Ge_{60} cages conserves the typical orbital structure of the neutral fullerene (i.e. a five-fold-degenerate HOMO and a three-fold-degenerate LUMO). Both the HOMO and LUMO are stabilized by the encapsulated cations, resulting in an increase in the ionization potentials and electron affinities (according to Koopmans' theorem). The HOMO–LUMO gap of Si_{60} is slightly reduced, but is almost unchanged for C_{60} and Ge_{60}. When an anion is placed within the cages the frontier orbitals are destabilized, giving rise even to negative electron affinities of the cages (see Table 12)[148].

(4) The stabilization energies of the X@Y_{60} systems as a result of the encapsulation (ΔE) are calculated by equation 43 (where $E_{(X@Y_{60})}$ is the energy of the endohedral complex whilst E_X and $E_{Y_{60}}$ are the energies of the free ion and of the fullerene, respectively) and are given in Table 12. The stabilization energies, ΔE, depend on the following factors: (i) the endohedral electrostatic potential; (ii) the ion-induced dipole interaction of the central ion with the polarizable cage and (iii) the electrostatic repulsions between the ion and the cage electrons. The stabilization energy sequences within a series of alkali metal ions or halide ions can be explained by using the 'hard'and 'soft' concept[148]. For Si_{60} and Ge_{60} the cations are strongly stabilizing whereas the anions are destabilizing. In the C_{60} cages all ionic species are stabilizing except for Rb^+, Br^- and I^-, which have ionic radii close to the radius of the C_{60} cage so that steric repulsions destabilize the endohedral complex[148]. Note the significant stabilizing effect of an encapsulated F^- in the C_{60} cage (Table 12). Geerlings and coworkers developed an analytical expression (within the framework of the density functional theory) for the endohedral complexation energy of various ions to Y_{60} cages, and the interested reader is referred to their paper for the detailed derivation of this expression[148].

$$\Delta E = E_{(X@Y_{60})} - (E_X + E_{Y_{60}}) \tag{43}$$

Bühl and Thiel used the chemical shifts of a ^{3}He atom (see above)[132,133] encaged within a fullerene for evaluating the degree of aromaticity of carbon fullerenes. A similar study is required for evaluating the degree of aromaticity of Si_{60}.

In an attempt to construct a new polymorph of silicon carbide, Osawa and coworkers employed the semi-empirical PM3 method and *ab initio* methods to study a hypothetical double fullerene C_{60}@Si_{60} (**117**, Figure 17) in which a C_{60} fullerene is encapsulated within a Si_{60} cage[147]. However, geometry optimization shows the generation of 60 new Si–C bonds connecting the inner C_{60} shell and the outer Si_{60} shell, forming a new

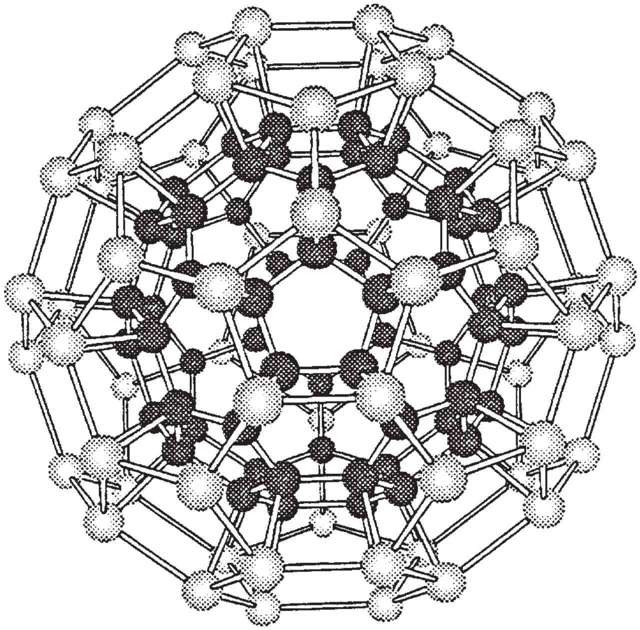

(117)

FIGURE 17. PM3 optimized structure of $C_{60}@Si_{60}$ **(117)**. Reprinted from Reference 147, by courtesy of Marcel Dekker, Inc.

molecule rather than an encapsulated fullerene pair. The C_{60} and Si_{60} radii in the optimized $C_{60}@Si_{60}$ structure have expanded relative to the isolated fullerenes from 3.22 Å to 3.73 Å for C_{60} and from 5.24 Å to 5.75 Å for Si_{60}, forming an inter-shell distance of 2.02 Å. Consequently, the Si−Si and C−C bond lengths became considerably longer as is expected of a sp^2 to sp^3 rehybridization; i.e. the Si−Si $r(6-6)$ and $r(5-6)$ bond distances in **117** are 2.309 and 2.327 Å, respectively, relative to 1.879 and 2.247Å, respectively, in Si_{60} (PM3), whilst the C−C $r(6-6)$ and $r(5-6)$ bond distances are 1.492 and 1.513 Å in **117** relative to 1.384 and 1.457 Å in C_{60}. The calculated bond-order and electron density map also clearly support the formation of new Si−C σ-bonds. As expected, the electron distribution along the Si−C bonds is shifted towards the more electronegative carbon atoms. Hence **117** is electron-deficient on the outer surface and electron-rich in the inner shell. **117** is still a hypothetical molecule, but the authors believe that it may be formed by the reaction of silicon with C_{60} by CVD techniques[147].

C. Si_{70}

An AM1 comparison of the geometry and electronic structure of D_{5h} Si_{70} (**118**, Figure 18) with that of C_{70}, Si_{60} and C_{60} was reported by Piqueras and coworkers[151]. The calculated bond lengths and bond orders, which are given in Table 13, suggest that the silicon clusters have a more localized structure than the carbon clusters, and that Si_{70}

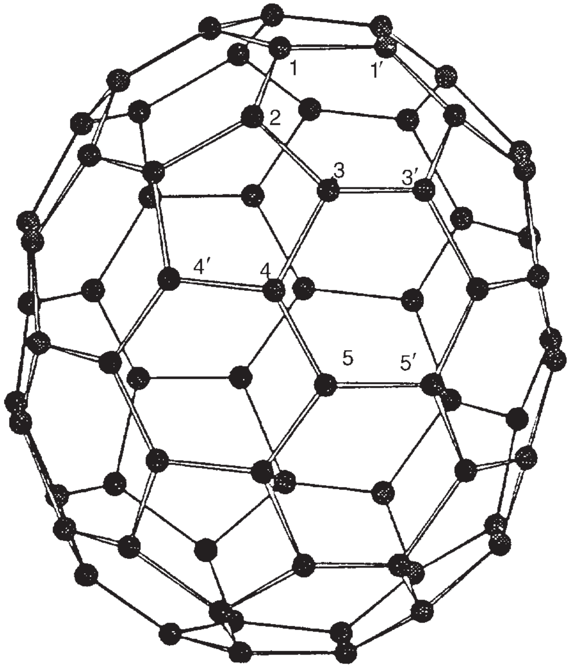

(118)

FIGURE 18. AM1 optimized structure of Si_{70} **(118)**. Reprinted from Reference 151, Copyright (1995) by permission of Elsevier Science-NL, Sara Burgerhartstraat 25, 1055 KV Amsterdam, The Netherlands

TABLE 13. AM1 bond lengths and bond orders for Si_{70} and C_{70}[a]

Bond[b]	Bond length (Å)		Bond order	
	Si_{70}	C_{70}	Si_{70}	C_{70}
$X_{(1)}-X'_{(1)}$	2.297	1.464	1.079	1.105
$X_{(1)}-X_{(2)}$	2.094	1.387	1.677	1.480
$X_{(2)}-X_{(3)}$	2.296	1.460	1.079	1.109
$X_{(3)}-X'_{(3)}$	2.067	1.375	1.715	1.526
$X_{(3)}-X_{(4)}$	2.304	1.467	1.049	1.065
$X_{(4)}-X'_{(4)}$	2.218	1.434	1.374	1.302
$X_{(4)}-X_{(5)}$	2.196	1.414	1.369	1.306
$X_{(5)}-X'_{(5)}$	2.296	1.465	1.078	1.094

[a] From Reference 151.

[b] For atom numbering see Figure 18.

is more delocalized than Si_{60}. A similar trend was found for C_{70} vs C_{60} based on their NICS values[132]. Among the four studied clusters, Si_{70} has the lowest ionization potential (7.63 eV), highest electron affinity (3.61 eV) and smallest HOMO–LUMO gap of 4.02 eV. The Koopmans' ionization potential of Si_{70} is by 0.37 eV lower than for Si_{60} and the authors argue that this is due to the more efficient electron delocalization in Si_{70} compared to Si_{60}[151]. The HOMO–LUMO gap for Si_{70} (4.02 eV) is smaller than for Si_{60} (4.62 eV), suggesting that the electrons in Si_{70} are more polarizable than in Si_{60}.

Si_{70} and higher silicon fullerenes, e.g. Si_{78} and Si_{84}, are more stable thermodynamically than Si_{60} because they have a larger number of hexagons and therefore they may be even better candidates for synthesis than Si_{60}[61,137].

VII. SILICON COMPOUNDS WITH POTENTIAL 'THREE-DIMENSIONAL AROMATICITY'

The concept of 'aromaticity' is not restricted only to planar conjugated systems. The '$4n + 2$ interstitial electron rule' extends the concept of aromaticity to three-dimensional delocalized systems[13a,91,152a]. Such systems have marked thermodynamic stability and favour substitution over addition reactions, a property characteristic of planar delocalized aromatic systems. For instance, ferrocene undergoes electrophilic substitution reactions in analogy to benzene[153]. Pyramidal molecules with three-dimensional aromaticity can be divided conceptually into caps (X) and rings (see **119**). The π-electrons of the ring, and the electrons available from the cap that form the cap-ring binding, constitute the interstitial electrons. A system with $4n + 2$ delocalized interstitial electrons is considered to have aromatic properties. Several examples of charged compounds which have potential 'three-dimensional aromaticity' have already been discussed in this review, i.e. **59**, **63a**, and **68–73**.

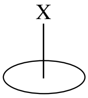

(119)

In this section we will discuss three families of neutral silicon compounds with potential 'three-dimensional aromaticity'.

A. Silicocenes

The synthesis of decamethylsilicocene **(120)**, which is regarded as the first stable silylene known, was reported by Jutzi and coworkers in 1986[154a]. This remarkable molecule can be formally described as being formed from 3 units, 2 units of cyclopentadienyl anions (Cp*) and Si^{2+}, which share 14 electrons (12 from the cyclopentadienyl rings and 2 from the Si). In terms of the cap-ring description, 6 interstitial electrons hold each of the rings to the 'sandwiched' silicon atom and the 2 remaining electrons reside in a lone-pair orbital on Si. The molecular orbital picture of **120**, which is discussed below, is analogous to that in ferrocene[152b], and therefore silicocene can be regarded as an aromatic molecule.

Crystal structure analysis of **120** indicated the presence of two structures, **120a** and **120b**, in a ratio of 1 : 2, respectively. In **120a**, the rings are parallel while in **120b** they form a tilt angle θ of 167.4°[154]. According to electron diffraction studies, also in the gas phase **120** has a bent metallocene-type structure with a tilt angle of 169.6°[154b]. Thus, the tilting of the rings in **120b** is not due to crystal packing forces.

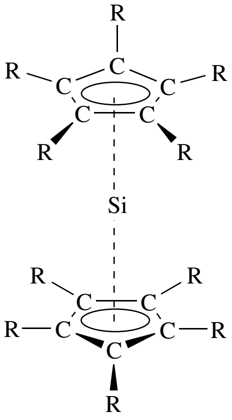

R = CH_3 **(120a)** D_{5d}

R = H **(121a)** D_{5d}

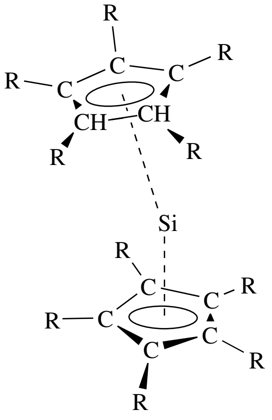

(120b) C_s

(121b) C_s

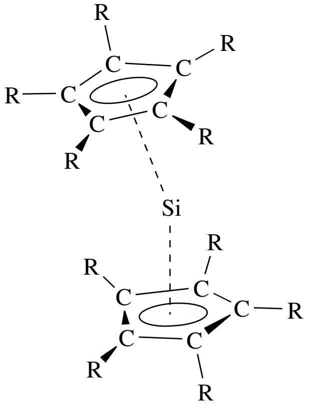

(121c) C_{2v}

These findings have stimulated computational studies of several possible isomers of the parent silicocene **121**, i.e. **121a–c** and their possible rotamers[154b,155] and the η^1,η^5-isomer (the η^1,η^1-isomer was considered, but was not studied due to computational problems)[154b]. For geometry optimizations these studies used the HF/STO-3G[154,155], HF/STO-3G*[154b,155], HF/DZ+d (in which one set of d orbitals is added only on Si) and HF/DZP[155] (with two sets of d orbitals on the Si and one set of d orbitals on C) methods. Electron correlation was introduced only in single-point energy calculations, using the MP2, CISD and CISD+Q methods[155]. The results of the calculations showed that: (a) With all the methods used the most stable structures are the bent C_s or C_{2v} conformers, **121b** or **121c** (or their C_2 rotamers). All these structures are quite close in energy and their relative energies depend on the level of calculation. **121a** is found to be less stable, i.e. the calculated energy difference between **121a** and **121b** at HF/DZ+d, HF/DZP, MP2/DZ+d and CISD+Q/DZ+d are 15.4, 11.2, 5.7 and 13.8 kcal mol^{-1}, respectively[155]. These findings are in agreement with the experimental electron diffraction results according to which decamethylsilicocene **(120)** has a bent structure[154b]. The η^1,η^5-isomer is much higher in energy; e.g. it is by 52.8 kcal mol^{-1} (at HF/STO-3G*) higher in energy than **121b**[154b]. (b) Addition of polarization functions to the basis set stabilizes the more symmetric structures, and thus decreases the energy difference between the D_{5d} isomer and the bent isomers. This is due to the participation of the low-lying d-orbitals of silicon in the bonding, a participation which is larger in more symmetric structures[155]. (c) The D_{5d} isomer **(121a)** is not a minimum on the SCF PES, and geometry optimization using correlated levels of theory have not been yet reported.

The most general conclusion from the calculations is that the PES of the parent silicocene **121** is flat with respect to the motion of the cyclopentadienyl rings, and the authors' prediction is that calculations at higher levels of theory will find that **121a**, **121b** and **121c** have similar energies[155]. This conclusion may explain the presence of two structures, **120a** and **120b**, in the solid state of decamethylsilicocene[154].

The calculated (HF/DZP) geometry[155] of **121b** and the X-ray structure of **120b**, which are shown in Figure 19, differ significantly in several parameters: (1) The Si−x2 distance is by as much as 0.4 Å longer than the experimental value. (2) the calculated and experimental C−C bond lengths in one of the cyclopentadienyl rings (x1 in Figure 19) differ by as much as 0.07 Å. Furthermore, the experimental C−C bond lengths in both cyclopentadienyl rings show little bond alternation with a typical average aromatic bond length of *ca* 1.4 Å. In contrast, the calculated C−C bond lengths show equalization in one of the cyclopentadienyl rings (x2) but significant localization in the second ring (x1). (3) The calculated tilt angle θ in **121b** of 152.4° is considerably smaller than the experimental value of 167.4° found in **120b**. This difference is probably due to the steric repulsions associated with the methyl groups, which increase the tilt angle relative to the parent silicocene[154b,155].

How can the bonding in silicocenes be described? The seven highest occupied molecular orbitals of **120a**, in which the 14 relevant electrons reside, are drawn schematically in Figure 20. Most of the bonding between the Si atom and the cyclopentadienyl rings is associated with the two lowest occupied MOs of a_{1g} and a_{2u} symmetry, which are the bonding combinations of the two cyclopentadienyl $2p_\pi$ MOs and the 3s-orbital ($1a_{1g}$) and one of the 3p-orbitals (a_{2u}) of the Si atom. Additional bonding interactions are associated with the e_{1u}-orbitals, which are the bonding linear combinations between the silicon 3p-orbitals and the $2p_\pi$-MOs of the cyclopentadienyl ligands of e_{1u} symmetry. The two highest occupied MOs of e_{1g} symmetry which are localized on the cyclopentadienyl ligands, and the $2a_{1g}$ orbital which is an antibonding combination of the Si 3s-orbital and the $2p_\pi$ MOs on the ligands, contribute little, if at all, to the bonding in the silicocene. This bonding picture, with several bonding orbitals which bind the 3 fragments together, topped by essentially non-bonding orbitals, is similar to the bonding picture of ferrocene[152].

The PE spectrum of **120b** reveals 3 major vertical ionization bands at 6.7, 7.5 and 8.1 eV (very similar ionization energies were calculated at HF/STO-3G* for **121b**, but this good agreement is probably fortuitous[154b]). The first and third ionization potentials were assigned to ionization from the weakly bonding e_{1g} and e_{1u} π-MOs and the ionization energy at 7.5 eV was assigned to ionization from the $2a_{1g}$ orbital[154b].

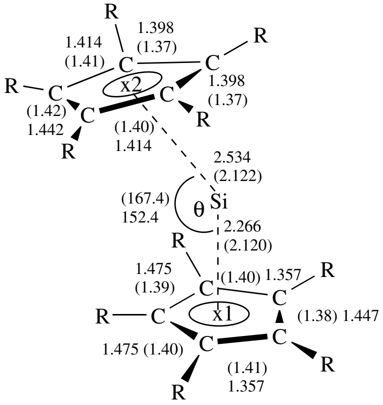

FIGURE 19. The HF/DZP[155] optimized structure of **121b** and the experimental X-ray structure of **120b** (in parentheses)[154]. Bond lengths in Å, bond angles in degrees. x1 and x2 specify the centres of the cyclopentadienyl rings

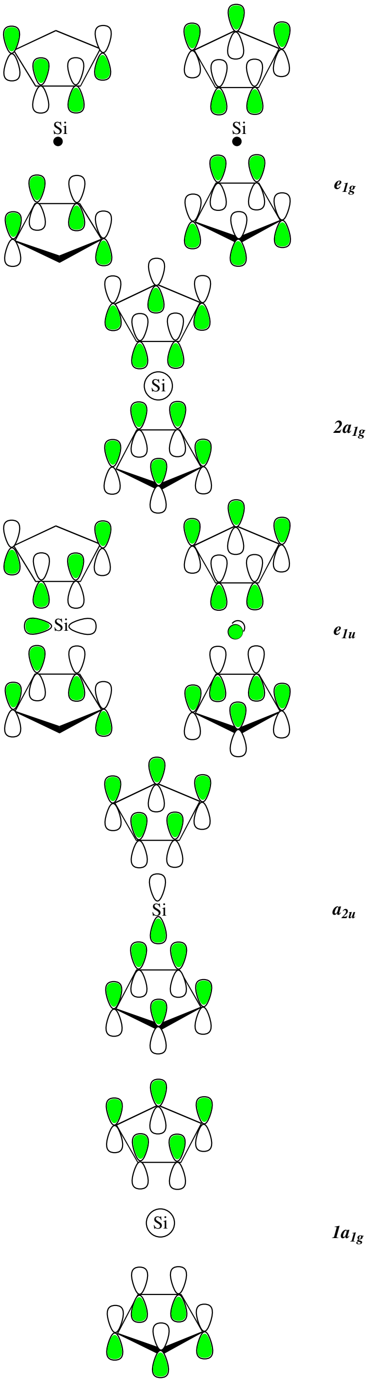

FIGURE 20. Schematic drawing of the seven highest occupied MOs of the parent silicocene, **120a**

B. Persilaferrocene, $(H_5Si_5)_2Fe$

In contrast to the well known ferrocene **122**[153], persilaferrocene $(H_5Si_5)_2Fe$ **(123)** is not known experimentally. However, **123** was studied computationally at the HF and MP2 levels of theory, using DZ and DZP quality basis sets (with ECP for Si and Fe). All-electron calculations were carried out only at the HF level[156].

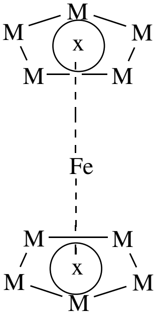

(122) M = CH
(123) M = SiH

The HF calculations show that persilaferrocene adopts the highly symmetric D_{5d} structure in analogy to ferrocene. In **123**, *r*(Fe−x) (where x is a point at the centre of the cyclopentadienyl rings) ranges from 2.060 to 2.175 Å, depending on the basis set. In **122**, *r*(Fe−x) is significantly shorter and varies from 1.869 to 1.898 Å. Comparison with experimental data for **122**, where *r*(Fe−x) is 1.65 Å, shows that the calculated *r*(Fe−x) distance is significantly overestimated by HF calculations and this conclusion probably holds also for **123**. The Si−Si bond lengths in **123** are all equal and they vary between 2.184 and 2.242 Å as a function of the basis set. This indicates the existence of some Si−Si double-bond character, which is also supported by the calculated Si−Si bond-order of 1.266. The planarity of the Si_5H_5 ligands is noteworthy, since the free cyclic Si_5H_5 radical has a non-planar structure. The calculated vibrational frequencies and relative energies suggest, however, that the D_{5d} structure of **123** lies in a rather shallow minimum and that its transformation to structures of lower symmetry (e.g. C_{2v} or C_{2h}), which involve non-planar Si_5H_5 rings, should therefore be facile[156].

The binding energy of the Fe atom to the two cyclopentadienyl rings is smaller in **123** than in **122**, i.e. 113.6 vs 144.1 kcal mol^{-1}, respectively, at MP2/DZP//HF/DZP. The vibration frequencies for the Fe-ring stretchings, of 103 cm^{-1} for **123** and 236 cm^{-1} for **122**, also indicate that the interaction of the Fe atom with the Si_5H_5 rings is smaller than with the C_5H_5 rings.

The positive charge on the Fe in $(H_5Si_5)_2Fe$ is about half of that in **122**, and the ring Si atoms of **123** are almost neutral. On this basis, it was predicted that the electrophilic reactivity of $(H_5Si_5)_2Fe$ towards polar reagents should be lower than that of $(H_5C_5)_2Fe$, where the cyclopentadienyl rings carry a significant negative charge[156].

C. Aromaticity in *closo*-Silaboranes, $B_3Si_2H_3$

Two bonding alternatives are possible for the *closo*-boranes 1,5-$X_2B_3H_3$ (X = SiH, CH, N, P, BH^-), i.e. the classical representation **124** and the non-classical representation

125. Theoretical studies which used Bader's 'Atoms in Molecules' bonding analysis[109] or Mulliken population analysis suggested that these members of the *closo*-borane family favour the classical Lewis representation **124**[157]. In contrast, a more recent study by Schleyer and coworkers[158] concluded that these *closo*-boranes are best represented by the non-classical representation **125** and that these compounds have 'three-dimensional aromaticity'. These conclusions were based on their calculated B−B and B−X distances and the corresponding Wiberg's bond indices (WBI) and natural atomic bond orders (NAO), as well as on their calculated aromatic stabilization energies (ASE) and magnetic properties (susceptibility exaltation and NICS values). Table 14 lists some of these values for the $1,5\text{-}X_2B_2H_3$ *closo*-boranes, with X = SiH, CH and BH^- (for X = P and N see Reference 158), which show clearly their non-classical aromatic character. Natural localized molecular orbital analysis reveals significant electron delocalization on each deltahedral face of the $1,5\text{-}X_2B_3H_3$ *closo*-boranes, also favouring representation **125** over **124**.

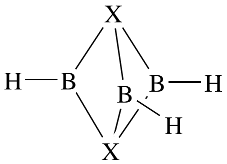

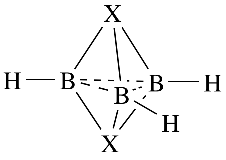

(124) X=SiH, CH, N, P, BH^- **(125)**

The degree of the 'three-dimensional aromaticity' and the preference for the non-classical structure **125** over the classical structure **124** follow the electronegativity of X in each row, i.e. the degree of aromaticity follows the order: X = $BH^- > SiH > P$

TABLE 14. Bonding, energetic and magnetic properties of *closo*-$1,5\text{-}X_2B_3H_3$ (**125**, X = SiH, CH and BH^-)[a]

Property	X		
	SiH	CH	BH^-
r(B−X)[b]	1.941	1.554	1.684
r(B−B)[b]	2.078	1.844	1.811
WBI(B−X)[c]	0.92	0.933	0.93
WBI(B−B)[c]	0.44	0.202	0.45
NAO(B−X)[d]	0.87	0.89	0.88
NAO(B−B)[d]	0.44	0.35	0.49
ASE[e]	−29.2	−19.8	−34.8
Λ[f]	−36.6	−6.9	−46.1
NICS[g]	−22.4	−17.1	−28.1

[a] From Reference 158.
[b] At MP2/6-31+G*, in Å.
[c] Wiberg's bond index.
[d] Natural atomic bond orders.
[e] In kcal mol^{-1} at MP2/6-31G*+ZPE.
[f] Diamagnetic susceptibility exaltation, calculated at CSGT-HF/6-311+G**//MP2/6-31+G*.
[g] At the cage centre, using GIAO-HF/6-311+G**//MP2/6-31+G*.

$>$ CH $>$ N, being the highest for **125**, X = BH^{-}[158]. According to the calculated ASE, *closo*-disilaborane (**125**, X = SiH) has 84% of the aromaticity of **125**, X = BH^{-} but it is by *ca* 50% more aromatic than the carbon analogue **125**, X = CH.

VIII. POTENTIAL SILAANTIAROMATIC COMPOUNDS

A. Silacyclobutadienes

Several sila-analogues of cyclobutadiene, the prototype of Hückel 4*n* antiaromatic systems, were studied computationally. The available studies on mono- and disilacyclobutadiene are quite old and therefore use relatively low levels of theory, and their results should therefore be treated with caution.

1. Monosilacyclobutadiene

Monosilacyclobutadiene **126** was first studied by Gordon at the HF/6-31G*//HF/3-21G level of theory[159]. More extensive calculations for the lowest singlet and triplet states of **126** were later carried out by Colvin and Schaefer[160] and a detailed HF/6-31G*//HF/6-31G* study of the C_3SiH_4 PES was later reported by Gordon and coworkers[161].

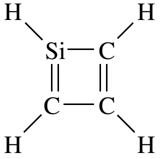

(126)

The optimized geometries (at HF/DZ+d and HF/6-31G*) of the singlet and triplet states of **126** are given in Figures 21a and 21b, respectively. Vibrational frequencies of **126** were also reported[160]. The singlet ground state of **126** is predicted to possess a planar geometry with alternating single and double bonds (Figure 21a). At HF/DZ+d, the C−Si bonds are calculated to be 1.866 and 1.688 Å (1.884 and 1.685 Å, respectively, at HF/6-31G*), close to those in methylsilane and silaethylene, respectively. This indicates little π-conjugation, as suggested also by the vibrational frequencies[160]. The structure of the $^3A'$ triplet state of **126** (Figure 21b) is very different. The shortest C−C and C−Si bonds are geminal, and not on opposite sides of the ring as in singlet **126**. Furthermore, the Si−C bond lengths are comparable to those of regular Si−C single bonds, while the C−C bond lengths are closer to those of C=C double bonds. Although silicon substitution rules out a truly square structure, the geometry of triplet **126** is much more 'square-like' than is the singlet monosilacyclobutadiene[160].

The singlet−triplet energy difference is, as expected, strongly dependent on the level of the calculations. At the CISD level the triplet is found to lie only 5 kcal mol^{-1} above the singlet[160]. This singlet−triplet splitting is about 16 kcal mol^{-1} smaller than the calculated splitting of cyclobutadiene at the same level of theory[160].

The 'antiaromatic' destabilization of singlet **126** was estimated (using equation 44) to be 49.1 kcal mol^{-1} (HF/DZ[160]; 53.5 kcal mol^{-1} at HF/6-31G*//HF/3-21G[159]), by *ca* 17 kcal mol^{-1} smaller than the destabilization calculated for cyclobutadiene at

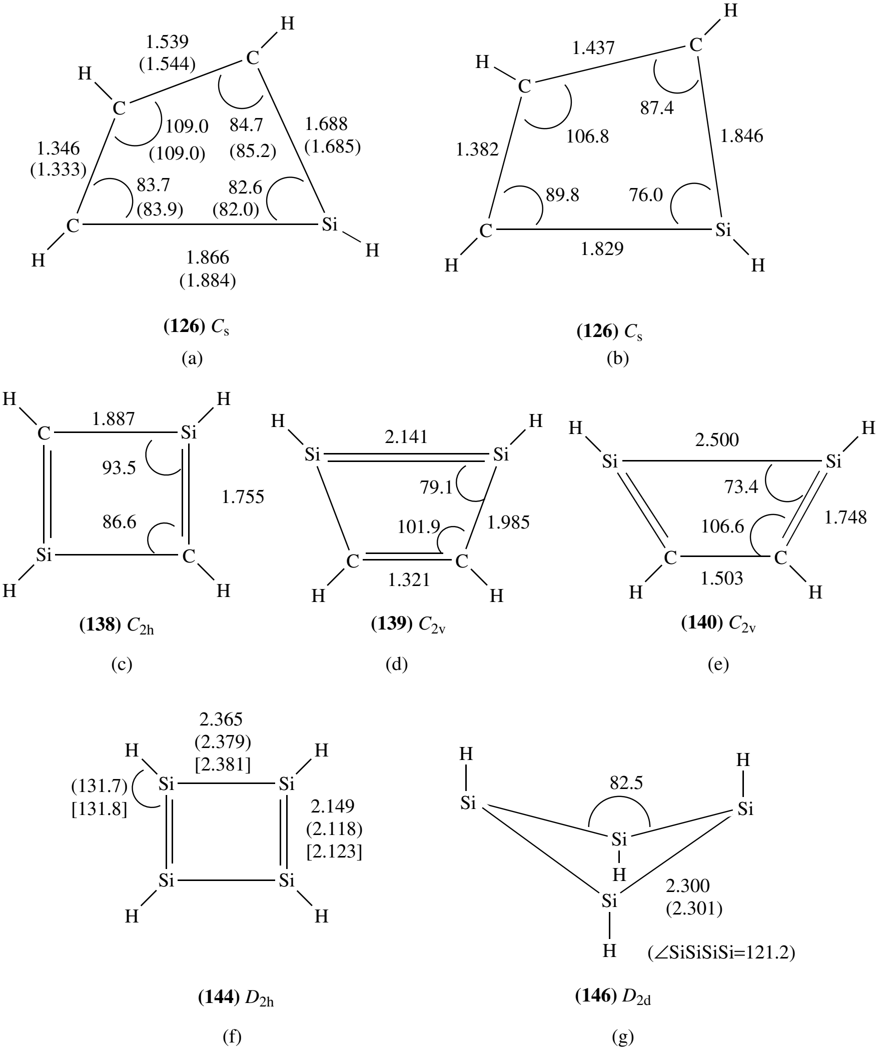

FIGURE 21. (a) Optimized geometries of the lowest $^{1}A'$ singlet state of monosilacyclobutadiene, **126**; (b) optimized geometries of the lowest $^{3}A'$ triplet state of **126**, both at HF/DZ+d[160] (HF/6-31G*[161] values in parentheses); (c), (d), (e) optimized geometries of disilacyclobutadienes **138**–**140** at HF/3-21G[162]; (f) and (g) optimized geometrics of tetrasilacyclobutadienes **144** (D_{2h}) and **146** (D_{2d}), respectively, at MP2/6-31G**[52], HF/DZP[165a] (in round parentheses) and at HF/6-31G*[164] (in square brackets). Bond lengths in Å, bond angles in degrees

a comparable level of theory[160]. However, note that equation 44 cannot distinguish destabilizing conjugation effects from angle strain or 1,3-interactions[160].

$$\mathbf{126} + 3CH_4 + SiH_4 \longrightarrow CH_3SiH_3 + CH_3CH_3 + H_2C{=}CH_2 + H_2C{=}SiH_2 \qquad (44)$$

The relative energies at HF/6-31G*//HF/6-31G* of various isomers of monosilacyclobutadiene are given in Figure 22[161]. The global minimum on the C_3SiH_4 PES is silylene **127**, which is stabilized by the interaction of the vacant p-orbital on silicon with the C=C π-bond to form a 2π-aromatic system. Four other silylenes **128–131** follow **127**. These silylenes are all lower in energy than the isomeric structures which possess a C=Si double bond or strained rings, such as **132–137**. This stability order contrasts with

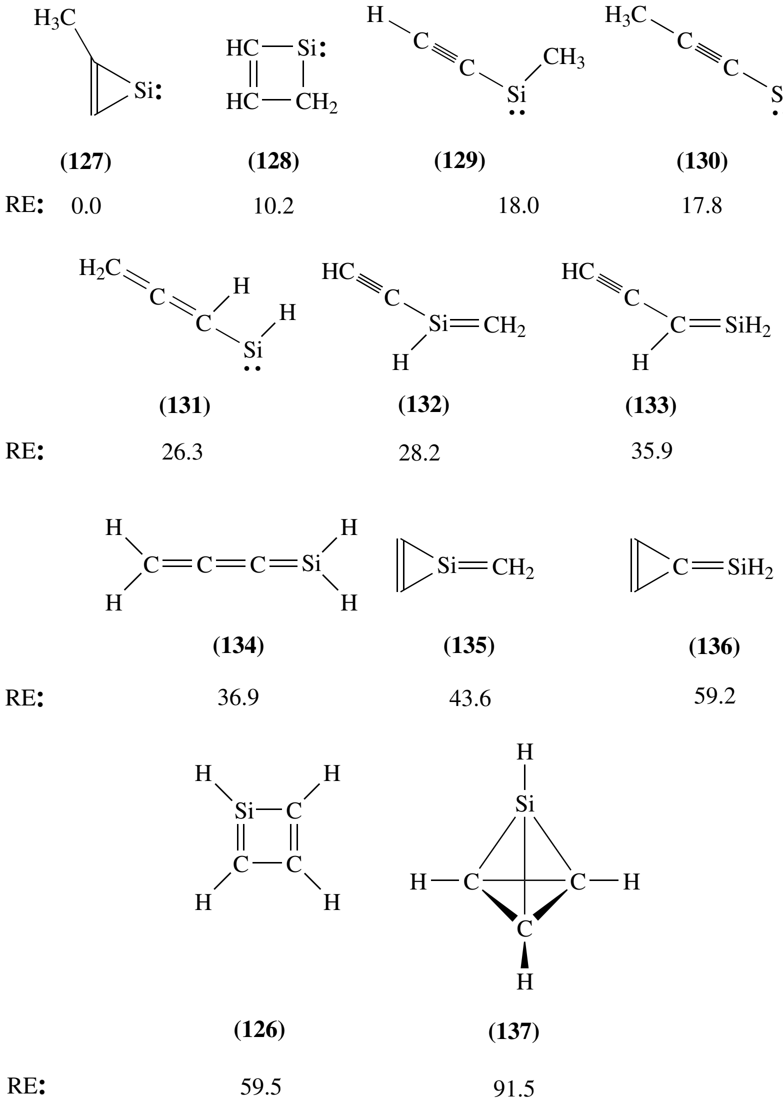

FIGURE 22. Relative energies (RE, in kcal mol^{-1}) calculated at HF/6-31G*//HF/6-31G* of C_3SiH_4 isomers. Data from Reference 161

that in the isoelectronic C_4H_4 system, where structures with multiple bonds are substantially more stable than the corresponding carbenes. Monosilacyclobutadiene **(126)** is by 59.5 kcal mol^{-1} less stable than the silylene, **127**, but it is by 32.0 kcal mol^{-1} more stable than the isomeric, highly strained silatetrahedrane **137**[161]. Due to the high degree of unsaturation or strain in many of the C_3SiH_4 isomers, it is clear that a correlated level of theory is required to obtain more reliable information on the relative energies of these isomers.

2. Disilacyclobutadienes

Holmes, Gordon and coworkers[162] studied at the HF/3-21G//HF/3-21G level (and for some isomers also at MP3/6-31G*//HF/3-21G) the three possible disilacyclobutadienes **138**, **139** and **140**, along with other $C_2Si_2H_4$ isomers. The HF/3-21G optimized structures (within the indicated symmetry constraints) of **138**, **139** and **140** are shown in Figures 21c, 21d and 21e, respectively. All three structures reflect bond localization, as expected for antiaromatic compounds. Of special interest is the Si−Si bond length in **140** of 2.50 Å, which is considerably longer even than a typical Si−Si single bond length of 2.35 Å, indicating the instability of the structure. Indeed, upon full geometry optimization, **140** decays to a disilylene structure with a C_1 symmetry **(141)**, which has a very long Si−Si bond of 2.860 Å.

Of the three disilacyclobutadiene isomers **(138–140)**, only **138** is a minimum on the HF/3-21G surface and is estimated to be by 49.7 kcal mol^{-1} (at MP3/6-31G*//HF/3-21G) higher in energy than the isomeric aromatic silylene **142**, which is the most stable $C_2Si_2H_4$ isomer (in analogy to **127**), **138** possesses, in analogy to cyclobutadiene, a high diradical character and it therefore cannot be adequately described at the RHF level of theory. The inclusion of the contribution of electron correlation using the MCSCF level or UHF-NO CI methods stabilizes **138**, but **142** is still by *ca* 20 kcal mol^{-1} more stable[162]. The disilylene **141** is by 7.0 kcal mol^{-1} more stable than **138** and by 42.7 kcal mol^{-1} less stable than **142** (at MP3/6-31G*//HF/3-21G)[162]. **138** is by 37.7 kcal mol^{-1} more stable than disilatetrahedrane **143**, which is the least stable $C_2Si_2H_4$ isomer.

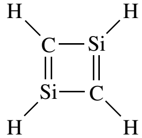
(138) C_{2h}

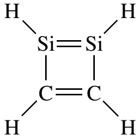
(139) C_{2v}

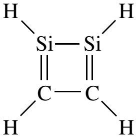
(140) C_{2v}

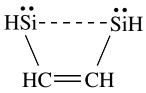
(141) C_1

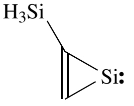
(142) C_s

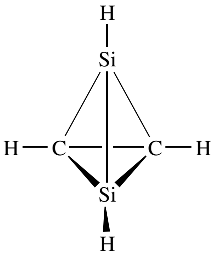
(143) C_2v

3. Tetrasilacyclobutadiene

The PES of tetrasilacyclobutadiene, **144**, the full silicon analogue of cyclobutadiene, was studied extensively using relatively high levels of theory which include the contributions of polarization functions and of electron correlation[52,163–165]. The calculations revealed a very complex Si_4H_4 PES.

What is the structure of Si_4H_4? Is it a delocalized square or a distorted planar rectangle, or does it possess a three-dimensional structure? The propensity of a planar square Si_4H_4 to distort to the rectangular D_{2h} structure **144** was studied by a valence bond approach (see Section III.F.1). Shaik and coworkers[15b,c] found that the π-distortion energies of square Si_4H_4 are approximately the same as for Si_6H_6, but the resistance of the σ-framework to distortion is smaller for the square than for the hexagon, due to the smaller number of bonds. The total outcome is that Si_4H_4 is more distorted (resulting in alternating bond lengths) than Si_6H_6 and that this distortion is dominated by the σ-framework.

The square and the rectangular **144** (see Figure 21f) are both not local minima on the Si_4H_4 PES at all levels of calculation[52,164,165]. Upon geometry optimization the planar D_{2h} structure **(144)** collapses to a C_{2h} structure, **145**, which lies 1.0 kcal mol^{-1} below **144** (CISD/DZP//HF/DZP[165a]). However, **145** is also not a minimum on the HF PES, and following its a_u imaginary frequency it collapses to a puckered D_{2d} minimum **(146)** which lies 17.4 kcal mol^{-1} below **144** (at CISD/DZP//HF/DZP[165a]; 34.8 kcal mol^{-1} at MP2/6-31G**//MP2/6-31G**[52], 4.7 kcal mol^{-1} at HF/DZP[165a], reflecting a very large electron correlation effect). **146** is thus the most stable $(SiH)_4$ isomer[165a]. The high stability of **146** is due to a large extent to its reduced strain, i.e. the calculated MP2/6-31G** strain energies of **144** and **146** are 38.7 and 8.3 kcal mol^{-1}, respectively[52]. **146** is by 4.5 kcal mol^{-1} less stable than the [1.1.0] bicyclic tetrasilane **147** (MC8SDQCI/TZP)[163b]. The most stable isomer on the Si_4H_4 PES is **148**, which is by 7.5 kcal mol^{-1} more stable than **147** [CISD(Q)/DZP//HF/DZP][165b].

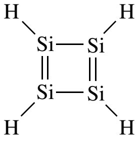

(144) D_{2h}

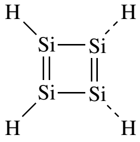

(145) C_{2h}

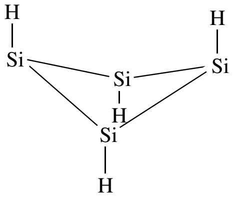

(146) D_{2d}

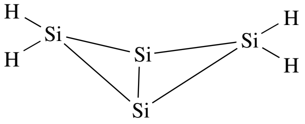

(147) C_{2v}

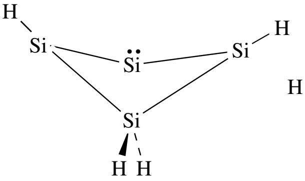

(148) C_s

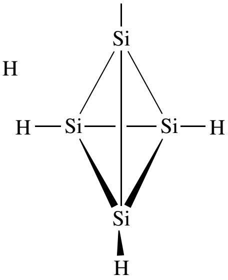

(149) T_d

The least stable isomer on the Si_4H_4 PES is tetrasilatetrahedrane (**149**), which is a local minimum at the HF level but has two imaginary vibrational frequencies at the MP2 level[52]. **149** is by only 7.9 kcal mol^{-1} less stable than **144** but by 33.4 kcal mol^{-1} less stable than **146**, at CI/6-31G*//HF/6-31G*[164] (40.9 and 21.9 kcal mol^{-1} at MP2/6-31G**//MP2/6-31G**[52] and CISD/DZP//HF/DZP[165a], respectively). Tetrasilatetrahedrane is also unstable kinetically, and it isomerizes to **146** with a negligible barrier of only 0.6 kcal mol^{-1} [HF/6-31G(2d,p)+ZPE[164]]. However, despite the high predicted reactivity of the parent tetrasilatetrahedrane, a stable derivative of tetrasilatetrahedrane, substituted with 4 bulky *t*-Bu_3Si groups, was recently synthesized and identified by X-ray crystallography by Wiberg and coworkers[166].

The geometries of **144** and **146** are shown in Figures 21f and 21g, respectively. The planar tetrasilacyclobutadiene (**144**) has a rectangular geometry with typical Si=Si and Si−Si bond lengths of 2.149 and 2.365 Å (MP2/6-31G**[52], 2.123 and 2.381 Å at HF/6-31G*[164], respectively). On the other hand, **146** has 4 equivalent Si−Si bonds of 2.300 Å (MP2/6-31G*; 2.301 Å at HF/DZP[165a] and 2.298 Å at HF/6-31G*[164]).

B. Charged Silaantiaromatic Compounds

1. The silirenyl anion, $C_2SiH_3^-$

The antiaromaticity of three-membered ring anions, **150**, at their ground and excited states was determined by Malar[167] by the bond-order definition of aromaticity suggested by Jug, which relates the lowest bond order in the ring with aromatic ring currents[168]. According to this method the aromaticity index of a ring is defined as being equal to the smallest bond order in the ring[168].

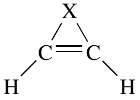

(**150**) X = SiH$^-$, CH$^-$

The geometries of the ground states and of the first excited singlet and triplet states of **150** with X = SiH$^-$, CH$^-$, NH, O, PH and S were calculated by the CI version of the semi-empirical SINDO1 method[167]. We will discuss here only the silirenyl anion (**150**, X = SiH$^-$) and compare the properties of this anion to those of the analogous cyclopropenyl anion (**150**, X = CH$^-$). The calculated optimized geometries and bond orders for **150**, X = SiH$^-$ and CH$^-$ are given in Table 15.

In the ground state of the silirenyl anion (**150**, X = SiH$^-$) the C=C and C−Si bond lengths are 1.325 and 1.867 Å, respectively, typical values of regular C=C and C−Si bonds. The Si centre in **150**, X = SiH$^-$ is highly pyramidal. The geometries of the excited triplet and singlet states do not differ significantly from that of the ground state, except for the Si centre which becomes less pyramidal upon excitation (Table 15).

The calculated vertical excitation energies to the T_1 and S_1 states are 2.3 and 3.0 eV, respectively (using SINDO1). The C−X bond order in the ground state of **150**, X = SiH$^-$ is 1.21, a typical value for strong single bonds[167] and in the range of non-aromatic systems[168], leading to the conclusion that the ground state of the silirenyl anion is non-aromatic[167]. Upon excitation, the C−Si bond-order is reduced to 0.99 and 1.03 for the S_1 and T_1 states, respectively, leading to the conclusion that the excited states of **150**, X = SiH$^-$ are highly antiaromatic. Generation of the singlet and triplet excited states of

TABLE 15. Calculated geometries and bond orders of the silirenyl anion (**150**, X = SiH$^-$) and the cyclopropenyl anion (**150**, X = CH$^-$) in their ground and first excited singlet and triplet states[a]

State	C−C	C−X	C−H	X−H	CCX	CCH	CXH	HCCX	CCXH
					X = SiH$^-$				
	Geometry								
S_0	1.325	1.867	1.058	1.474	69.2	134.0	103.8	175.0	96.0
S_1	1.336	1.875	1.060	1.484	69.1	131.0	155.4	178.3	146.3
T_1	1.333	1.856	1.067	1.477	68.9	132.5	158.5	182.5	167.6
	Bond order								
S_0	2.05	1.21[b,c]							
S_1	1.96	0.99[b,d]							
T_1	1.95	1.03[b,d]							
					X = CH$^-$				
	Geometry								
S_0	1.313	1.505	1.062	1.138	64.1	140.5	115.0	193.0	101.3
S_1	1.393	1.415	1.089	1.096	60.6	152.4	129.0	235.5	118.2
T_1	1.482	1.427	1.079	1.088	58.7	132.0	126.0	232.0	116.2
	Bond order								
S_0	2.10	1.14[b,e]							
S_1	1.39[b,f]	1.42							
T_1	1.43[b,f]	1.46							

[a] From Reference 167, using the CI/SINDO1 method. Bond lengths in Å, bond angles in degrees.
[b] Aromaticity index determined by the lowest ring bond order.
[c] Non-aromatic.
[d] Highly antiaromatic.
[e] Moderately antiaromatic.
[f] Moderately aromatic.

the silirenyl anion involves a $\sigma(a_1) \rightarrow \pi^*(a_2)$ transition. Both the σ and π^* orbitals are bonding along the C−C bond and antibonding along the C−X bond, but the antibonding along the C−X bonds is more pronounced in the π^* orbital. Thus, excitation weakens the C−X bonds and the S_1 and T_1 states of **150**, X = SiH$^-$ become antiaromatic. In contrast to **150**, X = SiH$^-$, the geometry of **150**, X = CH$^-$ varies from a localized structure in the S_0 ground state (moderately antiaromatic according to its bond order aromaticity index), to a delocalized structure in the S_1 and T_1 states, which are moderately aromatic (Table 15). Excitation of **150**, X = CH$^-$ involves a transition from the $\sigma(a_1)$ orbital to a $\pi^*(b_1)$ orbital. The $\sigma(a_1)$ orbital of **150**, X = CH$^-$ is bonding along the C−C bond and antibonding along the C−X bonds whilst the $\pi^*(b_1)$ orbital is antibonding along the C−C bond and non-bonding along the C−X bonds. Hence excitation weakens, and thus elongates, the C−C bond and strengthens, and thus shortens, the C−X bonds (Table 15)[167].

2. *Silacyclopentadienyl cations*

a. $C_4H_4SiH^+$. The degree of the antiaromaticity of singlet $C_4H_4SiH^+$, **151** (C_{2v}), a 4π-electron system, in comparison to the aromaticity/antiaromaticity of other five-membered C_4H_4X ring systems was estimated by Schleyer and coworkers using several criteria:

structural (Julg parameter), energetic (ASE, according to equation 21, Section IV.D.2a) and magnetic [i.e. magnetic susceptibility anisotropy (χ_{anis}), diamagnetic susceptibility exaltation (Λ) and NICS values]^{26,31a}. These calculated properties for **151** and those of the analogous **152**, X = CH^+, CH^- and SiH^- are given in Table 16. A graphical presentation of the correlation between the various criteria for the aromaticity/antiaromaticity of five-membered C_4H_4X ring systems is shown in Figure 1 (Section II.D).

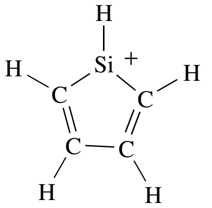

(151)

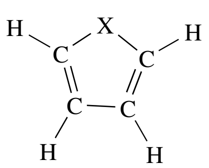

(152)

$C_4H_4SiH^+$ (C_{2v}) is a minimum on the MP2/6-31G* PES, with a C=C bond length of 1.357 Å, resembling that in polyenes. On the other hand, the conjugated C−C single bond length of 1.518 Å is significantly longer than in polyenes (1.450 Å in *trans*-1,3-butadiene). The Si−C bond lengths of 1.820 Å are very close to those of regular Si−C single bonds. This localized structure results in a small Julg parameter of 0.346. The pronounced bond length alternation points to a significant antiaromatic character of **151**. This conclusion is strongly supported by the relatively high destabilization energy of −24.1 kcal mol^{-1} and by the magnetic properties, i.e. $\chi_{\text{anis}} = -0.8 \times 10^{-6}$ cm^3 mol^{-1}, $\Lambda = 13.2 \times 10^{-6}$ cm^3 mol^{-1} and NICS = 12.8 ppm of **151**, which are all characteristic of an antiaromatic compound^{26,31e}. Table 16 shows, however, that the antiaromaticity of **151** is smaller than that of $C_5H_5^+$. In analogy, the aromaticity of *c*-$C_4H_4SiH^-$ (**152**, X = SiH^-) is smaller than that of its carbon analogue **152**, X = CH^-.

b. $Si_5H_5^+$. A detailed study at MP2/6-31G*^{169} of the potentially 4π-antiaromatic $Si_5H_5^+$ reveals a complex PES, which is very different from that of $C_5H_5^{+169,170}$. Several important isomers on the PES of $Si_5H_5^+$, **153–160**, arranged according to their relative energies at MP2/6-31G*, are presented in Figure 23 (additional isomers are discussed in Reference 169).

TABLE 16. Calculated structural, energetic and magnetic properties of *c*-C_4H_4X, **152**^{a}

X	Symmetry	A^b	ASE^c	χ^d_{anis}	Λ^d	NICS^e
SiH^+	C_{2v}	0.346	−24.1	−0.8	13.2	12.8
CH^+	C_{2v}	−0.084	−56.7	58.1	32.6	
SiH^-	C_s	0.926	13.8	−41.5	−7.7	−6.7
CH^-	D_{5h}	1.000	28.8	−45.8	−17.2	−14.3

^{a}From Reference 31a; all species are minima at MP2/6-31G*.
^{b}Julg's parameter.
^{c}In kcal mol^{-1}.
^{d}In 10^{-6} cm^3 mol^{-1}.
^{e}In ppm, at GIAO-SCF/6-31+G*.

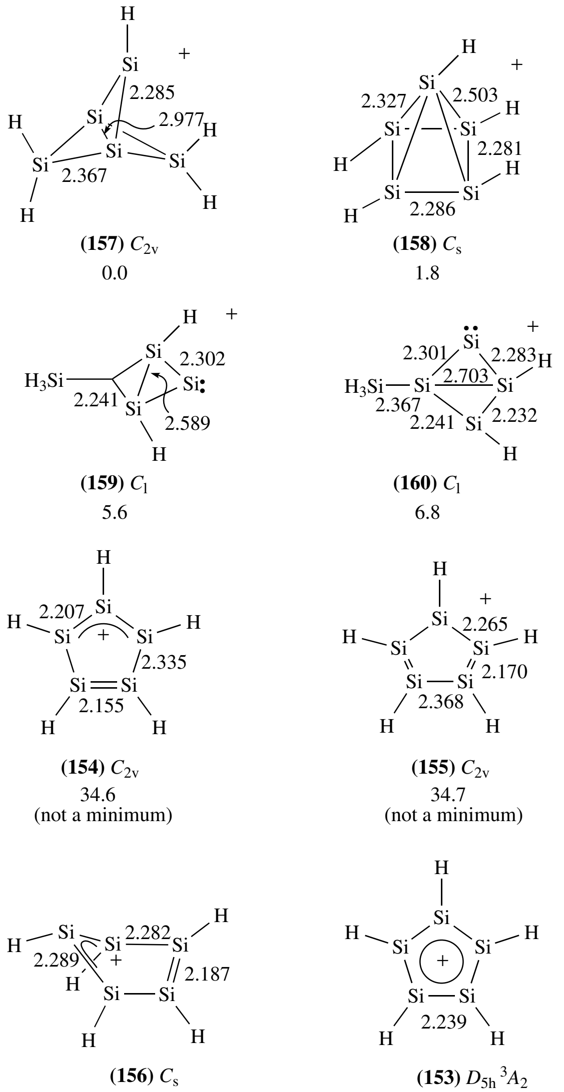

(157) C_{2v}
0.0

(158) C_s
1.8

(159) C_1
5.6

(160) C_1
6.8

(154) C_{2v}
34.6
(not a minimum)

(155) C_{2v}
34.7
(not a minimum)

(156) C_s
21.0

(153) D_{5h} $^3A_2$
24.1
(not a minimum)

FIGURE 23. Optimized structures (MP2/6-31G*) and relative energies (at MP2/6-31G* + ZPE, in kcal mol^{-1}) of $Si_5H_5^+$ isomers. Bond lengths in Å, bond angles in degrees. Data from Reference 169

The singlet and triplet states of the antiaromatic D_{5h} $Si_5H_5^+$ **(153)** are not minima on the $Si_5H_5^+$ PES. When the D_{5h} symmetry of the singlet is released, it first collapses to the C_{2v} isomers **154** and **155** which are also not minima on the PES, and upon release of the C_{2v} constraints they further collapse to the C_s structure **156**, which is the only minimum on the $Si_5H_5^+$ PES. The pentasila-allylic-type cation **156**, which has a structural resemblance to that of the classical antiaromatic D_{5h} $Si_5H_5^+$, is by 21.0 kcal mol^{-1} less stable than the pentasila[1.1.1]propellanyl cation **157**, which is the most stable $Si_5H_5^+$ isomer. Several other $Si_5H_5^+$ isomers, i.e. the C_s pyramidal cation **158** (the pyramidal C_{4v} structure is not a minimum) and the bicyclic cation-silylenes **159** and **160**, lie only a few kcal mol^{-1} above **157** and are more stable than the monocyclic **156**.

The calculated Si−Si bond lengths in **156** are 2.187, 2.282 and 2.289 Å, all in the range intermediate between that of double (2.14 Å) and single (2.35 Å) Si−Si bond lengths. This indicates a certain degree of charge delocalization in the ring, which is also supported by the calculated charge distribution. **156** can be described as being essentially non-aromatic, as the energy change resulting from the presence of the Si=Si double bond is small, only 2 kcal mol^{-1} (equation 45). In contrast, the corresponding antiaromatic carbon analogue is strongly destabilized (35.3 kcal mol^{-1}, according to an equation analogous to equation 45)[169].

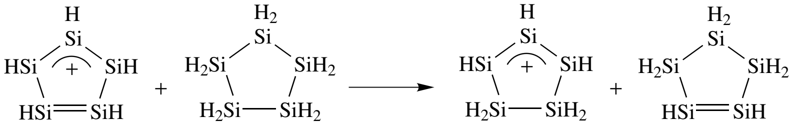
(45)

The contrast with the $C_5H_5^+$ surface is interesting. The global minimum on the $C_5H_5^+$ PES (all energies below are at MP2/6-31G*//MP2/6-31G*)[169] is a $^3A_2$ state having D_{5h} symmetry **(161)**. The D_{5h} singlet of **161** is not a minimum on the PES and it collapses to the planar singlet C_{2v} cyclopentadienyl cation **162**, which is by 11 kcal mol^{-1} less stable than **161**. The isomeric allylic cation **163** is not a minimum and has nearly the same energy as **162**. The C_{4v} pyramidal structure **(164)** is by 15.6 and 4.6 kcal mol^{-1} less stable than **161** and **162**, respectively. The most stable $C_5H_5^+$ isomer on the singlet surface is the vinylcyclopropeniun ion **(165)**, which is by only 1.7 kcal mol^{-1} less stable than **161**.

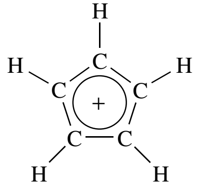
(161) D_{5h}, $^3A_2$

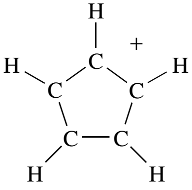
(162) C_{2v}

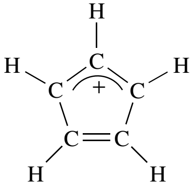
(163) C_{2v}

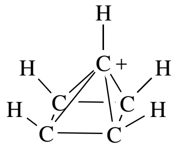
(164) C_{4v}

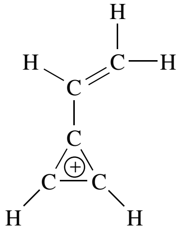
(165) C_s

The relative high stabilities of the pyramidal, bridged and silylenic structures in the case of $Si_5H_5{}^+$ result from several electronic effects typical of silicon, which were already discussed in detail in this review, such as the reluctance to form multiple bonds, high divalent state stabilization, preference for bridged bonding etc. These effects lead in the case of $Si_5H_5{}^+$, as in many other examples discussed in this chapter, to stable three-dimensional structures which are not minima on the PES of the analogous carbon compounds.

IX. CONCLUSIONS

Silicon compounds exhibit aromaticity and antiaromaticity in analogy to the corresponding carbon compounds. However, in general, the degree of their aromaticity and antiaromaticity is smaller than that of the analogous carbon compounds.

The reluctance of silicon to form multiple bonds, its high divalent state stabilization, its preference for bridged bonding and other factors result in the existence of compounds which have no stable carbon analogues.

Many important achievements have been reached in the last 20 years in this field, yet the study of aromatic silicon compounds is still in its infancy and much remains to be learned and understood. Quantum chemistry is a particularly powerful tool for studying these intriguing molecules and for directing the difficult and challenging experimental research in this field. The study of aromaticity and antiaromaticity of silicon compounds presents also a major theoretical challenge, as many of their properties are difficult to calculate and the potential energy surfaces on which they reside are extremely complex. As stated throughout the review, many of the currently available theoretical studies are quite old and consequently have not been performed at the appropriate level of theory. New high-level calculations which will lead to more reliable predictions are highly desired.

X. ACKNOWLEDGEMENTS

The authors would like to thank P. v. R. Schleyer, H. Jiao, S. Nagase, R. Kobayashi, W. Thiel, M. Bühl and D. Tilley for preprints of their manuscripts prior to publication. M. Karni thanks her family for their patience during writing this review. The financial support of the German Federal Ministry of Science, Research, Technology and Education and the Minerva Foundation and of the US–Israel Binational Science Foundation (BSF) is gratefully acknowledged.

XI. LIST OF ABBREVIATIONS

Ad	adamantyl
Ar	aryl
ASE	aromatic stabilization energy
B3LYP	Becke's 3-parameter hybrid with Lee, Young and Parr's correlation functional
BSE	bond separation energy
CCSD(T)	coupled cluster with single and double excitations (followed by a perturbation treatment of triple excitations)
CI	configuration interaction
CISD	configuration interaction with single and double excitations
Cp	cyclopentadienyl
CSA	chemical shift anisotropy

CSGT	continuous set of gauge transformations
DFT	density functional theory
DZ	double zeta
DZ+d	double zeta + polarization functions on heavy atoms
DZP	double zeta + polarization functions on all atoms
ECP	electron core potential
GIAO	gauge-independent atomic orbitals
HF	Hartree–Fock
HOMO	highest occupied molecular orbital
IGLO	individual gauge for localized orbitals
IP	ionization potential
LUMO	lowest unoccupied molecular orbital
MBPT	many-body perturbation theory
MCn	multi-configuration; n=number of configurations
MCSCF	multi-configuration self-consistent field
MO	molecular orbital
MP	Møller–Plesset
n-MR	n-membered ring
NAO	natural atomic bond-order
NICS	nucleus-independent chemical shift
NPA	natural population analysis
PES	potential energy surface
QMRE	quantum molecular resonance energy
RE	resonance energy
SCF	self-consistent field
SINDO	symmetrically orthogonalized intermediate neglect of differential overlap
TSB	trisilabenzene
TZP	Triple zeta + polarization
UHF	unrestricted Hartree–Fock
UHF–NO	unrestricted Hartree–Fock –natural orbitals
UMP	unrestricted Møller–Plesset
WBI	Wiberg bond index
ZPE	zero-point vibrational energy

XII. REFERENCES

1. (a) G. Raabe and J. Michl, in *The Chemistry of Organic Silicon Compounds* (Eds. S. Patai and Z. Rappoport), Chap. 17, Wiley, New York, 1989, p. 1015.
   (b) Y. Apeloig, in *The Chemistry of Organic Silicon Compounds* (Eds. S. Patai and Z. Rappoport), Chap. 2, Wiley, New York, 1989, p. 103.
   (c) Y. Apeloig and M. Karni, *Chem. Rev.* (1998), in preparation.

2. Chapters in this book by:
   (a) T. Müller, W. Ziche and N. Auner, Chapter 16.
   (b) H. Sakurai, Chapter 15.
   (c) N. Tokitoh and R. Okazaki, Chapter 17.
   (d) G. Maier, Chapter 19.
   (e) P. Gaspar and R. West, Chapter 43.
3. (a) A. G. Brook and K. M. Baines, *Adv. Organomet. Chem.*, **25**, 1 (1986).
   (b) A. G. Brook and M. A. Brook, *Adv. Organomet. Chem.*, **39**, 71 (1996).
   (c) R. Okazaki and R. West, *Adv. Organomet. Chem.*, **39**, 232 (1996).
   (d) I. Hemme and U. Klingebeil, *Adv. Organomet. Chem.*, **39**, 159 (1996).
   (e) M. Driess, *Adv. Organomet. Chem.*, **39**, 193 (1996).
   (f) N. Auner, G. Fearon and J. Weis in *Organosilicon Chemistry III* (Eds. N. Auner and J. Weis), VCH, Weinheim, 1997.
4. A. G. Brook, F. Abdesaken, B. Gutekunst, G. Gutekunst and R. K. Kallury, *J. Chem. Soc., Chem. Commun.*, 191 (1981).
5. R. West, M. J. Fink and J. Michl, *Science*, **214**, 1343 (1981).
6. G. E. Miracle, J. L. Ball, D. R. Powell and R. West, *J. Am. Chem. Soc.*, **115**, 11598 (1993).
7. (a) S. Bailleaux, M. Bogey, C. Demuynck, J. Destombes and A. Walters, *J. Chem. Phys.*, **101**, 2729 (1994).
   (b) M. Bogey, B. Delcroix, A. Walters and J.-C. Guillemin, *J. Mol. Spectrosc.*, **175**, 421 (1996).
   (c) R. Srinivas, D. K. Böhme, D. Sülzle and H. Schwarz, *J. Phys. Chem.*, **95**, 9836 (1991).
8. N. Tokitoh, K. Wakita, R. Okazaki, S. Nagase and P. v. R. Schleyer, *J. Am. Chem. Soc.*, **119**, 6951 (1997).
9. G. Märkel and W. Schlosser, *Angew. Chem., Int. Ed. Engl.*, **27**, 963 (1988).
10. (a) W. P. Freeman, D. Tilley, L. M. Liable-Sands and A. L. Rheingold, *J. Am. Chem. Soc.*, **118**, 10457 (1996).
    (b) R. West, H. Sohn, U. Bankwitz, J. Calabrese, Y. Apeloig and T. Müller, *J. Am. Chem. Soc.*, **117**, 11608 (1995).
    (c) J.-H. Hong, P. Boudjouk and S. Castellino, *Organometallics*, **13**, 3387 (1994).
    (d) W. P. Freeman, D. Tilley and A. L. Rheingold, *J. Am. Chem. Soc.*, **116**, 8428 (1994). See also references cited in these papers.
11. E. Hückel, *Z. Phys.*, **70**, 204 (1931); E. Hückel, *Z. Phys.*, **72**, 310 (1931).
12. P. v. R. Schleyer, H. F. Schaefer III and N. C. Handy (Eds.), *Encyclopedia of Computational Chemistry*, Wiley, New York, 1998.
13. (a) V. I. Minkin, M. N. Glukhovtsev and B. Ya. Simkin, *Aromaticity and Antiaromaticity*, Wiley, New York, 1994.
    (b) P. J. Garratt, *Aromaticity*, Wiley, New York, 1986.
14. M. N. Glukhovtsev, *J. Chem. Educ.*, **74**, 132 (1997).
15. (a) S. S. Shaik, A. Shurki, D. Danovitch and P. C. Hiberty, *J. Mol. Struct (Theochem)*, **398–399**, 155 (1997) and references cited therein.
    (b) S. S. Shaik, P. C. Hiberty, G. Ohanessian and J.-M. Lefour, *J. Phys. Chem.*, **92**, 5086 (1988).
    (c) G. Ohanessian, P. C. Hiberty, J.-M. Lefour, J.-P. Flament and S. S. Shaik, *Inorg. Chem.*, **27**, 2219 (1988).
16. P. v. R. Schleyer and H. Jiao, *Pure Appl. Chem.*, **68**, 209 (1996).
17. (a) A. Julg and P. Fracois, *Theor. Chim. Acta*, **7**, 249 (1967).
    (b) S. M. Van den Kerk, *J. Organomet. Chem.*, **215**, 315 (1981).
18. P. W. Fowler and E. Steiner, *J. Phys. Chem. A*, **101**, 1409 (1997).
19. P. v. R. Schleyer, H. Jiao, N. v. E. Hommes, V. G. Malkin and O. Malkina, *J. Am. Chem. Soc.*, **119**, 12669 (1992).
20. F. Bernardi, A. Bottoni and A. Venturini, *J. Mol. Struct. (Theochem)*, **163**, 173 (1988) and references cited therein.
21. (a) W. J. Hehre, R. Ditchfield, L. Radom and J. A. Pople, *J. Am. Chem. Soc.*, **92**, 4796 (1970).
    (b) P. George, M. Trachtman, C. W. Bock and A. M. Brett, *Theor. Chim. Acta*, **38**, 121 (1975).
    (c) P. George, M. Trachtman, C. W. Bock and A. M. Brett, *J. Chem. Soc., Perkin Trans. 2*, 1222 (1976).
    (d) B. A. Hass and L. J. Schaad, *J. Am. Chem. Soc.*, **105**, 7500 (1983).
22. Experimental data taken from: H. M. Rosenstock, K. Draxl, B. W. Steiner and J. T. Herron, *J. Phys. Chem. Ref. Data*, **6**, Suppl. 1 (1977); N. Cohen and S. W. Benson, *Chem. Rev.*, **93**, 2419 (1993).

23. (a) D. H. Hutter and W. H. Flygare, *Top. Curr. Chem.*, **63**, 89 (1976) and references cited therein.
(b) H. Jiao and P. v. R. Schleyer, *J. Chem. Soc., Perkin Trans. 2*, 407 (1994).
24. H. J. Dauben Jr., J. D. Wilson and J. L. Laity, *J. Am. Chem. Soc.*, **90**, 811 (1968); **91**, 1991 (1969); H. J. Dauben Jr., J. D. Wilson and J. L. Laity, in *Non-Benzenoid Aromatics*, Vol. 2 (Ed. J. P. Snyder), Academic Press, New York, 1971.
25. F. London, *J. Phys. Radium*, **8**, 397 (1933).
26. P. v. R. Schleyer, C. Maerker, A. Dransfeld, H. Jiao and N. v. E. Hommes, *J. Am. Chem. Soc.*, **118**, 6317 (1996) and references cited therein.
27. M. Bühl, W. Thiel, H. Jiao, P. v. R. Schleyer, M. Saunders and F. A. L. Anet, *J. Am. Chem. Soc.*, **116**, 7429 (1994); M. Bühl and C. van Wüllen, *Chem. Phys. Lett.*, **247**, 63 (1995).
28. R. C. Haddon, *J. Am. Chem. Soc.*, **101**, 1722 (1979).
29. A. R. Katritzky, P. Barczynski, G. Masummarra, D. Pisano and M. Szafran, *J. Am. Chem. Soc.*, **111**, 7 (1989).
30. K. Jug and A. M. Köster, *J. Phys. Org. Chem.*, **4**, 163 (1991).
31. (a) P. v. R. Schleyer, P. Freeman, H. Jiao and B. Goldfuss, *Angew. Chem., Int. Ed. Engl.*, **34**, 337 (1995).
(b) K. N. Houk and M. Mendel, *Chemtracts Organic Chemistry*, **9**, 118 (1996).
(c) C. W. Bird, *Tetrahedron*, **52**, 9945 (1996).
32. Silatoluene: (a) T. J. Barton and D. Banasink, *J. Am. Chem. Soc.*, **99**, 5199 (1977).
(b) C. L. Kreil, O. L. Chapman, G. T. Burns and T. J. Barton, *J. Am. Chem. Soc.*, **102**, 841 (1980).
(c) H. Bock, R. A. Bowling, B. Solouki, T. J. Barton and G. T. Burns, *J. Am. Chem. Soc.*, **102**, 429 (1980).
33. Silabenzene: (a) T. J. Barton and G. T. Burns, *J. Am. Chem. Soc.*, **100**, 5246 (1978).
(b) G. Maier, G. Mihm and H. P. Reisenauer, *Angew. Chem., Int. Ed. Engl.*, **19**, 52 (1980).
(c) B. Solouki, P. Rosmus, H. Bock and G. Maier, *Angew. Chem., Int. Ed. Engl.*, **19**, 51 (1980).
(d) G. Maier, G. Nihm and H. P. Reisenauer, *Chem. Ber.*, **115**, 801 (1982).
34. P. Jutzi, M. Meyer, H. P. Reisenauer and G. Maier, *Chem. Ber.*, **122**, 1227 (1989).
35. Y. van den Winkel, B. L. M. van Baar, F. Bickelhaupt, W. Kulik, C. Sierakowski and G. Maier, *Chem. Ber.*, **124**, 185 (1991).
36. G. Maier, K. Schöttler and H. P. Reisenauer, *Tetrahedron Lett.*, **26**, 4079 (1985).
37. A. Bjarnason and I. Arnason, *Angew. Chem., Int. Ed. Engl.*, **31**, 1633 (1992).
38. M. J. S. Dewar, D. H. Lo and C. A. Ramsden, *J. Am. Chem. Soc.*, **97**, 1311 (1975).
39. P. H. Blustin, *J. Organomet. Chem.*, **166**, 21 (1979).
40. J. Chandrasekhar, P. v. R. Schleyer, R. O. W. Baumgartner and M. T. Reets, *J. Org. Chem.*, **48**, 3453 (1983).
41. (a) M. S. Gordon, P. Boudjouk and F. Anwari, *J. Am. Chem. Soc.*, **105**, 4972 (1983).
(b) K. K. Baldridge and M. S. Gordon, *Organometallics*, **7**, 144 (1988).
42. H. B. Schlegel, B. Coleman and M. Jones Jr., *J. Am. Chem. Soc.*, **100**, 6499 (1978).
43. (a) K. K. Baldridge and M. S. Gordon, *J. Am. Chem. Soc.*, **110**, 4204 (1988).
(b) P. George, C. W. Bock and M. Trachtman, *Theor. Chim. Acta*, **71**, 289 (1987).
44. H. Bock, P. Rosmus. B. Solouki and G. Maier, *J. Organomet. Chem.*, **271**, 145 (1984).
45. (a) C. W. Bock, P. George and M. Trachtman, *J. Mol. Struct (Theochem)*, **109**, 1 (1984).
(b) C. W. Bock, P. George and M. Trachtman, *J. Phys. Chem.*, **88**, 1467 (1984).
46. (a) R. S. Grev, G. E. Scuseria,, A. C. Sheiner, H. F. Schaefer III and M. S. Gordon, *J. Am. Chem. Soc.*, **110**, 7337 (1988).
(b) S. Schroder and W. Thiel, *J. Am. Chem. Soc.*, **107**, 4422 (1985).
47. Y. Apeloig and M. Karni, *J. Am. Chem. Soc.*, **106**, 6676 (1984).
48. Y. Apeloig, M. Bendikov and S. Sklenak, unpublished results.
49. R. A. King, G. Vacek and H. F. Schaefer III, *J. Mol. Struct. (Theochem)*, **358**, 1 (1995).
50. (a) K. K. Baldridge and M. S. Gordon, *J. Organomet. Chem.*, **271**, 369 (1984).
(b) J. Chandrasekhar and P. v. R. Schleyer, *J. Organomet. Chem.*, **289**, 51 (1985).
51. (a) W. Ando, T. Shiba, T. Hidaka, K. Morihashi and O. Kikuchi, *J. Am. Chem. Soc.*, **119**, 3629 (1997).
(b) W. Ando, unpublished results.
52. M. Zhao and B. M. Gimarc, *Inorg. Chem.*, **35**, 5378 (1996).

53. (a) N. Matsunaga, T. R. Cundari, M. W. Schmidt and M. S. Gordon, *Theor. Chim. Acta*, **83**, 57 (1992).
    (b) N. Matsunaga and M. S. Gordon, *J. Am. Chem. Soc.*, **116**, 11407 (1994).
54. (a) W. J. Stevens, H. Basch and M. Kraus, *J. Chem. Phys.*, **81**, 6026 (1984).
    (b) W. J. Stevens, M. Kraus and P. Jasian, *Can. J. Chem.*, **70**, 612 (1992).
55. Y. Apeloig and J. Hrusàk, unpublished results.
56. S. Nagase, T. Kudo and M. Aoki, *J. Chem. Soc. Chem. Commun.*, 1121 (1985).
57. D. A. Clabo and H. F. Schaefer III, *J. Chem. Phys.*, **84**, 1664 (1986).
58. A. F. Sax and R. Janoschek, *Angew. Chem., Int. Ed. Engl.*, **25**, 651 (1986).
59. S. Nagase, H. Teramae and T. Kudo, *J. Chem. Phys.*, **86**, 4513 (1987).
60. A. F. Sax, J. Kalcher and R. Janoschek, *J. Comput. Chem.*, **9**, 564 (1988).
61. (a) S. Nagase, *Pure Appl. Chem.*, **65**, 675 (1993).
    (b) S. Nagase, *Polyhedron*, **10**, 1299 (1991).
62. P. v. R. Schleyer, unpublished.
63. J. M. Schulman and R. L. Disch, *J. Am. Chem. Soc.*, **107**, 5059 (1985).
64. H. Jacobson and T. Ziegler, *J. Am. Chem. Soc.*, **116**, 3667 (1994).
65. M. Karni and Y. Apeloig, *J. Am. Chem. Soc.*, **112**, 8589 (1990).
66. (a) R. Grev and H. F. Schaefer III, *J. Chem. Phys.*, **97**, 7990 (1992).
    (b) D. E. Goldberg, P. B. Hitchcock, M. F. Lappert, K. M. Thomas, A. J. Thorne, T. Fjeldberg, A. Haaland and B. E. R. Schilling, *J. Chem. Soc., Dalton Trans.*, 2387 (1986).
    (c) G. Trinquier and J.-P. Malrieu, *J. Phys. Chem.*, **94**, 6184 (1990).
    (d) G. Trinquier, *J. Am. Chem. Soc.*, **112**, 2130 (1990).
    (e) G. Trinquier, J.-P. Malrieu and P. Riviére, *J. Am. Chem. Soc.*, **104**, 4529 (1982).
67. N. Nagase, K. Kobayashi and T. Kudo, *Main Group Metal Chemistry*, **17**, 171 (1994).
68. L. Nyulászi, T. Kárpáti and T. Veszprémi, *J. Am. Chem. Soc.*, **116**, 7239 (1994).
69. T. Veszprémi, L. Nyulászi and T. Kárpáti, *J. Phys. Chem.*, **100**, 6262 (1996).
70. E. D. Jemmis, G. N. Srinivas, J. Leszczynski, J. Kapp, A. Korkin and P. v. R Schleyer, *J. Am. Chem. Soc.*, **117**, 11361 (1995).
71. A. Korkin, M. Glukhovtsev and P. v. R. Schleyer, *Int. J. Quantum Chem.*, **46**, 137 (1993).
72. (a) S. Murthy, Y. Nagano and J. L. Beauchamp, *J. Am. Chem. Soc.*, **114**, 3573, (1992).
    (b) Y. Nagano, S. Murthy and J. L. Beauchamp, *J. Am. Chem. Soc.*, **115**, 10805 (1993).
73. (a) A. Nicolaides and L. Radom, *J. Am. Chem. Soc.*, **118**, 10561 (1996).
    (b) A. Nicolaides and L. Radom, *J. Am. Chem. Soc.*, **116**, 9769 (1994).
    (c) R. L. Jarek and S. K. Shin, *J. Am. Chem. Soc.*, **119**, 6376 (1997).
74. (a) L. A. Curtiss, K. Raghavachari, G. W. Trucks and J. A. Pople, *J. Chem. Phys.*, **94**, 7221 (1991).
    (b) L. A. Curtiss, K. Raghavachari, G. W. Trucks and J. A. Pople, *J. Chem. Phys.*, **98**, 1293 (1993).
    (c) L. A. Curtiss and K. Raghavachari, in *Quantum Mechanical Electronic Structure Calculations with Chemical Accuracy* (Ed. S. R. Langhoff), Kluwer Academic Publishers, Dordrecht, 1995.
    (d) K. Raghavachari and L. A. Curtiss, in *Modern Electronic Structure Theory* (Ed. D. R. Yarkony), World Scientific, Singapore, 1995.
    (e) B. J. Smith and L. Radom, *J. Phys. Chem.*, **99**, 6468 (1995).
    (f) L. A. Curtiss, P. C. Redfern, B. J. Smith and L. Radom, *J. Chem. Phys.*, **104**, 5148 (1996).
75. R. Srinivas, J. Hrusák, D. Sülzle, D. K. Böhme and H. Schwarz, *J. Am. Chem. Soc.*, **114**, 2802 (1992).
76. (a) K. Krogh-Jespersen, J. Chandrasekhar and P. v. R. Schleyer, *J. Org. Chem.*, **45**, 1608 (1980).
    (b) B. J. Aylett and H. M. Colquhoun, *J. Chem. Res. (S)*, **148**, (1977); *J. Chem. Res. (M)*, 1674 (1977).
77. (a) J. Dubac, A. Leporterie and G. Manue, *Chem. Rev.*, **90**, 215 (1990).
    (b) J. Dubac, C. Guerin and P. Meunier, Chapter 34 in this book.
78. K. Tamao and A. Kawachi, *Adv. Organomet. Chem.*, **38**, 1 (1995).
79. J.-H. Hong and P. Boudjouk, *J. Am. Chem. Soc.*, **115**, 5883 (1993).
80. J.-H. Hong, P. Boudjouk and I. Stoenescu, *Organometallics*, **15**, 2179 (1996).
81. W. P. Freeman, D. Tilley, A. L. Rheingold and R. L. Ostrander, *Angew. Chem., Int. Ed. Engl.*, **32**, 1744 (1993).

82. W. P. Freeman, D. Tilley, G. P. A. Yap and A. L. Rheingold, *Angew. Chem., Int. Ed. Engl.*, **35**, 882 (1996).
83. W.-C. Joo, J.-H. Hong, S.-B. Choi, H.-E. Son and C.-H. Kim, *J. Organomet. Chem.*, **391**, 27 (1990).
84. U. Bankwitz, H. Sohn, D. R. Powell and R. West, *J. Organomet. Chem.*, **499**, C7 (1995).
85. R. West, H. Sohn, D. R. Powell, T. Müller and Y. Apeloig, *Angew. Chem., Int. Ed. Engl.*, **35**, 1002 (1996).
86. W. P. Freeman, D. Tilley, F. P. Arnold, A. L. Rheingold and P. K. Gantzel, *Angew, Chem., Int. Ed. Engl.*, **34**, 1887 (1995).
87. J. R. Damewood Jr., *J. Org. Chem.*, **51**, 5028 (1986).
88. B. Goldfuss and P. v. R. Schleyer, *Organometallics*, **14**, 1553 (1995).
89. B. Goldfuss and P. v. R. Schleyer, *Organometallics*, **16**, 1543 (1997).
90. (a) G. A. Olah and R. J. Hundai, *J. Am. Chem. Soc.*, **102**, 6989 (1980).
    (b) For a review on silyl anions see: K. Tamao and A. Kawachi, *Adv. Organomet. Chem.*, **38**, 1 (1995) and J. Beltzner and U. Dehnert, Chapter 14 in this book.
91. E. D. Jemmis and P. v. R. Schleyer, *J. Am. Chem. Soc.*, **104**, 4781 (1982).
92. H. Jiao and P. v. R. Schleyer, *Angew. Chem., Int. Ed. Eng.*, **32**, 1760 (1993).
93. (a) B. Goldfuss, P. v. R. Schleyer and F. Hampel, *Organometallics*, **15**, 1755 (1996).
    (b) T. Müller, Y. Apeloig, H. Son and R. West, in *Organosilicon Chemistry III* (Eds. N. Auner and J. Weis), VCH, Weinheim, 1997.
94. For reviews see:
    (a) Carbenes: O. M. Nefedov, M. P. Egorov, A. I. Joffe, C. G. Menchkov, P. S. Zuev, V. I. Minkin. B. Y. Simkin and M. N. Glukhovtsev, *Pure Appl. Chem.*, **64**, 265 (1992).
    (b) Silylenes: P. P. Gaspar, in *Reactive Intermediates* (Eds. M. Jones and R. A. Moss), Wiley, New York, 1978, Vol. 1, pp. 229–278; 1981, Vol. 2, pp. 335–385; 1985, Vol. 3, pp. 333–427.
    (c) Germylenes: J. Barrau, J. Escudie and J. Satge, *Chem. Rev.*, **90**, 283 (1990); W. P. Neumann, *Chem. Rev.*, **91**, 311 (1991).
95. (a) A. J. Arduengo III, R. L. Harlow and M. Kline, *J. Am. Chem. Soc.*, **113**, 361 (1991).
    (b) A. J. Arduengo III, H. V. Rasika Dias, R. L. Harlow and M. Kline, *J. Am. Chem. Soc.*, **114**, 5530 (1992).
    (c) A. J. Arduengo III, J. R. Goerlich and W. J. Marshall, *J. Am. Chem. Soc.*, **117**, 11027 (1995).
    (d) J. Cioslowski, *Int. Quantum Chem., Quant. Chem. Symp.*, **27**, 309 (1993).
    (e) A. J. Arduengo III, D. A. Dixon, R. L. Harlow, K. K. Kumashiro, C. Lee, W. P. Power and K. W. Zilm, *J. Am. Chem. Soc.*, **116**, 6361 (1994).
    (f) A. J. Arduengo III, H. V. Rasika Dias, D. A. Dixon, R. L. Harlow, W. T. Klooster and T. F. Koetzle, *J. Am. Chem. Soc.*, **116**, 6812 (1994),
    (g) C. Heinemann and W. Thiel, *Chem. Phys. Lett.*, **217**, 11 (1994),
    (h) D. A. Dixon and A. J. Arduengo III, *J. Phys. Chem.*, **95**, 4180 (1991).
96. A. J. Arduengo III, H. Bock, H. Chen, M. Denk, D. A. Dixon, J. C. Green, W. A. Herrmann, N. L. Jones, M. Wagner and R. West, *J. Am. Chem. Soc.*, **116**, 6641 (1994).
97. W. A. Herrmann, M. Denk, J. Behn, W. Scherer, F. R. Klingan, H. Bock, B. Solouki and M. Wagner, *Angew. Chem., Int. Ed. Engl.*, **31**, 1485 (1992).
98. (a) M. Denk, R. Lennon, R. Hayashi, R. West, A. V. Belyakov, H. P. Verne, A. Haaland, M. Wagner and N. Metzler, *J. Am. Chem. Soc.*, **116**, 2691 (1994).
    (b) M. Denk, J. C. Green, N. Metzler and M. Wagner, *J. Chem. Soc., Dalton Trans.*, 2405 (1994).
    (c) R. West and M. Denk, *Pure Appl. Chem.*, **68**, 785 (1996).
    (d) M. Denk, R. West, R. K. Hayashi, Y. Apeloig, R. Paunz and M. Karni in *Organosilicon Chemistry II. From Molecules to Materials* (Eds. N. Auner and J. Weis), VCH, Weinheim, 1996, p. 251.
99. (a) B. Gehrhus, M. Lappert, J. Heinicke, R. Boese and D. Bläser, *J. Chem. Soc., Chem. Commun.*, 1931 (1995).
    (b) B. Gehrhus, P. B. Hitchcock, M. Lappert, J. Heinicke, R. Boese and D. Bläser, *J. Organomet. Chem.*, **521**, 211 (1996).
    (c) P. Blakeman, B. Gehrhus, J. C. Green, J. Heinicke, M. Lappert, M. Kindermann and T. Veszprémi, *J. Chem. Soc., Dalton Trans.*, 1475 (1996).
100. (a) C. Heinemann, T. Müller, Y. Apeloig and H. Schwarz, *J. Am. Chem. Soc.*, **118**, 2023 (1996).
101. M. Veith, E. Werle, R. Lisowsky, R. Köppe and H. Schnöckel, *Chem. Ber.*, **125**, 1375 (1992).

102. Y. Apeloig, M. Karni and T. Müller, in *Organosilicon Chemistry II. From Molecules to Materials.* (Eds N. Auner and J. Weis), VCH, Weinheim, 1996, p. 263.
103. C. Boehme and G. Frenking, *J. Am. Chem. Soc.*, **118**, 2039 (1996).
104. C. Heinemann, W. A. Herrmann and W. Thiel, *J. Organomet. Chem.*, **475**, 73 (1994).
105. (a) R. Ditchfield, *Mol. Phys.*, **27**, 789 (1974).
    (b) J. Gauss, *J. Chem. Phys.*, **99**, 3629 (1993) and references cited therein.
106. (a) W. Kutzelnigg, U. Fleischer and M. Schindler, in *NMR—Basic Principles and Progress*, Vol. 23, Springer, Berlin, 1991.
    (b) W. Kutzelnigg, *Isr. J. Chem.*, **19**, 193 (1980).
    (c) M. Schindler and W. Kutzelnigg, *J. Chem. Phys.*, **76**, 1979 (1982).
107. R. West, J. J. Baffy, M. Haaf, T. Müller, B. Gehrhus, M. F. Lappert and Y. Apeloig, *J. Am. Chem. Soc.*, **120**, 1639 (1998).
108. A. E. Reed,, R. B. Weinstock and F. Weinhold, *J. Chem. Phys.*, **83**, 735 (1985).
109. (a) R. W. F. Bader, *Acc. Chem. Res.*, **8**, 34 (1975).
    (b) R. W. F. Bader, in *Atoms in Molecules. A Quantum Theory*, Clarendon Press, Oxford, 1990;
    (c) R. W. F. Bader, *Chem. Rev.*, **91**, 893 (1991); R. W. F. Bader, *Angew. Chem., Int. Ed. Engl.* **33**, 620 (1994).
110. Y. Apeloig and T. Müller, *J. Am. Chem. Soc.*, **117**, 5363 (1995).
111. J. Maxka and Y. Apeloig, *J. Chem. Soc., Chem. Commun.*, 737 (1990).
112. (a) G. Trinquier, and J.-C. Barthelat, *J. Am. Chem. Soc.*, **112**, 9121 (1990).
    (b) G. Trinquier, *J. Am. Chem. Soc.*, **113**, 144 (1991).
    (c) G. Trinquier and J.-P. Malrieu, *J. Am. Chem. Soc.*, **113**, 8634 (1991).
113. (a) R. Walsh, in *The Chemistry of Organic Silicon Compounds* (Eds. S. Patai and Z. Rappoport), Chap. 5, Wiley, Chichester, 1989, p. 371.
    (b) D. R. Lide (Ed.), *CRC Handbook of Chemistry and Physics, 71th edition*, CRC Press, Boca Raton, 1990.
114. L. Nyulászi, D. Szieberth and T. Veszprémi, *J. Org. Chem.*, **60**, 1647 (1995).
115. (a) D. J. Husain and P. E. Norris, *J. Chem. Soc., Faraday Trans. 1*, **74**, 106 (1978).
    (b) S. C. Basu and D. Husain, *J. Photochem. Photobiol. A.*, **42**, 1 (1988).
116. R. Srinivas, D. Sulzle, T. Weiske and H. Schwarz, *Int. J. Mass Spectrom. Ion Processes*, **107**, 369 (1991).
117. (a) G. Maier, H. P. Reisenauer and H. Pacl, *Angew. Chem., Int. Ed. Engl.*, **33**, 1248 (1994).
    (b) G. Maier, H. Pacl, H. P. Reisenauer, A. Meudt and R. Janoschek, *J. Am. Chem. Soc.*, **117**, 12712 (1995);
    (c) M. Izuha, S. Yamamoto and S. Saito, *Can. J. Phys.*, **72**, 1206 (1994).
118. (a) G. Frenking, R. B. Remington and H. F. Schaefer III, *J. Am. Chem. Soc.*, **108**, 2169 (1986).
    (b) G. Vacek, B. T. Colegrove and H. F. Schaefer, III, *J. Am. Chem. Sec.*, **113**, 3192 (1991).
    (c) T. J. Lee, A. Bunge and H. F. Schaefer, III, *J. Am. Chem. Soc.*, **107**, 137 (1985).
119. C. D. Sherrill, C. G. Brandow, W. D. Allen and H. F. Schaefer III, *J. Am. Chem. Soc.*, **118**, 7158 (1996).
120. (a) M.-D. Su, R. D. Amos and N. C. Handy, *J. Am. Chem. Soc.*, **112**, 1499 (1990).
    (b) M. S. Gordon and R. D. Koob, *J. Am. Chem. Soc.*, **103**, 2939 (1981).
121. S. Wlodek, A. Fox and D. K. Böhme, *J. Am. Chem. Soc.*, **113**, 4461 (1991).
122. (a) J. D. Presilla-Márquez, W. R. M. Graham and R. A. Shepherd *J. Chem. Phys.*, **93**, 5424 (1990); R. A. Shepherd and W. R. M. Graham, *J. Chem. Phys.*, **88**, 3399 (1988); R. A. Shepherd and W. R. M. Graham, *J. Chem. Phys.*, **82**, 4788 (1985); J. Oddershede, J. R. Sabin, G. H. F. Diercksen and N. E. Grüner, *J. Chem. Phys.*, **83**, 1702 (1985); W. Weltner, Jr. and D. McLeod Jr., *J. Chem. Phys.*, **41**, 235 (1964); B. Kleman, *Astrophys. J.*, **123**, 162 (1956).
    (b) G. Fitzgerald, S. J. Cole and R. J. Bartlett, *J. Chem. Phys.*, **85**, 1701 (1986).
    (c) R. S. Grev and H. F. Schaefer III, *J. Chem. Phys.*, **80**, 3552 (1984).
123. M. C. Ernst, A. F. Sax, J. Kalcher and G. Katzer, *J. Mol. Struct*, **334**, 121 (1995).
124. (a) H. W. Kroto, J. R. Heath, S. C. O'Brien, R. F. Curl and R. E. Smalley, *Nature*, **318**, 162 (1985).
    (b) J. R. Heath, S. C. O'Brien, Q. Zhang, Y. Liu, R. F. Curl, H. W. Kroto, F. K. Tittel and R. E. Smalley, *J. Am. Chem. Soc.*, **107**, 7779 (1985).
    (c) Q. Zhang, S. C. O'Brien, J. R. Heath, Y. Liu, H. W. Kroto and R. E. Smalley, *J. Phys. Chem.*, **90**, 525 (1986).
125. W. Kräschmer, F. Fostiropoulos and D. R. Huffman, *Nature*, **347**, 354 (1990); W. Kräschmer, F. Fostiropoulos and D. R. Huffman, *Chem. Phys. Lett.*, **170**, 167 (1990).

126. M. S. Dresselhaus, G. Dresselhaus and P. C. Eklund, *Science of Fullerenes and Carbon Nanotubes*, Academic Press, San Diego, 1996.
127. R. C. Haddon, *Science*, **261**, 1545 (1993) and references cited therein.
128. R. C. Haddon, *Nature*, **378**, 249 (1995) and references cited therein.
129. M. Bühl, W. Thiel, H. Jiao, P. v. R. Schleyer, M. Saunders and F. A. L. Anet, *J. Am. Chem. Soc.*, **116**, 6005 (1994).
130. R. C. Haddon, L. F. Schneemeyer, J. V. Waszczak, S. H. Glarum, R. Tycko, G. Dabbagh, A. R. Kortan, A. J. Muller, A. M. Mujsce, M. J. Rosseinsky, S. M. Zahurak, A. V. Makhija, F. A. Thiel, K. Raghavachari, E. Cockayne and V. Elser, *Nature*, **350**, 46 (1991).
131. (a) A. Pasquerello, M. Schlüter and R. C. Haddon, *Science*, **257**, 1660 (1992).
    (b) A. Pasquerello, M. Schlüter and R. C. Haddon, *Phys. Rev. A*, **47**, 1783 (1993).
    (c) R. C. Haddon, *Nature*, **367**, 214 (1994).
132. M. Bühl and W. Thiel, *Chem. Eur. J.*, submitted
133. M. Bühl and W. Thiel, *Chem. Phys. Lett.*, **233**, 585 (1995).
134. (a) Q. L. Zhang, T. Liu, R. F. Curl, F. K. Tittle and R. E. Smalley, *J. Phys. Chem.,* **88**, 1670 (1988).
    (b) M. F. Jarrold and E. C. Honea, *J. Phys. Chem.,* **95**, 9181 (1991).
135. D. A. Jelski, Z. C. Wu and T. F. George, *J. Cluster Sci.*, **1**, 143 (1990).
136. C. Zybill, *Angew. Chem., Int. Ed. Engl.*, **31**, 173 (1992).
137. S. Nagase and K. Kobayashi, *Fullerene Science and Technology*, **1**, 299 (1993).
138. Z. Slanina, S.-L. Lee, K. Kobayashi and S. Nagase, *J. Mol. Struct.*, **312**, 175 (1994).
139. (a) H. W. Kroto, *Nature*, **329**, 529 (1987).
    (b) T. G. Schmaltz, W. A. Seitz, D. J. Klein and G. E. Hite, *J. Am. Chem. Soc.*, **110**, 1113 (1988).
    (c) D. E. Manolopoulos, *J. Chem. Soc., Faraday Trans.*, **87**, 2861 (1991).
140. M. Menon and K. R. Subbaswamy, *Chem. Phys. Lett.*, **219**, 219 (1994).
141. M. C. Piqueras, R. Crespo, E. Ortí and F. Tomàs, *Chem. Phys. Lett.*, **213**, 509 (1993).
142. R. Crespo, M. C. Piqueras and F. Tomàs, *Synth. Met.*, **77**, 13 (1996).
143. S. Nagase and K. Kobayashi, *Chem. Phys. Lett.*, **187**, 291 (1991)
144. D. Bakowies and W. Thiel, *J. Am. Chem. Soc.*, **113**, 3704 (1991).
145. M. Häser, J. Almlöf and G. E. Scuseria, *Chem. Phys. Lett.*, **181**, 497 (1991).
146. K. Hedberg, L. Hedberg, D. S. Bethune, C. A. Brown, H. Dorn, R. D. Johnson and M. de Vries, *Science*, **254**, 410 (1991).
147. S. Osawa, M. Harada and E. Osawa, *Fullerene Science and Technology*, **3**, 225 (1995).
148. F. De Proft, C. Van Alesony and P. Geerlings, *J. Phys. Chem.*, **100**, 7440 (1996).
149. J. Cioslowsky and E. D. Fleischmann, *J. Chem. Phys.*, **94**, 3730 (1991).
150. J. Cioslowsky, *J. Am. Chem. Soc.*, **113**, 4139 (1991).
151. M. C. Piqueras. R. Crespo, and F. Tomàs, *J. Mol. Struct. (Theochem)*, **330**, 177 (1995).
152. (a) T. A. Albright, J. K. Burdett and M.-H. Whangbo, *Orbital Interactions in Chemistry*, Wiley, New York, 1984.
    (b) The orbital diagram of ferrocene is discussed on pp. 392–394.
153. J. P. Collman, L. S. Hegedus, J. R. Norton and R. G. Finke, *Principles and Applications of Organotransition Metal Chemistry*, University Science Books, Mill Valley, California, 1987; P. L. Pauson, in *Non-Benzenoid Aromatic Compounds* (Ed. D. Ginsburg), Interscience Publishers, New York, 1959.
154. (a) P. Jutzi, D. Kanne and C. Krüger, *Angew. Chem., Int. Ed. Engl.*, **25**, 164 (1986).
    (b) P. Jutzi, U. Holtmann, D. Kanne, C. Krüger, R. Blom, R. Gleiter and I. Hyla-Krispin, *Chem. Ber.*, **122**, 1629 (1989).
155. T. J. Lee and J. E. Rice, *J. Am. Chem. Soc.*, **111**, 2011 (1989).
156. T. Kudo and S. Nagase, *J. Mol. Struct., (Theochem)*, **311**, 111 (1994).
157. For X = SiH see:
    (a) E. D. Jemmis, G. Subramanian, I. H. Srivastava and S. R. Gadre, *J. Phys. Chem.*, **98**, 6445 (1994).
    (b) E. D. Jemmis and G. Subramanian, *J. Phys. Chem.*, **98**, 9222 (1994).
    (c) J. K. Burdett and O. Eisenstein, *J. Am. Chem. Soc.*, **117**, 11939 (1995).
158. P. v. R. Schleyer, G. Subramanian and A. Dransfeld, *J. Am. Chem. Soc.*, **118**, 9988 (1996).
159. M. S. Gordon, *J. Chem. Soc., Chem. Commun.*, 1131 (1980).
160. M. E. Colvin and H. F. Schaefer III, *Faraday Symp. Chem. Soc.*, **19**, 39 (1984).
161. G. W. Schriver, M. J. Fink and M. S. Gordon, *Organometallics*, **6**, 1977 (1987).

162. T. A. Holmes, M. S. Gordon, S. Yabushita and M. W. Schmidt, *Organometallics*, **3**, 583 (1984).
163. (a) A. F. Sax and J. Kalcher, *J. Chem. Soc., Chem. Commun.*, 809 (1987).
(b) A. F. Sax and J. Kalcher, *J. Comput. Chem.*, **10**, 309 (1989).
164. S. Nagase and M. Nakano, *Angew. Chem., Int. Ed. Engl.*, **27**, 1081 (1988).
165. (a) B. F. Yates, D. A. Calbo and H. F. Schaefer III, *Chem. Phys. Lett.*, **143**, 421 (1988).
(b) B. F. Yates and H. F. Schaefer III, *Chem. Phys. Lett.*, **155**, 563 (1989).
166. N. Wiberg, C. M. M. Finger and K. Polborn, *Angew. Chem., Int. Ed. Engl.*, **32**, 1054 (1993).
167. E. J. P. Malar, *Tetrahedron*, **52**, 4709 (1996).
168. K. Jug, *J. Org. Chem.*, **48**, 1344 (1983).
169. A. A. Korkin, V. V. Murashov, J. Leszczynski and P. v. R. Schleyer, *J. Phys. Chem.*, **99**, 17742 (1995).
170. (a) W. T. Borden and E. R. Davidson, *J. Am. Chem. Soc.*, **101**, 3771 (1979).
(b) E. D. Jemmis and P. v. R. Schleyer, *J. Am. Chem. Soc.*, **104**, 4781 (1982).
(c) S. Koseki, M. Arai, Y. Fujimura and T. Nakajima, *Chem. Phys.*, **108**, 33 (1986).
(d) J. Fabian, A. Mehlhorn and N. Tyutyulkov, *J. Mol. Struct. (Theochem)*, **151**, 355 (1987).
(e) J. Leszczynski, F. Weisman and M. C. Zerner, *Int. J. Quantum Chem., Quantum Chem. Symp.*, **22**, 117 (1988).
(f) J. Feng, J. Leszczynski, B. Weiner and M. C. Zerner, *J. Am. Chem. Soc.*, **111**, 4648 (1989).
(g) D. J. Wales and R. G. A. Bone, *J. Am. Chem. Soc.*, **114**, 5399 (1992).
(h) M. N. Glukhovtsev and P. v. R. Schleyer, *Mendeleev Commun.*, **100** (1993) and references cited therein.

CHAPTER **2**

A molecular modeling of the bonded interactions of crystalline silica

G. V. GIBBS and M. B. BOISEN, Jr

Departments of Geological Sciences, Materials Science and Engineering and Mathematics, Virginia Tech, Blacksburg, VA 24061, USA

I. INTRODUCTION

The chemistry of the animal and plant worlds is dominated by C, O, H and N whereas that of the mineral world is dominated by Si and O. Indeed, more than 80% of the volume of the earth's crust is believed to consist of the framework silicates quartz (Figure 1a see Plate 1) and feldspar (Figure 1b) with the remaining rock forming silicates mica, amphibole, pyroxene and olivine (Figures 1c, 1d, 1e and 1f, respectively, see Plates 2 and 3) bringing the grand total volume to more than 96%[1]. Therefore, it is not surprising that a knowledge of the bonded interactions that govern the structures and the properties of silicates is of central importance in attempts to understand inorganic materials in the natural environment and to find new uses for minerals in meeting the ever increasing materials needs of mankind.

The bonded interactions in silicates were recently examined in a survey of observed and calculated structures and electron density distributions reported for siloxane and silicic acid molecules and silica polymorph crystals[2]. Employing relatively robust basis sets that include polarization functions, the Si−O bond lengths and Si−O−Si angles of the silica polymorphs were reported to be reproduced in molecular orbital calculations to within a few percent. As observed in earlier studies, polarization functions were found to be a necessary ingredient in the generation of the observed geometries and spectra for silicate crystals. A topological analysis of the observed and calculated electron density distributions of the Si−O bond shows that the valence shell concentration of the oxide ion is locally depleted where the shell crosses the Si−O bond vector, while it is concentrated in the direction of the Si cation. The cross section of the bond was found to become more circular as the Si−O−Si angle widens and the Si−O bond length shortens, a result that can be ascribed to the formation of a weak π-bond involving two of the p-type orbitals on the oxide ion with an increase in the value of the electron density at the bond critical point. The close similarity of the bond length and angle data and the electron density distributions reported for silicate crystals and siloxane molecules were taken to indicate that the bonded interactions that govern the structure of a silicate can be treated as if localized as in a molecule and largely independent of the long-range forces of the ions that comprise the periodic field of a silicate crystal.

One of the goals of this paper is to provide a basis for understanding why the bonded interactions of a silicate crystal can be treated as localized and modeled with a molecular-based potential energy function. Another is to provide a basis for understanding why it is possible to reproduce the crystal structures and the bulk moduli of the known silica polymorphs with such a potential and why it is possible to generate many of the known structures of silica together with a large number of new structure types starting with a random arrangement of Si and O atoms in a unit cell with triclinic $P1$ symmetry, again using a molecular-based potential energy function. In Section II, the bond lengths recorded for silicate and related oxide minerals are compared with those calculated for chemically similar molecules. The Si−O bond lengths and Si−O−Si angles observed for the silica polymorphs are examined in Section III in terms of a potential energy surface calculated for the Si−O−Si skeletal unit of a disilicic acid molecule. Bond critical point properties of an electron density distribution calculated for the Si−O−Si unit is compared with that observed for a silica polymorph in Section IV. A modeling of the structures and the bulk moduli of the known polymorphs, using a potential energy function based on the molecule, is discussed in Section V, while in Section VI, the generation of large numbers of new structure types for silica is examined.

II. BOND LENGTH–BOND STRENGTH VARIATIONS IN SILICATES AND RELATED MOLECULES

More than 60 years ago, the important proposal[3] was made that the strength, s, of an X−O bond in an XO_n-coordinated polyhedron in a crystal like a silicate should depend on the valence, z, and the coordination number, n, of the X^{+z} metal cation such that $s = z/n$. With this simple definition, it was found for instance that the sum of the strengths of each of the t bonds in a crystal reaching a given oxide ion,

$$\zeta = \sum_{i=1}^{t} s_i,$$

often equals 2.0, the valence of the anion with its sign changed. Hence, for a silicate like quartz where each Si^{+4} cation resides in a SiO_4 tetracoordinate polyhedron and each oxide ion is bonded to two Si cations, the strength of the Si−O bond is 1.0 and the sum

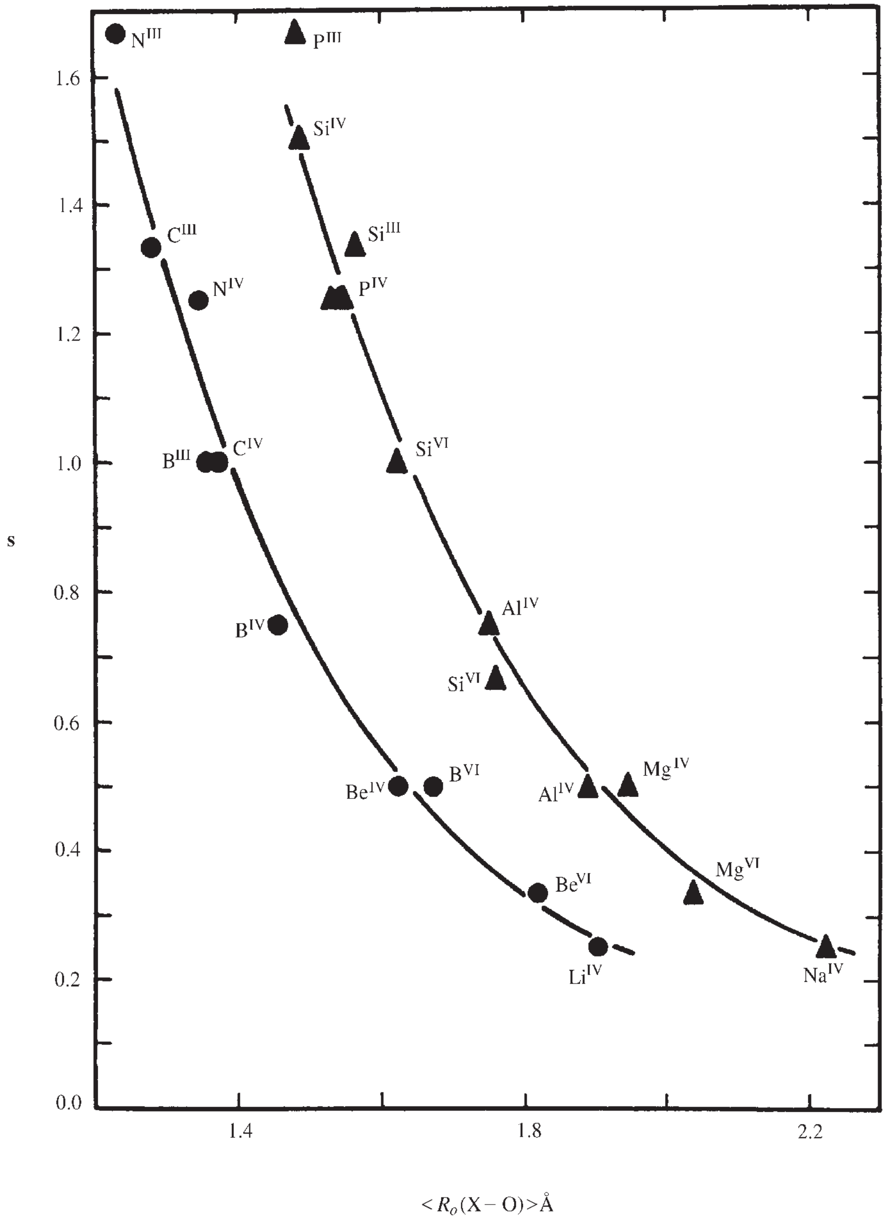

FIGURE 2. A plot of the average bond lengths, $<R_o(\mathrm{X{-}O})>$, of the XO_n coordination polyhedra observed for silicate and oxide crystals vs the Pauling bond strength, s, of the X$-$O bond. The Roman numeral superscript denotes the coordination number of the X-cation

of the bond strengths reaching each oxide ion is 2.0, matching exactly the valence of the oxide ion with its sign changed. A plot of s versus the average X—O bond length, $<R_o(\text{X—O})>$, observed for the XO_n-coordination polyhedra in silicate and oxide crystals shows for first-row (Li, Be, B, ...) and second-row (Na, Mg, Al, ...) X-cations that $<R_o(\text{X—O})>$ decreases nonlinearly in two separate but essentially parallel trends from left to right across each row of the periodic table as the strength of the bond increases[4,5] (Figure 2).

In an examination of whether the trends displayed in Figure 2 hold for molecules, molecular orbital calculations were completed[6] on a set of hydroxyacid $\text{H}_{2n-m}\ \text{X}^{+m}\ \text{O}_n$ molecules with XO_n-coordination polyhedra containing first and second-row X-cations using a 6-31G* basis set. The energies of the molecules were minimized with the X—O and the O—H bond lengths and the X—O—H angles each treated as single variables. The O—X—O angles were fixed at ideal values (120° for $\text{H}_{6-m}\ \text{X}^{+m}\ \text{O}_3$ molecules, 109.47° for

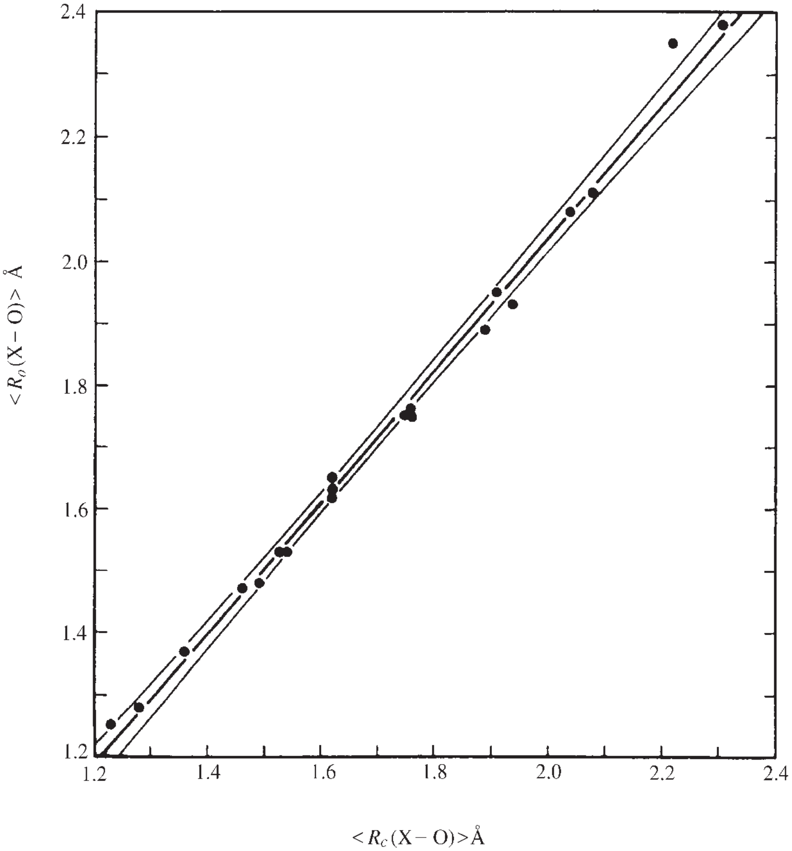

FIGURE 3. A plot of the observed bond length data, $<R_o(\text{X—O})>$, used to prepare Figure 1 vs bond length data, $<R_c(\text{X—O})>$, calculated for hydroxyacid $\text{H}_{2n-m}\ \text{X}^{+m}\text{O}_n$ molecules with XO_n-coordination polyhedra. The minimum energy X—O bond lengths were calculated with a 6-31G* basis set. A regression analysis of the data yielded the straight line drawn through the data points and its two upper and lower curved 2.7σ-confidence limits

H_{8-m} X^{+m} O_4 molecules and 90° for H_{12-m} X^{+m} O_6 molecules). The minimum energy X–O bond lengths, $<R_c(X{-}O)>$, calculated for the molecules were found to reproduce observed $<R_o(X{-}O)>$ bond length data for silicate and oxide crystals to within *ca* 0.02 Å, on average (Figure 3). Indeed, a statistical analysis shows that more than 99% of the variation in the experimental $<R_o(X{-}O)>$ bond lengths can be explained in terms of a linear dependence on $<R_c(X{-}O)>$. As expected, the s vs $<R_c(X{-}O)>$ data obtained for the molecules closely parallel the two trends displayed in Figure 2.

Similar calculations have yet to be completed for molecules with the main group X-cations for rows in the periodic table beyond the second. Nonetheless, it was found[6] that the observed bond length data for the main group cations for all six rows of the periodic table correlate with s in six separate but essentially parallel trends similar to those displayed in Figure 2. In a search for a parameter that would rank all of the bond length data in a single trend, a bond order parameter $p = s/r$ was defined where $r = 1, 2, 3, \ldots$ for first-, second-, third-, … row main group X-cations, respectively[6]. When the $<R_c(X{-}O)>$-values for row one and two X-cations are plotted against this bond order parameter (Figure 4a), it is apparent that p ranks the calculated bond length data in a single trend with shorter bonds involving larger p-values. The data in the figure are observed to conform with a simple power law expression of the form $R(X{-}O) = \kappa p^{-\beta}$ where $\beta > 0$. It is noteworthy that when $R(X{-}O)$ is plotted against the value of the electron density at the bond critical point, $\rho(\mathbf{r}_c)$, for each X–O bond the R(X–O) vs $\rho(\mathbf{r}_c)$ data also conform with a power law expression.

A regression analysis of the calculated bond length data used to prepare Figure 4a vs p yields the expression $R(X{-}O) = 1.39p^{-\beta}$ where $\beta = ca\ 2/9$. The observed X–O bond length data reported for main-group cations from all six rows of the periodic table are plotted in Figure 4b against p. Not only does the trend parallel that calculated for the molecules, but a regression analysis of the observed data set yields a statistically identical expression with the one obtained for the calculated data displayed in Figure 4a.

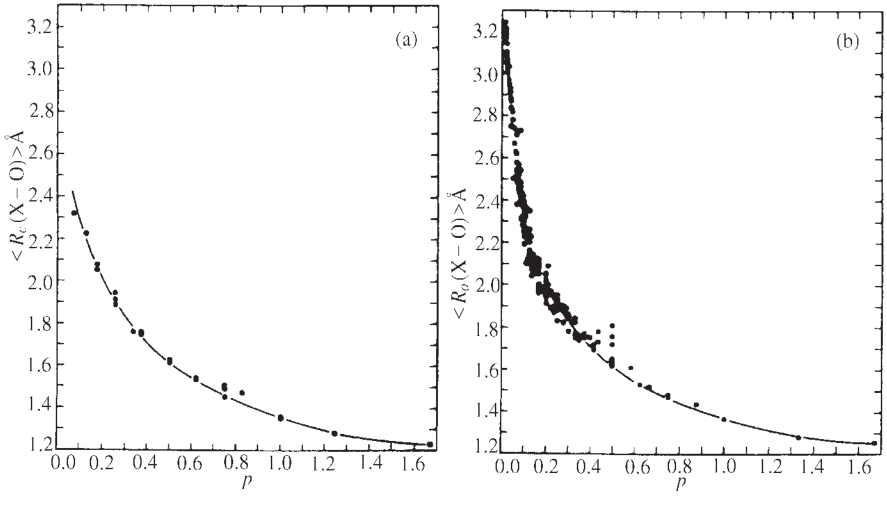

FIGURE 4. Scatter diagrams of bond length data (a) calculated for H_{2n-m} $X^{+m}O_n$ molecules and (b) observed for main group cations vs the bond order parameter p. The expression $R(X{-}O) = 1.39p^{-2/9}$ serves to model both sets of data equally well

In addition, a statistical analysis of the observed bond length data shows that more than 99% of the variation of $\ln(<R_o(\mathrm{X{-}O})>)$ can be explained in terms of a linear dependence upon $\ln(p)$. The observation that the same expression can be used to model the observed and calculated data sets indicates that the bond lengths in oxide molecules and crystals are similar with p playing a similar role in both systems despite the smaller size and density of a molecule.

A graph-theoretic study[7] of the bond length variations observed for 10 different silicate crystals has since yielded a similar expression connecting bond length and resonance bond number, n. A resonance bond number is defined to be the average number of times a bond appears in the family of subgraphs of the connectivity graph that are constrained to have the degree of each node equal to the valence of the atom represented by that node. In the study, resonance bond numbers were calculated for all of the nonequivalent bonds in representative blocks of atoms isolated from the structures of ten different silicate crystals, using an algorithm based on graph theory. A scatter diagram of the resulting n-values versus the individual observed $<R_o(\mathrm{X{-}O})>$ bond lengths (Figure 5) not only matches the trends discussed above when n is equated with s, but a regression analysis of the data set yields the expression $R(\mathrm{X{-}O}) = 1.39(n/r)^{-\beta}$ where $\beta = ca$ 2/9, in agreement with the form of the expression obtained for the data in Figure 4. A statistical analysis shows that more than 95% of the variation of the bond lengths in the silicate crystals can be explained in terms of the resonance bond numbers calculated for the X—O bonds in the representative fragments of the crystals. Despite the different roles attached to the valence electrons, it is apparent that both models yield similar numbers for the strength of a particular bond.

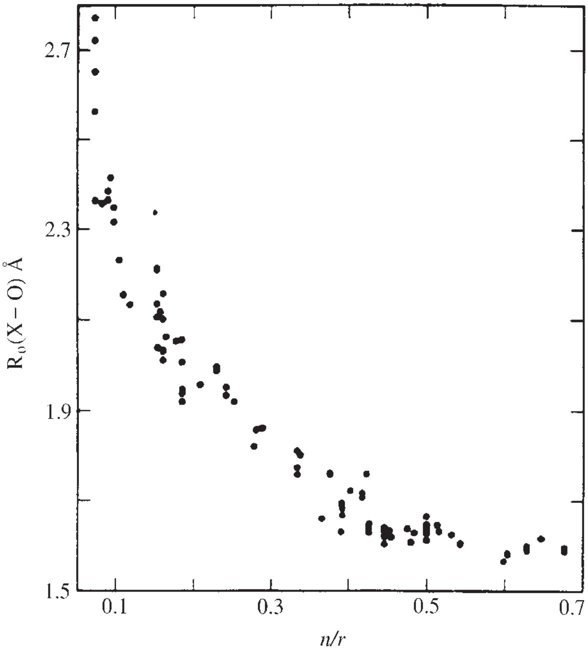

FIGURE 5. A scatter diagram of resonance bond numbers, n, calculated for the individual bonds in ten silicate crystals vs the observed bond lengths where r is the row number of the X-cation

With the discovery that an expression of the form $R(\mathrm{X{-}O}) = \kappa p^{-\beta}$ can be used to model the average bond lengths in oxide molecules and crystals, it was subsequently found that the average bond lengths observed for the coordination polyhedra in sulfide, nitride and fluoride crystals and molecules can also be modeled with a power law expression with essentially the same β-value (*ca* 2/9) but with κ-values of 1.93, 1.49 and 1.37, respectively[8−10]. In addition, bond length data calculated for cation-containing polyhedra in chemically similar molecules yielded expressions that are statistically identical to those obtained for each set of crystal data. As the relative change of the expression $f(p) = \kappa p^{-\beta}$, as a function of bond order p, is $-\beta/p$ and as β is the same for the bonds in oxide, sulfide, nitride and fluorides molecules and crystals, one can conclude that the relative change in bond length as a function of p, for any given bond order, is the same for all four anions. In short, if a given cation forms a bond of a given bond order in a coordination polyhedron and if it is replaced by another cation, then the relative change in bond length is indicated to be the same, regardless of whether the cation comprises a molecule or a crystal or whether it is bonded to an oxide, nitride, sulfide or a fluoride anion.

III. A POTENTIAL ENERGY SURFACE FOR THE Si−O−Si SKELETON OF THE DISILICIC ACID MOLECULE

The geometry of the disilicic acid $H_6Si_2O_7$ molecule has been partially optimized a number of times ranging from an SCF Hartree–Fock method with an STO-3G basis set to a hybrid density functional Becke3LYP method with a 6-311G(2d,p) basis set. To gain insight into the force field and the energetics of the skeletal Si−O−Si unit, a potential energy surface has been generated with energies calculated for the molecule for more than 70 different combinations of Si−O bridging bond lengths and Si−O−Si angles using a STO-3G basis set and assuming C_{2v} point symmetry[4] (Figure 6). The point of minimum energy (denoted by a '+' sign in the figure) defines an equilibrium Si−O bond length of 1.60 Å and an equilibrium Si−O−Si angle of 142°. Experimental Si−O bond lengths, R(Si−O), and Si−O−Si angle data, observed for the Si−O−Si units of the silica polymorphs quartz, cristobalite (Figure 1g), tridymite (Figure 1h, Plate 4) and

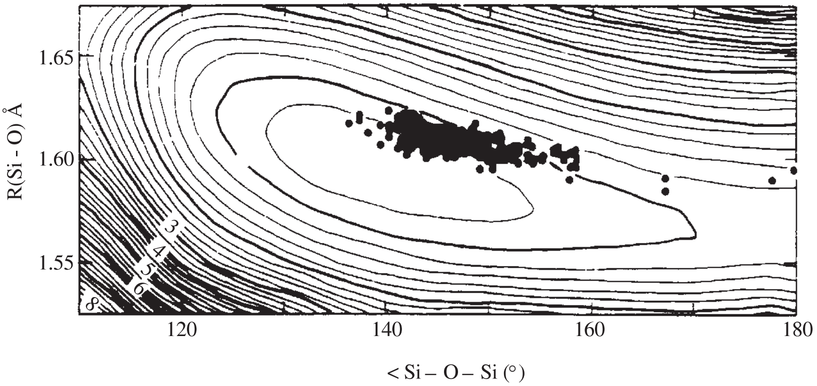

FIGURE 6. A potential energy surface calculated as a function of the Si−O bond length and the Si−O−Si bond angle of the Si−O−Si skeletal unit of the disilicic acid $H_6Si_2O_7$ molecule with a STO-3G basis set. The level contour lines are drawn at intervals of 2.6 kJ mol^{-1}. The bullets represent Si−O bond lengths and Si−O−Si angle data observed for the silica polymorphs. The minimum energy Si−O bond length (1.60 Å) and Si−O−Si angle geometry of the molecule is plotted as a '+' sign

coesite (Figure 1i, Plate 5), are plotted on the surface. The data follow the general trend of the surface, but the observed Si—O bond lengths are, for a given Si—O—Si angle, *ca* 0.015 Å longer, on average, than generated for the molecule. Also, for a given bond length, the data are shifted to wider angles by *ca* 5°. The Si—O bond lengths recorded for the silica polymorphs show a relatively small range of values between *ca* 1.58 Å and *ca* 1.63 Å while the Si—O—Si angles show a relatively wide range of values between *ca* 135° and 180°. The shape of the surface conforms with this result with the minimum energy conformation of the molecule lying at the bottom of a relatively narrow, cirque-shaped valley, bounded laterally on both sides by steeply rising energy barriers encountered with a departure of the Si—O bond length from its minimum energy value of 1.60 Å. The valley is blocked on the narrow angle side of the valley floor by a steeply rising headwall while the valley floor extends virtually unimpeded as the Si—O—Si angle widens with the slope along the valley floor, increasing very gradually from the valley bottom with an opening of the angle. The trace of valley floor shows a slight but well-defined curvature which conforms with the curvilinear R(Si—O) vs <Si—O—Si correlation observed for the silica polymorphs[11], a trend that is reproduced by MP2/6-31G* and Becke3LYP/6-311G(2d,p) level calculations on the disilicic acid molecule[5]. The topography of the valley floor indicates that the Si—O—Si energy barrier to linearity is small. If the binding forces that govern the Si—O—Si unit in the disilicic acid molecule and the silica polymorphs are similar, then the force required to deform the angle from its minimum energy value is expected to be small in both systems. Thus, a broad continuum of angles is expected to occur in agreement with the relatively large range of angles observed for the silica polymorphs and observed and calculated for silicic acid and siloxane molecules[12–14]. Also, because of the steeply rising energy headwall at the narrow angle end of the valley, Si—O—Si angles less than *ca* 120° are indicated to destabilize a structure in agreement with the fact that the Si—O—Si angles reported for a large number of silicate crystals[15] are observed in the range between 120 and 180°.

Like the disilicic acid molecule and silica, the minimum energy Si—O and X—O bond lengths and Si—O—X angles calculated for the skeletal Si—O—X units of a number of $(H_6SiX^{+n}O_7)^{-4+n}$ (X = B, Al, Be) molecules conform with those reported for framework silicate crystals[4,16]. Also, the relatively narrow range of angles observed for the Si—O—B (120–142°) units, the relatively moderate range observed for Si—O—Be (118–152°) units and relatively wide range observed for the Si—O—Al (115–180°) units of each crystal conforms with the shape of the well of the <Si—O—X–potential energy curve calculated for each molecule, the deeper and the narrower the well, the smaller the observed range of angles. The minimum energy angle of each curve (< Si—O—B = 125°, < Si—O—Be = 131°, < Si—O—Al = 139°) also agrees to within a few degrees of each respective average observed value of a silicate (< Si—O—B = 129°, < Si—O—Be = 127°, < Si—O—Al = 138°). This evidence indicates that the bonded interactions that govern the variability and average value of the angle adopted by an Si—O—X unit in a silicate crystal are similar to those that govern the unit in a chemically similar molecule.

The apparent Si—O bond lengths (uncorrected for thermal motion) observed for the silica polymorphs have been found to be shorter than the actual interatomic bond lengths (the bonded and nonbonded interatomic separations that exist between the atoms at their equilibrium positions), with apparent bond lengths decreasing with increasing temperature[17]. When the apparent bond lengths are corrected for thermal motion, the corrected bond lengths for the bonds described in Figure 6 are estimated to be *ca* = 0.01 Å longer than those plotted. As shown in the figure, the bridging Si—O bond length calculated for disilicic acid molecule at absolute zero (without zero-point vibration) with an STO-3G basis set is about 0.01–0.02 Å shorter than the apparent Si—O bond lengths for the silica polymorphs and consequently substantially shorter than the corrected bond lengths.

The geometry of the disilicic acid molecule has since been partially optimized with the relatively more accurate hybrid Becke3LYP method with a 6-311G(2d,p) basis set assuming a staggered structure with C_s point symmetry with its H atoms constrained so as to avoid the formation of bonded interactions between the H atoms of one tetrahedron of the molecule and the O atoms of the other. The calculations yielded a minimum energy Si−O bridging bond length of 1.612 Å and a Si−O−Si angle of 145°. The thermally corrected $<$Si−O$>$ average bond lengths calculated for the silica polymorphs quartz (1.615 Å), cristobalite (1.615 Å) and coesite (1.612 Å) match the minimum energy bond calculated for the molecule rather well. Also, the minimum energy Si−O−Si angle is only 2.5° narrower than the average value (147.4°) recorded for the silica polymorphs[18]. Thus, if a potential energy surface like the one in Figure 6 were recalculated at the Becke3LYP/6-311G(2d,p) level, then one might expect that the thermally corrected individual <Si−O> bond lengths for the silica polymorphs would lie along the energy valley of the surface rather closely in better agreement than that displayed by the data in the figure.

The two orthogonal curvatures of the energy surface evaluated at the point of minimum energy in Figure 6 indicate that the harmonic stretching force constant of the bridging Si−O bond of the disilicic acid molecule is roughly two orders of magnitude larger than the bending force constant of its Si−O−Si angle, in conformity with the narrow range of Si−O bond lengths and wide range of Si−O−Si angles observed for the silica polymorphs. As is well known, the force constant of a bond can provide useful information about the 'stiffness' of a bond, its 'variability' and the binding forces that exist between a pair of bonded atoms like Si and O. With the proposal that a Morse curve can be used to characterize the electronic energy of a diatomic molecule, it was also proposed that the force constant of the bond can be related to bond length, R, by the power expression $f(R) = \kappa R^{-\alpha}$ where α was taken to be *ca* 6 and κ is a constant that depends on the identity of the bond[19]. With spectroscopic force constant data determined for the Si−O bonds in a variety of molecules and crystals, together with scaled harmonic force constant data calculated for the molecules H_2SiO_3, H_4SiO_4, $H_6Si_2O_7$ and $H_{12}Si_5O_{16}$ with a 6-31G* basis set, the expression $f(\text{Si–O}) = 7.5 \times 10^3 R(\text{Si–O})^{-5.4}$ Newtons/meter (N/m) was calculated that relates the force constant of an Si−O bond, $f(\text{Si–O})$, to its length[20]. When used to generate the force constant for the Si−O bond of quartz, it yielded a value of 593 N/m compared with that observed (597 N/m)[21] and that calculated (600 N/m) for the H_4SiO_4 molecule at the MP2/6-31G** level. It was also reported in the study that the polyhedral compressibilities calculated for oxide, nitride and sulfide coordination polyhedra are similar to those reported for crystals[20].

Of the 3000 known minerals, more than 900 are silicates. Almost all silicates contain the silicate SiO_4 tetrahedra while about 20 are known to contain the SiO_6 octahedra, but none is known to contain an SiO_5 5-coordinate polyhedra. A few exceptions like wadeite (Figure 1j, Plate 5) contain both SiO_4 and SiO_6 polyhedra. Those with SiO_4 tetrahedra either contain monomeric and/or condensed corner sharing SiO_4 tetrahedra with the bulk of silicates containing condensed SiO_4 tetrahedra linked together by Si−O−Si units. The fact that the chemistry of the mineral world is dominated by Si and O certainly must play a role in determining the preponderance and the large number of different kinds of silicates that occur in nature. But the compliant nature of the Si−O−Si unit has also been argued to play a role as well[5,16,22]. Given that the Si−O−Si unit can be easily deformed from its equilibrium value without expending much energy, silicate tetrahedra can be linked together with other such tetrahedra in numerous ways as oligosilicates, cyclosilicates, inosilicates and phyllosilicate anions of various types and as a large variety of tectosilicate structures (see Reference 15 for elegant drawings of many of the condensed anionic units that silicate tetrahedra can adopt) without excessive destabilization unless the structure either requires an Si−O−Si angle that is less than *ca* 120° or unless the bond length–bond strength requirements of the bonds of the structure are poorly satisfied. The glass-forming tendencies of silica and the ability for silica to adopt a large variety of structure types can also be ascribed in part to the flexible nature of the Si–O–Si unit and the ease with which the Si–O–Si unit can be bent without excessively destabilizing the resulting structure[5,16,22]. The relatively high compressibility and expansion properties of quartz, cristobalite and tridymite can also be related to the compliant nature of the Si–O–Si angle.

As observed earlier, in modeling the Si–O–Si unit of silica and related silicates, the geometry of the $H_6Si_2O_7$ molecule was constrained during its optimization so that the terminating H atoms of each of the silicate groups were directed away from the O atoms of the other group so as to avoid the formation of one or more O···H bonded interactions. If such a constraint is not made, then O···H bonded interactions can be

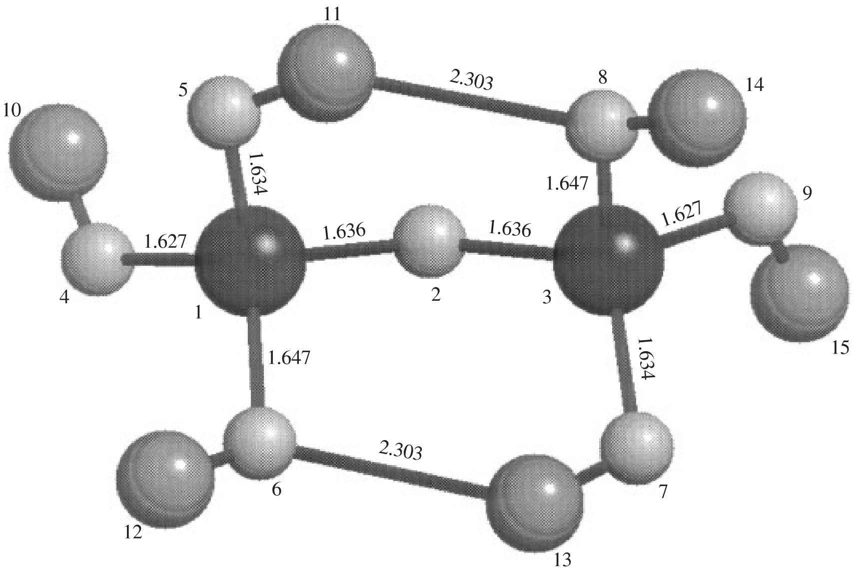

$H_6Si_2O_7$

FIGURE 7. A drawing of a ball and stick model of a minimum energy structure of the disilicic acid molecule, $H_6Si_2O_7$. The large dark gray spheres represent Si, the small light gray spheres represent O and the intermediate-size, darker gray spheres represent H. Bond lengths in Å are given next to each of the SiO bonds and the separations between the H and O atoms that define the two O···H interactions are given. The dihedral angles for the molecule, defined in terms of the integers assigned to each atom, are as follows: *D*(Si3,O2,Si1,O4), −172.38; *D*(Si3,O2,Si1,O5), 66.12; *D*(Si3,O2,Si1,O6), −55.44; *D*(O7,Si3,O2,Si1), 66.12; *D*(O8,Si3,O2,Si1), −55.43; *D*(O9,Si3,O2,Si1), −172.37; *D*(H10,O4,Si1,O2), −84.53; *D*(H10,O4,Si1,O5), 37.73; *D*(H10,O4,Si1,O6), 161.5; *D*(H11,O5,Si1,O2), −29.36; *D*(H11,O5,Si1,O4), −153.72; *D*(H11,O5,Si1,O6), 85.76; *D*(H12,O6,Si1,O2), 179.41; *D*(H12,O6,Si1,O4), −60.16; *D*(H12,O6,Si1,O5), 60.47; *D*(H13,O7,Si3,O2), −29.35; *D*(H13,O7,Si3,O8), 85.77; *D*(H13,O7,Si3,O9), −153.71; *D*(H14,O8,Si3,O2), 179.34; *D*(H14,O8,Si3,O7), 60.39; *D*(H14,O8,Si3,O9), −60.24; *D*(H15,O9,Si3,O2), −84.56; *D*(H15,O9,Si3,O7), 37.69; *D*(H15,O9,Si3,O8), 161.48. The predicted energy of the molecule is *E*(RB + HF -LYP) =-1109.83245 au

expected to form in the calculation with a concomitant lengthening of the Si–O bridging bonds and a narrowing of the Si–O–Si angle[23–25]. Because O···H bonds are absent in the silica polymorphs and in almost all silicates, an unconstrained molecule with O···H bonds is not considered to be a satisfactory moiety for modeling the structure and the elastic properties of crystalline silica.

As a matter of interest, the geometry of the $H_6Si_2O_7$ molecule was fully optimized for this study at the Becke31yp 6-311G(2d,p) level, assuming C_1 point symmetry without any restrictions imposed on the positions of its atoms. A drawing of a ball and stick model of the resulting minimum energy structure is displayed in Figure 7, where the bonded atoms are connected by the sticks. The minimum energy Si–O (br) bridging bond lengths (1.636 Å) of the molecule are *ca* 0.02 Å longer and the Si–O–Si angle (126.8°) is *ca* 20° narrower than that calculated for the constrained molecule (see above). The relatively large change in the angle is expected, given its compliant nature. The longer Si–O (br) bond lengths and the narrower Si–O–Si angle can be ascribed to the reduction of the electron density at the bond critical point of the Si–O bond induced by the two O···H bonded interactions, O6···H13 and O8···H11 (Figure 7). The atoms comprising these interactions are at a separation of 2.303 Å. Because a bond critical point exists in the electron density distribution between these atoms at a distance of *ca* 1.42 Å from each O atom, both O6···H13 and O8···H11 qualify as bonded interactions. But, since the value of the electron density at the critical point, $\rho(\mathbf{r}_c)$, is only 0.08 e Å^{-3}, the bond is indicated to be relatively weak with an $\nabla^2\rho(\mathbf{r}_c)$ value of 1.0 e Å^{-5}. As expected from the $\rho(\mathbf{r}_c)$ values calculated for the molecule, the Si–O bonds involving O6 and O8 are longer (1.647 Å) than either of the two remaining Si–O bonds (1.627, 1.634 Å) of the silicate groups. It is noteworthy that bonds in the molecule with identical environments have identical bond lengths. The dihedral angles and the predicted energy of the molecule are given in Figure 7.

IV. BOND CRITICAL POINT PROPERTIES OF THE ELECTRON DENSITY DISTRIBUTION OF THE SKELETAL Si–O–Si UNIT

If the electron density distribution of a crystal is similar to that of a chemically similar molecule, it can be concluded that the force fields of the two structures are similar. In a mapping of the electron density of coesite[26], deformation electron density distributions, $\Delta\rho(\mathbf{r})$, were generated from experimental X-ray diffraction data to learn whether any of the features in the distribution can be related to the observed bond length and angle variations and the character of the Si–O bond. As the observed Si–O bond lengths in coesite decrease with increasing Si–O–Si angle, it was expected that the heights of the peaks along the bonds in the maps would increase in value as the Si–O bond decreases in length. Although the resulting maps display peaks along each of the Si–O bonds, ranging in height between *ca* 0.3 and *ca* 0.5 e Å^{-3}, no statistically significant trend between peak height and bond length could be established.

Because of the nonquantitative nature of $\Delta\rho(\mathbf{r})$ maps[27,28], the X-ray diffraction data recorded for coesite[26] was used to generate a total electron density distribution, $\rho(\mathbf{r})$, for the mineral. In an analysis of the bond critical point properties of the distribution, Downs[29] located the critical points along each of its Si–O bonds, determined the value of the electron density and the Laplacian of $\rho(\mathbf{r})$ at each of these critical points, $\nabla^2\rho(\mathbf{r}_c)$, and mapped $-\nabla^2\rho(\mathbf{r})$ over the domain of each of its Si–O–Si skeletal units. A mapping of the total electron density distribution and its topological properties has a distinct advantage over a mapping of the deformation density in that *'The derivation of a unique and physically meaningful difference (deformation) electron density is a problem that cannot be solved since the choice of the promolecular reference density always implies some* *arbitrariness'*. This statement[30] seems to be borne out by the following results obtained for coesite: (1) The heights of the peaks in the experimental deformation maps recorded along its Si–O bonds fail to show any obvious trends with the observed bond lengths, and (2) The heights of the peaks in deformation maps calculated for the Si–O bridging bonds of the H_6 Si_2 O_7 molecule actually increase in height as the lengths of the bonds increase (and the Si–O–Si angle decreases) (see Reference 19, Figure 6). But, on the other hand, the value of $\rho(\mathbf{r}_c)$ provided by calculations of the total electron density distribution for a number of silicic acid molecules including the disilicic acid molecule shows that the value of $\rho(\mathbf{r}_c)$ increases in a regular way as the Si–O bond decreases in length (Figure 8).

For purposes of comparison with the results obtained for coesite[29], the electron density distribution of the partially, optimized conformer of $H_6Si_2O_7$ (shown in Figure 8) has been generated using the wave functions obtained in a density functional Becke3LYP/6-311G(2d,p) level calculation. The total electron density distribution measured for coesite attains an average value of 1.05 e Å^{-3} at an average distance of 0.936 Å from the bridging O atom to the critical point, $\mathbf{r}_c$, measured along the Si–O bonds from the oxide ions with an average $\nabla^2\rho(\mathbf{r}_c)$-value at this point of +20.4 e Å^{-5}. These observations together with the relationship between the bonded radius of the oxide ion and the electronegativity of

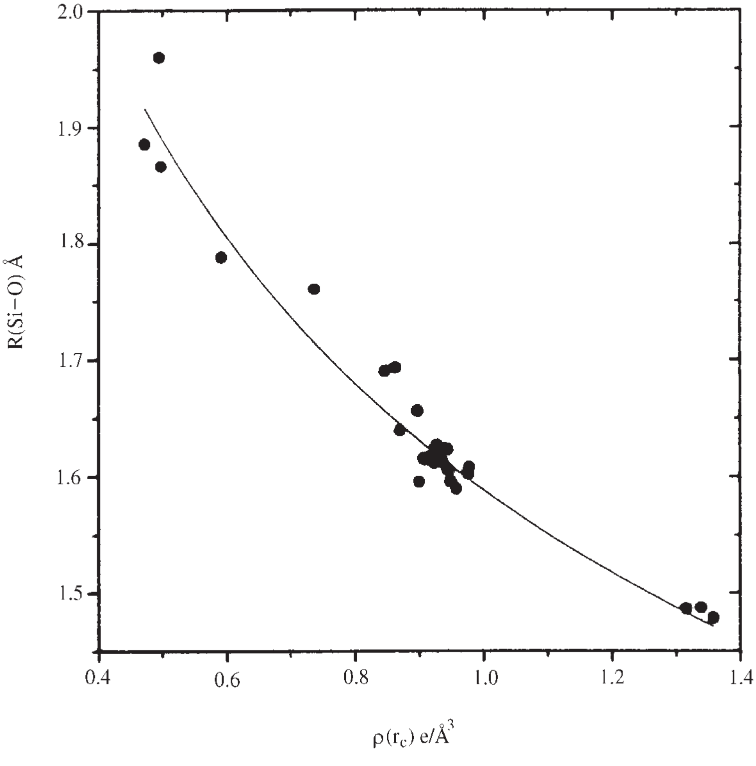

FIGURE 8. A scatter diagram of the minimum energy Si–O bond length, R(Si–O), calculated for a number of hydroxyacid molecules vs the value of the electron density, $\rho(r_c)$, evaluated at (3,−1) critical points. The geometries of the hydroxyacid molecules used to prepare the plot were those of minimum energy at the Hartree–Fock 6-31++G** level

the cation to which it is bonded[2] and the negative value of the local energy density, $H(\mathbf{r}_c)$, at $\mathbf{r}_c$ (ca – 0.3H Å^{-3}) indicate that the Si–O bonds in coesite have significant covalent character[27,30]. In addition, the curvatures of $\rho(\mathbf{r}_c)$, λ_1 and λ_2, measured at $\mathbf{r}_c$, perpendicular to the Si–O bonds, are −7.2 and −6.8 e Å^{-5}, respectively, on average, while the average curvature of $\rho(\mathbf{r})$ at $\mathbf{r}_c$ along the bond path, λ_3, is observed[29] to be 34.4 e Å^{-5}, resulting in a $\nabla^2(\mathbf{r}_c)$ value of 20.4 e Å^{-5}. The electron density distribution calculated for the molecule has a value of 1.00 e Å^{-3} (*ca* 5% less than that observed on average for coesite) at the critical point along each Si–O bond at a distance of 0.943 Å from the bridging oxide ion (*ca* 1% larger than observed on average for coesite). The curvatures, λ_1, λ_2 and λ_3 evaluated at $\mathbf{r}_c$ are −7.41, −7.35 and 35.6 e Å^{-5}, respectively, resulting in a $\nabla^2\rho(\mathbf{r_c})$-value of 20.9 e Å^{-5} (*ca* 2% larger than observed, on average, for coesite). As the curvature of $\rho(\mathbf{r})$ is a very sensitive probe of the topology of $\rho(\mathbf{r})$, as discussed above, it is apparent that a close connection exists between the topological properties of the electron density distribution observed for the crystal and those calculated for the model molecule.

V. A REPRODUCTION OF THE STRUCTURES AND RELATED PROPERTIES OF THE KNOWN SILICA POLYMORPHS

It has been stressed[31] in a study of chemical bonds in crystals that the bonding in molecules differs from that in crystals because bonds are less well defined in crystals and because most crystals are usually denser, much larger and more symmetrical than molecules. Despite these differences, it was acknowledged in the study that a wide range of data *'Shows that nearest neighbor interactions determine most of the properties of a material'*. At the very least, the evidence examined in this review conforms with this statement. For example, the force field that governs the geometry and the electron density distribution of the Si–O–Si skeleton of the disilicic acid molecule can be treated as virtually identical with that of a silica polymorph. The evidence upon which this assertion is based is twofold. First, the Si–O bond length and the Si–O–Si angle variations observed for the silica polymorphs conform in large part with the topographic features of a potential energy surface of the Si_2O_7 skeleton calculated for the disilicic acid molecule. Second, the bond critical point properties of the electron density distribution observed for the Si–O–Si units of a silica polymorph agrees to within a few percent with that calculated for the molecule. This evidence taken with the observation that spectroscopically determined force constants of a silica polymorph agree well with that calculated for the molecule provides a basis for believing that a silica polymorph like quartz can be viewed as a giant molecule bound together by the same forces that act between the Si and O atoms of the disilicic acid molecule[5]. It also provides a basis for understanding why it has been possible to reproduce the crystal structure of quartz to within *ca* 2% and its bulk modulus to within *ca* 5%, using a potential energy function calculated for the disilicic acid molecule[32]. Since then, a number of other workers have been successful not only in reproducing the structures and volume compressibilities of quartz and cristobalite using a potential energy function based on a molecule, but they have also been successful in reproducing the structures and bulk moduli of coesite and stishovite (Figure 1k, Plate 6) and modeling the observed properties of the α–β transition of quartz and the negative Poisson ratio observed for cristobalite[33–40].

VI. A GENERATION OF NEW STRUCTURE TYPES FOR SILICA

It is one thing to reproduce the known structure of a crystalline material like silica using a molecular potential energy function, but it is quite another to generate the possible crystal structures that silica can adopt with a molecular-based potential energy function, starting with a random arrangement of Si and O atoms in a structure with $P1$ symmetry. To attack this problem, we used simulated annealing. Simulated annealing is a physically inituitive strategy that can be used to search for global and local minimum energy crystal structures for silica using a molecular potential energy function based on that calculated for the Si_2O_7 skeleton of the $H_6Si_2O_7$ molecule[37,38]. Simulated annealing strategies accept all downhill steps but, unlike Newton and quasi-Newton methods, allow some uphill steps that increase the value of a potential energy function in a search for viable, low energy structures[37,38].

Calculations have been completed starting with four, six and eight formula units of SiO_2 randomly distributed in a structure with triclinic $P1$ symmetry[38]. Of the several thousand periodic structure types that have been generated, more than two-thirds were found to be framework structures where each Si atom is 4-coordinate and each O atom is 2-coordinate. Further study shows that these framework structures can be classified into a wide variety of distinct structure types. Despite the assumption in the calculations of $P1$ triclinic symmetry, more than two-thirds of the structures possess symmetries higher than $P1$ ranging between the monoclinic space group symmetry Pc and the tetragonal space group symmetry $I\bar{4}2d$. The resulting structures exhibit symmetrically equivalent cell dimensions that agree to within 0.0001 Å and equivalent interaxial angles that agree to within 0.0001°. A large number of low energy structure types match those observed for the left- and right-handed polymorphs (calculated in equal numbers) of quartz and cristobalite, mixed stacking sequences of tridymite and cristobalite and the molecular crystal silica-W. Several exhibit the framework structures of several known aluminosilicates including monoclinic $CaAl_2Si_2O_8$ and the orthorhombic zeolites Li-A(BW) and NaI[42]. Others exhibit structures that are similar to those of cancrinite, sodalite and bikitaite (Figure 11 Plate 6). In addition, the networks defined by the Si atoms of a number of the structures match those enumerated by earlier workers[43,44]. However, many of the remaining structures represent new structure types for silica yet to be synthesized or discovered in nature. Several of the structures generated in the calculations on silica are displayed in Figure 9 (Plates 7 and 8). In the study, two silica structures were considered to be equivalent if their energies are equal and the Schläfli symbols calculated for the 4-connected nets of Si atoms and the coordination sequences of the Si atoms out to the 10th coordination shell for the two are identical[41].

VII. CONCLUDING REMARKS

The notion that molecules can be used to model bonded interactions in crystals is not new. Indeed, it is an idea that has been around for more than 50 years when J. C. Slater[45] concluded, on the basis of the similar types of rigidity and geometry exhibited by several aliphatic molecules and diamond, that *'A diamond is really a molecule of visible dimensions held together by just the same forces acting in small molecules'*. More recently, with the completion of an accurate gas-phase structural determination of disiloxane, it was concluded[43] that the bonding picture of the skeletal Si−O−Si unit of the molecule is similar to that of a silicate crystal because the geometry of the unit [$R(\text{Si}-\text{O}) = 1.632$ Å; $< \text{Si}-\text{O}-\text{Si} = 142.2°$] is similar to that observed, on average, for a silicate crystal [$R(\text{Si}-\text{O}) = 1.626$ Å; $< \text{Si}-\text{O}-\text{Si} = 144°$]. It is noteworthy that a structural analysis of a disiloxane crystal grown at liquid nitrogen temperatures reveals that the geometry of the molecule in the crystal is not significantly different from that in the gas phase, despite differences between the forces acting on the atoms in the gas-phase molecule and those in the crystal[47]. In addition, a survey of the literature shows that the average Si−O bond length (1.634 Å) and Si−O−Si angle (144°) observed for a large variety of siloxane molecules are also similar to those observed for disiloxane and for silicates. Indeed, the structures of the condensed tetrahedral anions of organosiloxanes and silicates are so similar that they can be classified with the well known scheme used by Bragg to classify silicates[48]. Further, as observed above, the calculated geometry and the topological properties of the electron density distribution of the Si_2O_7 skeleton of disilicic acid are strikingly similar to those observed for a silica polymorph. Collectively, these results not only suggest that the force fields that govern the structures and electron density distributions of silicic acid molecules and silicates are not all that different, but they also suggest that the silica polymorphs can be viewed, as asserted earlier[5], as giant molecules bound together by the same forces that bind the Si and O atoms of the Si_2O_7 skeleton of the disilicic molecule, despite the greater size, density and symmetry of the former. It also provides a basis for understanding why the structures and the elastic properties of the silica polymorphs can be modeled with a molecular potential energy function and why a large number of new silica structure types can be generated using simulated annealing strategies and a molecular potential energy function.

Finally, as observed above, the evidence suggests that the forces that bind Si and O ions together in a silicate crystal can be treated as if localized as in a molecule. If the Si−O bond is of intermediate type as asserted by Pauling and others, then it would appear that the effective charges on the ions of the crystal would either be relatively small in conformity with his electroneutrality principle[49] or that the Si cation forms such a strong bonded interaction with its coordinating oxide ions that the field of the crystal has little effect on the geometry and the electron density distribution of a silicate tetrahedral oxyanion. In short, any model that is proposed for the Si−O bond ought to explain why the forces that govern the structure, the elastic properties and the electron density distribution of the Si−O bond of a silicate behave as if in a molecular environment[2].

VIII. ACKNOWLEDGMENTS

This paper was written when GVG was a JSPS Fellow and Invited Research Professor at Kyoto University, Kyoto, Japan and MBB was on Research Leave at UC Berkeley. In particular, GVG wishes to thank Professor Osamu Tamada and Dr. Masanobu Matsumoto for making his stay in Japan a very pleasant and stimulating experience. He also wishes to thank Professors Shegio Sueno, Satoshi Sasaki, Nobuo Ishizwara, Fumikuki Marumo and Yoshi Takeuchi for their kind hospitality. MBB wishes to thank Professor Mark Bukowinski at UC Berkeley for his hospitality and for making his stay an enjoyable and productive one. Dr. F. C. Hill is thanked for reading the manuscript and for her helpful comments. This work was supported by NSF Grant EAR-9627458.

IX. REFERENCES

1. K. H. Wedepohl, *Geochemistry*, Holt, Reinhart and Winston, New York, 1983.
2. G. V. Gibbs, J. W. Downs and M. B. Boisen, Jr., in *SILICA: Physical Behavior, Geochemistry and Materials Applications* (Eds. P. J. Heany, C. T. Prewitt and G. V. Gibbs), Chap. 10, American Mineralogist, Washington, D.C., 1994, p. 331.
3. L. Pauling, *J. Am. Chem. Soc.*, **51**, 1010 (1929).
4. I. D. Brown and R. D. Shannon, *Acta Cryst.*, **A29**, 266 (1973).
5. G. V. Gibbs, *Am. Mineral.*, **67**, 421 (1982).
6. G. V. Gibbs, L. W. Finger and M. B. Boisen, Jr., *Phys. Chem. Min.*, **14**, 327 (1987).
7. M. B. Boisen, Jr., G. V. Gibbs and Z. G. Zhang, *Phys. Chem. Min.*, **15**, 409 (1988).
8. K. L. Bartelmehs, G. V. Gibbs and M. B. Boisen, Jr., *Am. Mineral.*, **74**, 620 (1989).
9. L. A. Buterakos, G. V. Gibbs and M. B. Boisen, Jr., *Phys. Chem. Min.*, **19**, 127 (1992).
10. J. S. Nicoll, G. V. Gibbs, M. B. Boisen, R. T. Downs and K. L. Bartelmehs, *Phys. Chem. Min.*, **20**, 617 (1994).

11. G. V. Gibbs, C. T. Prewitt and K. J. Baldwin, *Z. Kristallogr.*, **145**, 108 (1977).
12. B. C. Chakoumakos, R. J. Hill and G. V. Gibbs, *Am. Mineral.*, **66**, 1237 (1981).
13. I. L. Karle, J. M. Karle and C. J. Nielson, *Acta Cryst.*, **C42**, 64 (1986).
14. H. B. Burği, K. W. Törnroos, G. Calzaferri and H. Bürgy, *Inorg. Chem.*, **32**, 4914 (1993).
15. F. Liebau, *Structural Chemistry of Silicates: Structure, Bonding, and Classification*, Springer-Verlag, Berlin, 1985.
16. K. L. Geisinger, G. V. Gibbs and A. Navrotsky, *Phys. Chem. Min.*, **11**, 266 (1985).
17. R. T. Downs, G. V. Gibbs, and M. B. Boisen, Jr., *Am. Mineral.*, **75**, 1253 (1990).
18. E. P. Meagher, J. A. Tossell and G. V. Gibbs, *Phys. Chem. Min.*, **4**, 11 (1979).
19. P. M. Morse, *Phys. Rev.*, **34**, 57 (1929).
20. F. C. Hill, G. V. Gibbs and M. B. Boisen, Jr., *Struct. Chem.*, **6**, 349 (1994).
21. J. Etchepare, M. Merian, and L. Smetarkine, *J. Chem. Phys.*, **60**, 1873 (1974).
22. K. L. Geisinger and G. V. Gibbs, *Phys. Chem. Min.*, **7**, 204 (1981).
23. D. J. M. Burkhart, B. H. W. S. DeJong, A. J. H. M Meyer and J. H. van Lenthe, *Geochim. Cosmochim. Acta*, **55**, 3453 (1991).
24. J. D. Kubicki and D. Sykes, *Am. Mineral.*, **78**, 253 (1993).
25. B. J. Teppen, D. M. Miller, S. Q. Newton and L. Schafer, *J. Phys. Chem.*, **98**, 12545 (1994).
26. K. L. Geisinger, M. A. Spackman and G. V. Gibbs, *J. Phys. Chem.*, **91**, 3237 (1987).
27. D. Cremer and E. Erakar, *Angew. Chem., Int. Ed. Engl.*, **23**, 627 (1984).
28. M. A. Spackman and E. N. Maslen, *Acta Cryst.*, **A41**, 347 (1985).
29. J. W. Downs, *J. Phys. Chem.*, **99**, 6849 (1995).
30. D. Cremer, in *Modelling of Structure and Properties of Molecules* (Ed. Z. D. Maksić), Chap. 7, Halsted Press, New York, 1987, p. 125.
31. J. C. Phillips, in *Treatise on Solid State Chemistry*, Vol. 1 (Ed. N. B. Hannay), Chap. 1, Plenum Press, New York, 1973, p. 1.
32. A. C. Lasaga and G. V. Gibbs, *Phys. Chem. Min.*, **14**, 107 (1987).
33. L. Stixrude and M. S. T. Bukowinski, *Phys. Chem. Min.*, **15**, 199 (1988).
34. S. Tsuneyuki, H. Aoki, T. Tsukada and M. Matsui, *Phys. Rev. Lett.*, **64**, 776 (1990).
35. G. V. Gibbs, M. B. Boisen, Jr., R. T. Downs and A. C. Lasaga, in *Better Ceramics Through Chemistry, III* (Eds. C. J. Brinker, D. E. Clark and D. R. Ulrich), Mat. Res. Soc. Symp. Proc., Vol. 121, 1988, p. 155.
36. B. W. H. van Beest, G. J. Kramer and R. A. Santen, *Phys. Rev. Lett.*, **64**, 129 (1990).
37. J. R. Chelikowsky, H. E. King, Jr., N. Troullier, J. L. Martins and J. Glinnemann, *Phys. Rev.*, **B44**, 489 (1991).
38. G. J. Kramer and R. A. van Santen, *Phys. Rev. Lett.*, **64**, 1955 (1990).
39. N .R. Keskar and J. R. Chelikowsky, *Phys. Rev.*, **B46**, 1 (1992).
40. M. B. Boisen, Jr. and G. V. Gibbs, *Phys. Chem. Min.*, **20**, 123 (1994).
41. M. B. Boisen, Jr., G. V. Gibbs and M. S. T. Bukowinski, *Phys. Chem. Min.*, **21**, 269 (1994).
42. M. O'Keeffe, *Phys. Chem. Min.*, **22**, 504 (1995).
43. J. V. Smith, *Am. Mineral.*, **62**, 703 (1977).
44. M. O'Keeffe, *Z. Kristallogr.*, **196**, 21 (1991)
45. J. C. Slater, *Introduction to Chemical Physics*, McGraw-Hill, New York, 1939.
46. A. Almennigen, O. Bastiansen, V. Ewing, K. Hedberg and M. Traetteberg, *Acta Chem. Scand.*, **17**, 2455 (1963).
47. M. J. Barrow, E. A. V. Ebsworth and M. M. Harding, *Acta Cryst.*, **B35**, 2093 (1979).
48. W. Noll, *Chemistry and Technology of Silicones*, Academic Press, New York, 1968.
49. L. Pauling, *The Nature of the Chemical Bond*, Cornell University Press, Ithaca, New York, 1960.

CHAPTER **3**

Polyhedral silicon compounds

AKIRA SEKIGUCHI

Department of Chemistry, University of Tsukuba, Tsukuba, Ibaraki 305, Japan
Fax: +81-298-53-4314; e-mail: sekiguchi@staff.chem.tsukuba.ac.jp

and

SHIGERU NAGASE

Department of Chemistry, Graduate School of Science, Tokyo Metropolitan University, Hachioji. Tokyo 192-03, Japan
Fax: +81-426-77-2525; e-mail: nagase@SNL70.chem.metro-u.ac.jp

---

I. INTRODUCTION

Polyhedral carbon compounds such as tetrahedrane, prismane, and cubane have long fascinated chemists because of their unique properties and aesthetic appeal due to their high symmetry[1,2]. In an effort to enrich silicon chemistry, synthesis of the silicon analogues is a great challenge since it could lead to novel physical and chemical properties unexpected from the carbon compounds. However, such synthesis was believed to be impossible until recently. Triggered by the first successes in synthesizing an octasilacubane derivative[3] and a hexagermaprismane derivative[4], the chemistry of polyhedral compounds of the heavier group 14 atoms has progressed by rapid strides in the last few years and many new derivatives have been prepared[5−11]. At present, only the tin analogues of tetrahedrane and prismane and the entire series of the lead compounds are missing in the series. In this review the successful syntheses, isolation and characterization of polyhedral silicon compounds such as tetrasilatetrahedrane, hexasilaprismane and octasilacubane are summarized together with related theoretical calculations[9,10]. These are also compared with those for the germanium and tin analogues.

II. THEORETICAL STUDIES

A. Strain Energies

Polyhedranes ($C_{2n}H_{2n}$) such as tetrahedrane ($n = 2$), prismane ($n = 3$) and cubane ($n = 4$) have long been interesting synthetic targets. These are highly strained, as is apparent from their carbon bond angles that deviate greatly from the normal tetrahedral value of 109.5°. For instance, the strain energies of tetrahedrane and cubane are evaluated to be as large as 140.0 and 154.7 kcal mol^{-1}, respectively[12]. Since no experimental value is available for the silicon analogues, their strain energies were calculated at the HF/6-31G* level from the appropriate homodesmotic reactions[13]. Table 1 compares the calculated strain energies of the carbon and silicon compounds. The strain energies of 141.4 and 158.6 kcal mol^{-1} calculated for tetrahedrane and cubane are in close agreement with the experimental values[12]. The strain energy of tetrasilatetrahedrane is as large as that of tetrahedrane. However, as the number of four-membered rings increases, the strain of the silicon compounds is significantly decreased while it tends to increase in the carbon compounds. It is noteworthy that hexasilaprismane and octasilacubane are 32 and 65 kcal mol^{-1} less strained than prismane and cubane, respectively.

Also given in Table 1 are the strain energies of the still heavier germanium and tin compounds calculated at the HF/DZ(d) level[14]. Substitution of carbon or silicon by germanium

TABLE 1. Strain energies (kcal mol^{-1}) calculated using homodesmotic reactions[a]

M_nH_n	C	Si[b]	Ge	Sn
Tetrahedrane (M_4H_4, T_d)	141.4	140.9	140.3	128.2
Prismane (M_6H_6, D_{3h})	145.3	113.8	109.4	93.8
Cubane (M_8H_8, O_h)	158.6	93.5	86.0	70.1

[a] $M_nH_n + (3n/2)M_2H_6 \rightarrow n(MH_3)_3MH$.
HF/6-31G* for M = C and Si. HF/DZ(d) for M = Ge, Sn and Pb.
[b] The HF/DZ(d) values are 140.3 (Si_4H_4), 118.2 (Si_6H_6) and 99.1 (Si_8H_8) kcal mol^{-1}.

or tin atoms has again only a small effect on the relief of strain in the tetrahedrane system. This is because three-membered germanium and tin rings are as highly strained as three-membered silicon rings, as is apparent from the strain energies of cyclotrigermane (39.4 kcal mol^{-1}) and cyclotristannane (36.6 kcal mol^{-1})[14] which differ only slightly from that of cyclotrisilane (38.9 kcal mol^{-1})[13]; all of these strain energies are significantly larger than that of cyclopropane (28.7 kcal mol^{-1})[13]. However, the strain energies of hexasilaprismane and octasilacubane containing four-membered rings are further decreased upon substitution of the silicon atoms by germanium and tin atoms. Such relief of strain in the prismane and cubane systems reflects the fact that the strain energies of four-membered rings decrease successively in the order: cyclobutane (26.7 kcal mol^{-1})[13] > cyclotetrasilane (16.7 kcal mol^{-1})[13] > cyclotetragermane (15.2 kcal mol^{-1})[14] > cyclotetrastannane (12.2 kcal mol^{-1})[14]. It is a general trend that the strain of polyhedral compounds is progressively relieved as the number of four-membered rings increases and the skeletal atoms become heavier.

The above trend is also applicable to the larger members of the [n]prismane family ($M_{2n}H_{2n}$, $n > 4$). As Figure 1 shows[5,10,15], the strain energies of persila[n]prismanes

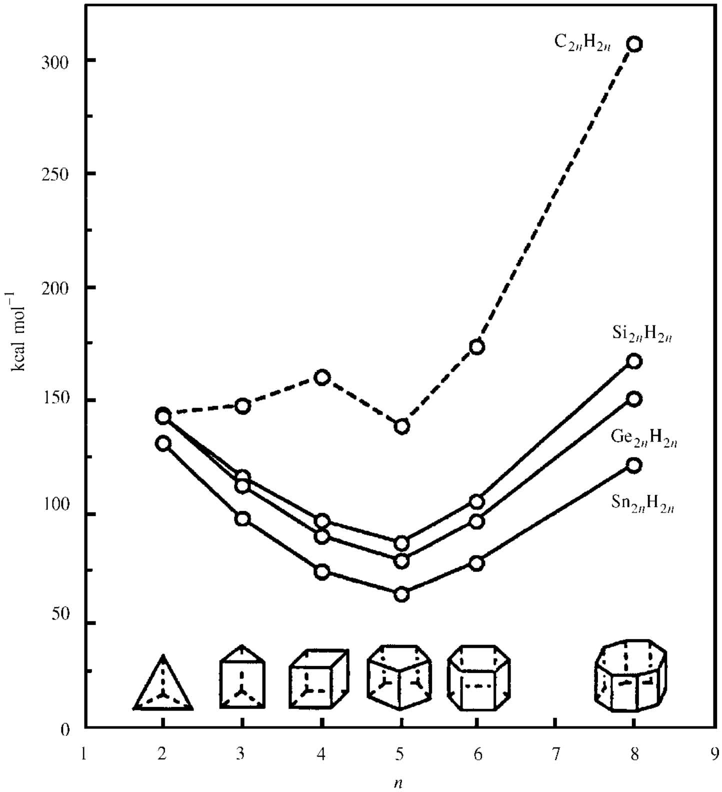

FIGURE 1. The strain energies of the tetrahedrane and [n]prismane system ($M_{2n}H_{2n}$) calculated at the HF/6-31G* level for M = C and Si and the HF/DZ(d) level for M = Ge and Sn. Reprinted with permission from Reference 10. Copyright 1995 American Chemical Society

($Si_{2n}H_{2n}$) are 53.2 ($n = 5$), 70.1 ($n = 6$) and 141.0 ($n = 8$) kcal mol^{-1} smaller than those of the corresponding $C_{2n}H_{2n}$, and even more so as M changes from Si to Ge and to Sn. The strain decreases when n increases from 2 to 5, because the number of four-membered rings increases and the bond angles in the n-membered rings at the top and bottom approach the ideal tetrahedral angle of 109.5°. However, the strain increases sharply with a further increase in n from $n = 5$, despite the increasing number of four-membered rings, because of the increasing deviation of the bond angles (120.0° for $n = 6$ and 135.0° for $n = 8$) in the n-membered rings from the tetrahedral angle. As a result, the strain energy is the smallest when $n = 5$. This suggests that a persila[5]prismane derivative is a reasonable synthetic target. It is interesting that a perstanna[5]prismane derivative was recently synthesized and isolated[16].

The concept of 'hybridization' is most helpful for an intuitive and unified understanding of the important differences in chemical bonding between carbon compounds and their heavier analogues. The size of the valence 2s atomic orbital of a carbon atom is almost equal to that of the 2p atomic orbitals, as measured by the atomic radii (r) of maximal electron density: $r_s = 0.646$ Å and $r_p = 0.644$ Å[17]. However, the valence s and p atomic orbitals differ successively in size for the heavier atoms: $r_p - r_s = 0.203$ (Si), 0.249 (Ge), 0.285 (Sn) and 0.358 (Pb) Å[17]. Therefore, the heavier atoms have a lower tendency to form s–p hybrid orbitals with high p character, and they tend to maintain the $n\mathrm{s}^2\ n\mathrm{p}^2$ electronic valence configuration[5,14,18]. This property of the heavier atoms is favourable for forming bond angles of *ca* 90° and thus for forming four-membered rings with low strain. In contrast, formation of three-membered rings with bond angles of *ca* 60° becomes unfavourable since hybrid orbitals with sufficiently high p character are essential for a description of the 'bent-bond' orbitals[19].

This property is also reflected in the relative stability of the M_6H_6 valence isomers. As is well known, benzene (C_6H_6) has a unique stability due to cyclic delocalization of its 6π electrons and it is much more stable than its strained isomers such as Dewar benzene, benzvalene and prismane[1,2]. However, this situation changes drastically in the heavier system. As Table 2 shows, the heavier atoms prefer the isomers with a smaller number of double bonds, since they must hybridize highly to form double bonds[20]. As a result, the saturated prismane structure becomes much more stable than the benzene structure as M

TABLE 2. Relative energies (kcal mol^{-1}) of M_6H_6 valence isomers

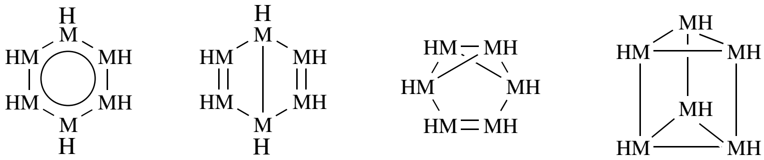

M	Benzene D_{6h}	Dewar benzene C_{2v}	Benzvalene C_{2v}	Prismane D_{3h}
C^a	0.0	81.1	74.9	117.6
Si^b	0.0 (−0.0)^c	4.1	−2.0	−8.1
Ge^b	0.0 (−9.1)^c	1.8	−1.2	−13.5
Sn^b	0.0 (−23.1)^c	−6.5	−11.0	−31.3

^{a}MP2/6-31G*//HF/6-31G*.

^{b}MP2/DZ(d)//HF/DZ(d) from Reference 15.

^{c}Values in parentheses are for chair-like puckered structures of D_{3d} symmetry from Reference 5.

becomes heavier[15,21,22]. This creates another interesting difference between the chemistry of carbon and in heavier congeners.

B. Bond Lengths and Angles

Figure 2 shows the calculated optimized structures of tetrasilatetrahedrane (Si_4H_4), hexasilaprismane (Si_6H_6) and octasilacubane (Si_8H_8) at the HF/6-31G* level[13]. The Si−Si bond lengths in Si_4H_4 are shorter than the single bond length of 2.352 Å calculated for $H_3Si{-}SiH_3$, and it increases in the order Si_4H_4 (2.314 Å) < Si_6H_6 (2.359 Å and 2.375 Å) < Si_8H_8 (2.396 Å). It is interesting that the Si−Si bond lengths are shorter in the three-membered rings than in the four-membered rings, as is also calculated for the monocyclic rings: cyclotrisilane (2.341 Å) vs cyclotetrasilane (2.373 Å)[13,23]. This trend is enhanced in the heavier compounds.

However, bond lengths are not necessarily correlated with bond strengths; the bonds in three-membered rings are weaker than those in four-membered rings[5]. This is because the heavier atoms are forced to hybridize to a considerable extent in order to achieve and maintain the three-membered skeletons of a given symmetry, at the expense of a large energy loss. To compensate for this energy loss, the bond lengths between skeletal atoms shorten in order to form bonds as effectively as possible. However, the cost for hybridization is too large to be offset just by bond shortening, leading to higher strain and weaker bonds in the three-membered rings.

As a result of the high strain and weak bonds, the heavier polyhedral compounds consisting of only three-membered rings easily undergo bond stretching or bond breaking. As Figure 3 shows, for example, bicyclo[1.1.0]tetrasilane consisting of two fused three-membered rings is subject to 'bond-stretch' isomerism[24,25], unlike bicyclo[2.2.0]hexasilane consisting of four-membered rings which has only one isomer[24d]. The isomer with a longer central bond is more stable than that with a normal short bond length. Since in the 'bond-stretch' isomer, two bridgehead hydrogens approach one another closely to form a H−Si−Si bond angle of 93°, bulky substituents cannot be accommodated at the bridgeheads. It is interesting that a bicyclo[1.1.0]tetrasilane derivative with a normal central bond was synthesized by introducing bulky *t*-Bu groups at the bridgeheads[26].

Tetrasilatetrahedrane was calculated to correspond to a local minimum on the potential energy surface[27]. However, because of the fusion of four three-membered rings it collapses, almost without a barrier, by breaking two skeletal bonds, to an isomer having one four-membered ring of tetraradical character[28]. As shown schematically in Figure 4 (see also Figure 3), it is general that bond stretching and bond breaking take place so as to decrease the number of three-membered rings and instead increase the number of the less strained four-membered rings.

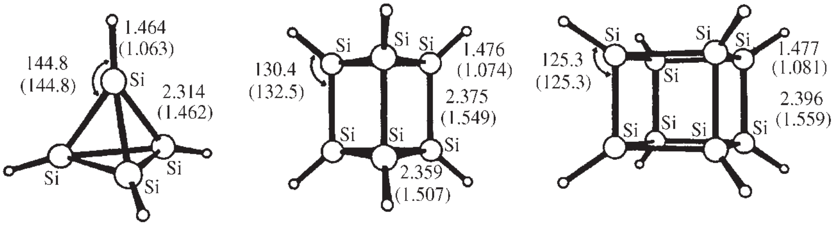

FIGURE 2. The HF/6-31G* optimized geometries of Si_4H_4, Si_6H_6 and Si_8H_8; bond lengths in Å and bond angles in degrees. The values in parentheses are for the corresponding carbon compounds. Reprinted with permission from Reference 13. Copyright 1995 The Chemical Society

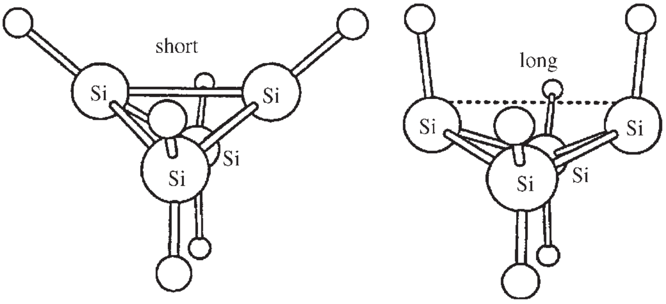

FIGURE 3. Two isomers of Si_4H_6

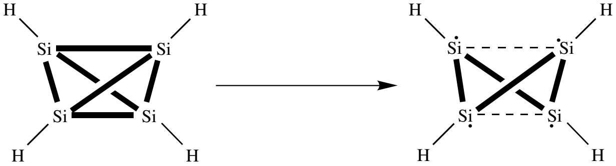

FIGURE 4. Bond stretch in Si_4H_4

C. Substituent Effects

Because of the high strain and weak bonds, the heavier three-membered rings may be regarded as unfavourable as building blocks for polyhedral compounds. In this context, it is important to disclose the role of substituents[8,10,29]. As already mentioned, the strain energy of cyclotrisilane (c-Si_3H_6) is *ca* 10 kcal mol^{-1} larger than that of cyclopropane (c-C_3H_6). As Table 3 shows, the strain energy decreases only by 1.3 kcal mol^{-1} when the H atoms are substituted by Me groups. In contrast, substitution by SiH_3 groups remarkably decreases the strain energy, c-$Si_3(SiH_3)_6$ being 11 kcal mol^{-1} less strained than c-Si_3H_6, reaching a strain energy as low as that of c-C_3H_6. This suggests that even three-membered rings are not unfavourable as building blocks when they bear suitable substituents.

Accordingly, the strain energies of polyhedral compounds can be also decreased remarkably by substitution, as shown in Table 3; the effect of SiH_3 groups is again larger than that of Me groups. Charge analyses show that the SiH_3 group acts as an electropositive substituent while the Me group is electronegative. The advantage of electron-donating

TABLE 3. Effect of substituents on the strain energies (kcal mol^{-1}) at the HF/6-31G* level

	R = H	R = Me	R = SiH_3
Cyclopropane (c-C_3R_6, D_{3h})	28.7	35.5	34.8
Cyclotrisilane (c-Si_3R_6, D_{3h})	38.9	37.6	28.1
Tetrasilatetrahedrane (Si_4R_4, T_d)	140.9	134.6	114.5
Hexasilaprismane (Si_6R_6, D_{3h})	113.8	105.6	95.7
Octasilacubane (Si_8R_8, O_h)	93.5	88.9	77.9

substituents over electron-accepting ones in the relief of strain is ascribed to the fact that the increased negative charges on the skeletal atoms decrease the size difference between valence s and p atomic orbitals and make s–p hybridization favourable. In addition, the s–p promotion energies are also decreased by the increased negative charges at the skeletal atoms[30].

III. SYNTHESIS

A. Substituents

The choice of substituents is of crucial importance for the successful synthesis and isolation of polyhedral silicon compounds. The Si–Si bonds of the small-ring compounds are readily oxidized because of the existence of high-lying orbitals and their inherent high strain. Therefore, the full protection of the skeleton by bulky substituents is required to suppress the attack by external reagents.

B. Precursors and Reducing Reagents

The most reasonable precursors for the synthesis of polyhedral silicons are halogenated cyclotrisilanes and cyclotetrasilanes. Compounds of the $RSiX_3$ and $RSiX_2{-}SiX_2R$ types can also serve as precursors of polyhedral silicons through the multi-step reactions when the R group is judiciously selected. The steric bulkiness of the R group determines the ring size and the shape of polyhedral silicons.

The role of metals as the reducing reagent is also crucial. In general, alkali metals such as Li, Na, Na/K, K and lithium naphthalenide (LiNp) are employed as coupling reagents for chlorosilanes. However, these reducing reagents are sometimes such powerful reagents that they cleave the resulting Si–Si bond. In contrast, magnesium metal does not cleave strained Si–Si bonds. $Mg/MgBr_2$ is a particularly useful reagent in this context. The reactive species is presumed to be MgBr, where Mg is at oxidation state +1[31]. The first step of the reaction involves one electron transfer from MgBr to the chlorosilane. For the preparation of tetrasilatetrahedrane, *t*-Bu_3SiNa was used as the electron transfer reagent[32].

IV. TETRASILATETRAHEDRANE

The reductive reaction of 1,2-bis(2,6-diisopropylphenyl)-1,1,2,2-tetrachlorodisilane **(1)** with LiNp led to several products from which **4** was isolated after hydrolytic workup (Scheme 1)[23]. Compound **4** is believed to be formed by the hydrolysis of the intermediate **3**, which arises from the cleavage of an Si–Si bond of the tetrasilatetrahedrane **2.**

The intermediacy of **2** was confirmed by the formation of 1,2,5,6-tetrakis(2,6-diisopropylphenyl)-1,2,5,6-tetrasilatricyclo[3.1.0.0^{2,6}]hexane **(6)** (Scheme 2)[33] in the reductive coupling reaction of 2,6-triisopropylphenyltrichlorosilane **(5)** by the $Mg/MgBr_2$ reagent (which was generated *in situ* by the reaction of Mg and $BrCH_2CH_2Br$). The tricyclic **6** is presumed to be derived from the insertion of ethylene (formed *in situ*, see Scheme 2) into the reactive Si–Si bond of **2.** None of **6** was formed after the complete removal of ethylene from the reaction system.

As pointed out in Section II.B, tetrasilatetrahedrane (Si_4R_4) collapses with no significant barrier to a 'two-bond broken' isomer when R = H, the latter being 37.3 kcal mol^{-1} more stable at the BLYP/6-31G* level[10,28,34]. This energy difference is decreased by 8.9 kcal mol^{-1} with R = Me, but the two bonds still remain broken. However, when R = SiH_3, the 'bond-stretch' isomer is by only 10.4 kcal mol^{-1} more stable than the corresponding tetrasilatetrahedrane, having only one bond stretched. As Figure 5 shows, the structural features of the two isomers, especially the close contact between the substituents

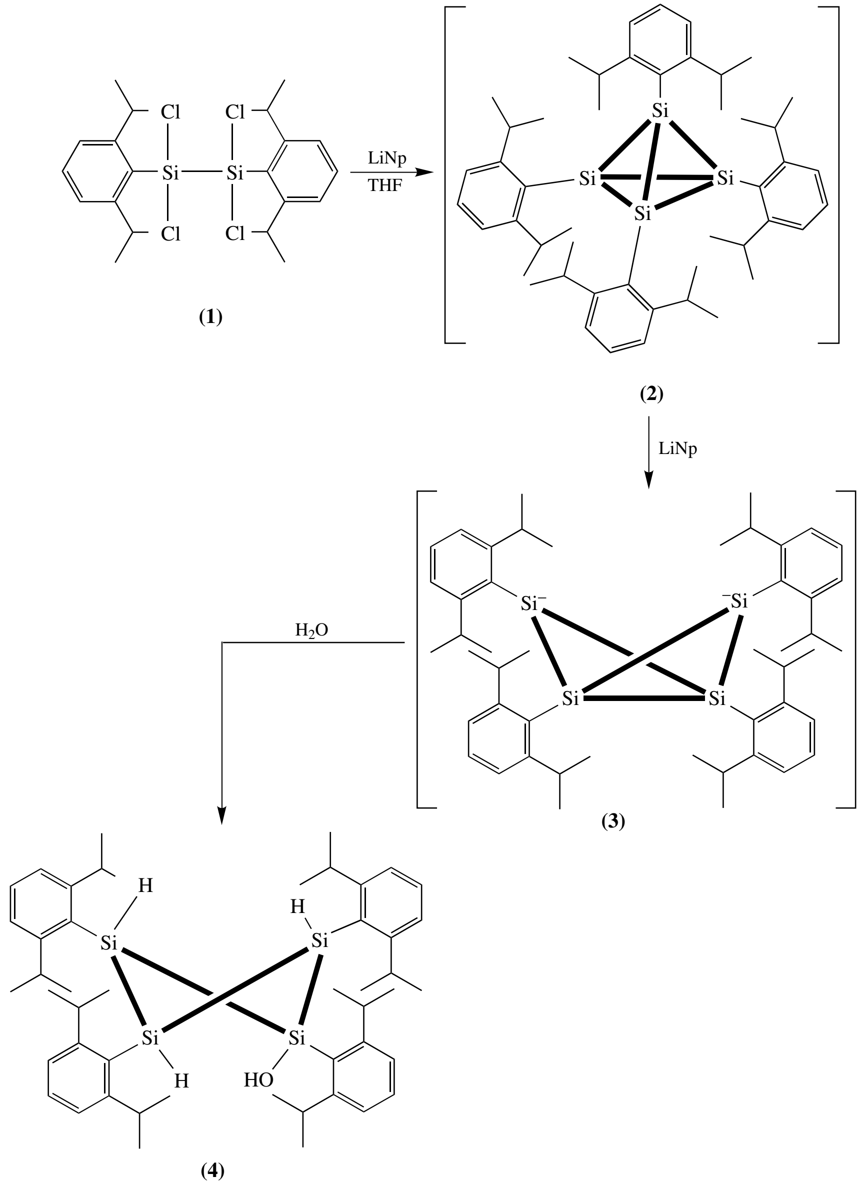

SCHEME 1

in the bond-stretch isomer, closely resembles the ‘bond-stretch’ isomer of bicyclo[1.1.0]tetrasilane in Figure 3 (as well as of **3** in Scheme 1). It is therefore expected that it should be possible to prepare a tetrasilatetrahedrane derivative by placing bulky silyl groups on the stretched atoms. This has recently been beautifully accomplished by using the ‘supersilyl’ group (t-Bu_3Si)[32].

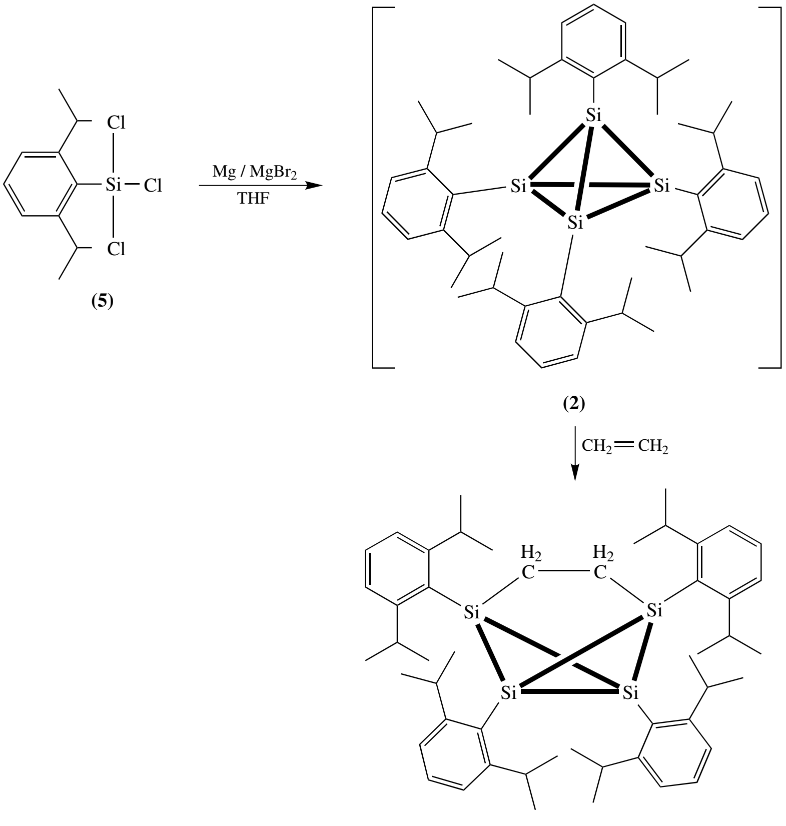

(5)

(2)

(6)

Mg + BrCH$_2$CH$_2$Br $\longrightarrow$ MgBr$_2$ + CH$_2$═CH$_2$

SCHEME 2

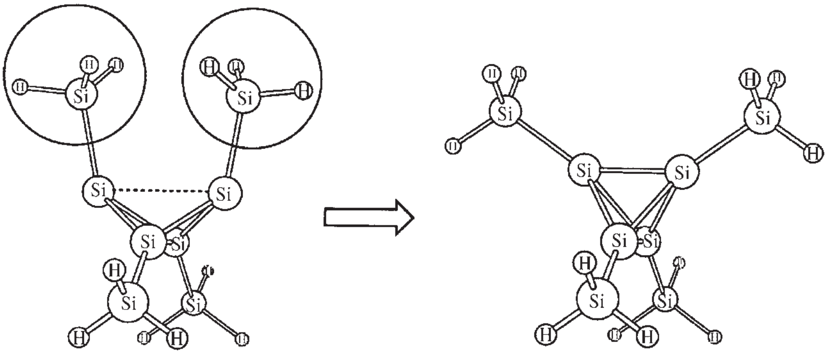

FIGURE 5. Possible conversion of the ‘bond-stretch’ isomer to a tetrasilatetrahedrane upon replacement of the substituents in circles by more bulky silyl groups. Reproduced with permission from Reference 10. Copyright 1995 American Chemical Society

The dehalogenation of t-Bu$_3$Si−SiCl$_3$ (**7**) with sodium at 80 °C led to the formation of various products such as 1,2-bis(supersilyl)disilane (**8**) and tris(supersilyl)cyclotrisilane (**9**). Bromination of **8** gave the tetrabromodisilane **10**. By the reaction of **10** with the supersilyl anion (t-Bu$_3$SiNa) in THF at −20 °C, tetrakis(tri-t-butylsilyl)tricyclo[1.1.0.0^{2,4}]tetrasilane (**11**) was obtained as yellow-orange crystals (Scheme 3)[32]. While the successful synthesis of **11** may be simply ascribed to the stabilizing effect of silyl groups, it should be emphasized that the large steric size of the t-Bu$_3$Si groups also plays an important role by preventing the collapse of the skeleton to the 'bond-stretch' isomer and by protecting it against reactive reagents[10]. The reaction mechanism that leads to **11** is not clear. However, the reactive disilyne t-Bu$_3$Si−Si≡Si−SiBu-t_3 which undergoes dimerization to give tetrasilacyclobutadiene, thereby leading to **11**, is a possible intermediate.

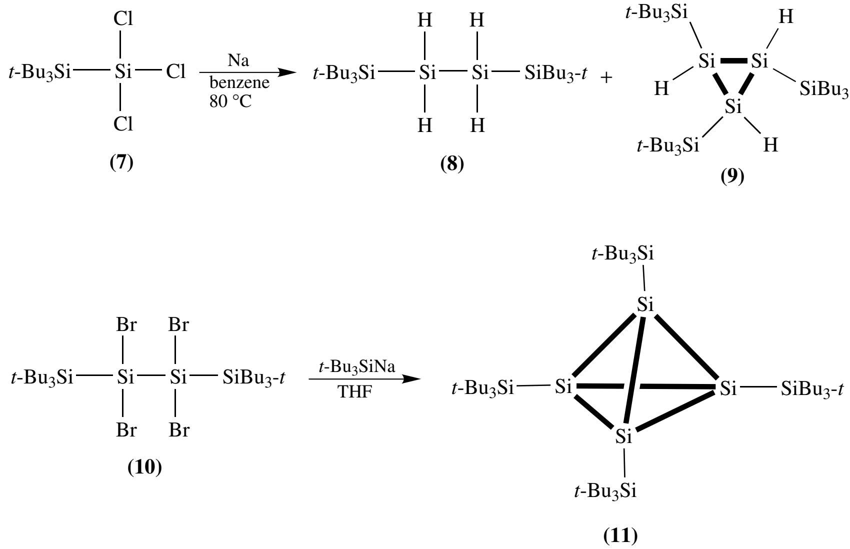

SCHEME 3

Tetrasilatetrahedrane **11** is unexpectedly stable to water, air and light. It cannot be reduced by sodium, but reacts with TCNE and Br$_2$[32]. Unlike t-butyl substituted tetrahedrane of carbon[35], **11** is thermally stable and its crystals do not melt below 350 °C. The bulky t-Bu$_3$Si substituents evidently prevent the collapse of the tetrahedrane skeleton. UV-Vis absorptions were observed at 210 ($\varepsilon = 76000$), 235 ($\varepsilon = 71000$), 310 ($\varepsilon = 20000$) and 451 ($\varepsilon = 3600$) nm.

Recrystallization of a mixture of **11** and hexa-t-butyldisilane from C$_6$D$_6$ leads to $2(t-\mathrm{Bu_3Si})_4\mathrm{Si_4}\bullet(t-\mathrm{Bu_3Si})_2\bullet\mathrm{C_6D_6}$ whose structure was established by X-ray crystallography (Figure 6). The cubic unit cell contains two sets of four molecules of **11** (**11A** and **11B**). The skeleton has two different Si−Si distances of 2.320 and 2.315 Å for **11A** and 2.326 and 2.341 Å for **11B**, while the Si−Si−Si bond angles in **11A** and **11B** are 59.9 and 60.4°, respectively. Their Si−Si bond lengths are somewhat longer than those of 2.314 (HF), 2.328 (B3LYP), 2.314 (B3P) and 2.315 (MP2) Å calculated for Si$_4$H$_4$ at several theoretical levels[13,34] with the 6-31G* basis, probably due to steric reasons.

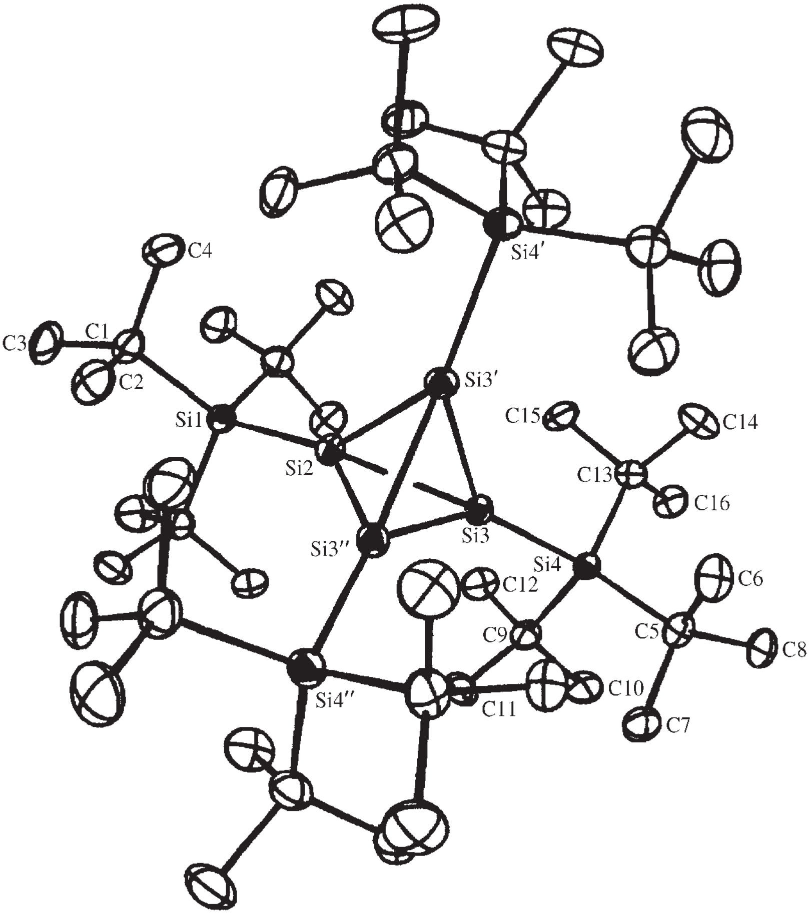

FIGURE 6. ORTEP drawing of tetrasilatetrahedrane (**11**). Reprinted with permission from Reference 32. Copyright 1993 VCH

However, the Si−Si bonds in **11** are shorter than the typical single Si−Si bond (2.34 Å). The exocyclic Si−Si bonds of 2.355 and 2.365 Å for **11A** and 2.371 and 2.356 Å for **11B** are stretched compared with the normal Si−Si bond. A tetragermatetrahedrane derivative was also prepared by using the *t*-Bu_3Si substituent[36].

V. HEXASILAPRISMANE

A. Synthesis

For the synthesis of hexasilaprismane, tetrachlorodisilane ($RSiCl_2-SiCl_2R$) and trichlorosilane ($RSiCl_3$) are utilized as the starting compounds. The Mg/$MgBr_2$ reagent is quite useful also for the synthesis of hexasilaprismane. A hexasilaprismane derivative, hexakis(2,6-diisopropylphenyl)tetracyclo[2.2.0.0^{2,6}.0^{3,5}]hexasilane (**12**), was successfully

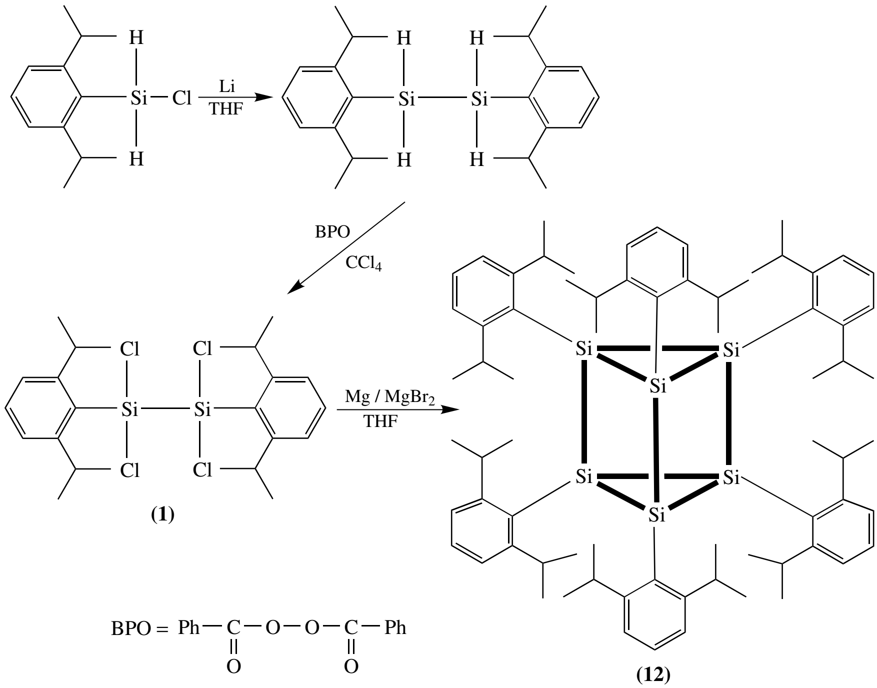

SCHEME 4

prepared by the dechlorinative coupling reaction of 1,2-bis(2,6-diisopropylphenyl)-1,1,2,2-tetrachlorodisilane (**1**) with the Mg/$MgBr_2$ reagent (Scheme 4)[37]. **12** was isolated as orange crystals (mp > 220 °C), by silica gel chromatography with hexane/toluene of the reaction mixture. On the other hand, the reaction of **1** with LiNp did not give **12**[23]. This demonstrates that the choice of the reducing reagent is critical, as mentioned in Section IV. The reaction of (2,6-diisopropylphenyl)trichlorosilane (**5**) with Mg/$MgBr_2$ also gave **12**. The tricyclic derivative **6** was also formed in the presence of ethylene (equation 1)[33]. In the solid state, **12** is thermally and oxidatively fairly stable; no change is observed even after several months in air.

The ^{1}H NMR spectrum of **12** at 25 °C shows that the two isopropyl and the aryl protons are not equivalent due to the restricted rotation of the aryl groups. One set of the methine protons appears at 3.45 ppm along with the two methyl protons at 0.64 and 1.10 ppm. The other set of the methine protons appears at 4.82 ppm with the two methyl protons at 1.01 and 1.62 ppm. The barrier for the rotation of the aryl groups ($\Delta G^{\neq}$) was estimated to be 16.5 kcal mol^{-1}[37].

B. Structure

Figure 7 shows the ORTEP drawing of the hexasilaprismane **12**[37]. Its structural parameters are listed in Table 4. The crystal has a two-fold axis of symmetry. The skeleton has a slightly distorted prismane structure with two triangular units [Si–Si = 2.374–2.387 Å (av. 2.380 Å) and ∠Si–Si–Si = 59.8–60.3° (av. 60.0°)] and three rectangular units [Si–Si′ = 2.365–2.389 Å (av. 2.373 Å) and ∠Si–Si–Si′ = 89.6–90.5° (av. 90.0°)]. The exocyclic Si–C_{ar} lengths are 1.901–1.920 Å (av. 1.908 Å). The exocyclic bond angles are significantly expanded: ∠Si–Si–C_{ar} = 126.9–138.7° (av. 133.5°) and ∠Si′–Si–C_{ar} = 124.2–129.2° (av. 126.9°).

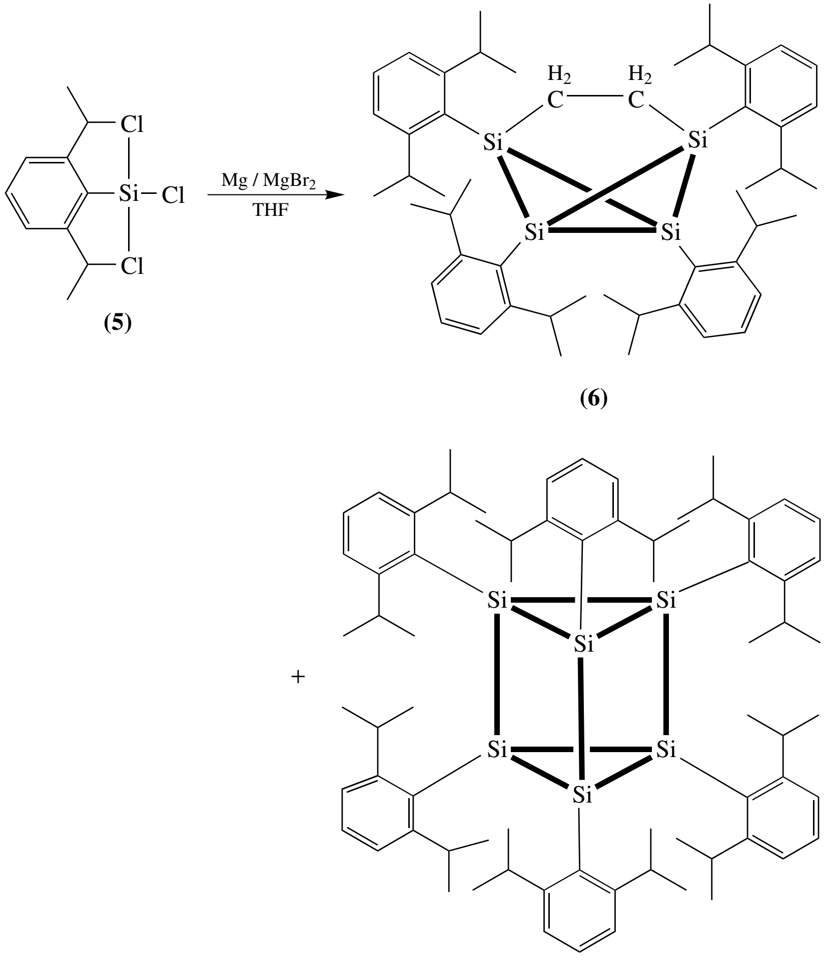

(5)

(6)

(1)

(12)

$$\text{Mg} + \text{BrCH}_2\text{CH}_2\text{Br} \longrightarrow \text{MgBr}_2 + \text{CH}_2{=}\text{CH}_2$$

All the Si–Si bonds in **12** are elongated from the normal Si–Si bond length (2.34 Å), but are shorter than those in cyclotrisilane $(R_2Si)_3$ (R = 2,6-dimethylphenyl: av. 2.407 Å)[38]. The Si–Si bond lengths of **12** are somewhat longer than those calculated with the 6-31G* basis set for Si_6H_6 [2.359 (HF), 2.369 (B3LYP), 2.354 (B3P) and 2.356 (MP2) Å for the triangular units and 2.375 (HF), 2.376 (B3LYP), 2.361 (B3P), and 2.361 (MP2) Å for the rectangular units][13,34]. The aryl planes are arranged in a screw-shaped

TABLE 4. Selected bond lengths and bond angles of hexasilaprismane **12**

Bond lengths (Å)		Bond angles (deg)	
Si1–Si2	2.374(2)	Si2–Si1–Si3	60.3(0)
Si1–Si3	2.379(2)	Si1–Si2–Si3	60.0(0)
Si2–Si3	2.387(2)	Si1–Si3–Si2	59.8(0)
Si1–Si1′	2.389(2)	Si2–Si1–Si1′	89.6(0)
Si2–Si3′	2.365(2)	Si3–Si1–Si1′	89.9(0)
Si3–Si2′	2.365(2)	Si1–Si2–Si3′	90.5(0)
Si–C_{ar}	1.901(7)	Si3–Si2–Si3′	90.4(0)
	≀		
	1.920(6)	Si1–Si3–Si2′	90.0(0)
		Si2–Si3–Si2′	89.6(0)
		Si–Si–C_{ar}	126.9(2)
			≀
			138.7(2)
		Si′–Si–C_{ar}	124.2(2)
			≀
			129.2(2)

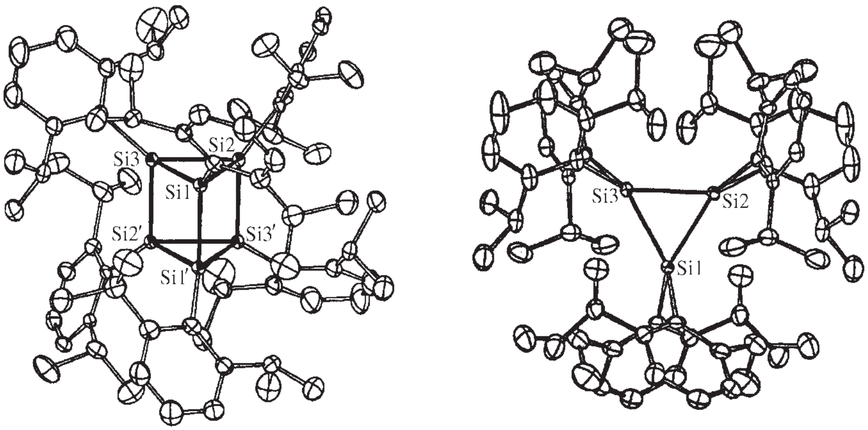

FIGURE 7. ORTEP drawing of hexasilaprismane **12**. Reprinted with permission from Reference 9. Copyright 1995 Academic Press, Inc.

manner around the three-membered rings so that the skeleton is effectively ‘covered’ by the six 2,6-diisopropylphenyl groups.

Table 5 summarizes the observed structural parameters of prismanes (M_6R_6, M = C, Si, Ge) together with the calculated values for R = H. The M–M bonds within and between the three-membered units are denoted by *a* and *b*, respectively. As calculated for R = $H^{13,14}$, *a* is shorter than *b* in prismane ($C_6H_6{}^{39}$) and its derivatives C_6R_6 (R = Me^{40}

TABLE 5. Structural parameters of prismanes comprising group 14 element

M	R	***a*** (Å)	***b*** (Å)	Method
C	H	1.507	1.549	Calcd.[a]
		1.500	1.585	ED[b]
	Me	1.540	1.551	ED[c]
	$SiMe_3$	1.510	1.582	XRD[d]
Si	H	2.359	2.375	Calcd.[a]
	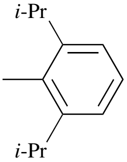	2.380 (2.374–2.387)	2.373 (2.365–2.389)	XRD[e]
Ge	H	2.502	2.507	Calcd.[f]
	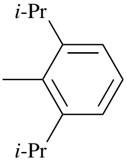	2.503 (2.497–2.507)	2.468 (2.465–2.475)	XRD[e]
	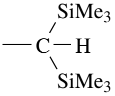 $-CH(SiMe_3)_2$	2.580 (2.578–2.584)	2.522 (2.516–2.526)	XRD[g]

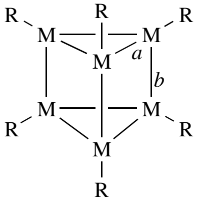

ED: electron diffraction

XRD: X-ray diffraction

[a] From Reference 13.
[b] From Reference 39.
[c] From Reference 40.
[d] From Reference 41.
[e] From Reference 37.
[f] From Reference 14.
[g] From Reference 4.

and $SiMe_3$[41]). The calculation shows that the length difference between a and b decreases significantly as M becomes heavier. Thus, $|a - b| = 0.042$ (C_6H_6), 0.016 (Si_6H_6), 0.005 (Ge_6H_6) Å. In this context, it is interesting that b is observed to be shorter than a in Si_6R_6 (**12**: R = 2,6-*i*-$Pr_2C_6H_3$) ($a = 2.380$ Å, $b = 2.373$ Å) and Ge_6R_6 [R = 2,6-*i*-$Pr_2C_6H_3$[37], $a = 2.503$ Å, $b = 2.468$ Å; R = $CH(SiMe_3)_2$[4], $a = 2.580$ Å, $b = 2.522$ Å].

C. Absorption Spectra

The prismanes with Si and Ge skeletons are yellow to orange. Figure 8 shows the UV-Vis spectra of **12** and its germanium analogue. These prismanes have absorptions tailing into the visible region. For example, **12** has an absorption band with a maximum at 241 ($\epsilon = 78000$) nm tailing to *ca* 500 nm. The absorption band of Ge_6R_6 (R = 2,6-*i*-$Pr_2C_6H_3$) has a maximum at 261 ($\epsilon = 84000$) nm, which is red-shifted compared to that of **12** because of the higher-lying orbitals of the Ge−Ge bonds.

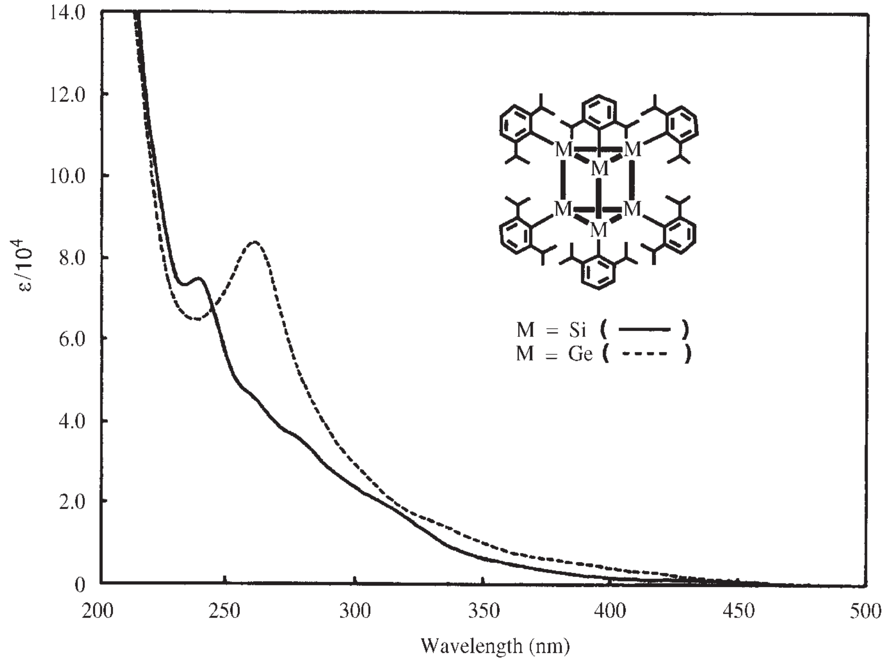

FIGURE 8. Electronic absorption spectra of hexasilaprismane **12** and hexagermaprismane in hexane

D. Photochemical Reaction

Hexasilaprismane **12** is photosensitive. On irradiation in solution at low temperature, with light having wavelengths of 340–380 nm, new absorption bands appeared at 335, 455 and 500 nm assignable to the absorption bands of hexasila-Dewar benzene **13** (equation 2)[37]. Upon excitation of these bands with wavelengths longer than 460 nm, **12** was immediately regenerated. A single chemical species was produced during the photochemical reaction since the bands of **12** and those assigned to **13** appeared and disappeared simultaneously.

The folding angle of the parent hexasila-Dewar benzene (Si_6H_6) with C_{2v} symmetry is 120° at the HF/6-31G* level. The through-space interaction between the Si=Si double bonds splits the π MOs into bonding (π_S) and antibonding (π_A) sets, as shown in Figure 9[42]. Likewise, their π^* MOs split into $\pi^*{}_S$ and $\pi^*{}_A$. The allowed transitions from π_S to $\pi^*{}_S$ and from π_A to $\pi^*{}_A$ correspond to the experimental absorption bands at 455 and 335 nm, respectively. The lowest energy transition from π_A to $\pi^*{}_S$ is forbidden. However, it is allowed if the C_{2v} symmetry is lowered. The relatively weak absorption at 500 nm is assigned to the π_A–$\pi^*{}_S$ transition.

The hexasila-Dewar benzene **13** is thermally stable at −150 °C, but it gradually reverted to the hexasilaprismane **12**[43]. The half-life is $t_{1/2} = 0.52$ min at 0 °C in 3-methylpentane. The activation parameters for the isomerization of **13** to **12** are $E_a = 13.7$ kcal mol^{-1}, $\Delta H^{\neq} = 13.2$ kcal mol^{-1} and $\Delta S^{\neq} = -17.8$ cal K^{-1} mol^{-1}. The small E_a value is consistent with the high reactivity of Si=Si double bonds. Most probably, the small HOMO–LUMO gap of **13** makes it possible that the Si=Si double bonds undergo a formally symmetry forbidden [2 + 2] thermal reaction. Hexasila-Dewar benzene is a key

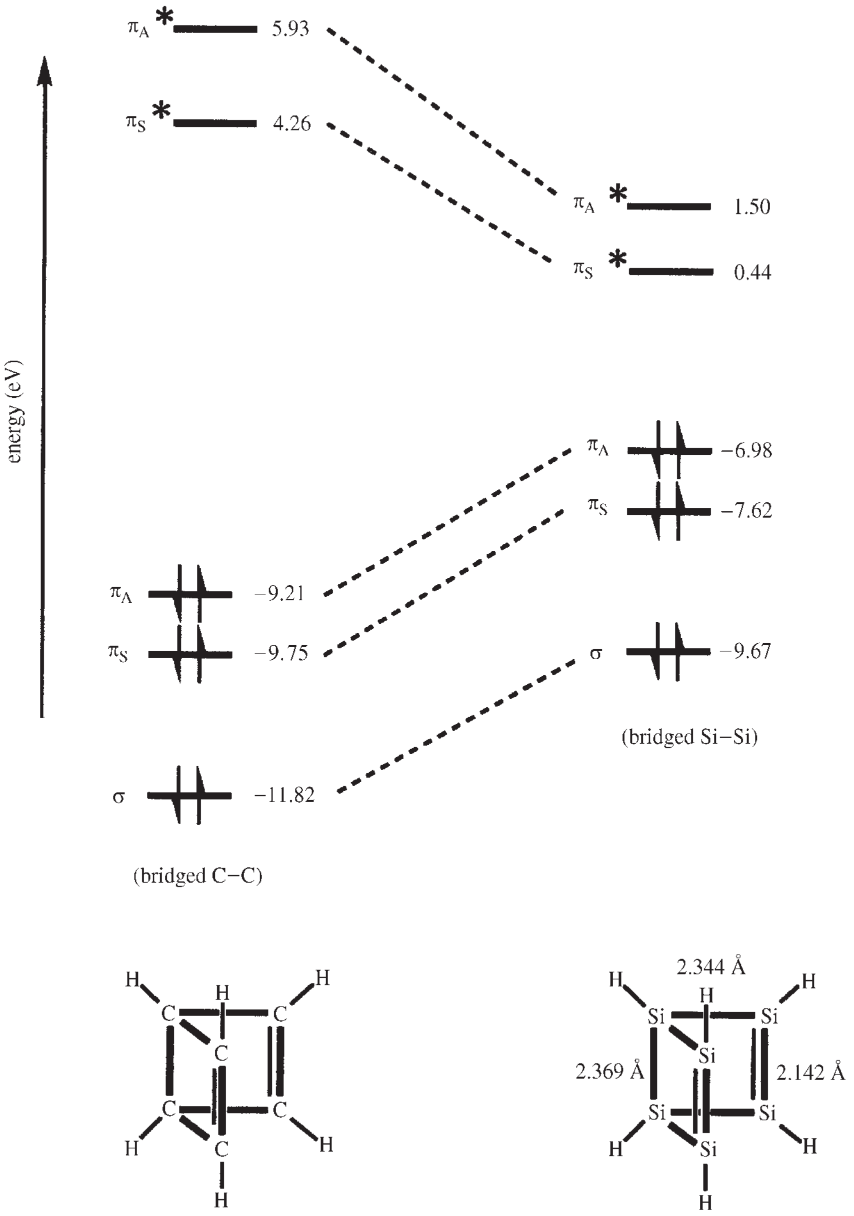

FIGURE 9. Energy diagram of Dewar benzene and of hexasila-Dewar benzene calculated at the HF/6-31G* level

intermediate in the reductive oligomerization of $RCl_2SiSiCl_2R$ and $RSiCl_3$ (R = 2,6-*i*-$Pr_2C_6H_3R$).

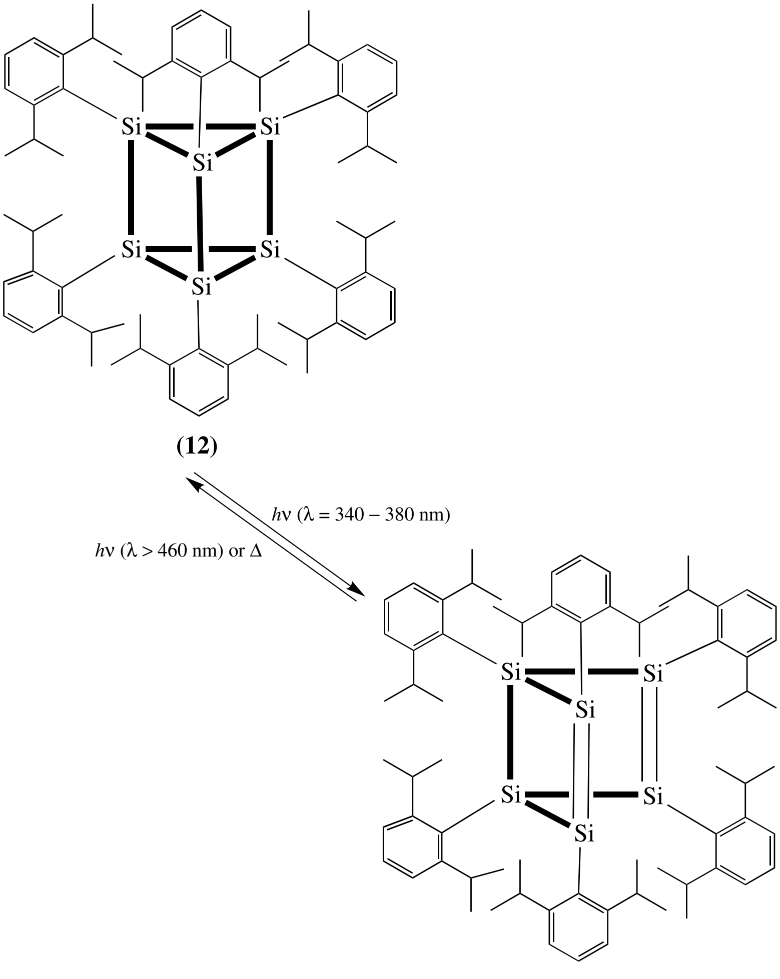

(12)

(2)

(13)

VI. OCTASILACUBANE

A. Synthesis

Trihalosilanes ($RSiX_3$) and tetrahalodisilanes ($RSiX_2{-}SiX_2R$) bearing appropriate substituents R can serve as precursors to octasilacubane by reductive coupling reactions. As pointed out in Section II.C, the strain of octasilacubane is significantly decreased by electropositive silyl groups[8,29]. Accordingly, a silyl-substituted octasilacubane, octakis(*t*-butyldimethylsilyl)pentacyclo$[4.2.0.0^{2,5}.0^{3,8}.0^{4,7}]$octasilane **(16)** was synthesized as bright yellow crystals by condensation of 1,1,1-tribromo-2-*t*-butyl-2,2-dimethyldisilane **(14)** and 2,2,3,3-tetrabromo-1,4-di-*t*-butyl-1,1,4,4-tetramethyltetrasilane **(15)** with sodium in toluene (equation 3)[3].

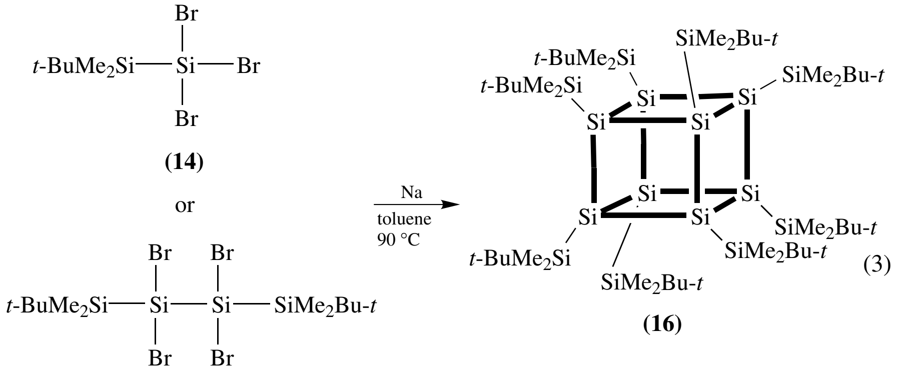

(14) or **(15)** → **(16)** (3)

Alkyl-substituted octasilacubanes, octakis(*t*-butyl)octasilacubane **(18a)**[44] and octakis(1,1,2-trimethylpropyl)octasilacubane **(18b)**[45], were also prepared. The condensation of *t*-butyltrichlorosilane with sodium in the presence of 12-crown-4 produced **18a** as a purple crystalline compound sparingly soluble in organic solvents (equation 4). On the other hand, **18b** was formed as red-orange prisms by the condensation of (1,1,2-trimethylpropyl)trichlorosilane with sodium in toluene (equation 4).

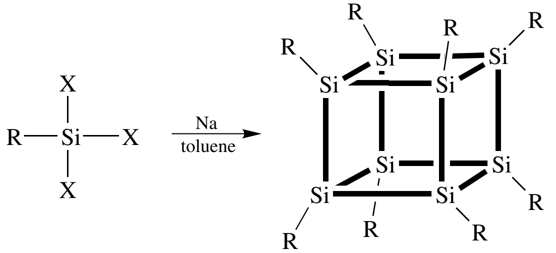

(4)

(17a) R = *t*-Bu
(17b) R = CMe_2CHMe_2

(18a) R = *t*-Bu
(18b) R = CMe_2CHMe_2

Aryl-substituted octasilacubanes **20** and **22** were prepared by the dechlorinative reactions of $ArCl_2SiSiCl_2Ar$ (equation 5) and of $ArSiCl_3$ (equation 6), respectively. Octakis(2,4,6-trimethylphenyl)octasilacubane **(20)** was isolated as orange crystals by a dechlorinative reaction of 1,2-bis(2,4,6-trimethylphenyl)-1,1,2,2-tetrachlorodisilane with $Mg/MgBr_2$ reagent (equation 5)[46]. In a similar manner, 2,6-diethylphenyl-substituted octasilacubane **22** was prepared by the reaction of (2,6-diethylphenyl)trichlorosilane **(21)** with $Mg/MgBr_2$ (equation 6)[47]. The cubane **20** is sparingly soluble in organic solvents, whereas **22** is soluble.

B. Structure

Figure 10 shows the ORTEP drawing of the 1,1,2-trimethylpropyl-substituted octasilacubane **18b**[45]. Its skeleton is slightly distorted from an ideal cubic form by the steric congestion of the eight bulky 1,1,2-trimethylpropyl groups. The Si−Si bond lengths range from 2.398(2) to 2.447(2) Å, and the Si−Si−Si bond angles vary from 87.2(1) to 92.6(1)°. X-ray diffraction analysis revealed that **18a** also has a slightly distorted cubic structure: the Si−Si bond lengths are 2.374–2.400 Å (av. 2.390 Å) and the Si−Si−Si bond angles are 89.3–90.9° (av. 90.0°)[44b].

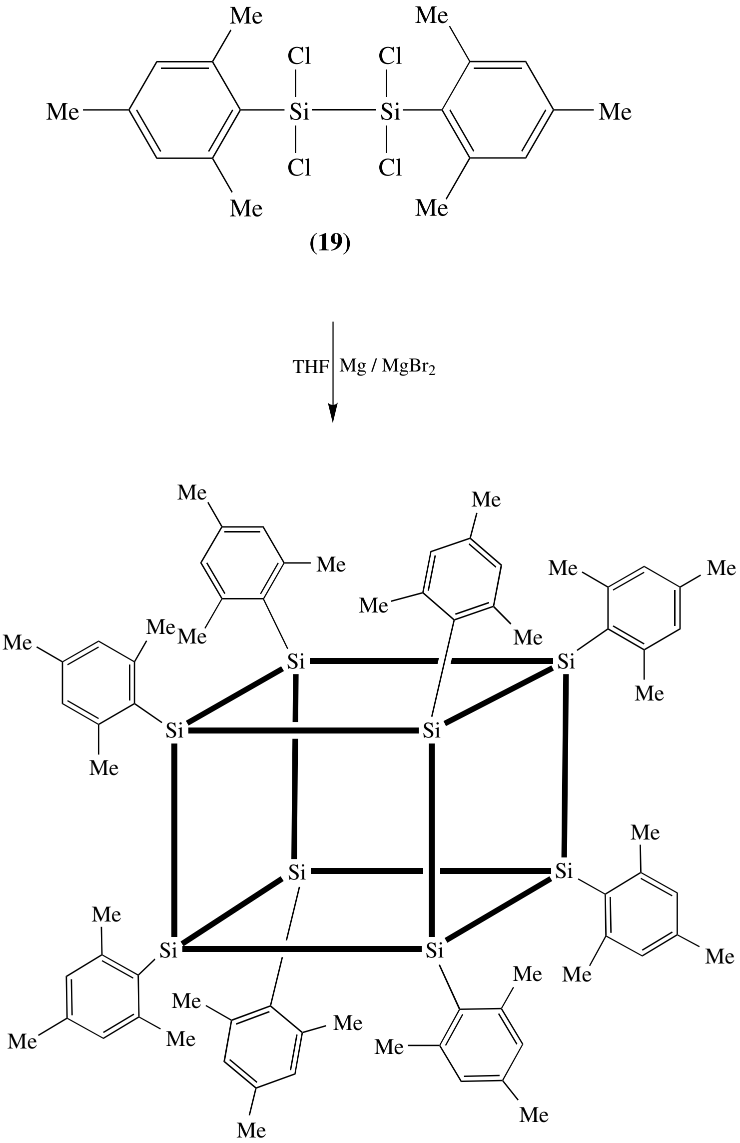

(19)

(5)

(20)

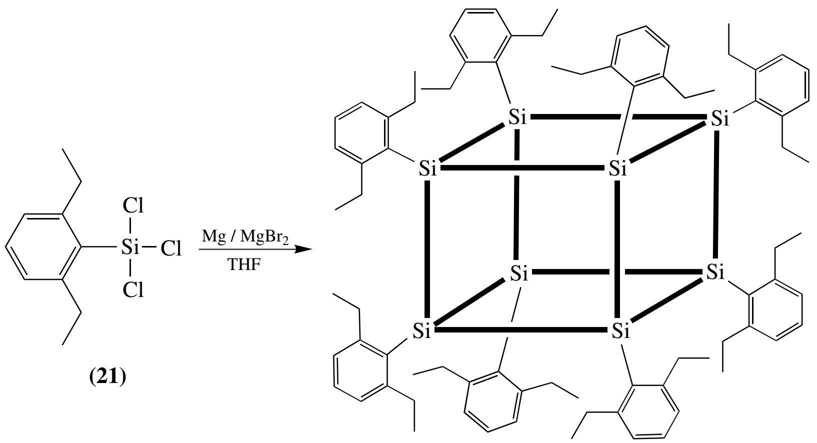

(21)

(22)

(6)

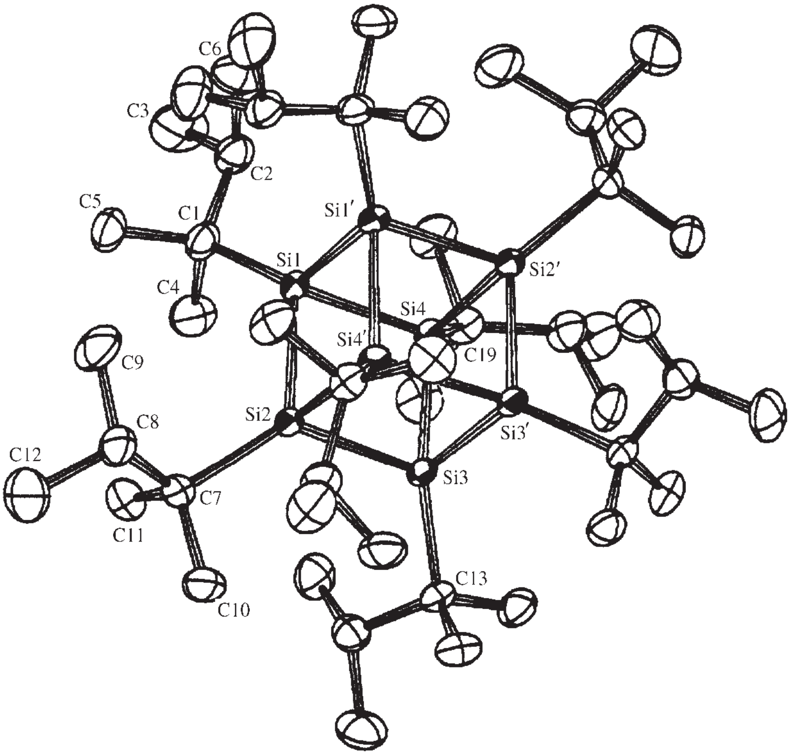

FIGURE 10. ORTEP drawing of octasilacubane **18b**. Reprinted with permission from Reference 45. Copyright 1992 VCH

Figure 11 shows the ORTEP drawing of 2,6-diethylphenyl-substituted octasilacubane **22**[47]. Its structural parameters are listed in Table 6. The X-ray structure indicates that its skeleton is almost perfect cubic. The Si−Si−Si bond angles are 88.9–91.1° (av. 90.0°). The Si−Si bond lengths are in the range of 2.384–2.411 Å (av. 2.399 Å), somewhat longer than the normal Si−Si bond length (2.34 Å). The Si−Si bond lengths of **22** are in close agreement with those calculated for Si_8H_8 of 2.396 (HF/6-31G*), 2.398 (B3LYP/6-31G*), 2.383 (B3P/6-31G*) and 2.385 (MP2/6-31G*) Å[13,14]. The exocyclic $Si-C_{ar}$ bond lengths of 1.911 Å (av) are somewhat longer than the normal Si−C bond length (1.88 Å). The $Si-Si-C_{ar}$ bond angles of 124.4° are significantly expanded due to the endocyclic angular constraint. The aryl substituents form dihedral angles of *ca* 90° between the benzene ring and the Si−Si bond: ring (Si1)/Si1-Si4′, ring (Si2)/Si2-Si3, ring (Si3)/Si3-Si2′ and (Si4)/Si4-Si1 being all *ca* 90°. As a result the cubic skeleton of **22** is effectively protected by the eight 2,6-diethylphenyl groups.

Octasilacubanes (Si_8H_8) bearing alkyl, aryl and silyl substituents of various sizes were calculated using the semiempirical AM1 method (Table 7)[10,48]. X-ray structures are available for R = 2,6-$Et_2C_6H_3$[47], CMe_2CHMe_2[45] and *t*-Bu[44b]. Both the calculated and the X-ray structures show almost perfect cubic skeletons. In addition, the experimental skeletal Si−Si bond lengths are reasonably well reproduced by the calculations, taking into account the overestimation of the Si−Si bond distances by *ca* 0.05 Å. As Table 7 shows, the O_h symmetry of Si_8H_8 is lowered as the substituents become more bulky. Nevertheless, all of the calculated structures still retain relatively high symmetry (Table 7), in contrast with the available experimental structures in crystals. This suggests that packing forces significantly affect the favourable conformations of bulky substituents around the cubane skeleton, probably because the energy loss due to the conformational changes is very small.

As Table 7 shows, the skeletal bond lengths increase by 0.02–0.05 Å upon substitution by alkyl and aryl groups. This bond lengthening is somewhat enhanced as the substituents become more bulky: e.g. 2.446 Å (R = Ph) vs 2.470 Å (R = 2,6-$Et_2C_6H_3$). There is also a good correlation between the Si−Si bond lengthening and the increased positive charges on the skeletal atoms (Table 7). The skeletal bonds are lengthened even on substitution by the small Me group. It appears that both steric and electronic effects are responsible for

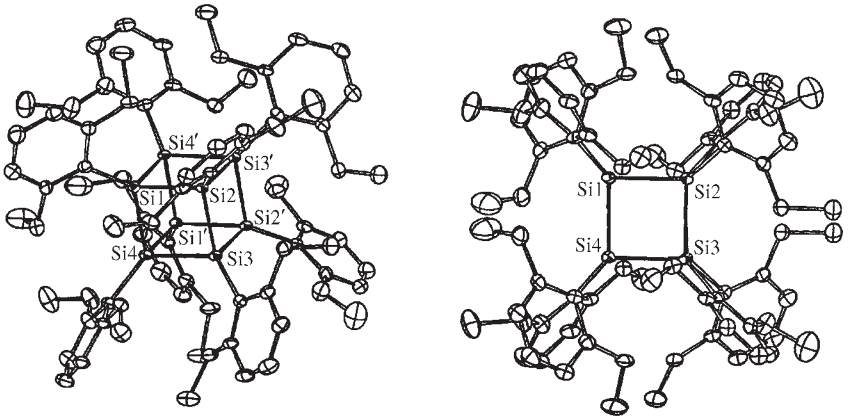

FIGURE 11. ORTEP drawing of octasilacubane **22**. Reprinted with permission from Reference 9. Copyright 1995 Academic Press, Inc.

TABLE 6. Selected bond lengths and bond angles of octasilacubane **22**

Bond lengths (Å)		Bond angles (deg)	
Si1–Si2	2.384(2)	Si2–Si1–Si4	90.8(0)
Si2–Si3	2.399(2)	Si2–Si1–Si4′	90.3(0)
Si3–Si4	2.411(2)	Si4–Si1–Si4′	91.1(0)
Si4–Si1	2.400(2)	Si1–Si2–Si3	89.8(0)
Si1–Si4′	2.406(2)	Si1–Si2–Si3′	90.3(0)
Si2–Si3′	2.396(2)	Si3–Si2–Si3′	89.1(0)
Si–C_{ar}	1.900(7) ≀ 1.924(7)	Si2–Si3–Si4	90.2(0)
		Si2–Si3–Si2′	90.8(0)
		Si4–Si3–Si2′	89.9(0)
		Si1–Si4–Si3	89.1(0)
		Si1–Si4–Si1′	88.9(0)
		Si3–Si4–Si1′	89.4(0)
		Si–Si–C_{ar}	120.7(2) ≀ 128.3(2)

TABLE 7. Symmetries, Si–Si bond lengths, charges and HOMO energies of octasilacubane derivatives (Si_8R_8) calculated at the AM1 level[a]

R	Symmetry	Si–Si (Å)[b]	Charge[c]	HOMO (eV)
H	O_h	2.421	0.045 (0.068)	−9.70 (−8.13)
Me	O_h	2.437	0.255 (0.343)	−8.68 (−6.65)
t-Bu	D_2	2.445	0.264 (0.481)	−8.68 (−6.71)
CMe_2CHMe_2	D_2	2.462	0.242 (0.435)	−8.54 (−6.51)
Ph	D_2	2.446	0.366 (0.393)	−8.26 (−6.27)
2,6-$Et_2C_6H_3$	C_2	2.470	0.343 (0.389)	−8.22 (−6.31)
$Si(SiH_3)_3$	D_2	2.414	0.021 (0.054)	−9.22 (−7.99)
SiH_3	O_h	2.402	−0.216 (−0.115)	−9.48 (−8.14)
$SiMe_2CHMe_2$	D_2	2.408	−0.324 (−0.188)	−8.48 (−7.08)
$SiMe_3$	O_h	2.395	−0.343 (−0.185)	−8.47 (−7.09)
SiF_3	O_h	2.391	−0.539 (−0.313)	−9.81 (−10.89)

[a] In parentheses are the HF/3-21G* values calculated on the AM1 optimized structures.

[b] Average skeletal bond lengths.

[c] Average Mulliken charges on the skeletal atoms.

the skeletal bond lengthening. It is noteworthy that substitution by alkyl and aryl groups raises the HOMO levels (localized on the skeletons) and therefore is expected to increase the reactivity. This makes the presence of bulky groups very important since they can fully protect the cubane skeleton, as clearly shown in Figure 12.

Table 7 reveals that the skeletal bond lengths tend to shorten with an increase in the negative charges on the skeletal atoms due to silyl substituents, regardless of their steric bulk. This is also confirmed by the geometry optimization at the HF/3-21G* level of

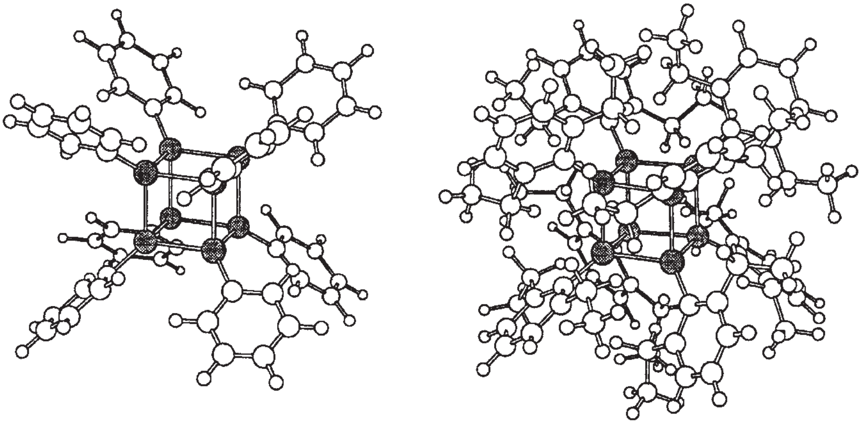

FIGURE 12. Examples of the steric protection of the cubic silicon skeleton by phenyl and 2,6-diethylphenyl groups. The 2,6-diethylphenyl group is apparantly more effective for steric protection. Reprinted with permission from Reference 10. Copyright 1995 American Chemical Society

TABLE 8. Calculated data for octasilacubane derivatives (Si_8R_8) optimized at the HF/3-21G* level

R	Symmetry	Si–Si (Å)[b]	Charge[c]	HOMO (eV)
H	O_h	2.386	0.065	−8.23
Me	O_h	2.391	0.328	−7.05
SiH_3	O_h	2.383	−0.112	−8.31
$SiMe_3$	O_h	2.390	−0.169	−7.45
SiF_3	O_h	2.369	−0.373	−10.42

[a] Mulliken charges on the skeletal atoms.

several substituted octasilacubanes as shown in Table 8[10,48]. The SiF_3 group which places the largest charge on the skeletal silicon atoms provides the shortest skeletal bond lengths and the lowest HOMO level while the $SiMe_3$-substituted octasilacubane has a relatively high HOMO level.

The geometries of C_8H_8[49] and M_8R_8 (M = Si[47], Ge[47] and Sn[50], R = 2,6-$Et_2C_6H_3$) are compared in Table 9. The M–M–M bond angles in M_8R_8 range from 89–91°, indicating that all these skeletons are almost perfect cubic. The M–M bond lengths of 2.399 Å for Si, 2.490 Å for Ge and 2.854 Å for Sn are in close agreement with those calculated for the corresponding M_8H_8 (2.382 Å for Si, 2.527 Å for Ge and 2.887 Å for Sn)[14]. The range of the M–M–C_{ar} bond angles increases in the order: 121–128° for Si $<$120–130° for Ge $<$117–133° for Sn. This implies that the steric congestion between the neighbouring ligands is relaxed by the longer M–C_{ar} bond as M becomes heavier: 1.911 Å for Si $<$1.982 Å for Ge $<$2.193 Å for Sn.

C. Absorption Spectra

All cubanes of Si, Ge and Sn are coloured from yellow to purple. The silyl substituted **16** is yellow[3], while the *t*-butyl substituted **18a** is purple[44]. A diffuse reflection absorption

TABLE 9. Structural parameters of cubanes comprising group 14 elements

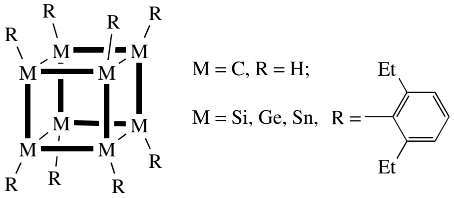

M = C, R = H;

M = Si, Ge, Sn, R =

	C_8H_8[a]	Si_8R_8[b]	Ge_8R_8[b]	Sn_8R_8[c]
M−M (Å)				
X-ray	1.551 (av.) (1.549–1.553)	2.399 (av.) (2.384–2.411)	2.490 (av.) (2.478–2.503)	2.854 (av.) (2.839–2.864)
Calculated[d]	1.559	2.382	2.527	2.887
M−C_{ar} (Å)	1.06 (av.)	1.911 (av.)	1.982 (av.)	2.193 (av.)
M−M−M (°)	89.3–90.5	88.9–91.1	88.9–91.1	89.1–91.1
M−M−Car (°)	123–127	121–128	120–130	117–133

[a] From Reference 49.
[b] From Reference 47.
[c] From Reference 50.
[d] From Reference 14.

spectrum of **18a** shows a broad absorption between 450 and 650 nm[44a]. The colour of **18b** is red-orange[45]. The UV/Vis spectrum of **18b** exhibits absorption bands at 252 ($\epsilon = 30800$), 350 ($\epsilon = 850$) and around 500 ($\epsilon = 70$) nm, as shown in Figure 13[45]. The aryl substituted **20** and **22** are orange. The spectrum depends on the type of the aryl substituent[46,47]. Thus, **20** exhibits three absorption bands at 246 ($\epsilon = 73000$), 280 ($\epsilon = 48500$) and 379 ($\epsilon = 4900$) nm[46], while **22** shows bands at 234 ($\epsilon = 87000$), 284 ($\epsilon = 42000$) and 383 ($\epsilon = 5000$) nm, as shown in Figure 14[47]. The absorption band at around 240 nm is attributed to the σ–σ^* transition, while the absorption at around 280 nm is caused by transition from a σ–π mixing between the orbitals of the Si−Si σ bonds and the aromatic π orbitals.

The lowest energy absorption is forbidden when the cubane has high symmetry, but becomes weakly allowed when the symmetry is lowered. CNDO/S calculations show that the spectrum shape in the low energy region depends strongly on the substituents[51]. Among *t*-butyl-, trimethylsilyl- and phenyl- substituted octasilacubanes, the *t*-butyl substituted cubane **18a** has the lowest energy absorption band.

Octasilacubanes were used as a model in an attempt to understand the optical properties of porous silicon because both porous silicon and octasilacubane show a broad photoluminescence spectra and large Stokes shifts[52]. **16** for example, shows an absorption edge at *ca* 3.2 eV and a broad photoluminescence spectrum with a peak at 2.50 eV.

D. Reactivity

The kinetic stability of octasilacubanes depends strongly on the steric bulkiness of the substituents. The silyl-substituted **16** is stable in an inert atmosphere, but is oxidized in air to give colourless solids[3]. The 1,1,2-trimethylpropyl-substituted **18b** is very stable even in air and survives for two weeks in the solid state[45]. The aryl-substituted **20** and **22** are gradually oxidized in the atmospheric air[46,47].

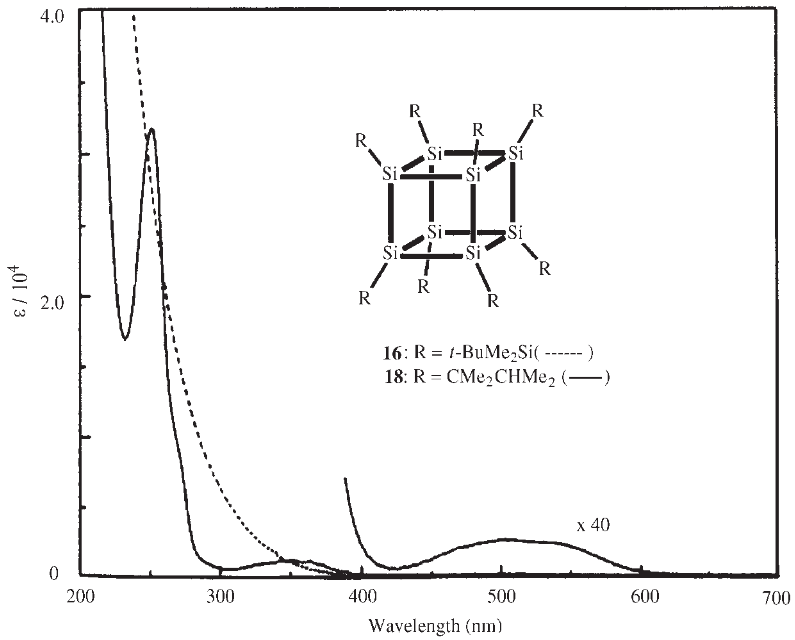

FIGURE 13. Electronic absorption spectra of octasilacubanes **16** and **18b** in hexane. Reproduced with permission from Reference 45. Copyright 1992 VCH

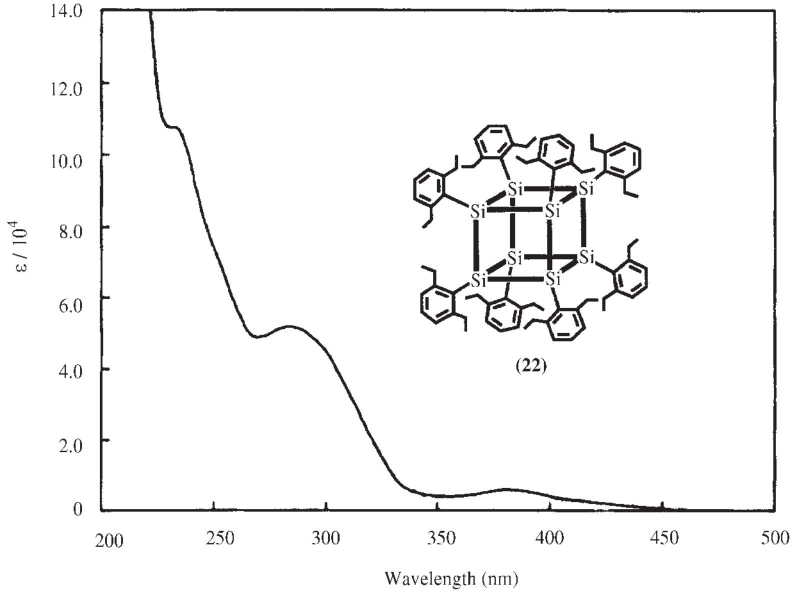

FIGURE 14. Electronic absorption spectrum of octasilacubane **22** in hexane

Despite its low oxidation potential of 0.43 V [vs saturated calomel electrode (SCE) in CH_2Cl_2], **18b** is very air-stable. Upon irradiation of **18b** in the presence of dimethyl sulphoxide with a high pressure mercury lamp, 9-oxaoctasilahomocubane **(23)** and 5,10-dioxaoctasilabishomocubane **(24)** were formed (equation 7)[53]. Without irradiation, neither **23** nor **24** was formed even at 115 °C.

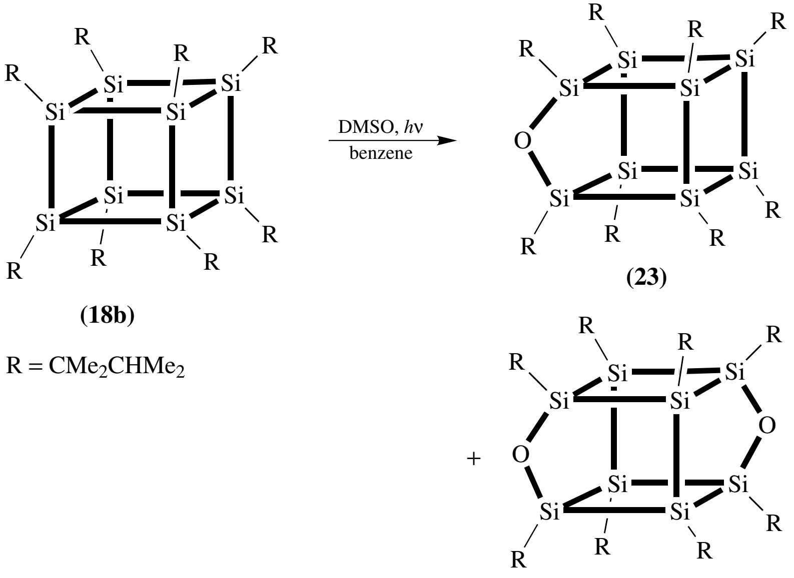

(18b)

R = CMe_2CHMe_2

(23)

(24)

(7)

The chlorination of **18b** with PCl_5 results in skeletal rearrangement to give three streoisomers of 4,8-dichlorooctakis(1,1,2-trimethylpropyl)tetracyclo[3.3.0.$0^{2,7}$.$0^{3,6}$]octasilanes **(25)** (equation 8)[54]. Three stereoisomers (*endo–exo*, *exo–exo*, *endo–endo*) were isolated in a pure form and characterized by X-ray diffractions. The mechanism by which **25** is formed is not clear, but the first step involves the electrophilic attack by PCl_5 on the strained Si−Si bond, followed by an intramolecular skeletal rearrangement. Bromo and iodo derivatives of **25** are also formed by the reactions of **18b** with Br_2 and with I_2[55].

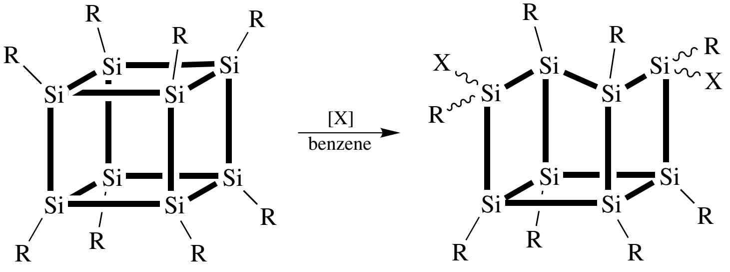

(18b)

[X] = PCl_5, Br_2, I_2

(25)

(8)

R = CMe_2CHMe_2

X = Cl, Br, I

Reductive dehalogenation of **25** with a large excess of sodium metal at 110–120 °C in toluene reverted to **18b** with formation of a reduced product **26** (equation 9)[55]. Interestingly, all of the three isomers could be used as precursors to **18b**.

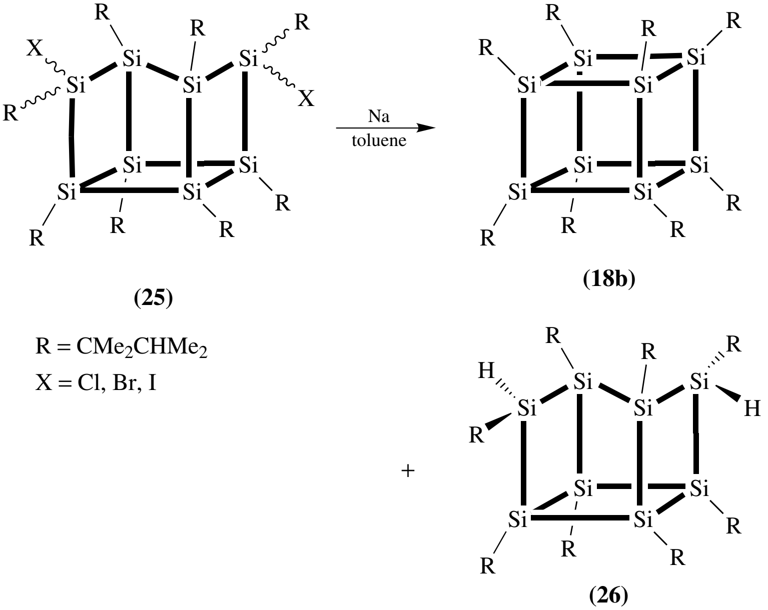

(25)

R = CMe_2CHMe_2
X = Cl, Br, I

(18b)

(26)

(9)

VII. ^{29}Si NMR SPECTRA

NMR spectroscopy is a powerful tool for structural analysis. The chemical shifts of polyhedral silicons range from −22 to 39 ppm. The ^{29}Si chemical shifts of tetrasilatetrahedrane **11**[32], hexasilaprismane **12**[37] and octasilacubanes (**16**[3], **18a**[44b], **18b**[45], **20**[46] and **22**[47]) are listed in Table 10.

^{29}Si NMR spectroscopy of **12** in solution demonstrated that the six skeletal silicons are equivalent, with a single resonance appearing at −22.3 ppm. However, cross polarization magic-angle spinning (CPMAS) ^{29}Si NMR in the solid state shows two signals at −22.2 and −30.8 ppm with relative intensity of 2 : 1[37]. Similarly, CPMAS ^{29}Si NMR of **18a**

TABLE 10. ^{29}Si NMR chemical shifts of poyhedral silicon compounds

Polyhedral silicon	^{29}Si (ppm)	Solvent
$[(t\text{-Bu})_3Si]_4Si_4$ **11**	38.89 (53.07 for $Si(t\text{-Bu})_3$)	C_6D_6
$(2,6\text{-}i\text{-Pr}_2C_6H_3)_6Si_6$ **12**	−22.3	C_6D_6
$(t\text{-BuMe}_2Si)_8Si_8$ **16**	−35.03 (5.60 for t-Bu Me_2Si)	C_6D_6
$t\text{-Bu}_8Si_8$ **18a**	13.04	o-xylene-d_{10}
$(Me_2CHCMe_2)_8Si_8$ **18b**	22.24	C_6D_6
$(2,4,6\text{-Me}_3C_6H_2)_8Si_8$ **20**	0.99	$CDCl_3$
$(2,6\text{-Et}_2C_6H_3)_8Si_8$ **22**	0.36	C_6D_6

gives two peaks at 6.6 and 10.6 ppm with relative intensity of 1 : 2[44a]. The solid state ^{29}Si NMR spectra of **12** and **18a** indicate that in distorted skeletons the silicon atoms are non-equivalent.

The static solid-state NMR can produce a broad pattern to give the three principal values of the shielding tensors for polyhedral silicons. Figures 15 and 16 show the static powder spectra of octasilacubane **22** and of the hexasilaprismane **12**, respectively[56]. The values of the σ_{11}, σ_{22} and σ_{33} tensors are given in Table 11 together with the calculated values for the methyl substituted compounds[57].

The principal axis of **22**, the least shielded principal value ($\sigma_{11} = 80$ ppm), corresponds to the diagonal of the cube in the direction parallel to the substituent. The other two axes corresponding to σ_{22} and σ_{33} are perpendicular to this axis and must have the same value. However, due to the different orientations of the 2,6-$Et_2C_6H_4$ groups, σ_{22} and σ_{23} are not equivalent. This is readily understood from the crystal structure of **22**, as shown in Figure 11. The isotropic chemical shift (σ_{iso}) of -0.3 ppm is consistent with the ^{29}Si chemical shift in solution of 0.36 ppm. The remarkable deshielding of σ_{11} is probably attributable to the paramagnetic term which is mainly caused by the low excitation energy, as depicted in Figure 14. As shown in Table 11, **22** shows an anisotropy spread ($\sigma_{11} - \sigma_{33}$) of 134 ppm. This is somewhat larger than those for ordinary cyclotetrasilanes[58].

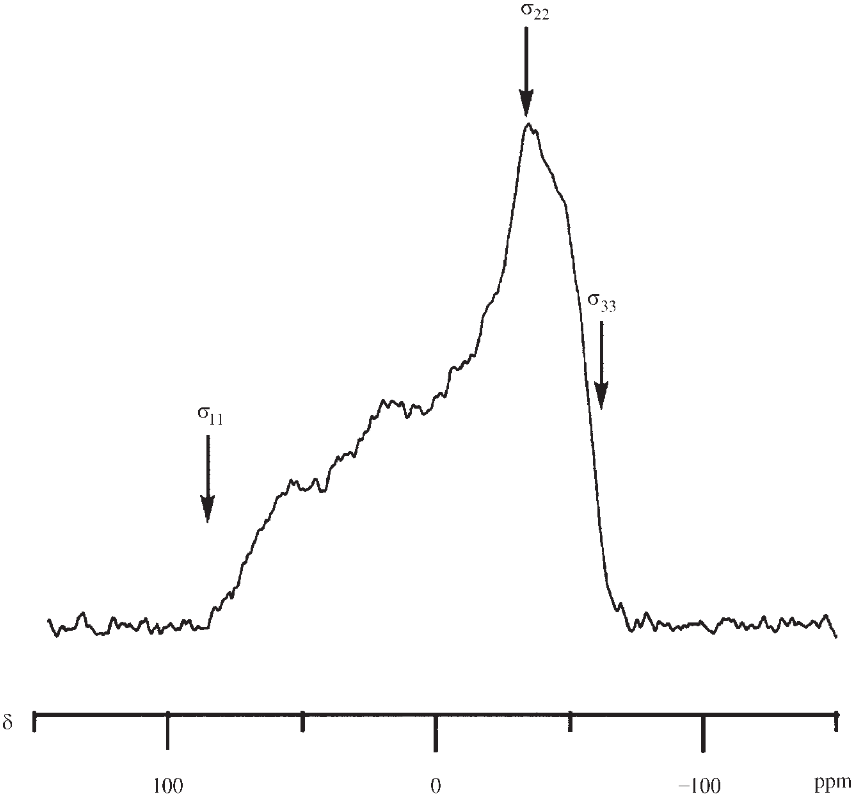

FIGURE 15. Static solid state ^{29}Si NMR spectrum of octasilacubane **22**

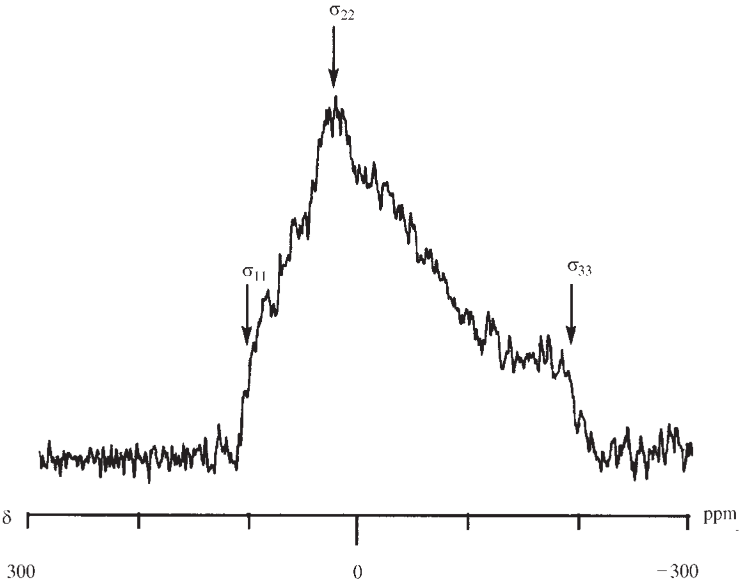

FIGURE 16. Static solid state ^{29}Si NMR spectrum of hexasilaprismane **12**

TABLE 11. Experimental and calculated principal values of shielding tensors for hexasilaprismane and octasilacubane

Tensors	$(2,6\text{-}i\text{-}Pr_2C_6H_3)_6Si_6$ **12**	Me_6Si_6 $(D_{3h})^a$	$(2,6\text{-}Et_2C_6H_3)_8Si_8$ **22**	Me_8Si_8 $(O_h)^a$
σ_{11}	98	101	80	86
σ_{22}	18	92	−27	−35
σ_{33}	−182	−221	−54	−35
σ_{iso}	−22	−29	−0.3	4.8
$\sigma_{11} - \sigma_{33}$	280	322	134	121

[a] GIAO-B3LYP calculations at B3LYP/6-31G (d) optimized geometries. The basis sets are 6-311G(3d) for Si and 6-311(d) for C and H.

In **12**, the principal axis corresponding to σ_{33}, the most shielded principal value (−182 ppm), is perpendicular to the three-membered rings. High shielding in this direction can be found in all types of cyclotrisilanes[58]. The hexasilaprismane **12** has an unprecedented spread anisotropy of 280 ppm; a high value of 322 ppm is also found theoretically for Me_6Si_6 (Table 11).

VIII. SPHERICAL CAGE COMPOUNDS

According to Figure 1, the strain energies of persila[*n*]prismanes increase highly with an increase in *n* because the bond angles in the *n*-membered rings at the top and bottom of the persila[*n*]prismanes deviates greatly from the ideal tetrahedral angle. In persila[10]prismane (**27**, $Si_{20}H_{20}$), the bond angles are as large as 144.0°. This great deviation from tetrahedral angles is reflected in the large strain energy of 252.1 kcal mol^{-1}, although this value is much smaller than that of 492.1 kcal mol^{-1} for $C_{20}H_{20}$[10,15]. For $Si_{20}H_{20}$, the less strained

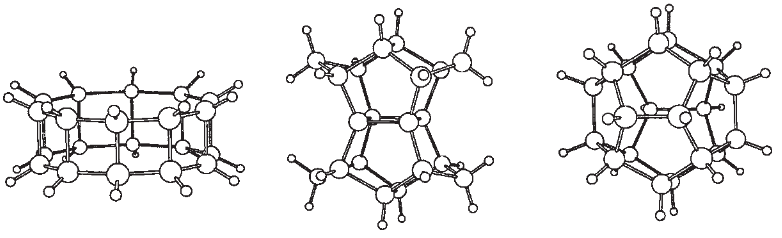

FIGURE 17. Three isomers of $Si_{20}H_{20}$ having the [10]prismane, pagodane, and dodecahedrane structures. Reprinted with permission from References 10. Copyright 1995 American Chemical Society

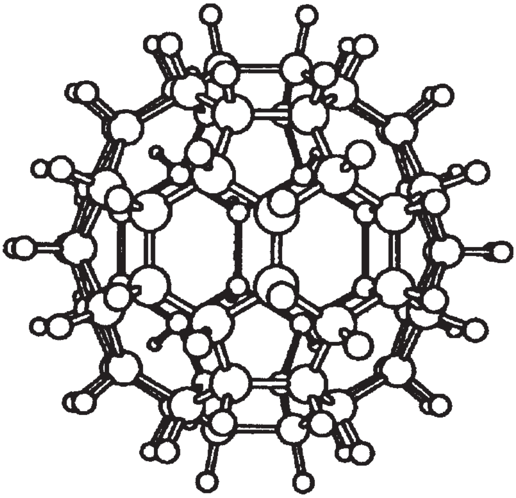

FIGURE 18. $Si_{60}H_{60}$ with I_h symmetry. Reprinted with permission from Reference 8. Copyright 1993 IUPAC

[1.1.1.1]pagodane **(28)** and dodecahedrane **(29)** structures shown in Figure 17 are 200 and 220 kcal mol^{-1} more stable than **27**[10,15]. In the I_h cage structure of **29**, skeletal silicons can form bond angles close to the ideal tetrahedral value and consequently the strain energy become as small as 32.3 kcal mol^{-1}. This is considerably smaller than the value of 43.6 kcal mol^{-1} for dodecahedrane. It may be an interesting challenge to chemists to synthesize persiladodecahedrane[10,15], as it was once to synthesize dodecahedrane[59].

In view of the great progress in the chemistry of fullerenes (spherical carbon clusters consisting of pentagonal and hexagonal rings, C_n), the silicon analogues are also interesting. It has been suggested that silicon clusters (Si_n) have a tendency to take on fullerene-like cage structures as the cluster size increases, as do carbon clusters[8,60]. The diameter (11.1 Å[60a]) of the hollow spherical cage of Si_{60} is much larger than that of C_{60} (7.1 Å[61]). In addition, the electrons of Si_{60} are more polarizable, as expected from the higher HOMO and lower LUMO levels: −6.5 and −2.1 eV for Si_{60}[60a] vs −8.0 and −0.3 eV for C_{60}[62]. The complete hydrogenation of Si_{60} leads to the saturated $Si_{60}H_{60}$ molecule, as shown in Figure 18. The strain energies of $Si_{60}H_{60}$ equal to 114 (AM1) and

207 (HF/DZ//HF/DZ) kcal mol^{-1} calculated from the homodesmotic reactions are much smaller than that of 530 (AM1) kcal mol^{-1} for $C_{60}H_{60}$. This may reflect the fact that Si_{60} is significantly less strained than C_{60}.

IX. EPILOGUE

Polyhedral silicon compounds were once thought to be synthetically inaccessible. However, this view has been drastically changed in the last few years through a close interplay of theoretical predictions and experimental tests. Many new types of polyhedral compounds including Si, Ge and Sn have been synthesized, characterized and isolated, showing novel structures and properties which are often unexpected from the carbon counterparts. These accomplishments have greatly enhanced our understanding of the bonding nature in the heavier systems.

X. ACKNOWLEDGEMENT

We thank Professors Hideki Sakurai, Robert West and Zvi Rappoport for helpful discussions and useful advise. We are also grateful to C. Kabuto, T. Yatabe, S. Doi and H. Kamatani for their experimental contributions and to K. Kobayashi, M. Nakano, T. Kudo, M. Souma and M. Nagashima for theoretical calculations. This work was supported in part by a Grant-in-Aid from the Ministry of Education, Science, Sports, and Culture of Japan.

XI. REFERENCES

1. A. Greenberg and J. F. Liebman, *Strained Organic Molecules*, Academic Press, New York, 1978.
2. A. T. Balaban, M. Banciu and V. Ciorba, *Annulenes, Benzo-, Hetero-, Homo-Derivatives, and Their Valence Isomers*, CRC Press, Florida, 1987.
3. H. Matsumoto, K. Higuchi, Y. Hoshino, H. Koike, Y. Naoi and Y. Nagai, *J. Chem. Soc., Chem. Commun.*, 1083 (1988).
4. A. Sekiguchi, C. Kabuto and H. Sakurai, *Angew. Chem., Int. Ed. Engl.*, **28**, 55 (1989).
5. S. Nagase, *Polyhedron*, **10**, 1299 (1991).
6. A. Sekiguchi and H. Sakurai, in *The Chemistry of Inorganic Ring Systems* (Ed. R. Steudel), Chap. 7, Elsevier, New York, 1992.
7. H. Sakurai and A. Sekiguchi, in *Frontiers of Organogermanium, -Tin and -Lead Chemistry.* (Eds. E. Lukevics and L. Ignatovich), Latvian Institute of Organic Synthesis, Riga, 1993.
8. S. Nagase, *Pure Appl. Chem.*, **65**, 675 (1993).
9. A. Sekiguchi and H. Sakurai, *Adv. Organomet. Chem.*, **37**, 1 (1995).
10. S. Nagase, *Acc. Chem. Res.*, **28**, 469 (1995).
11. L. R. Sita, *Acc. Chem. Res.*, **27**, 191 (1994).
12. K. B. Wiberg, *Angew. Chem., Int. Ed. Engl.*, **25**, 312 (1986).
13. S. Nagase, M. Nakano and T. Kudo, *J. Chem. Soc., Chem. Commun.*, 60 (1987).
14. S. Nagase, *Angew. Chem., Int. Ed. Engl.*, **28**, 329 (1989).
15. S. Nagase, K. Kobayashi and T. Kudo, *Main Group Metal Chem.*, **17**, 171 (1994).
16. L. R. Sita and I. Kinoshita, *J. Am. Chem. Soc.*, **113**, 1856 (1991).
17. J. P. Desclaux, *At. Data Nucl. Data Tables*, **12**, 311 (1973).
18. W. Kutzelnigg, *Angew. Chem., Int. Ed. Engl.*, **23**, 272 (1984). For a similar trend for group 15 elements, see: S. Nagase, in *The Chemistry of Organic Arsenic, Antimony and Bismuth Compounds* (Ed. S. Patai), Chap. 1, Wiley, New York, 1994.
19. D. Cremer, J. Gauss and E. J. Cremer, *J. Mol. Struct. (Theochem)*, **169**, 531 (1988).
20. For the successful synthesis of silicon–silicon double bonds, see:
    (a) R. West, *Pure Appl. Chem.*, **56**, 163 (1984).
    (b) G. Raabe and J. Michl, *Chem. Rev.*, **85**, 419 (1985).
    (c) R. West, *Angew. Chem., Int. Ed. Engl.*, **26**, 1201 (1987).

(d) G. Raabe and J. Michl, in *The Chemistry of Organic Silicon Compounds* (Eds. S. Patai and Z. Rappoport), Chap. 17, Wiley, New York, 1989.
(e) R. Okazaki and R. West, in *Adv. in Organomet. Chem.*, **39**, 232 (1996).

21. (a) S. Nagase, T. Kudo and M. Aoki, *J. Chem. Soc., Chem. Commun.*, 1121 (1985).
(b) A. Sax and R. Janoschek, *Angew. Chem., Int. Ed. Engl.*, **25**, 651 (1986).
(c) A. Sax and R. Janoschek, *Phosphorus Sulfur*, **28**, 151 (1986).
(d) S. Nagase, H. Teramae and T. Kudo, *J. Chem. Phys.*, **86**, 4513 (1987).
(e) N. Matsunaga and M. S. Gordon, *J. Am. Chem. Soc.*, **116**, 11407 (1994).
22. For a similar trend for group 15 elements, see: K. Kobayashi, H. Miura and S. Nagase, *J. Mol. Struct. (Theochem)*, **311**, 69 (1994).
23. For several experimental and calculated data, see: T. Tsumuraya, S. A. Batcheller and S. Masamune, *Angew. Chem., Int. Ed. Engl.*, **30**, 902 (1991).
24. (a) P. v. R. Schleyer, A. F. Sax, J. Kalcher and R. Janoschek, *Angew. Chem., Int. Ed. Engl.*, **26**, 364 (1987).
(b) T. Dabisch and W. W. Schoeller, *J. Chem. Soc., Chem. Commun.*, 896 (1986).
(c) W. W. Schoeller, T. Dabisch and T. Busch, *Inorg. Chem.*, **26**, 4383 (1987).
(d) S. Nagase and T. Kudo, *J. Chem. Soc., Chem. Commun.*, 54 (1988).
(e) J. A. Boatz and M. S. Gordon, *J. Phys. Chem.*, **93**, 2888 (1989).
(f) D. B. Kitchen, J. E. Jackson and L. C. Allen, *J. Am. Chem. Soc.*, **112**, 3408 (1990).
(g) J. A. Boatz and M. S. Gordon, *Organometallics*, **15**, 2118 (1996).
25. For calculations of the Ge, Sn and Pb analogues, see:
(a) S. Nagase and M. Nakano, *J. Chem. Soc., Chem. Commun.*, 1077 (1988).
(b) T. Kudo and S. Nagase, *J. Phys. Chem.*, **96**, 9189 (1992).
26. (a) S. Masamune, Y. Kabe, S. Collins, D. J. Williams and R. Jones, *J. Am. Chem. Soc.*, **107**, 5552 (1985).
(b) R. Jones, D. J. Williams, Y. Kabe and S. Masamune, *Angew. Chem., Int. Ed. Engl.*, **25**, 173 (1986).
27. (a) D. A. Clabo, Jr. and H. F. Schafer III, *J. Am. Chem. Soc.*, **108**, 4344 (1986).
(b) A. F. Sax and J. Kalcher, *J. Chem. Soc., Chem. Commun.*, 809 (1987).
(c) A. F. Sax and J. Kalcher, *J. Comput. Chem.*, **10**, 309 (1989).
28. S. Nagase and M. Nakano, *Angew. Chem., Int. Ed. Engl.*, **27**, 1081 (1988).
29. S. Nagase, K. Kobayashi and M. Nagashima, *J. Chem. Soc., Chem. Commun.*, 1302 (1992).
30. M. Kaupp and P. v. R. Schleyer, *J. Am. Chem. Soc.*, **115**, 1061 (1993).
31. (a) M. Gomberg, *Recl. Trav. Chim. Pays-Bas*, **48**, 847 (1929).
(b) M. Gomberg and W. E. Bachmann, *J. Am. Chem. Soc.*, **49**, 236 (1927).
32. (a) N. Wiberg, C. M. M. Finger and K. Polborn, *Angew. Chem., Int. Ed. Engl.*, **32**, 1054 (1993).
(b) N. Wiberg, C. M. M. Finger, H. Auer and K. Polborn, *J. Organomet. Chem.*, **521**, 377 (1996).
33. A. Sekiguchi, S. Doi and H. Sakurai, to appear.
34. S. Nagase and K. Kobayashi, to appear.
35. G. Maier, *Angew. Chem., Int. Ed. Engl.*, **27**, 309 (1988).
36. N. Wiberg, W. Hochmuth, H. Nöth, A. Appel and M. Schmidt-Amelunxen, *Angew. Chem., Int. Ed. Engl.*, **35**, 1333 (1996).
37. A. Sekiguchi, T. Yatabe, C. Kabuto and H. Sakurai, *J. Am. Chem. Soc.*, **115**, 5853 (1993).
38. S. Masamune, Y. Hanzawa, S. Murakami, T. Bally and J. F. Blount, *J. Am. Chem. Soc.*, **146**, 1150 (1982).
39. R. R. Karl, K. L. Gallaher, Y. C. Wang and S. H. Bauer, unpublished results cited in *J. Am. Chem. Soc.*, **96**, 17 (1974).
40. R. R. Karl, Y. C. Wang and S. H. Bauer, *J. Mol. Struct.*, **25**, 17 (1975).
41. A. Sekiguchi, K. Ebata, C. Kabuto and H. Sakurai, to appear.
42. S. Nagase, A. Sekiguchi, S. Doi and H. Sakurai, to appear.
43. A. Sekiguchi, T. Yatabe, S. Doi and H. Sakurai, *Phosphorus, Sulfur, and Silicon and the Related Elements*, **93 & 94**, 193 (1994).
44. (a) K. Furukawa, M. Fujino and N. Matsumoto, *Appl. Phys. Lett.*, **60**, 2744 (1992).
(b) K. Furukawa, M. Fujino and N. Matsumoto, *J. Organomet. Chem.*, **515**, 37 (1996).
(c) H. Tachibana, M. Goto, M. Matsumoto, H. Kishida and Y. Tokuda, *Appl. Phys. Lett.*, **64**, 2509 (1994). However, the crystal structure reported by Tachibana and coworker was questioned by K. Furukawa, M. Fujino and N. Matsumoto, *Appl. Phys. Lett.*, **66**, 1291 (1995).
45. H. Matsumoto, K. Higuchi, S. Kyushin and M. Goto, *Angew. Chem., Int. Ed. Engl.*, **31**, 1354 (1992).

46. A. Sekiguchi, S. Doi and H. Sakurai, to appear.
47. A. Sekiguchi, T. Yatabe, H. Kamatani, C. Kabuto and H. Sakurai, *J. Am. Chem. Soc.*, **114**, 6260 (1992).
48. K. Kobayashi and S. Nagase, to appear.
49. E. B. Fleischer, *J. Am. Chem. Soc.*, **86**, 3889 (1964).
50. L. R. Sita and I. Kinoshita, *Organometallics*, **9**, 2865 (1990).
51. K. Furukawa, H. Teramae and N. Matsumoto, *65th Annual Meeting of Japan Chemical Society*, Tokyo, March 1993, Abstract I 4F 342 (1993).
52. (a) Y. Kanemitsu, K. Suzuki, H. Uto, Y. Masumoto, T. Matsumoto, S. Kyushin, K. Higuchi and H. Matsumoto, *Appl. Phys. Lett.*, **61**, 2446 (1992).
    (b) Y. Kanemitsu, K. Suzuki, H. Uto, Y. Masumoto, K. Higuchi, S. Kyushin and H. Matsumoto, *Jpn. J. Appl. Phys.*, **32**, 408 (1993).
    (c) S. Kyushin, H. Matsumoto, Y. Kanemitsu and M. Goto, *J. Phys. Soc. Jpn.*, **63**, 46 (1994).
    (d) Y. Kanemitsu, K. Suzuki, M. Kondo, S. Kyushin and H. Matsumoto, *Phys. Rev. B*, **51**, 10666 (1995).
53. M. Unno, T. Yokota and H. Matsumoto, *J. Organomet. Chem.*, **521**, 409 (1996).
54. M. Unno, K. Higuchi, M. Ida, H. Shioyama, S. Kyushin and H. Matsumoto, *Organometallics*, **13**, 4633 (1994).
55. M. Unno, H. Shioyama, M. Ida and H. Matsumoto, *Organometallics*, **14**, 4004 (1995).
56. A. Sekiguchi, S. Doi, H. Sakurai and R. West, to appear.
57. S. Nagase, to appear.
58. (a) R. West, J. D. Cavalieri, J. Duchamp and K. W. Zilm, *Phosphorus, Sulfur, and Silicon and the Related Elements*, **93 & 94**, 213 (1994).
    (b) J. D. Cavalieri, R. West, J. C. Duchamp and K. W. Zilm, *J. Am. Chem. Soc.*, **115**, 3770 (1993).
59. L. A. Paquette, *Chem. Rev.*, **89**, 1051 (1989).
60. (a) S. Nagase and K. Kobayashi, *Chem. Phys. Lett.*, **187**, 291 (1991).
    (b) S. Nagase and K. Kobayashi, *Fullerene Sci. Technol.*, **1**, 299 (1993).
    (c) K. Kobayashi and S. Nagase, *Bull. Chem. Soc. Jpn.*, **66**, 3334 (1993).
    (d) Z. Slanina, S.-L. Lee, K. Kobayashi and S. Nagase, *J. Mol. Struct. (Theochem)*, **312**, 175 (1994).
61. K. Hedberg, L. Hedberg, D. S. Bethune, C. A. Brown, H. C. Dorn, R. D. Johnson and M. de Vries, *Science*, **254**, 410 (1991).
62. J. Cioslowski and E. D. Fleischmann, *J. Chem. Phys.*, **94**, 3730 (1991).

CHAPTER 4

Thermochemistry

ROSA BECERRA

Instituto de Quimica Fisica 'Rocasolano', CSIC, C/Serrano, 119, 28006 Madrid, Spain

and

ROBIN WALSH

Department of Chemistry, University of Reading, Whiteknights, PO Box 224, Reading RG6 6AD, UK

I. INTRODUCTION

A knowledge of molecular heats of formation and chemical bond dissociation energies has always been regarded as fundamental to the understanding of chemical structure and reactivity. This chapter deals with the extent and reliability of our knowledge of these quantities for silicon-containing compounds. The information and material presented here represent an update of an earlier review[1] in this series on the same subject. Whilst we were surveying the work published in the intervening seven years since the previous review, we were initially struck by how few experimental papers there were in this area. Indeed we even wondered whether, with the shortage of material, a review was justified. There is no doubt that the traditional science of calorimetry has virtually died out. Just a few laboratories in the world are left in this area. *Equilibrium studies* also have dropped out of fashion, in the direct sense, but if this is taken to include *kinetic studies* of matched pairs of forward and reverse processes, then the view is not so bleak. In this article, as in the previous one[1] and other reviews[2–6], we have always taken the view that thermochemistry should be inclusive of information derived from as wide a range of techniques and sources as possible. As anticipated, the impact of theoretical calculations through the development and implementation of molecular orbital theory *ab initio* methods has been substantial. Calculations of heats of formation through widespread use of computerized packages have become sufficiently routine that many experimental groups use them as a supplement to interpretation of their results. The quality of these calculations appears to have reached a point where they can seriously challenge experimental numbers in some cases (but see caveat below). Thus, in sum, there appears to be sufficient new information, including revisions of earlier results, to make this enterprise worthwhile. But if current trends continue we foresee both a benefit and a danger. The benefit is the increasing ease of calculation of once difficult-to-obtain thermochemical quantities. The danger will be the shortage of a sufficiently broad foundation of reliable experimental values with which to secure the theoretical edifice.

This chapter concentrates on results rather than the details of experimental techniques. These can be found either in the reviews[1–6] already mentioned or in original articles. Nevertheless it is worth recording that the application of oxygen-bomb calorimetry to organosilicon compounds continues to pose problems. The difficulties have been much discussed[1,7] and led to exclusion of most of the older (pre-1970) data on heats of formation[8] from earlier data compilations[7,9] (with one exception[10]). In the last decade or so the group of Voronkov has developed and exploited a method designed to overcome earlier problems of incomplete combustion, whereby the sample is initially vaporized prior to ignition. The initial results of these studies were flagged in our earlier review[1], and since then a series of seven papers has appeared covering the thermochemistry of polyalkylsilanes[11], polyalkoxysilanes[11], organylsilatranes[12], S-containing alkoxysilanes and silatranes[13], silacyclobutanes (siletanes)[14], oligocyclosiloxanes[15], silylamines[16] and cyclosilazanes[17]. These are an impressive series of studies and almost all of the data looks extremely self-consistent. The difficulty is that in some selected cases there are differences with either published data from other sources or reasonable chemical expectations (*vide infra*). This leads to the suspicion that in spite of the claims, there may still be some unassessed source of systematic error in the method. Unfortunately most of the papers do not give sufficient experimental details to enable such an evaluation. This is one of the continuing problems of data republished in western journals from largely unread Russian original sources. Data from other laboratories are relatively sparse and we reiterate that there is still a crying need for more, and reliable, experimentation in this field.

Amongst the theoretical calculations on organosilicon thermochemistry the work of Melius' group is noteworthy[18–25]. For each species a total atomization enthalpy is calculated by means of fourth-order Moller–Plesset (MP4) perturbation theory using the 6-31G** basis set at the HF/6-31G* calculated geometry. Bond additivity corrections (BAC) are then applied to these enthalpies to overcome the deficiencies of truncated wave functions and incomplete basis sets. These corrections require the use of experimental data on reference compounds. Thus the theory is not 'pure' in the sense of totally independent of experiment. Nevertheless the range of species and variety of compounds explored is impressive as is the general consistency and agreement with experiment. Melius and coworkers have studied compounds of Si/H[18,19], Si/Cl[18], Si/H/Cl[18], Si/F[20], Si/H/F[20], Si/H/N/F[21], Si/C/H[22], Si/C/Cl/H[23], Si/O/H/C[24] and Si/O/H[25].

In addition to our previous reviews of this subject, there is a recent review of theoretical investigations of the thermochemistry of organosilicon compounds[26]. An article on three methods to measure RH bond energies by Berkowitz, Ellison and Gutman[27] is a valuable up-to-date source of many bond dissociation energies and Chatgilialoglu's article[28] on structural and chemical properties of silyl radicals contains a useful discussion of silyl radical thermochemistry. In this review we have tried to concentrate on the recent work, but inevitably there is some overlap with the earlier review[1]. This is necessary to bring out a number of data comparisons. If the coverage in some parts is a little thin, due to shortage of new data, readers are urged to refer to the previous article[1]. We have structured this review similarly to the previous one for ease of back reference. As previously, all standard enthalpies of reaction or formation refer to the gas phase at 298.2 K.

II. COMPOUNDS OF TETRAVALENT SILICON

A. General Considerations, Additivity Rules and Electronegativity Correlations

It is now widely recognized that enthalpies of formation for each compound do not exist in isolation from one another. They can be judged by how well they fit into additivity schemes. Most authors of both experimental and theoretical papers recognize this. There are many additivity schemes, but most of them are variants on the same theme. We have used the laws of bond and group additivity devised by Benson and colleagues[29–31] to assess organosilicon compounds[1] and we again take this approach here.

1. Bond additivity

The law of bond additivity[29] states that for a bond redistribution (or disproportionation) reaction (these days called an isodesmic reaction) such as:

$$2\mathrm{SiX}_n\mathrm{Y}_{4-n} \rightleftharpoons \mathrm{SiX}_{n+1}\mathrm{Y}_{3-n} + \mathrm{SiX}_{n-1}\mathrm{Y}_{5-n}$$

overall thermodynamic changes (such as ΔH°) should be zero. Another way of stating this (for enthalpy changes) is to say that X- for -Y replacement enthalpies in a sequence of $\mathrm{SiX}_n\mathrm{Y}_{4-n}$ compounds should be constant. For X = Me, Y = H, i.e. the methylsilanes,

TABLE 1. Standard enthalpies of formation ($\Delta H_f{}^\circ$/kJ mol^{-1}) of fluoro- and chlorosilanes

Compound	Experiment[a]	Theory
SiH_3F	-377 ± 42	-359^b, $-358^{c,d}$
SiH_2F_2	-791 ± 33	-779^b, -780^c, -777^d
$SiHF_3$	-1200 ± 21	-1206^b, -1208^c, -1204^d
SiF_4	-1615 ± 1	
SiH_3Cl	-136 ± 10	-134^e, -134^c
SiH_2Cl_2	-315 ± 8	-310^e, -311^c
$SiHCl_3$	-499 ± 6	-489^e, -490^c
$SiCl_4$	-663 ± 5	

[a] Reference 3. [b]Reference 32. [c]Reference 20. [d]Reference 33. [e]Reference 34.

this is known to work very well[1,4]. This is not altogether surprising since the Si−C and Si−H bonds in these compounds are not very polar. A more demanding test is to examine silyl halides where X = F, Y = H or X = Cl, Y = H.

Enthalpies of formation of these compounds are listed in Table 1. Experimental values are taken from one of our earlier reviews[3]: values listed by JANAF[35] are in essential agreement (within experimental error). For the SiH_nF_{4-n} series, apart from $\Delta H_f{}^\circ$ (SiF_4), there is very little experimental information and the recommended values have been obtained by interpolation. Theoretical values are, however, all in close agreement with one another. The disproportionation enthalpies (kJ mol^{-1}) are −27 (SiH_3F), −6 (SiH_2F_2) and +16 ($SiHF_3$) based on the values of Ignacio and Schlegel[32]. Although not zero (as they would be if bond additivity were obeyed), they are relatively small and follow the same trend as for the analogous CH_nF_{4-n} series[3]. Thus the theoretical values for $\Delta H_f{}^\circ$ (SiH_nF_{4-n}) (uncertainties quoted at ± 8 kJ mol^{-1}) are certainly more reliable than experiment at the present time. For the SiH_nCl_{4-n} series, experimental and theoretical values are in reasonable agreement (except for $SiHCl_3$, see below). The disproportionation enthalpies (kJ mol^{-1}) are: for SiH_3Cl, −9.6 (expt), −8 (theory); for SiH_2Cl_2, −4.6 (expt), −1.7 (theory); for $SiHCl_3$, +21 (expt), +4 (theory). Here the values follow the same trends as for both SiH_nF_{4-n} and CH_nCl_{4-n}[31], whether experimental or theoretical values are used. Our expectation would be that the disproportionation values should be less for SiH_nCl_{4-n} than for SiH_nF_{4-n}. This seems to be the case except for $SiHCl_3$. This suggests that the experimental value for $\Delta H_f{}^\circ$ ($SiHCl_3$) may be slightly too low, although it has been determined by several groups[3]. For redistribution reactions involving other groups on silicon, we would thus expect bond additivity to work quite well, with deviations not exceeding the values just discussed.

2. Group additivity

The effectiveness of group additivity as a means to calculate unknown $\Delta H_f{}^\circ$ values depends on an extensive data base. The data base has been substantially enlarged in recent years by the work of Voronkov and coworkers[11−17a] who have shown good consistency using the Tatevsky[17b] as well as a version of Benson's additivity schemes[29]. Because we have reservations about some of the data from Voronkov's work (*vide infra*) and because there are not enough independent checks, we do not feel that substantial extension of the existing set of group contributions[1] is a worthwhile exercise. However, in the Appendix we provide a table showing the current values of the group contributions. These are slightly modified from previously[1] to provide a best fit to the data recommended in this review.

3. Enthalpy/electronegativity correlations

Starting from the classic work of Pauling[36], there have been many attempts to link quantitative measurements of bond energies (and reaction enthalpy changes) to fundamental properties of the bonded atoms, such as electronegativity. One of the most recent, by Luo and Benson[37,38], employs a new scale of electronegativity called 'unshielded core potential' or more simply 'covalent potential', V_x. In a series of papers[37–45], Luo and Benson have applied the covalent potential to the correlation of enthalpies of formation and argued that it is more successful in this exercise than other scales of electronegativity[45]. Some of these papers have been devoted to organosilicon compounds[41–44]. The correlations are generally good and have been exploited by Luo and Benson[43] to obtain new $\Delta H_f°$ values for Me_3SiF, Me_3SiNH_2 and Me_3SiSH and a revised $\Delta H_f°$ value for SiH_3I. In addition, they have suggested a revision of $\Delta H_f°$ (Si_2H_6)[44]. These claims led us to examine the correlations more closely[46]. Our conclusion is that, while this scale may be used *generally* to correlate the thermochemistry of silicon and organosilicon compounds, it has to be exercised with caution, particularly where the availability of data is very limited.

We can illustrate this with the example of the correlation of $\Delta_1 = [\Delta H_f°(SiH_3X) - \Delta H_f°(HX)]$ versus V_x. This is shown in Figure 1. The original plot of Luo and Benson[42] featured X = H, I, Br, Cl, F. We have added X = SiH_3 and CH_3. The 'best fit' line ignores the points we have added. For X = I the fit is clearly not good and this supports revision of $\Delta H_f°$ (SiH_3I). For X = SiH_3, the situation is more complicated. Luo and

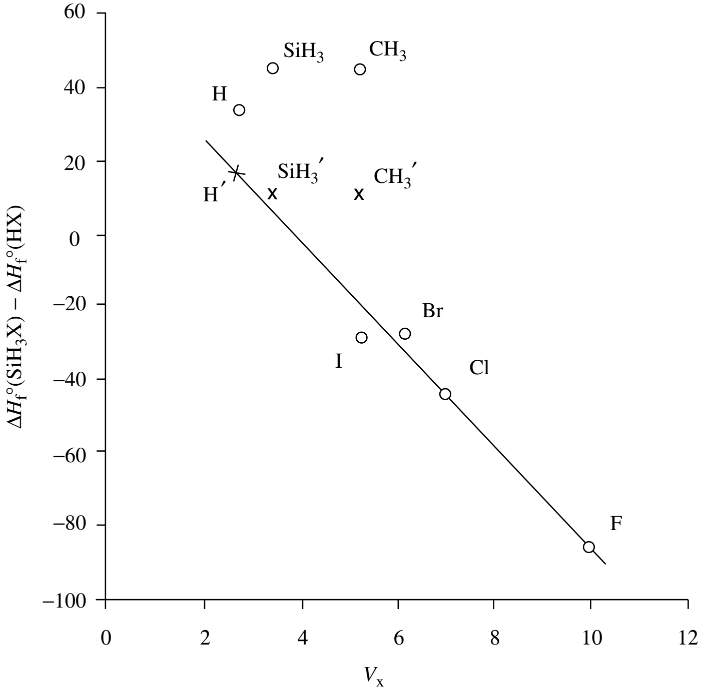

FIGURE 1. Correlation of selected $\Delta H_f°$ differences (Δ_1, kJ mol^{-1}) with covalent potential, V_x(Å^{-1}); ○, direct differences , Δ_1; ×, scaled differences, Δ_1/p (see text for definition of p). Primed substituents (H′,SiH_3',CH_3') indicate compounds with scaled differences

TABLE 2. Standard enthalpies of formation ($\Delta H_f{}^\circ$/kJ mol^{-1}) for selected silicon compounds obtained by correlations with the covalent potential

Compound	Luo and Benson[a]	Re-evaluated[b]
Me_3SiF	−572	−568
Me_3SiNH_2	−289	−291
Me_3SiSH	−269	−273
SiH_3I	+9.2	+8.6

[a] Reference 43. [b] Reference 46, see text.

Benson[39,42] argue that the true correlation test requires the use of a parameter p (= number of H atoms in the HX molecule), such that the real correlation should be between Δ_1/p and V_x, not Δ_1 and V_x. Thus $\Delta_1(X = H) = [\Delta H_f{}^\circ(SiH_4) - \Delta H_f{}^\circ(H_2)]$ is divided by 2 and $\Delta_1(X = SiH_3) = [\Delta H_f{}^\circ(Si_2H_6) - \Delta H_f{}^\circ(SiH_4)]$ is divided by 4. If the deviation of the $X = SiH_3$ point is taken as significant, then to fit perfectly requires the suggested alteration[44] in $\Delta H_f{}^\circ(Si_2H_6)$. We have added the further point $\Delta_1(X = CH_3) = [\Delta H_f{}^\circ(SiH_3CH_3) - \Delta H_f{}^\circ(CH_4)]$ and we note that (even after division by 4) the departure from the plot is significant and well beyond any experimental error. Our conclusion is thus that these correlations have to be treated with caution. There may be deep-seated factors causing them to break down for too wide a range of examples. For species of a similar kind (e.g. the halides) they seem to be all right. The revision of $\Delta H_f{}^\circ(SiH_3I)$ is supported by the correlation[43] of $\Delta_2 = [\Delta H_f{}^\circ(Me_3SiX) - \Delta H_f{}^\circ(SiH_3X)]$ versus V_x for X = I, Br, Cl and F. The values of $\Delta H_f{}^\circ$ for Me_3SiF, Me_3SiNH_2 and Me_3SiSH were obtained from the correlation[43] of $\Delta_3 = [\Delta H_f{}^\circ(Me_3SiX) - \Delta H_f{}^\circ(CH_3X)]$ versus V_x for X = I, Br, Cl and OH. For both these correlations, the examples where X = H, SiH_3 and CH_3 deviate substantially, attributed in the case of Δ_3 vs V_x[43], to p_π–d_π bonding. We have tried[46] to extend these ideas to $\Delta_4 = [\Delta H_f{}^\circ(Me_3SiX) - \Delta H_f{}^\circ(HX)]$ versus V_x and find the correlation neither so good, nor the deviations easily interpretable. Luo and Benson[44] extended the use of V_x to calculate group additivity values and enthalpies of formation for $SiMe_mH_{3-m}X$ compounds. This would be a very worthwhile exercise if the data base were more substantial, but with so few concrete values this exercise is dependent on too few reliable figures. The values obtained by Luo and Benson are shown in Table 2, together with minor revisions found by us[46] by use of slightly revised original data in the correlation plots.

B. Experimental Data and Preferred $\Delta H_f{}^\circ$ Values

1. Silicon hydrides (Si/H)

The heats of formation of silane[47], disilane[47] and trisilane[48] were determined in an explosive decomposition calorimeter by Gunn and Green in the 1960s and, apart from a small revision of the reference enthalpy of formation of amorphous silicon[35] are not thought to be in serious error. However, it is interesting to note that in the most state-of-the-art theoretical calculations yet performed on the silicon hydrides, SiH_n, Grev and Schaefer[49] have suggested the possibility of error in $\Delta H_f{}^\circ(SiH_4)$. Specifically they have calculated the atomization enthalpy of SiH_4 to be *ca* 6.2 kJ mol^{-1} higher than experiment[35]. Thus the difference $\Delta H_f{}^\circ(Si) - \Delta H_f{}^\circ(SiH_4)$ needs to be raised to match the theory. The combined experimental uncertainties of these quantities is ±8.2 kJ mol^{-1} and so the discrepancy is within experimental error. Nevertheless, this points to the fact that

TABLE 3. Standard enthalpies of formation ($\Delta H_\mathrm{f}^\circ$/kJ mol^{-1}) of silanes

Compound	$\Delta H_\mathrm{f}^\circ$[a]
SiH_4	34.3 ± 1.2
Si_2H_6	80 ± 1.5
Si_3H_8	121 ± 4.4

[a] Reference 1.

refinement of uncertainties in $\Delta H_\mathrm{f}^\circ(SiH_4)$ and $\Delta H_\mathrm{f}^\circ(Si)$ would be a worthwhile experimental exercise. The current values for SiH_4, Si_2H_6 and Si_3H_8 are shown in Table 3. They form a consistent set and are reasonably matched by the theoretical calculations of Ho and coworkers[19], Sax and Kalcher[50] and Leroy and coworkers[51]. As mentioned already Luo and Benson[44] have questioned the value of $\Delta H_\mathrm{f}^\circ(Si_2H_6)$ in Table 3 and suggested instead a figure less than 64.9 kJ mol^{-1} based on empirical correlations. There is no other evidence in favour of this figure, and it is clearly inconsistent with the other silicon hydrides.

2. Alkyl and related organosilanes (Si/C/H)

There are no new experimental data for the methylsilanes since the earlier review[1]. The original data are listed in Table 4. It is worth re-emphasizing that the listed values are

TABLE 4. Standard enthalpies of formation ($\Delta H_\mathrm{f}^\circ$/kJ mol^{-1}) of methyl, ethyl and propyl silanes

Compound	Experiment	Additivity[b,c,d]	*Ab initio*
SiH_4	34.3 ± 2.0[a]		
$MeSiH_3$	−29.1 ± 4.0[b]	−29.1[i]	−28.5[j], −30.5[k], −26.8[l]
Me_2SiH_2	−94.7 ± 4.0[b]	−94.7[i]	−94.6[j], −97.1[k], −96.2[l]
Me_3SiH	−163.4 ± 4.0[b]	−163.4[i]	−163.6[j], −164.8[k]
Me_4Si	−233.2 ± 3.2[e] −229 ± 3.0[f]	−233.2[i]	
$EtSiH_3$	−143[g]	−46.1[c]	−37.7[c], −34.3[l]
$PrSiH_3$		−66.8[c]	−61.5[c]
$EtSiH_2Me$		−111.7[c]	−106.3[c]
Et_2SiH_2	−182 ± 6[h]	−128.7[c]	−117.2[c]
i-$PrSiH_3$		−73.3	−59.0[l]
t-$BuSiH_3$			−86.6[l]
Et_3SiH	−201 ± 15[h] −217.5 ± 5[f]	214.4	
Pr_3SiH	−280 ± 6[f]	−276.5	
$MeSiHEt_2$	−200 ± 5[f]	−197.4	
$MeSiHPr_2$	−240 ± 6[f]	−238.8	
$MeSiHPr$-i_2	−255 ± 6[f]	−251.8[i]	
$EtSiHPr_2$	−259 ± 6[f]	−255.8	
$EtSiHPr$-i_2	−270 ± 6[f]	−268.8[i]	

[a] Reference 35. [b] Reference 4. [c] Reference 52. [d] Reference 1. [e] Reference 53. [f] Reference 11. [g] Reference 54. [h] Reference 9. [i] Used to fix additivity groups. [j] Reference 26. [k] Reference 22. [l] Reference 51.

related to, and therefore dependent upon, Steele's value[53] for $\Delta H_f°(Me_4Si)$ of −233.2 ± 3.2 kJ mol^{-1}. This is supported by a more recent value from Voronkov and coworkers[11] of −229 ± 3 kJ mol^{-1}, virtually within experimental error. Theoretical calculations using isodesmic reactions[26] and BAC-MP4 calculations by Allendorf and Melius[22] are in essential agreement, although just as with the experimental data for $MeSiH_3$, Me_2SiH_2 and Me_3SiH, they are pinned to the value for $\Delta H_f°(Me_4Si)$. Semi-empirical[55] and empirical correlations[44] are also in reasonable agreement.

For higher alkylsilanes there have been recent combustion measurements by Voronkov and coworkers[11] of a variety of trialkyl and tetraalkylsilanes. These are shown in Tables 4 and 5. Included also are some of the older data listed in earlier compilations[54]. We have pointed out in the previous review[1] and elsewhere[52] the unreliability of these data on ethylsilanes on the basis of lack of fit to additivity rules[1] and also to *ab initio* values combined with homodesmic reactions. The data of Voronkov are truly astonishing. Tables 4 and 5 include only organosilane molecules with alkyl groups up to C_3. This publication[11] contains 30 triorganyl and 14 tetraorganyl silanes. Within the cited data the fits to group additivity[1] show very small deviations. Indeed, if the $Si-(C)_3(H)$ group value were lowered by 2.6 kJ mol^{-1} and the $Si-(C)_4$ group value raised by 4 kJ mol^{-1} all compounds would fit to better than ±2 kJ mol^{-1} (see Table 27 in the Appendix for group values). Within the *total* data set, almost none of the evaluated experimental enthalpies of atomization deviates by more than 2 kJ mol^{-1} from values calculated on the authors' own additivity scheme (similar to groups increments). It is somewhat frustrating that the authors do not provide more details in their papers. The authors have seemingly republished their results in the *Journal of Organometallic Chemistry* after the original publications in *Izvestiya Akademii Nauk SSSR*[56]. The data, however, are not *identical* between the two publications (see Table 5), and many more compounds appear in the second publication. What is a pity is that there is no reference to the earlier publication[56] in the second[11], nor any mention of the changes (albeit small) in the values listed or error limits obtained. The biggest change (+7 kJ mol^{-1}) in Table 5 is the value for $\Delta H_f°(Pr_3SiMe)$. This value was the one previously furthest out of line with the authors' additivity scheme.

Apart from the importance of the individual data, increments which reveal aspects of bonding are particularly significant. We previously[1] emphasized the importance of the methyl to ethyl increment of −17 kJ mol^{-1}, which was based on an earlier analysis[4] of electronegativity trends and found to be consistent with the data of Voronkov and coworkers[11,56]. Luo and Benson[44,41] suggest −13 kJ mol^{-1} from their own analysis on

TABLE 5. Standard enthalpies of formation ($\Delta H_f°$/kJ mol^{-1}) of tetraalkylsilanes

Compound	Voronkov and coworkers[a]	Voronkov and coworkers[b]	Additivity[c]
Me_4Si	−230 ± 6	−229 ± 3	−233
Et_2SiMe_2	−264 ± 6	−263 ± 5	−267
Et_3SiMe	−287 ± 5	−281 ± 5	−284
Et_4Si	−297 ± 6	−297 ± 5	−301
Pr_2SiMe_2	−305 ± 7	−306 ± 5	−309
Pr_3SiMe	−350 ± 7	−343 ± 5	−346
$PrSiEt_3$		−319 ± 6	−322
Pr_2SiEt_2	−342 ± 6	−341 ± 5	−343
Pr_3SiEt		−360 ± 6	−363
Pr_4Si	−379 ± 6	−378 ± 5	−384

[a] Reference 56. [b] Reference 11. [c] Reference 1.

metal alkyl enthalpies of formation. An even less negative value of −5.4 (±10.5) kJ mol^{-1} has been recently suggested by Jardine and coworkers[57]. The *ab initio* calculations of Boatz, Gordon and Walsh[52] give −8.8 kJ mol^{-1} for this quantity and those of Leroy and coworkers[51] −7.5 kJ mol^{-1}. To be able to use the additivity rules with confidence there is a considerable need to confirm the value of this quantity, which corresponds to the group value C−(Si)(C)(H)$_2$. Another group which comes from fitting the Voronkov data is C−(Si)(C)$_2$(H) which has the value −4.2 kJ mol^{-1}, but for which Luo and Benson[44] recommend +7.1 kJ mol^{-1}. The theoretical work of Leroy and coworkers[51] implies +12.9 kJ mol^{-1}.

We have commented previously[1] on $\Delta H_f^\circ(\mathrm{Me_3SiC_2H_3})$ and $\Delta H_f^\circ(\mathrm{(C_2H_3)_4Si})$, determined by Voronkov and coworkers[11,56]. The interest here concerns whether there is any thermochemical evidence for a $d_\pi - p_\pi$ type interaction between the Si atom and the π-bond of the vinyl group. The combustion values for these compounds suggest that it should be *ca* 65 kJ mol^{-1} per vinyl group which we previously questioned[1]. Our argument was based on enthalpies of hydrogenation. There are no new thermochemical data on these compounds since the last review[1]. However, two sets of theoretical calculations by Allendorf and Melius[22], and Ketvirtis and coworkers[58] bear on this question. The relevant data are shown in Table 6. This shows that there is relatively little difference between estimates based on enthalpies of hydrogenation (or isodesmic reactions) and the *ab initio* calculations for the model compounds, vinyl- and ethynylsilane. Thus it would be surprising if the experimental thermochemical data were correct here. Electron diffraction studies of $\mathrm{Me_3SiC_2H_3}$[63] reveal no structural (or geometrical) evidence of any special interaction. It is also worth adding that there is no evidence for any strong π-type interaction between the phenyl ring and the Si atom in tetraphenylsilane[1].

One very useful experimental number to have been obtained recently is that for $\Delta H_f^\circ(\mathrm{Me_3SiSiMe_3}) = 303.7 \pm 5.5$ kJ mol^{-1} by reaction solution calorimetry[64]. This involved measuring ΔH° for the reaction $\mathrm{Br_2 + Me_3SiSiMe_3 \rightarrow 2Me_3SiBr}$. The reaction stoichiometry was verified and the calorimetry carried out under conditions with each reagent independently in excess, and furthermore $\Delta H_f^\circ(\mathrm{Me_3SiBr})$ was checked by measurement of the hydrolysis enthalpy of $\mathrm{Me_3SiBr}$ [to give $\mathrm{(Me_3Si)_2O}$] which was in agreement with the literature value. It is gratifying to see this important quantity now reliably established, after our plea in the previous review[1]. This compound provides one of the reference points in bond dissociation energy discussions and also for establishing silylene thermochemistry. Prior to this measurement, values for $\Delta H_f^\circ(\mathrm{Me_3SiSiMe_3})$ ranged from −295 to −359 kJ mol^{-1}. One of us[65] was responsible for one of the less accurate earlier values (−347 kJ mol^{-1}), while the better estimates, from kinetic

TABLE 6. Standard enthalpies of formation (ΔH_f°/kJ mol^{-1}) of vinyl and ethynyl substituted silanes

Compound	Experiment[a]	Additivity[b]	*Ab initio*
$\mathrm{(C_2H_3)_4Si}$	-81.6 ± 6.8	+199	
$\mathrm{Me_3SiC_2H_3}$	-190 ± 5	−125	
$\mathrm{H_2C{=}CHSiH_3}$		79 ± 6[c]	86.6 ± 4.2[e] 84.5[f], 108 ± 15[g]
$\mathrm{HC{\equiv}CSiH_3}$		243 ± 8[d]	221.8 ± 4.6[e] 215[f], 253 ± 13[h]

[a] References 11 and 56. [b] Based on ΔH° (hydrogenation) and isodesmic reactions. [c] Reference 59. [d] Reference 60. [e] Reference 22. [f] Reference 58. [g] Reference 61. [h] Reference 62.

TABLE 7. Standard enthalpies of formation ($\Delta H_f{}^\circ$/kJ mol^{-1}) of methyl substituted disilanes

Compound	Experiment[a]	Allen scheme[a]	Kinetics[b]	*Ab initio*[c]
Si_2H_6	80.3 ± 1.5	80.3		
MeH_2SiSiH_3		18.4	20.9	18.0
$Me_2HSiSiH_3$		−45.8	−46.0	−48.5
MeH_2SiSiH_2Me		−43.6	−37.7	−43.9
Me_3SiSiH_3		−111.8	−112.5	−116.3
$Me_2HSiSiH_2Me$		−107.7	−104.2	−110.0
Me_3SiSiH_2Me		−173.7	−172.8	−176.6
$Me_2HSiSiHMe_2$		−171.8	−171.1	−174.9
$Me_3SiSiHMe_2$		−237.9	−240.6	−244.8
$Me_3SiSiMe_3$	−303.7 ± 5.5	−303.9	−313.8	−313.8

[a]Reference 64. [b]Reference 55. [c]Reference 66.

studies, were provided by O'Neal and coworkers[55]. The details of the discussion of $\Delta H_f{}^\circ(Me_3SiSiMe_3)$ may be found in the original references[1,55,64,65] and are not reproduced here (they may provide aficionados with some entertainment on the subject of how scientists try to cope in the absence of concrete information!). The values have been used to derive $\Delta H_f{}^\circ$ values for the partially methylated disilanes. These values are reproduced in Table 7 together with the theoretical (*ab initio*) values of Boatz and Gordon[66]. Other theoretical values[51] for some of these disilanes are less accurate.

The situation for strained silicon-containing ring compounds has become if anything, more confusing since the previous review[1]. The only new experimental data, are those for a series of siletanes[14] (silacyclobutanes), shown in Table 8. From these, strain enthalpies in the range of 109–120 kJ mol^{-1} can be calculated. These are slightly larger than an

TABLE 8. Standard enthalpies of formation ($\Delta H_f{}^\circ$/kJ mol^{-1}) of some siletanes and their strain enthalpies

Compound	Experiment[a]	Strain enthalpy[b]
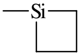	−23.0	109.4
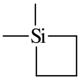	−85.0	117.2
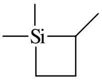	−110.0	122.2
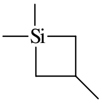	−113.0	119.2
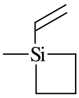	−8.0	—

[a]Reference 14. [b]Based on Group Additivity; see Table 27 and Reference 31.

TABLE 9. Standard enthalpies of formation (ΔH_f°/kJ mol^{-1}) and strain enthalpies (kJ mol^{-1}) of some silacycloalkanes[a] and their 1,1-dimethyl derivatives

Compound	ΔH_f°	Strain enthalpy	ΔH_f° (1,1-dimethyl compound)	
			additivity	experiment
Siletane	39	103	−99	−108.7 ± 6[b] −138 ± 11[c] −82.8 ± 5.9[d] −85.0[e]
Silacyclopentane	−66	19	−204	−182 ± 12[b]
Silacyclohexane	−88	17	−227	

[a] For silirane see Table 10. [b] Reference 68. [c] Reference 9. [d] Reference 69. [e] Reference 14.

ab initio estimate (at the MP2/6-31G* //3-21G* level) by Gordon and coworkers[52,67] of 103 kJ mol^{-1}, and also those corresponding to a number of other experimentally based ΔH_f° values shown in Table 9. For 1,1-dimethylsiletane, the experimental values for ΔH_f° correspond to strain enthalpies in the range 64–120 kJ mol^{-1}. The most recent analyses[70,71] of the kinetics of the thermal decomposition of this compound require a value of the strain enthalpy of 92 ± 12 kJ mol^{-1} corresponding to a ΔH_f° value of −110 ± 12 kJ mol^{-1}. For this reason we are still inclined to prefer Steele's (unpublished) value[68] of −108.7 ± 6 kJ mol^{-1}.

The need for thermochemistry for the three membered rings, silirane and silirene, is also driven, in part, by the desire to understand the complexities of gas-phase kinetics, in this case of addition reactions of SiH_2 with C_2H_4[59] and C_2H_2[60] (these reactions are more experimentally accessible than the reverse reactions of the thermal decompositions of silirane and silirene). Theoretical modelling of the pressure dependencies of rate constants has been used to obtain approximate (±12 kJ mol^{-1}) estimates of ΔH_f° values for these rings. These values are very consistent with those of the *ab initio* calculations of Gordon and coworkers[52,67,72] shown in Table 10. These values correspond to ring strain enthalpies of *ca* 167 kJ mol^{-1} (silirane) and 207 kJ mol^{-1} (silirene).

It has long been assumed that ring strain enthalpies are functions of the ring alone and independent of substituents. However, recent evidence suggests that for methyl-substituted siliranes this may not be so. Berry[74] has found that hexamethylsilirane has a strain enthalpy of *ca* 237 kJ mol^{-1} from a study of the kinetics of its decomposition: studies in our labs[75] also suggest increased ring strain in 2-methyl, 2,2-dimethyl and 1,1-dimethyl siliranes, compared with silirane itself.

TABLE 10. Standard enthalpies of formation (ΔH_f°/kJ mol^{-1}) of three-membered silicon heterocycles

Compound	*Ab initio*	Experiment
Silirane	126[a] 144[b] 153 ± 6[c]	124 ± 12[f]
Silirene	289[d], 302[e]	289 ± 12[g]

[a] References 52 and 67. [b] Reference 73. [c] Reference 61. [d] Reference 72. [e] Reference 62. [f] Reference 59. [g] Reference 60.

TABLE 11. Standard enthalpies of formation ($\Delta H_f{}^\circ$/kJ mol^{-1}) of methylchlorosilanes and methyl (hydrido) chlorosilanes

Compound	Recommended[a]	Gadzhiev + Agarunov[b]	*Ab initio*[c]
Me_3SiCl	-354 ± 3	-354 ± 3	-361 ± 4
Me_2SiCl_2	-466 ± 10	-464 ± 2	-476 ± 4
$MeSiCl_3$	-569 ± 11	-585 ± 4	-577 ± 4
$MeSiH_2Cl$	-210 ± 7	—	-210 ± 4
$MeSiHCl_2$	-393 ± 9	-414 ± 3	-394 ± 4
Me_2SiHCl	-282 ± 3	-305 ± 3	-285 ± 4

[a]Reference 1. [b]Reference 76. [c]Reference 23.

3. Halogen-containing organosilanes (Si/C/H/X)

There are virtually no new experimental data on this class of compounds. Earlier experimental data were discussed in detail in the previous review[1]. The only new information is the BAC-MP4 calculated data of Allendorf and Melius[23] for the chloromethylsilanes. These are compared with our earlier recommended values[1] in Table 11, which shows agreement within the stated uncertainties.

A new enthalpy of hydrolysis measurement[64] gives $\Delta H_f{}^\circ$ (Me_3SiBr) $= -298 \pm 4$ kJ mol^{-1}, which differs very little from the previous value[9,77] of -293 ± 4 kJ mol^{-1}. However we recommend the new value because it is slightly more consistent with the relative thermochemistry of ion breakdown from Me_3SiBr and Me_4Si[1,78]. This small change also implies modification[79] of $\Delta H_f{}^\circ$ (Me_3SiI). The revised value is -222 ± 4 kJ mol^{-1}, compared to -217 ± 4 kJ mol^{-1} previously[1].

4. Oxygen-containing compounds (Si/C/H/O)

This review is concerned with organosilanes and therefore purely inorganic Si/O/H species are not considered. Nevertheless, because of the importance of silane oxidation and of oxidized silicon coatings there is considerable interest and activity in this area. Four theoretical papers[25,80–82] have been published concerning stabilities of the potentially important molecules in these processes. Needless to say there are very few experimental data in the area under consideration.

There have been two experimental studies by Voronkov and colleagues[11,15], another by van der Vis and coworkers[83,84], and some theoretical calculations by Ho and Melius[24]. Previously we noted[1] (as with Si/C/H compounds reviewed here) the consistency of the Voronkov data from combustion calorimetry of silyl alkyl ethers. Once again the newer publication[11] gives figures which are slightly different from the old (without comment). The consistency is just as good. The authors[11] claim to check the reliability of their procedure using hexamethyldisiloxane, $(Me_3Si)_2O$, for which several independent determinations exist, but the data are missing from the new publication[11], although present in the old[56]. However, there is now an independent check possible on the compound tetraethoxysilane (commonly called TEOS) investigated by van der Vis and Cordfunke[83] by means of calorimetric measurements on the aqueous solution reaction:

$$Si(OEt)_4 + 6HF \longrightarrow H_2SiF_6 + 4EtOH$$

The data are shown in Table 12. This latter study obtained a value some 41 kJ mol^{-1} lower than the combustion value[11], well outside the quoted error limits of both studies.

TABLE 12. Standard enthalpies of formation ($\Delta H_f{}^\circ$/kJ mol^{-1}) of O-containing organosilanes

Compound	Experimental	BAC-MP4(MP2)[a]
Me_3SiOH	-500 ± 3^b	-500
$(Me_3Si)_2O$	-777 ± 6^c	$(-785)^g$
$Si(OMe)_4$	-1180 ± 5^d	-1190
$Si(OEt)_4$	-1315 ± 6^d, -1356 ± 6^e	-1328
$HSi(OEt)_3$	-912 ± 8^f	-975

[a] Reference 24. [b] References 7 and 9. [c] References 1 and 7. [d] Reference 11. [e] References 83 and 84. [f] Reference 10. [g] Estimated in Reference 24.

It is instructive to compare the implications of each value for the other's measurements. If the combustion value is correct, it implies that the ΔH_f° value for the aqueous solution reaction is -245.9 kJ mol^{-1} instead of -200.1 kJ mol^{-1} as measured, an error of *ca* 23%, well outside the quoted ±0.7%. If the -245.9 kJ mol^{-1} value is correct, then ΔH_f° (combustion) $= -5538$ kJ mol^{-1} instead of -5583 kJ mol^{-1} as measured, an error of 0.8% compared to the quoted ±0.07%. To the impartial assessor, the second scenario seems more likely than the first. A more detailed discussion of potential sources of uncertainty is contained in the paper of van der Vis and Cordfunke[83], which also lists earlier measurements. The BAC-MP4 calculation[24], while nearer to combustion value, is probably not definitive, since there are too few reliable reference compounds on which to base the Bond Additivity corrections.

The consequences of this are to undermine confidence in the previous analysis[1] of the thermochemistry of siloxanes and alkyl silyl ethers. Thus another study by Voronkov and coworkers[15] of perorganyloligocyclosiloxanes is therefore not easy to assess. This consists of combustion of 12 cyclosiloxanes with various differing ring sizes and substituents (methyl or phenyl groups). We may illustrate these data with hexamethylcyclotrisiloxane, c-$(Me_2SiO)_3$, for which $\Delta H_f{}^\circ = -1568$ kJ mol^{-1} in the gas phase has been obtained. According to the author's own additivity scheme this compound has a ring strain enthalpy of 80 kJ mol^{-1}. Our own estimate, based on our earlier group additivity scheme[1], is 108 kJ mol^{-1}. Since these figures depend on groups derived from the silylalkyl ethers, there must be a question as to their validity. The data for the three simple permethylated cyclic siloxanes (sometimes known as D_3 , D_4 and D_5) are shown in Table 13. Other lower estimates are obtained for the strain enthalpies if the van der Vis and coworkers value[83,84] for $\Delta H_f{}^\circ$ (TEOS) is used as the basis of an additivity scheme (see Appendix). Whatever the values of these strain enthalpies it seems that they decrease in magnitude with increasing ring size.

TABLE 13. Standard enthalpies of formation ($\Delta H_f{}^\circ$/kJ mol^{-1}) and strain enthalpies (kJ mol^{-1}) of selected permethylcyclosiloxanes

Compound	$\Delta H_f^{\circ a}$	Strain enthalpy		
		Voronkov[a]	additivity[b,c]	
c-$(Me_2SiO)_3$	-1568 ± 11	80	108^b	65^c
c-$(Me_2SiO)_4$	-2138 ± 11	60	97^b	40^c
c-$(Me_2SiO)_5$	-2708 ± 13	40	86^b	14^c

[a] Reference 15. [b] Reference 1. [c] This review (see text).

TABLE 14. Standard enthalpies of formation ($\Delta H_f{}^\circ$/kJ mol^{-1}) of methylsilylamines

Compound	Baldwin and coworkers[77]	Voronkov and coworkers[16]
$Me_3SiNHMe$	−227 ± 4	−238 ± 7
Me_3SiNMe_2	−248 ± 4	−246 ± 8
$(Me_3Si)_2NH$	−477 ± 5	−451 ± 10
$(Me_3Si)_2NMe$	−449 ± 8	−456 ± 10
$(Me_3Si)_3N$	−671 ± 12	−656 ± 11

5. Nitrogen-containing compounds (Si/C/H/N)

Only organo silylamines are considered here. There are again new combustion data from Voronkov and coworkers[16]. These may be compared with those previously obtained by Pedley's group[25] using solution calorimetry, as shown in Table 14. Only a selection of Voronkov and coworkers' data[16] is shown. There is some agreement here (within experimental error), although not in all cases. Previously[1] we evaluated group redistribution energies for these compounds and noted the variations. With Voronkov's data the variations are less. However, in view of the smaller enthalpy changes associated with solution calorimetry compared to combustion (as discussed in the previous section), it would be rash to prefer the combustion values. A deficiency in Voronkov's paper[16] is the failure to specify the final oxidized form of nitrogen in the combustion calorimetry.

Because of previously[1] and presently expressed doubts about earlier work[10,56] we do not discuss $\Delta H_f{}^\circ$ values for other nitrogen containing compounds[12]. There are as yet no theoretical calculations for this class of compounds, although the purely inorganic silyl amines(Si/N/H system) have been investigated by Melius and Ho[21].

6. Other organosilicon compounds

Amongst Si/C/H/S compounds only Me_3SiSBu has been studied[77] ($\Delta H_f{}^\circ = -381 \pm 3$ kJ mol^{-1}). However, Voronkov and coworkers[13] have investigated a series of (organylthioalkyl) trialkoxysilanes and 1-(organylthioalkyl) silatranes, viz compounds in the Si/C/H/S/O and Si/C/H/S/O/N classes. In view of the complexity of these molecules and the lack of comparisons with any related substances, these results are not reviewed here.

III. FREE RADICALS AND BOND DISSOCIATION ENTHALPIES

A. General Comments

Since our last review of values of Si−H bond dissociation energies[1] there have been small but significant changes in values. This has come about because of the experimental removal of one of the assumptions underlying earlier values[2,5]. The basis of determination of these values was the study of the kinetics of the reversible reaction:

$$X + RH \underset{r}{\overset{f}{\rightleftarrows}} R + HX$$

where X was usually I, an iodine atom. For this reaction we may write the exact enthalpic equation

$$DH^\circ(R{-}H) = DH^\circ(H{-}X) + E_f - E_r$$

where E_f and E_r represent forward and reverse activation energies; E_f was measured experimentally[2], but E_r was only estimated to lie in the range 4–8 kJ mol^{-1}. From measurements with carbon-centred (i.e. alkyl) radicals[85] it has emerged that E_r has small but negative values for many radicals, R, with both HI[85] and HBr[86,87] (X = I, Br). This is also true of silicon centred radicals, although thus far only R = SiH_3, and $SiMe_3$ have been investigated fully[88,89]. Because chemical bond energies are one of the most fundamental quantities of chemistry, this problem has been widely discussed in the literature in the past six years[5,6,27,28,90], and so no further general discussion is given here. However, this does imply that all Si−H bond dissociation energies previously listed[1] require an increase in value, and also that $\Delta H_f{}^\circ$ values for radicals are also higher. As a consequence, previously derived bond dissociation energies evaluated from thermochemical cycles[1] also need revision.This is carried out in this review.

B. Experimental Data: Measured Dissociation Energies and Radical Enthalpies of Formation

Table 15 shows the new values of bond dissociation energies and radical enthalpies of formation derived using the relationship

$$\Delta H_f{}^\circ(\mathrm{R}^\bullet) = \Delta H_f{}^\circ(\mathrm{RH}) - \Delta H_f{}^\circ(\mathrm{H}^\bullet) + D(\mathrm{R{-}H})$$

where $\Delta H_f{}^\circ$(RH) values used are those recommended in this review . For comparison, the earlier values[1] of D(R−H) are also included in Table 15. The value listed for $\Delta H_f{}^\circ$ (SiH_3) is that of Seetula and coworkers[88], which is the most precise, although other recent experimental determinations exist[95]. Numerous theoretical calculations[6,20,22,32,49,50,96–98] are well within the experimental error of the listed value. The values listed for $\Delta H_f{}^\circ$ ($Me_3Si^\bullet$)[89,92] indicate a substantial increase (18 kJ mol^{-1}) over that found previously[1]. The increased value of D(Me_3Si−H) implies an activation energy for the reaction of Me_3Si + HI of -12 kJ mol^{-1}, a value more negative than that for any radical + HI reaction yet studied. The values are, however, consistent with theoretical estimates by Marshall[90,99] and also by Allendorf and Melius[22] who obtained $\Delta H_f{}^\circ(MeSiH_2{}^\bullet) = 138 \pm 4$ kJ mol^{-1}, $\Delta H_f{}^\circ(Me_2SiH^\bullet) = 77 \pm 4$ kJ mol^{-1} and $\Delta H_f^\circ(Me_3Si^\bullet) = 13 \pm 4$ kJ mol^{-1} using the BAC-MP4 method. In addition to the new measured values, we may reasonably assume that the other, as yet uninvestigated, radical + HI reactions will all have negative activation energies. Using estimated values we have obtained revised values for other

TABLE 15. Measured Si−H bond dissociation energies for silanes (kJ mol^{-1}) and derived enthalpies of associated radicals ($\Delta H_f{}^\circ$/kJ mol^{-1})

Bond	D(old)[a]	D(new)	$\Delta H_f{}^\circ(\mathrm{R}^\bullet)$[i]
$H_3Si{-}H$	378 ± 5	384 ± 2[b]	200.5 ± 2
$MeSiH_2{-}H$	375 ± 8	388 ± 5[c]	141 ± 6
$Me_2SiH{-}H$	374 ± 8	391 ± 5[c]	78 ± 6
$Me_3Si{-}H$	378 ± 5	397 ± 2[d], 395 ± 9[e]	15 ± 7
$H_3SiSiH_2{-}H$	361 ± 8	372 ± 5[f], 374[g]	234 ± 6
$C_6H_5SiH_2{-}H$	369 ± 5	(382 ± 5)[h]	(ca 274)[j]
$Me_3SiCH_2{-}H$	415 ± 5	(419 ± 5)[h]	(−32 ± 6)
$Me_3SiCMe_2CH_2{-}H$	405 ± 5	(409 ± 5)[h]	(ca −121)[j]
$Cl_3Si{-}H$	382 ± 5	(395 ± 5)[h]	(−322 ± 8)
$F_3Si{-}H$	419 ± 5	(432 ± 5)[h]	(−987 ± 20)

[a] Reference 1. [b] Reference 88. [c] Reference 91. [d] Reference 89. [e] Reference 92. [f] Reference 93. [g] Reference 94. [h] Based on revised assumptions (see text) [i] Calculated using $\Delta H_f{}^\circ$(RH) from this review. [j] Based on bond additivity estimate for $\Delta H_f{}^\circ$(RH).

bond dissociation energies previously listed. The values for $\Delta H_f°(R^\bullet)$ corresponding to these are in reasonable agreement with recent theoretical values [$\Delta H_f°(Me_3SiCH_2^\bullet) = -29 \pm 6$ kJ mol^{-1}[22], $\Delta H_f°(SiCl_3^\bullet) = -318 \pm 7$ kJ mol^{-1}[20,100], $\Delta H_f°(SiF_3^\bullet)$ values in the range -976 to -1007 kJ mol^{-1}[26]], and also a recent experimental value of Armentrout and coworkers[101] [$\Delta H_f°(SiF_3^\bullet) = -997 \pm 5$ kJ mol^{-1}].

What emerges from these revised values is the fact that methyl substitution at silicon leads to a strengthening of Si−H bonds, whereas the old data showed no trend. Marshall has pointed out[89,90] that this is completely in accord with the relative electronegativities of carbon and silicon, a point invoked by one of us[2] to account for trends in other cases. Relative values remain unaffected so that, for instance, the SiH_3 group weakening effect manifests itself in the reduced Si−H dissociation energy of Si_2H_6 compared with SiH_4. This is again supported by other experimental[94] and theoretical calculations[20,50,90,93,102–104].

Studies of electron affinities of organosilyl radicals combined with gas-phase acidities have been used by Brauman and coworkers[105] to obtain bond dissociation energies. The values obtained are generally in excellent agreement with those of Table 15, although uncertainties tend to be greater (±8–12 kJ mol^{-1}). In addition to data in Table 15, other values for Si−H bond dissociation energies have been obtained by means of photoacoustic calorimetry[106–108]. These are shown in Table 16. We have increased the values by 19 kJ mol^{-1} on the grounds that the value for $D(Et_3Si{-}H)$ should be the same as that for $D(Me_3Si{-}H)$. Chatgilialoglu[28] has reviewed uncertainties in this method and concluded that while absolute values may be subject to systematic errors, relative values should be reliable. Thus these data show clearly that silyl substitution at the silicon centre systematically weakens Si−H bonds (by *ca* 12–20 kJ mol^{-1}) per silyl group. This is borne out by the theoretical calculations of Sax and Kalcher[50] who have obtained values for $D(H_3Si{-}H)$, $D(H_3SiSiH_2{-}H)$ and $D((H_3Si)_2SiH{-}H)$ of 383, 374 and 361 kJ mol^{-1}, respectively. The explanation for this effect is not clear. Stabilization by silyl groups is even more marked in silyl anions[109]. Calculations suggest that there is an increase in p character in the Si−Si bonds upon anion formation with the anion electron pair located on silicon in an orbital with substantial s character[109]. This type of explanation has been used by us to explain the stabilities of silylenes[5,110], but for the radicals a simple inductive effect from the silyl substituent to the silicon bearing the odd electron[2] seems equally appealing.

The data also suggest that phenyl substitution weakens Si−H bonds, but only by a small amount (*ca* 4–8 kJ mol^{-1}) per phenyl group. The difficulty here is that since methyl

TABLE 16. Bond dissociation energies (kJ mol^{-1}) for silanes obtained by photoacoustic calorimetry

Bond	D(old)	D(new)[d]
$Et_3Si{-}H$	377 ± 4[a]	396 ± 4
$Me_3SiSiMe_2{-}H$	357 ± 4[a]	376 ± 4
$(Me_3Si)_3Si{-}H$	331 ± 4[a]	350 ± 4
$(Me_3Si)_3Si{-}H$	345 ± 3[b]	364 ± 3
$PhMe_2Si{-}H$	358 ± 7[c]	377 ± 7
$Ph_2SiH{-}H$	360 ± 6[c]	379 ± 6
$Ph_2MeSi{-}H$	342 ± 10[c]	361 ± 10
$Ph_3Si{-}H$	352 ± 2[c]	371 ± 2

[a] Reference 106. [b] Reference 107. [c] Reference 108. [d] See text for discussion of these values.

groups strengthen the Si—H bonds, the effects of methyl and phenyl substitution tend to cancel out. This is also supported by $D(\text{PhMeSiH—H}) = 382 \pm 13\ \text{kJ mol}^{-1}$ from the electron affinity measurements[105]. Despite the revision of these values, the small effect of phenyl substitution remains indicative of very little π-type interaction between the aromatic ring and the odd-electron orbital on the silicon[2]. Silyl stabilization of a carbon-centred radical is very small. New values of bond dissociation energies do not affect these quantities, which were determined by us by relative means. Thus values for α-silyl and β-silyl stabilization of primary alkyl radicals $\text{Me}_3\text{SiCH}_2^\bullet$ and $\text{Me}_3\text{SiCMe}_2\text{CH}_2^\bullet$ are 2 and 12 kJ mol^{-1} respectively[1,111,112]. *Ab initio* calculations give 5 kJ mol^{-1} for the α-silyl stabilization in $\text{SiH}_3\text{CH}_2^\bullet$[103]. Higher values (11 kJ mol^{-1}) for α-stabilization[113] came from a different comparative basis which includes other effects, and cannot be strictly compared with these numbers[1].

The determination of an Si—N bond dissociation energy has been carried out by Krasnoperov and coworkers[114] who studied directly the gas-phase equilibrium:

$$\text{Me}_3\text{Si} + \text{NO} \rightleftharpoons \text{Me}_3\text{SiNO}$$

The value for ΔH° gives directly $D(\text{Me}_3\text{Si—NO})$. A value of $190.2 \pm 3.6\ \text{kJ mol}^{-1}$ was obtained using the third law method, and is in excellent agreement with the *ab initio* (BAC-MP4) value of 191.4 kJ mol^{-1}[114]. The same calculation[114] gives a value for $D(\text{H}_3\text{Si—NO})$ of 149.9 kJ mol^{-1}, slightly higher than the previous value[115]. This provides a more dramatic example of bond strengthening of Si—X bonds by methyl group. These Si—NO bonds are significantly weaker than those of the more typical Si—N bonds in silylamines obtainable only indirectly and discussed in the next section.

C. Derived Bond Dissociation Energies

A set of bond dissociation energies for representative Si—C, Si—Si, Si—halogen, Si—O and Si—N bonds are derived from the molecular and radical heats of formation of the previous sections and, where necessary, those in the Appendix. These are shown in Tables 17–19. The selection of molecules is identical to that of the earlier review[1], but the values are of course revised to take account of the new results. The most significant change is the general increase in values arising from the higher values for the enthalpies of formation of the silicon-centred radicals, particularly $\text{Me}_3\text{Si}^\bullet$. The changes do not affect significantly the trends in values discussed in earlier reviews[1,2]. The bond strengthening effect of methyl groups (at silicon centres), noted already here for Si—H bonds, is also clearly apparent for Si—C bonds, and also evident for Si—Si bonds. The effect was also found previously[1,2] for Si—halogen bonds, but it is even more marked than thought then. The bond weakening effect of silyl groups (at the silicon centres), noted already for Si—H bonds, is also evident for Si—Si bonds. A recent experimental study[92] of the pyrolysis of $\text{Me}_3\text{SiSiMe}_3$ yielded an estimate of $D(\text{Me}_3\text{SiSiMe}_2\text{—Me}) = 372\ \text{kJ mol}^{-1}$. When compared with the values of Table 17 it can be seen that the trimethylsilyl group is exerting a bond weakening effect on the Si—C bond.

The halogen substituent effects, as noted earlier[1], are more complex. Fluorine (as in F_3SiX) strengthens the Si—X bond (relative to H and Me). Chlorine and bromine are in between, $D(\text{H}_3\text{Si—X})$ and $D(\text{X}_3\text{Si—X})$ being equal within experimental error, and iodine weakens Si—X bonds. Si—OR and Si—NR_2 bonds, just like Si—halogen bonds, are very strong in comparison with analogous C—O, C—N and C—X bonds. The figures in parentheses in Table 19 were obtained indirectly by use of estimates of the radical heats of formation, $\Delta H_\text{f}^\circ(\text{Me}_3\text{SiO}) = -223\ \text{kJ mol}^{-1}$ and $\Delta H_\text{f}^\circ((\text{Me}_3\text{Si})_2\text{N}) = -231\ \text{kJ mol}^{-1}$.

TABLE 17. Derived silicon–carbon and silicon–silicon bond dissociation energies (kJ mol^{-1})

Bond	D	Bond	D
H_3Si-CH_3	375 ± 5	$H_3Si-SiH_3$	321 ± 4
$MeSiH_2-CH_3$	381 ± 7	$H_3Si-Si_2H_5$	313 ± 8
$Me_2SiH-CH_3$	387 ± 7	$H_3SiH_2Si-SiH_2SiH_3$	306 ± 10
Me_3Si-CH_3	394 ± 8	$Me_3Si-SiMe_3$	332 ± 12[a]

[a] Based on the directly measured data of Reference 92.

TABLE 18. Derived silicon–halogen bond dissociation energies (kJ mol^{-1})[a]

Halogen(X)	$D(H_3Si-X)$	$D(Me_3Si-X)$	$D(X_3Si-X)$
F	638 ± 5	662 ± 11	697 ± 6
Cl	458 ± 7	490 ± 8	462 ± 9
Br	376 ± 9	425 ± 8	376 ± 22
I	299 ± 8	344 ± 8	284 ± 26

[a] For $\Delta H_f{}^\circ$ values for SiH_3X and SiX_4 see Table 29.

TABLE 19. Derived silicon–oxygen and silicon–nitrogen bond dissociation energies (kJ mol^{-1})[a]

Bond	D	Bond	D
Me_3Si-OH	555 ± 8	Me_3SiO-H	(495)
$Me_3Si-OMe$[b]	513 ± 11	$Me_3SiO-Me$[b]	(403)
$Me_3Si-OEt$[b]	512 ± 11	$Me_3SiO-Et$[b]	(412)
$Me_3Si-OSiMe_3$	(569)		
$Me_3Si-NHMe$	419 ± 8	$(Me_3Si)_2N-H$	(464)
$Me_3Si-NMe_2$	408 ± 8	$(Me_3Si)_2N-Me$	(364)
$Me_3Si-N(SiMe_3)_2$	(455)		

[a] Figures in parentheses have been estimated (see text).

[b] $\Delta H_f{}^\circ$ values for Me_3SiOMe (-480 ± 8 kJ mol^{-1}) and Me_3SiOEt (-514 ± 8 kJ mol^{-1}) were estimated using additivity.

These were obtained, as previously[1], by assuming that sequential Si–O and Si–N dissociation energies in $(Me_3Si)_2O$ and $(Me_3Si)_3N$ follow the same proportionate relationships as O–H and N–H dissociation energies in H_2O and NH_3. It is interesting to note that the derived values for O–H and N–H dissociation energies in Me_3SiOH and $(Me_3Si)_2NH$ are very similar to $D(HO-H) = 499$ kJ mol^{-1} and $D(H_2N-H) = 453$ kJ mol^{-1}. As a substituent on these electronegative atoms, clearly the Me_3Si group is similar to the H atom itself in its electronic effects. Although there are no theoretically calculated *(ab initio)* values for the bond dissociation energies of Table 19, values of Si–O and Si–N dissociation energies have been obtained by the Melius group[21,24,25], Darling and Schlegel[81] and Zachariah and Tsang[82]. For the prototype molecules H_3SiOH and H_3SiNH_2, the following values (kJ mol^{-1}) have been found: $D(H_3Si-OH) = 505$[81], 514[25]; $D(H_3SiO-H) = 522$[81], 517[82], 513[25]; $D(H_3Si-NH_2) = 439$[21]; $D(H_3SiNH-H) = 480$[21].

Many other bond dissociation energies have been derived from theoretically calculated enthalpies of formation of radicals in recent years. These include Si–H, Si–C, Si–Si, Si–halogen, Si–O and Si–N. These are too many examples to consider in the context of this (mainly) experimentally orientated account. Where comparisons exist, as indicated, there has been a convergence in recent years, so that agreement between experiment and theory is generally good.

IV. OTHER SILICON CONTAINING SPECIES

There is great interest in silicon-containing transient species. This is because they are invariably involved in the thermal and photochemical breakdown mechanisms of more stable organosilicon compounds. Apart from SiX_3 free radical species dealt with in the previous section, these include the silylenes, SiX_2, and the π-bonded analogues of organic alkenes and carbonyl compounds containing Si=C, Si=Si and Si=O double bonds. An excellent account of the structure and energetics of these compounds has been given by Grev[116].

A. Silylenes

There has been a great deal of discussion about the thermochemistry of silylenes, particularly SiH_2, MeSiH and $SiMe_2$.

1. SiH_2

Together with Jasinski, we have recently reviewed[6] $\Delta H_f{}^\circ(SiH_2)$. Even more recently we have listed further published values[117] as part of a study of the kinetics and mechanism of the reaction

$$SiH_2 + SiH_4 \rightleftharpoons Si_2H_6$$

The latest data are shown in Table 20. In the previous article[1] we reported $\Delta H_f{}^\circ(SiH_2) = 273 \pm 6$ kJ mol^{-1} and the current experimentally preferred value[117] is the same but with a reduced uncertainty of ± 2 kJ mol^{-1}. This refinement has come about because the new kinetic data are extensive enough in their temperature and pressure ranges to be used to obtain the equilibrium constant for the above reaction without the need for extrapolation. A number of previous analyses of the kinetics of this system and also that of $SiH_2 + H_2 \rightleftarrows SiH_4$ have given very similar values[118–122], although the most recent study[123] seems to have given two different values (288 and 275 kJ mol^{-1}). The higher

TABLE 20. Recent values for $\Delta H_f{}^\circ(SiH_2)$/kJ mol^{-1}

Experimental values			Theoretical values		
year	value	Reference	year	value	Reference
1986	273 ± 6	118	1985	265	128
1986	289 ± 13	125	1985	285	18
1987	273 ± 3	127	1986	273	129
1987	287 ± 6	95	1986	287	19
1987	269 ± 1	119	1988	272	96
1987	268–287	120	1988	266	97
1988	274 ± 7	126	1990	271 ± 9	20
1989	267 ± 8	55	1991	275 ± 8	32
1991	274 ± 4	121	1991	277	50
1991	266 ± 6	64	1992	271 ± 9	22
1992	273 ± 2	5	1992	273	49
1992	269 ± 4	122	1992	267	49
1994	285 ± 13	124			
1995	273 ± 2	117			
1996	288, 275	123			

value is associated with an RRKM modelling analysis of the high temperature, shock tube pyrolysis of SiH_4[124]. This could have a number of uncertainties associated with energy transfer and pressure dependence and is therefore not definitive. Other experimental values of $\Delta H_f{}^\circ(SiH_2)$ from ion cyclotron resonance mass spectrometry[125] , Si^+ ion beam reaction thresholds[95], electronic excitation spectroscopy[126] and photoionization mass spectrometry[127] are in reasonable agreement with the preferred value[117] of $273\ kJ\,mol^{-1}$. On the theoretical side, advances have reflected the increasing use of electron-correlated wavefunctions and large basis sets. The highest level calculations by Grev and Schaefer[49] are in precise agreement with experiment[117] assuming $\Delta H_f{}^\circ(SiH_4)$ is correct. However, as indicated earlier, the discrepancy between $\Delta H_f{}^\circ(SiH_4)$ and $\Delta H_f{}^\circ(Si)$ means that a lower value of $267\ kJ\,mol^{-1}$ is obtained for $\Delta H_f{}^\circ(SiH_2)$ starting from $\Delta H_f{}^\circ(Si)$.

2. MeSiH

These data are shown in Table 21. In 1988 Walsh published a value[130] for $\Delta H_f{}^\circ(MeSiH\colon)$ of $184 \pm 13\ kJ\,mol^{-1}$. This was based on an analysis of the decomposition reactions of certain methyl substituted disilanes and was included in the previous review[1]. At the same time ion cyclotron resonance studies[131] gave a value of $222 \pm 17\ kJ\,mol^{-1}$. The next year we extended our analysis[65] but with no different outcome, although O'Neal and coworkers[55], using the same basic kinetic data, obtained $201 \pm 8\ kJ\,mol^{-1}$. The essential difference lay in the choice of values for $\Delta H_f{}^\circ$ for methyl substituted disilanes which were at that time rather uncertain. This problem was resolved by the calorimetric measurement of $\Delta H_f{}^\circ(Si_2Me_6)$ by Pilcher and coworkers[64] from which the securely based value of $\Delta H_f{}^\circ(MeSiH)$ of $201 \pm 6\ kJ\,mol^{-1}$ was obtained. Theoretical calculations[22,132,144] give values in reasonable agreement with this. More recently Becerra and coworkers[133] have obtained a value of $202 \pm 6\ kJ\,mol^{-1}$ from analysis of the same kinetic systems but incorporating new and directly measured kinetic data for MeSiH insertion reactions. Although the analysis is now more complete, there remains enough experimental uncertainty that it is not realistic to reduce error limits below $\pm 6\ kJ\,mol^{-1}$.

3. Me_2Si

The data are shown in Table 22. Just as with $\Delta H_f{}^\circ(MeSiH)$, Walsh published[130] a value of $\Delta H_f{}^\circ(SiMe_2)$ equal to $109 \pm 8\ kJ\,mol^{-1}$ in 1988 based on an analysis including

TABLE 21. Recent values for $\Delta H_f{}^\circ(MeSiH)/kJ\,mol^{-1}$

Year	Value	Reference
1988	184 ± 13	130[a]
1988	222 ± 17	131[a]
1989	206	144[b]
1989	184 ± 13	65[a]
1989	201 ± 8	55[a]
1990	212	132[b]
1991	201 ± 6	64[a]
1992	204 ± 10	22[b]
1993	201.8 ± 6	133[a]

[a]Experimental value. [b]Theoretical value.

TABLE 22. Recent values for $\Delta H_f{}^\circ(\mathrm{Me_2Si})$/kJ mol^{-1}

Year	Value	Reference
1988	109 ± 8	130[a]
1988	155 ± 25	131[a]
1989	136 ± 13	144[b]
1989	108 ± 13	65[a]
1989	134 ± 8	55[a]
1990	134–138	132[b]
1991	140 ± 6	64[a]
1992	135 ± 10	22[b]
1995	135 ± 8	134[a]

[a] Experimental value. [b] Theoretical value.

erroneous values for $\Delta H_f{}^\circ$ for methyl substituted disilanes. This was the value cited in our earlier review[1]. Once again, O'Neal and coworkers[55] were more foresighted and obtained a value of 134 ± 8 kJ mol^{-1}. Ion cyclotron resonance studies[131] gave an even higher value. The problem was resolved, as in the case of MeSiH, with the calorimetric determination of $\Delta H_f{}^\circ(\mathrm{Si_2Me_6})$[64]. Theory[22,132,144] is in excellent agreement with our current best estimate of 135 ± 8 kJ mol^{-1}.

4. H_3SiSiH

The only experimental value for $\Delta H_f{}^\circ(\mathrm{H_3SiSiH})$ is 312 ± 8 kJ mol^{-1}[135]. However, theoretical calculations have yielded values (kJ mol^{-1}) of 349[96], 313 ± 11[20], 305[132], 317[50] and 300[102]. Agreement is thus tolerable if not perfect.

5. Silicon dihalides

The thermochemistry of these species was reviewed by Walsh[3] some years ago. Since then new data have appeared for $\mathrm{SiF_2}$ and $\mathrm{SiCl_2}$. This has been recently reviewed again by Gordon and coworkers[26]. Theoretical values for $\Delta H_f{}^\circ(\mathrm{SiF_2})$, all in good agreement[20,32,136], have placed its value some 42 kJ mol^{-1} lower than the earlier experimental values[3,35]. Recent experimental ion-beam studies[101] have confirmed the theoretical values. $\Delta H_f{}^\circ(\mathrm{SiCl_2})$ seems to be experimentally well established[3,35] at 169 ± 3 kJ mol^{-1}. A more recent value[137] is in reasonable agreement, as are theoretical calculations[20,100]. $\Delta H_f{}^\circ$values for $\mathrm{SiBr_2}$ and $\mathrm{SiI_2}$ have not changed since earlier[3,35]. No theoretical calculations have been carried out on these species. The data are shown in Table 23.

TABLE 23. Standard enthalpies of formation ($\Delta H_f{}^\circ$/kJ mol^{-1}) of silicon dihalides

Silylene	Experiment	Theory
$\mathrm{SiF_2}$	−588 ± 13[a], −638 ± 6[b]	−627 ± 17[c], −640 ± 8[d], −642 (−638)[e]
$\mathrm{SiCl_2}$	−169 ± 3[a], −165 ± 14[f]	−151 ± 16[c], −163[g]
$\mathrm{SiBr_2}$	−52 ± 17[a], −46 ± 8[h]	
$\mathrm{SiI_2}$	93 ± 8[a], 92 ± 8[h]	

[a] Reference 35. [b] Reference 101. [c] Reference 20. [d] Reference 32. [e] Reference 136. [f] Reference 137. [g] Reference 100. [h] Reference 3.

TABLE 24. Recommended standard enthalpies of formation ($\Delta H_f{}^\circ$/kJ mol^{-1}) for silylenes together with DSSE values

Silylene	$\Delta H_f{}^{\circ a}$	DSSE[b]
SiH_2	273 ± 2	94 ± 4
MeSiH	202 ± 6	113 ± 11
$SiMe_2$	135 ± 8	128 ± 11
H_3SiSiH	312 ± 8	76 ± 10
SiF_2	-638 ± 6	259 ± 8
$SiCl_2$	-169 ± 3	188 ± 10
$SiBr_2$	-46 ± 8	161 ± 27
SiI_2	92 ± 8	152 ± 27

[a] See text and Tables 20–23 for source values.
[b] See text for definition.

Values for the important index of reactivity for silylenes, DSSE (= divalent state stabilization energy) defined as follows:

$$\mathrm{DSSE(SiR_2)} = D(\mathrm{R_3Si{-}R}) - D(\mathrm{R_2Si{-}R})$$

where R is the substituent, are shown in Table 24. This updates earlier estimates[3,5,110,134]. It can be generally seen that DSSE increases with the electronegativity of the substituent, as noted previously[5,110].

B. π-Bonded Species

There has been considerable attention paid to the thermochemistry of these species by theoreticians, but very little by experimentalists, since the earlier review[1].

1. Sila-alkenes

Experimental data for these Si=C double bonded species come from ion-cyclotron resonance measurements[131] or thermochemical analyses of siletane (silacyclobutanes) decomposition[71]. Our own previous estimate[78] was based on the latter approach. The value of $\Delta H_f{}^\circ(\mathrm{Me_2Si{=}CH_2}) = 36 \pm 7$ kJ mol^{-1} determined by Brix and coworkers[71] is the current best available value for any of the sila-alkenes, having reduced considerably the uncertainties and assumptions of our earlier analyses[78]. It is still, however, dependent on the value[68] for $\Delta H_f{}^\circ$ for 1,1-dimethylsiletane (-108.7 ± 6 kJ mol^{-1}) discussed elsewhere in this review (Section II.B.2). If the value of the latter is taken as -85 kJ mol^{-1} as obtained by Voronkov and coworkers[14], then $\Delta H_f{}^\circ(\mathrm{Me_2Si{=}CH_2})$ becomes 61 kJ mol^{-1} as suggested recently by Ahmed and coworkers[138]. Theoretical values of $\Delta H_f{}^\circ$ have been calculated for all the methylsila-alkenes ($H_2Si{=}CH_2$, $MeSiH{=}CH_2$, $Me_2Si{=}CH_2$) by the BAC-MP4 method[22] and these show a Me-for-H replacement enthalpy of -59 kJ mol^{-1}, a rather smaller value than might be expected from examination of other methyl-substituted silicon species (e.g. -67 kJ mol^{-1} for the methyl silanes, -69 kJ mol^{-1} for the methylsilylenes). Most theoretical activity has focused on $\Delta H_f{}^\circ(\mathrm{H_2Si{=}CH_2})$ for which the highest level calculation[139] has yielded a value 15 kJ mol^{-1} lower than for $\Delta H_f{}^\circ$(MeSiH). From

TABLE 25. Standard enthalpies of formation ($\Delta H_f{}^\circ$/kJ mol^{-1}) of sila-alkenes

Sila-alkene	Experiment	Theory
$H_2Si{=}CH_2$	155 ± 20^a, 180 ± 13^b 187 ± 6^c	170 ± 10^d, 194^e, 190^f
$MeSiH{=}CH_2$	88 ± 20^a	110 ± 8^d
$Me_2Si{=}CH_2$	21 ± 20^a, 36 ± 7^g $(61 \pm 7)^h$	51 ± 6^d

[a] Reference 1. [b] Reference 131. [c] Estimated from $\Delta H_f{}^\circ$(MeSiH); see text. [d] Reference 22. [e] Reference 132. [f] Reference 58. [g] Reference 71. [h] Reference 138.

our own experimental value for the latter, this would mean $\Delta H_f{}^\circ(H_2Si{=}CH_2) = 187 \pm 6$ kJ mol^{-1}. At the G-1 level of theory, Boatz and Gordon[132] have obtained a value of 194 kJ mol^{-1}. These are somewhat higher than the Allendorf and Melius (BAC-MP4) value[22] of 170 ± 10 kJ mol^{-1}. On the other hand, comparison of the highest of these values with $\Delta H_f{}^\circ(Me_2Si{=}CH_2)$ discussed above implies a rather high Me-for-H replacement (79 kJ mol^{-1}). There is thus room for further refinement of the enthalpies of formation for these species. The values are listed in Table 25. Earlier theoretical values are discussed by Gordon, Francisco and Schlegel[26].

2. Disilene

Our value[135] for $\Delta H_f{}^\circ(H_2Si{=}SiH_2)$ of 261 ± 8 kJ mol^{-1} is in conflict with the photoionization studies of Ruscic and Berkowitz[94] who obtained a value of 275 ± 4 kJ mol^{-1}. The discrepancy is not large but tends to be supported by theoretical values (kJ mol^{-1}) of 281[50], 272[132] and 270[102]. Ho and Melius[20] with 263 ± 10 are in between, and Horowitz and Goddard's value[96] of 322 looks to be too high. Our experimental value[135] is based on a mechanistic interpretation and is less direct than the photoionization value[94] which should therefore be the best available experimental estimate.

3. Silanone

An experimental value for $\Delta H_f{}^\circ(H_2Si{=}O)$ is urgently needed. None currently exists. In the previous review[1] we estimated a value of -90 ± 30 kJ mol^{-1} which we have revised to -92 ± 20[140] based on subsequent theoretical values. Hartman and coworkers[141] have estimated a value of -115 kJ mol^{-1} from bond energy arguments and recent theoretical values[25,81,82] are in agreement at -98 kJ mol^{-1}.

Values for the important index of reactivity, the π-bond energy, $D_\pi(Si{=}X)$, may be obtained from:

$$D_\pi(Si{=}X) = D_\sigma(Si{-}H) + D_\sigma(X{-}H) - D_\sigma(H{-}H) + \Delta H_{hyd}$$

where ΔH_{hyd} is the enthalpy of hydrogenation of the species $H_2Si{=}X$. $D_\pi(Si{=}X)$ values for several Si=X bonds are shown in Table 26.

There are many other important reactive silicon-containing species, for example the ground state 'butterfly' Si_2H_2 molecule, $Si(H_2)Si$. There is virtually no experimental thermochemistry on such species. However, theoretical values of $\Delta H_f{}^\circ$ for many other species have been calculated in the articles on theory cited in this review. Since the

TABLE 26. Recommended standard enthalpies of formation (ΔH_f°/kJ mol^{-1}) of unsaturated silicon-containing molecules and π-bond energies[a]

Species	ΔH_f°	π-Bond energy (D_π)[b]
$H_2Si{=}CH_2$	187 ± 6	146 ± 9
$MeHSi{=}CH_2$	116 ± 10	154 ± 12
$Me_2Si{=}CH_2$	46 ± 10	161 ± 12
$H_2Si{=}SiH_2$	275 ± 4	113 ± 8
$H_2Si{=}O$	−92 ± 20	256 ± 26

[a] See text and Table 25 for references.
[b] See text for definition.

emphasis is on experimental values we do not extend this article to include them. Interested readers are referred to the original articles.

V. APPENDIX

Group increments for silicon compounds based on the data reviewed here, and derived in accordance with the group additivity scheme[29–31], are shown in Table 27. Radical and atomic heats of formation for non-silicon-containing species used in this chapter to derive bond dissociation energies are shown in Table 28. Miscellaneous inorganic silane heats of formation are included in Table 29.

TABLE 27. Group increment contributions to standard enthalpies of formation (ΔH_f°/kJ mol^{-1}) for organosilicon compounds

Group	ΔH_f°
Si−(C)(H)$_3$	13.7
Si−(C)$_2$(H)$_2$	−9.1
Si−(C)$_3$(H)	−35.0
Si−(C)$_4$	−62.0
C−(Si)(H)$_3$	−42.8[a]
C−(Si)(C)(H)$_2$	−17.0
C−(Si)(C)$_2$(H)	−4.2
O−(Si)(H)	−309.2
O−(Si)$_2$	−396.6
O−(Si)(C)	−246.8
Si−(C)$_3$(O)	−62.0[b]
Si−(C)$_2$(O)$_2$	−62.2
Si−(C)(O)$_3$	−61.4
Si−(O)$_4$	−61.6
C−(C)(H)$_3$	−42.8
C−(C)$_2$(H)$_2$	−20.7
C−(O)(C)(H)$_2$	−33.9
C−(O)(C)$_2$(H)	−30.1

[a] Arbitrary value: C−(Si)(H)$_3$ set equal to C−(C)(H)$_3$.
[b] Arbitrary value: Si−(C)$_3$(O) set equal to Si−(C)$_4$.

TABLE 28. Standard enthalpies of formation (ΔH_f°/kJ mol^{-1}) for various atoms and free radicals

Species	ΔH_f°	Species	ΔH_f°
H	218.0[a]	C	716.7[a]
CH_3	145.6[b]	Si	450.6[a]
C_2H_5	120.9[b]	F	79.4[a]
OH	39.0[a]	Cl	121.3[a]
OMe	17.2[b]	Br	111.9[a]
OEt	−15.5[b]	I	106.8[a]
NH_2	185[c]		
NHMe	177[c]		
NMe_2	145[c]		

[a] Reference 35. [b] Reference 27. [c] Reference 142.

TABLE 29. Standard enthalpies of formation (ΔH_f°/kJ mol^{-1}) of silicon hydrides and halides

Molecule	$\Delta H_f^{\circ a}$	Molecule	ΔH_f°	Molecule	$\Delta H_f^{\circ d}$
SiH_4	34.3 ± 1.2	SiH_3F	−359 ± 8[c]	SiF_4	−1615 ± 1
Si_2H_6	80 ± 1.5	SiH_3Cl	−134 ± 6[c]	$SiCl_4$	−663 ± 5
Si_3H_8	121 ± 4.4	SiH_3Br	−64 ± 9[d]	$SiBr_4$	−415 ± 8
Si_4H_{10}	(162)[b]	SiH_3I	+8.6 ± 8[e]	SiI_4	−110 ± 16

[a] References 1 and 143. [b] Additivity estimate. [c] See Table 1. [d] Reference 3. [e] See Table 2.

VI. REFERENCES

1. R. Walsh, in *The Chemistry of Organic Silicon Compounds* (Eds. S. Patai and Z. Rappoport), Chap. 5, Wiley, Chichester, 1989, p. 371.
2. R. Walsh, *Acc. Chem. Res.*, **14**, 246 (1981).
3. R. Walsh, *J. Chem. Soc., Faraday Trans. 1*, **79**, 2233 (1983).
4. A. M. Doncaster and R. Walsh, *J. Chem. Soc., Faraday Trans. 2*, **82**, 707 (1986).
5. R. Walsh, in *Energetics of Organometallic Species* (Ed. J. A. Martinho Simões), NATO-ASI Series C, Vol. 367, Chap. 11, Kluwer, Dordrecht, 1992, p. 171.
6. J. M. Jasinski, R. Becerra and R. Walsh, *Chem. Rev.*, **95**, 1203 (1995).
7. J. D. Cox and G. Pilcher, *Thermochemistry of Organic and Organometallic Compounds*, Academic Press, London, 1970.
8. S. Tannenbaum, *J. Am. Chem. Soc.*, **76**, 1027 (1954).
9. J. B. Pedley and J. Rylance, *Sussex-NPL Computer Analysed Thermochemical Data: Organic and Organometallic Compounds*, University of Sussex, 1977.
10. V. I. Tel'noi and I. B. Rabinovitch, *Russ. Chem. Rev.*, **49**, 603 (1980).
11. M. G. Voronkov, V. P. Baryshok, V. A. Klyuchnikov, T. F. Danilova, V. I. Pepikin, A. N. Korchagina and Yu. I. Khudobin, *J. Organomet. Chem.*, **345**, 27 (1988).
12. M. G. Voronkov, V. P. Baryshok, V. A. Klyuchnikov, A. N. Korchagina and V. I. Pepikin, *J. Organomet. Chem.*, **359**, 169 (1989).
13. M. G. Voronkov, M. S. Sorokin, V. A. Klyuchnikov, G. N. Shvets and V. I. Pepikin, *J. Organomet. Chem.*, **359**, 301 (1989).
14. M. G. Voronkov, V. A. Klyuchnikov, E. V. Sokolova, T. F. Danilova, G. N. Shvets, A. N. Korchagina, L. E. Gusel'nikov and V. V. Volkova, *J. Organomet. Chem.*, **401**, 245 (1991).
15. M. G. Voronkov, V. A. Klyuchnikov, E. V. Mironenko, G. N. Shvets, T. F. Danilova and Yu. I. Khudobin, *J. Organomet. Chem.*, **406**, 91 (1991).
16. M. G. Voronkov, V. A. Klyuchnikov, L. I. Marenkova, T. F. Danilova, G. N. Shvets, S. I. Tsvetnitskaya and Yu. I. Khudobin, *J. Organomet. Chem.*, **406**, 99 (1991).

17. (a) M. G. Voronkov, V. A. Klyuchnikov and L. I. Marenkova, *J. Organomet. Chem.*, **510**, 263 (1996).
    (b) V. M. Tatevskii, *The Structure of Molecules*, Khimaya Publishers, Moscow, 1978, p. 51.
18. P. Ho, M. E. Coltrin, J. S. Binkley and C. F. Melius, *J. Phys. Chem.*, **89**, 4647 (1985).
19. P. Ho, M. E. Coltrin, J. S. Binkley and C. F. Melius, *J. Phys. Chem.*, **90**, 3399 (1986).
20. P. Ho and C. F. Melius, *J. Phys. Chem.*, **94**, 5120 (1990).
21. C. F. Melius and P. Ho, *J. Phys. Chem.*, **95**, 1410 (1991).
22. M. D. Allendorf and C. F. Melius, *J. Phys. Chem.*, **96**, 428 (1992).
23. M. D. Allendorf and C. F. Melius, *J. Phys. Chem.*, **97**, 720 (1993).
24. P. Ho and C. F. Melius, *J. Phys. Chem.*, **99**, 2166 (1995).
25. M. D. Allendorf, C. F. Melius, P. Ho and M. R. Zachariah, *J. Phys. Chem.*, **99**, 15285 (1995).
26. M. S. Gordon, J. S. Francisco and H. B. Schlegel, *Advances in Silicon Chemistry*, **2**, 137 (1993).
27. J. Berkowitz, G. B. Ellison and D. Gutman, *J. Phys. Chem.*, **98**, 2744 (1994).
28. C. Chatgilialoglu, *Chem. Rev.*, **95**, 1229 (1995).
29. S. W. Benson and J. H. Buss, *J. Chem. Phys.*, **29**, 546 (1958).
30. S. W. Benson, F. R. Cruickshank, D. M. Golden, G. R. Haugen, H. E. O'Neal, A. S. Rodgers, R. Shaw and R. Walsh, *Chem. Rev.*, **69**, 279 (1969).
31. S. W. Benson, *Thermochemical Kinetics*, 2nd edn., Wiley-Interscience, New York, 1976.
32. E. W. Ignacio and H. B. Schlegel, *J. Chem. Phys.*, **92**, 5404 (1990).
33. D. A. Dixon, *J. Phys. Chem.*, **92**, 86 (1988).
34. M-D. Su and H. B. Schlegel, *J. Phys. Chem.*, **97**, 8732 (1993).
35. M. W. Chase, C. A. Davies, J. R. Downey, D. J. Frurip, R. A. McDonald and A. N. Syverud, *JANAF Thermochemical Tables 3rd Edn., J. Phys. Chem. Ref. Data*, **14** (1985), supplement 1.
36. L. Pauling, *The Nature of the Chemical Bond*, 3rd edn., Cornell University Press, Ithaca, New York, 1960.
37. Y-R. Luo and S. W. Benson, *Acc. Chem. Res.*, **25**, 375 (1992).
38. Y-R. Luo and S. W. Benson, *J. Phys. Chem.*, **92**, 5255 (1988).
39. Y-R. Luo and S. W. Benson, *J. Am. Chem. Soc.*, **111**, 2480 (1989).
40. Y-R. Luo and S. W. Benson, *J. Phys. Chem.*, **93**, 3304 (1989).
41. Y-R. Luo and S. W. Benson, *J. Phys. Chem.*, **93**, 3306 (1989).
42. Y-R. Luo and S. W. Benson, *J. Phys. Chem.*, **93**, 1674 (1989).
43. Y-R. Luo and S. W. Benson, *J. Phys. Chem.*, **93**, 4643 (1989).
44. Y-R. Luo and S. W. Benson, *J. Phys. Chem.*, **93**, 3791 (1989).
45. Y-R. Luo and S. W. Benson, *J. Phys. Chem.*, **94**, 914 (1990).
46. R. Becerra and R. Walsh, unpublished calculations.
47. S. R. Gunn and L. G. Green, *J. Phys. Chem.*, **65**, 779 (1961).
48. S. R. Gunn and L. G. Green, *J. Phys. Chem.*, **68**, 946 (1964).
49. R. S. Grev and H. F. Schaefer III, *J. Chem. Phys.*, **97**, 8389 (1992).
50. A. F. Sax and J. Kalcher, *J. Phys. Chem.*, **95**, 1768 (1991).
51. G. Leroy, M. Sana, C. Wilante and D. R. Temsamani, *J. Mol. Struct. (Theochem)*, **259**, 369 (1992).
52. M. S. Gordon, J. A. Boatz and R. Walsh, *J. Phys. Chem.*, **93**, 1584 (1989).
53. W. V. Steele, *J. Chem. Thermodyn.*, **15**, 595 (1983).
54. D. D. Wagman, W. H. Evans, V. B. Parker, R. H. Shumm, I. Halow, S. M. Bailey, K. L. Churney and R. L. Nuttall, *J. Phys. Chem. Ref. Data, 1982 Supplement*, **11**, 2 (1982).
55. H. E. O'Neal, M. A. Ring, W. H. Richardson and G. F. Licciardi, *Organometallics*, **8**, 1968 (1989).
56. M. G. Voronkov, V. A. Klyuchnikov, T. F. Danilova, A. N. Korchagina, V. P. Baryshok and L. M. Landa, *Bull. Acad. Sci. USSR, Div. Chem. Sci.*, 1790, 1795 (1986).
57. R. E. Jardine, H. E. O'Neal, M. A. Ring and M. E. Beatie, *J. Phys. Chem.*, **99**, 12507 (1995).
58. A. E. Ketvirtis, D. K. Bohme and A. C. Hopkinson, *J. Phys. Chem.*, **99**, 16121 (1995).
59. N. Al-Rubaiey and R. Walsh, *J. Phys. Chem.*, **98**, 5303 (1994).
60. R. Becerra and R. Walsh, *Int. J. Chem. Kinet.*, **26**, 45 (1994).
61. D. Sengupta and M. T. Nguyen, *Mol. Phys.*, **89**, 1567 (1996).
62. M. T. Nguyen, D. Sengupta and L. G. Vanquickenborne, *Chem. Phys. Lett.*, **240**, 513 (1995).
63. E. M. Page, K. Hagen, D. A. Rice and R. Walsh, *J. Mol. Struct.*, in press (1997).
64. G. Pilcher, M. L. P. Leitâo, Y. Meng-Yan and R. Walsh, *J. Chem. Soc., Faraday Trans.*, **87**, 841 (1991).

65. R. Walsh, *Organometallics*, **8**, 1973 (1989).
66. J. A. Boatz and M. S. Gordon, *J. Phys. Chem.*, **94**, 3874 (1990).
67. J. A. Boatz, M. S. Gordon and R. L. Hildebrandt, *J. Am. Chem. Soc.*, **110**, 352 (1988).
68. W. V. Steele, unpublished results (private communication).
69. V. G. Genchel, N. V. Demidova, N. S. Nametkin, L. E. Gusel'nikov, E. A. Volnina, E. N. Burdasov and V. N. Vdovin, *Izv. Akad. Nauk SSSR, Ser. Khim.*, **10**, 2337 (1976).
70. R. T. Conlin, M. Namavari, J. S. Chickos and R. Walsh, *Organometallics*, **8**, 168 (1989).
71. Th. Brix, N. L. Arthur and P. Potzinger, *J. Phys. Chem.*, **93**, 8193 (1989).
72. J. A. Boatz, M. S. Gordon and L. R. Sita, *J. Phys. Chem.*, **94**, 5488 (1990).
73. D. A. Horner, R. S. Grev and H. F. Schaefer III, *J. Am. Chem. Soc.*, **114**, 2093 (1992).
74. D. H. Berry, unpublished results (private communication).
75. N. Al-Rubaiey, I. W. Carpenter and R. Walsh, unpublished results.
76. S. N. Gadzhiev and M. J. Agarunov, *J. Organomet. Chem.*, **11**, 415 (1968); **22**, 305 (1970).
77. J. C. Baldwin, M. F. Lappert, J. B. Pedley and J. A. Treverton, *J. Chem. Soc. (A)*, 1980 (1967).
78. R. Walsh, *J. Phys. Chem.*, **90**, 389 (1986).
79. A. M. Doncaster and R. Walsh, *J. Phys. Chem.*, **83**, 3037 (1979).
80. D. J. Lucas, L. A. Curtiss and J. A. Pople, *J. Chem. Phys.*, **99**, 6697 (1993).
81. C. L. Darling and H. B. Schlegel, *J. Phys. Chem.*, **97**, 8207 (1993).
82. M. R. Zachariah and W. Tsang, *J. Phys. Chem.*, **99**, 5308 (1995).
83. M. G. M. van der Vis and E. P. H. Cordfunke, *J. Chem. Thermodyn.*, **25**, 1205 (1993).
84. M. G. M. van der Vis, E. P. H. Cordfunke and R. J. M. Konings, *J. Phys. IV*, **C3**, 75 (1993).
85. J. A. Seetula, J. J. Russell and D. Gutman, *J. Am. Chem. Soc.*, **112**, 1347 (1990).
86. J. J. Russell, J. A. Seetula, R. S. Timonen, D. Gutman and D. F. Nava, *J. Am. Chem. Soc.*, **110**, 3084 (1988).
87. J. J. Russell, J. A. Seetula and D. Gutman, *J. Am. Chem. Soc.*, **110**, 3092 (1988).
88. J. A. Seetula, Y. Feng, D. Gutman, P. W. Seakins and M. J. Pilling, *J. Phys. Chem.*, **95**, 1658 (1991).
89. I. J. Kalinovski, D. Gutman, L. Krasnoperov, A. Goumri, W-J. Yuan and P. Marshall, *J. Phys. Chem.*, **98**, 9551 (1994).
90. P. Marshall, *J. Mol. Struct. (Theochem)*, **313**, 19 (1994).
91. L. Ding and P. Marshall, *J. Chem. Soc., Faraday Trans.*, **89**, 419 (1993).
92. W. J. Bullock, R. Walsh and K. King, *J. Phys. Chem.*, **98**, 2595 (1994).
93. A. Goumri, W-J. Yuan, L. Ding and P. Marshall, *Chem. Phys. Lett.*, **204**, 296 (1993).
94. B. Ruscic and J. Berkowitz, *J. Chem. Phys.*, **95**, 2416 (1991).
95. B. H. Boo and P. B. Armentrout, *J. Am. Chem. Soc.*, **109**, 3549 (1987).
96. D. S. Horowitz and W. A. Goddard III, *J. Mol. Struct. (Theochem)*, **163**, 207 (1988)
97. L. A. Curtiss and J. A. Pople, *Chem. Phys. Lett.*, **144**, 38 (1988).
98. L. A. Curtiss, K. Raghavachari, G. W. Trucks and J. A. Pople, *J. Chem. Phys.*, **94**, 7221 (1991).
99. L. Ding and P. Marshall, *J. Am. Chem. Soc.*, **114**, 5754 (1992).
100. C. L. Darling and H. B. Schlegel, *J. Phys. Chem.*, **97**, 1368 (1993).
101. E. R. Fischer, B. L. Kickel and P. B. Armentrout, *J. Phys. Chem.*, **97**, 10204 (1993).
102. L. A. Curtiss, K. Raghavachari, P. W. Deutsch and J. A. Pople, *J. Chem. Phys.*, **95**, 2432 (1991).
103. M. B. Coolidge and W. T. Borden, *J. Am. Chem. Soc.*, **110**, 2298 (1988).
104. Y-D. Wu and C-L. Wong, *J. Org. Chem.*, **60**, 821 (1995).
105. D. M. Wetzel, K. E. Salomon, S. Berger and J. I. Brauman, *J. Am. Chem. Soc.*, **111**, 3835 (1989).
106. J. M. Kanabus-Kaminska, J. A. Hawari, D. Griller and C. Chatgilialoglu, *J. Am. Chem. Soc.*, **109**, 5267 (1987).
107. C. Chatgilialoglu, M. Guerra, A. Guerrini, A. Seconi, K. B. Clark, D. Griller, J. M. Kanabus-Kaminska and J. A. Martinho Simões, *J. Org. Chem.*, **57**, 2427 (1992).
108. A. R. Dias, H. P. Diogo, D. Griller, M. E. Pinas de Piedade and J. A. Martinho Simões, *Bonding Energetics in Organometallic Compounds*, ACS Symposium Series No. 428 (Ed. T. Marks), Chap. 14 *(Metal Bond Dissociation Enthalpies from Classical and Nonclassical Calorimetric Studies)*, 1990, p. 205.
109. E. A. Brinkman, S. Berger and J. I. Brauman, *J. Am. Chem. Soc.*, **116**, 8304 (1994).
110. R. Walsh, *Pure Appl. Chem.*, **59**, 69 (1987).
111. A. M. Doncaster and R. Walsh, *J. Chem. Soc., Faraday Trans. 1*, **72**, 2908 (1976).
112. N. Auner, R. Walsh and J. Westrup, *J. Chem. Soc., Chem. Commun.*, 207 (1986).
113. I. M. Davidson, T. J. Barton, K. J. Hughes, S. Ijadi-Maghsoodi, A. Revis and G. C. Paul, *Organometallics*, **6**, 644 (1987).

114. L. N. Krasnoperov, J. T. Niiranen, D. Gutman, C. F. Melius and M. D. Allendorf, *J. Phys. Chem.*, **99**, 14347 (1995).
115. P. Marshall, *Chem. Phys. Lett.*, **201**, 493 (1993).
116. R. S. Grev, *Adv. Organomet. Chem.*, **33**, 125 (1991).
117. R. Becerra, H. M. Frey, B. P. Mason, R. Walsh and M. Gordon, *J. Chem. Soc., Faraday Trans.*, **91**, 2723 (1995).
118. H. M. Frey, R. Walsh and I. M. Watts, *J. Chem. Soc., Chem. Commun.*, 1189 (1986).
119. J. G. Martin, M. A. Ring and H. E. O'Neal, *Int. J. Chem. Kinet.*, **19**, 715 (1987).
120. K. F. Roenijk, K. F. Jensen and R. W. Carr, *J. Phys. Chem.*, **91**, 5732 (1987).
121. H. K. Moffat, K. F. Jensen and R. W. Carr, *J. Phys. Chem.*, **95**, 145 (1991).
122. H. K. Moffat, K. F. Jensen and R. W. Carr, *J. Phys. Chem.*, **96**, 7683 (1992).
123. H. J. Mick, P. Roth and V. N. Smirnov, *Kinet. Katal.*, **37**, 5 (1996).
124. H. J. Mick, P. Roth and V. N. Smirnov and I. S. Zaslonko, *Kinet. Katal.*, **35**, 485 (1994).
125. S. K. Shin and J. L. Beauchamp, *J. Phys. Chem.*, **90**, 1507 (1986).
126. C. M. Van Zoeren, J. W. Thoman, J. I. Steinfeld and N. Rainbird, *J. Phys. Chem.*, **92**, 9 (1988).
127. J. Berkowitz, J. P. Greene, H. Cho and B. Ruscic, *J. Chem. Phys.*, **86**, 1235 (1987).
128. J. A. Pople, B. T. Luke, M. J. Frisch and J. S. Binkley, *J. Phys. Chem.*, **89**, 2198 (1985).
129. M. S. Gordon, D. R. Gano, J. S. Binkley and M. J. Frisch, *J. Am. Chem. Soc.*, **108**, 2191 (1986).
130. R. Walsh, *Organometallics*, **7**, 75 (1988).
131. S. K. Shin, K. K. Irikura, J. L. Beauchamp and W. A. Goddard III, *J. Am. Chem. Soc.*, **110**, 24 (1988).
132. J. A. Boatz and M. S. Gordon, *J. Phys. Chem.*, **94**, 7331 (1990).
133. R. Becerra, H. M. Frey, B. P. Mason and R. Walsh, *J. Chem. Soc., Faraday Trans.*, **89**, 411 (1993).
134. R. Becerra and R. Walsh, *Kinetics and mechanisms of silylene reactions: a prototype for gas-phase acid/base chemistry*, in *Research in Chemical Kinetics* (Eds. R. G. Compton and G. Hancock), Vol. 3, Elsevier, Amsterdam, 1995, p. 263.
135. R. Becerra and R. Walsh, *J. Phys. Chem.*, **91**, 5765 (1987).
136. H. H. Michels and R. H. Hobbs, *Chem. Phys. Lett.*, **207**, 389 (1993).
137. E. R. Fischer and P. B. Armentrout, *J. Phys. Chem.*, **95**, 4765 (1991).
138. M. Ahmed, P. Potzinger and H. Gg. Wagner, *J. Photochem. Photobiol. A*, **86**, 33 (1995).
139. R. S. Grev, G. E. Scuseria, A. C. Scheiner, H. F. Schaefer III and M. S. Gordon, *J. Am. Chem. Soc.*, **110**, 7337 (1988).
140. R. Becerra, H. M. Frey, B. P. Mason and R. Walsh, *Chem. Phys. Lett.*, **185**, 415 (1991).
141. J. R. Hartman, J. Famil-Ghiria, M. A. Ring and H. E. O'Neal, *Combust. Flame*, **68**, 43 (1987).
142. D. F. McMillan and D. M. Golden, *Annu. Rev. Phys. Chem.*, **33**, 493 (1982).
143. J. B. Pedley and B. S. Iseard, *CATCH Tables for Silicon Compounds*, University of Sussex, 1972.
144. M. S. Gordon and J. A. Boatz, *Organometallics*, **8**, 1978 (1989).

CHAPTER 5

The structural chemistry of organosilicon compounds

MENAHEM KAFTORY, MOSHE KAPON and MARK BOTOSHANSKY

Department of Chemistry, Technion–Israel Institute of Technology, Haifa 32000, Israel

---

I. INTRODUCTION

The question of how closely do the properties of organic compounds of silicon resemble those of derivatives of its congener carbon atom was raised more than a century ago. A question that follows is how close are the structural chemistry of the two atoms in their analogue compounds. The major properties that distinguish silicon from carbon and have a direct effect on the structural chemistry of the compounds of the two atoms are compared in Table 1. From the differences between these properties it is seen that, since the silicon atom is about 50% larger than the carbon atom, the bond lengths involving silicon are expected to be longer than the lengths of similar bonds involving carbon. The longer distance between silicon and its bonded element will cause a weakening of the π-bonding and lowering the barrier to rotation about the bonds will influence the out-of-plane bending, which will in turn affect the planarity of the silicon atom. The smaller electronegativity of silicon will affect the bond polarity and ionicity, which will in turn have a major influence on the bond lengths involving silicon. Steric effects caused by bulky substituents will, on the one hand be less important than in the carbon analogues because of the longer bond lengths, but, on the other hand, will have a greater effect because of the lower barrier to distortion. One of the striking differences between silicon and carbon atoms is the ease of formation of hypervalent species with silicon. Five- and six-coordinate silicon compounds are stable and the role of d orbitals in the bonding of silicon in these compounds is a subject of continuing debate[7,8].

TABLE 1. A comparison of some properties of carbon and silicon

Property	C	Si
Atomic radius (Bragg–Slater)[1] (Å)	0.7	1.1
Covalent radius[2] (Å)	0.772	1.169
Van der Waals radius[3] (Å)	1.70	2.17
Ionization energies (eV)[4]		
E_1	11.26	8.15
E_2	24.38	16.34
E_3	47.89	34.49
Electron affinity[5] (eV)	1.12	1.39
Electronegativity[2]	2.746	2.138
Dipole polarizability[6] (a.u.)	11.8	36.3

This review is not the first to discuss the structural chemistry of organosilicon compounds. There have been a few earlier reviews discussing various aspects of the structural chemistry of organosilicon compounds. The stereochemistry of elements of Group 15 and 16 bonded to silicon was reviewed in 1973[9,10]. In 1985 the geometry of silatranes was reviewed[11] and simulation of the reaction pathway for S_N2 substitution reactions at tetrahedral silicon using structural data was published[12]. Later on, in 1986, the structural chemistry of tricoordinate silicon was reviewed[13], and the X-ray and NMR studies on penta- and hexacoordinate silicon compounds were summarized[14]. The most comprehensive review on the structural chemistry of organosilicon compounds was published in 1989 by W. S. Sheldrick[15].

In the last decade we have been witnessing an explosion of information on the geometry of organosilicon compounds extracted from X-ray crystal structure determination (later referred to as XRD). The histogram given in Figure 1 shows the growth in the number of organosilicon compounds whose structures have been determined by XRD. Until 1980 the structure of only 525 such compounds were known, and most of the structural data were obtained by other methods such as electron diffraction (ED) or microwave spectroscopy (MW). Both methods were restricted to small and symmetric compounds. The crystal structures of 1446 compounds were known at the time that Sheldrick was writing his review. At the time of writing the present review the crystal structures of more than 6300 organosilicon compounds are known.

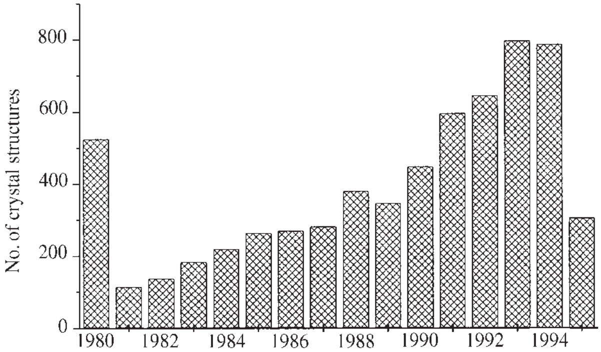

FIGURE 1. Annual growth in X-ray crystal structure determination of organosilicon compounds (the value for 1980 is the number of structures available in that year; not all compounds of 1995 are included)

Since most of the geometric parameters discussed in this review are obtained from X-ray crystal structure determination, it is important that the reader be familiar with some facts regarding the method. X-ray diffractions obtained from crystalline materials are being used to produce a model structure. The accuracy of the model and the refined structure is achieved by a least-squares procedure that minimizes the difference between the calculated and experimental structure factors (derived from the diffraction intensities). The accuracy of the refined structure is determined by the agreement factor (R); the smaller the R value, the better the experimentally determined structure. The reader should keep in mind that the position of the atom is determined by the centre of its electron density. However, comparison with the results of neutron diffraction, that provides the position of an atom as its centre of mass, shows that the shift of the centre of electron density from the centre of mass is in most cases of the order of only 0.001 Å. It should also be noted that in the presence of 'heavy' atoms (atoms with many electrons) in the molecule, the positions of the 'light' atoms are less accurate. The main disadvantage of the X-ray diffraction method for the structural determination of molecules and crystals is that the compound should be in its crystalline state. Consequently, the structures of unstable compounds and of small gaseous compounds are usually missing from XRD data. It means that calculated geometry by *ab initio* methods that are regularly conducted on small model molecules should be compared with caution with the experimental XRD molecular structures. The advantage of the method is evident from its extensive use and the data it provides form the base for every discussion related to molecular geometry. It should also be mentioned that, unlike isolated molecules in the gaseous state, molecules in the crystal are imposed on intermolecular forces that, when they are strong, they might affect the molecular geometry. The vast amount of XRD structural data available today, the ease of extracting the relevant parameters from computerized data banks and the possibility to perform statistical analysis of the data, all determine the character of the current review. The structural chemistry of organosilicon compounds reviewed here is mainly based on XRD structural data gathered from the Cambridge Structural Database (CSD)[16]. Comparison of the experimental geometry with optimized calculated geometry is given as well[17–29]. Statistical analysis was executed in most cases for the relevant geometric parameter. The review covers Si−X structural chemistry where X = C, Si, N, P, O, S, Hal. Silicon may be either tri-, tetra-, penta- or hexacoordinate and X may have different coordination numbers. For each type of Si−X bond, typical and exceptional compounds are shown and the relevant geometric parameters are listed in tables. Histograms are provided whenever statistical analysis was performed. Each compound that appears in the tables is designated by a six-letter code called Refcode, which is used in the CSD system. A complete list of Refcodes, IUPAC names and chemical formulae of all compounds appearing in this review can be obtained on request from the authors. The statistical analysis was executed with the Origin Program[30], the average value of a geometric parameter, its standard deviation (s.d.) and the standard deviation of the mean (s.m.) values were calculated according to equations 1–3:

$$d(\text{mean}) = (1/N)\Sigma d_i \tag{1}$$

where d(mean) is the calculated average, N is the number of data points; the sum is taken over all data points; d_i is the experimental value;

$$\text{s.d.} = \{[1/(N-1)]\Sigma[d_i - d(\text{mean})]^2\}^{1/2} \tag{2}$$

where s.d. is the standard deviation;

$$\text{s.m.} = (\text{s.d.})/(N)^{1/2} \tag{3}$$

where s.m. is the standard deviation of the mean.

II. SINGLE BONDS TO SILICON

A. Structural Chemistry of the Si−C Bond

Most of the organosilicon compounds contain bonds between the silicon and carbon atom. In the following paragraph the structural chemistry of the Si−C single bond is discussed, mostly in compounds with tetracoordinate silicon and tetracoordinate carbon atoms. The structural chemistry of the Si−C bond in compounds where the carbon coordination state is different, is also discussed. The Si−C bond is markedly polarized and the increase of the bond ionicity by attaching different substituents to either the silicon or the carbon atoms may affect its length. The electronic and steric effects are discussed later.

1. Si–C(sp) bonds

A single bond between a silicon and dicoordinate carbon atom involves a carbon atom in sp hybridization. XRD crystal structure analysis provided 238 individual Si−C(sp) bond lengths and Si−C(sp)−X bond angles. The average Si−C(sp) bond length was calculated from 226 values to be 1.839 Å (s.d. 0.02 Å, s.m. 0.001 Å). There were few exceptionally longer or shorter bonds; however, in almost all cases they resulted from disorder in the crystal or inaccurate crystal structure refinement. The histogram of Si−C(sp) bond lengths is shown in Figure 2. A list of Si−C(sp) bond lengths and Si−C(sp)−X bond angles for selected acyclic and cyclic compounds is given in Table 2. The histogram for the bond angles (Figure 2) shows that in most compounds the Si−C(sp)−X moiety is practically linear. The bonds that deviate from linearity are those in small cyclic molecular systems: Figure 3 shows the correlation between the Si−C(sp)−X bond angle and the ring size. Linearity is reached at a ring size of 10−12 atoms. No correlation was found between bond lengths and bond angles.

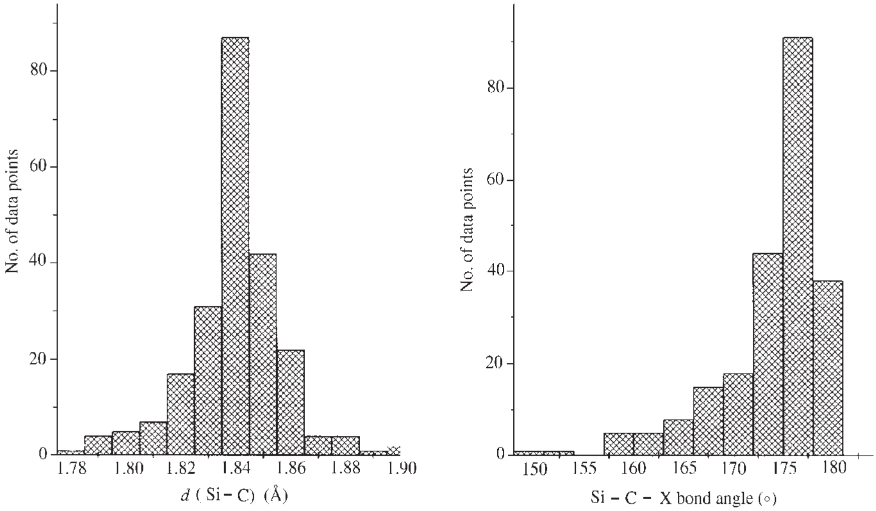

FIGURE 2. Histograms of Si−C(sp) bond lengths (left) and Si−C(sp)−X bond angles (right)

TABLE 2. Geometry of the Si−C(sp) bond in acyclic and cyclic compounds

Refcode	Compound	d(Si−C) (Å)	Si−C−X (°)	Reference
Acyclic				
HACLAY[a]	**1**	1.828	173.4	31
HEGGUV[a]	**2**	1.837	175.8	32
JUGBIW	**3**	1.840	179.0	33
JUGBOC[a]	**4**	1.855	174.3	33
SULMIV[a]	**5**	1.837	175.8	34
SUMTUP	**6**	1.807	177.6	35
VOBREJ[a]	**7**	1.837	177.1	36
WAWRER[a]	**8**	1.845	173.9	37
Cyclic				
KUPLAI[a]	**9**	1.843	148.7	38
TACKEN[a]	**10**	1.822	160.9	39
KUCVEJ[a]	**11**	1.842	166.7	40
KUCVIN[a]	**12**	1.832	164.3	40
BUXJUZ[a]	**13**	1.844	166.0	41
DUWCAZ[a]	**14**	1.842	177.0	42
DUWCED[a]	**15**	1.844	173.6	42
LENHUH[a]	**16**	1.840	173.1	43
DUWCIH[a]	**17**	1.850	179.4	42
DUWCON[a]	**18**	1.844	178.2	42
JALGOS[a]	**19**	1.843	177.5	44
SAYJIL[a]	**20**	1.821	176.3	45
PEZFOP[a]	**21**	1.839	177.9	46
JOHJUL	**22**	1.834	178.5	47

[a] Average values are given.

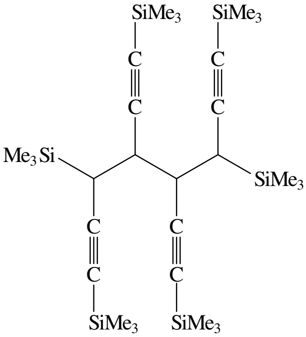

(1)

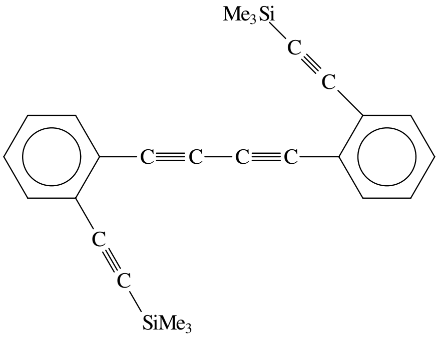

(2)

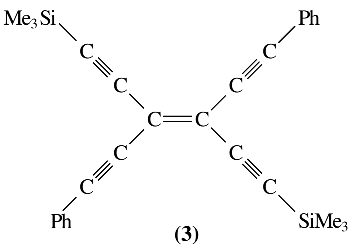

(3)

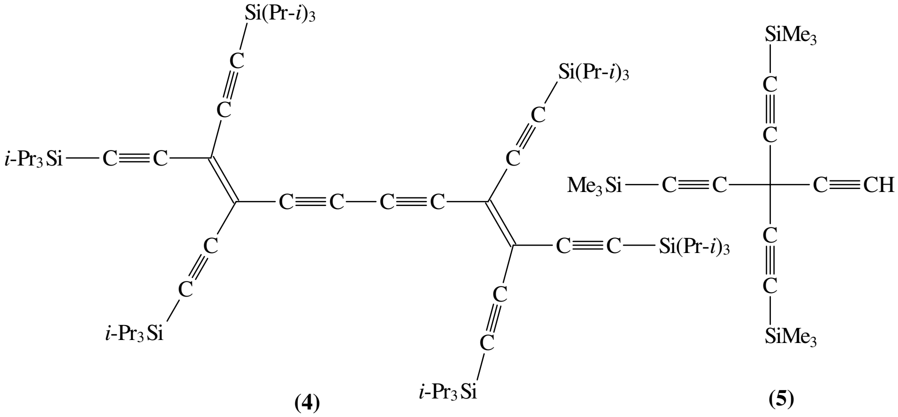

(4)

(5)

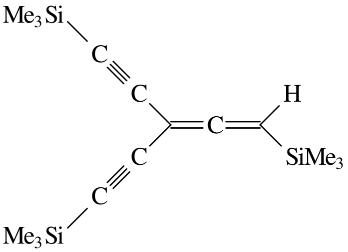

(6)

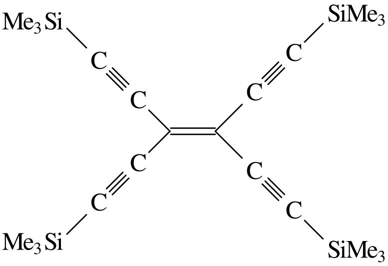

(7)

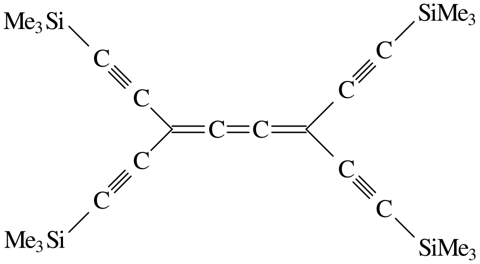

(8)

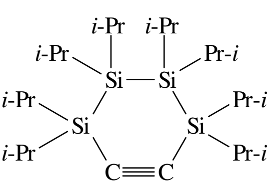

(9)

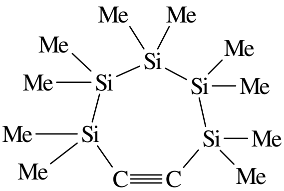

(10)

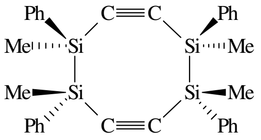

(11)

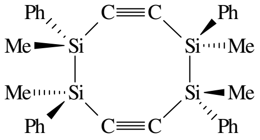

(12)

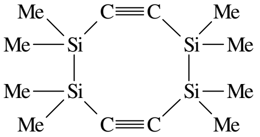

(13)

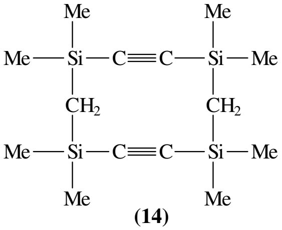

(14)

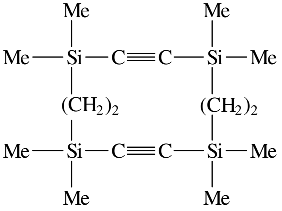

(15)

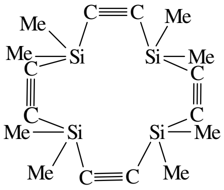

(16)

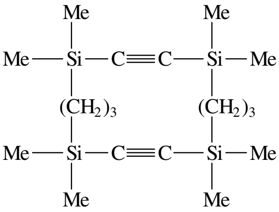

(17)

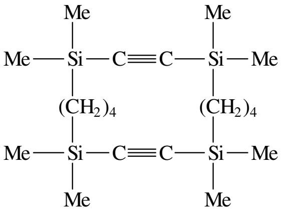

(18)

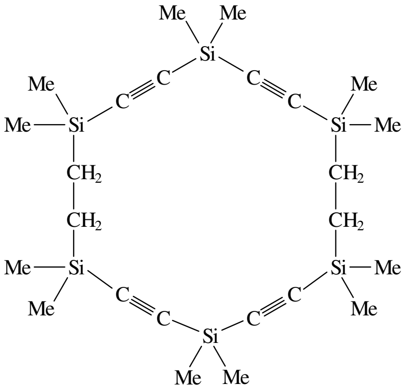

(19)

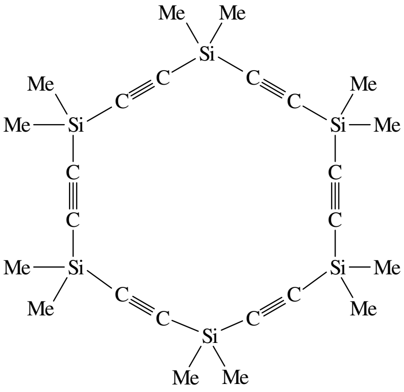

(20)

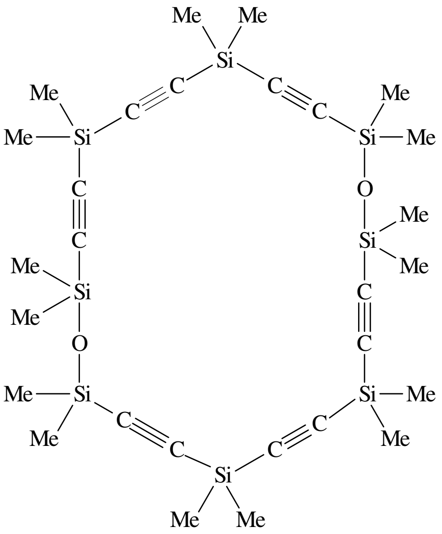

(21)

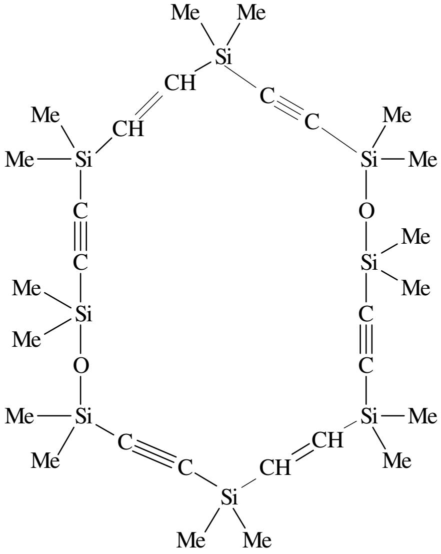

(22)

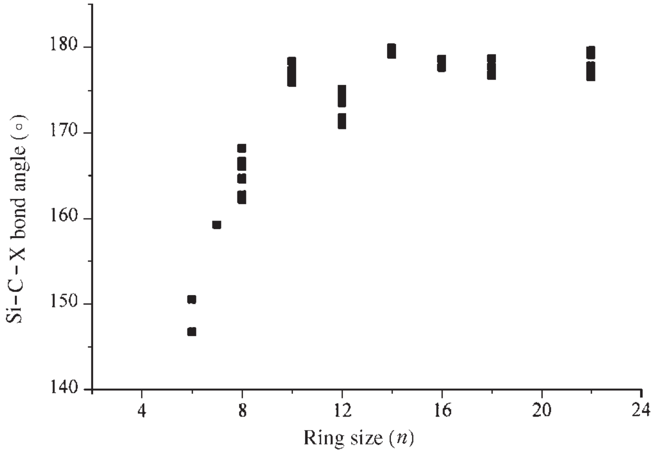

FIGURE 3. Correlation between Si−C(sp)−X bond angle and ring size

2. Si−C(sp^2) bonds

Replacing an sp carbon atom by an sp^2 carbon affects the lengthening of the Si−C bond by only 0.04 Å. The average length of the bond was calculated from 633 individual values obtained from XRD to be 1.878 Å (s.d. 0.03 Å, s.m. 0.001 Å). The histogram is shown in Figure 4. A list of Si−C (sp^2) bond angles and the sum of valence bond angles at the carbon atom are given in Table 3. Exceptionally longer bond lengths have

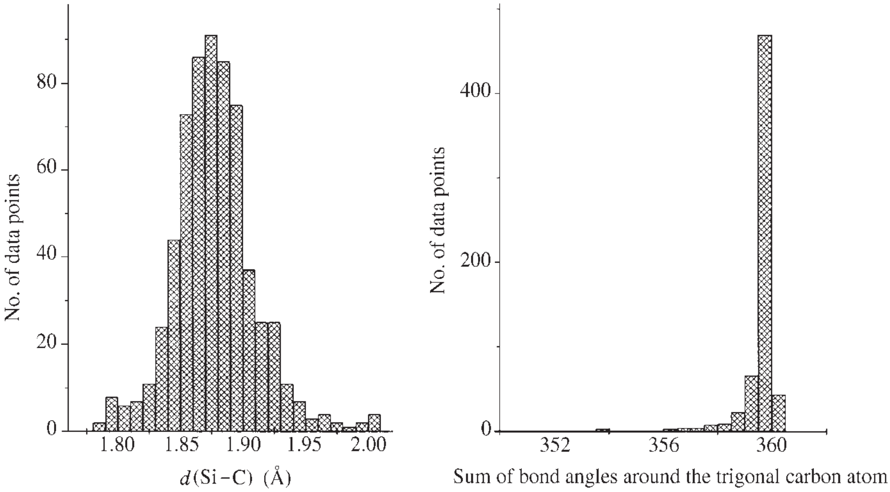

FIGURE 4. Histograms of Si−C(sp^2) bond lengths d (left) and the sum of Si−C(sp^2)−X bond angles (right)

been detected in compounds such as **29** and **30**, where the bond ionicity is reduced by the substitution on the carbon atom. Compound **31** provides a very good example of the effect of attachment of electronegative substituents on silicon on the bond length. Two different groups are bonded to the same sp^2 carbon atom, $SiMe_3$ and $SiCl_2Bu$-*t*. The Si−C bond length in the first is 1.867 Å, and 1.784 Å in the second. The shortening is a result of the attachment of two chlorine atoms to the same silicon atom. The planarity of the sp^2 carbon atom was checked by calculating the sum of its valence bond angles (see Figure 4). In almost all the compounds the sp^2 carbon is practically planar. The exceptional pyramidality of the sp^2 carbon found in **32** with the sum of valence angles equal to 323.8° is suspicious and might be in error.

TABLE 3. Geometry of Si−C(sp^2) bonds

Refcode	Compound	d (Si−C) (Å)	Σ Si−C−X (°)	Reference
Typical				
VOLZAX	**23**	1.879	360.0	48
WEGBAL	**24**	1.880	360.0	49
SUCVAN[a]	**25**	1.840	359.6	50
YIMYEY[a]	**26**	1.873	358.0	51
YIMYIC[a]	**27**	1.878	357.6	51
YOSSUU	**28**	1.906	360.0	52
Exceptions				
FERMIY	**29**	2.006	360.0	53
PESICR	**30**	2.003	360.0	54
LEBPIR	**31**	1.784	359.7	55
LEBPIR	**31**	1.867	359.7	55
KIZDUS	**32**	1.909	323.8	56

[a] Average values are given.

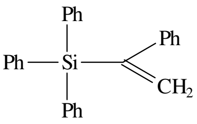

(23)

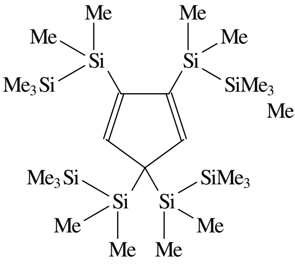

(24)

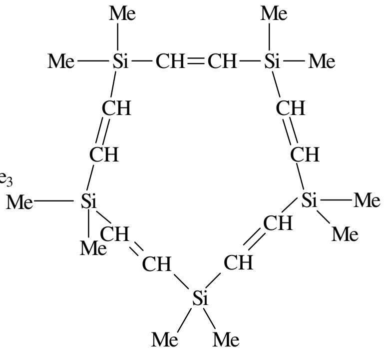

(25)

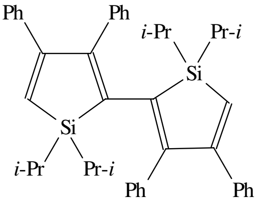

(26)

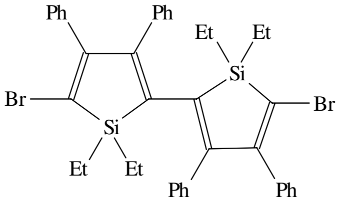

(27)

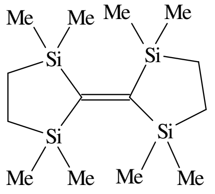

(28)

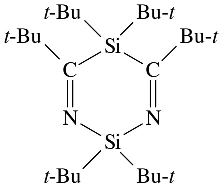

(29)

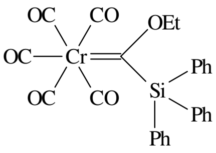

(30)

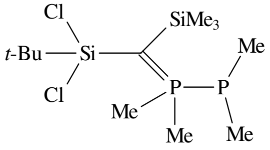

(31)

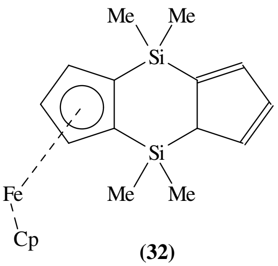

(32)

3. Si–C(aryl) bonds

The average Si–C(aryl) bond length was calculated from 3371 individual values to be 1.879 Å (s.d. 0.03 Å, s.m. 0.0004 Å). The histogram is shown in Figure 5. The experimental Si–C(aryl) bond length is in very good agreement with the calculated value.

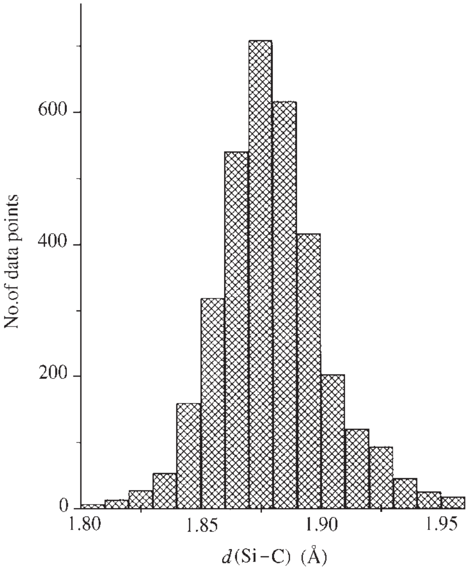

FIGURE 5. Histogram of Si—C(aryl) bond lengths

Ab initio computations at the Hartree–Fock level were carried out on two conformations of silylbenzene[17] and the Si—C(phenyl) bond length was calculated to be 1.8729 Å. Longer Si—C(aryl) bonds have been found in only a few compounds, such as **33**[57] (1.941, 1.954 and 1.972 Å) and **34**[58] (1.910 and 1.993 Å). In both cases the lengthening may be attributed to steric congestion.

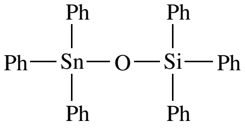

$Ph_3Sn{-}O{-}SiPh_3$

(33)

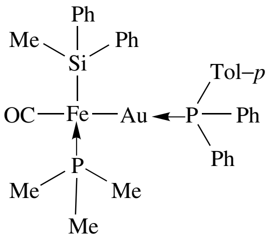

(34)

4. Si—C(sp^3) bonds

Perhaps the most abundant organosilicon fragment is trimethylsilyl. The average Si—C(sp^3) bond length was calculated from 19169 individual XRD experimental values to be 1.860 Å (s.d. 0.02 Å, s.m. 0.0002 Å). The histogram is shown in Figure 6a. The strong effect of electronegative groups attached to the silicon atom is shown in Figure 6b. The average Si—CH_3 bond is significantly shorter by 0.014 Å, upon attachment of at least one fluorine atom to the silicon.

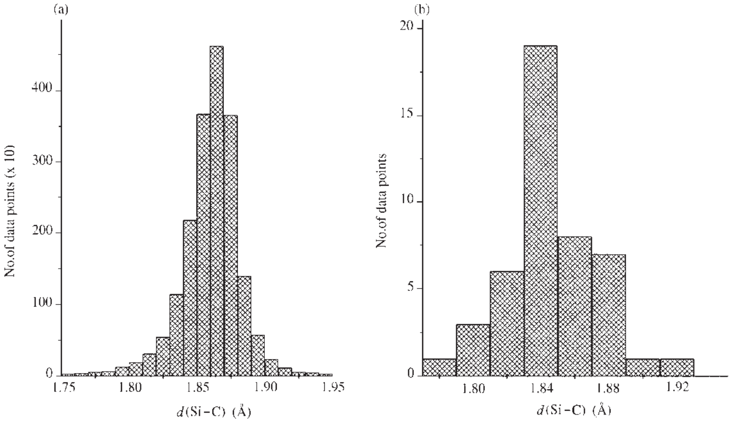

FIGURE 6. Histograms of Si−C(sp^3) bond lengths in trimethylsilyl (a) and Si−CH_3 bond lengths in fluorosilanes (b)

Replacement of a methyl by *t*-Bu causes a marked lengthening of the Si−C(sp^3) bond length (by 0.047 Å) to 1.907 Å (calculated from 889 XRD bond lengths, s.d. 0.03 Å, s.m. 0.001 Å). The histogram is shown in Figure 7. The effect of electronegative substituents is demonstrated by three compounds, **35**[59], **36**[60] and **37**[61]. In **35**, where a fluorine atom is attached to silicon, increasing the Si−C bond ionicity, the bond length is 'short' (1.888 Å); additional shortening is observed (1.801, 1.823 Å) when three fluorine atoms are attached to the silicon atom, as in **36**. In **37**, where a fluorine atom is bonded to the carbon atom, the Si−C bond length is 'long' (1.923 Å).

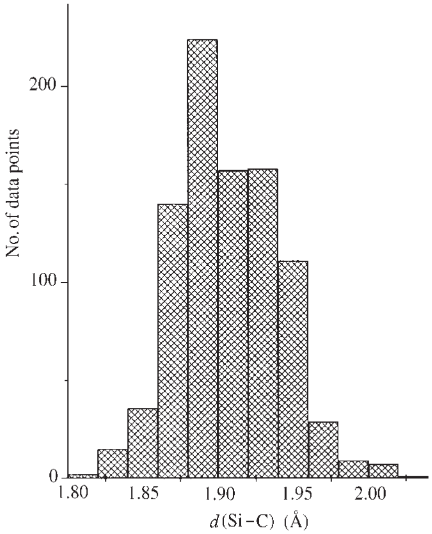

FIGURE 7. Histogram of Si−C(*t*−Bu) bond lengths

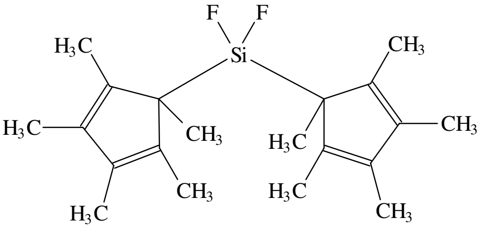

(35)

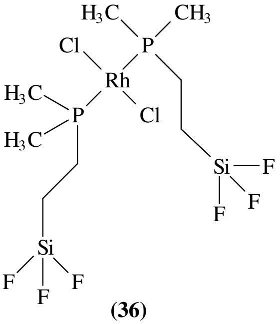

(36)

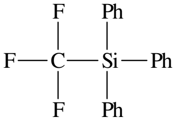

(37)

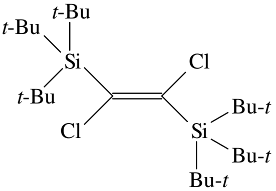

(38)

The lengthening of the Si—C(sp^3) bond length can also be a result of steric congestion, which is demonstrated by **38**[62] containing tri-*tert*-butylsilyl moieties. The average Si—C bond length in **38** is 1.953 Å, compared to 1.907 Å in compounds with a single *t*-Bu bonded to silicon.

5. Si—C bonds in silacyclopropanes and silacyclopropenes

Si—C bond lengths in silacyclopropanes are only slightly shorter (1.84–1.87 Å; see Table 4) than in any other Si—C(sp^3) bonds, such as with methyl (1.860 Å). However, the same bond in silacyclopropenes is significantly shorter (1.81–1.82 Å) than that found for Si—C(sp^2) bonds (1.879 Å). In both silacyclopropanes and silacyclopropenes C—Si—C bond angles are smaller than 60° due to the longer Si—C than C—C bond length. Since the C=C bond lengths in silacyclopropenes are even shorter than the C—C bond lengths in silacyclopropanes, the C—Si—C bond angle in the former (42–44°) is smaller than in the latter (47–52°).

TABLE 4. Geometry of Si—C bond in silacyclopropanes and in silacyclopropenes

Refcode	Compound	*d*(Si—C) (Å)	C—Si—C (°)	Reference
Cyclopropane				
GIMNUL[a]	**39**	1.869	50.2	63
WARREM[a]	**40**	1.843	46.9	64
KIPDES[a]	**41**	1.868	49.5	65
Cyclopropene				
FIBJUV[a]	**42**	1.811	43.0	66
YOSZEL[a]	**43**	1.817	43.7	67
SUJGOT	**44**	1.827[b]	42.7	68

[a] Average values are given.

[b] The second bond length seems to be in error.

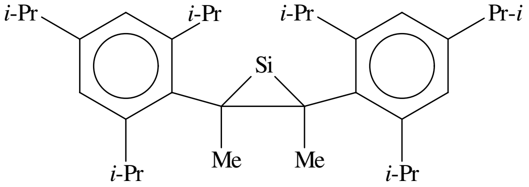

(39)

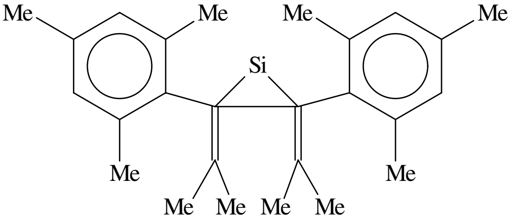

(40)

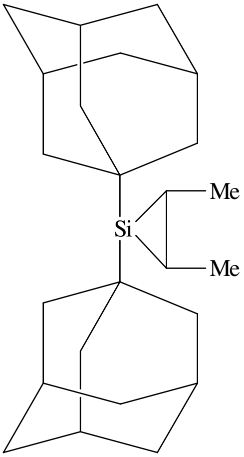

(41)

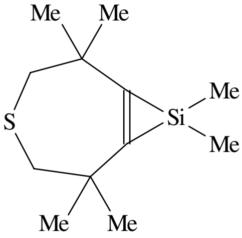

(42)

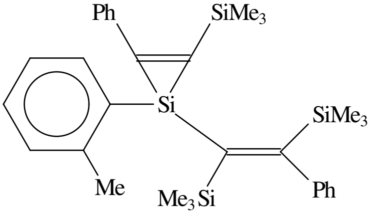

(43)

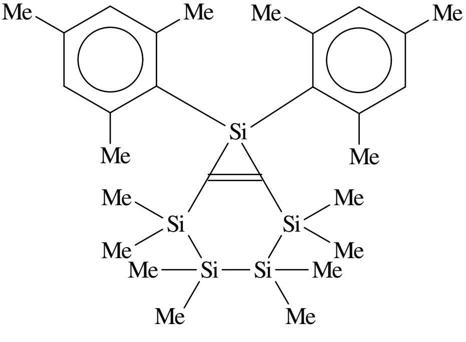

(44)

6. Structural chemistry of Si bonds with special functional groups

The structural chemistry of silicon bonded to special functional groups such as acetyl group, cyanide and isocyanide deserves special attention. Acylsilanes having the general formula R_3SiCOR constitute an interesting class of chemical compounds. They are sensitive to light and rather unstable, particularly in a basic environment, where they react to give aldehydes and more complex rearrangement products. Furthermore, their electronic and vibrational spectra display some unusual features. The enhanced reactivity of substituents attached to the carbon atom in the α-position to silicon is referred to as the α-silicon effect. The experimental Si$-$C(sp^2) bond length in these compounds containing acetyl groups is 1.925 Å, significantly longer (by 0.05 Å) than the regular Si$-$C(sp^2) bonds of 1.878 Å. A list of selected compounds is given in Table 5. Optimization[24] of the geometry of SiH_3CHO at the Hartree–Fock 6-31++G** level reveals a Si$-$CO bond length of 1.930 Å, slightly longer than the experimental value. The lengthening is attributed to the effect of attachment of the electronegative oxygen atom to the carbon atom, thus lowering the Si$-$C bond ionicity.

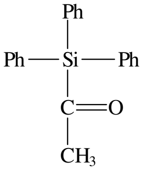

(45)

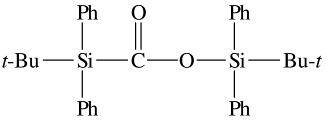

(46)

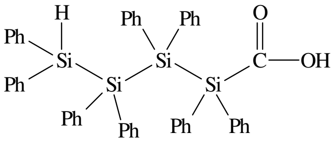

(47)

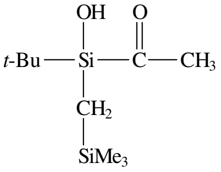

(48)

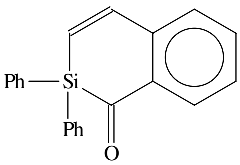

(49)

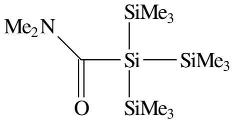

(50)

The crystal structures of only three silyl cyanides **51–53** are known. The Si$-$CN bond length in **51**[75] is 1.823 Å, the CN triple bond length is 1.211 Å and the Si$-$C$-$N bond angle is 178.7°. In the dicyanide **52**[76] the Si$-$CN bond length increases to 1.862 and 1.873 Å while CN triple bonds decrease to 1.121 and 1.148 Å. The Si$-$C$-$N bond angle is unchanged (178.0, 178.1°). When the silicon is pentacoordinate, as in **53**[77], the Si$-$CN bond length is elongated to 2.051 Å, the CN triple bond is unchanged (1.144 Å) and the Si$-$C$-$N bond angle is 175.0°. The silyl cyanide[78] H_3SiCN was used as a model for calculating the geometry of the Si$-$C and the CN triple bond lengths which resulted in values of 1.872 Å and 1.141 Å, respectively.

Agreement between the calculated[78] geometry and experimental geometry of silyl isocyanide is poor. The calculated Si$-$N bond length in H_3SiNC is 1.745 Å, and the NC triple bond length is 1.165 Å. The experimental values are 1.819 and 1.785 Å for the

TABLE 5. Geometry of Si$-$C bonds

Refcode	Compound	d(Si$-$C) (Å)	Σ Si$-$C$-$X (°)	Reference
ACTPSI	**45**	1.925	360.0	69
GIFPUG	**46**	1.925	359.8	70
JEMXII	**47**	1.925	360.0	71
JOPDUN	**48**	1.925	360.0	72
PSITET	**49**	1.921	360.0	73
VIGZOA[a]	**50**	1.907	360.0	74

[a] Average values are given.

Si−N bond, 1.087 and 1.152 Å for the N−C triple bond, and 175.1 and 169.9° for the Si−N−C bond angles in **54**[79] and **55**[80], respectively.

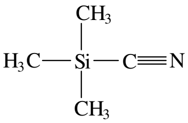

$H_3C-\overset{CH_3}{\underset{CH_3}{Si}}-C\equiv N$

(51)

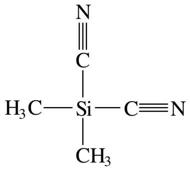

$H_3C-\overset{N\equiv C}{\underset{CH_3}{Si}}-C\equiv N$

(52)

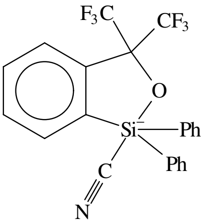

(53)

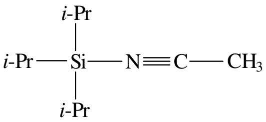

$i\text{-Pr}-\overset{i\text{-Pr}}{\underset{i\text{-Pr}}{Si}}-N\equiv C-CH_3$

(54)

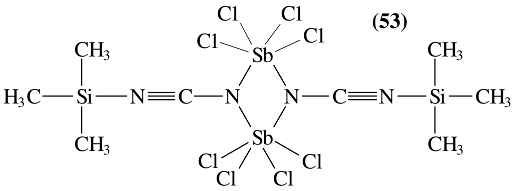

(55)

B. Structural Chemistry of the Si−Si Bond

1. Si–Si bonds in compounds with tetracoordinate silicon atoms

The sum of covalent radii for the Si−Si bond length in disilanes is 2.341 Å. The average bond length in acyclic disilanes was calculated from 541 individual XRD values to be 2.358 Å (s.d. 0.02 Å, s.m. 0.0009 Å). The histogram is shown in Figure 8. Bond lengths

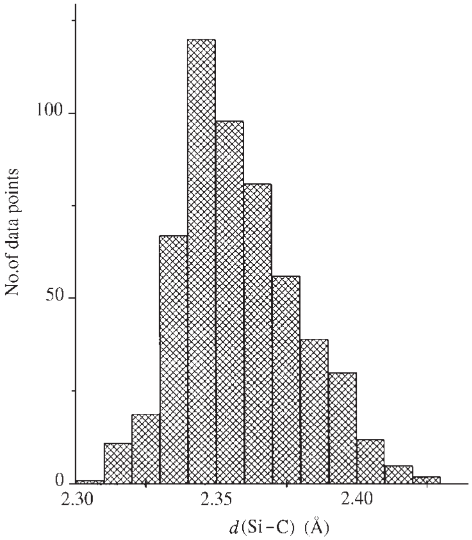

FIGURE 8. Histogram of Si−Si bond lengths in acyclic compounds

for selected compounds whose XRD data were published between 1990 and 1995 are listed in Table 6. Compounds with exceptionally long Si−Si bond lengths are also listed in Table 6. The significant lengthening (0.23 Å on average) of the Si−Si bond in **64–67** is attributed to the steric effect. In all four compounds the silicon atoms are substituted by more than one bulky group such as *t*-Bu or iodine atoms.

Slightly longer Si−Si bond lengths are found in cyclic disilane compounds. The average of this bond was calculated from 472 XRD values to be 2.372 Å (s.d. 0.04 Å, s.m. 0.002 Å). The histogram is shown in Figure 9. The cyclopolysilanes show a range of unique electronic and spectroscopic properties, which arise from electron delocalization in the Si−Si σ framework. Examples of cyclopolysilanes with ring sizes of 3, 4, 5, 6, 7, 13 and 16 are shown in **68–74**. Si−Si bond lengths and Si−Si−Si bond angles for these compounds are given in Table 7. Figure 10 shows the dependence of the Si−Si−Si bond angles on the ring size. The ring strain is relieved when the ring size is larger than 8.

Exceptionally long Si−Si bonds in cyclopolysilanes are found in compounds such as **75–79** which are bearing bulky substituents such as *t*-Bu.

C. Structural Chemistry of the Si−N Bond

More than 700 individual Si−N bond lengths were known at the time Sheldrick[15] wrote his review (1989). Although he did not make any remark on the source of the data, it seems that most were available from X-ray crystal structure analysis. At the time of writing the present review (July 1996) more than 3000 individual experimental Si−N bond lengths were obtained from the CSD bank for crystal structure data. It is not possible to present a comprehensive list in this review and therefore we provide a statistical analysis of the data and mention a few typical and exceptional compounds together with their Si−N structural features.

The Schomaker-Stevenson corrected sum of covalent radii of silicon and nitrogen is 1.80 Å and, in general, it was shown[15] that shorter bonds have been found for compounds in which the ionicity of the bond is enhanced by the attachment of either a very

TABLE 6. Typical and exceptional Si−Si bond lengths in acyclic compounds

Refcode	Compound	*d*(Si−Si) (Å)	Reference
Typical			
PERPAD	**56**	2.346	81
JUKYIX[a]	**57**	2.388	82
PAFNOZ[a]	**57**	2.363	83
PERPOR[a]	**57**	2.375	83
LINKAU[a]	**58**	2.362	84
YASYEW[a]	**59**	2.395	85
YASYIA[a]	**60**	2.373	85
JUXPIB	**61**	2.368	86
WAJZUC	**62**	2.335	87
WIGNUV	**63**	2.391	88
Exceptional			
TAGNOE	**64**	2.453	89
DIVKIC	**65**	2.697	90
FAPBON[a]	**66**	2.614	91
GERSEB	**67**	2.593	92

[a] Average values are given.

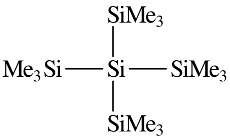

$\mathrm{Me_3Si{-}\overset{SiMe_3}{\underset{SiMe_3}{Si}}{-}SiMe_3}$

(56)

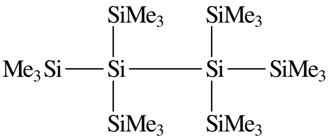

$\mathrm{Me_3Si{-}\overset{SiMe_3}{\underset{SiMe_3}{Si}}{-}\overset{SiMe_3}{\underset{SiMe_3}{Si}}{-}SiMe_3}$

(57)

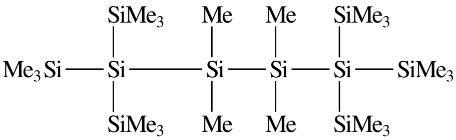

$\mathrm{Me_3Si{-}\overset{SiMe_3}{\underset{SiMe_3}{Si}}{-}\overset{Me}{\underset{Me}{Si}}{-}\overset{Me}{\underset{Me}{Si}}{-}\overset{SiMe_3}{\underset{SiMe_3}{Si}}{-}SiMe_3}$

(58)

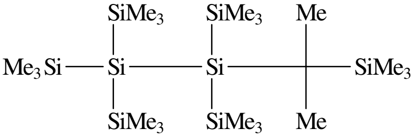

$\mathrm{Me_3Si{-}\overset{SiMe_3}{\underset{SiMe_3}{Si}}{-}\overset{SiMe_3}{\underset{SiMe_3}{Si}}{-}\overset{Me}{\underset{Me}{+}}{-}SiMe_3}$

(59)

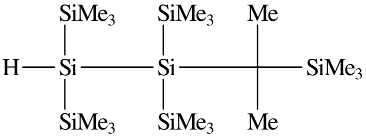

$\mathrm{H{-}\overset{SiMe_3}{\underset{SiMe_3}{Si}}{-}\overset{SiMe_3}{\underset{SiMe_3}{Si}}{-}\overset{Me}{\underset{Me}{+}}{-}SiMe_3}$

(60)

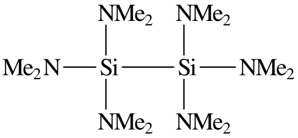

$\mathrm{Me_2N{-}\overset{NMe_2}{\underset{NMe_2}{Si}}{-}\overset{NMe_2}{\underset{NMe_2}{Si}}{-}NMe_2}$

(61)

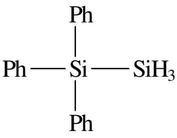

$\mathrm{Ph{-}\overset{Ph}{\underset{Ph}{Si}}{-}SiH_3}$

(62)

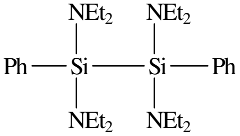

$\mathrm{Ph{-}\overset{NEt_2}{\underset{NEt_2}{Si}}{-}\overset{NEt_2}{\underset{NEt_2}{Si}}{-}Ph}$

(63)

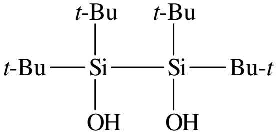

$\mathrm{\mathit{t}\text{-}Bu{-}\overset{\mathit{t}\text{-}Bu}{\underset{OH}{Si}}{-}\overset{\mathit{t}\text{-}Bu}{\underset{OH}{Si}}{-}Bu\text{-}\mathit{t}}$

(64)

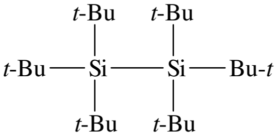

$\mathrm{\mathit{t}\text{-}Bu{-}\overset{\mathit{t}\text{-}Bu}{\underset{\mathit{t}\text{-}Bu}{Si}}{-}\overset{\mathit{t}\text{-}Bu}{\underset{\mathit{t}\text{-}Bu}{Si}}{-}Bu\text{-}\mathit{t}}$

(65)

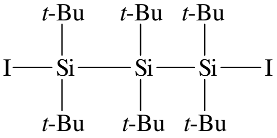

$\mathrm{I{-}\overset{\mathit{t}\text{-}Bu}{\underset{\mathit{t}\text{-}Bu}{Si}}{-}\overset{\mathit{t}\text{-}Bu}{\underset{\mathit{t}\text{-}Bu}{Si}}{-}\overset{\mathit{t}\text{-}Bu}{\underset{\mathit{t}\text{-}Bu}{Si}}{-}I}$

(66)

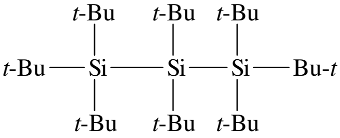

$\mathrm{\mathit{t}\text{-}Bu{-}\overset{\mathit{t}\text{-}Bu}{\underset{\mathit{t}\text{-}Bu}{Si}}{-}\overset{\mathit{t}\text{-}Bu}{\underset{\mathit{t}\text{-}Bu}{Si}}{-}\overset{\mathit{t}\text{-}Bu}{\underset{\mathit{t}\text{-}Bu}{Si}}{-}Bu\text{-}\mathit{t}}$

(67)

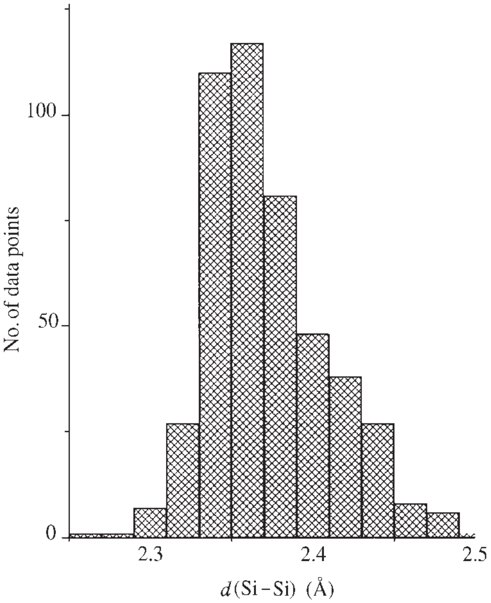

FIGURE 9. Histogram of Si—Si bond lengths in cyclic compounds

electronegative substituent to silicon or an electropositive metal to nitrogen. Long Si—N bonds are due to the reduction of the ionicity by the attachment of a substituent in the opposite manner, namely attachment of either an electronegative substituent to nitrogen or an electropositive substituent to silicon. Long bonds may also be a result of steric effects. In cases where the nitrogen atom is involved in a very strong hydrogen bond, the Si—N bond may lengthen.

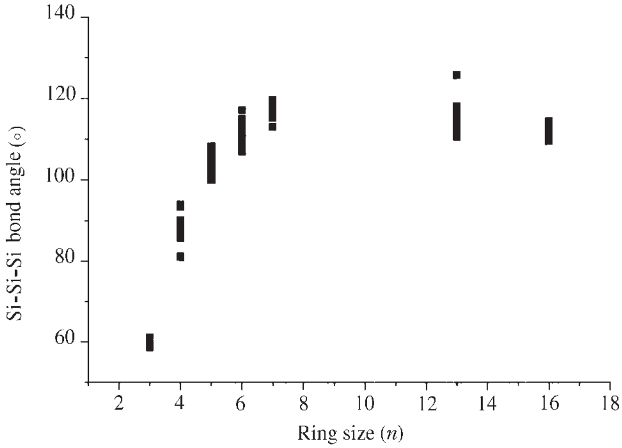

FIGURE 10. The dependence of Si—Si—Si bond angles on ring size in cyclopolysilanes

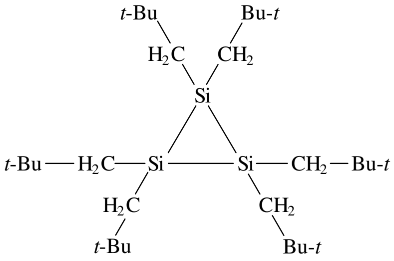

(68)

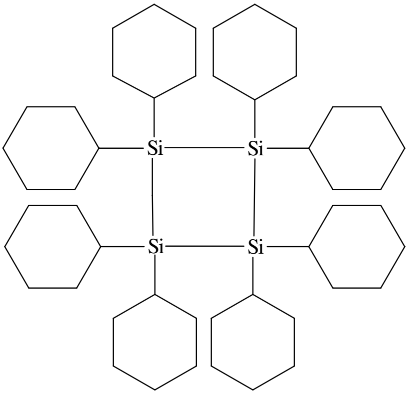

(69)

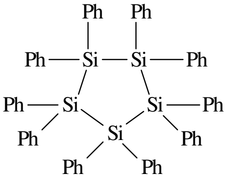

(70)

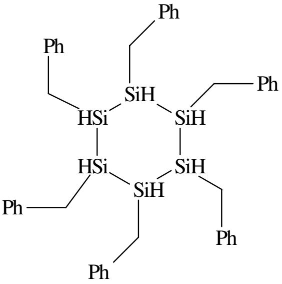

(71)

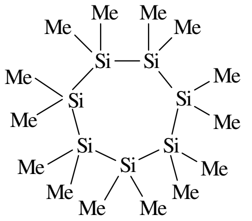

(72)

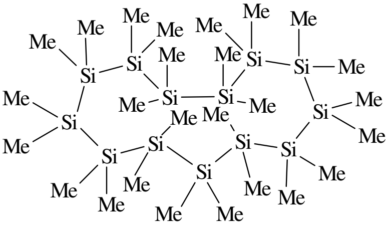

(73)

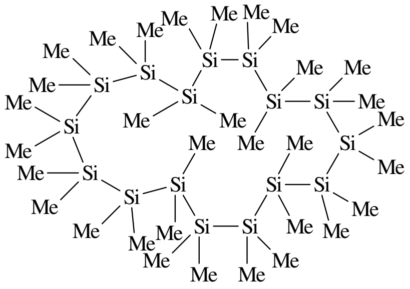

(74)

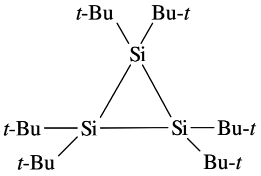

(75)

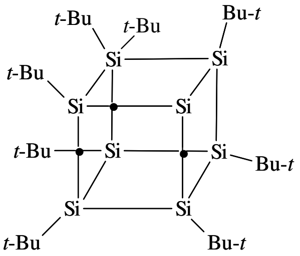

(76)

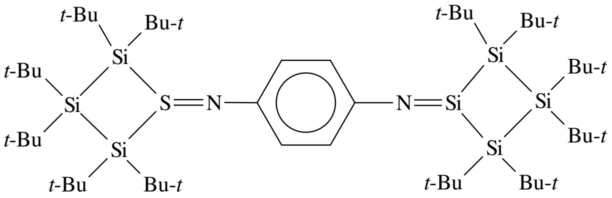

(77)

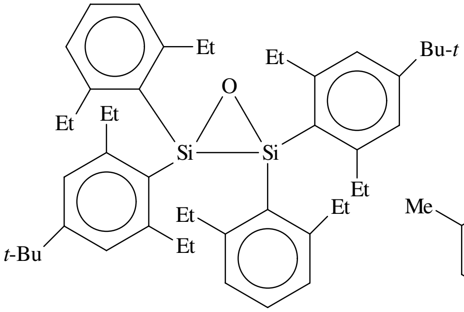

(78)

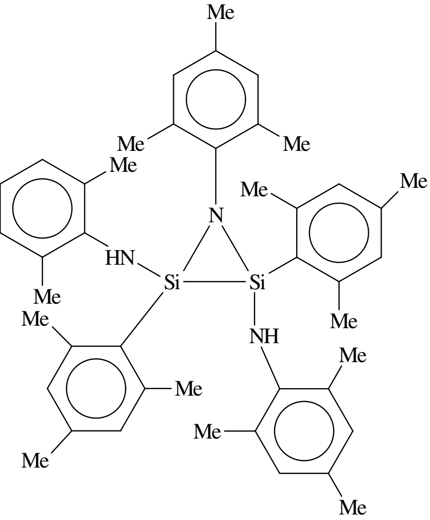

(79)

TABLE 7. Typical and exceptional Si–Si bond lengths in cyclic compounds with tetracoordinate silicon atoms

Refcode	Compound	d(Si–Si) (Å)	Si–Si–Si(°)	Reference
Typical				
COHBIC[a]	**68**	2.385	59.1	93
SOWBEL[a]	**69**	2.391	88.4	94
DPHPSI[a]	**70**	2.394	104.5	95
HASKAN[a]	**71**	2.332	117.0	96
DIDJOP[a]	**72**	2.341	116.2	97
FALSEQ[a]	**73**	2.355	115.7	98
FALSIU[a]	**74**	2.355	111.9	98
Exceptional				
CIHRAM	**75**	2.511	60.0	99
YISJUF[a]	**76**	2.494	90.1	100
SUDJEG[a]	**77**	2.500	78.8	101
LANLAN	**78**	2.214	—	102
LAWZIS	**79**	2.228	—	103

[a] Average values are given.

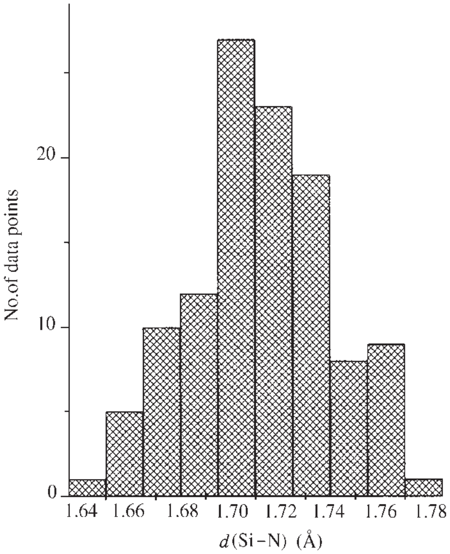

FIGURE 11. Histogram of Si—N bond lengths in compounds with tetracoordinate silicon and dicoordinate nitrogen atoms

1. Si—N bonds in compounds with tetracoordinate silicon and dicoordinate nitrogen atoms

The average Si—N bond length in this class of compounds was calculated from 115 individual experimental values obtained by XRD, and was found to be 1.713 Å (s.d. 0.03 Å and s.m. 0.003 Å). The histogram is shown in Figure 11. Selected typical and outlying Si—N bond lengths and Si—N—X bond angles are listed in Tables 8 and 9, respectively. The calculated[25] (3-21G*) Si—N(sp^2) bond length in H_3SiNCH_2 of 1.755 Å is significantly longer than the experimental value. In **80–84** Si=N double bonds are also present, but such bonds are discussed later in this review.

TABLE 8. Geometry of Si—N bonds in compounds with tetracoordinate silicon and dicoordinate nitrogen atoms

Refcode	Compound	d(Si—N) (Å)	Si—N—X (°)	Reference
DOKWUV	**80**	1.696	177.8	104
DOKXEG[a]	**81**	1.660	161.2	104
JIWGAX	**82**	1.661	174.2	105
GEVRII	**83**	1.678	169.4	104
LENVUV	**84**	1.662	149.8	106
POHXEP[a]	**85**	1.689	158.9	107
WECWIK	**86**	1.725	119.9	108
YEFJUO[a]	**87**	1.758	129.8	109
WEDDOY[a]	**88**	1.728	149.2	110
YOVLEA	**89**	1.739	155.7	111
LECDIG[a]	**90**	1.707	155.0	112

[a] Average values are given.

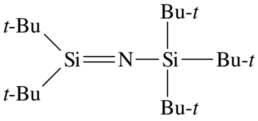

(80)

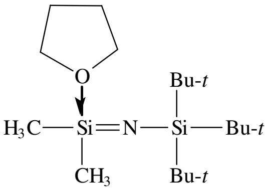

(81)

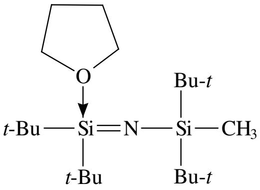

(82)

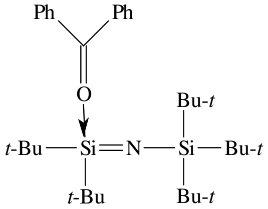

(83)

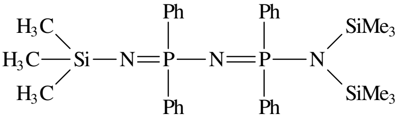

(84)

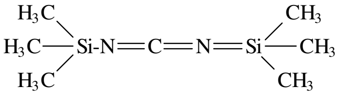

(85)

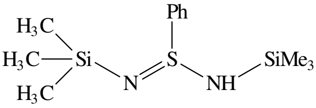

(86)

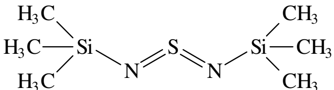

(87)

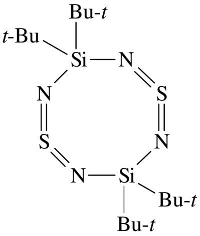

(88)

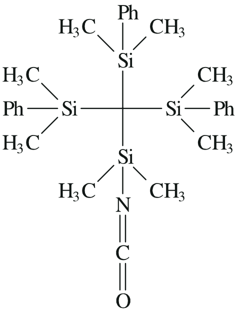

(89)

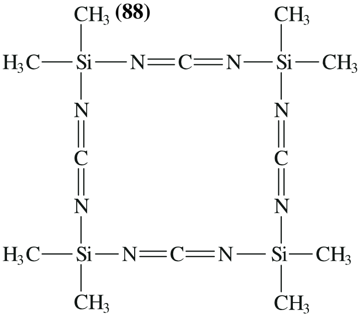

(90)

TABLE 9. Exceptionally long and short Si−N bonds in compounds with tetracoordinate silicon and dicoordinate nitrogen atoms

Refcode	Compound	d(Si−N) (Å)	Si−N−X (°)	Reference
Long bonds				
JALSUK	**91**	1.798	109.7	113
KEGTIZ[a]	**92**	1.808	168.0	114
KETMON	**93**	1.822	178.3	115
TMSIDM	**94**	1.807	120.0	116
Short bonds				
YEBVAC	**95**	1.673	136.0	117
YEBVAC	**95**	1.791	130.4	117
SETYEV	**96**	1.649	151.1	118

[a] Average values are given.

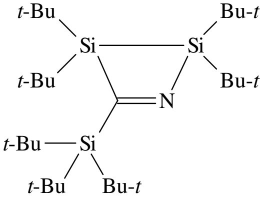

(91)

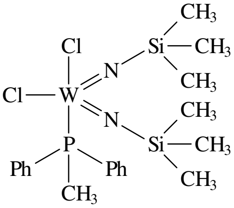

(92)

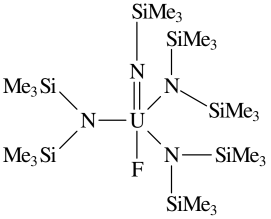

(93)

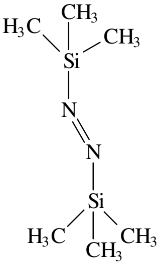

(94)

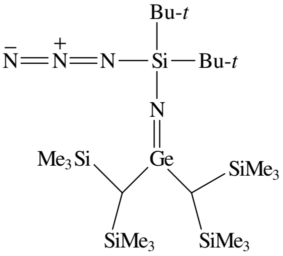

(95)

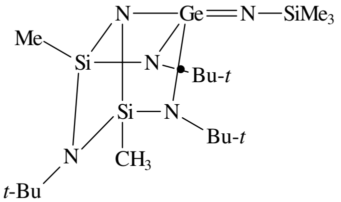

(96)

Si−N=X bond angles are wider than in the carbon analogues. Upon bending, the HOMO (which effectively contains the lone pair of nitrogen) and a σ^* orbital of higher energy can interact, leading to the stabilization of a bent geometry provided that the gap in energy between the two orbitals is small. Upon increasing the electronegativity on going from carbon to silicon, the energy gap will increase and the Si−N=X bond angle will widen. A similar effect will occur by the attachment of more electropositive substituent to nitrogen. Examples of the two extremes are seen in **80** where, by attachment of an electropositive Si atom to the nitrogen, the Si−N=Si bond angle widens to 177.8°, while in **86** where the electronegative substituent, the sulphur atom, is attached to nitrogen, the Si−N=S bond angle closes to 119.9°. It is also evident from the Si−N bond lengths listed in Table 8 that the Si−N bond length shortens upon linearization of the Si−N=X bond.

91–96 are compounds with exceptionally long or short Si−N bond lengths. Compound **95** provides an interesting example in which both long and short Si−N bonds exist in the same molecule. The attachment of the more electropositive germanium atom to nitrogen imposes an increase of ionicity and Si−N bond shortening (1.673 Å). The attachment of the azide to silicon causes a lengthening of the bond (1.791 Å). The shortening of the Si−N bond length caused by the attachment of germanium to the nitrogen atom is also seen in **96** (1.649 Å).

2. Si−N bonds in compounds with tetracoordinate silicon and tricoordinate nitrogen atoms

There are about 3000 individual experimental Si−N bond lengths obtained by XRD. Histograms of the Si−N bonds and of the sum of valence angles around the nitrogen atom are given in Figure 12. Selected typical and exceptional Si−N bond lengths and the sum of valence bond angles are listed in Tables 10 and 11, respectively. The average Si−N bond length was calculated from 2908 individual values to be 1.739 Å (s.d. 0.03 Å, and s.m. 0.0006 Å). Lengthening of the Si−N bond was observed in many compounds such as **112–120**, where the substituent at the nitrogen atom has a comparable electronegative character to that of nitrogen. Boron and phosphorus are most frequently found to be the substituents on nitrogen that cause the lengthening. On the other hand, the attachment of a strong electropositive atom to nitrogen increases the ionicity of the bond and the extent of its shortening. The effect is exemplified by compounds **124,125** and **126** where Li or Ca are the atoms attached to nitrogen. The same effect may also be achieved by the attachment of a strong electronegative atom or group to the silicon atom. Thus, in **121** and **122** where chlorine atoms are attached to silicon, the Si−N bonds are short (1.678 and 1.679 Å, respectively), while in a similar compound lacking the chlorine atoms **123** the Si−N bond is longer (1.703 Å).

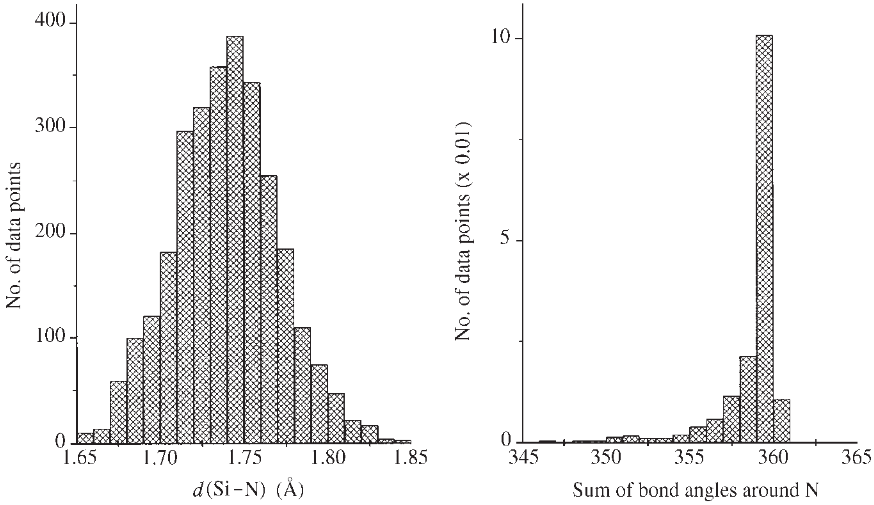

FIGURE 12. Histograms of Si−N bonds (left) and sum of valence bond angles around nitrogen atoms (right)

TABLE 10. Geometry of the Si–N bond in compounds with tetracoordinate silicon and tricoordinate nitrogen atoms

Refcode	Compound	d(Si–N) (Å)	Σ (X–N–X) (°)	Reference
PECBUU	**97**	1.710	351.9	119
LEHHEL[a]	**98**	1.700	360.0	120
LINTIL[a]	**99**	1.733	359.3	121
YEPTUI[a]	**100**	1.724	360.0	122
JUXPIB[a]	**101**	1.716	359.1	123
WIGNUV[a]	**102**	1.726	359.4	124
YEPTOC	**103**	1.718	358.8	122
PEWDAW[a]	**104**	1.738	360.0	125
WAHGOB[a]	**105**	1.728	358.7	126
WAJLOI[a]	**106**	1.729	359.0	127
WAJLUO[a]	**107**	1.729	359.8	127
PECCEF[a]	**108**	1.711	350.3	119
WEHMAX[a]	**109**	1.736	359.1	128
WEHLOK[a]	**110**	1.740	359.9	128
YUDLAK[a]	**111**	1.717	360.0	129

[a] Average values are given.

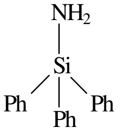

(97)

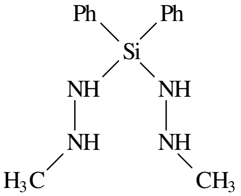

(98)

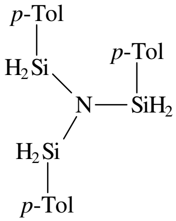

(99)

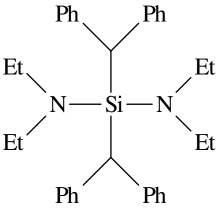

(100)

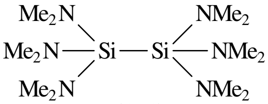

(101)

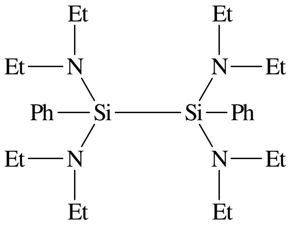

(102)

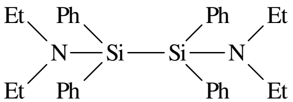

(103)

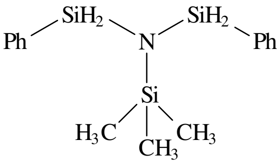

(104)

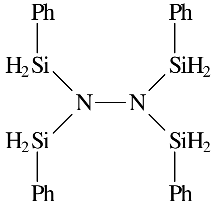

(105)

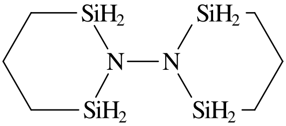

(106)

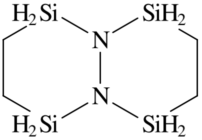

(107)

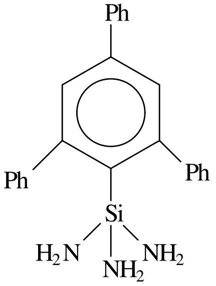

(108)

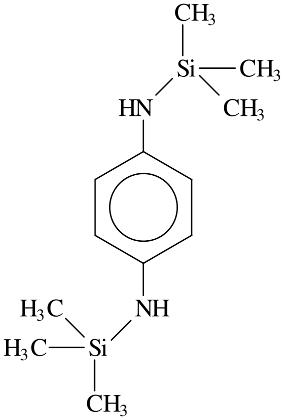

(109)

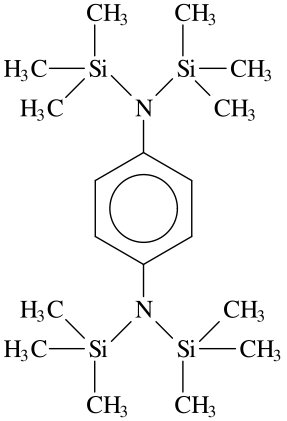

(110)

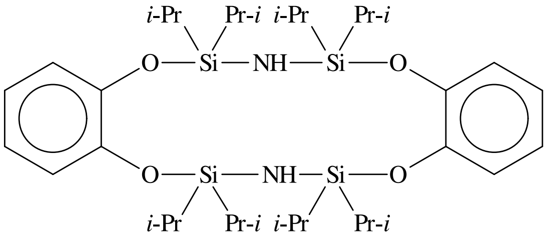

(111)

It is interesting to note that, with no exception, the tricoordinate nitrogen atom that is bonded to the tetracoordinate silicon atom is not pyramidal. The theoretical sum of valence angles in tetrahedral geometry (sp^3 for nitrogen atom) is 329.5°, and 360° for trigonal geometry (sp^2 for nitrogen atom). The histogram shown, in Figure 12 (right) shows very clearly that the nitrogen atom is practically planar. The average value is

TABLE 11. Geometry of exceptionally long and short Si−N bonds in compounds with tetracoordinate silicon and tricoordinate nitrogen atoms

Refcode	Compound	d(Si−N) (Å)	Σ (X−N−X) (°)	Reference
Long bonds				
LAWNAY[a]	**112**	1.804	359.9	130
LEMMIZ[a]	**113**	1.791	357.6	131
PEFPEV[a]	**114**	1.768	360.0	132
PEFPOF[a]	**115**	1.780	360.0	132
PEFRAT	**116**	1.756	358.2	132
PEPNON	**117**	1.795	357.1	133
PODSUW[a]	**118**	1.770	359.0	134
YERWOH[a]	**119**	1.816	358.2	135
YOVYEN	**120**	1.825	360.0	136
Short bonds				
HEZBUJ	**121**	1.679	359.8	137
HEZCEU[a]	**122**	1.678	354.7	137
HEZCIY[a]	**123**	1.703	356.1	137
LEZREN[a]	**124**	1.678	360.0	138
SUPSUR	**125**	1.675	358.8	139
WAKGIY	**126**	1.650	359.9	140

[a] Average values are given.

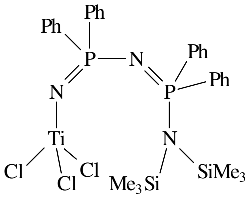

(112)

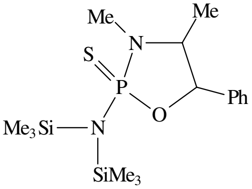

(113)

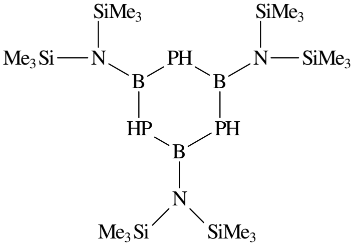

(114)

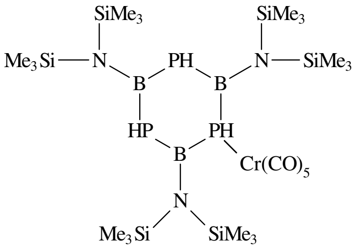

(115)

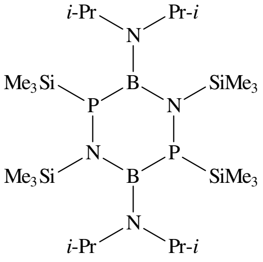

(116)

calculated to be 358.4° (s.d. 9.3°, s.m. 0.2°). The planarity of the tricoordinate nitrogen atom bonded to the silicon atom was established more than 40 years ago. The interaction of nitrogen 2p-orbitals normal to the NSi_3 plane in $(H_3Si)_3N$ with silicon 3d-orbitals of appropriate symmetry provided a simple explanation for both the planarity of nitrogen and the shortening of the bond compared with the corrected sum of the covalent radii (1.80 Å).

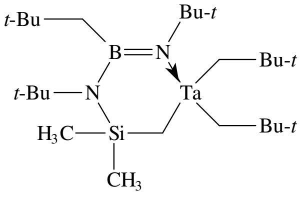

(117)

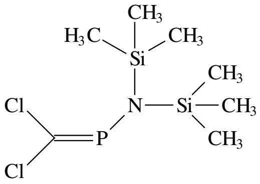

(118)

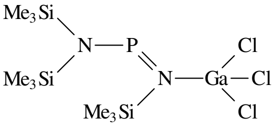

(119)

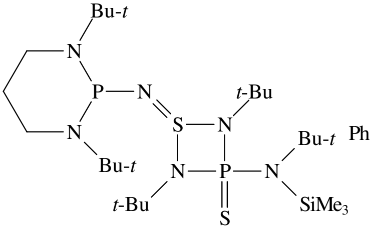

(120)

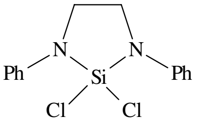

(121)

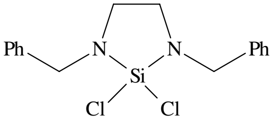

(122)

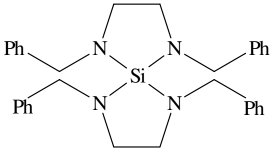

(123)

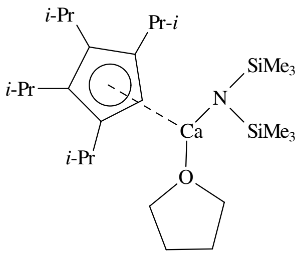

(124)

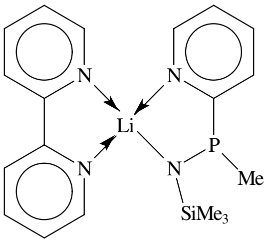

(125)

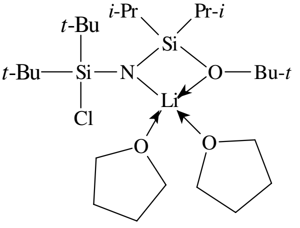

(126)

3. Si–N bonds in compounds with pentacoordinate silicon and tricoordinate nitrogen atoms

Pentacoordinate silicon forms two types of bonds with tricoordinate nitrogen atoms, a pure covalent bond and a N → Si dative bond. The first is significantly shorter than the second. The average covalent Si–N bond length in compounds where pentacoordinate silicon atom is bonded to tricoordinate nitrogen atom was calculated from 48 XRD experimental values to be 1.761 Å (s.d. 0.06 Å, s.m. 0.009 Å). An example of the difference in bond length is shown in **127**[141] where the covalent Si–N bond lengths are 1.766 and 1.770 Å and the dative bond is 2.333 Å.

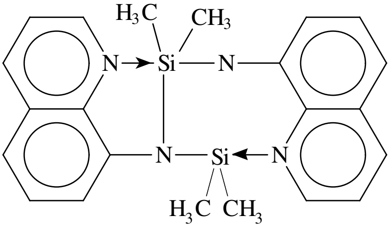

(127)

4. *Si−N bonds in compounds with hexacoordinate silicon and tricoordinate nitrogen atoms*

All Si−N bonds in compounds where hexacoordinate silicon atom is bonded to tricoordinate nitrogen atoms are dative bonds, where the nitrogen atom provides its lone-pair electrons to the bond. The average Si → N bond was calculated from 31 individual values to be 1.969 Å (s.d. 0.05 Å and s.m. 0.008 Å).

D. Structural Chemistry of the Si−P Bond

1. *Si−P bonds in compounds with tetracoordinate silicon and dicoordinate phosphorus atoms*

There are only five known X-ray crystal structures of compounds containing a tetracoordinate silicon atom that is bonded to a dicoordinate phosphorus atom. In three, **128**–**130**, the phosphorus atom is singly bonded to silicon and doubly bonded to either carbon or phosphorus atoms while in the remaining two, **131** and **132**, the phosphorus atom is singly bonded to both substituents. The Si−P bond lengths and the Si−P−X bond angles are given in Table 12. On the average the Si−P bond length in the first three compounds is longer by 0.1 Å than the average in the last two compounds. The double bond of phosphorus has the same effect as two single bonds in regards to the Si−P bond length and can be compared to compounds with tricoordinate phosphorus atoms.

2. *Si−P bonds in compounds with tetracoordinate silicon and tri- or tetracoordinate phosphorus atoms*

The sum of the covalent radii of silicon and phosphorus is 2.27 Å and, since the ionic character of the Si−P bond is relatively limited, no significant difference of the Si−P bond length is expected. The average of the experimental (X-ray diffraction) Si−P bond

TABLE 12. Geometry of the Si−P bond in compounds with tetracoordinate silicon and dicoordinate phosphorus atoms

Refcode	Compound	*d*(Si−P) (Å)	Si−P−X (°)	Reference
DARPOB	**128**	2.237	106.2	142
KAXZOY	**129**	2.269	98.6	143
PINZIV	**130**	2.263	109.3	144
KITKEV[a]	**131**	2.161	103.5	145
VEJNED	**132**	2.167	105.4	146

[a] Average values are given.

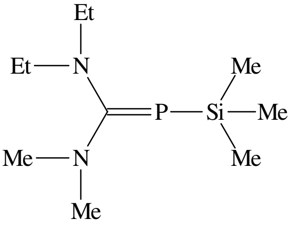

(128)

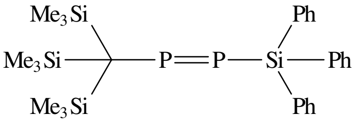

(129)

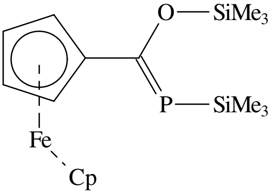

(130)

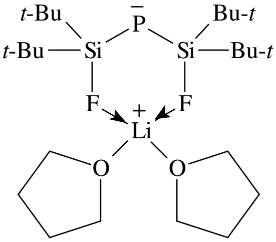

(131)

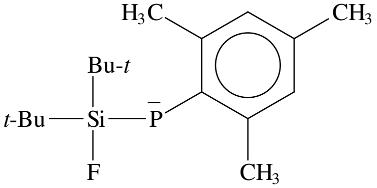

(132)

length in silylphosphines containing a tricoordinate phosphorus atom is calculated for 165 values to be 2.265 Å (s.d. 0.02 Å, s.m. 0.002 Å). The histogram for the Si−P bond lengths is shown in Figure 13. The geometry of typical compounds **133–142** is given in Table 13. In contrast to nitrogen, the tricoordinate phosphorus atom is pyramidal as shown by the sum of the bond angles it forms (Tables 13 and 14). The planar tricoordinate phosphorus atom has not been observed. The closest to planarity are observed whenever the phosphorus atom is bonded to a phenyl ring such as in **137** or in **148**, as indicated by the sum of bond angles involving the phosphorus atom, 345.2° and 351.7°, respectively.

The geometry of exceptionally long or short Si−P bond lengths is given in Table 14 for compounds **143–145** and **146–148**, respectively. The lengthening may be attributed to strain and steric congestion in compounds **144** and **145** and to the reduction of polarity in **143**. An electropositive substituent on the phosphorus atom will reduce the Si−P bond length as found in **147** and **148**.

The average Si−P bond length in compounds containing a tetracoordinate phosphorus atom was calculated with 144 individual bond lengths obtained experimentally by X-ray crystal structures. The Si−P bond length is 2.265 Å (s.d. 0.02 Å and s.m. 0.002 Å). The histogram is shown in Figure 14. Selected Si−P bond lengths for typical compounds **149–153** are listed in Table 15.

Exceptionally long and short Si−P bond lengths are found in **154–156** and in **157–163**, respectively, and the X-ray experimental values are summarized in Table 16. Most of the

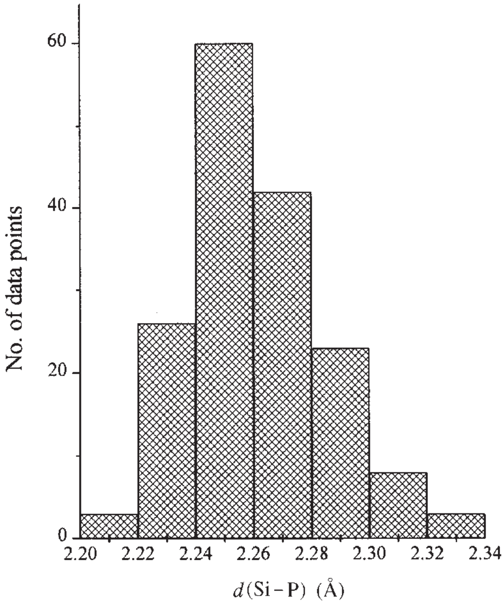

FIGURE 13. Histogram of the Si−P bond lengths in compounds containing tetracoordinate silicon and tricoordinate phosphorus atoms

TABLE 13. Geometry of the Si−P bond in compounds with tetracoordinate silicon and tricoordinate phosphorus atoms

Refcode	Compound	d(Si−P) (Å)	Σ (Si−P−X) (°)	Reference
HAZKUO	**133**	2.246	328.1	147
HAZLAV	**134**	2.298	301.4	147
JIXZAR[a]	**135**	2.228	201.6	148
SENLAY[a]	**136**	2.280	231.1	149
SIFMEZ[a]	**137**	2.264	345.2	150
SIYXUT[a]	**138**	2.278	333.0	151
VIXVAZ	**139**	2.256	290.4	152
VOBSOU[a]	**140**	2.245	294.3	153
WAPLOO[a]	**141**	2.293	304.6	154
WAPLUU[a]	**142**	2.257	321.3	154

[a] Average values are given.

short Si−P bonds are detected in compounds where the phosphorus is bonded to a very electropositive atom such as lithium, thus increasing the ionicity of the Si−P bond and its shortening.

E. Structural Chemistry of the Si−O Bond

In 1976, Si−O structural data were available for only 51 organosilicon compounds. The structural features of Si−O bonds have been reviewed by Voronkov and colleagues[172] in

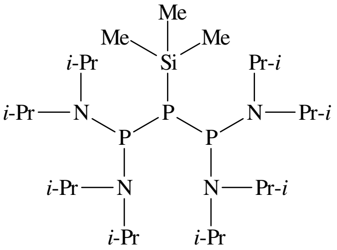

(133)

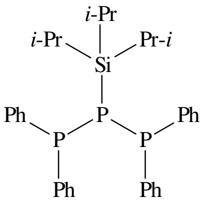

(134)

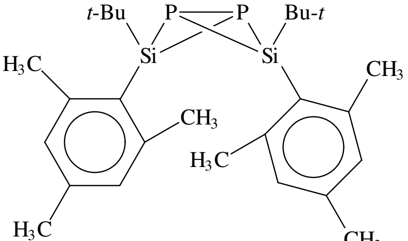

(135)

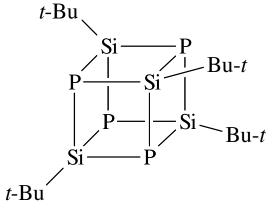

(136)

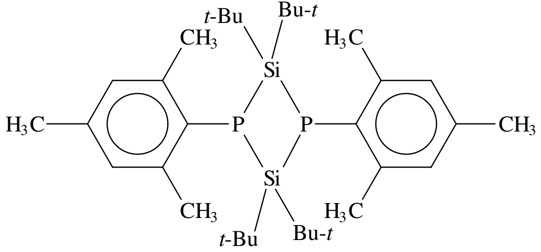

(137)

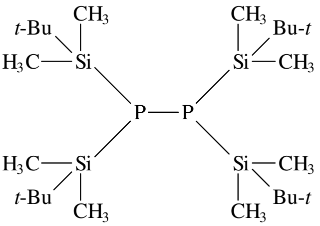

(138)

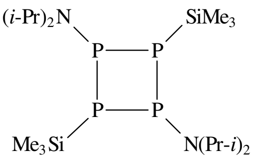

(139)

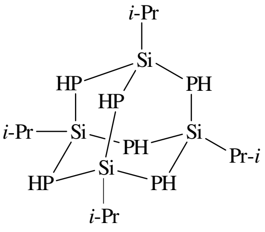

(140)

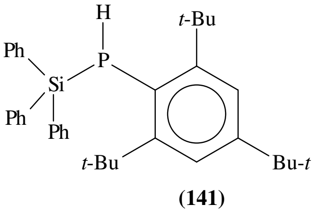

(141)

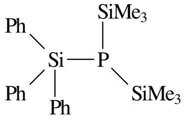

(142)

TABLE 14. Exceptionally long and short Si−P bonds in compounds with tetracoordinate silicon and tricoordinate phosphorus atoms

Refcode	Compound	d(Si−P) (Å)	Σ (P−Si−X) (°)	Reference
Long bonds				
DABLAT	**143**	2.306	301.3	155
JUWJAM[a]	**144**	2.318	331.4	156
VENKUU[a]	**145**	2.300	260.7	157
Short bonds				
DETTAX	**146**	2.227	307.7	158
FOWLOS[a]	**147**	2.218	325.4	159
WAPLEE	**148**	2.223	351.7	154

[a] Average values are given.

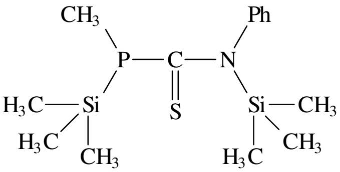

(143)

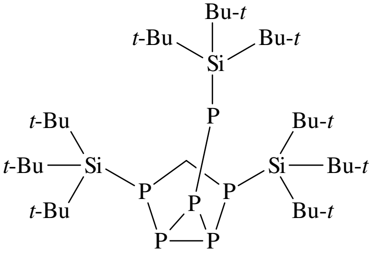

(144)

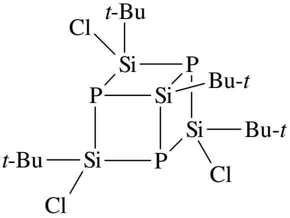

(145)

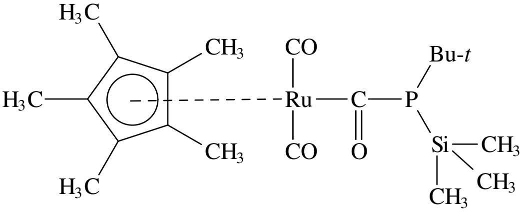

(146)

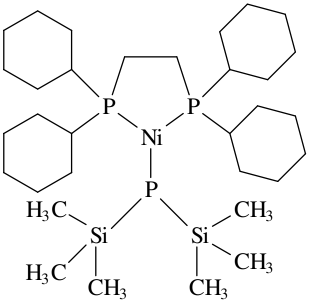

(147)

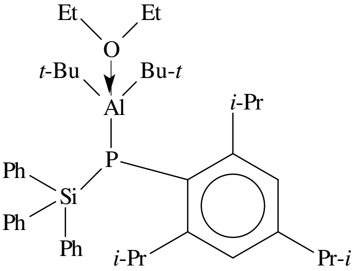

(148)

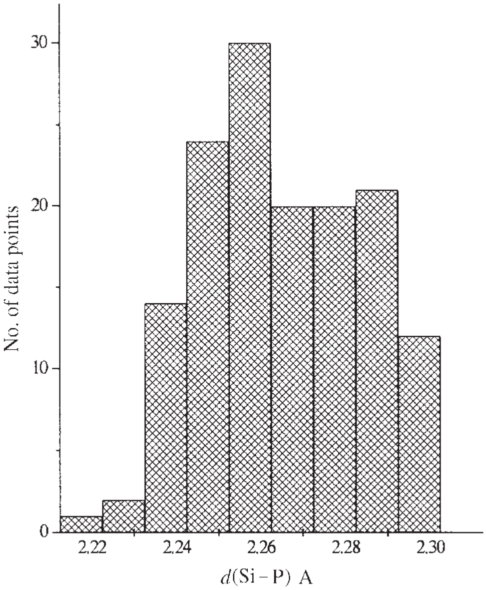

FIGURE 14. Histogram of the Si−P bond lengths in compounds containing tetracoordinate silicon and tetracoordinate phosphorus atoms

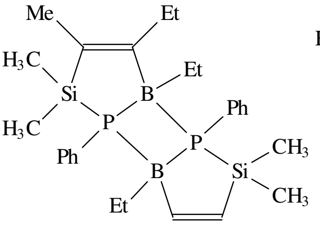

(149)

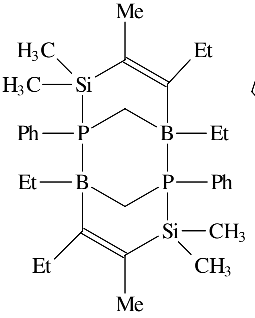

(150)

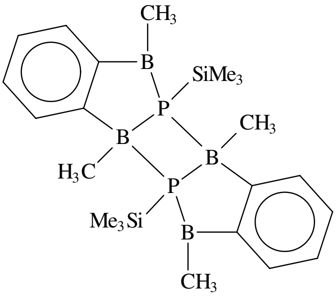

(151)

TABLE 15. Geometry of the Si−P bond in compounds with tetracoordinate silicon and tetracoordinate phosphorus atoms

Refcode	Compound	d(Si−P) (Å)	Reference
KAKFAD	**149**	2.242	160
KAKFEH	**150**	2.248	160
KUDXAI	**151**	2.254	161
TADFIN[a]	**152**	2.259	162
TADFOT[a]	**153**	2.265	162

[a] Average values are given.

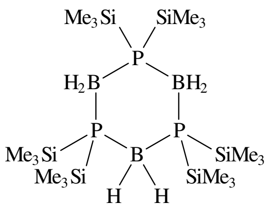

(152)

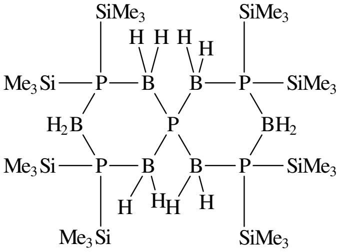

(153)

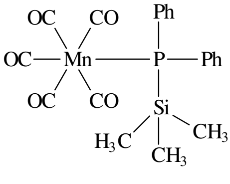

(154)

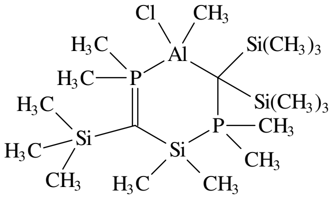

(155)

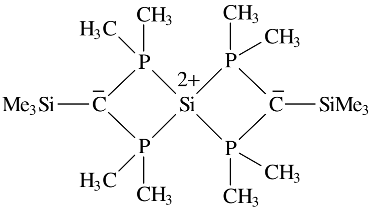

(156)

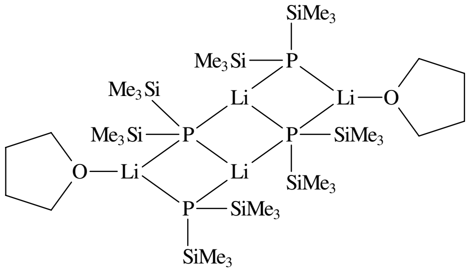

(157)

TABLE 16. Exceptionally long and short Si–P bonds in compounds with tetracoordinate silicon and tetracoordinate phosphorus atoms

Refcode	Compound	d(Si–P) (Å)	Reference
Long bonds			
GANRAO	**154**	2.328	163
KIBSAP	**155**	2.329	164
SEVRIE[a]	**156**	2.416	165
Short bonds			
FOFFUB[a]	**157**	2.211	166
FOFGAI[a]	**158**	2.194	166
SEHHOC	**159**	2.205	167
PADDED[a]	**160**	2.211	168
VAFWEE[a]	**161**	2.200	169
LAJLAJ[a]	**162**	2.220	170
YEZGOZ[a]	**163**	2.214	171

[a] Average values are given.

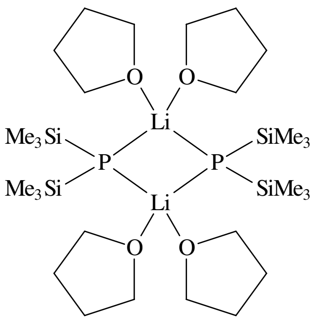

(158)

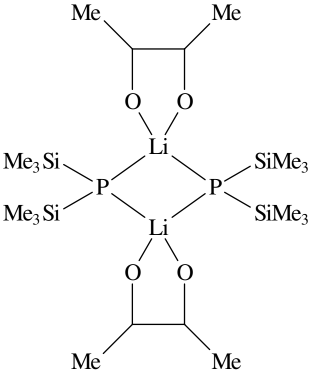

(159)

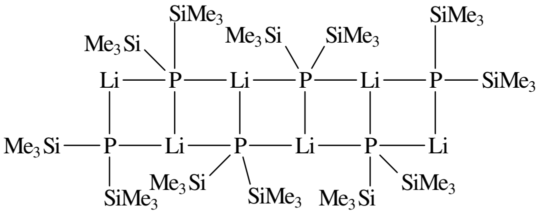

(160)

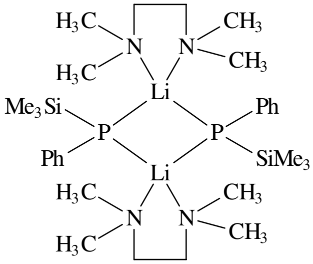

(161)

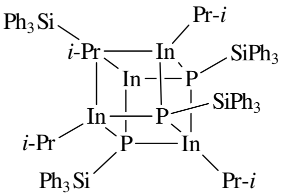

(162)

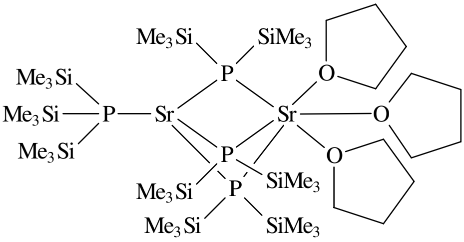

(163)

1978. At that time the calculated Si−O bond length was 1.64(3) Å. In 1989, Sheldrick[15] indicated in his review that the additional data available at the time he wrote his review confirmed this finding. This value is smaller than the Stevenson-Schomaker corrected sum of the covalent radii of silicon and oxygen (1.76 Å). The large amount of XRD structural data available today enables more accurate statistical analysis and the ability to verify it by theoretical calculation.

1. Si−O bonds in compounds with tetracoordinate silicon and dicoordinate oxygen atoms

The 3276 bond lengths obtained by XRD have been used to calculate the average Si−O bond length in compounds containing tetracoordinate silicon atom bonded to a dicoordinate oxygen atom. The average Si−O bond length is 1.629 Å (s.d. 0.03 Å, s.m.

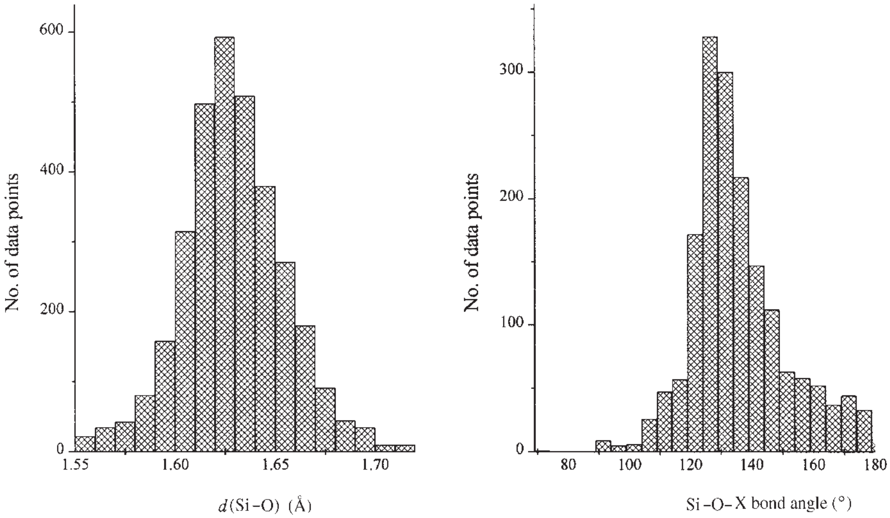

FIGURE 15. Histograms of Si−O bond lengths (left) and Si−O−X (X ≠ Si) (right) in compounds with tetracoordinate silicon and dicoordinate oxygen atoms

0.0005 Å). An average value for the Si−O−X (X = silicon was excluded) bond angle was calculated from 1722 individual values to be 135.4° (s.d. 15.8°, s.m. 0.4°). The histograms of the bond lengths and bond angles are given in Figure 15. A list of Si−O bond lengths and bond angles for typical compounds that have been published in the scientific literature since 1993, and their crystal structures, were very accurately refined ($R < 0.05$) are given in Table 17.

Most of the exceptional bond lengths were obtained for compounds that were found to be disordered in their crystalline state. Shorter bond lengths have been found to belong to similar systems as presented by **174–176**. The average Si−O bond lengths in these compounds are 1.552, 1.551 and 1.503 Å in **174**[183], **175**[184] and **176**[185], respectively. The attachment of an electronegative sulphur atom to the silicon atom increases the Si−O bond ionicity and therefore the bond tends to become shorter.

TABLE 17. Si−O bond lengths and Si−O−X bond angles in compounds with tetracoordinate silicon and dicoordinate oxygen atoms

Refcode	Compound	d(Si−O) (Å)	Si−O−X (°)	Reference
HMDSIX[a]	**164**	1.631	148.2	173
PODJIB	**165**	1.613	180.0	174
WEHJOI	**166**	1.635	148.7	175
WEHJOI[a]	**167**	1.616	141.2	176
PITHOP	**168**	1.642	121.7	177
YECTEF[a]	**169**	1.666	126.4	178
WEKFEX[a]	**170**	1.597	138.7	179
WEKTOV	**171**	1.627	117.9	180
PIJJIB[a]	**172**	1.621	147.5	181
LIJGUG[a]	**173**	1.606	147.4	182

[a] Average values are given.

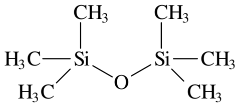

(164)

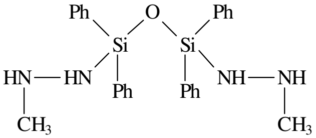

(165)

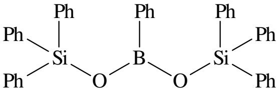

(166)

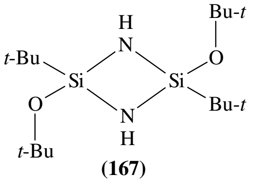

(167)

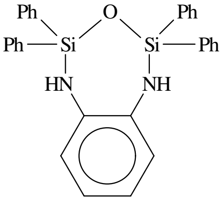

(168)

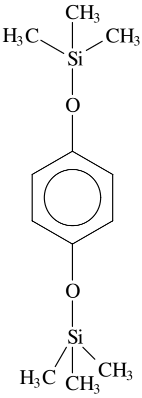

(169)

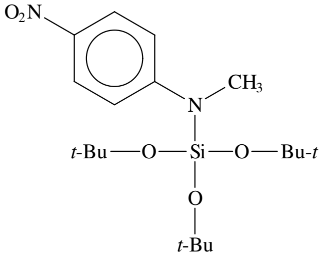

(170)

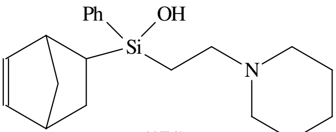

(171)

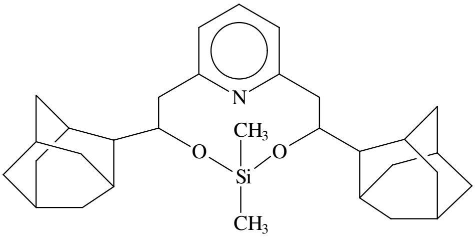

(172)

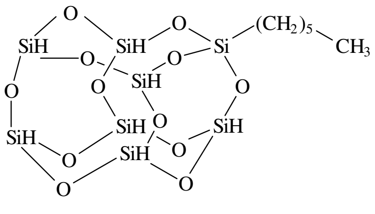

(173)

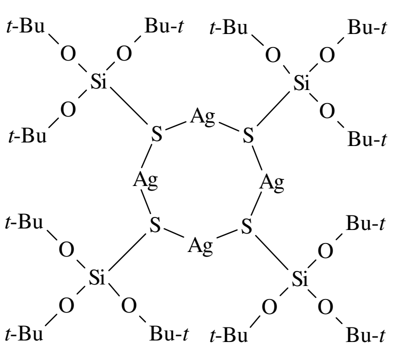

(174)

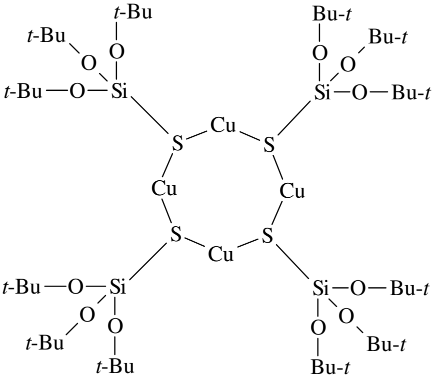

(175)

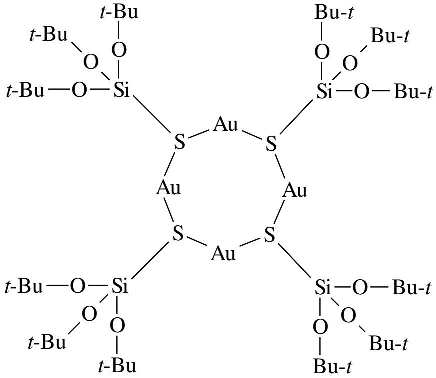

(176)

2. Si–O bonds in silanols

The geometry of silanols was the subject of many theoretical investigations. The Si–OH bond length in methylsilanol was calculated[18] by use of the 3-21G basis set to be 1.679 Å, significantly longer than the experimental value (1.636 Å). Shorter bond lengths were found[19] by optimization of the geometry using *ab initio* calculation at the 3-21G* (modified) level, 1.653 and 1.657 Å in H_3Si-OH and CH_3SiH_2-OH, respectively. Geometry optimization of silanol and methanol at the self-consistent field (SCF) level was carried out[20] and revealed a Si–OH bond length of 1.646 Å. Optimization of the geometry of silanol at the restricted Hartree–Fock (RHF) level with a series of basis sets of increasing quality was undertaken to determine the dependence of the structure on the basis set[21]. Starting with the STO-3G basis set the Si–OH bond length was calculated to be 1.686 Å. Further optimization using the double-zeta and triple-zeta split valence basis sets, both with and without polarization functions, reduces the bond length to a value of 1.631 Å. The histogram of the experimental (XRD) Si–OH bond lengths in silanols is given in Figure 16. The average bond length was calculated from 116 individual parameters to be 1.636 Å (s.d. 0.01 Å, s.m. 0.001 Å). The bond lengths for selected compounds are listed in Table 18. The Si–O bond lengths in silanols are only slightly longer than the average bond length found for alkoxysilanes (1.629 Å).

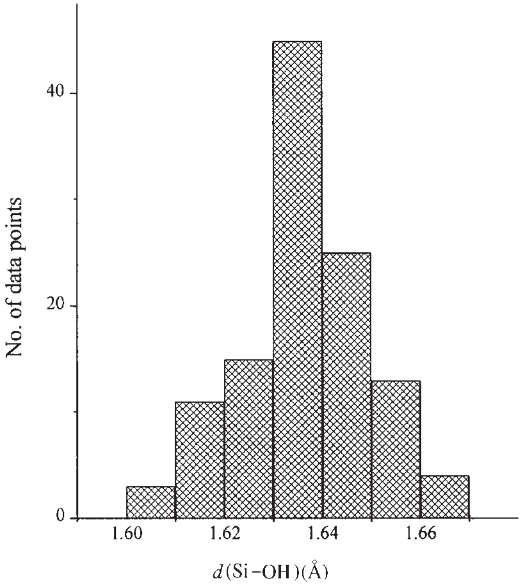

FIGURE 16. Histogram of Si—O bond lengths in silanols

TABLE 18. Geometry of Si—O bond lengths in silanoles

Refcode	Compound	d(Si—O) (Å)	Reference
JODYAC[a]	**177**	1.637	186
SELFIY	**177**	1.632	187
SITKEL[a]	**177**	1.645	188
VUFKEM[a]	**178**	1.627	189
JODYEG	**179**	1.636	186
VOZJOJ	**179**	1.638	190
VOZJUP	**179**	1.637	190
VOZKAW	**179**	1.642	190
VOZKEA	**179**	1.642	190
JODFAJ	**180**	1.646	191
KOMROT	**181**	1.631	192
KOSFUT	**182**	1.617	193
VAFWII[a]	**183**	1.632	194
WEKTUB	**184**	1.622	195
WEKTOV	**184**	1.627	195

[a] Average values are given.

3. Si—O bonds in disiloxanes

The geometry of disiloxane was a subject of many theoretical investigations. The molecular structure of $H_3Si—O—SiH_3$ was calculated at the 3-21G* level[19] and it was shown that the Si—O bond length is 1.645 Å and the Si—O—Si bond angle is 149.5°. Analyses of the Cambridge Structural Database and results of *ab initio* molecular orbital calculations[22] provide insights into the bond-angle widening at oxygen as compared to the alkyl ethers.

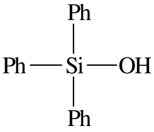

(177)

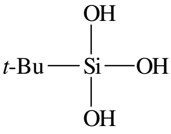

(178)

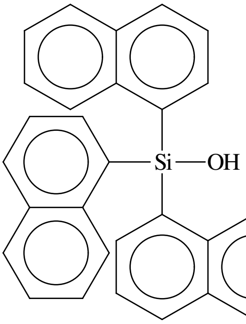

(179)

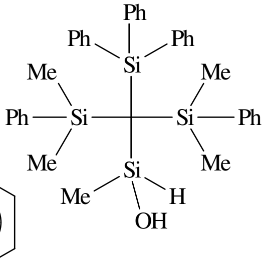

(180)

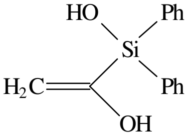

(181)

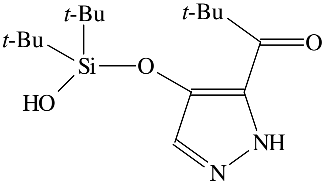

(182)

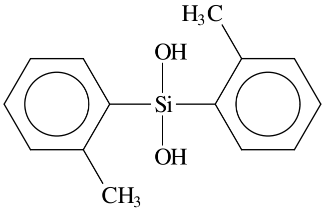

(183)

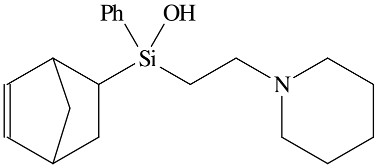

(184)

The XRD data of the acyclic Si−O−C(sp^3) fragments provided the basis for calculating the average bond angle of 134.2° and average Si−C bond distance of 1.62 Å. A trend of decreasing bond lengths with increasing bond angle was also shown. Optimization of the geometry of methoxysilane and disiloxane by calculation (at 6-31G) show that the Si−O−C and Si−O−Si bond angles are 125.0° and 170.1°, respectively, and the Si−O bond lengths are 1.640 and 1.626 Å, respectively. For both molecules the bond angles differ significantly from the experimental values. The calculated Si−O bond length in disiloxane is in very good agreement with the XRD experimental value (1.621 Å).

Optimization of the geometry of disiloxane at the restricted Hartree−Fock (RHF) level with a series of basis sets of increasing quality was conducted to determine the dependence of the structure on the basis set[21]. Starting with the STO-3G basis set, the Si−O bond length and Si−O−Si bond angle were calculated to be 1.658 Å and 124.0°; further optimization using the double-zeta and triple-zeta split valence basis sets, both with and without polarization functions, reduces the bond length and angle to values of 1.620 Å and 147.4°. The bond length is in very good agreement with the XRD experimental average (1.621 Å). No comparison is made with the XRD experimental bond angle because of the large scattering of the data (for more details see below). Linear disiloxanes and cyclosiloxanes of the general formula $(R^1R^2Si)_2O$ and $(R^1R^2SiO)_n$ were the subject of intensive XRD structural investigations. Karle and coworkers[196] found that the Si−O bond length in linear disiloxanes tends to shorten upon opening of the Si−O−Si bond angle. A linear correlation between the two parameters was found by applying a least-squares procedure to eight disiloxanes. XRD of such compounds provide more than 140 individual values for the Si−O−Si bond angles in disiloxanes. The trend of shortening the bond upon linearization of the bond angle can still be seen, but it is not as clear as that shown by Karle and coworkers. The average bond length for disiloxanes was calculated from 147 bond lengths to be 1.621 Å (s.d. 0.02 Å, s.m. 0.002 Å).

The average Si−O bond length in cyclosiloxanes was calculated from 161 individual values to be 1.618 Å. Both values are not significantly different from the average Si−O bond length calculated for the whole set of data mentioned above. In his review, Sheldrick[15] summarizes briefly the development in the study of structural chemistry since an earlier review[197] on organocyclosiloxanes published in 1980. The main structural features that are mentioned concern the dependence of the Si−O bond length and Si−O−Si bond angle on ring size. We have used geometric data selected on the basis of simplicity of the ring system, with $n = 3, 4, 6, 7, 8$. It is interesting to note that while the scattering of the O−Si−O XRD experimental bond angles is very small (105–114°, see also the histogram in Figure 17), the scattering of the Si−O−Si bond angle is very large (129–177°). It seems that the barrier to linearization of the Si−O−Si bond may be reduced by the attachment of different substituents on silicon, and therefore linearization of various degrees are detected. The average of the O−Si−O bond angle was calculated for 161 individual values to be 108.9° (s.d. 1.7°, s.m. 0.1°). Since the O−Si−O bond angle remains unchanged upon changing the ring size, the Si−O−Si bond angle must be varied with the ring size. The average Si−O−Si bond angles for $n = 3, 4, 6, 7$ and

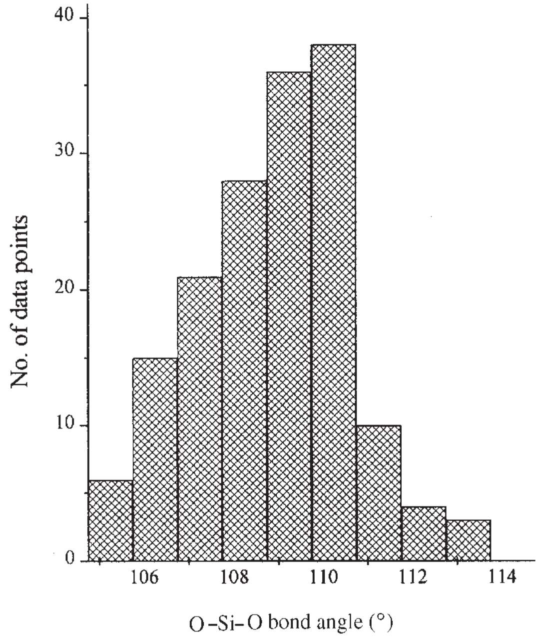

FIGURE 17. Histogram of O−Si−O bond angles in selected cyclosiloxanes

8 are 132.8, 148.9, 152.9, 164.9 and 153.3°, respectively. It should be emphasized that although it seems that the trend is real, a direct proof for it and for the correlation will be available only when cyclosiloxanes of different ring sizes with identical substituents are prepared and analysed structurally.

4. Si–O bonds in compounds with pentacoordinate silicon and dicoordinate oxygen atoms

The pentacoordinate silicon atom appears either as a neutral complex with Lewis base or as an anion. The average Si–O bond length for this coordination was calculated from 481 individual values to be 1.699 Å (s.d. 0.05 Å, s.m. 0.002 Å). The histogram is shown in Figure 18 and a list of selected compounds with Si–O bond lengths is given in Table 19. Compounds **185–190** are examples of neutral Lewis base complexes with N → Si dative bonds. In these compounds the Si–O bond length range is 1.650–1.666 Å. Compounds **191–194** are representative of anionic compounds where the silicon is negatively charged, and therefore the Si–O bond length is significantly longer. Upon increasing the number of oxygen atoms attached to the same silicon atom, the Si–O bond length shortens as a result of increasing bond ionicity. Thus, when the silicon atom is bonded to two oxygen atoms as in **191**, the Si–O bond length is 1.834 Å; when two additional oxygen atoms are attached to silicon, such as in **192** and **193**, the Si–O bond length shortens to 1.752 and 1.738 Å, respectively. The bond length is further shortened to 1.716 Å when the silicon atom is attached to five oxygen atoms as in **194**.

Exceptionally long Si–O bond lengths are found in compounds **195–198**. The longer bond lengths are the dative O → Si bonds such as in **195** (2.040 Å). In **196–198** two

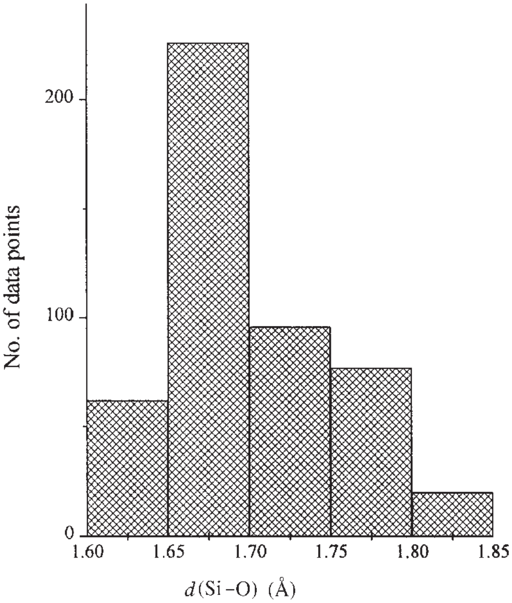

FIGURE 18. Histogram of Si–O bond lengths in compounds with pentacoordinate silicon and dicoordinate oxygen atoms

TABLE 19. Si−O bond lengths in compounds with pentacoordinate silicon and dicoordinate oxygen atoms

Refcode	Compound	*d*(Si−O) (Å)	Reference
MSILTR[a]	**185**	1.666	198
SITBEC[a]	**186**	1.663	199
TALVUX[a]	**187**	1.650	200
VIFVAH[a]	**188**	1.657	201
WABDIM[a]	**189**	1.661	202
WABDIM[a]	**190**	1.661	202
KELSAV[a]	**191**	1.834	203
KELSEZ[a]	**192**	1.752	203
KUXPIC[a]	**193**	1.738	204
YEVWOL[a]	**194**	1.716	205
PENDOB	**195**	2.050	206
PENDUH	**196**	2.242	206
WENBOG	**197**	1.778	207
WENBOG	**197**	2.227	207
WENCAT	**198**	1.787	207
WENCAT	**198**	2.077	207

[a] Average values are given.

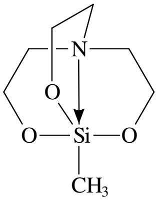

(185)

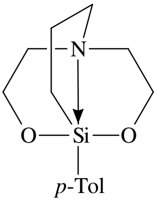

(186)

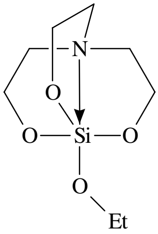

(187)

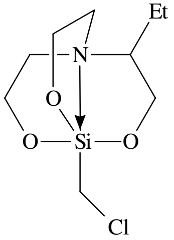

(188)

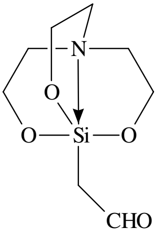

(189)

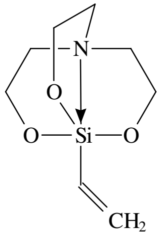

(190)

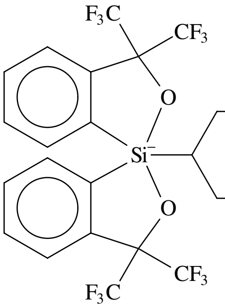

(191)

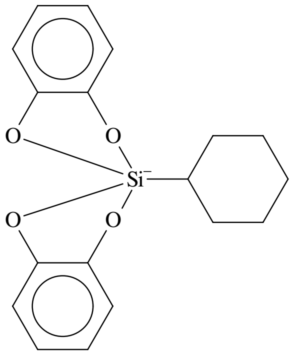

(192)

types, i.e. covalent and dative bonds, are found and the distinction between the two is easily conducted on the basis of the differences in the Si−O bond length. In **197** the covalent Si−O bond length is 1.778 Å and the dative O → Si bond is 2.227 Å. In **198** these bonds are 1.787 and 2.077 Å respectively.

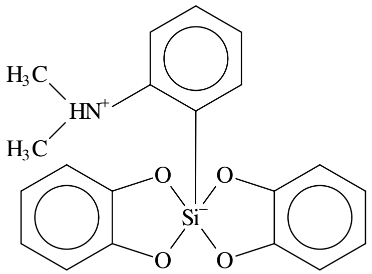

(193)

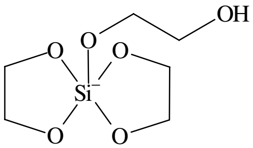

(194)

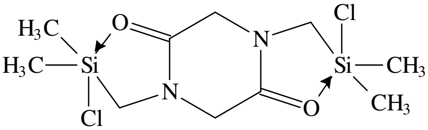

(195)

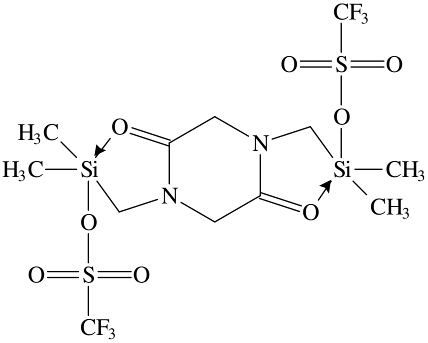

(196)

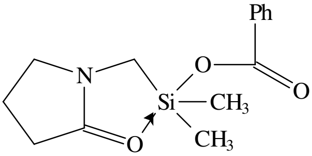

(197)

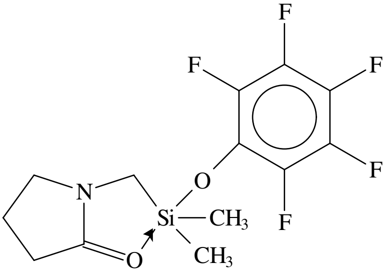

(198)

5. Si–O bonds in compounds with hexacoordinate silicon and dicoordinate oxygen atoms

Three types of compounds with hexacoordinate silicon atom bonded to dicoordinate oxygen atom are found; neutral Lewis acid–base complexes, such as **199**, compounds with positively charged silicon atom, such as **200**, and compounds with negatively charged silicon atoms, such as **201** and **202**. A list of Si–O bond lengths in these compounds is given in Table 20. It is clear that the Si–O bond length increases as one goes from positively charged silicon **200** to negatively charged silicon **201** and **202**, in accordance with the increase of ionicity of the bond.

TABLE 20. Si−O bond lengths in compounds with tetracoordinate silicon and hexacoordinate oxygen atoms

Refcode	Compound	*d*(Si−O) (Å)	Reference
YOMCEA[a]	**199**	1.724	208
BIPSTI[a]	**200**	1.643	209
PYPHSI[a]	**201**	1.784	210
JUVJEP[a]	**202**	1.785	211

[a] Average values are given.

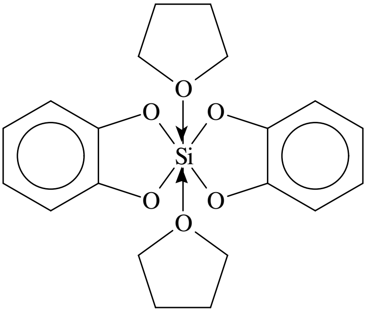

(199)

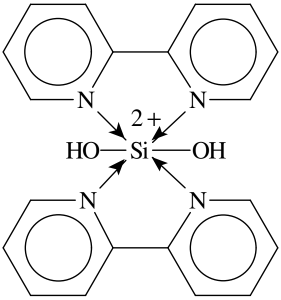

(200)

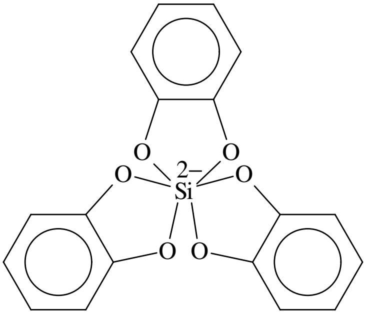

(201)

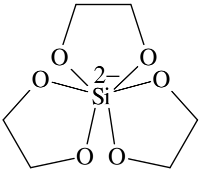

(202)

F. Structural Chemistry of the Si−S Bond

The sum of the covalent radii[3] for silicon and sulphur is 2.21 Å. The electronegativity of the sulphur atom is smaller than that of its congener oxygen atom and therefore the expected polarization and ionicity of the Si−S bond is smaller than that of the Si−O bond. As a result it is expected that the shortening of the Si−S bond length from the sum of covalent radii will be significantly smaller than that observed for the Si−O bond.

The Si−S−X bond angle is highly dependent on the HOMO-LUMO gap and it is expected that the barrier to linearization will be greater for sulphur than for oxygen.

The crystal structures of over 70 different compounds possessing Si−S bonds have been determined. These structures provide more than 90 bond lengths and bond angles. The complexity and diversity of the compounds do not allow fruitful discussion of all of them.

We therefore discuss three different classes of compounds and also analyse statistically the whole set of data.

1. Si−S bonds in compounds containing the Si−S−Si group

The fragment Si−S−Si was found in compounds **203–216** and contributed 39 Si−S bond lengths and bond angles. The geometric parameters are summarized in Table 21. Statistical analysis in the form of a histogram is given in Figure 19. The range of bond lengths is 2.07–2.19 Å with an average of 2.141 Å (s.d. 0.02 Å, s.m. 0.003 Å). We shall not compare and discuss Si−S−Si bond angles here because in some cases the fragment is confined within a cyclic compound, and therefore the Si−S−Si bond angles are determined by the ring size. We discuss these bond angles below.

2. Si−S bonds in compounds containing the $(t\text{-BuO})_3$−Si−S−X group

Compounds containing the $(t\text{-BuO})_3$−Si−S−X group may be regarded as a special group because they clearly show shortening of the Si−S bond length. The geometric data are given in Table 22. The average Si−S bond length is 2.100 Å (s.d. 0.03 Å, s.m. 0.01 Å). The remarkable shortening of the bonds is mainly observed for compounds where X is a metal such as Cu, Cd, V, Co as well as Pb and Tl[15]. Shortening of the Si−S bond length may be attributed to the increase of ionicity and polarization of the bond caused by the electron-withdrawing substituents at the silicon atom and the presence of a metal bonded to the sulphur atom.

3. Si−S bonds in compounds containing the $(Ph)_3$−Si−S−X group

There are only a few compounds containing triphenylsilanethiol derivatives of type **224a–e** that can be used to examine the effect of substitution at the sulphur atom on the Si−S−X geometry. It was found that the Si−S bond lengths range between 2.138 Å (for **224a**) to 2.161 Å (for **224e**) in accordance with the increase of the electronegative properties of the substituent on sulphur.

TABLE 21. Geometric parameters in compounds containing the Si−S−Si fragment

Refcode	Compound	*d*(Si−S) (Å)	Si−S−Si (°)	Reference
CADLOI	**203**	2.152	82.4	212
CUKFUJ	**204**	2.131	82.1	213
DEBYAK[a]	**205**	2.151	111.9	214
DIXJUP	**206**	2.169	94.9	215
DOBCEC[a]	**207**	2.118	110.5	216
FAPYAW[a]	**208**	2.148	104.0	217
FEKGAD[a]	**209**	2.147	108.8	218
FIGJIO[a]	**210**	2.139	105.4	219
FIGJOU[a]	**211**	2.109	108.0	219
FIGJUA[a]	**212**	2.136	107.7	219
GINCEL[a]	**213**	2.148	108.7	220
JITKIG[a]	**214**	2.172	82.9	221
MSISUL[a]	**215**	2.130	104.6	222
TMTPSS[a]	**216**	2.143	106.2	223

[a] Average values are given.

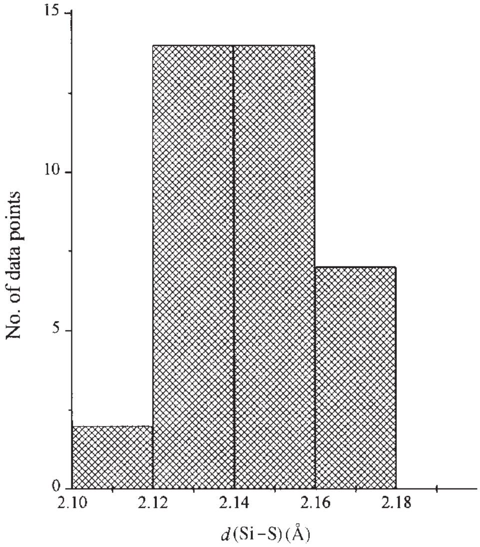

FIGURE 19. Histogram of Si−S bond lengths in compounds containing Si−S−Si fragments

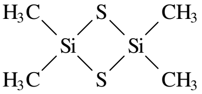

(203)

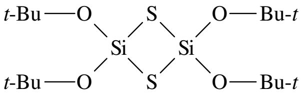

(204)

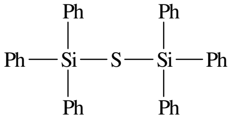

(205)

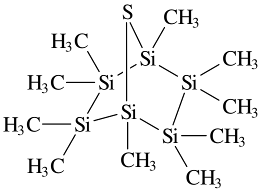

(206)

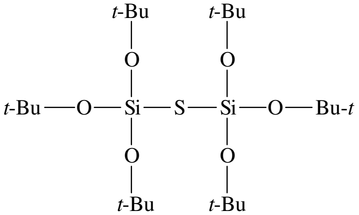

(207)

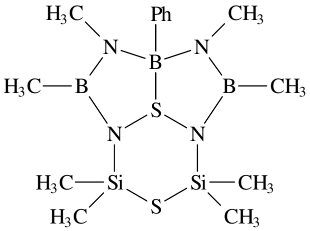

(208)

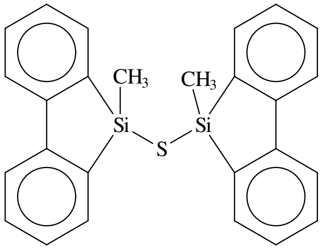

(209)

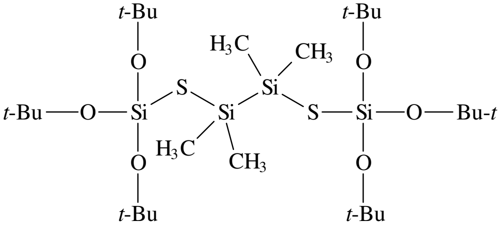

(210)

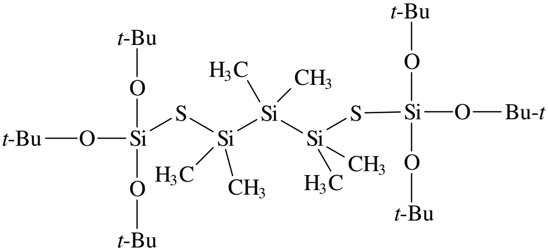

(211)

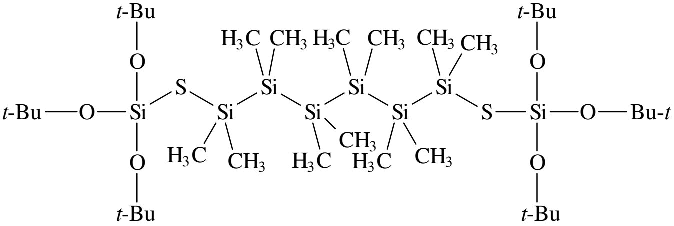

(212)

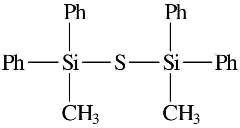

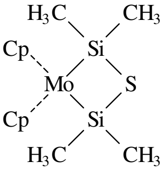

(213) **(214)**

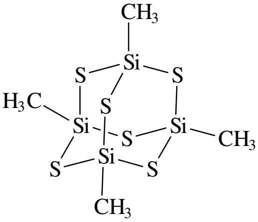

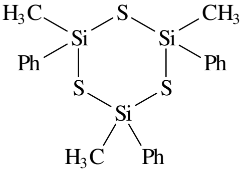

(215) **(216)**

TABLE 22. Geometric parameters in compounds containing the (t-BuO)$_3$−Si−S−X fragment

Refcode	Compound	d(Si−S) (Å)	Si−S−Si (°)	Reference
GAJBAU	**217**	2.111	110.9	224
KACBIZ[a]	**218**	2.131	100.8	225
KIJLUK[a]	**175**	2.132	98.3	184
LEBZIB	**219**	2.075	103.7	226
PAFZUR	**220**	2.085	102.1	227
PAGBAA[a]	**221**	2.075	91.7	228
POHXOZ	**176**	2.169	101.9	185
VIHPIL[a]	**222**	2.058	82.8	229
YOYNIJ	**223**	2.068	85.2	230

[a] Average values are given.

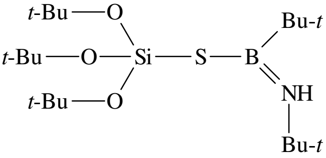

(217)

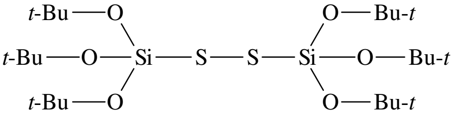

(218)

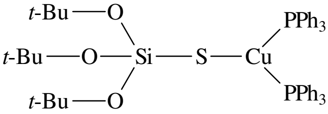

(219)

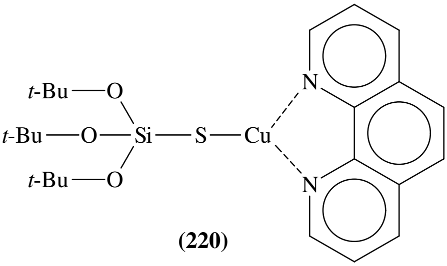

(220)

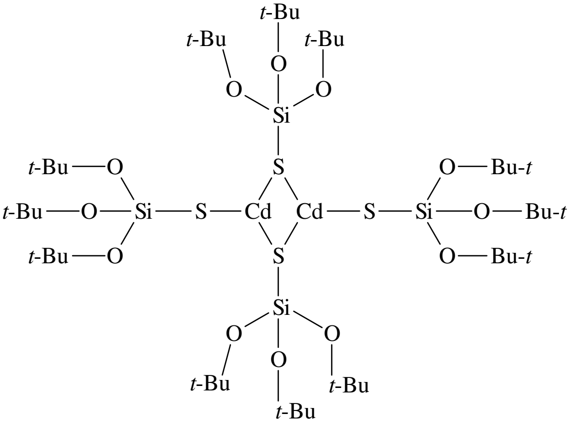

(221)

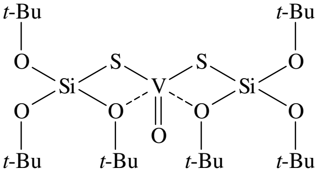

(222)

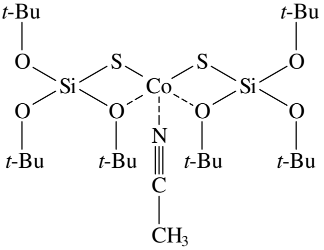

(223)

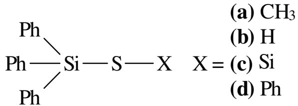

(224)

4. *Si—S bonds in compounds containing the Si—S—X group*

The average Si—S bond length obtained by statistical analysis of 95 data points is 2.144 Å (s.d. 0.03 Å, s.m. 0.004 Å). The results are shown in Figure 20. The average of 41 Si—S—X bond angles in acyclic derivatives is 108.3° (s.d. 4.7°, s.m. 0.7°) and the histogram is also shown in Figure 20.

G. Structural Chemistry of the Si–Halogen Bond (Si—F, Cl, Br, I)

Most of the available X-ray experimental geometry data for compounds containing silicon–halogen bonds are those with fluorine and chlorine atoms. The X-ray crystal structure of only a few compounds containing Si—Br and Si—I bonds are known.

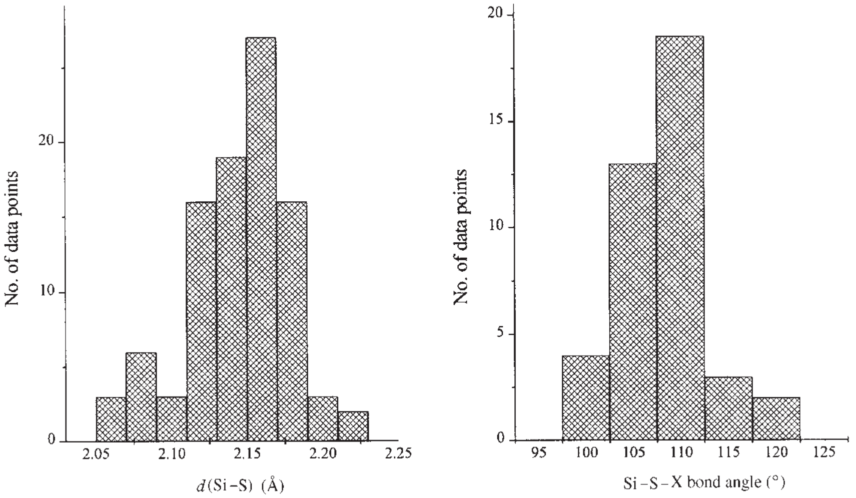

FIGURE 20. Bond lengths in silanethiol derivatives (left) and Si—S—X bond angles in acyclic silanethiol derivatives (right)

1. Si–F bond in compounds with tetracoordinate silicon

The geometries of fluorosilanes were fully optimized[23] at the Hartree–Fock level with the 3-21G and 6-31G* basis sets using analytical gradient methods. The latter basis set was shown to provide better agreement with experimental geometry. The calculated Si–F bond length in SiH_3F is 1.5941 Å, and 1.605 Å when the 6-31++G** basis set is being used for geometry optimization[24]. The Si–F bond length becomes shorter on increasing substitution by fluorine atoms to 1.5570 Å in SiF_4. The sum of the covalent radii for silicon and fluorine atoms is 1.69 Å, which is significantly longer than the experimental value. Sheldrick in his review[15] pointed out that the addition of fluorine atoms on the same silicon atom causes a progressive shortening of the Si–F bond length. The experimental data obtained by microwave spectroscopy shows that the Si–F bond length is 1.593 Å in SiH_3F[234], 1.577 Å in SiH_2F_2[235], 1.562 Å in $SiHF_3$[236] and 1.556 Å in SiF_4[237] (obtained by electron diffraction). The average Si–F bond length was calculated using 168 values obtained by X-ray crystal structures with no distinction between the different numbers of fluorine atoms attached to the same silicon atom. The results are shown in Figure 21. The average Si–F bond length is 1.594 Å (s.d. 0.02, s.m. 0.002 Å). Bond lengths for typical compounds are given in Table 23. The shortening of the bond caused by the increase in the number of fluorine substituents on the same silicon atom can be seen by comparing the Si–F bond length in **226** (1.607 Å), where a single fluorine atom is attached to silicon, with that in **225, 227** and **228** (1.590, 1.587 and 1.581 Å, respectively), where two fluorine atoms are bonded to the same silicon atom.

Exceptionally long Si–F bond lengths in the tetracoordinate silicon atom are found in compounds such as **232**[241] (1.656 Å), **233**[242] (1.684 Å on the average) and **234**[243] (1.667 Å). The first two are compounds having bulky substituents and the lengthening might be attributed to a steric effect. The third is an example of compounds where the Si–F bond ionicity decreases due to the negatively charged nitrogen atom attached to the same silicon atom.

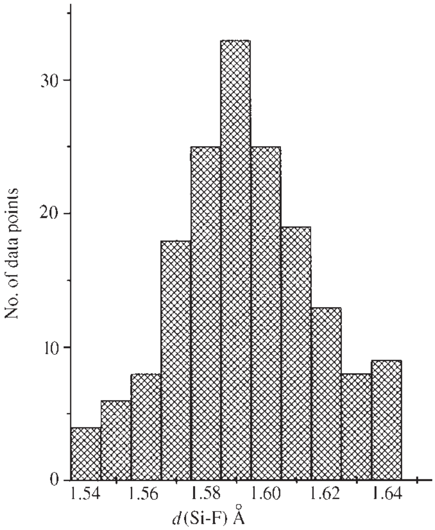

FIGURE 21. Histogram of Si–F bond lengths in compounds with a tetracoordinate silicon atom

TABLE 23. Si–F bond lengths in compounds with a tetracoordinate silicon atom

Refcode	Compound	d(Si–F) (Å)	Reference
JESLOI[a]	**225**	1.586	238
JESLUO	**226**	1.607	238
JESMAV[a]	**227**	1.593	238
JESMEZ[a]	**228**	1.584	238
JIXXIX	**229**	1.601	239
JIYNUA[a]	**230**	1.575	240
JIYPAI[a]	**231**	1.599	240

[a] Average values are given.

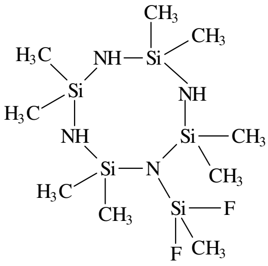

(225)

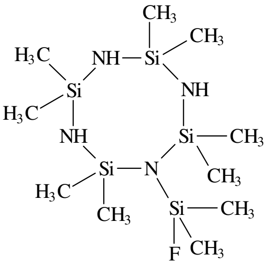

(226)

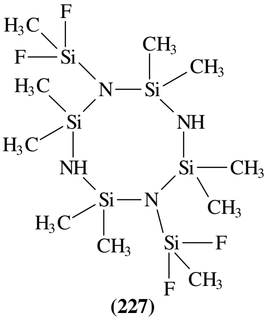

(227)

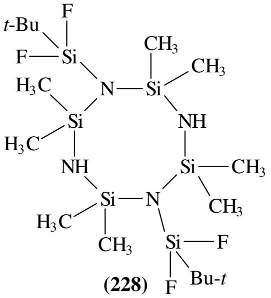

(228)

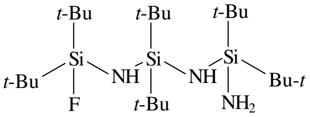

(229)

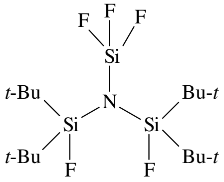

(230)

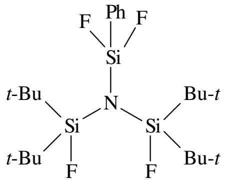

(231)

2. Si–F bond in compounds with pentacoordinate silicon

Three types of halogenosilanes (**235, 236** and **237**) with pentacoordinate silicon atom are considered. The first comprises anions of type **235**, the second is a neutral species containing a Lewis base (D) **(236)** and the last is a cation formed and stabilized by a chelate ligand of a Lewis base character **(237)**.

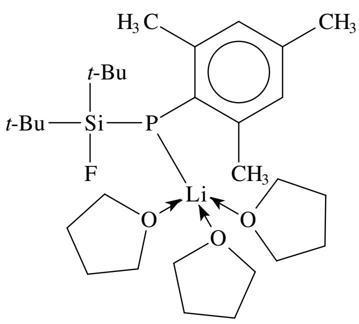

(**232**)

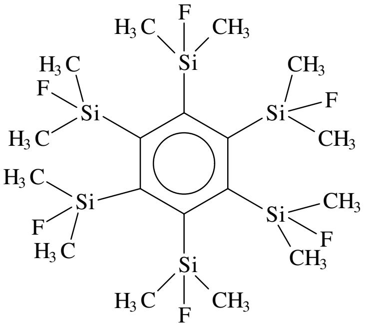

(**233**)

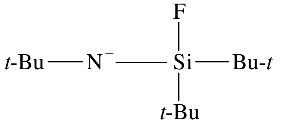

(**234**)

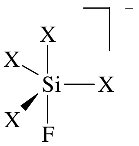

(**235**)

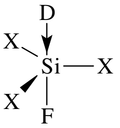

(**236**)

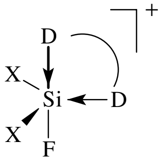

(**237**)

The average Si−F bond length in pentacoordinate silicon compounds was calculated from 153 XRD experimental bond lengths to be 1.631 Å (s.d. 0.04 Å, s.m. 0.004 Å) from 60 values obtained by X-ray crystal structure determination and its histogram is shown in Figure 22. Some typical values for compounds of type **236** are given in Table 24. All compounds **238**–**247** show much shorter Si−F bond lengths, resulting from the attachment of three fluorine atoms to the same silicon.

Si−F bond lengths in the anions of type **235** show significant lengthening, as can be seen in Table 25 for compounds **248**–**254**.

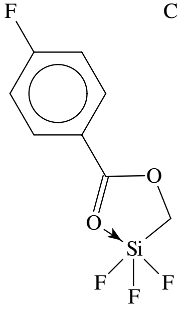

(**238**)

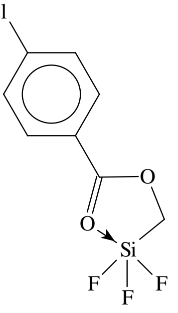

(**239**)

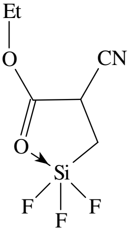

(**240**)

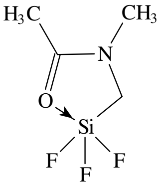

(**241**)

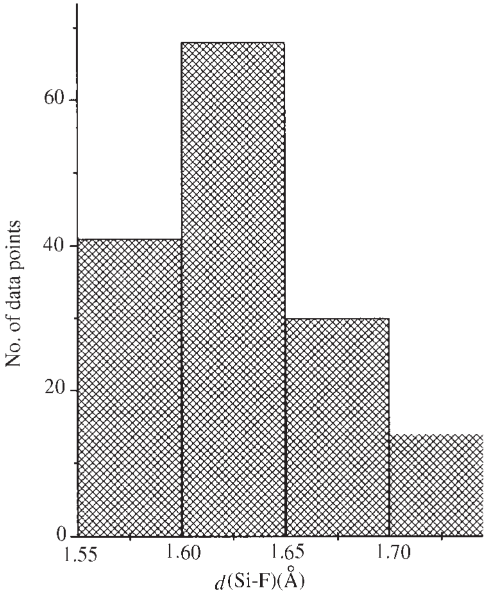

FIGURE 22. Histogram of Si−F bond lengths in compounds with a pentacoordinate silicon atom

TABLE 24. Si−F bond lengths in compounds with a pentacoordinate silicon atom

Refcode	Compound	d(Si−F) (Å)	Reference
BABZAF[a]	**238**	1.591	244
BABZEJ[a]	**239**	1.595	244
HEPCUA[a]	**240**	1.571	245
HEPDEL[a]	**241**	1.605	245
HEPDIP[a]	**242**	1.595	245
KEZROW[a]	**243**	1.591	246
VILJUV[a]	**244**	1.601	247
WEDKOF[a]	**245**	1.605	248
WEDKUL[a]	**246**	1.604	248
WIHYER[a]	**247**	1.591	249

[a] Average values are given.

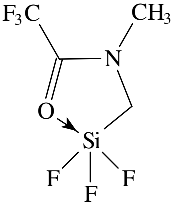

(242)

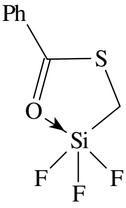

(243)

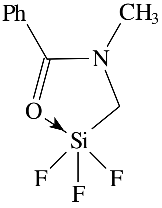

(244)

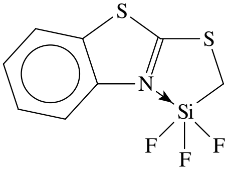

(245)

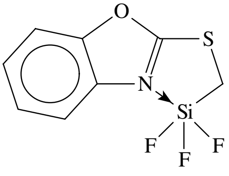

(246)

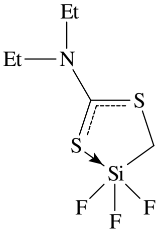

(247)

TABLE 25. Si−F bond lengths in anions of type **235**

Refcode	Compound	d(Si−F) (Å)	Reference
BEPCAA	**248**	1.670	250
FEDDUN	**249**	1.707	251
FESCOV[a]	**250**	1.671	252
FESCUB[a]	**251**	1.721	252
PERROT[a]	**252**	1.685	253
PERRUZ[a]	**253**	1.677	253
PILKEA[a]	**254**	1.757	251

[a] Average values are given.

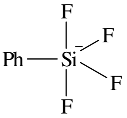

(248)

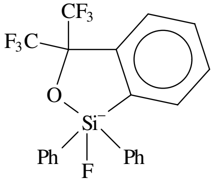

(249)

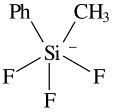

(250)

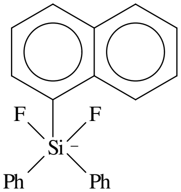

(251)

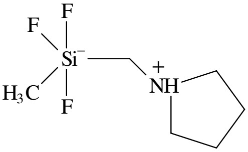

(252)

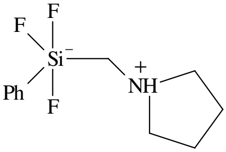

(253)

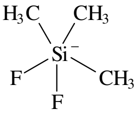

(254)

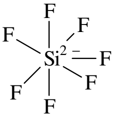

(255)

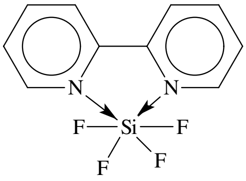

(256)

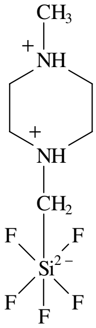

(257)

3. Si–F bond in compounds with hexacoordinate silicon

X-ray crystal structures of 24 compounds containing a hexacoordinate silicon atom bonded to a fluorine atom are known in the literature. Most of them contain the commonly used $[SiF_6]^{2-}$ anion **255** and similar anions with various numbers of fluorine atoms replaced by other substituents. The second type is the neutral species based on **237**. An average Si–F bond length of 1.677 Å (s.d. 0.02 Å, s.m. 0.004 Å) was calculated from 26 available bond lengths. The shortest Si–F bond length, within this family of compounds, was detected in **256**[254] (1.632 Å), and the longest was observed in **257**[255] (1.717 and 1.740 Å). Such a lengthening may be attributed to the involvement of fluorine in strong hydrogen bonding.

The average of all Si–F bond lengths for compounds with hexacoordinate silicon was calculated from 100 experimental values to be 1.675 Å (s.d. 0.02 Å, s.m. 0.002 Å) and the histogram is given in Figure 23.

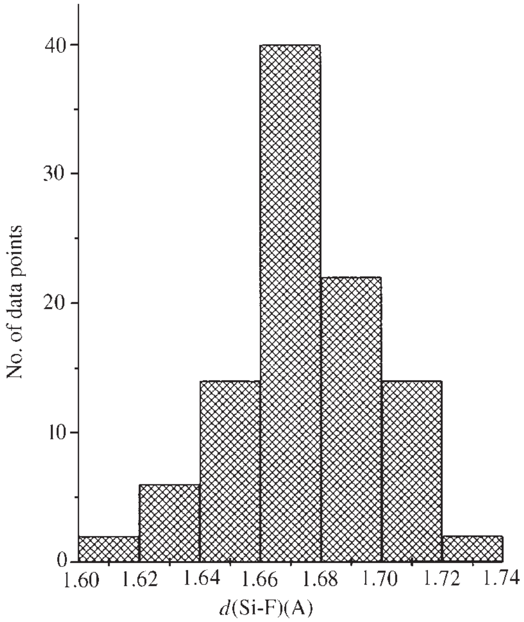

FIGURE 23. Histogram of Si–F bond lengths in compounds with a hexacoordinate silicon atom

4. Si–Cl bond in compounds with tetracoordinate silicon

The geometries of chlorosilanes were fully optimized[23] at the Hartree–Fock level with the 3-21G and 6-31G* basis sets using analytical gradient methods. The latter basis set was shown to provide better agreement with experimental geometry. The calculated Si–Cl bond length in SiH_3Cl is 2.0666 Å; the Si–Cl bond length becomes shorter when the number of chlorine atoms attached to Si is increasing such as in $SiCl_4$ (2.0290 Å). The sum of the covalent radii of chlorine and silicon is 2.05 Å. The X-ray crystal structure of compounds with a tetracoordinate silicon atom containing Si−Cl bonds provides 423 bond lengths that have been used for the statistical analysis. The average of the experimental Si−Cl bond lengths is 2.050 Å (s.d. 0.03 Å, s.m. 0.002 Å), in very good agreement with the sum of covalent radii. A histogram of the bond lengths is given in Figure 24. Bond lengths for the simplest representative compounds (**258**–**261**) are given in Table 26. As was pointed out for the Si−F bond lengths, Si−Cl bond lengths also become shorter upon increasing the number of chlorine atoms bonded to the same silicon atom. Therefore, the bond length in **260** is shorter than in the other representatives.

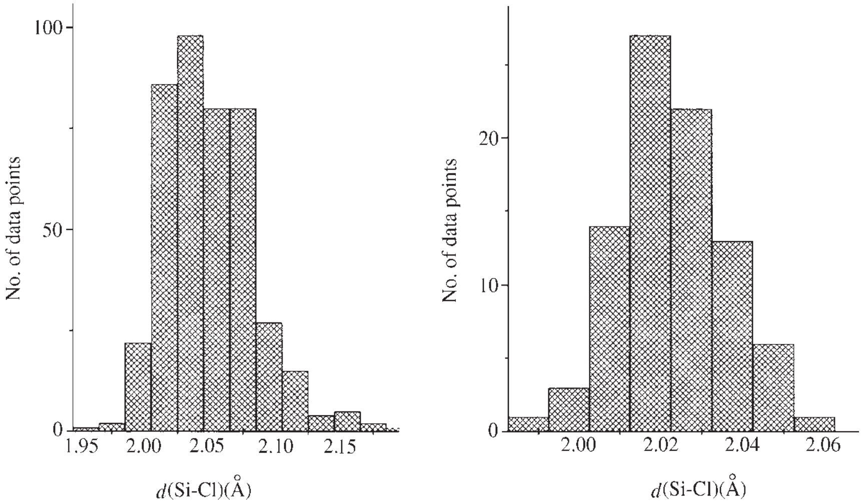

FIGURE 24. Histogram of Si−Cl bond lengths in compounds with a tetracoordinate silicon atom: (left) all 423 bond lengths are used, (right) data from compounds with multiple Si−Cl bonds

TABLE 26. Si−Cl bond lengths in compounds with a tetracoordinate silicon atom

Refcode	Compound	d(Si−Cl) (Å)	Reference
BARNUD[a]	**258**	2.077	256
COJKIV	**259**	2.075	257
JIRMAY[a]	**260**	2.020	258
LEFTEV	**261**	2.087	259

[a] The average value is given.

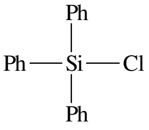

Ph_3SiCl

(258)

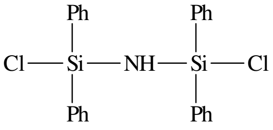

$ClPh_2Si{-}NH{-}SiPh_2Cl$

(259)

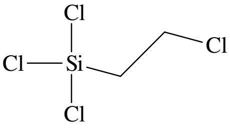

(260)

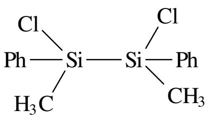

(261)

TABLE 27. Si−Cl bond lengths in compounds with multiple Si−Cl bonds

Refcode	Compound	d(Si−Cl) (Å)	Reference
LAYBES[a]	**262**	2.018	260
LAYBIW[a]	**263**	2.023	260
LEGKEN[a]	**264**	2.018	261
LEGKIR[a]	**265**	2.001	261
WIHJAY[a]	**266**	2.032	262
WIHJEC[a]	**267**	2.043	262
WIHJIG[a]	**268**	2.044	262
WILHUJ	**269**	2.005	263
WILXEU[a]	**270**	2.016	263
WILXIY[a]	**271**	2.020	263

[a] The average value is given.

Statistics on Si−Cl bonds extracted from the X-ray crystal structure of compounds **262–271** that contain several groups of silicon atoms, each bonded to at least two chlorine atoms, show that the average Si−Cl bond length is 2.022 Å (s.d. 0.01 Å, s.m. 0.001 Å), indeed shorter than found in compounds with a single Si−Cl bond. Bond lengths for **262–271** are given in Table 27 and the statistics is shown in Figure 24.

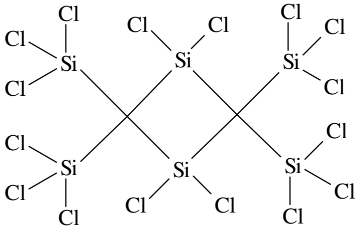

(262)

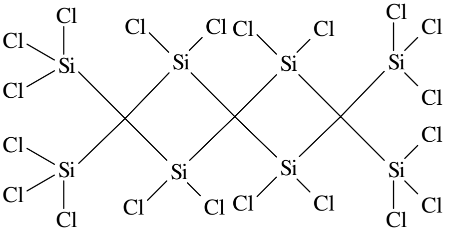

(263)

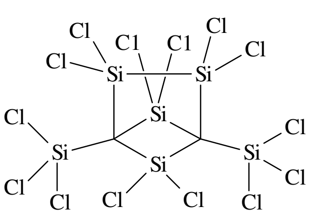

(264)

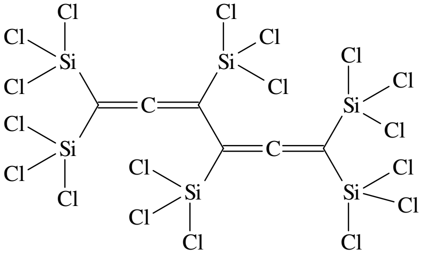

(265)

Longer Si−Cl bonds are found in compounds such as **272–275**[264−267], where the bond lengths are 2.137, 2.146, 2.124 and 2.112 Å, respectively.

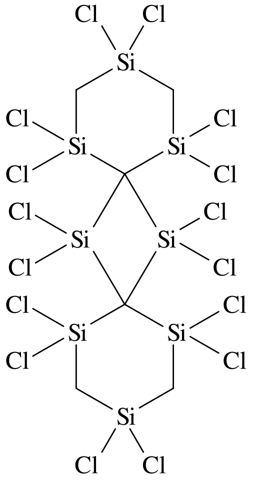

(266)

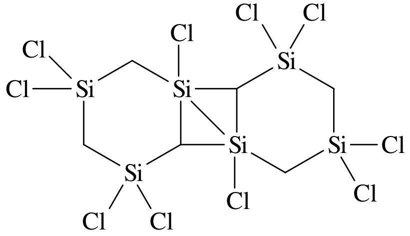

(267)

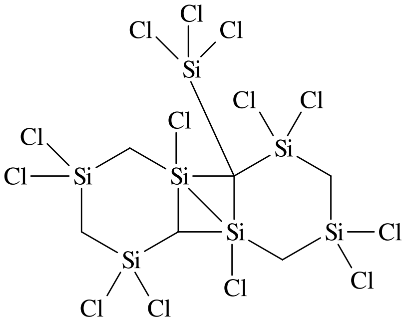

(268)

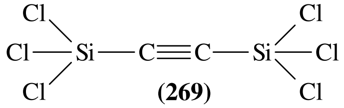

(269)

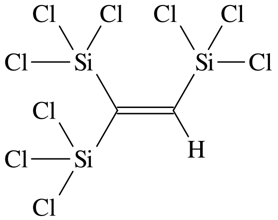

(270)

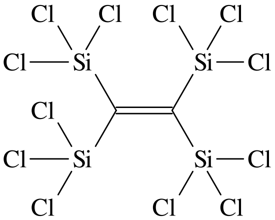

(271)

5. Si—Cl bond in compounds with pentacoordinate silicon

In contrast to fluorosilanes with pentacoordinate silicon systems such as **235–237**, it is very difficult to find similar compounds of chlorosilanes to establish the Si—Cl bond length in similar cases. X-ray crystal structure is available for only few of these compounds and only typical cases of the shortest and longest Si—Cl bonds are given. The shortest bond lengths are found in compounds where the silicon is bonded to a metal such as

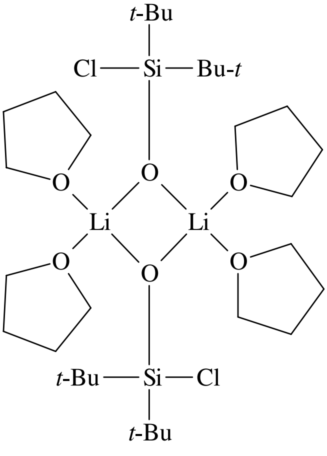

(272)

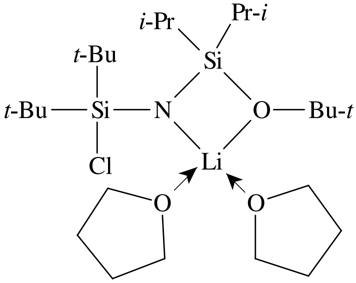

(273)

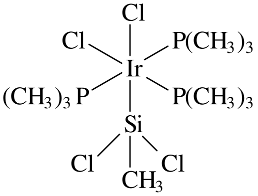

(274)

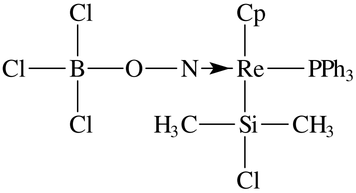

(275)

Mn **276**[268] or Cr **277**[269] with an average bond length of 2.062 and 2.072 Å, respectively. The longest bond lengths are found in compounds of the chloro analogue of **236**. On average, the Si–Cl bond length is 0.5 Å longer in **278–286** with the exception of **284** in which there are three chlorine atoms on the same silicon. The geometrical parameters for **278–286** are given in Table 28.

TABLE 28. Si–Cl bond lengths in compounds with pentacoordinate silicon atom

Refcode	Compound	d(Si–Cl) (Å)	Reference
FUPBOH	**278**	2.432	270
FUSYIB	**279**	2.307	271
GEGDAX	**280**	2.315	272
GEGDEB[a]	**281**	2.310	273
GILYIJ	**282**	2.624	274
VEKROS	**283**	2.609	275
VEKRUY	**284**	2.129	275
YAMSOU	**285**	2.678	276
YIJWOD	**286**	2.423	277

[a] The average value is given.

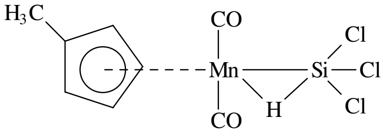

(276)

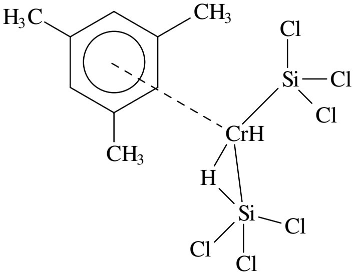

(277)

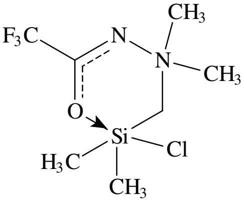

(278)

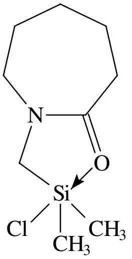

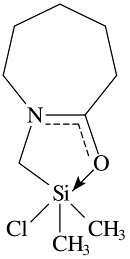

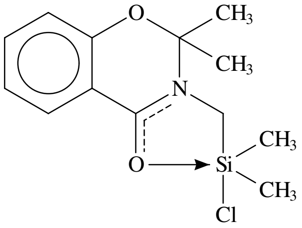

(279) **(280)** **(281)**

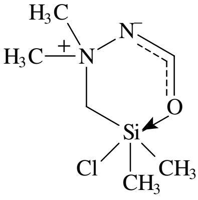

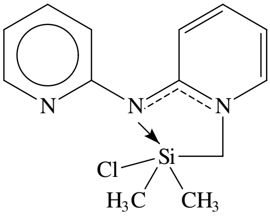

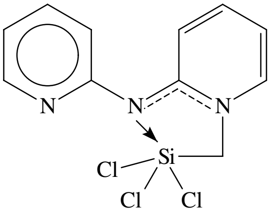

(282) **(283)** **(284)**

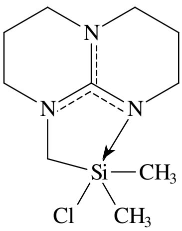

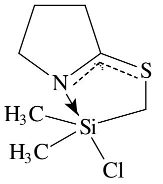

(285) **(286)**

6. Si−Cl bond in compounds with hexacoordinate silicon

The average Si−Cl bond length in compounds with a hexacoordinate silicon atom was determined from 17 experimental values to be 2.184 Å (s.d. 0.02 Å, s.m. 0.006 Å). The results are shown in Figure 25 and Table 29.

7. Si−Br and Si−I bonds

The crystal structures of only three compounds containing Si−Br bonds and only two with Si−I bonds are known. Si−Br bond length in tetracoordinate silicon is 2.197 and 2.284 Å in **295**[284] and **296**[285], respectively. The bond is significantly longer (3.122 Å) in **297**[286] when the silicon is pentacoordinate (analogous to **235**). Si−I bond lengths are 2.527 and 2.574 Å in **298**[287], and 2.487 Å in **299**[288].

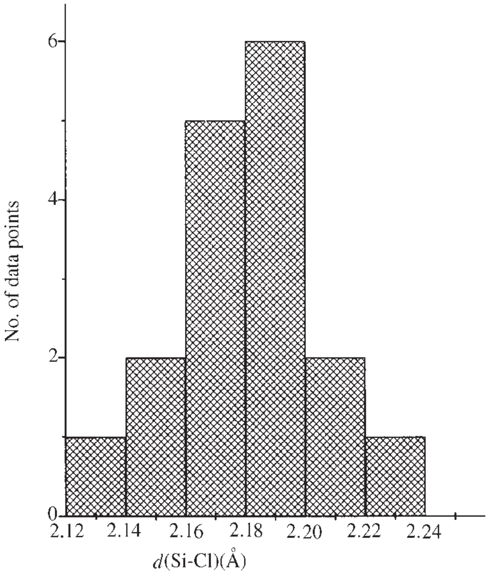

FIGURE 25. Si−Cl bond lengths in compounds with a hexacoordinate silicon atom

TABLE 29. Si−Cl bond lengths in compounds with a hexacoordinate silicon atom

Refcode	Compound	d(Si−Cl) (Å)	Reference
JEPCOW	**287**	2.184	278
CELFUU	**288**	2.198	279
FUMFAU[a]	**289**	2.169	280
SINBEW[a]	**290**	2.205	281
KENHUG[a]	**291**	2.196	282
KENJAO[a]	**292**	2.175	282
KENJES[a]	**293**	2.205	282
KUJFAW	**294**	2.140	283

[a] The average value is given.

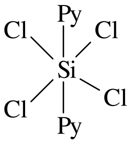

(287)

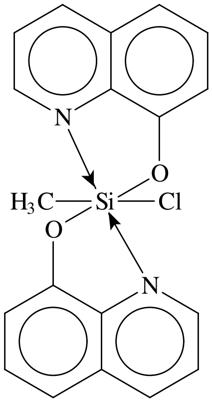

(288)

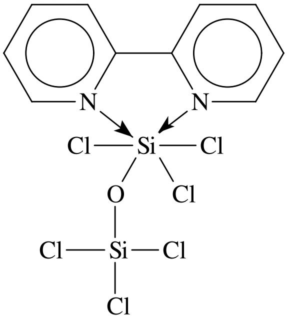

(289)

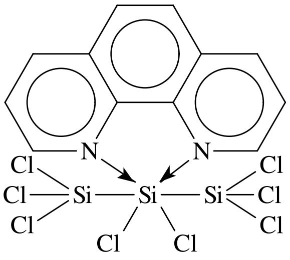

(290)

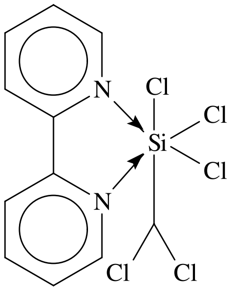

(291)

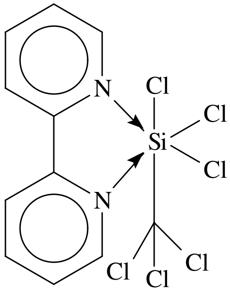

(292)

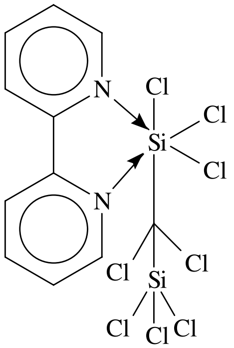

(293)

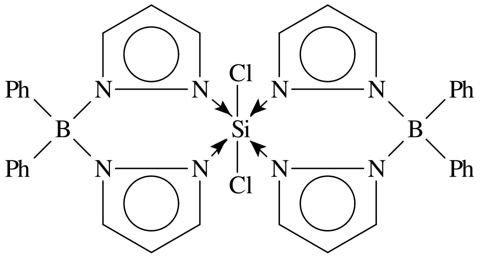

(294)

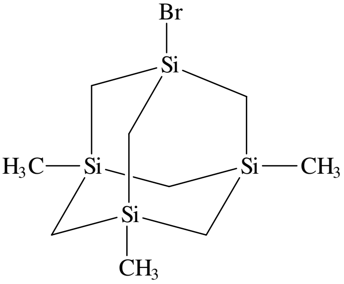

(295)

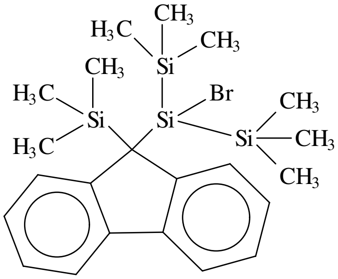

(296)

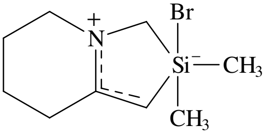

(297)

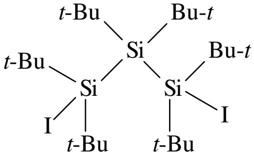

(298)

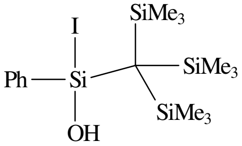

(299)

III. DOUBLE BONDS TO SILICON

A. Disilenes (>Si=Si<)

Stabilization of disilenes is achieved by the use of bulky substituents. Only a few disilenes have been prepared and X-ray diffraction studies were available for only three compounds when Sheldrick[15] published his review. A few other relevant reviews were published at the same time by West[289–291], Michl[292], Cowley[293,294] and their coworkers. There are crystallographic data for 14 crystal structures of disilenes in the CSD[16] updated on January 1996. Those 14 crystal structures provide geometric data for only 11 unique compounds. The most interesting geometric parameters are the bond lengths between the silicon atoms, the pyramidalization of the silicon atoms expressed by the sum of bond angles involving those atoms and the twist angle τ, signifying the bending at the double bond. The last two parameters are related to the steric congestion imposed by the substituents. The structural parameters are summarized in Table 30.

Disilenes are considered to be planar, but are very floppy in the sense that pyramidalization on silicon up to quite large angles (20°) lead to structures which are essentially equal in energy[295], within 4 or 8 kJ mol^{-1}. Raabe and Michl[292] suggested that such floppy molecules are likely to explore a large part of the nuclear configuration space at elevated temperatures, and since the $\pi\pi^*$ excitation energy is likely to decrease with pyramidalization and twisting, they can be expected to be thermochromic. Indeed, tetramesityldisilene[296] is bright orange at room temperature and pale yellow at $-100\,^{\circ}$C. The bond length between the silicon atoms is calculated[297] to be 2.125 Å,

TABLE 30. Structural parameters for disilenes

Refcode	Compound	d(Si=Si) (Å)	$\Sigma^a(Si_1)$ (°)[a]	$\Sigma(Si_2)$ (°)	τ (°)[b]	Sym.[g]	Reference
BUYYOJ[c,d]	**300**	2.160	356.3	356.3	6.5	Ci	291
CELSER	**301**	2.140	360.0	360.0	9.6	Ci	298
CIJRAO	**302**	2.143	359.9	359.9	0.0	Ci	291
GICSAM	**303**	2.145	360.1	359.9	1.6	none	299
JAXSAC	**304**	2.138	359.9	359.9	0.0	Ci	300
JUMSEP	**305**	2.153	360.0	360.0	0.0	Ci	301
JUMSIT	**306**	2.156	360.0	360.0	0.0	Ci	301
SESSUE[c,e]	**300**	2.142	358.7	358.4	3.1	none	302
SESSUE01[e,f]	**300**	2.142	358.4	358.0	2.9	none	302
WICVEJ	**307**	2.201	360.0	360.0	8.9	Ci	303
WICVAF	**308**	2.226	359.7	359.7	0.0	Ci	303
WICVIN	**309**	2.252	358.9	358.9	0.0	Ci	303
HATDOV	**310**	2.229	358.8	357.3	8.7	none	304

[a] Σ(Si) = sum of bond angle at Si.

[b] The average torsion angle in the general structure **311** (R^2SiSiR^3 and R^1SiSiR^4).

[c] Structural data from tetramesityldisilene obtained from different crystals.

[d] The crystal contains toluene.

[e] Crystal modification without solvent; data collected at room temperature.

[f] The same crystal modification as in footnote *e*; data collected at −100 °C.

[g] Ci = inversion centre.

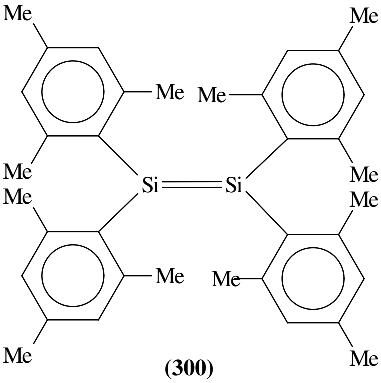

(300)

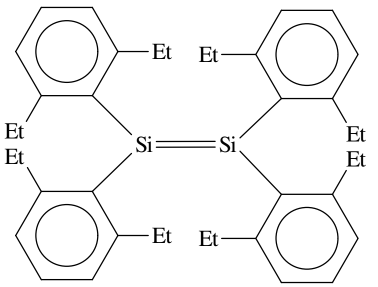

(301)

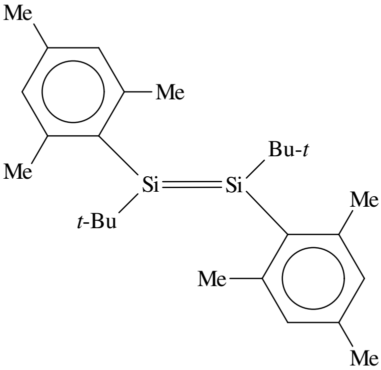

(302)

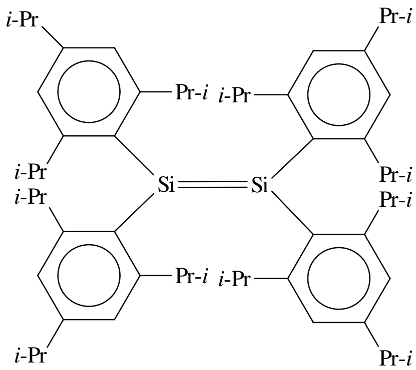

(303)

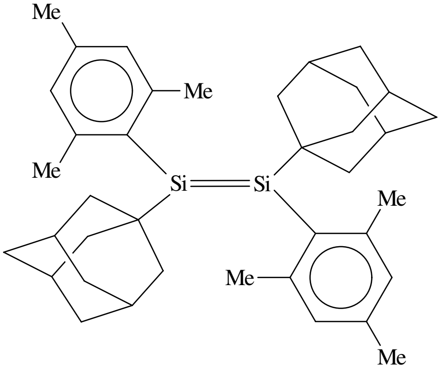

(304)

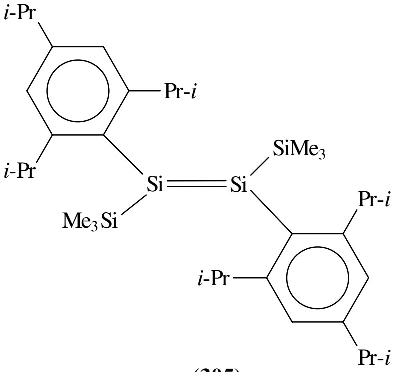

(305)

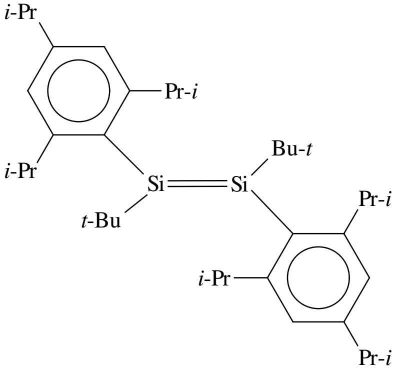

(306)

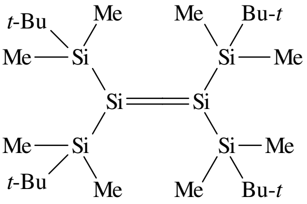

(307)

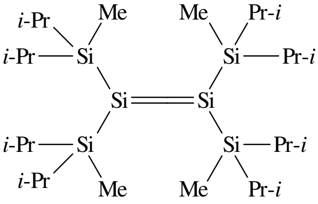

(308)

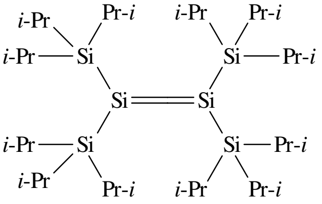

(309)

and recently[26] a Si=Si bond length of 2.150 Å was calculated, based on approximate density functional theory within the local density approximation and augmented by non-local exchange and correlation corrections. The experimental bond lengths obtained by X-ray crystal structure show two distinct ranges of values: 2.138–2.160 Å and 2.201–2.261 Å. The somewhat longer bond lengths were observed in compounds where all the substituents are alkylsilyls. The lengthening is attributed to an electronic effect. The same lengthening was also found where the substituents are extremely bulky, such

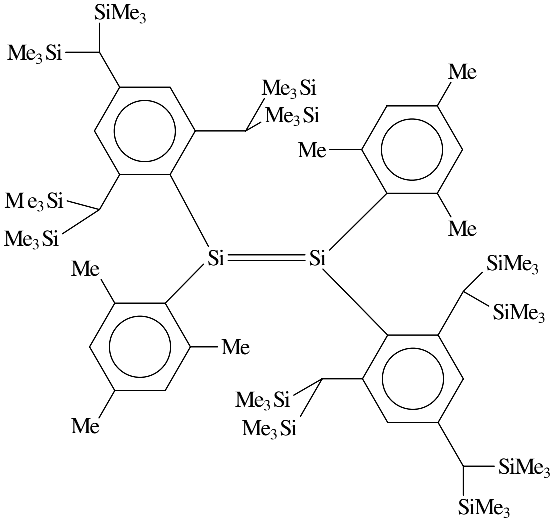

(310)

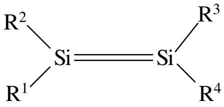

(311)

as 2,4,6-tris(bis(trimethylsilyl)methylphenyl) (HATDOV). The lengthening can be a result of steric congestion as manifested in the pyramidalization of the silicon atoms, deduced by the sum of bond angles at the silicon atoms (358.8 and 357.3°).

B. Silenes (>Si=C<)

The first stable silene was reported in 1981 by Brook and coworkers[305]. The X-ray crystal structures of four stable silenes have been published up to 1987[306–311]. In the last decade the X-ray crystal structures of only two more compounds possessing double bonds between silicon and carbon were published as well as two organometallic compounds containing Si double-bonded to carbon. The shorter Si=C bond length was found in **312**[309] (1.703 Å) and **313**[312] (1.704 Å). Significantly longer bonds were found in **314**[307] (1.764 Å) and **315**[313] (1.758 Å) and the longest ones in the organometallic compounds **316**[314] (1.799, 1.783 Å in the two crystallographically independent molecules) and **317**[315] (1.750 Å). The predicted bond length for $Me_2Si{=}CH_2$ based on *ab initio* MO calculation[316] was 1.692 Å, and later results of Si=C bond length obtained by *ab initio* calculations are 1.703[27] and 1.718[28] Å, while the sum of the double-bond radii of the participant atoms is 1.74 Å[3]. There are two possible explanations for the significant differences in the Si=C bond lengths. The first suggests that the differences between the bond lengths are the result of steric congestion, while the second attributes the differences to electronic effects[317–319]. According to the latter, the polarization of the Si=C bond is the dominant effect and substitution that alters the degree of polarization (and hence the degree of ionicity) will also cause variation of the bond lengths. Therefore, the presence of a Me_3SiO group that includes the very electronegative oxygen atom as the substituent on the carbon atom in **314** results in the withdrawal of charge from the carbon atom, thus reducing the polarity of the Si=C bond. Consequently, the bond lengthens compared to that found in **312**. The shortening of the Si=C bond in the latter is a result of the increase of polarity compared with the calculated value for the model molecule $Me_2Si{=}CH_2$.

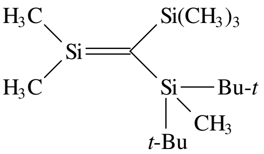

(312)

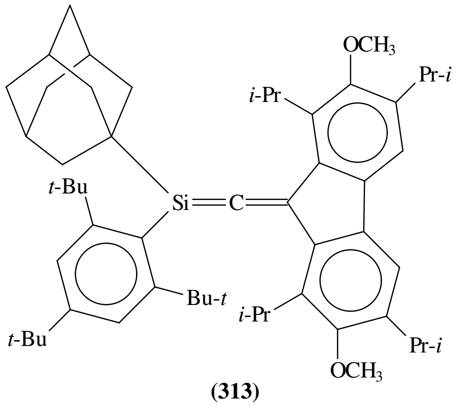

(313)

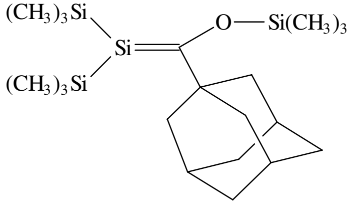

(314)

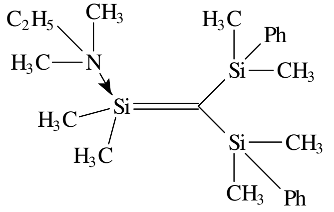

(315)

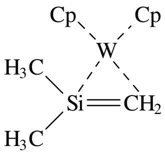

(316)

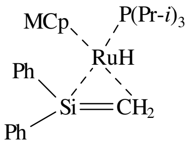

(317)

Of particular interest is the lengthening of the Si=C bonds in **316** (1.799 Å) and in **317** (1.783 and 1.790 Å). These values lie between typical Si=C double and Si−C single bond lengths, which can presumably be attributed to a partially double-bond character. The shortening of the similar bond in silaallene **313** (1.704 Å) exhibits a partial 'reversed polarity' of the Si=C double bond, comparable in effect to that of an electron-donating oxygen substituent on carbon, as in **314**, without bond elongation. This 'reversed polarity' of the Si=C π-bond is believed to be 'the most important single electronic factor that reduces the reactivity of silenes'[318]. Another group of silenes that should be mentioned are those including substituents with increasing Lewis basicity which leads to a Si=C bond lengthening, such as in **315** (1.758 Å).

C. Silanimines (>Si=N−)

Theoretical calculations[320] of the geometry in $H_2Si{=}NH$ were carried out at the SCF (3-21G* and 6-31G**), SCF-MP4 (6-31G**) and MCSCF+CI (6-31G*) levels and suggest that the molecule is planar with a Si=N bond length of 1.576 Å and a large SiNH valence angle of 129.5°. Further calculation[321] using a 6-31G* basis set with d-functions on Si and N atoms was carried out for $H_2Si{=}NSiH_3$ as a model molecule. The bond lengths were calculated to be 1.549 and 1.688 Å for the double and the single SiN bonds, with a Si=N−Si bond angle of 175.6°. The widening of the bond angle was attributed to an electronic effect. The potential energy surface for widening the bond angle is flat and the barrier for linearization of the bond is only 13.8 kJ mol^{-1}, ten times smaller than for the carbon analogue. The difference stems from the larger electronegativity differences between silicon and nitrogen compared with carbon and nitrogen. Experimental geometry obtained by the X-ray crystal structure of the first stable silanimine[322] was published in 1986[323]. Structural parameters in silanimines are given in Table 31.

It is interesting to compare the relevant geometries of compounds **318**–**322** as they all consist of identical Si=N−Si skeleton. The bond lengths in **319**–**321**, where the silicon is also complexed to THF, lie in a very small range: the Si=N bond length in the range 1.593 to 1.597 Å, and the Si−N bond length in the range 1.653 to 1.667 Å. In **318**, on the other hand, where the silicon is purely tricoordinated, the double bond decreases to 1.568 Å and the single bond increases to 1.696 Å. It should also be noted that in **318** the Si=N−Si bond angle is 177.8° while in the other compounds it is in a range between 160.9 and 174.2°. Upon linearization, the Si=N double bond is strengthened due to the increase of the s contribution to nitrogen hybridization. In compounds of the type Si=N−X, where X = sulphur (**325** and **326**) the Si=N bond length is significantly longer (1.714 and 1.704 Å, respectively).

TABLE 31. Structural parameters for silanimines

Refcode	Compound	d(Si=N) (Å)	d(Si−N) (Å)	Si=N−X[a] (°)	Reference
DOKWUV	**318**	1.568	1.696	177.8	324
DOKXAC	**319**	1.588	1.654	161.5	323
DOKXAC	**319**	1.574	1.667	161.0	323
DOKXEG	**320**	1.589	1.653	161.5	324
DOKXEG	**320**	1.573	1.666	160.9	324
JIWGAX	**321**	1.597	1.661	174.2	325
GEVRII	**322**	1.601	1.678	169.4	324
KIDRUK	**323**	1.605	—	—	326
FEWYAH	**323**[a]	1.619	—	172.1	327
YETNVG	**324**	1.599	—	134.6	328
KUCCIV	**325**	1.714	—	135.6	329
KUCCOA	**326**	1.704	—	137.1	329

[a] Similar to **323**, but at the silicon the CH_3 and *t*-Bu are replaced by *i*-Pr.

D. Silanephosphimines (>Si=P−)

There is a theoretical investigation of silanephosphimine $H_2Si{=}PH$ and of its isomer $HSiPH_2$[330]. Experimental X-ray crystal structure are known for only two silanephosphimines: **327**[331] and **328**[332]. The Si=P bond lengths are 2.094 and 2.063 Å in **327** and **328**, respectively. The trigonal silicon is planar in **328** [Σ(Si) is 359.9°] while it is slightly pyramidal in **327** [Σ(Si) is 356.7°].

E. Silanones (>Si=O) and Silanethiones (>Si=S)

The silanone molecule is calculated[333] to be planar and to contain the very polar and strong Si=O double bond. The bond length in silanone is calculated[334] to be 1.545 Å,

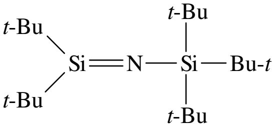

(318)

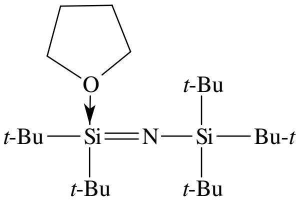

(319)

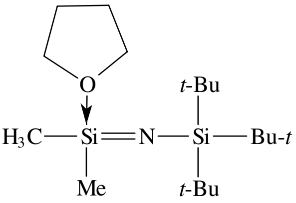

(320)

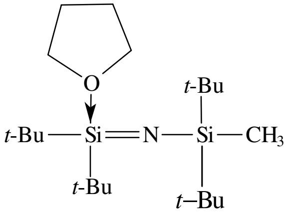

(321)

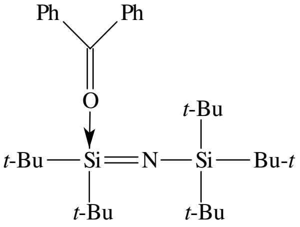

(322)

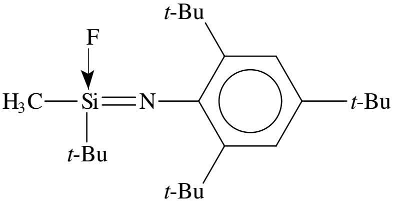

(323)

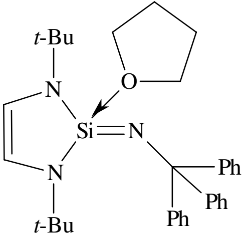

(324)

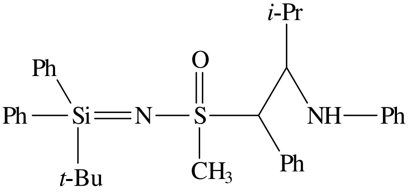

(325)

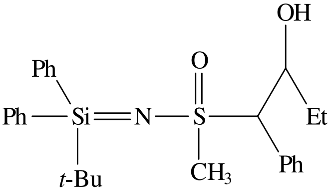

(326)

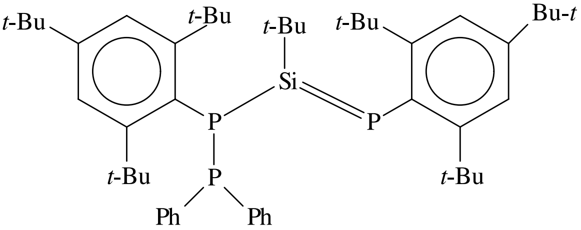

(327)

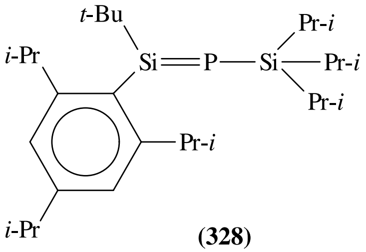

(328)

and later it was calculated[29] using gradient techniques with 3-21G to be 1.599 Å; the addition of the DZ + P basis set causes a shortening of the calculated bond to 1.499 Å. Few XRD structures of compounds possessing Si=O double bonds are known, but in all of them the silicon atom is tetracoordinate, such as in **329**–**332**. The average Si=O bond length in **329**[335] is 1.664 Å, and it is 1.687 Å in **330**[336], 1.622 Å in **331**[337] and 1.615 Å in **332**[337]. Those bond lengths are significantly longer than the calculated ones, which signify that these are not purely double bonds but dative bonds.

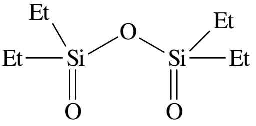

(329)

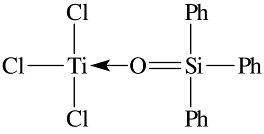

(330)

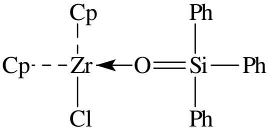

(331)

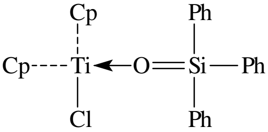

(332)

Unfortunately there are no structural data for silanethiones.

IV. SUMMARY

All Si−X bond lengths obtained by X-ray crystal structures of the organosilicon compounds discussed in this review are summarized in Table 32.

TABLE 32. Summary of bond lengths in organosilicon compounds

X	Si−X	d(Si−X) (Å)
C(sp)	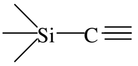	**1.839**
C(sp^2)	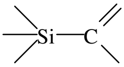	**1.878**

TABLE 32. (*continued*)

C(C=O)	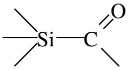	**1.925**
C(aryl)	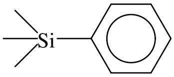	**1.879**
C(methyl)	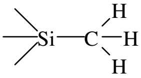	**1.860**
C(t-Bu)	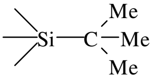	**1.907**
C	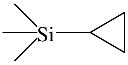	**1.855**
C	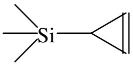	**1.815**
C(sp^2)	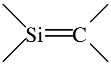	**1.703–1.764**
Si(acyclic)	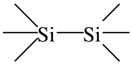	**2.358**
Si(cyclic)	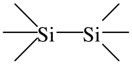	**2.372**
Si	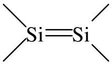	**2.138–2.261**
N(sp^2)	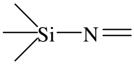	**1.713**
N(sp^3)	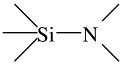	**1.739**
N(sp^3)	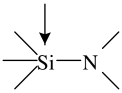	**1.761**
N(sp^3)	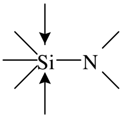	**1.969**
N(sp^2)	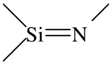	**1.568–1.619**
P	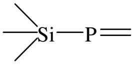	**2.161–2.269**

(*continued overleaf*)

TABLE 32. (*continued*)

X	Si−X	*d*(Si−X) (Å)
P	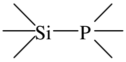	**2.265**
P	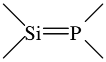	**2.063–2.094**
O	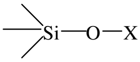	**1.629**
O	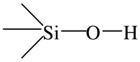	**1.636**
O(acyclic)	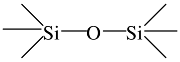	**1.621**
O(cyclic)	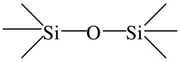	**1.618**
O	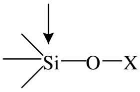	**1.699**
S	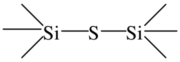	**2.141**
S	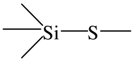	**2.144**
F	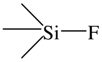	**1.594**
F	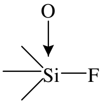	**1.631**
F	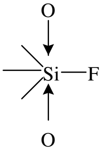	**1.677**
Cl	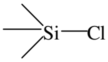	**2.050**
Cl	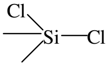	**2.022**
Cl	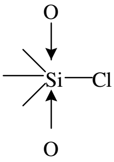	**2.184**

TABLE 32. (*continued*)

Br	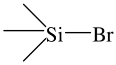	**2.200**
I	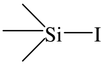	**2.55**

V. REFERENCES

1. J. C. Slater, *J. Chem. Phys.*, **41**, 3199 (1964).
2. R. T. Sanderson, *J. Am. Chem. Soc.*, **105**, 2259 (1983).
3. L. Pauling, *The Nature of the Chemical Bond*, 3rd ed., Cornell University Press, Ithaca, 1960.
4. C. E. Roore, *Ionization Potentials and Ionization Limits Derived from the Analysis of Optical Spectra*, NSRDS-NBS34, National Bureau of Standards, Washington, DC, 1970.
5. M. C. Day, Jr. and J. Selbin, *Theoretical Inorganic Chemistry*, Reinhold, New York, 1969.
6. M. J. S. Dewar, D. H. Lo and C. A. Ramsden, *J. Am. Chem. Soc.*, **97**, 1311 (1975).
7. H. Kwart and K. G. King, *d-Orbitals in the Chemistry of Silicon, Phosphorus and Sulfur*, Springer-Verlag, Berlin, 1977.
8. W. Kutzelnigg, *Angew. Chem., Int. Ed. Engl.*, **23**, 272 (1984).
9. C. Glidewell, *Inorg. Chim. Acta Rev.*, **7**, 69 (1973).
10. H. Bürger, *Angew. Chem., Int. Ed. Engl.*, **12**, 474 (1973).
11. P. Hencsei and L. Parkanyi, *Rev. Silicon, Germanium, Tin, Lead Compd.*, **8,** 191 (1985).
12. G. Klebe, *J. Organomet. Chem.*, **293**, 147 (1985).
13. G. Müller, *Nachr. Chem. Tech. Lab.*, **34**, 778 (1986).
14. S. N. Tandura, M. G. Voronkov and N. V. Alekseev, *Top. Curr. Chem.*, **131**, 99 (1986).
15. W. S. Sheldrick, in *The Chemistry of Organic Silicon Compounds* (Eds. S. Patai and Z. Rappoport), Wiley, Chichester, 1989
16. CSD, Cambridge Structural Database System, version April 1996, Cambridge Crystallographic Data Centre, Cambridge, England.
17. D. C. McKean, I. Torto, J. E. Boggs and K. Fan, *J. Mol. Spectrosc.*, **152**, 389 (1992).
18. M. S. Gordon and C. George, *J. Am. Chem. Soc.*, **106**, 609 (1984).
19. S. Grigoras and T. H. Lane, *J. Comput. Chem.*, **9,** 25 (1987).
20. P. Ugliengo, A. Bleiber, E. Garone and A. M. Ferrari, *Chem. Phys. Lett.*, **191**, 537 (1992).
21. J. B. Nicholas, R. E. Winans, R. J. Harrison, L. E. Iton, L. A. Curtiss and A. J. Hopfinger, *J. Phys. Chem.*, **96**, 10247 (1992).
22. S. Shambayati, J. F.Blake, S. G. Wierschke, W. L. Jorgensen and S. L. Schreiber, *J. Am. Chem. Soc.*, **112,** 697 (1990).
23. E. W. Ignacio and H. B. Schlegel, *J. Phys. Chem.*, **96**, 5830 (1992).
24. H. B. Schlegel and P. N. Skancke, *J. Am. Chem. Soc.*, **115**, 10916 (1993).
25. C. Guimon and G. Pfister-Guillouzo, *Organometallics*, **6**, 1387 (1987).
26. H. Jacobsen and T. Ziegler, *J.Am. Chem. Soc.*, **116**, 3667 (1994).
27. M. S. Gordon, *J. Am. Chem. Soc.*, **104**, 4352 (1982).
28. M. E. Colvin, J. Kobayashi, J. Bicerano and H. F. Schaefer III, *J. Chem. Phys.*, **85**, 4563 (1986).
29. D. A. Dixon and J. L. Gole, *Chem. Phys. Lett.*, **125**, 179 (1986).
30. ORIGIN, software for technical graphics and data analysis, Microcal Software Inc.
31. A. S. Dreiding, J. H. Bieri, R. Prewo, A. Linden and E. Gesing, private communication.
32. Li Guo, J. D. Bradshaw, C. A. Tessier and W. J. Youngs, *J. Chem. Soc., Chem. Commun.*, 243 (1994).
33. A. M. Boldi, J. Anthony, C. B. Knobler and F. Diederich, *Angew. Chem., Int. Ed. Engl.*, **31**, 1240 (1992).
34. K. S. Feldman, C. K. Weinreb, W. J. Youngs and J. D. Bradshaw, *J. Am. Chem. Soc.*, **116**, 9019 (1994).
35. K. S. Feldman, C. K. Weinreb, W. J. Youngs and J. D. Bradshaw, *J. Org. Chem.*, **59**, 1213 (1994).
36. Y. Rubin, C. B. Knobler and F. Diederich, *Angew. Chem., Int. Ed. Engl.*, **30**, 698 (1991).
37. J.-D. van Loon, P. Seiler and F. Diederich, *Angew. Chem., Int. Ed. Engl.*, **32**, 1187 (1993).

38. Y. Pang, A. Schneider, T. J. Barton, M. S. Gordon and M. R. Carroll, *J. Am. Chem. Soc.*, **114**, 4920 (1992).
39. W. Ando, N. Nakayama, Y. Kabe and T. Shimizu, *Tetrahedron Lett.*, **31**, 3597 (1990).
40. M. Ishikawa, T. Hatano, Y. Hasegawa, T. Horio, A. Kunai, A. Miyai, T. Ishida, T. Tsukihara, T. Yamanaka, T. Koike and J. Shioya, *Organometallics*, **11**, 1604 (1992).
41. H. Sakurai, Y. Nakadaira, A. Hosomi, Y. Eriyama and C. Kabuto, *J. Am. Chem. Soc.*, **105**, 3360 (1983).
42. G. A. Eliassen, E. Kloster-Jensen and C. Romming, *Acta Chem. Scand., Ser. B*, **40**, 574 (1986).
43. A. Baumegger, E. Hengge, S. Gamper, E. Herdtweck and R. Janoschek, private communication.
44. M. G. Voronkov, Yu. E. Ovchinnikov, V. E. Shklover, Yu. T. Struchkov, I. A. Zamaev, O. G. Yarosh, G. Yu. Turkina and V. Yu. Vitkovskii, *Dokl. Akad. Nauk SSSR*, **296**, 130 (1987); *Chem. Abstr.*, **109**, 93118b (1988).
45. R. Bortolin, S. S. D. Brown and B. Parbhoo, *Inorg. Chim. Acta*, **158**, 137 (1989).
46. Yu. E. Ovchinnikov, Yu. T. Struchkov, M. G. Voronkov, O. G. Yarosh, G. Yu. Turkina and T. M. Orlova, *Metalloorg. Khim.*, **5**, 1280 (1992); *Chem. Abstr.*, **119**, 226033a (1993).
47. I. A. Zamaev, Yu. E. Ovchinnikov, V. E. Shklover, Yu. T. Struchkov, O. G. Yarosh, M. G. Voronkov, G. Yu. Turkina and T. M. Orlova, *Metalloorg. Khim.*, **1**, 1265 (1988); *Chem. Abstr.*, **110**, 163900x (1989).
48. L. N. Lewis, K. G. Sy, G. L. Bryant Jr. and P. E. Donahue, *Organometallics*, **10**, 3750 (1991).
49. P. Jutzi, J. Kleimeier, R. Krallmann, H.-G. Stammler and B. Neumann, *J. Organomet. Chem.*, **462**, 57 (1993).
50. Yu. E. Ovchinnikov, V. A. Igonin, I. A. Zamaev, V. E. Shklover, Yu. T. Struchkov, O. G. Yarosh, M. G. Voronkov and G. Y. Turkina, *J. Struct. Chem.*, **32**, 250 (1991).
51. K. Tamao, S. Yamaguchi and M. Shiro, *J. Am. Chem. Soc.*, **116**, 11715 (1994).
52. A. Sekiguchi, M. Ichinohe, C. Kabuto and H. Sakurai, *Organometallics*, **14**, 1092 (1995).
53. M. Weidenbruch, A. Schaefer, K. Peters and H. G. von Schnering, *J. Organomet. Chem.*, **314**, 25 (1986).
54. E. O. Fischer, H. Hollfelder, P. Friedrich, F. R. Kreissl and G. Huttner, *Chem. Ber.*, **110**, 3467 (1977).
55. H. H. Karsch, R. Richter and A. Schier, *Z. Naturforsch., Teil B*, **48**, 1533 (1993).
56. M. Fritz, J. Hiermeier, N. Hertkorn, F. H. Kohler, G. Muller, G. Reber and O. Steigelmann, *Chem. Ber.*, **124**, 1531 (1991).
57. B. Morosin and L. A. Harrah, *Acta Crystallogr., Sect. B*, **37**, 579 (1981).
58. G. Reinhard, B. Hirle and U. Schubert, *J. Organomet. Chem.*, **427**, 173 (1992).
59. P. Jutzi, D. Kanne, M. Hursthouse and A. J. Howes, *Chem. Ber.*, **121**, 1299 (1988).
60. J. Grobe, R. Martin, G. Huttner and L. Zolnai, *Z. Anorg. Allg. Chem.*, **607**, 79 (1992).
61. H. Beckers, D. J. Brauer, H. Burger and C. J. Wilke, *J. Organomet. Chem.*, **356**, 31 (1988).
62. M. Weidenbruch, H. Flott, B. Ralle, K. Peters and H. G. von Schnering, *Z. Naturforsch., Teil B*, **38**, 1062 (1983).
63. W. Ando, M. Fujita, H. Toshida and A. Sekiguchi, *J. Am. Chem. Soc.*, **110**, 3310 (1988).
64. Y. Yammamoto, Y. Kebe and W. Ando, *Organometallics*, **12**, 1996 (1993).
65. Dong Ho Pae, M. Xiao, M. Y. Chiang and P. P. Gaspar, *J. Am. Chem. Soc.*, **113**, 1281 (1991).
66. M. Yu. Antipin, A. V. Polyakov, Yu. T. Struchkov, M. P. Egorov, A. L. Gal'minas, S. P. Golensnikov and O. M. Nefedov, *Metalloorg, Khim.*, **2**, 593 (1989); *Chem. Abstr.* **112**, 118996p (1990).
67. A. Kunai, Y. Matsuo, J. Ohshita, M. Ishikawa, Y. Aso, T. Otsubo and F. Ogura, *Organometallics*, **14**, 1204 (1995).
68. F. Hojo, S. Sekigawa, N. Nakayama, T. Shimizu and W. Ando, *Organometallics*, **12**, 803 (1993).
69. P. C. Chien and J. Trotter, *J. Chem. Soc. (A)*, 1778 (1969).
70. S. J. Rettig and J. Trotter, *Acta Crystallogr., Sect. C*, **44**, 1850 (1988).
71. Y. E. Ovchinnikov, V. E. Shklover, Yu. T. Struchkov, T. M. Frunze, V. V. Dement'ev, B. A. Antipova and T. M. Ezhova, *J. Struct. Chem.*, **30**, 281 (1989).
72. R. Tacke, H. Hengelsberg, E. Klingner and H. Henke, *Chem. Ber.*, **125**, 607 (1992).
73. J. P. Vidal, J. L. Galigne and J. Falgueirettes, *Acta Crystallogr., Sect. B*, **28**, 3130 (1972).
74. S. S. Al-Juaid, Y. Derouiche, P. B. Hitchcock, P. D. Lickiss and A. G. Brook, *J. Organomet. Chem.*, **403**, 293 (1991).
75. M. J. Barrow, *Acta Crystallogr., Sect. B*, **38**, 150 (1982).
76. J. Konnert, D. Britton and Y. M. Chow, *Acta Crystallogr., Sect. B*, **28**, 180 (1972).

77. D. A. Dixon, W. R. Hertler, D. B. Chase, W. B. Farnham and F. Davidson, *Inorg. Chem.*, **27**, 4012 (1988).
78. W. R. Hertler, D. A. Dixon, E. W. Matthews, F. Davidson and F. G. Kitson, *J. Am. Chem. Soc.*, **109**, 6532 (1987).
79. Z. Xie, D. J. Liston, T. Jelinek, V. Mitro, R. Bau and C. A. Reed, *J. Chem. Soc., Chem. Commun.*, 384 (1993).
80. G. Rajca, W. Schwarz and J. Weidlein, *Z. Naturforsch., Teil B*, **39**, 1219 (1984).
81. A. Heine, R. Herbst-Irmer, G. M. Sheldrick and D. Stalke, *Inorg. Chem.*, **32**, 2694 (1993).
82. F. R. Fronczek and P. D. Lickiss, *Acta Crystallogr., Sect. C*, **49**, 331 (1993).
83. S. P. Mallela, I. Bernal and R. A. Geanangel, *Inorg. Chem.*, **31**, 1626 (1992).
84. J. B. Lambert, J. L. Pflug, A. M. Allgeier, D. J. Campbell, T. B. Higgins, E. T. Singewald and C. L. Stern, *Acta Crystallogr., Sect. C*, **51**, 713 (1995).
85. H. Oehme, R. Wustrack, A. Heine, G. M. Sheldrick and D. Stalke, *J. Organomet. Chem.*, **452**, 33 (1993).
86. J. Wan and J. G. Verkade, *Inorg. Chem.*, **32**, 341 (1993).
87. A. Haas, R. Sullentrup and C. Kruger, *Z. Anorg. Allg. Chem.*, **619**, 819 (1993).
88. K. Tamao, A. Kawachi, Y. Nakagawa and Y. Ito, *J. Organomet. Chem.*, **473**, 29 (1994).
89. R. West and E. K. Pham, *J. Organomet. Chem.*, **403**, 43 (1991).
90. N. Wiberg, H. Schuster, A. Simon and K. Peters, *Angew. Chem., Int. Ed. Engl.*, **25**, 79 (1986).
91. M. Weidenbruch, B. Flintjer, K. Peters and H. G. von Schnering, *Angew. Chem., Int. Ed. Engl.*, **25**, 1129 (1986).
92. M. Weidenbruch, B. Flintjer, K. Kramer, K. Peters and H. G. von Schnering, *J. Organomet. Chem.*, **340**, 13 (1988).
93. H. Watanabe, M. Kato, T. Okawa, Y. Nagai and M. Goto, *J. Organomet. Chem.*, **271**, 225 (1984).
94. M. Weidenbruch, K.-L. Thom, S. Pohl and W. Saak, private communication.
95. L. Parkanyi, K. Sasvari, J. P. Declercq and G. Germain, *Acta Crystallogr., Sect. B*, **34**, 3678 (1978).
96. H. Li, I. S. Butler and J. F. Harrod, *Organometallics*, **12**, 4553 (1993).
97. F. Shafiee, J. R. Damewood Jr., K. J. Haller and R. West, *J. Am. Chem. Soc.*, **107**, 6950 (1985).
98. F. Shafiee, K. J. Haller and R. West, *J. Am. Chem. Soc.*, **108**, 5478 (1986).
99. A. Schafer, M. Weidenbruch, K. Peters and H. G. von Schnering, *Angew. Chem., Int. Ed. Engl.*, **23**, 302 (1984).
100. H. Tachibana, M. Goto, M. Matsumoto, H. Kishida and Y. Tokura, *Appl. Phys. Lett.*, **64**, 2509 (1994).
101. M. Weidenbruch, J. Hamann, S. Pohl and W. Saak, *Chem. Ber.*, **125**, 1043 (1992).
102. W. Ando, M. Kako, T. Akasaka and S. Nagase, *Organometallics*, **12**, 1514 (1993).
103. J. L. Shibley, R. West, C. A. Tessier and R. K. Hayashi, *Organometallics*, **12**, 3480 (1993).
104. G. Reber, J. Riede, N. Wiberg, K. Schurz and G. Muller, *Z. Naturforsch., Teil B*, **44**, 786 (1989).
105. S. Walter, U. Klingebiel and D. Schmidt-Base, *J. Organomet. Chem.*, **412**, 319 (1991).
106. R. Hasselbring, H. W. Roesky, M. Rietzel and M. Noltmeyer, private communication.
107. M. Jansen and H. Jungermann, *Z. Kristallogr.*, **209**, 779 (1994).
108. S. Freitag, W. Kolodziejski, F. Pauer and D. Stalke, *J. Chem. Soc., Dalton Trans.*, 3479 (1993).
109. M. Herberhold, S. Gerstmann, B. Wrackmeyer and H. Bormann, *J. Chem. Soc., Dalton Trans.*, 633 (1994).
110. M. Herberhold, S. Gerstmann, W. Milius and B. Wrackmeyer, *Z. Naturforsch., Teil B*, **48**, 1041 (1993).
111. S. S. Al-Juaid, A. A. Al-Nasr, G. A. Ayoko, C. Eaborn and P. Hitchcock, *J. Organomet. Chem.*, **488**, 155 (1995).
112. A. Kienzle, A. Obermeyer, R. Riedel, F. Aldinger and A. Simon, *Chem. Ber.*, **126**, 2569 (1993).
113. M. Weidenbruch, B. Flintjer, S. Pohl and W. Saak, *Angew. Chem., Int. Ed. Engl.*, **28**, 95 (1989).
114. J. D. Lichtenhan, S. C. Critchlow and N. M. Doherty, *Inorg. Chem.*, **29**, 439 (1990).
115. C. J. Burns, W. H. Smith, J. C. Huffman and A. P. Sattelberger, *J. Am. Chem. Soc.*, **112**, 3237 (1990).
116. M. Veith and H. Barnighausen, *Acta Crystallogr., Sect. B*, **30**, 1806 (1974).
117. W. Ando, T. Ohtaki and Y. Kabe, *Organometallics*, **13**, 434 (1994).
118. M. Veith, S. Becker and V. Huch, *Angew. Chem., Int. Ed. Engl.*, **29**, 216 (1990).
119. K. Ruhlandt-Senge, R. A. Bartlett, M. Olmstead and P. P. Power, *Angew, Chem., Int. Ed. Engl.*, **32**, 425 (1993).

120. J. He, Hua Qin Liu, J. F. Harrod and R. Hynes, *Organometallics*, **13**, 336 (1994).
121. N. W. Mitzel, J. Riede, A. Schier and H. Schmidbaur, *Acta Crystallogr., Sect. C*, **51**, 756 (1995).
122. F. Huppmann, M. Noltmeyer and A. Meller, *J. Organomet. Chem.*, **483**, 217 (1994).
123. Y. Wan and J. G. Verkade, *Inorg. Chem.*, **32**, 341 (1993).
124. K. Tamao, A. Kawachi, Y. Nakagawa and Y. Ito, *J. Organomet. Chem.*, **473**, 29 (1994).
125. N. W. Mitzel, J. Riede, A. Schier, M. Paul and H. Schmidbaur, *Chem. Ber.*, **126**, 2027 (1993).
126. N. W. Mitzel, P. Bissinger and H. Schmidbaur, *Chem. Ber.*, **126**, 345 (1993).
127. N. W. Mitzel, P. Bissinger, J. Riede, K.-H. Dreihaupl and H. Schmidbaur, *Organometallics*, **12**, 413 (1993).
128. H. Bock, J. Neuret, C. Nather and U. Krynitz, *Tetrahedron Lett.*, **34**, 7553 (1993).
129. L. Marcus, U. Klingebiel and M. Noltmeyer, *Z. Naturforsch., Teil B*, **50**, 687 (1995).
130. R. Hasselbring, I. Leichtweis, M. Noltmeyer, H. W. Roesky, H.-G. Schmidt and A. Herzog, *Z. Anorg. Allg. Chem.*, **619**, 1543 (1993).
131. V. Sum, C. A. Baird, T. P. Kee and M. Thornton-Pett, *J. Chem. Soc., Perkin Trans. 1*, 3183 (1994).
132. D. Dou, M. Westerhausen, G. L. Wood, G. Linti, E. N. Duesler, H. Noth and R. T. Paine, *Chem. Ber.*, **126**, 379 (1993).
133. H. Braunschweig, P. Paetzold and T. P. Spaniol, *Chem. Ber.*, **126**, 1565 (1993).
134. M. Yu. Antipin, A. N. Chernega and Yu. T. Struchkov, *Phosphorus, Sulfur & Silicon*, **78**, 289 (1993).
135. R. Oberdorfer, M. Nieger and E. Niecke, *Chem. Ber.*, **127**, 2397 (1994).
136. B. Wrackmeyer, C. Kohler, W. Milius and M. Herberhold, *Phosphorus, Sulfur & Silicon*, **89**, 151 (1994).
137. Th. Schlosser, A. Sladek, W. Hiller and H. Schmidbaur, *Z. Naturforsch., Teil B*, **49**, 1247 (1994).
138. D. J. Burkey, E. K. Alexander and T. P. Hanusa, *Organometallics*, **13**, 2773 (1994).
139. A. Steiner and D. Stalke, *Angew. Chem., Int. Ed. Engl.*, **34**, 1752 (1995).
140. K. Dippel, U. Klingebiel and D. Schmidt-Base, *Z. Anorg. Allg. Chem.*, **619**, 836 (1993).
141. L. M. Englehardt, P. C. Junk, W. C. Patalinghug, R. E. Sue, C. L. Raston, B. W. Skelton and A. H. White, *J. Chem. Soc., Chem. Commun.*, 930 (1991).
142. A. N. Chernega, M. Yu. Antipin, Yu. T. Struchkov, I. E. Boldeskul, T. V. Sarina and V. D. Romanenko, *Dokl. Akad. Nauk SSSR*, **278**, 1146 (1984); *Chem. Abstr.*, **102**, 149379n (1984).
143. A. H. Cowley, P. C. Knuppel and C. M. Nunn, *Organometallics*, **8**, 2490 (1989).
144. A. Grunhagen, U. Pieper, T. Kottke and H. W. Roesky, *Z. Anorg. Allg. Chem.*, **620**, 716 (1994).
145. U. Klingebiel, M. Meyer, U. Pieper and D. Stalke, *J. Organomet. Chem.*, **408**, 19 (1991).
146. M. Andrianarison, D. Stalke and U. Klingebiel, *J. Organomet. Chem.*, **381**, C38 (1990).
147. H. R. G. Bender, M. Nieger and E. Niecke, *Z. Naturforsch., Teil B*, **48**, 1742 (1993).
148. M. Driess, H. Pritzkow and M. Reisgys, *Chem. Ber.*, **124**, 1923 (1991).
149. K.-F. Tebbe and M. Feher, *Acta Crystallogr., Sect. C*, **46**, 1071 (1990).
150. M. Andrianarison, U. Klingebiel, D. Stalke and G. M. Sheldrick, *Phosphorus, Sulfur & Silicon*, **46**, 183 (1989).
151. H. Westermann and M. Nieger, *Inorg. Chim. Acta*, **177**, 11 (1990).
152. R. Appel, D. Gudat, E. Niecke, M. Nieger, C. Porz and H. Westermann, *Z. Naturforsch., Teil B*, **46**, 865 (1991).
153. M. Baudler, W. Oehlert and K.-F. Tebbe, *Z. Anorg. Allg. Chem.*, **598/599**, 9 (1991).
154. M. A. Petrie and P. P. Power, *J. Chem. Soc., Dalton Trans.*, 1737 (1993).
155. G. Becker, W. Massa, R. E. Schmidt and G. Uhl, *Z. Anorg. Allg. Chem.*, **520**, 139 (1985).
156. I. Kovacs, G. Baum, G. Fritz, D. Fenske, N. Wiberg, H. Schuster and K. Karaghiosoff, *Z. Anorg. Allg. Chem.*, **619**, 453 (1993).
157. M. Baudler, G. Schlotz and K.-F. Tebbe, *Z. Anorg. Allg. Chem.*, **581**, 111 (1991).
158. L. Weber, K. Reizig and R. Boese, *Organometallics*, **4**, 2097 (1985).
159. H. Schafer, D. Binder, B. Deppisch and G. Mattern, *Z. Anorg. Allg. Chem.*, **546**, 79 (1987).
160. R. Koster, G. Seidel, G. Muller, R. Boese and B. Wrackmeyer, *Chem. Ber.*, **121**, 1381 (1988).
161. P. Frankhauser, M. Driess, H. Pritzkow and W. Siebert, *Chem. Ber.*, **125**, 1341 (1992).
162. G. L. Wood, D. Dou, D. K. Narula, E. N. Duesler, R. T. Paine and H. Noth, *Chem. Ber.*, **123**, 1455 (1990).
163. G. Effinger, W. Hiller and I.-P. Lorenz, *Z. Naturforsch., Teil B.*, **42**, 1315 (1987).
164. H. H. Karsch, K. Zellner and G. Muller, *Organometallics.*, **10**, 2884 (1991).

165. H. H. Karsch, U. Keller, S. Gamper and G. Muller, *Angew. Chem., Int. Ed. Engl.*, **29**, 295 (1990).
166. E. Hey, P. B. Hitchcock, M. F. Lappert and A. K. Rai, *J. Organomet. Chem.*, **325**, 1 (1987).
167. G. Becker, H.-M. Hartmann and W. Schwartz, *Z. Anorg. Allg. Chem.*, **577**, 9 (1989).
168. E. Hey-Hawkins and E. Sattler, *J. Chem. Soc., Chem. Commun.*, 725 (1992).
169. E. Hey, C. L. Raston, B. W. Skelton and A. H. White, *J. Organomet. Chem.*, **362**, 1 (1989).
170. D. A. Atwood, A. H. Cowley, R. A. Jones and M. A. Mardones, *J. Organomet. Chem.*, **449**, C1 (1993).
171. M. Westerhausen, *J. Organomet. Chem.*, **479**, 141 (1994).
172. M. G. Voronkov, V. P. Mileshkevich and Yu. A. Yuzhelevskii, *The Siloxane Bond*, Consultants Bureau, New York, London, 1978.
173. A. N. Chernega, M. Yu. Antipin, Yu. T. Struchkov and D. F. Nikson, *Ukr. Khim. Zh.*, **59**, 196 (1993); *Chem. Abstr.*, **118**, 95614 (1993).
174. J. He, J. F. Harrod and R. Hynes, *Organometallics*, **13**, 2496 (1994).
175. D. Murphy, J. P. Sheehan, T. R. Spalding, G. Ferguson, A. J. Lough and J. F. Gallagher, *J. Mater. Chem.*, **3**, 1275 (1993).
176. S. Dielkus, D. Grosskopf, R. Herbst-Irmer and U. Klingebiel, *Z. Naturforsch., Teil B*, **50**, 844 (1995).
177. T. R. Prout, M. L. Thompson, R. C. Haltiwanger, R. Schaeffer and A. D. Norman, *Inorg. Chem.*, **33**, 1778 (1994).
178. H. Bock, J. Meuret, J. W. Bats and Z. Havlas, *Z. Naturforsch., Teil B*, **49**, 288 (1994).
179. W. Wojnowski, J. Pikies, K. Peters, E.-M. Peters, D. Thiery and H. G. von Schnering, *Z. Anorg. Allg. Chem.*, **620**, 377 (1994).
180. R. Tacke, J. Pikies, F. Wiesenberger, L. Ernst, D. Schomburg, M. Waelbroeck, J. Christophe, G. Lambecht, J. Gross and E. Mutchler, *J. Organomet. Chem.*, **466**, 15 (1994).
181. J. J. Edema, R. Libbers, A. Ridder, R. M. Kellog and A. L. Spek, *J. Organomet. Chem.*, **464**, 127 (1994).
182. G. Galzaferri, R. Imhof and K. W. Tornroos, *J. Chem. Soc., Dalton Trans.*, 3123 (1994).
183. W. Wojnowski, M. Wojnowski, K. Peters, E.-M. Peters and H. G. von Schnering, *Z. Anorg. Allg. Chem.*, **530**, 79 (1985).
184. B. Becker, W. Wojnowski, K. Peters, E.-M. Peters and H. G. von Schnering, *Polyhedron*, **9**, 1659 (1990).
185. W. Wojnowski, B. Becker, J. Sassmannshausen, E.-M. Peters, K. Peters and H. G. von Schnering, *Z. Anorg. Allg. Chem.*, **620**, 1417 (1994).
186. S. A. Bourne, L. Johnson, C. Marais, L. R. Nassimbeni, E. Weber, K. Skobridis and F. Toda, *J. Chem. Soc., Perkin Trans. 2*, 1707 (1991).
187. E. A. Babaian, M. Huff, F. A. Tibbals and D. C. Hrncir, *J. Chem. Soc., Chem. Commun.*, 306 (1990).
188. S. A. Bourne, L. R. Nassimbeni, K. Skobridis and E. Weber, *J. Chem. Soc., Chem. Commun.*, 282 (1991).
189. N. Winkhofer, H. W. Roesky, M. Noltemeyer and W. T. Robinson, *Angew. Chem., Int. Ed. Engl.*, **31**, 599 (1992).
190. S. A. Bourne, L. R. Nassimbeni, E. Weber and K. Skobridis, *J. Org. Chem.*, **57**, 2438 (1992).
191. S. S. Al-Juaid, A. K. A. Al-Nasr, C. Eaborn and P. B. Hitchcock, *J. Chem. Soc., Chem. Commun.*, 1482 (1991).
192. J. D. Buynak, J. B. Strickland, G. W. Lamb, D. Khasnis, S. Modi, D. Williams and H. Zhang, *J. Org. Chem.*, **56**, 7076 (1991).
193. A. Fronda, F. Krebs, B. Daucher, T. Werle and G. Maas, *J. Organomet. Chem.*, **424**, 253 (1992).
194. S. S. Al-Juaid, C. Eabron, P. B. Hitchcock and P. D. Lickiss, *J. Organomet. Chem.*, **362**, 17 (1989).
195. R. Tacke, J. Pikies, F. Eiesenberger, L. Ernst, D. Schomburg, M. Waelbroeck, J. Christophe, G. Lambrecht, J. Gross and E. Mutschler, *J. Organomet. Chem.*, **466**, 15 (1994).
196. I. L. Karle, J. M. Karle and C. J. Nielsen, *Acta Crystallogr., Sect. C*, **42**, 64 (1986).
197. V. E. Shklover and Yu. T. Struchkov, *Usp. Khim.*, **49**, 518 (1980); *Chem. Abstr.*, **92**, 198795d (1980).
198. W.-J. Lay, M.-S. Hong, M.-S. Huang and S.-J. Hu, *Jiegou Huaxue O. Struct. Chem.*, **10**, 258 (1991); *Chem. Abstr.*, **116**, 266136f (1992).
199. L. Parkanyi, V. Fulop, P. Hencsei and I. Kovacs, *J. Organomet. Chem.*, **418**, 173 (1991).
200. R. J. Garant, L. M. Daniels, S. K. Das, M. N. Janakiraman, R. A. Jacobson and J. G. Verkade, *J. Am. Chem. Soc.*, **113**, 5728 (1991).

201. Y. Yang, C. Yin, G. Chen and C. He, *Gaodeng Xuexiao Huaxue Xuebao (Chem. J. Chin. Uni.)*, **11**, 102 (1990).
202. M. Nasim, V. S. Petrosyan, G. S. Zeitseva, L. J. Lorbeth, S. Wocadlo and W. Massa, *J. Organomet. Chem.*, **441**, 27 (1992).
203. K. C. K. Swamy, V. Chandrasekhar, J. J. Harland, J. M. Holmes, R. O. Day and R. R. Holmes, *J. Am. Chem. Soc.*, **112**, 2341 (1990).
204. R. Tacke, F. Wiesenberger, A. Lopez-Mras, J. Sperlich and G. Mattern, *Z. Naturforsch., Teil B*, **47**, 1370 (1992).
205. K. Y. Blohowiak, D. R. Traedwell, B. L. Mueller, M. L. Hoppe, S. Jouppi, P. Kansal, K. W. Chew, C. L. S. Scotto, F. Babonneau, J. Kampf and R. M. Laine, *Chemistry of Materials*, **6**, 2177 (1994).
206. A. O. Mozzhurkhin, M. Y. Antipin, Y. T. Struchkov, A. G. Shipov, E. P. Kramerova and Y. T. Baukov, *Metalloorg. Khim.*, **5**, 906 (1992); *Chem. Abstr.*, **118**, 102109q (1993).
207. Yu. E. Ovchinnikov, A. A. Macharashvili, Yu. T. Struchkov, A. G. Shipov and Yu. T. Baukov, *J. Struct. Chem.*, **35**, 91 (1994).
208. F. E. Hahn, M. Keck and K. N. Raymond, *Inorg. Chem.*, **34**, 1402 (1995).
209. G. Sawitzki, H. G. von Schnering, D. Kummer and T. Seshadri, *Chem. Ber.*, **111**, 3705 (1978).
210. J. J. Flynn and F. P. Boer, *J. Am. Chem. Soc.*, **91**, 5756 (1969).
211. M. L. Hoppe, R. M. Laine, J. Kampf, M. S. Gordon and L. W. Burggraf, *Angew. Chem., Int. Ed. Engl.*, **32**, 287 (1993).
212. W. E. Schklower, Y. T. Struchkov, L. E. Guselnikow, W. W. Wolkowa and W. G. Awakyan, *Z. Anorg. Allg. Chem.*, **501**, 153 (1983).
213. W. Wojnowski, K. Peters, D. Weber and H. G. von Schnering, *Z. Anorg. Allg. Chem.*, **519**, 134 (1984).
214. W. Wojnowski, K. Peters, E.-M. Peters and H. G. von Schnering, *Z. Anorg. Allg. Chem.*, **525**, 121 (1985).
215. W. Wojnowski, B. Dreczewski, A. Herman, K. Peters, E.-M. Peters and H. G. von Schnering, *Angew Chem., Int. Ed. Engl.*, **24**, 992 (1985).
216. W. Wojnowski, W. Bochenska, K. Peters, E.-M. Peters and H. G. von Schnering, *Z. Anorg. Allg. Chem.*, **533**, 165 (1986).
217. C. Habben, A. Meller, M. Noltmeyer and G. M. Sheldrick, *Angew. Chem., Int. Ed. Engl.*, **25**, 741 (1986).
218. B. Becker, R. J. P. Corriu, B. J. L. Henner, W. Wojnowski, K. Peters and H. G. von Schnering, *J. Organomet. Chem.*, **312**, 305 (1986).
219. W. Wojnowski, B. Dreczewski, K. Peters, E.-M. Peters and H. G. von Schnering, *Z. Anorg. Allg. Chem.*, **540**, 271 (1986).
220. W. Wojnowski, B. Becker, K. Peters, E.-M. Peters and H. G. von Schnering, *Z. Anorg. Allg. Chem.*, **563**, 48 (1988).
221. D. H. Berry, J. Chey, H. S. Zipin and P. J. Carroll, *Polyhedron*, **10**, 1189 (1991).
222. J. C. J. Bart and J. J. Daly, *J. Chem. Soc., Dalton Trans.*, 2063 (1975).
223. L. Pazdernik, F. Brisse and R. Rivest, *Acta Crystallogr., Sect. B*, **33**, 1780 (1977).
224. W. Wojnowski, K. Przyjemska, K. Peters and H. G. von Schnering, *Z. Anorg. Allg. Chem.*, **556**, 92 (1988).
225. W. Wojnowski, M. Wojnowska, B. Becker and M. Noltmeyer, *Z. Anorg. Allg. Chem.*, **561**, 167 (1988).
226. B. Becker, W. Wojnowski, K. Peters, E.-M. Peters and H. G. von Schnering, *Inorg. Chim. Acta*, **214**, 9 (1993).
227. B. Becker, W. Wojnowski, K. Peters, E.-M. Peters and H. G. von Schnering, *Polyhedron*, **11**, 613 (1992).
228. W. Wojnowski, B. Becker, L. Waltz, K. Peters, E.-M. Peters and H. G. von Schering, *Polyhedron*, **11**, 607 (1992).
229. F. Preuss, M. Steidel and R. Exner, *Z. Naturforsch., Teil B*, **45**, 1618 (1990).
230. B. Becker, K. Radacki, A. Konitz and W. Wojnowski, *Z. Anorg. Allg. Chem.*, **621**, 904 (1995).
231. G. D. Andreetti, G. Calestani and P. Sgarabotto, *J. Organomet. Chem.*, **273**, 31 (1984).
232. R. Minkwitz, A. Kornath and H. Preut, *Z. Anorg. Allg. Chem.*, **619**, 877 (1993).
233. C. R. Lucas, M. J. Newlands, E. J. Gabe and F. L. Lee, *Can. J. Chem.*, **65**, 898 (1987).
234. R. Kewley, P. M. McKinney and A. G. Robiette, *J. Mol. Spectrosc.*, **34**, 309 (1970)
235. V. W. Laurie, *J. Chem. Phys.*, **26**, 1359 (1973).

236. A. R. Hoy, M. Bertram and I. M. Mills, *J. Mol. Spectrosc.*, **46**, 429 (1973).
237. B. Beagley, D. P. Brown and J. M. Freeman, *J. Mol. Struct.*, **18**, 337 (1973).
238. K. Dippel, U. Klingebiel, T. Kottke, F. Pauer, G. M. Sheldrick and D. Stalke, *Z. Anorg. Allg. Chem.*, **584**, 87 (1990).
239. T. Kottke, U. Klingebiel, M. Noltemeyer, U. Pieper, S. Walter and D. Stalke, *Chem. Ber.*, **124**, 1941 (1991).
240. S. Walter, U. Klingebiel, M. Noltemeyer and D. Schmidt-Base, *Z. Naturforsch., Teil B*, **46**, 1149 (1991).
241. M. Andrianarison, U. Klingebiel, D. Stalke and G. M. Sheldrick, *Phosphorus, Sulfur & Silicon*, 46, 183 (1989).
242. K. Ebata, T. Inada, C. Kabuto and H. Sakurai, *J. Am. Chem. Soc.*, **116**, 3595 (1994).
243. U. Pieper, D. Stalke, S. Vollbrecht and U. Klingebiel, *Chem. Ber.*, **123**, 1039 (1990).
244. E. A. Zelbst, V. E. Shklover, Yu. T. Struchkov, Yu. L. Frolov, A. A. Kashaev, L. I. Gubanova, V. M. D'yakov and M. G. Voronkov, *J. Struct. Chem.*, **22**, 377 (1981).
245. Yu. E. Ovchinnikov, A. O. Mozzhukhin, M. Yu. Antipin, Yu. T. Struchkov, V. P. Baryshok, N. F. Lazareva and M. G. Voronkov, *J. Struct. Chem.*, **34**, 888 (1993).
246. E. A. Zelbst, V. S. Fundamenskii, A. A. Kashaev, L. I. Gubanova, and M. G. Voronkov, *Dokl. Akad. Nauk SSSR*, **312**, 612 (1990); *Chem. Abstr.*, **113**, 174207y (1989).
247. M. G. Voronkov, E. A. Zelbst, V. S. Fundamenskii, A. A. Kashaev and L. I. Gubanova, *Dokl. Akad. Nauk SSSR*, **305**, 1124 (1989); *Chem. Abstr.*, **111**, 174207y (1989).
248. Yu. E. Ovchinnikov, Yu. T. Struchkov, N. F. Chernov, O. M. Trofimova and M. G. Voronkov, *J. Organomet. Chem.*, **461**, 27 (1993).
249. Yu. E. Ovchinnikov, M. S. Sorokon, Yu. T. Struchkov and M. G. Voronkov, *Dokl. Akad. Nauk SSSR*, **330**, 337 (1993); *Chem. Abstr.*, **119**, 282716n (1993).
250. D. Schomburg, *J. Organomet. Chem.*, **221**, 137 (1981).
251. D. A. Dixon, W. B. Farnham, W. Heilemann, R. Mews and M. Noltmeyer, *Heteroatom Chemistry*, **4**, 287 (1993).
252. J. J. Harland, J. S. Payne, R. O. Day and R. R. Holmes, *Inorg. Chem.*, **26**, 760 (1987).
253. R. Tacke, J. Becht, A. Lopez-Mras, W. S. Sheldrick and A. Sebald, *Inorg. Chem.*, **32**, 2761 (1993).
254. A. D. Adley, P. H. Bird, A. R. Fraser and M. Onyszchuk, *Inorg. Chem.*, **11**, 1402 (1972).
255. R. Tacke and M. Muhleisen, *Angew. Chem., Int. Ed. Engl.*, **33**, 1359 (1994).
256. E. B. Lobkovski, V. N. Fokin and K. N. Semeneko, *J. Struct. Chem.*, **22**, 603 (1981).
257. S. N. Gurkova, A. J. Gusev, N. V. Alexeev and Yu. M. Varezhkin, *J. Struct. Chem.*, **25**, 655 (1984).
258. N. A. Avdyukhina, E. B. Chuklanova, I. A. Abronin, A. I. Gusev, V. I. Zhun and V. D. Sheludyakov, *Metalloorg. Khim.*, **1**, 878 (1988); *Chem. Abstr.*, **111**, 153893d (1989).
259. A. Sekiguchi, I. Maruki and H. Sakurai, *J. Am. Chem. Soc.*, **115**, 11460 (1993).
260. G. Fritz, S. Lauble, R. Befurt, K. Peters, E.-M. Peters and H. G. von Schnering, *Z. Anorg. Allg. Chem.*, **619**, 1494 (1993).
261. G. Fritz, A. G. Beetz, E. Matern, K. Peters, E.-M. Peters and H. G. von Schnering, *Z. Anorg. Allg. Chem.*, **620**, 136 (1994).
262. G. Fritz, P. Fusik, E. Matern, K. Peters, E.-M. Peters and H. G. von Schnering, *Z. Anorg. Allg. Chem.*, **620**, 1253 (1994).
263. C. Rudinger, H. Beruda and H. Schmidbaur, *Z. Naturforsch., Teil B*, **49**, 1348 (1994).
264. D. Schmidt-Base and U. Klingebiel, *Chem. Ber.*, **123**, 449 (1990).
265. K. Dippel, U. Klingebiel and D. Schmidt-Base, *Z. Anorg. Allg. Chem.*, **619**, 836 (1993).
266. A. A. Zlota, F. Frolow and D. Milstein, *J. Chem. Soc., Chem. Commun.*, 1826 (1989).
267. K. E. Lee, A. M. Arif and J. A. Gladysz, *Chem. Ber.*, **124**, 309 (1991).
268. U. Schubert, K. Ackermann, G. Kraft and B. Worle, *Z. Naturforsch., Teil B*, **38**, 1488 (1983).
269. B. R. Jagirdar, R. Palmer, K. J. Klabunde and L. J. Radonovich, *Inorg. Chem.*, **34**, 278 (1995).
270. M. Yu. Antipin, A. A. Macharashvili, Yu. T. Struchkov and V. E. Shklover, *Metalloorg. Khim.*, **3**, 998 (1990); *Chem. Abstr.*, **114**, 102172 (1991).
271. A. A. Macharashvili, Y. I. Baukov, E. P. Kramarova, G. I. Olenova, V. A. Pestunovich, Y. T. Struchkov and V. E. Shklover, *J. Struct. Chem.*, **28**, 730 (1987).
272. A. A. Macharashvili, V. E. Shklover, Yu. T. Struchkov, V. A. Pestunovich, Yu. I. Baukov, E. P. Kramarova and G. I. Olenova, *J. Struct. Chem.*, **29**, 759 (1988).
273. A. A. Macharashvili, V. E. Shklover, Yu. T. Struchkov, G. I. Olenova, E. P. Kramarova, A. G. Shipov and Yu. I. Baukov, *J. Chem. Soc., Chem. Commun.*, 683 (1988).

274. A. A. Macharashvili, V. E. Shklover, Yu. T. Struchkov, B. A. Gostevskii, I. D. Kalikhman, O. B. Bannikova, M. G. Voronkov and V. A. Pestunovich, *J. Organomet. Chem.*, **356**, 23 (1988).
275. D. Kummer, S. C. Chaudhry, J. Seifert, B. Deppisch and G. Mattern, *J. Organomet. Chem.*, **382**, 345 (1990).
276. D. Kummer, S. H. A. Halim, W. Kuhs and G. Mattern, *J. Organomet. Chem.*, **446**, 51 (1993).
277. A. A. Macharashvili, Yu. E. Ovchinnikov, Yu. T. Struchkov, V. N. Sergeev, S. V. Pestunovich and Yu. I. Baukov, *Izv. Akad. Nauk SSSR, Ser. Khim.*, 189 (1993).
278. O. Bechstein, B. Ziemer, D. Hass, S. I. Trojanov, V. B. Rybakov and G. N. Maso, *Z. Anorg. Allg. Chem.*, **582**, 211 (1990).
279. G. Klebe and D. Tranqui, *Acta Crystallogr., Sect. C*, **40**, 476 (1984).
280. D. Kummer, S. C. Chaudhry, U. Thewalt and T. Debaerdemaeker, *Z. Anorg. Allg. Chem.*, **553**, 147 (1987).
281. D. Kummer, S. C. Chaudhry, W. Dempeier and G. Mattern, *Chem. Ber.*, **123**, 2241 (1990).
282. D. Kummer, S. C. Chaudhry, T. Debaerdemaeker and U. Thewalt, *Chem. Ber.*, **123**, 945 (1990).
283. V. O. Atwood, D. A. Atwood, A. H. Cowley and S. Trofimenko, *Polyhedron*, **11**, 711 (1992).
284. S. N. Gurkova, A. I. Gusev, V. A. Sharapov, T. K. Gar and N. V. Alexeev, *J. Struct. Chem.*, **20**, 302 (1979).
285. U. Schubert and C. Steib, *J. Organomet. Chem.*, **238**, C1 (1982).
286. A. A. Macharashvili, Yu. I. Baukov, E. P. Kramarova, G. I. Olenova, V. A. Shestunovich, Yu. T. Struchkov and V. E. Shklover, *J. Struct. Chem.*, **28**, 552 (1987).
287. M. Weidenbruch, B. Blintjer, K. Peters and H. G. von Schnering, *Angew. Chem., Int. Ed. Engl.*, **25**, 1129 (1986).
288. S. S. Al-Juaid, A. K. A. Al-Nasr, C. Eaborn and P. B. Hitchcock, *J. Organomet. Chem.*, **429**, C9 (1992).
289. R. West, *Pure Appl. Chem.*, **56**, 163 (1984).
290. R. West, *Science*, **225**, 1109 (1984).
291. R. West, M. J. Fink, M. J. Michaczyk and D. J. De Young, in *Organisilicon and Bioorganosilicon Chemistry* (Ed. H. Sakurai), Ellis Horwood, Chichester, 1985, p. 3.
292. G. R. Raabe and J. Michl, *Chem. Rev.*, **85**, 419 (1985).
293. A. H. Cowley, *Acc. Chem. Res.*, **17**, 386 (1984).
294. A. H. Cowley and N. C. Norman, *Prog. Inorg. Chem.*, **34**, 1 (1986).
295. K. Krogh-Jespersen, *J. Am. Chem. Soc.*, **107**, 537 (1985).
296. B. D. Shepherd, C. F. Campana and R. West, *Heteroatom Chemistry*, **1**, 1 (1990).
297. R. S. Grev, H. F. Schaefer and K. M. Baines, *J. Am. Chem. Soc.*, **112**, 9458 (1990).
298. S. Masamune, S. Murakami, J. T. Snow, H. Tobita and D. J. Williams, *Organometallics*, **3**, 333 (1984).
299. H. Watanabe, K. Takeuchi, N. Fukawa, M. Kato, M. Goto and Y. Nagai, *Chem. Lett.*, 1341 (1987).
300. B. D. Shepherd, D. R. Powell and R. West, *Organometallics*, **8**, 2664 (1989).
301. R. S. Archibald, Y. van der Winkel, A. J. Millevolte, J. M. Desper and R. West, *Organometallics*, **11**, 3276 (1992).
302. B. D. Shepherd, C. F. Campana and R. West, *Heteroatom Chemistry*, **1**, 1 (1990).
303. M. Kira, T. Maruyama, C. Kabuto, K. Ebata and H. Sakurai, *Angew. Chem., Int. Ed. Engl.*, **33**, 1489 (1994).
304. N. Tokitoh, H. Suzuki and R. Okazaki, *J. Am. Chem. Soc.*, **115**, 10428 (1993).
305. A. G. Brook, F. Abdesaken, B. Gutekunst, G. Gutekunst and R. K. Kallury, *J. Chem. Soc., Chem. Commun.*, 191 (1981).
306. A. G. Brook, S. C. Nyburg, F. Abdesaken, B. Gutekunst, G. Gutekunst, R. Krishna, M. R. Kallury, Y. C. Poon, Y.-M. Chang and W. Wong-Ng, *J. Am. Chem. Soc.*, **104**, 5667 (1982).
307. S. C. Nyburg, A. G. Brook, F. Abdesaken, G. Gutekunst and W. Wong-Ng, *Acta Crystallogs.*, **C41**, 1632 (1985).
308. N. Wiberg, G. Wagner and G. Müller, *Angew. Chem.*, **97**, 220 (1985).
309. N. Wiberg, G. Wagner, J. Riede and G. Müller, *Organometallics*, **6**, 32 (1987).
310. N. Wiberg, G. Wagner, J. Riede and G. Müller, *J. Organomet. Chem.*, **271**, 381 (1984).
311. N. Wiberg, G. Wagner, G. Reber, J. Riede and G. Müller, *Organometallics*, **6**, 35 (1987).
312. G. E. Miracle, J. L. Ball, D. R. Powell and R. West, *J. Am. Chem. Soc.*, **115**, 11598 (1993).
313. N. Wiberg, K.-S. Joo and K. Polborn, *Chem. Ber.*, **126**, 67 (1993).
314. T. S. Koloski, P. J. Carrol and D. H. Berry, *J. Am. Chem. Soc.*, **112**, 6405 (1990).

315. B. K. Campion, R. H. Heyn, T. D. Tilley and A. L. Rheingold, *J. Am. Chem. Soc.*, **115**, 5527 (1993).
316. H. F. Schaefer, *Acc. Chem. Res.*, **15**, 283 (1982).
317. Y. Apeloig and M. Karni, *J. Chem. Soc., Chem. Commun.*, 768 (1984).
318. Y. Apeloig and M. Karni, *J. Am. Chem. Soc.*, **106**, 6676 (1984).
319. B. T. Luke, J. A. Pople, M.-B. Krogh-Jespersen, Y. Apeloig, M. Karni, J. Chandrasekhar and P. v. R. Schleyer, *J. Am. Chem. Soc.*, **108**, 270 (1986).
320. M. S. Gordon and T. N. Truong, *Chem. Phys. Lett.*, **142**, 110 (1987).
321. P. v. R. Schleyer and P. D. Stout, *J. Chem. Soc., Chem. Commun.*, 1373 (1986).
322. N. Wiberg, K. Schurz and G. Fischer, *Angew. Chem.*, **97**, 1058 (1985).
323. N. Wiberg, K. Schurz, G. Reber and G. Müller, *J. Chem. Soc., Chem. Commun.*, 591 (1986).
324. G. Reber, J. Riede, N. Wiberg, K. Schurz and G. Müller, *Z. Naturforsch., Teil B*, **44**, 786 (1989).
325. S. Walter, U. Klingebiel and D. Schmidt-Base, *J. Organomet. Chem.*, **412**, 319 (1991).
326. R. Boese and U. Klingebiel, *J. Organomet. Chem.*, **315**, C17 (1986).
327. D. Stalke, U. Pieper, S. Vollbrecht and U. Klingebiel, *Z. Naturforsch., Teil B*, **45**, 1513 (1990).
328. M. Deak, R. K. Hayashi and R. West, *J. Am. Chem. Soc.*, **116**, 10813 (1994).
329. S. G. Pyne, B. Dikic, B. W. Skelton and A. H. White, *Aust. J. Chem.*, **45**, 807 (1992).
330. K. J. Dykema, T. N. Truong and M. S. Gordon, *J. Am. Chem. Soc.*, **107**, 4535 (1985).
331. H. R. G. Bender, E. Niecke and M. Nieger, *J. Am. Chem. Soc.*, **115**, 3314 (1993).
332. M. Driess, S. Rell and H. Pritzkow, *J. Chem. Soc., Chem. Commun.*, 253 (1995).
333. R. Jaquet, W. Kutzelnigg and V. Staemmler, *Theor. Chim. Acta*, **54**, 205 (1980).
334. T. Kudo and S. Nagase, *J. Phys. Chem.*, **88**, 2833 (1984).
335. A. P. Polishchuk, M. Y. Antipin, T. V. Timofeeva, N. N. Makarova, N. A. Golovina and Yu. T. Struchkov, *Soriet Phys. Crystallogr.*, **36**, 50 (1991).
336. T. Rubenstahl, D. W. von Grudenberg, F. Weller, K. Dehnicke and H. Goesmann, *Z. Naturforsch., Teil B*, **49**, 15 (1994).
337. D. W. von Grudenberg, H.-C. Kan, W. Massa, K. Dehnicke, C. Maichle-Mossmer and J. Strahle, *Z. Anorg. Allg. Chem.*, **620**, 1719 (1994).

CHAPTER 6

^{29}Si NMR spectroscopy of organosilicon compounds

YOSHITO TAKEUCHI

Department of Chemistry, Faculty of Science, Kanagawa University, 2946 Tsuchiya, Hiratsuka, Japan 259-12
Fax: +81 463 58 9684;   e-mail: yoshito@info.kanagawa-u.ac.jp

and

TOSHIO TAKAYAMA

Department of Applied Chemistry, Faculty of Engineering, Kanagawa University, 3-27-1 Rokkakubashi, Yokohama, Japan 221
Fax: +81 45 413 9770;   e-mail: takayama@cc.kanagawa-u.ac.jp

I. INTRODUCTION

Apart from ^{1}H and ^{13}C NMR ^{29}Si is one of the most frequently used method for NMR spectroscopy. The natural abundance is 4.7%, and its gyromagnetic ratio is -5.314 (10^7 radian T^{-1} s^{-1}), which is about one-fifth of that of the proton. Hence, in the advent of NMR spectroscopy, ^{29}Si NMR spectroscopy has been difficult if not esoteric. The increase in the magnetic field produced by the NMR instruments together with rapid development in computer hardware and software has gradually made ^{29}Si NMR spectroscopy more feasible.

Excellent reviews have occasionally been published on this topic. In the previous volume of this book the topic was also reviewed[1]. Hence in the present review, advances made mostly after that review, i.e. literature for the last ten years (*ca* 1985–1995), will be covered.

The advances in NMR spectroscopy in the last ten years were enormous. Thus, almost all laboratories which produce papers are equipped with SCM (Super Conducting Magnet) instruments with 400–500 MHz magnets, and 2D or multidimensional NMR experiments are now routinely employed. In addition, solid-state NMR and NMR imaging (MRI) have widened their scope to a considerable extent. ^{29}Si NMR has enjoyed this general progress.

A very noticeable change was found in the methodology associated with NMR. Previously NMR spectroscopies were used for structure elucidation with other spectroscopic means such as UV or IR. During the last decade, the partner of NMR was changed from conventional spectrometry to X-ray analysis. As expected, this combination is very much more powerful and often produces results which cannot be expected from the use of other combinations of methodologies.

At the same time, advances in the field of organosilicon chemistry have also been incredibly large[2]. Characterization of unstable species such as divalent silylenes or compounds with silicon-containing double bonds were successfully achieved for many compounds. Advances in the field of siloxanes and other polymeric materials are also remarkable.

Under such circumstances it would be difficult to cover all the literature of the last ten years. Rather, topics which, from the viewpoint of the authors of this review, demonstrate this fruitful period will be selected and discussed. Thus, firstly, new developments in NMR techniques will be discussed in relation to ^{29}Si NMR. Discussion of the ^{29}Si NMR spectra of novel and hypervalent organosilicon compounds will follow. New data on ^{29}Si NMR parameters are preceded by the recent development in the theory of ^{29}Si NMR. In most of the reviews on NMR, this section will come first. We have inverted this order because the purpose of this review is not to cover all the literature, but to bring to the attention of organosilicon chemists the most crucial points of recent ^{29}Si NMR spectroscopy. The development of solid-state ^{29}Si NMR will be described in a separate section. We deliberately make this section independent since the use of solid-state ^{29}Si NMR is increasing particularly rapidly. This tendency will no doubt be accelerated owing to the relevance of silicon chemistry to materials science.

A compilation of chemical shifts and other spectroscopic data was not intended, since the amount of newly reported data is much too large for a review of reasonable length. In addition such data can be found in previously published reviews and references cited therein[1,3]. Readers who are interested in a compilation of chemical shifts and coupling constants can consult Williams's review in Vol. 1 of this book.

II. NEW TECHNIQUES

A. Modern Pulse Sequences

Recent improvements in high resolution NMR of solutions have added a new dimension to the structural study of silicon compounds. Many new methods in measuring ^{29}Si NMR have been reported. The low sensitivity of ^{29}Si can be circumvented by isotopic enrichment and/or the use of very high fields. For aqueous ^{29}Si-enriched (99%) sodium silicate solutions, experiments at high field (11.7 T) have been reported by Harris and coworkers[4]. Furthermore, a large number of species have been identified[5] using two-dimensional (2D) experiments such as COSY for observation of ^{29}Si−^{29}Si correlations in chemical exchange studies.

For an effective measurement of ^{n}J(SiH) ($1 < n < 4$) values in silylated silyl enol ethers, a selective population transfer experiment was modified so that selective decoupling was applied during acquisition. ^{1}H−^{29}Si heteronuclear COSY confirmed the presence of silylated groups in the molecule[6].

Another way to improve sensitivity is to use NMR methods such as INEPT and DEPT[7−9] which, through scalar spin−spin coupling, will allow polarization to be transferred from the abundant high-γ protons to the rare low-γ ^{29}Si nuclei. Some ten years ago, measurements of ^{29}Si NMR spectra of trimethylsilyl derivatives by employing the INEPT technique were reported[10]. The authors suggested that the use of this technique will substantially shorten the measuring time and widen the scope of the analytical applications of ^{29}Si NMR spectroscopy.

Until now the double-quantum coherence spectroscopy has not often been used for silicon frameworks. In double-quantum coherence spectroscopy the silicon nucleus is almost ten times as sensitive as the ^{13}C nucleus because of the higher natural abundance of ^{29}Si (4.7% compared with 1.1% ^{13}C). Disadvantages of the ^{29}Si nucleus are the long relaxation times (T_1) and the negative nuclear Overhauser effect (NOE). In practice, this means that a very long recording time is necessary unless a relaxation reagent such as $Cr(acac)_3$ is used.

The usefulness of ^{29}Si-INADEQUATE spectroscopy has been demonstrated by Hengge and Schrank[11] for the four known cyclosilanes: trimethylsilylnonamethylcyclopentasilane ($Si_5Me_9-SiMe_3$, **1**), dimethylsilylnonamethylcyclopentasilane ($Si_5Me_9-SiMe_2H$, **2**), bis(undecamethylcyclohexasilanyl) ($(Si_6Me_{11})_2$, **3**) and bis(undecamethylcyclohexasilanyl) dimethylsilane ($(Si_6Me_{11})_2-SiMe_2$, **4**).

The chemical shifts and the ^{29}Si−^{29}Si coupling constants (determined from the 1D-INADEQUATE spectra) are summarized in Table 1. Figure 1 shows the 1D-INADEQUATE spectrum of **4**. If all the ^{29}Si−^{29}Si couplings can be determined, the structure of the compound can be easily derived.

When resonance frequencies are very close, overlapping or extinguishing (both satellite signals are in antiphase) of signals might occur. In such cases the 2D-INADEQUATE experiment provides the desired information about the structure, though the long recording time is sometimes a serious disadvantage. The applicability of the 2D-INADEQUATE technique to organosilicon compounds is demonstrated by the spectrum of **1** shown in Figure 2. Note, however, that in this case all the required information can be obtained from the 1D experiment[10].

A second means of enhancing sensitivity is to increase the concentration of the sample in solution. Thus, 2D-INADEQUATE studies of ^{29}Si−^{29}Si correlations on polysilanes at natural ^{29}Si abundance at high concentrations (1−2 M) was reported[12]. Sophisticated solid-state NMR studies (see Section V) have also been performed, including two-dimensional

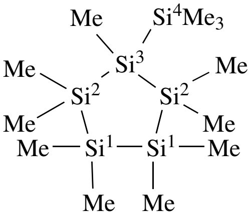

(**1**)

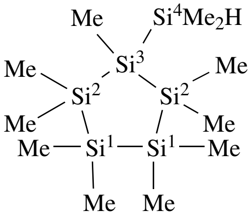

(**2**)

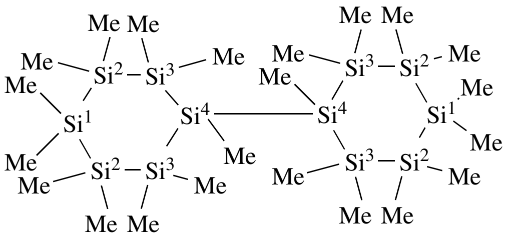

(**3**)

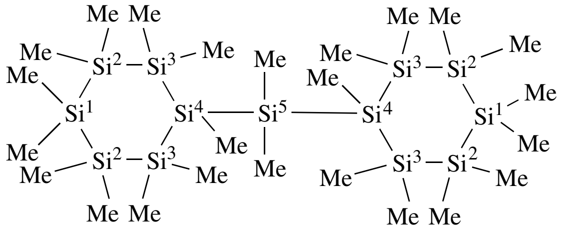

(**4**)

TABLE 1. ^{29}Si NMR data of compounds **1–4**

	Chemical shifts (ppm)				^1J (^{29}Si–^{29}Si) (Hz)		
1[a]	1 : −40.9	2 : −36.1	3 : −83.2	4 : −10.2	1,2 : 61.1	2,3 : 51.1	3,4 : 62.5
2[b]	1 : −41.0	2 : −36.2	3 : −83.3	4 : −34.2	1,2 : 61.6	2,3 : 51.8	3,4 : 60.5
3[c]	1 : −42.6	2 : −39.6	3 : −36.3	4 : −68.2	1,2 : 61.4	2,3 : 59.6	3,4 : 51.1
4[d]	1 : −42.5	2 : −40.3	3 : −36.6	4 : −73.5	1,2 : 61.4	2,3 : 59.8	3,4 : 50.7
	5 : −23.4				4,5 : 46.3		

[a] D2 40 µs, 900 mg, $T = 20\,^{\circ}$C.

[b] D2 60 µs, 950 mg, $T = 20\,^{\circ}$C.

[c] D2 50 µs, 650 mg, $T = 60\,^{\circ}$C.

[d] D2 60 µs, 500 mg, $T = 60\,^{\circ}$C.

Reproduced by permission of Elsevier Science from Reference 11.

COSY magic angle spinning NMR experiments on silicate glasses[13] and COSY and 2D-INADEQUATE measurements on Zeolites[14–16].

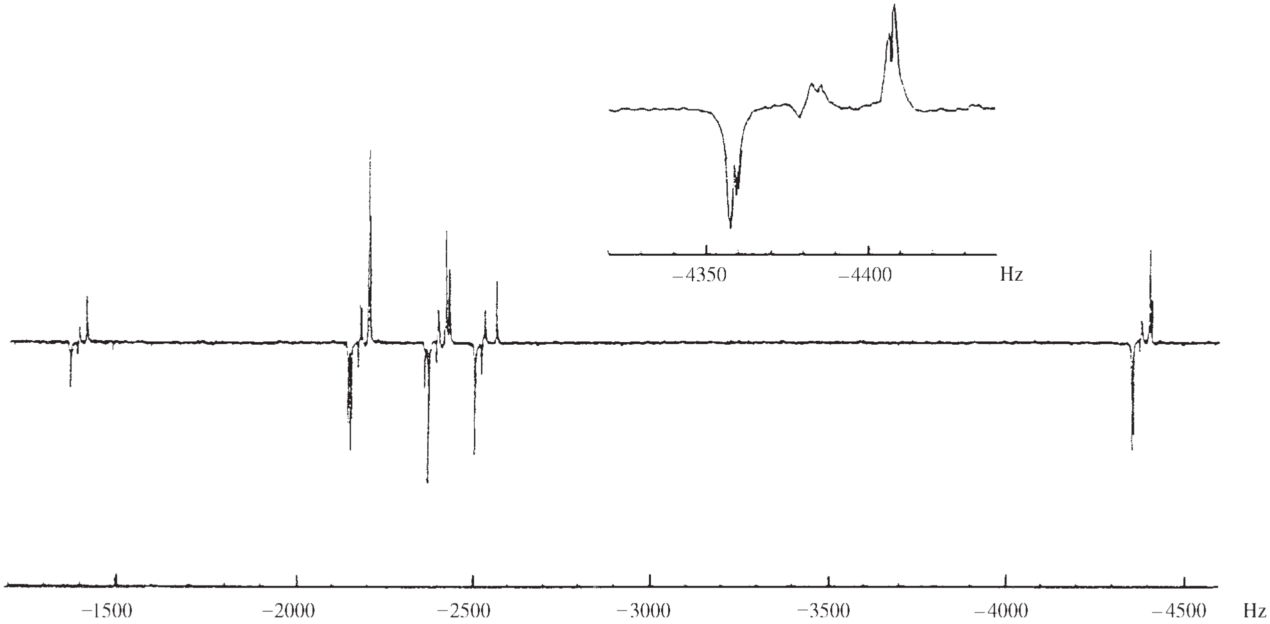

FIGURE 1. ID-INADEQUATE spectrum of $(Si_6Me_{11})_2SiMe_2$ (**4**): 500 mg silane in 2 ml C_6D_6, 30 mg $Cr(acac)_3$ added; $T = 333$ K; 6400 FIDs accumulated; gentle exponential multiplication; insert shows the couplings at Si^4 in an expanded scale. Reproduced by permission of Elsevier Science from Reference 11

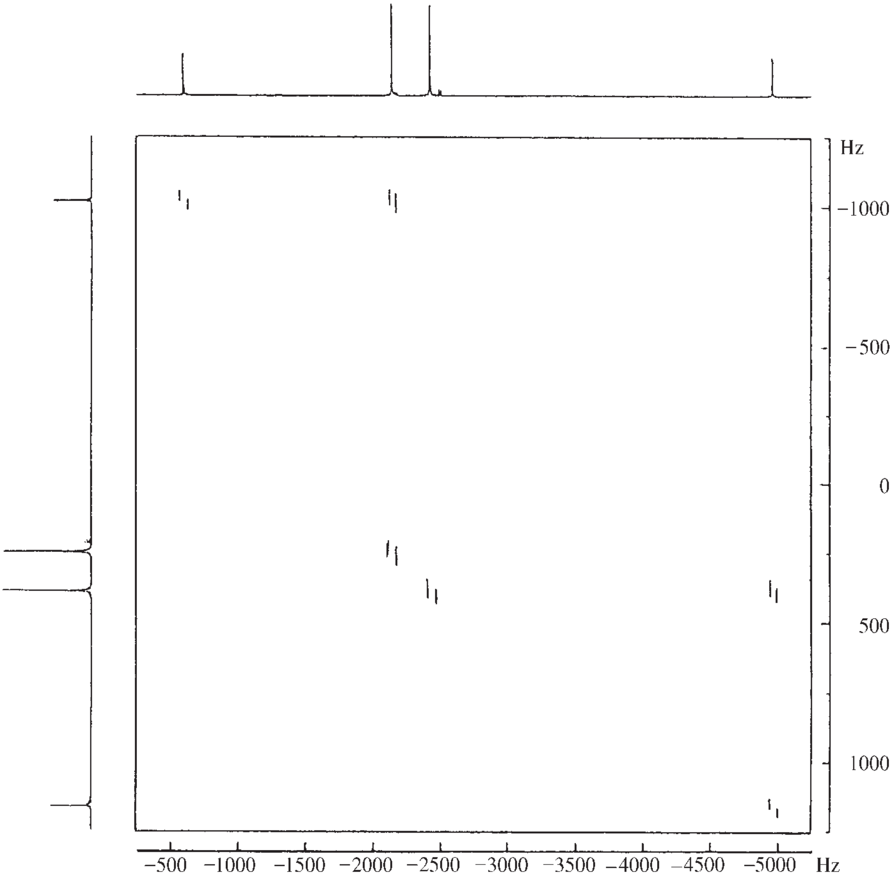

FIGURE 2. 2D-INADEQUATE spectrum of ($Si_5Me_9{-}SiMe_3$) (**1**); 900 mg silane in 2 ml C_6D_6 containing 30 mg $Cr(acac)_3$; $^{29}Si{-}^{1}H$ couplings refocused; 256 rows recorded, each 96 FIDs accumulated; 4 × 4 K data matrix, spectral width in F1-dimension is 6000 Hz (2.9 Hz digital resolution); mild gaussian multiplication in both dimensions; 24 h performance time. Reproduced by permission of Elsevier Science from Reference 11

^{13}C 2D-INADEQUATE spectroscopy can conveniently disclose the connectivity of each carbon atom embedded in a molecule and has found widespread use in structural elucidation of organic compounds[17]. This technique is extremely powerful when the size of $^{13}C{-}^{13}C$ one-bond coupling (^{1}J) is much larger than that of long-range couplings (^{n}J, $n \geqq 2$), which is usually the case in the acyclic and unstrained alicyclic systems so far investigated[18]. Using the INEPT INADEQUATE technique specifically modified for ^{29}Si nuclei[19], Masamune and coworkers[12] examined $^{29}Si{-}^{29}Si$ couplings in strained polycyclic compounds such as tetracyclo[3.3.0.0$^{2.7}$0$^{3.5}$]octasilane (**5**) and tricyclo[2.2.0.0$^{2.5}$]hexasilane (**6**).

The 2D NMR spectrum of the tetracycle **5a** (Figure 3a) reveals the presence of 15 $^{29}Si{-}^{29}Si$ couplings in the range of *ca* 20 to 40 Hz. Since this system is constructed

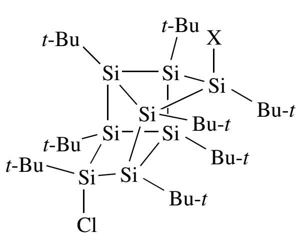

(**5**) **a**, X = Me
b, X = Cl

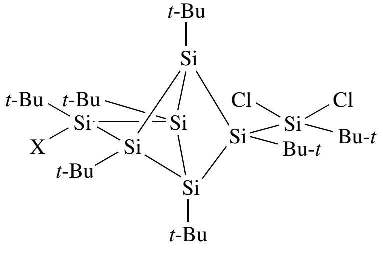

(**6**)

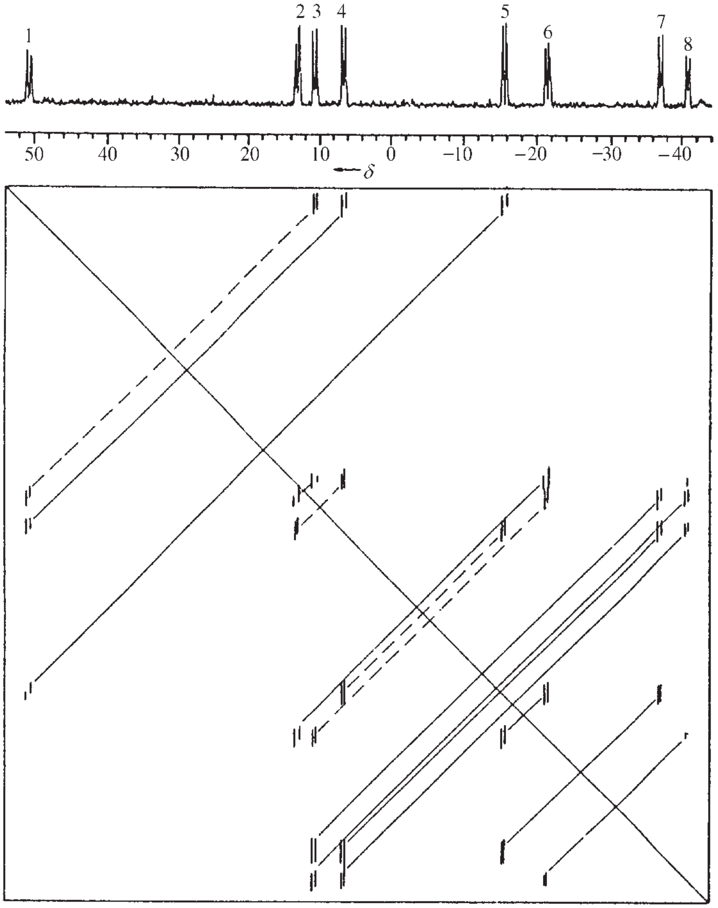

(a)

FIGURE 3. 53.7-MHz ^{29}Si−^{29}Si 2D-INEPT-INADEQUATE spectrum (a) Tetracycle **5a** in C_6D_6. (b) Tricycle **6** in $CDCl_3$ (40 °C). and projection of the 2D spectrum on the F2 axis (top). Signals connected by solid lines correspond to one-bond interactions (^1J); those connected by dotted lines denote long-range couplings (^nJ). Reproduced by permission of VCH Verlagsgesellschaft from Reference 12

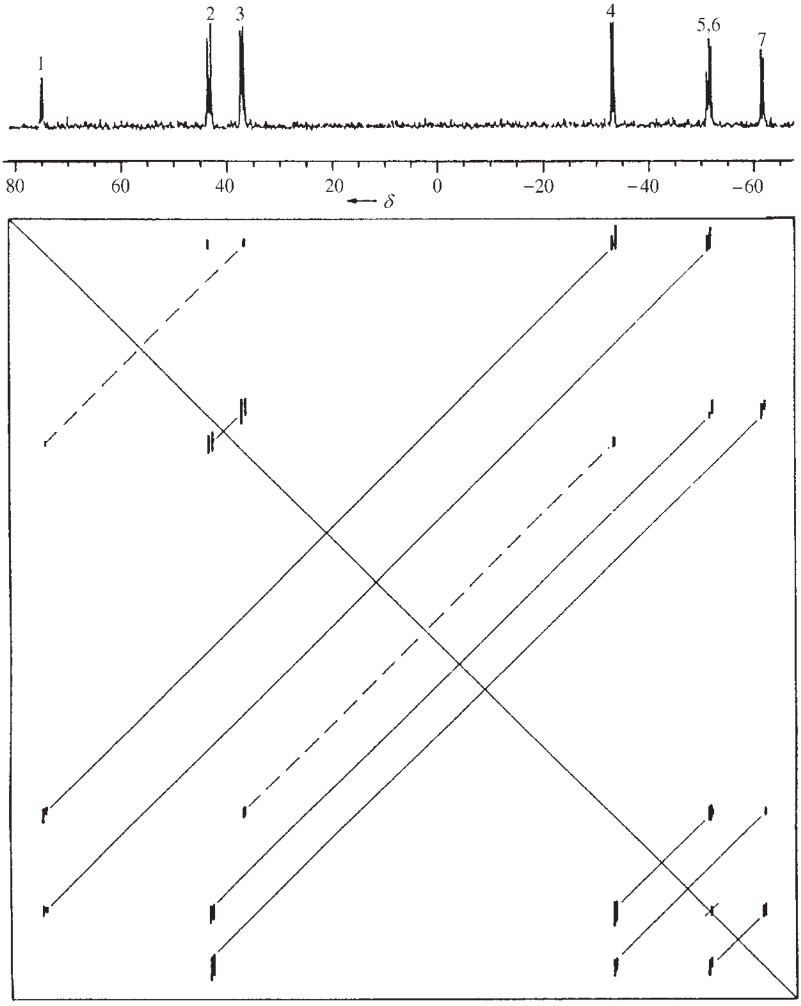

(b)

FIGURE 3. *(continued)*

from eleven Si—Si bonds, four of the 15 couplings must be long-range (^nJ). Through somewhat lengthy but logical arguments[20], ^{29}Si signals 1−8 are assigned to the Si nuclei of compound **5a** in the manner shown in Figure 3a. With the aid of the spectral assignment of **5a**, the assignment of signals of **5b** (having a C_2 axis) is now feasible. In **5b** there are three pairs of observable, significant long-range couplings of which a pair of couplings is rather small (5.8 Hz). Compound **6** also exhibits two sizable long-range couplings demonstrated by its spectrum (Figure 3b) as there are eleven observed Js of approximately 15 to 40 Hz while only nine Si—Si bonds build the framework of **6**. The ^{29}Si−^{29}Si coupling constants for **5** and **6** are tabulated in Table 2.

TABLE 2. ^{29}Si–^{29}Si coupling constants for the polycyclic polysilanes **5a**, **5b** and **6**[a]

Compound	^{1}J(Hz)		^{2}J ($n \geqq 2$) (Hz)
5a	42.2(2–6)	41.8(1–5)	24.1 (1–3)
	41.0(2–3)	33.4(1–4)	23.1(4–5)
	30.8(4–7)	28.9(3–8)	22.5(3–6)
	28.3(3–7)	25.7(4–8)	19.9(2–4)
	25.7(5–6)	18.0(5–7)	
	17.3(6–8)		
5b	41.0(1–3, 1′–3′)		23.5(1–2′, 1′–2)
	35.1(1–2, 1′–2′)		23.5(2–3, 2′–3′)
	29.3(2–4, 2′–4, or 2′–4′)		5.8(1–4, 1′–4′)
	17.5(3–4, 3′–4′)		
6	43.0(2–3)	36.1(1–4)	13.7(1–3)
	34.1(2–6)	32.2(2–7)	16.6(3–4)
	29.3(1–5)	27.4(5–7)	
	24.5(4–6)	23.4(4–7)	
	not determined(5–6)[b]		

[a] The silicon nuclei of each molecule are numbered according to the order of their chemical shifts as shown in the structures below. [b] The chemical shifts of these ^{29}Si nuclei were too close to permit accurate measurement of the coupling constant between them. Reproduced by permission of VCH Verlagsgesellschaft from Reference 12.

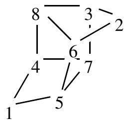

(5a)

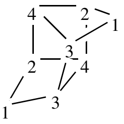

(5b)

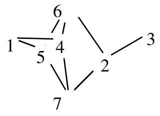

(6)

B. Combination of NMR and Other Techniques

It is usual for NMR spectroscopy to be employed together with other physicochemical methods in a complementary manner. Combined use of NMR and X-ray crystallography is already a main stream among the methodologies of physical organic chemistry. It must be pointed out that not only the combination of solution NMR and X-ray analysis but also that of solid-state NMR and X-ray analysis is possible.

Thus, Brook and coworkers[21] prepared a series of tetrakis(trimethylsilyl)ethynyl derivatives of Si, Ge, Sn and Pb and studied their structure by means of NMR, Mössbauer and X-ray methods. The combined results clearly indicated that there exists an electronic interaction between the central metal atom and distal Me_3Si groups, leading to a strong shielding of the central atom which was clearly demonstrated by chemical shifts of respective nuclei (Figure 4). The presence of the four distal Me_3Si groups serves to increase substantially the upfield shifts of the central atom. The chemical shifts reported here are −101.6, −188.5, −384.5 [−356.3 for $(HC\equiv C)_4Sn$], and −760.7 ppm for ^{29}Si, ^{73}Ge, ^{119}Sn and ^{207}Pb respectively.

Many other examples of this combination of techniques will be found in various parts of this review. Probably the most persuasive example of this combination are the criteria applied in attempts to establish the structure of silicenium ions. This topic will be discussed in the next section.

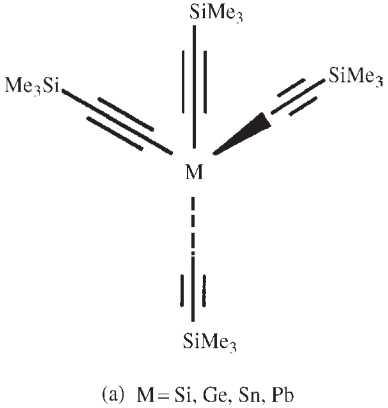

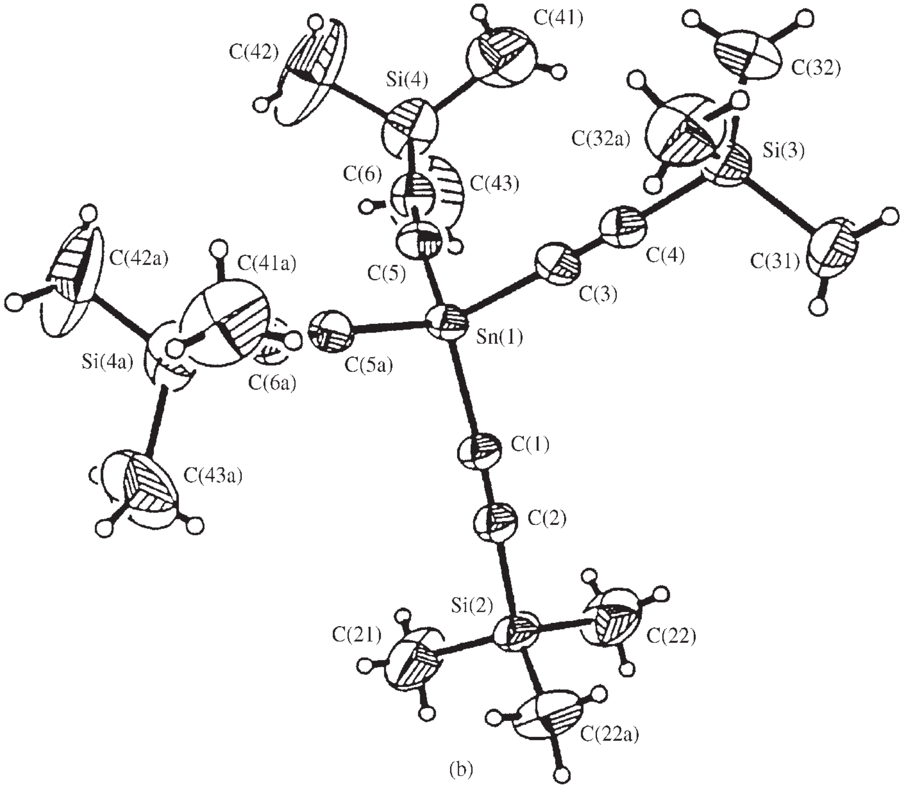

FIGURE 4. (a) The structure of the compounds investigated; (b) ORTEP plot from the X-ray crystal structure of $(Me_3SiC{\equiv}C)_4Sn$. Reproduced by permission of the Canadian Chemical Society from Reference 21

III. NEW COMPOUNDS

A. Some Interesting Compounds

The last ten years have experienced a great advance in the synthesis of novel and unusual organosilicon compounds which are interesting in view of their structure or relevance to theory. ^{29}Si NMR study of such interesting and unusual compounds will be treated in this section.

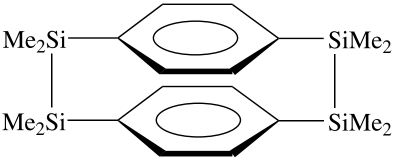

(**7**)

The first [2.2]paracyclophane bridged by silicon, tetrasila[2.2]paracyclophane (**7**) was prepared and characterized by Sakurai and coworkers[22] with the aid of UV, IR, ^{1}H, ^{13}C and ^{29}Si NMR spectra ($\delta = 6.45$) together with X-ray crystallographic data. Cyclophane **7** displays a strong σ–π mixing between Si–Si bonds and aromatic rings as evidenced by a large red shift in the UV spectra.

Ando and coworkers[23] reacted C_{60} with bis(2,6-diisopropylphenyl)silylene generated *in situ* by the photolysis of the corresponding trisilane. The dark brown powder obtained (58%) exhibits ^{29}Si signal at $\delta - 72.74$ which, together with other experimental evidence, supports the silirane structure **(8a)** rather than the bridged annulene structure **(8b)**.

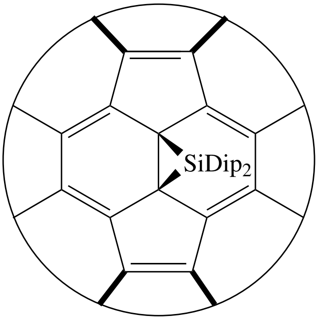

(8a)

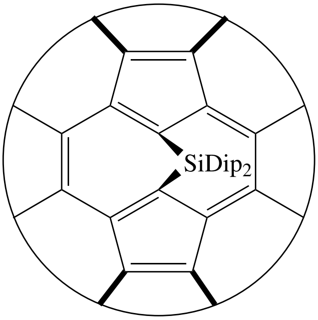

(8b)

Dip = 2,6-(i-Pr)$_2$C$_6$H$_3$

A photochemical 1 : 1 addition of bis(alkylidene)silacyclobutanes to C_{60} was reported (equation 1)[24] . The structure of adducts **9a** and **9b** were identified by various means including ^{29}Si NMR spectra (**9a**; $\delta = -14.30$, 4.20; **9b**; -11.47, 8.12). A Si–H HMBC heteronuclear shift correlation NMR spectra of **9a** was also taken. A photochemical addition of octaarylcyclotetrasilane to C_{60} was also reported, together with full ^{29}Si NMR data, by Ando and coworkers[25].

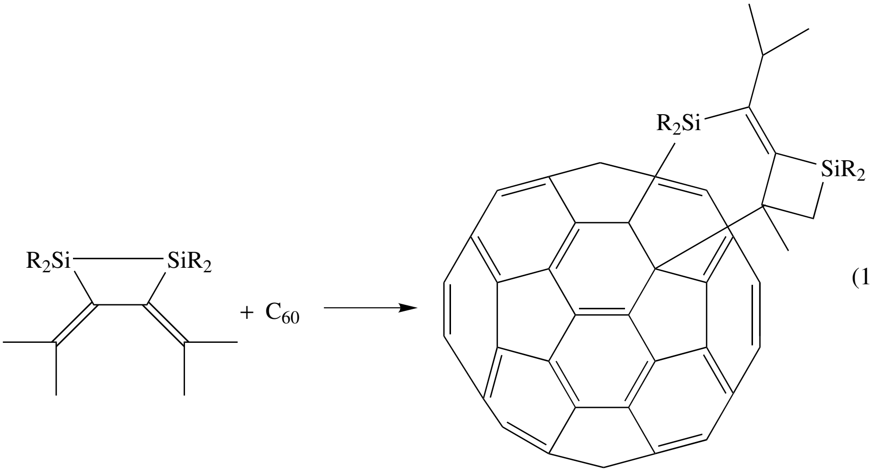

(1)

9a: R = *n*-Pr
9b: R = Et

Another interesting class of compounds reported by Ando and coworkers is tetrasilacyclohexynes and polysilabridged allenes. Thus, 1,1,2,2,3,3,4,4-octaalkyl-1,2,3,4-tetrasilacyclohexynes (**10a** and **10b**) were prepared and their ^{29}Si NMR spectral data were reported (**10a**; δ = −30.8, −19.2; **10b**: −17.7, −8.3)[26]. ^{29}Si NMR spectral data (−32.2, −7.9) were also reported for 1,3,5,5-tetraphenyl-4,4,6,6-tetramethyl-4,5,6-trisilacyclohexa-1,2-diene **(11)**[27].

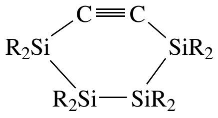

(**10**)

a, R = M
b, R = Et

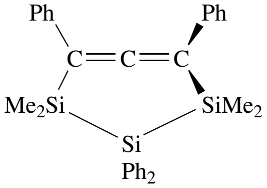

(**11**)

West and coworkers[28] used J(SiSi) to discuss the structure of long-debated 1,3- cyclodisiloxanes **(12a)** for which a few alternative structures were proposed. One such structure retains the σ bond between two silicon atoms **(12b)**. In a structure such **12a** as **12b**, the J(SiSi) should be close to the standard values of 80–90 Hz while for **12a** ^{2}J(Si–O–Si) will be observed with values of about 4 ppm. The values observed for a variety of 1,1,3,3-tetraaryl-1,3-cyclodisiloxanes are in the range of 3.85–4.02 Hz, which support structure **12a**. There is another proposal for the structure of 1,3-cyclodisiloxanes (dibridged π complex) and the authors suggested this structure is also consistent with the observed coupling constants.

The ^{1}J(Si=Si) values of a variety of unsymmetrically substituted disilenes were first reported in the same paper. The values are in the range 155–158 Hz, which is *ca* 1.8

times the standard ^{1}J(SiSi) values for organodisilanes. This is to be compared with the corresponding values in the carbon series (1.98 times; 67.6 Hz for ethylene and 34.6 Hz for ethane).

Watanabe and coworkers[29] reported a ^{29}Si chemical shift of a cyclotrisilane, i.e, hexaneopentylcyclotrisilane ($\delta - 81.68$), which is substantially upfield as compared with the values for larger rings.

Hengge and coworkers[30] assigned the structure and ^{29}Si δ values of halodimethylsilylnonamethylcyclopentasilanes and halononamethylcyclopentasilanes based on ^{1}J(SiSi) and ^{2}J(SiSi) derived from ^{29}Si INADEQUATE and ^{29}Si INEPT INADEQUATE spectra. The compounds exhibit good correlations between ^{1}J(SiSi) chemical shifts and Pauling electronegativities. Some ^{29}Si NMR spectral data were also reported for a series of cyclopolysilanes ($R^1R^2Si)_n(n = 3–6)$[31].

Watanabe and coworkers reported the synthesis and structure of a variety of polysilacycloalkanes in which other heteronuclei are also incorporated in the ring. An example is a series of peralkyl-1-germa-2,3,4-trisilacyclobutanes[32]. ^{29}Si NMR spectral data are as follows: 1,1-bis(trimethylsilyl)methyl-1-germa-2,2,3,3,4,4-hexaisopropyl-2,3,4-trisilacyclobutane, δ 1.13, 2.23. 5.78; 1,1-bis(trimethylsilyl)methyl-1-germa-2,2,3,3,4,4-hexaneopentyl-2,3,4-silacyclobutane, −23.45, −11.82, 1.83. A germanium analogue of the above compounds, 1,1-diphenyl-1-germa-2,2,3,3,4,4,5,5- octaisopropyl-2,3,4,5-tetrasilacyclopentane, was also reported by Watanabe and coworkers[33]. The ^{29}Si δ values for the compound are −13.76 and −12.16, respectively.

Stable disilenes have long been an intriguing target for organosilicon chemists. The first successful isolation of a stable disilene derivative, tetramesityldisilene was reported by West and coworkers[34] as early as 1981. Since then several investigators worked toward this target. Watanabe and coworkers[35] reported an air-stable disilene, tetrakis(2,4,6-triisopropylphenyl)disilene. ^{29}Si chemical shift of this compound was reported as $\delta + 53.4$.

Okazaki and coworkers[36] reported some extremely hindered and stable disilenes, (E)- and (Z)-Tbt(Mes)Si=Si(Mes)Tbt where Tbt = 2, 4, 6-tris[bis(trimethylsilyl)methyl]-phenyl and Mes = 2, 4, 6-trimethylphenyl. ^{29}Si chemical shifts of the (E)-isomer showed only one signal at δ 66.49 while that of the (Z)-isomer exhibited four peaks with roughly equal intensity at 56.16, 56.74, 57.12 and 58.12, for which the authors claimed the possible existence of two or more conformational isomers on the NMR time scale.

Silylenes, the carbene equivalent of organosilicon compounds, has been another intriguing target. Okazaki and coworkers carried out thermolysis of the hindered disilenes mentioned above with the expectation that a silylene, Tbt(Mes)Si:, will be formed. The thermolysis was monitored by means of ^{29}Si NMR spectra, but the generation of silylene was not proved by NMR, although trapping experiments established the generation of silylene[37].

West and coworkers[38] isolated a silylene **(13)** stable enough to be distilled at 85 °C/0.1 Torr and reported ^{29}Si (and other nuclei) NMR chemical shift ($\delta + 78.3$). The structure was also confirmed by X-ray crystallographic analysis (Figure 5) and quantum chemical calculations. It was suggested that the compound has an aromatic ground state.

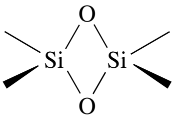

(**12a**)

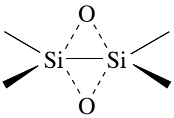

(**12b**)

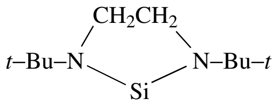

(13)

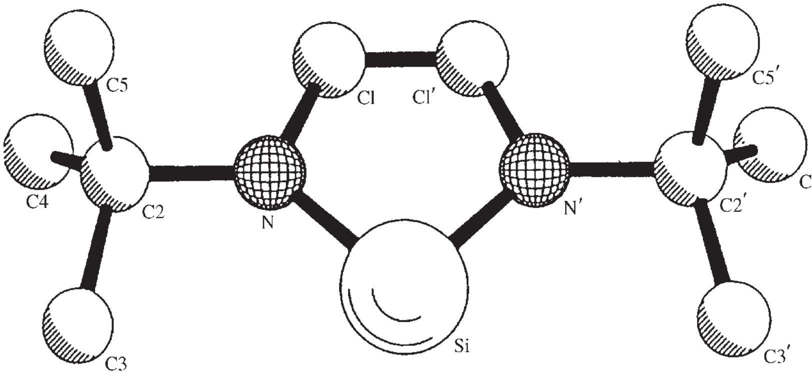

(13)

FIGURE 5. Molecular model of **13**. Hydrogen atoms have been omitted for clarity. Reprinted with permission from Reference 38. Copyright 1994 American Chemical Society

B. Silicenium Ions

There has been much dispute on the question whether triorganosilicenium cations, (R_3Si^+), can be generated in solution and whether some of the features found in the rich carbocation chemistry can also be found in silyl cation chemistry[39] (See Schleyer, Chapter 10, and Lickiss, Chapter 11 in this book).

In a recent publication, Lambert and Zhang[40] have presented a promising new procedure for isolating silicenium cations (equation 2)

$$Ph_3C^+X^- + R_3Si{-}H \longrightarrow Ph_3C{-}H + R_3Si^+X^- \qquad (2)$$

by using as a counterion the weakly coordinating anion tetrakis(pentafluorophenyl)borate, $(C_6F_5)_4B^-$ (TPFPB$^-$), in aromatic solvents such as benzene. From measured ^{29}Si NMR chemical shifts, they concluded that they had obtained R_3Si^+ (R = Me, Et, Pr, Me_3Si) ions which do not have interaction with anions but have weak interaction with the aromatic solvent, and therefore with a nearly free cationic structure. Lambert and coworkers[41] added further support to the postulated existence of silicenium ions by investigating the crystal structure of Et_3Si^+ TPFPB$^-$ **(14a)**. The unit cell of the crystal contains four molecules of **14a** and eight molecules of the aromatic solvent toluene, which was used for recrystallizing **14a**. Each molecule of **14a** has one associated toluene molecule with the closest contact between Si and a toluene C atom being 2.18 Å. The geometry at the Si atom is not planar, as expected for a silicenium cation, but pyramidal, while the toluene ring is essentially planar and does not indicate any stronger interactions with the triethylsilyl moiety[41].

Furthermore, Lambert and coworkers[42] obtained a white solid from the reaction of silanes and Ph_3C^+ TPFPB$^-$, which was examined as a solid or in solution. ^{29}Si chemical shift is highly dependent on the nucleophilicity of the solvent, with large downfield shifts. The shift in toluene is *ca* 100 ppm, far short of the expectation for a fully trigonal silicenium ion. For $(Me_3Si)_3Si^+$ TPFPB$^-$ **(14c)** the shift is 111 ppm, much closer to the trigonal ideal. ^{29}Si shifts for the solid are almost identical to those in benzene solution. Based on the X-ray crystallographic data of **14a** which is coordinated with toluene in the solid state, they proposed that the ions are best termed silicenium cations with weak η^1–π coordination to toluene.

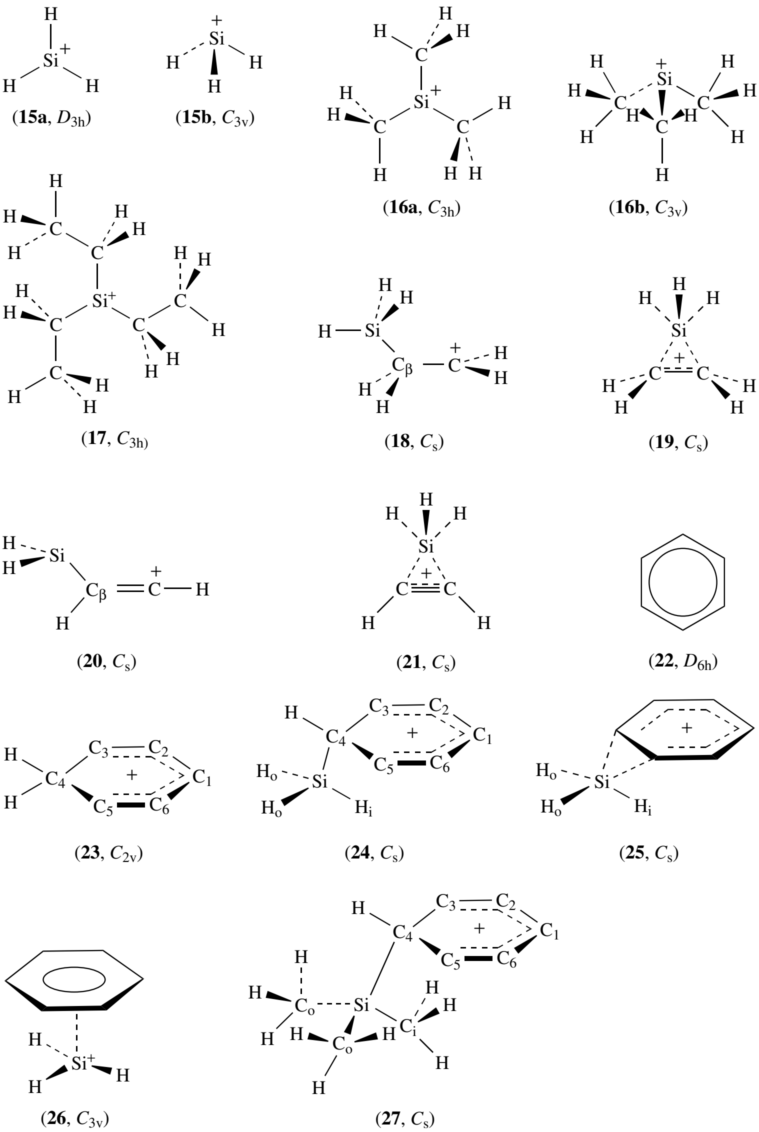

(**15a**, D_{3h}) (**15b**, C_{3v}) (**16a**, C_{3h}) (**16b**, C_{3v})

(**17**, C_{3h}) (**18**, C_s) (**19**, C_s)

(**20**, C_s) (**21**, C_s) (**22**, D_{6h})

(**23**, C_{2v}) (**24**, C_s) (**25**, C_s)

(**26**, C_{3v}) (**27**, C_s)

FIGURE 6. Structure and equilibrium conformation of compounds **15–27**. Reproduced by permission of Elsevier Science from Reference 43

A thorough theoretical study was carried out to cast light on this problem[43]. Olsson and Cremer calculated IGLO (individual gauge for localized orbitals) NMR chemical shifts (^{13}C and ^{29}Si) for molecules **15–27** shown in Figure 6, namely silicenium cations **15–17**, reference compounds **18–23** and silicenium–benzene interaction complexes **24–27** employing the [7s6p2d/5s4p1d/3s1p] basis set recommended by Kutzelnigg and Schindler[44].

TABLE 3. IGLO/7s6p2d/5s4p1d/3s1p] NMR chemical shifts[a]

Molecule		Symmetry	Chemical shifts				
			δ^{29}Si	δ^{13}C			
$SiH_3{}^+$	**15a**	D_{3h}	270.2				
	15b	C_{3v}	363.1				
$(CH_3)_3Si^+$	**16a**	C_{3h}	355.9	9.0			
	16b	C_{3v}	397.1	23.5			
$(CH_3CH_2)_3$ Si^+	**17**	C_{s}	376.9	16.5(Cα)	7.5(Cα)		
$H_3SiCH_2CH_2{}^+$	**18**	$\mathrm{C_s}$	−29.8	80.9(Cα)	262.8(C^+)		
	19	$\mathrm{C_s}$	−54.1	139.5			
H_3Si $CHCH^+$	**20**	$\mathrm{C_s}$	−51.7	63.6(Cα)	288.3(C^+)		
	21	C_{2v}	−31.9	89.1			
C_6H_6	**22**	C_{6h}		135.8			
$C_6H_7{}^+$	**23**	C_{2v}		205.2(C1)	134.2(C2)	199.9(C3)	43.8(C4)
H_3Si $C_6H_6{}^+$	**24**	C_{s}	−23.8	176.7(C1)	136.5(C2)	180.8(C3)	77.3(C4)
	25	C_{s}	10.5	152.1(Cγ)	145.0(Cβ)	126.3(Cα)	
	26	C_{3v}	201.9	138.3			
$(CH_3)_3SiC_6H_6{}^+$	**27**	C_{s}	83.1	166.2(C1)	137.1(C2)	163.1(C3)	91.7(C4)
			(83.6)[b]			−4.4(Me_i)	4.5(Me_o)

[a] All shifts in ppm relative to TMS. For the numbering of atoms, see structures. The IGLO calculations for **26** have been conducted with the 6-31 G (d) basis set.

[b] Experimental δ^{29}Si value.

Reproduced by permission of Elsevier Science from Reference 43.

The calculated chemical shifts are tabulated in Table 3. They imply the three conclusions given below.

(1) The postulated silicenium cations are covalently bonded C-centered π-complexes between SiR_3^+ and aromatic solvents. Formally, these may be described as Wheland σ complexes, in which the silicenium cation character is totally lost.

(2) Nevertheless, the use of the $TPFPB^-$ in connection with aromatic solvents opens an intriguing route to nearly free silicenium ions in the form of ring-centered SiR_3^+-arene van der Waals complexes with δ^{29}Si values of about 310–320 ppm. These complexes can be best generated if both the Si and the benzene ring are substituted by sterically demanding groups.

(3) Compound **14c** investigated by Lambert and Zhang realizes by 70% the situation of a free tricovalent silicenium cation in a condensed phase. These authors further suggested that experiments with properly substituted aromatic solvents and **14c** will generate a free silicenium cation in solution. Another interesting theoretical study was reported by Frenking and coworkers[45] for a series of silaguanidium $Si(NH_2)_3^+$ ions and derivatives in order to clarify the effective stabilization by the heteroatoms.

Reed and coworkers[46] employed hexahalocarboranes ($X_6B_{11}H_6$; X = Cl, Br, I) as counterions to stabilize and characterize $i\text{-}Pr_3Si^+$. They employed, as others did, two experimental criteria of developing silicenium ion character: (i) downfield ^{29}Si chemical shifts and (ii) the geometrical approach of silicon toward planarity. They reported that the chemical shift of $i\text{-}Pr_3Si(Cl_6B_{11}H_6)$ is 115 ppm while the upper limit of the expectation value for $i\text{-}Pr_3Si^+$ is around 220 ppm, and concluded that their compound may have >50% silicenium ion character. The C–Si–C angle as determined by X-ray crystallographic analysis of these carborane derivatives is in the range of 111–120°, in good agreement with the ideal angle for tricoordination.

Lambert and Zhao[47] chose a new compound, Mes_3Si^+ $TPFPB^-$ (**14d**) for preparing a free silyl cation. According to their molecular mechanics calculations, the *ortho* methyl groups shield the silicon center from attack by the large nucleophile but are prohibited by their geometry from interacting with the silicon. The ^{29}Si chemical shift of **14d** is $\delta = 225.5$ in C_6D_6. This is the highest value ever observed for species with silicenium ion character. The authors remarked that though the possibility of existence of interaction between the silicenium ion and TPFTB anion still remains to some extent, the chemical shift strongly favors a nearly free, tricoordinate silicenium ion.

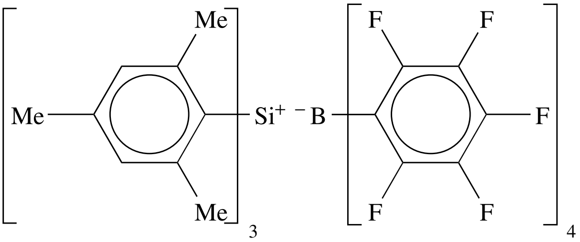

(**14d**)

It must be added that a new theoretical calculation of triarylsilicenium moieties nicely reproduced the experimental results of **14d**[48]. The calculated ^{29}Si chemical shift is 251.4. The 25.0 ppm difference may be the result of the applied computational method. Thus, the long debated controversy of the silicenium cation problem seems to be solved[49].

TABLE 4. ^{29}Si NMR data for silylnitrilium species

Species generated[a]	^{29}Si (δ)[b]
$[(t\text{-Bu})_2(s\text{-Bu})_2\text{Si(NCPr)}]^+$ TFPB^-	30.39
$[t\text{-BuMe}_2\text{Si(NCPr)}]^+$ TFPB^-	36.50
$[\text{Et}_3\text{Si(NCPr)}]^+$ TFPB^-	37.01
$[\text{Ph}_2\text{MeSi (NCCD}_3)]^+$ TFPB^-	4.23
$[(t\text{-Bu})_2$ $\text{SiH(NCCD}_3)^+$ TFPB^-	19.3 (d, $J_{\text{SiH}} = 242$ Hz)
$[(\text{PrCN})\text{Si(OCH}_2\text{CH}_2)_3\text{N}]^+$ TFPB^-	−94.9

[a] TFPB = [bis(3,5-trifluoromethyl)phenyl] borate.

[b] All ^{29}Si NMR spectra were taken in butyronitrile except for Ph_2MeSiH and $t\text{-Bu}_2\text{SiH}_2$, which were taken in CD_3CN.

Reproduced by permission of the American Chemical Society from Reference 50.

^{29}Si chemical shift of a nitrile-stabilized silicenium ion (silylnitrilium ion), $\text{R}_3\text{Si(NCC}_3\text{H}_7)^+\text{B[C}_6\text{H}_3(\text{CF}_3)_2\text{-3,5]}^{4-}$ is reported[50]. The compound was prepared by the reaction between trityl tetrakis [bis(3,5-trifluoromethyl)phenyl] borate and trialkylsilanes in butyronitrile. ^{29}Si chemical shifts are summarized in Table 4. All of the ^{29}Si NMR shifts for the alkylated or phenylated silicenium cations are consistently 12–30 ppm downfield of that of the starting hydrosilanes. Considering that only one nitrile group is coordinating with the bulky $(t\text{-Bu})_2(s\text{-Bu})$ Si moiety but that two or three nitrile groups may coordinate with the less bulky silyl moieties, the shifts for the five- or six-coordinate silicon species would be expected to be further upfield than the values observed. The authors suggested that the silicenium cation generated in their study was four-coordinate, with stabilization resulting from only one nitrile group.

C. Compounds with Hypervalent Si Nuclei

Penta- and hexacoordinate silicon compounds have recently attracted a great deal of interest from structural and mechanistic points of view[51]. In particular, pentacoordinate anionic siliconates have long been recognized as the reaction intermediates in nucleophilic substitution at silicon atoms[52]. The geometry of pentacoordinate anionic siliconate was first confirmed in 1981, by Schomburg[53], who performed an X-ray structural analysis of $[\text{PhSiF}_4][n\text{-Pr}_4\text{N}]$ and found that the geometry about the silicon atom was trigonal bipyramidal with two fluorine nuclei preferentially occupying the apical positions.

Since then a large number of reports have dealt with the structure and stability of anionic pentacoordinate mono(siliconates), which contain only one silicon atom in a molecule. Damrauer and his coworkers first reported nonhygroscopic fluorosiliconates as the K^+. 18-crown-6 salts[54]. Subsequently, Holmes and his coworkers have reported the isolation and structural analysis of a series of $[\text{R}_n\text{SiF}_{5-n}]^-$ species[55,56], especially sterically crowed fluorosiliconates such as $[\text{Mes}_2\text{SiF}_3]^-$ and $[(\text{TTBP})\text{SiF}_4]^-$, where TTBP stands for the 2,4,6-tri-t-butylphenyl group. These studies demonstrated that the bond parameters around the silicon atom depend highly on the steric hindrance of the organic groups R and on the number of fluorine ligands[55]. A number of pentacoordinate mono(siliconates) containing anionic chelate ligands such as catecholate, pinacolate, and Martin ligands[57] which involve the first examples of cyanosiliconates[58], silylsiliconates[59] and pentaalkoxysiliconate[60] have also been studied.

One interesting example of pentacoordinate silicon is a 1,2-oxasiletanide, reported by Okazaki and coworkers[61], which can be regarded as the intermediate of the Peterson reaction. Thus, treatment of a β-hydroxysilane **(28)** with butyllithium afforded oxasiletanide

(29). A large upfield shift of ^{29}Si chemical shift from **28** (δ 10.66) to **29** (δ − 72.45) strongly supports the structure of a pentacoordinate silicate.

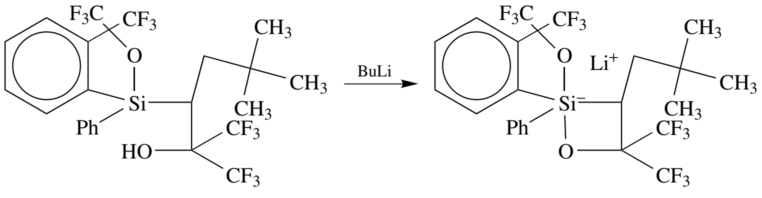

(**28**) (**29**)

Evans and coworkers[62] described the synthesis and structural study of a series of pentacoordinate bis(catecholate) complexes of silicon(IV). The crystal structure of the anion of $[Et_3NH][SiMe(3,5\text{-dncat})_2]$ $[H_2(3,5\text{-dncat}) = 3,5\text{-dinitrocatechol}]$ is reported (Figure 7).

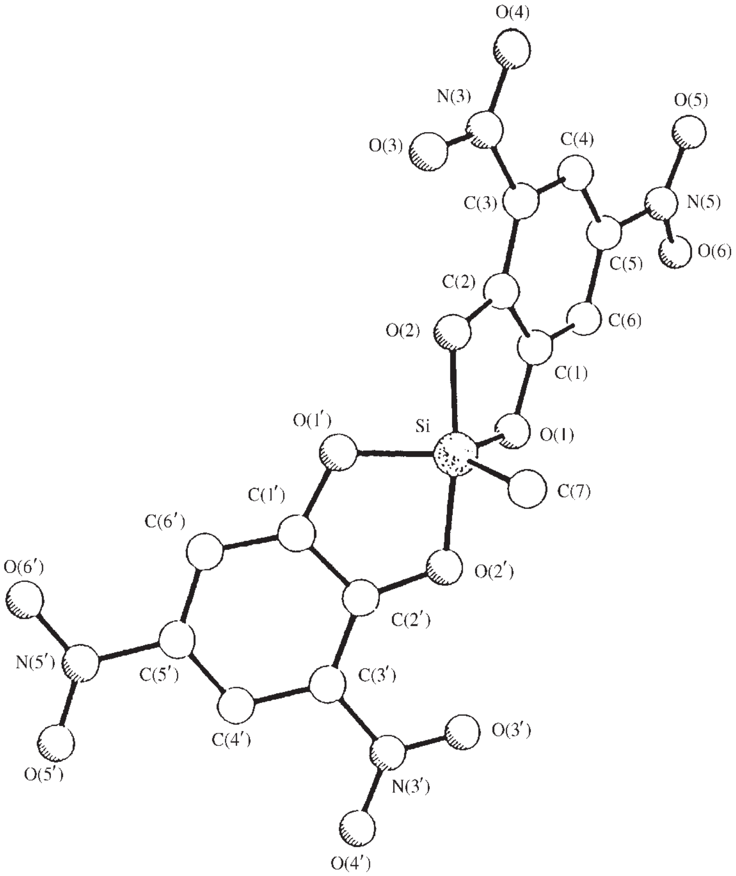

FIGURE 7. The crystal structure of the anion in $[Et_3NH][SiMe(3,5\text{-dncat})_2]$. Reproduced by permission of the Royal Society of Chemistry from Reference 62

Further analysis of the NMR data of these compounds reveals that the 'stronger', i.e. more electronegative, catechols give rise to complexes with more square pyramidal character. Conversely, the effect of the R group may be steric, i.e. the phenyl moiety twists the catechols out of the square plane, thus increasing the trigonal bipyramidal character. Two mixtures were prepared by dissolution of equivalents of each of two complexes in Me_2SO for ^{29}Si NMR analysis. Mixture A {K[SiPh(cat)$_2$] and K[SiPh(tccat)$_2$]}. (cat: catechol, tccat: tetrachlorocatechol) contained two complexes with symmetric catechols and each complex gave its own characteristic ^{29}Si NMR (δ $-$ 87.5 and $-$83.9, respectively). The equilibrated mixture contained a high, nonstatistical proportion of the $[SiPh(cat)(tccat)]^-$ species. This was characterized by a ^{29}Si NMR resonance appearing between those of the individual complexes at δ $-$ 85.3 (Figure 8). Equilibrium was achieved at ambient temperature over a period of *ca* 24 h.

Mixture B {K[SiPh(3-fcat)$_2$ and K[SiPh(dbcat)$_2$]} (3-fcat: 2,3-dihydroxybenzaldehyde, dbcat: 3,5-di-*t*-butylcatechol) contained two complexes with asymmetric catechols. Each complex showed the presence of two resonances due to the isomerism described above. The equilibrated mixtures showed the presence of two further species (Figure 9). These are attributed to isomers of the $[SiPh(3\text{-fcat})\ (dbcat)]^-$ anion. Equilibrium was not established even after 8 weeks, whereupon decomposition prevented a more quantitative kinetic analysis. However, it is apparent from the two experiments described that the kinetics of redistribution of ligands between complexes varies dramatically according to the catecholate involved. It is reasonable to conclude that the rate of redistribution decreases as the 'strength' of the catecholate derivative increases. The nonstatistical distribution of complexes in a mixture indicates a thermodynamic stability of the complexes in Me_2SO. The likely explanation lies in the electronic rather than the steric effects in the complex, since the five-coordination imposes little steric constraint.

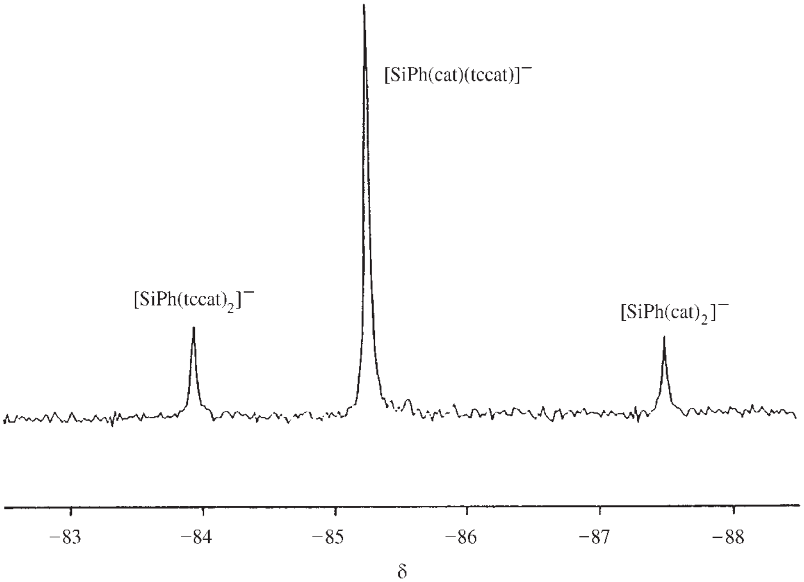

FIGURE 8. The ^{29}Si NMR spectrum of a mixture of K[SiPh(cat$_2$)] and K[SiPh(tccat)$_2$] [53.7 MHz, Me_2SO, internal $SiMe_4$, 0.08 mol dm^{-3} $Cr(acac)_3$ relaxant]. Reproduced by permission of the Royal Society of Chemistry from Reference 62]

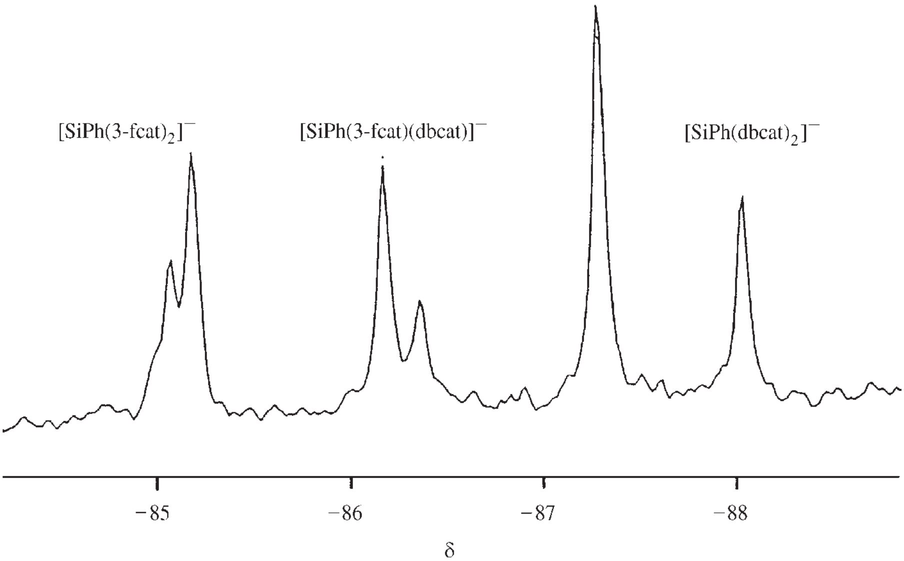

FIGURE 9. The ^{29}Si NMR spectrum of a mixture of K[SiPh(3-fcat)$_2$] and K[SiPh(dbcat)$_2$]. Details as in Figure 8. Reproduced by permission of the Royal Society of Chemistry from Reference 62

The silicon–hydrogen bond in pentacoordinate complexes has an enhanced reactivity compared with the equivalent bond in the related tetracoordinate compounds, as has been convincingly demonstrated by many investigators (e.g. Chopra and Martin[63]). It is established that the active hydrogen is normally expected to be in an equatorial position in trigonal bipyramidal complexes[64]. Bassindale and Jiang[65] were interested in pentacoordinate silicon hydrides as intermediates, or models for intermediates, in nucleophilic substitutions at silicon, and, with varying ligands around silicon, as potentially 'tunable' reducing agents. Most of the species in which they were interested were only available in solution and therefore were not susceptible to definitive structure determination by X-ray crystallography. Hence they employed ^{29}Si NMR extensively, and established the effect of coordination on ^1J(SiH) and δ (^{29}Si) for some reactions of the type shown in equation 3.

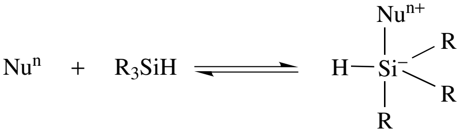

(3)

Thus, the formation of adducts R$_3$SiH/Nu produces changes in the ^{29}Si NMR chemical shift and ^1J(SiH) that follow similar trends. Coordination of highly electronegative, soft ligands is accompanied by the strongest low frequency shifts and the greatest increase in ^1J(SiH). Formal coordination of hard electropositive ligands such as methyl can result in high frequency shifts and a decrease in ^1J(SiH). The ^{29}Si chemical shift range for the pentacoordinate neutral, anionic and cationic adducts is about $\delta - 110$ to -47 ppm, whereas the range for the related tetracoordinate silanes is greater at $\delta + 24$ to -76 ppm.

As a part of a study on persilylated π-electron systems, particularly on persilylated benzenes[66], Sakurai and coworkers[67] were interested in hexakis(fluorodimethylsilyl)benzene **(30)** for its possible dynamic properties as a gear-meshed structure[68] and for the possible presence of nonclassical neutral pentacoordinate silicon atoms[52]. The X-ray analysis of **30** was also reported (Figure 10).

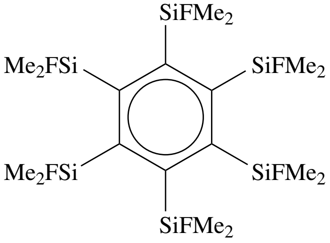

(30)

At 273 K, the ^{29}Si NMR of **30** shows a triplet [J(SiF) = 127 Hz], indicating that each of the silicon nuclei interacts with two fluorine nuclei in accord with the solid-state structure. This triplet did not change to a doublet of doublets at the low-temperature limit; however, these signals transformed at higher temperatures to a septet [J(SiF) = 43 Hz at 328 K] as shown in Figure 11. Correspondingly, all the ^{1}H and ^{13}C NMR signals which are triplets at 273 K become septets at 328 K. Noteworthy is the fact that chemical shifts in these NMR spectra did not change at all; only the coupling pattern changed. This unusual dynamic behavior can be explained by a mechanism where, at the low temperature, rotation of the silyl groups is frozen but fluorine atom transfer between vicinal silyl groups is rapid. This process corresponds to a cyclic network of

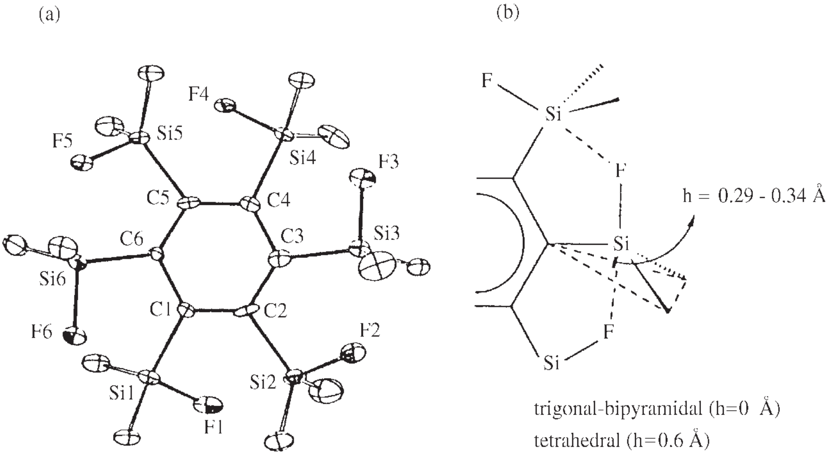

FIGURE 10. Molecular structure of hexakis(fluorodimethylsilyl)benzene **30**: (a) top view and (b) geometry around silicon. Reprinted with permission from Reference 67, Copyright 1994 American Chemical Society

intramolecular consecutive S_N2(Si)-type Walden inversions which are very rapid because each silicon atom already forms a quasipentacoordinate structure. As a consequence, triplet signals are observed. From a symmetry perspective, Si—F bond alternation in this study is analogous to the inversion mechanism studied by Mislow and coworkers[68], for hexakis(dimethylamino)benzene, although the molecular mechanism of the exchange is quite different.

Septet signals mean that silicon and other nuclei interact equally with six fluorine nuclei at the higher temperature. At high temperatures, rotation of the silyl groups is allowed and all the fluorine nuclei migrate throughout the ring by a combination of Si—F bond alternation and rotation. Although not proven in a strict sense, the gear-meshed motion is highly likely as the mechanism of rotation, since the molecule already takes the gear-meshed structure in the solid state. Fluorine nuclei thus move like in a merry-go-round.

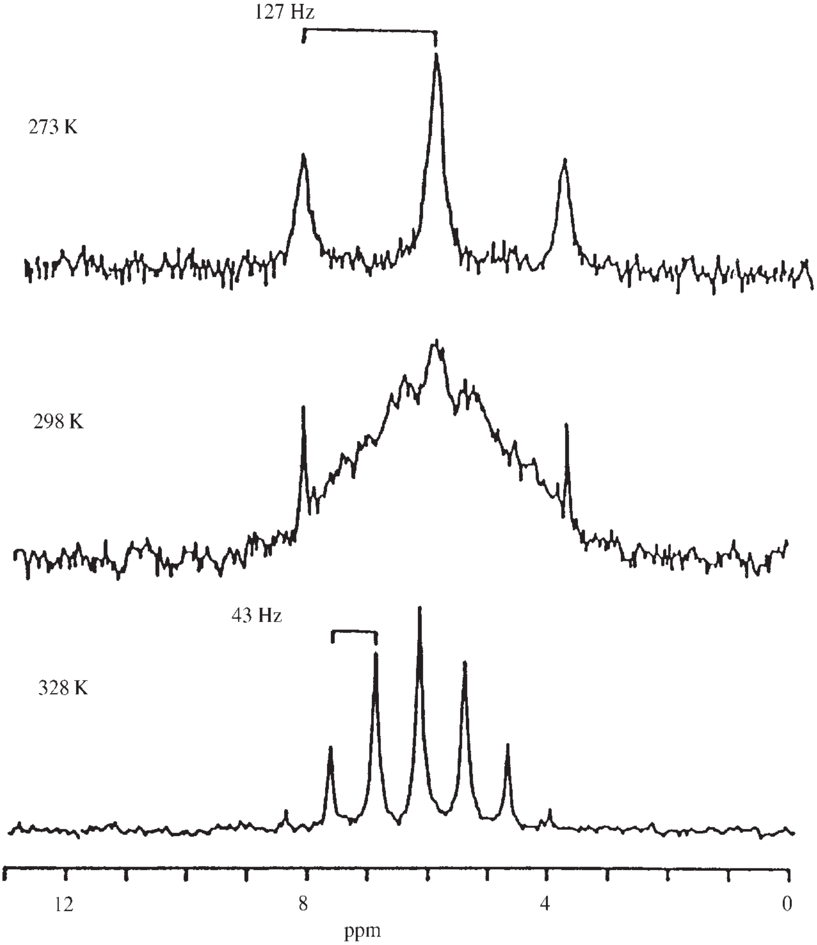

FIGURE 11. Temperature-dependent ^{29}Si NMR sepctra of hexakis(fluorodimethylsilyl)benzene in toluene-d$_8$. Reprinted with permission from Reference 67. Copyright 1994 American Chemical Society

D. Organically Modified Silicates

Organically modified silicates(ormosils) constitute an important new family of amorphous solids. Since the successful preparation of these new ormosils using the sol–gel method[69,70], there has been increasing interest in making new organic/inorganic hybrid materials. These materials are synthesized by chemically incorporating organic polymers into inorganic networks, resulting in improved mechanical properties such as ductility and toughness. Recently, structure-related rubber-like ormosils of the polydimethylsiloxane (PDMS)/tetraethoxysilane (TEOS) system have been reported and some characterization studies of these ormosils have been made[71–73]. The sol-gel reaction mechanisms of these ormosils are still unclear, though ^{29}Si NMR spectroscopy has proven to be a powerful tool for the structural characterization of organic and inorganic silicon compounds. Iwamoto and coworkers[74] investigated the reaction mechanisms leading to the formation of the ormosils of the PDMS/TEOS system by liquid-state ^{29}Si NMR spectroscopy.

In order to assign the ^{29}Si chemical shift relevant to the bonding between PDMS and TEOS relative to TMS, the liquid-state ^{29}Si NMR spectrum of the solution of the dimethyldiethoxysilane (DMDES)/TEOS system was recorded. DMDES is a "monomer" of PDMS and can form chains (equations 4 and 5), rings (especially cyclic D_4 tetramers in this acid catalyzed system[75]) (equation 6) and copolymerized species with condensed TEOS (equation 7).

$$\mathrm{SiMe_2(OR)_2 + 2H_2O \longrightarrow SiMe_2(OH)_2}, \tag{4}$$

$$\mathrm{-O-SiMe_2-OH + HO-SiMe_2-O- \longrightarrow -O-SiMe_2-O-SiMe_2-O- + H_2O} \tag{5}$$

$$\mathrm{4SiMe_2(OH)_2 \longrightarrow [SiMe_2-O-]_4(cyclic) + 4H_2O} \tag{6}$$

$$\mathrm{-O-SiMe_2-OH + HO-Si(-O-)_3 \longrightarrow -O-SiMe_2-O-Si(-O-)_3 + H_2O} \tag{7}$$

For clarity, the various silicate structures are shown in Figure 12. The ^{29}Si NMR spectra of the solutions whose starting compositions were TEOS: PDMS: H_2O: HCl = 1 : 0.082 : 2 : 0.1 at 70 °C are shown in Figure 13.

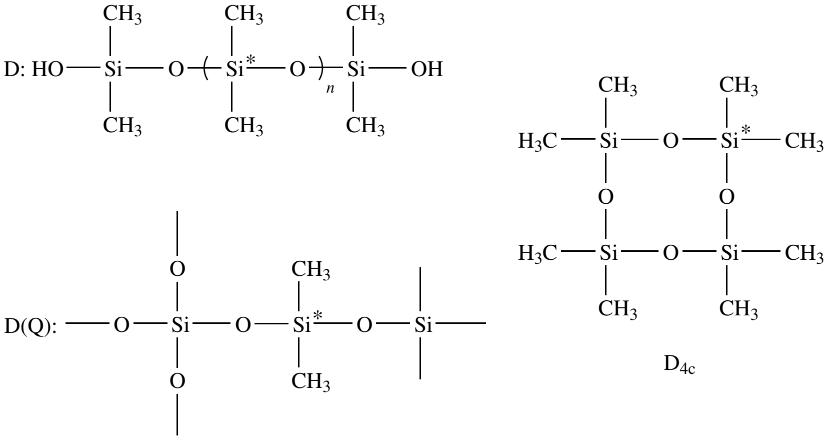

FIGURE 12. Various silicate structures. The asterisks denote the peaks for silicon. Reproduced by permission of Elsevier Science from Reference 74

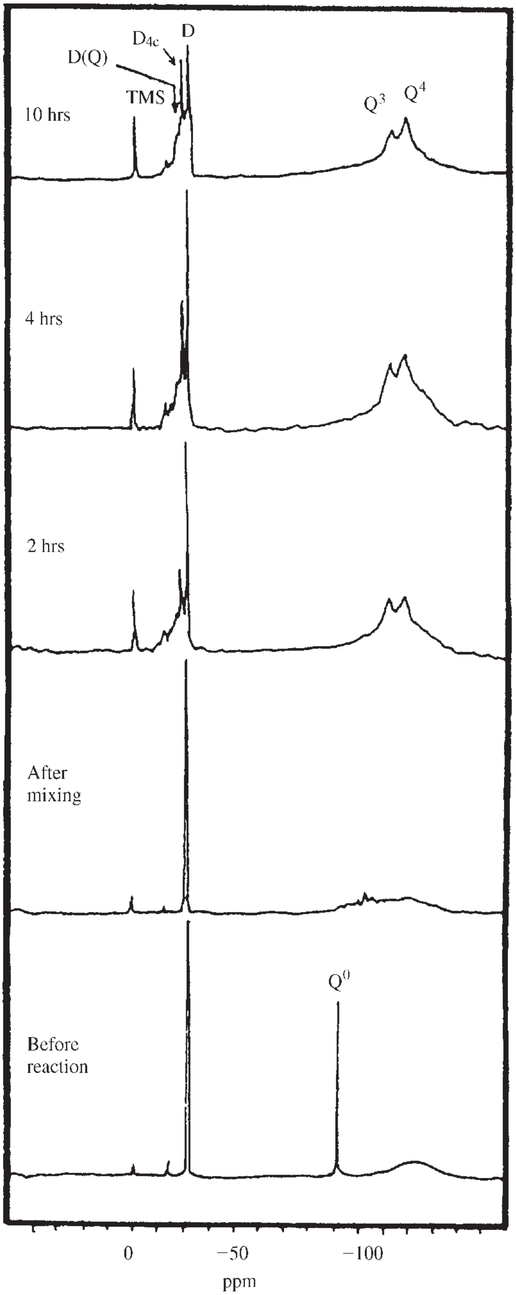

FIGURE 13. ^{29}Si NMR spectra of solutions with a TEOS: PDMS: H_2O: HCl = 1 : 0.082 : 2 : 0.1 composition at varying reaction times at 70 °C. Reproduced by permission of Elsevier Science from Reference 74

The self-condensation reaction of TEOS was predominant rather than copolymerization between PDMS and TEOS immediately after mixing. As the reaction proceeded, D decreased and D(Q) increased. Furthermore, the presence of D_{4c} was observed. These observations indicate that bonds between PDMS and TEOS are formed in the ormosils of the PDMS/TEOS system and that the PDMS chains which contained $-O-SiMe_2-O-$ units were broken into shorter chains and/or cyclic D_{4c} tetramers. These facts indicate that hydrolyzed TEOS reacted with $-O-SiMe_2-O-$ in the middle of PDMS chains as well with the silanol end groups, $HO-SiMe_2-O-$, of PDMS. D and D_{4c} remained after 10 h at 70 °C (Figure 13). The peak intensity of D after 10 h at 70 °C was about one-tenth of the peak intensity before reaction, and the peak intensity of D_{4c} after 10 h was also

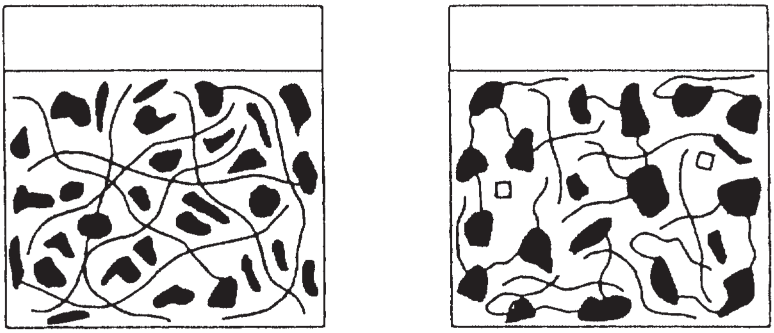

(I) Self-condensation of TEOS

(II) Copolymerization

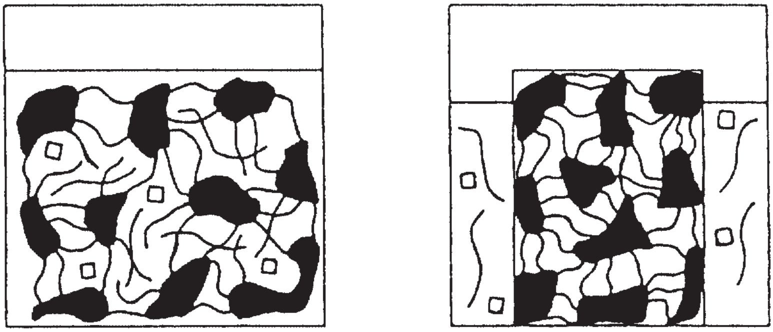

(III) Gelation

(IV) Syneresis

(▲ : condensed TEOS, ~ : PDMS, □ : cyclic D_4 tetramer)

FIGURE 14. Structural models of the sol-gel reaction products of ormosils. Reproduced by permission of Elsevier Science from Reference 74

about one-tenth of the peak intensity of D before reaction. Three peaks, D, D_{4c} and D(Q), appeared in the region of −14.5 to −22.0 ppm in Figure 13. Therefore, the intensity of the broad D(Q) peak was about 8/10 of the peak intensity of D before reaction. Since more PDMS would be copolymerized with TEOS until the solution gelled, the amount of PDMS that was copolymerized with TEOS in this solution can be estimated to be more than 80%.

Condensation of TEOS could be controlled by the reaction rate and/or the diffusion of water, while copolymerization could be controlled solely by the diffusion rate of PDMS. Proposed structural models of ormosils based on the reaction mechanisms before gelation are shown in Figure 14. The TEOS/PDMS ratio of the ormosils was 1/0.082. Immediately after mixing, the self-condensation of TEOS(I) was predominant over copolymerization between PDMS and TEOS. As the reaction time increased, copolymerization between PDMS and TEOS(II) was promoted. At this time, the PDMS chains were broken into shorter chains and/or cyclic D_{4c} tetramers. As copolymerization and condensation reactions of TEOS proceeded, the solution gelled (III). After gelation, syneresis (IV) occurred and nonbridging PDMS chains and cyclic D_{4c} tetramers were released from the gel.

IV. NMR PARAMETERS

A. Theory of ^{29}Si NMR Parameters

The widespread interest in ^{13}C NMR spectroscopy has ensured that the chemical shift of this nucleus has received much attention at both the semiempirical MO- and *ab initio* MO-level approaches, and comparison of the calculated and experimental ^{13}C chemical shifts has provided useful information on the electronic distribution and molecular structure[76,77]. On the other hand, in spite of the fact that ^{29}Si NMR spectroscopy is widely used for investigating molecular structures and electronic distributions in organosilicon compounds, theoretical investigation has been carried out only by using a rough approximate theory such as the averaged excitation energy (ΔE) method. This method has an ambiguity in the estimation of the value of ΔE as a parameter in the paramagnetic term by which ^{29}Si chemical shift is predominantly governed. According to our best knowledge, there have been few ^{29}Si chemical shift calculations using sophisticated methods. In this chapter, therefore, we show calculations of the ^{29}Si chemical shifts of several organic compounds containing a silicon atom by the use of semiempirical MO and *ab initio* MO methods.

Takayama and Ando[78] discussed the relationship between the ^{29}Si chemical shift and the electronic structure through a composition of the calculated finite perturbation theory (FPT) within the CNDO/2 framework, which successfully reproduced the experimental trend for the ^{13}C chemical-shift values. The diamagnetic, paramagnetic and total contributions for the ^{29}Si chemical shift calculated by using the 'new' value of $\beta_{\mathrm{Si}} = -12$ eV), together with the experimental values, are listed in Table 5 for several silicon derivatives.

As may be seen from Table 5, the diamagnetic term, σ^{d}, etc. moves upfield by about 2 ppm in going from SiH_4 to $SiHEt_3$. This variation is quite small, and the chemical shift displacement is in the opposite direction compared with the experimental one. On the other hand, the paramagnetic term, σ^{p}, moves downfield by up to 54 ppm. This means that the ^{29}Si chemical shift is predominantly governed by the paramagnetic term. Next, the authors examined the ^{29}Si chemical shift behavior of organic silicon compounds containing fluorine atoms. The electronegative fluorine nuclei are responsible for a higher electron unbalance in the Si−F bond and may lead to a wider range of ^{29}Si chemical shifts as compared with the case of silicon−hydride compounds. In the ^{29}Si chemical shift calculation, the value of β_{Si} determined above in silicon−hydride compounds was used; also, the authors adopted as the β_{F} parameter for the fluorine atom a value of −20 eV, by

TABLE 5. Calculated ^{29}Si chemical shifts of silicon hydrides[a,b]

Compound	d	σ^{d}	σ^{p}	σ^{Total}	$\delta_{calcd}{}^{c,d}$	$\delta_{exp}{}^{d}$
SiH_4	3.4578	66.78	−321.64	−254.86	−63.87	−92.5
SiH_3Me	3.5050	67.43	−336.78	−269.35	−49.38	−65.2
SiH_3Ph	3.5236	67.69	−333.55	−265.87	−52.86	−60.0
SiH_3Bz	3.5175	67.60	−341.22	−273.62	−45.11	−56.0
SiH_2Me_2	3.5376	67.88	−348.38	−280.50	−38.23	−40.0
SiH_2MePh	3.5546	68.11	−346.13	−278.02	−40.71	−36.9
SiH_2Ph_2	3.5874	68.56	−341.51	−272.95	−45.78	−33.6
$SiHMePh_2$	3.6058	68.80	−358.63	−289.82	−28.91	−19.5
$SiHPh_3$	3.6286	69.11	−352.99	−283.88	−34.85	−17.8
$SiHMe_2Ph$	3.5715	68.34	−367.09	−298.75	−19.98	−17.6
$SiHMe_3$	3.5577	68.15	−360.83	−292.67	−26.06	−16.3
$SiHPr_3$	3.5918	68.62	−375.43	−306.82	−11.91	−8.5
$SiHEt_3$	3.5798	68.45	−372.51	−304.05	−14.68	0.2

[a] Data taken from E. A. Williams and J. D. Cargioli, in *Annual Reports on NMR Spectroscopy,* Vol. 9, Academic Press, New York, p. 287, (1979).

[b] The bonding parameters used are $\beta_H = -13$ eV, $\beta_C = -15$ eV and $\beta_{Si} = -12$ eV.

[c] Values given in ppm. Chemical shifts calculated with respect to TMS.

[d] The negative sign means an upfield shift from TMS.

Reproduced by permission of the Chemical Society of Japan from Reference 78.

the use of which the ^{19}F chemical shift calculation reproduced the experiment reasonably well. The diamagnetic, paramagnetic and total contributions calculated by using these β parameters are listed, together with the experimental chemical shift values, in Table 6. It may be seen that the chemical shift range is much expanded relative to the case of silicon–hydride compounds.

TABLE 6. Calculated ^{29}Si chemical shifts of fluorosilanes[a,b]

Compound	d	σ^{d}	σ^{p}	σ^{Total}	$\delta_{calcd}{}^{c,d}$	$\delta_{exp}{}^{d}$
SiF_4	2.1098	45.17	−254.38	−209.20	−109.53	−111.0
SiF_3Ph	2.5888	53.50	−296.91	−243.41	−75.32	−73.7
$SiF_3C_6H_4Me$-*p*	2.5952	53.61	−297.43	−243.83	−74.90	−72.0
SiF_3CH_4OMe-*p*	2.5892	53.50	−297.29	−243.78	−74.95	−71.4
SiF_3Bz	2.5805	53.36	−303.18	−249.82	−68.91	−64.2
SiF_3Me	2.5345	52.59	−296.31	−243.72	−75.01	−51.8
SiF_2Ph_2	2.9720	59.64	−331.09	−271.45	−47.28	−30.5
SiF_2MePh	2.9314	59.01	−337.96	−278.95	−39.78	−12.4
$SiFPh_3$	3.3213	64.85	−351.88	−278.03	−31.70	−4.7
SiF_2Et_2	2.9258	58.93	−335.45	−276.52	−42.21	0.5
SiF_2Me_2	2.9006	58.53	−336.55	−278.02	−40.71	6.2
$SiFMePh_2$	3.2980	64.51	−358.52	−294.01	−24.72	7.7
$SiFMe_2Ph$	3.2633	64.01	−367.00	−302.99	−15.74	19.8
$SiFPr_3$	3.2819	64.28	−375.19	−310.91	−7.82	28.8
$SiFMe_3$	3.2426	63.71	−359.88	−296.17	−22.56	31.9

[a] Data taken from E. A. Williams and J. D. Cargioli, in *Annual Reports on NMR Spectroscopy*, Vol. 9, Academic Press, New York, p. 287 1979.

[b] The bonding parameters used are $\beta_H = -13$ eV, $\beta_C = -15$ eV, $\beta_{Si} = -12$ eV and $\beta_F = -20$ eV.

[c] Values given in ppm. Chemical shifts calculated with respect to TMS.

[d] The negative sign means an upfield shift from TMS.

Reproduced by permission of the Chemical Society of Japan from Reference 78.

It can also be seen that the relative chemical shift is predominantly governed by the paramagnetic term, although the diamagnetic term is much more varied by the degree of fluorine substitution than the value in the case of silicon–hydride compounds. A plot of the experimental chemical shifts vs the calculated values is shown in Figure 15. It can be seen that data points deviate slightly from the theoretical line with the slope of 1.0, but the overall trend of the calculation reasonably reproduce the experimental data. In particular, it can be said that it has been established that the ^{29}Si chemical shift in SiR_nF_{4-n} moves upfield as the degree of fluorine substitution is increased. (It is notable that the upfield shift with an increase in the degree of fluorine substitution is opposite to the case of the ^{13}C chemical shift in CR_nF_{4-n}.)

Tossell and Lazzeretti[79] have recently applied *ab initio* coupled Hartree–Fock perturbation theory (CHFPT) to the calculation of ^{29}Si NMR shifts in SiH_4, SiF_4 and other molecules. They also carried out CHFPT calculations of ^{29}Si chemical shielding tensors for SiH_4, Si_2H_6, Si_2H_4 and H_2SiO. Experimental geometries were employed for SiH_4 and Si_2H_6 (D_{3h} symmetry was utilized for Si_2H_6 in order to shorten the calculation time) and optimized geometries from high level *ab initio* SCF calculations were employed for Si_2H_4[80] and H_2SiO.

Total energies and atomization energies refereed to Hartree–Fock nuclei are shown in Table 7. For SiH_4 and Si_2H_6 a comparison can be made with experiment using tabulated bond dissociation energies. Calculated values were roughly 90% of experiment. It is evident that the calculated atomization energy for Si_2H_4 is only slightly greater than that for

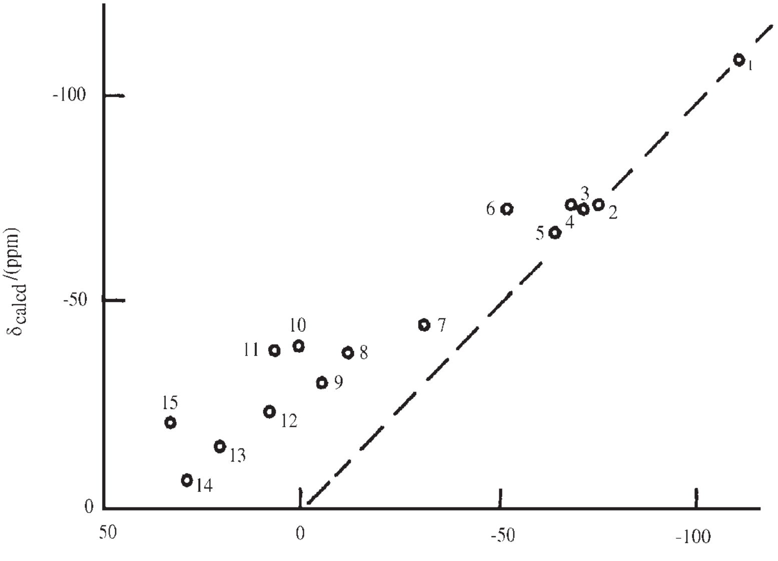

FIGURE 15. A plot of the calculated ^{29}Si chemical shifts vs experimental values in fluorosilanes. β bonding parameters are: ($\beta_H = -13$ eV, $\beta_C = -15$ eV, $\beta_{Si} = -12$ eV and $\beta_F = -20$ eV). The negative sign means upfield shift relative to TMS. The numbers refer to the following compounds: 1, SiF_4; 2, SiF_3Ph; 3, $F_3SiC_6H_4Me$-*p*; 4, SiF_3 C_6H_4OMe-*p*; 5, SiF_3Bz; 6, SiF_3Me; 7, SiF_2Ph_2; 8, SiF_2MePh; 9, $SiFPh_3$; 10, SiF_2Et_2; 11, SiF_2Me_2; 12, $SiFMePh_2$; 13, $SiFMe_2Ph$; 14, $SiFPr_3$; 15, $SiFMe_3$. Reproduced by permission of the Chemical Society of Japan from Reference 78

TABLE 7. Calculated total energies E (hartree) and heats of atomization (kcal mol^{-1}) for several silicon derivatives

	SiH_4	Si_2H_6	Si_2H_4	H_2SiO
E	−291.260	−581.365	−580.1355	−364.987
heat of atomization, calc.	279	461	317	222
exp.	304	509	—	—

Reproduced by permission of Elsevier Science from Reference 79.

SiH_4, indicative of the weakness of the Si=Si bond. (Note that the calculated minimum energy geometry rather than the experimental one was used for Si_2H_4; this should stabilize with respect to SiH_4 and Si_2H_6, for which the experimental geometries were used.) Indeed, the reaction $Si_2H_4 + H_2 \rightarrow Si_2H_6$ is exothermic by about 34 kcal mol^{-1} (assuming a calculated H_2 atomization energy of about 100 kcal mol^{-1}). The calculated Si=O atomization energy in H_2SiO (assuming the calculated Si−H atomization energy value of 70 kcal mol^{-1} from SiH_4) is only 82 kcal mol^{-1}, less than the experimental Si−O atomization energy of 108 kcal mol^{-1}.

Calculated chemical shielding tensors $\sigma_{\alpha\beta}$ are given in Table 8 for SiH_4, Si_2H_6, Si_2H_4 and H_2SiO. Comparison can be made with experimental chemical shift values for SiH_4 and Si_2H_6 and for $(Mes)_2Si{=}Si(Mes)_2$. For each molecule, σ and its components are given with the Si as gauge origin.

An example of the use of IGLO calculations was already mentioned[43].

B. Coupling Constants

One-bond nuclear spin−spin coupling constants (^1J) are a valuable source of information on the nature of chemical bonding[81]. The sign and magnitude of $^1J(^{29}Si^{15}N)$ were first reported for ^{15}N-enriched $(H_3Si)_3N$ (+6 Hz) in 1973[82]. Very few studies of these couplings appeared during the next decade, mainly due to a low natural abundance of both ^{15}N (0.36%) and ^{29}Si (4.7%) isotopes[83]. As a result, only scattered values of $^1J(SiN)$ had been reported in preliminary communications[84,85]. This is in contrast with the current upsurge of interest in Si−N bonding explored by both theoretical[86−88] and experimental[89,90] methods. Such attention is largely accounted for by the controversial assumption of d_π−p_π interaction along the Si−N bond[91]. Attempts to invoke ^{15}N and ^{29}Si chemical shifts in order to explore this phenomenon have met with little success so far[89].

^1H, ^{13}C and ^{29}Si NMR spectral analyses carried out earlier for bis(trimethylsilyl)ethylenes[92] and some types of vinylsilanes[93] indicate an interaction between the vacant d-orbitals on the silicon atom and the π-electron system of the vinyl group. In an effort to broaden these notions and in continuation of previous studies concerned with the influence of electronic effects of silicon and vinyl substituents on the chemical shifts as well as the coupling constants, Lukevics and coworkers[94] determined the ^1H, ^{13}C, ^{29}Si and ^{17}O NMR spectra for the following chlorinated silylethylenes **(31–34)** and 1,2-disilylethylenes **(35)**:

$$Me_{3-n}X_nSiCH{=}CHCl\ (\mathbf{31} = trans, \mathbf{32} = cis)$$

$$Me_{3-n}X_nSiCH{=}CCl_2\ (\mathbf{33})$$

$$Me_{3-n}X_nSiCCl{=}CCl_2\ (\mathbf{34})$$

$$Me_{3-n}X_nSiCH{=}CHSiX_nMe_{3-n}\ (n = 0\text{–}3, X = Cl, OEt, OMe)\ (\mathbf{35})$$

TABLE 8. Calculated diamagnetic, paramagnetic and total ^{29}Si chemical shielding tensors σ (in ppm, gauge origin at Si) compared with experimental chemical shifts, τ

	SiH_4	Si_2H_6			Si_2H_4				H_2SiO			
	xx, *yy*, *zz*	*xx*, *yy*	*zz*	av[a]	*xx*	*yy*	*zz*	av[a]	*xx*	*yy*	*zz*	av[a]
calc.												
σ^{d}	899.8	985.4	907.4	959.4	990.5	977.6	895.9	954.6	967.3	952.4	889.9	936.5
σ^{p}	−420.0	−476.6	−421.3	−458.2	−523.5	−801.6	−501.4	−608.8	−593.3	−819.6	−414.4	−609.1
σ^{Total}	479.8	508.7	486.2	501.2	467.0	176.0	394.5	345.8	374.0	132.8	475.5	327.4
exp.												
τ	−93		−104.8			+64						

[a] $\text{av} = (xx + yy + zz)/3$

Reproduced by permission of Elsevier Science from Reference 79.

TABLE 9. ^{29}Si−^{13}C and ^{29}Si−^{1}H spin−spin coupling constants (Hz) in silylethylenes

Compound	X	*n*	^{29}Si−^{13}CH$_3$	^{29}Si−^{13}C$_\alpha$	^{29}Si−^{13}C$_\beta$	^{29}Si−C−^{1}H	^{29}Si−C$_\alpha$−^{1}H	^{29}Si−C$_\alpha$=C$_\beta$−^{1}H
31a	Cl	0	53.33	59.32	5.76	6.81	4.25	2.34
31b	Cl	1	60.69	69.87	7.42	7.14	5.71	4.76
31c	Cl	2	73.00	86.11	9.03	7.93	6.75	6.81
31d	Cl	3	—	111.86	11.54	—	8.22	8.50
31e	OEt	1	62.64	68.20	7.06	6.81	2.83	4.75
31f	OEt	2	78.38	86.90	7.01	7.40	3.02	4.30
31g	OEt	3	—	114.56	7.79	—	3.22	5.06
31h	OMe	3	—	115.68	8.05	3.76(^3J(SiOCH))	3.03	5.13
32a	Cl	0	53.49	61.82	—	6.85	—	—
32b	Cl	1	60.49	73.02	—	7.31	2.17	13.40
32c	Cl	2	72.28	89.62	—	8.10	3.25	17.23
32d	Cl	3	—	115.58	—	—	7.69	21.76
32e	OEt	1	62.64	71.24	—	6.92	1.48	11.76
32f	OEt	2	78.54	89.68	—	7.51	1.20	13.25
32g	OEt	3	—	117.08	—	—	0.4	15.32
32h	OMe	3	—	116.74	—	3.95(^3J(SiOCH))	1.03	15.53
33a	Cl	0	54.24	58.60	—	6.85	1.46	—
33b	Cl	1	61.77	70.19	—	7.25	1.10	—
33c	Cl	2	74.37	87.81	—	8.17	1.60	—
33d	Cl	3	—	114.62	—	—	5.13	—
33f	OEt	2	81.19	87.35	—	7.58	1.13	—
33g	OEt	3	—	115.67	—	—	0.81	—
34a	Cl	0	55.49	60.81	6.07	6.89	—	—
34b	Cl	1	63.82	74.80	8.08	7.36	—	—

34c	Cl	2	77.58	96.77	10.72	8.39	—	—
34d	Cl	3	—	130.77	13.42	—	—	—
34f	OEt	2	84.34	91.30	8.64	7.73	—	—
34g	OEt	3	—	127.28	9.75	—	—	—
35a	Cl	0	51.89	63.34		6.63	—	—
35b	Cl	1	59.30	71.11		7.07	—	7.55
35c	Cl	2	71.01	84.42		7.74	—	7.66
35d	Cl	3	—	107.46		—	—	7.90
35g	OEt	3	—	115.96		—	—	8.10
$Me_3SiCH{=}CHBr$		*trans*	53.05	57.10	4.91	6.77	—	—
		cis	53.48	62.19	—	6.85	0.70	10.93
$Et_3SiCH{=}CHCOOEt$			53.48($SiCH_2$)	57.86	8.28	8.00($SiCH_2$) 6.60($SiCH_2$)	4.30	6.00
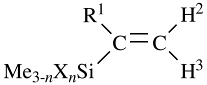	Cl	0	52.25	64.16	—	—	6.19	15.12(SiH_2)
	Cl	1	—	—	—	—		8.17(SiH_2)
	Cl	1	—	—	—	—	6.42	15.26 8.59
	Cl	2	70.40	89.70	—	—	11.80	23.81(SiH_2) 12.53(SiH_2)
	Cl	3	—	112.40	—	—	15.44	30.61(SiH_2) 15.54(SiH_2)

Reproduced by permission of Elsevier Science from Reference 94.

The $^{1}J(^{29}\text{Si}^{13}\text{C})$ coupling constants of **31–34** increase with increasing number of substituents X in the molecules. According to Bent's hypothesis[95], the value of this coupling depends on the s-character of both silicon and carbon. This is supported by the fact that $^{1}J(^{29}\text{SiC}_\alpha) > {}^{1}J(^{29}\text{SiMe})$ (Table 9). Nearly linear correlations were found between the $^{1}J(^{29}\text{SiC}_\alpha)$ coupling constants and the sum of the electronegativities of substituents attached to the silicon atom ($\sum E$) (equations 8–11).

$$^{1}J(^{29}\text{SiC}_\alpha) = -71.0 + 20.2\sum E \qquad n = 8;\ r = 0.964\ (\mathbf{31}) \tag{8}$$

$$^{1}J(^{29}\text{SiC}_\alpha) = -69.6 + 20.4\sum E \qquad n = 8;\ r = 0.969\ (\mathbf{32}) \tag{9}$$

$$^{1}J(^{29}\text{SiC}_\alpha) = -62.2 + 19.0\sum E \qquad n = 6;\ r = 0.984\ (\mathbf{33}) \tag{10}$$

$$^{1}J(^{29}\text{SiC}_\alpha) = -89.7 + 23.5\sum E \qquad n = 6;\ r = 0.978\ (\mathbf{34}) \tag{11}$$

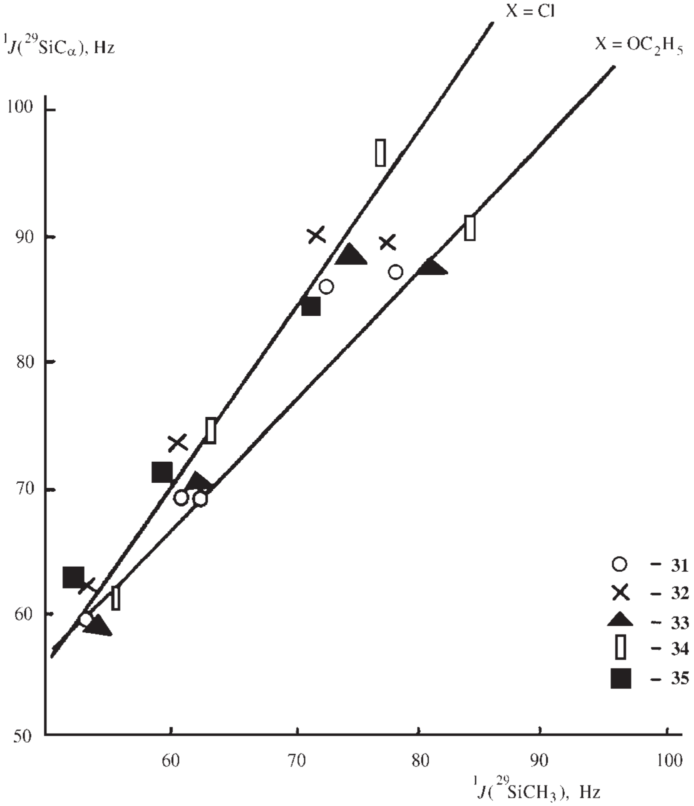

FIGURE 16. $^{1}J(^{29}\text{SiC}_\alpha)$ as a function of the $^{1}J(^{29}\text{SiCH}_3)$ coupling constants in silylethylenes; X = Cl, $^{1}J(^{29}\text{SiC}_\alpha) = -13.7 + 1.39\,^{1}J\ (^{29}\text{SiCH}_3)$ ($r = 0.980$); X = OEt, $^{1}J(^{29}\text{SiC}_\alpha) = 5.1 + 1.02\,^{1}J(^{29}\text{SiCH}_3)$ ($r = 0.979$) . Reproduced by permission of Elsevier Science from Reference 94

These equations indicate the predominant role of positive charge in determining $^1J(^{29}SiC_\alpha)$ coupling constants. The long-range coupling constants ^nJ(SiH) in vinylsilanes have been studied[96,97]. Based on this argument, the authors measured these coupling constants in compounds **31–35** (Table 9). There is a certain decrease in the geminal $^2J(^{29}SiC_\alpha H)$ coupling constants in compounds **31–33** as compared to $Me_3SiC_\alpha H = CH_2$ [$^2J(^{29}SiC_\alpha H)$ 6.42 Hz[98]] and $N(CH_2CH_2O)_3SiC_\alpha H = CH_2$ [^2J ($^{29}SiC_\alpha H$) 5.74 Hz[21]]. This can possibly be attributed not only to the influence of electronic charge on chlorine, but also to changes in the Si–C–H valence angle. The role of the latter factor can be deduced from NMR data obtained for organotin compounds[99].

As was shown above, SiOR and SiCl substituents exert a completely different effect on the chemical shifts. The same difference clearly comes out in the case of coupling constants. Thus, comparing the two sets of $^1J(^{29}SiC_\alpha)$ and $^1J(^{29}SiCH_3)$ values measured for the same SiCl-substituted molecule, one can find a linear correlation between these quantities with a slope coefficient close to unity (Figure 16). However, compounds bearing SiOR substituents form another straight line, showing additional electronic and/or steric effects. The same picture is found when comparing $^1J(^{29}Si^{13}CH_3)$ and $^2J(^{29}Si^{13}CH)$ coupling constants. Here, too, SiOR-substituted compounds account for a separate correlation line (Figure 17).

These findings can possibly be explained by a stronger $(p-d)_\pi$ conjugation in the Si–O bond in comparison with the Si–Cl bond. It is, however, necessary to take into account also the steric differences of the SiOR and SiCl substituents. The importance of the steric

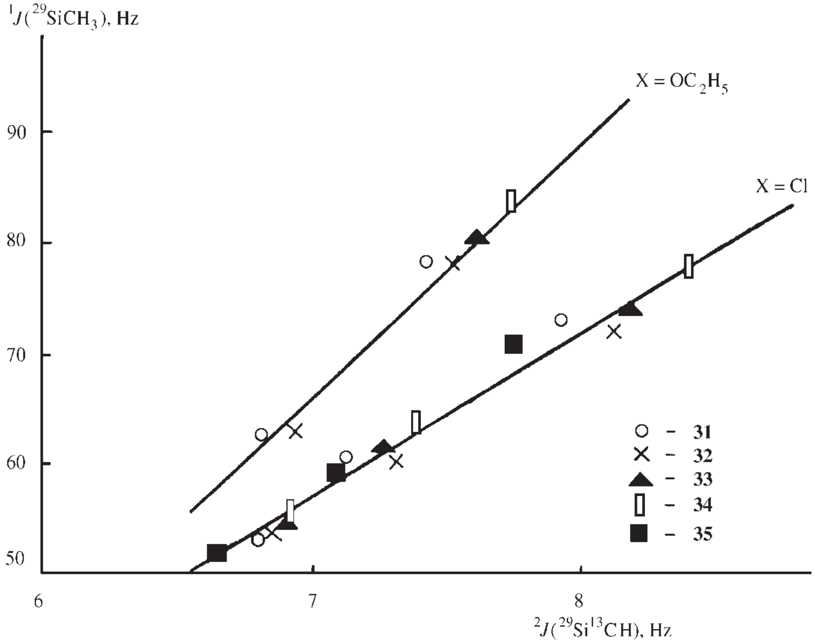

FIGURE 17. Correlation between $^1J(^{29}Si^{13}CH_3)$ and $^2J(^{29}Si^{13}CH)$ coupling constants in silylethylenes; X = Cl, $^1J(^{29}Si^{13}CH_3) = -49.5 + 15.2\ ^2J(^{29}Si^{13}CH)$ ($r = 0.989$); X = OC_2H_5, $^1J(^{29}Si^{13}CH_3) = -110.5 + 25.2\ ^2J(^{29}Si^{13}CH)$ C,H) ($r = 0.990$). Reproduced by permission of Elsevier Science from Reference 94

contribution can be inferred from the lack of correlation between the ${}^{1}J({}^{29}SiC_{\alpha})$ and ${}^{2}J({}^{29}SiC_{\alpha}H)$ couplings.

Measurements of spin–spin coupling constants make it possible to obtain information on electron distribution in molecules. ${}^{29}Si-{}^{15}N$ spin–spin coupling constants were, as mentioned previously, first measured in 1973[78]. The development of polarization transfer methods (INEPT, DEPT etc.) allowed their measurements under natural isotope abundance. As a result, systematic investigation of these spin–spin coupling constants and their application for structural studies became important[100–103]. Kupce, Lukevics and coworkers conducted an extensive study on ${}^{29}Si-{}^{15}N$ coupling constants in silazanes **36–51**, along with studies on ${}^{29}Si$ and ${}^{15}N$ chemical shifts, ${}^{15}N-H$, ${}^{29}Si-{}^{13}C$ and ${}^{29}Si-{}^{29}Si$ coupling constants and ${}^{15/14}N$ isotope effects on ${}^{29}Si$ chemical shifts[104]. This enabled the authors to attain a more reliable interpretation of ${}^{29}Si-{}^{15}N$ coupling constants scarcely studied so far and to characterize in detail the structure of the investigated compounds.

$(R_3Si)_2NH$

(36) $R_3 = Me_3$
(37) $R_3 = Me_2Ph$
(38) $R_3 = MePh_2$
(39) $R_3 = Me_2Cl$
(40) $R_3 = Me_2O(SiMe_2O)_5SiMe_3$

$(Me_3Si)_2NNa$

(41)

$Me_3SiNHOSiMe_3$

(42)

$Ph_2MeSiNH_2$

(43)

$Ph_2MeSiNHBu\text{-}t$

(44)

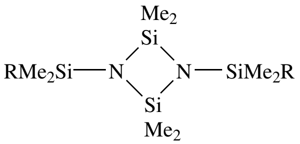

(**45**) R = Cl
(**46**) R = NH_2
(**47**) R = OEt

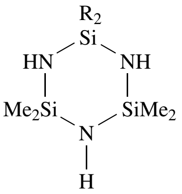

(**48**) R = Me
(**49**) R = Ph

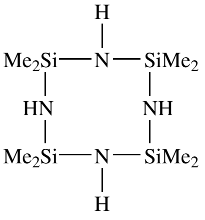

(**50**)

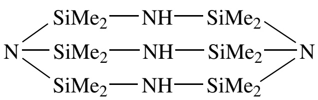

(**51**)

The spin–spin coupling constants and chemical shifts of the compounds studied are presented in Table 10. An increase in ${}^{1}J(SiN)$ with the electronegativities of the substituents on the Si atom in the SiR series Me < Ph < Cl < OR (compounds **36–40** and **46–48**) is indicative of positive ${}^{1}J(SiN)$ values $[{}^{1}J(SiN) > 0]$. Since the variation in the electronegativities of the substituents on the N atom is insignificant, it can be

TABLE 10. ^{29}Si NMR data of silazanes **36–51**[a]

Compound	Solvent	Position	δ (^{15}N)	δ (^{29}Si)	^{1}J(NH)	^{1}J (SiC)[b]	^{1}J(SiN)	$^{1}\Delta$ ($^{15/14}$N)[c]	Other data
36	acetone $-d_6$		−354.2	2.1	69.6	56.2	13.5	10.7	
37	$CDCl_3$		−357.8	−3.5	66.1	58.2	13.8	10.5	^{1}J(SiC) = 72.2 (Ph)
38	$CDCl_3$		−361.5	−9.4	66.3	60.0	14.2	8.5	^{1}J(SiC) = 74.6 (Ph)
39	$CDCl_3$		−334.3	13.3	68.1	68.1	14.4	8.2	
40	$CDCl_3$		−335.7	−11.9	nm[d]	69.4	17.4	5.9	
41	C_6D_6		nm[d]	−14.6		51.9	7.8	11.6	
42	C_6D_6		−255.6	10.9	64.8	56.7	6.5	14.3	δ (^{29}Si) 20.9 ($OSiMe_3$)
43	C_6D_6		−373.8	−10.2	74.0	59.8	17.5	10.8	^{1}J(SiC) = 74.4 (Ph)
44	acetone-d_6		−327.3	−15.4	75.0	nm	19.8	nm[d]	
45	$CDCl_3$	*endo*	−322.1	7.3		61.9	7.1	10.5	^{2}J(SiSi) = 2.2 (*exo–endo*)
		exo		6.2		67.2	16.9	4.0	
46	C_6D_6	*endo*	−323.8	3.0		60.9	7.4	10.0	^{2}J(SiSi) = 2.3 (*exo–endo*)
		exo	−363.1	−6.7	72.8	63.9	17.8	nm[d]	^{1}J(SiN) = 18.4 (NH_2) ^{3}J(SiN) = 3.1
47	$CDCl_3$	*endo*	−325.4	3.8		61.2	7.3	9.5	^{2}J(SiSi) = 2.0 (*exo–endo*)
		exo		−8.9		68.1	18.3	4.5	
48	$CDCl_3$		−347.3	−4.6	69.4	63.0	15.4	nm[d]	
49	$CDCl_3$	($SiMe_2$)	−347.6	−3.1	69.2	63.1	16.0	nm[d]	
		($SiPh_2$)	−351.0	−21.7	70.1	83.8	18.1	nm[d]	^{1}J(SiN) = 15.3 ($SiMe_2$) ^{3}J(SiN) = 2.8
50	$CDCl_3$		−341.7	−8.2	67.0	64.0	16.9	8.2	
51	$CDCl_3$	(NSi_3)	nm[d]	−6.8	nm[d]	64.1	9.8	8.7	
		(NSi_3)					14.3		

[a] Chemical shifts (δ) in ppm relative to TMS(^{29}Si) and $MeNO_2$(^{15}N).

[b] For the SiMe group.

[c] Isotope shift in ppb.

[d] nm = not measured.

Reproduced by permission of Elsevier Science from Reference 104.

suggested that the increase of $^{1}J(\mathrm{SiN})$ in this series is related to enhanced s character of the Si−N bond according to Bent's law[105]. A parallel increase in the $^{29}\mathrm{Si}{-}^{13}\mathrm{C}$ spin–spin coupling constants supports this suggestion. No general correlation exists between these coupling constants although, as in the case of aminosilanes[102], such correlation can be found for compounds with identical substituents at the N atom [e.g. disilazanes **36–40** (equation 12)]. Deviation from this relation occurs in the case of compound **39**.

$$^{1}J(\mathrm{SiN}) = 0.31\,^{1}J(\mathrm{SiC}) - 4.0 \qquad r = 0.993 \tag{12}$$

The less steep slope of the correlation line, as compared with the slope found for the analogous relation in aminosilanes [$^{1}J(\mathrm{SiN}) = 0.41\,^{1}J(\mathrm{SiC}) - 7.3$][103], results from the lower electronegativities of substituents on the N atom in the silazanes.

Much attention has been devoted in recent years to studies of isotope shifts in NMR spectra caused by the replacement of ^{12}C isotopes with ^{13}C in the molecule. As for the ethynylsilanes, the $^{13/12}$C isotope shifts in the ^{29}Si NMR spectra have so far been determined only for three derivatives. Therefore, in order to study this phenomenon more thoroughly Lukevics and coworkers[104] synthesized a wide range of ethynylsilanes: $\mathrm{Me_3SiC{\equiv}CX}$, where X = H, Br, I, SMe, SEt, $\mathrm{SC_6F_5}$, Me, $\mathrm{CH_2Cl}$, $\mathrm{CH_2OEt}$, $\mathrm{CH_2NEt_2}$, $\mathrm{CH_2SiMe_3}$, $\mathrm{CH_2Sn(Bu\text{-}\mathit{t})_3}$, $\mathrm{CF_3}$, CN, Ph, $\mathrm{C_6F_5}$, $\mathrm{SiMe_3}$, $\mathrm{GeMe_3}$, $\mathrm{GeEt_3}$, $\mathrm{SnMe_3}$, $\mathrm{Sn(Bu\text{-}\mathit{t})_3}$, and examined their ^{29}Si NMR spectra.

The isotope shifts $^{n}\Delta^{29}\mathrm{Si}\ (^{13/12}\mathrm{C})$ measured in the ^{29}Si NMR spectra of ethynylsilanes are listed in Table 11. For some of these ethynylsilanes the coupling constants $^{n}J(\mathrm{SiC})$ have been reported[106] but not discussed. Lukevics and coworkers[107] showed that the values of the $^{1}J(\mathrm{SiC_\alpha})$ coupling constants largely depend on the electronic properties of substituent X according to equation 13.

$$^{1}J(\mathrm{SiC_\alpha}) = 82.9 - 21.7\sigma^{\mathrm{p}} \qquad n = 12;\ r = 0.98 \tag{13}$$

Coupling constants over two bonds $^{2}\mathrm{J}(^{29}\mathrm{Si}^{13}\mathrm{C}_\beta)$ are influenced similarly by the substituent X. This is demonstrated by the correlation between $^{1}J(^{29}\mathrm{Si}^{13}\mathrm{C}_\alpha)$ and $^{2}J(^{29}\mathrm{Si}^{13}\mathrm{C}_\beta)$:

$$^{2}J(^{29}\mathrm{Si}^{13}\mathrm{C}_\beta) = -3.44 + 0.23\,^{1}J(^{29}\mathrm{Si}^{13}\mathrm{C}_\alpha) \qquad n = 15; r = 0.94 \tag{14}$$

Thus, an increase in the electron-accepting ability of the substituent X leads to a decrease in the coupling constant. A correlation similar to that in equation 14 has been reported for the coupling constants $^{n}J\ (^{119}\mathrm{Sn}^{13}\mathrm{C})$ in the ethynylstannanes $\mathrm{Me_3SnC{\equiv}CX}$. The slope of this correlation for the tin derivatives (0.28) is very close to that found for the ethynylsilanes (0.23), which indicates that the transmission of electronic effects of the substituent X through the triple bond is very similar for both classes of compounds.

It is noteworthy that the points obtained for ethynylsilanes with X = $\mathrm{SiMe_3}$, $\mathrm{GeMe_3}$, $\mathrm{SnMe_3}$ deviate strongly from correlations 13 and 14. In the case of equation 13, one can speculate that the σ^{p} values for $X = \mathrm{MMe_3}$ (M = Si, Ge, Sn) substituents inadequately describe the electronic effects in ethynylsilanes; however, the analogous deviations in the case of correlation 14 make this explanation questionable. These effects may be connected both with the violation of the nonlinearity of $\mathrm{R_3MC{\equiv}CM'R_3}$ acetylenides[108] and/or with the existing additional concurrent hyperconjugation effect $\mathrm{H_3{\equiv}C{-}M{-}C{\equiv}}$ in these molecules[109]. The latter effect must affect the state of π- and σ-electrons in the triple bond, which are involved in the transmission of spin information between the various nuclei.

In contrast to the $^{1}J(^{29}\mathrm{Si}^{13}\mathrm{C}_\alpha)$ and the $^{2}J(^{29}\mathrm{Si}^{13}\mathrm{C}_\beta)$, the $^{1}J(^{29}\mathrm{Si}^{13}\mathrm{CH_3})$ coupling constants increase with increasing acceptor properties of substituent X. Such changes can be

TABLE 11. ${}^nJ$ (${}^{29}Si-{}^{13}C$) coupling constants (Hz) and ${}^{13/12}C$ isotope shifts (ppb) in the ${}^{29}Si$ NMR spectra of ethynylsilanes $Me_3SiC_\alpha\equiv C_\beta X$

No.	X	${}^1\Delta^{29}Si\ ({}^{13/12}C_\alpha)$	${}^1J\ ({}^{29}Si^{13}C_\alpha)$	${}^1\Delta^{29}Si\ ({}^{13/12}C_\beta)$	${}^1J({}^{29}Si^{13}C_\beta)$	${}^1\Delta^{29}Si\ ({}^{13/12}C_{Me})$	${}^1J({}^{29}Si^{13}C_{Me})$
1	H	−16.4	81.47	−5.2	15.41	−1.2	56.28
2	Me	−14.8	85.75	−4.2	15.74	−1.3	56.28
3	CH_2SiMe_3	−13.3	89.54	−3.1	17.86	−1.8	56.06
4	CH_2GeMe_3	−12.9	88.31	−3.0	17.69	−2.0	56.01
5	$CH_2Sn(Bu\text{-}t)_3$	−13.5	90.80	−3.1	18.02	−1.8	55.91
6	CH_2NEt_2	−15.0	93.84	−4.3	15.75	−1.1	56.24
7	CH_2OEt	−15.3	80.57	−4.0	15.49	−1.1	56.41
8	CH_2Cl	−16.7	80.77	−5.0	15.42	−1.1	56.51
9	SMe	−16.2	82.63	−4.8	15.54	−1.0	56.44
10	SC_6F_5	−17.2	78.50	−4.9	14.61	−0.1	56.70
11	SEt	−16.2	82.73	−4.5	16.67	−0.9	56.39
12	Ph	−15.6	83.12	−4.7	16.01	−1.1	56.28
13	C_6F_5	−19.0	77.62	−6.2	14.00	−0.8	56.57
14	Br	−16.7	80.22	−5.5	15.05	−1.0	56.68
15	I	−17.9	77.73	−5.5	13.15	−0.6	56.49
16	CN	−21.8	68.10	−7.6	13.14	−0.5	57.27
17	CF_3	−20.9	71.77	*a*	*a*	−0.2	57.33
18	$SiMe_3$	−16.1	76.75	−4,2	12.37	−1.4	56.13
19	$GeMe_3$	−15.4	78.25	−4,1	12.20	−1.3	56.09
20	$GeEt_3$	−15.0	78.30	−4,3	12.30	−1.3	55.99
21	$SnMe_3$	−15.3	78.83	*a*	*a*	−1.3	55.92
22	$Sn(Bu\text{-}t)_3$	−14.3	78.66	*a*	*a*	−1.3	55.79

[a] Not recorded.

Reproduced by permission of Elsevier Science from Reference 107.

attributed to the occurrence of the same hyperconjugation effect. This shows that both types of Si—C bond are interrelated: a change in the properties of substituent X strengthens the Si—C_α and weakens the Si—Me bond. However, the data in Table 11 show that the $^1J(^{29}Si^{13}CH_3)$ values are subject to minor variations, thus making a more detailed discussion impossible.

Isotope shifts $^1\Delta^{29}Si(^{13/12}C_\alpha)$ in the ^{29}Si NMR spectra of ethynylsilanes reveal the same tendencies as the $^1\Delta^{119}Sn(^{13/12}C_\alpha)$ values in the ^{119}Sn NMR spectra of ethynylstannanes (equation 15 and Figure 18).

$$^1\Delta^{119}Sn(^{13/12}C_\alpha) = 0.59 + 3.6\,^1\Delta^{29}Si(^{13/12}C_\alpha) \qquad n = 11;\ r = 0.966 \qquad (15)$$

The correlation 15 suggests that the changes in the isotope shifts are uniform regardless of the type of the central atom in the group 14 acetylenides.

C. Relaxation Times and Exchange Phenomena

The high structural sensitivity of chemical shifts makes ^{29}Si NMR a powerful tool for determination of the structure of oligomeric and polymeric siloxanes. Detailed information can be obtained for the characterization of the different structural units, for the

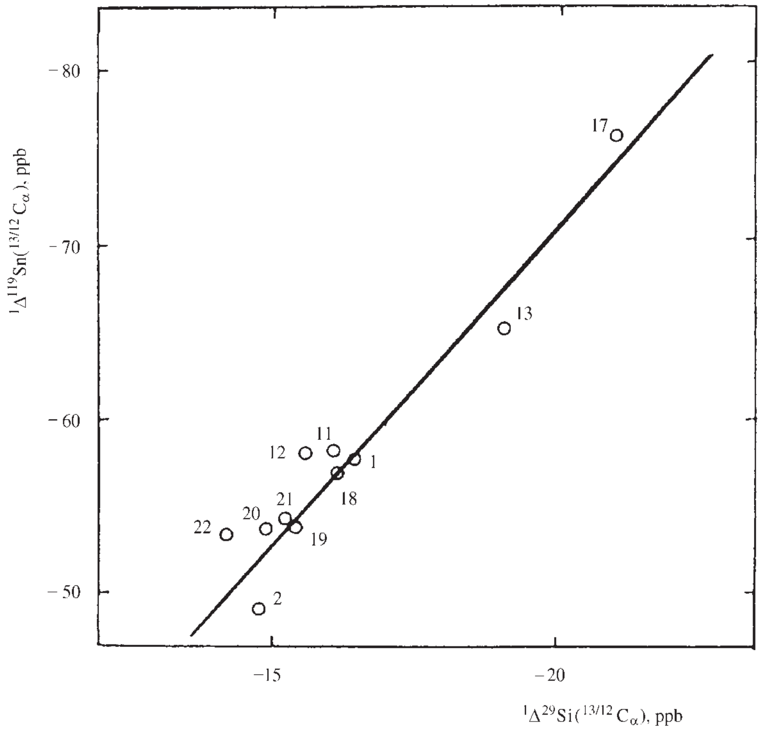

FIGURE 18. The correlation between one-bond $^1\Delta$ M($^{13/12}$C) isotope shifts in the ^{29}Si and ^{119}Sn NMR spectra of isostructural acetylenes $(CH_3)_3$ $MC_\alpha{\equiv}C_\beta$ X (M = ^{29}Si, ^{119}Sn). The numbering of the compounds corresponds to that in Table 11. Reproduced by permission of Elsevier Science from Reference 107

determination of average chain lengths or for the degree of condensation of the siloxane framework. Both the ^{29}Si chemical shifts as well as the spin–lattice relaxation times (T_1) of the silicon nuclei in low molecular weight linear polydimethylsiloxane, $Me_3SiO[Me_2SiO]_nSiMe_3(MD_nM)$, have been determined[110]. In the ^{29}Si NMR spectra of the oligomers MD_nM, $n = 1–8$, individual resonance lines can be found for each distinct silicon nucleus. This degree of chemical shift resolution surpasses that observed in the ^{13}C or ^{1}H NMR of the same materials. Spin–lattice relaxation times give information about the mobility at different points in polymer chains. The relatively high values of the ^{29}Si T_1 values found in MD_nM are consistent with high mobility of these polymer chains[111].

In the case of polymethylhydrosiloxanes, $Me_3SiO[MeHSiO]_nSiMe_3$ (MD^H_nM), some of the long-range substituent chemical shifts are obscured[112]. These complications result from the asymmetry of the MeHSiO(D^H) unit. In the ^{29}Si NMR spectra the terminal trimethylsilyl (M) groups and the D^H moieties exhibit resonances in substantially different regions. Tacticity effects are essential in understanding the stereochemical features of substituted vinyl polymer chains. Tacticity and end group effects were used to interpret the observed fine structure in the proton decoupled spectrum of MD^H_5M, i.e. the appearance of a triplet and a doublet. Analogous features in the ^{29}Si NMR of MD^H_{50} M were explained as resulting from either complete atacticity or from the presence of equal amounts of oligomers of different tacticities.

Pai and coworkers[113] investigated in detail both the ^{29}Si chemical shifts and the first spin–lattice relaxation times reported of these systems (Table 12). The spin–lattice relaxation time (T_1) for all ^{29}Si nuclei were measured simultaneously by the

TABLE 12. ^{29}Si chemical shifts and T_1 values for polymethylhydrosiloxanes [δ^a, $(T_1)^b$]

Compound[c]	M	D^H_a	D^H_b	D^H_c	D^H_x
MD^H_3M	10.00(50)	−35.84(42)	−35.67		
		−35.87(42)	−35.70(30)		
			−35.72		
MD^H_4M	10.22(50)	−35.60(44)	−35.11(32)		
		−35.65(38)	−35.15(36)		
			−35.19(41)		
MD^H_5M	10.21(52)	−35.61(43)	−35.06(44)	−34.69(42)	
		−35.65(43)	−35.10(39)	−34.76(42)	
			−35.20(38)	−34.82(41)	
MD^H_6M	10.15(47)	−35.64(44)	−35.08	−34.72	
		−35.69(46)	−35.12(42)	−34.76(43)	
			−35.16	−34.81	
MD^H_7M	10.21(48)	−35.60(48)	−35.02	−34.65(35)	
		−35.64(43)	−35.06(41)	−34.66(35)	
			−35.10	−34.69(32)	
MD^H_8M	10.26(45)	−35.58(46)	−34.96	−34.56	
		−35.61(48)	−34.99(42)	−34.58(36)	
			−35.04	−34.60	
$MD^H_{35}M$	10.07(59)	−35.84	−35.15		−34.66(37)
		−35.87	−35.18		−34.70(37)
			−35.23		−34.75(37)

[a] chemical shifts (ppm).

[b] In seconds; experimentally determined T_1 values are given in parentheses.

[c] For the definition of the symbols, see the text. The D units are identified as follows: $MD^H_aD^H_bD^H_c\ldots$.

Reproduced by permission of Elsevier Science from Reference 113.

inversion-recovery pulse method [$(180^\circ - t - 90^\circ - T)_n$] under conditions of proton noise decoupling. The delay between the pulse sequence (T) was set at 300 s. The ^{29}Si spectrum of $\mathrm{MD}_n^{\mathrm{H}}\mathrm{M}$ ($n = 5$–8, 35) oligomers shows four distinct regions of absorption, M at 10.00 to 10.26 ppm, $\mathrm{D}_a^{\mathrm{H}}$ from -35.58 to -35.84 ppm, $\mathrm{D}_b^{\mathrm{H}}$ from -34.96 to -35.72 ppm and $\mathrm{D}_x^{\mathrm{H}}$ ($x = 3$ to $n - 2$) from -34.56 to -34.82. The predominant feature, a triplet at -34.66 to -34.75 ppm, can be assigned to the D^{H} groups which are three or more D^{H} groups away from the terminal M group of the oligomer. These coalesce to a triplet structure. Hence there is no detectable change in these chemical shifts and no new stereochemical effects for oligomers $\mathrm{MD}_n^{\mathrm{H}}\mathrm{M}$ beyond $n = 5$ (Figure 19).

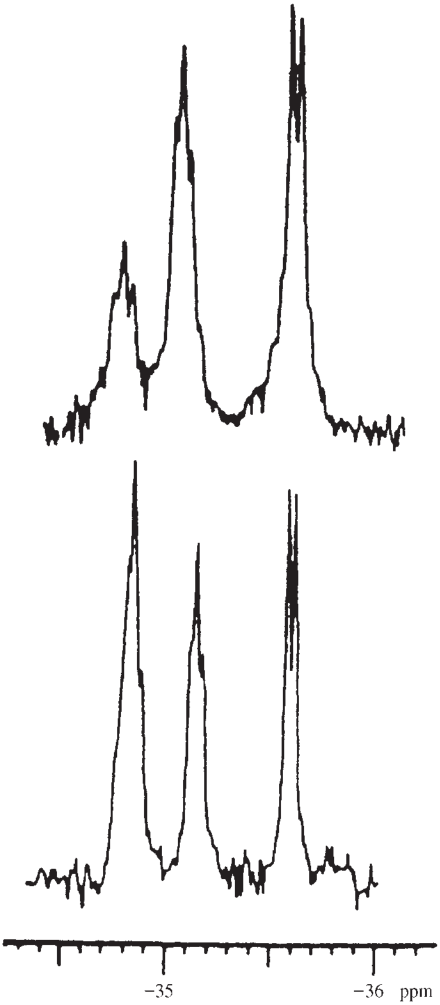

FIGURE 19. ^{29}Si {^{1}H} NMR of the D^{H} region of $\mathrm{MD_5{}^{H}M}$ (upper) and $\mathrm{MD_7{}^{H}M}$ (lower) oligomers. Reproduced by permission of Elsevier Science from Reference 113

The ^{29}Si spin–lattice relaxation times of these polymethylhydrosiloxanes were determined in order to provide information about their molecular motion. The general trends in T_1 values can be seen in Table 12. The T_1 for the M end groups are longest. The D_α^H units have longer relaxation times than those of more internal D^H units. It is reasonable that M has the longest T_1 because M units are able to spin freely at the ends of the chain while D^H units may only rotate through a restricted angle which obviously decreases their T_1 values. These values decrease gradually as the D^H units approach the middle of the chain. All D^H units have comparable relaxation times. This implies that the motional processes along the chains are similar. The relatively long values of T_1 make it clear that these systems are quite mobile. This is to be expected in the absence of crosslinking of linear MD_n^HM chains. Finally, the T_1 values of the different stereoisomers do not change significantly in oligomers and polymer systems. This implies that tacticity and chain length have little effect on the motion occurring in these systems. The ^{29}Si T_1 measurements on the series of MD_n^HM oligomers demonstrate that localized motions along segments of the oligomer backbone result in ^{29}Si relaxation that rapidly becomes independent of chain length.

For comparison, the T_1 values for the D^H groups in the MD_n^HM oligomers are consistently shorter than the T_1 values for the D groups in MD_nM oligomers. The Si–H groups present in the MD_n^HM oligomers provide a dipolar contribution to the relaxation mechanism which shortens the ^{29}Si T_1 relaxation times.

V. SOLID-STATE ^{29}Si NMR

A. Introduction

In recent years the literature has furnished a wealth of information concerning chemical structures from solid-state ^{29}Si NMR studies of crystalline and noncrystalline silicates and aluminosilicate, polysiloxanes, polysilanes and other organosilicon compounds.

Most spectroscopic techniques (e.g. infrared and Raman spectroscopy) provide a 'snapshot' view of the structure of a liquid because the timescale of the techniques is of the order of lattice vibration. However, NMR can probe much lower frequency motions, motions which are important in the glass transition and the viscosity of a silicate liquid. In addition, the timescale of the NMR experiment may be varied (by changing the magnetic field, or the type of experiment, T_1 or $T_{1\rho}$, or observing quadrupolar effects) from a few hertz to several hundred megahertz.

The advent of pulse Fourier Transform (FT) NMR techniques in the middle 1970s set the stage for the use of ^{29}Si NMR for qualitative and quantitative analysis in liquids. However, for solid samples the effects of ^{1}H–^{29}Si magnetic dipole–dipole interactions and ^{29}Si chemical shift anisotropies and the time bottleneck of long ^{29}Si spin–lattice relaxation times render the direct application of the liquid-state ^{29}Si NMR technique essentially useless yielding broad, featureless spectra of low intensity. For understanding the aspects for solid-state ^{29}Si NMR, those for solid-state NMR will be briefly presented.

Pines, Gibby and Waugh introduced the technique of high-power ^{1}H decoupling for eliminating the broadening effect of ^{1}H–^{13}C dipolar interactions, with ^{13}C–^{1}H cross-polarization (CP) to circumvent the ^{13}C T_1 bottleneck[114]. Schaefer and Stejskal[115] then introduced the use of magic angle spinning (MAS) to average out the ^{13}C chemical shift anisotropy[116,117] and demonstrated that the CPMAS combination provides an approach that is capable of yielding high-resolution ^{13}C NMR spectra of solid samples. Line widths of the order of 1 ppm or less can be achieved by this method on crystalline samples, often providing a higher order of structural discrimination than one can achieve in a corresponding liquid (e.g. because of motional averaging of different conformations in the liquid state)[118].

In solid-state high-resolution NMR spectra with MAS, line broadening due to chemical shift anisotropy and dipolar coupling is removed by magic angle spinning and rf irradiation, respectively, for attaining high resolution. Such anisotropy parameters, however, give information about static and dynamic molecular structures in more detail than isotropic chemical shifts do. In a static powder sample, an anisotropic interaction yields a peculiar line shape well known as a powder pattern[119], whose singularities give the principal values of the tensorial interaction. In general, however, the existence of some inequivalent nuclei results in an extensive overlap of their powder patterns, making interpretation almost impossible.

Alternatively, the spectral resolution can be increased at the expense of the angular resolution by MAS in particular in ^{29}Si NMR spectroscopy to allow discrimination between the different carbon residues in the sample. In order to retain the information about the anisotropic interactions, the spinning angular velocity ω_R must be low enough to produce a sufficient number of spinning sidebands[119]. The use of sideband patterns for studying molecular motions was demonstrated by Maricq and Waugh[120]. Not until 1986 was it realized how spinning sidebands can be exploited to study the degree of molecular alignment in partially ordered samples by applying two-dimensional NMR spectroscopy[121,122].

In fact, two-dimensional solid-state NMR is far superior to one-dimensional techniques for studying structure and dynamics[123]. In particular, the two-dimensional exchange NMR spectrum[124] of a static sample is identical with a two-time distribution function[125]. Thus a two-dimensional NMR spectrum, which is detected for a fixed mixing time, is an image of the state of the dynamic process under study at that time.

Experimental examples were first provided through ^{2}H NMR in powder samples of molecular crystals[126,127] and in polymers at their glass transition[128,129]. Switching-Angle Sample Spinning(SASS)[130,131] has some advantages: it can be applied to complex systems contrary to spinning side band analysis[132] or off-magic-angle spinning[133]; it requires no critical adjustments for the experimental parameters, contrary to the rotation-synchronized pulse methods, and, moreover, provides reliable principal values from nondistorted powder patterns.

Solid-state NMR methods allow the investigation of local orientation, dynamics and conformational order of polymer chain segments. ^{29}Si chemical shifts contain information about molecular moieties and about the conformation of chain segments. The line width of a ^{1}H wideline spectrum characterizes the strength of the dipolar couplings among protons and, therefore, the molecular mobility. ^{1}H spin diffusion, mediated by the homonuclear dipolar couplings, is a powerful technique to obtain information about the spatial proximity of molecular moieties. These concepts have recently been combined in a two-dimensional ^{1}H–^{13}C Wideline Separation Experiment (WISE-NMR spectroscopy) by Spiess and coworkers,[134]. They present the results of applying WISE-NMR and proton spin diffusion experiments to stiff macromolecules with flexible side chains. The WISE-NMR spectra demonstrate the existence of rigid and mobile side-chain domains and characterize them with respect to the predominant chain conformations and the local chain mobility. Proton spin diffusion experiments with ^{13}C detection are used to obtain morphological data, like the typical sizes of such domains. Under the normal conditions, to obtain a solid-state ^{13}C spectrum one might observe ^{29}Si signals. The other methods of obtaining ^{13}C NMR spectra are practical techniques for molecules containing multiple silicon atoms. These techniques would be applicable to a wide range of solid-state ^{29}Si NMR methods.

B. New Techniques

^{1}H–^{29}Si dipolar-dephasing experiments (Figures 20 and 21) indicate that various hydroxyl groups of silanols in silica gel undergo rapid ^{1}H spin exchange and that the most strongly coupled protons provide the dominant source of cross-polarization to geminal-silanol silicons. The ^{1}H–^{1}H dipolar dephasing prior to ^{1}H $\rightarrow$ ^{29}Si cross-polarization shows a rapid ^{1}H spin exchange between ^{1}H reservoirs of single-silanol groups and of geminal-silanol groups; however, the ^{1}H spin exchange rate is too fast to be measured by this strategy. A slower ^{1}H–^{1}H dipolar-dephasing decay due to ^{1}H spin exchanges is found for the ^{1}H spin reservoir of single-silanol groups[135].

Much of the power of MAS NMR has come from the ability of exploiting cross-polarization for facile signal detection and spectral editing for insensitive and rare-spin nuclei. To date, protons have almost invariably constituted the abundant-spin reservoir for cross-polarization experiments, although, most recently, ^{19}F has found increasing use.

There has been only a single CP study using any other nucleus (^{31}P) as the abundant-spin magnetization reservoir, but even that study benefited from the presence of highly abundant ^{1}H spins(which were detected). Thus, to date solid-state NMR spectroscopy of inorganic materials that are devoid of protons has been mostly limited to Bloch decay and spin echo studies. The spin–lattice relaxation times encountered in such systems are often excessively long, resulting in poor signal-to-noise ratios and long measurement times. Furthermore, the line shapes of disordered inorganic solids are frequently rather broad, poorly resolved and thus hard to interpret in the absence of spectral editing experiments.

Recently, various heteronuclear X–Y double resonance approaches have helped to increase the informational content of static and MAS NMR spectra of such systems. Frank and coworkers[136] demonstrate, for the first time, that cross-polarization from ^{31}P to insensitive ^{29}Si nuclei is possible in conjunction with MAS results in significant sensitivity enhancements, and can provide important insights into the structure of inorganic

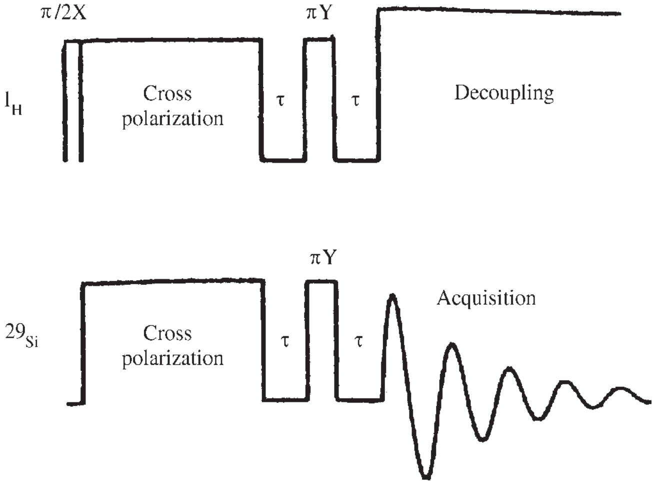

FIGURE 20. A ^{1}H–^{29}Si dipolar-dephasing ^{29}Si CPMAS NMR experiment. Reprinted with permission from Reference 135. Copyright 1992 American Chemical Society

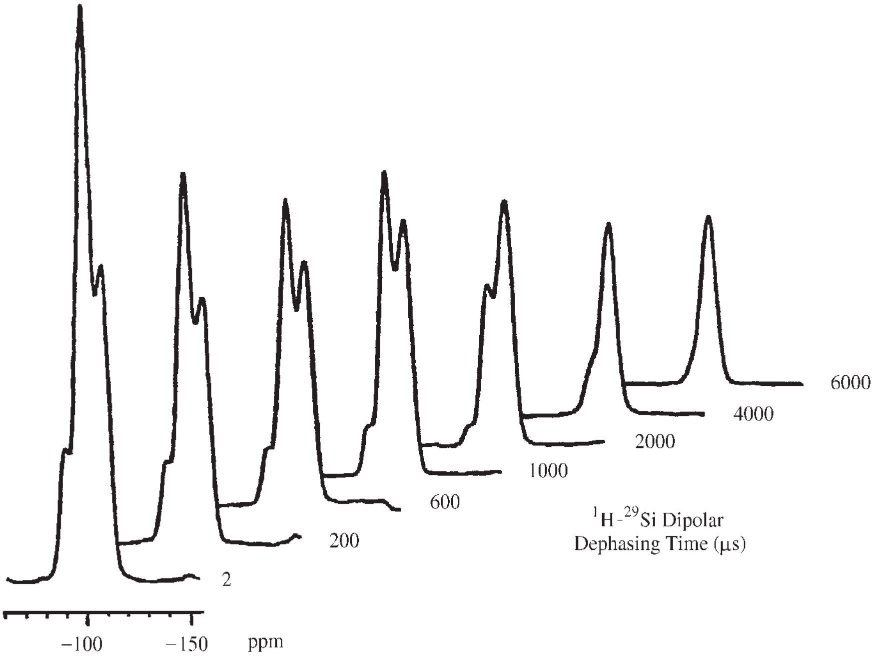

FIGURE 21. 39.75-MHz ^{1}H$-$^{29}Si dipolar dephasing ^{29}Si CPMAS NMR spectra of Fisher S-679 silica gel, with ^{1}H$-$^{29}Si dipolar-dephasing times shown. Cross-polarization contact times, 5 ms; magic angle spinning speed, 2.0 kHz. Each spectrum is the result of 3000 accumulations. Reprinted with permission from Reference 135. Copyright 1992 American Chemical Society

semiconductors. Figure 22 compares single-pulse ^{29}Si CPMAS NMR spectra obtained in crystalline $CdSiP_2$ with the corresponding ^{31}P$-$^{29}Si CPMAS NMR spectra, illustrating the expected sensitivity advantage of CPMAS NMR. This advantage is especially critical for the detection of the ^{29}Si nuclei which have excessively long spin–lattice relaxation times.

Silica gel has frequently been used as a convenient, inert, high-surface-area and non-swelling support that can be easily removed by filtration from the reaction medium if necessary. In these systems, the bonding of the reactant functionality, R, to the surface is via a bridging silicon attached to the silica surface by an Si—O—Si linkage. These functionalized silica gels are usually made by activating the silica surface to produce hydroxyl groups and then reacting it with a trichloro (or trialkoxy) silane. The reaction is often represented as in equation 16. However, the trifunctional silane can also be considered as a trifunctional monomer molecule that would polymerize to give a highly cross-linked polysiloxane polymer as in equation 17. Reaction 16 may be favored by making the system as anhydrous as possible, but this is difficult to do because of the hydrophilic nature of the silica surface, and in practice there may well be an unknown amount of self-condensation of the organosilane occurring, giving oligomeric polysiloxane species bonded to the surface, making the reproducibility of these reactions somewhat variable. Fyfe and coworkers[137] outline the use of an alternative preparation of functionalized materials of this general type and characterization of the systems formed by two-dimensional

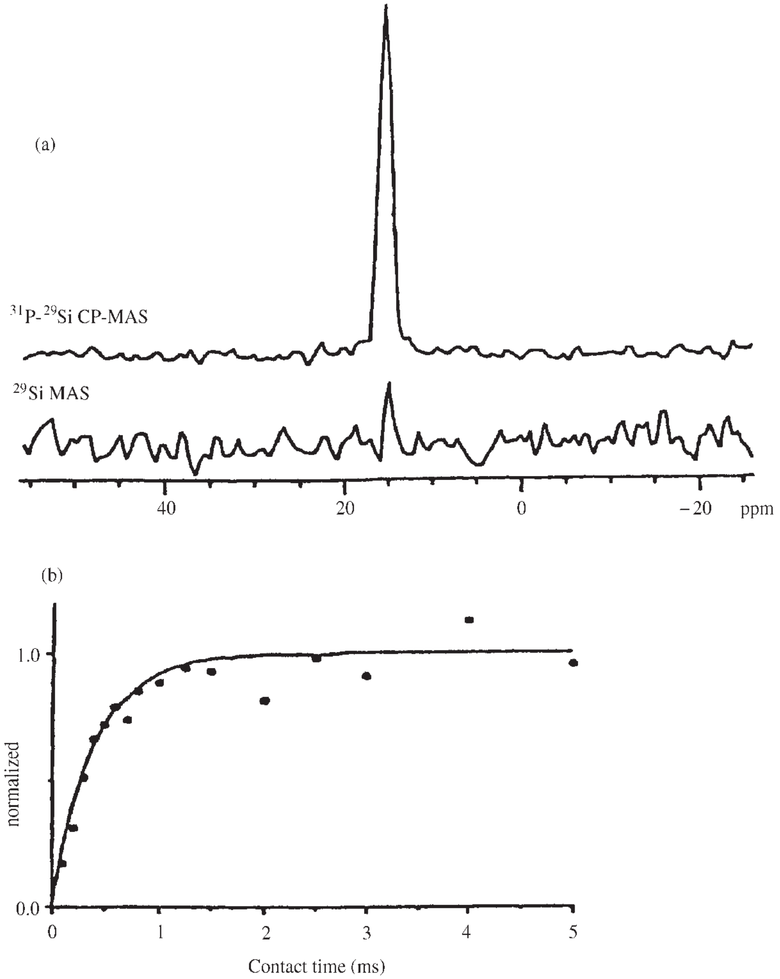

FIGURE 22. ^{31}P–^{29}Si CPMAS in crystalline $CdSiP_2$. (a) Comparison of single-pulse spectrum (bottom trace) and CPMAS spectrum (top trace). The spectrum is recorded by 16 scans with a 2-min relaxation delay and a single-pulse ^{29}Si spectrum (two scans, 15-min relaxation delay). The CPMAS contact times was 5.5 ms for the ^{29}Si detection. (b) Variable contact time ^{31}P–^{29}Si (MAS at 3.0 kHz) CPMAS experiment. The solid curve is a fit to an exponential cross-relaxation process time of 0.4 ms (^{31}P–^{29}Si). Reprinted with permission from Reference 136. Copyright 1992 American Chemical Society

solid-state NMR techniques.

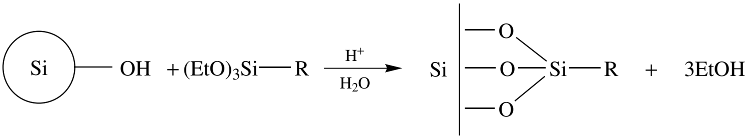

(16)

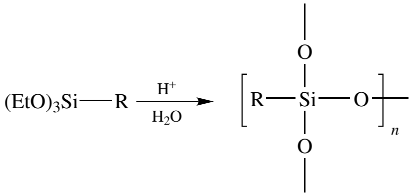

$$(EtO)_3Si\text{—}R \xrightarrow[H_2O]{H^+} \left[R\text{—}\overset{\overset{|}{O}}{\underset{\underset{|}{O}}{Si}}\text{—}O\right]_n \qquad (17)$$

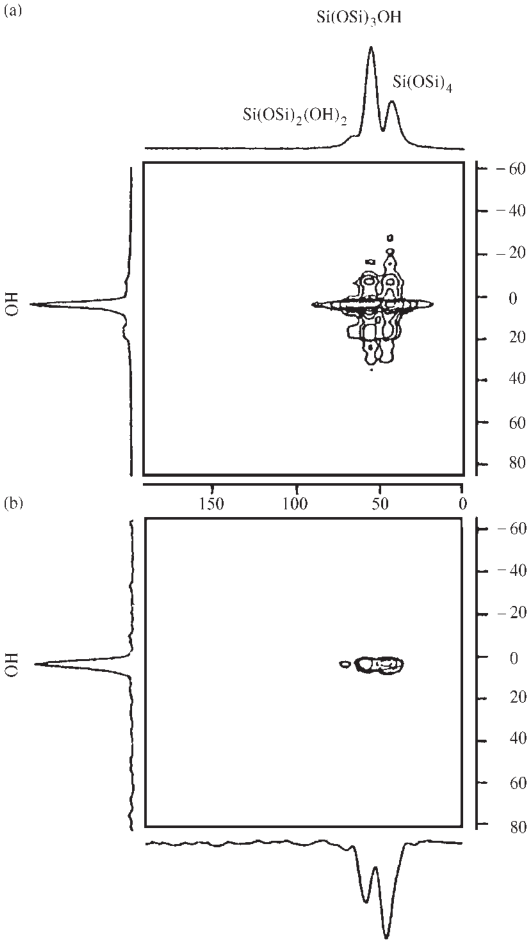

FIGURE 23. Contour plots of the 2D ^1H–^{29}Si correlation experiments on silica gel obtained with a 22.0 ms contact time, a 3.0 s repetition time and a 4.0 kHz sample spinning rate. The vertical axis represents the proton chemical-shift scale and the horizontal axis the ^{29}Si chemical-shift scale. The spectra above and at the side of the figures are the one-dimensional projections. The 2D spectrum was obtained from 64 individual experiments: (a) unwashed silica gel, 80 scans for each individual experiment; (b) D_2O washed sample, 200 scans for each experiment. Reprinted with permission from Reference 137. Copyright 1988 American Chemical Society

The viability of an experiment of this type between ^{1}H and ^{29}Si has previously been demonstrated by Vega[138]. At first sight, it might seem that this two-dimensional experiment would be limited by the same factors as the one-dimensional CP experiments. However, because the proton spins are relatively isolated MAS alone gives enough resolution to clearly distinguish the OH and Me signals, thus making it possible to identify the source of the polarization transfers. The isolation of the proton spins also limits ^{1}H–^{1}H spin diffusion. In addition, because there are two related frequency scales in the experiment, the chemical shift resolution is better than in the simple one-dimensional experiment. Figure 23 shows the results of the ^{1}H/^{29}Si connectivity experiments carried out on unfunctionalized silica gel using the experimental conditions detailed in the figure caption. The one-dimension spectra shown in the figure are projections of the data onto the F1 and F2 axes and can be used to establish the connectivities. However, the intensities of the signals do not reflect those of the corresponding 1D spectra.

In Figure 23a, the gel has not been deuterium-exchanged and an intense signal is observed due to OH protons in the ^{1}H projection. There is, as expected, a series of intense connectivities to the three silicon environments in the gel.

In Figure 23b, the gel has been exchanged twice with D_2O and dried at 100 °C, with considerable care being taken to avoid subsequent water adsorption. As can be seen from the figure, there is a very marked decrease in the intensity of the heteronuclear connectivity, but there is still a residual interaction arising from the trace amounts of hydroxy protons indicated in the projection of F1. It is this situation that leads to the possible ambiguities in the one-dimensional experiments described above.

Figure 24 shows experiments carried out on a simple physical mixture of unfunctionalized silica gel and polymethylsiloxane whose one-dimensional ^{29}Si MAS NMR spectrum is shown in Figure 25. In this case, there should be no connectivity between the methyl protons and any of the silicon nuclei in the gel. Figure 24a shows the experimental results when no deuterium exchange has been carried out. There are clear connectivities to both groups of silicon. In the case of the lower-field methyl-substituted silicon signal, the connectivity is mainly from the methyl protons, and there is substantial intensity from spinning sidebands consistent with this. In the case of the three high-field signals due to the silica gel, the connectivities must be to hydroxyl protons, as is borne out by the limited sideband pattern. Most importantly, however, the sources of polarization can be unambiguously identified from the chemical shifts. Thus, as indicated in the figure, the two different sets of silicon nuclei are polarized from two distinct proton sources: methyl groups for the polymethylsiloxane and hydroxyl groups for the silica gel. The projection on F1 identifies their proton chemical shifts as $\delta = 0.45$ ppm and $\delta = 1.9$ ppm, respectively. Consistent with this interpretation, D_2O exchange of the mixture removes the connectivities to the silica gel, while a very strong connectivity to the polymethylsiloxane silicons with its associated sideband pattern remains (Figure 24b).

The layered alkali metal silicate magadiite (Figure 26) is analyzed by solid-state 2D MAS NMR techniques (Figure 27). The ^{1}H peak at δ3.5 can be attributed to water molecules, whereas that at δ14.9 must arise from strongly hydrogen-bonded protons that presumably involve −Si−OH groups in unusual environments. The ^{29}Si projection spectrum consists of four peaks at δ−99.2, −109.5, −111.2 and −113.6. These can confidently be assigned to one Q3 site and three Q4 sites respectively. It has been proposed that the three Q4 sites may differ by their average Si−O−Si bond angles.

C. NMR and X-ray Studies

^{29}Si shielding tensor information may reflect the structure of organosilicon compounds while the structure might have been determined by X-ray crystallographic analysis. Thus,

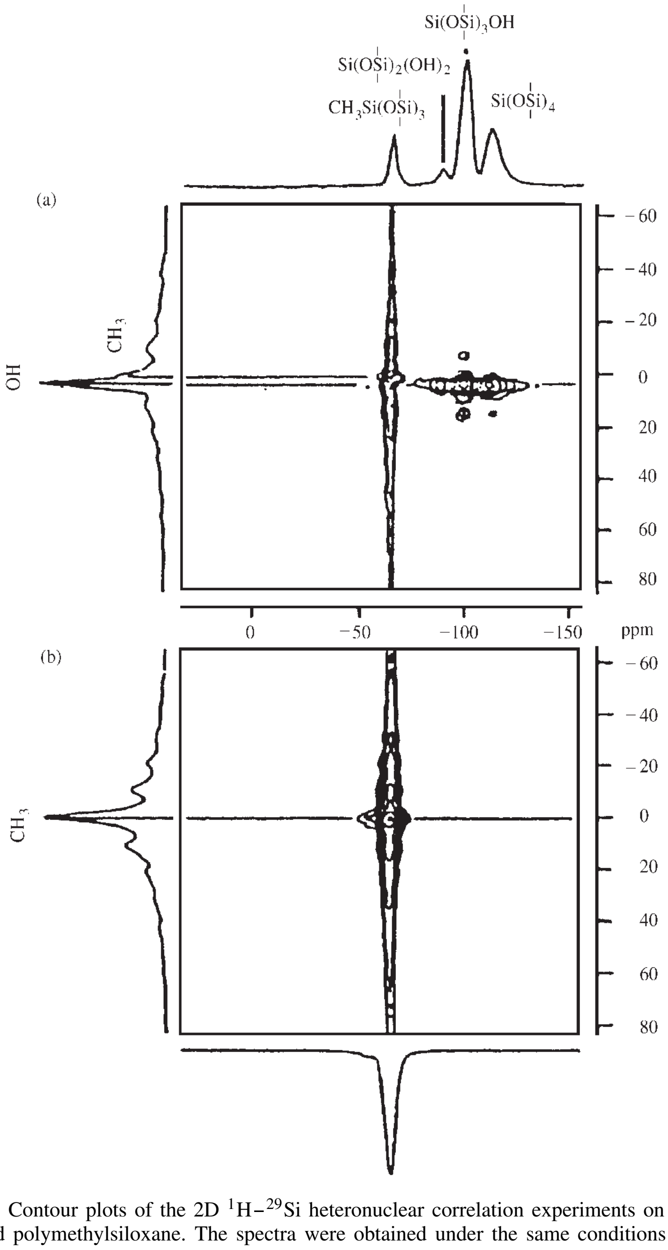

FIGURE 24. Contour plots of the 2D $^1H-^{29}Si$ heteronuclear correlation experiments on a mixture of silica gel and polymethylsiloxane. The spectra were obtained under the same conditions described in Figure 23: (a) untreated sample, 120 scans for each individual experiment: (b) D_2O washed sample, 200 scans for each individual experiment. The spinning rate used (4.3 kHz) was high enough to prevent overlap of spinning sidebands and isotropic peaks between the two sets of resonances. Reprinted with permission from Reference 137. Copyright 1988 American Chemical Society

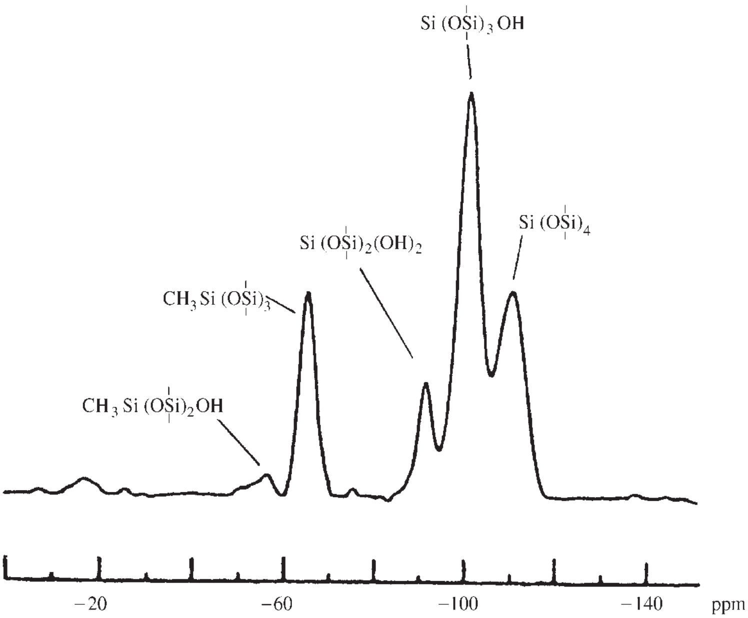

FIGURE 25. ^{29}Si CPMAS NMR spectrum of mechanical mixture of silica gel and polymethylsiloxane. Reprinted with permission from Reference 137, Copyright 1988 American Chemical Society

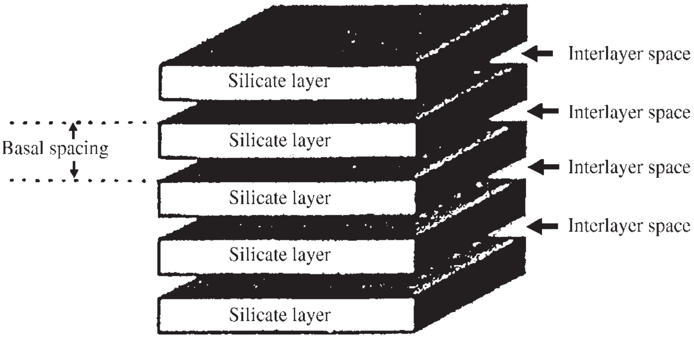

FIGURE 26. A schematic diagram of the layered alkali metal silicate magadiite. Reproduced by permission of the Royal Society of Chemistry from Reference 139

much work has been concerned with the measurement of isotropic chemical shift, and the correlation of these with various structural parameters. One difficulty with such an approach is that, in rapid magic-angle spinning experiments, only the isotropic part of the second-rank shielding tensor (σ) is generally obtained for ^{29}Si since shielding anisotropies are relatively small (less than 50 ppm in magnitude, which is smaller than typical spinning rates). Information concerning the principal compounds is lost. Harris and coworkers[140] have used slow MAS (i.e. at rates of *ca* 200 Hz) in order to obtain extensive spinning sideband manifolds from which shielding tensor components can be derived. The

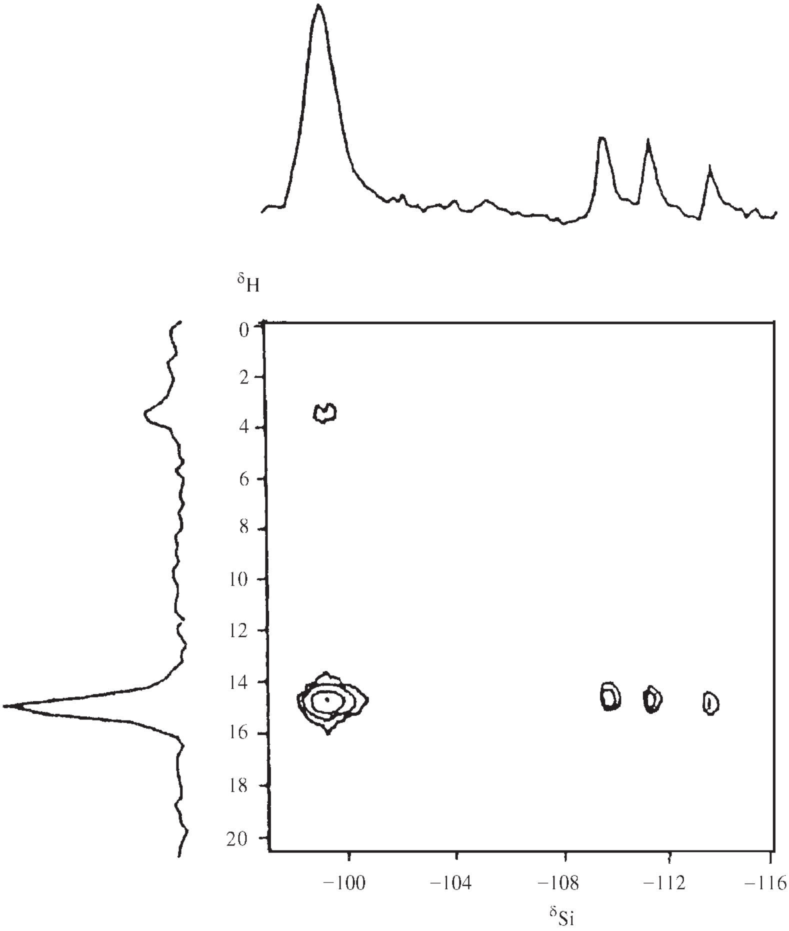

FIGURE 27. Two-dimensional $^{1}H-^{29}Si$ correlation spectrum (contour mode) of carefully-dried magadiite. Experimental conditions: recycle time 0.5 s, contact time 8 ms, number of experiments 128, number of transients per t_1 point 432, spinning rate 4.87 kHz. ^{1}H and ^{29}Si projections are shown along the axes. Reproduced by permission of the Royal Society of Chemistry from Reference 139

determination of the principal components of the tensor σ is important for several reasons. Firstly, it may help to provide a better explanation for and physical description of the trends observed in ^{29}Si chemical shifts. Secondly, the tensor components provide data which may be used to test theories of shielding. Finally, shielding tensor information may give evidence of molecular motion. They presented results on the isotropic chemical shifts and ^{29}Si shielding tensor components for a number of organosilicon compounds, in an attempt to investigate the various factors which influence the shielding anisotropy observed.

It is assumed that shielding is the only magnetic influence on spinning sideband intensities. The isotropic chemical shift $\sigma_{iso} = -\delta$ Si/ppm is defined as equal to one-third of the trace of the shielding tensor (Trσ/3). The principal values of the shielding tensor (σ_{11},

TABLE 13. ^{29}Si shielding tensor data for organosilicon compounds[a]

Compound	δ (^{29}Si) (ppm)		$\Delta\sigma$	σ_{11}	σ_{22}	σ_{33}	η[b]
	solution	solid	(ppm)	(ppm)	(ppm)	(ppm)	
$Ph_3Si{-}\mathit{Si}Me_3$	−18.4(23)	−18.9	21.9	11.6	11.6	33.5	0.00
$Ph_3\mathit{Si}{-}SiMe_3$	−21.0(23)	−21.0	−33.6	32.2	32.2	−1.4	0.00
$Ph_3Si{-}SiPh_3$	−26.61(24)	−25.4	−25.4	37.2	37.2	1.8	0.00
$Ph_3Si{-}O{-}SiPh_3$	−18.5	−17.0	27.9	1.5	13.9	35.6	0.67
Ph_3SiH	−21.1(25)	−21.4	45.0	−0.4	13.2	51.4	0.45
Ph_8Si_4	−20.93(26)	−24.2	−44.8	51.7	26.6	−5.7	0.84
$(PhCH_2)_3SiH$	−3.83(27)	−4.5	11.6	−2.8	4.1	12.2	0.90

[a] The errors in σ_{11} values are typically *ca* ± 2 ppm.

[b] A typical error in η is ±0.1.

Reproduced by permission of the Royal Society of Chemistry from Reference 140.

σ_{22} and σ_{33}) are designated by equation 18.

$$|\sigma_{33} - \sigma_{\text{iso}}| \geqq |\sigma_{11} - \sigma_{\text{iso}}| \geqq |\sigma_{22} - \sigma_{\text{iso}}| \tag{18}$$

The shielding anisotropy ($\Delta\sigma$) is defined by equation 19

$$\Delta\sigma = \sigma_{33} - (\sigma_{11} + \sigma_{22})/2 \tag{19}$$

and the asymmetry parameter (η) by equation 20

$$\eta = (\sigma_{22} - \sigma_{11})/(\sigma_{33} - \sigma_{\text{iso}}) \tag{20}$$

The results of these studies are summarized in Table 13. Some typical ^{29}Si CPMAS NMR spectra are displayed in Figures 28–30.

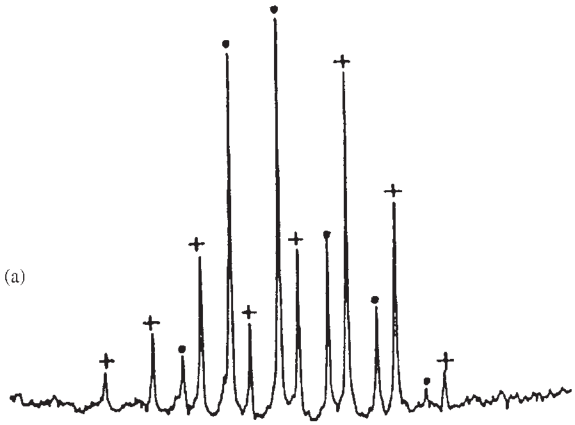

FIGURE 28. 39.758-MHz CPMAS ^{29}Si NMR spectrum of solid 1,1,1-trimethyltriphenyldisilane. (a) Slow spinning (206 Hz). (b) Fast spinning (3.2 kHz). The two spinning sideband manifolds in (a) are indicated by different symbols. Experimental conditions: contact time 8 ms, recycle time 10 s, number of transients 2090 (a) and 405 (b). Reproduced by permission of the Royal Society of Chemistry from Reference 140

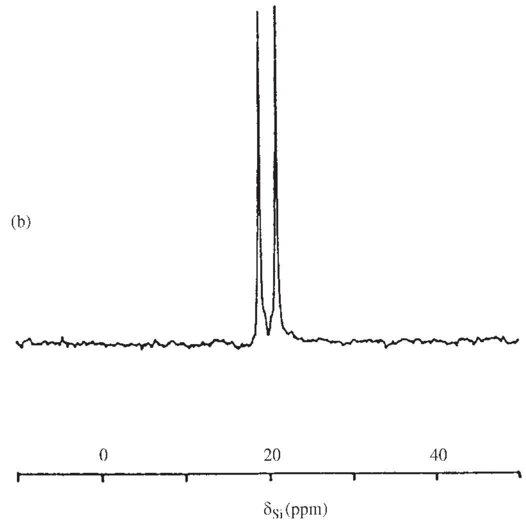

FIGURE 28. (*continued)*

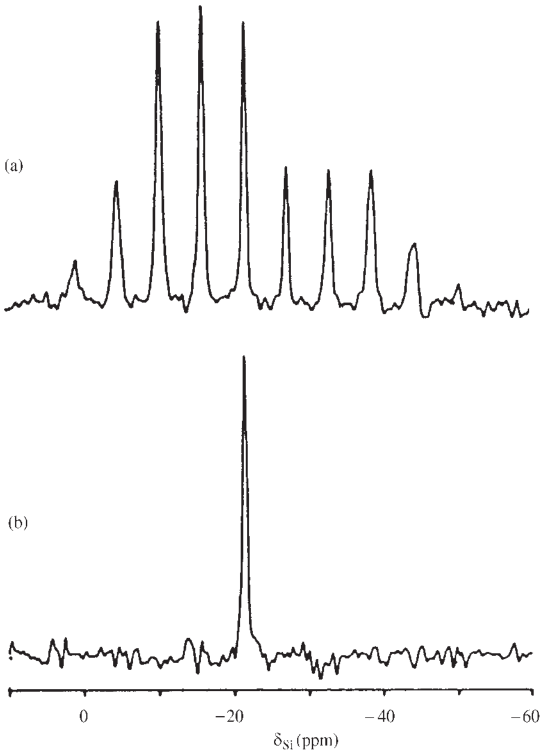

FIGURE 29. 39.758-MHz CPMAS ^{29}Si NMR spectrum of solid triphenylsilane. (a) Slow spinning (228 Hz). (b) Fast spinning (3.1 kHz). Experimental conditions: contact time 3 ms, recycle time 30 s, number of transients 1782 (a) and 24 (b). Reproduced by permission of the Royal Society of Chemistry from Reference 140

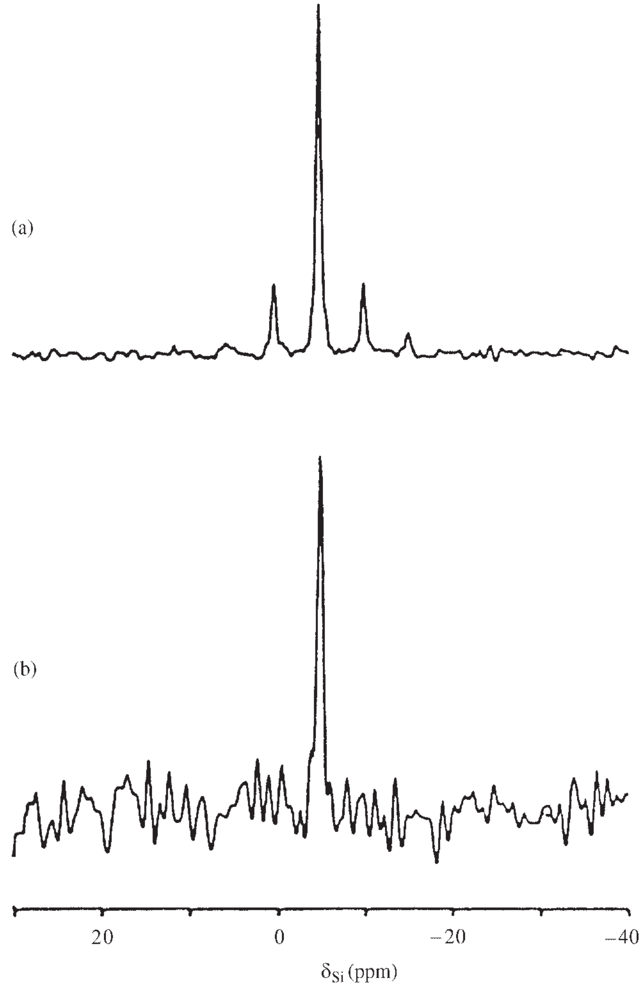

FIGURE 30. 39.758-MHz CPMAS ^{29}Si NMR spectrum of solid tribenzylsilane. (a) Slow spinning (196 Hz). (b) Fast spinning (3.2 kHz). Experimental conditions: contact time 1 ms, recycle time 30 s, number of transients 1480 (a) and 170 (b). Reproduced by permission of The Chemical Society from Reference 140

It is noticeable that the isotropic chemical shifts of the molecules do not change appreciably from the solution to the solid state. Therefore, effects caused by intermolecular interactions may be considered as negligible, and there are no major structural changes with phase. The ^{29}Si CPMAS spectra displayed two resonances at −18.9 and −21.0 ppm, which were assigned to silicon nuclei present within the Me_3Si and Ph_3Si moieties, respectively. The crystal structure of this compound has been published. It has space group P_3 and the asymmetric unit has been shown to consist of one molecule. Each of the silicon nuclei lies on an axis of C_{3v} symmetry. Hence slow-spinning ^{29}Si CPMAS NMR experiments reveal spinning sideband manifolds resulting from axially symmetric shielding tensors. The results (Table 13) obtained in this work are a positive anisotropy being observed for the Me_3Si while a negative anisotropy is seen for the silicon atom of the Ph_3Si group. Figure 31 summarizes the data on shielding tensor components for the six compounds studied. It is remarkable that for the four results involving Ph_3Si groups, the value of the lowest shielding component varies only to a small extent (within the range −1.5 to +1.8 ppm) whereas the other components vary widely. The relatively constant component is known to be directed along the Ph_3Si axis in two of the cases. However, the atom to which this group is bonded differs, being Si for the two disilanes, O for the disiloxane and H for triphenylsilane.

The low-temperature reaction (Figure 32) of (*E*)-1,2-dimesityl-1,2-di-*t*-butyldisilene **(52a)** with dioxgen gives (*E*)-1,2-dimesityl-1,2-di-*t*-butyl-1,2-disiladioxethane **(53a)**, the structure of which has been established by X-ray crystallographic analysis (Figure 33).

This result establishes that both oxidation of **52a** and rearrangement of **53a** to 1,3-cyclodisiloxane **55a** take place with retention of configuration at silicon. Disiladioxethane **53a** forms monoclinic crystals with space group C2/c. Extra electron density found above

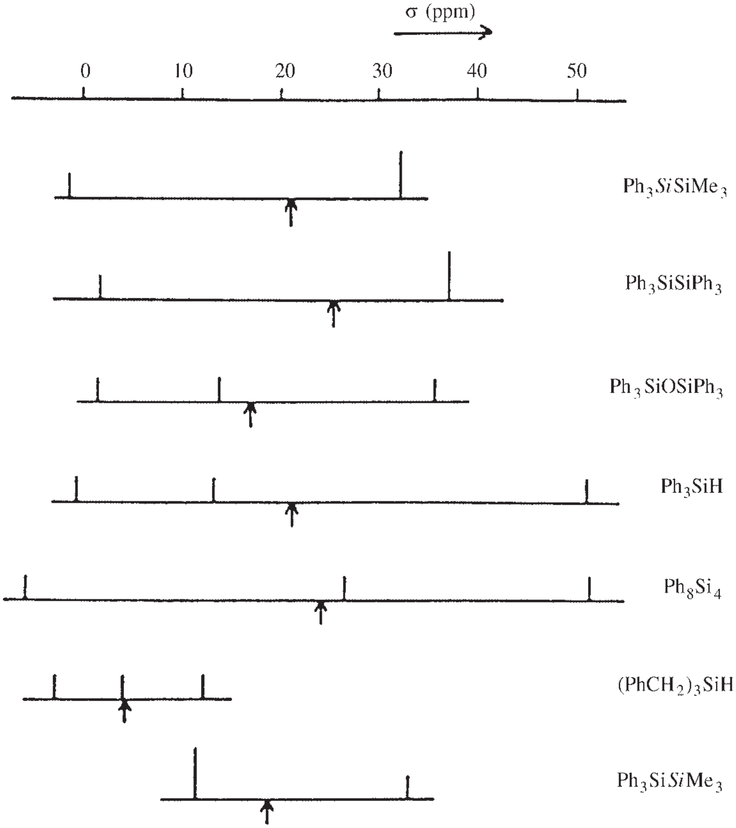

FIGURE 31. Summary chart of the principal components for the ^{29}Si shielding tensors of the compounds studied. Axial symmetry is indicated by the double intensity of lines at $\sigma_\perp$. The arrows indicate the isotropic values. The shielding scale is relative to the isotropic value for tetramethylsilane. Reproduced by permission of the Royal Society of Chemistry from Reference 140

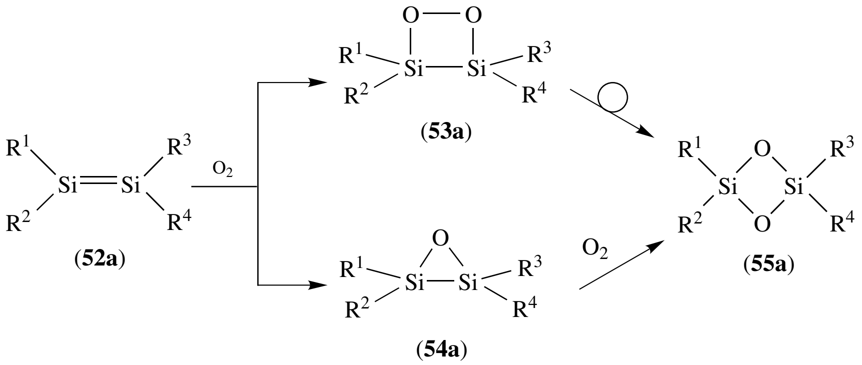

FIGURE 32. Oxidation of disilenes with $^3O_2$. Reprinted with permission from Reference 141. Copyright 1992 American Chemical Society

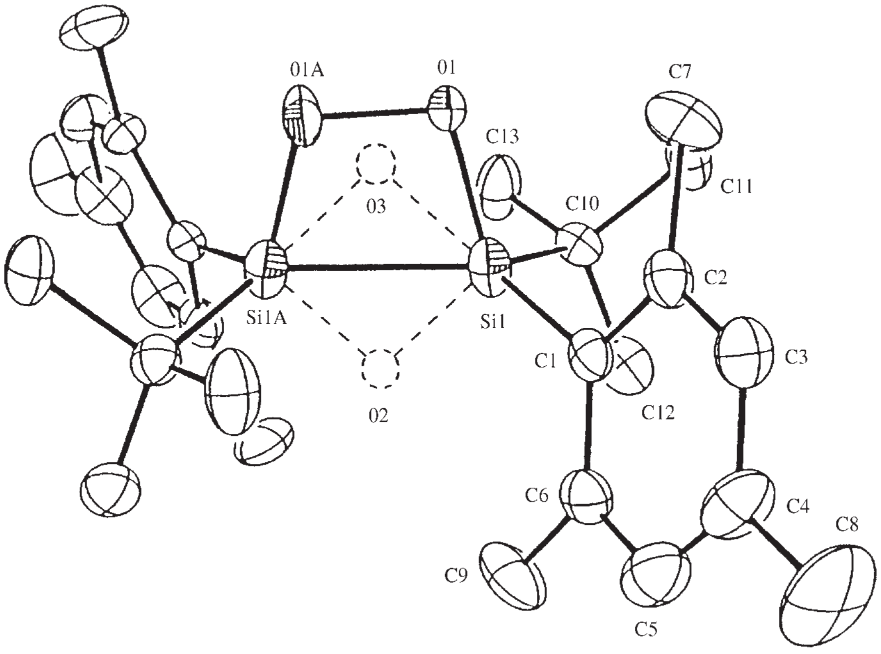

FIGURE 33. Thermal ellipsoid drawing of the crystal structure of 1,2-dimesityl-1,2-di-*t*-butyldisiladioxethane **(53a)** with hydrogen atoms omitted for clarify. Dotted lines indicate the 5.6% **55a** present. Selected bond distances (pm) and angles (deg) are as follows: Si(1)−Si(1A), 233.1(2); O(1)−O(1A), 148.2(5); Si(1)−O(1), 173.2(3); Si(1)−C(10), 189.4(3); Si(1)−C(1), 188.7(4); Si(1)−O(3), 170.2(2); Si(1)−O(2), 170.2(2); Si(1A)−Si(1)−O(1), 75.5(1); Si(1)−O(1)−O(1A), 103.7(1); Si(1)−O(3)−Si(1A), 86.5(1); Si(1)−O(2)−Si(1A), 86.4(1); O(3)−Si(1)−O(2), 93.6(1); C(10)−Si(1)−Si(1A), 123.0(1); C(1)−Si(1)−C(10), 112.9(2); C(1)−Si(1)−Si(1A), 119.5(1). Reprinted with permission from Reference 141. Copyright 1992 American Chemical Society

TABLE 14. ^{29}Si NMR chemical shifts δ (ppm) for **53** and **55**

System	Substitution[a]	**53**	**55**
a	$R^1 = R^4 =$ Mes; $R^2 = R^3 = t$-Bu	+54.80	+13.22
b	$R^1 = R^2 = R^3 = R^4 =$ Mes	+41.37	−3.35
c	$R^1 = R^2 = R^3 = R^4 =$ Xyl	+40.96	−3.30
d	$R^1 = R^2 = R^3 = R^4 =$ Dmt	+41.19	−2.46
e[b]	$R^1 = R^2 =$ Mes; $R^3 = R^4 =$ Xyl	+41.46, +40.67	−3.63, −2.33
f[c]	$R^1 = R^2 = R^3 =$ Xyl; $R^4 =$ Mes	+41.26, +40.77	−3.49, −2.75
g	$R^1 = R^3 =$ Mes; $R^2 = R^4 =$ Xyl	+41.16, +41.15	
h	$R^1 = R^3 =$ Ad; $R^2 = R^4 =$ Mes	+49.10	+8.1

[a] Mes = 2,4,6-trimethylphenyl, Xyl = 2,6-dimethylphenyl, Dmt = 2,6-dimethyl-4-(*t*-butyl)phenyl, Ad = 1-adamantyl.

[b] ^1J(SiSi) = 98 Hz for **52e**.

[c] ^1J(SiSi) = 94 Hz for **52f**.

Reproduced by permission of the American Chemical Society from Reference 141.

and below the Si−Si bond was shown by ^{1}H and solid-state ^{29}Si NMR to be due to **55a** (Table 14), arising from rearrangement of **53a** in the solid[141]. In the presence of phospines or sulfides, **53a** is partly deoxygenated to form disilaorirane **54a**, which was characterized by means of ^{29}Si NMR.

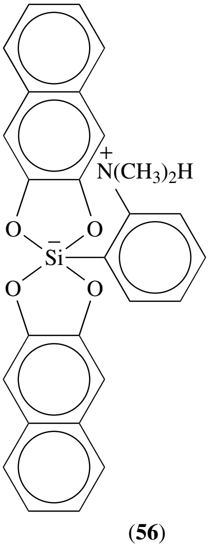

(**56**)

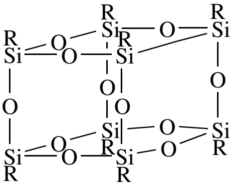

(**58**)

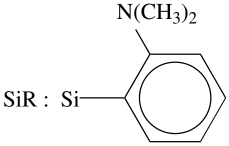

The zwitterion λ^5-spirosilicate bis[2,3-naphthalendiolato][2-(dimethylammonio)phenyl]silicate (**56**; isolated as **57** = **56**•1/2 MeCN) was synthesized by reaction of [2-(dimethylamino)phenyl]dimethoxyorganosilanes with 2,3-dihydroxynaphthalene in acetonitrile at room temperature. Reaction of **57** or of [2-(dimethylamino)phenyl]trimethoxysilane with water in acetonitrile yielded the cage-like silasesquioxane **58** ($R = 2 - \mathrm{Me_2NC_6H_4}$). The crystal structures of **57** and **58** were studied by X-ray diffraction. In addition, **57** and **58** were characterized by solid-state ^{29}Si CPMAS NMR[142] (Figure 34).

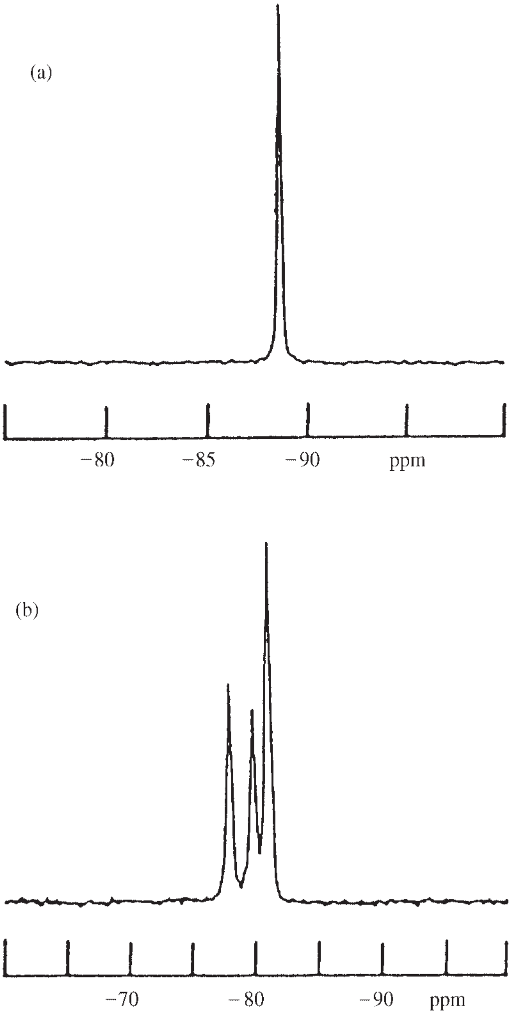

FIGURE 34. ^{29}Si CPMAS NMR spectra of **57** (a) and **58** (b). (a) δ^{29}Si $= -88.6$, $\nu_{1/2} = 12$ Hz, (b) δ^{29}Si $= -77.9, -79.7, -80.9$. Reproduced by permission of Johann Ambrosius Barth from Reference 142

D. Relaxation Times

Understanding of the physical chemistry of silicate liquids is important in both earth sciences and materials science: the chemical and physical behavior of magmas dominates many geological processes, and most technological glasses and glass ceramics start off in the molten state. The ability of NMR measurements to give information about the dynamics of systems (as well as about their structure) through the measurement of relaxation times and line shapes over a range of temperature is well known. Farnan and Stebbins[143] have applied a variable-temperature study over a temperature range of 1200 °C to silicate systems with different SiO_2 contents. Samples were prepared with SiO_2 which was enriched to 95% in ^{29}Si and high-purity Na_2CO_3, Al_2O_3, K_2CO_3, Li_2CO_3. These samples were albite ($NaAlSi_3O_8$) and potassium tetrasilicate ($K_2Si_4O_9$) glasses, and a mixture of crystalline lithium orthosilicate and metasilicate (Li_4SiO_4/Li_2SiO_3) with a near-eutectic composition. Each represents a different bridging and nonbridging oxygen distribution, from framework Q^4 (albite) to Q^2 and Q^0 (lithium orthosilicate/metasilicate). In the Q^n nomenclature, n refers to the number of oxygens per SiO_4 unit (Q) which are shared with another SiO_4 unit. The glass samples were made by heating stoichiometric amounts of their components to about 1200 °C above the melting point for several hours; they were then quenched, reground and remelted until homogeneous. The crystalline sample was made by slow cooling from the melt. In each preparation the weight loss at each stage was carefully monitored to ensure that there was only a negligible loss

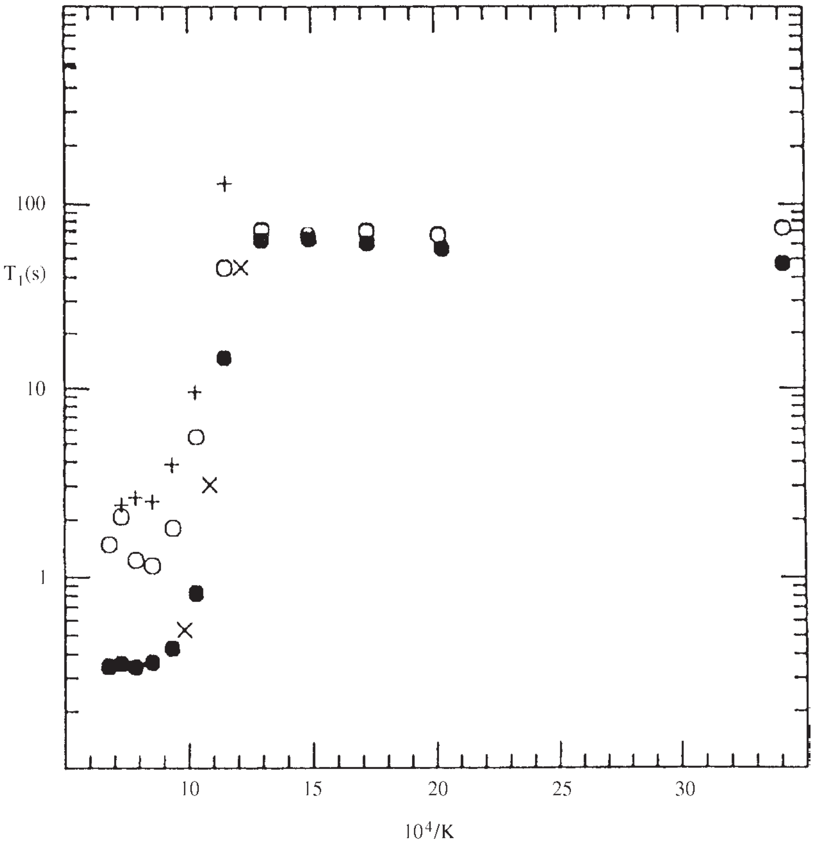

FIGURE 35. ^{29}Si T_1 versus inverse temperature for potassium tetrasilicate glass: undoped sample measured with increasing temperature (○), undoped sample measured with decreasing temperature (+); sample doped with 500 ppm Fe_2O_3 measured with increasing temperature (●); measured with decreasing temperature (×). Reprinted with permission from Reference 143. Copyright 1990 American Chemical Society

of alkalis. High-temperature (up to 1250 °C) ^{29}Si NMR T_1 and line-shape measurements were conducted on silicate samples with varying SiO_2 contents. The samples represented a range of bridging and nonbridging oxygen distributions from Q^4 in albite ($NaAlSi_3O_8$) to Q^2 and Q^0 in a mixture of lithium orthosilicate and metasilicate (Li_4SiO_4/Li_2SiO_3). T_1 relaxation data as a function of temperature for glassy samples showed a dramatic increase in efficiency at the glass transition (Figure 35). This was ascribed to relaxation by paramagnetic impurities becoming more efficient as silicon nuclei and impurity ions begin to diffuse through the material at temperatures above T_g.

In each sample chemical exchange was observed at high temperature, indicating that the lifetime of a silicate tetrahedron in the melt is short on the NMR timescale, i.e. a few microseconds. Variable-temperature line-shape data for potassium tetrasilicate ($K_2Si_4O_9$) allowed the exchange process to be modeled and spectra to be simulated (Figures 36 and 37) yielding an activation energy for the process. This was in good agreement with the activation energy for viscous flow derived from viscosity measurements. It appears that

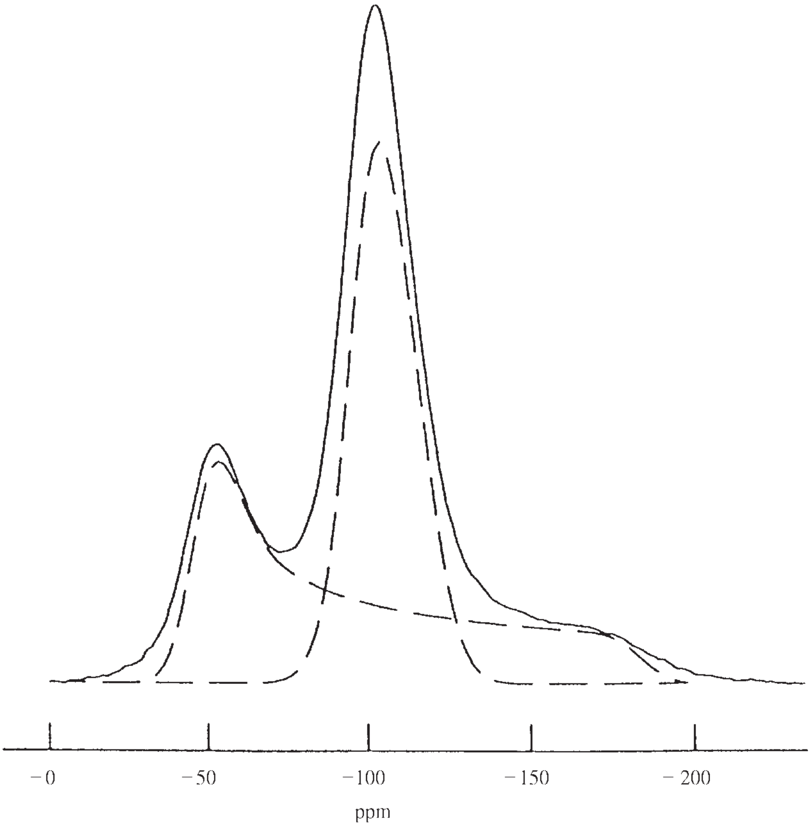

FIGURE 36. ^{29}Si NMR spectrum of potassium tetrasilicate glass (doped with 500 ppm of Fe_2O_3) at 20 °C: 128 pulses ($\pi/2$) with a delay of 300 s. The dashed lines show the two resonances (Q^3 and Q^4) which compose the total line shape. Reprinted with permission from Reference 143. Copyright 1990 American Chemical Society

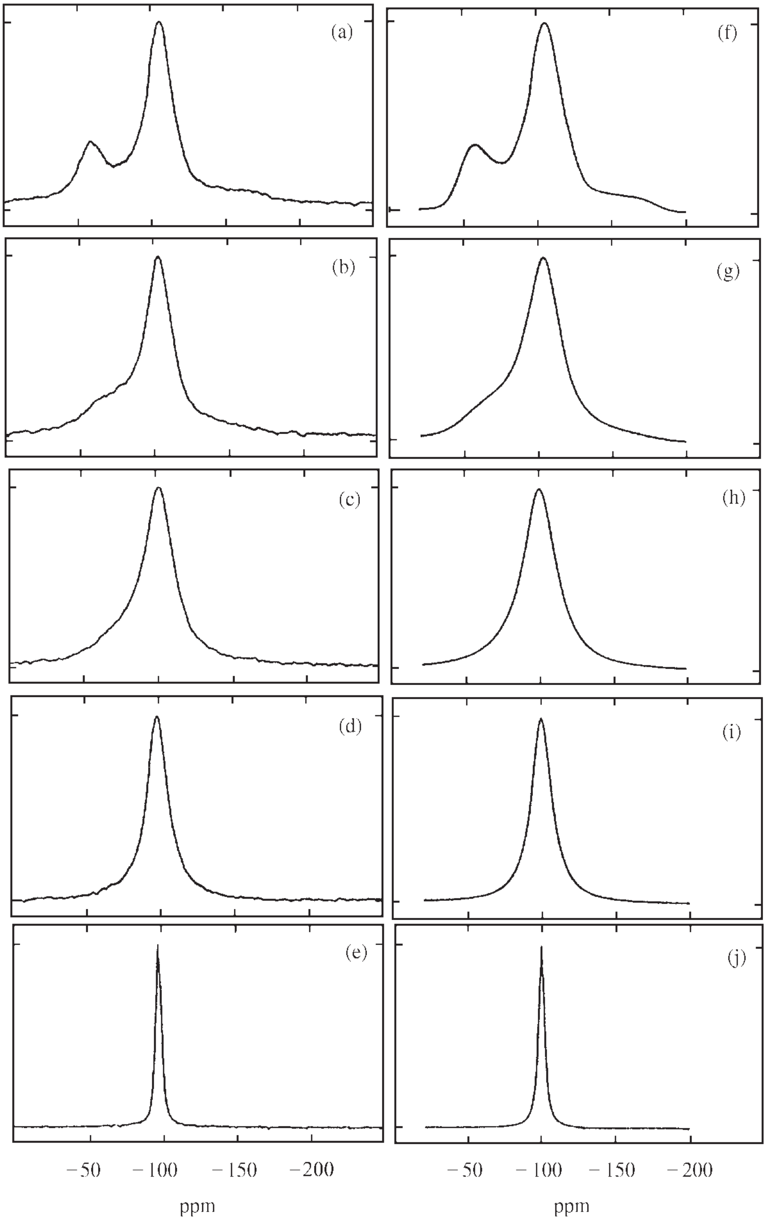

FIGURE 37. ^{29}Si NMR spectra (a−e) of potassium tetrasilicate glass and simulations (f−j). Spectra were recorded with 64 pulses ($< \pi/6$) and delays determined from the T_1 data at (a) 697 °C, (b) 774 °C, (c) 800 °C, (d) 847 °C, (e) 997 °C. Simulations of these spectra were judged 'by eye' to be the best match with exchange rates of (f) 2,000 Hz, (g) 10,000 Hz, (h) 25,000 Hz, (i) 50,000 Hz, (j) 500,000 Hz. Reprinted with permission from Reference 143, Copyright 1990 American Chemical Society

^{29}Si NMR comes close to detecting the fundamental step in viscous flow in silicates with good agreement between the time constant of the exchange process determined by NMR and the shear relaxation time of the $K_2Si_4O_9$ liquid.

High-resolution ^{29}Si NMR spectra and ^{29}Si NMR relaxation times of a polysiloxane containing rigid groups, namely copoly(tetramethyl-*p*-silaphenylenesiloxane/dimethylsiloxane) (CPTMPS/DMS) (equation 21) in the solid state, were measured over a wide range of temperature in order to obtain information about the conformation and dynamics[144]. The ^{29}Si T_1 values of CPTMPS/DMS in the solid state using the inversion recovery method at −90, −60, −30, 27 and 80 °C were determined. Figure 38 shows the ^{29}Si stack spectrum of CPTMPS/DMS at 80 °C. The plots of ^{29}Si T_1 against 1/T (K^{-1}) for the TMPS (tetramethyl-*p*-silaphenylene siloxane) and DMS (dimethylsiloxane) moieties from −90 to 80 °C are shown in Figure 39.

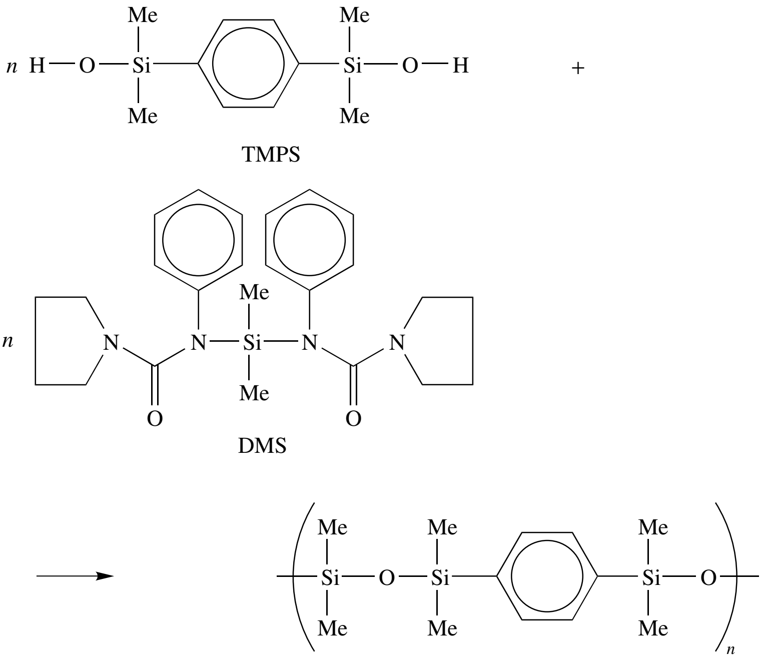

(21)

The T_1 value for the TMPS moiety decreased as the temperature increased from −90 to 80 °C. This indicates that the molecular motion is in the slow-motion region in this temperature range. However, the T_1 value for the DMS moiety is increased as the temperature is increased from −67 to 80 °C, becomes a minimum at −67 °C and is increased again as the temperature is decreased from −67 to −90 °C. This indicates that the molecular motion is in the extreme narrow region above −67 °C. The copolymer retains both rigid and soft parts in the main chain.

E. Dynamics

Solid-state NMR experiments showed the dynamic nature of the disordering. It has been possible to monitor the type and the changes of segmental motions within the mesomorphic phase and at the corresponding phase transitions for typical examples. The thermal

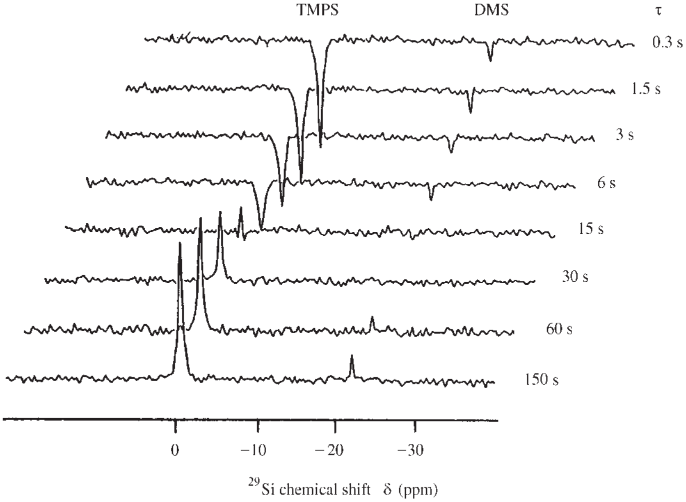

FIGURE 38. ^{29}Si GHDMAS NMR spectra of CPTMPS/DMS in the solid state at 80 °C using the inversion recovery method (180° — τ — 90° — 150 s) as a function of τ. Reproduced by permission of Elsevier Science from Reference 144

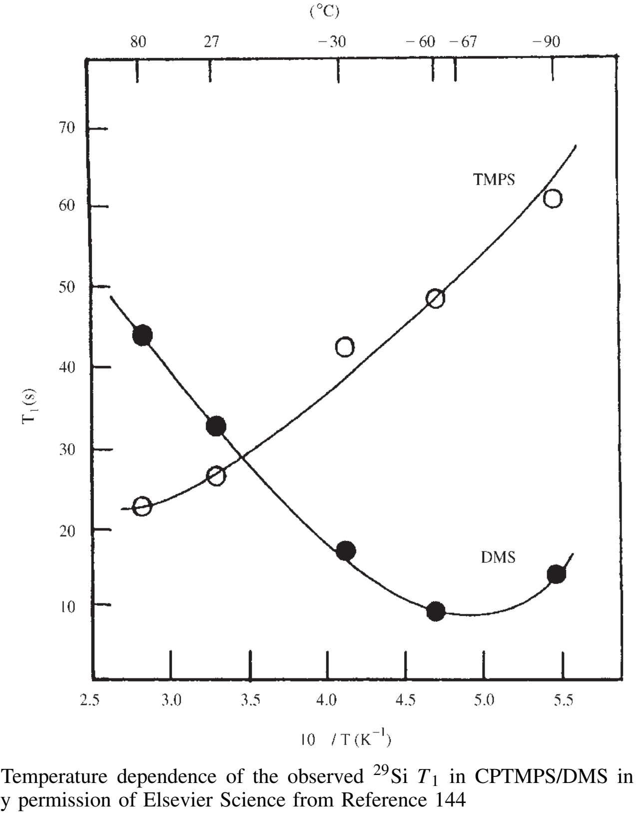

FIGURE 39. Temperature dependence of the observed ^{29}Si T_1 in CPTMPS/DMS in the solid state. Reproduced by permission of Elsevier Science from Reference 144

behavior of poly(diethylsiloxane) (PDES)[145] is summarized schematically in Figure 40. High-resolution solid-state ^{29}Si NMR spectra of PDES are shown in Figure 41.

The temperature-dependent MAS spectra were obtained by heating pure β-PDES (a) and also by heating a mixture of the α- and β-modification (b). The β-polymorph gave one sharp signal at -17.9 ppm for the fully ordered crystalline state at 190 K, which did not change on raising the temperature until the $\beta_1-\beta_2$ transition was reached. At the $\beta_1-\beta_2$ transition the resonance was shifted upfield by $\Delta\nu = 3.3$ ppm to -21.2 ppm. Increasing the temperature further resulted in a gradual upfield shift from -21.2 ppm at 220 K to -22.2 ppm at 280 K, which is directly below the $\beta_2-\mu$ transition. On passing the $\beta_2-\mu$ transition, the isotropic chemical shift of the silicon nuclei was shifted to -23.6 ppm. Further heating, even above the melt transition (isotropization), did not result in further variation of the chemical shift. The chemical shift remained the same at 298, 315 and 325 K.

The observed upfield shifts indicate changes in the molecular packing and the bond conformation as the sample is converted from a highly ordered crystal to the isotropic melt. In the melt, the ^{29}Si resonance gives the fast exchange-averaged chemical shift for a dynamic equilibrium between different rotational isomeric states of the Si−O and Si−C bonds. The fact that the ^{29}Si chemical shift is identical for the melt and the μ-phase demonstrates a dynamically disordered conformational state also below the isotropic transition. This is confirmed by ^{29}Si spin−lattice relaxation experiments. The T_1 time was 23 s for the melt at 330 K and 25 s for the μ-phase at 300 K. Thus, the motional state and the conformational equilibrium of the molecular segments remain very much the

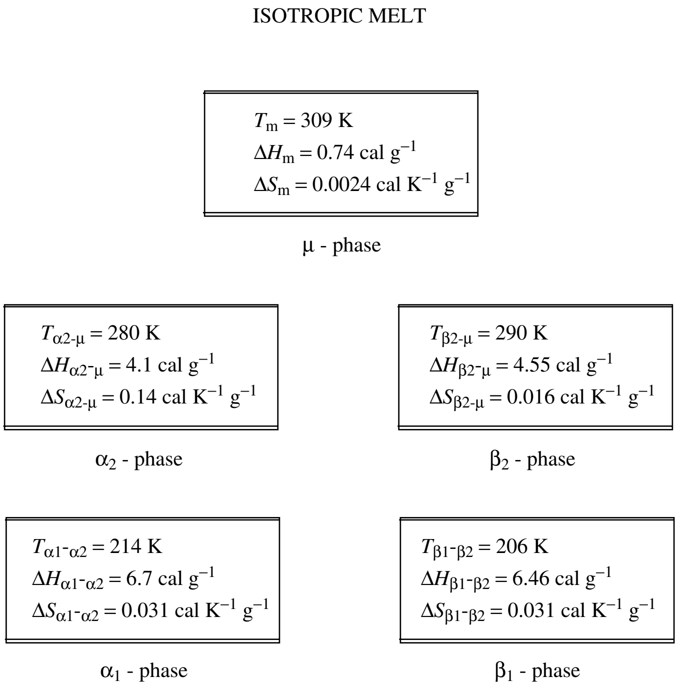

FIGURE 40. Polymorphism and melting of poly(diethylsiloxane). Reprinted with permission from Reference 145. Copyright 1989 American Chemical Society

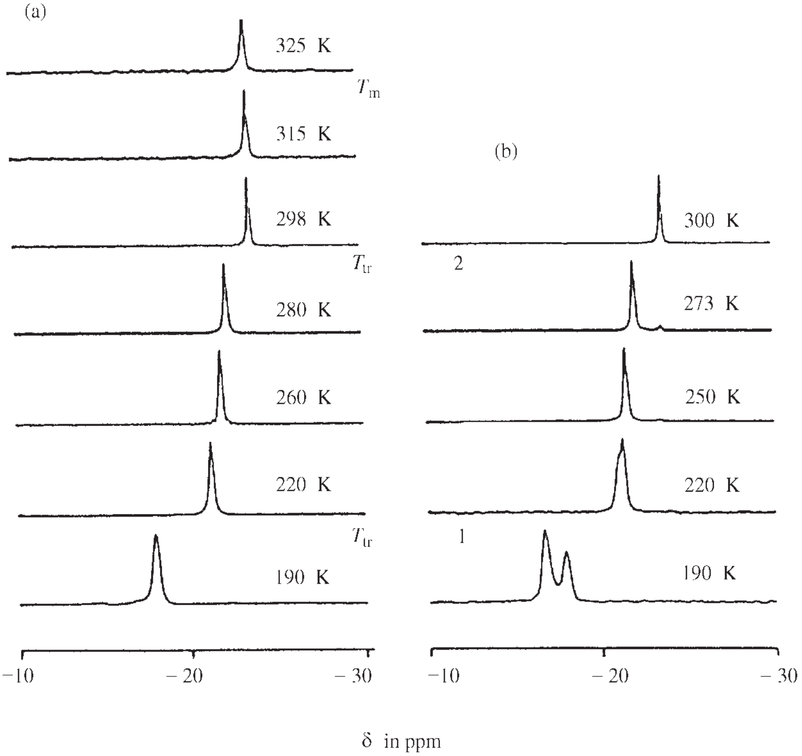

FIGURE 41. Temperature variation of the MAS ^{29}Si NMR spectrum of poly(diethylsiloxane): (a) spectra of the pure β-modification; (b) spectra of a mixture of α and β-modification. Spectra were recorded by stepwise heating of the samples. Reprinted with permission from Reference 145. Copyright 1989 American Chemical Society

same. The downfield shift of the ^{29}Si signal on cooling below the μ–β_2 transition may be explained by a change of the segmental conformations and the molecular packing. Below the β_1–β_2 transition, the silicon nuclei appear to be locked in a single state, which is represented by the -17.6 ppm ^{29}Si resonance. Thus, finally in the β_1-phase, the PDES molecules are packed rigidly in an ordered crystal lattice.

Figure 41b shows the ^{29}Si MAS NMR spectra of a sample that was quenched rapidly from the μ-phase and thus contains both the α- and β-modifications. Two signals could be resolved for the rigid crystal at 190 K. The -16.6 ppm signal was assigned to the α-polymorph while the -17.6 ppm signal is identical with the 190 K ^{29}Si NMR resonance in Figure 41b and represents the β-modification. The fraction of the α_1-modification was calculated to be 64% from the signal intensities as the relaxation and cross-polarization behavior of the two modifications did not differ significantly. Raising the temperature above the lower disordering transitions resulted in an upfield shift of the ^{29}Si resonances. Up to 220 K, two signals were resolved. This is demonstrated more clearly in the enlargement in Figure 42a.

The -20.9 ppm signal can be assigned to the α_2- and the resonance at -21.2 ppm to the β_2-modification by comparison with the corresponding spectrum of Figure 42b. Thus,

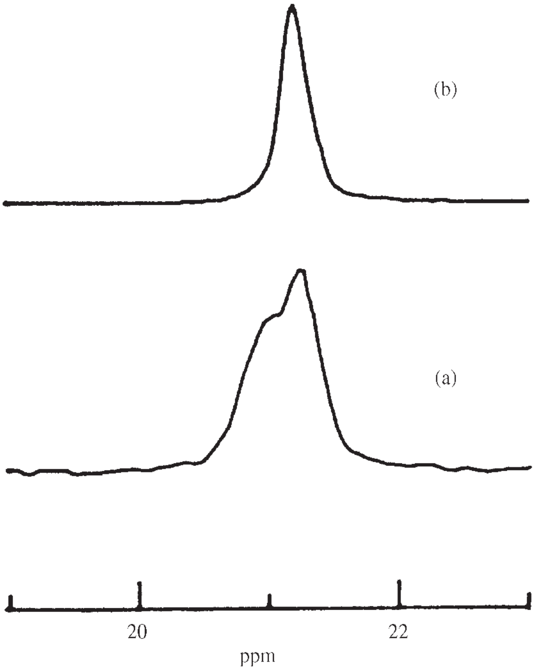

FIGURE 42. Enlargement of the MAS ^{29}Si NMR resonance of pure β-PDES (b) and a mixture of α- and β-PDES (a), $T = 220$ K. Reprinted with permission from Reference 145. Copyright 1989 American Chemical Society

the α_2- and β_2-modifications are clearly distinguished by the ^{29}Si NMR chemical shift. The deconvolution of the 220 K resonances yielded only 60% α_2-PDES, which is only little less than the value obtained from the spectrum at 190 K. When the temperature was raised further, the shoulder disappeared, and only one signal could be resolved. The slow rates for the conversion of α_2- to β_2-PDES as demonstrated by the calorimetric experiments cannot explain this phenomenon.

High-resolution solid-state ^{29}Si and ^{13}C NMR spectroscopy have been used to investigate the dynamic properties of tetrakis(trimethylsilyl)silane [Si(SiMe$_3$)$_4$:TTMSS]^{146}. It is clear from the temperature dependence of the spectra as a function of temperature that TTMSS shows the spectral changes associated with the phase transition. ^{29}Si chemical shifts are given relative to SiMe$_4$ as an external standard. The spectrum recorded at 153 K contains two peaks for the SiMe$_3$ environments (δ – 8.7 and −9.6) with 1 : 3 intensity ratio; coalescence of these peaks occurs at 206 K (δ – 9.5), and there are further changes of chemical shift on heating to 304 K (δ – 9.8). The spectrum contains a single peak for the central Si environment at δ – 140.8 (153 K), −138.8 (206 K) and −135.3 (304 K). As a result, the following represent two plausible types of motion that may be occurring in the low-temperature phase of solid TTMSS: (a) rotation of the whole molecule around a space-fixed crystallographic axis parallel to one of the Si−Si bonds, and (b) rotation of each SiMe$_3$ group about the local C$_3$ symmetry axis coincident with the relevant Si−Si bond. Rotation of each Me group around the relevant Si−C bond is assumed to be rapid on the experimental timescale at all temperatures studied here.

F. Hypervalent Silicon

An interesting question is whether hypervalent silicon nuclei can be monitored by ^{29}Si NMR spectroscopy. A systematic ^{29}Si MAS NMR measurement of nine silicates containing hexacoordinate silicon nuclei shows that a decrease in the mean Si−O bond distance $d(\mathrm{Si}^{\mathrm{VI}}\mathrm{-O})$ corresponds to an increase in the magnetic shielding of the $\mathrm{Si}^{\mathrm{VI}}$ nucleus. All isotropic chemical shifts lie within the range −142 to −220 ppm. The spectrum of $Si_5O(PO_4)_6$ (Figure 43) also shows a broad (*ca* 400 Hz) signal centered at −112 ppm and a narrow signal (*ca* 60 Hz) at −119.9 ppm; these lines are characteristic of tetrahedrally coordinated silicon, $\mathrm{Si}^{\mathrm{VI}}$.

The high-field signals between −142 and −220 ppm reflect the presence of octahedral silicon[147]. ^{29}Si MAS NMR is capable of detecting hexacoordinated silicon in heterogeneous phase in catalysts and other materials. Compounds **59** and **60** (R = Me, Ph) are zwitterionic (ammonioalkyl)organotrifluorosilicates. The zwitterionic organofluorosilicates contain a tetracoordinate nitrogen atom (formally positively charged). In the crystal, the coordination polyhedrons around the Si nuclei can be described as distorted trigonal bipyramids: two of the F nuclei occupy the axial sites, whereas the third F atom and two C nuclei are in the equatorial positions. In solution, the zwitterionic species display a rapid ligand exchange at room temperature (one ^{19}F resonance). Solid-state ^{15}N and ^{29}Si NMR studies on authentic tetrafluoro(pyrrolidiniomethyl)silicate $[F_4SiCH_2N(H)C_4H_8]$ **(61)** and on (3-ammoniopropyl)tetrafluorosilicate $[F_4Si(CH_2)_3NH_3]$ **(62)** revealed evidence that **62** is indeed the earlier postulated product formed in the reaction of (3-aminopropyl)triethoxysilane $[EtO)_3Si(CH_2)_3)NH_2]$ with HF in ethanol/HF [**61**, $\delta(^{15}\mathrm{N}) = -318.5$ ppm, $\delta(^{29}\mathrm{Si}) = -121.1$ ppm; **62**, $\delta(^{15}\mathrm{N}) = -345.3$ ppm, $\delta(^{29}\mathrm{Si}) = -112.4$ ppm][148,149] (Figure 44).

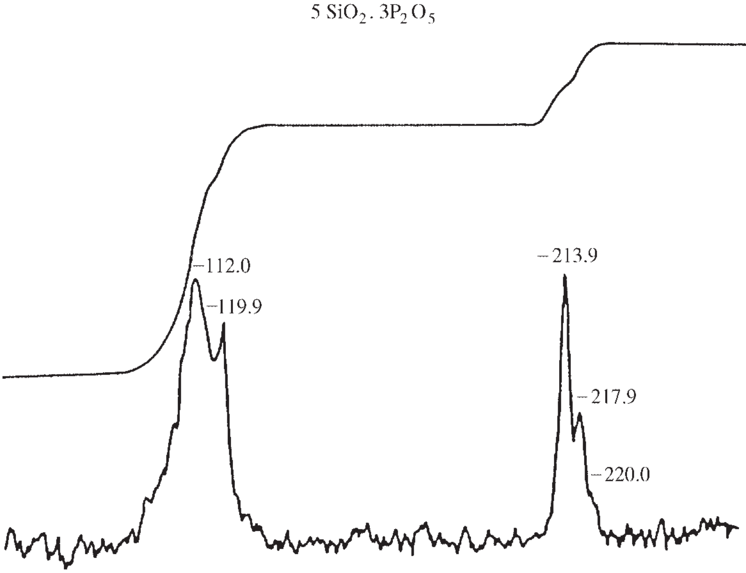

FIGURE 43. ^{29}Si NMR MAS spectrum of $Si_5O(PO_4)_6$. The chemical shift is referenced to the M signal of the Q_8M_8 external standard (+11.5 ppm). Delay between 30° pulses is 20 s, number of scans is 2242 and the frequency is 39.74 MHz. Reproduced by permission of Elsevier Science from Reference 147

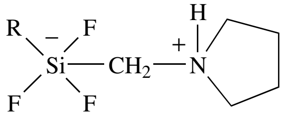

(**59**) R = Me
(**60**) R = Ph

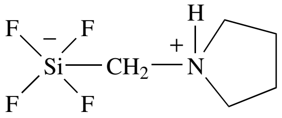

(**61**)

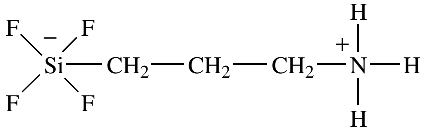

(**62**)

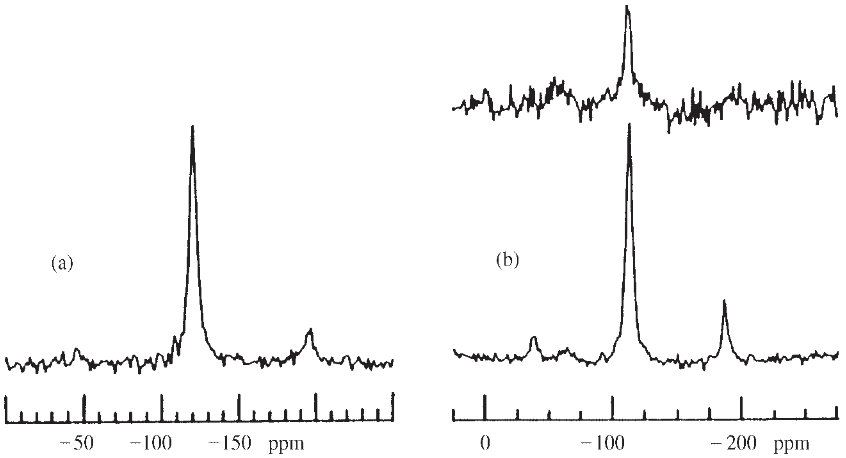

FIGURE 44. ^{29}Si MAS spectrum of **61** (a) and ^{29}Si MAS and ^{19}F →^{29}Si CP/MAS spectra of **62** (b) Key: (a) ^{19}F high-power decoupled ^{29}Si MAS spectrum of **61**, spinning rate = 4.5 kHz, 30°^{29}Si pulse, recycle delay time = 30 s, 2271 transients, exponential line broadening of 25 Hz, $\delta(^{29}\text{Si}) = -121.1$ ppm, $\nu_{1/2} = 350$ Hz; (b) ^{19}F → ^{29}Si CP/MAS spectra of **62** (top), with spinning rate = 4.5 kHz, contact time = 10 ms, recycle delay time = 15 s, 1167 transients, exponential line broadening of 25 Hz and ^{19}F high-power decoupled ^{29}Si MAS spectrum of **62** (bottom) with spinning rate = 4.5 kHz, 30°^{29}Si pulse, recycle delay time = 30 s, 2165 transients, exponential line broadening of 25 Hz, $\delta(^{29}\text{Si}) = -112.4$ ppm, $\nu_{1/2} = 300$ Hz. Reproduced by permission of VCH Weinheim from Tacke *et al., Chem. Ber.*, **126**, 851 (1993)

The isotropic chemical shift is the average value of the diagonal elements of the chemical shift tensor. Advances in solid state NMR spectroscopy allow one to determine the orientation dependence, or anisotropy, of the chemical shift interaction. It is now possible to determine the principal elements of a chemical shift powder pattern conveniently, and the orientation of the principal axes with more effort. Hence, instead of settling for just the average value of the chemical shift powder pattern, one can now aim for values of the three principal elements and the corresponding orientations in a molecular axis system.

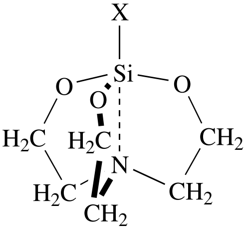

(**63**)

The chemical shift parameters of the ^{13}C, ^{15}N and ^{29}Si resonances in a set of 2,8,9-trioxa-5-aza-1-silabicyclo[3.3.3]undecanes (silatranes) **(63)** were determined from powdered, crystalline samples with and without magic angle spinning. Silatranes are a class of organosilicon compounds that feature a silicon atom that can be discussed as nominally pentacoordinate. The interest in silatranes is due to their intriguing molecular structure, biological activity and patterns of chemical reactivity. The most intriguing aspect of this structure is the existence of and influence of a 'transannular bond' between the silicon and nitrogen atoms, as indicated by the dashed line drawn between the silicon and nitrogen nuclei in structure **63**. Not surprisingly, because the substituent is directly attached to silicon, the chemical shift tensor for ^{29}Si yields a more striking dependence on substituent variation than that for ^{15}N. Although the correlations are not as 'clean' as for the ^{15}N chemical shift, the observed variation in the ^{29}Si chemical shift is much larger. ^{29}Si chemical shift powder patterns are shown in Figure 45. They correspond to chemical shift tensors that are nearly axially symmetric and exhibit wider variation in their anisotropies than do the ^{15}N chemical shift powder patterns.

For ^{29}Si, $\delta_{33} - \delta_{11} = \Delta\delta$ (the anisotropy) varies from 112 to 32 ppm for the chloro and ethyl derivatives of **63**, respectively, with all of the principal elements exhibiting a dependence on the substituent. δ_{11} and δ_{22} increase by approximately 40 ppm with increasing $r_{\mathrm{Si-N}}$, and δ_{33} decreases by approximately 20 ppm with increasing $r_{\mathrm{Si-N}}$.

The result of these trends is that δ_{iso} shows a slight dependence on $r_{\mathrm{Si-N}}$, increasing by approximately 30 ppm as $r_{\mathrm{Si-N}}$ increases. The ^{29}Si chemical shift powder patterns exhibit a trend that is the reverse of what is seen with the ^{15}N chemical shift powder patterns; the more electron-withdrawing substituents give the widest ^{29}Si chemical shift powder patterns and the least electron-withdrawing substituents give the narrowest ^{29}Si chemical shift powder patterns. As in the case of the ^{15}N chemical shift parameters, the ^{29}Si chemical shift parameters show general trends with respect to $r_{\mathrm{Si-N}}$. Figure 46 displays a set of chemical shift correlation curves for δ_{iso}, $\delta_{33} - \delta_{11}$, δ_{33}, δ_{22} and δ_{11} vs $r_{\mathrm{Si-N}}$. The correlations show some scatter as those discussed above for the ^{15}N data. The added complication is the presence and the local effect of the directly-attached substituent. Thus, the substituent effect on the ^{29}Si chemical shift can be viewed as having three types of origins:

(1) the geometry-structure effect associated with variations in the ∠OSiO bond angle;

(2) the substituent effect due to variations in the N•Si transannular interaction;

(3) the direct substituent effect that would be induced even in the absence of the first two, e.g. in an analogous system without nitrogen but with the substituent attached to silicon.

This third type of effect is, of course, absent in the ^{15}N case, so one can expect that interpretation of chemical shift data in terms of the transannular bond should be more

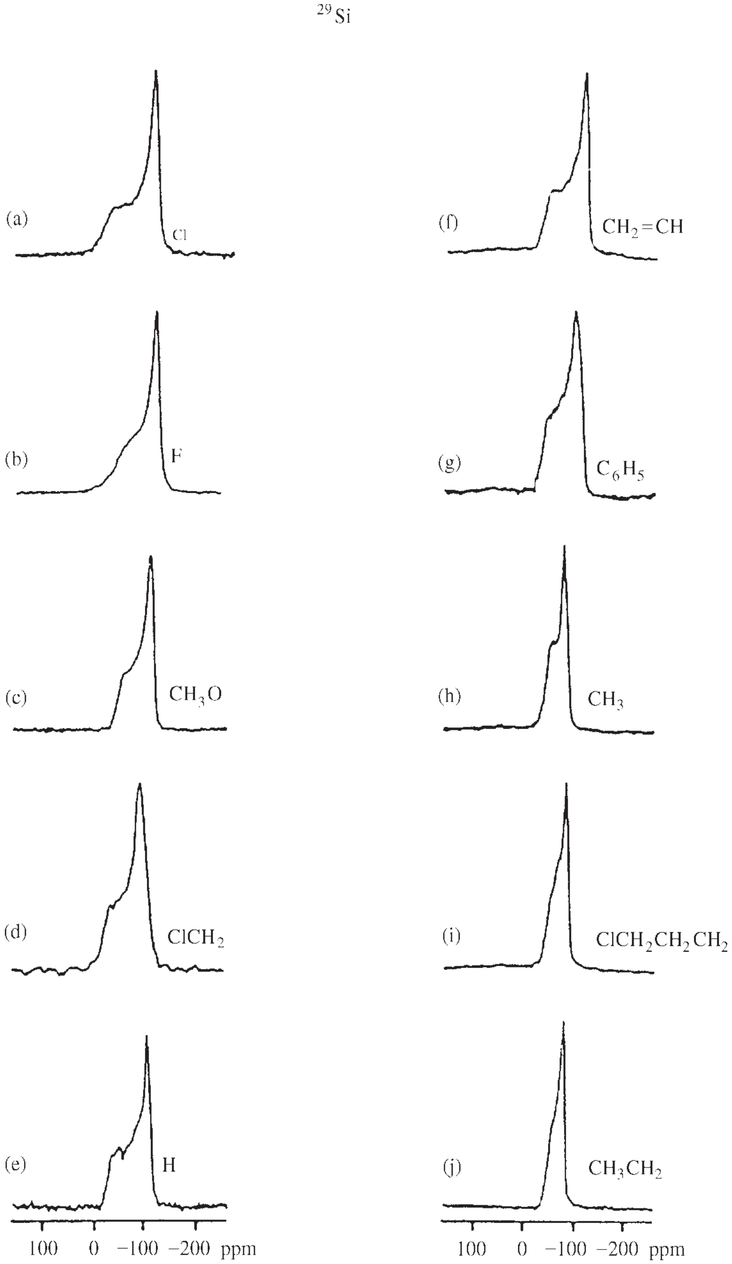

FIGURE 45. ^{29}Si chemical shift powder patterns collected under cross-polarization conditions at 39.8 MHz on X-substituted silatranes **63** with X indicated. The fluorosilatrane chemical shift powder pattern was collected under high-power ^{1}H and ^{19}F decoupling conditions at 200 MHz. Reprinted with permission from Reference 150. Copyright 1993 American Chemical Society

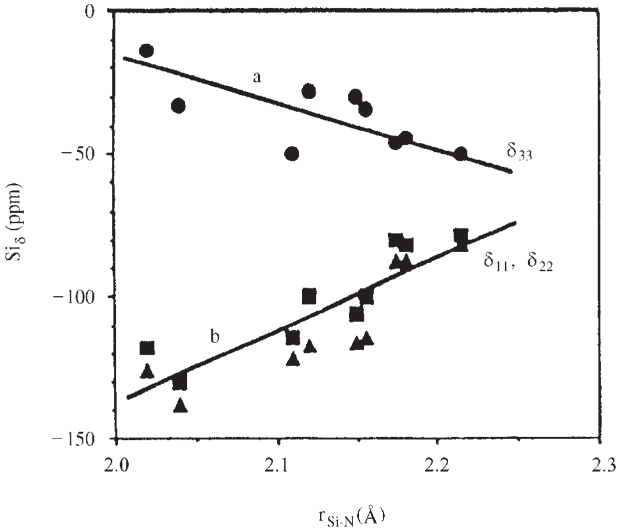

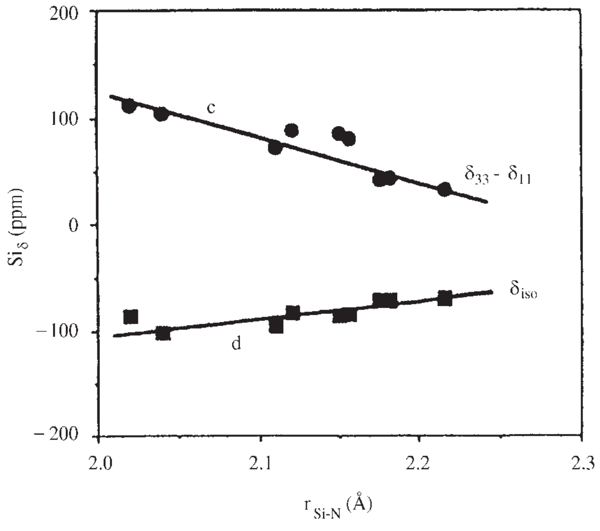

FIGURE 46. Correlation curves for some ^{29}Si chemical shift parameters vs r_{Si-N}: (a) δ_{33}, (b) δ_{11} (▲), δ_{22}(■), (c) $\delta_{33} - \delta_{11}$ and (d) δ_{iso}. Reprinted with permission from Reference 150. Copyright 1993 American Chemical Society

difficult for ^{29}Si than for ^{15}N. Nevertheless, the plots in Figure 46 indicate that as r_{Si-N} decreases in length, $\delta_{33} - \delta_{11}$ increases, the values of δ_{11} and δ_{22} decrease and δ_{33} increases, with the overall result that δ_{iso} decreases. In contrast to the ^{15}N data, each of the principal elements of the ^{29}Si chemical shift tensor shows a rough dependence on r_{Si-N}, with the δ_{11} and δ_{22} elements being more sensitive to changes in r_{Si-N} than the δ_{33} element[150].

Tamao and coworkers[151] presented the first example of a bis(siliconate) containing an Si–F–Si bond, [o-$C_6H_4(SiPhF_2)_2F]^-$, $K^+\bullet$ 18-crown-6 (**64**). This report describes the full details of the solid-state structures of **64** and the unsymmetrical analogues [o-$C_6H_4(SiF_3)(SiPh_2F)F]^-$, $K^+\bullet$ 18-crown-6 (**65**) and [o-$C_6H_4(SiPhF_2)(SiPh_2F)F]^-$, $K^+\bullet$ 18-crown-6 (**66**). For clarity, these bis(siliconates) **64–66** may be abbreviated to $[F2\{F\}F2]^-$, $[F\{F\}F3]^-$ and $[F\{F\}F2]^-$, respectively, in which the central $\{F\}$ represents the bridging fluorine atom while the left and right sides represent the number of fluorine nuclei on the two silicon atoms. An X-ray structural analysis of the three bis(siliconates) has afforded new significant information about bond lengths and bond angles (Figures 47–49).

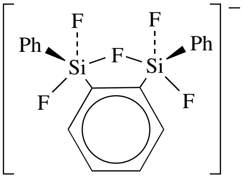

K^+ - 18-crown-6

(**64**) $[F2\{F\}F2]^-$

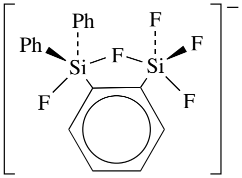

K^+ - 18-crown-6

(**65**) $[F\{F\}F3]^-$

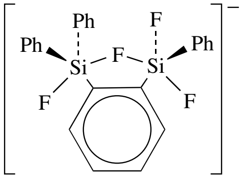

K^+ - 18-crown-6

(**66**) $[F\{F\}F2]^-$

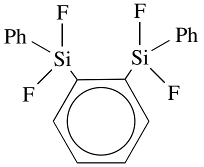

(**67**)

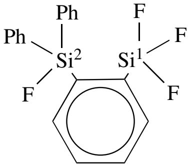

(**68**)

The ^{29}Si chemical shift and coupling constant, ^1J(SiF), for $[F2\{F\}F2]^-$ (**64**) are compared with data for other pertinent compounds in Table 15.

Three significant features should be mentioned.

(1) At 20 °C, the ^{29}Si NMR peak appears as a sextet for two silicon atoms, consistent with the fast exchange of all five fluorine nuclei.

(2) The ^{29}Si chemical shift (δ – 90.0 ppm) of **64** is intermediate between those of the tetracoordinate precursors o-bis(difluorphenylsilyl)benzene (**67**; δ – 30.21 ppm) and Ph_2SiF_2 (δ – 29.0 ppm) and that of the pentacoordinate mono(siliconate) $[Ph_2SiF_3]^-$ (δ – 109.5 ppm).

(3) The Si–F coupling constant [$^1J(SiF) = 134.7$ Hz] is smaller than those of Ph_2SiF_2 [$^1J(SiF) = 291.2$ Hz] and $[Ph_2SiF_3]^-$ [$^1J(SiF) = 238.0$ Hz] and is comparable with the calculated average value (130 Hz) on the assumption of $^1J(SiF) = 291$ Hz ($\times$ 2F), $^1J(SiF) = 238$ Hz ($\times$ 3F) and ^4J (SiF) $= 0$ ($\times$5F). Thus, these data strongly support fast fluoride transfer between tetracoordinate and pentacoordinate silicon atoms. The unsymmetrical bis(siliconates) **65** and **66** showed no detectable peaks of the silicon nuclei in solution.

Solid-state MAS ^{29}Si NMR data for the pentacoordinate bis(siliconates) **64** and **65** and mono(siliconate) $[PhSiF_4]^-$, $K^+\bullet$18-crown-6 are also summarized in Table 15 for comparison. The solid-state spectrum of **64** shows an uncharacterizable multiplet, possibly due to the slightly unsymmetrical structure. In contrast to the absence of peaks in solution,

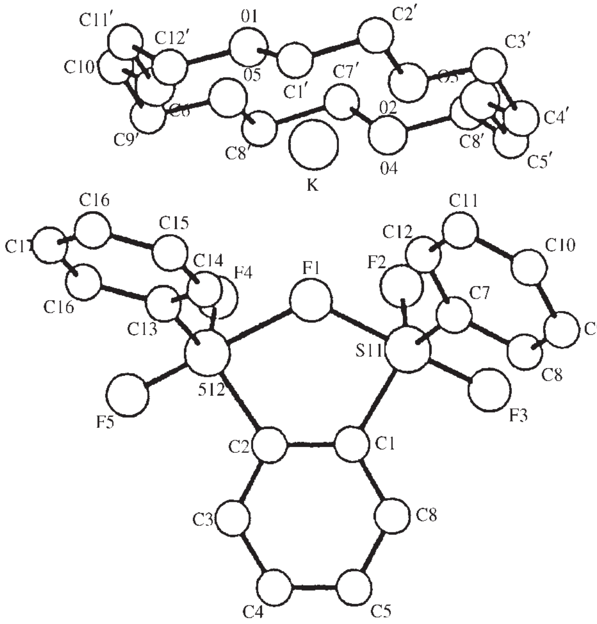

FIGURE 47. X-ray crystal structure of $[o\text{-}C_6H_4(SiPhF_2)_2F]^-$, K^+•18-crown-6 (**64**). Reprinted with permission from Reference 151. Copyright 1990 American Chemical Society

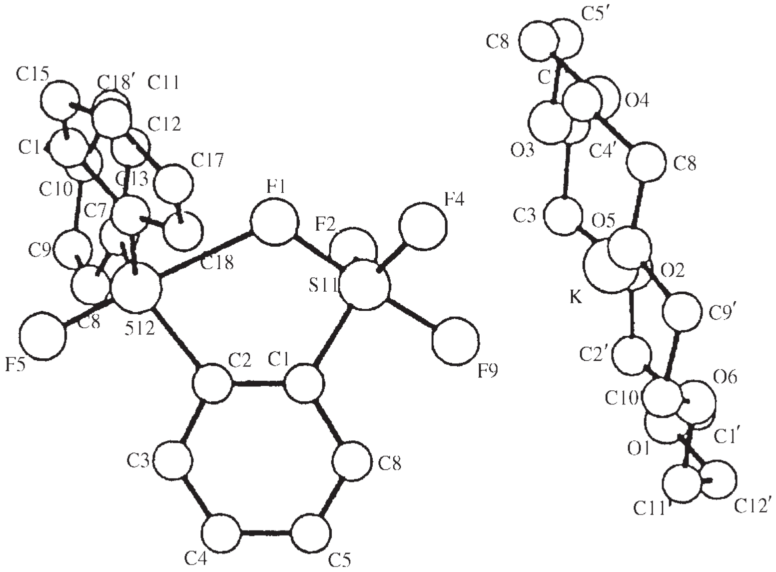

FIGURE 48. X-ray crystal structure of $[o\text{-}C_6H_4(SiF_3)(SiPh_2F)F]^-$, K^+•18-crown-6 (**65**). Reprinted with permission from Reference 151. Copyright 1990 American Chemical Society

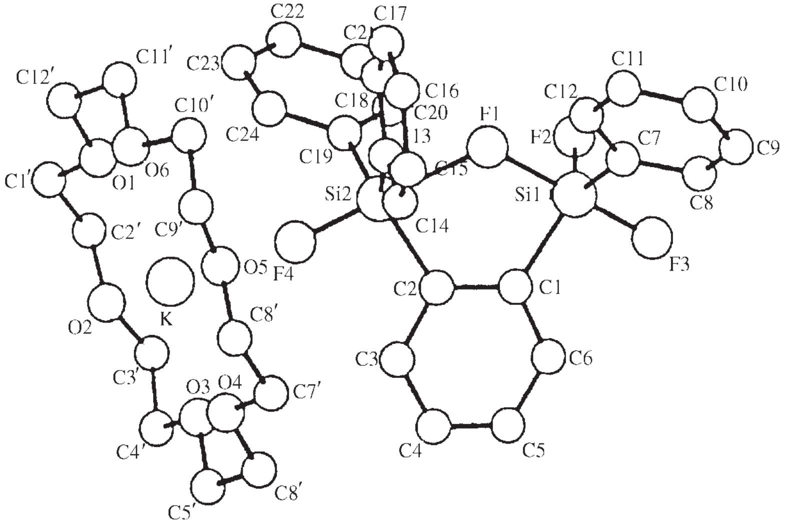

FIGURE 49. X-ray crystal structure of [o-C_6H_4(SiPh F_2)($SiPh_2F$) F]$^-$, K$^+$•18-crown-6 **(66)**. Reprinted with permission from Reference 151. Copyright 1990 American Chemical Society

TABLE 15. ^{29}Si NMR spectroscopic data for bis(siliconates) and mono(siliconates) and their precursors, fluorosilanes, in solution and/or in the solid state[a]

Siliconate and precursor[b]	Chemical shift (ppm)	Multiplicity	J(SiF) coupling constant (Hz)
anion of **64**	−90.03	sextet	134.74
	[−75 to −105]	[multiplet]	
anion of **65**	[−129.3(Si1)]	[triplet]	207.9
	[−31.3 (Si2)]	[doublet]	256.5
67	−30.21	triplet	293.9
68	−73.46(Si1)	quintet	265.4
	−3.63(Si2)	doublet	282.1
[Ph_2SiF_3]$^-$	−109.55	quartet	238.06
	−128.28	triplet	200.2
[$PhSiF_4$]$^-$	−125.90	quintet	210
	[−129.28]	[triplet]	200.2
Ph_2SiF_2	−29.00	triplet	291.20
$PhSiF_3$	−72.42	quintet	266.8

[a] Spectra were recorded at 20 °C in acetone-d$_6$ unless otherwise stated. Solid-state spectral data are given in brackets.

[b] The counterion of the siliconate is K$^+$•18-crown-6.

[c] No signal in solution.

Reproduced by permission of the American Chemical Society from Reference 151.

the solid-state spectrum of [F{F}F3]$^-$ **(65)** shows two distinct silicon peaks at −31.3 ppm as a doublet [^1J(SiF) = 256.5 Hz] for Si^2 and at −129.3 ppm as a triplet [^1J(SiF) = 207.9 Hz] for Si^1, as shown in Table 15 and in Figure 50. While Si^2 couples with only one fluorine, the Si^1 couples with only two of the four fluorine nuclei on Si^1 to appear as a triplet. It may be noted here that the silicon atom in the mono(siliconate) [$PhSiF_4$]$^-$ also appears as a triplet in the solid state (Table 15), although it cannot readily be deduced

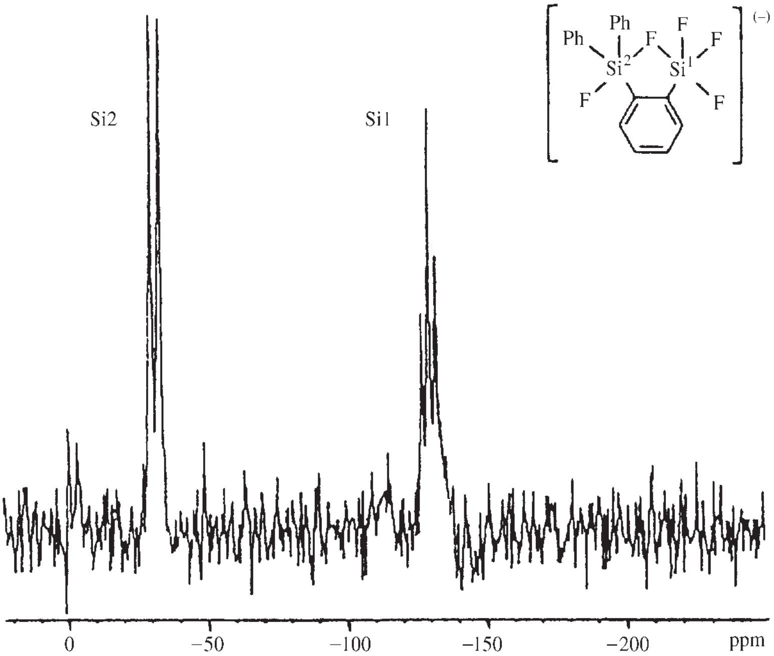

FIGURE 50. Solid-state ^{29}Si NMR spectrum for **65** (79.46 MHz, external standard DSS at δ 0 ppm). Reprinted with permission from Reference 151. Copyright 1990 American Chemical Society

whether the triplet arises from coupling with two apical or two equatorial fluorines. The Si^1 signal of **65** appears *ca* 56 ppm upfield from that of the $-SiF_3$ group in the precursor *o*-(fluorodiphenylsilyl)(trifluorosilyl)benzene (**68**). This difference is nearly equal to that (56.8 ppm) between $[PhSiF_4]^-$ in the solid state and $PhSiF_3$ in acetone-d_6, as shown in Table 15. Similarly, the chemical shift of Si^2 in **65** also shows a 27.7 ppm upfield shift from that of the $-SiPh_2F$ group in **68**, but the chemical shift difference is less than half of that for Si^1. Thus, it may be deduced that the Si^1 side is almost completely pentacoordinated, as for the trigonal-bipyramidal mono(siliconate) $[PhSiF_4]^-$, while the Si^2 side is of low pentacoordination character, in accordance with the results obtained by X-ray structural analysis. The $^{29}Si-^{19}F$ spin–spin coupling constant observed in the solid-state ^{29}Si NMR spectrum also provides useful information on the degree of interaction of the bridging fluorine atom with silicon atoms, i.e. on the pentacoordination character. ^1J (SiF) in the bis(siliconate) **65** and ^1J (SiF) in the precursor **68** are 207.9 and 265.4 Hz, respectively. Thus, the coupling constant in **65** is 57.5 Hz smaller than that in **68**. This suggests that Si^1 in **65** is highly pentacoordinated, since the difference in ^1J (SiF) between $[PhSiF_4]^-$ and $PhSiF_3$ is 66.5 Hz. In contrast, the coupling constant of ^1J (Si_2F) in **65** is 256.5 Hz, which is 25.6 Hz smaller than $^1J(Si_2F) = 282.1$ Hz in **68**, suggesting lower pentacoordination character of Si^2 in **65**. On the basis of the X-ray structural analysis of **65**, pentacoordination characters of Si^1 and Si^2 have been estimated to be 93% and 50%, respectively. Thus, the geometries about the silicon nuclei estimated from the ^{29}Si chemical shifts and ^{29}Si$-^{19}$F coupling constants by solid-state ^{29}Si NMR spectroscopy are consistent with the geometries found by the X-ray structural analysis (Figure 50).

G. Miscellaneous

In many applications of reversed-phase high-performance liquid chromatography (RP-HPLC), stationary-phase degradation is a major drawback when using alkylsilane-modified silica surfaces because of the hydrolytic instability of siloxane bonds. The lifetime of one column packing may not even be sufficient to perform adequate experimental designs for optimizing separation efficiencies. Consequently, much research was conducted in order to identify the most important factors involved in phase deterioration and to design new stationary phases with improved stability. The bulky substituents in the silanizing reagent (for example, diisobutyl-*n*-octadecylsilane instead of dimethyl-*n*-octadecylsilane) would result in a more efficient steric protection of the silica surface and, in particular, the ligand siloxane bond. These so-called stable bond phases indeed exhibit superior hydrolytic stability at low pH. However, the improved steric protection was not observed as such; it was postulated using the increased chromatographic stability as a criterion. Concerning the physicochemical methods used to investigate chromatographic silica surfaces, solid-state NMR has proven to be a powerful tool that enables identification of different chemical surface structures. The goal of much research has been to relate NMR characteristics of the detected chemical surface species to the observed chromatographic behavior of silica surfaces.

Scholten and coworkers[152] present ^{29}Si CPMAS NMR evidence for a decreased contribution of hydrogen bonding groups to the ligand silane signal in diisobutyl-*n*-octadecylsilane-modified silica gel, compared to the dimethyl-*n*-octadecylsilane analogue. This lower extent of hydrogen bonding is brought about by steric protection of the ligand siloxane bond by the bulky isobutyl substituents. Figure 51 displays the ^{29}Si CPMAS NMR spectra of the Aerosil samples in the silane ligand region for four different degrees of trimethylsilylation. Clearly, the chemical shift of the maximum of the ligand signal decreases with increasing surface coverage. Also, the asymmetry of the signals due to a shoulder at the left of the peak maximum is evident. Figure 52 displays the ^{29}Si CP MAS NMR spectra of the two Zorbax C_{18} phases. Before considering the asymmetry of the silane ligand NMR signals, it should be noted that the peak maximum of the SB-C_{18} ligand signal is shifted 2 ppm upfield from the maximum of the Rx-C_{18} ligand signal. This is due to the β effect on ^{29}Si upon substitution of two hydrogen nuclei for two isopropyl groups. This chemical shift difference is, however, irrelevant in the following discussion. The attention is focused on the degree of asymmetry of both signals. It appears that the shoulder in the SB-C_{18} spectrum is much less pronounced, indicating that the ligand siloxane bond is involved in hydrogen bonding only to a small extent. In the Rx-C_{18} spectrum, on the other hand, the shoulder is clearly discernible. It should be noted that the surface coverage by the diisobutyl-*n*-octadecylsilane ligands is much lower than that of the dimethyl-*n*-octadecylsilane ligands.

Bearing in mind the result of the trimethylsilylated Aerosil surfaces, where increasing surface coverage is accompanied by a decreasing hydrogen bonding contribution to the NMR signal, the slight asymmetry of the SB-C_{18} ligand NMR signal strongly suggests the superior steric shielding properties of the isobutyl groups. This is schematically illustrated in Figure 53.

Contact time dependences of signal intensities in ^{29}Si and ^{13}C CP MAS NMR spectrum (Figure 54) were measured for kaolinite and kaolinite-DMSO and kaolinite-DMSO-d_6

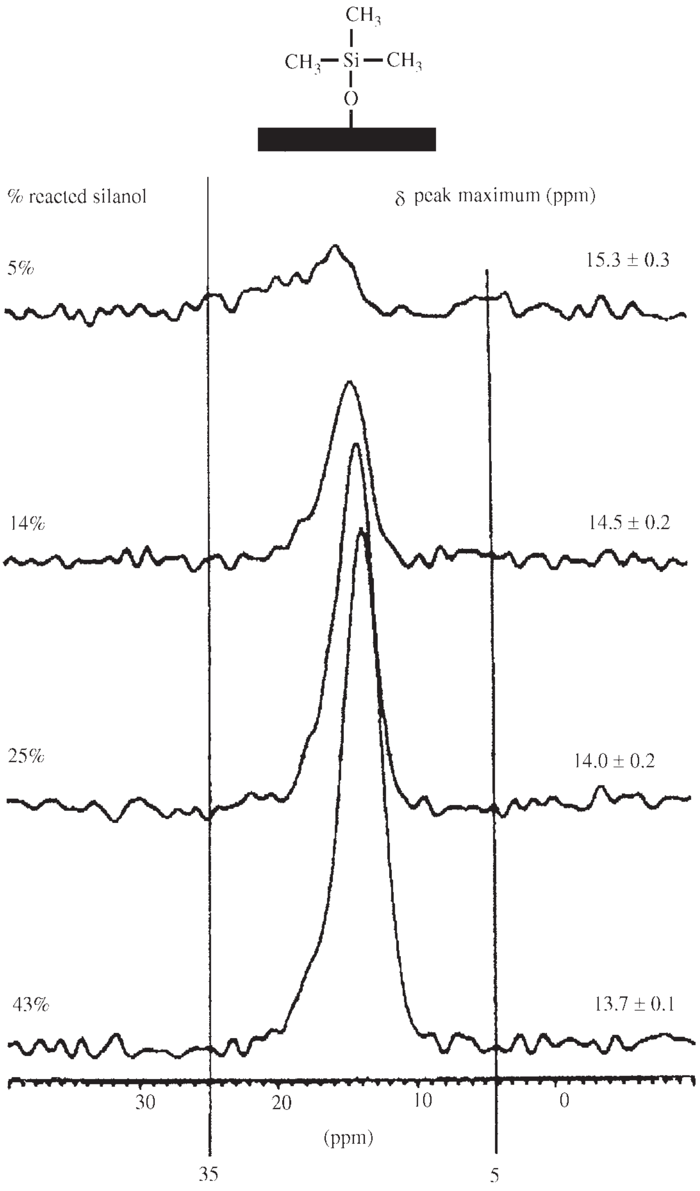

FIGURE 51. ^{29}Si CPMAS NMR spectra of Aerosil A-200 with trimethylsiloxane surface coverage and chemical shifts of the peak maxima (± maximum error) as indicated. All spectra are on the same intensity scale. Reproduced by permission of Elsevier Science from Reference 152

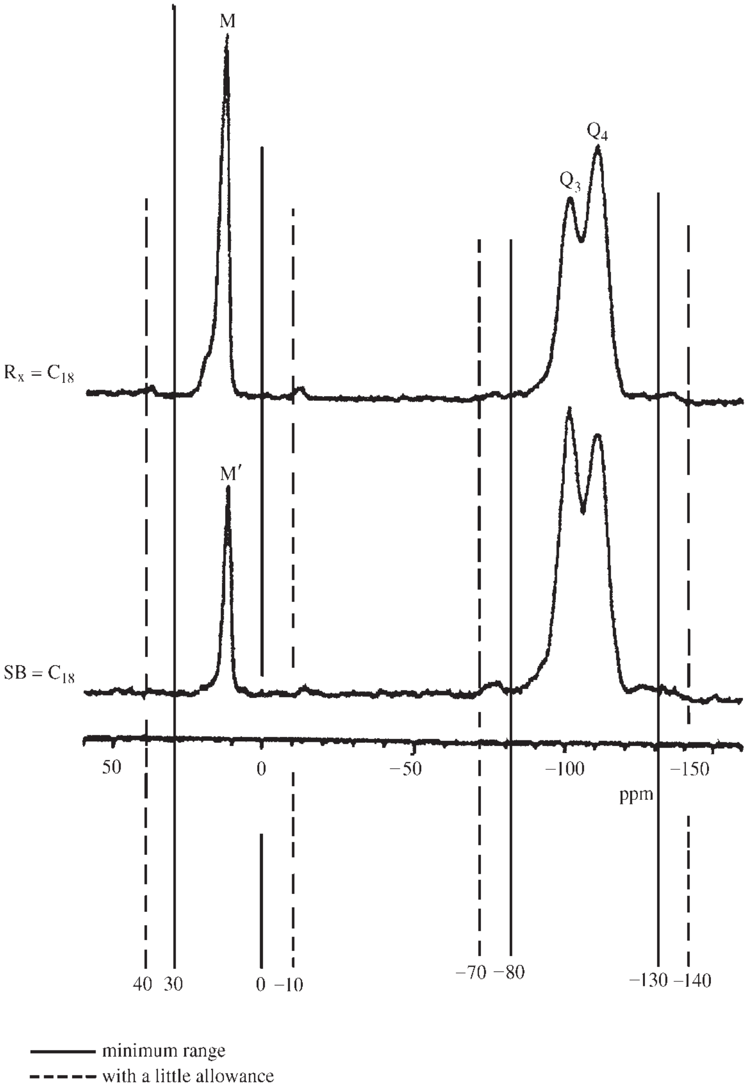

FIGURE 52. ^{29}Si CPMAS NMR spectra of the Zorbax octadecyl RP-HPLC phases. Both spectra are on the same intensity scale. M = dimethyl-*n*-octadecylsiloxane, M′ = diisobutyl-*n*-octadecylsiloxane, Q_3 = single silanol, Q_4 = siloxane. Reproduced by permission of Elsevier Science from Reference 152

intercalation compounds. Cross-relaxation times between ^{1}H and ^{29}Si and between ^{1}H and ^{13}C were estimated experimentally, which reflect the internuclear distances. Relaxation times were calculated theoretically using reported crystal structure models (Figure 55), and the validity of those models is discussed[153].

In 1997, West and coworkers[154] reported the solid-state NMR study of the ^{29}Si chemical shift tensors for a series of disilenes with different substitution at the Si=Si double bond

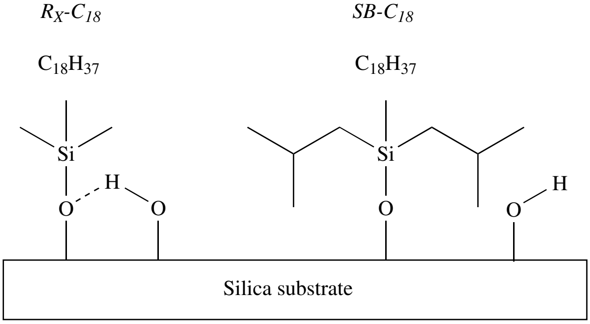

FIGURE 53. Schematic drawing of the dimethyl-*n*-octadecylsiloxane and the diisobutyl-*n*-octadecylsiloxane surface structures, illustrating the increased steric protection of the ligand siloxane bond by the bulky side groups in the latter. Reproduced by permission of Elsevier Science from Reference 152

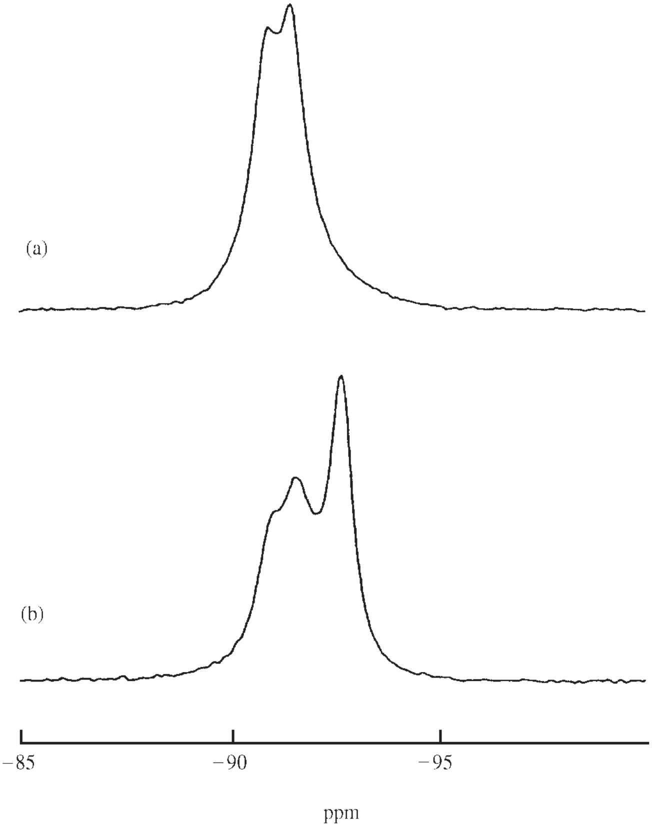

FIGURE 54. ^{29}Si CPMAS NMR spectra of (a) kaolinite and (b) kaolinite-DMSO. The spinning rate of the sample was 3.00 kHz. Reproduced by permission of Elsevier Science from Reference 153

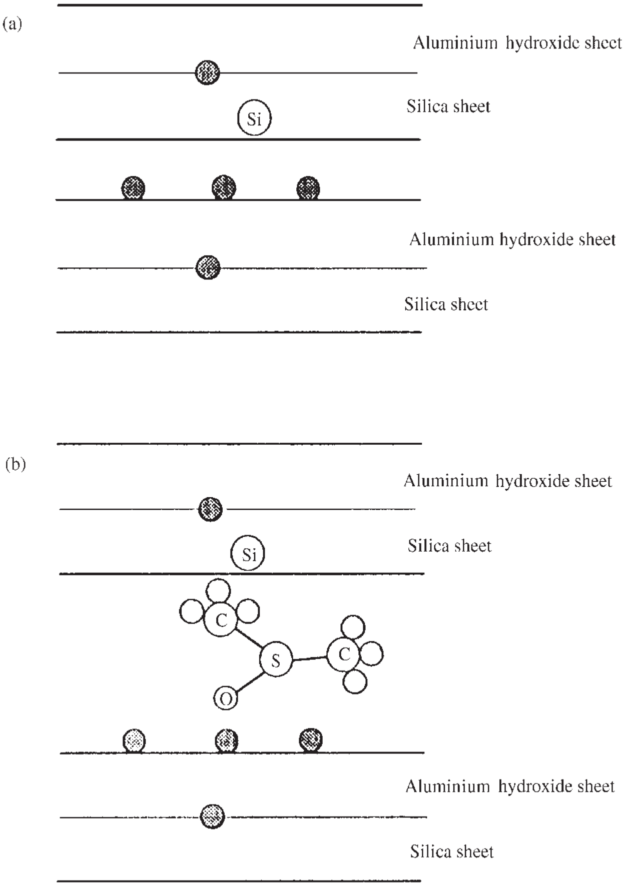

FIGURE 55. Schematic representation of layered structures in (a) kaolinite and (b) kaolinite-DMSO. Dark circles indicate hydrogen atoms. Reproduced by permission of Elsevier Science from Reference 153

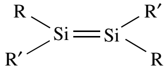

(69) R = R′ = mesityl
(70) R = R′ = 2,4,6-triisopropylphenyl
(71) R = mesityl, R′ = *t*-butyl
(72) R = R′ = $(Me_3Si)_2CH$
(73) R = Me_3Si, R′ = 2,4,6-triisopropylphenyl
(74) R = R′ = *i*-Pr_2MeSi
(75) R = R′ = *i*-Pr_3Si

FIGURE 56. Structures of disilenes studied by ^{29}Si NMR. Reprinted with permission from Reference 154. Copyright 1997 American Chemical Society

TABLE 16. Chemical shift tensors and structural parameters for disilenes

				δ_{iso}				Si=Si[b]
Disilene	δ_{11}	δ_{22}	δ_{33}	solid	soln	$\Delta\delta$	CSA[a]	(pm)
69	181	31	−22	63.2	63.3	203	176	214
69•C_7H_8	185	34	−22	65.0	63.3	207	179	216
69•THF$^-$	165	40	−25	59.6	63.0	190	157	215
70	155	30	−31	50.8	53.4	186	155	214
				53.2				
71	178	77	3	86.1	90.3	175	138	214
72	182	55	21	86.1	90.4	161	144	
	199	54	9	87.4		190		
73	296	46	−59	94.5	94.4	355	168	215
74	414	114	−100	143	144.5	514	408	228
75	412	149	−69	164	154.5	481	372	225

[a] $CSA = \delta_{11} - (\delta_{22} + \delta_{33})/2$.
[b] Data from Reference 159.

(Figure 56)[155]. Compounds investigated included three forms of tetramesityldisilene: the solvent-free form **69**[156], the toluene adduct **69**•C_7H_8[157] and the tetrahydrofuran solvate **69**•THF[158]. Also studied were a second tetraaryldisilene **(70)**[159] dialkyldiaryl-substituted disilene, **71**[160], and the only tetraalkyldisilene known to be stable as a solid, **72**[161]. Three silyl-substituted disilenes, **73**, **74** and **75**, were also investigared[162,163]. To assist in the interpretation of the experimental results, *ab initio* molecular orbital calculations of the ^{29}Si chemical shift tensors were carried out for model disilene molecules.

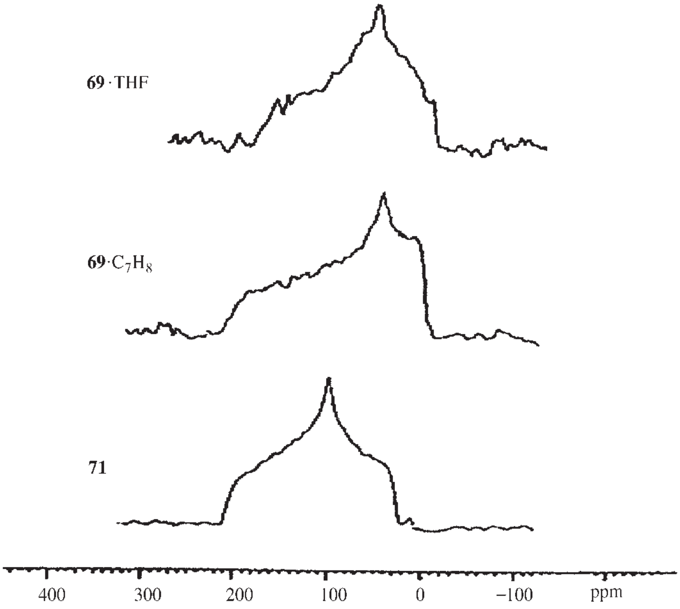

FIGURE 57. Static ^{29}Si NMR spectra of disilenes. Reprinted with permission from Reference 154. Copyright 1997 American Chemical Society

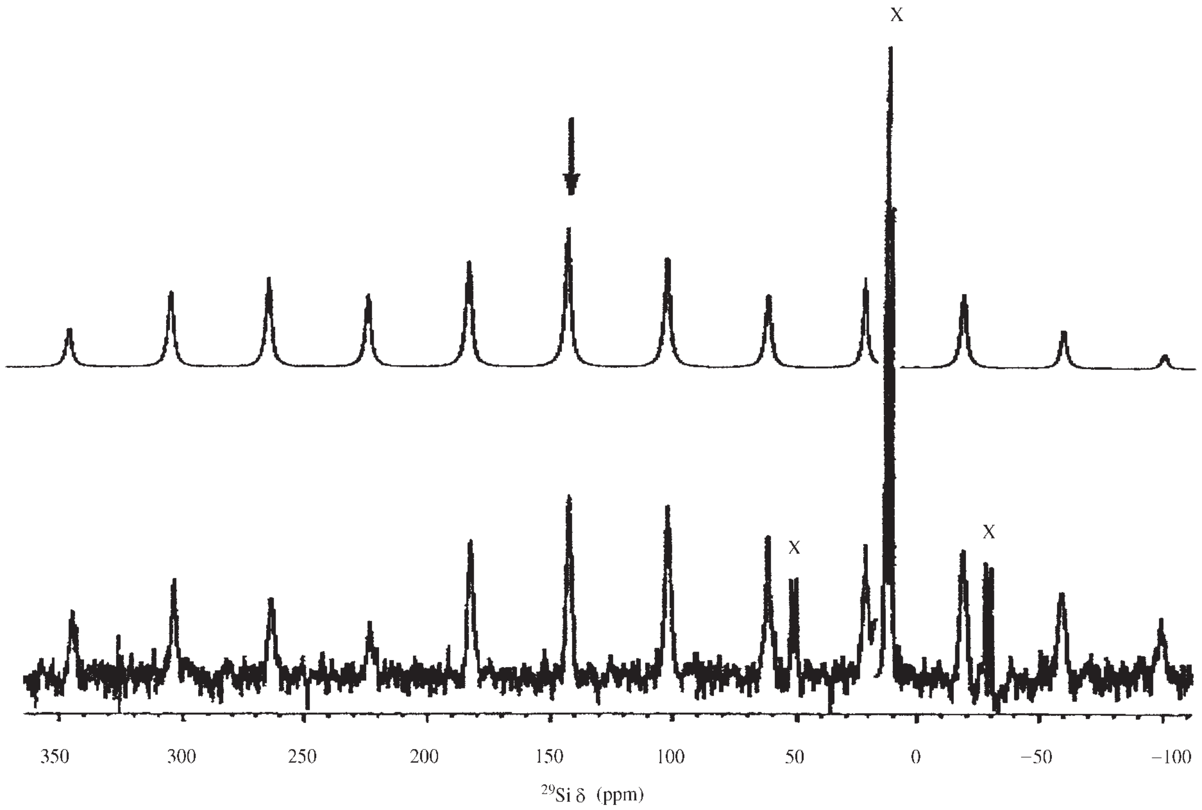

FIGURE 58. Slow-spinning MAS ^{29}Si NMR spectrum for $(i\text{-PrMe}_2)_2\text{Si}_2\text{Si}{=}\text{Si}(\text{SiMe}_2\text{Pr-}i)_2$ (**74**): below, recorded spectrum; above, computer simulation for the doubly-bonded silicons. The isotropic peak for the disilene silicons is marked with an arrow. Peaks marked x are due to the *i*-Pr−Si silicons; these isotropic peaks are shown at reduced gain. Reprinted with permission from Reference 154. Copyright 1997 American Chemical Society

Chemical shift tensors for the doubly-bonded silicon atoms in the nine disilene samples are given in Table 16. Typical powder patterns are shown in Figure 57, and the slow-spinning spectrum for **75** is illustrated in Figure 58. All of the disilenes show significant deshielding along one axis (δ_{11}). For tetrasilyldisilenes this deshielding is extreme, +414 ppm for **75**. Together with greater shielding in the δ_{33} direction, these lead to $\Delta\delta$ values ($\Delta\delta = \delta_{11} - \delta_{33}$) more than a factor of 2 greater than any previously reported for ^{29}Si[164]. The $\Delta\delta$ values for the doubly-bonded silicon atoms in all of the disilenes are significantly larger than those for singly-bonded silicon compounds, which typically have $\Delta\delta$ values of 0–60 ppm[165]. For disilenes **74** and **75**, tensors for the four-coordinate silicon atoms were also determined: for **74**, $\delta_{11} = 36.4$, $\delta_{22} = -0.9$ and $\delta_{33} = -4.2$ ppm; and for **75**, the corresponding values are 46.0, 21.1 and 17.8 ppm, giving $\Delta\delta$ values of about 30 ppm, as expected for sp^3-type silicons.

The MO calculations on model disilenes indicate that the deshielding results from a paramagnetic contribution along the in-plane axis perpendicular to the Si−Si vector. Implications of the NMR data and the theoretical computations for Si=Si bonding are discussed.

VI. REFERENCES

1. E. A. Williams, in *The Chemistry of Organic Silicon Compounds*, Vol. 1 (Eds. S. Patai and Z. Rappoport), Chap. 8, Wiley, New York, 1989, pp. 511–544.
2. A. R. Bassindale and P. P. Gasper (Eds.) *Frontiers of Organosilicon Chemistry*, The Royal Society of Chemistry, 1991.
3. H. Marsmann, in *NMR Basic Principles and Progress*, **17** (Eds. P. Diehl, E. Fluck and R. Kosfeld), Springer-Verlag, Berlin, 1981, p. 235; H. C. Marsmann, 'Silicon-29 NMR', and G. Engelhardt, 'Silicon-29 NMR of Solid Silicates', in *Encyclopedia of Nuclear Magnetic Resonance*, Wiley, New York, 1996; *Specialist Periodical Report, Nuclear Magnetic Resonance*, Vols 1–24, The Royal Society of Chemistry, These volumes are useful since most of them contain some ^{29}Si NMR results.
4. R. K. Harris, N. J. O'Connor, E. H. Curzon and O. W. Howarth, *J. Magn. Reson.*, **57**, 115 (1984).
5. G. Engelhardt and D. Michel, *High Resolution Solid State NMR of Silicates and Zeolites*, Wiley, New York, 1987.
6. V. Baudrillard, D. Davoust and G. Ple, *Magn. Reson. Chem.*, **32**, 40 (1994).
7. G. A. Morris and R. Freeman, *J. Am. Chem. Soc.*, **101**, 760 (1979).
8. Th. Blinka, B. J. Helmer and R. West, *Adv. Organomet. Chem.*, **23**, 193 (1984).
9. O. W. Sorensen, *Prog. Nuclear Magn. Reson. Spectrosc.*, **21**, 503 (1989).
10. J. Schraml, *Collect. Czech. Chem. Commun.*, **48**, 3402 (1983).
11. E. Hengge and F. Schrank, *J. Organomet. Chem.*, **362**, 11 (1989).
12. M. Kuroda, Y. Kabe, M. Hashimoto and S. Masamune, *Angew. Chem., Int. Ed. Engl.*, **27**, 1727 (1988).
13. C. T. G. Knight, R. J. Fitzpatrick and E. Oldfield, *J. Non-Cryst. Solids*, **116**, 140 (1990).
14. C. A. Fyfe, H. Grondey, Y. Feng and G. T. Kokotailo, *Chem. Phys. Lett.*, **173**, 211 (1990).
15. C. A. Fyfe, H. Grondey, Y. Feng and G. T. Kokotailo, *J. Am. Chem. Soc.*, **112**, 8812 (1990).
16. C. A. Fyfe, H. Grondey, Y. Feng and G. T. Kokotailo, *Nature (London)*, **341**, 223 (1989).
17. M. R. Churchill, J. W. Ziller, J. H. Freudenberger and R. R. Scrock, *Organometallics*, **3**, 1554 (1984).
18. J. Okuda, R. C. Murray, J. C. Dewan and R. R. Schrock, *Organometallics*, **5**, 1681 (1986).
19. R. R. Schrock, S. F. Pedersen, M. R. Churchill and J. W. Ziller, *Organometallics*, **3**, 1574 (1984).
20. T. M. Sivavec and T. J. Katz, *Tetrahedron Lett.*, **26**, 2159 (1985).
21. C. Dallaire, M. A. Brook, A. D. Bain, C. S. Frampton and J. F. Britten, *Can. J. Chem.*, **71**, 1676 (1993).
22. H. Sakurai, S. Hoshi, A. Kamiya and A. Hosomi, *Chem. Lett.*, 1781 (1986).
23. K. Akasaka, W. Ando, K. Kobayashi and S. Nagase, *J. Am. Chem. Soc.*, **115**, 1605 (1993).
24. T. Kusakawa, Y. Kabe, T. Erata, B. Nestler and W. Ando, *Organometallics*, **13**, 4186 (1994).

25. T. Kusakawa, Y. Kabe and W. Ando, *Organometallics*, **14**, 2142 (1995).
26. W. Ando, F. Hojo, S. Sakigawa, N. Nakayama and T. Shimizu, *J. Am. Chem. Soc.*, **115**, 3111 (1993).
27. T. Shimizu, F. Hojo and W. Ando, *Organometallics*, **11**, 1009 (1992).
28. H. B. Yokelson, A. J. Millevolte, B. R. Adams and R. West, *J. Am. Chem. Soc.*, **109**, 4116 (1987).
29. H. Watanabe, T. Okawa, M. Kato and Y. Nagai, *J. Chem. Soc., Chem. Commun.*, 781 (1983).
30. P. K. Jenkner, A. Spielberger, M. Eibl and E. Hengge, *Spectrochim. Acta*, **49A**, 161 (1993).
31. H. Watanabe, M. Kato, T. Okawa, Y. Kougo, Y. Nagai and M. Goto, *Appl. Organometal. Chem.*, **1**, 157 (1987).
32. H. Suzuki, K. Okabe, R. Kato, N. Sato, Y. Fukuda, H. Watanabe and M. Goto, *Organometallics*, **12**, 4833 (1993).
33. H. Suzuki, N. Kenmotu, K. Tanaka, H. Watanabe and M. Goto, *Chem. Lett.*, 811 (1995).
34. For a review see: R. West, *Angew. Chem., Int. Ed. Engl.*, **26**, 1201 (1987).
35. H. Watanabe, K. Takeuchi, N. Fukawa, M. Kato, M. Goto and Y. Nagai, *Chem. Lett.*, 1341 (1987).
36. H. Suzuki, N. Tokitoh, R. Okazaki, J. Harada, K. Ogawa, S. Tomoda and M. Goto, *Organometallics*, **14**, 1016 (1995).
37. N. Tokitoh, H. Suzuki, R. Okazaki and K. Ogawa, *J. Am. Chem. Soc.*, **115**, 10428 (1993).
38. M. Denk, R. Lennon, R. Hayashi, R. West, A. V. Belyakov, H. P. Verne, A. Haaland, M. Wagner and N. Metxler, *J. Am. Chem. Soc.*, **116**, 2691 (1994).
39. J. B. Lambert, L. Kania and S. Zhang, *Chem. Rev.*, **95**, 1191 (1995); P. D. Lickiss, *J. Chem. Soc., Dalton Trans.*, 1333 (1992).
40. J. B. Lambert and S. Zhang, *J. Chem. Soc., Chem. Commun.*, 383 (1993).
41. J. B. Lambert, S. Zhang, C. L. Stern and J. C. Huffman, *Science*, **260**, 1917 (1993).
42. J. B. Lambert, S. Zhang and S. M. Ciro, *Organometallics*, **13**, 2430 (1994).
43. L. Olsson and D. Cremer, *Chem. Phys. Lett.*, **215**, 433 (1993).
44. W. Kutzelnigg, M. Schindler and U. Fleischer, in *NMR Basic Principles and Progress*, Vol. 23, Springer, Berlin, 1989.
45. U. Pidum, M. Stahl and G. Frenking, *Chem. Eur. J.*, **2**, 1996 (1997).
46. Z. Xie, J. Manning, R. W. Reed, R. Mathur, P. D. W. Boyd, A. Benesi and C. A. Reed, *J. Am. Chem. Soc.*, **118**, 2922 (1996).
47. J. B. Lambert and Y. Zhao, *Angew. Chem., Int. Ed. Engl.*, **36**, 400 (1997).
48. T. Müller, Y. Zhao and J. Lambert, private communication.
49. P. v. R. Schleyer, *Science*, **275**, 39 (1997).
50. S. R. Bahr and P. Boudjouk, *J. Am. Chem. Soc.*, **115**, 4514 (1993).
51. For a review, see: R. J. P. Corriu and J. C. Young, in *The Chemistry of Organic Silicon Compounds*, Vol. 1 Part 2 (Eds. S. Patai and Z. Rappoport), Chap. 20, Wiley, Chichester, 1989; St. N. Tandura, N. V. Alekseev and M. G. Voronkov, *Top. Curr. Chem.*, **131**, 99 (1986).
52. R. R. Holmes, *Chem. Rev.*, **90**, 17 (1990); R. J. P. Corriu, *J. Organomet. Chem.*, **400**, 81 (1990); R. J. P. Corriu, C. Guerin and J. J. E. Moreau, in *The Chemistry of Organic Silicon Compounds*, Vol. 1, Part 1 (Eds. S. Patai and Z. Rappoport), Chap. 4, Wiley, Chichester, 1989; A.R. Bassindale and P. G. Taylor, in *The Chemistry of Organic Silicon Compounds*, Part 1 (Eds. S. Patai and Z. Rappoport), Chap. 13, Wiley, Chichester, 1989; C. E. DePuy, R. Damrauer, J. H. Bowie and J. C. Sheldon, *Acc. Chem. Res.*, **20**, 127 (1987).
53. D. J. Schomburg, *J. Organomet. Chem.*, **221**, 137 (1981).
54. R. Damrauer and S. E. Danahey, *Organometallics*, **5**, 1490 (1986); R. Damrauer, B. O'Connell, S. E. Danahey and R. Simon, *Organometallics*, **8**, 1167 (1989).
55. J. Harland, J. S. Payne, R. O. Day and R. R. Holmes, *Inorg. Chem.*, **26**, 760 (1987).
56. S. E. Johnson, J. A. Deiters, R. O. Day and R. R. Holmes, *J. Am. Chem. Soc.*, **111**, 3250 (1989); S. E. Johnson, R. O. Day and R. R. Holmes, *Inorg. Chem.*, **28**, 3182 (1989); S. E. Johnson, J. S. Payne, R. O. Day, J. M. Holmes and R. R. Holmes, *Inorg. Chem.*, **28**, 3190 (1989).
57. W. H. Stevenson, III, S. Wilson, J. C. Martin and W. B. Farnham, *J. Am. Chem. Soc.*, **107**, 6340 (1985); W. H. Stevenson, III and J. C. Martin, *J. Am. Chem. Soc.*, **107**, 6352 (1985).
58. D. A. Dixon, W. R. Hertler, D. B. Chaseand, W. G. Farnham and F. Davidson, *Inorg. Chem.*, **27**, 4012 (1988).
59. M. Kira, K. Sato, C. Kabuto and H. Sakurai, *J. Am. Chem. Soc.*, **111**, 3747 (1989).
60. S. K. C. Kumara, V. Chandraskhar, J. J. Harland, J. M. Holmes, R. O. Day and R. R. Holmes, *J. Am. Chem. Soc.*, **112**, 2341 (1990).

61. T. Kawashima, N. Iwama and R. Okazaki, *J. Am. Chem. Soc.*, **114**, 7599 (1992).
62. D. F. Evans, A. M. Z. Slawin, D. J. Williams, C. Y. Wong and J. D. Woollins, *J. Chem. Soc., Dalton Trans.*, 2383 (1992).
63. S. K. Chopra and J. C. Martin, *J. Am. Chem. Soc.*, **112**, 5342 (1990).
64. C. Breliere, F. Care, R. J. P. Corriu, M. Poirier and G. Royo, *Organometallics*, **5**, 388 (1986).
65. A. R. Bassindale and J. Jiang, *J. Organomet. Chem.*, **446**, C3 (1993).
66. H. Sakurai, K. Ebata, C. Kabuto and A. Sekiguti, *J. Am. Chem. Soc.*, **112**, 1799 (1990); A. Sekiguti, K. Ebata, C. Kabuto and H. Sakurai, *J. Am. Chem. Soc.*, **113**, 1464 (1991); A. Sekiguti, K. Ebata, C. Kabuto and H. Sakurai, *J. Am. Chem. Soc.*, **113**, 7081 (1991); A. Sekiguti, K. Ebata, Y. Terui and H. Sakurai, *Chem. Lett.*, 1417 (1991).
67. K. Ebata, T. Inada, C. Kabuto and H. Sakurai, *J. Am. Chem. Soc.*, **116**, 3595 (1994).
68. J. M. Chance, B. Kahr, A. B. Buda, J. P. Toscano and K. Mislow, *J. Org. Chem.*, **53**, 3226 (1988) and references cited therein.
69. G. Philipp and H. Schmidt, *J. Non-Cryst. Solids*, **63**, 283 (1984).
70. G. L. Wilkesg, B. Orler and H. Huang, *Polym. Prepr.*, **26**, 300 (1985).
71. H. Huang, B. Orler and G. L. Wilkesg, *Polym. Bull.*, **14**, 557 (1985).
72. H. Huang, B. Orler and G. L. Wilkesg, *Macromolecules*, **20**, 1322 (1987).
73. H. Huang, R. H. Glaser and G. L. Wilkesg, *Polym. Prepr.*, **28**, 434 (1987).
74. T. Iwamoto, K. Morita and J. D. Mackenzie, *J. Non-Cryst. Solids*, **159**, 65 (1993).
75. T. W. Zerda, I. Artaki and J. Jonas, *J. Non-Cryst. Solids*, **81**, 365 (1986).
76. K. A. K. Ebraheen and W. A. Webb, *Prog. Nucl. Magn. Reson. Spectrosc.*, **11**, 149 (1977).
77. I. Ando and W. A. Webb, *Theory of NMR Parameters*, Academic Press, London, 1983.
78. T. Takayama and I. Ando, *Bull. Chem. Soc. Jpn.*, **60**, 3125 (1987).
79. For a more extensive paper see: J. A. Tossell and P. Lazzeretti, *Chem. Phys. Lett.*, **128**, 420 (1986).
80. H. Lischka and H. -J. Kohler, *Chem. Phys. Lett.*, **85**, 467 (1982).
81. J. Kowalewski, *Annu. Rep. NMR Spectrosc.*, **12**, 81 (1982); A. Laaksonen, Specialist Periodical Report, *Nucl. Magn. Reson.*, **14**, 62 (1985); **13**, 64 (1984); I. Ando and G. A. Webb, *Theory of NMR Parameters*, Academic Press, London, 1983, p. 83.
82. D. W. N. Anderson, J. E. Bentham and D. W. H. Rankin, *J. Chem. Soc., Dalton Trans.*, 1215 (1973).
83. B. Wrackmeyer, *J. Magn. Reson.*, **61**, 536 (1985).
84. E. Kupce, E. Liepins, O. Pudova and E. Lukevics, *J. Chem. Soc., Chem. Commun.*, 581 (1984).
85. E. Kupce, E. Liepins and E. Lukevics, *Angew. Chem.*, **97**, 588 (1985); *Angew. Chem., Int. Ed. Engl.*, **24**, 568 (1985).
86. T. N. Truong and M. S. Gordon, *J. Am. Chem. Soc.*, **108**, 1775 (1986).
87. P. v. R. Schleyer and P. D. Stout, *J. Chem. Soc., Chem. Commun.*, 1373 (1986).
88. M. S. Gordon, *Chem. Phys. Lett.*, **126**, 451 (1986).
89. R. H. Cragg and R. D. Lane, *J. Organomet. Chem.*, **294**, 7 (1985).
90. B. Wrackmeyer, S. Kerschl, C. Stader and K. Horchler, *Spectrochim. Acta, Part A*, **42**, 1113 (1986).
91. B. Coleman, in *NMR of Newly Accessible Nuclei*, Vol. 2 (Ed. P. Laszlo), Academic Press, New York, 1983, p. 197.
92. E. Lippmaa, M. Magi, V. Chvalovsky and J. Schraml, *Collect. Czech. Chem. Commun.*, **42**, 318 (1977).
93. H. Schmidbaur, J. Ebenhoch and G. Muller, *Z. Naturforsch.*, **42**, 142 (1987).
94. E. Liepins, I. Birgele, E. Lukevics, V. D. Sheludyakov and V. G. Lahtin, *J. Organometal. Chem.*, **385**, 185 (1990).
95. H. A. Bent, *Chem. Rev.*, **61**, 275 (1961).
96. E. Liepins, I. Birgele, P. Tomsons and E. Lukevics, *Magn. Reson. Chem.*, **23**, 485 (1985).
97. M. Grignon-Dubois and M. Laquerre, *Organometallics*, **7**, 1443 (1988).
98. H. J. Jacobsen, P. J. Kanyha and W. S. Brey, *J. Magn. Reson.*, **54**, 134 (1983).
99. B. De Poorter, *J. Organomet. Chem.*, **128**, 361 (1977).
100. E. Kupce, E. Liepins and E. Lukevics, *Angew. Chem.*, **97**, 588 (1985); *Angew. Chem., Int. Ed. Engl.*, **24**, 568 (1985).
101. E. Kupce, E. Liepins, E. Lukevics and B. Astapov, *J. Chem. Soc., Dalton Trans.*, 1593 (1987).
102. B. Wrackmeyer, S. Kerschl, C. Stader and K. Horchler, *Spectrochim. Acta*, *Part A*, **42A**, 1113 (1986).

103. E. Kupce and E. Lukevics, *J. Magn. Reson.*, **76**, 63 (1988).
104. E. Kupce, E. Lukevics, Y. M. Varezhkin, A. N. Mikhailova and V. D. Sheludyakov, *Organometallics*, **7**, 1649 (1988).
105. V. A. Chertkov and N. M. Sergeyev, *J. Magn. Reson.*, **52**, 400 (1983).
106. K. Kamenska-Trela, Z. Biedrzicka, R. Machinek, B. Knieren and W. Luttke, *Org. Magn. Reson.*, **22**, 317 (1984).
107. E. Liepins, I. Birgele, E. Lukevics, E. T. Bogoradovsky and V. S. Zavgovodny, *J. Organomet. Chem.*, **393**, 11 (1990).
108. K. Kamenska-Trela, H. Ilcewicz, M. Rospenk, M. Pajdowska and L. Sobczyk, *J. Chem. Res.(S)*, 122 (1987).
109. G. A. Ranzuvaev, A. N. Egorochkin, S. E. Skobeleva, V. A. Kuzenetsov, V. S. Zavgorodny and E. T. Bogoradovsky, *J. Organomet. Chem.*, **222**, 55 (1981).
110. G. C. Levy, J. D. Cargioli, P. C. Juliano and T. D. Mitchell, *J. Magn. Reson.*, **8**, 399 (1972).
111. C. G. Levy, J. D. Cargioli, P. C. Juliano and T. D. Mitchell, *J. Am. Chem. Soc.*, **95**, 3445 (1973).
112. R. K. Harris and B. J. Kimber, *J. Organomet. Chem.*, **70**, 43 (1974).
113. Y. M. Pai, W. P. Weber and K. L. Servis, *J. Organomet. Chem.*, **288**, 269 (1985).
114. A. Pines, M. G. Gibby and J. S. Waugh, *J. Chem. Phys.*, **59**, 569 (1973).
115. J. Schaefer and E. O. Stejskal, *J. Am. Chem. Soc.*, **98**, 1031 (1976).
116. E. R. Andrew, *Prog. Nucl. Magn. Reson. Spectrosc.*, **8**, 1 (1971).
117. J. Schaefer and E. O. Stejskal, in *Topics in Carbon-13 NMR Spectroscopy*, Vol. 3 (Ed. G.C. Levy), Wiley-Interscience, New York, 1979, p. 283.
118. M. J. Sullivan and G. E. Maciel, *Anal. Chem.*, **54**, 1606 (1982).
119. M. Mehring, *High Resolution NMR in Solids*, Springer-Verlag, Berlin, 1983.
120. M. M. Maricq and J. S. Waugh, *J. Chem. Phys.*, **70**, 3300 (1979).
121. G. S. Harbison and H. W. Spiess, *Chem. Phys. Lett.*, **124**, 128 (1986).
122. G. S. Harbison, V. -D. Vogt and H. W. Spiess, *J. Chem. Phys.*, **86**, 1206 (1987).
123. B. Blumich and H. W. Spiess, *Angew. Chem., Int. Ed. Engl.*, **27**, 1655 (1988).
124. R. R. Ernst, G. Bodenhausen and A. Wokaun, *Principles of Nuclear Magnetic Resonance in One and Two Dimensions*, Oxford Univ. Press (Clarendon), London and New York, 1987.
125. S. Wefing and H. W. Spiess, *J. Chem. Phys.*, **89**, 1219 (1988).
126. C. Schmidt, S. Wefing, B. Blumich and H. W. Spiess, *Chem. Phys. Lett.*, **130**, 84 (1986).
127. C. Schmidt, B. Blumich and H. W. Spiess, *J. Magn. Reson.*, **79**, 269 (1988).
128. S. Wefing, S. Kaufmann and H. W. Spiess, *J. Chem. Phys.*, **89**, 1234 (1988).
129. A. Hagemeyer, K. Schmidt-Rohr and H. W. Spiess, *Adv. Magn. Reson.*, **13**, 85 (1989).
130. T. Terao, T. Fujii, T. Onodera and A. Saika, *Chem. Phys. Lett.*, **107**, 145 (1984); J. Ashida, T. Nakai and T. Terao, *Chem. Phys. Lett.*, **168**, 523 (1990).
131. A. Bax, N. M. Szeverenyi and G. E. Maciel, *J. Magn. Reson.*, **55**, 494 (1983).
132. M. M. Maricq and J. S. Waugh, *J. Chem. Phys.*, **70**, 3300 (1979); J. Herzfeld and A. Berger, *J. Chem. Phys.*, **73**, 6021 (1989); W. P. Aue, D. J. Ruben and R. G. Griffin, *J. Magn. Reson.*, **43**, 472 (1981); A. C. Kolbert, H. J. M. de Groot and R. G. Griffin, *J. Magn. Reson.*, **85**, 60 (1989).
133. E. O. Stejskal, J. Schafer and R. A. McKay, *J. Magn. Reson.*, **25**, 569 (1977).
134. J. Clauss, K. Schmidt-Rohr, A. Adam, C. Boeffel and H. W. Spiess, *Macromolecules*, **25**, 5208 (1992).
135. S. Chuang, D. R. Kinney, C. E. Bronnimann, R. Zeigler and G. E. Maciel, *J. Phys. Chem.*, **96**, 4027 (1992).
136. D. Frank, C. Hudalla, R. Maxwell and H. Eckert, *J. Phys. Chem.*, **96**, 7506 (1992).
137. C. A. Fyfe, Y. Zhang and P. Aroca, *J. Am. Chem. Soc.*, **114**, 3252 (1992).
138. A. J. Vega, *J. Am. Chem. Soc.*, **110**, 1049 (1988).
139. G. G. Almond, R. K. Harris and P. Graham, *J. Chem. Soc., Chem. Commun.*, 851 (1994).
140. R. K. Harris, T. N. Pritchard and E. G. Smith, *J. Chem. Soc., Faraday Trans. 1*, **85**, 1853 (1989).
141. K. L. McKillop, G. R. Gillette, D. R. Powell and R. West, *J. Am. Chem. Soc.*, **114**, 5203 (1992).
142. R. Tacke, A. Lopez-Mras, W. S. Sheldrick and A. Sebald, *Z. Anorg. Allg. Chem.*, **619**, 347 (1993).
143. I. Farnan and J. F. Stebbins, *J. Am. Chem. Soc.*, **112**, 32 (1990).
144. T. Takayama and I. Ando, *J. Mol. Struct.*, **271**, 75 (1992).
145. G. Koegler, A. Hasenhindl and M. Moeller, *Macromolecules*, **22**, 4190 (1989).
146. A. E. Aliev, K. D. M. Harris and D. C. Apperley, *J. Chem. Soc., Chem. Commun.*, 251 (1993).
147. A. R. Grimmer, F. Von-Lampe and M. Magi, *Chem. Phys. Lett.*, **132**, 549 (1986).

148. R. Tacke, J. Becht, A. Lopez-Mras, W. S. Sheldrick and A. Sebald, *Inorg. Chem.*, **32**, 2761 (1993).
149. R. Tacke, A. Lopez-Mras, J. Sperlich, C. Strohmann, W. F. Kuhs, G. Mattern and A. Sebald, *Chem. Ber.*, **126**, 851 (1993).
150. J. H. Iwamiya and G. E. Maciel, *J. Am. Chem. Soc.*, **115**, 6835 (1993).
151. K. Tamao, T. Hayashi, Y. Ito and M. Shiro, *Organometallics*, **11**, 2099 (1992).
152. A. B. Scholten, J. W. de Haan, H. A. Claessens, L. J. M. von de Ven and C. A. Cramers, *J. Chromatogr. A*, **688**, 25 (1994).
153. S. Hayashi and E. Akiba, *Chem. Phys. Lett.*, **226**, 495 (1994).
154. R. West, J. D. Cavalieri, J. J. Buffy, C. Fry, K. W. Zilm, J. C. Duchamp, M. Kira, T. Iwamoto, T. Mullerand and Y. Apeloig, *J. Am. Chem. Soc.*, **119**, 4972 (1997).
155. Experimental data for a few disilenes were reported earlier in a communication. See: J. D. Cavalieri, R. West, J. C. Duchamp and K. W. Zilm, *Phosphorus, Sulfur, Silicon*, **93–94**, 213 (1994).
156. B. D. Shepherd, C. F. Campana and R. West, *Heteroat. Chem.*, **1**, 1 (1990).
157. M. J. Fink, M. J. Michalczyk, K. J. Haller, R. West and J. Michl, *J. Chem. Soc., Chem. Commun.*, 1010 (1983).
158. M. Wind, D. J. Powell and R. West, *Organometallics*, **15**, 5772 (1996).
159. H. Watanabe, K. Takeuchi, N. Fukawa, M. Kato, M. Goto and Y. Nagai, *Chem. Soc. Jpn., Chem. Lett.*, 1341 (1987).
160. M. J. Fink, M. J. Michalczyk, K. J. Haller, R. West and J. Michl, *Organometallics*, **3**, 793 (1984).
161. S. Masamune, Y. Eriyama and T. Kawase, *Angew. Chem., Int. Ed. Engl.*, **26**, 584 (1987).
162. R. S. Archibald, Y. van den Winkel, A. Millevolte, D. R. Powell and R. West, *Organometallics*, **11**, 3276 (1992).
163. M. Kira, T. Maruyama, C. Kabuto, K. Ebata and H. Sakurai, *Angew. Chem., Int. Ed. Engl.*, **33**, 1489 (1994).
164. T. M. Duncan, *A Compliation of Chemical Shift Anisotropies*, Farragut Press, Chicago, 1990.
165. R. Okazaki and R. West, *Adv. Organomet. Chem.*, **39**, 232 (1995).

CHAPTER **7**

Activating and directive effects of silicon

ALAN R. BASSINDALE, SIMON J. GLYNN and PETER G. TAYLOR

Department of Chemistry, The Open University, Milton Keynes, MK7 6AA, UK

I. INTRODUCTION

This chapter extends and updates our previous review in *The Chemistry of Organic Silicon Compounds*[1]. Each section starts by summarizing some of the key conclusions of the previous review, then goes on to discuss the work that has been published since 1989.

In Section II we begin by surveying the factors that lead to activation and direction. In Section III these concepts are then applied to the various systems in which silicon exerts a stabilizing or destabilizing effect. Where possible we have tried to give quantitative information on the size of the effect. In the final sections we survey reactions which exemplify the activating and directing effects of silicon.

II. ELECTRONIC EFFECTS OF R_3Si

A. Introduction

Under appropriate conditions a proximate silicon atom may exhibit electron-donating or electron-accepting properties, stabilizing positive or negative charge.

The electronic effects of an R_3Si group can be divided into four components: (i) inductive effects, (ii) field effects, (iii) (p–d) π bonding and (iv) hyperconjugative effects. The total electronic effect of an R_3Si group in a molecule or intermediate will be a combination of these effects, and much effort has been made in the last ten years to quantify the contributions of the various effects to certain properties of silicon compounds, particularly as regards the importance of (p–d) π bonding and hyperconjugative effects.

The four electronic effects are defined in the following sections.

B. Inductive Effects

Inductive effects are generally considered to act through the σ-framework of a molecule, and the electronegativity of an element is taken as a measure of the tendency of the element to attract σ-electrons. Ebsworth[2] cited twelve electronegativity scales, all of which agree that carbon is more electronegative than silicon. The most commonly referenced values are those of Pauling[3]; C, 2.5; Si, 1.8; H, 2.1, and Allred and Rochow[4]; C, 2.55; Si, 1.93. The electronegativity of hydrogen is intermediate between that of silicon and carbon.

Therefore the polarity of the silicon–carbon bond is $Si^{+}C^{-}$, and silicon–carbon bonds are generally observed to cleave in this direction, either via electrophilic attack at carbon, or nucleophilic attack at silicon.

Trialkylsilyl and triarylsilyl groups are electron-supplying through inductive effects. The inductive effect is short-range in character, having the greatest effect on atoms directly bonded to silicon, and falling off rapidly after two or three atoms.

C. Field Effects

Field effects describe the response of a neighbouring π-system to the dipole moment of the R_3Si group. There are two types of π-inductive effects[5,6]. The first, known as π_S, is a consequence of charge differences in the σ-system brought about by inductive effects. For example, a substitutent Y which is more electronegative than H will induce a fractional positive charge at C-1 in a benzene ring, and this may induce a redistribution of the π-system that can be predicted by consideration of the resonance canonicals shown in equation 1. Thus, through the π_S effect, the electron density is diminished at C-2 and C-4, and enhanced at C-1, by an electron-withdrawing substituent Y.

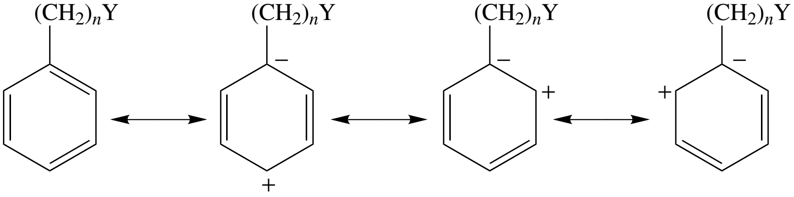

(1)

The second π-inductive effect is the field effect, π_F, which arises through polarization of the whole π-system due to the electric dipole of $(CH_2)_n$ Y, as shown in **1**.

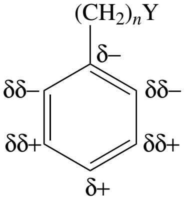

(1)

Both these effects contribute to the overall π-electron density, but are difficult to separate, particularly as they both operate mainly at C-1.

D. (p–d) π Bonding

The chemical and physical properties of the R_3Si group show that it can act as a π-electron-withdrawing group; however, the mechanism by which this electron withdrawal takes place has been open to dispute. The first explanation is that the relatively low-lying, unoccupied silicon d orbitals can participate in (p–d) π bonding. In this way electron density from the p orbital on X can be partially devolved onto silicon through a donor–acceptor interaction with the vacant silicon 3d-orbitals. The conceptually simple (p–d) π bonding model was introduced by Pauling[7] to account for the unexpected shortness of silicon–oxygen and silicon–halogen bonds, and is most easily applied to systems in which electron density, in a p-type orbital adjacent to silicon, is transferred partially onto silicon.

An important feature of the (p–d) π-bonding model is the lack of conformational requirements. The degree of (p–d) π overlap is constant, regardless of rotation around the Si−X bond, as a consequence of the symmetry of the five 3d orbitals on silicon.

E. Hyperconjugation

Hyperconjugation[8], also known as vertical stabilization[9], has been advanced as an alternative to (p–d) π bonding[8]. If two adjacent molecular orbitals are relatively close in energy and have appropriate symmetry, they can undergo interaction so that the energy of one is lowered and that of the other is raised. For example, the hyperconjugative interaction of a π orbital with a Si−C σ^* orbital is shown in Figure 1.

The magnitude of the hyperconjugative interaction is dependent on the energy difference between the orbitals and the orbital coefficients. To evaluate fully the effect of hyperconjugation it is necessary to also consider the σ^*–π^*, σ–π and σ^*–π^* interactions. However, in many cases the overall effect of hyperconjugation can be predicted simply by the use of resonance canonicals and knowledge of the polarity of bonds to silicon. The hyperconjugative effect of a methyl group can be represented as shown in equation 2.

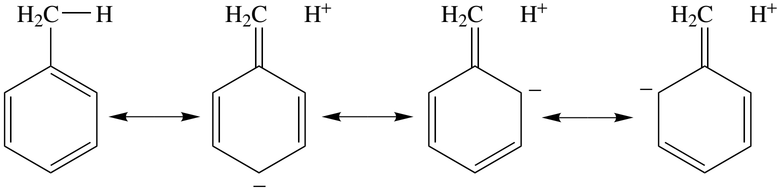

(2)

Based on the polarity of the C−H bond being C^-H^+, the resonance canonicals predict that the methyl group activates the *ortho* and *para* carbons in an aromatic ring to electrophilic substitution. For SiH_3 or $SiMe_3$ the polarities are Si^+H^- and Si^+C^-, which gives the resonance canonicals, shown in equation 3.

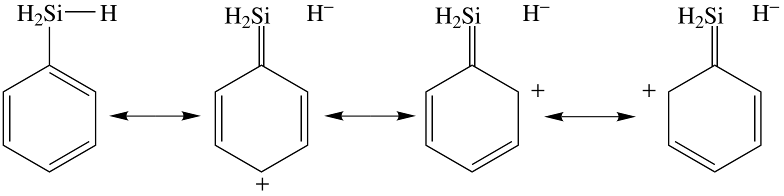

(3)

These suggest that, in contrast to a methyl group, the hyperconjugative effect of a SiH_3 or a $SiMe_3$ group will act to deactivate the *ortho* and *para* positions, although the electron-supplying inductive effect will complicate this.

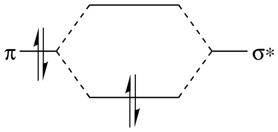

FIGURE 1. The hyperconjugation interaction of a π and σ^* orbital

Hyperconjugation also predicts that the R_3SiCH_2 group will be electron releasing at the *ortho* and *para* positions of an aromatic ring, and activating to electrophilic aromatic substitution, as shown in equation 4.

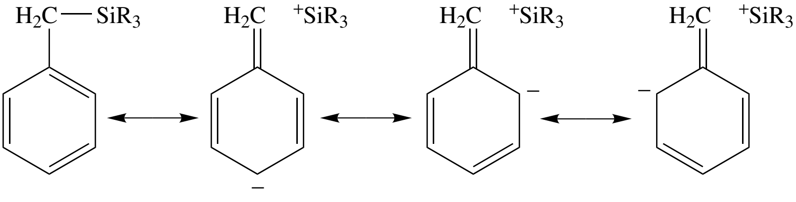

(4)

The simple hyperconjugation approach also predicts the stabilization of carbocations $R_3SiCH_2CH_2^+$, and of carbanions $R_3SiCH_2^-$, as shown in equations 5 and 6, respectively.

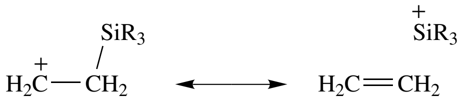

$$\overset{+}{H_2C}-\overset{SiR_3}{CH_2} \longleftrightarrow \overset{\overset{+}{SiR_3}}{H_2C{=}CH_2} \qquad (5)$$

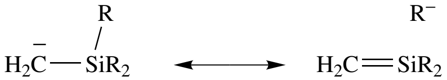

$$\overset{-}{H_2C}-\overset{R}{SiR_2} \longleftrightarrow \overset{R^-}{H_2C{=}SiR_2} \qquad (6)$$

No hyperconjugative stabilization is predicted, on the basis of bond polarities, for α-silylcarbocations or for β-silylcarbanions, as shown in equations 7 and 8, respectively.

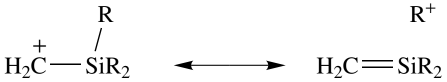

$$\overset{+}{H_2C}-\overset{R}{SiR_2} \longleftrightarrow \overset{R^+}{H_2C{=}SiR_2} \qquad (7)$$

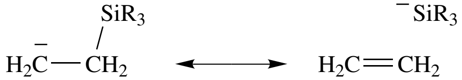

$$\overset{-}{H_2C}-\overset{SiR_3}{CH_2} \longleftrightarrow \overset{^-SiR_3}{H_2C{=}CH_2} \qquad (8)$$

Unlike (p–d) π bonding, hyperconjugation has strict conformational requirements. For hyperconjugation to be at a maximum the C–Si bond must be coplanar with the p orbital with which it is interacting[9]. When the C–Si bond is orthogonal to the p orbital, hyperconjugation is necessarily zero. This marked difference in conformational dependence between hyperconjugation and (p–d) π bonding has been utilized in attempts to determine which is the more important effect.

III. THE MEASUREMENT AND INTERPRETATION OF R_3Si ACTIVATING AND DIRECTIVE PARAMETERS

A. R_3Si as a Substituent in Aromatic Compounds

The first quantitative measures of the electronic effect of R_3Si groups were obtained through application of the Hammett equation[10] which is usually expressed in the forms:

$$\log k = \log k_0 + \rho\sigma$$

$$\log K = \log K_0 + \rho\sigma$$

where k or K is the rate or equilibrium constant for a side-chain reaction of a *meta*- or *para*-substituted benzene derivative. The quantities k_0 and K_0 approximate to k or K for the unsubstituted or parent compound. The substituent constant σ measures, for a *meta* or *para* substituent, the polar electronic effect relative to hydrogen. The σ-constant is, in principle, independent of the nature of the reaction provided there is no conjugation between the reaction centre and the substituent. Electron-withdrawing substituents have positive σ-values, and electron-supplying substituents have negative σ-values. The reaction constant ρ is a measure of the susceptibility of the reaction to polar effects and varies from reaction to reaction.

The σ_m and σ_p values for R_3Si groups have been measured in a variety of ways for a variety of reactions. Hansch, Leo and Taft[11] have surveyed Hammett substituent constants, resonance and field parameters and a selection of values of σ_m and σ_p for R_3Si groups are presented in Table 1.

The values of $\sigma_m = -0.04$ and $\sigma_p = -0.07$ for the trimethylsilyl substituent compare with values of −0.07 and −0.17 for the methyl substituent and values of −0.10 and −0.20 for the *t*-butyl substituent[11]. Hence compared with alkyl groups the Me_3Si group has a modest electronic effect in both the *meta* and *para* positions. The σ_m and σ_p constants suggest that Me_3Si will be a weakly activating substituent, but will not have a significant directing effect in aromatic substitutions.

It is clear from Table 1 that the nature of R is important in determining the electronic effect of R_3Si. Unlike $SiMe_3$, SiH_3 is found to be electron-withdrawing in both *meta*

TABLE 1. Selected Hammett substituent constants, resonance and field parameters for silicon-based substituents

R	σ_m	σ_p	F	R	$\sigma_p{}^+$	$\sigma_p{}^-$
SiH_3	0.05	0.10	0.06	0.04	0.14	
$SiMe_3$	−0.04	−0.07	0.01	−0.08	0.02	0.11
$SiHMe_2$	0.01	0.04	0.03	0.01	−0.04	
$SiPhMe_2$	0.04	0.07	0.06	0.01	0.08	
$SiMePh_2$	0.10	0.13	0.11	0.02	−0.04	
$SiPh_3$	−0.03	0.10	−0.04	0.14	0.12	0.29
$SiMe_2(OMe)$	0.04	−0.02	0.09	−0.11	−0.02	
$SiMe(OMe)_2$	0.04	−0.10	0.05	0.05	0.01	
$Si(OMe_3)$	0.09	0.13	0.10	0.03	0.13	
$Si(OEt)_3$	0.02	0.08	0.03	0.05	0.17	
$SiMe_2(OSiMe_3)$	0.00	−0.01	0.04	−0.05		
$SiMe(OSiMe_3)_2$	−0.02	−0.01	0.01	−0.02		
$Si(OSiMe_3)_3$	−0.09	−0.01	−0.08	0.07		
$Si(NMe_2)_3$	−0.04	−0.04	0.00	−0.04		
$SiMe_2F$	0.12	0.17	0.12	0.04	0.17	
$SiMe_2Cl$	0.16	0.21	0.16	0.05	0.02	
$SiMeF_2$	0.29	0.23	0.32	−0.09	0.23	
$SiMeCl_2$	0.31	0.39	0.29	0.10	0.08	
SiF_3	0.54	0.69	0.47	0.22		
$SiCl_3$	0.48	0.56	0.44	0.12	0.57	
$SiBr_3$	0.48	0.57	0.44	0.13	0.41	

and *para* positions. The triphenylsilyl group appears to be slightly activating in the *meta* position, but deactivating in the *para* position. Substitution of halogen atoms for methyl groups causes incremental increases in both σ_m and σ_p. This is mainly due to σ-electron withdrawal by the halogen atom, although enhanced (p−d) π bonding or hyperconjugation will also make a contribution. Replacement of methyl groups by methoxy groups on the silicon has a much lesser deactivating effect, whereas replacement by trimethylsilyloxy appears to show no simple trend.

The Hammett σ_p constants are inadequate for aromatic reactions in which cross-conjugation between substituents is possible. For example, when the substituent X is electron-supplying by resonance and Y is electron-accepting, cross-conjugation is possible as shown in equation 9. This direct cross-conjugation is not possible for *meta* substituents. To allow for these interactions the σ-constants ${\sigma_p}^+$ and ${\sigma_p}^-$ have been defined[12] for resonance electron-withdrawing and resonance electron-supplying substituents respectively, and some values for these constants are shown in Table 1.

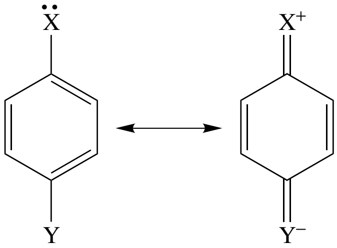

(9)

Unlike alkyl groups, the Me_3Si group does not show a much increased ${\sigma_p}^+$ value compared to σ_p. In alkyl groups C−H or C−C hyperconjugation is usually invoked to explain the enhanced electron supply. For the trimethysilyl group hyperconjugation in this direction is not favoured.

By contrast, ${\sigma_p}^-$ for Me_3Si has a value of +0.11, compared to −0.07 for σ_p. This is attributed to the Me_3Si group being electron-withdrawing by resonance, as predicted by (p−d) π bonding or hyperconjugation. The $SiPh_3$ group also shows a greatly enhanced ${\sigma_p}^-$ value.

The Hammett σ-values contain contributions from both inductive/field effects and the resonance effect. The σ-constant can be separated quantitatively into a resonance component R, which operates mainly in the *para* position, and an inductive component F, which is assumed to be equal in the *meta* and *para* positions. Hansch, Leo and Taft[11] have calculated the F and R values of Me_3Si to be 0.01 and −0.08, respectively, as quoted in Table 1. These values seem somewhat at odds with experimentally determined values[12−18] for the inductive and resonance parameters, which give mean values of −0.08 and 0.06, respectively. These values confirm the generally accepted view that Me_3Si is electron-supplying by inductive effects and electron-withdrawing by resonance effects.

B. R_3SiCH_2 as a Substituent in Aromatic Compounds

In contrast to the R_3Si group, R_3SiCH_2 is quite strongly electron-supplying to the aromatic ring; Hammett σ-values of $\sigma_m = -0.16$ and $\sigma_p = -0.21$ are quoted by Hansch, Leo and Taft[11] for Me_3SiCH_2. By comparison values of $\sigma_m = -0.05$ and $\sigma_p = -0.17$ are quoted for Me_3CCH_2. Initially it was thought that the trimethylsilylmethyl substituent was electron-releasing through inductive effects only, but the measurement of a ${\sigma_p}^+$ value of −0.62 indicated a large degree of resonance contribution due to hyperconjugative release[19].

Schaefer and coworkers[20] have used long-range NMR coupling constants to investigate rotational barriers about the C(sp^2)$-$C(sp^3) bonds in benzyl compounds. The barrier for benzylsilane was found to be 1.77 kcal mol^{-1}, compared to 1.2 kcal mol^{-1} for ethylbenzene. The increased barrier for benzylsilane is attributed to increased stabilization of the stable conformer, in which the C$-$Si bond lies in a plane perpendicular to the benzene plane, by a hyperconjugative interaction between the C$-$Si bond and the π-system.

On this evidence the Me_3SiCH_2 group attached to an aromatic ring should be quite strongly activating and *ortho/para* directing. Crestoni and Fornarini[21] have studied the gas-phase reactivity of benzyltrimethylsilane and have confirmed that it is highly activated towards electrophilic attack directed to the *ortho/para* positions.

C. The Effect of R_3Si on α-Silylcarbocations

Despite the electron-releasing inductive effect of trialkylsilyl groups, silicon does not have a large stabilizing effect on $R_3SiCH_2{}^+$. An often cited observation is that Me_3SiCMe_2Br has been found to solvolyse 38,000 times more slowly than Me_3CCMe_2Br[22]. Eaborn and coworkers[23] found that there was little rate increase in the solvolyses of Me_3SiCH_2Cl, $(Me_3Si)_2CHCl$ and $(Me_3Si)_3CCl$, compared to the large rate increases observed in the carbon substituted series ethyl, propyl and *t*-butyl. In the carbon series, the rate increase is attributed to C$-$H hyperconjugation, $\sigma-\pi$ delocalization leading to a carbon$-$carbon double bond and a positively charged hydrogen. The lack of a rate increase on silyl substitution is therefore attributable to the poor ability of the Si$-$C bond to hyperconjugate, as shown in equation 10.

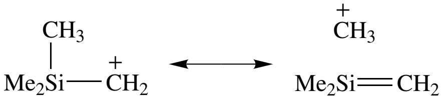

$$Me_2\overset{\overset{\displaystyle CH_3}{|}}{Si}-\overset{+}{C}H_2 \longleftrightarrow Me_2\overset{\overset{+}{CH_3}}{Si}=CH_2 \qquad (10)$$

α-Silyl carbocations generated in the gas phase by chloride elimination were observed to rearrange to silicenium ions with migratory aptitudes Ph>H$\gg$Me[24] (equation 11).

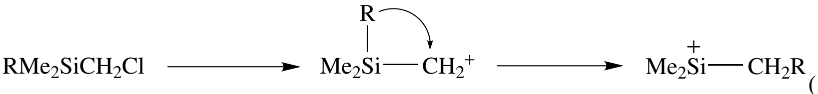

$$RMe_2SiCH_2Cl \longrightarrow Me_2\overset{\overset{\displaystyle R}{|}}{Si}-CH_2{}^+ \longrightarrow Me_2\overset{+}{Si}-CH_2R \qquad (11)$$

Cho has calculated[25], using *ab initio* methods (MP2/6-31G*), that all three of the above groups migrate from silicon to the adjacent α-carbon with no energy barrier. However, Hartee–Fock calculations (HF/6-31G*) predict small energy barriers of 1.4 kcal mol^{-1} and 1.5 kcal mol^{-1} for hydrogen and methyl migrations respectively.

The solvolysis of Me_3SiCH_2Br is observed to be enhanced relative to Me_3CCH_2Br, with a rate ratio of 2600 : 1 in basic ethanol[26]. However, further studies[27] showed that the reaction took place without formation of the carbocation. The solvolysis of Me_3CCH_2X ($X =$ triflate or tosylate) took place with almost total rearrangement, whereas no rearrangement was observed in the silicon case, although calculations indicated that this should take place on formation of the α-silyl carbocation. Together with kinetic information, these observations led to the conclusion that the α-silyl compound undergoes solvolysis by a S_N2 mechanism whilst the corresponding carbon compound involves considerable neighbouring group participation.

Calculations at the 6-31G* level[27] predicted $CH_3CH_2{}^+$ to be more stable than $H_3SiCH_2{}^+$ by 13.2 kcal mol^{-1}, and $Me_3SiCH_2{}^+$ to be less stable than $Me_3CCH_2{}^+$ by

11 kcal mol^{-1}. However, $H_3SiCH_2^+$ was more stable than CH_3^+ by 16.1 kcal mol^{-1}[27]. High level calculations using polarization functions and electron correlation at the MP3/6-31G* level have been performed for the isodesmic reaction shown in equation 12a.

$$XCH_2^+ + CH_4 \longrightarrow XCH_3 + CH_3^+ \tag{12a}$$

From the calculations it was found that when X = CH_3 the cation is 34 kcal mol^{-1} more stable than when X = H. However, when X = SiH_3 the cation is only 17.8 kcal mol^{-1} more stable than when X = H[28].

For the vinyl cation, using the isodesmic reaction shown in equation 12b, it was found that CH_3 and SiH_3 were 27 and 24 kcal mol^{-1} more stabilizing than H, respectively[28]. In this case the alpha effect of silicon is comparable to that of carbon.

$$H_2C{=}CX^+ + H_2C{=}CH_2 \longrightarrow H_2C{=}CHX + H_2C{=}CH^+ \tag{12b}$$

This has been supported by the mass spectroscopic experiments of McGibbon, Brook and Terlouw[29], who determined the stabilization of the trimethylsilylvinyl cation to be 29.5 kcal mol^{-1} relative to the vinyl cation. The trimethylsilyl group was stabilizing by 2 kcal mol^{-1} relative to a methyl group. These values are in good agreement with the theoretical figures above.

Bausch and Gong[30] have experimentally derived values for the free energies of the heterolytic C−H bond cleavage in the substituted fluorenes **2**. The α-$SiMe_3$ group and the α-CMe_3 groups have near-equal effects on the free energies of C−H heterolysis. The α-Me substituent is found to stabilize the fluorenium cation by 6 kcal mol^{-1} compared to the α-$SiMe_3$, whereas the α-$SiMe_3$ substituent gives a stabilization of 2 kcal mol^{-1} relative to hydrogen.

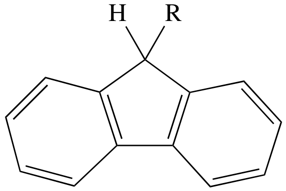

(2)

R = H, Me, $SiMe_3$, CMe_3

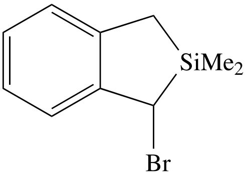

(3)

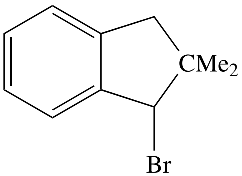

(4)

2,2-Dimethyl-2-sila-1-indanyl bromide **3** was found to solvolyse 4.98 × 10^2 times less rapidly than the carbon reference 2,2-dimethyl-1-indanyl bromide **4**[31]. This corresponds to the solvolytic generation of the α-silylated benzylic cation being some 4 kcal mol^{-1} less favourable than the α-alkylated benzylic cation.

Apeloig and coworkers studied solvolysis rates of Me_3CX and $(Me_3Si)Me_2CX$ in 97% trifluoroethanol and derived a value of 4.8 kcal mol^{-1} for the stability of the *t*-butyl cation over the 2-trimethylsilylpropyl cation[32a].

Apeloig and coworkers have also studied the effect of silyl substituents on keto−enol equilibria (equation 13)[32b,32c].

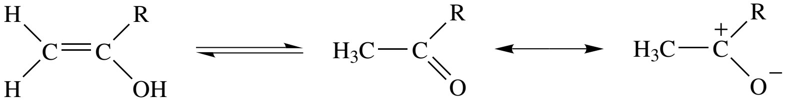

(5a) **(5b)** **(5c)** (13)

The equilibrium between the enol **(5a)** and the keto **(5b)** forms depends upon the nature of R, electropositive substituents destabilizing the keto form **5b**. This destabilization is due to the adjacent carbon having some carbocationic character, as can be seen in the resonance form **5c**.

Calculations at the 6-31G*//3-21G level showed ΔE (keto–enol) for R = SiH_3 to be 12.9 kcal mol^{-1}, which is 6.1 kcal mol^{-1} lower than ΔE for R = Me. The silyl group was calculated to destabilize the keto form by 3.8 kcal mol^{-1} relative to R = H. The theoretical predictions were confirmed experimentally.

The gas-phase basicities of α-trimethylsilylstyrenes were determined by Mishima and coworkers by measurement of proton transfer equilibrium constants[33]. The basicity of α-trimethylsilylstyrene was found to be comparable to that of α-alkyl styrenes, which was taken to suggest that an α-trimethylsilyl group stabilizes a carbocation.

D. The Effect of R_3SiCH_2 on Adjacent Carbocations

In this section we concentrate mainly on mechanistic aspects of reactions involving β-silylcarbocations. The structure and properties of β-silylcarbocations are discussed in detail in Chapter 12 on Silicon-substituted Carbocations in this volume. The strong stabilization of β-silylcarbocations is of particular importance in relation to activating and directing effects in organic syntheses using silicon compounds, and is still an important area for mechanistic, theoretical and synthetic studies.

The β-effect was first noted by Ushakov and Itenberg in 1937[34], and in 1946 Sommer, Whitmore and coworkers reported the high reactivity of β-chlorosilyl systems to elimination (equation 14), compared to the corresponding α- and γ-systems[35,36].

$$R_3Si{-}CH_2CH_2{-}X \longrightarrow CH_2{=}CH_2 + R_3SiX \qquad (14)$$

The current evidence supports a carbocationic (E1) mechanism for this reaction. However, the nature of the carbocationic intermediate has caused much interest. There are two possibilities:

(i) Interaction of silicon by a purely hyperconjugative mechanism. In this case there is no significant movement of the silicon atom, and the process is termed ‘vertical’ participation (of **6a**).

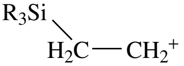

(6a)

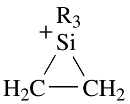

(6b)

(ii) Interaction of silicon by internal neighbouring group participation, to form a three-membered ring siliconium ion **6**. This is termed ‘non-vertical’ participation.

Studies by Jarvie and coworkers[37] showed that solvolysis of *erythro*- $Me_3SiCHBrCHBr$-CH_3 led predominantly to *cis*-1-bromopropene, via an antiperiplanar elimination. This was taken to be evidence in favour of the cyclic siliconium intermediate, although the open-chain cation could also maintain the antiperiplanar geometry if hyperconjugation disfavours rotation about the C−C bond.

A further study[38] found that the treatment of $Me_3SiCH_2CD_2OH$ with PBr_3 gave the products $Me_3SiCH_2CD_2Br$ and $Me_3SiCD_2CH_2Br$ in equal amounts. The deuterium scrambling again appears to support the cyclic siliconium intermediate, although again the open cation would also be consistent provided that it undergoes a rapid 1,2 migration of the trimethylsilyl group, as shown in equation 15.

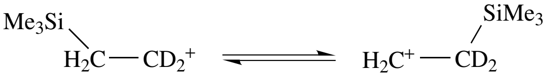

$$\overset{Me_3Si}{H_2C}{-}CD_2^+ \rightleftharpoons H_2C^+{-}\overset{SiMe_3}{CD_2} \qquad (15)$$

Calculations by Jorgensen and co-workers[28] on primary systems assessed the size of the β-effect by calculation of the energy change for the isodesmic reaction shown in equation 16.

$$CH_4 + H_3SiCH_2CH_2^+ \longrightarrow H_3SiCH_2CH_3 + CH_3^+ \qquad (16)$$

The energies at the MP3/6-31G* level of the three geometries cyclic **(7)**, parallel open **(8)** and orthogonal open **(9)** were calculated.

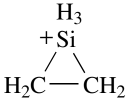

cyclic
(7)

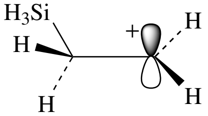

parallel
(8)

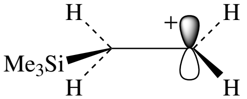

orthogonal
(9)

The cyclic form **7** had a stabilization of 74.4 $kcal\,mol^{-1}$ relative to CH_3^+, the parallel form **8**, 72.0 $kcal\,mol^{-1}$, and the orthogonal form **9**, 42.4 $kcal\,mol^{-1}$. The lesser stability of the orthogonal form is attributable to the lack of hyperconjugation in this geometry.

Compared to the ion $HCH_2CH_2^+$, $H_3SiCH_2CH_2^+$ in the parallel geometry is stabilized by 38 $kcal\,mol^{-1}$, this stabilization arising from a combination of hyperconjugative and inductive effects. In the orthogonal geometry, the cation is stabilized by 8.9 $kcal\,mol^{-1}$ which must necessarily arise from angle-independent inductive effects. The hyperconjugative stabilization in the parallel geometry is therefore around 29 $kcal\,mol^{-1}$.

Further calculations[39] on secondary and tertiary systems at the MP2/6-31G(d) level showed that for the 2-propyl cation, a β-silyl group in the bisected orientation provides 22.1 $kcal\,mol^{-1}$ of stabilization compared to a β-hydrogen, as opposed to 6.6 $kcal\,mol^{-1}$ provided by a β-methyl group. For the secondary system, the bridged carbocation was found to have a stabilization of 18.4 $kcal\,mol^{-1}$, i.e. less than the open form.

The lesser magnitude of the β-effect in the secondary cation (22.1 $kcal\,mol^{-1}$ compared to 38 $kcal\,mol^{-1}$ for the primary cation) is attributed to reduced electron demand in the secondary cation, as a consequence of the stabilizing effect of alkyl substituents.

β-Effects for the tertiary butyl carbocation were also calculated and, as would be expected, the value for β-silicon stabilization was smaller than in the secondary system, having a value of 15.9 $kcal\,mol^{-1}$. For comparison, the β-methyl stabilization was 5.0 $kcal\,mol^{-1}$.

In all these calculations SiH_3 has been used as a model for $SiMe_3$, which is the more common group used in practice. Recently, calculations by Adcock and coworkers have shown that the two silyl groups can have markedly different stabilizing effects[40].

Lambert and coworkers[41] studied the solvolysis reactions of the two cyclohexyl systems **10** and **11**.

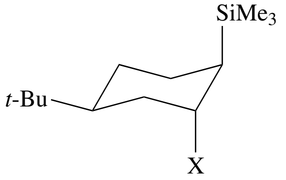

(10)

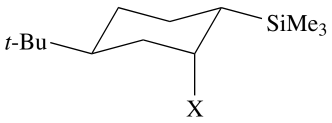

(11)

$X = CF_3CO_2$

It was found that the rate of solvolysis of the trifluoroacetate of the *trans* isomer **10** was 10^{12} times faster than that of cyclohexyl trifluoroacetate, whereas the rate acceleration of the trifluoroacetate of the *cis* isomer **11** was only 10^4. In the *trans* isomer, the Me_3Si group is frozen into the antiperiplanar (diaxial) relationship with respect to the leaving group, due to the *t*-butyl group. This is the ideal conformation for maximal hyperconjugation, whereas in the *cis* isomer, the dihedral angle between the two substituents is around 60°, and a much smaller contribution from hyperconjugation would be expected. Analysis of the various contributing effects gave rate accelerations of a factor of 10^2 in both cases arising from inductive effects. Hyperconjugative contributions were shown to be 10^{10} for the *trans* isomer and 10^2 for the *cis* isomer.

Norbornyl systems were used to study the β-effect in the synperiplanar geometry[42]. The solvolyses of the mesylates ($X = MeSO_2O$) of *endo*-3-(trimethylsilyl)-*endo*-2-norborneol **12** and *endo*-2-norborneol **13** were shown to take place via carbocationic mechanisms, and the trimethylsilyl-substituted system showed a rate acceleration of 10^5.

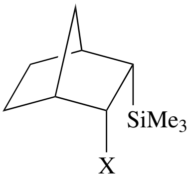

(12)

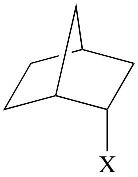

(13)

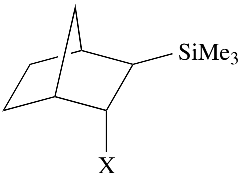

(14)

A direct comparison of *exo*-3-trimethylsilyl-*endo*-2-norbornyl mesylate **14** with **12** and **13** could not be obtained because of solubility problems. However, measurements of the acid catalysed elimination of the corresponding alcohols suggested that **14**, which has an anticlinal stereochemistry (dihedral angle = 120°), has a β-effect of a similar or slightly larger magnitude to that in **12**.

These studies imply that the synperiplanar β-effect is considerably less than the antiperiplanar β-effect. Although the synperiplanar β-effect was measured in a norbornyl system and the antiperiplanar β-effect measured in a cyclohexyl system, it is unlikely that the skeletal differences between the two systems could cause such a large difference. The β-effect of $10^4 - 10^5$ observed for the synperiplanar, synclinal and anticlinal geometries is of too great a magnitude to be attributed solely to inductive effects. Non-vertical participation cannot contribute at dihedral angles of 0° and 60°, so the β-effect at these geometries necessarily arises from hyperconjugation. However, from this study it cannot be determined whether the large β-effect in the antiperiplanar geometry contains a contribution from non-vertical participation, or whether the β-effect in the synperiplanar geometry is attenuated by reduced orbital overlap arising from steric and/or electronic factors.

To ascertain the origin of the large β-effect in the antiperiplanar geometry, α-secondary deuterium isotope effects were measured for the solvolysis of **15**[43].

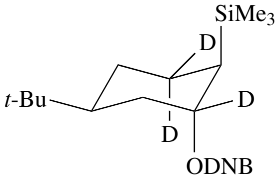

(15)

ODNB = 3,5-$(O_2N)_2C_6H_3CO_2$

For a vertical mechanism, the hybridization of the β-carbon atom changes from sp^3 to sp^2, for which the α-hydrogen/deuterium kinetic isotope effect is normally in the range 1.15–1.25.

For the non-vertical mechanism, the transition state is analogous to a S_N2 reaction, for which the isotope effect is negligible or inverse, in the range 0.95–1.05.

Solvolysis of **15** in 97% trifluoroethanol gave a secondary isotope effect of 1.17, which indicates a vertically stabilized transition state. Thus the highly unsymmetrical dihedral dependence of silicon participation can almost entirely be attributed to the hyperconjugation model with little non-vertical involvement of the silicon nucleophile.

A recent investigation has involved a system in which the vacant p orbital of the carbocation has an orthogonal relationship with the Si–C bond (equation 17)[44].

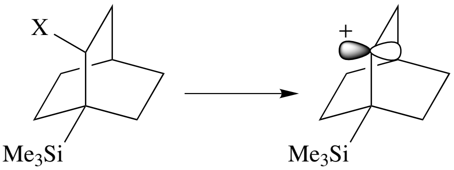

(17)

(16)

In the ion **16** neither bridging nor hyperconjugation is possible and any stabilization must result from inductive effects.

Solvolysis of the tosylates **17** and **18** in 97% trifluoroethanol gave a rate ratio β-silyl/β-H of 1.31.

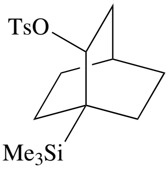

(17)

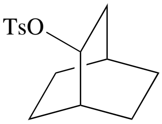

(18)

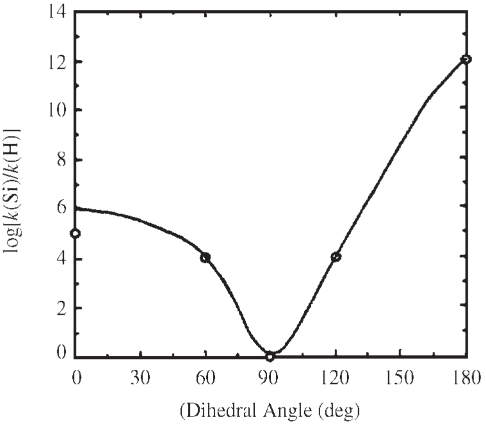

FIGURE 2. The dihedral angle dependence of the β effect of silicon

In the absence of hyperconjugative and internal participation, there is essentially no silicon β-effect. The inductive effect of the Me_3Si group is essentially zero. This agrees with the calculations of Ibrahim and Jorgensen[39], which predict no inductive stabilization for secondary systems.

From these data the dependence of the β-silicon effect on the dihedral angle can be represented graphically as shown in Figure 2, and resembles a cosine-squared curve with a highly flattened left side.

A variety of methods have been used to determine the energy of stabilization of a carbocation by a β-silicon substituent. Li and Stone[45] studied the association of the trimethylsilicenium ion with alkenes in a mass spectrometer and have calculated the β-silyl stabilization energies for the carbocations produced as shown in Table 2.

These data show a decrease in the extent of β-silyl stabilization with successive methyl substitution. The methyl (and phenyl) substituents stabilize the carbocation by polarization and inductive effects, resulting in a delocalization of positive charge away from the carbocation, and therefore a reduction in hyperconjugative interaction with the β-substituent bond.

Mass spectral studies have also shown that the vinyl cation $Me_3SiCH{=}CH^+$ is stabilized by 43.5 kcal mol^{-1} relative to $CH_2{=}CH^+$[29]. The association of trimethylsilicenium ion

TABLE 2. Thermodynamic data for the reaction $Me_3SiX^+ + XH_2 = Me_3SiXH + XH^+$

X	ΔH° (kcal mol^{-1})
Ethene	48.2
1-Propene	38.4
2-Butene	38.2
2-Methylpropene	28.1
2-Methyl-2-butene	28.8
2,3-Dimethyl-2-butene	25.8
Styrene	21.8

TABLE 3. Stabilization of vinyl cations by β-trimethylsilyl groups

Cation	β-Silicon stabilization (kcal mol^{-1})
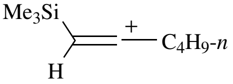 (**19**)	11
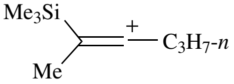 (**20**)	12
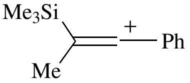 (**21**)	9

with alkynes gave stabilization energies (kcal mol^{-1}) as shown in Table 3 for some further vinyl cations **19**–**21**[46].

The smaller stabilizations of the vinyl cations **19**–**21** compared to the alkyl cations in Table 2 is attributed to the α-aryl or alkyl substituents having a greater stabilizing effect on the vinylic systems.

Kresge and Tobin[47] found that the protonation of phenyl(trimethylsilyl)acetylene in superacid media was only 300 times faster than that of phenylacetylene, corresponding to a stabilization of 3.4 kcal mol^{-1} for the β-trimethysilylvinyl cation. This small stabilization was attributed to a reduction of the hyperconjugative interaction. Although the dihedral angle in the system has the optimum value of 0°, the angle φ between the C$-$SiMe$_3$ bond and the adjacent C$-$C bond varies from 180° in the reactant **22** to 120° in the product **23** (equation 18). Hyperconjugative interaction would be expected to be maximum when $\varphi = 90°$. Thus, the small β-effect in this system arises from a large φ value in the transition state.

(18)

$\varphi = 180°$ **(22)** $\varphi = 120°$ **(23)**

Kresge and Tobin[48] also studied the hydrolysis of vinyl ethers and found a rate ratio of 130 between methyl vinyl ether and ethyl *cis*-trimethylsilylvinyl ether, corresponding to a stabilization of the β-silyl carbocation of 2.9 kcal mol^{-1}. In this case the small rate acceleration (compared to the cyclohexyl systems studied by Lambert) can be attributed to the unfavourable dihedral angle. The dihedral angle in the vinyl ether is 90° **(24)**, and on protonation it drops to 60° **(25)**, whereas maximum hyperconjugative interaction requires a dihedral angle of 0°.

The rate accelerations $k(X = SiMe_3)/k(X = H)$ and corresponding free energy differences produced by trimethylsilyl substituents in alkene and alkyne protonation reactions are shown in Table 4[49].

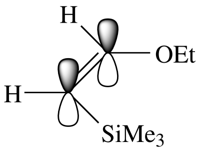

(24)

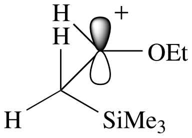

(25)

TABLE 4. Rate accelerations and free energy differences in the protonation of alkenes and alkynes

Substrate, X = H, SiMe_3	$k(\mathrm{X}=\mathrm{SiMe}_3/k(\mathrm{X}=\mathrm{H})$	$\delta(\Delta G)$ (kcal mol^{-1})
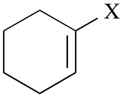 X	15,300	5.7
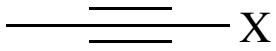 X	54,300	6.5
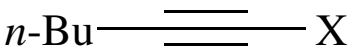 n-Bu, X	56,800	6.5
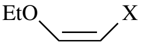 EtO, X	129	2.9
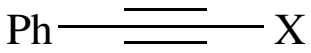 Ph, X	312	3.4

The β-silyl effects are much greater for the purely aliphatic systems than the vinyl ether or phenylacetylene, indicating that the stabilization in these latter systems is attenuated by the carbocation-stabilizing ability of the ethoxy and phenyl groups, respectively.

However, the β-effects in the aliphatic systems are still much smaller than the 10^{12} rate acceleration observed in the cyclohexyl system. As mentioned earlier, this is due to the unfavourable dihedral angle θ in the alkene protonations and the angle φ in the acetylene protonations.

A variety of other methods have been used to measure the β-silicon stabilization of carbocations. From gas-phase studies, Hajdasz and Squires[50] derived a value of 39 kcal mol^{-1} for the stabilization of the cation $\mathrm{Me_3SiCH_2CH_2}^+$ relative to the ethyl cation. This is in agreement with calculations by Ibrahim and Jorgenson[39]. Siehl and Kaufmann[51] have used carbon-13 NMR spectroscopic data to give an indication of the β-silyl stabilizing effect in some aryl vinyl cations.

Shimizu and coworkers have extensively studied the solvolyses of β-silyl benzyl systems. They observed a rate acceleration of 3×10^5 for solvolysis of 1-phenyl-2-(trimethylsilyl) ethyl trifluoroacetate **26** compared to the corresponding β-t-butyl system **27**. This indicates that the solvolytic generation of the β-silyl carbocation is about 7.5 kcal mol^{-1} more favourable[52].

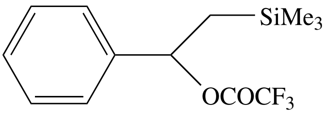

(26)

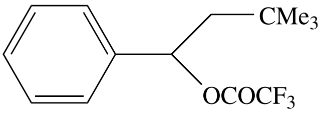

(27)

The rate of hydrolysis of the disilanyl benzyl bromide **28** is about 1 × 10^5 larger than that of **29**[53]. Thus the β-effect of **28** is similar in magnitude to **26**.

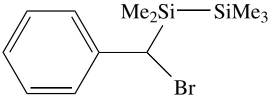

(**28**)

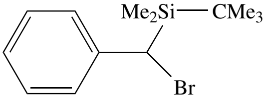

(**29**)

The effect of a methoxy substituent at the *para* position in **30** was found to be different from that in **31**[54].

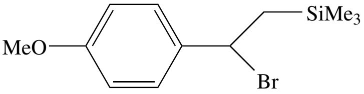

(**30**)

k(Y=MeO/Y=H) = 269

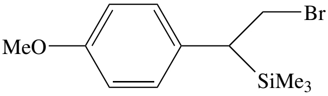

(**31**)

k(Y=MeO/Y=H) = 2.1

This was taken to indicate that solvolysis of the two substrates does not give the same cyclic siliconium ion intermediate **32**, but that one (if not both) has an open β-carbocation form.

However, the studies of Fujiyama and Munechika[55] on the solvolyses of 2-(aryldimethylsilylethyl) chlorides **33** revealed aryl substituent effects which were consistent with the formation of a cyclic siliconium ion **34**.

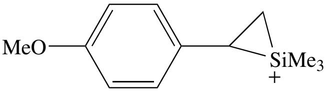

(**32**)

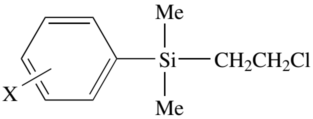

(**33**)

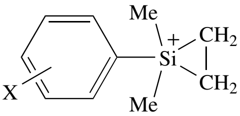

(**34**)

Shimizu and coworkers also compared the rates of solvolysis of β-silyl benzyl trifluoroacetates **35**, and chlorides **36**, with varying substituents at silicon[56]. The relative rates of solvolysis observed are given in Table 5 and 6.

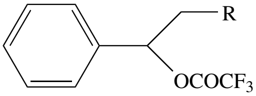

(**35**)

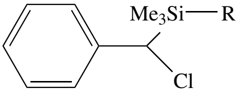

(**36**)

TABLE 5. Relative rates of solvolysis for compounds having structure **35**

R	k_{rel}
Me_3Si	1.0
Me_3SiMe_2Si	5.57
$PhMe_2Si$	0.31

TABLE 6. Relative rates of solvolysis for compounds having structure **36**

R	k_{rel}
Me_3Si	1.0
Me_3SiMe_2Si	7.65
(i-PrO)Me_2Si	0.50
(CH_3OCH_2)Me_2Si	0.29

The γ-substituent data in Tables 5 and 6 show that phenyl and alkoxy substituents at silicon are less effective than methyl at stabilizing the partial positive charge build-up on β-silicon by hyperconjugation. However, the γ-trimethylsilyl group does stabilize this build-up of positive charge.

The effect of the substituents at silicon to stabilize a β carbocation has also been investigated by Brook and Neuy[57], who studied the degree of *syn* addition to (E)-β-silylstyrenes. Addition of bromine to vinyltrimethylsilanes normally proceeds in an *anti* sense as shown in Scheme 1, the *trans* vinylsilane **37** giving the *cis* product **38**.

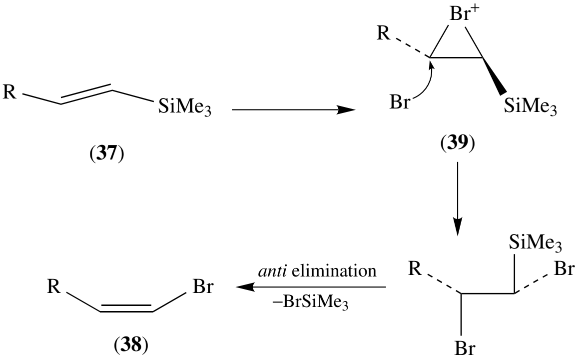

SCHEME 1

However, when R is phenyl, the bromonium ion **39** is found to open to give a β-silyl carbocation **40**. Overall *syn* addition can then occur, followed by *anti* elimination to give the *trans* alkene **41**, as seen in Scheme 2.

Table 7 shows *syn/anti* ratios obtained for a variety of styrylsilanes, together with group electronegativities.

It was concluded that for halogen and methyl substituted silyl groups, the magnitude of the β-effect is directly related to the electron-withdrawing ability of the ligands.

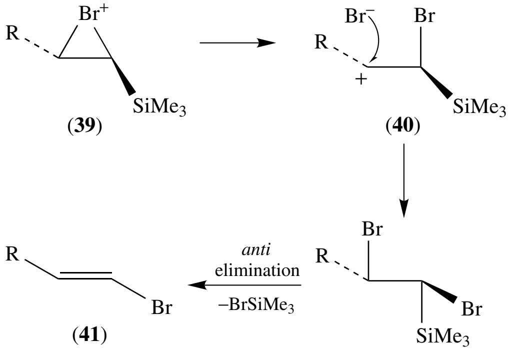

SCHEME 2

TABLE 7. *Syn/anti* ratio in the bromination of styrylsilanes

Ligands on Si	*syn/anti*	Group electronegativity
Me_3	100/0	2.06
Me_2Cl	100/0	2.12
Me_2F	85/15	2.18
$MeCl_2$	75/25	2.19
Cl_3	55/45	2.26
MeF_2	40/60	2.32
F_3	15/85	2.46

In addition to the stabilization of β-carbocations, the β-effect of silicon can also be observed in the ground states of neutral molecules. Lambert and Singer[58] studied compounds of the type **42** where hyperconjugation should be enhanced by increasing the electron-accepting properties of the substituent X (MeO < Me < H < CN). $\sigma-\pi$ overlap in this system gives the resonance structure **43** shown in equation 19.

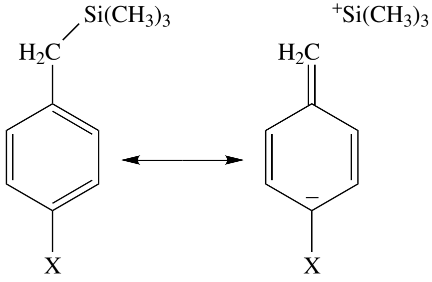

(**42**) (**43**)

(19)

Hyperconjugation should raise the bond order between the *ipso* and benzylic carbons, and lower the bond order between the benzylic carbon and the silicon atom. As the *ipso*-benzylic bond length decreases, the $^{13}C-^{13}C$ coupling constant should increase, and as the benzylic carbon–silicon bond length increases, the $^{13}C-^{29}Si$ coupling constant should decrease. The observed coupling constants are shown in Table 8, and demonstrate the expected variations.

Kirby and coworkers[59,60] obtained crystal structures of the esters **44** and **45**.

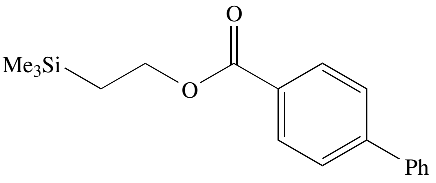

(**44**)

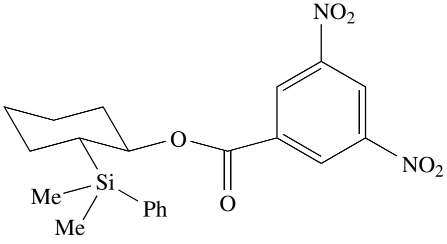

(**45**)

In 2-trimethylsilylethyl 4-phenylbenzoate **44**, the C—Si and C—O ester bonds are in an antiperiplanar conformation, and the C—O ester bond is significantly longer than expected for an alkyl ester bond at a primary centre. This is consistent with a $\sigma_{\mathrm{C-Si}}$–$\sigma^*_{\mathrm{C-O}}$ interaction in the ground state. In *trans*-2-(dimethylphenylsilyl)cyclohexyl-3,5-dinitrobenzoate **45**, the dihedral angle between the C—Si and C—O ester bonds is found to be just over 60°, and there appears to be little lengthening of the C—O bond.

White and coworkers have made further studies in this area[61–64]. The crystal structures of seven β-trimethylsilyl-substituted cyclohexylnitrobenzyl esters were obtained, together with two silicon-free model compounds[62]. In the molecules where Si—C and C—O bonds were antiperiplanar, the C—O bond lengths were found to be increased by an average of 0.014 Å. For the molecules where the Si—C and C—O bonds were *gauche*, no such systematic lengthening of the C—O bonds is observed.

NMR analysis of the conformational change in the ester **46** (equation 20) revealed the equilibrium data given in Table 9[63].

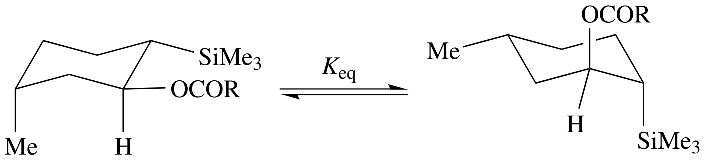

(**46a**) (**46b**) (20)

All the substrates show a preference for the diaxial conformation, **(46b)**. It appears that there is a relationship between the increasing electronegativity of the ester function and the increasing preference for the diaxial conformation.

TABLE 8. Coupling constants in trimethylsilylbenzyl systems **42**

1X	^1J ($^{13}C_{ipso}$–$^{13}CH_2$) (Hz)	^1J ($^{13}CH_2$–^{29}Si) (Hz)
MeO	41.5	46.9
Me	41.1	46.5
H	40.9	46.1
CN	40.4	43.8

TABLE 9. Ratio of diequatorial **(46a)** and diaxial **(46b)** conformers of 2-trimethysilyl cyclohexyl esters

R	Diaxial (%)	Diequatorial (%)	$\log K_{eq}$
Me	58.0	42.0	0.140
$ClCH_2$	70.0	30.0	0.367
Cl_2CH	80.8	19.2	0.624
Cl_3C	87.0	13.0	0.825
Ph	68.5	31.5	0.337
3-$MeOC_6H_4$	70.0	30.0	0.367
4-$MeOC_6H_4$	67.0	33.0	0.307
3-$O_2NC_6H_4$	70.0	30.0	0.367
4-$O_2NC_6H_4$	72.9	27.1	0.429
2,4-$(O_2N)_2C_6H_3$	81.8	18.2	0.647
3,4-$(O_2N)_2C_6H_3$	74.5	25.5	0.466
3,5-$(O_2N)_2C_6H_3$	73.0	27.0	0.431

The results demonstrate the presence of significant σ–σ^* interactions between the σ_{C-Si} orbital and the σ^*_{C-O} orbital, which stabilizes the diaxial conformation, in a similar fashion to the anomeric effect between an oxygen p-type lone pair and a σ^*_{C-X} orbital. The effect of increasing the electronegativity of the ester function is to decrease the energy of the σ^*_{C-O} orbital, resulting in a closer energy match with the σ_{C-Si} orbital, and therefore a greater interaction.

Analysis of the crystal structure of the *p*-nitrobenzoate and 2,4-dinitrobenzoate derivatives of *endo*-3-(trimethylsilyl)-*endo*-2-norborneol **47**, in which the Si—C and C—O bonds are in the synperiplanar geometry, showed that there was no significant lengthening of the C—O bond in these cases[64]. By comparison, the cyclohexyl ester **48**, in which the Si—C and C—O bonds are in the antiperiplanar conformation, did show a significant lengthening of the C—O bond compared to model compounds[64].

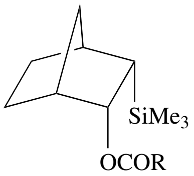

(**47**)

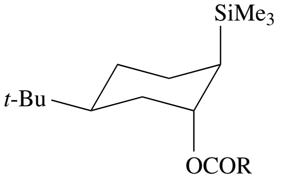

(**48**)

The small ground state effect of a β-silicon in the synperiplanar geometry compared to an antiperiplanar geometry is presumably the result of much poorer overlap between the σ_{C-Si} orbital and the neighbouring σ^*_{C-O} orbital in the synperiplanar geometry **(49)** compared to the antiperiplanar geometry **(50)**.

E. The Effect of $R_3SiCH_2CH_2$ on Adjacent Carbocations

Sommer, Whitmore and their coworkers were the first to recognize, in 1946, that a γ silicon atom could interact with a positive charge. They found that $ClCH_2CH_2CH_2SiCl_3$

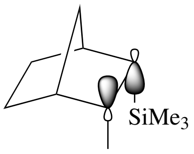

(**49**)

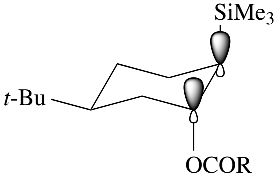

(**50**)

underwent hydrolysis faster than the corresponding α isomer, though slower than the β isomer[35].

The magnitude of the γ-effect was reported by Shiner and coworkers, who studied the solvolyses of the three cyclohexyl brosylates **51**–**53**[65].

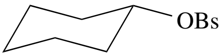

(**51**)

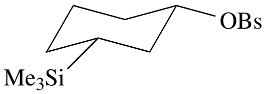

(**52**)

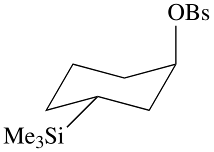

(**53**)

The *cis* isomer **52** was found to react about 450 times faster than its unsilylated analogue **51** in 97% trifluoroethanol. However, the *trans* isomer **53** showed essentially no acceleration. The secondary deuterium isotope effect observed with the β tetradeuterated analogue of the *cis* isomer **52** confirmed that the molecule reacts via the diequatorial conformation. In this conformation the back lobes of the Si—C bond at the 3-position can interact with the developing p orbital at the 1-position. This through-space interaction is often referred to as homohyperconjugation.

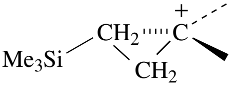

This interaction can also be modelled by the simple hyperconjugation approach, as shown in equation 21.

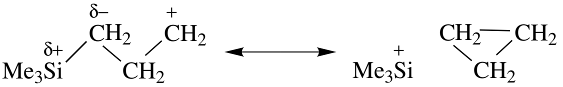

(21)

Solvolysis of the optically active $Me_3SiCH_2CH_2CH(CH_3)OBs$ had a rate acceleration of 130 relative to the carbon analogue, and gave a racemic substitution product, which indicates that the cationic intermediate is attacked equally from both sides[66].

Grob and Sawlewicz examined the effect of γ-trimethylsilyl groups using the adamantyl systems **54**[67].

Compared with hydrogen (**54**; $R = R' = H$), one trimethylsilyl group (**54**; $R = H$, $R' = SiMe_3$) accelerated the ethanolysis by a factor of 8.6 and two trimethylsilyl groups gave a further acceleration by a factor of 3.8, giving a total acceleration of 33, and forming the doubly γ-silyl stabilized ion **55**.

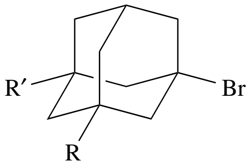

(**54**)

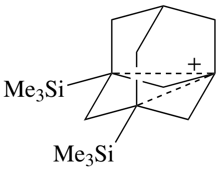

(**55**)

Further studies by Shiner and coworkers on the diastereomeric 4-(trimethylsilyl)-3-methyl-2-butyl brosylates **56** showed that solvolysis of one diastereomer gave mainly substitution products with a retained configuration[68]. A minor product is a cyclopropane resulting from nucleophilic attack at silicon in the ionic intermediate. From the stereochemistry of the cyclopropanes obtained it was deduced that the 'W' conformation is favoured over the '*endo*-sickle', as shown in Figures 3a and 3b.

Kirmse and Sollenbohmer[69] studied the trifluoroethanolysis of the norbornyl *p*-nitrobenzoate **57**, and observed the formation of the intermediate **58**, followed by a 6,2 migration of silicon and Wagner–Meerwein shifts to give a mixture of products. The solvolysis of the norbornyl system **57** is accelerated by a factor of 3 × 10^4 compared to unsubstituted 2-norbornyl *p*-nitrobenzoate.

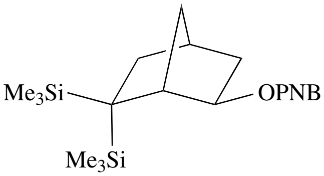

(**57**)

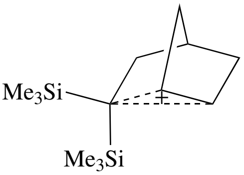

(**58**)

Ground state γ-effects of silicon may be responsible for the elongated C(alkyl)-O(ester) bond in *cis*-3-trimethylsilylcyclohexyl *p*-nitrobenzoate **59** relative to the silicon-free derivative[61]. It is suggested that the ground state γ-effect could be due either to homohyperconjugation, **60**, or to inductively enhanced C−C hyperconjugation where the trimethylsilyl substituent increases the importance of the resonance form **61** relative to the silicon-free derivative.

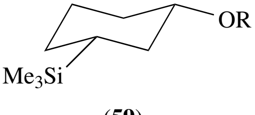

(**59**)

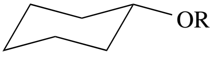

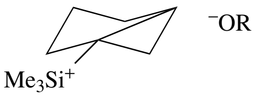

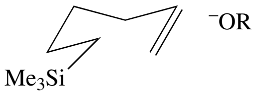

(**60**) (**61**)

OR = $OCOC_6H_4NO_2$-*p*

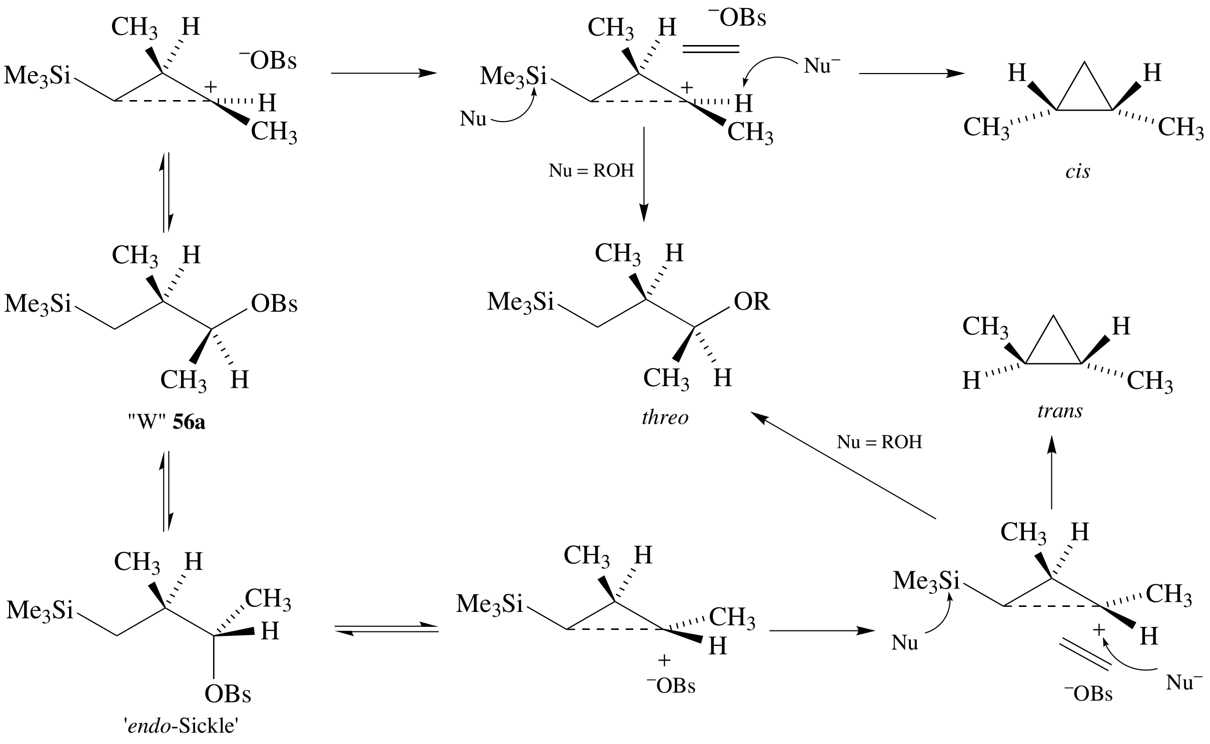

FIGURE 3a. Mechanism for the solvolysis of *threo*-4-(trimethylsilyl)-3-methyl-2-butyl brosylate, **56a**

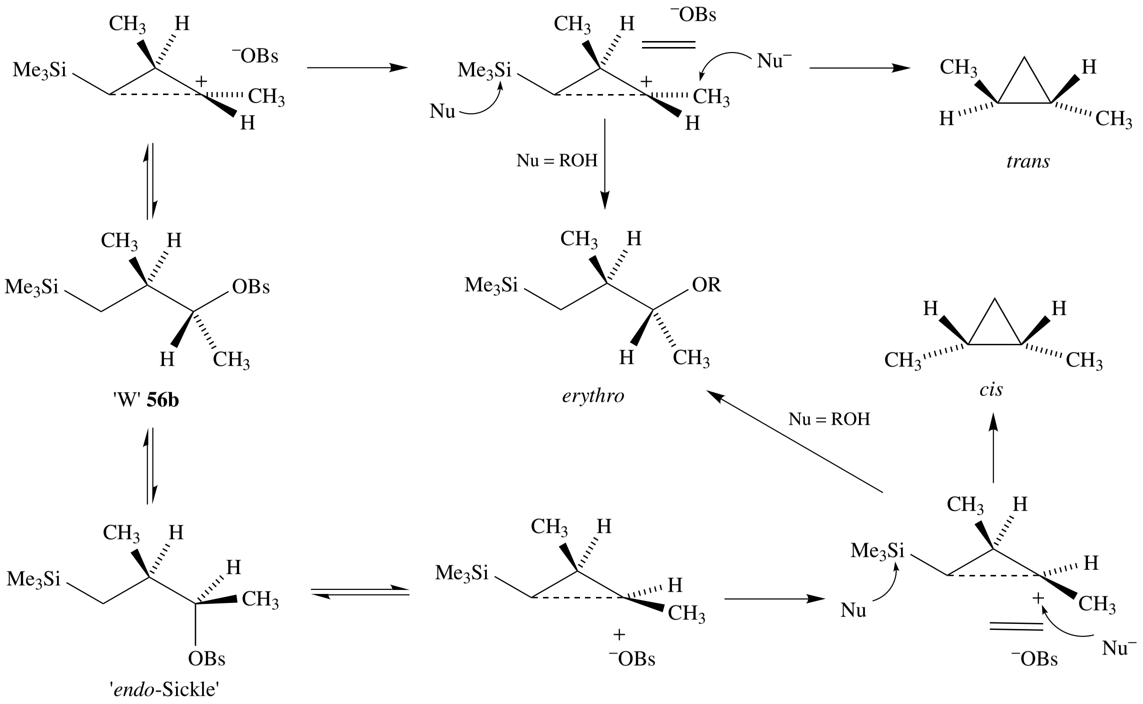

FIGURE 3b. Mechanism for the solvolysis of *erythro*-4-(trimethylsilyl)-3-methyl-2-butyl brosylate, **56b**

Adcock and Kok have analysed the ^{19}F chemical shifts of a range of 3-substituted 1-fluoroadamantane derivatives **62**. The substituent chemical shift (^{19}F SCS) can be factorized into polar field ($\rho_F\sigma_F$) and residual contributions (^{19}F SCS - $\rho_F\sigma_F$). A significant solvent-independent residual contribution is observed when R = $SiMe_3$, and is attributed to homohyperconjugation[70].

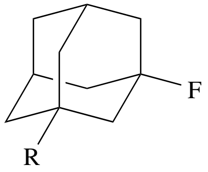

(**62**)

F. The Effect of $R_3SiCH_2CH_2CH_2$ on Adjacent Carbocations

Until recently it was thought that silicon substituents beyond the γ-position have no effect on reactivity[71]. Fessenden and coworkers[72] found that the rates of ethanolysis of *cis*- and *trans*-4-(trimethylsilyl)cyclohexyl tosylates were almost identical to those of the *cis*- and *trans*-4-*tert*-butylcyclohexyl tosylates.

However, Adcock, Shiner and coworkers found increased rates of solvolysis for 4-metalloidal-substituted bicyclo[2.2.2]-oct-1-yl *p*-nitrobenzenesulphonates and methanesulphonates, in the order tin>germanium>silicon[73], as also observed for the β-effect. The relative rate of solvolysis of the 4-trimethylsilyl mesylate **63** compared to the non-substituted parent compound was 49 : 1.

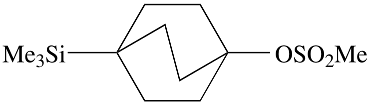

(**63**)

The stabilization of a positive charge by δ-silicon is believed to be through double hyperconjugation, represented by the resonance structures shown in equation 22.

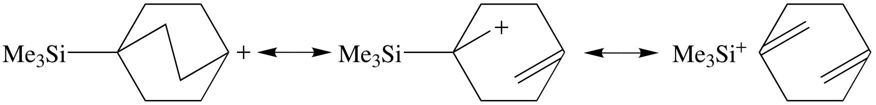

(22)

This mechanism also accounts for the very large δ-deuterium isotope effect observed for the solvolysis of (4-D)bicyclo[2.2.2]oct-1-yl mesylate. This mechanism is also supported by theoretical calculations of 4-substituted bicyclo[2.2.2]oct-1-yl cations[74].

^{19}F NMR studies on 5-substituted 2-fluoroadamantanes **64** showed residual contributions which suggest contributions from the resonance structures **65** and **66** to the ground-state structure (equation 23)[75].

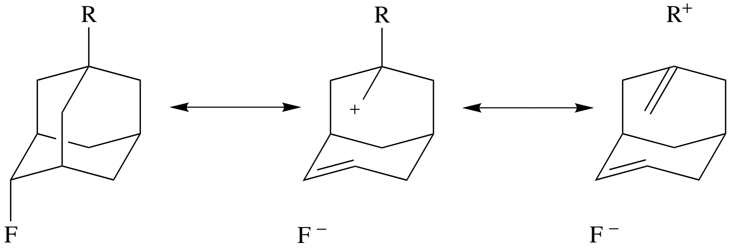

(23)

(64) **(65)** **(66)**

Similar conclusions are obtained from the ^{19}F NMR of 4-substituted bicyclo[2.2.2]oct-1-yl fluorides[76].

An X-ray crystal structure analysis of *trans*-4-trimethylsilylcyclohexyl *p*-nitrobenzenesulphonate **67** reveals an elongated C(alkyl)-O(ester) bond, compared to the non-silicon substituted derivative[61].

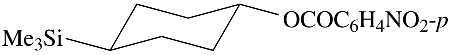

(67)

G. The Effect of R_3Si on α-Silylcarbanions

It is a general observation in organosilicon chemistry that R_3Si tends to stabilize an adjacent negative charge. In the series $(Me_3Si)_nH_{3-n}CH$ the ease of metallation increases as n increases from 0 to 3[77].

The stabilization of α-carbanions by silicon has been the subject of several theoretical studies. Using *ab initio* calculations, Hopkinson and Lien[78] calculated the proton affinities of $C_2H_5^-$ and $H_3SiCH_2^-$. They found a difference of 31.5 kcal mol^{-1}, which represents the stabilization of the carbanion by the SiH_3 group relative to methyl. The α-methyl group was found to be weakly destabilizing, by 2.2 kcal mol^{-1}, relative to hydrogen, such that for the isodesmic proton-transfer reaction in equation 24, the proton affinity relative to methane is 29.3 kcal mol^{-1}.

$$CH_4 + H_3SiCH_2^- \longrightarrow CH_3^- + H_3SiCH_3 \qquad (24)$$

Glidewell and Thomson[79] calculated the proton affinities for a variety of silyl substituted carbanions. In the series $H_3SiCH_2^-$, $(H_3Si)_2CH^-$ and $(H_3Si)_3C^-$, stability increased by about 20 kcal mol^{-1} per silyl substituent.

The proton affinity of the trimethylsilylmethyl anion was also calculated from measurements of the electron affinity of the trimethylsilylmethyl radical[80]. This gave a proton affinity of 25.7 kcal mol^{-1} for $Me_3SiCH_2^-$, relative to methane. This compares well with the calculated value for $H_3SiCH_2^-$ given earlier.

Brinkman and coworkers[81] obtained a value of around 30 kcal mol^{-1} from a similar gas-phase study for the same proton affinity relative to methane. Calculations at the 6-311+G(d,p) level gave a value of 25 kcal mol^{-1} (for $H_3SiCH_2^-$). The proton affinities of $(H_3Si)_2CH^-$ and $(H_3Si)_3C^-$ relative to methane were calculated to be 47 and 66 kcal mol^{-1}, respectively. The experimental proton affinity of $(Me_3Si)_2CH^-$ was found to be approximately 43 kcal mol^{-1}.

The computed geometries of the anionic and neutral species reveal a decrease in carbon–silicon bond length by approximately 0.1 Å on deprotonation. This is consistent with the important role played by hyperconjugation in stabilizing the carbanion. In addition, Mulliken population analysis indicates that in the neutral molecule, the central atom has close to a full negative charge. Upon deprotonation, most of the charge is picked up throughout the rest of the molecule. Previous studies have shown that the inclusion of silicon d-functions in calculations of the energies of α-silyl carbanions has little effect on the results[78–80], indicating that the d orbitals on silicon are not involved in the stabilization of anions by α-silicon. This suggests that the stabilization arises solely through hyperconjugation, as shown in equation 25.

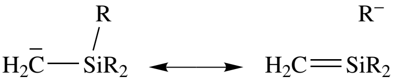

$$H_2\overset{-}{C}{-}\overset{R}{\overset{/}{Si}}R_2 \longleftrightarrow H_2C{=}\overset{R^-}{Si}R_2 \qquad (25)$$

Sieburth and Somers[82] studied the product ratio of metallation of *t*-butyl-*N*-phenylmethyl-*N*-trimethylsilylmethyl carbamate **68** (equation 26). This ratio reflects the relative abilities of an α-phenyl and α-trimethylsilyl group to stabilize an adjacent carbanion. It was found that metallation α to silicon **(70)** was slightly favoured kinetically, but at equilibrium the α-phenyl anion **69** was strongly favoured.

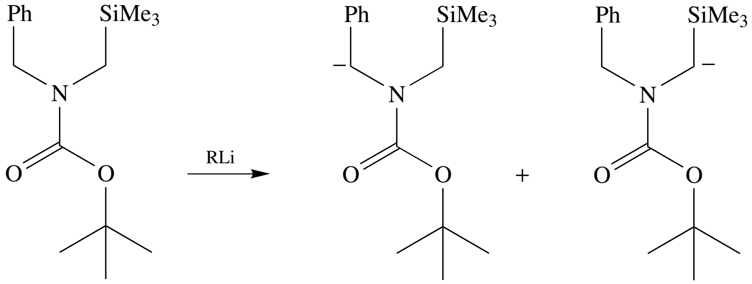

(26)

(68) **(69)** **(70)**

Bordwell and coworkers[83] investigated the deprotonation of 9-trimethylsilylfluorene and trimethylsilylmethyl phenyl sulphones. The presence of an α- trimethylsilyl group increased the acidity by 2 and 4.2 kcal mol^{-1}, respectively. Introduction of a Ph_3Si group increased the acidity by 5.9 and 10.5 kcal mol^{-1}, respectively.

H. The Effect of R_3SiCH_2 on Adjacent Carbanions

Very little experimental or theoretical work has been reported on the stability of $R_3SiCH_2CH_2^-$. All available evidence points to the formation of $R_3SiCH_2^-$ instead of $R_3SiCH_2CH_2^-$, where there is a choice.

IV. ACTIVATING AND DIRECTIVE EFFECTS OF SILICON IN ELECTROPHILIC AROMATIC SUBSTITUTION

A. Reactions of Compounds with SiR_3 Directly Bonded to the Aromatic Ring

Electrophilic aromatic substitution normally proceeds via a positively charged intermediate **71** (known as a Wheland intermediate or σ-complex) (equation 27)[84].

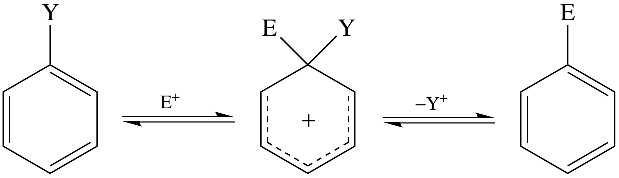

(27)

(71)

The transition states in both steps of the reaction are not likely to be far removed in energy or structure from the intermediate, which may be used as a model to rationalize variations in the rates and products of such reactions. If silicon is in a position such that it is β to the positive charge in one of the resonance forms, this might be expected to lower the energy and increase the rate, provided the carbon−silicon bond can overlap with the vacant π-orbital.

Substitution of a trimethylsilyl group directly onto an aromatic ring does lead to a rate increase relative to hydrogen, however the reaction usually occurs via *ipso* substitution (equation 28).

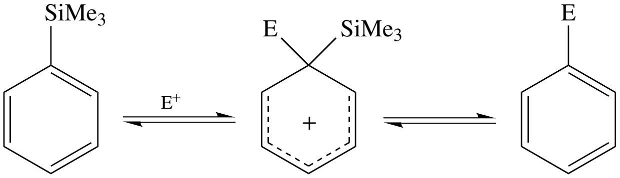

(28)

Cleavage of the C−Si bond is in the direction $C^{-}SiR_3{}^{+}$, in the same sense as aryl−H bonds are broken $C^{-}H^{+}$. Activation to electrophilic attack arises from β-stabilization of the carbocation in one of the resonance forms **(72)** of the intermediate[85,86].

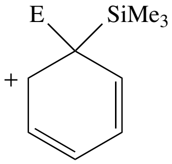

(72)

For each *ipso* substitution there is a competing electrophilic substitution of hydrogen (equation 29).

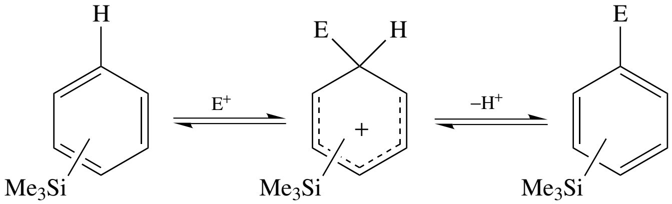

(29)

For most electrophiles substitution of the silyl group is faster than replacement of hydrogen.

As would be expected, substituents on the silicon have a profound effect on the reactivity of the arylsilicon compound. Increased electron supply from R in R_3Si increases the rate of reaction. Aryl−SiX_3 bonds are cleaved much less readily than aryl−$SiMe_3$ bonds when X is a more electronegative element than carbon. When X is halogen, desilylation is deactivated to such an extent that ring substitution occurs without loss of silicon. In the presence of other substituents the degree of Si−C cleavage compared to C−H bond cleavage depends upon the relative ability of the silyl group and the other directing group to stabilize the intermediate. The hydroxy, amino, methoxy and dimethylamino groups usually have a more powerful directing effect than the $-SiMe_3$ group (equation 30)[87,88], whereas the directing effect of the methyl group is often less (equation 31)[89].

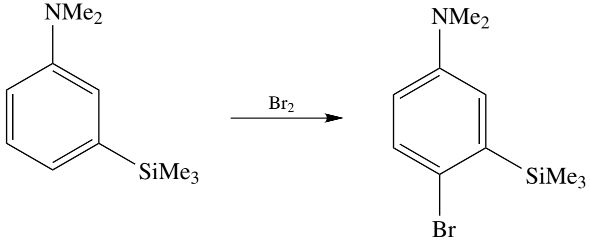

(30)

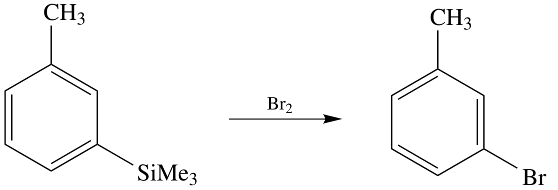

(31)

The ability of the silyl group to direct substitution in competition with other directing groups is also found to depend on the nature of the electrophile (equation 32).

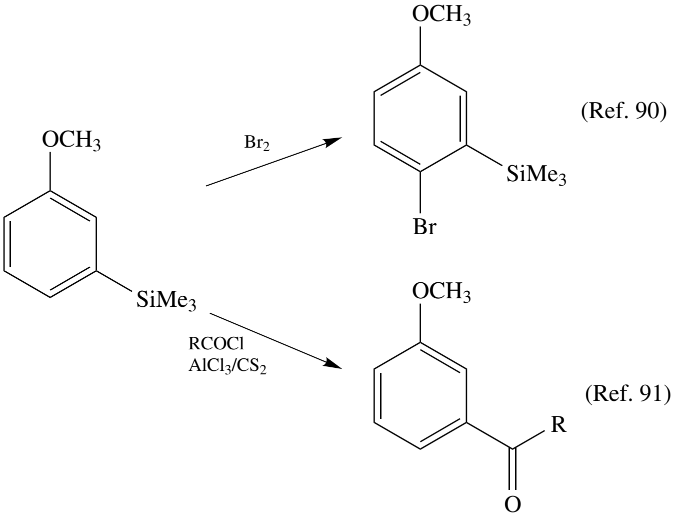

(32)

As expected, electronegative substituents on silicon decrease the preference for *ipso* substitution and silicon substituents in normally activated sites are not substituted, as shown in equation 33[92].

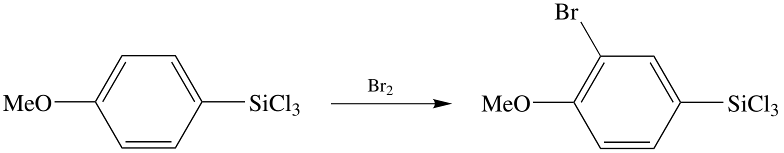

(33)

Silicon-substituted arenes have particular usefulness in organic synthesis. *Ipso* substitution always gives a single isomer, and desilylation can be carried out on deactivated systems, or systems that would undergo side-reactions under normal conditions (equations 34–36). *Ipso* substitution also provides a useful route to labelled compounds (equation 37)[95–97].

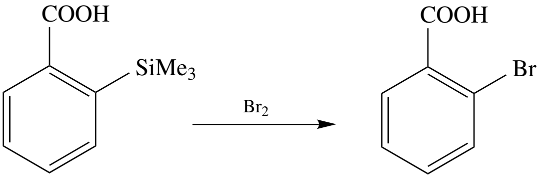

(Ref. 93) (34)

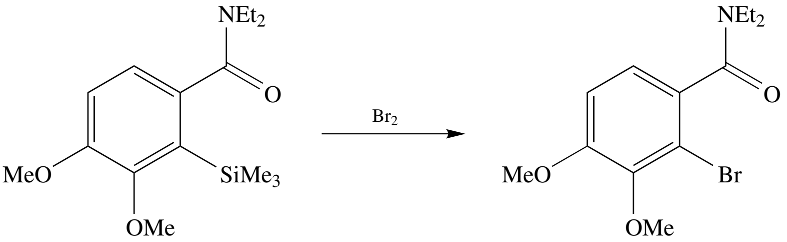

(Ref. 94) (35)

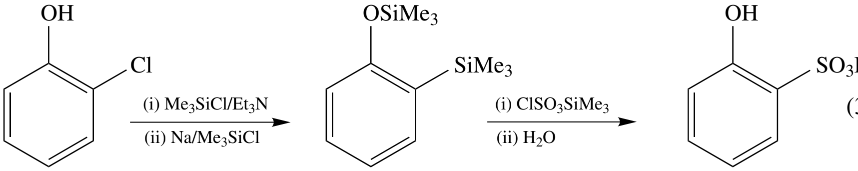

(36)

(Ref. 95)

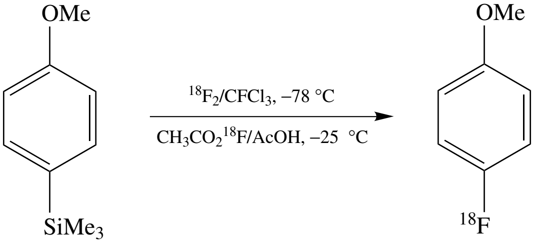

(Ref. 96) (37)

Felix, Dunogues and Calas[98–101] have extended this strategy such that a range of disubstituted benzene derivatives **74** can be regiospecifically synthesized starting from the readily accessible *o*-, *m*- or *p*-bis(trimethylsilyl)benzenes **73** (equation 38).

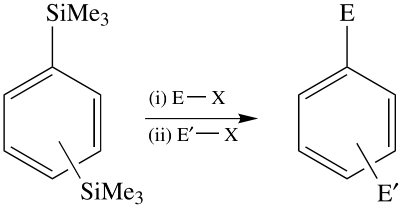

(73) **(74)**

(38)

Since trimethylsilylarenes can be prepared by metallation of the arene followed by treatment with chlorotrimethylsilane, this provides an alternative route into a range of difficult substitution patterns. For example, the *ortho/para* directing effects of the methoxy groups in 1,3-dimethoxybenzene **75** direct the electrophile to the 4-position. However, lithiation of 1,3-dimethoxybenzene takes place at the 2-position. Reaction with chlorotrimethylsilane then gives the 2-trimethylsilyl compound **76**, which undergoes *ipso* substitution with the electrophile to give the 1,2,3-trisubstituted product **77** (equation 39)[101,102].

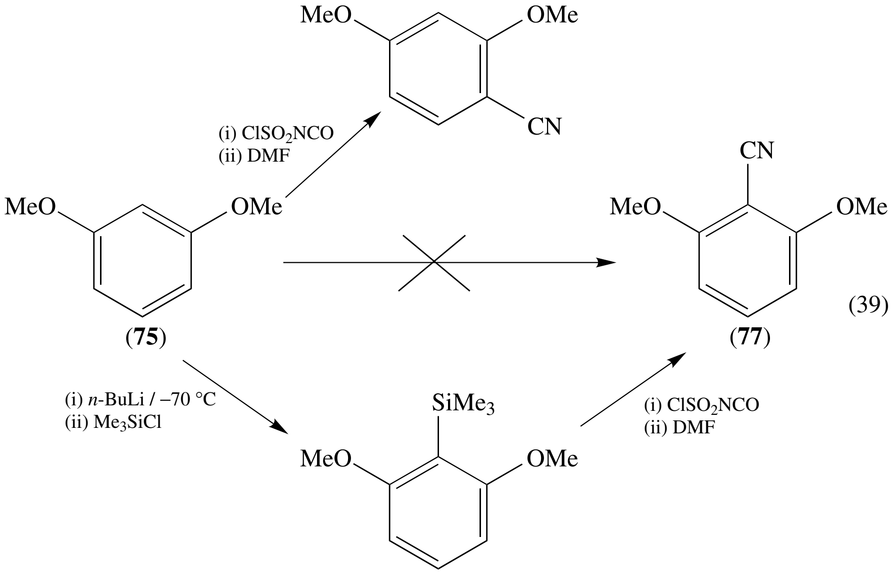

(**75**) (**77**) (**76**)

(39)

Mills, Taylor and Snieckus[103] describe a methodology based on the preferred *o*-metallation of benzamides (equation 40). In this case the trimethylsilyl group is used to block one of the *ortho* positions, directing the electrophile to the other.

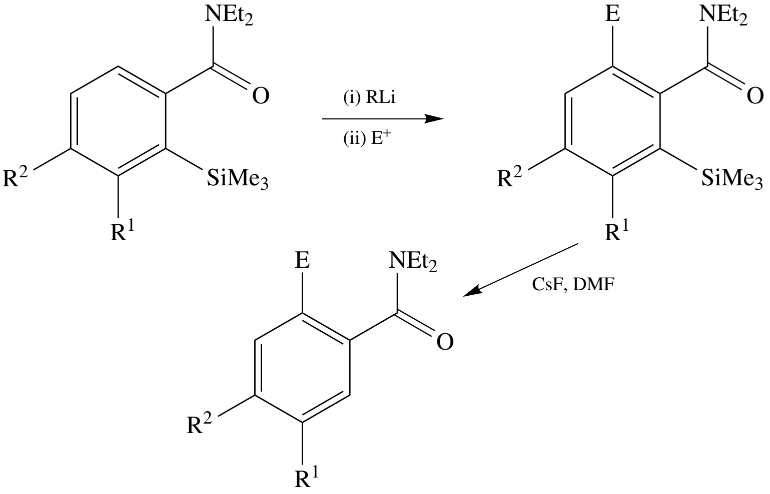

(40)

In the absence of desilylation the $-SiMe_3$ group is very slightly activating with no discernable directing effect on electrophilic aromatic substitution. Although electrophilic attack at the *meta* position generates a β-carbocation **78**, the carbon–silicon bond and the vacant p orbital are orthogonal, which precludes any stabilization by hyperconjugation.

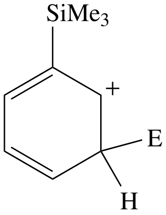

(**78**)

A recent study by Ishibashi and coworkers[104] found that the reaction of trimethylphenylsilane with methyl chloro(methylthio)acetate in the presence of tin(IV) chloride gave no *ipso* substitution (equation 41). This was attributed to steric factors, since when the primary chloride $ClCH_2SCH_2CO_2Et$ was used, a 20% yield of *ipso*-substituted product was obtained.

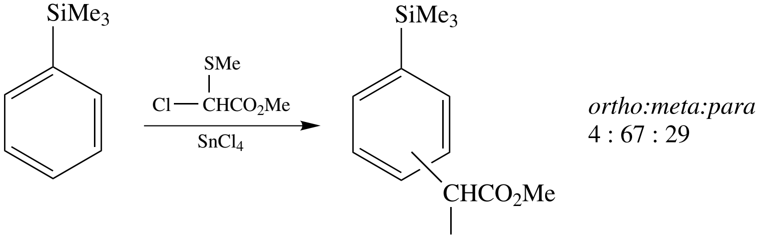

(41)

TABLE 10. Partial rate factors for the reaction of arenes with methyl chloro (methylthio)acetate

Ph-X	$k_{Ar}/k_{benzene}$	% *ortho*	% *meta*	% *para*	f_{ortho}	f_{meta}	f_{para}
$X = Me_3Si$	3.81	4.6	65.8	30.0	0.53	7.53	6.87
$X = Me$	152.4	11.7	0.3	88.0	52.4	1.5	804

The rate of electrophilic addition relative to the rate of reaction of benzene and of toluene was measured in this study, and the partial rate factors f calculated, as shown in Table 10. These data demonstrate the weak activating effect of Me_3Si compared to methyl.

Substitution of R in R_3Si by more electronegative groups both decreases the extent of desilylation and increases the proportion of *meta* substitution. The overall rate of electrophilic substitution is also decreased as the R_3Si group becomes more electron-withdrawing.

B. Electrophilic Aromatic Substitution in $ArCH_2SiR_3$ Compounds

The p-CH_2SiMe_3 group has a large activating effect in protiodetritiation and protiodesilylation, the $-CH_2SiMe_3$ substituted compound reacting up to 180 times faster than the corresponding methyl compound[105,106]. Presumably this is due to β-stabilization of the resonance form **79**.

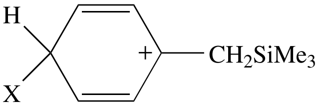

(**79**)

The $-CH_2SiMe_3$ group is *ortho/para* directing, as mentioned earlier.

V. ACTIVATING AND DIRECTIVE EFFECTS IN ALIPHATIC ELECTROPHILIC REACTIONS

A. Reactions of Vinylsilanes

1. Introduction

Electrophilic addition to carbon–carbon double bonds normally occurs through cationic intermediates. As discussed previously, β-silylcarbocations are strongly stabilized, whereas α-silylcarbocations are not stabilized. Thus, if the R_3Si group is arranged so that it can be β to the carbocation, then hyperconjugative stabilization may be possible, and this will affect the regio- and stereochemical outcome of the reaction.

Vinylsilanes react readily with a variety of electrophiles either by addition to the double bond or substitution of the R_3Si group. The addition product **80** often undergoes subsequent elimination to give the substitution product **81**, as shown in equation 42.

The first step in substitution or addition is normally addition of the electrophile to the carbon bearing the silicon to give a β-silylcarbocation (equation 43).

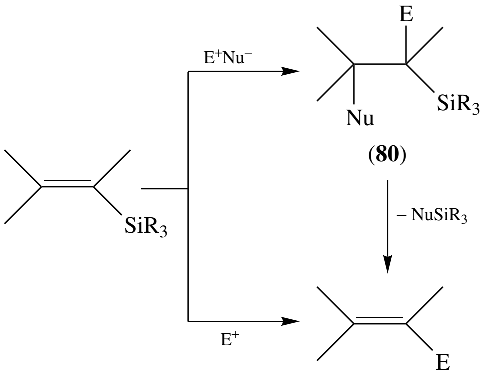

(80)

(81)

(42)

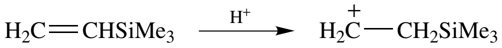

$$H_2C{=}CHSiMe_3 \xrightarrow{H^+} H_2\overset{+}{C}{-}CH_2SiMe_3 \qquad (43)$$

However, the directing influence of silicon can be overcome if the vinylsilane contains another substituent that can stabilize a carbocation more strongly than silicon. For example, when the silyl group is attached to C-2 of a terminal alkene, reaction occurs to give the more substituted carbocation **82** (equation 44)[107]. Similarly, if the silicon is bound to the same carbon atom as a phenyl group, reaction occurs via the benzyl cation to give the product shown in equation 45[108].

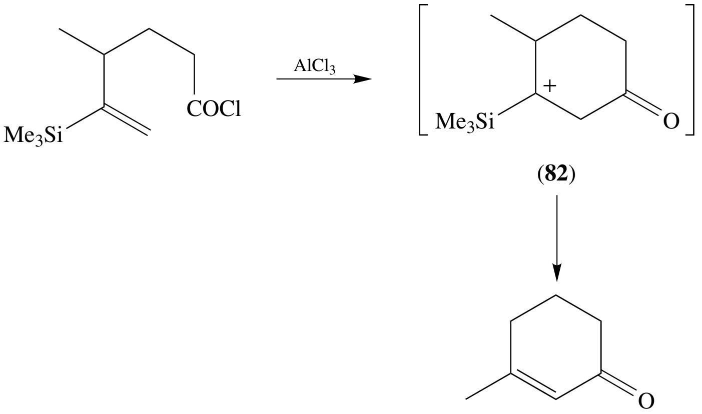

(82)

(44)

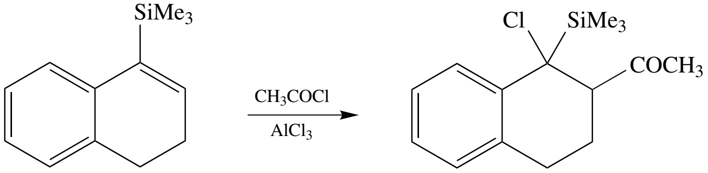

(45)

2. Addition to vinylsilanes

As with alkenes, in general, *anti*-addition is often the course of reaction, especially when halonium ions are involved[109–112]. However, as mentioned earlier, *syn* addition can take place in the bromination of β-silylstyrenes. This stereochemistry is explained by stabilization of the open-chain carbocation by the aromatic group, compared to the cyclic bromonium ion. In this case the conformer **83** has the maximum hyperconjugative stabilization, and is formed by the least motion rotation about the carbon–carbon bond.

Attack of bromide then takes place on the less hindered side of the cation, *anti* to the β-silyl group, to give overall *syn* addition (equation 46).

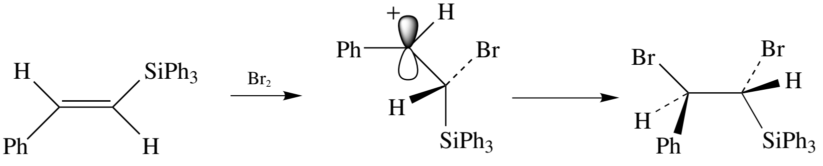

(**83**)

(46)

Miura and coworkers have studied the intramolecular addition of alcohols to vinylsilanes[113]. 5-Silyl-4-penten-1-ols **84** are readily transformed into 2-substituted tetrahydrofurans **(85)** in the presence of a catalytic amount of *p*-toluenesulphonic acid or titanium tetrachloride (equation 47).

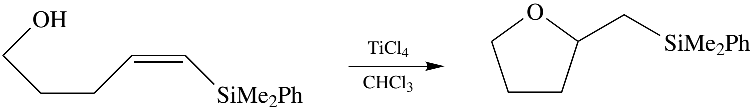

(**84**) (**85**)

(47)

Such cyclization does not take place in the absence of the silyl group.

The *syn* stereochemistry of the addition is revealed when 5-deuteriated vinylsilanes **86** are employed, as shown in equation 48.

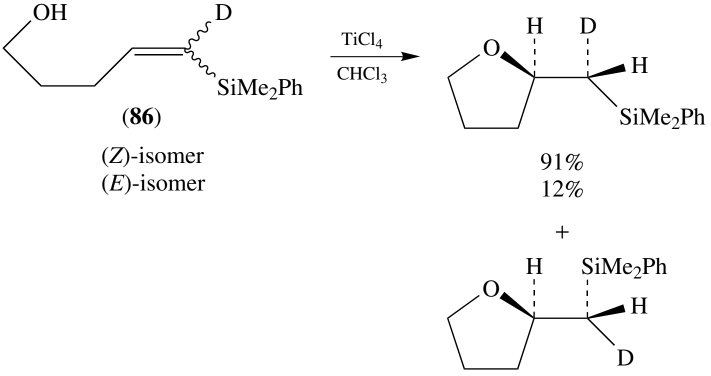

(**86**)

(*Z*)-isomer
(*E*)-isomer

91%
12%

9%
88%

(48)

Under identical conditions, 6-silyl-5-penten-1-ols **87** cyclize to give 2-substituted tetrahydropyrans **88** and **89**. Again *cis* addition is strongly favoured, as shown in

equation 49.

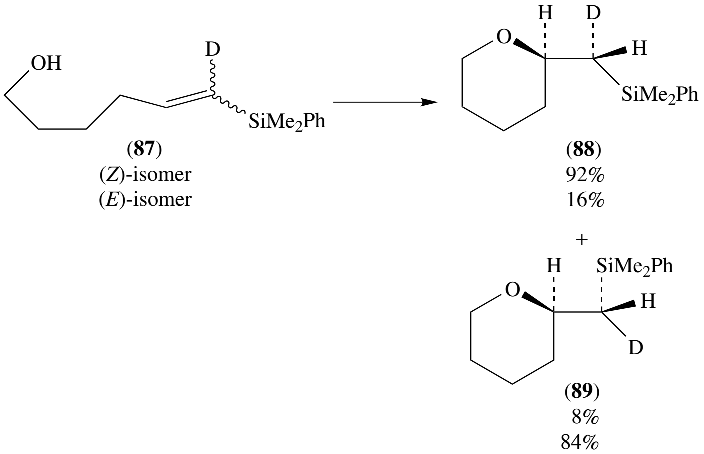

(**87**)
(*Z*)-isomer
(*E*)-isomer

(**88**)
92%
16%

(**89**)
8%
84%

(49)

The cyclization of (*Z*)-1-substituted-5-silyl-4-penten-1-ols **90**, shown in equation 50, gave 2,5-disubstituted tetrahydrofurans **91** and **92** with a high *trans*-selectivity (% *trans* > 86 for R = Ph, *i*-Pr, C_6H_{13})[114].

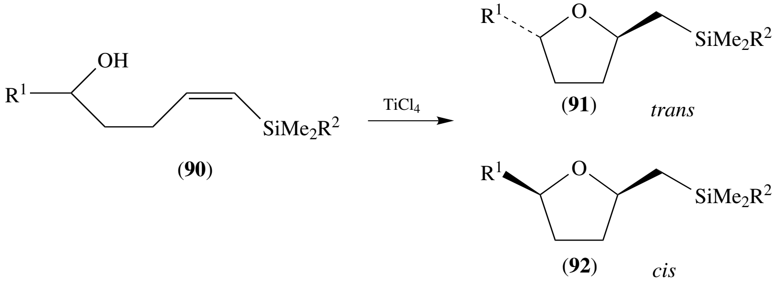

(**90**)

(**91**) *trans*

(**92**) *cis*

(50)

Addition to vinylsilanes is favoured over substitution by (i) the presence of bulky spectator ligands which hinder nucleophilic attack at silicon, and (ii) when the presence of electron-withdrawing groups on silicon lowers its leaving group ability.

Brook and coworkers have studied the effects of electronegative groups on silicon on the reactivities of vinylsilanes[115]. Unlike the substitution reaction of 1-trimethylsilylprop-1-ene with acetyl chloride (equation 51a) the major product of the reaction of β-trichlorosilylstyrene with phenylacetyl chloride arises from addition, as shown in equation 51b.

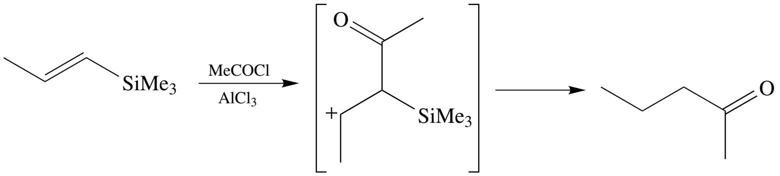

(51a)

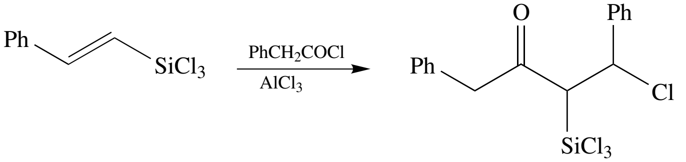

(51b)

The reduced leaving ability of electron-poor silicon is demonstrated by the reactions of styrene derivatives with trifluoromethanesulphonic acid, as shown in Scheme 3. When the silicon has one or zero electronegative substituents, protiodesilylation takes place. However, when two chloro substituents are present, the loss of the silyl group is disfavoured such that an intramolecular cyclization of the intermediate β-carbocation **93** takes place[116,117].

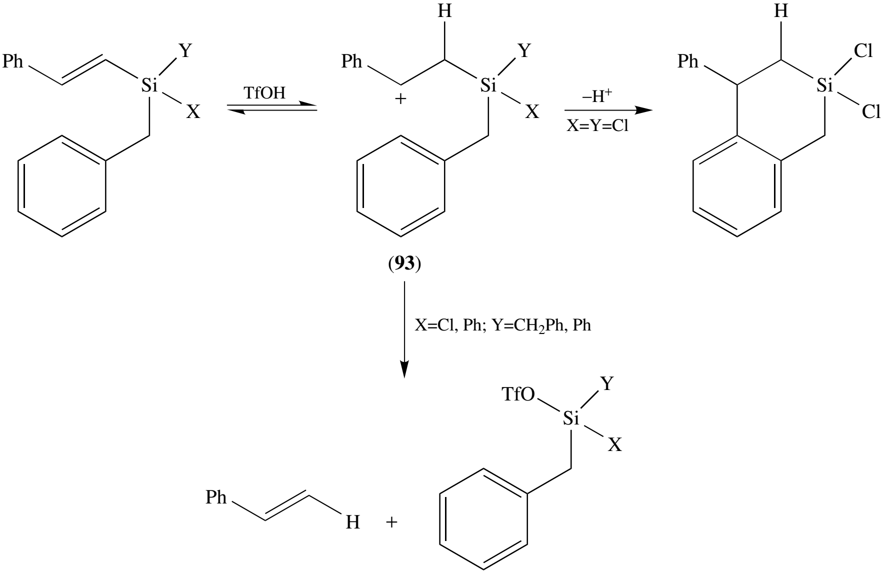

SCHEME 3

3. Substitution in vinylsilanes

The electrophilic substitution of vinylsilanes has been reviewed in detail by Fleming, Dunogues and Smithers[118]. In most cases, substitution of vinylsilanes take place with retention of configuration. This can be rationalized as follows. If the electrophile attacks on the top face of the π-bond, as shown in Scheme 4, the silyl group will then rotate into a conformation in which there is a maximum hyperconjugative interaction between the C−Si bond and the vacant p orbital[119]. There are two ways the silyl group can rotate into the plane of the vacant p orbital — either via a 120° counterclockwise rotation, which would give inversion of configuration in the product **94**, or via rotation through 60° clockwise, which gives the observed retention product **95**. This shorter path would be expected to be the more likely, especially when the effects of hyperconjugation are taken into account. In the 60° rotation, hyperconjugation increases as the silyl group moves into the plane of the p orbital. However, in the 120° rotation, hyperconjugative stabilization will initially decrease to zero as the silyl group passes through an orientation perpendicular to the p orbital.

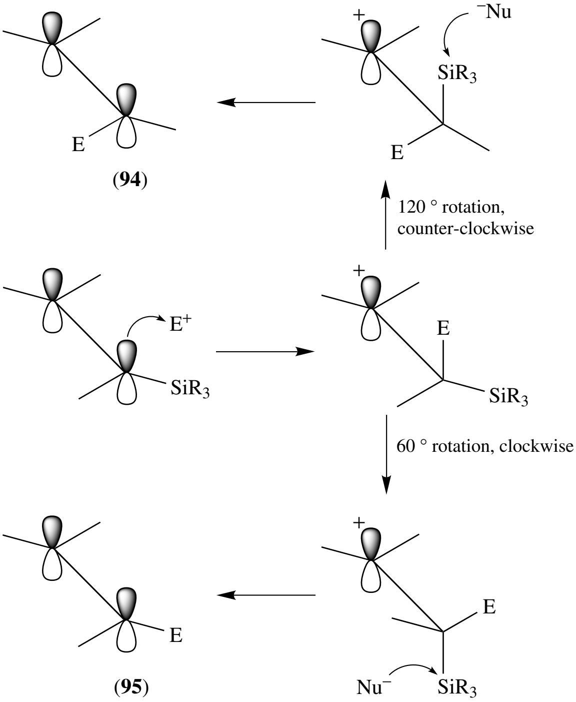

SCHEME 4

With halogen electrophiles both retention and inversion of stereochemistry have been observed. In this case the addition of the electrophile may lead to the β-silicon cation, or a cyclic halonium ion. Scheme 5 shows a generalized mechanism for the reaction of vinylsilanes with electrophilic reagents[120].

The position of the equilibrium A depends upon which provides the greater stabilization, hyperconjugation or onium ion bridging.

When the electrophile E^+ is a proton, the equilibrium A lies to the left, and the routes B (addition of nucleophile X at carbon to give overall *syn* addition, followed by *anti* elimination of Me_3SiX in D) and C (attack of nucleophile X at silicon) are followed. Both these routes give overall retention of configuration.

When R is phenyl, the stabilizing effect of the phenyl group on an α-cation drives the equilibrium A to the left, and substitution with retention of configuration dominates, whatever the electrophile.

For other vinylsilanes, the reaction with chlorine or bromine usually proceeds with inversion of configuration, i.e. the equilibrium A lies to the right.

The situation is more complicated with electrophiles such as iodine[121], cyanogen bromide and cyanogen chloride[122] in the presence of aluminium chloride. In these cases products with retained stereochemistry are obtained, despite the equilibrium A lying to the right. This is because the addition step F does not take place, and reaction occurs via the minor β-silylcarbocation species **96**. When E^+ is I^+, changing the nature of X^-

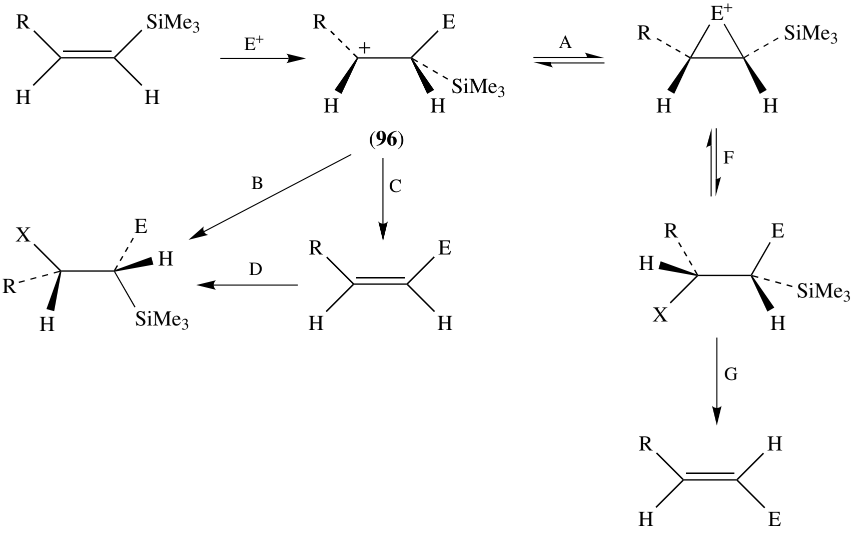

SCHEME 5

to F$^-$[123] or Cl$^-$[111] favours the addition reaction F and the expected inverted product is observed.

Some recent examples of vinylsilane substitutions demonstrating the synthetic utility of such reactions follow.

The reaction of the (*E*)-α,β-disubstituted vinylsilane **97** with the glyoxalate **98** gives exclusively the (*E*)-trisubstituted product with the 2*S* configuration **99** (equation 52)[124].

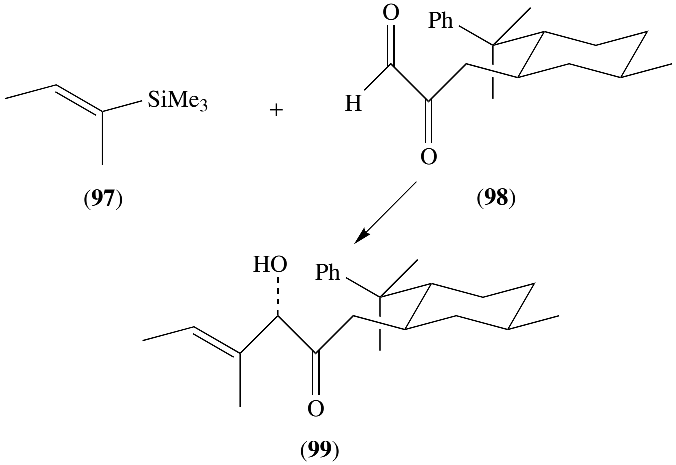

(52)

Kishi, Mikami and Nakai[125] have studied the intramolecular acylation of trimethylsilyl alkenoyl chlorides, using aluminium trichloride. They found two possible outcomes. 5-Trimethylsilylhept-5-enoyl chloride **100** cyclized in the expected fashion (α-cyclization) via the β-silyl carbocation **101**, to give the cyclopentanone **102** (equation 53).

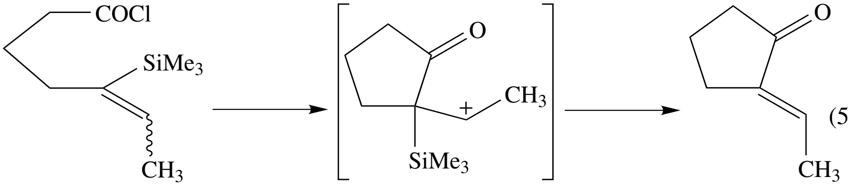

(**100**) (**101**) (**102**)

(53)

However, 4-methyl-5-trimethylsilylhex-5-enoyl chloride **103** gave a cyclohexenone product **104**, as shown in equation 54.

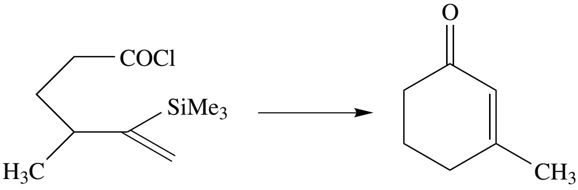

(**103**) (**104**)

(54)

This product must arise from β-cyclization followed by migration of the methyl group to give a β-silyl carbocation intermediate **106**, as shown in equation 55.

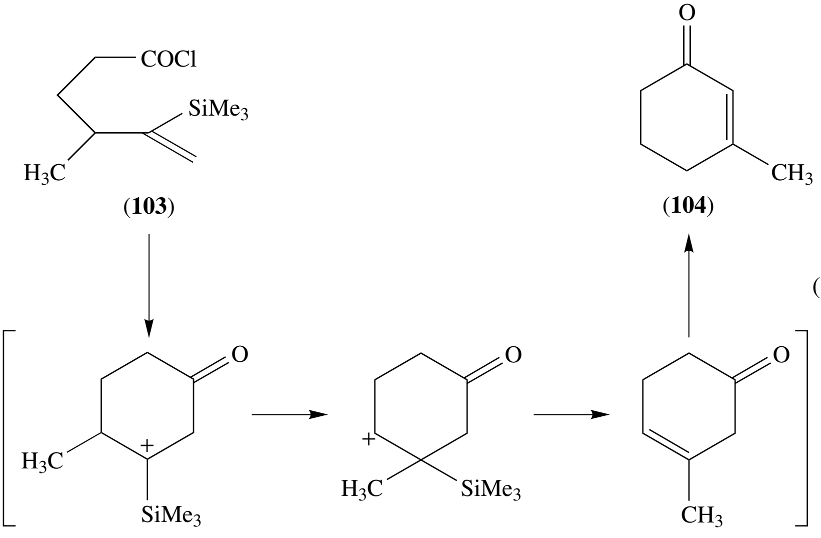

(**103**) (**104**)

(55)

(**105**) (**106**)

These results suggest that the tertiary α-silyl carbocation **105** has a higher stability than the primary β-silyl cation **107**, formed by α-cyclization. This shows that the β-effect does not always dominate the regioselectivity of reactions of vinylsilanes.

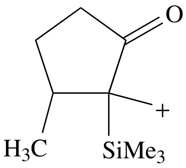

(**107**)

Another example of an important cyclization is the intramolecular addition of iminium ions to vinylsilanes, as shown in equation 56. This synthetically important cyclization has been studied in detail by Overman and coworkers[126–130].

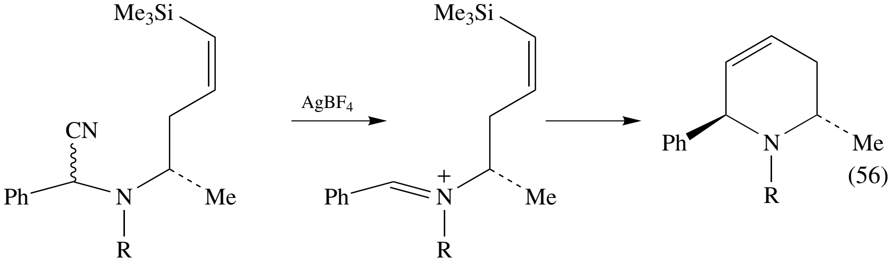

Brook and Henry[131] studied the reactivity of aryldimethylsilyl styrenes towards acetyl chloride. They found that when the aryl group was phenyl **(108)**, the expected vinylsilane substitution reaction took place to give the ketone **109** (equation 57). However, when a mesityl group was used **(110)**, *ipso* substitution on the aromatic ring occurred (equation 58). Although the reactivity of the aryl group would be expected to increase with increasing alkylation, it would not be expected to surpass the reactivity of the styryl group. The cleavage of the silicon–aryl bond is facilitated in this case by the relief of steric congestion.

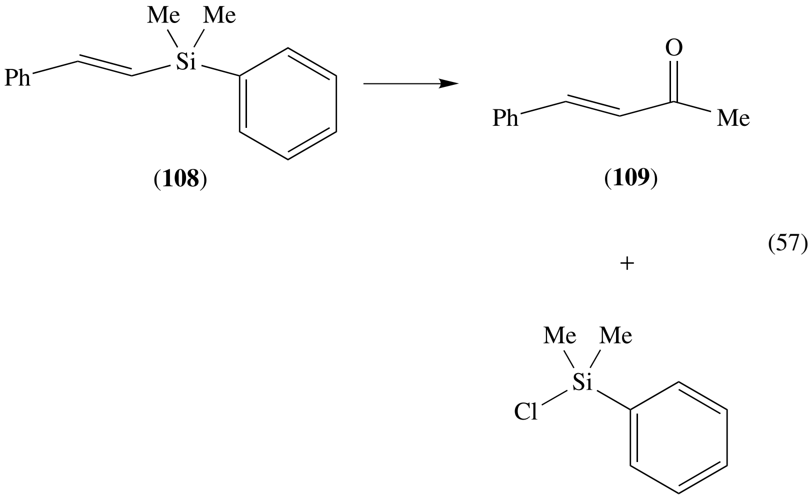

(**108**) (**109**)

(57)

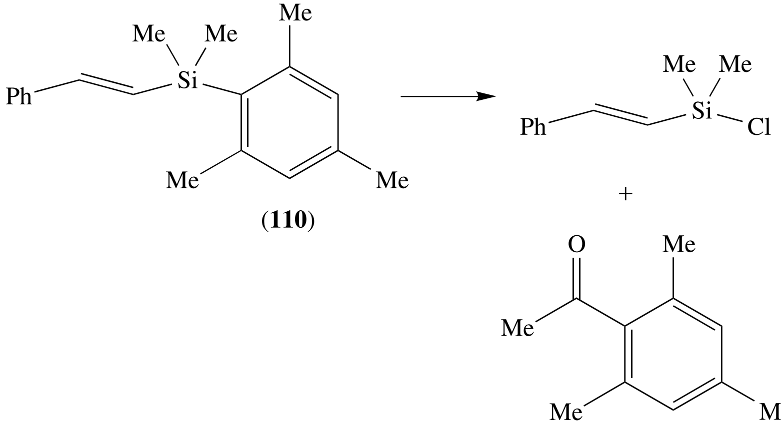

(**110**)

(58)

B. Reactions of Alkynylsilanes

Alkynylsilanes have been studied less than vinylsilanes. Electrophilic addition to an alkynylsilane can give a α- or β-silyl-substituted vinyl cation, in the first step (equation 59).

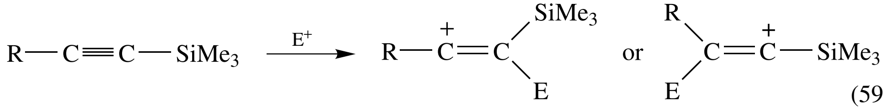

$$\mathrm{R{-}C{\equiv}C{-}SiMe_3} \xrightarrow{\mathrm{E^+}} \mathrm{R{-}\overset{+}{C}{=}C(SiMe_3)(E)} \quad \text{or} \quad \mathrm{(R)(E)C{=}\overset{+}{C}{-}SiMe_3} \qquad (59)$$

Provided that the silicon–carbon bond can be coplanar with the vacant p orbital, the β-silyl substituted carbocation should be stabilized by hyperconjugation, and this has been demonstrated by Kresge and coworkers[47,49].

Overall electrophilic addition to alkynes is rare, although bromination of alkynylsilanes has been described and takes place in the *trans* sense (equation 60)[132].

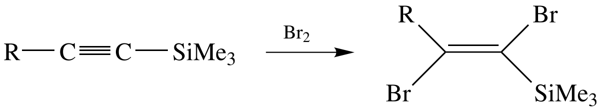

(60)

Substitution reactions normally predominate, as shown in equations 61[132] and 62[133].

$$\mathrm{Me_3Si{-}C{\equiv}C{-}SiMe_3} \xrightarrow{\mathrm{ICl}} \mathrm{Me_3Si{-}C{\equiv}C{-}I} \qquad (61)$$

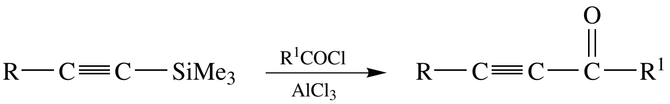

$$\mathrm{R{-}C{\equiv}C{-}SiMe_3} \xrightarrow[\mathrm{AlCl_3}]{\mathrm{R^1COCl}} \mathrm{R{-}C{\equiv}C{-}\overset{\overset{\displaystyle O}{\|}}{C}{-}R^1} \qquad (62)$$

The titanium tetrachloride catalysed addition of alkenes to the alkynylsilane **111** selectively produces cyclopentene products via a β-silylcarbocation **112** (equation 63)[134].

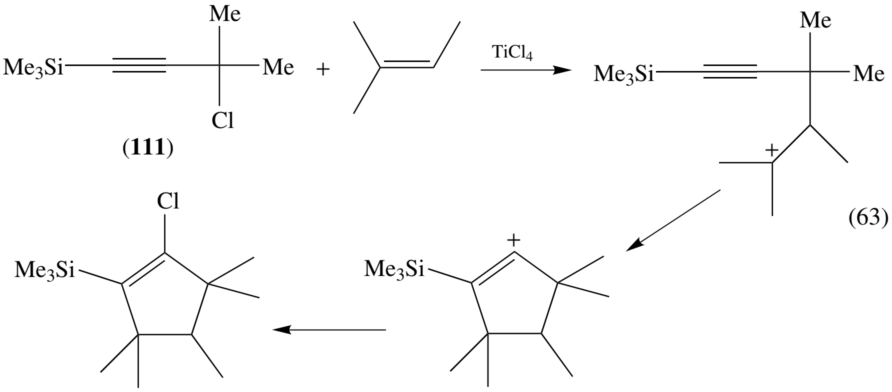

(**111**)

(63)

(**112**)

C. Reactions of Allylsilanes

Electrophilic substitution reactions of allylsilanes have been reviewed in detail by Fleming, Dunogues and Smithers[118].

In general, allylsilanes undergo electrophilic addition or substitution via an intermediate β-silylcarbocation (equation 64).

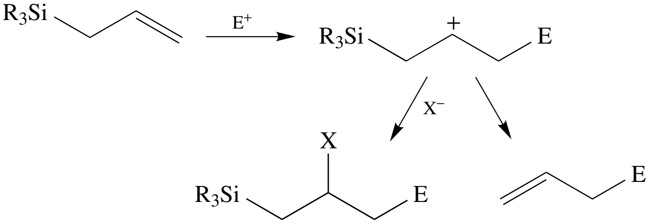

(64)

If a substituent is present that can stabilize the cationic intermediate more effectively than the silicon, this may alter the course of the reaction. For example, deuterionation of the allylsilane **113** leads to a mixture of the expected product **114** and an anomalous product **115** (equation 65)[135].

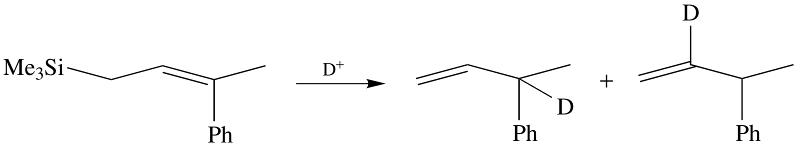

(65)

(**113**) (**114**) (**115**)

in ratio of 2:3

This can be explained if the initial attack on **113** forms a carbocation α to the phenyl group **(116)** (Markovnikov attack), followed by a 1,2 shift of hydride or deuteride to give the β-silyl carbocations **117** and **118** respectively, and hence the alkenes **114** and **115** (Scheme 6).

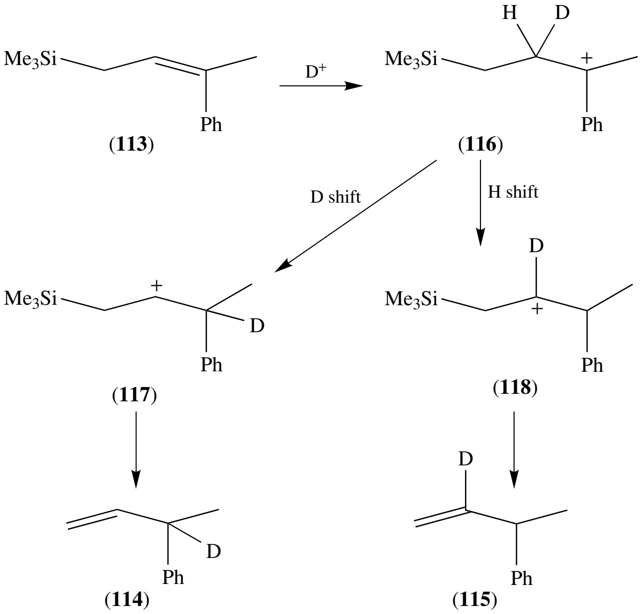

SCHEME 6

As with vinylsilanes and alkynylsilanes, substitution is favoured over addition for allylsilanes. However, this can be affected by the steric and electronic effects of the silicon substituents. Mayr and Hagen have studied the reactivities of allylsilanes towards the *p*-methoxy substituted diphenylcarbocation (Scheme 7)[136,137]. Relative rate data and observed products are summarized in Table 11 for allylsilanes of the structures **119–122**, with various silicon substituents.

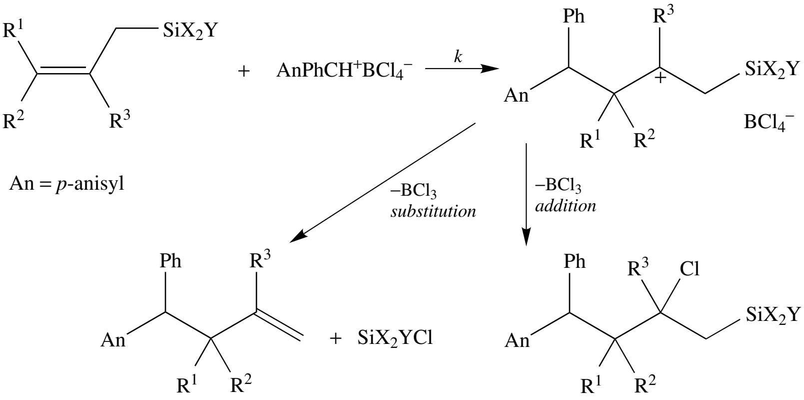

SCHEME 7

From these data it seems that steric hindrance at the silicon atom is responsible for the course of the reaction, whilst the electronegativity of the substituents affects the reaction

TABLE 11. Rate data and reaction process for the reaction of allysilanes with $AnPhCH^+$

Allylsilane	X	k (l mol^{-1} s^{-1})[a]	Process
119	$SiCl_3$	no reaction	—
119	$SiClMe_2$	0.276	substitution
119	$SiPh_3$	3.21	add:subst 1.5 : 1
119	$SiMe_2Ph$	38.7	substitution
119	$SiMe_3$	197	substitution
119	$SiMe_2Bu$-t	204	addition
119	$SiEt_3$	313	substitution
119	Si(Pr-i)$_3$	439	addition
119	Si(Bu-n)$_3$	507	substitution
119	Si(Hex-n)$_3$	542	substitution
120	$SiCl_3$	0.066	substitution
120	$SiPh_3$	1.91×10^4	substitution
120	$SiMe_3$	$>10^5$	substitution
121	$SiMe_3$	4.15×10^3	substitution
122	$SiMe_3$	1.56×10^3	substitution

[a] Reference rate constant 23.8 l mol^{-1} s^{-1} for 2-methylpropene.

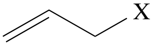

(**119**)

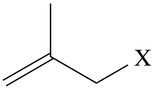

(**120**)

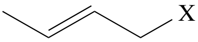

(**121**)

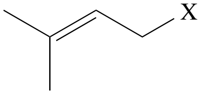

(**122**)

rates. As expected, nucleophilic attack at silicon, as necessary for the substitution pathway, is slow when the silicon atom is surrounded by bulky groups. Addition is favoured in these cases. The overall rate of both reactions depends on the stability of the intermediate carbocation which is increased by electron-supplying groups on silicon and decreased by electron withdrawal.

Allylsilanes undergo reactions with a large range of electrophiles, although catalysis by Lewis acids is often necessary. Some recent examples of substitution reactions of allylsilanes are discussed below.

Hosomi and coworkers found that β-cyclopropyl allylsilanes undergo substitution without affecting the cyclopropyl group, as shown in equation 66[138].

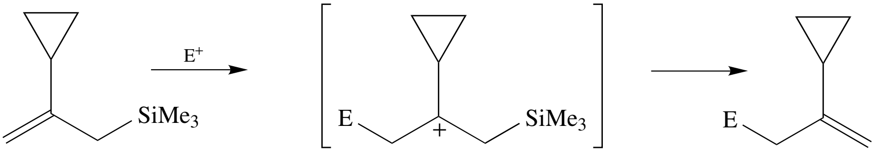

(66)

Generally, systems in which a carbocation is formed next to a cyclopropyl group are avoided, as this leads to isomerization of the cyclopropyl group (equation 67).

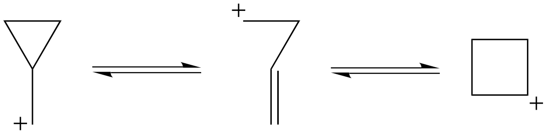

(67)

The increased stabilization by the β-silicon of the carbocation α to the cyclopropyl ring presumably disfavours the isomerizations in which the charge is located on other carbon atoms in the molecule.

Aluminium chloride is often used as a Lewis acid catalyst (equations 68 and 69), although there are many other suitable catalysts (equations 70 and 71). Strong electrophiles such as chlorosulphonyl isocyanate or an aluminium salt do not require catalysis (equations 72 and 73).

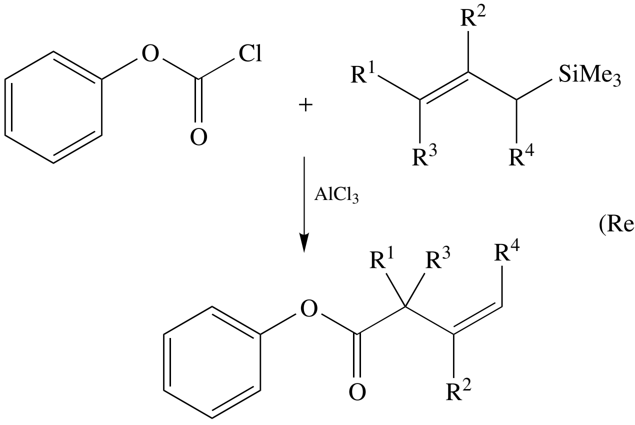

(Ref. 139) (68)

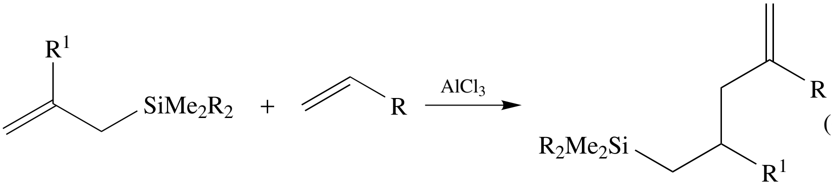

(69)

(Ref. 140)

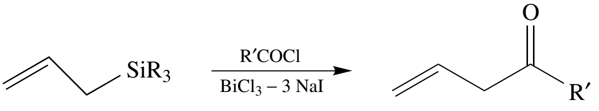

(Ref. 141) (70)

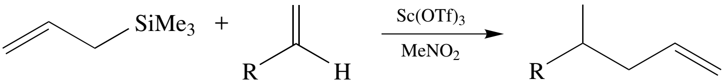

(71)

(Ref. 142)

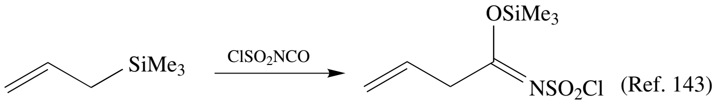

(72)

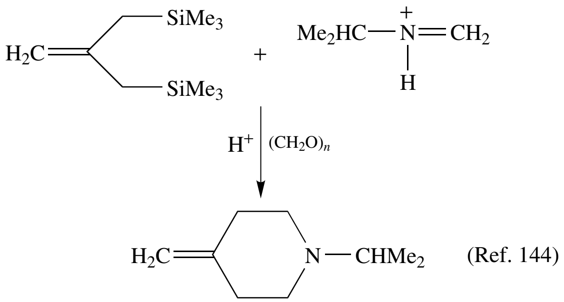

(73)

As reactions 68 and 69 above exemplify, the substitution of the allylsilane usually takes place with an allylic shift (S_E2'). This can be synthetically useful, for example in the isomerization of allyl sulphones **123** to vinyl sulphones **124** (equation 74)[145]. The reaction is also highly stereospecific (>90% *E*) (*vide infra*).

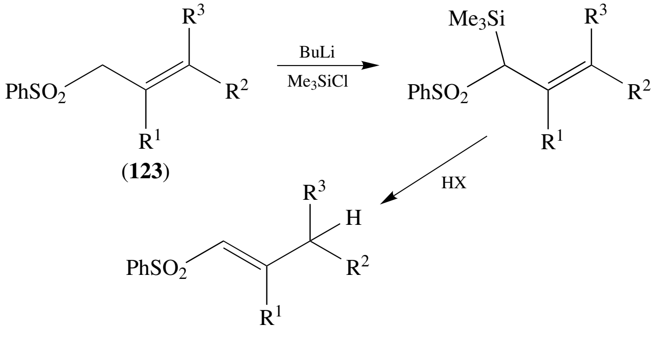

(**123**)

(**124**)

(74)

Occasionally the allylic shift is not observed (equations 75–80).

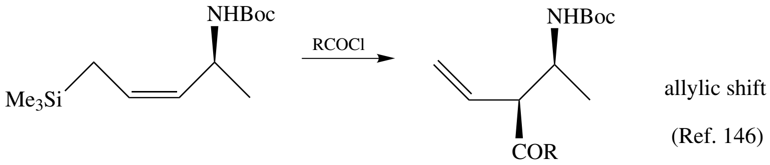

(75)

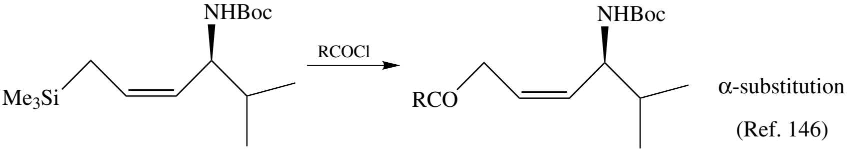

(76)

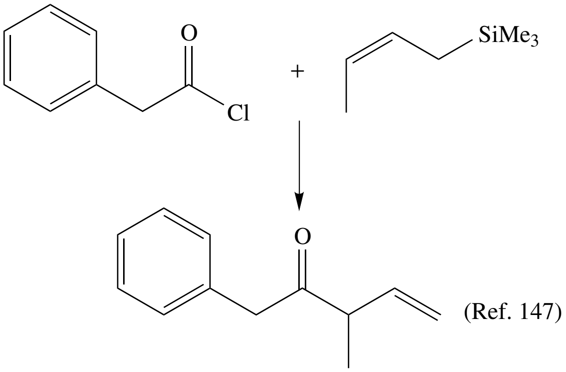

(77)

(Ref. 147)

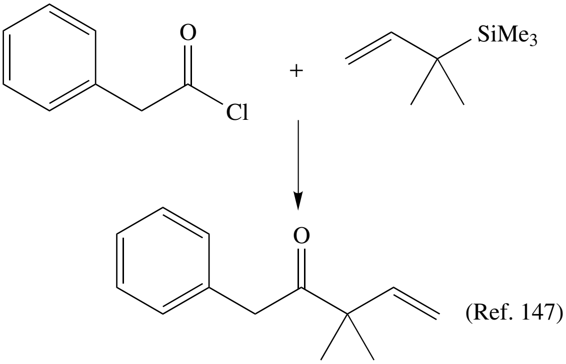

(78)

(Ref. 147)

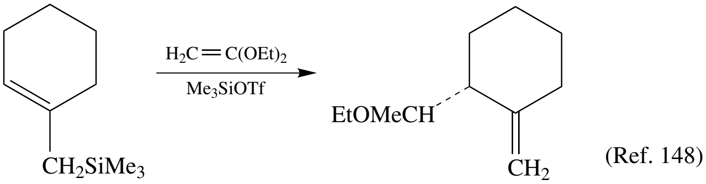

(79)

(Ref. 148)

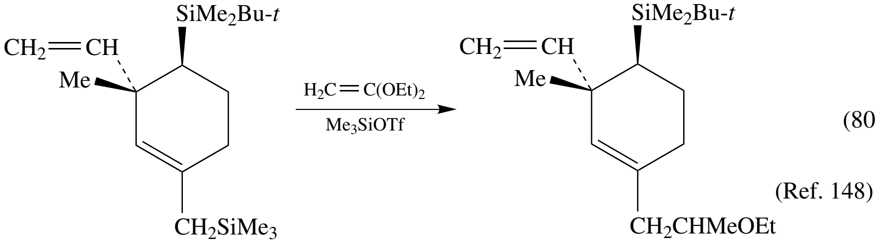

(80)

(Ref. 148)

An increase in steric hindrance at the γ-position appears to favour α-substitution in equations 76 and 80, compared to γ-substitution in equations 75 and 79. However, this does not explain the α-substitution in equation 78. Polla and Frejd[148] attribute the α-substitution shown in equation 80 to protiodesilylation followed by electrophilic alkylation of the resulting olefin.

With α, β-unsaturated carbonyl compounds as the electrophile, 1,4-addition of the allylsilane to the α,β-unsaturated carbonyl is often observed, as shown in equation 81.

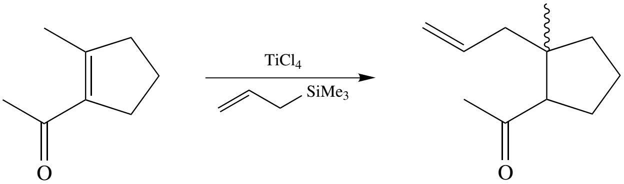

(81)

This synthetically important reaction is known as the Sakurai or Hosomi–Sakurai reaction[149]. The intramolecular Sakurai reaction is useful for the synthesis of spiro **(125)** and fused **(126)** ring systems, as shown in equations 82 and 83[150].

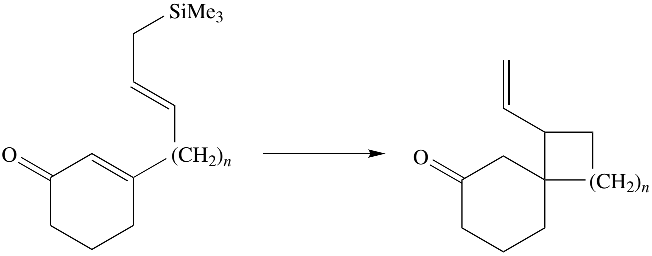

(82)

(**125**)

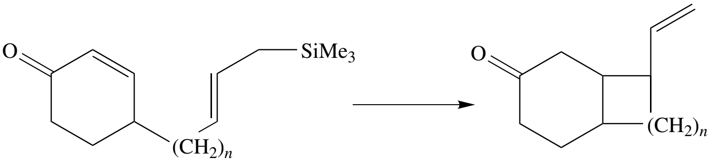

(83)

(**126**)

In some cases, a minor silicon-containing product is observed, which has been shown to be a cyclopentane derivative. An example is shown in equation 84[151].

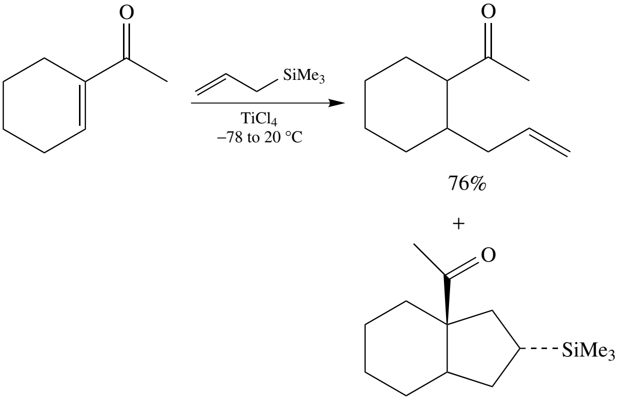

(84)

18%

When bulky groups are present on silicon, this reaction pathway dominates (equations 85 and 86).

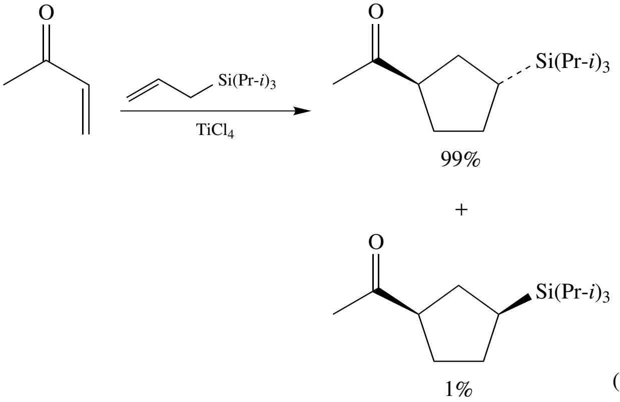

(85)

(Ref. 152)

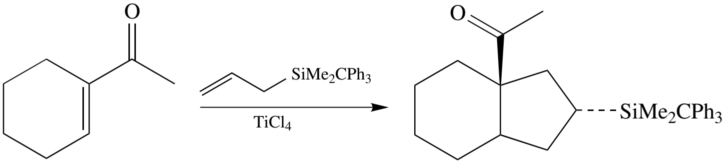

(86)

(Ref. 153)

The formation of these products can be explained by consideration of the reaction mechanism, which is most usefully pictured as proceeding via a cyclic siliconium ion **128** (equation 87).

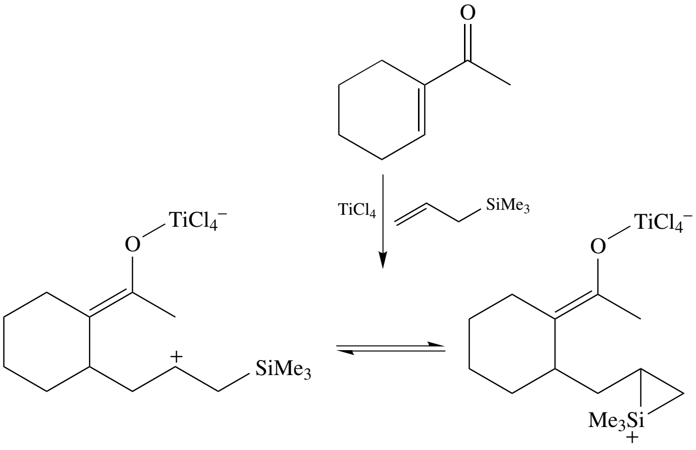

(87)

(**127**) (**128**)

Attack of a nucleophile on the β-silyl carbocation **127** or the cyclic siliconium ion **128** leads to desilylation and formation of the Sakurai product. When nucleophilic attack is disfavoured by steric hindrance at the silicon, competing intramolecular attack by the enolate becomes important. This 5-*exo-tet* cyclization gives the trimethylsilylcyclopentane product with high stereospecificity, the trimethylsilyl group having undergone a 1,2 shift.

It has recently been found that replacement of ketones by esters in this reaction leads to the production of cyclobutanes, sometimes as the major product, arising from intramolecular attack of the enolate at the secondary carbon of the siliconium ion (equation 88)[154].

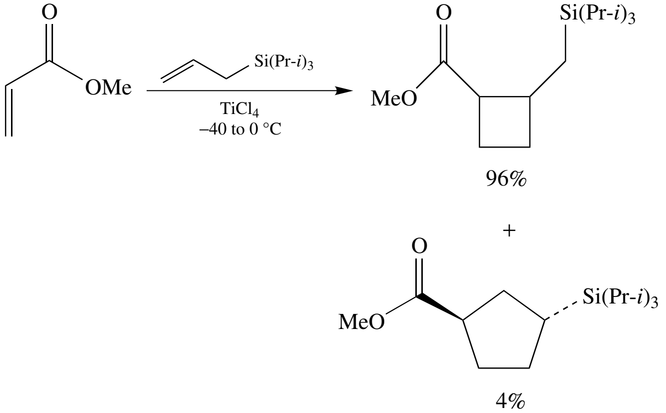

(88)

Majetich and coworkers[155] have investigated the effects of substitution and catalyst on the conjugated dienones, which can cyclize by 1,6-addition. Increased substitution at the terminal carbon of a conjugated system leads to the favouring of 1,2-addition over 1,6-addition, as does increasing the strength of the Lewis acid (equations 89–91).

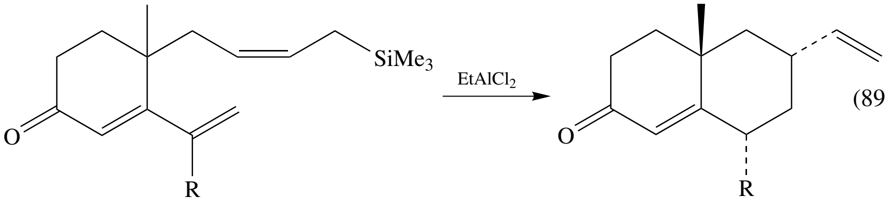

(89)

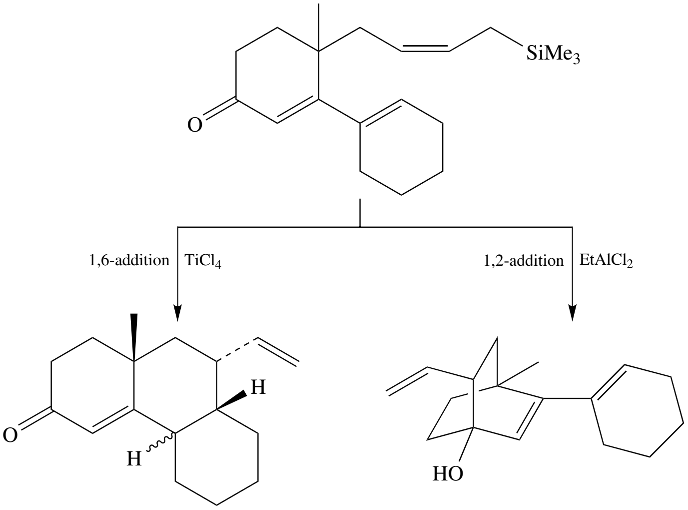

(90)

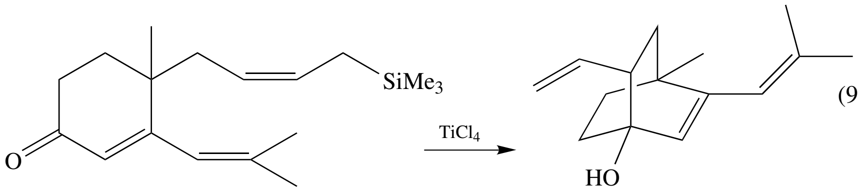

(91)

In most cases, open-chain allylsilanes react with electrophiles with *anti* stereoselectivity[156–162]. The simple explanation for this observation follows from the probable conformation of the allylsilane. The preferred conformation **129** will have the small substituent H eclipsing the double bond.

The large and electropositive silyl group encourages attack of the electrophile on the lower surface as shown in equation 92, and only a 30° rotation is necessary to give the β-silyl cation **130** with the optimum geometry for hyperconjugative stabilization. This stabilization is probably large enough that the configuration is maintained until the silyl group is lost in the second step, to give a product **131** containing a *trans* double bond, with the overall reaction being stereoselectively *anti*.

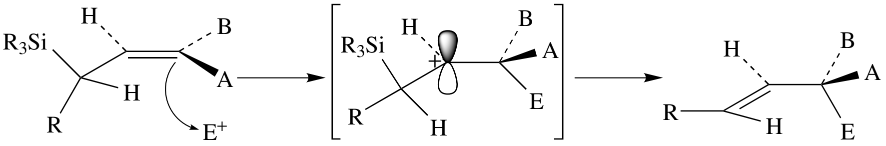

(**129**) (**130**) (**131**) (92)

However, several factors can result in this simple pattern of stereospecific *anti* attack not being followed. The difference in size between the substituents H and R may not be sufficient to prevent reaction through the alternative conformation **132** (equation 93). This is most common when the substituent A is a proton.

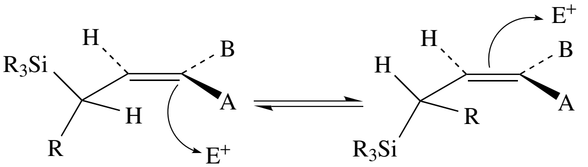

(93)

(**129**) (**132**)

The alternative conformation **132** may also be favoured when the electrophile is a very bulky species, in which case interactions between the electrophile and R are minimized. Increasing the size of the R group might also be expected to change the direction of electrophilic attack as its hindrance to the incoming electrophile becomes similar to that of the silyl group. This also acts to disfavour the conformation **132** due to increased 1,3 interactions.

Fleming and Higgins[163] studied the protiodesilylation of the two cyclohexene derivatives **133** and **134**. If protonation takes place as described in the simple picture above, then the protiodesilylation products should be **135** and **136**, respectively, as shown in equations 94a and 94b.

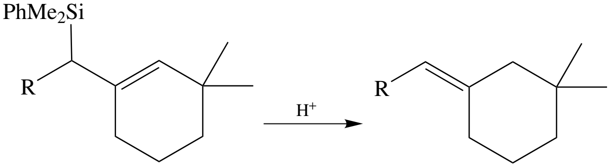

(**133**) (**135**)

(94a)

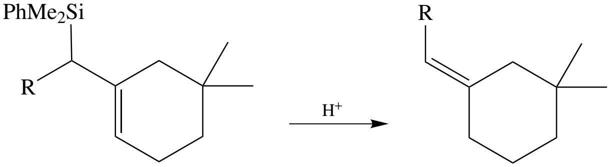

(**134**) (**136**)

(94b)

The protonations of the two cyclohexenes were not completely stereospecific, both **135** and **136** being formed in both cases. The product ratios observed for various substituents R are given in Table 12.

Selectivity is found to be negligible when R is methyl, and surprisingly not much improved when R is phenyl. However, the isopropyl group gives a substantial degree of stereoselectivity in the expected sense.

Another study by Fleming and coworkers examined the stereoselectivity of the titanium tetrachloride catalysed reaction of the allylsilane **137** with 1-adamantyl chloride (equation 95)[164].

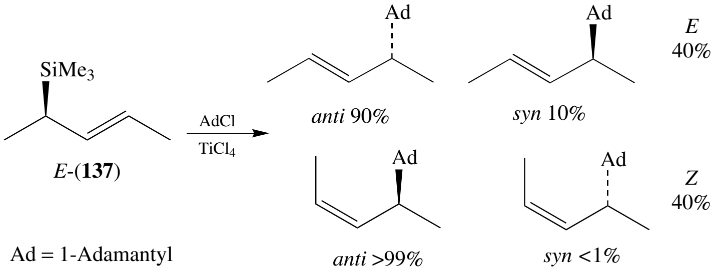

(95)

TABLE 12. Product ratios in the protiodesilylations of allylsilanes **133** and **134**

Allylsilane	R	Product ratio **135 : 136**
133	Me	57 : 43
134	Me	38 : 62
133	Ph	69 : 31
134	Ph	38 : 62
133	*i*-Pr	91 : 9
134	*i*-Pr	8 : 92

The Z product is enantiomerically pure, but the E isomer is formed in a 90 : 10 ratio of enantiomers. One reason for this was revealed by considering the relevant conformations of the allylsilane, shown in equation 96.

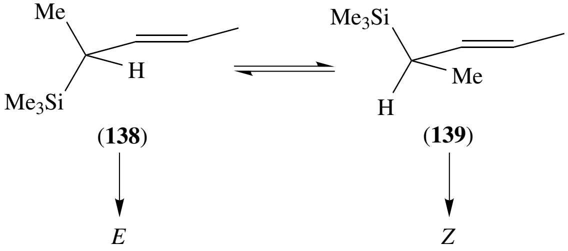

(96)

Attack in the conformation **139** which leads to the Z-isomer takes place from the upper surface of the molecule, *anti* to the trimethylsilyl group. This face is occupied by a hydrogen group. In the conformation **138** which leads to the E-isomer, this surface is occupied by a methyl group. The greater steric effect of this group leads to the small amount of attack on the other surface.

In order to determine whether attack *anti* to silicon was due to steric effects or electronic effects, Fleming and coworkers studied the attack of electrophiles on the pentadienylsilanes **140**, in which the electrophile attacks at the second double bond, as shown in equation 97[165].

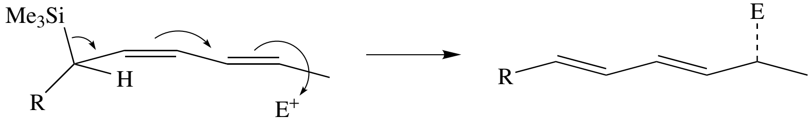

(**140**) (97)

The electrophiles isobutyraldehyde and its dimethyl acetal gave surprisingly high ratios of *syn* : *anti* attack, around 10 : 90. Since the silicon centre is more removed from the reactive site, this could be taken to indicate that electronic effects predominate. However, the intramolecular cyclization of **141** (equation 98) was found to take place with an enantiomeric excess of only 20%.

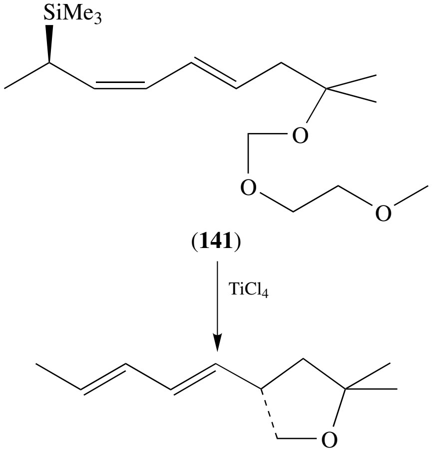

(98)

The corresponding allyl system reacts to give a product with an enantiomeric excess of 90%. The small electrophilic centre in this reaction is very unlikely to experience any steric interaction with the silyl group, and the small *anti* stereoselectivity (60 : 40) in this reaction was taken to be an indication of the size of the electronic effect. The high stereoselectivities observed for the reactions of isobutyraldehyde and isobutyraldehyde dimethyl acetal were thought to be due to steric interactions. Following these and other studies Fleming and coworkers concluded: 'whether the high levels of *anti* stereoselectivity seen with allylsilanes are largely steric or electronic in origin remains unknown'[165].

The reactions of chiral allylsilanes with electrophiles to give diastereoselective products has recently been extensively reviewed by Masse and Panek[166]. An example is shown in equation 99. The reaction of the chiral allylsilanes **142** with phenylsulphenyl chloride (PSC) and chlorosulphonyl isocyanate (CSI) takes place with a diastereoselectivity which increases with the increasing steric bulk of the substituent R[167].

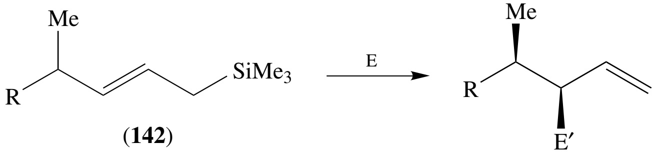

(**142**)

E = PhSCl; E′ = PhS
E = $ClSO_2NCO$;
E′ = CN
(99)

The product diastereomeric excesses (de) obtained with various R substituents in **142** are summarized in Table 13.

The increasing diastereoselectivity, as the steric requirements of R increase, can be rationalized by considering the conformation of the allylsilane. Again the smallest group (H) is positioned in the plane of the double bond **(143)**, and the steric influence of R determines the ratio of attack on the two faces of the allylsilane.

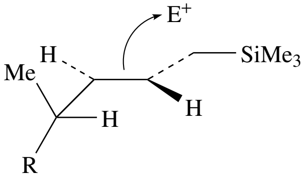

(**143**)

Allylsilanes are more reactive than vinylsilanes. Firstly, hyperconjugative overlap of the C—Si bond with the π bond raises the energy of the HOMO, making it more

TABLE 13. Diastereomeric excesses (de) in the products of the reactions of the allylsilane **142** with electrophiles E

R	E	de
Et	PSC	20%
Ph	PSC	90%
t-Bu	PSC	98%
Et	CSI	24%
Ph	CSI	90%
t-Bu	CSI	98%

reactive towards electrophiles, and secondly, the C−Si bond can stabilize the positive charge buildup throughout electrophilic addition to allylsilanes. This is in contrast with vinylsilanes, where full hyperconjugative stabilization is only possible after rotation of the C−C bond through 90°. For these reasons, systems which are both an allylsilane and a vinylsilane generally react as an allylsilane. An example is the cyclohexene **144**, which reacts with acetyl chloride as an allylsilane (equation 100)[168].

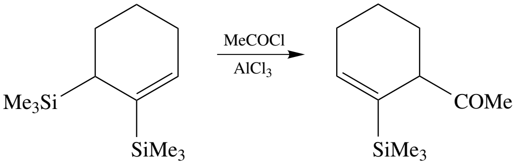

(**144**)

(100)

D. Reactions of Propargylsilanes

Propargylsilanes undergo addition to give a *β*-silylcarbocation, which can then react further to give either addition or substitution, as shown in equation 101.

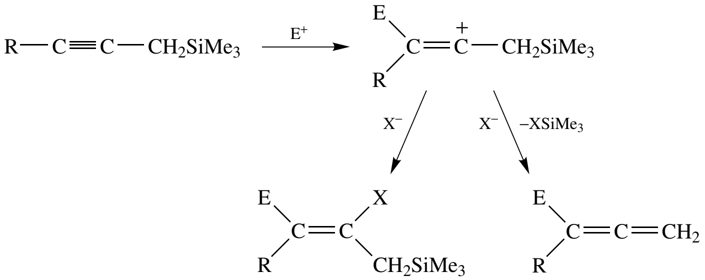

(101)

As with allylsilanes, substitution is found to be the dominant reaction pathway (equation 102)[169].

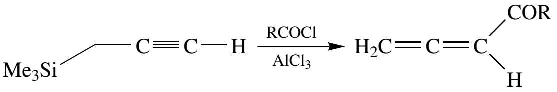

(102)

Electrophilic substitution of propargylsilanes is an important route to allenes. Cyclization gives allene-substituted cyclic compounds as shown in equations 103 and 104.

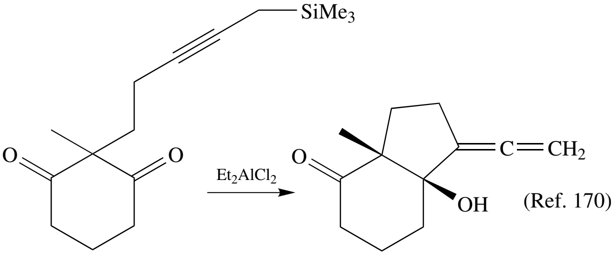

(Ref. 170)

(103)

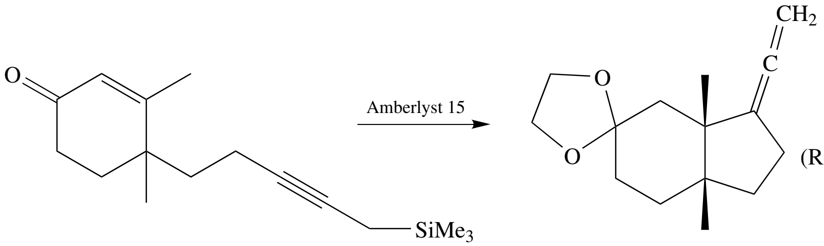

(Ref. 171)

(104)

As with allylsilanes, increased steric hindrance at silicon favours annulation (equation 105)[172] rather than the Sakurai reaction (equations 103 and 104).

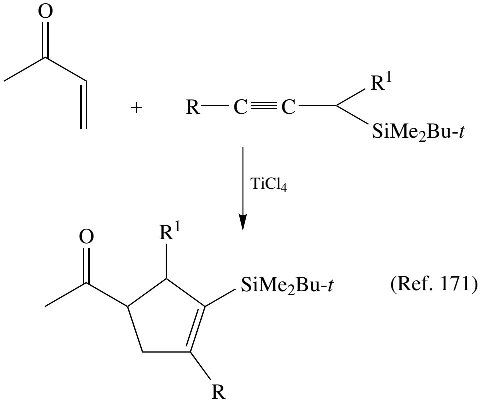

(Ref. 171)

(105)

E. Reactions of Allenylsilanes

Allenylsilanes may behave as allyl or vinylsilanes. In general, allylsilane behaviour dominates over vinylsilane behaviour. The reactions of allenylsilanes with electrophiles have been comprehensively reviewed by Fleming, Dunogues and Smithers[118].

Electrophilic substitution of allenylsilanes gives alkynes (equation 106)[173].

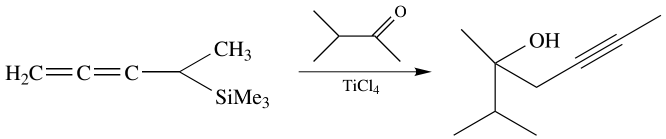

(106)

Allenylsilanes with α-alkyl substituents undergo annulation reactions, as in equation 107[174].

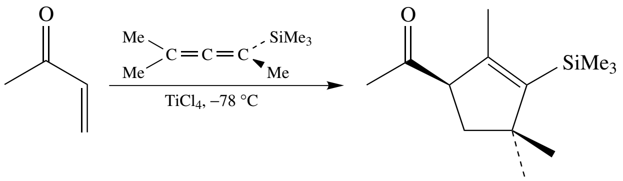

(107)

Buckle and Fleming studied the reactions of the allenylsilane **145** with 1-adamantyl chloride (equation 108) and with isobutyraldehyde and found these S_E2 reactions to be stereospecifically *anti* to a very high degree[175].

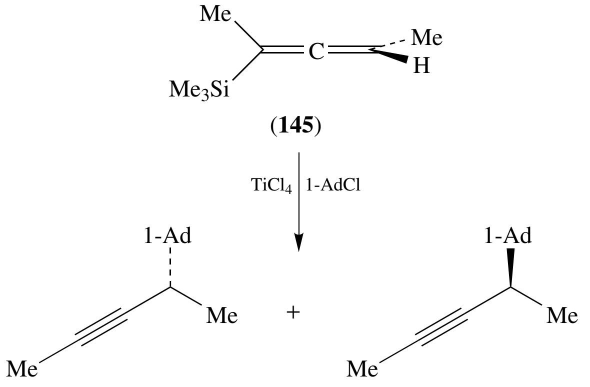

(**145**)

anti 99% *syn* 1%

(108)

F. Miscellaneous Reactions Controlled by the Formation of a β-Silylcarbocation

There are a number of reactions in which the chemical and stereochemical outcome is controlled by the formation of a β-silylcarbocation.

One example is the Baeyer–Villiger reaction. The migratory aptitude of groups in the Baeyer–Villiger reaction depends on their ability to bear a positive charge[176]. Hudrlik and coworkers have shown that the presence of a silicon substituent β to a ketone stabilizes the incipient carbocation leading to a regiospecific oxygen insertion, as shown in equation 109[177].

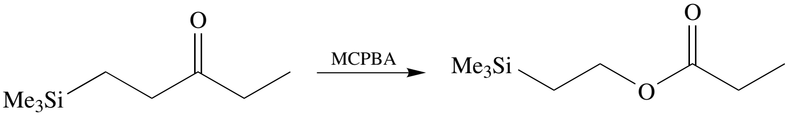

(109)

This regioselectivity has been useful in ring expansions (equation 110)[178].

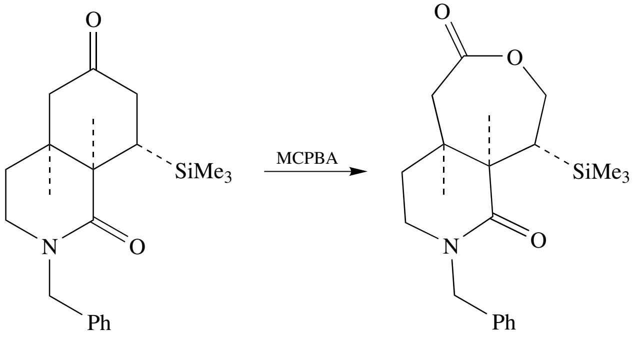

(110)

The ring contraction shown in equation 111 is also promoted by formation of a β-silyl carbocation in the intermediate **146**[179].

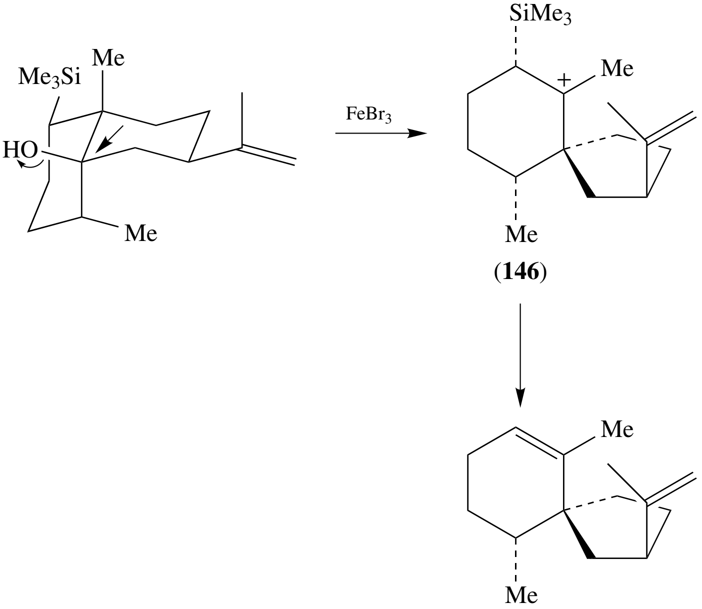

(**146**)

(111)

G. Reactions Involving γ-Silylcarbocations

The γ-effect of silicon has so far found little application in organic synthesis, apart from the solvolysis studies described previously.

Hwu and Gilbert have shown the Nef conversion of nitro compounds to ketones to be promoted by a γ-silyl substituent (equation 112)[180].

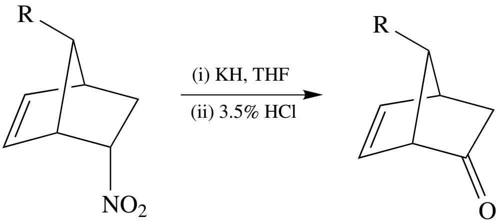

(112)

When R is hydrogen or methoxymethyl, no reaction is observed, but for R = $SiMe_3$, reaction takes place in a 64% yield. Similar results have been demonstrated for other systems[180].

Engler and Reddy found the titanium tetrachloride-catalysed arylation of 1,4-benzoquinones **147** to be promoted by γ-silyl substituents in the aryl component, via stabilization of the carbocationic intermediate **148** (equation 113)[181].

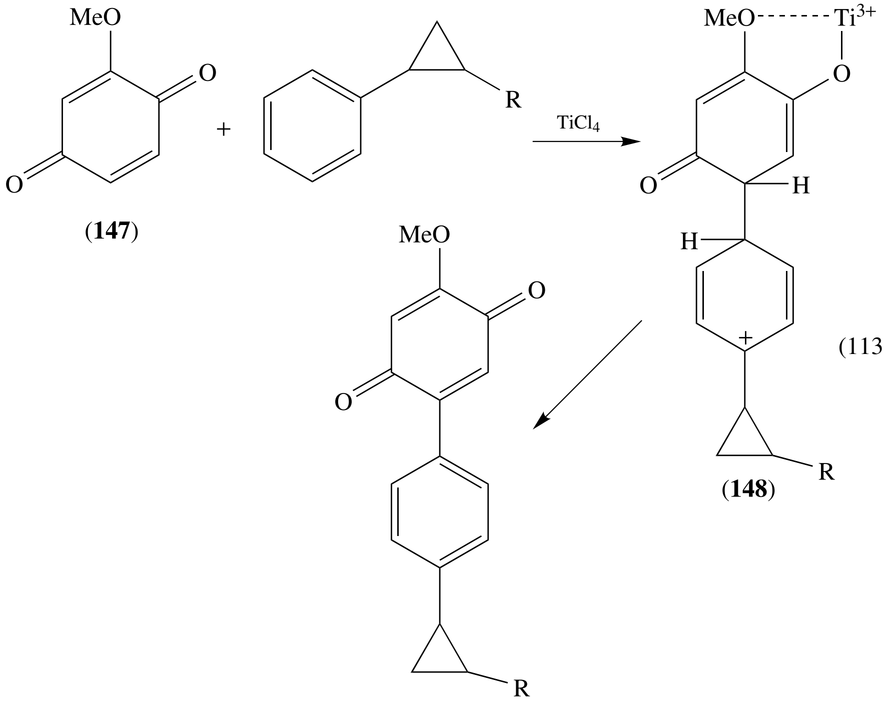

(**147**)

(**148**)

(113)

The yield in this reaction increased from 46% (R = H) to 69% (R = $SiMe_3$).

VI. ACTIVATING AND DIRECTIVE EFFECTS OF SILICON IN CARBANIONIC REACTIONS

A. Methods of Formation of α-Silylcarbanions

Silicon stabilizes an adjacent C−metal bond despite being more electropositive than hydrogen or carbon. Stabilization of the free anion is often discussed, although it should be noted that the free ion is rarely involved. The generation of α-silylcarbanions is discussed in detail in Ager's review of the Peterson olefination reaction[182]. A selection of methods for generating α-silylcarbanions are illustrated below.

1. Proton abstraction (equation 114)[183]

$$\mathrm{Me_3SiCH_2R} \xrightarrow{\text{BuLi/TMEDA}} \mathrm{Me_3Si\overset{-}{C}HR} + \mathrm{Li^+} \qquad (114)$$

Generally, the direct metallation of unactivated alkyl groups is not a synthetically useful reaction. However, under certain circumstances unactivated α-silylcarbanion formation has been reported. Treatment of *ortho*-silylated benzamides **149** with LDA gave an α-silyl carbanion **150**, stabilized by a complex-induced proximity effect, which then underwent intramolecular attack on the amide group (equation 115)[184].

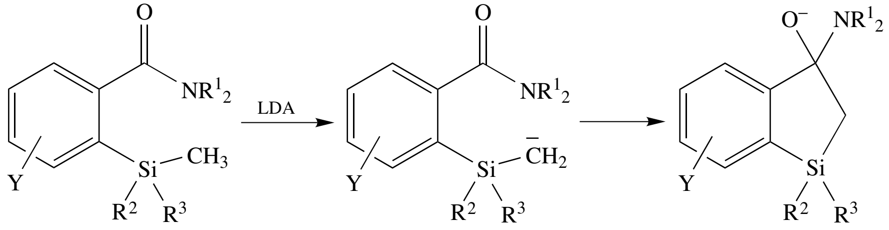

(**149**) (**150**)

(115)

The TBDMS ether **151** also undergoes deprotonation of the silyl methyl group, again due to chelation control (equation 116)[185].

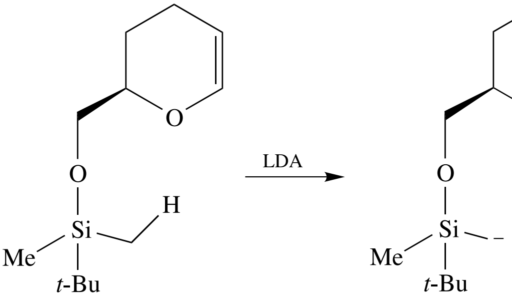

(**151**)

(116)

2. Metal–halogen exchange (equation 117)[186,187]

$$\mathrm{Me_3SiCHIR} \xrightarrow{\mathrm{BuLi}} \mathrm{Me_3Si\bar{C}HR} + \mathrm{Li^+} \qquad (117)$$

3. Transmetallation (equation 118)[188]

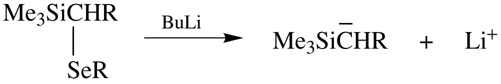

$$\begin{array}{c}\mathrm{Me_3SiCHR}\\ |\\ \mathrm{SeR}\end{array} \xrightarrow{\mathrm{BuLi}} \mathrm{Me_3Si\bar{C}HR} \quad + \quad \mathrm{Li^+} \qquad (118)$$

Included in this category are desilylations of bis(silyl) compounds with fluoride or alkoxide ions which is a particularly clean method of anion production (equation 119)[189].

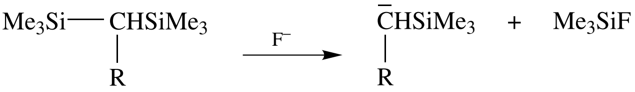

$$\begin{array}{l}\mathrm{Me_3Si{-}CHSiMe_3}\\ \qquad\quad |\\ \qquad\quad \mathrm{R}\end{array} \xrightarrow{\mathrm{F^-}} \begin{array}{l}\mathrm{\bar{C}HSiMe_3}\\ |\\ \mathrm{R}\end{array} \quad + \quad \mathrm{Me_3SiF} \qquad (119)$$

4. *Organometallic addition to vinylsilanes*

Organolithium[190–192] and Grignard reagents[193] react with vinylsilanes to give α-silylcarbanions (equation 120). Such reactions are difficult with unsubstituted vinylsilanes.

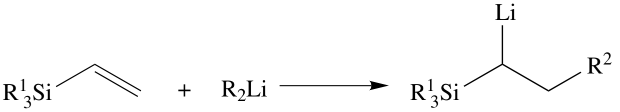

(120)

The $SiMe_3$ group does not stabilize an α-carbanion to the same extent as a nitro group, as shown by the regioselectivity of the reaction shown in equation 121[194].

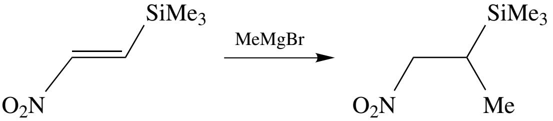

(121)

The stability of an α-silyl carbanion is responsible for the improved synthetic utility of the Stork annulation over other annulations[195,196]. These reactions involve the Michael addition of an enolate ion to an enone, and in the absence of a α-silyl substituent suffer drawbacks due to the reversibility of the Michael reaction. However, the addition of enolate ions to α-trimethylsilylvinyl ketones is not reversible, owing to α-silicon stabilization of the canonical form **152** shown in equation 122.

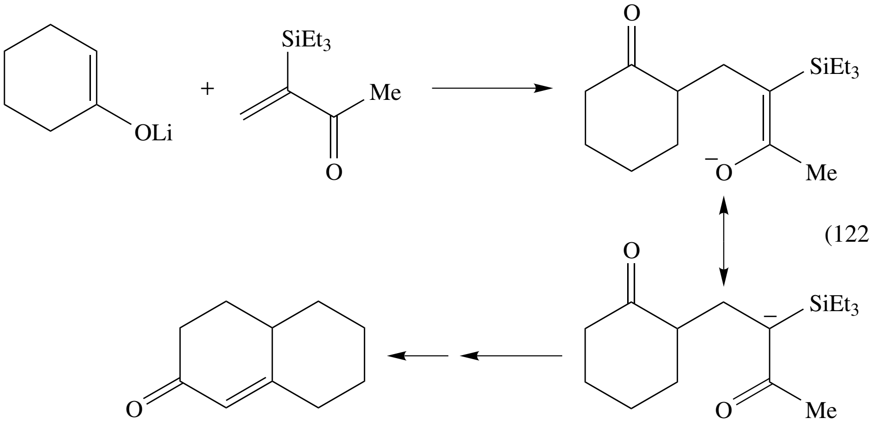

(122)

(**152**)

B. The Peterson Reaction

α-Silylcarbanions undergo the normal range of carbanion reactions. Of particular importance is their reaction with carbonyl compounds (equation 123). Depending on the counterion, the β-silyl alkoxide **153** can undergo protonation to give the corresponding β-silyl alcohol **154**, or can eliminate R_3SiO^- to give the alkene **155**. This latter route is the Peterson olefination[183], which has great synthetic utility and is often used in situations where the Wittig reaction has failed. The carbonyl compound can be an aldehyde or a ketone and a range of carbanions have been used. The Peterson reaction has two general advantages over the Wittig reaction: (i) the silanolate ion is water-soluble, which makes the reaction cleaner than the Wittig; and (ii) the silyl carbanion is less sterically hindered and more reactive than the Wittig reagent. The Peterson reaction has recently been comprehensively reviewed by Ager[182].

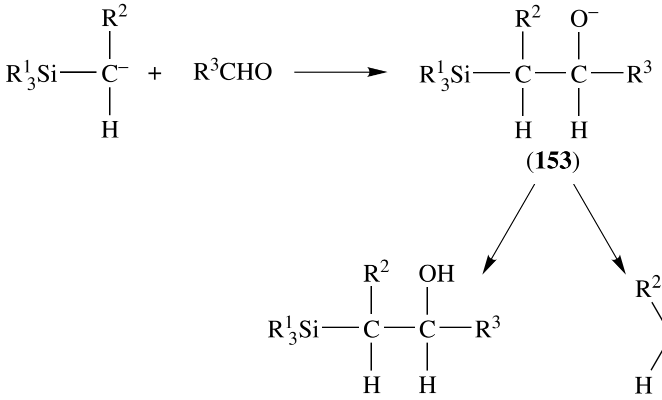

(**153**)

(**154**) (**155**)

(123)

The detailed mechanism of the Peterson reaction has not yet been revealed. When only alkyl, hydrogen or electron-donating substituents are present on the carbon atom bonded to silicon, the β-hydroxysilane **156** can be isolated, usually as a diastereomeric mixture (equation 124), which can be separated using the usual physical methods.

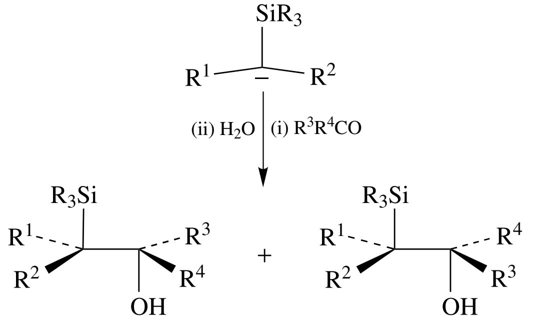

(124)

(**156**)

Treatment of the β-hydroxysilane **156** with acid gives an *anti* elimination, as shown in equation 125.

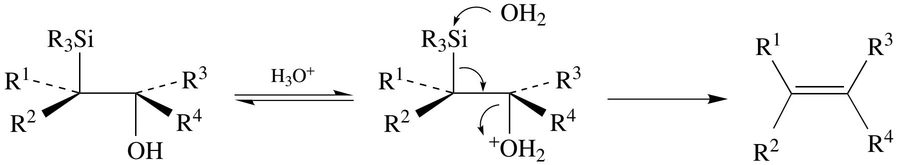

(**156**)

(125)

Treatment of the β-hydroxysilane **156** with base gives *syn* elimination[197], producing the isomeric alkene (equation 126).

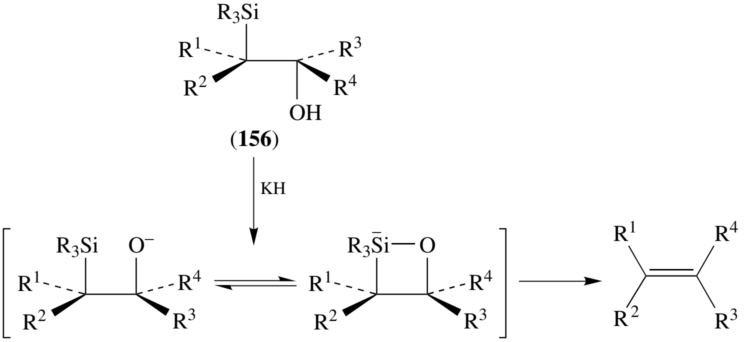

(126)

Using these routes either alkene is available from each diastereoisomer of the β-hydroxysilane[197].

To avoid the need for separation of the diastereoisomers of the β-hydroxysilane, various stereoselective routes to β-hydroxysilanes have been developed.

When an electron-withdrawing, carbanion-stabilizing group (Z) is present on the carbon-bearing silicon, the olefin is generally isolated directly from the reaction mixture, usually as a mixture of isomers (equation 127).

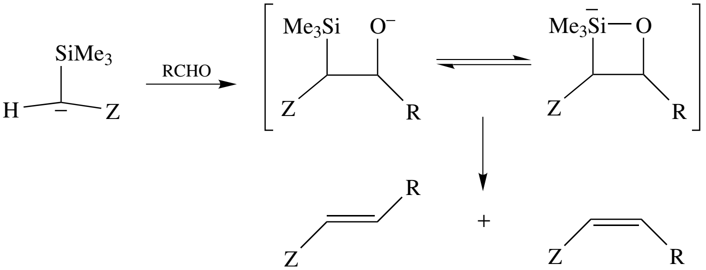

(127)

The nature of the intermediate in equation 127 and in the base-promoted elimination of β-hydroxysilanes is still uncertain. Hudrlik and co-workers have shown that the β-oxidosilane may not be an intermediate[198]. When the β-oxidosilane **158** was generated by deprotonation of the β-hydroxysilane **157** or by hydride opening of the epoxide **159**, the product arising from elimination from the β-oxidosilane was exclusively the *trans* alkene **160** (Scheme 8).

However, the reaction of benzaldehyde with bis(trimethylsilyl)methyllithium gave a mixture of *trans* and *cis* isomers in a ratio of 1.4 : 1 (equation 128). If this reaction involved the β-oxidosilane intermediate **158**, the same stereochemical outcome would be expected. This was taken to suggest that, in this particular Peterson olefination reaction at least, the β-oxidosilane **158** is not a major intermediate, and that the oxasiletane anion is formed directly by simultaneous formation of C−C and Si−O bonds.

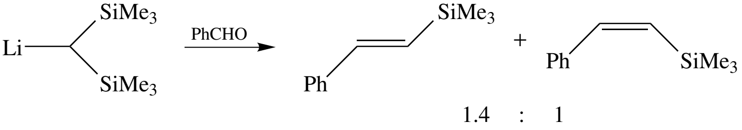

(128)

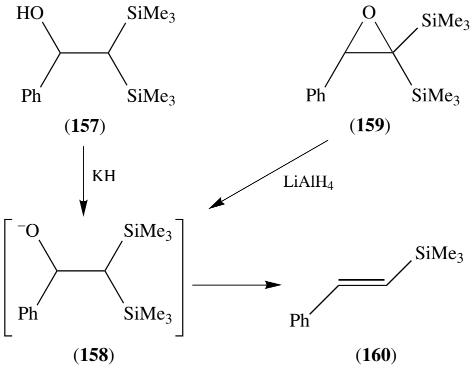

SCHEME 8

1,2-Oxasiletanide **161a** has been synthesized and its structure determined by X-ray crystallographic analysis[199]. On slight heating a similar oxasiletanide **161b** was observed to decompose to the alkene and lithium silanoxide, as shown in equation 129.

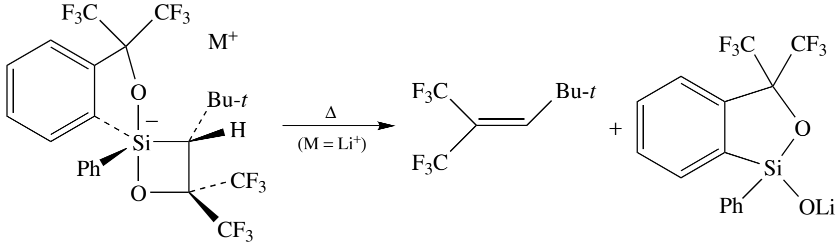

(129)

(**161a**) M = K (18-crown-6)
(**161b**) M = Li

The stereochemical outcome of the Peterson reaction between unsymmetrically substituted α-silyl carbanions and aldehydes or unsymmetrical ketones is determined by the relative rates of formation of the *threo* and *erythro* β-oxidosilanes. Often the rates are similar, to give a product alkene $E : Z$ ratio of $1 : 1$, although some workers report a predominance of *cis* olefins in the reactions of aldehydes.

The $E : Z$ ratio is found to vary as the steric bulk of R_3Si increases, the Z isomer becoming more favoured. This is easily rationalized by consideration of the attack of the carbanion on the carbonyl compound[200,201]. The two possible attacks of the α-silylbenzyl anion on benzaldehyde are shown in **162a** and **162b**.

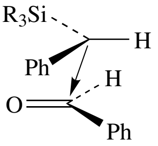

(*erythro*)
(**162a**)

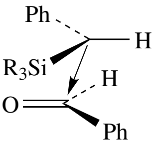

(*threo*)
(**162b**)

TABLE 14. Effect on the Z/E product ratio of electron-withdrawing aryl substituents on silicon in the Peterson reaction

Ar	$Z:E$ ratio
Ph	1 : 0.55
m-C_6H_4F	1 : 0.88
p-$C_6H_4CF_3$	1 : 1.22

The smallest group on the anion is placed between the substituents on the aldehyde to minimize steric repulsion. The other two groups are placed so that the largest group is placed opposite the bulky phenyl group on the aldehyde. Thus as the steric bulk at silicon is increased, the transition state **162a** leading to the *erythro* isomer and the Z alkene becomes increasingly favoured.

However, electronic factors can also have an effect. It was found that placing electron-withdrawing groups on the aryl substituents at silicon led to an increase in the proportion of E-alkene formed, as shown by the data in Table 14[202].

The slight increase in steric bulk on going from phenyl to fluorophenyl to trifluoromethylphenyl would be expected to increase the proportion of Z isomer. However, this is not observed. It was proposed that the increased electrophilicity of silicon when electron-withdrawing substituents are present causes an increase in the degree of silicon–oxygen interaction in the transition state and a concomitant modification of the geometry of the transition state to allow this. If a decrease in the dihedral angle between silicon and oxygen is considered in the two transition states **162a** and **162b**, the steric repulsion will increase in the *erythro* transition state **162a** as the two phenyl groups become closer to being eclipsed, whereas in the *threo* transition state **162b**, steric repulsion will decrease. Therefore, the proportion of E-alkene product increases accordingly.

C. Variations of the Peterson Reaction

An intramolecular Peterson reaction led to cycloalkene products (equation 130)[203].

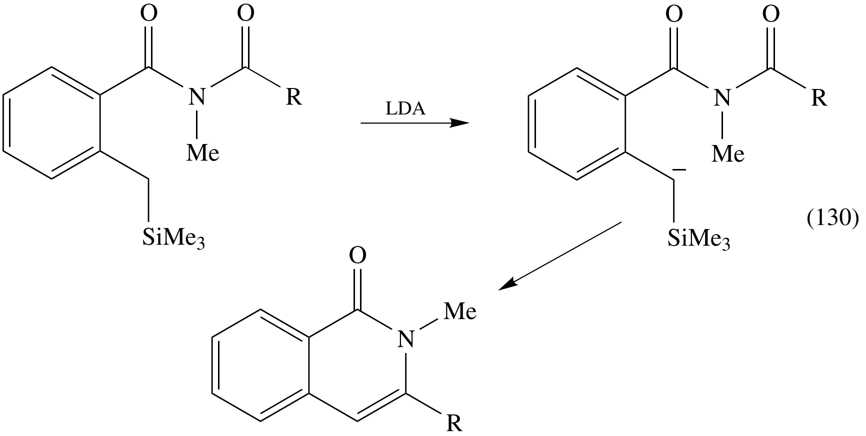

(130)

α-Silylcarbanions with α-halo groups **163** may give epoxides **164**, as shown in equation 131[204].

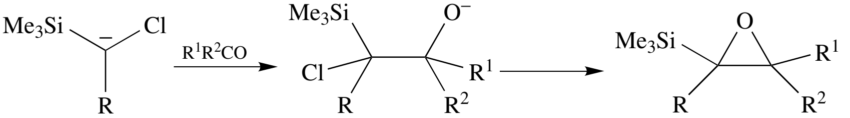

(**163**) (**164**) (131)

α-Silylallyl anions **165** have been used in the Peterson reaction and often give γ-attack (equation 132)[205].

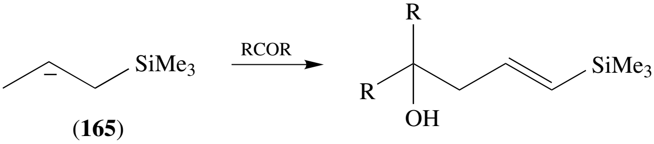

(**165**) (132)

Under certain conditions α-attack is favoured (equation 133)[206].

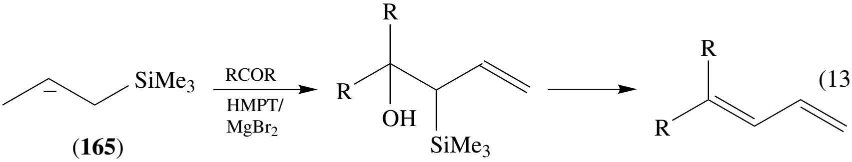

(**165**) (133)

Reaction of α-silylcarbanions with epoxides has led to observation of the homo-Peterson reaction (equation 134)[207].

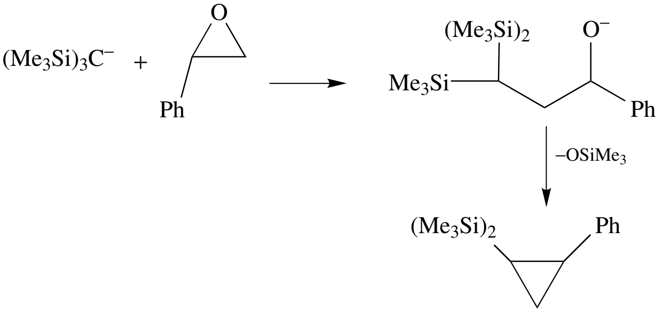

(134)

A vinylogous Peterson reaction has also been described, and the elimination has been found to be stereospecifically *syn*, as shown in equations 135 and 136[208].

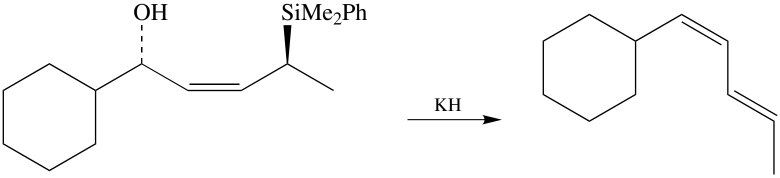

(135)

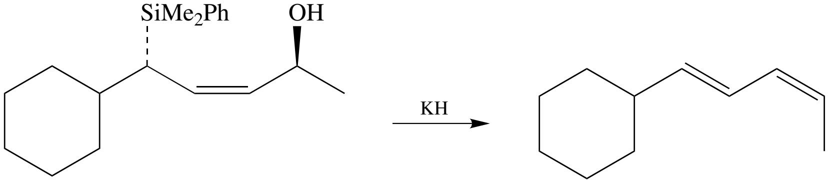

(136)

The *cis* double bond is found to be selectively placed adjacent to the carbon that originally carried the hydroxy group.

A recent modification of the Peterson reaction involves the use of fluoride ion catalysts. Reaction of bis(trimethylsilyl)methyl derivatives **166** and carbonyl compounds gives the expected alkenes **167** (as shown in equation 137) in high yields, especially for non-enolisable carbonyl compounds, and in some cases with high stereoselectivity[209].

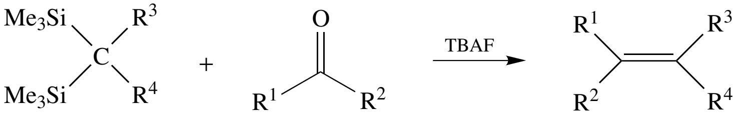

(**166**) (**167**)

(137)

In a similar catalysed reaction alkenes are produced by the addition of monosilylated derivatives **168** to aldehydes in the presence of a catalytic amount of caesium fluoride in dimethyl sulphoxide (equation 138)[210].

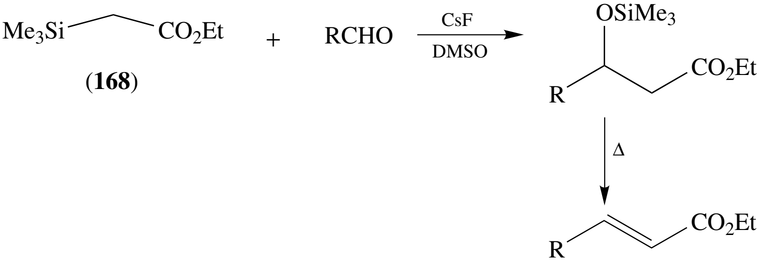

(**168**)

(138)

VII. STABILIZATION OF DEVELOPING NEGATIVE CHARGE BY SILICON

A. α-Silylepoxides

In addition to stabilizing an α-carbanion, silicon also stabilizes negative charge build-up on the α-carbon in a transition state. This situation is found in nucleophilic substitutions where substantial Nu$-$C bond formation precedes C$-$X bond cleavage. One example of this phenomenon is the ring-opening reactions of α,β-epoxysilanes. In the absence of stronger activating effects, α,β-epoxysilanes undergo α C$-$O bond cleavage in both nucleophilic and electrophilic ring opening (equation 139).

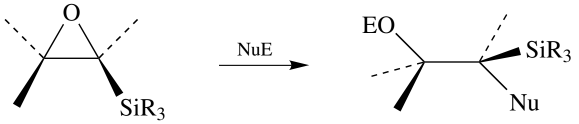

(139)

It might be predicted that electrophilic attack would take place by a S_N1 - type process, to give a β-silyl carbocation on cleavage of the β C−O bond. However, the relative orientations of the C−Si bond and the developing positive charge are such that hyperconjugative overlap is minimal **(169)**.

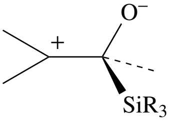

(169)

Consequently, the predominant reaction of α-silylepoxides is α-cleavage, due to the stabilization of the transition state for the S_N2 reaction α to silicon. Some recent examples are shown in equations 140[211] and 141[212].

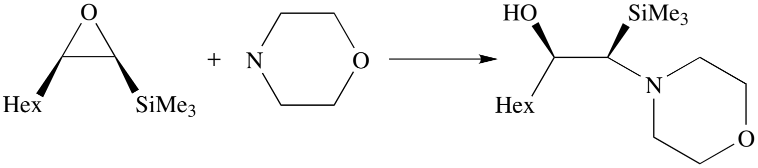

(140)

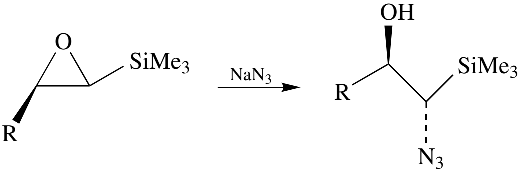

(141)

However, β-cleavage is observed in some cases, especially when steric factors are important. The regioselectivity of the reaction of epoxysilane **170** with α-sulphonyl anions derived from **171** (Scheme 9) was found to depend upon the substitution in the anion[213].

The ratios of products **172** and **173** arising from α-attack and β-attack are shown in Table 15 for sulphones with varying R^1 and R^2 groups.

Due to steric hindrance by the trimethylsilyl group, attack at the α-carbon becomes increasingly disfavoured as the steric bulk of the carbanion increases. With cyclohexyl phenyl sulphone the hindrance is such that exclusive β-attack is observed.

Replacement of the trimethylsilyl group by a triphenylsilyl group gave exclusive addition in the β-position for all sulphones studied[214].

TABLE 15. Products formed in the reaction of trimethylsilylepoxide **170** with α-sulphonyl anions

R^1, R^2	% Yield **172** (α-attack)	% Yield **173** (β-attack)
n-C_5H_{11}, H	57	—
i-Pr, H	35	40
Me, Me	31	45
$-(CH_2)_5-$	—	73

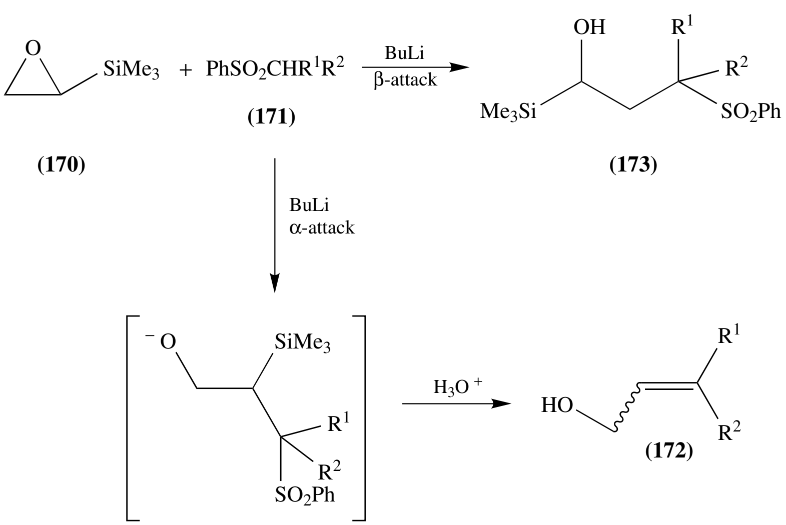

SCHEME 9

The reaction of triphenylsilylepoxide **174** with Grignard reagents gives the unexpected product **175** (equation 142)[215].

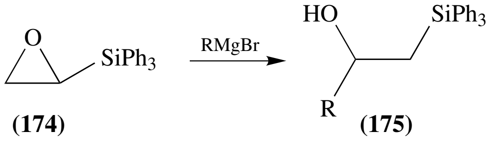

(142)

Magnesium halides are known to promote rearrangement of α, β-epoxysilanes **176** to β-silyl carbonyl compounds **177**, as shown in equation 143[216,217].

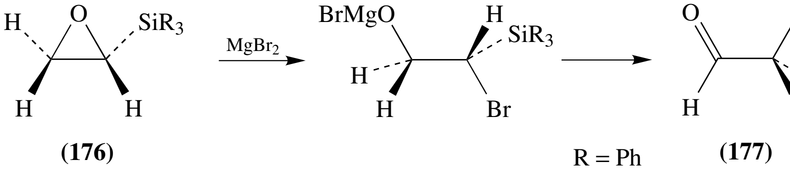

(143)

In the reaction in equation 142, the aldehyde **177**, R = Ph, produced by the magnesium halide promoted rearrangement, is then trapped by the Grignard reagent to give the observed product **175** (equation 144).

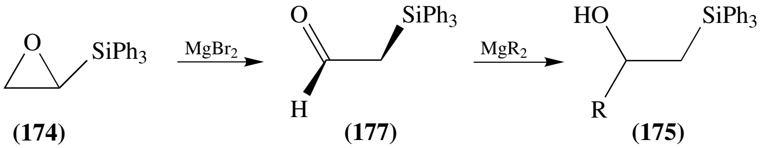

(144)

VIII. REFERENCES

1. A. R. Bassindale and P. G. Taylor, in *The Chemistry of Organic Silicon Compounds*, Vol. 1, Part 2 (Eds. S. Patai and Z. Rappoport), Wiley, Chichester, 1989, pp. 893–964.
2. E. A. V. Ebsworth, in *Organometallic Compounds of the Group IV Elements*, Vol. 1 (Ed. A. G. MacDiarmid), Dekker, New York, 1968, pp. 1–104.
3. L. Pauling, *The Nature of the Chemical Bond and the Structure of Molecules and Crystals*, 3rd edn., Cornell Univ. Press, Ithaca, New York, 1960, p. 93.
4. A. L. Allred and E. G. Rochow, *J. Inorg. Nucl. Chem.*, **5**, 264 (1958).
5. R. D. Topsom, in *Prog. Phys. Org. Chem.*, **12**, 1 (1976).
6. M. J. S. Dewar and P. J. Grisdale, *J. Am. Chem. Soc.*, **84**, 3539 (1962).
7. L. Pauling, *The Nature of the Chemical Bond*, 2nd edn., Cornell Univ. Press, New York, 1950.
8. C. G. Pitt, *J. Organomet. Chem.*, **61**, 49 (1973).
9. T. G. Traylor, W. Hanstein, H. J. Berwin, N. A. Clinton and R. S. Brown, *J. Am. Chem. Soc.*, **93**, 5715 (1971).
10. L. P. Hammett, *Physical Organic Chemistry*, 2nd edn., McGraw-Hill, New York, 1970.
11. C. Hansch, A. Leo and R. W. Taft, *Chem. Rev.*, **91**, 165 (1991).
12. H. C. Brown and Y. Okamoto, *J. Am. Chem. Soc.*, **80**, 4979 (1958).
13. O. Exner, *Coll. Czech. Chem. Commun.*, **31**, 65 (1966).
14. J. Lipowitz, *J. Am. Chem. Soc.*, **94**, 1582 (1972).
15. W. F. Reynolds, G. K. Hamer and A. R. Bassindale, *J. Chem. Soc., Perkin Trans. 2*, 971 (1977).
16. S. Ehrenson, R. T. C. Brownlee and R. W. Taft, *Prog. Phys. Org. Chem.*, **10**, 1 (1973).
17. W. Adcock, J. Alste, S. Q. A. Rizvi and M. Auranagzeb, *J. Am. Chem. Soc.*, **98**, 1701 (1976).
18. A. R. Katritzky, R. F. Pinelli, M. V. Sinnott and R. D. Topsom, *J. Am. Chem. Soc.*, **92**, 6801 (1970).
19. A. R. Bassindale, C. Eaborn, D. R. M. Walton and D. J. Young, *J. Organomet. Chem.*, **20**, 49 (1969).
20. T. Schaefer, R. Sebastian and G. H. Penner, *Can. J. Chem.*, **69**, 496 (1991).
21. M. E. Crestoni and S. Fornarini, *J. Organomet. Chem.*, **465**, 109 (1994).
22. F. R. Cartledge and J. P. Jones, *J. Organomet. Chem.*, **67**, 379 (1974).
23. M. A. Cook, C. Eaborn and D. R. M. Walton, *J. Organomet. Chem.*, **29**, 389 (1971).
24. R. Bakhtiar, C. M. Holznagel and D. B. Jacobson, *J. Am. Chem. Soc.*, **114**, 3227 (1992).
25. S. G. Cho, *J. Organomet. Chem.*, **510**, 25 (1996).
26. I. Dostrovsky and E. D. Hughes, *J. Chem. Soc.*, 157 (1946).
27. P. J. Stang, M. Ladika, Y. Apeloig, A. Stanger, M. D. Schiavelli and M. R. Hughey, *J. Am. Chem. Soc.*, **104**, 6852 (1982).
28. S. G. Wierschke, J. Chandrasekhar and W. L. Jorgensen, *J. Am. Chem. Soc.*, **107**, 1496 (1985).
29. G. A. McGibbon, M. A. Brook and J. K. Terlouw, *J. Chem. Soc., Chem. Commun.*, 360 (1992).
30. M. J. Bausch and Y. Gong, *J. Am. Chem. Soc.*, **116**, 5963 (1994).
31. N. Shimizu, E. Osijama and Y. Tsuno, *Bull. Chem. Soc. Jpn.*, **64**, 1145 (1991).
32. (a) Y. Apeloig, R. Biton and A. Abufreih, *J. Am. Chem. Soc.*, **115**, 2522 (1993).
    (b) Y. Apeloig, D. Arad and Z. Rappoport, *J. Am. Chem. Soc.*, **112**, 9131 (1990).
    (c) E. Nadler, Z. Rappoport, D. Arad and Y. Apeloig, *J. Am. Chem. Soc.*, **109**, 7873 (1987).
33. M. Mishima, T. Ariga, Y. Tsuno, K. Ikenaga and K. Kikukawa, *Chem. Lett.*, 489 (1992).
34. S. N. Ushakov and I. M. Itenberg, *Zh. Obshch. Khim.*, **7**, 2495 (1937); *Chem. Abstr.*, **32**, 2083 (1938).
35. L. H. Sommer, E. Dorfman, G. M. Goldberg and F. C. Whitmore, *J. Am. Chem. Soc.*, **68**, 488 (1946).
36. L. H. Sommer, D. L. Bailey and F. C. Whitmore, *J. Am. Chem. Soc.*, **70**, 2869 (1948).
37. A. W. P. Jarvie, *Organometal. Chem. Rev. A*, **6**, 153 (1970).
38. A. W. P. Jarvie, A. Holt and J. Thompson, *J. Chem. Soc. (B)*, 746 (1970).
39. M. R. Ibrahim and W. L. Jorgensen, *J. Am. Chem. Soc.*, **111**, 819 (1989).
40. W. Adcock, C. I. Clark and C. H. Schiesser, *J. Am. Chem. Soc.*, **118**, 11541 (1996).
41. J. B. Lambert, G. Wang, R. B. Finzel and D. H. Teramura, *J. Am. Chem. Soc.*, **109**, 7838 (1987).
42. J. B. Lambert and E. C. Chelius, *J. Am. Chem. Soc.*, **112**, 8120 (1990).
43. J. B. Lambert, R. W. Emblidge and S. Malony, *J. Am. Chem. Soc.*, **115**, 1317 (1993).
44. J. B. Lambert and X. Liu, *J. Organomet. Chem.*, **521**, 203 (1996).
45. X. Li and J. A. Stone, *J. Am. Chem. Soc.*, **111**, 5586 (1989).
46. W. Zhang, J. A. Stone, M. A. Brook and G. A. McGibbon, *J. Am. Chem. Soc.*, **118**, 5764 (1996).

47. A. J. Kresge and J. B. Tobin, *Angew. Chem., Int. Ed. Engl.*, **32**, 721 (1993).
48. A. J. Kresge and J. B. Tobin, *J. Phys. Org. Chem.*, **4**, 587 (1991).
49. V. Gabelica and A. J. Kresge, *J. Am. Chem. Soc.*, **118**, 3838 (1996).
50. D. Hajdasz and R. Squires, *J. Chem. Soc., Chem. Commun.*, 1212 (1988).
51. H.-U. Siehl and F.-P. Kaufmann, *J. Am. Chem. Soc.*, **114**, 4937 (1992).
52. N. Shimizu, S. Watanabe and Y. Tsuno, *Bull. Chem. Soc. Jpn.*, **64**, 2249 (1991).
53. N. Shimizu, C. Kinoshita, E. Osajina, F. Hayakawa and Y. Tsuno, *Bull. Chem. Soc. Jpn.*, **64**, 3280 (1991).
54. F. Hayakawa, S. Watanabe, N. Shimizu and Y. Tsuno, *Bull. Chem. Soc. Jpn.*, **66**, 153 (1993).
55. R. Fujiyama and T. Munechika, *Tetrahedron Lett.*, **34**, 5907 (1993).
56. N. Shimizu, S. Watanabe, F. Hayakawa, S. Yasuhara, Y. Tsuno and T. Inazu, *Bull. Chem. Soc. Jpn.*, **67**, 500 (1994).
57. M. A. Brook and A. Neuy, *J. Org. Chem.*, **55**, 3609 (1990).
58. J. B. Lambert and R. A. Singer, *J. Am. Chem. Soc.*, **114**, 10246 (1992).
59. M. J. Doyle, A. J. Kirby, J. M. Percy and P. R. Raithby, *Acta Crystallogr., Sect. C*, **48**, 866 (1992).
60. P. G. Jones, A. J. Kirby and J. K. Parker, *Acta Crystallogr., Sect. C*, **48**, 868 (1992).
61. J. M. White, *Aust. J. Chem.*, **48**, 1227 (1995).
62. J. M. White and G. B. Robertson, *J. Org. Chem.*, **57**, 4638 (1992).
63. Y. Kuan and J. M. White, *J. Chem. Soc., Chem. Commun.*, 1195 (1994).
64. A. J. Green, Y. Kuan and J. M. White, *J. Org. Chem.*, **60**, 2734 (1995).
65. V. J. Shiner, Jr., M. W. Ensinger, G. S. Kriz and K. A. Halley, *J. Org. Chem.*, **55**, 653 (1990).
66. V. J. Shiner, Jr., M. W. Ensinger and R. D. Rutkowske, *J. Am. Chem. Soc.*, **109**, 804 (1987).
67. C. A. Grob and P. Sawlewicz, *Tetrahedron Lett.*, **28**, 951 (1987).
68. V. J. Shiner, Jr., M. W. Ensinger and J. C. Huffman, *J. Am. Chem. Soc.*, **111**, 7199 (1989).
69. W. Kirmse and F. Sollenbohmer, *J. Am. Chem. Soc.*, **111**, 4127 (1989).
70. W. Adcock and G. B. Kok, *J. Org. Chem.*, **52**, 356 (1987).
71. J. B. Lambert, *Tetrahedron*, **46**, 2677 (1990).
72. R. J. Fessenden, K. Seiles and M. Dagani, *J. Org. Chem.*, **31**, 2433 (1966).
73. W. Adcock, A. R. Krstic, P. J. Duggan, V. J. Shiner, Jr., J. Coope and M. W. Ensinger, *J. Am. Chem. Soc.*, **112**, 3140 (1990).
74. D. Hrovat and W. T. Borden, *J. Org. Chem.*, **57**, 2519 (1992).
75. W. Adcock and N. A. Trout, *J. Org. Chem.*, **56**, 3229 (1991).
76. W. Adcock, H. Gangodawila, G. B. Kok, V. S. Iyer, W. Kitching, G. M. Drew and D. Young, *Organometallics*, **6**, 156 (1987).
77. I. Fleming, in *Comprehensive Organic Chemistry*, Vol. 3 (Eds. D. H. R. Barton and W. D. Ollis), Chap. 13, Pergamon Press, Oxford, 1979.
78. A. C. Hopkinson and M. H. Lien, *J. Org. Chem.*, **46**, 998 (1981).
79. C. Glidewell and C. Thomson, *J. Comput. Chem.*, **3**, 495 (1982).
80. D. M. Wetzel and J. I. Brauman, *J. Am. Chem. Soc.*, **110**, 8333 (1988).
81. E. A. Brinkman, S. Berger and J. I. Brauman, *J. Am. Chem. Soc.*, **116**, 8304 (1994).
82. S. McN. Sieburth and J. J. Somers, *Tetrahedron*, **52**, 5683 (1996).
83. S. Zhang, X-M. Zhang and F. G. Bordwell, *J. Am. Chem. Soc.*, **117**, 602 (1995).
84. E. Berliner, *Prog. Phys. Org. Chem.*, **2**, 253 (1964).
85. C. Eaborn, *J. Chem. Soc., Chem. Commun.*, 1255 (1972).
86. R. W. Bott, C. Eaborn and P. M. Greasley, *J. Chem. Soc.*, 4804 (1964).
87. T. Hashimoto and M. Seki, *Yakugaku Zasshi*, **81**, 204 (1961); *Chem. Abstr.*, **55**, 14340 (1961).
88. Y. Sakata and T. Hashimoto, *Yakugaku Zasshi*, **80**, 730 (1960); *Chem. Abstr.*, **54**, 24480 (1960).
89. C. Eaborn and D. E. Webster, *J. Chem. Soc.*, 4449 (1957).
90. C. Eaborn and D. E. Webster, *J. Chem. Soc.*, 179 (1960).
91. G. V. Motsarev, V. T. Inshhakova, V. I. Kolbasov and V. R. Rosenberg, *Zh. Obshch. Khim.*, **44**, 1053 (1974); *Chem. Abstr.*, **81**, 105611 (1974).
92. T. Hashimoto, *Yakugaku Zasshi*, **87**, 528 (1967); *Chem. Abstr.*, **61**, 54206 (1967).
93. R. J. Mills and V. Snieckus, *Tetrahedron Lett.*, **25**, 483 (1984).
94. P. Babin, B. Bennetau, P. Bourgeois, F. Rajarison and J. Dunogues, *Bull. Soc. Chim. Fr.*, **129**, 25 (1992).
95. G. W. Kalbalka and R. S. Varma, *Tetrahedron*, **45**, 6601 (1989).
96. S. M. Moerlein, W. Beyer amd G. Stocklin, *J. Chem. Soc., Perkin Trans. 1*, 779 (1988).

97. M. Speranza, C-Y. Shiue, A. P. Wolf, D. S. Wilbur and J. Angelini, *J. Fluorine Chem.*, **30**, 97 (1985).
98. G. Felix, J. Dunogues and R. Calas, *Angew. Chem., Int. Ed. Engl.*, **18**, 402 (1979).
99. G. Felix, M. Laguerre, J. Dunogues and R. Calas, *J. Chem. Res.*, 236 (1980).
100. R. Calas, *Compt. Rend. Acad. Sci., Ser. 2*, **301**, 1289 (1985).
101. B. Bennetau and J. Dunogues, *Synlett*, 171 (1993).
102. B. Bennetau, F. Rajarison, J. Dunogues and P. Babin, *Tetrahedron*, **49**, 10843 (1993).
103. R. J. Mills, N. J. Taylor and V. Snieckus, *J. Org. Chem.*, **54**, 4372 (1989).
104. H. Ishibashi, H. Sakashita and M. Ikeda, *J. Chem. Soc., Perkin Trans. 1*, 1953 (1992).
105. C. Eaborn, T. A. Emokpae, V. I. Sidorov and R. Taylor, *J. Chem. Soc., Perkin Trans. 2*, 1454 (1974).
106. R. W. Bott, C. Eaborn and R. Taylor, *J. Chem. Soc.*, 4927 (1961).
107. K. Mikami, K. Nishi and T. Nakai, *Tetrahedron Lett.*, **24**, 795 (1983).
108. I. Fleming and A. Pearce, *J. Chem. Soc., Perkin Trans. 1*, 2485 (1980).
109. F. Duboudin, *J. Organomet. Chem.*, **156**, C25 (1978).
110. R. B. Miller and T. Reichenbach, *Tetrahedron Lett.*, 543 (1974).
111. R. B. Miller and G. McGarvey, *Synth. Commun.*, **8**, 291 (1978).
112. R. B. Miller and G. McGarvey, *Synth. Commun.*, **7**, 475 (1977).
113. K. Miura, S. Okajima, T. Hondo and A. Hosomi, *Tetrahedron Lett.*, **36**, 1483 (1995).
114. K. Miura, T. Hondo, S. Okajima and A. Hosomi, *Tetrahedron Lett.*, **37**, 387 (1996).
115. M. A. Brook, C. Henry, R. Jueschke and P. Modi, *Synlett*, 97 (1993).
116. C. Henry, R. Juschke and M. A. Brook, *Inorg. Chim. Acta*, **220**, 145 (1994).
117. C. Henry and M. A. Brook, *Tetrahedron*, **50**, 11379 (1994).
118. I. Fleming, J. Dunogues and R. Smithers, *Org. React.*, **37**, 57 (1989).
119. K. E. Koenig and W. P. Weber, *J. Am. Chem. Soc.*, **95**, 3416 (1973).
120. T. H. Chan and T. Fleming, *Synthesis*, 761 (1979).
121. T. H. Chan and K. Koumaglo, *Tetrahedron Lett.*, **27**, 883 (1986).
122. T. H. Chan, P. W. K. Lau and W. Mychajlowskij, *Tetrahedron Lett.*, 3317 (1977).
123. T. H. Chan and K. Koumaglo, *J. Organomet. Chem.*, **285**, 109 (1985).
124. K. Mikami, H. Wakabayashi and T. Nakai, *J. Org. Chem.*, **56**, 4337 (1991).
125. N. Kishi, K. Mikami and T. Nakai, *Tetrahedron*, **47**, 8111 (1991).
126. L. E. Overman and A. T. Robichard, *J. Am. Chem. Soc.*, **111**, 300 (1989).
127. G. W. Daub, D. A. Heerding and L. E. Overman, *Tetrahedron*, **44**, 3919 (1988).
128. R. M. Lett, L. E. Overman and J. Zablocki, *Tetrahedron Lett.*, **29**, 6541 (1988).
129. R. M. Burk and L. E. Overman, *Heterocycles*, **35**, 205 (1993).
130. P. Castro, L. E. Overman, X. M. Zhang and P. S. Mariano, *Tetrahedron Lett.*, **34**, 5243 (1993).
131. M. A. Brook and C. Henry, *Tetrahedron*, **52**, 861 (1996).
132. M. I. Alhassan, *J. Organomet. Chem.*, **372**, 183 (1989).
133. D. R. M. Walton and F. Waugh, *J. Organomet. Chem.*, **37**, 45 (1972).
134. H. Mayr, E. Bauml, G. Cibura and R. Koschinsky, *J. Org. Chem.*, **57**, 768 (1992).
135. I. Fleming and S. K. Patel, *Tetrahedron Lett.*, **22**, 2321 (1981).
136. H. Mayr and G. Hagen, *J. Chem. Soc., Chem. Commun.*, 91 (1989).
137. G. Hagen and H. Mayr, *J. Am. Chem. Soc.*, **113**, 4954 (1991).
138. M. Hojo, K. Ohsumi and A. Hosomi, *Tetrahedron Lett.*, **33**, 5981 (1992).
139. G. A. Olah, D. S. Van Vliet, Q. Wang and G. S. Prakash, *Synthesis*, 159 (1995).
140. S. H. Yeon, B. W. Lee, B. R. Yoo, M-Y. Suk and I. N. Jung, *Organometallics*, **14**, 2361 (1995).
141. C. LeRoux and J. Dubac, *Organometallics*, **15**, 4646 (1996).
142. V. K. Aggarwal and G. P. Vennall, *Tetrahedron Lett.*, **37**, 3745 (1996).
143. E. W. Colvin and M. Monteith, *J. Chem. Soc., Chem. Commun.*, 1230 (1990).
144. B. Guyot, J. Pornet and L. Miginiac, *Tetrahedron*, **47**, 3981 (1991).
145. R. L. Funk, J. Umstead-Daggett and K. M. Brummond, *Tetrahedron Lett.*, **34**, 2867 (1993).
146. M. Franciotti, A. Mann, A. Mordini and M. Taddei, *Tetrahedron Lett.*, **34**, 1355 (1993).
147. H. Mayr, A. O. Gabriel and R. Schumacher, *Justus Liebigs Ann. Chem.*, 1583 (1995).
148. M. Polla and T. Frejd, *Acta Chem. Scand.*, **47**, 716 (1993).
149. A. Hosomi and H. Sakurai, *J. Am. Chem. Soc.*, **99**, 1673 (1977).
150. D. Schinzer, *Synthesis*, 263 (1988).
151. H. J. Knolker, N. Foitzik, R. Graf and J-B. Pannek, *Tetrahedron*, **49**, 9955 (1993).
152. R. L. Danheiser, B. R. Dixon and R. W. Gleason, *J. Org. Chem.*, **57**, 6094 (1992).

153. G. P. Brengal and A. I. Meyers, *J. Org. Chem.*, **61**, 3230 (1996).
154. H. J. Knolker, G. Baum and R. Graf, *Angew. Chem., Int. Ed. Engl.*, **33**, 1612 (1994).
155. G. Majetich, K. Hull, A. M. Casares and V. Khetani, *J. Org. Chem.*, **56**, 3958 (1991).
156. H. Wetter and P. Scherer, *Helv. Chim. Acta*, **66**, 118 (1983).
157. T. Hayashi, M. Konishi, H. Ito and M. Kumada, *J. Am. Chem. Soc.*, **104**, 4962 (1982).
158. T. Hayashi, M. Konishi and M. Kumada, *J. Am. Chem. Soc.*, **104**, 4963 (1982).
159. T. Hayashi, H. Ito and M. Kumada, *Tetrahedron Lett.*, **23**, 4605 (1982).
160. G. Wickham and W. J. Kitching, *J. Org. Chem.*, **48**, 612 (1983).
161. I. Fleming and N. K. Terrett, *J. Organomet. Chem.*, **264**, 99 (1984).
162. S. D. Khan, C. F. Pau, A. R. Chamberlin and W. J. Hehre, *J. Am. Chem. Soc.*, **109**, 650 (1987).
163. I. Fleming and D. Higgins, *J. Chem. Soc., Perkin Trans. 1*, 3327 (1992).
164. M. J. C. Buckle, I. Fleming and S. Gil, *Tetrahedron Lett.*, **33**, 4481 (1992).
165. I. Fleming, G. R. Jones, N. D. Kindon, Y. Landais, C. P. Leslie, I. T. Morgan, S. Peukert and A. K. Sarkar, *J. Chem. Soc., Perkin Trans. 1*, 1171 (1996).
166. C. E. Masse and J. S. Panek, *Chem. Rev.*, **95**, 1293 (1995).
167. C. Nativi, G. Palio and M. Taddei, *Tetrahedron Lett.*, **32**, 1583 (1991).
168. M. Laguerre, M. Grignon-Dubois and J. Dunogues, *Tetrahedron*, **37**, 1161 (1981).
169. J. P. Pillot, B. Bennetau, J. Dunogues and R. Calas, *Tetrahedron Lett.*, **22**, 3401 (1981).
170. D. Schinzer and G. Panke, *J. Org. Chem.*, **61**, 4496 (1996).
171. D. Schinzer, J. Kabbara and K. Ringe, *Tetrahedron Lett.*, **33**, 8017 (1992).
172. R. L. Danheiser, B. R. Dixon and R. W. Gleason, *J. Org. Chem.*, **57**, 6094 (1992).
173. R. L. Danheiser and D. J. Carini, *J. Org. Chem.*, **45**, 3925 (1980).
174. R. L. Danheiser, D. J. Carini and A. Basak, *J. Am. Chem. Soc.*, **103**, 1604 (1981).
175. M. J. C. Buckle and I. Fleming, *Tetrahedron Lett.*, **34**, 2383 (1993).
176. P. A. Smith, in *Molecular Rearrangements*, Part 1 (Ed. P. de Mayo), Wiley-Interscience, New York, 1963, pp. 577–589.
177. P. F. Hudrlik, A. M. Hudrlik, G. Nagandrappa, T. Yimenu, E. T. Zellers and E. Chin, *J. Am. Chem. Soc.*, **102**, 6894 (1980).
178. S. R. Wilson and M. J. diGrandi, *J. Org. Chem.*, **56**, 4766 (1991).
179. J. R. Hwu and J. M. Wetzel, *J. Org. Chem.*, **57**, 922 (1992).
180. J. R. Hwu and B. A. Gilbert, *J. Am. Chem. Soc.*, **113**, 5917 (1991).
181. T. A. Engler and J. P. Reddy, *J. Org. Chem.*, **56**, 6491 (1991).
182. D. J. Ager, *Org. React.*, **38**, 1 (1990).
183. D. J. Peterson, *J. Org. Chem.*, **33**, 780 (1968).
184. P. A. Brough, S. Fisher, B. Zhao, R. C. Thomas and V. Snieckus, *Tetrahedron Lett.*, **37**, 2915 (1996).
185. H. Imanieh, P. Quayle, M. Voaden, J. Conway and S. D. A. Street, *Tetrahedron Lett.*, **33**, 543 (1992).
186. A. G. Brook, J. M. Duff and D. G. Anderson, *Can. J. Chem.*, **48**, 561 (1970).
187. A. G. M. Barrett and J. A. Flygare, *J. Org. Chem.*, **56**, 638 (1991).
188. W. Dumont and A. Krief, *Angew. Chem., Int. Ed. Engl.*, **15**, 161 (1976).
189. A. R. Bassindale, R. J. Ellis and P. G. Taylor, *Tetrahedron Lett.*, **25**, 2705 (1984).
190. D. Seyferth, T. Wada and G. Raab, *Tetrahedron Lett.*, 20 (1960).
191. D. Seyferth and T. Wada, *Inorg. Chem.*, **1**, 78 (1962).
192. M. R. Stober, K. W. Michael and O. L. Speier, *J. Org. Chem.*, **32**, 2740 (1967).
193. K. Tomao, R. Kanatani and M. Kumada, *Tetrahedron Lett.*, **25**, 1905 (1984).
194. T. Hayama, S. Tomoda, Y. Takeuchi and Y. Nomura, *Tetrahedron Lett.*, **24**, 2795 (1983).
195. G. Stork and J. Singh, *J. Am. Chem. Soc.*, **96**, 6181 (1974).
196. R. K. Boeckman Jr., *J. Am. Chem. Soc.*, **96**, 6179 (1974).
197. H. O. House, *Acc. Chem. Res.*, **9**, 59 (1976).
198. P. F. Hudrlik, E. L. O. Agwaramgbo and A. M. Hudrlik, *J. Org. Chem.*, **54**, 5613 (1989).
199. T. Kawashima, N. Iwama and R. Okazaki, *J. Am. Chem. Soc.*, **114**, 7598 (1992).
200. A. R. Bassindale, R. J. Ellis, J. C-Y. Lau and P. G. Taylor, *J. Chem. Soc., Chem. Commun.*, 98 (1986).
201. H. B. Burgi and J. D. Dunitz, *Acc. Chem. Res.*, **16**, 153 (1983).
202. A. R. Bassindale, R. J. Ellis and P. G. Taylor, *J. Chem. Res (S)*, 34 (1996).
203. A. Couture, H. Cornet and P. Grandclaudon, *J. Organomet. Chem.*, **440**, 7 (1992).
204. C. Burford, F. Cooke, E. Ehlinger and P. Magnus, *J. Am. Chem. Soc.*, **99**, 4536 (1977).

205. E. Ehlinger and P. Magnus, *J. Am. Chem. Soc.*, **102**, 5004 (1976).
206. P. W. K. Lau and T. H. Chan, *Tetrahedron Lett.*, 1137 (1978).
207. I. Fleming and C. D. Lloyd, *J. Chem. Soc., Perkin Trans. 1*, 969 (1981).
208. I. Fleming, I. T. Morgan and A. K. Sarkar, *J. Chem. Soc., Chem. Commun.*, 1575 (1990).
209. C. Palomo, J. M. Aizpurua, J. M. Garcia, I. Ganboa, F. P. Cossio, B. Lecea and C. Lopez, *J. Org. Chem.*, **55**, 2498 (1990).
210. M. Bellassoued and N. Ozanne, *J. Org. Chem.*, **60**, 6582 (1995).
211. P. F. Hudrlik, A. M. Hudrlik and A. K. Kulkarni, *Tetrahedron Lett.*, **26**, 139 (1985).
212. A. R. Bassindale, P. G. Taylor and Y. Xu, *Tetrahedron Lett.*, **37**, 555 (1996).
213. P. Jankowski, S. Marczak, M. Masnyk and J. Wicha, *J. Chem. Soc., Chem. Commun.*, 297 (1991).
214. P. Jankowski and J. Wicha, *J. Chem. Soc., Chem. Commun.*, 802 (1992).
215. P. F. Hudrlik, M. E. Ahmed, R. R. Roberts and A. M. Hudrlik, *J. Org. Chem.*, **61**, 4395 (1996).
216. A. G. Brook, D. McRae and A. R. Bassindale, *J. Organomet. Chem.*, **86**, 185 (1975).
217. P. F. Hudrlik, R. N. Misra, G. P. Withers, A. M. Hudrlik, R. J. Rona and J. P. Arcoleo, *Tetrahedron Lett.*, 1453 (1976).

CHAPTER **8**

Steric effects of silyl groups

R. JIH-RU HWU, SHWU-CHEN TSAY and BUH-LUEN CHENG

Organosilicon and Synthesis Laboratory, Institute of Chemistry, Academia Sinica, Nankang, Taipei, Taiwan 11529, Republic of China and Department of Chemistry, National Tsing Hua University, Hsinchu, Taiwan 30043, Republic of China
Fax: 886-2-7881337; e-mail: JRHWU@chem.nthu.edu.tw

I. INTRODUCTION

Triorganosilyl groups are frequently used in organic reactions. Appropriate placement of those groups in substrates, in reagents or in catalysts can control the stereochemical outcome of the reactions because of their steric influence. The most popular silyl group is the Me$_3$Si, which is referred to as the ‘bulky proton’[1−3]. In 1989, a review was published on the steric effect of the Me$_3$Si group[2].

In this chapter, the influence resulting from many different silyl groups on organic compounds and reactions will be discussed. Topics are selected from papers published mainly between mid-1988 and mid-1996. During this period of time, several informative reviews and articles on organosilicon chemistry have been published by Chan and Wang[4,5], Fleming[6], Page and coworkers[7], Cirillo and Panek[8], Rücker[9] and Steinmetz[10]. The chemistry discussed in those papers will not be emphasized in this chapter although some crucial information is cited in the text or listed in Table 1.

II. AN ORDER IN INCREASING SIZE OF SILYL GROUPS

A comparison of steric influence resulting from more than 80 different silyl groups is summarized in Table 1. The trend is established on the basis of reaction yields, rates and selectivity, as well as on reactivity and physical properties of organosilanes. Two different effects may be involved: (a) the effect of a silyl group on reactions taking place at the neighboring centers, and (b) the effect of the groups attached to silicon on the nucleophilic attack at the silicon atom.

The results from analyses of many research groups' reports published in the past decade indicate that often both effects display a parallel trend. An order of the bulk of 44 silyl groups is thus established as follows:

smaller ⟶ bulkier
(less influence) (greater influence)

Me$_2$HSi < Me$_3$Si < PhMe$_2$Si < Ph$_2$MeSi < EtMe$_2$Si < (PhCH$_2$)Me$_2$Si < (*n*-Pr)Me$_2$Si ∼ Ph$_3$Si ∼ (*t*-Bu)$_2$HSi < Et$_2$MeSi ∼ (*n*-Bu)Me$_2$Si ∼ (*n*-C$_6$H$_{13}$)Me$_2$Si < (Me$_3$Si)Me$_2$Si < (*i*-Bu)Me$_2$Si < (cyclopentyl)Me$_2$Si ∼ (*n*-Pr)$_2$MeSi < (*n*-Bu)$_2$MeSi < Et$_3$Si < (*i*-Pr)Me$_2$Si < (cyclohexyl)Me$_2$Si < (*s*-Bu)Me$_2$Si < (*n*-Bu)(*i*-Pr)MeSi ∼ (*n*-Pr)$_3$Si < (*i*-Pr)(−CH$_2$CH$_2$CH$_2$CH$_2$−)Si < [(*t*-Bu)$_2$CH]Me$_2$Si ∼ (*t*-Bu)Me$_2$Si ∼ (*i*-Pr)$_2$MeSi < (EtMe$_2$C)Me$_2$Si < (*n*-PrMe$_2$C)Me$_2$Si < (*i*-PrMe$_2$C)Me$_2$Si < (*n*-Bu)$_3$Si < (*n*-hexyl)$_3$Si < (*i*-Bu)$_3$Si < [(*t*-Bu)CH$_2$]$_3$Si < [(*t*-Bu)EtMeC]Me$_2$Si < (*i*-Pr)$_3$Si < (*t*-Bu)Ph$_2$Si < (*t*-Bu)(−CH$_2$CH$_2$CH$_2$CH$_2$−)Si < (*t*-Bu)(*i*-Pr)EtSi < (*t*-Bu)(*i*-Pr)$_2$Si < (*t*-Bu)$_2$MeSi < (*t*-Bu)$_3$Si < (*t*-Bu)(cyclohexyl)$_2$Si < (cyclohexyl)$_3$Si

TABLE 1. Order of the size of organosilyl groups on the basis of their influence on various reactions

Entry	Reaction or property studied	Selectivity basis	Order of the size	References
1	1,2-addition	%ee and yield	$(i\text{-Pr})_3\text{Si} < (t\text{-Bu})\text{Ph}_2\text{Si}$	11
2	1,2-addition	rate and diastereoselectivity	$\text{Me}_3\text{Si} < \text{Et}_3\text{Si} < (t\text{-Bu})\text{Me}_2\text{Si} < (t\text{-Bu})\text{Ph}_2\text{Si} < (i\text{-Pr})_3\text{Si}$	12,13
3	1,2-addition	regioselectivity	$\text{Ph}_3\text{Si} < (t\text{-Bu})\text{Ph}_2\text{Si} < \text{Et}_3\text{Si} < (i\text{-Pr})_3\text{Si}$	14
4	Mukaiyama addition	stereoselectivity	$\text{Me}_3\text{Si} < \text{Et}_3\text{Si} < (t\text{-Bu})\text{Me}_2\text{Si} < (i\text{-Pr})_3\text{Si}$	15
5	Mukaiyama addition	stereoselectivity	$\text{Me}_3\text{Si} < \text{Et}_3\text{Si} < (t\text{-Bu})\text{Me}_2\text{Si} < \text{PhMe}_2\text{Si} < \text{Ph}_2\text{MeSi}$	16
6	addition	cone angle	$\text{Me}_3\text{Si} < \text{ClMe}_2\text{Si} < \text{PhMe}_2\text{Si} < \text{Et}_3\text{Si} < (n\text{-Bu})_3\text{Si} \sim (n\text{-hexyl})_3\text{Si} < (n\text{-Bu})\text{Me}_2\text{Si} < \text{Ph}_3\text{Si} < (i\text{-Pr})_3\text{Si}$	17
7	alkylation	yield	$\text{Me}_3\text{Si} < \text{PhMe}_2\text{Si} < \text{Ph}_2\text{MeSi} < \text{Ph}_3\text{Si}$	18
8	alkylation	γ/α site of alkylation	$\text{Me}_3\text{Si} < \text{Ph}_3\text{Si} < \text{Et}_3\text{Si} < (n\text{-Pr})_3\text{Si}$	19
9	allylation vs dihydrofuranation	ratio	$\text{Me}_3\text{Si} < \text{PhMe}_2\text{Si} < (i\text{-Pr})_3\text{Si}$	20
10	allylation	regio-selectivity	$(t\text{-Bu})\text{Me}_2\text{Si} < (i\text{-Pr})_3\text{Si}$	21
11	dihydrofuranation	yield	$\text{Me}_3\text{Si} < \text{PhMe}_2\text{Si} < (i\text{-Pr})_3\text{Si}$	20
12	cyclization	stereoselectivity	$\text{Me}_3\text{Si} < \text{Et}_3\text{Si}$	22
13	iodolactonization	diastereoselectivity	$(t\text{-Bu})\text{Me}_2\text{Si} < (t\text{-Bu})\text{Ph}_2\text{Si} < (i\text{-Pr})_3\text{Si}$	23
14	iodolactonization	diastereoselectivity	$(t\text{-Bu})\text{Me}_2\text{Si} < (t\text{-Bu})\text{Ph}_2\text{Si} < (i\text{-Pr})_3\text{Si}$	24
15	iodolactonization	diastereoselectivity	$(t\text{-Bu})\text{Me}_2\text{Si} < (i\text{-Pr})_3\text{Si}$	25
16	cyclization	*cis/trans* ratio	$\text{Me}_3\text{Si} < \text{Ph}_2\text{MeSi} < \text{Ph}_3\text{Si}$	26
17	cyclization	product distribution	$\text{PhMe}_2\text{SiMe}_2\text{Si} < \text{PhMe}_2\text{SiEt}_2\text{Si} < \text{PhMe}_2\text{SiPh}_2\text{Si} < \text{PhMe}_2\text{Si}(i\text{-Bu})_2\text{Si} < \text{PhMe}_2\text{Si}(i\text{-Pr})_2\text{Si}$	27
18	decomposition	product distribution	$\text{Me}_3\text{Si} < \text{Et}_3\text{Si} < (t\text{-Bu})\text{Me}_2\text{Si} < (i\text{-Pr})_3\text{Si}$	28
19	desilylation	rate	$\text{Et}_3\text{Si} < (t\text{-Bu})\text{Me}_2\text{Si} < (i\text{-PrMe}_2\text{C})\text{Me}_2\text{Si} \sim (t\text{-Bu})\text{Ph}_2\text{Si}$	29
20	desilylation	rate	$(t\text{-Bu})\text{Me}_2\text{Si} < (i\text{-PrMe}_2\text{C})\text{Me}_2\text{Si} < (i\text{-Pr})_3\text{Si} < (t\text{-Bu})\text{Ph}_2\text{Si}$	30
21	desilylation	rate	$\text{Me}_3\text{Si} < (t\text{-Bu})\text{Me}_2\text{Si} \sim (i\text{-Pr})_3\text{Si} < (t\text{-Bu})\text{Ph}_2\text{Si}$	31
22	dehydrogenolysis	rate	$(t\text{-Bu})\text{Me}_2\text{Si} < (i\text{-Pr})_3\text{Si} < (t\text{-Bu})\text{Ph}_2\text{Si}$	32
23	desilylation	chemoselectivity	$(t\text{-Bu})\text{Me}_2\text{Si} < (i\text{-Pr})_3\text{Si}$	33
24	desilylation	chemoselectivity	$(t\text{-Bu})\text{Me}_2\text{Si} < (t\text{-Bu})\text{Ph}_2\text{Si}$	34,35
25	elimination	rate	$\text{Me}_3\text{Si} < \text{PhMe}_2\text{Si} < \text{Ph}_2\text{MeSi} < \text{Ph}_3\text{Si}$	36
26	ene reaction	stereoselectivity	$(t\text{-Bu})\text{Me}_2\text{Si} < (t\text{-Bu})\text{Ph}_2\text{Si}$	37

TABLE 1. (*continued*)

Entry	Reaction or property studied	Selectivity basis	Order of the size	References
27	epoxidation	stereoselectivity	$Me_3Si < (Me_3Si)Me_2Si$	38
28	hydroboration	stereoselectivity	$Me_3Si < Et_3Si < (t\text{-Bu})Me_2Si < (i\text{-Pr})_3Si$	39
29	hydroformylation	regioselectivity	$Me_3Si < (t\text{-Bu})Me_2Si < Ph_3Si < (t\text{-Bu})Ph_2Si$	40
30	hydrosilylation	reactivity	$Ph_2HSi << PhMe_2Si < Ph_2MeSi < Ph_3Si$	41
31	isomerization	ratio	$(t\text{-Bu})Ph_2Si < (t\text{-Bu})Me_2Si < (i\text{-Pr})_3Si$	42
32	Brook vs. Wittig rearrangements	chemoselectivity	$Me_3Si < (t\text{-Bu})Ph_2Si < Et_3Si < (i\text{-PrMe}_2C)Me_2Si$ and $(i\text{-Pr})_3Si$	43
33	silyl migration	yield	$Me_3Si < Et_3Si < (n\text{-Pr})_3Si < (i\text{-Pr})_3Si$	44
34	intermolecular migration	product distribution	$Me_3Si < Et_3Si < (i\text{-Pr})Me_2Si < (t\text{-Bu})Me_2Si < (i\text{-Pr})_3Si$	45
35	osmylation	stereoselectivity	$Me_3Si < PhMe_2Si < Et_3Si < (t\text{-Bu})Me_2Si < Ph_2MeSi$	46
36	oxymercuration	diastereoselectivity	$(t\text{-Bu})Me_2Si < (t\text{-Bu})Ph_2Si$	47
37	ozonolysis	stereoselectivity	$Me_3Si < (i\text{-Pr})_3Si < (t\text{-Bu})Me_2Si$	48
38	ozonolysis	rate	$(n\text{-Bu})_2HSi < (i\text{-Pr})_2HSi < Et_2MeSi < (i\text{-Pr})_2MeSi < (n\text{-Bu})_2MeSi < Et_3Si < (n\text{-Pr})_3Si < (n\text{-Bu})_3Si < (t\text{-Bu})(\text{cyclohexyl})_2Si < (\text{cyclohexyl})_3Si$	49,50
39	Peterson olefination	diastereomeric ratio	$Me_3Si < Et_3Si < (\text{cyclohexyl})_2MeSi < (t\text{-Bu})Me_2Si < (t\text{-Bu})Ph_2Si < Ph_3Si$	51
40	Peterson olefination	diastereomeric ratio and yield	$Me_3Si < Et_3Si < (t\text{-Bu})Me_2Si < (t\text{-Bu})Ph_2Si$	52,53
41	Peterson olefination	*E/Z* ratio	$Me_3Si < Et_3Si < (i\text{-Pr})_3Si$	54
42	phosphonylation	diastereoselectivity	$Et_3Si < (t\text{-Bu})Me_2Si < (t\text{-Bu})Ph_2Si < (i\text{-Pr})_3Si$	55
43	reduction	product distribution	$Me_3Si < Et_3Si$	56
44	substitution	Taft's E_s value	$Me_3Si < EtMe_2Si < (n\text{-Pr})Me_2Si < (n\text{-Bu})Me_2Si < (i\text{-Bu})Me_2Si < (\text{cyclopentyl})Me_2Si < (i\text{-Pr})Me_2Si < (\text{cyclohexyl})Me_2Si < (s\text{-Bu})Me_2Si$	57
45	epoxidation	stereoselectivity	$Ph_3Si < (t\text{-Bu})Me_2Si$	58
46	1,4-addition	stereoselectivity	$Me_3Si < (Me_3Si)Me_2Si$	38
47	[3 + 2] cycloaddition	yield	$Me_3Si < PhMe_2Si < (t\text{-Bu})Me_2Si$	59
48	hydrosilylation	product distribution	$(n\text{-}C_5H_{11})H_2Si < Ph_2HSi < (n\text{-Pr})_2HSi < (n\text{-Bu})MeHSi < Et_2MeSi < Et_3Si$	60

(*continued overleaf*)

TABLE 1. (*continued*)

Entry	Reaction or property studied	Selectivity basis	Order of the size	References
49	hydrosilylation	rate	$EtMe_2Si < Et_2MeSi < Et_3Si < (n\text{-}Pr)_2MeSi < (i\text{-}Pr)_3Si < (i\text{-}Pr)_2MeSi$	61
50	[2 + 1] insertion	rate and yield	$Ph_3Si < Et_3Si$	62
51	insertion	regioselectivity	$(t\text{-}Bu)Me_2Si < (i\text{-}Pr)_3Si$	63
52	olefination	regioselectivity	$Me_3Si < Et_3Si < (t\text{-}Bu)Me_2Si < Ph_3Si$	64
53	silylation	heat of reaction and rate	$Ph_2MeSi < Me_3Si < (t\text{-}Bu)Ph_2Si < (i\text{-}Pr)_3Si$	65
54	solvolysis of $PhCH(SiR_3)OTs$	rate	$Me_3Si < Et_3Si < (t\text{-}Bu)Me_2Si$	66
55	solvolysis of R_3SiOPh	rate (H^+, aq EtOH)	$Me_3Si < (t\text{-}Bu)Me_2Si < Et_3Si < (n\text{-}Pr)_3Si < (n\text{-}Bu)_3Si$	67,68
56	solvolysis of R_3SiOPh	rate (OH^-, aq EtOH)	$Me_3Si < Et_3Si < (t\text{-}Bu)Me_2Si < (n\text{-}Pr)_3Si < (n\text{-}Bu)_3Si$	67,68
57	solvolysis of triorganochlorosilanes	rate (aq dioxane)	$Me_2HSi < Me_2(Cl_2HC)Si < (CF_3CH_2O)Me_2Si < (ClH_2C)Me_2Si < [MeO(CH_2)_2O]Me_2Si < (p\text{-}O_2NC_6H_4)Me_2Si < [NC(CH_2)_3]Me_2Si < Me_3Si < (MeO)Me_2Si < [MeO(CH_2)_3]Me_2Si < EtMe_2Si < (EtO)Me_2Si < (PhCH_2)Me_2Si < (n\text{-}Pr)Me_2Si < (i\text{-}PrO)Me_2Si < (n\text{-}Bu)Me_2Si < (Me_3Si)Me_2Si < (i\text{-}Bu)Me_2Si < PhMe_2Si < (n\text{-}C_{18}H_{37})Me_2Si < (t\text{-}BuCH_2O)Me_2Si < (p\text{-}MeC_6H_4)Me_2Si < (Me_3SiCH_2)Me_2Si < (t\text{-}BuCH_2)Me_2Si < (i\text{-}Pr)Me_2Si < (s\text{-}Bu)Me_2Si < (n\text{-}Bu)_2MeSi < (cyclohexyl)Me_2Si < (t\text{-}BuO)Me_2Si < (EtO)_3Si < (Et_2CH)Me_2Si < Et_3Si < Ph_2MeSi < (n\text{-}Bu)_3Si < (i\text{-}Pr)_2MeSi < Ph_3Si < (t\text{-}Bu)Me_2Si < (i\text{-}PrMe_2C)Me_2Si < (i\text{-}Pr)_3Si < (t\text{-}Bu)Ph_2Si$	69
58	solvolysis of triorganochlorosilanes	reactivity (aq dioxane)	$Me_2HSi < (CF_3CH_2O)Me_2Si < (p\text{-}O_2NC_6H_4)Me_2Si < Me_3Si < (MeO)Me_2Si < (EtO)Me_2Si < EtMe_2Si < (PhCH_2)Me_2Si < (PhO)Me_2Si < (n\text{-}PrO)Me_2Si < (n\text{-}Pr)Me_2Si < (n\text{-}Bu)Me_2Si \sim (n\text{-}C_6H_{13})Me_2Si < (Me_3Si)Me_2Si < (i\text{-}PrO)Me_2Si < (n\text{-}C_{18}H_{37})Me_2Si < PhMe_2Si < (i\text{-}Bu)Me_2Si \sim (Me_3SiO)Me_2Si < (t\text{-}BuCH_2O)Me_2Si < (p\text{-}MeC_6H_4)Me_2Si < (Me_3SiCH_2)Me_2Si < (t\text{-}BuCH_2)Me_2Si < (i\text{-}Pr)Me_2Si < (n\text{-}Bu)_2MeSi < (s\text{-}Bu)Me_2Si < (cyclohexyl)Me_2Si$	70

TABLE 1. (*continued*)

Entry	Reaction or property studied	Selectivity basis	Order of the size	References
			< (Et$_2$CH)Me$_2$Si < [(*i*-Pr)MeCH]Me$_2$Si < (*t*-BuO)Me$_2$Si < Ph$_2$MeSi < [(*i*-Pr)Me$_2$CO]Me$_2$Si < (EtO)$_3$Si < Et$_3$Si < [(*t*-Bu)MeCH]Me$_2$Si < [(*i*-Pr)$_2$CH]Me$_2$Si < (*n*-Bu)$_3$Si < Ph$_3$Si < (*i*-Pr)$_2$MeSi < [(*t*-Bu)$_2$CH]Me$_2$Si < (*t*-Bu)Me$_2$Si < (EtMe$_2$C)Me$_2$Si < (*i*-PrMe$_2$C)Me$_2$Si < (Et$_3$C)Me$_2$Si < [(*t*-Bu)Me$_2$C]Me$_2$Si < [(*t*-Bu)CH$_2$]$_3$Si < [(*t*-Bu)EtMeC]Me$_2$Si < (*i*-Pr)$_3$Si < (*t*-Bu)Ph$_2$Si < (*t*-Bu)(*i*-Pr)EtSi < (*t*-BuO)$_3$Si < (*t*-Bu)(*i*-Pr)$_2$Si < (*t*-Bu)$_2$MeSi < (*t*-Bu)$_3$Si	
59	solvolysis of R$_3$SiF	rate (aq acetone)	Et$_2$MeSi < Et$_3$Si < (*n*-Bu)(*i*-Pr)MeSi < (*n*-Bu)$_3$Si < (*i*-Pr)$_3$Si	71
60	solvolysis of R$_3$SiH	rate (H$^+$, aq EtOH)	(cyclohexyl)H$_2$Si < (*n*-Pr)$_2$HSi < (ClH$_2$C)Me$_2$Si < (*n*-Pr)Me$_2$Si < (*n*-Pr)$_2$MeSi < Et$_3$Si < (*n*-Pr)$_3$Si < (*n*-Bu)$_3$Si < (*i*-Bu)$_3$Si < (*i*-Pr)$_3$Si	72,73
61	solvolysis of R$_3$SiH	rate (OH$^-$, aq EtOH)	EtMe$_2$Si < (*n*-Pr)Me$_2$Si < Et$_2$MeSi < (*n*-Pr)$_2$MeSi < Et$_3$Si < (*i*-Pr)Me$_2$Si < (*n*-Pr)$_3$Si < (*i*-Pr)$_2$MeSi < (*t*-Bu)Me$_2$Si < (*i*-Pr)$_3$Si	74
62	distortion of geometry	degree of distortion	Me$_3$Si < Et$_3$Si < Ph$_3$Si ∼ (*t*-Bu)$_2$HSi	75
63	complexation	bond length	Me$_2$HSi < Me$_3$Si < (*t*-Bu)$_2$HSi	76
64	complexation	physical data	PhMe$_2$Si ∼ Ph$_2$MeSi < Me$_3$Si < Ph$_3$Si	77
65	complexation	bond length	Me$_3$Si < (Me$_3$Si)Me$_2$Si < (Me$_3$Si)$_2$MeSi	78
66	ring flip	*A* value	Me$_3$Si < (Me$_3$Si)$_3$Si < (Me$_3$Si)$_3$C	79
67	decay	rate	Me$_3$Si < Et$_3$Si < (*i*-Pr)$_3$Si	80
68	^{1}H NMR spectroscopy	peak broadening	Me$_3$Si < Et$_3$Si < (*t*-Bu)Me$_2$Si	81
69	^{1}H NMR spectroscopy	coupling constant	Me$_3$Si < PhMe$_2$Si < (*t*-Bu)Ph$_2$Si	82
70	1,2-addition	diastereoselectivity	(*i*-Pr)Me$_2$Si < (*t*-Bu)Me$_2$Si < (*i*-Pr)$_3$Si	83
71	1,2-addition	selectivity	Me$_3$Si < Et$_3$Si < (*t*-Bu)Me$_2$Si < (*i*-Pr)$_3$Si < (*t*-Bu)Ph$_2$Si	84
72	Diels–Alder reaction	selectivity	Me$_3$Si < (*t*-Bu)Me$_2$Si < (*i*-Pr)$_3$Si	85
73	Diels–Alder reaction	chemoselectivity	Me$_3$Si < (*t*-Bu)Me$_2$Si < (*i*-Pr)$_3$Si	86
74	ene reactions	selectivity	(*i*-Pr)Me$_2$Si < (*i*-PrMe$_2$C)Me$_2$Si < (*i*-Pr)$_3$Si < (*t*-Bu)Ph$_2$Si	87
75	rearrangement	regioselectivity	Me$_3$Si < (*t*-Bu)Me$_2$Si < (*i*-Pr)$_3$Si	88

(*continued overleaf*)

TABLE 1. (*continued*)

Entry	Reaction or property studied	Selectivity basis	Order of the size	References
76	[3 + 2] cycloaddition	selectivity	$(t\text{-Bu})Me_2Si < (i\text{-Pr})_3Si < (t\text{-Bu})Ph_2Si$	89
77	deoxygenation	diastereoselectivity	$(t\text{-Bu})Me_2Si < (i\text{-Pr})_3Si$	90
78	epoxide opening	regioselectivity	$Et_3Si \sim (i\text{-Pr})Me_2Si < PhMe_2Si < (t\text{-Bu})Me_2Si < Ph_3Si < (i\text{-Pr})_3Si$	91
79	Ireland–Claisen rearrangement	selectivity	$Me_3Si \sim Et_3Si < (n\text{-PrMe}_2C)Me_2Si < (t\text{-Bu})Me_2Si < (i\text{-Pr})_3Si$	92
80	oxidation	enantioselectivity	$(t\text{-Bu})Me_2Si < (i\text{-Pr})_3Si$	93
81	photolysis	quantum yield	$Me_3Si < Et_3Si < (i\text{-Pr})_3Si$	94

The trend of increasing the bulk agrees with most of the information listed in Table 1, as well as with the order established in 1989[2]. The current order is, however, much more informative than that (including 23 silyl groups) published earlier.

III. COMPARISON OF ORGANOSILYL GROUPS IN SUBSTRATES

A. General Considerations

Different silyl groups in substrates exert steric influence on organic reactions in various degrees. Evidence for this exists in the following 29 types of important organic reactions, which can be controlled by bulky silyl groups. Their steric effect often dominates the outcome of those reactions. Nevertheless, the electronic or the stereoelectronic effect may simultaneously also play a minor role.

B. Organic Reactions of Various Types

1. Acylation

With an unsubstituted phenyl group on silicon, *trans*-PhCH=CHSiMe$_2$Ph is converted to *trans*-PhCH=CHC(=O)R upon reaction with RC(=O)Cl in the presence of TiCl$_4$[95]. This reaction involves transfer of a styryl group to acyl chlorides. Introduction of methyl groups into the *ortho* positions of the phenyl group attached to silicon results in synergistic activation through relief of steric strain. Thus dearylation becomes preferable.

2. Addition[83,84]

Diethylzinc adds to α-silyloxyaldehydes **1** in the presence of a catalytic amount of (1*R*,2*R*)-bis(trifluoromethanesulfonamido)cyclohexane (**2**) and Ti(OPr-*i*)$_4$ (2 equiv) in toluene at −20 °C (equation 1)[11]. The yields of the 1,2-adducts **3** and the enantioselectivity of the transformation depend upon the steric environment resulting from the silyl group (see entry 1 of Table 1). The asymmetric addition involving the substrate bearing an $(i\text{-Pr})_3Si$ group gives 89% yield of the corresponding alcohol with 85 %ee. The enantioselectivity can be increased to 92 %ee, although the yield drops to 78%, by use of a bulky $(t\text{-Bu})Ph_2Si$ group to shield the aldehydic oxygen.

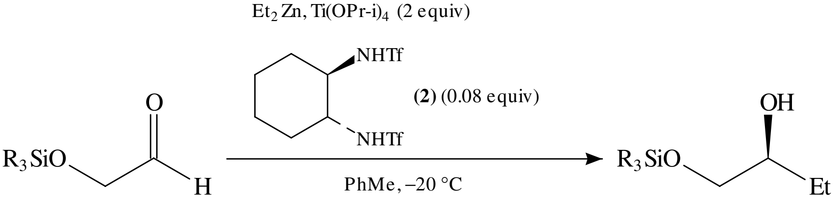

(1) **(3)** (1)

R_3Si	Chemical yield (%)	%ee
(i-Pr)$_3$Si	89	85
(t-Bu)Ph$_2$Si	78	92

On the other hand, specific rates of 1,2-additions of Me_2Mg to ketones $PhCOCH(OSiR_3)Me$ **(4)** parallel the diastereoselectivity of the reactions, as predicted by Cram's rule[12]. Experimental results from complexation and kinetics (equation 2) indicate a steady decrease in chelating ability upon an increase in size of the silyl groups[13,96]. The order is shown in entry 2 of Table 1.

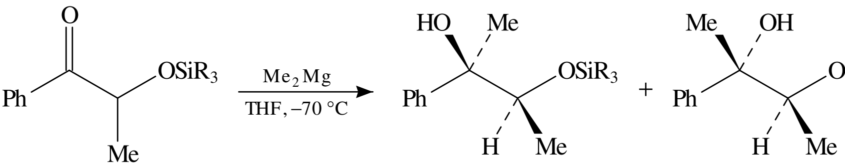

(2)

(4)
(excess)

(RS/SR)

(RR/SS)

'Cram's rule product'

R_3Si	$k_2(\times 10^2\ M^{-1}\,s^{-1})$	$(RS/SR)/(RR/SS)$
Me$_3$Si	100 ± 30	99/1
Et$_3$Si	8 ± 1	96/4
(t-Bu)Me$_2$Si	2.5 ± 0.3	88/12
(t-Bu)Ph$_2$Si	0.82 ± 0.06	63/37
(i-Pr)$_3$Si	0.45 ± 0.04	42/58

Furthermore, organobarium reagents, prepared from anhydrous BaI_2 and (silyloxy)allyllithium, react with carbonyl compounds at the least sterically hindered terminus (i.e. the γ position)[14]. The ratio of γ- to α-products depends upon the size of the silyl group and follows the order shown in entry 3 of Table 1.

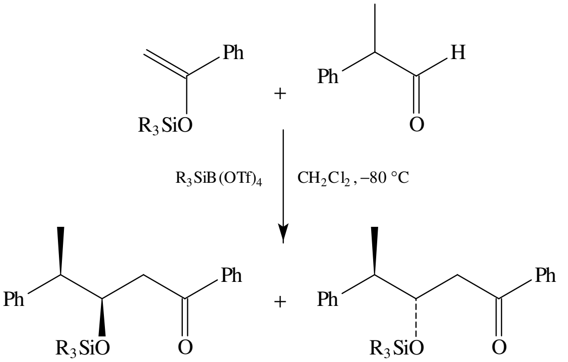

(3)

(RS/SR) (RS/RS)

R_3Si	Overall yield (%)	Selectivity (RS/SR) : (RS/RS)
Me_3Si	44	8 : 1
Et_3Si	60	18 : 1
(*t*-Bu)Me_2Si	82	25 : 1
(*i*-Pr)$_3$Si	71	97 : 1

The Mukaiyama addition of a silyl enol ether to an aldehyde can be catalyzed by $TiCl_4$, $TiCl_3(OPr\text{-}i)$[97], and 'supersilylating agents' $R_3SiB(OTf)_4$ (equation 3)[15]. The steric bulk of the silyl groups in enol ethers controls the 'Cram-type' selectivity, ranging from 8:1 to 97:1, and follows the order shown in entry 4 of Table 1. Similarly, $SnCl_4$-catalyzed additions of a silyl enol ether to various silyl-substituted acyclic acetals give diastereomeric ketones with ratios ranging from 5.0:1 to 13.0:1 (equation 4)[16]. The diastereoselectivity depends upon the size of silyl groups, as shown in entry 5.

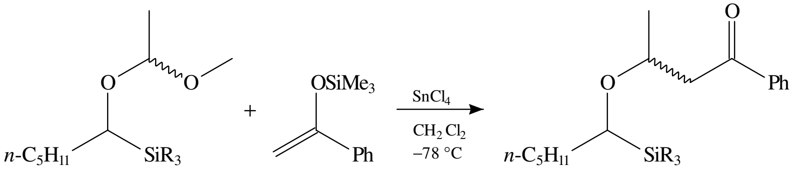

(4)

R_3Si	Yield (%)	Selectivity
Me_3Si	71	5.0 : 1
Et_3Si	73	5.5 : 1
(*t*-Bu)Me_2Si	66	6.6 : 1
$PhMe_2Si$	83	11.6 : 1
Ph_2MeSi	59	13.0 : 1

Addition followed by silylation of *O*-silylcyanohydrins **5**, **7** and **9** gives disilyl enamines **6**, **8** and **10**, respectively (equations 5–7)[98]. In all instances, the *C*-Me_3Si group of the starting cyanohydrins is transferred to the nitrogen atom in the products. The original *O*-silyl groups are also transferred to the nitrogen atom except for the highly hindered

(i-Pr)$_3$Si group[99].

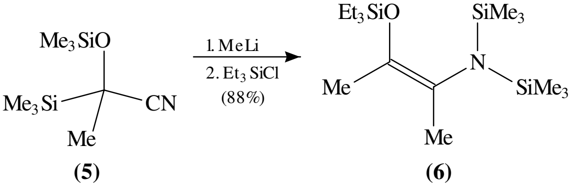

(5)

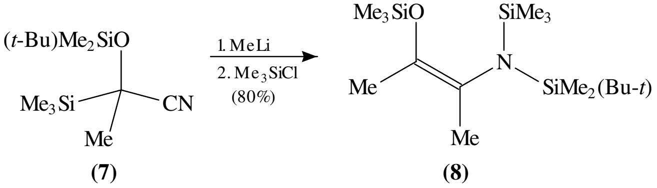

(6)

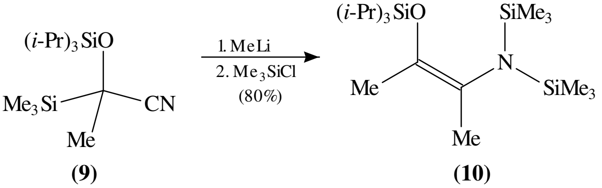

(7)

A different way to determine the steric size of various silyl groups is to use the values of cone angle θ^{100}, which are listed in equation 8[17]. It illustrates the mechanism of addition of the (p-anisyl)phenyl methyl ion **(11)** to allylsilanes[101]. The rate of addition depends on the size of the silyl groups. Bulky silyl groups, the size of which is reflected by their θ values can accelerate the addition process. Given the θ values, the size of the silyl groups follows the order shown in entry 6 of Table 1.

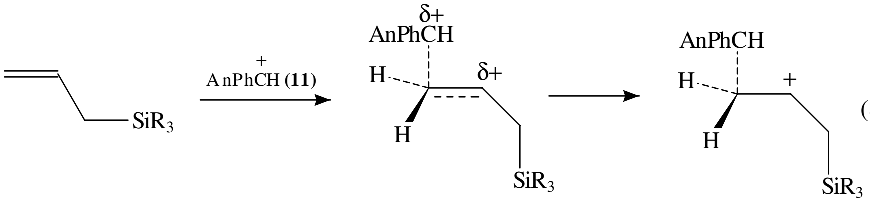

(8)

An = p-MeOC$_6$H$_4$

R$_3$Si	θ	R$_3$Si	θ	R$_3$Si	θ
Me$_3$Si	118	Et$_3$Si	132	(n-Bu)Me$_2$Si	139
ClMe$_2$Si	120	(n-Bu)$_3$Si	136	Ph$_3$Si	145
PhMe$_2$Si	122	(hexyl)$_3$Si	136	(i-Pr)$_3$Si	160

3. Aldol condensation[102]

Reaction of lithium enolates of α-silyloxyketones with benzaldehyde may yield opposite diastereoselection depending upon the size of the silyl group[103–105]. The corresponding titanium enolates, however, lead to high diastereofacial selectivities[106]. Replacement of the Me_3Si group in acyl silanes by $(t\text{-Bu})Me_2Si$, Et_3Si and $(n\text{-Pr})_3Si$ groups leads to diastereoselectivity increase from 1 : 1 to > 20 : 1 in the aldol condensation with aldehydes[107].

4. Alkylation

The size of silyl groups influences the carbon–carbon bond formation between silylalkenes and ketones. Treatment of allylsilanes **12** or vinylsilanes **14** with ketones in the presence of MnO_2 and acetic acid at elevated temperature gives α-alkylation products **13** and **15**, respectively (equations 9 and 10)[18]. The steric effect resulting from the silyl groups plays an essential role on the exclusive C–C bond formation at the terminal sp^2 carbon of silylalkenes **12** and **14**. The yield of the alkylation is inverse to the size of silyl groups and follows the order listed in entry 7 of Table 1.

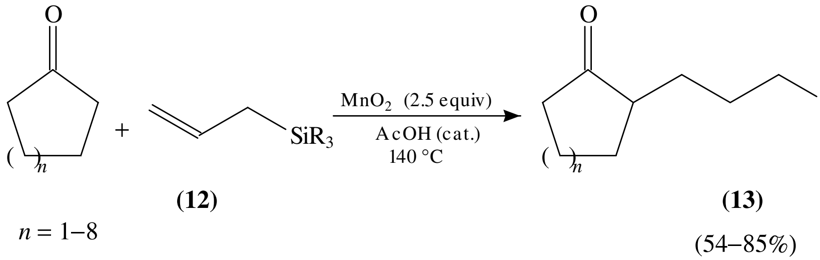

(9)

$(R_3Si = Me_3Si, PhMe_2Si, Ph_2MeSi, Ph_3Si)$

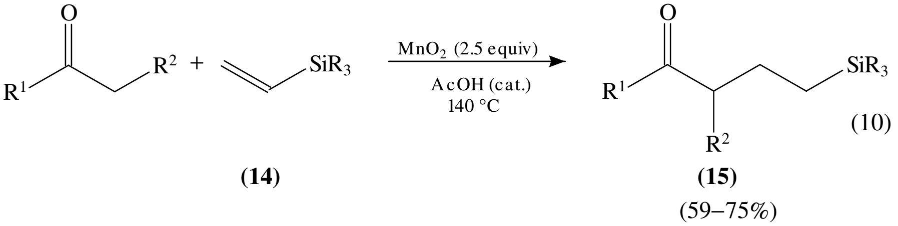

(10)

$R^1, R^2 = Alkyl; R_3Si = Me_3Si, Et_2MeSi$

On the other hand, methylaluminum bis(4-bromo-2,6-di-*tert*-butylphenoxide) can effect the α-alkylation of enol silyl ethers of a variety of ketones, esters and some aldehydes[108]. Use of the $(t\text{-Bu})Me_2Si$ group is recommended in the ketene silyl acetal substrates. Use of a less bulky Me_3Si or Et_3Si group leads to a mixture of monoalkylation products and rearranged α-silyl esters.

Reaction of silylallyl anions **16** with alkyl halides gives a mixture of α- and γ-alkylated products **17** and **18**, respectively (equation 11)[19]. The ratio of γ/α alkylation increases along with the bulk of the silyl groups by following the order shown in entry 8 of Table 1.

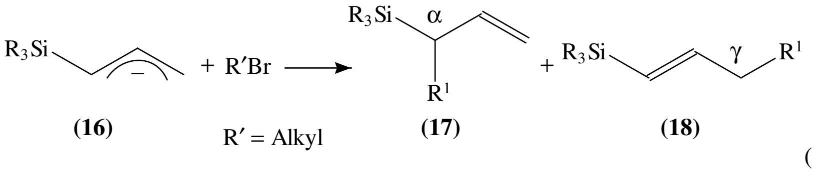

(11)

R_3Si	$\alpha : \gamma$
Me_3Si	1 : 5.5
Ph_3Si	1 : 16
Et_3Si	1 : 18
$(n\text{-Pr})_3Si$	1 : 46

5. Allylation

Allylsilanes **12** react with β-ketoester **19** in the presence of ceric ammonium nitrate **(20)** in methanol to give allylated ketoesters **21** or silylated dihydrofurans **22** or both in 76–84% overall yields (equation 12)[20]. The ratio of **21/22** depends upon the steric bulk of the silyl groups in the order listed in entry 9 of Table 1. A larger silyl group offers a greater chance to form a dihydrofuran through an intramolecular cyclization.

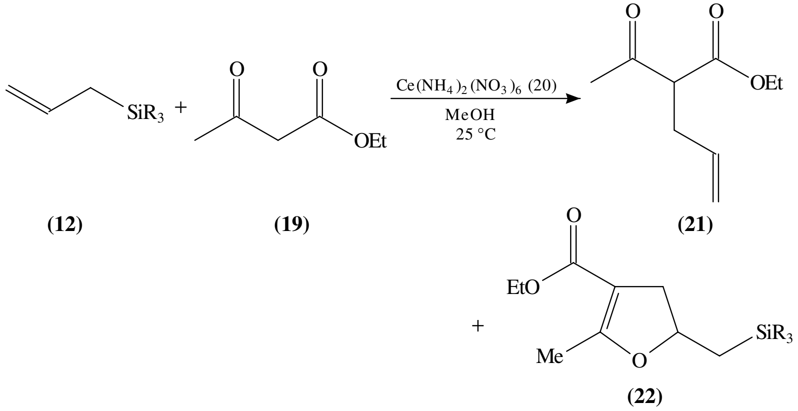

(12)

R_3Si	Overall yield (%)		Ratio	
		21	:	**22**
Me_3Si	84	100	:	0
$PhMe_2Si$	80	16	:	1
$(i\text{-Pr})_3Si$	76	0	:	100

In the ruthenium-catalyzed allylation of terminal propargylic silyl ethers, a regioisomeric mixture of 1,4-dienes is produced[21]. Their ratio can reflect the size of the silyl groups as shown in entry 10 of Table 1.

Furthermore, regioselective (α versus γ) allylation and propargylation by use of Grignard, organozinc and tin reagents can be accomplished by use of acylsilanes as electrophiles[109–111]. Because of the bulkiness of the $(i\text{-Pr})_3Si$ group, its use results in a greater extent of regiocontrol than that involving the Me_3Si group.

6. Cyclization

Allylsilanes **12** react with β-ketoester **19** in the presence of $Mn(OAc)_3 \cdot 2H_2O$ and acetic acid to give dihydrofurans **22** in 76–85% yields (equation 13)[20]. Efficiency of the dihydrofuran formation depends upon the steric bulk of the silyl groups shown in entry 11 of Table 1.

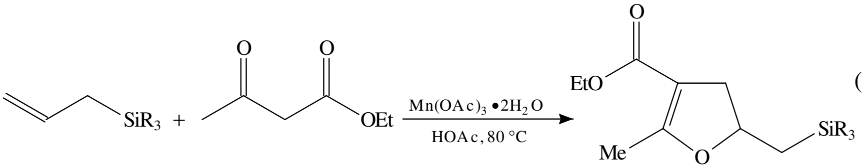

(13)

(12) **(19)** **(22)**

R_3Si	Yield (%)
Me_3Si	85
$PhMe_2Si$	82
$(i\text{-}Pr)_3Si$	76

An example involving intramolecular cyclization is the treatment of silyl ethers **23** with I_2 and triethylamine in acetonitrile at 0 °C to give diastereomeric tetrahydrofurans **24** and **25** (equation 14)[22]. The Me_3Si and Et_3Si groups are expelled in the reaction and do not appear in the final cyclization products. In comparison with the Me_3Si group, cyclization of the substrate carrying a Et_3Si group gives a much higher selectivity (entry 12 of Table 1). Moreover, iodolactonizations of silyloxy-containing alkenylcarboxylic acids also give diastereomeric mixtures[23–25]. Their ratio often depends upon the size of the silyl groups as shown in entries 13–15.

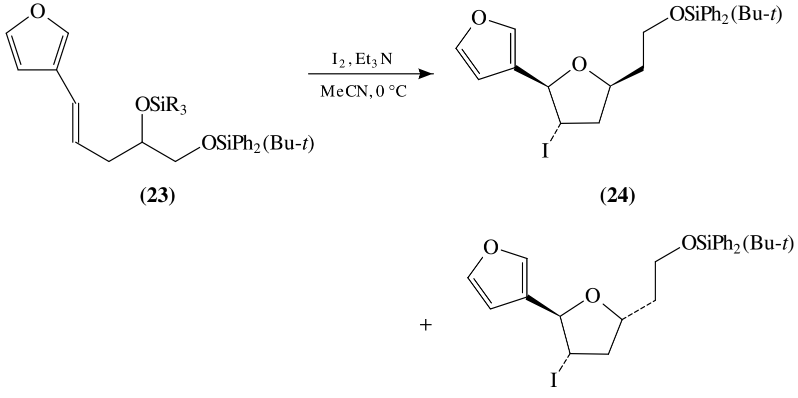

(23) **(24)** **(25)**

(14)

R_3Si	Yield (%)	Ratio 24 : 25
Me_3Si	93	6 : 1
Et_3Si	91	75 : 1

N-Bromosuccinimide can also initiate an intramolecular cyclization. Thus vinylsilane alcohols **26** are converted to a mixture of 2,5-*cis*- and *trans*-furans **27** in a ratio ranging from 1 : 1 to 1 : 2.3 (equation 15)[26]. The thermodynamically favored 2,5-*trans*-isomer can be generated in a higher ratio by increasing the bulk of the silyl group in the order shown in entry 16 of Table 1.

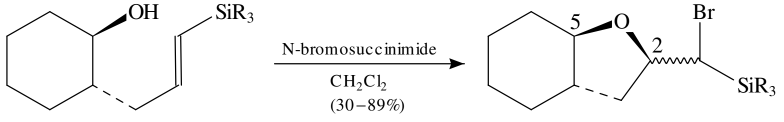

(26)
R = Me or Ph

(27)
cis/*trans*
1:1–1:2.3

(15)

Furthermore, intramolecular bis-silylative cyclization of dienes **28** with face selectivity gives a diastereomeric mixture of **29** and **30** (equation 16). The size of the substituents on the nonterminal silicon influences the ratio of **29/30**, which follows the order Me < Et < Ph < *i*-Bu < *i*-Pr (cf. entry 17 of Table 1)[27].

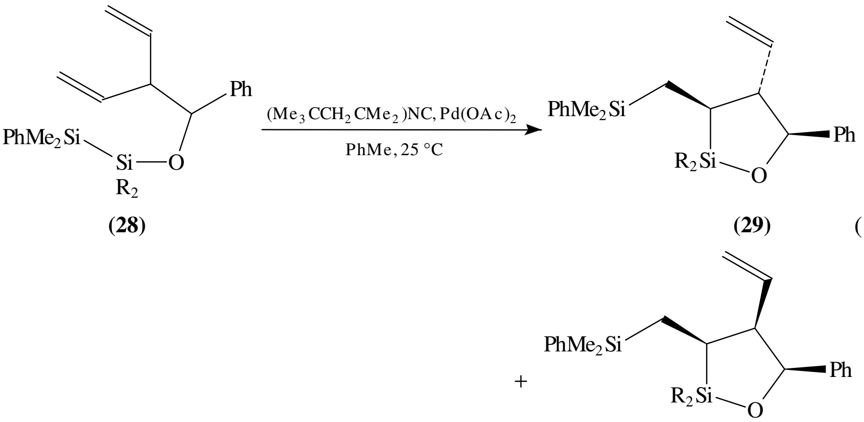

(28) **(29)** (16)

(30)

R	Yield (%)	**29**	:	**30**
Me	98	59	:	41
Et	82	75	:	25
Ph	87	83	:	17
i-Bu	90	88	:	12
i-Pr	27	92	:	8

7. [2 + 2] Cycloaddition

In certain reactions, introduction of a bulkier silyl group in substrates may decrease the stereoselectivity. For example, photolysis of a mixture of benzaldehyde and silyl vinyl ethers **31** affords a mixture of diastereomeric [2 + 2] cycloadducts **32** and **33** (equation 17)[112]. The stereoisomeric ratio of 10 : 1 obtained by use of **31a** containing a Me_3Si group drops to 5.7 : 1 by use of **31b**, which contains a (*t*-Bu)Me_2Si group.

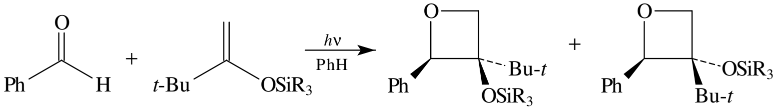

(31) **(32)** **(33)**

(17)

R_3Si	Yield (%)		Ratio	
		32	**:**	**33**
(a) Me_3Si	65	10	:	1
(b) (*t*-Bu)Me_2Si	61	5.7	:	1

On the other hand, upon reaction with methyl glyoxalate imines, an increase in bulk of the silyl moiety [i.e., $PhMe_2Si$, Ph_2MeSi, Ph_3Si and (*t*-Bu)Ph_2Si] in *β*-(triorganosilyl)alkanoyl chlorides causes a moderate increase in the *anti/syn* ratio of the [2 + 2] *cis*-adducts[113]. Little effect on the *cis/trans* ratio is observed.

8. [4 + 2] Cycloaddition[85,86]

Diorganylsilyl ethers of sorbyl alcohol **(34)** undergo a smooth intramolecular Diels–Alder reaction to give a mixture of bicyclic products **35** and **36** (equation 18)[114]. The *endo/exo* selectivity depends upon the steric influence resulting from the substituent on silicon atom.

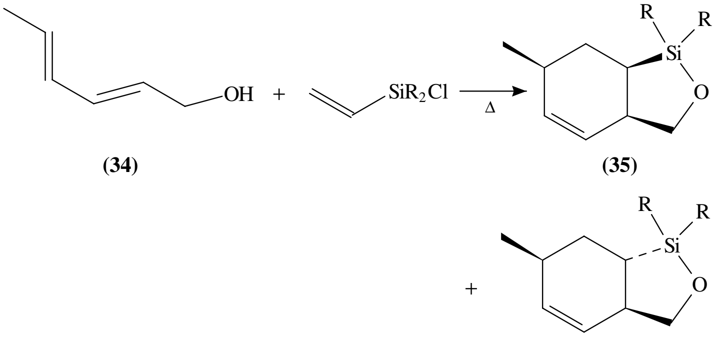

(34) **(35)**

(18)

(36)

R	Ratio		
	35		**36**
Me	2	:	1
Ph	1	:	1
t-Bu	1	:	4

9. Decomposition

The size of the silyl groups in compounds $R_3SiC(N_2)COOMe$ influences their decomposition by copper(I) triflate, dirhodium tetraacetate and dirhodium tetrakis(perfluorobutyrate)[28]. These reactions may lead to $R_2(MeO)SiC(R){=}C{=}O$, carbene dimers, azines and 5,5-dimethoxy-3,4-bis(organosilyl)-2(5*H*)-furanones. As the silyl groups become larger (see entry 18 of Table 1), the azine formation becomes preferable.

10. Deprotonation

Steric bulk of various silyl groups, including Me_3Si, (*i*-Pr)Me_2Si, (*t*-Bu)Me_2Si, (*t*-Bu)Ph_2Si and (*i*-Pr)$_3$Si, at the C-2 position can effectively block a base to coordinate the oxygen atom of the furan ring[115]. Thus, coordination occurs between a base and a hydroxymethyl group at the C-3 position and consequently results in C-4 deprotonation.

11. Desilylation

Tetrafluorosilane can cleave various silyl ethers in CH_2Cl_2 or MeCN at 23 °C to give the corresponding alcohols via trifluorosilyl ethers (equation 19)[29]. The steric bulk of the series of silyl groups, shown in entry 19 of Table 1, is opposite to the relative rates of desilylation of the silyl ethers.

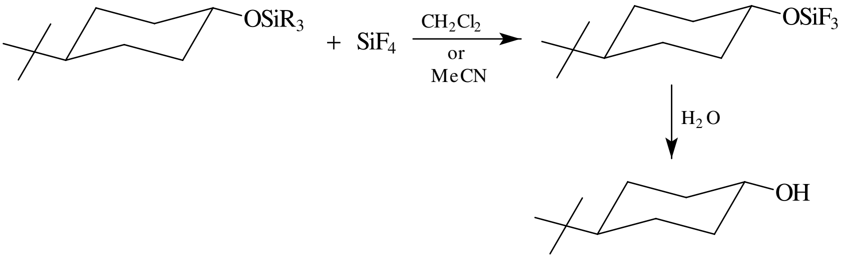

(19)

Very recently, the bulk of various silyl groups[116] was also determined by the time required for desilylation of 5′-*O*-silylthymidine **37** with a complex of Bu_4NF and $BF_3 \cdot OEt_2$ in MeCN at room temperature (equation 20)[30]. The size follows the order listed in entry 20 of Table 1. Furthermore, the steric bulk of silyl groups is determined independently, as shown in entry 21, by utilization of neutral alumina for selective cleavage of various primary and secondary silyl ethers[31]. Catalytic transfer dehydrogenolysis by Pd(II)O has also been used to cleave silyl protecting groups selectively[32]. The rate of deprotection appears to be sensitive to the steric bulk of the silyl groups by following the order listed in entry 22.

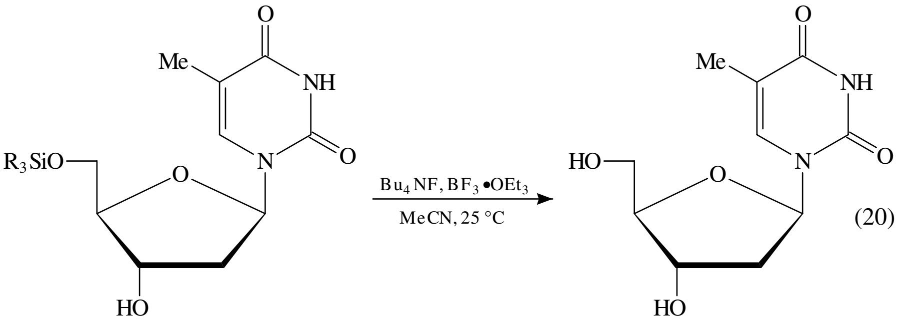

(37)

(20)

Selective removal of a (t-Bu)Me_2Si group in the presence of the (i-Pr)$_3$Si group in disilylated p-xylene-α,α'-diol **38** can be accomplished by use of a stoichiometric amount of fluorosilicic acid (H_2SiF_6) in *tert*-butanol (equation 21). Alcohol **39** is thus obtained in 91% yield[33,117]. The results indicate that the (i-Pr)$_3$Si group is sterically bulkier than the (t-Bu)Me_2Si group (entry 23 of Table 1).

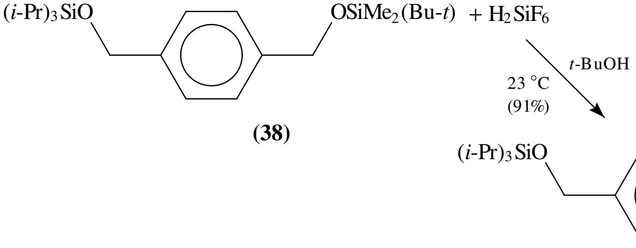

(38)

(39)

(21)

In addition to fluorosilicic acid[34], pyridinium p-toluenesulfonate can selectively remove the less bulky (t-Bu)Me_2Si group in the presence of the (t-Bu)Ph_2Si group from the corresponding silyl ethers (entry 24 of Table 1)[35]. In contrast, under basic conditions involving sodium hydride in HMPA, the rate of cleavage of t-butyldiphenylsilyl ethers is significantly faster than that of the corresponding t-butyldimethylsilyl ethers[118]. Furthermore, sodium azide in DMF effects the cleavage of the methyldiphenylsilyl ether bond, yet t-butyldimethylsilyl ethers and t-butyldiphenylsilyl ethers survive[119].

12. Elimination

Upon thermolysis, *erythro*-silyl ethers **40** undergo 1,2-*syn*-elimination. The ratio of the possible products **41** and **42** depends upon the bulk of the silyl groups (equation 22). These reactions involve four-membered ring transition states[81].

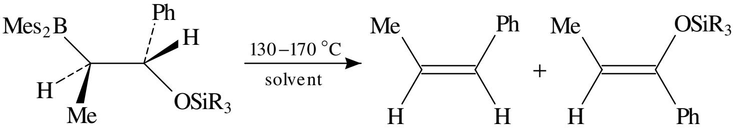

(22)

(40) **(41)** **(42)**

Mes = 2,4,6-trimethylphenyl

R_3Si	Solvent	Ratio **41**	:	Ratio **42**
Me_3Si	C_6D_6	100	:	0
Et_3Si	C_6D_6	32	:	68
(t-Bu)Me_2Si	toluene-d_8	<5	:	95

In a different study, the rates (k) are measured at 600 K for a thermal elimination of R_3SiCH_2COOEt to give R_3SiOEt and $CH_2{=}C{=}O$[36]. The k values are 1.98, 2.12, 1.86 and 1.42×10^{-2} s^{-1} for Me_3SiCH_2COOEt, $PhMe_2SiCH_2COOEt$, $Ph_2MeSiCH_2COOEt$ and Ph_3SiCH_2COOEt, respectively. Increase in the electrophilicity of silicon through replacement of one methyl group by a phenyl group causes a minor increase in reactivity[36]. Furthermore, the similar replacements result in a rate decrease, which is attributed to steric hindrance as shown in entry 25 in Table 1.

13. Ene reaction[87,120]

Intramolecular ene reaction takes place in activated 1,6-dienes **43** to give diastereomeric cyclopentanes **44** and **45** (equation 23)[37]. The stereoselectivity of ene adducts increases with the steric bulk of the silyl groups on oxygen atom by following the order shown in entry 26 of Table 1.

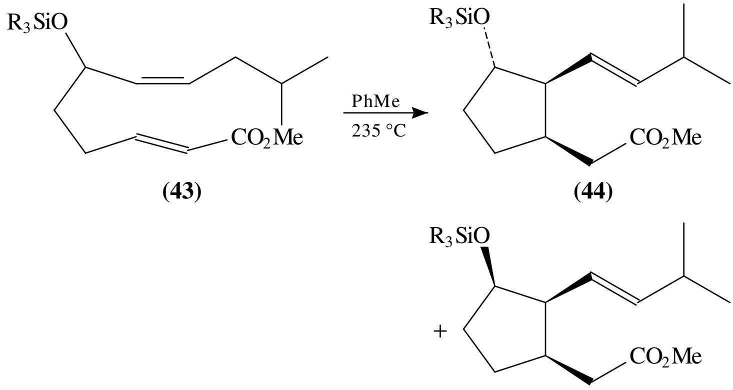

(43) **(44)** **(45)**

(23)

R_3Si	Yield (%)	Ratio **44** **45**
(t-Bu)Me_2Si	83	79 : 21
(t-Bu)Ph_2Si	79	88 : 12

A profound steric effect resulting from the Me_3Si group also exists in the regio- and diastereoselective ene reaction between 4-methyl-1,2,4-triazoline-3,5-dione and electronically activated vinylsilanes[121]. The steric effect resulting from t-Bu, Me_3Si, and Me_3Sn groups attached to a 1,2-dimethylvinyl moiety also influences the regioselectivity in photooxygenation with singlet oxygen[122]. The influence increases in the order $Me_3Sn < Me_3Si < t$-Bu; a longer carbon–metal bond would decrease the effective size of the substituents[123].

14. Epoxidation

Epoxidation of diene **46a** with MCPBA occurs at the more electron-rich trisubstituted $C_4{-}C_5$ double bond, instead of at the isopropenyl unit (equation 24)[38,124]. The Me_3Si group with α configuration prevails over the β-angular methyl group in directing epoxidation. Thus β-epoxide **47a** is obtained as the major product along with the corresponding α-epoxide as the by-product (ratio = 35 : 1). The bulkier $(Me_3Si)Me_2Si$ group in **46b**, however, can fully dominate the epoxidizing orientation (cf. entry 27 of Table 1). Accordingly, β-epoxide **47b** is obtained exclusively from **46b** under the same epoxidation conditions.

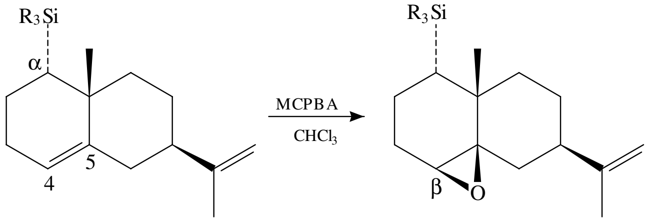

(46) **(47)**

(24)

	R_3Si	Yield (%)	Selectivity
(a)	Me_3Si	64	β/α = 35 : 1
(b)	Me_3SiMe_2Si	59	β exclusively

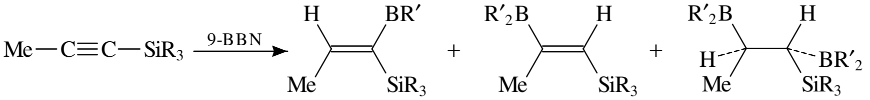

(48) **(49)** **(50)** **(51)**

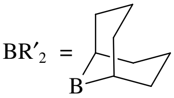

(25)

R_3Si	**49**	:	**50**	:	**51**
					Ratio
Me_3Si	100	:	0		
		54		:	23
Et_3Si	97	:	3		
		70		:	15
$(t\text{-Bu})Me_2Si$	95	:	5		
		71		:	14
$(i\text{-Pr})_3Si$	0	:	100		
		100		:	0

15. Hydroboration

The size of the silyl groups in alkynylsilanes **48** effects their regio- and chemoselectivity in hydroboration with 9-borabicyclo[3.3.1]nonane[125] (9-BBN). Alkynylsilanes

48 bearing a silyl group smaller than (i-Pr)$_3$Si (see entry 28 of Table 1) are led to (α-borylvinyl)silanes **49** in high regioisomeric purity (equation 25)[39]. The use of the (i-Pr)$_3$Si substituent not only provides the (β-borylvinyl)silane **50** exclusively, but also completely suppresses the formation of 1,2-diboryl adduct **51**.

16. Hydroethoxycarbonylation

The steric hindrance created by the silyl group, including Me$_3$Si and (t-Bu)Me$_2$Si, influences the efficiency of stereo-defined hydroethoxycarbonylation of silylacetylenes[126]. In the presence of PdCl$_2$[1,1′-bis(diphenylphosphino)ferrocene] and SnCl$_2$ · H$_2$O, silylacetylenes react with CO and ethanol to give (E)-β-ethoxycarbonylvinylsilanes in good to excellent yields.

17. Hydroformylation

Regiochemistry of hydroformylation of alkenes can be controlled by use of bulky silyl groups directly attached to the sp^2 carbon. Treatment of silylalkenes **52** with an initial pressure of 400 psi of H$_2$ and CO (1 : 1 molar ratio) in the presence of HRhCO(PPh$_3$)$_3$ and PPh$_3$ provides a mixture of aldehydes **53** and **54**[40,127]. The regioselectivity increases dramatically as the bulk of the silyl groups increases in the order shown in entry 29 of Table 1 and equation 26. Moreover, sterically demanding silyl substituents can efficiently control the regioselectivity of hydrocyanation of alkynes[128].

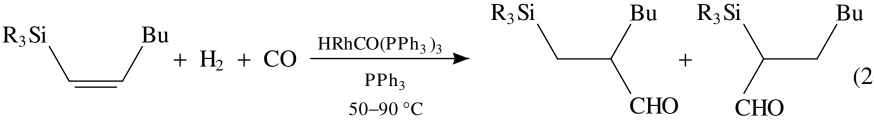

(52) **(53)** **(54)**

(26)

R$_3$Si	Yield (%)	Ratio		
		53	:	**54**
Me$_3$Si	81	50	:	50
(t-Bu)Me$_2$Si	87	70	:	30
Ph$_3$Si	69	90	:	10
(t-Bu)Ph$_2$Si	80	96	:	4

18. Hydrosilylation

The fluoride ion-catalyzed reduction of 2-methylcyclohexanone by various hydrosilanes gives the corresponding silyl ethers in 40–99% yields (equation 27)[41]. The reactivity, markedly influenced by the steric bulk of hydrosilanes (see entry 30 of Table 1), decreases in the order of Ph$_2$SiH$_2$ >>PhMe$_2$SiH > Ph$_2$MeSiH > Ph$_3$SiH.

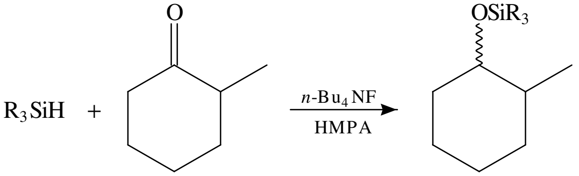

(27)

R_3Si	Temp (°C)	Time (h)	Yield (%)
Ph_2HSi	0	5	74
$PhMe_2Si$	0	24	99
Ph_2MeSi	0	24	81
Ph_3Si	25	12	40

19. Isomerization

(1-Diazo-2-oxoalkyl)silanes **55** react with cyclopropene **56** to give a mixture of diazabicyclohexenes **57** and 1,4-dihydropyridazines **58** (equation 28)[42]. Steric interactions between the vicinal acyl and silyl groups exist in **58**. Therefore the monocyclic isomer **58** is increasingly destabilized and isomerized to give **57** as the more bulky these silyl groups are (see entry 31 of Table 1).

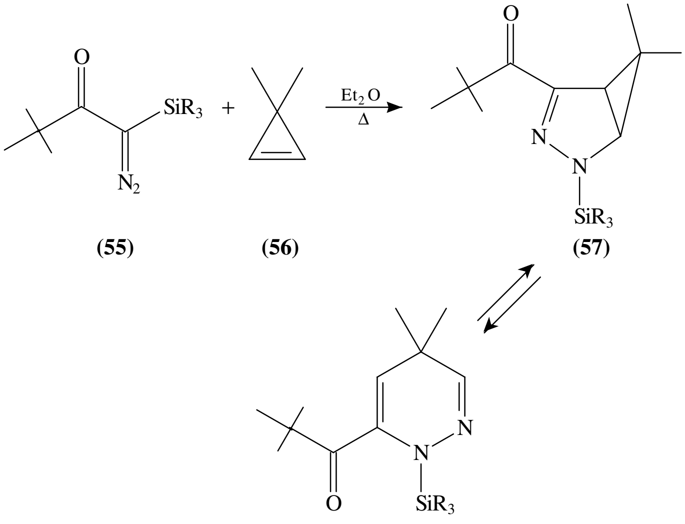

(58)

(28)

R_3Si	Ratio **57**	:	**58**
(*t*-Bu)Ph_2Si	30	:	70
(*t*-Bu)Me_2Si	52	:	48
(*i*-Pr)$_3$Si	>97	:	3

20. Migration and rearrangement[88]

Palladium(0)-catalyzed rearrangement of 2-silyl-3-vinyloxiranes **59** depends upon the size of the silyl groups[129]. The substrates containing a bulky (*t*-Bu)Me_2Si or (*i*-Pr)$_3$Si group give α-silyl-β,γ-unsaturated aldehydes **60** (equation 29). In contrast, substrates bearing a less steric congested group, such as Me_3Si, Et_3Si and $PhMe_2Si$, are led to silyldienol ethers **61** through the Brook rearrangement[130].

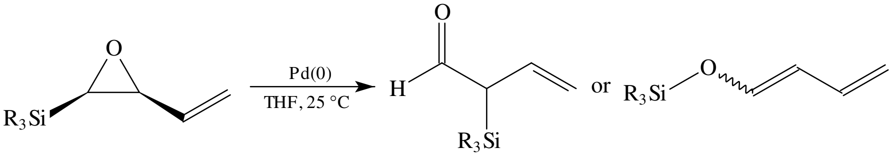

(59) **(60)** **(61)** (29)

Upon treatment with lithium naphthalenide, silyloxy *O*,*S*-acetals **62** may lead to α-silyl ethers **63** through a retro [1,4]-Brook rearrangement or to 1,3-diol **64** through a [2,3]-Wittig rearrangement (equation 30)[43]. With a small (e.g. Me_3Si) or a medium-sized silyl group [e.g. $(t\text{-Bu})Ph_2Si$], the retro Brook rearrangement prevails. Contrarily, protection of **62** with a bulkier $(i\text{-PrMe}_2C)Me_2Si$ or $(i\text{-Pr})_3Si$ group gives Wittig products. Use of the Et_3Si group affords a mixture of **63** and **64** in a *ca* 4 : 1 ratio (see entry 32 of Table 1).

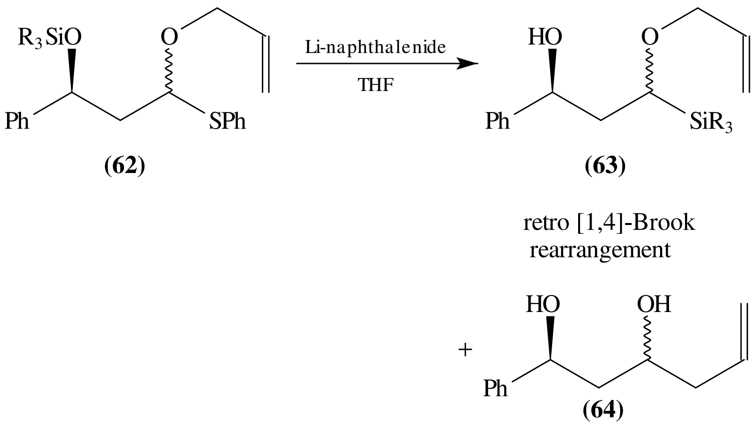

(62) **(63)**

retro [1,4]-Brook rearrangement (30)

(64)

[2,3]-Wittig rearrangement

R_3Si	Yield (%) **63**	**64**
Me_3Si	81	0
$(t\text{-Bu})Ph_2Si$	77	0
Et_3Si	49	12
$(i\text{-PrMe}_2C)Me_2Si$	0	66
$(i\text{-Pr})_3Si$	0	59

Migratory aptitude, however, highly depends on the bulk of the substituents on silicon[131,132], and is opposite to the size of the silyl groups in the order listed in entry 33 of Table 1[44]. As shown in equation 31, homoallylic silyl ethers **65** react with lithium di-*tert*-butylbiphenylide to give allylsilanes **66**. The trend of migratory aptitude of silyl groups parallels the corresponding yields of **66**.

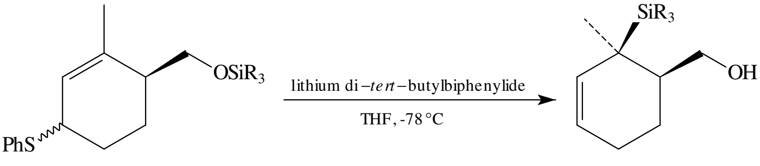

(31)

(65) **(66)**

R_3Si	Yield (%)
Me_3Si	83
Et_3Si	70
$(n\text{-}Pr)_3Si$	49
$(i\text{-}Pr)_3Si$	0

Furthermore, upon treatment with lithium diisopropylamide (LDA) and HMPA in THF at −78 °C, 3-(silyloxycarbonyl)furans **67** undergo 1,4 O→C silyl migration to give the corresponding 2-silyl-3-carboxyfurans (**68**, equation 32)[133–135]. The yields, ranging from 43–72%, are silyl group dependent. Similar migrations also occur to the corresponding 3-silyloxymethylfurans and thiophenes[134] as well as 1-iodo-2-silyloxyalkenes[135].

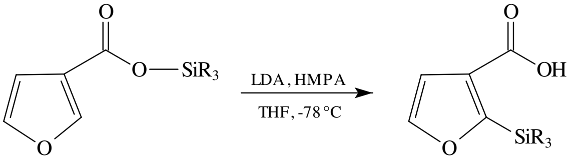

(32)

(67) **(68)**

R_3Si	Yield (%)
$(t\text{-}Bu)Me_2Si$	72
Et_3Si	57
$(i\text{-}Pr)_3Si$	56
$(n\text{-}Bu)_3Si$	51
$(t\text{-}Bu)Ph_2Si$	43

Under basic conditions, 1,3-migration of triorganosilyl groups (i.e., Me_3Si, $PhMe_2Si$ and Ph_2MeSi) from carbon to oxygen takes place in highly crowded organosilanols[136]. These migrations $(\mathbf{R_3Si})(R'_3Si)_2C{-}SiR''_2{-}OH \rightarrow H(R'_3Si)_2C{-}SiR''_2{-}O{-}\mathbf{SiR_3}$ are facilitated, in part, by relief of steric strain created by silyl groups.

On the other hand, an intermolecular migration of silyl groups also takes place among 5-methyl-2-(trialkylsilyl)thiophenetricarbonylchromium(0) complexes under basic conditions[45]. Increased steric hindrance from the silyl groups (see entry 34 of Table 1) results in preferential deprotonation.

21. Osmylation

Osmium-catalyzed vicinal hydroxylations of various allylic silanes **69** give a mixture of *anti*- and *syn*-diols **70** and **71** (equation 33)[46]. The silyl groups participate in vicinal hydroxylation reactions with useful levels of selectivity[137-140]. The *anti* selectivity (i.e., **70/71**) improves as the size of the silyl group increases as shown in entry 35 of Table 1.

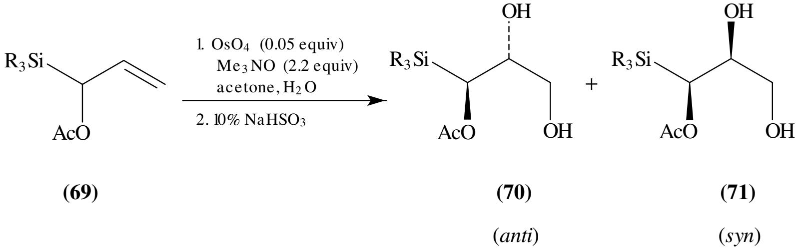

(69) **(70)** (*anti*) **(71)** (*syn*) (33)

R_3Si	Yield (%)	Ratio **70** : **71**
Me_3Si	57	6.5 : 1
$PhMe_2Si$	70	7.0 : 1
Et_3Si	67	7.5 : 1
(t-Bu)Me_2Si	70	11.3 : 1
Ph_2MeSi	58	11.5 : 1

22. Oxymercuration

Use of remote allylic silyl ethers, such as **72b,c**, rather than of allylic alcohol **72a** in intramolecular oxymercurations leads to a higher 1,3-*syn*-diastereoselectivity (equation 34)[47]. The overall yields for *syn*-**73** and *anti*-**74** range between 85–93%. The best selectivity reaches 7 : 1 involving the (t-Bu)Ph_2Si group (entry 36 of Table 1).

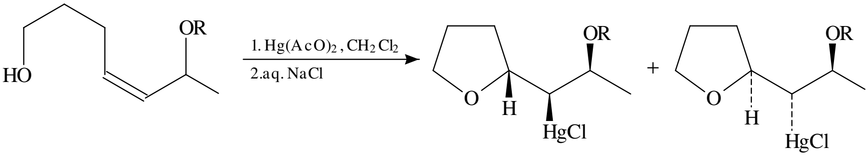

(72) **(73)** (*syn*) **(74)** (*anti*) (34)

R	Yield (%)	Ratio **73**	:	**74**
(a) H	85	2.5	:	1
(b) (t-Bu)Me_2Si	89	6	:	1
(c) (t-Bu)Ph_2Si	93	7	:	1

23. Ozonolysis

Ozonolysis of silyl ethers of 1-cyclopenten-3-ol gives a high selectivity in favor of the *exo*-substituted ozonide[48]. The bulkier silyl blocking groups, as shown in entry 37 of Table 1, exhibit a somewhat higher degree of stereoselection. Furthermore, the size of the silyl groups in R_3SiH influences their ozonolysis rates in CCl_4[49,50]. The order is listed in entry 38 of Table 1.

24. Peterson olefination[141]

The diastereomeric ratio of *cis*- to *trans*-stilbenes formed in the Peterson olefination of $Ph\bar{C}HSiR_3$ with benzaldehyde increases significantly as the bulk of silyl groups increases (see entry 39 of Table 1)[51]. Upon reaction with *n*-decanal, the steric bulk of the silyl groups in reagent, **75**[142,143] also affects the E/Z ratio and the yields of the product **76**[52,53]. Increased steric congestion by the order shown in entry 40 results in higher diastereoselectivity, but at the expense of the yield (equation 35). Those outcomes are in accord with those of the addition of prochiral carbanions, including α-silyl carbanions, to aldehydes[144]. Furthermore, the Peterson olefination between a ketone and bis-heterocycles bearing various silyl groups [e.g. Me_3Si, Ph_3Si and $(t\text{-Bu})Me_2Si$] is applied as a key step in the synthesis of BRL 49467, an anti-bacterial compound[145].

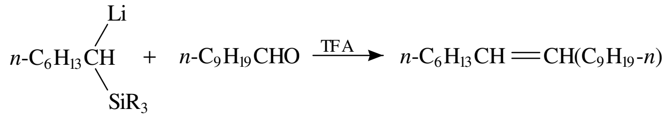

$$n\text{-}C_6H_{13}CH(Li)(SiR_3) + n\text{-}C_9H_{19}CHO \xrightarrow{\text{TFA}} n\text{-}C_6H_{13}CH{=}CH(C_9H_{19}\text{-}n) \qquad (35)$$

(75) **(76)**

R_3Si	Yield (%)	E/Z
Me_3Si	76	1 : 2
Et_3Si	60	1 : 2
$(t\text{-Bu})Me_2Si$	51	6 : 1
$(t\text{-Bu})Ph_2Si$	47	6 : 1

In addition, the Peterson olefination of 3-phenylthioketones by use of R_3SiCH_2COOR' gives α,β-unsaturated esters. An increase in size of the substituent at the silicon atom in R_3SiCH_2COOR' [e.g., $R_3Si = Me_3Si$, Et_3Si, $(i\text{-Pr})_3Si$, $PhMe_2Si$, Ph_2MeSi and Ph_3Si] only results in a slight decrease in Z/E ratio of the products (cf entry 41 of Table 1)[54,146].

25. Phosphonylation

Nucleophilic phosphonylations of α-silyloxy aldehydes (e.g. **77**) with phosphite **78** give a mixture of **79** and **80** with moderate to good diastereoselectivity (equation 36)[55]. The ratio of **79/80** depends greatly upon the size of the silyl groups in **77**, according to the order shown in entry 42 of Table 1.

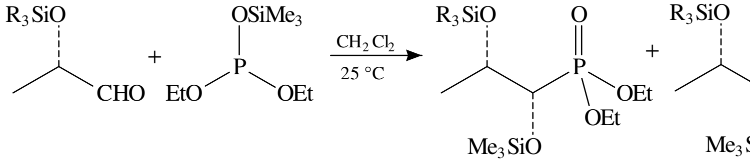

(77) **(78)** **(79)** **(80)**

(36)

R_3Si	Yield (%)		Ratio	
		79	:	**80**
Et_3Si	55	63	:	37
(t-Bu)Me_2Si	71	71	:	29
(t-Bu)Ph_2Si	66	90	:	10
(i-Pr)$_3Si$	67	92	:	8

26. Polymerization

A $(MeO)_3Si$ or $(i\text{-PrO})_3Si$ group attached at the C-2 position of 1,3-butadienes enables anionic polymerization to take place under various conditions and to give a stable propagating end[147]. The geometry of the monomer units in the polymers is influenced by the steric hindrance on the silyl group; 1,4-E geometry is the predominant micro-structure of the resultant polymers.

For co-polymerization, various silyl methacrylates ($CH_2{=}C(Me)CO_2SiR_3$) can react with methyl methacrylate in bulk at 60 °C[148]. Their reactivity depends upon, in part, the steric effect resulting from the silyl groups including (t-Bu)Me_2Si, (t-Bu)Ph_2Si, Ph_2MeSi and Ph_3Si.

27. Reduction

The steric bulk of the silyl groups in acylsilanes influences their asymmetric reduction to give chiral secondary alcohols by borane complexed with (S)-(−)-2-amino-3-methyl-1,1-diphenylbutan-1-ol[149]. The enantiomeric excess increases from 50% to 94% by replacement of the $PhMe_2Si$ group with the Ph_3Si group.

Palladium(0)-catalyzed reduction of trialkylsilylallyl esters **81** in the presence of n-BuZnCl leads to a mixture of allylsilanes **82**, vinylsilanes **83** and dienylsilanes **84** (equation 37). Because the Et_3Si group exerts a greater steric influence than the Me_3Si group (cf entry 43 of Table 1), the yields for allylsilanes are higher for Et_3Si-containing products[56].

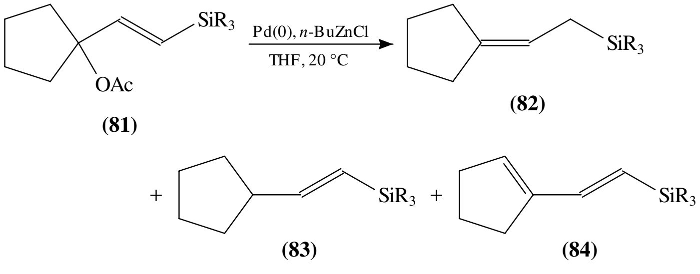

(37)

R_3Si			Ratio		
	82	:	**83**	:	**84**
Me_3Si	37	:	16	:	47
Et_3Si	67	:	17	:	16

28. Simmons–Smith reaction

Reaction of γ-silyl allylic alcohols **85** with Et_2Zn and CH_2I_2 in the presence of (+)-diethyl tartrate as a chiral auxiliary affords the corresponding cyclopropylmethyl

TABLE 2. Taft's E_s values for alkyl and cycloalkyl groups R^1 and relative rate constants $k(R^1Me_2SiCl)/k(Me_3SiCl)$ for the reaction of the two chlorides with lithium silanolates and lithium isopropylate in Et_2O at 20 °C

R^1	E_s (R^1)	Relative rate constants for their reactions with		
		Me_3SiOLi	$PhMe_2SiOLi$	Me_2CHOLi
Me	0.0	1.00	1.00	1.00
Et	−0.28	0.40	0.25	0.46
n-Pr	−0.36	0.30	0.25	0.38
n-Bu	−0.39	0.29	0.22	0.33
i-Bu	−0.55	0.08	0.17	0.25
Cyclopentyl	−0.70	0.10	—	0.14
i-Pr	−0.76	0.10	0.07	0.11
Cyclohexyl	−0.79	0.08	0.07	0.09
s-Bu	−0.87	0.09	0.06	0.07

alcohols **86** with high stereoselectivity (equation 38)[150]. The effective silyl groups for these Simmons–Smith reactions include the Me_3Si, $PhMe_2Si$ and Ph_3Si groups.

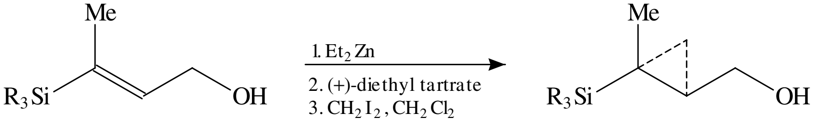

(85) **(86)** (38)

R_3Si	Yield (%)	%ee
Me_3Si	53	87
$PhMe_2Si$	88	92
Ph_3Si	82	90

29. Substitution

Data listed in Table 2 include the substituent constants R^1 of trialkylchlorosilanes and the relative rate constants $k(R^1Me_2SiCl)/k(Me_3SiCl)$ for the reactions of the two chlorides with lithium silanolates and isopropylate (equation 39)[57]. The reaction rates of silanes are influenced almost exclusively by the steric effects of the alkyl groups attached to the silicon atom. The $\log(k_{rel})$ values of the compounds with various R^1 groups give a satisfactory correlation with Taft's E_s values[151]. Thus the steric hindrance of silyl groups follows the order listed in entry 44[57] of Table 1.

$$R^1Me_2SiCl + R^2OLi \longrightarrow R^1Me_2SiOR^2 + LiCl \qquad (39)$$

IV. COMPARISON OF THE INFLUENCE RESULTING FROM HYDROGEN ATOM AND ALKYL GROUPS VERSUS SILYL GROUPS

A. General Considerations

Replacement of a hydrogen atom or an alkyl group, such as Me, Et, *i*-Pr, *t*-Bu and Ph, in organic compounds with a silyl group selected with deliberation often gives improved stereoselectivity. The following reactions of 23 types represent different ways to use a silyl group in stereochemical control. The silyl groups include Me_3Si, $(t\text{-Bu})Me_2Si$, $(i\text{-Pr})_3Si$, $PhMe_2Si$, Ph_3Si, $(Me_3Si)Me_2Si$ and $(i\text{-PrO})Me_2Si$.

B. Organic Reactions of Various Types

1. Addition

Replacement of the aldehydic hydrogen with a Me_3Si group in **87** increases the diastereofacial selectivity in nucleophilic addition[152–154]. An example is shown in equation 40, in which the ratio of **88** to **89** is increased from 5 : 1 to >100 : 1. Furthermore, the γ-Me_3Si group in α-methyl-α,β-cyclopentenone provides stereocontrol of the Michael addition by use of $PhCH_2OCH_2CH_2CMe_2MgCl$ in the presence of $CuBr\cdot SMe_2$, Me_3SiCl and HMPA[155]. The desired β,γ-*trans* adduct is generated in *ca* 63% yield. In addition, the Me_3Si group at the C-5 position of cyclohexenone **90** influences 1,4-addition by organometallic reagents to give *trans* adducts **91** as the major or even the exclusive products (equation 41)[156].

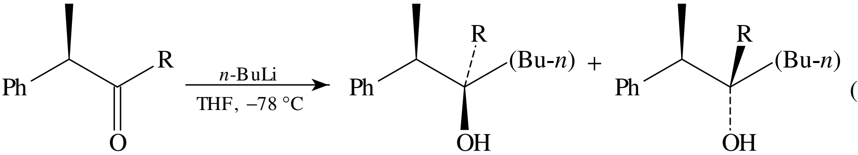

(40)

(87) **(88)** **(89)**

R	Yield (%)	Ratio 88	:	89
H	91	5	:	1
Me_3Si	92	>100	:	1

In asymmetric syntheses, the bulky $(i\text{-Pr})_3Si$ group can direct 1,2-addition of phosphite **92** to (*S*)-triisopropylsilyloxy lactaldehyde **(93)** to afford adduct **94** preferentially along with the by-product **95** (equation 42)[157]. The stereochemical outcome results from the bulk of the $(i\text{-Pr})_3Si$ protecting group[9]. Furthermore, the steric congestion in allylic cyanohydrin trimethylsilyl and *tert*-butyldimethylsilyl ethers influences their regioselective 1,2- and 1,4-additions to carbonyl compounds under basic conditions[158].

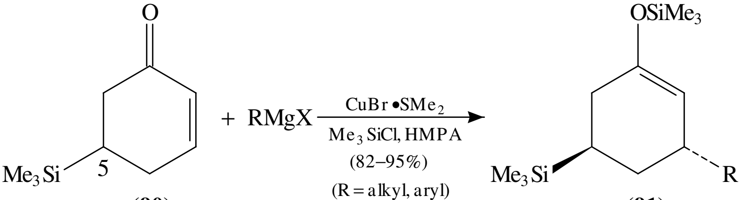

(41)

(90) **(91)**

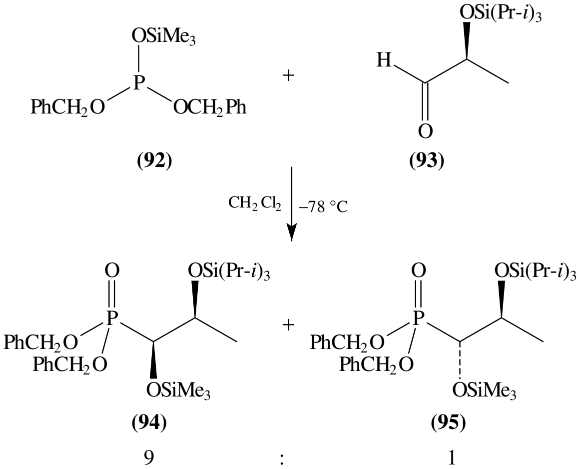

(42)

The asymmetric addition of ethyl azidoformate (N_3CO_2Et) to an optically active enamine, prepared from cyclohexanone and (*S*)-2-pyrrolidinemethyl methyl ether, followed by photolysis produces 2-(ethoxycarbonylamino)cyclohexanone with modest enantiomeric excess (18 %ee) in 40% yield[159]. Use of (*S*)-2-pyrrolidinemethyl trimethylsilyl ether as a chiral auxiliary increases the steric hindrance and provides the same product with the highest value of %ee (35%) in 51% yield.

2. Aldol reaction

A $PhMe_2Si$ group at the β position of open-chain enolates enables a highly diastereoselective aldol reaction to take place upon treatment with aldehydes[160]. Change of the silyl group results in a small but not always consistent effect on selectivity of related methylation by MeI[161].

3. Alkylation

Regioselective functionalization of metallated 2-aza-1,1-disilylimine allyl anion **96** with an electrophile depends upon competition between the steric and the electronic effects offered by the C-1 Me_3Si groups (equation 43)[162]. Reaction of **96** with alkyl iodides occurs at the C-1 position to give **97** (52–63%); this is because the two Me_3Si groups can stabilize the α-carbanion. In contrast, with bulkier electrophiles such as Me_3SiCl and ClCOOEt, functionalization of **96** takes place at the C-3 position to give **98** in 59–60% yields. Thus the steric congestion created by the Me_3Si groups prevails over the electronic effect. Moreover, a higher level of stereocontrol on alkylation of enol acetates can be accomplished by introduction of a Me_3Si group at the α position[163].

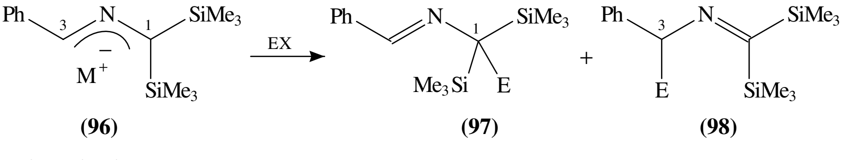

(43)

$M^+ = Li^+, K^+$

EX = MeI, EtI, BuI, Me_3SiCl, ClCOOEt

4. Allylboration

Homochiral borolanes **99–102** can asymmetrically allylborate aldehydes[164]. The better enantioselectivity exhibited by borolane **102** than others is due to the steric origin offered by the Me_3Si group.

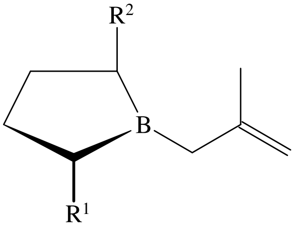

	R^1	R^2	%ee
(99)	Me	Me	27
(100)	*i*-Pr	H	24
(101)	*t*-Bu	H	72
(102)	Me_3Si	H	81

5. Allylsilylation

In the $AlCl_3$-catalyzed allylsilylation, the silyl group of allyltrimethylsilane adds regioselectively to the terminal carbon of phenylacetylene (equation 44)[165]. The allyl group adds to the inner carbon to form a 1,4-diene, in which the allyl moiety is *cis* to the silyl group. In contrast, allyltrimethylsilane adds to diphenylacetylene to give the corresponding *trans* adduct. Steric interaction is greater between two phenyl groups than between the phenyl and the Me_3Si groups in a *cis* configuration.

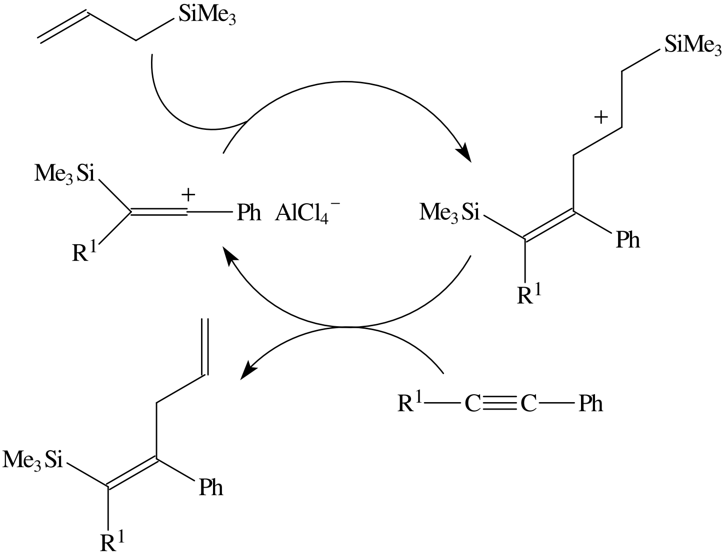

(44)

6. Carbenoid rearrangement

Reaction of 1,1-dihalo-2-*t*-butyldimethylsilyloxyalkanes with lithium diisopropylamide in ether gives (*Z*)-1-halo-2-*t*-butyldimethylsilyloxy-1-alkenes regio- and stereoselectively via carbenoids through α-elimination[166]. Replacement of the (*t*-Bu)Me_2Si group with a Me_3Si or Et group results in the formation of a by-product through β-elimination.

7. Cyclization

Various types of cyclizations can be controlled by the silyl group present in the substrates or reagents. Thus the desired products with a four-, five-, six- or seven-membered ring can be produced stereoselectively. An example shown in equation 45 includes cyclization of (2-pyridylthio)glycosidic *t*-butyldimethylsilyl enol ethers **103**, initiated by silver trifluoromethanesulfonate, to give bicyclic ketooxetanes **104**[167]. The steric crowding resulting from the (*t*-Bu)Me_2Si group in the transition state dominates the stereoselectivity during the four-membered ring formation.

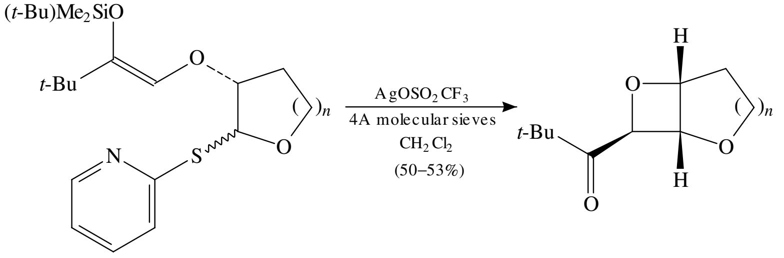

(45)

(103) **(104)**

The *t*-Bu group has a condensed bulk, yet it is spatially smaller than the Me_3Si group. The example shown in equation 46 indicates this phenomenon. Induced by dibenzoyl peroxide, the free radical cyclization takes place on iodo *t*-butylacetylenic ester **105a** to give a mixture of (*E*)- and (*Z*)-iodoalkylidene lactones **106a** (51%) and **107a** (*ca* 5%)[168]. The Me_3Si-containing iodo acetylenic ester **105b**, however, undergoes cyclization to generate a high yield of (*E*)-iodoalkylidene lactone **106b** (92%) exclusively.

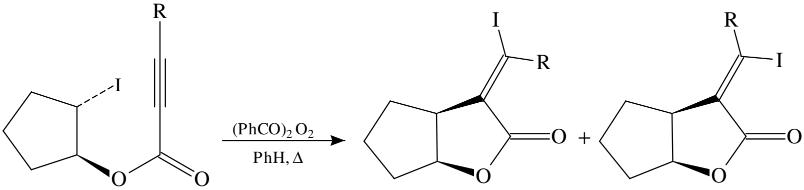

(46)

(105) *E*-**(106)** *Z*-**(107)**

R	*E*-**(106)**	*Z*-**(107)**
(a) *t*-Bu	51%	(*ca* 5%)
(b) $SiMe_3$	92%	—

In a total synthesis of (−)-β-vetivone, the key step involves intramolecular alkylation of the bromo ketone **108** to give spiro ketone **111** (equation 47)[169]. The 5-*Exo*-Tet cyclization taking place preferentially on intermediate **110** over **109** is due to the steric effect of the methyl group, which is fixed in the pseudoaxial position by the bulky Me_3Si group. Moreover, 5-*Exo*-Trig cyclization occurs with silyloxyalkene **112** to give diol **113** (equation 48)[170]. This radical cyclization with steric and stereochemical control provides an efficient avenue to introduce an angular hydroxymethyl group in organic compounds.

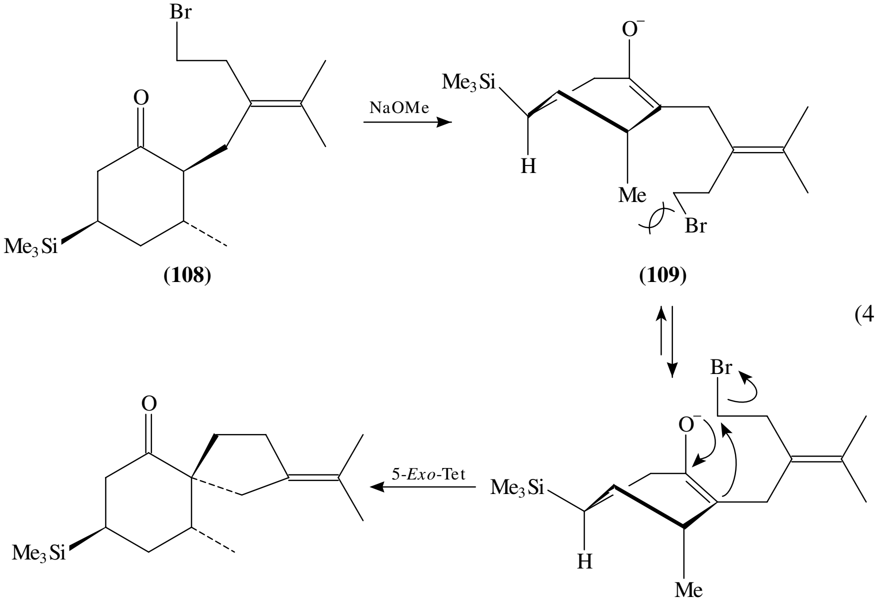

(108) **(109)**

(47)

(111) **(110)**

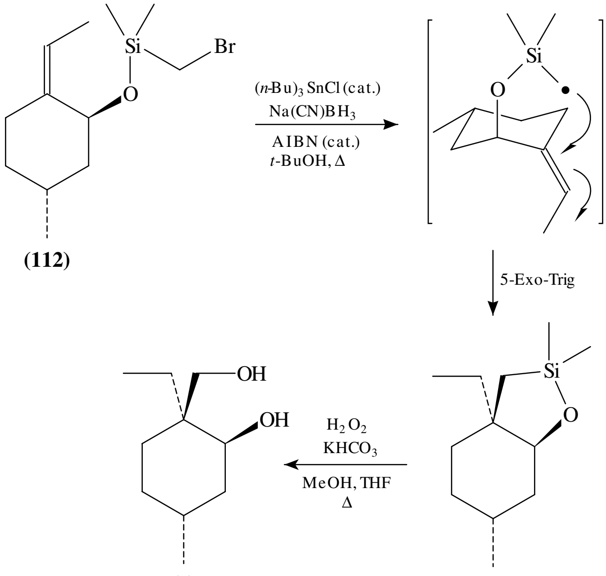

(112)

(48)

90%

(113) 87%

Polyene cyclization of epoxy trienylsilanes **114** by use of $TiCl_4$ in CH_2Cl_2 containing 2,6-di-*tert*-butylpyridine at −78 °C gives a mixture of 9,10-*syn* and 9,10-*anti* bicycles **117** and **118** in comparable amounts (equation 49)[171]. The formation of six-membered ring products proceeds through a chair/chair or a chair/boat transition state (i.e. **115** and **116**) with similar steric interactions. These results contrast sharply with the consistent bias favoring the chair/chair orientation in the cyclization of polyene epoxides lacking the Me_3Si substituent[172–174].

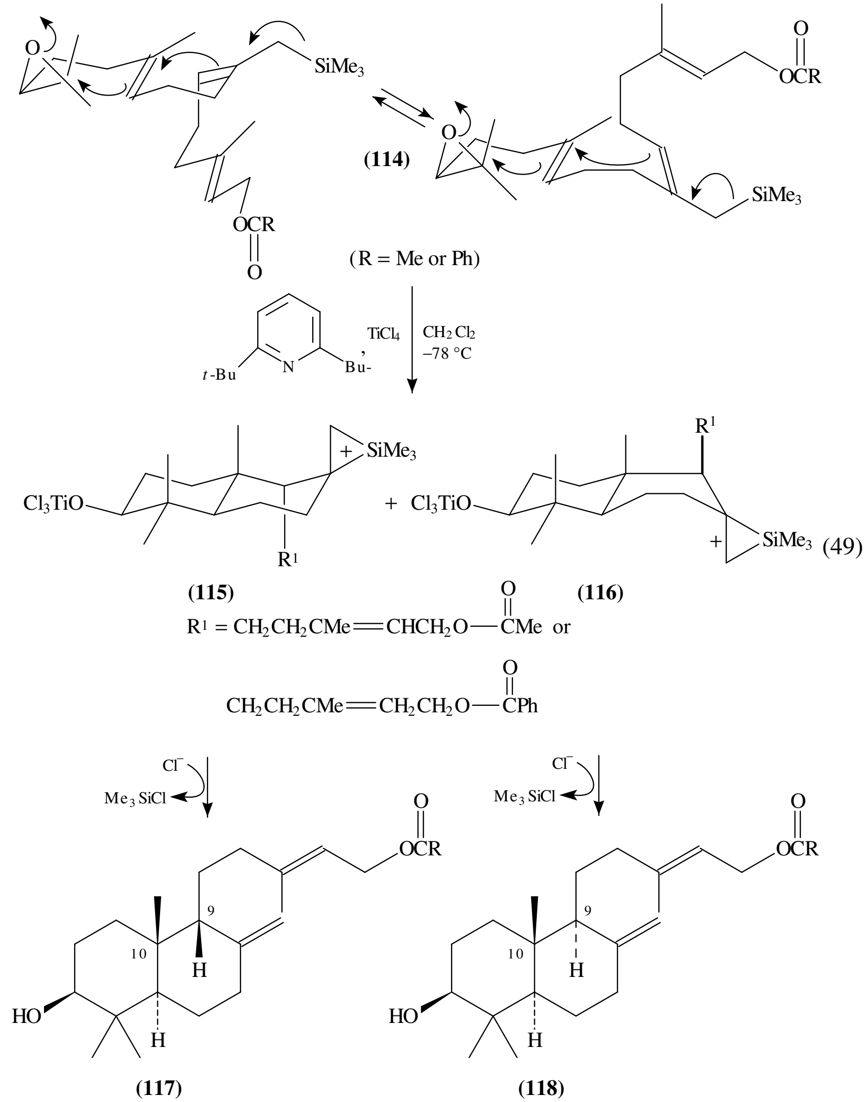

$$R^1 = CH_2CH_2CMe{=}CHCH_2O{-}\overset{O}{\overset{\|}{C}}Me \text{ or } CH_2CH_2CMe{=}CH_2CH_2O{-}\overset{O}{\overset{\|}{C}}Ph$$

Recently a [1,7] cyclization has been reported for the diazostyryl compounds **119** (equation 50)[175]. It leads to a diastereomeric pair of 1*H*-2,3-benzodiazepines **120** and **121**. Modification of the allylic hydroxyl group can promote attack from either face of the C−C double bond. Its lithium alcoholate gives a selectivity of 85 : 15 for one face and its *tert*-butyldimethylsilyl ether gives a selectivity of 9 : 91 for the other face.

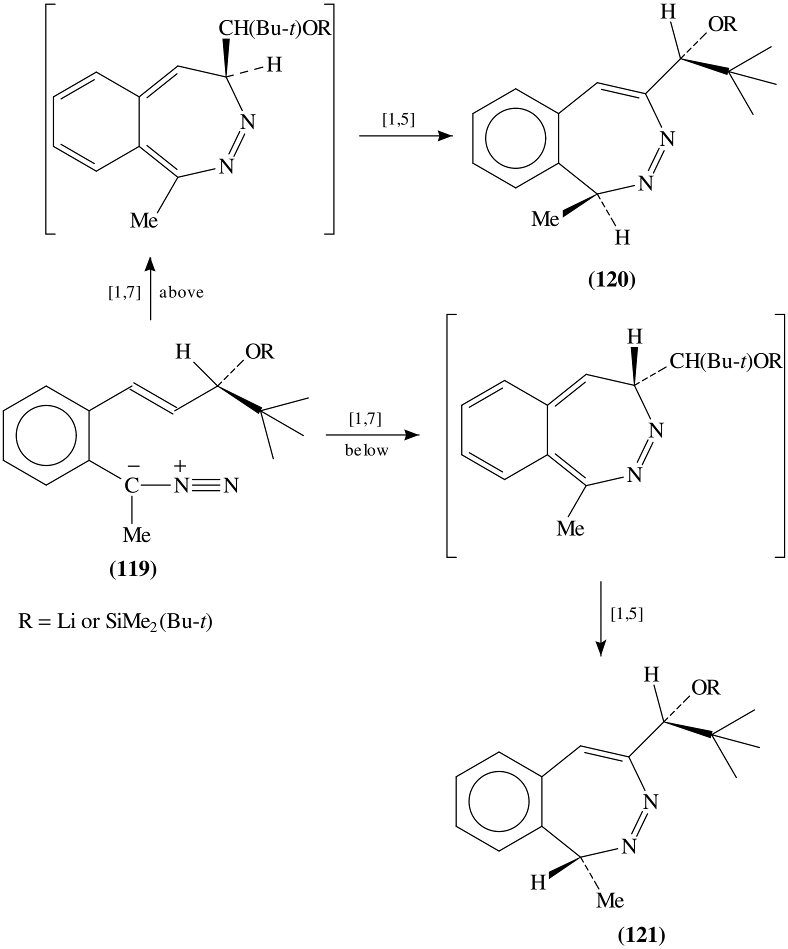

R = Li or $SiMe_2(Bu\text{-}t)$

(50)

8. [2 + 2] Cycloaddition

Reaction of (trimethylsilyl)vinyl selenide **122** with methyl vinyl ketone catalyzed by $SnCl_4$ gives the [2 + 2] adduct **123** in 66% yield (equation 51)[176]. Replacement of the Me_3Si group with a hydrogen atom or a methyl group produces a complex mixture. Thus, the Me_3Si group can suppress side reactions by its steric effect.

9. [3 + 2] Cycloaddition[89]

The intermolecular cycloaddition of *N*-(azidomethyl)benzisothiazolone **124** with various electron-deficient acetylenes **125** generates potential inhibitors of human leukocyte elastases 1,2,3-triazoles **126** and their regioisomers **127** in 72–99% overall yields (equation 52)[177]. As the steric effect increases due to the increase size of R in **125**, the adducts **127** prevail over adducts **126** and become the predominant products. The substituent rank order obtained on the basis of the STERIMOL program (the Verloop steric parameters) is H < Ph < SO_2Ph< *t*-Bu ~ Me_3Si[178]. A similar type of dominating effect by a Me_3Si substituent is also noted in the cycloaddition of diazoalkanes[179].

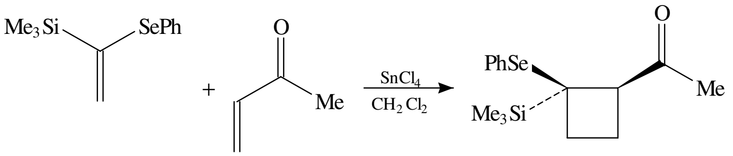

(122) **(123)** 66% (51)

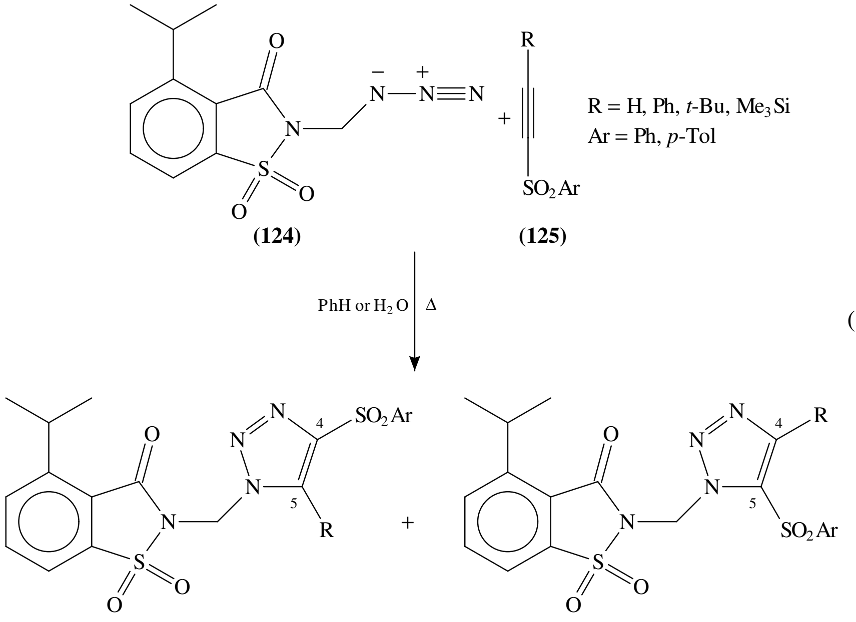

(124) **(125)** (52)

(126) **(127)**

In a different class, palladium(0)-catalyzed diastereo-controlled [3 + 2] cycloaddition of vinyl sulfone **128a** with allylsilyl acetate **129** gives a mixture of spiranes **130a** and **131a** in a ratio of 4.2 : 1 (equation 53)[180]. The diastereomeric ratio increases to >100 : 1 for **130b/131b** by introduction of a (*t*-Bu)Me_2SiO group in the vinyl sulfone (i.e. **128b**).

10. [4 + 2] Cycloaddition

Introduction of a silyl group, such as Me_3Si and (*t*-Bu)Me_2Si, on the oxygen of a propargylic alcohol[181,182] or on vinylallenes[183] affects the feasibility and the stereochemical course of intramolecular Diels–Alder reactions with an alkynyl diene, maleic anhydride or *N*-methylmaleimide. A possible explanation involves steric effects.

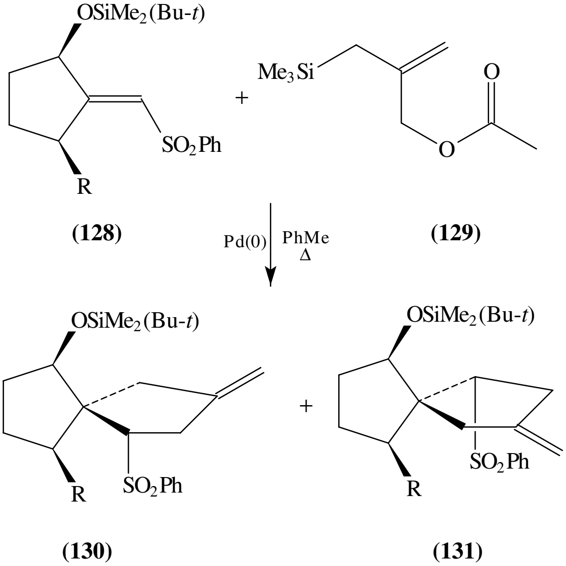

(53)

	R	Yield (%)	Ratio 130	:	131
(a)	H	67	4.2	:	1
(b)	$OSiMe_2(Bu\text{-}t)$	76	>100	:	1

Moreover, enone **132** reacts with (t-Bu)Me_2SiOTf and Et_3N to give the Diels–Alder adduct **134** in 82% yield via intermediate **133** (equation 54)[184]. Lactam **134** with a *cis* fused ring is more stable than the corresponding *trans* isomer, in which the Me_3Si group must rotate into an axial position. The secondary orbital overlap and the steric requirements of the Me_3Si group on the dienophile moiety in **133** also appear to be critical to the observed stereoselectivity.

In addition, protection of the hydroxyl group of chiral naphthyl alcohols with a Me_3Si group increases the steric crowding. Consequently, the rate decreases for their [4 + 2] cycloaddition with singlet oxygen[185]. [4 + 2] Cycloaddition also takes place between N-phenylmaleimide and trimethylsilyl enol ether of N-methyl-2-acetylpyrrole in toluene at 115 °C to give the corresponding adduct in 34% yield[186]. Nevertheless, the same reaction does not proceed by use of N-trimethylsilyl-2-acetylpyrrole as the substrate. Results from a model study indicate that the bulk of the Me_3Si group suppresses a requisite cisoid conformation.

For substrates containing a larger silyl group, the stereocontrol in intramolecular [4+2] cycloaddition of **135** is achieved by use of a sterically demanding $PhMe_2Si$ group to affect *endo*-selectivity in the production of **136** as the major product (equation 55)[187]. Absence of this group leads to a 1 : 8 selectivity in favor of the *exo*-product **137**.

11. Cyclopropanation

Attachment of a Me_3Si group to the terminal sp^2 carbon of allylic alcohols can influence diastereoselective cyclopropanation involving Sm and CH_2I_2[188].

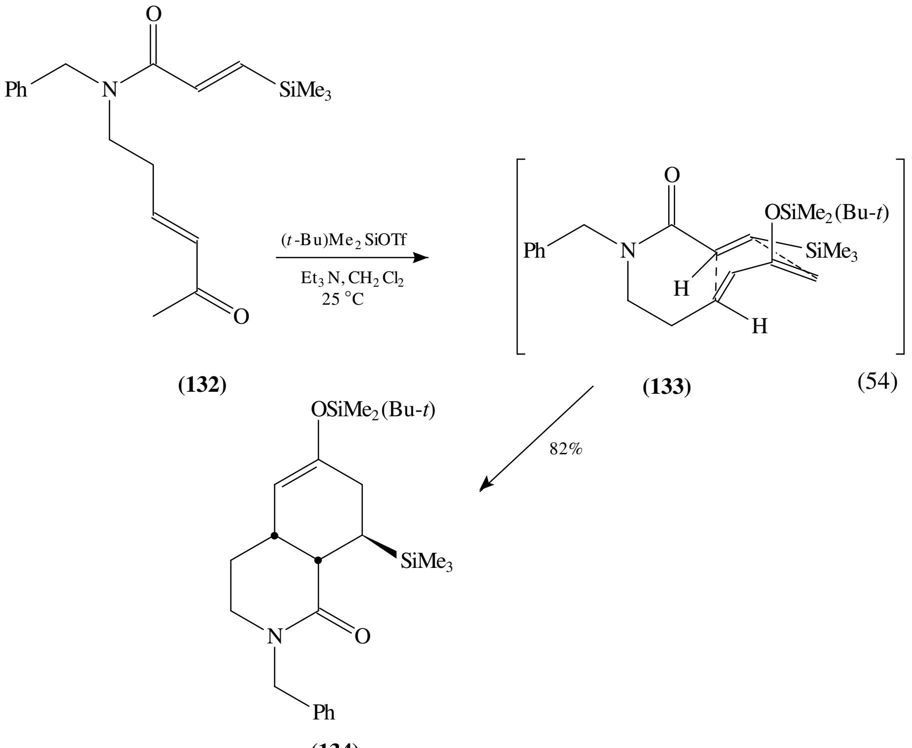

(132) **(133)** (54)

(134)

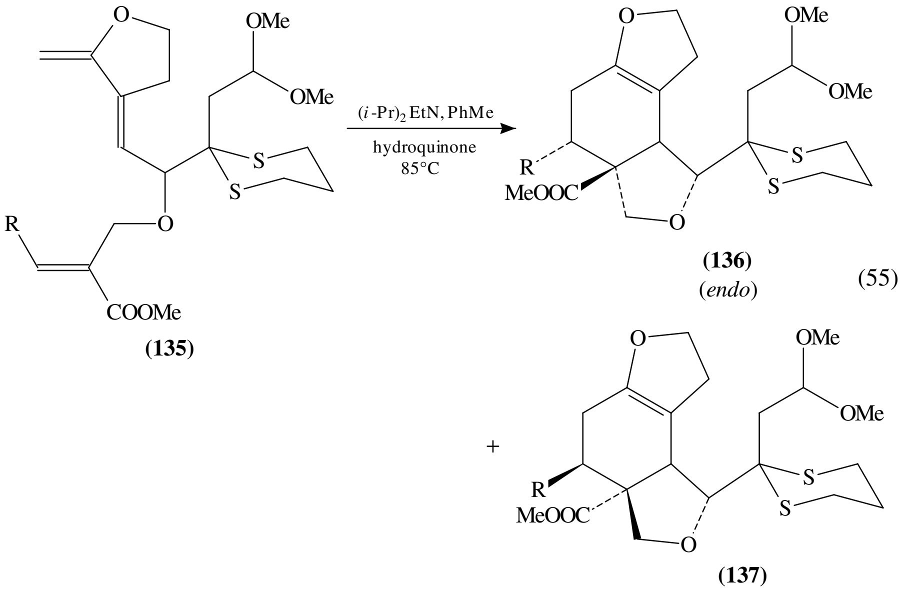

(135)

(136)
(*endo*) (55)

(137)
(*exo*)

R	**136**	Ratio	**137**
$PhMe_2Si$	5	:	2
H	1	:	8

12. Dehydration

Dehydration of α-hydroxy-γ-oxoalkyltrimethylsilanes under acidic conditions gives a mixture of (*E*)- and (*Z*)-γ-oxoalkenyltrimethylsilanes[189]. The thermodynamically more stable (*Z*)-isomer, according to *ab initio* calculation, is isolated as the major component. The ratio of (*Z*)/(*E*) isomers ranges from 4.5 : 1 to 27 : 1. The Me_3Si group stabilization of the (*Z*)-isomer is due to steric along with electronic influence.

13. Ene reaction

Carbonyl–ene reactions involving vinylsilanes promoted by a Lewis acid provide an avenue for regio- and stereocontrolled introduction of a vinyl functionality. The selectivity changes dramatically by placement of a Me_3Si group into the substrates as shown in equations 56 and 57[190]. Similarly, upon reaction with aldehydes in the presence of Me_2AlCl, the (*t*-Bu)Me_2Si group in optically pure **138** assists the chirality transfer to give adducts **139** in 80–99 %ee (equation 58)[191,192].

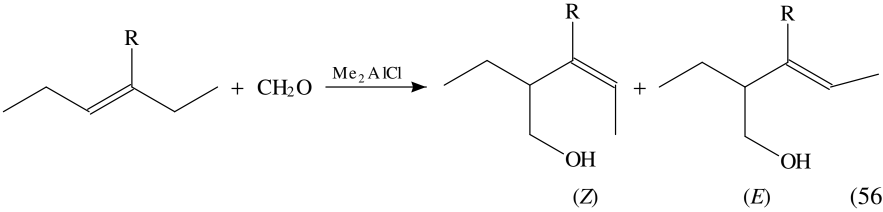

(56)

R	Ratio (*Z*)		(*E*)
H	15	:	85
Me_3Si	98	:	2

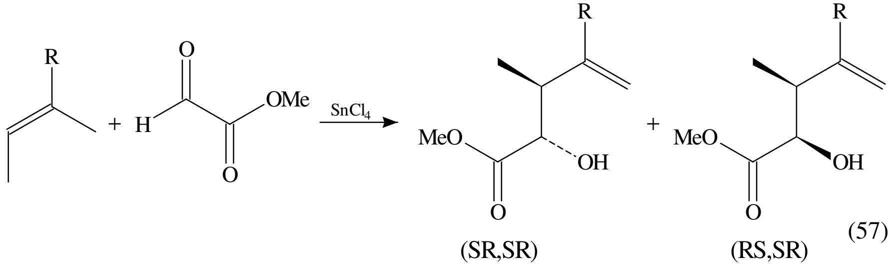

(57)

R	Ratio (SR, SR)		(RS,SR)
H	72	:	28
Me_3Si	7	:	93

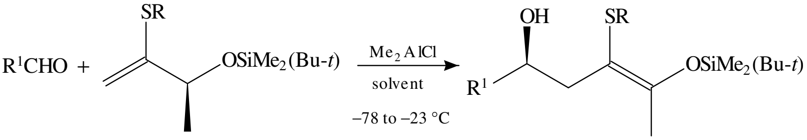

(58)

(138) **(139)**

R = Et, Ph (70–98%) (80–99 %ee)

R′ = Alkyl, Aryl, 2-Furyl

14. Epoxidation[193,194]

Epoxidation of 4-(hydroxymethyl)cyclopent-1-ene **(140a)** with *m*-CPBA gives a mixture of *syn*- and *anti*-epoxides in 1 : 1.1 ratio (equation 59)[58]. This ratio is slightly raised to 1 : 2.3 in the epoxidation of the corresponding benzoate **140b**. Protection of the hydroxyl group in **140a** with a (*t*-Bu)Me$_2$Si group increases the steric hindrance significantly. Consequently, conversion of **140c** to a mixture of *syn*- and *anti*-epoxides affords a ratio of 1 : 8.2 (entry 45 of Table 1). The selectivity drops to 1 : 4 when the less sterically congested Ph$_3$Si group replaces the (*t*-Bu)Me$_2$Si group (i.e. **140d**).

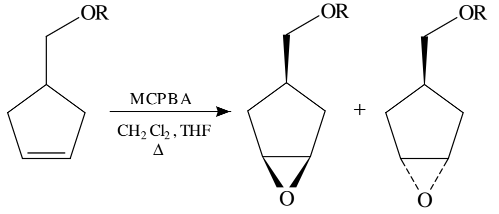

(59)

(140) *syn* *anti*

	R	Ratio *syn*	:	*anti*
(a)	H	1	:	1.1
(b)	COPh	1	:	2.3
(c)	(*t*-Bu)Me$_2$Si	1	:	8.2
(d)	Ph$_3$Si	1	:	4.0

In a related reaction, stereochemical control during epoxidation of Δ^4-*cis*-1,2-disubstituted cyclohexenes **141** with MCPBA depends upon the hydroxyl functionality[195]. A free alcohol **(141a)** or an acetate **(141b)** affords *syn*-epoxides exclusively. Epoxidation of a *t*-butyldimethylsilyl ether **(141c)** gives predominantly the *anti*-epoxide (54%).

15. Hydride reduction

The Me$_3$Si group can direct stereoselective synthesis of 2-vinyl-1,3-diols. Reduction of 3-hydroxy-2-vinylketone **142a** with LiBEt$_3$H produces a mixture of diastereomers **143a** and **144a** in a ratio of 1 : 49 (equation 60)[196]. Introduction of a Me$_3$Si group to the vinyl moiety of the substrate completely reverses the selectivity. This is evidenced by reduction of **142b** to give a mixture of **143b** and **144b** in a ratio of >99 : 1.

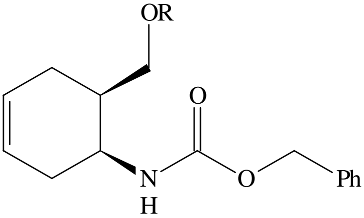

(141)

R =
(a) H
(b) Ac
(c) $SiMe_2(Bu\text{-}t)$

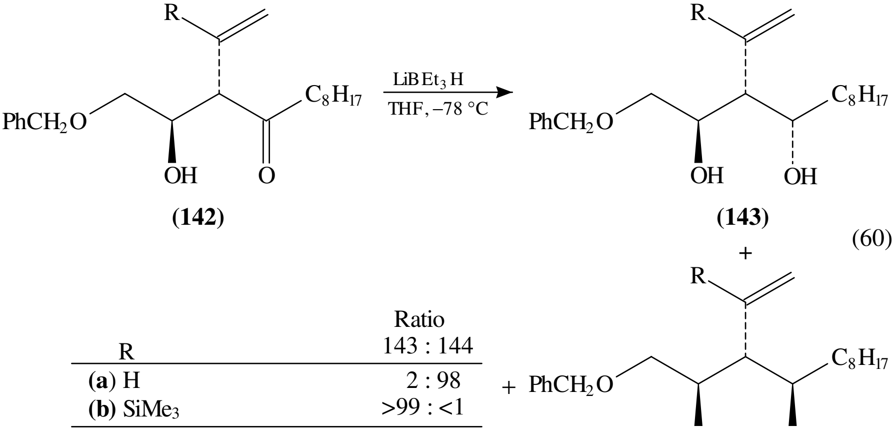

(142) **(143)** **(144)** (60)

R	Ratio 143 : 144
(a) H	2 : 98
(b) $SiMe_3$	>99 : <1

Furthermore, simple reduction of Me_3Si-containing norcamphor **145a** with $LiAlH_4$ gives the corresponding *endo* alcohol **146a** in 98% yield (equation 61)[197]. Under the same conditions, reduction of substrate **145b** possessing geminal di-Me_3Si groups produces a mixture of *endo* alcohol **146b** (83%) and silyl ether **147** (15%). Conversion of **146b** to **147** can also be achieved in 80–82% yields by use of MeLi (2 equiv) in ether or *t*-BuOK (0.01 equiv) in THF. The diverse results of reduction indicate that the unusual cleavage of an Si−Me bond is assisted by steric compression resulting from the Me_3Si groups.

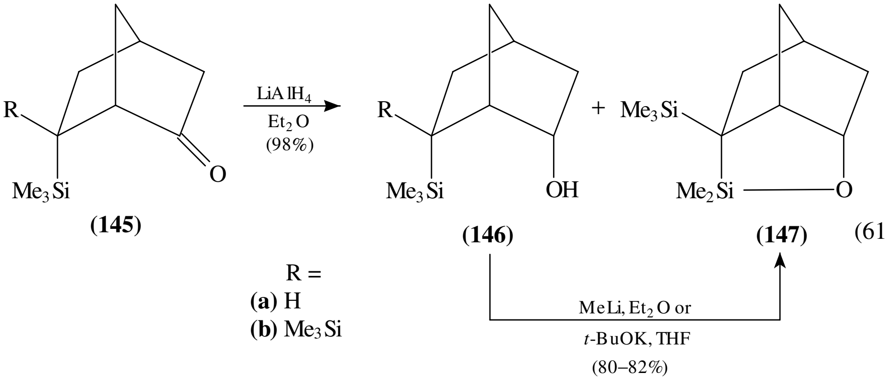

(145) **(146)** **(147)** (61)

R =
(a) H
(b) Me_3Si

A very recent report discloses that regio- and stereoselective deuteriation of allylic chlorides can be controlled by a neighboring hydroxyl, acetoxyl or silyl ether group[198]. Protection of a free hydroxyl group in **148**, R = H with a (t-Bu)Me_2Si group gives, however, a completely different regioselectivity (equation 62). Similarly, reductive ring opening of bicyclic ether **149a** with DIBALH in the presence of MeLi produces homoallylic alcohol **150a** as the major product along with by-product **151a** (equation 63)[199]. Reduction of the corresponding *tert*-butyldimethylsilyl ether **(149b)** by the same reducing agent in the absence of MeLi gives homoallylic alcohol **151b** as the major product along with by-product **150b**. The opposite regioselectivity results from the bulky (t-Bu)Me_2Si protecting group.

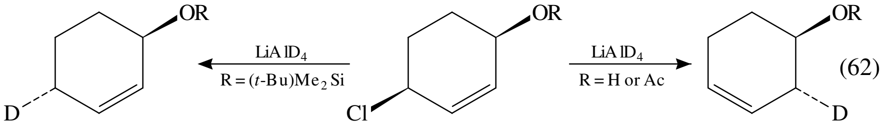

(62)

(78%) **(148)** (83–86%)

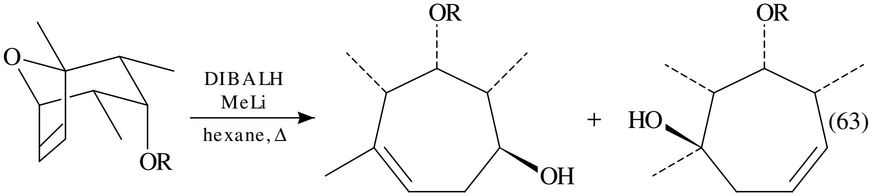

(63)

(149) **(150)** **(151)**

R		Ratio	
	150	:	**151**
(a) H	9.5	:	1
(b) (t-Bu)Me_2Si	1	:	6.4

Moreover, introduction of the (i-PrO)Me_2Si group to ketones at an α position assists their selective reduction by L-*Selectride*[200]. Upon treatment with $KF/KHCO_3$ and H_2O_2, the resultant α-silyl alcohols give vicinal diols.

16. Hydroboration

The steric hindrance caused by the $PhMe_2Si$ group in allylsilanes **152** influences the orientation of hydroboration by 9-BBN, NaOH and H_2O_2 (equation 64)[139]. The corresponding alcohols **153** are produced stereoselectively in 79–96% yields.

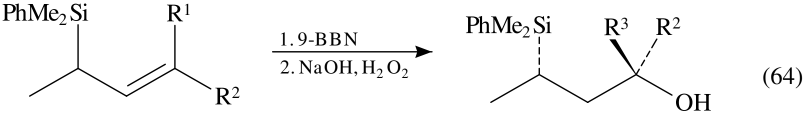

(64)

(152) **(153)**

	R^1	R^2		R^3	R^4	
(a)	H	Me	**(a)**	OH	H	(96%)
(b)	Me	H	**(b)**	H	OH	(79%)

17. Hydrogenation

Hydroxy-directed hydrogenation of (phenyldimethylsilyl)allyl alcohols with a cationic rhodium complex provides a highly diastereoselective route to β-silyl alcohols[201,202].

18. Lithiation

Introduction of a bulky (t-Bu)Me_2Si group at the C-2 position of 3-furoic acid allows regioselective lithiation at the C-4 position with 2.5 equiv of BuLi[203]. In comparison, lithiation of 3-furoic acid without the (t-Bu)Me_2Si group takes place at the C-2 position with 2.0 equiv of LDA[204].

19. Oxidation

The (t-Bu)Me_2Si group in ketones **154** directs their diastereoselective oxidation to the corresponding α-silyloxy ketones **155** with m-CPBA or 3-phenyl-2-(phenylsulfonyl)oxaziridine (equation 65)[205]. The oxidizing agents approach *anti* to the (t-Bu)Me_2Si group. This process compares well with other silicon-directed electrophilic reactions at an alkene C−C double bond[206].

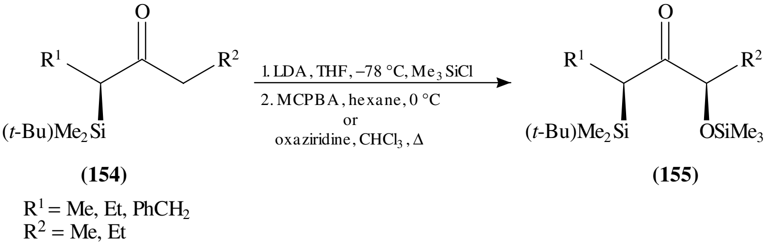

(65)

20. Photocyclization

Photoinduced cyclizations of phenyl triphenylsilyl thioketone **(156)** with *cis*- and *trans*-1,2-dichloroethene give a mixture of silyl thietanes **157** and **158** in a regio- and stereoselective manner (equation 66)[207]. These reactions involving biradical intermediates and ring closure are governed by the steric effect. The steric hindrance between the Ph_3Si group and the vicinal chlorine atom ensures their *trans* relationship in the thietane products.

For a different class of compounds, cyclization of *ortho*- and *meta*-substituted 1-benzyl-1-pyrrolinium perchlorates **159** and **160** under photolytic conditions gives benzopyrrolizidines or benzindolizidines or both[208]. The product distribution is highly influenced by the steric effect resulting from the silyl groups at the benzylic position[209].

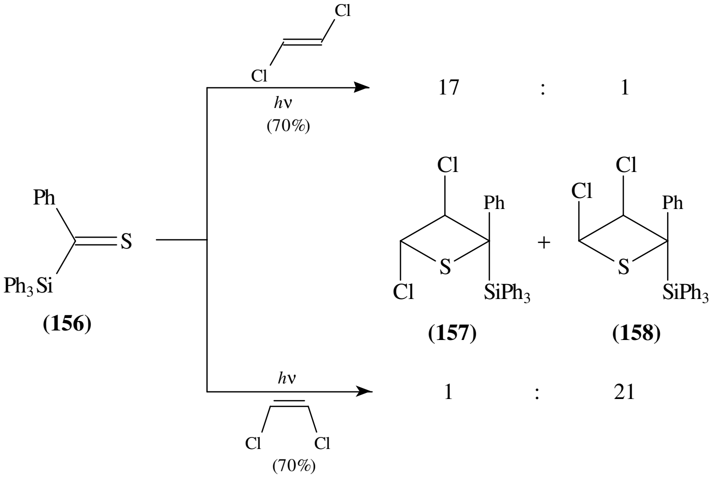

(156) **(157)** **(158)**

(66)

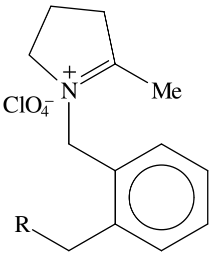

(159)

R = H, Me_3Si, (*t*-Bu)Me_2Si

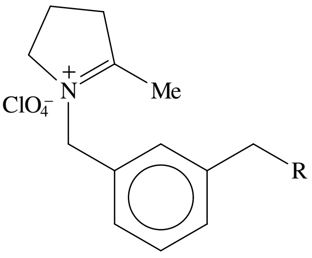

(160)

R = H, Me_3Si, (*t*-Bu)Me_2Si

21. Reduction

A sterically demanding $PhMe_2Si$ group at the C-3 position of 1-cyclohexanone derivatives affects a highly stereoselective reduction of the C-1 carbonyl group by $NaBH_4$ in methanol[187]. The 3-silyl-1-cyclohexanol product holds a *cis* configuration.

22. [2,3]-Sigmatropic rearrangement

A stereoselective [2,3]-sigmatropic rearrangement can be achieved by introduction of a Me_3Si or (*i*-Pr)$_3$Si group at the terminal *sp*-carbon in a prop-2-ynyl-2-(trimethylsilyl)allyl ether[210]. It generates vinylsilanes in the *E* form.

23. Substitution

A sterically demanding group at one terminus of the allyl moiety blocks the incoming nucleophile in palladium-catalyzed allylic substitutions. The Me_3Si group in **161** can fulfil such a purpose and prevails over the phenyl group as a controlling element in the preparation of optically active γ-silylallylamines (**162**, equation 67)[211].

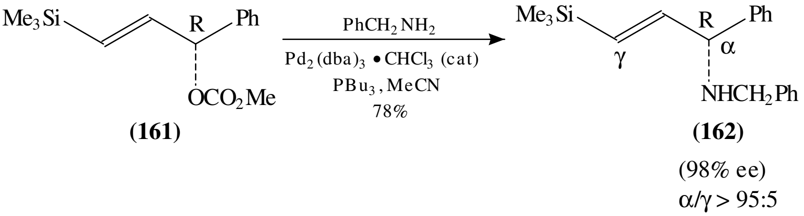

(161) (162)

(98% ee)
α/γ > 95:5

(67)

V. REACTIVITY OF SILICON-CONTAINING REAGENTS

A. General Considerations

The size of a silyl group in silicon-containing reagents greatly influences their reactivity[212] and selectivity. Some prominent examples are discussed in the following reactions of 12 classes.

B. Organic Reactions of Various Types

1. Addition and substitution

A complete stereocontrol is achieved by addition of the bulky silyl radical $(Me_3Si)_3Si^\bullet$ to a chiral and conformationally flexible electron-deficient olefin **163**, as shown in equation 68[213]. Replacement of $(Me_3Si)_3Si^\bullet$ with a less sterically hindered $(n\text{-}Bu)_3Sn^\bullet$ gives a mixture of *syn* and *anti* diastereomeric adducts **164** and **165** in a ratio of 7 : 3. The A values (kcal mol^{-1}) of the tin, carbon and silicon species follow the order $(n\text{-}Bu)_3Sn$ (1.1) < Me (1.7) < Me_3Si (2.5), and the bond length for C−Sn (2.2 Å) is longer than that for C−Si (1.85 Å)[214,215].

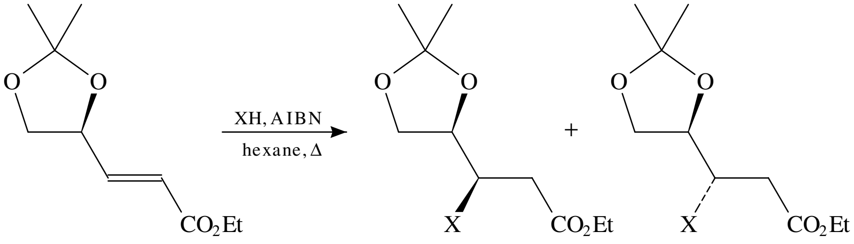

(68)

(163) **(164)** (*syn*) **(165)** (*anti*)

X	Overall yield (%)	Ratio **164**	:	**165**
$(Me_3Si)_3Si$	>95	100	:	0
n-Bu_3Sn	93	7	:	3

Recent reports indicate that the size of silyl groups, including Ph_3Si and Ph_2MeSi, influences the 1,2-addition of an imine by α-silyl organocopper reagent[216] and the S_N2 displacement of a styrene oxide by α-silyl organolithium reagents[217]. On the other hand, 1,4-addition of a silyl anion to an α,β-unsaturated enone moiety provides an efficient way to introduce the silicon element onto organic molecules. Reaction of Me_3SiLi with dienone **166** at the C_1 position gives enone **167a** as the major product along with its α-epimer in a ratio of 19 : 1 (equation 69)[38,124]. Reagent $(Me_3Si)Me_2SiLi$, sterically more hindered than Me_3SiLi, reacts with **166** to afford exclusively enone **167b** in 63% yield (cf entry 46 of Table 1).

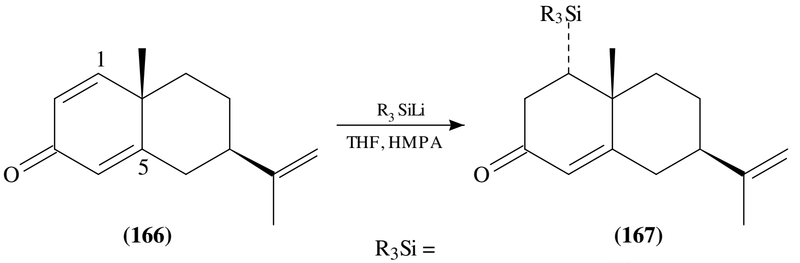

(166) **(167)** (69)

R_3Si =
(a) Me_3Si (66%; 19:1)
(b) Me_3SiMe_2Si (63%)

Silylcuprate reagents add diastereoselectively to various types of functional groups[91,218], including α-alkylidenelactones[219], *N*-acryloyl lactams[220], *N*-enoyl sultams[221], 2-phenylselenocyclopent-2-en-1-one[222] as well as α,β-unsaturated enones, amides and esters[218,223,224]. The level of diastereoselection of the addition to *N*-enoyl sultams **168** giving a mixture of **169** and **170** (equation 70) greatly depends on the nature of silyl cuprates and invariably increases when the higher-order silylcyanocuprates are used. The stereofacial discrimination ability follows the sequence: $(R_3Si)_2CuLi \ll R_3SiCu < (R_3Si)_2Cu(CN)Li_2$[225].

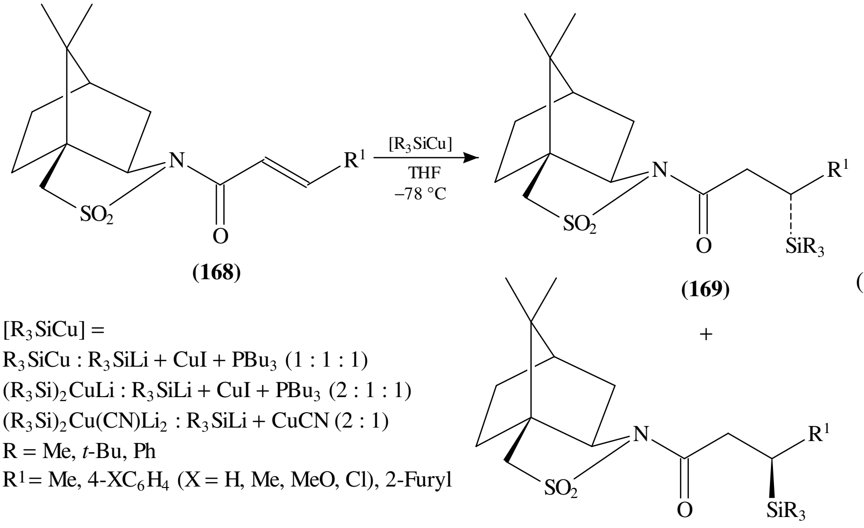

(168) **(169)** (70) **(170)**

$[R_3SiCu]$ =
R_3SiCu : R_3SiLi + CuI + PBu_3 (1 : 1 : 1)
$(R_3Si)_2CuLi$: R_3SiLi + CuI + PBu_3 (2 : 1 : 1)
$(R_3Si)_2Cu(CN)Li_2$: R_3SiLi + CuCN (2 : 1)
R = Me, *t*-Bu, Ph
R^1 = Me, 4-XC_6H_4 (X = H, Me, MeO, Cl), 2-Furyl

The diastereoselection levels are uniformly appealing (93–99%) for crotonates and cinnamates when higher (dimethylphenylsilyl)cyano cuprates are used as reagents. Other more hindered silyl groups, such as Ph_2MeSi and (t-Bu)Ph_2Si groups, show somewhat lower diastereoselection levels.

Depending upon the steric nature of the alkyl groups attached to tin and silicon in $R_3Sn{-}SiR'_2R''$, these silylstannanes undergo ligand exchange upon treatment with a higher-order cuprate (n-Bu)$_2$Cu(CN)Li_2 to afford trialkylsilyl mixed cuprates (equation 71)[226]. The resultant cuprates RMe_2Si(n-Bu)Cu(CN)Li_2 (R = t-Bu or thexyl) can participate in substitution and addition reactions.

$$RMe_2SiSnMe_3 + (n\text{-Bu})_2Cu(CN)Li_2 \xrightarrow[\text{THF}]{25\,°C} RMe_2Si(n\text{-Bu})Cu(CN)Li_2 \qquad (71)$$

R = t-Bu or thexyl;
R^1 = H or Me

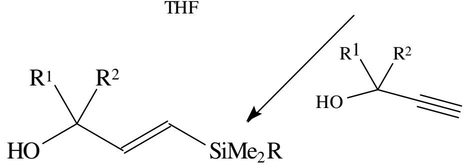

2. Condensation

The chiral reagents [(1R,2S)-ephedrine]$POSiR_3$ **(172)** are prepared through the reaction of [(1R,2S)-ephedrine]PCl **(171)** with R_3SiOH in the presence of NEt_3 (equation 72)[227]. The epimers **172** and **173** exist as an equilibrium mixture with a diastereoselectivity (86–94%) that is dependent upon the nature of the substituents on silicon.

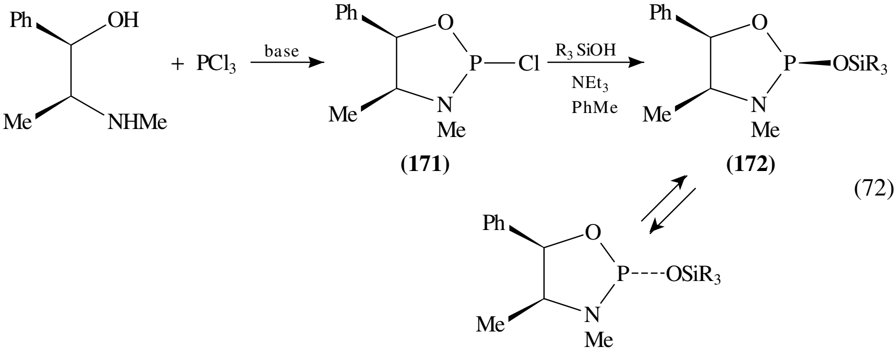

(171) **(172)** **(173)**

(72)

R_3Si	Yield (%)	Diastereoselectivity (%) of **172/173**
Et_3Si	82	86
(t-Bu)Me_2Si	78	88
Ph_3Si	91	94

3. [3 + 2] Cycloaddition

Allylsilanes **12** react with α-ketoesters **174** to give [3 + 2] cycloadducts **175** in 50–85% yields through 1,2-silyl migration (equation 73)[59,228]. Use of an allylic trimethylsilane produces an allyl alcohol by-product through a competing silyl elimination process. It can be circumvented by use of a bulkier silicon-containing reagent, such as the

$CH_2{=}CHCH_2SiMe_2(Bu\text{-}t)$ (cf entry 47 of Table 1). Given a similar concern, a new sterically demanding allylsilane, $CH_2{=}CHCH_2SiMe_2(CPh_3)$, has been developed recently as a mild and efficient reagent for hydroxypropyl annulation of electron-deficient alkenes[229].

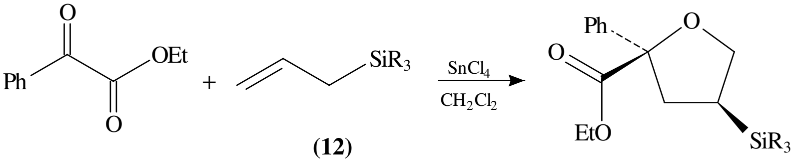

(174) **(12)** **(175)**

(73)

R_3Si	Yield (%)
Me_3Si	50
$PhMe_2Si$	54
$(t\text{-Bu})Me_2Si$	85

4. [4 + 2] Cycloaddition

The Me_3Si group in (*E*)-1,3-bis(trimethylsilyloxy)buta-1,3-diene (**177**) provides the necessary steric requirement to react with 10-amino-9-hydroxy-1,4-anthraquinone derivatives **176** in a regio- and stereospecific manner (equation 74)[230]. Thus a single anthracyclinone derivative (**178**) is obtained in an excellent yield through the Diels–Alder process.

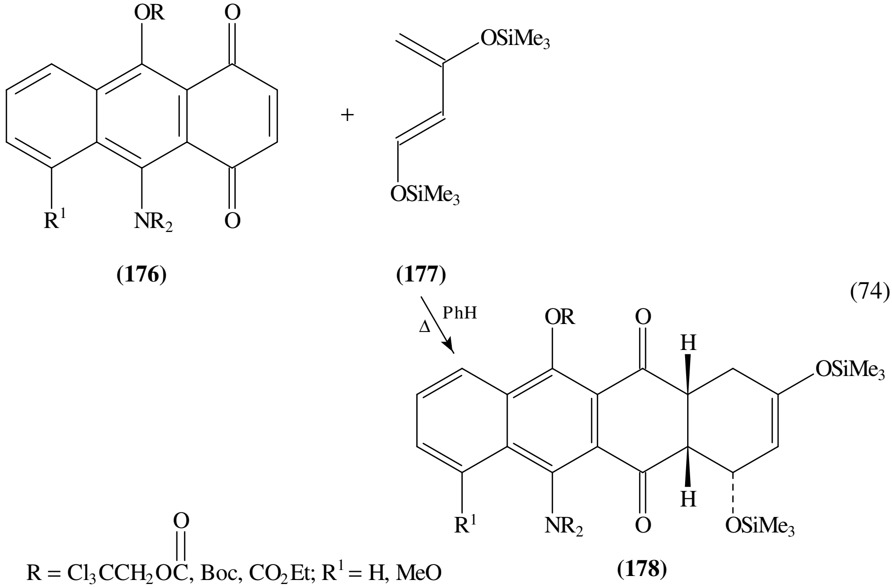

(176) **(177)** **(178)**

(74)

$R = Cl_3CCH_2O\overset{\overset{\displaystyle O}{\|}}{C}$, Boc, CO_2Et; $R^1 = H$, MeO

5. Hydrosilylation

Various organosilanes, including (n-C_5H_{11})SiH_3, (n-Bu)$MeSiH_2$, (n-Pr)$_2SiH_2$, Ph_2SiH_2, Et_3SiH and Et_2MeSiH, are used in hydrosilylation of 2,2,4,4-tetramethyl-1,3-cyclobutanedione in the presence of the Wilkinson catalyst [i.e., $Rh(PPh_3)_3Cl$]. These reactions lead to a mixture of the corresponding *cis* and *trans* diols as well as 3-hydroxylcyclobutanone[60]. The selectivity of the reductions depends greatly upon the bulk of silane reagents. The order of the silyl groups in these reagents is listed in entry 48 of Table 1.

For hydrosilylation of 1-hexyne with R_3SiH in the presence of H_2PtCl_6, the trend of steric influence of silyl groups is shown in entry 49 of Table 1[61]. The steric hindrance resulting from various substituents on the silicon of vinylsilanes also influences their hydrosilylation by Et_3SiH in the presence of Ni(acac)$_2$ as a catalyst[231].

6. Insertion reaction

Alkenyl Fischer carbene complexes (e.g. **179**) undergo a [2 + 1] insertion reaction with Et_3SiH or Ph_3SiH to give allylsilanes (e.g. **180**) in 68–87% yields (equation 75)[62]. In comparison with Et_3SiH, use of Ph_3SiH shows a significant (*ca* 10-fold) rate enhancement and a yield improvement of *ca* 20%. The Ph_3Si group, although 'bigger' than the Et_3Si group, is less hindered as a result of the 'propeller effect' of the phenyl rings (entry 50 of Table 1).

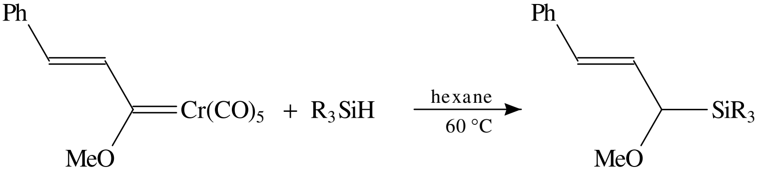

(75)

(179) **(180)**

R_3Si	Yield (%)
Et_3Si	68
Ph_3Si	87

On the other hand, rhodium(II) can catalyze intramolecular C–H insertion of 1-methyl-3-silyloxy-1-(diazoacetyl)cyclohexanes[63]. The ratio of the products through C_5–H versus C_3–H insertions increases from 2.2 : 1 to 6 : 1 when the bulkier (i-Pr)$_3$Si group is used to replace the (t-Bu)Me_2Si group (entry 51 of Table 1).

7. Nitrone formation

'Bulky proton'-containing reagent $Me_3SiN(Me)OSiMe_3$ **(181)** reacts with aldehydes and ketones to give the corresponding nitrones **182** in good to excellent yields (equation 76)[232,233]. This reagent is sensitive towards steric hindrance as exemplified by reacting it with dicarbonyl compound 5α-pregnan-3,20-dione (**183**, equation 77). Treatment of a 1 : 1 ratio of $Me_3SiN(Me)OSiMe_3$ **(181)** with **183** in benzene at reflux affords mono-nitrone **184** in 71% yield. In comparison with the C-20 carbonyl group, the

C-3 carbonyl moiety in **183** is less sterically congested[3].

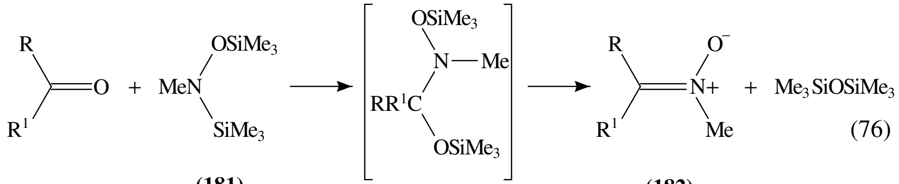

(181) **(182)**

(76)

R = H, Me; R^1 = Me, $CHMe_2$, CMe_3, $(CH_2)_3CH=CH_2$, p-XC_6H_4 (X = H, NH_2, NO_2), 2-Furyl

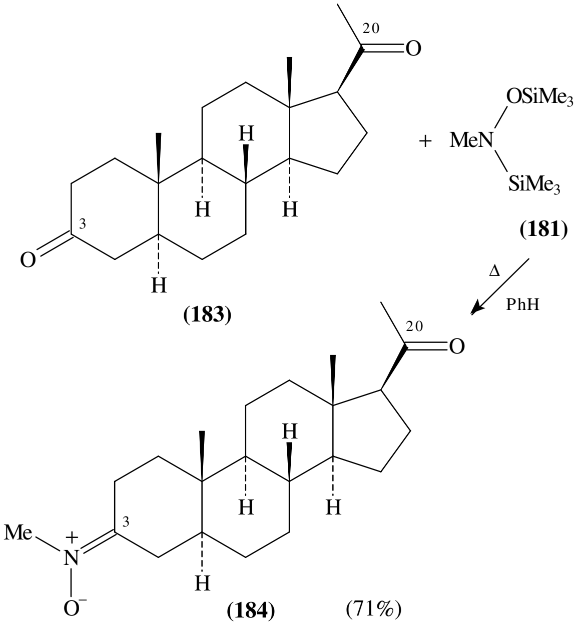

(183) **(181)** **(184)** (71%)

(77)

8. Olefination

Various silyl groups in Grignard reagents **185** mediate their addition to aldehydes to generate mainly *Z*-enynes **186** (equation 78)[64]. The ratios of **186** to its *E*-isomer **187** depends upon the size of silyl groups according to the order listed in entry 52 of Table 1.

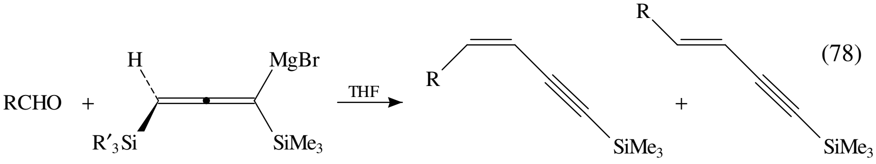

(185) **(186)** **(187)**

(78)

R'_3Si = Me_3Si, Et_3Si, $(t\text{-}Bu)Me_2Si$, Ph_3Si

9. Oxygen–oxygen bond cleavage

Phenylethynyllithium (**188**) reacts with silylperoxides **189a–d** to give C-silylated products **190a–d** or silyl ethers **191a–d** or both in 48–90% overall yields (equation 79)[234]. The distribution of the products and the yields depend upon the steric hindrance created by the substituents attached to the silicon atom.

$$\underset{\textbf{(188)}}{PhC{\equiv}C{-}Li} + \underset{\textbf{(189)}}{(R_3Si{-}O{\rightarrow}_2} \longrightarrow \underset{\textbf{(190)}}{PhC{\equiv}C{-}SiR_3} + \underset{\textbf{(191)}}{PhC{\equiv}C{-}OSiR_3} \qquad (79)$$

	R_3Si	Overall yield (%)	Ratio		
			190	:	**191**
(a)	Me_3Si	86	100	:	0
(b)	$(n\text{-}Pr)_3Si$	67	3	:	2
(c)	$(n\text{-}Bu)_3Si$	90	3	:	2
(d)	Ph_2MeSi	48	>9	:	1

10. Silylation

The steric effect resulting from trisubstituted silyl chlorides influences their capability in silylation of alkali phenolates[65]. As the size of the silyl groups increases with the trend shown in entry 53 of Table 1, the activity of the silyl chlorides decreases.

Substitution with a *t*-Bu functionality in the *ortho* position of the phenolate ring retards the reactivity through steric crowding of the reaction site. Moreover, the feasibility of reactions of azasilatranes with CF_3SO_3Me can be rationalized on steric grounds[235].

11. Silylformylation

Dirhodium(II) perfluorobutyrate [i.e. $Rh_2(pfb)_4$] catalyzes the silylformylation of terminal alkynes with carbon monoxide and organosilanes to afford β-silylacrylaldehydes **192** in moderate to excellent yields (equation 80)[236]. Use of organosilanes Et_3SiH and $PhMe_2SiH$ provides appealing stereocontrol for the (*Z*)-isomer (>10 : 1). Hydrosilylation, however, competes with the silylformylation. The steric effect between the organosilanes and alkynes plays a role in determining the relative rates of these two competitive processes.

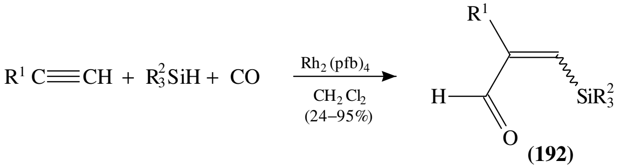

(192)
(*Z*/*E* > 10:1)

(80)

R^1 = Ph, *p*-Tol, *p*-*i*(-Bu)C_6H_4, 6-MeO-Naph-2,
n-Hex, $AcOCH_2$, $MeOCH_2$, $Me_2C(OH)$
R^2_3Si = Et_3Si, $PhMe_2Si$

12. Silylstannation

Silylstannation of alkenes with organosilylstannanes in the presence of bis(dibenzylideneacetone)palladium [Pd(dba)$_2$] and trialkylphosphine as catalysts affords 1,2-adducts in 36–97% yields (equation 81)[237]. The organosilylstannane reagents include $Me_3SiSnMe_3$, $Me_3SiSn(Bu\text{-}n)_3$, $(MeO)Me_2SiSn(Bu\text{-}n)_3$, $(t\text{-}Bu)Me_2SiSnMe_3$, and $(t\text{-}Bu)Me_2SiSn(Bu\text{-}n)_3$. The steric congestion seems to affect the reaction significantly.

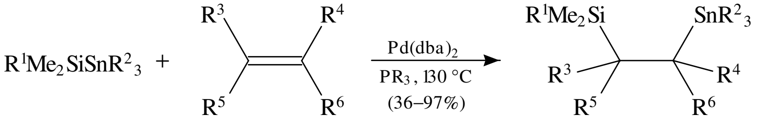

(81)

R^1 = Me, t-Bu, OMe
R^2 = Me, n-Bu

$R^3R^5C{=}CR^4R^6$ = ethylene, norbornene

VI. SOLVOLYSIS OF VARIOUS ORGANOSILANES

A. Adamantane *p*-Nitrobenzoates

The Me_3Si and the Me groups exhibit similar effective sizes in 2-adamant-2-yl *p*-nitrobenzoate[238]. The conclusion is drawn on the basis of solvolysis of its derivatives bearing a Me_3Si and a Me group as well as on the results of *ab initio* and force-field calculations. The solvolysis rate of the adamant-2-yl derivatives is not sterically accelerated by a 2-Me_3Si group, yet it is greatly accelerated by a 2-*t*-Bu group[239].

B. Benzylic *p*-Toluenesulfonates

A pronounced rate-retardation of 1.65×10^4-fold by an α-Me_3Si group relative to Me in the solvolysis of benzylic *p*-toluenesulfonates is due to a steric effect[66]. The rate increment in ethanol decreases with increasing steric size of the α-silyl group attached to the benzylic position and follow the order listed in entry 54 of Table 1.

C. Silyl Ethers

Complexation of silyltetralol **193** with $Cr(CO)_6$ gives a mixture of *syn*- and *anti*-complexes (**194**/**195** = 45 : 55; equation 82)[240]. The *anti*-isomer is favored because the steric effect of the $(t\text{-}Bu)Me_2SiO$ group outweighs any chelation effect. A greater desilylation rate for **195** than for **194** by use of $Bu_4NF{\cdot}3H_2O$ is due to the steric bulk around the silicon in **194** caused by the $Cr(CO)_3$ moiety at the *syn*-position.

The k_2 values ($M^{-1}\,s^{-1}$) of the solvolysis of various R_3SiOPh in aqueous ethanol at 25 °C were determined under acidic and basic conditions[67,68]. The size of the silyl groups influences the rate and follows the order listed in entries 55 and 56 of Table 1. The correlation between the Si–O–C angle and the oxygen basicities may be completely different, or even reversed, in comparison with trimethylsilyl and *tert*-butyldimethylsilyl ethers[241]. The relative hydrolysis rates may be simply controlled by steric hindrance to solvent assistance for the Si–O bond cleavage following the protonation step.

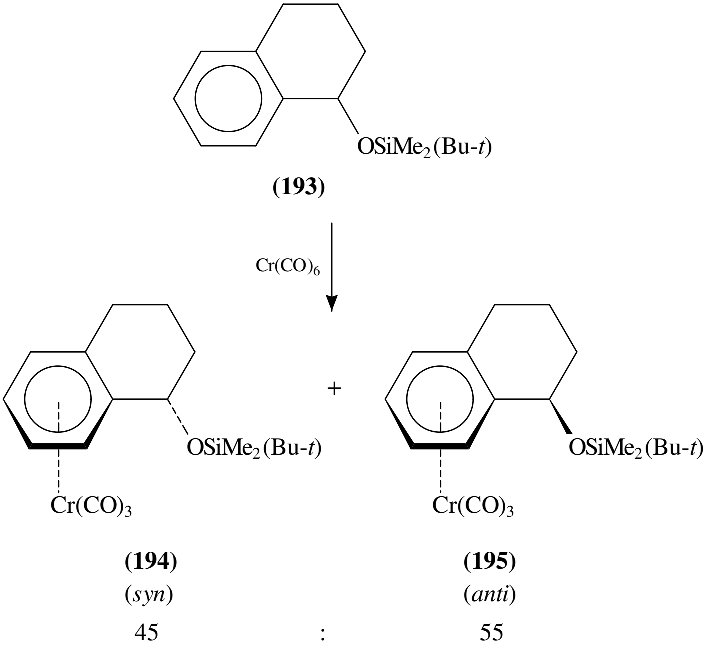

(193)

(194) (*syn*) 45 : **(195)** (*anti*) 55

(82)

D. Triorganosilyl Chlorides and Fluorides

A quantitative scale for the structural effect of various silyl groups is established, as shown in entry 57 of Table 1, by the rates of solvolysis of 40 triorganosilyl chlorides in aqueous dioxane under neutral conditions[69]. The structural effect involves the steric effect and, in some examples, the electronic effect. Because little difference exists in the electronic effect among alkyl groups, their steric effect at silicon follows the order primary < secondary < tertiary substituents.

Moreover, reactivities for 54 triorganosilyl groups toward nucleophilic displacement at silicon have been predicted on the basis of their solvolysis rates in aqueous dioxane (see entry 58)[70]. In addition, results from solvolysis of R_3SiF in aqueous acetone are listed in entry 59[71] of Table 1.

E. Triorganosilyl Hydrides

Two similar orders listed in entries 60 and 61 of Table 1 are established by solvolysis of R_3SiH. Those reactions are performed in aqueous ethanol at 34.5 °C under acidic[72,73] or basic conditions[74].

VII. CHANGE OF PHYSICAL, CHEMICAL AND SPECTROSCOPIC PROPERTIES BY INTRODUCTION OF SILYL GROUPS

Replacement of an H, Me, Et, *i*-Pr, or *t*-Bu unit with a bulky silyl group in organic compounds may change their physical or spectroscopic properties to a great extent. The changes in the following systems clearly come from the steric congestion created by the silyl groups.

A. Change of Physical and Chemical Properties

1. Conformation, bond angles and bond lengths

An extreme example reflecting the steric congestion is the replacement of all hydrogens in benzene by six Me_3Si groups to cause a large ring distortion into a chair form[242]. A strong σ(C−Si)−π conjugation becomes important. At elevated temperature (e.g. 200 °C), the relative amount of the boat form increases to 70%[243]. Thermolysis of the highly distorted hexakis(trimethylsilyl)benzene results in rupture of the aromatic ring[244]. The internal benzene ring bond angles also reflect the distortion of molecule **196**, resulting from the bulk of the substituents and the size of the Me_3Si groups at the C-4 and the C-6 positions[245].

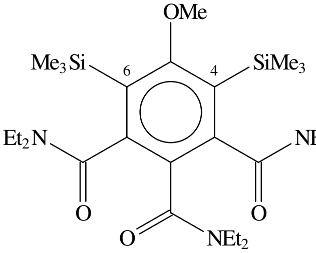

(196)

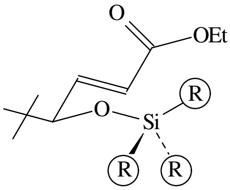

(197)
(eclipsed)
R_3Si =
(a) Me_3Si
(b) Et_3Si

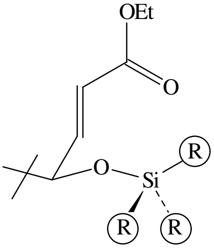

(198)
(staggered)
R_3Si =
Ph_3Si =
(i-Pr)$_3$Si

Another example includes replacement of two or four methyl groups in N,N,N',N'-tetramethyl-p-phenylenediamine (i.e. Wurster's Blue) with Me_3Si groups. It results in distortion of the SiHN−C_6H_4−NHSi skeleton[246]. The nitrogen lone pairs of the planar Me_3SiNH units in N,N'-disilylated derivatives are co-axial with the π-vector perpendicular to the benzene ring. The p-type electron pairs of the flattened $(Me_3Si)_2N$ groups in the overcrowded N,N,N',N'-tetrakis(trimethylsilyl)-p-phenylenediamine are twisted into the plane of the benzene ring. Thus it provides the possibility for one-electron reduction to a Wurster's Blue radical anion.

In addition, trimethylsilyl ether **197a** and triethylsilyl ether **197b** have conformations different from those of compounds **198a** and **198b**[247], which bear a bulky Ph_3Si or a (i-Pr)$_3$Si group, respectively. The change of conformation is due to the steric hindrance from these two bulky silyl groups.

Furthermore, reactions of R_3SiNH_2 with R'_3Al in hexane at reflux afford dimeric aluminum silylamides $[R'_2AlNHSiR_3]_2$ [R_3 = Me_3, Et_3, Ph_3 or $(t\text{-Bu})_2H$; R′ = Me or (i-Bu)][75]. A distorted-tetrahedral geometry at nitrogen of the resultant complexes places the silyl groups nearly in the plane of the Al_2N_2 ring. The degree of distortion depends on the steric bulk of the silyl groups by following the order shown in entry 62 in Table 1.

In metal complexes, good correlation exists between the size of the silyl ligand and the metal−Si bond distance. For example, the Mo−Si bond distances are 2.538(2), 2.560(1) and 2.604(1) Å for $(Cp)_2Mo(H)(SiMe_2H)$, $(MeCp)_2Mo(H)(SiMe_3)$ and $(MeCp)_2Mo(H)[Si(Bu\text{-}t)_2H]$, respectively (cf. entry 63 in Table 1)[76]. Complexes containing a bulky silyl ligand [i.e. $(t\text{-Bu})_2HSi$] exhibit hindered rotation around the metal−Si bond in solution as determined by variable temperature ^1H NMR spectroscopy. Moreover, the steric bulk of the silyl groups in (ferrocenylacyl)silanes, (η^5-C_5H_5) Fe (η^5-C_5H_4) $COSiR_3$, is in the order of $PhMe_2Si = Ph_2MeSi < Me_3Si < Ph_3Si$ (entry 64)[77].

For the η^5-indenyl complexes (η^5-C_9H_7)$Fe(CO)_2(Si_nMe_{(2n+1)})$, the Fe−Si bond length increases regularly in the order of increasing silyl group bulk as the sequence listed in entry 65 of Table 1[78]. Moreover, the readily accessible ligands $-N(SiMe_2Ph)_2$ and $-N(SiMePh_2)_2$ are capable of stabilizing two coordinations in the solid state for the metals Mn, Fe and Co[248].

Comparison of two extremely bulky groups[249,250], [i.e. $(Me_3Si)_3Si$ and $(Me_3Si)_3C$], is made on the basis of their *A* values. The structures of enols $Mes_2C{=}C(OH)R$ [Mes = 2, 4, 6-trimethylphenyl; R = Me_3Si, $(Me_3Si)_3Si$, $(Me_3Si)_3C$ and *tert*-Bu] and two-ring flip barriers have been calculated by the MM2* force field[79]. The *A* values are estimated as 2.5, 4.89, 13.3 and 4.9 kcal mol^{-1} for the Me_3Si, $(Me_3Si)_3Si$, $(Me_3Si)_3C$ and *tert*-Bu groups, respectively. Thus the $(Me_3Si)_3Si$ and the *tert*-Bu groups have similar effective size; the $(Me_3Si)_3C$ group is significantly larger (entry 66 of Table 1).

In related studies, characteristic structural parameters including dihedral angles of $X_3{-}Y{-}Y{-}X_3$ as well as bond distances between Y−Y and Y−X are determined for molecules containing bulky half-shell substituent groups. The molecules include $(Me_3Si)_3Si{-}Si(SiMe_3)_3$[251,252], $(Me_3C)_3Si{-}Si(CMe_3)_3$[253], *p*-$(Me_3Si)_3C{-}C_6H_4{-}C(SiMe_3)_3$[254] and $(Me_3Si)_3C{-}C{\equiv}C{-}C(SiMe_3)_3$[254]. They often adopt staggered conformations of their sterically congested $(Me_3X)_3Y$-half shells along substituent axes of C_3-symmetry at different distances Y−Y.

2. Stability, free energy of activation and reaction rates

Steric crowding among the Me_3Si groups in boraazatrane **199**, in contrast to the methyl analog **200**, leads to enantiomers sufficiently long-lived to be observed at room temperature on the NMR time scale[255]. The enantiomers racemize by a concerted mechanism rather than by the stepwise process found for silatranes[256]. Moreover, by increasing the bulk of R in compounds **201** to Me_3Si (when E = Si and Z = Me), the transannular bond is essentially broken[257].

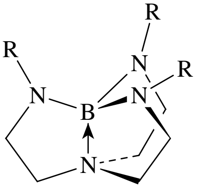

(199) R = Me_3Si
(200) R = Me

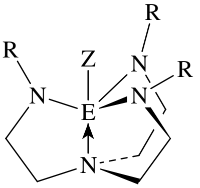

(201) E = Si, Ge, Sn, Ti, V
Z = NMe_2, N-(Bu-*t*)

On the other hand, an intramolecular reversible rotation of the two mesityl rings in 2,2-dimesityl-1-(trimethylsilyl)ethenol **(202)** occurs to give **203** (equation 83)[258]. The free energy of activation for the rotation ($\Delta G_c{}^{\ddagger}$) leading to the enantiomerization is

11.1 kcal mol^{-1}, which is intermediate between the $\Delta G_c{}^{\ddagger}$ values for the corresponding 1-isopropyl enol (10.4 kcal mol^{-1}) and 1-*t*-butyl enol (11.7 kcal mol^{-1}). Charton's υ values, proportional to the van der Waals radii, are 0.76, 1.24 and 1.40 for *i*-Pr, *t*-Bu and Me_3Si groups, respectively[259]. According to Charton's values, the Me_3Si group occupies more space than the *t*-Bu group. The lower rotational barrier for 2,2-dimesityl-1-(trimethylsilyl)ethenol than for the corresponding 1-*t*-butyl enol may reflect small differences in the ground state geometry.

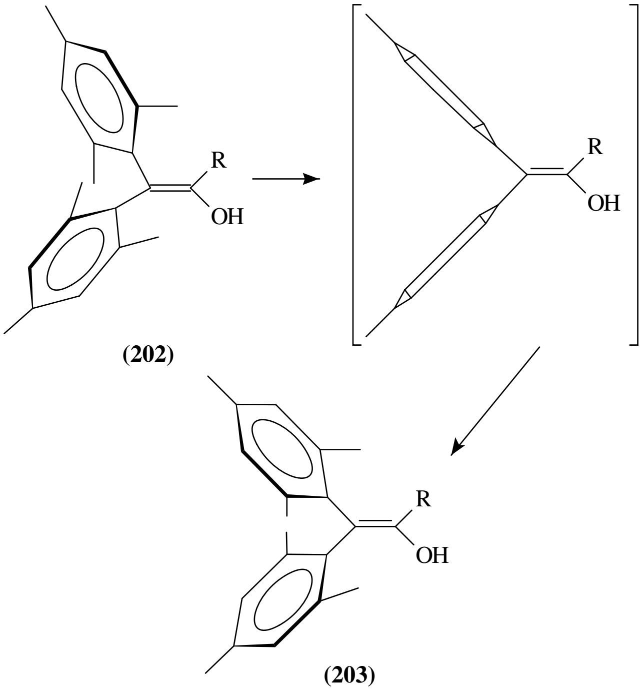

(202)

(203)

(83)

R	$\Delta G_c{}^{\ddagger}$ (kcal mol^{-1})	Charton's υ value
i-Pr	10.4	0.76
Me_3Si	11.1	1.40
t-Bu	11.7	1.24

Rates of decay for (*p*-methoxybenzyl)trialkylsilane cation radicals, which bear a Me_3Si, Et_3Si or $(i\text{-Pr})_3Si$ group, are determined in acetonitrile as 2.3×10^6, 1.3×10^6 and $< 4 \times 10^3$ s^{-1}, respectively[80]. Thus the lifetimes of silane cation radicals increase as the size of the silyl group increases, as shown in entry 67 of Table 1.

Furthermore, the relative steric bulk of the hindered bases 2,4,6-tris[bis(trimethylsilyl)methyl]phenyllithium and 2,4,6-tri-*tert*-butylphenyllithium is determined by investigating the kinetic versus thermodynamic enolate formation from benzyl methyl ketones[260]. The results indicate that the 2,4,6-$[(Me_3Si)_2CH]_3C_6H_2$ (Tb) group is bulkier than the 2,4,6-$(t\text{-Bu})_3C_6H_2$ (Bp) group[261]. The high steric demand of the Tb group is used in the synthesis of extremely hindered and kinetically stable *cis*- and *trans*-disilenes

Tb(Mes)Si=Si(Mes)Tb (Mes = mesityl) by reductive coupling of Tb(Mes)SiBr$_2$ with lithium naphthalenide[262].

The steric size of the substituent R on silenes (Me$_3$Si)RSi=C(OSiMe$_3$)R′ influences their photochemical reactivity[263]. When R = Me$_3$Si or Me, head-to-head dimerization occurs to give 1,2-disilacyclobutanes. When R = Ph or bulky *t*-Bu, the silenes are stable. Although the Me$_3$Si group is also bulky, the long Si−C single bond reduces markedly the effective steric hindrance.

3. Migratory aptitudes of organic groups

A relative ranking of the migratory aptitudes of the σ-bound ligands is established in the study of the regioselective insertions of CO into the W−C σ bonds of complexes (η^5-C$_5$Me$_5$)W(NO)(R)(R′) (R,R′ = alkyl, aryl). The trend, Me < Ph < *o*-toluenesulfonyl < CH$_2$SiMe$_3$ < CH$_2$CMe$_3$, primarily reflects steric effects[264]. This trend agrees with the results found from kinetic studies on carbonylation of Cp$_3$ThR complexes to form η^2-acyl products. The rate increases in the order PhCH$_2$ < Me < CH$_2$SiMe$_3$ $\ll$ *n*-Bu < CH$_2$CMe$_3$ $\ll$ *s*-Bu < *i*-Pr[265]. A similar trend is also noted for the insertion rates of CpFe(CO)$_2$R in DMSO solution to form η^1-acyls. The trend follows the order Me < Et < *n*-Bu < CH$_2$SiMe$_3$ < *i*-Pr < *s*-Bu < CH$_2$CMe$_3$ $\ll$ CH(SiMe$_3$)$_2$[266].

B. Change of Spectroscopic Properties

1. ^{1}H, ^{13}C, ^{19}F and ^{29}Si NMR spectroscopy

In the ^{1}H NMR spectra of compound **40**, the signals are broad for the *ortho*-CH$_3$ of two mesityl groups. This is because of the hindered rotation of the mesityl groups caused by the silyl groups[81]. The degree of broadening increases in the order **40a** < **40b** < **40c** with an increase in the bulk of the silyl groups by following the order shown in entry 68 of Table 1.

As the silyl group becomes larger (see entry 69 of Table 1) in 2-methoxy-3-silylhex-4-en-1-oic acids, the coupling constant $^3J_{2,3}$ for the 2,3-*syn* diastereomer increases (7.57, 8.00 and 9.80 Hz)[82]. Yet the $^3J_{2,3}$ values of 2,3-*anti* diastereomers decrease (3.17, 3.10 and 2.40 Hz).

In a different system, 1-(trimethylsilyl)cycloocta-1,5-diene forms complexes with Ag(I), Rh(I), Pd(II) and Pt(II), in which the metals are pushed away from the Me$_3$Si group[267]. The distortion in their structures, in comparison with the near-symmetrical structures of the corresponding 1,5-cyclooctadiene complexes, changes the characteristics of their ^{1}H and ^{13}C NMR spectra.

Substituent contributions to the exchange barrier are determined by ^{19}F NMR for silicates RR′SiF$_3{}^-$, which are prepared as their K$^+$-18-crown-6 salts[268]. Their free energies of activation range from 9.3–14 kcal mol^{-1}. The steric comparison can be made in two series: Ph$_2$SiF$_3{}^-$ < Ph(2,6-Me$_2$C$_6$H$_3$)SiF$_3{}^-$ < (2,6-Me$_2$C$_6$H$_3$)$_2$SiF$_3{}^-$ and Ph(2,6-Me$_2$C$_6$H$_3$)SiF$_3{}^-$ < (2-MeC$_6$H$_4$)(2,6-Me$_2$C$_6$H$_3$)SiF$_3{}^-$ < (2,6-Me$_2$C$_6$H$_3$)$_2$SiF$_3{}^-$. Moreover, the steric effect resulting from a silyl group can be used for structure determination of hydroxy steroids by means of ^{29}Si NMR spectroscopy[269].

2. X-ray crystallography

Results from X-ray crystallography analyses indicate that the Si−Si bond distance is 2.539 Å in di-thexyl-substituted disilane **204** and 2.476 Å in di-*tert*-butyl disilane

205[270]. These values are much larger than the typical Si–Si bond length of 2.34 Å[271]. These distances result from mutual repulsions between the bulky thexyl, *tert*-butyl, and diethylamino groups. In addition, the bulk of the (*t*-Bu)Me_2Si group severely restricts its bending back in icosahedral *closo*-dicarbaborane 1-phenyl-2-(*t*-butyldimethylsilyl)-1,2-dicarba-*closo*-dodecaborane (12), $C_{14}H_{30}B_{10}Si$. In consequence, some deformation of the cage has resulted[272].

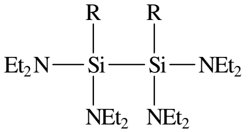

$$Et_2N{-}\overset{R}{\underset{NEt_2}{Si}}{-}\overset{R}{\underset{NEt_2}{Si}}{-}NEt_2$$

R =
(204) CMe_2(Pr-*i*)
(205) *t*-Bu

On the other hand, a series of tetrasilylethylenes **206–210** is prepared and their structures are studied spectroscopically. Nonplanar distortion (i.e., twisting) is the main factor for relieving the severely crowded environment for **207**[273] and **208**[274], but slight pyramidalization starts to occur for **209**[275] in addition to twisting. Compound **210**[276] is the most twisted and congested olefin and **206** is an untwisted tetrasilylethylene.

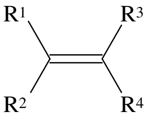

(206) $R^1 = R^2 = R^3 = R^4 = HMe_2Si$
(207) $R^1 = R^2 = R^3 = R^4 = Me_3Si$
(208) $R^1 = R^2 = Me_3Si$; $R^3 = R^4 =$ (*t*-Bu)Me_2Si
(209) $R^1 = R^3 = Me_3Si$; $R^2 = R^4 =$ (*t*-Bu)Me_2Si
(210) $R^1 = Me_3Si$; $R^2 = R^3 = R^4 =$ (*t*-Bu)Me_2Si

VIII. CONCLUSION

Triorganosilyl groups can control stereochemistry in organic reactions through a steric, an electronic or a stereoelectronic effect. More than one of these effects may exist simultaneously in some chemical processes. The trend listed in Section II could provide chemists with a clear guideline, yet definitive order, to choose a silyl group with appropriate size in control of reactions based on the steric effect.

IX. ACKNOWLEDGMENT

The authors wish to thank Mr. Chun-Chieh Lin and Miss Shu-Mei Liao for their assistance in the preparation of the manuscript.

X. REFERENCES

1. J. R. Hwu and J. M. Wetzel, *J. Org. Chem.*, **50**, 3946 (1985).
2. J. R. Hwu and N. Wang, *Chem. Rev.*, **89**, 1599 (1989).
3. J. R. Hwu, K. P. Khoudary and S.-C. Tsay, *J. Organomet. Chem.*, **399**, C-13 (1990).
4. T. H. Chan and D. Wang, *Chem. Rev.*, **92**, 995 (1992).
5. T. H. Chan and D. Wang, *Chem. Rev.*, **95**, 1279 (1995).
6. I. Fleming, *Chemtracts: Organic Chemistry*, **9**, 1 (1996).
7. P. C. B. Page, S. S. Klair and S. Rosenthal, *Chem. Soc. Rev.*, **19**, 147 (1990).
8. P. F. Cirillo and J. S. Panek, *Org. Prep. Proc. Int.*, **24**, 555 (1992).
9. C. Rücker, *Chem. Rev.*, **95**, 1009 (1995).
10. M. G. Steinmetz, *Chem. Rev.*, **95**, 1527 (1995).
11. C. Eisenberg and P. Knochel, *J. Org. Chem.*, **59**, 3760 (1994).
12. X. Chen, E. R. Hortelano, E. L. Eliel and S. V. Frye, *J. Am. Chem. Soc.*, **114**, 1778 (1992).
13. X. Chen, E. R. Hortelano, E. L. Eliel and S. V. Frye, *J. Am. Chem. Soc.*, **112**, 6130 (1990).

14. A. Yanagisawa, K. Yasue and H. Yamamoto, *Synlett*, 686 (1993).
15. A. P. Davis and S. J. Plunkett, *J. Chem. Soc., Chem. Commun.*, 2173 (1995).
16. R. J. Linderman and T. V. Anklekar, *J. Org. Chem.*, **57**, 5078 (1992).
17. J. S. Panek, A. Prock, K. Eriks and W. P. Giering, *Organometallics*, **9**, 2175 (1990).
18. J. R. Hwu, B.-L. Chen and S.-S. Shiao, *J. Org. Chem.*, **60**, 2448 (1995).
19. T. H. Chan and K. Koumaglo, *J. Organomet. Chem.*, **285**, 109 (1985).
20. J. R. Hwu, C. N. Chen and S.-S. Shiao, *J. Org. Chem.*, **60**, 856 (1995).
21. B. M. Trost and A. Indolese, *J. Am. Chem. Soc.*, **115**, 4361 (1993).
22. S. H. Kang and S. B. Lee, *Tetrahedron Lett.*, **34**, 7579 (1993).
23. F. Bennett and D. W. Knight, *Tetrahedron Lett.*, **29**, 4865 (1988).
24. F. Bennett, D. W. Knight and G. Fenton, *J. Chem. Soc., Perkin Trans. 1*, 133 (1991).
25. F. Bennett, D. W. Knight and G. Fenton, *J. Chem. Soc., Perkin Trans. 1*, 1543 (1991).
26. G. Adiwidjaja, H. Flörke, A. Kirschning and E. Schaumann, *Justus Liebigs Ann. Chem.*, 501 (1995).
27. M. Suginome, Y. Yamamoto, K. Fujii and Y. Ito, *J. Am. Chem. Soc.,* **117**, 9608 (1995).
28. G. Maas, M. Gimmy and M. Alt, *Organometallics*, **11**, 3813 (1992).
29. E. J. Corey and K. Y. Yi, *Tetrahedron Lett.*, **33**, 2289 (1992).
30. S.-I. Kawahara, T. Wada and M. Sekine, *Tetrahedron Lett.*, **37**, 509 (1996).
31. J. Feixas, A. Capdevila and A. Guerrero, *Tetrahedron*, **50**, 8539 (1994).
32. J. F. Cormier, M. B. Isaac and L.-F. Chen, *Tetrahedron Lett.*, **34**, 243 (1993).
33. A. S. Pilcher and P. DeShong, *J. Org. Chem.*, **58**, 5130 (1993).
34. A. S. Pilcher, D. K. Hill, S. J. Shimshock, R. E. Waltermire and P. DeShong, *J. Org. Chem.*, **57**, 2492 (1992).
35. C. Prakash, S. Saleh and I. A. Blair, *Tetrahedron Lett.*, **30**, 19 (1989).
36. S. E. Chapman and R. Taylor, *J. Chem. Soc., Perkin Trans. 2*, 1119 (1991).
37. T. K. Sarkar, B. K. Ghorai, S. K. Nandy and B. Mukherjee, *Tetrahedron Lett.*, **35**, 6903 (1994).
38. J. R. Hwu and J. M. Wetzel, *J. Org. Chem.*, **57**, 922 (1992).
39. J. A. Soderquist, J. C. Colberg and L. D. Valle, *J. Am. Chem. Soc.*, **111**, 4873 (1989).
40. M. M. Doyle, W. R. Jackson and P. Perlmutter, *Aust. J. Chem.*, **42**, 1907 (1989).
41. M. Fujita and T. Hiyama, *J. Org. Chem.*, **53**, 5405 (1988).
42. R. Munschauer and G. Maas, *Chem. Ber.*, **125**, 1227 (1992).
43. R. Hoffmann and R. Brückner, *Chem. Ber.*, **125**, 1471 (1992).
44. S. Marumoto and I. Kuwajima, *J. Am. Chem. Soc.*, **115**, 9021 (1993).
45. M. S. Loft, D. A. Widdowson and T. J. Mowlem, *Synlett*, 135 (1992).
46. J. S. Panek and P. F. Cirillo, *J. Am. Chem. Soc.*, **112**, 4873 (1990).
47. K. Bratt, A. Garavelas, P. Perlmutter and G. Westman, *J. Org. Chem.*, **61**, 2109 (1996).
48. W. H. Bunnelle and T. A. Isbell, *J. Org. Chem.*, **57**, 729 (1992).
49. L. Spialter, L. Pazdernik, S. Bernstein, W. A. Swansiger, G. R. Buell and M. E. Freeburger, *J. Am. Chem. Soc.*, **93**, 5682 (1971).
50. Y. A. Aleksandrov and B. I. Tarunin, *Dokl. Akad. Nauk SSSR, Ser. Khim.*, **212**, 869 (1973); *Chem. Abstr.*, **80**, 2930d (1974).
51. A. R. Bassindale, R. J. Ellis and P. G. Taylor, *Tetrahedron Lett.*, **25**, 2705 (1984).
52. A. G. M. Barrett, J. M. Hill, E. M. Wallace and J. A. Flygare, *Synlett*, 764 (1991).
53. A. G. M. Barrett and J. A. Flygare, *J. Org. Chem.*, **56**, 638 (1991).
54. Cf B. Santiago, C. Lopez and J. A. Soderquist, *Tetrahedron Lett.*, **32**, 3457 (1991).
55. A. Bongini, M. Panunzio, E. Bandini, G. Martelli and G. Spunta, *Synlett*, 461 (1995).
56. J. Ollivier and J. Salaün, *Synlett*, 949 (1994).
57. K. Käppler, U. Scheim, K. Rühlmann and K. Porzel, *J. Organomet. Chem.*, **441**, 15 (1992).
58. L. Agrofoglio, R. Condom and R. Guedj, *Tetrahedron Lett.*, **33**, 5503 (1992).
59. T. Akiyama, K. Ishikawa and S. Ozaki, *Chem. Lett.*, 627 (1994).
60. B. Török, K. Felföldi, Á. Molnár and M. Bartók, *J. Organomet. Chem.*, **460**, 111 (1993).
61. M. G. Voronkov, V. B. Pukhnarevich, L. I. Kopylova, V. A. Nestunovich, E. O. Tsetlina, B. A. Trofimov, I. Pola and V. Khvalovskii, *Dokl. Akad. Nauk SSSR, Ser. Khim.*, **227**, 91 (1976); *Chem. Abstr.*, **85**, 5012v (1976).
62. C. C. Mak and K. S. Chan, *J. Chem. Soc., Perkin Trans. 1*, 2143 (1993).
63. P. Wang and J. Adams, *J. Am. Chem. Soc.*, **116**, 3296 (1994).
64. Y. Yamakado, M. Ishiguro, N. Ikeda and H. Yamamoto, *J. Am. Chem. Soc.*, **103**, 5568 (1981).
65. J. C. Ellington Jr. and E. M. Arnett, *J. Am. Chem. Soc.*, **110**, 7778 (1988).

66. N. Shimizu, E. Osajima and Y. Tsuno, *Bull. Chem. Soc. Jpn.*, **64**, 1145 (1991).
67. E. Akerman, *Acta Chem. Scand.*, **10**, 298 (1956).
68. E. Akerman, *Acta Chem. Scand.*, **11**, 373 (1957).
69. N. Shimizu, N. Takesue, A. Yamamoto, T. Tsutsumi, S. Yasuhara and Y. Tsuno, *Chem. Lett.*, 1263 (1992).
70. N. Shimizu, N. Takesue, S. Yasuhara and T. Inazu, *Chem. Lett.*, 1807 (1993).
71. L. H. Sommer, *Stereochemistry, Mechanism, and Silicon*, McGraw-Hill, New York, 1965, p. 142.
72. J. E. Baines and C. Eaborn, *J. Chem. Soc.*, 1436 (1956).
73. O. W. Steward and O. R. Pierce, *J. Am. Chem. Soc.*, **83**, 4932 (1961).
74. W. P. Barie Jr., Ph.D. Dissertation, Pennsylvania State University, 1954.
75. D. M. Choquette, M. J. Timm, J. L. Hobbs, M. M. Rahim, K. J. Ahmed and R. P. Planalp, *Organometallics*, **11**, 529 (1992).
76. T. S. Koloski, D. C. Pestana, P. J. Carroll and D. H. Berry, *Organometallics*, **13**, 489 (1994).
77. H. K. Sharma, S. P. Vincenti, R. Vicari, F. Cervantes and K. H. Pannell, *Organometallics*, **9**, 2109 (1990).
78. K. H. Pannell, S.-H. Lin, R. N. Kapoor, F. Cervantes-Lee, M. Pinon and L. Parkanyi, *Organometallics*, **9**, 2454 (1990).
79. J. Frey, E. Schottland, Z. Rappoport, O. Bravo-Zhivotovskii, M. Nakash, M. Botoshansky, M. Kaftory and Y. Apeloig, *J. Chem. Soc., Perkin Trans. 2*, 2555 (1994).
80. J. P. Dinnocenzo, S. Farid, J. L. Goodman, I. R. Gould, W. P. Todd and S. L. Mattes, *J. Am. Chem. Soc.*, **111**, 8973 (1989).
81. T. Kawashima, N. Yamashita and R. Okazaki, *Chem. Lett.*, 1107 (1995).
82. M. A. Sparks and J. S. Panek, *J. Org. Chem.*, **56**, 3431 (1991).
83. H. Yoda, K. Shirakawa and K. Takabe, *Tetrahedron Lett.*, **32**, 3401 (1991).
84. M. Carda, F. González, S. Rodríguez and J. A. Marco, *Tetrahedron: Asymmetry*, **3**, 1511 (1992).
85. P. A. Jacobi and G. Cai, *Tetrahedron Lett.*, **32**, 1765 (1991).
86. P. A. Jacobi and G. Cai, *Heterocycles*, **35**, 1103 (1993).
87. M. Shimizu and K. Mikami, *J. Org. Chem.*, **57**, 6105 (1992).
88. N. Iwasawa and M. Iwamoto, *Chem Lett.*, 1257 (1993).
89. Y. Horiguchi, I. Suehiro, A. Sasaki and I. Kuwajima, *Tetrahedron Lett.*, **34**, 6077 (1993).
90. H. Yoda, H. Kitayama, W. Yamada, T. Katagiri and K. Takabe, *Tetrahedron: Asymmetry*, **4**, 1451 (1993).
91. D. C. Chauret and J. M. Chong, *Tetrahedron Lett.*, **34**, 3695 (1993).
92. K. Araki, and J. T. Welch, *Tetrahedron Lett.*, **34**, 2251 (1993).
93. T. Nakamura, N. Waizumi, Y. Horiguchi and I. Kuwajima, *Tetrahedron Lett.*, **35**, 7813 (1994).
94. M. Okabe, R.-C. Sun and S. Wolff, *Tetrahedron Lett.*, **35**, 2865 (1994).
95. M. A. Brook and C. Henry, *Tetrahedron*, **52**, 861 (1996).
96. E. L. Eliel and H. Satici, *J. Org. Chem.*, **59**, 688 (1994).
97. K. Ishihara, H. Yamamoto and C. H. Heathcock, *Tetrahedron Lett.*, **30**, 1825 (1989).
98. R. F. Cunico and C. P. Kuan, *J. Org. Chem.*, **55**, 4634 (1990).
99. F. K. Cartledge, *Organometallics*, **2**, 425 (1983).
100. For the definition of the cone angle sec C. A. Tolman, *Chem. Rev.*, **77**, 313 (1977).
101. H. Mayr and G. Hagen, *J. Chem. Soc., Chem. Commun.*, 91 (1989).
102. A. Vulpetti, A. Bernardi, C. Gennari, J. M. Goodman and I. Paterson, *Tetrahedron*, **49**, 685 (1993).
103. C. Panyachotipun and E. R. Thornton, *Tetrahedron Lett.*, **31**, 6001 (1990).
104. A. Choudhury and E. R. Thornton, *Tetrahedron Lett.*, **34**, 2221 (1993).
105. C. Mukai, S. Hashizume, K. Nagami and M. Hanaoka, *Chem. Pharm. Bull.*, **38**, 1509 (1990).
106. C. Siegel and E. R. Thornton, *J. Am. Chem. Soc.*, **111**, 5722 (1989).
107. D. Schinzer, *Synthesis*, 179 (1989).
108. K. Maruoka, J. Sato and H. Yamamoto, *J. Am. Chem. Soc.*, **114**, 4422 (1992).
109. A. Yanagisawa, S. Habaue and H. Yamamoto, *J. Org. Chem.*, **54**, 5198 (1989).
110. M. Suzuki, Y. Morita and R. Noyori, *J. Org. Chem.*, **55**, 441 (1990).
111. A. Yanagisawa, S. Habaue and H. Yamamoto, *Tetrahedron*, **48**, 1969 (1992).
112. T. Bach and K. Jödicke, *Chem. Ber.*, **126**, 2457 (1993).
113. C. Palomo, J. M. Aizpurua, R. Urchegui and M. Iturburu, *J. Org. Chem.*, **57**, 1571 (1992).
114. S. M. Sieburth and L. Fensterbank, *J. Org. Chem.*, **57**, 5279 (1992).
115. E. J. Bures and B. A. Keay, *Tetrahedron Lett.*, **29**, 1247 (1988).

116. I. Fleming, J. Dunoguès and R. Smithers, in *Organic Reactions*, Vol. 37 (Ed. A. S. Kende), Chap. 2, Wiley, New York, 1989.
117. S. J. Shimshock, R. E. Waltermire and P. DeShong, *J. Am. Chem. Soc.*, **113**, 8791 (1991).
118. M. S. Shekhani, K. M. Khan, K. Mahmood, P. M. Shah and S. Malik, *Tetrahedron Lett.*, **31**, 1669 (1990).
119. S. J. Monger, D. M. Parry and S. M. Roberts, *J. Chem. Soc., Chem. Commun.*, 381 (1989).
120. H. Shoda, T. Nakamura, K. Tanino and I. Kuwajima, *Tetrahedron Lett.*, **34**, 6281 (1993).
121. W. Adam and M. Richter, *Chem. Ber.*, **125**, 243 (1992).
122. W. Adam and P. Klug, *J. Org. Chem.*, **58**, 3416 (1993).
123. W. Kitching, D. Doddrell and J. B. Grutzner, *J. Organomet. Chem.*, **107**, C-5 (1976).
124. J. R. Hwu, J. M. Wetzel, J. S. Lee and R. J. Butcher, *J. Organomet. Chem.*, **453**, 21 (1993).
125. K. K. Wang, Y. G. Gu and C. Liu, *J. Am. Chem. Soc.*, **112**, 4424 (1990).
126. R. Takeuchi and M. Sugiura, *J. Chem. Soc., Perkin Trans. 1*, 1031 (1993).
127. M. M. Doyle, W. R. Jackson and P. Perlmutter, *Tetrahedron Lett.*, **30**, 233 (1989).
128. N. Fitzmaurice, W. R. Jackson and P. Perlmutter, *J. Organomet. Chem.*, **285**, 375 (1985).
129. F. Le Bideau, F. Gilloir, Y. Nilsson, C. Aubert and M. Malacria, *Tetrahedron Lett.*, **36**, 1641 (1995).
130. R. Hoffmann and R. Brückner, *Chem. Ber.* **125**, 2731 (1992).
131. M. Lautens, P. H. M. Delanghe, J. B. Goh and C. H. Zhang, *J. Org. Chem.*, **60**, 4213 (1995).
132. M. Lautens, P. H. M. Delanghe, J. B. Goh and C. H. Zhang, *J. Org. Chem.*, **57**, 3270 (1992).
133. G. Beese and B. A. Keay, *Synlett*, 33 (1991).
134. Cf. E. J. Bures and B. A. Keay, *Tetrahedron Lett.*, **28**, 5965 (1987).
135. Cf. K. D. Kim and P. A. Magriotis, *Tetrahedron Lett.*, **31**, 6137 (1990).
136. A. I. Al-Mansour, M. A. M. R. Al-Gurashi, C. Eaborn, F. A. Fattah and P. D. Lickiss, *J. Organomet. Chem.*, **393**, 27 (1990).
137. E. Vedejs and C. K. McClure, *J. Am. Chem. Soc.*, **108**, 1094 (1986).
138. I. Fleming, A. K. Sarkar and A. P. Thomas, *J. Chem. Soc., Chem. Commun.*, 157 (1987).
139. I. Fleming and N. J. Lawrence, *Tetrahedron Lett.*, **29**, 2077 (1988).
140. D. A. Evans and S. W. Kaldor, *J. Org. Chem.*, **55**, 1698 (1990).
141. P. F. Hudrlik and A. M. Hudrlik, in *Advances in Silicon Chemistry*, Vol. 2 (Ed. G. L. Larson), JAI Press, London, 1993, pp. 1–89.
142. T. Cohen, J. P. Sherbine, J. R. Matz, R. R. Hutchins, B. M. McHenry and P. R. Willey, *J. Am. Chem. Soc.*, **106**, 3245 (1984).
143. D. J. Ager, *J. Org. Chem.*, **49**, 168 (1984).
144. A. R. Bassindale, R. J. Ellis, J. C.-Y. Lau and P. G. Taylor, *J. Chem. Soc., Chem. Commun.*, 98 (1986).
145. D. Bell, E. A. Crowe, N. J. Dixon, G. R. Geen, I. S. Mann and M. R. Shipton, *Tetrahedron*, **50**, 6643 (1994).
146. N. Y. Grigorieva, O. A. Pinsker and A. M. Moiseenkov, *Mendeleev Commun.*, 129 (1994).
147. K. Takenaka, T. Hattori, A. Hirao and S. Nakahama, *Macromolecules*, **22**, 1563 (1989).
148. P. Durand, A. Margaillan, M. Camail and J. L. Vernet, *Polymer*, **35**, 4392 (1994).
149. J. D. Buynak, J. B. Strickland, T. Hurd and A. Phan, *J. Chem. Soc., Chem. Commun.*, 89 (1989).
150. Y. Ukaji, K. Sada and K. Inomata, *Chem. Lett.*, 1227 (1993).
151. K. Käppler, A. Porzel, U. Scheim and K. Rühlmann, *J. Organomet. Chem.*, **402**, 155 (1991).
152. M. Nakada, Y. Urano, S. Kobayashi and M. Ohno, *J. Am. Chem. Soc.*, **110**, 4826 (1988).
153. P. F. Cirillo and J. S. Panek, *J. Org. Chem.*, **55**, 6071 (1990).
154. G. L. Larson, J. A. Soderquist and M. R. Claudio, *Synth. Commun.*, **20**, 1095 (1990).
155. M. Asaoka, K. Obuchi and H. Takei, *Tetrahedron*, **50**, 655 (1994).
156. M. Asaoka, K. Shima, N. Fujii and H. Takei, *Tetrahedron*, **44**, 4757 (1988).
157. E. Bandini, G. Martelli, G. Spunta and M. Panunzio, *Tetrahedron: Asymmetry*, **6**, 2127 (1995).
158. S. Hünig and M. Schäfer, *Chem. Ber.*, **126**, 177 (1993).
159. S. Fioravanti, M. A. Loreto, L. Pellacani and P. A. Tardella, *Tetrahedron: Asymmetry*, **1**, 931 (1990).
160. I. Fleming and J. D. Kilburn, *J. Chem. Soc., Perkin Trans. 1*, 3295 (1992).
161. I. Fleming, *J. Chem. Soc., Perkin Trans. 1*, 3363 (1992).
162. A. Ricci, A. Guerrini, G. Seconi, A. Mordini, T. Constantieux, J.-P. Picard, J.-M. Aizpurua and C. Palomo, *Synlett*, 955 (1994).
163. J. P. Gilday, J. C. Gallucci and L. A. Paquette, *J. Org. Chem.*, **54**, 1399 (1989).

164. R. P. Short and S. Masamune, *J. Am. Chem. Soc.*, **111**, 1892 (1989).
165. S. H. Yeon, J. S. Han, E. Hong, Y. Do and I. N. Jung, *J. Organomet. Chem.*, **499**, 159 (1995).
166. H. Shinokubo, K. Oshima and K. Utimoto, *Tetrahedron Lett.*, **34**, 4985 (1993).
167. D. Craig and V. R. N. Munasinghe, *J. Chem. Soc., Chem. Commun.*, 901 (1993).
168. G. Haaima, M.-J. Lynch, A. Routledge and R. T. Weavers, *Tetrahedron*, **49**, 4229 (1993).
169. M. Asaoka, K. Takenouchi and H. Takei, *Chem. Lett.*, 1225 (1988).
170. M. Koreeda and D. C. Visger, *Tetrahedron Lett.*, **33**, 6603 (1992).
171. N. K. N. Yee and R. M. Coates, *J. Org. Chem.*, **57**, 4598 (1992).
172. E. E. van Tamelen, *Acc. Chem. Res.*, **8**, 152 (1975).
173. E. E. van Tamelen and J. R. Hwu, *J. Am. Chem. Soc.*, **105**, 2490 (1983).
174. J. R. Hwu and E. J. Leopold, *J. Chem. Soc., Chem. Commun.*, 721 (1984).
175. A. J. Blake, M. Harding and J. T. Sharp, *J. Chem. Soc., Perkin Trans. 1*, 3149 (1994).
176. S. Yamazaki, H. Fujitsuka and S. Yamabe, *J. Org. Chem.*, **57**, 5610 (1992).
177. D. J. Hlasta and J. H. Ackerman, *J. Org. Chem.*, **59**, 6184 (1994).
178. A. Verloop, W. Hoogenstraaten and J. Tipker, in *Drug Design*, Vol. 7 (Ed. E. J. Ariens), Chap. 4, Academic Press, New York, 1976.
179. A. Padwa and M. W. Wannamaker, *Tetrahedron*, **46**, 1145 (1990).
180. B. M. Trost and M. Acemoglu, *Tetrahedron Lett.*, **30**, 1495 (1989).
181. B. M. Trost and R. C. Holcomb, *Tetrahedron Lett.*, **30**, 7157 (1989).
182. For a related intermolecular reaction, see L. Strekowski, S. Kong and M. A. Battiste, *J. Org. Chem.*, **53**, 901 (1988).
183. H. J. Reich, E. K. Eisenhart, W. L. Whipple and M. J. Kelly, *J. Am. Chem. Soc.*, **110**, 6432 (1988).
184. S. R. Wilson and M. J. Di Grandi, *J. Org. Chem.*, **56**, 4766 (1991).
185. W. Adam and M. Prein, *Tetrahedron Lett.*, **35**, 4331 (1994).
186. M. Ohno, S. Shimizu and S. Eguchi, *Tetrahedron Lett.*, **31**, 4613 (1990).
187. H. C. Kolb, S. V. Ley, A. M. Z. Slawin and D. J. Williams, *J. Chem. Soc., Perkin Trans. 1*, 2735 (1992).
188. M. Lautens and P. H. M. Delanghe, *J. Org. Chem.*, **57**, 798 (1992).
189. K. Nakatani, T. Izawa and S. Isoe, *J. Org. Chem.*, **59**, 5961 (1994).
190. K. Mikami, T.-P. Loh and T. Nakai, *J. Am. Chem. Soc.*, **112**, 6737 (1990).
191. K. Tanino, H. Shoda, T. Nakamura and I. Kuwajima, *Tetrahedron Lett.*, **33**, 1337 (1992).
192. K. Tanino, T. Nakamura and I. Kuwajima, *Tetrahedron Lett.*, **31**, 2165 (1990).
193. R. F. W. Jackson, S. P. Standen, W. Clegg and A. McCamley, *Tetrahedron Lett.*, **33**, 6197 (1992).
194. A. B. Bueno, M. C. Carreño and J. L. G. Ruano, *Tetrahedron Lett.*, **34**, 5007 (1993).
195. D. P. Rotella, *Tetrahedron Lett.*, **30**, 1913 (1989).
196. K. Suzuki, M. Miyazawa, M. Shimazaki and G.-I. Tsuchihashi, *Tetrahedron*, **44**, 4061 (1988).
197. W. Kirmse and F. Söllenböhmer, *J. Chem. Soc., Chem. Commun.*, 774 (1989).
198. P. G. Andersson, *J. Org. Chem.*, **61**, 4154 (1996).
199. M. Lautens, *Pure Appl. Chem.*, **64**, 1873 (1992).
200. D. Enders and S. Nakai, *Helv. Chim. Acta*, **73**, 1833 (1990).
201. M. Lautens, C. H. Zhang and C. M. Crudden, *Angew. Chem., Int. Ed. Engl.*, **31**, 232 (1992).
202. M. Lautens, C. H. Zhang, B. J. Goh, C. M. Crudden and M. J. A. Johnson, *J. Org. Chem.*, **59**, 6208 (1994).
203. S. Yu and B. A. Keay, *J. Chem. Soc., Perkin Trans. 1*, 2600 (1991).
204. D. W. Knight and A. P. Nott, *J. Chem. Soc., Perkin Trans. 1*, 1125 (1981).
205. B. B. Lohray and D. Enders, *Helv. Chim. Acta*, **72**, 980 (1989).
206. I. Fleming, *Pure Appl. Chem.*, **60**, 71 (1988).
207. B. F. Bonini, M. C. Franchini, M. Fochi, G. Mazzanti, A. Ricci, P. Zani and B. Zwanenburg, *J. Chem. Soc., Perkin Trans. 1*, 2039 (1995).
208. A. J. Y. Lan, R. O. Heucheroth and P. S. Mariano, *J. Am. Chem. Soc.*, **109**, 2738 (1987).
209. I.-S. Cho and P. S. Mariano, *J. Org. Chem.*, **53**, 1590 (1988).
210. J. E. Crawley, A. D. Kaye, G. Pattenden and S. M. Roberts, *J. Chem. Soc., Perkin Trans. 1*, 2001 (1993).
211. H. Inami, T. Ito, H. Urabe and F. Sato, *Tetrahedron Lett.*, **34**, 5919 (1993).
212. D. W. H. Rankin, in *Frontiers of Organosilicon Chemistry* (Eds. A. R. Bassindale and P. P. Gaspar), Royal Society of Chemistry, Cambridge, 1991, pp. 253–262.

213. W. Smadja, M. Zahouily and M. Malacria, *Tetrahedron Lett.*, **33**, 5511 (1992).
214. C. Chatgilialoglou, *Acc. Chem. Res.*, **25**, 180 (1992) and references cited therein.
215. M. Pereyre, J. P. Quintard and A. Rahm, *Tin in Organic Synthesis*, Butterworths, London, 1987.
216. F. L. van Delft, M. de Kort, G. A. van der Marel and J. H. van Boom, *J. Org. Chem.*, **61**, 1883 (1996).
217. E. J. Corey and Z. Chen, *Tetrahedron Lett.*, **35**, 8731 (1994).
218. R. A. N. C. Crump, I. Fleming, J. H. M. Hill, D. Parker, N. L. Reddy and D. Waterson, *J. Chem. Soc., Perkin Trans. 1*, 3277 (1992).
219. W. Amberg and D. Seebach, *Chem. Ber.*, **123**, 2439 (1990).
220. I. Fleming and N. J. Lawrence, *Tetrahedron Lett.*, **31**, 3645 (1990).
221. W. Oppolzer, R. J. Mills, W. Pachinger and T. Stevenson, *Helv. Chim. Acta*, **69**, 1542 (1986).
222. S. Kusuda, Y. Ueno, T. Hagiwara and T. Toru, *J. Chem. Soc., Perkin Trans. 1*, 1981 (1993).
223. I. Fleming and N. D. Kindon, *J. Chem. Soc., Chem. Commun.*, 1177 (1987).
224. M. R. Hale and A. H. Hoveyda, *J. Org. Chem.*, **59**, 4370 (1994).
225. C. Palomo, J. M. Aizpurua, M. Iturburu and R. Urchegui, *J. Org. Chem.*, **59**, 240 (1994).
226. B. H. Lipshutz, D. C. Reuter and E. L. Ellsworth, *J. Org. Chem.*, **54**, 4975 (1989).
227. V. Sum and T. P. Kee, *J. Chem. Soc., Perkin Trans. 1*, 2701 (1993).
228. J. S. Panek and M. Yang, *J. Am. Chem. Soc.*, **113**, 9868 (1991).
229. G. P. Brengel and A. I. Meyers, *J. Org. Chem.*, **61**, 3230 (1996).
230. F. Fariña, P. Noheda and M. C. Paredes, *J. Org. Chem.*, **58**, 7406 (1993).
231. B. Marciniec and H. Maciejewski, *J. Organomet. Chem.*, **454**, 45 (1993).
232. J. A. Robl and J. R. Hwu, *J. Org. Chem.*, **50**, 5913 (1985).
233. J. R. Hwu, J. A. Robl, N. Wang, D. A. Anderson, J. Ku and E. Chen, *J. Chem. Soc., Perkin Trans. 1*, 1823 (1989).
234. S. Florio and L. Troisi, *Tetrahedron Lett.*, **34**, 3141 (1993).
235. J. Woning and J. G. Verkade, *J. Am. Chem. Soc.*, **113**, 944 (1991).
236. M. P. Doyle and M. S. Shanklin, *Organometallics*, **13**, 1081 (1994).
237. Y. Obora, Y. Tsuji, M. Asayama and T. Kawamura, *Organometallics*, **12**, 4697 (1993).
238. Y. Apeloig and A. Stanger, *J. Am. Chem. Soc.*, **107**, 2806 (1985).
239. Y. Apeloig, R. Biton and A. Abu-Freih, *J. Am. Chem. Soc.*, **115**, 2522 (1993).
240. S. G. Davies and C. L. Goodfellow, *J. Organomet. Chem.*, **340**, 195 (1988).
241. S. Shambayati, J. F. Blake, S. G. Wierschke, W. L. Jorgensen and S. L. Schreiber, *J. Am. Chem. Soc.*, **112**, 697 (1990).
242. A. Sekiguchi, K. Ebata, C. Kabuto and H. Sakurai, *J. Am. Chem. Soc.*, **113**, 1464 (1991).
243. H. Sakurai, K. Ebata, C. Kabuto and A. Sekiguchi, *J. Am. Chem. Soc.*, **112**, 1799 (1990).
244. A. Sekiguchi, K. Ebata, Y. Terui and H. Sakurai, *Chem. Lett.*, 1417 (1991).
245. R. J. Mills, N. J. Taylor and V. Snieckus, *J. Org. Chem.*, **54**, 4372 (1989).
246. H. Bock, J. Meuret, C. Näther and U. Krynitz, *Tetrahedron Lett.*, **34**, 7553 (1993).
247. B. W. Gung, J. P. Melnick, M. A. Wolf and A. King, *J. Org. Chem.*, **60**, 1947 (1995).
248. H. Chen, R. A. Bartlett, H. V. R. Dias, M. M. Olmstead and P. P. Power, *J. Am. Chem. Soc.*, **111**, 4338 (1989).
249. Cf N. Wiberg, in *Frontiers of Organosilicon Chemistry* (Eds. A. R. Bassindale and P. P. Gaspar), Royal Society of Chemistry, Cambridge, 1991, pp. 263–270.
250. Cf. H. Bock, J. Meuret, C. Näther and K. Ruppert, in *Organosilicon Chemistry: From Molecules to Materials* (Eds. N. Auner and J. Weis), VCH, New York, 1994, pp. 11–19.
251. W. S. Sheldrick, in *The Chemistry of Organic Silicon Compounds* (Eds. S. Patai and Z. Rappoport), Wiley, New York, 1989, pp. 227–304.
252. E. Lukevics, O. Pudowa and R. Sturkovich, *Molecular Structure of Organosilicon Compounds*, Wiley, New York, 1989.
253. G. Raabe and J. Michl, in *The Chemistry of Organic Silicon Compounds* (Eds. S. Patai and Z. Rappoport), Wiley, New York, 1989, pp. 1015–1142.
254. H. Bock, J. Meuret and K. Ruppert, *J. Organomet. Chem.*, **462**, 31 (1993).
255. J. Pinkas, B. Gaul and J. G. Verkade, *J. Am. Chem. Soc.*, **115**, 3925 (1993).
256. K.-J. Lee, P. D. Livant, M. L. McKee and S. D. Sorley *J. Am. Chem. Soc.*, **107**, 9901 (1985).
257. D. Gudat, L. M. Daniels and J. G. Verkade, *J. Am. Chem. Soc.*, **111**, 8520 (1989).
258. E. B. Nadler and Z. Rappoport, *Tetrahedron Lett.*, **32**, 1233 (1991).
259. M. Charton, *J. Am. Chem. Soc.*, **97**, 1552 (1975).
260. M. Yoshifuji, T. Nakamura and N. Inamoto, *Tetrahedron Lett.*, **28**, 6325 (1987).

261. R. Okazaki, M. Unno and N. Inamoto, *Chem. Lett.*, 791 (1989).
262. N. Tokitoh, H. Suzuki, R. Okazaki and K. Ogawa, *J. Am. Chem. Soc.*, **115**, 10428 (1993).
263. K. M. Baines, A. G. Brook, R. R. Ford, P. D. Lickiss, A. K. Saxena, W. J. Chatterton, J. F. Sawyer and B. A. Behnam, *Organometallics*, **8**, 693 (1989).
264. J. D. Debad, P. Legzdins, R. J. Batchelor and F. W. B. Einstein, *Organometallics*, **12**, 2094 (1993).
265. T. J. Marks, E. A. Mintz and D. C. Sonnenberger, *J. Am. Chem. Soc.*, **106**, 3484 (1984).
266. J. D. Cotton, G. T. Crisp and L. Latif, *Inorg. Chim. Acta*, **47**, 171 (1981).
267. B. S. Bandodakar and G. Nagendrappa, *J. Organomet. Chem.*, **430**, 373 (1992).
268. R. Damrauer, B. O'Connell, S. E. Danahey and R. Simon, *Organometallics*, **8**, 1167 (1989).
269. J. Schraml, J. Čermák, V. Chvalovsky, A. Kasal, C. Bliefert and E. Krahé, *J. Organomet. Chem.*, **341**, C-6 (1988).
270. M. Unno, M. Saito and H. Matsumoto, *J. Organomet. Chem.*, **499**, 221 (1995).
271. W. S. Sheldrick, in *The Chemistry of Organic Silicon Compounds* (Eds. S. Patai and Z. Rappoport), Chap. 3, Wiley, New York, 1989.
272. T. D. McGrath and A. J. Welch, *Acta Crystallogr.*, **C51**, 654 (1995).
273. H. Sakurai, Y. Nakadaira, H. Tobita, T. Ito, K. Toriumi and H. Ito, *J. Am. Chem. Soc.*, **104**, 300 (1982).
274. H. Sakurai, H. Tobita, Y. Nakadaira and C. Kabuto, *J. Am. Chem. Soc.*, **104**, 4288 (1982).
275. H. Sakurai, K. Ebata, Y. Nakadaira and C. Kabuto, *Chem. Lett.*, 301 (1987).
276. H. Sakurai, K. Ebata, K. Sakamoto, Y. Nakadaira and C. Kabuto, *Chem. Lett.*, 965 (1988).

CHAPTER 9

Reaction mechanisms of nucleophilic attack at silicon

ALAN R. BASSINDALE, SIMON J. GLYNN and PETER G. TAYLOR

Department of Chemistry, The Open University, Milton Keynes, MK7 6AA, UK

I. INTRODUCTION

The mechanism of reactions involving silicon have proved to be a most fruitful area of research for almost fifty years. Silicon engages in nucleophilic and radical reactions covering almost all known reaction mechanisms.

In this review we have chosen to limit the scope to nucleophilic substitution at silicon. A short overview is given of material covered in detail in our previous review in 'The Chemistry of Organic Silicon Compounds'[1], with recent advances covered in greater depth.

Recently, the stereochemistry of nucleophilic substitution at silicon has been reviewed by Holmes[2], and the role of pentacoordinate silicon compounds as reaction intermediates has been reviewed by Corriu and coworkers[3].

II. DIRECT SUBSTITUTION OF A LEAVING GROUP BY A NUCLEOPHILE

A. Stereochemistry of Substitution

We begin by examining the direct exchange of a leaving group X by a nucleophile Y. Much of the discussion in this area has centred on whether the five-coordinate species **1** is an activated complex, as in the elementary mechanism A, or an intermediate, as in mechanism B (equation 1).

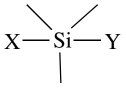

(1)

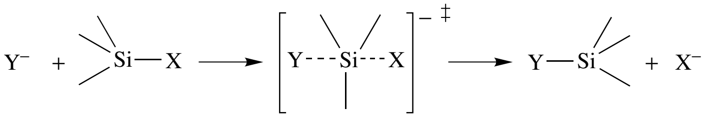

Mechanism A

(1)

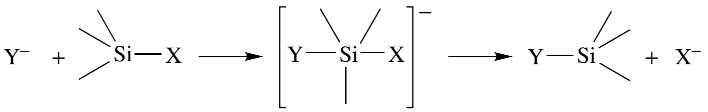

Mechanism B

As in substitution at carbon, stereochemical and kinetic data provide the means of differentiating between these two possibilities. The stereochemical data are examined first. Substitution at silicon leads to both retention and inversion of configuration and the stereochemical outcome depends upon the nature of the leaving group, the nucleophile, solvent, complexing agents and whether or not the silicon is part of a ring.

1. The effect of nucleophile and leaving group

When the leaving group at a chiral silicon is chlorine, inversion of configuration invariably occurs. Fluorine may lead to inversion, retention or a mixture of products. Si−H bond cleavage occurs primarily with retention of configuration. Sommer[4] and Corriu and Guerin[5,6] have both suggested that bond polarization and ease of Si−X stretching during nucleophilic attack may be important factors in the stereochemical outcome. An empirical relationship between the observed stereochemistry and the ability of the leaving group to be displaced has been suggested by Corriu and Guerin[5,6], to give a series Cl, Br, OAc > F, SR > OMe, H where leaving group ability decreases and degree of retention increases towards the right.

It was suggested by Sommer and coworkers[7,8] that retention occurs when the counterion is able to assist the departure of the leaving group. For poor leaving groups such as RO^-, it is difficult to displace the leaving group as the free ion, and Sommer proposed a cyclic mechanism involving electrophilic assistance by the E of E-Y (cf. **2**)[4].

This electrophilic assistance could account for the observed solvent and counterion effects. The stereochemistry of substitution of alkoxy, mercapto and fluorosilanes with alkoxide ion depends dramatically on the composition of the solvent[4]. As the percentage

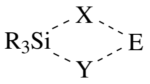

(2)

of alcohol in the benzene solution increases, there is a move from retention of stereochemistry to inversion. Sommer suggested that in benzene, electrophilic assistance from the counterion is required to enable the leaving group to be expelled. However, as the alcoholic content of the solution increases, hydrogen bonding to the solvent provides sufficient electrophilic assistance for removal of the poor leaving group, thus allowing inversion to proceed.

When the counterion is varied from lithium to sodium to potassium, the proportion of inversion increases. The relatively covalent lithium–oxygen bond favours a retentive mechanism. However, as the metal–oxygen bond becomes more ionic, the components may function more independently, allowing attack of RO^- on the back face of the silicon tetrahedron while electrophilic assistance by M^+ of the leaving group aids inversion of configuration.

The stereochemistry of substitution is also dependent on the nucleophile. Corriu and coworkers have related the preference for retention to the hardness of the nucleophile[5,6,9]. A hard nucleophile such as CH_3CH_2Li, where the negative charge is concentrated on the carbon, gives retention whereas the soft nucleophile $PhCH_2Li$, where the charge is delocalized, leads to inversion. These ideas have received a theoretical justification from the work of Anh and Minot[10], who carried out perturbational studies on substitution at silicon with either retention or inversion. More recently, Deiters and Holmes[11] have performed molecular orbital calculations on the $[SiH_3XY]^-$ species. The experimentally observed tendency of leaving groups towards retention ($H^- > OH^- > SH^- \sim F^- > Cl^-$) is found to correlate with a decrease in the overlap population of the silicon–leaving group bond. The nucleophile was found to influence the apicophilicity of the leaving group, soft nucleophiles increasing the leaving group apicophilicity and favouring inversion.

Corriu has also used the hard/soft nucleophile concept to explain the solvent and countercation effects[5,6,9]. He suggests that in benzene the RO^- M^+ species have a localized negative charge on the oxygen atom and thus are hard and react with retention. On increasing the alcohol content the charge on the anion is dispersed by hydrogen bonding producing a softer species which reacts with inversion.

2. The effect of substrate structure

The structure of the alkyl or aryl groups on the silicon has been found to have little effect on the stereochemical outcome of substitution[4]. Changes in both electronic and steric factors leave the stereochemical outcome unchanged[4]. However, there is a significant effect when the silicon is part of a strained-ring structure. When the leaving group is exocyclic there is a move to retention as the angle strain at silicon increases[12,13]. The opposite stereochemical trend is observed with endocyclic leaving groups. In this case angle strain favours inversion[6,14]. These observations can be rationalized by considering the requirements of small rings to be axial/equatorial with respect to a pentacoordinate silicon. With exocyclic leaving groups, axial entry of the nucleophile give the intermediate **3** which results in retention. When the leaving group is endocyclic, the small ring provides extra incentive for the leaving group to be axial. With axial entry this leads to preferred inversion as shown in **4**.

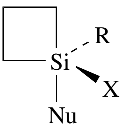

(3)

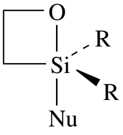

(4)

Anh and Minot[10] have forwarded an alternative explanation involving considerations of orbital overlap as the s character of the Si−X bond varies with the bond angle.

B. Kinetics of Substitution

The rates of hydrolysis of *p*-methoxyphenyltriphenylsilane and methoxytriphenylsilane were found by Eaborn and coworkers[15] to be first-order with respect to base concentration. This is consistent with (i) a concerted S_N2 mechanism, (ii) a mechanism involving a pentacoordinate intermediate where loss of alkoxide is not catalysed by HO^- or (iii) a mechanism where such a step is not kinetically significant. Detailed kinetic studies on the solvolyses of silyl ethers have been interpreted by Dietze and coworkers[16−19] as not supporting a mechanism in which there is a pre-equilibrium formation of a pentacoordinate intermediate which then collapses to produce products. They favour a mechanism in which solvent attack occurs on a tetravalent silicon atom with simultaneous breaking of the silicon leaving group bond (S_N2). They suggested that the observation of general acid catalysis, general base catalysis and bifunctional catalysis all arise from a common mechanism involving the transition state **5**, in which A = acid, B = base, OR^1 is the leaving group and HOR^2 is the nucleofuge.

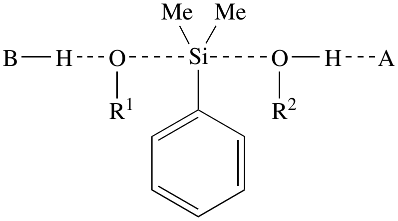

(5)

The dependence of the rate of reaction on leaving group has been measured by a number of workers. In solvolysis reactions, Sommer found that the rate of reaction decreases as the basicity of the leaving group increases[4]. However, using organolithium and Grignard nucleophiles, Corriu and coworkers found only a very small variation of rate with leaving group[20,21]. This was taken to suggest that the rate-determining step in this case does not involve Si−X bond cleavage; thus, a mechanism involving a single elementary step could be eliminated.

C. The Geometry of the Intermediate/Transition State

1. Inversion

The simplest model for the transition state and/or intermediate leading to inversion is a distorted trigonal bipyramid with the entering and leaving groups both apical.

Recent theoretical studies of the S_N2(Si) reaction and pentacoordinate silicon intermediates or transition states show that d-orbitals are unlikely to have any significant involvement in the bonding in such species. Using valence bond computations of curve-crossing diagrams, Sini and coworkers[22] have shown that the stability of SiH_5^- relative to CH_5^- originates from the ability of silicon to utilize its Si−H σ^* orbitals for bonding to a much greater degree than carbon does. Consequently, pentavalent silicon has two resonating H−Si−H axial bonds, one arising from the axial p-orbital of the silicon and the other from the equatorial $\sigma^*(SiH_3)$ orbital of the central SiH_3 fragment. Due to the bonding nature of this σ^* orbital SiH_5^- can delocalize the fifth valence–electron pair into the equatorial Si−H bonds. For carbon this delocalization is prohibited by the high p-σ^* promotion energy, and by poor overlap of the σ^* orbital with the axial hydrogens. Thus, the fifth valence electron pair is localized in the H−C−H axial bonds, which are elongated and raise the energy of the system.

Shi and Boyd[23] have compared the reaction pathway of CH_3X with SiH_3X by calculating the Laplacian of the charge density, which gives an indication of differences in bonding and electron distributions. The bonding in CH_3X is essentially completely covalent. In S_N2 reactions, the uncharged carbon atom is always attacked from the area of greatest charge depletion, which is found opposite the C−X bond (see contour map, Figure 1) — hence the reaction takes place with inversion. The pentacoordinate species is a high energy transition state. In the case of SiH_3X, it is found that the bonding has more ionic character with a considerable positive charge on silicon. This positive charge makes nucleophilic attack easier, hence the increased reactivity of silicon with nucleophiles. Additionally, the large positively charged centre can attract nucleophiles from all directions. The stereochemistry is then dependent on the extent of charge depletion in different regions of space (Figure 2) which varies with the substrate. The significant ionic bonding increases the stability of the pentacoordinate species, which is therefore found to lie at the bottom of the potential energy surface.

A similar conclusion was reached by Streitwieser and coworkers[24], who used integrated population analyses to indicate that bonds between Si and H, C, O and F are extensively polarized in the sense $Si^+ X^-$ with significant charge transfer. As a result Si−O and Si−F

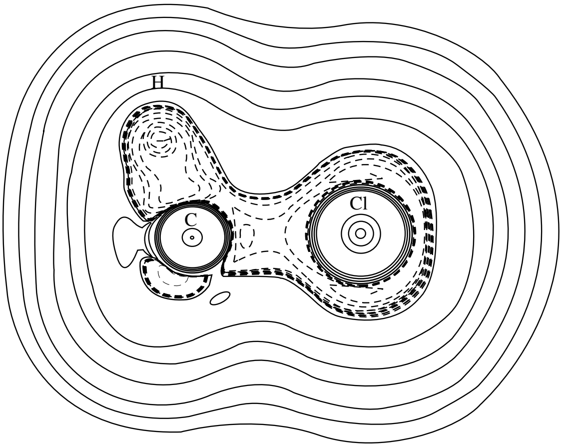

FIGURE 1. Laplacian of the charge density contour map of CH_3Cl in the HCCl plane. Reprinted with permission from Z. Shi and R. J. Boyd, *J. Phys. Chem.*, **95**, 4698. Copyright (1991) American Chemical Society

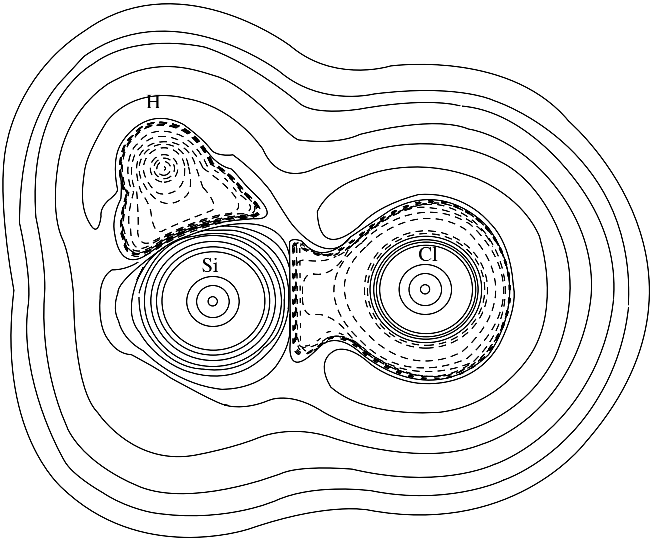

FIGURE 2. Laplacian of the charge density contour map of SiH_3Cl in the HSiCl plane. Reprinted with permission from Z. Shi and R. J. Boyd, *J. Phys. Chem.,* **95**, 4698. Copyright (1991) American Chemical Society

bonds are dominated by ionic interactions, and Si−H and Si−C bonds have an important ionic character. The ionic nature of these bonds allows silicon to expand its coordination sphere to form stable pentacoordinate species.

The increased ionic character of the bonding in SiH_5^- was also described by Carroll, Gordon and Windus[25]. They studied the addition of H^- to MH_4 to form MH_5^-. When M = Si, stabilization of the incoming hydride was dominant over the destabilization of the original MH_4, and ΔE for the addition was negative. When M = C, the destabilization of the atoms originally comprising CH_4 is greater than the stabilization of the incoming hydride and ΔE is positive.

Structural studies of pentacoordinate silicon compounds give valuable insight into the S_N2 process at silicon. Macharashvili and coworkers[26] obtained the X-ray crystal structures of a series of (halodimethylsilylmethyl) lactams. The Si−O and Si−X distances were found to vary over a wide range (1.749–2.461 and 3.734–1.630 Å, respectively) in the series X = I, Br, Cl, F. The compounds can be regarded as models of intermediate stages of the S_N2 substitution process at silicon. The silicon atom coordination changes from a slightly distorted tetrahedron with a long Si−X bond (X = I), through a trigonal bipyramid, and back to a distorted tetrahedron, inverted, with a long Si−O distance (X = F).

Similar studies have been carried out by Bassindale and Borbaruah[27] in the solution phase for a series of N-(halodimethylsilylmethyl) pyridones **(6)** (equation 2). The structures of the pyridones can be envisaged as points on the reaction profile of a nucleophilic substitution of X^- by the carbonyl oxygen (**6**, **7**, **8**). Analysis of the pyridone ring carbon-13 NMR chemical shifts can, using a mapping method, give a measure of the extent of silicon−oxygen bond formation in each pyridone.

The extent of Si−O bond formation is found to increase as X becomes a better leaving group ($F<Cl<Br<OSO_2CF_3$). Additionally, substituents Y on the pyridone ring

also affect the extent of Si−O bond formation. With a strongly electron-withdrawing substituent, 3-NO_2, the extent of Si−O bond formation for each leaving group was significantly less than for the unsubstituted series.

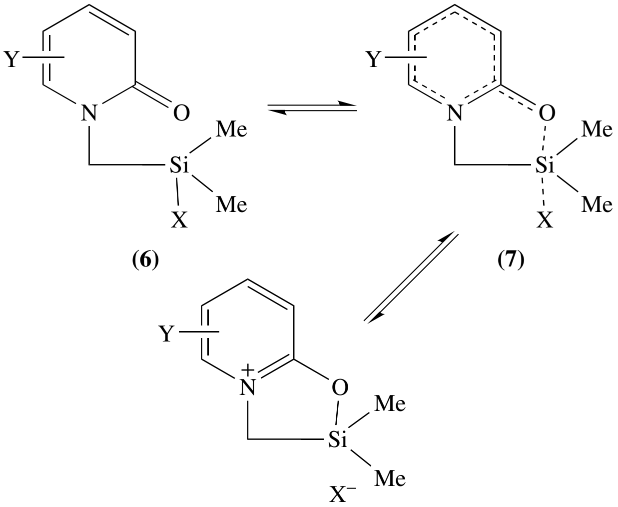

(6) **(7)** **(8)**

(2)

Sidorkin and coworkers[28] have used quantum chemical (MNDO) methods to model the pathway of intramolecular S_N2 substitution at silicon, as shown in equation 3.

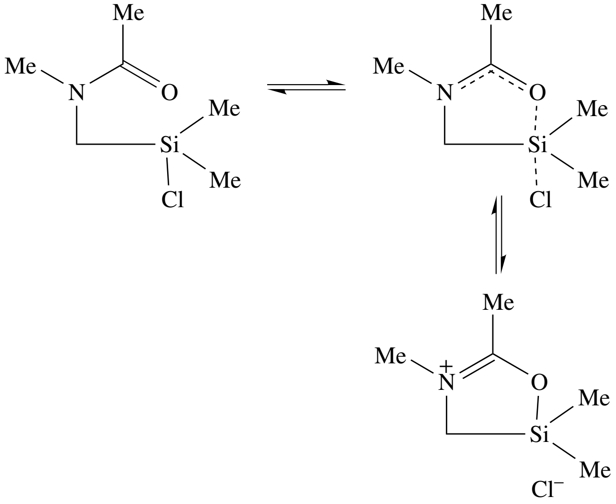

(3)

The changes in the geometric parameters of the $ClSiC_3O$ coordination centre are typical of a bimolecular nucleophilic substitution reaction at a tetrahedral atom and consistent with the results obtained using the Burgi–Dunitz structure correlation method with the experimental results of Macharashvili and coworkers[26].

These studies show the simultaneous lengthening of the silicon–leaving group bond as the silicon–nucleophile interaction increases. Molecular orbital calculations at the STO-3G level by Deiters and Holmes[29] also show that as the nucleophile approaches from an apical position, the *trans* axial bond to the leaving group increases in length. However, there is little conclusive evidence as to whether a pentacoordinate intermediate with a finite lifetime is involved in such invertive processes.

2. Retention

Retention requires the nucleophile to attack from the same side as the leaving group in **9** and this can give rise to two different trigonal bipyramidal structures, **10** and **11**.

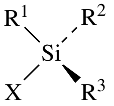

(9)

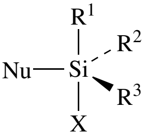

(10)

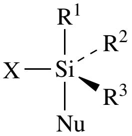

(11)

10 is the result of attack of the nucleophile at the R^1–X edge of the tetrahedron **9** whereas **11** is formed by attack on the lower XR^2R^3 face of the tetrahedron **9**. Loss of the leaving group directly from the axial position in **10** gives the retention product. For **11**, retention could result from direct loss of the leaving group from the equatorial position, or by pseudorotation to give an intermediate in which the leaving group is axial and the nucleophile equatorial, followed by loss of the leaving group from the axial position. This latter mechanism is generally accepted for substitution with retention at phosphorus[30].

Molecular-orbital calculations by Deiters and Holmes[29] suggest that for silicon, edge attack is very unlikely. Using a number of different reaction pathways, *ab initio* calculations at the STO-3G level for the reaction shown in equation 4 suggest that edge attack has a higher energy than face attack.

$$SiH_3X + H^- \longrightarrow (HSiH_3X)^- \longrightarrow SiH_3H + X^- \qquad (4)$$

$$X = Cl \text{ or } F$$

In fact, for edge attack, as the reaction progresses the incoming nucleophile slips over to a lower-energy tetrahedral face and follows the course of axial entry. Calculations also suggest that, using the square pyramidal form **12** as the transition state, the pseudorotation has a relatively low energy, such that axial entry, of a nucleophile A followed by pseudorotation and axial exit of a leaving group C or D is a viable pathway (equation 5).

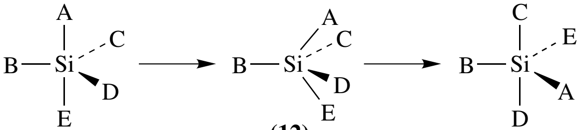

(12)

(5)

The calculations also suggest that face attack leading to inversion and face attack leading to retention were similar in energy for fluorine, but for chlorine inversion was preferred. This agrees with the experimental stereochemical behaviour of fluorine and chlorine. The Si–Cl bond stretched under the influence of the nucleophile to a larger extent than the Si−F bond. The authors proposed that with a good leaving group such as chlorine, the Si−Cl bond breaks as the Si−Nu bond forms, leading to inversion. However, with poor leaving groups such as fluorine, a tightly bound intermediate is formed allowing ligand rearrangement, so that the inversion and retention routes have similar energies. It was also found that the calculated apicophilicities of the leaving groups correlated with the experimentally determined tendency for inversion, with groups of low apicophilicity tending towards retention. Furthermore, the apicophilicities of the leaving groups were found to be dependent on the nucleophile, such that soft nucleophiles increase the apicophilicity of the leaving group and hence favour inversion.

By definition, the retention mechanism involving axial attack and axial exit must involve a pentacoordinated intermediate of sufficient lifetime to allow pseudorotation. The evidence for pseudorotation in the retentive process is now reviewed.

D. Pseudorotation in Pentacoordinate Silicon Species

The possibility of pseudorotation at silicon was first suggested by Klanberg and Muetterties[31] in their study of pentacoordinate fluorosilicates SiF_5^-, $RSiF_4^-$ and $R_2SiF_3^-$. Recently there have been a number of studies on the pseudorotation of pentacoordinate silicon species.

Corriu and coworkers[32] have used compounds of the type **13** to distinguish between two possible routes of ligand exchange — pseudorotation and a dissociative process involving cleavage of the Si−N bond.

The two N-methyl groups are diastereotopic owing to the chirality of the benzyl group. A pseudorotation process will cause equivalence of the fluorines but not of the two N-methyl groups. However, a dissociative pathway as shown in equation 6 causes the fluorines and the methyl groups to be made equivalent.

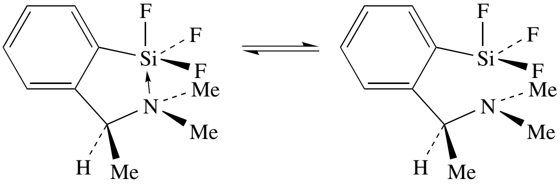

(13)

(6)

Variable-temperature studies using fluorine-19 NMR show an equivalence mechanism with a $\Delta G^{\ddagger}$ of 13.1 kcal mol^{-1}, whereas proton DNMR shows that the NMe_2 groups are made equivalent via a process with a $\Delta G^{\ddagger}$ of 15.8 kcal mol^{-1}. The authors propose that the lower-energy pathway shown by fluorine-19 NMR arises from pseudorotation, whereas the higher-energy process shown by proton NMR is due to a dissociative process. Silicon–fluorine coupling is retained in all cases, showing that intermolecular fluorine exchange does not occur.

The interconversion of diastereomeric pentacoordinate organosilanes **14** was found to have an activation energy which had only a small dependence on the nature of the equatorial X substituent, despite large changes in the electronic effect of the ligand (X = H, F, Cl, OCOR, OPh, Ph)[33].

It is observed that on heating, the NMe_2 methyl signals become equivalent with the same $\Delta G^{\ddagger}$ values as the methyl groups of the pinacoxy moiety. This implies a symmetrical geometry in the transition state. The only pseudorotation mechanism which involves the degree of symmetry required for the equivalence of the methyl groups is shown in

equation 7.

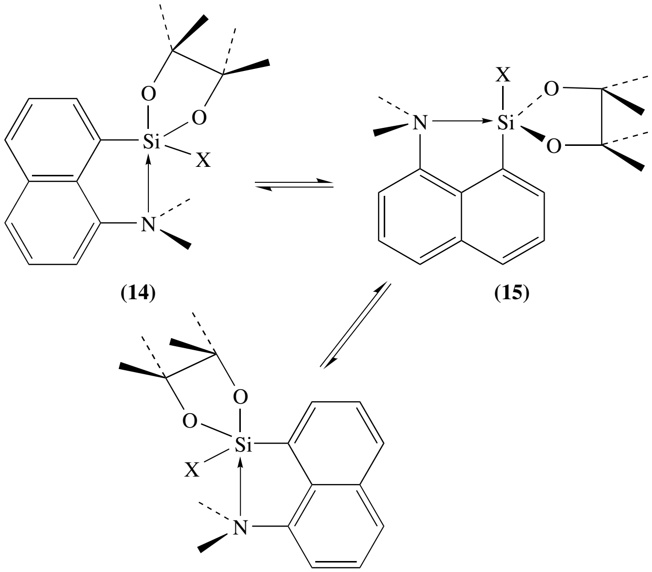

(14) **(15)** (7)

In conformation **15**, X is apical (which can be favourable) but the pinacoxy moiety is in the highly unfavourable diequatorial position. The authors suggest that this discourages pseudorotation such that the interconversion of diastereomers with $\Delta G^{\ddagger}$ values between 15 and 19 kcal mol^{-1} is thought to result from dissociation and recoordination of the Si−N bond.

Kalikhman, Kost and coworkers[34] have studied ligand exchange reactions in the system **16**.

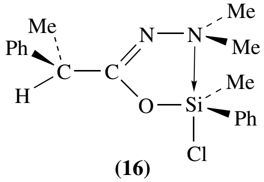

(16)

Two diastereomers are observed at the slow-exchange limit, due to the different relative configurations at the two chiral centres. As the temperature increases the four N-methyl singlets first coalesce into two singlets. This corresponds to a N-methyl interchange process without interconversion of diastereomers. This is attributed to exchange of N-methyls via Si−N bond cleavage, followed by rotation around the N−N bond and reclosure of the chelate ring, without concomitant epimerization at the silicon. $\Delta G^{\ddagger}$ for this process is 11.4 kcal mol^{-1}. On raising the temperature, a second exchange process is observed in which all the signal pairs of the diastereomers coalesce, i.e. epimerization at the silicon centre becomes rapid relative to the NMR time scale. This epimerization process, presumably occuring via a pseudorotation reaction, has a remarkably high activation barrier of 18.7 kcal mol^{-1}. This large activation energy is attributed to two factors: (i) in the pseudorotation process, the electronegative Cl ligand is forced out of the apical position and replaced by a less electronegative carbon ligand, to give a much less stable arrangement, and (ii) the chelate ring may be forced into a diequatorial position, generating considerable ring strain.

Corriu and coworkers have found that the barrier to pseudorotation seems to depend on the number of electronegative groups present[35]. For species with one electronegative substituent, $\Delta G^{\ddagger} > 20$ kcal mol^{-1}. With two electronegative groups, the barrier decreases to *ca* 9–12 kcal mol^{-1}, and when three electronegative substituents are present, the pseudorotation barrier has $\Delta G^{\ddagger} < 7$ kcal mol^{-1}.

Gordon and coworkers have studied the pseudorotation of SiH_5^- using *ab initio* and semiempirical calculations[36]. Both AM1 and MP2/6-31++G(d,p) calculations predict a pseudorotation barrier of 2.4 kcal mol^{-1}. In a further study[37], detailed *ab initio* investigations of the pseudorotation of the pentacoordinated silicon anions $SiH_{5-n}X_n^-$ ($X = F$, Cl; $n = 0–5$) were made. The barriers to pseudorotation of SiF_5^- and $SiCl_5^-$ were also found to be less than or equal to 3 kcal mol^{-1}. In fact, pseudorotation is less energetically demanding than loss of X^- for SiH_5^-, $SiH_3F_2^-$, $SiX_2X_3^-$, $SiHX_4^-$ and SiX_5^-. Cramer and Squires[38] have described the conformational potential energy surface for the dihydroxysiliconate ion $H_3Si(OH)_2^-$. They found it to be remarkably flat with six minima lying within 2.7 kcal mol^{-1} of one another. Interconversions of the minima have pseudorotation barriers of less than 6 kcal mol^{-1}, suggesting that $H_3Si(OH)_2^-$ may be considered to be essentially without structure as regards ligand location.

These results show that pseudorotation is to be expected with silicon, and Martin and coworkers[39] have shown that it has a lower barrier than pseudorotation involving phosphorus. Thus axial entry, pseudorotation and axial exit, which is generally accepted for phosphorus, is a viable mechanism for silicon.

Myers and coworkers[40,41] have shown evidence for a pseudorotational mechanism in the reaction of the O-silyl ketene *N*,*O*-acetal **17** with aromatic aldehydes (equation 8).

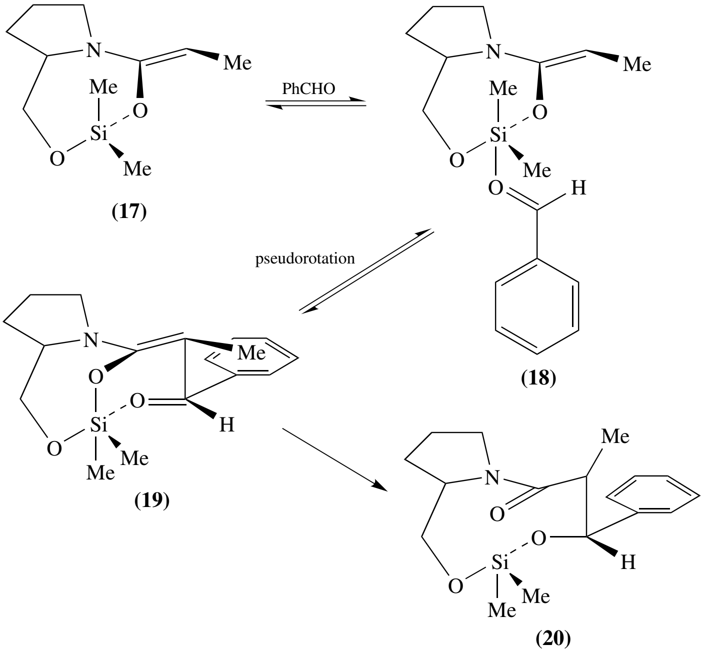

(8)

Kinetic studies were consistent with an associative mechanism involving pentacoordinate silicon. X-ray crystallographic data for the product **20** suggests the trigonal bipyramid **19** as a reasonable precursor. Axial attack of benzaldehyde on the starting material **17** gives the trigonal bipyramid **18**, which can be converted to **19** by a pseudorotation.

Gung and coworkers[42] have located (at the MP2/6-31 G* level of theory) the transition state for the silicon-directed aldol reaction between a silyl enol ether and formaldehyde. They found it to be a boatlike six-membered ring **21** with a pentacoordinate silicon (equation 9).

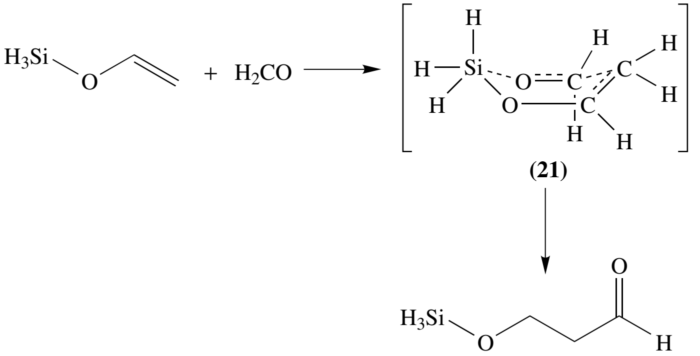

(21)

(9)

The formaldehyde oxygen occupies the apical position with a Si−O bond length of 2.01 Å. The enol silane oxygen assumes the equatorial orientation with a Si−O bond length of 1.81 Å.

A similar transition state **22** is calculated for the reaction of allylsilanes with aldehydes (equation 10)[43]. In this case, however, the calculations show that the oxygen attacks at an apical site of the silicon centre, while the allyl group departs directly from an equatorial position without causing a pseudorotation, in contrast to the mechanisms previously discussed.

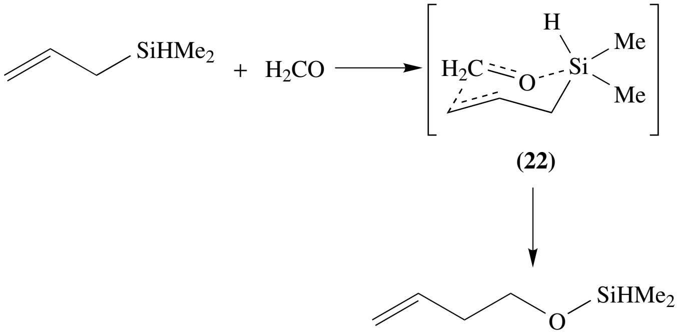

(22)

(10)

In these reactions the pentacoordinate species is a high-energy transition state, not an intermediate.

III. NUCLEOPHILE-CATALYSED SUBSTITUTION AT SILICON AND RACEMIZATION

Nucleophilic substitution at silicon has frequently been found to be catalysed by the presence of other nucleophiles. Corriu and coworkers have found that the hydrolysis of a range of chlorosilanes is first order in nucleophilic catalysts such as pyridines, HMPA, DMSO and DMF[44]. The stereochemistry of this type of reaction has been shown to be retentive, even with chlorosilanes where direct nucleophilic substitution normally gives inversion[45].

A reaction related to the nucleophile-catalysed hydrolysis of silanes is the nucleophile-catalysed racemization of silanes. The racemization of a range of halosilanes was found to have an order with respect to nucleophile varying from 1 to 3[46,47]. The reactions have entropies of activation which are large and negative, and enthalpies of activation which are small and sometimes negative. Both racemization and hydrolysis are slowed by increasing steric crowding at silicon.[48]

It was proposed by Sommer and Bauman that the methanol-catalysed racemization of 1-naphthylphenylmethylfluorosilane involves formation of a pentacoordinate intermediate followed by pseudorotation[49]. Three successive pseudorotations are required for racemization, followed by axial loss of the solvent. However, this mechanism is not consistent with the reaction being subsequently reported to be third order with respect to nucleophile[46,47].

Corriu and coworkers have proposed[50] an alternative mechanism involving extension of the coordination of the silicon atom. The first step involves rapid and reversible attack by a molecule of the nucleophilic catalyst, Nu^-, to give the pentacoordinate species **23** (equation 11).

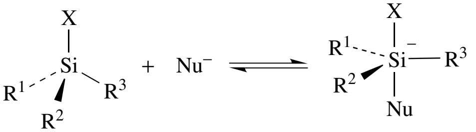

(23)

(11)

The slow step in the process is then the attack by a second nucleophile at an R−X edge to give a hexacoordinate intermediate or transition state. The second nucleophile is the alcohol in the case of alcoholysis or the nucleophilic catalyst in the case of racemization (equations 12 and 13).

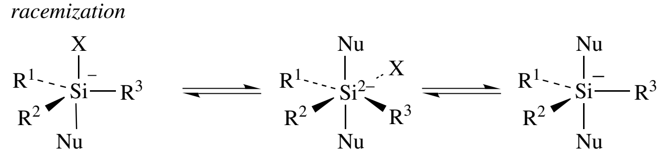

(23) **(24)** **(25)**

(12)

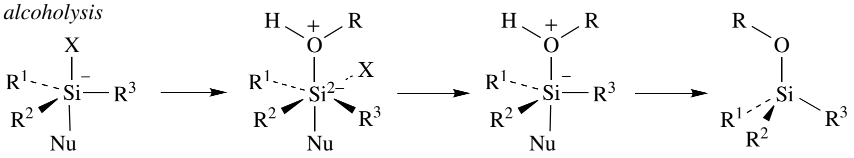

(23) **(26)** **(27)** **(28)**

(13)

For alcoholysis, collapse of **23** via **26** and **27** then leads to the substitution product **28** with retention. For racemization, since both **24** and **25** have a plane of symmetry, the reversible formation of such species leads to retention and inversion. It is not certain whether racemization involves solely the intermediate **24** or whether this is a transition state leading to **25** as the only intermediate.

In addition to explaining the stereochemistry, this mechanism is also in agreement with the kinetics. Corriu has found[48,51] that racemization is second order with respect to the nucleophile, whereas alcoholysis is first order in the alcohol and nucleophile. Both of these rate equations are in agreement with the pre-equilibrium formation of an intermediate followed by rate-limiting attack by a second nucleophile. The small values obtained for $\Delta H^{\ddagger}$ and the large negative values for $\Delta S^{\ddagger}$ show the reaction to be entropy controlled with a highly organized transition state, as would be expected for a hexacoordinate transition state/intermediate.

Corriu's proposed mechanisms were criticised by Frye and coworkers[52], who considered the observed rate enhancements to be irreconcilable with intermediates of increased coordination number. Frye maintained that steric effects would retard attack on a pentacoordinate silicon compared to a tetracoordinate silicon, and nucleophilic attack would also be disfavoured on pentacoordinate silicon as the silicon bears a formal negative charge due to the formation of an essentially dative bond with the nucleophile.

However, recent studies have shown that pentacoordinate silicon centres are indeed more reactive than tetracoordinate silicon centres. Theoretical studies have shown that the positive charge on the central silicon atom is at least maintained[53] and may well be increased[54] by coordination of an additional ligand, even when the ligand is anionic. Calculations by Deiters and Holmes[53] also show a lengthening of bonds, particularly axial bonds, in pentacoordinate silicon species compared to tetracoordinate silicon species. As there is no decrease in positive charge at the central silicon atom on coordination of an anionic ligand, the negative charge on the ligands is increased in the pentacoordinate silicon species compared to the corresponding tetracoordinate species. Thus the leaving group ability of the ligands in the pentacoordinate system is increased.

Numerous experimental observations of the increased reactivity of pentacoordinate silicon over tetracoordinate silicon have been reported. Corriu and coworkers have found that the relative reactivity of $PhMeSiF_3^-$ and $PhMeSiF_2$ towards t-BuMgBr was >1000:1[55]. The pentacoordinate species **29** reacts with alcohols and acids to give mono- or disubstitution products whereas the corresponding four-coordinate species **30** does not react at all[56].

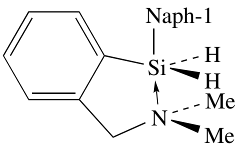

(29)

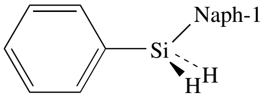

(30)

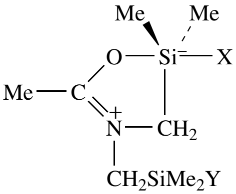

(31)

Bassindale and Borbaruah have studied the reactivities of bis-halo N,N-bisdimethylsilylmethylacetamides **31** towards nucleophiles[57]. In these systems there are two silicon centres that, when X = Y, differ only in the coordination at silicon. Investigations were carried out at both centres at the same time and under the same conditions.

It was found that silicon–bromine and silicon–chlorine bonds were thermodynamically activated towards substitution by coordination of an oxygen nucleophile, whereas coordination was found to deactivate the silicon–fluorine bond.

A further mechanism for nucleophile-catalysed racemization and substitution has been proposed by Chojnowski and coworkers[58]. They proposed that the HMPA catalysed substitution of halogen at silicon may involve the transient formation of a phosphonium cation **(32)** containing a four-coordinate silicon. The retention of the configuration observed would then be the result of two consecutive inversions (equation 14).

$$R_3SiCl \underset{\text{inversion}}{\overset{\text{HMPA}}{\rightleftharpoons}} R_3SiO{-}\overset{+}{P}(NMe_2)_3Cl^- \xrightarrow[\text{inversion}]{R'OH} R_3SiOR' \qquad (14)$$

(**32**)

The HMPA adducts of trimethylchlorosilane (**32**, R = Me) and trimethylbromosilane were isolated and found to be ionic as shown. If the first step shown in equation 14 is a pre-equilibrium, the observed order for substitution is first order as expected. For racemization, the rate-limiting step is invertive attack of the second HMPA molecule on **32**, such that the reaction is second-order overall with respect to nucleophile.

A wide range of four-coordinate adducts have been formed from the reaction of nucleophiles with Me_3SiX (X = I, Br, OSO_2CF_3)[59,60]. As expected, these salts are highly susceptible to nucleophilic attack[61].

Corriu and coworkers suggest that Chojnowski's mechanism may only operate with very labile Si−Br and Si−I bonds and good nucleophiles[62]. They also criticize the mechanism as it cannot account for the nucleophile-induced epimerization of chlorocyclobutanes. As mentioned earlier, in small rings with exocyclic leaving groups, retentive substitution predominates, so that two consecutive substitutions by HMPA would only lead to retention.

Bassindale and coworkers[63,64] have studied the nucleophile-assisted racemizations of $PhCHMeSiMe_2X$ where X = Cl or Br. Thermodynamic and kinetic studies led to the conclusion that intermediates involving extracoordinate silicon were not being formed. The results were interpreted in terms of two competing mechanisms for racemization: (a) halide–halide exchange, with inversion of configuration (equation 15) and (b) displacement of halide by nucleophile followed by nucleophile–nucleophile exchange, followed by displacement of nucleophile by halide, each step proceeding by inversion of configuration (equation 16).

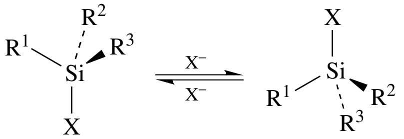

(15)

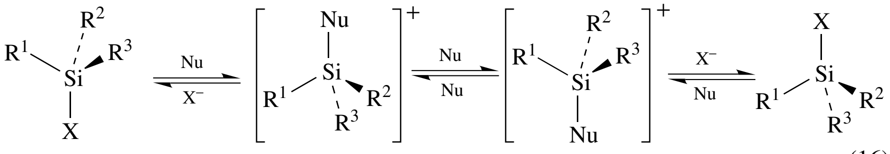

(16)

Substitution with inversion and retention of the pentacoordinate species **33** has been interpreted in terms of two competing dissociative mechanisms: Si−O cleavage and Si−NMI cleavage[65]. A hexacoordinate intermediate is not implicated.

However, Corriu and coworkers[66] postulate a hexacoordinate intermediate (or transition state) in the hydrolysis of organic silicates, with the rate-determining step in the reaction being the coordination of water to a pentacoordinate intermediate formed by initial nucleophilic attack.

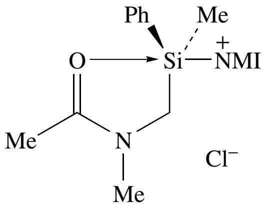

(33) NMI = *N*-methyl imidazole

A hexacoordinate transition state **34** is also postulated in the reaction of allyltrichlorosilanes with aldehydes in the presence of DMF (equation 17)[67].

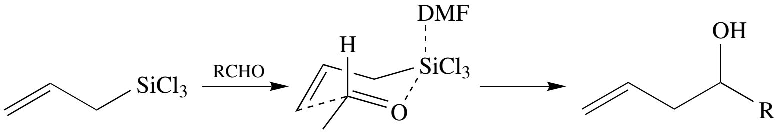

(34)

(17)

IV. REFERENCES

1. A. R. Bassindale and P. G. Taylor, in *The Chemistry of Organic Silicon Compounds*, Part 1 (Eds. S. Patai and Z. Rappoport), Wiley, Chichester, 1989, pp. 839–892.
2. R. R. Holmes, *Chem. Rev.*, **90**, 17 (1990).
3. C. Chuit, R. J. P. Corriu, C. Reye and J. C. Young, *Chem. Rev.*, **93**, 1371 (1993).
4. L. H. Sommer, *Intra-Sci. Chem. Rep.*, **7**, 1 (1973).
5. R. J. P. Corriu and C. Guerin, *J. Organomet. Chem.*, **74**, 1 (1980).
6. R. J. P. Corriu and C. Guerin, *Adv. Organomet. Chem.*, **20**, 265 (1982).
7. L. H. Sommer and W. D. Korte, *J. Am. Chem. Soc.*, **89**, 5802 (1967).
8. L. H. Sommer, J. McLick and C. M. Golino, *J. Am. Chem. Soc.*, **94**, 669 (1972).
9. R. J. P. Corriu, C. Guerin and J. J. E. Moreau, *Top. Stereochem.*, **15**, 43 (1984).
10. N. T. Anh and C. Minot, *J. Am. Chem. Soc.*, **102**, 103 (1980).
11. J. A. Deiters and R. R. Holmes, *J. Am. Chem. Soc.*, **109**, 1692 (1987).
12. B. G. McKinnie, N. S. Bhacca, F. K. Cartledge and J. Fayssoux, *J. Org. Chem.*, **41**, 1534 (1976).
13. F. K. Cartledge, J. M. Wolcott, J. Dubac, P. Mazerolles and M. Joly, *J. Organomet. Chem.*, **154**, 203 (1978).
14. R. Corriu, C. Guerin and J. Masse, *J. Chem. Res. (M)*, 1877 (1977).
15. C. Eaborn, R. Eidenschink and D. R. M. Walton, *J. Chem. Soc., Chem. Commun.*, 388 (1975).
16. P. E. Dietze, *J. Org. Chem.*, **57**, 6843 (1992).
17. P. E. Dietze, *J. Org. Chem.*, **58**, 5653 (1993).
18. Y. Xu and P. E. Dietze, *J. Am. Chem. Soc.*, **115**, 10722 (1993).
19. P. E. Dietze, C. Foerster and Y. Xu, *J. Org. Chem.*, **59**, 2523 (1994).
20. R. J. P. Corriu and B. J. L. Henner, *J. Organomet. Chem.*, **102**, 407 (1975).
21. G. Chauviere, R. J. P. Corriu and B. J. L. Henner, *J. Organomet. Chem.*, **86**, C1 (1975).
22. G. Sini, G. Ohanessian, P. C. Hiberty and S. S. Shaik, *J. Am. Chem. Soc.*, **112**, 1407 (1990).
23. Z. Shi and R. J. Boyd, *J. Phys. Chem.*, **95**, 4698 (1991).
24. S. Gronert, R. Glaser and A. Streitwieser, *J. Am. Chem. Soc.*, **111**, 3111 (1989).
25. M. T. Carroll, M. S. Gordon and T. L. Windus, *Inorg. Chem.*, **31**, 825 (1992).
26. A. A. Macharashvili, V. E. Shklover, Yu. T. Struchkov, G. I. Oleneva, E. P. Kramarova, A. G. Shipov and Yu. I Baukov, *J. Chem. Soc., Chem. Commun.*, 683 (1988).
27. A. R. Bassindale and M. Borbaruah, *J. Chem. Soc., Chem. Commun.*, 1501 (1991).
28. V. F. Sidorkin, V. V. Vladimirov, M. G. Voronkov and V. A. Pestunovich, *J. Mol. Struct.*, **228**, 1 (1991).
29. J. A. Deiters and R. R. Holmes, *J. Am. Chem. Soc.*, **109**, 1686 (1987).

30. R. Luckenbach, *Dynamic Stereochemistry of Pentacoordinate Phosphorus and Related Elements*, George Thieme Publ., Stuttgart, 1973.
31. F. Klanberg and E. L. Muetterties, *Inorg. Chem.*, **7**, 155 (1968).
32. R. J. P. Corriu, A. Kpoton, M. Poirier, G. Royo and J. Y. Corey, *J. Organomet. Chem.*, **277**, C5 (1986).
33. F. H. Carre, R. J. P. Corriu, G. F. Lanneau and Z. Yu, *Organometallics*, **10**, 1236 (1991).
34. I. Kalikhman, S. Krivinos, A. Ellern and D. Kost, *Organometallics*, **15**, 5073 (1996).
35. J. Boyer, R. J. P. Corriu, A. Kpoton, M. Mazhar, M. Poirier and G. Royo, *J. Organomet. Chem.*, **301**, 131 (1986).
36. M. S. Gordon, T. L. Windus, L. W. Burggraf and L. P. Davis, *J. Am. Chem. Soc.*, **112**, 7167 (1990).
37. T. L. Windus, M. S. Gordon, L. P. Davis and L. W. Burggraf, *J. Am. Chem. Soc.*, **116**, 3568 (1994).
38. C. J. Cramer and R. R. Squires, *J. Am. Chem. Soc.*, **117**, 9285 (1995).
39. W. H. Stevenson III, S. Wilson, J. C. Martin and W. B. Farnham, *J. Am. Chem. Soc.*, **107**, 6340 (1985).
40. A. G. Myers, K. L. Widdowson and P. J. Kukkola, *J. Am. Chem. Soc.*, **114**, 2765 (1992).
41. A. G. Myers, S. E. Kephart and H. Chen, *J. Am. Chem. Soc.*, **114**, 7922 (1992).
42. B. W. Gung, Z. Zhou and R. A. Fouch, *J. Org. Chem.*, **60**, 2860 (1995).
43. K. Omoto, Y. Sawada and H. Fujimoto, *J. Am. Chem. Soc.*, **118**, 1750 (1996).
44. R. J. P. Corriu, G. Dabosi and M. Martineau, *J. Organomet. Chem.*, **150**, 27 (1978).
45. R. J. P. Corriu, G. Dabosi and M. Martineau, *J. Organomet. Chem.*, **154**, 33 (1978).
46. R. J. P. Corriu and M. Henner-Leard, *J. Organomet. Chem.*, **64**, 351 (1974).
47. F. K. Cartledge, B. G. McKinnie and J. M. Wolcott, *J. Organomet. Chem.*, **118**, 7 (1976).
48. R. J. P. Corriu, F. Larcher and G. Royo, *J. Organomet. Chem.*, **104**, 293 (1976).
49. L. H. Sommer and D. L. Bauman, *J. Am. Chem. Soc.*, **91**, 7045 (1969).
50. R. J. P. Corriu, F. Larcher and G. Royo, *J. Organomet. Chem.*, **129**, 299 (1977).
51. R. J. P. Corriu and M. Henner-Leard, *J. Organomet. Chem.*, **65**, C39 (1974).
52. H. K. Chu, M. D. Johnson and C. L. Frye, *J. Organomet. Chem.*, **271**, 327 (1984).
53. J. A. Deiters and R. R. Holmes, *J. Am. Chem. Soc.*, **112**, 7197 (1990).
54. M. S. Gordon, M. T. Carroll, L. P. Davis and L. W. Burggraf, *J. Phys. Chem.*, **94**, 8125 (1990).
55. J. L. Brefort, R. J. P. Corriu, C. Guerin, B. J. L. Henner and W. W. C. Wong Chi Man, *Organometallics*, **9**, 2080 (1990).
56. B. J. Helmer, R. West, R. J. P. Corriu, M. Poirier, G. Royo and A. De Saxce, *J. Organomet. Chem.*, **251**, 295 (1983).
57. A. R. Bassindale and M. Borbaruah, *J. Chem. Soc., Chem. Commun.*, 352 (1993).
58. J. Chojnowski, M. Cypryk and M. Michalski, *J. Organomet. Chem.*, **161**, C31 (1978).
59. A. R. Bassindale and T. Stout, *J. Chem. Soc., Perkin Trans. 2*, 221 (1986).
60. A. R. Bassindale and T. Stout, *J. Organomet. Chem.*, **238**, C41 (1982).
61. A. R. Bassindale, J. C-Y. Lau, T. Stout and P. G. Taylor, *J. Chem. Soc., Perkin Trans. 2*, 227 (1986).
62. R. J. P. Corriu, G. Dabosi and M. Martineau, *J. Organomet. Chem*, **186**, 25 (1980).
63. A. R. Bassindale, J. C-Y. Lau and P. G. Taylor, *J. Organomet. Chem.*, **490**, 75 (1994).
64. A. R. Bassindale, J. C-Y. Lau and P. G. Taylor, *J. Organomet. Chem.*, **499**, 137 (1995).
65. A. R. Bassindale, S. J. Glynn, J. Jiang, D. J. Parker, R. Turtle, P. G. Taylor and S. S. D. Brown, in *Organosilicon Chemistry II. From Molecules to Materials* (Eds. N. Auner and J. Weiss), VCH, Weinheim, 1996, pp. 411–425.
66. R. J. P. Corriu, C. Guerin, B. J. L. Henner and Q. Wang, *Organometallics*, **10**, 3200 (1991).
67. S. Kobayashi and K. Nishio, *J. Org. Chem.*, **59**, 6620 (1994).

CHAPTER 10

Silicenium ions: Quantum chemical computations

CHRISTOPH MAERKER and PAUL VON RAGUÉ SCHLEYER[†]

Computer Chemistry Center of the Institute of Organic Chemistry, The University of Erlangen-Nürnberg, Henkestrasse 42, 91054 Erlangen, Germany
Fax: 49-9131-85-9132, e-mail: pvrs@ccc.uni-erlangen.de

[†] New postal address: Center for Computational Quantum Chemistry The University of Georgia, Athens, GA 30602 USA. Fax: +1-706-542-0406

I. ABBREVIATIONS

B	Becke's exchange functional
B3LYP	three-parameter hybrid exchange-correlation-density functional
BII	standard basis set of triple-zeta quality, including polarization functions for all elements, often employed in IGLO calculations
BII′	same basis set as BII for non-hydrogen atoms, combined with a double-zeta quality sp-basis set for hydrogen atoms
9-BBN	9-borabicyclo[3.3.1]nonyl group
CCSD	coupled-cluster theory with single and double excitation terms
CCSD(T)	same as CCSD plus a perturbative estimate of triple excitation terms
DFT	density functional theory
DFPT	density functional perturbation theory
ΔZPE	differential zero-point vibrational energy
E_h	computed total energy in Hartree
ϵ	dielectric constant
fc	frozen-core approximation
GIAO	gauge-including atomic orbitals
HF	Hartree–Fock
http	hypertext transfer protocol
IGLO	individual gauge for localized orbitals
KS	Kohn–Sham
LYP	gradient-corrected correlation functional by Lee, Yang and Parr
MBPT	many-body perturbation theory
Me	methyl group
Mes	mesityl group
MP2	second-order Møller–Plesset perturbation theory
Ng	noble gas
NPA	natural population analysis
PG	(symmetry) point group
π-SE	π-electron stabilization energy
$\rho(\mathbf{r})$	electron density distribution
$\nabla^2\rho(\mathbf{r})$	Laplacian of the electron density distribution
TMS	tetramethyl silane, Me_4Si
URL	uniform resource locator
WBI	Wiberg bond index
WWW	world wide web
ZPE	zero-point vibrational energy

II. INTRODUCTION

Since 1989, when the first volume of *The Chemistry of Organosilicon Compounds* appeared[1], large strides have been made in preparing silicenium cations. The first X-ray structures[2,3] of solvent stabilized silicenium cations are among the most notable successes. Most recently, a free silicenium cation has been prepared in solution[4,5]. In addition to experimental techniques for structure elucidation, e.g. X-ray single-crystal structure analysis, and nuclear magnetic resonance (NMR) spectroscopy, *quantum theory* is now a widely accepted *practical tool* for the exploration of chemical entities and their reaction behaviour. In particular, quantum chemistry has played a major role in exploring and predicting the structure and energetics of organosilicon compounds[6], especially of silenes[7], which very often behave quite differently from their lighter carbon analogues[7,8]. Apeloig[9,10], Gordon[11], Nagase[12] and Morokuma[13], to name but a few, have recently reviewed quantum chemical studies on neutral and ionic silicon compounds.

This chapter focuses almost exclusively on the most recent theoretical investigations of silicenium ions, i.e. of trivalent, positively charged silicon ions, which have not been covered in earlier reviews[6,9]. When appropriate, experimental work on silicenium ions and studies on closely related carbenium ions will be mentioned. This chapter is organized as follows: Section III summarizes briefly recent developments in quantum mechanical methodology pertinent to organosilicon chemistry. Section IV highlights recent computational studies, and Section V presents conclusions and an outlook of future work. The reader is also referred to the accompanying review by Lickiss which describes recent experimental work on silicenium ions.

III. COMPUTATIONAL METHODS

In the past decade quantum chemical investigations of organosilicon compounds have progressed substantially due to the benefits from hardware speed-up and new software developments. Modern RISC processors and new parallel machines facilitate computations on large molecular systems which one could not have imagined even five years ago. Today, routine high-level computational ‘experiments’ can be carried out on ‘real’ systems, i.e. the actual system carrying the experimental substituents, rather than on simple model species. Very recently, a massively parallel Intel^{TM} computer reached unprecedented 2.5 Teraflops per second, which is 1000 times faster than in currently used supercomputers. In addition to these hardware achievements, new software and methodology developments are equally important. Density functional theory based methods have become more widely used[14,15]; see the discussion below. Faster algorithms, such as the Fast Multipole Method (FMM)[16], facilitate an efficient linear-scaling computation of the Coulomb problem, both in quantum mechanics[17] (QM) and in molecular[18] mechanics (MM) computations. Combined QM/MM methods[19] are currently under development, mainly in the field of biomedical research[20]. In QM/MM, the active part of the molecule (e.g. the reaction site) is treated quantum mechanically, whereas the outer spheres are described by well-parametrized force fields. Similar computational techniques in principle can be applied to silicon compounds, e.g. in the simulation of semiconductor surface–gas phase interactions. In summary, it is not too far fetched to say that a computational revolution is taking off with ever-increasing speed.

A. ‘Traditional’ *ab initio* Molecular Orbital (MO) Techniques

A wealth of texts, e.g. those by Clark[21] and by Pople and coworkers[22], and the series *Reviews in Computational Chemistry*[23] provide comprehensive overviews on the whole field of computational chemistry, in particular on quantum chemistry. The *Encyclopedia of Computational Chemistry*[24], to appear in 1998, will provide a comprehensive review on state-of-the-art computational chemistry, written by world-leading experts in the field. The Internet also provides an online forum of computational chemistry related sites, e.g. the Fourth Electronic Computational Chemistry Conference (ECCC4)[25] and the *Journal* *of Molecular Modeling*[26]. Thus, it suffices here to comment shortly on more recent developments such as quantum mechanical calculations using density functional theory[14,15] (DFT) and *ab initio* computations of magnetic properties[27].

B. Density Functional Theory (DFT) Based Methods

'The physicists have been trying to persuade us for years that we ought to study density functional theory. We ought have listened more carefully, especially since it was one of our own, J. C. Slater who pushed them in that direction with his 1951 contribution[28] ... So although I think we have all worked hard and made great progress ... I rather wonder if we are up against it and the physicists were right after all[29]'. This very emphatic statement by Handy, one of the leading proponents of traditional *ab initio* MO theory, gives the reader an impression to what extent the DFT-based methods have influenced the quantum chemists' thinking since they have plunged into the quantum theory of molecules some years ago.

The key theorems of modern density functional theory were introduced by Hohenberg, Sham and Kohn in the mid-1960s[30]. DFT theory is based on the fact that the total energy E of a chemical species (either in its electronic ground or in its excited states) can in principle be expressed via functionals of the electron density ρ. However, the exact form of these functionals, in particular that of the exchange-correlation functional, $E_{\mathrm{XC}}[\rho]$, is unknown[14,15]. Nevertheless, currently-employed DFT-based methods often rival high-level molecular orbital procedures in accuracy, and their computational efficiency (with a formal scaling in computer time of N^3, where N is the number of electrons) provides a superior accuracy per computational cost ratio[14,15]. Excellent monographs on recent implementations and applications of DFT methods are available, where the interested reader can obtain further information[14,15]. Fast multipole methods[16], as mentioned earlier, are now being incorporated into quantum chemical programs[17] and will provide further speed-ups.

C. Computations of Magnetic Properties

NMR spectroscopy is an ubiquitous and indispensable tool for modern structure elucidation. During the last two decades quantum mechanical procedures for the computation of nuclear magnetic shielding constants and the derived chemical shifts have become available. Questionable experimental assignments can now be verified by means of computed data[27]. In addition, high-level computations even allow reliable predictions for yet-to-be prepared species. The recently developed computations of spin–spin coupling constants[31] have analytical and predictive potential, as do computations of chemical shifts.

Despite the importance of theoretical NMR data, magnetic property computations have only become possible recently. The gauge dependence problem of finite basis set calculations is best handled via 'local gauge origin' methods. The most widely employed approaches are the 'individual gauge for localized orbitals' (IGLO)[32], the 'localized orbital/local origin' (LORG)[33] and the 'gauge-including atomic orbitals' (GIAO)[34] methods. The IGLO method (and program), developed by Kutzelnigg and coworkers[32] at the beginning of the 1980s, was the first practical tool for *ab initio* computations of the magnetic properties of medium-sized molecules.

Schleyer and coworkers have shown[35] that in order to use effectively the IGLO/NMR approach to structure elucidation, it is necessary to employ high-level optimized geometries (e.g. at the correlated MP2/6-31G* or DFT levels of theory) in order to obtain best agreement between computed and experimental chemical shifts. Early GIAO-SCF calculations some 20 years ago[36] were hampered by an inefficient implementation which prohibited computations on larger molecules. Improved gradient algorithms in the GIAO scheme[37] enabled GIAO/NMR calculations on large organic molecules at a speed comparable with that of IGLO calculations.

It soon became apparent that the inclusion of electron correlation in the computation of chemical shielding tensors would improve the results considerably[38]. The contributions by Oddershede[39], Galasso[40], Kutzelnigg[41], Gauss[42,43] and their coworkers are noteworthy. In particular the reader is referred to the impressive series of benchmark calculations by Gauss and coworkers[43] of chemical shielding tensors at hierarchically increased electron correlated levels employing the GIAO approach (GIAO-MBPT[n], $n = 2$–4; GIAO-CCSD and GIAO-CCSD(T)), which have also been reviewed recently[27]. However, the inherent scaling problem of these highly correlated levels prevents their application even to medium-sized organic species. Thus, the burgeoning field of DFT-based methods for the computation of magnetic properties might be a valuable alternative for larger systems, and implementations of density functional theory based computer codes for the calculation of magnetic properties have already appeared recently[44].

IV. QUANTUM MECHANICAL STUDIES OF SILICENIUM CATIONS

A. Thermodynamic Stability of Silicenium Cations

Unlike carbocations[45–47], for which the first quantum mechanical studies were reported in the 1950s[48,49], computational studies on silicenium ions only date back some 20 years[50–54]. Schleyer, Apeloig and coworkers were the first to report comprehensive investigations on the structure and stability of α-substituted silicenium cations[51,54]. Although those early computations only employed modest SCF levels, the authors were able to analyse the importance of the various properties of α-substituents, such as σ-inductive effects, lone pair π-donation, conjugation and hyperconjugation, in stabilizing silicenium ions[51,54]. The relative stabilities of silicenium ions were explored by means of isodesmic reactions 1 to 3. Isodesmic reactions, where the same type and number of bonds appear on both sides of the equation, were introduced by Pople and coworkers[55] in order to reduce errors, particularly when using lower theoretical levels.

$$R_nSiH_{3-n}^+ + SiH_4 \longrightarrow R_nSiH_{4-n} + SiH_3{}^+ \qquad n = 0\text{–}3 \qquad (1)$$

$$R_nCH_{3-n}^+ + CH_4 \longrightarrow R_nCH_{4-n} + CH_3{}^+ \qquad n = 0\text{–}3 \qquad (2)$$

$$R_nSiH_{3-n}^+ + R_nCH_{4-n} \longrightarrow R_nSiH_{4-n} + R_nCH_{3-n}^+ \qquad n = 0\text{–}3 \qquad (3)$$

Equation 1 compares the stability of substituted silicenium ions versus the parent $SiH_3{}^+$ (**1**). Equation 2 compares the stabilities of the correspondingly substituted carbocations versus $CH_3{}^+$. Equation 3 compares the stabilities of silicenium ions with those of the corresponding carbocations. The calculated energies of equations 1–3 are presented in Table 1, and the following conclusions can be drawn[51]:

(1) Relative to hydrogen, all the first-row substituents, with the exception of fluorine, stabilize the silicenium ion. The greater stability of α-substituted silicenium cations versus their corresponding carbocations can be attributed in part to the lower electronegativity of silicon (1.7) compared to carbon (2.5). Equation 3 also takes into account the relative stability of alkanes versus silanes, i.e. the stability of C—H versus Si—H bonds. The Si—H bond is weaker than the C—H bond by *ca* 13 kcal mol^{-1} in the gas phase, e.g. the bond dissociation energy DH_{298}^0(C—H) in CH_4 is 104.9 kcal mol^{-1}[56], compared

TABLE 1. Computed stabilization energies of α-substituents on carbenium $RCH_2{}^+$ and silicenium $RSiH_2{}^+$ cations (kcal mol^{-1})

R	Equation 1		Equation 2		Equation 3	
	this group[a]	Ref. 9[b]	this group[a]	Ref. 9[b]	this group[a]	Ref. 9[b]
H	0.0	0.0	0.0	0.0	57.4	54.9
Li	57.8		75.3		39.8	
BeH	14.3		15.1		56.5	
BH_2, planar		8.3		2.7		60.4
BH_2, perp.	13.7	13.9	25.9	25.8	45.1	43.0
CH_3	15.1	15.1	40.6	34.1	31.8	35.9
NH_2, planar	37.5	36.8	100.5	97.8	−5.6	−6.1
NH_2, perp.		11.9		15.9		50.9
OH, planar	19.1	17.9	66.3	62.7	10.1	10.1
F	−1.1	−2.3	25.3	21.5	31.0	31.1
SiH_3	12.3	12.6	16.5	17.7	53.2	49.8
PH_2, planar	17.6	13.5	63.4	60.0	11.6	8.4
SH, planar	18.5	18.4	63.6	60.9	12.2	12.4
SH, perp.		0.4		8.1		47.3
Cl	2.2	2.0	29.2	26.6	30.3	30.3

[a] MP2(fc)/6-31G*//MP2(fc)/6-31G* level of theory, Reference 6.
[b] MP3/6-31G*//HF/6-31G*.

to DH^0_{298}(Si−H) of 91.9 kcal mol^{-1} in SiH_4[57]. Trimethyl substitution decreases the difference in dissociation energies DH^0_{298}(E−H) slightly: 96.4 kcal mol^{-1} in $Me_3C{-}H$[58], compared to 90.3 kcal mol^{-1} in $Me_3Si{-}H$[59]. Thus, hydride transfer from silicon to carbon in the gas phase is favoured by the weaker silicon–hydrogen bonds. Hydride transfer from organosilicon compounds to trityl salts in solution was first reported and utilized by Corey and coworkers[60] in an attempted preparation of silicenium ions. In this context it is important to note that commonly employed leaving groups other than hydrogen, e.g. halides, do not lead to silicenium ions, and only Lewis acid–organosilane adducts are formed[61].

(2) First-row α-substituents are more effective in stabilizing carbocations than in stabilizing silicenium ions. In particular, lone pair π-electron donation, e.g. by a planar amino group in $SiH_2NH_2{}^+$, is *ca.* 60 kcal mol^{-1} less effective than in $CH_2NH_2{}^+$. This dramatic decrease in the stabilizing power of π-donors was attributed to the unfavorable interaction (reduced overlap) between the 2p lone pair donor and the 3p(Si^+) acceptor orbitals[62]. One might therefore assume that second-row substituents are more effective in stabilizing silicenium ions, either due to a better 3p lone pair to 3p(Si^+) overlap or due to a reduced inductive destabilization caused by the less electronegative second-row substituents. In particular, the SH group even competes in its stabilizing power for silicenium ions with the OH group, whereas chlorine substitution gives a stabilizing effect contrary to the destabilization found for fluorine. Noteworthy is also the remarkable stabilization of silicenium and carbenium ions by electropositive substituents, e.g. by Li, BeH and by BH_2.

The *intrinsic* π-donation capabilities of heavy element atoms (group 15 to group 17), compared to first-row atoms, has been investigated recently by Schleyer and coworkers[63]. The superior ability of nitrogen to act as a π-donor in α-substituted carbocations

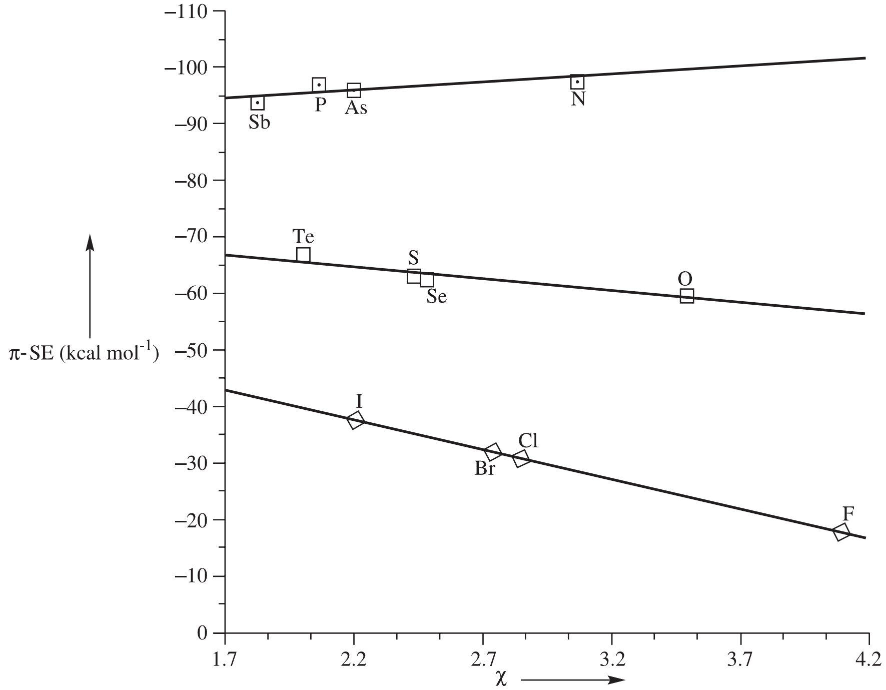

FIGURE 1. $CH_2{-}XH_n^+$ ($n = 0, 1, 2$) π-stabilization energies (π-SE) [kcal mol^{-1}; at QCISD(T)/-DZ++PP//MP2/DZ+P+ZPE] versus the electronegativity χ of X. Reproduced by permission of Wiley-VCH from Reference 63

$H_2C{-}XH_n{}^+$ relative to heavier group 15 substituents, e.g. comparing $-NH_2$ with $-PH_2$, was found to be due to the small planarization energy of the amino group relative to that of the PH_2 group. Thus, the *inherent* π-donor stabilization energies of the heavy element group 15 atoms is *not* reduced compared to first-row substituents, as long as a planarized, sp^2-hybridized $-XH_2$ group is taken into account, although such idealized groups might be of little practical relevance. Group 16 −XH and group 17 −X heavy element atoms (X = S, Se, Te; and Cl, Br, I, respectively) even were found to stabilize carbocations better than the parent first-row substituents −OH and −F, respectively (Figure 1). The authors concluded that: 'In contrast to the still common misconception that 2p/3p/4p/5p overlap is ineffective, our comparison emphasizes that the *inherent* π-donor capabilities of the heavier elements are as large as or even larger than their first-row counterparts'[63].

B. Towards Free Silicenium Ions in Solution: How Can They be Prepared?

While appropriate substitution can enhance the thermodynamic stability of silicenium ions, this does not suffice to produce stable silicenium ions in solution. The propensity of silicon to form intermediates with higher coordination numbers[64], in combination with the large positive charge on silicon, makes any free silicenium ion an inviting target for Lewis bases, e.g. solvent molecules or counterions. Hence, both electronic stabilization and steric shielding of the cationic silicon centre, e.g. by bulky groups, are necessary simultaneously. The following approaches towards the generation of silicenium ions in solution have been proposed, and most of them have already been examined:

- substitution with alkyl groups R (e.g. R = methyl, ethyl and especially the sterically demanding isopropyl and *t*-butyl), which provide electronic stabilization via both inductive and hyperconjugative (C−H and C−C hyperconjugation) effects.
- electronic stabilization by lone pair donor atoms (e.g. by N, O or S),
- substitution by bulky boraorganyl substituents, e.g. the 9-borabicyclo[3.3.1]nonyl group,
- stabilization via conjugation with aryl groups, which might provide resonance stabilization and steric shielding simultaneously,
- incorporation of the silicenium ion function into an aromatic ring, a strategy which has worked well in many other cases, e.g. in preparing silanol anions[65], isolable carbenes[66] and stable nitrenium ions[67].

Let us first have a closer look at trialkyl-substituted silicenium ions[2,3] since, four years ago, the X-ray structures of these species started a lively debate on silicenium ions.

C. Trialkyl-substituted Silicenium Ions

1. Energetic stabilization by multiple alkyl substitution

Successive methyl substitution of SiH_3^+ was investigated in a 1989 ion cyclotron resonance (ICR) study[68]. The first, second and third methyl substitution decreases the experimental hydride affinity of the corresponding silicenium ions by 15.5, 15.8 and 9.6 kcal mol^{-1}, respectively, relative to SiH_3^+ (equation 1)[68]. Apeloig reported computed values of 15.1, 12.9 and 10.6 kcal mol^{-1} (MP3/6-31G*//6-31G*)[9], respectively, which fit the experimental numbers quite well. Thus, the incremental stabilization by the methyl substituent decreases with increasing degree of substitution (Table 2). Note that a similar trend of decreasing incremental methyl stabilization is also known for carbenium ions[68] (Table 2). According to equation 3, the trimethyl silicenium cation is only 21.0 kcal mol^{-1} more stable than the corresponding *t*-butyl cation, compared to 57.4 kcal mol^{-1} for the parent species SiH_3^+ vs CH_3^+ [at MP2(fc)/6-31G*]. Nevertheless, hydride transfer from trialkyl silanes to trialkyl carbenium ions still is favoured thermodynamically.

2. The first X-ray structures: The first stable tricoordinate silicenium ions?

X-ray crystal structures of ‘silicenium ion candidates’ have been reported as early as in 1983[69], but in all cases it turned out that the silicon atom formed a covalent bond to a neighbouring solvent molecule or to the counterion[70,71]. In 1993, both Lambert’s[2] and

TABLE 2. Effect of multiple methyl substitution on the stability of carbenium $R_nCH_{3-n}^+$ and silicenium $R_nSiH_{3-n}^+$ ions (kcal mol^{-1})

Species	Equation 1		Equation 2		Equation 3	
	calc[a]	exp[b]	calc[a]	exp[b]	calc[a]	exp[b]
R = Me						
$n = 1$	15.1 (15.1)[c]	15.5	40.6	43.9	31.8 (27.4)[c]	24.8
$n = 2$	27.9 (28.0)[c]	31.3	58.7	62.9	26.6 (17.4)[c]	21.8
$n = 3$	38.4 (38.6)[c]	40.9	74.8	80.8	21.0 (12.9)[c]	12.9

[a] At MP2(fc)/6-31G*//MP2(fc)/6-31G*, from Reference 6.

[b] Data taken from Reference 68.

[c] MP3/6-31G*//6-31G* from Reference 9.

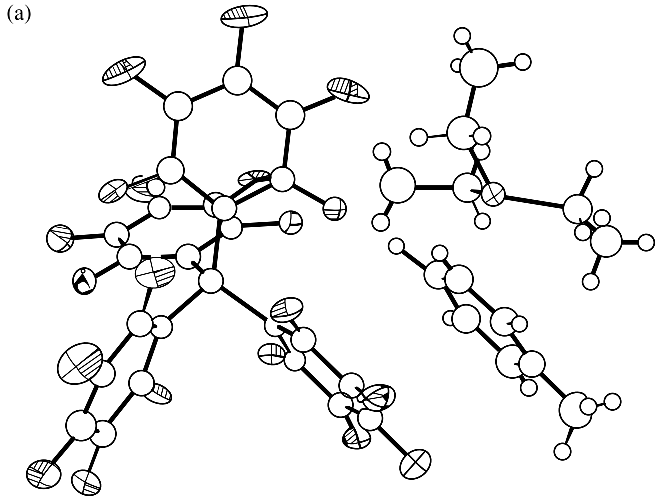

(2)

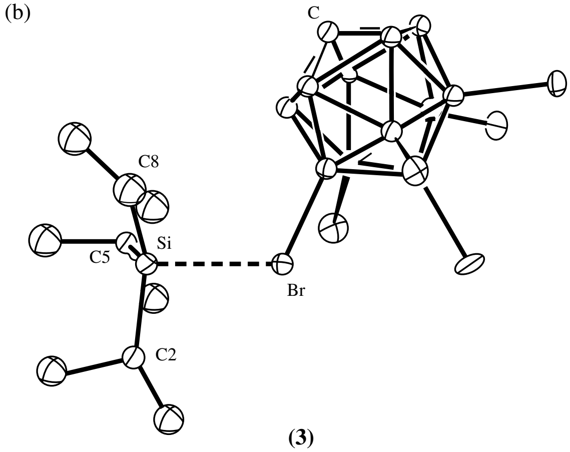

(3)

FIGURE 2. (a) Experimental molecular structure (ORTEP) of Et_3Si^+ $(C_6F_5)_4B^-$ (**2**). Silicenium ion upper right, anion left; the toluene solvent molecule, lower right. Reproduced by permission of the American Association for the Advancement of Science from Reference 2a. (b) Experimental molecular structure (ORTEP) of i-$Pr_3Si^+(Br_6CB_{11}H_6)^-$ (**3**). Bond distances (Å): Si−Br = 2.479(9) (dashed); Si−C(2) = 1.860(27); Si−C(5) = 1.908(27); and Si−C(8) = 1.799(35). Bond angles (deg): C(2)−Si−C(5) = 102.2(12); C(2)−Si−C(8) = 111.2(14); and C(5)−Si−C(8) = 119.6(13). Reproduced by permission of the American Association for the Advancement of Science from Reference 3a

Reed's[3] groups reported single-crystal X-ray structures of alkyl-substituted 'silicenium ion candidates', namely $Et_3Si^+B[C_6F_5]_4^-$ (**2**) and i-Pr_3Si^+ $Br_6CB_{11}H_6^-$ (**3**), as shown in Figures 2a and 2b, respectively. Their claims to have prepared tricoordinate positively charged silicon ions in the solid state[2,3] opened a lively discussion[72–78]. Note that

Lambert and his coworkers have made similar claims earlier, based on insufficient evidence in solution[79,80,81]. Lambert's 1993 study[2a], for example, showed an organosilyl moiety with no coordination to the anion, but with a toluene molecule close nearby ($R(Si{-}C) = 2.18$ Å). Lambert and coworkers claimed that in **2** "covalent bonding is weak or absent"[2a] i.e. there is no fourth coordination between the silicon atom and toluene. The elongated $Si{-}C_{ipso}$ distance in **2** led Lambert and his coworkers to the stable silicenium ion description[2a]. The X-ray structure of **3**, reported by Reed and coworkers, showed a $Si^+ \cdots Br$ distance of 2.48 Å, 0.24 Å longer than a normal Si−Br single bond[3a].

Pauling, in one of his last scientific contributions, pointed out that, based on the observed Si−C bond length, there is a covalent silicon−carbon (of the toluene) bonding in the triethylsilicenium−toluene complex **2**[72]. The bond number, n, is 0.35, according to equation 4,

$$D(n) = D(1) - 0.60 \log n \qquad (4)$$

where $D(n)$ is the bond length in question and $D(1)$ is the bond length of a 'normal' covalent single bond (i.e. n equals 1), whilst n is the bond number of the bond length in question. Pauling further noted that 'It has been [his] experience that calculated bond numbers as small as 0.10 (which represent an increase of bond length as great as 0.60 Å) need to be taken into account'[72]. Thus, the 2.18 Å Si−C bond length observed by Lambert and coworkers[2a] can *not* be regarded as being 'well outside the range (1.9 to 2.0 Å) of "long" Si−C bonds that unusually involve Si−*t*-butyl' bonds[2], as stated by Lambert and coworkers.

Similar conclusions were drawn by Schleyer, Apeloig, Siehl and coworkers, whose calculated structures for the $[Me_3Si{-}toluene]^+$ complex **(4)** and the $[H_3Si{-}benzene]^+$ complex **(5)** are shown in Figure 3[73]. These authors reported a Wiberg bond index[82] of 0.44 for the Si−C bond and described the silicenium ion−toluene complexes **4** and **5** as silylated arenium ions (Figure 3), i.e. σ-bonded Wheland-type species, with considerable charge delocalization to the aromatic ring[73]. The long $Si{-}C_{ipso}$ bond distance is due to extensive Si−C hyperconjugation, as represented by the stabilizing resonance forms shown in Figure 4[73]. Reed's group acknowledged the presence of some covalent interactions between the arene and the silyl moiety, e.g. in **2**, but interpreted the structure of the adduct as reflecting a weak π-complex[76].

The X-ray structure of **2** (Figure 2a) showed an average CSiC bond angle of 114° (the toluene was essentially planar), and the silicon atom was 0.4 Å above the plane of the three adjacent ethyl carbons[2a]. *Ab initio* Hartree−Fock and DFT geometry optimizations of **4** by Schleyer and coworkers[6,73], by Olah and coworkers[77] and by Cremer's group[83] reproduced these structural details quite well. A comparison between the calculated and some of the experimental structural parameters is given in parentheses in **4** (Figure 3). Lambert and coworkers attributed the significant non-planarity of the silicenium moiety in **2** to 'a combination of steric effects, long-range orbital interaction, and crystal packing forces. ... the silyl cation herein easily distorts from the plane to relieve external sources of strain'. However, even these arguments were refuted by *ab initio* computations[77,83]. Pyramidalization towards the observed CSiC bond angle of 114° *raises* the energy of the silicenium ion by 9.3 $\mathrm{kcal\,mol^{-1}}$ (MP2/6-31G*)[77]. Moreover, IGLO NMR computations showed that pyramidalization leads to a *deshielded* silyl resonance (see below)[77,83] and not to an increased shielding as surmised by Lambert and coworkers[2a].

Olah and coworkers[77] further characterized Reed's silicenium ion **3** as a silylated bromonium ion[6] [exp. $R(Si{-}Br) = 2.479$ Å]. Despite all the criticism and theoretical evidence, both Lambert and Reed defended their own interpretation of structures **2** and **3** as being chemical entities with predominant silicenium ion character[75,76].

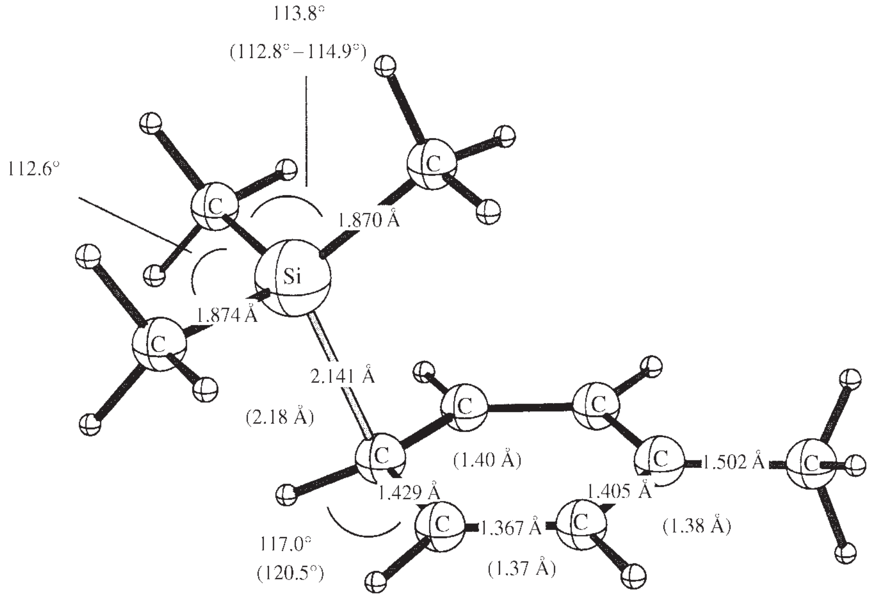

(4)

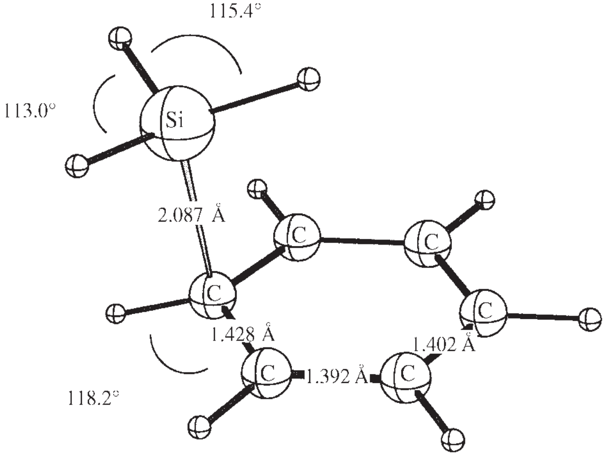

(5)

FIGURE 3. *Ab initio* optimized geometries of the [Me$_3$Si–toluene]$^+$ complex **(4)** (HF/6-31G*, top) and of the [H$_3$Si–benzene]$^+$ complex **(5)** [MP2(fc)/6-31G*, bottom]. Values in parentheses correspond to experimental X-ray data of Et$_3$Si$^+$ (C$_6$F$_5$)$_4$B$^-$ **(2)**. Reproduced by permission of Wiley-VCH from Reference 73

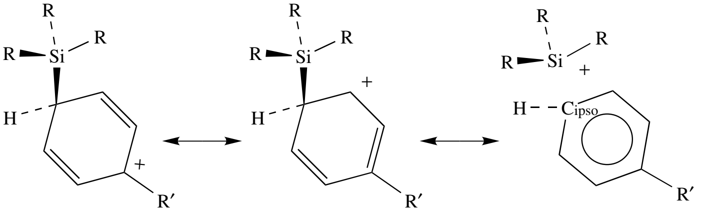

FIGURE 4. Resonance structures of silyl-substituted arenium ions

3. Interactions with Lewis bases: Binary and ternary complexes

Previously attempted preparations of silicenium ions in condensed phases gave structures with silicon covalently bonded to perchlorate, e.g. in triphenylsilyl perchlorate **(6)**[70], to pyridine, e.g. in $[Me_3Si{-}pyridine]^+$-I^- **(7)**[69] (Figures 5 and 6) and to acetonitrile, e.g. in $[Me_3Si{-}NCMe]^+$ **(8)**[3b]. Recently, Reed and coworkers reported on the X-ray structure of the 1 : 1 $(t\text{-Bu})_3Si^+$–water complex **9** (Figure 7), formed by protonation of $(t\text{-Bu})_3SiOH$[71]. The latter complex featured a Si–O bond length of 1.779 Å, and a ^{29}Si NMR chemical shift of 46.7 ppm versus TMS[71] (see below).

Quantum theory sheds more light on the character of such silicenium ion–Lewis base complexes, e.g. on the nature of the bonds formed. Are they covalent? Do d-orbitals contribute? How large are the complexation energies and how do they change upon substitution? Can free tricoordinate silicenium ions be formed at all in π-donor or aromatic solvents?

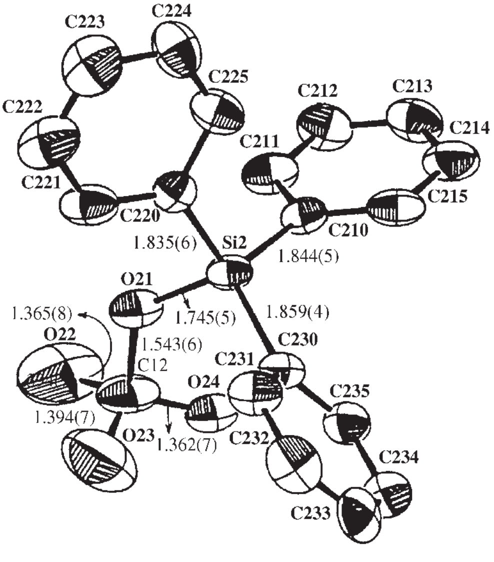

(6)

FIGURE 5. ORTEP drawing of the experimental structure of triphenylsilyl perchlorate **(6)**. Hydrogen atoms are omitted for clarity. Bond lengths in Å. Reprinted with permission from Reference 70. Copyright (1987) American Chemical Society

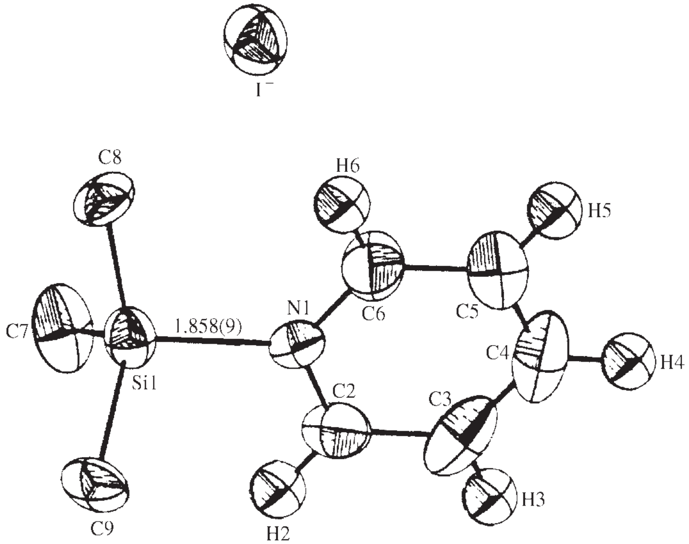

(7)

FIGURE 6. ORTEP drawing of the experimental structure of the trimethylsilyl–pyridine complex (**7**). Si–N bond length in Å. Reproduced by permission of Wiley-VCH from Reference 69

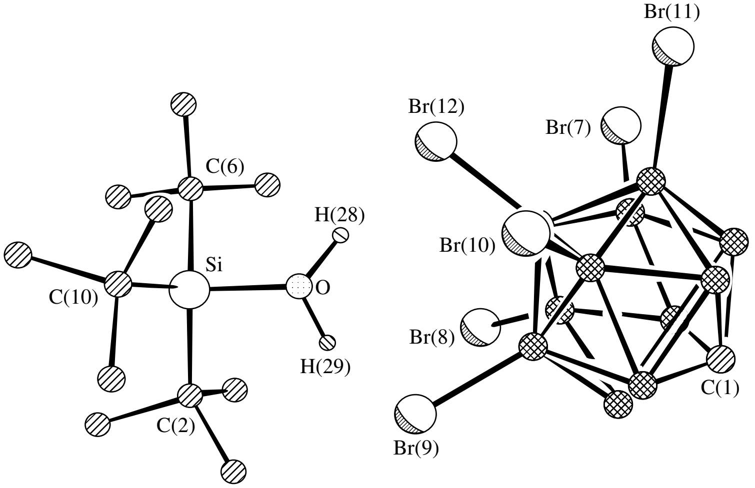

(9)

FIGURE 7. Experimental molecular structure of $[t\text{-Bu}_3\text{Si(OH}_2)]^+$ $[\text{Br}_6\text{CB}_{11}\text{H}_6]^-$. Bond distances (Å): Si–O 1.779(9), Si–C(2) 1.897(17), Si–C(6) 1.897(15), Si–C(10) 1.884(12). Bond angles (deg): C(2)–Si–C(6) 116.0(6), C(2)–Si–C(10) 116.1(6), C(6)–Si–C(10) 115.9(7), O–Si–C(2) 100.7(5). Reproduced by permission of the Royal Society of Chemistry from Reference 71

The myth that d-orbitals contribute significantly to silicon bonds has been discredited, e.g. by Schleyer and coworkers[6]. Natural population analysis (NPA)[85] of the bonds to silicon reveals no d-orbital participation in the SiX_3^+, SiX_4, SiX_5^-, SiX_6^{2-} species **1**, **10–12** (X = H), and **13–16** (X = F); see Figure 8. Even the tetrahedral SiH_4 **(10)** and SiF_4 **(14)** do not show the expected sp^3 hybridization, since H and F substituents, which are more electronegative than Si, withdraw more electrons from the higher-lying silicon p-orbitals. The bonds between silicon and first-row elements are both covalent and highly polar[6].

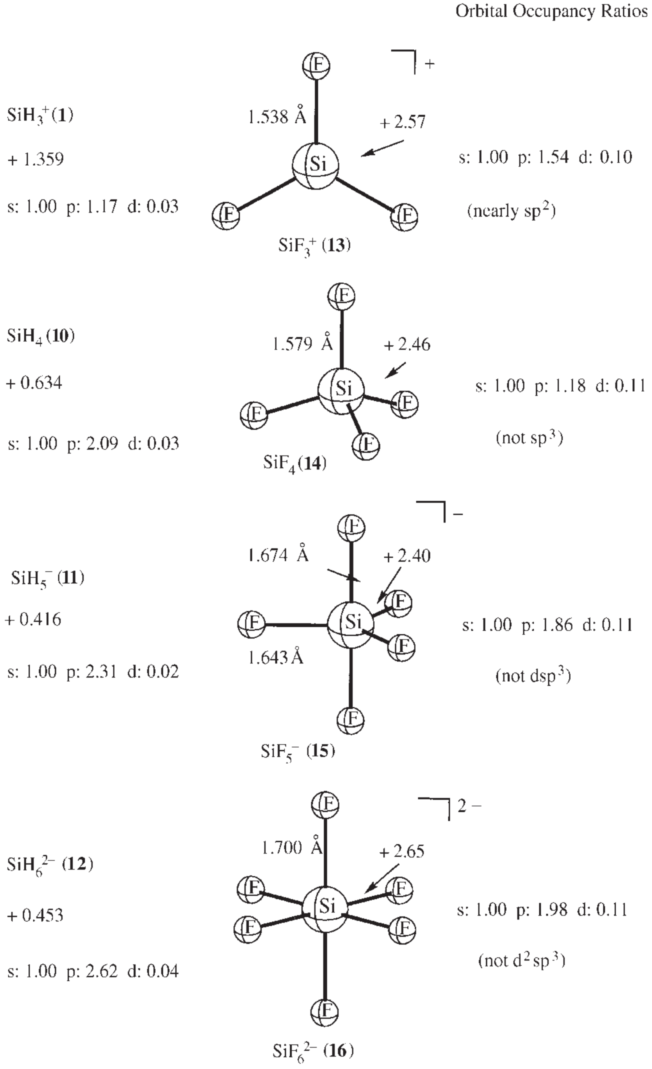

FIGURE 8. Silicon hybridizations and silicon NPA charges in species **1** and **10–16**. Reproduced by permission of Wiley-VCH from Reference 6

The complexation energies of silicenium ions with Lewis bases have been studied in detail by several groups[6,83,86]. Schleyer and coworkers reported a decrease in the interaction energies between silicenium ions and Lewis bases in the order: haloalkanes (or haloalkenes)[6] > arenes[73] > alkanes (e.g. methane)[6] > noble gases[6] (Table 3). Both the computed and experimental data show large complexation energies between silicenium ions and arenes, i.e. the silophilicity of arenes even competes with those of *n*-donors such as fluoroalkanes. It is not expected that such interactions will be suppressed totally in solution. Hence, the triethyl silicenium–toluene aggregate in **2** is best described as a covalent σ-complex with some ionic character[73]. The data in Table 3 show that the more stable the silicenium ion becomes the smaller is its complexation energy with Lewis bases.

TABLE 3. Interaction energies ΔE in binary complexes between silicenium ions and different Lewis bases (kcal mol^{-1}). Coordinating atoms are underlined

R^+	Base	PG[i]	ΔE[a]	Reference
$SiH_3{}^+$	$HN\underline{C}$	C_{3v}	61.4	83a
$SiH_3{}^+$	$HC\underline{N}$	C_{3v}	59.9	83a
$SiMe_3{}^+$	$HC\underline{N}$	C_{3v}	40.1	83a
$SiH_3{}^+$	$\underline{N}H_3$	C_{3v}	76.6	83a
$SiMe_3{}^+$	$\underline{N}H_3$	C_{3v}	54.4	83a
$SiH_3{}^+$	$H\underline{Cl}$	C_s	26.0	83a
$SiMe_3{}^+$	$H\underline{Cl}$	C_s	12.2	83a
$SiH_3{}^+$	$H_2\underline{O}$	C_s	56.4	83a
$SiMe_3{}^+$	$H_2\underline{O}$	C_s	38.8	83a
$SiH_3{}^+$	$Me{-}\underline{O}{-}Me$	C_s	70.2	83a
$SiH_3{}^+$	$Me\underline{Cl}$	C_s	40.6	83a
$SiH_3{}^+$	$Me\underline{F}$	C_s	44.9[b]	6
$SiMe_3{}^+$	$Me\underline{F}$	C_s	30.0[b]	6
$SiH_3{}^+$	$Me\underline{Br}$	C_s	43.1[c]	6
$SiMe_3{}^+$	$Me\underline{Br}$	C_s	28.4[c]	6
$SiMe_3{}^+$	$MeC\underline{N}$	C_{3v}	50.6	83a
$SiH_3{}^+$	*cis*-$CHF{=}CH\underline{F}$	C_1	36.5[b]	6
$SiMe_3{}^+$	*cis*-$CHF{=}CH\underline{F}$	C_1	23.7[b]	6
$SiH_3{}^+$	C_6H_6	C_s	54.8[d]	73
$SiMe_3{}^+$	C_6H_6	C_s	31.1[e]; 23.9[f]	73
$SiMe_3{}^+$	4-Me-C_6H_5	C_s	34.2[e]; 28.4[g]	73
$Si(NH_2)_3{}^+$	$H_2\underline{O}$	C_s	32.6[d] (28.8)[h]	86
$Si(NMe_2)_3{}^+$	$H_2\underline{O}$	C_s	17.3[h]	86
$SiH_3{}^+$	CH_4	C_1	16.4[d]	6
$SiH_3{}^+$	He; Ne; Ar	C_{3v}	0.3; 6.8; 7.1	6[d]
$SiMe_3{}^+$	He; Ne; Ar	C_{3v}	0.4; 4.4; 2.6	6[d]

[a] At HF/TZ+P, unless noted otherwise.

[b] At MP2(fc)/6-31+G*.

[c] At MP2(fc)/ECP; C,Si/Br: 4/7-ve-MWB-ECP and DZ+P valence basis; H: DZ basis.

[d] At MP2(fc)/6-31G*.

[e] At MP2(fc)/6-31G*//HF/6-31G*.

[f] Experimental gas-phase value taken from A. C. M. Wojtyniak and J. A. Stone, *Int. J. Mass Spectrom. Ion Process.*, **74**, 59 (1986).

[g] Experimental gas-phase value taken from J. M. Stone and J. A. Stone, *Int. J. Mass spectrom. Ion Process.*, **109**, 247 (1991).

[h] HF/6-31G*.

[i] Point-group symmetry.

The comprehensive studies by Cremer and coworkers of silicenium ions and their interactions with Lewis bases and solvent molecules are particularly noteworthy[83]. Nonspecific solvation effects on calculated ^{13}C and ^{29}Si NMR chemical shifts were probed via the PISA continuum model[87] (see discussion below). According to the authors, silicenium ions react in weak or normal nucleophilic media with one or more solvent molecules to form covalently bonded tetra- and penta-coordinate silicon complexes, in which any silicenium ion character is lost[83]. The complexation energies can be as high as 100 kcal mol^{-1} for ternary complexes (see Table 4), e.g. 104.7 kcal mol^{-1} for $SiH_3(NH_3)_2^+$ (at HF/6-311G**)[83]. Similar values have been reported by Schleyer and coworkers[6]. Competitive base coordination to silicenium ion reduces the effectiveness of substituent stabilization; e.g. note the trend in HF/TZ+P computed methyl stabilization energies (in kcal mol^{-1}): Me_3Si^+ (36.0) > Me_3Si^+/ClH (22.7) > Me_3Si^+/OH_2 (18.3) > Me_3Si^+/H_3N (13.8)[83a].

Cremer and coworkers have also investigated the effect of increasing the number of 'solvent molecules' in the model complexes $SiH_3^+{-}(H_2O)_n$ ($n = 1, 2, 3, 5$)[83a]. The equilibrium Si−O bond lengths in $H_3Si{-}OH_2^+$ **(17)** and in $Me_3Si{-}OH_2^+$ **(18)**, computed at HF/6-31G*, are 1.859 Å and 1.910 Å, respectively[83a], compared to an experimental value of 1.779(9) Å in $(t\text{-Bu})_3Si{-}OH_2^+$ **(9)**[71]. One would have expected that the presence of the sterically more demanding alkyl groups in **9** correlates with a longer Si−O bond length. Therefore, we attribute the short experimental Si−O bond distance in **9** to crystal packing forces. In any event, the covalent character of the Si−O bond results in a highly shielded δ ^{29}Si of 99.0 ppm (computed at IGLO/BII[83a]). Based on calculated electron density distributions $\rho(r)$, its associated Laplacian concentration $-\nabla^2\rho(r)$ and the energy density distribution $H(r)$[88], the authors differentiated between covalent and ionic bonding patterns for a large number of silicon compounds and silicenium ions[83a]. Analysis of the electron density in highly hydrated silicenium cations showed that only the axially but not the equatorially positioned water molecules are covalently bonded to silicon. Cremer and coworkers concluded: 'This suggests that only the 1 : 1 and 1 : 2 adducts of water are chemically distinct species, which can be isolated and investigated while additional water molecules do not enlarge the coordination sphere of Si but lead to solvation of the 1 : 2 adduct'[83a]. Thus, one can speak of different 'solvation shells' of the silicenium ion: the first one containing a maximum of two solvent molecules, and a second shell with up to 12 solvent molecules[83b].

Frenking's group investigated the solvation of the silaguanidinium ion, $(H_2N)_3Si^+$ **(19)**, by a water molecule[86]. Compared to the H_2O binding energies of the parent H_3Si^+

TABLE 4. Interaction energies ΔE in ternary complexes between silicenium ions and different Lewis bases (kcal mol^{-1}). Coordinating atoms are underlined

R^+	Base (2x)[a]	PG[b]	ΔE^c	Reference
SiH_3^+	$HC\underline{N}$	D_{3h}	80.0	83a
SiH_3^+	$\underline{N}H_3$	D_{3h}	105.0; 122.3[d]	83a, 6
$SiMe_3^+$	$\underline{N}H_3$	C_{3h}	65.7	83a
$SiMe_3^+$	$H_2\underline{O}$	C_s	47.7	83a
SiH_3^+	$H_2\underline{O}$	C_{2v}	79.9	83a
SiH_3^+	$H_2\underline{O}$ (3x)	C_{2v}	87.7	83a
SiH_3^+	$H_2\underline{O}$ (5x)	C_{2v}	97.8	83a

[a] The number of the base molecules is given in parentheses (2 molecules, unless stated otherwise).
[b] Point-group symmetry.
[c] At HF/TZ+P, unless stated otherwise.
[d] At MP2(fc)/6-31G*.

(57.7 kcal mol^{-1}) and of trialkyl-substituted silicenium ions, e.g. Me_3Si^+ (40.6 kcal mol^{-1}), the $(NH_2)_3Si^+$ cation interacts with water to a much smaller extent, i.e. the binding energy is 28.8 kcal mol^{-1}. Hexamethyl substitution on all three nitrogens reduces the water binding energy further to 17.3 kcal mol^{-1}. Thus, the silaguanidinium cation **19** should coordinate to solvent molecules less strongly than alkyl-substituted silicenium ions[86].

Trialkylsilicenium ions and their Lewis base complexes have also been studied by the groups of Olah[77,89], Reed[90,91] and Schleyer[6,73]. Olah and coworkers plotted (see Figure 9) the dependence of the complexation energy (computed at B3LYP/6-31G*//B3LYP/3-21G) in the Me_3Si^+–benzene complex **(20)** on the Si–C$_{ipso}$ distance[89] (see also Figure 4, with R = Me, R′ = H). The authors found an 'anharmonic' energy potential with a computed equilibrium Si–C$_{ipso}$ distance of 2.250 Å[89]. The computed distance in **20** fits nicely the experimental value of 2.18 Å found in **2**[2a], and underlines the reliability of the computational level chosen in this study. The interaction energy between Me_3Si^+ and the benzene in **20** vanishes only at a distance as large as 4.5 Å[89], illustrating that the 'myth of non-coordinating counterions'[92] or solvent molecules is not valid. Thus, it seems very unlikely that 'free' tricoordinate silicenium ions can exist with Si–C bond distances of *ca* 2.2 Å to a nearby arene moiety[89].

Reed's group reported the X-ray structures of trialkyl-silicenium ions R_3Si^+ complexed to low-nucleophilic hexahalo carborane anions[90,91]. The authors varied systematically both the alkyl substituents R (R = Me, Et, *i*-Pr and *t*-Bu) and the halogen substitution of the $X_6CB_{11}H_6^-$ (X = Cl, Br, I) counterions. The degree of silicenium ion character in the

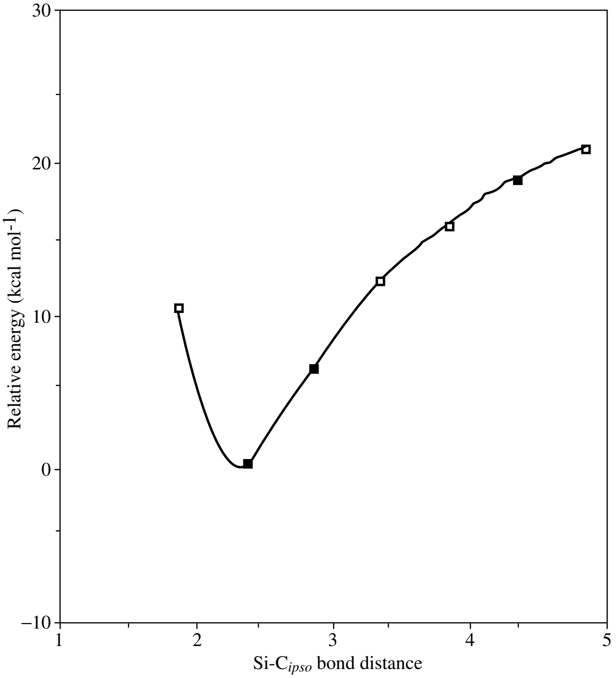

FIGURE 9. Plot of the relative energy vs the Si–C$_{ipso}$ bond distance (Å) in the benzene complex of Me_3Si^+ **(20)**. Reproduced by permission of Elsevier Science from Reference 89

R_3Si^+ moiety was estimated from the sum of the bond angles around silicon, which should reach the ideal 360° value in a free tri-coordinate silicenium ion[90]. Surprisingly, the closest approach to planarity was found for the tri-*iso*-propyl derivatives, rather than for the tri-*tert*-butyl species. The authors also concluded that hyperconjugative stabilization of the cationic silicon centre is not negligible, although it is less pronounced than in carbocations[90]. The hexachloro carborane anion was found to be the least coordinating and, based on structural, energetic and NMR criteria, more than 50% silicenium ion character was assigned to the i-$Pr_3Si^{\delta+}$ $(Cl_6CB_{11}H_6)^{\delta-}$ complex[91] **21**. The experimental structure of **21** is shown in Figure 10. This viewpoint was challenged by Olah and coworkers, who regard such species as halonium ions[74,89].

The infrared (IR) spectrum of $SiH_7{}^+$ **(22)**, formally a complex of H_3Si^+ and two molecules of H_2, was reported in 1993 by Okumura and coworkers[93]. The IR spectrum displayed a single band centred around 3866 cm^{-1}, which was red-shifted by 295 cm^{-1} with respect to free molecular hydrogen[93]. The absence of a second band in the 3500 to 4200 cm^{-1} region suggested a symmetric complex with the structure $H_2{-}SiH_3{}^+{-}H_2$, i.e. a planar $SiH_3{}^+$ species with two equidistant H_2 ligands bound to opposite faces of the silicenium ion[93]. Moreover, the authors suggested a preferred side-on ligation of the H_2 moieties, since such an arrangement would maximize the electron donation from the σ H−H bonds into the empty 3p-orbital on silicon[93]. Based on an empirical correlation between the lowering of the H−H stretching mode and the binding energy of molecular hydrogen–ion cluster complexes, a crude binding energy estimate of 7–9 kcal mol^{-1} was obtained[93]. The symmetric structure of $SiH_7{}^+$ is in sharp contrast to that found for the closely related $CH_7{}^+$ complex[94] **(23)**, which exhibits an unsymmetric equilibrium geometry. Indeed, **23** has a structure of a protonated methane $CH_5{}^+$[95] **(24)** complexed with an additional, but weakly bound molecule of hydrogen, attached to one of the electron-deficient hydrogens of the three-centre–two-electron bond. Consequently, two different H−H stretching frequencies are observed in the IR spectrum of $CH_7{}^+$[94].

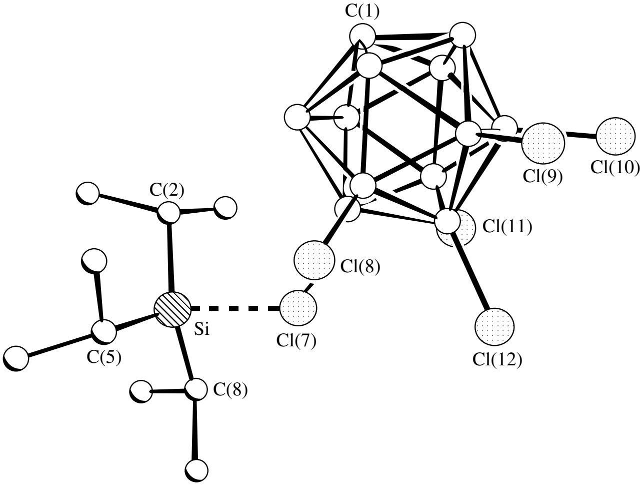

FIGURE 10. Experimental structure of i-$Pr_3Si^+(Cl_6CB_{11}H_6)^-$ **(21)**. The Si−Cl(7) bond length is 2.323(3) Å. Reprinted with permission from Reference 91. Copyright (1996) American Chemical Society

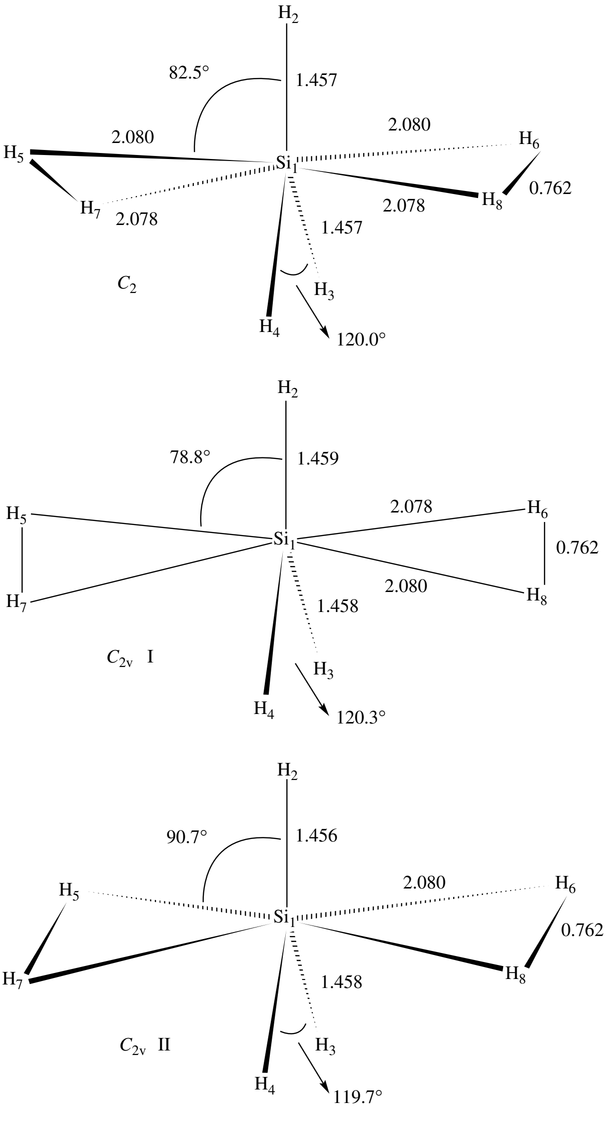

FIGURE 11. Three different structures of SiH_7^+ **(22)**, optimized at CCSD(T). Bond lengths in Å, bond angles in deg. Reprinted with permission from Reference 98. Copyright (1994) American Chemical Society

Subsequent high level computations on both CH_7^+[96] and SiH_7^+[97,98] confirmed the conclusions drawn from the experimental data. The calculated structures of three different SiH_7^+ species are shown in Figure 11. The quite remarkable structural and energetic differences between the CH_7^+ and SiH_7^+ species could be related to the differences between the CH_3^+/SiH_3^+ and CH_5^+/SiH_5^+ pairs. The greater thermodynamic stability of the SiH_3^+ cation (see the previous discussion) requires less stabilization by the ligands, which is reflected in the first complexation energies: CH_3^+ binds molecular hydrogen by 40.0–42.0 kcal mol^{-1}[95] whereas the formation of SiH_5^+ (**25**) from H_3Si^+ and H_2 is much less exothermic (calculated: 10–15 kcal mol^{-1}[99]; experimental: 17.8 kcal mol^{-1}[100]). The calculated equilibrium geometries of SiH_5^+ and of CH_5^+ are also quite different: CH_5^+ is a rather fluxional species in which the electron deficiency is spread over all hydrogens via a non-classical three-centre–two-electron bond[95]. In contrast, SiH_5^+ is best described as a side-on complex between molecular hydrogen and the parent SiH_3^+ cation[99]. The second hydrogen complexation energies, however, show a contrasting trend: they are 4.6 kcal mol^{-1} for SiH_5^+[98,99] but only 1.2 kcal mol^{-1} for CH_5^+[95]. Thus, ligation of a second molecular hydrogen to SiH_3^+ is *ca* 50% as effective as the first binding, whereas for CH_3^+ second ligation contributes nearly zero. These remarkable differences can be rationalized on both electronic and steric grounds. The more electronegative carbon in CH_3^+ coordinates the first molecular hydrogen more strongly than SiH_3^+, but a hypothetical symmetric $H_2{-}CH_3^+{-}H_2$ complex is sterically more crowded than its silicon congener[98].

D. ^{29}Si NMR Chemical Shifts of Silicenium Ions

Nuclear magnetic resonance is very sensitive to structural variations. Thus, ^{29}Si NMR chemical shifts should be one of the best tools for measuring the degree of silicenium ion formation. IGLO NMR computations predict ^{29}Si NMR chemical shifts δ of 264.7 ppm and 346.7 ppm for SiH_3^+ and $SiMe_3^+$ (**26**), respectively[6]. The observed chemical shifts of trialkylsilicenium ions in arene solvents, however, were found at much higher fields (83.6 ppm for $SiMe_3^+$ in d_6-benzene[2b], 81.8 ppm for $SiEt_3^+$ in toluene[2b] and 109.8 ppm for $i\text{-}Pr_3Si^+$ in the solid state[3a]). A summary of calculated and experimental ^{29}Si NMR chemical shifts of silicenium ions and related compounds is given Table 5. Note, for instance, the computed large deshieldings in the isolated silyl-substituted silicenium ions (e.g. $\delta^{29}Si = 925$ ppm for $(Me_3Si)_3Si^+$)[77], compared to the experimental δ^{29}Si of 111.1 ppm in benzene solution[101]. Hence, the alleged preparation of free $(Me_3Si)_3Si^+$ cations in arene solutions[101] must be questioned.

Lambert and coworkers attributed the 200–250 ppm upfield deviation from the computed gas-phase values of the free silicenium ions to 'distortion from the plane to relieve external sources of strain'[2]. Contrary to these speculations, IGLO computations by Olah's[77] and Cremer's[83] groups predict a *downfield* shift upon pyramidalization, as shown in Figure 12. A similar deshielding of the ^{13}C NMR chemical shift upon pyramidalization of CH_3^+ has been reported by Schindler and Kutzelnigg[32b,c]. The distortion of the HCH bond angle from 120° to 117° results in a downfield shift of 20 ppm. Due to the pyramidalization, the empty p_π-orbital (either on C^+ or on Si^+) mixes with the σ-orbitals gaining partial s-character. The energy of the p_π-orbital is lowered, giving larger paramagnetic contributions since the local $\sigma{-}\pi$ excitation energies are reduced. Therefore, the central carbon or silicon nuclei in the XH_3^+ species ($X = C$, Si) are deshielded upon bending[32b,c].

^{29}Si NMR chemical shifts of silicenium ions show a remarkable long-range dependence on the distance to neighbouring molecules (either Lewis bases or solvent molecules). Schleyer and coworkers[6] first noticed that δ^{29}Si in the H_3Si^+–methane adduct **27** is considerably shielded at C–Si distances below 4.0 Å, e.g. 56.8 ppm at the equilibrium

TABLE 5. Compilation of calculated and measured δ^{29}Si NMR values (ppm) of silicenium ions and of related compounds

Species (PG)	δ^{29}Si, calc.[a]	Reference	δ^{29}Si, exp.
H_3Si^+ (D_{3h})	270.2 (310.8)	83a	
	264.7[b]	6	
H_3Si^+/Ng (C_{3v})	Ng = He: 253.7[b]	6	
	Ng = Ne: 188.2[b]		
	Ng = Ar: 112.1[b]		
H_3Si^+/NH_3 (C_{3v})	−28.7	83a	
$H_3Si^+/(NH_3)_2$ (D_{3h})	−127.7	83a	
H_3Si^+/NCH (C_{3v})	−26.2	83a	
$H_3Si^+/(NCH)_2$ (D_{3h})	−102.8	83a	
$H_3Si^+/NCMe$ (C_{3v})	−35.3	83a	
H_3Si^+/OH_2 (C_s)	13.4	83a	
$H_3Si^+/(OH_2)_3$ (C_{2v})	−64.3	83a	
$H_3Si^+/(OH_2)_5$ (C_{2v})	−51.5	83a	
H_3Si^+/ClH (C_s)	26.7	83a	
MeH_2Si^+ (C_s)	299.1[b]	119	
Me_2HSi^+ (C_2)	325.1[b]	119	
Me_3Si^+ (C_{3h})	355.9	83a	
	346.7	6	
	354.2[c]	89	
Me_3Si^+/Ng (C_{3v})	Ng = He: 345.0[b]	6	
	Ng = Ne: 311.0[b]		
	Ng = Ar: 275.0[b]		
Me_3Si^+/C_6H_6 (C_s)	60[b,d], 80.0[c]	6, 89	83.6 (Ref. 2)
Me_3Si^+/NH_3 (C_{3v})	52.8	83a	
Me_3Si^+/NCH (C_{3v})	67.0	83a	
$Me_3Si^+/NCMe$ (C_{3v})	52.2	83a	
Me_3Si^+/OH_2 (C_s)	99.0, 101.9[c]	83a, 89	
Me_3Si^+/ClH (C_s)	183.5	83a	
Me_3Si^+/BrH	154.4[c]	89	
$Me_3Si^+/BrMe$ (C_s)	102.1[b] [−1.9][f], 117.5[c]	6; 89	
Me_3Si^+/FMe (C_s)	134.4[b] [49.6][f]	6	
$Me_3Si^+/CFH{=}CFH$ (C_1)	178.0[b] [74.6][f]	6	
Me_3SiBr (C_{3v})	33.9[e]	89	26.4 (Ref. 118)
$Et_3Si^+/$(C_{3h})	371.3[c]	89	
Et_3Si^+/C_3H_6 (C_1)	70.0[c]	89	
Et_3Si^+/C_6H_6 (C_s)	104.6[g]	77	92.3 (Ref. 2)
Et_3Si^+/C_6H_5Me (C_s)	79.8[c]	89	81.8 (Ref. 2) 83.2 (Ref. 89)
$NH_2SiH_2^+$ (C_{2v})	122.2[h]	86	
$(NH_2)_3Si^+$ (D_3)	40.0[h]	86	
$(NH_2)_3Si^+/OH_2$ (C_1)	−21.0[h]	86	
Me_3SiOH	15.1[c]	89	
$(Me_3Si)_2OH^+$	67.6[c]	89	
$Me_3Si^+/NCCH_3$	51.5[c]	89	
$(H_3Si)_3SiH$	−139.2[g]	77	

(*continued overleaf*)

TABLE 5. (*continued)*

Species (PG)	δ^{29}Si, calc.[a]	Reference	δ^{29}Si, exp.
$(H_3Si)_3Si^+$	865.7[g]	77	
$(Me_3Si)_3SiH$	−124.2[g]	77	−117.4 (Ref. 77)
$(Me_3Si)_3Si^+$	925.3[g]	77	
$(H_3Si)_3Si^+/C_6H_6$	55.6[g]	77	

[a] All data at IGLO/BII/HF/6-31G* (values in parentheses at GIAO-MP2/BII), unless noted otherwise.

[b] IGLO/BII//MP2/6-31+G*, except the values of the H_3Si^+ and Me_3Si^+ noble gas (Ng) complexes, which are at IGLO/BII//MP2/6-31G*.

[c] IGLO/BII′//B3LYP/6-31G*.

[d] Using a HF/6-31G* geometry.

[e] IGLO/BII′//B3LYP/6-311+G*.

[f] Data in square brackets refer to the corresponding H_3Si^+ complexes.

[g] IGLO/BII′//HF/6-31G*.

[h] IGLO/BII+sp//MP2/6-31G*.

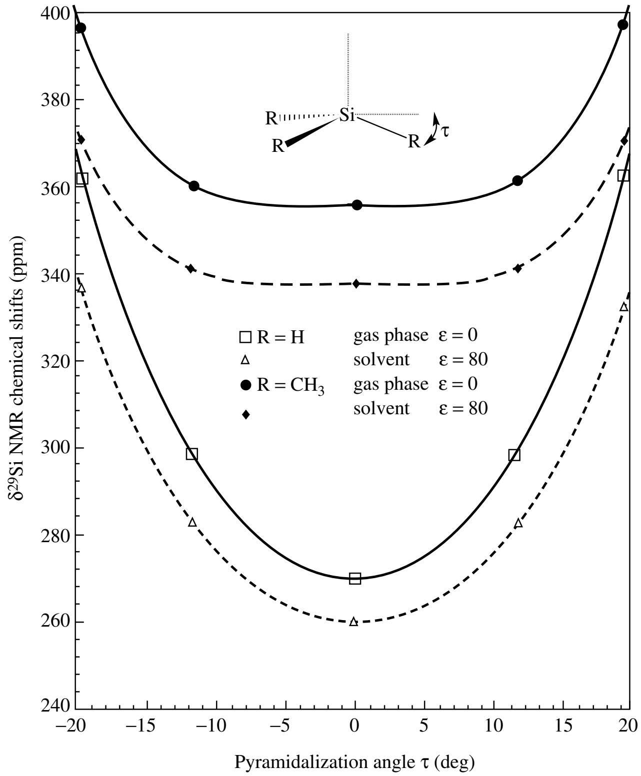

FIGURE 12. Dependence of the calculated δ^{29}Si chemical shifts of $SiR_3{}^+$ (R = H, CH_3) on the pyramidalization angle τ at Si. Solid lines denote IGLO/[7s6p2d/5s4p1d/3s1p] (basis II) calculations, dashed lines denote PISA-IGLO/[7s6p2d/5s4p1d/3s1p] (basis II) calculations. Reprinted with permission from Reference 83a. Copyright (1995) American Chemical Society

distance of 2.26 Å [MP2(fc)/6-31G* geometry; see Figure 13]. Thus, the highly deshielded ^{29}Si NMR values, which have been computed for 'naked' silicenium ions and also are anticipated for free silicenium ions in solution, are practically hard to achieve. A similar distance dependence of the ^{29}Si NMR chemical shifts in $H_3Si^+{-}S_n$ complexes ($S = H_2O$, NH_3 and HCN; $n = 1, 2$) was also reported by Cremer's group[83a] and their results are shown in Figure 14.

Even non-nucleophilic media, such as nobel gases, were shown to influence the ^{29}Si NMR chemical shifts of silicenium ions to a remarkable extent[6], e.g. in $Me_3Si^+{-}Ng$ complexes, where Ng = He **(28)**, Ne **(29)** and Ar **(30)** (Figure 15), compared to the isolated Me_3Si^+ ion.

A recent achievement by Cremer's group[83] is the direct incorporation of continuum solvent effects, via the PISA self-consistent reaction field (SCRF) model[87], in the computation of chemical shifts. Cremer and his coworkers found that computed solvent effects on ^{29}Si NMR chemical shifts can be as large as 20 ppm *upfield* in highly polar media ($\epsilon = 80$)[83]. The expected ^{29}Si NMR chemical shift range of silicenium cations[83a] as a function of the strength of interaction with nucleophiles, predicted by Cremer and his coworkers, are given in Table 6. The largest δ^{29}Si values, i.e. *ca* 410 ppm, have been estimated for free alkyl-substituted silicenium ions in the gas phase or in non-coordinating solvents. Weakly interacting solvents, i.e. with donicities D^{84} ranging between 0 and 1,

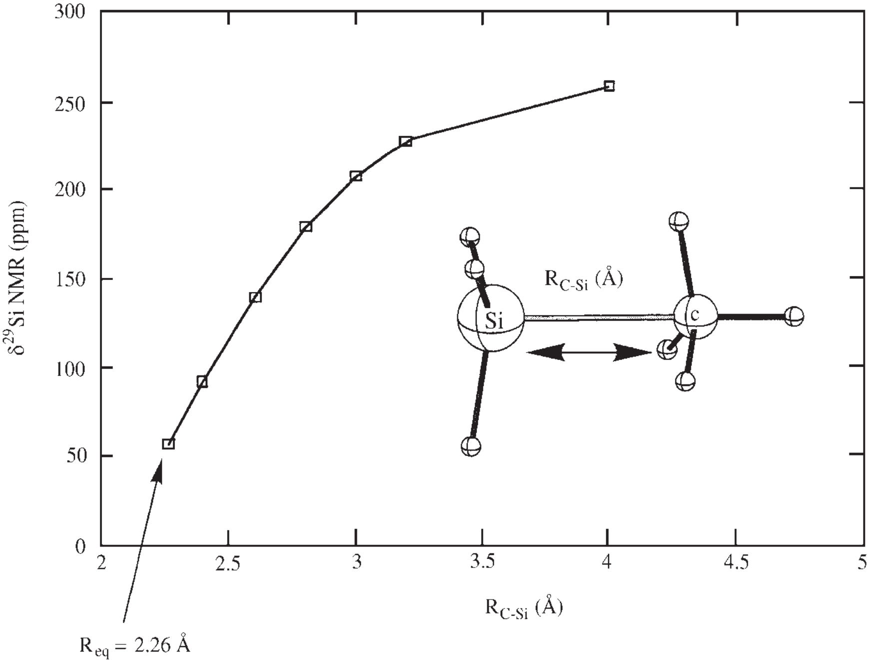

FIGURE 13. Dependence of the computed δ^{29}Si chemical shifs on the Si−C distance in the H_3Si^+−methane complex **(27)**; data at IGLO/BII//MP2(fc)/6-31G* versus TMS. Reproduced by permission of Wiley-VCH from Reference 6

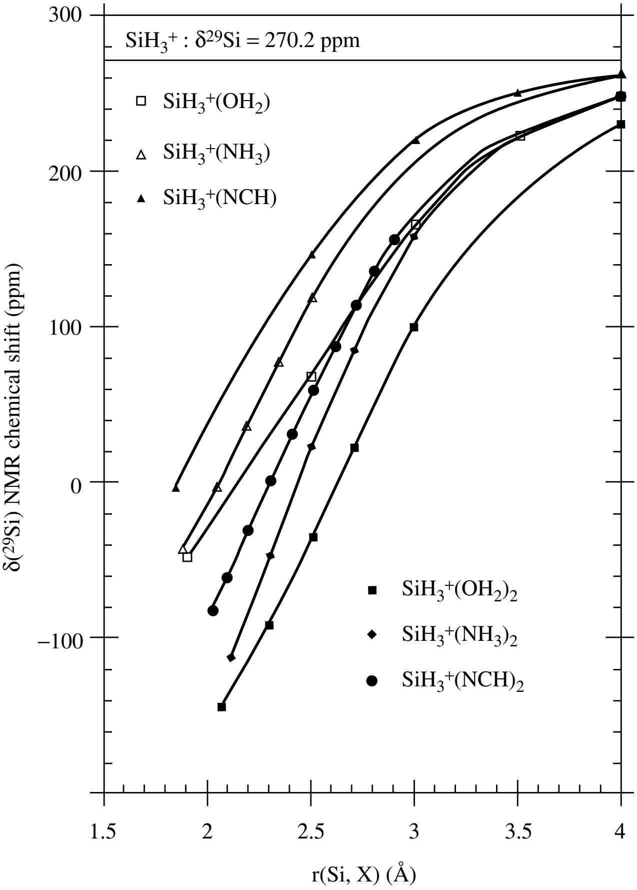

FIGURE 14. Dependence of the δ^{29}Si chemical shifts of $SiH_3(S)_n{}^+$ cations, for $n = 1$ (S = HCN, NH_3, H_2O, HCl) and for $n = 2$ (S = HCN, NH_3, H_2O), on the Si–S distance, IGLO/[7s6p2d/5s4p1d/3s1p] //HF/6-311G(d,p) calculations. Reprinted with permission from Reference 83a. Copyright (1995) American Chemical Society

lead to a partial loss of silicenium ion character due to van der Waals interactions (with the most deshielded δ^{29}Si values being between 220 and 390 ppm), implying some charge transfer. Weakly and strongly coordinating solvents, i.e. solvents having donicities larger than 1, result in a total loss of silicenium ion character, as indicated by the strongly shielded δ^{29}Si values ranging between −130 and +110 ppm[83a].

The preparation of a species which can be described as a free silicenium ion in solution has been finally achieved recently by Lambert's group[4]. The experimentally determined, strongly deshielded δ^{29}Si of 225.5 ppm for the trimesitylsilyl cation Mes_3Si^+ (Mes = 2,4,6-trimethylphenyl), **31**, could also be verified computationally[5] (see discussion below).

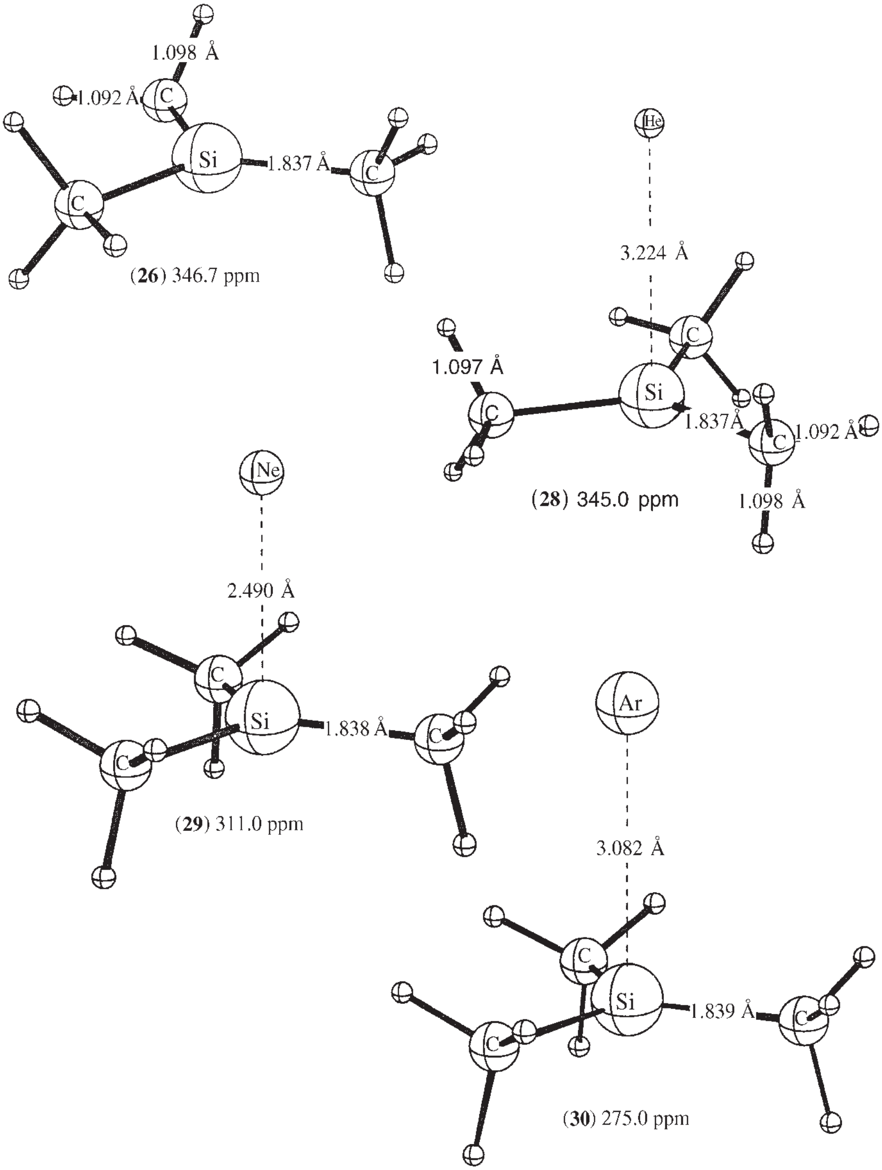

FIGURE 15. Computed δ^{29}Si chemical shifts and geometries of Me_3Si^+ (**26**) and noble gas complexes, **28–30**. Calculated NMR data at IGLO/BII//MP2(fc)/6-31G* versus TMS. Reproduced by permission of Wiley-VCH from Reference 6

TABLE 6. Estimated ranges of δ^{29}Si chemical shifts (ppm) for silicenium cations in the gas phase and in solution[a,b]

R_3Si^+	Gas phase	Non-coordinating solvent ($0 < \epsilon \leqslant 80$)	Weakly interacting solvents ($0 < D \leqslant 1$)	Weakly coordinating solvents ($0 < D \leqslant 10$)	Strongly coordinating solvents ($D > 10$)
R = H	300[c]	290–300	120–290	10–110	−130 to 10
R = CH_3	385[c]	370–385	200–370	90–190	−50 to 90
R = C_2H_5	410[c]	390–410	220–390	110–210	−30 to 110
Si−S interaction		solvation[d]	van der Waals[e]	weakly bonding	stronger bonding
Ion character		free silicenium ions	partial loss of silicenium ion character	total loss of silicenium ion character	

[a] Data from Reference 83a.

[b] The solvent is characterized by a dielectric constant ϵ and a donicity D (see Reference 84).

[c] Including estimated correlation corrections of 30 ppm (see Reference 83a for details).

[d] Solvation without any charge transfer from S to R_3Si^+.

[e] Van der Waals interactions imply some charge transfer.

E. π-Donor Stabilized Silicenium Ions

1. The silaguanidinium ion

In continuation of their previous computational work on Y-conjugated compounds[102], Frenking and his coworkers presented a detailed study on the silaguanidinium cation $(H_2N)_3Si^+$ **(19)** and related species[86]. The computations predict an equilibrium geometry with an overall D_3 symmetry, i.e. the amino groups are planar but rotated about the Si−N bonds by 19.6° at MP2/6-31G* (12.9° at HF/6-31G*)[86]. The calculated Si−N bond lengths of 1.658 Å are intermediate between those of Si=N double (1.568 Å) and Si−N single (1.748 Å) bonds. The planar D_{3h} form, which has one imaginary frequency, is only 0.7 kcal mol^{-1} higher in energy than the D_3 minimum (at MP4/6-311G**//MP2/6-31G*)[86]. The calculated out-of-plane rotation barrier about the Si−N bond of 5.5 kcal mol^{-1} (same level) is by 6.6 kcal mol^{-1} lower than the corresponding value in the parent guanidinium carbocation $(H_2N)_3C^+$. Thus, there is a higher π-contribution to the C−N bonds of the guanidinium ion than to the Si−N bonds in the silaguanidinium ion. The topological analysis of the electron density in **19**, which is shown in Figure 16, reveals highly polar Si−N bonds with large ionic contributions, but the weakly negative value for the energy density at the Si−N bond critical point also indicates moderate covalent character[86].

The stabilization energies due to the amino groups were evaluated by means of the homodesmotic reactions shown in Scheme 1[86]. The incremental stabilization by amino groups becomes less effective upon higher degree of substitution (equations 5–7), but the attenuation is less pronounced for the silicenium ions. Similar conclusions were drawn earlier by Apeloig[9,10]. The cumulative stabilizing effect of the three amino groups in the silaguanidinium ion, computed via the sum of equations 5–7, namely −77.6 kcal mol^{-1}, amounts to *ca* 44% of the corresponding value in the analogous guanidinium carbocation (−174.8 kcal mol^{-1}). The total stabilizing effect of triple substitution shows that amino groups (equation 8) are much more effective than methyl groups (equation 9). Thus, the authors concluded that amino-substituted silicenium ions are better targets in the search for stable silicenium ions in solution than alkyl-substituted species[86]. In particular, they

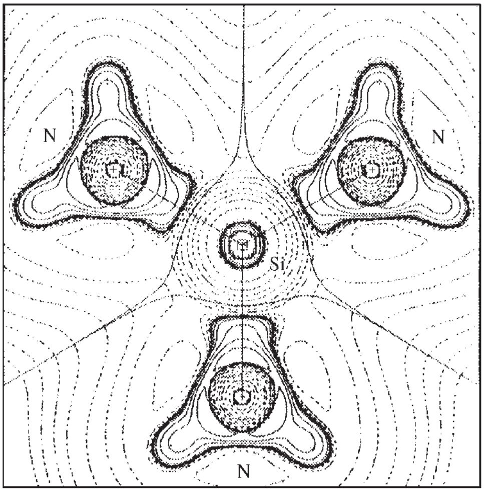

FIGURE 16. Contour line diagrams of the Laplacian distribution $\nabla^2\rho(r)$, at MP2/6-31G(d), of the silaguanidinium ion **19** in the SiN_3 plane. Dashed lines indicate charge depletion [$\nabla^2\rho(r) > 0$], solid lines indicate charge concentration [$\nabla^2\rho(r) < 0$]. The solid lines connecting the atomic nuclei are the bond paths; the solid lines separating the atomic nuclei indicate the zero-flux surfaces in the plane. The crossing points of the bond paths and zero-flux surfaces are the bond critical points r_b. Reproduced by permission of Wiley-VCH from Reference 86

suggested that the bis(pyrrolidino)(2,5-di-*tert*-butylpyrrolidono)silicenium ion **32**, whose calculated structure is shown in Figure 17, should benefit from both strong electronic stabilization and steric protection of the cationic centre[86].

Stabilization energies (kcal mol^{-1}) for:			X = S;	X = C	
$XH_3^+ + H_3XNH_2$	$\longrightarrow$	$XH_2NH_2^+ + XH_4$	−37.5	−103.4	(5)
$XH_2NH_2^+ + H_3XNH_2$	$\longrightarrow$	$XH(NH_2)_2^+ + XH_4$	−23.3	−44.3	(6)
$XH(NH_2)_2^+ + H_3XNH_2$	$\longrightarrow$	$X(NH_2)_3^+ + XH_4$	−16.8	−27.1	(7)
Σ (5) − (7)			−77.6	−174.8	
$XH_3^+ + HX(NH_2)_3$	$\longrightarrow$	$X(NH_2)_3^+ + XH_4$	−63.5	−159.3	(8)
$XH_3^+ + HX(Me)_3$	$\longrightarrow$	$X(Me)_3^+ + XH_4$	−36.0	−67.7	(9)

SCHEME 1

The silicon atom in the silaguanidinium ion bears a high positive charge (+2.24) while the nitrogens carry a high negative charge (−1.35)[86]. The large positive charge on silicon is not reflected in a downfield shift of the ^{29}Si NMR chemical shift of the silaguanidinium ion. IGLO calculations for $(H_2N)_3Si^+$ predict a highly shielded ^{29}Si NMR chemical shift of 40 ppm[86]. The upfield shift of the ^{29}Si NMR resonance, relative to SiH_3^+ (270.2 ppm), is due to a significant electron population of the formally empty 3p-orbital on silicon[86]. Recently, the effect of π-back donation on the NMR resonance of the X atom in a series of Me_nXCl_{4-n} (X = C, Si, Ti; $n = 0$–4)[103] compounds has been found to vary

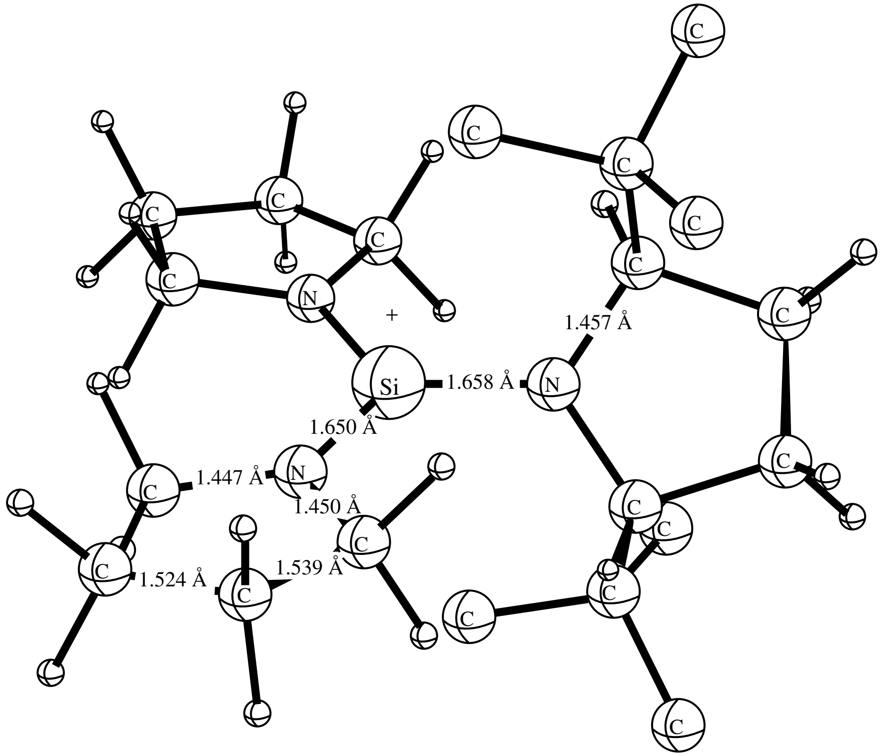

(32)

FIGURE 17. AM1 optimized geometry of the C_2 bis(pyrrolidono)(2,5-di-*tert*-butylpyrrolidino)silicenium ion (**32**), originally reported in C_1 symmetry in Reference 86. For clarity, all hydrogens of the *tert*-butyl groups were omitted from the plot. Bond lengths are given in Å

strongly for different atoms X. In general, there is no simple charge density–chemical shift relationship, although such correlations were found for series of closely related compounds, e.g. for the neutral H_nSiMe_{4-n} compounds[83a].

2. Resonance stabilization by aromatic substituents

The alleged preparation of triphenylsilicenium (sityl) ions in different solvents, e.g. in sulpholane or dichloromethane[79,80], was reported by Lambert and coworkers in the mid-1980s. Based on conductance measurements and $^{35}Cl/^{37}Cl$ NMR spectra of the sityl perchlorate solutions, the authors concluded that the species which they observed were 'free' silicenium ions[80]. Unfortunately, Lambert and his coworkers did not report the ^{29}Si NMR spectra of the silyl compounds. Lambert's claims were challenged by Olah and coworkers[70] and by Eaborn[104] based on experimental data on related compounds. In particular, the reported silicon chemical shift of 3.0 ppm[70] was that of a normal covalently bound, i.e. non-dissociated, triphenylsilyl perchlorate. In the case of $Me_3Si{-}OClO_3$ ($\delta^{29}Si = 43.4{-}47.0$ ppm)[105] and (i-PrS)$_3$Si$-$OClO$_3$ ($\delta^{29}Si = 18$ ppm)[81], similar highly shielded δ^{29}Si NMR chemical shifts have been measured, and these values were confirmed by the subsequent IGLO NMR computations on such silicenium ion–Lewis base complexes (see discussion above).

Nevertheless, aryl rings can provide significant conjugative stabilization to silicenium ions. A single phenyl substituent, for instance, stabilizes $C_6H_5SiH_2{}^+$ by 31.5 kcal mol^{-1} (HF/6-31G*)[6], compared to hydrogen in the parent $SiH_3{}^+$.

'Internally solvated' (chelated) silicenium ions, e.g. **33** shown in Figure 18, have been prepared, both by Corriu's[64,106] and by Belzner's[107] groups, who employed aryl rings with electron-donating amino groups in the *ortho*-positions to stabilize coordinatively the silicenium ion. In essence, the silicenium ion function interacts internally with the *ortho* dimethylamino groups to form a pentacoordinate siliconium ion. The observed δ^{29}Si NMR values in *internally solvated* silicenium ions are highly shielded (ranging from *ca* −10 to −60 ppm)[106,107]. IGLO computations on 2,6-diaminophenyl-substituted silicenium ions confirmed the upfield ^{29}Si NMR chemical shift (−80.5 ppm) in these pentacoordinate species[108].

A detailed theoretical study of phenyl- and anthryl-substituted silicenium ions was reported by Ottosson and Cremer[108]. The silicenium ion **34**, substituted with a 1,8-dimethylanthryl group, whose optimized geometry is shown in Figure 19, has a computed δ^{29}Si of 187 ppm, which is *ca* 150 ppm upfield from the corresponding gas-phase value of $SiHMe_2{}^+$ (334 ppm)[108]. Thus, the $-SiMe_2{}^+$ group in **34**, which is positioned between two methyl groups, retains much more silicenium ion character than amino-coordinated

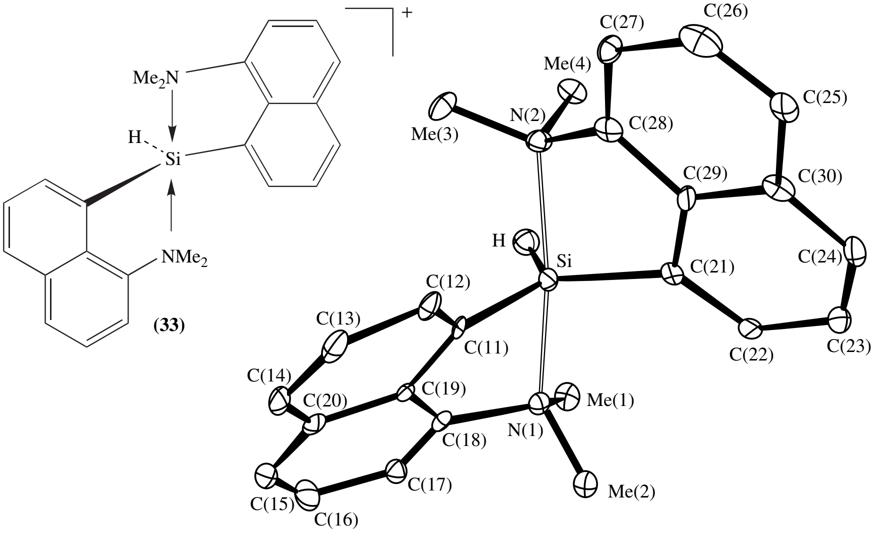

(**33**)

FIGURE 18. ORTEP drawing of the cation **33** showing the molecular conformation and atom numbering. Selected bond lengths (Å) and angles (deg): Si−H 1.73(12), Si−C(11) 1.90(1), Si−C(21) 1.85(1), Si−N(1) 2.08(1), Si−N(2) 2.06(1), N(1)−Si−N(2) 167.8(4), C(11)−Si−C(21) 118.4(6), C(11)−Si−H 126(4), C(21)−Si−H 114(4), Si−C(11)−C(19) 106.5(9), Si−C(21)−C(29) 110.2(9), N(1)−C(18)−C(19) 110.6(1.0), N(2)−C(28)−C(29) 113.4(1). Reproduced by permission of The Royal Society of Chemistry from Reference 106b

silicenium ions (e.g. **33**). Note also that the less nucleophilic methyl groups cannot stabilize the silicenium ion centre via dative lone pair-donation, as is the case with amino groups, although the steric shielding might be similar. Maerker, Kapp and Schleyer showed that even methane can coordinate to silicenium cations[6], and the intramolecular methyl group interactions in **34** are similar.

Very recently, Lambert and Zhao[4] prepared the trimesityl silicenium ion **31** by protonation of allyltrimesityl silane. It had been found earlier that protonation of allylsilanes removes the allyl group (as its corresponding alkene), and this is a good way to generate silicenium ion intermediates[109]. The cleavage of the C−Si bond is rationalized in terms of extensive C−Si hyperconjugation in the initially formed carbocation[6,73]. Unfortunately, Lambert and Zhao were not able to obtain a crystal structure of the trimesityl silicenium tetrakis(pentafluorophenyl)borate salt[4]. However, they could measure the ^{29}Si NMR spectrum of **31** and observed a highly deshielded ^{29}Si NMR absorption at $\delta = 225.5$ ppm[4]. The extent of solvent coordination was further probed by using mixtures of different aromatic solvents, but no significant change in the ^{29}Si chemical shifts was observed[4]. The authors concluded that nucleophilic coordination to the arene moieties is almost completely inhibited sterically by the *ortho*-methyl groups of the mesityl substituents. C_6D_6/CH_3CN (1/3) and C_6D_6/Et_3N (1/1) solvent mixtures, in contrast, result in δ^{29}Si of 37.0 and 47.1 ppm, respectively[4]. Hence, the much smaller alkyl nitriles and amines can bind directly to the silicenium ion centre of **31**.

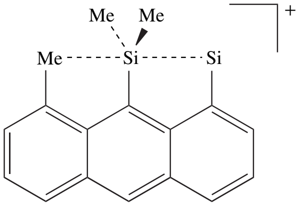

(34)

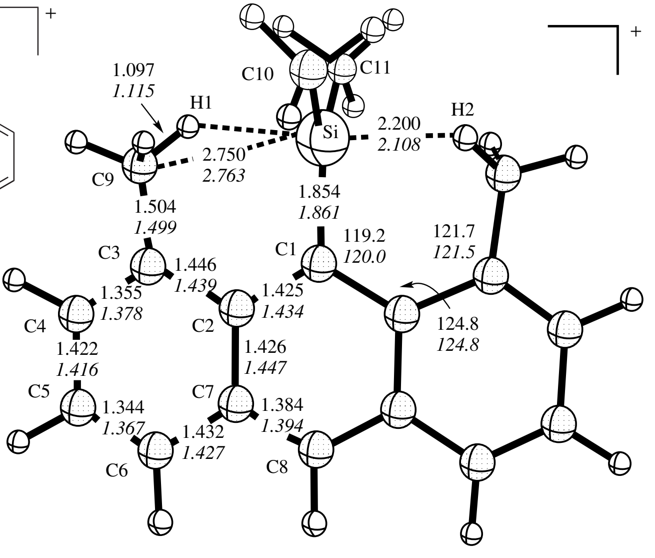

(34)

FIGURE 19. HF/6-31G* (normal print) and B3LYP/6-31G* (italics) geometrical parameters of cation **34**. Selected bond lengths (Å), bond and torsion angles (deg): Si−C(10) 1.869 *1.878*, C(10)−Si−C(1) 123.0 *123.1*, H(1)−Si−H(2) 175.5 *175.0*, C(10)−Si−C2−C3 84.3 *82.4*, Si−C(1)−C(2)−C(3) 0.0 *0.3*, C(1)−C(2)−C(3)−C(9) −4.9 *−6.0*, H(1)−C(9)−C(3)−C(2) 50.9 *47.3*, H(1)−C(9)−Si−C(10) 115.3 *110.8*, H(1)−C(9)−Si−C(11) 1.0 *2.9*. Reprinted with permission from Reference 108. Copyright (1996) American Chemical Society

Subsequent *ab initio* computations by Müller and coworkers[5] on triarylsilicenium ions confirmed the formation of a free tricoordinate trimesitylsilicenium ion **31** in solution. The calculated equilibrium geometries of triarylsilicenium ions exhibit considerably twisted aryl rings and propeller-like shapes. The C−H bonds of the *ortho*-methyl groups, however, are too far from the silicon centre to interact (2.990 Å at B3LYP/6-31G*)[5]. Employing B3LYP/6-31G* optimized geometries, the following ^{29}Si NMR chemical shifts were calculated, using GIAO-B3LYP/6-311+G(2df,p) [Si], 6-31G* [C,H]//B3LYP/6-31G*: 205.0 (triphenylsilicenium) and 243.9 ppm (trimesitylsilicenium **31**), respectively[5]. The 18.4 ppm difference between experiment and theory for **31** was attributed to deficiencies in the computational method[5], since GIAO-DFT seems to overestimate the paramagnetic contributions to $\sigma(^{29}\text{Si})$. In the parent triphenylsilicenium ion there is a strong dependence of δ^{29}Si on the twist angle; the larger the dihedral angle the larger the downfield shift of δ^{29}Si. A δ^{29}Si of 290.2 ppm is predicted for the D_{3h} symmetric all-perpendicular triphenylsilicenium ion geometry[5]. The authors concluded: 'This computational study strongly corroborates the experimental finding that the trimesitylsilicenium ion **(31)** is the first free trigonal silyl cation lacking any coordination to solvent or counterion'[5].

3. Intramolecular π-stabilization

In 1995, Schleyer and coworkers reported the results of calculations for the silicon congeners of a number of non-classical carbocations: the 2-norbornyl cation, $C_7H_{11}{}^+$ **(35)**, the 7-norbornadienyl cation, $C_7H_7{}^+$ **(36)** and cyclopropylcarbinyl cation, $C_4H_7{}^+$ **(37)**[6]. The MP2(fc)/6-31G* calculations predicted that the silicenium ion analogs, **38**−**40** are more stable than the corresponding parent carbocations **35**−**37**, respectively. Thus, the 6-sila-2-norbornyl cation **(38)** is more stable than **32** by 18.1 kcal mol^{-1}; the 7-sila-7-norbornadienyl cation **39** is by 15.1 kcal mol^{-1} more stable than **36** and the cyclopropylsilicenium ion **(40)** is by 12.6 kcal mol^{-1}, more stable than **37**[6]. IGLO/BII′//MP2(fc) /6-31G* chemical shift calculations predicted that the sila-analogs of the two bicyclic carbocations should show unusually shielded ^{29}Si NMR chemical shifts of 1 ppm for **38** and −148.6 ppm for **39**[6]. Thus, the higher coordination number of the silicon atoms in these cations is reflected directly in their ^{29}Si NMR resonances.

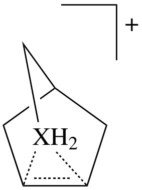

(35) X = C
(38) X = Si

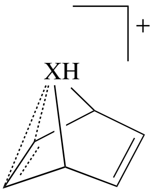

(36) X = C
(39) X = Si

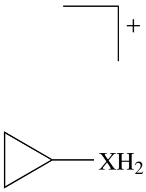

(37) X = C
(40) X = Si

More recently, Auner's and Schleyer's groups in a joint effort reported the experimental observation of an alkyl-substituted 6-sila-2-norbornyl cation[110]. The 6,6-Dimethyl-5-neopentyl-6-sila-2-norbornyl cation **41** was prepared by a hydride transfer reaction via the 'π-route'[111] from a suitable cyclopentenyl silane derivative at room temperature (equation 10). The toluene solution of the tetrakis(pentafluorotetraborate) salt of **41** showed a sharp single peak at $\delta(^{29}Si)$ of 87.7 ppm versus TMS[110]. As this value is also in the range of silicenium ion–arene σ-complexes[73], and no X-ray quality crystals could be obtained, the 6-sila-2-norbornyl cation structure of **41** had to be confirmed by quantum chemical computations. Calculations using the hybrid density functional B3LYP/6-31G* method confirmed that **41** indeed has the 'closed' form of a true sila-analog of the non-classical 2-norbornyl cation. Calculations of the effect of interaction with a benzene molecule on the relative stabilities of an 'open' **(42)** and of a 'closed' **(43)** cation show that, although the 'open' arenium ion form benefits much more from solvation by benzene (20.8 kcal mol^{-1}) than the closed form (5.0 kcal mol^{-1}), the latter remains by 6.3 kcal mol^{-1} more stable (see Figure 20)[110].

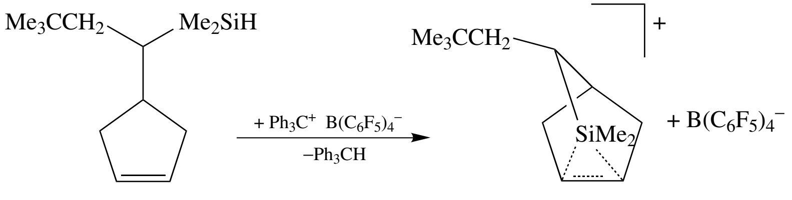

(10)

(41)

Due to computational savings, the 'open' and 'closed' forms of the 6,6-dimethyl-6-sila-2-norbornyl cation, **42** and **43**, the 'closed' 5,6,6-trimethyl-6-sila-2-norbornyl cation **(44)** and their corresponding benzene complexes **45, 46** and **47**, respectively, were optimized

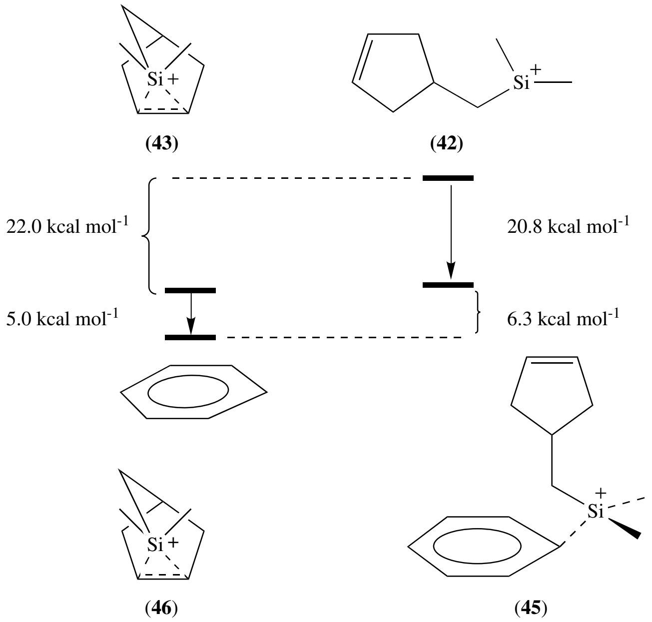

FIGURE 20. Energetics (kcal mol^{-1}) of benzene complexation to cations **42** and **43**, forming complexes **45** and **46**, respectively. Reproduced by permission of Wiley-VCH from Reference 110

as reasonable realistic theoretical models[110] of cation **41** in toluene solution. Despite the unsymmetrical substitution pattern, an almost symmetrically bridged 'closed' silicenium ion is predicted to be the most stable structure at B3LYP/6-31G* of **44**, as shown in Figure 21[110]. Benzene coordination has only minor structural consequences, resulting mainly in a slight lengthening (by 0.13 to 0.16 Å) of the Si6−Cl/C2 bonds in **47** compared to those in **44**[110]. The B3LYP/6-31G* optimized geometries of **44, 45** and **47** are shown in Figure 21.

The most important support for the 'closed' structure of **41** was given, however, by comparison of the computed and measured ^{29}Si and ^{13}C NMR chemical shifts and the $^{1}J_{\mathrm{CH}}$ coupling constants. In particular, the deshielding of the 'olefinic' carbons C1 and C2 upon ionization are only reproduced well by the 'closed' structures **43** and **44**. Similarly, the shielded methyl groups are found only in the 'closed' structures. In contrast, the computations predict a strongly deshielded methyl signal for the 'open' silicenium ion isomer **42**[110]. The non-classically bridged bicyclic nature of silicenium ion **41** is further confirmed by the computed $^{1}J_{\mathrm{Cl/C2-H}}$ of 167.4 Hz (in **44**), which is in reasonable agreement with the experimental $^{1}J_{\mathrm{Cl/C2-H}}$ of 174 Hz[110] (in **41**). Relative to the corresponding silane,

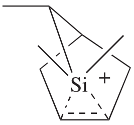

(44)

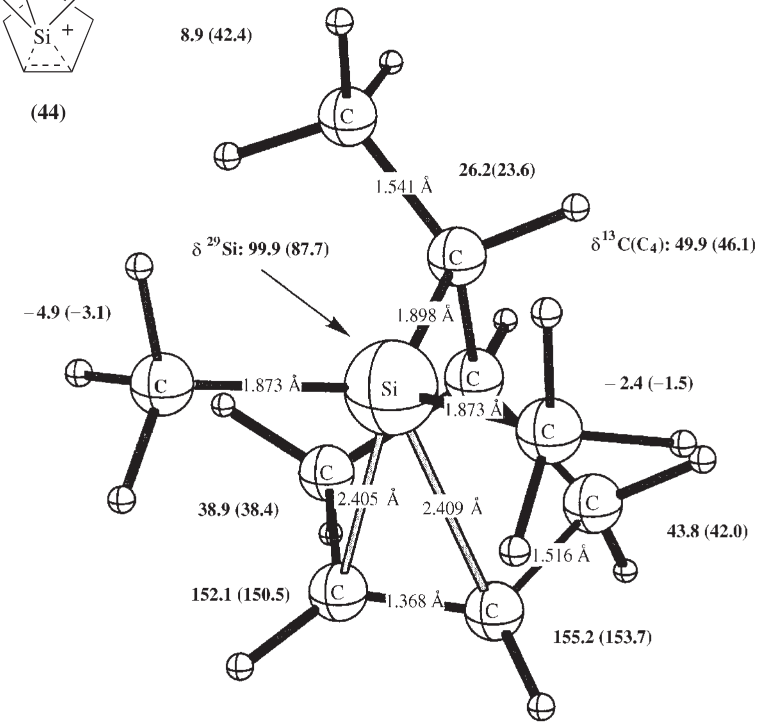

(44)

FIGURE 21. B3LYP/6-31G* optimized geometries of species **44, 45** and **47**. Bond lengths in Å; computed ^{13}C and ^{29}Si NMR data in boldface (**44:** IGLO-DFPT/BIII; **45, 47:** IGLO-DFPT/BII), experimental NMR data for species **41** given in parentheses. Reproduced by permission of Wiley-VCH from Reference 110

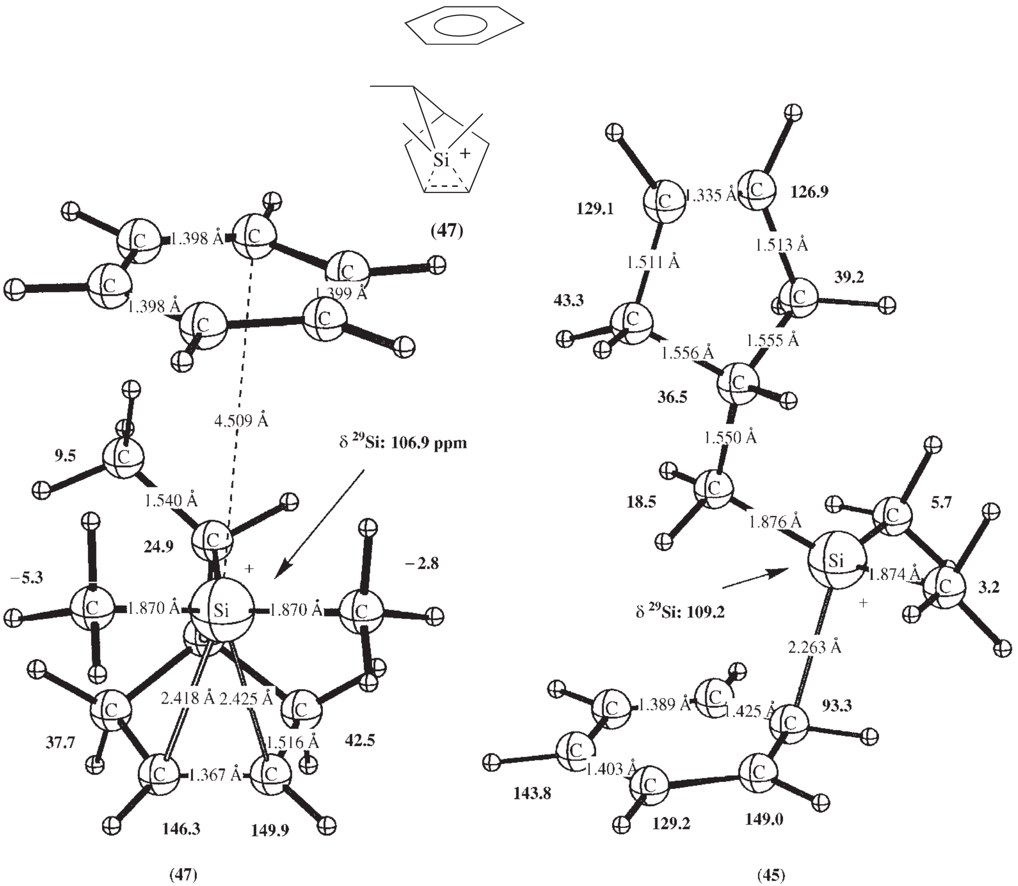

FIGURE 21. (*continued*)

this is an increase in $^1J_{\mathrm{CH}}$ of by 22 Hz. The corresponding difference in $^1J_{\mathrm{CH}}$ between the 2-norbornyl cation and cyclopentene is 26.2 Hz (experimental data)[110]. The authors concluded about **41**: '... there is strong evidence for the preparation of the first intramolecularly π-stabilized silanorbornyl cation in solution that is not coordinated to solvent or a counterion'[110]. An alternative description of **41** is: 'a nearly symmetrically bridged β-silyl carbocation with siliconium ion character'[110]. Interestingly, such non-classical pentavalent silicon ('siliranium') ions have been postulated before by Knölker and coworkers in the sila-Wagner–Meerwein rearrangement of organosilicon compounds[112].

F. Stabilization by Organoboryl Groups

It has been shown theoretically by several groups that the tetra- or pentacoordination of trialkylsilicenium ions to counterions or solvent molecules in solution cannot be easily prevented. Thus, the preservation of a major silicenium ion character might be obtained only by combining internal stabilization and steric blocking of the silicon centre. Cremer and coworkers have shown that strong electron-donor groups, such as amino groups (see also Section IV. E.1)[86], are not entirely suitable for this purpose, since π-donation to the formally empty $3p_\pi$ (Si^+) orbital is so extensive that the silicenium ion character is essentially lost[108,113]. This is indicated by the strongly shielded ^{29}Si NMR chemical shifts, usually around 40 ppm or lower[86].

Cremer and coworkers have recently explored the stabilization of silicenium ions by electropositive substituents[83,113]. The trimethylsilyl or tris(trimethylsilyl)silyl groups, which have also been used experimentally[2b,101], are thought to stabilize an electron-deficient centre mainly by hyperconjugation and by inductive effects. However, the calculations reveal that the rather long $Si{-}Si^+$ bonds (*ca* 2.34–2.40 Å) in $(Me_3Si)_3Si^+$ result in little hyperconjugative stabilization by the terminal groups. Figure 22 shows the optimized geometry of $(Me_3Si)_3Si^+$.

In contrast to silyl groups, boron substituents have the following advantages[113]: (a) boron has a lower electronegativity (2.01) than carbon (2.50), which results in smaller distortions of the frontier molecular orbital energies; (b) the Si−B bonds (*ca* 1.98 to 2.03 Å) are shorter than Si−Si bonds, facilitating interactions between the pseudo-π orbitals of the substituent's alkyl groups and the formally empty $3p_\pi(Si^+)$ orbital, transmitted via the empty $2p_\pi(B)$ orbital.

Following this reasoning, Cremer's group studied computationally several organoboryl-substituted silicenium ions[113]. The tris(dimethylboryl)silicenium ion, $(Me_2B)_3Si^+$ (**48**), is by 61.9 kcal mol^{-1} more stable than the parent H_3Si^+ (B3LYP/6-31G*), compared to a stabilization energy of only 43.2 kcal mol^{-1} provided by three methyl groups as in Me_3Si^+[113]. The $(Me_2B)_3Si^+$ cation adopts a twisted D_3 equilibrium structure, where the BC bonds are rotated by 86° (relative to a planar structure), rather close to the 90° rotated D_{3h} structure. Presumably, the slight distortion from the ideal orthogonal arrangement reduces the steric repulsions between the organoboryl groups. The barrier to rotation around the Si−B bonds is 6.7 kcal mol^{-1} per each substituent[113]. If one assumes that the rotational barrier is mainly due to the loss of the hyperconjugative stabilization resulting from the interaction of the $3p_\pi(Si^+)$ orbital and the $B{-}CH_3$ bond, then 20 kcal mol^{-1} can be attributed to this stabilization while *ca* 40–42 kcal mol^{-1} of the total 61.9 kcal mol^{-1} stabilization energy of **48** (versus H_3Si^+) can be attributed to inductive contributions[113].

The tris-(9-borabicyclo[3.3.1]nonyl)silicenium ion, $(9\text{-BBN})_3Si^+$ (**49**), adopts a D_{3h} equilibrium geometry, perhaps due to the greater rigidity of the bicyclic cages. Based on non-bonded H−H distances it was estimated that an opening with a diameter of 2.34 Å, through which nucleophiles might interact with the silicenium ion centre, exists in **49**[113].

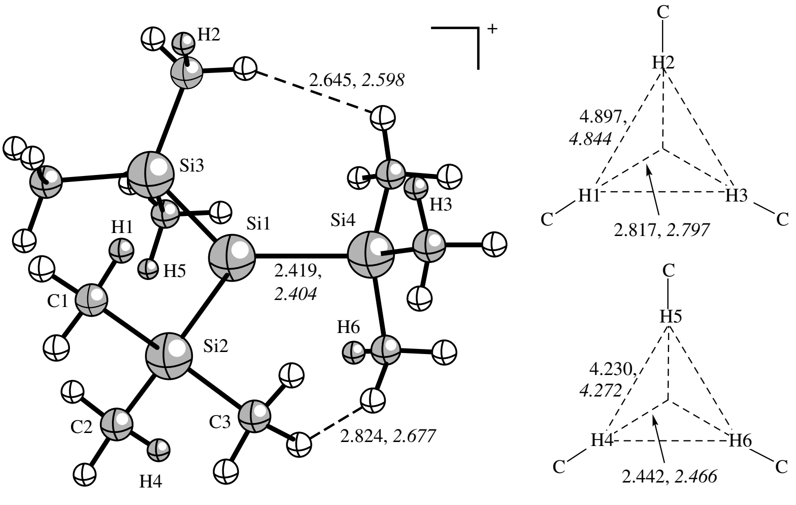

Si2-Si1-Si3 = 119.9, *119.9*
C1-Si2-Si1 = 107.6, *107.1*
C2-Si2-Si1 = 104.0, *104.5*
C3-Si2-Si1 = 110.0, *110.7*
C1-Si2-Si1-Si3 = −54.8, *−56.6*
C2-Si2-Si1-Si3 = 64.7, *61.9*
C3-Si2-Si1-Si3 = −175.8, *−178.2*

FIGURE 22. HF/6-31G* and B3LYP/6-31G* (values in italics) optimized geometries of $(Me_3Si)_3Si^+$. Bond lengths in Å, bond angles in deg. The two inserts on the right side indicate the dimensions of the opening above and below the central Si atom formed by non-bonded hydrogen contacts. Reprinted with permission from Reference 113. Copyright (1997) American Chemical Society

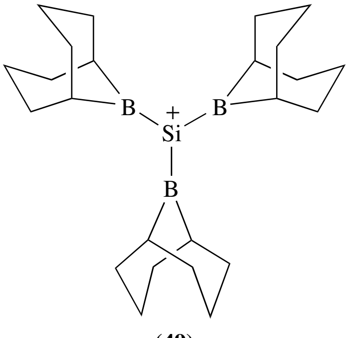

(49)

The complexation of **49** with benzene, forming **50**, has been further examined at HF/6-31+G*[113]. Frequency calculations confirmed that the C_1 structure, which is shown in Figure 23, is a minimum. The shortest $Si-C_{benzene}$ bond length in **50** is 2.57 Å, which is 0.1–0.3 Å longer than silicon–carbon distances in other silicenium ion–arene complexes. At HF/6-31G*, the complexation energy of benzene to **49** is only 4.4 kcal mol^{-1}, which is roughly 20 kcal mol^{-1} lower than the complexation energies of tertiary alkylsilicenium ions to benzene or toluene. The low interaction energy of **49** with benzene was attributed by Cremer and coworkers to the large stabilization of silicenium ion **49** by the three 9-BBN substituents[113]. However, the coordination of **49** to benzene forces the three boryl groups towards each other, increasing the steric interactions within the silicenium cation moiety. Thus, one might speculate whether the energetically unfavourable steric effects in **50** partially compensate the stabilization provided by the interaction of the silicenium ion with benzene. In any event, a low solvent interaction of the silicenium ion with benzene is the outcome. The weak interaction of **49** with benzene was further confirmed by the computed geometries, e.g. the relatively long Si−C distance and the small C−C bond alternation in the benzene moiety (see Figure 23)[113].

Due to computational limitations, the ^{29}Si NMR chemical shift could be computed only for the benzene complex of (Me$_2$B)$_3$Si$^+$, whose interaction energy with benzene of 8.9 kcal mol^{-1} is almost two-fold greater than that of **49**[113]. The computed δ^{29}Si NMR chemical shift for the (Me$_2$B)$_3$Si$^+$−benzene complex is 116.4 ppm versus TMS, corresponding to *ca* 28% silicenium ion character[113]. A better model for the (9-BBN)$_3$Si$^+$−benzene complex was constructed by adjusting the (Me$_2$B)$_3$Si$^+$−benzene geometry to that of the (9-BBN)$_3$Si$^+$−benzene complex, i.e. the bicyclic cages of the latter complex were ‘deleted’, and the free valencies were saturated by hydrogens, whose positions were partially optimized. The estimated silicenium ion character for this model of the (9-BBN)$_3$Si$^+$−benzene complex is 41%. This estimation is based on the computed ^{29}Si NMR chemical shift of 189 ppm in (Me$_2$B)$_3$Si$^+$−benzene, compared to δ of 571.8 ppm for the free (Me$_2$B)$_3$Si$^+$ cation[113]. The reported 41% silicenium-ion character is much higher than estimated for any other R$_3$Si$^+$−solvent complex. However, note that even the (9-BBN)$_3$Si$^+$ ion **(49)** is not a ‘free’ silicenium ion in benzene solution, since it forms a rather weak cation−solvent complex.

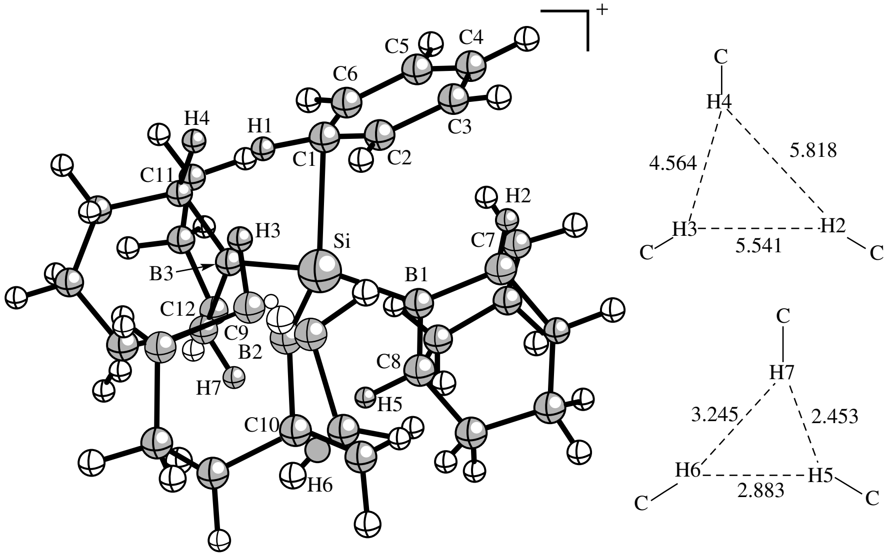

FIGURE 23. HF/6-31G* calculated geometry of the complex (9-BBN)$_3$Si−C$_6$H$_6$$^+$ **(50)**. The two inserts on the right side indicate the dimensions of the opening above the central Si atom formed by atoms H2, H3, H4 (black atoms), and below the central Si atom by atoms H5, H6, H7 (black atoms). Distances in Å. Reprinted with permission from Reference 113. Copyright (1997) American Chemical Society

V. CONCLUDING REMARKS AND OUTLOOK

The experimental search for free stable silicenium ions in solution seems to have finally succeeded, at least for triaryl-substituted species[4,5]. However, computational studies will continue to augment, to verify and to guide the interpretations of experimental findings, as well as to suggest new experiments for preparing other silicenium ions. Schleyer and coworkers, for instance, have recently explored a silicenium ion 'within a cage', namely

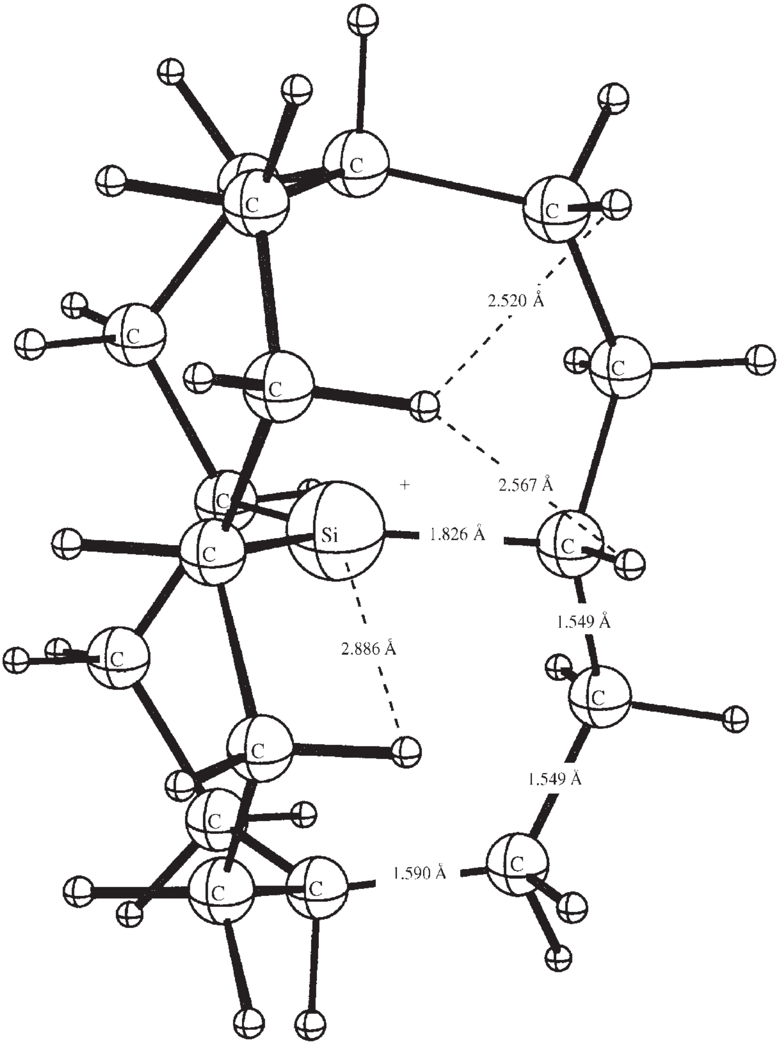

(51)

FIGURE 24. B3LYP/6-31G* optimized geometry of a fully 'caged' silicenium ion **51**. Bond lengths in Å. Non-bonded H−H and H−Si contacts (Å) shown as dashed lines

$C_{17}H_{29}Si^+$ (**51,** C_{3h} symmetry), which corresponds to a local minimum at HF/3-21G*[114]. The B3LYP/6-31G* optimized geometry of **51** is shown in Figure 24. In **51**, the silicenium ion centre is extremely shielded sterically, and the closest non-bonded H−H distances at the peripheral methylene linkages are 2.52–2.57 Å (Figure 24). GIAO-SCF/3-21G//B3LYP/6-31G* chemical shift computations for **51** predict a strongly deshielded δ^{29}Si of 303 ppm[114]. However, the very efficient steric protection of the deeply buried ionic centre might also hamper the ion's preparation!

Another future direction might be the theoretical exploration of the reactions of silicenium ions with other species, e.g. the application of silicenium ions in cationic polymerization. Work on the heavier analogs of silicenium ions has also progressed significantly during the last three years[115], leading to the isolation and X-ray characterization of the first aromatically stabilized trigermanium ion[116,117]. The fruitful interplay between experiment and theory provides a most promising pathway to new chemical structures and insights, as was demonstrated so clearly for silicenium ions.

VI. REFERENCES

1. S. Patai and Z. Rappoport (Eds.), *The Chemistry of Organic Silicon Compounds*, Wiley, New York, 1989.
2. (a) J. B. Lambert, S. Zhang, C. L. Stern and J. C. Huffman, *Science*, **260**, 1917 (1993),
   (b) J. B. Lambert and S. Zhang, *J. Chem. Soc., Chem. Commun.*, 383 (1993).
3. (a) C. A. Reed, Z. Xie, R. Bau and A. Benesi, *Science*, **262**, 402 (1993),
   (b) Z. Xie, D. J. Liston, T. Jelinek, V. Mitro, R. Bau and C. A. Reed, *J. Chem. Soc., Chem. Commun.*, 384 (1993).
4. J. B. Lambert and Y. Zhao, *Angew. Chem.*, **109**, 389 (1997); *Angew. Chem., Int. Ed. Engl.*, **36**, 400 (1997).
5. T. Müller, Y. Zhao, and J. B. Lambert, *Organometallics*, **17**, 278 (1998).
6. C. Maerker, J. Kapp and P. v. R. Schleyer, in *Organosilicon Chemistry: From Molecules to Materials*, Vol. II (Eds N. Auner and J. Weis), VCH, Weinheim, 1995, pp. 329–359.
7. (a) B. J. DeLeeuw, R. S. Grev and H. F. Schaefer III, *J. Chem. Educ.*, **69**, 441 (1992).
   (b) H. F. Schaefer III, *Acc. Chem. Res.*, **15**, 283 (1982).
8. See also the first chapter by Y. Apeloig and M. Karni in this volume.
9. Y. Apeloig, in *Heteroatom Chemistry* (Ed. E. Block), VCH, Weinheim, 1990, pp. 27–46.
10. Y. Apeloig, in *The Chemistry of Organic Silicon Compounds*, Vol. 1 (Eds. S. Patai and Z. Rappoport), Wiley, New York, 1989, p. 57.
11. M. S. Gordon, in *Molecular Structure and Energetics* (Eds. J. F. Liebman and A. Greenberg), VCH, Deerfield Beach, FL, 1986, p. 101.
12. S. Nagase, *Acc. Chem. Res.*, **28**, 469 (1995).
13. K. Morokuma, in *Organosilicon and Bioorganosilicon Chemistry: Structure, Bonding, Reactivity and Synthetic Applications* (Ed. H. Sakurai), Ellis Horwood, Chichester, 1985, p. 33.
14. Leading texts are:
   (a) J. M. Seminario and P. Politzer (Eds.), *Modern Density Functional Theory: A Tool for Chemistry; Theoretical and Computational Chemistry*, Vol. 2, Elsevier, Amsterdam, 1995.
   (b) D. R. Salahub, R. Fournier, P. Mlynarski, I. Papai, A. St-Amant and J. Ushio, *Density Functional Methods in Chemistry*, Springer-Verlag, Berlin, 1991.
   (c) R. M. Dreizler and E. K. Gross, *Density Functional Theory*, Springer-Verlag, Berlin, 1990.
   (d) R. G. Parr and Y. Wang, *Density Functional Theory of Atoms and Molecules*, Oxford University Press, Oxford, 1989.
15. T. Ziegler, *Chem. Rev.*, **91**, 651 (1991).
16. L. Greengard, *Science*, **265**, 909 (1994).
17. M. C. Strain, G. E. Scuseria and M. J. Frisch, *Science*, **271**, 51 (1996).
18. (a) T. Darden, D. M. York and L. Pedersen, *J. Chem. Phys.*, **98**, 10089 (1993).
   (b) D. M. York, T. Darden and L. Pedersen, *J. Chem. Phys.*, **99**, 8345 (1993).
   (c) D. M. York, A. Wlodawer, L. G. Pedersen and T. A. Darden, *Proc. Natl. Acad. Sci. U.S.A.*, **91**, 8715 (1994).

19. (a) J. Gao, *Acc. Chem. Res.*, **29**, 298 (1996).
    (b) J. Gao, in *Reviews in Computational Chemistry*, Vol. 7 (Eds. K. B. Lipkowitz and D. B. Boyd), Verlag Chemie, Weinheim, 1996, p. 119.
20. R. L. Martino, C. A. Johnson, E. B. Suh, B. L. Trus and T. K. Yap, *Science*, **265**, 902 (1994).
21. T. Clark, *A Handbook of Computational Chemistry. A Practical Guide to Chemical Structure and Energy Calculations*, Wiley, New York, 1985.
22. W. J. Hehre, L. Radom, P. v. R. Schleyer and J. A. Pople, *Ab Initio Molecular Orbital Theory*, Wiley, New York, 1986.
23. K. B. Lipkowitz and D. B. Boyd (Eds.), *Reviews in Computational Chemistry*, Vols. 1–8, Verlag Chemie, Weinheim, 1990–1996.
24. P. v. R. Schleyer, H. F. Schaefer III and N. C. Handy (Eds.), *Encyclopedia of Computational Chemistry*, Wiley, New York, to appear in 1998. Look also at: http://www.ccc.uni-erlangen.de/info/ECC/
25. Browse the following URL: http://hackberry.chem.niu.edu/ECCC4/
26. Browse at http://www.ccc.uni-erlangen.de/info/JMOLMOD/jmolinfo.html
27. J. Gauss, *Ber. Bunsenges. Phys. Chem.*, **99**, 1001 (1996).
28. J. C. Slater, *Phys. Rev.*, **81**, 385 (1951).
29. N. C. Handy, in *Lecture Notes in Quantum Chemistry II*, Vol. 58 (Ed. B. O. Roos), Springer-Verlag, Berlin–Heidelberg, 1994, p. 91.
30. (a) P. C. Hohenberg and W. Kohn, *Phys. Rev.*, **B136**, 864 (1964).
    (b) W. Kohn and L. J. Sham, *Phys. Rev.*, **A140**, 1133 (1965).
    (c) A recent review is: P. C. Hohenberg, W. Kohn and L. J. Sham, *Adv. Quantum Chem.*, **21**, 7 (1990).
31. See, for example, V. G. Malkin, O. L. Malkina, L. A. Eriksson and D. R. Salahub, in *Modern Density Functional Theory: A Tool for Chemistry; Theoretical and Computational Chemistry*, Vol. 2 (Eds. J. M. Seminario and P. Politzer), Elsevier, Amsterdam, 1995, p. 273 and references cited therein.
32. (a) W. Kutzelnigg, C. van Wüllen, U. Fleischer, R. Franke and T. von Mourik, in *Nuclear Magnetic Shieldings and Molecular Structure* (Ed. J. A. Tossell), Kluwer Academic Publishers, Dordrecht, 1993, p. 141.
    (b) W. Kutzelnigg, U. Fleischer and M. Schindler, in *NMR Basic Principles and Progress*, Vol. 23, Springer-Verlag, Berlin–Heidelberg, 1990, p. 165.
    (c) M. Schindler and W. Kutzelnigg, *J. Chem. Phys.*, **76**, 1919 (1982).
    (d) W. Kutzelnigg, *Israel J. Chem.*, **19**, 193 (1980).
33. A. E. Hansen and T. D. Bouman, *J. Chem. Phys.*, **82**, 5035 (1985).
34. R. Ditchfield, *Mol. Phys.*, **27**, 789 (1974).
35. For summaries on the application of the *ab initio*/IGLO/NMR method see:
    (a) For applications on carbocations: P. v. R. Schleyer and C. Maerker, *Pure Appl. Chem.*, **67**, 755 (1995), especially footnote #4.
    (b) For boranes and carboranes: M. Bühl and P. v. R. Schleyer, *J. Am. Chem. Soc.*, **114**, 477 (1992).
    (c) An extensive bibliography has also been given by M. Diaz, J. Jaballas, J. Arias, H. Lee and T. Onak, *J. Am. Chem. Soc.*, **118**, 4405 (1996).
36. R. Ditchfield and D. P. Miller, *J. Am. Chem. Soc.*, **93**, 5287 (1971).
37. K. Wolinski, J. F. Hinton and P. Pulay, *J. Am. Chem. Soc.*, **112**, 8251 (1990).
38. M. Bühl, J. Gauss, M. Hofmann and P. v. R. Schleyer, *J. Am. Chem. Soc.*, **115**, 12385 (1993).
39. (a) S. P. A. Sauer, I. Paidorova and J. Oddershede, *Mol. Phys.*, **81**, 87 (1994).
    (b) S. P. A. Sauer, I. Paidorova and J. Oddershede, *Theor. Chim. Acta*, **88**, 351 (1994).
40. (a) V. Galasso and G. Fronzoni, *J. Chem. Phys.*, **84**, 3215 (1986).
    (b) V. Galasso, *J. Mol. Struct. (THEOCHEM)*, **10**, 201 (1983).
41. C. v. Wüllen and W. Kutzelnigg, *Chem. Phys. Lett.*, **205**, 563 (1993).
42. (a) J. Gauss, *Chem. Phys. Lett.*, **191**, 614 (1992).
    (b) J. Gauss, *J. Chem. Phys.*, **99**, 3629 (1993).
43. (a) D. Sundholm, J. Gauss and A. Schäfer, *J. Chem. Phys.*, **105**, 11051 (1996).
    (b) J. Gauss and J. F. Stanton, *J. Chem. Phys.*, **104**, 2574 (1996).
    (c) J. Gauss and J. F. Stanton, *J. Chem. Phys.*, **103**, 3561 (1995).
    (d) J. Gauss and J. F. Stanton, *J. Chem. Phys.*, **102**, 251 (1995).
    (e) J. Gauss, *Chem. Phys. Lett.*, **229**, 198 (1994).

44. (a) J. R. Cheeseman, G. W. Trucks, T. A. Keith and M. J. Frisch, *J. Chem. Phys.*, **104**, 5497 (1996).
    (b) G. Rauhut, S. Puyear, K. Wolinski and P. Pulay, *J. Phys. Chem.*, **100**, 6310 (1996).
    (c) V. G. Malkin, O. L. Malkina, M. E. Casida and D. R. Salahub, *J. Am. Chem. Soc.*, **116**, 5898 (1994).
    (d) A. M. Lee, N. C. Handy and S. M. Colwell, *J. Chem. Phys.*, **103**, 10095 (1995).
    (e) A. M. Lee, S. M. Colwell and N. C. Handy, *Chem. Phys. Lett.*, **229**, 225 (1994).
45. G. A. Olah and P. v. R. Schleyer (Eds.), *Carbonium Ions*, Vols. 1–5, Wiley, New York, 1968–1976; *Stable Carbocation Chemistry*, P.v.R. Schleyer and G. K. S. Prakash (Eds.), Wiley, New York, 1997.
46. P. Vogel, *Carbocation Chemistry*, Elsevier, Amsterdam, 1985.
47. M. Hanack, D. Lenoir, H.-U. Siehl and L. R. Subramanian, in *Methoden der Organischen Chemie (Houben-Weyl)*, Vol. **E19c** (Ed. M. Hanack), Georg Thieme Verlag, Stuttgart, 1990.
48. N. Muller and R. S. Mulliken, *J. Am. Chem. Soc.*, **80**, 3489 (1958).
49. J. Higuchi, *J. Chem. Phys.*, **31**, 563 (1959).
50. B. Wirsam, *Chem. Phys. Lett.*, **18**, 578 (1973).
51. Y. Apeloig and P. v. R. Schleyer, *Tetrahedron Lett.*, 4647 (1977).
52. A. C. Hopkinson and M. H. Lien, *J. Org. Chem.*, **46**, 998 (1981).
53. S. A. Godleski, D. J. Heacock and J. M. McKelvey, *Tetrahedron Lett.*, **23**, 4453 (1982).
54. Y. Apeloig, S. A. Godleski, D. J. Heacock and J. M. McKelvey, *Tetrahedron Lett.*, **22**, 3297 (1981).
55. W. J. Hehre, R. Ditchfield, L. Radom and J. A. Pople, *J. Am. Chem. Soc.*, **92**, 4796 (1970).
56. J. Berkowitz, G. B. Ellison and D. Gutman, *J. Phys. Chem.*, **98**, 2744 (1994).
57. J. A. Seetula, Y. Feng, D. Gutman, P. W. Seakins and M. J. Pilling, *J. Phys. Chem.*, **95**, 1658 (1991).
58. P. W. Seakins, M. J. Pilling, J. T. Niiranen, D. Gutman and L. N. Krasnoperov, *J. Phys. Chem.*, **96**, 9847 (1992).
59. R. Damrauer, S. R. Kass and C. H. DePuy, *Organometallics*, **7**, 637 (1988).
60. (a) J. Y. Corey, *J. Am. Chem. Soc.*, **97**, 3237 (1975).
    (b) J. Y. Corey, D. Gust and K. Mislow, *J. Organomet. Chem.*, **101**, C7 (1975).
61. See for example, the attempted ionization of $(Me_2N)_3SiCl$ with $AlCl_3$: H. Cowley, M. C. Cushner and P. E. Riley, *J. Am. Chem. Soc.*, **102**, 624 (1980).
62. W. J. Pietro and W. J. Hehre, *J. Am. Chem. Soc.*, **104**, 4329 (1982).
63. J. Kapp, C. Schade, A. M. El-Nahas and P. v. R. Schleyer, *Angew. Chem.*, **108**, 2373 (1996); *Angew. Chem., Int. Ed. Engl.*, **35**, 2236 (1996).
64. C. Chuit, R. J. P. Corriu, C. Reyé and J. C. Young, *Chem. Rev.*, **93**, 1371 (1993).
65. For recent reviews see:
    (a) H. Grützmacher, *Angew. Chem.*, **107**, 323 (1995); *Angew. Chem., Int. Ed. Engl.*, **34**, 295 (1995).
    (b) M. Drieβ and H. Grützmacher, *Angew. Chem.*, **108**, 900 (1996); *Angew. Chem., Int. Ed. Engl.*, **35**, 829 (1996) and references cited therein.
66. A. J. Arduengo III, R. L. Harlow and M. Kline, *J. Am. Chem. Soc.*, **113**, 361 (1991).
67. G. Boche, P. Andrews, K. Harms, M. Marsch, K. S. Rangappa, M. Schimeczek and C. Willeke, *J. Am. Chem. Soc.*, **118**, 4925 (1996).
68. S. K. Shin and J. L. Beauchamp, *J. Am. Chem. Soc.*, **111**, 900 (1989).
69. K. Hensen, T. Zengerly, P. Pickel and G. Klebe, *Angew. Chem.*, **95**, 739 (1983); *Angew. Chem. Int. Ed. Engl.*, **22**, 725 (1983).
70. G. K. S. Prakash, S. Keyaniyan, R. Aniszfeld, L. Heiliger, G. A. Olah, R. C. Stevens, H.-K. Choi and R. Bau, *J. Am. Chem. Soc.*, **109**, 5123 (1987).
71. Z. Xie, R. Bau and C. A. Reed, *J. Chem. Soc., Chem. Commun.*, 2519 (1994).
72. L. Pauling, *Science*, **263**, 983 (1994).
73. P. v. R. Schleyer, P. Buzek, T. Müller, Y. Apeloig and H.-U. Siehl, *Angew. Chem.*, **105**, 1558 (1993); *Angew. Chem., Int. Ed. Engl.*, **32**, 1471 (1993).
74. G. A. Olah, G. Rasul, X.-y. Li, H. A. Buchholz, G. Sandford and G. K. S. Prakash, *Science*, **263**, 983 (1994).
75. J. B. Lambert and S. Zhang, *Science*, **263**, 984 (1994).
76. C. A. Reed and Z. Xie, *Science*, **263**, 985 (1994).
77. G. A. Olah, G. Rasul, H. A. Buchholz, X.-y. Li and G. K. S. Prakash, *Bull. Soc. Chim. Fr.*, **132**, 569 (1995).

78. K. N. Houk, *Chemtracts Org. Chem.*, **6**, 360 (1993).
79. J. B. Lambert, J. A. McConnell and W. J. J. Schulz, *J. Am. Chem. Soc.*, **108**, 2482 (1986).
80. (a) J. B. Lambert, W. J. J. Schulz, J. A. McConnell and W. Schilf, *J. Am. Chem. Soc.*, **110**, 2201 (1988).
    (b) J. B. Lambert and W. Schilf, *J. Am. Chem. Soc.*, **110**, 6364 (1988).
81. J. B. Lambert and W. J. Schulz, *J. Am. Chem. Soc.*, **105**, 1671 (1983).
82. K. B. Wiberg, *Tetrahedron*, **24**, 1083 (1968).
83. (a) L. Olsson, C.-H. Ottosson and D. Cremer, *J. Am. Chem. Soc.*, **117**, 7460 (1995).
    (b) M. Arshadi, D. Johnels, U. Edlund, C.-H. Ottosson and D. Cremer, *J. Am. Chem. Soc.*, **118**, 5120 (1996).
84. V. Gutmann, *Coord. Chem. Rev.*, **18**, 225 (1976).
85. A. E. Reed, L. A. Curtiss and F. Weinhold, *Chem. Rev.*, **88**, 899 (1988).
86. U. Pidun, M. Stahl and G. Frenking, *Chem. Eur. J.*, **2**, 869 (1996).
87. (a) S. Miertus, E. Scrocco and J. Tomasi, *Chem. Phys.*, **55**, 117 (1981).
    (b) R. Bonaccorsi, R. Cimiraglia and J. Tomasi, *J. Comput. Chem.*, **4**, 567 (1983).
    (c) R. Bonaccorsi, P. Pala and J. Tomasi, *J. Am. Chem. Soc.*, **106**, 1945 (1984).
    (d) J. L. Pascual-Ahuir, E. Silla, J. Tomasi and R. Bonaccorsi, *J. Comput. Chem.*, **8**, 778 (1987).
    (e) F. Floris and J. Tomasi, *J. Comput. Chem.*, **10**, 616 (1989).
88. (a) R. F. W. Bader, *Atoms in Molecules*, Oxford University Press, Oxford, New York, 1990.
    (b) R. F. W. Bader, *Acc. Chem. Res.*, **18**, 9 (1985).
89. G. A. Olah, G. Rasul and G. K. S. Prakash, *J. Organomet. Chem.*, **521**, 271 (1996).
90. Z. Xie, R. Bau, A. Benesi and C. A. Reed, *Organometallics*, **14**, 3933 (1995).
91. Z. Xie, J. Manning, R. W. Reed, R. Mathur, P. D. W. Boyd, A. Benesi and C. A. Reed, *J. Am. Chem. Soc.*, **118**, 2922 (1996).
92. M. R. Rosenthal, *J. Chem. Educ.*, **50**, 33 (1973).
93. Y. Cao, J.-H. Choi, B.-M. Hass, M. S. Johnson and M. Okumura, *J. Phys. Chem.*, **97**, 5215 (1993).
94. D. W. Boo and Y. T. Lee, *Chem. Phys. Lett.*, **211**, 358 (1993).
95. (a) P. R. Schreiner, S.-J. Kim, H. F. Schaefer III and P. v. R. Schleyer, *J. Chem. Phys.*, **99**, 3716 (1993).
    (b) P. v. R. Schleyer and J. W. de. M. Carneiro, *J. Comput. Chem.*, **13**, 997 (1992).
    (c) see also W. Klopper and W. Kutzelnigg, *J. Phys. Chem.*, **94**, 5625 (1990).
96. S.-J. Kim, P. R. Schreiner, P. v. R. Schleyer and H. F. Schaefer III, *J. Phys. Chem.*, **97**, 12232 (1993).
97. R. Liu and X. J. Zhou, *J. Phys. Chem.*, **97**, 9555 (1993).
98. (a) C.-H. Hu, P. R. Schreiner, P. v. R. Schleyer and H. F. Schaefer III, *J. Phys. Chem.*, **98**, 5040 (1994).
    (b) P. R. Schreiner, H. F. Schaefer III and P. v. R. Schleyer in *Advances in Gas Phase Ion Chemistry*, N. G. Adama and L. G. Babcock (Eds.), JAI Press, Inc., London, Vol. 2, pp. 125–160.
99. (a) P. v. R. Schleyer, Y. Apeloig, D. Arad, B. T. Luke and J. A. Pople, *Chem. Phys. Lett.*, **95**, 477 (1983).
    (b) C.-H. Hu, M. Shen and H. F. Schaefer, *Chem. Phys. Lett.*, **190**, 543 (1992).
    (c) E. Delrio, M. I. Menendez, R. Lopez and T. L. Sordo, *J. Chem. Soc., Chem. Commun*, 1779 (1997).
100. B. H. Boo and P. B. Armentrout, *J. Am. Chem. Soc.*, **109**, 3549 (1987).
101. J. B. Lambert, S. Zhang and S. M. Ciro, *Organometallics*, **13**, 2430 (1994).
102. (a) A. Gobbi and G. Frenking, *J. Am. Chem. Soc.*, **115**, 2362 (1993).
    (b) A. Gobbi, P. J. MacDougall and G. Frenking, *Angew. Chem.*, **103**, 1023 (1991); *Angew. Chem., Int. Ed. Engl.*, **30**, 1001 (1991).
103. S. Berger, W. Bock, G. Frenking, V. Jonas and F. Müller, *J. Am. Chem. Soc.*, **117**, 3820 (1995).
104. C. Eaborn, *J. Organomet. Chem.*, **405**, 173 (1991).
105. G. A. Olah, G. Rasul, L. Heiliger, J. Bausch and G. K. S. Prakash, *J. Am. Chem. Soc.*, **114**, 7737 (1992).
106. (a) C. Chuit, R. J. P. Corriu, A. Mehdi and C. Reyé, *Angew. Chem.*, **105**, 1372 (1993); *Angew. Chem., Int. Ed. Engl.*, **32**, 1311 (1993).
    (b) C. Brelière, F. Carré, R. Corriu and M. W. C. Man, *J. Chem. Soc., Chem. Commun.*, 2333 (1994).

(c) F. Carré, C. Chuit, R. J. P. Corriu and A. Mehdi, *Angew. Chem.*, **106**, 1152 (1994); *Angew. Chem., Int. Ed. Engl.*, **33**, 1097 (1994).
(d) M. Chauhan, C. Chuit, R. J. P. Corriu and C. Reyé, *Tetrahedron Lett.*, **37**, 845 (1996).

107. J. Belzner, D. Schär, B. O. Kneisel and R. Herbst-Irmer, *Organometallics*, **14**, 1840 (1995).
108. C.-H. Ottosson and D. Cremer, *Organometallics*, **15**, 5309 (1996).
109. W. Uhlig, in *Organosilicon Chemistry: From Molecules to Materials*, Vol. II (Eds. N. Auner and J. Weis), VCH, Weinheim, 1995, p. 21.
110. H.-U. Steinberger, T. Müller, N. Auner, C. Maerker and P. v. R. Schleyer, *Angew. Chem.*, **109**, 667 (1997); *Angew. Chem., Int. Ed. Engl.*, **36**, 626 (1997).
111. (a) R. G. Lawton, *J. Am. Chem. Soc.*, **83**, 2399 (1961).
    (b) S. Winstein and P. Carter, *J. Am. Chem. Soc.*, **83**, 4485 (1961).
    (c) P. D. Bartlett and S. Bank, *J. Am. Chem. Soc.*, **83**, 2591 (1961).
    (d) P. D. Bartlett, S. Bank, R. J. Crawford and G. H. Schmid, *J. Am. Chem. Soc.*, **87**, 1288 (1965).
112. (a) H.-J. Knölker, G. Baum and R. Graf, *Angew. Chem.*, **106**, 1705 (1994); *Angew. Chem., Int. Ed. Engl.*, **33**, 1612 (1994).
    (b) H.-J. Knölker, N. Foitzik, H. Goesmann and R. Graf, *Angew. Chem.*, **105**, 1104 (1993); *Angew. Chem., Int. Ed. Engl.*, **32**, 1081 (1993).
    (c) H.-J. Knölker, P. G. Jones and J.-B. Pannek, *Synlett*, 429 (1990).
113. C.-H. Ottosson, K. J. Szabó and D. Cremer, *Organometallics*, **16**, 2377 (1997).
114. N. J. R. van Eikema Hommes, C. Maerker and P. v. R. Schleyer, unpublished results.
115. E. D. Jemmis, G. N. Srinivas, J. Leszczynski, J. Kapp, A. A. Korkin and P. v. R. Schleyer, *J. Am. Chem. Soc.*, **117**, 11361 (1995).
116. A. Sekiguchi, M. Tsukamoto and M. Ichinohe, *Science*, **275**, 60 (1997).
117. For recent reviews see:
    (a) P. v. R. Schleyer, *Science*, **275**, 39 (1997).
    (b) J. Belzner, *Angew. Chem.*, **109**, 1331 (1997); *Angew. Chem., Int. Ed. Engl.*, **36**, 1277 (1997).
118. R. K. Harris and B. E. Mann, *NMR and The Periodic Table*, Academic Press, London, 1978, p. 313.
119. H. Jiao and P. v. R. Schleyer, unpublished data.

CHAPTER **11**

Silicenium ions — experimental aspects

PAUL D. LICKISS

Department of Chemistry, Imperial College of Science, Technology and Medicine, London SW7 2AY, UK
Fax: +44 (0)171 594 5804; e-mail: p.lickiss@ic.ac.uk

I. INTRODUCTION

There have been a large number of comparative studies of the chemistry of analogous carbon and silicon compounds over the last 50 years, many of which were carried out in order to ascertain whether silicon compounds could be demonstrated to exhibit similar chemical properties to those of their more well-known carbon analogues. Such studies have, for example, during the last 15 years led to the successful isolation of compounds containing multiple bonds to silicon and to a much improved knowledge of compounds containing polysilane linkages (see Chapters 15, 16 and 17 by Sakurai, Auner, and Tokitoh and Okazaki respectively for multiple bonding and Chapter 37 by Hengge and Stüger for polysilanes). One of the remaining, and one of the most difficult, practical challenges to silicon chemists has been to demonstrate the existence of, and to isolate, three-coordinate, trivalent cationic species R_3Si^+, analogous to the well known R_3C^+ cations in either solution or the solid state. Even the naming of R_3Si^+ species has been the subject of some discussion; the terms siliconium, silylium, silicenium, silylenium, silyl cation and silico cation have all been used. The current recommendation by IUPAC[1] is silylium, but silicenium will be used here in order to be consistent with other chapters in this volume.

The Pauling scale of electronegativities gives values of 2.5 and 1.8, respectively, for carbon and silicon. The more electropositive nature of silicon would suggest that it should be easier to form R_3Si^+ species than analogous R_3C^+ and this is indeed the case in the gas phase where, for example, R_3Si^+ ions are abundant in the mass spectra of organosilicon compounds[2,3] and ionization potentials for silyl radicals are lower than for alkyl radicals, e.g. 9.84 and 8.01 eV for $H_3C^\bullet$ and $H_3Si^\bullet$ and 6.34 and 5.93 eV for $Me_3C^\bullet$ and $Me_3Si^\bullet$ radicals, respectively (see Table 1 in Reference 4). Silicon is also more polarizable and larger than carbon and might again, therefore, be expected to form more stable R_3Si^+ ions than the analogous carbon species. Why then was there little real progress in preparing silicenium ions in condensed phases until very recently and why do unambiguous examples of such species still remain to be prepared? It is not due to a thermodynamic instability, as gas-phase silicenium ions are readily prepared[2,3] (tables of calculated relative stabilities of carbenium and silicenium ions are given in Reference 4) and a determination by FT ion cyclotron resonance spectroscopy of the hydride affinities for H_2MeSi^+, HMe_2Si^+ and Me_3Si^+ in the gas phase gives values of 245.9, 230.1 and 220.5 kcal mol^{-1}, respectively, which, when compared with the values of 270.5, 251.5 and 233.6 kcal mol^{-1} for the corresponding carbenium ions, shows that the silicenium ions are thermodynamically significantly more stable[5]. The instability is actually kinetic in origin due to the high electrophilicity of R_3Si^+ ions which, in solution or the solid state, leads to such species interacting with a wide variety of both π- and σ-electron donors, such as solvents and other potential nucleophiles such as oxygen- and halogen-containing counter anions. The false notions of non-coordinating solvents and anions are particularly highlighted in this field, the strongly electrophilic silicenium ions being found to interact with many species that in other areas of chemistry are found to be relatively innocent. Unlike carbon which readily forms compounds containing three-coordinate sp^2 carbon and which tends not to increase its coordination number above four, silicon has a tendency to increase its coordination number to five or six which has traditionally been thought to be due to formal hybridization states of sp^3d and sp^3d^2. Calculations, however, indicate that the orbital participations for five and six-coordinate silicon species are in fact approximately sp^2 with no significant d-orbital participation, and that the bonding to silicon is better regarded as partially ionic[4]. These factors, together with the poorer π–π overlap between Si and first-row π-donor substituents containing N or O, and the longer Si–R compared to C–R bond lengths which mean that R_3C^+ ions are sterically better protected from anions than R_3Si^+, all militate against the formation of R_3Si^+ ions. The work described below shows how various factors such as solvent, anion, steric and electronic effects of the substituents at silicon, and reaction byproducts can be manipulated in potential preparations of silicenium ions so that the chances of success are maximized. Even with the best current knowledge on the important factors a recent review concludes that ‘the prospects for obtaining and observing truly ‘free’ silyl cations in condensed phases are very poor’[4].

One further problem that arises in the search for a ‘free’ silicenium ion is what the term ‘free’ means in this context. In the case of R_3C^+ ions there are crystallographic studies that show that for free ions such as Me_3C^+ there is a separation of about 3 Å or greater between the cationic centre and the closest atoms of its counter anion $Sb_2F_{11}^-$, and that the ions are planar[6] and so it might be expected that a similar or even greater separation might be found between a silicenium ion and its related anion and that R_3Si^+ will be planar. Such separations and planar geometry have yet to be found (see Section IV). The arguments presented in recent years for the existence of silicenium ions have focused on the anion cation separation (ideally greater than 3 Å), the R−Si−R angles in the R_3Si^+ species (ideally 120°), the out-of-plane displacement of the silicon atom (ideally zero) and the ^{29}Si NMR chemical shift values (according to calculations, these should be about 350 ppm or even greater for simple trialkyl silicenium ions). As there may be species isolated that successfully satisfy one of the criteria better than the others, the question of whether a 'free' silicenium ion has been prepared or can be prepared may depend on the definition chosen. Certainly none of the species so far isolated or observed spectroscopically satisfies any of these criteria, and calculations carried out in the last few years have shown that most, if not all, of the species proposed to be silicenium ions are actually better described in other ways. Much discussion has therefore been directed towards the degree or extent of cationic character in cationic silicon-containing species.

The long history of the search for silicenium ions has meant that there have been several reviews or critical comments published on the problem. Early work was reviewed by O'Brien and Hairston[7] and by Corriu and Henner[8] while more recent studies have been reviewed by various authors[3,4,9−19]. This chapter will concentrate on work reported in the last few years, particularly since 1988.

Running in parallel with the numerous experimental attempts to prepare silicenium ions in recent years, there has been a considerable number of computational studies carried out on them. The computational work is described in detail in the chapter by Schleyer and Maerker and this chapter will describe experimental work, concentrating mainly on solution and solid state experimental work with only occasional reference to calculations when necessary.

II. GAS-PHASE STUDIES

The abundance of silicenium ions in the gas phase has allowed many studies to be carried out on their formation and chemistry and much of this work has been reviewed[2,3] (see also the chapter by Goldberg and Schwarz). This chapter will concentrate on studies carried out in condensed phases but some gas-phase studies, particularly where they give information relevant to some of the current work on condensed-phase species, will be described briefly below.

The importance of silicenium ion reactions in the gas phase has become better appreciated in recent years as the use of chemical vapour deposition techniques for the preparation of materials such as silicon carbide[20] and silicon nitride[21−24] has increased. Silicenium ions have been generated in the gas phase by several ionization techniques, often using mass spectrometric methods; see, for example, Reference 25. The methods involved will not be described here but some of the physical characteristics and the chemistry of the derived ions will be discussed. A study of the gas-phase IR spectrum of H_3Si^+ shows the ν_2 and ν_4 fundamentals to be at 838.0669(24) and 938.3969(36) cm^{-1}, respectively[26], while an IR laser absorption spectroscopy shows that, as expected, H_3Si^+ is planar, and gives a value for the ν_2 band centre of 838.0674(7) cm^{-1}, a ground state rotational constant of 5.2153(1) cm^{-1}, and an Si−H bond length of 1.462 Å[27]. The heat of formation of H_3Si^+ generated by the reaction of ground state silicon ions with SiH_4 was found to be 237.1(2) kcal mol^{-1}, in good agreement with earlier photoionization measurements and calculations[28]. More recent photoionization mass spectrometry studies give heats of formation for H_3Si^+, D_2MeSi^+, HMe_2Si^+ and Me_3Si^+ of 235.3, 204 ± 1, 173.2 and 145.0 kcal mol^{-1}, respectively[29]. Low energy electron impact dissociation of both SiH_4 and Si_2H_6 gives H_3Si^+ as a primary product[30] and cluster cations containing up to nine silicon atoms in the gas phase are formed in the reactions between disilane and cations

D_nSi^+ ($n = 0-3$) and $D_nSi_2^+$ ($n = 0-6$)[31-33]. Calculations on the clustering reactions of H_3Si^+ with SiH_4 and D_3Si^+ with SiD_4 have also shown that only small clusters seem to be formed by this mechanism and that such clustering is not the route to the hydrogenated silicon dust formed in SiH_4 plasmas[34,35]. However, if a few percent of water is present, then larger clusters leading to the formation of hydrogenated particles of silicon are formed[36]. The reaction rates of H_3Si^+ with D_4Si and D_3Si^+ with H_4Si have been measured and two different mechanisms for the reactions were found, one involving ion–molecule formation, the other 'long-range hydride stripping', which together combine to give a reaction rate that is greater than the collision rate. The overall rate depends significantly on the number of H and D substituents present[37]. Gas-phase reactions in SiH_4/GeH_4 proceed via both H_3Si^+ and H_3Ge^+ ions to give species containing Si–Ge bonds[38] and reactions between H_3Si^+ and PH_3 give a variety of ions containing Si, P and H as determined by mass spectrometry[39]. A study of the association reactions of primary, secondary and tertiary amines with Me_3Si^+ applying high pressure mass spectrometry shows that the Me_3Si^+ affinities (46.5 and 59.5 kcal mol^{-1} for NH_3 and n-$BuNH_2$, respectively) increase in the order $NH_3 < MeNH_2 < EtNH_2 < n\text{-}BuNH_2$, the values increasing linearly with the proton affinity of the amines. The affinities for *sec*- and *tert*-butylamines are lower than for the *n*-butyl isomer which is attributed to steric effects and the Me_3Si^+ affinities also increase in the order primary < secondary < tertiary amine[40].

An FT ion cyclotron resonance study shows that in the reactions of H_3SiCl with $H_nCl_{3-n}Si^+$ ions ($n = 1$, 2 or 3), H_2ClSi^+ participates in both disproportionation and hydride transfer reactions but H_3Si^+ and HCl_2Si^+ only participate in hydride transfer. The disilylchloronium ion $(H_3Si)_2Cl^+$ is thought to be an intermediate (perhaps analogous to the silylated halonium ions found in condensed phases, see Section IV) in the reaction between H_3Si^+ and H_3SiCl and to have a lifetime at room temperature of several tenths of a second[41]. The values of the chloride affinities for chlorosilyl cations are similar and fall in the order $H_2ClSi^+ > HCl_2Si^+ \approx Cl_3Si^+$ while the hydride affinities are in the order $Cl_3Si^+ > HCl_2Si^+ > H_2ClSi^+$[42]. Fourier transform mass spectrometric studies show that the predominant mechanism of decomposition for MeH_2Si^+ is dehydrogenation and that of $Me(Cl)HSi^+$ to be a 1,2-elimination of HCl[43]. The dominant reaction between H_3Si^+ and CH_3Cl, CH_2Cl_2 and $CHCl_3$ is chloride abstraction to give SiH_3Cl and H_3C^+, H_2ClC^+ and HCl_2C^+ ions, respectively[44]. Generation of the highly reactive Cl_3Si^+ ion in the gas phase under plasma conditions allows polymeric surfaces such as polyester, polypropylene and polytetrafluoroethylene, that are normally regarded as inert, to be modified by replacement of H, OH or F[45,46].

The silicenium ions derived from the methylsilanes Me_nSiH_{4-n} ($n = 0-3$) have been studied by photoionization mass spectrometric techniques[29] and have been shown to undergo rapid Me/H exchange reactions with propene and with 2-methylpropene[47]. The most stable isomer of formula $SiC_2H_7^+$ has been calculated[48] to be Me_2HSi^+ and this ion has also been found to be thermodynamically more stable than its isomer EtH_2Si^+ using Fourier transform mass spectrometry[49]. Such gas-phase spectrometric techniques have also shown that, after collisional activation, Me_3Si^+ undergoes a rearrangement to $EtMeHSi^+$ followed by extrusion of $H_2C{=}CH_2$ to give MeH_2Si^+[50]. The silicenium ions i-$PrMe_2Si^+$ and n-$PrMe_2Si^+$ can be generated in the gas phase from i-$PrMe_2SiCl$ and n-$PrMe_2SiCl$, respectively, by chemical ionization using isobutane. Both ions undergo rearrangements to give isomeric α- and β-silyl substituted carbenium ions which then undergo elimination of C_2H_4 and C_3H_6 to give a mixture of Me_3Si^+ and Me_2HSi^+, respectively, Me_3Si^+ predominating for i-$PrMe_2Si^+$, and Me_2HSi^+ for n-$PrMe_2Si^+$[51]. The ions i-$PrMe_2Si^+$ and n-$PrMe_2Si^+$ are also formed in the high pressure (50–760 torr) γ-radiolysis of mixtures of CH_4 and $Me_3SiCH{=}CH_2$ after initial protonation both α and β to the silicon and subsequent rearrangement of the resulting carbenium ions. Both silicenium ions can be trapped using methanol to give *i*-$PrMe_2SiOMe$ and *n*-$PrMe_2SiOMe$[52]. A recent theoretical study of the migratory aptitude of H, Me and Ph groups from silicon to an α carbon atom to give silicenium ions is consistent with the experimental results determined by mass spectrometry in the gas phase[53]. Ionization of $Me_3SiOCH_2CH_3$ in the gas phase followed by alkene elimination leads to $Me_2(OH)Si^+$ formation (equation 1). This cation can then be used to generate the $Me_2(OH)Si^\bullet$ radical by collisional neutralization[54]. The unimolecular reactions of $Me_3SiOSiMe_2{}^+$ and deuterium labelled analogues have been studied using mass-analysed ion kinetic energy spectrometry. Scrambling of the methyl groups occurs initially and this is followed by losses of CH_4 and $Me_2Si{=}O$. This is in contrast to the carbon analogue $Me_3COCMe_2{}^+$, the most significant reaction of which is loss of $CH_2{=}CMe_2$[55]. A related study has shown that electron impact induced fragmentation of $Me_2Si(OEt)_2$ leads to formation of $MeSi(OH)_2{}^+$ and $Me_2Si{=}OH^+$[56]. The differences between the relative stabilities and the decomposition pathways of the products formed in the reactions between Me_3Si^+ and the *cis* and the *trans* isomers of 1,2-cyclopentanediol can be used to distinguish between the two isomers. The *cis* isomer decomposes to give the hydrated trimethylsilicenium ion $Me_3SiOH_2^+$[57], which is also formed in the reaction between Me_3Si^+ and water[58]. The *t*-Bu analogue of the hydrated ion *t*-$Bu_3SiOH_2{}^+$ has been prepared in solution and its solid state structure has been determined[59] (Section IV).

$$Me_3SiOCH_2CH_3{}^{+\bullet} \longrightarrow Me_2\overset{+}{Si}OCH_2CH_3 \longrightarrow Me_2\overset{+}{Si}OH + CH_2{=}CH_2 \qquad (1)$$

Studies carried out on reactions in the gas phase also offer the opportunity to investigate species that interact strongly with solvents etc. in condensed phases. It has thus been possible to study reactions of silicenium ions in the gas phase, solution state analogues of which have become of significant interest. One such type of reaction is that of electrophilic aromatic silylation which was a reaction unknown in solution [but see the discussion of the structure of $Et_3Si(toluene)^+$ in Sections III.C.2 and IV for a recent solution and solid state example] due to the strong influence of both solvent and anion on silicenium ion formation. A mass spectrometric study of the reactions of Me_3Si^+, generated by the reaction between $CH_5{}^+$ and $C_2H_5{}^+$ with Me_4Si, with aromatic compounds, concluded that there was no aromatic substitution with the formation of a Si−C bond to give **1**, but rather that a π-complex of type **2** was formed[60]. A more recent collision-assisted dissociation study of Me_3SiArH^+ (Ar = benzene or toluene) formed by either silylation of the aromatic or by protonation of $ArSiMe_3$ failed to resolve the question of whether **1** or **2** represents the gas-phase structure best[61].

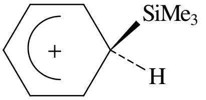

(1)

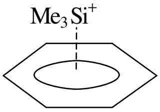

(2)

Radiolytic studies have now demonstrated that the Wheland intermediate type **1** does in fact form and that earlier work had neglected the possibility that rapid desilylation by bases present in the mass spectrometric study would compete effectively with, and prevent, deprotonation, i.e. that reaction 2 is faster than reaction 3. This would therefore give the appearance that an Si−C bond was not formed[62−65]. If a nitrogen-centred base such as Et_3N is added to the system for the generation of Me_3Si^+, then this does cause deprotonation and this competes effectively with the trace amounts of oxygen containing impurities present that cause desilylation. This then does allow the formation of neutral arylsilane products. If, however, larger amounts of amine are added, then this intercepts the Me_3Si^+ and $C_nH_5^+$ ($n = 1$ or 2) precursor ions thus reducing arylsilane yields[63]. Yields of less than 2% of silylated arenes can be achieved in solution if a similar strategy is used and a hindered base is present to abstract the proton (equation 4). For example, trimethylsilylation of toluene gives an overall yield of 1.0%, the *o*-, *m*- and *p*-isomers being formed in a 0.6 : 34.6 : 64.8 ratio. The very low overall yields are due in part to the disproportionation of the products in the presence of the $AlCl_3$[66].

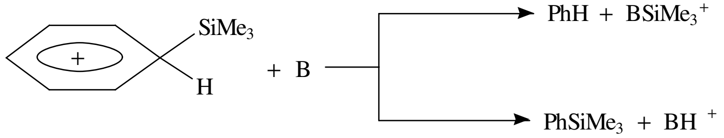

(2)

(3)

B = oxygenated base, e.g. H_2O, MeOH or CH_2O

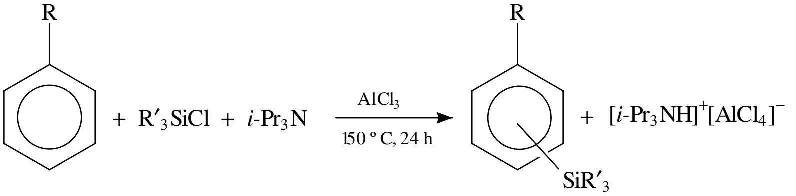

(4)

The selectivity of the gas-phase electrophilic aromatic substitution appears to be dominated by the steric requirements of the silyl substituent, the *meta* : *para* ratio for toluene substitution by Me_3Si^+ is 14 : 86, while mesitylene, in which any substitution is forced to be *ortho* to two methyl groups, is unreactive[62,66]. This substitution pattern is similar to that found in work on the solution or solid state products from the reaction between Et_3Si^+ and toluene in which there is apparently 100% *para* substitution[67] (see Section IV). Once formed, species of type **1** appear to be stable towards 1,2-H shifts as judged by radiolytic techniques[68]. The existence of ions of type **1** has been further confirmed (although not excluding the possibility of ions **2** in equilibrium with **1**) by ion cyclotron resonance mass spectrometry studies. This work shows that transfer of D^+ from $[Et_3SiC_6D_6]^+$ to Et_3N does occur, this type of reaction being unknown for the π-type complex, but being consistent with the σ-structure which can undergo both reactions 2 and 3[69]. The existence of long-lived $[Me_3Si(toluene)]^+$ ions with the σ-bound structure **1** is also confirmed by the observation of a primary kinetic isotope effect in competition reactions of Me_3Si^+ with $C_6H_5CH_3$ and $C_6D_5CD_3$[70].

III. SOLUTION STUDIES

A. Conductance Measurements

Early attempts to demonstrate that silicenium ions were components of conducting solutions relied on methods analogous to those used successfully in carbon chemistry. In solvents, such as liquid SO_2, pyridine or nitrobenzene/$AlBr_3$, in which Ph_3CCl was found to be ionized, there was no significant ionization of Ph_3SiCl[71,72]. There is also no ionization of Ph_3SiOH in liquid HCl, a solvent that does promote ionization of

Ph_3COH to give Ph_3C^+[73]. This and other early work has been reviewed by Corriu and Henner[8]. More recent work by Lambert and coworkers has focused on the possibility that organosilicon perchlorates (prepared from the reaction between silanes R_3SiH and Ph_3CClO_4[74]) might be ionized in suitable solvents. The perchlorates Me_3SiClO_4[75–77], $PhMe_2SiClO_4$[77], $Ph_2MeSiClO_4$[77], Ph_3SiClO_4[75,78], $(RS)_3SiClO_4$ (where R = Me[76], Et[76], or *i*-Pr[76,79]) and $(Me_2N)_nMe_{3-n}SiClO_4$ (where $n = 1$, 2 or 3)[80] have been studied using CH_2Cl_2, MeCN, sulpholane and 1,2-dichloroethane solutions. In concentrated solutions in sulpholane or in the solvents of lower ionizing power, CH_2Cl_2 and 1,2-dichloroethane, the perchlorates R_3SiClO_4 (where R = Me or Ph) are thought to be covalent R_3SiClO_4 species or $R_3Si^+ClO_4^-$ ion pairs in equilibrium with free ions, but in dilute (less than 0.01 M) sulpholane solution conductance measurements suggest that free ions are present. The organosulphur derivative $(i\text{-PrS})_3SiClO_4$ was found to give a conducting solution in CH_2Cl_2[79]. By comparison, the azide Me_3SiN_3 gave negligible conductance in CH_2Cl_2, MeCN or sulpholane and the triflate $Me_3SiOSO_2CF_3$ gave very low conductance in CH_2Cl_2 but high conductance in MeCN and sulpholane. The interpretations of the results from these conductance studies have been questioned[13,81–83] and they have been proposed to be due not to ionized silyl perchlorates but to hydrolysis, to give free ClO_4^- ions, by residual water in the solvents used, some of which are particularly difficult to dry adequately for studies using very low concentrations of highly moisture sensitive materials. Lambert and coworkers have countered these criticisms[18,77] and have argued that integration of the ^1H NMR signals due to hydrolysis products show that the concentration of water present is only about one-tenth of that of the silicon-containing substrate. Hydrolysis is clearly a problem in some of the NMR studies that have been reported (see below) and if free R_3Si^+ ions are present there seems to be a contradiction between the conductance results and those of ^{29}Si NMR studies on similar solutions which indicate the silicon to be four coordinate[13,18]. Most recent attempts to study silicenium ions have not used conductance as a measure of potential ion formation. The very bulky perchlorate $(Me_3Si)_3CSiMe_2ClO_4$ has been shown to undergo methanolysis relatively slowly with a half-life at 27.5 °C of about 24 min, and little if any solvolysis in CF_3CH_2OH[12,84]. Although this perchlorate is far bulkier than those used by Lambert, the relief of steric strain on formation of the three-coordinate $[(Me_3Si)_3C]Me_2Si^+$ ion might be expected to aid ionization. It would be expected that in such good ionizing solvents, and at the concentrations used, ionization would occur and there would then be very rapid solvolysis. As rapid solvolysis does not occur, this also seems to cast doubt on the proposal that silyl perchlorates undergo ionization in solution at low concentrations.

A further complication in solution-phase measurements is the possibility that the solvent molecules may play an important role such that even if the silyl perchlorate were to ionize, the silyl moiety may still be four coordinate by interaction with the solvent to give species $R_3Si{-}S^+$ (S = solvent) such as **3** which is both four coordinate and ionic and which might be consistent with both conductance and some NMR measurements.

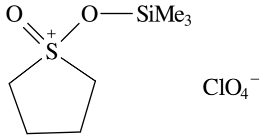

(3)

Several studies[75,78,85] including the use of conductometric titration[18,76,77] showed that for pyridine and *N*-methylpyrrole in CH_2Cl_2 complex formation occurs, but for the weaker nucleophiles MeCN and sulpholane solvent complexes were unimportant. Unfortunately, it is likely that in CH_2Cl_2 solution, sulpholane and MeCN cannot displace perchlorate from the substrate due to poor solvation by CH_2Cl_2. It is thus possible that the ions in sulpholane solution are of the form shown in **3**. This interpretation of the conductance measurements is not unreasonable as there are many $R_3Si{-}S^+$ (S = solvent) type complexes known (for a review of the work in this area see Reference 3). For example, for R = Me, complexes with $(Me_2N)_3P$[86], Ph_3PO[86], pyridine[87,88] and 3-methyl and 3-(trimethylsilyl)imidazole[87] are all well described. The ions $[R_3Si(MeCN)]^+$ (where $R_3 = Me_3$, Ph_3 or $PhMe_2$) are also thought to be generated electrochemically from the corresponding disilanes $(R_3Si)_2$ in MeCN solution[89]. A recent study of over sixty combinations of silyl halides, perchlorates, triflates and tetraarylborates in solvents such as CH_2Cl_2, pyridine, DMSO, MeCN, HMPA and sulpholane concluded that in all cases weak covalent Si-solvent bonds were formed, and that no free silicenium ions were generated[90]. Intramolecular stabilitation of a cationic species to give a five-coordinate ion **4** can also be achieved, ^{29}Si NMR spectroscopy indicating that the same five-coordinate species is present both in solution and in the solid state[91]. Multinuclear NMR studies have, however, shown that the cationic species **5**, with no Si−H group present, is in fact an equilibrium mixture of the two four-coordinate silylammonium cations **6** and **7** in CD_3OD, $CDCl_3$ and CD_3CN solutions[92]. More recently it has been shown that the nature of the cations without an Si−H group present is dependent on the anion, the more nucleophilic anions chloride and iodide give four-coordinate silylammonium species **8**, the less nucleophilic tetraarylborate giving a silicon-centred cationic species **9**, and the Ph_4B anion giving a mixture of the four-and the five-coordinate species that slowly converts into the four-coordinate species in CD_3CN solution[93,94]. Calculations have also shown that in aryl-substituted silicenium ions bearing substituents in the *ortho* position, e.g. $[R_2SiC_6H_3(CH_2NMe_2)_2\text{-}2,6]^+$ (R = H or Me), intramolecular coordination of the silicon by the amine functions is strong, and that this may prevent intermolecular solvation of the ion by solvent molecules[95].

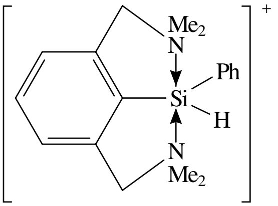

(4)

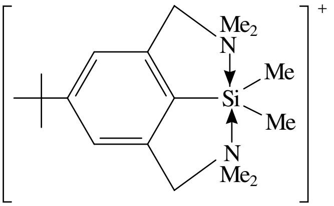

(5)

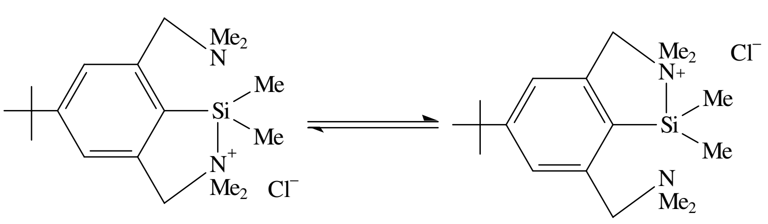

(6) **(7)**

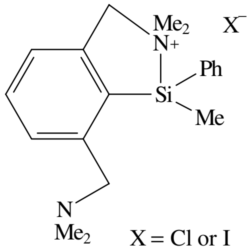

(8)

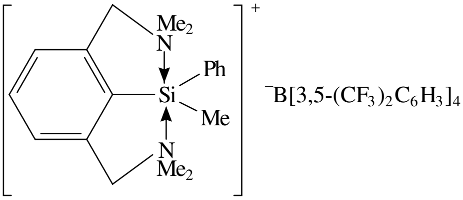

(9)

B. Cryoscopic Measurements

Early, unsuccessful work to demonstrate ionization of organosilicon compounds by cryoscopic methods has been reviewed by Corriu and Henner[8]. More recent work has again focused on the possible dissociation of silyl perchlorates, particularly in sulpholane and in CH_2Cl_2. The perchlorates $(i\text{-PrS})_3SiClO_4$, $Ph_nMe_{3-n}SiClO_4$ (n = 0, 1 or 3) and $(Me_2N)_nMe_{3-n}SiClO_4$ ($n = 1$, 2 or 3) were all found to give the expected molecular weights, within about 5–10% accuracy, for two-particle systems in sulpholane rather than those expected for either covalent perchlorates or for hydrolysis products such as silanols or siloxanes[18]. The apparent accuracy of these results is surprising as, together with the silyl perchlorate present, there will also be an equivalent number of moles of Ph_3CH (formed during the synthesis of the silyl perchlorate), and some $R_3SiOSiR_3$ and $HClO_4$. The ionic and covalent forms of the silyl perchlorate are also in equilibrium and, at the concentrations at which the experiments were carried out, only about 45–65% free ions are thought to be present[13,18,75]. It is also possible that the cryoscopic measurements can be explained by the presence of solvent complexes of the type $R_3Si{-}S^+ClO_4^-$ (S = solvent) rather than $R_3Si^+ClO_4^-$ species. The importance of such solvent complexes is discussed in the previous section.

C. Spectroscopic Measurements

1. Electronic spectroscopy

In acidic solution the carbinol $[4\text{-}(Me_2N)C_6H_4]_3COH$ ionizes to give the deep violet cation $[4\text{-}(Me_2N)C_6H_4]_3C^+$ but the corresponding silanol $[4\text{-}(Me_2N)C_6H_4]_3SiOH$ shows very little change on protonation, this being due to protonation of the NMe_2 groups rather than to ionization[96]. Similarly, simple perchlorates such as R_3SiClO_4 (R = Ph, *p*-tolyl) are colourless whereas the analogous crystalline carbon analogues are highly coloured[97]. Both of these studies thus indicated that silicenium ions did not seem to be present in systems where carbon analogues were well known. Electronic spectroscopy does not seem to have been widely used in silicenium ion studies in more recent years, although for $Et_3SiB(C_6F_5)_4$ in benzene solution a spectrum comprising one broad absorption, $\lambda_{max} = 303$ nm, has been reported[67].

2. NMR spectroscopy

NMR spectroscopy has, in the last ten years, become one of the most important tools in the search for silicenium ions in condensed phases. Studies involving ^1H, ^{11}B, ^{13}C, ^{19}F, ^{29}Si and ^{35}Cl have all been carried out, with particular recent interest focused on the ^{29}Si nucleus.

a. ^{1}H and ^{13}C NMR spectroscopy. Proton NMR spectroscopy has been used relatively little in silicenium ion studies, despite its high sensitivity (especially when compared with ^{29}Si), but it is useful in determining the extent of hydrolysis of simple species such as Me_3SiClO_4 for which the hydrolysis product, $Me_3SiOSiMe_3$ (after initial formation of Me_3SiOH and its condensation), has a simple and distinct ^{1}H NMR signal[77]. A series of ^{1}H and ^{13}C chemical shift values for Me_3SiClO_4, $MePh_2SiClO_4$ and $Me_2PhSiClO_4$ in sulpholane containing 10% CD_2Cl_2[77] and ^{13}C shifts for Ph_3SiClO_4 in CD_2Cl_2[76] have been reported, but there is only a small change of about 0.1 ppm in ^{1}H chemical shift on changing the concentration of the silyl perchlorate from 0.27 to 0.009 mol dm^{-3} and about 0.2 ppm ^{13}C chemical shift change on changing the concentration from 0.27 to 0.01 mol dm^{-3} [77]. These changes could be attributed to an increasing ionic content, but such small changes could also readily be attributed to dilution effects.

A study of i-Pr_2MeSi derivatives by ^{1}H and ^{13}C NMR spectroscopy has led to an estimation of the strength of interaction between a silicenium ion and a coordinating solvent[67]. The methyl groups of i-Pr_2MeSiH and other covalent derivatives are diastereotopic and this can be observed by both ^{1}H and ^{13}C NMR spectroscopy, but if the perchlorate were either dissociated into a planar three-coordinate cation, or formed a four-coordinate species that could dissociate to a planar form, then the methyl groups would become homotopic. In C_6D_6 solution both Pr_2MeSiH and i-$Pr_2MeSiClO_4$ show diastereotopic methyls in the NMR spectra, but for i-$Pr_2MeSiClO_4$ in CD_2Cl_2 and i-$Pr_2MeSiB(C_6F_5)_4$ in C_6D_6, CD_3CN or a pyridine/C_6D_6 mixture the methyl groups are observed to be homotopic. If the methyl groups are rendered equivalent by a dissociative exchange of the solvent molecules and formation of an intermediate planar silicenium ion, then the upper limit for the dissociation energy has been calculated to be about 13 kcal mol^{-1}. This value compares with 28.4 kcal mol^{-1} measured by mass spectrometry for the association of Me_3Si^+ with toluene in the gas phase[98] which would be greater than that expected in solution as solvation would help to stabilize free ions. Both the solution-and gas-phase values are significantly less than that for a covalent Si−C bond for which bond energies are about 90 kcal mol^{-1} [99]. It is also possible for the methyl groups in the isopropyl groups to be equivalent if a five-coordinate species with a trigonal bipyramidal structure with two solvent molecules in the axial positions is formed. This possibility has not been disproved for these species, but for other systems involving nitrile exchange there is evidence against a five-coordinate, associative exchange mechanism[100,101].

b. ^{35}Cl NMR spectroscopy. The ^{35}Cl nucleus is quadrupolar with a spin of 3/2, which means that covalent perchlorates exhibit a ^{35}Cl NMR signal that may be hundreds or thousands of Hz wide. In contrast, symmetrical ionic species such as Cl^- and ClO_4^- have much narrower signals. This difference in linewidths has been used to probe the possible ionization of silyl perchlorates in solution. For a 0.584 mol dm^{-3} solution in sulpholane the ^{35}Cl NMR signal for Me_3SiClO_4 is −28 ppm and has a width at half height of 1960 Hz. As the concentration of the silyl perchlorate is reduced there is a concomitant reduction in linewidth until, at a concentration of 0.0047 mol dm^{-3}, it is only 24 Hz[75]. These results were interpreted as being due to the rapid equilibrium between an associated (covalent or ion pair) species, giving a broad signal and free ions that would give a sharp signal. The degrees of ionization for both Me_3SiClO_4 and Ph_3SiClO_4 were both calculated to be about 50% at a concentration of 0.03 mol dm^{-3} and to be essentially complete below about 0.005 mol dm^{-3} [75]. Unfortunately, the lower concentration samples in this study were made up by taking a fraction of the original sample and diluting with fresh solvent, thus adding new water from incompletely dried solvent. Using such a technique it is clearly possible to introduce sufficient water into the sample to cause complete hydrolysis for dilute solutions[13]. The ^{35}Cl NMR results also do not seem to agree well with those from a ^{29}Si NMR study of Me_3SiClO_4, which showed that there was little change in the chemical shift over a similar range of concentrations[81].

c. ^{11}B and ^{19}F NMR spectroscopy. Spectra from ^{11}B and ^{19}F nuclei have mainly been used for compounds containing $[B(C_6F_5)_4]$ as the anion. One of the potential problems with anions containing halogens is coordination between the anion and the cation via a halogen atom. If this were the case for $B(C_6F_5)_4$ containing species, then a shift in a fluorine resonance would be expected; there is, however, no significant difference in ^{19}F chemical shifts for the anion in either the trityl or the Et_3Si^+ species, suggesting that there is no significant interaction between Si and F. The linewidth and the chemical shift for the boron resonance in the trityl and the Et_3Si^+ salts is also the same, again indicating little interaction between the anion and the cation[67,102]. The ^{11}B resonance for *i*-$Pr_3Si(Br_5CB_9H_5)$ ($Br_5CB_9H_5$ = *closo*-6,7,8,9,10-$Br_5CB_9H_5^-$) is essentially the same as that for the $Br_5CB_9H_5^-$ anion in ionic species, suggesting that although X-ray crystallography shows only one Si$\cdots$Br interaction in the solid state (thus rendering the boron atoms inequivalent), that in toluene solution there is rapid rotation of the anion via the four equivalent bromines so that the boron atoms appear equivalent, even down to −40 °C[103].

d. ^{29}Si NMR spectroscopy. The wide availability of high-field FT NMR spectrometers during the last ten years has brought ^{29}Si NMR spectroscopy to the fore in the search for silicenium ions in solution. Clearly a cationic species with the positive charge largely located on a silicon atom should give a distinctive chemical shift, deshielded with respect to related four-coordinate species. More recently, solid state NMR studies have also become important (see Section IV). The availability of reliable computational methods for the calculation of ^{29}Si chemical shifts has also allowed comparisons to be made between experimentally observed shifts and those expected for free ionic species, and there has been considerable discussion about the degree of ionic character indicated by particular chemical shifts. Calculations of chemical shifts are discussed in detail in the chapter by Schleyer and coworkers, but they will be mentioned here where relevant. Chemical shifts for Me_3Si^+ and Ph_3Si^+ have been predicted to be 250 ± 25 and 125 ± 25 ppm, respectively, from correlations with carbon analogues[104]. IGLO calculations, however, predict a chemical shift of 355.7 ppm for Me_3Si^+[83] while an estimate including correlation effects using the GIAO-MP2 method gives a value of 385 ± 20 ppm[105]; other calculations give 354 (GIAO) and 382 (SOS-DFPT) ppm[106]. Similar calculations give values of 371.2 (GIAO) and 415.6 (SOS-DFPT) ppm for Et_3Si^+ and 342.3 (GIAO) and 371.0 (SOS-DFPT) ppm for *i*-Pr_3Si^+[106]. It is unlikely that the highly deshielded values for calculations on free ions in the gas phase will be closely approached for ions in condensed phases, and even at the best levels of theory there is a discrepancy of between 17 and 30 ppm between the calculated and observed values for Me_3C^+[107].

For the simple silyl perchlorates Me_3SiClO_4 and Ph_3SiClO_4 the ^{29}Si chemical shifts are about 47 and 3 ppm, respectively, the values depending a little on the solvent used[18,77]. Reliable chemical shifts for $(i\text{-PrS})_3SiClO_4$ and other thioalkyl derivatives have not been obtained because of the poor stability of these ions in solution[18]. The chemical shift of Me_3SiClO_4 varies little for either neat liquid or sulpholane solutions at concentrations of 0.584, 0.29 and 0.15 mol dm^{-3}, clearly indicating covalency over this range of concentrations[81]. This seems to contradict the results of the ^{35}Cl NMR study described above which indicated that at these three concentrations there were 20 ± 5, 29 ± 5 and

$35 \pm 7\%$ free ions, respectively[75]. Such degrees of free-ion formation would, according to an IGLO-type calculation value of 355.7 ppm, lead to average chemical shifts of about 108.7, 136.5 and 155.0 ppm, respectively[83]. The discrepancy between these results can be resolved if hydrolysis (which would lead to increasing concentrations of $HClO_4$ being formed as the concentration of the silyl perchlorate was reduced) of the perchlorates is taken into account in the case of the ^{35}Cl NMR measurements.

Table 1 shows ^{29}Si chemical shift values for a variety of silicon species in which there was thought to be a significant degree of positive character to the silicon atom together with some less polar species for comparison. One of the criteria that has been used to argue for the development of cationic character at a silicon centre has been the downfield chemical shift change on going from a silyl hydride R_3SiH, to the analogous cationic species R_3Si^+ after hydride abstraction using a trityl salt. This change is about 101.1, 92.1, 95.5 and 228.5 ppm for methyl, ethyl, isopropyl and trimethylsilyl substituents, respectively. These changes are considerably less than those expected for the Me, Et, and *i*-Pr derivatives, suggesting that species with predominantly silicenium ion character are not present. However, it has been reported that the large change for the Me_3Si derivative was 'in accord with a substantially free silylium ion'[102]. From comparisons between SiH_4 and H_3Si^+ it has been predicted that a δ ^{29}Si value (for the central silicon) for free $(Me_3Si)_3Si^+$ would be *ca* 245 ppm and that for the π-complex $(Me_3Si)_3SiC_6H_6{}^+$, δ $^{29}Si = 175$ ppm[108]. The experimentally observed value of δ $^{29}Si = 111$ ppm for $(Me_3Si)_3SiC_6H_6{}^+$ in benzene solution has thus been proposed to indicate 'that a nearly free silylium cation is realized up to 70% by $(Me_3Si)_3SiC_6H_6{}^+$ TPFPB$^-$'[108]. This optimistic conclusion does not seem to be borne out by more recent calculations which give values of 925.3[109] and 920.4 ppm[110] for $(Me_3Si)_3Si^+$ indicating that a change of over 1000 ppm would be expected on free cation formation, and that in fact the change of 228.5 ppm is indicative of relatively little cationic character to the silicon in the species formed. Calculations also give a value of 205.8 ppm for the central silicon in $(Me_3Si)_3SiC_6H_6{}^+$ in the gas phase, which is much closer to that of the experimentally determined solution species than the value for $(Me_3Si)_3Si^+$[110]. (Early work by Lambert and Sun on the potential of silyl substitution for the stabilization of silicenium ions derived from silyl perchlorates also concluded that 'Silyl substitution offers no palpable stabilisation of positive charge on trivalent silicon'[111].) The argument that very large chemical shift changes should be associated with a change from R_3SiH to $R_3Si(solvent)^+$ to R_3Si^+ should also be used with caution if the substituents R are not simple alkyl groups. For example, the ^{29}Si chemical shifts for $(Me_2N)_3SiH$, $(Me_2N)_3Si(H_2O)^+$ and $(Me_2N)_3Si^+$ are calculated to be -20.8, -20.5 and 42.1 ppm respectively[112]. Relatively little experimental work has been carried out recently using non-alkyl or aryl substituents and careful comparisons should be made between experimental and calculated ^{29}Si chemical shift values before conclusions can be drawn. It should be noted that Ph_3SiH, $EtMe_2SiH$, $Me_2(Me_3SiCH_2)SiH$ and $Ph_2(Me_3SiCH_2)SiH$ also react with $Ph_3CB(C_6F_5)_4$, but to give, as judged by ^{29}Si NMR spectroscopy, a variety of unidentified products, none of which have a ^{29}Si resonance at lower field than 60 ppm[67]. It is unclear why such relatively closely similar substrates to those that do seem to give single species should undergo apparently significantly different reactions. The reactions of the trityl salt with *t*-Bu_3SiH and with *t*-$Bu_2(C_6H_{11}$-*c*)SiH are very slow and are also reported to give unidentified mixtures of products[67]. It is clear that further work needs to be carried out to ascertain the influence of a range of substituents at silicon and to determine what other products are formed in the reactions with trityl salts.

The ^{29}Si NMR data described above and detailed in Table 1 are derived mainly from solution state spectra for which it is difficult to take into account the effect that the solvent

TABLE 1. Solution ^{29}Si chemical shifts for various compounds with some cationic character containing silicon, together with calculated values and related species for comparison[a]

Compound	Solvent	Chemical shift (δ, ppm from Me_4Si)	References
Me_3SiH	C_6D_6	-17.5^b	102
	CD_2Cl_2, at −70 °C	-15.5	113
Me_3SiClO_4	CH_2Cl_2	44.0	77
	sulpholane	46.5	77
	none	47	81
	C_5D_5N	42.6	90
	calc. value	40.2	83
	calc. value	58.6	114
Me_3SiOTf	none	43.54	115
	CH_2Cl_2	43.7	90
	CH_2Cl_2/sulpholane	46.6	90
	C_5D_5N	40.8	90
Me_3SiCl	CH_2Cl_2	31.1	90
	C_5D_5N	31.8	90
Me_3SiBr	CH_2Br_2	27.3	104
	benzene	26.41	116
	calc. value	33.9	117
$Me_3SiBr.AlBr_3$	CH_2Br_2	62.7	104
Me_3SiBrH^+	calc. value	154.4	117
$Me_3SiBrMe^+$	calc. value	117.5	117
$Me_3Si[B(C_6F_5)_4]$	C_6D_6	83.6	67
$Me_3SiC_6H_6{}^+$	calc. value	77.9	109,117
$Me_3SiC_6H_5Me^+$	calc. value	60.4	109
Me_3SiOH	acetone	14.9	118
	calc. value	15.1	117
$Me_3Si(OH_2)^+$	calc. value	101.9	117
$[Me_3SiOEt_2]^+$ $\{B[C_6H_3(CF_3)_2\text{-}3,5]_4\}$	CD_2Cl_2, at −70 °C	66.9	113
$[(Me_3Si)_2OEt]^+$	CD_2Cl_2	59.0	113
$(Me_3Si)_2OH^+$ $\{B[C_6H_3(CF_3)_2\text{-}3,5]_4\}$	calc. value	67.6	117
$(Me_3Si)_3O[B(C_6F_5)_4]$	CD_2Cl_2	51.1	119
$Me_3Si(MeCN)^+$	CD_2Cl_2, at −10 °C	38.5	120
	calc. value	51.5	117
$Me_3Si(C_5H_5NO)^+$	CD_2Cl_2	49.4	121
$Me_3Si(C_5H_5N)^+$	CD_2Cl_2	42.3	121
$[Ph_2C{=}O\text{-}SiMe_3]^+$ $\{B[C_6H_3(CF_3)_2\text{-}3,5]_4\}$	CD_2Cl_2	52.3	122
Me_3Si^+	calc. value	354	106
	calc. value	354.2	117
	calc. value	355.7	83
	calc. value	382	106
	calc. value	385 ± 20	105
Et_3SiH	C_6D_6	0.2	102
	MeCN	6.0	102
Et_3SiOTf	none	44.46	115
$Et_3SiOTf.BCl_3$	none	76.72	115
$Et_3Si[B(C_6F_5)_4]$	C_6D_6	92.3	67
	C_6D_6/C_6H_5Me (3 : 1)	87.1	67
	p-$(CD_3)_2C_6H_4$	85.6	67
	$C_6D_5CD_3$	81.8	67

(*continued overleaf*)

TABLE 1. (*continued*)

Compound	Solvent	Chemical shift (δ, ppm from Me_4Si)	References
	sulpholane	58.4	67
	CD_3CN	36.7	67
$Et_3SiC_6H_5Me^+$	calc. value	79.7	117
$[Et_3SiCH_2CPh_2]\ [B(C_6F_5)_4]$	C_6D_6	46.2	123
$Et_3SiC_3H_6{}^+$	calc. value	70.0	117
$[Et_3Si(NCPr)]^+\ \{B[C_6H_3(CF_3)_2\text{-}3,5]_4\}^-$	PrCN	37.01	101
Et_3Si^+	calc. value	371.2	106
	calc. value	371.3	117
	calc. value	376.6	109
	calc. value	415.6	106
$Et_3Si(C_6H_6)^+$	calc. value	104.6	109
$Et_3Si(C_6H_5Me)^+$	calc. value	82.1	109
$i\text{-}Pr_3SiH$	$C_6D_5CD_3$	12.1	103
$i\text{-}Pr_3SiBr$	$C_6D_5CD_3$	45.4	103
$i\text{-}Pr_3SiBr.AlBr_3$	$C_6D_5CD_3$	55.8	103
$i\text{-}Pr_3Si(Br_5CB_9H_5)$	$C_6D_5CD_3$	97.9	103
$[i\text{-}Pr_3Si(MeCN)][Br_5CB_9H_5]$	CD_2Cl_2	33.8	103
$i\text{-}Pr_3Si[B(C_6F_5)_4]$	C_6D_6	107.5	67
	$C_6D_5CD_3$	94.0	103
$i\text{-}Pr_3Si^+$	calc. value	342.3	106
	calc. value	371.0	106
Bu_3SiClO_4	CH_2Cl_2	44.6	90
	CH_2Cl_2/sulpholane	46.3	90
$Bu_3Si[B(C_6F_5)_4]$	CH_2Cl_2	33.4^c	90
	CH_2Cl_2/HMPA-d_{18}	32.8^c	90
$i\text{-}Bu_3Si[B(C_6F_5)_4]$	C_6D_6	99.5	67
$i\text{-}Pr_2MeSi[B(C_6F_5)_4]$	C_6D_6	96.9	67
	CD_3CN	41.9	67
	pyridine/C_6D_6	44.3	67
$(C_6H_{13})_3Si[B(C_6F_5)_4]$	C_6D_6	90.3	67
	mesitylene	65	67
$MePh_2SiH$	CD_2Cl_2, at −40°C	−17.4	113
$[MePh_2SiOEt_2]\ \{B[C_6H_3(CF_3)_2\text{-}3,5]_4\}$	CD_2Cl_2	38.0	113
$MePh_2Si[B(C_6F_5)_4]$	C_6D_6	73.6	67
	CD_3CN	4.2	67
$[MePh_2Si(NCR)]^+\ \{B[C_6H_3(CF_3)_2\text{-}3,5]_4\}$	MeCN	4.23	103
$(mesityl)_3Si[B(C_6F_5)_4]$	C_6D_6	225.5	124
	C_6D_6/toluene (1 : 3)	225.6	124
	C_6D_6/p-xylene (1 : 1)	225.6	114
	C_6D_6/MeCN (1 : 3)	37	114
	C_6D_6/Et_3N (1 : 1)	47.1	114
$(Me_3Si)_3SiH$	C_6D_6	−117.4^b	102
	calc. value	−124.2	109
	calc. value	−119.6	110
$(Me_3Si)_3Si^+$	calc. value	925.3	109
	calc. value	920.4	110
$(Me_3Si)_3Si[B(C_6F_5)_4]$	C_6D_6	111.1	67
	C_6H_5Me	96.1	67
$(Me_3Si)_3Si(C_6H_6)^+$	calc. value	205.8	110
11	*e*	87.7	125
$(Me_2N)_3Si[B(C_6F_5)_4]$	C_6D_6	−30.8	126
	CH_2Cl_2	−39.3	126

TABLE 1. (*continued*)

Compound	Solvent	Chemical shift (δ, ppm from Me_4Si)	References
$(Me_2N)_3Si^+$	calc. value	42.1	112
$[Cp_2Zr(\mu\text{-}H)(SiHPh)]_2{}^{2+f}$	C_6D_6	105.9	127
	$C_2D_2Cl_4$	110.0	127
$[Cp_2Zr(\mu\text{-}H)(SiHCH_2Ph)]_2{}^{2+f}$	$C_6D_5CD_3$	110.9	127
$[CpCp^*Zr(\mu\text{-}H)(SiHPh)]_2{}^{2+f}$	C_6D_6	106.0	127
$[(MeCp)_2Zr(\mu\text{-}H)(SiHPh)]_2{}^{2+g}$	C_6D_6	101.5	127
$[(p\text{-tolylS})_2SiRu(PMe_3)_2Cp^*][BPh_4]$	CH_2Cl_2, at −60 °C	259.4	128
$[(EtS)_2SiRu(PMe_3)_2Cp^*][BPh_4]$	CH_2Cl_2, at −60 °C	264.4	128
$[(EtS)_2Si(trans\text{-}PtH(PCy_3)_2][BPh_4]$	*e*	308.65	129
$[Me_2SiRu(PMe_3)_2Cp^*][B(C_6F_5)_4]$	CH_2Cl_2, low temp.	311	130
$[Ph_2SiRu(PMe_3)_2Cp^*][B(C_6F_5)_4]$	CH_2Cl_2, low temp.	299	130
12	*e*	−12.1	131

[a] The structural formulae are mostly written as given by the original authors, but, in the light of recent calculations, the species shown as silicenium ions in solution are probably better represented as arenium, bromonium ions etc.; see text for a more detailed description.

[b] The value of *ca* 17.5 given for Me_3SiH in some reports is incorrect.

[c] Reaction with the solvent gives Bu_3SiCl.

[d] The value of *ca* 117.4 given for $(Me_3Si)_3SiH$ in several reports is incorrect.

[e] Solvent not reported.

[f] Counter anion, $[B(Bu)_n(C_6F_5)_{4-n}]_2{}^{2-}$.

[g] Counter anion, $[BH(C_6F_5)_3]_2{}^{2-}$.

has on chemical shifts. It is clear from computational work carried out in the last few years that solvents do play a crucial role by forming species in which there is a significant and well defined interaction or bond between the silicon and a solvent molecule, and that these species are calculated to have ^{29}Si NMR chemical shift values close to those found experimentally in solution. (The nature of the Et_3Si^+ species in aromatic solvents has been particularly controversial and is discussed in more detail in Section IV.) Thus, the ^{29}Si NMR data may better be attributed to species described as $R_3Si(solvent)^+$ rather than a silicenium ion salt dissolved in a non-interacting solvent. Details of the many calculations carried out in this area are discussed more fully in the chapter by Schleyer and coworkers. X-ray crystallographic structure determinations have been carried out on some of the species given in Table 1 and they do indeed show interactions between the silicon and either a solvent molecule or the anion; these are described in more detail in Section IV.

The potential for solvent and anion complexation to a cationic silicon centre has led to a move away from the solvents and anions traditionally regarded as potential nucleophiles to both solvents (for example benzene and toluene) and anions (for example $[B(C_6F_5)_4]^-$ and halogenated carboranes) that are less nucleophilic. The reactions between chlorosilanes with $Na\{[3,5\text{-}(CF_3)_2C_6H_3]_4B\}$ or hydrosilanes with $Ph_3C\{[3,5\text{-}(CF_3)_2C_6H_3]_4B\}$ in CD_2Cl_2 in the presence of ethers gives oxonium salts, for example $[Me_3SiOEt_2]^+\{[3,5\text{-}(CF_3)_2C_6H_3]_4B\}^-$, which has a ^{29}Si NMR chemical shift of 66.9 ppm (cf 46 ppm for Me_3SiClO_4), indicative of a significant degree of positive charge buildup on the silicon[113]. Since the silyl perchlorates are not attacked by Et_2O alone, these results suggest that it is a silicenium ion that is attacked by the ether. Trisilyloxonium ions, for example $(Me_3Si)_3O^+$, are formed as relatively long-lived (at −70 °C) products from the reaction between Me_3SiH and $Ph_3CB(C_6F_5)_4$ in the presence of a siloxane[119]. Again the use of an anion with low coordinating ability allows the formation of silicenium ions which silylate the siloxane present to give the novel oxonium ions. The ^{29}Si NMR chemical shift for the Me_3Si group in $(Me_3Si)_3O^+$ is 43.4 ppm deshielded compared with $(Me_3Si)_2O$, again indicative of the positive charge buildup on the silicon. If the same reaction is carried out with $Ph_3C\{[3,5\text{-}(CF_3)_2C_6H_3]_4B\}$ the more nucleophilic fluorines in the aryl ligand are abstracted by the trisilyloxonium ions to give fluorosilanes[119]. This also occurs in the reaction between $Ph_3C\{[3,5\text{-}(CF_3)_2C_6H_3]_4B\}$ and hydrosilanes in CH_2Cl_2, but, in the presence of a more strongly coordinating solvent such as butyronitrile, silylnitrilium salts $[R_3Si(NCC_3H_7)]^+\{[3,5\text{-}(CF_3)_2C_6H_3]_4B\}^-$ are formed (R_3 = Et_3, Me_2Bu-*t*, *t*-Bu_2Bu-*s* etc.) which undergo exchange of the nitrile on the NMR timescale indicating a relatively weak Si−N interaction[101]. A crystalline acetonitrilium salt *i*-$Pr_3Si(MeCN)]^+$[*closo*-6,7,8,9,10-$Br_5CB_9H_5]^-$ was isolated by Xie and coworkers from a similar reaction[103]. The positive character of the silicon in this case was indicated by both the ^{29}Si NMR chemical shift of 37.2 ppm in CD_2Cl_2 solution, and the C−Si−C angle in the cation being opened up to an average of 115.8° (see Section IV)[103]. Reaction between R_3SiH [R_3 = Me_3, Ph_2Me, (2-thienyl)$_2$Me, or (3,5-*t*-$Bu_2C_6H_3)_3$] and $Ph_3C\{[3,5\text{-}(CF_3)_2C_6H_3]_4B\}$ in CD_2Cl_2 solution containing excess MeCN gives $[R_3Si(MeCN)]^+\{[3,5\text{-}(CF_3)_2C_6H_3]_4B\}^-$ which has, in the case for $R_3 = Me_3$, a ^{29}Si NMR chemical shift that varies with the amount of MeCN present. If less than two equivalents are present, then the shift is about 38 ppm, but if a large excess is present then the shift is about 28 ppm, which can be attributed to an equilibrium being set up with the five-coordinate species $[R_3Si(MeCN)_2]^+\{[3,5\text{-}(CF_3)_2C_6H_3]_4B\}^-$ containing two coordinated MeCN molecules[120]. This effect has also been proposed to explain the difference in chemical shifts (see Table 1) between the spectra of [*i*-$Pr_3Si(MeCN)][Br_5CB_9H_5]$ in CD_2Cl_2 and MeCN[103]. The use of the weakly coordinating *closo*-7,8,9,10,11,12-$Br_6CB_{11}H_6{}^-$ anion has also allowed the first protonated silanol [*t*-$Bu_3SiOH_2]^-$ to be prepared[59]. The compounds shown in Table 1 in which there is a halogenated carborane as the anion do not seem to show an interaction between the silicon and a solvent molecule in the solid state but rather a halogen atom in the anion. This may also persist in solution as is indicated by ^{11}B NMR studies as described above. This type of interaction would also explain why the chemical shifts in solution (and in the solid state) are also considerably more upfield than free silicenium ions would be, in a similar manner to the $R_3Si(solvent)^+$ species. A more detailed discussion of these compounds is given below in Section IV.

Perhaps the most interesting ^{29}Si NMR data to be reported recently is that on a species thought to be (mesityl)$_3Si[B(C_6F_5)_4]$[124]. The species seems to be a product from several reactions (Scheme 1), although not from the reaction between (mesityl)$_3$SiH and trityl cation, the cleanest product being obtained from the reaction between (mesityl)$_3SiCH_2CH{=}CH_2$ and the *β*-silylcarbocation $(Et_3SiCH_2)Ph_2C^+$. The product may be obtained as an oil [unfortunately $B(C_6F_5)_4$-containing species rarely seem to give material suitable for X-ray crystallography in this field] and solutions in various aromatic solvents (see Table 1) give ^{29}Si chemical shifts of *ca* 225.5 ppm. In mixed solvents containing a good donor such as Et_3N, the shift (see Table 1) is what might be expected for an $R_3Si(solvent)^+$ species. It is currently unclear exactly what the nature of the species responsible for the strongly deshielded value for the silicon is, but the ^{29}Si NMR chemical shift would seem to be consistent with the presence of a substantially free silicenium ion[132]. Unfortunately, there have been few calculations on triarylsilicon species such as Ar_3Si^+ or $Ar_3Si(solvent)^+$ reported. If the value for Ph_3Si^+ derived from comparison with Ph_3C^+[104] similarly underestimates the chemical shift compared with calculation, as does Me_3Si^+ (250 ± 25 ppm by comparison with the carbon analogue, versus *ca* 370 ± 15 ppm for more recently calculated values), then a value for Ph_3Si^+ might tentatively be given as *ca* 245 ± 25 ppm, quite close to the observed value for the (mesityl)$_3$Si-containing species. Recent preliminary calculations[133] on Ph_3Si^+ and on $(2,6\text{-}Me_2C_6H_3)_3Si^+$ show that the ^{29}Si NMR chemical shift depends strongly on the aryl twist angle and that the chemical shifts predicted for such species are indeed close to that found experimentally for (mesityl)$_3$Si$^+$. It should also be noted that there is very little change in the ^{29}Si chemical shift for the species in several different aromatic solvent mixtures (Table 1). This seems to be in contrast to the work reported for Et_3Si^+ in various solvents where changing the nature of the aromatic solvent has a small but apparently significant effect on the chemical shift (Table 1). The (mesityl)$_3$Si species may thus be interacting relatively little with the solvent, or there may be a strong interaction between the cation and the anion, to the exclusion of the solvent, or a strong interaction between the silicon and C_6D_6 which is not affected by addition of other aromatic solvents. It would be of interest to record the chemical shift in toluene alone to see if the same shift is obtained in the absence of C_6D_6. These arguments can only be regarded as speculative at this stage and further computational work needs to be carried out to estimate chemical shifts for Ar_3Si^+ and $Ar_3Si(solvent)^+$ species together with an investigation of the effect of substituents on the aromatic rings. It may be that the steric protection afforded by the *ortho* substituents in a (mesityl)$_3$Si-containing species prevents the close approach of any solvent or the counter anion to the silicon and that a three-coordinate silicon species is indeed present. (Steric effects are clearly important in the gas-phase silylations of aromatic molecules where sites *ortho* to a methyl substituent are strongly shielded from attack.) Pidun, Stahl and Frenking have suggested a similar approach to steric protection of a three-coordinate silicon centre by the use of the 2,5-*t*-Bu$_2$-pyrrolidino group as a substituent[112].

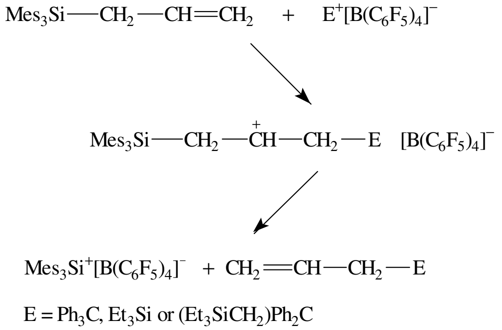

SCHEME 1

Another recent attempt to generate a silicenium ion has followed from the computational result that the symmetrically bridged 6-sila-2-norbornyl cation is a local minimum on the potential surface and that it is more stable than the 2-norbornyl cation[4]. Auner, Schleyer, Müller and coworkers have reported that treatment of the silicon hydride **10** with a stoichiometric amount of trityl cation affords a species thought to be the bridged cation **11** (equation 5) having a ^{29}Si chemical shift of 87.7 ppm[125]. The calculated value for the fully open, three-coordinate cation is 364.2 ppm but the value for the bridged structure is calculated to be only 101.4 ppm, the sum of the angles at silicon being 350.6°[125]. Although in this case the silicon atom is pseudo-five-coordinate, the relatively good agreement between the experimental and calculated values for the ^{29}Si NMR chemical shift suggests that the species formed in solution does indeed have a structure similar to that shown for the cationic species **11**, and that there is little, if any, specific interaction between the cation and the solvent. Clearly, a solid state structure determination of the norbornyl derviative **11** would be of great interest.

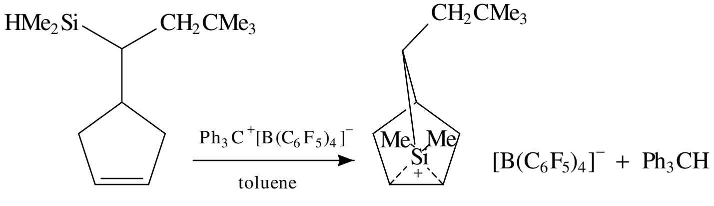

(5)

(10) **(11)**

The reaction of decamethylsilicocene with catechol gives the unusual silicon hydride **12**, the structure of which was determined by NMR spectroscopy (equation 6)[131]. The ^{29}Si NMR chemical shift for **12** is 386 ppm deshielded when compared with Cp_2^*Si and the Si−H coupling constant is 302 Hz both of which could be regarded as consistent with a silicenium ion. However, although the silicon in **12** is formally only bound to three substituents, its coordination number can be regarded as higher because the Cp* groups are π- rather than σ- bonded.

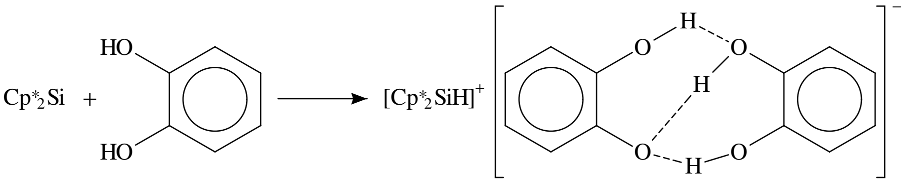

(6)

(12)

Dinuclear zirconium complexes **13** and **14** that are part of a catalytic cycle in the polymerization of silanes such as $PhSiH_3$ by Cp'_2 $MCl_2/2BuLi/B(C_2F_5)_3$ (where Cp′ can be C_5H_5 or a substituted cyclopentadienyl ligand, and M = Ti, Zr or Hf) can be prepared according to equations 7 and 8. Although no crystallographic data for the complexes are available, the IR and spectroscopic data (the ^{29}Si NMR chemical shifts are all greater than 100 ppm. see Table 1) available suggest that the cationic parts of the complexes exist as a hybrid of two mesomeric structures **15** and **16** which can be thought of as a cationic zirconocene with a α-agostic Si−H or an intramolecularly stabilized silicenium ion, respectively[127,134,135]. Solid state structural data for these complexes would be of obvious interest.

$$Cp'_2ZrCl_2 \xrightarrow[3.\ RSiH_3]{1.\ 2BuLi,\ 2.\ B(C_6F_5)_3} [Cp'_2Zr(\mu\text{-}H)(SiHR)]_2{}^{2+}\ [BBu_n(C_6F_5)_{4-n}]_2{}^{2-} \qquad (7)$$

(13)

$Cp' = C_5H_5$; R = Ph, $PhCH_2$ etc.

$$(MeCp)_2ZrH_2 \xrightarrow[2.\ PhSiH_3]{1.\ B(C_6F_5)_3} [(MeCp)_2Zr(\mu\text{-}H)(SiHPh)]_2{}^{2+}[BH(C_6F_5)_3]_2{}^{2-} \qquad (8)$$

(14)

A range of transition metal complexes (see Table 1) have been prepared by Tilley and coworkers in recent years that contain three-coordinate silicon[128−130]. The ^{29}Si NMR

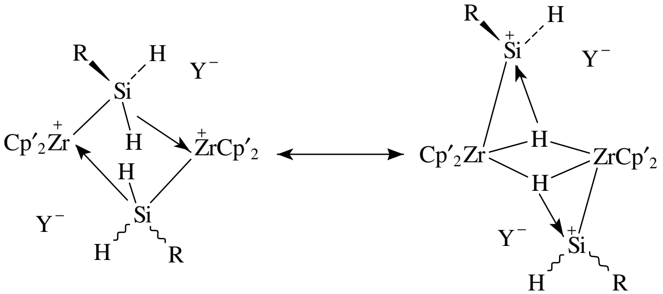

(15)

(16)

chemical shifts for these complexes are highly deshielded, possibly indicative of cationic character, and the geometry around the silicon is trigonal planar, also consistent with silicenium ion character. Calculations to estimate the effect of a transition metal substituent on the chemical shifts do not yet seem to have been carried out. There are several possible resonance forms for the complex cations (Scheme 2); the short metal–Si distances found in the solid state, however, are consistent with double bond character between the metal and silicon, and **17** is probably the main contributor. These compounds may therefore best be regarded as silylene complexes even though they fulfil some of the criteria that are often associated with silicenium ions.

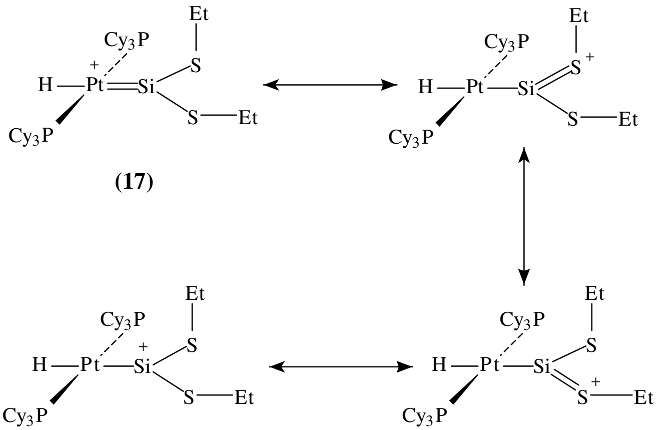

(17)

SCHEME 2

D. Silicenium Ions as Reaction Intermediates

The mechanism of the now widely used hydride transfer reaction for the formation of possible silicenium ions has been investigated in some detail. Studies of the reactions between R_3SiH (R = Et, Ph, *n*-Bu etc.) and trityl salts such as Ph_3CBF_4 and Ph_3CSbF_6 led Chojnowski and coworkers to conclude, on the basis of steric, substituent, kinetic isotope and ring strain effects, that the mechanism involves in the rate-determining step a single electron transfer process which, in a second fast step, yields a silicenium-like species[136,137] (equation 9). This conclusion was, however, questioned by Apeloig[11] who showed by calculations that the experimentally observed substituent effects on the hydride transfer rates are fully consistent with a rate-determining formation of a silicenium-like species. Mayr and coworkers have carried out further detailed studies on the reactions between R_3SiH compounds and diarylcarbenium ions Ar_2HC^+ (Ar = Ph, *p*-tolyl, *p*-$MeOC_6H_4$, *p*-$PhOC_6H_4$)[138]. They concluded, in contrast to Chojnowski and coworkers, that, based on deuterium labelling studies as well as steric and electronic arguments, the mechanism is not a single electron transfer process but involves formation of a silicenium ion in the rate-determining step (equation 10). It was also shown, using a series of β-substituted silanes such as $(Me_3MCH_2)Me_2SiH$ (M = C, Si, Ge or Sn), that both electronic and steric effects are important in determining the reaction rate, and that hyperconjugation is also effective in stabilizing silicenium ions, but that the effect is much smaller than that for comparable carbenium ions[139]. More recent computational work also shows that the mechanism is not a single electron transfer process but is actually a barrierless synchronous hydride transfer (SHT, equation 10), and that the single electron transfer mechanism is calculated to be highly disfavoured[140].

$$R_3SiH + R'_3C^+X^- \xrightarrow[\text{slow}]{\text{SET}} R_3SiH^{+\bullet}X^-//R'_3C^\bullet \xrightarrow{\text{fast}} R_3Si^+X^- + R'_3CH \tag{9}$$

$$R_3SiH + R'_3C^+X^- \xrightarrow{\text{SHT}} R_3Si^+X^- + R'_3CH \tag{10}$$

Work by Apeloig and Stanger on adamantyl substituted silanes has provided another example of a reaction in which formation of a silicenium ion seems to represent the best interpretation of the experimental results. Solvolysis of the adamantyl derivatives **18** in aqueous $(CF_3)_2CHOH$ proceeds (Scheme 3) to give a mixture of products, one of which, **20**, is a simple substitution product from carbenium ion **19** but the second, **22**, appears to be the result of a 1,2-methyl migration from the silicon to the ring carbon to which it is attached to give silicenium ion **21**[141,142]. The ratios of the products can be interpreted as due to the reactions of solvent separated ion pairs, but it is also possible that a bridged

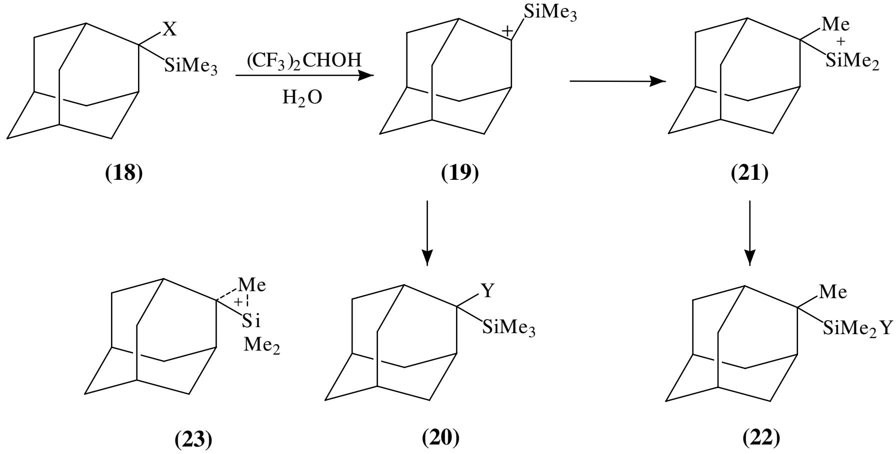

$X = Cl$ or $O_2CC_6H_4NO_2$–*p*

$Y = OH$ or $OCH(CF_3)_2$

SCHEME 3

cation such as **23**, which could be attacked by the solvents at either end of the bridge, could be involved[12,143]. The rearrangement of **19** to **21** is consistent with the relative thermodynamic stabilities for carbenium and silicenium ions found in the gas phase as described in Section II and calculations, for example on $Me_3CSiMe_2{}^+$ and $Me_3SiCMe_2{}^+$ which show that the silicenium ion is more stable by 9.7 kcal mol^{-1}[11].

The involvements of 1,3-bridged silicenium ion intermediates, analogous to the 1,2-bridged species **23**, has been proposed for a range of reactions involving silicon compounds bearing the exceptionally bulky $(Me_3Si)_3C$ group. Eaborn and coworkers have found that compounds of the type $(Me_3Si)_3CSiRR'X$ and $(Me_3Si)_2C(SiMe_2X)(SiRR'X)$ (where R = Me, Et, Ph etc. and X = halogen, H etc.) undergo reactions (e.g. equation 11) with some electrophiles including silver salts AgY(Y = $MeCO_2$, CF_3CO_2, ClO_4 etc.), CF_3CO_2H and ICl to give, in the case of $(Me_3Si)_3C$-containing precursors, rearranged products $(Me_3Si)_2C(SiMe_2Y)(SiRR'Me)$ if the substituents R and R′ are large (e.g. Ph), or a mixture of the rearranged and the unrearranged products $(Me_3Si)_3CSiRR'Y$ if the R and R′ groups are smaller, e.g. Et (for a review see Reference 144). Such reactions are thought to proceed via a bridged cationic intermediate of type **24**, which may be attacked by an incoming nucleophile at either end of the bridge, attack at Si(1) leading to unrearranged products and attack at Si(2) leading to rearranged products. (Calculations also reveal that structures of type **24** do correspond to local energy minima[4].) The difference in size between the substituents on the silicon atoms at either end of the bridge would then have a significant effect in determining at which end a nucleophile would attack larger groups, e.g. Ph on Si(1), would prevent attack at that silicon leading to exclusive attack at Si(2) to give rearranged products. This work has been extended to include other groups than Me as the bridging or migrating group, for example Ph[145–149], $CH{=}CH_2$[150], OMe[151,152], Cl[153] and N_3[153,154] have all been found to undergo similar rearrangements. It is now clear, however, that steric effects may not be the overriding factors in determining the degree of rearrangement and that electronic factors may dominate if the electronic environment at each of the two ends of a bridged cation is very different. For example, $(Me_3Si)_3CSi(OMe)_2I$ reacts with ICl to give only the unrearranged product $(Me_3Si)_3CSi(OMe)_2Cl$[155], $(Me_3Si)_3CSiPh(OMe)I$ reacts with AgOCN to give $(Me_3Si)_3CSiPh(OMe)NCO$[156] and $(Me_3Si)_3CSiH_2I$ reacts with $AgBF_4$ in Et_2O solution to give $(Me_3Si)_3CSiH_2F$ [the same reaction in CH_2Cl_2 gives a 1 : 1 ratio of $(Me_3Si)_3CSiH_2F$ and $(Me_3Si)_2C(SiMe_2F)(SiH_2Me)$][157]. The inadequacy of a simple steric argument for rearrangements of this type of bulky silane has also been shown in recent studies using isotopically labelled compounds in which the two ends of the bridged cation are the same size, i.e. by using $(Me_3Si)_3CSi(CD_3)_2I$ as a precursor. In reactions of this bulky iodide with silver salts such as $AgClO_4$, $AgNO_3$ and AgO_2CCF_3, products that are predominantly unrearranged are formed and it is now clear that as more data are accumulated on this type of reaction, more complicated reaction mechanisms involving several intermediates will have to be invoked[158].

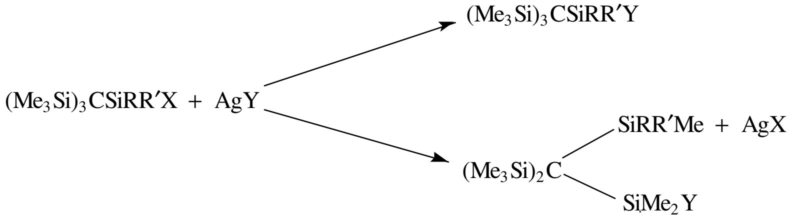

(11)

Y = $MeCO_2$, CF_3CO_2, ClO_4, etc.

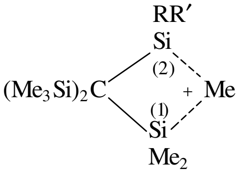

(24)

The reaction between polysilylacylsilanes $(Me_3Si)_3SiCOR$ (R = *t*-Bu, adamantyl or bicyclo[2.2.2]octyl) with $TiCl_4$ in CH_2Cl_2 solution gives rise, after an aqueous workup, to the 1,3-bis(silanols) **25.** The products may result from either of the routes shown in Scheme 4, both of which involve 1,2-migrations of methyl groups to a silicenium ion centre and of silyl groups to a carbocationic centre[159].

The reaction between Ph_3SiH and $Ph_3CB(OTeF_5)_4$ in CH_2Cl_2 solution leads to formation of $Ph_3SiOTeF_5$ and $B(OTeF_5)_3$ due to breakdown of the bulky anion. This may be due to attack by the strongly electrophilic Ph_3Si^+ although further evidence for the existence of the silicenium ion in this reaction is lacking[160]. Silicenium ions are also thought to be short-lived intermediates in the fluorination of silanes R_3SiH (R = Me, Et, *t*-Bu, $PhCH_2$, Ph etc.) by $NOBF_4$ or NO_2BF_4 (equation 12), although as the reaction is carried out in MeCN solution the formation of $[R_3Si(MeCN)]^+$ species is also likely[161]. The species $[R_3Si(MeCN)]^+$ are thought to be present as short-lived intermediates in the reaction between R_3SiCl (R_3 = $PhMe_2$, Bu_2H, Ph_2Bu-*t* etc.) and $NaBF_4$ in MeCN solution (equation 13)[162].

$$R_3SiH \xrightarrow{NOBF_4 \text{ or } NO_2BF_4} R_3SiF + BF_3 + HNO \text{ or } HNO_2 \qquad (12)$$

$$R = \text{Me, Et, } t\text{-Bu, Ph, } PhCH_2 \text{ etc.}$$

$$R_3SiCl + NaF \text{ or } NaBF_4 \xrightarrow{MeCN} R_3SiF + NaCl \text{ or } MeCN{\bullet}BF_3 \qquad (13)$$

$$R_3 = t\text{-}Bu_2H,\ t\text{-}BuMe_2,\ Ph_2Me \text{ etc.}$$

The reactions between the silylenes SiX_2 (X = F, Cl, Br or I), generated in the gas phase, and condensed into toluene solutions containing I_2 or ICl at −90 °C, afford mixtures of the *ortho*, *meta* and *para* isomers of $SiX_2I(C_6H_4Me)$ probably due to an electrophilic attack on the aromatic ring by short-lived X_2ISi^+ species[163]. *Ortho*-substituted products are favoured in these reactions, the *o* : *p* : *m* ratio for the Cl_2Si/I_2/toluene system being 10 : 4 : 3, but if ethylbenzene is used in place of toluene the proportion of *ortho*-substituted product is reduced and the ratio is 4 : 2 : 3. This was attributed to steric effects and is also consistent with the formation of only the *para* isomer in the $[Et_3Si(toluene)]\ [B(C_6F_5)_4]$ compound as described above, which results from the silylation of toluene by the relatively bulky Et_3Si^+.

The reaction between $(ArS)_3SiCl$ (Ar = 2,4,6-*t*-$Bu_3C_6H_2$) and $AgClO_4$ in benzene solution at 50 °C gives several unexpected sulphur-containing compounds such as (3,5-*t*-$Bu_2C_6H_3S)_2$ that are thought to arise from the initial formation of covalent $(ArS)_3SiClO_4$ in equilibrium with its ionic form $(ArS)_3Si^+ClO_4{}^-$, which then undergoes fragmentation and rearrangement to give the observed products[164]. Attempts to generate silicenium ions from sterically hindered aryloxy and arylthio silanes $(ArO)_2(MeO)SiX$ (X = H or Cl), $(ArS)_3SiH$ or $(Ar'S)_3SiH$ (Ar = 2,4,6-*t*-$Bu_3C_6H_2$, Ar′ = 2,4,6-*i*-$Pr_3C_6H_2$) have been unsuccessful[165] and no clear evidence was found for the intermediacy of silicenium ions

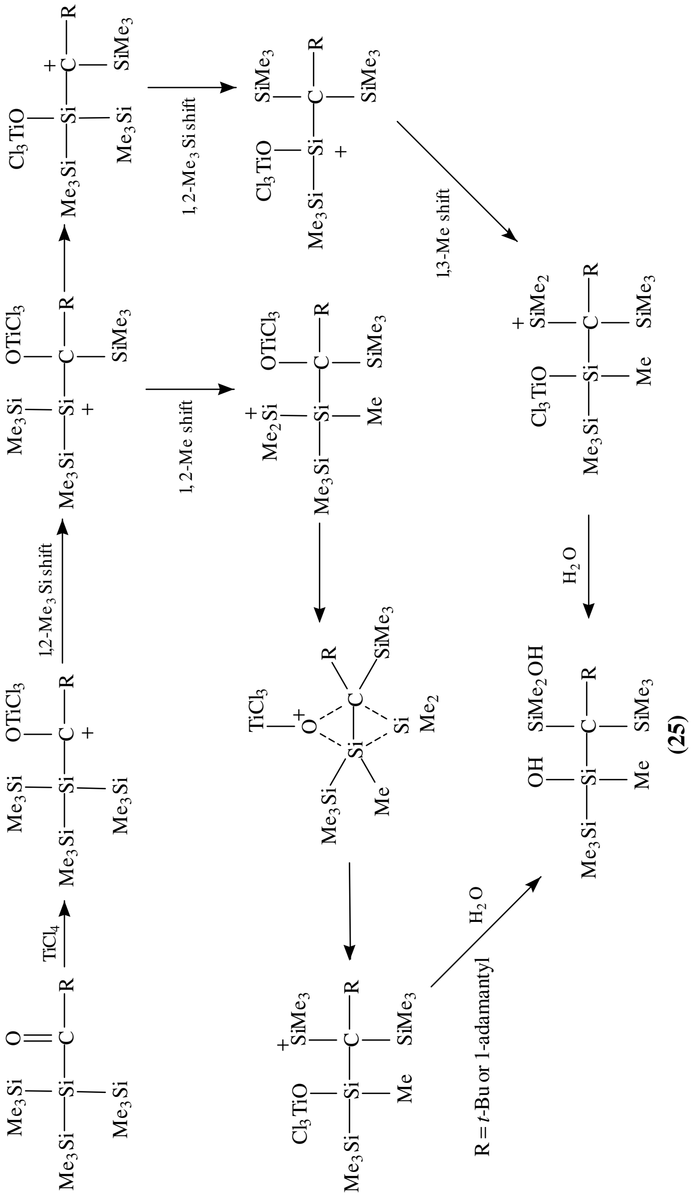

(25)

R = *t*-Bu or 1-adamantyl

SCHEME 4

in the reaction of Me_3SiX/BX_3 (X = Cl, Br or I) with alcohols[166]. The reaction between glycidyl methacrylate and chlorosilanes is proposed to proceed via an electrophilic attack by R_3Si^+ on an epoxide ring, although in the DMF solution used the ion is undoubtedly solvated and is not a free silicenium ion[167].

A silicenium ion might potentially be stabilized by being coordinated to a $Cr(CO)_3$ unit, but there is no reaction between $(Ph_3SiH)Cr(CO)_3$ and Ph_3CBF_4 and, in contrast to the reaction of $(Ph_3CH)Cr(CO)_3$ with triflic acid which gives the $[(Ph_3C)Cr(CO)_3]^+$ cation, the reactions between $(Ph_3SiH)[Cr(CO)_3]_n$ (n = 1, 2 or 3) and triflic acid are thought to give protonated silanols (which are themselves unusual species) as judged by NMR spectroscopy[168]. Extended Hückel molecular orbital calculations also suggest that a silicenium ion can be significantly stabilized by interaction with a suitable transition metal fragment such as $CpMo(CO)_2$ or $Co(CO)_3$, but, so far, no stable complexes of this type containing a silicenium ion seem to have been isolated[169].

A study of the kinetic and thermodynamic aspects of the radiation-induced polymerization of 'super-dry' cyclic siloxanes $(Me_2SiO)_n$ (n = 3, 4 or 5) suggests that the reactions proceed via silicenium ions. Initial ionization proceeds via loss of a methyl group to give silicenium ions, which may then either be involved in backbiting reactions in which the silicenium centre is internally solvated by oxygen atoms in the chain **26**, or in propagation in which more reactive unsolvated ions **(27)** participate[170,171]. The formation of $(EtO)_3Si^+$ during the hydrolysis of $(EtO)_4Si$ has been postulated[172,173], but this seems highly unlikely and a mechanism involving five-coordinate intermediates is much more probable[174].

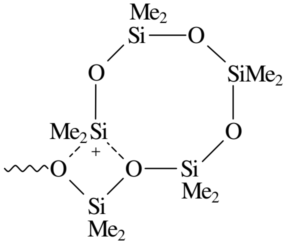

(26)

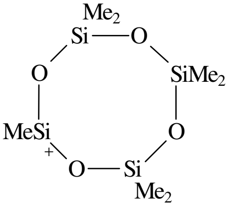

(27)

A recent patent[175] claims that $Et_3SiB(C_6F_5)_4$ is formed as a white solid from the reaction between Et_3SiH and $Ph_3CB(C_6F_5)_4$ in the absence of a solvent. The silicenium salt can then be used as a co-catalyst with group 4 transition metal complexes in the polymerization of olefins. Unfortunately, neither the precise nature of the silicenium cation nor its exact role in the polymerization process has been reported. An ether adduct $[Me_3Si(OEt_2)]^+[B(C_6F_5)_4]^-$, also of unknown structure, was reported to be formed from the reaction of Me_3SiCl and $LiB(C_6F_5)_4 \cdot 2.5\ Et_2O$ and could similarly be used as a polymerization co-catalyst. The same patent also describes an electrochemical method for the preparation of $Me_3SiB(C_6F_5)_4$ from $Me_3SiSiMe_3$ in 1,2-difluorobenzene with n-$Bu_4NB(C_6F_5)_4$ as supporting electrolyte. Again, the precise nature of the active species produced is unclear, but reactions in the absence of solvent and electrochemical methods of generation may have some synthetic potential[175]. The 9,10-dicyanoanthracene sensitized photolytic cleavage of aryldisilanes $ArMe_2SiSiMe_3$ (Ar = Ph, 4-MeC_6H_4 or 4-$MeOC_6H_4$) in MeCN gives initially disilane radical cations; subsequent Si−Si bond fission gives radicals $ArMe_2Si^\bullet$ or $Me_3Si^\bullet$ and silicenium ions $ArMe_2Si^+$ or Me_3Si^+ (presumably coordinated to the MeCN solvent), which can then undergo reaction with any water present to give silanols and siloxanes[176]. The $[Et_3Si(C_6H_6)]$ $[B(C_6F_5)_4]$ species has recently been used as a useful reagent because it is able to silylate $Ph_2C{=}CH_2$ to give the first example of a stable β-silyl carbocation $[Et_3SiCH_2CPh_2][B(C_6F_5)_4]$[123].

One further method for the preparation of silicenium ions that is independent of the phase in which the reaction occurs and which is not sensitive to solvent, pressure or temperature is to use a nuclear decay to generate a good leaving group from silicon. Russian workers have studied the process of β-decomposition of a tritium nucleus to helium which, if it occurs for tritium bonded to silicon, gives a molecular ion which then loses helium to give a silicenium ion as shown for Me_2SiT_2 (equation 14). The Me_2TSi^+ ion formed in this way reacts with MeOH to give $Me_2TSiOMe$, and with (t-BuO)Me_2SiH and $Me_3SiOSiMe_2H$ to give $Me_2TSiOSiMe_2H$[9]. The reaction between T_3C^+ and $Me_3SiOSiMe_3$ affords Me_3SiOCT_3 and Me_3Si^+, apparently via the intermediate formation of the oxonium ion $(Me_3Si)_2(T_3C)O^+$ [177]. Although only small amounts of material may be generated and detected in this way, it would be of interest to apply the method to molecules bearing larger and more stabilizing groups than methyl and hydrogen.

$$Me_2SiT_2 \xrightarrow{\beta} [Me_2SiTHe]^+ \longrightarrow Me_2TSi^+ + He^0 \qquad (14)$$

IV. SOLID STATE STUDIES

A variety of compounds containing four-, five- or six-coordinate silyl cations in which the silicon centre is stabilized by N→Si interactions have been prepared and structurally characterized, but they do not fulfil the criteria for description as silicenium ions. The four-coordinate **28** has an Si−N distance of 1.821(2) Å and C−Si−C angles averaging 113.4°, while the five-coordinate **29** is also stabilized intermolecularly, this time by two N-methylimidazole molecules with Si−N distances of 2.034(3) and 2.005(3) Å and a planar geometry at silicon[178]. Intramolecular stabilization of a silicon cation is also possible to give the five-coordinate **30** with Si−N distances of 2.06(1) and 2.08(1) Å and a near-planar geometry at silicon in the equatorial plane[179]. The triflate salt **31** has Si−N distances of 2.072(2) and 2.052(2) Å and has a nearly trigonal bipyramidal geometry at silicon[180]. All of these Si−N distances are significantly longer than would be expected for a covalent bond (1.70–1.76 Å) but are shorter than dative interactions found in neutral species with an intramolecular N→Si interaction, for example 2.291(2) Å in the five-coordinate $[2\text{-}(Me_2NCH_2)C_6H_4]_2SiCl_2$[181].

The first, and probably the most controversial crystallographic study of a compound thought to contain a silicon with substantial silicenium ion character, was that described by Lambert and coworkers who isolated, after crystallization from toluene, the colourless $[Et_3Si(toluene)]^+[B(C_6F_5)_4]^-$, from the reaction between Et_3SiH and $Ph_3CB(C_6F_5)_4$[67,182]. The original description of the compound was that of 'a silyl cation with no coordination to anion and distant coordination to solvent'[182]. The closest approach between the anion and the cation is an Si···F distance of 4.04 Å, indicative of negligible interaction between them. Figure 1 does, however, show that the geometry at silicon in the Et_3Si group is not planar and that the fourth coordination site at silicon is occupied by a toluene molecule (for structural details see Table 2). It is the nature of the interaction between the silicon and the toluene molecule that has been the point of most contention. There are two crystallographically independent molecules in the unit cell, the distance between the silicon and the *para* carbon atom of the toluene molecule averaging 2.18 Å, which

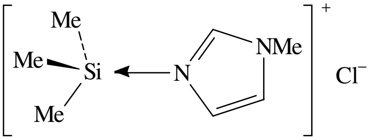

(28)

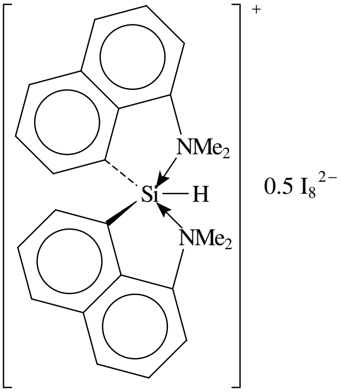

(30)

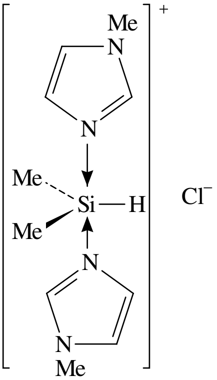

(29)

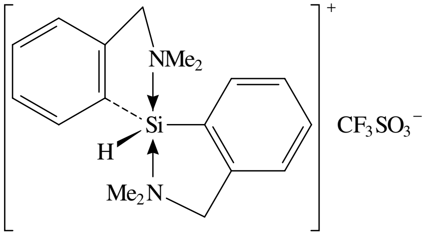

(31)

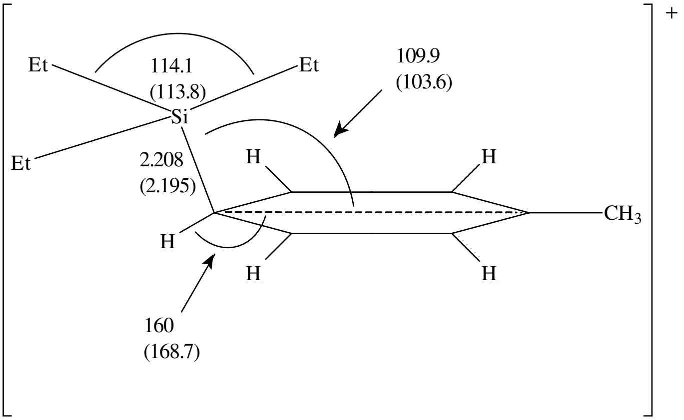

FIGURE 1. Calculated and experimental (in parentheses) parameters for one of the two crystallographically independent cations of $[Et_3Si(toluene)]^+$. Distances are in Å, angles are in degrees

TABLE 2. Structural data for compounds reported to have silicenium ion character[a]

Compound	Si–L distance (Å)		Pauling bond order[b]	Σ C–Si–C (°)[c]	Out-of-plane distance (Å)[d]	References
	obs.	covalent				
Compounds of the type [R_3Si(solvent)] [anion][e]						
[Et_3Si(toluene)] [$B(C_6F_5)_4$][f]	2.18	1.85	0.28	342	0.462	67,182
[Me_3Si(pyridine)] [Br]	1.856	1.73	0.62			88
[Me_3Si(pyridine)] [I]	1.858	1.73	0.61		0.485	88
[i-Pr_3Si(MeCN)] [$Br_5CB_9H_5$]	1.82(2)	1.73	0.71	346.7	0.410	103
[t-$Bu_3Si(H_2O)$] [$Br_6CB_{11}H_6$]	1.779(9)	1.64	0.58	348		59
Compounds of the type [R_3Si] [anion][g]						
[Et_3Si] [$Br_6CB_{11}H_6$][h]	2.444(7)	2.24	0.46	345.0(10)	0.419	185
[Et_3Si] [$Br_6CB_{11}H_6$][h]	2.430(6)	2.24	0.48	349.0(9)	0.348	185
[i-Pr_3Si] [$Cl_6CB_{11}H_6$]	2.323(3)	2.08	0.39	351.8(4)	0.307	106
[i-Pr_3Si] [$I_6CB_{11}H_6$]	2.661(6)	2.46	0.46	346.8(9)	0.400	106
[i-Pr_3Si] [$Br_6CB_{11}H_6$]	2.479(9)	2.24	0.40	351.0(13)	0.300	185
[i-Pr_3Si] [$Br_5CB_9H_5$]	2.46(1)	2.24	0.43	347.5	0.40	103
[t-Bu_2MeSi] [$Br_6CB_{11}H_6$]	2.466(12)	2.24	0.42	345.8(21)	0.408	185
[t-Bu_3Si] [$Br_6CB_{11}H_6$]	2.465(5)	2.24	0.42	348.7(7)	0.371	185
Ph_3SiClO_4	1.74	1.64	0.68	340.9	0.479	82

[a] Table adapted, with additions, from Reference 18; Ph_3SiClO_4 is included for comparison.

[b] Calculated according to the Pauling equation, $0.60 \log n = D(l) - D(n)$, where $D(l)$ is the distance for a covalent bond order of one, and $D(n)$ is the observed bond distance for a bond order n.

[c] Sum of three C–Si–C angles at silicon, tetrahedral $\Sigma = 328.5^\circ$, trigonal planar $\Sigma = 360^\circ$.

[d] The distance of the silicon atom from the plane containing the 3α-carbons.

[e] L = carbon for toluene, nitrogen for pyridine and MeCN, and oxygen for water.

[f] Values are average for two crystallographically independent molecules.

[g] L = halogen for carborane anions and oxygen for perchlorate.

[h] Two crystallographically independent molecules.

is significantly longer than the previously longest known Si−C bond of 2.03 Å found in the sterically crowded cyclic $t\text{-Bu}_2\overline{\text{Si}(t\text{-Bu})_2\text{SiOPh}_2\text{C}}$[183] and even more so compared to the sum of the covalent radii, 1.88 Å, of Si and C. Other noteworthy features of the structure are that the C−Si−C angles in the Et_3Si groups of the two molecules range from 112.8–114.9°, that the aromatic ring is nearly planar (the largest dihedral angle being 3°), and that the bond lengths within the ring fall in a relatively narrow range. These features are in contrast to those known for Wheland-type complexes containing alkyl rather than silyl substituents, in which severe distortions are found in the aromatic ring[184].

The crystallographic parameters clearly indicate the absence of a 'free' silicenium ion as the geometry at silicon is not planar (indeed the Et−Si−Et angle of 114° is closer to the tetrahedral than to the trigonal planar value), and the fourth coordination site is occupied by a toluene molecule. The solid state ^{29}Si NMR chemical shift is also not indicative of a 'free' ion according to the value expected by calculations. Conversely, it was argued that the relatively long distance between the silicon and the toluene molecule suggested insignificant σ-complexation and that, as the toluene molecule is relatively little perturbed from its normal geometry, there is little positive charge on the carbon atoms[182]. These factors would seem to suggest that there is some significant degree of silicenium ion character to the cation. These arguments have, however, been countered in numerous papers, many of them presenting detailed computational studies that indicate that bonding between the silicon and the toluene molecule is significant and that the species is best described as an arenium ion $[\text{Et}_3\text{Si(toluene)}]^+$ in which the positive charge is largely on the ring with very little silicenium ion character present. A detailed description of this computational work is provided in the chapter by Schleyer; only a brief outline of the arguments will be given here for comparison with the experimental studies. Pauling[186] and Lambert and Zhang[187] have both calculated the bond order n for the Si···toluene interaction using the equation $D(n) = D(1) - 0.60 \log n$ [where $D(1)$ is the distance for a full single bond and $D(n)$ the distance for a bond of order n] using different values for $D(1)$ to give values of n of 0.35 and 0.28, respectively, i.e. about one-third of a normal covalent bond. Further experimental evidence for a significant σ interaction, analogous to that found in the gas-phase work described in Section II, comes from the reaction between the $[\text{Et}_3\text{Si(toluene)}]^+$ species with the hindered base $i\text{-Pr}_2\text{NH}$ which gives, along with $(\text{Et}_3\text{Si})_2\text{O}$, a 7% yield of *p*- and *m*-triethylsilyltoluenes in a 2 : 1 ratio, respectively[109,187]. Thus the *meta*-silylated arenium ion is present in solution even though this isomer is not detected in the solid state. Although the yield of triethylsilyltoluenes is low, their formation does suggest that deprotonation competes with desilylation of a σ complex as is found in the gas phase. Another puzzling aspect of the Et_3Si derivatives is that the solid state ^{29}Si NMR chemical shift values for $[\text{Et}_3\text{Si (toluene)}]^+$ and for $\text{Et}_3\text{SiB}(\text{C}_6\text{F}_5)_4$ prepared in the absence of solvent are so similar[67] (see Table 3). This could be due to the species prepared in the absence of a solvent interacting with the Ph_3CH formed as a byproduct from the reaction to give $[\text{Et}_3\text{Si(Ph}_3\text{CH)}]^+$, which as a silylated monosubstituted aromatic system might be expected to have a similar chemical shift to that of $[\text{Et}_3\text{Si(toluene)}]^+$.

Calculations by Olah and coworkers[109,117,188], Schleyer and coworkers[4,189] and Olsson and Cremer and coworkers[105,108,114] have, however, shown that the experimentally determined structure is close to that calculated for arenium ions $[\text{R}_3\text{Si(arene)}]^+$ (R = Me or Et, arene = benzene or toluene). The various bond lengths and angles are generally reproduced well as are the ^{29}Si NMR chemical shift data. The unusually long $\text{Si}-\text{C}_{para}$ bond length can be attributed to β-silicon hyperconjugation as shown in Scheme 5[117,189]. The experimental and calculated structural parameters for $[\text{Et}_3\text{Si (toluene)}]^+$ are shown in Figure 1. Thus, although some of the experimental data do, at first sight, seem to be

TABLE 3. Solid state ^{29}Si chemical shifts for various compounds containing silicon with some cationic character

Compound	Chemical shift (δ, ppm from Me_4Si)	References
$Me_3Si[B(C_6F_5)_4]$	84.8	67
t-$BuMe_2Si(Br_6CB_{11}H_6)$	112.8	185
$Et_3Si[B(C_6F_5)_4]$	94.3	67
$[Et_3Si(toluene)]\ [B(C_6F_5)_4]$	93.5	67
$Et_3Si(Br_6CB_{11}H_6)$	106.2, 111.8	185
i-$Pr_3Si[B(C_6F_5)_4]$	107.6	67
i-$Pr_3Si(Cl_6CB_{11}H_6)$	115	106
i-$Pr_3Si(Br_6CB_{11}H_6)$	110	106
i-$Pr_3Si(I_6CB_{11}H_6)$	97	106
i-$Bu_3Si[B(C_6F_5)_4]$	89.4	67
$[t$-$Bu_3Si(OH_2)]\ [(Br_6CB_{11}H_6)]$	46.7	59

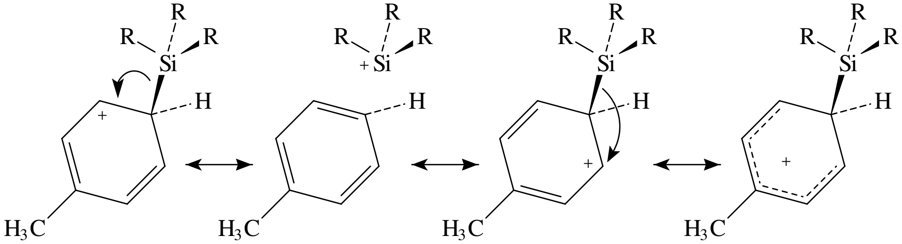

SCHEME 5

consistent with the presence of a significantly silicenium ion like species, the calculations show that the data are, in fact, very similar to those predicted for arenium ions. Lambert and Zhang have, however, countered the theoretical interpretations of their results and point out the deviations between experiment and theory. In particular, there is a pronounced alternation of C−C bond lengths in the arene ring found in the experimentaly derived structure which, although the same trend is reproduced by the calculations, is much less pronounced. Also, the Si−$C_{para} \cdots C_{ipso}$ angle (Figure 1) is less well reproduced by theory than other important parameters[187]. A more detailed discussion of the theoretical arguments is given in the chapter by Schleyer. More recent calculations, however, at the correlated level of MP2/6-31G* for $[Me_3Si(toluene)]^+$ do agree significantly better than earlier calculations, in particular reproducing the Si−$C_{para} \cdots C_{ipso}$ angle in $[Et_3Si(toluene)]^+$ well[109]. It would thus seem that fully optimized calculations can reproduce experimental data well for these compounds, and that the $[Et_3Si(toluene)]^+$ species is best described as an arenium rather than a silicenium ion in the solid state. Such small discrepancies that do still exist between the experimental and calculated structures may well be inevitable. Other calculations have investigated how the bonding in $R_3M(arene)^+$ (M = Si, Ge, Sn and Pb) species varies and these results also suggest that the $Et_3Si(toluene)^+$ complex is best described as a σ-bonded arenium complex in which the positive charge is delocalized on the aromatic ring, rather than a π-bonded complex in which the positive charge is mainly found on silicon. This situation changes on descending group 14 with the π-bonded complex structure being favoured for lead[190].

The solid state work on $[Et_3Si(toluene)]^+[B(C_6F_5)_4]^-$ was quickly followed by related work by Reed and coworkers who have used halogenated carboranes as anions of low nucleophilicity in the place of $[B(C_6F_5)_4]^-$. Structural data for the compounds prepared in this work are given in Table 2. The first of these compounds to be reported were i-$Pr_3Si(Br_5CB_9H_5)$ and $[i\text{-}Pr_3Si(MeCN)][Br_5CB_9H_5]$, prepared in a similar manner to Lambert's compounds, by treating i-Pr_3SiH with the trityl salt of the carborane anion in toluene and in MeCN, respectively[103]. The structural data for the $[i\text{-}Pr_3Si(MeCN)]^+$ cation show C−Si−C angles that are about half way between those expected for tetrahedral and trigonal planar and an Si−N distance of 1.82(2) Å, which while slightly longer than a typical Si−N bond length which fall in the range 1.70–1.76 Å, is similar to that found in $[Me_3Si(pyridine)]I$ (1.858 Å)[88]. These values together with the ^{29}Si NMR shift of only 33.8 ppm in MeCN solution suggest that the species is best regarded as an N-tri-isopropylacetonitrilium ion. The other compounds containing halogenated carborane anions detailed in Table 2 (apart from the $[t\text{-}Bu_3SiOH_2]^+$-containing compound which can be regarded as a silaoxonium ion) have been the subject of similar discussion to that for the $[R_3Si(arene)]^+$ species, i.e. do the structural and NMR parameters indicate silicenium or silahalonium ion character? Perhaps the most obvious difference between these compounds and those studied by Lambert and coworkers is the absence of any solvent molecules coordinated to the silicon; even when prepared and crystallized from toluene solution, an ion pair is isolated rather than a silylated toluene product. The structural data for the series of compounds $[R_3Si]$ $[Br_6CB_{11}H_6]$ are given in Table 2 and the general structure for such compounds is shown in Figure 2.

The Si−Br bond distances are 2.430(6)–2.479(9) Å, the relatively narrow range suggesting that the effect of the substituents is small[185]. These values are about 0.2 Å greater than the Si−Br bond lengths in unhindered silyl bromides, e.g. Me_3SiBr [2.235(2) Å][191], $(BrH_2SiCH_2)_2$ [2.2362(12) Å][192] and 1-bromo-3,5,7-trimethyl-1,3,5,7-tetrasilaadamantane (2.197 Å)[193], and also significantly longer than in the bulky bromo-9-(9-trimethylsilylfluorenyl)-bis(trimethylsilyl)silane [2.284(5) Å][194]. Although the values

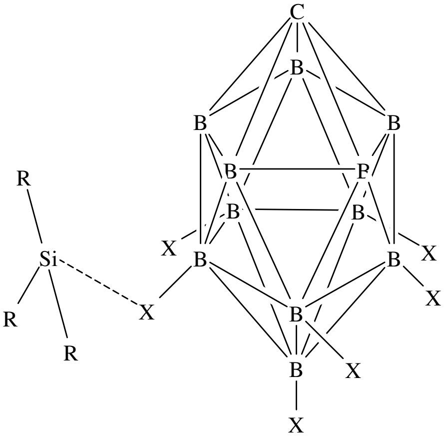

FIGURE 2. A schematic representation of $[R_3Si][X_6CB_{11}H_6]$ compounds where for X = Br, R = Me, Et, i-Pr or i-Bu and for X = Cl or I, R = i-Pr

for the bromocarborane derivatives are significantly longer than the other reported Si−Br distances in four-coordinate compounds, they are much shorter than the value of 3.122 Å found in the five-coordinate 1-[(bromo)dimethylsilylmethyl]-piperid-2-one[195] and well within the value of 3.5 Å estimated for complete charge separation[185]. Another argument for significant silicenium ion character in these compounds is that the halocarborane anion is very little distorted. The B−Br distance for the bromines coordinated to the silicon atoms lie in the range 1.99(2)–2.05(2) Å while those uncoordinated to Si lie in the range 1.92(2)–2.02(3) Å, i.e. there is perhaps a small, but barely significant, increase in B−Br distance on coordination to silicon which perhaps suggests little covalent bonding between the Si and the bromine. The individual C−Si−C angles within a particular R_3Si group may vary by up to 8 or 9°, and so it is probably more instructive to consider the sum of the C−Si−C angles and the deviation of the silicon from the plane of the three carbons to which it is attached (Table 2). There are some significant differences in the parameters for the two independent $Et_3Si(Br_6CB_{11}H_6)$ molecules and these presumably represent some degree of the flexibility of the species under crystal packing forces. Perhaps the most surprising aspects of the structures of the $R_3Si(Br_6CB_{11}H_6)$ compounds are that the sum of the C−Si−C angles and the Si−Br distance are not maximized in the most sterically demanding and electron-releasing *t*-Bu_3Si derivative. This has been attributed[185] to the flexibility of the Si−Br−B angle which readily opens up to 125° in the *t*-Bu_3Si derivative compared to only 114.7° in the *i*-Pr_3Si analogue. The *i*-Pr_3Si derivative thus seems to be the closest approach to a silicenium ion for a structurally characterized species, as it has the largest sum of C−Si−C angles and is closest to planarity at silicon. It should be noted that the correlation between the C−Si−C angle and the Si displacement from the C_3 plane is not linear, and a distortion from 120° to 117° gives more than half of the full displacement on going from a trigonal planar to a tetrahedral geometry at silicon[15]. The geometry of the substituents R in the $R_3Si(Br_6CB_{11}H_6)$ compounds, particularly for the ethyl and the isopropyl derivatives, is, in the case of at least one of the alkyl substituents on each silicon, highly distorted. This is manifested in large Si−C−C angles, some greater than 120°, and a near-planar geometry at the carbon attached to the silicon. These features have been attributed to C−H bond hyperconjugation, which gives some double bond character to the Si−C bond[185].

A further study by Reed and coworkers has concentrated on the coordinating ability of the carborane anion and the halogenated series *i*-$Pr_3Si(X_6CB_{11}H_6)$ (X = Cl, Br, I) have been prepared[106]. Structural data are given in Table 2. Again, as in the case of varying the alkyl substituents, there is an unexpected trend and the hexachloro derivative is found to be less coordinating in this case than the more bulky, softer, hexaiodo derivative. This has been explained using the argument that, as the stability of halonium ions is known to follow the trend iodonium > bromonium > chloronium, then the iodo derivative will have the greatest halonium ion character and the chloronium ion the least halonium ion (and consequently the most silicenium ion) character[106]. The average C−Si−C angle, the sum of the C−Si−C angles and the distance the Si is away from the C_3 plane for the chloro and bromo derivatives are very similar, although it does seem that the chloro-containing anion is slightly less strongly coordinated. It has thus been argued that *i*-$Pr_3Si(Cl_6CB_{11}H_6)$ is an 'ion-like' species and is the closest to a silicenium ion in the condensed phase to be structurally characterized so far[106]. The structural parameters together with the ^{29}Si NMR data have led Reed and coworkers to conclude that *i*-$Pr_3Si(Cl_6CB_{11}H_6)$ 'may have >50% silylium ion character' and that the term 'silylium ion-like' is most appropriate to describe the structure[106].

Further evidence proposed to support the predominance of silicenium ion character in these compounds is provided by their chemistry, because they react as if they were silicenium ions. For example, they react with nucleophiles such as CH_2Cl_2 and C_6H_5F

to form R_3SiX[196] and with water to give $R_3Si(OH_2)^+$[59]. In none of these reactions is the B-halogen bond seen to be cleaved. These interpretations of Reed and coworkers' results have, however, as was the case for $[Et_3Si(toluene)]$ $[B(C_6F_5)_4]$, been criticized, the alternative explanation being that the compounds are, in fact, halonium ions[117,186]. Olah and coworkers[117] argue that a species such as i-Pr_3Si with significant silicenium ion character could not be isolated from toluene solution without reaction occurring, as indeed seems to be the case for Et_3Si^+ in Lambert's work. It does seem surprising that, if the species are predominantly ionic when generated in the presence of Reed's weakly coordinating halocarborane anions, in the presence of a large excess of toluene silylation of the solvent does not occur. It is unclear why Et_3Si^+ should not react with solvent and bind to a less coordinating anion than $[B(C_6F_5)_4]^-$ in preference. This might, however, be the case if the product is a halonium ion rather than a silicenium ion.

Another argument against a silicenium ion formulation for the $R_3Si(X_6CB_{11}H_6)$ species is that their ^{29}Si NMR chemical shifts, given in Table 3, which generally fall in the range of 85–115 ppm, are well short of the range, 350–400 ppm, calculated for R_3Si^+ ions (cf Section III.C.2). The calculated values for free gas-phase R_3Si^+ ions may not be good yardsticks by which to estimate the degree of ionicity in condensed phases. For example, calculations on the $Me_3Si\cdots Cl$ system show that approach of the Cl^- ion any closer than the van der Waals distance of 3.3 Å reduces the ^{29}Si NMR chemical shift from a 'free' value of 388 ppm to only about half of this value[106]. Related calculations on the effect of species such as argon and methane, that can be regarded as some of the least nucleophilic potential solvents, also show that the ^{29}Si NMR chemical shift for R_3Si^+ is significantly reduced in their presence[4]. This would suggest that there is very little chance of observing 'free' silicenium ions in solution or the solid state with chemical shifts greater than 350 ppm unless, perhaps, the silicon bears substituents that sterically hinder the approach of solvent molecules. Unfortunately, large and elaborate substituents may well lead to intramolecular coordination. Such calculations have led Reed and coworkers to suggest a value of about 220 ppm as the upper limit to be expected for R_3Si^+ ions (R = alkyl) in condensed phases, and hence his halocarborane derivatives would have about 50% ionic character based on this parameter.

Calculations of the chemical shift for the bromonium ion $[Me_3SiBrMe]^+$ give a value of 117.5 ppm, which is close to the observed values for $Et_3Si(Br_6CB_{11}H_6)$. This again suggests that Reed's compounds may better be regarded as halonium ions[117]. Calculations on the structure of $[Me_3SiBrMe]^+$ give values of 2.523 Å and 116.4° for the Si–Br bond distance and C–Si–C angle, respectively, which are close to those (2.444 Å and 116.3°) for the comparable parameters in $Et_3Si(Br_6CB_{11}H_6)$, also consistent with the formulation of $Et_3Si(Br_6CB_{11}H_6)$ as a bromonium ion[117]. The lack of significant B–Br bond elongation for the bromine involved in an interaction with the silicon compared to the uncoordinated B–Br bonds has also been used to support the proposition that $R_3Si(X_6CB_{11}H_6)$ species have significant silicenium ion character. However, the C–Br bond length of 1.996 Å in $[Me_3SiBrMe]^+$ is not very much longer than that, 1.939 Å, in free MeBr[197], and can be compared, for example, with the similar lengthening of the B–Br distances for uncoordinated [1.92–1.98(2) Å] to coordinated [1.99(2) Å] in $Et_3Si(Br_6CB_{11}H_6)$[185]. Thus, all of the important structural parameters of $Et_3Si(Br_6CB_{11}H_6)$ seem to be reasonably well reproduced in calculations of a bromonium ion structure for $[Me_3SiBrMe]^+$ and this has led Olah and coworkers to conclude that $Et_3Si(Br_6CB_{11}H_6)$, and by implication other $R_3Si(X_6CB_{11}H_6)$ species, 'has very little triethylsilicenium character and is de facto a bromonium zwitterion'[117].

V. CONCLUSIONS

It can be seen from the work described above that there are a whole series of criteria such as $R_3Si\cdots X$ distance, Si−R distance, R−Si−R angle, distance of the Si from the C_3 plane and ^{29}Si NMR chemical shift that have been used as measures of the degree of ionicity in cationic silicon compounds. The degree of silicenium ion character is thus definition-dependent, and in no case does an experimentally observed species satisfy any definition completely. These various experimentally derived parameters have led to a wide range (*ca* 20–75%) of ionic character being assigned to $R_3Si(X_6CB_{11}H_6)$ species, and this has, in turn, led to conflicts with computational interpretations. The current state of work on these compounds seems to reflect that they best be described as halonium ions but with some silicenium ion character, the degree of which varies with the definition chosen but which probably does not yet exceed 50% in any case. Similarly, the $Et_3Si(toluene)^+[B(C_6F_5)_4]$ compound is probably best regarded as an arenium ion in the light of high level computational studies. Perhaps the most promising candidate for a free silicenium ion is the recently described $(mesityl)_3Si^+$ for which solution ^{29}Si NMR data are in reasonably close agreement with the calculated value (see Section III.C.2). Solid state studies on this ion, perhaps in conjunction with the use of a halogenated carborane as anion, may well lead to convincing evidence that a free silicenium ion can exist in a condensed phase.

It should also be noted here that recent work in Japan has shown that a free germanium cation can be prepared and structurally characterized. Thus, the reaction of tetrakis (tri-*t*-butylsilyl)cyclotrigermene with trityl tetraphenylborate affords $(t\text{-}Bu_3SiGe)_3^+\ BPh_4^-$ as a yellow crystalline solid. X-ray crystallography shows that there is no close interaction between the anion and the cation. The stability of the compound is presumably due not only to the steric protection afforded by the bulky $t\text{-}Bu_3Si$ substituents, but also to the fact that it contains a 2π-electron aromatic ring.[198]

Finally, it is perhaps well to be reminded of the comment made by Grant Urry[199] more than 25 years ago when describing the chemistry (or lack of it at that time) of polysilanes, and apply it to the field of silicenium ion chemistry: ‘It is perhaps appropriate to chide the polysilane (silicenium ion) enthusiast for milking the horse and riding the cow in attempting to adapt the successes of organic chemistry in the study of polysilanes (silicenium ions). A valid argument can be made for the point of view that the most effective chemistry of silicon arises from the differences with the chemistry of carbon compounds rather than the similarities’.

VI. ACKNOWLEDGEMENTS

The author wishes to thank Professor C. Eaborn for the many stimulating discussions concerning silicenium ions over the years, and Professors N. Auner, A. R. Bassindale, J. B. Lambert and P. v. R. Schleyer, and Dr. T. Müller for kindly supplying information prior to publication.

VII. REFERENCES

1. G. J. Leigh (Ed.), *Nomenclature of Inorganic Chemistry*, Blackwell, Oxford, 1990, p. 106.
2. H. Schwarz, in *The Chemistry of Organic Silicon Compounds* (Eds. S. Patai and Z. Rappoport), Part 1, Wiley, Chichester, 1989, pp. 445–510.
3. J. Chojnowski and W. A. Stanczyk, *Adv. Organomet. Chem.*, **30,** 243 (1990).
4. C. Maerker, J. Kapp and P. v R. Schleyer, in *Organosilicon Chemistry II* (Eds. N. Auner and J. Weis), VCH, Weinheim, 1996, pp. 329–359.

5. S. K. Shin and J. L. Beauchamp, *J. Am. Chem. Soc.*, **111,** 900 (1989).
6. S. Hollenstein and T. Laube, *J. Am. Chem. Soc.*, **115,** 7240 (1993).
7. D. H. O'Brien and T. J. Hairston, *Organomet. Chem. Rev. A*, **7**, 95 (1971).
8. R. J. P. Corriu and M. Henner, *J. Organomet. Chem.*, **74,** 1 (1974).
9. V. D. Nefedov, T. A. Kochina and E. N. Sinotova, *Russian Chem. Rev.*, **55**, 426 (1986).
10. J. B. Lambert and W. J. Schulz Jr., in *The Chemistry of Organic Silicon Compounds* (Eds. S. Patai and Z. Rappoport), Part 2, Wiley, Chichester, 1989, pp. 1007–1014.
11. Y. Apeloig, in *Heteroatom Chemistry* (Ed. E. Block), VCH, New York, 1990, pp. 27–46.
12. C. Eaborn, *J. Organomet. Chem.*, **405**, 173 (1991).
13. P. D. Lickiss, *J. Chem. Soc., Dalton Trans.*, 1333 (1992).
14. K. N. Houk, *Chemtracts, Org. Chem.*, **6**, 360 (1993).
15. S. H. Strauss, *Chemtracts, Inorg. Chem.*, **5**, 119 (1993).
16. S. Borman, *Chem. Eng. News*, Nov. 8, 1993, p. 41.
17. J. Chojnowski and W. A. Stanczyk, *Main Group Chem. News*, **2**, 6 (1994).
18. J. B. Lambert, L. Kania and S. Zhang, *Chem. Rev.*, **95**, 1191 (1995).
19. G. Rong, R. Ma, L. Long and C. Zhou, *Huaxue Tongbao*, 19 (1996); *Chem. Abstr.*, **125**, 221889 (1996).
20. A. Tachibana, S. Kawauchi, T. Yano, N. Yoshida and T. Yamabe, *J. Mol. Struct., (THEOCHEM)*, **119**, 121 (1994).
21. L. Operti, R. Rabezzana, G. A. Vaglio and P. Volpe, *J. Organomet. Chem.*, **509**, 151 (1996).
22. J.-F. Gal, R. Grover, P.-C. Maria, L. Operti, R. Rabezzanna, G.-A. Vaglio and P. Volpe, *J. Phys. Chem.*, **98**, 11978 (1994).
23. I. Haller, *J. Phys. Chem.*, **94**, 4135 (1990).
24. A. Tachibana, S. Kawauchi, N. Yoshido, T. Yamabe and K. Fukui, *J. Mol. Struct.*, **300**, 501 (1993).
25. M. Yamamoto, M. Tanaka, Y. Yokota and T. Takeuchi, *J. Mass Spectrom. Soc. Jpn.*, **41**, 277 (1993).
26. P. B. Davies and D. M. Smith, *J. Chem. Phys.*, **100**, 6166 (1994).
27. D. M. Smith, P. M. Martineau and P. B. Davies, *J. Chem. Phys.*, **96**, 1741 (1992).
28. B. H. Boo and P. B. Armentrout, *J. Am. Chem. Soc.*, **109**, 3549 (1987).
29. S. K. Shin, R. R. Corderman and J. L. Beauchamp, *Int. J. Mass Spectrom. Ion Processes*, **101**, 257 (1990).
30. T. Motooka, P. Fons, H. Abe and T. Tokuyama, *Jpn. J. Appl. Phys. Part 2b*, **32**, L879 (1993).
31. W. D. Reents, Jr., M. L. Mandich, and C. R. C. Wang, *J. Chem. Phys.*, **97**, 7226 (1992).
32. M. L. Mandich, W. D. Reents Jr. and K. D. Kolenbrander, *Pure Appl. Chem.*, **62**, 1653 (1990).
33. M. L. Mandich, W. D. Reents Jr. and K. D. Kolenbrander, *J. Chem. Phys.*, **92**, 437 (1990).
34. K. Raghavachari, *Adv. Met. Semicond. Clusters*, **2**, 57 (1994).
35. K. Raghavachari, *J. Chem. Phys.*, **92**, 452 (1990).
36. M. L. Mandich and W. D. Reents Jr., *J. Chem. Phys.*, **96**, 4233 (1992).
37. W. D. Reents Jr. and M. L. Mandich, *J. Chem. Phys.*, **93**, 3270 (1990).
38. L. Operti, M. Splendore, G. A. Vaglio and P. Volpe, *Spectrochim. Acta, Part A*, **49A**, 1213 (1993).
39. P. Antoniotti, L. Oporti, R. Rabezzana, G. A. Vaglio, P. Volpe, J.-F. Gal, R. Grover and P.-C. Maria, *J. Phys. Chem.*, **100**, 155 (1996).
40. X. Li and J. A. Stone, *Int. J. Mass Spectrom. Ion Processes*, **101**, 149 (1990).
41. S. Murthy and J. L. Beauchamp, *J. Phys. Chem.*, **99**, 9118 (1995).
42. S. Murthy and J. L. Beauchamp, *J. Phys. Chem.*, **96**, 1247 (1992).
43. R. Bakhtiar, C. M. Holznagel and D. B. Jacobson, *J. Phys. Chem.*, **97**, 12710 (1993).
44. K. P. Lim and F. W. Lampe, *Int. J. Mass Spectrom. Ion Processes*, **92**, 53 (1989).
45. F. Denes, Z. Q. Hua, C. E. C. A. Hop and R. A. Young, *J. Appl. Polym. Sci.*, **61**, 875, (1996).
46. Z. Q. Hua, F. Denes and R. A. Young, *J. Vac. Sci. Technol.*, **14**, 1339 (1996).
47. K. A. Reuter and D. B. Jacobson, *Organometallics*, **8**, 1126 (1989).
48. I. S. Ignatyev and T. Sundius, *Organometallics*, **15**, 5674 (1996).
49. R. Bakhtiar, C. M. Holznagel and D. B. Jacobson, *Organometallics*, **12**, 621 (1993).
50. R. Bakhtiar and C. M. Holznagel, *Organometallics*, **12**, 880 (1993).
51. Y. Apeloig, M. Karni, A. Stanger, H. Schwarz, T. Drewello and G. Czekay, *J. Chem. Soc., Chem. Commun.*, 989 (1987).
52. G. Angelini, Y. Keheyan, G. Laguzzi and G. Lilla, *Tetrahedron Lett.*, **29**, 4159 (1988).

53. S. G. Cho, *J. Organomet. Chem.*, **510**, 25 (1996).
54. V. Q. Nguyen, S. A. Shaffer, F. Turecek and C. E. C. A. Hop, *J. Phys. Chem.*, **99**, 15454 (1995).
55. S. Tobita, S. Tajima, F. Okada, S. Mori, E. Tabei and M. Umemura, *Org. Mass Spectrom.*, **25**, 39 (1990).
56. S. Tobita, S. Tajima and F. Okada, *Org. Mass. Spectrom.*, **24**, 373 (1989).
57. W. J. Meyerhoffer and M. M. Bursey, *Org. Mass Spectrom.*, **24**, 246 (1989).
58. J. A. Stone, A. C. M. Wojtyniak, *Can. J. Chem.*, **64**, 575 (1986).
59. Z. Xie, R. Bau and C. A. Reed, *J. Chem. Soc., Chem. Commun.*, 2519 (1994).
60. A. C. M. Wojtyniak and J. A. Stone, *Int. J. Mass Spectrom. Ion Processes*, **74**, 59 (1986).
61. X. Li and J. A. Stone, *Can. J. Chem.*, **70**, 2070 (1992).
62. F. Cacace, M. E. Crestoni, S. Fornarini and R. Gabrielli, *Int. J. Mass Spectrom. Ion Processes*, **84**, 17 (1988).
63. S. Fornarini, *J. Org. Chem.*, **53**, 1314 (1988).
64. F. Cacace, *Acc. Chem. Res.*, **21**, 215 (1988).
65. M. Speranza, *Mass Spectrom. Rev.*, **11**, 73 (1992).
66. G. A. Olah, T. Bach and G. K. S. Prakash, *J. Org. Chem.*, **54**, 3770 (1989).
67. J. B. Lambert, S. Zhang and S. M. Ciro, *Organometallics*, **13**, 2430 (1994).
68. F. Cacace, M. E. Crestoni and S. Fornarini, *J. Am. Chem. Soc.*, **114**, 6776 (1992).
69. F. Cacace, M. Attinà and S. Fornarini, *Angew. Chem., Int. Ed. Engl.*, **34**, 654 (1995).
70. M. E. Crestoni and S. Fornarini, *Angew. Chem., Int. Ed. Engl.*, **33**, 1094 (1994).
71. A. B. Thomas and E. G. Rochow, *J. Inorg. Nucl. Chem.*, **4**, 205 (1957).
72. N. N. Lichtin and P. D. Bartlett, *J. Am. Chem. Soc.*, **73**, 5530 (1951).
73. M. E. Peach and T. C. Waddington, *J. Chem. Soc.*, 1238 (1961).
74. J. Y. Corey, *J. Am. Chem. Soc.*, **97**, 3237 (1975).
75. J. B. Lambert and W. Schilf, *J. Am. Chem. Soc.*, **110**, 6364 (1988).
76. J. B. Lambert, W. J. Schulz, J. A. McConnell and W. Schilf, *J. Am. Chem. Soc.*, **110**, 2201 (1988).
77. J. B. Lambert, L. Kania, W. Schilf and J. A. McConnell, *Organometallics*, **10**, 2578 (1991).
78. J. B. Lambert, J. A. McConnell and W. J. Schulz, *J. Am. Chem. Soc.*, **108**, 2482 (1986).
79. J. B. Lambert and W. J. Schulz, *J. Am. Chem. Soc.*, **105**, 1671 (1983).
80. J. B. Lambert, L. Kania, B. Kuhlmann and J. A. McConnell, unpublished results, cited in Reference 18.
81. G. A. Olah, L. Heiliger, X. Y. Li and G. K. S. Prakash, *J. Am. Chem. Soc.*, **112**, 5991 (1990).
82. G. K. S. Prakash, S. Keyaniyan, R. Aniszfeld, L. Heiliger, G. A. Olah, R. C. Stevens, H. K. Choi and R. Bau, *J. Am. Chem. Soc.*, **109**, 5123 (1987).
83. G. A. Olah, G. Rasul, L. Heiliger, J. Bausch and G. K. S. Prakash, *J. Am. Chem. Soc.*, **114**, 7737 (1992).
84. C. Eaborn and F. M. S. Mahmoud, *J. Chem. Soc., Perkin Trans. 2*, 1309 (1981).
85. J. B. Lambert, J. A. McConnell, W. Schilf and W. J. Schulz Jr., *J. Chem. Soc., Chem. Commun.*, 455 (1988).
86. J. Chojnowski, M. Cypryk and J. Michalski, *J. Organomet. Chem.*, **161**, C31 (1978).
87. A. R. Bassindale and T. Stout, *J. Chem. Soc., Perkin Trans. 2*, 221 (1986).
88. K. Hensen, T. Zengerley, P. Pickel and G. Klebe, *Angew. Chem., Int. Ed. Engl.*, **22**, 725 (1983).
89. M. Okano and K. Mochida, *Chem. Lett.*, 819 (1991).
90. M. Arshadi, D. Johnels, U. Edlund, C.-H. Ottosson and D. Cremer, *J. Am. Chem. Soc.*, **118**, 5120 (1996).
91. C. Chuit, R. J. P. Corriu, A. Mehdi and C. Reye, *Angew. Chem., Int. Ed. Engl.*, **32**, 1311 (1993).
92. V. A. Benin, J. C. Martin and M. R. Willcott, *Tetrahedron Lett.*, **35**, 2133 (1994).
93. M. Chauhan, C. Chuit, R. J. P. Corriu and C. Reyé, *Tetrahedron Lett.*, **37**, 845 (1996).
94. M. Chauhan, C. Chuit, R. J. P. Corriu, A. Mehdi and C. Reyé, *Organometallics*, **15**, 4326 (1996).
95. C.-H. Ottosson and D. Cremer, *Organometallics*, **15**, 5309 (1996).
96. H. Gilman and G. E. Dunn, *J. Am. Chem. Soc.*, **72**, 2178 (1950).
97. U. Wannagat and W. Liehr, *Angew. Chem.*, **69**, 783 (1957).
98. J. M. Stone and J. A. Stone, *Int. J. Mass Spectrom. Ion Processes*, **109**, 247 (1991).
99. R. Walsh, in *The Chemistry of Organic Silicon Compounds* (Eds. S. Patai and Z. Rappoport), Part 1, Wiley, Chichester, 1989, pp. 371–391.
100. D. A. Strauss, C. Zhang, G. E. Quimbita, S. D. Grumbine, R. H. Heyn, T. D. Tilley, A. L. Rheingold and S. J. Geib, *J. Am. Chem. Soc.*, **112**, 2673 (1990).

101. S. R. Bahr and P. Boudjouk, *J. Am. Chem. Soc.*, **115**, 4514 (1993).
102. J. B. Lambert and S. Zhang, *J. Chem. Soc., Chem Commun.*, 383 (1993).
103. Z. Xie, D. J. Liston, T. Jelinek, V. Mitro, R. Bau and C. A. Reed, *J. Chem. Soc., Chem. Commun.*, 384 (1993).
104. G. A. Olah and L. Field, *Organometallics*, **1**, 1485 (1982).
105. L. Olsson, C.-H. Ottosson and D. Cremer, *J. Am. Chem. Soc.*, **117**, 7460 (1995).
106. Z. Xie, J. Manning, R. W. Reed, R. Mathur, P. D. W. Boyd, A. Benesi and C. A. Reed, *J. Am. Chem. Soc.*, **118**, 2922 (1996).
107. S. Sieber, P. Buzek, P. v. R. Schleyer, W. Koch, J. W. d. M. Carneiro, *J. Am. Chem. Soc.*, **115**, 259 (1993).
108. L. Olsson and D. Cremer, *Chem. Phys. Lett.*, **215**, 433 (1993).
109. G. A. Olah, G. Rasul, H. A. Buchholz, X.-Y. Li and G. K. S. Prakash, *Bull Chem. Soc. Fr.*, **132**, 569 (1995).
110. C.-H. Ottosson and D. Cremer, *Organometallics*, **15**, 5495 (1996).
111. J. B. Lambert and H.-n. Sun, *J. Am. Chem. Soc.*, **98**, 5611 (1976).
112. U. Pidun, M. Stahl and G. Frenking, *Chem. Eur. J.*, **2**, 869 (1996).
113. M. Kira, T. Hino and H. Sakurai, *J. Am. Chem. Soc.*, **114**, 6697 (1992).
114. D. Cremer, L. Olsson and H. Ottosson, *J. Mol. Struct. (THEOCHEM)*, **313**, 91 (1994).
115. G. A. Olah, K. Laali and O. Farooq, *Organometallics*, **3**, 1337 (1984).
116. E. V. Van Den Berghe and G. P. Van Der Kelen, *J. Organomet. Chem.*, **59**, 175 (1973).
117. G. A. Olah, G. Rasul and G. K. S. Prakash, *J. Organomet. Chem.*, **521**, 271 (1996).
118. A. R. Bassindale, personal communication.
119. G. A. Olah, X.-Y. Li, Q. Wang, G. Rasul and G. K. S. Prakash, *J. Am. Chem. Soc.*, **117**, 8962 (1995).
120. M. Kira, T. Hino and H. Sakurai, *Chem. Lett.*, 153 (1993).
121. A. R. Bassindale and T. Stout, *Tetrahedron Lett.*, **26**, 3403 (1985).
122. M. Kira, T. Hino and H. Sakurai, *Chem. Lett.*, 555 (1992).
123. J. B. Lambert and Y. Zhao, *J. Am. Chem. Soc.*, **118**, 7867 (1996).
124. J. B. Lambert and Y. Zhao, *Angew. Chem., Int. Ed. Engl.*, **36**, 400 (1997) and personal communication
125. N. Auner, paper OB20, XIth International Symposium on Organosilicon Chemistry, Montpellier, September 1996; H.-U. Steinberger, T. Müller, N. Auner, C. Maerker and P. v. R. Schleyer, *Angew. Chem., Int. Ed. Engl.*, **36**, 626 (1997).
126. J. B. Lambert, personal communication to G. Frenking, cited in Reference 107.
127. V. K. Dioumaev and J. F. Harrod, *Organometallics*, **15**, 3859 (1996).
128. D. A. Strauss, S. D. Grumbine and T. D. Tilley, *J. Am. Chem. Soc.*, **112**, 7801 (1990).
129. S. D. Grumbine, T. D. Tilley, F. P. Arnold and A. L. Rheingold, *J. Am. Chem. Soc.*, **115**, 7884 (1993).
130. S. K. Grumbine, T. D. Tilley, F. P. Arnold and A. L. Rheingold, *J. Am. Chem. Soc.*, **116**, 5495 (1994).
131. P. Jutzi and E.-A. Bunte, *Angew. Chem., Int. Ed. Engl.*, **31**, 1605 (1992).
132. P. v. R. Schleyer, *Science*, **275**, 39 (1997).
133. T. Müller, personal communication.
134. V. K. Dioumaev and J. F. Harrod, *J. Organomet. Chem.*, **521**, 133 (1996).
135. V. K. Dioumaev and J. F. Harrod, *Organometallics*, **13**, 1548 (1994).
136. J. Chojnowski, W. Fortuniak and W. A. Stanczyk, *J. Am. Chem. Soc.*, **109**, 7776 (1987).
137. J. Chojnowski, L. Wilczek and W. Fortuniak, *J. Organomet. Chem.*, **135**, 13 (1977).
138. H. Mayr, N. Basso and G. Hagen, *J. Am. Chem. Soc.*, **114**, 3060 (1992).
139. N. Basso, S. Görs, E. Popowski and H. Mayr, *J. Am. Chem. Soc.*, **115**, 6025 (1993).
140. Y. Apeloig, O. Merin-Aharoni, D. Danovich, A. Ioffe and S. Shaik, *Isr. J. Chem.*, **33**, 387 (1993).
141. Y. Apeloig, *Stud. Org. Chem.*, **31**, 33 (1987).
142. Y. Apeloig and A. Stanger, *J. Am. Chem. Soc.*, **109**, 272 (1987).
143. D. N. Kevill, *J. Chem. Res. (S)*, 272 (1987).
144. A. R. Bassindale and P. G. Taylor, in *The Chemistry of Organic Silicon Compounds* (Eds. S. Patai and Z. Rappoport), Part 1, Wiley, Chichester, 1989, pp. 839–892.
145. M. A. M. R. Al-Gurashi, G. A. Ayoko, C. Eaborn and P. D. Lickiss, *Bull. Soc. Chim. Fr.*, **132**, 517 (1995).
146. C. Eaborn, P. D. Lickiss, S. T. Najim and W. A. Stanczyk, *J. Chem. Soc., Chem. Commun.*, 1461 (1987).

147. C. Eaborn, K. L. Jones and P. D. Lickiss, *J. Chem. Soc., Chem. Commun.*, 595 (1989).
148. C. Eaborn, K. L. Jones and P. D. Lickiss, *J. Chem. Soc., Perkin Trans. 2*, 489 (1992).
149. C. Eaborn, K. L. Jones, P. D. Lickiss and W. A. Stanczyk, *J. Chem. Soc., Perkin Trans. 2*, 59 (1993).
150. A. Ayoko and C. Eaborn, *J. Chem. Soc., Perkin Trans. 2*, 1047 (1987).
151. N. H. Buttrus, C. Eaborn, P. B. Hitchcock, P. D. Lickiss and S. T. Najim, *J. Chem. Soc., Perkin Trans. 2*, 891 (1987).
152. C. Eaborn, P. D. Lickiss, S. T. Najim and M. N. Romamelli, *J. Chem. Soc., Chem. Commun.*, 1754 (1985).
153. C. Eaborn, P. D. Lickiss, S. T. Najim and M. N. Romanelli, *J. Organomet. Chem.*, **315**, C5 (1986).
154. C. Eaborn and M. N. Romanelli, *J. Organomet. Chem.*, **451**, 45 (1993).
155. C. Eaborn and D. E. Reed, *J. Chem. Soc., Perkin Trans. 2*, 1695 (1985).
156. Z. H. Aiube and C. Eaborn, *J. Organomet. Chem.*, **421**, 159 (1991).
157. S. M. Whittaker, Ph. D. Thesis, University of Salford (1993).
158. A. I. Almansour, J. R. Black, C. Eaborn, P. M. Garrity and D. A. R. Happer, *J. Chem. Soc., Chem. Commun.*, 705 (1995).
159. A. G. Brook, M. Hesse, K. M. Baines, R. Kumarathasan and A. J. Lough, *Organometallics*, **12**, 4259 (1993).
160. D. M. Van Seggan, P. K. Hurlburt, M. D. Noirot, O. P. Anderson and S. H. Strauss, *Inorg. Chem.*, **31**, 1423 (1992).
161. G. K. S. Prakash, Q. Wang, X.-y. Li and G. A. Olah, *New J. Chem.*, **14**, 791 (1990).
162. Y. Apeloig and O. Merin-Aharoni, *Croat. Chem. Acta*, **65**, 757 (1992).
163. S. R. Church, C. G. Davies, R. Lümen, P. A. Mounier, G. Saint and P. L. Timms, *J. Chem. Soc., Dalton Trans.*, 227 (1996).
164. N. Tokitoh, T. Imakubo and R. Okazaki, *Tetrahedron Lett.*, **33**, 5819 (1992).
165. A. Schäfer, M. Weidenbruch, S. Pohl and W. Saak, *Z. Naturforsch. Teil B*, **45B**, 363 (1990).
166. M. Labrouillère, C. Le Roux, A. Oussaid, H. Gaspard-Ilhoughmane and J. Dubac, *Bull. Soc. Chem. Fr.*, **132**, 522 (1995).
167. V. A. Kovyazin, I. B. Sokol'skaya, V. M. Kopylov, I. A. Abronin, Yu. T. Efimov, O. V. Shtefan and V. Yu. Kapustin, *Organomets. in USSR*, **4**, 652 (1991).
168. K. L. Malisza, L. C. F. Chao, J. F. Britten, B. G. Sayer, G. Jaouen, S. Top, A. Decken and M. J. McGlinchy, *Organometallics*, **12**, 2462 (1993).
169. R. Ruffolo, A. Decken, L. Girard, H. K. Gupta, M. A. Brook and M. J. McGlinchey, *Organometallics*, **13**, 4328 (1994).
170. P. Sigwalt and V. Stannett, *Makromol. Chem., Macromol. Symp.*, **32**, 217 (1990).
171. D. M. Naylor, V. T. Stannett, A. Deffieux and P. Sigwalt, *Polymer*, **35**, 1764 (1994).
172. S. S. Jada, *J. Am. Ceram. Soc.*, **70**, C298 (1987).
173. S. S. Jada, *J. Am. Ceram. Soc.*, **71**, C413 (1988).
174. L. D. David, *J. Am. Ceram. Soc.*, **71**, C412 (1988).
175. D. D. Devore, D. R. Neithamer, R. E. Lapointe and R. D. Mussell, World Patent, No. WO 9608519 A2 960321, 1996.
176. K. Mizuno, T. Tamai, I. Hashida and Y. Otsuji, *J. Org. Chem.*, **60**, 2935 (1995).
177. I. S. Ignatyev and T. A. Kochina, *J. Mol. Struct. (THEOCHEM)*, **236**, 249 (1991).
178. K. Hensen, T. Zengerley, T. Müller and P. Pickel, *Z. Anorg. Allg. Chem.*, **558**, 21 (1988).
179. C. Brelière, F. Carré, R. Corriu and M. W. C. Man, *J. Chem. Soc., Chem. Commun.*, 2333 (1994).
180. J. Belzner, D. Schär, B. O. Kneisel and R. Herbst-Irmer, *Organometallics*, **14**, 1840 (1995).
181. R. Probst, C. Leis, S. Gamper, E. Herdtweck, L. Zybill and N. Auner, *Angew. Chem., Int. Ed. Engl.*, **30**, 1132 (1991).
182. J. B. Lambert, S. Zhang, C. L. Stern and J. C. Huffman, *Science*, **260**, 1917 (1993).
183. A. Schäfer, M. Weidenbruch and S. Pohl, *J. Organomet. Chem.*, **282**, 305 (1985).
184. F. Effenberger, F. Reisinger, K. H. Schöwälder, P. Bäuerle, J. J. Stezowski, K. H. Jogun, K. Schöllkopf and W.-D. Stohrer, *J. Am. Chem. Soc.*, **109**, 882 (1987).
185. Z. Xie, R. Bau, A. Benesi and C. A. Reed, *Organometallics*, **14**, 3933 (1995).
186. L. Pauling, *Science*, **263**, 983 (1994).
187. J. B. Lambert and S. Zhang, *Science*, **263**, 984 (1994).
188. G. A. Olah, G. Rasul, X.-Y. Li, H. A. Buchholz, G. Sandford and G. K. S. Prakash, *Science*, **263**, 983 (1994).

189. P. v. R. Schleyer, P. Buzek, T. Müller, Y. Apeloig and H.-U. Siehl, *Angew. Chem., Int. Ed. Engl.*, **32**, 1471 (1993).
190. H. Basch, *Inorg. Chim. Acta*, **242**, 191 (1996).
191. M. D. Harmony and M. R. Strand, *J. Mol. Spectrosc.*, **81**, 308 (1980).
192. N. W. Mitzel, J. Reide and H. Schmidbaur, *Acta Crystallogr. Sect. C*, **52**, 980 (1996).
193. S. N. Gurkova, A. I. Gusev, V. A. Sharapov, T. K. Gar and N. V. Alexeev, *Zh. Strukt. Khim.*, **20**, 356 (1979); English translation: *J. Struct. Chem.*, **20**, 302 (1979).
194. U. Schubert and C. Steib, *J. Organomet. Chem.*, **238**, C1 (1982).
195. A. A. Macharashvili, Yu. I. Baukov, E. P. Kramarova, G. I. Oleneva, V. A. Shestunovich, Yu. T. Struchkov and V. E. Shklover, *Zh. Strukt. Khim.*, **28**, 107 (1987); English translation: *J. Struct. Chem.*, **28**, 552 (1987).
196. C. A. Reed, Z. Xie, R. Bau and A. Benesi, *Science*, **262**, 402 (1993).
197. S. L. Miller, L. C. Aamodt, G. Dousmanis, C. H. Townes and J. Kraitchman, *J. Chem. Phys.*, **20**, 1112 (1952).
198. A. Sekiguchi, M. Tsukamoto, and M. Ichinoke, *Science*, **175**, 60 (1997).
199. G. Urry, *Acc. Chem. Res.*, **3**, 306 (1970).

CHAPTER **12**

Silyl-substituted carbocations

HANS-ULLRICH SIEHL

Abteilung für Organische Chemie I der Universität Ulm, D-86069 Ulm, Germany
Fax: +49-(0)731-502-2800; e-mail: ullrich.siehl@chemie.uni-ulm.de

and

THOMAS MÜLLER

Fachinstitut für Anorganische und Analytische Chemie der Humboldt Universität Berlin, D-10115 Berlin, Germany
Fax: +49(0)30-2903-6966; e-mail: h0443afs@rz.hu-berlin.de

I. INTRODUCTION

This chapter deals with silyl-substituted carbocations. In Section II results of quantum chemical *ab initio* calculations of energies and structures of silyl-substituted carbocations are summarized[1]. Throughout the whole chapter results of *ab initio* calculations which relate directly to the experimental observation of silyl-substituted carbocations and their reactions are reviewed. Section III reports on gas phase studies and Section IV on solvolytic investigations of reactions which involve silyl-substituted carbocation intermediates and transition states. Section V summarizes the structure elucidation studies on stable silyl-substituted carbocations. It includes ultra-fast optical spectroscopic methods for the detection of transient intermediates in solution, NMR spectroscopic investigations of silyl-substituted carbocations in superacids and non-nucleophilic solvents, concomitant computational studies of model cation and X-ray crystallography of some silyl-substituted carbocations which can be prepared as crystals of salts.

II. CALCULATIONAL RESULTS

In this brief part only the most important results of *ab initio* calculations regarding the energies and structures of silyl-substituted carbocations are summarized[1].

The simplest α-silyl-substituted carbenium ion $H_3SiCH_2^+$ (**1**) is not a minimum on the potential energy surface and it rearranges without a barrier to the more stable (by 49 kcal mol^{-1} at MP4/6-31G(d)//3-21G(d)) silylium ion H_2Si^+Me (**2**)^2. For α-silylethyl cation (**3**) and α-silylvinyl cation (**4**) calculations at the correlated MP2(fu)/6-31G(d,p) level predict hydrogen bridged structures just as for the parent ethyl and vinyl cations^{3,4}. **3** is separated by a barrier of only 5.2 kcal mol^{-1} from the ethylsilylium ion **5**, which is by 25.9 kcal mol^{-1} more stable [at MP2(fu)/6-31G(d,p)]. Similarly, the activation barrier for the 1,2-H shift from the α-silylvinyl cation (**4**) to the isomeric 1-silaallyl cation (**6**) is only 8.9 kcal mol$^{-1^{3,4}}$.

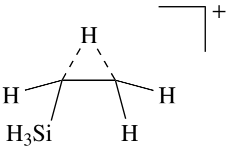

(3)

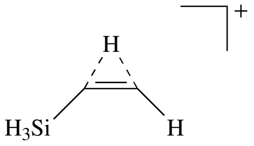

(4)

$\overset{+}{H_2Si}CH_2Me$

(5)

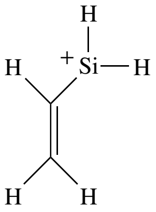

(6)

According to *ab initio* calculations by Wierschke, Chandrasekhar and Jorgensen a silyl-substituent stabilizes a directly attached positively charged carbon compared with hydrogen, but it destabilizes it compared with a methyl substituent. Thus, the calculated reaction energies of the isodesmic reaction 1 are 17.8 kcal mol^{-1} ($R = SiH_3$) and 34.0 kcal mol^{-1} ($R = Me$) [at MP3/6-31G(d)//3-21G(d)]^5.

$$H_2\overset{+}{C}{-}R + CH_4 \longrightarrow CH_3^+ + CH_3{-}R \qquad (1)$$

$$H_2C{=}\overset{+}{C}{-}R + H_2C{=}CH_2 \longrightarrow H_2C{=}\overset{+}{C}{-}H + H_2C{=}CHR \qquad (2)$$

For dicoordinated cations the situation is slightly different. Apeloig and Stanger showed, using the isodesmic reaction 2, that an α-silyl group, i.e. in **7**, stabilizes the vinyl cation by *ca* 24.9 kcal mol^{-1} (HF/3-21G//3-21G) relative to hydrogen^6. This value remains nearly unchanged at higher levels of calculations [24.1 kcal mol^{-1} at MP3/6-31G(d)//3-21G(d)^5 and 25 kcal mol^{-1} at QCISD(T)/6-31G(d)//MP2(fu)/6-31G(d)]^7. More interesting is the comparison with the methyl group. It is found that α-silyl and α-methyl groups stabilize the vinyl cation nearly to the same extent: the difference between the calculated reaction energies of equation 2 for $R = Me$ and $R = SiH_3$ is only 2.5 kcal mol^{-1} at QCISD(T)/6-31G(d)//MP2(fu)/6-31G(d)^7, 0.2 kcal mol^{-1} (HF/3-21G//3-21G)^6 and 2.9 kcal mol^{-1} [MP3/6-31G(d)//3-21G(d)]^5, with the 2-propenyl cation **8** being the more stable.

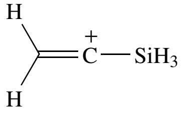

(7)

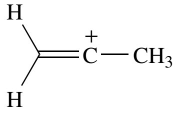

(8)

The destabilizing effect of a silyl group compared with a methyl group in trivalent carbocations was explained by the weaker SiH (relative to CH) hyperconjugation and by electrostatic repulsion between the adjacent positively charged cationic carbon and the electropositive silicon[8]. In the vinyl cation the stronger hyperconjugation with the β-vinylic hydrogens diminishes the demand for hyperconjugative stabilization from the α-substituent, thus reducing the advantage of an α-methyl group. In addition, the vinyl cation is more sensitive to the σ-effects of the α-substituent than an alkyl cation, and the stabilizing σ-donation by the electropositive silyl group is therefore more important for the vinyl cation than for the tricoordinated carbenium ion[6].

In contrast, β-silyl-substitution is predicted by the calculations to be far more stabilizing than β-alkyl substitution. Thus, the isodesmic equation 3 predicts for **9** a stabilization by the β-silyl group of 38 kcal mol^{-1}, while the β-methyl substitution in **10** gives only a stabilization of 28 kcal mol^{-1} [MP3/6-31G(d)//3-21G(d)][5]. The stabilization by the silyl substituent is markedly orientation-dependent. Thus, the perpendicular conformation of the β-silylethyl cation **9p** is higher in energy by 29.6 kcal mol^{-1} compared with the bisected conformation **9** [MP3/6-31G(d)//3-21G(d)][5]. The open β-silyl-substituted vinyl cation **11** is lower in energy by 28.6 kcal mol^{-1} and 20.5 kcal mol^{-1} [MP3/6-31G(d)//3-21G(d)] compared with the vinyl cation (equation 4, R = H) and the 1-propenyl cation (equation 4, R = Me), respectively[5].

$$H_2\overset{+}{C}{-}CH_2R + C_2H_6 \longrightarrow H_3C{-}CH_2R + H_3CCH_2{}^+ \qquad (3)$$

$$H\overset{+}{C}{=}CHR + C_2H_6 \longrightarrow H_2C{=}CHR + H_3CCH_2{}^+ \qquad (4)$$

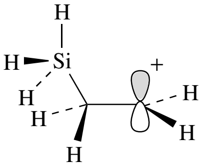

(9)

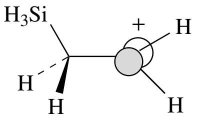

(9p)

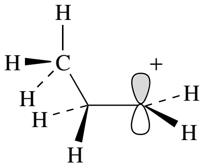

(10)

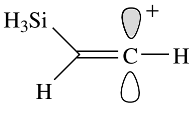

(11)

The β-silyl effect is dependent on the electron demand of the electron-deficient centre and it decreases with the increased stability of the silicon-free cation. Thus, the stabilization energy is reduced from the value for the primary cation **9** (33.2 kcal mol^{-1} compared with the ethyl cation) to the secondary cation **12** (22.1 kcal mol^{-1} compared with the isopropyl cation) and finally attains an additional stabilization of only 15.9 kcal mol^{-1} for the tertiary cation **13** [compared with the *t*-butyl cation; all values calculated at MP2(fc)/6-31G(d)//6-31G(d)][9]. The additional stabilization gained by β-silyl substitution is reduced from 33 kcal mol^{-1} for the primary vinyl cation **11** to only *ca* 10 kcal mol^{-1} for the strongly stabilized α-phenyl-substituted vinyl cation **14** [at MP2(fc)/6-31G(d)//MP2(fc)/6-31G(d)][7].

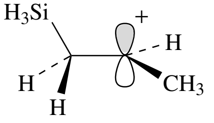

(12)

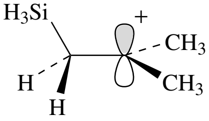

(13)

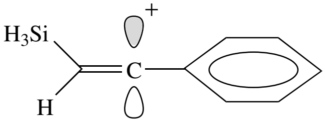

(14)

The hyperconjugative interaction between the σ-Si−C bond and the formally empty 2p(C^+) orbital leads to marked geometrical effects. For example, in the calculated equilibrium structure of the secondary ion **12** (Figure 1) the calculated Si−C bond is distinctly longer than in the perpendicular conformation **12p**, in which the $SiCC^+$ hyperconjugation is switched off [2.070 Å versus 1.938 Å, at HF/6-31G(d)[9]]. Furthermore, the calculated C^+−C distance shortens from 1.461 Å in the perpendicular **12p** to 1.386 Å in the bisected conformation **12**, which is by 22 kcal mol^{-1} more stable. The series of calculated structures of vinyl cations shown in Figure 2 demonstrates nicely the geometrical consequences of β-C−Si hyperconjugation in vinyl cations. Apeloig, Siehl, Schleyer, and coworkers[7,10] calculated at the correlated MP2/6-31G(d) level the structures of β-silylvinyl cations **14**−**20** possessing various α-substituents including methyl, hydroxy, vinyl, isobuten-1-yl, phenyl, cyclopropyl and silyl. The degree of bridging in these β-silyl-substituted vinyl

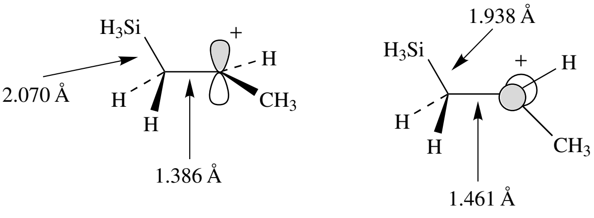

(12) **(12p)**

FIGURE 1. Calculated structures of bisected ion **12** and perpendicular ion **12p** (HF/6-31G(d))

cations (taking the $SiC_{\beta}C^{+}$ bond angle α as a measure) was found to decrease (i.e. increases) with increasing electron-donating ability of the α-substituent. Thus, on going from the strongly electron-donating isobuten-1-yl substituent in **16** to a methyl group in **19**, α decreases from 117.5° to 91.9° and closes even further to 76.3° for an α-silyl group in **20**.

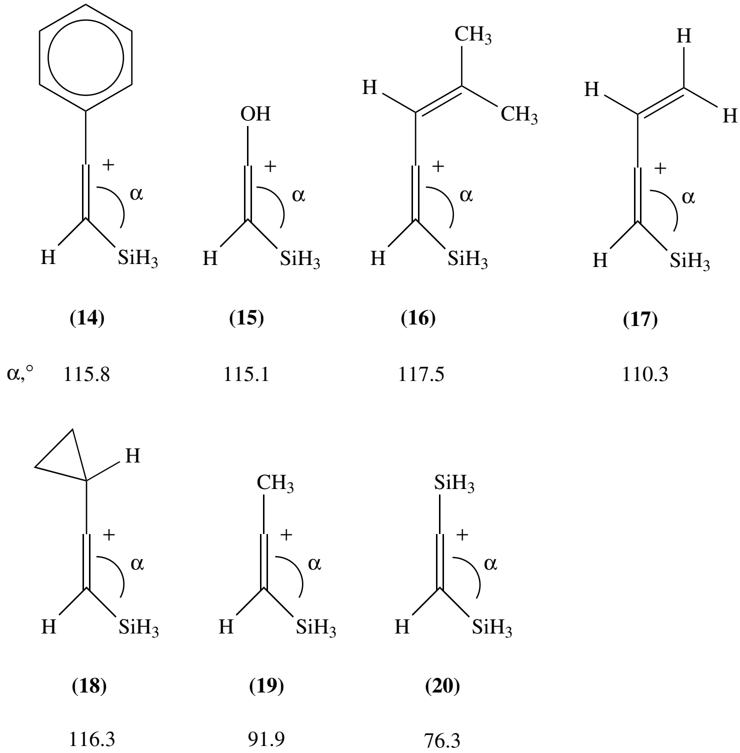

	(14)	**(15)**	**(16)**	**(17)**
α,°	115.8	115.1	117.5	110.3

	(18)	**(19)**	**(20)**
α,°	116.3	91.9	76.3

FIGURE 2. Geometrical consequences of β-C–Si hyperconjugation in vinyl cations (MP2/6-31G(d))

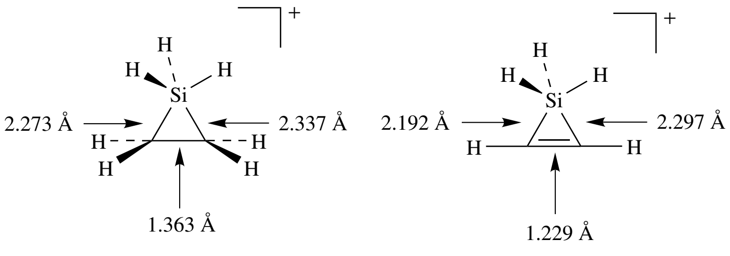

(21) **(22)**

FIGURE 3. Calculated structures of **21** and **22** (MP2/6-31G(d,p))

The 'classical' open β-silylethyl cation **9** and β-silylvinyl cation **11** are no minima at higher level of theory[3,4]. They collapse to the bridged protonated silacyclopropane **21** and silacyclopropene **22**, respectively. On the basis of their calculated structures (Figure 3) both cyclic molecules are best described as π-complexes between a silylium ion and ethene or acetylene, respectively.

Silyl substituents have also distinct effects on the stability of aryl cations. For example, the disilyl **(23)** and trisilyl-substituted **(24)** phenyl cations are calculated to be more stable than the parent phenyl cation **25** by 25 kcal mol^{-1} (HF3-21G)[11] and by 22.4 kcal mol^{-1} (HF6-31G(d))[12], respectively.

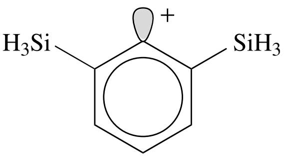

(23)

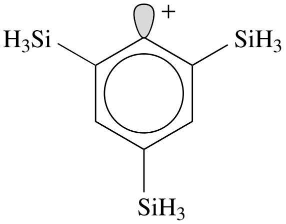

(24)

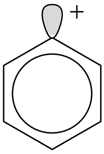

(25)

III. GAS PHASE STUDIES

A. α-Substitution

In agreement with the calculations, all gas phase studies of α-silyl-substituted carbenium ions show that these intermediates exist only in a very flat potential well. They undergo fast 1,2-H- or 1,2-alkyl shifts, producing the more stable silylium or β-silyl-substituted carbenium ions. For example, Apeloig, Schwarz and coworkers[13] employed elegant gas phase ion techniques combined with *ab initio* MO theory to study the unimolecular dissociation of nascent $C_5H_{13}Si^+$ ions. Their results indicate that the nascent α-silyl-substituted $H_3C{-}CH^+Si(CH_3)$ ion **26** undergoes a fast 1,2-methyl migration forming the silylium ion **27** with little or no barrier (Figure 4). The 1,2-H shift yielding the β-silyl-substituted carbenium ion **28** is connected with an appreciable barrier of *ca* 10 kcal mol^{-1}, which results from the fact that the 1,2-H shift produces the eclipsed conformation **28a** which lies 37 kcal mol^{-1} higher in energy than the ground-state conformation **28**. This agrees nicely with the results of isotopic labeling experiments which demonstrate that, prior to dissociation to C_2H_4 and Me_3Si^+, the nascent ion **26** rapidly undergoes 1,2-methyl migrations leading to an almost complete exchange of the four methyl groups[13,14]. It is notable that the tertiary silyl-substituted carbenium ion $Me_2C^+SiMe_3$ **29** also exchanges, prior to loss of propene, its five methyl groups in a nearly quantitative way. Thus, the methyl migration to the silylium ion $Me_3CSi^+Me_2$ **30** is still relatively facile while the hydrogen shift to produce the β-silyl-substituted carbenium ion $H_2C^+MeCHSiMe_3$ **31** involves a significant barrier[14].

Ion–molecule reactions were used to identify the structure of the predominant ion resulting from ionization of $MeCHXSiMe_3$ ($X = Cl$, OR, OH). While Hajdasz and Squires[15] concluded from their afterglow study that ions **27** and **28** are formed in the ionization of the chloride in a 4 : 1 ratio, Jacobson and coworkers[16] clearly identified the exclusively formed $SiC_5H_{13}{}^+$ ion in their FTMS study as the silylium ion **27**. This disparity was explained by the different reactant gas pressures used in the experiments[16]. The high

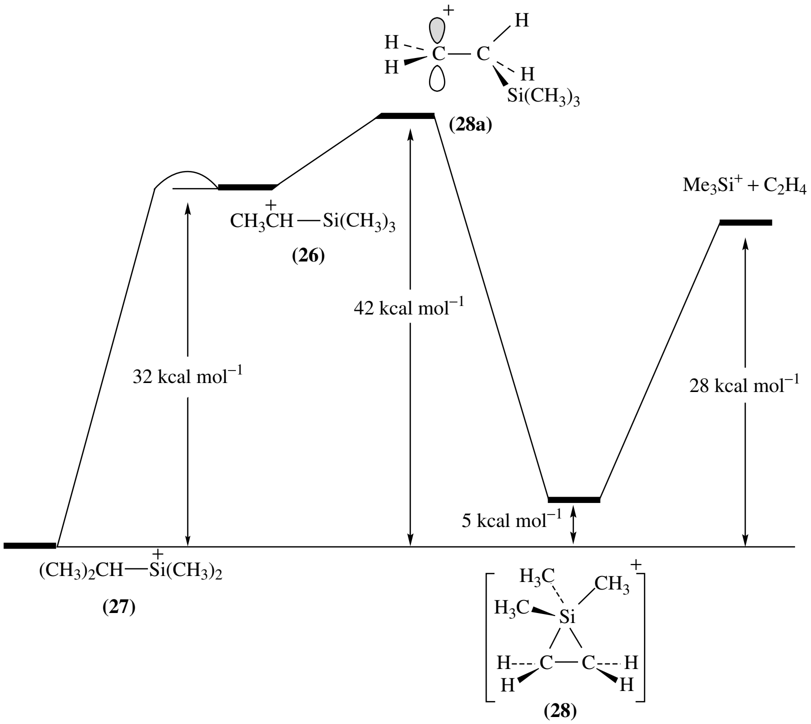

FIGURE 4. Schematic potential energy diagram of some $C_5H_3Si^+$ isomers and their dissociation products. The relative energies are given in parentheses and are based on HF/6-31G(d)//3-21G(d), corrected for substituent effects obtained from MP2/6-31G(d)//6-31G(d) calculations of the smaller $C_2H_7Si^+$ system

pressure used in the afterglow experiment allows the relaxation of the complex ion **28** prior to monomolecular dissociation into C_2H_4 and Me_3Si^+. This relaxation process is not favoured in the low pressure FTMS conditions[16].

In a FTMS study Jacobsen and coworkers[16] produced incipient α-silyl-substituted carbenium ions **32**–**34** by chloride elimination from the corresponding α-chloroalkylsilanes. They studied the rearrangement of **32**–**34** to silylium ions by direct 1,2-group migration (H, Me, Ph) from silicon to carbon (equations 5–7). The structures of the resulting silylium ions **35**–**38** were determined by specific ion/molecule reactions with methanol and isotopically labeled ethene. The product ratio **37**/**38** (resulting from nascent **34**) and the exclusive formation of **35** from **32** suggested the following relative migratory aptitude: phenyl > hydrogen >> methyl. However, several factors which may contribute to the observed migration distribution, like the relative thermodynamic stability of the products or the orientation of the migrating group in the neutral silane as the elimination of chloride occurs, could not be determined[16]. A theoretical study at the MP2/6-31+G(d)//HF/6-31G(d) level by Cho[17] revealed that all three α-silyl-substituted carbenium ions **32**–**34** are not minima on the potential energy surface but rearrange spontaneously to **35**–**38**. According to these calculations the experimentally observed migratory aptitude is determined by the activation energy for the simultaneous C−Cl bond heterolysis of the α-chlorosilanes and the concurrent 1,2-silyl migration[17].

$$\underset{\textbf{(32)}}{(H_3C)_2HSi{-}\overset{+}{C}H_2} \longrightarrow \underset{\textbf{(35)}}{(H_3C)_2\overset{+}{Si}{-}CH_3} \tag{5}$$

$$\underset{\textbf{(33)}}{(H_3C)_3Si{-}\overset{+}{C}H_2} \longrightarrow \underset{\textbf{(36)}}{(H_3C)_2\overset{+}{Si}{-}CH_2CH_3} \tag{6}$$

$$\underset{\textbf{(34)}}{(C_6H_5)(H_3C)HSi{-}\overset{+}{C}H_2} \longrightarrow \underset{\textbf{(37)}\ \ 6\%}{(C_6H_5)(H_3C)\overset{+}{Si}{-}CH_3} + \underset{\textbf{(38)}\ \ 94\%}{(H_3C)H\overset{+}{Si}{-}CH_2C_6H_5} \tag{7}$$

Gas phase basicities defined by the reaction of alkenes with acids (equation 8) can be used to determine the relative stabilities of the resulting carbenium ions. Tsuno and coworkers found in pulsed ICR gas phase protonation experiments of α-trimethylsilylstyrenes **39** that benzyl cation **40** is exclusively formed. The measured gas phase basicities for **39** are comparable to those of α-alkylstyrenes and they are significantly higher than for styrene[18].

$$Ar{-}CR{=}CR'_2 + BH^+ \longrightarrow Ar\overset{+}{C}R{-}CHR'_2 + B \tag{8}$$

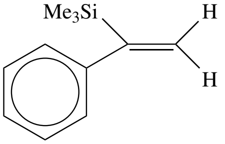

(39)

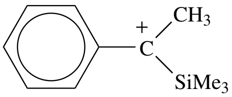

(40)

Using the isodesmic equations 9a–c Tsuno and coworkers calculated from the experimental gas phase basicities that the α-trimethylsilyl group stabilizes the styryl cation by 4.5 kcal mol^{-1} (equation 9a). Equations 9b and 9c which compare the effect of the α-trimethylsilyl group with those of the t-butyl- and the methyl substituent, respectively, are nearly thermoneutral, indicating the order Alkyl = SiMe$_3$ > H of styryl cation stabilization ability[18].

$$\begin{aligned} &PhC(SiMe_3){=}CH_2 + Ph\overset{+}{C}HMe \longrightarrow Ph\overset{+}{C}(SiMe_3)Me \\ &\qquad +PhCH{=}CH_2 \qquad\qquad \Delta G^\circ = -4.5 \end{aligned} \tag{9a}$$

$$\begin{aligned} &PhC(SiMe_3){=}CH_2 + Ph\overset{+}{C}(Me)Bu\text{-}t \longrightarrow Ph\overset{+}{C}(SiMe_3)Me \\ &\qquad +PhC(Bu\text{-}t){=}CH_2 \qquad\qquad \Delta G^\circ = -0.2 \end{aligned} \tag{9b}$$

$$\begin{aligned} &PhC(SiMe_3){=}CH_2 + Ph\overset{+}{C}Me_2 \longrightarrow Ph\overset{+}{C}(SiMe_3)Me \\ &\qquad +PhC(Me){=}CH_2 \qquad\qquad \Delta G^\circ = 0.7 \end{aligned} \tag{9c}$$

This seems to be in disagreement with theoretical calculations, which predict a smaller stabilization of carbenium ions by silyl groups compared with alkyl groups[1,5–7,9]. The calculations, however, utilize SiH$_3$ groups instead of trialkylsilyl groups. The lower electron-donating capacity of the silyl group might be the reason for this apparent theoretical–experimental disagreement.

While simple α-silyl-substituted trivalent carbenium ions could be detected in the gas phase only as nascent species and their existence as such is very unlikely, substituted α-silylvinyl cations could be produced in the gas phase and their thermodynamic stability could be measured. MS experiments by McGibbon, Brook and Terlouw showed that $Me_3Si{-}C^+{=}CH_2$ **41** formed by ionization of $Me_3SiCl{=}CH_2$ is stabilized by 29.5 kcal mol^{-1} compared with hydrogen[19]. This experimental finding is in agreement with recent calculations which found that $Me_3Si{-}C^+{=}CH_2$ is more stable than the parent (bridged) vinyl cation $HC(H)CH^+$ by 30.1 kcal mol^{-1} at MP2/6-311G(2d,p)//MP2(fu)/6-31G(d) (further corrections for higher order correlation effects and zero-point energy differences lead to an estimate of 33.3 kcal mol^{-1})[7]. On the other hand, according to the same experiments, $Me_3Si{-}C^+{=}CH_2$ is by only 2 kcal mol^{-1} more stable than $H_2C{=}C^+{-}CH_3$[19], while the calculations predict, using the hydride transfer reaction 10, a value of 11.7 kcal mol^{-1} at MP4SDTQ/6-31G(d)//MP2(fu)/6-31G(d)[7] (15.3 kcal mol^{-1} at HF/3-21G//3-21G[6]). This large experimental–theoretical discrepancy reflects in our view experimental errors rather than the inadequacy of the calculations.

$$H_2C{=}\overset{+}{C}{-}SiMe_3 + H_2C{=}CHMe \longrightarrow H_2C{=}\overset{+}{C}{-}Me + H_2C{=}CHSiMe_3 \qquad (10)$$

B. β-Substitution

Most of the gas phase studies concerning the β-silyl-substituted carbocations were directed towards a quantification of the β-silyl group effect and to assign a structure to the observed ions. We will first report the results of the experiments in which only the energy of these type of cations have been determined and we will then discuss the results of the structure elucidations.

The simplest β-trimethylsilyl-substituted carbenium ion was studied by Hajdasz and Squires[15]. They found that α-protonation of $Me_3SiHC{=}CH_2$ **42** yields exclusively the β-trimethylsilylethyl cation **43** which undergoes collision-induced dissociation by C_2H_4 loss and reacts with MeOH, C_6H_6 and other Lewis bases by exclusive ethylene displacement. The measured proton affinity (PA) of 199 kcal mol^{-1} ranks **42** among isobutene (PA 196), tetramethylethylene (PA 199) and styrene (PA 202 kcal mol^{-1}) with respect to base strength. Therefore, the total stabilization energy of **43** relative to the bridged ethyl cation is similar to that of tertiary and benzylic carbenium ions.

The authors computed from the measured PA, using the hydride transfer reaction 11, a relative stabilization energy of the β-Me_3Si group compared with hydrogen of 39 kcal mol^{-1}. This is in perfect agreement with the results of earlier *ab initio* calculations which predict a stabilization of 38 kcal mol^{-1} [MP3/6-31G(d)//3-21G(d)] for $H_3SiCH_2CH_2{}^+$, **44**, compared with the open ethyl cation[5]. Note, however, that at higher level **44** is not stable but closes to the bridged silylethyl cation **21**, which is more stable by 30.0 kcal mol^{-1} than the bridged ethyl cation[5,9,10].

$$Me_3SiCH_2CH_3 + H_2C(H)CH_2{}^+ \longrightarrow \underset{\textbf{(43)}}{Me_3SiCH_2{-}\overset{+}{C}H_2} + C_2H_6 \qquad (11)$$

Theory predicts that the stabilizing effect by a β-silicon group is slightly larger for the vinyl cation than for the ethyl cation. Thus, at MP2(fu)/6-31G(d)//MP2(fu)/6-31G(d) the bridged silylvinyl cation **22** is stabilized by 33.5 kcal mol^{-1} compared with the bridged vinyl cation[7]. Higher level calculations predict a stabilization of 33.1 kcal mol^{-1} for **22** compared with the bridged vinyl cation [QCISD(T)/6-31G(d)//MP2(fu)/6-31G(d)][7]. The stabilizing effect of a trimethylsilyl group is even larger, 51.3 kcal mol^{-1}

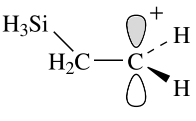

(44)

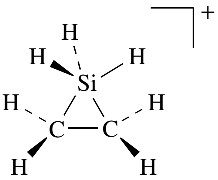

(21)

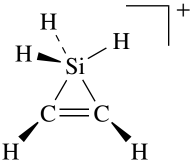

(22)

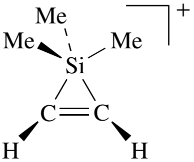

(45)

at MP4(SDTQ)/6-31G(d)//MP2(fu)/6-31G(d), as given by equation 12, for R = Me[7]. Corrections for the restricted basis set size and zero-point energy differences lead to a theoretical value of 49.6 kcal mol^{-1} [7], in agreement with the results of an experimental study by McGibbon, Brook and Terlouw[19] who calculated from their appearance energy measurements of $HC(SiMe_3)^+CH$ **45** formed by ionization of $Me_3Si(H)C{=}CHI$ **46** a value of 43.5 kcal mol^{-1}.

$$\underset{(\mathbf{22}\text{ or }\mathbf{45})}{H_2C{=}CH_2 + HC(SiR_3)^+CH} \longrightarrow HCH^+CH + H_2C{=}CHSiR_3 \tag{12}$$

Stone and coworkers determined the β-silicon effect in α-alkyl- and aryl-substituted carbenium ions[20] and vinyl cations[21] by measuring in a high-pressure mass spectrometer the thermodynamic data for the association of various alkenes and alkynes with trimethylsilylium ion. From their measured thermodynamic data they calculated, by using equations 13 and 14, the β-silyl stabilization energies listed in Table 1.

$$R^1R^2HC{-}\overset{+}{C}R^3R^4 + Me_3SiR^1R^2C{-}CHR^3R^4 \longrightarrow R^1R^2HC{-}CHR^3R^4 + Me_3SiR^1R^2C{-}\overset{+}{C}R^3R^4 \tag{13}$$

$$Me_3SiR^1C{=}CHR^2 + R^1HC{=}\overset{+}{C}R^2 \longrightarrow Me_3SiR^1C{=}\overset{+}{C}R^2 + R^1HC{=}CHR^2 \tag{14}$$

The measured stabilization energies are consistent with the theoretically predicted large hyperconjugative interaction between the Si−C σ-bond and the formally empty 2p(C) orbital. The results for the trivalent carbenium ions show a consistent decrease of 10 kcal mol^{-1} with each successive methyl group substitution on the carbenium carbon (Table 1, entries 1,4,6). Even the very stable *t*-butyl cation Me_3C^+ is stabilized by an additional 24 kcal mol^{-1} by a β-Me_3Si substituent (Table 1, entry 6). The stabilization of vinyl cations due to the presence of a β-Me_3Si group is found to be smaller than for

TABLE 1. Experimental stabilization energies (kcal mol^{-1}) of β-silyl-substituted carbocations $Me_3SiCHR^1R^2{-}\overset{+}{C}R^3R^4$ and $Me_3Si{-}CR^1{=}\overset{+}{C}R^2$ according to equations 13 and 14, respectively

Entry	Cation		β-Silyl-stabilization energy	Reference
Carbenium ions	(equation 13)			
	R^1, R^2	R^3, R^4		
1	H, H	H, H	44	20[a]
2	H, H	H, H	39	16
3	H, H	n-C_4H_9, H	26	21
4	H, H	CH_3, H	34	20[a]
5	CH_3, H	CH_3, H	34	20[a]
6	H, H	CH_3, CH_3	24	20[a]
7	CH_3, H	CH_3, CH_3	25	20[a]
8	CH_3, CH_3	CH_3, CH_3	22	20[a]
9	H, H	H, C_6H_5	17	20[a]
Vinyl cations	(equation 14)			
	R^1	R^2		
10	H	n-C_4H_9	11	21
11	CH_3	n-C_3H_7	12	21
12	H	C_6H_5	9	21
13	H	H	43.5	19

[a] Original value was corrected by −4 kcal mol^{-1}; for details see Reference 21.

similar carbenium ions (i.e. compare Table 1, entries 3 and 10 or 9 and 12). This seems to be in disagreement with the simple argument that hyperconjugative interactions between the C−Si bond and the formally empty 2p(C) orbital should be more efficient in vinyl cations than in carbenium ions due to the shorter C=C bond and the coplanar alignment of the interacting orbitals in the vinyl cations[22]. Very early calculations of Apeloig, Schleyer and Pople[23] have already suggested that vinyl cations are more sensitive to α-stabilizing effects than trivalent carbenium ions. This is corroborated by the gas phase protonation studies of several alkynes and alkenes by Stone and coworkers[20,21]. These studies show that the same α-alkyl or α-aryl substituent stabilizes a carbenium ion less than a vinyl cation[20]. The total stabilization afforded by both the α-alkyl or α-aryl substituent and a β-Me_3Si substituent appears to be approximately the same in both alkyl and vinyl cations and hence the β-silicon effect is considerably smaller for the vinyl cations. Unfortunately, the equilibrium constants for the association between acetylene and trimethylsilicenium ion could not be measured due to the low basicity of acetylene toward Me_3Si^+. However, Stone and coworkers extrapolated from their study of α-substituent effects on the alkyl cations a lower limit of 20 kcal mol^{-1} on the β-silicon effect for the unsubstituted vinyl cation[21]. This small extrapolated value is in contrast with the most recent high level computations and with the experimental study of Terlouw and coworkers[19] (Table 1, entry 13). Clearly, an additional experimental determination of the stabilization due to the β-silicon in $HC(SiMe_3)^+CH$ ion **(45)** is desirable.

The structure determination of the observed species is not straightforward since the only direct information from the gas phase MS studies are the m/z values of the species. Further structural details have to be obtained by indirect methods like deuterium labeling experiments and consecutive reactions of the investigated ions. High energy collision activation experiments by Ciommer and Schwarz[24] with ^{13}C- and CD_2-labelled $C_5H_{13}Si^+$ ions formed by dissociative ionization of $Me_3SiCH_2CH_2OPh$ show that the methylene groups in the ethene ligand become equivalent prior to or during collisional activation decomposition (CAD). This finding was originally advanced as proof for the bridged structure **28** of the $Me_3SiCH_2CH_2^+$ ion, but this finding was later interpreted as being consistent with either the open ion **47** or the bridged ion **28**[14]. The bimolecular reactions of the $Me_3SiCH_2CH_2^+$ ion with n- and π-Lewis bases are relatively rapid and result mainly or exclusively in ethene displacement. This behaviour is indicative of an ion structure with an intact but labile ethene ligand. Again, both the open **47** and silicon-bridged **28** structures are consistent with the observed reactivity.

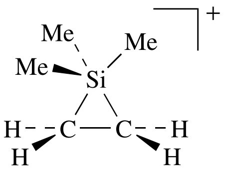

(28)

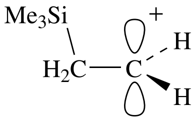

(47)

The gas phase reactions between the simplest silylium ion H_3Si^+ and ethene[25], acetylene[26] and benzene[27,28] and the fate of the formed adducts in the high pressure MS (HPMS) were studied by Mayer and Lampe[25]. By using tandem and high pressure mass spectrometry they found that H_3Si^+ adds to ethene yielding the persistent complex $SiC_2H_7^+$, which successively adds two more molecules of ethene yielding the ion $(C_2H_5)_3Si^+$. Based on the reactivity of the initially formed $SiC_2H_7^+$ adduct Mayer and Lampe concluded that it has an alkylsilylium ion $C_2H_5SiH_2^+$ **48** structure and that no silyl-substituted carbenium ion is formed[25]. This is in line with recent *ab initio* calculations by Hopkinson and coworkers[3] (Figure 5) which show that ethylsilylium ion **48** is more stable [at MP2/(fu)/6-31G(d,p)] than the bridged silylethyl cation **21** by 6 kcal mol^{-1}. According to these calculations ion **21** is stabilized by 43.2 kcal mol^{-1} compared with both separated fragments ethene and SiH_3^+. The activation barrier of 10.2 kcal mol^{-1} for the 1,2-H shift to **48** is small but significant. Thus, the calculations suggest that both ions are formed by the addition of H_3Si^+ to ethene with the silylium ion **48** being the more abundant species. In the absence of any efficient collisional deactivation **21** will rearrange to the more stable **48**. Formation of the hydrogen-bridged species **49** is very unlikely, considering the unfavourable thermochemistry.

Mayer and Lampe made no hypothesis concerning the structure of the adduct formed in their HPMS experiments with acetylene and H_3Si^+[26]. More definite answers are given by theory. The initially formed acetylene–H_3Si^+ complex, e.g. the silyl-bridged vinyl cation **22**, is a minimum at MP2(fu)/6-31G(d,p), but it undergoes a facile two-step isomerization to the more stable (by 22.4 kcal mol^{-1}) 1-silaallyl cation **50**. The overall barrier for this transformation, 17.2 kcal mol^{-1}, is smaller than the energy of its dissociation into H_3Si^+

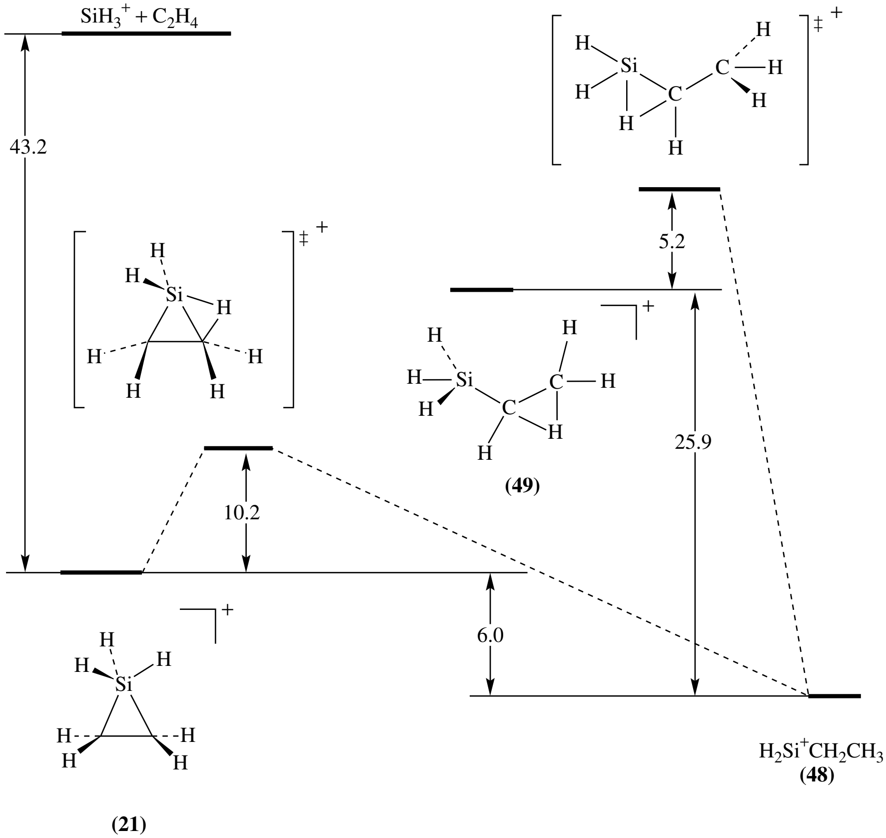

FIGURE 5. Part of the $SiC_2H_7^+$ potential energy surface (MP2/6-31G(d,p), relative energies in kcal mol^{-1})

and acetylene (Figure 6). It is therefore predicted that **22** which is initially formed by the addition of H_3Si^+ to acetylene, has enough excess energy (39.6 kcal mol^{-1}) to equilibrate with **50**, which is the most stable ion on the potential energy surface. This suggests that the species which is formed under high pressure MS conditions[26] is **50** and not the bridged vinyl cations **22** or **51**[4].

The addition of H_3Si^+ to benzene (equation 15) appears to follow a mechanism that is completely analogous to that proposed for the addition of carbenium ions to aromatics[26,27]. The energy-rich complex H_3Si^+/C_6H_6 can be collisionally stabilized and analysed in a tandem-MS. H_3Si^+/C_6H_6 eliminates hydrogen molecule, producing the phenylsilylium ion **52**. The predominant loss of HD from the initially formed complex of D_3Si^+ and benzene (70%) suggests that the formed ion has the structure of a β-silyl-substituted dienyl cation **53**[26,27].

Fornarini and colleagues gave also experimental evidence that in the reaction of trimethylsilicenium ion with arenes, σ-complexes such as **54** are produced[29–31]. The kinetic isotope effect of the gas phase deprotonation reaction and specific deuterium labeling

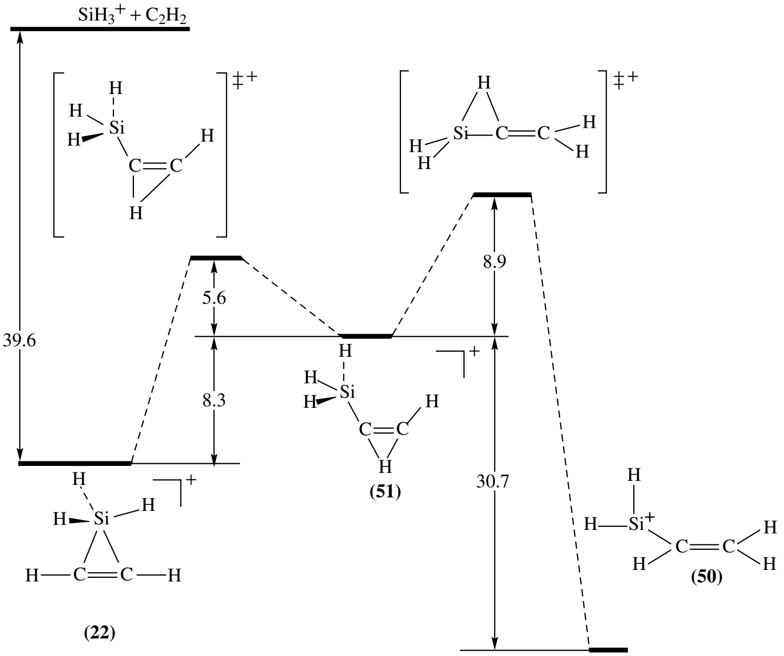

FIGURE 6. Part of the $SiC_2H_5^+$ potential energy surface (MP2/6-31G(d,p), relative energies in kcal mol^{-1})

experiments discard the possibility of a π-complex like **55**[32] and confirm the dienyl cation-type structure **54** of Me_3Si^+/C_6H_6.

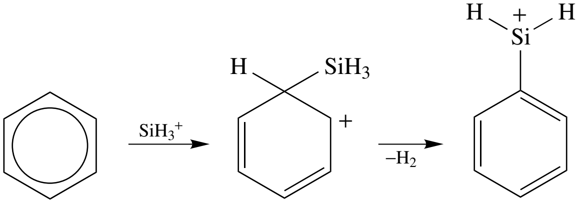

(53) **(52)**

(15)

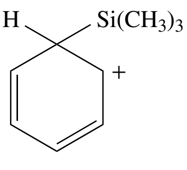

(54)

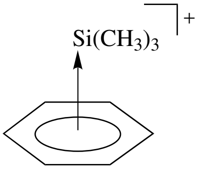

(55)

Tsuno and coworkers measured the gas phase affinity of substituted styrenes toward trimethylsilylium ions based on Me_3Si^+ transfer equilibria between different styrenes[33]. The substituent effect on the stability of the Me_3Si^+/styrene complex has been analysed by means of the LArSR equation and gave a ρ value of -5.76 and an r value of 0.41. These results imply that the long-lived Me_3Si^+/styrene ions have only little need for stabilization by additional π-donation from the aryl ring. Therefore, the classical open structure **56** for the Me_3Si^+/styrene complex was discarded in favour of a partially bridged structure **57**[33].

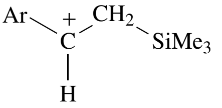

(56)

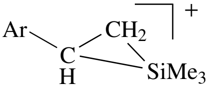

(57)

IV. SOLVOLYTIC STUDIES

In this section, solvolysis reactions are described which are thought to proceed via silyl-substituted carbocations. The reader should be aware of the fact that nearly all effects which are described here are of purely kinetic origin and therefore refer to energy differences between ground states and transition states. Hence they are not strictly applicable to the intermediate silyl-substituted carbocations, although the Hammond postulate suggests a close structural resemblance between the transition state for the ionization and the formed carbocation.

A. α-Silicon-substituted Carbocations in Solvolysis

The first report of a distinct effect of silicon on a neighbouring carbenium ion was published as early as 1946. Sommer, Whitmore and coworkers[34,35] reported that under conditions of basic hydrolysis, (1-chloroethyl)trichlorosilane **58** and (1-chloropropyl)trichlorosilane **59** failed to give cleavage of the α-C−Cl bond, while under the same conditions the analogous 2-chloroethyl **60** and 2-chloropropyl compounds **61** hydrolyse rapidly.

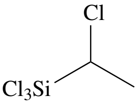

(58)

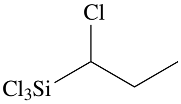

(59)

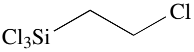

(60)

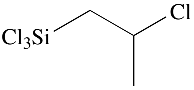

(61)

Since then the kinetic α-silicon effect has been measured in solvolysis of various systems that are considered to involve ionization in the rate-determining step. The results are compiled in Table 2, which also includes for comparison data for the α-silicon effect

TABLE 2. Kinetic α-silicon effects in solvolysis

Compound	10^5k (s^{-1})	Reference group R	k (compound)/ k (reference compound)	Reference
S_N1 solvolysis				
65				
X = Br	^{a}	*t*-Bu	2.6×10^{-5}	37
	^{b}	Me	3.3×10^{-4}	40
X = Cl	^{b}	Me	1.3×10^{-3}	40
X = OPBN	^{b}	Me	0.33	40
66				
X = OPBN	3.82^{c}	Me	0.46	39
		t-Bu	2.8×10^{-6}	39
		H	10^8	39
	72.70^{d}	Me	1.08	39, 40
X = Cl	^{a}	Me	70	40
73				
X = Br	0.0313^{e}	Me	6.06×10^{-5}	41
X = OTs	$2.06\ 10^3$	*t*-Bu	1.53	41
80				
X = Br	3.17^{f}	CMe_2	2.01×10^{-3}	41
88				
X = OTf	6.34^{g}	Me	118	45
		i-Pr	0.75	45
93				
X = OTf	0.0282^{g}	*t*-Bu	0.021	45
		H	61	45
99				
X = OTf	0.153^{g}	*t*-Bu	0.019	45
		H	31	45
Protonation				
83				
	$24{,}200^{h}$	*t*-Bu	0.018	42
		H	1.8	42
	^{i}	*t*-Bu	0.014	43
		H	15.1	43
S_N2 solvolysis				
62				
X = OTs	0.144^{j}	*t*-Bu	1830	8
X = OTf	$21{,}400^{j}$	*t*-Bu	957	8
X = OTs	2.249^{k}	*t*-Bu	0.96	8
X = OTf	18.3^{l}	*t*-Bu	0.42	8

[a] In 60% EtOH.
[b] In 97% TFE.
[c] In 80% acetone at 125.8 °C.
[d] In 97% TFE at 100.2 °C.
[e] In 97% TFE at 25 °C.
[f] In 60% acetone.
[g] In 50% EtOH at 25 °C.
[h] In 80% acetone at 25 °C.
[i] In H_2O at 25 °C.
[j] In 60% EtOH at 25.0 °C.
[k] In 97% TFE at 97 °C.
[l] In 97% TFE at 35 °C.

in S_N2-type substitution experiments. In most cases the α-silicon effect is evaluated by comparing the rate for an α-trimethylsilyl-substituted substrate with that for the silicon-free, the α-methyl or the α-t-butyl analogues.

The effect of α-silyl substitution on the stability of a carbenium ion was qualitatively unclear for a long time. Early solvolytic studies by the groups of Eaborn[36] and Cartledge[37] suggest a destabilizing effect of α-silyl substitution compared with alkyl. The measurement and interpretation of the kinetic α-silicon effect in solvolysis reactions is, however, often complicated by the fact that steric and ground state effects may play an important role and that, in addition, the rates of ionization often involve a contribution from nucleophilic solvent assistance.

For example, the experimental finding by Dostrovsky and Hughes[38] that compound **62**, X = Br solvolyses 2600 times more rapidly than the neopentyl analog **63**, X = Br in basic ethanol could be explained by a change of the reaction mechanism. In α-silicon-substituted systems S_N2 reactions are favoured. Stang, Apeloig, Schiavelli and their coworkers[8] found that **62**, X = OTf, OTs ethanolysed 957 and 1830 times faster, respectively, without rearrangement, than the analogous **63** which yield in a k_Δ mechanism (i.e. with neighbouring group participation) almost only rearranged products. The extremely low Grunwald–Winstein m values for **62** (0.34 and 0.23 for X = OTf and OTs, respectively) are also consistent with a bimolecular mechanism for the solvolysis of these silicon derivatives. Furthermore, in aqueous trifluoroethanol the relative solvolysis rates are reversed: $k(\mathbf{62})/k(\mathbf{63}) = 0.42$ and 0.96 for X = OTf and OTs, respectively. This serves as strong evidence for a bimolecular mechanism without the intermediacy of an ionic species. The theoretical calculations further corroborate the S_N2-type displacements in neopentyl-like silylmethyl sulphonates. According to the calculations, if an α-trimethylsilylcarbenium ion is formed in a k_C mechanism it should rearrange to the more stable silylium ion. Thus the transient formation of $Me_3SiCH_2^+$ **33** should yield substantial amounts of rearranged products as well. In addition, the calculations also indicate that a Me_3Si group lowers the barrier for S_N2 displacements relative to t-Bu by 20 kcal mol^{-1} (at 3-21G//3-21G). This dramatic effect is due to a better σ-electron-accepting ability of the trimethylsilyl group and the comparably long Si–C bonds which alleviates the steric effects that inhibit the S_N2 reaction in neopentyl systems[8].

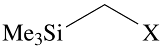

(62)

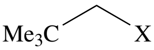

(63)

Another complication concerning the kinetic α-silicon effect arises from large ground-state effects in the α-silyl sulphonates or carboxylates used for the kinetic experiments. Cartledge and Jones[37] found that the bromide **64**, X = Br reacted 38000 times faster than bromide **65**, X = Br in 60% aqueous ethanol at 25 °C, in agreement with a strong destabilizing effect of the α-silyl substituent. In contrast, Apeloig and Stanger[39] found comparable reaction rates for Me_3Si and methyl substitution in the k_C solvolysis of tertiary adamantyl systems **66**, X = OPNB and **67**, X = OPNB, i.e. $k(\alpha\text{-Me}/k(\alpha\text{-Me}_3\text{Si}) = 2.18$ in 80% aqueous acetone and 0.97 in 97% TFE. This very small solvent effect strongly supports a rate-limiting k_C solvolysis for both compounds. The secondary **68**, X = OPNB solvolyses 10^8 times slower than either tertiary system. The authors argued that the nearly identical solvolysis rates of **66** and **67**, X = OPNB are not due to the similar stabilities of the corresponding carbenium ions but rather reflect that the α-silylcarboxylates are electronically destabilized relative to the corresponding α-alkylcarboxylates. Their calculations corroborate the interpretation of the solvolysis experiments. Thus the α-silylmethanol **69** (which serves as a model for the carboxylate) is destabilized by a geminal interaction between the oxygen and the silyl group relative to the corresponding alkyl alcohols by 6–8 kcal mol^{-1} [at MP2/6-31G(d)//3-21G(d)]. By combining these ground-state energy differences with the similar solvolysis rates of **66** and **67**, X = OPNB the authors concluded that in solution an α-Me_3Si substituent destabilizes the 2-adamantyl cation **70** by 6–8 kcal mol^{-1} but that it is by 12.4 kcal mol^{-1} more stabilizing than hydrogen[39].

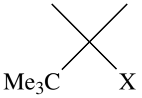

(64)

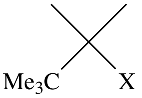

(65)

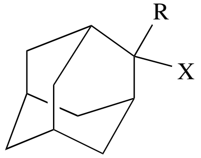

(66) R = $SiMe_3$
(67) R = Me
(68) R = H

H_3SiCH_2OH

(69)

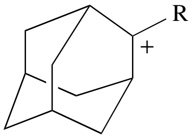

(70)

Further *ab initio* calculations at the MP2/3-21G(d)//3-21G(d) level by the group of Apeloig[40] indicate that the destabilizing geminal interactions between the α-silyl substituent and the leaving group become less important for halogens as the leaving groups. Thus, while the destabilization of **71** compared with **72** due to geminal interactions is 7.8 kcal mol^{-1} for X = formate or 5.6 kcal mol^{-1} for X = sulphonate, it decreases to 4.4 kcal mol^{-1} for X = Cl and becomes very small for X = Br or I (1.9 and 1.0 kcal mol^{-1}, respectively). These theoretical predictions were supported by accompanying solvolysis experiments, which show that the relative rate ratio $k(\mathbf{64})/k(\mathbf{65})$ increases from 3 for X = OPNB to 792 for X = Cl and to 3010 for X = Br[40].

A similar dependence of k(α-Alkyl)/k(α-$SiMe_3$) on the leaving group was observed in the solvolysis of benzylic substrates. Thus, Shimizu and coworkers[41] found that the $k(\mathbf{74})/k(\mathbf{73})$ ratio in 97% TFE (25 °C) is 0.66 for X = OTs but the $k(\mathbf{75})/k(\mathbf{73})$ ratio is 16400 for X = Br. The authors argued that the steric repulsion between the *t*-butyl group and the *ortho* hydrogens in the nearly planar incipient benzyl cation **76** is larger than the steric effect in **76**. This actually slows the solvolysis rate of **74**, resulting in a nearly identical solvolysis rate to that of **73**. These destabilizing steric interactions are absent in **78**, thus leading to a faster solvolysis[41]. However, the arguments given by Apeloig and coworkers[39,40] suggest that ground state effects should also be taken into account in explaining the observed solvolysis rates of the benzyl tosylates studied by Shimizu and coworkers[41].

H_3SiCH_2X

(71)

$MeCH_2X$

(72)

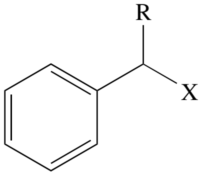

(73) R = $SiMe_3$
(74) R = *t*-Bu
(75) R = Me

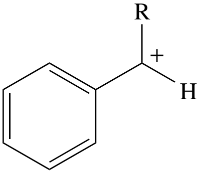

(76) R = $SiMe_3$
(77) R = *t*-Bu
(78) R = Me

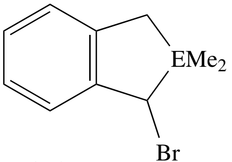

(79) E = C
(80) E = Si

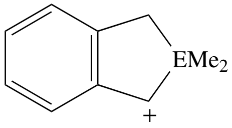

(81) E = C
(82) E = Si

In order to minimize the complications due to steric effects Shimizu and coworkers[41] investigated also the solvolysis reactions of 1-indanyl bromides **79** and **80**. **79** solvolyses via a cationic intermediate **81**. The characteristics of the solvolysis of **80** in aqueous acetone ($m = 0.93$, no skeletal rearrangement during the solvolysis) are consistent with a k_C mechanism involving the rate-determining formation of the 2-silaindanyl cation **82**. **80** solvolysed 498 times slower than the carbon analogue **79**, i.e., approximately 30-fold slower than the relative solvolysis rate ratio $k(\mathbf{75})/k(\mathbf{73})$ of 16,400 for the open benzylic system. This comparison suggests that the electronic α-silyl effect in benzyl cations leads to a rate retardation of approximately 500-fold, while steric repulsion between the *ortho* hydrogen and the trimethylsilyl group is responsible for another factor of 30. These experiments suggest that in solution an α-silyl group is *ca* 4 kcal mol^{-1} less effective than an alkyl substituent in stabilizing benzyl cation **78**. The smaller destabilizing effect on **78** compared with that in RC^+Me_2 probably reflects the reduced electronic demand of the carbenium ion centre in the former cation[41].

The small α-silyl effect found by Soderquist and Hassner[42] and by Kresge and Tobin[43] in the protonation of methoxyvinyl ethers **83–85** [$k(\alpha\text{-H}) : k(\alpha\text{-SiMe}_3) : k(\alpha\text{-}t\text{-Bu}) = 1 : 1.8 : 100$ in aqueous acetone at 33 °C[42] and 1 : 15 : 1025 in H_2O at 25 °C][43] (equation 16) might also be explained by the inherent stability of the formed α-methoxy-stabilized carbocations **86a–c**. Destabilization due to geminal interaction between the $SiMe_3$ and the MeO group in the α-silyl-substituted vinyl ether **83** (R = $SiMe_3$) might, however, also contribute to the apparently small α-silyl effect. The relative rate ratio **83** : **87** of 30 : 1 is consistent with smaller stabilization of the α-methoxy-α-triphenylethyl cation by the less electropositive $SiPh_3$ group[42].

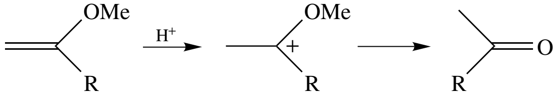

(16)

(83) R = $SiMe_3$
(84) R = H
(85) R = *t*-Bu

(86a) R = $SiMe_3$
(86b) R = H
(86c) R = *t*-Bu

Theory predicts that β-hyperconjugation across the double bond of vinyl cations is more effective than in carbenium ions. In addition, due to the higher electronegativity of the positively charged sp-carbon atom, vinyl cations are more sensitive to σ-hyperconjugative effects than trivalent carbenium ions[22,23,44]. Consequently, it is predicted that α-silyl substitution will stabilize a vinyl cation to the same extent as does a methyl group[44]. Solvolysis studies by Schiavelli, Stang and coworkers[45] revealed that the α-silyl triflate, **88**, which forms an intermediate vinyl cation in the rate-determining step, reacts 118 times faster than its methyl-substituted analogue **89**, but it solvolyses slightly slower than the α-isopropylalkenyl triflate **90** [k(**88**)/k(**90**) $= 0.75$]. Ground-state and steric effects complicate the interpretation of these experiments[6]. The α-silyl-substituted enol $H_2C{=}C(SiH_3)OH$ (**91**), which is a model for the solvolytically investigated vinyl triflates, is calculated to be destabilivzed by 3.8 kcal mol^{-1} (at HF/3-21G//3-21G) relative to $H_2C{=}C(CH_3)OH$ (**92**) due to unfavourable α-geminal interactions in **92**. According to these calculations α-silylvinyl triflates are predicted to solvolyse faster than α-alkylvinyl triflates, although the corresponding carbenium ions have nearly the same energy[6]. Therefore, the solvolysis studies by Stang, Schiavelli and coworkers[45] support the calculational results. The deactivating influence of the α-trimethylsilyl substituent in **88** compared with the α-isopropyl group in **90** might result from acceleration of the solvolysis of the α-isopropyl derivative by steric effects. In combination with the calculations[6] it became evident from the solvolysis experiments[45] that α-silyl substitution stabilizes a vinyl cation relative to hydrogen and that it is as effective as an alkyl group.

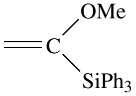

(87)

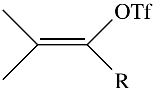

(88) R = SiMe$_3$
(89) R = Me
(90) R = i-Pr

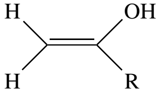

(91) R = SiH$_3$
(92) R = Me

Ethanolysis of the α-ethynyl-substituted vinyl triflates **93–95** proceeds via the intermediacy of the cumulenic dicoordinated cations **96–98** (equation 17) and suggests the following stability order for the carbocations: **98** > **96** > **97**[45]. The same relative reactivity order was found for the triflates **99–101**[45].

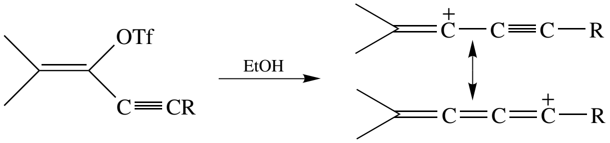

(17)

(93) R = SiMe$_3$
(94) R = H
(95) R = t-Bu

(96) R = SiMe$_3$
(97) R = H
(98) R = t-Bu

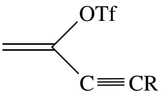

(99) R = SiMe$_3$
(100) R = H
(101) R = t-Bu

Dallaire and Brook[46] studied the protiodemetallation reaction of the bis(silyl) alkynes **102**, E = R_3Si to give **104** shown in equation 18. They found small differences in the relative rates for R_3E = $SiMe_2Bu$-*t*, $SiMe_3$ and $SiPh_3$ [*k*(**102**, $SiMe_2Bu$-*t*) : *k*(**102**, $SiMe_3$) : *k*(**102**, $SiPh_3$) = 1.2 : 1 : 0.04]. Assuming that the β-stabilization by the trimethylsilyl group in the intermediate vinyl cation **103** is constant for the three different α-silyl groups, these relative rates provide an estimate of the inductive effects, showing the $SiPh_3$ group to be destabilizing compared with trialkylsilyl groups[46].

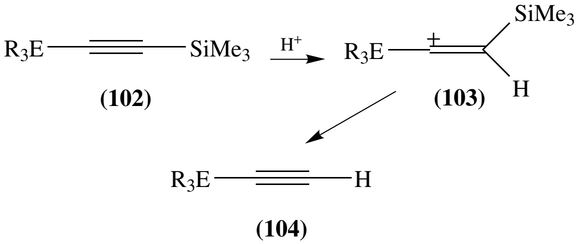

(18)

B. β-Silicon-substituted Carbocations in Solvolysis

The dramatic β-effect of silicon in reactions which involve carbocations was noted already in 1937 by Ushakov and Itenberg[47]. During the ensuing sixty years mechanistic, theoretical and synthetic studies have established the β-silicon effect as one of the largest neighbouring group effects which is exceeded only by those of the silicon congeners germanium and tin.

In solvolysis reactions, a silicon at the β-position greatly facilitates the heterolysis of a C−X bond, often affording exclusively elimination products (equation 19). Thus, already Sommer, Whitmore and coworkers[34,35] described a greatly enhanced reactivity of **60** and **61** in their basic hydrolysis in comparison with the corresponding α- and γ-substituted systems.

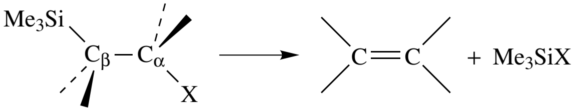

(19)

It is now commonly accepted that in polar solvents the elimination to the alkene **107** takes place by an E1-like mechanism involving a cationic intermediate[48]. The major issue still in need of clarification is the structure of the intermediate β-silicon carbocation which will be close to the structure of the transition state of the solvolysis reaction. An open carbocation **105** in which the silicon interacts purely by hyperconjugation without significant movement in the transition state (vertical stabilization)[49−52] is as possible as a three-membered siliconium ion **106** formed by neighbouring group participation (non-vertical stabilization). The terms vertical and non-vertical stabilization are referred to here for historical reasons only. They should no longer be used to describe hyperconjugative stabilization which implies no or little reorganization of the atoms, and hypercoordination with bridging, respectively. High level quantum chemical *ab initio* calculations reveal that all electronic stabilization is accompanied by geometrical distortions of the molecule. The stabilization and reorganization of the molecular framework depend on the electronic demand of the positively charged centre[53]. The mechanism via **105** involves a simple rate-determining ionization (k_C mechanism, equation 20), while the latter route via **106** involves a rate-determining nucleophilic attack of the β-silicon substituent at C_α during generation of the incipient carbenium ion (k_Δ mechanism, equation 20).

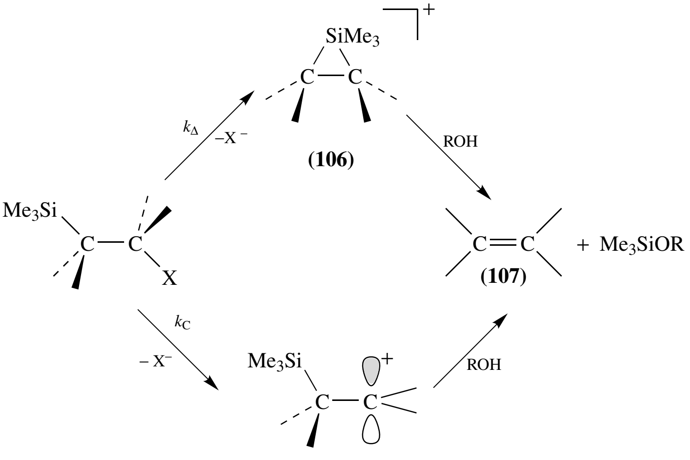

(20)

Both mechanisms are equally compatible with the high E1 character found by Sommer and Baughman for the solvolysis of the primary chloride **108**[54]. The negative Hammett ρ values, found by Vencl and coworkers[55] and Fujiyama and Munechika[56] for the ethanolysis of the primary aryldimethylsilylethyl chloride **109** (-1.2 and -2.3 in 92% EtOH and 80% EtOH, respectively) which indicates a significant build-up of positive charge at the silicon atom in the transition state of the solvolysis, also do not allow one to distinguish between both mechanisms.

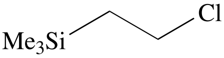

(108)

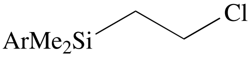

(109)

The stereochemistry of the elimination of Me_3SiX from β-trimethylsilyl-substituted precursors has been studied by Jarvie and coworkers[57]. They found that solvolysis of *erythro*-$Me_3SiCHBrCHBrMe$ **110** lead predominately to *cis*-1-brompropene **111** (equation 21).

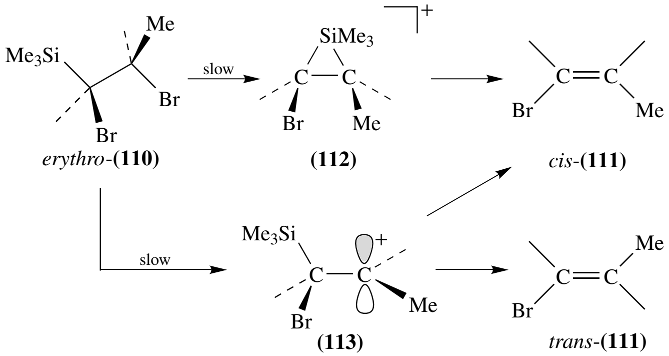

(21)

The solvent effects found for this reaction excluded an E2 mechanism in favour of an E1 reaction with a rate-determining cleavage of the C−Br bond. Thus, the elimination of bromine from **110** must proceed from an antiperiplanar conformation. Independent hydrolysis experiments by Hudrlik and Peterson[58] gave further support for this mode of the silicodehalogenation. They found that *threo*-**114** gave >90% *cis*-4-octene **115** (equation 22), as expected for an antiperiplanar stereochemistry for the elimination. The stereochemical outcome of the reaction of **110** can be explained most conveniently by the intermediacy of silicon-bridged species **112**. Increasing amounts of *trans*-1-brompropene (*trans*-**111**) were, however, detected in solvent mixtures with increasing ionization power parameter Y[0.3% of *trans*-**111** in pure ethanol ($Y = -2.033$) and 15% in 100% formic acid ($Y = 2.05$)]. This behaviour might be explained by an equilibrium between the bridged **112** and the open ion **113** (equation 21)[57]. However, Lambert[48] argues that a high barrier for the rotation around the C−C bond in **113** resulting from strong β-Si$^-$ hyperconjugation could enforce the antiperiplanar mode for the elimination from **113**. His arguments are supported by the significant rotation barrier of 22 kcal mol^{-1} calculated for ion **116** [at MP2/6-31G(d)//6-31G(d)] in the gas phase[9].

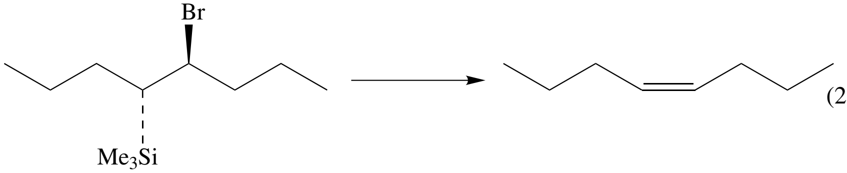

(114) **(115)**

(22)

Jarvie and coworkers[59] studied the secondary deuterium isotope effects on the solvolysis rates of bromides **117**, **118** and **119** and concluded from the value of the k_H/k_D of 1.10 for **117** that a C−Br bond cleavage was rate-determining, 'possibly assisted by the β-silicon'[59]. Their arguments were supported by the very small secondary isotope effects found for **118** and **119** ($k_H/k_D = 1.02$ and 0.995, respectively). Interestingly, they found that the reaction of **120** with PBr_3 gave equal amounts of **121** and **122** (equation 23), i.e. the CD_2 and CH_2 groups became equivalent during the reaction. A similar result was obtained by Eaborn and coworkers[60]. Similarly to the non-classical ion debate[61], this can be explained either by the intermediacy of a bridged ion **123** or by a fast equilibrium between two open cation structures **124** and **125** (equation 24) as suggested by Lambert[48]. Eaborn and coworkers favoured the cyclic siliconium ion, based on the fact that **126** solvolyses faster than predicted from its σ_p^+ constant [$\sigma_p^+(Me_3SiCH_2) = -0.54$][60].

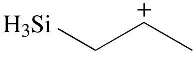

(116)

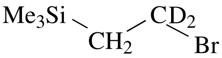

(117)

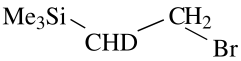

(118)

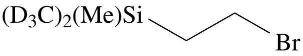

(119)

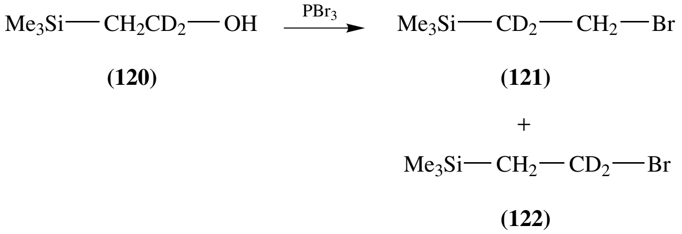

$$\mathrm{Me_3Si{-}CH_2CD_2{-}OH} \xrightarrow{\mathrm{PBr_3}} \mathrm{Me_3Si{-}CD_2{-}CH_2{-}Br} + \mathrm{Me_3Si{-}CH_2{-}CD_2{-}Br} \qquad (23)$$

(120) **(121)** **(122)**

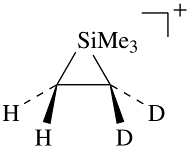

(123)

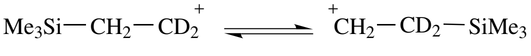

$$\mathrm{Me_3Si{-}CH_2{-}}\overset{+}{\mathrm{CD_2}} \rightleftharpoons \overset{+}{\mathrm{C}}\mathrm{H_2{-}CD_2{-}SiMe_3} \qquad (24)$$

(124) **(125)**

Experiments by Davis and Jacocks[62] shed a new light on the problem. They found for the deoxysilylation reaction of substituted β-hydroxyalkylsilanes **127**–**130** a relative rate ratio of k(**127**) : k(**128**) : k(**129**) : k(**130**) $= 1 : 10^{3.3} : 10^{5.92} : 10^{6.77}$. The substituent effect on the rate was analysed by considering the sum of the σ^+ values of the substituents on the alcohol carbon ($\sum \sigma^+$). From the linear free energy relationship for this reaction ($\log k_{rel} = \rho^+ \sum \sigma^+$) a ρ^+ value of -11 is obtained. The second CH_2SiMe_3 group in **129** leads to a rate acceleration of $10^{5.92}$ compared with **127**, resulting in $\sigma^+ = -0.54$ for the second CH_2SiMe_3 group, identical with that of the first group in **127**. This suggests an additivity of the substituent effects on the relative rates[62] which is inconsistent with an anchimeric effect of the β-trimethylsilyl group on the solvolysis reaction, since only one silyl group can engage in a neighbouring group participation in the transition state of the solvolysis of **129**[62].

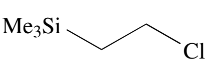

(126)

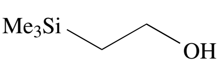

(127)

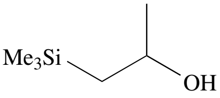

(128)

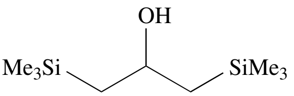

(129)

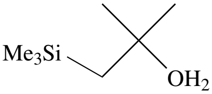

(130)

A good tool to distinguish between the neighbouring group assisted route (k_Δ) with a silicenium ion-like intermediate, and the formation of an open β-silyl carbocation which is only stabilized by hyperconjugation without significant geometrical changes, is the conformational dependence of the rate acceleration by the β-silicon in the solvolysis reactions.

It is well established that hyperconjugation exhibits a cosine-squared dependency on the dihedral angle Θ between the interacting orbitals [for an open cation like **105**, the 2p(C) and the σ(C−Si)][63]. A siliconium ion structure like **106** can only be formed by a backside attack on the carbon attached to the leaving group in an antiperiplanar conformation. Thus, both mechanisms should display a maximum acceleration when Θ is 180°, i.e. at the antiperiplanar arrangement. Smaller angles between the leaving group X and the β-Si−C bond will severely hamper the formation of the three-membered ring and will slow down the solvolysis rate in a k_Δ mechanism. In contrast, for the k_C mechanism, there will be a substantial rate acceleration for all angles Θ, except for $\Theta = 90^\circ$ at which the interacting orbitals are orthogonal and no hyperconjugative stabilization of the transition state can occur. A pure inductive β-silicon effect should show no angular dependency. The qualitative relationship between all three modes of stabilization is shown in Figure 7[64].

The experiments by Jarvie and coworkers[59] have established the antiperiplanar mode for the rate-determining ionization. The rate enhancement by the β-trimethylsilyl group compared with a non-substituted reference [$k(\beta\text{-SiMe}_3)/k(\beta\text{-H})$] was typically about 10^6–10^7 for acyclic substrates. The elimination of the leaving group can, however, also occur from a less favoured conformation and will show a lower rate enhancement. In a series of papers Lambert and coworkers[64–68] examined cyclic systems **131**–**139** with well defined dihedral angles (except **131** and **133**) between the leaving group and the β-trimethylsilyl group and measured the kinetic enhancement of their solvolysis by the latter. The solvolytic results are summarized in Table 3. Solvent effect studies revealed that all the silicon-containing substrates solvolysed by a k_C mechanism

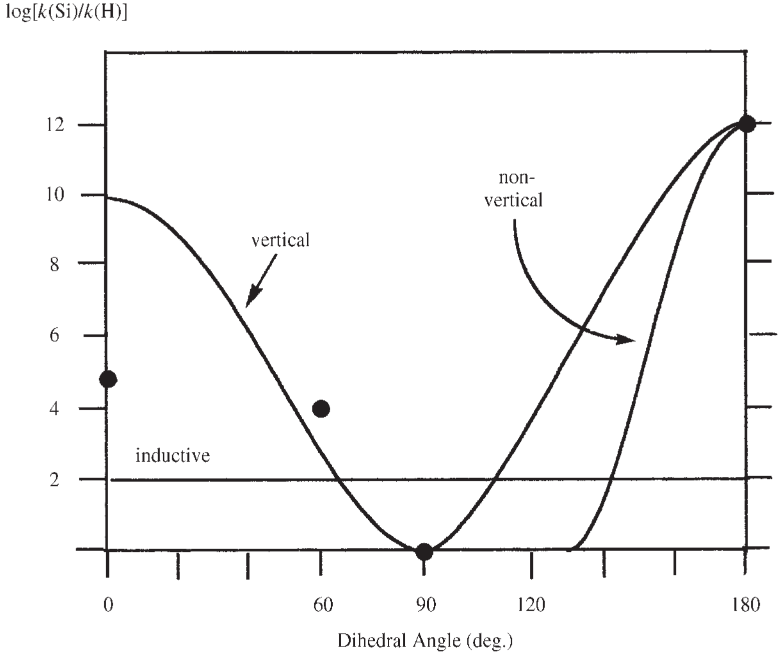

FIGURE 7. Qualitative dihedral dependences for the inductive, vertical and nonvertical modes of the kinetic β-silicon effect. Reprinted with permission from Reference 64. Copyright (1990) American Chemical Society. Experimental data[64,66,67] are indicated with solid dots

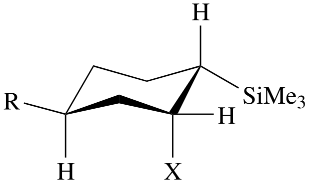

(131) R = H
(132) R = *t*-Bu

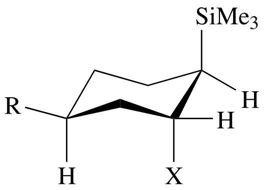

(133) R = H
(134) R = *t*-Bu

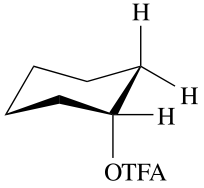

(135)

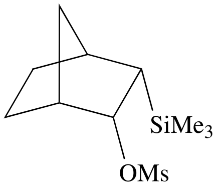

(136)

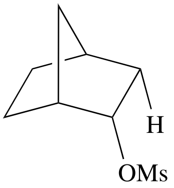

(137)

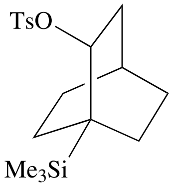

(138)

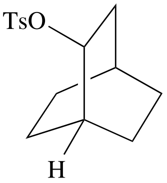

(139)

TABLE 3. Kinetic *β*-silicon effects in solvolysis

Compound	$k(\mathrm{s}^{-1})$	Reference group R	k(compound)/ k(reference compound)	Reference
(131) X = OTFA	2.36×10^{-5a}	H	3.3×10^{4b}	65
(132) X = OTFA	2.84×10^{-5a}	H	4.0×10^{4b}	66
(133) X = OTFA	4.0^{a}	H	5.7×10^{9b}	66
(134) X = OTFA	1.72×10^{3a}	H	2.4×10^{12b}	66
(134) X = ODNB	7.1×10^{-3a}	H	1.0×10^{7b}	66
(136) X = OMs	0.335^{a}	H	9.4×10^{4}	64
(138) X = OTs	1.64×10^{-3c}	H	1.3^{b}	67
(141) X = OTFA	3.68^{d}	*t*-Bu	2.99×10^{5}	72
		H	1.05×10^{5}	72
(150) X = OTs	6.7×10^{2}	Me	9.9×10^{10b}	73
(179) X = OTFA	1.4×10^{5}	H	27	82

[a] In 97% TFE at 25 °C.
[b] The reference solvolyses by a k_S mechanism.
[c] In 97% TFE at 35 °C.
[d] In 30% dioxane at 25 °C.

involving a silyl-substituted carbocation as an intermediate, whereas most of the reference compounds solvolysed by a k_S mechanism[65–67]. Thus, the introduction of even an entirely perpendicular trimethylsilyl group in **138** brings about a change in the mechanism from k_S to k_C[67]. While the solvolytic results of the cyclohexyl trifluoroacetates **131** and **133**, X = OTFA were inconclusive due to the not well defined stereochemical relation between the leaving group and the silyl group[65], the results for the stereochemically biased systems **132** and **134** are highly interesting[66]. **134** (X = OTFA), in which the leaving group and the trimethylsilyl group are in antiperiplanar orientation, reacts in 97% TFE 10^{12} more rapidly than the reference compound cyclohexyl−OTFA **135**[66]. This rate acceleration is equivalent to a relative stabilization of the transition state by the β-silicon compared with β-hydrogen of 16.5 kcal mol^{-1}. Even **131** (X = OTFA)[65] and **132** (X = OTFA)[66] in both of which a *syn*-clinal arrangement (Θ = 60°) exists between the leaving group and the trimethylsilyl group solvolysed about 4×10^4 times faster than **135** in TFA at 25 °C. Similar results were obtained in five-membered ring systems[68,69]. The β-silicon effect in a *syn*-periplanar geometry, studied in the *endo*-norbornane system **136**, is of the same magnitude[64]. The relative rate for the solvolysis of the mesylates in 97% TFE, k [**136** (OMs)]: k [**137** (OMs)], is $9.4 \times 10^4 : 1$. Provided that ground state effects are negligible, this suggest a free energy difference between the transition states of 6.8 kcal mol^{-1}. A dihedral angle of $\Theta = 0°$ was modeled in the 1-trimethylsilyl[2.2.2]bicyclooctane-2-tosylate **138** (X = OTs)[67]. The very low relative rate ratio k (**138**, X = OTs): k(**139**, X = OTs) = 1.34 : 1 ($\Delta\Delta G^{\ddagger}$ = 0.2 kcal mol^{-1}) was ascribed to the absence of any β-silicon effect, especially an inductive stabilization of the incipient carbocation by the β-silyl group[67]. This interpretation is hampered by the fact that the reference molecule **139** solvolyses by a k_S mechanism under the applied reaction conditions. The measured rate ratio is therefore only a lower estimate of the β-silicon effect on the transition state stabilization for a k_C solvolysis. *Ab initio* calculations by Ibrahim and Jorgensen[9], however, do support the experimental finding by Lambert and Liu[67]. According to their MP2/6-31G(d)//6-31G(d) calculations the perpendicular conformation in the β-silyl carbocation **12** is not stabilized compared with the isopropyl cation $(CH_3)_2CH^+$ **140**[9].

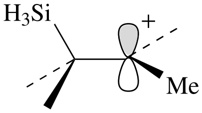

(12)

The experimental dependency of the β-silyl effect on Θ in solvolysis reactions is sketched in Figure 7[64]. Obviously, it differs from that anticipated for a k_Δ mechanism with rate-determining formation of siliconium ion or from the cosine-squared function expected for the pure hyperconjugative stabilization model. Apparently, the β-silyl effect is operative in the solvolysis of both the *syn*- and *anti*-periplanar conformations. The rate acceleration in the latter might be ascribed to a more favourable geometry for the σ-anchimeric assistance.

The α-secondary deuterium isotope effect in the solvolysis of **134** ($k_H/k_D = 1.17$) is similar to these for model reactions proceeding via an open carbocation-like transition state with hyperconjugative stabilization ($k_H/k_D = 1.2$)[70]. The isotope effect is, however, markedly different from effects observed for model reactions proceeding via internal oxygen participation (where ($k_H/k_D < 1.08$)[71]. Thus, although strong hyperconjugative β-silyl stabilization is involved in the solvolysis reaction, the measured kinetic isotope effect was thought to exclude a rate-determining formation of a bridged silicenium ion-like transition state.

On the other hand, calculations have shown that hyperconjugative interaction of the β-Si$-$C σ-bond with an empty 2p(C) orbital does have pronounced structural consequences[9]. Thus, in the secondary cation **12** the silyl group is bent towards the positively charged carbon. A *syn* leaving group might prevent the molecule from adopting the optimal geometry for maximum β-silyl stabilization already in the transition state, leading to the observed lower reactivity of **136** compared with **134**[64]. From these arguments it is obvious that a clear distinction between hyperconjugative and bridging stabilization modes is not made easily, since there is always a subtle interplay between the electron demand of the carbocation and the magnitude of the β-silyl effect.

The question arises whether a k_C process can be distinguished kinetically from the k_Δ mechanism for the ionization of β-silicon-containing molecules. Mechanistic studies by Shimizu, Tsuno and coworkers showed that for some systems it is possible to distinguish between the two mechanisms[72,73]. The benzyl trifluoroacetate **141**, X = OTFA solvolyses more rapidly than both the silicon-free substrate **142** and the β-*t*-butyl analogue **143**, X = TFA in 30% dioxane at 25 °C by factors of 1.05×10^5 and 2.99×10^5, respectively, revealing a marked β-silyl effect even in a benzylic system[72]. These $k(\mathbf{141})/k(\mathbf{142})$ and $k(\mathbf{141})/k(\mathbf{143})$ rate ratios amount to β-silyl stabilization energies of 6.9 and 7.5 kcal mol^{-1}, respectively, relative to β-hydrogen or β-*t*-butyl in the solvolysis leading to the cationic benzylic intermediate. The relative small stabilization due to β-silyl-substitution compared with the cyclohexyl system **134** reflects the reduced electronic demand of the α-methylbenzyl cation **144** relative to the secondary cyclohexyl cation **145**[72]. The solvolysis rates of **141** in dioxane–water mixtures are as sensitive to the solvent ionizing power as those for the 1-tolylethyl trifluoroacetate **146**, a reference standard undergoing k_C solvolysis. The solvolysis of **141** and **146** exhibits almost identical secondary α-deuterium isotope effects ($k_H/k_D = 1.18$–1.19 and 1.178, respectively), in line with a change from sp^3 to sp^2 hybridization at the benzylic carbon atom in the transition state. Substituent effects on the solvolysis of **141** in 90% dioxane indicate that the resonance interaction of the aryl ring with a positive charge at the benzylic position is as effective as in an α-methylbenzyl cation. Thus, all these mechanistic criteria of solvent effects, kinetic isotope effects and substituent effects support a simple k_C mechanism

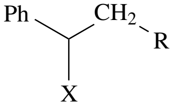

(141) R = SiMe$_3$
(142) R = H
(143) R = *t*-Bu

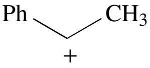

(144)

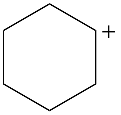

(145)

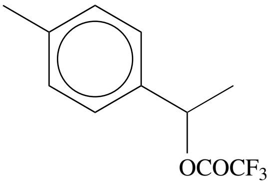

(146)

via the open *β*-silyl-substituted carbocation **147** and are inconsistent with a k_{Δ} mechanism involving a cyclic siliconium ion **148**[72]. It is noteworthy that Tsuno and coworkers did not find in the gas phase any effective *π*-delocalization of the positive charge into the aryl *π*-system for a series of 2-trimethylsilyl 1-arylethyl cations having different aryl substituents[33]. This indicates that the thermodynamic stabilities of 2-trimethylsilyl 1-arylethyl cations are only very little influenced by the *π*-donor ability of the aryl ring. Hence, they concluded that the ground state structure of these cations is not the open structure **147** but a partially bridged structure **149**. The obvious disagreement between gas phase studies[33] and the solvolytic experiments[72] was rationalized by suggesting that in the rate-determining transition state for the bond cleavage step in the solvolysis experiment, no neighbouring group assistance by the *β*-trimethylsilyl group is operative and that **147** is formed. However, after the bond cleavage takes place a partially bridged ion **149** is formed without any significant barrier [33].

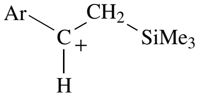

(147)

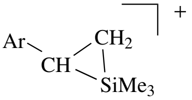

(148)

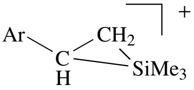

(149)

In contrast, **150** is 2.7×10^4-fold less reactive than **141**, X = OTFA, corresponding to an energy difference of 6.1 kcal mol^{-1} between the transition states provided that the ground state energies are similar . The ethanolysis of **150** gives 1,2-silyl rearranged products in addition to styrene. The substituent effects for the reaction of **150** are remarkably small (i.e. the $k_{p\text{-MeO}}/k_{\text{H}}$ rate ratio is 2.11, compared with 269 for **141**). These facts are more consistent with the formation of a bridged siliconium ion **151** than of an open *β*-silyl cation **152**[73].

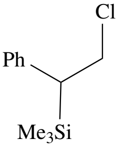

(150)

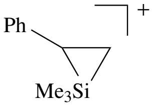

(151)

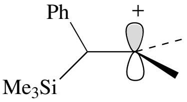

(152)

Competition experiments by Mayr and Pock[74] showed that allylsilane **153** is at −78 °C 30700 times more reactive towards diarylcarbenium ions than propene **154**. Thus, in the

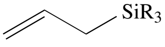

(153) R = Me
(157) R = Ph
(161) R = Et
(162) R = *i*-Pr
(163) R = *n*-Bu
(164) R = *n*-Hex

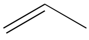

(154)

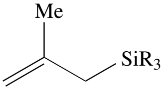

(158) R = Me
(159) R = Ph
(160) R = Cl

transition state for the addition of an electrophile to an allylsilane a β-silicon provides only a stabilization of 4.2 kcal mol^{-1}[74]. In subsequent studies Mayr and Hagen[75,76] examined the influence of the substituent on silicon on the rate of the electrophilic addition of p-anisylphenylcarbenium ion **155** to allysilanes to give ion **156** (equation 25) and their results are summarized in Table 4.

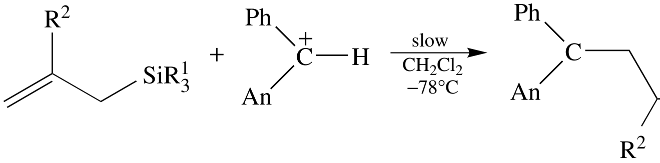

(25)

(155) **(156)**

An = p-MeOC$_6$H$_4$, R^2 = H, Me

They found a correlation between Taft inductive constants σ_I for the substituents on silicon and the reactivity of the allylsilane towards **155**[76]. Inductively electron-withdrawing substituents at silicon greatly reduce the reaction rates, i.e. $k(\mathbf{158}) : k(\mathbf{159}) : k(\mathbf{160}) = 1 : 0.11 : 1.8 \times 10^{-7}$ at −78 °C in CH$_2$Cl$_2$[76]. Thus, the trichlorosilyl substituent is actually slightly deactivating for the addition of the carbocation to the C=C double bond compared with hydrogen. [$k(\mathbf{160})$: k(isobutene) = 355 : 1)][76]. Replacement of the methyl by larger (branched or unbranched) alkyl groups leads to a slight increase in the reactivity [$k(\mathbf{153}) : k(\mathbf{164}) = 1 : 2.75$, see Table 4]. The stability of the formed carbocation also influences the extent of the kinetic β-silicon effect in this reaction. Thus, while **153**

TABLE 4. Relative rate constants for the reaction of substituted allyl element compounds R$_3{}^1$ECH$_2$C(R^2)=CH$_2$ with bisarylcarbenium ions in CH$_2$Cl$_2$[74–76] at −70 °C.

Compound	E	R^1	k_{rel}
157 [a]	Si	Ph	0.017
153 [a]	Si	Me	1.0
161 [a]	Si	Et	1.59
162 [a]	Si	i-Pr	2.23
163 [a]	Si	n-Bu	2.57
164 [a]	Si	n-Hex	2.75
170 [a]	Ge	Ph	0.096
171 [a]	Sn	Ph	27.7
160 [b]	Si	Cl	1.8×10^{-7}
158 [b]	Si	Me	1
159 [b]	Si	Ph	0.113
168 [b]	Ge	Ph	0.283
169 [b]	Sn	Ph	4.91

[a] Addition of p-anisylphenylcarbenium ion; reference: propene $k = 5.0 \times 10^{-6}$.
[b] Addition of bis(p-anisyl)carbenium ion; reference: isobutene $k = 6.4 \times 10^{-5}$

reacts 2×10^5 times faster with **155** than propene, yielding the secondary carbocation **156** (R^2=H) (equation 26) the reaction of **165** with dianisylcarbenium ion **166** yielding the tertiary carbocation **167** (equation 27) is only 15600 times faster than the addition of **155** to isobutene[76,77].

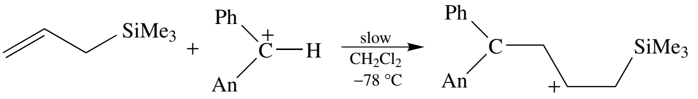

(26)

(153) **(155)** **(156** R^2 = H)

An = p-C_6H_4OMe

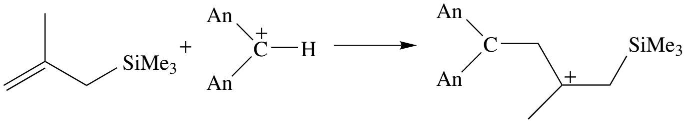

(27)

(165) **(166)** **(167)**

The kinetic β-silyl effect for the reactions shown in equations 25 and 26 is smaller than the kinetic effect of β-germanium and β-tin substituents. The relative rate ratio for the addition of **166** is k(**159**) : k(**168**) : k(**169**) = 1 : 2.5 : 43. The reactivity differences are, however, larger in the propene series, reflecting the higher electron demand in the transition state of the addition in the secondary system [k(**157**) : k(**170**) : k(**171**) = 1 : 5.6 : 1614].

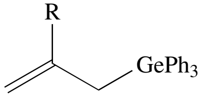

(168) R = Me
(170) R = H

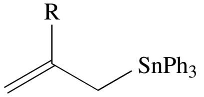

(169) R = Me
(171) R = H

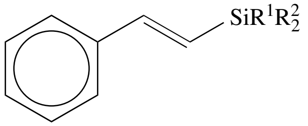

(172)

A similar dependence of the kinetic β-silicon effect on the electronegativity of the substituents at silicon was found by Brook, Hadi and Neuy[78,79] They analysed the degree of *syn* addition of bromine to a series of (E)-β-silylstyrenes **(172)** as a measure of the stabilizing ability of the silyl group (equation 28). While they recovered from the reaction of **172**, $R^1 = R^2$ = Me with bromine exclusively the *trans*-β-bromostyrene **173**, suggesting a *syn*-addition of the bromine to the C=C double bond, the yield of *trans*-**173** is reduced to only 17% for **172**, $R^1 = R^2 = F$[78]. Furthermore, the same authors found a linear correlation between the group electronegativity of the silyl substituent and the percentage of *syn* addition[79]. This was interpreted as an indication of a reduced β-silyl effect on the intermediate carbocation **174** for electronegative substituents at the silicon.

Kresge and Tobin[80] investigated the β-silicon effect on the hydrolysis of vinyl ethers (equation 29) and found a rate acceleration on the hydrolysis of **175** compared with **176**, and hence a stabilizing effect of the β-silyl group on the intermediate α-ethoxy carbocation **177** compared with **178**. The acceleration is small: the rate factor k(**175**) : k(**176**) of 129 is equivalent to a free energy of activation difference $\Delta\Delta G^{\ddagger}$ of 2.9 kcal mol^{-1}, whereas the solvolytic studies for the generation of a cyclohexyl cation **145** gave $\Delta\Delta G^{\ddagger} = 16.5\ \mathrm{kcal\,mol^{-1}}$[76].

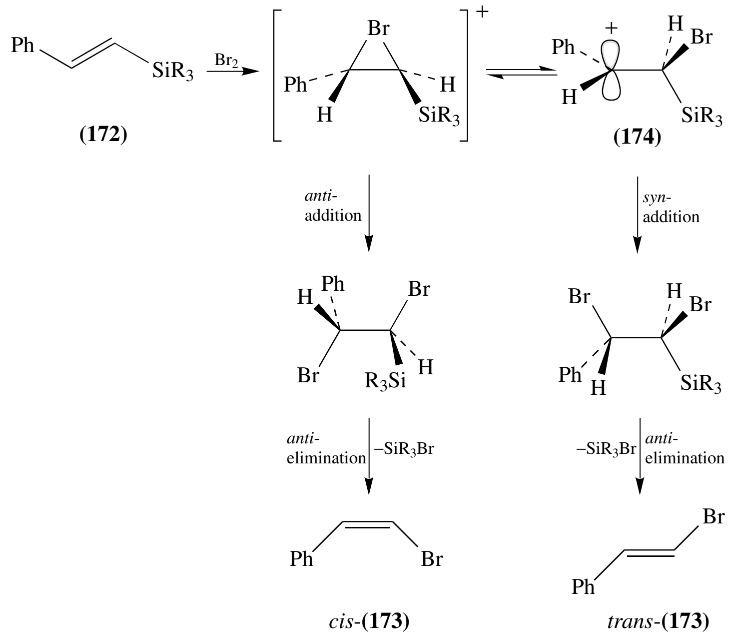

(28)

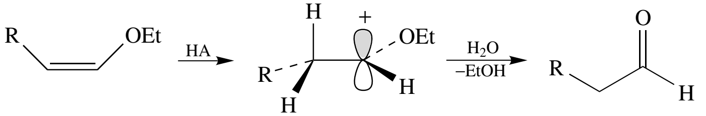

(29)

(175) R = $SiMe_3$ **(177)** R = $SiMe_3$

(176) R = H **(178)** R = H

This difference was originally attributed solely to a transition state conformation in the vinyl ether hydrolysis reaction that is unfavourable for hyperconjugative stabilization[80]. The authors argued that the protonation reaction starts at a dihedral angle $\Theta = 90°$ between the β-Si−C bond and the developing empty $2p(C_\alpha)$ orbital that, even in a product-like very late transition state **TS-175** would never decrease to less than $\Theta = 60°$. The cosine-squared dependence of the hyperconjugation interaction would therefore explain the low observed reaction rate[80]. Another important factor which attenuates the β-silyl effect in **177** is the inherent stability of the ethoxy-stabilized carbocation **178**. The interaction with lone pair at the oxygen will lower the energy of the formally empty $2p(C^+)$ orbital in **177** and **178**. Thus, the hyperconjugative interaction with the β-Si−C bond is smaller in **177** than in secondary cyclohexyl cations, which is shown by the smaller additional β-silyl stabilization for **177**. In a subsequent paper Gabelica and Kresge also agreed on the contribution of this effect to an observed small acceleration in the hydrolysis of **175**[81].

The small β-silicon effect found by DeLucca and Paquette[82] in the solvolysis of the cyclopropylmethyl trifluoroacetate **179** (equation 30) might be a result of the inherent stability of the cationic intermediate **180** and its delocalized structure. The 27-fold rate acceleration of **179** compared with cyclopropylmethyl trifluoroacetate is equivalent to a β-silyl stabilization of only 2.2 kcal mol^{-1}.

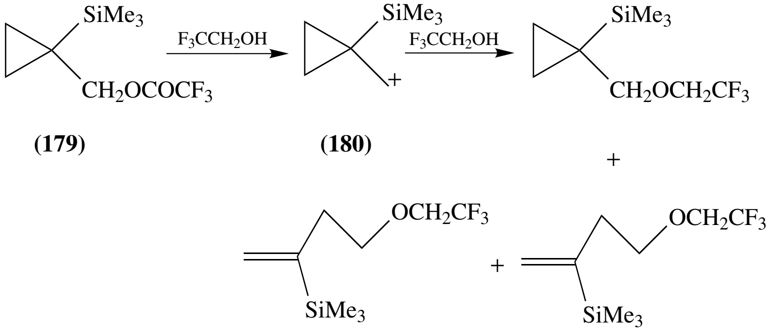

(179) **(180)**

(30)

Kresge and coworkers[81,83] studied also the β-silyl effect on the rate of protonation of simple alkynes and alkenes. They found for the protonation of phenyl(trimethylsilyl)acetylene **181** in aqueous perchloric acid a rate acceleration compared with **182** of only a factor of 300[83]. They attributed this to a ‘surprisingly weak stabilization of a carbocation by a trimethylsilyl group’[83]. They explained this apparently small rate acceleration (which is equivalent to $\Delta\Delta G^{\ddagger} = 3.4$ kcal mol^{-1}) by assuming a transition state geometry for the protonation of **181**, which is not optimal for silyl stabilization of the developing positive charge. In contrast to the transition state (**TS-175**) of the protonation of the vinyl ether **175**, the dihedral angle Θ in the transition state (**TS-181a**) for the protonation of phenyltrimethylsilylacetylene already has the optimum value of $\Theta = 0°$, due to the linear geometry of the alkyne and the incipient vinyl cation. The authors argued, however, that the Me$_3$Si$-$C=C$^+$ bond angle α begins with an initial value of 180° which will finally reach 120° in the fully formed vinyl cation, but will remain considerably greater than that in the early stages of the protonation of **175**. During the course of the protonation of the alkyne the β-trimethylsilyl group is bent far away, as shown in **TS-181b** (side view), from the developing empty 2p(C$^+$) orbital, leading to a sizable reduction of hyperconjugation interaction between the 2p(C$^+$) orbital and the β-Si$-$C bond.

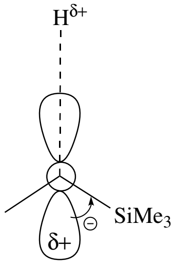

(TS-175)

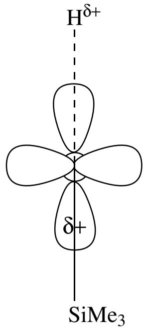

(TS-181a)

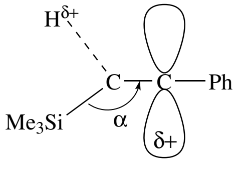

(TS-181b)

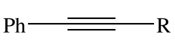
(181) R = $SiMe_3$
(182) R = H

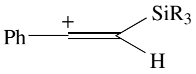
(183) R = Me
(184) R = H

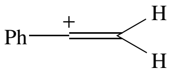
(185)

However, it must be taken into account that the α-phenylvinyl cation **185** is already highly stabilized by the phenyl substituent, leading consequently to a smaller β-silicon effect in the vinyl cation **183**. *Ab initio* calculations by Buzek predicted for **184** an additional stabilization of 10 kcal mol^{-1} by the silyl group[7]. The thermodynamic stabilization of **183** compared with **185**, experimentally determined by Stone and coworkers in the gas phase, is 9 kcal mol^{-1}[21]. Thus, the kinetically determined stabilization of the transition state is only about 6 kcal mol^{-1} smaller than the β-silyl effect for stabilization of the ground state carbocation.

Similar comparisons between the thermodynamic β-silyl stabilization measured in the gas phase[20,21] and the kinetic β-silicon effect[81,83] found in protonation experiments in solution are possible for the acetylenes **186** and **188** and for the alkene **190**. The data for both solution study and gas phase equilibrium measurements are summarized in Table 5.

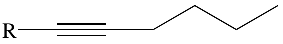
(186) R = $SiMe_3$
(187) R = H

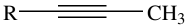
(188) R = $SiMe_3$
(189) R = H

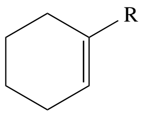
(190) R = $SiMe_3$
(191) R = H

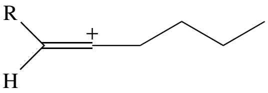
(192) R = $SiMe_3$
(193) R = H

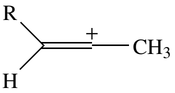
(194) R = $SiMe_3$
(195) R = H

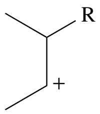
(196) R = $SiMe_3$
(197) R = H

TABLE 5. Comparison between the kinetic β-silyl effect ($\Delta\Delta G^{\ddagger}$) derived from protonation experiments and thermodynamic β-silyl stabilization (ΔH°) of small carbocations[20,21,81,83]

System	$\Delta\Delta G^{\ddagger}$	ΔH°
181/182	3.5	
183/185		9
186/187	6.5	
188/189	6.5	
192/193		11
190/191	5.7	
196/197		34

In solution the alkynes **186–189** undergo a rate-determining carbon protonation to yield the corresponding vinyl cations **192–195**, as is evident from the measured deuterium isotope effects and the linear Cox–Yates plots[81,83]. The rate accelerations due to the β-silyl substitution of 56,800 and 54,300 measured for **186** and **188**, respectively, reflect stabilization of the transition states for the protonation by $\Delta\Delta G^{\ddagger} = 6.5\ \text{kcal mol}^{-1}$ for both compounds. These effects are considerably greater than those found for protonation of **181**, indicating that the β-silyl effect in **183** is attenuated by the strongly electron-donating phenyl substituent. They are, however, significantly smaller than the $\Delta H^{\circ} = 11\ \text{kcal mol}^{-1}$ found for **192** in the gas phase, and Gabelica and Kresge[81] attributed the difference between the small $\Delta\Delta G^{\ddagger}$ found in their protonation experiments and the nearly three times larger effect for the kinetic β-effect found for the fixed antiperiplanar stereochemistry in **134** to an unfavourable geometry in the transition state for the protonation, and used arguments similar to those discussed for the protonation of **181**. The question, however, arises as to whether solvent or ground state effects might play an important role in the solution phase protonation.

The large difference between the $\Delta\Delta G^{\ddagger} = 5.7\ \text{kcal mol}^{-1}$ found for the cyclohexene system **190/191**[81] and the $\Delta H^{\circ} = 34\ \text{kcal mol}^{-1}$ for the similar ions **196/197**[20] point to drastic differences in the mode of stabilization of the transition state for the protonation in solution and the free silyl-substituted carbocation in the gas phase.

Dallaire and Brook[46] studied the protiodemetallation of silyl-, germyl- and stannyl-alkynes **198–200** in order to compare the β-effect of these groups on vinyl cations. The first step of the protiodemetallation (equation 31), i.e. the protonation of the triple bond, was found to be rate-determining for all alkynes. The relative kinetic β-effect arising from the second-order rate constants for EMe_3, $Me_3Sn : Me_3Ge : Me_3Si$ ($1.5 \times 10^8 : 525 : 1$), follows the order found for tricoordinated carbenium ions.

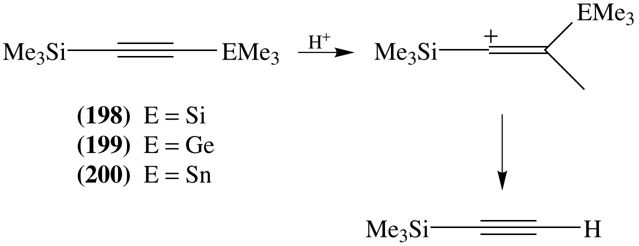

(198) E = Si
(199) E = Ge
(200) E = Sn

(31)

The first solvolytic generation of an aryl cation by Sonoda and coworkers[84] following theoretical predictions by Apeloig and Arad[11] highlights the exceptional stabilization of a carbocation by a β-silyl substituent. Apeloig and Arad pointed out that a 2,6-disilylphenyl cation **201** is calculated to be stabilized compared with the unsubstituted phenyl cation **202** by 25 kcal mol^{-1} (at 3-21G). Thus, it is as stable as the 2-propenyl cation **195**, which is one of the least stable vinyl cations produced in solvolysis reaction. The solvolytic generation of 2,6-bis(trimethylsilyl)-substituted aryl cation **203** should thus be amenable[11]. This theoretical prediction was verified by Sonoda and coworkers[84] who showed that triflate **204** gives at 100 °C in trifluoroethanol, **205**, quantitatively the trifluoroethyl ether **206**. The reactions followed first-order kinetics and isotopic labeling experiments proved an aryl–oxygen cleavage of **204** during the solvolysis. The kinetic data and the observed low selectivity toward external nucleophiles support a S_N1 mechanism for the solvolysis of **204** proceeding via the aryl cation **203** (equation 32)[84].

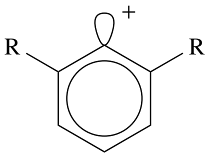

(201) R = SiH_3
(202) R = H
(203) R = $SiMe_3$

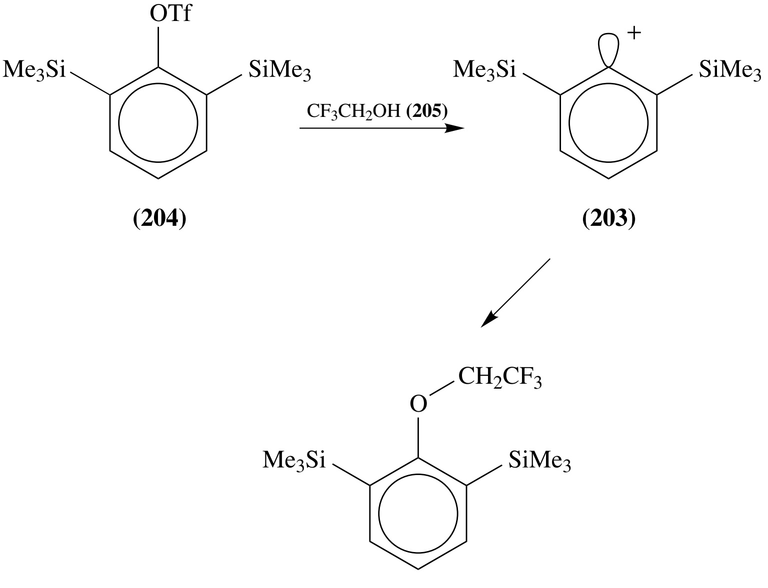

(204) **(203)** **(206)**

(32)

Thermodynamic stabilization of carbocations can be accurately determined by calculating the free energies of bond homolysis and bond heterolysis from experimentally measured ionization constants $pK_{(R^+)}$ and standard potentials $E_{NHE}(R^-/R^\bullet)$ and $E_{NHE}(R^\bullet/R^+)$ in a thermodynamic cycle. Bausch and Gong used such a thermochemical cycle to determine in solution the free energies of C−H bond heterolysis in 9-substituted fluorenes[85]. Their data (Table 6) show that the C−H bond is destabilized by an α-methyl group (in **208**) by 8 kcal mol^{-1} compared with the unsubstituted fluorene **207**. An α-trimethylsilyl group (in **210**) weakens the C−H bond by only 2 kcal mol^{-1}. The same small effect on the free energy for the C−H bond was found for the α-*t*-butylfluorene **209**. These very small α-effects might be due to destabilization of the fluorenyl cations by steric interactions between the bulky α-substituents and the 1- and 8-*peri* hydrogens of the fluorene ring.

The β-trimethylsilyl group in **212** weakens the C−H bond by 16 kcal mol^{-1} compared with the C−H bond in fluorene **207**. Comparing the data for the tertiary C−H bonds from Table 6, the β-H-substituted fluorenyl cation (from **208**) is less stable by 8 kcal mol^{-1}, and

TABLE 6. Free energy data (in kcal mol^{-1}) for the C−H bond heterolysis of fluorenes[85]

Compound	ΔG°(R−H)
207	105
208	97
209	103
210	103
211	95
212	89

the β-*t*-butyl-substituted carbocation (from **211**) is less stable by 6 kcal mol^{-1}, compared with the β-trimethylsilyl-substituted carbocation (from **212**). The thermochemical solution data for the β-silyl effect are therefore in qualitative agreement with theoretical predictions and data from kinetic experiments[85].

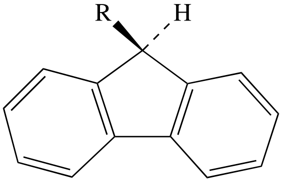

(207) R = H
(208) R = Me
(209) R = *t*-Bu
(210) R = $SiMe_3$

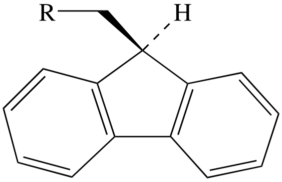

(211) R = *t*-Bu
(212) R = $SiMe_3$

1. α-Disilanyl carbocations in solvolysis

The intriguing combination of an α-silyl and a β-silyl substituent in the disilanyl group ($-SiR_2SiR_3$) prompted Shimizu, Tsuno and coworkers to study the effect of a β-Si−Si bond on the stability of carbocations[86]. They studied the solvolysis of the benzylic bromides **213**–**215** and found that the β-$SiMe_3$ substituent in **213** increases the solvolysis rate by a factor of 1.07×10^5 compared with the *t*-butyl-substituted reference compound **214** (Table 7).

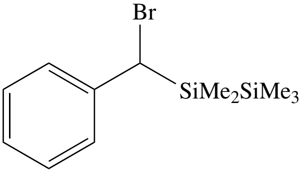

(213)

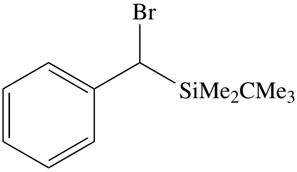

(214)

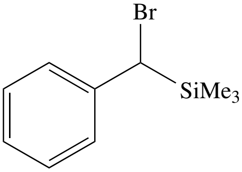

(215)

TABLE 7. Kinetic effect of the disilanyl group in solvolysis

Compound	$k(\mathrm{s}^{-1})^a$	Reference group R	k(compound)/k(R)	Reference
213	6.2×10^{-2}	$-\mathrm{SiMe_2Bu}$-t^b	1.07×10^5	86
		$-\mathrm{SiMe_3}^b$	1.98×10^5	86
		$-\mathrm{Me}^b$	1.20×10^1	86
220	3.86×10^{-4}	$-\mathrm{SiMe_2CH_2}$	0.209	86

[a] In 97% TFE at 25 °C.
[b] R replacing $\mathrm{Me_3SiMe_2Si}$.
[c] R replacing the $\mathrm{SiMe_2SiMe_2}$.

Unlike the β-alkyl substituted bromides **214** and **215** which give substitution products without skeletal rearrangements, the solvolysis of the disilanyl compound **213** in various solvents gives exclusively 1,2-trimethylsilyl rearranged products irrespective of the solvent nucleophilicity (equation 33). The Grunwald–Winstein solvent effects for the solvolysis of **213** ($m = 0.91-0.98$) suggest a k_C mechanism with a rate-determining formation of a carbocation. The measured α-deuterium effect (1.16–1.17) and the substituent effects ($\rho = -3.71$, $\sigma = 1.16$) are consistent with the formation of an open sp^2-hybridized benzylic carbocation **216** which undergoes a fast 1,2-trimethylsilyl shift, yielding the rearranged product **217** after capture by the solvent. The experimental findings rule out a k_Δ mechanism via the siliconium ion **218**[86].

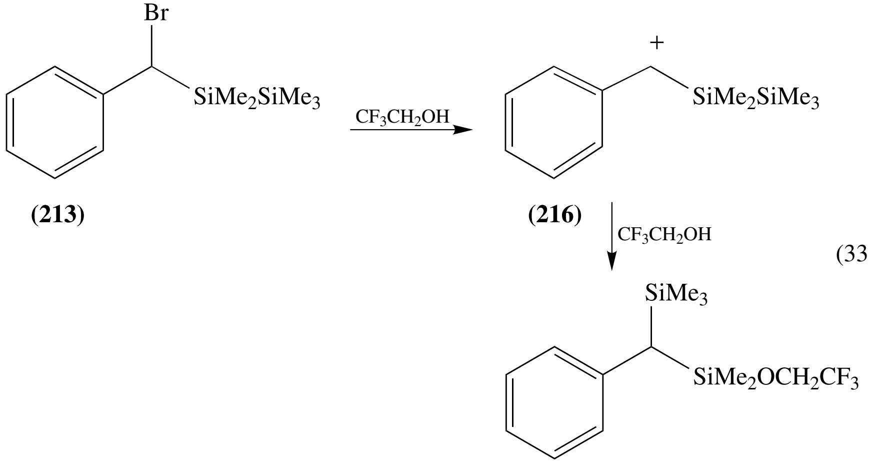

(213) **(216)** **(217)**

(33)

From the relative solvolysis rates of **213** and **215**, Shimizu and coworkers calculated a stabilization by 7 kcal mol^{-1} of the benzyl cation by the β-Si–Si bond compared with a β-C–Si bond. Due to the antagonistic effects of the α- and the β-silyl groups, the net effect of the disilanyl group is relatively small[86]. Thus, **213** is only 12 times as reactive as α-methylbenzyl bromide **219**, X = Br (Table 7; in 30% acetone the relative rate is decreased to 0.66). This might be compared with the rate acceleration of 1.05×10^5 by the CH_2SiMe_3 group found for the solvolysis of **141** (X = OTf) relative to **142** (X = OTf) (see Table 3). Calculation, however, reveals no stabilizing effect of an α-disilanyl group on the positive charge in carbocations. These theoretical results are supported by solvolysis experiments. 2-Disilanyl-substituted 2-adamantyl sulphonates solvolyse with the same rate as the corresponding 2-trimethylsilyl-2-adamantyl derivatives **66**[87].

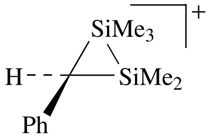

(218)

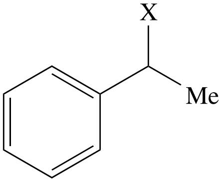

(219)

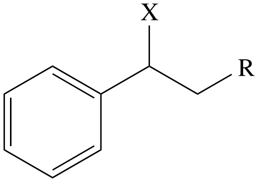

(141) R = $SiMe_3$
(142) R = H

Similar to the β-Si effect of a σ(C−Si) bond, the stabilizing effect of a $\beta-\sigma$(Si−Si) bond is not operative in an orthogonal arrangement with the 2p(C^+) orbital. Thus, the indanyl compound **220** solvolyses via the carbocation intermediate **221** without skeletal rearrangement yielding **222** (equation 34), but **220** is slightly less reactive than its β-alkyl analogue **223** [k(**220**)/k(**223**) = 0.209]. This rate retardation compared with the large accelerating effect found for **213** provides experimental evidence that the β-silicon effect of a $\beta-\sigma$(Si−Si) bond in benzylic cations is exclusively hyperconjugative in origin and contributions of inductive effects are insignificant[86].

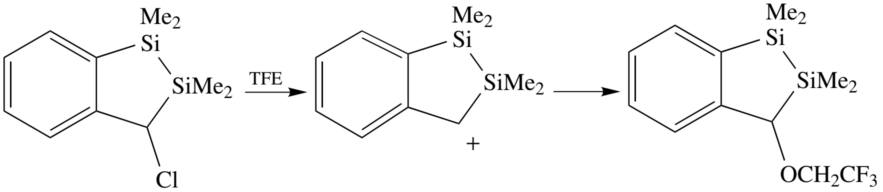

(220) **(221)** **(222)** (34)

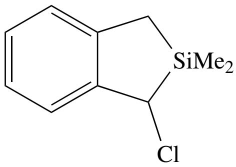

(223)

A remarkable change of the mechanism was observed by Shimizu and coworkers[88] in the solvolysis of the disilanyl-substituted cyclopropyl bromide **224c**. While the cyclopropyl bromides **224b** and **224c** give, upon solvolysis, the open allylic ethers **227**, in line with a σ-assisted mechanism $(k_\Delta)^{86}$ via the allyl cations **228**, **224c** predominantly yielded the cyclopropyl ring-retained product **225** and only smaller amounts of **227c** (product ratio **225**/**227c** = 1.18; equation 35). These findings suggest that the β-silyl effect stabilizes the incipient cyclopropyl cation **226** enough to compete with the σ-assisted ring opening to the allyl cation **228c**[88].

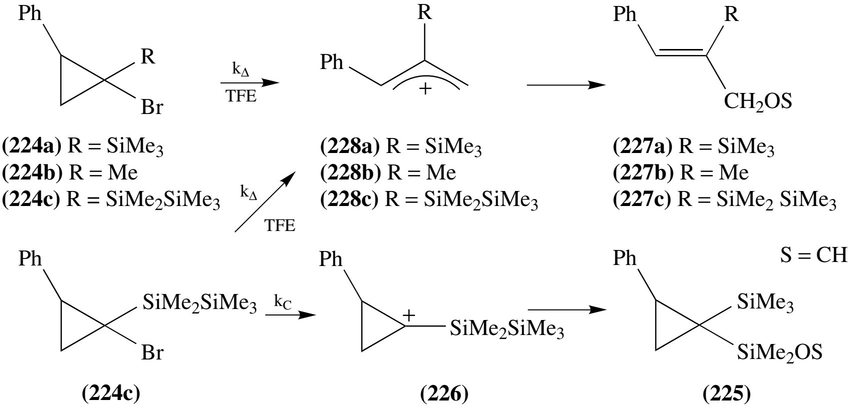

(35)

The overall kinetic effect of the disilanyl group is, however, small due to the different solvolysis mechanisms. **224** solvolyses only 3.48 times faster than **226** in TFE at 100 °C. For the k_Δ process Shimizu and coworkers calculated the relative rates for **224** : **225** : **226** to be 1.60 : 1.0 : 10.7. They concluded that these small silicon effects reflect the concerted nature of the k_Δ solvolysis involving transition states with a highly delocalized charge distribution[88].

C. γ-Silicon Effect

Sommer, Whitmore and coworkers already recognized the stabilizing effect of a γ-silyl group on a positively charged carbon[34,35]. In the basic hydrolysis they found an enhanced reactivity of **229** compared with the α-substituted chlorosilane **58**, although **229** was found to be less reactive than the β-isomer **59**.

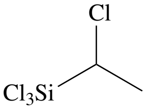

(58)

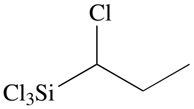

(59)

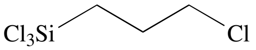

(229)

Shiner and coworkers were the first to study quantitatively the γ-silyl effect in solvolysis[90–95]. They found a distinct kinetic acceleration of the solvolysis of *cis*-3-(trimethylsilyl)cyclohexyl brosylate **230** compared with the alkyl reference **231** in TFA [k(**230**)/k(**231**) = 462] which is equivalent to a lowering of the ionization barrier by 3.7 kcal mol^{-1}[90,91]. This kinetic γ-silicon effect has striking stereochemical requirements. For example, the *trans* isomer **232** solvolyses by β-H participation similar to the *t*-Bu analogues **231** and **233** as evident from the large β-d$_4$ isotope effects ($k_H/k_D = 2-3$) and **232** is only as reactive as the *t*-Bu substituted cyclohexyl brosylate **233** [k(**232**)/k(**233**) = 1.2]. In contrast, the β-tetradeuterio analogue of **230** exhibits a small or even inverse secondary isotope effect ($k_H/k_D = 0.972-1.005$). The α-d$_1$ isotope effect is also smaller than expected for the formation of an open sp^2-hybridized carbenium ion. This indicates a participation of the γ-Si—C bond in the rate-determining step of the solvolysis of **230**[90,91].

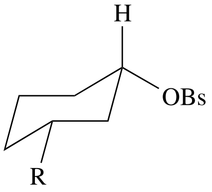

(230) R = $SiMe_3$
(231) R = *t*-Bu

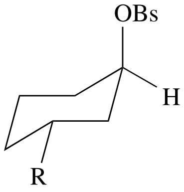

(232) R = $SiMe_3$
(233) R = *t*-Bu

Further support was given by the formation of small amounts of bicyclo[3.1.0]hexane **234** and by the retained configuration at C_α in the substitution product **235**. On the basis of these experimental data Shiner and coworkers suggested that the solvolysis of **230** proceeds via a 1,3-bridged carbonium ion **236** as intermediate (equation 36). The preferred conformation of **230** is a 'W' conformation with respect to the orientation of the leaving group and the silyl substituent. The incipient carbocation **236** is stabilized by the silyl group through the so-called 'percaudal' interaction involving overlap of the back lobe of the $C_\gamma-Si$ bond and the developing 2p(C) orbital on the positively charged carbon atom[90,91].

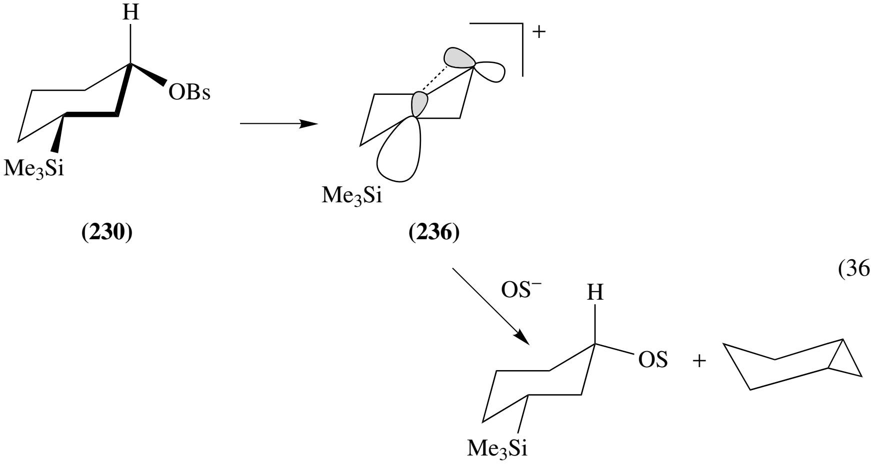

(230) **(236)** **(235)** **(234)**

(36)

A theoretical analysis of the γ-silicon effect at the HF/6-31G(d) level of theory by Davidson and Shiner[92] showed that a γ-silyl-substituted cation strongly favoured the *trans* perpendicular structure **237**. In the optimized structure of **237** the γ-carbon approaches the positively charged carbon to within a distance of only 1.75 Å [at HF/6-31G(d)]. This geometry and the γ-stabilizing effect and its orientation dependence were attributed to a significant contribution from the canonical structure **238C**. Consequently, the γ-silyl group stabilizes the carbocation **238** more than a methyl group because SiH_3^+ is more stable than CH_3^+[92].

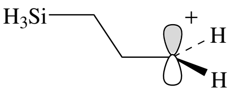

(237)

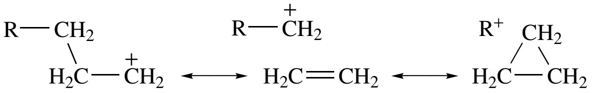

(238A) **(238B)** **(238C)**

R = H_3C, SiH_3

TABLE 8. Kinetic γ-silicon effect in solvolysis

Compound	k(s^{-1})	Reference group R[e]	k(compound)/ k(reference compound)	Reference
230	176.3[a]	t-Bu	462	91
232	1.99[a]	t-Bu	1.2	91
239	1100[a]	H	138	94
240	84.37[a]	H	129	93
241	0.144[a]	H	21 800	95
242	707[a]	H	4600	95
245	6.15×10^{-4}[b]	H	8.6	96
247	2.36×10^{-3}[b]	H	33	97
248 (R = OMs)	0.103[c]	H	33 000	98
249 (R = OMs)	1.5×10^{-4}[c]	H	48	98
251 (R = OBs)	3.8×10^{-6}[d]	H	2.4	98
252 (R = OBs)	1.7×10^{-8}[d]	H	0.01	98
257	3.8×10^{-7}[d]	H	0.24	98
260	7.1×10^{-2}[c]	H	23 000	98

[a] In 97% TFE at 25 °C.
[b] In 80% EtOH at 70 °C.
[c] In EtOH at 25 °C.
[d] In 80% EtOH at 25 °C.
[e] Group R replacing the Me_3Si group in the compound.

Shiner and coworkers also studied optically active acyclic secondary sulphonate esters and found rate accelerations of about 100 in solvolysis in TFA at 25 °C compared with the alkyl reference (Table 8)[93–95]. From the product distribution and the stereochemical outcome of the solvolysis Shiner and coworkers proposed the reaction course outlined in equation 37 for the brosylate **239**[94]. The transition state for the ionization adopts the 'W' conformation and, to a smaller extent, the '*endo*-Sickle' conformation and results in the formation of γ-silicon carbocation which is stabilized by a percaudal interaction. The incoming nucleophile attacks the bridged ion from the front side[94].

A remarkably high rate acceleration by a γ-silyl group was found for the acyclic primary sulphonate **241**, which is 21 800 times more reactive than its silicon-free analogue. In this case a 1,2-migration of Me_3SiCH_2 occurs after the rate-limiting formation of the carbocation **243**, yielding the more stable tertiary carbocation **244** (equation 38). For the secondary sulphonate **242** a smaller kinetic γ-silicon effect was detected[95].

In the adamantyl framework the γ-silicon effect was studied by Grob and coworkers[96,97]. The first-γ-trimethylsilyl substituent (cf **245**) enhances the solvolysis rate of 1-bromoadamantane **246** by a factor of only 8.6 and the second trimethylsilyl group in

247 leads to an overall enhancement of 33[96,97].

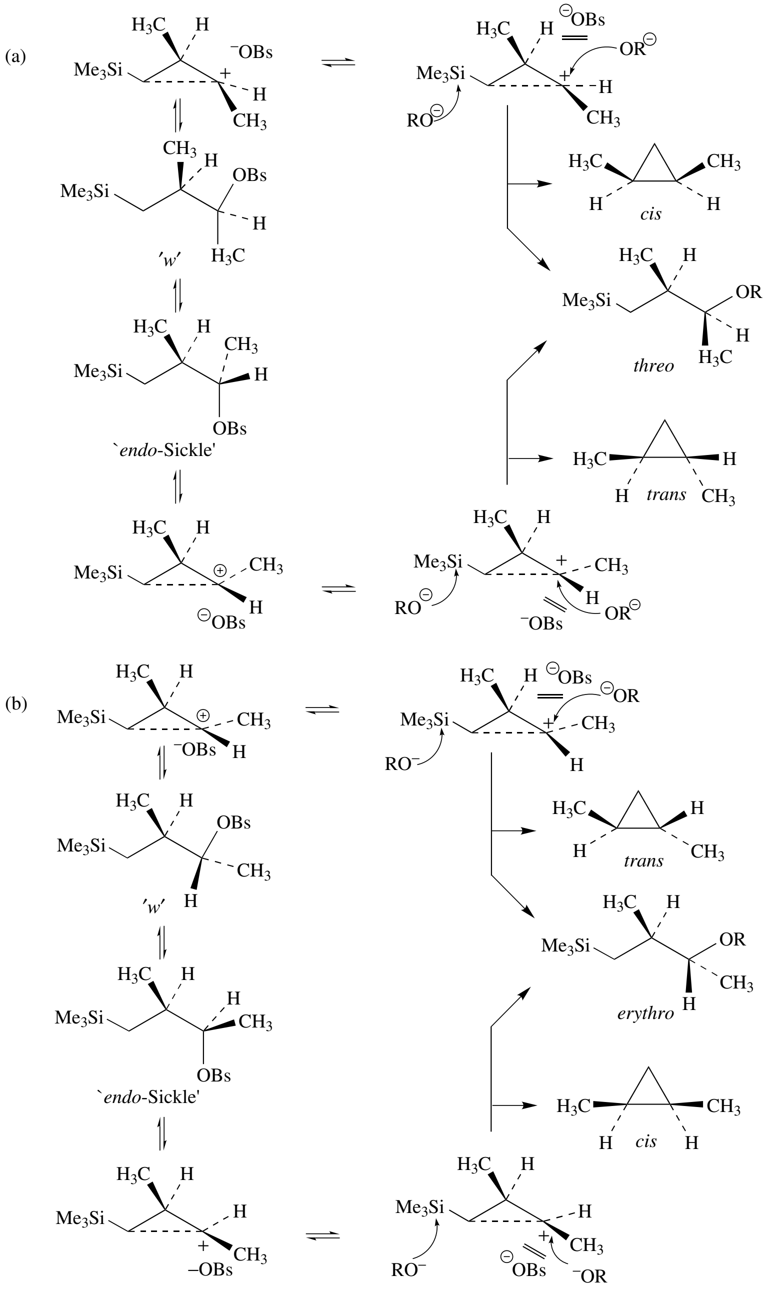

(37)

(a) Mechanism for the solvolysis of *threo*-4-(trimethylsilyl)-3-methyl-2-butyl-brosylate
(b) Mechanism for the solvolysis of *erythro*-4-(trimethylsilyl)-3-methyl-2-butyl-brosylate

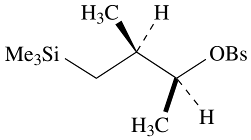

(239)

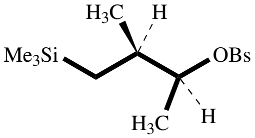

***threo*-(239)**
′W′ conformation

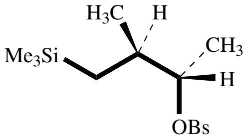

***threo*-(239)**
′*endo*-Sickle′ conformation

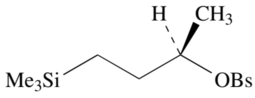

(240)

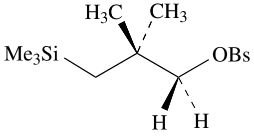

(241)

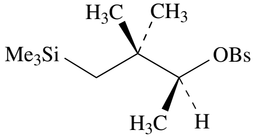

(242)

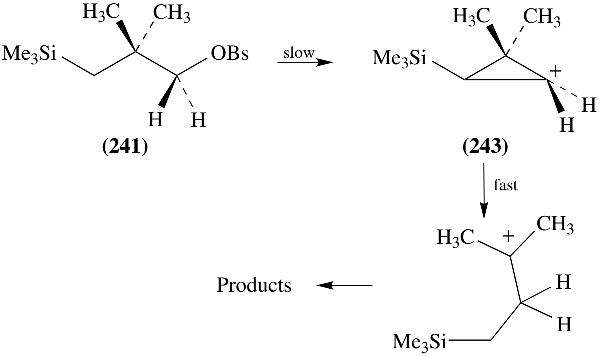

(241) **(243)** **(244)**

(38)

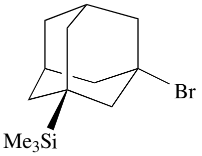

(245)

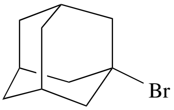

(246)

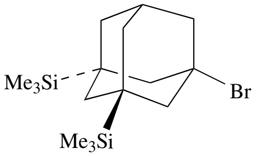

(247)

Further convincing evidence for the strong orientational preference of a 'W' -like geometry for the kinetic γ-silicon effect was given by Bentley, Kirmse and coworkers[98–100]. By using the rigid geometric arrangement in 2,6-disubstituted norbornyl derivatives, they found that for the 2-*exo* substituted compound the 6-*exo* trimethylsilyl substituent in **248** (R = Ms) causes a rate acceleration of 33 000 relative to hydrogen, while the 6-*endo*-Me_3Si compound **249** (R = Ms) solvolyses only 48 times faster than the unsubstituted reference compound **250** (R = Ms)[98]. In contrast, in the solvolysis of the corresponding 2-*endo*-mesylate **251** (R = Bs) the 6-*exo*-Me_3Si substituent shows only a 2–4-fold rate enhancement and the 6-*endo*-Me_3Si substituent in **252** (R = Bs) actually shows a rate retardation. The large kinetic effect of the *exo*-Me_3Si substituent in **248** (R = Ms) and the absence of a similar rate enhancement for the *endo* isomer **249** (R = Ms) are consistent with specially favourable interaction of the γ-silicon group with the incipient empty

$2p(C^+)$ orbital in the transition state for the solvolysis. The weak deactivating effect of the 6-*endo*-Me_3Si group in **252** (R = Ms) was ascribed to steric hindrance to departure and/or solvation of the leaving group[98,99].

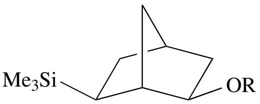

(248)

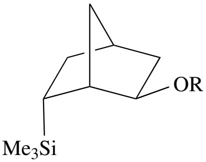

(249)

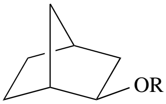

(250)

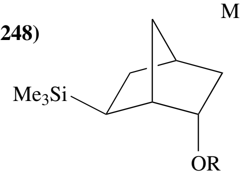

(251)

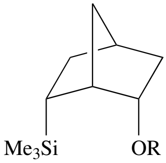

(252)

The solvolysis of **252** is one of the rare examples for a norbornyl–norpinyl rearrangement. While the *exo*-trimethylsilyl brosylate **251** yields mainly substitution and elimination products **253–255** with an intact norbornyl framework, **252** gives nearly 86% of norpinene **256** (equation 39). The bis-(trimethylsilyl)substituted compound **257** gives almost exclusively the norpinene derivative **258** (equation 40). While the trimethylsilyl group(s) in **252** and **257** exert no kinetic effect on the reaction rate, the β-effect on the intermediate carbocations **252A** and **259**, respectively, determines the product distribution[99].

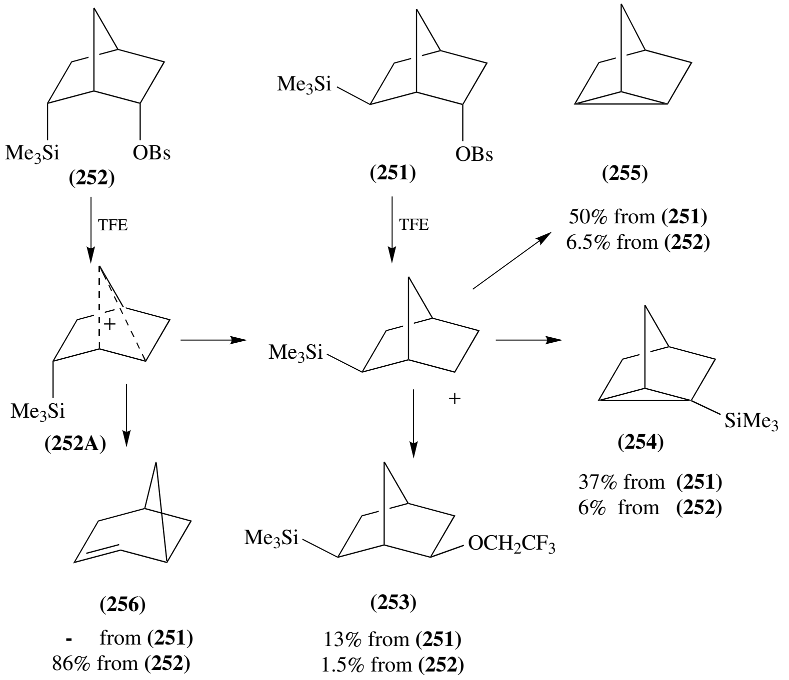

(39)

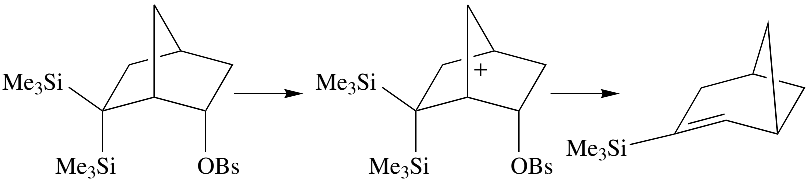

(257) **(259)** **(258)**

(40)

In the 2-*exo* isomer **260** the measured rate enhancement of 23 000 compared with **250** indicates a large γ-silicon effect. The intermediate **261** undergoes a fast 2,6 migration and Wagner-Meerwein shifts to give the products via ion **262** (equation 41)[100].

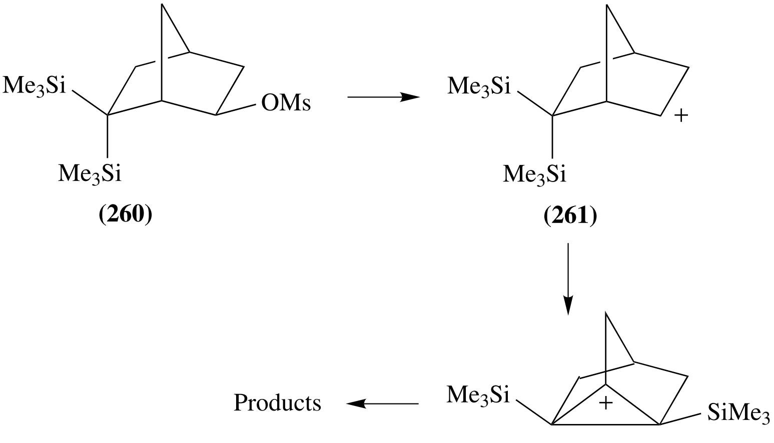

(260) **(261)**

(41)

(262)

D. δ-Silicon Effect

The kinetic influence of a δ-silicon substituent on the solvolysis of cyclohexyl tosylates is insignificant. Fessenden and coworkers[101] found virtually identical rates of ethanolysis of *cis* and *trans* **263** to those of the *t*-butyl reference compounds **264**. However, no evidence for a rate-determining k_c solvolysis was provided.

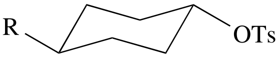

trans-**(263)** Me$_3$Si
trans-**(264)** *t*-Bu

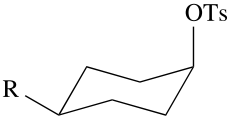

cis-**(263)** Me$_3$Si
cis-**(264)** *t*-Bu

Adcock, Shiner and coworkers found a significant 48.6-fold rate enhancement for the 4-trimethylsilyl bicyclo[2.2.2]octyl mesylate **265** compared with the silicon-free analogue **266**[102]. The effects of trimethylgermyl and trimethyltin groups in the 4-position (in **267**

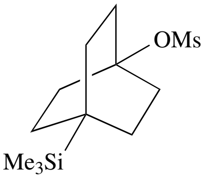

(265)

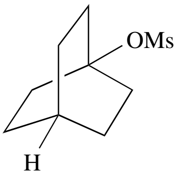

(266)

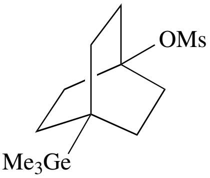

(267)

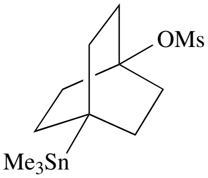

(268)

and **268**, respectively) are even larger, i.e. the trimethyltin mesylate **268** solvolyses 2841 times faster than **266** (Table 9).

The remarkable δ-effect on the transition state of the solvolysis was ascribed to the occurrence of double hyperconjugation (through bond coupling), i.e. **269A** $\leftrightarrow$ **269B** $\leftrightarrow$ **269C** in the intermediate cation **269**. The large δ-deuterium effect ($k_H/k_D = 1.05$ in TFE) found for **266**-d^4 indicate a substantial lowering of the C−H force constants and corroborates the idea of through bond coupling in **269**[102]. The alternative explanation in terms of homohyperconjugation[103−105] or back-lobe (percaudal) participation through space (**269A** $\leftrightarrow$ **269D**) was discarded on the basis of previous ^{19}F NMR studies on bicyclo[2.2.2]octanes. According to the authors a pure transmission of polar effects through space could also not account for the relatively large kinetic effects in solvolysis of **265**, **267** and **268**[102].

Similar large δ-effects were found in the adamantyl framework, although the stereochemical arrangement of δ-substituent and leaving group is very different[106,107]. Thus, *E*-5-trimethylsilyl-2-adamantyl brosylate **270** undergoes ionization 23 times more rapidly than 2-adamantyl brosylate **271**. Again the trimethyltin substituent exerts an even larger effect [k(**272**)/k(**270**) = 9000] (Table 9)[106]. The major product of the solvolysis of the tin compound **272** was **273**, the result of a five-bond heterolytic Grob fragmentation. Together with the similarity of the kinetic acceleration to the bicyclo[2.2.2]octyl case this was taken as an indication that the effect is transmitted through the bonds rather than

TABLE 9. Kinetic δ-silicon, δ-germanium and δ-tin effects in solvolysis

Compound	$k(s^{-1})$	k(compound)/ k(reference compound)^a	Reference
265	80.7^b	48.6	102
267	177.9^b	71.1	102
268	4713^b	2841	102
270	23.13^b	51	106
272	3200^b	7000	106
274	3.69^b	8	106
275	44.83^b	98	106
278	$1.14 \times 10^{-4^b}$	1319.4	108
280	$1.77 \times 10^{-4^b}$	20486	108
286	316^c	108.9	109

[a] Reference compound is hydrogen instead of the R_3E (E = Si, Ge, Sn) derivative.
[b] In 97% TFE at 25 °C.
[c] In MeOH at 25 °C.

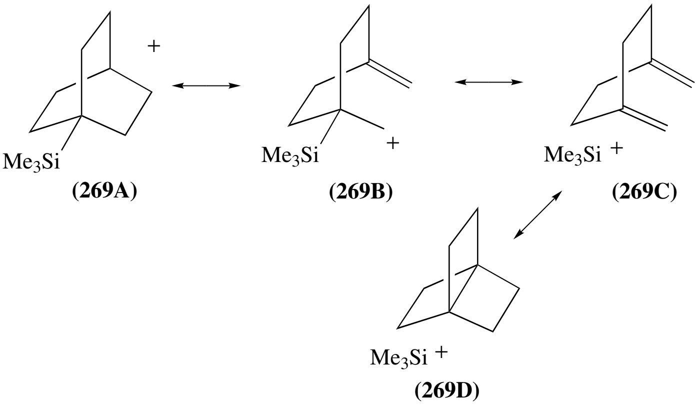

(269A) **(269B)** **(269C)** **(269D)**

through space[106]. It was postulated[106] that the smaller effect found for the Z-isomers **274** and **275** (Table 9) is due to isomerization of the pyramidal Z-cation, e.g. of **276** to the more stable E-cation **277**[107].

A large kinetic silicon γ,δ-effect was found in the solvolysis of 4-trimethylsilylnorbornane triflate. Adcock and coworkers[108] found a 1319-fold acceleration for **278** compared with **279**. For the tin compound **280** the relative solvolysis rate was even 20486, while a 4-methyl group in **281** causes only a modest acceleration $[k(\mathbf{281})/k(\mathbf{279}) = 7.41]$[108].

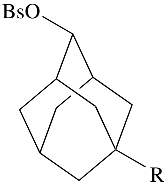

(270) R = SiMe$_3$
(271) R = H
(272) R = SnMe$_3$

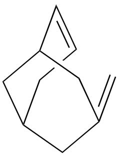

(273)

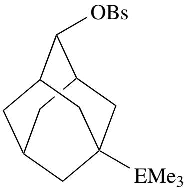

(274) R = SiMe$_3$
(275) R = SnMe$_3$

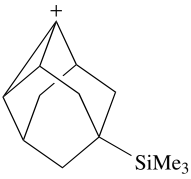

(276)

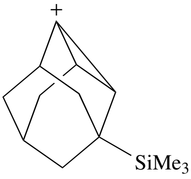

(277)

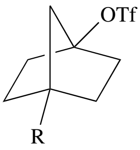

(278) R = SiMe$_3$
(279) R = H
(280) R = SnMe$_3$
(281) R = CH$_3$

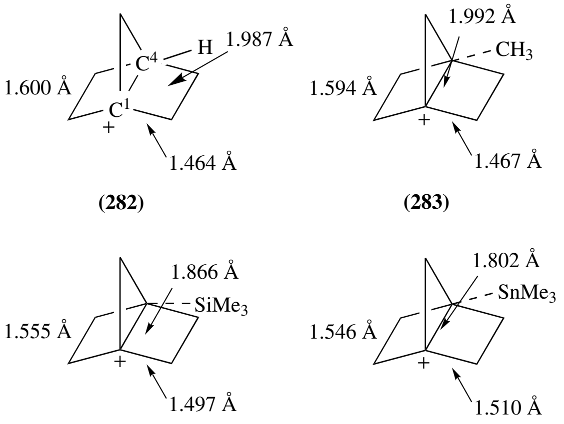

(282) **(283)**

(284) **(285)**

FIGURE 8. Optimized geometries of cations **282–285** (at MP2/6-31G(d)/[DZP])

High level computations[108]. on the cations **282–285** at the correlated MP2(6-31G(d))/[DZP] level of theory show that cation **284** is by 11.1 kcal mol^{-1} more stable than its unsubstituted analogue, the 1-norbornyl cation **282**. Furthermore, the calculations reveal that in the norbornyl system the silyl-effect is transmitted by back-lobe interactions (homohyperconjugation), while stabilization by double hyperconjugation is of minor importance. Thus, the optimized structures of **282–285** (Figure 8) show smaller C1–C4 distances for the highly stabilized **284** and **285** than for **282**, indicating the importance of C1–C4 interaction as described in the canonical structures **284B–D**. In contrast, on the basis of the calculated structures, the occurrence of double hyperconjugation (see canonical structures **284 E–F**) was discarded for the 1-norbornyl cation system[108].

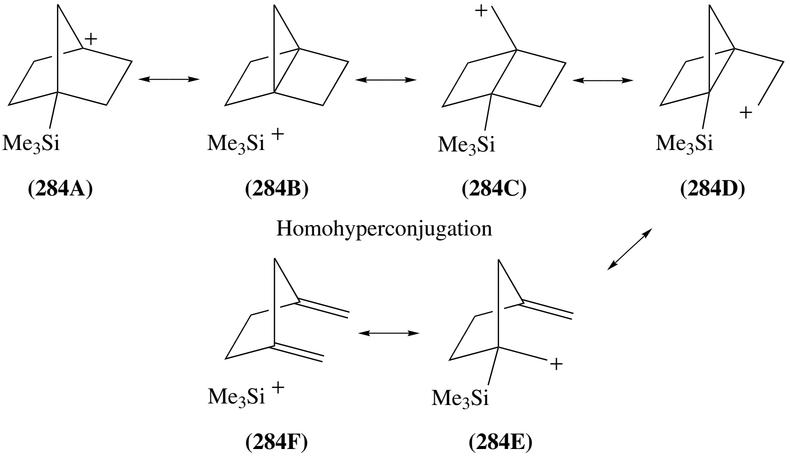

(284A) **(284B)** **(284C)** **(284D)**

Homohyperconjugation

(284F) **(284E)**

Double Hyperconjugation

Eaton and Zhou[109] found in the cubyl system a rate enhancement by a δ-trimethylsilyl group of $k(\mathbf{286})/k(\mathbf{287}) = 109$. For the trimethyltin substituent in **288** a factor of 2800 was extrapolated. This measured δ-effect seems to be too large for the transmission of pure polar effect through the cubyl cage, as suggested by Moriarty, Kevill and coworkers[110,111]. Eaton and Zhou argued that the relatively large δ-effects of silicon and tin are connected with the delocalized structure of the cubyl cation **289** as shown schematically in **289A**–**289C**, originally suggested by Hrovat and Borden[112].

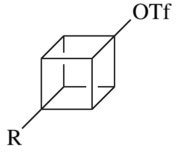

(286) R = $SiMe_3$
(287) R = H
(288) R = $SnMe_3$

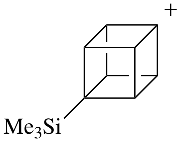

(289)

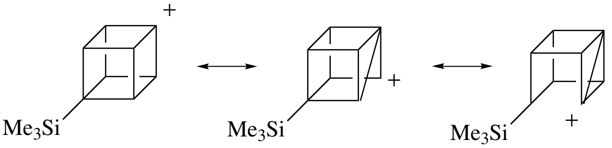

(289A) **(289B)** **(289C)**

V. STABLE ION STUDIES

This section summarizes the structure elucidation studies on silyl-substituted carbocations. It includes ultra-fast optical spectroscopic methods for the detection of transient intermediates in solution with life-times of about 10^{-7} s. A summary of NMR spectroscopic investigations of silyl-substituted carbocations and concomitant computational studies of model cations is given. A number of reactive silyl-substituted carbocations can be obtained as persistent species in superacids and non-nucleophilic solvents. Some of them have life-times of hours or even longer at low temperatures, and in some cases silyl-substituted carbocations can be prepared which are stable even at room temperature. Some silyl-substituted carbocations form crystals which were investigated by X-ray crystallography at room temperature.

A. α-Silyl Substitution

1. NMR spectroscopic characterization of α-silyl-substituted carbocations

a. 1-Phenyl-1-trimethylsilylethyl cation. Early attempts to generate the 1-phenyl-1-trimethylsilylethyl cation **290** by ionization of the 1-phenyl-1-trimethylsilyl ethanol **291** with SbF_5/FSO_3H at −78 °C have failed. Only the cumyl cation **292** was observed instead (equation 42)[113].

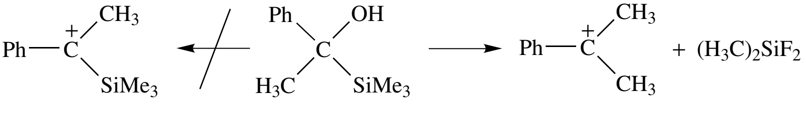

(42)

(290) **(291)** **(292)**

When 1-phenyl-1-trimethylsilylethyl chloride **293** is reacted with SbF_5 under carefully controlled experimental conditions at −125 °C, the 1-phenyl-1-trimethylsilylethyl cation

290 is exclusively generated as indicated by ^{1}H and ^{13}C NMR spectra (equation 43)[114,115].

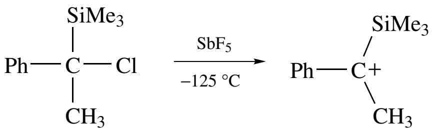

$$\mathrm{Ph{-}C(SiMe_3)(CH_3){-}Cl}\ \xrightarrow[-125\,^\circ\mathrm{C}]{\mathrm{SbF_5}}\ \mathrm{Ph{-}C^+(SiMe_3)(CH_3)} \tag{43}$$

(293) **(290)**

Due to the benzylic p$-\pi$ resonance stabilization, the C^+-C_{ipso} bond has partial double bond character and the *ortho*, *ortho′* and *meta*, *meta′* CH groups *syn* and *anti* to the silyl group are non-equivalent. The ^{1}H NMR spectrum (Table 10) shows two separate signals for the *ortho* protons at $\delta = 8.80$ and 8.72 ppm and additional signals at 8.63 (*para*-H), 8.02 (*meta*-H), 3.75 ($C^+-C\underline{H}_3$) and 0.65 (Si−Me) ppm.

The ^{13}C NMR spectrum (Table 11) exhibits signals at $\delta = 292.82$ (C^+), 37.27 ($C^+-\underline{C}H_3$) and −0.21 ($Si\underline{C}H_3$) ppm and six signals for the aromatic carbons at $\delta = 158.91$ (C_{para}), 148.12 (C_{ipso}), 148.34/138.25 (C_{ortho} *anti/syn* to $SiMe_3$), 133.59/133.07 (C_{meta} *anti/syn* to $SiMe_3$).

The effect of an α-silyl group on the positive charge in benzyl cations can be estimated by comparing the NMR spectroscopic data for the 1-phenyl-1-trimethylsilylethyl cation **290** with those for the phenyl ethyl cation **78** and the cumyl cation **292** prepared under identical conditions from the corresponding chlorides with SbF_5. The ^{1}H and ^{13}C NMR data for **78**, **290** and **292**[114] measured under comparable conditions are given in Tables 10 and 11.

TABLE 10. ^{1}H NMR chemical shifts (δ, ppm) for various benzylic carbocations, $Ph-C^+RR'$ in SO_2ClF/SO_2F_2 at $-117\,^\circ C$[a]

Ion	R,R′	R	R′	*o*	*m*	*p*
78	R = Me, R′ = H	3.39	10.1	8.88/8.47 *anti/syn*	8.02	8.73
290	R = Me, R′ = $SiMe_3$	3.75	0.65	8.80/8.72 *anti/syn*	8.02	8.63
292	R = R = Me	3.46		8.77	7.92	8.52

[a] 250 MHz, internal reference $\delta(NMe_4^+) = 3.00$ ppm.

TABLE 11. ^{13}C NMR chemical shifts (δ, ppm) for various benzylic carbocations, $Ph-C^+RR'$ in SO_2ClF/SO_2F_2

Ion	R,R′	C^+	C_o	C'_o	C_m	C'_m	C_p	C_{ipso}	R
78	R = Me, R′ = H[a]	231.28	155.36	144.14	134.25	134.01	161.92	141.91	28.05
290	R = Me, R′ = $SiMe_3$[b]	292.82	148.34 *anti*	138.25	133.59 *anti* to Si	133.07 *syn*	158.91	139.43	R(37.27) R′(−0.21)
292	R = R′ = Me[a]	255.85	142.22		132.96		156.14	140.25	33.46
	[c]	256.33	142.79		133.56		156.70	140.91	34.14

[a] 63 MHz at $-117\,^\circ C$ in SO_2ClF/SO_2F_2, internal reference $\delta(NMe_4^+) = 55.65$ ppm.

[b] 100 MHz at $-124\,^\circ C$, internal reference $\delta(CD_2Cl_2) = 53.80$ ppm.

[c] 100 MHz at $-110\,^\circ C$.

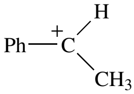

(78)

The low field shift of the resonance for the C$^+$ carbon of the 1-phenyl-1-trimethylsilylethyl cation **290** is noteworthy. This is the most deshielded shift of a benzyl cation carbon observed so far. NMR chemical shifts are dependent not only on the charge densities but also upon the substituent effect of the neighbouring groups. Consequently, the chemical shift of the C$^+$ carbon is not a good measure of the relative charge in these type of benzyl cations because the substituent effect on chemical shift is different for the substituents R = H, $SiMe_3$ and CH_3. The trimethylsilyl substituent has a large deshielding effect on the chemical shift of an adjacent sp^2-hybridized carbon.

The carbonyl carbon signal in trimethylsilyl phenyl ketone **294** ($\delta = 238$ ppm) is 42 ppm deshielded compared with that in acetophenone **295** ($\delta = 196$ ppm)[113]

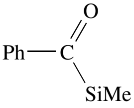

(294)

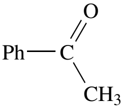

(295)

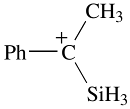

(296)

The *para* carbon in benzyl cations is remote from the substitution site at the benzylic position and has an approximately similar environment in all the three carbocations **78, 290** and **292**. Hence, the *para* carbon chemical shift can be used to monitor the demand for delocalization of the positive charge into the aromatic ring. Semiempirical (AM1) and *ab initio* calculations [B3LYP/6-31G(d)] for the benzyl cation-type structures (Ph$-$C$^+$ MeR) with R = H, Me, SiH_3, $SiMe_3$ show that the aryl π-system and the vacant 2p(π)-orbital in the phenylethyl **(78)**, the 1-phenyl-1-silylethyl **(296)**, the 1-phenyl-1-trimethylsilylethyl **(290)** and the cumyl **(292)** cations are almost coplanar in all systems, thus p$-\pi$-conjugative overlap is not hindered even in **290** which is substituted by the rather bulky $SiMe_3$ group. The better the α-substituent at the C$^+$-carbon stabilizes the positive charge, the less charge needs to be delocalized into the aryl ring, and a less deshielded NMR signal for the *para* carbon is expected. The chemical shift of the *para* carbon in the 1-phenyl-1-trimethylsilylethyl cation **290** ($\delta = 158.9$ ppm) is in between the values of C_{para} in the phenylethyl cation **78** ($\delta = 161.9$ ppm) and the cumyl cation **292** ($\delta = 156.7$ ppm)[116–118]. This shows that the α-trimethylsilyl group is stabilizing compared with α-hydrogen, but destabilizing compared with the α-methyl group in these carbocations. This is confirmed by comparison of the ^{1}H chemical shifts for the *para* hydrogens, which are $\delta = 8.73$, 8.63 and 8.52 ppm in the phenylethyl **(78)**, the 1-phenyl-1-trimethylsilylethyl **(290)** and the cumyl **(292)** cation, respectively[114]. These findings are in accord with earlier calculations on model systems, with solvolysis data and also with recent quantum chemical *ab initio* calculations of charge distribution in α-silyl-substituted carbocations[11,13,119]. The ^{29}Si chemical shift of the 1-phenyl-1-trimethylsilylethyl cation **290** ($\delta = 9.61$ ppm in SO_2ClF/SO_2F_2 at $-127\,^\circ$C) is similar to that of the neutral progenitor, 1-phenyl-1-trimethylsilylethyl chloride **293** (δ^{29}Si $= 9.08$ ppm)[115]. Charge delocalization to the silyl group is not important in **290**, contrary to the case of β-silyl-substituted carbocations (Section V.B).

b. Diphenyl(trimethylsilyl)methyl cations. The diphenyl(trimethylsilyl)methyl cation **297** can be generated from the corresponding alcohol by reaction with FSO_3H in SO_2ClF[113].

The ^{13}C NMR chemical shift of the C^+ carbon is at $\delta = 259$ ppm, 30–60 ppm deshielded from the shift of the C^+ carbon in the 1,1-diphenylethyl cation **(298)**, $\delta = 222.9$ ppm and the diphenylmethyl cation **(299)**, $\delta = 200.6$ ppm, respectively. The *para*-carbons of the aromatic rings show slightly shielded chemical shifts compared with the methyl and hydrogen analogues [$\delta = 147.4$, 148.1 and 150.9 ppm, respectively, for the $SiMe_3$, CH_3 and H derivatives]. This was taken as an indication of a smaller positive charge delocalization into the aromatic ring in the trimethylsilyl-substituted analogue **(297)**. However, as evident from the results obtained for the 1-phenyl-1-trimethylsilylethyl cation **(290)**, this does not imply that the α-trimethylsilyl group is a better stabilizer of the positive charge than the α-methyl or α-hydrogen analogues. The non-planarity of the two phenyl rings does not allow a conclusive comparison for the cations $(C_6H_5)_2C^+R$ (**297, 298** and **299**) with R = $SiMe_3$, CH_3 and H, respectively

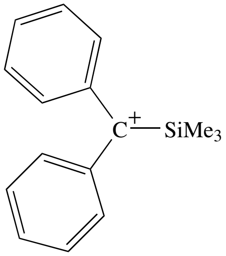

(297)

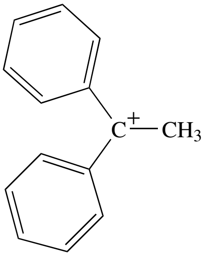

(298)

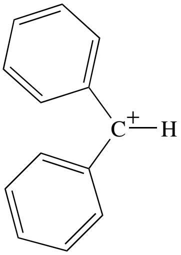

(299)

2. X-ray structure analysis of the tris(trimethylsilyl)cyclopropenylium cation

The tris(trimethylsilyl)cyclopropenylium hexachloroantimonate **300**•$SbCl_6^-$ forms crystals which are stable at room temperature[121].

The X-ray structure shows slight distortions of the ring due to the close vicinity of one of the chlorine atoms of the anion. One silyl group is bent out of the ring plane and away from the anion. The tris(silyl)cyclopropenylium cation **301** serves as a close model in quantum chemical *ab initio* calculations for the experimentally investigated trimethylsilyl-substituted carbocation **300**. At both the HF/6-31G(d) and the correlated MP2(fc)/6-31G(d) levels a highly symmetric C_{3h} structure of **301** is a minimum. This is consistent with ^{13}C NMR measurements of the trimethylsilyl-substituted cation **300** in solution which indicate that it has a C_{3h} symmetry[122]. The calculated C–C bond length in the three-membered ring of the SiH_3 model **301** (1.388 Å) is in agreement within experimental error with the average value found in the X-ray structure of the $SiMe_3$-substituted cation salt **300**•$SbCl_6^-$ (1.384 Å). The other geometrical data also show good agreement between the experimental and calculated data for the model cation. According to a NBO analysis of the HF/6-31G(d) wave function all the ring carbons in cyclopropenylium cations carry the same charge. The charge decreases with decreasing electronegativity of the substituent [**302** (CH_3) +0.2, **303** (H) +0.025 and **301** (SiH_3) −0.243]. With silyl substitution the ring carbons are actually negatively charged, although formally they represent the carbocation centres, and the positive charge resides on the silyl groups. As the Me_3Si group is probably a better σ-electron donor than H_3Si, the total negative charge on the ring carbons is expected to be even higher in the experimentally studied cation **300**. The smaller π-orbital occupation of 2.04 e for SiH_3 substitution in **301** as compared with 2.12 e for methyl substitution in **302** indicates a less effective hyperconjugative electron donation from the silyl group across the longer Si–C^+ bond in **301**, compared with the $C^+{-}CH$ hyperconjugation in the trimethyl-substituted cation **302**. The calculated ^{13}C NMR chemical shift of $\delta = 218.3$ ppm for the ring carbons, calculated for a geometry of **301** obtained at the MP2(fc)/6-31G(d) level using the IGLO method and basis set II, agrees very well with the value measured experimentally for the $SiMe_3$-substituted cation **300** ($\delta = 214.3$ ppm). The thermodynamic stabilities of tris-substituted cyclopropenylium cations was evaluated from isodesmic reactions. Three silyl groups as in **301** stabilize the parent cyclopropenylium cation **303** by 22.4 kcal mol^{-1} at MP3(fc)/6-311G(d,p)//6-31G(d)+ZPVE. The tris-methyl-substituted carbocation **302** is 31.4 kcal mol^{-1} more stable than the parent cation **303**. The order of substituent stabilizing abilities Me $>$ H_3Si $>$ H found for cyclopropenylium ions **302, 301** and **303** is thus the same as that observed for other carbocations with a corresponding substitution pattern. However, due to the inherent higher stability of the 2π-Hückel aromatic system, the magnitude of the stabilizing effect is smaller than in ordinary alkyl cations. The $pK_{(R^+)}$ value of the tris-silyl-substituted cyclopropenylium cation **301** is estimated to be 4 as compared with 7.4 for the tris-methyl-substituted cyclopropenylium cation **302.**

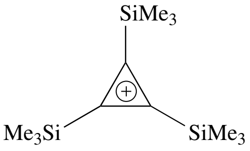

(300)

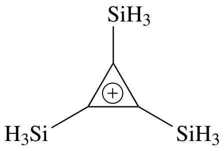

(301)

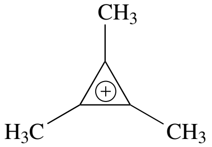

(302)

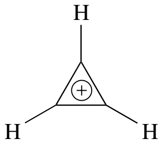

(303)

B. β-Silyl-substituted Carbocations

1. sp^2-Hybridized carbocations

a. Photochemical generation and UV characterization of transient β-silyl-substituted carbocations. i. 9-(Trimethylsilylmethyl)fluoren-9-yl cations. When 9-(trimethylsilylmethyl)fluoren-9-ol **304** at ca. 10^{-4} molar concentrations in TFE is submitted to photolysis, both dehydroxylation and desilylation take place (equation 44)[123].

The only product observable after short irradiation times is 9-methylenefluorene **305.** At longer times 9-methyl-9-trifluorethyl ether **306** is detected as a secondary product formed by protonation of the exocyclic double bond of 9-methylenefluorene **305** to give the 9-methylfluoren-9-yl-cation **307**, which then reacts with the TFE solvent. The transient absorption spectrum obtained upon laser flash photolysis of 9-(trimethylsilylmethyl)fluoren-9-ol **304** shows three bands with λ_{max} 340, 370 and 425 nm, all decaying with the same rate constant, 2.4×10^7 s^{-1} in TFE at 25 °C. The transient spectrum is different from the spectrum of 9-methylfluoren-9-yl cation **307**, which can be obtained as a stable cation in 96% H_2SO_4 from the corresponding alcohol **308**. Picosecond experiments reveal that the transient is formed on a 25 ps time scale directly from the silyl-substituted precursor **304** and shows the characteristics of a cationic intermediate, being unaffected by oxygen but sensitive to the nucleophilicity of the medium. This leads to the conclusion that the 9-(trimethylsilylmethyl)fluoren-9-yl cation **309** is the observed intermediate of the desilylation. The rate constant decreases on proceeding from TFE to the more weakly nucleophilic 1,1,1,3,3,3-hexafluoro-2-propanol (HFIP). It was concluded that the desilylation is a one-step process proceeding via a transition state **310** with participation of the solvent or other added nucleophiles. The marked different absorptions of the 9-(trimethylsilylmethyl)fluoren-9-yl cation **309** compared with simple 9-alkylfluoren-9-yl cations such as **307** indicate that the interaction of the β-silyl group with the positive charge has a significant perturbing effect. If all the charge would be transferred from the fluorenyl moiety to the silicon, a 9-methylenefluorene/Me_3Si^+ complex would result. The spectrum of the transient **309** is, however, quite different from that of 9-methylenefluorene **305** and thus the geometry was suggested to be intermediate between a 9-alkylfluoren-9-yl cation and a 9-methylenefluorene-Me_3Si^+ complex.

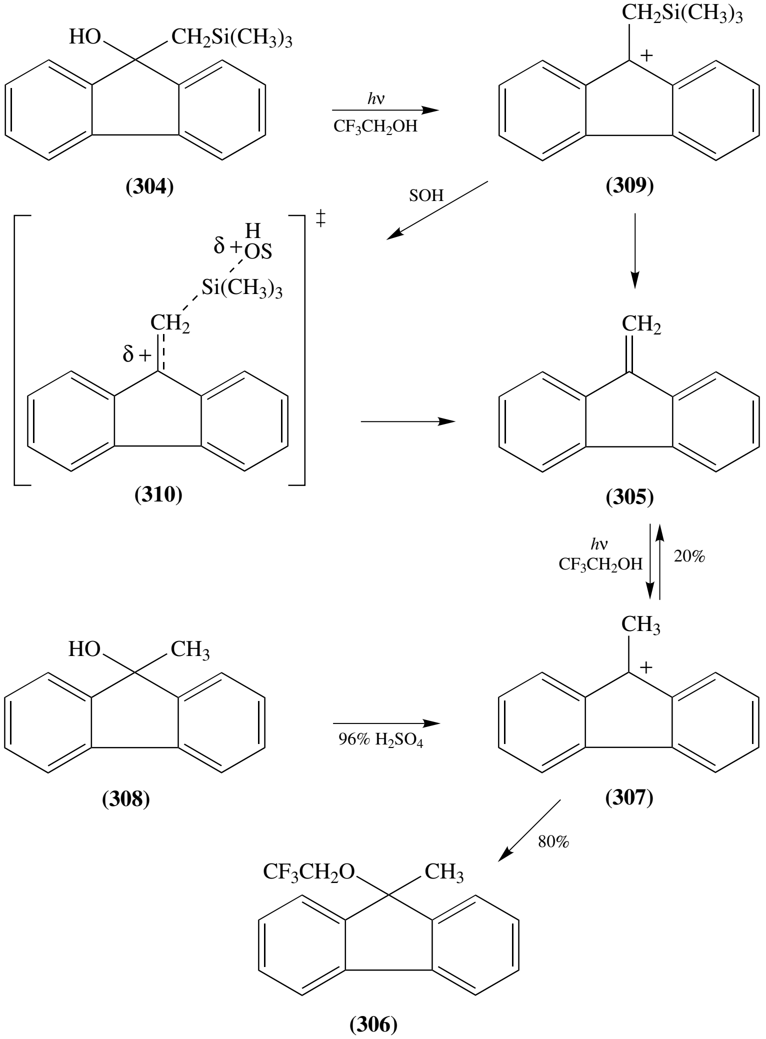

(44)

ii. Silyl-substituted cyclohexadienyl cations. 2-Silyl-substituted 1,3-dimethoxybenzenes **311** undergo a desilylation reaction upon photoexcitation in HFIP[124]. The only products observed are 1,3-dimethoxybenzene **312** and the silyl ether $R_3SiOCH(CF_3)_2$ (equation 45). The reaction proceeds via selective protonation at the 2-position.

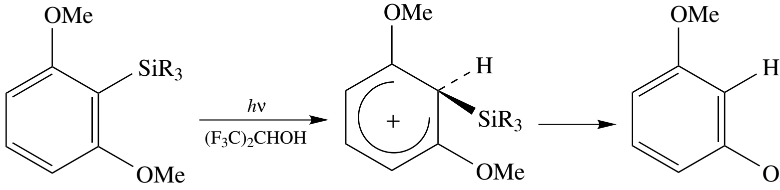

(45)

(311) **(313)** **(312)**

When the reaction was conducted in O-deuteriated HFIP, $(CF_3)_2CHOD$, as a solvent, the deuterium was found exclusively at the 2-position of the 1,3-dimethoxybenzene **312**. Laser flash photolysis at 248 nm irradiation carried out with 10^{-3} M solutions of substrates **311** with different silyl groups ($SiMe_3$, $SiMe_2Ph$, $SiMePh_2$, $SiMe_2C_6H_4X$-4: X = OMe, Me, F, I) show absorptions of the transient cations **313** with maxima at 380–390 nm and a weak band at 300 nm. The absorption spectra are similar to that of the parent 2,6-dimethoxybenzenium ion **314** (R = H) ($\lambda_{max} = 410$ nm) but show a slight hypsochromic shift.

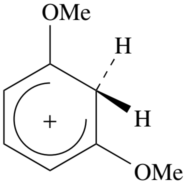

(314)

The exponential decay is uniform across the entire spectrum, indicating that a single transient species is being produced. The decay rate at 25 °C varies between 8×10^3 for the $SiMe_3$ and 1×10^5 for the $4\text{-}MeC_6H_4(Me)_2Si$ group. The decay is unaffected by oxygen, an efficient quencher of radicals and triplets. Despite its photochemical generation the transient **313** is a ground state species. The relative long life of the transient implies that it cannot be a singlet excited state while the lack of quenching by oxygen mitigates against a triplet. However, the decay is accelerated by added nucleophiles such as alcohols, which is characteristic for cations. The transient is assigned the structure of a β-silyl-substituted cyclohexadienyl cation **313**. The hypsochromic shift compared with the parent cyclohexadienyl cation **314** reflects a perturbation of the cyclohexadienyl π-system induced by the interaction of the silyl substituent with the positive charge. The mechanism suggested initiates by a photoprotonation of the excited 2-silyl-1,3-dimethoxybenzenes **311** at C2 to give the intermediate $1\text{-}R_3Si$-2,6-dimethoxybenzenium ions **313** which undergo desilylation via transition state **316** to give 1,3-dimethoxybenzene **312** and the protonated silyl ethers **315** (equation 46). Kinetic analysis demonstrates that these cations undergo preferentially desilylation over deprotonation. The desilylation occurs with nucleophilic participation. Quantitative agreement between the kinetics and the product analysis as well as the entropies of activation determined for the reaction with the solvent serve as evidence for a bimolecular reaction.

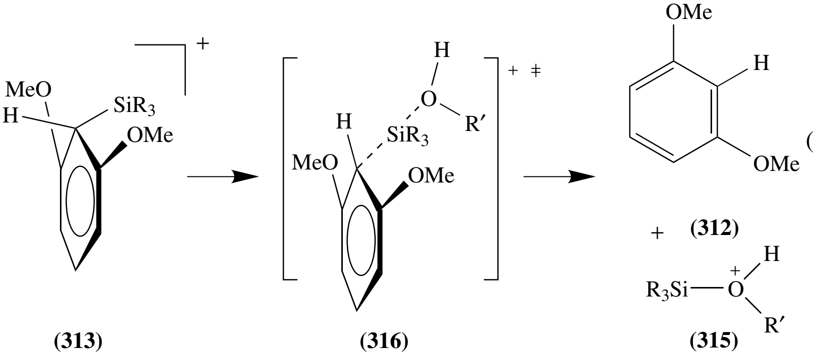

(313) (316) (312) (315) (46)

The observation that added alcohol accelerates the decay supports the interpretation that the reaction is associative, with concerted Si—C bond breaking and Si—O bond making. A dissociative pathway with initial cleavage of the C—Si bond to 1,3-dimethoxybenzene and the silylium ion R_3Si^+ is inconsistent with the results. Although a free silyl cation does not form even for the reaction with the less nucleophilic *t*-BuOH and HFIP, the ρ-values obtained for different R_3Si substituents offer evidence for some silyl cation character in the transition state **316**. The silicon in carbocation **313** bears a partial positive charge due to its interaction with the neighbouring π-system. In an associative transition state **316** this charge can either decrease or increase, depending on the relative amount of C—Si bond breaking and Si—O bond making. For the reaction with methanol, ρ is 0.0, indicating no charge formation at the transition state. The *t*-BuOH and HFIP reactions, however, have negative ρ values (−0.8 and −1.3, respectively), pointing to an increase in the positive charge at silicon as the reaction proceeds. With these nucleophiles C—Si bond breaking is more advanced than Si—O bond making at the transition state **316** and the silicon has some Si^+ character. This study gives direct evidence that β-silyl-substituted carbocations react with nucleophilic participation in the Si—C_β bond-breaking process. This is in accord with the observation made in superacids that bulky substituents at silicon increase the stability of β-silyl carbocations, i.e. that the rate-determining step of the β-C—Si bond cleavage in superacids is the attack of the nucleophile, which is retarded by the large alkyl groups at silicon.

b. X-ray crystallographic study of β-silylcyclohexadienyl cations. When trityl tetrakis(pentafluorophenyl)borate **317** was reacted with triethylsilane in toluene, a compound with the composition $Et_3Si(C_6F_5)_4B\text{-}(PhMe)_2$ was isolated as a solid and investigated by X-ray crystallography[125,126]. The crystal data, in particular the nearly planar geometry of the closer toluene moiety, as well as the relatively long Si–C(ring) distance (2.18 Å) were interpreted as due to a structure of a silylium ion with no coordination to anion and a distant coordination to the solvent. This interpretation was heavily disputed by several authors (see Lickiss' chapter on silylium ions) and the structure was suggested to correspond instead to the *p*-triethylsilyltoluenium ion **318**[127–131].

The structural data reported from the X-ray analysis are very similar to the *ab initio* calculated structural data for silyl-substituted arenium cations. The calculations of the *p*-trimethylsilyl **(319)** (Figure 9) and *p*-triethylsilyl toluenium ions **(318)** [HF/6-31G(d)] and the silylbenzenium ion **53** [MP2(fc)6-31G(d)] all show similar geometries and the characteristic geometric data resemble closely the main features found in the crystal structure.

$Ph_3C^+ \ B(C_6F_5)_4^-$

(317)

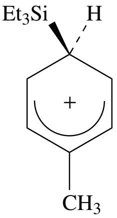

(318)

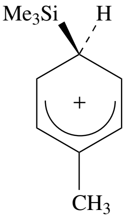

(319)

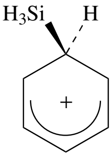

(53)

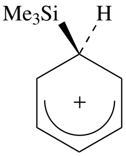

(54)

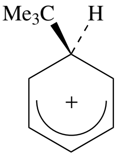

(320)

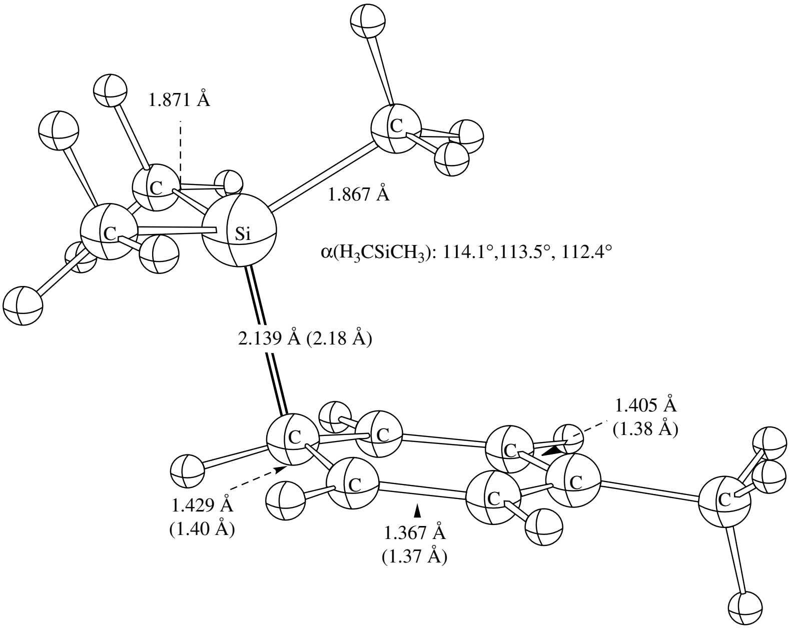

FIGURE 9. Calculated structure of **319** at HF/6-31G* (bond distances in Å, angles in deg), experimental data for **318** in parentheses

The calculated Si−C_{ipso} distances of 2.14, 2.087 and 2.197 Å, the 113.8° average angle at silicon in the silyl groups and the near planarity of the six-membered rings are just like those reported for the X-ray structure.

Furthermore, the ^{29}Si NMR chemical shift ($\delta = 81.8$ ppm) measured in toluene differed very much from what is expected by quantum chemical calculation of model compounds for planar trialkylsilylium ions (Me_3Si^+, $\delta^{29}Si = 355.7$ ppm; Et_3Si^+, $\delta^{29}Si = 354.6$ ppm). For distorted trimethylsilylium ions with C−Si−C angles of 114.0° and 109.5°, even more deshielded ^{29}Si chemical shifts of 368.2 and 397.0 ppm were calculated [IGLO basis II at HF/6-31 G(d) level].

IGLO calculation of the ^{29}Si NMR chemical shift [DZ basis (C,H), basis II (Si)//HF/6-31G(d)] for the *p*-trimethylsilyltoluenium ion **319** and the trimethylsilylbenzenium ion **54** give δ^{29}Si = 60 and 80.9 ppm. These results are in line with the expected trend that more charge will be delocalized towards silicon in the trimethylsilylbenzenium ion **54** compared with the *p*-trimethylsilyltoluenium ion **319**. The chemical shift of $\delta = 82.1$ ppm calculated for the *p*-triethylsilyltoluenium ion **318** agrees very well with the experimental value of $\delta = 81.8$ ppm in toluene.

Contrary to the original interpretation, the structures investigated by X-ray crystallography are regarded as silyl-substituted arenium ions. The characteristic geometric features accompanying the β-silyl stabilization of these carbocations are rationalized as follows. The long Si$-$C$_{ipso}$ bond is the result of hyperconjugative stabilization of the cyclohexadienyl cation by the β-silyl effect. The silyl group bends over towards the dienyl π-system and the hydrogen at the *ipso*-carbon moves up, thus resulting in a flattening of the ring. The alternation of the ring bond lengths arising from π-resonance stabilization of the positive charge is reduced compared with alkyl-substituted cyclohexadienyl cations. β-Silyl stabilization is more efficient than β-alkyl stabilization and thus the demand for π-resonance stabilization is lower in the β-silyl-substituted carbocations. For the *t*-butyl analogue, i.e. the 6-*t*-butylcyclohexa-2,4-dienyl cation **320**, ring bond lengths with more pronounced alternation are calculated.

A closely related X-ray structure *i*-$Pr_3Si(Br_6CB_{11}H_6)$ **321** (Figure 10) also displays similar features[132]. The brominated carborane anion $Br_6CB_{11}H_6^-$ was considered to be the least nucleophilic anion and the structure was interpreted as having about one third silylium ion character.

Consideration of the X-ray structure (with a Si$-$Br bond distance of 2.479 Å and average CSiC bond angles of 115.8°) and the relevant ^{29}Si NMR shift of δ^{29}Si = 109.8 ppm indicate, however, that no R_3Si^+ species was observed, but rather a structure in which

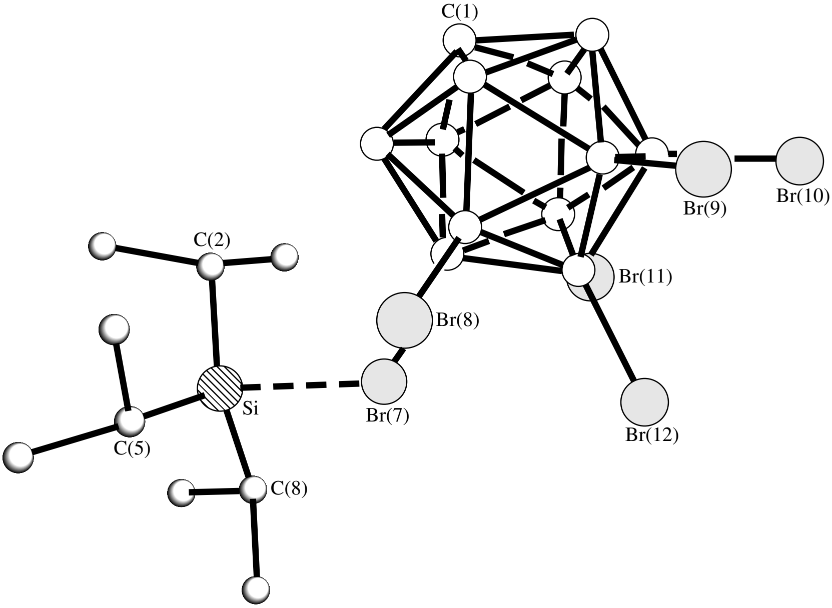

FIGURE 10. X-ray structure of **321**

a single bromine atom was in bonding distance to a silyl group, which resulted in a polarized silylbromonium zwitterion.

c. NMR spectroscopic characterization of β-silyl-substituted carbocations. i. β-Silyl-substituted secondary p-methoxybenzyl cations. α. 1-p-Anisyl-2-triisopropylsilylethyl cations. Protonation of *E*-1-*p*-anisyl-2-triisopropylsilylethene **322** with FSO_3H in SO_2ClF/SO_2F_2 yields a mixture of *anti*- and *syn*-**323** 1-*p*-anisyl-2-triisopropylsilylethyl cations **323** (equation 47)[115,133].

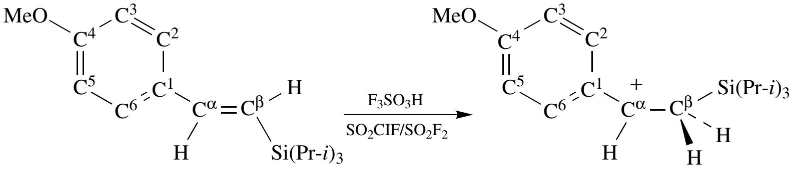

(47)

(322) **(323)**

The *para*-methoxy group is involved in the *p*-*π*-resonance delocalization of the positive charge as shown in the resonance structure **323B** of the limiting structures **323A**–**323D**. Hence, the C4–oxygen bond in **323** has a partial double bond character.

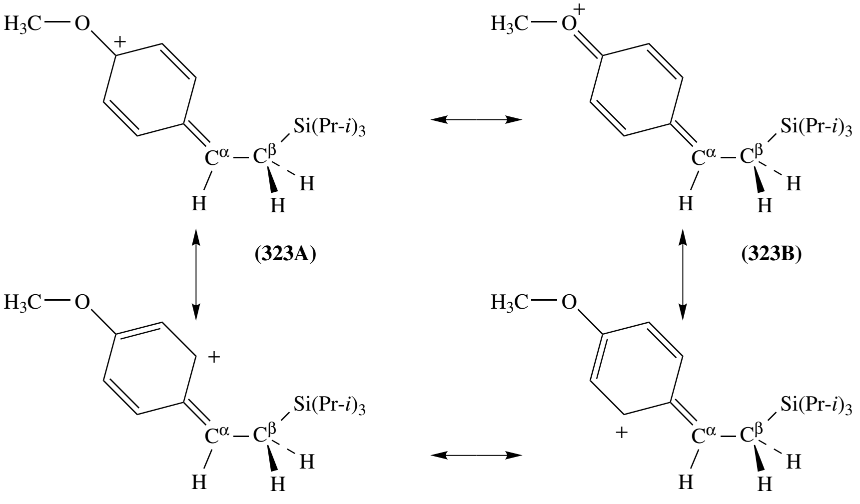

(323A) **(323B)**

(323D) **(323C)**

Two isomers with the O-methoxy group in the plane of the aryl ring are possible. The O-methoxy group can be in an *anti* or *syn* orientation relative to the $-CH_2SiR_3$ group at the benzylic carbon as in *anti*-**323** or *syn*-**323** (equation 48).

Below 120 °C the interconversion of the *syn* and *anti* isomers is slow on the NMR time scale. The *ortho*, *ortho*′ and *meta*, *meta*′ positions in the two isomers are non-equivalent. Two sets of four lines are observed, one for the C2 and C6 *ortho* and C3 and C5 *meta* carbons in the *anti* isomer (*anti*-**323**) and another set with lower intensity for the C2′ and C6′ *ortho* and C3′ and C5′ *meta* carbons in the *syn* isomer (*syn*-**323**). Upon warming above the coalescence temperature of about −110 °C the chemical shift for the non-equivalent positions in the two isomers is averaged and only four lines for the aromatic methine carbons are observable. A barrier $\Delta G^{\#}$ (−110 °C) of about 7 −8 kcal mol^{-1} was estimated from a line shape analysis.

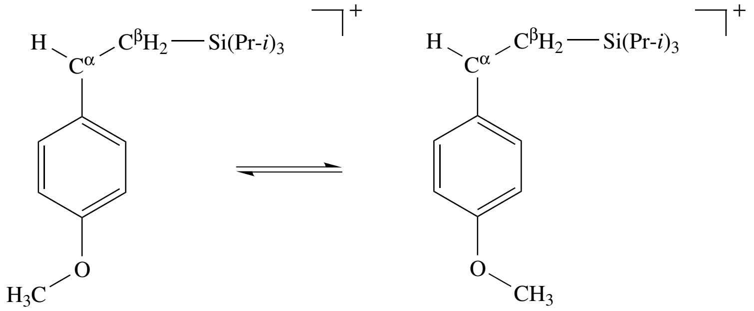

(48)

anti-**(323)** *syn*-**(323)**

Ab initio DFT calculations were performed using the B3LYP/6-31G(d) hybrid method for the analogous 1-*p*-anisyl-2-SiH_3-substituted ethyl cation **324**, which is a close model for the experimentally observed cation **323** with alkyl groups at silicon. It has been shown that different alkyl groups at silicon have no significant impact on the electronic stabilization in α-aryl-β-silyl-substituted carbocations.

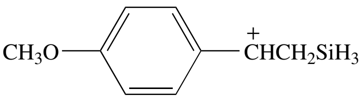

(324)

The optimized structures for the *anti* and *syn* isomers of **324** (Figure 11) have very similar energies, the *syn* isomer *syn*-**324** being only 0.3 kcal mol^{-1} less stable than the *anti* isomer *anti*-**324**.

The C_{β}−Si bond is perpendicular to the aryl ring plane and thus a maximum β-silyl stabilization is possible. In the transition state for the interconversion of the *syn* and *anti* isomers (TS-**324**) the oxygen−methyl bond of the *p*-methoxy group is oriented perpendicularly to the plane of the aryl ring and cannot conjugate with the aromatic π-system. This is the most favourable transition structure for the *syn/anti* isomerization (equation 48). Rotation around the C1−C^{+} bond in benzyl-type cations is known to be higher in energy as compared to rotation around the C4−OCH_3 bond.

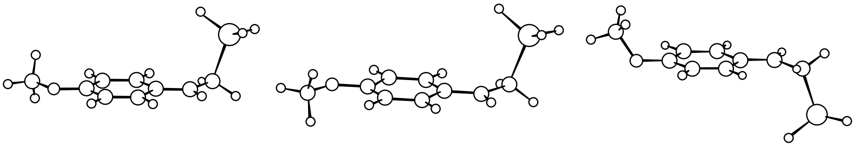

syn-**(324)** *anti*-**(324)** TS-(324)

FIGURE 11. Structures of *syn, anti* and TS-**324**

The energy difference between the transition structure TS-**324** with a perpendicular OCH_3 group and the *syn* and *anti* structures of **324** is a measure of the barrier for the methoxy group rotation around the C4–oxygen bond. The transition structure TS-**324** is calculated to be higher in energy by 10.3 kcal mol^{-1} than the *anti* isomer (*anti*-**324**). This is in satisfactory agreement with the experimentally observed energy barrier. The energy barrier for methoxy group rotation is a measure of the electronic demand of the carbocation. The better the β-substituent stabilizes the positive charge, the less delocalization into the aryl ring is necessary and thus the lower the barrier expected for the rotation around the C4–methoxy bond.

The corresponding barriers in the parent anisylmethyl cation **325**, the 1-anisylethyl cation **326**, the anisyl phenylmethyl cation **327** and the anisyl cyclopropylmethyl cation **328** were determined experimentally to be $\Delta G^{\#} = 12$, 10.6, 8.9 and 8 kcal mol^{-1}, respectively. This shows that a β-silyl substituent, here the R_3SiCH_2 group in **323**, is much more efficient than a methyl group in **326** and about as efficient as an α-phenyl or α-cyclopropyl ring in delocalizing the positive charge in **327** and **328**, respectively. This is in accord with the experimentally observed chemical shift of the *para* carbon C4, which is less deshielded in the R_3SiCH_2- substituted cation **323** ($\delta = 178.84$ ppm) compared with $\delta = 185.84$ ppm in the 1-*p*-anisylethyl cation **326** and $\delta = 181.93$ ppm in the 1-*p*-anisylpropyl cation **329** (see below).

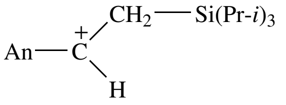

(323)

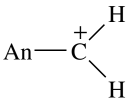

(325)

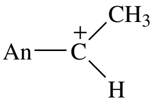

(326)

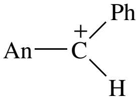

(327)

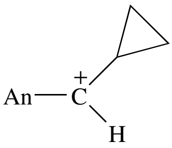

(328)

An = *p*-$MeOC_6H_4$

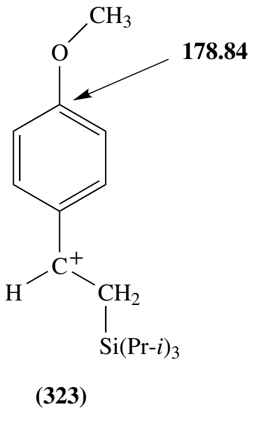

(323)

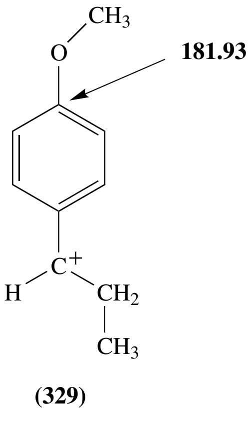

(329)

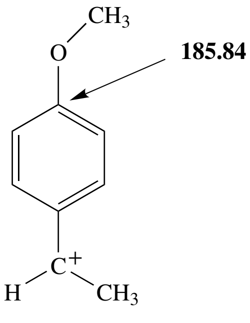

(326)

NMR chemical shift calculations for the B3LYP/6-31G(d) optimized geometries of the *anti* and *syn* SiH_3-substituted model cations *anti*-**324** and *syn*-**324** were performed using various levels of theory (Table 12).

The NMR chemical shifts calculated with the B3LYP/6-31G(d) DFT/SCF hybrid method using the GIAO method implemented in the Gaussian 94 program show deviations for both *syn*-**324** and *anti*-**324** of more than 10 ppm and up to about 20 ppm for the SiH_3-substituted methylene group compared with the corresponding experimental values observed for *syn*-**323** and *anti*-**323**. The deviations from experiment are smaller (<8 ppm) when the 6-311G(d,p) basis set is used. The SOS DFT IGLO III method implemented in the DeMon program which uses the Perdew-Wang91 DFT functional gives small deviations from experiment (<6 ppm, excluding the β-methylene carbon chemical shift)[134]. Computational experience with smaller carbocations, where calculations at higher levels are feasible, have shown that an appropriate level of theory for the optimization of the molecular geometry is very important in order to obtain useful results

TABLE 12. Experimental ^{13}C NMR chemical shifts of 1-*p*-anisyl-2-(trialkylsilyl)ethyl cations (at 100 MHz, $T = -126\,^{\circ}C$) in SO_2ClF (external capillary TMS, $\delta = 0$ ppm)[a]

NMR method		C1	C_α	C_β	C6	C2	C5	C3	C4	OCH_3
exp **(323)**										
	anti				152.18	138.12	114.98	123.85		
		132.20	205.30	43.17					178.84	58.93
	syn				148.49	141.65	121.95	116.57		
calc **(324)**										
GIAO	*anti*[b]	120.8	185.71	29.0	142.0	127.9	105.5	115.6	167.3	53.5
BLYP/	Δ	11.4	19.6	14.2	10.2	10.2	9.5	8.3	11.6	5.4
6-31G(d)										
GIAO	*anti*[c]	136.9	206.5	37.1	158.8	144.0	118.9	131.5	187.1	61.8
B3LYP/	Δ	−4.7	−1.2	6.0	−6.6	−5.9	−3.9	−7.7	−8.3	−2.9
6-311G(d,p)										
SOS DFT/	*anti*[d]	136.8	198.31	39.9	155.1	140.7	118.3	129.8	182.9	63.4
IGLO III	Δ	−4.6	7	3.3	−2.9	−2.6	−3.3	−6.0	−4.0	−4.5
GIAO	*syn*[b]	120.6	185.73	28.8	138.6	131.0	114.1	107.0	167.2	53.4
BLYP/	Δ	11.6	19.6	14.4	9.9	10.7	7.9	9.6	11.7	5.5
6-31G(d)										
GIAO	*syn*[c]	136.8	206.6	36.9	155.2	147.3	129.8	120.4	187.0	61.7
B3LYP/		−4.6	−1.3	6.3	−6.7	−5.8	−7.9	−3.8	−8.2	−2.8
6-311G(d,p)										
SOS DFT/	*syn*[d]	136.6	198.34	38.8	151.7	143.5	128.1	119.9	183.1	63.2
IGLO III	Δ	−4.4	7	4.4	−3.2	−1.9	−6.2	−3.3	−4.3	−4.3

[a] All geometries calculated at SCF/DFT level using B3LYP Functional and 6-31G(d) basis set. For numbering see equation 47.

[b] Reference TMS $\delta^{13}C(calc) = 186.01$ ppm, geometry (C_1): B3LYP/6-31G(d);NMR calculation: GIAO BLYP/6-31G(d).

[c] Reference TMS $\delta^{13}C(calc) = 183.9$ ppm, geometry (T): B3LYP/6-31G(d);NMR calculation: GIAO B3LYP/6-311G(d,p) ^{13}C.

[d] Reference TMS $\delta^{13}C(calc) = 183.5$ ppm, geometry (C1): B3LYP/6-31G(d);NMR calculation: SOS DFT PW91 (Perdew-Wang 91) IGLO III.

from the calculation of NMR chemical shifts. The general good agreement between the calculated and observed chemical shifts obtained show that DFT-based *ab initio* calculations are practical and reliable methods for the computational investigation of this type of benzyl-substituted carbocations. The calculated differences between the chemical shifts of the two sets of signals for the two isomers allow unequivocal assignment of the experimental signals to the *syn* and *anti* isomers even using the data obtained at the lowest level of the chemical shift calculations.

ii. Other β-silyl-substituted secondary benzyl cations. α. β-Silyl-substituted tolyl- and phenylmethyl cations. The protonation of styrenes normally leads to facile oligomerization and polymerization. β-Silyl-substituted styrenes lacking the strong electron-donating *p*-OCH_3 group but having bulky alkyl groups at silicon, such as 1-phenyl-2-triisopropylsilylethene **330**, are protonated under strong acidic conditions using FSO_3H/SbF_5 at low temperatures in SO_2ClF/SO_2F_2 solution to form β-silyl-α-aryl-substituted ethyl cations such as **331** (equation 49)[115,135].

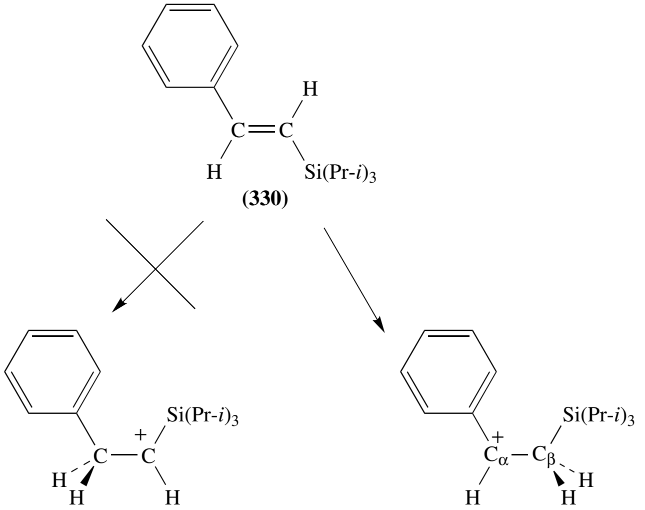

(332) **(331)**

(49)

The protonation of silyl-substituted styrenes is regioselective and leads to secondary benzyl cations with a β-silyl substituent (equation 49). The isomeric carbocation **332** is not formed.

Likewise, the 1-*p*-tolyl-2-triisopropylsilylethyl cation **333** is obtained by protonation of 1-*p*-tolyl-2-triisopropylsilylethene **334** (equation 50). Less acidic conditions, i.e. FSO_3H without addition of SbF_5, are sufficient to generate the carbocation **333** while they are insufficient to generate **331**.

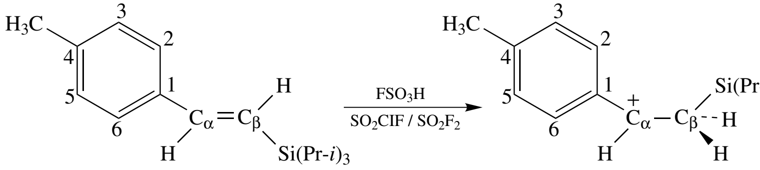

(334) **(333)**

(50)

Styrenes with less bulky alkyl groups at silicon, such as 1-phenyl-2-trimethylsilylethene **335**, 1-*p*-tolyl-2-trimethylsilylethene **337** and even the relatively more bulky substituted 1-*p*-tolyl-2-dimethylisopropylsilyl ethene **338**, on protonation using either FSO_3H/SbF_5 or FSO_3H, do not lead to solutions of persistent *β*-trimethylsilyl-substituted carbocations such as **336** from **335** but undergo fast *β*-silyl fragmentation to silyl-free cations such as **78** (equation 51).

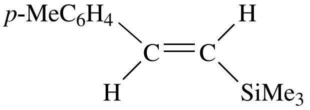

(337)

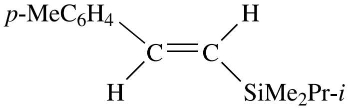

(338)

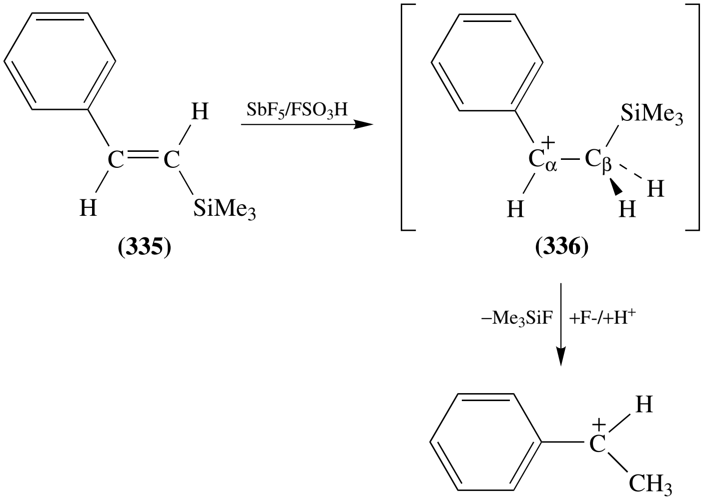

(335) **(336)** **(78)**

(51)

^{29}Si NMR spectroscopy is a suitable tool to monitor the electron demand in *β*-silyl-substituted carbocations. The ^{29}Si NMR chemical shifts in the *α*-phenyl-, *α*-*p*-tolyl,*α*-*p*-anisyl- and *α*-ferrocenyl-substituted *β*-silylethyl cations **331**, **333**, **323** and **339** are $\delta = 66.3$, 56.9, 38.9 and 23.5 ppm, respectively, decreasing regularly as expected on increasing the electron-donating capability of the *α*-substituent.

β. 1-Ferrocenyl-2-triisopropylsilylethyl cations. The 1-ferrocenyl-2-triisopropylsilylethyl cation **339** can be generated from 1-ferrocenyl-2-triisopropylsilylethene **340** with trifluoroacetic acid in SO_2ClF (equation 52)[115,135]. Cation **339** is the only *β*-silyl-substituted secondary carbocation which can be generated without *β*-silyl fragmentation even in trifluoroacetic acid, a less non-nucleophilic solvent than superacids.

The ^{13}C NMR chemical shifts (ppm) of **339** (−95 °C in SO_2ClF/SO_2F_2) are at $\delta =$ 139.4 (C^+), 98.83 (C1), 76.67/79.29 (C2,5), 90.99/91.64 (C3,4), 80.12 (C1′–5′), 25.29 (CH_2), 18.06 (*i*-Pr–CH_3) and 11.12 (*i*-Pr–CH). The positive charge in *α*-ferrocenyl-substituted carbocations is highly delocalized into the ferrocenyl moiety and the demand for hyperconjugative stabilization by the β-silyl-substituent is reduced. This is confirmed by comparing the ^{29}Si NMR chemical shift of $\delta = 23.5$ ppm in the 1-ferrocenyl-2-triisopropylsilylethyl cation **339** with $\delta^{29}\text{Si} = 66.3$ ppm for the corresponding 1-phenyl-2-triisopropylsilylethyl cation **331**. The β-silyl effect in α-ferrocenyl-substituted carbocations is, however, still verifiable.

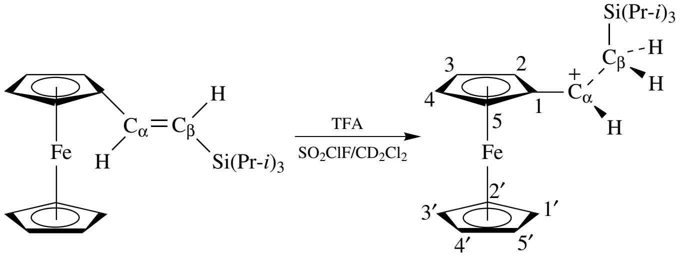

(340) **(339)**

(52)

The signals for the C2,5, C3,4 and C1′–5′ positions in the 1-ferrocenyl-2-triisopropylsilylethyl cation **339** are shielded by −7.5, −4.3 and −3.2 ppm, respectively, compared with the parent ferrocenylmethyl cation **341**. The corresponding shieldings for the *t*-butyl-(**342**) and isopropyl-(**343**) substituted ferrocenylmethyl cations, and the ferrocenylethyl cation **344** are smaller; **342**: −3.7, −0.4, −2.1 ppm; **343**: −4.6, −0.8, −2.0 ppm and **344**: −3.3, −0.35, +0.1 ppm, respectively[136]. This shows that even in carbocations with 2p(C$^+$)–π conjugative stabilization by a very good electron donor like the α-ferrocenyl group, hyperconjugative stabilization by the β-σ-bonds is operative and the stabilization by 2p(C$^+$)–σ(C–Si) interaction of a silyl group (as in **339**) is stronger than the 2p(C$^+$)–σ(C–H) hyperconjugation (as in **344**) or 2p(C$^+$)–σ(C–C) hyperconjugation (as in **342** and **343**).

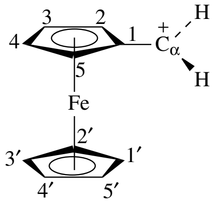

(341)

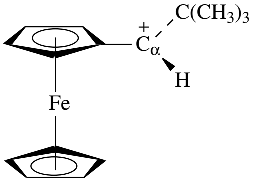

(342)

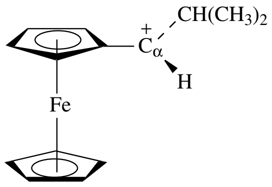

(343)

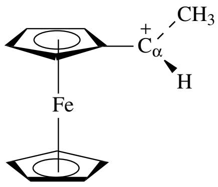

(344)

iii. β-Silyl-substituted tertiary benzyl cations. Earlier attempts to prepare the 1,1-diphenyl-2-trimethylsilylethyl cation **345** by ionization of 1,1-diphenyl-2-trimethylsilylethanol in FSO_3H/SO_2ClF at both −78 °C and −140 °C failed and led only to the formation of 1,1-diphenylethyl cation **298** along with trimethylsilyl fluorosulphate[113].

$$Ph_2C^+CH_2SiMe_3$$

(345)

α. 1,1-Diphenyl-2-(triethylsilyl)ethyl cations. When the benzene complex of triethylsilyl tetrakis(pentafluorphenyl)borate ($[Et_3Si^+(PhH)TPFPB^-]$) **346** was added to a benzene or toluene solution of 1,1-diphenylethene at room temperature, a highly coloured product was formed which was assigned to the 1,1-diphenyl-2-(triethylsilyl)ethyl cation **347** (equation 53)[137].

$$\underset{\textbf{(346)}}{[Et_3Si^+(PhH)TPFPB^-]} + H_2C{=}CPh_2 \longrightarrow \underset{\textbf{(347)}}{Et_3SiCH_2CPh_2{}^+\,TPFPB^-} + PhH \qquad (53)$$

The room temperature ^{13}C NMR spectrum in benzene-d_6 showed a peak at $\delta = 225.4$ ppm, in addition to signals at $\delta = 130.3$, 135.2, 137.6 and 141.1 ppm which were attributed to carbons in *meta*, *ortho*, *ipso* and *para* positions. The methylene signal was at $\delta^{13}C = 56.2$ ppm and the ethyl groups at silicon at $\delta^{13}C = 5.2$ and 6.3 ppm. A ^{29}Si NMR resonance was reported at $\delta = 46.2$ ppm. UV spectra show a strong absorption maximum at 432 nm and a weaker maximum at 310 nm, resembling those observed for the diphenylmethyl and diphenylethyl cations **299** and **298** at 442 nm and 300 nm, respectively.

In comparison with the 1,1-diphenylethyl cation **298** ($\delta^{13}C = 229.2$, C^+; 131.5, C_{meta}; 141.2, C_{ortho}; 141.5, C_{ipso} and 148.1, C_{para}) the 7 ppm high field shift of the *para* position may indicate the stabilizing effect of the β-silyl substituent. The C^+ carbon in cation **347** is about 4 ppm less deshielded compared to that in **298**. It is dangerous, however, to base interpretations on small differences of chemical shifts obtained under vastly different conditions; **347** was measured in benzene while **298** was measured in FSO_3H/SO_2ClF at very different temperatures. Since diphenyl-substituted carbocations are stabilized very efficiently by π-aryl resonance of the two phenyl rings, the β-silyl effect in **347** is diminished compared with carbocations with higher electron demand, such as cyclohexadienyl and phenylethyl cations.

The ^{29}Si NMR chemical shift for the *p*-triethyltoluenium ion **318** [δ (exp) = 81.8 ppm, δ(calc) = 82.1 ppm] and the 1-phenyl-2-triisopropylsilylethyl cation **331** ($\delta = 66.34$ ppm) indicate a larger hyperconjugative charge delocalization towards the silyl group in these carbocations. The ^{29}Si NMR chemical shift in the 1,1-diphenyl-2-(triethylsilyl)ethyl cation **347** ($\delta = 46.2$ ppm) is in between the shift for 1-(*p*-tolyl)-2-triisopropylsilylethyl cation **333** ($\delta^{29}Si = 56.92$ ppm) and the 1-(*p*-anisyl)-2-triisopropylsilylethyl cation **323** ($\delta^{29}Si = 38.88$ ppm).

iv. β-Silyl-substituted allyl cations. α. 2-[1′-(Trimethylsilyl)ethenyl]adamant-2-yl cations. The 2-[1′-(trimethylsilyl)ethenyl]adamant-2-yl cation **348a** can be obtained by the reaction of [1′-(trimethylsilyl)ethenyl]-2-adamantanol with FSO_3H/SbF_5 at −130 °C[138].

The ^{1}H and ^{13}C NMR data measured at $-100\,^\circ$C are in accord with the formation of the carbocation structure (equation 54).

The trimethylsilyl substituent in 2-(trimethylsilyl)allyl cations is enforced into a perpendicular conformation and thus β-C$-$Si hyperconjugative stabilization is essentially not possible. The carbocationic centre C1 (δ^{13}C $= 295.0$ ppm) and the terminal methylene carbon C3 of the allyl system (δ^{13}C $= 166.6$ ppm) in **348a** are deshielded by 11.5 and 1.2 ppm, respectively, compared with the silicon-free analogue **348** (δ^{13}C = C1 283.5; C3 165.7 ppm). The deshielding was inferred to arise from a neighbouring silicon-induced anisotropic effect or from the trimethylsilyl group induced twisted π-system. ^{13}C chemical shift calculations [IGLO at the DZ/6-31G(d) level, geometry at 6-31G(d)] of the parent allyl cation $C_3H_5{}^+$ and 2-SiH_3- and 2-$SiMe_3$-substituted allyl cations show a deshielding of the same magnitude (10 ppm) for the cationic centres in the silyl-substituted allyl cation model structures (δ^{13}C = C1, C3: 2-SiH_3 $= 238.6$ ppm; 2-$SiMe_3$ $= 235.1$ ppm) as in the parent allyl cation (δ^{13}C = C1, C3: 228.8 ppm). MM2 and MNDO calculations of the 1-adamantyl-2-trimethylsilylallyl cation **348a** show that the bulky trimethylsilyl substituent severely hinders the coplanarity of the carbocationic carbon and the vinylic π-system. This reduces the allylic stabilization due to a reduced overlap of the π-electrons with the cationic centre compared with the system lacking the silyl group. Thus the interplay of electronic and steric effects produces a slight deshielding of the signal for the C^+ carbon and indicates an overall destabilizing effect of the trimethylsilyl group in this cation. The silicon-substituted central carbon of the 1-adamantyl-2-trimethylsilylallyl cation **348a** (δ^{13}C $= 161.2$ ppm vs 140.7 ppm for **348b**) is deshielded by 20.5 ppm in accordance with other experimental observations on acylsilanes. For the central carbon of 2-R-substituted allyl cations $C_3H_4R^+$, ^{13}C chemical shifts of $\delta = 136.9$, 144.4 and 151.7 ppm for 2-R = H, SiH_3 and $SiMe_3$, respectively, were calculated by IGLO at the DZ/6-31G(d) level using 6-31G(d) geometries.

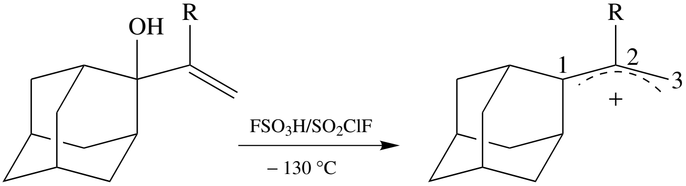

(54)

R = $Si(CH_3)_3$
R = H

(348) (a) R = $Si(CH_3)_3$
(b) R = H

At $-100\,^\circ$C the β-C$-$H carbons of the adamantyl moiety are equivalent, indicating a rapid rotation across the bond between the cationic carbon and the central carbon of the allyl cation. However, in the parent 2-ethenyladamantyl cation **348b** these carbons are non-equivalent, indicating a high barrier for such a rotational process. The low rotational barrier in the silyl-substituted cation can be rationalized by assuming the intermediacy of a perpendicular allyl cation conformation **348ap** in which the β-silyl group is aligned in the plane with the vacant p orbital at the cationic carbon. This conformation lacks stabilization by $\pi$$-$p allyl conjugation but is hyperconjugatively stabilized by the β-silyl effect. The perpendicular conformation of the β-silyl-substituted allyl cation **348ap** is thus lower in energy compared with the perpendicular conformation of the allyl cation **348bp** lacking the *β*-silyl group (equations 55 and 56). Therefore the barrier for allyl rotation is smaller for the *β*-silyl-substituted allyl cation **348a** as compared with **348b**, leading at −100 °C to a fast exchange on the ^{13}C NMR time scale and an averaged signal for the *β*−CH carbons of the adamantyl moiety.

2. sp-Hybridized carbocations (vinyl cations)[139,140]

a. β-Silyl-substituted dienyl cations. The silyl-substituted vinyl cations **349** and **350** are formed by the reaction of the silyl-substituted allenyl alcohols **351** with SbF_5 at temperatures below −130 °C[141,142]. At about −110 °C cations **349** and **350** fragment with cleavage of the *β*-C−Si bond and expulsion of the silyl group, forming the silicon-free cations **352** and **353** (equation 57). The ^{13}C NMR chemical shifts of **349** and **350** (Table 13) are in general similar to those in the other *α*-vinyl-substituted vinyl cations.

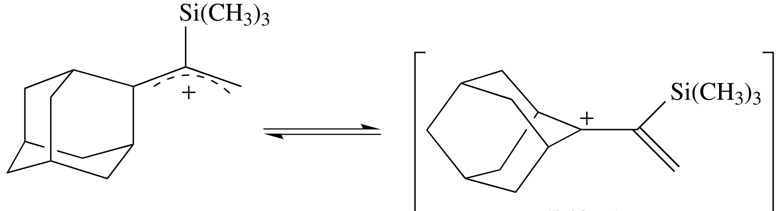

(348a) **(348ap)** (55)

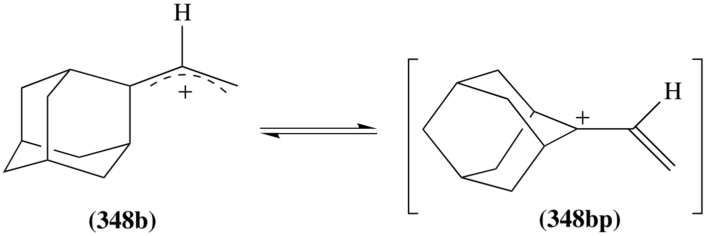

(348b) **(348bp)** (56)

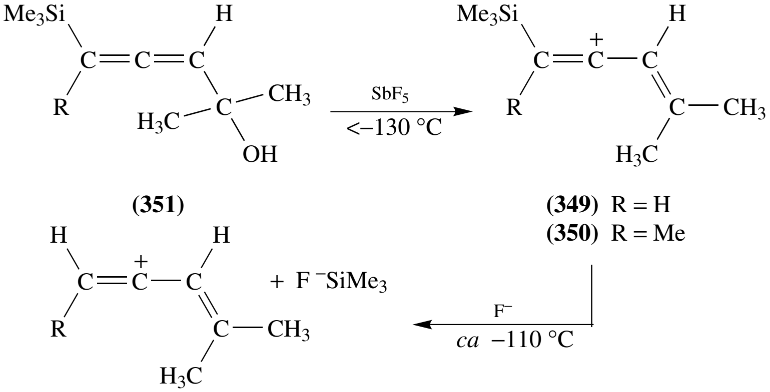

(57)

(352) R = H
(353) R = Me

The shielding of the C_α and $C_{\gamma'}$ resonances in **349** and **350** indicates allyl resonance delocalization of the positive charge. The unusual high field resonance of the signals for the sp^2-hybridized carbons C_β and $C_{\beta'}$ in accord with those for other vinyl cations, are due to the sp-hybridization of the geminal C_α carbon. The methyl groups at $C_{\gamma'}$ are non-equivalent because of the partial double bond character of the $C_\alpha{-}C_{\beta'}$ bond.

A closer comparison of the silyl-substituted cations **349** and **350** with the analogous non-silyl-substituted cations **352**, **353** and **355** reveals significant differences. The charge-dispersing effect of the β-trimethylsilyl group is evident when **349** and **350** are compared with their non-silyl-substituted counterparts. The positively charged C_α in **349** is about 33–36 ppm and, in **350**, 54–57 ppm less deshielded than the corresponding carbon in **352**, **353** and **355** (Table 13). The chemical shift of the C_α carbon is, however, not only dependent on the charge density at C_α, but is also influenced by a $\beta{-}\pi$ substituent effect on the chemical shift from the different substituents at C_β. The composite effect of the charge-density effect and C_β-substituent effect precludes a direct correlation of the chemical shift of the C_α signal with the charge delocalization. The γ'-carbon is, however, remote from the substitution site C_β and the changes of the chemical shift for $C_{\gamma'}$ in dienyl cations are related only to the charge delocalization abilities of the different C_β substituents. The 28 ppm and 25 ppm shielding of $C_{\gamma'}$ in **349** compared with **352** and **353**, respectively, can thus be attributed to the superior electron-donating ability of a β-trimethylsilyl group compared with a β-hydrogen or β-methyl group, respectively. The high field shift for the signals of the γ'-methyl groups in **349** and **350** as compared with those in **352**, **353** and **355** reflects a lower demand for a C−H hyperconjugative stabilization of a positive charge at the γ-carbon by the γ-methyl groups because less charge is localized at this site in **349** and **350**. The signal of the methyl carbons on the silicon group shows no significant shift differences compared with the neutral precursor molecules, and hence the contribution of the alkyl groups at silicon to the delocalization of the positive charge in this type of carbocation is not significant. Both positively charged carbons of the allyl moiety in **349** and **350**

TABLE 13. ^{13}C NMR chemical shifts (δ, ppm) for dienyl cations of type **354** in SO_2ClF/SO_2F_2[a]

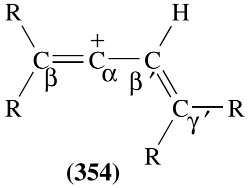

(354)

	C_α	C_β	$C_\beta{}'$	$C_\gamma{}'$	$C_\beta{-}R$	$C_\gamma{}'{-}R$	
352[b]	242.50	79.40	114.70	262.10		33.23, 37.22	
353[c]	244.30	90.50	114.51	259.40	9.30	32.53, 36.56	
355	245.39	101.55	113.9	257.64	16.29	32.43, 36.44	
356	202.66	63.66	111.72	228.92	39.63	27.15, 30.62	
349[b]	208.72	80.83	108.94	234.32		28.48, 32.52	−0.4 $SiMe_3$
350[c]	188.43	86.42	107.85	221.72	11.09	26.84, 30.68	−1.17 $SiMe_3$

[a] 100.62 MHz, internal reference $\delta(NMe_4{}^+) = 55.65$ ppm, $T = -120\,^\circ C$, chemical shifts $\delta(\pm 0.03)$ ppm.

[b] At $-137\,^\circ C$.

[c] At $-126\,^\circ C$.

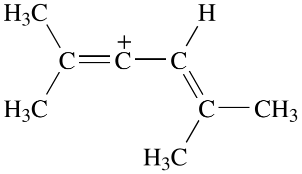

(355)

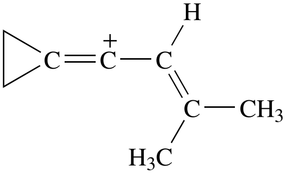

(356)

are more shielded than the corresponding carbons in **352**, **353** and **355**. This indicates that the positive charge is delocalized away from0 the allylic system **357A** ↔ **357C** towards the β-trimethylsilyl group, as described by the hyperconjugative resonance structure **357B.**

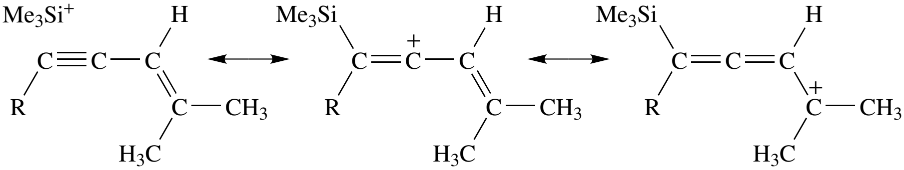

(357B) **(357A)** **(357C)**

The electron donating ability of a β-C−Si bond in **349** is nearly as large as the effect of the strained C−C bond of a β-cyclopropylidene substituent in **356**. The difference in the chemical shift of $C_{\gamma'}$ in **356** (228.92 ppm) and in **349** (234.32 ppm) is only 5.4 ppm. The additional methyl substitution at C_β in the dienyl cation **350** causes an unexpectedly large effect on the chemical shifts, and the signals of both positively charged carbons C_α and $C_{\gamma'}$ are shifted upfield compared with **349**. For the dienyl cations **352**, **353** and **355** an additional methyl group leads to a downfield shift for C_α and an upfield shift for $C_{\gamma'}$ of about 1.5 ppm per methyl group (Table 13). This indicates an internal shift of the positive charge in **352**, **353** and **355** between the two terminal carbon atoms of the resonating allylic system from the γ'-site to the α-site in the order **355**, **353** and **352**. However, for the geminal β-methyl and β-trialkylsilyl-substituted dienyl cation **350**, C_α and $C_{\gamma'}$ absorb at 20.3 ppm and 12.6 ppm higher field, respectively, as compared with cation **349**, which has only the trialkylsilyl substituent at C_β. The ^{13}C NMR chemical shifts for cation **350** indicate that the additional methyl group at the β-carbon enhances the hyperconjugative interaction of the β-Si−C bond with the formally empty (2p)π orbital of the vinyl cation C_α carbon. This effect can be rationalized by theoretical calculations. The additional methyl substituent at C_β in the model cation structure **358** decreases the C_α−C_β−Si bond angle as compared with the model structure **359**. This geometrical distortion towards more bridging enhances the hyperconjugative effect of the β-silyl group in cations of type **358**.

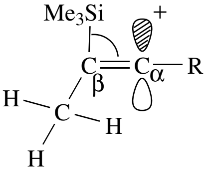

(358)

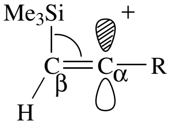

(359)

When the ^{13}C NMR chemical shift of the $C_{\gamma'}$ carbon in dienyl cations **349, 350, 352, 353, 355** and **356** is used as a probe for the ability of β-substituents to hyperconjugatively donate electrons to the formally empty 2p(π) orbital of the vinyl cation C_α, the order in Scheme 35 is obtained;

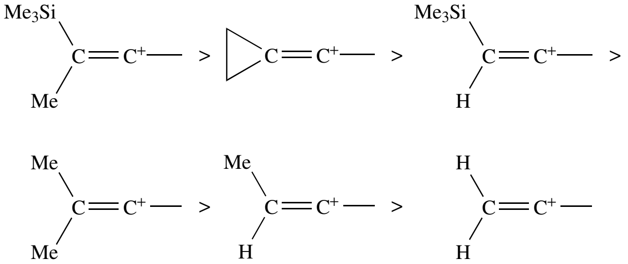

SCHEME 35

b. β-Silyl-substituted α-arylvinyl cations. i. α-Ferrocenyl-β-silyl-substituted vinyl cations. ^{1}H NMR spectroscopy was used in 1977 to search for β-silyl-substituted ferrocenyl cations[143]. 1-(1′,2-Dimethylferrocenyl)-2-(trimethylsilyl)ethyne **360** was converted in trifluoroacetic acid solution into 1-(1′,2-dimethylferrocenyl)vinyl cation **363**, which quickly captured the solvent to form the 1-(1′,2-dimethylferrocenyl)-1-trifluoracetoxyethyl cation **364**. The reaction was followed by ^{1}H NMR spectroscopy. The first-formed β-silyl-substituted vinyl cation **361**, which was not observed under experimental conditions, presumably fragments to ferrocenylalkyne **362** and trimethylsilyl trifluoroacetate. The alkyne **362** is protonated to give the 1-ferrocenylvinyl cation **363**, which is quickly converted by the acid solvent to cation **364** (equation 58). Related fragmentations of benzyltrimethylsilanes in trifluoroacetic acid are known.

Protonation of 1-ferrocenyl-2-trimethylsilylalkyne **365** by trifluoroacetic acid in SO_2ClF at $< -80\,^\circ$C yielded the α-ferrocenyl-β-trimethylsilylvinyl cation **366**. Cation **366** decomposes slowly at $-80\,^\circ$C to the parent α-ferrocenylvinyl cation **367** and trimethylsilyl trifluoroacetate (equation 59)[144].

Steric shielding of the silicon atom increases the stability of the initially formed β-silyl vinyl cations. The 1-ferrocenyl-2-(triisopropylsilyl)vinyl cation **368** and the 1-ferrocenyl-2-(dimethyl-*tert*-hexylsilyl)vinyl cation **369** are formed when the corresponding alkynes are protonated with trifluoroacetic acid in SO_2ClF. These cations show no fragmentation at comparable low temperatures[144].

The general ^{13}C NMR spectroscopic data of the β-silyl α-ferrocenylvinyl cations are similar to those of the β-*tert*-butyl-substituted α-ferrocenylvinyl cation **370** (Table 14)[145]

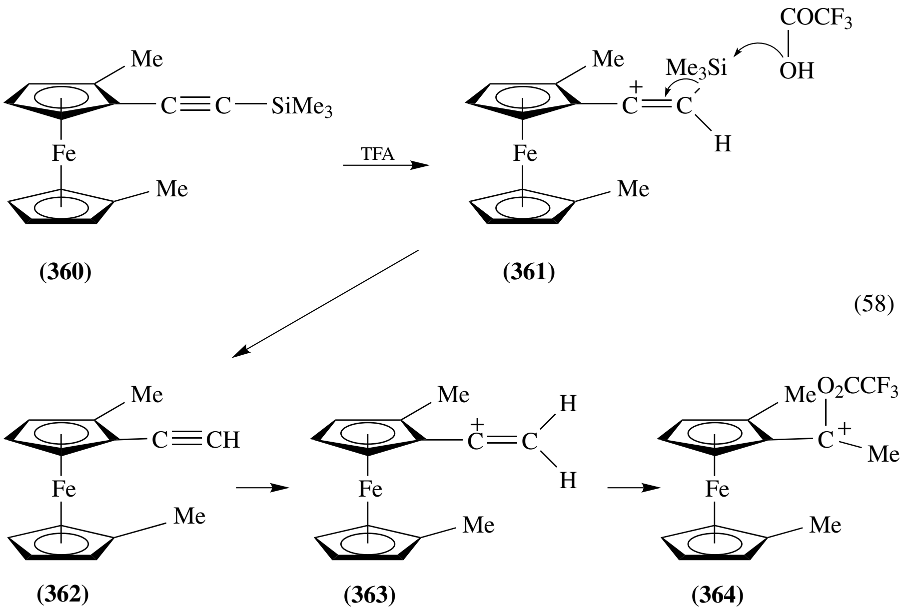

(58)

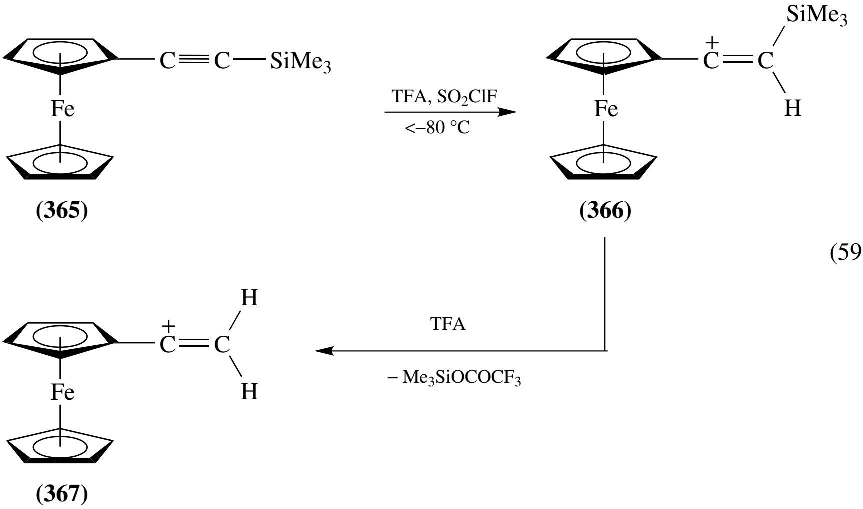

(59)

A detailed comparison of the chemical shifts of the ring carbons in the β-H **(367)**, β-*tert*-butyl- **(370)** and β-trialkylsilyl-substituted α-ferrocenylvinyl cations (**366, 368** and **369**) reveals that the β-silyl group is superior to β-alkyl groups in stabilizing the positive charge. In the β-silyl-substituted vinyl cations the C3, C4 signals are about 2.5 ppm shielded as compared with the β-H or β-*tert*-butyl-substituted vinyl cations. The chemical shifts in the silyl-substituted ferrocenylvinyl cations exhibit only minor variations on changing the alkyl groups at silicon, showing that the latter do not contribute significantly to the charge delocalization in these carbocations.

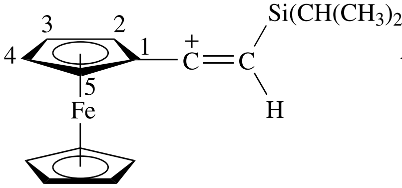

(368)

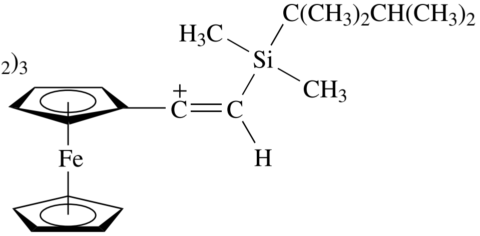

(369)

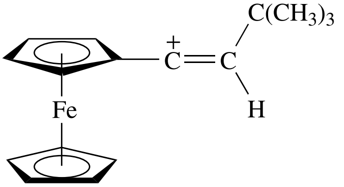

(370)

The β-silyl effect is attenuated in α-ferrocenyl-substituted vinyl cations because the strong electron-donating effect of the α-ferrocenyl group renders the cation centre less electron-deficient and thus lowers the demand for hyperconjugative stabilization by substituents at the β-carbon[149].

TABLE 14. ^{13}C NMR chemical shifts (δ, ppm) for α-ferrocenyl-substituted vinyl cations **366–370**

	R in Fc-$\overset{+}{C}$ = CHR	C_α	C_β	C3,4	C2,5	C1	C1′–5′
367	H	183.7	99.2	95.9	81.9	72.5	84.9
370	CMe_3	177.1	126.6	96.1	83.1	74.7	85.2
366	$SiMe_3$	183.2	105.1	93.4	79.7	63.1	83.1
369	Si(Me)$_2$(Hex-*t*)	181.9	104.4	93.3	79.6	62.6	83.1
368	Si(Pr-*i*)$_3$	181.8	99.4	93.3	79.4	62.2	83.1

ii. α-Mesityl-β-silyl-substituted vinyl cations. Steric shielding by bulky alkyl groups at silicon and special experimental precautions are essential for the successful preparation of β-trialkylsilyl-substituted α-arylvinyl cations in solution, which otherwise easily undergo a C_β–Si bond fragmentation. The α-mesityl-β-silyl-substituted vinyl cations **372–375** are accessible by protonation of the corresponding alkynes with FSO_3H/SbF_5 in SO_2ClF/SO_2F_2 at −130 °C (equation 60)[114,147] Figure 12 shows as a typical example the ^{13}C NMR spectrum of the α-mesityl-β-(triisopropyl)silylvinyl cation **375**.

Attempts to generate the β-trimethylsilylvinyl cation **376** by protonation of mesityltrimethylsilyl ethyne **377** (equation 61) were unsuccessful[114,148].

The β-unsubstituted mesitylvinyl cation **378** is not accessible by direct protonation of mesitylethyne **379** (equation 62). All attempts to generate vinyl cations by direct

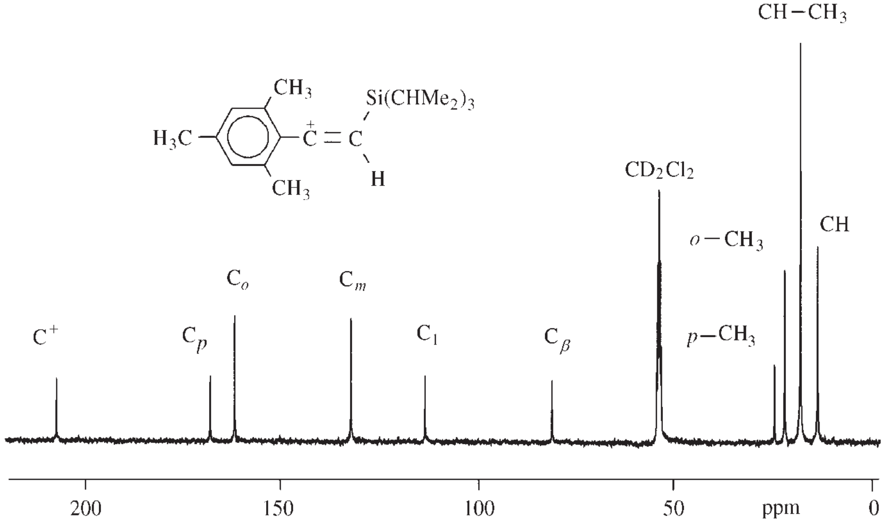

FIGURE 12. ^{13}C NMR of α-mesityl-β-(triisopropyl)silylvinyl cation **375** at −135 °C in SO_2ClF/SO_2F_2, internal reference CD_2Cl_2.

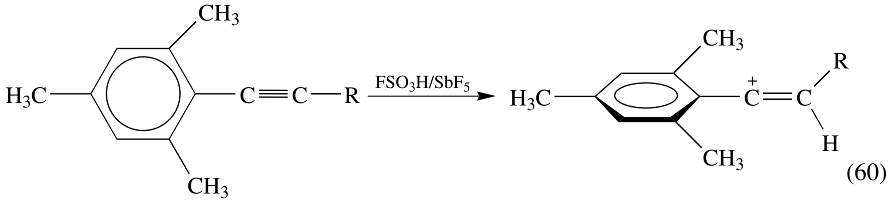

(60)

(371)

(372) R = $SiMe_2Pr$-*i*
(373) R = $SiMe_2Bu$-*t*
(374) R = $SiMe_2Hex$-*t*
(375) R = Si(Pr-*i*)$_3$

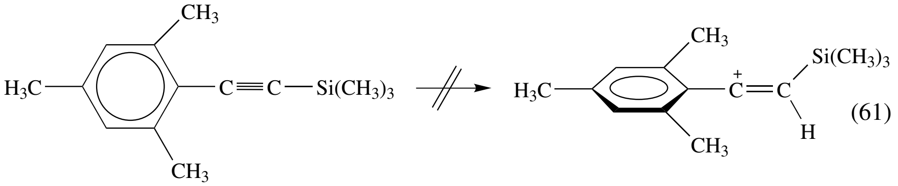

(61)

(377)

(376)

protonation of monosubstituted alkynes with superacids have failed and led instead only to the formation of rather complex mixtures and partial polymerization.

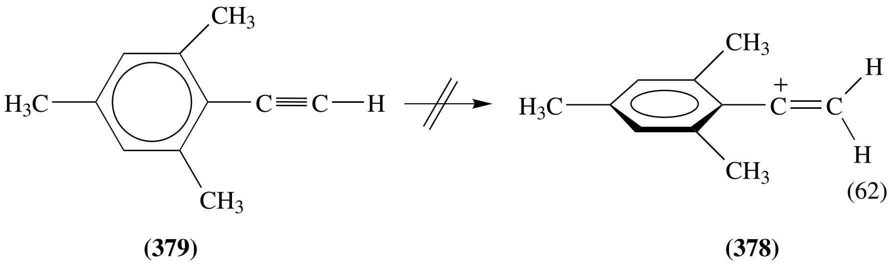

(62)

The mesitylvinyl cation **378** is obtained, however, without apparent formation of any side products, when a solution of α-mesityl-β-dimethylisopropylsilylvinyl cation **372** is warmed up from -130 to $-100\,^{\circ}$C for 10 minutes. This reaction can be explained as outlined in equation 63.

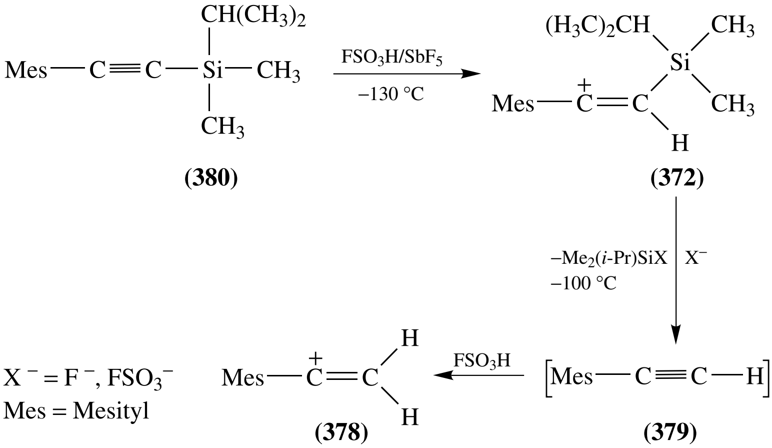

(63)

Protonation of the fairly sterically congested 1-mesityl-2-dimethylisopropylsilyl alkyne **380** at $-130\,^{\circ}$C leads to a clean formation of the α-mesityl-β-silyl-substituted vinyl cation **372**. The hyperconjugative interaction of the β-C$-$Si bond with the formally vacant p orbital at C_α increases the partial positive charge at silicon, thus increasing its susceptibility to nucleophilic attack by the anions present in the superacid solution. Fragmentation of the β-silyl group in **372** occurs at somewhat higher temperatures ($-100\,^{\circ}$C). The nucleophile attacks at silicon likely via an S_N2(Si) transition state, which subsequently leads to fast cleavage of the β-C$-$Si bond. This cleavage is facile because the vinyl cation moiety is strongly electron-withdrawing, thus acting as a good leaving group to form the trialkylsilane i-PrMe$_2$SiX (X $=$ OSO$_3$F or F). The monosubstituted alkyne **379** formed as a transient in the presence of a large excess of superacid is immediately protonated to yield the silicon-free vinyl cation **378**.

An alternative mechanism, proceeding through a double protonation reaction sequence followed by silyl fragmentation, could be envisaged in the highly acidic media (equation 64). The first step at $-130\,^{\circ}$C leads to C_β protonation of the alkyne **380** with formation of the vinyl cation **381** ($=$ **372**). At the higher temperature ($-100\,^{\circ}$C) the large excess of superacid permits a second proton to attack the vinyl cation **381**, presumably at the p orbital at C_β which is orthogonal to the vacant p orbital at C_α. This leads to a highly reactive gitonic dication intermediate **382** with two formal positive charges at the C_α carbon. Further reaction to give stable products could occur by concerted attack of the gegen ion X^- at silicon and a C_β–Si bond cleavage to form $XSiR_3$ and the β-unsubstituted mesitylvinyl cation **378**.

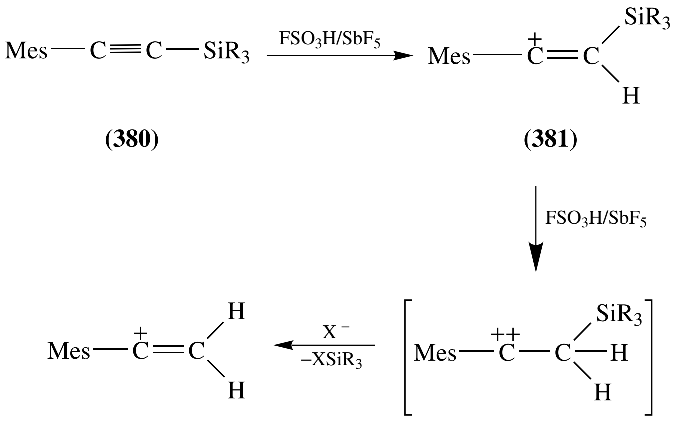

(380) **(381)** **(378)** **(382)**

(64)

The silyl fragmentation in superacids initiated by a controlled temperature increase is a method to generate persistent carbocations, such as the vinyl cation **378**, which are not accessible by direct protonation of unsaturated hydrocarbons because of excessive formation of oligomeric and polymeric products.

For the β-trialkylsilyl-substituted mesitylvinyl cations **373–375** with larger alkyl groups at silicon, fragmentation to the silicon-free vinyl cations is not observed. Cations with larger groups are stable at relatively higher temperatures compared with those substituted by less bulkier alkyl groups at silicon. The β-silyl fragmentation reaction in superacids is controlled, at least in part, by steric crowding caused by the alkyl groups at silicon. However, this is not the only factor controlling the stability of β-silyl-substituted arylvinyl cations towards C_β–Si bond cleavage. Depending on the ability of the α-aryl substituent to delocalize a positive charge, more or less partial positive charge is localized at the silicon centre as a result of the hyperconjugative electron donation from the β-C–Si bond to the formally vacant $2p(\pi)$ orbital at the C^+ carbon. This changes the susceptibility of the silicon towards nucleophilic attack which is followed by cleavage of the β-C–Si bond.

The NMR spectroscopic data of the β-silyl-substituted α-mesitylvinyl cations corroborate the hyperconjugative charge-delocalizing ability of β-silyl groups. Comparison with β-alkyl- and β-H-substituted α-mesitylvinyl cations gives a measure of the magnitude of the β-silyl effect in these type of carbocations. The ^{13}C NMR spectroscopic data of the α-mesitylvinyl cations **372–375** and **378, 383–385** with various β-substituents together with data for the sp^2-hybridized mesityl carbocations **386** and **387** are summarized in Table 15.

The ^{13}C NMR chemical shifts of the positively charged carbon in the vinyl cations in Table 15 cover a range from 239 to 192 ppm. The difference of the chemical shift for

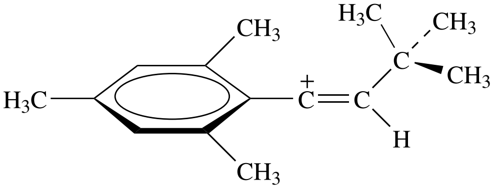
(383)

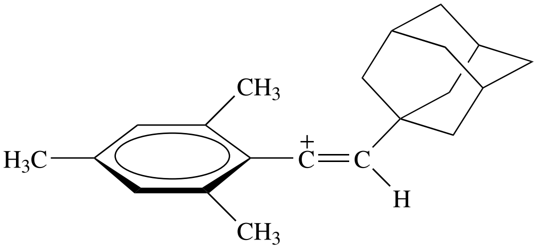
(384)

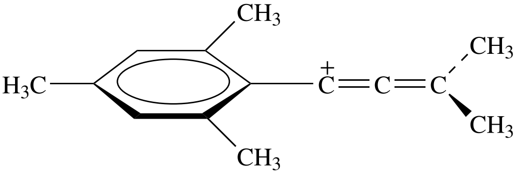
(385)

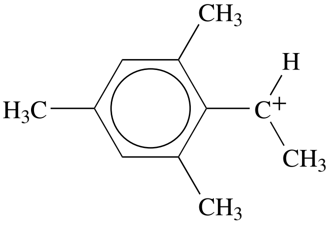
(386)

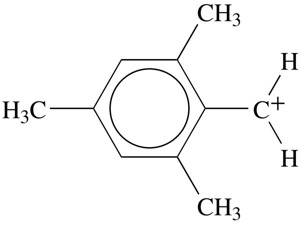
(387)

the C^+ carbon in the β-silylvinyl cations **372–375** and in the silicon free analogues **378** and **383–385** is 30–33 ppm. Silyl substituents cause a pronounced shielding effect on the C_β carbon shift ($\Delta\delta$: *ca* −24 ppm) as compared with alkyl groups. The aromatic C1 position in the vinyl cations **372–375**, **378** and **383–385** display a large shielding effect of 20–30 ppm relative to the 1-mesitylethyl **(386)** and the mesitylmethyl cation **(387)**. This is due to the different hybridization of the adjacent C^+ carbon which is sp-hybridized in the vinyl cations but sp^2-hybridized in the trigonal carbocations **386** and **387**. Analogous high field shift has been observed for the C1 aryl carbon adjacent to the sp-hybridized C^+ carbon of the benzoyl cation **388**.

TABLE 15. ^{13}C NMR chemical shifts (δ, ppm) of vinyl cations **372-375**, **378**, **383-385** and cations **386** and **387** in SO_2ClF/SO_2F_2^{a,b}

Cation	C_α	C_β	C1	C_{ortho}	C_{meta}	C_{para}	*o*-Me	*p*-Me	Other
378	238.5	82.3 (177)	116.6	167.8	133.8 (166)	180.0	21.7 (130)	26.1 (131)	
383	237.3	107.1 (174)	118.4	166.4	133.4 (165)	178.5	21.5 (130)	25.8 (129)	Cq 40.9, Me 30.0 (125)
384	238.7	106.3 (169)	118.7	166.1	133.2 (166)	177.9	21.5 (130)	25.7 (131)	C1' 45.0, C2', 8', 9' 43.4, C3', 5', 7' 29.2 (128), C6', 4', 10' 35.6 (125)
372	206.0	83.6 (183)	113.5	162.7	132.5 (166)	168.5	21.4 (131)	24.4 (129)	Si-Me −4.2 (122), CH 16.5 (129), C-Me 16.7 (129)
373	206.0	83.2 (182)	113.2	162.3	132.2 (165)	168.2	21.3 (127)	24.2 (124)	Si-Me −5.4 (122), Cq 19.8, C-Me 24.9 (122)
374	207.3	84.3 (184)	113.5	162.3	132.3 (165)	168.1	21.4 (131)	24.3 (129)	Si-Me −2.9 (128), Cq 26.6, Cq-Me 17.8 (125), CH 33.6 (156), CH-Me 18.0 (132)
375	207.8	81.1 (175)	113.6	162.3	132.6 (166)	168.5	21.8 (134)	24.4 (132)	CH 13.4 (118), Me 17.8 (125)
385	192.2	136.2	119.5	155.7	131.6 (160)	165.3	21.0 (129)	23.7 (130)	C_γ 213.9, Me 34.9(132)
387	172.0 (166)		144.1	168.3	135.3 (170)	189.6	20.9 (135)	27.3 (131)	
386	204.3 (154)	27.1 (129)	140.5	166.4 163.9	136.5 134.4 (165) (171)	179.6	26.6 25.3 (130) (127)	21.6 (131)	

[a] 100.6 MHz, $\delta(\pm 0.1$ ppm) at $-120\,^\circ$C; internal reference: CD_2Cl_2: $\delta = 53.8$ or NMe_4^+: $\delta = 55.7$,

[b] $^1J_{CH}$, coupling constants (± 1.8 Hz) in parentheses.

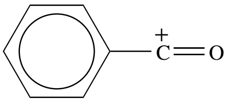

(388)

The chemical shift of the C^+ carbon in the vinyl cations **372–375**, **378**, **383–385** is dependent not only on the charge density, but is also influenced by a substituent effect on the chemical shift from the different substituents at C_β. Thus the shift of the C^+ carbon is not a good probe to evaluate the effect of a β-silyl group on a positive charge in **372–375**. Similar to sp^2-hybridized benzyl cations the shift of the *para* carbon, however, is a suitable probe to monitor the demand for delocalization of the positive charge into the aromatic ring. Figure 13 shows a comparison of the ^{13}C NMR chemical shift of the *para* carbon in the vinyl cations **372–375**, **378**, **383–385** and the sp^2-hybridized model cations **386** and **387**[149]. The better the positive charge is stabilized by σ-electron donation of the substituent at the β-carbon as in **372–375** and **383–384** or by π-electron donation of the β-vinylidene substituent as in the allenyl cation **385**, the less is the demand for charge delocalization by π-conjugation with the aromatic ring and thus the *para* carbon becomes less deshielded.

The chemical shift for the *para* carbon in the parent mesitylvinyl cation **378** (180.0 ppm) and in the mesitylethyl cation **386** (179.6 ppm) is similar, indicating that the electronic demand is about the same. Both carbocations are stabilized by σ-bond hyperconjugative interaction with the β-hydrogens as compared with the mesitylmethyl cation **387** (189.6 ppm) which lacks a β-substituent. A pronounced upfield shift of the *para* carbon (10–12 ppm) is observed for the β-silylvinyl cations **372–375** relative to the silyl-free vinyl cations **378**, **383** and **384**, indicating a decrease in the electron demand when the β-substituent is changed from β-H or β-alkyl to a β-silyl group. This shows that β-C−Si hyperconjugation is more efficient than β-C−H or β-C−C hyperconjugation.

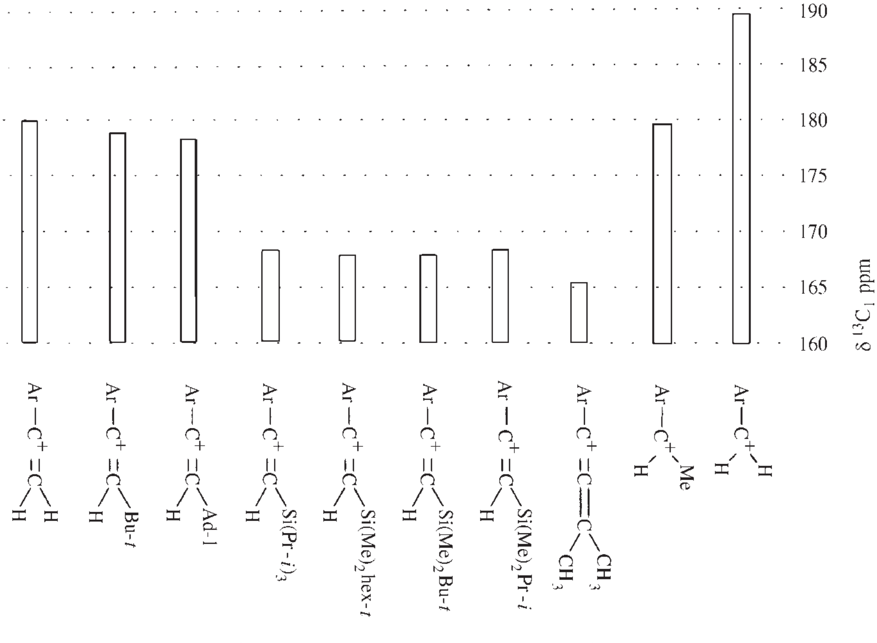

FIGURE 13. Comparison of the *para* carbon NMR chemical shift (ppm) in mesitylvinyl cations **372–375**, **378**, **383–385** and model cations **386** and **387** (Ar = mesityl).

The close resemblance of the *para* carbon shift of the silyl-substituted cations **372–375** (168–170 ppm) to that of the mesitylallenyl cation **385** (165.9 ppm), which in addition to aryl conjugation is stabilized by β-allyl resonance, shows that hyperconjugative interaction of a β-C–Si σ-bond with the 'vacant' 2p(π) orbital on C^+ in **372–375** is about as efficient as β-π-conjugation in **385**.

iii. α-Tolyl- and α-phenyl-β-silyl-substituted vinyl cations. Protonation of 1-(*p*-tolyl)-2-triisopropylsilylethyne **388a** leads to formation of the α-(*p*-tolyl)-β-triisopropylsilylvinyl cation **389a** (equation 65)[114,140]. The ^{13}C NMR chemical shifts and $^1J_{CH}$ coupling constants are summarized in Table 16.

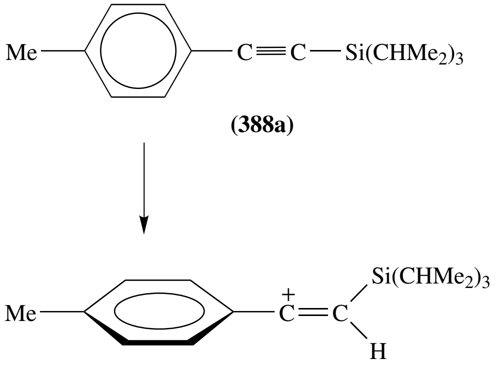

(388a)

(389a)

(65)

The dimethylisopropylsilyl-substituted 1-*p*-tolylvinyl cation **389b** can be prepared from the corresponding alkyne **388b** at temperatures below −125 °C. At somewhat higher temperature (−105 °C) the cleavage of the β-silyl carbon bond occurs rapidly and the α-(*p*-tolyl)vinyl cation **390** is formed as the only detectable product (equation 66). The β-fragmentation is faster and occurs at lower temperatures compared with that of the

TABLE 16. ^{13}C NMR chemical shifts (δ, ppm) of α-tolyl and α-phenyl-substituted vinyl cations **389a, 389b**, **390** and **393** in SO_2ClF/SO_2F_2[a,b]

	C_α	C_β	C1	C_{ortho}	C_{meta}	C_{para}	*p*-Me	Other
390	250.94	77.10	114.24	152.78	135.44	181.11	26.79	
		(177)		(175)	(172)		(134)	
389a	205.84	73.82	111.23	148.11	133.69	167.25	24.45	CH 13.55
		(187)		(170)	(170)		(129)	Me 17.33
					(9.0)			
389b[c]	—	—	—	147.89	133.57	—	24.40	
393	205.84	73.82	114.16	148.18	132.51	164.6		CH 14.12
	(4.0)	(192)	(8.4)	(170)	(172)	(6.4)		(116.7)
					(6.3)			Me 17.35
								(126.6)

[a] 100.6 MHz, δ(± 0.1 ppm) at −120 °C; internal reference: CD_2Cl_2 $\delta = 53.8$ or NMe_4^+ $\delta = 55.7$.

[b] J_{CH} coupling constants (±1.8 Hz) in parentheses.

[c] Weak signals.

corresponding α-mesityl-substituted vinyl cation **372**.

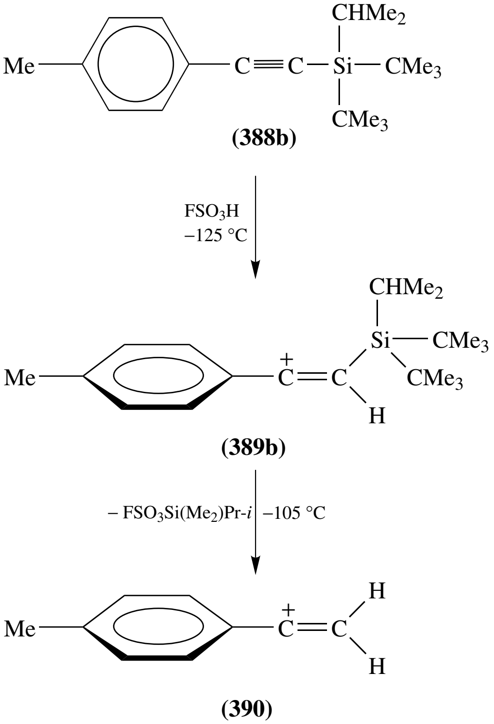

(66)

A comparison of the ^{13}C NMR chemical shift of the *para* carbon in α-(p-tolyl)vinyl cations **389a** and **390** and the sp^2 hybridized 1-(p-tolyl)ethyl cations with an additional 1-cyclopropyl- **(391)** or 1-methyl substituent **(392)** (Figure 14)[150,151] gives a qualitative measure of the electron demand of various 1-p-tolyl- substituted sp^2- and sp-hybridized carbocations.

The demand for π-aryl delocalization of the positive charge is decreasing as the hyperconjugative σ-stabilization of the positive charge by the β-substituents is increasing from β-H in **390** and **392** to a β-silyl group in **389a** and the strained cyclopropane C—C bonds in **391**.

The α-phenyl-β-triisopropylsilylvinyl cation **393** can be prepared by protonation of the corresponding alkyne **394** (equation 67). The ^{13}C NMR spectroscopic data are given in Table 16[114,140].

Attempts to protonate 1-phenyl-2-(trialkylsilyl)alkynes **395** with alkyl groups smaller than isopropyl, in order to prepare 1-phenylvinyl cations **396**, were unsuccessful (equation 68)[114].

The ^{13}C NMR chemical shifts of the *para* carbon for various phenyl-substituted sp^2-and sp-hybridized carbocations (Figure 15) indicate that the demand for π-aryl delocalization of the positive charge for the β-silyl-substituted vinyl cation **393** is lower compared with that in α-phenylethyl **(78)**, α-methyl-α-phenylpropyl **(397)** and cumyl **(292)** cations[150,153]. The stabilizing effect of the β-silyl group in **393** is comparable to that of the cyclopropyl substituent in 1-cyclopropylbenzyl cation **(398)**. The *para* carbon shift in the β-σ-silyl

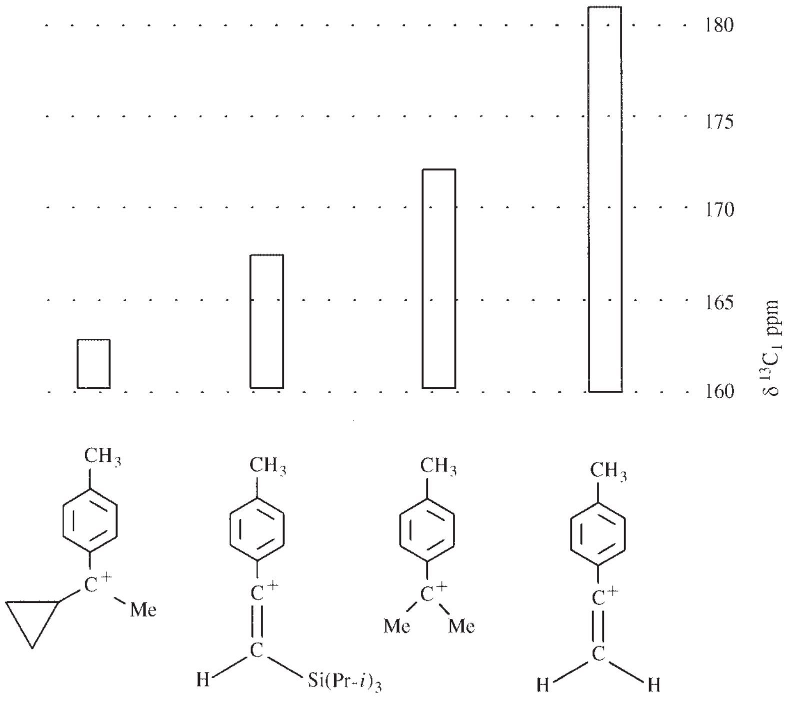

(391) **(389a)** **(392)** **(390)**

FIGURE 14. Comparison of the *para* carbon NMR chemical shift (ppm) in α-(p-tolyl)vinyl cations **389a** and **390** and sp^2-hybridized p-tolyl model cations **391** and **392**.

stabilized vinyl cation **393** is at about 5 and 4 ppm lower field compared with the β-π-resonance-stabilized phenylallenyl cation **399**, or the sp^2-hybridized carbocation **400**, respectively.

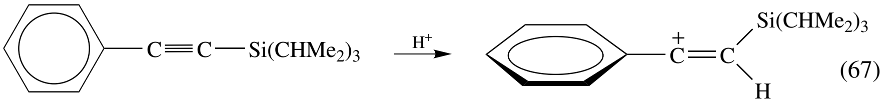

(67)

(394) **(393)**

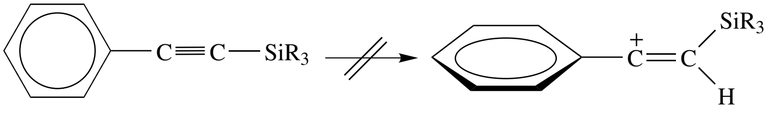

(68)

(395) **(396)**

R$_3$ < (i-Pr)$_3$

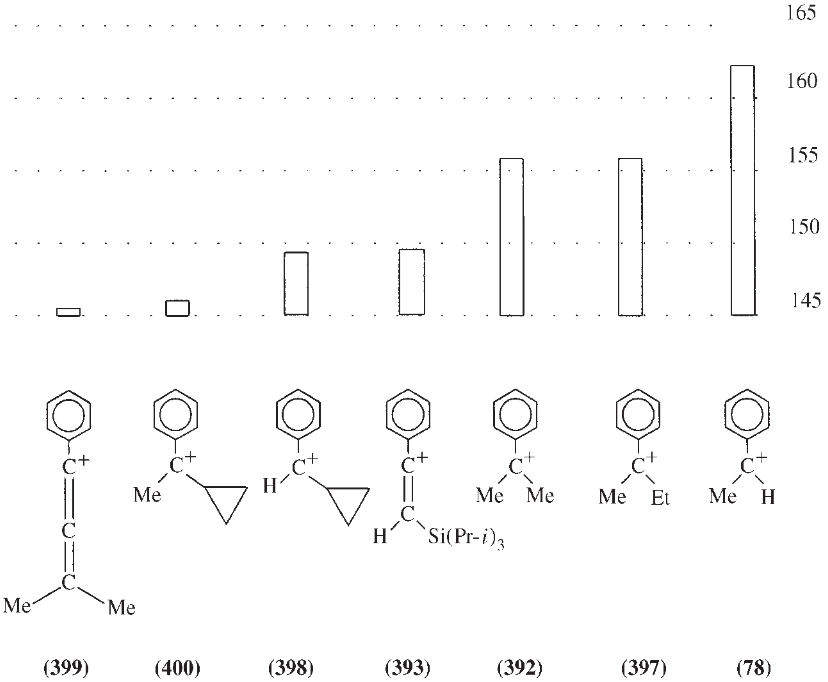

FIGURE 15. Comparison of the ^{13}C NMR chemical shift (ppm) of the *para* carbon in phenylvinyl cations **393** and **399** and selected sp^2-hybridized phenyl cations.

iv. α-Anisyl-β-silyl-substituted vinyl cations. The α-(*p*-anisyl)-β-triisopropylsilylvinyl cation **401** is accessible by protonation of the corresponding alkyne **402** at very low temperatures (equation 69)[154]. The β-silyl group in **401** is readily cleaved, and at temperatures above −115 °C complete conversion to 1-(*p*-anisyl)vinyl cation **(403)** takes place in a few minutes (equation 70). The ^{1}H NMR and ^{13}C NMR spectra of cation **401** are shown in Figures 16 and 17.

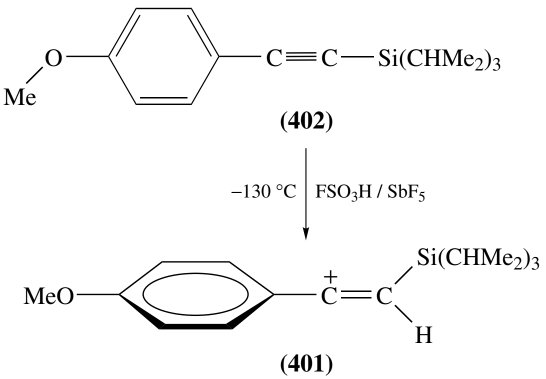

(69)

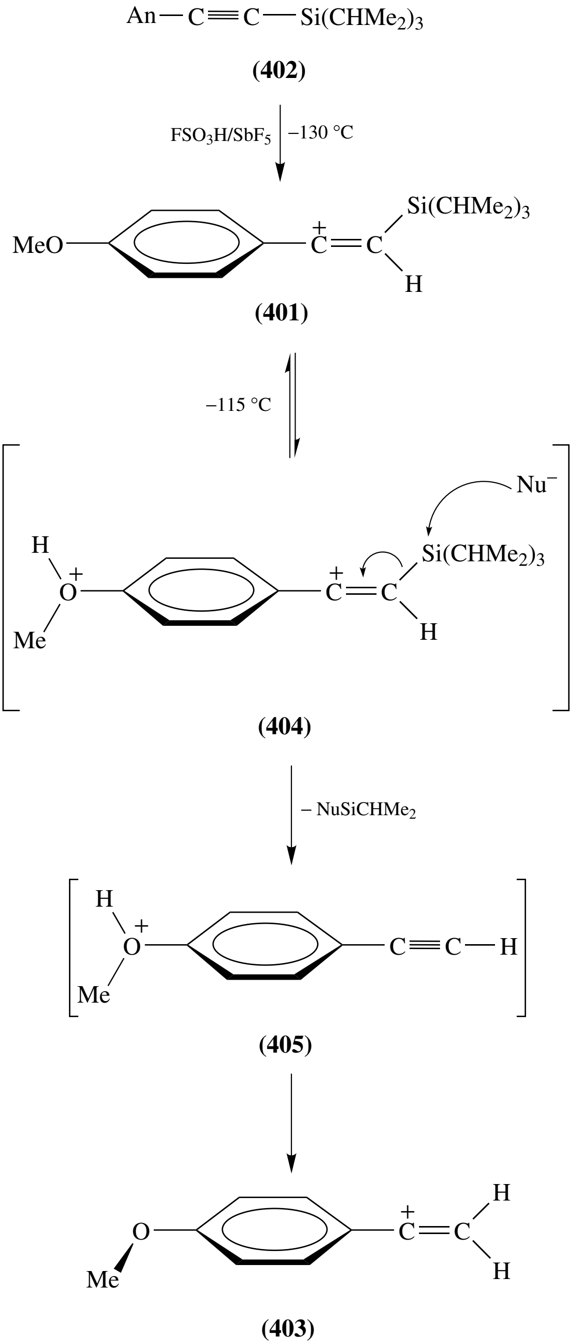
An—C≡C—Si(CHMe2)3
(402)
FSO3H/SbF5
−130 °C
MeO
Si(CHMe2)3
H
(401)
−115 °C
Nu−
H
Me
Si(CHMe2)3
H
(404)
− NuSiCHMe2
H
Me
C≡C—H
(405)
O
Me
H
H
(403)

(70)

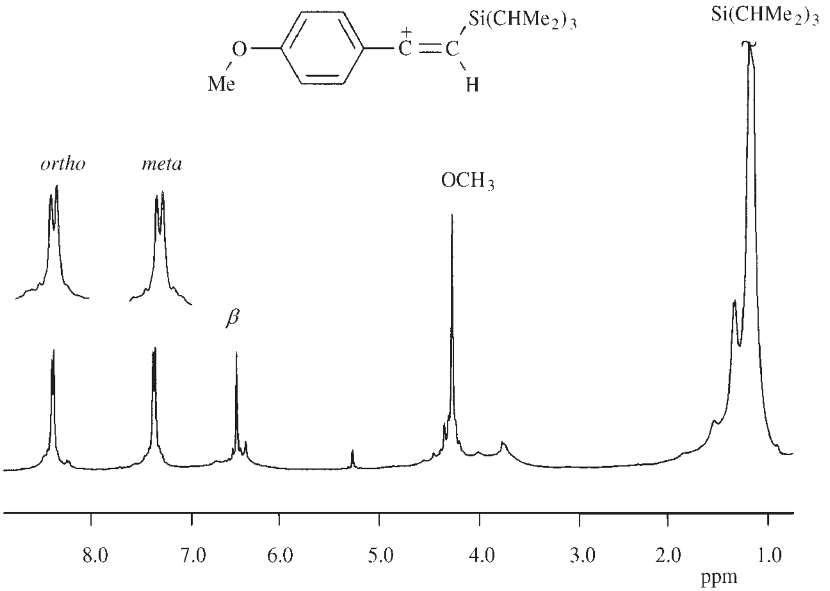

FIGURE 16. 400-MHz ^{1}H NMR spectrum of cation **401** in SO_2ClF/SO_2F_2 at −120 °C

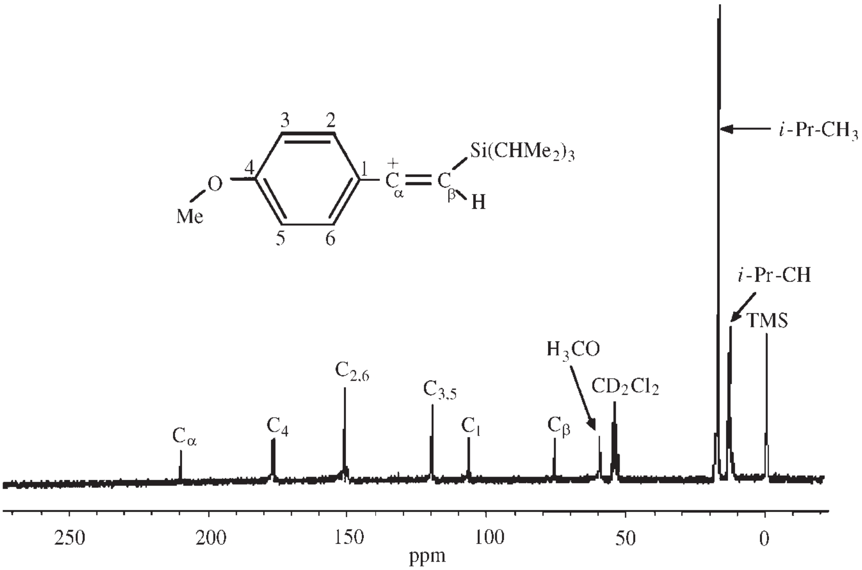

FIGURE 17. 63-MHz ^{13}C NMR spectrum of cation **401** in SO_2ClF/SO_2F_2 at −124 °C.

The C_β−Si bond fragmentation in cation **401** occurs already at temperatures where the corresponding 1-mesityl-, 1-(*p*-tolyl)- and 1-phenylvinyl-β-(triisopropyl)silyl-substituted vinyl cations **375**, **389a** and **393** are stable. The facile formation of the 1-(*p*-anisyl)vinyl cation **403** can be ascribed to a second protonation of **401** at the oxygen of the anisyl group.

At −130 °C the highly sterically hindered alkyne **402** is protonated at C_β to form cation **401**. When the temperature is raised above about −115 °C, the large excess of superacid leads to a reversible protonation at the oxygen of the methoxy group to form a doubly charged carbo-oxonium dication **404**. This dication is not observable, presumably since only a minor fraction of it is in equilibrium with **401** (equation 70). The protonated *p*-methoxy group in **404** is no longer a good electron-releasing group. Therefore, in the protonated **406** resonance hybrids like **406D** and **406E**, which in **401** contribute significantly to the delocalization of the positive charge, are of minor importance for **404**.

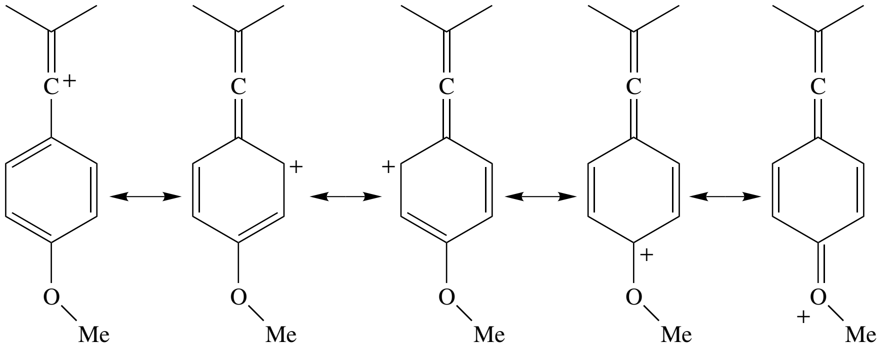

(406A) **(406B)** **(406C)** **(406D)** **(406E)**

As the delocalization of the charge at C_α by π-conjugation into the aromatic ring is lower in **404**, the demand for charge delocalization by β-C−Si hyperconjugation (cf **407A** ↔ **407B**) is increased. The formal no-bond hyperconjugative resonance structure **407B** gains more importance and the partial positive charge at silicon is increased. The silicon therefore becomes more susceptible to nucleophilic attack by the gegen ions which led to its expulsion via an S_N2(Si) transition state. The intermediate O-protonated alkyne **405** formed *in situ* is converted in the superacid media to the silicon-free vinyl cation **403** (equation 70). The ^1H and ^{13}C NMR spectra of the 1-(*p*-anisyl)vinyl cation **403** are remarkably different from those of the corresponding β-silyl-substituted vinyl cation **401**.

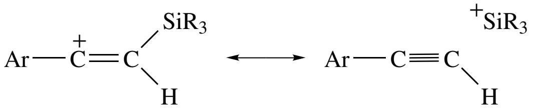

(407A) **(407B)**

The ^{13}C NMR chemical shift (Table 17) of the positive charged carbons in **401** (209.8 ppm) and **403** (239.7 ppm) is comparable to the C^+ carbon shift in 1-mesitylvinyl cations with analogous β-substituents (207.8 ppm for **375** and 238.5 ppm for **378**, respectively). The chemical shift of the signal for the sp^2-hybridized β-carbon in **401** (76.0 ppm) and **403** (78.4 ppm) is in accord with that in other vinyl cations and with IGLO

TABLE 17. ^1H and ^{13}C NMR chemical shifts (δ, ppm) for cations **401** and **403** in SO_2ClF/SO_2F_2[a]

	C_α	C_β	C1	C2, C6		C3, C5		C_{para}	OMe
401[b]	209.8	75.9	106.8	151.3		119.8		177.0	59.9
		(179)		(172)		(172)			(152)
		[6.51]		[8.41]		[7.37]			[4.29]
403[c]	239.7	78.4	108.9	156.1	150.9	118.0	124.9	184.4	60.7
		(176)		(174)	(173)	(174)	(173)		(150)
		[6.42]		[8.51]	[8.26]	[7.30]	[7.46]		[4.37]

[a] 400-MHz ^1H NMR data in square brackets, δ ($\pm$0.01 ppm) at $-120\,^\circ C$, internal reference: $CHDCl_2$: $\delta = 5.32$ ppm.
[b] 63-MHz ^{13}C NMR δ ($\pm$0.05 ppm) at $-124\,^\circ C$, $^1J_{CH}$ coupling constants ($\pm$1.8 Hz) are given in parentheses.
[c] 100.6-MHz ^{13}C NMR at $-102\,^\circ C$.

calculations of model vinyl cations. A shielding of 4–5 ppm is observed as compared with the corresponding C_β signals of 1-mesitylvinyl cations **375** (81.1 ppm) and **378** (82.3 ppm). Due to the sp-hybridization of the C^+-carbon in the vinyl cations **401** and **403** the aromatic C1 position shows an upfield shift of about 25–30 ppm compared with 1-(*p*-anisyl)-substituted carbocations with an sp^2-hybridized C^+-carbon.

As in other benzylic-type carbocations, the chemical shift of the *para* carbon is a probe to the electronic demand of the carbocation centre and it can be used to evaluate the effect of a β-silyl group on the positive charge.

The signal for the *para* carbon in the β-silyl-substituted cation **401** (177.0 ppm) appears about 7 ppm upfield compared with the signal in the silicon-free cation **403** (184.4 ppm), indicating a lower demand for charge delocalization into the aryl ring when the β-substituent is changed from β-H to a β-silyl group. This shows that the β-silyl stabilization effect is operative even in highly conjugatively stabilized carbocations with α-anisyl substituents. The *para* carbon shift in **401** may be compared with those in 1-phenyl **(408)** or 1-cyclopropyl **(409)** substituted *p*-anisylmethyl (R = H) or 1-(*p*-anisyl)ethyl (R = Me) cations (176–181 ppm)[155]. The similar shifts suggest that β-silyl stabilization in the vinyl cation **401** is about as efficient in dispersing the positive charge as 2p(π)-conjugation of an additional phenyl ring in **408** or a σ-C–C hyperconjugation of an additional cyclopropyl group in **409**.

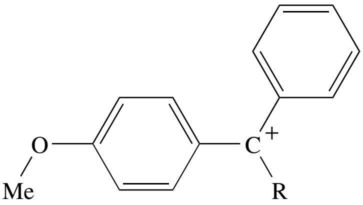

(408)

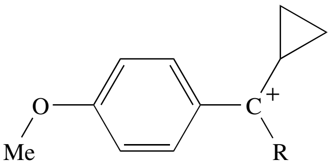

(409)

Whereas the NMR spectra for the 1-(*p*-anisyl)vinyl cation **403** show magnetically non-equivalent signals for the C2 and C6 *ortho* and C3 and C5 *meta* carbon and proton signals, these positions remain equivalent in the ^1H and ^{13}C NMR spectra of the β-silyl-substituted cation, even at the lowest temperatures.

As in other 1-(*p*-anisyl)-substituted carbocations, in the 1-(*p*-anisyl)vinyl cations **401** and **403** there exists a torsional barrier for a methoxy group rotation around the phenyl–C4–oxygen bond which is due to delocalization of the positive charge to the methoxy group. This is illustrated by the contribution of the valence bond resonance structure **406E**. This rotational barrier is lower than the other barrier around the C1–C$^+$ bond which is due to contributions of resonance structures **406B–406E**.

The demand for delocalizing positive charge into the aryl moiety is higher in **403** than in **401**, as is evident from the *para* carbon chemical shifts (Table 15). In **403** the enhanced participation of the *p*-methoxy group in delocalizing the positive charge results in higher double bond character of the phenyl–C4–oxygen bond as compared with **401**. The free energy of activation ($\Delta G^{\#} = 9.0 \pm 1$ kcal mol^{-1} at $-100\,^{\circ}$C) for the dynamic process was determined from kinetic line broadening in the ^{13}C NMR spectra. The fact that the rotation around the C4–O bond in **403** is slow, but is fast in **401**, clearly demonstrates that **401** is stabilized by the β-silyl effect and thus needs less π-aryl stabilization compared with **403**.

Quantum chemical *ab initio* calculations were performed to reveal additional details of the structures and charge stabilization of 1-(*p*-anisyl)vinyl cations. The 1-(*p*-anisyl)vinyl cation **403** and the model cation structures **410** and **411** with β-SiH$_3$ and β-CH$_3$ groups, respectively, were calculated along with the corresponding transition state structures **403-TS**, **410-TS** and **411-TS** for the rotation of the *p*-methoxy group around the C4–oxygen bond.

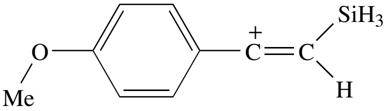

(410)

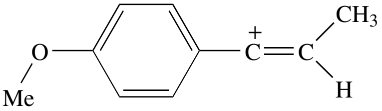

(411)

The geometries were calculated at the HF/6-31G level. Figure 18 shows the structure of vinyl cation **403** and the transition state structure **403-TS**. Computational experience with more electron-deficient, smaller vinyl cation structures lacking π-conjugative stabilizing α-substituents, indicate that at higher level of calculations, which is feasible for the smaller structures, the effects of σ-stabilization by β-σ-C–H, β-σ-C–C and β-σ-C–Si bonds are more pronounced while the relative order for hyperconjugation is not changed. The α-arylvinyl cations **403**, **410** and **411** have an inherently lower demand for β-σ hyperconjugative stabilization than vinyl cations lacking α-π-conjugating substituents, and the

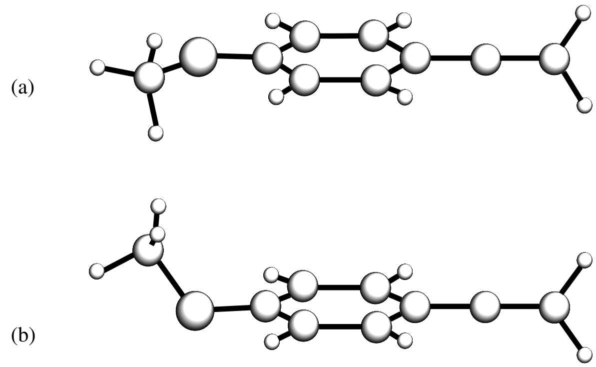

FIGURE 18. Calculated geometry of (a) **403-TS** and (b) **403**

level of the basis set used for the *ab initio* calculation is thus not as crucial. Model calculations for **403** using the 6-31G(d) basis set and for **410** using the 6-31G basis set with inclusion of d orbitals at silicon show that the data obtained at the 6-31G level are qualitatively reliable and thus adequate to allow comparison of a consistent set of calculated data with the experimental NMR results.

In the optimized geometry for the vinyl cations **403**, **410** and **411** the β-C$-$R bonds are confined to the same plane with the formally vacant 2p(C^+) orbital, allowing optimum overlap of the latter with the π-orbitals of the aromatic system as well as with the β-C$-$R σ-bond.

In the most stable conformation for the 1-(p-anisyl)-substituted vinyl cations **403**, **410** and **411** the O$-$methyl bond of the C4$-$$OCH_3$ group is calculated to be coplanar with the plane of the aryl ring (Figure 18), as expected due to the contributions of resonance forms **406E**. The calculated geometrical data reveal that charge dispersal to the aryl ring and to the p-methoxy group becomes more important as the hyperconjugative interaction of the formally vacant 2p(C^+) orbital with the β-σ-bond is decreasing in the order **410** > **411** > **403**, where the β-substituent changes from β-SiH_3 to β-CH_3 and β-H. The C4$-$OMe and C1$-$$C^+$ bond lengths decrease in the same order. Also, the bond length alternation for the aromatic C$-$C bonds, i.e. shorter C2,C3 and C5,C6 bonds and elongated C1,C2/C1,C6 and C3,C4/C4,C5 bonds, due to increasing importance of quinonoid resonance structures of the type **406B**$-$**406E**, becomes more pronounced.

The calculated data confirm the interpretation of the NMR data that, even in highly π-stabilized α-anisyl carbocations, β-σ-bond hyperconjugation contributes to the dispersal of positive charge. The computational data also confirm the relative order of the hyperconjugative electron-donor ability of β-σ bonds to be C$-$Si > C$-$C > C$-$H. The energy differences between the transition state structures and the most stable structures were calculated to be 8.3, 7.9 and 7.4 kcal mol^{-1} for **403**, **411** and **410**, respectively, and they are a measure of the barrier for methoxy group rotation around the C4$-$oxygen bond. The order obtained is in agreement with the other calculated data, as well as with the observed chemical shifts for **401** and **403**.

c. The 1-bis(trimethylsilyl)methyl-2-bis(trimethylsilyl)ethenyl cation. Protonation of tetrakis(trimethylsilyl)allene **412** with HSO_3F/SbF_5 gives the 1-[bis(trimethylsilyl)]methyl-2-bis(trimethylsilyl)ethenyl cation **413**[156]. The isomeric allyl cation **414** is not formed (equation 71).

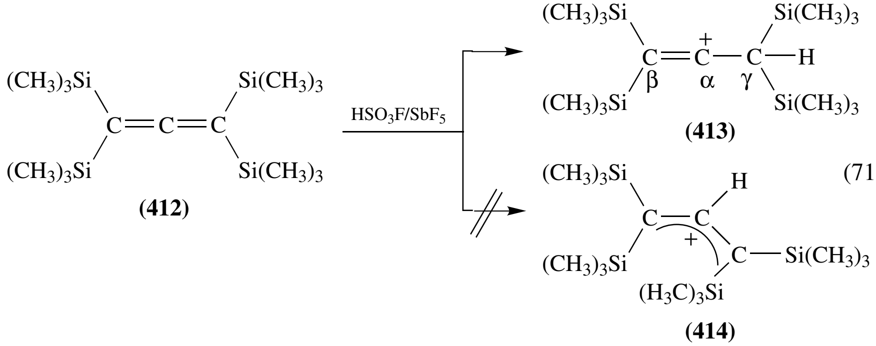

(71)

This contrasts with the protonation occurring at the central allene carbon of 1,3-dimethyl-, 1,1,3,3-tetramethyl- and 1,3,3-trimethyl-1-phenyl allenes **415** (R = H, Me, Ph) with HSO_3F/SbF_5, which yields the corresponding allyl cations **416** (equation 72)[157].

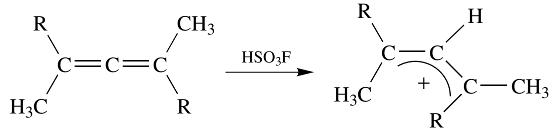

(72)

(415) R = H, CH_3, Ph **(416)**

The different reaction course followed by the silyl- and alkyl-substituted allenes is fully consistent with the hyperconjugation model, which predicts that a β-silyl group stabilizes carbenium ions better than a β-alkyl group, and with previous conclusions that α-silyl substitution in carbocations is destabilizing relative to α-methyl substitution. The larger space requirements of the trimethylsilyl groups compared with methyl groups may also contribute to the kinetic stability of **413**.

At $-100\,^\circ C$ the ^{13}C NMR spectrum of **413** shows five signals (Figure 19, Table 18). The signal of the C^+-carbon C_α in **413** appears at 208.7 ppm. This value is comparable with the chemical shift in vinyl cations stabilized by 2p-π-conjugation or by hyperconjugation with cyclopropyl substituents. The signal of the C^+-carbon in simple α-alkyl-substituted vinyl cations $H_2C{=}C^+{-}CH_3$ and $H_2C{=}C^+{-}CH_2CH_3$ have been estimated by IGLO chemical shift calculations to be about 200 ppm more deshielded.

The strong shielding effect for C_α in the tetrasilyl-substituted vinyl cation **413** can be attributed mainly to the hyperconjugative charge dispersal by the silyl groups. At

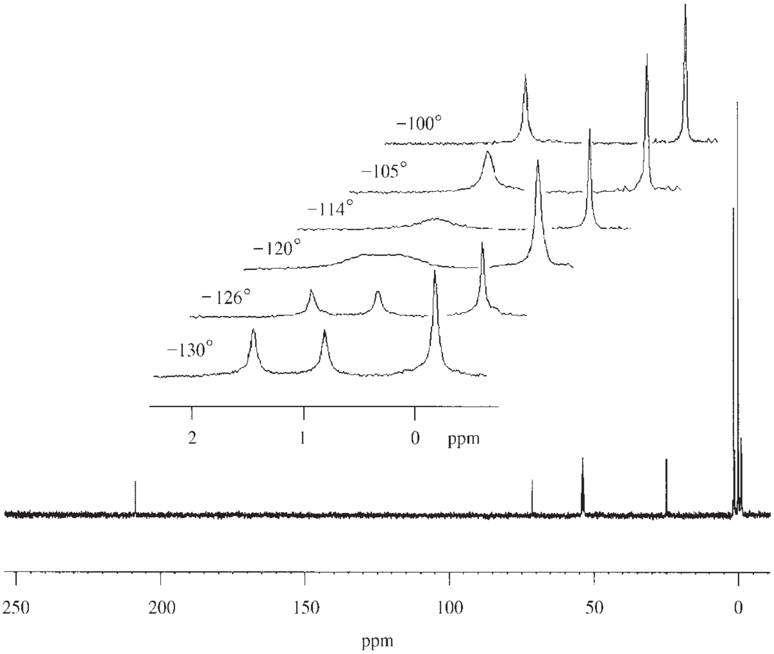

FIGURE 19. 100.6-MHz ^{13}C NMR spectrum of **413** ($-100\,^\circ C$, SO_2ClF/SO_2F_2, reference CD_2Cl_2, $\delta = 53.80$ ppm), and an expanded region (2–0.5 ppm) showing the temperature dependence of the $(CH_3)_3Si$ signals at -130 to $-100\,^\circ C$)

TABLE 18. ^{13}C NMR chemical shifts (δ, ppm) of **413** in SO_2ClF/SO_2F_2[a]

T(°C)	C_α	C_β	CH	β-C$-$SiMe$_3$	CH$-$SiMe$_3$
-100	208.73	71.39	25.00	1.59	0.14
-136	208.74	70.58	25.27	1.35/0.70	-0.30

[a] 100.62 MHz, internal standard CD_2Cl_2, $\delta = 53.80$ ppm.

temperatures $< -100\,°$C the low field peak of the two signals for the four trimethylsilyl groups broadens and below the coalescence temperature of *ca* $-114\,°$C it splits into two signals at 1.35 and 0.75 ppm. This peak is assigned to the trimethylsilyl groups at the methine carbon which is connected to C_α by a single bond. The observed dynamic process is due to rotation around the $C^+-CH(SiMe_3)_2$ bond which renders the two $SiMe_3$ groups at the methine carbon non-equivalent. The torsional barrier, $\Delta G^\# = 7.7$ kcal mol^{-1} at $-114\,°$C, is determined by the dihedral angle dependence of the hyperconjugative stabilization of the positive charge by the β-CH-silyl groups.

Whereas the $SiMe_3$ groups at the double bonded β-carbon are always in an optimal position for hyperconjugation, the $SiMe_3$ groups at the methine carbon are conformationally mobile. At low temperatures the cation prefers a conformation in which the hyperconjugation between the empty 2p(C^+) orbital and the C$-$Si bond is maximized. The non-equivalence of the two $SiMe_3$ groups at the methine carbon indicate that the conformation in which one silyl group is fully conjugated with the empty orbital and the other has a dihedral angle of about 60° is the most favourable conformation. This conformation would also render the $SiMe_3$ groups at the sp^2 C_β carbon non-equivalent. Any ^{13}C NMR chemical shift difference for these groups is likely to be small and was not observed.

Theoretical calculations performed on smaller model cations with SiH_3 groups confirm the dihedral dependence of the β-silyl effect. In disilyl-substituted model cation $H_2C{=}C^+{-}CH(SiH_3)_2$ **417** the difference between conformation **417b** where each of the C$-$Si bonds forms a dihedral angle, θ, of *ca* 30° with the empty 2p(C^+) orbital, and conformation **417a** with different dihedral angles θ of 0° and 60°, is small, about 3 kcal mol^{-1} [HF/6-31G(d)] in favour of **417b**. A detailed analysis of the computational results leads to the prediction that at higher levels of calculations and with inclusion of electron correlation, conformation **417a** is likely to be the more stable conformation of **417**. The model calculations reveal that the silyl groups involved in hyperconjugation show strong geometric distortions towards bridging. The Si$-$CH$-$C$^+$ bond angle is smaller (102.4°) and the C$-$Si bond is elongated [r(CH$-$Si) $= 2.03$ Å] for the SiH_3 group in **417a** which is aligned for optimal interaction with the empty 2p orbital, compared with the other silyl group at $\theta = 60°$ for which the Si$-$CH$-C_\alpha$ bond angle is 117.1° and the r(CH$-$Si) bond length is 1.96 Å. According to calculations [3-21G(d)] the rotational barrier around the $C_\alpha$$-$CH-bond of **417** is 5.9 kcal mol^{-1}, in very good agreement with the experimental value of 7.5 kcal mol^{-1}. The theoretical calculations are also consistent with the experimental observation at $-130\,°$C in indicating the appearance of two signals for the $CH(SiMe_3)_2$ group. Similar, though less pronounced structural distortions have been observed in tricoordinated carbocations stabilized through C$-$C hyperconjugation[158].

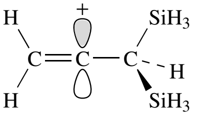

(417a)

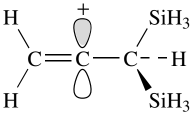

(417b)

C. Silyl-substituted Hypercoordinated Carbocations

1. The α- and γ-silyl effect in bicyclobutonium ions

The structure and dynamics of the cyclopropylmethyl/cyclobutyl cation system $[C_4H_7]^+$ and its 1-methyl-substituted analogue $[C_4H_6CH_3]^+$ have been a subject of controversy for many years[159,160]. Depending on the substitution pattern, these types of carbocations are prone to undergo facile rearrangements. A three-fold degenerate bicyclobutonium/cyclopropylmethyl cation rearrangement (equation 73) would render the CH_2 carbons equivalent.

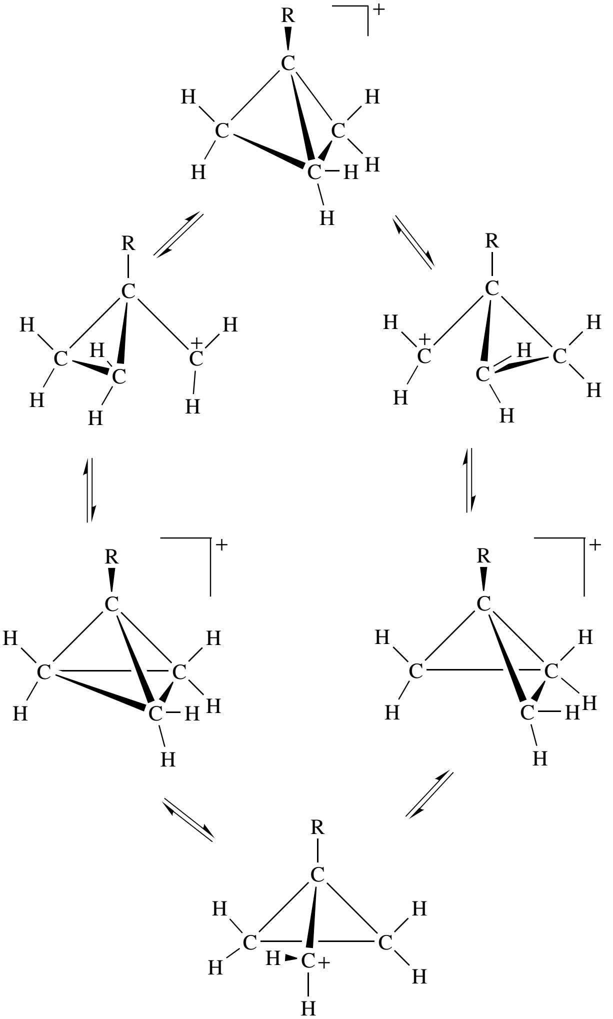

(73)

The rate of another dynamic process, a conformational ring inversion, depends in particular on the nature of the substituent R at the α-carbon. The geminal *exo* and *endo* methylene hydrogens are interchanged by opening of the bridging bond and planarization to a cyclobutyl cation intermediate, followed by closure of the bridging bond to a mirror image bicyclobutonium ion (equation 74).

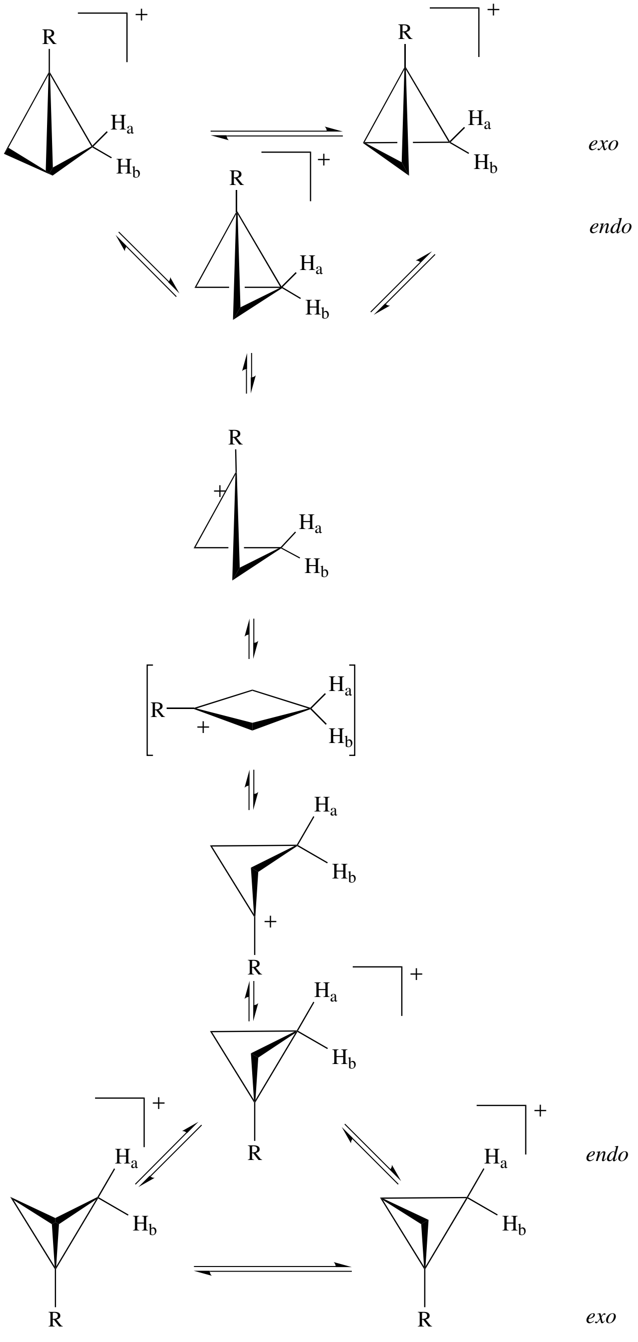

(74)

Depending on the rates of these processes and related to the NMR time scale, only an averaged signal for the methylene carbons and/or an averaged signal for the geminal *exo/endo* methylene hydrogens are observed in the ^{13}C and ^{1}H NMR spectrum, respectively.

According to contemporary high field NMR spectroscopic measurements, investigations of equilibrium isotope effects on NMR spectra and quantum chemical calculations which include electron correlation, the parent system $[C_4H_7]^+$ is now best described as a degenerate set of rapidly interconverting bicyclobutonium ions **418** with minor contributions from another degenerate set of rapidly equilibrating cyclopropylmethyl cations **419** which are only marginally higher in energy (by <1 kcal mol^{-1}) than **418**[161–165].

For the analogous 1-methyl-substituted cation $[C_4H_6CH_3]^+$, recent experimental investigations and quantum chemical *ab initio* calculations agree that the dynamics of this cation system can be adequately described by considering only one degenerate set of cations, which have the hypercoordinated puckered methylbicyclobutonium ion structure **420** without contributions from a degenerate set of (1′-methylcyclopropyl)methyl cation structures **421**[7,166,167].

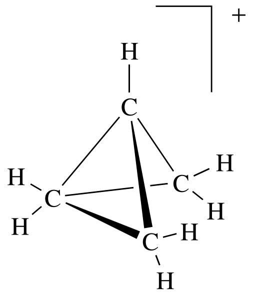

(418)

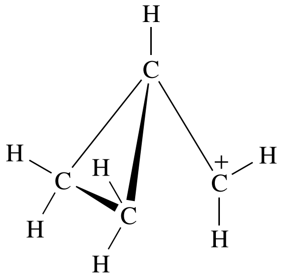

(419)

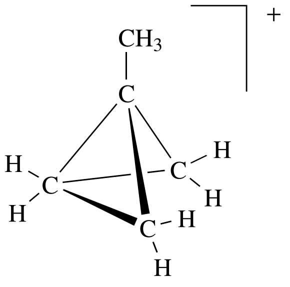

(420)

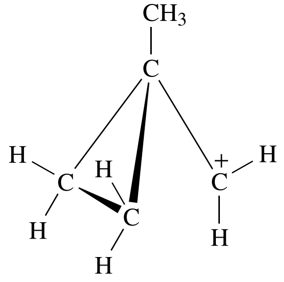

(421)

Recently, trialkylylsilyl-substituted bicyclobutonium ions have been generated in superacid solution and were characterized by NMR spectroscopy.

a. 1-(Trimethylsilyl)bicyclobutonium ion. The 1-(trimethylsilyl)bicyclobutonium ion **422** is obtained from (1′-trimethylsilylcyclopropyl)methanol **423** by reaction with SbF_5

(equation 75)[168].

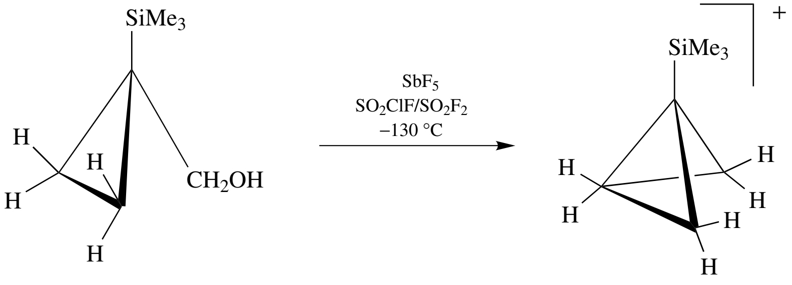

(75)

(423) **(422)**

Analogous cations **424** with the alkyl groups R at silicon larger than methyl can be prepared more easily. The NMR spectroscopic data of **422** in SO_2ClF/SO_2F_2 solution at $-128\,^{\circ}C$ is in accord with a bridged puckered bicyclobutonium structure undergoing a three-fold rapid degenerate rearrangement (equation 76, R = $SiMe_3$) that renders the two β-and one γ-methylene groups equivalent, thus leading to one averaged ^{13}C NMR signal for the CH_2 groups at 48.9 ppm (Figure 20).

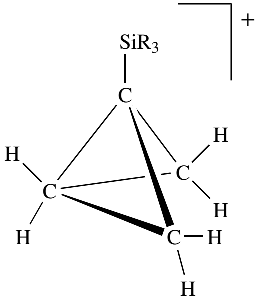

(424)

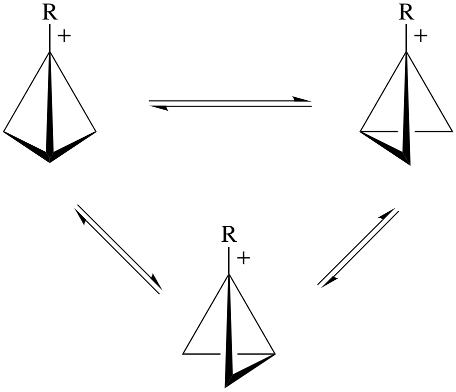

(76)

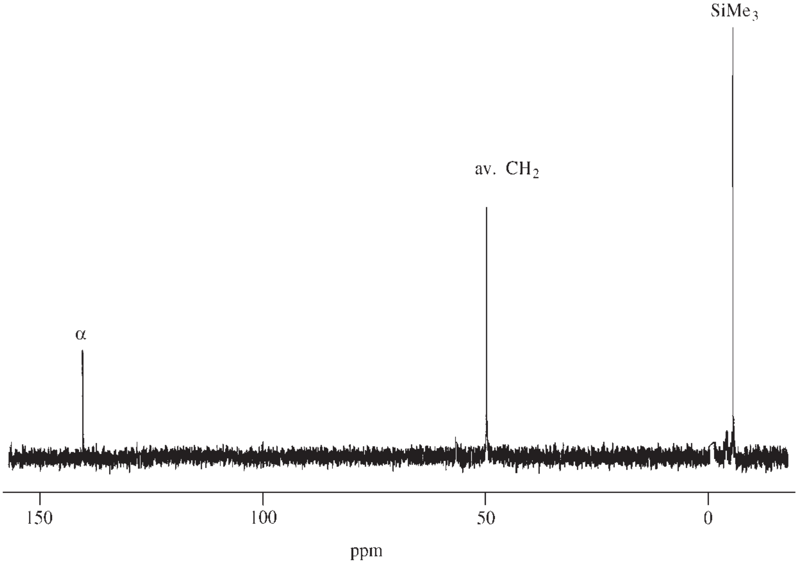

FIGURE 20. ^{13}C NMR spectrum of 1-(trimethylsilyl)bicyclobutonium ion **422** at −125 °C

Conformational ring inversion for cation **422** (equation 74, R = SiMe$_3$) is slow, so that two separate signals for the three averaged *endo*-CH$_2$ (4.04 ppm) and three averaged *exo*-CH$_2$ hydrogens (3.24 ppm) are observed. The deuterium equilibrium isotope effects for *exo*- and *endo*-CHD-labeled cations are different in sign and magnitude and can be explained by assuming different *endo* and *exo* C−H bond force constants at the pentacoordinated carbon. NMR chemical shift calculations for MP2/6-31G(d) optimized geometries of the 1-silylbicyclobutonium ion **425** and the (1′-silylcyclopropyl)methyl cation **426** were performed by the GIAO-SCF and GIAO-MP2 method (Figure 21).

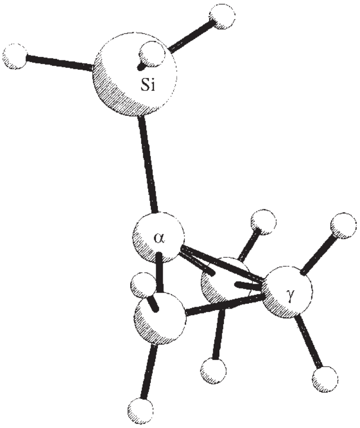

(425)

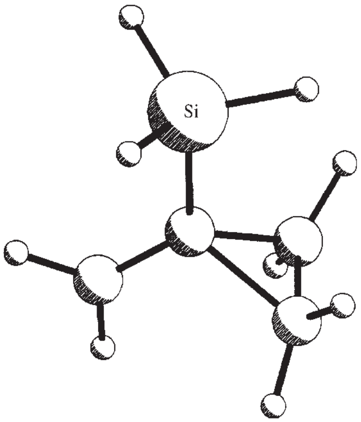

(426)

FIGURE 21. Calculated structures of **425** and **426**

The experimental shifts are satisfactorily reproduced by GIAO-MP2//tzp/dz calculated shifts for the 1-silylbicyclobutonium structure **425**. This good agreement between theory and experiment supports a fully degenerate set of interconverting 1-trimethylsilylbicyclobutonium ions for **422** and **424** (R = Me_2Bu-*t*), respectively, and excludes contributions from the other isomers, the 1′-trialkylsilylcyclopropylmethyl cations **427**, to the observed equilibrium process.

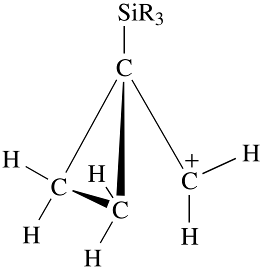

(427)

The geometric and electronic properties of the 1-trialkylsilylbicyclobutonium cations, as concluded from a comparison of the experimental data for **422** and **424** and the calculated data for **425**, are intermediate between that of the parent bicyclobutonium ion **418** and that of the 1-methylbicyclobutonium ion **420**.

b. 3-endo-(Trialkylsilyl)bicyclobutonium ions. The 3-*endo*-(*t*-butyldimethylsilyl)bicyclobutonium ion **428** is accessible from [1′-(*t*-butyldimethylsilyl)cyclopropyl]methanol **429** (equation 77)[169].

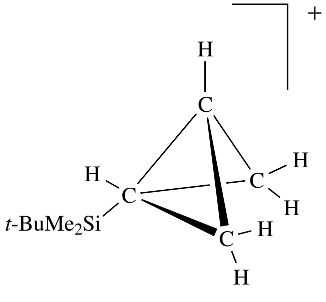

(428)

Reaction of [1′-(*t*-butyldimethylsilyl)cyclopropyl]methanol **429** with SbF_5 at −130 °C initially leads to formation of the 1-(*t*-butyldimethylsilyl)bicyclobutonium ion **430**. At −115 °C cation **430** is completely converted to the 3-*endo*-(*t*-butyldimethylsilyl)bicyclobutonium ion **428** in a few minutes.

The 3-*endo*-(trimethylsilyl)bicyclobutonium ion **431** is also obtained directly from a four-membered-ring progenitor, i.e. 3-(trimethylsilyl)cyclobutyl chloride **432**, by reaction with SbF_5 at −130 °C (equation 78).

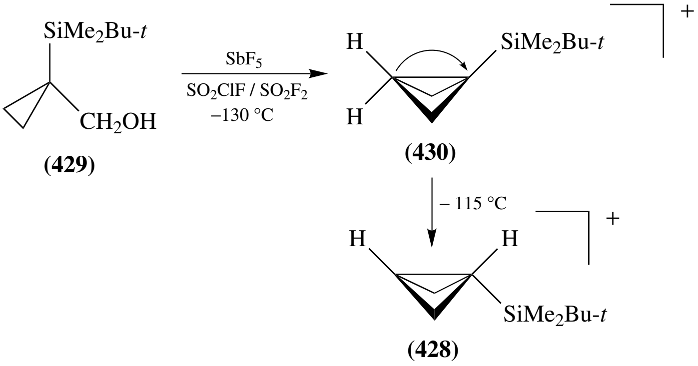

(77)

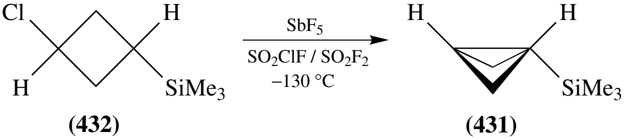

(78)

The ^{13}C NMR spectrum of the 3-*endo*-(*t*-butyldimethylsilyl)bicyclobutonium ion **428** in $SO_2ClF/SO_2F_2/CCl_3F$ solution at −120 °C (Figure 22) shows three distinct signals for C_α (99.6 ppm), $C_\beta/C_{\beta'}$ (66.3 ppm) and C_γ (−21.0 ppm).

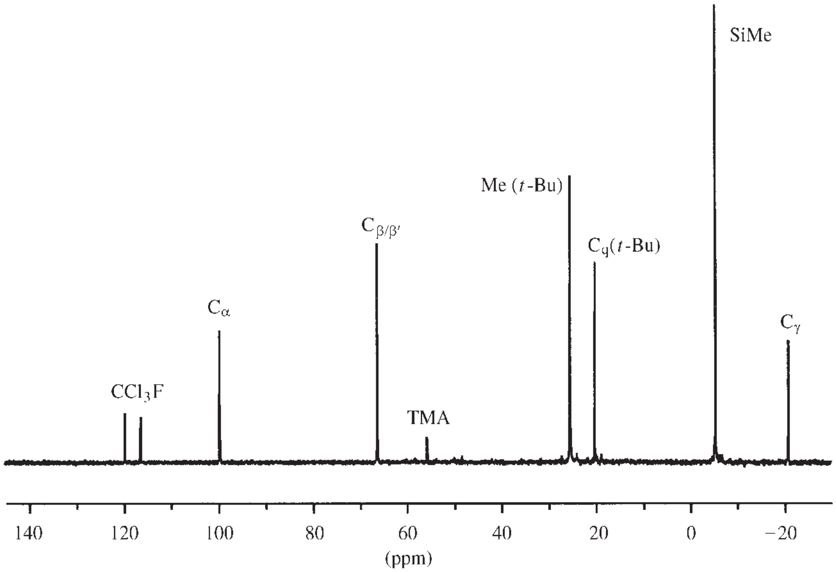

TMA = Me_4N^+

FIGURE 22. ^{13}C NMR spectrum of **428** in $SO_2ClF/SO_2F_2/CCl_3F$ at −120 °C

The ^{1}H NMR spectrum shows resonances for H_α (5.95 ppm), H_β/$H_{\beta'}$ *exo* (4.01 ppm), H_β/$H_{\beta'}$ *endo* (3.12 ppm) and H_γ (0.30 ppm). The NMR data are in accord with a bridged, puckered bicyclobutonium ion structure that is static on the NMR time scale. The ^{29}Si NMR chemical shift of 43.1 ppm for ion **428** indicates that the silicon is involved in stabilization of the positive charge. The stabilization occurs by shifting electron density from the $C_\gamma{-}Si$ σ-bond across the bridging bond to the formal carbenium carbon C_α. This γ-silyl- type of interaction may be termed silicon homohyperconjugation.

Quantum chemical calculations at MP2/6-31G(d) level for SiH_3-substituted model structures predict that only the 3-*endo*-silylbicyclobutonium cation structure **433** is at a minimum on the potential energy surface, while the 3-*exo* cation structure *exo*-**433** has one imaginary frequency and thus corresponds to a transition state. The calculated structures of *endo*- and *exo*-**433** are given in Figure 23.

For the model bicyclobutonium ion structure **433** with the SiH_3 substituent at the γ-*endo* position, the NMR chemical shifts calculated at the GIAO-MP2//tzp/dz level and the coupling constants calculated with an SOS-DFT approach are in good agreement with experimental results for **428** and **431**. The $^3J_{HH}$ coupling between H_α and H_γ, measured experimentally as 5.5 Hz, is calculated to be 5.9 Hz in the *endo*-SiH_3-substituted cation **433** but only 1.2 Hz for the *exo*-SiH_3-substituted cation *exo*-**433**. The observation of a cross bridge $^3J_{HH}$ coupling is direct proof for the bridged structure and the magnitude of the coupling constant confirms the *endo* arrangement of the silyl substituent in **428** and **431**.

The calculated $C_\alpha{-}C_\gamma$ bridging distance for the 3-*endo* ion **433** (1.642 Å) is shorter by 0.012 Å compared with the parent bicyclobutonium ion **418**. This indicates that the homohyperconjugative stabilization of the positive charge by the γ-*endo* C−Si σ-bond is more efficient than the stabilization by a γ-*endo* C−H σ-bond. In analogy with a β-silicon substituent, γ-silyl groups with a suitable stereoelectronic arrangement are superior to hydrogen in stabilizing the positive charge in carbocations.

2. Silanorbornyl cation

a. The 6,6-dimethyl-5-neopentyl-6-sila-2-norbornyl cation. This cation, **434**, was prepared as a tetrakis(pentafluorophenyl)borate salt by a hydride transfer reaction of 3-(3-cyclopentenyl)-2,5,5-trimethyl-2-silahexane **435** with trityl tetrakis(pentafluoro-

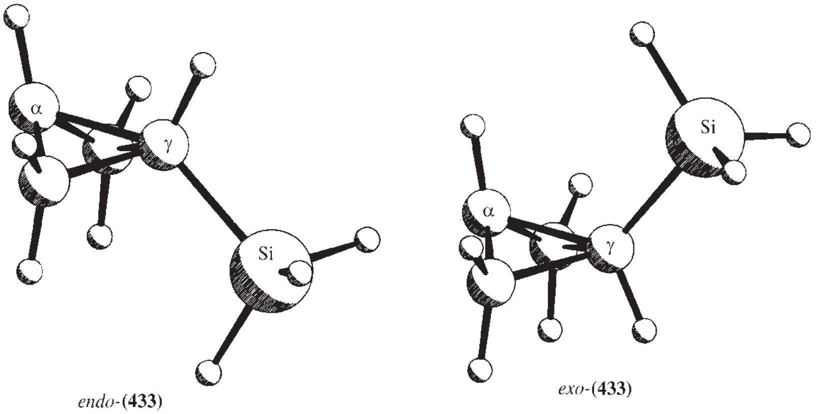

endo-(**433**)

exo-(**433**)

FIGURE 23. Calculated structures [MP2/6-31G(d)] of *endo*- and *exo*- **433**.

phenyl)borate in toluene (equation 79)[170].

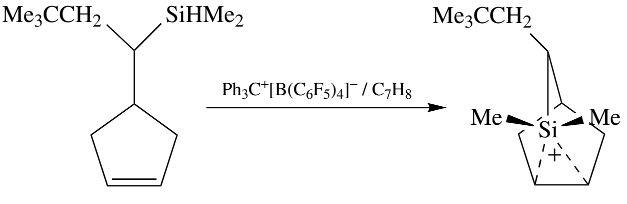

(435) **(434)** (79)

The single peak observed in the ^{29}Si NMR spectrum in toluene at 87.7 ppm is in the ^{29}Si chemical shift range expected for arene–silyl cation complexes (experimental or computed structures). However, the deshielding of the C1 and C2 carbons at 153.74 ($^1J_{CH}$ = 174 Hz) and 150.52 ($^1J_{CH}$ = 174 Hz) ppm compared with the corresponding signals in the starting silane at 130.57 ($^1J_{CH}$ = 156 Hz) and 130.41 ($^1J_{CH}$ = 156 Hz) provides evidence for an intramolecular π-complexation of the positively charged silicon. Quantum chemical calculations on ions **436** and **437** at the B3LYP/6-31G(d) level support the interpretation of the experimental findings. The C_s symmetric model cation structure, 5,6,6-trimethyl-6-sila-2-norbornyl cation **436**, is a local minimum (Figure 24).

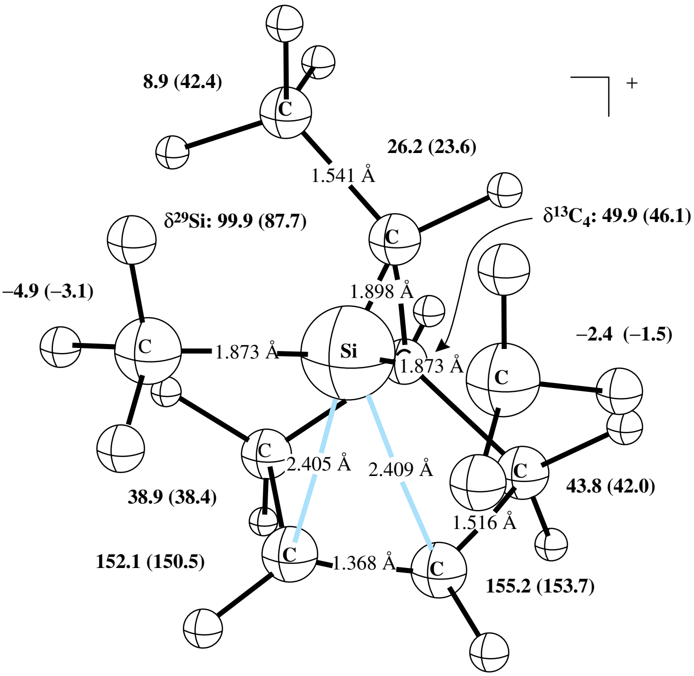

(436)

FIGURE 24. Calculated structure of ion **436** at B3LYP/6-31G(d). Bond lengths in Å, calculated chemical shifts at IGLO-DFPT/BIII in bold. Experimental chemical shifts for **434** in parenthesis

The deshielding of C1/C2 carbons and the $\delta^{13}C$ values of the methyl groups at silicon are well reproduced by the calculations of NMR chemical shifts in a model structure **437**.

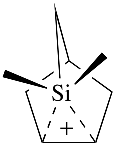

(437)

Further support comes from calculation of $^{1}J_{CH}$ spin–spin coupling constants at IGLO-DFPT/BIII level. The data were interpreted as giving strong evidence for intramolecularly π-stabilized silanorbornyl cation structure lacking coordination to solvent or counterion. The species can also be regarded as an almost symmetrically bridged β-silyl carbocation with siliconium ion character.

VI. CONCLUSIONS

The data presented in this chapter have resulted from quantum chemical *ab initio* calculations and various experimental studies performed in the gas phase, in nucleophilic solvents, in superacid media and in the soild state. Continued evolution of the techniques to study reactive intermediates and the advance of high-speed computers and sophisticated *ab initio* programs have yield rich rewards. The information gained provides very useful insights into the energetic and structural details of silyl substituted carbocations and the kinetics of their reactions. In particular much has been learned through these studies on the many aspects of σ-π-interactions of silicon with a positive charge in carbocationic intermediates, transition states and stable ions. The principles of the silicon interaction in carbocations are now quite well understood. The stabilizing effect of β- or γ-silyl groups have been used to synthesize hitherto elusive carbocations from silyl substituted precursors. The combined application of experimental and theoretical methods has been especially fruitful in the study of silicon substituted carbocations.

VII. ACKNOWLEDGEMENTS

H.-U. S. gratefully acknowledges financial support by the Deutsche Forschungsgemeinschaft (DFG) and the Fonds der Chemischen Industrie. T. M. thanks the Fonds der Chemischen Industrie for a Liebig scholarship.

VIII. REFERENCES

1. For a recent review see: Y. Apeloig, in *The Chemistry of Organic Silicon Compounds* (Eds. S. Patai and Z. Rappoport), Vol. 1, Chap. 2, Wiley, Chichester, 1989, p. 87.
2. J. A. Pople, Y. Apeloig and P. v. R. Schleyer, *Chem. Phys. Lett.*, **85**, 489 (1982).
3. A. E. Ketvirtis, D. K. Bohme and A. C. Hopkinson, *Organometallics*, **14**, 347 (1995).
4. A. E. Ketvirtis, D. K. Bohme and A. C. Hopkinson, *J. Phys. Chem.*, **98**, 13225 (1994).
5. C. Wierschke, J. Chandrasekhar and W. J. Jorgensen, *J. Am. Chem. Soc.*, **107**, 1496 (1985).
6. Y. Apeloig and A. Stanger, *J. Org. Chem.*, **47**, 1462 (1982); see also addition in *J. Org. Chem.*, **48**, 5413 (1983).
7. P. Buzek, Ph. D. Thesis, Erlangen, 1993.
8. P. J. Stang, M. Ladika, Y. Apeloig, A. Stanger, M. D. Schiavelli and M. R. Hughey, *J. Am. Chem. Soc.*, **104**, 6852 (1982).
9. M. R. Ibrahim and W. J. Jorgensen, *J. Am. Chem. Soc.*, **111**, 819 (1989).

10. T. Müller, Y. Apeloig and H.-U. Siehl, unpublished results.
11. Y. Apeloig and D. Arad, *J. Am. Chem. Soc.*, **107**, 5285 (1985).
12. P. v. R. Schleyer, H. Jiao, M. N. Gluk'hovtsev, J. Chandresekhar and E. Kraka, *J. Am. Chem. Soc.*, **116**, 10129 (1994).
13. Y. Apeloig, M. Karni, A. Stanger, H. Schwarz, T. Drewello and G. Czekay, *J. Chem. Soc., Chem. Commun.*, 989 (1987).
14. T. Drewello, P. C. Burgers, W. Zummack, Y. Apeloig and H. Schwarz, *Organometallics*, **9**, 1161 (1990).
15. D. Hajdasz and R. Squires *J. Chem. Soc., Chem. Commun.*, 1212 (1988).
16. R. Bakhtiar, C. M. Holznagel and D. B. Jacobson, *J. Am. Chem. Soc.*, **114**, 3227 (1992).
17. S. G. Cho, *J. Organomet. Chem.*, **510**, 25 (1996).
18. M. Mishima, T. Ariga, Y. Tsuno, K. Ikenaga and K. Kikukawa, *Chem. Lett.*, 489 (1992).
19. G. A. McGibbon, M. A. Brook and J. K. Terlouw, *J. Chem. Soc., Chem. Commun.*, 360 (1992).
20. X. Li and J. A. Stone, *J. Am. Chem. Soc.*, **111**, 5586 (1989).
21. W. Zhang, J. Stone, M. A. Brook and G. A. McGibbon, *J. Am. Chem. Soc.*, **118**, 5764 (1996).
22. Y. Apeloig and T. Müller, in *Divalent Carbocations*, (Eds. Z. Rappoport and P. J. Stang), Chap 2, Wiley, Chichester, 1997.
23. Y. Apeloig, P. v. R. Schleyer and J. A. Pople, *J. Am. Chem. Soc.*, **99**, 5901 (1977).
24. B. Ciommer and H. Schwarz, *J. Organomet. Chem.*, **244**, 319 (1987).
25. T. M. Mayer and F. W. Lampe, *J. Phys. Chem.*, **78**, 2433 (1974).
26. T. M. Mayer and F. W. Lampe, *J. Phys. Chem.*, **78**, 2645 (1974).
27. W. N. Allen and F. W. Lampe, *J. Chem. Phys.*, **65**, 3378 (1976).
28. W. N. Allen and F. W. Lampe, *J. Am. Chem. Soc.*, **99**, 2943 (1977).
29. S. Fornarini, *J. Org. Chem.*, **53**, 1314 (1988).
30. F. Cacace, M. E. Crestioni and S. Fornarini, *J. Am. Chem. Soc.*, **114**, 6776 (1992).
31. M. E. Crestioni and S. Fornarini, *Angew. Chem., Int. Ed. Engl.*, **33**, 1094 (1994).
32. A. C. M. Wojtyniak and J. A. Stone, *Int. J. Mass Spectrom. Ion Processes*, **74**, 59 (1986).
33. M. Mishima, C. H. Kang, M. Fujio and Y. Tsuno, *Chem. Lett.*, 2439 (1992).
34. L. H. Sommer, E. Dorfmann, G. M. Goldberg and F. C. Whitmore, *J. Am. Chem. Soc.*, **68**, 488 (1946).
35. L. H. Sommer and F. C. Whitmore, *J. Am. Chem. Soc.*, **68**, 485 (1946).
36. M. A. Cook, C. Eaborn and D. R. M. Walton, *J. Organomet. Chem.*, **29**, 389 (1971).
37. F. K. Cartledge and J. P. Jones, *Tetrahedron Lett.*, 2193 (1971).
38. I. Dostrovsky and E. D. Hughes, *J. Chem. Soc.*, 157 (1946).
39. Y. Apeloig and A. Stanger, *J. Am. Chem. Soc.*, **107**, 2807 (1985).
40. Y. Apeloig, R. Biton and A. Abu-Freih, *J. Am. Chem. Soc.*, **115**, 2522 (1993).
41. N. Shimizu, E. Osajima and Y. Tsuno, *Bull. Chem. Soc. Jpn.*, **64**, 1145 (1991).
42. J. A. Soderquist and A. Hassner, *Tetrahedron Lett.*, **29**, 1899 (1988).
43. A. J. Kresge and J. B. Tobin, *J. Phys. Org. Chem.*, **4**, 587 (1991).
44. Y. Apeloig, P. v. R. Schleyer and J. A. Pople, *J. Am. Chem. Soc.*, **99**, 1291 (1977).
45. M. D. Schiavelli, D. M. Jung, A. K. Vaden, P. J. Stang, T. E. Fisk and D. S. Morrison, *J. Org. Chem.*, **46**, 92 (1981).
46. C. Dallaire and M. A. Brook, *Organometallics*, **12**, 2332 (1993).
47. S. N. Ushakov and A. M. Itenberg, *Zh. Obshch. Khim.*, **7**, 2495 (1937); *Chem. Abstr.*, **32**, 2083^8 (1938).
48. J. B. Lambert, *Tetrahedron*, **46**, 2677 (1990).
49. W. Hanstein and T. G. Traylor, *Tetrahedron Lett.*, 4451 (1967).
50. W. Hanstein, H. J. Herwin and T. G. Traylor, *J. Am. Chem. Soc.*, **92**, 829 (1970).
51. T. G. Traylor, W. Hanstein, H. J. Berwin, N. A. Clinton and R. S. Brown, *J. Am. Chem. Soc.*, **93**, 5715 (1971).
52. T. G. Traylor, H. J. Berwin, J. Jerkunica and M. H. Hall, *Pure Appl. Chem.*, **30**, 599 (1972).
53. P. v. R. Schleyer, D. Lenoir, P. Mison, G. Liang, G. K. S. Prakash and G. A. Olah, *J. Am. Chem. Soc.*, **102**, 683 (1980).
54. L. H. Sommer and G. A. Baughman, *J. Am. Chem. Soc.*, **83**, 3346 (1961).
55. J. Vencl, J. Hetflej, J. Czermak and V. Chvalovsky, *Collect. Czech. Chem. Commun.*, **38**, 1256 (1973).
56. R. Fujiyama and T. Munechika, *Tetrahedron Lett.*, **34**, 5907 (1993).
57. A. W. P. Jarvie, A. Holt and J. Thompson, *J. Chem. Soc. (B)*, 852 (1969).

58. P. F. Hudrlik and D. Peterson, *J. Am. Chem. Soc.*, **97**, 1464 (1975).
59. A. W. P. Jarvie, A. Holt and J. Thompson, *J. Chem. Soc. (B)*, 746 (1970).
60. M. A. Cook, C. Eaborn and D. R. M. Walton, *J. Organomet. Chem.*, **24**, 301 (1970).
61. H. C. Brown, *The Non-Classical Ion Problem*, with comments by P. v. R. Schleyer, Plenum, New York, 1977.
62. D. D. Davis and H. M. Jacocks III, *J. Organomet. Chem.*, **206**, 33 (1981).
63. R. Hoffmann, L. Radom, J. A. Pople, P. v. R. Schleyer, W. J. Hehre and L. Salem, *J. Am. Chem. Soc.*, **94**, 6221 (1972).
64. J. B. Lambert and E. C. Chelius, *J. Am. Chem. Soc.*, **112**, 8120 (1990).
65. J. B. Lambert and R. B. Finzel, *J. Am. Chem. Soc.*, **104**, 2020 (1982).
66. J. B. Lambert, G.-T. Wang, R. B. Finzel and D. H. Teramura, *J. Am. Chem. Soc.*, **109**, 7838 (1987).
67. J. B. Lambert and X. Liu, *J. Organomet. Chem.*, **521**, 203 (1996).
68. J. B. Lambert and G.-T. Wang, *J. Phys. Org. Chem.*, **1**, 169 (1988).
69. G. -t. Wang, E. C. Chelius, D. Li and J. B. Lambert, *J. Chem. Soc., Perkin Trans. 2*, 331 (1990).
70. J. B. Lambert, R. W. Emblidge and S. Malany, *J. Am. Chem. Soc.*, **115**, 1317 (1993).
71. R. Eliason, M. Tomic, S. Borcic and D. E. Sunko, *J. Chem. Soc., Chem. Commun.*, 1490 (1968).
72. N. Shimizu, S. Watanabe and Y. Tsuno, *Bull. Chem. Soc. Jpn.*, **64**, 2249 (1991).
73. N. Shimizu, F. Hayakawa, S. Watanabe and Y. Tsuno, *Bull. Chem. Soc. Jpn.*, **66**, 153 (1993).
74. H. Mayr and R. Pock, *Tetrahedron*, **42**, 4214 (1986).
75. H. Mayr and G. Hagen, *J. Chem. Soc., Chem. Commun.*, 91 (1989).
76. G. Hagen and H. Mayr, *J. Am. Chem. Soc.*, **113**, 4954 (1991).
77. H. Mayr and M. Patz, *Angew, Chem., Int. Ed. Engl.*, **33**, 938 (1994).
78. M. A. Brook, M. A. Hadi and A. Neuy, *J. Chem. Soc., Chem. Commun.*, 957 (1989).
79. M. A. Brook and A. Neuy, *J. Org. Chem.*, **55**, 3609 (1990).
80. A. J. Kresge and J. B. Tobin, *J. Phys. Org. Chem.*, **4**, 587 (1991).
81. V. Gabelica and A. J. Kresge, *J. Am. Chem. Soc.*, **118**, 3838 (1996).
82. G. DeLucca and L. A. Paquette, *Tetrahedron Lett.*, **24**, 4931 (1983).
83. A. J. Kresge and J. B. Tobin, *Angew. Chem., Int. Ed. Engl.*, **32**, 721 (1993).
84. Y. Himeshima, H. Kobayashi and T. Sonoda, *J. Am. Chem. Soc.*, **107**, 5286 (1989).
85. M. J. Bausch and Y. Gong, *J. Am. Chem. Soc.*, **116**, 5963 (1994).
86. (a) N. Shimizu, C. Kinoshita, E. Osajima, F. Hayakawa and Y. Tsuno, *Bull. Chem. Soc. Jpn.*, **64**, 3280 (1991).
    (b) N. Shimizu, C. Kinoshita, E. Osajima and Y. Tsuno, *Chem. Lett.*, 1937 (1990).
87. (a) A. Abu-Freih, PhD Thesis, Technion, Haifa, 1997.
    (b) V. Braude, PhD Thesis, Technion, Haifa, 1995.
88. (a) N. Shimizu, C. Kinoshita, E. Osajima, F. Hayakawa and Y. Tsuno, *Bull. Chem. Soc. Jpn.*, **64**, 3280 (1991)
    (b) N. Shimizu, C. Kinoshita, E. Osajima and Y. Tsuno, *Chem. Lett.*, 1937 (1990).
89. (a) P. v. R. Schleyer, W. F. Sliwinski, G. W. Van Dine, U. Schöllkopf, J. Paust and K. J. Fellenberger, *J. Am. Chem. Soc.*, **94**, 125 (1972).
    (b) W. F. Sliwinski, T. M. Su and P. v. R. Schleyer, *J. Am. Chem. Soc.*, **94**, 133 (1972).
    (c) H. C. Brown, C. Gundu Rao and M. Ravindranathan, *J. Am. Chem. Soc.*, **100**, 7946 (1978).
90. V. J. Shiner, Jr., M. W. Ensinger and G. S. Kriz, *J. Am. Chem. Soc.*, **108**, 842 (1986).
91. V. J. Shiner, Jr., M. W. Ensinger, G. S. Kriz and K. A. Halley, *J. Org. Chem.*, **55**, 653 (1990).
92. E. D. Davidson and V. J. Shiner, Jr., *J. Am. Chem. Soc.*, **108**, 3135 (1986).
93. V. J. Shiner, Jr., M. W. Ensinger and R. D. Rutkowske, *J. Am. Chem. Soc.*, **109**, 802 (1987).
94. V. J. Shiner, Jr., M. W. Ensinger and J. C. Huffman, *J. Am. Chem. Soc.*, **111**, 7199 (1989).
95. J. Coope, V. J. Shiner, Jr. and M. W. Ensinger, *J. Am. Chem. Soc.*, **112**, 2834 (1990).
96. C. A. Grob and P. Sawlewicz, *Tetrahedron Lett.*, **28**, 951 (1987).
97. C. A. Grob, M. Gründel and P. Sawlewicz, *Helv. Chim. Acta.*, **71**, 1502 (1988).
98. T. W. Bentley, W. Kirmse, G. Llewellyn and F. Söllenböhmer, *J. Org. Chem.*, **55**, 1536 (1990).
99. W. Kirmse and F. Söllenböhmer, *Angew. Chem., Int. Ed. Engl.*, **28**, 1667 (1989).
100. W. Kirmse and F. Söllenböhmer,. *J. Am. Chem. Soc.*, **111**, 4129 (1989).
101. R. J. Fessenden, K. Seeler and M. Dagani, *J. Org. Chem.*, **31**, 2483 (1966).
102. W. Adcock, A. R. Krstic, P. J. Duggan, V. J. Shiner, Jr., J. Coope and M. W. Ensinger, *J. Am. Chem. Soc.*, **112**, 3140 (1990).
103. R. Hoffmann, A. Iwamura and W. J. Hehre, *J. Am. Chem. Soc.*, **90**, 1499 (1968).

104. R. Hoffmann, *Acc. Chem. Res.*, **4**, 1 (1971).
105. D. E. Sunko, S. Hirsl-Starcevic, S. Pollack and W. J. Hehre, *J. Am. Chem. Soc.*, **101**, 6163 (1979).
106. W. Adcock, J. Coope, V. J. Shiner, Jr. and N. A. Trout, *J. Org. Chem.*, **55**, 1411 (1990).
107. M. Xie and W. J. Le Noble, *J. Org. Chem.*, **54**, 3839 (1989).
108. W. Adcock, C. I. Clark and C. H. Schiesser, *J. Am. Chem. Soc.*, **118**, 11541 (1996).
109. P. E. Eaton and J. P. Zhou, *J. Am. Chem. Soc.*, **114**, 3119 (1992).
110. R. M. Moriarty, S. M. Tuladhar, R. Penmasta and A. K. Awasthi, *J. Am. Chem. Soc.*, **112**, 3228 (1990).
111. D. N. Kevill, M. J. D'Souza, R. M. Moriarty, S. M. Tuladhar, R. Penmasta and A. K. Awasthi, *J. Chem. Soc., Chem. Commun.*, 3228 (1990).
112. D. A. Hrovat and W. T. Borden, *J. Am. Chem. Soc.*, **112**, 3227 (1990).
113. G. A. Olah, A. L. Berrier, L. D. Field and G. K. S. Prakash, *J. Am. Chem. Soc.*, **104**, 1349 (1982).
114. F.-P. Kaufmann, Ph. D. Thesis, University of Tübingen, 1992.
115. B. Müller, Ph. D. Thesis, University of Tübingen, 1995.
116. G. A. Olah, R. J. Spear and D. A. Forsyth, *J. Am. Chem. Soc.*, **99**, 2615 (1977).
117. G. A. Olah and P. W. Westerman, *J. Am. Chem. Soc.*, **95**, 3706 (1973).
118. H. C. Brown, M. Periasamy, D. P. Kelly and J. J. Giansiracusa, *J. Org. Chem.*, **47**, 2089 (1982).
119. M. Karni, Y. Apeloig and H.-U. Siehl, unpublished results.
120. H.-U. Siehl, Y. Apeloig and T. Müller, unpublished results.
121. A. de Meijere, D. Faber, M. Noltemeyer, R. Boese, T. Haumann, T. Müller, M. Bendikov, E. Matzner and Y. Apeloig, *J. Org. Chem.*, **61**, 8564 (1996).
122. G. Maier, D. Volz and J. Neudert, *Synthesis*, 561 (1992).
123. C. S. Q. Lew, R. A. McClelland, L. J. Johnston and N. P. Schepp, *J. Chem. Soc., Perkin Trans. 2*, 395 (1994).
124. C. S. Q. Lew and R. A. McClelland, *J. Am. Chem. Soc.*, **115**, 1156 (1993).
125. J. B. Lambert, S. Zhang, C. L. Stern and J. C. Huffman, *Science*, **260**, 1917 (1993).
126. J. B. Lambert and S. Zhang, *J. Chem. Soc., Chem. Commun.*, 383 (1993).
127. P. v. R. Schleyer, P. Buzek, T. Müller, Y. Apeloig and H.-U. Siehl, *Angew. Chem., Int. Ed. Engl.*, **32**, 1471 (1993).
128. L. Pauling, *Science*, **263**, 983 (1994).
129. G. A. Olah, G. Rasul, X.-Y. Li, H. A. Buchholz, G. Sandford and G. K. S. Prakash, *Science*, **263**, 983 (1994).
130. G. A. Olah, G. Rasul, H. A. Buchholz, X.-Y. Li and G. K. S. Prakash, *Bull. Soc. Chim. Fr.*, **132**, 569 (1995).
131. C. Maerker, J. Kapp and P. v. R. Schleyer, in *Organosilicon Chemistry II* (Eds. N. Auner and J. Weis), VCH, Weinheim, 1996, p. 329.
132. C. A. Reed, Z. Xie, R. Bau and R. Benesi, *Science*, **262**, 402 (1993).
133. H.-U. Siehl, B. Müller and O. Malkina, in *Organosilicon Chemistry III* (Eds. N. Auner and J. Weis) VCH, Weinheim, 1997, p. 25.
134. (a) V. G. Malkin, O. L. Malkina and D. R. Salahub, *Chem. Phys. Lett.*, **261**, 335 (1996).
     (b) V. G. Malkin, O. L. Malkina, M. E. Casida and D. R. Salahub, *J. Am. Chem. Soc.*, **116**, 5898 (1994).
135. B. Müller and H.-U. Siehl, unpublished results.
136. S. Braun, T. S. Abram and W. E. Watts, *J. Organomet. Chem.*, **97**, 429 (1975).
137. J. B. Lambert and Y. Zhao, *J. Am. Chem. Soc.*, **118**, 7867 (1996).
138. G. K. S. Prakash, V. P. Reddy, G. Rasul, J. Casanova and G. A. Olah, *J. Am. Chem. Soc.*, **114**, 3076 (1992).
139. H.-U. Siehl, in *Dicoordinated Carbocations* (Eds. Z. Rappoport and P. Stang), Chap. 5, Wiley, Chichester, 1997.
140. H.-U. Siehl, in *Stable Carbocation Chemistry* (Eds. G. K. S. Prakash and P. v. R. Schleyer), Chap. 5, Wiley, New York, 1997.
141. T. Müller, Ph. D. Thesis, University of Tübingen, 1993.
142. H.-U. Siehl, *Pure Appl. Chem.*, **67**, 769 (1995).
143. T. S. Abram and W. E. Watts, *J. Chem. Soc., Perkin Trans. 1*, 1522 (1977).
144. K. Bertsch, Diplomarbeit, University of Tübingen, 1987.
145. E.-W. Koch, H.-U. Siehl and M. Hanack, *Tetrahedron Lett.*, **26**, 1493 (1985).

146. S. Braun, T. S. Abram and W. E. Watts, *J. Organomet. Chem.*, **97**, 429 (1975).
147. F.-P. Kaufmann and H.-U. Siehl, *J. Am. Chem. Soc.*, **114**, 4937 (1992).
148. F.-P. Kaufmann, Diplomarbeit, University of Tübingen, 1990.
149. H.-U. Siehl, B. Müller, M. Fuss and Y. Tsuji, in *Organosilicon Chemistry II* (Eds. N. Auner and J. Weis) VCH, Weinheim, 1996, p. 361.
150. G. A. Olah and P. W. Westerman, *J. Am. Chem. Soc.*, **95**, 3706 (1973).
151. H. C. Brown. M. Periasamy, D. P. Kelly and J. J. Giansiracusa, *J. Org. Chem.*, **47**, 2089 (1982).
152. H. C. Brown, M. Periasamy and K. T. Liu, *J. Org. Chem.*, **46**, 1646 (1981).
153. G. A. Olah, R. J. Spear and D. A. Forsyth, *J. Am. Chem. Soc.*, **99**, 2615 (1977).
154. H.-U. Siehl, F.-P. Kaufmann and K. Hori, *J. Am. Chem. Soc.*, **114**, 9343 (1992).
155. R. Jost, J. Sommer, C. Engdahl and P. Ahlberg, *J. Am. Chem. Soc.*, **102**, 7663 (1980).
156. H.-U. Siehl, F.-P. Kaufmann, Y. Apeloig, V. Braude, D. Danovich, A. Berndt and N. Stamatis, *Angew. Chem., Int. Ed. Engl.*, **30**, 1479 (1991).
157. C. U. Pittman Jr., *J. Chem. Soc., Chem. Commun.*, 122 (1969).
158. P. v. R. Schleyer, W. de M. Caneiro, W. Koch and D. A. Forsyth, *J. Am. Chem. Soc.*, **113**, 3990 (1991).
159. G. A. Olah, V. P. Reddy and G. K. S. Prakash, *Chem. Rev.*, **92**, 69 (1992).
160. (a) D. Lenoir and H.-U. Siehl, in *Houben-Weyl Methoden der Organischen Chemie*, (Ed. M. Hanack), Vol. E19c, Thieme, Stuttgart, 1990, p. 413.
    (b) G. A. Olah, G. K. S. Prakash and J. Sommer, *Superacids*, Wiley, New York, 1985, p. 143.
161. M. Saunders and H.-U. Siehl, *J. Am. Chem. Soc.*, **102**, 6860 (1980).
162. W. Koch, B. Liu and D. J. DeFrees, *J. Am. Chem. Soc.*, **110**, 7325 (1988).
163. M. L. McKee, *J. Phys. Chem.*, **90**, 4980 (1986).
164. (a) M. Saunders, K. E. Laidig, K. B. Wiberg and P. v. R. Schleyer, *J. Am. Chem. Soc.*, **110**, 7652 (1988).
    (b) C. S. Yannoni, P. C. Myhre and G. G. Webb, *J. Am. Chem. Soc.*, **112**, 8992 (1990).
165. J. S. Staral, I. Yavari, J. D. Roberts, G. K. S. Prakash, D. J. Donovan and G. A. Olah, *J. Am. Chem. Soc.*, **100**, 8016 (1978).
166. (a) H.-U. Siehl, *J. Am. Chem. Soc.*, **107**, 3390 (1985).
    (b) H.-U. Siehl in *Physical Organic Chemistry* 1986 (Ed. M. Kobayashi), Elsevier, Amsterdam, 1987, p. 25.
    (c) J. Gottaut, Diplomarbeit, University of Tübingen, 1990.
    (d) H.-V. Siehl, Habilitationsschvift, University of Tübingen, 1986.
167. M. Saunders and N. Krause, *J. Am. Chem. Soc.*, **110**, 8050 (1988).
168. H.-U. Siehl and M. Fuss, *J. Am. Chem. Soc.*, **117**, 5983 (1995).
169. H.-U. Siehl and M. Fuss, unpublished results.
170. H.-U. Steinberger, T. Müller, N. Auner, C. Maerker and P. v. R. Schleyer, *Angew. Chem., Int. Ed. Engl.*, **36**, 626 (1997).

CHAPTER **13**

Silicon-substituted carbenes

GERHARD MAAS

Abteilung Organische Chemie I, Universität Ulm, Albert-Einstein-Allee 11, D-89081 Ulm, Germany
Fax: (int.)+49(0)731-502-2803; e-mail: gerhard.maas@chemie.uni-ulm.de

---

I. INTRODUCTION

Carbenes are species which contain a divalent carbon atom with six electrons in its valence shell. Thus, the general formula of a carbene is CR_2, where R stands for a wide range of substituents, including silyl groups. Typically, carbenes are short-lived intermediates which are generated *in situ* from appropriate precursors and undergo fast intra- or intermolecular reactions. In this manner, silicon-substituted carbenes provide access to a variety of organosilicon compounds, such as silyl-substituted molecular frameworks, silaheterocycles and silaethenes.

Since the first reports in the 1960s, the interest of researchers in the chemistry of silicon-substituted carbenes has not ceased up to the present time. While the now classical books on carbene chemistry by Kirmse[1] and Jones and Moss[2] mentioned silylcarbenes only in passing, detailed reviews on the preparative chemistry of silylcarbenes[3] and on the synthesis of silylcyclopropanes by silylcarbene transfer to alkenes[4] have recently appeared in two volumes of the Houben-Weyl series. The chemistry of (trimethylsilyl)carbene has also been covered in further reviews[5,6].

All silicon-substituted carbenes that have been studied experimentally so far contain a SiR_3 group (as opposed to silicon with other coordination numbers); therefore, the expression ‘silylcarbenes’ will be used throughout this chapter.

II. GEOMETRIC AND ELECTRONIC STRUCTURE: THEORY AND EXPERIMENT

Depending on whether the two nonbonding electrons at a carbenic carbon atom are spin-paired or not, the carbene can exist either in a singlet or a triplet electronic state. The lowest-energy singlet state (S) has a bent structure with both electrons located in the nonbonding σ orbital, while the lowest triplet state (T) has one electron in each of the two nonbonding orbitals, one with σ- and one with π-character (Figure 1). Typical valence angles of monosubstituted singlet carbenes, according to experimental observations[7] and theoretical calculations[8], are in the range 100−110 deg, whereas those of the corresponding triplet carbenes are larger by at least 20−30 deg.

Methylene itself has a triplet ground state. The best experimental determinations of the singlet−triplet gap have furnished a value of 9.0−9.1 $\mathrm{kcal\,mol^{-1}}$[9,10], in excellent agreement with recent high-level calculations. Stabilization of the singlet state is achieved by heteroatom substituents such as Hal, OH and NH_2, which can denote electron density

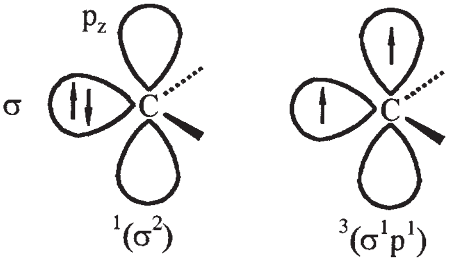

FIGURE 1. Lowest-energy singlet (S) and triplet (T) state of a carbene

from a nonbonding electron pair at the heteroatom to a formally empty p_z orbital of the carbenic carbon atom. On the other hand, triplet states are expected to be stabilized by substituents that are more electropositive than carbon as well as by an increase of the valence bond angle due to bulky substituents. Both substituent effects cause a higher amount of *s* character in the C−X bond(s) of the carbene. This in turn produces more *p* character in the nonbonding σ orbital at the carbene center, so that both nonbonding valence orbitals get closer in energy.

Along these lines, it is expected that a silyl substituent will stabilize the triplet ground state of a carbene. No experimental values for the singlet–triplet gap of silyl-substituted carbenes are available, but meaningful comparisons with other carbenes are now possible based on theoretical calculations[8,11] which take care of a balanced treatment of the two spin states. [Earlier calculations suffered from the problem of unbalanced electron correlation and a spin–coupling bias, both in favor of the triplet state, so that a too high value of the singlet–triplet gap was predicted for carbenes with a triplet ground state (e.g. $HCSiH_3$[12–14]) and a too low value for carbenes with a singlet ground state.] Some results so obtained for silylcarbenes and some other archetypical carbenes are given in Tables 1 and 2. These data are in reasonable agreement with available experimental values for CH_2, CHCl and other carbenes (CHF, CF_2) not mentioned in the Tables.

TABLE 1. Geometries of some carbenes (H−C−X−Y) according to theoretical calculations[a][8]

Carbene	Singlet			Triplet		
	C−X (Å)	H−C−X (deg)	H−C−X−Y (deg)	C−X (Å)	H−C−X (deg)	H−C−X−Y (deg)
CH_2	1.109	101.4		1.082	126.1	
HCCl	1.727	102.3		1.702	124.0	
$HCNH_2$	1.342	104.0		1.434	122.9	
$HCSiH_3$	1.950	109.0		1.858	144.8	
$HCSiH_2CH_3$	1.949	105.8	162.0	1.866	138.8	180.0
$HCSiH_2SiH_3$[b]	1.911	106.6	89.0	1.861	139.9	43.6
$HCCH_2SiH_3$	1.508	104.3	91.4	1.526	127.1	49.0
$HCCH_2CH_3$	1.546	102.6	180.0	1.530	126.6	60.2

[a] Double zeta plus polarization basis sets, two-configuration self-consistent field (singlets) or ROHF (triplet) wave functions using the Huzinaga MINI(d,p) basis set were used. For $HCSiH_2SiH_3$, the latter basis set was replaced by an effective core potential (ECP) together with a split valence plus polarization basis set.

[b] Geometry-optimized at CASSCF/ECP(d,p).

TABLE 2. Calculated singlet–triplet energy gaps ($\Delta E_{ST}{}^{a}$) for several carbenes (kcal mol^{-1})^{b}

Carbene	ΔE_{ST}			Carbene	ΔE_{ST}	
	6-31G(d,p)^{c}	ECP(d,p)^{c}	MRCI^{d}		6-31G(d,p)^{c}	ECP(d,p)^{c}
CH_2	8.7	6.8	9.0	$HCSiH_2CH_3$	18.1	
HCCl	−5.1	−6.0	−9.3	$HCSiH_2SiH_3$		14.7
$HCNH_2$	−32.9	−32.1		$HCCH_2CH_3$	3.4	
$HCSiH_3$	17.8	16.7	18.4	$HCCH_2SiH_3$	−1.2	−2.3

[a] $\Delta E_{ST} = E_S - E_T$; a positive sign means that the singlet is higher in energy.

[b] Structures were optimized at the theoretical level described in Table 1, footnote *a*. Final energies were obtained by using multi-reference configuration interaction (MRCI) wave functions including single and double excitations from the reference wave functions.

[c] From Reference 8.

[d] From Reference 11; individual basis sets were used for each atom.

Table 1 presents two remarkable features of silylcarbene geometry. First, the C−Si bond length is dramatically decreased in the triplet carbene with respect to the singlet species; this difference correlates with a higher *s* character of the $C_{carbene}$−X bonds for the triplet, but more *p* character for the singlet, as discussed above. The second feature concerns the dihedral angle H−C−X−Y: while (methylsilyl)carbene has an antiperiplanar arrangement in both spin states, (disilanyl)carbene shows torsion angles of 89 (singlet) and 43.6 (triplet) deg. Notably, the conformation of (silylmethyl)carbene is very similar to (disilanyl)carbene, whereas ethylcarbene has an antiperiplanar singlet state conformation. By analogy to the energetic stabilization of a carbenium ion by silyl groups in β-position (see the chapter by Siehl), the β-silicon effect can be invoked to explain the conformational differences. In the perpendicular conformation of (disilanyl)carbene and (methylsilyl)carbene, respectively, overlap of the σ(Si−Si) or σ(C−Si) orbitals with the carbenic π orbital is possible, and it is clear that this interaction is especially important energetically for the singlet carbene where the π orbital is essentially empty (Figure 2). In contrast to $HCCH_2SiH_3$, no σ/π-overlap is possible in $HCSiH_2CH_3$ (torsion angle, 162 deg). It has been suggested that the magnitude of the β-silicon effect is associated with the amount of overlap between the carbenic π orbital and the attached Si−Si or Si−C (or C−Si) bond[8]. If one takes the distance *d* between $C_{carbene}$ and the midpoint of X−Y, which is a function of the C−X bond length and the C−X−Y bond angle (Figure 2), as a qualitative measure, it becomes obvious why the β-silicon effect is of minor importance in disilanyl carbene (as suggested by the calculated singlet–triplet gap, see below), in spite of the favorable torsion angle.

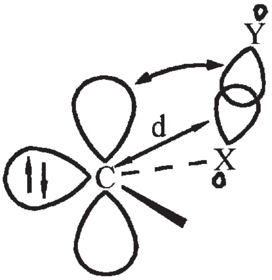

X−Y	*d* [Å]
SiH_2-SiH_3	2.478
CH_2-SiH_3	2.472
SiH_2-CH_3	1.948

FIGURE 2. The β-silicon effect in a singlet carbene

The calculated singlet–triplet splitting (Table 2) confirms that silylcarbene has a triplet ground state. The gap is about 9 kcal mol^{-1} higher than in methylene, a value which is much lower than in earlier calculations. Replacement of SiH_3 by SiH_2CH_3 does not affect ΔE_{ST} appreciably. However, the gap is already much smaller for (disilanyl)carbene, and in (silylmethyl)carbene the singlet state is so much stabilized with respect to the triplet state that a singlet ground state is predicted. Thus, the importance of the β-silicon effect for stabilization of a singlet state is also reflected in the calculated ΔE_{ST} values. The qualitative correlation between increasing Mulliken population of the carbenic π orbital and increasing stabilization of the singlet state for the carbenes mentioned in Table 2 underlines the importance of electron donation to the formally empty π orbital at the carbene center.

Calculations of relative energies on the CH_4Si potential surface established the following order of increasing energy[12]: silaethene ($H_2C{=}SiH_2$), singlet methylsilylene [$^1(H_3CSiH)$], triplet methylsilylene [$^3(H_3CSiH)$], $^3(HCSiH_3)$, $^1(HCSiH_3)$.

The geometries, relative energies and net atomic charges of fifteen structural isomers with the chemical formula C_2H_4Si have been calculated at the (6-31G*//3-21G) SCF level[15]. The four carbenes in this set, which also includes silylenes and Si,C double- and triple-bonded species, have by far the highest relative energy. Two of these carbenes are silicon-substituted carbenes, namely 2-silacyclopropylidene ($H_2\overline{SiCC}H_2$) and (1-silavinyl)carbene [$H_2C{=}Si(H)CH$]:

The silicenium-substituted carbene $HCSi^+H_2$ has been studied in the context of the potential energy surface for the unimolecular decomposition of the methylsilicenium ion ($H_3CSi^+H_2$)[16]. Calculated structures for the singlet and triplet species are shown in Figure 3. In both cases, a remarkably short Si−C distance is found, which points to some degree of π bonding. The linearity of the singlet carbene is remarkable (cf, Table 1) and suggests a description of this species as a silavinyl cation. At the UMP4/6-311++G(2df,2pd) level, triplet $HCSi^+H_2$ is 7.7 kcal mol^{-1} lower in energy than the singlet species. Thus, ΔE_{ST} is much lower than for the neutral carbene $HCSiH_3$ and even lower than for CH_2. According to the calculations of activation barriers, generation of the carbene by 1,1-dehydrogenation at carbon ($H_3CSi^+H_2 \rightarrow HCSi^+H_2 + H_2$ plays no role in the experimentally studied[17] thermal decomposition of the methylsilicenium ion, since 1,2-dehydrogenation and cleavage into CH_4 and SiH^+ occur more easily.

The geometries and relative energies of the singlet carboxycarbene **1** and carboxy(trimethylsilyl)carbene **2** (Figure 4) have been calculated and analyzed by *ab initio* methods[18]. The optimized geometries (RHF/6-31G*) of several conformations of **1** and **2**, i.e., **1-p** or **2-p** (perpendicular, C_1 symmetry), ***1-s-cis*** and ***1-s-trans*** and ***2-s-cis*** and ***2-s-trans*** (all planar, C_s symmetry), are shown in Figure 4. It was found that the perpendicular conformer represents the global minimum and that ***1-s-cis*** and ***1-s-trans*** are transition states for the rotation about the C−C bond. According to MP4/6-31G**//6-31G* calculations, the relative energy differences, $\Delta\Delta H_f$ (***1p*** − ***1-s-cis***) and $\Delta\Delta H_f$

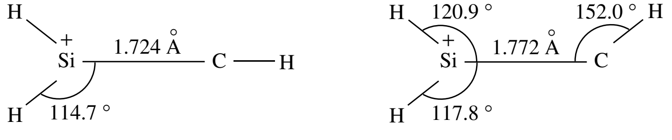

singlet (C_{2v}) triplet (C_s)

FIGURE 3. Structures for $HCSi^+H_2$; singlet species calculated at MP2/6-31G(d,p), triplet species at UMP2/6-31G(d,p))

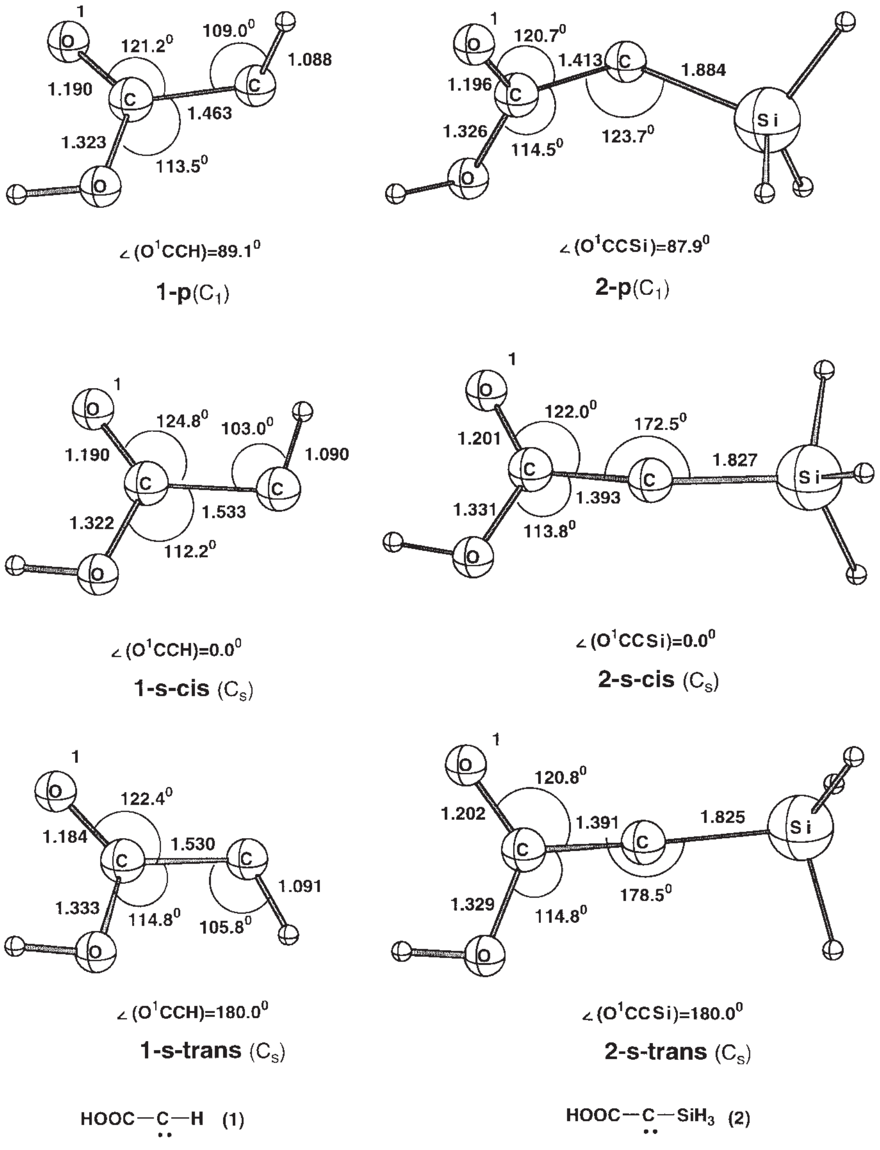

FIGURE 4. Geometry-optimized calculated structures of carbenes **1** and **2**

(***1p* – *1-s-trans***), are about 5–7 kcal mol^{-1} higher in the monosubstituted carbene **1** than in carboxy(silyl)carbene **2**. The geometries of the perpendicular conformation of carbenes **1** and **2** are not very different. In contrast, the planar *s-trans* and *s-cis* conformations of **2** differ from those of **1** as well as from the perpendicular conformation of **2** by having a nearly linear C–C–Si bond angle. The shortening of both the C–C and the C–Si bond lengths in the linear form may also be seen as a consequence of the increased *s* character of these bonds. Geometries and electronic properties of silylcarbene ($HCSiH_3$), (trimethylsilyl)carbene, and carboxy(silyl)carbene (**2**) had been calculated earlier with the MINDO/3 method[19]. The MINDO/3 optimized geometry of singlet **2** was similar to that of ***2-s-cis*** or ***2-s-trans*** which as pointed out above according to the *ab initio* calculations[18] are not local minima.

The matrix-isolation technique is the method of choice for the direct spectroscopic observation of carbenes[7]. However, efforts to generate and to observe silylcarbenes in solid matrices at cryogenic temperatures met with limited success. When (trimethylsilyl)diazomethane, (dimethylsilyl)diazomethane or bis(trimethylsilyl)diazomethane were irradiated in an argon matrix at $\leqslant$10 K, no IR spectra of the corresponding carbenes **3a**–**c** could be obtained[20,21]. However, weak ESR signals were observed which were typical for a linear carbene with a triplet ground state[21]. These results indicate that at least small amounts of carbenes **3a**–**c** were present in the matrix.

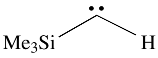

(**3a**)

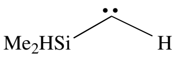

(**3b**)

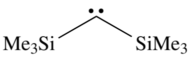

(**3c**)

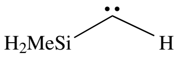

(**3d**)

Attempts to trap carbenes **3b** and **3d** with molecular oxygen, a reaction frequently used to characterize triplet carbenes, were successful at high (>5%) concentrations of O_2 in the argon matrix[22]. In both cases, the corresponding silyl formate was detected, and it was assumed that a carbonyl oxide and a dioxirane are intermediates in this carbene trapping reaction.

Photolysis of matrix-isolated (trimethoxysilyl)diazomethane at $\lambda \geqslant$ 305 nm produced carbene **3e** (equation 1), which was characterized by IR and UV-Vis spectroscopy[23]. Under these conditions, no other species besides the carbene could be detected spectroscopically. In an O_2-doped (1%) argon matrix, the carbene rapidly reacted with oxygen to give carbonyl oxide **4** which was further photoisomerized to formylsilane **5**. Again, the fast reaction of **3e** with $^3O_2$ points to a triplet ground state of the carbene.

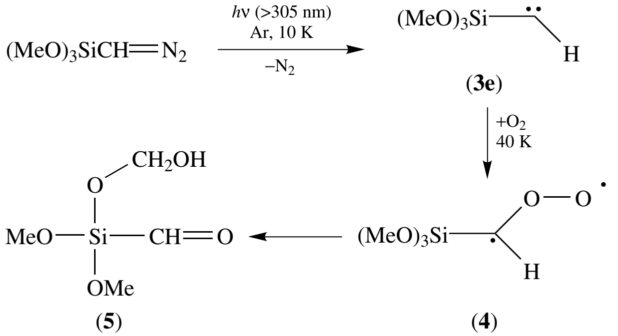

(1)

Considerable interest has been shown recently in so-called 'stable carbenes' of the type $(R_2N)_2P{-}C{-}SiR_3$[24]. Due to the ability of the phosphino group to share the lone electron pair at phosphorus with the carbenic carbon and to the ability of phosphorus to expand its valence shell, the basic question is whether these species in particular, and phosphinocarbenes in general, are to be considered indeed as carbenes I or better as phosphavinyl ylides II or λ^5-phosphaacetylenes III (Figure 5). The geometries predicted by theoretical calculations for the parent phosphinocarbene $H_2P{-}C{-}H$[25] and the silyl-substituted phosphinocarbenes $H_2P{-}C{-}SiH_3$ and $(H_2N)_2P{-}C{-}SiH_3$[26] are given in Figure 5. In all cases, the singlet is predicted to be planar while the triplet is calculated to have a nonplanar, C_s-symmetrical structure featuring a pyramidal phosphorus atom. The P−C distance in the singlet is much shorter than in the triplet and falls in the range of a P≡C triple bond for $(H_2N)_2P{-}C{-}SiH_3$, where electron donation by the phosphino group is particularly high. As discussed above, the introduction of a SiH_3 group at the carbene center increases the valence angle at this center both in the singlet and in the triplet, but a decrease of the C−Si bond length in the triplet with respect to the singlet (cf Table 1) is not observed.

In all cases, the calculations identify the singlet species as the more stable one; at the PMP-4 level, the singlet states of $H_2P{-}C{-}SiH_3$ and $(H_2N)_2P{-}C{-}SiH_3$ are 5.6 and 13.9 kcal mol^{-1}, respectively, below the triplet states. Thus, all computational evidence points to a description of $(R_2N)_2P{-}C{-}SiR_3$ as a species with a P,C multiple bond, with an emphasis on the ylide structure II in which both charges are stabilized by the respective neighboring substituents. An X-ray structure determination of one of the isolable [bis(dialkylamino)phosphino](silyl)carbenes is not yet available but, as will be shown in

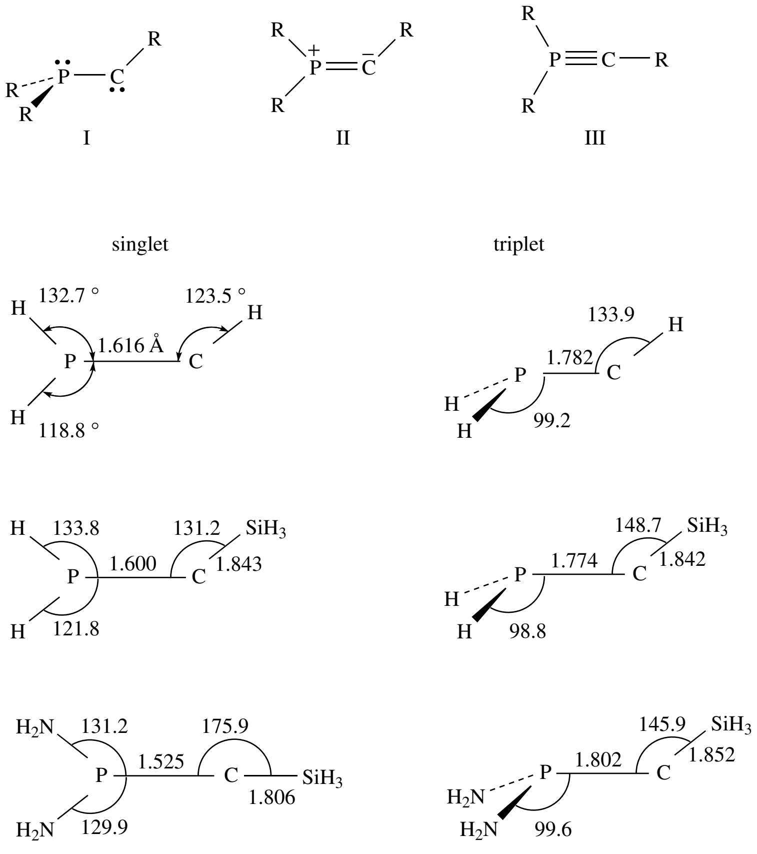

FIGURE 5. Possible structures of phosphinocarbenes and phosphino(silyl)carbenes and the calculated structures for singlet and triplet species; bond lengths (Å) and bond angles (°) are given

Section III.E.7, the chemical behavior has facets of carbene as well as P,C multiple bond chemistry.

III. SILICON-SUBSTITUTED CARBENES IN SYNTHESIS

A. Common Methods of Preparation and General Reactivity Patterns

The most common routes to carbenes[27] are also the major ones to generate silylcarbenes, namely dediazoniation of aliphatic diazo compounds and α-elimination reactions (Scheme 1). The extrusion of N_2 from silyl-substituted diazo compounds can be achieved by UV-irradiation or thermally. The thermal decomposition, however, is of less importance since these diazo compounds are thermally much more stable than their nonsilylated counterparts, so that thermal impact may stimulate noncarbene pathways.

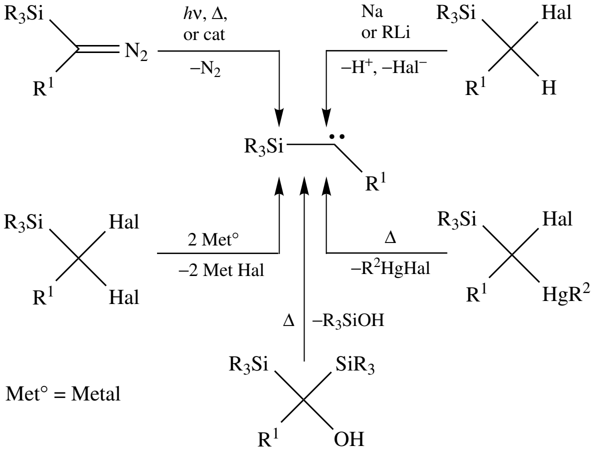

SCHEME 1

Transition-metal catalysis, especially by copper, rhodium, palladium and ruthenium compounds, is another approved method for the decomposition of diazo compounds. It is now generally accepted that short-lived metal–carbene intermediates are or may be involved in many of the associated transformations[28]. Nevertheless, these catalytic carbene transfer reactions will be fully covered in this chapter because of the close similarity in reaction modes of electrophilic carbenes and the presumed electrophilic metal–carbene complexes.

Suitable candidates for α-elimination reactions are silylmethyl halides (→ base-induced elimination of H-Hal), silylmethyl dihalides (→ halide/metal exchange followed by elimination of a metal halide) and stable carbenoid-type compounds such as (α-halo-α-silylalkyl)mercury compounds (→ thermal elimination of mercury(II) halide). Bis(phenylthio)(trimethylsilyl)methyl lithium (→ elimination of LiSPh) represents a borderline case (see Section III.E.8).

Further methods for the generation of silylcarbenes are available, but their application is usually limited to special types of silylcarbenes. Such methods will be discussed separately in Section III.F.

A specific silylcarbene may be generated from different precursors. Furthermore, these reactive intermediates may undergo different competing transformations. Therefore, this section is not classified by methods of generation nor reaction patterns, but rather according to the different types of silylcarbenes, i.e. to the substituent R^1 in a carbene with the general formula $R_3Si{-}C{-}R^1$.

With the exception of some phosphino(silyl)carbenes, which should only formally be considered as carbenes (see Section III.E.7), silylcarbenes are short-lived, electrophilic intermediates. They rapidly undergo intra- or intermolecular reactions which are typical of electrophilic carbenes in general, such as insertion reactions in C−H, X−H and other single bonds, $[1+2]$ cycloaddition to alkenes and alkynes, ylide-forming reactions with nonbonding electron pairs of heteroatoms and the formation of (formal) carbene dimers. Furthermore, the possibility to isomerize by a 1,2-migration of a substituent to the carbene center also applies to silylcarbenes. In a disubstituted carbene **6** both R^1 and R^2 can undergo such a migration, which in the case of R^1 generates a silyl-substituted alkene [or, in the Wolff rearrangement of acyl(silyl)carbenes, a silylketene] but a silicon−carbon double bond (silaethene, silene) in the case of R^2 (equation 2). It is obvious that the silylcarbene-to-silene rearrangement is a particularly appealing aspect in silylcarbene chemistry.

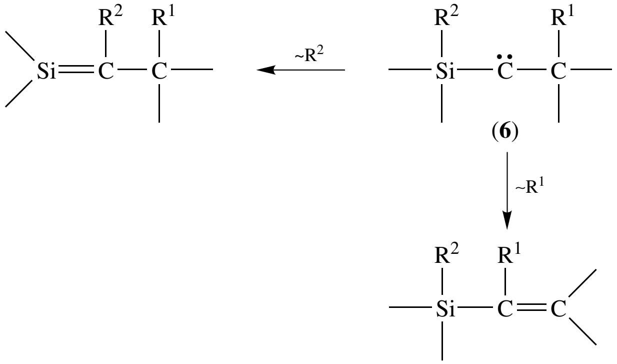

(2)

The spin state of a reacting carbene has consequences for the product formation[1,2]. Reactions such as 1,2-migration, concerted insertion into C−H and O−H bonds and stereospecific cyclopropanation are considered to be typical for a singlet state, whereas nonstereospecific cyclopropanation and H-abstraction originate from the triplet carbene. It must be taken into account, however, that the spin state of the reacting species is not necessarily the same as that of the electronic ground state. For example, simple UV irradiation of a diazo compound will first generate the singlet carbene, while irradiation in the presence of an appropriate triplet sensitizer populates the triplet state; the further reaction course depends on whether the reaction with spin conservation is faster or not than the (spin-forbidden) intersystem crossing. For silylcarbenes, these issues have not been looked at as closely as for some other carbene classes. In spite of the fact that a silyl substituent stabilizes the triplet state (see Section II), it appears, however, that silylcarbenes often undergo singlet carbene reactions. This is especially true for acyl(silyl)carbenes, which have a high tendency for the Wolff rearrangement (Section III.E.5) and add to 1,2-disubstituted alkenes with nearly complete retention of stereochemistry.

B. The Silylcarbene-to-Silene Rearrangement

Silylcarbenes, especially when generated by photochemical or thermal decomposition of diazo compounds or tosylhydrazone alkali salts or α-hydroxy-α-silylsilanes, tend to rearrange to silaethenes (silenes) by a 1,2(Si→C) migration of substituents such as H, alkyl, alkenyl, aryl and SiR_3 (equation 3). Several studies show the following migratory aptitude: H > Me[22], $SiMe_3$ > Me[29–31], $(Me_3Si)_3Si$ > Me[32], Ph > Me[31,33]; in all these cases, the first-mentioned substituent migrates exclusively. While the observation Ph > Me was obtained from the photochemical decomposition of methyl (dimethylphenylsilyl)diazoacetate, product studies of the photolysis of diazo compounds $Me_2(R)SiC(H)N_2$ in ethanol revealed the competitive migration of substituents in the following, statistically corrected order: Me > Ph > CH_2Ph[34]. Methoxy groups do not migrate at all[23].

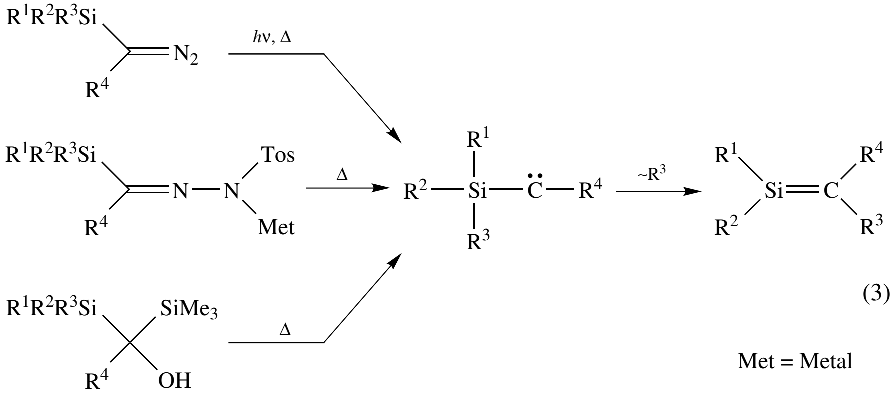

(3)

Met = Metal

All silenes generated so far on the silylcarbene route are reactive intermediates themselves, which were characterized by typical subsequent reactions[35] such as isomerization and dimerization or by trapping reactions (see below). However, photolysis of (silyl)diazo compounds in inert matrices at low temperature allowed the isolation and spectroscopic (IR, UV) characterization of several silenes (Scheme 2, Table 3). Irradiation of (diazomethyl)silanes **7** at $\lambda > 360$ nm produced both diazirine **8** and silenes **10**, but at shorter wavelength ($\lambda > 305$ nm) the silenes were produced cleanly from both precursors; the

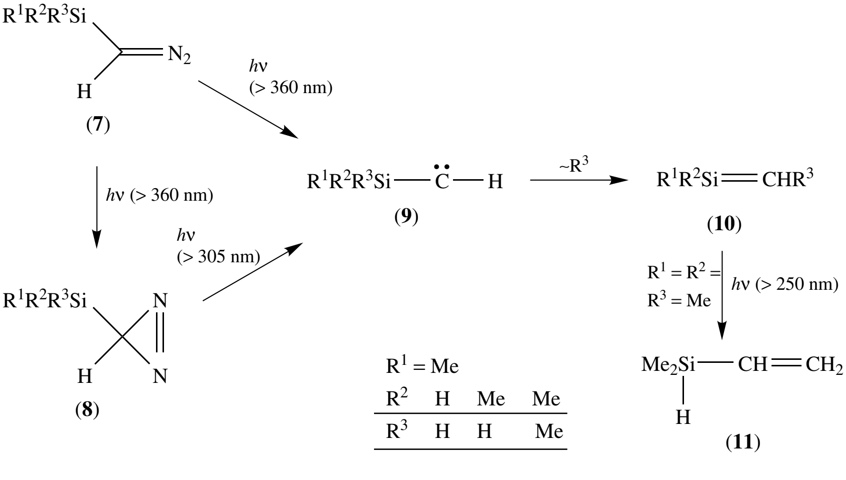

R²	H	Me	Me
R³	H	H	Me

SCHEME 2. Photochemistry of (silyl)diazo compounds in argon matrix

TABLE 3. Matrix isolation of silenes $R^1R^2Si{=}CR^3R^4$ by photolysis of (silyl)diazo compounds according to Scheme 2.

R^1	R^2	R^{3a}	R^4	Conditions[b]	Reference
Me	H	H	H	A	22
Me	Me	H	H	A	22
Me	Me	Me	H	A,B	20–22,31
Me	Me	Me	D	A	21
Me	Me	$SiMe_3$	H	B	29,31
Me	Me	Me	$SiMe_3$	B	29,31
Me	Me	$SiMe_3$	$SiMe_3$	B	29,31
Me	Me	Ph	COOMe	C	31
Me	Me	$SiMe_3$	COAd[c]	C	31
Me	Me	$SiMe_3$	COOEt	C	31,36

[a] R^3 is the substituent that has undergone the 1,2(Si→C) migration.

[b] A denotes argon matrix, 10 K, $\lambda > 305$ nm; B denotes 3-methylpentane matrix, 77 K, $\lambda > 300$ nm; C denotes 3-methylpentane matrix, 77 K, $\lambda > 360$ nm.

[c] Ad = 1-adamantyl.

carbenes **9** were probably too short-lived to be observed even under these conditions (see Section II)[20–22]. When matrix-isolated 1,1,2-trimethylsilene was irradiated at still shorter wavelengths, isomerization to dimethyl(vinyl)silane **(11)** took place[22].

Several transformations of silenes upon warming of the matrix have been described[20–22]. For example, dimerization of 1,1,2-trimethylsilene **(12)**, leading to 1,3-disilacyclobutanes **13**, occurs above 45 K[20–22], addition of methanol before warming to 20 °C yields **14**[22] and warming of an O_2-doped matrix (0.5–1%) gives silylhydroperoxide **15** and vinyloxysilanol **16** in temperature-dependent relative yields[22] (Scheme 3).

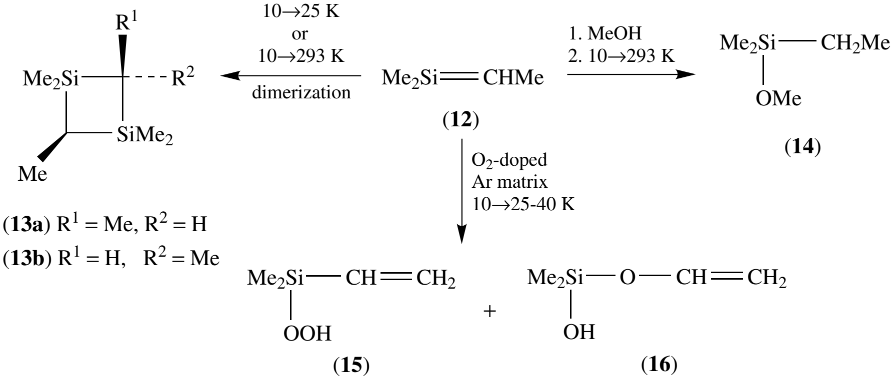

SCHEME 3. Reactions of matrix-isolated silene **12** on warming

Silaacrylate **17** is another example of a matrix-isolated silene[36]. It is formed simultaneously with ketene **18** on irradiation of methyl (pentamethyldisilanyl)diazoacetate in an argon matrix at 10 K (Scheme 4). At shorter wavelengths, the isomerization of **17** to **18** by a 1,3(C→Si) ethoxy shift takes place. Silene **17** does not react with methanol at 10 K, but above 35 K addition at the Si=C bond takes place and generates ethyl methoxydimethylsilyl–(trimethylsilyl)acetate. Similarly, irradiation of the diazoester in a methanol/tetrahydro-2-methylfuran glass at 77 K gave the (methoxysilyl)acetate (83%), **18** (11%) and methoxydimethylsilyl–(trimethylsilyl)ketene (4%) as the only isolable products.

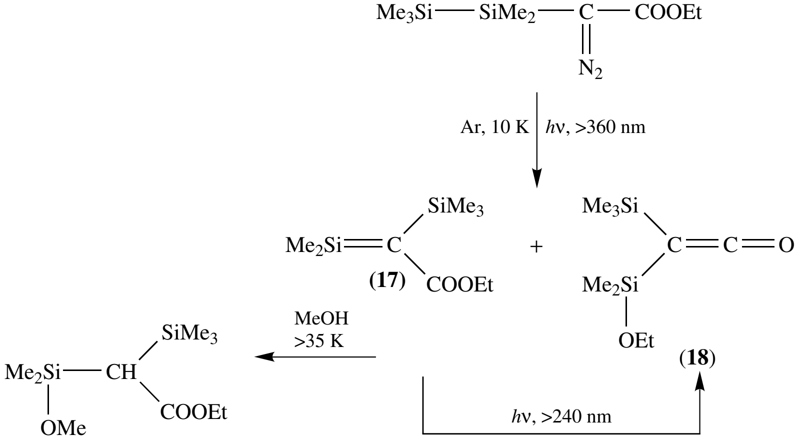

SCHEME 4. Preparation and reactions of silaacrylate **17** in an argon matrix

The following examples in this section illustrate that the silylcarbene-to-silene rearrangement and subsequent silene reactions are common also under nonmatrix conditions. The early research on this topic was reviewed in 1979[37].

When (trimethylsilyl)carbene **(3a)** is generated by photolysis of the diazo precursor **19** in an alcohol solution at room temperature, the rearrangement to the silene is so fast that only the addition products of the latter, but not the O,H insertion product of the carbene, can be isolated (equation 4)[34]. The same holds true for photolysis in diethylamine[38].

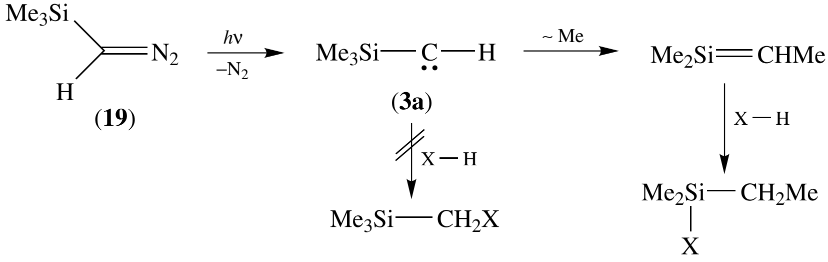

(4)

$X = OCEt_3, OCMe_3, OCHMe_2, NEt_2$

Analogously, copyrolysis of **19** with an alcohol at 425 °C also leads to the silene-derived product, but not to the O,H insertion product of the carbene[38]. The formation of 1-phenylpropene upon copyrolysis of **19** with benzaldehyde[38] (equation 5) corresponds to another well-established silene-trapping reaction, namely [2 + 2] cycloaddition between silene and carbonyl group and thermal [2 + 2] cycloreversion of the resulting silaoxetane.

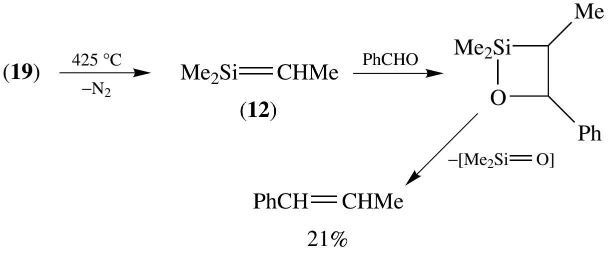

(5)

When phenyl(trimethylsilyl)diazomethane **(20)** is pyrolyzed in the gas phase, typical reactions of carbene **21** can be observed (see Section III.E.4). However, copyrolysis with alcohols or carbonyl compounds generates again products which are derived from silene **22**[39,40] (equation 6). Thus, alkoxysilanes **23** are obtained in the presence of alcohols and alkenes **24** in the presence of an aldehyde or a ketone. 2,3-Dimethylbuta-1,3-diene traps both the carbene (see Section III.E.4) and the silene.

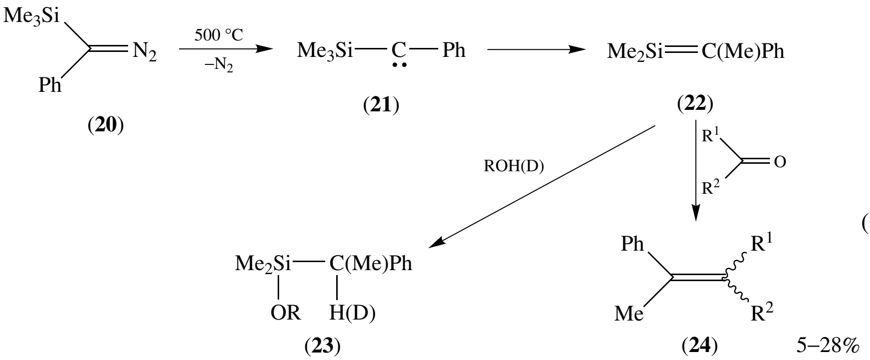

(6)

R = Me (16%), Et (16%)

R^1	Me	$(CH_2)_4$	$(CH_2)_3$	H	H
R^2	Me			Ph	Et

Bis(trimethylsilyl)diazomethane **(25)** represents an excellent source for silene **26**[41]. It appears that carbene **3c**, which is expected from the photochemical or thermal decomposition of **25**, escapes most trapping efforts due to rapid isomerization to silene **26** (equation 7). Photolysis of **25** in benzene solution yields **27** and **28** in a combined yield of 64% and disilazane **29** (10%); all these products are likely to be derived from **26**. Similarly, photolysis in the presence of methanol or D_2O traps the silene quantitatively (to give **31** and **32**).

Remarkably enough, epoxide **30** was identified among the products of the photolysis of **25** in benzene/benzaldehyde. This seems to be the only reported case where carbene **3c** has been intercepted. Pyrolysis of **25** in a nitrogen flow at 400 °C or vacuum pyrolysis at 500 °C led to the same product pattern as the photolysis. Copyrolysis with benzaldehyde or butadiene gave only trapping products of the silene intermediate[41].

Investigations similar to the ones just mentioned have focussed on (trimethylgermyl) (trimethylsilyl)carbene **34**[41]. Photolysis of diazo compound **33** in MeOD yielded a mixture of methoxysilane **37** and methoxygermane **38** in a 79 : 21 ratio (equation 8). This result suggests that carbene **34** underwent a 1,2(Si→C) and a 1,2(Ge→C) methyl shift competingly and that silaethene **35** as well as germaethene **36** were trapped by the alcohol. In contrast, copyrolysis of diazo compound **33** with benzaldehyde allowed one to isolate only compounds that are likely to be derived from the intermediary silaethene **35**[41] (equation 9).

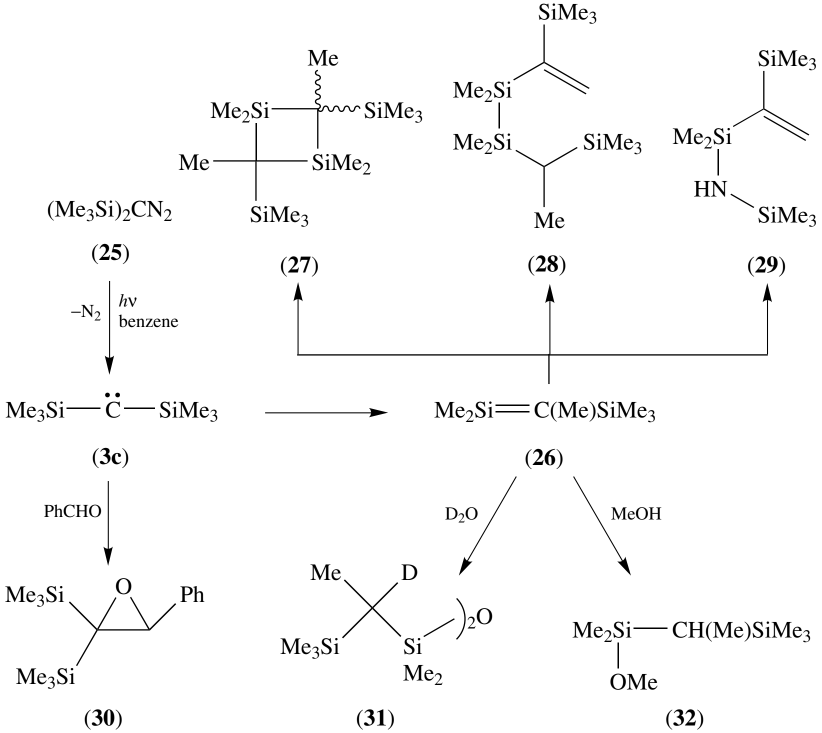

(7)

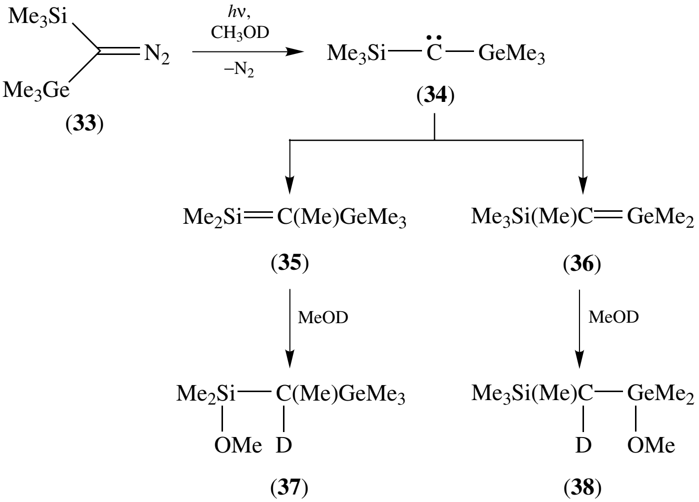

(8)

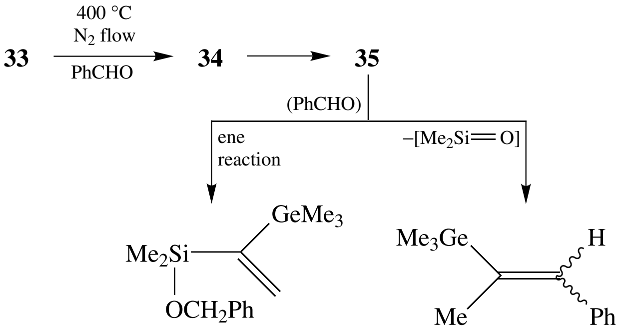

(9)

Taking into account the better migrating ability of $SiMe_3$ with respect to methyl, it comes as no surprise that carbenes **36** and **38**, when generated photochemically or thermally from the corresponding diazo compounds, immediately rearrange to silenes **37** and **39** (equation 10). Again, only the silenes are trapped in the presence of alcohols, benzaldehyde or acetone[29,30]. When **37** was generated through flash pyrolysis at 450 °C in the absence of another reagent, it underwent head-to-tail dimerization to the corresponding 1,3-disilacyclobutane[30]. Silylcarbene-to-silene rearrangements by 1,2(Si→C) silyl group migration are also assumed for the photochemical decomposition of 1,3-bis(diazomethyl)trisilanes and 1,4-bis(diazomethyl)tetrasilanes (see Section III.D).

$$\underset{(\mathbf{36})}{\mathrm{Me_3Si{-}SiMe_2{-}\ddot{C}{-}H}} \xrightarrow{\sim \mathrm{Me_3Si}} \underset{(\mathbf{37})}{\mathrm{Me_2Si{=}CHSiMe_3}}$$

$$\underset{(\mathbf{38})}{\mathrm{Me_3Si{-}SiR_2{-}\ddot{C}{-}SiMe_3}} \xrightarrow{\sim \mathrm{Me_3Si}} \underset{(\mathbf{39})}{\mathrm{R_2Si{=}C(SiMe_3)_2}} \qquad (10)$$

(a) R = Me, (b) R = $SiMe_3$

The last three entries of Table 3 tell us that 2-acylsilenes are accessible by irradiation of matrix-isolated (silyl)diazoketones and (silyl)diazoacetates. In fact, the same transformations can be reproduced in solution, but in all reported cases the 2-acylsilenes underwent fast intra- or intermolecular reactions or were trapped by added alcohols or enolizable as well as nonenolizable carbonyl compounds. Short-lived acyl(silyl)carbenes are generally assumed to be the immediate precursors of the 2-acylsilenes, but their intermediacy has never been proven. It appears that a clean silylcarbene-to-silene rearrangement for silyl-ketocarbenes **(40)** requires the presence of a disilanyl substituent (Si–Si) at the carbene, whereas silyl groups having only Si–C bonds favor the silylcarbene-to-silylketene isomerization **(40→41a**, Wolff rearrangement) (Scheme 5). Similarly, alkoxycarbonyl(disilanyl)carbenes (**43**, $R^1 = SiR_3$) rearrange only to 2-acylsilenes **45**, but alkoxycarbonyl(trialkylsilyl)carbenes (**43**, R^1 = alkyl, aryl) can undergo both types of rearrangement. Although acylsilenes **42** and **45** can be trapped (see below), it is also possible that they isomerize to ketenes **41b** and **46** respectively, by a fast 1,3 (C→Si) substituent migration. Thus, acyl(silyl)carbenes **40** and **43** may furnish not only the 'normal' ketenes **41a** and **44** from the Wolff rearrangement, but also the 'doubly

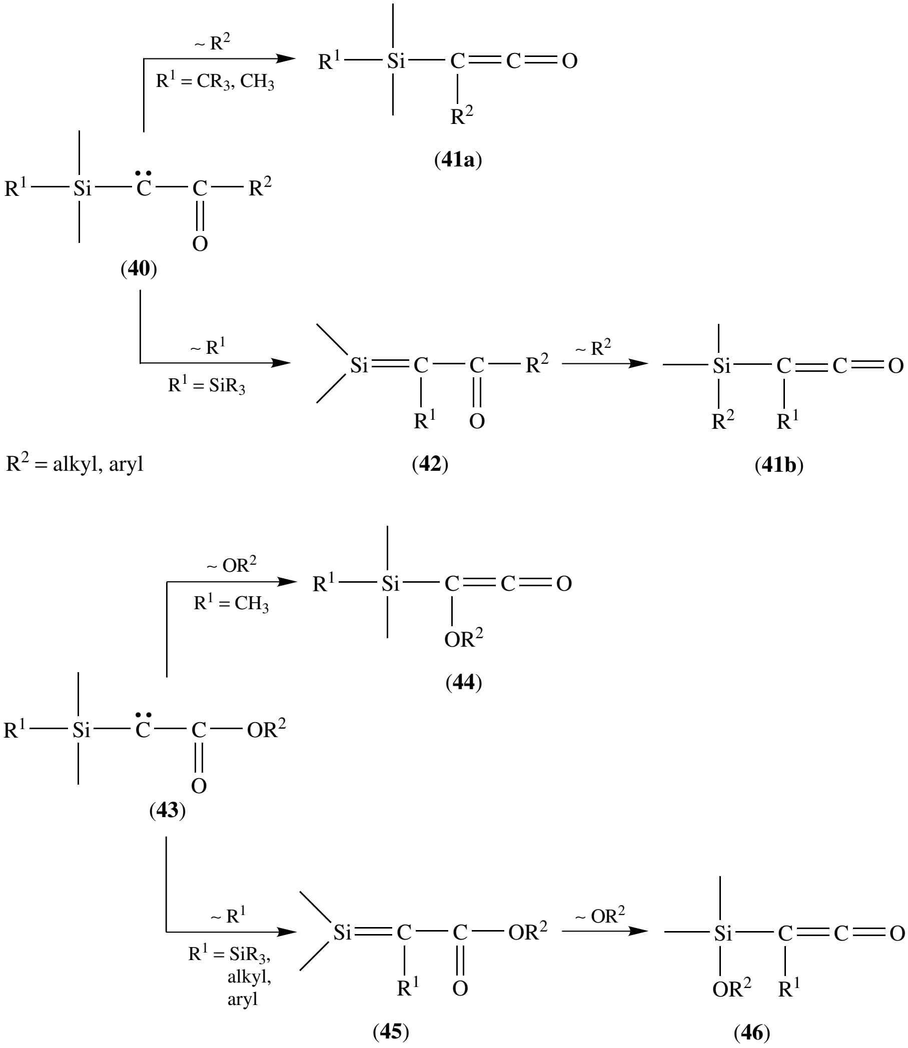

SCHEME 5

rearranged' ketenes **41b** and **46**. In this section, we look only at the acyl(silyl)carbene-to-acylsilene isomerization, and leave the Wolff rearrangement to Section III.E.5.

When acyl(disilanyl)carbenes **48** are generated by photolysis of diazoketones **47** in benzene solution, the acyl(silyl)carbene-to-acylsilene rearrangement appears to be the exclusive consequence. The further fate of the acylsilenes **49** depends on the nature of substituent R (equation 11). When R is bulky (1-adamantyl (1-Ad), *t*-Bu), 1,4-cyclization yields the 1,2-silaoxetanes **50**, which easily decompose to an alkyne and dimethylsilanone at elevated temperature[32,42,43]. Acylsilenes with sterically less demanding substituents undergo a [4+4] cyclodimerization leading to the eight-membered silaheterocycles **51**[32,43].

In some cases, the doubly rearranged (i.e. silene-derived, see Scheme 5) ketenes **52** could be detected as minor by-products[32].

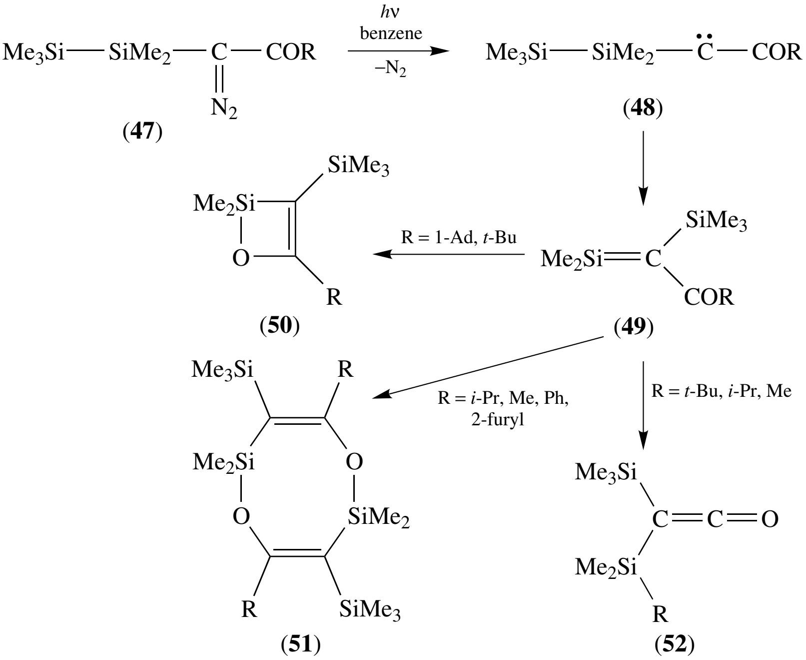

(11)

When carbonyl compounds were present during the photolysis of diazoketones **47**, the three acylsilene transformations displayed in equation 11 were partly or fully suppressed. (However, this was not the case for **47**, R = 1-Ad, which did not react with carbonyl compounds[42].) Thus, acylsilenes **49** reacted with enolizable ketones such as acetone, acetophenone and acetylacetone in an ene-type reaction forming silyl enol ethers, e.g. **54** (equation 12)[44]. With nonenolizable carbonyl compounds, such as benzophenone, crotonaldehyde and ethyl acetate, the acylsilenes where trapped in a hetero-[4+2] cycloaddition reaction forming 1,3-dioxa-4-sila-5-cyclohexenes **55**[44]. Surprisingly, the doubly rearranged ketenes **52** were no longer found in these reactions; rather, the 'normal' ketenes **53**, corresponding to a Wolff rearrangement, were formed in significant amounts and were characterized by addition of methanol[44]. It is not clear how the added carbonyl compounds partly redirect the reaction pathway from the exclusive silylcarbene-to-acylsilene to the silylcarbene-to-silylketene pathway. It would appear that at least some of these carbonyl compounds act as triplet sensitizers in the photolysis reaction, but it is well established that the Wolff rearrangement (i.e. **47** → **53** or **48** → **53**) occurs either from an excited singlet state of the diazoketone or from the singlet carbene.

In this context, it is worth mentioning that there is only one other, clear-cut example for the simultaneous occurrence of the acyl(silyl)carbene-to-acylsilene and the acylcarbene-to-silylketene rearrangement of an acylcarbene bearing a Si−Si substituent. Carbene **57**, generated by photolysis of diazoketone **56** in benzene, isomerized to both **58** and **59** in about equal amounts[44]. While the acylsilene cyclized to 1,2-silaoxetene **60**, the ketene was isolated and structurally characterized by X-ray diffraction analysis of the derived carboxylic acid **61** (equation 13).

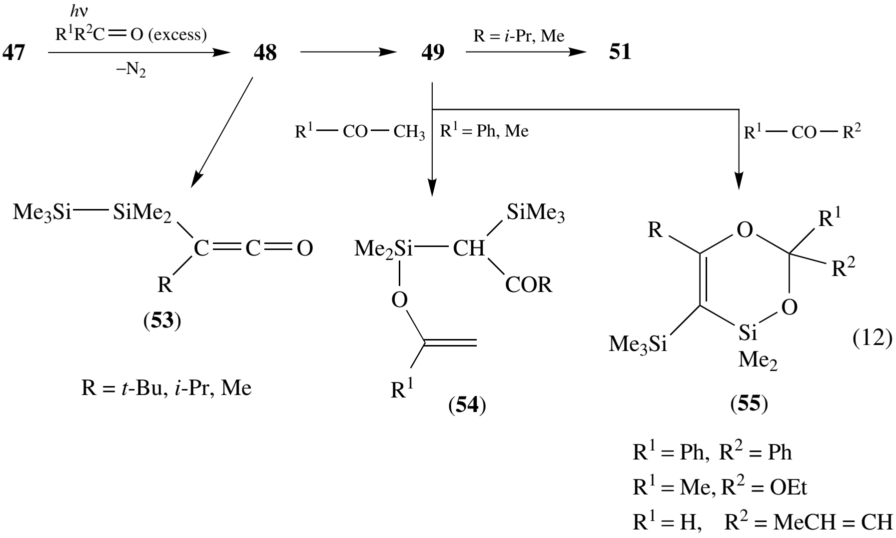

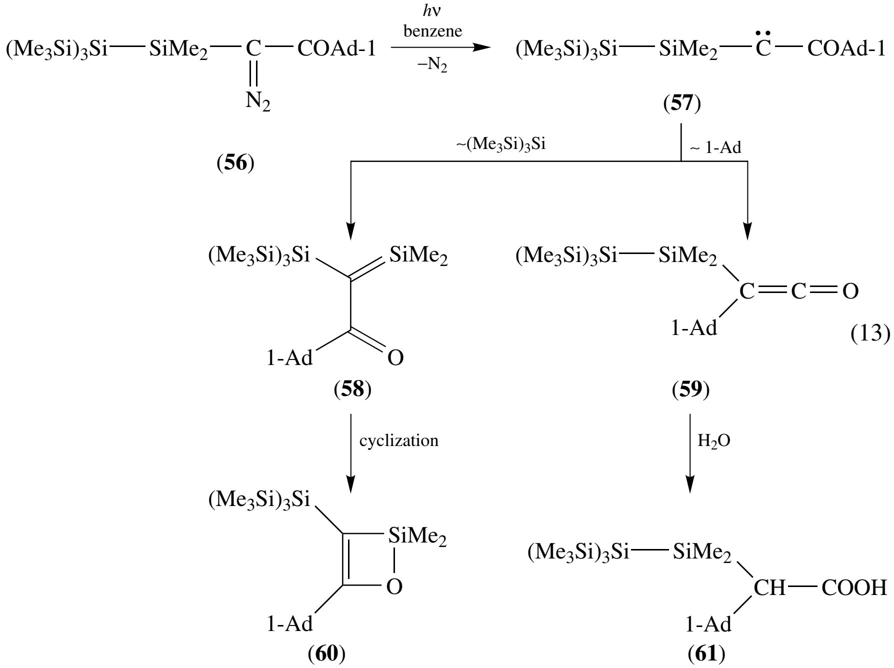

As stated above, an alkoxycarbonyl(disilanyl)carbene rearranges to an acylsilene, but not to a silylketene (Scheme 5). For diazoacetate **62**, the result of a matrix-isolation experiment (Table 3) can also be reproduced when the nitrogen extrusion is induced by vacuum pyrolysis at 360 °C, by thermolysis of the neat compound at 180 °C or by photolysis in

THF solution[36,45]. In all cases, the formation of the doubly rearranged ketene **65** in nearly quantitative yield suggests that an isomerization sequence carbene→ silene → ketene has taken place (equation 14). While no direct evidence for the participation of carbene **63** is available, the presumed acylsilene intermediate **64** could be trapped with alcohols, by an ene-reaction with enolizable ketones (cyclohexanone, cyclooctanone, 3-pentanone, 3-heptanone) and by alkene formation with benzophenone or 2-adamantanone. For example, the photolysis of **62** in methanol gave **66** (70% yield), obviously an addition product of methanol to silene **64**, together with ketene **67** (23%) and a small amount of ketene **65**[36]. Since **65** is stable in methanol, **67** cannot stem from direct alkoxy exchange in **65**. It has been suggested that (similar to the migration of alkoxy groups in the Wolff rearrangement, see Section III.E.5.b), the 1,3 (C→Si) alkoxy migration (**64** → **65**) proceeds via an ion pair, which could be susceptible to the alkoxy exchange.

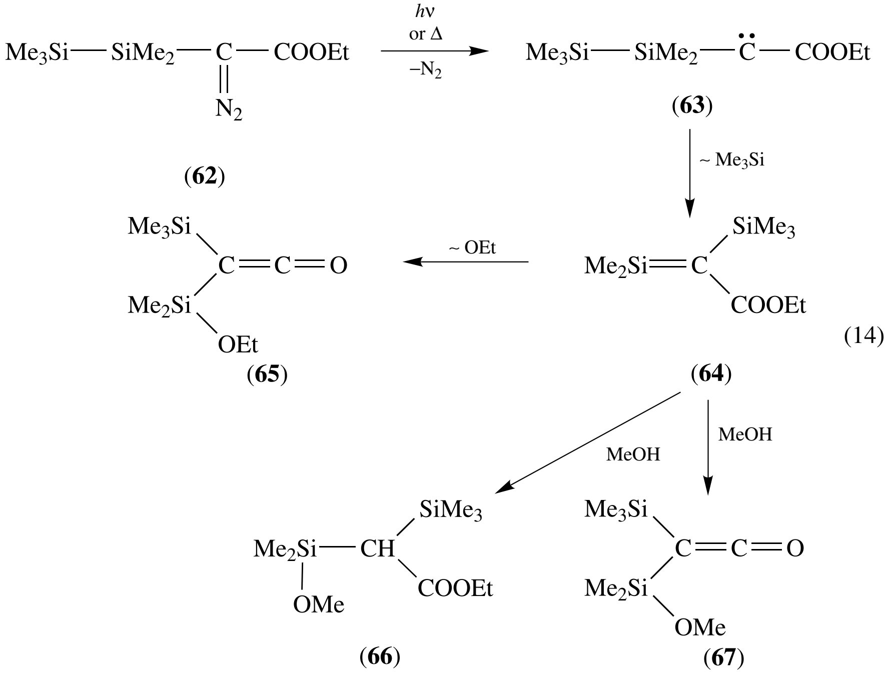

(14)

When diazoacetate **62** was thermolyzed in 7-norbornanone, the acylsilene **64** could be trapped again, this time in a formal [4 + 2] cycloaddition reaction to give **68** (equation 15)[46,47]. The simultaneous formation of **69** suggests a stepwise, ionic pathway providing both products.

The silylcarbene-to-silene rearrangement has also been considered for the construction of the Si=C bond of silabenzenes and silafulvenes. Thus, the photochemical decomposition of (diazomethyl)silole **70** in methanol produced a mixture of 1,2-dihydrosilin **74** (8%), 1,4-dihydrosilin **75** (8%) and silole **76** (19%)[48,49] (equation 16). Undoubtedly, the primarily formed silylcarbene **71** has undergone a ring expansion to form silabenzene **72**, and a 1,2(Si→C) methyl shift to form silafulvene **73**, and methanol has added to the Si=C bond of both intermediates. When the hydrogen atom in carbene **71** is replaced by a methyl group, an 1,2(C→C)H shift leading to a 1-vinylsilole takes over[49] (see Section III.E.2).

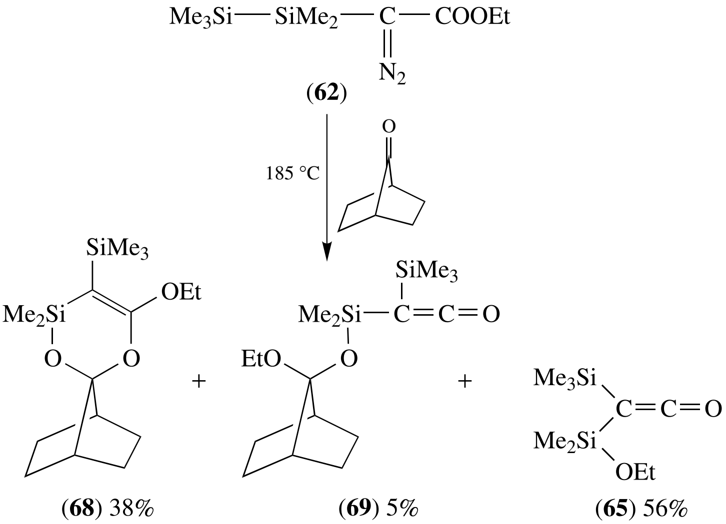

(**62**)

(**68**) 38% (**69**) 5% (**65**) 56%

(15)

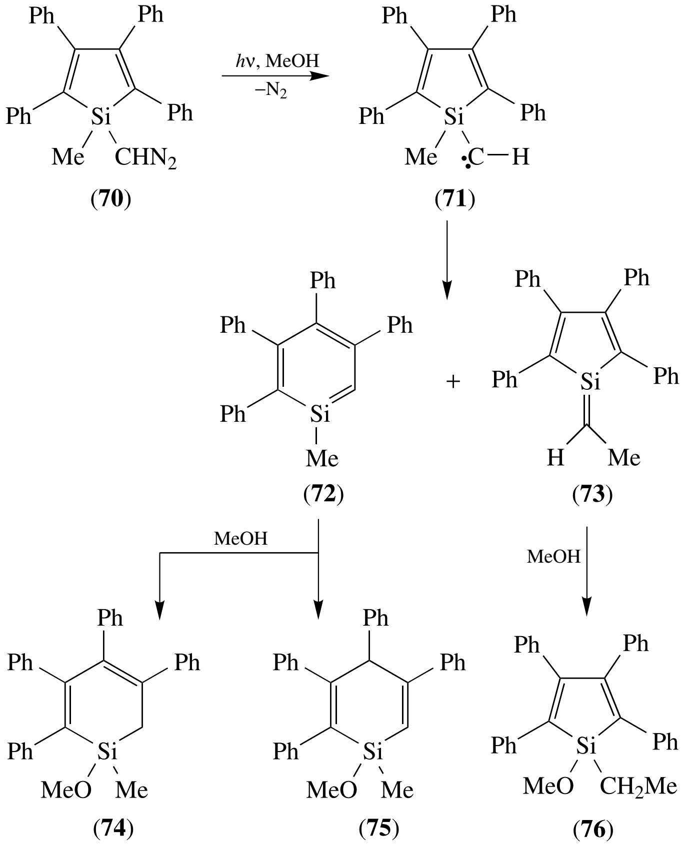

(**70**) (**71**)

(**72**) (**73**)

(16)

(**74**) (**75**) (**76**)

A silafulvene **(79)** was also formed when the 2-diazo-1,2-dihydrosilin **77** was decomposed under copper catalysis (equation 17)[49,50]. In the presence of *tert*-butanol, **79** was trapped as the (*tert*-butoxy)silane **81**. When **77** was decomposed in the presence of benzophenone or benzaldehyde, fulvenes **80** were obtained in another reaction typical for silenes.

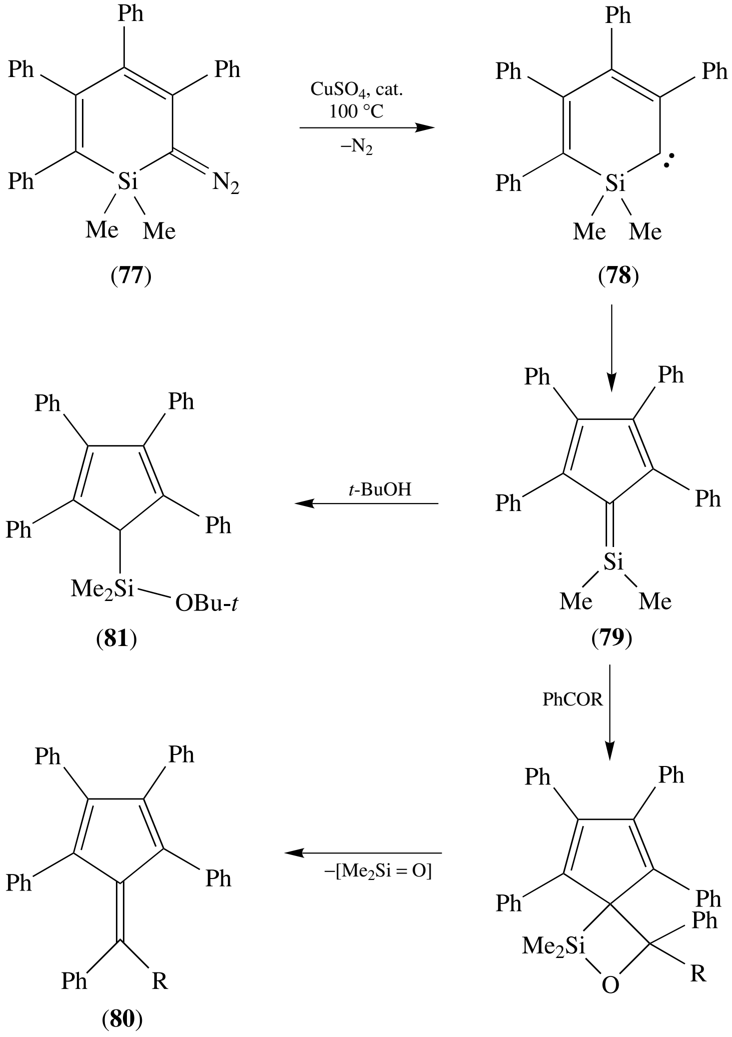

(17)

While formation of a silabenzene from carbene **78** failed probably because of the low tendency of methyl to undergo the 1,2 migration, this strategy was at least partly successful with carbene **83**, where the high migratory aptitude of a Me_3Si group has been exploited[51]. The result depends, however, very strongly on the reaction conditions for the decomposition of **82**; the products are shown, together with presumed intermediates, in equation 18. In a similar manner, silabenzene **84** was generated and could be observed by its IR and NMR spectra at $-100\,^{\circ}\mathrm{C}^{52}$.

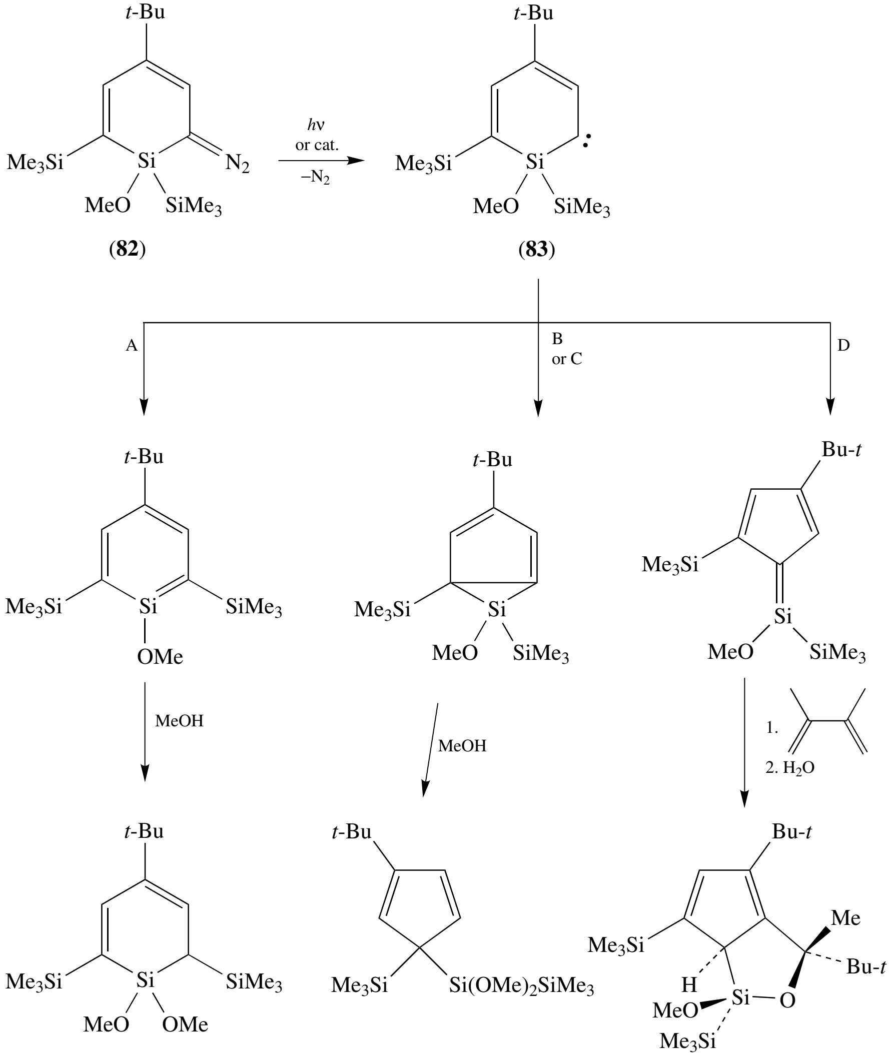

Conditions : A, $CuSO_4/Cu_2Cl_2$(cat.), benzene-MeOH, 25 °C, 8 days ;
B, $CuSO_4/Cu_2Cl_2$(cat.), benzene-MeOH, >25 °C ;
C, *h*ν, $\lambda \leq 385$ nm, MeOH-ether, −60 → 25 °C ;
D, *h*ν, $\lambda \leq 435$ nm, ether, 2,3-dimethylbuta-1,3-diene, 25 °C

(18 *continued*)

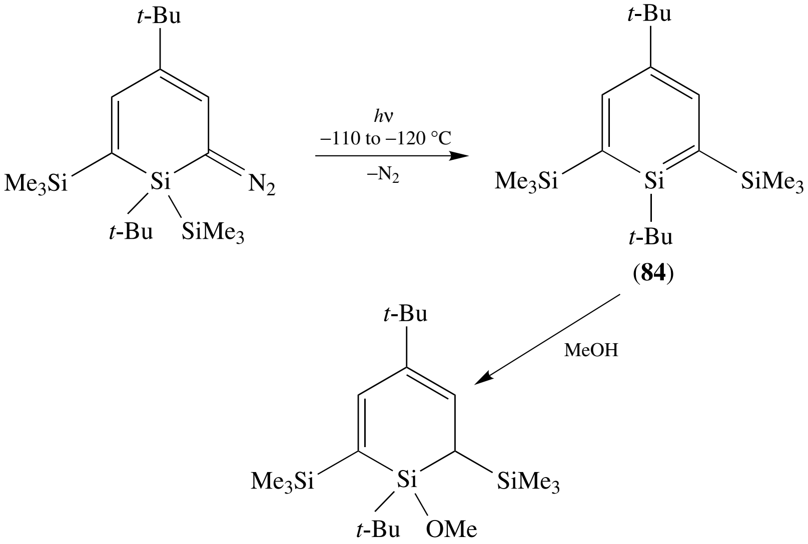

(18)

Photochemical or copper-catalyzed decomposition of diazo compound **85** failed to give a handle on 2-silanaphthalene **87** (equation 19)^{49,50}. Instead of the expected 1,2-Ph migration, carbene **86** apparently underwent simply an O,H insertion reaction with methanol in 96% yield.

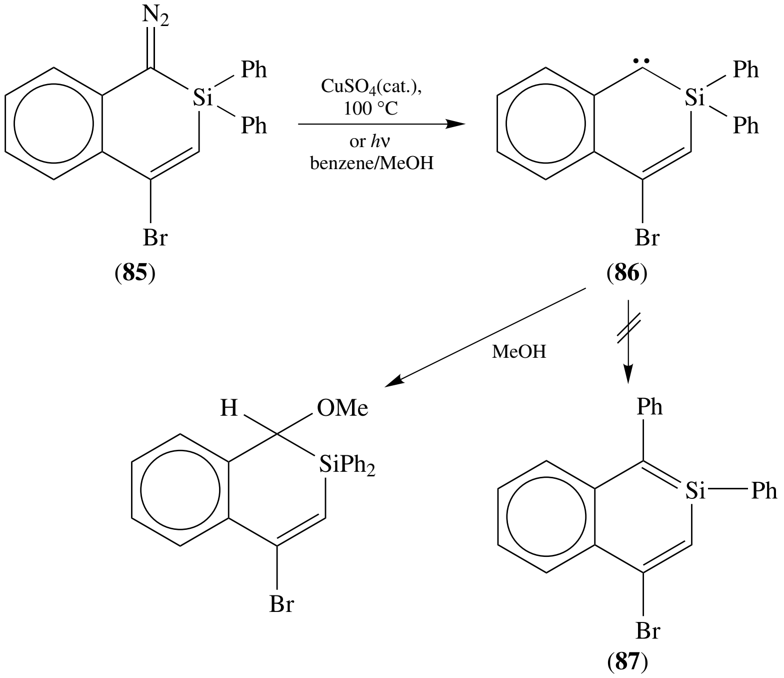

(19)

C. Intramolecular Carbene Reactions with Substituents Attached to Silicon

1. C,H insertion

a. 1,3-C,H insertion. In a silylcarbene, this reaction mode would lead to a silirane. Although silirane formation has been invoked as one of the reaction pathways of (trimethylsilyl)carbene[21,38,53,54], other (trialkylsilyl)carbenes[55,56] and phenyl(trimethylsilyl)carbene[40], a stable silirane has never been isolated from any of these reactions, probably because this strained ring system was not stable under the pyrolytic or nucleophilic reaction conditions. For example, flash vacuum pyrolysis of (trimethylsilyl)diazomethane at 440 °C yields the products **13, 89** and **90**[21,38] (equation 20). While **13** is obviously the dimer of silene **12** and two mechanistic proposals exist for the formation of **90**[21,54], a deuterium-labeling study[54] [flash-vacuum pyrolysis of $Me_3Si{-}C(D)N_2$ at 750 °C] supports the proposal that vinylsilane **89** is formed by isomerization partly of silene **12** and partly of silirane **88**. Extrusion of dimethylsilylene from **88** may be the source of ethylene[57], similar to the observation of a small amount of styrene in the pyrolytic decomposition of phenyl(trimethylsilyl)diazomethane[40].

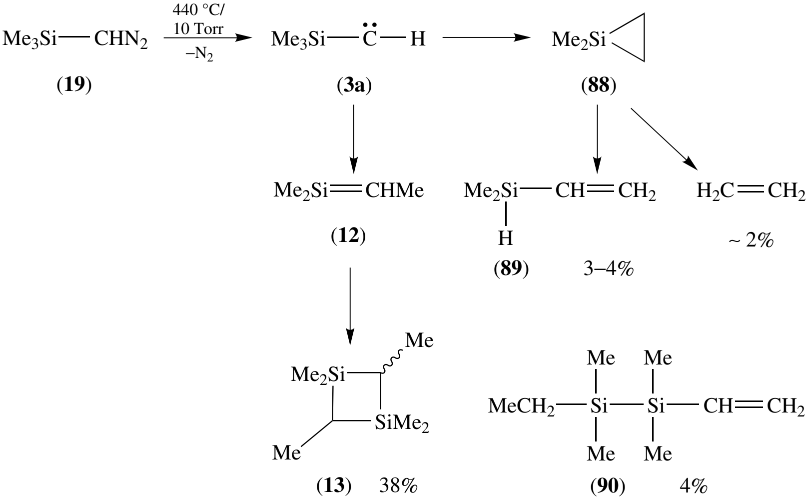

(20)

The silirane intermediate could also account for the formation of vinylsilane **89** when (trimethylsilyl)carbene is generated from dichloromethyl(trimethyl)silane and Na−K in a gas-phase reaction[53]. The transformations of (trialkylsilyl)carbenes, generated from (α-halomethyl)silanes by α-elimination with a strong base, may involve transient siliranes as well (equation 23 and Section III.E.1.b).

For an eventual 1,3-C,H insertion in the copper-catalyzed decomposition of diazoketone **190**, see Section III.E.5.a.

b. 1,4-C,H insertion. (Trimethoxysilyl)carbene **(3e)**, generated in an argon matrix by irradiation ($\lambda > 305$ nm) of (trimethoxysilyl)diazomethane (equation 1), undergoes clean 1,4-C,H insertion to form 1,2-silaoxetane **91** (equation 21) upon short-wavelength UV irradiation[23]. A carbenic 1,4-C,H insertion also accounts for the formation of silacyclobutanes **93** upon solution photolysis of diazoesters **92** (equation 22)[58]. Only one diastereomer of **93** was obtained in all cases, but the stereochemistry was not determined. The silacyclobutenes rearrange easily to the 1-oxa-2-silacyclohexenes **94** which in some cases

($X = N_3$, NCS) are already present in the reaction mixture.

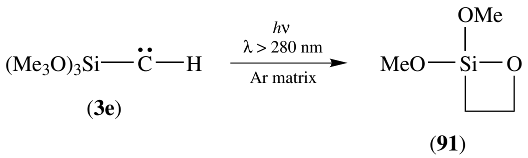

(21)

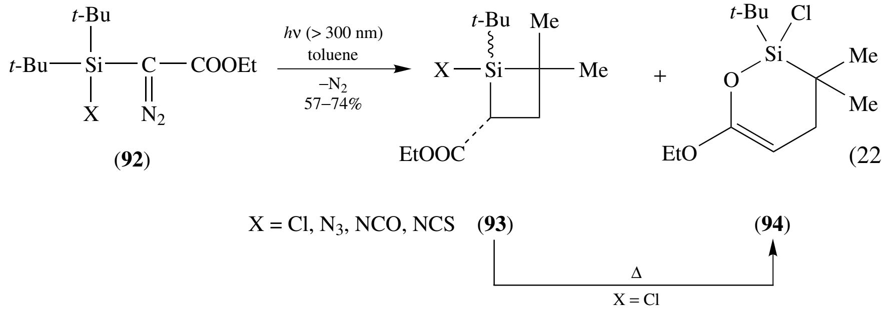

(22)

c. 1,5-C,H insertion. Alkyl (dimethylsilyl)carbenes **95**, generated from an alkyl(chloromethyl)dimethylsilane and sodium, can undergo both 1,3- and 1,5-C,H insertion (equation 23)[56], but 1,4- and 1,6-C,H insertion reactions are not observed. 1,3-C,H insertion can occur at a methyl or a methylene group of **95**. The ratio of the products formed on the silirane route suggests a 1°/2° selectivity of 1 : 2.5, which is to be compared with the ratio 1.0 : 1.3–1.9 reported for 2-butylcarbene undergoing 1,3-C,H insertion[1].

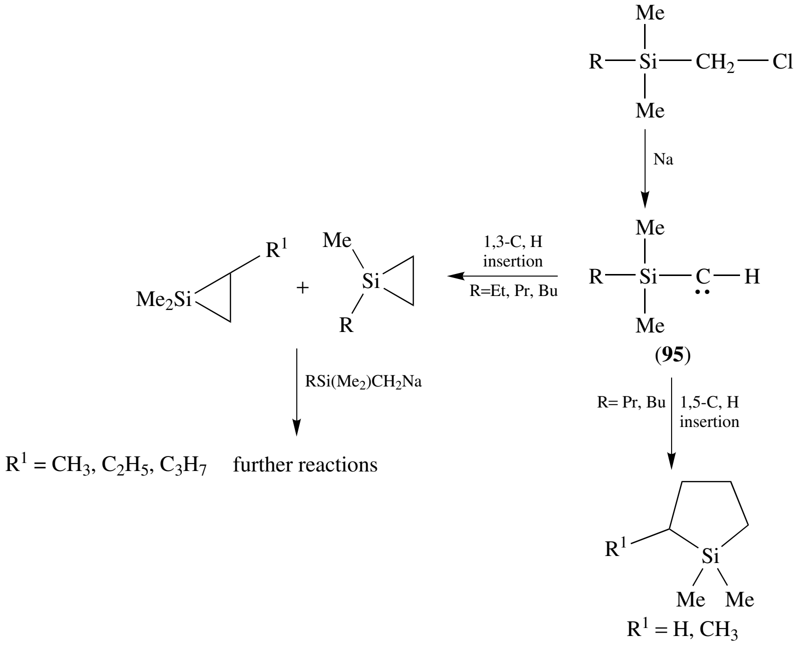

(23)

Similarly generated (*ω*-alkenyl)(dimethylsilyl)carbenes **96** (equation 24) undergo 1,5-C,H insertion reactions giving **97** in competition with intramolecular cyclopropanation to give **98**[59]; however, the yields of all these reactions are low.

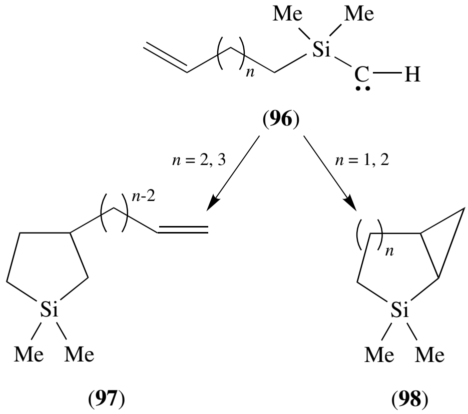

(24)

Carbenes **100**, generated by UV irradiation of methyl (alkoxysilyl)diazoacetates **99**, furnish 1-oxa-2-silacyclopentanes **101** by 1,5-C,H insertion (equation 25)[60]. In order to suppress competing reaction pathways of the carbene intermediate (e.g. formation of a ketazine with excess diazo compound), the photolysis was carried out at high dilution, but, even then, yields were rather modest. Carbene insertion at CH_2 seems to occur much more easily than at CH_3; a preference of 3 ± 0.6 : 1 for methylene insertion can be calculated from the isolated yields after correction for the number of C−H bonds. It should be noted that for both carbenes, **96** and **100**, C,H insertion occurs only in the 1,5 mode whereas no 1,3-, 1,4- or 1,6-C,H insertion products could be detected.

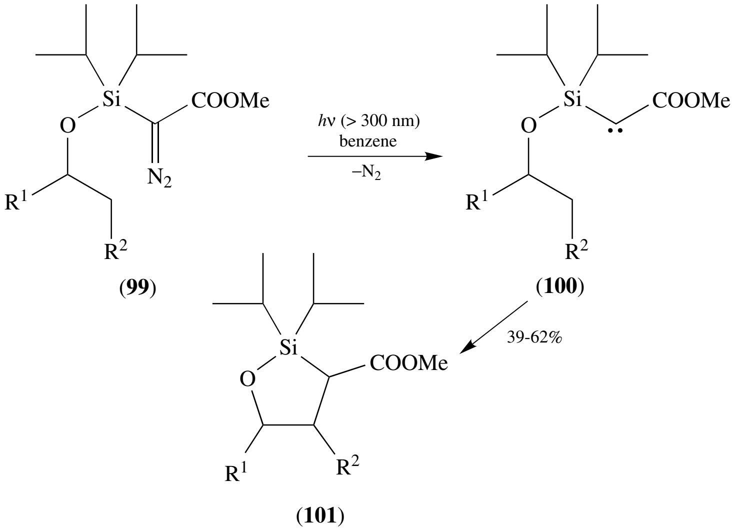

(25)

R^1	H	H	Me
R^2	H	Me	Me

2. Reactions at C=C bonds

[(3-Butenyl)-, (2,3-dimethyl-3-butenyl)- and (4-pentenyl)-dimethylsilyl)]carbene have been generated by treatment of the corresponding chloromethylsilanes with sodium. Intramolecular [1 + 2] cycloaddition of the carbenic carbon atom to the double bond leads to 1-silabicyclo[3.1.0]hexanes and 1-silabicyclo[4.1.0]heptanes, respectively, usually in competition with intramolecular C,H insertion (equation 24)[56]. In contrast, no carbene-derived product could be obtained from (allyldimethylsilyl)carbene. Finally, reaction of chloromethyldimethylvinylsilane with sodium provided, besides the typical products of a Wurtz reaction (**103** and **104**), a small amount of cyclopropane **106** (equation 26)[56]. It has been suggested that (dimethylvinylsilyl)carbene **(102)** isomerizes to silabicyclo[1.1.0]butane **105** by intramolecular cyclopropanation, and nucleophilic ring-opening finally leads to **106**.

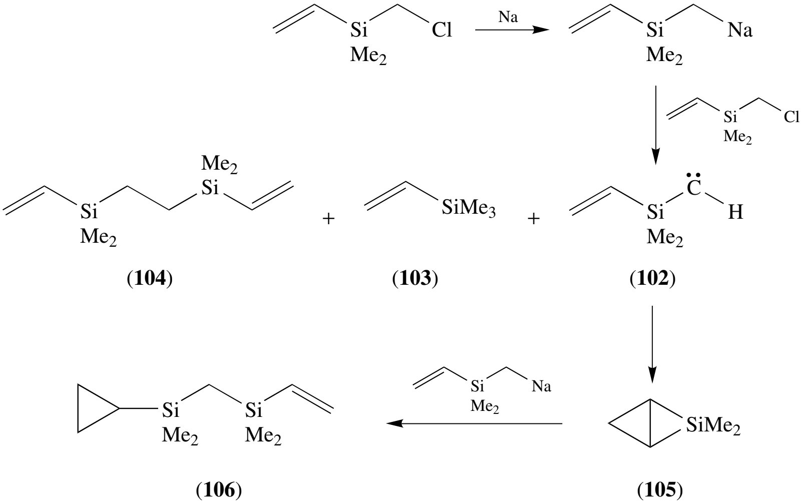

(26)

In contrast to the failure to observe an intramolecular reaction of (allyldimethylsilyl)carbene[56], photolysis of the (allyldiisopropyl)diazoacetate **107** furnishes 1-silabicyclo[2.1.0]pentane **109** in good yield[61] (equation 27). Obviously, the intramolecular cyclopropanation of carbene **108** accounts for this result. Altogether, the chemistry of (alkenylsilyl)carbenes (equations 24, 26 and 27) exhibits close similarities to that of the all-carbon analogues[1].

2-Oxa-1-silabicyclo[n.1.0]alkanes (n = 3: **111**; n = 4: **113**) were the only products isolated from the photochemical, thermal or transition-metal catalyzed decomposition of (alkenyloxysilyl)diazoacetates **110** and **112**, respectively (equation 28)[62]. The results indicate that intramolecular cyclopropanation is possible via both a carbene and a carbenoid pathway. The efficiency of this transformation depends on the particular system and on the mode of decomposition, but the copper triflate catalyzed reaction is always more efficient than the photochemical route. For the thermally induced cyclopropanation **112** → **113**, a two-step noncarbene pathway at the high reaction temperature appears as an alternative, namely intramolecular cycloaddition of the diazo dipole to the olefinic bond followed by extrusion of N_2 from the pyrazoline intermediate. A direct hint to this reaction mode is the formation of 3-methoxycarbonyl-4-methyl-1-oxa-2-sila-3-cyclopentenes instead of cyclopropanes **111** in the thermolysis of **110**.

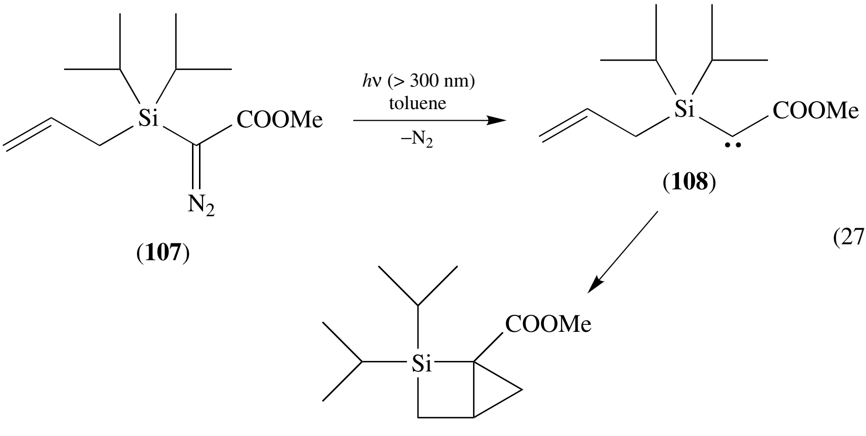

(**107**) (**108**) (**109**) 72%

(27)

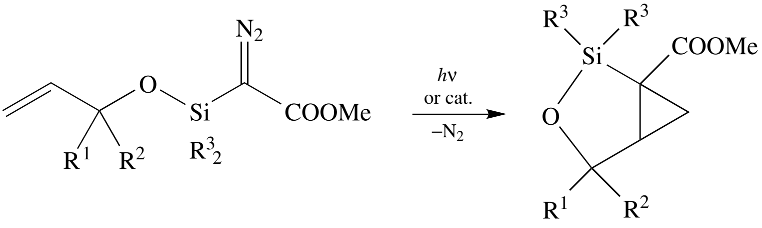

(**110**) (**111**)

R^1	R^2	R^3
H	H	Me
H	H	*i*-Pr
H	Me	*i*-Pr
Me	Me	*i*-Pr

(28)

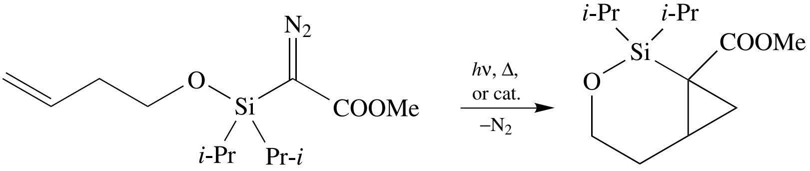

(**112**) (**113**)

hν, λ > 300 nm ; Δ, 140 °C ;
cat. CuOTf or $Rh_2(OOCC_3F_7)_4$

Photochemical or thermal decomposition of (vinyloxysilyl)diazoacetates **114** yields the 1-oxa-2-sila-3-cyclopentenes **118** as the major reaction products (equation 29), but much material is lost in the separation steps[61] (isolated yields: 12–24%). It is reasonable to assume that the zwitterion **116** is the direct precursor of **118**. It is open to speculation whether **116** is formed directly by attack of the electrophilic carbene on the electron-rich double bond in **115** or via cyclopropanation (by analogy to **108** → **109**, equation 27) and subsequent ring-opening of the so-formed push-pull-substituted cyclopropane. At least, the first-mentioned reaction mode is more likely when the decomposition of **114** is catalyzed by the highly electrophilic rhodium(II) perfluorobutyrate which leads to **117**, a structural isomer of **118**.

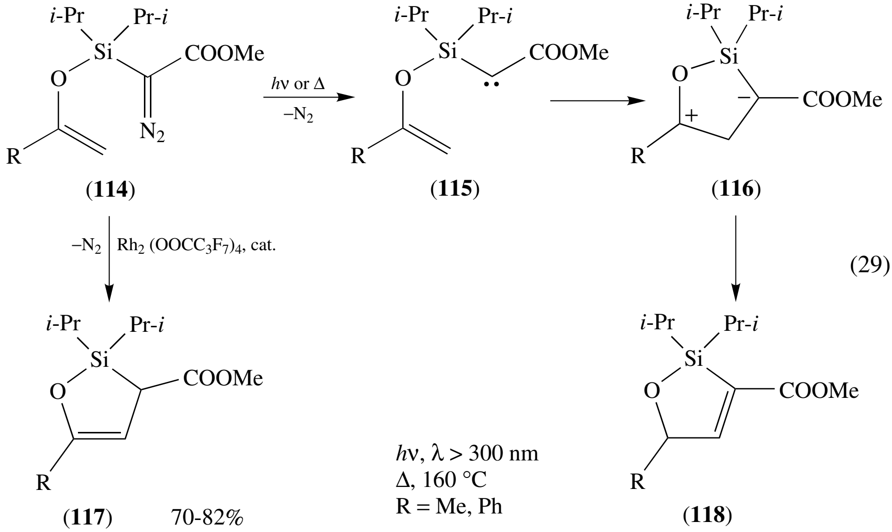

(29)

3. Reactions at C≡C bonds

The Cu(I)-catalyzed decomposition of (alkynyloxysilyl)diazoacetates **119** furnishes the silaheterocycles **120** and/or **121** (equation 30) in modest yield[63]. In these cases, the photochemical extrusion of nitrogen from **119** does not lead to defined products and the thermal reaction is dominated by the 1,3-dipolar cycloaddition ability of these diazo compounds. In mechanistic terms, carbene **122** or more likely a derived copper carbene complex, is transformed into cyclopropene **123** by an intramolecular [1 + 2] cycloaddition to the triple bond. The strained cyclopropene rearranges to a vinylcarbene either with an exocyclic **(124)** or an endocyclic **(125)** carbene center, and typical carbene reactions then lead to the observed products. Analogous carbene-to-carbene rearrangements are involved in carbenoid transformations of other alkynylcarbenes[64].

D. Carbene Reactions of Bis(diazomethyl)silanes and -polysilanes

When two carbene functions are separated by one or more silicon atoms, one can expect them to enter independently the usual inter- or intramolecular reactions. Among the intramolecular reactions, extensions of those which have been discussed in Sections III.B and III.C are particularly appealing, namely silylcarbene-to-silene rearrangement at one or both carbene centers and intramolecular carbene dimerization to form a C,C double bond and thus an unsaturated silaheterocycle.

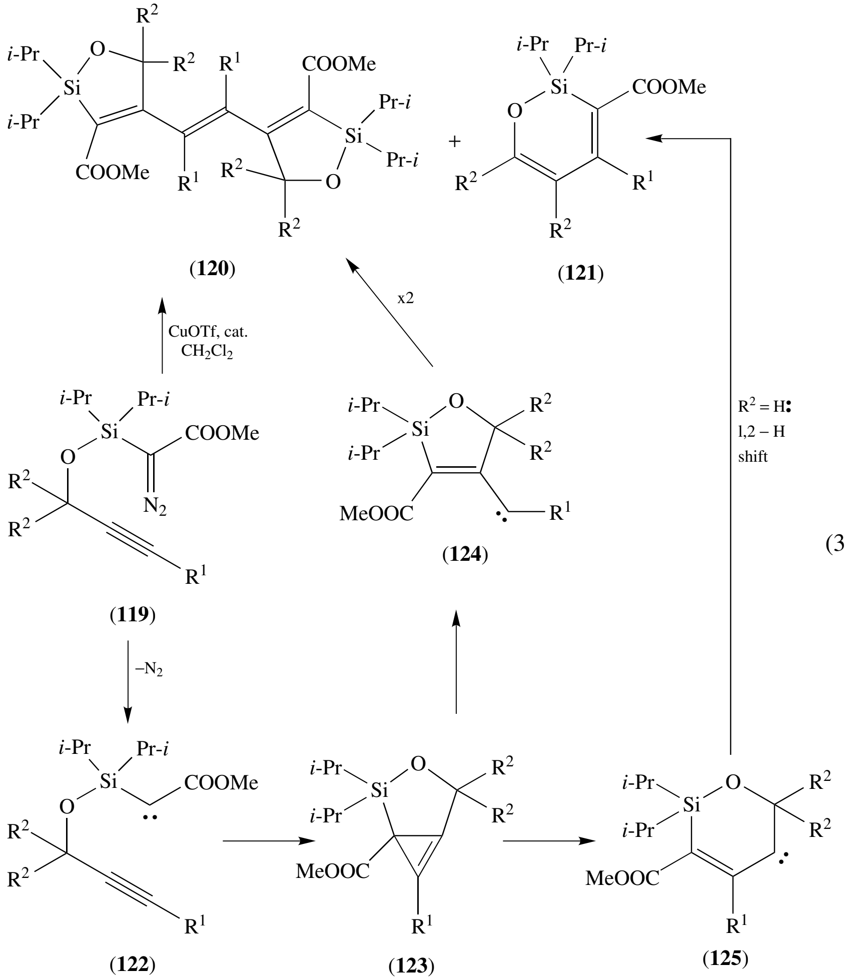

(30)

$R^1 = R^2 = H$: **(120)** 26% ; **(121)** 25%

$R^1 = H, R^2 = Me$: **(120)** 25%

$R^1 = Me, R^2 = H$: **(121)** 39%

To date, bis(diazomethyl)silanes represent the only precursors to silylene-dicarbenes. It should be noted, however, that the extrusion of N_2 from the two diazo functions can occur more or less simultaneously or successively. In the latter case, a diazocarbene is formed in the first place, which is supposed to undergo a fast carbene reaction before the generation of a carbene from the second diazo function occurs. This should be kept in mind for all transformations which are explained mechanistically with the participation of silylene-dicarbenes. There are even examples where only one of the two diazo groups enters carbene chemistry at all (see equations 35 and 36 below).

Various intramolecular transformations are conceivable for dicarbene **127**, which would result from twofold elimination of molecular nitrogen from bis(diazomethyl)silane **126**. HF energies, calculated by *ab initio* methods, for the possible rearrangement products **128–134** are given in Scheme 6[65].

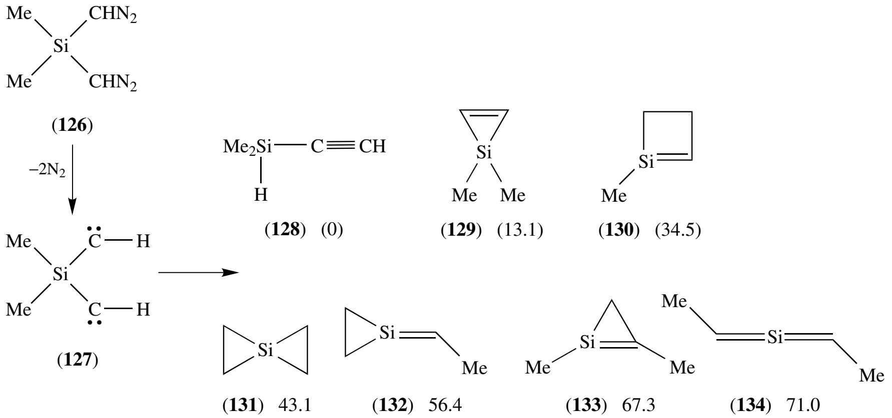

SCHEME 6. Possible intramolecular products from dicarbene **127**; HF energies relative to **128** (kcal mol^{-1}, calculated at the RHF/6-31G(d,p) level) are given in parentheses

Photolysis ($\lambda \geqslant 305$ nm) of **126** in an argon matrix at 10 K generated a single photoproduct to which the 1*H*-silirene structure **129** was assigned by comparison of the experimental with the calculated IR spectrum[65]. Short-wavelength irradiation ($\lambda > 254$ nm) of **129** caused its rearrangement to ethynylsilane **128**. The latter was also the main product of a flash vacuum pyrolysis of **126** at 500 °C. When **126** was photolyzed in ethanol (170 and 273 K) or in an EPA glass (77 K), products **135–138** (equation 31) were obtained in temperature-dependent yields. While **135, 136** and **138** are likely to be derived from 1*H*-silirene **129**, dicarbene **127** and 1-silacyclobutene **130** (formed from the carbene by 1,2-methyl shift followed by 1,4-C,H insertion of the second carbene center), respectively, diethoxysilane **137** could result from the intermediates **131, 132** or **134**.

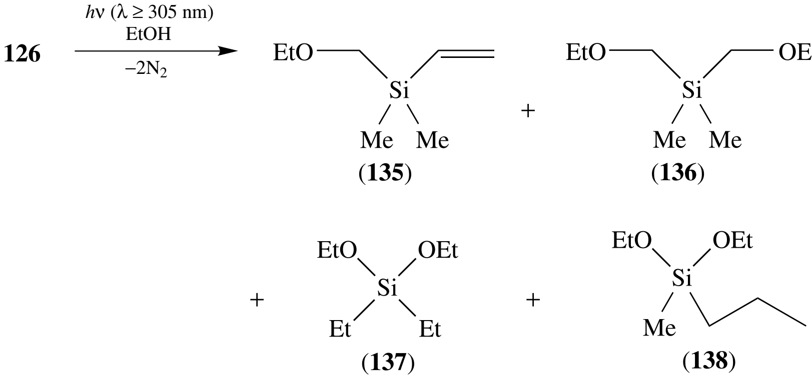

(31)

Silirenes (**140**, equation 32) could also be involved in the transition-metal catalyzed decomposition of bis(diazoketones) **139** which provides the electron-rich [4]radialenes **142**[66,67]. While the formation of **142** directly from silirene **140** cannot be excluded *a priori*, it is more reasonable to assume that **140** undergoes twofold ring-expansion to form the cyclic cumulene **141**, which then provides **142** by a cyclodimerization reaction. The intermediacy of **141** is corroborated by the isolation of the Diels–Alder product **143**[66].

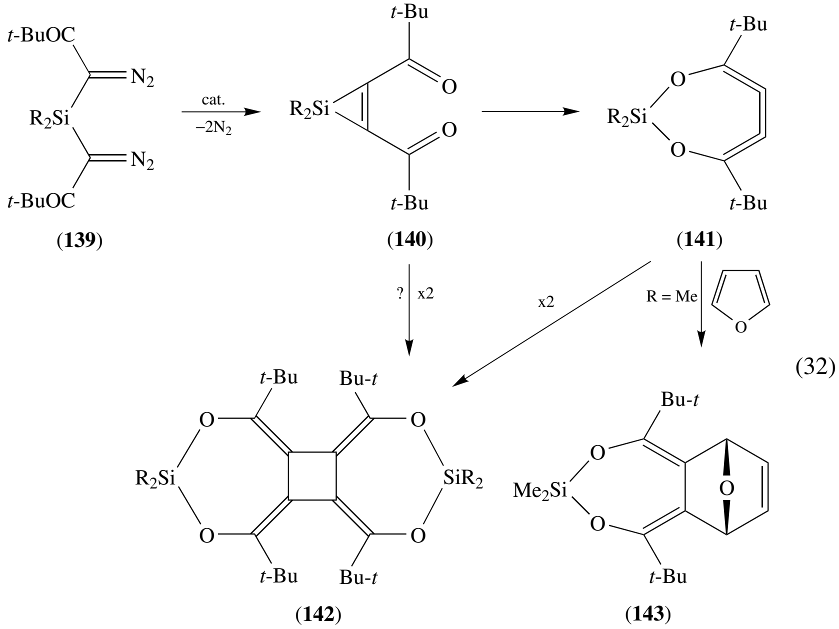

R = Me: 38-40%
R = *i*-Pr: 5-9%
cat.: CuOTf or Pd(OAc)$_2$

By analogy with the formation of a 1*H*-silirene from a silylene-dicarbene, a disilanediyl-1,2-dicarbene could isomerize to a 1,2-disilacyclobutene. Such a species **(147)** may be involved indeed in the photochemical or metal-catalyzed decomposition of bis(diazoketones) **144** (equation 33), from which silaheterocycles **145** and **146** were obtained in low yield[68]. Electrocyclic ring-opening of **147** and twofold cyclization of bissilene **148** could provide **145**, and twofold ring-expansion of **147** with subsequent hydrogenation of the resulting cyclic [3]cumulene could account for **146**. However, these mechanisms are still a matter of speculation. Apart from the fact that it is not known whether a diazocarbene or a dicarbene is the reacting species, it is also possible that a silylcarbene-to-silene rearrangement is involved in the formation of the products shown.

When the COR groups of bis(diazo) compound **144** are replaced by Ph or SiMe$_3$ substituents, the derived carbene chemistry leads to different results[69] (equation 34). The only identified product obtained from the flow pyrolysis of 1,2-bis(diazobenzyl)-tetramethyldisilane was 1,1,2,2-tetramethyl-3,4-diphenyl-1,2-disilacyclobutene, which rapidly reacts with air under insertion of an oxygen atom into the Si–Si bond. In contrast, the analogous 1,2-disilacyclobutene could not be directly isolated from the vacuum pyrolysis of 1,2-bis[diazo(trimethylsilyl)methyl]-tetramethyldisilane. However, exposure of the pyrolysate to air, *N*-methyl-1,2,4-triazolinedione or methanol furnished products that point to the presence of this 1,2-disilacyclobutene in the pyrolysate, perhaps in equilibrium with the corresponding bissilene.

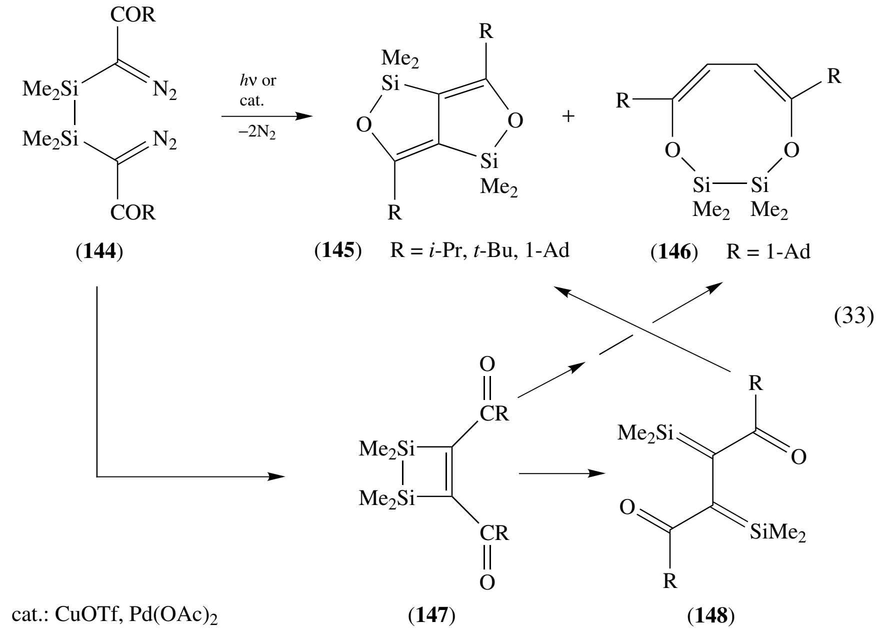

(**144**) (**145**) (**146**) (**147**) (**148**)

(33)

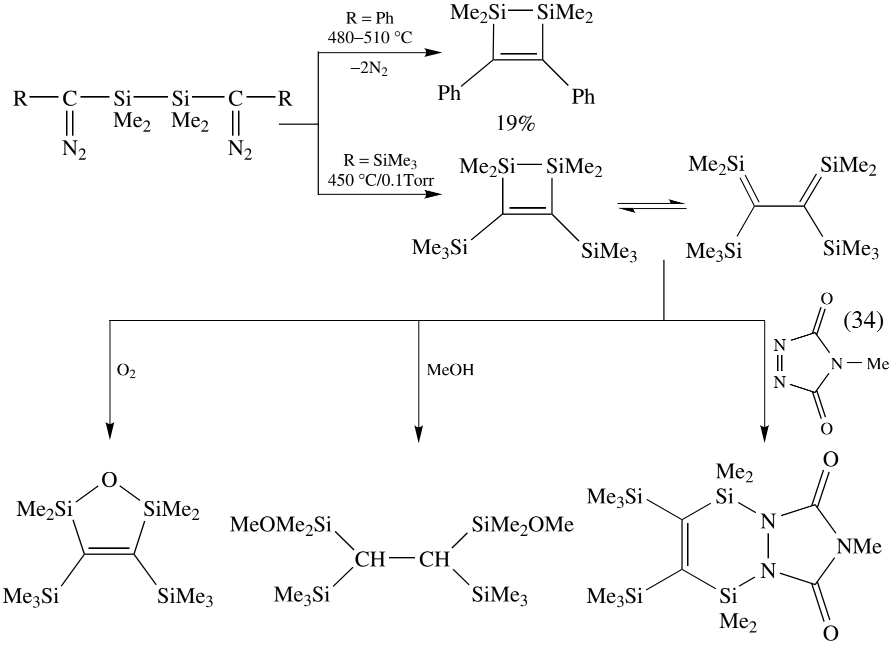

(34)

The photochemical decomposition of the same diazo compound in *tert*-butanol/benzene generated five products, in which either one or two alcohol molecules are incorporated and which are obviously derived from diazosilene and bissilene intermediates.

Photochemical or thermal decomposition of 1,3-bis(diazomethyl)trisilanes **149, 152** and of 1,4-bis(diazomethyl)tetrasilanes **155** begins with formation of only one carbene center followed by a silylcarbene-to-silene rearrangement[69–71] (equation 35; suggested intermediates are put in brackets for clarity). Intramolecular [3+2] cycloaddition of the resulting diazosilenes (e.g. **150**) would create bicyclic pyrazolines (e.g. **151, 153**) which can furnish the final isolated products with retention or loss of the azo moiety. Alternatively, the diazosilene intermediate can be transformed into a disilene (e.g. **154**). For the photolysis of **149**, only the pyrazoline route with retention of the azo moiety was observed[69,70]. UV-irradiation of bis(diazo)trisilanes **152** in cyclohexane yields mainly polymeric material, but also small amounts of a highly air-sensitive 2,3,5-trisilabicyclo[2.1.0]pentane and a 2,4,5-trisilabicyclo[1.1.1]pentane[69,70]. While the latter is considered to be the head-to-tail cyclodimer of disilene **154**, the former does not seem to be the corresponding head-to-head dimer but rather a product arising from pyrazoline **153**, by analogy with the pathways suggested for **149** and **155**[69]. Bissilene **154** (R = Me) could be trapped when the photolysis of **152** was carried out in the presence of a teriary amine or in *tert*-butanol[71].

A diazosilene is probably also involved in the photochemical or copper-catalyzed decomposition of bis(diazoacetate) **156** in benzene (equation 36). In both cases, diazoketene **157** was the only identified product[72]. Its formation was explained by the silylcarbene-to-acylsilene-to-silylketene sequence outlined in Scheme 5. Efforts to achieve the N_2 extrusion from the remaining diazo function by thermolysis in boiling toluene or by prolonged photolysis resulted only in unspecific decomposition.

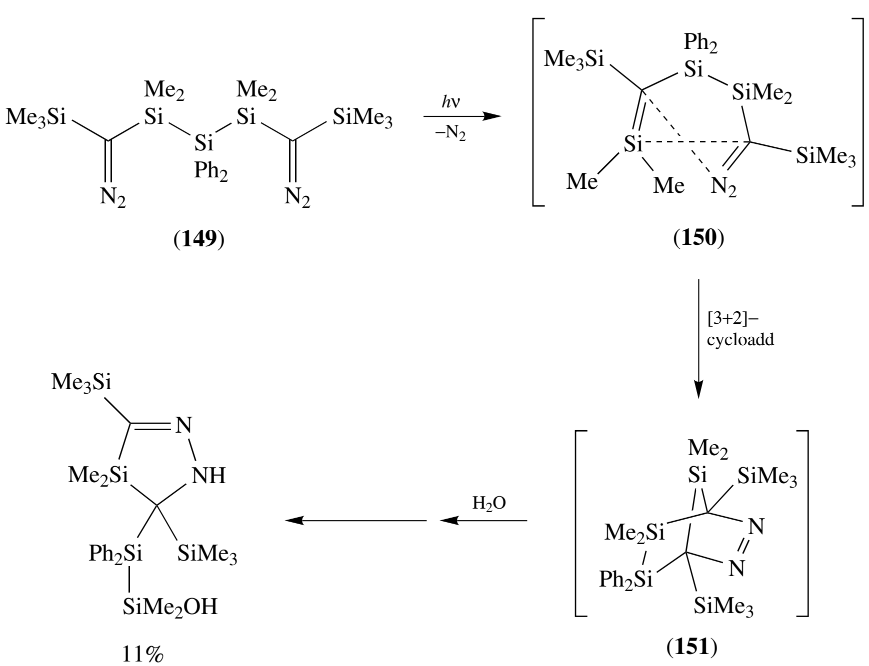

(**149**)

(**150**)

(**151**)

11%

(35 *continued*)

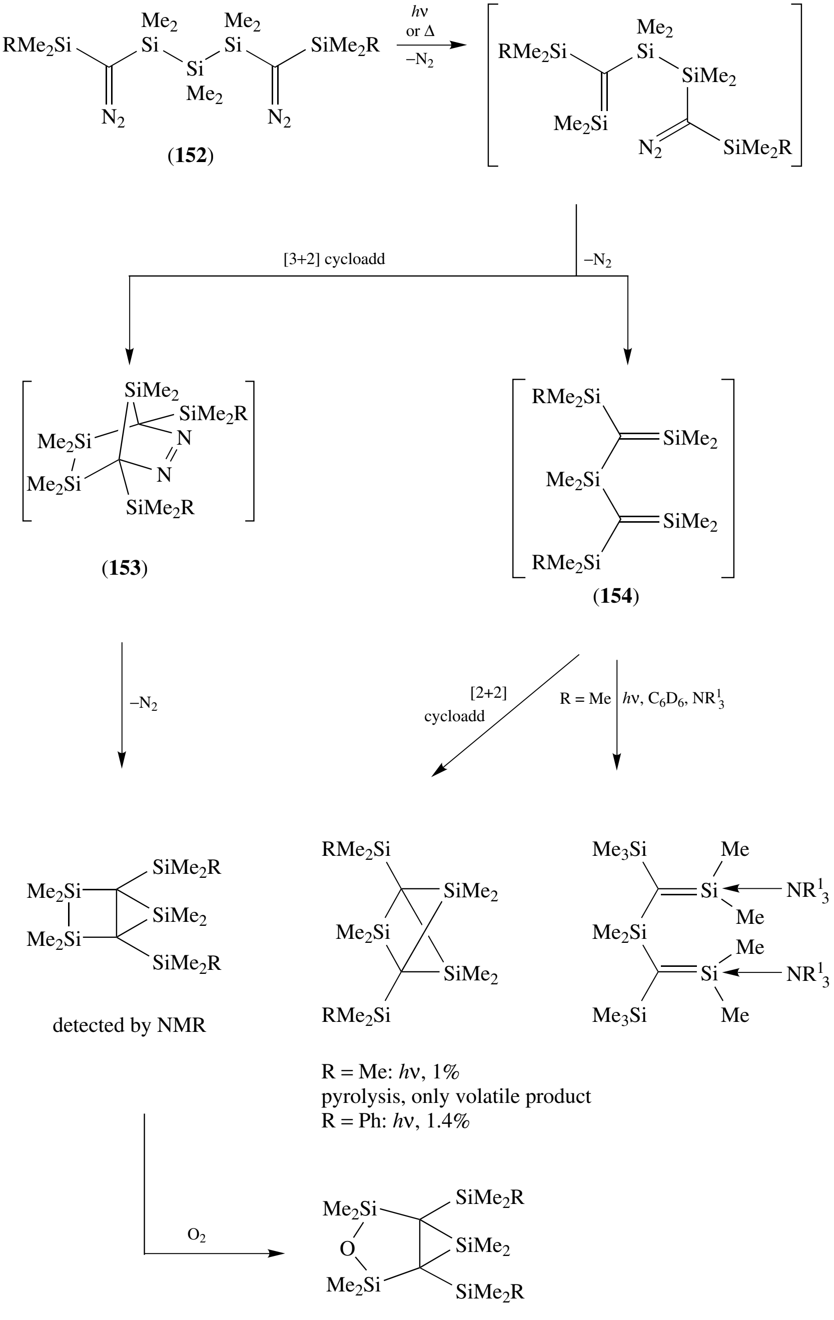

(**152**)

(**153**)

(**154**)

detected by NMR

R = Me: hν, 1%
pyrolysis, only volatile product
R = Ph: hν, 1.4%

R = Ph: hν, 6%

(35 *continued*)

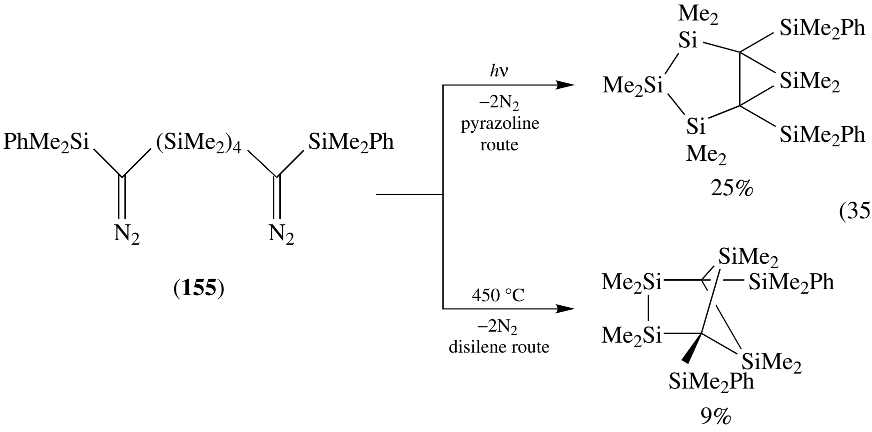

(35)

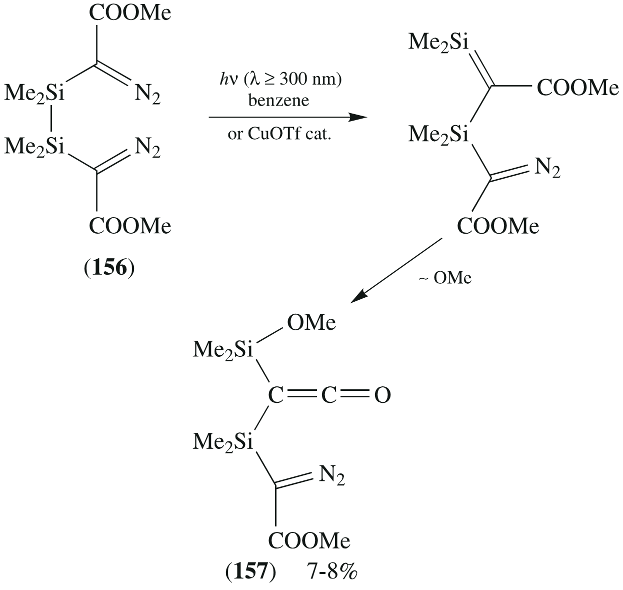

(36)

E. Silylcarbene Reactions not Involving the Silyl Group

1. Silylcarbenes without a second substituent

a. (Trimethylsilyl)carbene. This carbene is probably the best investigated silylcarbene. It is assumed to be an intermediate in the reactions of (dichloromethyl)trimethylsilane with Na−K in the gas phase[53] (equation 37, method A) and of (chloromethyl)trimethylsilane with alkali metals[55] (method B) or lithium 2,2,6,6-tetramethylpiperidide[73,74] (method C). Furthermore, the carbene can be generated by thermal decomposition of bis[bromo(trimethylsilyl)methyl]mercury[75] (method D) and by extrusion of molecular nitrogen from diazo(trimethylsilyl)methane[5,6] (method E). It is not clear, however, whether the carbenoid-type species phenylthio(trimethylsilyl)methyl lithium provides a source for this carbene by α-elimination[76] (method F, see also Section III.E.8).

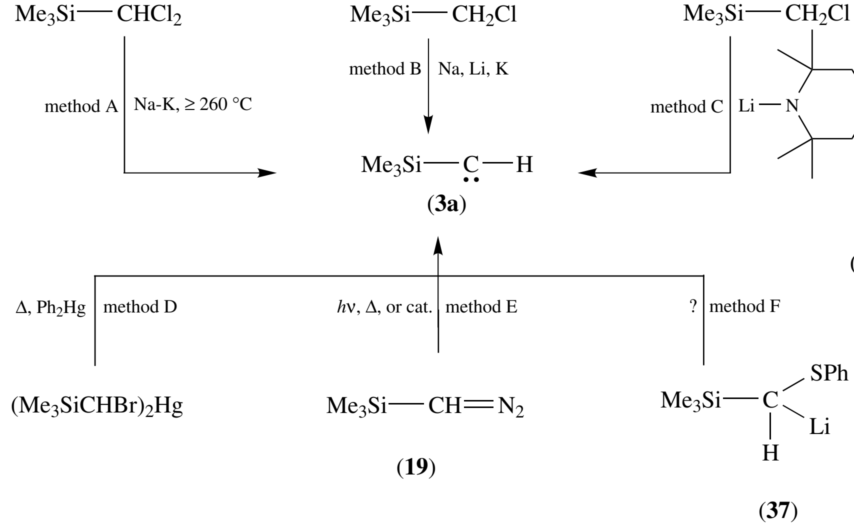

(37)

While method A furnished only dimethyl(vinyl)silane (see Section III.C.1.a), the Wurtz reaction (method B) in an inert solvent gave a mixture of products which stem either from the α-elimination generating **3a** or from the C,C coupling process leading to **158** (equation 38)[55]. It is assumed that **3a** forms 1,1-dimethylsilirane by 1,3-C,H insertion (cf equation 23) and that C,C and Si,C cleavage of this sensitive ring system by (trimethylsilyl)methyl sodium is responsible for the formation of **159–161** (combined yield: 32%). It is obvious that, due to the complexity of this reaction, method B cannot serve as a versatile entry into the chemistry of **3a**.

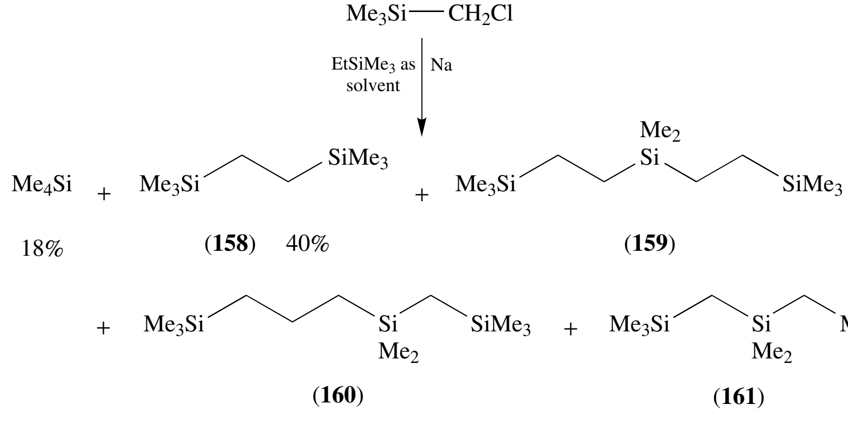

(38)

With respect to the complications of method B, it is remarkable that generation of carbene **3a** according to method C in the presence of *cis*-but-2-ene or various cycloalkenes gave the corresponding (trimethylsilyl)cyclopropanes in yields up to 30%[73,74]. Similarly, 1,2,3-tris(trimethylsilyl)cyclopropene was obtained in 15% yield by carbene transfer to bis(trimethylsilyl)acetylene[77]. The base is crucial for the success of the α-elimination; with *sec*-butyl lithium as a base, only $Me_3SiCH(Li)Cl$ is formed which is reluctant to the carbene-forming step.

Method D (equation 37) is neither a convenient nor an effective way to generate **3a**. After heating bis[bromo(trimethylsilyl)methyl]mercury for 7 days at 160 °C with cyclohexene and diphenylmercury, 7-trimethylsilylbicyclo[4.1.0]heptane was obtained in a yield of only 9%, accompanied by a trace of the carbene dimers (*cis*- and *trans*-bis(trimethylsilyl)ethene) and a large amount of starting material[75].

By far the best source for **3a** is (trimethylsilyl)diazomethane (**19**). It has already been mentioned that gas-phase pyrolysis of **19** alone[21,38,54] yields products which are derived from intramolecular carbene reactions such as 1,3-C,H insertion and silylcarbene-to-silene rearrangement (see equation 20). Also, copyrolysis of **19** with alcohols or benzaldehyde allowed one to trap the silene but not the carbene **33** (see equation 5). Furthermore, solution photolysis of **19** in the presence of alcohols or amines did not give the X,H insertion products of the carbene but rather trapping products of the silene[33,38]. On the other hand, photochemically generated carbene **3a** did undergo some typical intermolecular carbene reactions such as cyclopropanation of alkenes (ethylene, *trans*-but-2-ene, but not 2,3-dimethylbut-2-ene, tetrafluoroethene and hexafluoropropene), and insertion into Si−H and methyl-C−H bonds[78] (equation 39). The formal carbene dimer, *trans*-1,2-bis(trimethylsilyl)ethene, was a by-product in all photolyses in the presence of alkenes; it is generally assumed that such carbene dimers result from reaction of the carbene with excess diazo compound.

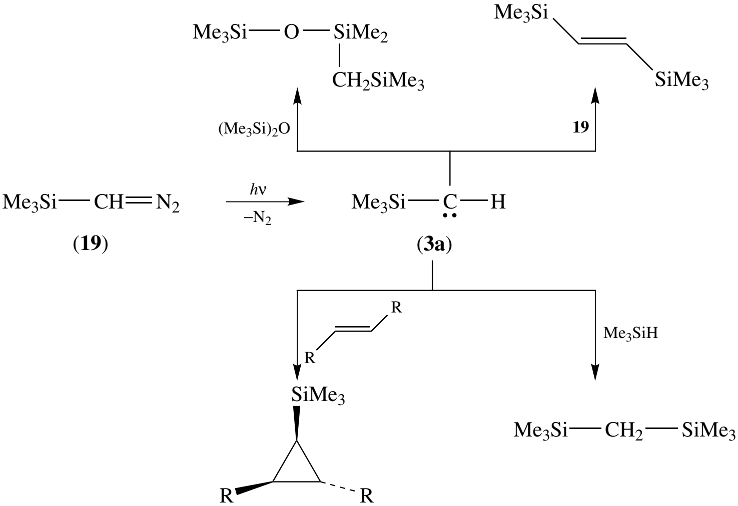

(39)

Transfer of carbene **3a** from **19** to a variety of alkenes and cycloalkenes has been achieved under catalysis by copper(I) chloride[74,79–82]. However, with the exception of cyclohexene[69,70] (72% yield), only moderate yields could be obtained. In all cases, the cyclopropanation was stereospecific with respect to the double bond configuration of the alkene and gave the sterically less crowded cyclopropane diastereomer in excess. As in the photochemical cyclopropanation, the formal carbene dimer *trans*-1,2-bis(trimethylsilyl)ethene is often formed as the major by-product. Cyclopropanation of *trans*-but-2-ene with **19** with copper(II) chloride as catalyst was found to be even less productive than the photochemical carbene transfer reaction[78] (13 vs 23% yield). Not unexpectedly, electron-deficient acyl-substituted alkenes could also be cyclopropanated when $PdCl_2$ was used as catalyst, whereas the copper- or rhodium-catalyzed carbene transfer failed[82] (equation 40).

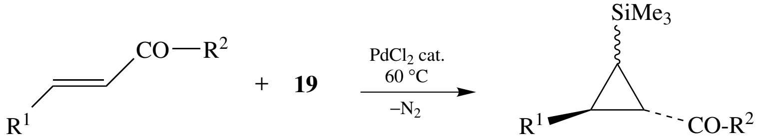

(40)

R^1 =	Ph	Ph	Ph	C_5H_{11}
R^2 =	OEt	Me	Ph	OEt
yield(%)	79	32	21	23

In connection with these catalytic cyclopropanation reactions, it should be mentioned that the isolable ruthenium–carbene complex **162**, which is obtained from **19**, $[RuCl_2(p\text{-cymene})]_2$ and 2,6-bis(4-isopropyl-1,3-oxazolin-2-yl)pyridine, reacts with styrene at elevated temperature in a carbene transfer reaction[83] (equation 41). Since complex **162** is also catalytically active for (alkoxycarbonyl)carbene transfer to olefins, this reaction represents one of the few connecting links between catalytic and stoichiometric carbene transfer reactions of metal–carbene complexes.

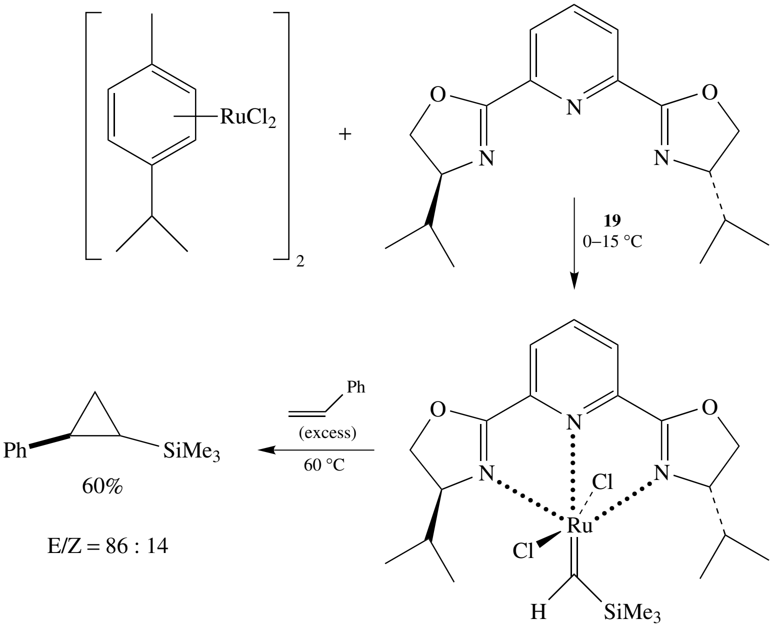

(**162**)

(41)

b. Other (alkylsilyl)carbenes. (Ethyldimethylsilyl)carbene, (propyldimethylsilyl)carbene and (butyldimethylsilyl)carbene have been generated from the corresponding trialkyl(chloromethyl)silane according to method B (equation 37), but no other transformations than their intramolecular C,H insertion reactions (cf equation 23) are known[56]. (Benzyldimethylsilyl)carbene and (dimethylphenylsilyl)carbene, when generated by UV irradiation of the corresponding diazomethylsilane in the presence of ethanol, did not seem to react with the alcohol, probably because of the high rate of the silylcarbene-to-silene rearrangement which led finally to the addition product of the alcohol to the silene[33].

c. (Alkenylsilyl)carbenes. The preparation of these carbenes and intramolecular reactions such as competitive C,H insertion and cyclopropanation have been discussed in Section III.C.2. No intermolecular chemistry has been reported.

d. (Trimethoxysilyl)carbene. Irradiation of (trimethoxysilyl)diazomethane in a CO-doped argon matrix at 35 K produced (trimethoxysilyl)ketene, which is a trapping product of carbene **3e**[21] (equation 42). For the reaction of **3e** with molecular oxygen, see equation 1. No solution chemistry of **3e** has been reported as yet.

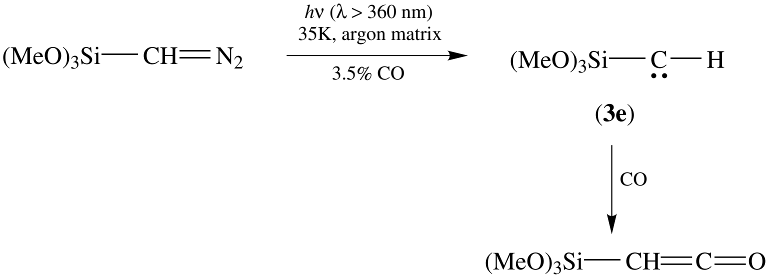

$$\mathrm{(MeO)_3Si{-}CH{=}N_2} \xrightarrow[\text{3.5\% CO}]{h\nu\ (\lambda > 360\ \text{nm}),\ \text{35K, argon matrix}} \mathrm{(MeO)_3Si{-}\underset{\bullet\bullet}{C}{-}H}\ \mathbf{(3e)} \xrightarrow{\text{CO}} \mathrm{(MeO)_3Si{-}CH{=}C{=}O} \qquad (42)$$

2. Alkyl(silyl)carbenes and cycloalkyl(silyl)carbenes

For alkyl(silyl)carbenes where the alkyl contains an α-C−H bond, 1,2(C→C) hydride shift leading to a vinylsilane is the common reaction pathway. Vinylsilane formation has been observed for free (photochemically or thermally generated) carbenes (equations 43[84], 44[48,49,50] and 45[85,86]) but also in carbenoid reactions. In the latter case, the configuration of the alkene could be controlled to a large extent by the choice of the catalyst: The E-alkene was formed nearly exclusively with copper(I) chloride as catalyst[87], whereas rhodium(II) pivalate[88] gave mainly the Z-alkene (equation 46).

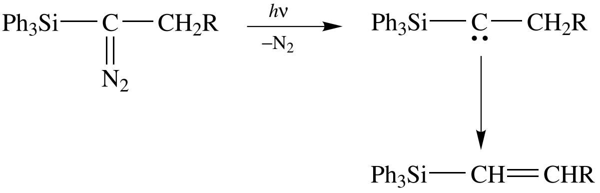

$$\mathrm{Ph_3Si{-}\underset{N_2}{\underset{\|}{C}}{-}CH_2R} \xrightarrow[-\mathrm{N_2}]{h\nu} \mathrm{Ph_3Si{-}\underset{\bullet\bullet}{C}{-}CH_2R} \longrightarrow \mathrm{Ph_3Si{-}CH{=}CHR} \qquad (43)$$

R = H: 55%
R = Ph: 75%; $E/Z = 2.6$

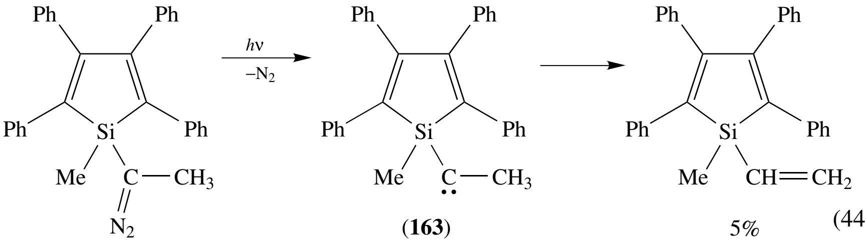

(**163**)

5%

(44)

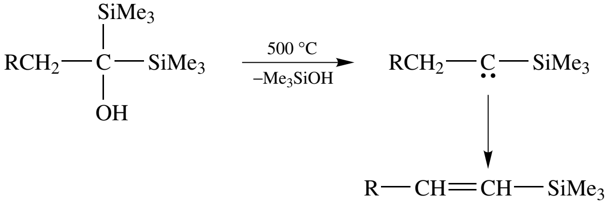

(45)

R = CH_2Ph (98%) ; *E/Z* = 1.0
R = C_6H_{13} (93%) ; *E/Z* = 1.0
R = C_8H_{17} (94%) ; *E/Z* = 0.77

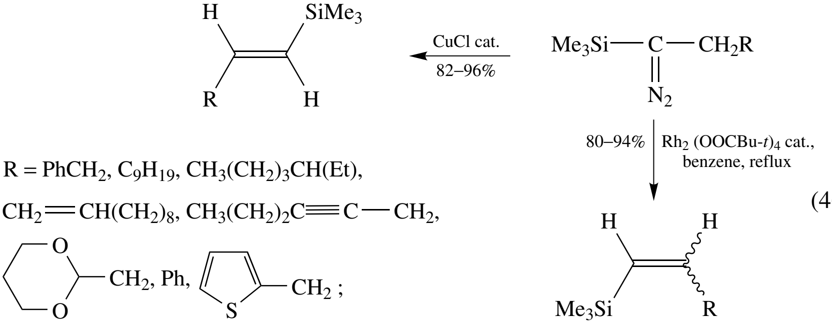

Z/E ≤ 6/94

(46)

R = $(CH_2)_8Me$, CH_2Ph, Ph,
1-naphthyl, 2-thienyl ;
Z/E = 78/22 to 97/3

The dramatic influence of a methyl group on the reaction pathway is exemplified by carbene **163** which rearranges to a vinylsilane. In the absence of this methyl group, however, the silylcarbene-to-silene rearrangement (equation 16) occurs[48,49].

Cycloalkyl(silyl)carbenes with an α-C−H bond have not yet been investigated systematically. When cyclohexyl(trimethylsilyl)carbene was generated by thermal α-elimination from cyclohexyl-bis(trimethylsilyl)methanol at 500 °C, only the (1,2) hydride shift took place, whereas cyclopentyl(trimethylsilyl)carbene, generated analogously, gave both the endocyclic alkene and the 1,3-C,H insertion product[85,86] (equation 47).

3. Alkenyl(silyl)carbenes and cycloalkenyl(silyl)carbenes

a. 1-Alkenyl(silyl)carbenes. Acyclic vinylcarbenes tend to rearrange to cyclopropenes. This transformation is also involved in the photochemical conversion of 3*H*-pyrazole **164** into cyclopropene **167**[89] (equation 48). Photochemical ring-opening of **164** generates diazo compound **165**, which on prolonged irradiation yields the carbene **166**.

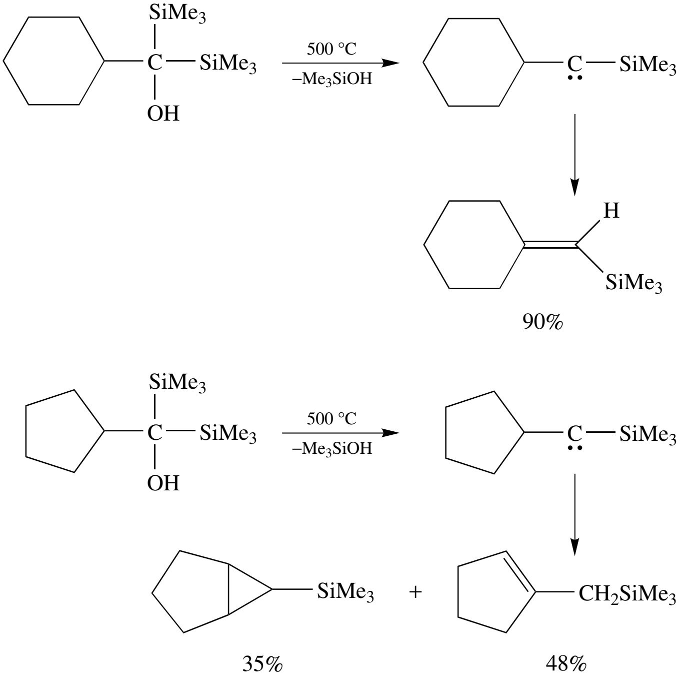

(47)

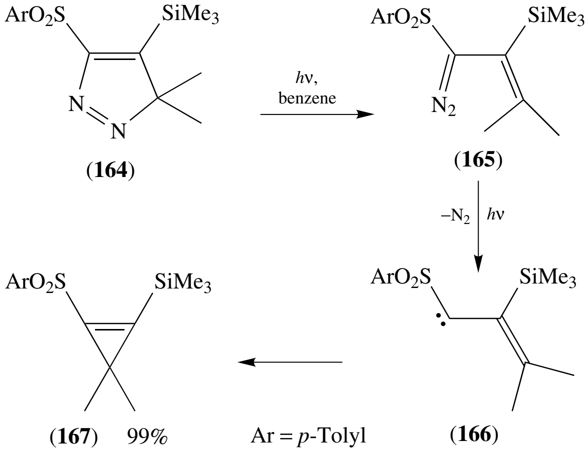

(48)

In principle, the vinylcarbene-to-cyclopropene isomerization is reversible. While this has not been reported for **167** (where ring-opening could produce not only alkenyl(sulfonyl)carbene **166**, but also the isomeric 1-alkenyl(silyl)carbene), it was found that 1-trimethylsilylcyclopropenone acetal **168** (equation 49) by thermal ring-opening yields the (trimethylsilyl)vinylcarbene **169** besides traces of the isomeric vinylcarbene **170**. Both carbenes are obviously nucleophilic since they are able to cyclopropanate the electron-poor double bond of acrylonitrile[90a].

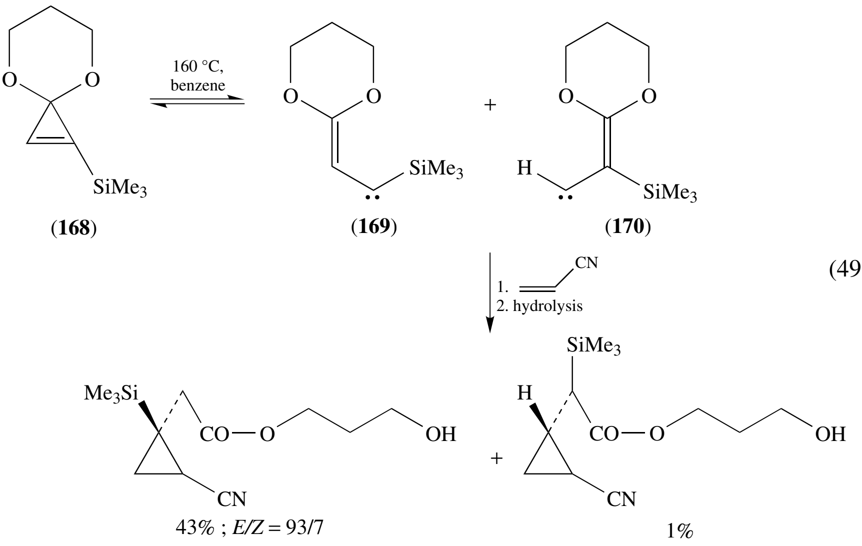

(**168**) (**169**) (**170**)

43% ; *E/Z* = 93/7 1%

(49)

In a similar manner, 3,3-disubstituted 1,2-bis(trimethylsilyl)cyclopropenes rearrange to 1,1-bis(trimethylsilyl)allenes, most likely by 1,2-silyl shift of primarily formed (1-silylvinyl)silylcarbenes. According to *ab initio* calculations, this reaction pathway is energetically more favorable than those including a 2,2-disilylcyclopropylidene or a 2,3-disilylpropylidene[90b].

b. 2-Alkenyl(silyl)carbenes. Carbenes **172** can be generated from α,α-dibromosilanes **171** and methyl lithium (equation 50). They undergo intramolecular cyclopropanation of the C=C bond to form silylbicyclo[1.1.0]butanes **173**[91]. It is remarkable that an 1,2(C→C) hydride shift to the carbene center plays no role here.

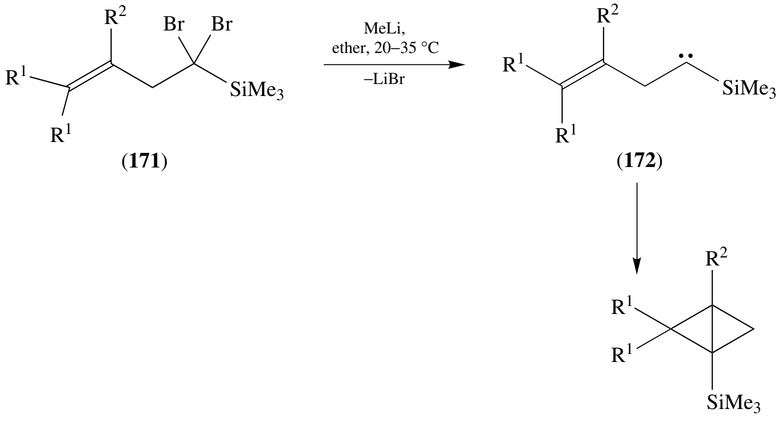

(**171**) (**172**)

(50)

$R^1 = R^2 = H$ (47%) ; $R^1 = Me, R^2 = H$ (53%) ; $R^1 = H, R^2 = Me$ (48%) (**173**)

Bicyclobutanes are also obtained from the catalytic decomposition of diazo compound **174**[92] (equation 51). Copper(I) iodide was the catalyst of choice, whereas rhodium(II) acetate did not show any activity in this case. When the related diazo compound **175** was decomposed, the product pattern depended in an unusually selective manner on the catalyst[92]. Intramolecular cyclopropanation leading to **176** is obviously less favorable than for carbene **172** and must yield to the 1,2-hydride shift not observed with the former carbene. The configuration of the resulting butadiene **177** can be completely reversed by the choice of the catalyst.

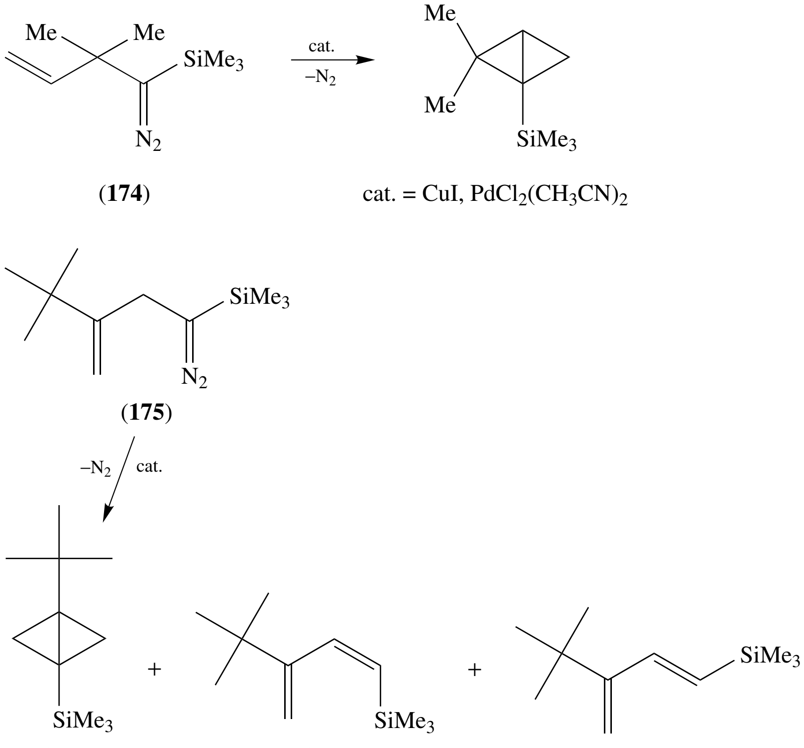

(**174**)

cat. = CuI, $PdCl_2(CH_3CN)_2$

(**175**)

(51)

(**176**) (*Z*-**177**) (*E*-**177**)

catalyst	%**176**	% *Z*-**177**	% *E*-**177**
$Rh_2(OAc)_4$	–	91	–
$PdCl_2(CH_3CN)_2$	–	–	74
CuI	33	–	49

c. Cycloalkeny(silyl)carbenes. Under UV-irradiation (in solution, in an organic glass at −196 °C or in argon matrix), the carbene generated from various [(2-cyclopropenyl)diazomethyl]silanes **178** (R = Me[93,94], Ph[95], OPr-*i*[95]) undergoes exclusive fragmentation to give two alkynes (equation 52). By analogy with experiments carried out with the analogue of **178** with COOR instead of $SiMe_2R$[96] it is assumed that this fragmentation is a triplet carbene reaction. As the related *tert*-butylcarbene (**178**, *t*-Bu instead of $SiMe_2R$) undergoes ring-expansion rather than fragmentation, it has been suggested that the silyl group enhances the rate of the intersystem crossing from the singlet to the triplet carbene. While the carbene fragmentation is also one of the pathways of the thermolysis of silylated diazo compounds **178**, the copper(I)-catalyzed decomposition generates the stable cyclobutadienes **179** (equation 52), which can be isolated in pure form after complexation of the copper salt with 1,2-(diphenylphosphino)ethane[93–95]. Obviously, a 1,2-carbon shift bringing about a ring-expansion has taken place at the stage of the intermediate metal carbene.

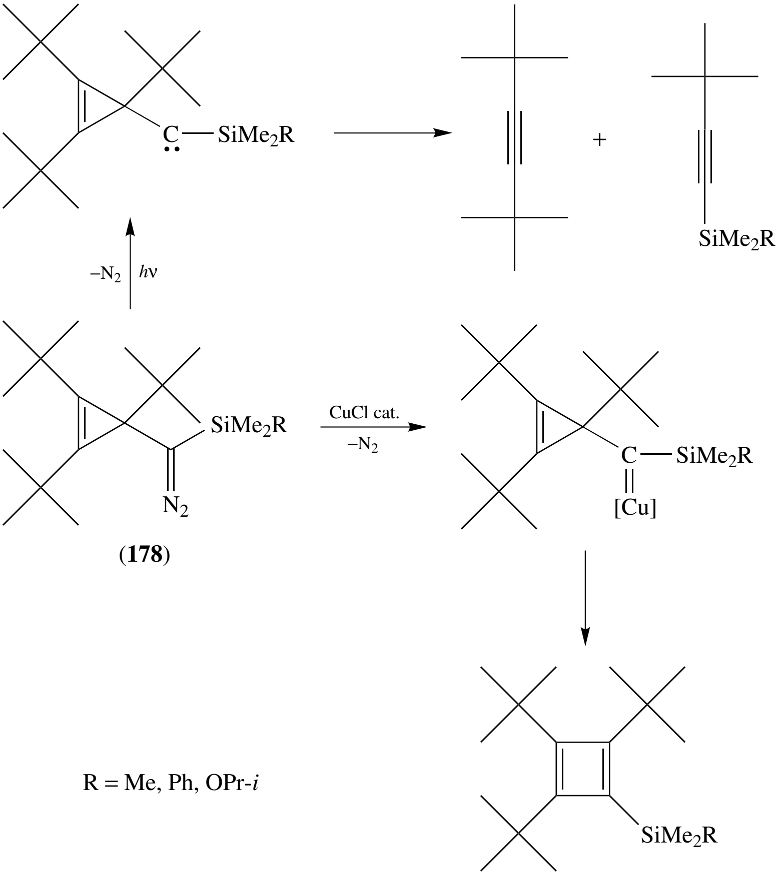

(**178**)

(**179**)

(52)

4. Aryl(silyl)carbenes

Phenyl(trimethylsilyl)carbene (**21**) has been generated from phenyl(trimethylsilyl)diazomethane (**20**) by gas-phase pyrolysis[39,40] as well as by thermolysis[97] or photolysis[33,40,98,99] in solution, by flash thermolysis of the tosylhydrazone lithium salt **180**[40], and by pyrolysis of α,α-bis(trimethylsilyl)benzyl alcohol **(181)**[85,86] (equation 53).

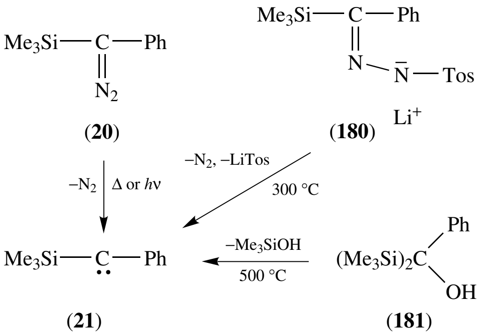

(53)

The gas-phase pyrolysis of **20**[40] in the absence of other reagents gave the products shown in equation 54. Olefin **182** is probably formed from two carbene molecules or from reaction of the carbene with **20**, and benzyltrimethylsilane is a typical product of a twofold H abstraction attributed to a triplet carbene. A carbene-to-carbene rearrangement, not uncommon for arylcarbenes, should account for the formation of **183**, and styrene

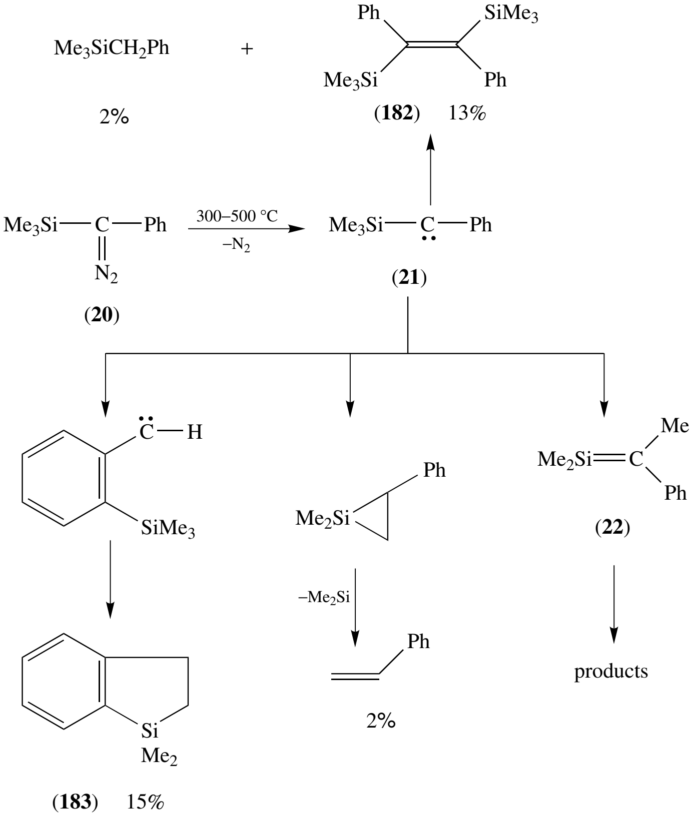

(54)

is probably a decomposition product of 1,1-dimethyl-2-phenylsilirane, formed by 1,3-C,H insertion at the carbene stage (cf Section III.C.1). The flash thermolysis of **180** led to **183** (20%) and styrene (5%)[40]. Products of the silylcarbene-to-silene rearrangement (**21** → **22**, equation 6) were not detected in these experiments; however, formation of silene **22** under the reaction conditions is suggested by various copyrolyses with alcohols, ketones and aldehydes, or 2,3-dimethylbuta-1,3-diene, which furnished trapping products of the silene[39,40] (see equation 6). Furthermore, gas-phase pyrolysis of **181** furnished, besides **183** and styrene, pentamethyl-(1-phenylethyl)disiloxane; the latter product appears to result from addition of trimethylsilanol to silene **22**[85,86].

When carbene **21** is generated from the diazo precursor photochemically in solution, it reacts with added alcohols by O,H insertion (equation 55), in contrast to the gas-phase copyrolysis where the silene intermediate is trapped[32,98]. Similarly, photolysis of **20** in the presence of 2,3-dimethylbutadiene gives mainly vinylcyclopropane **184**, while after copyrolysis of **20** and the same diene one finds that most of the vinylcyclopropane rearranged to the cyclopentene, together with the [4+2] cycloaddition product of diene and silene **22**[40]. Furthermore carbene **21**, generated photochemically[99] or thermally[97] (at 117–148 °C) in solution, undergoes [1 + 2] cycloaddition to alkynes to give cyclopropenes **185**.

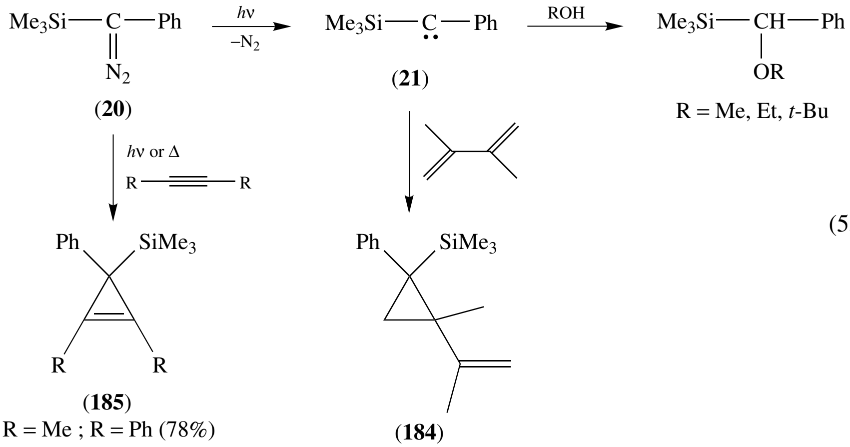

(55)

Phenyl(triphenylsilyl)carbene has also been trapped without the interference of a silylcarbene-to-silene rearrangement[84]. It undergoes O,H insertion with alcohols and is oxidized to the ketone by DMSO; the latter reaction is likely to include an S-oxide ylide (equation 56).

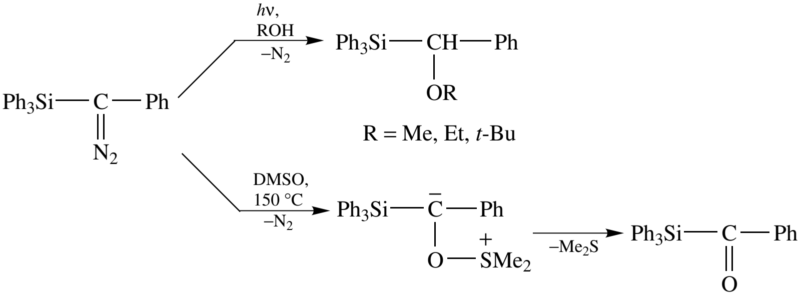

(56)

5. Acyl(silyl)carbenes

a. Silyl-substituted ketocarbenes. Wolff rearrangement yielding ketenes is a typical result of the photochemically or thermally induced elimination of N_2 from many α-diazocarbonyl compounds[100,101]. It is now generally accepted that this transformation normally proceeds via singlet acylcarbenes as reaction intermediates, but can also occur from an excited singlet state of the diazo compound itself by concerted N_2 loss and (1,2) migration of a substituent. Furthermore, there are many indications that the rearrangement is under conformational control, requiring the *s-cis* conformation at the (O=)C−C(N_2) bond of the diazo compound[100] or a *syn*-periplanar arrangement of the two substituents at the ketocarbene moiety[102]. Photochemical decomposition ($\lambda \geqslant 280$ nm) of (1-diazo-2-oxoalkyl)silanes **186** in benzene produced indeed silyl ketenes **188** as the result of a Wolff rearrangement (equation 57). These ketenes were either isolated or quenched with water or alcohols to give the corresponding acids or esters[103]. When R^1 was a *t*-Bu group, the β-silylcyclobutanones **189** were obtained as by-products; obviously, they result from an intramolecular γ-C,H insertion of carbene **187**.

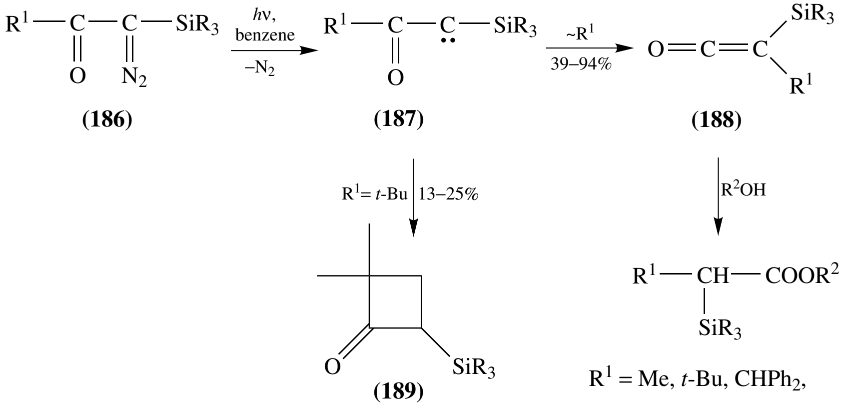

(57)

$R_3Si = SiMe_2{,}Bu\text{-}t$, $SiMe(Bu\text{-}t)_2$,
$SiPh_2{,}Bu\text{-}t$, $Si(Pr\text{-}i)_3$

R^1 = Me, *t*-Bu, $CHPh_2$,
1-adamantyl, Ph
R^2 = H, Me, Et
$R_3Si = SiEt_3$, $Si(Pr\text{-}i)_3$,
$SiMe_2Bu\text{-}t$, $SiMe(Bu\text{-}t)_2$,
$SiPh_2Bu\text{-}t$

Due to the bulkiness of the SiR_3 group, diazoketones **186** most likely adopt a *s-trans* conformation, which is prohibitive for a concerted Wolff rearrangement directly from **186**. Therefore, carbenes **187** are the common intermediates in the formation of both **188** and **189**. Furthermore, triplet-sensitized irradiation of **186** [R^1 = *t*-Bu, $SiR_3 = Si(Pr\text{-}i)_3$] (excess of benzophenone, $\lambda = 320$ nm) gave the same products in similar yields as the direct irradiation. It can be assumed, therefore, that a primarily formed triplet carbene interconverts rapidly with the singlet carbene which then rearranges to the ketene or undergoes intramolecular C,H insertion. Decomposition of diazo compounds **186a** by catalytic copper(I) triflate also gave silyl ketenes **188a** in several cases (equation 58); in contrast to the photochemical reaction, γ-C,H insertion was not observed[103]. A singular result is the formation of 1-oxa-2-sila-4-cyclopentene **191** in the Cu(I)-catalyzed decomposition of diazoketone **190**. It may be assumed that a copper−carbene intermediate undergoes

β-C,H insertion to form an acylsilirane, the ring-expansion of which leads to the final product **191**.

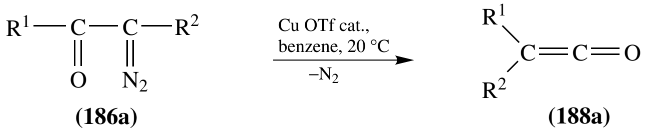

R^1	Me	*t*-Bu	Ph
R^2	$SiEt_3$	$SiMe_2$ Bu	Si(Pr-*i*)$_3$

(58)

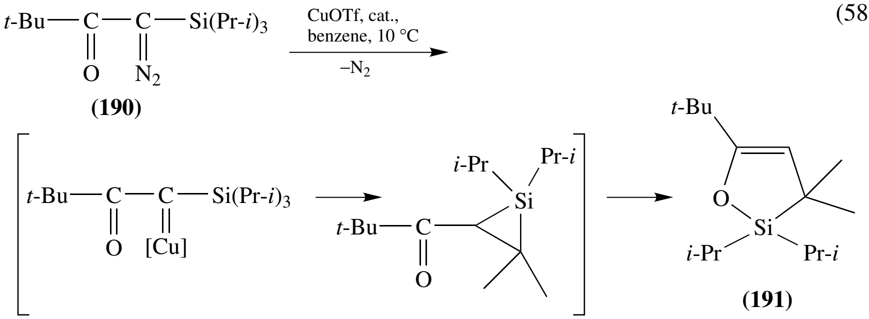

Remarkably, the thermal decomposition of (1-diazo-2-oxoalkyl)silanes **186** does not generate silylcarbenes. Instead, a 1,3(C→O) silyl shift takes place under rather mild conditions (20–80 °C, depending on the substituents) from which (β-siloxy)diazoalkenes **192** result (equation 59). These short-lived cumulenic diazo compounds rapidly split off molecular nitrogen, and the resulting β-siloxyalkylidene carbenes undergo typical intramolecular reactions, from which siloxyalkynes[104], 1-oxa-2-sila-4-cyclopentenes[103,105] or heptafulvene derivatives[106] result. The presumed diazoalkenes **192** can be trapped by [3 + 2] cycloaddition to electron-deficient alkenes[107], cyclopropenes[108] and phosphaalkenes[109].

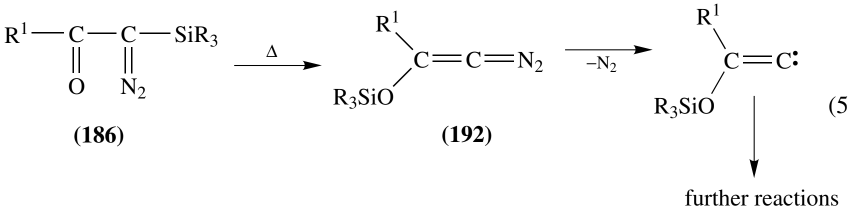

(59)

A transformation analogous to **190** → **191** was observed when diazoketone MeCO—C(N_2)$SiEt_3$ was heated in boiling cyclohexane in the presence of copper powder[110]. In the light of the preceding results, it must be assumed that a purely thermal decomposition via a diazoalkene intermediate is operating here, rather than the ketocarbenoid pathway outlined in equation 58.

b. Alkoxycarbonyl(silyl)carbenes. The photochemical[32,33,111–114], thermal[33,115] and transition-metal catalyzed[114] decomposition of readily available silyl-substituted diazoesters has been studied in much detail. While the first two methods represent a convenient source of carbenes **43** (equation 60), the metal-mediated transformation is likely to include metal–carbene intermediates *(vide infra)* in the product-forming step.

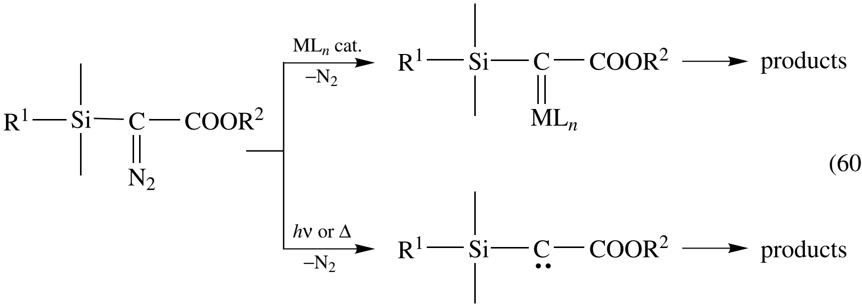

(43)

(60)

As already discussed in Section III.B, carbenes **43** can rearrange to a silene by migration of R^1 to the carbene center and to a ketene by migration of OR^2. The situation is complicated further by a subsequent 1,3(C→Si) shift of the OR^2 group in the silene to form a doubly rearranged ketene (see Scheme 5).

Photolysis of ethyl (trimethylsilyl)diazoacetate[112], methyl (triethylsilyl)diazoacetate[114] and methyl (*tert*-butyldiphenylsilyl)diazoacetate[114] in inert solvents did not provide useful information as to this question. More informative was the photolysis of **193** in various alcohols, leading to a similar mixture of products **194–197** in all cases[33,113] (equation 61). Compound **194** is the major product and probably represents the O,H insertion product of carbene **43**. Compound **195** could be derived from a silene intermediate (equation 62). Wolff rearrangement accounts for the alkoxyacetates **196** and **197**. The exchange of both alkoxy residues leading to **197** is rationalized by the assumption that the Wolff rearrangement of alkoxy groups can include an ion pair intermediate which either collapses or exchanges the alkoxy group with an external alcohol molecule.

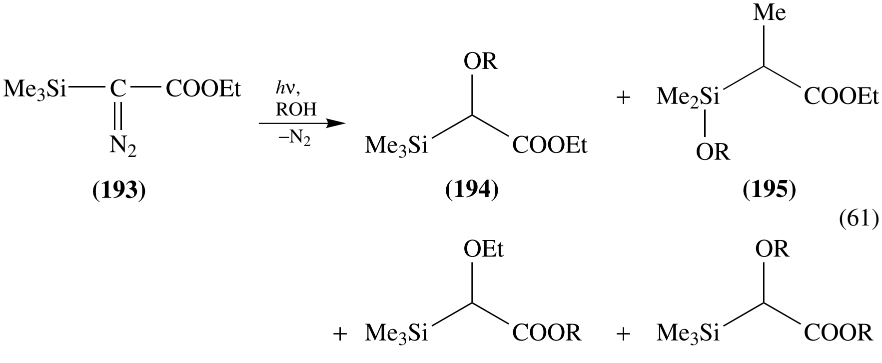

(193) **(194)** **(195)**

(61)

(196) **(197)**

R = Me, Et, *i*-Pr, *t*-Bu

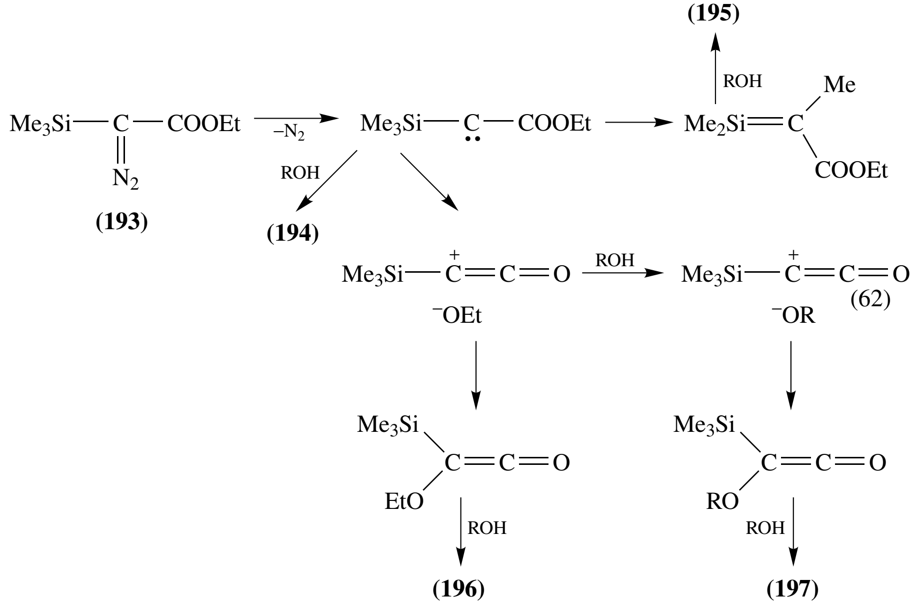
(62)

When diazoester **198** was subjected to gas-phase pyrolysis and ethanol was added afterwards, a partly different result was obtained[32] (equation 63). Alkoxyacetate **199** is again considered to result from the Wolff rearrangement, but since both ethoxy groups in **200** stem from the added alcohol, a silene cannot be the precursor. In a separate experiment, the doubly rearranged ketene **202** was isolated and shown to react quantitatively with ethanol to give **200**. Also interesting is the formation of a small amount (4%) of *β*-lactone **201**, which appears to result from 1,4-C,H insertion of the carbene. No product of an intramolecular C,H insertion could be found after photolysis of ethyl (trimethylsilyl)diazoacetate in an inert solvent[112].

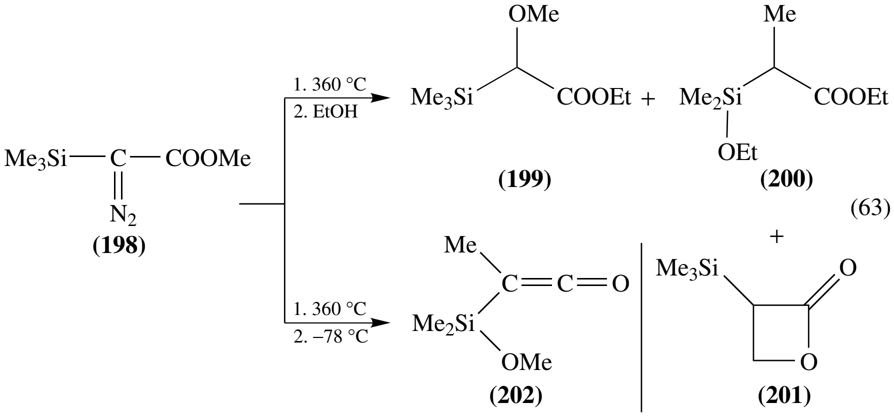
(63)

In the presence of appropriate substrates, a variety of other typical acylcarbene reactions took place with carbene **43** (equation 64). Photolysis of **193** in hydrocarbons (cyclohexane, butane, 2,3-dimethylbutane) yields C,H insertion products of the carbene in approximately 50% yield[111,112] with the following selectivities: 2°/1° = 3.5; 3°/1° = 1.5. The higher selectivity for insertion into secondary than into tertiary C,H bonds is unusual and may be attributed to unfavorable steric interactions between the disubstituted carbene and the substrate.

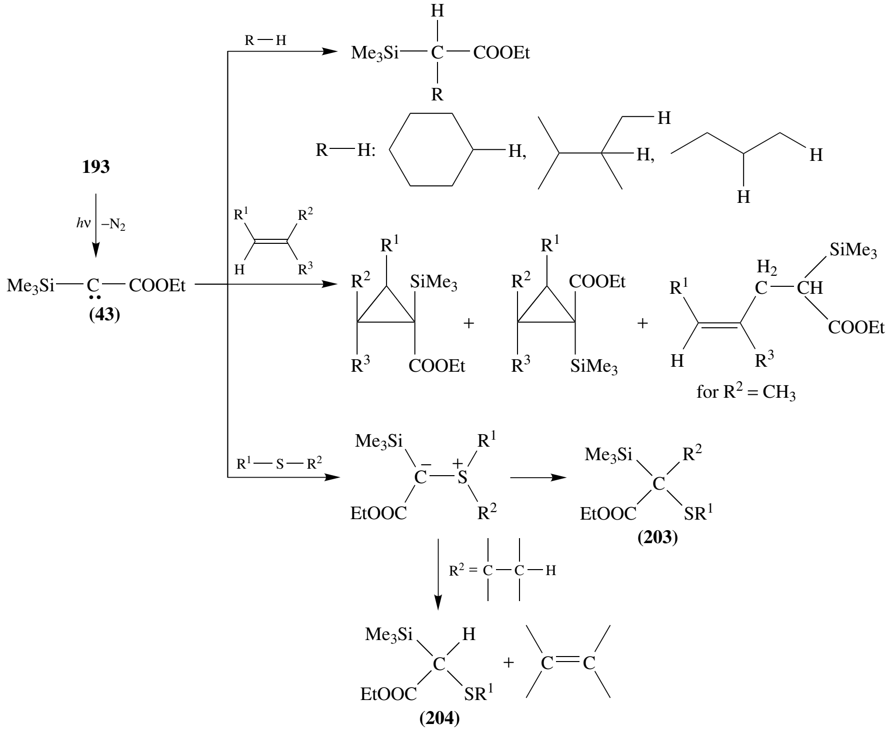

(64)

In the presence of alkenes, photolysis of alkyl (silyl)diazoacetates leads mainly to the formation of cyclopropanes as diastereomeric mixtures[4,111,112]. With (*Z*)- and (*E*)-but-2-ene, the cyclopropanation is not completely stereospecific with respect to the double bond configuration, but gives a small amount of the 'wrong' isomer; these results point to the participation of a triplet carbene in the cyclopropanation reaction. Allylic C,H insertion products are also formed; their yield increases in the series 1,1-, 1,2-, tri- and tetrasubstituted C=C bond. With 2,3-dimethyl-but-2-ene, the allylic C,H insertion product is formed at the complete expense of the cyclopropane.

Interaction of carbene **43** with thioethers leads first to a sulfonium ylide; a subsequent 1,2-R shift provides the formal C,S insertion product **203** and, if possible, β-elimination generates (alkylthio)acetate **204**[116].

For the transition-metal catalyzed decomposition of silyl-substituted diazoacetates **205** [silyl = $SiMe_3$, $SiEt_3$, $SiMe_2Bu$-*t*, $Si(Pr$-*i*$)_3SiPh_2Bu$-*t*, $SiMe_2SiMe_3$], copper(I) triflate and dirhodium tetrakis(perfluorobutyrate) proved to be the best catalysts[114]. While these two catalysts induce the elimination of N_2 at 20 °C even with bulky silyl substituents, dirhodium-tetraacetate even at 100 °C decomposes only the trimethylsilyl- and triethylsilyl-diazoacetates. When the decomposition reactions are carried out in tetrachloromethane or toluene solution, the formal carbene dimers **206**, azines **207** (probably formed from diazoester and the carbene or metal–carbene intermediate), furanone **208** and doubly rearranged ketenes **209** can be formed[114] (equation 65). The result depends on the catalyst, the solvent and the particular silyl group. Furanone **208** could result from [3 + 2] cycloaddition of the ketocarbene 1,3-dipole (or a metal complex thereof) to the ketene formed by a Wolff rearrangement.

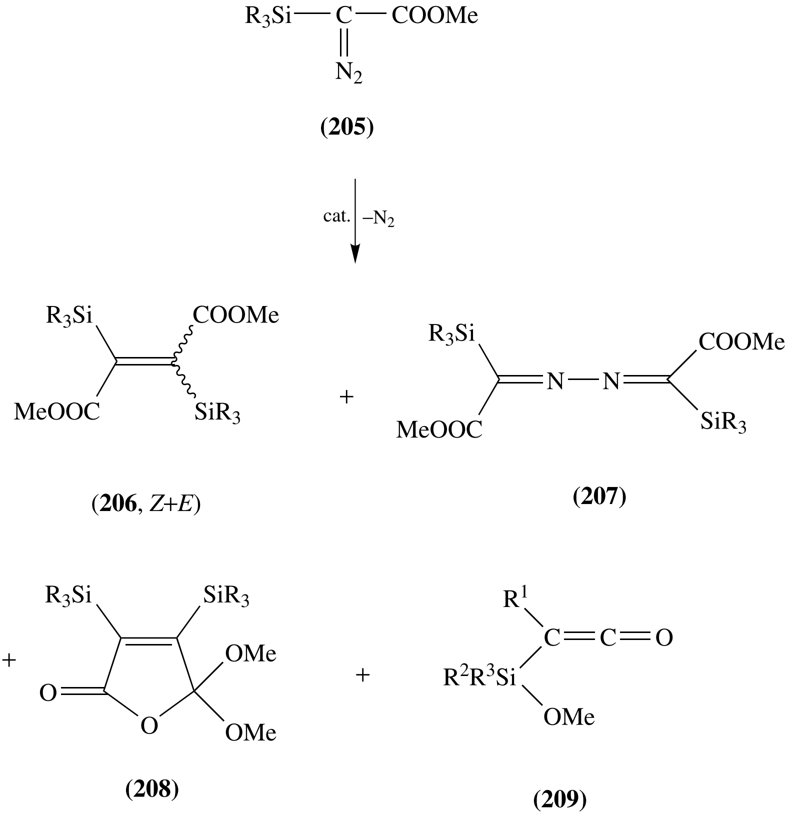

(205)

(**206**, *Z*+*E*)

(207)

(65)

(208)

(209)

$R_3Si = Me_3Si, Et_3Si, (i\text{-}Pr)_3Si, t\text{-}BuPh_2Si\ (R^1{=}Ph),$

$Me_3SiMe_2Si\ (R^1 = SiMe_3)$

With dirhodium tetrakis(perfluorobutyrate) as catalyst, only ketene **209** was obtained in practically all cases, except for the trimethylsilyl (unseparated product mixture) and triisopropylsilyl cases (no decomposition by this catalyst).

With the same catalysts, carbene transfer from diazoacetates **205** [silyl groups: $SiMe_3$, $SiEt_3$, $Si(Pr\text{-}i)_3$] to 1-hexene and styrene was studied[4,117]. The yields of cyclopropanes were usually higher in the metal-catalyzed than in the photochemical version. Interestingly, the metal-catalyzed procedure gave preferentially *E*-**210**, whereas with the photochemically generated carbene an E/Z ratio <1 was obtained (equation 66). The significance of these results needs further investigation. For the cyclopropanation of cyclohexene with diazoester **205** ($R_3Si = Me_3Si$), the complex $[Ru_2(CO)_4(\mu\text{-}OAc)_2]_n$ is the catalyst of choice[118], since only the allylic C,H insertion product of the carbene is obtained with copper(I) triflate and $Rh_2(OOCC_3F_7)_4$ as catalysts.

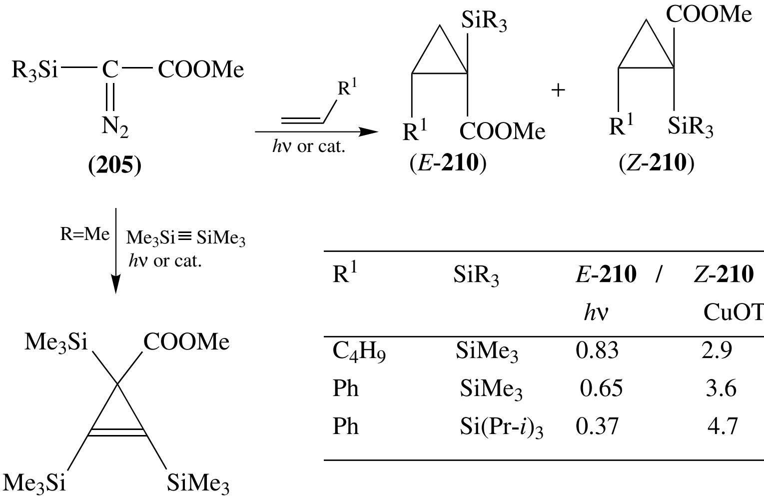

(66)

R^1	SiR_3	E-**210** /	Z-**210**
		$h\nu$	CuOTf cat.
C_4H_9	$SiMe_3$	0.83	2.9
Ph	$SiMe_3$	0.65	3.6
Ph	$Si(Pr\text{-}i)_3$	0.37	4.7

[1 + 2] Cycloaddition of the carbene derived from **205** to bis(trimethylsilyl)acetylene yields the expected cyclopropene in low yield both photochemically (20%) and under catalysis by copper(I) triflate at 80 °C (10–13%)[119]. The latter version of the reaction is accompanied by [3 + 2] cycloaddition of the diazo compound to the alkyne, and the photochemical route yields a by-product which obviously comes from carbenic C,H insertion at a $SiMe_3$ group of the alkyne.

Transition-metal mediated carbene transfer from **205** to benzaldehyde generates carbonyl ylides **211** which are transformed into oxiranes **216** by 1,3-cyclization, into tetrahydrofurans **212, 213** or dihydrofurans **214** by [3 + 2] cycloaddition with electron-deficient alkenes or alkynes, and 1,3-dioxolanes **215** by [3 + 2] cycloaddition with excess carbonyl compound[120] (equation 67). Related carbonyl ylide reactions have been performed with crotonaldehyde, acetone and cyclohexanone (equation 68). However, the ylide generated from cyclohexanone could not be trapped with dimethyl fumarate. Rather, the enol ether **217**, probably formed by 1,4-proton shift in the ylide intermediate, was isolated in low yield[120]. In this respect, the carbene transfer reaction with **205** is not different from that with ethyl diazoacetate[121], whereas a close analogy to diazomalonates is observed for the other carbonyl ylide reactions.

Efforts to trap the carbonyl ylide intermediate by intramolecular [3 + 2] cycloaddition to a C=C bond were unsuccessful. Rather, the decomposition of allyl (trimethylsilyl)diazoacetate **(218)** (equation 69) in the presence of aldehydes gave 1,3-dioxolan-4-ones **219**; their formation has been explained by 1,5-cyclization of the carbonyl ylide intermediate followed by a Claisen rearrangement[122]. With acetone as carbonyl component, the reaction proceeds analogously. Clean formation of **219** occurred only with $Rh_2(OOCC_3F_7)_4$ as catalyst, while the copper(I) triflate catalyzed version led to a mixture of **219**, an oxirane and the product of intramolecular carbenoid cyclopropanation. Carbonyl ylide reactions derived from homoallylic ester **220** are shown in equation 70[122].

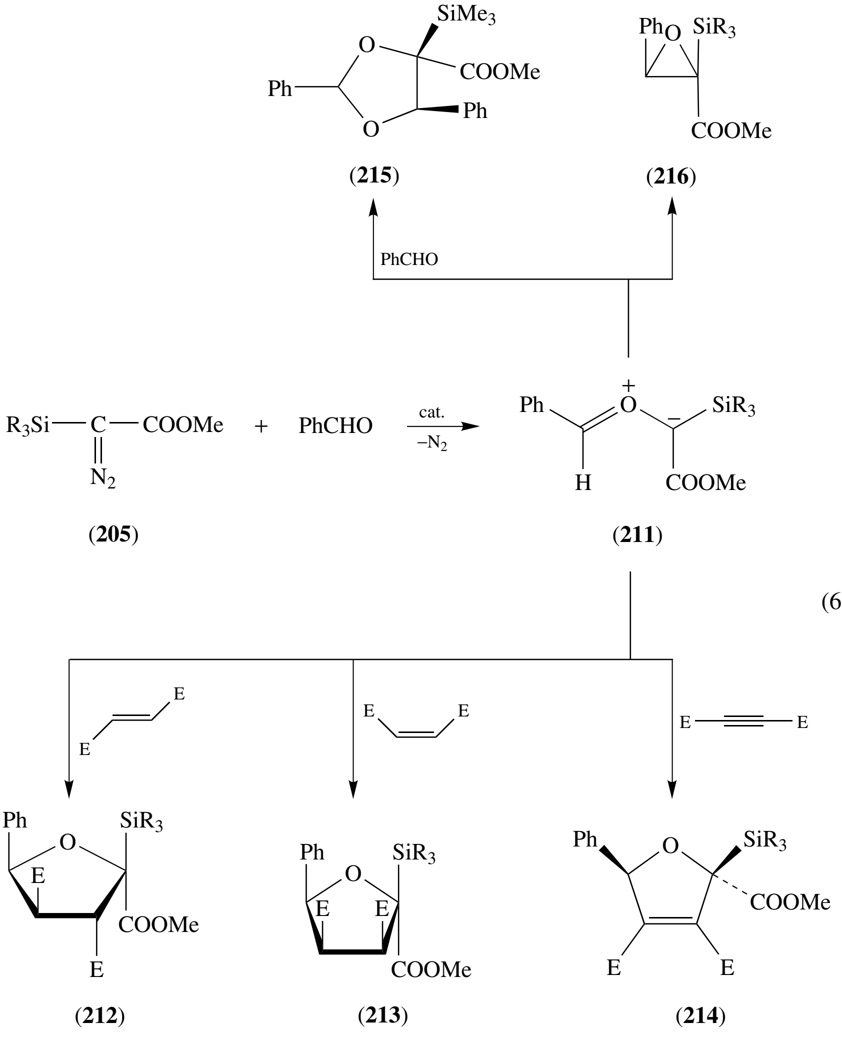

(67)

R = Me, Et
E = COOMe
cat. = CuOTf, $Rh_2(OOCC_3F_7)_4$, $[Ru_2(CO)_4(\mu\text{-}OAc)_2]_n$

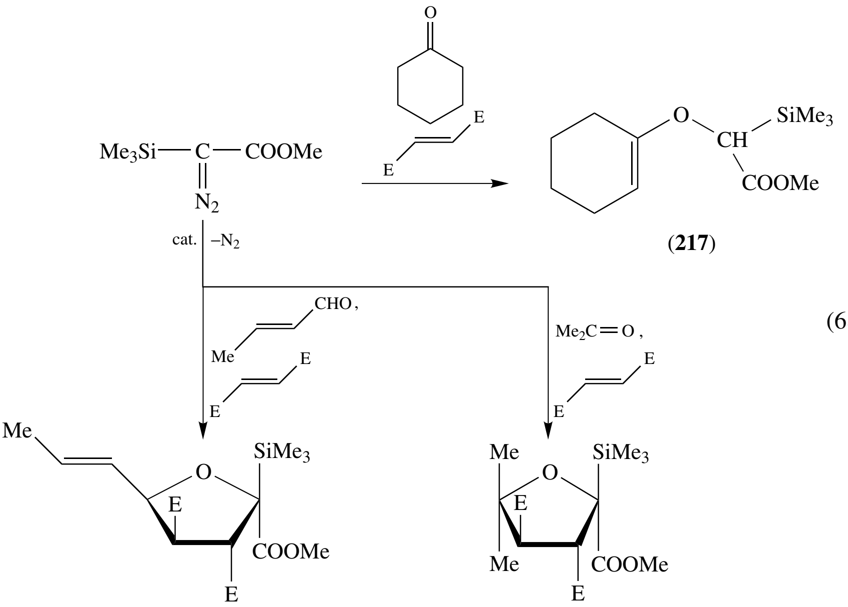

(217)

(68)

E = COOMe

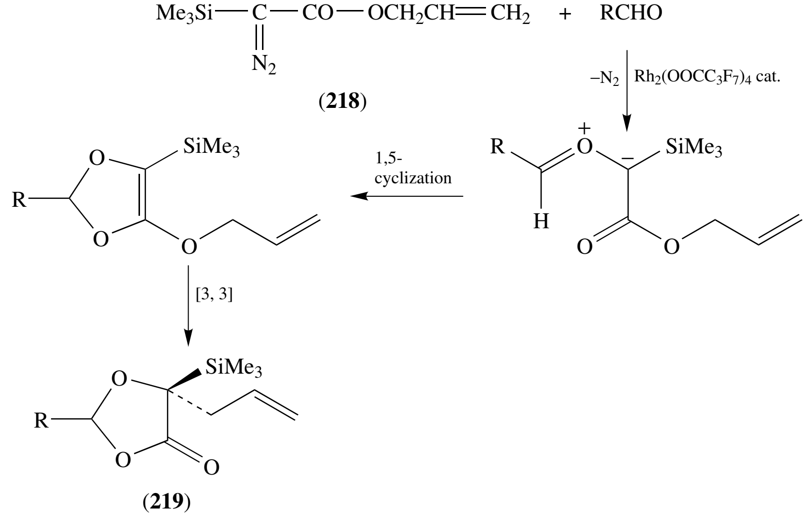

(218)

(219)

(69)

R = Me, CH = CHMe, Ph, 4-MeOC$_6$H$_4$, C$_6$H$_4$, 3,4,5-(MeO)$_3$C$_6$H$_2$

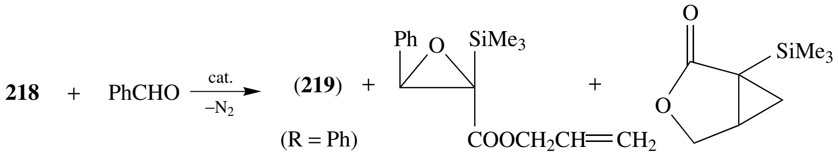

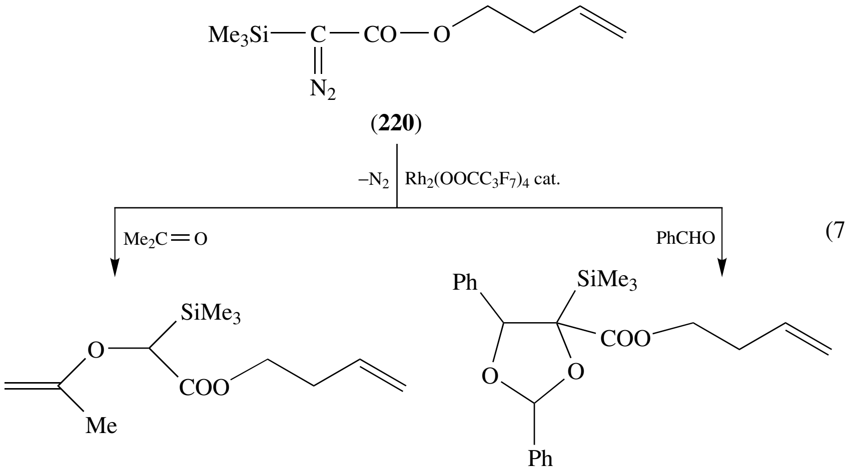

(**220**)

(70)

Transition-metal catalyzed transfer of acylcarbenes to nitriles leads to 1,3-oxazoles via nitrile ylide intermediates[123]. The corresponding nitrile ylide chemistry derived from acyl(silyl)carbenes still awaits a closer look, but it has been shown that the rhodium-catalyzed decomposition of **198** in the presence of methyl cyanoformate and benzaldehyde provides 1,3-oxazole **221** (equation 71) exclusively[120]. This implies that the carbene moiety has been transferred only to the nitrile but not to the aldehyde.

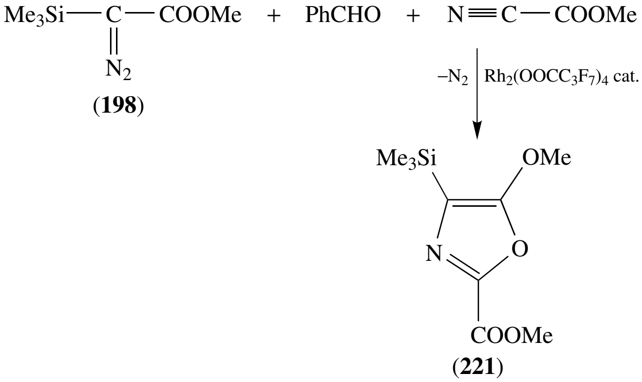

(**198**)

(**221**)

(71)

In another copper-mediated carbene transfer reaction, diazoester **222** has been decomposed in the presence of bis(triethylsilyl- or -germyl)mercury (equation 72); it was assumed that the obtained ketenes **223** result from the insertion of ethoxycarbonyl(trimethylsilyl)carbene into a Hg-element bond followed by a cyclic fragmentation process[110].

c. Aminocarbonyl(silyl)carbenes. UV-irradiation of *N*,*N*-diethyl diazo(triisopropylsilyl)acetamide (**224**) provides a mixture of β-lactam **225** and γ-lactam **226** in a 1 : 2 ratio[103] (equation 73). Both products may be considered to result from carbenic C,H insertion. For the analogous transformation of the nonsilylated diazoacetamide, however, it has been proposed that only the γ-lactam is formed on a carbene pathway, whereas the

β-lactam results directly from an excited singlet state of the diazo compound[124,125].

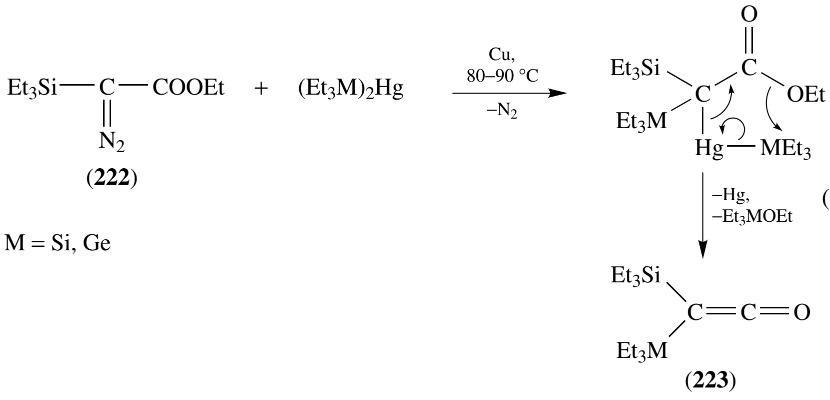

(222) (223)

M = Si, Ge

(72)

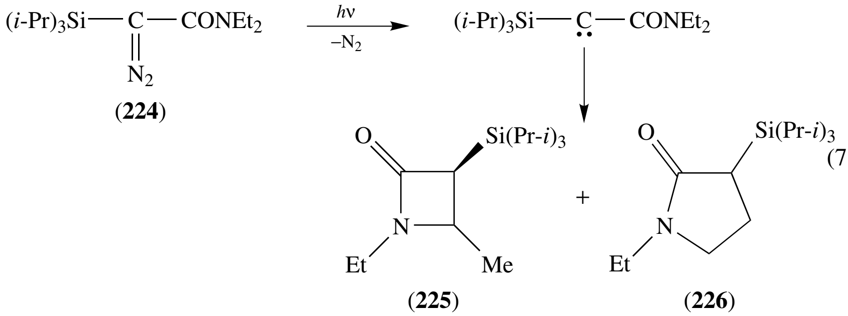

(224) (225) (226)

(73)

6. Imino(silyl)carbenes

Photolysis of 1,2,3-triazole **227** (equation 74) provides the bis(trimethylsilyl)ketenimine **229** in better than 80% yield[126]. As with other triazoles it can be assumed that the light-induced extrusion of nitrogen from **227** generates the iminocarbene **228** which undergoes a fast Wolff rearrangement by 1,2-migration of a trimethylsilyl group. It is remarkable that a 1,5-cyclization of the carbene does not compete with the rearrangement at all, in contrast to the behavior of those N-aryl iminocarbenes where phenyl or alkyl substituents are involved in the 1,2-migration.

7. Phosphino(silyl)carbenes and phosphoryl(silyl)carbenes

a. Phosphino(silyl)carbenes. In 1988, Bertrand and coworkers reported that the thermolysis of [bis(diisopropylamino) phosphino]-(trimethylsilyl)diazomethane (**230a**, equation 75) at 250 °C provides a red oily material which can be distilled at 75–80 °C/0.02 Torr and is stable for several weeks at room temperature in benzene solution[127]. This compound has the constitution **231a** and was therefore called a 'stable carbene'. Since this report, several other carbenes of the same type became known (**231b–e**[128,129], **231f**[130]). They are typically obtained by thermal extrusion of molecular nitrogen from their rather unstable diazo precursors at 25–70 °C. Photolysis of the diazo compounds also generates these carbenes, but a clean preparation was only possible for **231f**. At room temperature, carbenes **231a–d** and **f** are stable for several weeks, while **231e** survives for only a few hours. Together with the salt $[(i\text{-Pr})_2N]_2P{-}C{-}^{+}PH[N(Pr\text{-}i)_2]_2^{\bullet}\ CF_3SO_3^{-}$[131], **231a–f** represent the only known examples of this type of 'stable carbene', i.e. compounds in which a phosphino group is attached to a formally divalent carbon atom. By comparison with other substitution patterns, it becomes obvious that one or better two dialkylamino groups in the phosphino groups are important for stabilization of the phosphinocarbenes. Furthermore, the silyl group also contributes to stabilization. By comparison, the analogous stannyl-substituted carbenes $[(i\text{-Pr})_2N]_2P{-}C{-}SnR_3$ (R = Me, Ph, *c*-Hex) are only transient intermediates which could be trapped with *tert*-butylisonitrile or methyl acrylate[132].

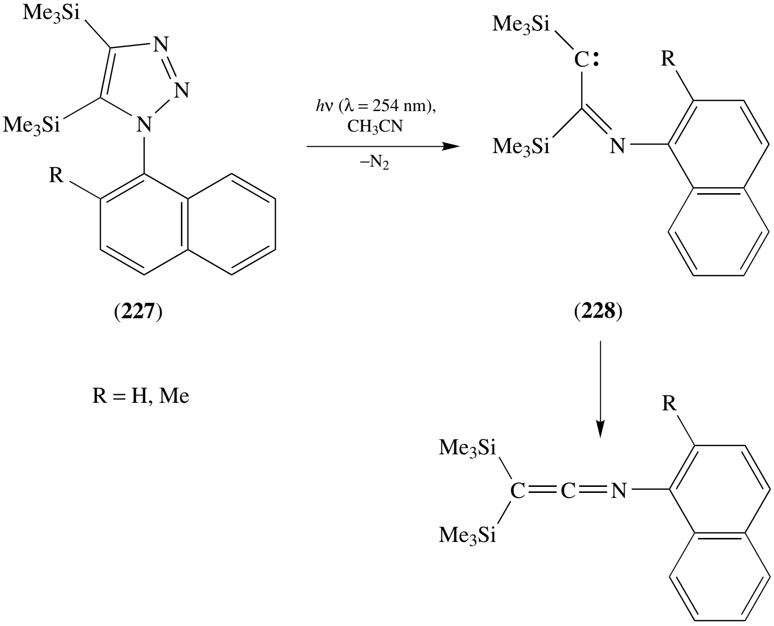

(**227**) (**228**) (74)

R = H, Me

(**229**)

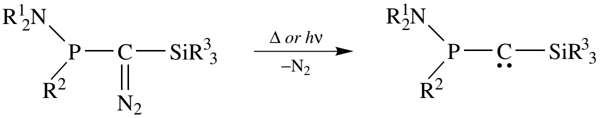

(**230**) (**231**) (75)

230, 231	**a**	**b**	**c**	**d**	**e**	**f**
R^1_2N	$(i\text{-Pr})_2N$	Tmp	Tmp	Tmp	Tmp	$(c\text{-Hex})_2N$
R^2	$(i\text{-Pr})_2N$	$(i\text{-Pr})_2N$	Me_2N	Me_2N	Ph	$(c\text{-Hex})_2N$
R^3	Me	Me	*i*-Pr	Me	Me	Me

Tmp = 2,2,6,6-tetramethylpiperidide

As carbenes are typically perceived by chemists as short-lived intermediates, the term ‘stable carbenes’ appears as a *contradictio in se*, and some debate arose about the true chemical nature of Bertrand’s stable phosphinocarbenes as well as Arduengo’s carbenes of the 1,3-imidazol-2-ylidene type[133]. It has been outlined already in Section II that resonance structures **232A** (carbene), **232B** (phosphavinyl ylide) and **232C** (λ^5-phosphaacetylene) (equation 76) can be used to describe the bond state of singlet phosphinocarbenes and that, according to theoretical calculations, the so-called stable carbenes **231** are best regarded as phosphavinyl ylides **(232B)**. For this structure, amino groups obviously stabilize the positive charge at phosphorus, and silyl groups can stabilize the negative charge at carbon by delocalization.

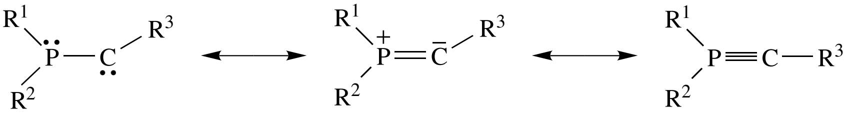

(**232A**) (**232B**) (**232C**)

(76)

The results of theoretical calculations, spectroscopic data and chemistry of phosphinocarbenes have been reviewed[22,134]. In the context of this chapter, it may suffice to mention that phosphino(silyl)carbenes **231** behave as chemical chameleons which in some of their transformations display a behavior that is thought to be typical for (nucleophilic) carbenes, whereas the reactivity of a species with a P,C multiple bond is perceived in other cases. Examples of carbene-type reactions of **231a** are given in equation 77, namely intramolecular C,H insertion[127], cyclopropanation of electron-deficient alkenes such as methyl acrylate and dimethyl fumarate[135] (dimethyl maleate does not react), stereospecific oxirane formation with aldehydes [135] and ketenimine formation with an isocyanide[135]. Other aminophosphino(silyl)carbenes react analogously[129]. In most cases, the first-formed phosphino-substituted products are rather unstable and were converted to the P-sulfides for isolation. Carbene **231f** undergoes a smooth [1 + 2] cycloaddition to benzonitrile leading to 2*H*-azirene **233**[136]. Under the catalytic action of dichloro(*p*-cymene)ruthenium(II), **233** undergoes ring-expansion to a 1,2(λ^5)-azaphosphete (equation 78).

Photochemically generated carbene **231a** reacts with (*tert*-butylmethylidyne)phosphine to form the stable 1(λ^5),2(λ^3)-diphosphete **234**[137]. It has been proposed that 2*H*-phosphirene **235** is a transient intermediate in this reaction (equation 79); it would be formed by [1 + 2] cycloaddition of **231a** to the P,C triple bond in complete analogy to azirene **233** and would undergo spontaneous ring-expansion to **234**.

It should be mentioned that alkenes **236**, which are often found as (formal) carbene dimers in reactions involving electrophilic carbenes, have never been observed in the context of phosphino(silyl)carbenes. UV-irradiation of a [bis(dialkylamino)phosphino](trimethylsilyl)diazomethane leads to a 1(λ^5),3(λ^5)-diphosphete **237** (equation 80) which can be regarded as the head-to-tail cyclodimer of a phosphavinyl ylide (cf **232B**), whereas irradiation of diphenylphosphino- or dimethoxyphosphino-(trimethylsilyl)diazomethane produces a 1,2(λ^5),4(λ^5),6(λ^5)-azatriphosphorin **238** in a sequence which may also include the corresponding diphosphete **237**[138].

Several other transformations have been reported which highlight either the carbene or the P,C multiple bond nature of compounds **231** or allow a mechanistic interpretation by more than one of the different reactivity patterns[24].

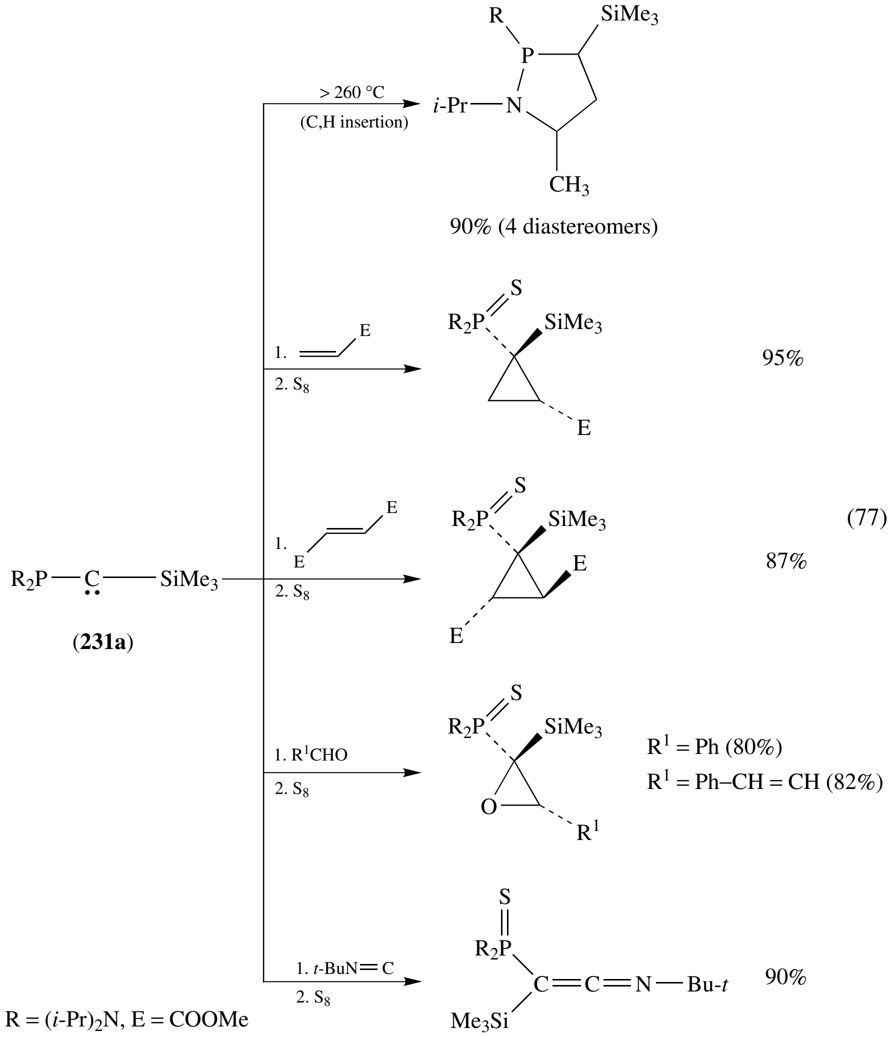
> 260 °C
(C,H insertion)
90% (4 diastereomers)
1. 2. S$_8$
95%
87%
1. R^{1}CHO
2. S$_8$
R^1 = Ph (80%)
R^1 = Ph–CH = CH (82%)
1. t-BuN≡C
2. S$_8$
90%
(231a)
R = (i-Pr)$_2$N, E = COOMe

(77)

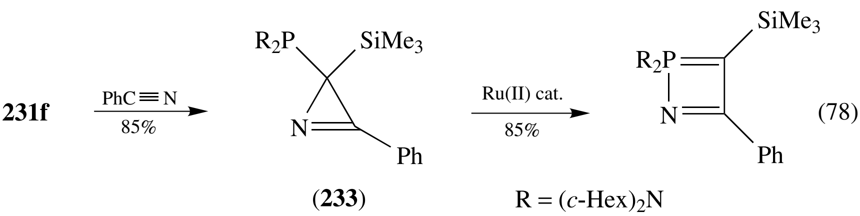
231f
PhC≡N
85%
(233)
Ru(II) cat.
85%
R = (c-Hex)$_2$N

(78)

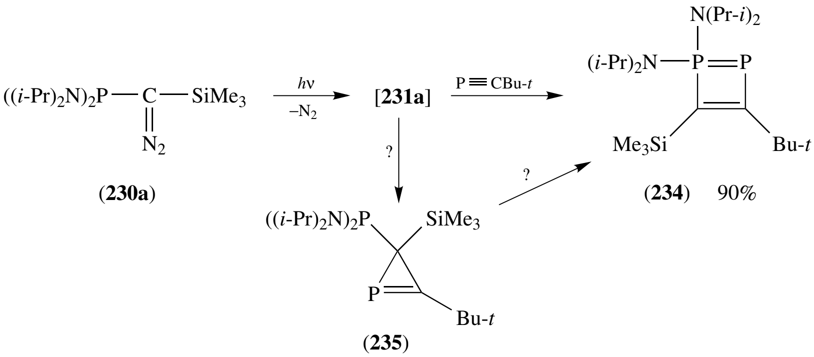

(79)

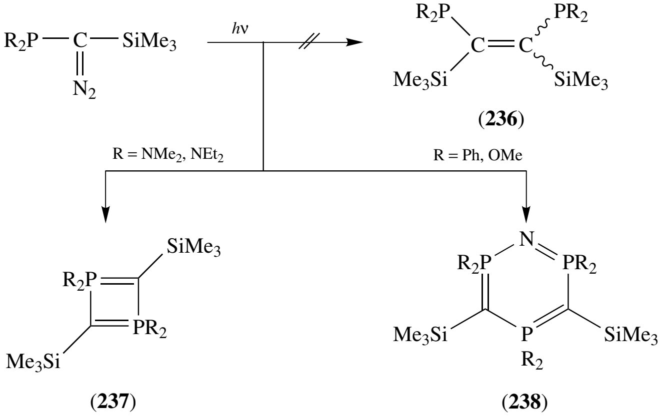

(80)

Bis[diazo(trimethylsilyl)methyl] phosphines **239** loose only one equivalent of dinitrogen on warming and are transformed into 1,2,4(λ^3)-diazaphospholes **240**[139] (equation 81). It is obvious to explain this cyclization by intramolecular ketazine formation of a diazocarbene intermediate, but in light of the preceding discussion, speculations about the bond state of this phosphinocarbene (phosphavinyl ylide or phosphaacetylene) are allowed.

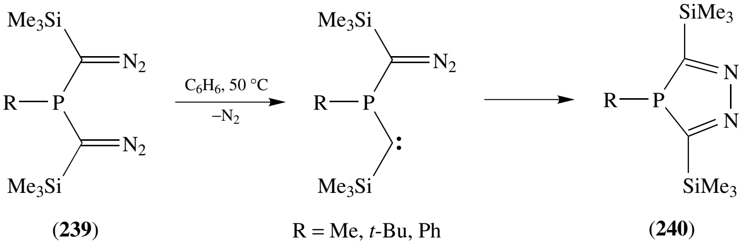

(81)

b. Phosphoryl(silyl)carbenes. Although the chemistry of phosphorylcarbenes is well developed[140], hardly anything is known about phosphoryl(silyl)carbenes. Some experiments in the author's laboratories were rather unproductive[141]. Thus, photolysis of diazo compound **241** in benzene produced an unseparable mixture with at least five major components, one of which is probably a cycloheptatriene according to NMR data, likely to be formed by [1+2] cycloaddition of the carbene to benzene and subsequent norcaradiene-to-cycloheptatriene isomerization. An unidentified product mixture with at least three major components was also obtained from the photolysis ($\lambda = 254$ nm) of **242** in benzene.

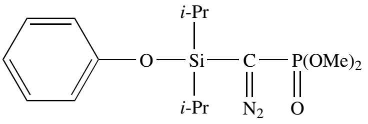

(**241**)

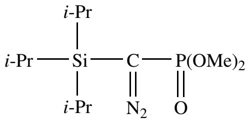

(**242**)

8. Sulfur-substituted silylcarbenes

The three-component reaction of bis(phenylthio)-(trimethylsilyl)methyl lithium **(243)**, phenyloxirane and a terminal alkene yields cyclopropanes **245**[142] (equation 82). It is assumed that α-elimination of LiSPh from the carbenoid-like species **243** generates phenylthio(trimethylsilyl)carbene **(244)** which is in equilibrium with **243**; although this equilibrium is probably far on the side of the latter, trapping of the thiophenolate ion by the

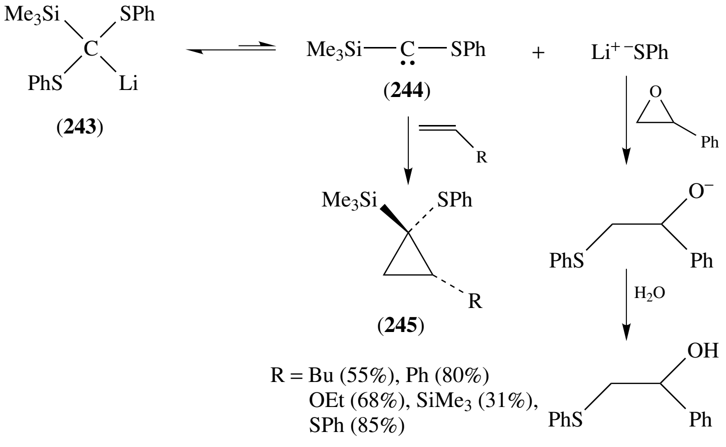

R = Bu (55%), Ph (80%)
OEt (68%), SiMe$_3$ (31%),
SPh (85%)

(82)

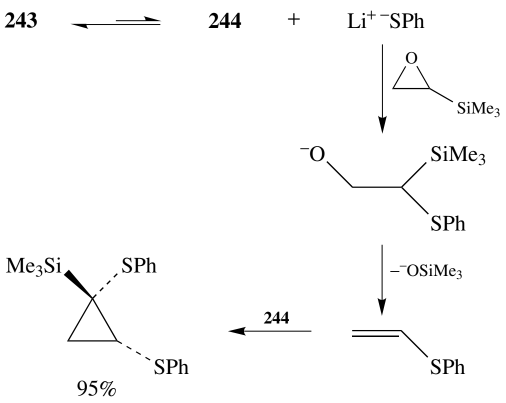

oxirane renders the carbene available for [1 + 2] cycloaddition to the alkene. The chosen alkenes were cyclopropanated diastereospecifically; their successful reaction indicates the electrophilic nature of carbene **244**. Related carbenes (**244**; $SiEt_3$, t-$BuMe_2Si$ instead of $SiMe_3$; Tol and 4-ClC_6H_4 instead of Ph) have been generated analogously[143].

Interestingly, cyclopropane **245** (R = SPh) is also formed when **243** is combined with (trimethylsilyl)oxirane. In this case, the necessary alkene (phenylthioethylene) is provided by silanolate elimination from the alkoxide arising from regiospecific ring-opening of the oxirane by thiophenolate (equation 82)[142].

It should be mentioned that this elegant method to generate a carbene appears to be of limited scope. Lithium salts related to **243**, e.g. $(Me_3Si)_2(PhS)CLi$, $Me_3Si(MeS)_2CLi$ and 2-trimethylsilyl-1,2,3-thiolan-2-yl lithium, do not undergo efficient α-elimation of a lithium thiolate but rather direct nucleophilic addition to the two oxiranes mentioned[142]. These observations are reminiscent of the reaction of phenylthio(trimethylsilyl)methyl lithium with olefins leading to (trimethylsilyl)cyclopropanes[76]; it is not clear whether this transformation really includes the transfer of free (trimethylsilyl)carbene or rather occurs by a Michael addition/ring closure sequence (see also Section III E.l.a).

9. Halo(silyl)carbenes

Carbenes of this type have been generated so far only by thermally induced α-elimination of RHgHal from suitable (α-halo)mercurials (see Section III.A). Thus, chloro(trimethylsilyl)carbene **(248)** can be generated by heating $(Me_3SiCCl_2)_2Hg$ **(246)** at *ca* 120 °C. It undergoes [1 + 2] cycloaddition with acyclic and cyclic alkenes and inserts into the Si−H bond of triethylsilane[75,144] (equation 83). The disadvantage that only one dichloro(trimethylsilyl) group of **246** is used for carbene formation can be overcome, with the consequence of better yields of the carbene transfer products, by the use of an equimolar mixture of **246** and Ph_2Hg. In this case, the mixed organomercury compound **247** is likely to be formed and to serve as the carbene precursor. Similarly, carbene **248** can be generated thermally from an equimolar mixture of Me_3SiCCl_2HgCl and Ph_2Hg[75]. In all cases, by-products were formed which are likely to be derived from the $Me_3SiCCl_2^\bullet$ radical. In fact, when **246** is decomposed at higher temperature (*ca* 220 °C), the homolytic cleavage of the Hg−C bond, generating this radical, becomes the major pathway.

Analogously to carbene **248**, bromo(trimethylsilyl)carbene **250** was generated by thermal decomposition of an equimolar mixture of **249** and Ph_2Hg (equation 84) and transferred to cyclohexene[75]. Although the α-elimination reaction of the carbene precursor occurs faster than in the chloro case, the obtained bromocyclopropane is less stable under the still harsh reaction conditions and is partly decomposed.

F. Special Methods to Generate Silylcarbenes

In this section, some individual transformations are mentioned in which silylcarbene intermediates have been suggested but which do not belong to any of the more familiar and more versatile methods to generate silylcarbenes as shown in Scheme 1 (Section III.A).

1. Silylcarbenes by rearrangement reactions

a. Isomerization of 2-silylfurans. 2-Silyl-substituted furans **251** undergo a remarkably clean photochemical isomerization reaction featuring a ring-opening process[145]. It has been suggested that the latter leads to (1-alkenyl)(trimethylsilyl)carbenes **252** which provide an 1-acyl-3-silylallene by a 1,2(C→C) H shift (equation 85). A similar mechanism has been proposed to explain the formation of a 1,2-oxasilin as one of the products from flash vacuum pyrolysis of **251** ($R^1 = R^2 = H$)[146]; in this case, a 1,2(Si→C) H shift in the intermediate carbene **253** was assumed.

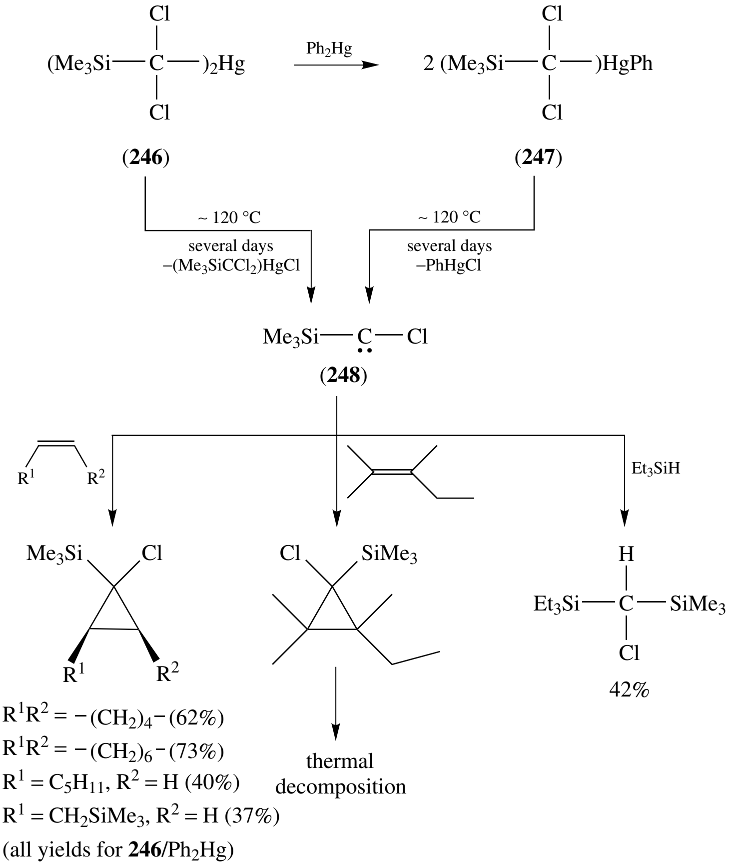

(83)

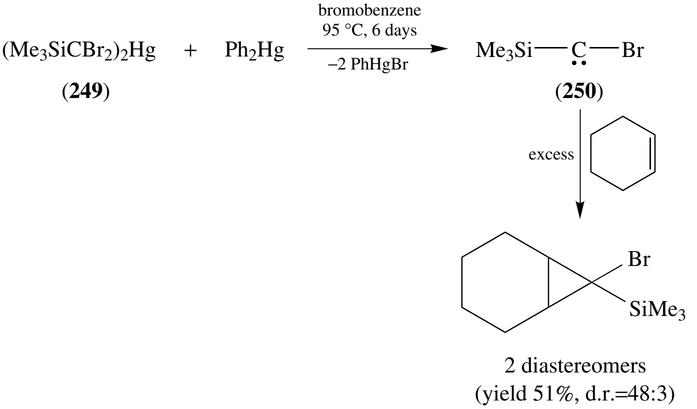

(84)

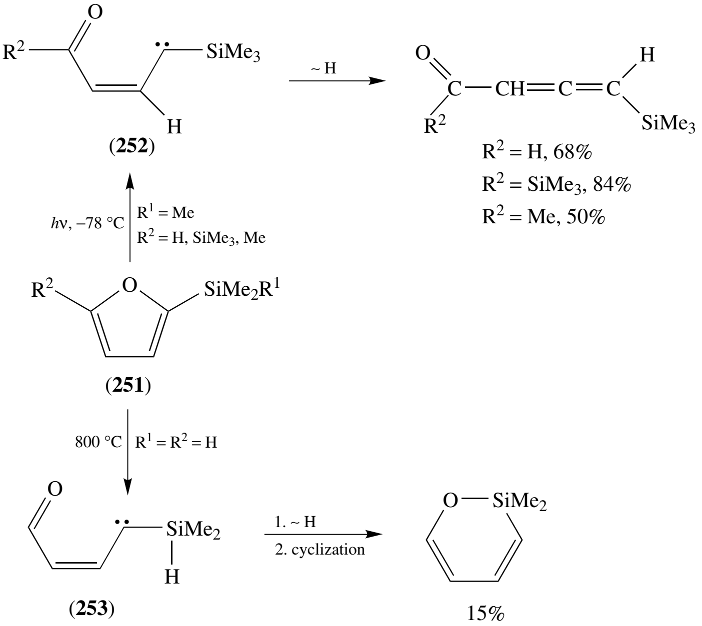

(85)

b. Olefin-to-carbene isomerization. Flash vacuum pyrolysis (FVP) at 700 °C of bis(silyl)ketenes **254** (equation 86) cleanly affords a silyl acetylene and a mixture of permethylcyclosiloxanes[147]. It has been suggested that the decomposition of **254** begins with a 1,2-silyl shift at the C═C bond to produce an acyl(silyl)carbene **255**, which then reacts further as shown in the equation. It should be noted that the proposed isomerization **254** → **255** represents a retro-Wolff rearrangement.

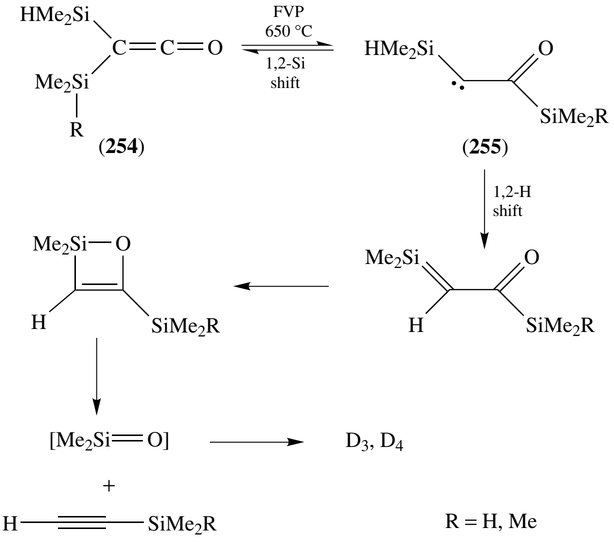

(86)

An analogous mechanistic scheme (equation 87) has been proposed for the flash vacuum pyrolysis of dimethylsilyl(trimethylsilyl)thioketene[148] (**256**). The pyrolysis of bis(trimethylsilyl)thioketene (**257**) leads to a more complicated product mixture (equation 88). With 47% conversion, a mixture of trimethylsilylacetylene, 1-trimethylsilyl-1-propyne, bis(trimethylsilyl)acetylene, (trimethylsilyl)thioketene, 2,2,4,4-tetramethyl-2,4-disila-1-thietane and 2,2,4,4-tetramethyl-2,4-disila-1,3-dithietane was obtained. All products can be rationalized, however, by the assumption that carbene **258** undergoes not only a silylcarbene-to-silene rearrangement (as in the preceding two cases) but also isomerization to 2-thiirene and insertion into a methyl-C, H bond.

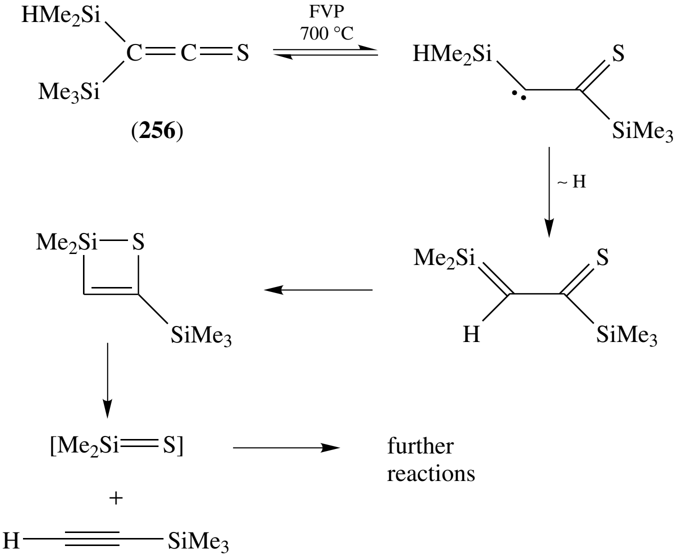

(87)

An in-depth experimental and theoretical study on the feasibility of the olefin-to-carbene rearrangement by a thermally induced 1,2-shift of H, Me or $SiMe_3$ has appeared[149]. In contrast to the hetero cumulenes **254**, **256** and **257**, acyclic vinylsilanes do not undergo this rearrangement. For example, flash vacuum pyrolysis (FVP) at 700–800 °C of 1,1-bis(trimethylsilyl)ethylene yields CH_4, Me_3SiH and trimethyl(vinyl)silane as the major products, but not 1,2-bis(trimethylsilyl)ethylene expected from an olefin-to-carbene rearrangement. In small rings bearing an *exo*-methylene group, the sought rearrangement could be assisted by the relief of ring strain on the way to the carbene. Therefore, the FVP of 2,4-dimethylene-1,3-disiletane **259** and of 2-methylenesiletane **262** was studied. In fact, the 1,2-silyl shift at the olefinic bond took place in both cases (equation 89). The Arrhenius parameters of these rearrangements were determined in a stirred flow reactor system as follows: **259** → **261** at 500–600°C: $E_a = 54.09 \pm 1.26$ kcal mol^{-1}, $\log A = 12.48 \pm 0.33$ s^{-1}; **262** → **264 (a+b)** at 530–590 °C: $E_a = 47.5 \pm 0.8$ kcal mol^{-1}, $\log A = 11.3 \pm 0.2$ s^{-1}. In both cases, the values are in accord with a concerted process, in which alkyl(silyl)carbene **260** and dialkylcarbene **263** are transition states rather than intermediates. For the process involving carbene **260** (SiH_2 instead of $SiMe_2$ an energy level of 60.8 kcal mol^{-1} for the transition state, represented by the carbene, has been calculated [MP2/6-31 G(d)//HF-6-31 G(d) + 0.89 ZPE(HF)] for carbene **260** (SiH_2 instead of $SiMe_2$). In another theoretical study[90b], isomerization pathways of 1,2-disilylcyclopropene were considered and it was found that the rearrangement to a 2,2-disilylcyclopropylidene, which would a also require a 1,2-silyl shift at the olefinic bond, cannot compete energetically with the ring-opening leading to (1-silylvinyl)silylcarbene.

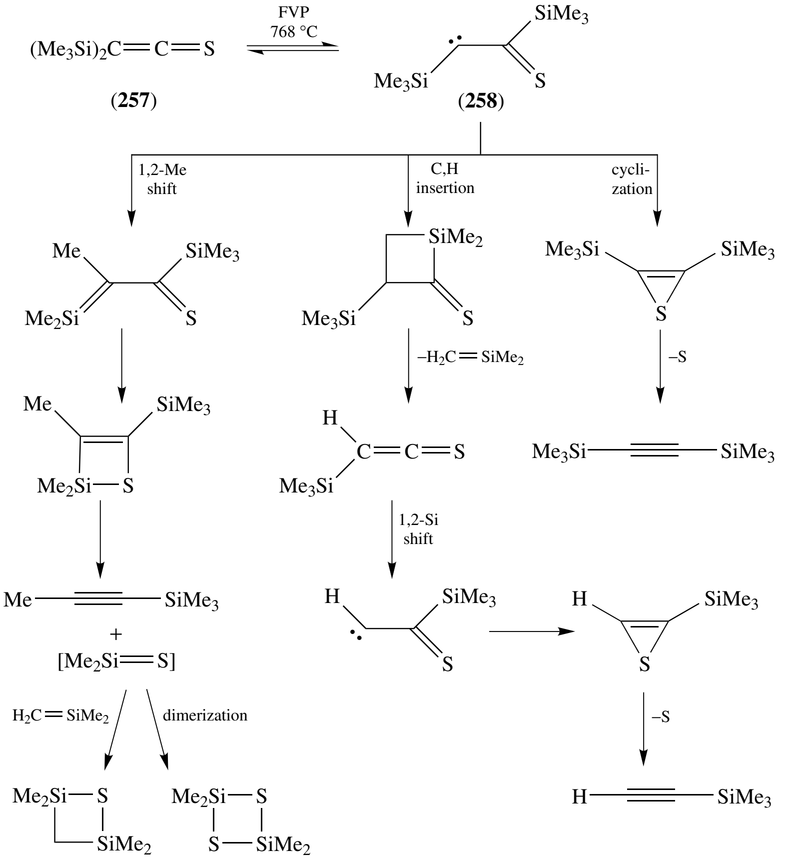

(88)

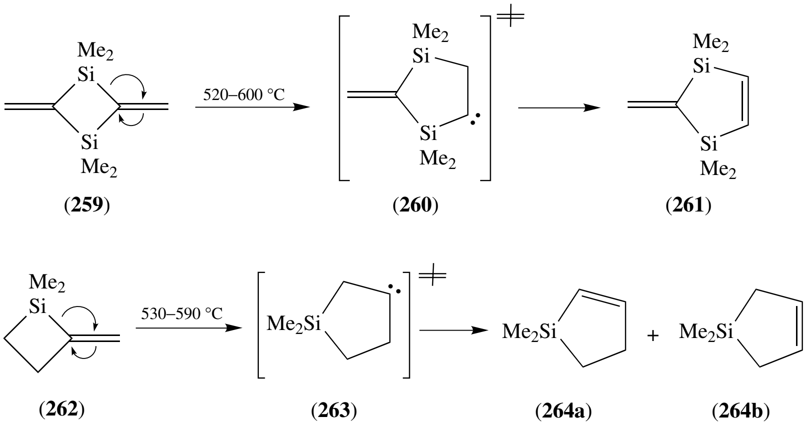

(89)

Notably, the carbon analogue of **259** (CMe_2 instead of $SiMe_2$) does not seem to undergo the olefin-to-carbene rearrangement[149]. A comparison of the energy surfaces for the two processes by *ab initio* methods including electron correlation shows that, in contrast to the rearrangement by 1,2-silyl migration (**259** → **260**), the process featuring a 1,2-alkyl migration has an early transition state with a substantial barrier. This fact seems to be prohibitive to the rearrangement, although the relief of ring strain would have been larger than for the silicon case (**259** → **261**) according to the calculations. The thermochemical differences mentioned do not appear to be a property of these cyclic systems. Electron-correlated *ab initio* methods predict an analogous difference for acyclic olefins as well[149], namely barrier-free thermal olefin-to-carbene rearrangements of vinylsilane (equation 90) as opposed to the analogous rearrangements of propene (cf equation 90, CH_3 instead of SiH_3).

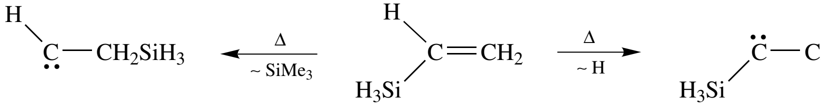

(90)

c. Ring-opening of 2-lithio-2-silyloxiranes.[150] 2-(Triphenylsilyl)oxiran-2-yl lithium **(265)** is obtained quantitatively by metalation of 2-(triphenylsilyl)oxirane with butyl or *tert*-butyl lithium in a donor solvent (THF, TMEDA) and can be quenched with various electrophiles, also at low temperature. However, at 25 °C **265** undergoes ring-opening, which can be considered as an α-elimination reaction of this carbenoid-type species to form the silylcarbene **266**. In the presence of excess butyl lithium or phenyl lithium, alkenes **268** are finally obtained. It is assumed that the carbene adds RLi to form the dilithiated intermediates **267**, which can readily eliminate lithium oxide (equation 91). No further trapping reactions of the carbene have been described.

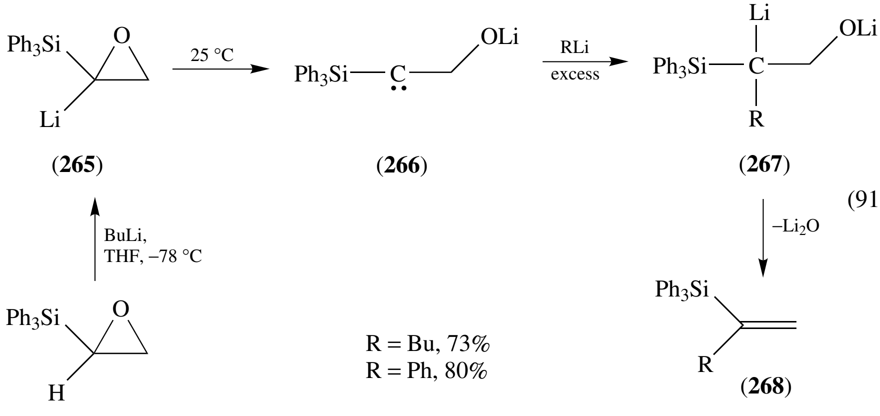

(91)

2. Silylcarbenes by intermolecular reactions

a. Photochemical reaction of (silyl)alkynones with alkenes. (1-Alkynyl)ketones react photochemically with simple alkenes in two directions, namely with formation of a 2-alkynyloxetane (Paterno–Büchi reaction) and by [3 + 1] cycloaddition to the alkene; for the latter reaction, a carbene intermediate has been proposed[151]. The first-mentioned reaction is attributed to an excited singlet state of the alkynone and the carbene route to a triplet state[152]. In this context, irradiation of a mixture of (silyl)alkynone **269** and

2,3-dimethylbut-2-ene in benzene (equation 92) furnished a 4-oxaspiro[2,4]heptane **272** (53%), which underwent thermal isomerization to dihydrofuran **273** rather easily, and the expected oxetane (12%)[153]. It was proposed that the photochemical [3 + 2] cycloaddition of **269** to the alkene generates silylcarbene **270**, which isomerizes to **272** via diradical **271** that arises from the triplet state of the carbene by intramolecular hydrogen abstraction. The $SiMe_3$ group has a decisive influence on the further fate of carbene **270,** since the analogous *tert*-butyl-(vinyl)carbene (**270**, *t*-Bu instead of $SiMe_3$) reacts in a different way; the difference may lie in the different spin states (triplet vs singlet) of the reacting carbenes.

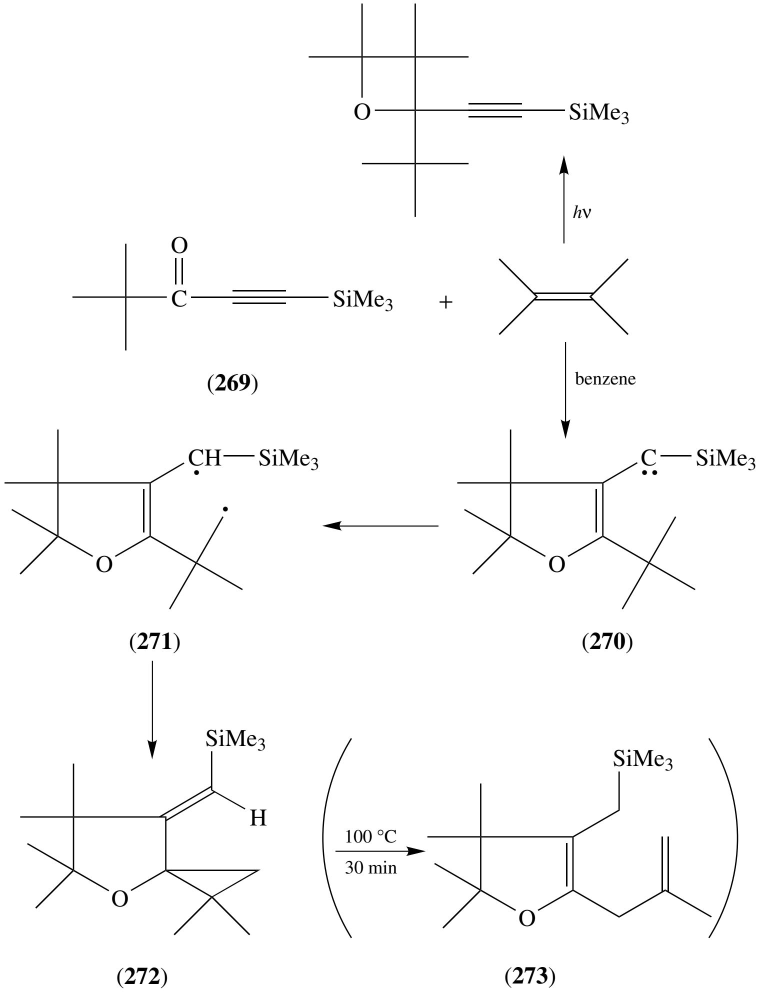

(92)

b. Insertion of carbon into a Si–H bond. When trimethylsilane and carbon vapor, generated by means of a 16-V electrical arc between graphite electrodes, were codeposited on a surface cooled at 77 K, tetramethylsilane and bis(trimethylsilyl)methane were formed in very low yield together with some other silicon-containing products (equation 93)[154]. It is assumed that the two products mentioned come from (trimethylsilyl)carbene by a twofold H abstraction and by insertion into a Si−H bond of another molecule of Me_3SiH, respectively. By analogy to the generation of alkylcarbenes by insertion of a carbon atom into a C−H bond[155], it is assumed that carbon insertion into the Si−H bond of trimethylsilane yields (trimethylsilyl)carbene.

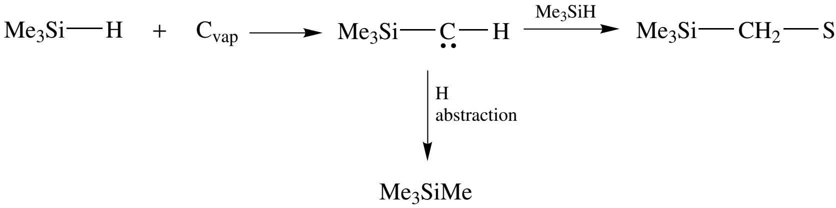

(93)

IV. CONCLUDING REMARKS

This review has shown that a silyl group attached to a carbene center is not simply an innocent bystander. In one way or the other, it is in most cases involved in the further transformation of the carbene. For example, it may influence the electronic properties of a carbene by stabilizing the triplet state. In Bertrand's phosphino(trimethylsilyl)carbenes, the fact that these compounds can be isolated at room temperature is due in part to the $SiMe_3$ group that seems to stabilize the bond structure of a phosphavinyl ylide by delocalization of a negative charge at the carbon atom. In other silylcarbenes, a substituent or a functional group at the silicon takes part in typical intramolecular carbene reactions; these reaction modes allow the synthesis of a great variety of organosilicon compounds that are often not easily available otherwise, such as silaethenes and silaheterocycles. Finally, in a silylcarbene bearing a different second substituent, the carbene transformation may be determined by the second substituent, but the presence of a bulky silyl group may still exert a more or less pronounced steric effect on product formation. With these principles in mind, silylcarbene pathways should be considered also in future syntheses of organosilicon compounds of new structural type or substitution pattern.

It was mentioned in the Introduction that among the whole class of silicon-substituted carbenes, only those bearing a silyl group (R_3Si) are known experimentally. Substituents containing Si with other coordination numbers [e.g. $R_2C{=}Si(R)$ and R_2Si^+] are, of course, unusual since silenes and even more silicenium ions are high-energy compounds themselves, and their combination in a corresponding carbene seems rather esoteric. Nevertheless, theoretical calculations on such species already exist (see Section II) and may stimulate the experimental quest.

V. ACKNOWLEDGMENTS

Our own work on silylcarbenes has been supported by the Deutsche Forschungsgemeinschaft and the Volkswagen-Stiftung.

VI. REFERENCES

1. W. Kirmse, *Carbene Chemistry*, 2nd ed., Academic Press, New York, 1971.
2. M. Jones, Jr. and R. A. Moss, *Carbenes*, Vol. I, Wiley, New York, 1973.
3. H. Tomioka, in *Methoden der organischen Chemie (Houben-Weyl)*, Vol. E19b (Ed. M. Regitz), Thieme Verlag, Stuttgart, 1989, pp. 1410–1459.
4. D. Mayer and G. Maas, in *Methoden der organischen Chemie (Houben-Weyl)*, Vol. E17a (Ed. A. de Meijere), Thieme Verlag, Stuttgart, 1997, pp. 811–842.

5. T. Shioiri and T. Aoyama, in *Advances in the Use of Synthons in Organic Chemistry*, Vol. 1 (Ed. A. Dondoni), JAI Press, London, 1993, pp. 51–101; T. Shioiri and T. Aoyama, *J. Synth. Org. Chem. Jpn.*, **44**, 149 (1986).
6. R. Anderson and S. B. Anderson, in *Advances in Silicon Chemistry*, Vol. 1 (Ed. G. L. Larson). JAI Press, London, 1991, pp. 303–325.
7. W. Sander, G. Bucher and S. Wierlacher, *Chem. Rev.*, **93**, 1583 (1993).
8. H. Shimizu and M. S. Gordon, *Organometallics*, **13**, 186 (1994).
9. A. R. W. McKellar, P. R. Bunker, T. J. Sears, K. M. Evenson, R. J. Saykally and S. R. Langhoff, *J. Chem. Phys.*, **79**, 5251 (1983).
10. D. G. Leopold, K. K. Murray and W. C. Lineberger, *J. Chem. Phys.*, **81**, 1048 (1984); D. G. Leopold, K. K. Murray, A. E. S. Miller and W. C. Lineberger, *J. Chem. Phys.*, **83**, 4849 (1985).
11. E. A. Carter and W. A. Goddard III, *J. Chem. Phys.*, **88**, 1752 (1988).
12. B. T. Luke, J. A. Pople, M.-B. Krogh-Jespersen, Y. Apeloig, M. Karni, J. Chandrasekhar and P.v.R. Schleyer, *J. Am. Chem. Soc.*, **108**, 270 (1986).
13. H. J. Köhler and H. Lischka, *J. Am. Chem. Soc.*, **104**, 4085 (1982).
14. J. D. Goddard, Y. Yoshioka and H. F. Schaefer III, *J. Am. Chem. Soc.*, **103**, 7366 (1981).
15. M. S. Gordon and R. D. Koob, *J. Am. Chem. Soc.*, **103**, 2939 (1981).
16. M. S. Gordon, L. A. Pederson, R. Bakhtiar and D. B. Jacobson, *J. Phys. Chem.*, **99**, 148 (1995).
17. S. Tobita, K. Nakajima, S. Tajima and A. Shigihara, *Rapid Commun. Mass Spectrom.*, **4**, 472 (1990).
18. Y. Apeloig and K. Albrecht, personal communication, 1994.
19. R. Nojori, M. Yamakawa and W. Ando, *Bull. Chem. Soc. Jpn.*, **51**, 811 (1978).
20. O. L. Chapman, C.-C. Chang, J. Kolc, M. E. Jung, J. A. Lowe, T. J. Barton and M. L. Tumey, *J. Am. Chem. Soc.*, **98**, 7844 (1976).
21. M. R. Chedekel, M. Skoglund, R. L. Kreeger and H. Shechter, *J. Am. Chem. Soc.*, **98**, 7846 (1976).
22. M. Trommer, W. Sander and A. Paryk, *J. Am. Chem. Soc.*, **115**, 11775 (1993).
23. M. Trommer and W. Sander, *Organometallics*, **15**, 736 (1996).
24. G. Bertrand and R. Reed, *Coord. Chem. Rev.*, **137**, 323 (1994).
25. (a) M. T. Nguyen, M. A. McGinn and A. F. Hegarty, *Inorg. Chem.*, **25**, 2185 (1986),
    (b) M. R. Hoffmann and K. Kuhler, *J. Chem. Phys.*, **94**, 8029 (1991).
26. D. A. Dixon, K. D. Dobbs, A. J. Arduengo III and G. Bertrand, *J. Am. Chem. Soc.*, **113**, 8782 (1991).
27. M. Regitz (Ed.), *Methoden der organischen Chemie (Houben-Weyl)*, Vol. E19b: *Carbene(oide), Carbine*, Thieme Verlag, Stuttgart 1989.
28. (a) M. P. Doyle, *Chem. Rev.*, **86**, 919 (1986).
    (b) G. Maas, *Top. Curr. Chem.*, **137**, 75 (1987).
29. A. Sekiguchi and W. Ando, *Organometallics*, **6**, 1857 (1987).
30. A. Sekiguchi and W. Ando, *Chem. Lett.*, 871 (1983).
31. A. Sekiguchi and W. Ando, *Chem. Lett.*, 2025 (1986).
32. K. Schneider, B. Daucher, A. Fronda and G. Maas, *Chem. Ber.*, **123**, 589 (1990).
33. W. Ando, A. Sekiguchi, T. Hagiwara, T. Migita, V. Chowdhry, F. H. Westheimer, S. L. Kammula, M. Green and M. Jones Jr., *J. Am. Chem. Soc.*, **101**, 6393 (1979).
34. W. Ando, A. Sekiguchi and T. Migita, *Chem. Lett.*, 779 (1976).
35. Recent review on silenes: G. Raabe and J. Michl, in *The Chemistry of Organic Silicon Compounds* (Eds. S. Patai and Z. Rappoport), Chap. 17, Wiley, Chichester, 1989, pp. 1015–1142; A. G. Brook and K. M. Baines, *Adv. Organomet. Chem.*, **25**, 1 (1986).
36. (a) A. Sekiguchi and W. Ando, *Tetrahedron Lett.*, **26**, 2337 (1985).
    (b) A. Sekiguchi, T. Sato and W. Ando, *Organometallics*, **6**, 2337 (1987).
37. L. E. Gusel'nikov and N. S. Nametkin, *Chem. Rev.*, **79**, 529 (1979).
38. R. L. Kreeger and H. Shechter, *Tetrahedron Lett.*, 2061 (1975).
39. W. Ando, A. Sekiguchi, J. Ogiwara and T. Migita, *J. Chem. Soc., Chem. Commun.*, 145 (1975).
40. W. Ando, A. Sekiguchi, A. J. Rothschild, R. R. Gallucci, M. Jones Jr., T. J. Barton and J. A. Kilgour, *J. Am. Chem. Soc.*, **99**, 6995 (1977).
41. T. J. Barton and S. K. Hoekman, *J. Am. Chem. Soc.*, **102**, 1584 (1980).
42. A. Sekiguchi and W. Ando, *J. Am. Chem. Soc.*, **106**, 1486 (1984).
43. G. Maas, K. Schneider and W. Ando, *J. Chem. Soc., Chem. Commun.*, 72 (1988).

44. G. Maas, M. Alt, K. Schneider and A. Fronda, *Chem. Ber.*, **124**, 1295 (1991).
45. W. Ando, A. Sekiguchi and T. Sato, *J. Am. Chem. Soc.*, **103**, 5573 (1981).
46. W. Ando, A. Sekiguchi and T. Sato, *J. Am. Chem. Soc.*, **104**, 6830 (1982).
47. T. J. Barton and G. P. Hussmann, *Organometallics*, **2**, 692 (1983).
48. W. Ando, H. Tanikawa and A. Sekiguchi, *Tetrahedron Lett.*, **24**, 4245 (1983).
49. A. Sekiguchi, H. Tanikawa and W. Ando, *Organometallics*, **4**, 584 (1985).
50. A. Sekiguchi and W. Ando, *J. Am. Chem. Soc.*, **103**, 3579 (1981).
51. G. Märkl, W. Schlosser and W. S. Sheldrick, *Tetrahedron Lett.*, **29**, 467 (1988).
52. G. Märkl and W. Schlosser, *Angew. Chem.*, **100**, 1009 (1988); *Angew. Chem., Int. Ed. Engl.*, **27**, 963 (1988).
53. P. S. Skell and E. J. Goldstein, *J. Am. Chem. Soc.*, **86**, 1442 (1964).
54. M.-H. Yeh, L. Linder, D. K. Hoffman and T. J. Barton, *J. Am. Chem. Soc.*, **108**, 7849 (1986).
55. J. W. Connolly and G. Urry, *J. Org. Chem.*, **29**, 619 (1964).
56. J. W. Connolly, *J. Organomet. Chem.*, **11**, 429 (1968).
57. D. Seyferth and D. C. Annarelli, *J. Am. Chem. Soc.*, **97**, 7162 (1975).
58. G. Maas and S. Bender, *J. Chem. Soc., Chem. Commun.*, 437 (2000).
59. J. W. Connolly and P. F. Fryer, *J. Organomet. Chem.*, **30**, 315 (1971).
60. T. Werle, Diploma Thesis, University of Kaiserslautern, 1991.
61. B. Daucher, Dissertation, University of Kaiserslautern, 1996.
62. G. Maas, F. Krebs, T. Werle, V. Gettwert and R. Striegler, *Eur. J. Org. Chem.*, 1939 (1999).
63. V. Gettwert, F. Krebs and G. Maas, *Eur. J. Org. Chem.*, 1213 (1999).
64. A. Padwa and M. D. Weingarten, *Chem. Rev.*, **96**, 223 (1996).
65. M. Trommer, W. Sander and C. Marquard, *Angew. Chem.*, **103**, 816 (1994); *Angew. Chem., Int. Ed. Engl.*, **33**, 766 (1994).
66. A. Fronda and G. Maas, *Angew. Chem.*, **101**, 1750 (1992); *Angew. Chem., Int. Ed. Engl.*, **28**, 1663 (1992).
67. A. Fronda, F. Krebs, B. Daucher, T. Werle and G. Maas, *J. Organomet. Chem.*, **424**, 253 (1992).
68. G. Maas and A. Fronda, *J. Organomet. Chem.*, **398**, 229 (1990).
69. W. Ando, M. Sugiyama, T. Suzuki, C. Kato, Y. Arakawa and Y. Kabe, *J. Organomet. Chem.*, **499**, 99 (1995).
70. W. Ando, H. Yoshida, K. Kurishima and M. Sugiyama, *J. Am. Chem. Soc.*, **113**, 7790 (1991).
71. W. Ando, *Bull. Chem. Soc. Jpn.*, **69**, 1 (1996).
72. A. Fronda, Dissertation, University of Kaiserslautern, 1991.
73. R. A. Olofson, D. H. Hoskin and K. D. Lotts, *Tetrahedron Lett.*, 1677 (1978).
74. R. G. Daniels and L. A. Paquette, *J. Org. Chem.*, **46**, 2901 (1981).
75. D. Seyferth and E. M. Hanson, *J. Organomet. Chem.*, **27**, 19 (1971).
76. E. Schaumann, C. Friese and S. Spanka, *Synthesis*, 1035 (1986).
77. P. J. Garratt and A. Tsotinis, *J. Org. Chem.*, **55**, 84 (1990).
78. R. N. Haszeldine, D. L. Scott and A. E. Tipping, *J. Chem. Soc., Perkin Trans. 1*, 1440 (1974).
79. D. Seyferth, A. W. Dow, H. Menzel and T. C. Flood, *J. Am. Chem. Soc.*, **90**, 1080 (1968).
80. D. Seyferth, H. Menzel, A. W. Dow and T. C. Flood, *J. Organomet. Chem.*, **44**, 279 (1972).
81. A. J. Ashe III, *J. Am. Chem. Soc.*, **95**, 818 (1973).
82. T. Aoyama, Y. Iwamoto, S. Nishigaki and T. Shioiri, *Chem. Pharm. Bull.*, **37**, 253 (1989).
83. S.-B. Park, H. Nishiyama, Y. Itoh and K. Itoh, *J. Chem. Soc., Chem. Commun.*, 1315 (1994).
84. A. G. Brook and P. F. Jones, *Can. J. Chem.*, **49**, 1841 (1971).
85. A. Sekiguchi and W. Ando, *Tetrahedron Lett.*, 4077 (1979).
86. A. Sekiguchi and W. Ando, *J. Org. Chem.*, **45**, 5286 (1980).
87. T. Aoyama and T. Shioiri, *Tetrahedron Lett.*, **29**, 6295 (1988).
88. T. Aoyama and T. Shioiri, *Chem. Pharm. Bull.*, **37**, 2261 (1989).
89. A. Padwa, M. W. Wannamaker and A. D. Dyszlewski, *J. Org. Chem.*, **52**, 4760 (1987).
90. (a) H. Tokuyama, T. Yamada and E. Nakamura, *Synlett*, 589 (1993).
    (b) Y. Apeloig, T. Müller, A. de Meijere and T. Faber, unpublished results.
91. M. S. Baird, S. R. Buxton and M. Mitra, *Tetrahedron Lett.*, **23**, 2701 (1982).
92. M. S. Baird and H. H. Hussain, *Tetrahedron*, **43**, 215 (1987).
93. G. Maier and D. Born, *Angew. Chem.*, **101**, 1085 (1989); *Angew. Chem., Int. Ed. Engl.*, **28**, 1050 (1989).
94. G. Maier D. Born, I. Bauer, R. Wolf, R. Boese and D. Cremer, *Chem. Ber.*, **127**, 173 (1994).
95. G. Maier, R. Wolf, H.-O. Kalinowski and R. Boese, *Chem. Ber.*, **127**, 191 (1994).

96. M. Regitz and P. Eisenbarth, *Angew. Chem.*, **94**, 935 (1982); *Angew. Chem., Int. Ed. Engl.*, **21**, 913 (1982).
97. B. Coleman, N. D. Conrad, M. W. Baum and M. Jones Jr., *J. Am. Chem. Soc.*, **101**, 7743 (1979).
98. W. Ando, A. Sekiguchi, T. Hagiwara and T. Migita. *J. Chem. Soc., Chem. Commun.*, 372 (1974).
99. H. G. Köser, G. E. Renzoni and W. T. Borden, *J. Am. Chem. Soc.*, **105**, 6359 (1983).
100. H. Meier and K.-P. Zeller, *Angew. Chem.*, **87**, 52 (1975); *Angew. Chem., Int. Ed. Engl.*, **14**, 32 (1975).
101. W. Ando, in *The Chemistry of Diazonium and Diazo Groups* (Ed. S. Patai), Part 1, Wiley, Chichester, 1978, p. 458.
102. M. Torres, J. Ribo, A. Clement and O. P. Strausz, *Can. J. Chem.*, **61**, 996 (1983).
103. R. Brückmann, K. Schneider and G. Maas, *Tetrahedron*, **45**, 5517 (1989).
104. G. Maas and R. Brückmann, *J. Org. Chem.*, **50**, 2801 (1985).
105. R. Brückmann and G. Maas, *Chem. Ber.*, **120**, 635 (1987).
106. R. Brückmann and G. Maas, *J. Chem. Soc., Chem. Commun.*, 1782 (1986).
107. R. Munschauer and G. Maas, *Angew. Chem.*, **103**, 312 (1991); *Angew. Chem., Int. Ed. Engl.*, **30**, 306 (1991).
108. R. Munschauer and G. Maas, *Chem. Ber.*, **125**, 1227 (1992).
109. B. Manz and G. Maas, *Tetrahedron*, **52**, 10053 (1996).
110. O. A. Kruglaya, I. B. Fedot'eva, B. V. Fedot'ev, I. D. Kalikhman, E. I. Brodskaya and N. S. Vyazankin, *J. Organomet. Chem.*, **142**, 155 (1977).
111. U. Schöllkopf and N. Rieber, *Angew. Chem.*, **79**, 906 (1967); *Angew. Chem., Int. Ed. Engl.*, **6**, 884 (1967).
112. U. Schöllkopf, D. Hoppe, N. Rieber and V. Jacobi, *Justus Liebigs Ann. Chem.*, **730**, 1 (1969).
113. W. Ando, T. Hagiwara and T. Migita, *J. Am. Chem. Soc.*, **95**, 7518 (1973).
114. G. Maas, M. Gimmy and M. Alt, *Organometallics*, **11**, 3813 (1992).
115. W. Ando, A. Sekiguchi, T. Migita, S. Kammula, M. Green, and M. Jones Jr., *J. Am. Chem. Soc.*, **97**, 3818 (1975).
116. W. Ando, T. Hagiwara and T. Migita, *Tetrahedron Lett.*, 1425 (1974).
117. M. Alt, Dissertation, University of Kaiserslautern, 1993.
118. G. Maas, T. Werle, M. Alt and D. Mayer, *Tetrahedron*, **49**, 881 (1993).
119. G. Maier, D. Volz and J. Neudert, *Synthesis*, 561 (1992).
120. M. Alt and G. Maas, *Tetrahedron*, **50**, 7435 (1994).
121. H. C. Lottes, J. A. Landgrebe and K. Larsen, *Tetrahedron Lett.*, **30**, 4089 and 4093 (1989).
122. M. Alt and G. Maas, *Chem. Ber.*, **127**, 1537 (1994).
123. R. D. Connell, M. Tebbe, A. R. Gangloff, P. Helquist and B. Åkermark, *Tetrahedron*, **49**, 5445 (1993) and references cited therein.
124. H. Tomioka, H. Kitagawa and Y. Izawa, *J. Org. Chem.*, **44**, 3072 (1979).
125. H. Tomioka, M. Kondo and Y. Izawa, *J. Org. Chem.*, **46**, 1090 (1981).
126. G. Mitchell and C. W. Rees, *J. Chem. Soc., Perkin Trans. 1*, 413 (1987).
127. A. Igau, H. Grützmacher, A. Baceiredo and G. Bertrand, *J. Am. Chem. Soc.*, **110**, 6463 (1988).
128. G. R. Gillette, A. Baceiredo and G. Bertrand, *Angew. Chem.*, **102**, 1486 (1990); *Angew. Chem., Int. Ed. Engl.*, **29**, 1429 (1990).
129. G. R. Gillette, A. Igau, A. Baceiredo and G. Bertrand, *New. J. Chem.*, **15**, 393 (1991).
130. G. Alcaraz, R. Reed, A. Baceiredo and G. Bertrand, *J. Chem. Soc., Chem. Commun.*, 1354 (1993).
131. M. Soleilhavoup, A. Baceiredo, O. Treutler, R. Ahlrichs, M. Nieger and G. Bertrand, *J. Am. Chem. Soc.*, **114**, 10959 (1992).
132. N. Emig, J. Tejeda, R. Réau and G. Bertrand, *Tetrahedron Lett.*, **36**, 4231 (1995).
133. (a) A. Arduengo, H. V. R. Dias, R. L. Harlon and M. Kline, *J. Am. Chem. Soc.*, **114**, 5530 (1992); A. D. Dixon and A. D. Arduengo, *J. Phys. Chem.*, **95**, 4180 (1991).
    (b) For a short résumé of recent developments with 'stable carbenes'. see M. Regitz, *Angew. Chem.*, **103**, 691 (1991); *Angew. Chem., Int. Ed. Engl.*, **30**, 674 (1991).
134. (a) G. Bertrand, *Heteroatom Chem.*, **2**, 29 (1991).
    (b) G. Bertrand, in *Multiple Bonds and Low Coordination in Phosphorus Chemistry* (Eds. M. Regitz and O. J. Scherer), Thieme Verlag, Stuttgart, 1990, pp. 443–461.
135. A. Igau, A. Baceiredo, G. Trinquier and G. Bertrand, *Angew. Chem.*, **101**, 617 (1989); *Angew. Chem., Int. Ed. Engl.*, **28**, 621 (1989).
136. G. Alcaraz, U. Wecker, A. Baceiredo, F. Dahan and G. Bertrand, *Angew. Chem.*, **107**, 1358 (1995); *Angew. Chem., Int. Ed. Engl.*, **34**, 1246 (1995).

137. R. Armbrust, M. Sanchez, R. Réau, U. Bergsträsser, M. Regitz and G. Bertrand, *J. Am. Chem. Soc.*, **117**, 10785 (1995).
138. H. Keller, Dissertation, University of Kaiserslautern, 1986.
139. H. Keller and M. Regitz, *Tetrahedron Lett.*, **29**, 925 (1988).
140. H. Heydt, M. Regitz and G. Bertrand, in *Methoden der organischen Chemie (Houben-Weyl)*, Vol. E19b (Ed. M. Regitz), Thieme Verlag, Stuttgart, 1989, pp. 1822–1900.
141. G. Maas, K. Schneider and S. Mayer, unpublished work.
142. E. Schaumann and C. Friese, *Tetrahedron Lett.*, **30**, 7033 (1989).
143. C. Friese, in *Methoden der organischen Chemie (Houben-Weyl)*, Vol. E17a (Ed. A. de Meijere), Thieme Verlag, Stuttgart, 1997, pp. 835–842.
144. D. Seyferth and E. M. Hanson, *J. Am. Chem. Soc.*, **90**, 2438 (1968).
145. T. J. Barton and G. P. Hussmann, *J. Am. Chem. Soc.*, **105**, 6316 (1983).
146. T. J. Barton and B. L. Groh, *J. Am. Chem. Soc.*, **107**, 8297 (1985).
147. T. J. Barton and B. L. Groh, *J. Am. Chem. Soc.*, **107**, 7221 (1985).
148. T. J. Barton and G. C. Paul, *J. Am. Chem. Soc.*, **109**, 5293 (1987).
149. T. J. Barton, J. Lin, S. Ijadi-Maghsoodi, M. D. Power, X. Zhang, Z. Ma, H. Shimizu and M. S. Gordon, *J. Am. Chem. Soc.*, **117**, 11695 (1995).
150. J. J. Eisch and J. E. Galle, *J. Organomet. Chem.*, **341**, 293 (1988).
151. S. Hussain and W. C. Agosta, *Tetrahedron*, **37**, 3301 (1981).
152. S. Saba, S. Wolff, C. Schröder, P. Margaretha and W. C. Agosta, *J. Am. Chem. Soc.*, **105**, 6902 (1983).
153. S. Wolff and W. C. Agosta, *J. Am. Chem. Soc.*, **106**, 2363 (1984).
154. P. S. Skell and P. W. Owen, *J. Am. Chem. Soc.*, **94**, 1578 (1972).
155. P. S. Skell and R. R. Engel, *J. Am. Chem. Soc.*, **87**, 4663 (1965); *J. Am. Chem. Soc.*, **88**, 4883 (1966).

CHAPTER 14

Alkaline and alkaline earth silyl compounds — preparation and structure

JOHANNES BELZNER and UWE DEHNERT

Institut für Organische Chemie der Georg-August-Universität Göttingen, Tammannstr. 2, D-37077 Göttingen, Germany

---

I. ABBREVIATIONS

DME	1,2-dimethoxyethane	Mes	2,4,6-trimethylphenyl
DMI	1,3-dimethylimidazolidine	PMDTA	pentamethyldiethylenetriamine
DMPU	*N*,*N*′-dimethylpropyleneurea	TBAF	tetrabutylammonium fluoride
HMPA	hexamethylphosphortriamide	THF	tetrahydrofuran
Tip	2,4,6-tris(*i*-propyl)phenyl	TMDAP	1,3-bis(dimethylamino) propane
LDMAN	lithium 1-(dimethylamino) naphthalenide	TMEDA	*N*,*N*,*N*′,*N*′-tetramethylethylenediamine

II. INTRODUCTION

This chapter will concentrate mainly on the chemistry of silyllithium compounds, i.e. neutral tetravalent silyl compounds bearing one or more lithium substituents at silicon. In addition, the chemistry of other organosilicon compounds containing alkaline and alkaline earth metals will be outlined in this chapter.

The chemistry of metalated organosilicon compounds has been the subject of several reviews[1], the most recent ones by Lickiss and Smith[1a] and Tamao and Kawachi[1b], which cover the literature up to the year 1994. This chapter will now take into account the developments in the chemistry of metalated silanes up to the middle of 1996; however, for completeness there will be some overlap with former reviews. The emphasis of this review is on the synthesis and structure of these metalated silanes. However, some examples of their utilization for synthetic purposes will also be given where appropriate. For more information about synthetic applications of silyl anions the reader is referred to some leading references in this field[1a,b,h–k].

Another point which needs to be clarified from the start is the nomenclature of metalated silanes: We will frequently use the term ‘silyl anion’ in this chapter when we talk about metalated silanes. Although the term ‘anion’ defines, literally taken, an ionic compound, this expression, when used by us, does not necessarily imply that the compound in question is of ionic nature, but covers, as well, in analogy to the use of the term ‘carbanion’, silicon compounds with a polarized covalent silicon–metal bond.

In order to organize the material to be presented in this chapter, we use a ranking system of substituents at silicon, which starts with hydrogen as the substituent of lowest priority (Section III) and will proceed through alkyl (Section IV), aryl (Section V) and silyl groups (Section VI) as substituents to functional groups (e.g. amino, hydroxy, Section VII) as the highest-ranked substituents; a compound which bears substituents of different priority will be found in the chapter dealing with the substituents of higher priority. The final section will treat metalated siloles and oligolithiated monosilanes.

III. HYDRIDOSILYL ANIONS

The reaction of SiH_4 with potassium in DME or diglyme yields silylpotassium[2]; silylrubidium and silylcesium are obtained analogously[3]. In contrast, the reaction of sodium with SiH_4 yields a mixture of metalated silanes $NaSiH_n(SiH_3)_{3-n}$ ($n = 1-3$)[4]; depending on the reaction conditions, either $NaSiH_3$[4a] or $NaSi(SiH_3)_3$[2f] is formed as the major product.

$KSiH_3$, $RbSiH_3$ and $CsSiH_3$ form a NaCl-type lattice[2b,3]; $KSiH_3$ is reported to crystallize also in an orthorhombic modification at low temperature[2e]. *Ab initio* calculations at the MP4/6-31G*//3-21G* level predict a molecular tetrahedral structure **1** for $NaSiH_3$[5]. An analogous structure was found for $LiSiH_3$. However, an inverted tetrahedron **2** was calculated at the MP4SDTQ/6-31G**//6-31G* level of theory to be by 2.4 kcal mol^{-1} more stable than **1**, because of more favourable electrostatic interactions[6].

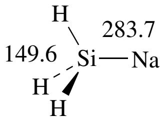

(**1**)

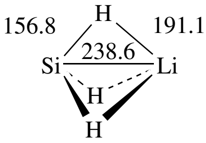

(**2**) bond lengths in pm

Interestingly, this type of inverted geometry around silicon has been found experimentally in a sodium–oxygen cage compound, $[Na_8(O_3C_5H_{11})_6(SiH_3)_2]$, which contains inverted $NaSiH_3$ moieties. A computational reinvestigation, using the complex $[(NaOH)_3NaSiH_3]$ as a model, has shown that in this environment the inverted geometry of $NaSiH_3$ is favored by 1.43 kcal mol^{-1} over the 'normal' tetrahedral structure[7].

IV. ALKYL-SUBSTITUTED SILYL ANIONS

A. Methods of Preparation

Three methods are available for the preparation of peralkylated silyl alkaline and alkaline earth compounds.

(1) Cleavage of the Si–Si bond of a disilane with nucleophiles such as organolithium compounds or alkali metal alkoxides or hydrides (equation 1):

$$R_3Si{-}SiR_3 + MNu \longrightarrow R_3SiM + NuSiR_3 \qquad (1)$$
$$M = Li, Na, K;\ Nu = Me, OMe, H$$

(2) Reaction of sodium or potassium hydride with a hydrogen-bearing silane (equation 2):

$$R_3SiH + MH \longrightarrow [R_3SiH_2]^-M^+ \longrightarrow R_3SiM + H_2 \qquad (2)$$
$$M = Na, K$$

This reaction, which initially was assumed to be a simple deprotonation[8a,b], was shown later by Corriu and coworkers[9] to proceed via a two-step mechanism. The initial step is the reversible formation of a pentacoordinated species, which decomposes irreversibly under formation of molecular hydrogen and the metalated silane.

(3) Transmetalation of silylmercury compounds with lithium (equation 3):

$$R_3SiCl \xrightarrow{Na/Hg} (R_3Si)_2Hg \xrightarrow{Li} 2R_3SiLi + Hg \qquad (3)$$

The silylmercury compounds are most conveniently available by reacting a chlorosilane with sodium amalgam. In contrast to the two methods mentioned above, which in most cases require polar, aprotic solvents such as THF, DME or HMPA, transmetalation reactions can be performed in nonpolar solvents and often result in better yields than when performed in ethereal solvents.

Two types of reaction allow the synthesis of silylmagnesium compounds:

(1) Transmetalation of a lithiated silane or of a silylcobalt compound by reaction with a magnesium halide or a Grignard reagent yields the corresponding silyl Grignard compound (equation 4). Silylmagnesium compounds can be also obtained from silylmercury compounds, which undergo metal–metal exchange with magnesium (equation 5).

$$R_3SiM \xrightarrow[\text{or RMgHal}]{\text{MgHal}_2} R_3SiMgHal \tag{4}$$

$$M = Li, Co(CO)_4$$

$$(R_3Si)_2Hg \xrightarrow{\text{Mg}} (R_3Si)_2Mg + Hg \tag{5}$$

(2) Silyl Grignard compounds can be obtained from highly reactive magnesium (given as Mg*) and halosilanes (equation 6).

$$R_3SiHal \xrightarrow{\text{Mg}^*} R_3SiMgHal \tag{6}$$

The most effective way to obtain Me_3SiLi on a preparative scale is the reaction of $Me_3Si{-}SiMe_3$ with MeLi in Et_2O with HMPA as cosolvent (equation 7)[10]. The driving force for this conversion is the formation of a Si–C bond, which is stronger than the Si–Si bond of the starting material[10b]. However, the formation of Me_3SiMe_2SiLi as a co-product in this reaction (up to 58%, depending on the reaction conditions[11d]) sometimes limits its usefulness[11] (see Section VI.B.1.) Alternatively, Me_3SiLi may be obtained by the reaction of $(Me_3Si)_2Hg$ with lithium metal[12]. Based on variable-temperature NMR studies, $LiHg(SiMe_3)_3$ and $Li_2Hg(SiMe_3)_4$ were postulated as intermediates in this reaction[12].

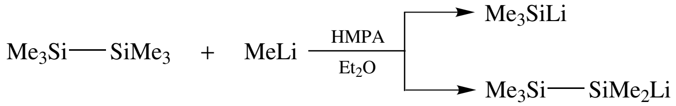

(7)

MeSiNa and Me_3SiK have been prepared by nucleophilic cleavage of $Me_3Si{-}SiMe_3$ using different nucleophile/solvent systems such as NaOMe/HMPA[13a], NaOMe/DMI[13b], KOMe/18-crown-6/benzene[13b], KOMe/18-crown-6/THF[13b], KOBu-*t*/THF[13c] and KOBu-*t*/DMPU[13c] (equation 8). These reactions are exergonic due to the formation of the strong Si–O bond.

$$Me_3Si{-}SiMe_3 + MOMe \longrightarrow Me_3SiM + Me_3SiOMe \tag{8}$$

$$M = Na, K$$

The metal hydrides NaH and KH have also been used to cleave $Me_3Si{-}SiMe_3$ forming Me_3SiM (M = Na, K) and Me_3SiH (Scheme 1)[8a] These reactions are frequently performed in HMPA. Using THF or benzene as solvent requires the presence of 18-crown-6. The initially formed Me_3SiH is transformed by reaction with excess metal hydride into another equivalent of Me_3SiM[8a,b]. On the whole, the reaction of $Me_3Si{-}SiMe_3$ with two equivalents of NaH or KH converts both silyl groups into the corresponding metalated silanes and thus is, in so far as the yield is concerned, often superior to the cleavage of disilanes with other nucleophiles.

When equivalent amounts of $Me_3Si{-}SiMe_3$ and tetrabutylammonium fluoride (TBAF) are dissolved in HMPA, an equilibrium between the starting material, a pentacoordinated

$$\begin{array}{lcl}
\mathrm{Me_3Si{-}SiMe_3} + \mathrm{MH} & \longrightarrow & \mathrm{Me_3SiM} + \mathrm{Me_3SiH} \\
\mathrm{Me_3SiH} + \mathrm{MH} & \longrightarrow & \mathrm{Me_3SiM} + \mathrm{H_2} \\
\hline
\mathrm{Me_3Si{-}SiMe_3} + 2\,\mathrm{MH} & \longrightarrow & 2\,\mathrm{Me_3SiM} + \mathrm{H_2}
\end{array}$$

$\mathrm{M = Na, K}$

SCHEME 1

species and a silyl anion with Bu_4N^+ as countercation is established according to ^1H NMR studies (equation 9)[14]. This mixture was used by Hiyama and coworkers to transfer the trimethylsilyl group to aldehydes[14], 1,3-dienes[14], and 3,3,3-trifluoropropenes[15].

$$\begin{tikzcd}
\mathrm{Me_3Si{-}SiMe_3} + \mathrm{TBAF} \arrow[r, shift left, ""] & \arrow[l, shift left] {[\mathrm{Me_3Si{-}SiMe_3F}]^-\mathrm{Bu_4N^+}} \arrow[d, shift left] \\
 & {[\mathrm{Me_3Si}]^-\mathrm{Bu_4N^+}} + \mathrm{Me_3SiF} \arrow[u, shift left]
\end{tikzcd} \tag{9}$$

Treatment of the trisilane $Me_3SiSiMe_2SiMe_3$ with TBAF in HMPA, however, does not proceed by formation of $SiMe_3{}^-$; instead, the more stable disilanyl anion $Me_3SiMe_2Si^-$ is formed in equilibrium, as was concluded from the products which were obtained when the reaction was performed in the presence of aldehydes[16].

Et_3SiLi is formed along with EtLi, when the mercury compound $EtHgSiEt_3$ is reacted with lithium in benzene (equation 10). However, when this reaction is performed in THF, Et_3SiLi is obtained as sole lithiated compound (equation 11)[17].

$$\mathrm{EtHgSiEt_3} \xrightarrow[\text{benzene}]{\text{Li}} \mathrm{Hg + EtLi + Et_3SiLi} \tag{10}$$

$$2\,\mathrm{EtHgSiEt_3} \xrightarrow[\text{THF}]{\text{Li}} 2\,\mathrm{Hg} + \mathrm{C_2H_4} + \mathrm{C_2H_6} + 2\,\mathrm{Et_3SiLi} \tag{11}$$

In contrast, Et_3SiK cannot be prepared by mercury–potassium exchange. Reaction of $(Et_3Si)_2Hg$ with potassium metal gives Et_3SiPh in 90% yield (equation 12). The reaction of $(Et_3Si)_2Hg$ with sodium proceeds analogously, albeit with a lower yield of Et_3SiPh[18]. It has been speculated that the initially formed, strongly basic Et_3SiM ($M = Na, K$) is protonated by benzene thereby forming PhM and Et_3SiH, which subsequently undergo a coupling reaction to yield eventually Et_3SiPh and the corresponding metal hydride[18].

$$\mathrm{(Et_3Si)_2Hg} + 2\,\mathrm{K} \xrightarrow{\text{benzene}} \mathrm{Hg} + 2\,\mathrm{KH} + 2\,\mathrm{Et_3SiPh} \tag{12}$$

t-Bu_3SiK and *t*-Bu_3SiNa are the only peralkylated silylmetal compounds which can be prepared directly by reaction of the appropriately substituted halosilane with the corresponding metal (equation 13)[19]. The coupling reaction of the formed silyl anion with the starting material to give a disilane, which has been observed when other alkylated halosilanes are treated with alkali metals, does not occur in this case due to the severe steric hindrance at the silicon center.

$$t\text{-}\mathrm{Bu_3SiHal} + 2\,\mathrm{M} \longrightarrow t\text{-}\mathrm{Bu_3SiM} + \mathrm{MHal} \tag{13}$$

$M = Na, K; Hal = Br, I$

A silyl compound with two different alkyl substituents, $(t\text{-Bu})_2\text{MeSiK}$, was prepared by Fürstner and Weidmann in low yield by the cleavage of the Si−Si bond of $(t\text{-Bu})_2\text{MeSi–SiMe}(t\text{-Bu})_2$ with C_8K[20]. This reaction is quite exceptional, as usually the Si−Si bond of peralkylated disilanes is not susceptible to reductive cleavage by alkali metals.

Silylstannanes having at least one bulky substituent can be cleaved with a high-order organocuprate yielding the corresponding silylcuprates (equation 14), which are used *in situ* as silylating agents in organic syntheses[21].

$$\text{RMe}_2\text{Si–SnMe}_3 \xrightarrow[-n\text{-BuSnMe}_3]{+n\text{-Bu}_2\text{Cu(CN)Li}_2} \text{RMe}_2\text{SiBu(Cu)(CN)Li}_2 \qquad (14)$$

$$\text{R} = t\text{-Bu, 1,1,2-trimethylpropyl}$$

Bis(trimethylsilyl)magnesium has been prepared by treatment of $(\text{Me}_3\text{Si})_2\text{Hg}$ with magnesium metal in either THF[22], DME[22] or 1,3-bis(dimethylamino)propane (TMDAP)/Et_2O[23]. When the reaction is carried out in THF, the initial product is $(\text{Me}_3\text{Si})_2\text{Mg•2THF}$, according to its ^1H NMR spectrum, but it readily looses one equivalent of THF to yield $(\text{Me}_3\text{Si})_2\text{Mg•THF}$. The product, which has been obtained in DME as solvent, can be recrystallized from cyclopentane to yield an adduct $(\text{Me}_3\text{Si})_2\text{Mg•DME}$. By treating this ethereal adduct with a 10-fold excess of TMEDA, the $(\text{Me}_3\text{Si})_2\text{Mg•TMEDA}$ complex has been prepared as well (equation 15)[24].

$$\begin{tikzcd}
(\text{Me}_3\text{Si})_2\text{Hg} + \text{Mg} \arrow[r, "\text{DME}"] & \text{Hg} + (\text{Me}_3\text{Si})_2\text{Mg•DME} \arrow[d, "-\text{DME}"', "+\text{TMEDA}"] \\
& (\text{Me}_3\text{Si})_2\text{Mg•TMEDA}
\end{tikzcd} \qquad (15)$$

Silyl Grignard compounds were suggested to be formed in the reaction of silyllithium and silylpotassium compounds with magnesium halides and they were used *in situ* for subsequent reactions[8a,b]. However, an unambiguous characterization of such species or their isolation was missing. The reaction of Me_3SiCl with Riecke magnesium does not lead to Me_3SiMgCl but yields instead the disilane $\text{Me}_3\text{SiSiMe}_3$. The formation of the latter via an initially formed silyl Grignard compound Me_3SiMgCl followed by a subsequent coupling with the starting material seems plausible[8c]. The first unambiguously identified silicon analogues of a Grignard compound were obtained by Ritter and coworkers when trimethylsilyl bromide or trimethylsilyl iodide were treated with highly reactive magnesium metal (synthesized by dehydrogenation of catalytically prepared MgH_2) in the presence of chelating ligands such as TMEDA or pentamethyldiethylenetriamine (PMDTA) (equation 16). In contrast to the classical Grignard synthesis, toluene had to be used as solvent, because ethereal solvents are quantitatively cleaved under the reaction conditions[25].

$$\text{R}_3\text{SiHal} \xrightarrow[\text{L}]{\text{Mg}^*} \text{R}_3\text{SiMgHal•L}$$

$$\text{Hal} = \text{Br, I; L} = \text{Me}_2\text{NCH}_2\text{CH}_2\text{NMe}_2\text{, MeN(CH}_2\text{CH}_2\text{NMe}_2)_2 \qquad (16)$$

B. Structural Studies

Studies of the structure of peralkylated silyl anions in solution by spectroscopic methods such as IR, UV or NMR spectroscopy are exceedingly rare, but some information on their structure in the solid is available.

Trimethylsilyllithium is a hexamer in the crystal (Figure 1)[26]. The Li_6 framework can be described as a six-membered ring, which adopts a 'folded-chair' conformation with an average Li—Li bond length of 270 pm. Alternatively, taking into account the considerably longer 1,3-Li$\cdots$Li distances within the six-membered ring (average: 327 pm), the Li_6 skeleton may be regarded as a strongly distorted octahedron. Above each Li_3 face a μ^3-bridging trimethylsilyl group is located. The silicon centers are hexacoordinated to three carbon substituents and three lithium centers with Si—Li distances averaging 268 pm. The interaction between silicon and lithium may be regarded as a four-center two-electron bonding. However, in view of more recent results concerning the nature of the Si—Li bond in metalated silanes (Section V.B), a predominately ionic character of the Si—Li interaction may be assumed as well.

When solvent-free $(Me_3SiLi)_6$ is recrystallized from TMEDA, the complex $(Me_3SiLi)_2$•3TMEDA is obtained[27]. Here the hexameric structure of $(Me_3SiLi)_6$ is broken down into a dimeric aggregate which is shown in Figure 2. The lithium centers are coordinated by one Me_3Si substituent and one chelating TMEDA ligand; the fourth coordination site is occupied by the dimethylamino group of another TMEDA molecule, the second amino terminus of which is bridging toward the second Me_3SiLi•TMEDA unit of the dimer.

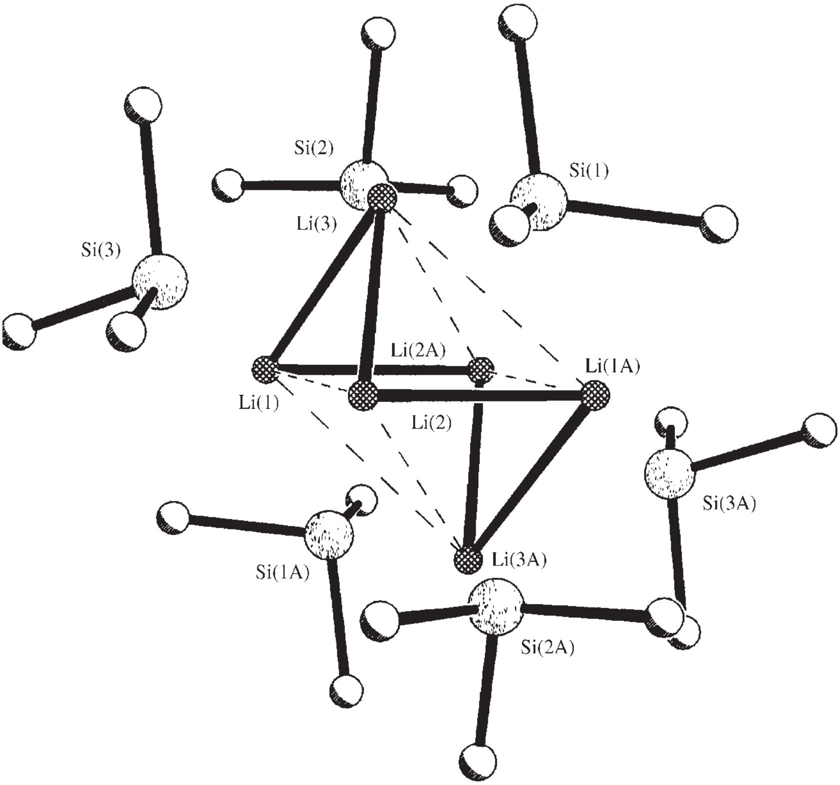

FIGURE 1. Solid state structure of $(SiMe_3Li)_6$ with hydrogen atoms omitted. Reprinted with permission from Reference 26. Copyright 1980 American Chemical Society

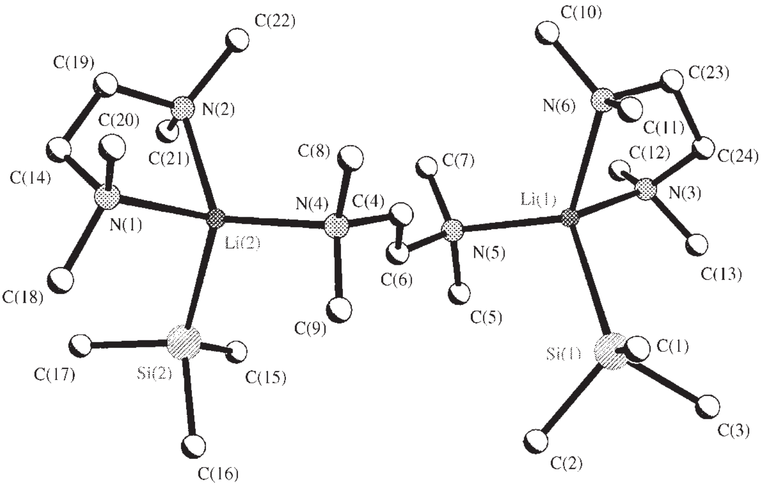

FIGURE 2. Solid state structure of $(Me_3SiLi\bullet TMEDA)_2\bullet TMEDA$ with hydrogen atoms omitted. Reprinted with permission from Reference 27. Copyright 1982 American Chemical Society

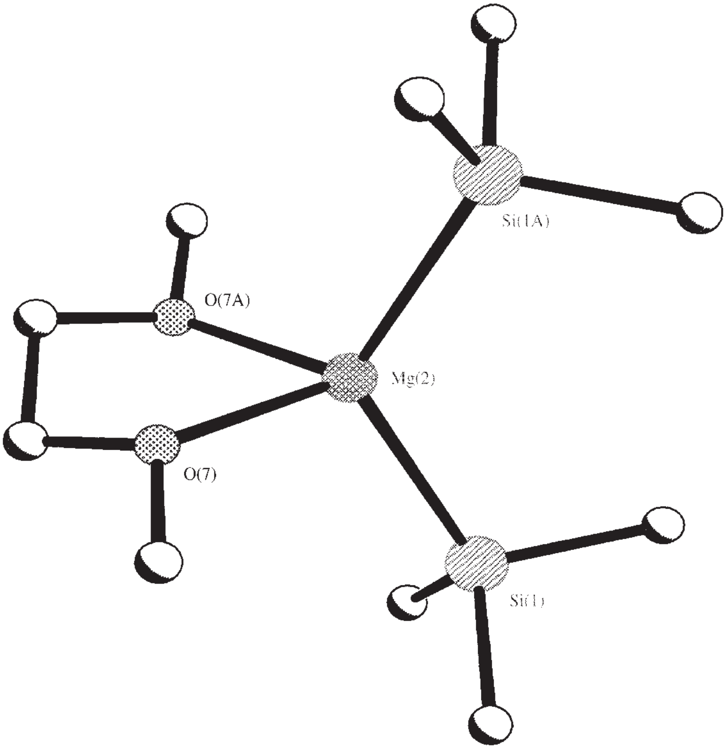

FIGURE 3. Solid state structure of $(Me_3Si)_2Mg\bullet DME$ with hydrogen atoms omitted. Reprinted with permission from Reference 22. Copyright 1977 American Chemical Society

To date, three bis(trimethylsilyl)magnesium compounds have been structurally characterized in the solid state. All of them are monomeric and show quite similar structural characteristics.

The molecular structure of $(Me_3Si)_2Mg{\bullet}DME$ exhibits C_2 symmetry[22] (Figure 3). The magnesium center is located at the twofold axis and is surrounded by two silicon and two oxygen atoms, thus adopting a distorted tetrahedral coordination sphere. The Mg−Si distance of 263.0 pm is about 9% longer than the sum of the covalent radii of both atoms (241 pm). The steric demand of the trimethylsilyl groups is reflected in the Si−Mg−Si angle of 125.2°, which is appreciably enlarged in comparison with the normal tetrahedral value (109.4°). In contrast, the O−Si−O angle is reduced to 76.3° in order to fit the 'bite angle' of DME. In $(Me_3Si)_2Mg{\bullet}TMEDA$, the deviation from tetrahedral geometry is smaller. The Si−Mg−Si and N−Mg−N angles are 115.3° and 82.8°, respectively. These changes may be explained by the larger 'bite angle' of TMEDA as well as repulsive interactions between the methyl groups at nitrogen and silicon[24]. The reduced strain of the chelating six-membered ring in $(Me_3Si)_2Mg{\bullet}TMDAP$ in comparison with the five-membered ring in $(Me_3Si)_2Mg{\bullet}TMEDA$ is reflected in the enlarged N−Mg−N angle of 93.8[23].

In contrast to these monomeric structures, $[Me_3SiMgBr{\bullet}TMEDA]_2$ is reported to form a centrosymmetrical dimer in the solid with two bromine atoms bridging two $Me_3SiMg{\bullet}TMEDA$ subunits (Figure 4)[25]. The two magnesium–bromine distances differ appreciably in length: The short Mg−Br bond length of 253.4 pm falls into the range of monomeric and dimeric Grignard compounds, whereas the $Mg^{*}\cdots Br$ distance of 322.0 pm is longer than the sum of the ionic radii of Mg^{2+} and Br^{-}, indicating that the interaction between the two $Me_3SiMgBr{\bullet}TMEDA$ units is quite weak. Substitution of the bidentate TMEDA ligand by the tridentate PMDTA ligand results in deaggregation,

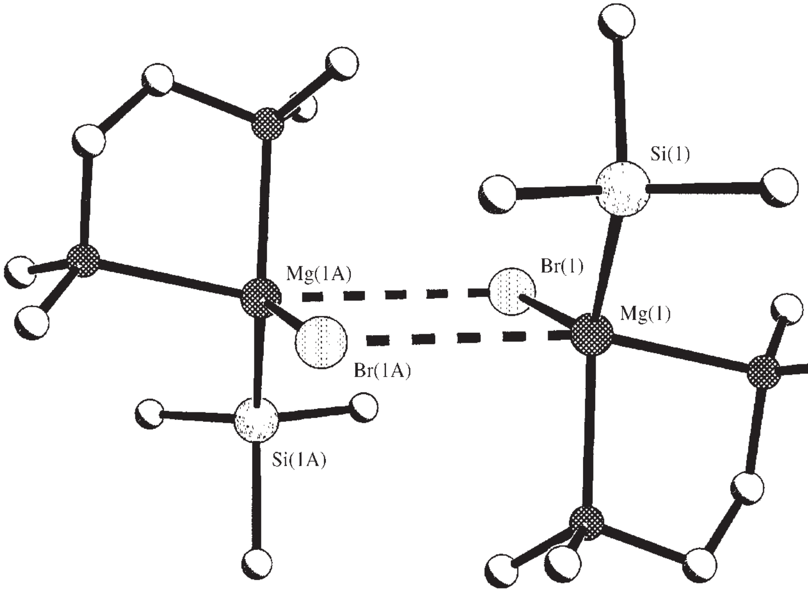

FIGURE 4. Solid state structure of $[Me_3SiMgBr{\bullet}TMEDA]_2$ with hydrogen atoms omitted. Reproduced from Reference 25 by permission of VCH Verlagsgesellschaft, Weinheim

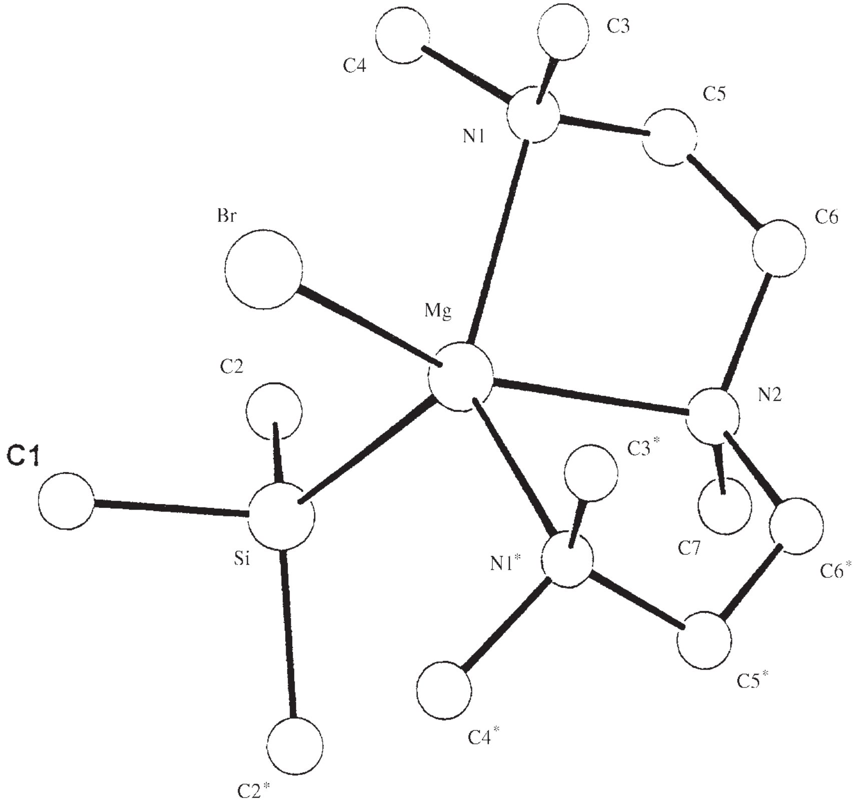

FIGURE 5. Solid state structure of $Me_3SiMgBr{\bullet}PMDTA$ with hydrogen atoms omitted. Reproduced from Reference 25 by permission of VCH Verlagsgesellschaft, Weinheim

and the monomeric, C_S-symmetric $Me_3SiMgBr{\bullet}PMDTA$ is formed (Figure 5), in which magnesium is pentacoordinated to bromine, silicon and three nitrogen centers.

V. ARYL-SUBSTITUTED SILYL ANIONS

A. Preparation

The most convenient method to prepare metalated arylsilanes is the reaction of a chlorosilane with lithium or potassium in polar solvents such as THF or DME (Scheme 2).

The first step of this conversion is assumed to be the formation of the silyl anion, which undergoes a subsequent nucleophilic attack on the starting material[28a]. The resulting disilane may be isolated, when stoichiometric amounts of metal are used. However, in contrast to peralkylated disilanes, disilanes which bear at least one aryl substituent at each silicon are susceptible to further reduction. Accordingly, the Si−Si bond of the fully or partially arylated disilane is easily cleaved under the reaction conditions by slow electron transfer from excess metal, eventually transforming both silyl units of the disilane into the desired metalated silane.

$$\begin{array}{lll}
Ar_3SiCl + 2\,M & \longrightarrow & Ar_3SiM + MCl \\
Ar_3SiM + Ar_3SiCl & \longrightarrow & Ar_3Si{-}SiAr_3 + MCl \\
Ar_3Si{-}SiAr_3 + 2\,M & \longrightarrow & 2\,Ar_3SiM \\
\hline
2\,Ar_3SiCl + 4\,M & \longrightarrow & 2\,Ar_3SiM + 2\,MCl
\end{array}$$

M = Li, Na, K, Rb, Cs

SCHEME 2

A variety of metalated silanes such as Ph_3SiLi[28a], (o-Tol)$_3$SiLi[28a], Ph_3SiNa[28b], Ph_3SiCs[28a], (o-Tol)$_3$SiCs[28a], Ph_3SiRb[28a], Ph_2(t-Bu)SiLi[28c], Ph_2(o-Tol)SiLi[28d] and Ph(o-Tol)$_2$SiLi[28e] has been obtained by this method from the corresponding halosilanes. A superior access to Ph_3SiK, Ph_2MeSiK and $PhMe_2SiK$ is the reaction of the corresponding chlorosilane with C_8K in THF. This method yields the silylpotassium compound in a few minutes and in high yield[20].

A disadvantage is that solutions of silyl anions prepared from the halosilanes by one of these methods inevitably contain metal halides as by-product. Salt-free perarylated silyl anions can be prepared by the reaction of a disilane with lithium, sodium or potassium in polar solvents such as THF or DME (Table 1)[28b,29]. Alternative procedures for the preparation of halide-free Ph_3SiK utilize the reductive cleavage of the Si−C bond of $Ph_3Si{-}CMe_2Ph$ by a sodium−potassium alloy in Et_2O (equation 17)[28f], as well as via the reaction of Ph_3SiH with KH in DME[8a].

$$Ph_3Si{-}CMe_2Ph \xrightarrow[Et_2O]{Na{-}K} Ph_3SiK + PhMe_2CK \tag{17}$$

A mixture of the disilane $Me_3Si{-}SiPh_3$ with TBAF in HMPA has been used by Hiyama and coworkers as a metal-free, synthetic equivalent of the triphenylsilyl anion[15] (equation 18).

$$Me_3Si{-}SiPh_3 + TBAF \rightleftharpoons Me_3SiF + [Bu_4N]^+[SiPh_3]^- \tag{18}$$

An analogous regioselectivity was observed by Buncel and coworkers[13d], when unsymmetrically substituted disilanes such as $Me_3Si{-}SiPh_3$, $Me_3Si{-}SiMePh_2$ or $Me_3Si{-}SiMe_2Ph$ were treated with potassium t-butoxide in THF or DME. The nucleophilic cleavage of the Si−Si bond proceeded in all three cases to yield exclusively the more stable silyl anion. A salt-free Ph_3SiLi has also been obtained by metal−metal exchange between a silyl−cobalt complex **3** and MeLi (equation 19)[28g,30]. The reaction of **3** with different Grignard reagents has also been used by Corriu and Colomer to generate the corresponding silyl Grignard compound **4** (equation 19)[28g,30].

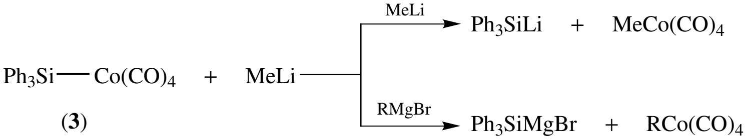

(19)

(**3**)

R = Me, Et, allyl

(**4**)

Analogously, the metal–metal exchange reaction of Ph_3SiK or Ph_3SiLi with $MgBr_2$ was assumed to yield **4**[8b,31]. In contrast, West and Selin found that the reaction of Ph_3SiCl with magnesium is not a practical way to prepare $Ph_3SiMgCl$ (**4**)[32]. The final product of this reaction is $Ph_3Si{-}SiPh_3$, which most likely arises from the coupling of an initially formed **4** with the starting material Ph_3SiCl. This produced disilane is stable in the presence of excess metal, because magnesium, unlike alkali metals, does not have a sufficiently high reducing potential to effect the cleavage of the Si–Si bond[28a].

Reductive cleavage of disilanes by alkali metals is the most versatile method to prepare metalated arylsilanes, which carry, in addition to the aromatic group, also an aliphatic, benzylic or allylic substituent. Table 1 reports all the metalated arylsilanes which have been prepared by reductive cleavage of disilanes with alkali metals.

Scheme 3 depicts the reaction sequence, which was developed by Sommer and Mason to show that the reductive cleavage of the Si–Si bond of disilanes by lithium proceeds under retention of configuration at a chiral silicon center[39]. The starting silane **5** was converted to the corresponding chlorosilane, which was coupled subsequently with $MePh_2SiLi$ to yield disilane **6**; these reactions are known to proceed with retention and inversion, respectively, i.e. disilane **6** has a configuration at Si* which is inverted in comparison to that of **5**. Cleavage of **6** with lithium metal and subsequent hydrolysis afforded silane *ent*-**5**, which has an inverted configuration of silicon relative to **5**. Because the hydrolysis of the silyllithium compound is assumed to proceed with retention, it has been concluded that the cleavage of the Si–Si bond of **6** by lithium does not invert the configuration at the chiral silicon center[39].

Optically active silyl anions were generated by Corriu and coworkers[28g,30] via the reaction of enantiomerically pure $(+)$-(α-Naph)PhMeSi*$Co(CO)_4$ with MeLi, which gave after hydrolysis $(+)$-(α-Naph)PhMeSi*H with 70% retention of configuration. The stereochemistry of the reaction is highly dependent on the nature of the organometallic reagent. With MeMgBr only 55% retention is observed, whereas the reaction with

TABLE 1. Metalated arylsilanes prepared by reductive cleavage of disilanes with alkali metals

Metalated silane	Precursor silane	Solvent	Reference
Ph_3SiLi	$Ph_3Si{-}SiPh_3$	DME	28b
Ph_3SiNa	$Ph_3Si{-}SiPh_3$	DME	28b
Ph_3SiK	$Ph_3Si{-}SiPh_3$	DME, Et_2O	28b, 29
$Ph_2MeSiLi$	$Ph_2MeSi{-}SiMePh_2$	THF	33
Ph_2MeSiK	$Ph_2MeSi{-}SiMePh_2$	THF	20[a]
$Ph_2(t\text{-}Bu)SiLi$	$Ph_2(t\text{-}Bu)Si{-}Si(t\text{-}Bu)Ph_2$	THF	34
$Ph_2(t\text{-}Bu)SiK$	$Ph_2(t\text{-}Bu)Si{-}Si(t\text{-}Bu)Ph_2$	THF, Et_2O	20[a], 35
$PhMe_2SiLi$	$PhMe_2Si{-}SiMe_2Ph$	THF	33
$PhMe_2SiK$	$PhMe_2Si{-}SiMe_2Ph$	THF, Et_2O, DME	20[a], 36
$Ph(i\text{-}Pr)_2SiLi$	$Ph(i\text{-}Pr)_2Si{-}Si(i\text{-}Pr)_2Ph$	THF	37
$Ph(PhCH_2)_2SiLi$	$Ph(PhCH_2)_2Si{-}Si(PhCH_2)_2Ph$	THF	37
$Me(H)C{=}C(Me)CH_2SiPh_2Li$	$[Me(H)C{=}C(Me)CH_2SiPh_2]_2$	THF	38
$(-)$-*neo*-$C_5H_{11}PhMeSiLi$	$[(-)$-*neo*-$C_5H_{11}PhMeSi]_2$	THF	39
Ph_2HSiLi	$Ph_2HSi{-}SiHPh_2$	THF	40, 45[b]
$[2\text{-}(Me_2NCH_2)C_6H_4]_2HSiLi$	$\{[2\text{-}(Me_2NCH_2)C_6H_4]_2HSi\}_2$	THF	41

[a] C_8K used as the reducing agent.

[b] Lithium 1-(dimethylamino)naphthalenide used as the reducing agent.

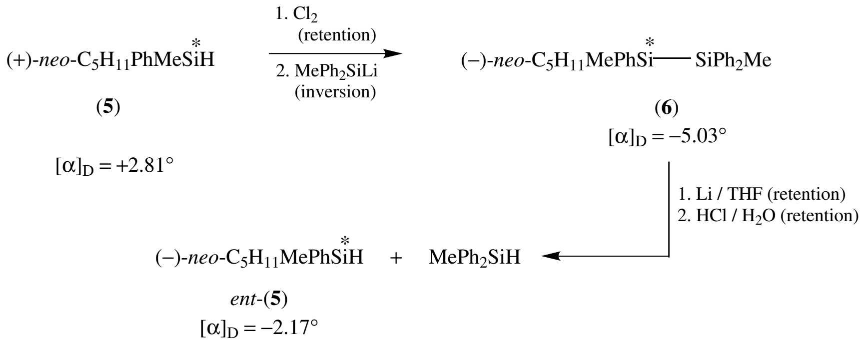

SCHEME 3

n-BuLi proceeds under total loss of chiral information. Similarly, racemic (±)-(α-Naph)PhMeSi*(n-Bu) is obtained when enantiomerically pure (+)-(α-Naph)PhMeSi*H is treated with KH in DME at 50 °C for 24 hours, and the resulting silylpotassium compound is reacted with n-BuBr[11]. The stereochemical course of the metalation is explained by an addition–elimination mechanism via an achiral pentacoordinated silicon compound **7** as the crucial intermediate (equation 20) (see also Section IV.A).

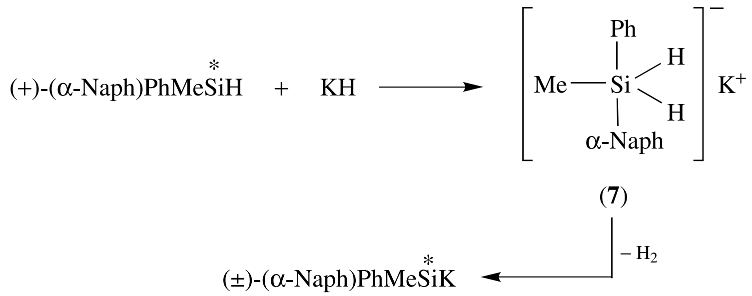

(20)

The cleavage of the Si—Si bond in the 9,10-disilanthracene **8** dimer by lithium metal in THF allows the synthesis of a dimetalated species **9** (Scheme 4)[42]. The reaction can be quenched at this point with electrophiles such as methyl iodide. Extended reaction times in the presence of excess metal produced 9,10-dimetalla-9,10-disilaanthracene **10** (M = Li). The corresponding potassium derivative **10** (M = K) was obtained directly from **8** upon treatment with excess metal. These 1,4-dimetalla species **10** have been used to synthesize a variety of *cis*-substituted disilaanthracene derivatives[42].

When $PhMe_2SiLi$ was reacted with CuCN[43a], CuX (X = Br, I)[43b] or MeCu(CN)Li[43c,d], a variety of silylcopper compounds and silylcuprates was formed: Depending on the stoichiometry used, compounds such as $(PhMe_2Si)_2CuLi{\bullet}LiX$[43b], $PhMe_2SiCu(CN)Li$[43a,c,d], $(PhMe_2Si)_2Cu(CN)Li_2$[43a,c,d], $Me(PhMe_2Si)Cu(CN)Li_2$[43c,d] and $(PhMe_2Si)_3CuLi_2$[43b–d] were identified by means of multinuclear NMR spectroscopy. These compounds have been used in organic synthesis as silylating agents. They undergo, *inter alia*, 1,4-addition to enones[43a–c] or may be used for silylcupration of alkynes[43a,c].

The synthesis of silyllithiums containing two aromatic substituents and a hydrogen has been accomplished by the reaction of Ar_2SiHCl (Ar = Ph[40], Mes[44]) with lithium metal or lithium 1-(dimethylamino)naphthalenide (LDMAN)[45] in THF. This reaction is assumed

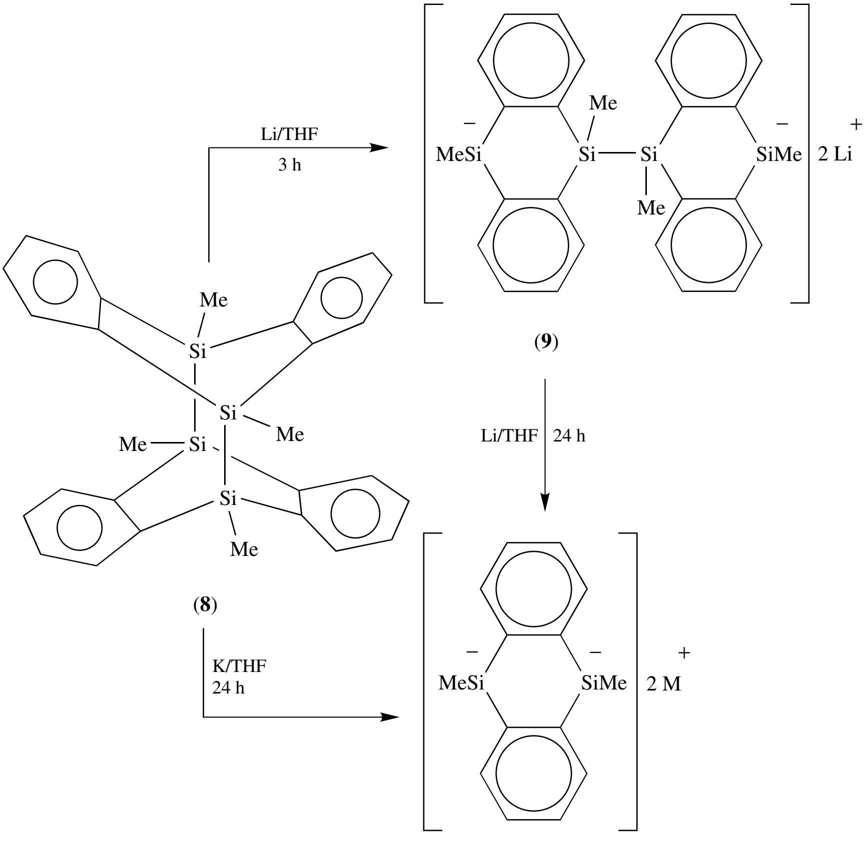

(**8**)

(**9**)

(**10**)

M = Li, K

SCHEME 4

to proceed via a disilane as intermediate (cf Scheme 2). Cleavage of the Si−Si bond of disilanes $Ar_2(H)Si-Si(H)Ar_2$ [Ar = Ph[40], 2-$(Me_2NCH_2)C_6H_4$[41]] by Li in THF is an alternative way to $Ar_2(H)SiLi$ (equation 21).

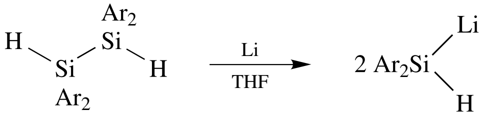

$$Ar_2(H)Si-Si(H)Ar_2 \xrightarrow[\text{THF}]{\text{Li}} 2\,Ar_2Si(Li)H \qquad (21)$$

Ar = Ph, 2-$(Me_2NCH_2)C_6H_4$

In addition, the silylpotassium compounds Ph_2SiHK and $PhSiH_2K$ have been obtained from Ph_2SiH_2 and $PhSiH_3$ by reaction with potassium (the yields were not reported)[46].

B. Structural Studies

IR, UV and, most importantly, NMR spectroscopy have proven to be excellent tools for elucidation of the molecular and electronic structures of silyl anions. Whereas ^{13}C NMR data of metalated alkylsilanes are quite rare, the wealth of ^{13}C NMR data which are available for metalated arylsilanes allows one to draw important conclusions concerning the question of charge delocalization in these compounds (Table 2)[36,47].

Comparing the chemical shift values of chlorosilanes with that of the corresponding silyl alkali metal compounds reveals a strong deshielding of the *ipso* carbons as well as a significant shielding of the *para* carbons; the shift changes of the *ortho* and *meta* carbons on going from the chlorosilane to the silyl anion are less pronounced. This pattern of chemical shift values indicates that charge delocalization into the phenyl ring via mesomeric effects, which would involve the interaction between suitable orbitals at the silicon and the aromatic π-system, is negligible. Instead, the charge distribution in these phenyl-substituted anions is governed by inductive π-polarization effects. Accordingly, the negative charge in phenyl-substituted silyl anions resides almost exclusively at the metalated silicon center in contrast to the corresponding carbon analogues, in which the negative charge density at the α-carbon is significantly reduced by mesomeric delocalization into the aromatic ring system. Similar conclusions have been drawn from UV-spectroscopic investigations, which provide corroborating evidence that there is almost no conjugation between silicon and the phenyl rings[46,48]. The reduced importance of resonance effects in silicon anions relative to carbanions is also reflected in the solid state structures of $Ph_3SiLi{\bullet}3THF$[49a], as well as of $[Ph_3SiCu(PMe_3)_2]$[49b], in which the silicon center is tetrahedrally surrounded by three carbon and one lithium atoms, whereas in the carbon analogue $Ph_3CLi{\bullet}Et_2O$ the carbon center exhibits a planar coordination sphere[50].

Spectroscopic studies have also been devoted to the question of ion-pairing phenomena in silyl anions. It was found that in arylated silyl anions the ^{13}C NMR as well as the ^{7}Li NMR chemical shifts are only slightly influenced by the polarity of the solvent[36,51]. This is in clear contrast to the NMR-spectroscopic behavior of aryl-substituted carbanions, which show a marked solvent dependence. This was interpreted in terms of a significant covalent interaction between silicon and lithium in metalated silanes[36]. Further evidence for a significant covalent nature of the Si−Li bond arises from the observation of a scalar

TABLE 2. ^{13}C NMR chemical shifts (in ppm) of metalated arylsilanes and related species (THF as solvent, cyclohexane (δ 27.7 ppm) as reference)[36]

Compound	*ipso*	*ortho*	*meta*	*para*	$\Delta\delta^a_{ipso}$	$\Delta\delta^a_{ortho}$	$\Delta\delta^a_{meta}$	$\Delta\delta^a_{para}$
Ph_3SiCl	133.8	135.9	128.9	131.5	—	—	—	—
$Ph_2MeSiCl$	134.4	134.0	128.1	130.5	—	—	—	—
$PhMe_2SiCl$	137.0	133.8	128.8	131.0	—	—	—	—
Ph_3SiLi	155.9	137.0	126.9	124.6	22.1	1.1	−2.0	−6.9
$Ph_2MeSiLi$	160.1	135.4	126.7	123.9	25.7	1.4	−1.4	−6.6
$PhMe_2SiLi$	166.0	133.8	126.5	122.7	29.0	0.0	−2.3	−8.3
Ph_3SiK	158.6	136.9	126.7	123.8	24.8	1.0	−2.2	−7.7
Ph_2MeSiK	163.2	135.1	126.5	123.0	28.8	1.1	−1.6	−7.5
$PhMe_2SiK$	170.1	133.6	126.4	121.6	33.1	−0.2	−2.4	−9.4

[a] $\Delta\delta = \delta(Ph_nMe_{3-n}SiM) - \delta(Ph_nMe_{3-n}SiCl)$, M = Li, K.

$^{29}Si-^{6}Li$ or $^{29}Si-^{7}Li$ coupling in various arylated silyllithium compounds[52]. For example, the ^{29}Si-NMR signal of Ph_3Si^6Li is resolved into a 1 : 1 : 1 triplet with a 17 Hz spacing at 173 K in 2-methyltetrahydrofuran[47b]; for Ph_3Si^7Li a quartet with a $^{29}Si-^{7}Li$ coupling constant of 45 Hz is observed in d_8-toluene at *ca* −80 °C[49a]. These coupling patterns as well as the magnitude of the coupling constants, which are close to values calculated by *ab initio* methods[53], are in good agreement with a monomeric structure of Ph_3SiLi and shows that the Si−Li bond, which was found in the solid state, remains essentially intact in solution at least at low temperatures. However, increase of temperature or changing the solvent to the more polar THF results, due to an acceleration of the intermolecular lithium–lithium exchange, in the disappearance of the $^{29}Si-^{6}Li$ coupling.

In contrast to these results, which argue in favor of a significant covalent contribution to the Si−Li bonding, other experiments point to a more ionic Si−Li bond. Thus, the fast exchange of lithium in mixtures of Ph_3SiLi and $Ph_2MeSiLi$ or $PhMe_2SiLi$ in THF at temperatures above −90 °C, as observed by ^7Li NMR spectroscopy, as well as the observation that the chemical shifts of the lithium nuclei of these compounds are quite similar, has been interpreted in terms of a predominantly ionic Si−Li interaction[51b]. In addition, it was argued that the occurrence of an observable $^{29}Si-^{6}Li$ or $^{29}Si-^{7}Li$ coupling speaks for a more ionic bonding, because in case of a covalent Si-Li bond one might expect that a fast quadrupole relaxation would quench the scalar coupling.

The temperature-dependent ^1H NMR spectra of $Ph(i\text{-}Pr)_2SiLi$ in various solvents were shown by Lambert and Urdaneta-Pérez to provide information on the configurational stability of silyllithium compounds[37]. The methyl groups of the isopropyl group are diastereotopic in this compound, and in diglyme they are observed as two separate signals at temperatures up to 185 °C (which is the upper experimental limit). Making the reasonable assumption that the rotation around the Si−C bond is fast on the NMR time scale (and therefore hindered rotation around the C−Si bond cannot account for the chemical inequivalence of the methyl groups) it has been concluded that the configuration of the silicon center is retained up to 185 °C. From this observation, a lower limit of 24 kcal mol^{-1} was calculated for the inversion barrier at silicon. This estimate is in good agreement with the inversion barrier of 26±6 kcal mol^{-1}, which was determined experimentally for SiH_3^- in the gas phase[54], as well as with theoretical calculation[1g].

VI. SILYL-SUBSTITUTED SILYL ANIONS

A. Preparation of Hydrido-Oligosilyl Anions $H_{2n+1}Si_nM$

The reaction of Na with SiH_4 in polar solvents such as mono- or diglyme has been reported to yield $NaSiH_3$[4a]; however, under carefully controlled conditions, $NaSi(SiH_3)_3$ has been obtained in good yield[4b]. KSi_2H_5 is formed as the major product when $KSiH_3$ is treated with excess SiH_4 in HMPA. This synthesis may be performed as a one-pot procedure, starting from SiH_4 and potassium in HMPA: After 1 h, $KSiH_3$ is formed almost exclusively, and if left for longer periods it undergoes subsequent homologization to yield the disilanyl anion. The branched silylpotassium compounds $KSiH(SiH_3)_2$ and $KSi(SiH_3)_3$ have been prepared by the reaction in HMPA of $KSiH_3$ with Si_2H_6 or Si_3H_8[2d,55].

B. Preparation and Properties of Acyclic Oligosilyl Anions

Three methods have been used to synthesize ‘organic’ metalated oligosilanes:

(a) Cleavage of a Si−Si bond of oligosilanes by nucleophiles such as organolithium or silyllithium compounds (Table 3).

TABLE 3. Metalated oligosilanes prepared by nucleophilic cleavage of a Si−Si bond

Compound	Starting material	Nucleophile	Reference
$[Me_3SiMe_2Si]^-[NBu_4]^+$	$Me_3SiMe_2Si{-}SiMe_3$	$[NBu_4]^+F^-$	16
Me_3SiMe_2SiLi	$Me_3SiMe_2Si{-}Me$	Me_3SiLi	10b,11
Me_3SiPh_2SiLi	$Me_3SiPh_2Si{-}SiMe_3$	MeLi	57
Me_3SiMes_2SiLi	$Me_3SiMes_2Si{-}SiMe_3$	MeLi	57
$(Me_3Si)_2MeSiLi$	$(Me_3Si)_2MeSi{-}SiMe_3$	MeLi	62c
$(Me_3Si)_2(t\text{-}Bu)SiLi$	$(Me_3Si)_2(t\text{-}Bu)Si{-}SiMe_3$	MeLi	62c
$(Me_3Si)_2PhSiLi$	$(Me_3Si)_2PhSi{-}SiMe_3$	MeLi	62b
$(Me_3Si)_2MesSiLi$	$(Me_3Si)_2MesSi{-}SiMe_3$	MeLi	62a
$(Me_3Si)_2TipSiLi$	$(Me_3Si)_2TipSi{-}SiMe_3$	MeLi	62b
$(Me_3Si)_3SiLi$	$(Me_3Si)_3Si{-}SiMe_3$	MeLi	63a,b,c
	$(Me_3Si)_3Si{-}SiMe_3$	Ph_3SiLi	68
	$(Me_3Si)_3Si{-}Si(SiMe_3)_3$	MeLi	34, 71a
	$(Me_3Si)_3Si{-}SiMe_2H$	MeLi	69b
	$(Me_3Si)_3Si{-}SiMe(SiMe_3)_2$	MeLi	69b[a]
	$(Me_3Si)_3Si{-}SiMeHSi(SiMe_3)_3$	MeLi	69b
	$(Me_3Si)_3Si{-}SiMe_2SiMe_3$	MeLi	69b[b]
	$(Me_3Si)_3Si{-}SiMe_2Si(SiMe_3)_3$	MeLi	69b
$(HMe_2Si)_3SiLi$	$(HMe_2Si)_3Si{-}SiMe_2H$	MeLi	68
	$(HMe_2Si)_3Si{-}SiMe_2H$	Ph_3SiLi	68
$t\text{-}BuMe_2Si(Me_3Si)_2SiLi$	$t\text{-}BuMe_2Si(Me_3Si)_2Si{-}SiMe_3$	MeLi	69a,b
$Me_3Si(t\text{-}BuMe_2Si)_2SiLi$	$Me_3Si(t\text{-}BuMe_2Si)_2Si{-}SiMe_3$	MeLi	69a
$Me_3SiMe_2Si(Me_3Si)_2SiLi$	$Me_3SiMe_2Si(Me_3Si)_2Si{-}SiMe_3$	MeLi	69b[b]
$t\text{-}BuMe_2SiSiMe_2Si(Me_3Si)_2SiLi$	$t\text{-}BuMe_2SiSiMe_2Si(Me_3Si)_2Si{-}SiMe_3$	MeLi	69b
$Me(Me_3Si)_2Si(Me_3Si)_2SiLi$	$Me(Me_3Si)_2Si(Me_3Si)_2Si{-}SiMe_3$	MeLi	69b[a]
$(Me_3Si)_3Si(SiMe_3)_2SiLi$	$(Me_3Si)_3Si(SiMe_3)_2Si{-}SiMe_3$	$(Me_3Si)_3SiLi$	34
	$(Me_3Si)_3Si(SiMe_3)_2Si{-}SiMe_3$	Ph_3SiLi	34,71a
$Li(Me_3Si)_2Si{-}Si(SiMe_3)_2Li$	$Me_3Si{-}Si(SiMe_3)_2(Me_3Si)_2Si{-}SiMe_3$	$(Me_3Si)_3SiLi$	34
	$Me_3Si{-}Si(SiMe_3)_2(Me_3Si)_2Si{-}SiMe_3$	Ph_3SiLi	34,71a
$Ph_3Si(Ph_2Si)_3Li$	$(Ph_2Si)_4$	PhLi	79
$Ph_3Si(Ph_2Si)_4Li$	$(Ph_2Si)_4$	Ph_3SiLi	79

[a] $(Me_3Si)_3SiLi$ and $Me(Me_3Si)_2Si(Me_3Si)_2SiLi$ are formed in a ratio 40 : 60.

[b] $(Me_3Si)_3SiLi$ and $Me_3SiMe_2Si(Me_3Si)_2SiLi$ are formed in a ratio 70 : 30.

(b) Cleavage of a Si−Si bond of oligosilanes by electron transfer from alkali metals (Table 4).

(c) Transmetalation of (oligosilyl)mercury compounds with alkali metal. It appears that only this method allows the use of nonpolar solvents such as toluene or alkanes (Table 5).

1. Linear oligosilyl anions

The formation of Me_3SiMe_2SiLi as a by-product in the reaction of $Me_3Si{-}SiMe_3$ with MeLi in HMPA/Et_2O (which yields mostly Me_3SiLi) has been mentioned earlier (Section IV.A). In a large-scale experiment the disilanyl anion has been reported to be

TABLE 4. Metalated oligosilanes prepared by reductive cleavage of a Si−Si bond by means of alkali metals

Compound	Starting material	Solvent	Reference
Me_3SiMes_2SiK	$(Me_3Si)_2Mes_2Si$	THF	57
$Me_3SiAr_2SiLi^a$	$Me_3SiAr_2Si{-}SiAr_2SiMe_3$	THF	41
$(Me_3Si)_3SiLi$	$(Me_3Si)_3Si{-}Si(SiMe_3)_3$	THF	71a
$(Me_3Si)_3SiK$	$(Me_3Si)_4Si$	not stated	71b
$Li(Ph_2Si)_4Li$	$(Ph_2Si)_4$	THF	72, 74
$Li(Ph_2Si)_5Li$	$(Ph_2Si)_5$	THF	73
$Li(SiAr_2)_3Li^a$	$(SiAr_2)_3$	1,4-dioxane	75
$Li(SiAr_2)_2Li^a$	$(SiAr_2)_3$	THF	75
$Li[(R_3Si)_2Si]_2Li^b$	$(R_3Si)_2Si{=}Si(SiR_3)_2$	THF	76
$K[(R_3Si)_2Si]_2K^b$	$(R_3Si)_2Si{=}Si(SiR_3)_2$	DME	76

[a] $Ar = 2\text{-}(Me_2NCH_2)C_6H_4$.

[b] $R_3Si = (i\text{-}Pr)_3Si$, $Me(i\text{-}Pr)_2Si$, $Me_2(t\text{-}Bu)Si$.

TABLE 5. Metalated oligosilanes prepared by mercury−metal exchange between silylmercury compounds and alkali metals

Compound	Starting material	Solvent	Reference
Me_3SiMe_2SiLi	$(Me_3SiMe_2Si)_2Hg$	toluene	56
$Me_3SiMe_2SiMe_2SiLi$	$(Me_3SiMe_2SiMe_2Si)_2Hg$	toluene	56
Ph_3SiPh_2SiK	$(Ph_3SiPh_2Si)_2Hg$	THF	83a
$Ph_3SiPh_2SiPh_2SiK$	$(Ph_3SiPh_2SiPh_2Si)_2Hg$	THF	83a
$(Me_3Si)_2MeSiLi$	$[(Me_3Si)_2MeSi]_2Hg$	toluene	56, 61
$(PhMe_2Si)_2MeSiLi$	$[(PhMe_2Si)_2MeSi]_2Hg$	toluene	61
$(Me_3Si)_3SiLi$	$[(Me_3Si)_3Si]_2Hg$	*n*-heptane	66b
$(Me_3Si)_3SiNa$	$[(Me_3Si)_3Si]_2Hg$	*n*-heptane	66b
$(Me_3Si)_3SiK$	$[(Me_3Si)_3Si]_2Hg$	*n*-pentane	66a,b
$(Me_3Si)_3SiRb$	$[(Me_3Si)_3Si]_2Hg$	*n*-pentane	66a,b
$(Me_3Si)_3SiCs$	$[(Me_4Si)_3Si]_2Hg$	*n*-pentane	66a,b
$(Me_3SiMe_2Si)_3SiLi$	$[(Me_3SiMe_2Si)_3Si]_2Hg$	THF or *n*-hexane	69c
$c\text{-}(Me_9Si_5)K$	$[c\text{-}(Me_9Si_5)]_2Hg$	THF	83c
$c\text{-}(Me_9Si_5)Me_2SiK$	$[c\text{-}(Me_9Si_5)Me_2Si]_2Hg$	THF	83b
$c\text{-}(Me_{11}Si_6)K$	$[c\text{-}(Me_{11}Si_6)]_2Hg$	THF	84

formed as the main product when MeLi or *n*-BuLi is used as the metalating agent[11d]. It has been suggested that Me_3SiMe_2SiLi results from a nucleophilic attack of the initially formed Me_3SiLi on excess disilane under cleavage of a peripheral Si−C bond[10b]; however, an unambiguous demonstration of this hypothesis is still missing.

Crystals of Me_3SiMe_2SiLi, which are suitable for X-ray crystallography, have been obtained by Sekiguchi and coworkers via a lithium−mercury exchange reaction of $(Me_3SiMe_2Si)_2Hg$ with lithium metal in toluene[56]. In contrast to hexameric $(Me_3SiLi)_6$ (Section IV.B), Me_3SiMe_2SiLi is a tetramer in the solid state (Figure 6). The four lithium

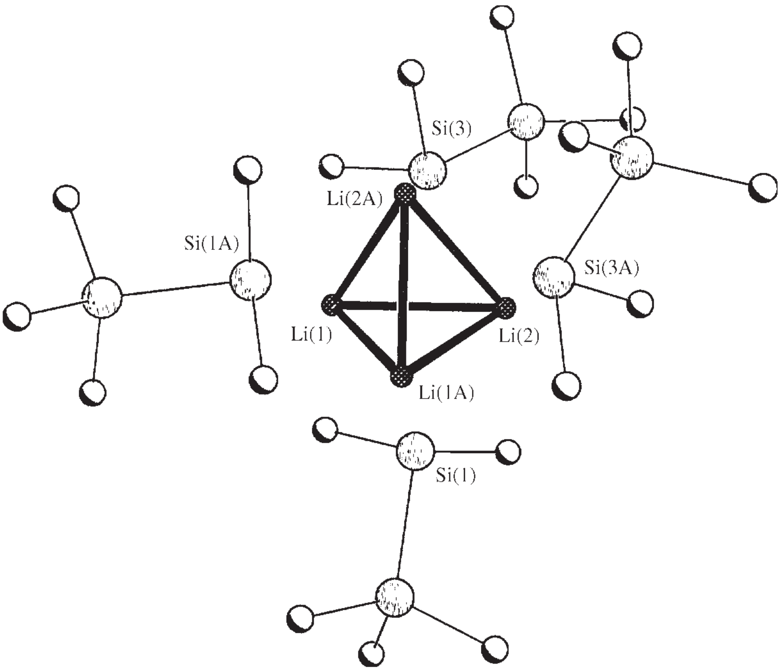

FIGURE 6. Solid state structure of $(Me_3SiMe_2SiLi)_4$ with hydrogen atoms omitted. Reprinted with permission from Reference 56. Copyright 1995 American Chemical Society

atoms build a central tetrahedron with an average Li—Li distance of 278.0 pm, which is about 20 pm longer than the distances found in tetrameric alkyllithiums; each of the disilyl moieties is located above one of the faces of the Li_4 tetrahedron with three nearly equal Si—Li distances averaging 268.3 pm. The broad ^{29}Si NMR signals of isotopically enriched $Me_3SiMe_2Si^6Li$ in toluene-d_8 imply the existence of oligomeric aggregates in toluene solution as well. However, in THF-d_8 a well resolved 1 : 1 : 1 triplet with 18.8 Hz spacing is observed at 180 K. This signal pattern indicates that the oligomeric aggregates, which exist in the solid as well as in nonpolar solvents, are broken down into a monomeric species by the more polar THF. Moreover, the observation of a $^{29}Si-^6Li$ coupling and its magnitude indicates that the Si—Li bond has a partially covalent character[56].

The aryl-substituted lithiated disilanes, Me_3SiPh_2SiLi and Me_3SiMes_2SiLi (Mes = 2, 4, 6-trimethylphenyl), have been prepared by Brook and coworkers from the corresponding trisilanes by nucleophilic cleavage of a Si—Si bond with MeLi in THF/Et_2O (equation 22)[57]; an alternative synthesis of Me_3SiPh_2SiLi utilizes the reaction of Me_3SiPh_2SiCl with the electron transfer reagent LDMAN[45].

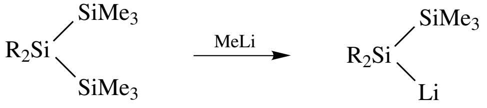

(22)

R = Ph, 2,4,6-trimethylphenyl(=Mes)

Me_3SiMes_2SiK has been obtained by treatment of the trisilane $(Me_3Si)_2SiMes_2$ with Na/K alloy in THF/Et_2O/HMPA[57]. The selective rupture of the central Si−Si bond of a symmetrical tetrasilane by lithium in THF allows access to a metalated disilane, bearing the chelating 2-(dimethylaminomethyl)phenyl substituent at the α-silicon (equation 23)[41].

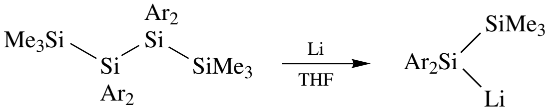

(23)

Ar = 2-$(Me_2NCH_2)C_6H_4$

The reaction of Ph_3SiPh_2SiCl with lithium metal was reported to produce Ph_3SiPh_2SiLi and it is likely to proceed via the tetrasilane $Ph_3Si(Ph_2Si)_2SiPh_3$ as an intermediate[58]. The selectivity of this reaction is surprising in view of the more recent report that the reaction of lithium metal with a related chlorosilane, $PhMe_2SiMe_2SiCl$, produces an equilibrium mixture of $PhMe_2SiMe_2SiLi$, $PhMe_2SiLi$ and $(Me_2Si)_6$ (equation 24)[59].

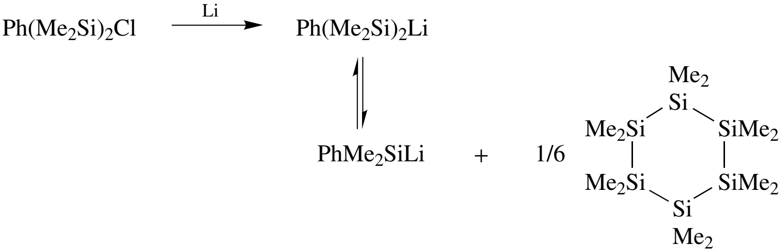

(24)

This reaction has been monitored by means of multinuclear NMR, ESR and UV spectroscopy as well as by HPLC, and four distinct stages have been recognized. In the first step the tetrasilane is formed, as expected. In the second stage, the tetrasilane is further reduced by excess lithium to produce via its radical anion metalated mono-, di- and trisilanes, which subsequently undergo coupling with the starting chlorodisilane to form α,ω-diphenyltri-, tetra- and pentasilanes. In the third stage, $(Me_2Si)_6$ is produced by the cleavage of the Si−Si bonds in the diphenylated oligosilanes by silyl anions; linear oligosilanes are produced as well at this point. In the final step, more electrons are transferred from the lithium metal to the system resulting in a complex equilibrium mixture of $PhMe_2SiMe_2SiLi$, $PhMe_2SiLi$ and $(Me_2Si)_6$. It should be mentioned at this point that the third step of the reaction sequence, i.e. the formation of $(Me_2Si)_6$ from oligosilanes and silyl anions, has been known also for other α,ω-phenylated permethyloligosilanes, e.g. $PhMe_2Si(SiMe_2)_nSiMe_2Ph$ or $Ph_3Si(SiMe_2)_nSiPh_3$ ($n = 1-3$)[60].

2-Lithiotrisilanes, which are used as precursors to polysilane dendrimers, have been obtained by a mercury−lithium exchange reaction (equation 25)[56,61]. The terminally metalated trisilane $Me_3Si(Me_2Si)_2Li$ has been synthesized analogously[56].

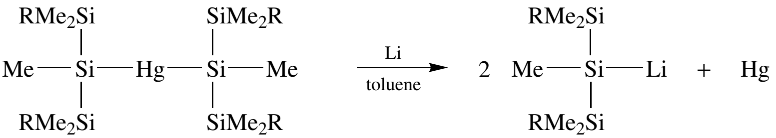

$$\mathrm{Me-\overset{RMe_2Si}{\underset{RMe_2Si}{Si}}-Hg-\overset{SiMe_2R}{\underset{SiMe_2R}{Si}}-Me} \xrightarrow[\text{toluene}]{\text{Li}} 2\ \mathrm{Me-\overset{RMe_2Si}{\underset{RMe_2Si}{Si}}-Li} + \mathrm{Hg}$$

(25)

R = Me, Ph

The reaction of MeLi in Et_2O with alkyl- and aryl-substituted branched tetrasilanes proceeds by cleavage of one Si−Si bond, thus affording various trisilanes, which are lithiated at the central silicon atom (equation 26)[62]. The outcome of these reactions apparently is insensitive as to whether halide-free MeLi or the MeLi•LiBr complex is used[62]. The decrease in the reaction rate in the order: R = Tip > Mes > Ph has been suggested by Fink and coworkers to reflect the relief of steric strain on converting the tetrasilane into the metalated silane[62b].

$$RSi(SiMe_3)_3 \xrightarrow[\text{MeLi•LiBr}]{\text{MeLi or}} RSi(SiMe_3)_2Li + SiMe_4 \qquad (26)$$

R = Me, Ph, Mes, Tip

2. Branched oligosilyl anions

The preparation of $(Me_3Si)_3SiM$ and derivatives thereof, which contain the *iso*-tetrasilabutyl subunit, is one of the best investigated topics in the chemistry of metalated oligosilanes.

The Si−Si bond of the easily available pentasilane $(Me_3Si)_4Si$ is smoothly cleaved by organometallic reagents such as MeLi[63] or Ph_3SiLi[63a] yielding $(Me_3Si)_3SiLi$ **(11)**. The most convenient access to this silyllithium compound on a large scale appears to be the reaction of $(Me_3Si)_4Si$ with MeLi•LiBr in THF/Et_2O[63b] (equation 27).

$$(Me_3Si)_4Si + MeLi \xrightarrow{\text{THF/Et}_2\text{O}} \underset{\textbf{(11)}}{(Me_3Si)_3SiLi} + SiMe_4 \qquad (27)$$

The ethereal solution of **11** obtained in this way is of limited stability, and therefore should be used immediately for further reactions. Alternatively, crystalline THF-solvated reagents, **11**•3THF, which can be stored for months without decomposition, may be isolated in a yield of 92% by replacing the ether solvent by *n*-pentane and cooling the resulting solution[63b]. This isolated complex has the further advantage of being soluble in nonpolar solvents such as pentane or toluene, in which, as a rule, subsequent coupling reactions of the anionic species with electrophilic substrates proceed more cleanly and with higher yield than in polar solvents. **11**•3THF is monomeric in the solid state[49a,64]. The Si−Si−Si bond angle is reduced from the ideal tetrahedral value of 109.5° to 102.4°. A similar distortion has been observed for **11**•1.5DME[65] and for the $(Me_3Si)_3SiLi$ unit in the cocrystal **11**•$(Me_3Si)_4Si$[64]. The significant compression of the Si−Si−Si bond angle in these $(Me_3Si)_3SiLi$ compounds was interpreted by Sheldrick and coworkers[64] as an indication of an appreciable ionic character of the Si−Li bond. However, an inherent covalent contribution to the Si−Li interaction is indicated by the $^{29}Si-^{7}Li$ coupling constant of 38.6 Hz measured in toluene-d_8 at room temperature[64]. The quartet pattern of the ^{29}Si NMR signal reveals the momomeric nature of **11** under these conditions.

The entire series of alkali metal compounds $(Me_3Si)_3SiM$ (M = Li, Na, K, Rb, Cs) have been prepared by Klinkhammer and coworkers via a metal−metal exchange reaction from bis[tris(trimethylsilyl)] derivatives of the zinc group, $[(Me_3Si)_3Si]_2M$ (M = Zn, Cd, Hg), and the corresponding alkali metal in *n*-pentane or *n*-heptane (equation 28)[66a,b].

$$M'[Si(SiMe_3)_3]_2 \xrightarrow{M} 2MSi(SiMe_3)_3 + M' \qquad (28)$$

M′ = Zn, Cd, Hg M = Li, Na, K, Rb, Cs

The formation of the cesium compound is complete after a few minutes, when the mercury derivative is used as the starting material. In contrast, the reaction of the zinc compound with potassium metal reaches only 60% conversion in 2 days[66a]. The rubidium and cesium compounds obtained by this method have been characterized in the solid as toluene and THF solvates[66a]. In addition, a cocrystallization product of $(Me_3Si)_3SiCs$ with biphenyl, the origin of which is not stated, is mentioned in Reference 66b. All these complexes are dimeric aggregates having a folded M_2Si_2 ring. The solvate-free lithium, sodium and potassium compounds form cyclic dimers in the solid state as well. The Li_2Si_2 and the K_2Si_2 rings are almost planar, whereas in the sodium compound a folding angle of 170.9° has been found[66b]. In benzene solutions aggregation numbers between 1 and 2 have been determined for all these compounds, which indicates that the dimers found in the solid are partially broken down in benzene solution[66a].

11•3THF has been converted by treatment with CuCl[67a] or CuBr[67b] into $[Li(THF)_4][Cu_5Cl_4(Si(SiMe_3))_2]$ and $[Cu_2(Si(SiMe_3))_2Li(THF)_3]$, respectively, which are the first lithium silylcuprates to be characterized in the solid state.

The synthesis of metalated *iso*-tetrasilanes via nucleophilic cleavage of a Si−Si bond by means of organolithium compounds is not restricted to the synthesis of $(Me_3Si)_3SiLi$ itself: $(HMe_2Si)_3SiLi$[68], $(t\text{-}BuMe_2Si)(Me_3Si)_2SiLi$[69a,b], $(t\text{-}BuMe_2Si)_2(Me_3Si)SiLi$[69a] as well as a stannyl derivative, $(Me_3Sn)_3SiLi$[70], have been prepared from the corresponding silane precursors by reaction with MeLi.

$(Me_3SiMe_2Si)_3SiLi$•3THF and the unsolvated dimer $[(Me_3SiMe_2Si)_3SiLi]_2$ were obtained most recently by Apeloig and coworkers upon treatment of $[(Me_3SiMe_2Si)_3Si]_2Hg$ with lithium metal in THF or hexane[69c]. Both lithiotrisilanes exhibit in the solid a Si−Li distance, which is significantly elongated (i.e. by *ca* 0.07 Å) in comparison to $(Me_3Si)_3SiLi$•3THF and $[(Me_3Si)_3SiLi]_2$, respectively. This observation as well as the highfield shift in the ^{29}Si NMR of the metalated silicon center upon changing the Me_3Si group to the Me_3SiMe_2Si group was interpreted in terms of an enhanced ionicity of the silyllithium compounds by β-silyl substitution[69c].

Whereas $(Me_3Si)_4Si$ is not susceptible to electron transfer from lithium (thus allowing its synthesis by lithium-mediated coupling of $SiCl_4$ with Me_3SiCl), hexasilane $(Me_3Si)_3Si{-}Si(SiMe_3)_3$ (**12**) undergoes smooth reaction with lithium in THF to yield **11** (Scheme 5)[71a]. Alternatively, the central Si−Si bond of **12** may be cleaved by MeLi leading to **11**[71a]. However, the attack of the more bulky Ph_3SiLi or $(Me_3Si)_3SiLi$ on **12** takes a different course. The central Si−Si bond is not broken, and instead one or even two trimethylsilyl groups at the periphery of the molecule are substituted by lithium atoms (Scheme 5)[34,71a].

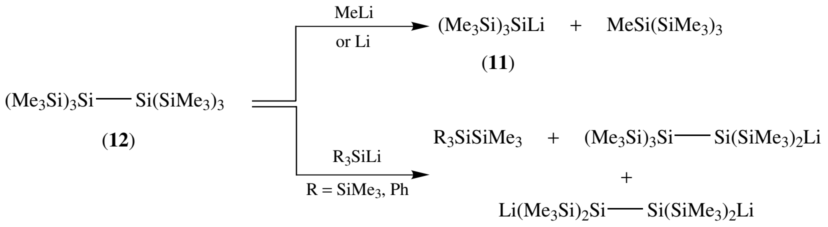

SCHEME 5

It may be concluded from the results of Scheme 5 that steric effects are responsible for the removal of the peripheral Me_3Si group. However, the cleavage of unsymmetrical disilanes such as $Me_3Si{-}SiPh_3$, $Me_3Si{-}SiMePh_2$ or $Me_3Si{-}SiMe_2Ph$ by potassium *t*-butoxide[13c] or by TBAF[15] appears to be governed by electronic effects, i.e. in these cases the more stable arylated silyl anion is formed.

A more recent study by Apeloig and coworkers of the reaction of MeLi with a variety of oligosilanes $(Me_3Si)_3Si{-}X$ has shed some more light on the factors which determine the course of the nucleophilic cleavage[69b]. When X is a group having a backbone of one or two silicon centers such as $-SiMe_2H$, $-SiMe_2(t\text{-}Bu)$, $-SiMe_2SiMe_3$ or $-SiMe_2SiMe_2(t\text{-}Bu)$, MeLi attacks preferentially the sterically less hindered silicon center. Thus $(Me_3Si)_3Si{-}SiMe_2H$ yields on treatment with MeLi almost exclusively $(Me_3Si)_3SiLi$ **(11)**, whereas the reaction of the same nucleophile with $(Me_3Si)_3Si{-}SiMe_2(t\text{-}Bu)$ proceeds to yield exclusively $Li(Me_3Si)_2Si{-}SiMe_2(t\text{-}Bu)$, i.e. the sterically more accessible trimethylsilyl group of the $(Me_3Si)_3Si$ moiety is cleaved by MeLi. In contrast, steric effects appear to be overridden by — not yet fully understood — electronic effects, when X is a branched oligosilyl group such as, *inter alia*, $-SiMe(SiMe_3)_2$ or $-Si(SiMe_3)_3$. In these cases attack of MeLi and cleavage occur preferentially at the silicon center, which is located in the α-position to the $(Me_3Si)_3Si$-moiety, thus yielding **11** as main product.

When the oligosilane $(Me_3Si)_3Si{-}X$ contains a chloro substituent which is geminal to the $(Me_3Si)_3Si$ group (i.e. $X = -SiR^1R^2Cl$), $Li(Me_3Si)_2SiSiR^1R^2Me$ was obtained, upon reaction with MeLi (Scheme 6). A two-step substitution–lithiation mechanism (a in Scheme 6) was ruled out by demonstrating that the initial substitution product yields a different product in the reaction with MeLi and an elimination–addition mechanism (b in Scheme 6) via a disilene as intermediate was tentatively suggested.

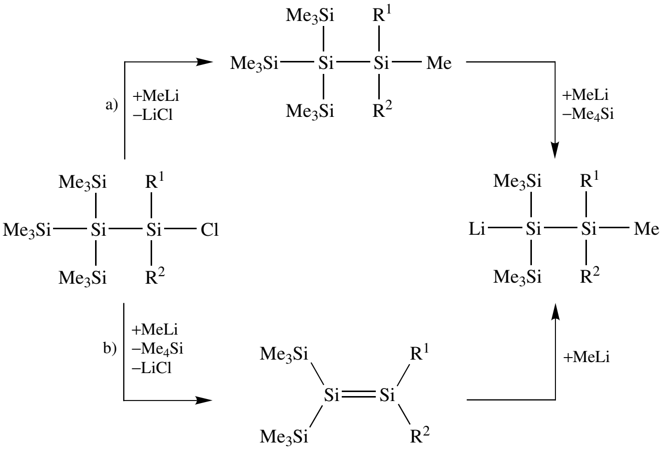

SCHEME 6

3. Oligosilyl anions via cleavage of cyclic silanes

The cleavage of a Si–Si bond in silacyclic compounds by lithium metal is the most versatile method to prepare linear, α,ω-dilithiated oligosilanes. The first dilithio compound obtained by Gilman and coworkers in this way was $Li(Ph_2Si)_4Li$ (equation 29)[72].

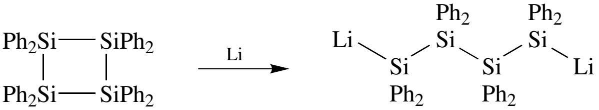

(29)

Analogously, Li(Ph$_2$Si)$_5$Li has been synthesized from the corresponding cyclopentasilane[73]. ^{29}Si NMR and ^{7}Li NMR measurements of Li(Ph$_2$Si)$_4$Li in THF solvents indicate the presence of three different adducts which, at temperatures above 294 K, undergo exchange reactions, which are fast on the NMR time scale[74]. At 173 K, the ^{29}Si NMR signals of the terminal silicon nuclei of each of the adducts show a scalar coupling to one ^{7}Li nucleus (coupling constants: 32.8, 40 and 42 Hz), thus reflecting the partially covalent character of the Si−Li bond. It was shown by X-ray structure determination that Li(SiPh$_2$)$_4$Li is a monomer in the solid state with a planar LiSi$_4$Li backbone with each of the lithium atoms of the centrosymmetrical molecule being bonded to a terminal silicon center in accordance with the solution structures, and adopting a distorted tetrahedral environment due to its coordination to three THF molecules.

1,3-Dilithiotrisilane **13** has been obtained by the reaction of a cyclotrisilane with two equivalents of lithium in 1,4-dioxane (Scheme 7)[75]. **13** is monomeric in the solid state and its structure is shown in Figure 7. Each lithium atom is bonded to a terminal silicon atom and in addition it is coordinated to the two amino groups of the neighboring (Me$_2$NCH$_2$)C$_6$H$_4$ substituents, as well as to an oxygen atom of the dioxane solvent molecule. The LiSi$_3$Li backbone adopts an approximately antiperiplanar conformation.

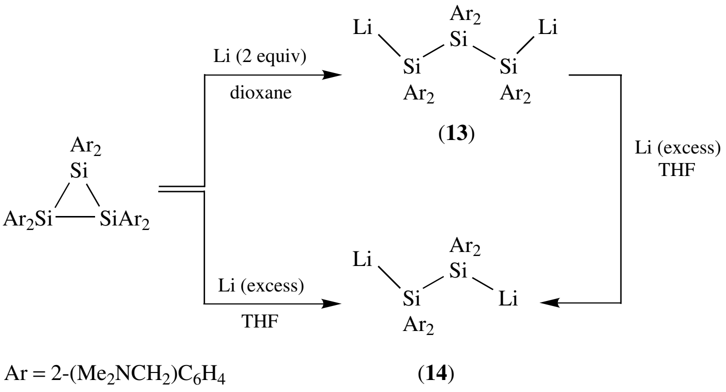

SCHEME 7

The reaction of **13** with excess lithium in THF results in the formation of 1,2-dilithiodisilane **14**, which can be obtained more conveniently directly by the reaction of the cyclotrisilane with lithium in THF. The mechanism of these reactions is still unknown. In contrast to 1,2-dilithioethane derivatives, the lithium atoms in **14** do not undergo a side-on coordination to the Si−Si bond, the length of which is typical for a Si−Si single bond (Figure 8). Instead, each lithium atom is bonded to a silicon atom; Li1 is further coordinated intramolecularly to two Me$_2$NCH$_2$ groups of the geminal aryl substituents and intermolecularly to a THF molecule, while Li2 interacts with only one dimethylamino group and two external THF molecules. **14** is monomeric at room temperature in THF, and the Si−Li bonding is retained in solution, as can be concluded from the ^{29}Si NMR spectrum, which exhibits a 1 : 1 : 1 : 1 quartet at $\delta = -32.8$ with a ^{29}Si−^{7}Li coupling constant of 36 Hz.

Various silyl-substituted disilenes undergo reaction with potassium in DME or with Li in THF to yield the corresponding vicinal dianions (equation 30)[76].

Another 1,2-dilithiodisilane **(16)** was obtained by Ando and coworkers from 1,2-dichlorodisilane **15** by reaction with excess lithium metal in THF under ultrasonic

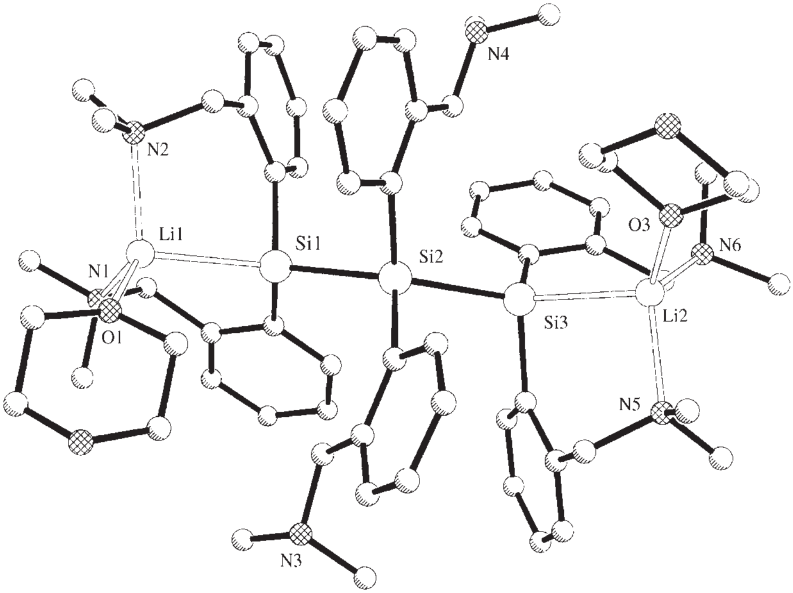

FIGURE 7. Solid state structure of **13** with hydrogen atoms omitted. Reproduced from Reference 75 by permission of VCH Verlagsgesellschaft, Weinheim

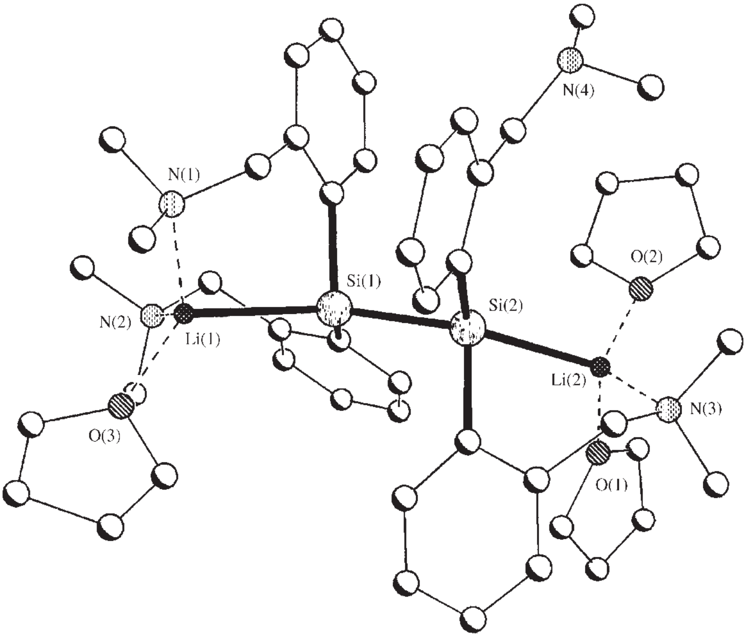

FIGURE 8. Solid state structure of **14** with hydrogen atoms omitted. Reproduced from Reference 75 by permission of VCH Verlagsgesellschaft, Weinheim

activation (equation 31)[77].

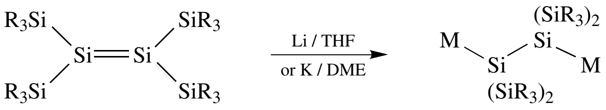

(30)

SiR_3 = Si(i-Pr)$_3$, Si(i-Pr)$_2$Me, SiMe$_2$(t-Bu); M = Li, K

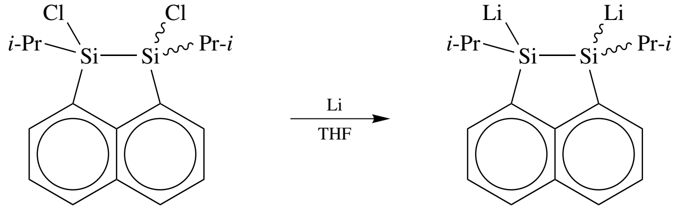

(31)

(**15**) (**16**)

One might assume that **16** is formed via a disilene, which is reduced subsequently by the excess metal. However, although the metal-mediated dehalogenation of vicinal dihalodisilanes is known to yield disilenes[78], the formation of such a species in reaction 31 appears unlikely in view of the geometric constraints, which are imposed by the disilaacenaphthene skeleton. Although both the starting material **15** and the products which were obtained on quenching of **16** with D_2O or MeI were shown by NMR spectroscopy to be mixtures of diastereomers, the fact that the NMR spectra of **16** did not show paired signal sets was interpreted in terms of the formation of a single diastereoisomer of **16**. However, the relative stereochemistry at the silicon centers remained undetermined. The ^{29}Si NMR signal of **16** is observed at $\delta = -1.24$ ppm, shifted to lower field compared to other silyl anions. This signal splits into a well-resolved 1 : 1 : 1 : 1 quartet at 173 K in THF-d$_8$ ($^1J_{^{29}\text{Si}-^7\text{Li}} = 43.5$ Hz). This finding has been interpreted in terms of a partially covalent character of the Si−Li bond, and is in agreement with calculations at the HF/3-21G* level, which found a minimum structure, in which each lithium interacts with one silicon atom[77].

The behavior of cyclic silanes toward nucleophiles is less uniform. The reactions of $(Ph_2Si)_4$ with PhLi or Ph_3SiLi have been reported to result in mixtures of $(Ph_2Si)_6$ and open-chained oligosilanes; $Ph_3Si(Ph_2Si)_3Li$ and $Ph_3Si(Ph_2Si)_4Li$ have been postulated as reaction intermediates[79]. However, when $(R_2Si)_4$ is reacted with $PhMe_2SiLi$ the initially formed ring-opening product $PhMe_2Si(R_2Si)_4Li$ can be trapped efficiently by $(PhMe_2Si)_2$, yielding the hexasilane $PhMe_2Si(R_2Si)_4SiMe_2Ph$. $PhMe_2SiLi$, which is regenerated in the last step of the sequence, attacks the remaining cyclotetrasilane thus making the overall reaction catalytic in $PhMe_2SiLi$ (Scheme 8)[80].

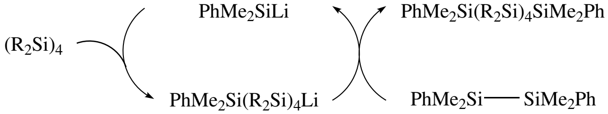

SCHEME 8

When the all-*trans* isomer of $(PhMeSi)_4$ is treated with catalytic amounts of nucleophiles such as n-BuLi, Me_3SiK or $(PhMe_2Si)_2CuLi$, a ring-opening polymerization occurs and polysilanes are formed[81]. Similar reactions were reported for phenylnonamethylcyclopentasilane **(17)** in polar solvents at low temperatures[82]. In this case the ring-opening of **17** proceeds regioselectively with cleavage of the Si−Si bond to the phenyl-bearing silicon center in each propagation step, eventually forming the ordered polymer **18** (equation 32). It was assumed that the regioselectivity of the Si−Si bond cleaving reaction is due to the formation of the thermodynamically more stable, phenyl-substituted silyl anion[82].

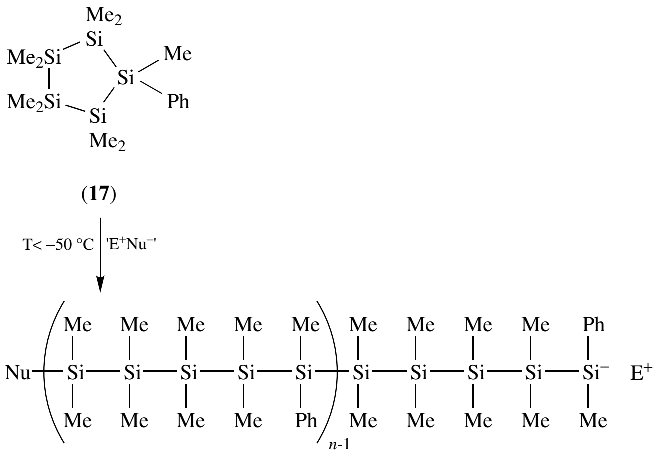

(**17**)

(**18**)

(32)

'E^+Nu^-' = Me_3SiK, $PhMe_2SiK$, Bu_4NF

C. Preparation and Properties of Cyclic Oligosilyl Anions

Transmetallation of silylmercury compounds, which are most easily available via the reaction of a silane with (t-Bu)$_2$Hg, appears to be the most convenient method for the preparation of cyclic potassium oligosilyl compounds: c-(Me_9Si_5)K **(19)**[83c] as well as c-($Me_{11}Si_6$)K **(20)**[84] were obtained by Hengge and coworkers from the corresponding mercury compound by means of a Na/K alloy in THF (equation 33).

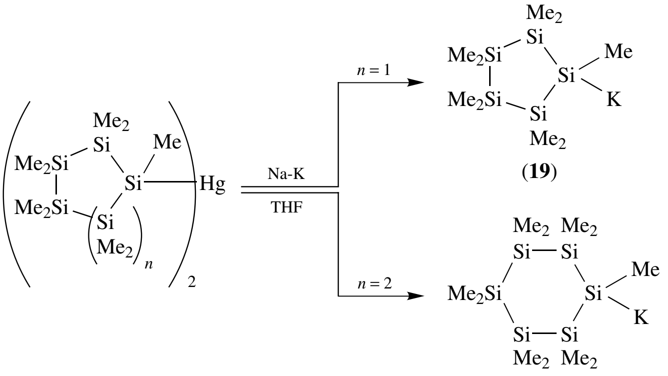

(**19**)

(**20**)

(33)

In addition, **20** is assumed to be formed as the initial product, when the silyl bromide **21** is treated with Na/K alloy in *n*-heptane. The fast coupling of intermediate **20** with bromide **21** results in the formation of dimer **22** in 80% yield (equation 34)[84].

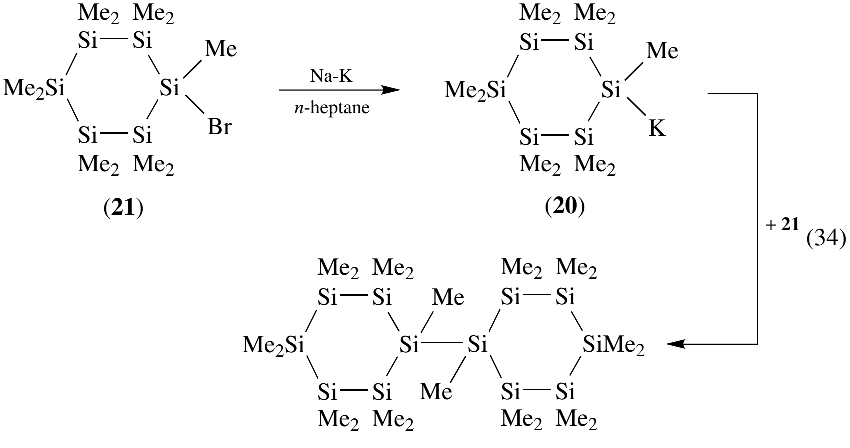

(**21**) (**20**) (**22**)

(34)

The reaction of cyclic silane **23** with lithium metal in THF opens an unexpected way to *c*-$(Me_{11}Si_6)Li$ (**24**). Whereas in tri-, tetra- and penta-cyclosilanes a Si—Si bond is cleaved under these conditions (Section VI.B.3), **23** reacts with cleavage of a exocyclic Si—C bond (equation 35)[85]. The reasons for the different behavior of **23** toward lithium remain unclear. It was, however, suggested that the facile formation of **24** is due to its thermodynamic stabilization by electron delocalization into the silicon framework[85].

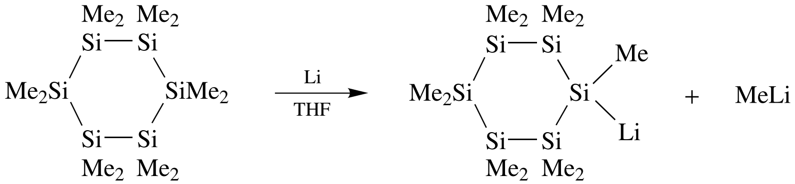

(**23**) (**24**)

(35)

24 is inert to further substitution of methyl groups by lithium, even in the presence of excess metal[85]. A variety of other reagents such as sodium or potassium metal, RLi (R = *n*-Bu, Ph), MOR (M = Na, K; R = Me, Et, *t*-Bu) and $KSiMe_3$ have been shown to metalate $(Me_2Si)_6$ in Et_2O/HMPA, inducing a loss of a methyl substituent. However, when using nucleophiles such as PhLi or $KSiMe_3$ concomitant ring cleavage is observed[85].

The lower homologue, *c*-$(Me_9Si_5)Li$, cannot be prepared from $(Me_2Si)_5$: Reaction with lithium metal proceeds under Si—Si bond cleavage to yield $Li(Me_{10}Si_5)Li$[73], whereas on treatment of $(Me_2Si)_5$ with MeLi in HMPA a complex mixture of acyclic silyl anions is formed[85]. Attempts to synthesize *c*-$(Me_9Si_5Li$ from *c*-$(Me_9Si_5)SiMe_3$ by cleavage of the exocyclic Si—Si bond with alkali metal alkoxides or organolithium species in various solvents were unsuccessful due to the stability of *c*-$(Me_9Si_5)SiMe_3$ toward these reagents[86]. However, KOBu-*t* in diglyme reacts with *c*-$(Me_9Si_5)SiMe_3$, but surprisingly a mixture of *c*-(Me_9Si_5)K (**19**) and *c*-($Me_{11}Si_6$)K (**20**) was formed[86]. A similar product mixture, albeit in low yield, is formed when *c*-($(Me_2Si)_5$ is treated either with NaOBu-*t* or KOBu-*t* in THF. It was shown, that *c*-$(Me_2Si)_5$ as well as *c*-($(Me_3Si)Me_9Si_5$) rearrange under the influence of alkoxides to *c*-$(Me_2Si)_6$, which subsequently undergoes metalation with cleavage of a Si−C bond to yield an equilibrium mixture of metalated cyclohexa- and cyclopenta silanes (Scheme 9)[86]. This equilibrium mixture reacts further with alkoxide. Eventually, an almost quantitative yield of potassium compound **19** was accomplished by the reaction of *c*-$(Me_2Si)_6$ with one equivalent of KOBu-*t* in DME or diglyme, and this is now the best route to prepare synthetically useful amounts of this silylpotassium compound[86].

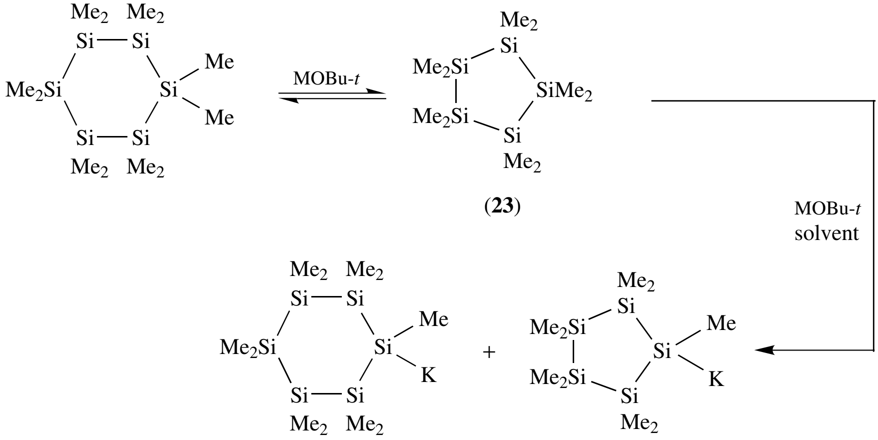

(**23**)

(**24**)

(**19**)

M/solvent = Na, K/THF	12-15%	2-5%
= K/diglyme	75-85%	< 5%

SCHEME 9

VII. FUNCTIONALIZED SILYL ANIONS

A. Lithium Silenolates

Silenolates **26**, i.e. silicon analogues of enolates, are formed, as shown by Ishikawa and coworkers, when sterically congested tris(trimethylsilyl)acylsilanes **25** are treated with silyllithium compounds (Scheme 10)[87a,b,c]: The silyllithium reagent does not add to the C=O bond but exclusively cleaves a Si−Si bond, yielding the corresponding silenolate **26**.

According to *ab initio* calculations at the CISD/6-31G*//6-31G* level the model reaction given in equation 36 is exothermic by -30.0 kcal mol^{-1}[87c].

The NMR chemical shift of the central silicon atom of the mesityl-substituted **26**, which is a stable compound at room temperature in THF, is shifted by 15.4 ppm to lower field in comparison to the starting material which resonates at $\delta = -59.9$ ppm. It was suggested that this lowfield shift reflects the sp^2 character of the central silicon atom in **26**[87c]. According to the ^{1}H and ^{29}Si NMR spectra, the Me_3Si groups are magnetically nonequivalent at $-40\,°C$ due to hindered rotation around the Si−C bond. From variable-temperature NMR

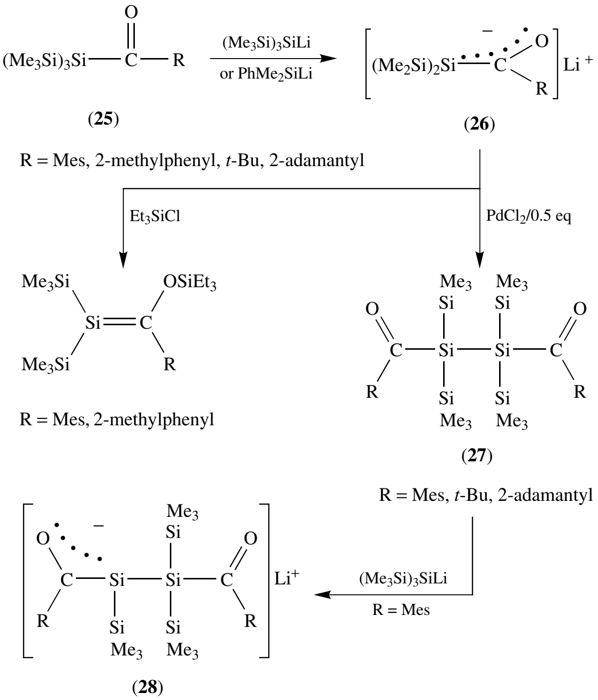

SCHEME 10

experiments, a rotation barrier of 14.3 kcal mol^{-1} has been determined[87c]. The silenolates **26** (R = Mes, 2-methylphenyl) can be converted to silenes by silylation of the anionic oxygen center with Et_3SiCl[87a,c]. On treatment of the silyl enolates with 0.5 equivalents of $PdCl_2$, a Si−Si coupling reaction occurs, and the corresponding bis(acyl)-substituted hexasilanes **27** are obtained[87b]. When R = Mes, addition of 1 equivalent of $(Me_3Si)_3SiLi$ **(11)** converts **27** (R = Mes) into a new silenolate **28** (Scheme 10). However, the adamantyl- and *t*-butyl-substituted **27** did not react with **11** even at room temperature[87b]. Attempts to prepare silenolates with sterically less demanding substituents such as Ph or Me at the carbonyl center were unsuccessful. The phenyl-substituted **26** was formed upon reaction of the corresponding acylsilane **25** with **11**, but it underwent rapid dimerization and subsequent reactions, whereas the methyl-substituted **25** was deprotonated at the methyl group by **11** yielding the corresponding carbon enolate[87c].

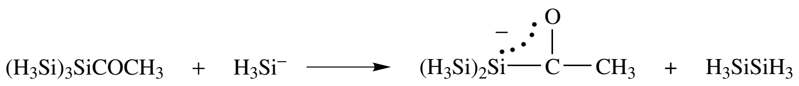

$$(H_3Si)_3SiCOCH_3 \; + \; H_3Si^- \longrightarrow (H_3Si)_2\overset{-}{Si}\cdots\overset{O}{C}-CH_3 \; + \; H_3SiSiH_3 \qquad (36)$$

B. Silyl Anions Bearing a Heteroatom in the α-Position

1. Amino-substituted silyl anions

Amino-substituted silyllithium compounds have been prepared by Tamao and coworkers from the corresponding chlorosilanes by treatment with either a dispersion of lithium metal in THF[88] (equation 37 and 38) or LDMAN[45] (equation 39).

$$\begin{array}{ccc} (Et_2N)_nPh_{3\text{-}n}SiCl & \xrightarrow[\text{THF}]{\text{Li}} & (Et_2N)_nPh_{3\text{-}n}SiLi \\ n = 1, 2 & & 97\text{-}98\% \end{array} \tag{37}$$

$$\begin{array}{ccc} (Et_2N)PhMeSiCl & \xrightarrow[\text{THF}]{\text{Li}} & (Et_2N)PhMeSiLi \\ & & 80\% \end{array} \tag{38}$$

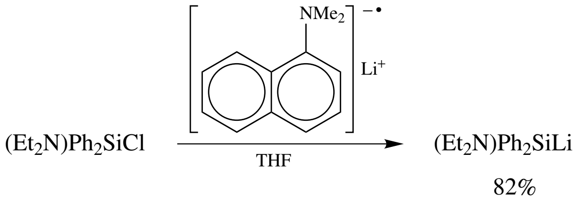

(39)

These α-functionalized lithiosilanes are stable for up to 6 days at 0 °C, when at least one substituent at silicon is an aryl group. Alkylated mono- or diaminochlorosilanes, however, undergo with lithium in THF homocoupling reactions to yield the corresponding symmetrical di- and tetraaminodisilanes (equation 40)[89].

$$\begin{array}{ll} (Et_2N)_nR_{3-n}SiCl & \xrightarrow[\text{THF}]{\text{Li}} (Et_2N)_nR_{3-n}SiSiR_{3-n}(NEt_2)_n \\ R = \text{alkyl},\ n = 1, 2 & \end{array} \tag{40}$$

(Amino)silyllithium compounds can be obtained alternatively by transmetalation of stannylated aminosilanes with *n*-BuLi or *t*-BuLi (equation 41)[90].

$$\begin{array}{ccc} (Et_2N)_nPh_{3-n}SiSnMe_3 & \xrightarrow[-RSnMe_3]{\text{RLi}} & (Et_2N)_nPh_{3-n}SiLi \\ n = 1,\ R = n\text{-Bu} & & 90\% \\ n = 2,\ R = t\text{-Bu} & & 77\% \end{array} \tag{41}$$

In sharp contrast to the aforementioned lithiated (amino)arylsilanes, 1,3-dilithio compounds **30**, which were prepared from the corresponding chlorosilanes **29** by treatment with lithium naphthalenide (equation 42), decompose completely after 3 h at 0 °C[91].

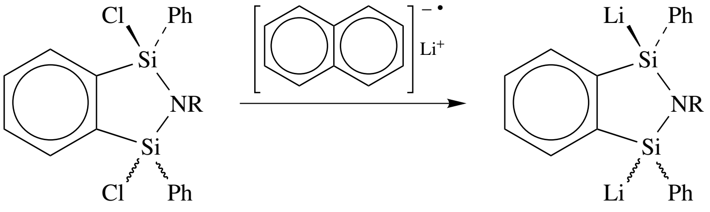

(42)

(**29**)
R = *n*-Bu, *t*-Bu

(**30**)

The ^{29}Si NMR signal of $(Et_2N)Ph_2SiLi$ is observed at $\delta = 19.34$ ppm. The ^{13}C NMR shifts of the aromatic carbon atoms resemble that of $MePh_2SiLi$, thus indicating that the charge distribution in both lithiosilanes is quite similar despite the fact that a methyl group was substituted by the electronically very different Et_2N group. $(Et_2N)Ph_2SiLi$ as well as $(Et_2N)Ph_2SiMgMe$ and $(Et_2N)Ph_2SiCu(CN)Li$, which are accessible from the corresponding lithium compound by reaction with MeMgBr or copper cyanide, respectively, have been used in reactions with allylsilanes, β-hydroxysilanes and vinylsilanes as synthetic equivalent of the hydroxy anion[92].

2. Alkoxy-substituted silyl anions

The first evidence for the existence of short-lived (alkoxy)silyl anions (e.g. **32**) was obtained by Watanabe and coworkers in the reaction of NaOMe with the corresponding disilanes **(31)**, which yielded in the presence of alkyl halides the expected trapping product of the intermediate (alkoxy)silyl sodium compounds **32** (equation 43)[93].

$$\begin{tikzcd}
(MeO)_nMe_{3\text{-}n}Si\text{—}SiMe_{3\text{-}n}(MeO)_n \arrow[r, "NaOMe"] & (MeO)_nMe_{3\text{-}n}SiNa \\
(\mathbf{31}) & (\mathbf{32}) \arrow[d, "RX"] \\
n = 1, 2 & (MeO)_nMe_{3\text{-}n}Si\text{—}R
\end{tikzcd} \qquad (43)$$

When the stannylated allyloxysilane **33** was treated with n-BuLi in THF at −78 °C, a rearranged product **36** was isolated after work-up with Me_3SiCl (equation 44). This reaction was assumed to proceed via the initial formation of the allyloxy-substituted silyllithium **34**, which subsequently — similar to a [2,3] Wittig rearrangement — undergoes a [2,3] sigmatropic rearrangement to yield the corresponding silanolate **35**[94].

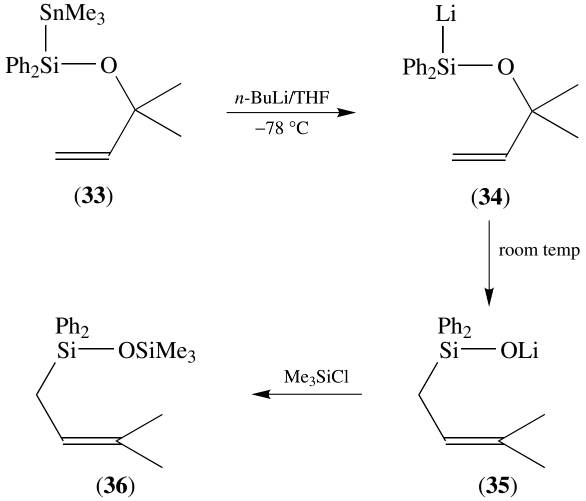

(**33**) (**34**) (**35**) (**36**)

(44)

(t-BuO)Ph_2SiLi **(37)** has been prepared by stannyl–lithium exchange from the corresponding silylstannane at low temperature (equation 45)[95]. In contrast to the analogous amino-substituted silyllithium $(Et_2N)Ph_2SiLi$, **37** is stable in THF at −78 °C only for several hours.

$$(t\text{-BuO})\mathrm{Ph_2Si{-}SnMe_3} \xrightarrow[\text{THF}/-78\,^\circ\text{C}]{n\text{-BuLi}} \underset{\mathbf{(37)}}{(t\text{-BuO})\mathrm{Ph_2SiLi}} \tag{45}$$

Other alkoxy-substituted silyllithium compounds such as (i-PrO)$\mathrm{Ph_2SiLi}$ and (MeO)$\mathrm{Ph_2SiLi}$ have been obtained by reduction of the corresponding chlorosilanes with LDMAN at −78 °C (equation 46)[45].

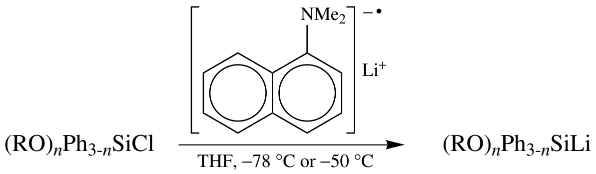

(46)

R = t-Bu (n = 1, 2), i-Pr (n = 1), Me (n = 1)

The use of LDMAN as the electron transfer reagent also allows (though a higher temperature of −50 °C is required) the preparation of a di(alkoxy)lithiosilane, (t-BuO)$_2$PhSiLi, from the corresponding chlorosilane[45]. Alternatively, this compound may be obtained from the chlorosilane by reaction with lithium metal at 0 °C[96].

The ^{29}Si nucleus of (t-BuO)$\mathrm{Ph_2SiLi}$ **(37)** resonates at $\delta = 11.3$ ppm, i.e. the ^{29}Si NMR signal is strongly lowfield shifted in comparison with (t-BuO)$\mathrm{Ph_2SiCl}$ ($\delta = -23.3$ ppm). Tamao and Kawachi[95] pointed out that the deshielding of the ^{29}Si nucleus of **37** is similar to the deshielding observed in the ^{13}C NMR spectra of carbenoids[97]. Moreover, the chemical properties of these alkoxy-substituted silyllithium compounds argue in favor of a silylenoid character of **37** (Scheme 11)[95]. Thus, when **37** is warmed to 0 °C, it undergoes a homocoupling reaction to yield, after work-up with $\mathrm{Me_3SiCl}$, the trisilane **38**; i.e. one molecule of **37** acts as a nucleophile, whereas a second molecule takes the role of the electrophile. Upon treatment with excess of n-BuLi in the presence of TMEDA, $\mathrm{BuPh_2SiLi}$, the result of a nucleophilic attack of n-BuLi on **37**, is obtained. However, the ambiphilic character of **37** is completely suppressed in the presence of 12-crown-6, which promotes the formation of a solvent-separated ion pair under these conditions. Self-condensation does not occur, and only reactions with electrophiles, such

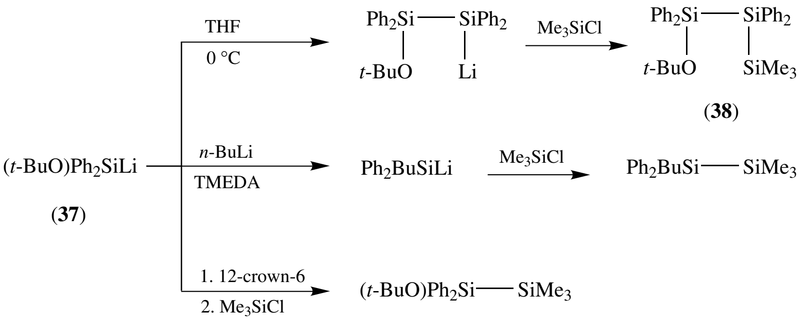

SCHEME 11

as Me_3SiCl, are observed. A similar ambiphilic reactivity was reported for (*i*-PrO)Ph_2SiLi and (MeO)Ph_2SiLi[45]. The di(alkoxy)lithiosilane (*t*-BuO)$_2$PhSiLi is thermally more stable than the lithiated monoalkoxy compounds: It can be kept in a THF solution at room temperature for longer periods without formation of even traces of the self-condensation product[45]. In addition, no nucleophilic substitution occurs with *n*-BuLi at this temperature, thus revealing the decreased electrophilicity of (*t*-BuO)$_2$PhSiLi relative to monoalkoxy silyllithium compounds.

3. Halogen-substituted silyl anions

Metalated halosilanes were postulated as intermediates in the reductive coupling reactions of dihalosilanes **39** to yield linear and cyclic oligo- and polysilanes (Scheme 12).

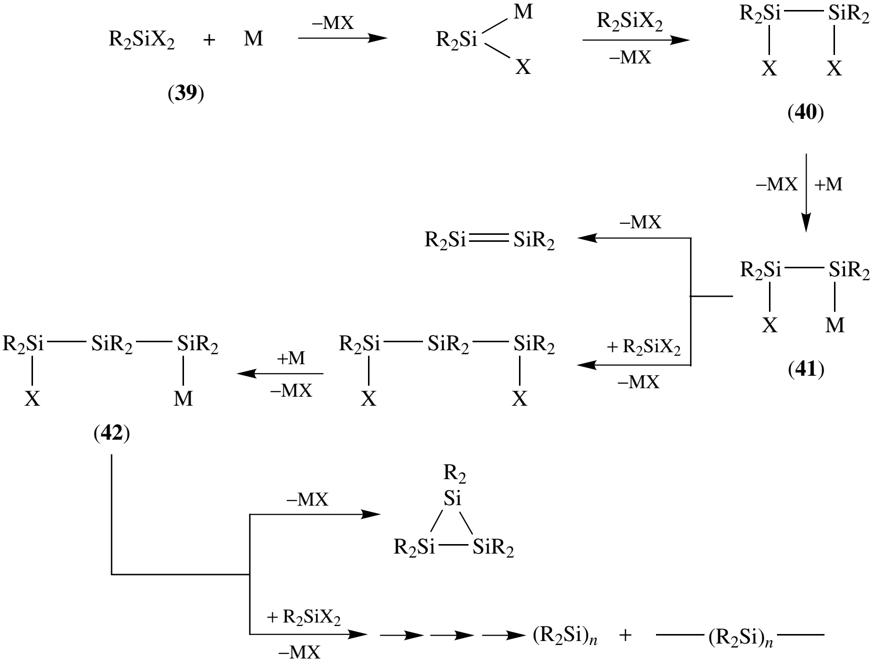

SCHEME 12

The 1,2-dihalodisilane **40**, which is formed by nucleophilic attack of the α-functionalized metalated silane on the starting material, is subsequently converted to the 1-halo-2-metalladisilane **41**. At this stage, the steric demand of the substituents at silicon strongly influences the outcome of the reaction[98]. With very bulky substituents (e.g. R = Tip[78]), elimination of metal halide forms a disilene[99]. Less bulky substituents such as *t*-butyl or *i*-propyl favor, via 1-halo-3-metallatrisilane **42**, the formation of cyclotri- and tetrasilanes[99a,100], whereas dihalosilanes with relatively small substituents such as methyl or phenyl undergo coupling reactions to yield larger rings and acyclic polysilanes[101].

$LiSiCl_3$ was probably formed by a halogen−metal exchange reaction, when an attempt was made to couple the highly hindered aryllithium compound **43** with $BrSiCl_3$

(equation 47)[102].

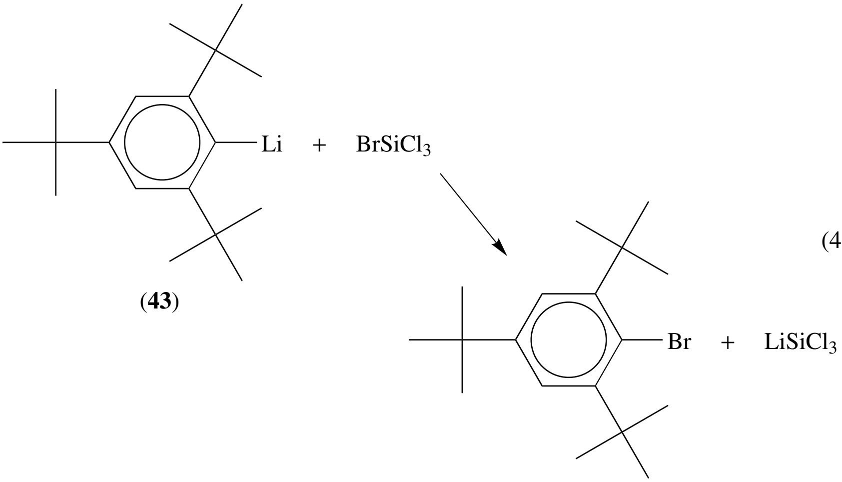

(**43**)

(47)

The formation of $(i\text{-Pr})_3NH^+$ upon treatment of $HSiCl_3$ with $(i\text{-Pr})_3N$ in refluxing CH_3CN indicates that $HSiCl_3$ is deprotonated by this and also by other amines such as $(n\text{-Bu})_3N$ or TMEDA[103,104]. According to ^1H NMR studies this proton transfer is reversible (equation 48).

$$HSiCl_3 + (i\text{-Pr})_3N \rightleftharpoons Cl_3Si^- + (i\text{-Pr})_3NH^+ \qquad (48)$$

Mixtures of tertiary amines with $HSiCl_3$ have been used to introduce the trichlorosilyl group, *inter alia*, into olefins[105a] (equation 49) or to convert aromatic carboxylic acids to the corresponding toluenes[105b] (equation 50).

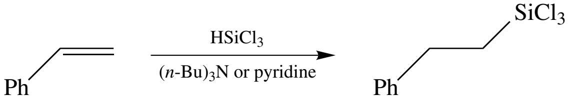

(49)

$$ArCO_2H \xrightarrow[CH_3CN]{\Delta,HSiCl_3} \xrightarrow[\Delta]{(n\text{-Pr})_3N} \xrightarrow[MeOH/H_2O]{\Delta,\ KOH} ArCH_3 \qquad (50)$$

Similarly, the mixture of TMEDA with RCl_2SiH ($R = Me, Ph$) was reported to act in the presence of copper(0), copper(I) or copper(II) catalysts as a useful synthetic equivalent of the corresponding RCl_2Si^- anion (equation 51)[104].

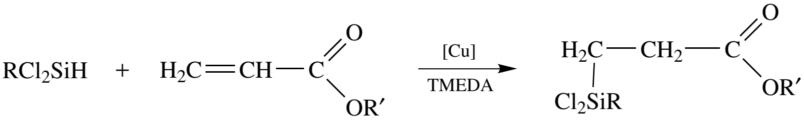

$$RCl_2SiH + H_2C{=}CH{-}C({=}O)OR' \xrightarrow[TMEDA]{[Cu]} H_2C(SiCl_2R){-}CH_2{-}C({=}O)OR' \qquad (51)$$

R = Me, Ph, Cl ; R′ = Me, Et

VIII. MISCELLANEOUS

A. Mono- and Dianions of Silacyclopentadienes

Remarkable advancements have been made in the chemistry of metalated silacyclopentadienes (siloles) during the last few years.

The interest in silole monoanions centers mainly on the question of aromaticity in these compounds. According to early 3-21G/STO-2G calculations by Gordon and coworkers, $[SiC_4H_5]^-$ is about 25% as aromatic as $[C_5H_5]^-$[106]. The optimized structure of the silole anion has C_s symmetry with a pyramidal silicon center. The calculated energy barrier for the inversion at silicon through a planar transition state of C_{2v} symmetry is 16.2 $kcal\,mol^{-1}$ at HF/6-31G*//6-31G*[107], significantly lower than the value of 26 $kcal\,mol^{-1}$ calculated for $[SiH_3]^-$, and it was proposed that this reflects the small, but not negligible, stabilization of the transition state by electron delocalization[107]. More recent calculations by Schleyer and Goldfuss using the considerably better RMP2/6-31+G*//RMP2/6-31+G* level reveal a silicon center of $[SiC_4H_5]^-$, which is still pyramidal, but strongly flattened (angle sum around Si is 321.6°). The calculated inversion barrier is reduced at this computational level to only 3.8 $kcal\,mol^{-1}$[108a]. These results, which imply a certain degree of aromaticity in $[SiC_4H_5]^-$, are in agreement with calculations of the magnetic properties of this anion such as the diamagnetic susceptibility exaltation, which is about 50% of that found for $[C_5H_5]^-$[108b]. Calculations on $[SiC_4H_5]Li$ at the RMP2/6-31+G*//RMP2/6-31+G* level found a C_s structure, which features a η^5 coordinated lithium atom. In C_4H_5SiLi, planarization at the silicon center has increased (angle sum around Si is 340.2°) and the ring C−C bond lengths are nearly equalized, as expected for an aromatic system[108a]. Moreover, the aromatic stabilization energy (ASE), which has been calculated by using appropriate isodesmic reactions, increases on going from the silole anion to the lithium compound: $[SiC_4H_5]^-$ exhibits 55% of the ASE of $[C_5H_5]^-$, whereas the ASE of $[SiC_4H_5]Li$ amounts to 80% of that computed for $[C_5H_5]Li$. In summary, according to these calculations, the silole anion $[SiC_4H_5]^-$ 'exhibits at least moderate aromaticity, which is enhanced strongly by η^5 coordination of Li^+'[108a].

The reaction of silole **44** with KH in THF or DME yields, after work-up with D_2O, quantitatively the corresponding deuteriated silole (equation 52); metalated siloles have been suggested as intermediates[8b]. In contrast, the analogous treatment of silole **45** with KH yields a mixture of three NMR spectroscopically characterized potassium compounds (equation 53). The main product of this reaction is the pentavalent silicate **46**, which results from the nucleophilic attack of a hydride at the silicon center[109]. The other two products result from hydride addition to one of the ring carbons.

The first metalated silole, **48**, which was characterized unambiguously by means of NMR spectroscopy, has been obtained by Boudjouk and coworkers via reductive cleavage of the Si−Si bond of disilane **47** with lithium or sodium under ultrasonic activation (equation 54)[110a].

Most significant is the appreciable deshielding of the silicon nucleus upon metalation: The ^{29}Si NMR signal is shifted to low-field on going from the disilane to the metalated silole [$\Delta\delta = 21.48$ (Li) and 22.50 (Na) ppm, respectively], which sharply contrasts with the upfield shift, which is characteristic for the conversion of aryl-substituted disilanes into the corresponding silyl anions (Section V.B). The deshielding of the silicon nucleus as well as the shielding of the C_α and C_β nuclei of the five-membered ring indicates appreciable charge transfer from the silicon center into the butadiene moiety. These trends are nicely reproduced by the calculated (IGLO) chemical shifts for $[SiC_4H_5]Li$[108a].

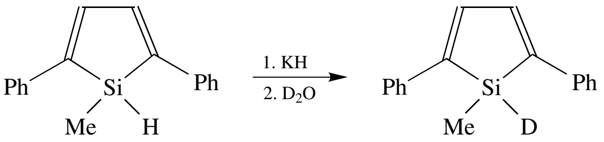

(**44**)

(52)

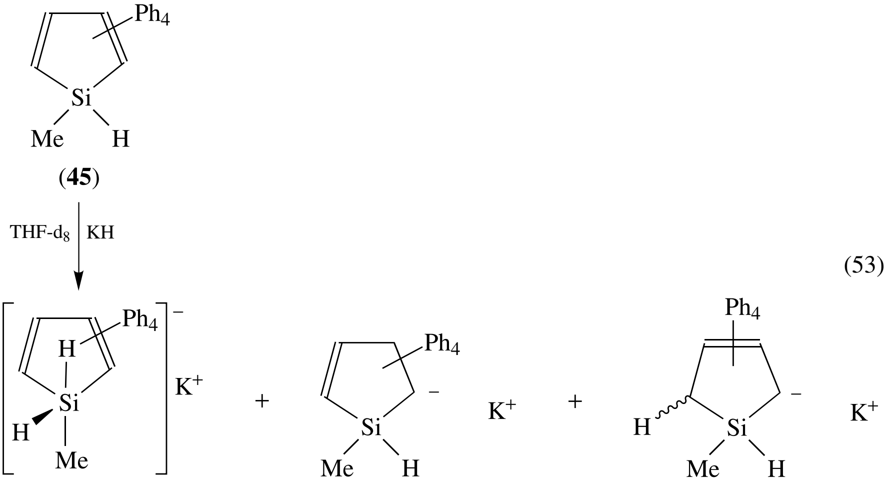

(**45**)

(53)

(**46**)

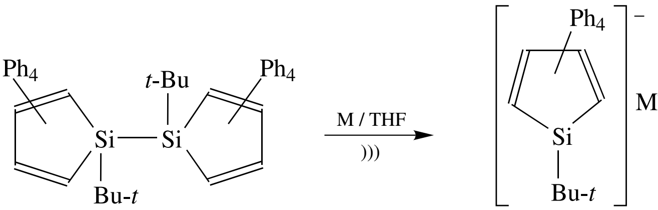

(54)

(**47**) (**48**)

In contrast to these experimental and computational results, lithiated 1-silafluorenide **50**, which was prepared by the reductive cleavage of the central Si−Si bond of disilane **49** with lithium under ultrasonic activation, provides some evidence for the existence of localized metalated siloles (equation 55)[111]. Thus, upon metalation of **49** to form **50**, a highfield shift of the ^{29}Si nucleus ($\Delta\delta = -47.9$ ppm) is observed. In addition, the chemical shifts of the phenyl carbons indicate that there is no accumulation of π electron density, which would be expected for a delocalized lithium silafluorenide[111].

The reductive dehalogenation of permethylated 1,1-dibromosilole **51** and the subsequent reactions were used by Tilley and coworkers to synthesize the metalated siloles

52–54 (Scheme 13)[112a].

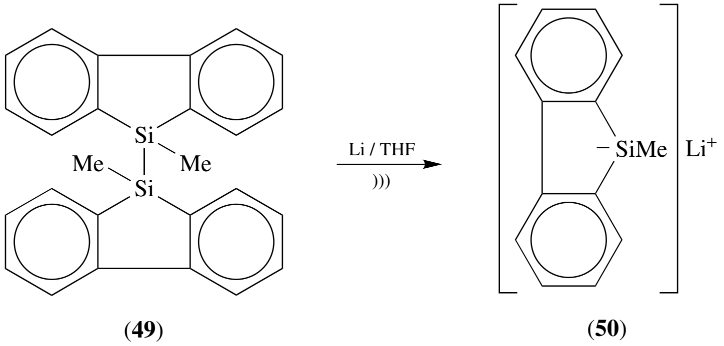

(55)

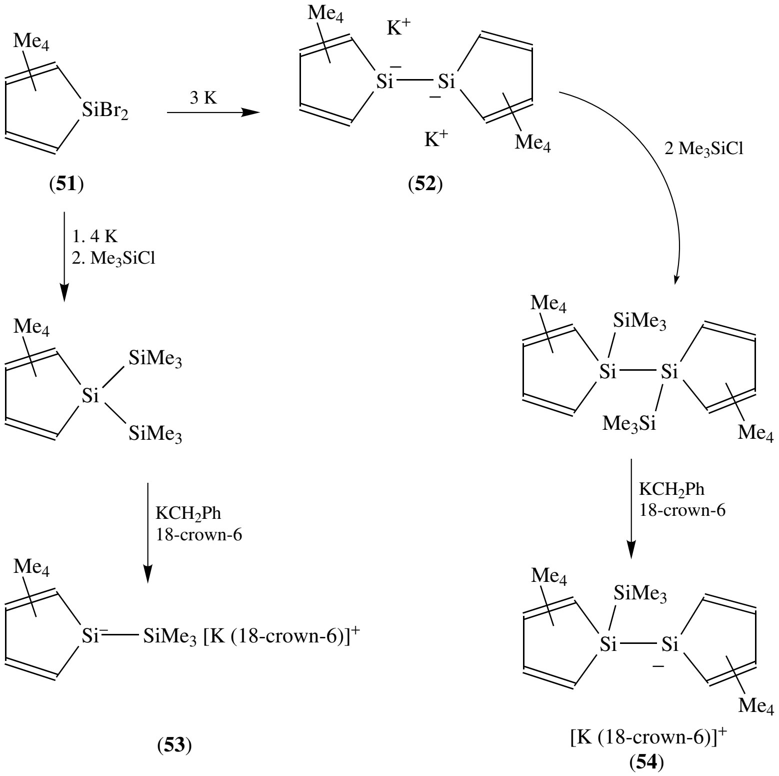

SCHEME 13

The highfield shifted ^{29}Si NMR signal of the 18-crown-6 complex of [$C_4Me_4(SiMe_3)Si$]K **(53)** in solution as well as the strongly pyramidalized silicon center (angle sum around Si is 279.3°) and the bond localization, which were found in the solid state (Figure 9), support a nonaromatic nature with fixed double bonds for the silole

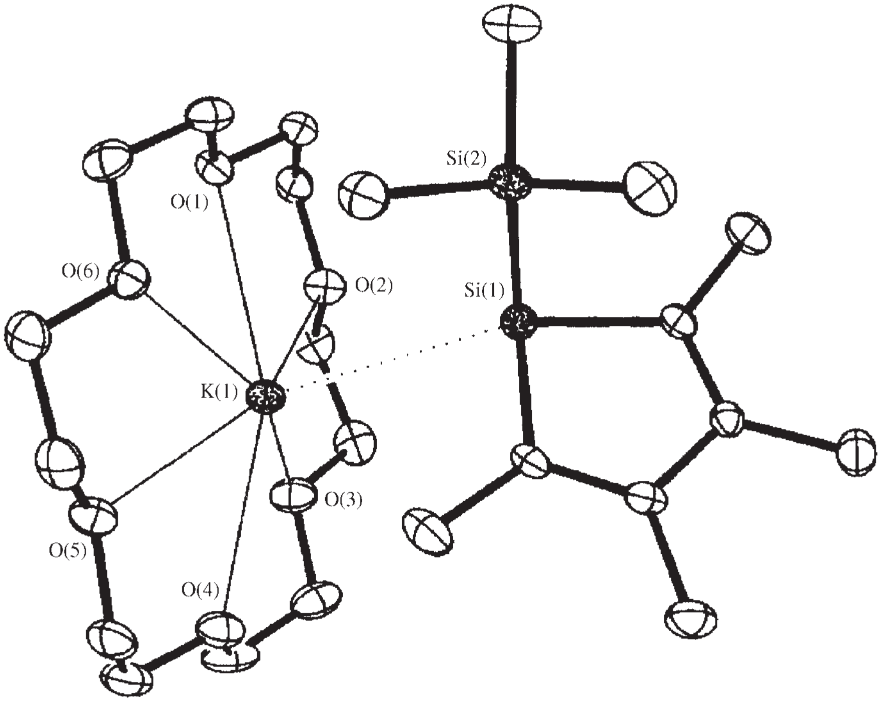

FIGURE 9. Solid state structure of **53** with hydrogen atoms omitted. Reprinted with permission from Reference 112b. Copyright 1996 American Chemical Society

ring[112b]. Variable-temperature NMR spectroscopy of the tetraethyl-substituted siloles, with potassium or the 18-crown-6 complex of potassium as countercations, allows one to estimate the inversion barrier of these compounds as being lower than 8 kcal mol^{-1}. These exceptionally low inversion barriers were attributed to stabilization of the planar transition state by delocalization of the π-electron density[112b]. In conclusion, when comparing the experimental results for siloles such as **48**, **50** and **53**, it appears that the electronic structure of metalated siloles is highly sensitive to the nature of the substituent at silicon and at the ring carbon atoms.

According to theoretical results, silole dianions and dimetalated siloles are aromatic compounds. The geometries of $[H_4C_4Si]^{2-}$, $[H_4C_4Si]Li^-$, $[H_4C_4Si]Li_2$, $[H_4C_4Si]Na_2$ and $[H_4C_4Si]K_2$ have been calculated by Schleyer and coworkers at the RMP2/6-31+G* level, and in all these compounds the five-membered C_4Si ring is planar[113]. The dimetalated siloles prefer an inverted C_{2v} sandwich-type structure, in which the metal centers are located above and below the C_4Si ring, thus adopting an η^5-coordination. The equalized ring bond lengths as well as the calculated aromatic stabilization energies point to a substantial degree of aromaticity in these compounds, which approaches the aromaticity of the $[C_5H_5]^-$ anion. The diamagnetic susceptibility exaltations, which may be used as a gauge for the aromaticity of a system, indicate large aromatic ring currents; these are responsible for the strong shielding of the ^{7}Li nucleus, which results in a calculated chemical shift (IGLO) of $\delta = -7.7$ ppm.

The first experimental evidence for the existence of a dimetalated silole **56** was obtained by Joo and coworkers from treatment of 1,1-dichlorosilole **55** with sodium in dioxane[114]. A red solid was isolated from this reaction, which yielded upon addition of electrophiles such as Me_2HSiCl or Me_3SiCl the corresponding **57**. Upon treatment with *t*-BuCl or Me_3SnCl, coupling products **58** were obtained (Scheme 14).

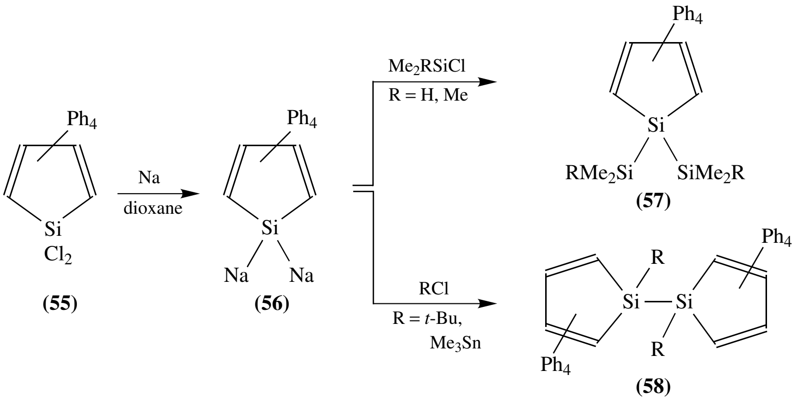

SCHEME 14

A mixture of analogous products was formed when **55** was treated with lithium metal in THF, and the resulting solution was worked up with Me_3SiCl (equation 56)[115].

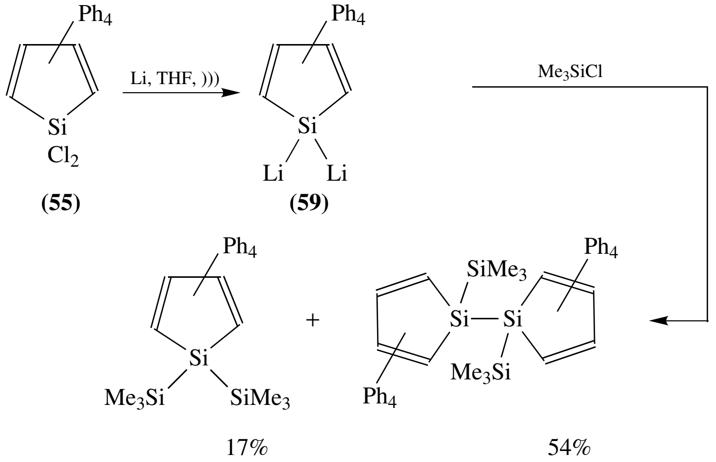

(56)

NMR studies showed that the only anionic intermediate which is present in solution is dilithiosilole **59**[115]. The marked downfield shift in the ^{29}Si NMR spectrum ($\delta = +68.4$ ppm) of **59** as well as the shielding of the C_α and C_β nuclei indicate, in agreement with calculations[113], an aromatic character of this compound. This conclusion is supported by the solid state structure of **59** (Figure 10)[116]. The silole ring in **59** is planar and exhibits nearly equal C−C distances, as one would expect for a delocalized system. However, in contrast to the computational results[113,116], the lithium atoms in **59** are not

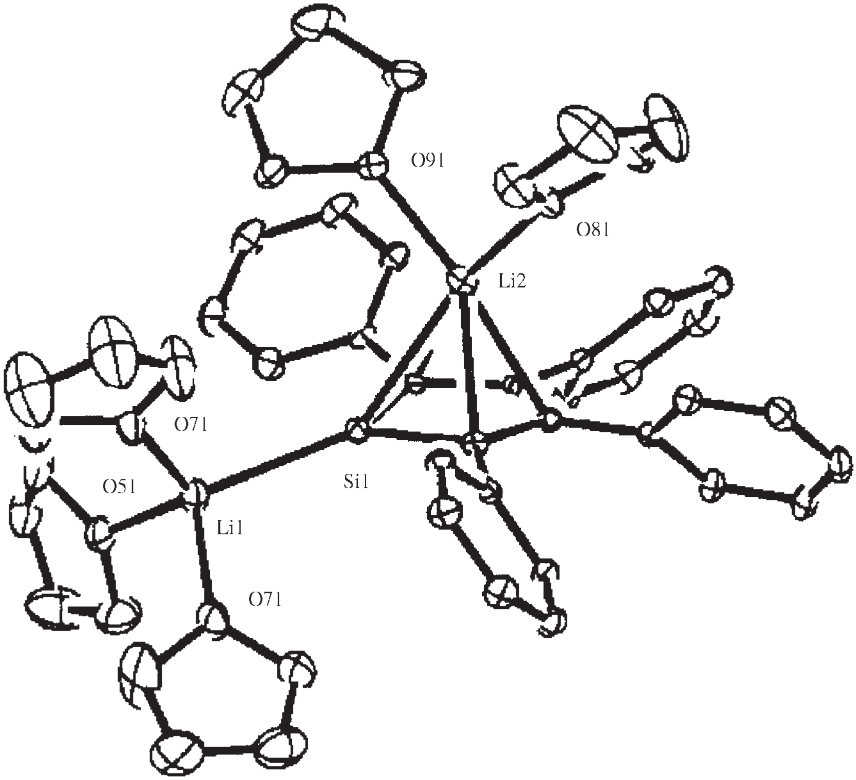

FIGURE 10. Solid state structure of **59** with hydrogen atoms omitted. Reprinted with permission from Reference 116. Copyright 1995 American Chemical Society

equivalent: one of them is η^5-coordinated to the planar silole ring, whereas the other is η^1-bonded to the silicon center. This is in clear contradiction to the calculated minimum structure of the parent bismetalated silole[113,116] for which a $\eta^1-\eta^5$ structure has been calculated to be 21 kcal mol^{-1} less stable than the C_{2v} symmetrical $\eta^5-\eta^5$ structure[116]. However, as pointed out by West and coworkers, solvation of the cationic centers by THF as well as crystal packing effects could reverse this stability order[116].

In contrast to these experimental findings, the 18-crown-6 complex of [Me_4C_4Si]K_2, which was prepared by the reaction of the corresponding dibromosilole with potassium metal in the presence of 18-crown-6 (2 equivalents), adopts in the solid state, in agreement with calculations[113,116], an inverted sandwich structure (Figure 11)[112], thus supporting the theoretical results[113] that the C_{2v} structure is more stable than the η^1-η^5 structure.

B. Oligolithiated Monosilanes

When lithium vapor was reacted with $SiCl_4$ in a Knudsen cell, and the reaction product was treated with excess methyl chloride, Me_4Si was obtained in 5–10% yield. This result was interpreted in terms of the formation of $SiLi_4$[117]. Interestingly, tetrahedral $SiLi_4$ is a saddle point of 3rd order at the 3-21G* level of theory[118]. The minimum structure of

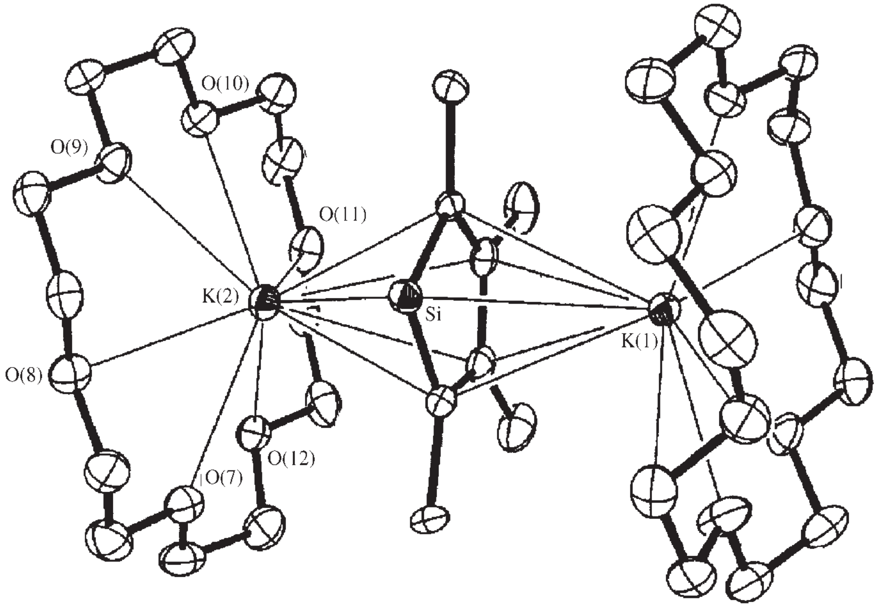

FIGURE 11. Solid state structure of $[(18\text{-crown-}6)\mathrm{K}]_2[\mathrm{SiC_4Me_4}]$ with hydrogen atoms omitted. Reproduced from Reference 112a by permission of VCH Verlagsgesellschaft, Weinheim

$\mathrm{SiLi_4}$ has $C_{2\mathrm{v}}$ symmetry and it exhibits an inverted tetrahedron **60** (Figure 11); the equatorial and axial lithium atoms exchange easily via a $C_{4\mathrm{v}}$ symmetrical transition state, which is only 3.2 kcal mol^{-1} higher in energy than **60** (bond lengths in pm)[118].

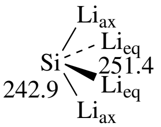

(**60**) $C_{2\mathrm{v}}$

Thermolysis of $(\mathrm{Me_3Si})_3\mathrm{SiLi}$ at 140–150 °C *in vacuo* for 4 h appears to result in the formation of 1,1-dilithiosilane $(\mathrm{Me_3Si})_2\mathrm{SiLi_2}$, which was quenched with $\mathrm{D_2O}$ to yield 35% of $(\mathrm{Me_3Si})_2\mathrm{SiD_2}$ (equation 57)[119].

$$\begin{array}{lcccc}
(\mathrm{Me_3Si})_3\mathrm{SiLi} & \xrightarrow[4\ \mathrm{h}]{140\text{-}150\ ^\circ\mathrm{C}}\ \xrightarrow{\mathrm{D_2O}} & (\mathrm{Me_3Si})_3\mathrm{SiD_2} & + & \mathrm{Me_3SiSiMe_3} \\
 & & 35\% & & \text{not stated}
\end{array} \qquad (57)$$

$$\begin{array}{cccccc}
+ & (\mathrm{Me_3Si})_3\mathrm{SiD} & + & (\mathrm{Me_3Si})_4\mathrm{Si} & + & (\mathrm{Me_3Si})_3\mathrm{SiSi(SiMe_3)_3} \\
 & 22\% & & 10\% & & 27\%\quad (\mathbf{12})
\end{array}$$

The major by-product in this reaction is the hexasilane **12**, which is formed at the expense of the dilithio compound, when the reaction time is extended. In the flash vaporization mass spectrum of solid $(Me_3Si)_2SiLi_2$ the parent ions of the monomer and dimer of the dilithiosilane have been observed. According to *ab initio* calculations for H_2SiLi_2 at the MP4SDTQ/6-31G**//6-31G** level, a structure **61** (bond lengths in pm) in which the lithium atoms are placed unsymmetrically with respect to the mirror plane of the SiH_2 moiety is 6.3 kcal mol^{-1} lower in energy than the conventional tetrahedral geometry[120].

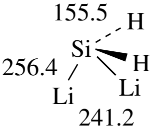

(**61**) C_s

IX. REFERENCES

1. Recent reviews on silyl anions:
   (a) P. D. Lickiss and C. M. Smith, *Coord. Chem. Rev.*, **145**, 75 (1995).
   (b) K. Tamao and A. Kawachi, *Adv. Organomet. Chem.*, **38**, 1 (1995).
   (c) M. Fujita and T. J. Hiyama, *Yuki Gosei Kagaku Kyokaishi*, **42**, 293 (1984); *Chem. Abstr.*, **101**, 55130b (1984).
   Structural studies of silyl anions:
   (d) W. S. Sheldrick, in *The Chemistry of Organic Silicon Compounds* (Eds. S. Patai and Z. Rappoport), Wiley, Chichester, 1989, pp. 268–272.
   (e) E. Lukevics, O. Pudova and R. Strukovich, *Molecular Structure of Organosilicon Compounds*, Ellis Horwood, Chichester, 1989, pp. 76–84.
   (f) J. B. Lambert and W. J. Schultz, Jr., in *The Chemistry of Organic Silicon Compounds* (Eds. S. Patai and Z. Rappoport), Wiley, Chichester, 1989, pp. 1007–1010.
   Theoretical studies of silyl anions:
   (g) Y. Apeloig, in *The Chemistry of Organic Silicon Compounds* (Eds. S. Patai and Z. Rappoport), Wiley, Chichester, 1989, pp. 80, 201–204.
   Synthetic applications of silyl anions:
   (h) D. D. Davis and C. E. Gray, *Organomet. Chem. Rev.*, **6**, 283 (1970).
   (i) I. Fleming, in *Comprehensive Organic Chemistry*, Vol. 3 (Eds. D. Barton and W. D. Ollis), Pergamon, Oxford, 1979, pp. 541–669.
   (j) P. D. Magnus, T. Sarkar and S. Djuric, in *Comprehensive Organometallic Chemistry*, Vol. 3 (Eds. G. Wilkinson, F. G. A. Stone and E. W. Abel), Pergamon, Oxford, 1982, pp. 608–614.
   (k) E. W. Colvin, *Silicon in Organic Synthesis*, Academic Press, London, 1988, pp. 51–55.
2. (a) M. A. Ring and D. M. Ritter, *J. Am. Chem. Soc.*, **83**, 802 (1961).
   (b) M. A. Ring and D. M. Ritter, *J. Phys. Chem.*, **65**, 182 (1961).
   (c) E. Amberger and E. Muehlhofer, *J. Organomet. Chem.*, **12**, 55 (1968).
   (d) H. Bürger, R. Eujen and H. C. Marsmann, *Z. Naturforsch., Teil B*, **29B**, 149 (1974).
   (e) O. Mundt, G. Becker, H.-M. Hartmann and W. Schwarz, *Z. Anorg. Allg. Chem*, **572**, 75 (1989).
   (f) T. Lobreyer, J. Oeler and W. Sundermeyer, *Chem. Ber.*, **124**, 2405 (1991).
3. E. Weiss, G. Hencken and H. Kuehr, *Chem. Ber.*, **103**, 2868 (1970).
4. (a) F. Fehér, M. Krancher and M. Fehér, *Z. Anorg. Allg. Chem*, **606**, 7 (1991).
   (b) T. Lobreyer, J. Oeler, W. Sundermeyer and H. Oberhammer, *Chem. Ber.*, **126**, 665 (1993).
5. B. T. Luke, J. A. Pople, M.-B. Krogh-Jespersen, Y. Apeloig, J. Chandrasekhar and P. v. R. Schleyer, *J. Am. Chem. Soc.*, **108**, 260 (1986).
6. P. v. R. Schleyer and T. Clark, *J. Chem. Soc., Chem. Commun.*, 1371 (1986).
7. W. Sundermeyer, T. Lobreyer, H. Pritzkow, N. J. R. v. E. Hommes and P. v. R. Schleyer, *Angew. Chem.*, **106**, 221 (1994); *Angew. Chem., Int. Ed. Engl.*, **33**, 216 (1994).

8. (a) R. J. P. Corriu and C. Guérin, *J. Chem. Soc., Chem. Commun.*, 168 (1980).
   (b) R. J. P. Corriu, C. Guérin and B. Kolani, *Bull. Soc. Chim. Fr.*, 973 (1985).
   (c) L. Rösch, W. Erb and H. Müller, *Z. Naturforsch., Teil B*, **31B**, 281 (1976).
9. R. J. P. Corriu, C. Guérin, J. L. Brefort and B. Henner, *J. Organomet. Chem.*, **370**, 9 (1989).
10. (a) W. C. Still, *J. Org. Chem.*, **41**, 3063 (1976).
    (b) E. B. Nadler and Z. Rappoport, *Tetrahedron Lett.*, **31**, 555 (1990).
11. (a) P. F. Hudrlik, M. A. Waugh and A. M. Hudrlik, *J. Organomet. Chem.*, **271**, 69 (1984).
    (b) P. F. Hudrlik, A. M. Hudrlik, T. Yimenu, M. A. Waugh and G. Nagendrappa, *Tetrahedron*, **44**, 3791 (1988).
    (c) L. Gong, R. Leung-Toung and T. T. Tidwell, *J. Org. Chem.*, **55**, 3634 (1990).
    (d) K. Krohn and K. Khanbabaee, *Angew. Chem.* **106**, 100 (1994); *Angew. Chem., Int. Ed. Engl.*, **33**, 99 (1994).
12. (a) T. F. Schaaf and J. P. Oliver, *J. Am. Chem. Soc.*, **91**, 4327 (1969).
    (b) E. Hengge and N. Holtschmidt, *J. Organomet. Chem.*, **12**, P5 (1968).
13. (a) H. Sakurai, A. Okada, M. Kira and K. Yonezawa, *Tetrahedron Lett.*, 1511 (1971).
    (b) H. Sakurai and F. Kondo, *J. Organomet. Chem.*, **92**, C46 (1975).
    (c) M. A. Shippey and P. B. Dervan, *J. Org. Chem.*, **42**, 2654 (1977).
    (d) E. Buncel, T. K. Venkatachalam and U. Edlund, *J. Organomet. Chem.*, **437**, 85 (1992).
14. T. Hiyama, M. Obayashi, I. Mori and H. Nozaki, *J. Org. Chem.*, **48**, 912 (1983).
15. T. Hiyama, M. Obayashi and M. Sawahata, *Tetrahedron Lett.*, **24**, 4113 (1983).
16. T. Hiyama and M. Obayashi, *Tetrahedron Lett.*, **24**, 4109 (1983).
17. N. S. Vyazankin, G. A. Razuvaev, E. N. Gladyshev and S. P. Korneva, *J. Organomet. Chem.*, **7**, 353 (1967).
18. E. N. Gladyshev, E. A. Fedorova, L. O. Yuntila, G. A. Razuvaev and N. S. Vyazankin, *J. Organomet. Chem.*, **96**, 169 (1975).
19. (a) N. Wiberg and K. Schurz, *J. Organomet. Chem.*, **341**, 145 (1988).
    (b) N. Wiberg, H. Schuster, A. Simon and K. Peters, *Angew. Chem.*, **98**, 100 (1986); *Angew. Chem., Int. Ed. Engl.*, **25**, 79 (1986).
20. A. Fürstner and H. Weidmann, *J. Organomet. Chem.*, **354**, 15 (1988).
21. B. H. Lipshutz, D. C. Reuter and E. L. Ellsworth, *J. Org. Chem.*, **54**, 4975 (1989).
22. A. R. Claggett, W. H. Ilsley, T. J. Anderson, M. D. Glick and J. P. Oliver, *J. Am. Chem. Soc.*, **99**, 1797 (1977).
23. L. Rösch, J. Pickardt, S. Imme and U. Börner, *Z. Naturforsch., Teil B*, **41B**, 1523 (1986).
24. J. P. Oliver, D. W. Goebel, Jr. and J. L. Hencher, *Organometallics*, **2**, 746 (1983).
25. R. Goddard, C. Krüger, N. A. Ramadan and A. Ritter, *Angew. Chem.*, **107**, 1107 (1995); *Angew. Chem., Int. Ed. Engl.*, **34**, 1030 (1995).
26. W. H. Ilsey, T. F. Schaaf, M. D. Glick and J. P. Oliver, *J. Am. Chem. Soc.*, **102**, 3769 (1980).
27. B. Teclé, W. H. Ilsley and J. P. Oliver, *Organometallics*, **1**, 875 (1982).
28. (a) M. V. George, D. J. Peterson and H. J. Gilman, *J. Am. Chem. Soc.*, **82**, 403 (1960).
    (b) A. G. Brook and H. J. Gilman, *J. Am. Chem. Soc.*, **76**, 278 (1954).
    (c) B. K. Campion, R. H. Heyn and T. D. Tilley, *Organometallics*, **12**, 2584 (1993).
    (d) H. Wagner and U. Schubert, *Chem. Ber.*, **123**, 2101 (1990).
    (e) J. Meyer, J. Willnecker and U. Schubert, *Chem. Ber.*, **122**, 223 (1989).
    (f) R. A. Benkeser and R. G. Severson, *J. Am. Chem. Soc.*, **73**, 1424 (1951).
    (g) E. Colomer and R. J. P. Corriu, *J. Chem. Soc., Chem. Commun.*, 176 (1976).
29. H. Gilman and T. C. Wu, *J. Am. Chem. Soc.*, **73**, 4031 (1951).
30. E. Colomer and R. J. P. Corriu, *J. Organomet. Chem.*, **133**, 159 (1977).
31. D. L. Comins and M. O. Killpack, *J. Am. Chem. Soc.*, **114**, 10972 (1992).
32. T. G. Selin and R. West, *Tetrahedron*, **5**, 97 (1959).
33. H. Gilman and G. D. Lichtenwalter, *J. Am. Chem. Soc.*, **80**, 608 (1958).
34. C. M. Smith and P. D. Lickiss, in *Xth International Symposium on Organosilicon Chemistry*, Poznań, Poland, 1993, P-142.
35. B. Reiter and K. Hassler, *J. Organomet. Chem.*, **467**, 21 (1994).
36. E. Buncel, T. K. Venkatachalam, B. Eliasson and U. Edlund, *J. Am. Chem. Soc.*, **107**, 303 (1985).
37. J. B. Lambert and M. J. Urdaneta-Pérez, *J. Am. Chem. Soc.*, **100**, 157 (1978).
38. I. Fleming and S. B. D. Winter, *Tetrahedron Lett.*, **34**, 7287 (1993).
39. L. H. Sommer and R. Mason, *J. Am. Chem. Soc.*, **87**, 1619 (1965).

40. H. Gilman and W. Steudel, *Chem. Ind. (London)*, 1094 (1959).
41. J. Belzner and U. Dehnert, unpublished results.
42. W. Ando, K. Hatano and R. Urisaka, *Organometallics*, **14**, 3625 (1995).
43. (a) S. Sharma and A. C. Oehlschlager, *Tetrahedron*, **45**, 557 (1989).
    (b) S. Sharma and A. C. Oehlschlager, *J. Org. Chem.*, **54**, 5383 (1989).
    (c) S. Sharma and A. C. Oehlschlager, *J. Org. Chem.*, **56**, 770 (1991).
    (d) R. D. Singer and A. C. Oehlschlager, *J. Org. Chem.*, **56**, 3510 (1991).
44. (a) M. Weidenbruch, K. Kramer, K. Peters and H. G. v. Schnering, *Z. Naturforsch., Teil B*, **40B**, 601 (1985).
    (b) D. M. Roddick, R. H. Heyn and T. D. Tilley, *Organometallics*, **8**, 324 (1989).
45. K. Tamao and A. Kawachi, *Organometallics*, **14**, 3108 (1995).
46. E. Buncel, R. D. Gordon and T. K. Venkatachalam, *J. Organomet. Chem.*, **507**, 81 (1996).
47. (a) G. A. Olah and R. J. Hunadi, *J. Am. Chem. Soc.*, **102**, 6989 (1980).
    (b) U. Edlund, T. Lejon, T. K. Venkatachalam and E. Buncel, *J. Am. Chem. Soc.*, **107**, 6408 (1985).
48. A. G. Evans, M. A. Hamid and N. H. Rees, *J. Chem. Soc. B*, 1110 (1971).
49. (a) H. V. R. Dias, M. M. Olmstead, K. Ruhlandt-Senge and P. P. Power, *J. Organomet. Chem.*, **462**, 1 (1993).
    (b) A. H. Cowley, T. M. Elkins, R. A. Jones and C. M. Nunn, *Angew. Chem.*, **100**, 1396 (1988); *Angew. Chem., Int. Ed. Engl.*, **27**, 1349 (1988).
50. R. A. Bartlett, H. V. R. Dias and P. P. Power, *J. Organomet. Chem.*, **341**, 1 (1988).
51. (a) U. Edlund, T. Lejon, P. Pyykkö, T. K. Venkatachalam and E. Buncel, *J. Am. Chem. Soc.*, **109**, 5982 (1987).
    (b) E. Buncel, T. K. Venkatachalam and U. Edlund, *Can. J. Chem.*, **64**, 1674 (1986).
52. For a comprehensive table, see: K. Tamao and A. Kawachi, *Adv. Organomet. Chem.*, **38**, 48–49 (1995).
53. T. Koizumi, K. Morihashi and O. Kikuchi, *Organometallics*, **14**, 4018 (1995).
54. M. R. Nimlos and G. B. Ellison, *J. Am. Chem. Soc.*, **108**, 6522 (1986).
55. H. Bürger and R. Eujen, *Z. Naturforsch., Teil B*, **29B**, 647 (1974).
56. A. Sekiguchi, M. Nanjo, C. Kabuto and H. Sakurai, *Organometallics*, **14**, 2630 (1995).
57. A. G. Brook, A. Baumegger and A. J. Lough, *Organometallics*, **11**, 310 (1992).
58. O. W. Steward, G. L. Heider and J. S. Johnson, *J. Organomet. Chem.*, **168**, 33 (1979).
59. K. E. Ruehl, M. E. Davis and K. Matyjaszewski, *Organometallics*, **11**, 788 (1992).
60. (a) M. Kumada, S. Sakamoto and M. Ishikawa, *J. Organomet. Chem.*, **17**, 231 (1969).
    (b) M. Kumada, S. Sakamoto, M. Ishikawa and S. Maeda, *J. Organomet. Chem.*, **17**, 223 (1969).
61. A. Sekiguchi, M. Nanjo, C. Kabuto and H. Sakurai, *J. Am. Chem. Soc.*, **117**, 4195 (1995).
62. (a) M. J. Fink and D. B. Puranik, *Organometallics*, **6**, 1809 (1987).
    (b) D. B. Puranik, M. P. Johnson and M. J. Fink, *Organometallics*, **8**, 770 (1989).
    (c) K. M. Baines, A. G. Brook, R. R. Ford, P. D. Lickiss, A. K. Saxena, W. J. Chatterton, J. F. Sawyer and B. A. Behnam, *Organometallics*, **8**, 693 (1989).
63. (a) H. Gilman and C. L. Smith, *J. Organomet. Chem.*, **14**, 91 (1968).
    (b) G. Gutekunst and A. G. Brook, *J. Organomet. Chem.*, **225**, 1 (1982).
    (c) W. Biffar and H. Nöth, *Z. Naturforsch., Teil B*, **36B**, 1509 (1981).
64. A. Heine, R. Herbst-Irmer, G. M. Sheldrick and D. Stalke, *Inorg. Chem.*, **32**, 2694 (1993).
65. G. Becker, H. M. Hartmann, A. Münch and H. Riffel, *Z. Anorg. Allg. Chem.*, **530**, 29 (1985).
66. (a) K. W. Klinkhammer and W. Schwarz, *Z. Anorg. Allg. Chem.*, **619**, 1777 (1993).
    (b) K. W. Klinkhammer, G. Becker and W. Schwarz, in *Organosilicon Chemistry II* (Eds. N. Auner and J. Weis), VCH, Weinheim, 1996, pp. 493–498.
67. (a) A. Heine and D. Stalke, *Angew. Chem.*, **105**, 90 (1993); *Angew. Chem., Int. Ed. Engl.*, **32**, 121 (1993).
    (b) A. Heine, R. Herbst-Irmer and D. Stalke, *J. Chem. Soc., Chem. Commun.*, 1729 (1993).
68. H. Gilman, J. M. Holmes and C. L. Smith, *Chem. Ind. (London)*, 848 (1965).
69. (a) Y. Apeloig, M. Bendikov, M. Yuzefovich, M. Nakash and D. Bravo-Zhivotovskii, *J. Am. Chem. Soc.*, **118**, 12228 (1996).
    (b) Y. Apeloig, M. Yuzefovich, M. Bendikov, D. Bravo-Zhivotovskii and K. Klinkhammer, *Organometallics*, **16**, 1265 (1997).
    (c) Y. Apeloig, personal communication.

70. (a) W. Biffar, T. Gasparis-Ebeling, H. Nöth, W. Storch and B. Wrackmeyer, *J. Magn. Reson.*, **44**, 54 (1981).
    (b) R. H. Heyn and T. D. Tilley, *Inorg. Chem.*, **29**, 4051 (1990).
71. (a) H. Gilman and R. L. Harrell, Jr., *J. Organomet. Chem.*, **9**, 67 (1967).
    (b) H. Gilman and C. L. Smith, *J. Organomet. Chem.*, **8**, 245 (1967).
72. H. Gilman, D. J. Peterson, A. W. Jarvie and H. S. J. Winkler, *J. Am. Chem. Soc.*, **82**, 2076 (1996).
73. H. Gilman and G. L. Schwebke, *J. Am. Chem. Soc.*, **85**, 1016 (1963).
74. G. Becker, H.-M. Hartmann, E. Hengge and F. Schrank, *Z. Anorg. Allg. Chem.*, **572**, 63 (1989).
75. J. Belzner, U. Dehnert and D. Stalke, *Angew. Chem.*, **106**, 2580 (1994); *Angew. Chem., Int. Ed. Engl.*, **33**, 2450 (1994).
76. M. Kira, T. Maruyama, C. Kabuto, K. Ebata and H. Sakurai, in *Xth International Symposium on Organosilicon Chemistry*, Poznań, Poland, 1993, P-66.
77. W. Ando, T. Wakahara, T. Akasaka and S. Nagase, *Organometallics*, **13**, 4683 (1994).
78. See e.g.: M. Weidenbruch, A. Pellmann, Y. Pan, S. Pohl, W. Saak and H. Marsmann, *J. Organomet. Chem.*, **450**, 67 (1993).
79. A. W. Jarvie and H. Gilman, *J. Org. Chem.*, **26**, 1999 (1961).
80. Y. Hatanaka and T. Hiyama, in *40th Symposium on Organometallic Chemistry*, Sapporo, Japan, 1993, p. 136
81. M. Cypryk, Y. Gupta and K. Matyjaszewski, *J. Am. Chem. Soc.*, **113**, 1046 (1991).
82. M. Suzuki, J. Kotani, S. Gyobu, T. Kaneko and J. Saegusa, *Macromolecules*, **27**, 2360 (1994).
83. (a) E. Hengge and F. K. Mitter, *Monatsh. Chem.*, **117**, 721 (1986).
    (b) E. Hengge, P. K. Jenkner, P. Gspaltl and A. Spielberger, *Z. Anorg. Allg. Chem.*, **560**, 27 (1988).
    (c) E. Hengge, A. Spielberger and P. Gspaltl, in *Xth International Symposium on Organosilicon Chemistry*, Poznań, Poland, 1993, P-145.
84. E. Hengge and P. K. Jenkner, *J. Organomet. Chem.*, **314**, 1 (1986).
85. A. L. Allred, R. T. Smart and D. A. V. Beek, Jr., *Organometallics*, **11**, 4225 (1992).
86. F. Uhlig, P. Gspaltl, M. Trabi and E. Hengge, *J. Organomet. Chem.*, **493**, 33 (1995).
87. (a) J. Oshita, Y. Masaoka, S. Masaoka, M. Ishikawa, A. Tachibana, T. Yano and T. Yamabe, *J. Organomet. Chem.*, **473**, 15 (1994).
    (b) J. Oshita, S. Masaoka and M. Ishikawa, *Organometallics*, **15**, 2198 (1996).
    (c) J. Oshita, S. Masaoka, Y. Masaoka, H. Hasebe, M. Ishikawa, A. Tachibana, T. Yano and T. Yamabe, *Organometallics*, **15**, 3136 (1996).
88. K. Tamao, A. Kawachi and Y. Ito, *J. Am. Chem. Soc.*, **114**, 3989 (1992).
89. K. Tamao, Y. Ito and A. Kawachi, *Organometallics*, **12**, 580 (1993).
90. K. Tamao, A. Kawachi, and Y. Ito, in *Xth International Symposium on Organosilicon Chemistry*, Poznań, Poland, 1993, I-9.
91. K. Tamao, G.-R. Sun and A. Kawachi, *J. Chem. Soc., Chem. Commun.*, 2070 (1995).
92. K. Tamao, A. Kawachi, Y. Tanaka, H. Othani and Y. Ito, *Tetrahedron*, **52**, 5765 (1996).
93. (a) H. Watanabe, K. Higuchi, M. Kobayashi, M. Hara, Y. Koike, T. Kitahara and Y. Nagai, *J. Chem. Soc., Chem. Commun.*, 534 (1977).
    (b) H. Watanabe, K. Higuchi, T. Goto, T. Muraoka, J. Inose, M. Kageyama, Y. Izuka, M. Nozaki and Y. Nagai, *J. Organomet. Chem.*, **218**, 27 (1981).
94. A. Kawachi, N. Doi and K. Tamao, *J. Am. Chem. Soc.*, **119**, 233 (1997).
95. K. Tamao and A. Kawachi, *Angew. Chem.*, **107**, 886 (1995); *Angew. Chem., Int. Ed. Engl.*, **34**, 818 (1995).
96. K. Tamao and A. Kawachi, *Organometallics*, **15**, 4653 (1996).
97. See e.g.:
    (a) D. Seebach, R. Hässig and J. Gabriel, *Helv. Chim. Acta*, **66**, 308 (1983).
    (b) G. Boche, F. Bosold, J. C. W. Lohrenz, A. Opel and P. Zulauf, *Chem. Ber.*, **126**, 1873 (1993).
98. H. Watanabe, T. Muraoka, M. Kageyama, K. Yoshizumi and Y. Nagai, *Organometallics*, **3**, 141 (1984).
99. (a) T. Tsumuraya, S. A. Batcheller and S. Masamune, *Angew. Chem.*, **103**, 916 (1991); *Angew. Chem., Int. Ed. Engl.*, **30**, 902 (1991) and references cited therein.
    (b) N. Tokitoh, H. Suzuki, R. Okazaki and K. Ogawa, *J. Am. Chem. Soc.*, **115**, 10248 (1993).

100. (a) R. West, *Angew. Chem.*, **99**, 1231 (1987); *Angew. Chem., Int. Ed. Engl.*, **26**, 1201 (1987) and references cited therein.
    (b) M. Weidenbruch, *Chem. Rev.*, **95**, 1479 (1995) and references cited therein.
101. (a) R. West, in *The Chemistry of Organic Silicon Compounds* (Eds. S. Patai and Z. Rappoport), Wiley, Chichester, 1989, pp. 1210–1217.
    (b) K. Matyjazewski, D. Greszta, J. S. Hrkach and H. K. Kim, *Macromolecules*, **28**, 59 (1995).
102. H. Öhme and H. Weis, *J. Organomet. Chem.*, **319**, C16 (1987).
103. R. A. Benkeser, *Acc. Chem. Res.*, **4**, 94 (1971) and references cited therein.
104. P. Boudjouk, S. Kloos and A. B. Rajkumari, *J. Organomet. Chem.*, **443**, C41 (1993).
105. (a) R. A. Pike, *J. Org. Chem.*, **27**, 2186 (1962).
    (b) R. A. Benkeser, K. M. Foley, J. M. Gaul and G. S. Li, *J. Am. Chem. Soc.*, **92**, 3232 (1970).
106. M. S. Gordon, P. Boudjouk and F. Anwari, *J. Am. Chem. Soc.*, **105**, 4972 (1983).
107. J. R. Damewood, Jr., *J. Org. Chem.*, **51**, 5028 (1986).
108. (a) B. Goldfuss and P. v. R. Schleyer, *Organometallics*, **14**, 1553 (1995).
    (b) P. v. R. Schleyer, P. K. Freeman, H. J. Jiao and B. Goldfuss, *Angew. Chem.*, **107**, 332 (1995); *Angew. Chem., Int. Ed. Engl.*, **34**, 337 (1995).
    (c) P. v. R. Schleyer and H. J. Jiao, *Pure Appl. Chem.*, **68**, 209 (1996).
109. J.-H. Hong and P. Boudjouk, *Organometallics*, **14**, 574 (1995).
110. (a) J.-H. Hong and P. Boudjouk, *J. Am. Chem. Soc.*, **115**, 5883 (1993).
    See also:
    (b) H. Gilman and R. D. Gorsich, *J. Am. Chem. Soc.*, **80**, 3243 (1958).
    (c) M. Ishikawa, T. Tabohashi, H. Ohashi, M. Kumada and J. Iyoda, *Organometallics*, **2**, 351 (1983).
    (d) P. Jutzi and A. Karl, *J. Organomet. Chem.*, **214**, 289 (1981).
111. J.-H. Hong, P. Boudjouk and I. Stoenescu, *Organometallics*, **15**, 2179 (1996).
112. (a) W. P. Freeman, T. D. Tilley, G. P. A. Yap and A. L. Rheingold, *Angew. Chem.*, **108**, 960 (1996); *Angew. Chem., Int. Ed. Engl.*, **35**, 882 (1996).
    (b) W. P. Freeman, T. D. Tilley, L. M. Liable-Sands and A. L. Rheingold, *J. Am. Chem. Soc.*, **118**, 10457 (1996).
113. B. Goldfuss, P. v. R. Schleyer and F. Hampel, *Organometallics*, **15**, 1755 (1996).
114. W.-C. Joo, J.-H. Hong, S.-B. Choi and H.-E. Son, *J. Organomet. Chem.*, **391**, 27 (1990).
115. J.-H. Hong, P. Boudjouk and S. Castellino, *Organometallics*, **13**, 3387 (1994).
116. R. West, H. Sohn, U. Bankwitz, J. Calabrese, Y. Apeloig and T. Müller, *J. Am. Chem. Soc.*, **117**, 11608 (1995).
117. J. A. Morrison and R. J. Lagow, *Inorg. Chem.*, **16**, 2972 (1977).
118. P. v. R. Schleyer and A. E. Reed, *J. Am. Chem. Soc.*, **110**, 4453 (1988).
119. S. K. Mehrotra, H. Kawa, J. R. Baran, Jr., M. M. Ludvig and R. J. Lagow, *J. Am. Chem. Soc.*, **112**, 9003 (1990).
120. A. Rajca, P. Wang, A. Streitwieser and P. v. R. Schleyer, *Inorg. Chem.*, **28**, 3064 (1989).

The Chemistry of Organic Silicon Compounds. Volume 2
Edited by Zvi Rappoport and Yitzhak Apeloig
ISBN: 0-471-96757-2

CHAPTER 15

Mechanism and structures in alcohol addition reactions of disilenes and silenes

HIDEKI SAKURAI

Department of Industrial Chemistry, Faculty of Science and Technology, Science University of Tokyo, Noda, Chiba 278, Japan

I. INTRODUCTION

Organosilicon chemistry has expanded its scope considerably in the last two decades. One of the most remarkable achievements is the progress which was made in the elucidation of the mechanisms in silicon chemistry, which now become comparable to those in carbon chemistry. The behavior of reactive intermediates such as silylenes[1], silyl radicals[2] and silyl anions[3,4] are well explored, although the chemistry of silyl cations is still controversial[5]. Doubly-bonded silicon species are now well understood[6−12] but triply-bonded silicon is still elusive.

The mechanism of substitution reactions at saturated silicon centers is well studied, regarding both kinetics and stereochemistry[13,14]. In contrast, addition reactions to unsaturated silicon centers, such as to disilenes and silenes, are relatively unexplored. The reason is clear: suitable substrates for investigations of regio- and stereochemistry and reaction kinetics are not readily available due to inherent kinetic instability of disilenes and silenes. Kinetically stabilized disilenes and silenes are now available, but these are not always convenient for studying the precise mechanism of addition reactions. For example, stable disilenes are usually prepared by the dimerization of silylenes with bulky substituents. Therefore, it is extremely difficult to prepare unsymmetrically substituted disilenes necessary for regio- and/or stereochemical studies.

Nevertheless, mechanistic investigations on the addition reaction to disilenes and silenes advanced considerably in recent years. In this chapter, the author tries to survey the progress achieved recently. The author will not try to review all aspects of the chemistry of silicon unsaturated species since many extensive reviews on this topic are already available[6–12].

II. DISILENES

A. *E*–*Z* Isomerization of Disilenes

After Roark and Peddle generated in 1972 tetramethyldisilene, $Me_2Si{=}SiMe_2$, as the first silicon–silicon unsaturated species[15], it was of major interest to examine the double-bond character of these reactive species. In 1979, Sakurai and coworkers generated independently the (*E*)- and the (*Z*)-1,2-dimethyl-1,2-diphenyldisilene and demonstrated

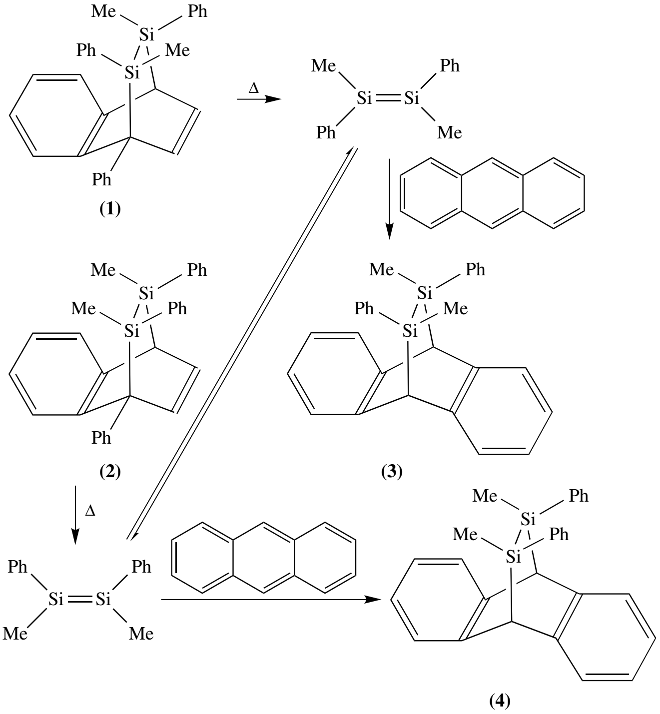

SCHEME 1

that these isomeric disilenes underwent only slow E–Z isomerization compared with trapping reactions by dienes as shown in Scheme 1[16]. The thermal decomposition of **1** at 300 °C in the presence of anthracene afforded a mixture of **3** (96%) and **4** (4%) in 81% yield. A similar thermolysis of the isomeric **2** gave **4** (94%) and **3** (6%) in 88% yield. Since 1,2-dimethyl-1,2-diphenyldisilene generated by the dimerization of PhMe$\ddot{\mathrm{Si}}$ gave a 1 : 1 mixture of **3** and **4** in the reaction with anthracene, [17], these results are remarkable and demonstrate clearly that the strength of the Si=Si double bond in 1,2-dimethyl-1,2-diphenyldisilene is sufficient to prevent the geometrical isomerism from occurring prior to the trapping reactions.

Upon increasing the reaction temperature to 350 °C, thermolysis gave slightly less stereospecific results. Thus **1** gave **3** (94%) and **4** (6%) in 84% yield, and **2** gave **3** (10%) and **4** (90%) in 85% yield, respectively. Later Olbrich, Walsh and coworkers estimated the E–Z isomerization energy of 1,2-dimethyl-1,2-diphenyldisilene to be 25.8 ± 5 kcal mol^{-1} on the basis of these and other data[18].

Thermal E–Z isomerization was also observed for kinetically stabilized disilenes **5–9** (equation 1)[19–22]. The π bond strength was estimated to range from 24.7 to 30.6 kcal mol^{-1}. These data are in good agreement with those of 1,2-dimethyl-1,2-diphenyldisilene and those predicted by *ab initio* calculations for $H_2Si{=}SiH_2$ (22–28 kcal mol^{-1})[23,24].

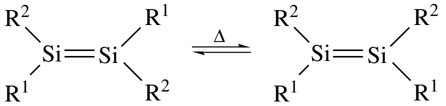

(**5**) R^1 = t-Bu; R^2 = Mes
(**6**) R^1 = Mes; R^2 = Ad
(**7**) R^1 = Mes; R^2 = N(SiMe$_3$)$_2$
(**8**) R^1 = Mes; R^2 = Dep (1)
(**9**) R^1 = Mes; R^2 = Dip

Ad = 1-adamantyl; Dep = 2,6-diethylphenyl; Dip = 2,6-diisopropylphenyl;
Mes = 2,4,6-trimethylphenyl

These E–Z isomerization studies of disilenes indicate that the π overlap between two 3p orbitals of silicon is sufficiently effective to retain the configuration around the double bond, although the π bonding of disilenes is significantly weaker than that of the C=C double bond. Therefore, it is expected that if appropriately substituted disilenes can be generated, regiochemistry as well as diastereochemistry of addition reactions to disilenes can be investigated even with transient reactive disilenes.

B. Generation of Phenyl-substituted Disilenes. Spectra and Kinetics of Addition of Alcohols

Several methods are available for generating disilenes[8] but photolysis of masked disilenes[25,26] is most convenient for mechanistic studies. 7,8-Disilabicyclo[2.2.2]octa-2,5-dienes, the formal adducts of the addition of disilenes to benzene, naphthalene, anthracene and biphenyl, are well established to generate the corresponding reactive disilenes by either thermolysis or photolysis. The parent 7,7,8,8-tetramethyl-7,8-disilabicyclo[2.2.2]octa-2,5-diene (**10**) generates tetramethyldisilene (**11**) in an argon matrix by photolysis at 10 K[27]. Tetramethyldisilene (**11**) was also observed at 344 nm in UV spectra by 3-methylpentane (3-MP) and EPA (ether: isopentane: ethanol = 5 : 5 : 2) matrices (equations 2 and 3, respectively)[27]. On annealing the EPA matrix, a product of addition of ethanol to **11**, 1-ethoxy-2-hydrotetramethyldisilane **(12)**, was obtained (equation 3).

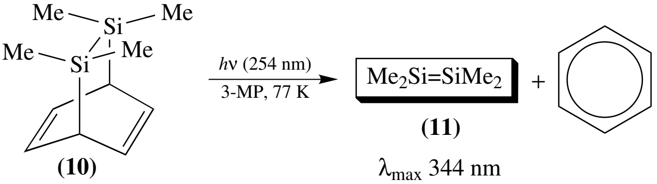

(10) **(11)** λ_{max} 344 nm (2)

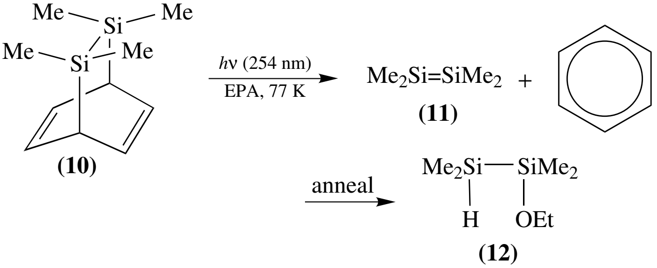

(10) **(11)** **(12)** (3)

Phenyltrimethyldisilene **(15)** and (*E*)- and (*Z*)-1,2-dimethyl-1,2-diphenyldisilene **(16)** were also generated (equation 4) by the photolysis of precursors **13**, (*E*)-**14** and (*Z*)-**14**, respectively[28]. Absorption maxima of **15**, (*E*)-**16** and (*Z*)-**16** were observed at 386, 417 and 423 nm, respectively. These absorption bands are also observed in an organic glass (3-MP, EPA), the ethanol addition products being detected after annealing of the EPA matrix, similar to the case of **11**.

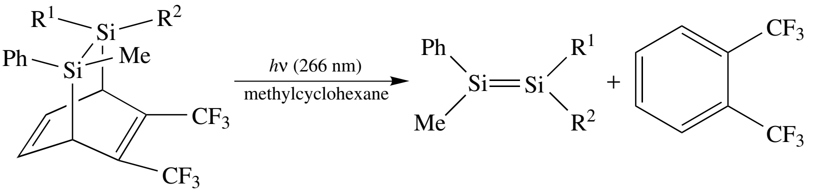

(4)

(13) $R^1 = R^2 = Me$
(*E*)-**(14)** $R^1 = Me, R^2 = Ph$
(*Z*)-**(14)** $R^1 = Ph, R^2 = Me$

(15) $R^1 = R^2 = Me$
(*E*)-**(16)** $R^1 = Me, R^2 = Ph$
(*Z*)-**(16)** $R^1 = Ph, R^2 = Me$

Phenyltrimethyldisilene **(15)** and (*E*)- and (*Z*)-1,2-dimethyl-1,2-diphenyldisilene **(16)** were also observed as transient absorption spectra by laser flash photolysis of the precursors in methylcyclohexanes[28]. The absorption band at 380 nm, assigned to the disilene **15**, reached maximum intensity at *ca* 10 ns after the excitation and then started to decrease. The half-life assigned to **15** was 700 ns. The logarithm of the decay profile of the transient absorption at 380 nm versus time shows a very good linear relationship, indicating that the decay of the transient absorption fits first-order kinetics. This result shows that intramolecular isomerization or proton abstraction from the solvent is the origin for the decay of the disilene **15**, which survives in solution only for several nanoseconds.

Photochemical generations of transient (*E*)- and (*Z*)-1,2-dimethyl-1,2-diphenyldisilenes (*E*)-**16** and (*Z*)-**16** in solution is also confirmed by laser flash photolysis of the precursors, (*E*)-**14** and (*Z*)-**14**, respectively, in degassed methylcyclohexane at 293 K[28]. The absorption bands at 415 and 417 nm are assigned to the disilenes (*E*)-**16** and (*Z*)-**16**, respectively.

TABLE 1. Rate constants for quenching of phenyl-substituted disilenes by alcohols[28]

Trapping agent	$k_2/M^{-1} \cdot s^{-1}$		
	(E)-PhMeSi=SiMePh	(Z)-PhMeSi=SiMePh	PhMeSi=SiMe$_2$
EtOH	1.7×10^8	1.9×10^8	1.9×10^8
EtOD	1.7×10^8	1.7×10^8	1.8×10^8
i-PrOH	1.2×10^8	1.2×10^8	1.3×10^8
t-BuOH	0.9×10^7	1.1×10^7	1.6×10^7

The half lives of (E)- and (Z)-**14** obtained from the decay profiles at 415 nm are 800 and 710 ns, respectively. These half-lives are almost the same, but both are slightly larger than that of **15**. The logarithms of decay profiles of the transient absorptions versus time also show very good linear lines, indicating a first-order kinetics for decay.

The transient absorption of **15** and of (E)- and (Z)-**16** are successfully quenched by addition of alcohols. The quenching rate constants for these disilenes, determined from the change in the half-lives in the presence of alcohols, give the second-order rate constants k_2, which are summarized in Table 1.

The second-order rate constants k_2 for the reactions of phenyl-substituted disilenes with various alcohols indicate several interesting points. First, the addition reaction of alcohols to the disilenes proceeds so rapidly that it is probable that these phenyl-substituted disilenes are quenched prior to E–Z isomerization. The order of **15** > (E)-**16** ~ (Z)-**16** is found for the relative reactivity of these disilenes. Rate constants of phenyltrimethyldisilene **15** are slightly larger than those of dimethyldiphenyldisilenes (E)-**16** and (Z)-**16**, probably due to steric factors. However, there is little difference in the reactivity among the (E)- and (Z)-isomers, the rate constants of these disilenes also being almost independent of the number of the attached phenyl group(s). Second, the relative rates decrease in the order of EtOH > *i*-PrOH $\gg$ *t*-BuOH, consistent with the increased steric bulkiness of the alcohols. In particular, the reactivity of *t*-BuOH toward the disilene is lowest, being only about one-tenth that of other alcohols. Third, the magnitude of the kinetic isotope effect (k_H/k_D) observed for the reaction with ethanol and ethanol-*d* is only 1.0 –1.1, indicating that there is no significant deuterium isotope effect in these reactions. This fact strongly indicates that the rate-determining step of the addition reaction must be the nucleophilic attack of the alcoholic oxygen on the coordinatively unsaturated silicon center.

C. Generation of Alkoxy- and Amino-substituted Disilenes

Alkoxy- and amino-substituted disilenes (**17**, **18** and **19**) are produced by photolysis of the corresponding masked disilenes (**20**, **21** and **22**)[29]. Thus, when a degassed 3-methylpentane (3-MP) matrix of **20** was irradiated at 77 K, the corresponding alkoxy-substituted disilene **17** was produced (equation 5) as indicated by its broad band at 373 nm.

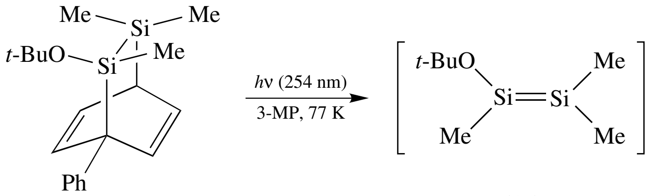

(20) **(17)** (5)

After similar irradiation of a mixture of **20** and ethanol in a mixed matrix of 3-MP and isopentane (4 : 1) at 77 K, GC-MS analysis of the solution showed the formation of the expected ethanol adduct of the disilene. The regiochemistry of the product will be discussed in the next section.

The formation of amino-substituted disilenes **18** and **19** was also confirmed in similar experiments using **21** and **22** (equations 6 and 7, respectively). Broad bands growing at 395 and 408 nm, respectively, were observed. Absorption maxima of several transient disilenes are summarized in Table 2, in which the absorption spectral data of the recently prepared (trimethylsilylmethyl)trimethyldisilene[30] is also included. The electronic spectral data of stable disilenes are well documented[8].

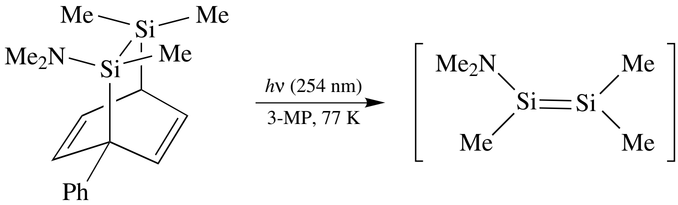

(21) **(18)**

(6)

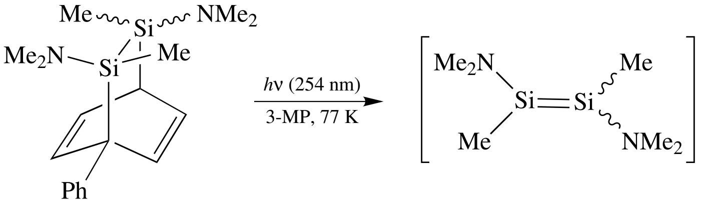

(22) **(19)**

(7)

It is clear that introduction of the functional groups to the silicon–silicon double bond causes a large red shift of the absorption maxima of disilenes. Similar substituent effects have been known for a variety of alkenes[31]. Qualitatively, the reason for the red shift should arise from destabilization of the HOMO of the disilene by an appreciable interaction between the n-orbital of the heteroatoms and the π-orbital of the disilene, although the effect of their distorted structure should also be considered as discussed later.

TABLE 2. Absorption maxima of some reactive disilenes

Disilene	Medium	λ_{max} (nm)	$\Delta\nu$ (cm^{-1})[a]	Reference
$Me_2Si{=}SiMe_2$	Argon matrix	344		27
$PhMeSi{=}SiMe_2$	Argon matrix	386	3160	28
(E)-PhMeSi=SiPhMe	Argon matrix	417	5090	28
(Z)-PhMeSi=SiPhMe	Argon matrix	423	5430	28
(t-BuO)MeSi=$SiMe_2$	3-MP matrix	373	2260	29
$(Me_2N)MeSi{=}SiMe_2$	3-MP matrix	395	3750	29
$(Me_2N)MeSi{=}SiMe(NMe_2)$	3-MP matrix	408	4560	29
$(Me_3SiCH_2)MeSi{=}SiMe_2$	3-MP matrix	360	1290	30

[a] Difference (in wave numbers) from the absorption of tetramethyldisilene.

There is rather little information about disilenes with substituents other than alkyl and aromatic groups. An example is the bis(trimethylsilylamino)-substituted disilene **23** which was isolated as a stable disilene by West and coworkers[19]. More recently, the dialkoxydisilenes **24** were generated by the dimerization of methoxy-substituted silylenes in matrices[32]. However, only the change of UV spectra through an annealing of the matrices containing alkoxysilylenes was observed; no trapping adducts, except for cyclotrisilane, were obtained. Other attempts to generate amino- or fluoro-substituted disilenes were unsuccessful[33].

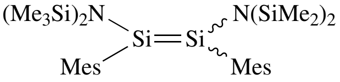

(23)

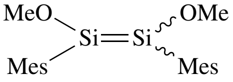

(24)

The formation of an intermediate difluorodisilene **25** (equation 8) was proposed by Jutzi and coworkers[34] in the reaction of decamethylsilicocene with tetrafluoroboric acid. The disilene which was characterized by the ^{29}Si NMR spectrum, then formed the isolable cyclotetrasilane by [2 + 2] cycloaddition.

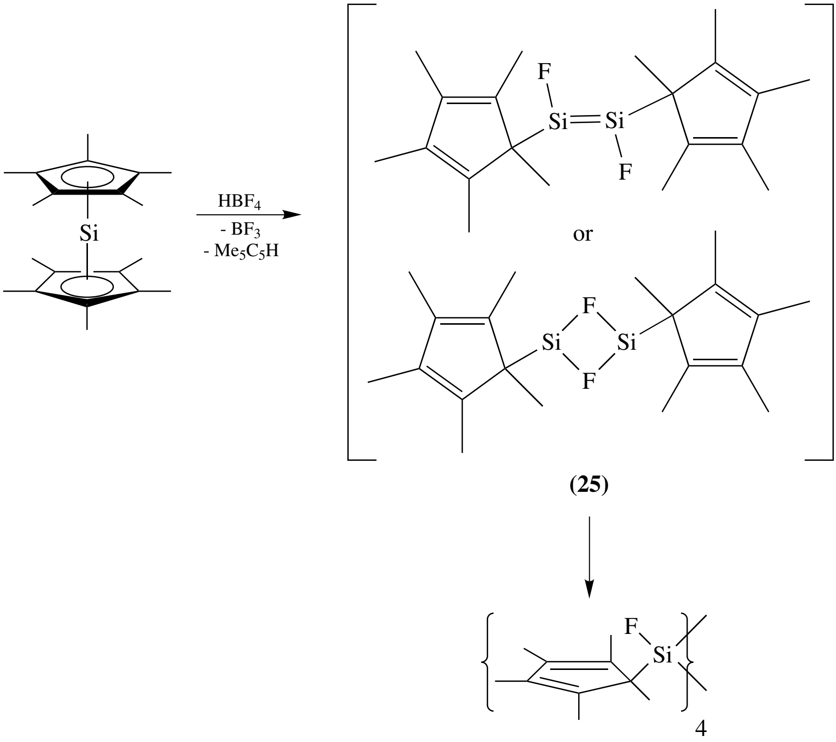

(8)

Later, Maxka and Apeloig calculated the geometry of $Si_2H_2F_2$ by an *ab initio* (6-31G*) method and suggested a nonclassical bridged structure for the fluorosilylene dimer[35]. Thus, even in this case, no clear evidence for generation of the disilene has been indicated. More recently, the existence of the nonclassical bridged structure of the tetraaminodisilene has been suggested in the dimerization reaction of diaminosilylene[36], where scrambling of amino groups occurs between differently substituted diaminosilylenes (see Scheme 2).

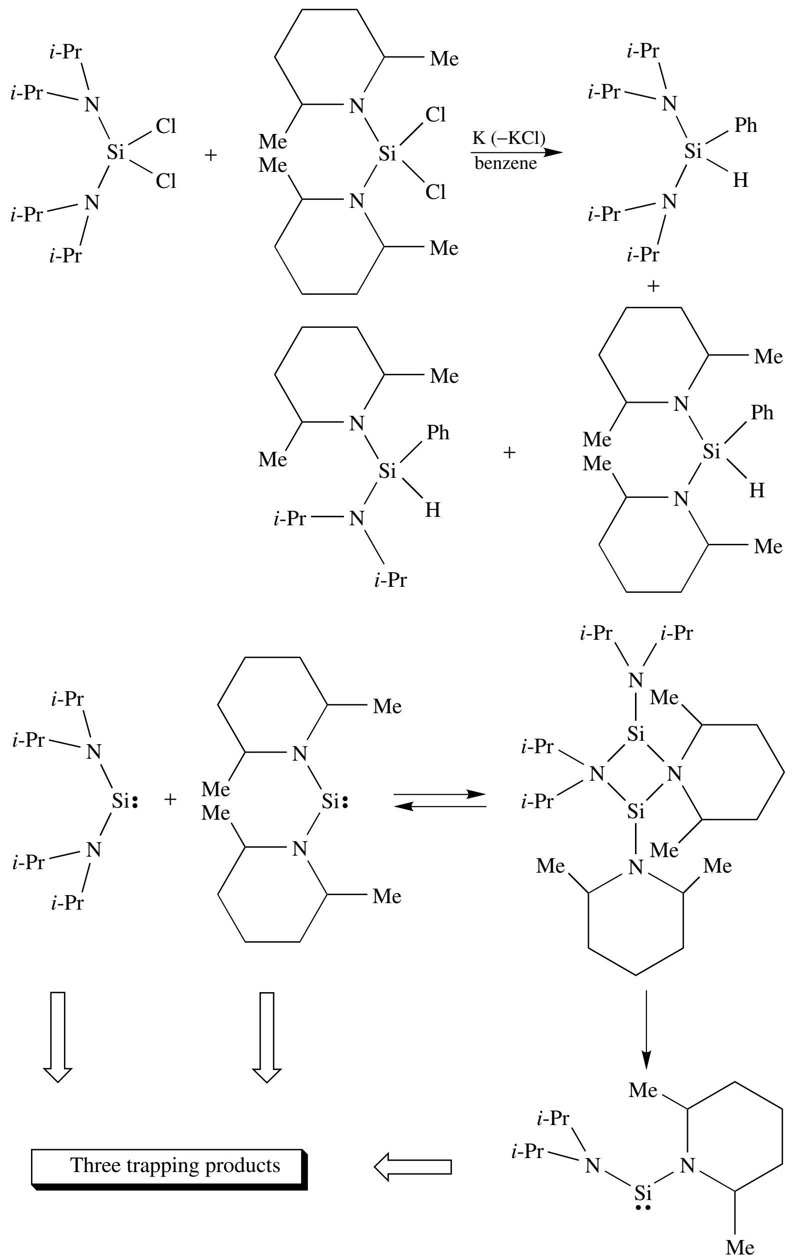

SCHEME 2

Diaminosilylenes generated by the reaction of the corresponding diaminodichlorosilane with potassium react with benzene to give products derived by insertion into the Ph−H bond. Interestingly, the reaction of simultaneously generated bis(diisopropylamino)- and bis(*cis*−2,6-dimethylpiperidino) silylenes gave three products due to scrambling of the amino substituents on silicon atoms.

In relation to the structure of disilene, several *ab initio* MO calculations of the geometry and energies of various disilenes have been reported[37−43]. Several possibilities regarding the conformations around the Si=Si double bond (planar, *trans*-bent, twist and bridged etc.) have to be considered. According to these calculations the most stable geometry depends significantly on the substituents. The parent $H_2Si{=}SiH_2$ adopts a *trans*-bent conformation, having a bent angle of 12.9°, whereas electropositive substituents such as Li, BH_2 and SiH_3 are predicted to give disilenes with a preferred planar geometry. In contrast, the electronegative and π-donating substituents such as NH_2, F and OH induce large distortions from planarity[35,43].

D. Regiochemistry of Addition of Alcohols to Disilenes

Generation of various phenyl-substituted disilenes by the photolysis of the masked disilenes, 7,8-disilabicyclo[2.2.2]octadiene derivatives, is quite useful, especially for unsymmetrically substituted disilenes. Investigation of the regiochemistry as well as the diastereochemistry of alcohol addition to phenyltrimethyldisilene was made possible for the first time by using this method[27].

Phenyltrimethyldisilene **15**, produced by irradiation of the precursor **13** ($\lambda > 280$ nm) in the presence of several alcohols, gives rise to the formation of 1-alkoxy-2-hydrido-1,1,2-trimethyl-2-phenyldisilane **(26)** as the major product along with a small amount of the isomeric 1-alkoxy-2-hydrido-1,2,2-trimethyl-1-phenyldisilane **(27)** (see Scheme 3). As shown in Table 3, very high regioselectivity was observed. This is the first example demonstrating a regioselective addition reaction to the unsymmetrically substituted disilenes.

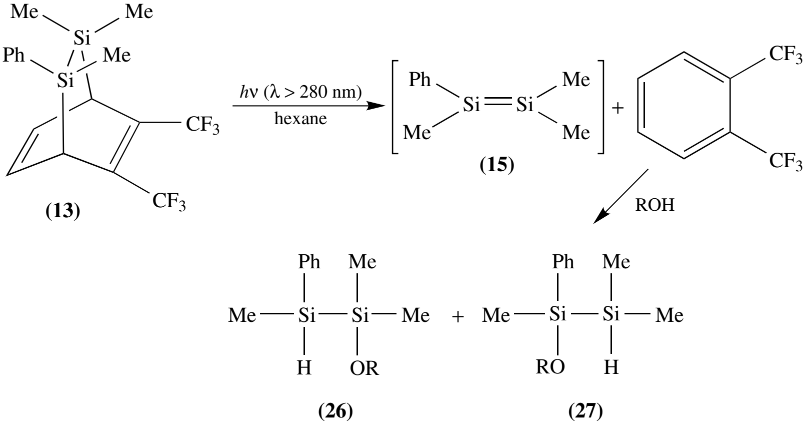

26a and **27a** R = Me
26b and **27b** R = Et
26c and **27c** R = *i*-Pr
26d and **27d** R = *t*-Bu

SCHEME 3

TABLE 3. Product ratio in the photolysis of **13** in the presence of various alcohols[28]

ROH	**26/27**
MeOH	92/8
EtOH	95/5
i-PrOH	97/3
t-BuOH	>99/<1

The results in Table 3 were explained as shown in Scheme 4. From the fact that no kinetic isotope effect was observed in the reaction of phenyl-substituted disilenes with alcohols (Table 1), it is assumed that the addition reactions of alcohols to phenyltrimethyldisilene proceed by an initial attack of the alcoholic oxygen on silicon (nucleophilic attack at silicon), followed by fast proton transfer via a four-membered transition state. As shown in Scheme 4, the regioselectivity is explained in terms of the four-membered intermediate, where stabilization of the incipient silyl anion by the phenyl group is the major factor favoring the formation of **26** over **27**. It is well known that a silyl anion is stabilized by aryl group(s)[44a]. Thus, the product **26** predominates over **27**. However, it should be mentioned that steric effects also favor attack at the less hindered $SiMe_2$ end of the disilene, thus leading to **26**.

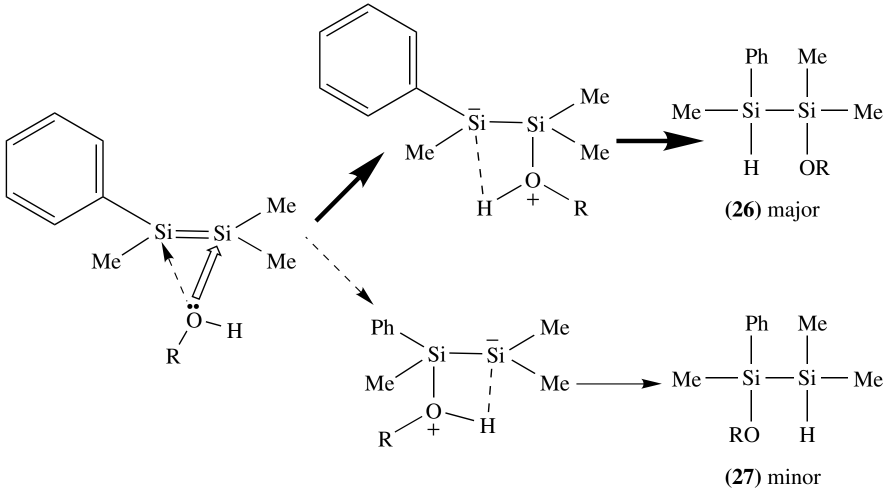

SCHEME 4

Methoxy- and amino-substituted disilenes behave differently from **15**[29]. Irradiation of a hexane solution of **20** in the presence of various alcohols at room temperature afforded 1,1-dialkoxyhydrodisilanes **28a-32a** together with a small amount of the regioisomers **28b-32b** (Scheme 5). Thus alkoxy groups direct the alcohol addition to the alkoxy-substituted silicon atom. The ratios of regioisomers (**a/b**) were 100/0 (EtOH, **28**), 96/4 (*i*-PrOH, **29**) and 93/7 (*t*-BuOH, **30**). Steric bulkiness is not the only factor that determines the regioselectivity, since bulky but acidic alcohols, such as 2,6-dimethylphenol and 1,1,1,3,3,3-hexafluoro-2-methyl-2-propanol, give products in higher regioselectivities (98/2, **31** and >99/<1, **32**, respectively) than *t*-BuOH (Table 4).

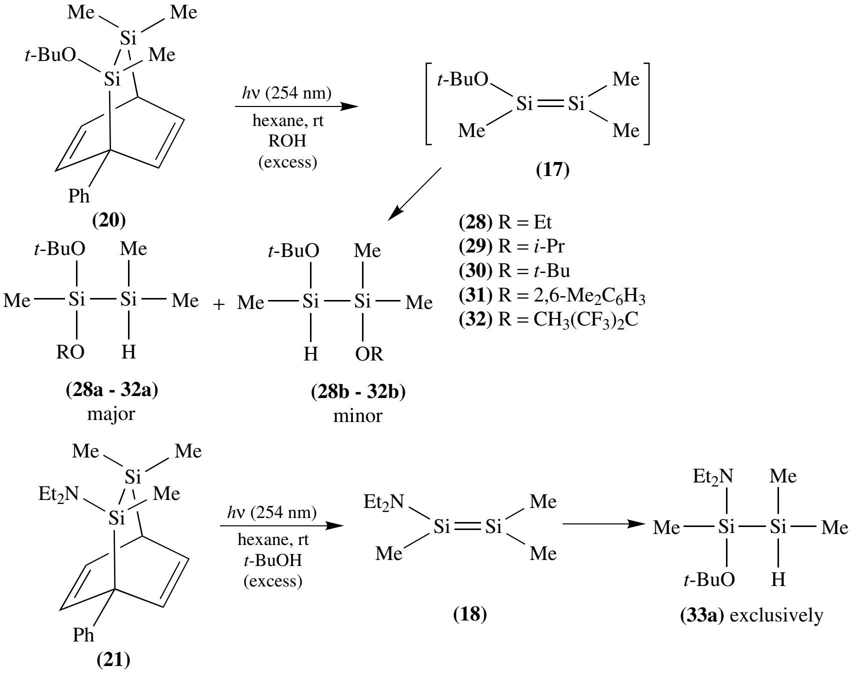

SCHEME 5

TABLE 4. Addition reaction of alcohols to silicon-substituted disilenes XMeSi=SiMe$_2$[29]

X	ROH	Product	a/b[a]
t-BuO	EtOH	**28**	100/0
	i-PrOH	**29**	96/4
	t-BuOH	**30**	93/7
	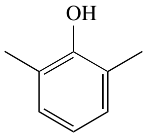	**31**	98/2
	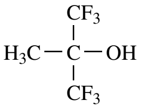 $H_3C-C(CF_3)_2-OH$	**32**	>99/<1
Et$_2$N	*t*-BuOH	**33a**	100/0

[a] Determined by ^{1}H NMR.

Addition of an alcohol to the amino-substituted disilene **18** proceeds with an even higher regioselectivity than that to the methoxy-substituted disilene **17**. Thus, the addition of *t*-BuOH to **18** is completely regioselective, where only 1-diethylamino-1-*t*-butoxy-2-hydro-1,2,2-trimethyldisilane **33a** is obtained.

A very high regioselectivity is indicated in the previous section in the addition reactions of alcohols to phenyl-substituted disilene **15**, where the alcoholic proton adds to the silicon atom bearing the phenyl group. Both electronic and steric factors favor this direction of addition. However, it should be noted that the direction of the addition is completely opposite in the case of alkoxy- and amino-substituted disilenes, where the alkoxy groups of the alcohols add to the hetero-substituted and the sterically more hindered silicon atom. The experimental observations indicate that the mechanisms should be quite different in the two cases. The regioselectivity observed for alkoxy- and amino-substituted disilenes may be explained in terms of a strong π-donation effect of the functional groups as shown in Scheme 6.

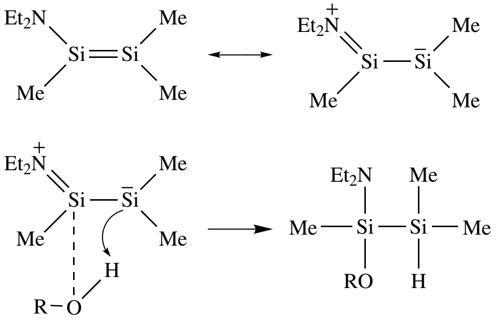

SCHEME 6

Donation of π-electrons from the alkoxy and amino groups makes the Si=Si bond very polar. Although it is uncertain whether nucleophilic interaction between the alcoholic oxygen and the silicon still operates in this mechanism, proton transfer (electrophilic process) is probably the rate-determining step. This suggestion has to be supported by kinetic isotope effect studies similar to those carried out in the case of phenyl-substituted disilenes. Unfortunately, at this point data on the kinetic isotope effect are not available in this system, but the fact that the more acidic but sterically similar 1,1,1,3,3,3-hexafluoro-2-methyl-2-propanol gives higher selectivity ($>99/<1$) than *t*-BuOH (93/7) supports the rate-determining proton transfer. To some extent the mechanism may be similar to that of the reaction of silyl enol ethers and enamines with electrophiles, since strongly π-donating groups destabilize olefinic systems favoring electrophilic attack[44b]. Therefore, alcohol addition to alkoxy- and amino-substituted disilenes is governed by electrophilic factors. This, however, does not necessarily exclude the formation of a four-centered transition state, even though electrophilic attack by the proton is the rate-determining step.

The trimethylsilylmethyl group (Me_3SiCH_2-) is a weaker electron-donating group than the amino and methoxy groups. The σ^+ value of the trimethylsilylmethyl group on the Brown–Okamoto scale was reported to be -0.66[45], which is smaller (in absolute value) than those of the amino (-1.7) and methoxy (-0.78) groups. Therefore, it was interesting to investigate the regioselectivity of the alcohol addition to the trimethylsilylmethyl-substituted disilene, $(Me_3SiCH_2)MeSi{=}SiMe_2$ (**34**). Indeed **34**, generated from the corresponding masked disilene, reacted with ethanol to give a 1 : 1 mixture of **35** and **36** (Scheme 7)[30]. In this case, probably both electronic and steric factors compete in determining the regiochemistry.

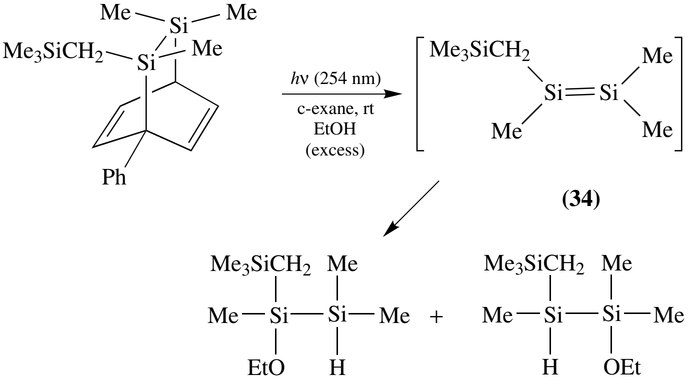

(34)

(35) **(36)**

50 : 50

SCHEME 7

E. Diastereochemistry of Addition of Alcohols to Disilenes

Although the chemistry of disilenes has been developed considerably after the isolation of stable disilenes by West, Finle and Michl[46], rather little has been known about the mechanism, especially on the stereochemistry for the addition reactions to Si=Si bonds of nucleophiles or electrophiles. West and coworkers reported that the addition reaction of ethanol to (*E*)-1,2-di-*t*-butyl-1,2-dimesityldisilene in THF gave a 1 : 1 mixture of two diastereomers of alkoxysilanes (equation 9), suggesting a stepwise mechanism[47]. However, the bulky substituents necessary to stabilize disilenes sometimes complicate the stereochemistry. In fact, for the addition reaction of water to the parent disilene ($H_2Si{=}SiH_2$), theoretical calculation predicted a concerted-type four-center-like transition state, leading to a *syn*-addition product[48].

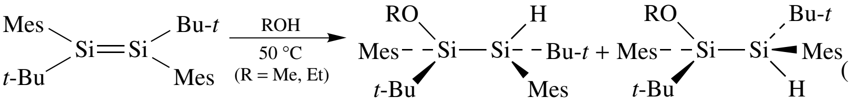

(9)

50 : 50

As stated before, there is little knowledge on the unsymmetrically substituted stable disilenes because stable disilenes are usually prepared by dimerization of silylenes, thus leading to symmetrical disilenes. Unsymmetrically substituted disilenes are produced mostly as transient species (see the preceding section), and it was found that (*E*)- and (*Z*)-1,2-dimethyl-1,2-diphenyldisilenes undergo the addition reaction with alcohols very rapidly ($k_2 = 10^7$–10^8 M^{-1} s^{-1}). The rates are only 1 to 2 orders of magnitude smaller than the diffusion rates and this guarantees that these disilenes can react with alcohols prior to rotation around the Si–Si bond or prior to *E*–*Z* isomerization[28]. This makes it possible to investigate the diastereoselectivity in the addition reaction of alcohols to these disilenes.

Irradiation ($\lambda > 280$ nm) of a hexane/isopropyl alcohol solution of the disilene precursor (*E*)-**14** (Scheme 8) in a quartz tube at room temperature produced *threo*-1-isopropoxy-1,2-dimethyl-1,2-diphenyldisilane **37a**, which is the product of *syn* addition of isopropyl alcohol to (*E*)-**16** together with a small amount of the *erythro*-isomer **38a** (**37a**/**38a** => 99/1, 62% yield). High *syn*-addition diastereoselectivity was also found for (*Z*)-**16** (**38a**/**37a** => 99/1, 49% yield). The diastereoselectivity in the addition of isopropyl alcohol depends on the concentration of the alcohol (Table 5). At lower concentrations a higher selectivity is indicated[28].

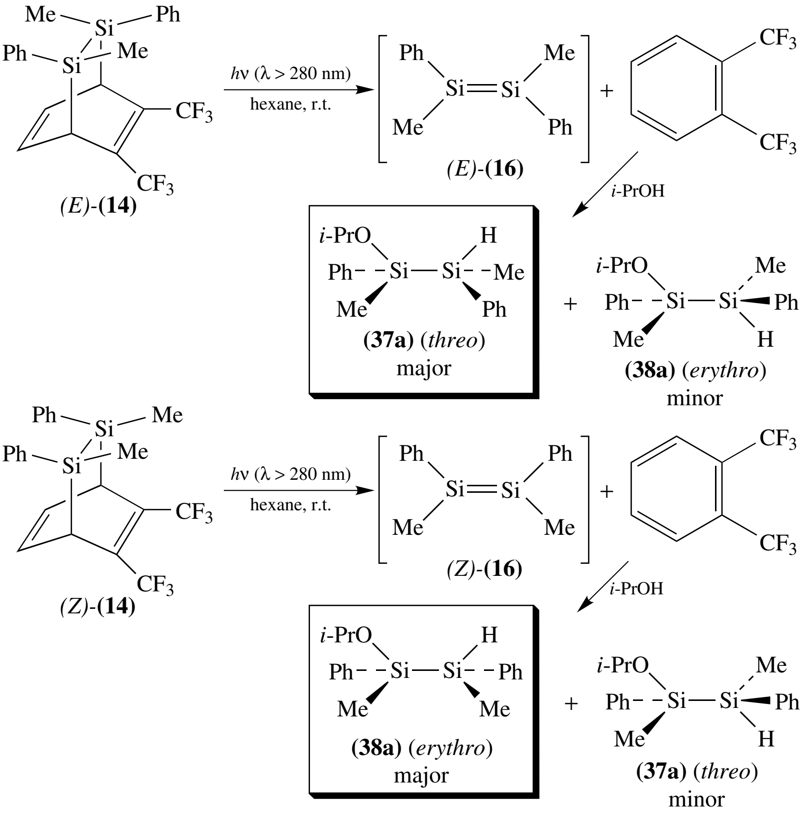

SCHEME 8

TABLE 5. Product ratio in the photolysis of (*E*)- and (*Z*)-**16** in the presence of alcohols[28]

Alcohol		Product ratio, **37/38**	
ROH	concentration (*M*)	(*E*)-**16**	(*Z*)-**16**
EtOH	0.85	92/8	8/92
EtOH	1.26	82/18	25/75
EtOH	1.69	78/22	27/73
EtOH	2.48	70/30	44/56
EtOH	5.65	51/49	49/51
i-PrOH	1.31	>99/<1	<1/>99
i-PrOH	4.33	89/11	9/91
t-BuOH	3.51	94/6	5/95

Similar high diastereoselectivities are observed for the addition reaction of *t*-butyl alcohol to (*E*)- and (*Z*)-**16**[28]. High diastereoselectivities are also observed for the reaction with ethanol at low concentration, but the selectivity decreases rather sharply by increasing the ethanol concentration. The diastereoselectivities for the reaction of ethanol, i.e. the [*syn*]/[*anti*] product ratios, are linearly and inversely correlated with the concentration of the alcohol:

$$[syn]/[anti] = (k_a/k_b)/[\mathrm{EtOH}]$$

Where k_a and k_b are the rate constants for intramolecular and intermolecular proton transfer reactions, respectively.

The high diastereoselectivity in the addition of *i*-PrOH, *t*-BuOH and EtOH (at low concentration) suggests that $E \rightleftarrows Z$ photoisomerization of (*E*)- or (*Z*)-**16** does not occur in solution at room temperature or that the trapping of (*E*)- or (*Z*)-**16** by alcohols proceeds faster than the $E \rightleftarrows Z$ isomerization. In addition, the results show that proton transfer in the intermediate adduct formed by the disilenes and alcohols occurs much faster than rotation around the Si−Si bond. However, in the reaction with ethanol, an appreciable amount of the *anti* addition product was formed. Thus, the diastereoselectivity remarkably depended on the concentration of ethanol.

A mechanism involving coordination of the alcoholic oxygen to a silicon atom, followed by a fast intramolecular proton transfer explains the predominant *syn* addition of alcohol to disilene. However, intermolecular proton transfer leading to the *anti*-product competes with intramolecular proton transfer at high alcohol concentrations. The proposed mechanism is presented in Scheme 9.

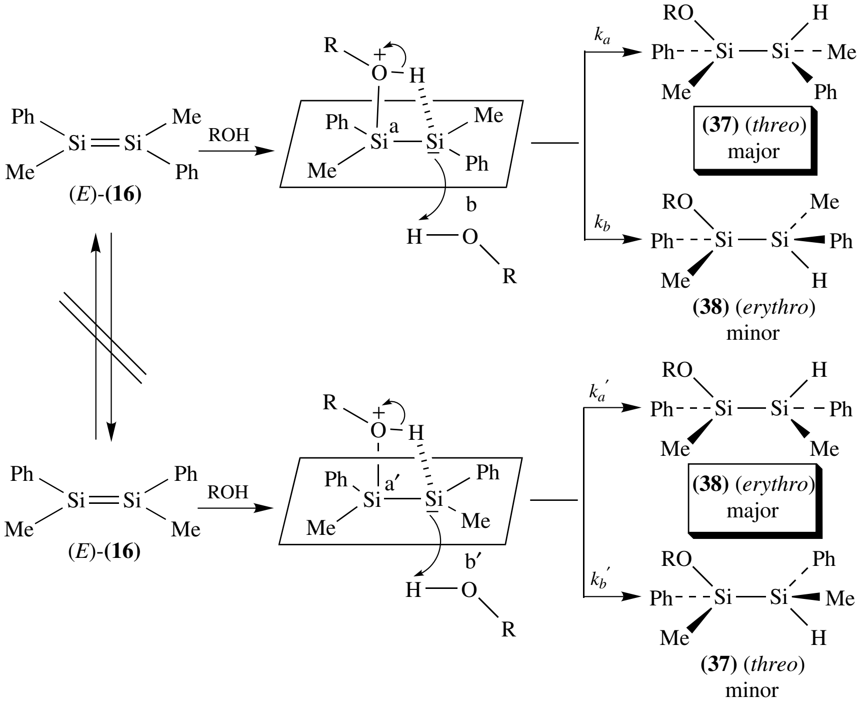

SCHEME 9

The difference in the selectivities as a function of the alcohol used is explained in terms of the differences in the acidities of the silyl alkoxy oxonium cations (protonated alkoxysilanes) formed as intermediate[28]. The rate of intramolecular proton transfer in the intermediate adduct is expected to increase by increasing the acidity of protonated alkoxysilanes. No data are available for acidities of protonated alkoxysilanes, but the pK_a values of protonated alcohols may be used instead. These are in the following order: EtO^+H_2 (−2.4) >> *i*-PrO^+H_2 (−3.2) > *t*-BuO^+H_2 (−3.8)[49]. Addition of *t*-BuOH gives rise to the most acidic intermediate (among those examined) and therefore gives the highest diastereoselectivity. Ethanol forms the least acidic intermediate, leading to *anti*-addition product competing with the intramolecular *syn* adduct, especially at high concentrations of the alcohol.

Recently, West and coworkers have reported similar diatereoselectivities in the reaction of stable disilenes, (*E*)-**5** and (*E*)- and (*Z*)-1,2-di-*t*-butyl-1,2-bis(2,4,6-triisopropyl phenyl) disilene, with ROH (R = Me, Et and *i*-Pr)[50]. In these studies, alkoxy oxygen-coordinated complexes have been suggested as key intermediates (Scheme 9). Computational studies on the reaction of $RSiH{=}SiH_2$ with water also suggest the importance of water coordinated disilene molecules as intermediate[51]. However, it should be noted that in the X-ray crystallographic structure of $Mes_2Si{=}SiMes_2$•THF complex, the THF molecule is not coordinated to silicon[52].

More recently, Apeloig and Nakash have studied diastereoselectivity in the reaction of (*E*)-**5** with *p*-methoxyphenol[53]. In both benzene and THF, the stereochemistry of the products was independent of the phenol concentration. The *syn/anti* ratios of the addition products were 90 : 10 in benzene and 20 : 80 in THF. They have suggested that intramolecular proton transfer after rotation of the Si−Si bond of the phenol-coordinated intermediate is responsible for the formation of the *anti*-addition rather than intermolecular proton transfer. This must be a special case due to much slower (by a factor of 10^9–10^{12}) rates of addition of phenol to (*E*)-**5**. Since phenolic oxygen is definitely less basic than alkyl alcoholic oxygen, coordination of oxygen in the zwitterionic intermediate in the reaction of (*E*)-**5** with phenol must be loose and hence the intermediates should have much chance of rotation around the Si−Si bond.

F. Competition Between Nucleophilic and Electrophilic Mechanisms

Apeloig and Nakash have reported recently a Hammett-type study for the addition reactions of seven *para*- and *meta*-substituted phenols to tetramesityldisilene **39** (equation 10)[54]. They used a large excess of the phenol to enforce pseudo-first-order kinetics. The addition reactions are indeed firstorder in both the disilene and the phenol.

The second-order rate constants ($k = 10^{-4}$–10^{-2} M^{-1} s^{-1}) are much lower compared with the rates of addition of alcohols to (*E*)- and (*Z*)-1,2-dimethyl-1,2-diphenyldisilene and 1,2,2-trimethyl-1-phenyldisilene ($k = 10^7$–10^8 M^{-1} s^{-1} (Table 1). The larger steric bulk of the mesityl substituents in **39** may account for this large reactivity difference, but the magnitude of the difference is indeed extremely large. The resulting Hammett plot (see Figure 1) has a concave shape with a minimum for the parent phenol. This means that all phenols, either with electron-donating or electron-withdrawing substituents, react faster than the parent unsubstituted phenol. The concave Hammett plot is formed by two intersecting straight lines having positive and negative ρ values.

The negative ρ value (−1.77) in the reaction of the tetramesityldisilene **39** with phenols with electron-donating substituents indicates that a positive charge is developing on the phenolic oxygen in the transition state, whereas the positive ρ value (1.72) observed

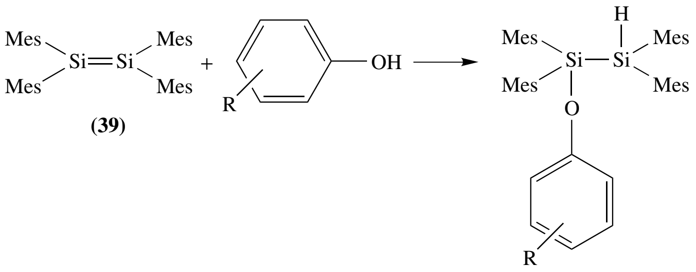

(10)

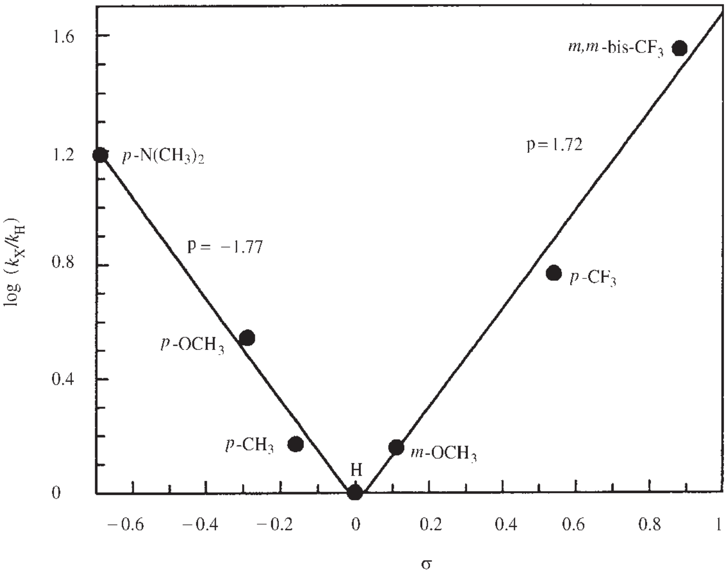

FIGURE 1. A Hammett plot for the addition of ArOH to $Mes_2Si{=}SiMes_2$

with electron-withdrawing substituents means that a negative charge develops on the phenolic oxygen in the transition state of the rate-determining step. Thus these opposite Hammett slopes indicate a change in mechanism of the reaction of **39** with phenols, from a rate-determining nucleophilic step for electron-rich phenols, to a rate-determining electrophilic step for electron-poor phenols (Scheme 10)[54].

Kinetic isotope effect measurements support this interpretation. A small kinetic isotope effect ($k_H/k_D = 0.71$) is observed for *p*-methoxyphenol in agreement with a rate-determining nucleophilic attack, while a large kinetic isotope effect ($k_H/k_D = 5.27$), observed for *p*-trifluoromethylphenol, strongly supports a mechanism in which a phenolic H (or D) is transferred to **39** in the rate-determining step. Unfortunately, **39** is a symmetric disilene so that diastereoselectivity could not be determined. It will be interesting to examine whether the diastereoselectivity will be effected by the change in the addition mechanism from electrophilic to nucleophilic.

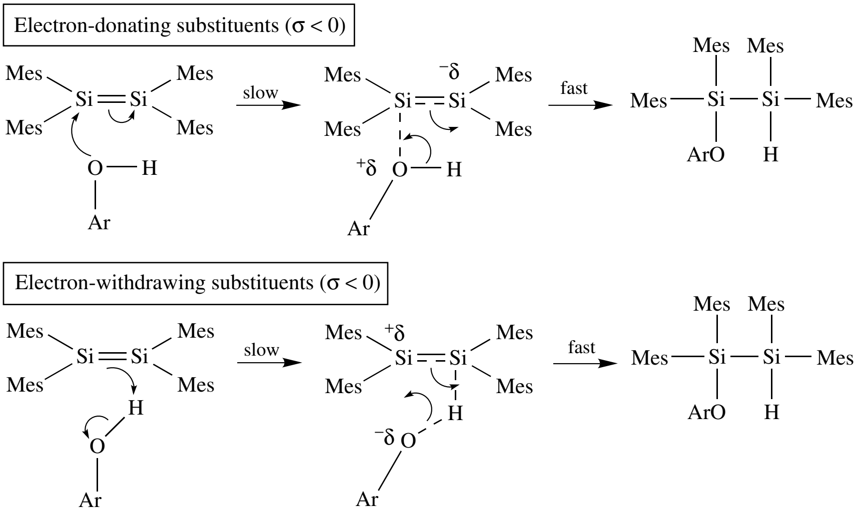

SCHEME 10

III. SILENES

A. Generation of Silenes

After the first recognition of generating silenes in vapor phase by thermolysis of silacyclobutane[55], a large number of reports appeared on the reactions of both reactive and stable silenes[6]. Sterically protected silenes are prepared by [1,3]-sigmatropic shift of a silyl group from silicon to the oxygen of the acylsilanes. Brook has isolated the first kinetically stabilized silenes by the photolysis of certain acylsilanes which lead to a [1,3]-sigmatropic shift[56]. Thermal 1,2-elimination of lithium fluoride from α-lithiated fluorosilanes also provides a variety of sterically hindered silenes[57−62]. Reactive silenes can be generated by 1,2-shift, 1,3-shift, electrocyclic ring-opening, $[2+2]$ cycloreversion, $[2+4]$ cycloreversion and disproportionation of silyl radicals. Raabe and Michl summarized these reactions in their extensive reviews[7,8]. Generation of geometric isomers of stable or of reactive silenes is difficult and therefore mechanistic studies on the reaction of silenes are still quite limited.

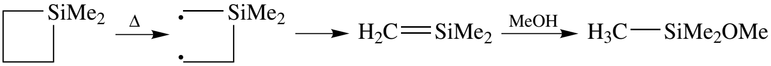

(11)

B. Nucleophilic Addition to Silenes

Unlike disilenes, silenes are dipolar species with the silicon and the carbon atoms charged positively and negatively, respectively. Hence, the silicon centers of silenes are strong Lewis acids which can form donor−acceptor complexes with Lewis bases. 1,1-Dimethyl-2,2-bis(trimethylsilyl)silene, for example, forms an adduct with trimethylamine (equation 12)[62]. Other Lewis bases can form adducts with silenes and it is possible to replace a weaker donor by a stronger donor. The order of donor strength thus determined is: $F^- > NMe_3 > NEt_3 > Br > THF$[62].

Silenes also react efficiently with alcohols to give addition products. Indeed, addition is the most characteristic reaction of silenes and has been used for trapping silenes. Alcohols react regiospecifically to form alkoxysilanes.

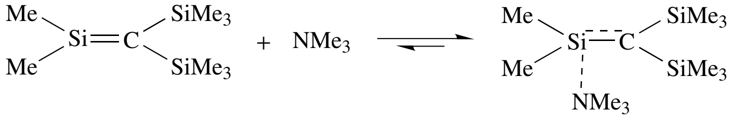

(12)

This is generally true, but it should be noted that silicon–carbon double bonds with inverse electron demand behave differently. Silatriafulvene, for example, did not react with alcohol but underwent 1,2-silyl migration followed by ring expansion reaction to silacyclobutadiene[63]. Silacalicene also adds alcohol in a reverse fashion[64].

C. Diastereochemistry of Addition of Alcohol to Silene

In the first stereochemical study, Brook has observed nonstereospecific addition of methanol to certain isolable silenes[65,66]. Although the precise stereochemistry of the products was not established, a 1/3 mixture of *syn/anti* or *anti/syn* isomers was obtained (equation 13). The results indicate a nonconcerted process for the addition of alcohol to silenes. Wiberg has proposed a two-step mechanism involving an initial formation of a silene–alcohol complex, in accord with the formation of nucleophilic adducts, followed by proton migration from the alcohol to the carbon of the silene (equation 14)[59,61]. This mechanism may be compatible with the results obtained by Brook and coworkers, if rotation around the silene's Si–C bond occurs faster than the proton migration.

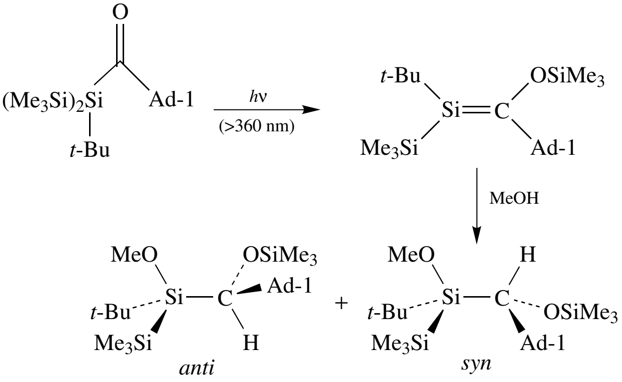

(13)

syn/*anti* or *anti*/*syn* = 1/3

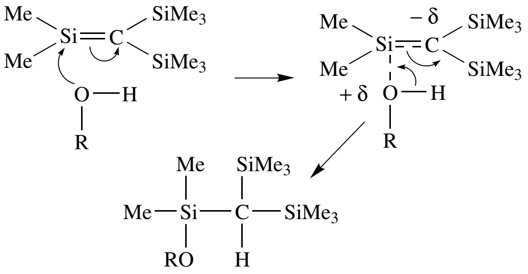

(14)

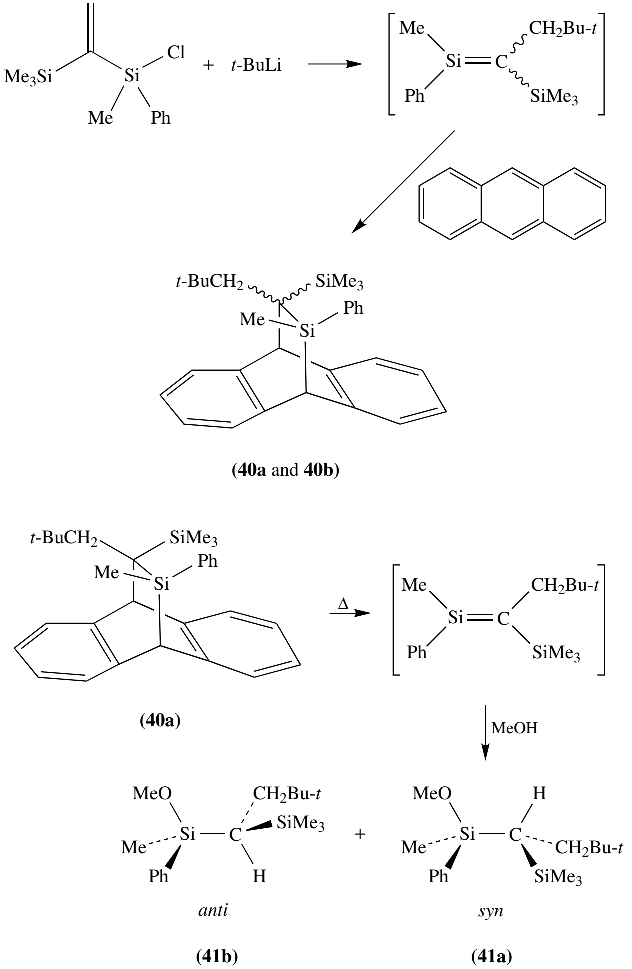

syn:*anti* = 100:0

SCHEME 11

Jones and coworkers developed a new method of generating silenes based on the addition–elimination reaction. Addition of *t*-BuLi to an appropriately substituted chloro(vinyl)silane produces a neopentyl-substituted silene[67,68]. Among many reactions, it has been shown that the transient silene adds to anthracene to afford stereoisomers, **40a** and **40b**, as isolable compounds (Scheme 11). Fractional crystallization of the adduct **40** from hexane gave pure **40a**, leaving a 69/31 mixture of **40a** and **40b**.

The adducts can produce silenes by thermolysis at 190 °C. Thermolysis of **40a** in the presence of a 9-fold excess of methanol gave only **41a**. Similar thermolysis by using a 69/31 mixture of **40a** and **40b** afforded a 69/31 mixture of **41a** and **41b**. Thus methanol adds to the silene stereospecifically[69]. A similar stereospecific addition of alkoxysilane to silene was reported by the same group[70]. The stereospecific *syn* addition can be explained to result from a concerted process involving a [4 + 2] ($\sigma + \text{n} + \pi$) 6-electron[71], but Jones and coworkers have concluded that the reaction must be a stepwise process similar to that proposed by Wiberg, where the intermediate adduct must have a substantial Si=C double-bond character. This is expected from the fact that the silene–THF adduct has a relatively short Si–C bond length as determined by X-ray crystallographic analysis[59].

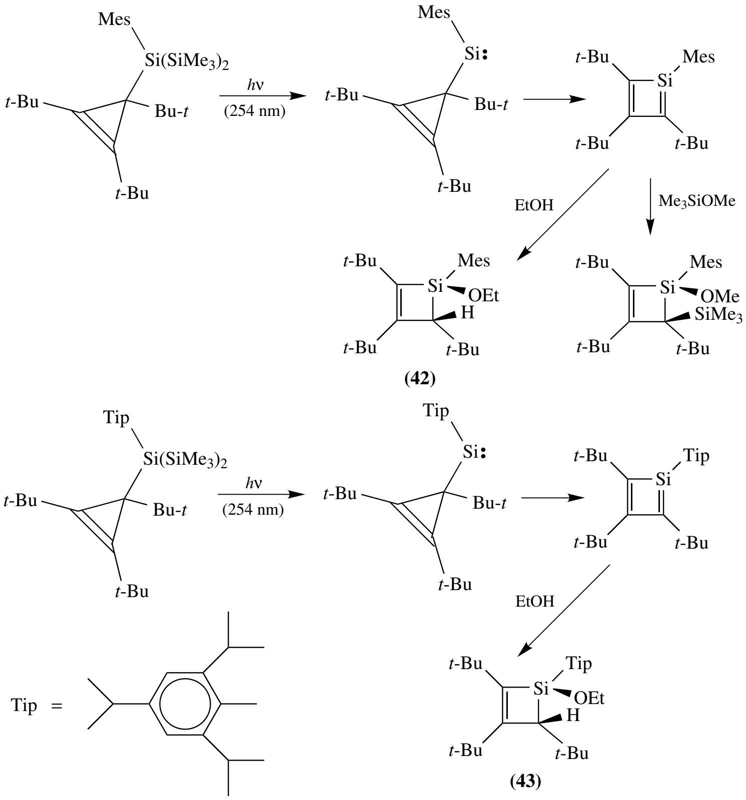

SCHEME 12

Stereospecific *syn* addition of methoxysilane to silacyclobutadiene was reported by Fink and coworkers (Scheme 12)[72]. Ethanol also adds the silacyclobutadiene stereospecifically in a *syn* fashion to give **42** (Scheme 12), but the ethanol adduct undergoes photoisomerization to a photostationary mixture of **42** and its stereoisomer. A similar system, but with the more bulky 2,4,6-triisopropylphenyl (Tip) groups, also gave the *syn* ethanol adduct **43**[73]. The rather complicated photochemical–thermal isomerization process was discussed by Fink[74].

Sakurai and coworkers[75] generated the five-membered silene **44** by a photochemical 1,3-silyl shift in the cyclic divinyldisilane **45** (Scheme 13). Since the silene **44** is constrained to be planar, no bond rotation is possible during the reaction. Contrary to the previous observations i.e. a simple two-step or a concerted four-centered mechanism, alcohols add to **44** nonstereospecifically, although in the cyclic silene bond rotation is prohibited.

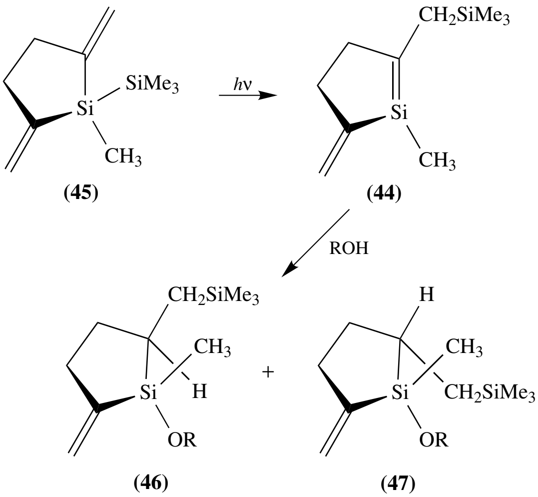

(**a**) R = CH_3; (**b**) R = $CH_2CH_2CH_3$;
(**c**) R = $CH(CH_3)_2$; (**d**) R = $C(CH_3)_3$

SCHEME 13

The stereochemical outcome for the addition of various alcohols to **44** depends markedly on the concentration and on the acidity of the alcohols used. The *syn/anti* **46/47** product ratio increased in the following order as a function of the alcohol: MeOH (27/73) $<$ n-PrOH (35/65) $<$ i-PrOH (46/54) $<<$ t-BuOH (100/0). t-Butyl alcohol gave only a *syn* adduct. Since no interconversion between **46** and **47** was observed under irradiation, the stereochemical outcome must reflect the inherent stereochemistry of the reaction.

Further interesting findings are the dependence of the **46/47** product ratio on the concentration of alcohol. Plots of **46/47** versus the inverse of alcohol concentration gave straight lines at the initial stage of the reaction. This was observed when **45** was irradiated in the presence of various amounts of alcohols in acetonitrile. The slope depended remarkably on the alcohol, i.e. the slopes were 4.6 for MeOH, 9.2 for n-PrOH and 32 for i-PrOH. An infinitely large slope was estimated for t-BuOH, because t-BuOH gave only the *syn* compound.

Based on these results, Sakurai and coworkers proposed for the addition of alcohols to the silene **44** the mechanism shown in Scheme 14. In the first stage the silene forms an alcohol–silene complex **48** as suggested by Wiberg[61], and this stage is followed by an intramolecular proton migration in **48** (the first-order rate constant, k_1) which competes with the intermolecular proton transfer from an additional external alcohol (the second-order rate constant, k_2). These two processes give the *syn* and *anti* addition products, respectively.

This mechanism is fully compatible with the observed linear relationship between the **46/47** product ratio and the reciprocal concentration of the alcohol, since the initial product ratio should be represented by the following equation:

$$d[\mathbf{46}]/d[\mathbf{47}] = (k_1/k_2)/[\mathrm{ROH}] \tag{15}$$

The relative rate constants (k_1/k_2) reflect the relative rates for intra- and intermolecular proton transfer, respectively. As discussed for disilene, the Brønsted catalysis law must be applied to determine the relative rates, where k_2 and k_1 are expected to increase with the

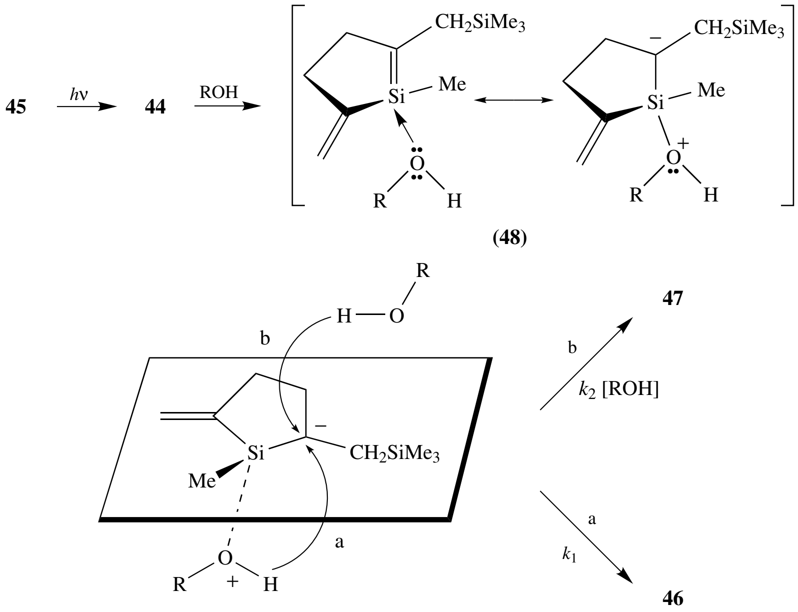

a, Intramolecular H$^+$ transfer
b, Intermolecular H$^+$ transfer

SCHEME 14

increasing acidity of ROH and of the protonated alcohol, respectively. The pK_a values of alcohols increase in the following order (in DMSO)[76]: MeOH (29.0) $<$ n-PrOH (29.8)[77] $<$ i-PrOH (30.25) $<$ t-BuOH (32.2). The inverse order is known for the pK_a values of the corresponding protonated alcohols, RO^+H_2: t-BuO^+H_2 $>$ i-PrO^+H_2 $>$ n-PrO^+H_2 $>$ MeO^+H_2[76]. The less acidic the alcohol is, the more acidic the corresponding protonated alcohol. Thus k_1/k_2 is expected to increase in the following order: MeOH $<$ n-PrOH $<$ i-PrOH $<$ t-BuOH, as observed[75].

The solvent effect on the diastereoselectivity of the reaction is noteworthy[79]. Figure 2 shows the relationship between the **46**/**47** product ratio and the reciprocal concentration of methanol, in various solvents. The k_1/k_2 values are: CH_3CN (4.8), 9 : 1 hexane/Et_2O (5.9) and C_6H_6 (11). The largest value was obtained in benzene, the most nonpolar solvent among those examined. This implies that the relative importance of intramolecular proton transfer (Scheme 14, process a) increases relative to the intermolecular bimolecular process (Scheme 14, process b) as the solvent polarity decreases. Since process a is a reaction starting from a dipolar reactant to give a nonpolar product, polar solvents should retard the rate. Interestingly, the **46**/**47** product ratio does not follow a linear relationship but shows a concave curve in ether. Ether can coordinate to the silene to give **49** (Scheme 15). The lower the concentration of methanol, the more important the role of the ether–silene complex becomes. Then intermolecular proton transfer gives adduct **50**. The complex **50** undergoes S_N2-like substitution by MeO^- or MeOH to give the *syn* adduct **46**.

By using nanosecond laser flash photolysis of **51**, Leigh and coworkers have studied alcohol addition reactions of the 1,3,5-(1-sila)hexatriene derivative **52** (Scheme 16)[80,81] and of 1,1-diphenylsilene[82–84].

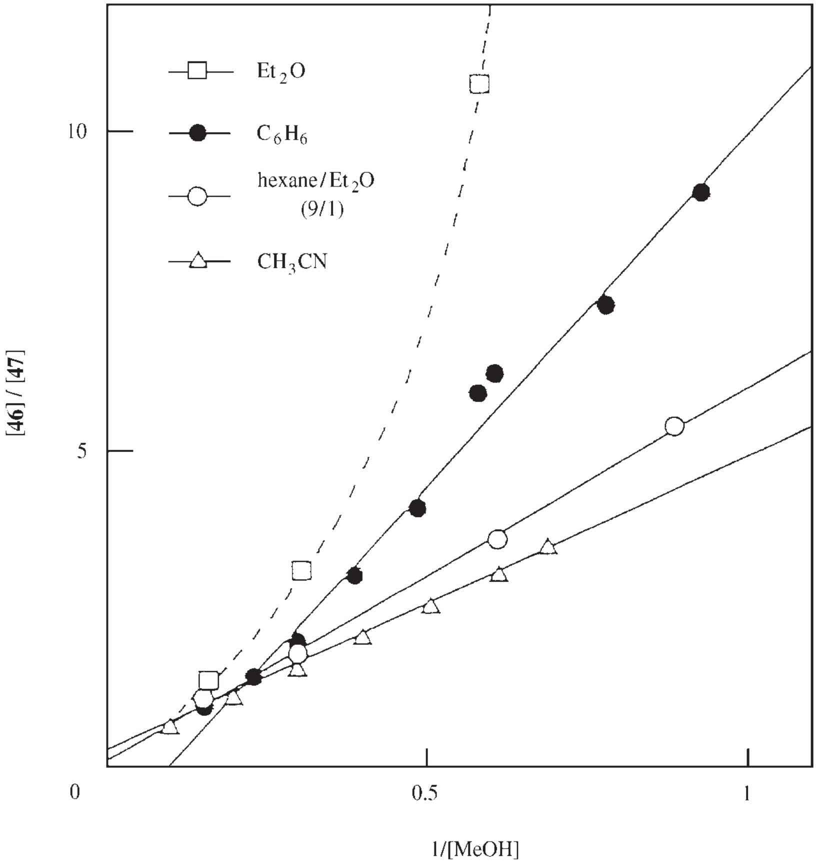

FIGURE 2. Relationship between the **[46]/[47]** ratio and 1/[MeOH] in various solvents

Although the products do not allow one to distinguish between intra- and intermolecular processes, they found that the plots of k_{decay} versus quencher (alcohol) concentration are nonlinear. They have analyzed the data according to the quadratic expression shown in equation 16, where $k_{\text{q}}^{(2)}$ is the third-order rate constant corresponding to transient quenching by two molecules of alcohol.

$$k_{\text{decay}} = k_o + k_q[\text{Q}] + k_{\text{q}}^{(2)}[\text{Q}]^2 \qquad (16)$$

From these spectroscopic and kinetic analyses, the authors proposed a mechanism of alcohol addition to **52** which is similar to one proposed earlier[75].

Rate constants for the reaction of silatrienes **52a–c** with alcohols are listed in Table 6. According to the proposed mechanism, k_{q} and $k_{\text{q}}^{(2)}$ correspond to k_1 and k_2 of equation 15, respectively. It is interesting to compare the very low value of $k_{\text{q}}/k_{\text{q}}^{(2)}$ (0.015–0.047) in the reaction of **52a–52c** with methanol with the corresponding k_1/k_2 value of 4.6 for the silene **44**. The latter is about two orders of magnitude greater than the former. Apparently, silatrienes derived from aryldisilanes behave very differently from **44**.

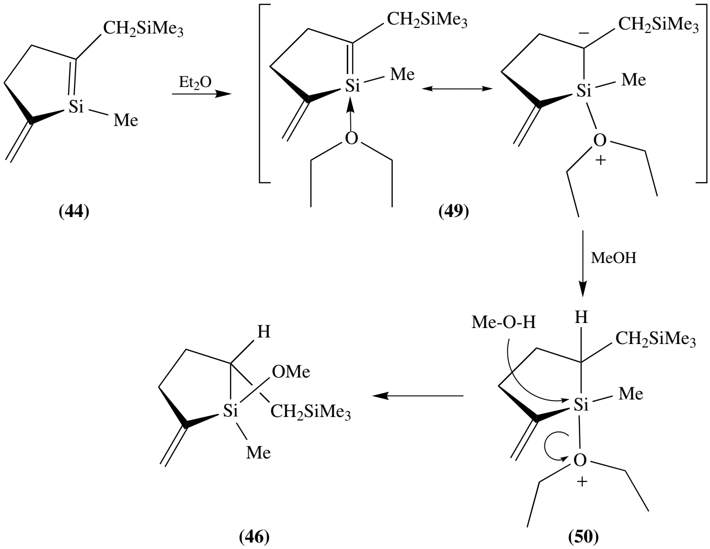

SCHEME 15

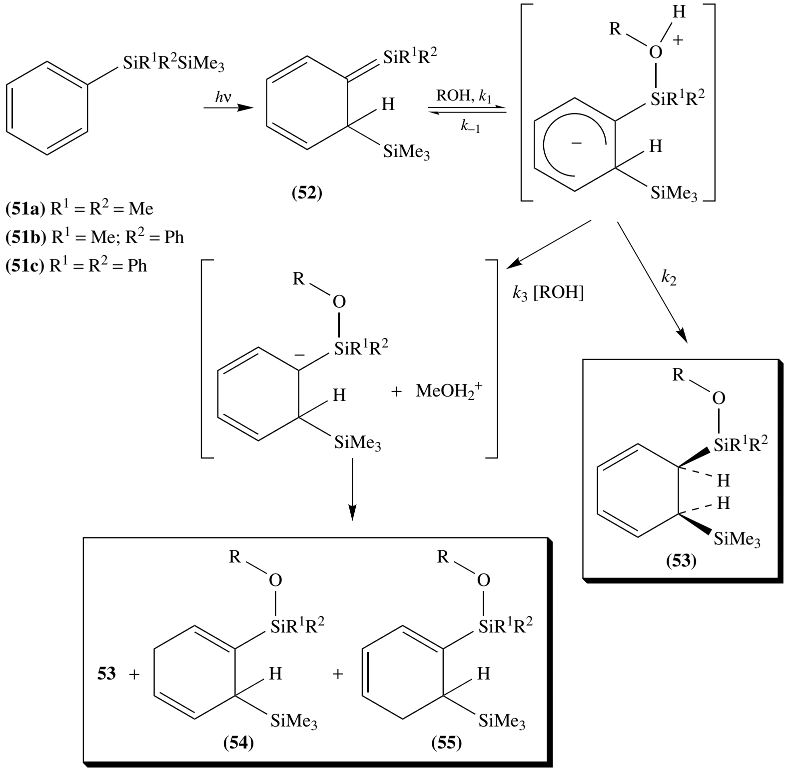

SCHEME 16

TABLE 6. Rate constants for reaction of silatrienes **51a, b, c** with alcohols in acetonitrile[84]

Reagent	Rate constant	**52a**	**52b**	**52c**
MeOH	$10^{-8}k_q$	2.3 ± 0.7	0.60 ± 0.25	0.17 ± 0.10
	$10^{-8}k_q^{[2]}$	49 ± 10	28 ± 5	11 ± 4
MeOD	$10^{-8}k_q$	1.2 ± 0.2	0.34 ± 0.08	0.09 ± 0.04
	$10^{-8}k_q^{[2]}$	51 ± 4	23 ± 2	7.9 ± 0.7
CF_3CH_2OH	$10^{-8}k_q$	0.236 ± 0.004	0.056 ± 0.001	0.017 ± 0.001

In the photolysis of pentamethyldisilane **51a** three methanol addition products are obtained. Compound **53a**, which has not been observed by previous workers[85], is attributed to be the product of intramolecular proton transfer. Photochemical reactions of aryldisilanes have been recently reviewed[86].

1,1-Diphenylsilene, generated by similar photolysis of silacyclobutane[82–84], also reacts very rapidly with water, alcohols and acetic acid (equation 17). Rate constants are only one order of magnitude slower than the diffusion-controlled limit and depend only slightly on the nucleophilicity or acidity of the quencher. Although it is not easy to distinguish kinetically unimolecular and bimolecular processes, a similar mechanism to that shown in Scheme 16 was suggested also for the addition of alcohols to 1,1-diphenylsilene.

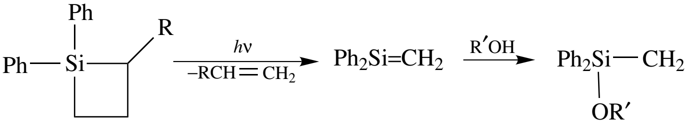

(17)

Bradaric and Leigh have also measured absolute rate constants for the reaction of a series of ring-substituted 1,1-diphenylsilene derivatives with methanol, *t*-butyl alcohol and acetic acid in acetonitrile by similar nanosecond laser flash photolysis techniques[87] (Table 7).

All the three reactions show small positive Hammett ρ-values at 23 °C. According to Scheme 17, the reaction constants for complexation of alcohols to silene should be positive, consistent with the mechanism involving initial, reversible nucleophilic attack

TABLE 7. Bimolecular rate constants, deuterium isotope effects and Hammett ρ-values for reactions of 1,1-diarylsilenes (**56**; R′ = H)[87] with MeOH, *t*-BuOH and AcOH in acetonitrile at 23 °C

58 ($R^1 = H$)	$k_{MeOH}/(10^9\ M^{-1}\ s^{-1})$	$k_{t-BuOH}/(10^9 M^{-1}\ s^{-1})$	$k_{AcOH}/(10^9 M^{-1}\ s^{-1})$
Ar = $4\text{-}CH_3C_6H_4$	1.12 ± 0.06	0.130 ± 0.006	1.41 ± 0.05
	$(k_H/k_D = 1.9 \pm 0.1)$	$(k_H/k_D = 1.9 \pm 0.2)$	$(k_H/k_D = 1.2 \pm 0.2)$
Ar = C_6H_5	1.5 ± 0.1	0.22 ± 0.02	1.5 ± 0.2
	$(k_H/k_D = 1.5 \pm 0.1)$	$(k_H/k_D = 1.6 \pm 0.1)$	$(k_H/k_D = 1.1 \pm 0.1)$
Ar = $4\text{-}F\text{−}C_6H_4$	1.89 ± 0.08	0.33 ± 0.022	1.8 ± 0.2
Ar = $4\text{-}Cl\text{−}C_6H_4$	2.13 ± 0.10	0.39 ± 0.02	2.0 ± 0.2
Ar = $4\text{-}CF_3\text{−}C_6H_4$	2.99 ± 0.16	0.75 ± 0.04	2.3 ± 0.4
	$(k_H/k_D = 1.0 \pm 0.1)$	$(k_H/k_D = 1.7 \pm 0.1)$	$(k_H/k_D = 1.1 \pm 0.1)$
ρ	+0.13 ± 0.05	+0.55 ± 0.084	+0.17 ± 0.02
	$(r^2 = 0.980)$	$(r^2 = 0.985)$	$(r^2 = 0.987)$

at silicon to form a σ-complex. Proton transfer within the complex is the rate-limiting process since relatively large kinetic isotope effects are observed. However, the polar nature of the proton transfer should be small and overall polar character of the reaction is governed by the initial complexation steps. They also found that proton transfer within the complex was entropy-controlled, resulting in negative activation energies for the reaction. However, the reaction of $Ph_2Si{=}CH_2$ ($E_a = +1.9 \pm 0.3$ kcal mol^{-1}) and more reactive $(p\text{-}CF_3C_6H_4)_2Si{=}CH_2$ ($E_a = +3.6 \pm 0.5$ kcal mol^{-1}) with acetic acid gave positive activation energies. They have suggested that acetic acid adds by a stepwise mechanism but with formation of the complex being rate-determining.

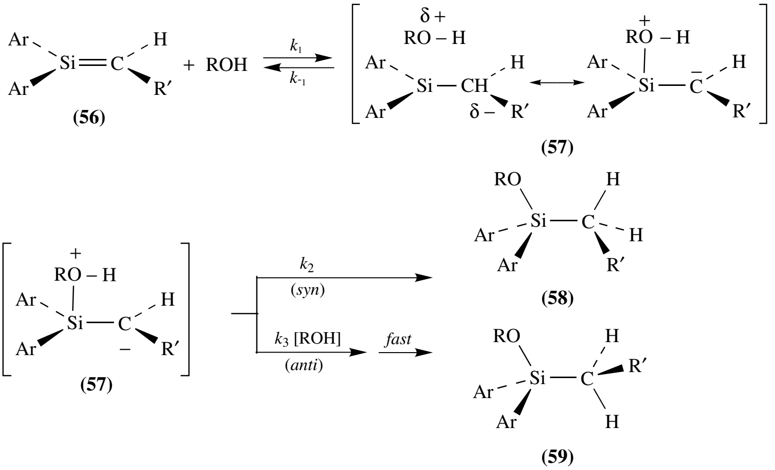

SCHEME 17

IV. CONCLUDING REMARKS

It is evident from the above discussion that much progress has been made in the past decade in deepening our understanding of the chemistry of silicon–silicon and silicon–carbon double bonds. However, the field is still in its infancy and many additional studies should be carried out in order to broaden our knowledge. Proper design of substrates combined with transient spectroscopy is needed. Theoretical studies will also assist the better understanding of the chemistry of multiple bonds to silicon. In this respect, the author did not discuss the theoretical aspects of silicon-containing double bonds, because an excellent review on this topic is available elsewhere[88].

V. ACKNOWLEDGMENTS

The author wishes to thank his colleagues for their indispensable contributions to the studies on the chemistry of silicon–silicon and silicon–carbon double bonds. Their names are cited in the references. The author also wishes to thank the Ministry of Education, Science, and Culture (Specially Promoted Research 02102004) and the Japan Society for the promotion of Sciences (RFTF95P00303) for financial support.

VI. REFERENCES

1. P. D. Gaspar, in *Reactive Intermediates* (Eds. M. Jones, Jr. and R. A. Moss), Vol. 1, Chap. 7 (1978); Vol. 2, Chap. 9 (1981); Vol. 3, Chap. 9 (1985), Wiley, New York.

2. (a) H. Sakurai, in *Free Radicals* (Ed. J. K. Kochi), Chap. 24, Wiley-Interscience, New York, 1975. (b) C. Chatgilialoglu, *Chem. Rev.*, **95**, 1229 (1995).
3. I. Fleming, in *Comprehensive Organic Chemistry* (Eds. D. Barton and W. D. Ollis), Vol. 3. (Ed. D. Neville Jones), Pergamon Press, Oxford, 1979.
4. K. Tamao and A. Kawachi, *Adv. Organomet. Chem.*, **38**, 1 (1995).
5. See chapters by P. v. R. Schleyer (Chapter 10) and P. D. Lickiss (Chapter 11) in this volume.
6. A. G. Brook and K. M. Bains, *Adv. Organomet. Chem.*, **25**, 1 (1985).
7. G. Raabe and J. Michl, in *The Chemistry of Organic Silicon Compounds*, Vol. 1, Part 2 (Eds. S. Patai and Z. Rappoport), Chap. 17, Wiley, New York, 1989.
8. G. Raabe and J. Michl, *Chem. Rev.*, **85**, 419 (1985).
9. R. West, *Pure Appl. Chem.*, **56**, 163 (1984).
10. R. West, *Angew. Chem., Int. Ed. Engl.*, **26**, 1201 (1987).
11. T. Tsumuraya, S. A. Batcheller and S. Masamune, *Angew. Chem., Int. Ed. Engl.*, **30**, 902 (1991).
12. R. Okazaki and R. West, *Adv. Organomet. Chem.*, **39**, 231 (1996).
13. A. R. Bassindale and P. G. Taylor, in *The Chemistry of Organic Silicon Compounds*, Vol. 1 Part 2 (Eds. S. Patai and Z. Rappoport), Chap. 17, Wiley, New York, 1989.
14. R. J. P. Corriu, C. Guerin and J. J. E. Moreau, in *The Chemistry of Organic Silicon Compounds*, Vol. 1 Part 2 (Eds. S. Patai and Z. Rappoport), Chap. 4, Wiley, New York, 1989.
15. D. N. Roark and G. J. Peddle, *J. Am. Chem. Soc.*, **94**, 5837 (1972).
16. H. Sakurai, Y. Nakadaira and T. Kobayashi, *J. Am. Chem. Soc.*, **101**, 487 (1979).
17. Y. Nakadaira, T. Kobayashi, T. Otsuka and H. Sakurai, *J. Am. Chem. Soc.*, **101**, 486 (1979).
18. G. Olbrich, P. Potzinger, B. Reinmann and R. Walsh, *Organometallics*, **3**, 1267 (1984).
19. M. J. Michalczyk, R. West and J. Michl, *Organometallics*, **4**, 826 (1985).
20. B. D. Shepherd, D. R. Powell and R. West, *Organometallics*, **8**, 2664 (1989).
21. S. A. Batcheller, T. Tsumuraya, O. Tempkin, W. Dacis and S. Masamune, *J. Am. Chem. Soc.*, **112**, 9394 (1990).
22. H. Jacobsen and T. Ziegler, *J. Am. Chem. Soc.*, **116**, 3667 (1994).
23. M. W. Schmidt, P. N. Truong and M. S. Gordon, *J. Am. Chem. Soc.*, **109**, 5217 (1987).
24. W. Kutzelnigg, *Angew. Chem., Int. Ed. Engl.*, **23**, 272 (1984).
25. H. Sakurai, K. Sakamoto, Y. Funada and M. Yoshidain, in *Inorganic and Organometallic Polymers II, Advanced Materials and Intermediates*, Chap. 2, ACS Symposium Series 572 (Eds. P. Wisian-Neilson, H. R. Allcock and K. J. Wynne), 1994.
26. K. Sakamoto, K. Obata, H. Hirata, M. Nakajima and H. Sakurai, *J. Am. Chem. Soc.*, **111**, 7641 (1989).
27. A. Sekiguchi, I. Maruki, K. Ebata, C. Kabuto and H. Sakurai, *J. Chem. Soc., Chem. Commun.*, 341 (1991).
28. A. Sekiguchi, I. Maruki and H. Sakurai, *J. Am. Chem. Soc.*, **115**, 11460 (1993).
29. H. Sakurai, K. Sakamoto and M. Yoshida, submitted for publication.
30. T. Hoshi, T. Shimada, T. Sanji and H. Sakurai, *Chem. Lett.*, submitted.
31. H. Suzuki, *Bull. Chem. Soc. Jpn.*, **33**, 619 (1960).
32. G. R. Gillette, G. Noren and R. West, *Organometallics*, **9**, 2925 (1990).
33. R. S. Archibald, Y. v. d. Winkel, A. J. Millevolte, J. M. Desper and R. West, *Organometallics*, **11**, 3276 (1992).
34. P. Jutzi, U. Holtmann, H. Bögge and A. Müller, *J. Chem. Soc., Chem. Commun.*, 305 (1988).
35. J. Maxka and Y. Apeloig, *J. Chem. Soc., Chem. Commun.*, 737 (1990).
36. K. Sakamoto, S. Tsutsui, H. Sakurai and M. Kira, *Bull. Chem. Soc. Jpn.*, **70**, 253 (1997).
37. B. T. Luke, J. A. Pople, M.-B. Krogh-Jesperson, Y. Apeloig, M. Karni, J. Chandrasekhar and P. v. R. Schleyer, *J. Am. Chem. Soc.*, **108**, 270 (1986).
38. H. Teramae, *J. Am. Chem. Soc.*, **109**, 4140 (1987).
39. J.-P. Malrieu and G. Trinquier, *J. Am. Chem. Soc.*, **111**, 5916 (1989).
40. G. Trinquier and J.-P. Malrieu, *J. Phys. Chem.*, **94**, 6184 (1990).
41. C. Liang and L. C. Allen, *J. Am. Chem. Soc.*, **112**, 1039 (1990).
42. R. S. Grev, *Adv. Organomet. Chem.*, **33**, 125 (1991).
43. M. Karni and Y. Apeloig, *J. Am. Chem. Soc.*, **112**, 8589 (1990).
44. (a) M. V. George, D. J. Peterson and H. Gilman, *J. Am. Chem. Soc.*, **82**, 403 (1960).
    (b) H. O. House, *Modern Synthetic Reactions*, 2nd ed., Benjamin, Menlo Park, CA, 1977, p. 568.
45. W. Hanstein, H. J. Berwin and T. G. Traylor, *J. Am. Chem. Soc.*, **92**, 829 (1970).
46. R. West, M. J. Fink and J. Michl, *Science (Washington, D.C.)*, **214**, 1343 (1981).

47. D. J. De Young, M. J. Fink, R. West and J. Michl, *Main Group Met. Chem.*, **10**, 19 (1987).
48. S. Nagase, T. Kudo and K. Ito, in *Applied Quantum Chemistry* (Eds. V. H. Smith Jr., H. F. Schaefer III and K. Morokuma), Reidel, Dordrecht, 1986.
49. E. M. Arnett, *Prog. Phys. Org. Chem.*, **1**, 223 (1963).
50. J. Budaraju, D. R. Powell and R. West, *Main Group Met. Chem.*, **19**, 531 (1996).
51. S. Tsutsui, K. Sakamoto, H. Sakurai, M. Kira, T. Veszprèmi, 72 Annual Meeting of the Chemical Society of Japan, March 27–30 (1997); Abstracts I, 2E313.
52. M. Wind, D. R. Powell and R. West, *Organometallics*, **15**, 5772 (1996).
53. Y. Apeloig and M. Nakash, *Organometallics*, in press.
54. Y. Apeloig and M. Nakash, *J. Am. Chem. Soc.*, **118**, 9798 (1996).
55. L. E. Gusel'nikov, N. S. Nametkin and V. M. Vdovin, *Acc. Chem. Res.*, **8**, 18 (1975).
56. A. G. Brook, S. C. Nyburg, W. F. Reynolds, Y. C. Poon, Y.-M. Chan, J.-S. Lee and J.-P. Picard, *J. Am. Chem. Soc.*, **101**, 6750 (1979).
57. N. Wiberg, G. Wagner and G. Muller, *Angew. Chem., Int. Ed. Engl.*, **24**, 229 (1985).
58. N. Wiberg and G. Wagner, *Angew. Chem., Int. Ed. Engl.*, **22**, 1005 (1983).
59. N. Wiberg, G. Wagner, G. Muller and J. Riede, *J. Organomet. Chem.*, **271**, 381 (1984).
60. N. Wiberg and G. Wagner, *Chem. Ber.*, **119**, 1467 (1986).
61. N. Wiberg, *J. Organomet. Chem.*, **273**, 141 (1984).
62. N. Wiberg and H. Köpf, *J. Organomet. Chem.*, **315**, 9 (1986).
63. K. Sakamoto, J. Ogasawara, H. Sakurai and M. Kira, *J. Am. Chem. Soc.*, **119**, 3405 (1997).
64. H. Sohn, J. Merritt and R. West, 30th Organosilicon Symposium, May 30–31, 1997, London, Ontario, Canada, Abstracts, A19.
65. A. G. Brook, K. D. Safa, P. D. Lickiss and K. M. Baines, *J. Am. Chem. Soc.*, **107**, 4338 (1985).
66. K. M. Baines, A. G. Brook, R. R. Ford, P. D. Lickiss, A. K. Saxena, W. J. Chatterton, J. F. Sawyer and B. A. Behnam, *Organometallics*, **8**, 693 (1989).
67. P. R. Jones and M. E. Lee, *J. Am. Chem. Soc.*, **105**, 6725 (1983).
68. P. R. Jones, M. E. Lee and L. T. Lin, *Organometallics*, **2**, 1039 (1983).
69. P. R. Jones and T. F. Bates, *J. Am. Chem. Soc.*, **109**, 913 (1987).
70. P. R. Jones, T. F. Bates, A. F. Cowley and A. M. Arif, *J. Am. Chem. Soc.*, **108**, 3122 (1986).
71. G. Bertrand, J. Dubac, P. Mazerolles and J. Ancelle, *Nouv. J. Chim.*, **6**, 381 (1982).
72. M. J. Fink, D. B. Puranik and M. P. Johnson, *J. Am. Chem. Soc.*, **110**, 1315 (1988).
73. D. B. Puranik and M. J. Fink, *J. Am. Chem. Soc.*, **111**, 5951 (1989).
74. M. J. Fink, in *Frontiers of Organosilicon Chemistry* (Eds. A. R. Bassindale and P. P. Gaspar), Royal Society of Chemistry, Cambridge, 1991.
75. M. Kira, T. Maruyama and H. Sakurai, *J. Am. Chem. Soc.*, **113**, 3986 (1991).
76. F. G. Bordwell, *Acc. Chem. Res.*, **21**, 456 (1988).
77. pK_a value of propanol in DMSO from Reference 78.
78. W. N. Olmsted, Z. Margolin and F. G. Bordwell, *J. Org. Chem.*, **45**, 3295 (1980).
79. T. Maruyama, M. Sc. Thesis, Tohoku University (1989).
80. G. W. Sluggett and W. J. Leigh, *J. Am. Chem. Soc.*, **114**, 1195 (1992).
81. W. J. Leigh and G. W. Sluggett, *J. Am. Chem. Soc.*, **116**, 10468 (1994).
82. W. J. Leigh, C. J. Bradaric and G. W. Sluggett, *J. Am. Chem. Soc.*, **115**, 5332 (1993).
83. C. J. Bradaric and W. J. Leigh, *J. Am. Chem. Soc.*, **118**, 8971 (1996).
84. W. J. Leigh, C. J. Bradaric, C. Kerst and J.-A. H. Banisch, *Organometallics*, **15**, 2246 (1996).
85. M. Ishikawa, T. Fuchikami and M. Kumada, *J. Organomet. Chem.*, **118**, 155 (1976).
86. M. G. Steinmetz, *Chem. Rev.*, **95**, 1527 (1995).
87. C. J. Bradaric and W. J. Leigh, *Can. J. Chem.*, **75**, 1393 (1997).
88. Y. Apeloig, in *The Chemistry of Organic Silicon Compounds*, Vol. 1 Part 1 (Eds. S. Patai and Z. Rappoport), Chap. 2, Wiley, New York, 1989.

CHAPTER **16**

Silicon–carbon and silicon–nitrogen multiply bonded compounds

THOMAS MÜLLER[†], WOLFGANG ZICHE and NORBERT AUNER[†]

Fachinstitut für Anorganische und Allgemeine Chemie der Humboldt Universität Berlin, D 10115 Berlin, FRG
Fax: +49-30-20936966; e-mail: h0443afs@joker.rz.hu-berlin.de, wolfgang=ziche@chemie.hu-berlin.de, norbert=auner@chemie.hu-berlin.de

---

[†] Present address: Institut fur Anorganische Chemie der J.W.-Goethe Universität Marie-Curie St. 11, D-60438 Frankfurt am Main, Germany

---

I. SILENES

Three decades after the publication of landmark papers by Gusel'nikov and Flowers[1,2] reporting evidence for a silicon–carbon doubly bonded species, the status of silenes has been changed from that of a laboratory curiosity to a not uncommon chemical compound. An impressive amount of information concerning silenes and the behaviour of the Si=C double bond has been discovered and published. While the early days of silene chemistry were marked by gas-phase studies, in the last fifteen years the emphasis of silene chemistry has moved from gas-phase investigations to studies of the reactivity and the physical properties of silenes in the condensed phase. Clearly, the isolation and structural characterization of stable silenes by Brook and coworkers[3] and subsequently by Wiberg and coworkers[4] are the highlights in the short history of silene chemistry, which are adequately followed by the recent synthesis of an air-stable 1-silaallene by West and coworkers[5] and the isolation of the first room-temperature stable silaaromatic compound, the 2-silanaphthalene, by Tokitoh, Okazaki and coworkers[6]. Reactivity studies of silenes and the isolation and characterization of novel organosilicon compounds arising from silene chemistry have been the focus of research in the late eighties and early nineties. Although silenes will, due to their inherent kinetic instability, never play such a dominant role in organosilicon chemistry as alkenes do in organic chemistry, there will be an increasing number of novel compounds and new materials arising from silene chemistry. Physical organic chemistry of silicon, which was restricted for a long time to gas-phase chemistry, has now been developed as an important tool, suggesting detailed mechanisms for the reactivity of silenes also in the condensed phase. Probably no other field of chemistry has been influenced so much by theory as the chemistry of multiple bonded silicon. Silene chemistry has been especially inspired from its infancy until now by the fruitful interplay between theory and experiment.

All these developments of the last thirty years have been well summarized in several accounts. The reviews by Raabe and Michl[7,8] cover most of the work in the silene area till 1988 and the review by Brook and Brook[9] extends this to 1994. The theoretical implications on silene chemistry are reviewed in several articles by Gordon[10a]. Grev[10b], Apeloig[11] and up to 1996 by Karni and Apeloig[12]. The photochemistry of organosilanes has received considerable attention in recent years and has also been well reviewed. *Organosilane photochemistry* by Steinmetz is a review that covers the literature from the mid-1980s till 1994[13]. The photolysis of silylene precursors is treated in a review by Gaspar and coworkers[14].

A. Synthesis

1. Cycloreversion reactions

Most of the pioneering and fundamental work of the last thirty years in silene chemistry has been conducted in the gas phase under thermolytic or photolytic conditions. The results of the last ten years in this area of silene chemistry are summarized together with related earlier reports in the next sections of the chapter. For more complete information, which includes the literature before 1987, the interested reader is referred in addition to the previous reviews by Raabe and Michl[7,8] and to references given therein.

The classical pyrolytic source of silenes is the [2 + 2] cycloreversion of silacyclobutanes performed at 700–1000 K at low pressure. Due to the high temperature employed, generally only silenes with small substituents (H, Me, vinyl) can be generated. The classical first evidence for the formation of a transient silene came from the thermolysis of dimethylsilacyclobutane **1**, which resulted in fragmentation into 1,1-dimethylsilene **2** and ethene (equation 1)[1,2]. This reaction proceeds for 1,1-disubstituted silacyclobutanes via an initial homolytic cleavage of a C–C bond followed by extrusion of ethene[15,16]. This mechanism is also favored by recent high level ab initio calculations[16b].

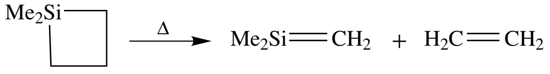

(1) **(2)** (1)

This fragmentation mode is not altered for silacyclobutanes bearing a vinyl group at the silicon[17], as the same Arrhenius parameters are found for the decomposition of **1** and of 1-methyl-1-vinylsilacyclobutane **3** ($\log A = 15.64\ \mathrm{s}^{-1}$, $E_A = 62.6\ \mathrm{kcal\,mol}^{-1}$), in sharp contrast to the pyrolysis of cyclobutanes where a vinyl group accelerates the pyrolysis by a factor of nearly 600[18]. 2-Silabuta-1,3-diene **4** was produced in a laser-photosensitized (SF_6) decomposition (LPD) of 1-methyl-1-vinylsilacyclobutane **3** (equation 2)[19] which, under these conditions, gave polymeric poly(silaisoprene) lacking any carbon–carbon double bonds. The measured Arrhenius parameters ($\log A$ (s^{-1}) = 16.0, $E_A = 59.7$ kcal mol^{-1} for the decomposition reaction are very close to those obtained in the low pressure pyrolysis[18] of **3**, suggesting that the rate-determining step of LPD is the same as that of the pyrolysis, which is assumed to be the cleavage of a C–C bond[19].

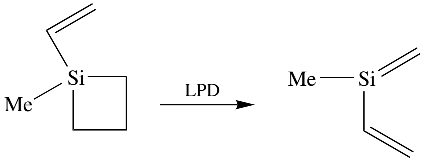

(3) **(4)**

(2)

Conlin and coworkers have prepared (*E*)- and (*Z*)-1,1,2,3-tetramethylsilacyclobutanes **5** and have studied the mechanism of their thermal decomposition in order to gain insight into the stereochemistry of the thermal decomposition of silacyclobutanes[20]. The occurrence of transient 1,4-biradicals like **6** in [2 + 2] fragmentations is accompanied by a loss of the reactant stereochemistry. This can be rationalized by rotational processes in the diradical **6** (**6a** → **6b**) which compete effectively with the *β*-scission steps yielding the silene **2** and *E*/*Z* 2-butene **7** (equation 3).

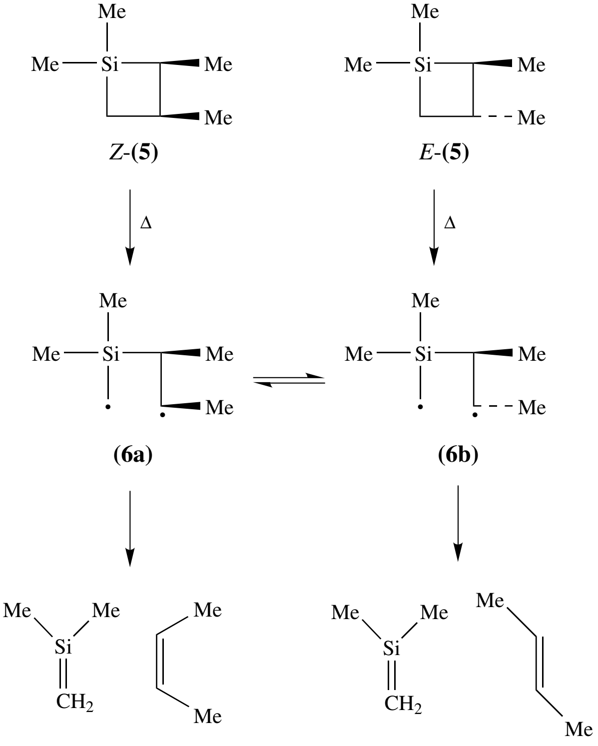

Z-(**5**) *E*-(**5**)

(6a) **(6b)**

(2) *Z*-(**7**) **(2)** *E*-(**7**)

(3)

TABLE 1. Kinetic data for the thermal decomposition of silacyclobutanes

Compound	$\log A$ (s^{-1})	E_A (kcal mol^{-1})	10^4k (s^{-1})	k_{rel}	Reference
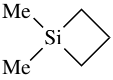 (**1**)	15.64	62.6	0.20	1	2, 21
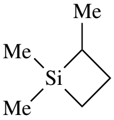 (**12**)	15.45	60.6	0.53	2.7	20
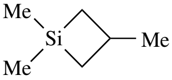 (**13**)	16.39	63.3	0.62	3.1	16
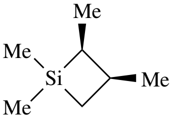 *Z*-(**5**)			7.0	35	20
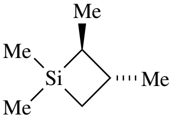 *E*-(**5**)			1.97	10	20
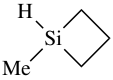 (**14**)	14.9	59.1			22
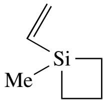 (**3**)	15.64	62.6			18
	16.0	59.7			19

Separate pyrolysis of (*E*)-**5** and (*Z*)-**5** led to the same products **2**, **7**–**11** in equation 4 in slightly different ratios: the major products were trimethylsilene **8** and propene **9**, indicating preferred cleavage of the most highly substituted C–C bond[20]. Comparison (see Table 1) with kinetic data for the pyrolysis of other small silacyclobutanes like **1** or **12**–**13** reveals an activating effect of the methyl substituents in **5**. The stereospecificity of the 2-butene formation is high in both cases: the fragmentation exhibits a fivefold preference for retention in the 2-butene fragment, indicating that the Si–C bond breaking in **6** is fast compared with bond rotation, if a diradical intermediate is assumed[20]. The results have been compared with pyrolysis data of substituted cyclobutanes. Silacyclobutanes were found to react faster than cyclobutanes and the activating effect of the methyl groups on the decompostion rate is larger in the former. Thus, ring splitting across the more substituted bond is more dominant in the silacyclobutane than in the cyclobutane series[20].

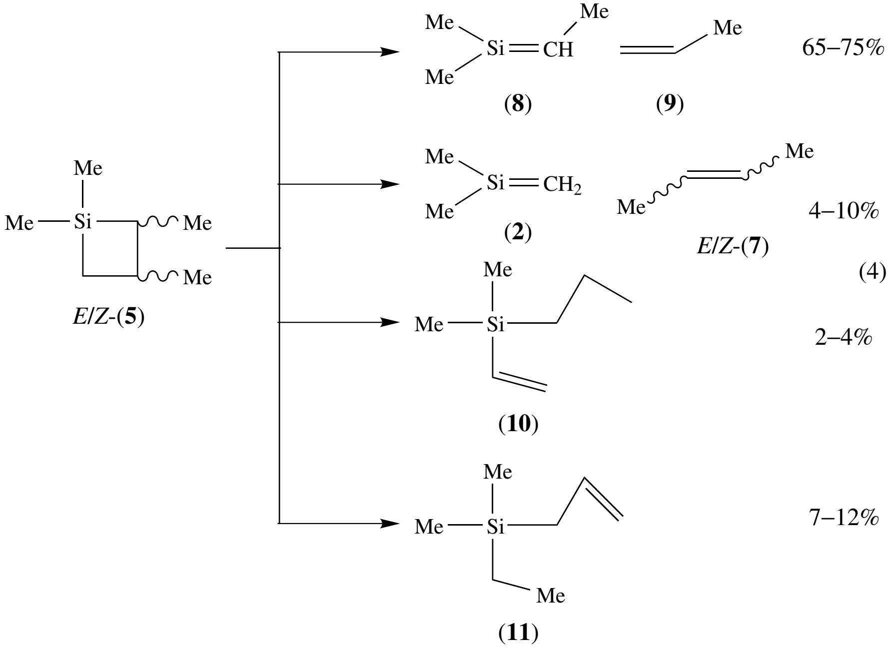

(4)

The very similar Arrhenius parameters measured for methylsilacyclobutane **14** suggest that **14** also decomposes by a multistep biradical mechanism similar to **1** and not by a unimolecular reaction as was originally proposed[22].

In contrast, in the excited state the primary cleavage mechanism in silacyclobutanes like **5** involves the breaking of a silicon–carbon bond[23]. The initially formed silyl radicals **15** and **16** are stabilized by an intramolecular disproportionation reaction giving the silenes **17** and **18** and the homoallylsilane **19**. **17** and **18** were identified by their trapping products (**20, 21**) with methanol (equation 5)[23]. From pyrolysis of *Z*-**5** a different set of products from 1,4-diradical disproportionation is obtained, which can be attributed to predominant cleavage of the carbon–carbon bond[23].

The laser flash photolysis of gaseous silacyclobutanes **22**[24] and **23**[25] and 1,3-disilacyclobutane **24** produced the transient silenes **25** (from **22** and **24**) and **26** (from **23**) as the major primary product. The silenes **25** and **26** were identified by their UV spectra with $\lambda_{max} \approx 260$ nm. Rate constants for the decay processes of the transient silenes were also measured.

Grobe, Auner and coworkers studied the thermal decomposition of **22**, **1** and methylsilacyclobutane **14** under low pressure flow pyrolysis conditions[26]. They characterized the transient silenes **2**, **25** and **26** by mass spectrometric methods and by low temperature NMR spectroscopy of the adducts **27**–**29** of the silenes with hexadeuteriomethyl ether (equation 6)[27].

For the generation of the parent silene $H_2Si{=}CH_2$ **25** the vacuum flash photolysis of 5,6-bis(trifluoromethyl)-2-silabicyclo[2.2.2]octa-5,7-diene **30** was shown to be the most

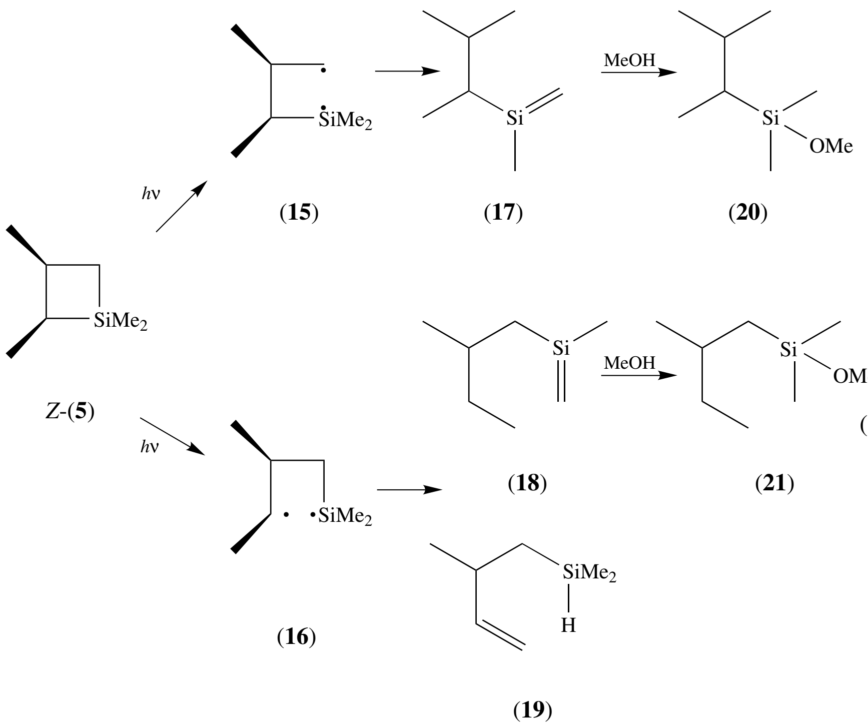

(5)

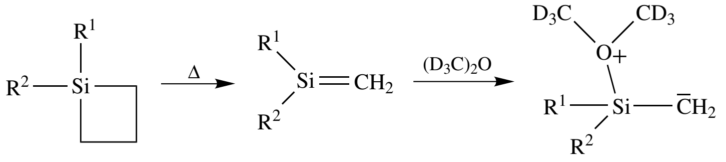

(6)

(**1**) $R^1=R^2=Me$	(**2**) $R^1=R^2=Me$	(**27**) $R^1=R^2=Me$
(**22**) $R^1=R^2=H$	(**25**) $R^1=R^2=H$	(**28**) $R^1=R^2=H$
(**23**) $R^1=H$; $R^2=Me$	(**26**) $R^1=H$; $R^2=Me$	(**29**) $R^1=H$; $R^2=Me$

favourable approach. IR and UV spectra of matrix isolated **25** have been reported[28,29] and the PES spectra[30] of **25** have also been obtained in the gas phase using **30** as precursor. Only recently Bogey, Bürger and coworkers obtained by pyrolysis of **30** a millimeter microwave spectrum from **25** in the gas phase, thereby characterising for the first time the transient **25** by high resolution spectroscopy[31–33]. Other precursors like silacyclobutane **22** or 1,3-disilacyclobutane **24** were also employed (equation 7), but the required temperatures for the generation of **25** from both molecules were much higher[31]. The structural details of **25** resulting from this study will be discussed in Section I.C.1.

Leigh and coworkers used laser flash photolysis to generate transient 1,1-diphenylsilene **31** from silacyclobutane **32** and measured its UV absorption[34,35]. The method was used to determine Arrhenius parameters for the addition of nucleophiles such as alcohols to **31**[25]

In the absence of a trapping agent the head-to-tail dimer **33** was isolated (equation 8).

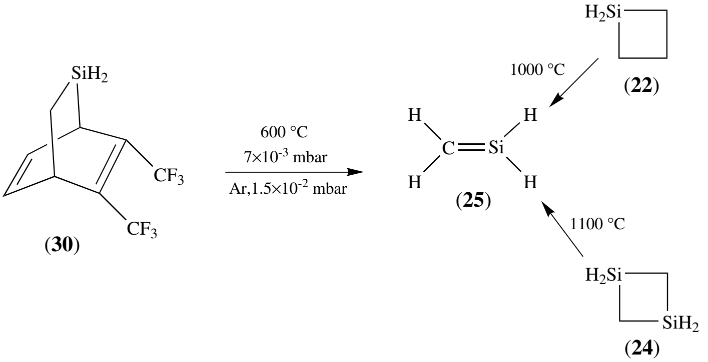

(7)

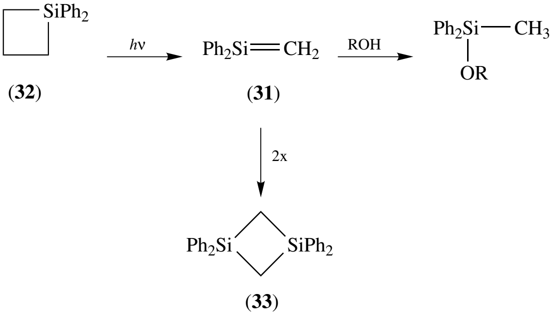

(8)

Pyrolysis of the bis-silacyclobutane **34** yields under chemical vapour deposition conditions polymeric material **37** (equation 9)^{38}. **37** is the mixed product of the

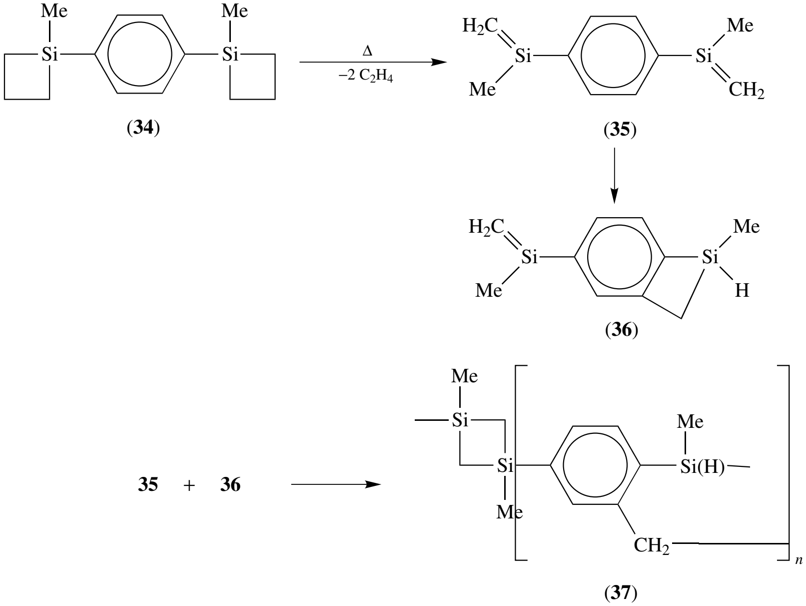

(9)

polydimerization of the intermediate bis-silene **35** and of the ring-opening polymerization of the benzosilacyclobutane **36**. **36** is formed by a sigmatropic 1,3-hydrogen shift from an aryl carbon to the sp^2 silene silicon atom in **35**, that results in a 1,4-diradical, which closes to **36**. This surprising rearrangement could be verified for the thermolysis of phenylsilacyclobutane **38**, which gives as one of the main products the benzo-annelated silacyclobutene **39** (equation 10)[38].

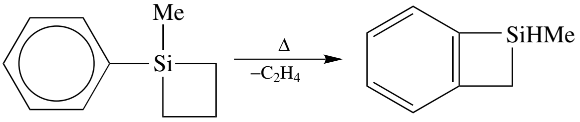

(10)

(**38**) (**39**)

Conlin and Bobbitt thermolyzed 3-vinyl-1-silacyclobutane **40** in order to liberate the silene **41**. In addition to the expected silene trapping products like **42**, several products **44**–**46** resulting from the biradical **43** were found (equation 11)[37].

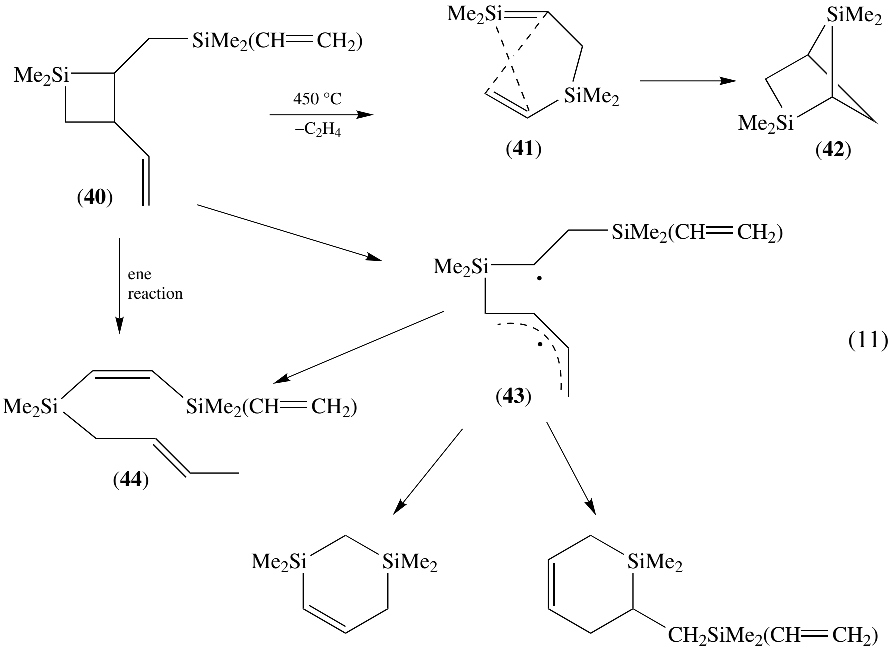

(**40**) (**41**) (**42**) (**43**) (**44**) (**45**) (**46**)

(11)

While several highly substituted 1,2-disilacyclobutanes are known to revert under very mild conditions to silenes[38,39], it is generally believed that 1,3-disilacyclobutanes need more drastic conditions to undergo the cycloreversion yielding silenes[40]. Kinetic data for the pyrolyses of several 1,3-disilacyclobutanes (**24**, **47**, **48**) have been reported by Davidson and coworkers and are summarized in Table 2[40]. Silene formation was inferred from detection of trapping products with TMSOMe and HCl. It was found that methyl substitution at silicon slows down the pyrolysis rate. The initial process for the decomposition of

TABLE 2. Kinetic data for the thermal decomposition of 1.3-disilacyclobutanes.[40].

Compound	log A (s^{-1})	E_A (kcal mol^{-1})	K_{rel}
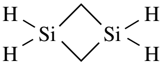 (**24**)	13.3	55.0	1220
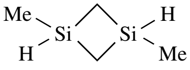 (**47**)	13.5	61.0	50
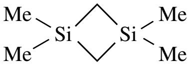 (**48**)	14.4	70.8	1

hydrogen substituted 1,3-disilacyclobutanes was shown to be the 1,2-hydrogen shift from silicon to carbon which results in a complex decomposition mechanism. Both modes of Si–C bond breaking processes, endo- and exocyclic, are shown to occur in the pyrolysis of the tetramethyl derivative **48**[40].

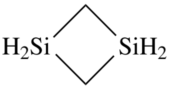

(**24**)

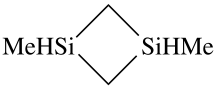

(**47**)

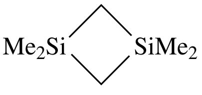

(**48**)

The cleavage of 1,1,3,3-tetraphenyl-2,4-dineopentyl-1,3-disilacyclobutane E/Z-**49** probably gives a 1,4-biradical species **50** in the first step, which may fragment to give silene **51** or reclose to the ring compound[41]. A competing reaction is the disproportionation of the diradical to give **52**. The silene **51** may be trapped to give the species **53** (equation 12).

When one of the phenyl groups is replaced by a vinyl group, a silaallylic diradical intermediate is formed, which produces a six-membered ring silene[42].

Okazaki and coworkers showed that photolysis of benzosilacyclobutenes **54** results in the formation of *ortho*-silaquinonoid compounds **55** (equation 13)[43].

Similarily, the intriguing *ortho* quinodisilane **56** was suggested as the key intermediate in the thermal reaction of benzodisilacyclobutene **57**, which gives a mixture of trisilacyclopentene **58** and the dibenzo-1,4-disilacyclohexadiene **59**[44]. Earlier reports of the formation of the dibenzotetrasilacycloocta-4,7-diene **60**[45,46] were based on wrong structural assignments[44]. The formation of product **58** can be explained in terms of a [4 + 2] dimerization of **56**, followed by elimination of benzosilacyclopropene **61** which would undergo dimerization to **59**[44]. Further evidence for the intermediate **56** was provided by the isolation of its trapping product with t-butanol **62** and with other trapping reagents (equation 14)[45,46].

Interestingly, **56** cannot be obtained photochemically from the benzodisilacyclobutene **57**; instead silastyrene **64** is formed as an intermediate[46]. **64** is produced by homolytic bond scission of the Si–Si bond in **57** followed by intramolecular disproportionation of the resulting biradical **65**. **64** can be intercepted by deuteriated *t*-butanol giving the silanol ether **66** in which the deuterium is incorporated in one ethyl group next to the *t*-butoxy group. In the absence of a scavenger reagent the disilane **67** is formed in 64% yield. The reaction proceeds in a somewhat unusual head-to-head coupling to the carbon centered biradical **68**, which abstracts hydrogens to give product **67** as shown (equation 15)[46] (for an alternative mechanism see Reference 9).

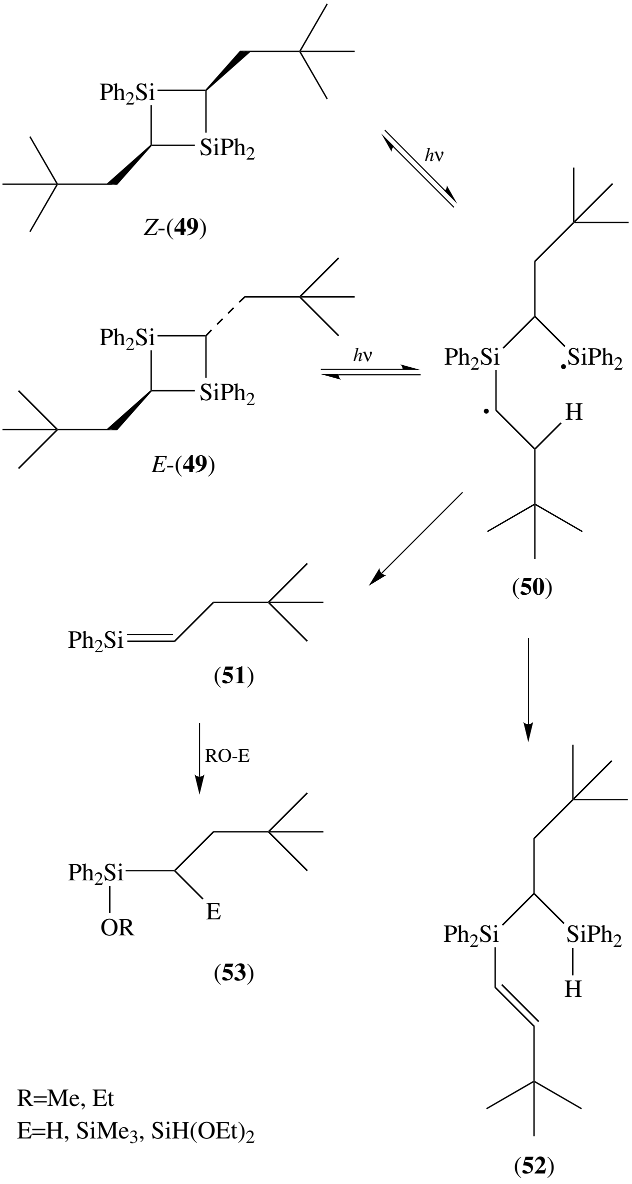

R=Me, Et
E=H, SiMe$_3$, SiH(OEt)$_2$

(12)

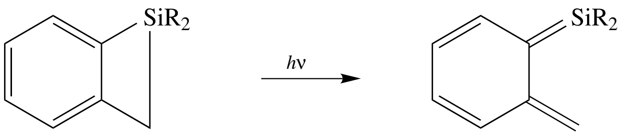

(13)

(**54**) R = Me,Ph (**55**)

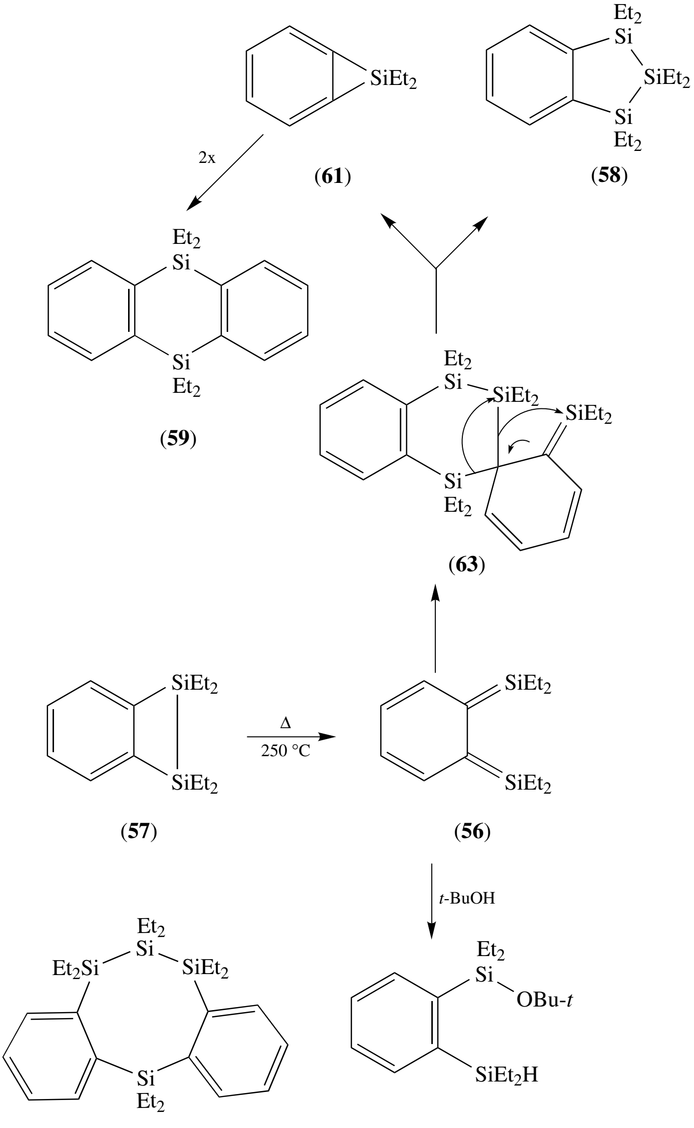

(**61**) (**58**)

(**59**)

(**63**)

(14)

(**57**) (**56**)

(**60**) (**62**)

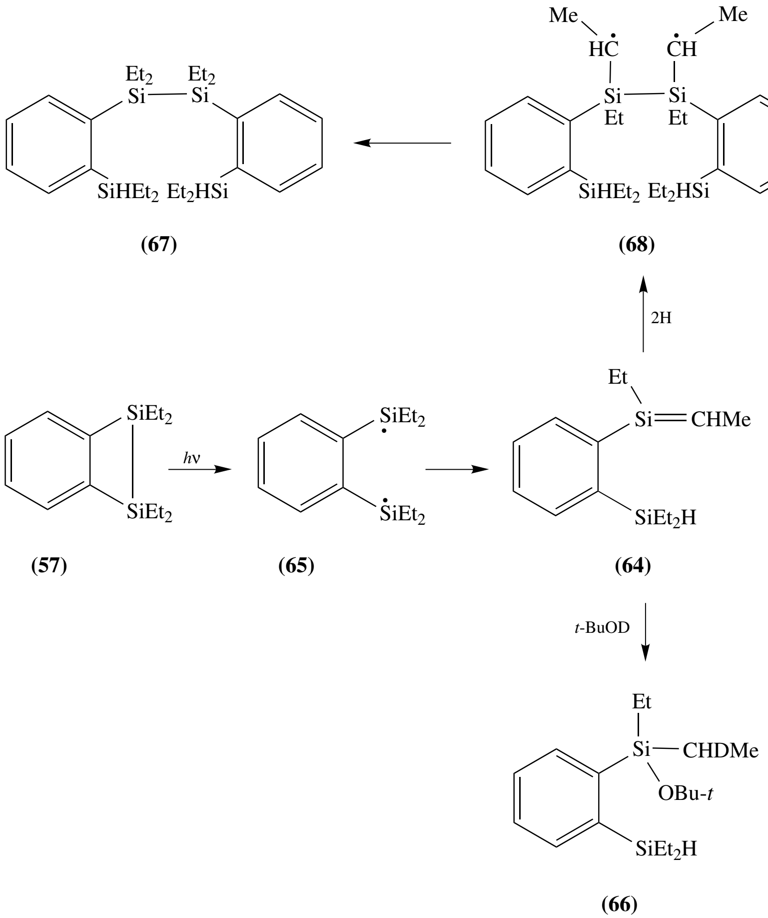

(15)

The ring opening of **57** can be achieved thermolytically at milder conditions using catalytic amounts of Ni[0][47], Pd[0][44] or Pt[0][48] catalysts. Under these conditions the reaction is believed to proceed via a metal[0] bissilene complex **69**. Depending on the metal used, different products **60**, **70** and **71** have been isolated from the thermolysis in benzene (equation 16). Catalyzed ring-opening reactions of **57** in the presence of carbonyl compounds[49], alkenes[50], dienes[50] and acetylenes[51] have also been reported.

Photolysis of 2,3-disiloxetanes **72** liberates the corresponding silene **73** and silanone **74** in a retro-[2 + 2] reaction[52]. The transient species are trapped by ethanol to give **75** and **76**. In the absence of traps the silene undergoes a 1,3-hydrogen shift to give **77**. Ene reaction of the initially formed intermediates, or cleavage of the 1,3-disiloxetane **78** yields the silyl ether **79** (equation 17).

The irradiation of a 1,2-disila-3-thietane gives products from a [2 + 2] cycloreversion, which may be trapped by ethanol[53].

Conlin and Namavari pyrolyzed dimethyl-1-silacyclobut-2-ene **80** in order to obtain 1,1-dimethylsilabutadiene **81**. In the presence of excess ethene two silacyclohexenes, **82** and **83**, were obtained in nearly quantitative yield (equation 18)[54].

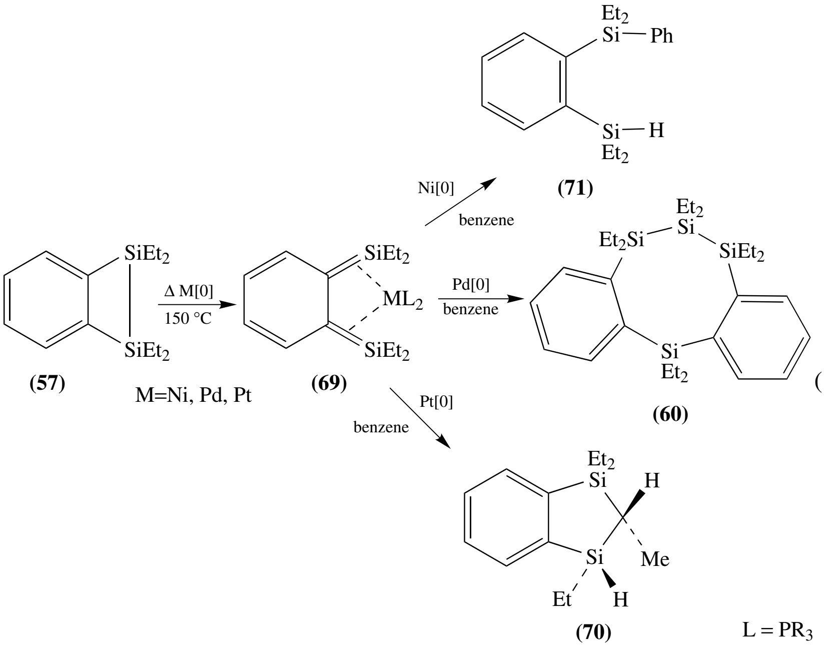
(57)
M=Ni, Pd, Pt
Δ M[0]
150 °C
(69)
ML2
Ni[0]
benzene
(71)
Pd[0]
benzene
(60)
Pt[0]
benzene
(70)
L = PR3

(16)

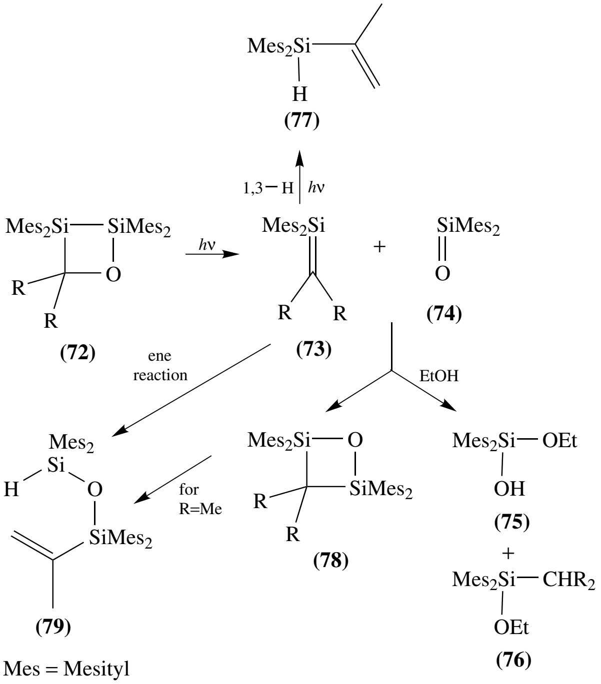
(77)
1,3−H
hν
(72)
(73)
(74)
ene reaction
EtOH
for R=Me
(79)
(78)
(75)
(76)
Mes = Mesityl

(17)

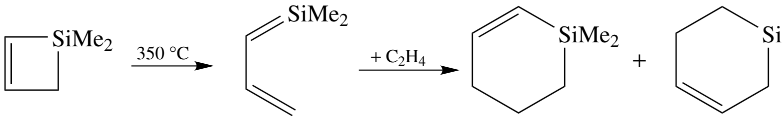

(80) **(81)** **(82)** **(83)**

(18)

Steinmetz and coworkers carried out mechanistic studies on the far-UV photochemical ring opening of 1-silacyclobut-2-ene **80**. The intermediates were trapped by alcohols to give **84**–**87** and by methoxytrimethylsilane to give **88** and **89**[55]. The main reaction is the formation of 1-silabuta-1,3-diene **81**, while the formation of silene **2**, probably via the carbene **90**, is a minor reaction (equation 19). The mechanism suggested was supported by deuterium labelling studies and *ab initio* calculations.

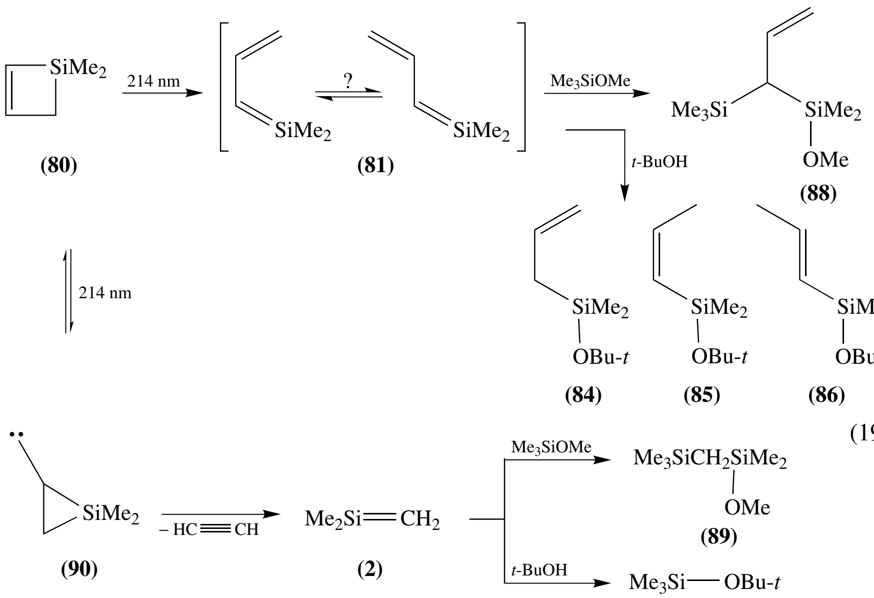

(80) **(81)** **(88)** **(84)** **(85)** **(86)** **(90)** **(2)** **(89)** **(87)**

(19)

The main reaction occuring in the gas-phase pyrolysis of diallyldimethylsilane **91** is the retro-ene elimination of propene with formation of 1-silabuta-1,3-diene **81** followed by a ring closure reaction to yield the 1-silacyclobut-2-ene **80** (equation 20)[56,57]. In the presence of methanol the adduct of **81** was observed[57]. The Arrhenius parameters for the retro-ene fragmentation of **91** ($\log A$ (s^{-1}) $= 11.2$, $E_A = 47.6$ kcal mol^{-1})[57] are very similar to those for the pyrolysis of the carbon analogue hepta-1,6-diene[58].

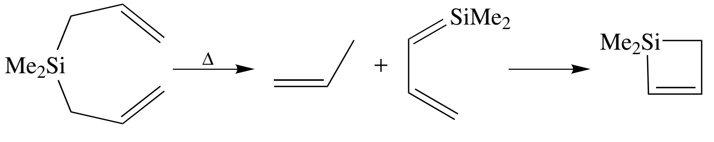

(91) **(9)** **(81)** **(80)**

(20)

The ‘Wiberg’-type silenes like **92**, available through salt elimination reactions from **93**, react with nonenolisable aldehydes, ketones and the corresponding imino derivatives to give in a first step donor adducts **94**[59], which are then transformed to the [2 + 2] and [2 + 4] cycloadducts **95** and **96**, respectively (equation 21)[60–62]. These cycloadducts may liberate the silene **92** upon heating and it can be trapped by suitable reagents.

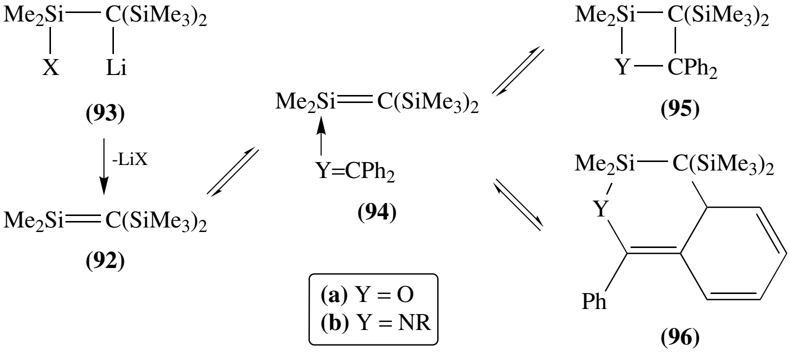

(21)

Silene $Ph_2Si{=}C(SiMe_3)_2$ **97** reacts with benzophenone and gives the [2 + 4] cycloproduct **98**, probably via the donor adduct **99**. **98** is, however, not a silene precursor but decomposes to the alkene **100** and diphenylsilanone **101** (equation 22)[63,64].

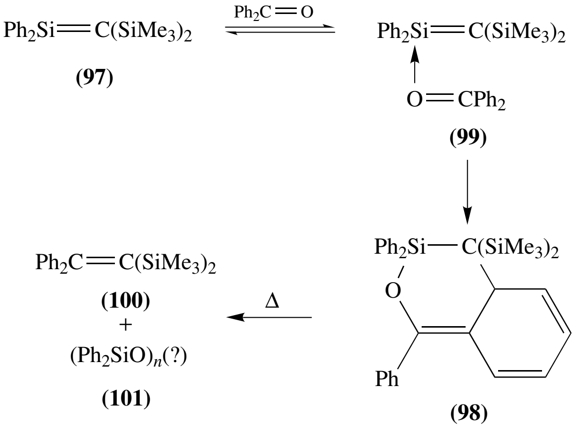

(22)

The primary product from the reaction of **97** with $Me_3Si{-}N{=}CPh_2$ is the [2+4] adduct **102**, which, above 80 °C, equilibrates with the [2+2] adduct **103**. **102** as well as **103** serve as silene sources when heated (equation 23)[63,64]. Trapping reactions and rearrangements of **97** are discussed in more detail below.

The attempted synthesis of **104** from its LiF adduct by salt elimination leads exclusively to the silene **104a**[65,66]. **104a** can be reacted with benzophenone to give the [2 + 4] and [2 + 2] cycloadducts **105** and **106**[67]. The [2 + 4] cycloadduct of silene **104** cannot be obtained directly. The adducts **105** and **106**, however, rearrange to the thermodynamically more stable **107**, probably via the donor adducts **108**, **109** and the free silenes **104** and **104a** (equation 24).

Jones and Bates used the combination of *t*-BuLi/vinylchlorosilane in the presence of anthracene to synthesize the *E* and *Z* isomers of the [4 + 2] cycloadducts **110** of the transient neopentylsilene **111** (equation 25)[68]. The thermal retro-Diels–Alder reaction proceeds stereospecifically. Photochemical reactions of similar compounds have been carried out[69].

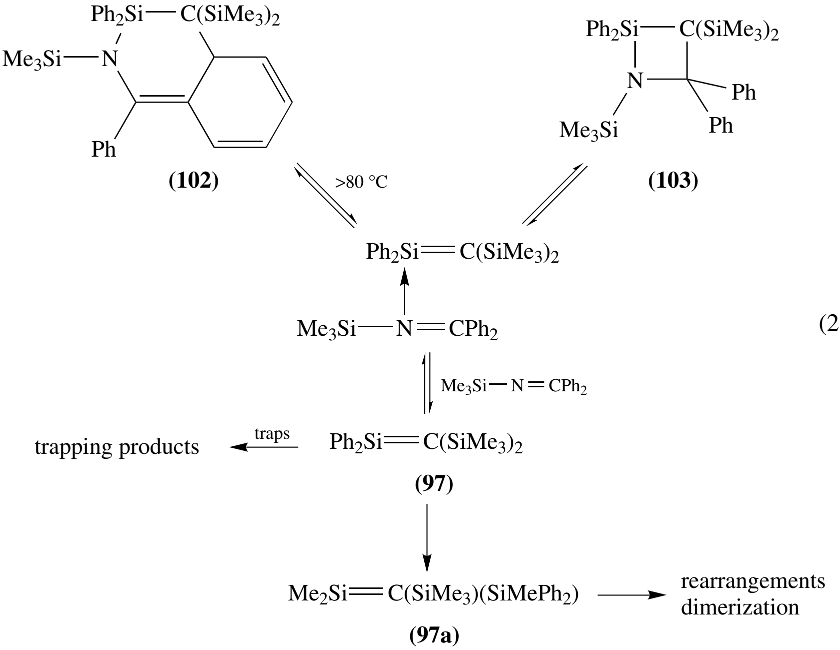

(23)

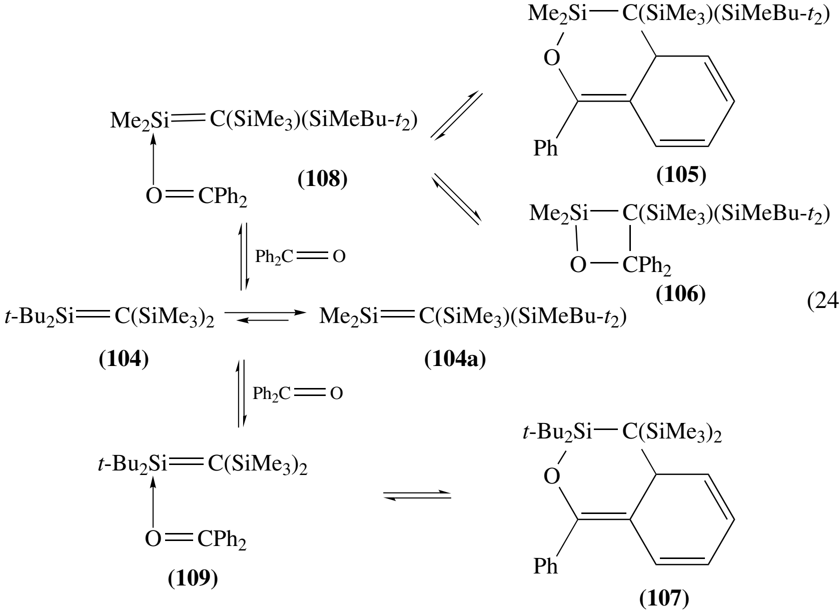

(24)

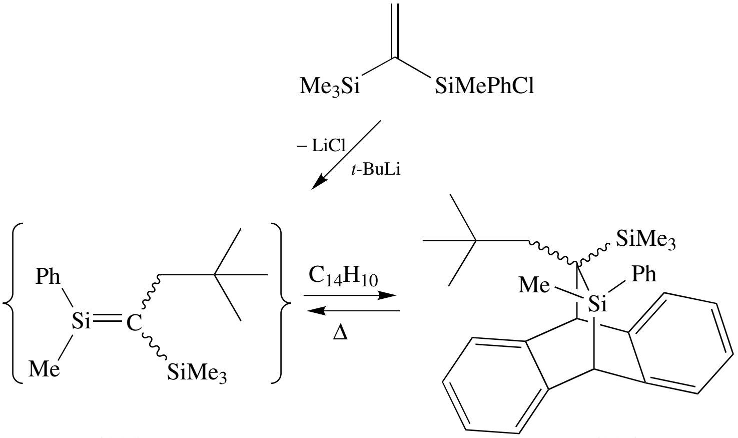

(25)

(111) **(110)**

The photochemical reactions of 2-silabicyclo[2.2.2]octanes **110** and **112** have been investigated[69]. Photolysis of **112** in the presence of methanol gives silyl methyl ether **113** as the main product, while **114** is only a minor byproduct (equation 26). This suggests that silene formation is a minor process and the main reaction proceeds via diradical intermediate similar to **115**. In agreement, interconvertion of E/Z **110**, probably via diradical **115**, is found during photolysis along with extensive polymerization (equation 27).

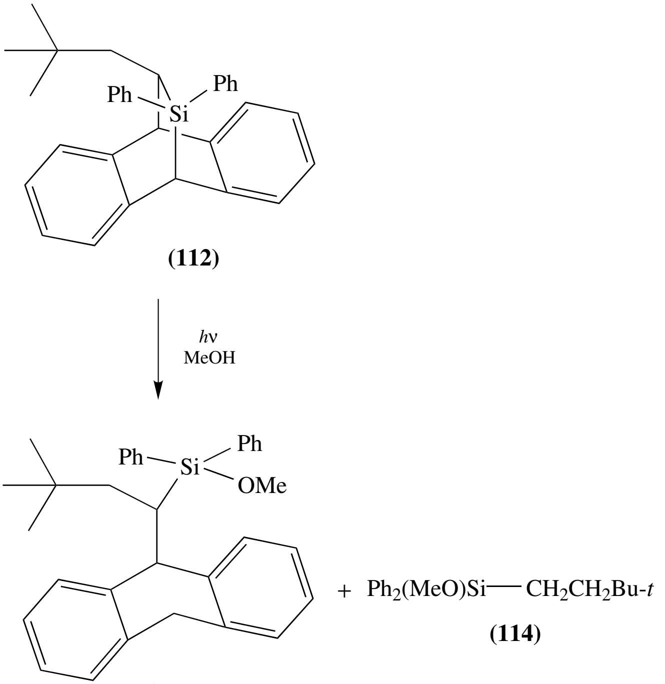

(112)

(26)

(113)

+ $Ph_2(MeO)Si—CH_2CH_2Bu$-t

(114)

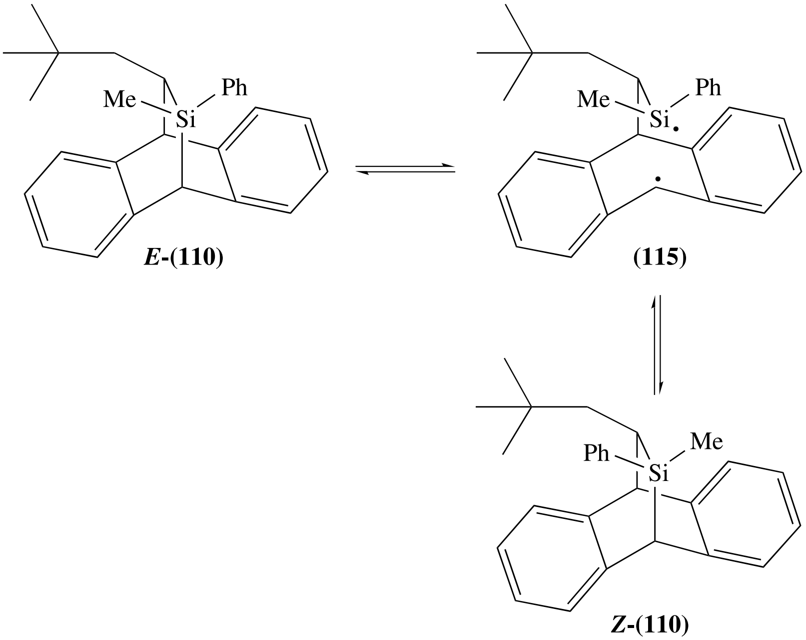

(27)

More reaction pathways are opened up when one of the substituents at silicon is a vinyl group as in **116** (equation 28)[70]. The intermediate silaallylic radical **117** (alternatively, the authors suggest an ionic mechanism) can be trapped directly by methanol to give the silyl ether **118**. Alternatively, **117** closes to the silene **119**, which was identified by its reaction product with methanol, **120**. A third reaction channel is the elimination of a silene, which again was identified by its trapping product **121** with methanol.

2. Salt elimination

The most straightforward synthesis of unsaturated Si=C compounds is the formation of the double bond by 1,2-elimination of a salt. This method has been widely used by N. Wiberg's and N. Auner's groups in recent years to produce a variety of different silenes.

The synthesis of the 'Wiberg'-type silenes is primarily achieved through the metalation of halogenotrisilylmethanes **122** with subsequent mild thermal salt elimination from the metalated species **92**•LiX, **97**•LiX and **104**•LiX[71–78]. The silenes formed, **92**, **97** and **104**, rearrange to the silenes **92a**, **97a** and **104a** or are trapped by suitable reagents (equation 29). In the case of R = *t*-Bu (**104a**) the silene is metastable[65,66] and its structure could be determined by X-ray diffraction[4].

The further increase in steric bulk is achieved in the potential silene precursors $Me_2Si(X)-C(Y)(SiMe_3)(SiBu\text{-}t_3)$[77]. For X = F and Y = Na the trisilylmethane **123** transforms into a silene/THF adduct **124•THF** in the presence of Me_3SiCl (equation 30). Removal of THF destabilizes the silene **124**, which can be either trapped or rearranged by a 1,3 H-shift to give **125**.

Recently, Wiberg and coworkers have answered the question whether the formation reaction for silenes of the type **126** can be analogously extended for silene types **127** and **128**[78].

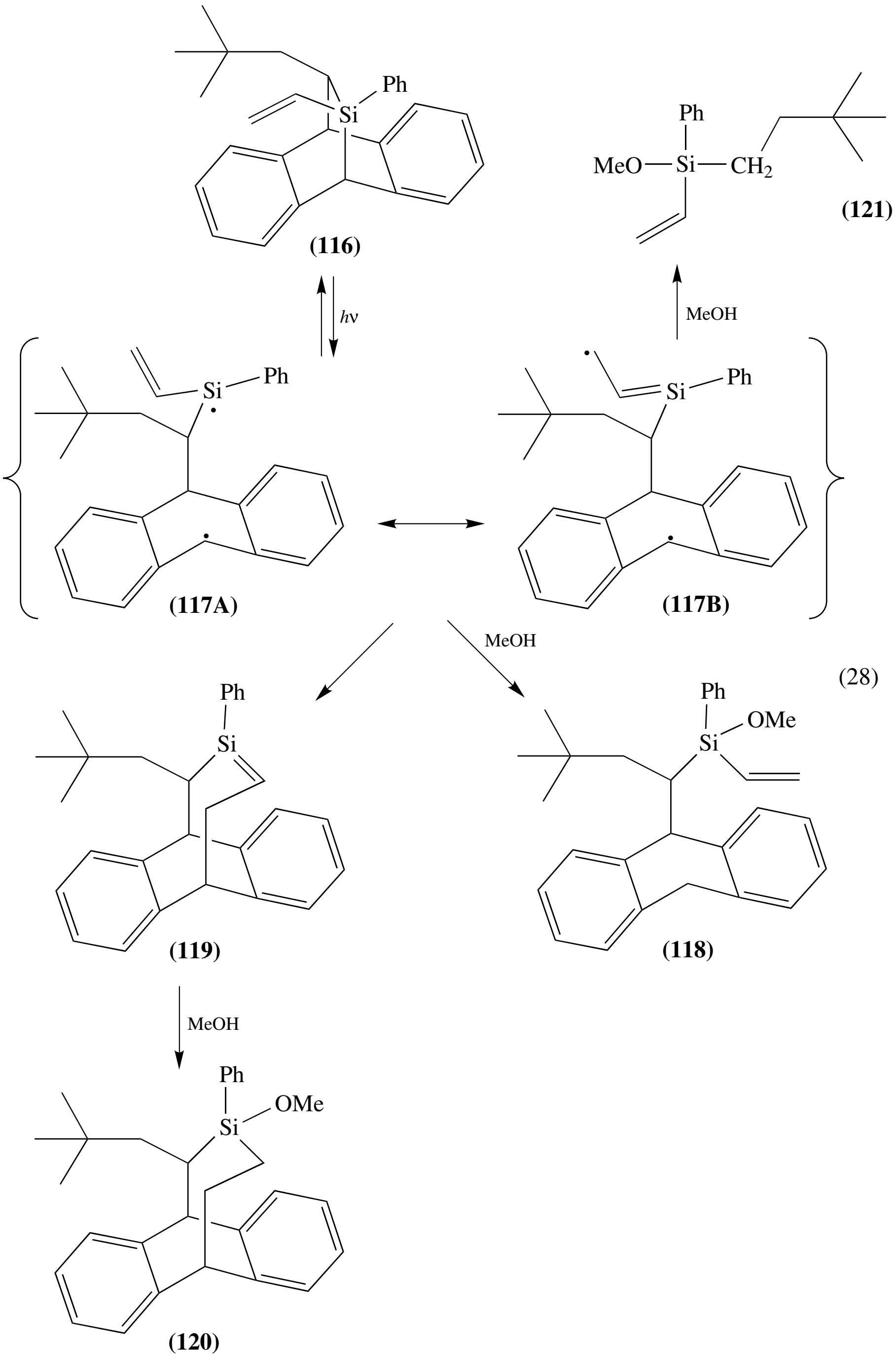
Ph
Si
(116)
hν
Ph
MeO
Si
CH2
(121)
MeOH
Si
Ph
Si
Ph
(117A)
(117B)
MeOH
Ph
Si
(119)
Ph
OMe
Si
(118)
MeOH
Ph
OMe
Si
(120)

(28)

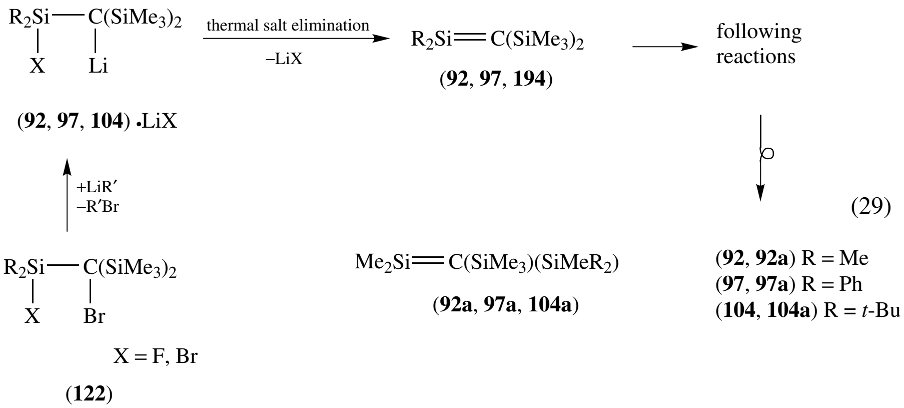

(29)

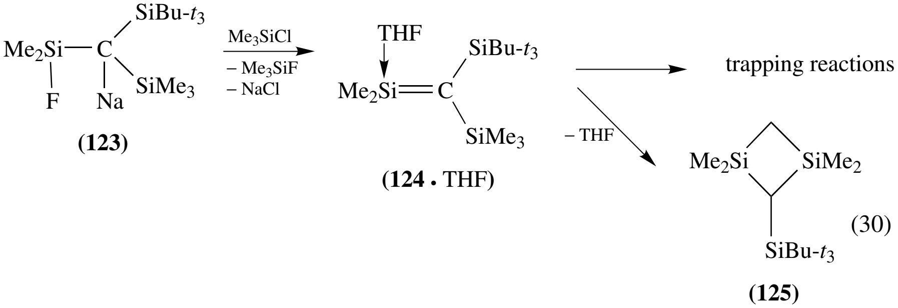

(30)

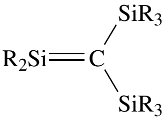

$R_2Si{=}C(SiR_3)_2$

(126)

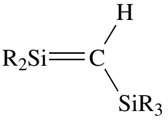

$R_2Si{=}C(H)(SiR_3)$

(127)

$R_2Si{=}CH_2$

(128)

$Me_2Si{=}CH(SiBu\text{-}t_3)$

(129)

This question can be answered positively for the sterically shielded silenes **129** and **130**. They not only form dimers, but can be trapped by dienes. In the case of **131**, no dimers or trapping products with dienes are obtained. The formation of the products from the reaction $t\text{-}Bu_2Si(Br){-}C(Br)H_2 + LiR$, however, is tentatively explained by the authors by the participation of a silene along the reaction pathway.

$t\text{-}BuMeSi{=}CH(SiBu\text{-}t_3)$ **(130)** $t\text{-}Bu_2Si{=}CH_2$ **(131)**

The formation of the α-metalated species in the case of the 'Auner/Jones Type' silenes (neopentylsilenes) **132** (which is deduced by formation of dimers **133** or by trapping) is achieved through addition of *t*-butyllithium to a vinylchlorosilane in an inert solvent[79,80]. The initially formed lithiated intermediate eliminates LiCl at *ca* 0 °C (equation 31), the exact temperature depends on the substituents R. The multitude of transient silenes that are available through this method will be discussed in Section I.B.4.b on the reactivity of neopentylsilenes. The basic reactions of $Cl_3Si{-}CH{=}CH_2$ with *t*-BuLi have been investigated[81].

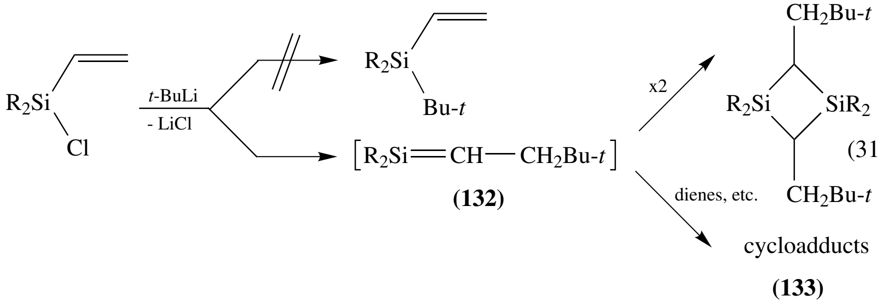

(31)

A stable neopentylsilene, 1,1-dimesityl-2-neopentyl-1-silene **134**, was synthesized by the Couret group from fluorodimesitylvinylsilane and *t*-BuLi[82]. It was characterized by NMR spectroscopy.

$$Mes_2Si{=}CHCH_2C(CH_3)_3$$

(134)

3. Donor cleavage

The silicon atom in Wiberg's silenes is a Lewis acidic center and can be coordinated with donors. These donors may be halide ions [like, e.g., in **104**•LiX(12-C-4)[83]], ethers or nitrogen bases[84]. Coordination with the donor stabilizes the silenes and, when the basicity suffices ($Et_2O < Br^-$, THF, NMe_3, F^-), the adducts serve as stock compounds from which the silenes may be liberated (equation 32). **92** decomposes at −100 °C, but its trimethylamine adduct is stable at room temperature[85]. Noticeable amounts of **97** are available from **97**•LiBr already at −78 °C, whereas from **97**•LiF the temperature has to be raised to +30 °C. Structures of such silene adducts will be discussed in Section I.C.1. The silene adduct **124**•THF has been discussed in Section I.A.2.

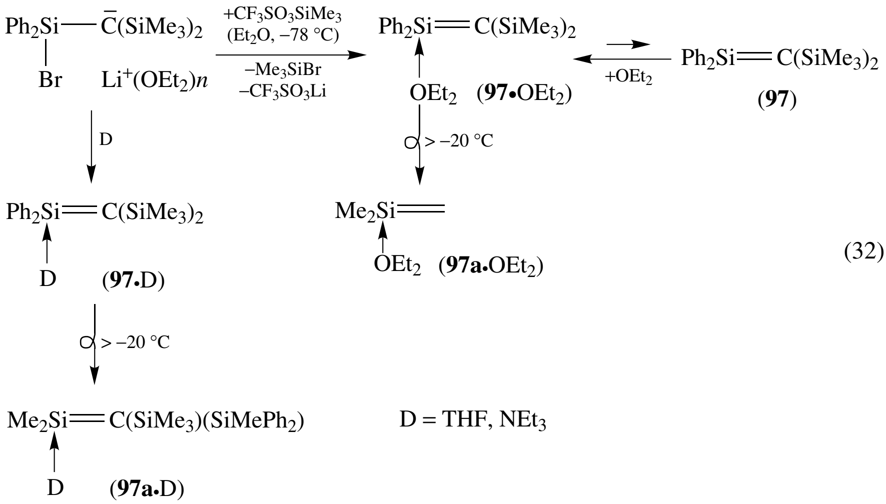

(32)

4. Isomerization of acylpolysilanes

The facile photochemical sigmatropic 1,3-trimethylsilyl shift in polysilylacylsilanes from silicon to oxygen (equation 33) was utilized historically to prepare the first relatively stable silenes[3,86,87]. Silenes prepared by isomerization of acylpolysilanes bear, due to the synthetic approach, a trimethylsiloxy group at the sp^2-hybridized carbon and relatively stable silenes of this type have in addition also at least one trimethylsilyl group at the silicon. These substituents strongly influence the physical properties and the chemical behaviour of these silenes. This is noticeable in many reactions in which these 'Brook'-type silenes behave differently from simple silenes or silenes of the 'Wiberg' type.

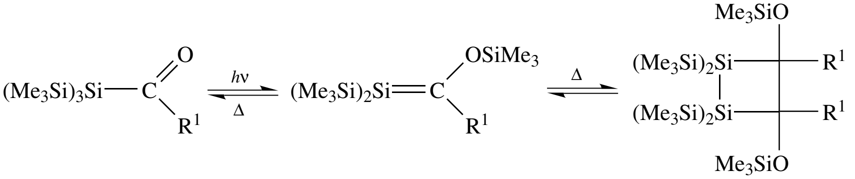

(33)

TABLE 3. Silenes synthesized by photolysis or thermolysis of acyl di- or polysilanes

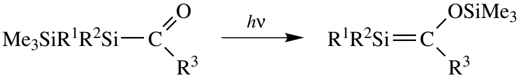

R^1	R^2	R^3	Silene characterized by	References
Me_3Si	Me_3Si	Me	dimerization	86, 88
Me_3Si	Me_3Si	Et	dimerization	89
Me_3Si	Me_3Si	*i*-Pr	dimerization	89
Me_3Si	Me_3Si	CH_2Ph	dimerization	90
Me_3Si	Me_3Si	*t*-Bu	dimerization, NMR	3, 38, 86
Me_3Si	Me_3Si	CEt_3	dimerization, NMR	3, 90
Me_3Si	Me_3Si	bco[a]	dimerization, NMR	90
Me_3Si	Me_3Si	1-Mecyhex[b]	dimerization, NMR	91
Me_3Si	Me_3Si	1-Ad[c]	NMR, X-ray	3
Me_3Si	Me_3Si	Ph	dimerization	86
Me_3Si	Me_3Si	C_6H_4Y or $C_6H_3Y_2$[d]	dimerization	92
Me_3Si	Me_3Si	CF_3	dimerization	92
Me_3Si	Me_3Si	Mes	NMR	91
Me_3Si	Me	1-Ad[c]	dimerization	90
Me_3Si	*t*-Bu	1-Ad[c]	NMR	90
Me_3Si	Ph	1-Ad[c]	dimerization, UV	90
Me_3Si	Ph	CEt_3	dimerization, NMR	90
Me_3Si	Ph	*t*-Bu	dimerization, NMR	90
Me_3Si	Ph	Mes	trapping	90
Me_3Si	Mes	1-Ad[c]	trapping, NMR	90
Me_3Si	Tip[e]	1-Ad[c]	trapping, NMR	93
Ph	Ph	1-Ad[c]	trapping	94
Mes	Mes	1-Ad[c]	trapping	94

[a] bco: bicyclooctyl.

[b] 1-Mecyhex: 1-methylcyclohexyl.

[c] 1-Ad: 1-adamantyl.

[d] Y = *p*-MeO, *o*-MeO, *p*-*t*-Bu, 3,5-dimethyl.

[e] Tip 2,4,6-triisopropylphenyl.

Depending on the bulk of the group R^1 the produced silenes are reactive intermediates (i.e. R^1 = Me[86,88], Et[89], *i*-Pr[89], CH_2Ph[89]), or they are in a temperature-sensitive equilibrium with their head-to-head dimers (e.g. R^1 = *t*-Bu)[3,38,86]. When R^1 = 1-adamantyl[3,87], no dimer was formed; rather the pure silene was isolated and its crystal structure was obtained.

Subsequently, this methodology was further widely exploited by Brook and coworkers and siloxysilenes with different substitution pattern have been prepared (see Table 3 for a list of silenes prepared along this route). Many of the siloxysilenes listed in Table 3 have been characterized by NMR spectroscopy. The identity of nearly all silenes is confirmed by the isolation of their dimerization products, the 1,2-disilacyclobutanes or by isolation of their trapping products with alcohols, dienes or acetylenes. Photolysis of acylsilanes of the type $(Me_3Si)_2R^2SiC(O)R^1$ gives rise to a mixture of *E* and *Z* isomers[93,95]. It has been reported that *t*-Bu(Me_3Si)Si=C($OSiMe_3$)Ad-1 **135** is formed as a single geometric isomer on the basis of NMR evidence[90]. Trapping experiments with acetylenes do, however, reveal that this silene must have also been formed as a pair of geometric isomers[93]. The geometrical isomers are conformationally stable even at higher temperatures, thus the (*E*/*Z*) isomers of Mes(Me_3Si)Si=C($OSiMe_3$)Ad-1 **136** do not interconvert even upon heating to 100 °C, when they slowly decompose[95].

Siloxysilenes Ar_2Si=C($OSiMe_3$)Ad-1 arising from photolysis of acyldisilanes are transient species and can only be identified by their trapping product or by isolation of consecutive isomerization products[94].

Silenes of the family Me_3SiR^1Si=C($OSiMe_3$)Ad-1 **137** undergo a complex silene-to-silene photoisomerization reaction[90,94,96]. When silenes **137** are generated by photolysis of acylsilanes **138**, the isomeric silenes **139** and **140** are formed in a subsequent reaction. The reaction was followed by UV and ^1H NMR spectroscopy. The disappearance of **138** cleanly follows first-order kinetics and the overall kinetics were consistent with the transformation **138** → **137** → **139**. **137** as well as **139** were characterized by NMR spectroscopy and, in addition, the structure of **137** was established by trapping with methanol. The identity of **139** and **140** was confirmed by the isolation of their head-to-tail dimers from which crystals, suitable for X-ray analyses, were isolated (equation 34)[90].

The complex reaction sequence shown in equation 34 might provide some rationalization. The formation of the silylcarbene **141** is suggested, based on experimental results from related reactions[94], but there is no evidence for the formation of **141** nor for a silylene intermediate. Thus, the transformation **137** → **142** might proceed via a dyotropic rearrangement as well. The facile 1,3-methyl shift in 2-trimethylsilylsilenes which interconverts **142** → **139** is well known from 'Wiberg'-type silenes[64,97]. **139** (R^1 = *t*-Bu) is stable in solution at room temperature over days and isomerizes only slowly to **140** (R^1 = *t*-Bu) which rapidly dimerizes giving a 1,3-disilacyclobutane[90].

A similar but thermal silene-to-silene rearrangement is reported for the sterically highly crowded silene **143**. Upon prolonged heating to 120° *E*/*Z*-**143** isomerizes cleanly to a single isomer of the new silene **144**, which was identified by NMR spectroscopy[93]. The silenes **145** and **146** were not detected, although they are regarded as intermediates (equation 35).

The thermolysis of neat acylpolysilanes usually gives mixtures of compounds. However, thermolysis in the presence of a scavenger such as an alcohol or an acetylene is much cleaner. Brook and coworkers showed that thermolysis of pivaloyltris(trimethylsilyl)silane **147** in the presence of 1-phenylpropyne yields the 2-silacyclobutene **148** in 72% yield, indicating the thermolytic generation of **149**[86]. (Note, however, that originally a different regiochemistry for the cycloaddition product **148**[86] was suggested[95]; equation 36.)

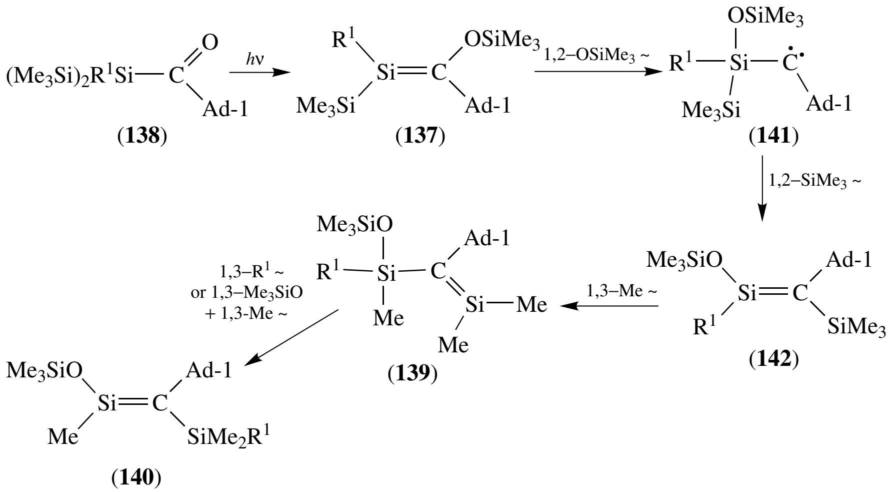

(34)

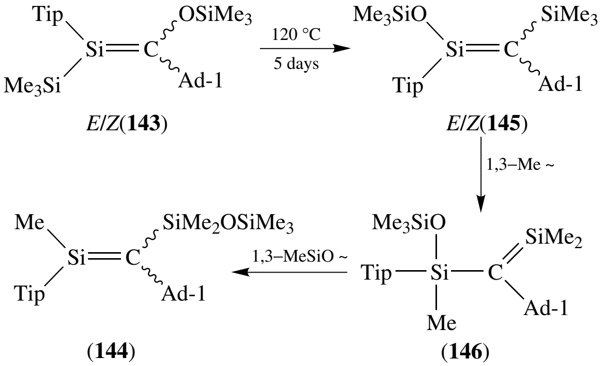

(35)

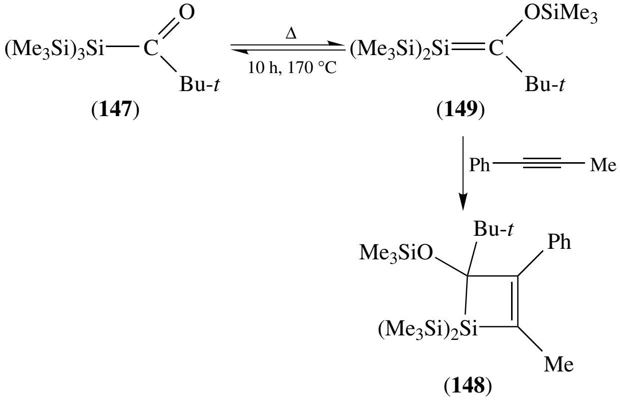

(36)

Recently, Ishikawa and coworkers again adopted this approach[98,99]. Silenes were formed from various substituted tris(trimethylsilyl)acylsilanes by heating them to 140 °C in benzene and they could be trapped by suitable scavenger reagents. For example, **150**, generated by thermolysis of **151**, reacts with acetone yielding the siloxetane **152** which is, however, not stable at the applied conditions (equation 37). In the presence of a Ni catalyst the thermolysis of **151** gives rise to products which can be rationalized by the intermediacy of Ni/silene complexes[98]. In the absence of any trapping agent the starting acylpolysilane was in some cases recovered unchanged[98,99].

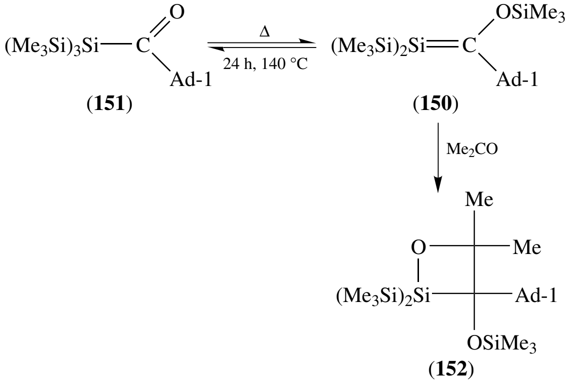

(37)

An intermediate siladiene **153** is formed during the thermolysis of an α,β-unsaturated acylsilane **154**. Addition of $(Me_3Si)_3Si^{\bullet}$ and subsequent hydrogen abstraction led to the isolation of the enol ether **155** formed, presumably, via radical **156** (equation 38). The identity of **155** was confirmed by an X-ray crystal structure[100].

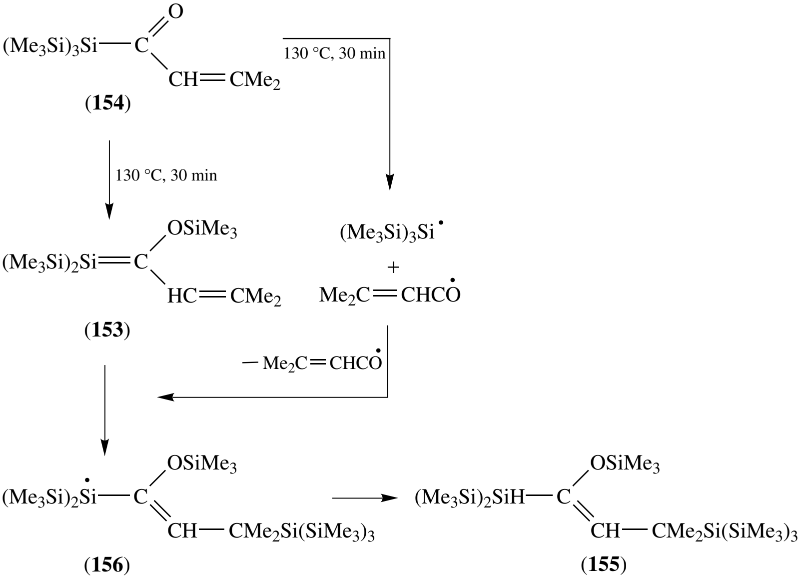

(38)

5. Silenes by the sila-Peterson reaction

A relatively new synthetic approach to silenes was established independently in the laboratories of Oehme[101–110], Apeloig[39,111] and Ishikawa[112,113]. The key-step is a base-initiated 1,2-elimination of silanolate from α-hydroxydisilanes **157** and formation of silenes **158** analogous to the original Peterson olefination reaction (equation 39).

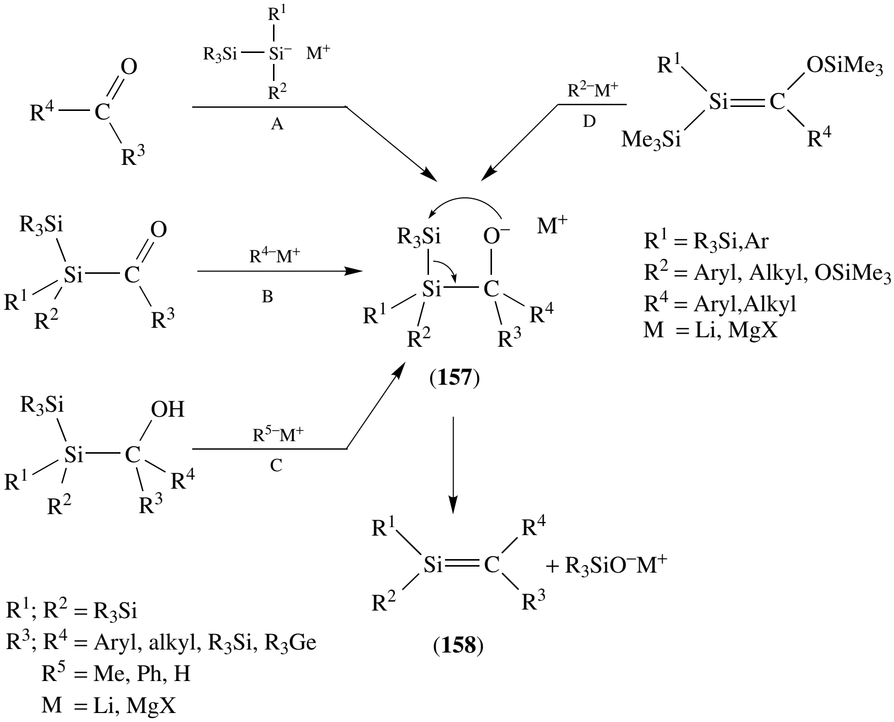

(39)

All silenes formed by the sila-Peterson elimination have a common, novel substitution pattern, bearing two silyl substituents at the tricoordinated silicon centre and a wide variety of substituents including hydrogen, alkyl, aryl and vinyl groups, at the doubly bonded carbon atom. This novel substitution pattern has consequences related to the physical properties and the chemical behaviour of the 'Apeloig–Ishikawa–Oehme' type of silenes. Almost all silenes formed via the sila-Peterson elimination reaction are only transient species. They can either be trapped by nucleophilic reagents or undergo cycloadditions with various dienes. In the absence of scavenger reagents they dimerize in a head-to-head fashion yielding 1,2-disilacyclobutanes or linear polysilanes.

Three different routes to the key compounds for the sila-Peterson elimination, the α-alkoxydisilanes **157**, are described in the literature, namely: A, reaction of silyllithium reagents with ketones or aldehydes; B, addition of carbon nucleophiles to acylsilanes; C, deprotonation of the polysilylcarbinols. In addition, method D, which already starts with the reaction of 2-siloxysilenes with organometallic reagents, leads to the same products. The silenes of the 'Apeloig–Ishikawa–Oehme' type synthesized so far are summarized in Table 4.

TABLE 4. Silenes $R^1R^2Si{=}CR^3R^4$ synthesized by the sila-Peterson reaction and related reactions

R^1	R^2	R^3	R^4	Method of preparation[a]	References
Me_3Si	Me_3Si	cypen[b]		A	114, 115
t-$BuMe_2Si$	t-$BuMe_2Si$	cypen[b]		A	114
Me_3Si	Me_3Si	2-Ad[c]		A	39, 111
t-$BuMe_2Si$	Me_3Si	2-Ad[c]		A	111
t-$BuMe_2Si$	t-$BuMe_2Si$	2-Ad[c]		A	111
Me_3Si	Me_3Si	Me	Me	A,B	107, 112
Me_3Si	Me_3Si	Me	Ph	B	112
Me_3Si	Me_3Si	Ph	Ar[d]	B	113
Me_3Si	Me_3Si	H	Sup[e]	A	109
Me_3Si	Me_3Si	H	Tip[f]	A,C	105
Me_3Si	Me_3Si	H	Ar[g]	C	g
Me_3Si	Me_3Si	H	t-Bu	C	104, 107
Me_3Si	Me_3Si	H	$CH{=}CMe_2$	C	106
Me_3Si	Me_3Si	H	$CH{=}CHPh$	C	106
Me_3Si	Me_3Si	cypheptene[h]		A	115
Me_3Si	Me_3Si	Me	p-DMAP[i]	C	110
Me_3Si	Me	Me_3Si	t-Bu	D	116
Me_3Si	Me	Me_3Si	Ph	D	116
Me_3Si	Me	Me_3Si	1-Ad[j]	D	116
Me_3Si	Et	Me_3Si	1-Ad[j]	D	116
Me_3Si	Me_3Si	Me_3Si	1-Ad[j]	D	116
Me_3Si	Ph	Me_3Si	1-Ad[j]	D	116
Me_3Si	$PhCH_2$	Me_3Si	1-Ad[j]	D	116
Ph	Me	Me_3Si	1-Ad[j]	D	116
Ph	Et	Me_3Si	1-Ad[j]	D	116

[a] See equation 39.

[b] cypen: 2,3 di-*t*-butylcyclopropenylidene.

[c] 2-Ad: 2-adamantylidene.

[d] Ar: Ph, *o*-tolyl, *p*-xylyl.

[e] Sup: 2,4,6-tri-*t*-butylphenyl.

[f] Tip: 2,4,6-triisopropylphenyl.

[g] Ar: 1,4-di-*t*-butylphenyl[109], 2,4,6-trimethylphenyl[107,108,117], 2,5-diisopropylphenyl[118], *o*-dimethylaminophenyl[110].

[h] cyheptene: [*a*,*e*]-dibenzocyclohepta-2,4,6-trienylidene.

[i] DMAP: dimethylaminophenyl.

[j] 1-Ad: 1-adamantyl.

a. Reaction of silyllithium reagents with ketones or aldehydes. Oehme and his group studied the reaction of $(Me_3Si)_3SiLi$ **159** with simple aliphatic ketones like acetone in THF (equation 40)[101–104]. They found that the reaction of acetone with an excess of **159** leads to α-alkoxypolysilane **160**, which spontaneously eliminates lithium silanolate. The intermediate silene **161** is immediately trapped by the excess of the silyllithium reagent forming polysilyl carbanion **162**. **162** undergoes a 1,3-silyl shift to the polysilaanion **163** and therefore, after hydrolytic work-up, products deriving from **163** were isolated[103].

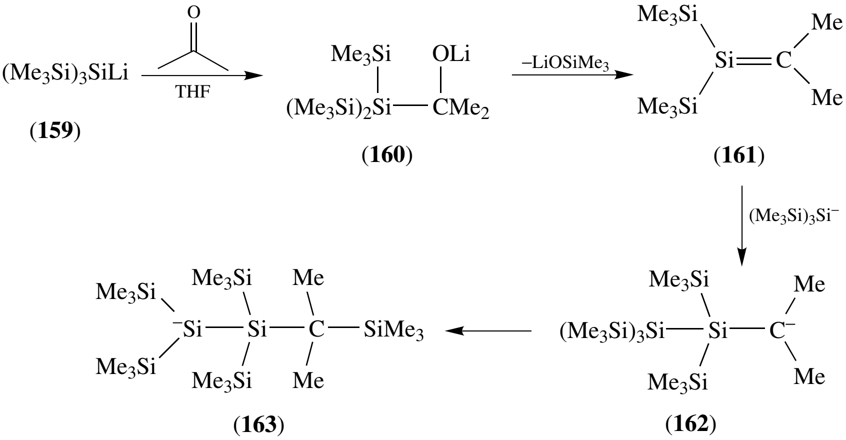

(40)

The use of equimolar amounts of a ketone in hydrocarbons prevents the addition of the silyl anion to the silene. Apeloig, Bravo-Zhivotovskii and coworkers found that tris(trimethylsilyl)silyllithium **159** gives in the reaction with 2-adamantanone the unusual head-to-head dimer **164** in 85% yield, suggesting the intermediate formation of silene **165** (equation 41)[39]. More bulky polysilyl anions react with 2-adamantanone to form at room temperature indefinitely stable silenes. Thus, (t-BuMe$_2$Si)(Me$_3$Si)$_2$SiLi **166** reacts with 2-adamantanone to give the silene (t-BuMe$_2$Si)(Me$_3$Si)Si=Ad-2 (2-Ad = 2-adamantylidene) **167** (equation 42), whose crystal structure was obtained (see Section I.C.1 for details)[111]. A second indefinitely stable silene bearing two (t-BuMe$_2$Si) groups at silicon was also obtained[111].

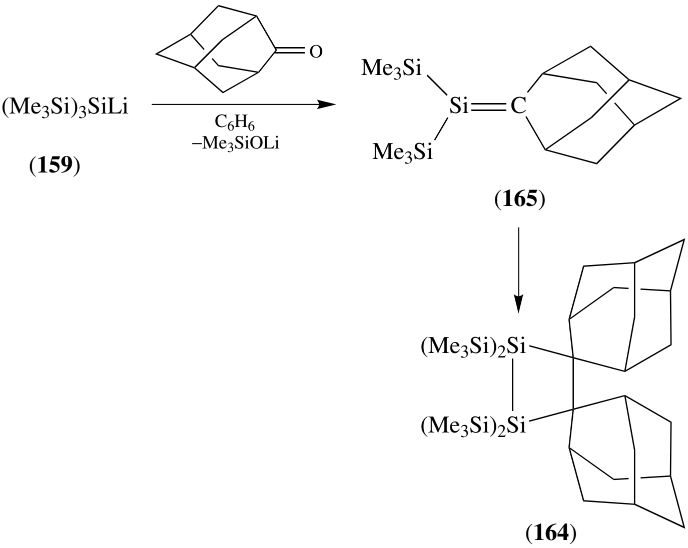

(41)

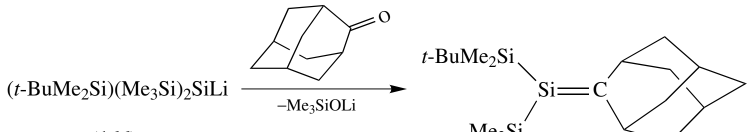

(**166**) (**167**) (42)

The sila-Peterson olefination reaction was also used to synthesize derivatives of 4-silatriafulvene **168**[114,119]. While the reaction of **159** with cyclopropenone **169** without any trapping reagents gives a complex mixture of products including several dimers of the transient silatriafulvene **170**, in the presence of 2,3-dimethylbuta-1,3-diene or anthracene **171** and **172**, respectively, are formed (equation 43). Since the anthracene adduct **172** undergoes a facile *retro* cycloaddition upon heating to 200 °C, **172** is a convenient storage compound of 4-silatriafulvene **170**[119]. The use of more bulky silyl anions like **173** allows the isolation of a stable silatriafulvene **174** as yellow crystals, the identity of which could be proven by NMR spectroscopy[114].

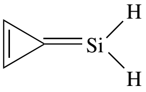

(**168**)

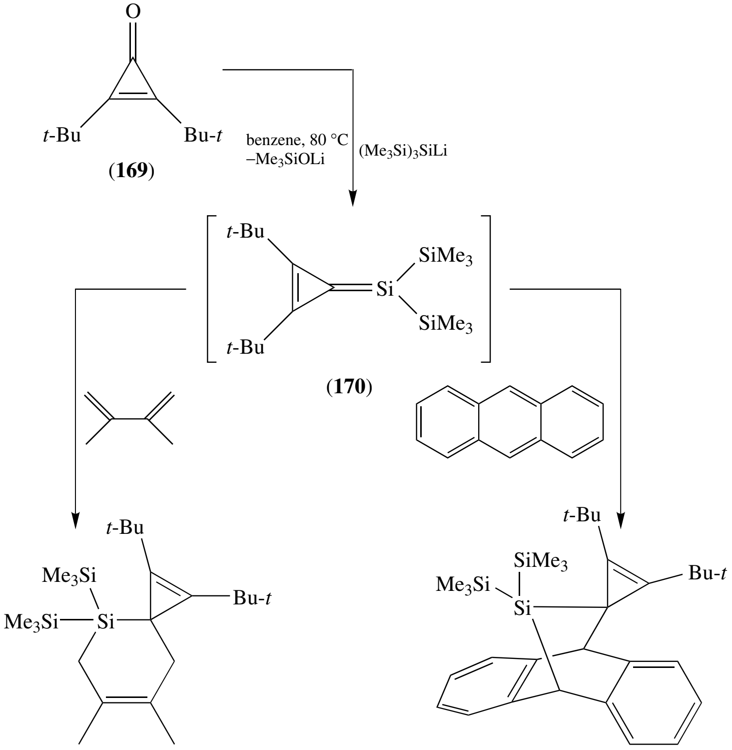

(**169**) (**170**) (**171**) (**172**) (43)

$(t\text{-BuMe}_2\text{Si})_3\text{Si}^-$

(173)

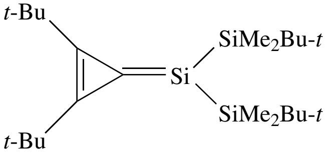

(174)

b. Reaction of polysilylacylsilanes with organometallic reagents. Ishikawa and coworkers studied the addition of organolithium reagents to polysilylacylsilanes such as $(\text{Me}_3\text{Si})_3\text{SiCOR}$ (R = Me, Ph) **175**[112,113]. In the reaction of **175a**, the initial adduct **176** eliminates spontaneously Me_3SiO^- and the intermediate silene **177** could be either trapped or dimerized, yielding head-to-head dimers **178** (equation 44). The scope of the organometallic reagent has been limited to MeLi[112] and ArLi[113].

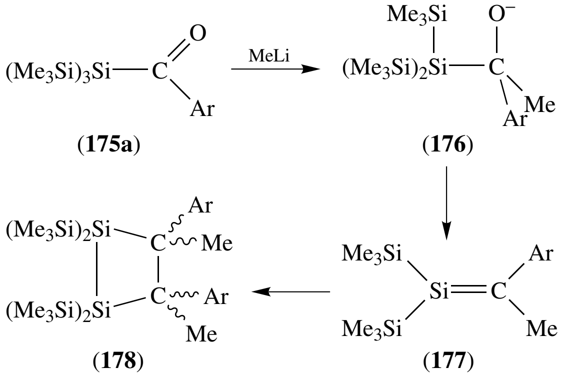

(44)

In contrast, silyl- or germyllithium reagents attack one of the trimethylsilyl groups attached to the central silicon atom rather than the carbonyl group of the acylsilanes **179**[120–122]. Subsequent elimination of disilane or germylsilane, respectively, results in the formation of lithium silenolate anions **180–183** (equation 45), which were characterized by NMR spectroscopy (see Section I.C.2)[120–122] and by trapping experiments[120–123].

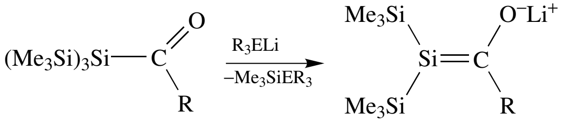

(179)

E = Ge, Si

(180) R = *t*-Bu
(181) R = 1-Ad
(182) R = Mes
(183) R = *o*-Tol

(45)

182 is thermally stable, while **180** and **181** could be analysed only by low temperature NMR spectroscopy[121]. Anions **182** and **183** can be silylated at the oxygen atom yielding the 'Brook-type' silenes **184** and **185** respectively, which could be trapped with 2,3-dimethylbuta-1,3-diene and thus identified. In addition, **184** could be characterized by NMR spectroscopy at −80 °C[121]. Interestingly, in the silylation reaction of the alkyl substituted silenolates **180** and **181** a different regiochemistry was observed: **180** and **181**

give acylpolysilanes **186** and **187** upon quenching with Et_3SiCl (equation 46)[121].

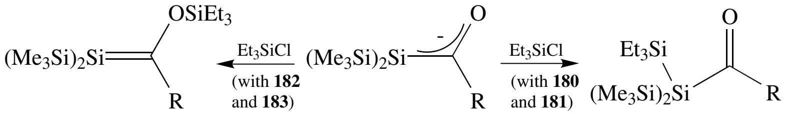

(46)

(**184**) R = Mes
(**185**) R = *o*-Tol

180-183

(**186**) R = *t*-Bu
(**187**) R = 1-Ad

c. Deprotonation of polysilylcarbinols. The reaction of tris(trimethylsilyl)silylmagnesium bromide **188** with carbonyl compounds offers easy and versatile access to isolable polysilylcarbinols **189**[106–110,117]. Polysilylcarbinols **189** can be subsequently deprotonated with various bases. Thus, addition of MeLi or RMgX to **189** in ether results in the elimination of silanolate and gives the transient silenes **190** (equation 47), which undergo dimerization reactions yielding various dimers depending on the substituents on carbon.

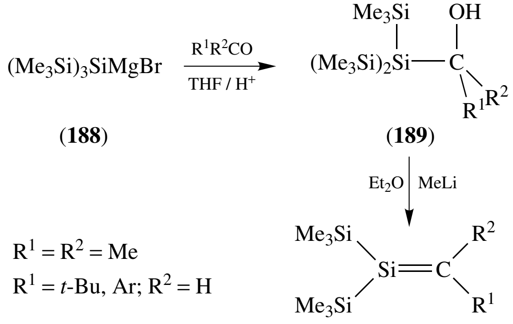

(**188**) (**189**) (**190**)

$R^1 = R^2 = Me$
$R^1 = t\text{-Bu, Ar}; R^2 = H$

(47)

The final product of the deprotonation depends strongly on the deprotonation reagent and/or the reaction conditions. Thus, in THF and using MeLi (or NaH) as base, an anionotropic 1,3-Si,O-trimethylsilyl migration occurs in the alkoxymethylsilane **191** with formation of the silyl anion **192** instead of elimination of silanolate. Therefore, after hydrolytic work-up only trimethylsiloxy(bis(trimethylsilyl)silyl)alkanes **193** were obtained (equation 48).[108,117]

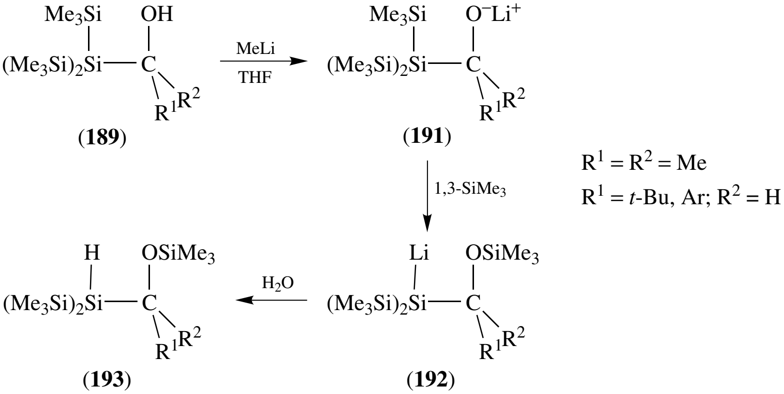

(**189**) (**191**) (**193**) (**192**)

$R^1 = R^2 = Me$
$R^1 = t\text{-Bu, Ar}; R^2 = H$ (48)

d. Reaction of 2-siloxysilenes with organometallic reagents. 'Brook-type' silenes **194**, generated by photolysis of acylsilanes **195**, react with Grignard or organolithium reagents giving new intermediate silenes **196** with a novel substitution pattern[116]. The key step in this reaction sequence is similar to the sila-Peterson reaction. The organometallic reagent is added to the Si=C bond forming the carbanion **197** which rearranges to the alkoxide **198**. In a Peterson-type elimination of silanolate the silene **196** is generated. The excess of the organometallic compound or the silanolate adds readily to the Si=C bond. Thus, after hydrolytic work-up products deriving from the carbanions **199** and **200** have been isolated (equation 49)[116].

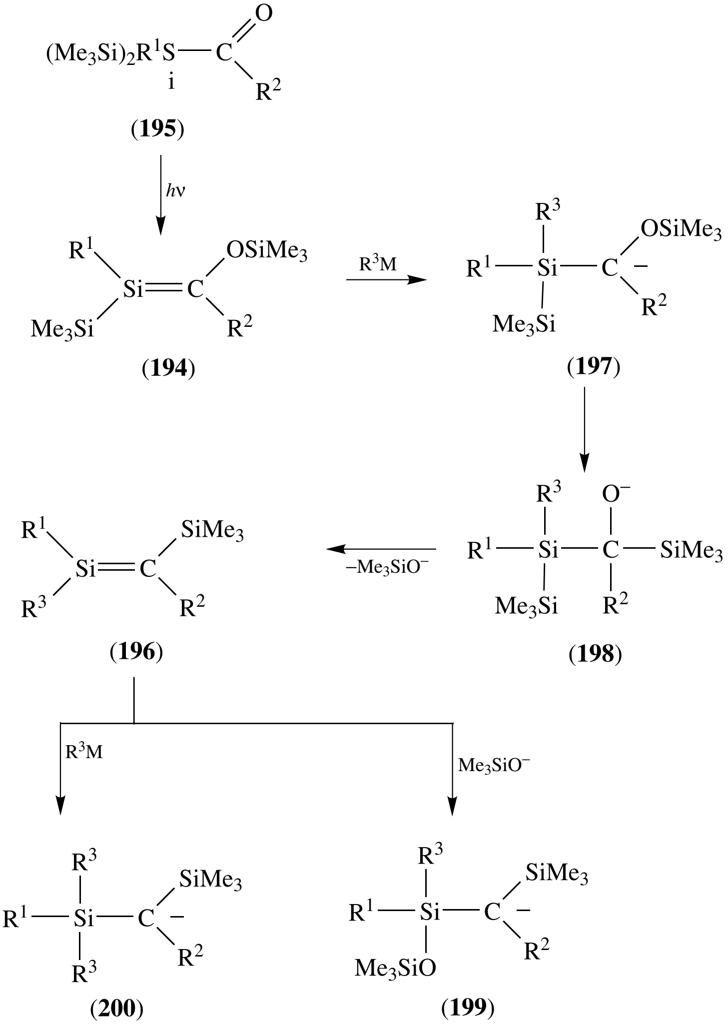

(49)

$R^1 = Me_3Si$, Ph; $R^2 = t$-Bu, 1-Ad, Ph;
$R^3 = Me$, Et, $OSiMe_3$; M = MgBr, Li

6. Photolysis of disilanes

The generation of silenes, e.g. **201** from aryl- or vinyl-substituted disilanes like **202**, is possible by irradiation, which may lead to a 1,3-silyl migration to the π-system (equation 50)[124,125].

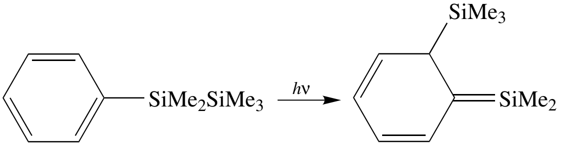

(202) **(201)** (50)

A number of disilanes have been investigated for their suitability as potential silene precursors. The formation of silenes by the 1,3-silyl migration pathway competes with dehydrosilylation, which also gives silenes, and with homolytic Si–Si bond cleavage to give silyl radicals.

In this connection Ishikawa and coworkers studied the photodegradation of poly(disilanylene)phenylenes **203**[126], and found that irradiation under the same conditions as in the photolysis of the aryldisilanes results in the formation of another type of nonrearranged silene **204** produced together with silane **205** from homolytic scission of a silicon–silicon bond, followed by disproportionation of the resulting silyl radicals **206** to **204** and **205** (equation 51).

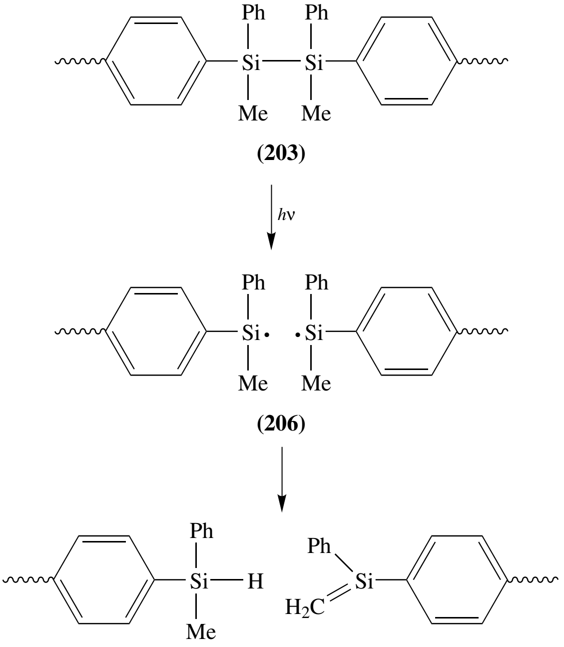

(203)

(206)

(205) **(204)** (51)

The gradual increase in chain length from monomeric 1,4-disilanylbenzenes to poly(disilanylene)phenylenes was investigated for a series of oligomers **207**[127]. For $n = 2$

and 3 the main route under photolysis conditions is to form rearranged silenes, which can, however, only be trapped in low yields. The homolytic scission of the Si−Si bond is a minor route. For the oligomer with $n = 4$, appreciable amounts of products arising from homolytic scission to give silyl radicals are obtained.

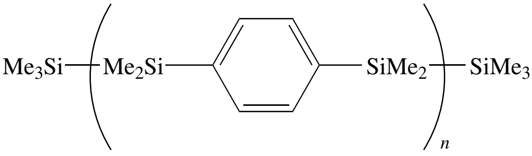

$n = 2, 3, 4$ **(207)**

In contrast, the study of isomeric bis(disilanyl)benzenes **208**–**210** showed that only products **211**–**213** from ene reaction of isobutene with rearranged silenes **214**–**216** were formed[128]. The silepines **217** and **218** result from a reaction of the initially formed silenes with isobutene (equation 52–54).

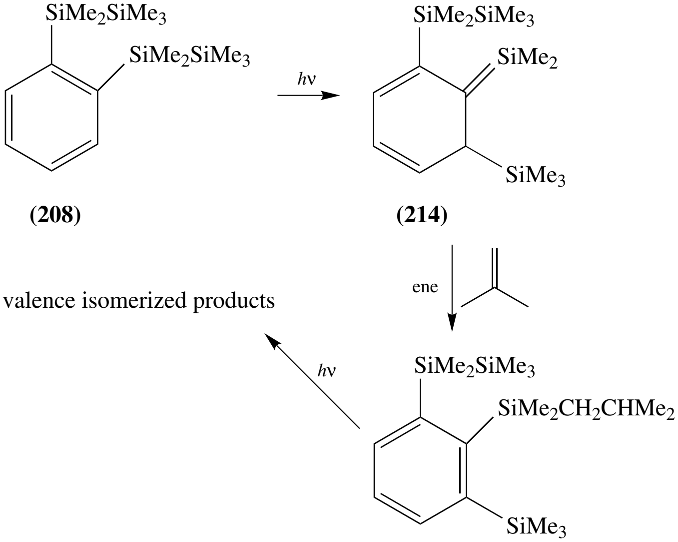

(52)

The irradiation of systems having two different π-electron systems[129] shows, in the case of 1,4-bis(1-phenyltetramethyldisilanyl)benzene, the exclusive migration to the phenylene ring but not to the phenyl ring. When the phenyl groups are in 2-position of the disilanyl moiety, a small fraction of silene formed from migration to this aryl ring is obtained[130].

Disilanyl substituted naphthalenes exhibit unusual photochemical reactivity[131]. 1,4-Bis(pentamethyldisilanyl)naphthalene **219** yields compound **220** in both the absence and presence of methanol, possibly via a biradical **221**. Noteworthy is the 1,8-silyl migration from position 1 to 8 of the naphthalene ring. In the presence of methanol, compound **222** is formed via an initial silene **223**, which then rearranges via **224** (equation 55). In a homogenous solution of methanol/benzene (1 : 1.5) only **225** is formed, probably by direct reaction of the photoexcited disilane with methanol, before migration of a trimethylsilyl group to the naphthalene ring (equation 56).

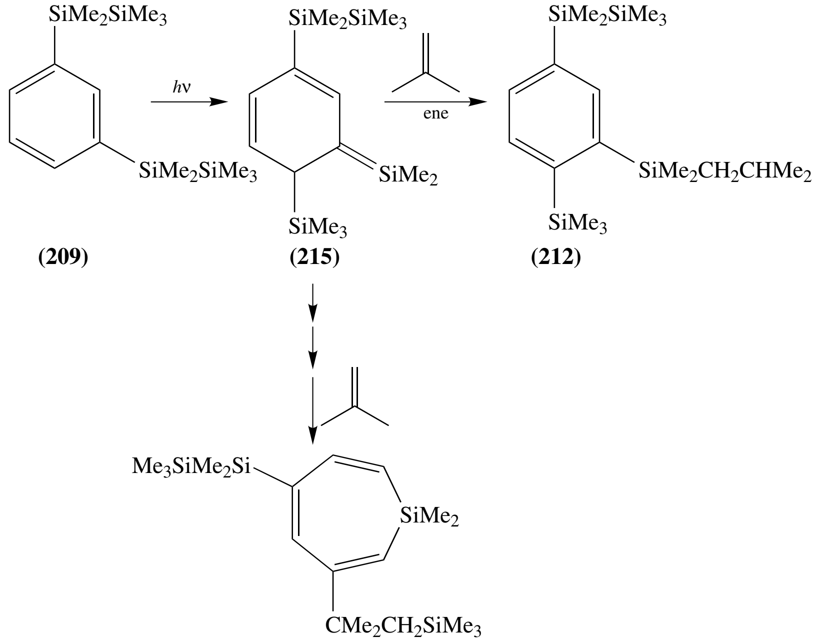

(209) **(215)** **(212)** **(217)**

(53)

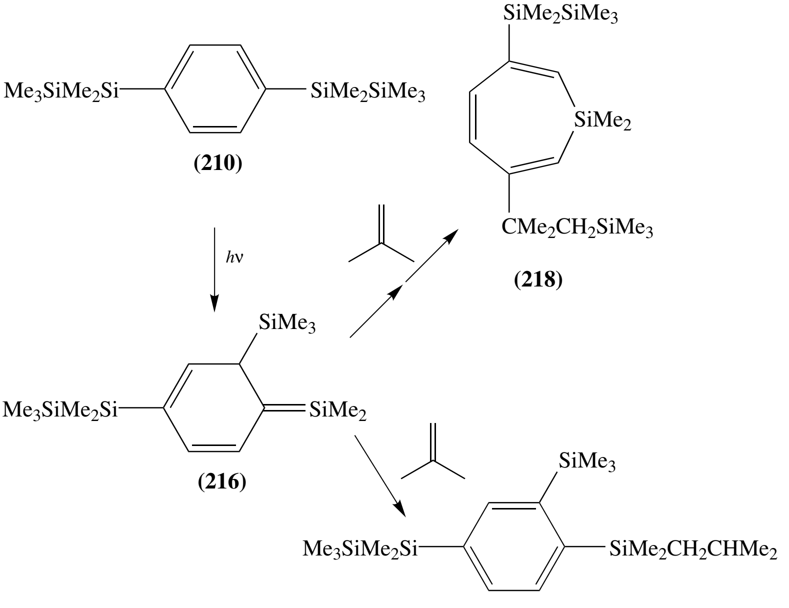

(210) **(218)** **(216)** **(213)**

(54)

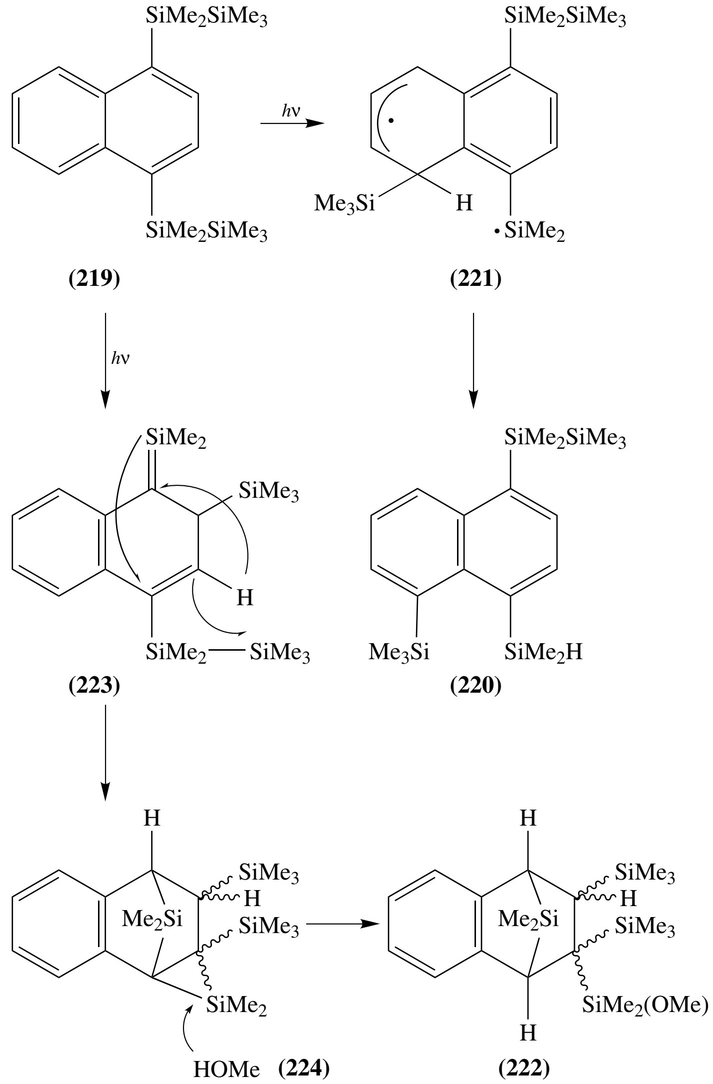
SiMe2SiMe3
hν
SiMe2SiMe3
Me3Si
H
SiMe2SiMe3
• SiMe2
(219)
(221)
hν
SiMe2
SiMe3
H
SiMe2
SiMe3
SiMe2SiMe3
Me3Si
SiMe2H
(223)
(220)
H
Me2Si
SiMe3
H
SiMe3
SiMe2
HOMe
(224)
H
Me2Si
SiMe3
H
SiMe3
SiMe2(OMe)
H
(222)

(55)

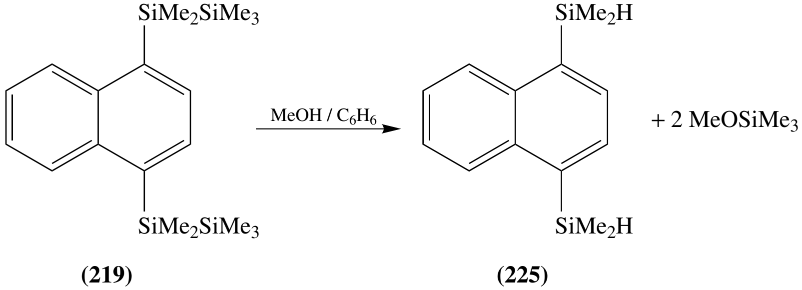
SiMe2SiMe3
SiMe2SiMe3
MeOH / C6H6
SiMe2H
SiMe2H
+ 2 MeOSiMe3
(219)
(225)

(56)

For 1,5-bis(pentamethyldisilanyl)naphthalene a 1,3-silyl migration does not occur. The products formed are analogous to **220** and **225**. 1-(Pentamethyldisilanyl)naphthalene undergoes silyl migration from position 1 to 8. 2-(Pentamethyldisilanyl)naphthalene **226** gives a silene **227** by a silyl shift from position 2 to 1. It can be trapped in an ene reaction with isobutene to yield **228** (equation 57).

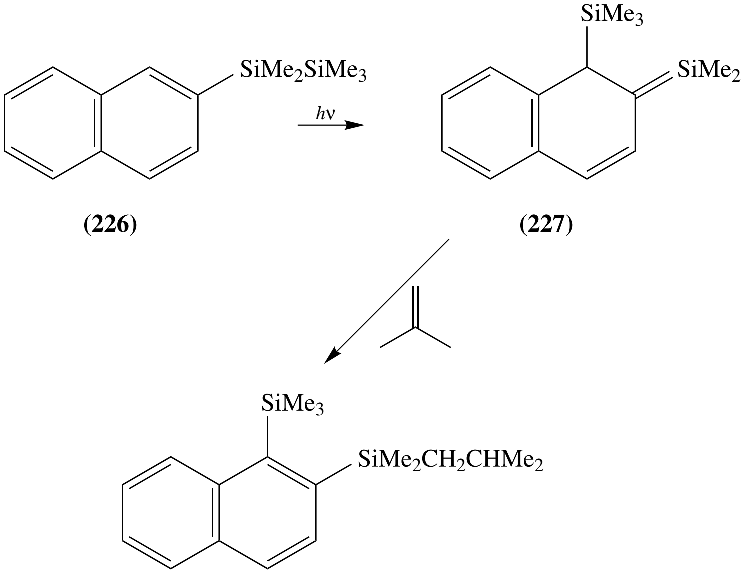

(226) **(227)** **(228)**

(57)

2,6-Bis(pentamethyldisilanyl)naphthalene **229** undergoes 1,3-silyl shift to the 1-position to give the rearranged silene **230**[132]. A siloxetane **231** is discussed as an intermediate in the reaction with acetone. It loses silanone to give **232**, and then restores aromaticity by a 1,3-silyl migration to give the naphthalene **233**. Alternatively, **231** may expand the ring and, along with a 1,2-silyl shift, produce siloxacyclopentanes **234**, which then rearrange photolytically to the cyclic allenes **235**. An ene by-product **236** is also formed in the reaction with acetone (equation 58). 2,7-Bis(pentamethyldisilanyl)naphthalene reacts analogously.

Ishikawa and coworkers investigated the relative ease of migration of a Me_3Si group to vinyl and phenyl groups in precursor compounds containing both groups[133]. In the case of the irradiation of compound **237** in the presence of methanol, silene **238** was found to be the major reactive intermediate, while with acetone and 2,3-dimethylbuta-1,3-diene the number and nature of different ene products can only be explained by the existence of silatriene **239** (equation 59).

Substitution of one of the methyl groups on silicon by an ethyl group gave similar results. The authors state that these findings indicate the existence of an equilibrium between the precursor and the silenes or between the silenes.

The regiochemistry of such reactions was further investigated for the dihydropyranyl-substituted phenyldisilane **240**[134]. It was found that two types of silene intermediates, **241** and **242**, are formed by 1,3-silyl shifts to the dihydropyranyl and the phenyl group, respectively (equation 60), and that the distribution of trapping products from these silenes depends on the trapping agent used.

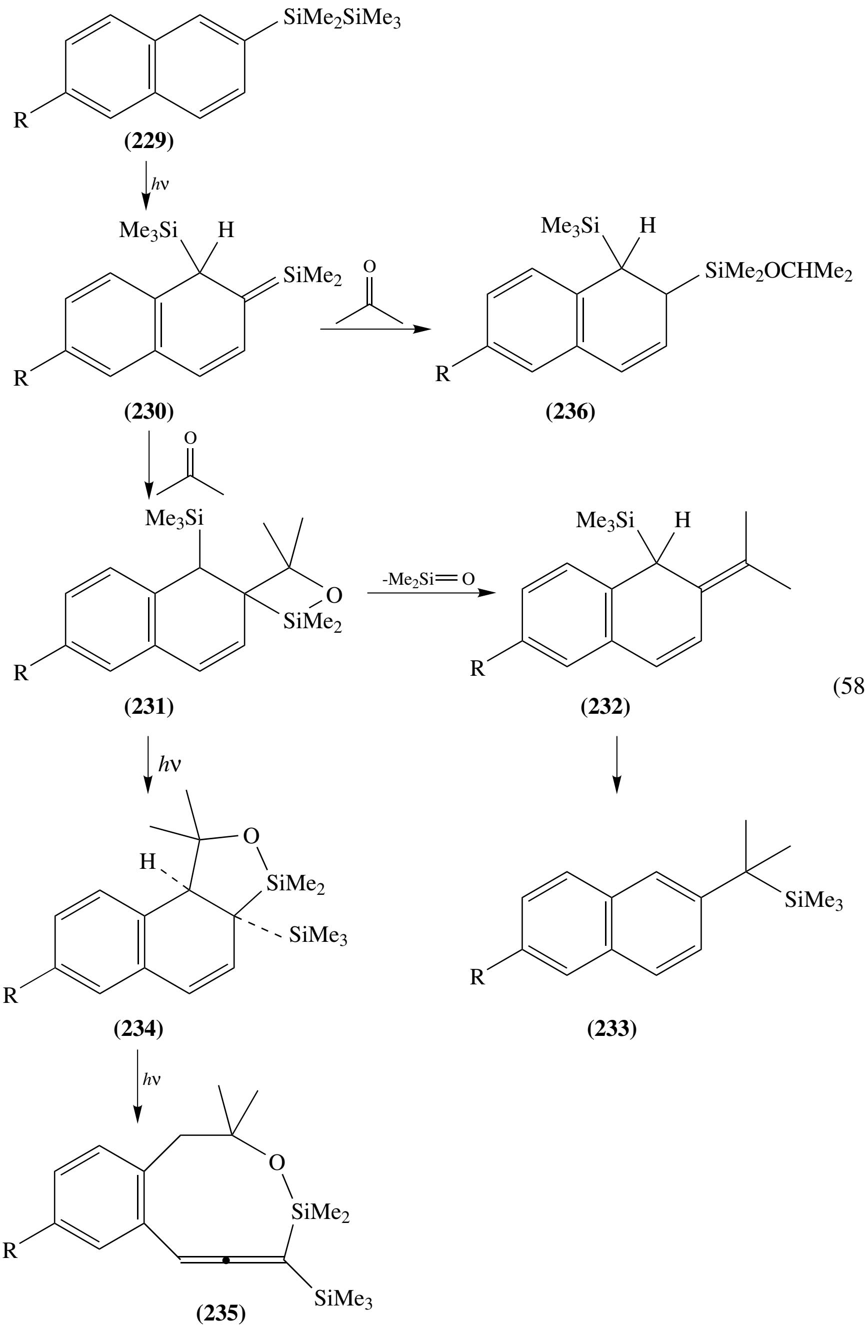

(58)

$R = Me_3SiMe_2Si$

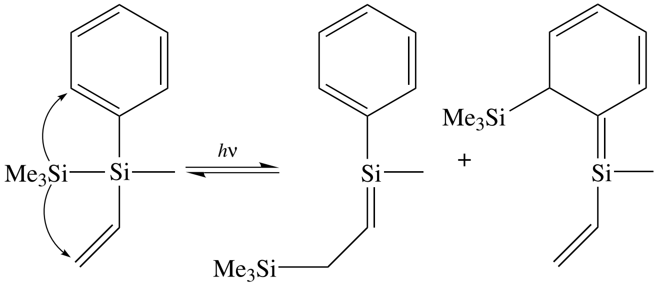

(237) **(238)** **(239)**

(59)

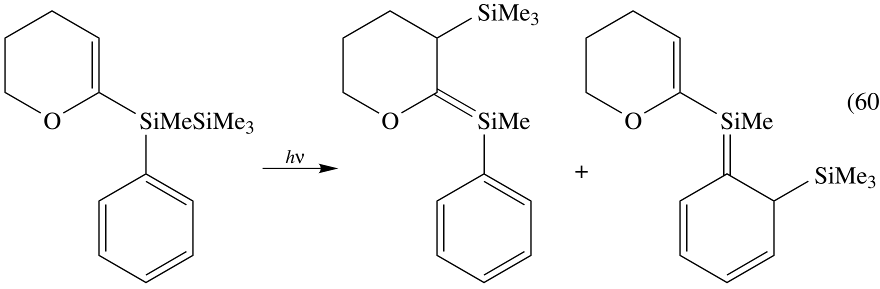

(240) **(241)** **(242)**

(60)

Sluggett and Leigh also used these reactions to obtain reactive intermediates, and studied these intermediates by nanosecond laser flash photolysis. Absorption spectra of the transient species were recorded, their decay rates were determined and kinetic studies were conducted. The photolysis of $Ph_3Si-SiMePh_2$ gives a low yield of the silatriene **243**[135], whose absorption spectrum could be recorded and found to be comparable to that of the well known silatriene obtained from $PhMe_2Si-SiMe_3$. Other species ($Ph_2Si=CH_2$, Ph_3SiH, $Ph_3Si^\bullet$ and $MePh_2Si^\bullet$) are also formed in the photolysis reaction. The relative yields depend on the solvent[136,137]. Silene species are formed from the lowest excited singlet state and are the major products in non-polar solvents, while silyl radicals stem from the lowest excited triplet state and are preferentially formed in polar solvents.

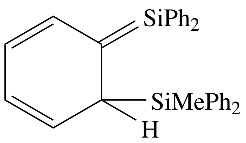

(243)

A photolytic study with trifluoromethyl-substituted phenyldisilanes in the presence of alcohols revealed the nature of the excited states responsible for the photoreactions: the 1,3-silyl migration occurs from an aromatic $\pi\pi^*$ (locally excited) state, while the direct alcoholysis of the aryldisilane takes place from the $\sigma\pi^*$ orthogonal intramolecular charge transfer state[138].

The product types vary as a function of the degree and type of alkyl/aryl substitution at silicon. Thus Ph_2t-BuSi$-$SiPh$_2$(t-Bu) only yields silyl radicals and no Si=C species when irradiated[139].

In the case of the disilane **244** 1,3-silyl migration to give silene **245** competes with dehydrosilylation to give silene **246**[140] (equation 61).

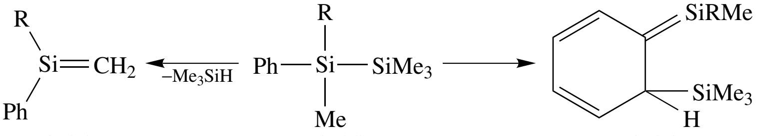

(246) **(244)** **(245)**

(61)

With the functional groups at different silicon atoms as in **247** only the migration to the vinyl group occurs. A competitive reaction is the cleavage to yield the silyl radicals **248** and **249**.

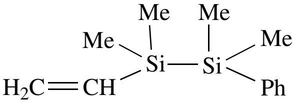

(247)

(248)

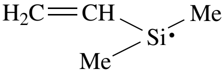

(249)

The photolysis of the rigid 1-silabicyclo[2.2.1]heptene **250**, which may be regarded as a cyclic vinylsilane, induces a 1,3-carbon shift to produce a cyclic silene intermediate **251**, which is trapped by alcohols to give **252** (equation 62)[141,142].

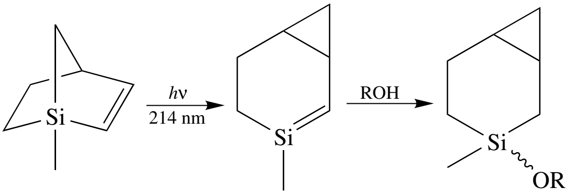

(250) **(251)** **(252)**

(62)

Sakurai, Kira and coworkers synthesized silene **253** from the cyclic divinyldisilane precursor **254** (equation 63)[143].

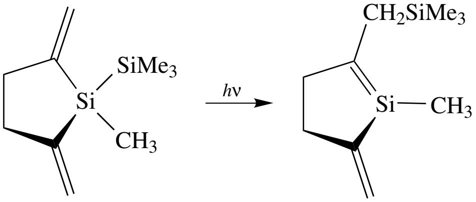

(**254**) (**253**)

(63)

The corresponding trisilane **255**, however, gives the expected silylene **256** (trapped as **257**) when photolysed, as the irradiation of trisilanes having a chromophore is a good method for the synthesis of silylenes[14]. Silene **258** is not obtained (equation 64).

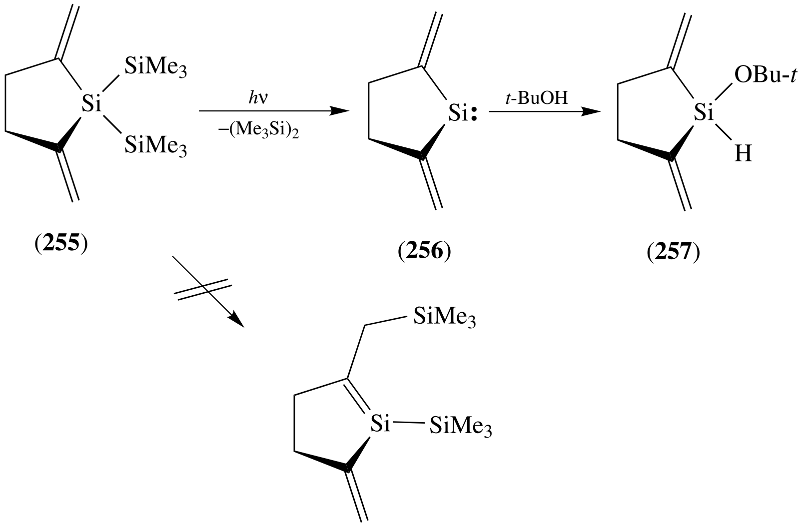

(**255**) (**256**) (**257**) (**258**)

(64)

The 1,3-silyl shift in aryl disilanes is suppressed when the aromatic ring is *ortho*-substituted[144]. An attempted silylene synthesis from 1,3-dimesitylhexamethyltrisilane **259**, however, led to low yields of silylene trapping products (*ca* 30% generation of $Me_2Si\colon$). The major pathway is the homolytic cleavage of the trisilane, followed by disproportionation of the radicals **260** and **261** to the silene **262** and the disilane **263** (equation 65).

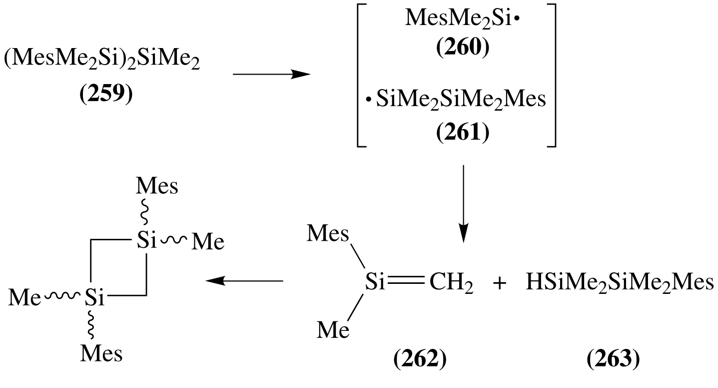

E/*Z*-(**264**)

(65)

The generation of these reactive species was supported by trapping experiments and the dimerization of the silene to E/Z isomeric 1,3-disilacyclobutanes **264**. The coproduct, 1,2-dimesityltetramethyldisilane **265**, of the $Me_2Si\colon$ extrusion is also photolabile. Silene

262 is also formed as intermediate in this case (equation 66)[145].

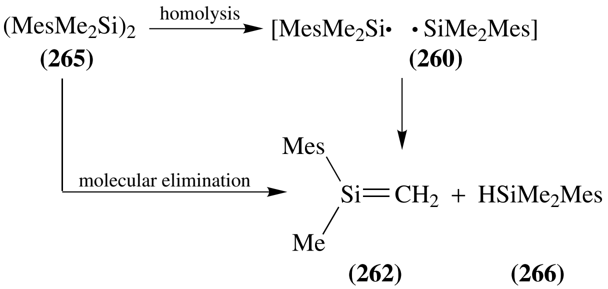

(66)

Similarly, the attempted synthesis of diadamantylsilylene by extrusion from a trisilane **267** did not give the wanted product[145]. The predominant photoreactions are silicon-silicon bond homolysis to give the radicals **268** and **269** (equation 67). Disproportionation of **268** and **269** results in the formation of silene **271** and silane **272**. The silene is identified by isolation of its head-to-tail dimer **273**. In the presence of scavenger reagents like 2,3-dimethylbuta-1,3-diene radical trapping products like **270** could be detected in low yields. Secondary photoprocesses involving the disilane **272** take place. Formation of silyl radicals **269** and **274** with subsequent disproportionation of the radicals explain the formation of diadamantylsilane **275.**

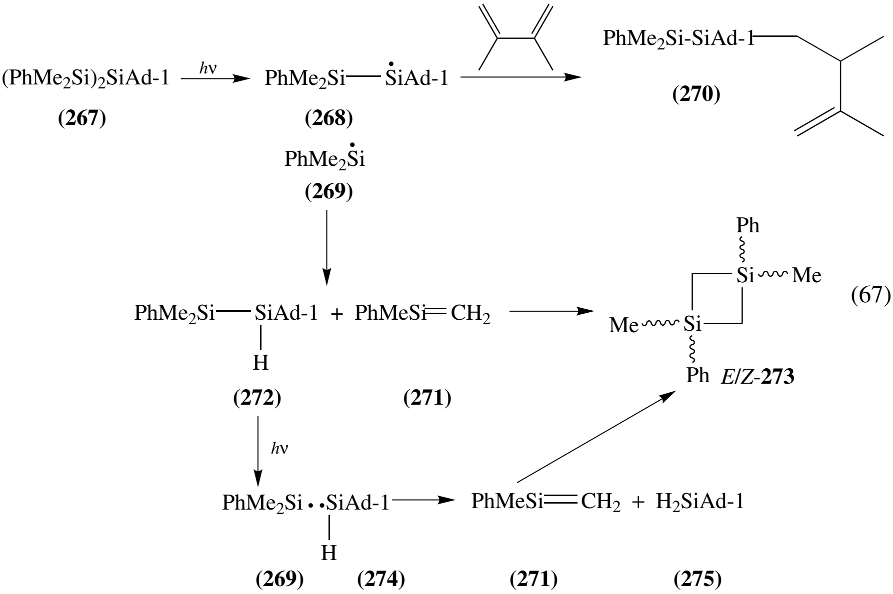

(67)

7. Silenes by rearrangement of silylenes and carbenes

In contrast to ethene which is separated by a high potential barrier from the isomeric methylcarbene, silene **25** can undergo a 1,2 shift to either methylsilylene **276** or, less favourably, to silylmethylene **277** (equation 68). The thermochemistry and the kinetics of these reactions have been a point of major disparity between theory and experiment[11,146] and much work has been done by theoreticians and experimentalists to settle this discrepancy. The recent developments have been summarized in great detail[11,12] and we will refer here only to the latest results.

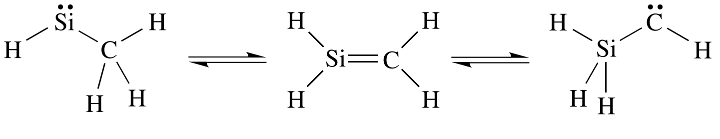

(276) **(25)** **(277)**

(68)

According to the best available calculations, silylcarbene **277** is higher in energy than silene **25** by 47.4 kcal mol^{-1} (MP4SDTQ/6-31G*//3-21G*)[147] while the best experimental value derived from calculated heats of formation is 52 kcal mol^{-1}[148]. In contrast, the silylene — silene rearrangement **25** → **276** is nearly thermoneutral, with the silene slightly more stable. A difference of *ca* 5 kcal mol^{-1} can be derived from the recent experimental heat of formations of **276** (48.3 kcal mol^{-1})[149] and of **25** (43 ± 3 kcal mol^{-1})[150], in agreement with high level calculations by Grev and coworkers which predict an energy difference of 4 kcal mol^{-1}[151].

The barrier for the 1,2-hydrogen shift was calculated by Kudo and Nagase to be 42.2 kcal mol^{-1} (MP3/6-31G*//6-31G*)[152]. This is considerably higher than the experimental values reported by Conlin and Kwak who reported an activation energy $E_{\text{A}} = 30.4 \pm 0.7$ kcal mol^{-1} ($\Delta H^{\ddagger} = 28.9 \pm 0.7$ kcal mol^{-1}) and a preexponential factor $\log A = 9.6 \pm 0.2$ s^{-1} ($\Delta S^{\ddagger} = -18.5 \pm 0.9$ cal deg^{-1} mol^{-1}) for the reaction **25** → **276**[22]. Higher quality calculations are clearly desirable to resolve this disagreement between theory and experiment[146].

Both silene isomers **278** and **279** are ideal precursors for the generation of silylene **284**, since their interconversion to **284** is spontaneous (in the case of **278**) or can be easily induced by irradiation (in the case of **279**). There are numerous well-established methods to prepare transient silylenes **279**. Three important examples are shown in equation 69, namely the photolytic generation from a trisilane **280**[153], thermolytic or photolytic decomposition of cyclic silanes **281**[14,154,155] and degradation of diazidosilanes **282**[153,156]. The photolysis of the diazido silane **282** is an especially clean reaction which has been used in several spectroscopic studies[157]. The photolysis of α-diazo compounds **283** is the only frequently used reaction path to silenes **284** via a carbene–silene rearrangement[8].

Maier and coworkers have shown that it is possible to induce by irridation using the appropriate absorption band, a 1,2-hydrogen shift in silenes and in silylenes[29,158]. Thus, it is possible to 'switch' photochemically between silylenes and silenes. Michl, West and coworkers have used this approach to isomerize dimethylsilylene **285** and 1-methylsilene **26** several times (equation 70). Due to the clean formation of **285** from the diazido precursor **286**[153] it was possible to measure the IR transition moment directions for both **26** and **285**[156].

Nefedov, Michl and coworkers reported the successful spectroscopic characterization of the 1-silacyclopenta-2,4-diene **287** and its photochemical transformation into the isomeric species **288**–**290** (equation 71)[159]. Gaspar and coworkers[160] had suggested that silole **287** might be formed by a rearrangement of the cyclic silylene **288** via the 1-silacyclopenta-1,3-diene **289**. This proposal was confirmed in an elegant UV-visible, IR-matrix isolation study[159]. The silylene **288** was generated by vacuum pyrolysis either of the spiro compound **291** or the diazide **292** or by UV-irradiation of matrix isolated **292**. The complex interrelationship between the silylene **288**, the isomeric silabutadienes **289**, **290** and the silole **287** has been established through matrix isolation, spectroscopic characterization and photoisomerization of the individual compounds. A 1,2-H shift transforms silylene **288** to silabutadiene **289**. Subsequent 1,3- or 1,5-H shifts interconvert the silabutadienes **289**–**290** and silole **287**. The final product after warmup of the argon matrix is **293**, the [4 + 2] dimer of **287** (equation 71).

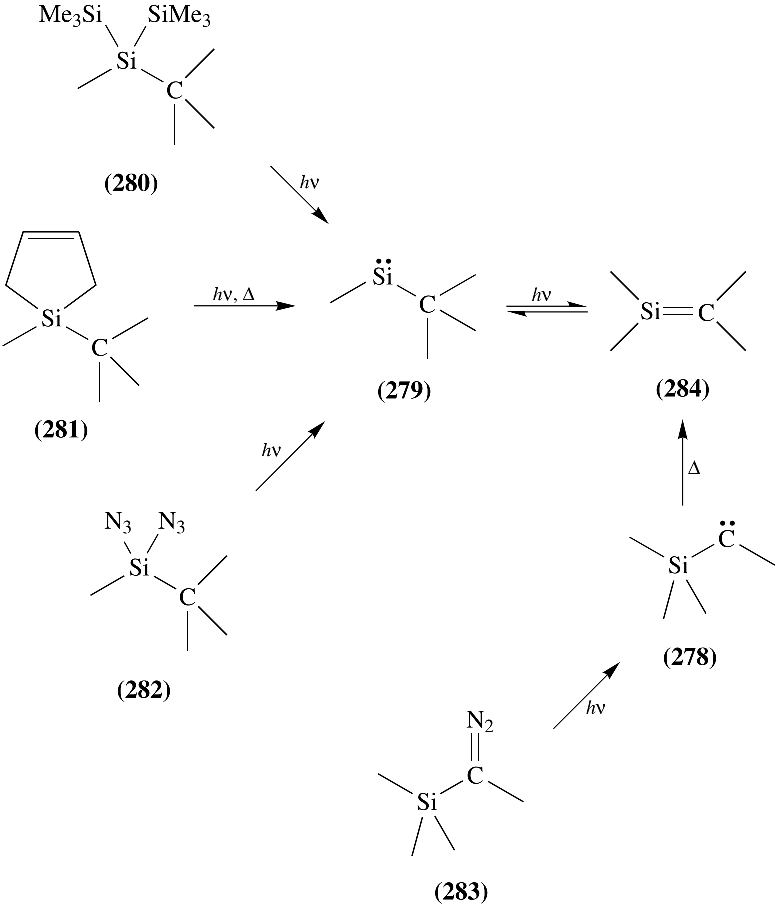

(69)

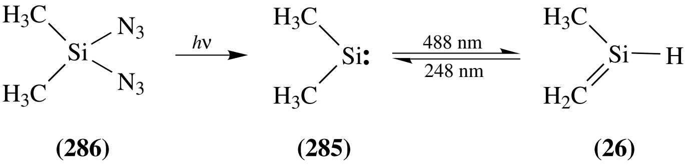

(70)

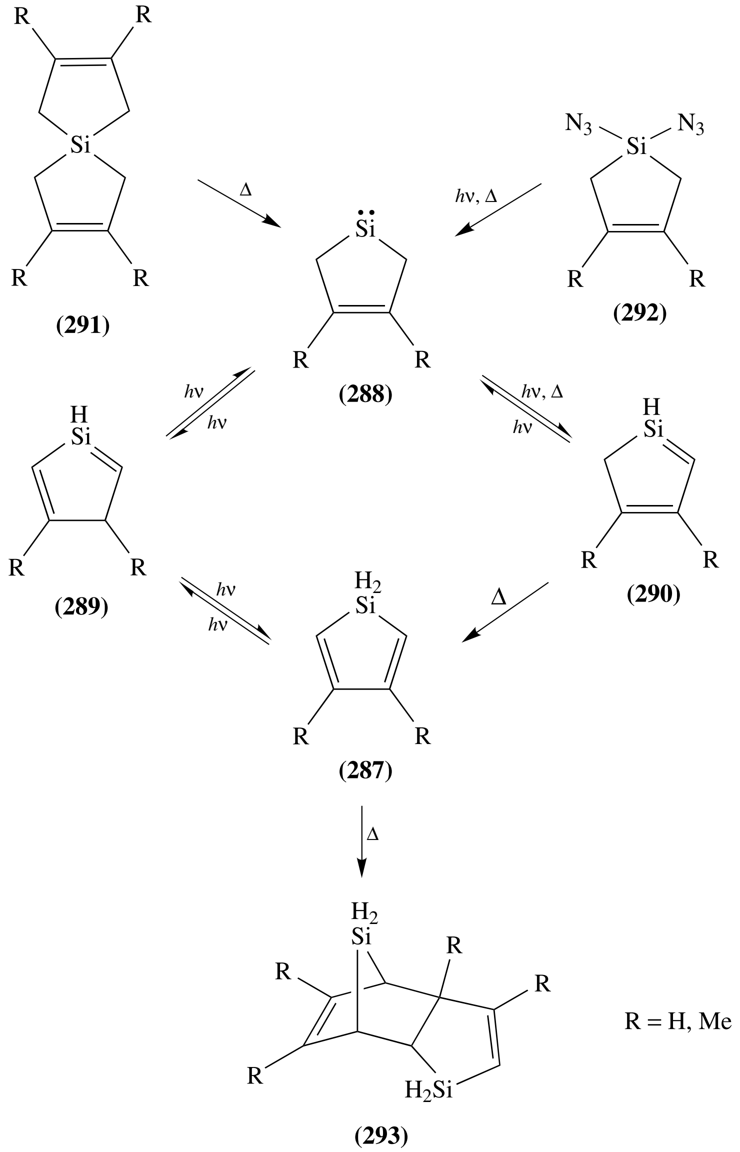

(71)

A photochemical approach via a silylene-to-silene rearrangement was followed by Fink and coworkers in their synthesis of silacyclobutadienes in a 3-methylpentane matrix at low temperatures[161]. Irradiation of the cyclopropenyltrisilane **294** gives the relatively stable cyclopropenylsilylene **295**. **295** can be efficiently converted to silacyclobutadiene **296** by irradiation into the visible absorption band of the silylene (equation 72)[161,162].

The structure of the trapping product with TMSOMe has been established by X-ray crystallography, thereby confirming the identity of **296**[161]. Further adducts with amines and alcohols have been isolated[161,163]. The [2 + 2] cycloadduct **297** of **296** with trimethylsilylacetylene (equation 73) is the first room-temperature stable Dewar silabenzene[163].

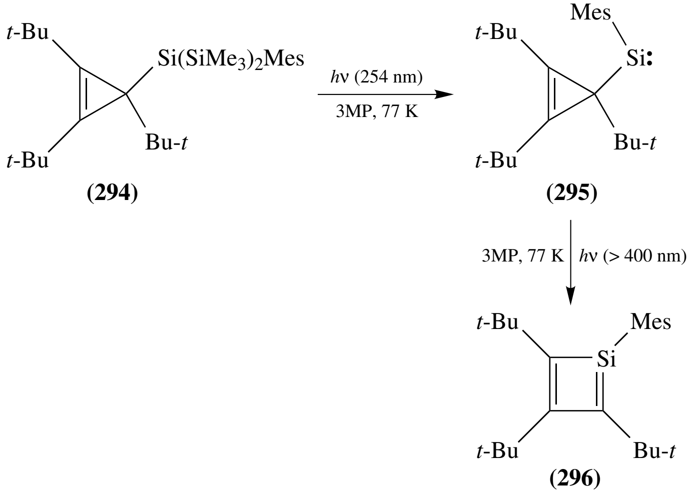

(294) **(295)** **(296)**

(72)

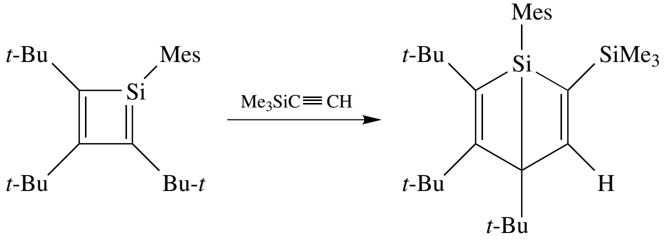

(296) **(297)**

(73)

Silenes are formed by rearrangement of silylcarbenes. If polysilylated diazomethanes **298–300** are employed, a selective migration of a silyl group to the carbene centre occurs and silenes **301**, **92** and **302** are formed (equations 74–76)[164]. The outcome of trapping reactions is independent of the mode of silene generation: photochemical and pyrolytic methods give the same results.

$$(\mathrm{Me_3Si})\mathrm{SiMe_2}-\underset{\underset{\displaystyle \mathrm{N_2}}{\|}}{\mathrm{C}}-\mathrm{H} \longrightarrow \mathrm{Me_2Si{=}CH(SiMe_3)}$$

(298) **(301)**

(74)

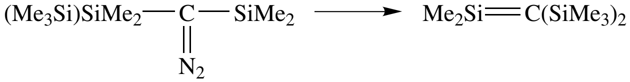

$$(\mathrm{Me_3Si})\mathrm{SiMe_2}-\underset{\underset{\displaystyle \mathrm{N_2}}{\|}}{\mathrm{C}}-\mathrm{SiMe_2} \longrightarrow \mathrm{Me_2Si{=}C(SiMe_3)_2}$$

(299) **(92)**

(75)

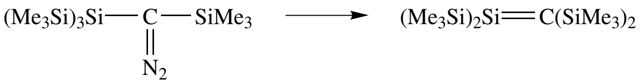

$$(\mathrm{Me_3Si})_3\mathrm{Si}-\underset{\underset{\displaystyle \mathrm{N_2}}{\|}}{\mathrm{C}}-\mathrm{SiMe_3} \longrightarrow (\mathrm{Me_3Si})_2\mathrm{Si{=}C(SiMe_3)_2}$$

(300) **(302)**

(76)

In the case of the disilanyldiazoacetate **303**, photolysis initially gives the carbene **304** that rearranges to the silaacrylate **305**[165], which then isomerizes to the bissilylketene **306** (equation 77). The trapping reaction with alcohols gives the products **307** and **308**. The latter is obviously formed via ion pair intermediates like **309**. The UV and IR spectra of irradiated matrices at 10 K have been measured. The band at 1670 cm^{-1} is tentatively assigned to the $\nu_{C=0}$ of **305**; λ_{max} is at 288 nm.

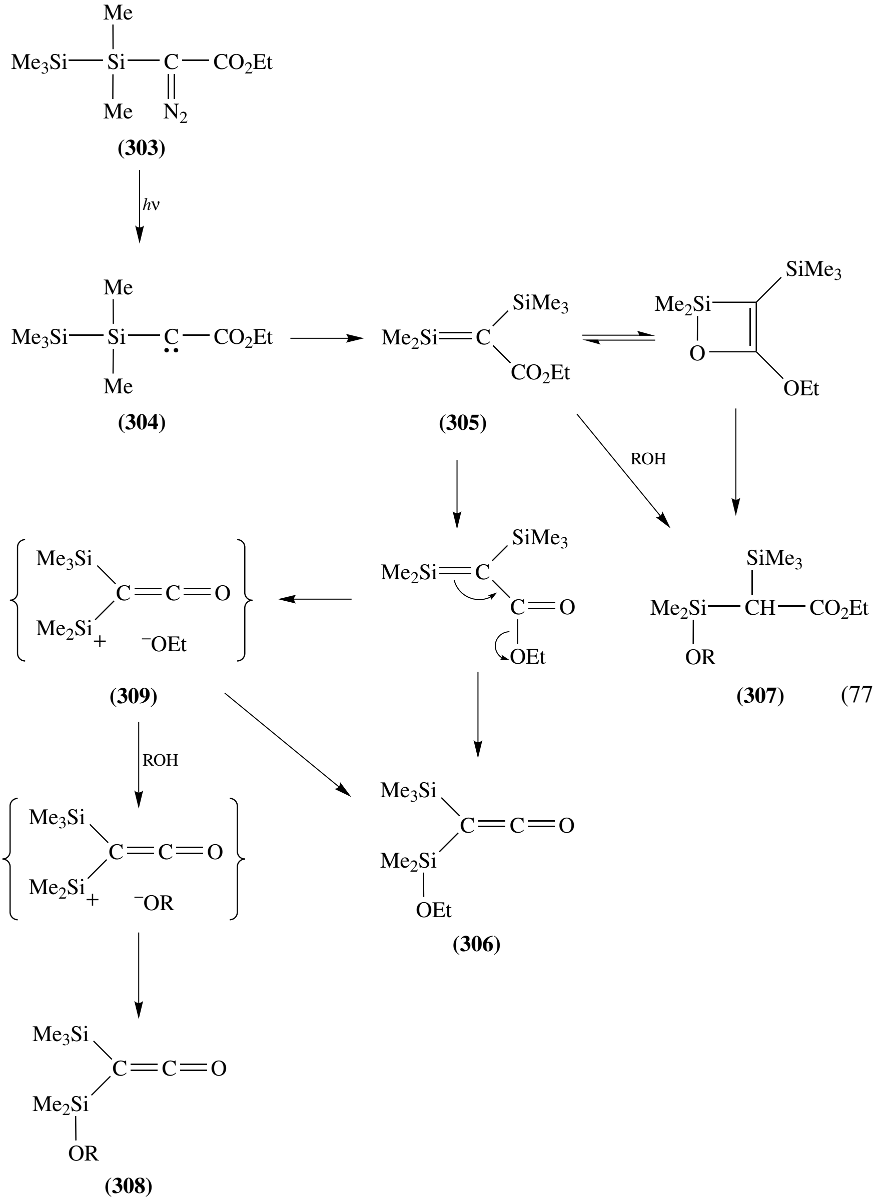

(77)

The integration of two carbene precursor groups, like in bis(1-diazo-2-oxoalkyl)disilane **310**, leads to interesting products upon irradiation[166,167]. Intermediate carbenes (**313** and **314**) formed through nitrogen loss and silenes (**315** and **316**) formed through 1,2-silyl migration to the carbene centre are discussed. The formation of the eight-membered ring **312** (R = 1-adamantyl) is not explained. Product **311** is obtained, probably via the intermediates **317**–**320** as shown in equation 78.

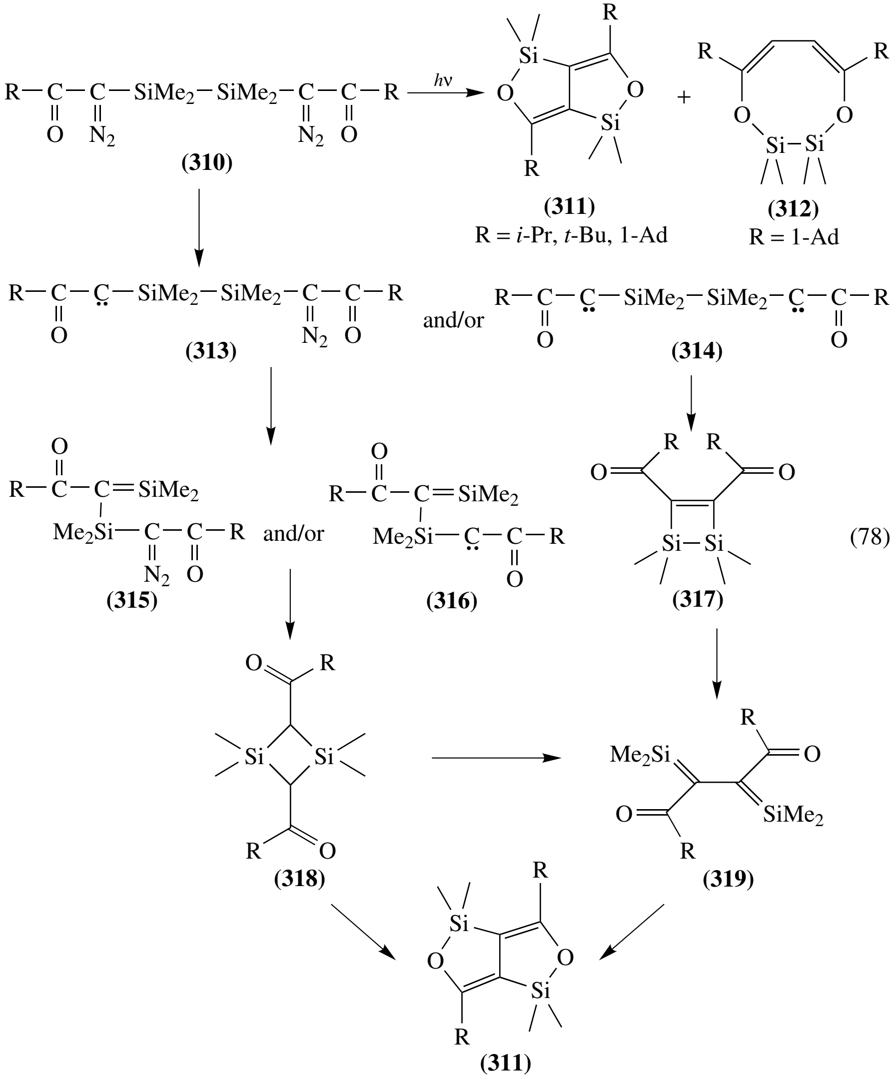

(78)

The photochemical decomposition of bis(silyldiazomethyl)tetrasilane **320** produces one silene group to give **321** followed by intramolecular [2 + 3] silene–diazo cycloaddition via **322** to give the bicyclic compound **323** as final product, while thermal decomposition gives a bis-silene **324** which then undergoes head-to-tail dimerization[168,169] to

325. Interestingly, compound **323** is one of the most stable siliranes having methyl substituents at silicon. However, under prolonged exposure to air **323** decomposes to give **326** (equation 79).

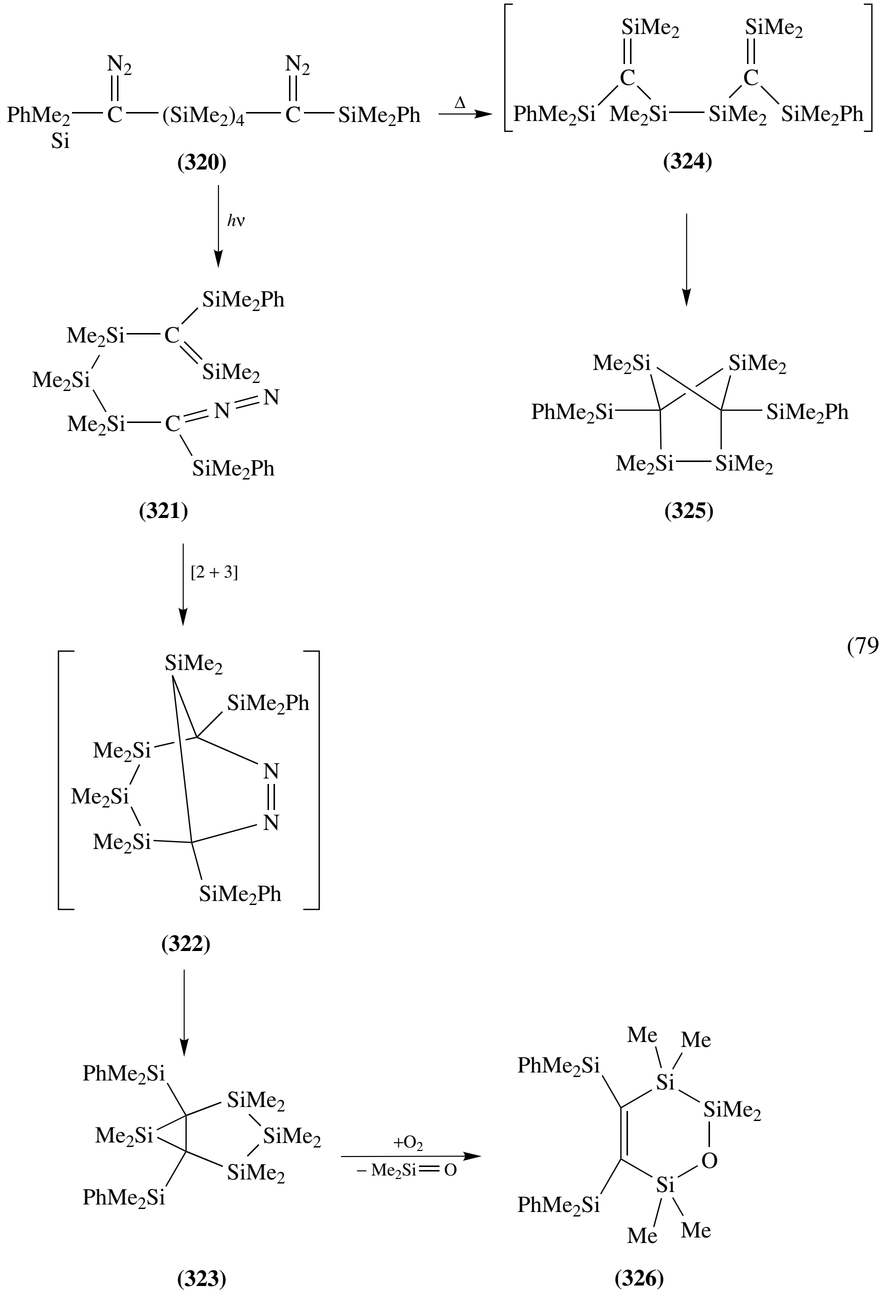

(79)

For a central hexamethyltrisilanyl unit in the precursor **327** a formal head-to-tail dimer **329** and a head-to-head dimer **330** are formed[169] under photolysis conditions. Thermal reaction gave only the bicyclic dimer **329** (equation 80).

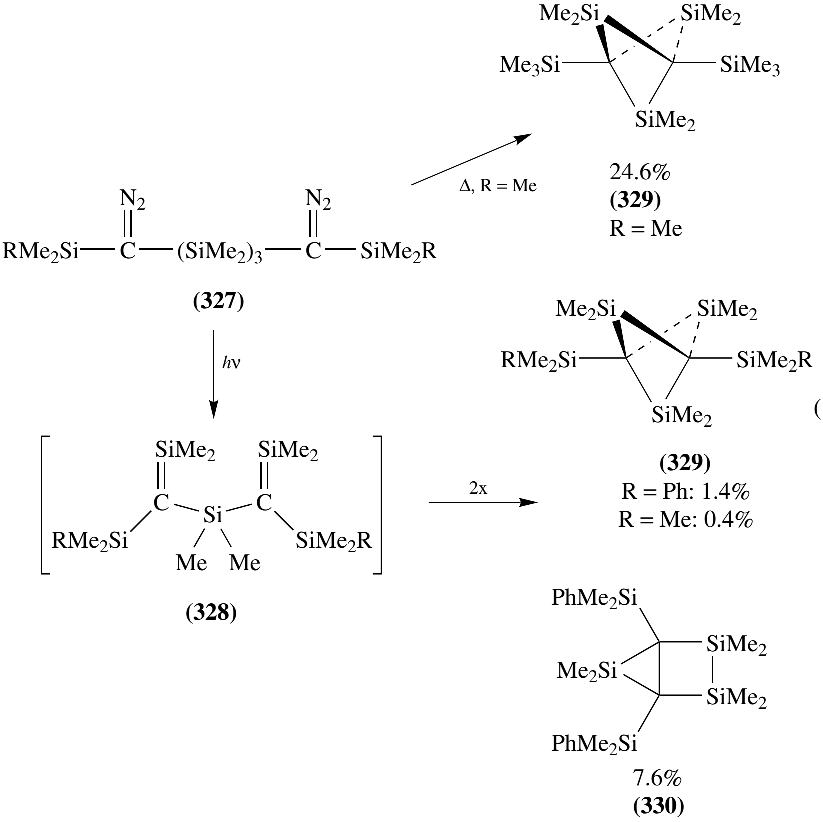

(80)

When the 1-diazo-2-silyl moiety is incorporated into cycles then endocyclic silicon–carbon double bonds should be formed. Most interesting in this connection is the decomposition of 1-diazo-2-sila-3,5-cyclohexadiene **331**, because the initial Si=C product should be silabenzene **332**[170]. The outcome of the nitrogen elimination depends on the conditions used. The products isolated are **333** (equation 81), **335** via bicyclic **334** (equation 82) and **338**, formed via silafulvenes and **336** (equation 83).

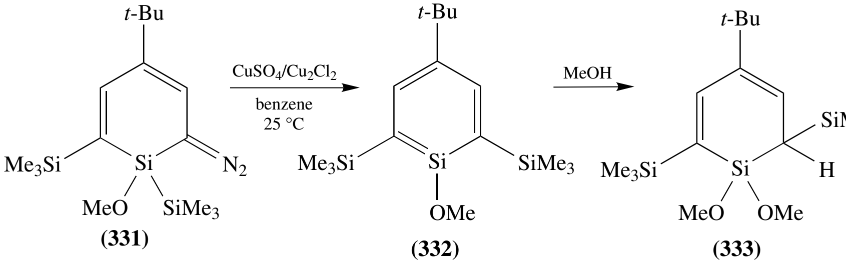

(81)

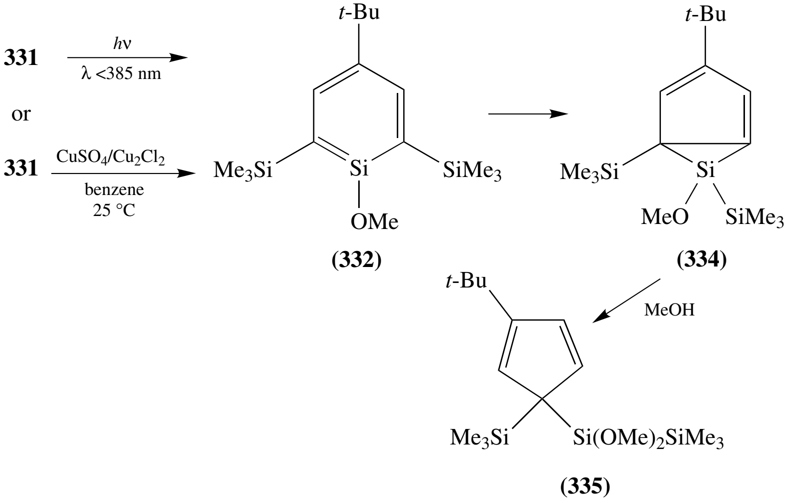

(82)

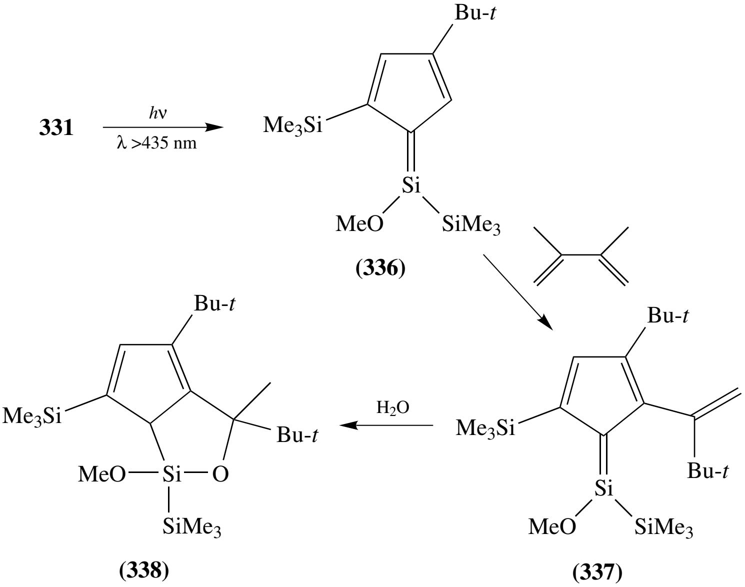

(83)

8. Other group 14 carbon double bonded species

Wiberg's group has prepared other species analogous to the silenes **92**, **97** and **104**, with tin or germanium instead of silicon. With tin and germanium the generation and reactivity of $Me_2E{=}C(SiMe_3)_2$ has been investigated (E = Sn[171], E = Ge[172]). With germanium a stable species was available: $Me_2Ge{=}C(GeMe_3)(SiMe\text{-}Bu_2\text{-}t)$ is formed from the germene source $t\text{-}Bu_2SiF{-}CLi(GeMe_3)_2{\cdot}2$ THF[173,174].

The group of Satgé has presented evidence for the formation of the chloro- or fluorogermenes $Me_5C_5(X)Ge{=}CR_2$, with CR_2 = fluorenylidene[175].

B. Reactivity

1. Rearrangements

a. Silene-to-silylene interconversions. An interesting isomerization reaction is reported for the reactive 4-silatriafulvene **170**. When **170** is generated by thermolysis of **172** in the presence of *t*-BuOH the silacyclobutenes **339** and **340** are formed quantitatively in a relative ratio of 3 : 1[119]. This result indicates a rearrangement of **170** to the silacyclobutadiene **341**, which is faster than the addition of *t*-BuOH to the Si=C double bond in **170**. This is especially interesting in the context that thermolysis of **172** in the presence of 2,3-dimethylbuta-1,3-diene yields **171** in quantitative yield (equation 84). Thus, **170** reacts with dienes faster than with *t*-BuOH[119]. This unusual behaviour of **170** is illustrated by comparison with the silene $Me_2Si{=}C(SiMe_3)_2$ **92**, which reacts with *t*-BuOH nearly 2000 times faster than with 2,3-dimethylbuta-1,3-diene[62,176].

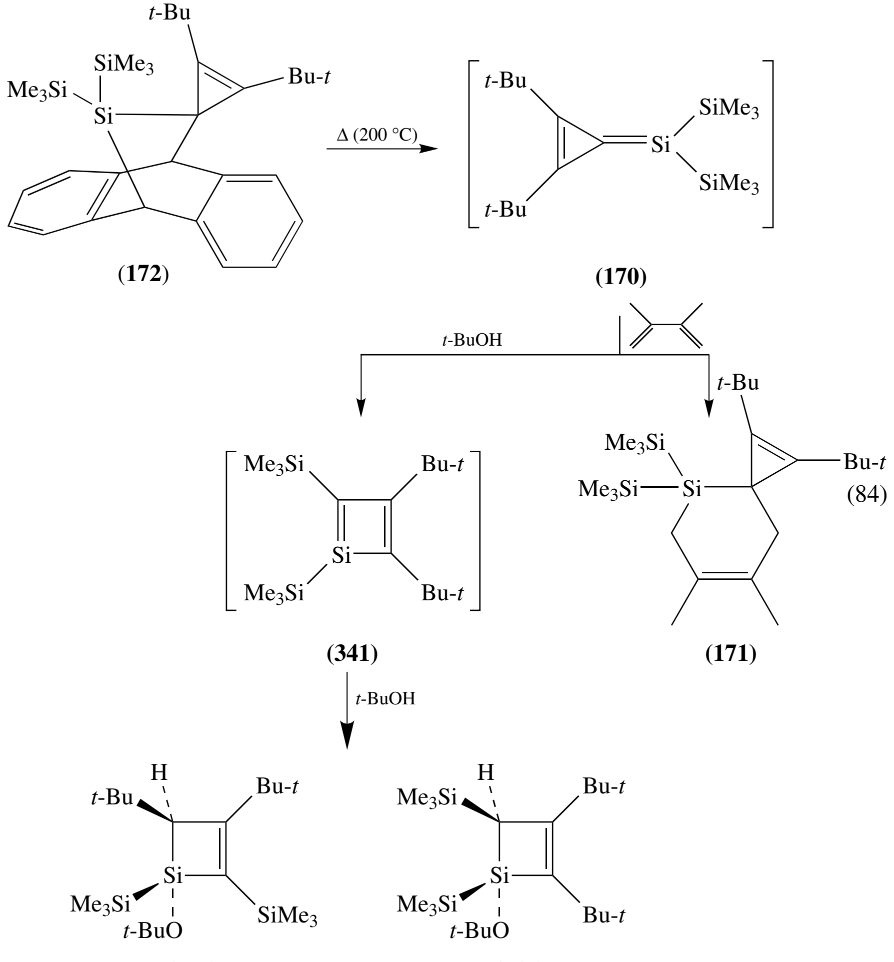

(172) (170) (341) (171) (339) (340)

(84)

The low reactivity of **170** toward alcohols would be explained by the reduced polarity of the Si=C double bond due to the contribution of the resonance structure **168B**, in addition to the silyl substituent effects. In agreement with experiment a theoretical study for the parent species **168** predicts that water addition to **168** is thwarted by an unusual high barrier (20.0 kcal mol^{-1} at MP2/6-311++G**)[119,177]. Furthermore, the calculations suggest that the transformation **170** → **341** proceeds in two steps via the cyclopropenylsilylene **342** (equation 85). The highest barrier for the isomerization of the parent **168** → **343** is calculated to be 17 kcal mol^{-1}. Thus, the isomerization can effectively compete with the water addition[177].

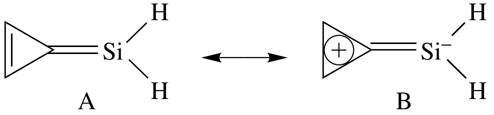

(168)

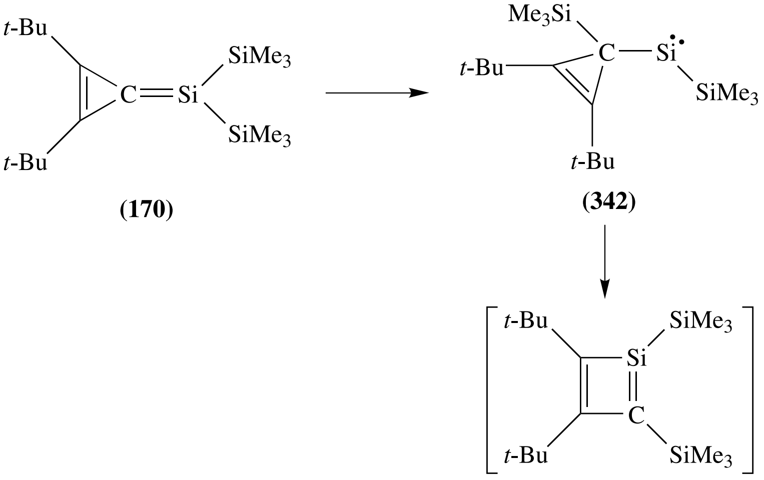

(170) **(342)** **(341)**

(85)

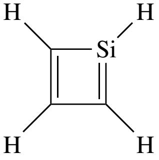

(343)

b. Silene-to-silene isomerization. The rearrangement process of the 'Wiberg' silenes **92**, **97** and **104** (formed, e.g., by equation 86) by methyl migration gives the silenes **92**, **97a** and **104a** as has already been mentioned in Section I.A.1. Equation 87 demonstrates this degenerate rearrangement.

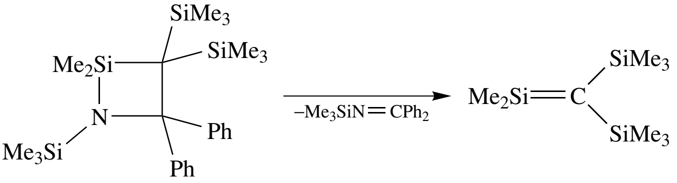

(95b) **(92)**

(86)

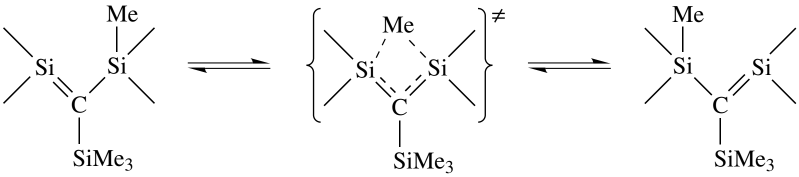

(92) **(92)**

(87)

The use of deuteriated **92** allows the observation of this process. So the deuteriated 1-aza-2-silacyclobutane **95b$_1$**-d$_6$ [from $(D_3C)_2SiF{-}CLi(SiMe_3)_2$ and $Ph_2C{=}N{-}SiMe_3$] releases $(D_3C)_2Si{=}C(SiMe_3)_2$ **92**-d$_6$ in a reversible [2 + 2] cycloreversion in minor amounts when slightly heated. Fortunately, the methyl migration is faster than intermolecular dimerization and a mixture of 1-aza-2-silacyclobutanes **95b**$_1$-d$_6$–**95b**$_4$-d$_6$ is formed by [2 + 2] cycloaddition reaction with imine.

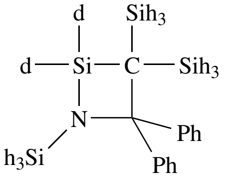

(**95b$_1$**-d$_6$)

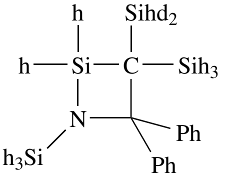

(**95b$_2$**-d$_6$)

h = CH_3
d = CD_3

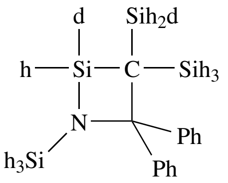

(**95b$_3$**-d$_6$)

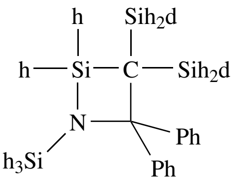

(**95b$_4$**-d$_6$)

When deuteriated **92** is generated from irreversibly decomposing precursors, just the head-to-tail dimer $[(D_3C)_2Si{-}C(SiMe_3)_2]_2$ is found[97]. An even faster reaction than the methyl migration is the reaction of the silene with silyl azides. Just one of the possible deuteriated dihydrotetrazoles **344**-d_6 is formed (equation 88).

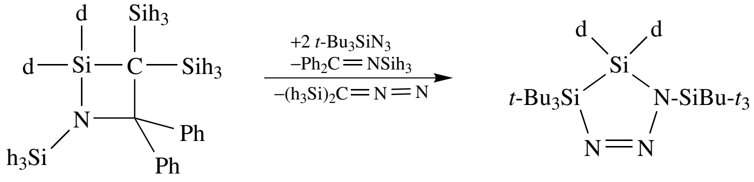

(**95b$_1$**-d_6)

$h = CH_3$
$d = CD_3$

(**344**-d_6)

(88)

Silene **124** having the very bulky tri-*tert*-butylsilyl group at the linking carbon atom undergoes hydrogen migration to give a disilacyclobutane, as has been mentioned above[77].

The tendency to isomerization by methyl migration is higher in $Ph_2Si{=}C(SiMe_3)_2$ **(97)**, because the less polar and acidic **97a** is formed[64].

A rearrangement quite similar to the above-mentioned methyl migrations is found for the initially formed dichloroneopentylsilene **345**, which possesses a *tert*-butoxy group. The higher electrophilicity of this silene's silicon atom in comparison with that of the resulting dimethylsilene **346** leads to a 1,3 migration of the *tert*-butoxy group[178,179]. The identity of **346** was established by isolation of the dimer **347** and the trapping product with quadricyclane **348** (equation 89).

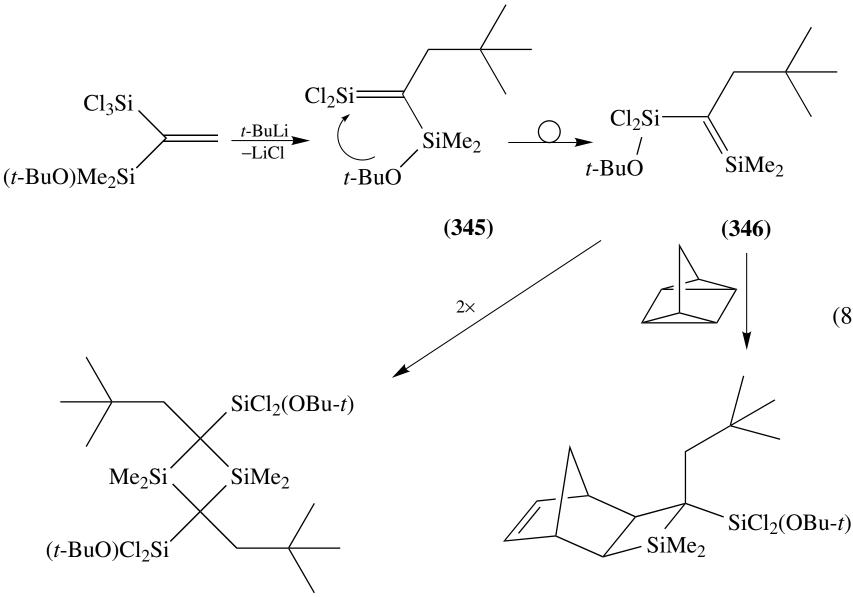

(345) **(346)**

(89)

(347) **(348)**

The thermal 1,3 shift of a trimethylsilyl group from oxygen to silicon in 2-siloxysilenes (equation 90) is the reversal of their photochemical formation from acylpolysilanes. The reaction occurs already at room temperature[38,180].

'Brook-type' silenes with less than two trimethylsilyl groups at the silicon tend to be photolabile[90,96]. Thus silenes $Me_3SiR^1Si{=}C(OSiMe_3)Ad\text{-}1$ **137** undergo a complex photoisomerization to novel silenes (Me$_3$SiO)MeSi=C(Ad-1)(SiMe$_2$R^1) **140** (equation 91). This has been summarized in detail together with the related thermal isomerization[93] in Section I.A.4.

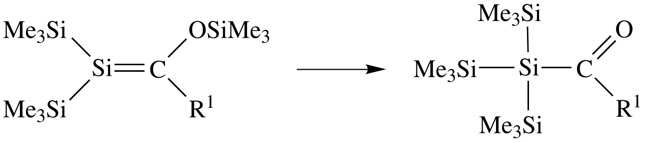

(90)

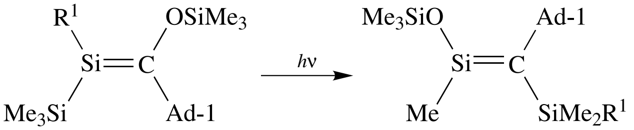

(137) **(140)**

(91)

c. Intramolecular insertion reactions. In a number of rearrangements of silenes the Si=C bond has been observed to insert into a C−H bond of an *ortho* methyl substituent of an adjacent mesityl group. For example, Brook and coworkers found that upon irradiation of the silene **349** the benzocyclobutane **350** is produced. Formally, this can be regarded as a $[2\pi + 2\sigma]$ cycloaddition; however, a 1,5-hydrogen migration with a consecutive electrocyclic ring closure via **351** can also account for the observed product (equation 92)[90,181]

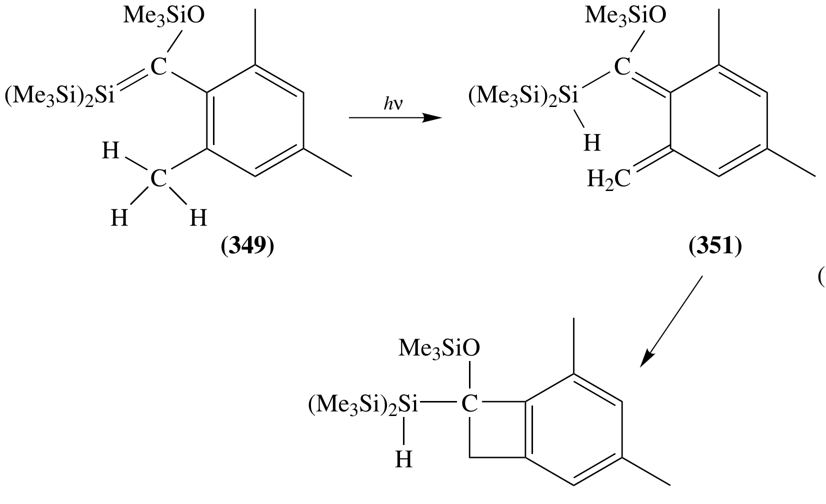

(349) **(351)** **(350)**

(92)

The transient silene **352** undergoes, under the photolytic conditions applied for its generation from **353**, a fast subsequent isomerization yielding the silaindane **354**. The silylcarbene **355** was suggested as short-lived intermediate (equation 93)[94]. Similar formal insertions of the Si=C bond into the C−H bond of an *ortho*-methyl group have been also observed for other 1-mesityl silenes[95] or 1-aminomesityl silenes[182].

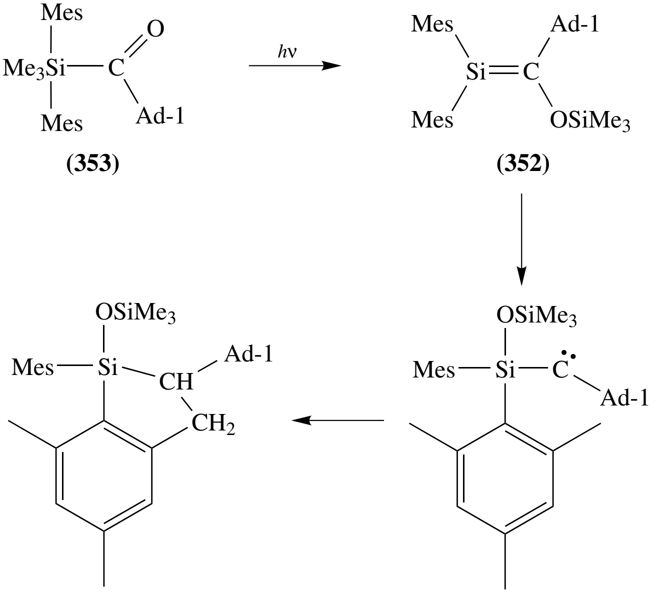

(353) **(352)**

(93)

(354) **(355)**

In an attempt to synthesize a kinetically stabilized silene, Oehme and coworkers used the sterically highly demanding 2,4,6-tri-*t*-butylphenyl (supermesityl = sup) substituent as a protecting group. Although the Si=C double bond in **356** is extremely sterically shielded, the silene is not stable under the applied conditions. The steric congestion of the molecule obviously prevents a dimerization, but the highly reactive silene group is inserted into the C–H bond of an *ortho*-*t*-Bu group of the supermesityl substituent and the bicyclic product **357** is obtained (equation 94)[199].

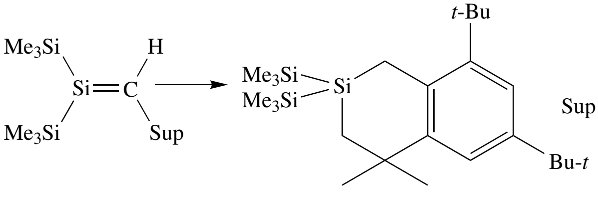

Sup = 2,4,6-t-BuC_6H_2 (94)

(356) **(357)**

Generally, the isomerization/dimerization behaviour of $Ph_2Si{=}C(SiMe_3)_2$ **(97)** is more complex than that of $Me_2Si{=}C(SiMe_3)_2$ **(92)**[64]. Silene **97**, formed from **97**•LiBr, isomerizes by fast methyl migration to $Me_2Si{=}C(SiMe_3)(SiMePh_2)$ **97a**, which undergoes a slower phenyl migration to $PhMeSi{=}C(SiMe_3)(SiMe_2Ph)$ **97b**, and finally a fast methyl migration gives $Me_2Si{=}C(SiMe_2Ph)_2$ **97c**. Simultaneously **97a** and **97c** dimerize and also irreversibly isomerize into disilaindanes **358a–b** (equation 95). The latter reaction is quantitative when the dimers of **97a** and **97c** are thermolysed.

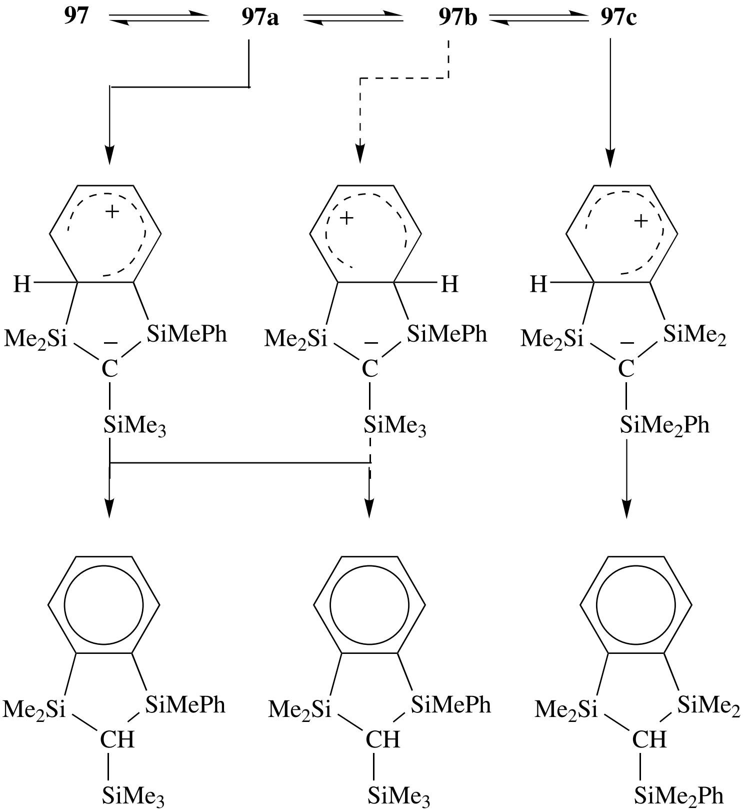

(95)

(**358a**) (**358a**) (**358b**)

The silene **124** is probably formed as its THF adduct and can be trapped by, e.g., 1,3-dimethyl 2,3-butadiene to give a [4+2] cycloadduct. The attempt to liberate the silene **124** from its donor adduct results in the formation of a disilacyclobutane **125**. This is ascribed to the prolonged life-time of the intermediate **359** formed by the methyl migration in the silene (equation 96), which allows for a hydrogen migration to take place.

Photolytically generated 1-silabuta-1,3-dienes undergo a thermal reverse reaction to 2-silacyclobutenes. Thus 2-phenylsilacyclobut-2-ene **360** is easily opened to the 2-phenylsilabuta-1,3-diene **361** by irradiation in 3-methylpentane matrix at 77 K or by flash photolysis at ambient temperature (equation 97)[183]. The rate for the thermal reverse reaction was measured at room temperature and the activation energy for the 1-siladiene ring closure was estimated to be 9.4 kcal mol^{-1} [183].

2. Dimerizations

The dimerization of silenes is probably *the* prominent type of reaction of silenes since the structures of most of the relatively stable and transient silenes have been established by isolation and identification of their dimers. The formation of disilacyclobutanes has now gained acceptance as evidence for the intermediate formation of a transient silene.

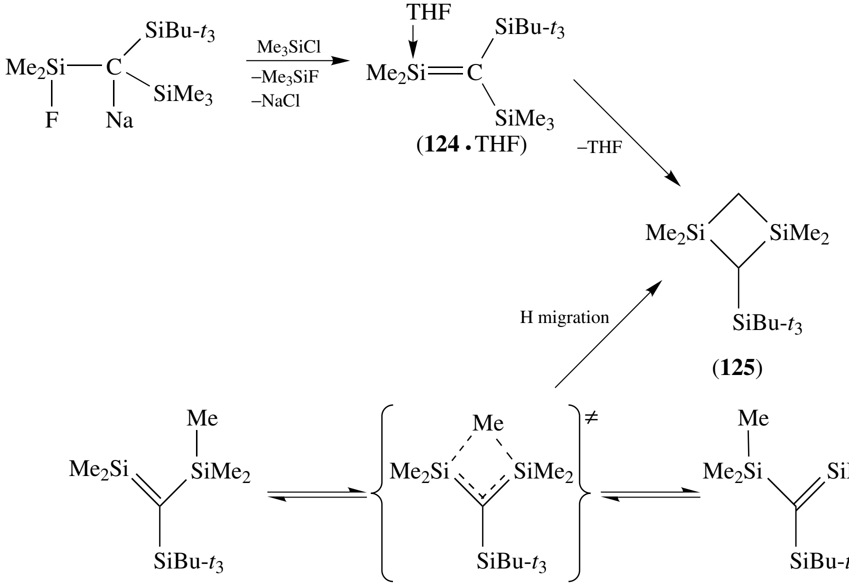

(**124**•THF)

(**125**)

(96)

(**124**) (**359**) (**124**)

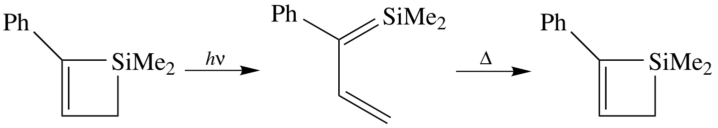

(97)

(**360**) (**361**) (**360**)

Simple silenes readily couple to yield the head-to-tail dimers, 1,3-disilacyclobutanes[1,2,15,157]. The dimerization is extremely facile and silenes bearing only small alkyl groups dimerize in an argon matrix even at 40 K, i.e., the dimerization proceeds at a diffusion controlled rate. Bulky substituents slow down the dimerization rate and allow the isolation of stable silenes. The head-to-tail dimerization (equation 98) is the predominant dimerization path for silenes, including those of the 'Auner–Jones'[79,80] and 'Wiberg' type[72,73,78].

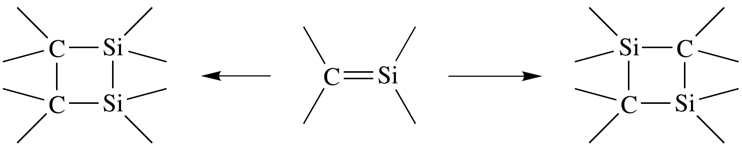

(98)

head-to-head head-to-tail

In contrast, 1,1-silylsilenes[39,104,107,108] and 2-siloxysilenes [3,86,90,180] i.e. silenes of the 'Apeloig–Ishikawa–Oehme' and 'Brook' type as well as some 1-silaallenes[184,185], dimerize in a head-to-head mode yielding 1,2-disilacyclobutanes (equation 98).

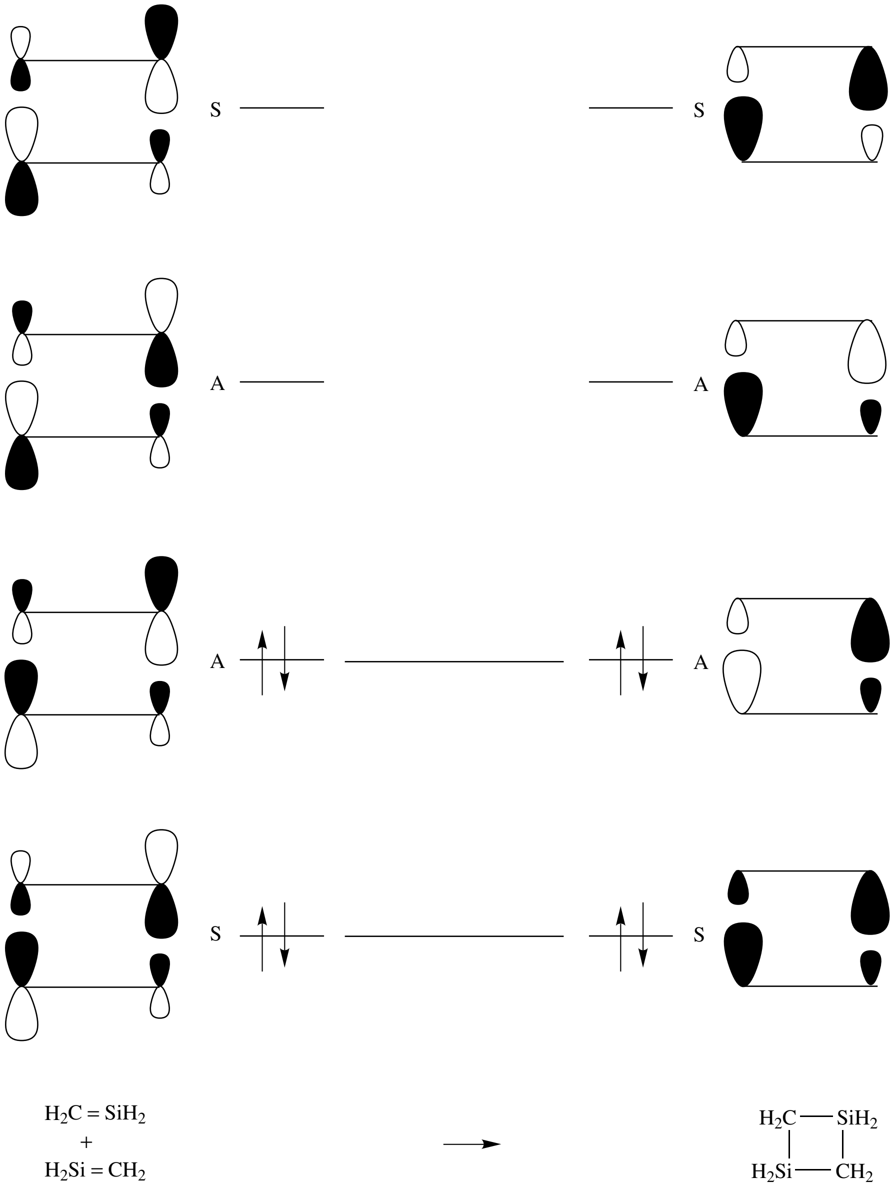

FIGURE 1. Correlation diagram for the head-to-tail dimerization reaction allowing for reduction in orbital symmetry. S and A designate a molecular orbital as symmetric or antisymmetric with respect to the C_2 axis perpendicular to the plane of the page. Reprinted with permission from Ref. 186. Copyright (1992) American Chemical Society

The principal questions arising from the facile occurrence of a formally forbidden concerted process like the dimerization of silenes attracted considerable interest from theoreticians. The theoretical work done is well summarized in several recent reviews[11,12] and we will only discuss briefly the very recent theoretical results on the silene dimerization reaction.

All recent *ab initio* studies on the head-to-tail dimerization reaction for the parent silene $H_2Si{=}CH_2$ predict a very exothermic reaction with a low barrier, despite the fact that the reaction is formally forbidden[12]. It is believed that the strong polarization of the Si=C double bond leads to a relaxation of the Woodward–Hoffmann rules. A detailed analysis of the symmetry of the head-to-tail silene dimerization reveals, however, that a concerted $[2\pi_s + 2\pi_s]$ reaction in the appropriate point group is not forbidden by symmetry (see Figure 1)[186].

Thus, Seidl, Grev and Schaefer found a barrier for a concerted fully synchronous $[2\pi_s+2\pi_s]$ reaction path of 5.2 kcal mol^{-1} (at CCSD/DZ+d+ZPE)[186]. At the same level of theory the head-to-tail dimerization is exothermic by 79.1 kcal mol^{-1}. The transition state for this reaction appears very early on the reaction coordinate, i.e., the silene geometry being nearly conserved, as expected for a highly exothermic reaction[186]. The calculated reaction path is shown in Figure 2a.

These conclusions of Schaefer and coworkers were severly challenged by Bernardi, Robb, Olivucci, and coworkers who concluded, based on multiconfigurational calculations at the CASSCF level, that in the course of the head-to-tail silene dimerization a conical intersection occurs[187,188]. That is, the reaction path does not proceed on a single energy surface but the formerly higher (π–π^*) doubly excited state intercepts with the ground state potential energy surface while the reaction proceeds. Thus, Bernardi and coworkers favoured a stepwise mechanism with a biradical intermediate, lying 18.9 kcal mol^{-1} lower in energy than the two separated silenes with a barrier for its formation of 5.3 kcal mol^{-1} (at CASSCF/DZ + d) (see Figure 2b). At this level of theory the transition state for the concerted reaction channel is 12.6 kcal mol^{-1} higher in energy than the reactants[187,188].

The head-to-head dimerization of $H_2C{=}SiH_2$ was also studied by both groups[186,188]. Schaefer and coworkers found the 1,2-disilacyclobutane to be less stable than the head-to-tail dimer, 1,3-disilacyclobutane by 19.8 kcal mol^{-1} (at SCF/DZ + d)[186]. Both theoretical studies predict for the head-to-head dimerization a stepwise reaction involving a carbon-centred biradical which is formed after the initial Si–Si bond formation. Bernardi and coworkers located a barrier of merely 2.5 kcal mol^{-1} for Si–Si bond formation to create the biradical[188]. Note that this barrier for the head-to-head dimerization is distinctively smaller than the barrier for the head-to-tail process (5.3 kcal mol^{-1}). This theoretical finding is totally at odds with the experimental experience that simple silenes including $H_2Si{=}CH_2$ dimerize to give the head-to-tail dimer[8]. Apparently, even more sophisticated computational methods are required to reproduce the correct course of these reactions.

a. Head-to-head dimerization. Head-to-head dimerization of silenes is the typical dimerization mode for silenes of the 'Brook' type, 'Apeloig–Ishikawa–Oehme' type and of 1-silaallenes. The reduced polarity of the Si=C double bond in these families of silenes seems to favour the head-to-head dimerization mechanism and to raise the barrier for the dimerization reaction.

Relatively little is known experimentally about the mechanism of the reaction. A widely accepted mechanism originally suggested by Brook and coworkers starts with the formation of a Si–Si bond, giving a carbon centred 1,4-biradical[86]. This 1,4-biradical then combines in a second step to the 1,2-disilacyclobutane. This mechanism is favoured by the calculations and is also corroborated by experiments: the relatively stable silene **149**

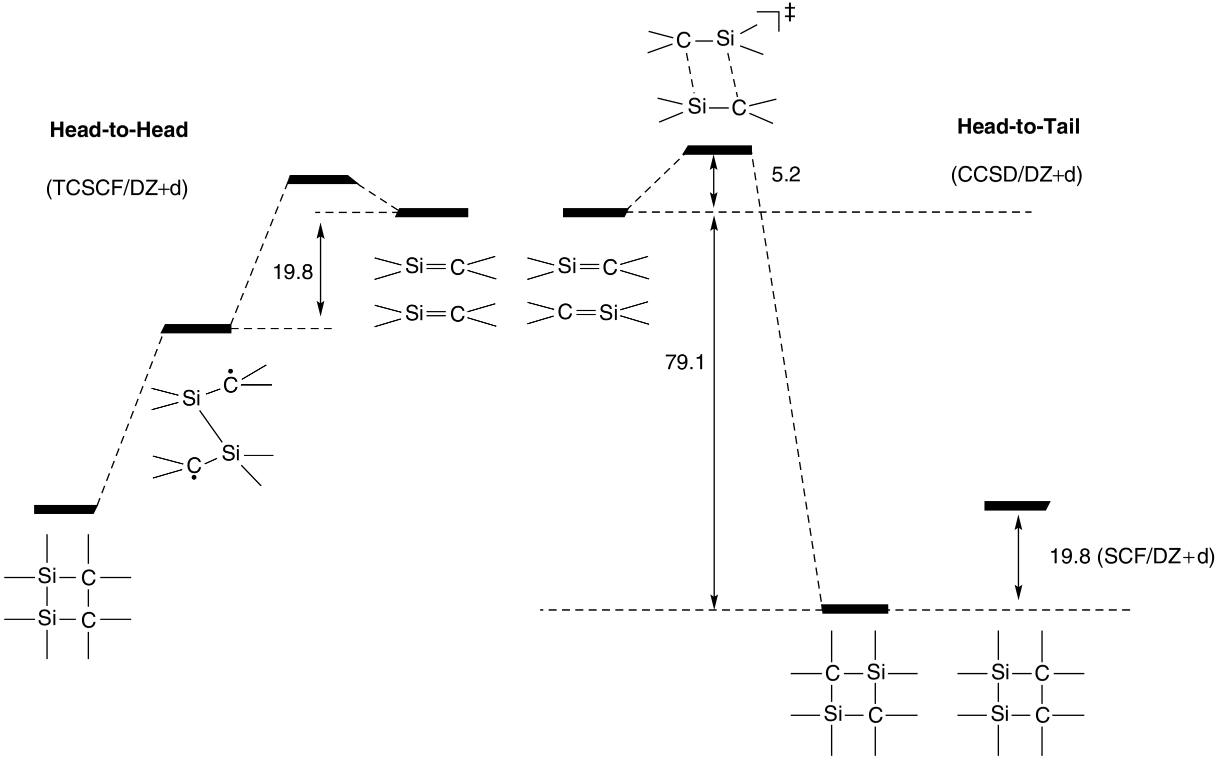

FIGURE 2a. Calculated reaction path for the head-to-head and head-to-tail dimerization of silene (at TCSCF/DZ + d or CCSD/DZ + d, respectively, relative energies in kcal mol^{-1})[186]

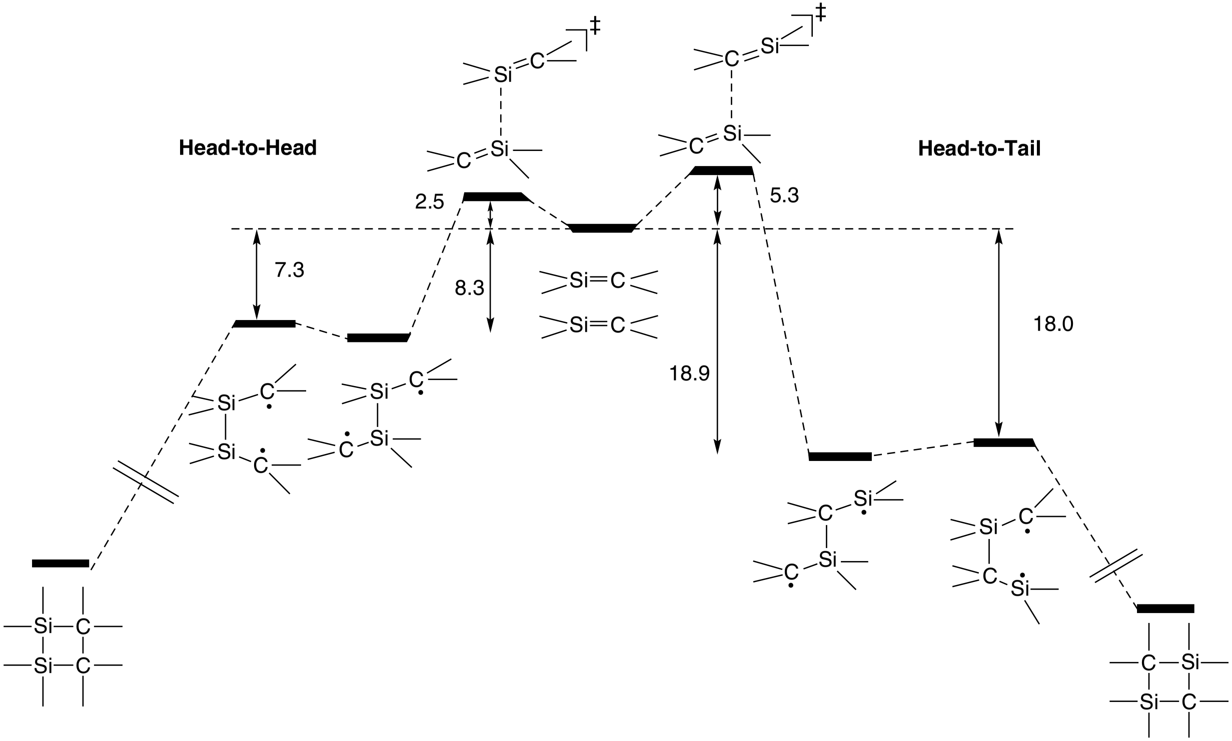

FIGURE 2b. Calculated reaction path for the head-to-head and head-to-tail dimerization of silene: biradical path (relative energies in kcal mol^{-1} at CASSCF/DZ + d)[187,188]

is in a temperature-sensitive equilibrium with its head-to-head dimer **362**, a solid whose crystal structure has been obtained (equation 99).

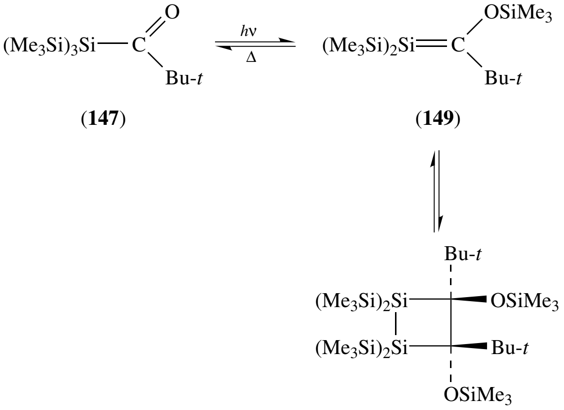

(**147**) (**149**)

(**362**)

(99)

The very long endocyclic C$-$C bond in **362** (1.66 Å) indicates already relatively facile homolytic C$-$C bond cleavage[38]. The solution of the dimer and the irradiated pivaloylacylsilane **147** gave rise to a strong broad ESR signal without a fine structure. Attempts to intercept a putative biradical like **363** failed, but they do not rule out the possible existence as an intermediate in low concentrations. A biradical species like **363** would also account for dimerization products isolated from other silenes (see below)[119].

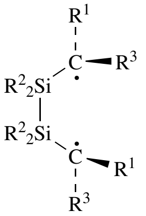

(**363**)

Clear evidence for radicals as intermediates in a somewhat unusual head-to-head dimerization of matrix isolated silacyclobutadiene **296** was given by Fink and coworkers[189]. Upon annealing of the 3-methylpentane matrix the unusual head-to-head dimer **364** is formed in 95% yield[190]. When the reaction was followed by ESR spectroscopy two distinctly different triplet biradicals have been identified[189]. This finding discards the originally suggested mechanism for the formation of **364**[190] and corroborates the reaction mode outlined in equation 100[163,189]. After initial formation of a Si$-$Si bond, the allylic biradical **365** undergoes an internal hydrogen atom abstraction to afford the new biradical species **366**. Ring closure of this ultimate biradical gives the observed dimer **364**.

Silenes, bearing an allylic hydrogen, frequently give 'linear' non-cyclic dimers, in which two silene molecules form a Si$-$Si bond[39,86,88,89,107,112]. This linear head-to-head dimer can be formed by intramolecular disproportionation of the initially formed biradical (path B in equation 101). Of course, an 'ene'-reaction (path A in equation 101) between two silenes would also account for the formation of the linear dimer. This dimerization mode is dominant for silenes of the type $(Me_3Si)_2Si{=}C(OSiMe_3)R^1$ and $(Me_3Si)_2Si{=}CR^2R^1$ (R^1 = alkyl). In some cases, such as for $(Me_3Si)_2Si{=}C(OSiMe_3)R^1$ (R^1 = *i*-Pr, CH_2Ph)[89] or $(Me_3Si)_2Si{=}CPhMe$[112], both the cyclic and linear dimer were formed in appreciable amounts. Table 5 gives more detailed data on the products formed in the head-to-head dimerization of silenes.

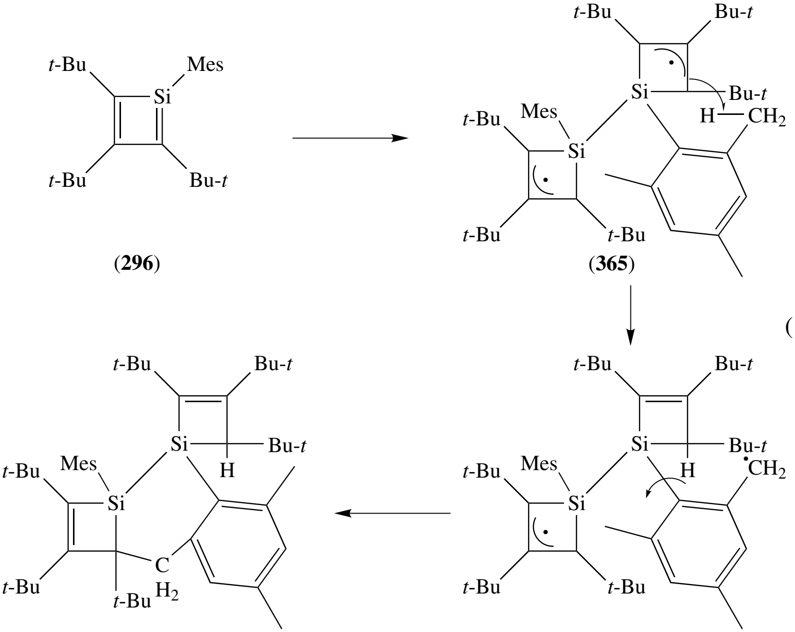

(**296**) (**365**)

(**364**) (**366**)

(100)

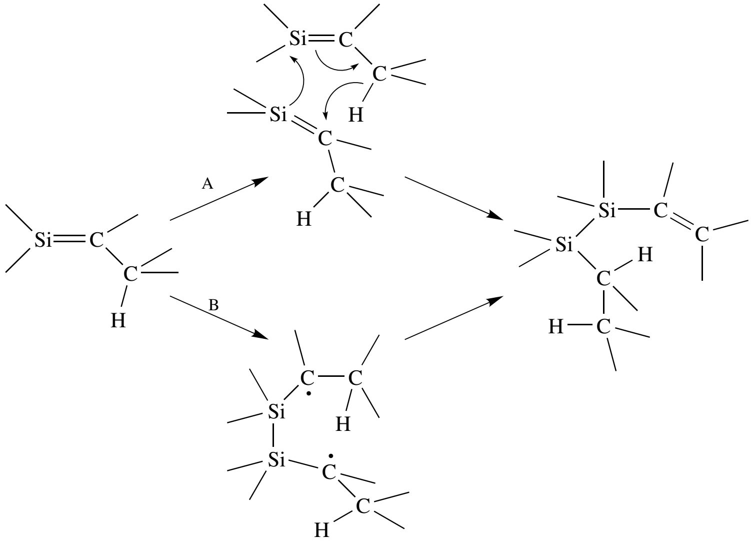

(101)

TABLE 5. Formation of different head-to-head dimers from silenes and silaallenes

Silene	Linear dimer	1,2-Sila-cyclobutane	Tetrahydro -2,3-disilanaphthalene	Remarks	References
$(Me_3Si)_2Si{=}C(OSiMe_3)R^1$					
$R^1 = Me$	exclusively				86,88
$R^1 = Et$	exclusively				89
$R^1 = i\text{-}Pr$	24%	76%			89
$R^1 = CH_2Ph$	20%	80%		see Ref. for details	89
$R^1 = t\text{-}Bu$		exclusively			86
$R^1 = Ph$		exclusively		equilibrium with silene	89
$R^1 = bco^a$		exclusively		equilibrium with silene	90
$R^1 = CF_3$		exclusively			92
$R^1 = Ar$		exclusively			92
$(Me_3Si)R^2Si{=}C(OSiMe_3)R^1$					
$R^1 = 1\text{-}Ad^b, R^2 = Me$		exclusively			90
$R^1 = t\text{-}Bu, R^2 = Ph$		exclusively			90
$R^1 = 1\text{-}Ad^b, R^2 = Ph$		exclusively			90
$Ph_2Si{=}C(OSiMe_3)1\text{-}Ad^b$		exclusively		equilibrium with silene	95
$(Me_3Si)_2Si{=}CMe_2$	exclusively				112
$(Me_3Si)_2Si{=}CPhMe$	67%	33%			112
$(Me_3Si)_2Si{=}cyhex^c$	exclusively				39

$(Me_3Si)_2Si{=}2\text{-}Ad$[d]		exclusively		reverts at 70°C	39
$(Me_2EtSi)(Me_3Si)Si{=}2\text{-}Ad$[d]		exclusively			191
$Ph_2Si{=}C{=}C(SiMe_3)_2$		exclusively			129, 192
$(Me_3Si)_2Si{=}CR^1R^2$					
R^1 = *p*-diethylaminophenyl, R^2 = Me	80%	20%			110
R^1 = 2, 4-di-*t*-Bu-phenyl, R^2 = H		88%	12%		109
R^1 = mesityl, R^2 = H			exclusively	MeLi, Et_2O, −78 °C	107, 117
		82%	18%	PhMgBr, THF, rt	108
R^1 = *t*-Bu, R^2 = H		exclusively			107
R^1 = Me, R^2 = Me	exclusively				104, 107
R^1 = 2,5-di-isopropylphenyl-, R^2 = H		46%	54%		118
R^1 = HC=CMe$_2$, R^2 = H		exclusively			106
R^1 = HC=CHPh, R^2 = H		exclusively			106
R^1 = Tip[e], R^2 = H		exclusively			105

[a] bco = bicyclooctyl.

[b] 1-Ad = 1-adamantyl.

[c] 2-cyhex = cyclohexenylidene.

[d] 2-Ad = 2-Adamantylidene

[e] Tip = 2,4,6-triisopropylphenyl.

Interestingly, dimerization of thermolytically generated **8** gives two products. The regular head-to-tail dimer **367** is formed preferentially, but minor amounts of the linear head-to-head dimer **368** could also be detected (equation 102)[20].

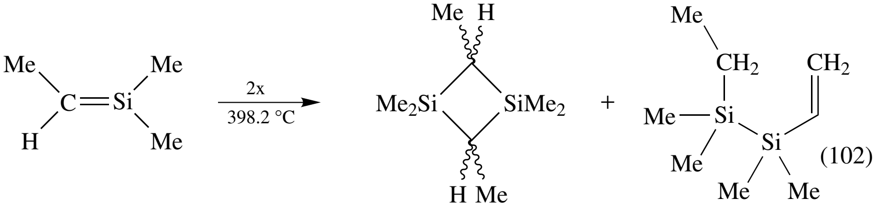

(102)

major minor

(**8**) (**367**) (**368**)

Conlin and coworkers have studied the kinetics of the dimerization of the silene **369** by laser flash photolysis. **369** gives in a clean reaction exclusively the linear dimer **370** (equation 103)[88]. Second-order kinetics were observed with a bimolecular rate constant of $k = 1.3 \times 10^7\ \text{M}^{-1}\,\text{s}^{-1}$. The temperature dependence of the rate constant k gave a preexponential factor $\log(\text{A/s}^{-1})$ of 7 ± 1 and an activation energy $E_\text{A} = 0.2 \pm 0.1$ kcal mol^{-1}. These activation parameters suggest a highly ordered transition state requiring only small enthalpic changes for reaction[88]. This low A value and the small E_A are more in accord with a concerted 'ene'-reaction than with an intermediate biradical. However, more experimental data are needed in order to draw more definite conclusions.

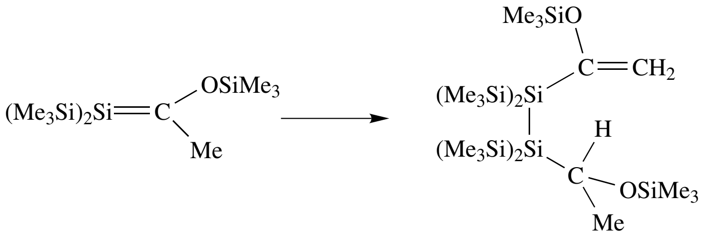

(103)

(**369**) (**370**)

The surprising product distribution of the dimerization of some silenes having a bulky aryl group at the doubly bonded carbon studied by Oehme and his group[107–109,117,118] might be rationalized by the occurrence of biradicaloid intermediates. Oehme and coworkers found that, for example, mesitylsilene **371** dimerizes in a kinetically controlled reaction to a formal head-to-head [4 + 2] cycloadduct, the tetrahydro-2,3-disilanaphthalene **372**[117]. **372** gradually decomposes to the thermodynamically more stable 1,2-disilacyclobutane **373** (equation 104)[108]. For other aryl groups [R = bis(2,4-di-*t*-Bu)phenyl[109], R = bis(2,5-di-*i*-Pr)phenyl[107,118]] both types of dimers have been isolated directly from the reaction mixture. In all cases the 2,3-disilanaphthalene could be converted by heating to the thermodynamically more stable 1,2-disilacyclobutane. An intermediate carbon-centred, 1,4-benzyl-type biradical **374** can account for both types of dimers[109]. 1,4-Recombination of **374** affords the 1,2-disilacyclobutane **373**.

Alternatively, the reaction may proceed via 1,6-ring closure giving the isolated 2,3-disilanaphthalene **372**[109]. It should be mentioned, however, that under the reaction conditions it is possible that silyl lithium compound **375** formed from the precursor of the silene **376** (obtained from metalation of **377**) by a 1,3-trimethylsilyl shift adds to the intermediate silene **371** and that subsequent ring closure with elimination of lithium silanolate gives rise to the observed products **372** and **373** (equation 105).

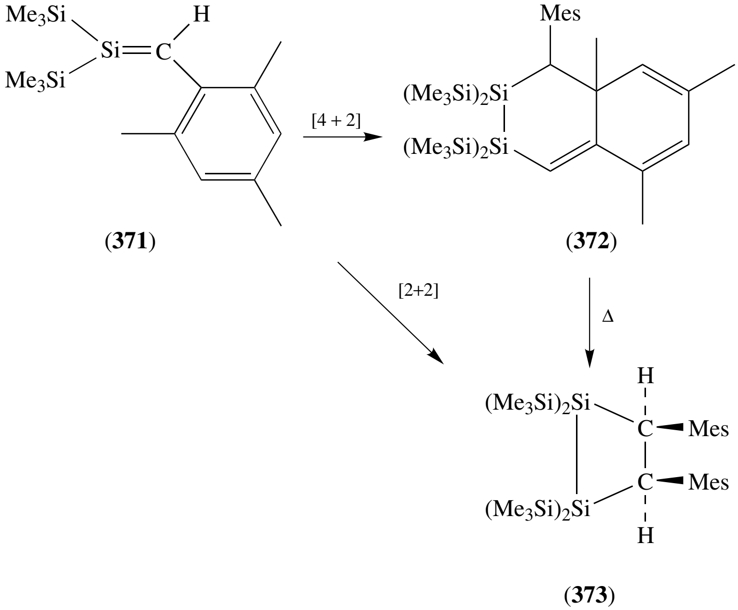

(104)

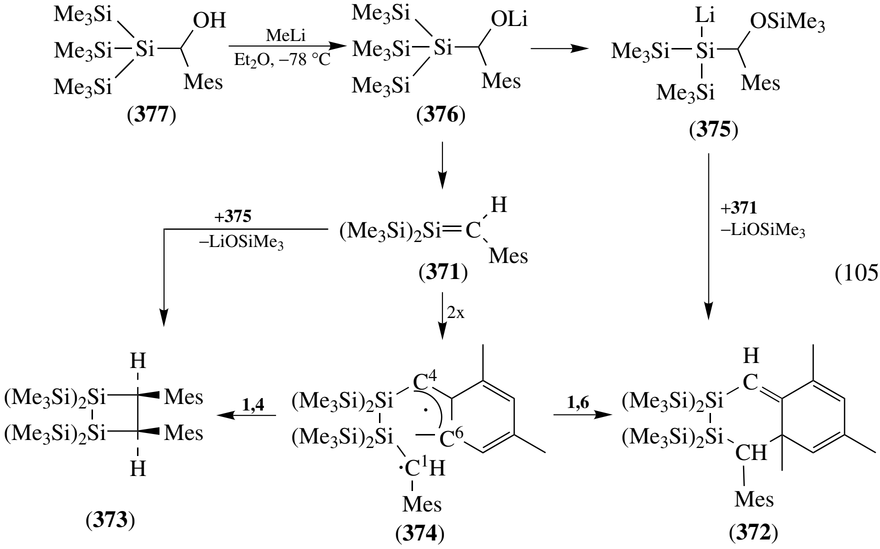

(105)

Head-to-head dimers with bulky substituents at the C−C bond tend to be thermolabile and they can be used as convenient sources for relatively stable or transient silenes. Examples are the already-mentioned dimer of the relatively stable silene **149**[86] and the 1,2-disilacyclobutane **164**, which liberates the adamantylidene silene **165** smoothly upon heating to 70 °C in benzene (equation 106)[39].

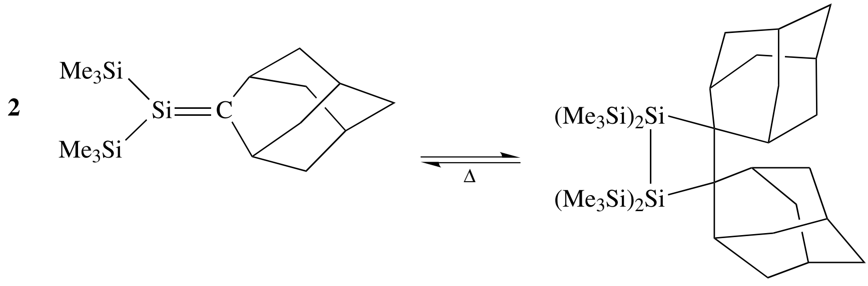

(**165**) (**164**)

(106)

In contrast, the cleavage of the 1,2-disilacyclobutane **378** needs more drastic conditions (250 °C) and yields the thermodynamically more stable linear dimer **379**. It was suggested that this reaction proceeds via the 1,4 biradical **380** (equation 107)[112].

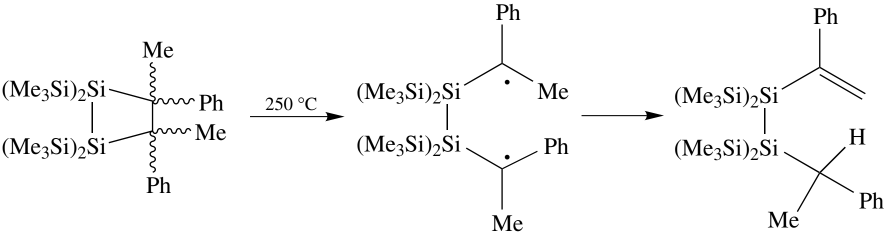

(**378**) (**380**) (**379**)

(107)

Obviously, the interplay between subtle steric and electronic effects determines the final product of the dimerization of 'Apeloig–Ishikawa–Oehme' silenes. Thus, the *p*-dimethylaminophenyl-substituted silene **381** gives the expected dimerization products, the 1,2-disilacyclobutane **382** and the linear dimer **383**, in a relative ratio of 1 : 4 (equation 108)[110]. In sharp contrast the very similar *o*-dimethylaminophenyl-substituted silene **384** gives in 63% yield a 1 : 2 mixture of the *E*/*Z*-1,3-disilacyclobutane **385** (equation 109)[110]. It was suggested that this peculiar regiospecific outcome of the dimerization of **384** results from a directive *intermolecular* donor–acceptor interaction between the *ortho*-dimethylamino group and the Si=C double bond[110]. Clearly, more work has to be done in order to understand the small effects which determine the dimerization behaviour of 'Apeloig–Ishikawa–Oehme' silenes[110].

The dimerization of silatrienes **216** obtained from photolysis of disilanylbenzenes **210** was studied by Ishikawa and coworkers[193,194]. A head-to-head dimerization takes place under participation of the vinylologous double bonds to give the isomers **386a** and **386b**.

A ring-opened isomer **387** is obtained through thermolysis of **386b** (equation 110).

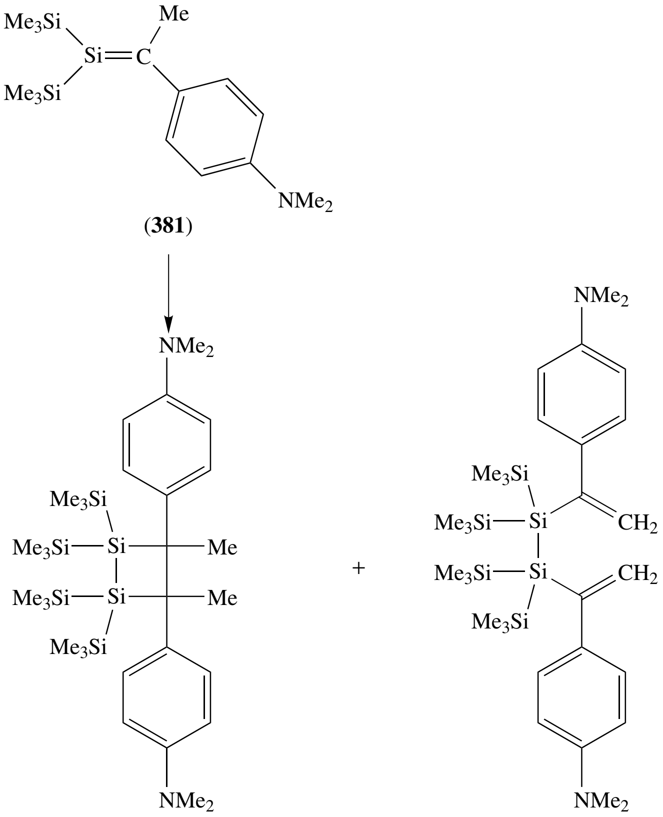

(**381**)

(**382**) (**383**)

(108)

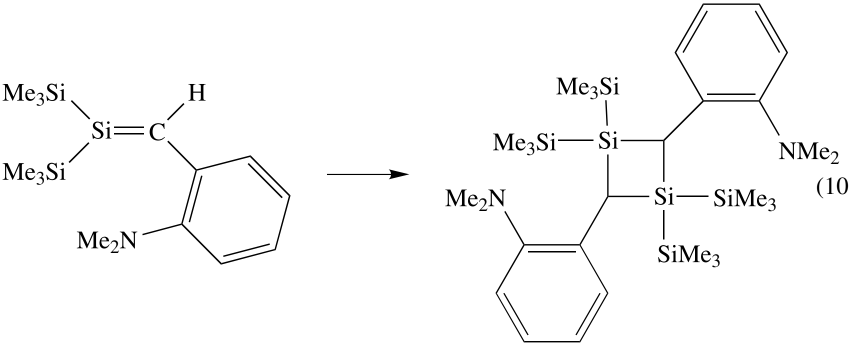

(**384**) (**385**)

(109)

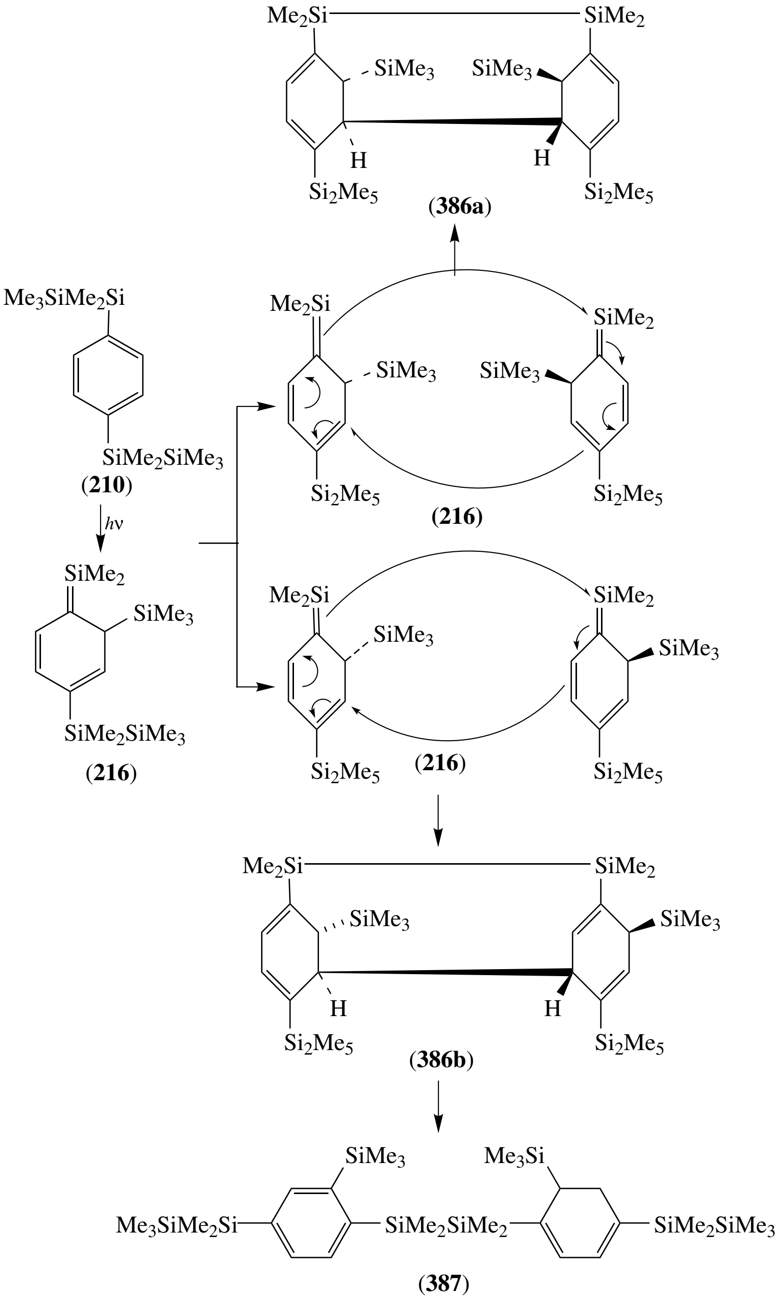
Me2Si
SiMe2
SiMe3
SiMe3
H
H
Si2Me5
Si2Me5
(386a)
Me3SiMe2Si
SiMe2SiMe3
(210)
hν
SiMe2
SiMe3
SiMe2SiMe3
(216)
Me2Si
SiMe2
SiMe3
SiMe3
Si2Me5
Si2Me5
(216)
Me2Si
SiMe2
SiMe3
SiMe3
Si2Me5
Si2Me5
(216)
Me2Si
SiMe2
SiMe3
SiMe3
H
H
Si2Me5
Si2Me5
(386b)
SiMe3
Me3Si
Me3SiMe2Si
SiMe2SiMe2
SiMe2SiMe3
(387)

(110)

b. Head-to-tail dimerization. The head-to-tail dimerization is found for 'Wiberg'-type[78] and neopentyl silenes[79,80].

Heating the azasiletane **95b** in the absence of trapping reagents for **92** gives **388**, the head-to-tail dimer of **92** (equation 111)[72,73]. This dimer is even formed at −100 °C when **92** is synthesized via salt elimination of $Me_2SiF{-}CLi(SiMe_3)_2$.

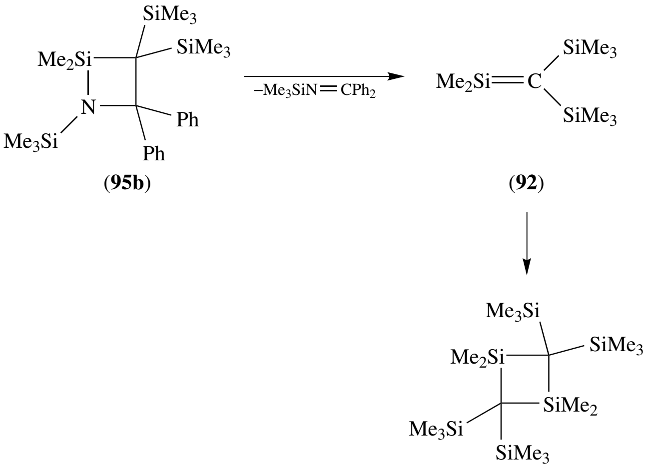

(**95b**) (**92**)

(111)

(**388**)

The mode of dimerization of silaacrylates **389** depends on the steric bulk of the substituents[195,196]. Large substituents R prevent formation of dimers **390** and lead to intramolecular [2 + 2] cycloaddition to give 1-oxa-2-silacyclobut-3-enes **391** (equation 112). Smaller substituents R allow head-to-tail dimerization to the eight-membered ring compound **390**.

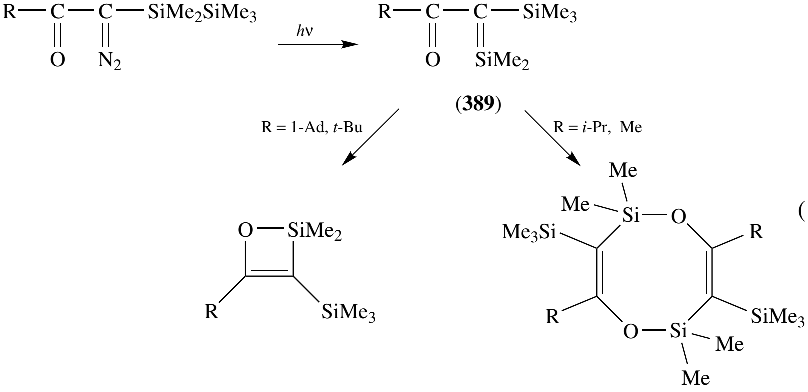

(**389**)

(112)

(**391**) (**390**)

For a central hexamethyltrisilanyl unit in the bisdiazomethyloligosilane **327** the silenes resulting from photolytic decomposition give a formal head-to-tail dimer **329** and a head-to-head dimer **330** (equation 80)[169].

3. Nucleophilic additions

Nucleophiles easily attack the Si=C double bond at the silicon. Complexes between diethyl ether and the parent silene $H_2Si{=}CH_2$ have been detected by low temperature NMR[27] and stable silenes of the 'Wiberg'-type form adducts with THF, triethylamine, pyridine and even with the fluoride anion[83,84,197]. These complexes have been structurally characterized by X-ray structure analysis and details are presented in Section I.C.1. Similarly, the initial step of the alcohol addition to silenes is the formation of a short-lived complex between the silene and the attacking alcohol[198], as is evident from the measured negative activation energy in the reaction of simple silenes with alcohols[35,34,199].

a. Reaction with alcohols. In the presence of trapping reagents of the general type A−H (O−H: water, alcohols, carbonic acids; S−H: thiols; N−H: amines, imines) addition across the Si=C bond takes place. The general reaction is shown for a 'Wiberg'-type silene in equation 113[62]

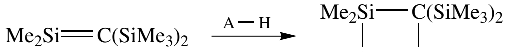

$$\underset{(\mathbf{92})}{\mathrm{Me_2Si{=}C(SiMe_3)_2}} \xrightarrow{\mathrm{A-H}} \underset{\mathrm{A}}{\mathrm{Me_2Si}}-\underset{\mathrm{H}}{\mathrm{C(SiMe_3)_2}} \qquad (113)$$

The addition reaction of alcohols to silenes is a strictly regiospecific process; the OR group in the product is always attached to the silicon. The reaction is of special importance since silenes are easily trapped by reagents like methanol and *t*-butanol, and isolation of the adducts is normally taken as evidence for an intermediate silene. Furthermore, the alcohol addition to silenes is the prototypical reaction for the 1,2-addition of polar bonds across the Si=C double bond. A complete account on the alcohol addition to silenes, including the most recent mechanistic implications, is given in the chapter by Sakurai. We will therefore give only a brief survey of the reactivity of several families of silenes towards alcohols.

The addition of methanol to Brook-type silenes at room temperature using an excess of methanol was found to be a non-stereospecific process, as is evident from its stereochemical outcome. Methanolysis of a 1 : 4 mixture of *E*/*Z*-**392** gives a mixture of two diastereomeric methanol adducts *SS*- and *RS*-**393** in a relative ratio of 2.5 : 1 (equation 114)[95].

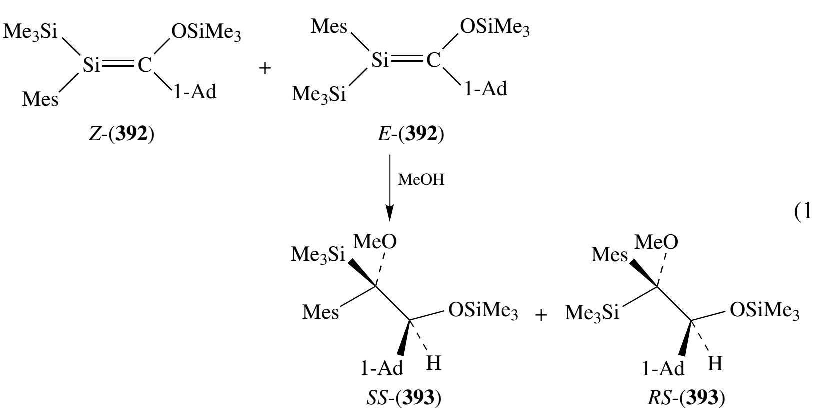

(114)

Fink and coworkers showed, however, that the ethanol addition to the sterically highly hindered silacyclobutadiene **296** is a stereospecific *syn* addition process[163]. When **296** is photolytically generated from the silylene **295** in the presence of ethanol, only the *syn* adduct *E*-**394** is formed (equation 115). Upon further photolysis the silacyclobutene **394** undergoes a photoisomerization process involving photolytic ring opening of *E*-**394** to give silabutadiene *EZ*-**395**, followed by a thermal ring closure to *Z*-**394** with the opposite stereochemistry[163]; a second cycle equilibrates the isomers *E*/*Z*-**394** via silabutadiene *ZZ*-**395** (equation 116).

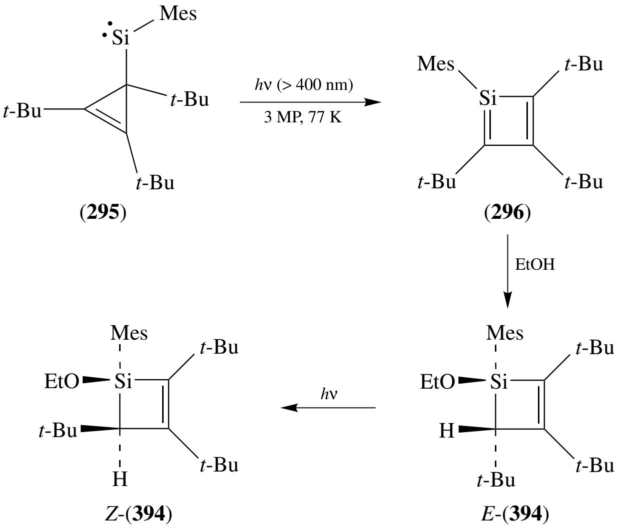

(115)

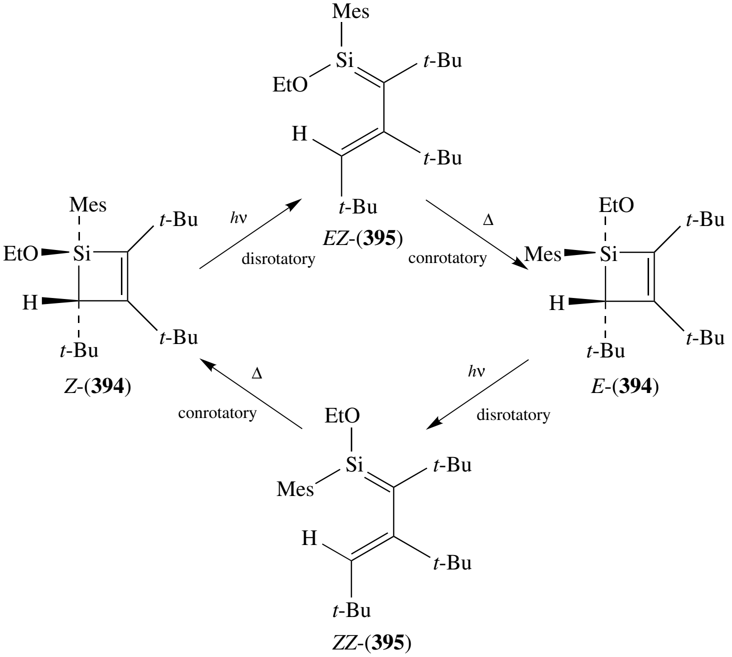

(116)

In agreement, the thermolytically generated silacyclobutadiene **341** reacts with *t*-butanol stereospecifically, yielding the regioisomers **339** and **340** (equation 84)[119].

The stereospecificity of methanol addition to neopentylsilenes has been investigated by Jones and Bates[68]. The mild thermal retro-Diels–Alder reaction (at *ca* 200 °C) of *E* and *Z* anthracene [4 + 2] cycloadducts **110** liberates stereospecifically the corresponding silenes **111**, which are trapped by methanol. The ratio of the diastereomeric products **396a/396b** coincides with the *E*/*Z* ratio of the precursors **110** (equation 117). In photochemical reactions of similar silene precursors, alcohols were used also to probe the decomposition mechanism[69].

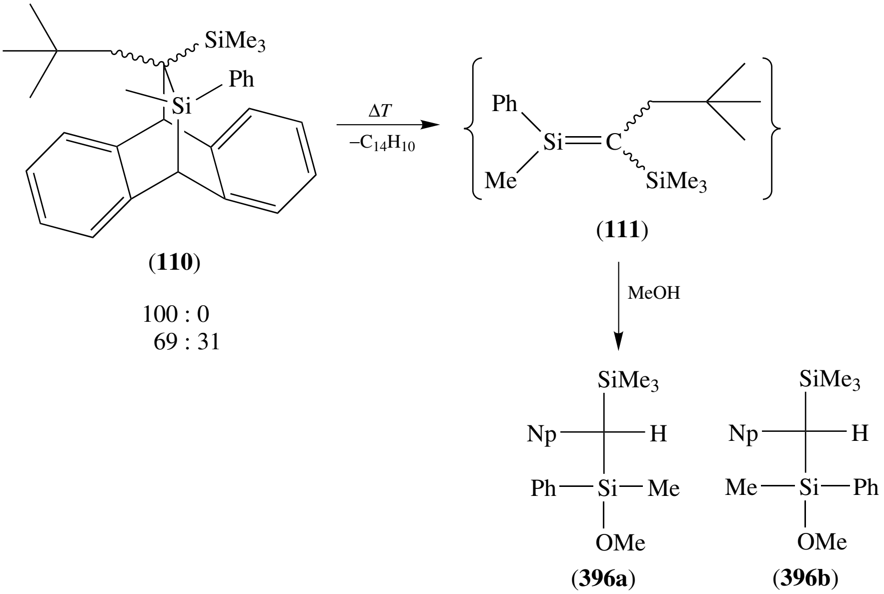

(**110**)

100 : 0
69 : 31

(**111**)

(**396a**) (**396b**)

100 : 0
69 : 31

Np: neopentyl

(117)

An alternative mechanism to explain the stereospecificity has been suggested in the review by Brook and Brook[9].

The most widely accepted and applicable mechanism for the alcohol addition was suggested by Kira, Maruyama and Sakurai[198]. They found that the ratio of the *syn* adduct **397** to the *anti* adduct **398** obtained by the reaction of the photolytically generated silene **253** is dependent on the alcohol concentration and on its acidity. Thus, the **397/398** ratio increased in the order MeOH $<$ *n*-PrOH $<$ *i*-PrOH $\ll$ *t*-BuOH. *t*-Butanol gave only *syn* adduct **397**[198]. At high concentrations of the alcohol the *anti* isomer **398** is preferentially formed. This is compatible with an initial formation of a complex **399** between the silene and the alcohol. Intramolecular proton migration in **399** (route b) competes with the intermolecular proton transfer from a second alcohol to **399** (route a). These two processes give the *syn* and *anti* isomers, **397** and **398**, respectively (equation 118). Higher concentrations of alcohol favour process (a) and higher acidity of the protonated alcohol and lower acidity of the alcohol facilitate the intramolecular proton transfer (b)[198]. Further detailed mechanistic studies were conducted by Leigh and coworkers[25,34,200] and these are summarized in the chapter by Sakurai.

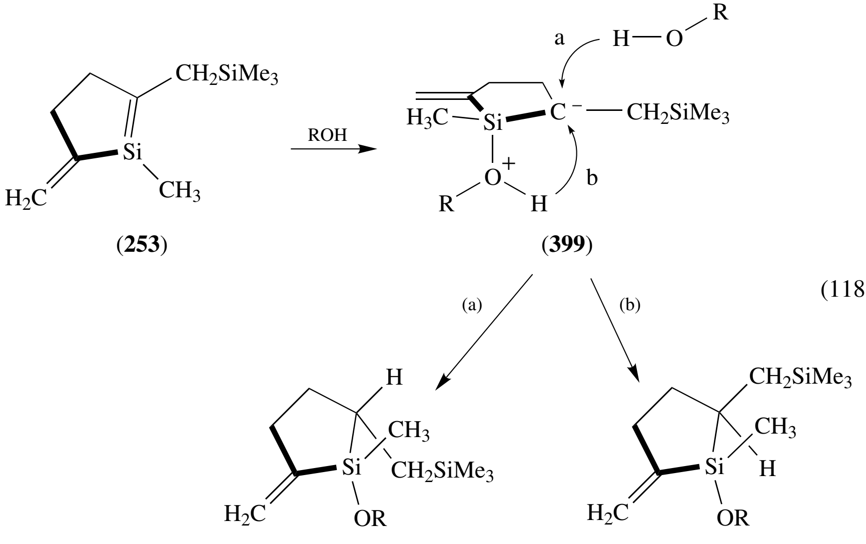

(**253**) (**399**) (**398**) (**397**)

(118)

The competitive migration to either a vinyl or phenyl group has been investigated by Ishikawa and coworkers[133]. While with traps other than methanol there is proof for the intermediacy of both silenes **238** and **239**, formed from **237** (of equation 53), just one product, i.e., **400**, is found for the reaction with the alcohol (equation 119).

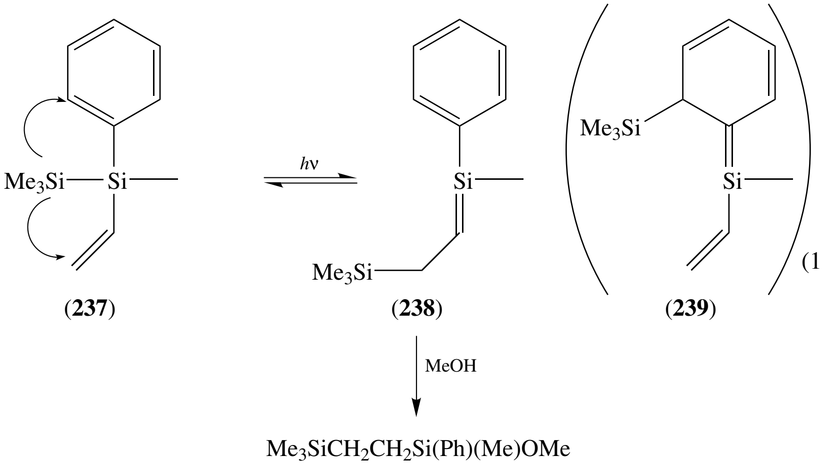

(**237**) (**238**) (**239**)

(119)

$Me_3SiCH_2CH_2Si(Ph)(Me)OMe$

(**400**)

With the dihydropyranyl-substituted phenyldisilane **240** Ishikawa and coworkers found the formation of both possible types of silenes **241** and **242**; they were formed and trapped by methanol giving adducts **401**–**403** (equation 120)[134].

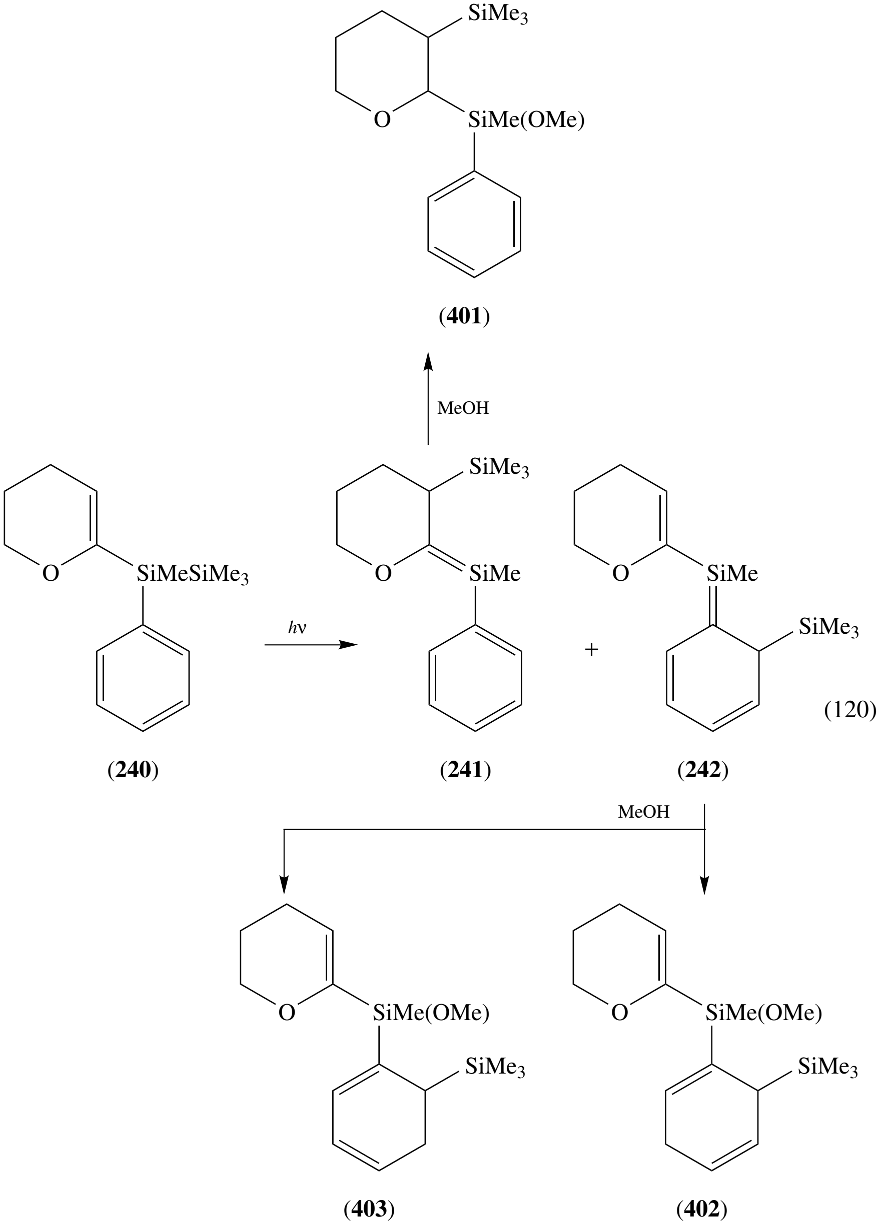

(120)

b. Reaction with alkoxysilanes. Polar single bond species, e.g., A−EMe$_3$ are also suitable for trapping silenes as long as one of the atoms has a free electron pair (E = Si, A = OR, NR$_2$, N=CPh$_2$; E = Ge, Sn, A = Cl). The general scheme is shown for the 'Wiberg'-type silene **92** (equation 121)[62].

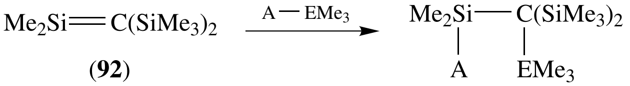

$$\mathrm{Me_2Si{=}C(SiMe_3)_2} \xrightarrow{\mathrm{A-EMe_3}} \mathrm{Me_2Si(A){-}C(SiMe_3)_2(EMe_3)}$$

(**92**)

(121)

Alkoxysilanes are frequently used as scavenger reagents for silenes. They add regiospecifically to the Si=C bond. In the case of silacyclobutadiene **296** the reaction was shown to be also stereospecific. Thus *Z*-**404** is the sole product of the addition of trimethylsilyl methyl ether (TMSOMe) to **296** (equation 122)[163]. Characteristically 'Brook'-type silenes do not react with alkoxysilanes like TMSOMe.

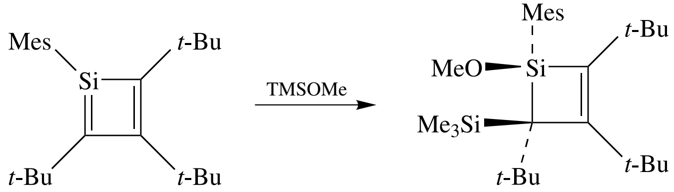

(**296**) *Z*-(**404**)

(122)

c. Reaction with organometallic reagents. In the course of the sila-Peterson reaction a nucleophilic addition of an organometallic reagent to the incipient silenes is often observed. Organolithium reagents[63,103,104,107,113,117,201], silyllithium reagents[103], lithium trimethylsilanolate[103,113,116], and Grignard reagents[103,105,116] add regiospecifically across the Si=C double bond. In each case the anionic part of the reagent adds to the silicon, yielding a carbanion which can be protonated, deuteriated by hydrolysis, or may rearrange prior to hydrolysis (equation 123). The addition of organometallic reagents to 'Brook-type' silenes is complicated by subsequent reactions leading to new silenes[116] (see Section I.A.5.d). Addition of silyl anions gives polysila-anions as final products which result from a silyl shift in the intermediate polysilyl carbanion[103] (see Section I.A.5.a for an example). More examples are summarized in Table 6.

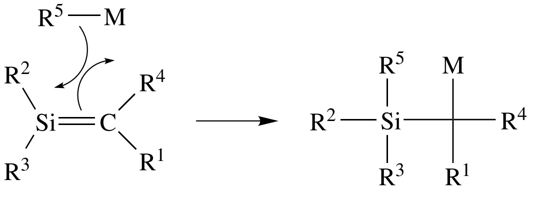

(123)

Addition reactions of lithium organyls have been investigated for **97**[63,201]. The reaction is not a nucleophilic substitution of Br$^-$ by R$^-$ in **97**•LiBr, but rather a two-step mechanism with an initial dissociation via **97** (equation 124). This was proven by the addition of the very efficient silene trap *t*-Bu$_2$MeSiN$_3$, that competes with the lithium organyl for the silene.

TABLE 6. Reactions of silenes with organometallic reagents

Silene	Organometallic reagent	Product after hydrolysis	Remarks	References
$(Me_3Si)_2Si{=}CPh_2$	PhLi	$(Me_3Si)_2PhSi{-}CHPh_2$		113
$(Me_3Si)_2Si{=}CPh_2$	Me_3SiOLi	$(Me_3Si)_2(Me_3SiO)Si{-}CHPh_2$		113
$Me_3SiMeSi{=}CSiMe_3Ad$-1	MeMgBr	$Me_3SiMe_2Si{-}CH(SiMe_3)Ad$-1		103
$(t\text{-}Bu)_2Si{=}CHCH_2Bu\text{-}t$	t-BuLi	$(t\text{-}Bu)_3Si{-}CH{=}CHBu\text{-}t$	product after LiH elimination	199
$(Me_3Si)_2Si{=}CHBu\text{-}t$	PhLi	$(Me_3Si)_2PhSi{-}CH_2Bu\text{-}t$		104, 200
$(Me_3Si)_2Si{=}CHMes$	PhLi	$(Me_3Si)_2PhSi{-}CH_2Mes$		117, 200
$(Me_3Si)_2Si{=}CHMes$	MeLi	$(Me_3Si)_2MeSi{-}CH_2Mes$		107, 200
$(Me_3Si)_2Si{=}CHTip$	$(Me_3Si)_3SiMgBr$	$(Me_3Si)_3Si(Me_3Si)_2Si{-}CH_2Tip$		105
$(Me_3Si)_2Si{=}CMe_2$	$(Me_3Si)_3SiLi$	$H(Me_3Si)_2Si(Me_3Si)_2Si{-}CMe_2SiMe_3$	product after 1,3-silyl shift	103
$(Me_3Si)_2Si{=}C(OSiMe_3)Ad$-1	Me_3SiOLi	$Me_3Si(Me_3SiO)_2Si{-}C(1\text{-}Ad)(SiMe_3)H$	formation of a new silene	116
$(Me_3Si)_2Si{=}C(OSiMe_3)$ Ad-1	MeMgBr	$Me_3SiMe_2Si{-}C(1\text{-}Ad)(SiMe_3)H$	formation of a new silene	116
$Ph_2Si{=}C(SiMe_3)_2$	PhLi	$Ph_3Si{-}C(SiMe_3)_2H$		63, 201
$Ph_2Si{=}C(SiMe_3)_2$	t-BuLi	$HPh_2Si{-}C(SiMe_3)_2H$	elimination of isobutene	63, 201

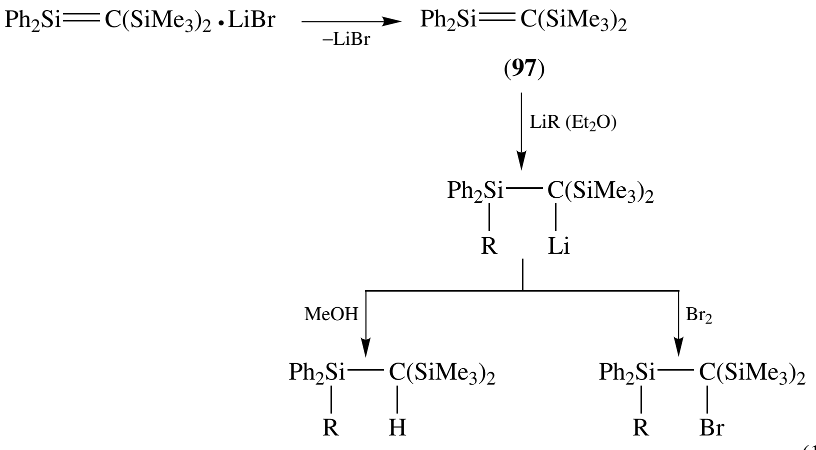

(124)

The stable adamantylsilene **150** was found to react with the phosphorous ylide $Ph_3P^+CH_2^-$ to form the zwitterion **405** which cyclizes to the silacyclopropane **406**, as shown by NMR spectroscopy and by derivatization with methanol or acetophenone (equation 125)[202].

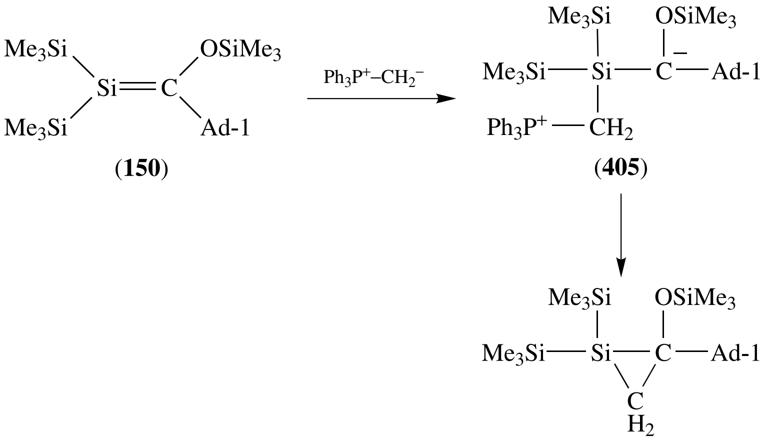

(**406**)

(125)

An interesting addition reaction to silenes was recently described by Oehme and coworkers. They found that at high concentrations of LiBr the dimerization of the transient silene **371** yields 33% of the head-to-head dimer **373** and the head-to-tail dimer **407** in a 1 : 5.6 relative ratio[108]. The formation of the unexpected dimer **407** was rationalized by the addition of LiBr to the Si=C bond and intermolecular cyclization of the α-lithiosilyl bromide **408** or its reaction with the transient silene **371** with subsequent cyclization to the 1,3-disilacyclobutane **407** (equation 126)[108].

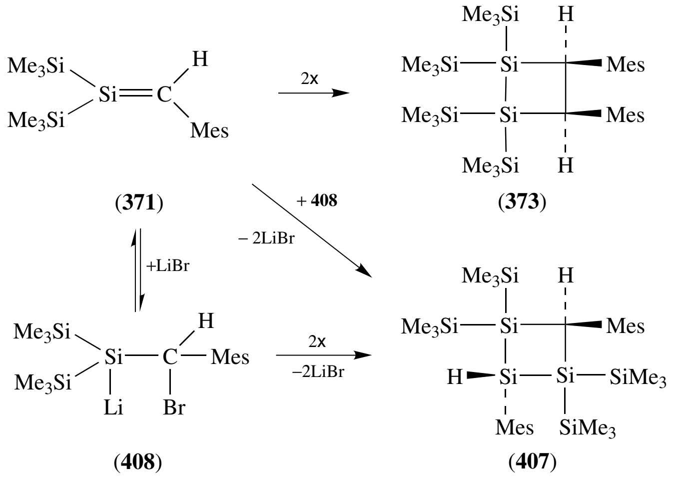

(126)

4. Cycloaddition reactions

In this section we will summarize bimolecular reactions of silenes with alkenes, alkynes and dienes which might be regarded nominally as cycloaddition reactions.

It is well accepted that silenes undergo concerted cycloadditions of various types[8]. Most silenes readily form $[4\pi + 2\pi]$ cycloadducts with dienes, although products arising from the 'ene' reaction are often present and may occasionally even be the major product. In contrast to carbon chemistry $[2\pi + 2\pi]$ cycloadditions compete with the above processes. Silenes react even with alkenes, giving products arising from a formal $[2\pi + 2\pi]$ cycloaddition, provided no allylic hydrogen is present. The presence of an allylic hydrogen results normally in the products of an 'ene' reaction. The [4+2] and 'ene' reactions of silenes are believed to be concerted processes, but the [2 + 2] addition reaction is often considered to be a stepwise process involving 1,4-biradicals or 1,4-zwitterionic species. It should be pointed out, however, that true mechanistic studies, both experimental and theoretical, on the cycloadditions of silenes are very rare[54,88], and most of the mechanistic conclusions are based on product studies.

It is evident that the relative proportions of products from [2 + 2], [4 + 2] and 'ene' reactions depend strongly on the polarity of the Si=C bond, on the polarization of the frontier orbitals and on steric factors both in the silenes and in the reactant. Therefore, we will first discuss cycloaddition reactions of silenes without separating them into subclasses like [2+2] or [2+4] cycloadditions, but we will concentrate on the cycloaddition behaviour of several classes of silenes towards alkenes, alkynes and dienes. We will then discuss some special cycloaddition reactions in subsequent sub-sections.

a. Wiberg-type silenes. i. $Me_2Si{=}C(SiMe_3)_2$ **92**. One of the greatest assets of Wiberg's silenes is that they may be stored as cycloadducts of, e.g., $Ph_2C{=}N{-}SiMe_3$, from which they are simply regenerated by heating (*vide supra*). The liberated silenes can then be studied in detail. $Me_2Si{=}C(SiMe_3)_2$ **(92)** has been investigated most closely[72–76,83,84,97] and the [2 + 2] imine adduct **95b** has been mostly used as its source.

α. [2+2] Cycloaddition reactions. The polar double bond of silene **92** can react in a [2 + 2] cycloaddition reaction with systems of the general formula a=b[62]. The cycloadducts **95a** and **95b** from $Ph_2C{=}Y$ ($Y = O$, $N{-}SiMe_3$) have already been mentioned in Section I.A.1. Their formation is reversible, and the concomitant formation of [2 + 4] cycloadducts is described below. With C=C bonds, [2 + 2] adducts **409** are formed when an electron-donating substituent is bound to the π-system as in vinyl ethers or *cis*-1-propenylethene (equation 127)

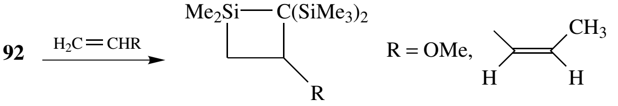

(409)

(127)

The formation of [2 + 2] cycloaddition products obviously occurs in a stepwise fashion via an adduct of the Lewis acid **92** and the Lewis base a=b. Kinetic data, investigation of isotope effects and the isolation of **92**•donor adducts support this assumption.

β. [2 + 4] Cycloaddition and ene reactions. Dienes >C=C–C=C< such as buta-1,3-diene, isoprene, 2,3-dimethylbuta-1,3-diene, *trans*-piperylene, cyclopentadiene or anthracene react with **92** in Diels–Alder fashion to give [2 + 4] cycloadducts **410** (equation 128)[62]. Ene products **411** are formed additionally when the relative reaction rates for the [2 + 4] cycloaddition reaction and the ene reaction are comparable (e.g. for isoprene and 2,3-dimethyl-1,3-butadiene); Alkenes with allylic hydrogen (propene, 2-butene, isobutene) give ene products see equation 129.

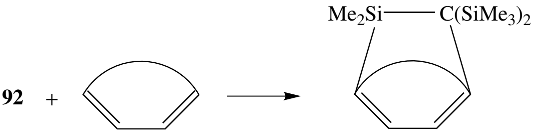

(410)

(128)

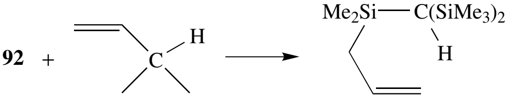

(411)

(129)

A one-step mechanism is proposed for the formation of the [2 + 4] cycloadducts and the ene products[62], since the sila-Diels–Alder and sila-ene reactions are regio- and stereo-selective. The stereospecifity of Diels–Alder reactions of **92** with hexadienes has been investigated[203], as well as the regio- and stereoselectivity and the relative reaction rates of ene reactions[176] and [2 + 4] cycloadditions[204]. A selection of relative reaction rates of **92** with trapping reagents is given in Table 7.

With heterodienes, like $Ph_2C{=}Y$ ($Y = O$, $N{-}SiMe_3$), [2 + 2] as well as [2 + 4] cycloadducts **95** and **96**, respectively, are obtained from the reaction with **92**.

When $Me_2SiX{-}CLi(SiMe_3)_2$ [$X = F$, Br, $(PhO)_2PO_2$] is decomposed in the presence of benzophenone, only the [2 + 4] cycloadduct **96a** is formed[60]. Similarly to **96b**, **96a** can be rearranged thermally to the [2 + 2] cycloadduct **95a** in quantitative yield; **95a** is the first example of an isolated oxasilacyclobutane[59]. The rearrangement occurs through the intermediate formation of **92**. This is supported by thermolysis reactions of **96a/95a** in the presence of trapping reagents, since the trapping products are essentially the same as those obtained from other sources of **92**.

TABLE 7. Relative rates of $Me_2Si{=}C(SiMe_3)_2$ **(92)** with trapping reagents[a]

Trapping reagent	Relative rate	Reaction type
i-$PrNH_2$	23000	addition
MeOH	21000	addition
i-PrOH	10000	addition
$Ph_2C{=}O$	3000	[2 + 2]
t-BuN_3	230	[2 + 3]
CpH[b]	2.9	[2 + 4]
Propene	2.9	ene
Buta-1,3-diene	1	[2 + 4]

[a] For a comprehensive compilation see References 62 and 176.
[b] Cyclopentadiene.

ii. [2 + 3] Cycloaddition reactions. Azides R—N_3 (R = Me_3C, Me_3Si, *t*-Bu_2MeSi, *t*-Bu_3Si) react with **92** (obtained from **95b** in Et_2O at 100 °C) to give [2+3] cycloadducts **412a**[62], which are, however, not stable under the reaction conditions. They decompose to the diazomethanes **413a** by rearrangement, or to $(Me_3Si)_2C{=}N{=}N$ and the silanimines **414a**. The latter can be trapped, e.g., by excess azide to give the addition product **415a** and/or the dihydrotetrazoles **344a** (see also Section III) (equation 130).

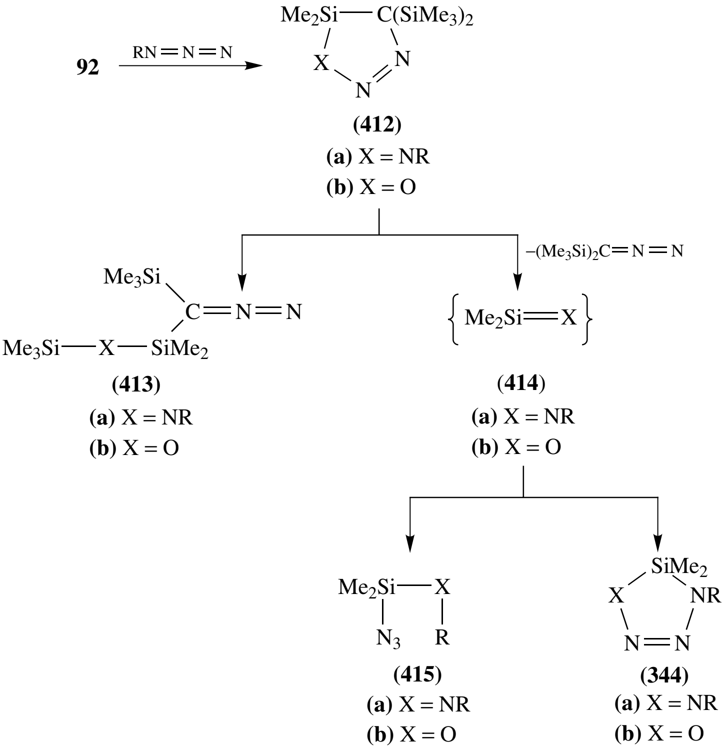

(130)

An analogous reaction is observed with N_2O: the [2 + 3] cycloadduct **412b** rearranges to **413b**, or, with elimination of $(Me_3Si)_2CN_2$, to the silanone **414b**. In the presence of Me_3SiCl, the insertion product of **414b**, $Me_2SiCl{-}OSiMe_3$ is obtained. No [2+3] adduct is formed with $(Me_3Si)_2CN_2$.

iii. $Ph_2Si{=}C(SiMe_3)_2$ **97**. The replacement of the two methyl groups at the silene silicon atom in **92** by two phenyl groups to give silene **97** is not accompanied by a profound change in silene reactivity[63,64]. The slight differences can be attributed to an electronically enhanced double bond polarity (i.e. a greater Lewis acidity of the silene silicon atom) and to a sterically greater shielding of the double bond. The differences in reactivity between **92** and **97** are therefore due to (a) more stable donor adducts of **97** due to the greater Lewis acidity, and (b) changes in the relative reactivity of the trapping reagents.

iv. t-$Bu_2Si{=}C(SiMe_3)_2$ **(104)**, *$Me_2Si{=}C(SiMe_3)[SiMe(t\text{-}Bu)_2]$* **(104a)** *and* **104a**•*donor*. By LiF elimination from *t*-$Bu_2SiF{-}CLi(SiMe_3)_2$ only **104a** instead of **104** is isolated[67]. With benzophenone, silene **104a** (from **104a**•THF) forms a [2+4] cycloadduct **416** and a [2+2] cycloadduct **417** at −78 °C. With increasing temperature **416** transforms to **417**, and **417** more slowly transforms to the [2+4] cycloadduct **418** of **104** with benzophenone. This means that an equilibrium exists between **104** and **104a** (equation 131). **418**, whose X-ray structure has been determined, serves as a source for **104**, which is trapped by acetone (to give an ene product) and by benzaldehyde (to form a [2+2] cycloadduct, unstable against cycloreversion into $PhCH{=}C(SiMe_3)_2$ and *t*-Bu_2SiO containing substances). Less reactive traps, like trimethylsilyl azide, allow for rearrangement of **104** (again formed from **418**) to **104a**, which then gives an unstable [2+3] cycloadduct **420**, which transforms into **421** and **422** (equation 132).

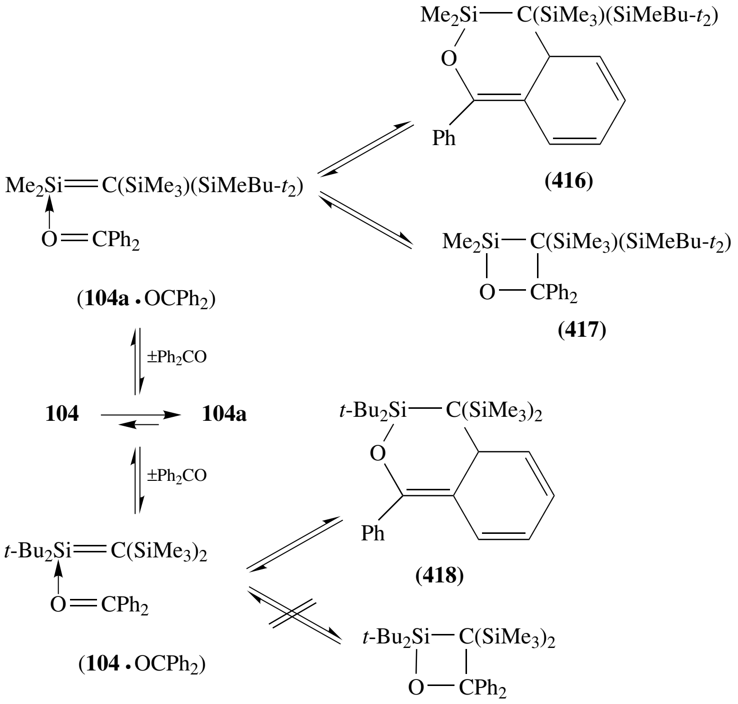

(131)

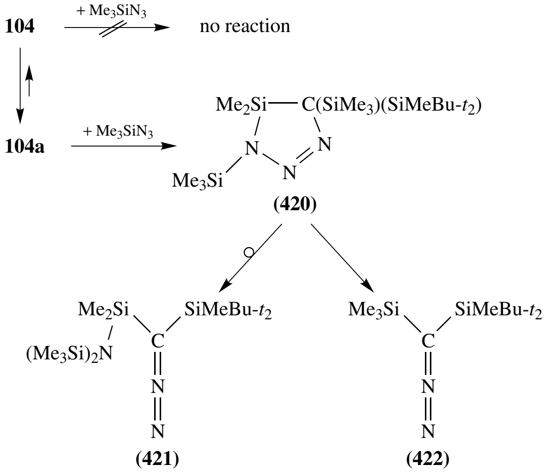

(132)

104a and its donor adducts **104a**•donor react in essentially the same manner; this implies that the reactions are preceded by the dissociation of the donor to give the free silene **104a**[83]. Most investigations have been conducted with the THF adduct[197]. The reactivity of **104a** is summarized in equation 133. Ene reactions with, e.g., propene, [2+4] reactions with butadiene, and [2 + 3] cycloadditions with silyl azides are principally the same as for other 'Wiberg-type' silenes.

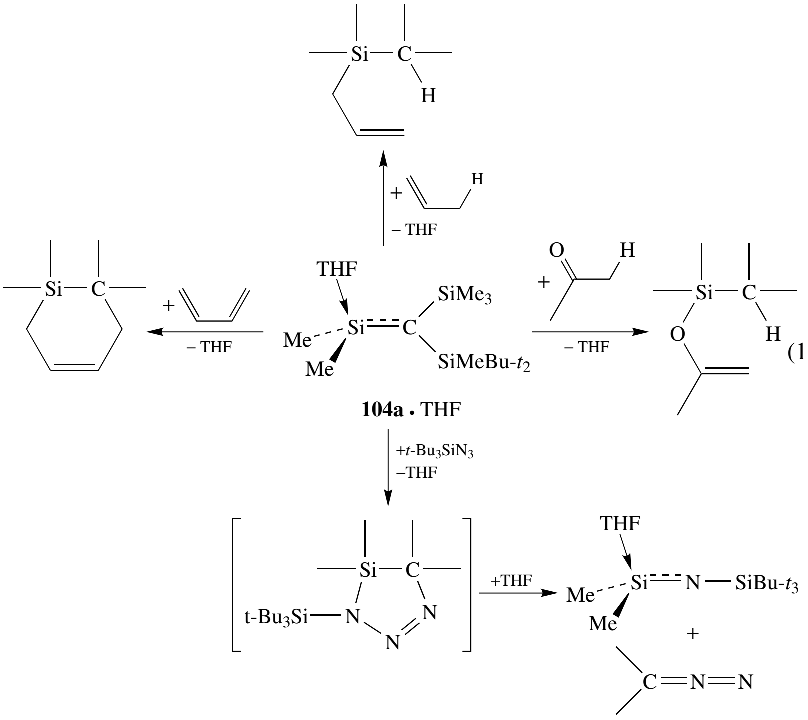

(133)

TABLE 8. Products from selected cycloaddition reactions of $R_2Si{=}CHCH_2Bu$-*t* **132** (R = *t*-Bu, Me, Ph)

R	Diene[a]	Dimer	[2 + 2]	[4 + 2]	Ene	Others	Reference
t-Bu	DMB			+			81
	Cp			+			81
Me	BD	+	+[b]	+		+[c]	79
	DMB	+		+		+[c]	79
	Cp	+		+		+[c]	79
	anthracene	+		+		+[c]	79
	CHD	+	+	+			205
Ph	MBD		+	+	+		206
	DB			+	+		206
	Cp			+			206
	CHD	+	+				206
	NBD	+				+[d]	206
	anthracene	+		+			206

[a] DMB : 2,3-dimethylbuta-1,3-diene; MBD : 2-methylbuta-1,3-diene; BD : buta-1,3-diene; Cp : cyclopentadiene; CHD : cyclohexadiene; NBD : norbornadiene.

[b] Two regioisomers.

[c] Coupling product from lithiated species to chlorosilane.

[d] [2 + 2 + 2] Cycloadducts.

b. Neopentylsilenes: $R_2Si{=}C(R')CH_2Bu$-t—**132**. *i. Diorgano-substituted neopentylsilenes*. The products formed in the system vinylchlorosilane/*t*-butyllithium/trap depend strongly on the substituents at the silicon atom. Diorgano-substituted neopentylsilenes tend to give predominantly 'normal', i.e. [4 + 2] cycloadducts, with diene systems (see Table 8). The cycloaddition reactions are mostly regiospecific, but give stereoisomers as far as the orientation of the neopentyl group is concerned.

For R_2 = cyclobutyl the results are not very much different from those for R = alkyl[207]. The substitution of one of the alkyl groups by $Cp(CO)_2Fe$ leads to the formation of the dimer only when the remaining alkyl group is methyl. The proposed intermediate silene may be trapped by dienes like DMB or Cp[208].

ii. π-Donor-substituted neopentylsilenes. The more interesting neopentylsilenes are those that have electronegative π-donor substituents like alkoxy, siloxy and, especially, chlorine. They have a quite pronounced tendency towards [2 + 2] cycloaddition and react even with reagents of only low reactivity, e.g. alkynes[209,210] (see Table 9). Thus, dichloroneopentylsilene **423** reacts with cycloheptatriene in [2 + 2] and [6 + 2] cycloaddition fashion[211]. No [4 + 2] cycloadducts are formed. The [2 + 2] cycloadducts **424** rearrange thermally into the [6+2] adduct **425** probably via a zwitterionic intermediate (equation 134).

The exceptional reactivity is explained by the authors as due to the enhanced polarity of the Si=C double bond. For a discussion of the effects see the references in the tables. In some cases, and preferably when R = Cl, the initially formed cycloadducts like *E*-**426** or **429** undergo ring enlargements to other silacycles like **427** or **430**. Interestingly,

TABLE 9. Products of cycloaddition reactions of $R_2Si{=}CHCH_2Bu\text{-}t$ (R = Cl, OBu-*t*, $OSiMe_3$)

R	Diene[a]	Dimer	[2 + 2]	[4 + 2]	Ene	Others	References
Cl	BD		+		+		212
	MBD		+				212
	DMB		+		+		212
	Cp			+			81
	Cp*			+			81
	furan	+		+		+[b]	213
	2-methylfuran	+		+		+[b]	213
	2,5-dimethylfuran	+		+		+[b]	213
	CHD		+	+			205, 214
	CHpD		+	+	+		211
	CHpT		+			+[c]	211
	NB		+				215
	NBD		+		+	+[d]	215
	naphthalene			+			214
	anthracene			+			81
	aldehydes					+[e]	216
	imines		+				217
	alkynes		+				209, 210
	vinyl ethers		+				218
	pentafulvenes		+	+	+		219, 220
	terpenes		+	+	+		221
	styrene		+	+			222
t-BuO	BD		+				223
$OSiMe_3$	BD		+				224
	DMB		+				224
	CHD		+	+			224
	CHpD		+	+			224
	NB		+		+		224
	NBD		+		+	+[d]	224
	QUC		+				224
	anthracene			+			224
	styrene		+				224

[a] See footnote *a* in Table 8; Cp* : pentamethylcyclopentadiene; CHpD : cycloheptadiene; CHpT : cycloheptatriene; NB : norbornene; QUC : quadricyclane.

[b] Oxasilaheptene from rearrangement of the [4 + 2] adduct; see scheme above.

[c] [6 + 2] Cycloadduct.

[d] [2 + 2 + 2] Cycloadducts.

[e] Rearranged non-cyclic product.

silacyclobutane *Z*-**426** does not give silacyclohexenes like **427**, but it isomerizes in a retro-ene reaction to the acyclic chlorosilane **428** (equations 135 and 136).

$$Cl_3Si{-}CH{=}CH_2 + t\text{-}BuLi \longrightarrow Cl_3Si{-}CH(Li){-}CH_2Bu\text{-}t \xrightarrow{-LiCl} Cl_2Si{=}CHCH_2Bu\text{-}t$$

(423)

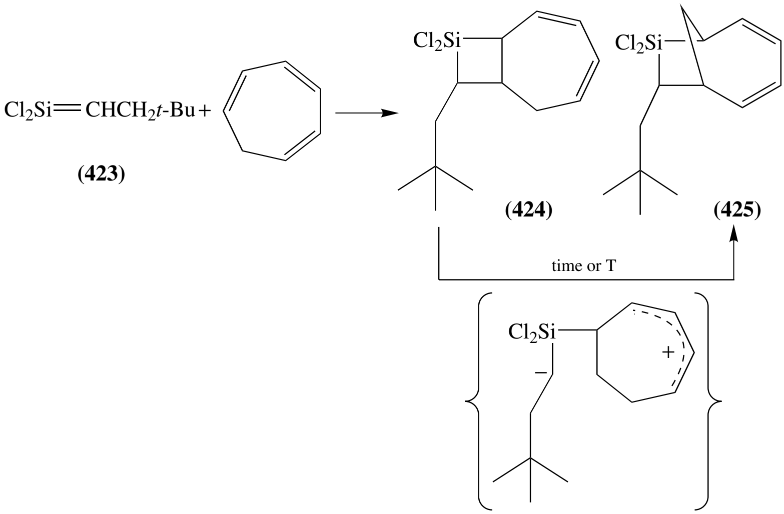

(423) **(424)** **(425)** (134)

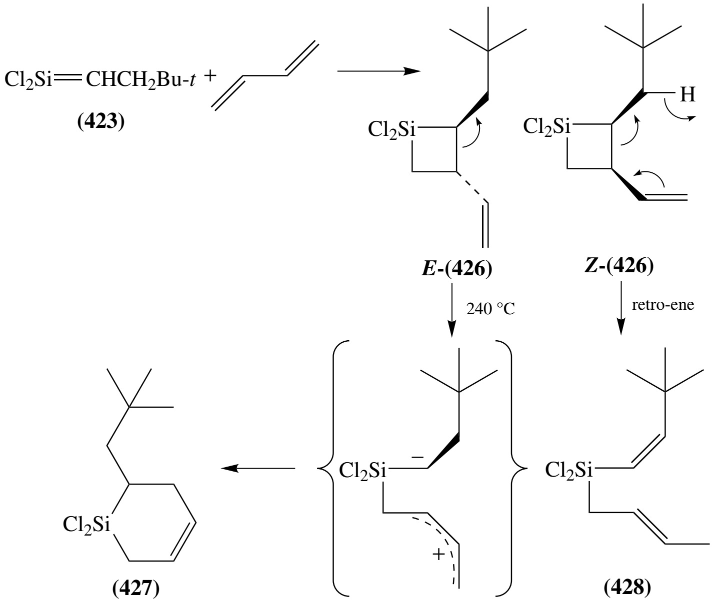

(423) ***E*-(426)** ***Z*-(426)** (135)

(427) **(428)**

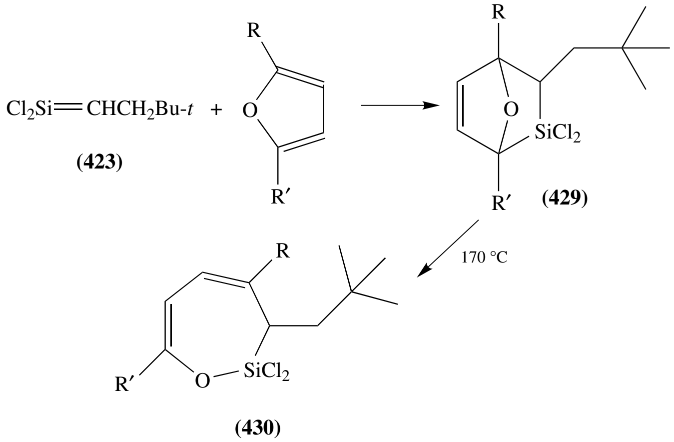

(136)

Nitrogen ligands can replace oxygen substituents bound to silicon and several aminocyclic precursors have been synthesized and their reaction towards *t*-BuLi has been investigated. The reactivity of the aminoneopentylsilenes is close to that of the well investigated dichloroneopentylsilene[225–228]. The substitution of just one chlorine atom by an amino group does not change much the resulting silene's reactivity[229]. Precursors for neopentylsilenes having one alkyl or aryl group and one amino group at silicon hardly yield cycloadducts in the presence of trapping agents but rather undergo dimerization upon reaction with *t*-BuLi.[229].

The substitution of one of the chlorine atoms by a vinyl group reduces the strong tendency to [2 + 2] cycloaddition reactions[225,230–232]. With the additional possibility of the formation of a second Si=C bond from dichlorodivinylsilane/2*t*-BuLi the intermediacy

TABLE 10. Products from cycloaddition reactions of $Cl_2Si{=}CR^1CH_2Bu$-*t* (R^1 = $SiMe_3$, Ph)

R^1	Diene[a]	[2 + 2]	[4 + 2]	Ene	Others	Reference
$SiMe_3$	BD	+				233
	DMB		+	+		
	Cp*		+			
	CHD		+			
	NBD			+	+[b], +[c]	
	QUC				+	
	anthracene		+			
Ph	BD		+	+		234
	MBD		+	+		
	DMB		+	+		
	CHD	+	+	+		
	NBE	+		+		
	NBD	+		+	+	
	QUC				+	
	styrene	+	+		+[d]	

[a] See footnotes *a* in Tables 8 and 9.

[b] [2 + 2 + 2] Cycloadducts.

[c] Coupling product.

[d] Rearomatized [4 + 2] cycloadduct.

of a 2-silaallene is conceivable[232]. An additional substitution of the vinyl group at the α-carbon atom is possible (see Table 10 and equation 137 for an example of cycloadducts with $R' = SiMe_3$)[233].

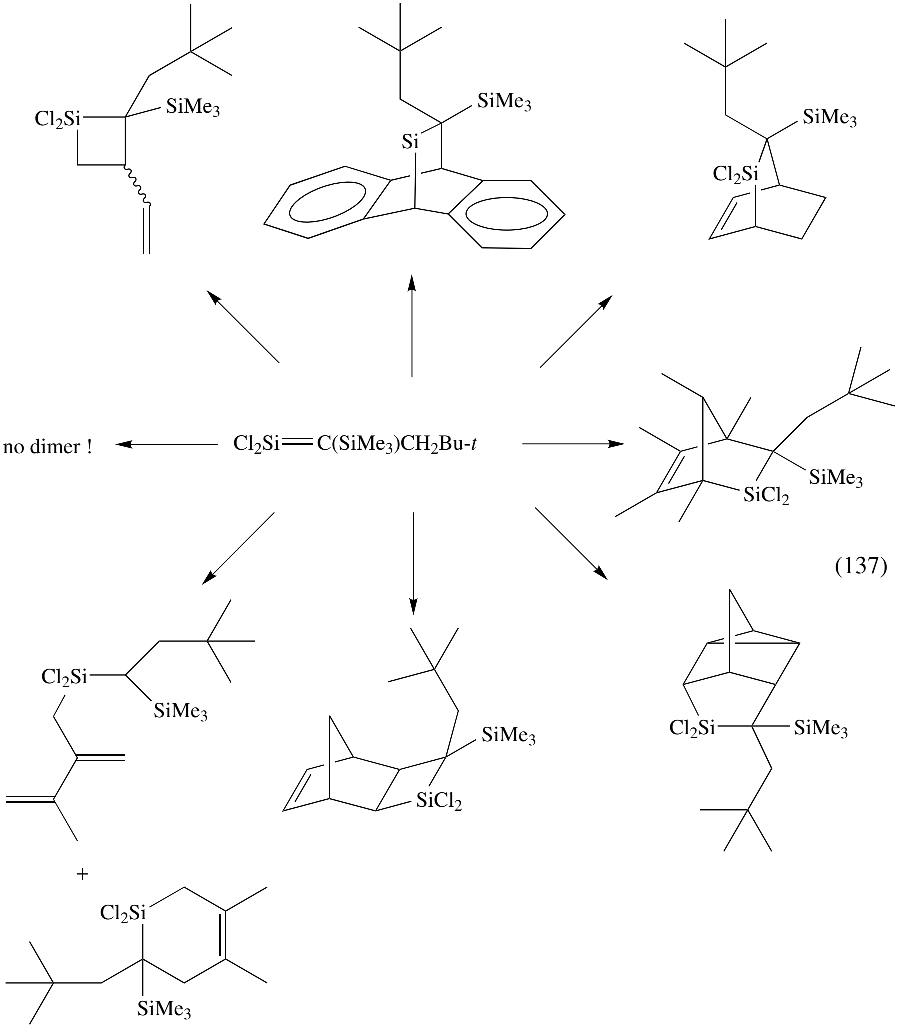

(137)

The rearrangement of the silene **345** to **346** has been described in Section I.B.1.b. **346** undergoes head-to-tail dimerization, [2 + 4] and [2 + 2 + 2] cycloaddition reactions[178,179].

c. Brook-type silenes. i. [2 +1] Cycloaddition reactions. The formal addition of silylenes to Si═C double bonds has been reported by Brook and Wessely[181]. They found that the reaction of silene **349** with hexamethylsilirane **431** in the dark yields the disilirane **432** which was identified by NMR spectroscopic methods as a main product. **432** was found to be thermally unstable. It isomerizes quantitatively into the disilaindane derivative **433** during 48 h. This reaction is photoreversible: upon photolysis of **433** the disilirane **432** is cleanly formed (equation 138; note that in the original paper a different assignment of the regiochemistry of the disilane unit was suggested[181,235]).

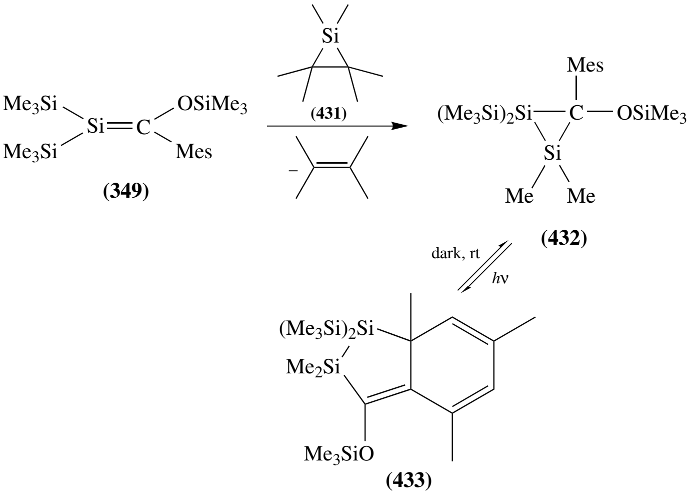

(138)

The products arising from the reaction of **431** with the alkyl-substituted silenes **149** and **150** suggest that the reaction occurs by a radical pathway, initiated by a homolytic Si−C bond cleavage of **431** and subsequent Si−Si bond formation giving the biradical **434**. Intramolecular disproportionation of **434** gives **435**, while **436** and **437** are the results of ring closure reactions without or with expulsion of tetramethylethene, respectively (equation 139)[181].

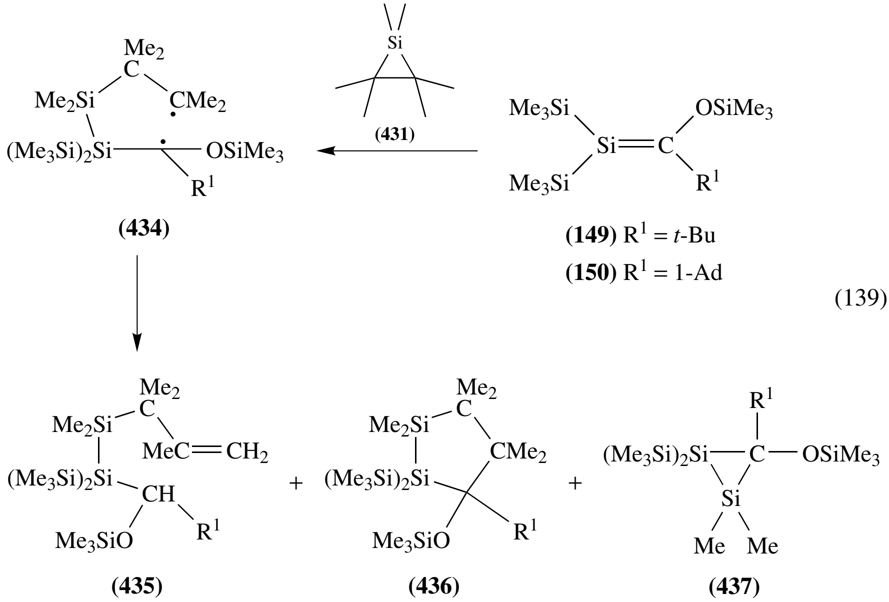

(139)

Alkylisocyanides do react readily with Brook-type silenes $(Me_3Si)_2Si{=}C(OSiMe_3)R^1$ giving silaaziridines **438** as isolated products[236,237]. The initially formed silacyclopropanimines **439** are very unstable. Only one could be detected in the reaction of **150** with *t*-butylisocyanide as a transient species by low temperature ^{1}H and ^{13}C NMR at −70 °C. At −40 °C, **439** (R^1 = 1-Ad) undergoes a rapid thermal rearrangement to the isomeric **438** (R^1 = 1-Ad)[236]. When one of the groups R^1 or R^2 is an aryl group, the first observed isolated products are 1-sila-3-azacyclobutanes **440** resulting from the dark reaction between **438** and a second molecule of isocyanide (equation 140)[237].

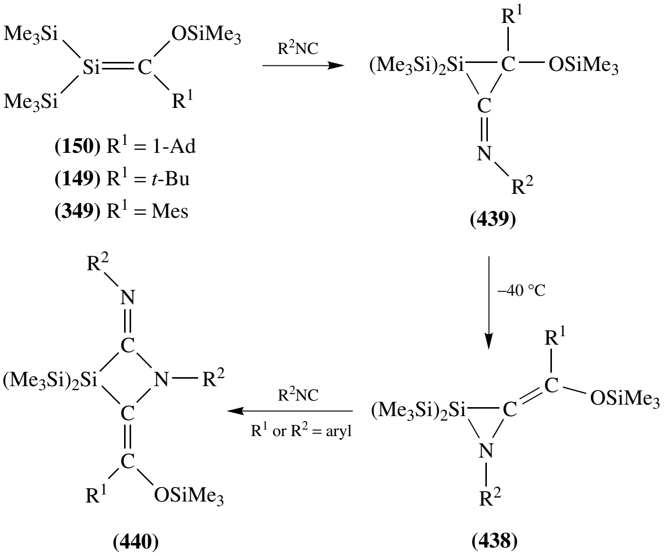

(140)

Ab initio calculations by Nguyen and coworkers for the principal reaction of $H_2Si{=}CH_2$ and HNC at the QCISDT/6-31G**//MP2(fc)/6-31G** + ZPE level of theory corroborate the experimental findings[238a]. The initial reaction between the HNC and the Si=C double bond giving the siliranimine **441** is a concerted but asynchronous [2 + 1] process in which the carbon lone pair of HNC attacks first the Si. The reaction is exothermic by *ca* 16 kcal mol^{-1} and has a barrier of 11.1 kcal mol^{-1} (see Figure 3). It was suggested that the electron-releasing substituents $OSiMe_3$ and Me_3Si in the experimentally investigated species will decrease the barrier for the cycloaddition[238a]. According to the calculation the isomerization of **441** to the silaaziridine **442**, which is 6.3 kcal mol^{-1} more stable, occurs in two distinct steps involving the four-membered cyclic carbene intermediate **443**[238a]. This is in contrast to the original suggestion by Brook[238b] who favoured a zwitterionic intermediate **444**. The carbene **443** is of nearly similar stability to **441** and its formation is the rate-determining step of the entire transformation **441** → **442**. Although **443** is a formal [2 + 2] cycloadduct of HNC + $H_2Si{=}CH_2$, the possibility of its direct formation was excluded based on experimental evidence.

Relatively stable adducts of sulphur and selenium can be prepared by direct addition to silenes, provided that the latter bear appropriate substituents. Thus, silene **392** reacts with sulphur or selenium at room temperature giving the silathiirane **445** or silaselenirane **446** in 70% or 60% yield, respectively (equation 141). In contrast, the reaction of other silenes of the $(Me_3Si)_2Si{=}C(OSiMe_3)R^1$ family give only complex mixtures with sulphur[239].

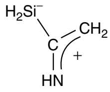

(444)

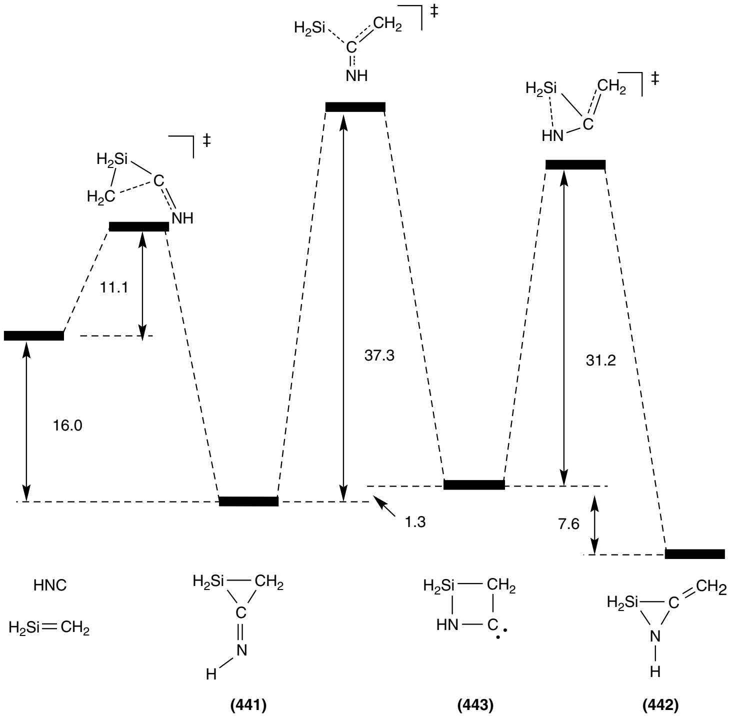

FIGURE 3. Schematic potential energy profile for the cycloaddition of $H_2Si{=}CH_2$ and HNC and the rearrangement to a silaziridine (calculated at QCISD(T)/6-31G**//MP2(fc)/6-31**)[238a]

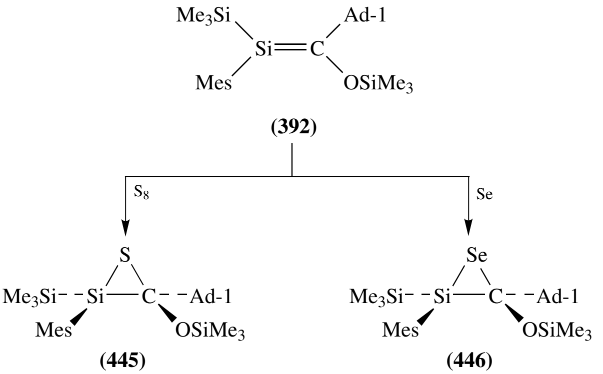

(141)

ii. Cycloadditions with alkenes, dienes and alkynes. The cycloaddition behaviour of some typical Brook-type silenes with alkenes, dienes and acetylenes is summarized in Table 11 and will be discussed only briefly. Experimentally, most of the reactions have been conducted in two different ways: (1) The diene was cophotolysed ($\lambda > 340$ nm) with the acylsilane precursor of the 2-siloxysilene and the reaction took place immediately during the photolysis. (2) The silene was preformed by photolysing the precursor acylsilane and only then is the reactant added. Thus, this is a 'dark' reaction and no photochemistry can interfere. Both experimental methodologies give in nearly all cases exactly the same results with respect to formed products and product distribution. Frequently, different reaction rates for the dark and for the photolytic reaction have been observed.

The 'Brook-type' silenes $(Me_3Si)_2Si{=}C(OSiMe_3)R^1$ give with dienes having an allylic hydrogen normally a mixture of the Diels–Alder cycloadduct 1-silacyclohex-3-ene and the product of the intermolecular 'ene' reaction[240]. Thus, **149** or **150** give with 2,3-dimethylbuta-1,3-diene 60 : 40 mixtures of **447** and **448** (equation 142)[240]. The amount of 'ene' product **448** is larger than that found for sterically less hindered silenes, i.e. the 'Wiberg'-type silene $Me_2Si{=}C(SiMe_3)_2$ **92** gave only 20% of 'ene' product[176]. Steric factors alone cannot account for the observed product distributions. For example, the mesitylsilene **349** gives exclusively the [4 + 2] cycloadduct **447** (R = Mes), although **349** is not less crowded than **149** (see Table 11)[240].

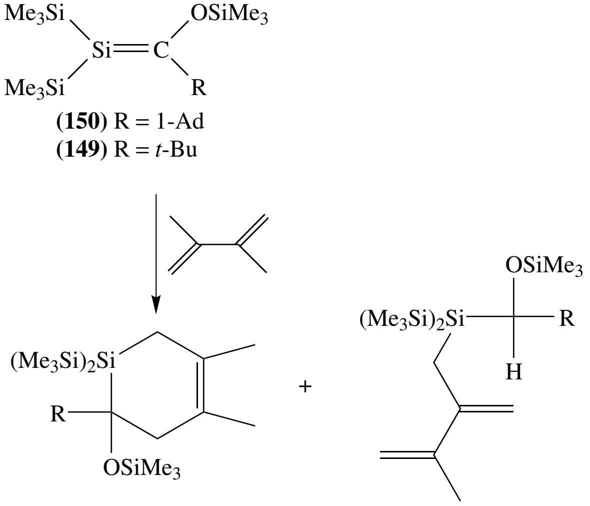

(150) R = 1-Ad
(149) R = t-Bu

(447) **(448)**

(142)

In the reaction of 'Brook-type' silenes with buta-1,3-diene the products **449** arising from a [2 + 2] cyclization are predominant (see Table 11). Silacyclohexenes like **450**, resulting from formal [4 + 2] cycloadditions are formed only as byproducts[240]. Furthermore, with the silenes E/Z-$(Me_3Si)MesSi{=}C(OSiMe_3)Ad$-1 **136** the [2 + 2] adduct is formed even exclusively as a mixture of 4 diastereomers. Usually, only the regioisomers **449** having the vinyl group attached to the C^3 atom of the ring are formed (equation 143). There is no experimental evidence for the other regioisomer **451**[240].

Brook and coworkers attempted to establish a mechanism for these formally forbidden [2 + 2] cycloadditions[240]. Attempts to intercept a possible biradical intermediate **452** in the reaction of **150** with buta-1,3-diene with tributyltin hydride failed. In addition, when

TABLE 11. Product distribution (given as % of characterized product) from the cycloaddition reactions of 2-siloxysilenes with dienes, alkenes and alkynes.

Silene[a]	Reactant	[2 + 4]	[2 + 2]	Ene	Reference
$(Me_3Si)_2Si{=}C(OSiMe_3)R$[a]	buta-1,3-diene	20	80 (2 stereoisomers, 1:1)		240
$(Me_3Si)_2Si{=}C(OSiMe_3)Mes$	buta-1,3-diene	25	75 (2 stereoisomers, 4 : 1)		240
E/*Z*-$(Me_3Si)MesSi{=}C(OSiMe_3)$Ad-1	buta-1,3-diene		100 (4 stereoisomers)		95
$(Me_3Si)_2Si{=}C(OSiMe_3)$Ad-1	isoprene	88 (2 regioisomers 3 : 1)		11	240
$(Me_3Si)_2Si{=}C(OSiMe_3)R$[a]	2,3-dimethylbuta-1,3-diene	60		40	240
$(Me_3Si)_2Si{=}C(OSiMe_3)Mes$	2,3-dimethylbuta-1,3-diene	100			240
E/*Z*-$(Me_3Si)MesSi{=}C(OSiMe_3)$Ad-1	2,3-dimethylbuta-1,3-diene		no reaction		95
$(Me_3Si)_2Si{=}C(OSiMe_3)R$[a]	cyclopentadiene	100 (1 stereoisomer)			240
$(Me_3Si)_2Si{=}C(OSiMe_3)R$[a]	cyclohexadiene	80 (2 stereoisomers)	20 (2 stereoisomers)		240
$(Me_3Si)_2Si{=}C(OSiMe_3)Mes$	cyclohexadiene	no reaction			240
$(Me_3Si)_2Si{=}C(OSiMe_3)$Ad-1	1-octene			100	240
$(Me_3Si)_2Si{=}C(OSiMe_3)Mes$	1-octene			no reaction	240
$(Me_3Si)_2Si{=}C(OSiMe_3)$ Ad-1	styrene		100 (2 stereoisomers of 1 regioisomer)		240
$(Me_3Si)_2Si{=}C(OSiMe_3)Mes$	styrene		100		240
$(Me_3Si)_2Si{=}C(OSiMe_3)R$[a]	$PhMeC{=}CH_2$			100	240
$(Me_3Si)_2Si{=}C(OSiMe_3)Mes$	$PhMeC{=}CH_2$			100	240
$(Me_3Si)_2Si{=}C(OSiMe_3)$ Bu-*t*	$PhC{\equiv}CMe$		100 (one regioisomer)		95
E/*Z*-$(Me_3Si)MesSi{=}C(OSiMe_3)$Ad-1[a]	$PhC{\equiv}CH$		100 (one regioisomer)		95
E/*Z*-$(Me_3Si)MesSi{=}C(OSiMe_3)$Ad-1[a]	$Me_3SiC{\equiv}CH$		100 (one regioisomer)		95

[a] R : *t*-Bu.

[b] 1-Ad : 1-adamantyl.

the reaction was performed in different solvents (pentane, benzene and diethyl ether) no significant change in the product distribution was observed. This led Brook and coworkers to discard also the zwitterionic species **453** as a possible intermediate. They concluded that the reaction of 2-siloxysilenes like **150** with buta-1,3-diene does not involve a two-step process but is consistent with a concerted [2 + 2] process[240].

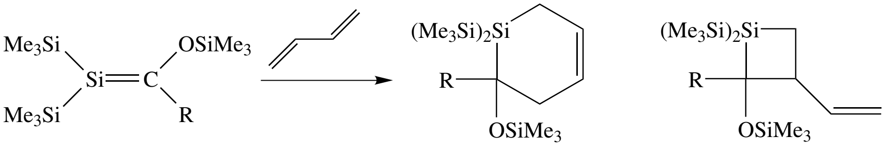

(450) **(449)**

(143)

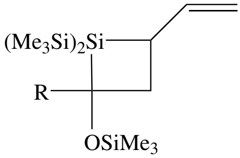

(451)

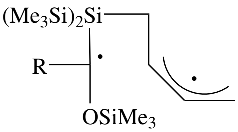

(452)

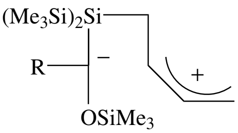

(453)

When simple alkenes were employed as reaction partners for silenes of the type $(Me_3Si)_2Si{=}C(OSiMe_3)R^1$, silacyclobutanes were obtained, provided that no allylic hydrogen is present in the alkene. In the reaction with alkenes with allylic hydrogens the 'ene' reaction becomes predominant (see Table 11). Thus, while the reaction with styrene exclusively gives the four-membered ring compound **454**, with 1-methylstyrene the 'ene' products **455** were obtained (equation 144). Similarly, from the reaction of **150** with 1-octene only the 'ene' product **456** was isolated (equation 145).

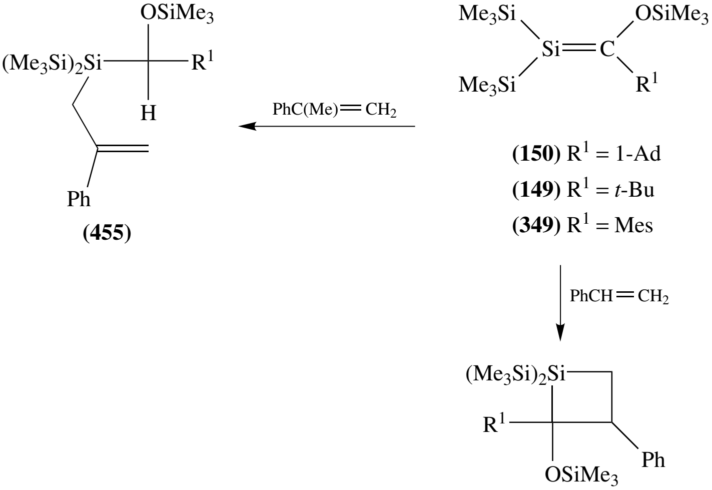

(455)

(150) R^1 = 1-Ad
(149) R^1 = *t*-Bu
(349) R^1 = Mes

(144)

(454)

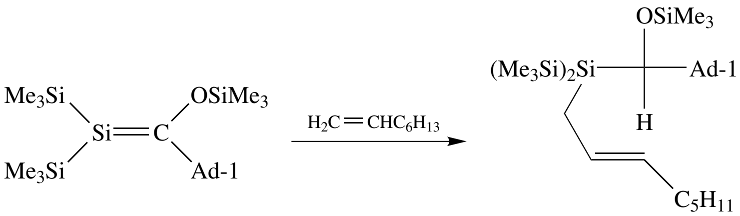

(150) **(456)**

(145)

Alkynes also react with sterically, highly hindered Brook-type silenes giving 1-silacyclobut-2-enes in high yields[95]. This reaction is strictly regiospecific: thus from *E*/*Z*-**136** only a *E*/*Z* mixture of **457** is formed, whereas the regioisomer **458** was not detected (equation 146)[95].

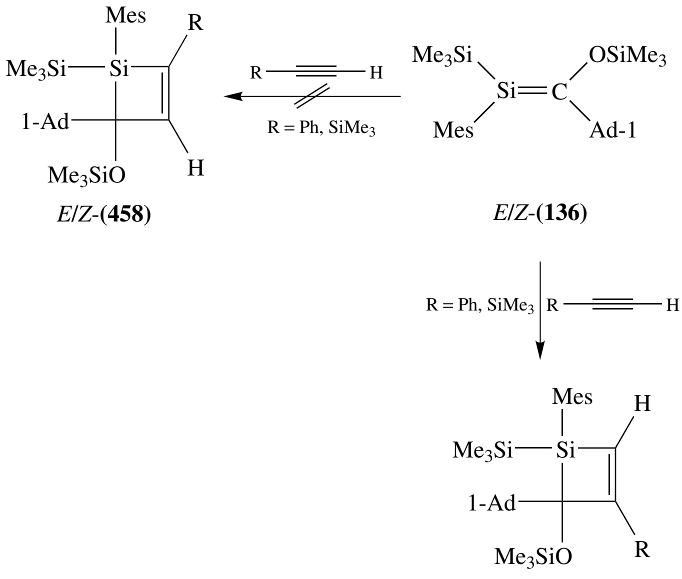

E/*Z*-**(458)** *E*/*Z*-**(136)**

(146)

E/*Z*-**(457)**

Similarly, it was shown by a crystal structure analysis that the adduct of silene **149** with phenylpropyne has the constitution **148** (equation 147)[95] in contrast to earlier reports which favoured the reversed regiochemistry[86].

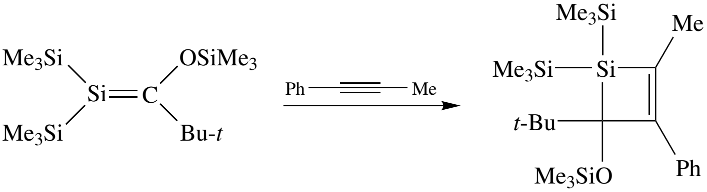

(147)

(149) **(148)**

d. Apeloig–Ishikawa–Oehme-type silenes. Compared with the well established cycloaddition chemistry of the 'Brook-type silenes, relatively little is known about the behaviour of 'Apeloig–Ishikawa–Oehme'-type silenes in these reactions. Characteristically these silenes undergo [4 + 2] cycloadditions with buta-1,3-dienes yielding silacyclohexenes; e.g. silene **459** gives with 2,3-dimethylbuta-1,3-diene the silacyclohexene **460** in 60% isolated yield (equation 148)[104].

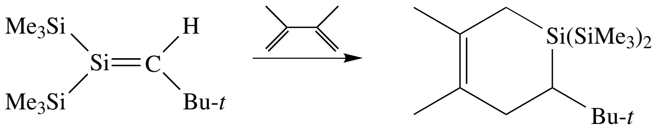

(**459**) (**460**)

(148)

There are, however, reports in which the formation of a [2 + 2] cycloadduct was also observed. Thus, the stable silene **167** reacts with 1-methoxybuta-1,3-diene yielding regiospecifically only one [4 + 2] regioisomer **461**[111]. The product **462** arising from a formal [2 + 2] cycloaddition is formed, however, in appreciable amounts (20–30% yield) (equation 149)[111].

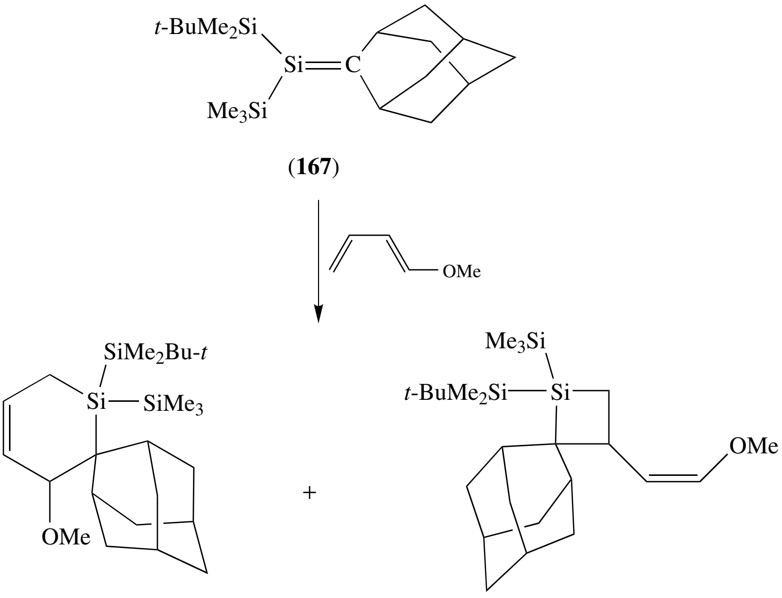

(**167**)

(149)

(**461**) (**462**)

The [4 + 2] reaction with dienes has been frequently used to establish the intermediacy of a silene in the sila-Peterson olefination reaction[39,107,112,119]. Thus, further examples for cycloadditions can be found in Section I.A.5.

Silenolates like **180** do react with 2,3-dimethylbuta-1,3-diene in a formal [4+2] fashion and, when the alkoxide **463** is trapped by triethylsilyl chloride, the 1-silacyclohex-3-ene

464 is isolated (equation 150)[120].

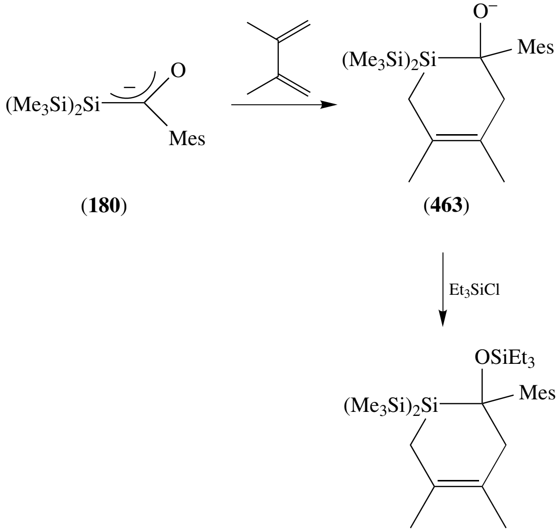

(**180**) (**463**) (**464**)

(150)

A very interesting reaction of a disilene with a silenolate forming a stable trisilacyclobutane was reported by Bravo-Zhivotovskii, Apeloig and coworkers[241]. The decomposition of **182**, prepared by the reaction of Brook's ketone $(Me_3Si)_3SiC(O)Ad$-1 with triethylgermyllithium, yields in a complex reaction sequence the trisilacyclobutane **465** in 54% isolated yield (equation 151). The key step in this reaction is believed to be the formal cycloaddition between the transient tetra(trimethylsilyl)disilene **466** and **182** giving the trisilacyclobutane **467** (equation 152).

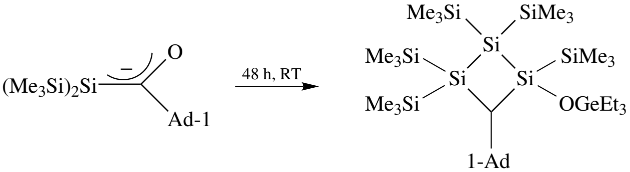

(**182**) (**465**)

(151)

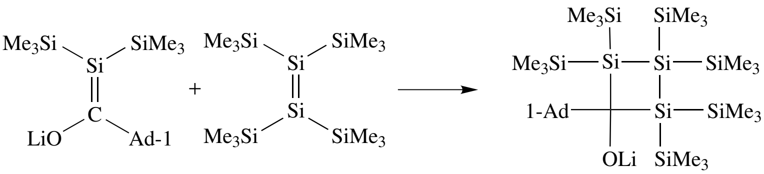

(**182**) (**466**) (**467**)

(152)

e. Cycloaddition reactions with carbonyl compounds and derivatives. The reaction of transient silenes with carbonyl compounds leads normally to an olefin and silanone oligomers[8]. It is usually assumed that a 2-siloxetane **468** is formed first and then fragments at the applied reaction conditions (equation 153). As pointed out by Raabe and Michl, a concerted 2-siloxetane formation is thermally not forbidden, when lone pair electrons of the carbonyl oxygen are involved; however, a two-step process is equally possible[8]. Streitwieser and Bachrach studied the reaction using *ab initio* methods[242]. They found that the overall reaction between $H_2Si{=}CH_2$ and H_2CO to produce $H_2C{=}CH_2$ and H_2SiO is exothermic by *ca* 30 kcal mol^{-1} (HF/3-21G*) and that the intermediate 2-siloxetane **468** is more stable than the products by at least 50 kcal mol^{-1}, thus indicating that siloxetanes similar to **468** are stable toward unimolecular decomposition and should therefore be isolable compounds[242].

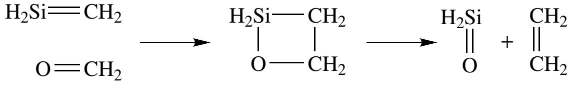
(153)

(**468**)

Reaction of simple aromatic aldehydes with 'Brook' - type silenes $(Me_3Si)_2Si{=}C(OSiMe_3)R^1$ gives exclusively a *cis/trans* mixture of the 2-siloxetanes **469**, the nominal [2 + 2] cycloadducts, which can be identified by NMR spectroscopy (equation 154)[235].

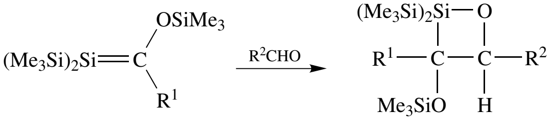
(154)

(**469**)

In contrast, the reactions with aromatic ketones are rather complex and hardly predictable. In some cases, only the [2 + 2] cycloadducts were formed, but they isomerized in the dark to the bicyclic [4 + 2] isomers. Thus, mesitylsilene **349** gives with benzophenone the 2-siloxetane **470**, which undergoes spontaneously a ring expansion reaction at room temperature in the dark to give a 1.8 : 1 mixture of **471** and unchanged **470** (equation 155)[235].

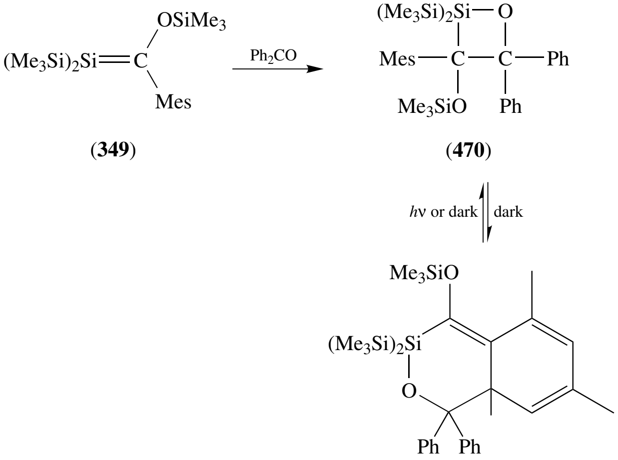
(**349**) (**470**)

(155)

(**471**)

When **349** is generated thermally at 140 °C from mesitoyl-tris(trimethylsilyl)silane, the silyl enol ether **472** was isolated as the sole product[99]. **472** results from isomerization of the siloxetane **470** (equation 156)[99].

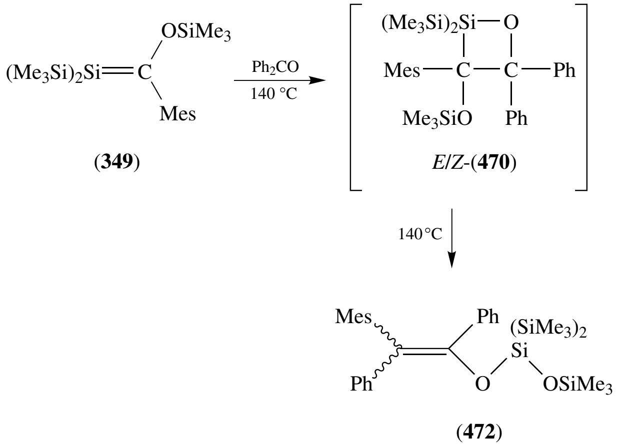

(156)

In contrast, the initial product of the reaction of phenylsilene **473** with aromatic ketones is the formal [4 + 2] cycloadduct **474** in which the silene serves as the 4π component and no evidence could be found that a siloxetane **475** is formed initially. On photolysis and also in the dark, although much more slowly, **474** isomerizes to the siloxetane **475**, indicating that **475** is the thermodynamically more stable isomer. This isomerization is not reversible[235]. When bis(p-tolyl) ketone was used in the reaction, the isomerization cascade did not end at the stage of the siloxetane but a second isomerization step giving **476** took place (equation 157). **476** is the formal [4 + 2] cycloadduct with the ketone serving as the diene and the silene as the dienophile[235].

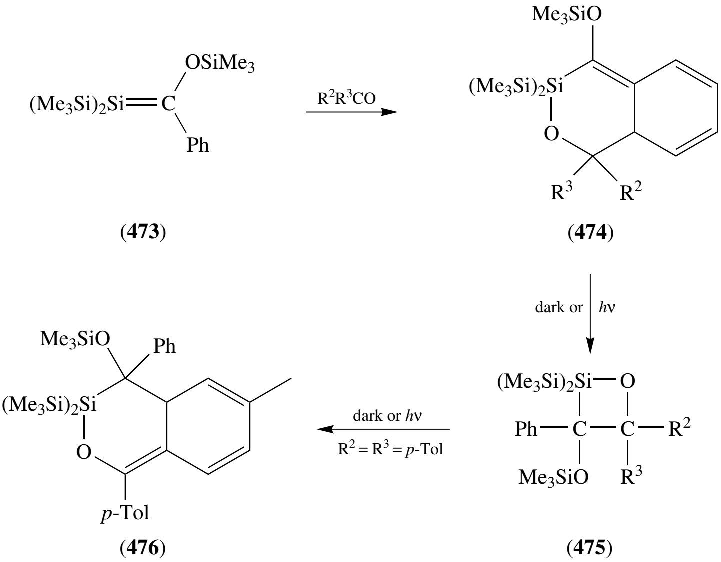

(157)

Reaction of phenylsilene **473** with benzophenone in boiling dioxane gives directly the silyl enol ether **477**, the thermal decomposition product of the initially formed oxasilirane *E/Z*-**478** (equation 158)[243].

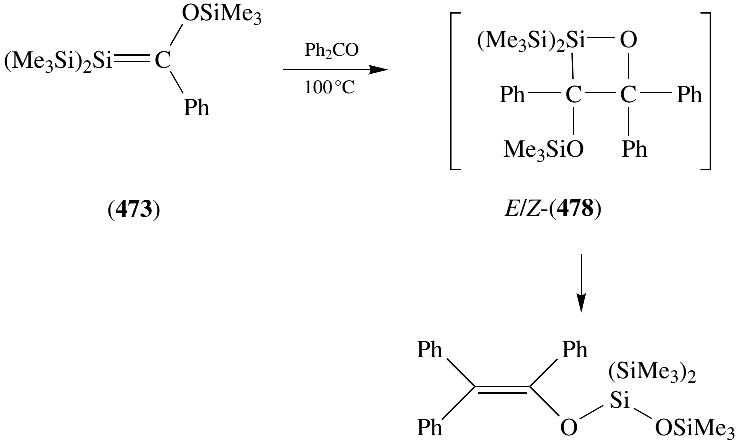

(**473**) *E/Z*-(**478**)

(158)

(**477**)

The same product was obtained in 52% yield along with considerable amounts of 1,2,2-triphenyl-1-(trimethylsilyl)ethene (22%) when the benzoyl-tris(trimethylsilyl)silane was thermolysed in the presence of benzophenone[99].

The [4π(ketone)–2π (silene)] reaction mode is dominant for the alkyl substituted silenes **149** and **150**: The initially formed product is **479**, which isomerizes in the dark in a non-reversible reaction to the siloxetane **480** (equation 159)[235].

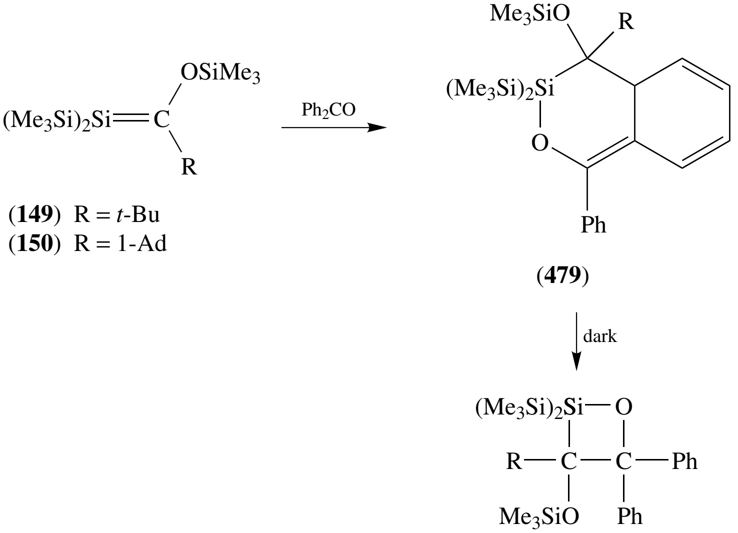

(**149**) R = *t*-Bu
(**150**) R = 1-Ad

(**479**)

(159)

(**480**)

Under thermolytic conditions the cycloheptatriene **481** and the silyl enol ether **482** were obtained in 46% and 24% yield, respectively, along with 29% of the unreacted starting compound, the acylpolysilane which is the precursor for the reactive silene (equation 160)[99].

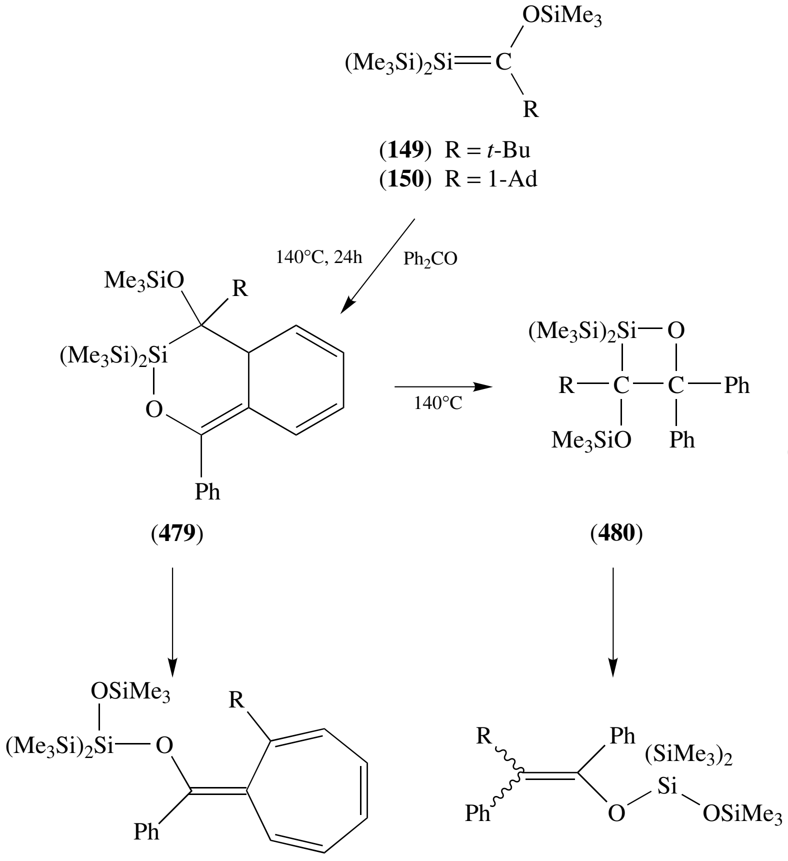

(160)

(**479**) (**480**)

(**481**) (**482**)

The reaction of thermolytically generated 'Brook'-type silenes with acetone is believed to give initially the siloxetane **483**, which undergoes diverse isomerizations or fragmentations depending on the substituent R, yielding products **484**–**491** (equation 161)[99].

The complexity of the reactions is even increased when α,β-unsaturated carbonyl compounds have been employed as reactants. Silenes of the family $(Me_3Si)_2Si{=}C(OSiMe_3)R^1$ react with propenal **492** ($R^2 = R^3 = H$) in a [4 + 2] manner giving surprisingly both possible regioisomers, the 1-sila-3-oxacyclohex-4-ene **493** as the major product and the 1-sila-2-oxocyclohex-3-ene isomer **494**. The siloxetane **495** was also formed in minor amounts[244]. Aldehydes **492** bearing a β-substituent (R^2 and/or $R^3 \neq H$) did not give the regioisomer **493** upon reaction with silenes of the type $(Me_3Si)_2Si{=}C(OSiMe_3)R^1$ but yield a mixture of the Si–O bonded isomer **494** and, as the minor component, **495**[244]. The reaction between the mesitylsilene **349** and cinnamaldehyde, however, gives exclusively the siloxetane **495** (R^1 = Mes, R^2 = Ph, R^3 = H) (equation 162)[244].

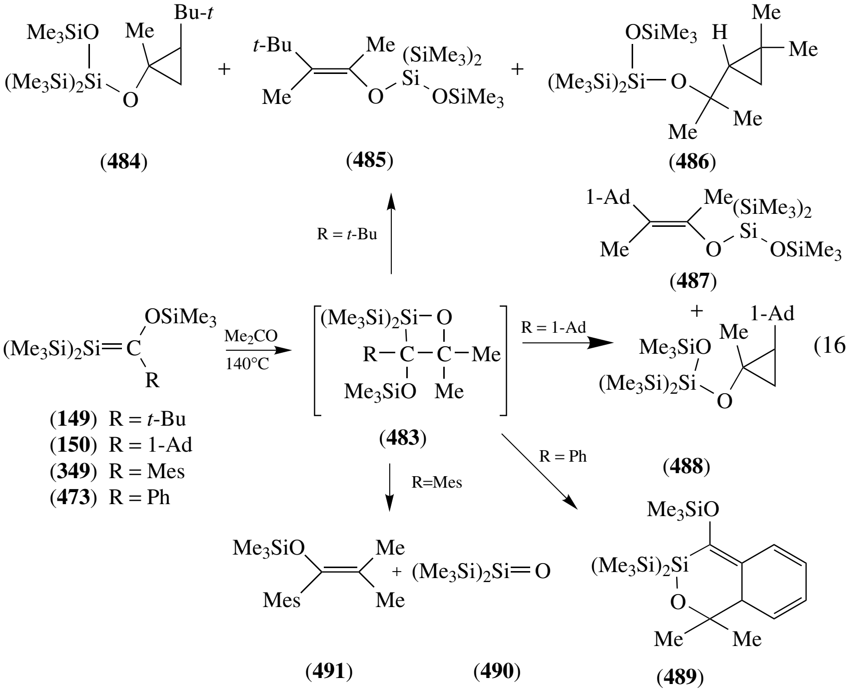

(161)

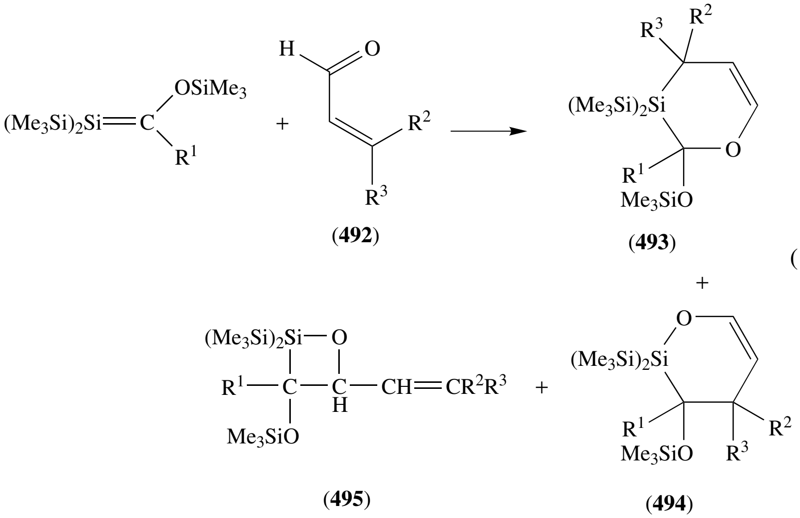

(162)

α,β-Unsaturated ketones behave similarly to aldehydes in their reaction with $(Me_3Si)_2Si{=}C(OSiMe_3)R$, i.e. in the reaction with methyl vinyl ketone, a ketone lacking a β-substituent, the 1-sila-3-oxocyclohex-4-enes are formed as major products[244]. The reaction of silenes $(Me_3Si)_2Si{=}C(OSiMe_3)R$ with β-substituted α,β-unsaturated ketones give exclusively the 1-sila-2-oxocyclohex-3-enes **496** (equation 163). In contrast to the reaction with aldehydes, in both cases no formation of a siloxetane similar to **495** was observed[244].

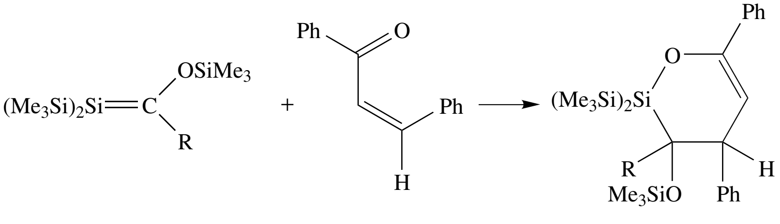

(**496**)

(163)

In contrast to all investigated α,β-unsaturated ketones, cyclopentadienones like **497** react with **149** and **473** exclusively to give the spiro compounds **498** i.e. the nominal $[2 + 2]$ cycloadduct, in 61 and 63% yield (equation 164)[243].

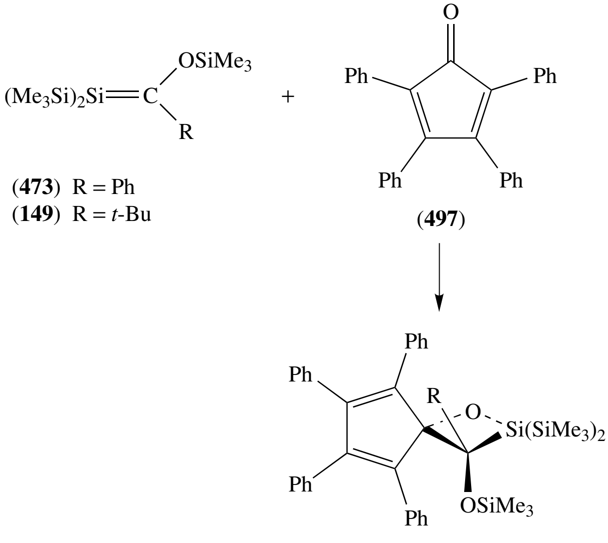

(**473**) R = Ph
(**149**) R = *t*-Bu

(**497**)

(164)

(**498**)

Brook-type silenes are unreactive toward simple esters such as ethyl acetate or methyl benzoate[245]. α,β-Unsaturated esters, however, readily undergo $[2 + 4]$ cycloaddition reactions with **149** or **150**. In these reactions no evidence was found for a product arising from a $[2 + 2]$ cycloaddition, neither involving the C=C bond nor the C=O double bond[245]. Anomalous behaviour was observed in the regiochemistry of the $[2 + 4]$ cyclizations. With acrylate esters only one type of regioisomer, the 1-sila-3-oxacyclohex-4-enes **499** having a new Si–C bond, were formed as the sole product (equation 165). In contrast, 1-sila-2-oxacyclohex-3-enes **500** having a new Si–O bond were the products of the reaction of **149** or **150** with ethyl cinnamate (equation 166). When diethyl maleate and diethyl fumarate were employed, diastereomeric mixtures of 1-sila-3-oxacyclohex-4-enes similiar to **499** were obtained[245].

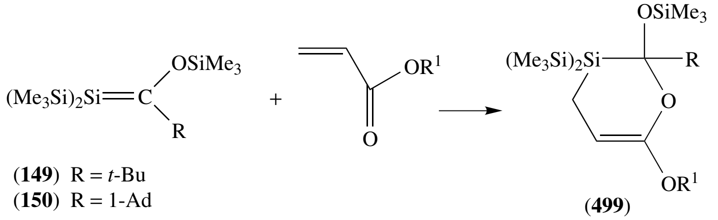

(**149**) R = *t*-Bu
(**150**) R = 1-Ad

(**499**)

(165)

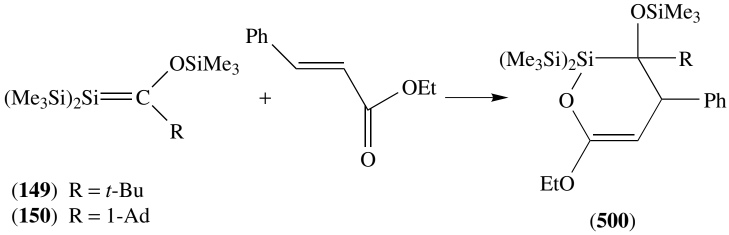

(**149**) R = *t*-Bu
(**150**) R = 1-Ad

(**500**)

(166)

When crotonate esters were employed the regioisomers **501** were mainly formed, accompanied by a significant amount of non-cyclic compounds **502** formally arising from insertion of the Si=C group in an allylic C–H bond (equation 167). The reaction of silenes **149** and **150** with crotonate esters are the only examples known so far where the product distribution is different when the reaction is conducted under photolytic conditions or in the absence of light. Thus, in the dark reaction of **150** with methyl crotonate the relative ratio **501** (R^1 = 1-Ad, R^2 = Me): **502** (R^1 = 1-Ad, R^2 = Me) = 3.75 : 1 was obtained, while under photolytic conditions only minor amounts of **501** were detected[245]. The nominal insertion product **503** is also the major product in the reaction of methacrylate esters with **149** and **150** (equation 168). The minor product in this reaction is the 1-sila-3-oxacyclohex-4-ene **504** (relative ratio **503** : **504** = 5.7 : 1)[245].

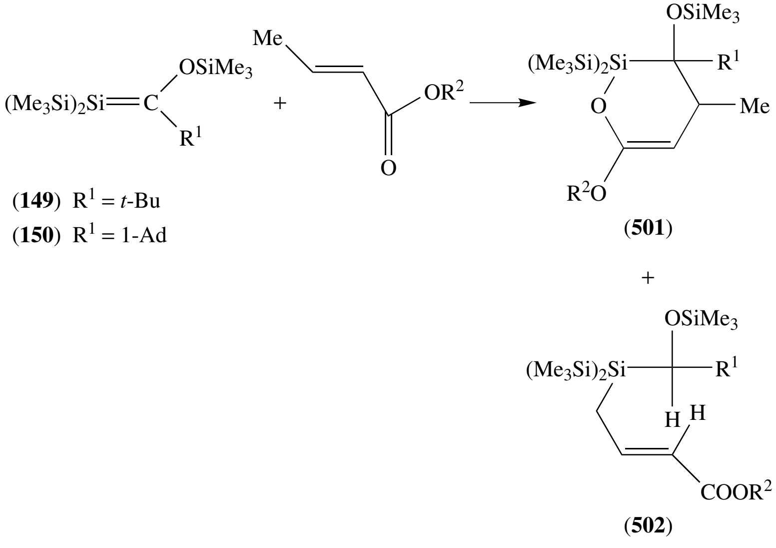

(**149**) R^1 = *t*-Bu
(**150**) R^1 = 1-Ad

(**501**)

(167)

(**502**)

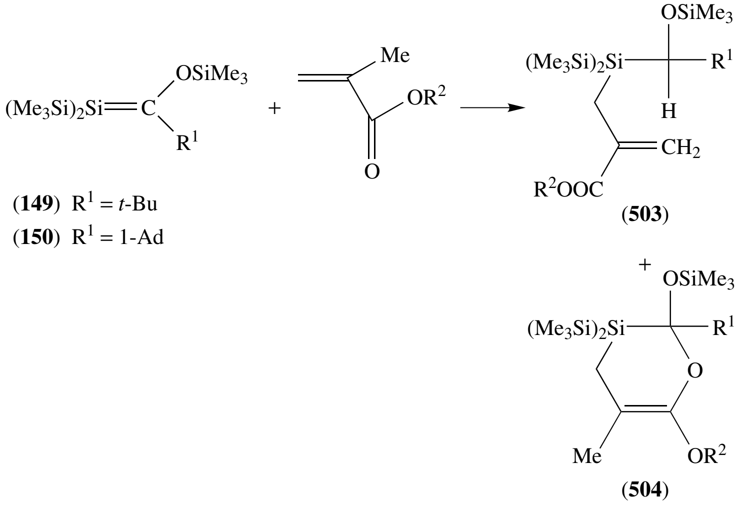

(**149**) $R^1 = t$-Bu

(**150**) $R^1 = 1$-Ad

(**503**)

(**504**)

(168)

Evidently, the reactivity of Brook-type silenes with α,β-unsaturated carbonyl compounds[243–245] is often very sensitive to factors other than polarities of the silene double bond and of the α,β-unsaturated system. Brook and coworkers pointed out that frontier orbital control of the [4 + 2] cyclization reactions might account for the predominant formation of 1-sila-3-oxacyclohex-4-enes like **505** in the reaction of acrylate esters or propenal with silenes $(Me_3Si)_3Si{=}C(OSiMe_3)R$ (equation 169)[244]. Thus, the HOMO of the silene $(H_3Si)_2Si{=}C(OSiH_3)R$ with its higher orbital coefficient located on silicon as calculated by Apeloig and Karni[246] will interact with the LUMO of the unsubstituted α,β-unsaturated carbonyl compound, where the higher orbital coefficient of the frontier orbital appears to be located on the terminal carbon atom of the C=C bond. The formation of 1-sila-2-oxacyclohex-3-ene like **506** from crotonaldehyde, crotonate esters or from ethyl cinnamate (equation 169) is in accord with a cyclization reaction dominated by the high affinity of oxygen towards silicon and is consistent with the polarity of the reagents, as most commonly prevails in [2+4] cycloadditions. Steric effects introduced by the β-substituents may also be important in determining the preferred regiochemistry[244]. The occurrence of significant amounts of byproducts in some reactions[245] suggest, however, that other non-concerted reaction routes with different intermediates may be important. More synthetic and theoretical work is clearly needed to understand in more detail the mechanism of this formal cycloaddition of silenes.

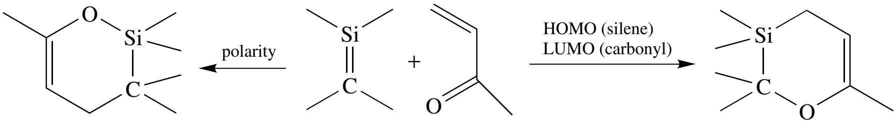

(**506**) (**505**)

(169)

In view of the evident reactivity of 'Brook'-type silenes toward carbonyl compounds and the fact that they are generated photochemically from acylpolysilanes, the question arises whether the silenes do react with their precursors. The very reactive silene **507** reacts in the absence of suitable trapping reagents with the acyldisilane **508** leading to the siloxetane **509**[94]. **509** is thermally unstable and rearranges to the siloxyalkene **510** (equation 170)[94].

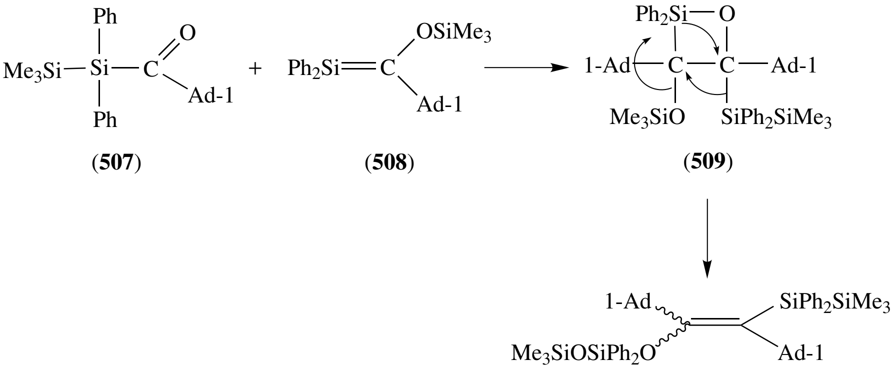

(**507**) (**508**) (**509**)

(**510**)

(170)

The reaction shown in equation 170 is, however, the only known example where a silene reacts with its acylpolysilane precursor. Whereas silenes of the type $(Me_3Si)_2Si{=}C(OSiMe_3)R^1$ do not react with their polysilane precursors, they readily react with less sterically congested acylsilanes[247]. Thus, mesitylsilene **349** gives with benzoyl trimethylsilane a mixture of the diastereomeric siloxetanes *E*/*Z*-**511** in 95% yield (equation 171). Typically, the adamantylsilene **150** gives with benzoyl trimethylsilane the nominal [4 + 2] cycloadduct **512** in 89% yield (equation 172). The silyl enol ether **513** is the result of an 'ene'-type reaction which occurs between **150** and acetyl triphenylsilane, a carbonyl compound having an activated hydrogen (equation 173)[247].

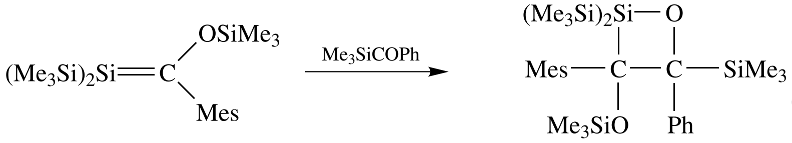

(171)

(**349**) *E*/*Z*-(**511**)

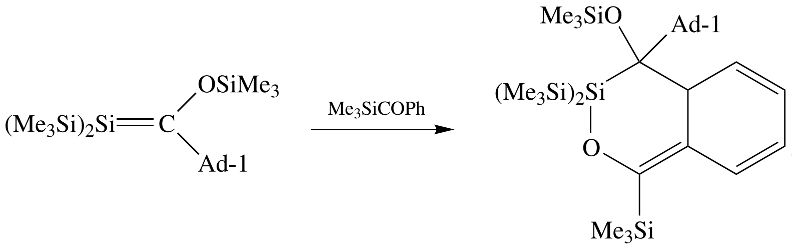

(172)

(**150**) (**512**)

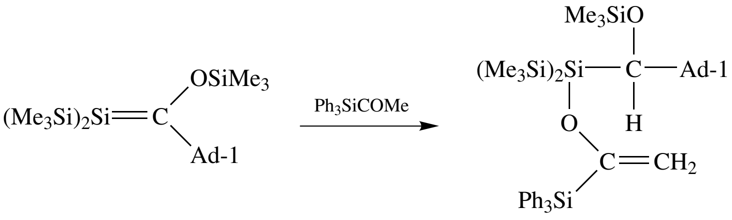

(173)

(**150**) (**513**)

'Brook'-type silenes have been found to undergo [4+2] and [2+2] cycloadditions with imines $R_2C{=}NR$ to give silatetrahydroisoquinolines or silaazetidines, respectively[248]. If formed, the [4 + 2] adducts generally rearrange slowly in the dark or more rapidly when photolysed to the thermodynamically more stable [2 + 2] isomers.

Thus, the alkyl-substituted silenes of the family $(Me_3Si)_2Si{=}C(OSiMe_3)R$ give with triphenylimine the unstable **514** which is converted completely, faster upon photolysis or more slowly in the dark, into the silaazetidine **515** (equation 174). For the adamantylsilene **150** the complete conversion from the acylpolysilane to **515** (R = 1-Ad) requires 5 days and proceeds in an overall yield of 94%[248]. The mesitylsilene **349** forms no [4 + 2] cycloadduct, and the only product of the reaction with triphenylimine detected after 24 h is the silaazetidine **515** (R = Mes)[248]. The imine component also influences the product distribution of the reaction. For example, no [4+2] cycloadducts are formed in the reaction of silenes $(Me_3Si)_2Si{=}C(OSiMe_3)R$ with *N*-fluorenylidineaniline and only silaazetidines have been detected[248].

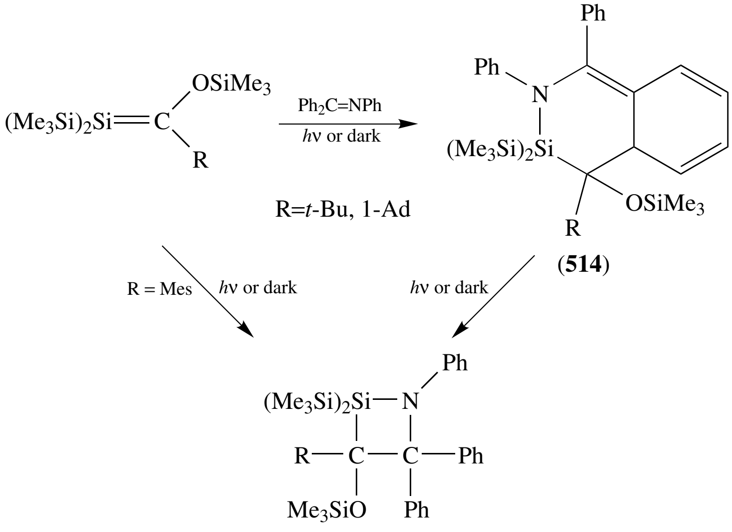

(**514**)

(174)

(**515**)

Most of the silaazetidines are remarkably stable and prolonged heating over days at 70 °C is required to reconvert them to precursors acylpolysilane and imine (equation 175)[248]. This is in contrast to the behaviour of silaazetidines deriving from

'Wiberg'-type silenes which can be easily cleaved thermolytically to the silene and the imine[60–64].

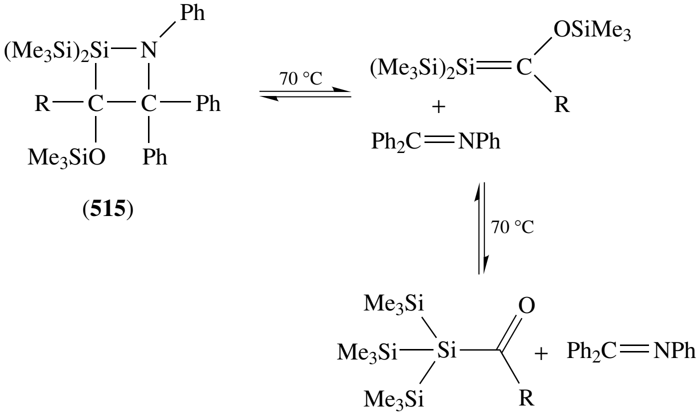

(**515**)

(175)

An exception is the silaazetidine **516** prepared from **349** and *N*-fluorenylidineaniline, which decomposes slowly already at room temperature, yielding the head-to-head dimer **517** of the intermediate silanimine **518** and siloxyalkene **519** (equation 176)[248].

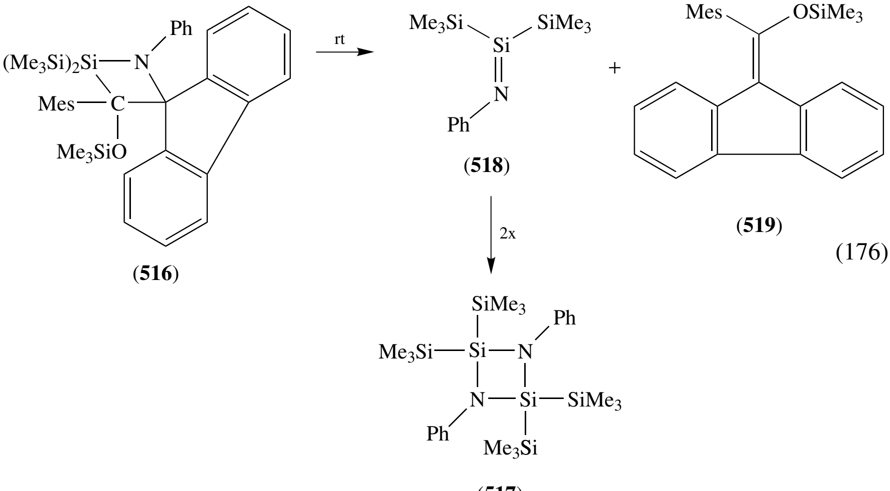

(**516**) (**518**) (**519**) (**517**)

(176)

Silaacrylate **305** undergoes reactions with ketones[165]. The initial coordination of the ketones is reminiscent of the donor adducts to silenes. The products **520–522** are formed by an ene or a formal $[2 + 2]$ cycloaddition reaction, depending on the substituents on the ketones (equation 177).

Leigh could prove the formation of siloxetanes **525** from carbonyl compounds and silatrienes **524** obtained through the photolysis of aryldisilanes **523** (equation 178)[136,137,140,249]. They are thermally and hydrolytically unstable but an unambiguous assignment was possible through NMR spectroscopy. The yield of siloxetanes

525 varies with the degree of aryl substitution at the silene's **524** silicon atom.

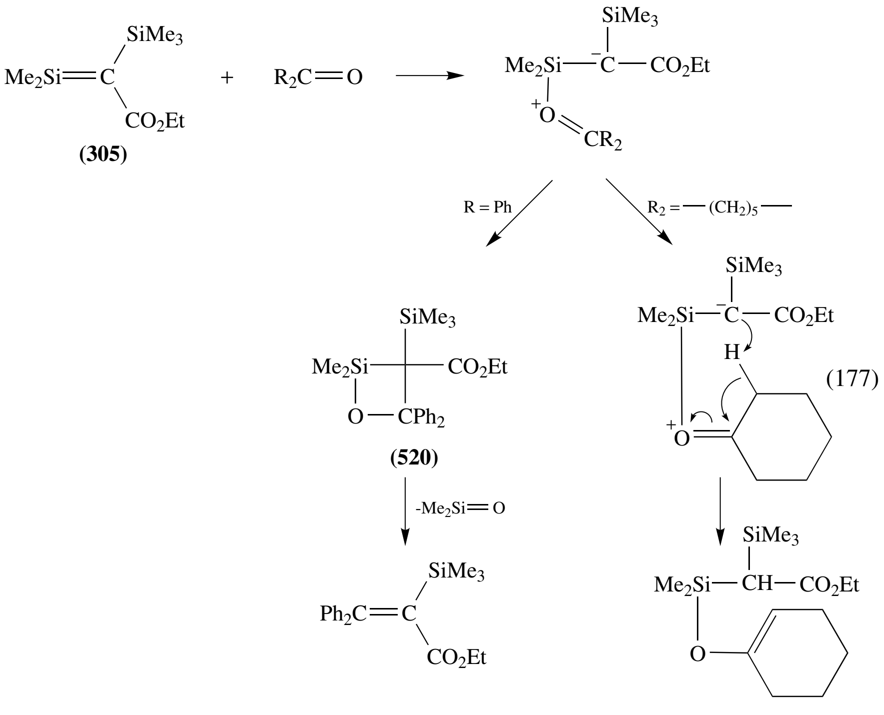

(305)

(520)

(177)

(521)

(522)

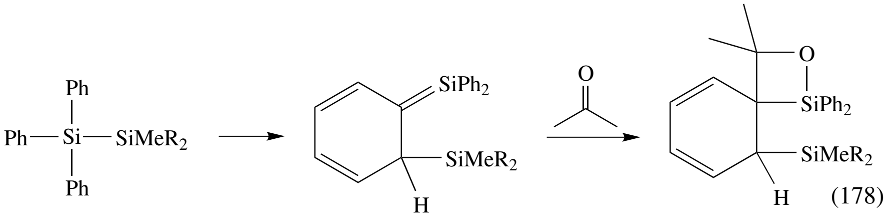

(178)

(523)

(524)

(525)

R = Me, Ph

A siloxetane **526** as an intermediate from a [2 + 2] cycloaddition of silene **241** with acetone has been formulated by lshikawa[134]. It extrudes a silanone equivalent to give the vinyl ether **527**. The second regioisomeric silene **242** generated together with **241** by photolysis of **240** undergoes an ene reaction instead (equation 179)[134].

f. Miscellaneous silenes. i. [2 + 2] Cycloaddition reactions. Conlin and Bobbitt photolysed the symmetric 1,2-divinyldisilane **528** and obtained silene **42** which was trapped by buta-1,3-diene to form the E/Z isomeric [2 + 2] cycloadducts **40**, along with minor amounts of the [4 + 2] cycloadduct (equation 180)[37].

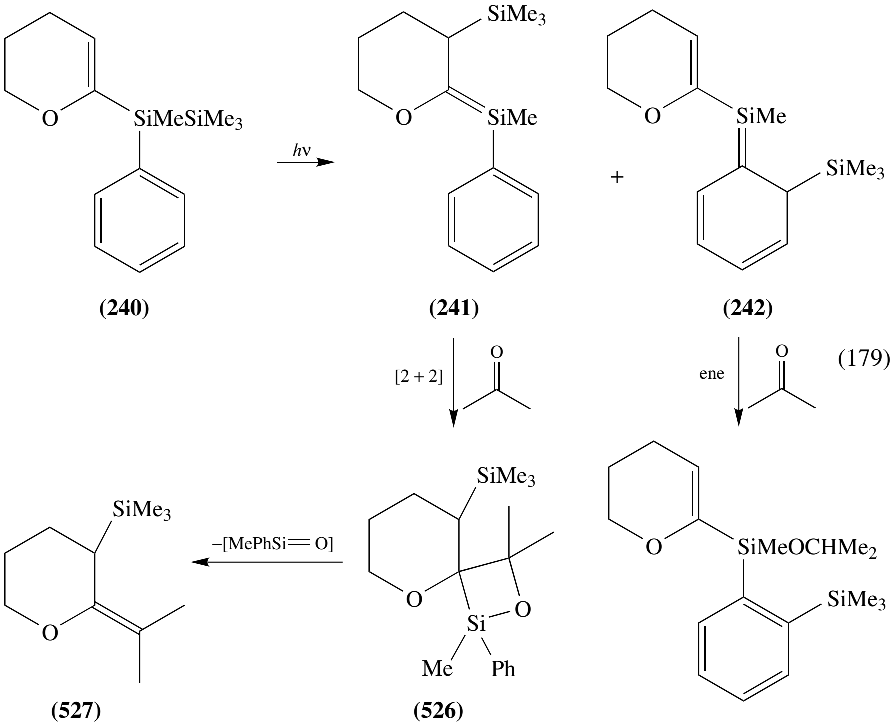

(179)

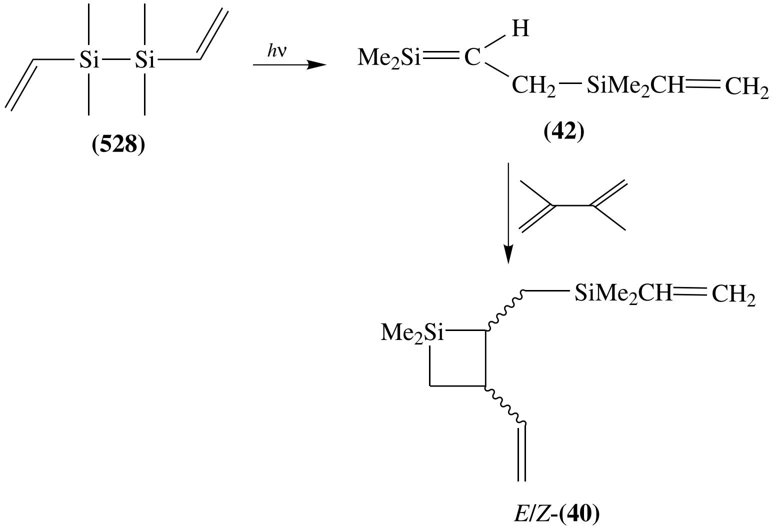

(180)

The silene **42** itself is liberated from the vinylsilacyclobutanes **40** and undergoes, in competition with other reactions, an intramolecular [2 + 2] addition giving **44** (equation 181).

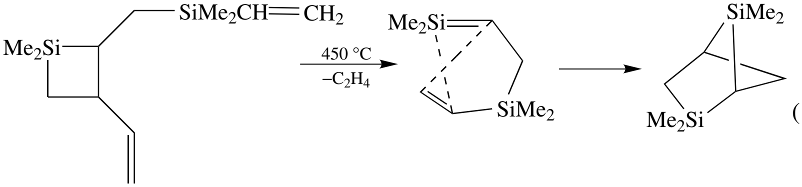

(40) **(42)** **(44)** (181)

The pyrolysis of 1,1-dimethyl-1-silacyclobut-2-ene **80** gives 1,1-dimethylsilabutadiene **81**[54,250]. The consecutive reactions of **81** yield several compounds **529–533** (with the yields given at 363 °C after 180 min of pyrolysis) (equation 182). While **529** is formed by the dimerization of **81**, the authors suggest a pathway to the formation of the formal dimers **530** and **531** that includes cycloaddition reactions with the starting compound **80**. A Diels-Alder-type reaction gives regiospecifically **530** and the [2+2] cycloreaction gives initially the bicyclic compound **534**, which undergoes subsequent ring expansions to **535** and to **531** (equation 183). In a secondary fragmentation reaction **535** decomposes into dimethylsilene **2** and **532**. The occurrence of small amounts of **533** can be rationalized by a [4 + 2] cycloaddition between **81** and **2**.

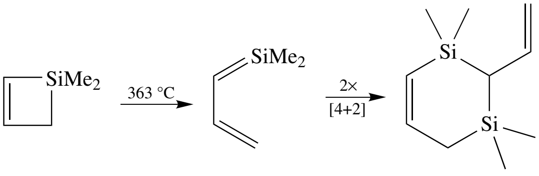

(80) **(81)** **(529)** 9% (182)

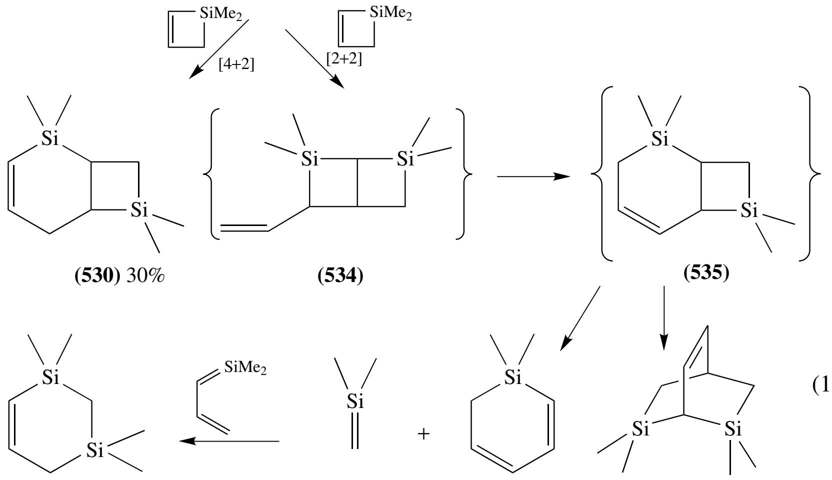

(183)

ii. [2 +3] Cycloaddition reactions. The photochemical decomposition of bis(silyldiazomethyltetrasilane **321** produces one silene group in **322** followed by [2 + 3] silene–diazo cycloaddition to give **323** and finally **324** (equation 184)[168,165].

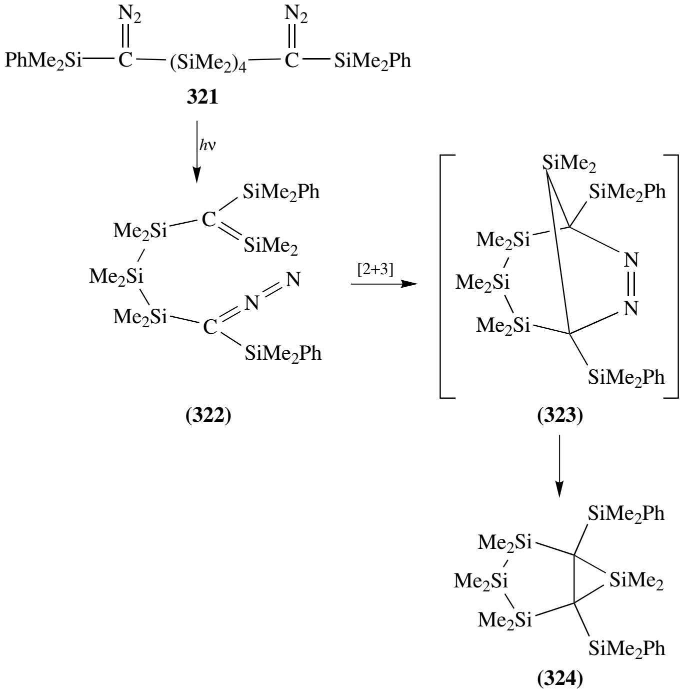

(184)

iii. [2 + 4] Cycloaddition reactions. Conlin and Namavari have demonstrated that 1-silabuta-1,3-dienes may undergo a stereospecific [4 + 2] and non-stereospecific [2 + 2] cycloaddition with alkenes[54]. Isomerization of 1,1-dimethylsilacyclobutene **80** in the presence of 20-fold excess of ethylene at 350 °C leads cleanly to a mixture of the isomeric silacyclohexenes **82** and **83** in nearly quantitative yields. Formation of the silacyclohex-2-ene **82** might be anticipated from a Diels–Alder-type reaction between ethylene and sila-1,3-diene **81** (equation 185).

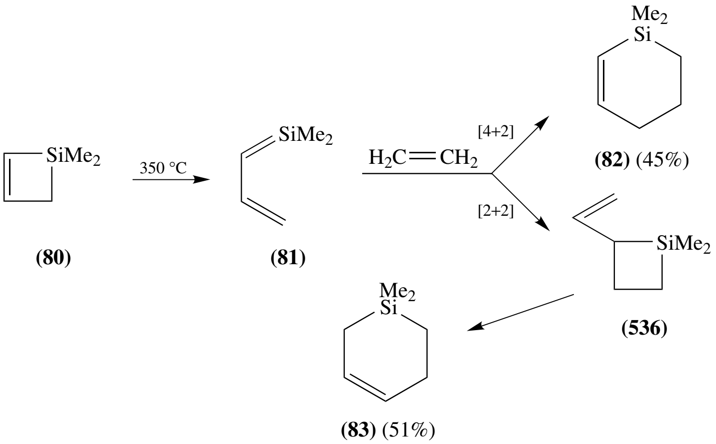

(185)

The observation of the silacyclohex-3-ene **83** was rationalized by a [2+2] cycloaddition of ethylene to give unusual 2-vinylcyclobutane **536**. A facile ring expansion via a 1,3-silyl shift to the terminal methylene group yields **83**. Surprisingly, the relative product ratio **82/83** suggests that $\Delta G^{\ddagger}$ for the forbidden [2 + 2] reaction is slightly smaller than for the stereospecific allowed Diels–Alder path[54].

The [4 + 2] reaction was shown to be stereospecific by the formation of only one geometric silacyclohex-2-ene isomer (**537** or **538**) in the reaction of **81** with *Z*- or *E*-but-2-ene, respectively, whereas the distribution of products deriving from the [2 + 2] cycloaddition (**539–541**, equation 186) suggests a non-stereospecific course of the reaction[54].

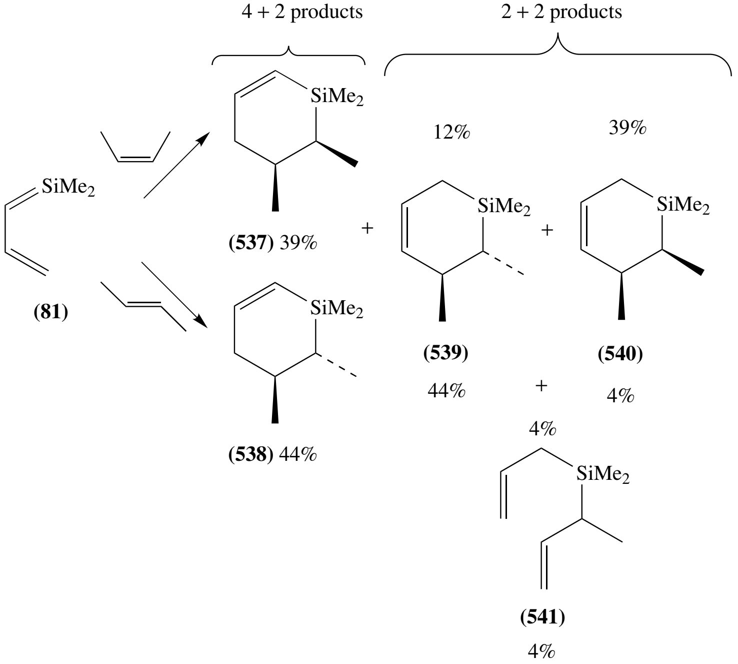

(186)

The *ortho* quinodisilane **57** reacts with acetylenes exclusively in a [4 + 2] fashion. The only product isolated in 89% yield from the reaction with phenylacetylene is **542** (equation 187)[46,45].

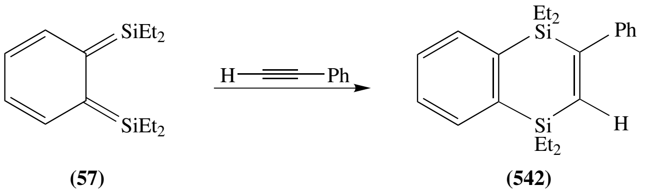

(187)

5. Ene reactions

The competitive silyl migration to either a vinyl or phenyl group in aryl- and vinyldisilanes has been investigated by Ishikawa and coworkers[133]. With 2,3-dimethylbuta-1,3-diene, two modes of ene reaction are possible for **238** to give **543** and **544**. Another ene product **547** arises from silene **239**. Both silenes react with acetone to give the respective ene products **545** and **546** (equation 188).

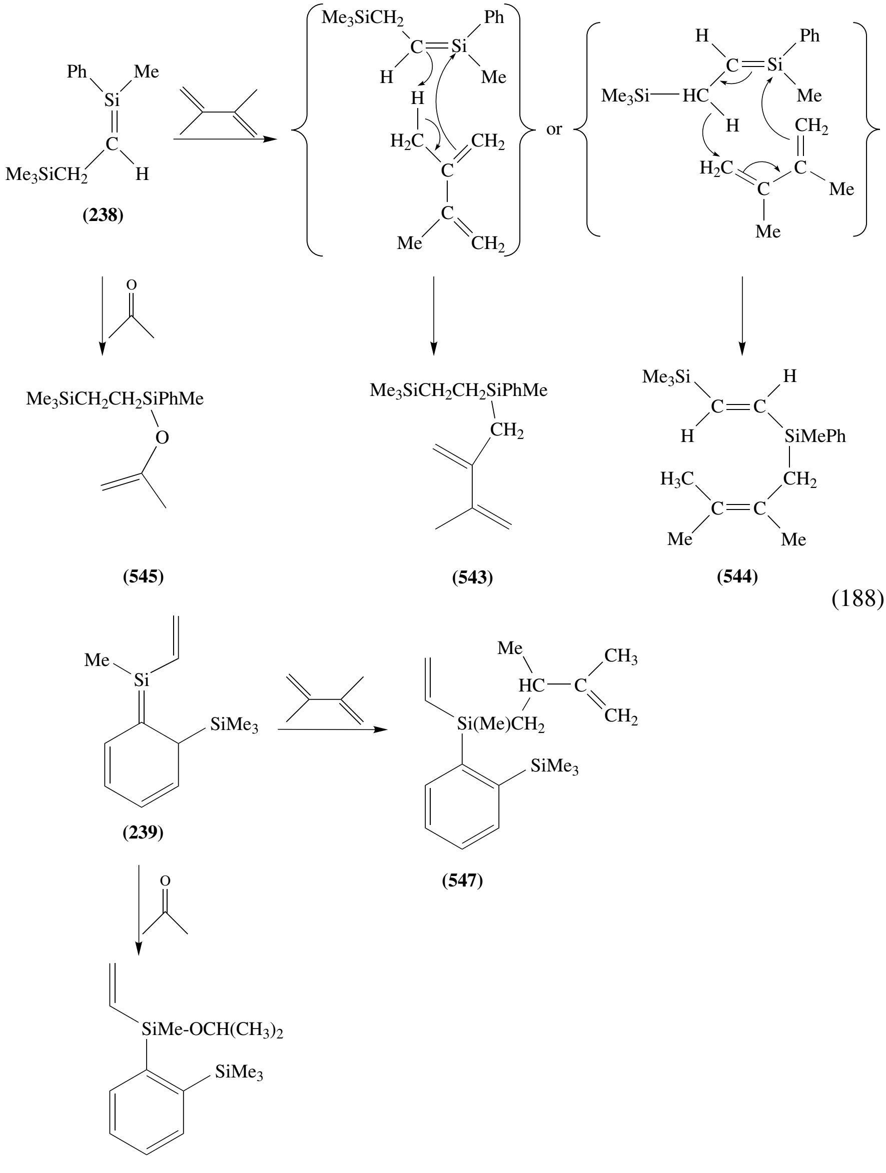

(238) **(545)** **(543)** **(544)** **(239)** **(547)** **(546)**

(188)

With dihydropyranyl-substituted phenyldisilane **240** Ishikawa and coworkers found the formation of both possible types of silenes **241** and **242**[134]. Both were trapped by acetone, but **242**, however, only through an ene reaction to give **549**. With isobutene only the silene **242** gives an ene product **548** (equation 189).

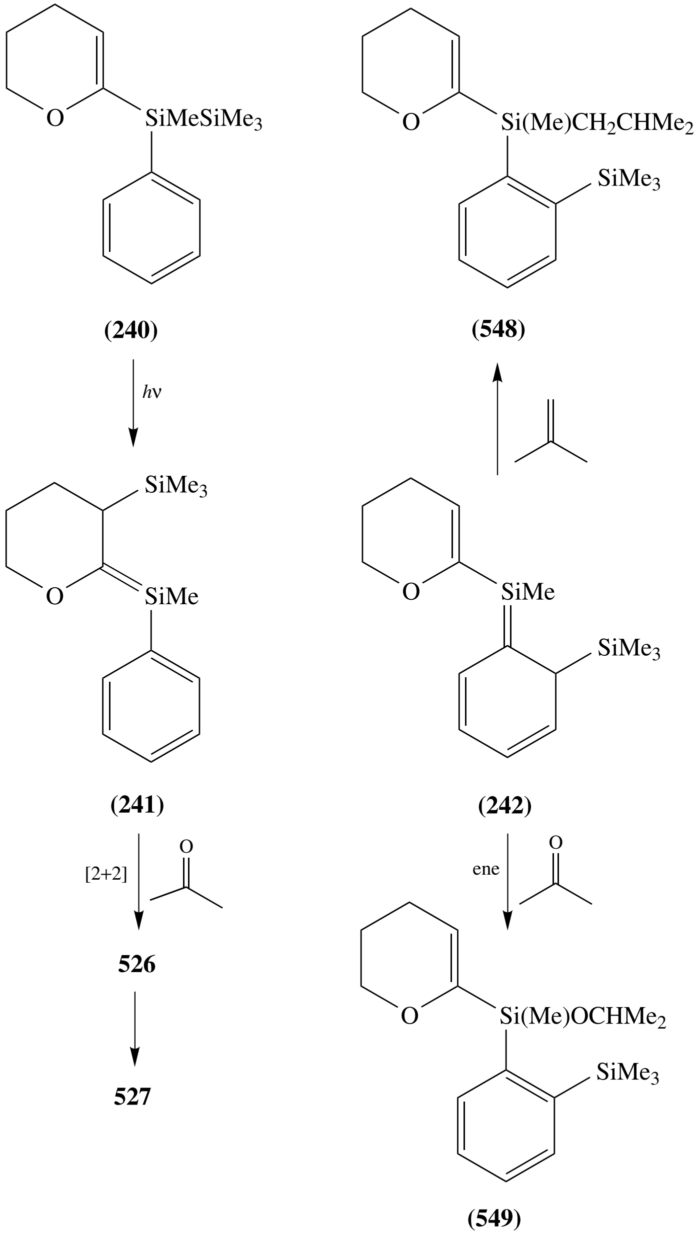

(189)

The stereochemistry of the ene reaction with carbonyl compounds has been investigated by Ishikawa and coworkers with *meso*-**(550)** and *rac*-Ph(Et)MeSi−SiMe(Et)Ph as silene precursors[251]. With acetone and acetaldehyde the reactions were found to be highly diastereoselective when run in ether or toluene. In electron-donating solvents like THF or acetonitrile the diastereoselectivity decreased, and this was ascibed to a stepwise reaction.

With benzophenone the reactions are stereoselective. Equation 190 outlines the reaction mechanism for the case of acetone ($R^1 = R^2 = Me$). The disilanes rearrange via a concerted suprafacial 1,3-silyl shift under the photochemical conditions to produce the silenes diastereospecifically.

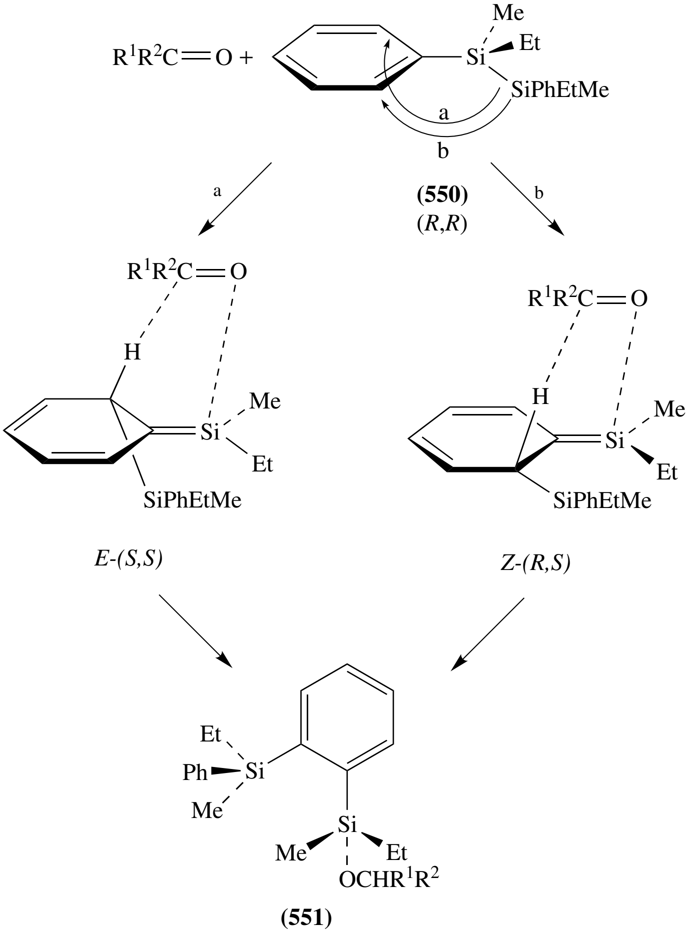

(190)

(551)

(R,S)

The ene reactions of the silatriene from $Ph_3Si{-}SiMe_3$ **552** with acetone and 2,3-dimethylbuta-1,3-diene have been investigated by Leigh and Sluggett[140]. In addition, a [2 + 2] cycloadduct is formed in the reaction with acetone.

6. Oxidations

All known silenes react violently with molecular oxygen with the exception of the stable 1-silaallenes which are air-stable. Along with carbonyl compounds the products of the oxidation of silenes are cyclic siloxanes from the corresponding silanone, depending on the reaction conditions[3,8,28]. For example, when the stable adamantylsilene **150** is exposed to dilute dry oxygen, the major products of the reaction are the cyclic trimer **553** and the trimethylsilyl ester **554**[3]. As an intermediate the disila-2,3-dioxetane **555** was suggested (equation 191)[13].

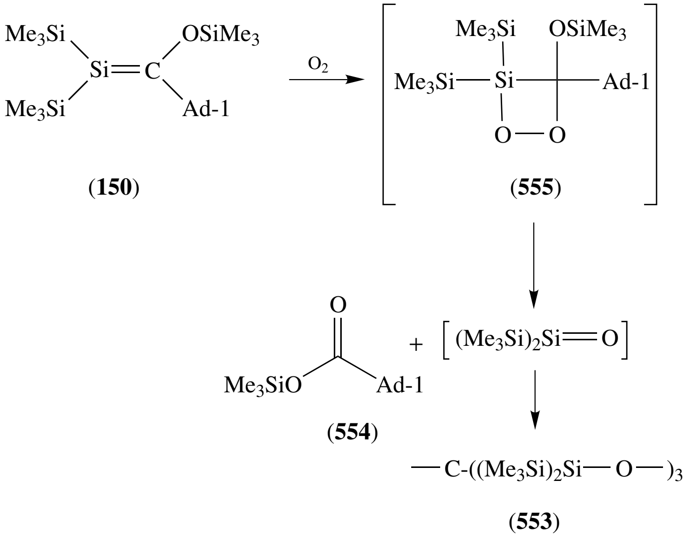

(191)

Only a recent matrix isolation study by Sander and coworkers gives further evidence for these type of intermediates[252,253]. They followed the reaction of small silenes with molecular oxygen in an argon matrix at 10–25 K with IR spectroscopy. Their results for the oxidation of $Me_2Si{=}CHMe$ **8** suggests the mechanism shown in equation 192. Initially the triplet biradical **T556** is formed. Intersystem crossing of **T556** to **S556** and fast exothermic ring closure gives the siladioxetane **557**. This opens easily, giving a complex **558** between dimethylsilanone and acetaldehyde. Finally, hydrogen transfer and silicon oxygen bond formation gives the product **559**, which could be identified by IR spectroscopy. The intermediacy of the biradical could be established by the spectroscopic identification of the hydroperoxide **560** (equation 192). A complex between methylsilanone and formaldehyde similar to **558** has been detected in the oxidation reaction of methylsilene. Although the existence of dioxetane intermediate **557** could not be proven directly, the identified oxidation product **559** gives strong evidence that siladioxetane **557** is an intermediate in the oxidation of silenes. Further support comes from the spectroscopic identification of complexes similar to **558** in the related oxidation of methylsilene[253]. Whether the excess energy produced in the exothermic formation of **557** leads to the fragmentation or if siladioxetanes like **557** are intrinsically unstable could, however, not be answered[253].

Some evidence for the intermediacy of a siladioxetane was given by Brook and coworkers, who detected in the careful oxidation of E/Z-**392** at $-70\,^{\circ}C$ a new species whose ^{29}Si NMR spectrum is consistent with a structure like **561**[95]. The originally proposed heterolytic ring opening to the peroxocarbene **562** and the consecutive reactions via the radicals **563** and **565**, followed by recombination to **564** which is the only product (equation 193)[95], is however not consistent with the results of the matrix isolation study by Sander and coworkers[252,253]. We suggest therefore that also in the oxidation of **392** a complex **566**, between a silanone and an ester, is formed as an intermediate which, after initial nucleophilic attack by the oxygen on the silicon and subsequent trimethylsilyl shift, yields **564** (equation 194).

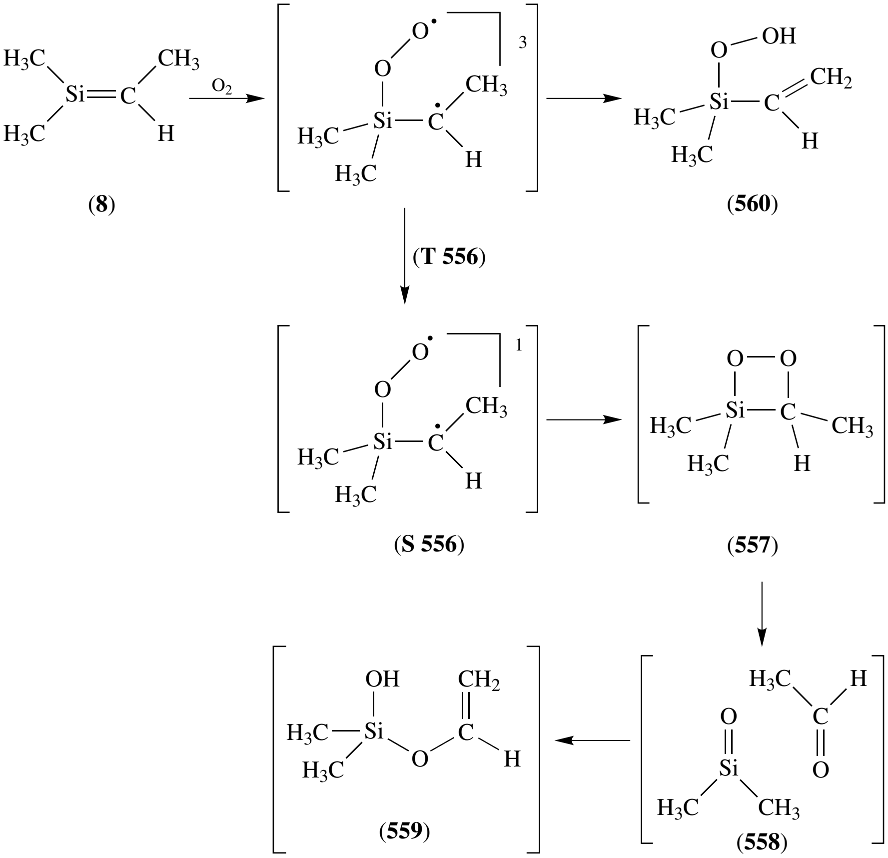

(192)

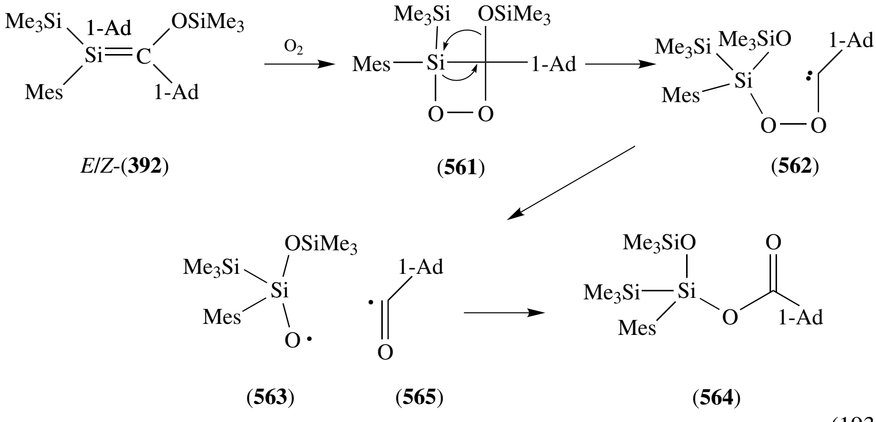

(193)

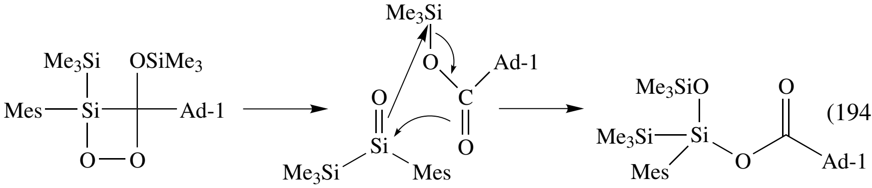

(561) **(566)** **(564)**

(194)

7. Miscellaneous

Different reaction modes between free **104a** and **104a**•donor adducts are found in two cases:

(a) The adduct **104a**•pyridine does not decompose in the regular way to give **104a** and pyridine, but isomerizes well below 0 °C by formation of the insertion product **567** into an *ortho* CH bond of pyridine (equation 195).

$$\mathrm{Py{\bullet}Me_2Si{=}C(SiMe_3)(SiMeBu\text{-}\mathit{t}_2)}$$

104•py

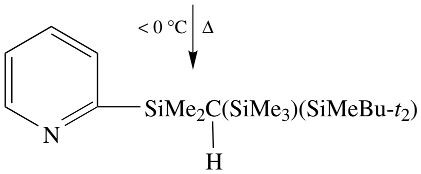

(567)

(195)

(b) The bromination of **104a** leads to the expected dibromo compound **568**, whereas with **104a**•THF, **568** and **569** — with incorporated THF — are formed in a 1 : 1 ratio (equation 196).

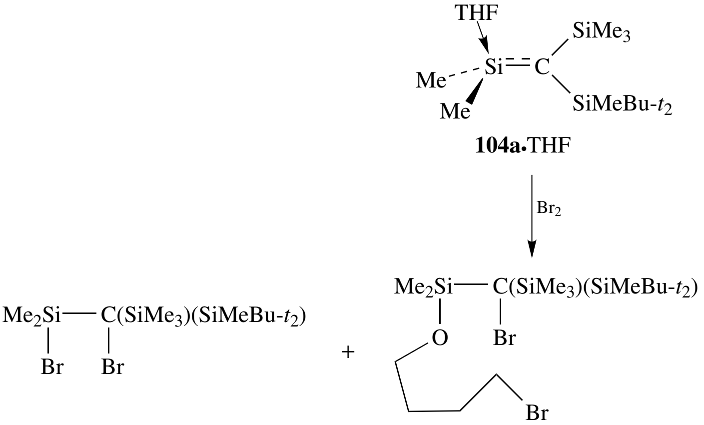

104a•THF

(568) **(569)**

(196)

C. Structure and Spectroscopic Properties of Silenes

1. Structural studies

In the early days of silene chemistry most of the structural data for simple silenes came from IR, UV[1,2,7,8,29,157,158,254–256] and microwave studies[257,258]. By 1997 only three X-ray studies of stable silenes had been published[3,4,111] and much of the information about structure and bonding in silenes came from *ab initio* molecular orbital calculations. These data are well summarized in several review articles by Brook and Brook[9] and by Michl and Raabe[7,8]. The important role which *ab initio* calculations play in this field is outlined in the comprehensive review by Apeloig[11] and by Karni and Apeloig[12]. We will therefore emphasize in this paragraph the new important findings and we will outline the general trends of structural silene chemistry. Some structural data and original references are summarized in Table 12.

Only very recently a millimeter microwave study by Bogey, Bürger and coworkers established finally the ground state geometry of the parent silene **25**[31–33]. **25** was generated

TABLE 12. Structural parameters of silenes and related compounds (bond length in Å)

Compound	*r* (Si=C)	Method	Remarks	References
Silenes				
$H_2Si{=}CH_2$ **25**	1.704	millimeter microwave		31–33
$Me_2Si{=}CH_2$ **2**	1.692	microwave		254, 257
$Me_2Si{=}C(SiMe_3)(SiMeBu\text{-}t_2)$ **104a**	1.702	X-ray	twisted by 1.6° $\Sigma SiCSi = 360^{\circ f}$	4
$(Me_3Si)_2Si{=}C(OSiMe_3)Ad\text{-}1$ **150**[a]	1.764	X-ray	twisted by 16°	3
$(Me_3Si)_2Si{=}Ad\text{-}2$ **167**[b]	1.741	X-ray	twisted by 4.6°	111
1-Silaallenes				
1-AdSupSi=C=fluorene-2 **571**[a,c,d]	1.704	X-ray	*trans* bent	5
$Tip_2Si{=}C{=}C(Ph)\ Bu\text{-}t$ **572**[e]	1.693	X-ray	Σ: 357.2[f]	259
Silaaromatics				
$(PhC)_4Si^{2-}$ **574a**	1.850	X-ray	dilithio compound	260
$(MeC)_4Si^{2-}$ **575**	1.830	X-ray	dipotassium compound	261, 262
Silene donor adducts				
$Me_2Si{=}C(SiMe_3)(SiMe\ Bu\text{-}t_2){\bullet}THF$ **104a**•THF	1.747	X-ray	$r(D \rightarrow Si) = 1.878^g$ $\Sigma SiCSi = 348.7^{\circ f}$	197
$Me_2Si{=}C(SiMe_3)(SiMe\ Bu\text{-}t_2){\bullet}F^-$ **104**•F^-	1.777	X-ray	$r(D \rightarrow Si) = 1.647^g$ $\Sigma SiCSi = 341.7^{\circ g}$	83
$Me_2Si{=}C(SiMe_2Ph)_2{\bullet}NEtMe_2$ **97**•$NEtMe_2$	1.761	X-ray	$r(D \rightarrow Si) = 1.988^g$	84

[a] 1-Ad = 1-adamantyl.

[b] 2-Ad = 2-adamantylidene.

[c] Sup = 2,4,6-tributylphenyl.

[d] fluoren = 1,3,6,8-tetraisopropyl-2,7-dimethoxyfluorenylidene.

[e] Tip = 2,4,6-tri-isopropylphenyl.

[f] pyramidalization.

[g] D = donor.

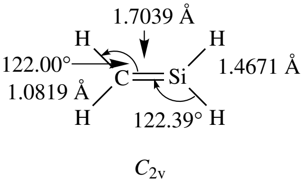

FIGURE 4. Experimental equilibrium structure of silene **25**, deduced from the rotational constants of six different isotopomers (for error margins see Table 13)[31-33].

by pyrolysis of 5,6-bis(trifluoromethyl)-2-silabicyclo[2.2.2]octa-5,7-diene **30** at 600 °C and at 1000 °C from silacyclobutane **22** and in traces also from 1,3-disilacyclobutane **24** in a flow of argon. The search for the millimeter wave transitions in the 180–473 GHz frequency range was guided by high level *ab initio* calculations of the rotational constants up to the CCSD(T) level of theory by Breidung, Thiel and coworkers[31]. The perfect agreement between the experimentally observed rotational constants A_0, B_0 and C_0 and the values predicted by the calculations (see Table 13) confirms beyond doubt that the rotational spectrum of $H_2C{=}SiH_2$ was observed[31]. From the rotational constants of six isotopomers of **25**, the experimental equilibrium structure shown in Figure 4 was deduced[32,33]. The geometric parameters are consistent with the results of *ab initio* calculations summarized in Table 13.

The Si=C bond length of 1.704 Å for **25** is in accord with a microwave study of $Me_2Si{=}CH_2$ **2** by Gutowsky and coworkers[257,258]. They found for **2** a Si=C bond length of 1.692 Å, in agreement with all *ab initio* calculations[246] but in contrast with a previous electron diffraction study which predicted an erroneously long Si=C bond length of 1.83 Å[263].

TABLE 13. Molecular constants of $H_2Si{=}CH_2$[31-33]

Parameter[a]	*Ab initio*					Experimental
	SCF[b]	MP2[b]	CCSD[b]	CCSD(T)[b]	CCSD(T)[c]	
r_e(C=Si)	1.6922	1.7085	1.7084	1.7167	1.7043	1.7039(18)[d]
r_e(CH)	1.0739	1.0777	1.0781	1.0799	1.0824	1.0819(12)[d]
r_e(SiH)	1.4684	1.4680	1.4713	1.4728	1.4670	1.4671(9)[d]
α_e(HCSi)	122.32	121.84	122.12	122.04	122.06	122.00(4)[d]
α_e(HSiC)	123.01	122.6	122.6	122.50	122.49	122.39(3)[d]
A_0	106554	105200	105119	104557	104945.0	104716.6
B_0	14944	14719	14700	14583	14772.6	14786.7
C_0	13082	12890	12875	12776	12927.9	12936.3
μ_e	1.114	0.867		0.810		0.700

[a] Equilibrium distances r_e in Å and angles α_e in deg; ground state rotational constants (A_0, B_0, C_0) in MHz; dipole moment μ_e in D.

[b] TZ2Pf basis set was used.

[c] cc-pVQZ(C,Si)/cc-pVTZ(H) basis set was used.

[d] The quoted accuracy corresponds to 15 standard deviations.

Three X-ray structures of stable silenes were published by 1997. All three silenes differ markedly in their substitution pattern and we will discuss them below in more detail. Historically, the first silene which was subjected to an X-ray analysis was the 'Brook'-type silene $(Me_3Si)_2Si{=}C(OSiMe_3)Ad\text{-}1$ **150**[3]. **150** had a relatively long Si=C bond length of 1.764 Å and its double bond is twisted by 16°. The increased bond length in **150** could be satisfactorily explained by Apeloig and Karni[246] by calculating the substituent effects on the Si=C bond length. The combined effect of two silyl substituents at silicon, and especially of the one siloxy substituent on carbon, lengthens the Si=C bond by 0.070 Å. Taking this substituent effect into account, the relatively long Si=C bond length is fully consistent with the Si=C bond length in the unsubstituted **25**[246]. This excellent experimental—theoretical agreement implies that in **150** the elongation of the Si=C bond due to the steric repulsion between the bulky substituents is small[246]. In contrast, the 16° twist in **150** is explained by steric interaction between the bulky groups at the ends of the double bond. Small twist angles in silenes have only minimal effects on the bond strengths[10]. Steric congestion in silenes leads to a twisting of the Si=C bond rather than to a bond elongation.

A much less perturbed Si=C bond is found in the Wiberg silene $Me_2Si{=}C(SiMe_3)(SiMe(Bu\text{-}t)_2)$ **104a**[4]. **104a** was shown to be nearly planar (twist angle of 1.8°), and the length of the Si=C bond was 1.702 Å, very near to the bond length of **25** and in perfect agreement with calculated substituent effects.

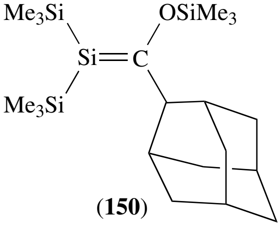

(**150**)

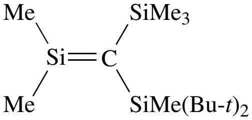

(**104a**)

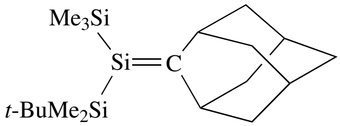

(**162**)

Only very recently Apeloig, Bravo-Zhivotovskii and coworkers published the X-ray structure of the indefinitely stable silene **162**, synthesized in a sila-Peterson reaction[111]. Due to the synthetic approach to it, **162** has a novel substitution pattern, and it bears two silyl groups at silicon and two alkyl substituents on carbon. **162** exhibits an essentially planar arrangement around the C=Si bond with a small twist angle of 4.6° around the Si=C bond. The Si=C bond length in **162** is 1.741 Å, intermediate between that in **150** and **104a**. Similar to **150** the elongation of the Si=C bond in **162** is due to electronic effects of the substituents and not to their steric bulk. Thus, the calculated (HF/6-31G*) r(Si=C) in **162** of 1.734 Å is only 0.005 Å longer than for the strain-free $Me_2C{=}Si(SiH_3)_2$ **570** (1.729 Å at HF/6-31G*)[111].

The Si=C bond lengths in the recently synthesized novel stable 1-silaallenes **571**[5] and **572**[259] are relatively short (1.704 Å and 1.693 Å in **571** and **572**, respectively). This might be expected for a Si=C double bond formed from a sp-hybridized carbon and a sp^2-hybridized silicon. Both 1-silaallenes are slightly bent at the central carbon [α(SiC^{1}C^2): 173.5° and 172.0° in **571** and **572**, respectively][5,259] and **571** is *trans* bent about the Si=C^1 bond in agreement with theoretical predictions[264].

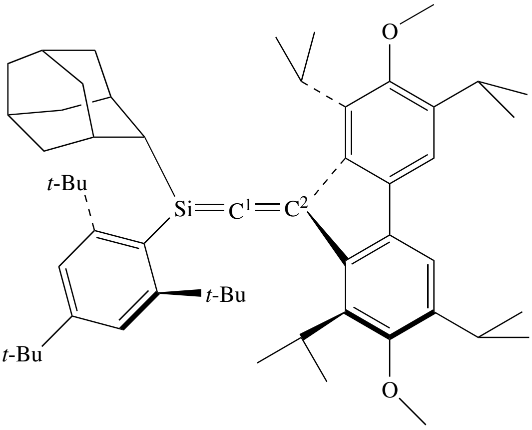

(571)

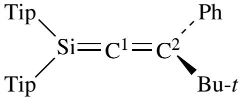

(572)

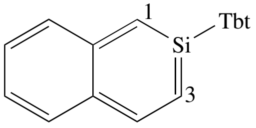

(573)

Tbt = 2,4,6-[$(Me_3Si)_2CH]_3C_6H_2$

Since 1994 several silaaromatic compounds have been synthesized[265] and structurally characterized[260–262]. The crystal structure of the remarkably stable 2-silanaphthalene **573** reveals planar environment around silicon, suggesting a delocalization of π-electrons in the 2-silanaphthalene ring system of **573**[6]. Further structural details were not reported due to severe disordering of the 2-silanaphthalene ring in the crystal. The crystal structures of the two silole dianions **574a**[260] and **575**[261] have been reported by the groups of West and Don Tilley. In both compounds the five-membered ring is planar and the inner-cyclic C−C bond lengths are nearly equalized, indicating the occurrence of cyclic conjugation in both compounds. The SiC bond lengths in **574a** and **575** are in the usual range for SiC single bonds. Calculations reveal, however, that silyl dianions are expected to have very long C−Si bonds, i.e. MeHSi^{2-}: 2.078 at MP2(fc)/6-31+G*)[266]. Thus the comparatively short Si−C$^\alpha$ distance in dianions **574a** and **575** indicates some degree of π-bonding. This view is supported by further theoretical analysis[266,267].

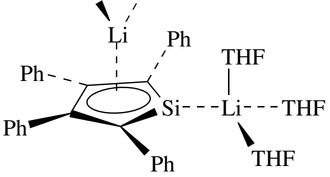

(574a)

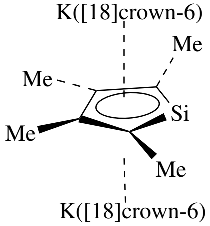

(575)

From the accumulated experimental and theoretical structural data one can draw the following general picture: The $R_2Si{=}CR_2$ unit is essentially planar with a Si=C bond length of about 1.70 Å. Electronic substituent effects do influence strongly the measured Si=C bond length. It is noteworthy that the substitution pattern is also important for r(Si=C). Thus, for $Me_2C{=}Si(SiH_3)_2$ **576** a much longer r(Si=C) is calculated than for the isomeric $Me_2Si{=}C(SiH_3)_2$ **577** [1.754 Å compared to 1.722 Å for **576** and **577** at MP2(fc)/6-31G*, respectively][111]. This theoretically predicted behaviour is supported by the structural data for **104a**[4] and **162**[111] (see Table 13). Steric interactions between the substituents at the Si=C bond do not contribute significantly to the Si=C[1] bond length but do enforce small twisting of the double bond. The Si=C[1] bond in 1-silaallenes is somewhat distorted towards a *trans* bent arrangement.

2. ^{29}Si and ^{13}C NMR spectroscopic data

a. ^{29}*Si NMR spectroscopy*. The chemical shifts of sp^2-hybridized silicon in silenes are found significantly downfield from the position normally observed for tetracoordinated, sp^3-hybridized silicon atoms. This is reminiscent of the carbon analogs alkanes and alkenes. Although the experimental data are limited to a small number of silenes with only small variances in the substitution pattern, the data summarized in Table 14 allows one to already draw some conclusions. The ^{29}Si chemical shift of silenes depends markedly on the substituents at silicon. Thus, silenes bearing two silyl substituents, i.e. silenes from the Brook family **149, 150, 578–580**[3,38,90,91,93,95] or those synthesized in the group of Apeloig[111] **162** and **585**, absorb in the relatively small region from 41 to 54 ppm (see Table 14). At the other extreme, two methyl groups at the silicon, like in Wiberg's silene **104a**[268] or in $Me_2Si{=}C(SiMe(t\text{-}Bu)OSiMe_3)Ad\text{-}1$ **583**[90], lead to an extremely deshielded ^{29}Si resonance ($\delta^{29}Si = 144$ ppm and 126.5 ppm in **104a** and **583**, respectively). This reflects already the different polarization of the Si=C bond in those silenes, which is also revealed in their different chemical behaviour. When in Brook-type silenes one trimethylsilyl group is replaced by an aryl group, little effect on the ^{29}Si chemical shift is observed (0.3 ppm for the mesityl substituent in *E*-**392**[95] and 7.3 ppm for the phenyl group in **581**[90], while the *t*-butyl group in **582** leads to a significant downfield shift by 32.3 ppm compared with **150**[91]. The neopentyl silene **134** recently isolated by Delpon-Lacaze and Couret with two aryl groups at the trigonal silicon resonates at 77.6 ppm[269].

A comparison with the substituent effects on the chemical shift in disilenes might be of interest here: The sp^2-hybridized silicon in tetramesityldisilene **590** has a ^{29}Si chemical shift ($\delta^{29}Si = 63.3$ ppm)[269,270] similar to that of the neopentylsilene **134**. In contrast with the relatively small shielding effect of two silyl groups on δ^{29}Si in silenes ($\delta^{29}Si =$ 49.7 ppm for **585**), silyl substitution in the disilenes leads to a markedly downfield shift. Thus, for tetra(triisopropylsilyl)disilene **591** $\delta^{29}Si = 164$ ppm is found[270,254]. Apparently, substituent effects on the ^{29}Si chemical shift found in silenes do not simply parallel those in disilenes.

$$R_2Si{=}SiR_2$$

(**590**) $R = Mes$

(**591**) $R = (i\text{-}Pr)_3Si$

Coupling constants across the Si=C bond are measured for some stable Brook-type silenes[29]. All $^1J_{Si=C}$ coupling constants cluster around 84 Hz, which is appreciably larger than $^1J_{SiC}$ between sp^3-hybridized silicon and attached methyl carbons (47–48 Hz), consistent with a double bond between carbon and silicon[91].

TABLE 14. $\delta^{29}Si$ and $\delta^{13}C$ chemical shifts (ppm) of silenes and related compounds

Compound	$\delta^{29}Si$	$\delta^{13}C$	Remarks	References
$(Me_3Si)_2Si{=}C(OSiMe_3)R$				
R = *t*-Bu **(149)**	41.5	212.7	$^1J_{C=Si} = 83.5$ Hz	38, 91
R = 1-Ad(**150**)[a]	41.4	214.2	$^1J_{C=Si} = 84.4$ Hz	3, 91
R = CEt_3 **(578)**	54.3	207.3	$^1J_{C=Si} = 83.9$ Hz	3, 91
R = (1-Me)cyhex **(579)**[b]	43.5	212.9	$^1J_{C=Si} = 85.0$ Hz	90, 91
R = bco **(580)**[c]	42.4	212.7		90
$(Me_3Si)_2Si{=}C(OSiMe_3)Mes$ **(349)**	37.8	197.7		181
$(Me_3Si)_2Si{=}C(OSiEt_3)Mes$ **(184)**	34.3	197.7		121
$(Me_3Si)(Ph)Si{=}C(OSiMe_3)CEt_3$ **(581)**	61.6	191.2		90
$(Me_3Si)(t\text{-}Bu)Si{=}C(OSiMe_3)Ad\text{-}1$ **(582)**[a]	73.7	195.6		90
E-$(Me_3Si)(Mes)Si{=}C(OSiMe_3)Ad\text{-}1$ **(*E*-392)**[a]	41.8	195.8		95
Z-$(Me_3Si)(Mes)Si{=}C(OSiMe_3)Ad\text{-}1$ **(Z-392)**[a]	44.0	191.6		95
E-$(Me_3Si)TipSi{=}C(OSiMe_3)Ad\text{-}1$ **(*E*-143)**[a,d]	40.3	195.9		93
Z-$(Me_3Si)TipSi{=}C(OSiMe_3)Ad\text{-}1$ **(*Z*-143)**[a,d]	43.3	191.0		93
$Me_2Si{=}C(SiMe(t\text{-}Bu)OSiMe_3)Ad\text{-}1$ **(583)**[a]	126.5	118.1		90
$Me_2Si{=}C(SiMePhOSiMe_3)CEt_3$ **(584)**	k	110.6		90
$Me_2Si{=}C(SiMe_3)SiMe(t\text{-}Bu)_2$ **(104a)**	144.2	77.2		268
$TipMeSi{=}C(SiMe_2OSiMe_3)Ad\text{-}1$ **(144)**[a,d]	108.1	127.3		93

$Mes_2Si{=}CHCH_2Bu$-*t* **(134)**	77.6	110.4	$\delta^1H(=CH) = 5.53$	82
(Me_3Si)(*t*-$BuMe_2Si)Si{=}Ad$-2 **(162)**[e]	51.7	196.8		111
(*t*-$BuMe_2Si)_2Si{=}Ad$-2 **(585)**[e]	49.7	198.2		111
(*t*-$BuMe_2Si)_2Si{=}Cypen$ **(174)**[f]	-71.0	157,160		114
Silaaromatics				
2-Tbt-Silanaphthalene[g] **(573)**	87.4	116.0(C1), 122.6(C3)	$^1J_{C1=Si} = 92$ Hz; $^1J_{C3=Si} = 76$ Hz	6
1,4-di-*t*-Bu-2,6-bis(Me_3Si)-1-silabenzene **(586)**	26.8	126–127		274
$(PhC)_4Si^{2-}$ **(574b)**	68.5	151.2[h]	dilithio compound in solution	265
$(PhC)_4Si^{2-}$ **(574a)**	87.3		dilithio compound in the solid state	260
1-Silaallenes				
1-AdSupSi=C=fluoren[a,i,j] **(571)**	48.4	225.7		5
$Tip_2Si{=}C{=}CPhBu$-*t* **(572)**[d]	13.1	213.6		259
t-BuSupSi=C=CPhBu-*t* **(587a)**[i]	55.1[l]	216.3	$^1J_{C=Si} = 142.4$ Hz	259
t-BuSupSi=C=CPh_2 **(587b)**[d]	58.7	227.9		259
t-BuSupSi=C=fluoren(a) **(588)**[d,l,m]	48.0			271
t-$Bu_2Si{=}C{=}$fluoren(b) **(589)**[n]	44.0			271

(*continued overleaf*)

TABLE 14. (*continued*)

Compound	δ^{29}Si	δ^{13}C	Remarks	References
Silenolate anions				
$(Me_3Si)_3Si{=}C(O^-)R$				
R = Mes **(182)**	−59.9	262.7		121
R = 1-Ad **(181)**[a]	−70.5	274.1		121
R = *t*-Bu **(180)**	−70.3	274.3		121
Silene donor adducts				
$Me_3N//Me_2Si{=}C(SiMe_3)_2$ (**92**•NMe_3)	36.9	56.5		83
$Me_3N//Me_2Si{=}C(SiMe_3)SiMe(Bu\text{-}t)_2$ **104a**•NMe_3)	34.7	[k]		83
$THF//Me_2Si{=}C(SiMe_3)SiMe\text{-}(Bu\text{-}t)_2$ (**104a**•THF)	52.4	[k]		83
$(D_3C)_2O//H_2Si{=}CH_2$ **(27)**	−25.2	10.8		27
$(D_3C)_2O//MeHSi{=}CH_2$ **(28)**	−1.8	[k]		27
$(D_3C)_2O//Me_2Si{=}CH_2$ **(29)**	16.8	[k]		27

[a] 1-Ad = 1-adamantyl.
[b] (1-Me)cyhex = 1-methylcyclohexyl.
[c] bco = bicyclooctyl.
[d] Tip = 2,4,6-trisopropylphenyl.
[e] 2-Ad = 2-adamantylidene.
[f] Cypen = 2,3-di-*t*-Bu-cyclopropenylidene.
[g] Tbt = 2,4,6-tris[bis(trimethylsilyl)methyl]phenyl.
[h] assignment according to Ref 267.
[i] Sup = 2,4,6-*t*-butylphenyl.
[j] fluoren = 1,3,6,8-tetraisopropyl-2,7-dimethoxyfluorenylidene.
[k] Not assigned.
[l] δ^{29}Si = 52.8 ppm reported in Ref. 271.
[m] fluoren(a) = octaisopropylfluorenylidene.
[n] fluoren(b) = fluorenylidene.

The silicon atom in the recently synthesized 4-silatriafulvene **174** is strongly shielded and therefore has a remarkably high field shifted ^{29}Si resonance (δ^{29}Si = −71 ppm)[114]. The cyclopropenyl carbons, however, were observed at relatively low field, suggesting substantial contribution from the canonical structure **174B** (equation 197)[114].

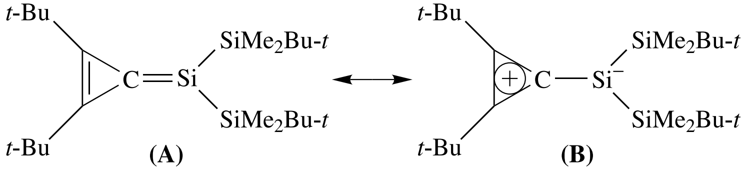

(197)

(174)

The trigonal silicon in the 1-silaallenes **571**[5], **587a-b**[259], **588** and **589**[271] gives rise to a signal in the region between 44.0–58.7 ppm. The unexpected high field shift of δ^{29}Si in **572**[259] might be reasonably explained by the substituent effect of the second aryl group which has in silenes a large shielding influence, i.e. $\Delta\delta \approx 32$ ppm for **582** compared with *E*-**392** (see Table 14). For **587a** an extremly large $^{1}J_{C=Si} = 142$ Hz is reported.

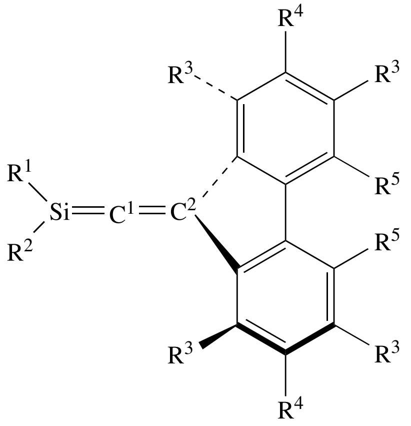

R^1/R^2	$R^3/R^4/R^5$
(571) Sup/1-Ad	*i*-Pr/OMe/H
(588) Sup/*t*-Bu	Me/Me/Me
(589) *t*-Bu/*t*-Bu	H/H/H

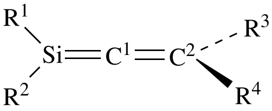

R^1/R^2	R^3/R^4
(572) Tip/Tip	Ph/*t*-Bu
(587a) Sup/*t*-Bu	Ph/*t*-Bu
(587b) Sup/*t*-Bu	Ph/Ph

The dicoordinated silicon in the aromatic silole dianion **574** resonates at an unexpectedly low field for a silyl dianion (δ^{29}Si = 68.5 ppm)[265]. The different chemical shifts in the solid state (δ^{29}Si = 87.3 ppm)[260] and in solution suggest different structures. While in the solid state a η^1,η^5 structure **574a** is proven by an X-ray structure, in solution a highly symmetric η^5,η^5 structure **574b** seems to dominate[260]. According to *ab initio* calculations both isomers show indications of cyclic conjugation[260].

The first neutral silaaromatic compound stable at room temperature was recently synthesized by Okazaki and coworkers[6,272]. The 2-silanaphthalene **573** is characterized by

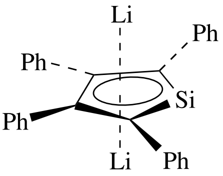

(574b)

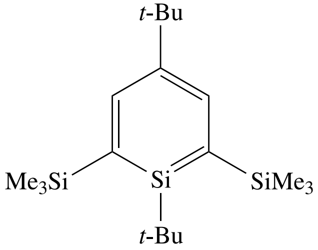

(586)

δ^{29}Si = 87.4 ppm, well in the region for trigonal sp^2-hybridized silicon. The coupling constants $^{1}J_{C=Si}$ to the neighbouring carbons C^1 and C^3 of 92 Hz and 76 Hz, respectively, are similar to those reported for the stable 'Brook' silenes. Schlosser and Märkl[274] reported that the ^{29}Si chemical shift of the highly substituted silabenzene **586** at −100 °C occurred at 26.8 ppm. It is not clear, however, if the relative high field shift of the ^{29}Si signal is characteristic for the silabenzene or is caused by complexation with the solvent THF.

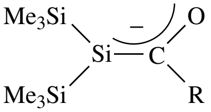

(**180**) R = *t*-Bu
(**181**) R = 1-Ad
(**182**) R = Mes

The silenolate anion **182** is characterized by a very high field shifted signal in the ^{29}Si NMR (δ^{29}Si = −59.9 ppm). It is shifted to a lower field by 15.4 ppm relative to that of the acylsilane $(Me_3Si)_3SiC(O)Mes$. Due to hindered rotation around the SiC(O) bond the two trimethylsilyl groups at the silicon in **182** are magnetically not equivalent and give rise to different signals in the NMR spectrum, which coalesce at 25 °C[121]. The barrier for rotation around the SiC(O) bond was calculated from these data to be 14.3 kcal mol^{-1}, considerably smaller than that for Si=C double bonds[121] (43±6 kcal mol^{-1} suggested by Jones and Lee)[273]. **181** and **180** have magnetically equivalent trimethylsilyl groups even at −80 °C, indicating free rotation around the SiC(O) bond[121]. [Note that for **181** and **180** quite different chemical shifts are reported by Ishikawa and coworkers[21] (δ^{29}Si(**181**) = −70.5 ppm) and by Bravo-Zhivotovskii, Voronkov and coworkers (δ^{29}Si(**181**) = 64.9 ppm)[122]; we will refer here only to results of the first group.

Auner, Grobe and coworkers could detect the complexes **27**–**29** of simple silenes with perdeuterio dimethyl ether by low temperature NMR spectroscopy[27]. The NMR spectra of the complex **27** recorded at −140 °C showed a triplet at −25.2 ppm in the ^{29}Si NMR spectra and a triplet at 10.8 ppm in the ^{13}C NMR spectra. The spectral data are consistent with the formation of a complex between silene **25** and dimethyl ether yielding the betain-like complex **27**. High level *ab initio* calculations of structure and NMR chemical shift for **27**–**29** strongly corroborate the experimental findings and establish the importance of both canonicals structures **27A** $\leftrightarrow$ **27B**[27].

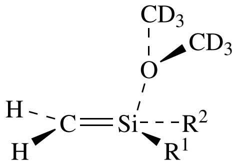

(**27**) $R^1 = R^2 = H$

(**28**) $R^1 = H, R^2 = Me$

(**29**) $R^1 = R^2 = Me$

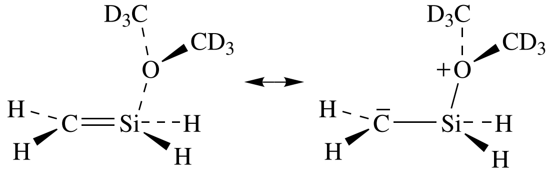

(**27A**) (**27B**)

The complexation of silene **104a** with THF or trimethylamine leads to a shielding of the silicon by 92 ppm or 110 ppm, respectively, indicating the strong interaction between the Si and the donor molecule[4].

b. ^{13}C NMR spectroscopy. The observed range for the ^{13}C resonance for stable silenes is very large (77–214 ppm), much larger than for most alkenes (95–155 ppm). For the group of silenes $(Me_3Si)_2{=}C(OSiMe_3)R$ **149**, **150**, **578–580**, the sp^2-hybridized carbon atom is observed in the range of 207–214 ppm. The carbon in silenolates absorbs at even lower field (262.7–274.1 ppm). Replacing one trimethylsilyl group at the silicon in silenes by an aryl or alkyl group shifts the ^{13}C resonance to higher field by 15–20 ppm. The trimethylsiloxy group in **149**, **150**, **578–580** is responsible for a deshielding of the carbon by approximatively 10–15 ppm compared with an alkyl group. Thus, the silenes **162** and **585**, having only alkyl substituents at the carbon, resonate at 197–198 ppm. The tertiary vinylic carbon in the neopentylsilene **134** is found at 110.4 ppm. The shielding influence of two directly attached trimethylsilyl groups is responsible for the relatively high field resonance of the doubly bonded carbon at 77.2 ppm in Wiberg's silene **104a**, although the different polarity of the Si=C bond might also contribute to the shielding of the carbon atom. The ^{13}C signal of the central carbon in 1-silaallenes ($\delta^{13}C = 213.6–227.9$ ppm) can be found at the lowfield end of the usual range for the ^{13}C resonance of the central allenic carbon ($\delta^{13}C = 195–215$ ppm).

3. Infrared spectroscopic data

Much IR data has been collected for simple silenes in matrix isolation work and these data are summarized in several previous reviews[7,8].

Simple silenes have a Si=C stretching frequency around 1000 cm^{-1} (see Table 15 for a few examples). Thus, for silene **25** a weak band is found at 985 cm^{-1} which is shifted by methyl substitution to higher frequencies. $Me_2Si{=}CH_2$ **2** has a $\nu_{Si=C}$ of 1003.5 cm^{-1}.

TABLE 15. UV [λ (nm) (ϵ_0)], IR [$\nu_{(Si=C)}$ (cm^{-1})] and PE [IP (eV)] data of silenes and related compounds

Compound	$\lambda_{max}(\epsilon_0)$	$\nu_{(Si=C)}$	$\nu_{(Si=H)}$	IP	Remarks	References
Silenes						
$H_2Si{=}CH_2$ **(25)**	258	985	2239,2219	8.85		28–30
$MeHSi{=}CH_2$ **(26)**	260	989	2187			156, 158
$Me(HO)Si{=}CH_2$ **(592)**		899			Si–O 777.5, 781	275
$Me_2Si{=}CH_2$ **(2)**	244	1001;1003.5		7.71(ad),7.98(v)		254–256, 276
						256
$Me_2Si{=}CHMe$ **(8)**	255	978				157, 164
$Me_2Si{=}CHSiMe_3$ **(301)**	265					164
$Me_2Si{=}CMeSiMe_3$ **(593)**	274					164
$Me_2Si{=}C(SiMe_3)_2$ **(92)**	278					164
$Me_2Si{=}CPhCO_2Me$ **(594)**	280					18, 165
$Me_2Si{=}CPhCO_2Et$ **(595)**	288					165, 277
$Me_2Si{=}C(SiMe_3)CO$ Ad-1 **(596)**	284					165, 277
$Me_2Si{=}C(OSiMeBu$-$t$$OSiMe_3)$ Ad-1 **(583)**^{a}	290					90
$Ph_2Si{=}CH_2$ **(31)**	325					35b
$(Me_3Si)_2Si{=}C(OSiMe_3)R$						
R = Me **(369)**	330 (6500)					88
R = 1-Ad **(150)**^{a}	340 (7400)			7.7		3, 91
R = CEt_3 **(578)**	342 (7060)					3, 91
R = t-Bu **(149)**	339 (5200)					3, 91
$(Me_3Si)(t$-$BuMe_2Si)Si{=}$Ad-2 **(162)**^{b}	322 (6300)					111
$(Me_3Si)t$-$BuSi{=}C(OSiMe_3)$Ad-1 **(582)**^{a}	340					90
Silaallenes						

Me_2Si=C=C$(SiMe_3)_2$ **(597)**	275,325				278
1-Ad(Sup)Si=C=fluoren^{a,c,d} **(571)**	267,276,297,318,334				5
Silabutadienes					
Me_2Si=CPh−CH=CH_2 **(361)**	338				183
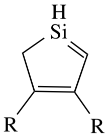	296	929	2210		159
R = H					
R = Me	312	917	2202		159
(**290**)					
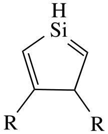					
R = H	270	936	2216		159
R = Me	274	933	2212		159
(**289**)					
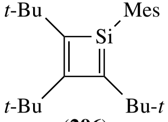 (**296**)	278			further λ_{max} at 328, 400	
Silatrienes					

(*continued overleaf*)

TABLE 15. (*continued*)

Compound	$\lambda_{max}(\epsilon_0)$	$\nu_{(Si=C)}$	$\nu_{(Si=H)}$	IP	Remarks	References
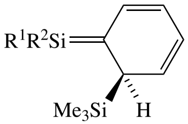						
R^1=R^2=Me (**201**)	425					137
R^2=Ph, R^2=Me (**524A**)	460					137
R^1=R^2=Ph (**524B**)						
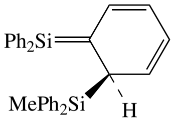						
(**598**)	490					137
Silaaromatics						
2-Tbt-silanaphthalene (**573**)[e]	267(20000),312(7000) 387(3000)				1368 cm^{-1} (Raman (C–C))	6
Silabenzene (**599**)	212,272,298,305,313,321				for IR see Ref.	279,281
1,4-Disilabenzene (**600**)	275,396,385,396,408					282
4-Silatoluene (**601**)	301,307,314,322					283

[a] 1-Ad = 1-adamantyl.
[b] 2-Ad = 2-adamantylidene.
[c] Sup = 2,4,6-*t*-butylphenyl.
[d] fluoren = 1,3,6,8-tetraisopropyl-2,7-dimethoxyfluorenylidene.
[e] Tbt = 2,4,6-tris[bis(trimethylsily) methyl]phenyl.

From that value a force constant of $k = 5.6$ mdyn Å^{-1} for the Si=C double bond is deduced[255]. This frequency is clearly higher than the usual range for Si–C stretch vibrations but substantially less than for C=C stretches, both because Si is heavier than C and because the Si=C bond is weaker than the C=C bond. More suitable for the experimental characterization is the vinylic Si–H stretch vibration which gives rise to a medium band at 2239 cm^{-1} (**25**) or 2187 cm^{-1} (**2**)[29], hypsochromically shifted by around 100 cm^{-1} relative to the Si–H stretch in simple silanes. A detailed analysis of the vibrational spectra of matrix-isolated $MeHSi{=}CH_2$ **26** using polarized IR spectroscopy established IR transition moment directions relative to the $\pi\pi^*$-transition moment (Si–C axis) in **26**[156]. These data provide detailed information about the vibrational modes and about the structure of **26**[156]. The bathochromic shift of the Si=C stretch in the isomeric 1,3-silabuta-1,3-dienes **289** and **290** by around 70 cm^{-1} compared with the Si=C stretch in simple silenes (Table 15), was interpreted as an indication of Si=C–C=C and C=Si–C=C π-conjugation[159].

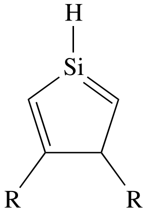

(289)

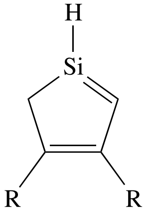

(290)

R = H, Me

Stable Brook silenes like $(Me_3Si)_2Si{=}C(OSiMe_3)Ad\text{-}1$ **150** are characterized by several bands in the region 1300–930 cm^{-1}, but it is not known with certainty which bond is associated with the Si=C bond[3]. The same is true for the heavily substituted 1-silaallene **571**. Several strong bands have been detected by IR spectroscopy but no assignment was given[5]. Two silabenzenes **599**[279–281] and **600**[282] and silatoluene **601**[283] have been investigated in the matrix at low temperatures and the IR spectra are reported without any assignment. For the 2-silanaphthalene **573**, an absorption at 1368 cm^{-1} for the C–C bond stretch is found in the Raman spectrum, which corresponds to the maximum absorption at 1382 cm^{-1} for naphthalene[6].

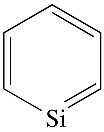

(599)

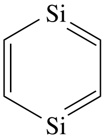

(600)

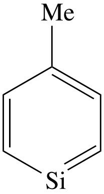

(601)

A matrix reaction of trimethylsilane with oxygen atoms (from ozone) at 14–17 K gives a product that was tentatively identified as the silenol $H_2C{=}Si(OH)Me$ **592** by IR spectroscopy[275]. The finding was supported by isotopic labeling with ^{18}O and D.

4. UV spectroscopic data

UV spectroscopic data have been summarized in detail in earlier reviews and we will outline only the fundamental UV characteristics of silenes and will concentrate on new achievements of interest.

Small silenes absorb in the region 245–260 nm, a region which is assigned to the $\pi\pi^*$ transition[89]. For example, the parent silene **25** is characterized by a UV transition at 258 nm[28,29]. $Me_2Si{=}CH_2$ **2** has a λ_{max} at 244 nm and further substitution at the vinylic carbon gives a bathochromic shift of the $\pi\pi^*$ band (see Table 15). The highly substituted stable silenes of the 'Brook' family have UV absorbtions around 340 nm and extinction coefficients ϵ_0 between 5200 and 7400[3,91]. Similarly, the stable 'Apeloig' silene **162** has a UV maximum at 322 nm (ϵ_0 = 6300)[111]. This indicates a relatively large bathochromic shift induced by the two silyl groups at the sp^2-hybridized silicon. Interestingly, silyl substitution at the carbon atom induces a smaller bathochromic shift, thus for $Me_2Si{=}C(SiMe_3)_2$ **92**, $\lambda_{max} = 278$ nm[164]. Conjugation with aryl or C=O groups gives expectedly a bathochromic shift. Thus the UV band is red shifted in **595** to $\lambda_{max} =$ 288 nm[165].

The UV absorption bands of the siladienes **289** and **290** attributed to $\pi\pi^*$ transition on the basis of multireference CI calculations are considerably red shifted in comparison with the absorptions of the parent silene **25** (Table 15) and suggest that π-conjugation is significant in these compounds[159]. The large difference between the 1-silabuta-1,3-diene **290** and the 2-silabuta-1,3-diene **289** was rationalized by the opposite influences of the small SiC resonance integral on the HOMO–LUMO gap in **290** (decreasing HOMO–LUMO gap) and **289** (increasing HOMO–LUMO gap). Phenyl substitution at the silabuta-1,3-diene moiety increases the bathochromic shift further: **361** absorbs at 338 nm (Table 15)[183]. Transient silacyclobuta-1,3-diene **296** is characterized by an UV absorption at 278 nm[161]. Further red-shifted to 425–490 nm is the $\pi\pi^*$ transition in a series of 1-silatrienes **201, 524** and **598** observed by Leigh and coworkers[137].

The transient 1-silaallene, $Me_2Si{=}C{=}C(SiMe_3)_2$ **597**, absorbs at 275 nm and 325 nm[278]. The *ca* 30 nm red shift of the spectral maximum for **597** relative to that of $Me_2Si{=}CH_2$ was ascribed to hyperconjugative interactions between the β-trimethylsilyl groups and the Si=C bond[278]. The UV spectrum of the stable 1-silaallene **571** was also reported, but no assignment of the bands was given (Table 15)[5].

For several silaaromatics (**573, 599–601**) UV spectra are reported (Table 15). The compounds were found to behave like perturbed benzenes (or naphthalenes).

5. Miscellaneous

Only a few photoelectron spectra of silenes have been measured. Silene **25** has a first vertical ionization energy of *ca.* 8.85 eV, in agreement with the theoretical value of 8.95 eV[30]. The assignment is further supported by the observed fine structure of the first band which is similar to that found for ethene. The first ionization potential of the stable 'Brook' silene **150** is 7.7 eV[3], similar to what is found for $Me_2Si{=}CH_2$ **2** (7.98 eV)[276].

Silene **2**, 1-fluorosilene **602** and 1,1-difluorosilene **603** have been examined by FT ion cyclotron resonance spectroscopy in order to estimate the π-bond strength. Bracketing studies with various bases (B) and fluoride acceptors (A) gave values for the proton and fluoride affinity of the silenes[284]. The π-bond energy was calculated by thermochemical cycles and found to increase with fluorine substitution. The data are given in Table 16.

TABLE 16. Thermochemical data for substituted silenes[284]

Silene	Proton affinity (kcal mol^{-1})	Fluoride affinity (kcal mol^{-1})	π-Bond energy (kcal mol^{-1})
$Me_2Si{=}CH_2$, **2**	228±2	37±2	39±6
$MeFSi{=}CH_2$, **602**	187±2	40±2	45±5
$F_2Si{=}CH_2$, **603**	178±2	46±2	50±5

The proton and fluoride silene adducts were produced according to equations 198−201.

$$Si(CH_3)_4 + e^- \longrightarrow Si(CH_3)_3^+ + CH_3 + 2\,e^-$$

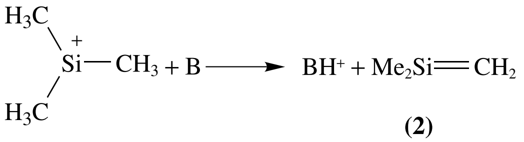

$$(H_3C)_2\overset{+}{Si}{-}CH_3 + B \longrightarrow BH^+ + Me_2Si{=}CH_2 \quad \text{proton affinity} \qquad (198)$$

(2)

$$NF_3 + e^- \longrightarrow F^- + NF_2 \qquad (199)$$

$$SiMe_4 + F^- \longrightarrow [FSiMe_4]^{-*} \longrightarrow FSiMe_2CH_2^- + CH_4 \quad \text{fluoride affinity} \qquad (200)$$

$$FSiMe_2CH_2^- + A \longrightarrow AF^- + Me_2Si{=}CH_2 \qquad (201)$$

II. SILAALLENES

A. Theoretical Studies

The isomeric 1- and 2-silaallenes have been the subject of numerous computational studies. According to calculations the 1-silaallene **604** is more stable than the isomeric **605** by 14.7 kcal mol^{-1} (at MP2/6-31G**//MP2/6-31G**)[285a], but both are relatively high lying minima on the C_2H_4Si potential energy surface. Thus, **604** is less stable than the *syn/anti-* isomeric silylenes **606** and **607** by 5.7 and 5 kcal mol^{-1}, respectively. Note that according to high level *ab initio* calculations silene $H_2Si{=}CH_2$ **25** is more stable than methylsilylene H_3CSiH **277** by *ca* 4 kcal mol^{-1}[151].

$H_2C{=}C{=}SiH_2$

(604)

$H_2C{=}Si{=}CH_2$

(605)

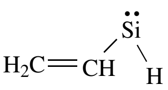

(606)

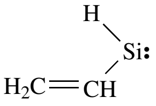

(607)

In contrast to carbon chemistry, the three-membered cyclic C_2H_4Si isomers are relatively stable. Thus, silacyclopropylidene **608** and 2-silacyclopropene **609** are more stable than **604** by 10.9 and 13.8 kcal mol^{-1}, respectively[285b], while cyclopropene **610** is by 22.4 kcal mol^{-1} less stable than allene **611** and more stable by 62.0 kcal mol^{-1} than singlet cyclopropylidene **612**[286].

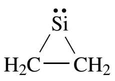
(608)

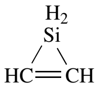
(609)

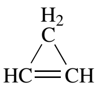
(610)

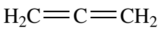
(611)

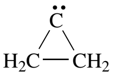
(612)

B. Synthesis

It was suggested that 1-silaallene [1-D] **604** is a short-lived intermediate in the isomerization of the isotopomeric vinylsilylenes [1-D] **606** and [2-D] **606** (equation 202) which have been generated in the high vaccum flash pyrolysis of 1,1,1-trimethyl-2-vinyldisilane[285b].

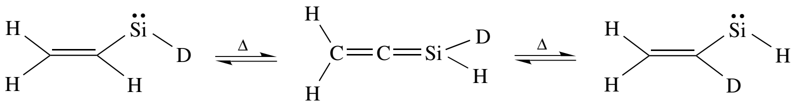

[1-D] **(606)** [1-D] **(604)** [2-D] **(606)**

(202)

1-Silaallenes **613** have been proposed by Ishikawa, Kumada and coworkers as transient reactive intermediates in the photolytic or thermolytic degradation of alkynyldisilanes **614** as minor byproducts, the main product being silacyclopropenes **615**[184,192,287] (equation 203).

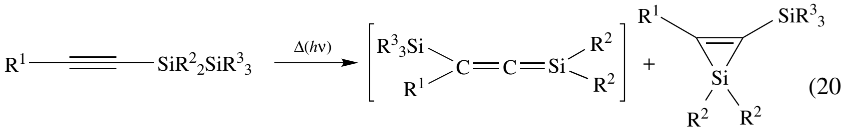

(203)

(614) **(613)** **(615)**

In the presence of scavenger reagents, consecutive products of 1-silaallenes **613** have been characterized[287,288]. Optimization of the substitution pattern in the precursor ethynylsilane increases the yield of the transient 1-silaallene. Also, silacyclopropenes themselves may serve as starting materials for 1-silaallenes[289,290]. Photolysis or thermolysis of 2-silacyclopropene **616** gives, after trapping of the intermediate silaallene **617** with methanol, the vinylsilane *Z*-**618** in 21% yield[291] (equation 204).

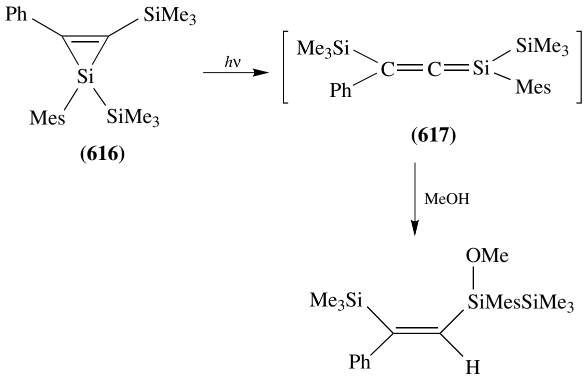

(616) **(617)**

(204)

Z-(618)

Following this reaction sequence established by Kumada and Ishikawa, Leigh and coworkers detected the transient 1-silaallene **597** in a laser flash photolysis of the ethynyldisilane **619**. **597** was identified by its characteristic UV absorptions at 275 nm and 325 nm[278] and by the trapping reaction with methanol. It is formed, however, in a mixture with silacyclopropene **620**, dimethylsilylene **621** and acetylene **622**. Based on the quantitative analysis of the products of methanolysis (**623–626**) a chemical yield of **597** of 12–15% was deduced[278] (equation 205).

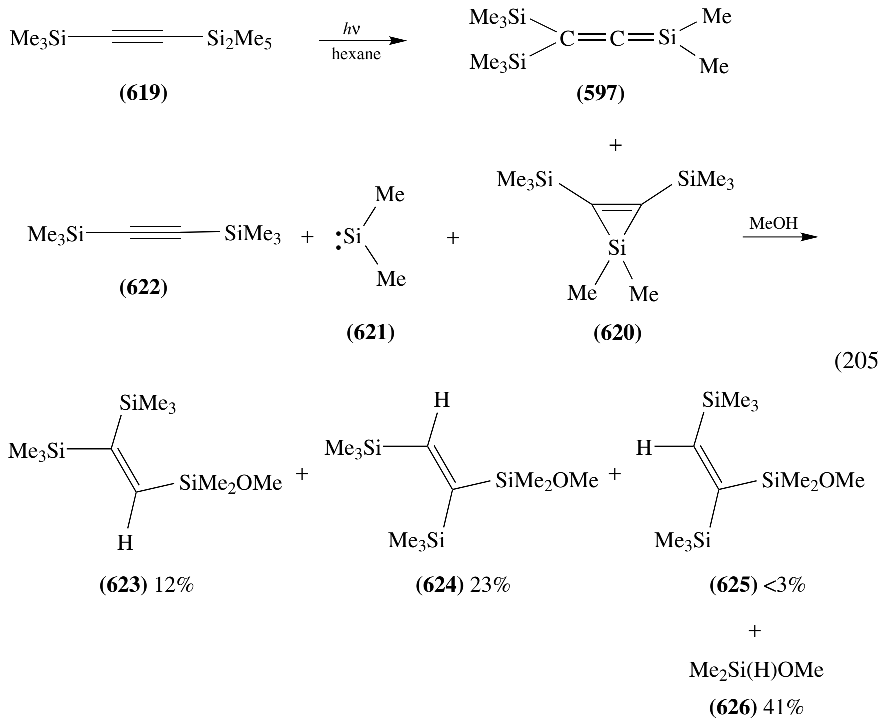

(205)

The first synthesis of stable 1-silaallenes follows closely an established route developed in carbon chemistry[292]. An overall nucleophilic 1,3 substitution at propargylic halides gives allenes in good yields (equations 206 and 207). In organosilicon chemistry, special attention must be paid to avoid direct substitution at the silicon which is the preferred site for nucleophilic attack.

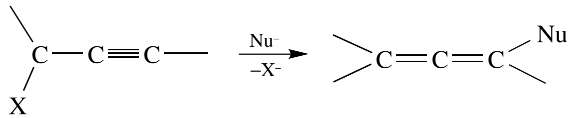

(206)

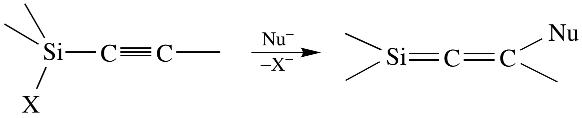

(207)

Two different approaches to solve this problem have been developed by the group of West[5,259,271]. In the steric method the substituents R^1 and R^2 at the silicon block the attack of the organometallic reagent by virtue of their bulkiness, thus attack occurs at the β-carbon atom[271]. Three 1-silaallenes **572, 587a** and **587b**, which are stable at room temperature, have been prepared from ethynylfluorsilanes **627** and **628** according to equation 208 and were identified by NMR spectroscopy[259]. From **572** a crystal structure was also obtained (see Section I.C.1). The organolithium compounds **629–631** can be detected by low temperature NMR and **629** is even stable around 0 °C and was clearly identified by trapping reactions and by X-ray crystal diffraction of its TMEDA complex[259].

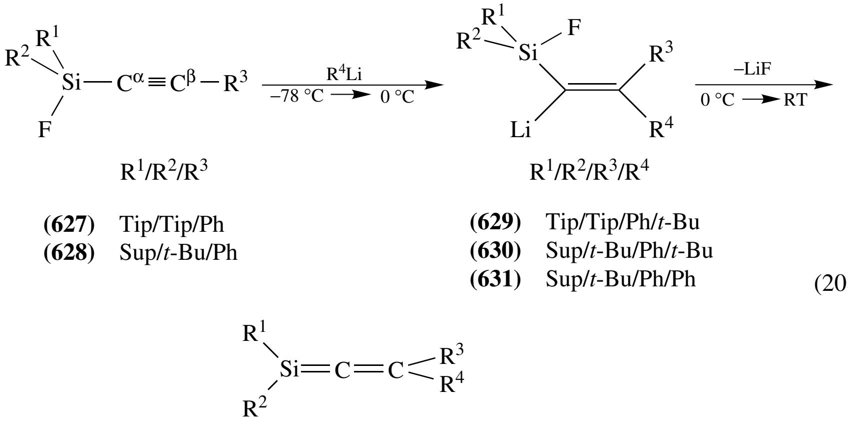

R¹/R²/R³

(627) Tip/Tip/Ph
(628) Sup/*t*-Bu/Ph

R¹/R²/R³/R⁴

(629) Tip/Tip/Ph/*t*-Bu
(630) Sup/*t*-Bu/Ph/*t*-Bu
(631) Sup/*t*-Bu/Ph/Ph (208)

R¹/R²/R³/R⁴

(572) Tip/Tip/Ph/*t*-Bu
(587a) Sup/*t*-Bu/Ph/*t*-Bu
(587b) Sup/*t*-Bu/Ph/Ph

In the intramolecular method the organometallic reagent is attached to the alkyne in such a way that it cannot reach the silicon atom intramolecularly, yet it can easily reach the β-carbon atom[271]. The synthesis of 1-silaallenes **571, 588, 589** by the dehalogenative intramolecular carbometalation–elimination (DICE) reaction is shown in equation 209. In the reaction of 2-bromo-2′[(fluorosilyl)]ethynyl]biphenyls **632–634** with 2 eq of *t*-butyllithium at 0 °C, the 1-silallenes **571, 588, 589** were obtained in nearly quantitative yields[5,192]. Due to extreme steric congestions, **571** is stable at air and moisture and can be dissolved in boiling ethanol without observable transformation[5].

Of the 2-silaallenes no sufficiently stable species have yet been isolated, so that no spectroscopic verification is available up to date. The synthesis of possible 2-silaallenes is therefore treated along with the description of their reactivity in Section II.C below.

C. Reactivity

1. 1-Silaallenes

The polarity of the Si=C bond in 1-silaallenes is reduced compared with that in silenes. Thus, for the parent 1-silaallene $H_2Si{=}C{=}CH_2$ **604** the calculated Mullikan atomic charges on Si and on the central C are +0.17 and -0.10[293], respectively, compared to 0.46 and -0.65 in $H_2Si{=}CH_2$ **25**. This is expected to reduce the reactivity of 1-silaallenes compared with silenes[246]. The theoretical prediction is strongly supported by kinetic data collected by Leigh and coworkers[278]. 1-Silaallene **597** exhibits a reactivity characteristic of the Si=C bond but the absolute rate constants for reaction of **597** towards characteristic silene trapping reagents like MeOH are significantly lower than those determined for other transient silenes. For example, $Ph_2Si{=}CH_2$ **31** reacts with MeOH more than 1000 times faster than **597** ($k_{MeOH} = 1.9{\pm}0.2{\times}10^9$ $M^{-1}s^{-1}$ for **31** $K_{MeOH} = 1.7{\pm}0.1{\times}10^6$ $M^{-1}s^{-1}$ for **597**[278]) (For the mechanistic details of the alcohol addition to silenes, see the chapter by Sakurai.) Also, the reactivity towards other silene scavenger reagents like HOAc, acetone, O_2 or octa-1,3-diene is strongly reduced[278]. Silylenes have also been employed as trapping reagents. Thus, the transient silylene Mes_2Si: **635** reacts with **636** giving the intriguing bissilacyclopropylidene **637** in 29% yield[185,288] (equation 210).

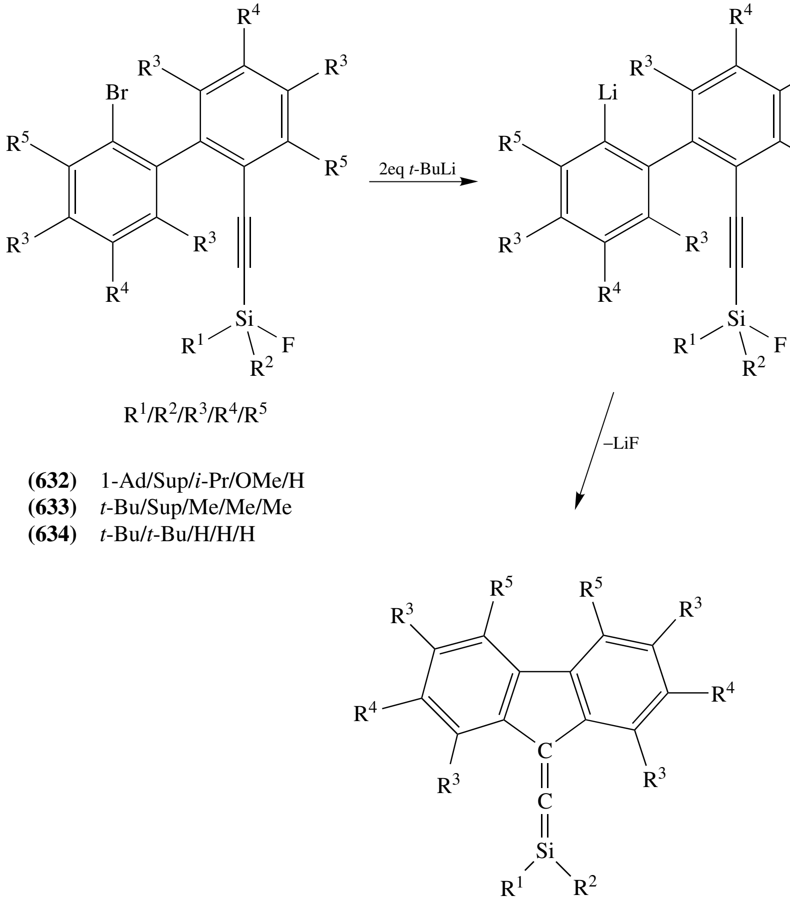

$R^1/R^2/R^3/R^4/R^5$

(632) 1-Ad/Sup/*i*-Pr/OMe/H
(633) *t*-Bu/Sup/Me/Me/Me
(634) *t*-Bu/*t*-Bu/H/H/H

(209)

$R^1/R^2/R^3/R^4/R^5$

(571) 1-Ad/Sup/*i*-Pr/OMe/H
(588) *t*-Bu/Sup/Me/Me/Me
(589) *t*-Bu/*t*-Bu/H/H/H

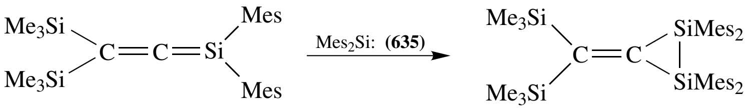

(210)

(636) **(637)**

In the absence of trapping reagents the transient 1-silapropadiene **638** dimerizes in contrast to usual simple silenes in a head-to-head fashion forming the 1,2-disilacyclobutane **639** in 18% yield[184,192]. This parallels the dimerization behaviour of 'Brook'-type and 'Apeloig–Ishikawa–Oehme'-type silenes in which the inherent polarity of the Si=C double bond is reduced by the substituents (see Section I.B.2.a). In contrast, the silene $Ph_2Si{=}C(SiMe_3)_2$ **97** cleanly gives the head-to-tail dimer[63,64]. **639** undergoes under diverse reaction conditions a further rearrangement, yielding the cummulenic 1,2-disilacyclobutane **640** (equation 211)[184,192]. 1-Silabutatrienes like $(Me_3Si)_2C{=}C{=}C{=}Si(o\text{-}Tol)_2$, however, dimerize in a head-to-tail fashion, like most simple silenes[192].

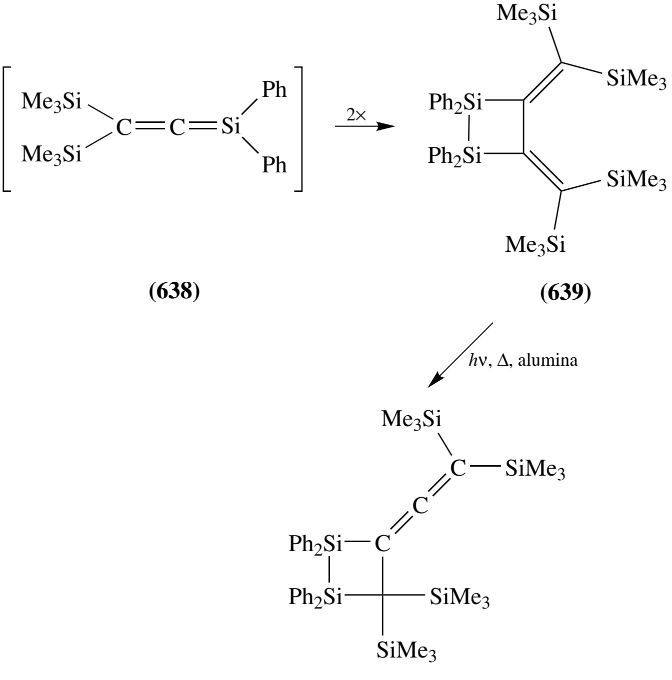

(638) **(639)**

(211)

(640)

The smaller polarity of the Si=C bond in 1-silaallenes probably contributes also to the remarkable kinetic stability of the stable silaallenes prepared by West and coworkers, but obviously steric factors play a dominant role in this case. Some product studies have been undertaken with the stable silaallene **572** and they are summarized in equation 212[259].

572 reacts instantaneously with water and methanol to yield hydroxyvinylsilane **641** and methoxylvinylsilane **642**, respectively. In each case the sterically less hindered *Z*-isomer was formed preferentially ($E : Z = 1 : 11$ and $1 : 15$ for **641** and **642**, respectively) (equation 212). The addition of alcohols proceeds probably by initial protonation of the central carbon atom; the incipient silicenium ion is trapped by the nucleophile or, alternatively, can be trapped intramolecularly. Thus, acidic ethanolysis of **587a** or **588** yields **645** or **646** (equations 213 and 214) in subsequent reactions of the transient silylium ions with the primary C–H bond of an adjoining *t*-Bu group[259].

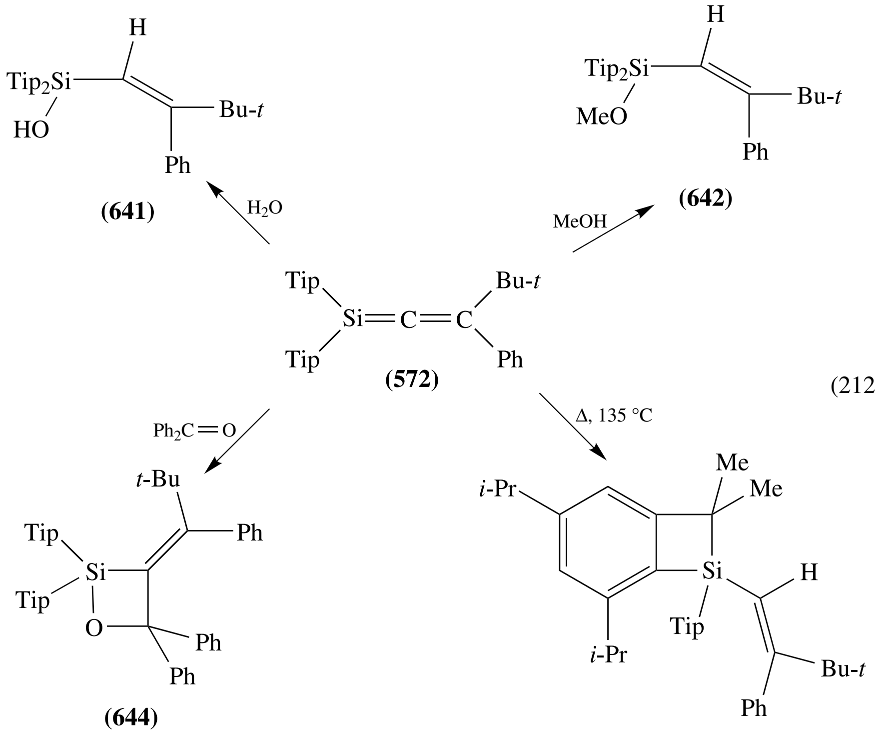

(641) **(642)** **(572)** **(644)** **(643)**

(212)

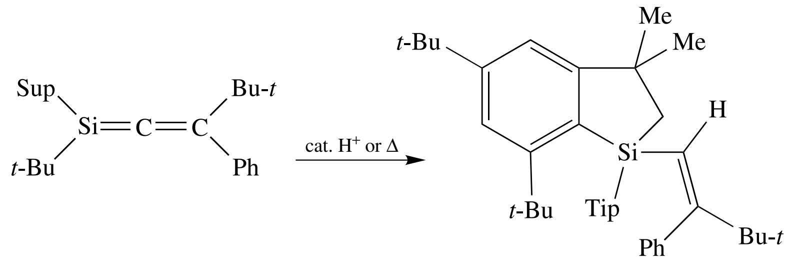

(213)

(**587a**) (**645**)

572 gives with benzophenone, in a formal [2 + 2] cycloaddition, a mixture of the stereoisomeric 1,2-oxasiletane E/Z-**644** ($E : Z = 6 : 1$) (equation 212). When **572** is heated in C_6D_6, an insertion of the Si=C double bond into one of the adjacent tertiary aliphatic C–H bonds of the isopropyl groups occurs yielding a mixture of the isomeric benzosilacyclobutenes E/Z-**643** (equation 212). Similarly, the benzosilacyclopentene **645**, the formal insertion product of Si=C in the primary C−H bond of the *ortho* *t*-butyl group of the supermesityl (Sup) substituent, is isolated when **587a** is heated in ether (equation 213)[259]. Related insertions of Si=X bonds in the *ortho* position of adjacent mesityl groups are well documented[90,181,259].

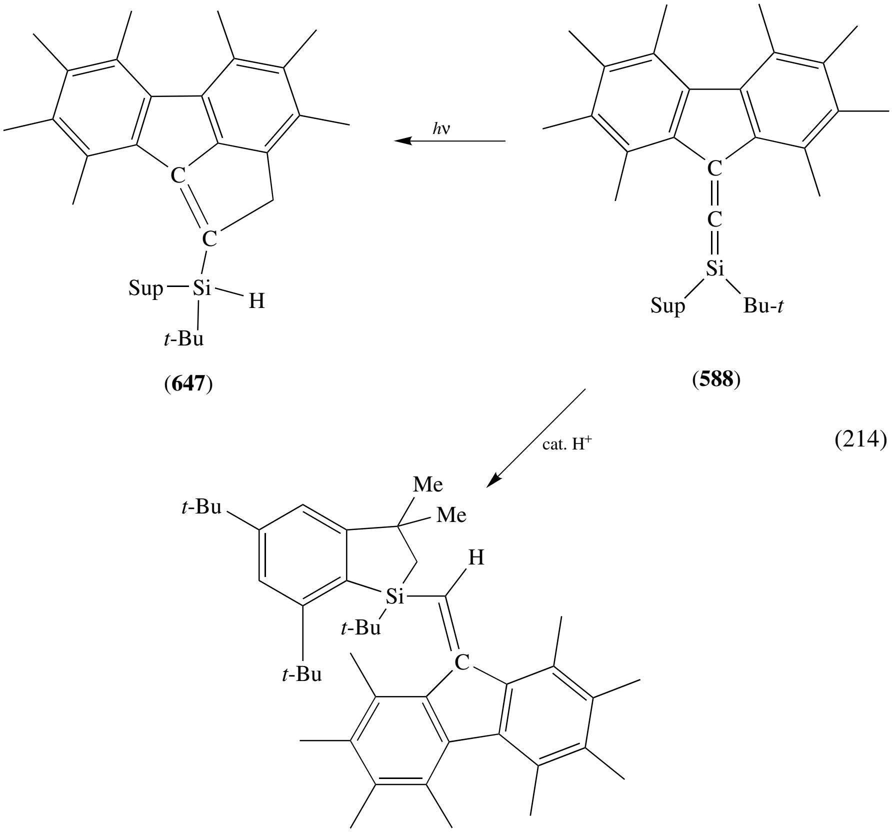

(**647**)

(**588**)

(214)

(**646**)

Interestingly, photolysis of fluorenylidenesilene **588** is reported to give insertion of the Si=C bond in one of the *ortho* methyl groups of the fluorenylidene substituent yielding the polycyclic compound **647** (equation 214). This product has the opposite regiochemistry in respect to the formal addition of a C−H bond across the Si=C double bond of the 1-silaallene moiety than that found in the protonation reaction[271].

A different decomposition channel is utilized by the silyl-substituted 1-silaallene **617**[289,290]. In the absence of trapping reagents the transient **617** formed in the thermolysis of **646** at 280 °C undergoes a 1,2-trimethylsilyl shift giving the silylene **648** and finally the 3,5-disilacyclopentene **649** in 25% yield. Alternatively **648** can also be formed from the silacyclopropene **616**. The silaindene **650**, the formal insertion product of the Si=C bond into the *ortho* C−H of the phenyl ring, is isolated in 18% yield[289]. The formation of **650** was rationalized by the intermediacy of the biradical **651** (equation 215)[289,290].

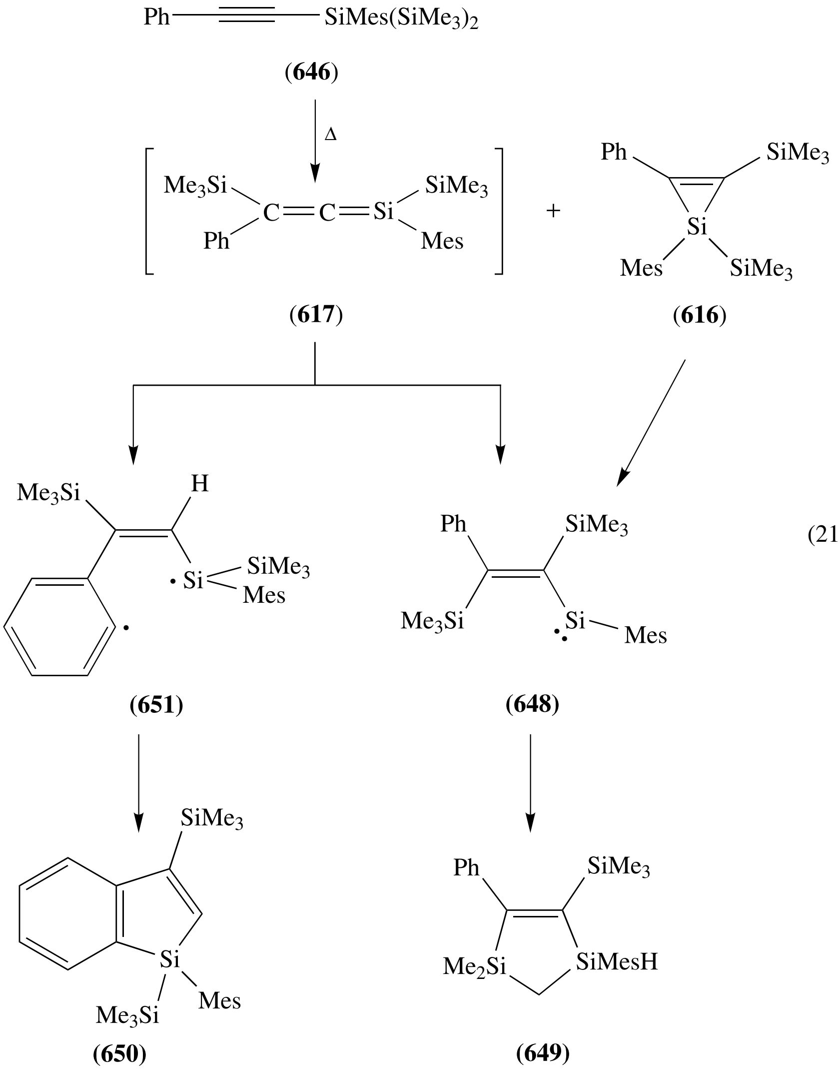

(215)

2. 2-Silaallenes

The first report about the possible formation of a short-lived 2-silaallene dated back to 1978. Bertrand and coworkers found as products from the pyrolysis of the silaspirocycle **652** in the presence of benzaldehyde, silica and styrene **653** as major products[294]. They suggested that 2-silaallene **605** is a possible intermediate in this reaction which can account for the formation of the observed products via **654** (equation 216)[296,294].

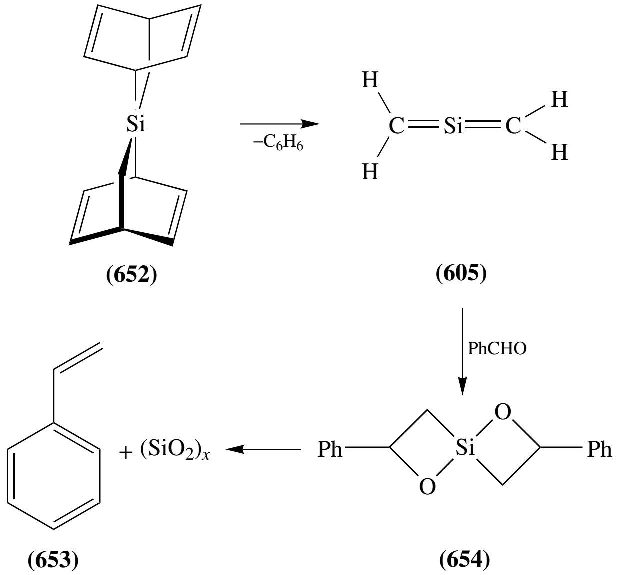

(216)

Silaspirocycles are the ideal precursors for 2-silaallenes. Thus, Pola and coworkers used 4-silaspiro[3,3]heptane **655** in a continuous-wave laser-photosensitized decomposition reaction in an attempt to generate 2-silaallene as an intermediate[295]. In the absence of scavenger reagents a transparent material is formed, which results from polymerization of the highly reactive intermediates **605, 656, 657** and **658**, which are produced either directly from the precursor **655** or from the silene **659** (equation 217). ESCA, Auger and FT-IR analysis of the SiC_2 polymer give indirect indications for transient species like **605** or its isomers. In the presence of alcohols as trapping reagents dimethyldialkoxysilanes **660** are formed, which might result from the double addition of ROH to **605** and/or **657, 660** (equation 218)[295].

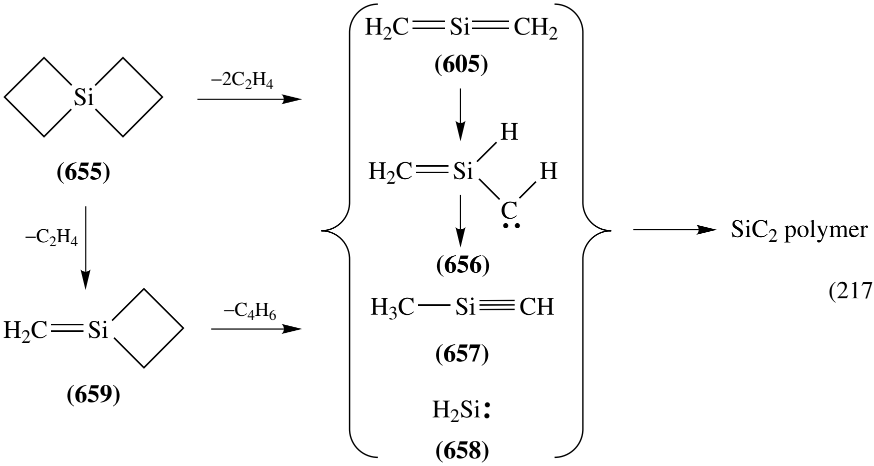

(217)

$$\underset{\textbf{(605)}}{H_2C{=}Si{=}CH_2} \xrightarrow{ROH} \underset{\textbf{(660)}}{(H_3C)_2Si(OR)_2} \xleftarrow{ROH} \underset{\textbf{(657)}}{H_3C{-}Si{\equiv}CH} \qquad (218)$$

A different approach to 2-silallenes was utilized by Auner and coworkers[232]. They found that in the reaction of dichlorodivinylsilane and 2 equivalents *t*-BuLi, highly reactive intermediates are formed, which could be trapped with suitable scavenger reagents like anthracene, TMSOMe and norbornadiene (equation 219).

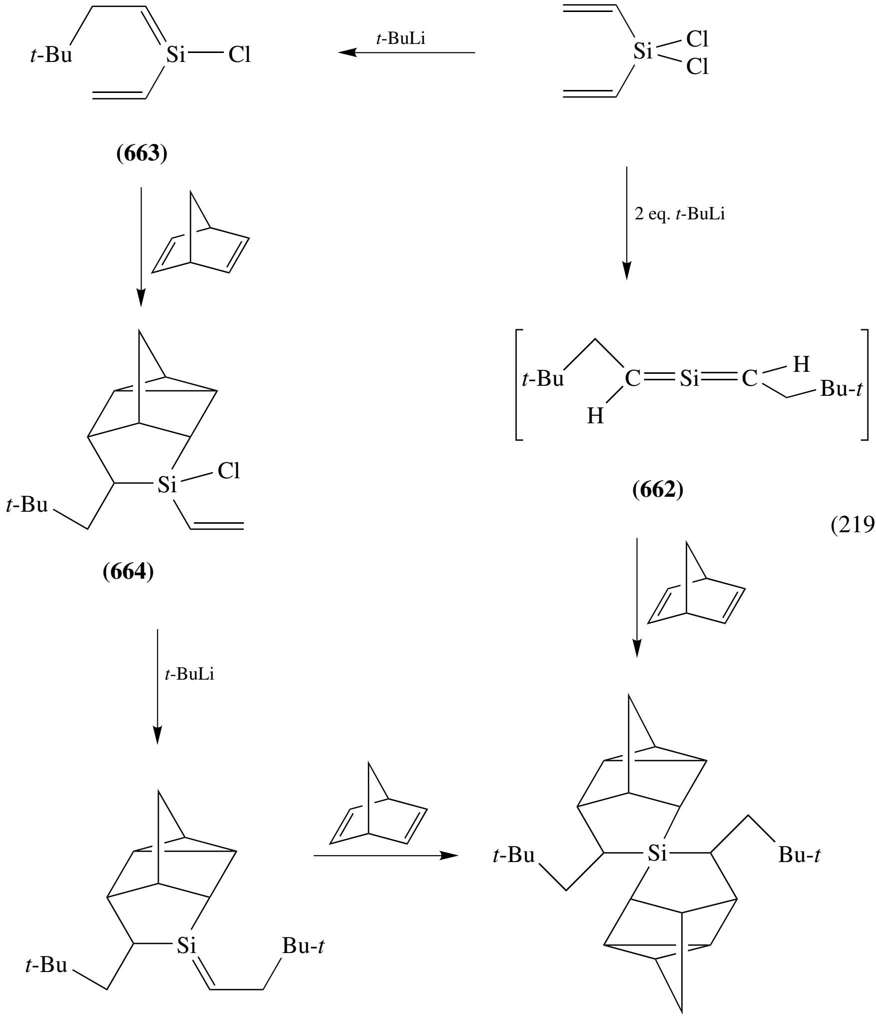

(219)

For example, in the presence of norbornadiene the spirocyclic compound **661** is formed. According to the authors this provides evidence for the intermediate formation of bisneopentyl-2-silaallene **662**. The stepwise formation of **661** via the 3-silabuta-1,3-diene **663**, vinylsilane **664** and silene **665** was excluded based on the different observed reactivities of dichlorodivinylsilane and **664** versus *t*-BuLi/norbornadiene. While dichlorodivinylsilane reacts immediately with 2 equivalents of *t*-BuLi in the presence of norbornadiene yielding **661**, the stepwise synthesized vinylsilane **664** reacts only sluggishly with 1 equivalent of *t*-BuLi in the presence of norbornadiene (equation 219)[232]. The experiments conducted by Auner and coworkers, however, do not exclude the possiblity that organolithium species like **666** and **667** give rise to the observed products. Nevertheless, the synthesized spirocycles like **661** are tailor-made molecules for the pyrolytic or photolytic generation of 2-silaallenes[232].

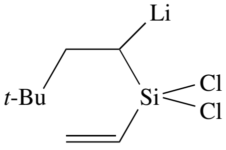

(666)

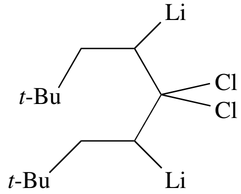

(667)

III. SiC TRIPLY BONDED COMPOUNDS: THEORETICAL RESULTS

Triple bonds to silicon still have the touch of unreachableness. At the time this review is being completed (summer 1997) no clear experimental evidence for a species containing a Si≡C bond is available. Some rather indirect evidence for the intermediacy of MeSi≡CH and XSi≡CH (X = F, Cl) in laser-induced decompositions of substituted silacyclobutanes is given by Pola and coworkers[295,296a]. Positively identified by spectroscopic methods were, however, several compounds with triple bonds between nitrogen and silicon (see Section IV.B) and dimethyldisilyne MeSi≡SiMe has been suggested as a transient intermediate[286b,c]. At the moment, the only reliable information about molecules with Si≡C bond comes from theory, which allows one to study their fundamental properties and reactions. However, theory also has faced considerable difficulties in describing triple bonds to silicon and the calculational results have been converging only in the last years to attain a uniform picture. These developments are well summarized in the reviews by Apeloig[11] and Karni and Apeloig[12] and we will give here only the most interesting and recent theoretical results for silynes and related compounds.

$H{-}C{\equiv}Si{-}H$

(668a)

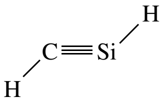

(668b)

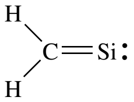

(668c)

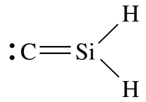

(668d)

All recent high level calculations predict that a classical linear silyne **668a**, the analogue to acetylene, is not a minimum on the potential energy surface (PES)[12,297]. The *trans*-bent isomer **668b** is, however, a local minimum, but it is thermodynamically and kinetically very unstable. The barrier for the isomerization to the global minimum, i.e, the silavinylidene **668c** which is by 34.1 kcal mol^{-1} more stable than **668b**, is very low. The most sophisticated calculations at the CCSD(T)/TZ2p(fd)//CCSD(T)/TZ2p+ZPE level predict a barrier of 5.1 kcal mol^{-1}[297b]. **668c** has been recently identified in a glow-discharge plasma of a gaseous mixture of SiH_4 and CO and rotational spectral lines of $H_2C{=}Si{:}$ have been observed[298a], confirming the calculated structures. In addition, vibrational frequencies of **668c** and its deuterio analogue $D_2C{=}Si{:}$ have been measured in a photoelectron study of the anion $SiCH_2^-$[298b]. The fourth isomer, **668d,** is a high-lying minimum *ca* 87−89 kcal mol^{-1} higher in energy than **668c**[12,297]. The PES of H_2SiC, calculated at the CCSD(T)/TZ2p(fd)//CCSD(T)/TZ2p+ZPE level of theory, is shown in Figure 5[297b]. A theoretical treatment of hydrogen tunneling across the small barrier of isomerization of **668b** to **668c** suggests a lifetime for **668b** and its deuterio analogue DSi≡CH of about 10^{-8} and 5×10^{-6} s, respectively[297a]. Thus, detection of **668b** or of DSi≡CH with a nanosecond resolution spectrometer might be feasible[297a].

The calculated Si≡C bond lengths in *trans*-bent silynes are distinctively shorter than Si=C bond lengths in silenes (i.e. 1.632 Å and 1.714 Å in HSi≡CH and in $H_2Si{=}CH_2$, respectively, at MP2/6-31G**)[297c]. A theoretical analysis in the framework of natural bond theory predicts for **668b** and substituted derivatives bond orders for the SiC bond which are intermediate between double and triple bonds with considerable ionic contributions[297b,c].

Apeloig and Karni investigated computationally the influence of substitution on the relative energies of the different silyne isomers **668a-d** and the barriers separating them[297c]. They found that fluorine and oxygen substitution at silicon stabilizes the *trans*-bent structure RSi≡CH relative to the silavinylidene isomer RHC=Si**:**. Thus, FSi≡CH is even more stable by 6.4 kcal mol^{-1} than HFC=Si**:**. These large substituent effects are best understood in terms of R−Si versus R−C bond energies. Thus, the larger Si−F bond energy compared with the C−F bond energy overrides the intrinsic preference of **668c** over **668b**. Furthermore, the barriers for the interconversion of both isomers are increased by substitution at silicon (from 9 kcal mol^{-1} for R = H to 17.5–25.0 kcal mol^{-1} for

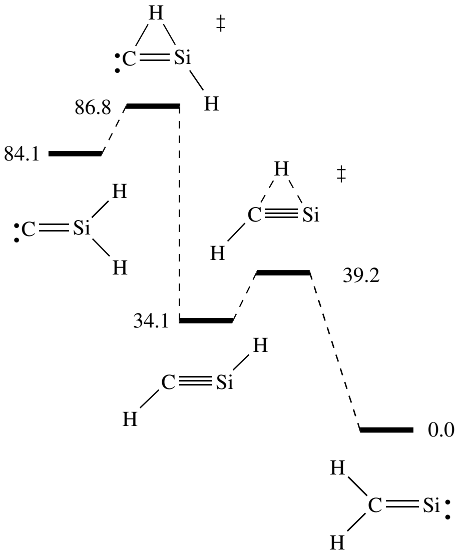

FIGURE 5. Calculated PES (relative energies kcal mol^{-1}) of H_2SiC at the CCSD(T)/TZ2p(fd)//CCSD (T)/ TZ2p+ZPE level of theory[297b]

R = F, Me, OH at MP4/6-31G**//MP2/6-31G**+ZPE), while the activation energies for the 1,2-hydrogen shift from RHSi=C:, forming the *trans*-bent isomer RSiCH, remain very small for different substituents (0.6–2.1 kcal mol^{-1} for R = Me, F, OH). According to Apeloig and Karni, a possible strategy for the synthesis of *trans*-bent silynes $R^2Si{\equiv}CR^1$ is to generate substituted 2-silavinylidenes $R^1R^2Si{=}C{:}$, preferently from suitable substituted silenes. An immediate 1,2-shift of the group R^1 might yield the *trans*-bent silyne $R^2Si{\equiv}CR^1$, which is kinetically stable towards unimolecular isomerization to the silavinylidenes $R^1R^2C{=}Si{:}$[297c].

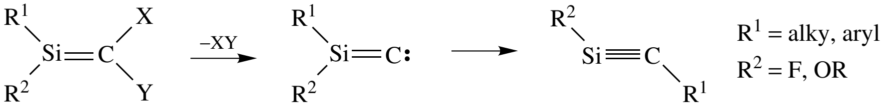

IV. SILICON–NITROGEN MULTIPLY BONDED COMPOUNDS

A. Introduction

This section deals with the literature since 1987 on silicon-nitrogen multiply bonded species as a sequel to Raabe and Michl's chapter in Vol 1 of *The Chemistry of Organic Silicon Compounds*[8]. A comprehensive treatment of silicon–nitrogen compounds has since appeared in 1989 in the *Gmelin Handbook of Inorganic Chemistry* covering the literature until the end of 1987[298]. A review on iminosilanes and related compounds was published by Hemme and Klingebiel in 1995[299].

The nomenclature of Si=N-systems used in the literature is somewhat confusing, especially for unusual systems. The nomenclature used in this review corresponds with the most commonly used description.

$R_2Si{=}NR$: iminosilane, silaketimine, silanimine
SiNR: iminosilylene, iminosilicon, silaisonitrile, silane isonitrile, isosilacyanide, silaisocyanide
RSiN: silanitrile, silane nitrile
RN=Si=NR: silanediimine
$RN{=}Si{=}NR^-$: silaamidide

B. Synthesis

This section comprises synthetic approaches to SiN multiply bonded systems. Whenever neccessary reactions of Si=N species have been included.

1. Si=N and Si≡N-systems

a. Salt elimination. Salt elimination is a well investigated route for the synthesis of unsaturated Group 14 species. Their stability depends on the size of the substituents at the Si–E skeleton and the subsequent replacement of small by bulky substituents eventually leads to stable sterically shielded Si=E species. This approach has been successfully exploited by Wiberg and coworkers in the field of silene chemistry (see Section I) and was later extended to silanimine synthesis. Instead of, or in addition to, the introduction of bulky substituents, stabilization of the Si=N moiety is also achieved by donor coordination to the Lewis acidic silicon atom. In this way Wiberg's group isolated adducts of $Me_2Si{=}NSi$*t*-Bu_3 **672** by salt elimination from N-metalated aminohalogenosilanes **670** (formed from **669**) in the presence of donors (Et_2O, THF, NR_3, X^-)[4]

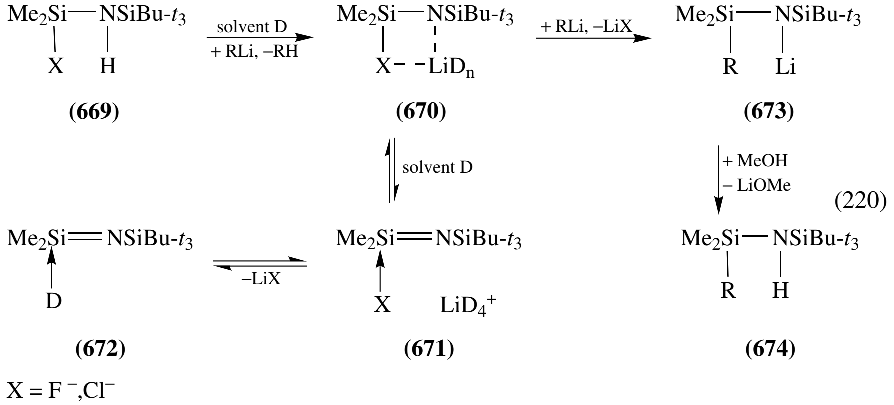

(220)

The LiX elimination equilibrium depends on the kind of solvent D used and it may be shifted via the ion pair **671** to the silanimine •D **(672)** side by the addition of $F_3CSO_3SiMe_3$ (which results in the formation of the weak base $LiOSO_2CF_3$ and removal of LiCl), of 12-crown-4 [causing formation of insoluble Li([12]-C-4)Cl] or of solvents in which LiCl is badly soluble. A side reaction may take place under unfavourable conditions (slow metalation of **669**, fast X/R exchange with **670** to give **673**); the rate ratio **669→670/670→673** is a function of the solvent. An X-ray structure of the adduct $Me_2Si{=}NSiBu\text{-}t_3$•THF has been published[301,302]. The further substitution of methyl groups by *tert*-butyl groups to give the sterically overloaded bis(silyl)amine $t\text{-}Bu_2Si(Cl){-}NHSiBu\text{-}t_3$ was not possible but the reverse reaction by addition of HX to the required silanimine leads to this amine. An elegant detour devised by the Wiberg group finally led to the stable silanimine **678** by the reaction of $NaSiBu\text{-}t_3$ with the azide **675**, probably via the triazenide **676** and the α-sodio chlorosilane **677** (equation 221)[303]

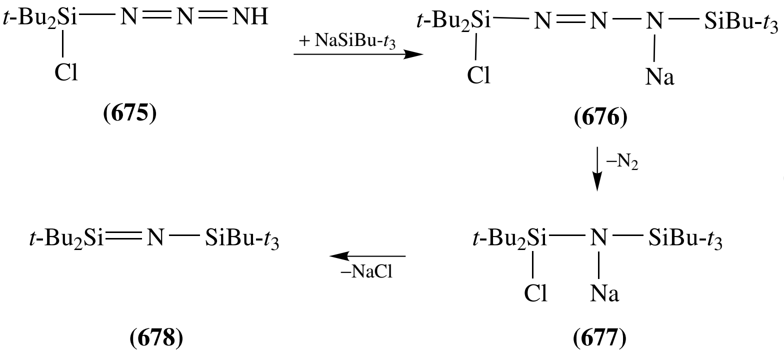

(221)

The X-ray structure of **678** has been determined (see below). The addition of donors leads, as expected, to adducts.

The synthesis of silanimines by salt elimination has been independently developed in the laboratories of Klingebiel[304–307]. An example of the synthesis of a stable donor adduct **(681)** is shown in equation 222 and equation 223 illustrates the general dimerization reaction of iminosilanes.

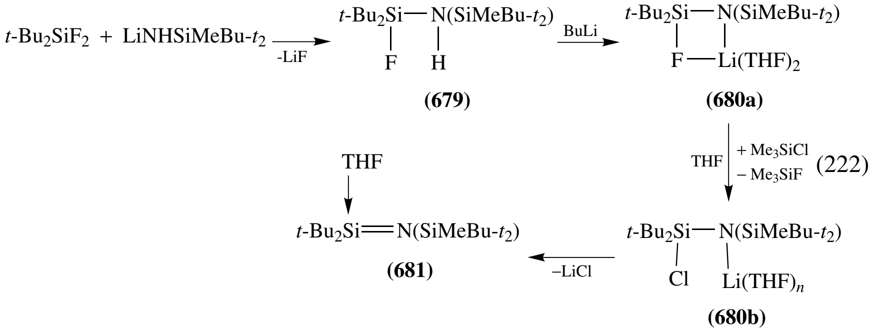

(222)

Aminofluorosilanes **679** are formed in the reaction of difluorosilanes with lithiated amines. **679** can then be metalated by RLi (R = Me, Bu) to give the corresponding lithium salts (e.g. **680a**). The structure of salts **680** depends on the basicity of the nitrogen atom and on the solvent. Representative structure types (**680a–c**) will be discussed in the subsection dedicated to structural features. The thermal elimination of LiF leads to silanimine dimers (e.g. **682** from **680c**), if sterically possible (equation 223), or to rearrangements.

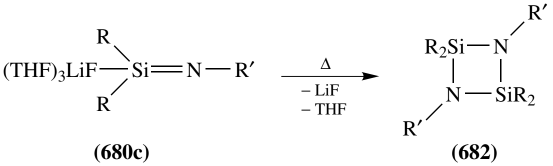

(223)

The mode of reaction of the salts **680** with Me_3SiCl depends on the bulk of the substituents. With less sterically demanding residues a trimethylsilyl group is introduced at the nitrogen atom, whereas F/Cl exchange takes place for larger substituents, provided that a Lewis base (e.g. THF) is present. In comparison with LiF the cleavage of LiCl is more facile. Thus, when compounds like **683c** are heated to 80 °C in a vacuum, THF is cleaved and the silanimine **684** (formed via **683b**) begins to sublime (equation 224)[306]. The donor adduct **681**, obtained in a similar fashion, can be distilled without decomposition.

b. Cycloreversion reactions. While the salt elimination method is only applicable without problems to systems having bulky substituents, the thermal cycloreversion reactions of suitable precursors are possible for a wide variety of substituents[308]. First results have been obtained by Wiberg and coworkers in the synthesis of the thermally labile silanimine **414a** from either the triazole **412a** or from the 2,3-diazasiletane **685** (equation 225)[309].

The synthesis of siladihydrotriazoles **412a** is easily achieved by the [2+3] cycloaddition reaction of azides RN_3 with the silenes $Me_2Si{=}C(SiMe_3)_2$ **92** (equation 226).

The thus formed heterocycles **412a** decompose or isomerize thermally; the required reaction temperature depends on the substituents. The isomerization leads to diazomethane derivatives **413a**, whereas the decomposition by [2 + 3] cycloreversion reaction gives bis(trimethylsilyl)diazomethane and short-lived silanimines **414a**, which dimerize in most cases. The ratio isomerization/cycloreversion depends on R, the solvent and the temperature and more cycloreversion is observed at higher temperature. An unfavourable side reaction is the insertion of $Me_2Si{=}NR$ into Si–N bonds (formation of **415a** and **686**; see below).

The formation of silanimines can further be proven by trapping reactions. One such reaction is the [2 + 3] cycloaddition with azides to give siladihydrotetrazoles **344a** (equation 227).

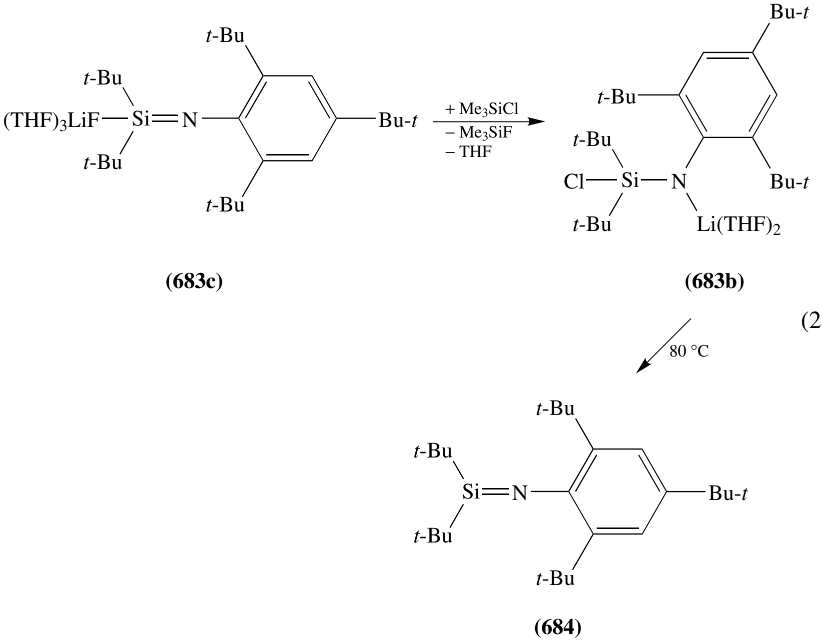

(224)

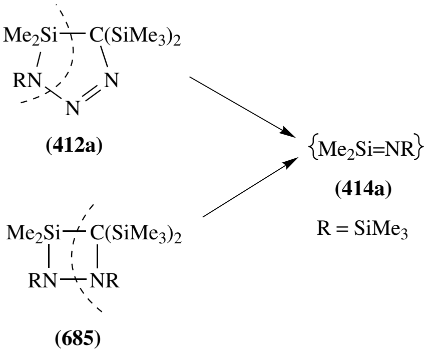

(225)

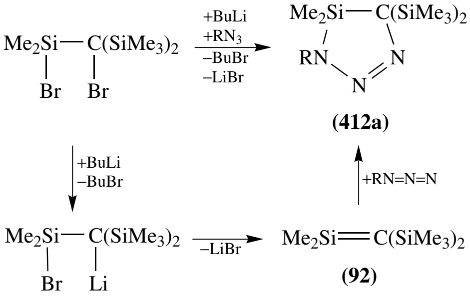

(226)

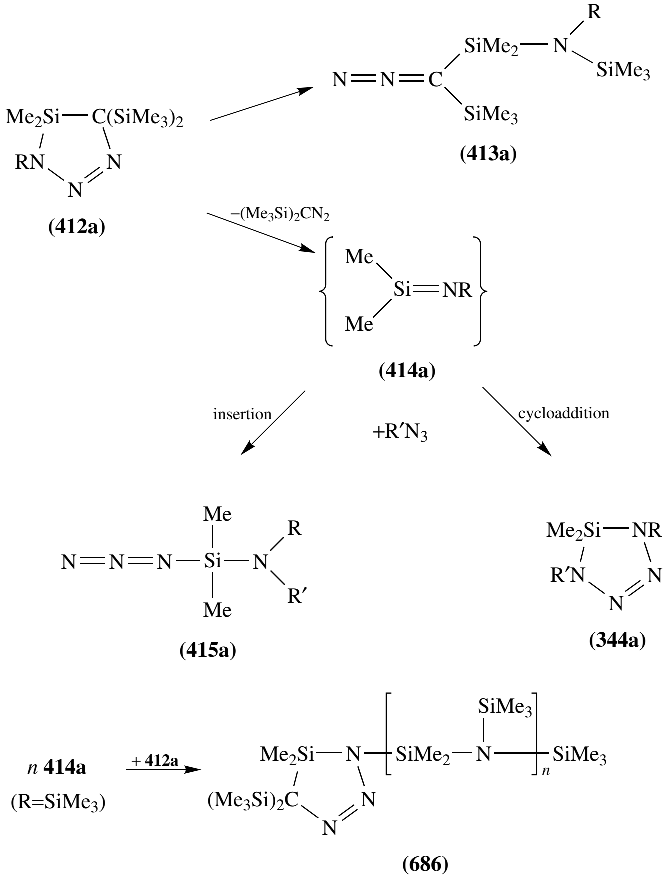

(227)

The yield of the [2 + 3] cycloadducts lies between 15 and 100%. The siladihydrotetrazoles **344a** are thermally quite stable and decompose in solution at temperatures higher than 130 °C in the reversal of their formation reaction to give silanimines and azides. The Si=N species dimerize to **687** or may be trapped by, e.g., acetone to give the ene product **688** (equation 228)[310].

The cleavage of unsymmetric siladihydrotetrazoles may lead to two different silanimines. The ease of formation increases in the order $Me_2Si{=}NSiMe_3$ < $Me_2Si{=}NSiMe_2Bu\text{-}t$ < $Me_2Si{=}NSiMeBu\text{-}t_2$ < $Me_2Si{=}NSiBu\text{-}t_3$, which might reflect the increasing stability of the silanimines.

The [2 + 2] cycloreversion of 1-aza-2-silacyclobutanes (silaazetidines) is a possible mode of silanimine preparation (equation 229).

While route B has been observed and utilized by Wiberg to synthesize silenes (see Section I), route A has been found to occur when less bulky substituents are used. Tamao and coworkers prepared the heterocycles (e.g. **689**) by intramolecular hydrosilylation of silylated allylamines and decomposed them in toluene solution at 204 °C[311]. From the thermolysis of **689** they obtained the corresponding *trans* alkene and the dimerization product **691**. In the presence of Me_3SiOEt the insertion product **690** was formed at the expense of the dimer **691** (equation 230).

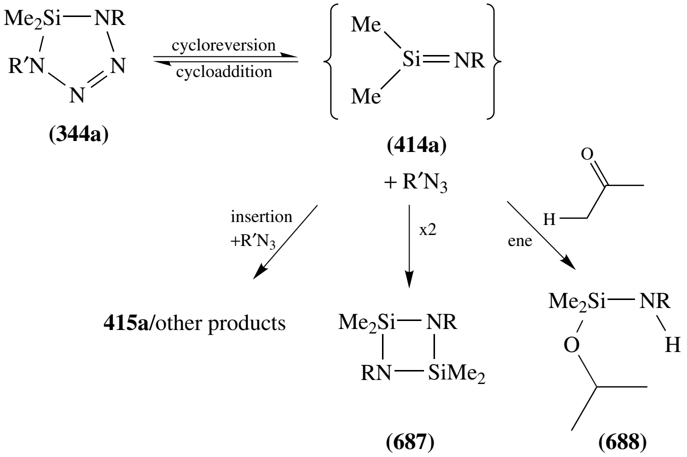

(344a) **(414a)** **(687)** **(688)**

(228)

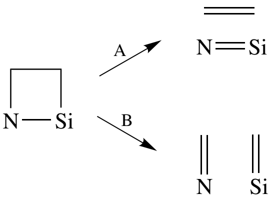

(229)

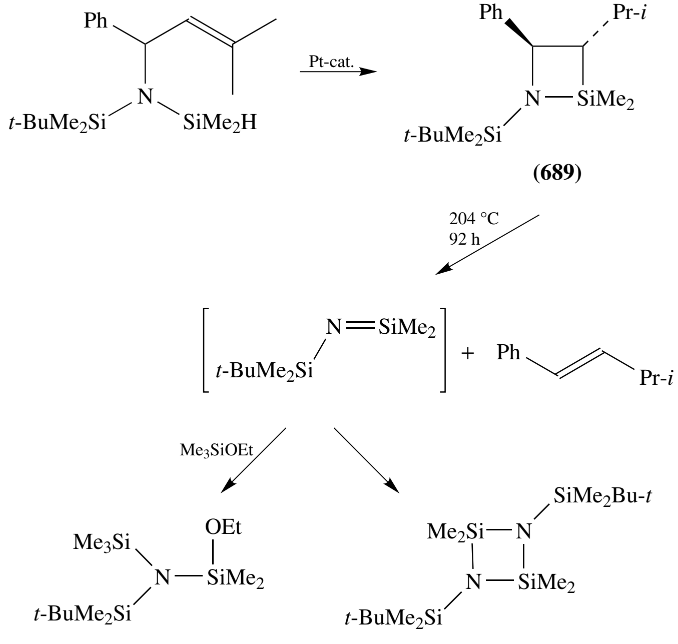

(689) **(690)** **(691)**

(230)

The [2 + 2] cycloreversion reaction proceeds stereospecifically with retention at carbon atoms, its rate obeys first-order kinetics and it depends on the stereochemistry and number of substituents at the ring carbon atoms. It is therefore concluded that the reaction mechanism is a concerted $[2_s + 2_a]$ cycloreversion.

Auner and coworkers synthesized dichlorosilaazetidines **692** by the reaction of $H_2C{=}CH{-}SiCl_3$/*t*-BuLi with imines[217,312]. The reaction possibly proceeds through the silene $Cl_2Si{=}CHCH_2Bu$-*t* **423** (equation 231). The attempted liberation of this silene from the silaazetidine analogous to one of Wiberg's silene syntheses failed, and instead reaction via pathway A of equation 229 took place. The silanimine **693a** obviously polymerizes, but can be trapped by $MeOSiMe_3$ and $Ph_2C{=}NBu$-*t* to give **694** and **695**, respectively (equation 232). In contrast to Tamao's results both stereoisomers of the alkene **696** were found (equation 233). This is explained by a stepwise reaction.

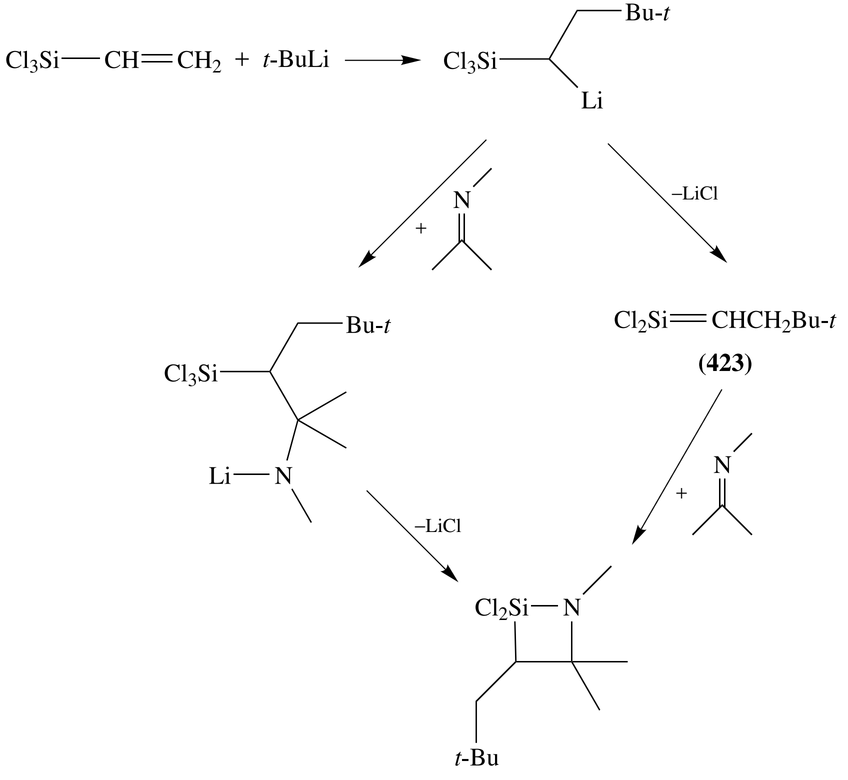

(692)

(231)

The cyclization of allyl silyl amine **697** by hydrosilylation led to silaazetidine **698**, which was subjected to flash vacuum thermolysis at 700–900 °C at 10^{-4} hPa[313]. The silanimines **699** and **700** themselves were too reactive to be observed by high resolution mass spectrometry of the reaction mixture, but their cyclic dimers, the cyclodisilazane **701** and **702** and a trapping product with *t*-BuOH **703**, were definitely confirmed (equation 234; see also the section on retro-ene reactions).

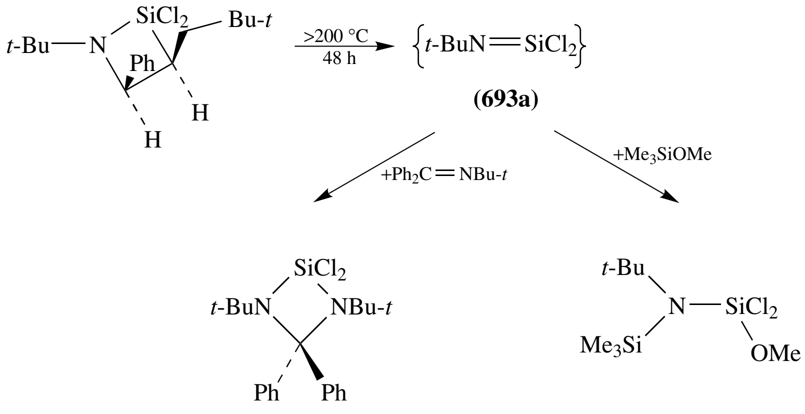

(693a)

(695)

(694)

(232)

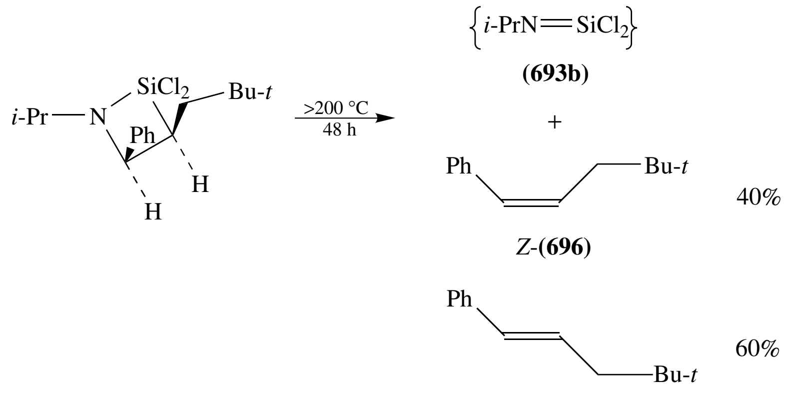

(693b)

Z-**(696)**

E-**(696)**

(233)

c. Photolysis and pyrolysis of silyl azides. For the study of highly reactive silicon species in the gas phase or at low temperatures in solution or matrix, azides are most suitable precursors, as the by-product of photolysis or pyrolysis is just molecular nitrogen that does not impede the spectroscopic characterization.

The first report of a silicon–nitrogen multiple bond molecule obtained from an azide is comparatively old: already in 1966 Cradock and Ogilvie isolated silaisocyanide **704** at 4 K (Ar matrix) after photolysis of H_3SiN_3[314].

The flash pyrolysis of trimethylsilyl azide **705** (1100 K, 0.01 mbar) was monitored by photoelectron spectroscopy, a method already successfully employed in the detection of phenylsilaisocyanide, PhNSi[315]. Accompanied by theoretical studies Guimon and Pfister-Guillouzo were able to assign the PE bands to two products: dimethylsilylimine **706** and silaisocyanide **704** (equation 235)[316].

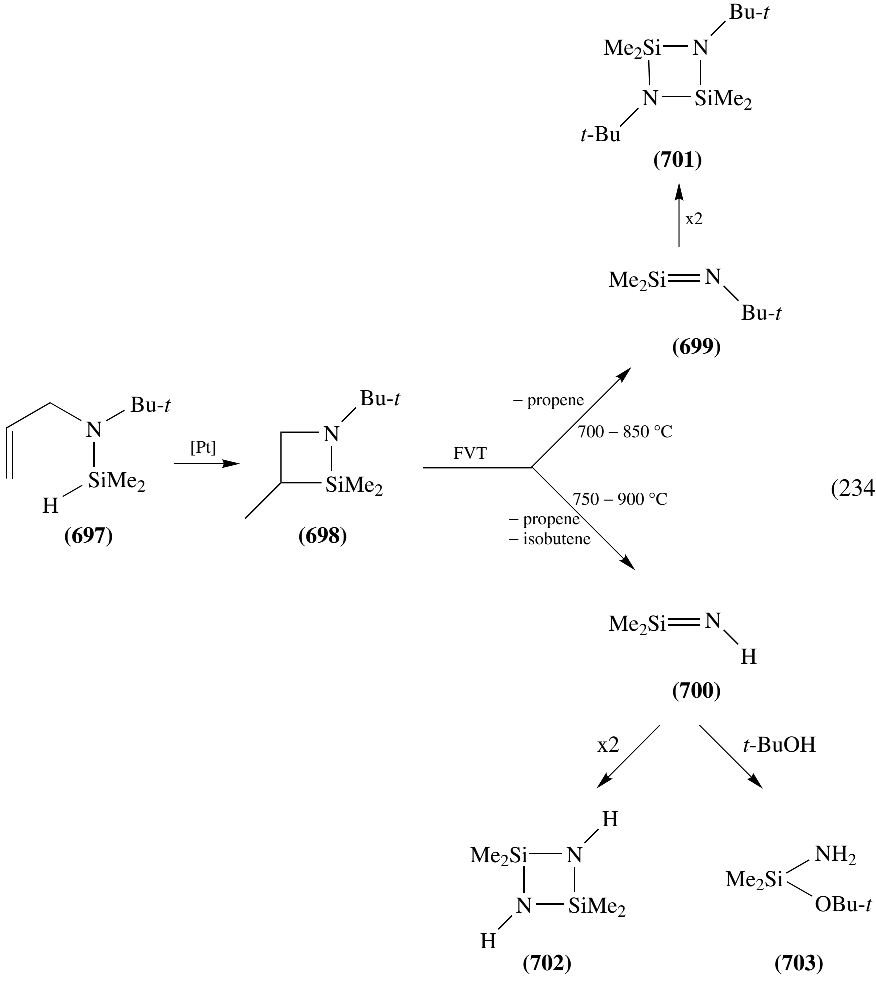

(234)

$$\underset{\mathbf{(705)}}{(CH_3)_3SiN_3} \xrightarrow[1100\text{ K},\ 10^{-2}\text{ mbar}]{} \underset{\mathbf{(706)}}{(CH_3)_2HSiN{=}CH_2} + N_2 + \underset{\mathbf{(704)}}{Si{\equiv}NH} \qquad (235)$$

West and coworkers photolysed a series of hindered azidosilanes **707**–**710** in a 3-methylpentane (3-MP) glass at 77 K and in solution at low temperatures[317]. The products were analysed by UV-Vis, GC/MS and ^{1}H NMR spectroscopy.

Trimesitylsilanimine **711** is identified by its UV absorption at 296 and 444 nm and by trapping experiments with alcohols. **711** is stable in solution up to *ca* $-125\,^\circ$C, as could be shown by the disappearence of its characteristic UV bands above this temperature. The major product of the photolysis, regardless of temperature, is, however, the C–H insertion compound **712** (55% yield) (equation 236).

Mes_3SiN_3

(707)

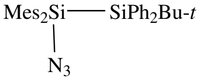

$Mes_2Si(N_3){-}SiPh_2Bu\text{-}t$

(708)

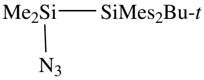

$Me_2Si(N_3){-}SiMes_2Bu\text{-}t$

(709)

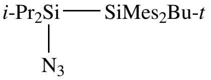

$i\text{-}Pr_2Si(N_3){-}SiMes_2Bu\text{-}t$

(710)

Mes = Mesityl

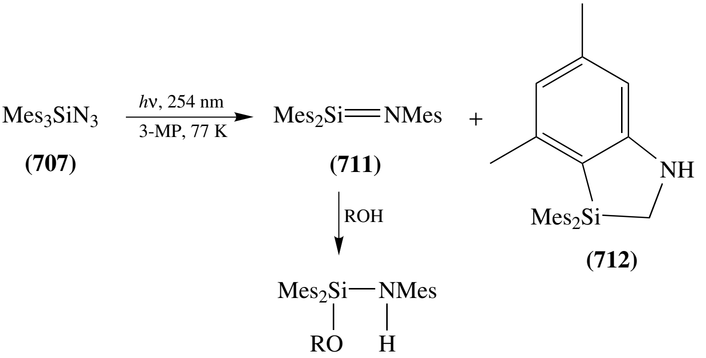

(236)

The photolysis of the three other azidosilanes **708–710** in 3-MP glass at 77 K produced no new UV bands, nor was a trapping product obtained in the presence of alcohols. In solution, however, the silanimines **711–713** were produced by photolysis and could be intercepted with alcohols (equation 237).

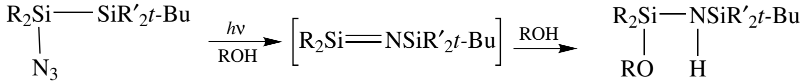

(237)

(708) R = Mes; R′ = Ph
(709) R = Me3; R′ = Mes
(710) R = *i*-Pr ; R′ = Mes

(711) R = Mes; R′ = Ph
(712) R = Me3; R′ = Mes
(713) R = *i*-Pr ; R′ = Mes

The authors propose that N-silanimines result from a migration of a silyl group with simultaneous loss of N_2 in the excited state of the azidosilane. This is in accordance with evidence published earlier by Kyba and Abramovich[318,319] that the photochemical decomposition of alkyl azides does not proceed via a nitrene intermediate (see also Reference 320).

An elegant study to probe the effects of π-bonding on the properties of the Si=N bond has been carried out with bridgehead silanimines **714–716**, in which the double bond is twisted[321].

The photolyses of the azides **717** and **718** and the trapping of the silanimines **714–716** was repeated according to an earlier study[322]. The irradiation (248 nm) of an argon matrix of **717** at 10 K led to a new absorption band at 397 nm and a new set of IR peaks. The experimental data are in good agreement with *ab initio* calculations. Trapping experiments and isotope labeling support the evidence of silanimine **714** as the primary photoproduct (equation 238).

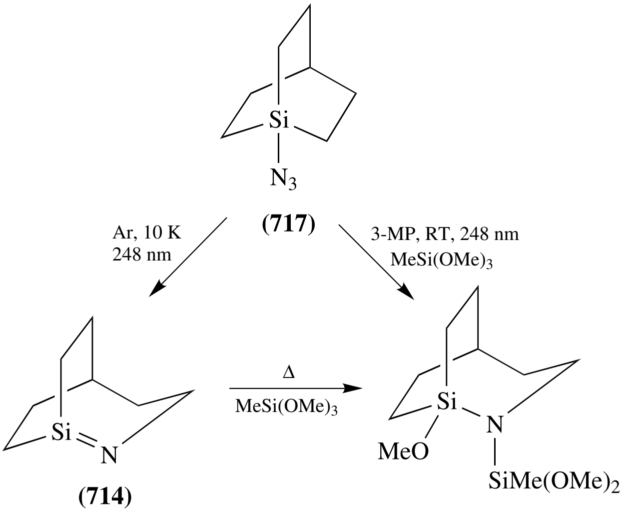

(238)

In the case of azide **718** the matrix containing the primary photoproducts, silanimines **715** and **716**, was also irradiated shortly at 514.5 nm; this obviously destroyed the more stable isomer **715** (equation 239).

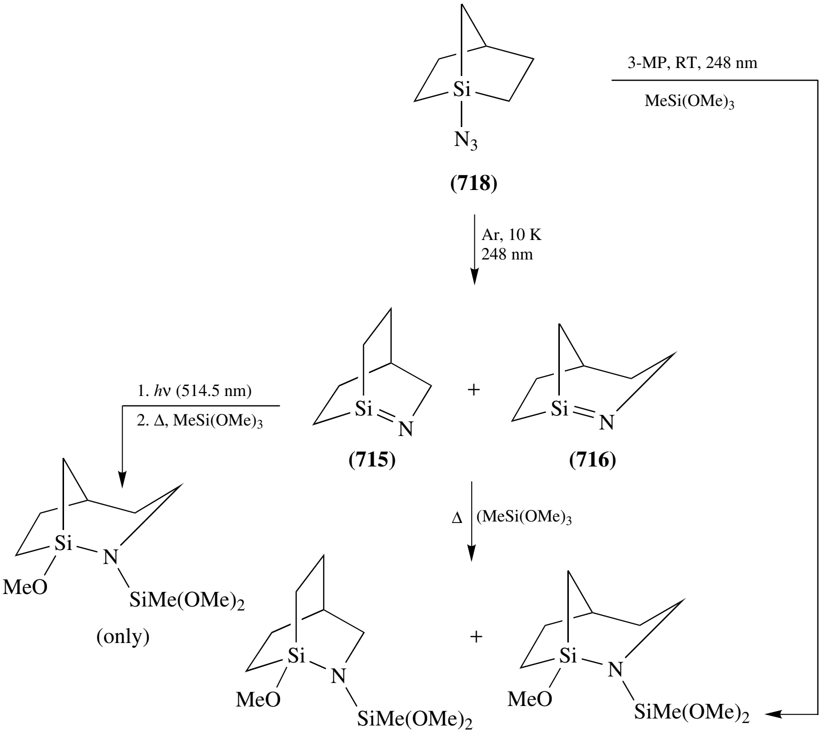

(239)

The authors stated that their results support the common belief[320] that the loss of N_2 is concerted with the rearrangement of the silyl group and that a singlet nitrene does not appear as a distinct intermediate. As far as the geometry of the silanimines is concerned the calculations (which predicted the IR spectra quite well) give optimized Si=N bond lengths which are *ca* 5 pm longer than in planar $Me_2Si{=}NMe$. This implies that the Si=N bond is weakened by twisting. Other geometric factors (e.g. pyramidalization) also play a role. The observed trends leave no doubt about the importance of π bonding in the electronic structure of the Si=N double bond, but they are not easily predictable.

The first spectroscopic observation of the radical SiN, a silicon compound that can be formulated as triply bonded in one of its formal valence-bond structures ($\cdot Si{\equiv}N{:}$) dates back to 1913[323–325]! Despite this early appearance it was not until recently that enhanced effort was applied to the synthesis of triply bonded silicon species. In this connection a group of authors photolysed and pyrolysed the geminal triazide, **719**, in the attempt to isolate a silicon analogue of a nitrile or an isocyanide.[326]

The pyrolysis at 900 °C and in a stream of argon gave the silaisocyanide **721** (also as the ^{15}N-labeled species) which could be trapped in a matrix (12 K), and characterized unequivocally by its UV and IR spectra and GC-MS of the trapping product with *t*-BuOH. The spectra correspond well to calculated values. The assignment of the structure of the pyrolysis product agrees with the prior attribution by photoelectron spectroscopy by Bock and Dammel[315]. Photolyses of matrices containing **719** also give **721**; it was ruled out that spectral features of minor impurities could be attributed to the silanitrile **720**. Chemical trapping experiments with *t*-BuOH, however, gave evidence for the intermediacy of a species still containing the C–Si–N skeleton: two volatile trapping products (**722** and **723**) were detected by GC-MS analysis (equation 240). The authors state that, although **722** could be formed by the addition of two equivalents of *t*-BuOH to **720**, this is not ultimate proof for the existence of the silanitrile. The structure of the silaisocyanide **721** as determined by *ab initio* methods (see Section IV.F) exhibits a linear C–N–Si group and a Si=N bond length of 1.587 Å, which coincides well with the measured length of the Si=N bond in hindered, stable silanimines (1.568 Å)[327]. The energy difference between **720** and **721** is 55 kcal mol^{-1} in favour of the silaisocyanide.

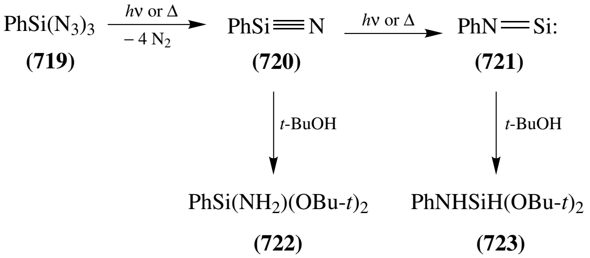

$$\begin{tikzcd}
PhSi(N_3)_3 \arrow[r, "h\nu \text{ or } \Delta", "-4\,N_2"'] & PhSi{\equiv}N \arrow[r, "h\nu \text{ or } \Delta"] \arrow[d, "t\text{-BuOH}"] & PhN{=}Si{:} \arrow[d, "t\text{-BuOH}"] \\
& PhSi(NH_2)(OBu\text{-}t)_2 & PhNHSiH(OBu\text{-}t)_2
\end{tikzcd} \tag{240}$$

(719) **(720)** **(721)** **(722)** **(723)**

This fact did not deter Maier and coworkers in the quest for the still ‘missing’ silanitriles, $R{-}Si{\equiv}N$[328–330].

After the elimination of four equivalents of nitrogen from methyltriazidosilane **(724)**, one nitrogen should remain on the silicon atom, i.e. a silanitrile or silaisocyanide could be formed. The photochemistry of **724** is relatively complex. The final product of 254 nm irradiation is silyl isocyanide **725**, which is in photoequilibrium with silyl cyanide **726**. It is assumed that the silanitrile **727** is an intermediate, which isomerizes by methyl migration to the silaisocyanide **728** (identified by IR). **728** then rearranges by three-fold 1,3-hydrogen shift to **725**. The latter compound is obtained in traces upon irradiation of the silanimine **729**, which is available from methylazidosilane **730**, along with aminosilylene

731, which itself is in equilibrium with 2-aminosilene **732** (equation 241).

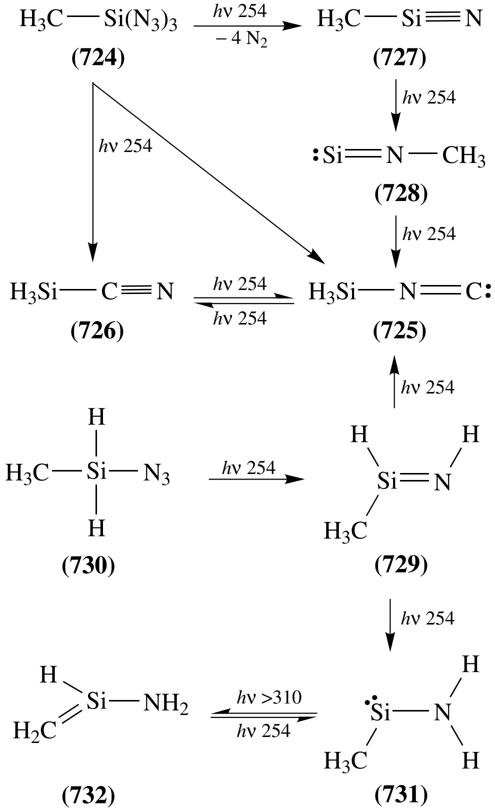

(241)

The ideal starting compound for the matrix studies of the parent silanitrile, H−Si≡N, is silyl azide **734**. By judicious choice of irradiation wavelengths the preparation and interconversion of a series of H,Si,N containing species **735**–**737**, characterized by UV and IR spectra, was possible. It was found that silanitrile **733** can indeed be obtained, at first in a mixture with the hydrogen associate **733**•H_2. Tempering the matrix to 30 K leaves only **733**. The interconversion of **737** and **733** is also possible (equation 242).

In addition, these experiments were the first proof for the simplest of all silanimines, $H_2Si{=}NH$ (**735**). The results were interpreted with the help of corresponding calculations and supported by deuterium labeling experiments. The bond orders, as determined from the force constants (experimental IR spectra), are 2.0 for HSi≡N **733** and 2.3 for HN=Si **737**.

d. Retro-ene reactions. The retro-ene reaction of allyldimethylsilyl ether, $H_2C{=}CHCH_2O$-$SiMe_2H$, has been successfully used to prepare dimethylsilanone, $Me_2Si{=}O$[331]. This led a group of French researchers to anticipate the silanamine **738** as a precursor of the silanimine **739**[332]. In fact, the flash vacuum thermolysis (FVT, 900 °C, 10^{-4} h Pa) of **738** mainly gave the expected products, namely propene and silanimine **739**. The formation of **739** was unambiguously shown by trapping it with *tert*-butanol to give **740** (equation 243). Direct evidence of the presence of **739** has been obtained by coupling the FVT oven with a high-resolution mass spectrometer (HRMS).

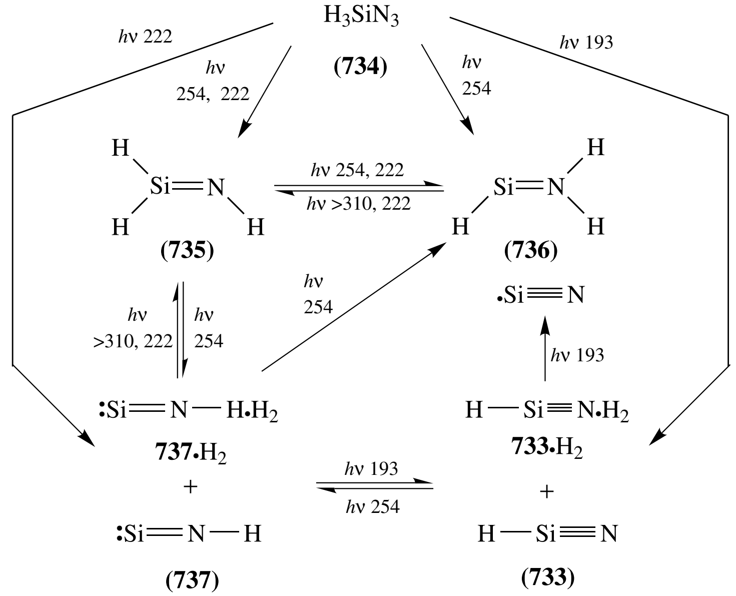

(242)

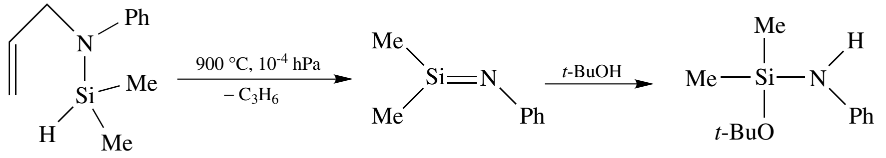

(738) **(739)** **(740)**

(243)

Other precursors like **741** and **742** were pyrolysed under similar conditions, but here the energetically favoured, competitive retro-ene process leading to the silyl imines **743** was predominant (equation 244).

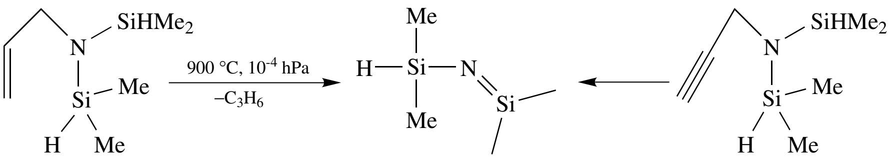

(741) **(743)** **(742)**

(244)

Similarly to the preparation of **739**, substituted silanimine **744** was prepared and characterized along with the silyl substituted analogue **745**[313]. HRMS showed **745** and the dimer **702** of **744**, which is expected to polymerize rapidly in the condensed phase. (equation 245).

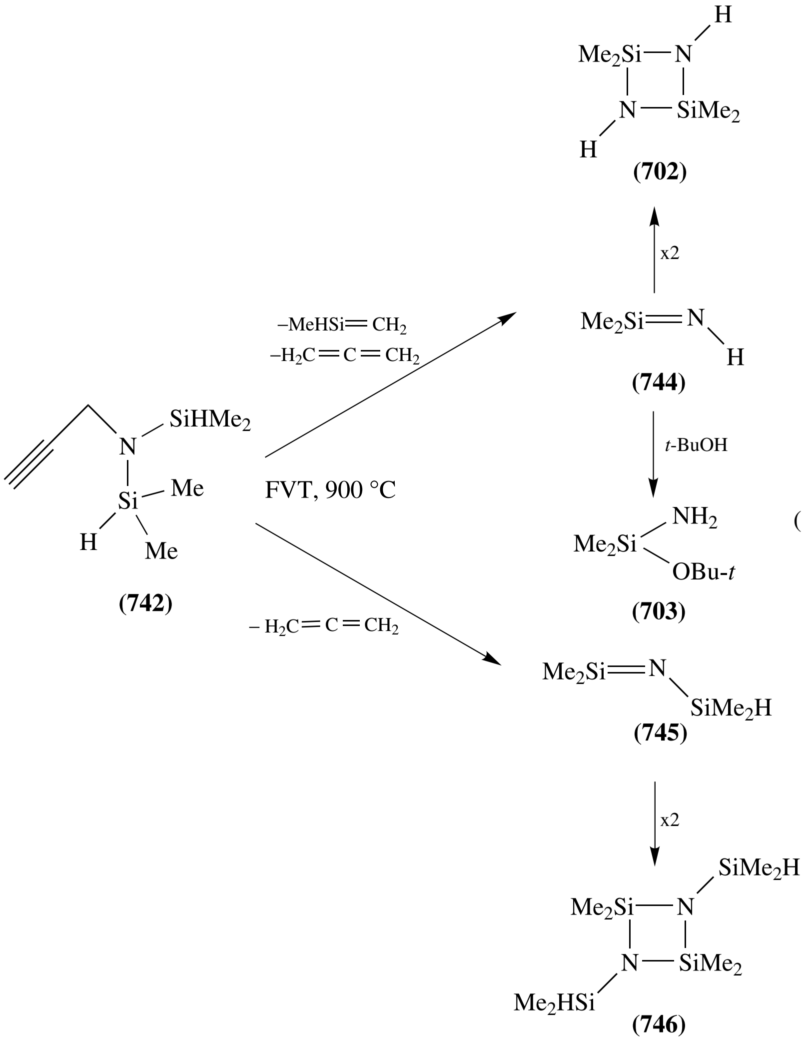

(245)

The detection of the *t*-BuOH trapping product **703** and of the dimer **746** gives further evidence for the intermediacy of **744** and **745**, respectively. Silanimine **735** is an intermediate in the synthesis of silaisocyanide **737** by retro-ene reaction from **747** under FVT conditions (equation 246)^{333}. **737** was characterized by millimeter wave spectroscopy.

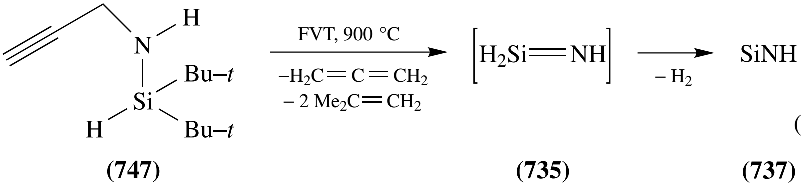

(246)

e. Dehydrochlorination. The dehydrochlorination of volatile halogenated silanimines by non-volatile bases in a vacuum gas solid reaction (VGSR)[332] is reminiscent of the salt elimination procedure used by Wiberg and Klingebiel for the synthesis of silanimines.

The compounds resulting from the reaction of **748** were characterized by HRMS directly coupled to the reactor. The stable products **750** and **751** were analysed by GC and ^{1}H NMR spectroscopy. The formation of the cyclodisilazane **750** is explained by dimerization of the unstable silanimine **749** only in the cold trap, as the reaction is carried out under high dilution conditions (equation 247). It was also shown that the hydrogen chloride elimination did not occur in the ion source of the mass spectrometer.

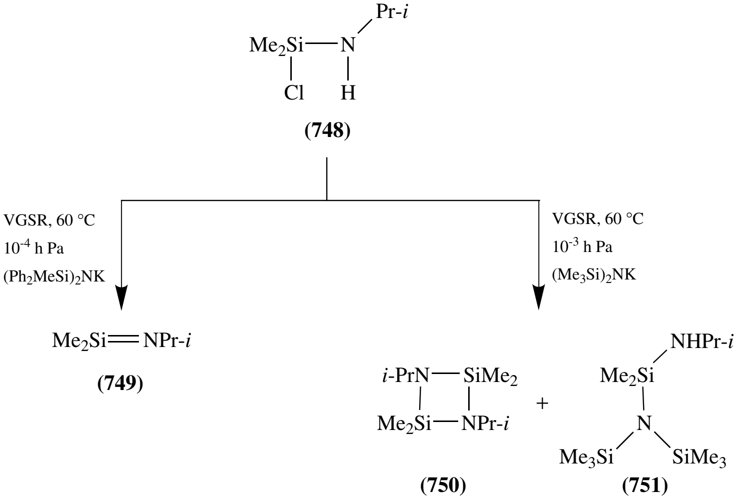

(247)

f. Silylene addition to azides. Weidenbruch and coworkers reacted silylenes, t-Bu$_2$Si: and Mes$_2$Si:, with sterically hindered t-Bu$_3$SiN$_3$ **752** in order to obtain either [2 + 1] or [3 + 1] cycloadducts[334]. With t-Bu$_2$Si: they obtained products (for **678** see above) already known from another synthesis (**753** by prolonged heating of **678**, or double ene reaction of **678** with isobutene) by Wiberg (equation 248)[303].

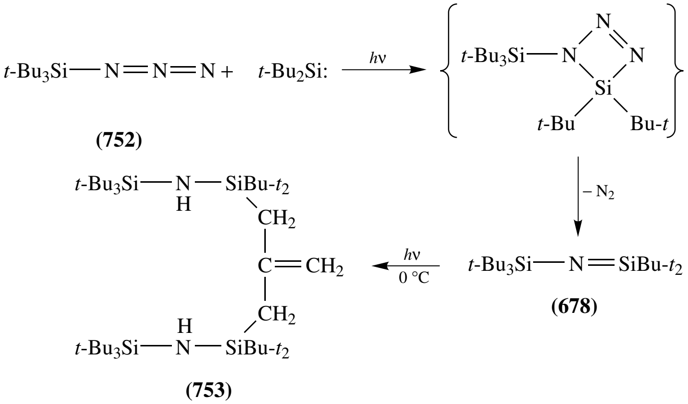

(248)

Under photolysis conditions silanimine **678** was always obtained along with its consecutive product **753**. With Mes_2Si**:** another silanimine **(754)** was formed in the reaction with the azide, but in this case it rearranged to give a benzosilacyclobutene **(755)**, that was characterized by X-ray diffraction (equation 249).

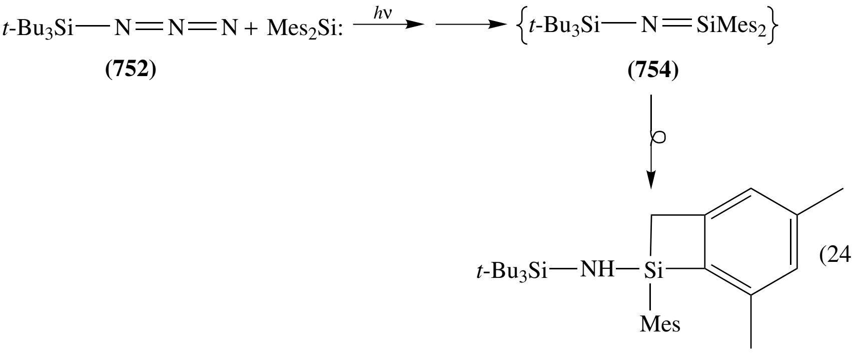

(752) **(754)** **(755)**

(249)

The stable silylene **756** was reacted with triphenylmethyl azide to give a silanimine **(757)** (equation 250)[335].

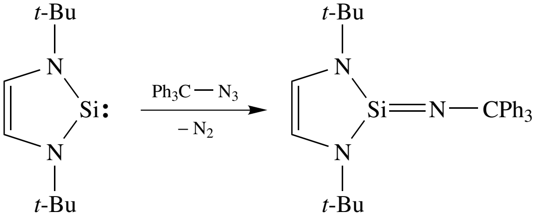

(250)

(756) **(757)**

g. Reaction of SiH_4 and N_2. A radio frequency excited discharge of a mixture of silane and nitrogen was monitored by Fourier transform spectroscopy. A band at 3584 cm^{-1} was assigned to the fundamental ν_1 band (NH stretch) of silaisocyanide, HNSi **737**[336]. This was the first observation of this molecule in the gas phase by high resolution infrared vibration rotation spectra. The experimental data fit the calculated values assuming a linear molecule.

h. Ionic Si=N compounds by gas phase reactions. i. Silicon-containing anions. Damrauer and coworkers have perfected the preparation of simple silicon-containing anions in the gas phase whose conjugate acids are highly reactive, low valent neutral silicon compounds[337,338]. These studies have the advantage that many anions are readily prepared in the gas phase, even though their conjugate acids would be expected to be exceptionally reactive in the gas and condensed phase. The reaction chemistry of anions is an indirect probe of the properties of their corresponding acids.

The technique used is the Flowing Afterglow Selected Ion Flow Tube (FA-SIFT), a short description of which is given elsewhere[337,338]; it allows the preparation of ions in a first flow tube, their separation from complex reaction mixtures with a quadrupole, the study of their reactivity in a second flow tube and the detection of the reaction products. It is demonstrated for $[HSiNH]^-$ in equation 251.

$$\begin{array}{lll}
\left.\begin{array}{rcl} NH_3 & \xrightarrow{EI} & H_2N^- \\ C_6H_5\,SiH_3 + H_2N^- & \longrightarrow & H_3SiNH^- + C_6H_6 \end{array}\right\} & & \text{flow tube 1} \\
\quad H_3SiNH^- \xrightarrow{CID} [HSiNH]^- + H_2 & & \text{flow tube 2} \\
\text{or} & & \qquad (251) \\
\quad C_6H_5SiH_3 + H_2N^- \longrightarrow [HSiNH]^- + H_2 + C_6H_6 & & \text{flow tube 1}
\end{array}$$

EI = electron impact
CID = collisionally induced dissociation

α. $[HSiNH]^-$: an anion related to silanimine $H_2Si{=}NH$[337]. Experimental verification of the connectivity for $[HSiNH]^-$ rests on labeling and H/D exchange reactions (equation 252).

$$\begin{array}{rcl}
D_3SiNH^- & \xrightarrow{CID} & [DSiNH]^- \text{ only product} \\
HSiNH^- & \xrightarrow[\text{or EtOD}]{CD_3OD} & [HSiND]^- \\
[DSiNH^-] & \xrightarrow{EtOH} & \text{no exchange} \\
 & \xrightarrow{EtOD} & [DSiND]^-
\end{array} \qquad (252)$$

The reactivity (see below) and the greater electronegativity of nitrogen with respect to silicon suggests that the charge will be concentrated on the nitrogen of $HSiNH^-$. The gas phase anion proton affinity has been determined by bracketing techniques and $\Delta G^0_{\text{acid}} = 352 \pm 3$ kcal mol^{-1} is found as the acidity of $HSiNH_2$. A variety of reactions with small neutral molecules, their reaction products, rate coefficients, efficiencies and branching ratios are reported. Equation 253 illustrates most of the important features of the reaction of $HSiNH^-$ **758** with COS.

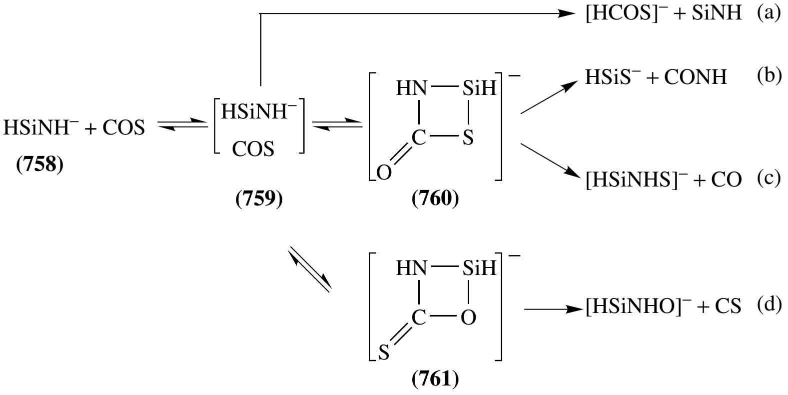

(253)

At first an ion–molecule complex **759** is formed from which either a hydride is transferred to COS (path a) or addition to COS takes place (paths b–d). Intermediate **760** can react by ring cleavage leading to $HSiS^-$ and CONH (path b), or by extrusion leading to $[HSiNHS]^-$ and CO (path c). Intermediate **761** can also undergo extrusion (path d).

Other neutral reaction partners used were CO_2, CS_2, O_2, C_6F_6 and alcohols. Computational studies of the $[H_2,Si,N]^-$ system show the *cis* and *trans* isomers $[HSiNH]^-$ to be more stable than either $[H_2SiN]^-$ (by 24 kcal mol^{-1}), or $[SiNH_2]^-$ (by 24 kcal mol^{-1}).

β. Silaformamide ion [HSi(O)NH]$^-$[338]. The reactions which can lead to the silaformamide ion are given in equation 254.

$$\left.\begin{array}{lcl} NH_3 & \xrightarrow{\mathrm{El}} & H_2N^- \\ C_6H_5SiH_3 + H_2N^- & \longrightarrow & H_2NSiH_2^- + C_6H_6 \\ H_2NSiH_2^- + H_2O & \longrightarrow & H_2NSiH_2O^- + H_2 \\ H_2NSiH_2O^- & \xrightarrow{\mathrm{CID}} & [H_2, Si, N, O]^- + H_2 \end{array}\right\}\text{flow tube 1} \qquad (254)$$

The connectivity of the silaformamide ion $[HSi(O)NH]^-$ **762** was established by deuteriation studies using both ND_2^- and D_2O. The reaction chemistry with neutral reagents such as CO_2, CS_2, COS, fluoro and aliphatic alcohols has been studied. An example is shown in equation 255, which displays the ambident reactivity versus COS.

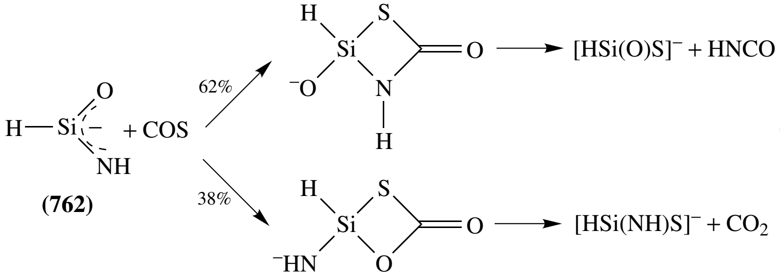

(255)

Ab initio calculations probed the stability of **762**: it was found to be less stable than the silylene isomer $[Si(O)NH_2]^-$ **763** by 1.32–7.5 kcal mol^{-1}, depending on the method. Calculation of the charge density shows nearly equal charges on oxygen and nitrogen in the anion **762** and suggests an explanation for its ambident behaviour. The gas phase acidity of the conjugate acid of **762** has been difficult to determine experimentally (*ca* 350–355 kcal mol^{-1}) but a value of 345 kcal mol^{-1} is given by calculation. Silaformamide $HSi(O)NH_2$ **764** itself is calculated to be the most stable $[H_3SiON]$ isomer.

ii. Silicon containing cations. Bohme and coworkers have reacted ground state (^2P) Si^+ ions, obtained by electron impact from tetramethylsilane, and have studied their reactivity in *ca* 100 ion/molecule reactions using the selected ion flow tube (SIFT) technique[339,340].

Reaction with ammonia initiates the sequence of equation 256 which, according to theoretical studies, selectively establishes hydrogen silaisocyanide, H−N=Si **737**[341].

$$\begin{aligned} &Si^+ + NH_3 \longrightarrow SiNH_2{}^+ + H\cdot \\ &\underset{\textbf{(765)}}{SiNH_2{}^+} + NH_3 \longrightarrow HNSi + NH_4{}^+ \end{aligned} \tag{256}$$

Calculated and experimentally determined proton affinities for HNSi (**737**) confirm its formation. The ion $SiNH_2{}^+$ **765** is best described as $:Si^+\text{-}NH_2$. It inserts into C−C and C−S bonds of $(H_3C)_2CO$ and $(H_3C)_2S$ or, in the case of $(H_3C)_2S$, in a side reaction a hydride H^- is transfered to form the aminosilylene $:Si(H)NH_2$ **736**.

Schwarz and coworkers have used the technique of neutralization−reionization mass spectrometry (NRMS) to structurally characterize numerous elusive silicon-containing molecules of interstellar interest[342]. The identification of HNSi was supported by *ab initio* calculations. The radical ion $[HNSi]^{\bullet +}$ was produced from N_2 and SiH_3I in the chemical ionization source of the mass spectrometer.

2. N=Si=N systems

a. Silanediimines. The first silanediimine was isolated in matrix by West and coworkers[343]. Photolysis of **766** in the presence of Me_3SiOMe in solution at room temperature gives **768** and further photolysis gives **770**. Both products probably result from addition of the alkoxysilane to intermediate silanimines **767** and **769** formed by 1,2-trimethylsilyl migration (equation 257).

$$\begin{tikzcd}
\underset{\textbf{(766)}}{(Me_3Si)_2Si(N_3)_2} \arrow[r, "h\nu\ 254\ \text{nm}"] & \underset{\textbf{(767)}}{[Me_3SiSi(N_3){=}NSiMe_3]} \arrow[d, "Me_3SiOMe"] \\
\underset{\textbf{(769)}}{[(Me_3Si)_2NSi(OMe){=}NSiMe_3]} \arrow[d, "Me_3SiOMe"] & \underset{\textbf{(768)}}{Me_3SiSi(OMe)(N_3)N(SiMe_3)_2} \arrow[l, "h\nu\ 254\ \text{nm}"'] \\
\underset{\textbf{(770)}}{[(Me_3Si)_2N]_2Si(OMe)_2} &
\end{tikzcd} \tag{257}$$

Irradiation of **766** in glassy 3-methylpentane at 77 K gave two new UV bands at 274 and 324 nm. The two species responsible for this spectrum were identified as **767** and **771**. The following experimental facts support the assignment: (i) the 274 nm band grows more rapidly, (ii) bleaching at >270 nm reduces the 274 nm band with a concomitant increase in the 324 nm band, (iii) trapping experiments give **768** and **770** (equation 258). The ratio depends on the irradiation conditions.

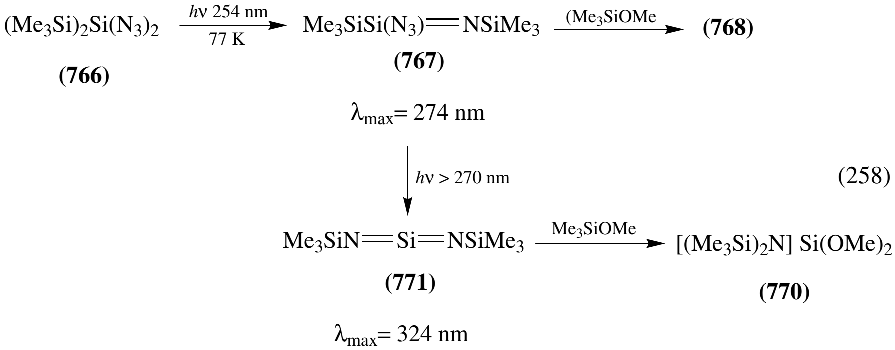

(258)

The photolysis of $Ph_2Si(N_3)_2$ **772** in the presence of *tert*-butanol has been reported to give one product from the migration of both phenyl groups to a nitrogen and the addition of 2 equivalents of alcohol. This was interpreted as evidence for the intermediacy of *N*,*N*′-diphenylsilandiimine PhN=Si=NPh **773**[344]. The above results, however, suggest that **773** is not formed, but that sequential migration–addition steps take place.

The irradiation of a similar diazidosilane **(774)** gives as the major product the silylene *t*-Bu_2Si**:**, which undergoes a subsequent photochemical C–H insertion to give the stable silacyclopropane **775**[345]. Evidence for the intermediacy of *t*-Bu_2SiN_2 **776** as a photochemical precursor to **775** (<5%) is presented and supported by calculations. Another minor product of the photolysis of **774** is *N*,*N*′-di-*tert*-butylsilanediimine (**777**, *ca* 10%), which exhibits UV bands at 240 and 385 nm; a definite IR spectrum was impossible to obtain (equation 259). Chemical trapping, isotope labeling (^{15}N) and calculations support the spectroscopic evidence.

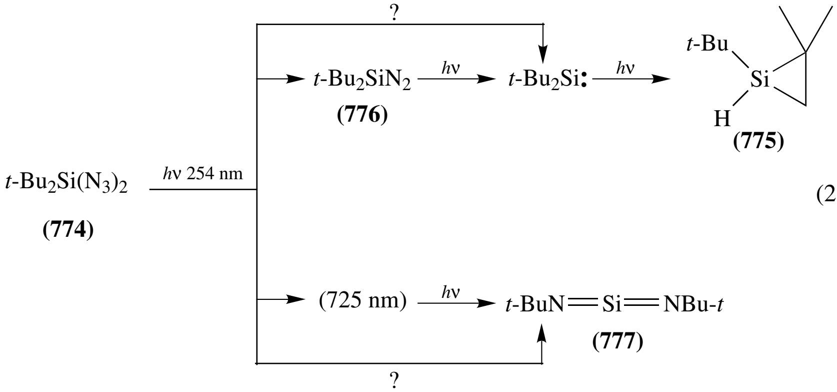

(259)

b. Silaamidides [(RN)$_2$SiR′]$^-$. The first silaamidide ion was isolated by Underiner and West[346]. The reaction of the silanediamine **778** with two equivalents of *t*-BuLi gives the silaamidide **779**. The ether-free salt **780** can be obtained by heating **779** in vacuo. The lithium cation may be complexed by 12-crown-4 to give **781** (equation 260). The NMR spectroscopic data are consistent with symmetric species. The ^{29}Si NMR chemical shifts reflect the extent of ion pair separation, e.g. $\delta^{29}Si$ is +7 ppm for $[SupN)_2SiPh]Li$

780 and −36.3 ppm for $[(SupN)_2SiPh][Li([12]\text{-}C\text{-}4)_2]$ **781**. An intense IR peak in the range of 1303–1284 cm^{-1} is assigned to ν_{as} of the $[N{-}Si{-}N]^-$ system and, as expected, these bands are at lower energy than for the Si=N stretching absorption. The crystal structure of $[SupN)_2SiBu\text{-}t]$ $[Li([12]\text{-}C\text{-}4)THF]$ (see Table 17) shows that there is indeed no interaction between the ions. The geometry around the tricoordinated silicon atom is planar. The Si–N bond lengths, 1.594 and 1.626 Å, are intermediate between single (*ca* 1.75 Å) and double bond lengths (*ca* 1.57 Å), but closer to a double bond, and are thus consistent with a considerable Si–N π bonding in the allylic system.

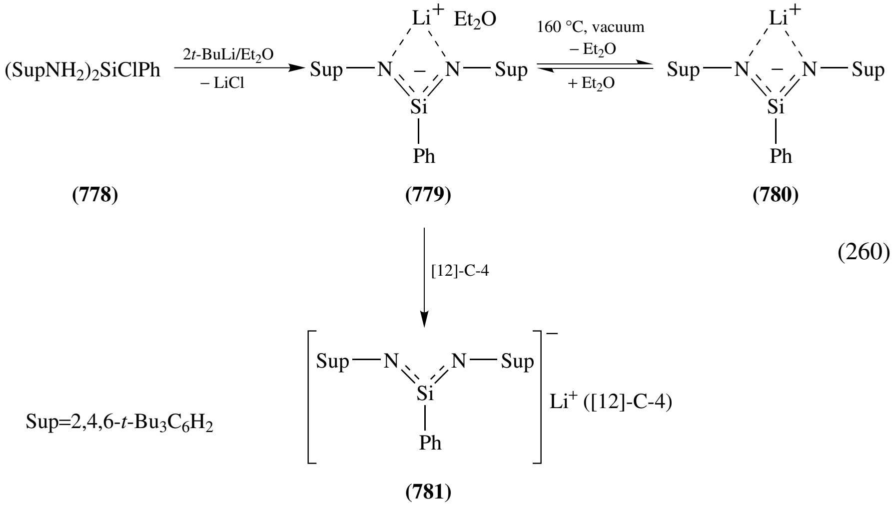

(260)

Sup=2,4,6-t-$Bu_3C_6H_2$

Salts **782** and **783** having chloro or triflate substituents at silicon could also be prepared by partial metal–halogen exchange[347]. The elimination of MX (X = Cl, OTf; M = Li, K) from these compounds to give silanediimines did not occur, but may lead to substitution products like **784** (equation 261). Addition reactions and a [2 + 2] cycloaddition are reported (equation 262 and 263).

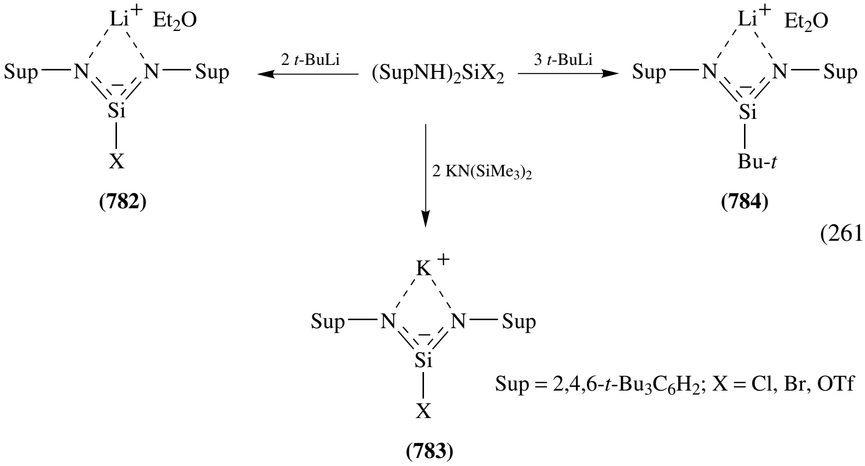

(261)

Sup = 2,4,6-t-$Bu_3C_6H_2$; X = Cl, Br, OTf

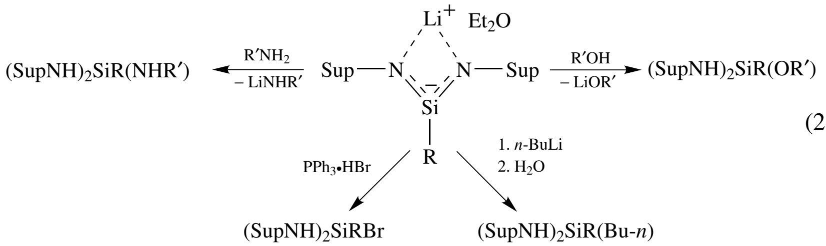

(262)

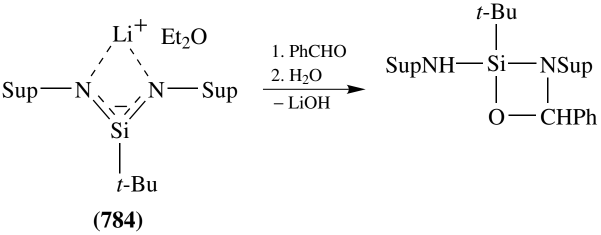

(263)

3. Si=N metal systems

The stabilization of small reactive species is mostly always possible by the coordination to transition metals. For silicon such complexes are known for silylenes, silenes and disilenes[348,349]. The first example of a metal silanimine complex was reported by Berry and coworkers in 1991[350]. The synthetic strategy employed involves formation of the unsaturated fragment by β-hydrogen abstraction and loss of alkane. Alkylation of the amido complex **785** with $LiCH_2SiMe_3$ gives **786**, which is observed as unstable intermediate by ^1H NMR. It decomposes in solution, probably via the reactive 16-electron intermediate **787**. In the presence of PMe_3 as a trapping ligand the silanimine complex **788** can be isolated (equation 264).

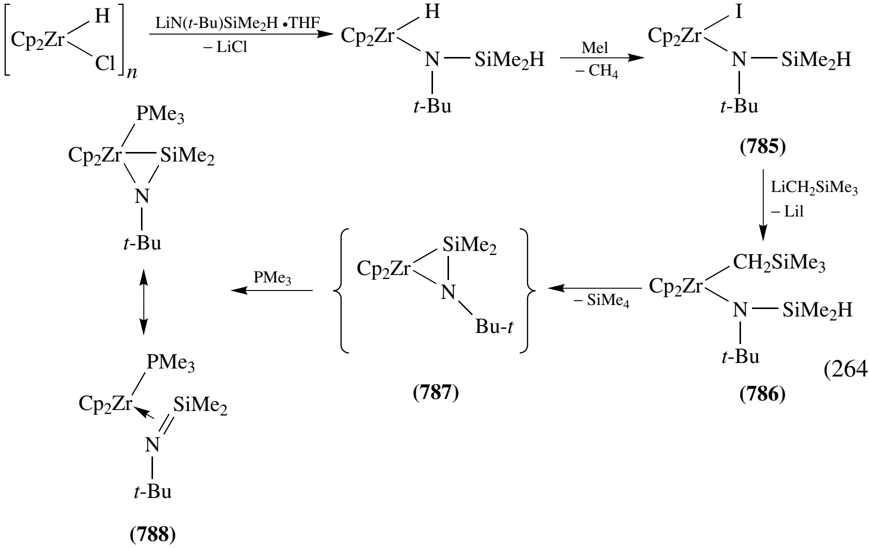

(264)

In analogy to metal alkene complexes, two extreme resonance forms (metallacycle, sp^3 Si; π-donor complex, sp^2 Si) can be formulated. X-ray structural analysis of **788** gives a Si–N bond length of 1.687 Å, which is within the normal range for Si–N single bonds (1.64–1.80 Å); Wiberg's silanimine t-$Bu_2Si{=}NSiBu$-t_3 (1.568 Å) and a donor adduct THF•$Me_2Si{=}NSiBu$-t_3 (*ca* 1.58 Å) show significantly shorter bonds[301,303]. Along with the short Zr–Si distance (2.654 Å) this implies that the best description of the complex is that of a metallacycle.

C. Reactivity

The reactivity of SiN multiply bonded species has in part been discussed in Section IV. B, dedicated to synthesis, because the existence of reactive and short-lived species is often proven by trapping experiments. This part of the review therefore focusses on more comprehensive reactivity studies of Si=N systems.

1. Donor addition

The addition of donors to the Lewis acidic sp^2-hybridized silicon in Si=N systems is a general method to stabilize the multiple bond, even when non-bulky substituents are used. In most cases the donor adduct reacts just like the free Si=N compound, obviously by initial dissociation of the donor molecule. In the absence of trapping agents and when the steric bulk allows it, silanimines dimerize[300,308,311], e.g. **672** gives cyclodisilazane **789** (equation 265).

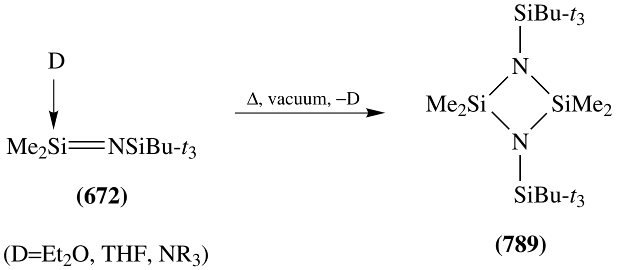

(672)

($D{=}Et_2O$, THF, NR_3)

(789)

(265)

The proximity of the donor to the reactive species does, however, lead to the reaction of the Si=N bond with the coordinated molecule. Wiberg has encountered several cases of such behaviour. When **672**•Et_2O is heated to 60 °C in diethyl ether, the dimer **789** is only formed in 10% yield; the other 90% are compound **790** (equation 266)[300]. Its formation may be understood as β-elimination reaction analogous to that occurring in oxonium salts, and subsequent insertion of the alcohol. No dimer is obtained when **672** ($D = Me_2EtN$) is heated: the products **791** and **793** are formed in the sense of a Stevens migration from the silanimine donor adducts **672** and **792**, respectively. In excess Me_2EtN the displacement of the amine donor ($D = Me_2EtN$) from **672** by **791** to give **792** does not occur (equation 267)[300].

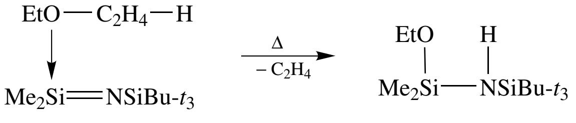

$$\overset{\displaystyle EtO-C_2H_4-H}{\downarrow}\atop{Me_2Si{=}NSiBu\text{-}t_3} \xrightarrow[-C_2H_4]{\Delta} Me_2\overset{\displaystyle EtO}{\overset{|}{Si}}-\overset{\displaystyle H}{\overset{|}{N}}SiBu\text{-}t_3 \qquad (266)$$

(672) $D{=}Et_2O$ **(790)**

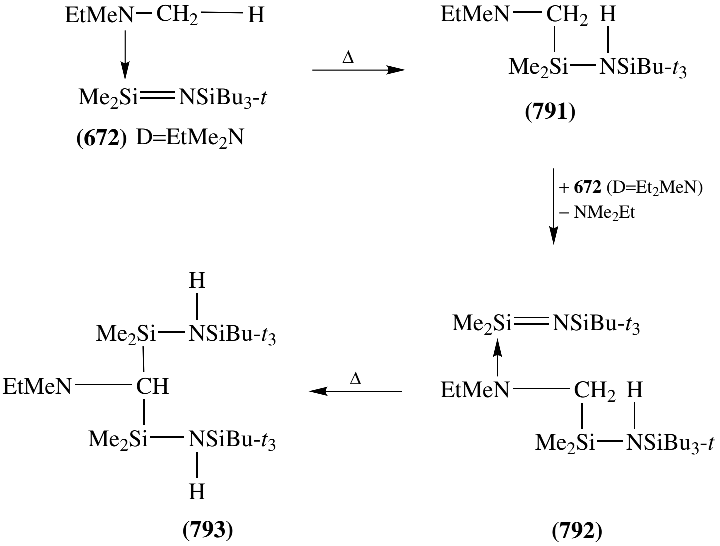

(267)

The expected exchange of donors does not take place with compound **678**•THF and NMe_2Et; instead the THF ring is cleaved, ethylene is eliminated and compound **794** is formed (equation 268). The reaction of **678**•THF with N_2O, in which the THF ligand also participates, will be described below.

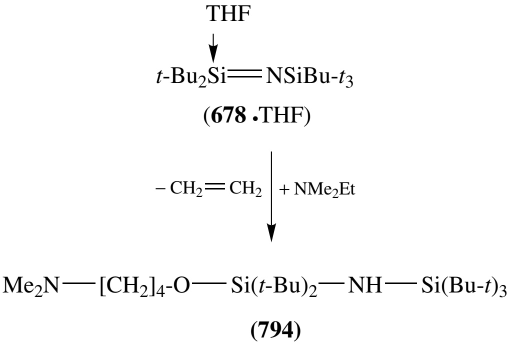

(268)

2. Insertion reactions

Insertion of the Si=N bond into polar bonds is the most used reaction for the characterization of very reactive and transient silanimines. Especially, the reaction with alcohols is often the first reaction to be carried out with silicon−nitrogen multiple bond systems. Other reagents used for insertion reactions are amines, water and alkoxysilanes (equation 269)[300,303,306,311,351–353]. The insertion into E−X bonds (E = Si, Ge, Sn; X = Cl, OR, NR_2, N_3) has been shown earlier in this review for the insertion into the Si−N bond of silyl azides[310,351]. A reaction reported is the insertion of **678** into the C−H bond of benzene at elevated temperatures[303].

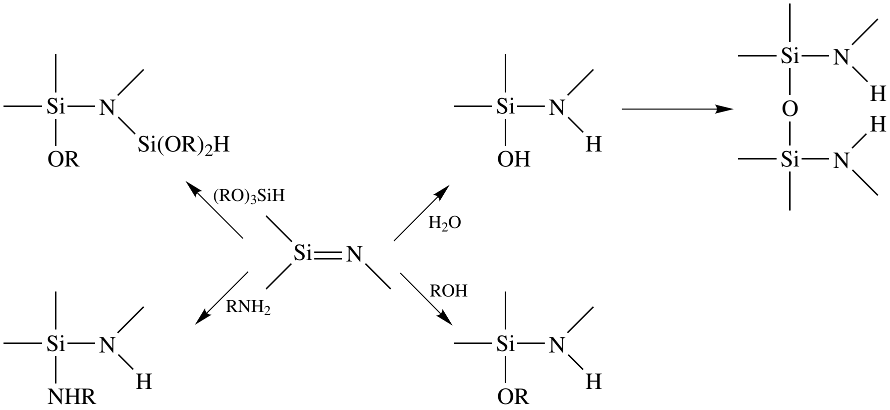

(269)

3. Ene reactions

In contrast to the silenes, silanimines undergo ene reactions (equation 270) rather than $[2 + 4]$ cycloaddition reactions with diene reagents. $Me_2Si{=}NSiBu\text{-}t_3{\cdot}D$) (**672·D**)[300] and $Me_2Si{=}NR$ [$R = SiMe_nBu\text{-}t_{3-n}$, $SiPh_3$, $EMe_2N(SiMe_3)_2$ with E = Si, Ge][351] react with propene, isobutene, 2,3-dimethylbuta-1,3-diene and cyclopentadiene; $t\text{-}Bu_2Si{=}NSiBu\text{-}t_3$ **(678)**, its donor adducts, and $Me_2Si{=}NR$ react also with acetone[303,351].

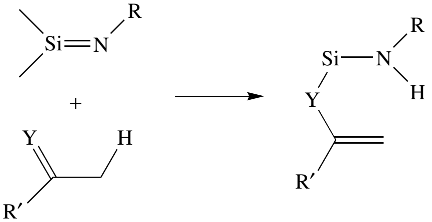

(270)

($Y{=}CH_2$, O; $R'{=}H$, Me, $CH_2{=}CMe$; $R = SiMe_nt\text{-}Bu_{3\text{-}n}$, $SiPh_3$, $EMe_2N(SiMe_3)_2$, E = Si, Ge)

4. Cycloaddition reactions

a. [2 + 2] Cycloadditions. The dimerization reaction as a special case of the $[2 + 2]$ cycloaddition reaction has already been mentioned above. It was mentioned that the dimerization occurs when the steric bulk allows the reaction. In the case of **795** a direct dimerization is thus not possible. The system seeks to gain stability in another way. The authors suggest an interaction between the Lewis acidic silicon atom in **795** and the oxygen atom of the siloxy group of a second molecule of **795**, which leads to an isomerized silanimine **796** that then dimerizes to give the head-to-tail dimer **797** (equation 271)[354].

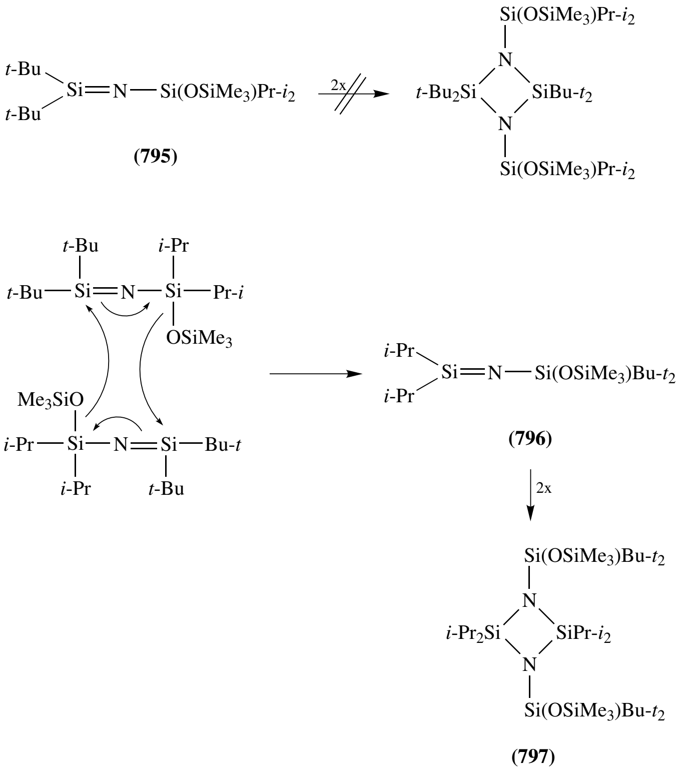

(271)

Silanimine **672**•D reacts with benzophenone to give a cycloadduct **798**, which cannot be isolated, and eliminates the benzophenoneimine $Ph_2C{=}NSiBu\text{-}t_3$, giving the cyclus **799** with another equivalent of **672**•D (equation 272)[300].

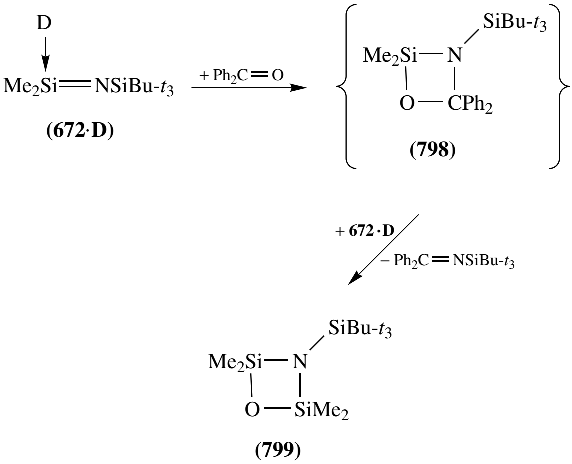

(272)

678 just gives an adduct with benzophenone, while with the less bulky benzaldehyde a [2 + 2] cycloadduct **800** is obtained (equation 273)[59].

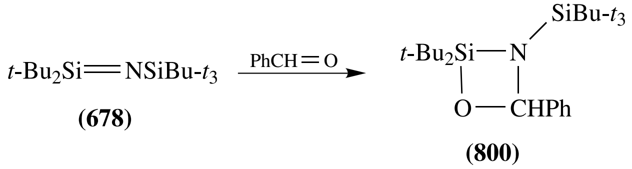

(678) **(800)**

(273)

Lithiated fluorosilanes such as **801** and **802** may be considered as fluoride donor adducts to silanimines and behave as the free silanimines (e.g. **803**) in cycloaddition reactions with C=O compounds. The stability of the four-membered cycloadducts obviously depends on the substituents (equation 274)[355].

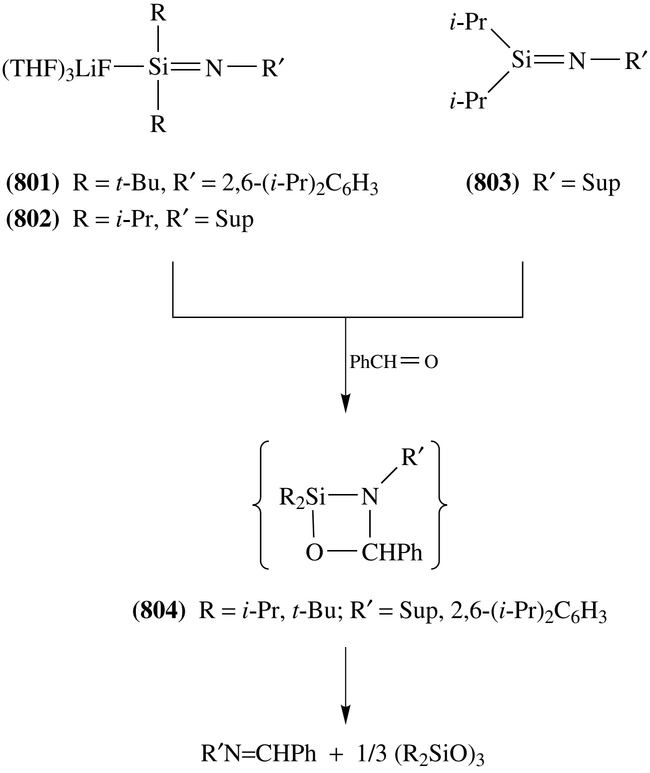

(801) R = t-Bu, R′ = 2,6-(i-Pr)$_2$C$_6$H$_3$

(802) R = i-Pr, R′ = Sup

(803) R′ = Sup

(804) R = i-Pr, t-Bu; R′ = Sup, 2,6-(i-Pr)$_2$C$_6$H$_3$

(274)

The choice of other differently substituted silanimine precursors like **805** and **806** allows the isolation of stable cycloadducts, e.g. **807** and **808** (equation 275). While **808** slowly decomposes at room temperature (equation 276), **807** can even be distilled at 110 °C/10^{-2} mbar.

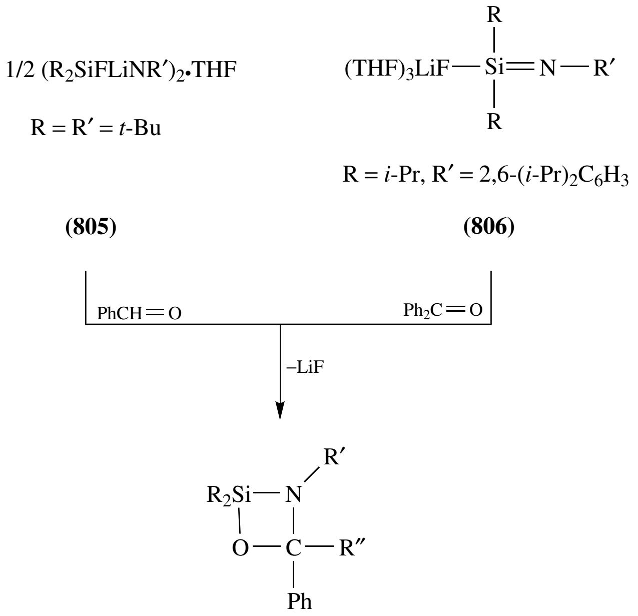

(805) **(806)**

(275)

(807) $R = R' = t\text{-Bu}, R'' = H$

(808) $R = i\text{-Pr}, R' = 2,6\text{-}(i\text{-Pr})_2C_6H_3, R'' = Ph$

$$\mathbf{808} \xrightarrow{25\,^{\circ}\mathrm{C}} R'N{=}C(Ph)R'' + 1/3\,(R_2SiO)_3 \qquad (276)$$

The lithiated aminofluorosilane $[t\text{-}Bu_2Si{-}N{-}Si(OSiMe_3)Pr\text{-}i_2\text{•}LiF]_2$ **809** behaves in the same way, and its cycloadduct with benzaldehyde decomposes into the respective imine and cyclotrisiloxane above 105 °C[354].

Silanimine **678** reacts with methyl vinyl ether in a clean reaction to give the [2 + 2] cycloadduct **810** (equation 277)[303].

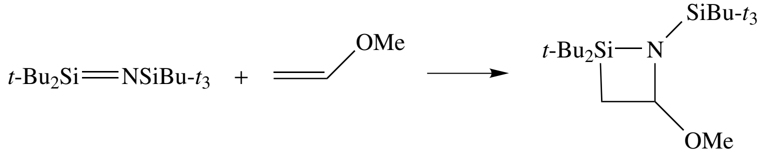

(678) **(810)**

(277)

b. [2 + 3] Cycloadditions. The silanimine **414a** reacts with azides $R'N_3$ ($R' = t$-Bu, silyl) to give siladihydrotetrazoles **344a**[300,310,351]. As a byproduct the insertion product **415a** is also formed (equation 278).

Silanimines **678**[303], $t\text{-}Bu_2Si{=}NSiBu\text{-}t_2Ph$ **(811)** and $t\text{-}Bu_2Si{=}NSiBu\text{-}t_2Me\text{•}THF$[353] (**812**•THF) also react with silyl azides in the same way as shown in equation 278. The reaction of **678** with N_2O obviously gives the [2 + 3] cycloadduct **813** as the initial product, but **813** then decomposes, probably via the silanone $t\text{-}Bu_2Si{=}O$, to give **814** as main product (equation 279)[356].

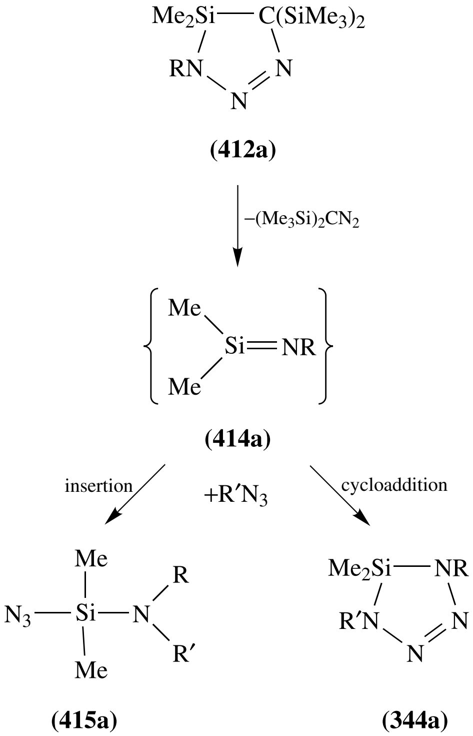

(278)

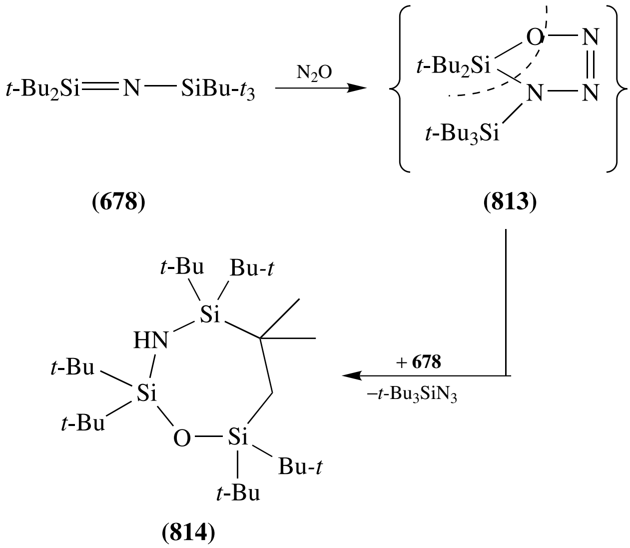

(279)

The authors suggest that the formation of **814** probably proceeds via the silanone t-$Bu_2Si{=}O$ and an insertion into one C–H bond of a *tert*-butyl group.

A different reaction occurs when the donor adduct **678**•THF is used for the reaction with N_2O. In this reaction the THF ring is incorporated into the product **815** (equation 280)[303].

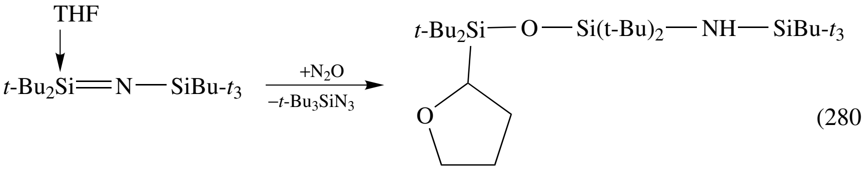

(280)

(678)•THF **(815)**

c. [2+4] Cycloadditions. With the Wiberg silanimines [2+4] cycloaddition reactions do not occur, rather ene reaction takes place. There is one example by Klingebiel and coworkers who obtained [2+2] and [2+4] cycloadducts **816** and **817** in a 1 : 3 ratio respectively, in the reaction of $t\text{-Bu}_2\text{Si}{=}\text{N}(2,6\text{-C}_6\text{H}_3i\text{-Pr}_2)^*\text{LiF(THF)}_3$ (**801**•LiF(THF)_3) with 2-methyl-2-propen-1-al (equation 281)[355]. The [2 + 2] adduct decomposes as described above.

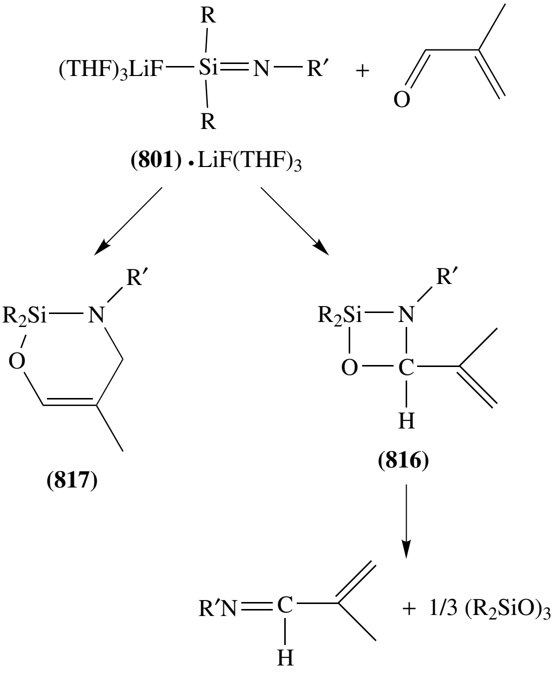

(801) • LiF(THF)_3

(817)

(816)

(281)

R = t-Bu, R′ = 2,6-(i-Pr)$_2$C$_6$H$_3$

5. Metal silanimine complexes

Berry describes a variety of reactions of the silanimine complex **788** to give **818**–**821**[348–350]. The phosphine ligand is quite labile and can be replaced by CO yielding the carbonyl complex **818** (equation 282).

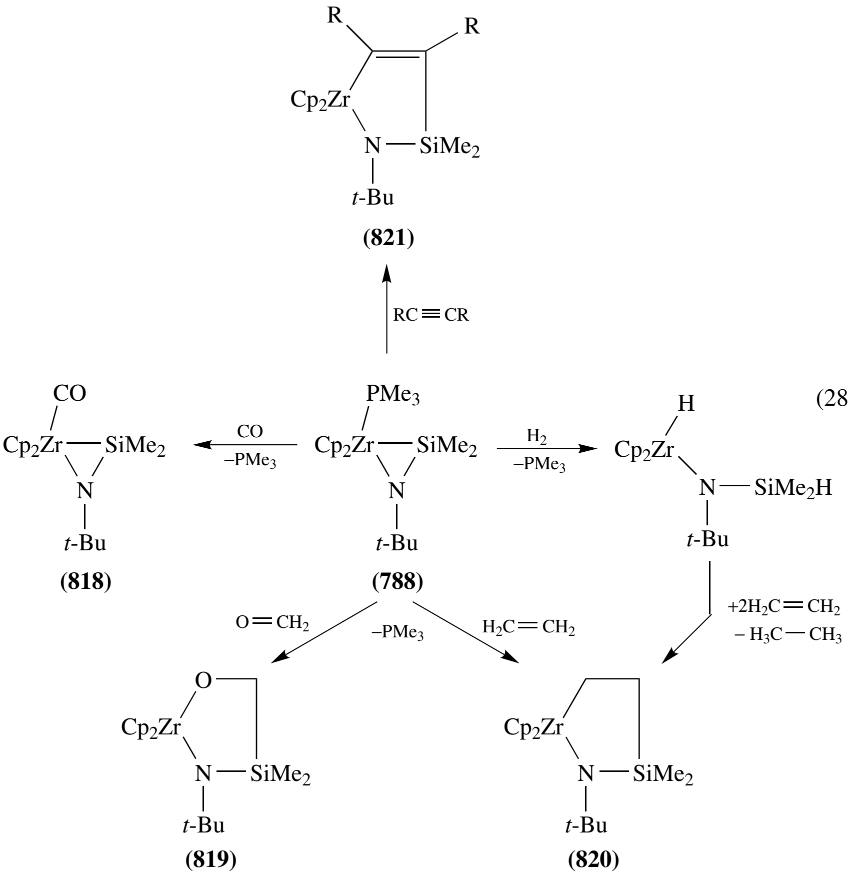

(821)

(818) **(788)**

(819) **(820)**

(282)

The carbonyl adduct **818** might be expected to react with PMe_3 in the reversal of its formation reaction, but the product isolated after prolonged reaction at 50 °C is the five-membered metallacycle **822** (equation 283).

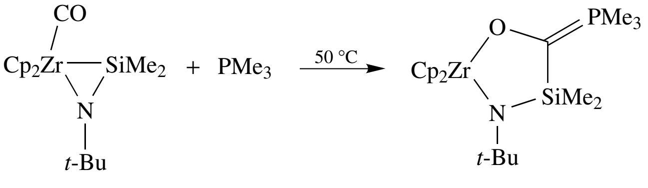

(818) **(822)**

(283)

In particular, the insertion of C=X compounds giving metallacycles like **819, 820** and **813** suggested that molecules with cumulenic bonds might insert in a similar fashion. CO_2, however, leads to a net oxygen atom insertion into the Zr–Si bond and the dimeric complex **823** is formed. The initial intermediate *cyclo*-$Cp_2Zr[O(C{=}O)SiMe_2NBu$-*t*] **824**, formed by insertion of CO_2 into the Zr–Si bond, has been observed by low temperature NMR studies (equation 284).

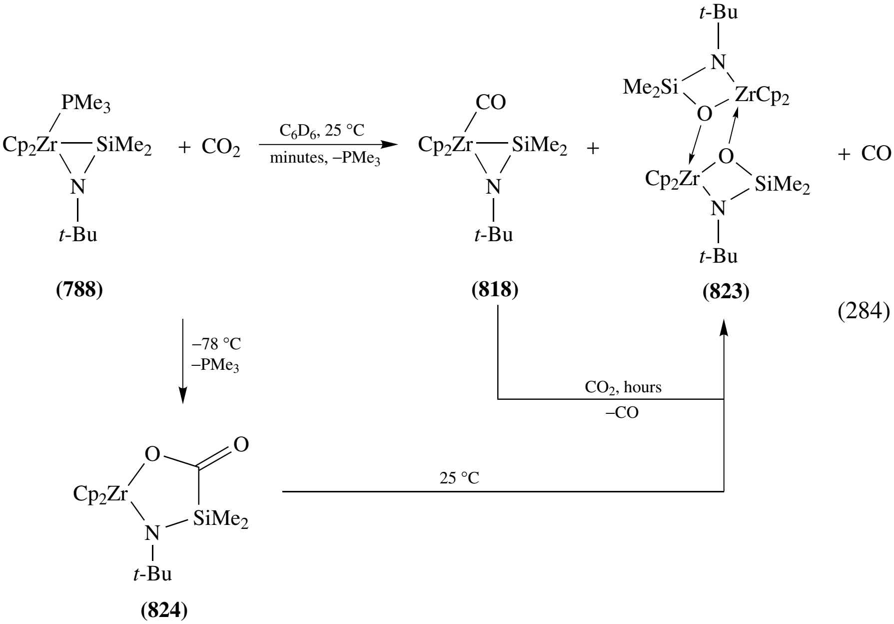

(284)

The reaction with CS_2 led to a monomeric sulphur insertion product **825** (equation 285). With COS, a mixture of the oxygen and sulphur insertion products (**823** and **825**) and the carbonyl adduct **818** are obtained.

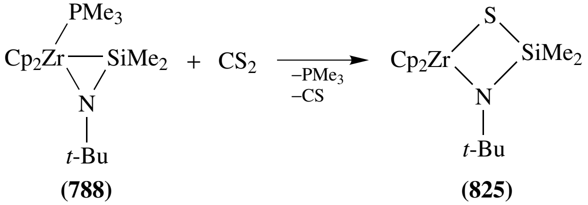

(285)

D. X-ray Structures

A comparison of the calculated Si=N bond length with that measured by single crystal X-ray diffraction was possible for just one compound, Wiberg's silanimine $t\text{-Bu}_2Si{=}N{-}SiBu\text{-}t_3$[327]. The Si=N bond length was determined to be 1.568 Å (Table 17) and, despite the bulky groups in this molecule, this value corresponds well with the calculated length for $H_2Si{=}NMe$ (1.569 Å, Table 21)[316].

The coordination of donors lengthens the Si=N bond and leads to pyramidalization at the silicon centre, as can be seen from the deviation of the sum of angles around the silicon atom from 360° (see examples in Table 17). Coordination of silanimines to transition metal centres also increases the silicon–nitrogen bond length to 1.66–1.69 Å, which corresponds to a Si–N single bond. It has already been mentioned above that these metal compounds are best described as metallacycles[349,350].

TABLE 17. Structural data of silanimines and related compounds (bond distances r in Å, angles α in deg)

Compound	r(Si=N)	α(Si=N−R)	r(Si→ D)	$\alpha(\angle\mathrm{Si})$[b]	References
t-$\mathrm{Bu_2Si{=}NSiBu}$-t_3	1.568	177.8		359.9	327
$\mathrm{Me_2Si{=}NSiBu}$-t_3•THF[a]	1.588	161.5	1.888	349.5	327
	1.57	161.0	1.866	349.2	
t-$\mathrm{Bu_2Si{=}NSiBu}$-t_3• $\mathrm{Ph_2C{=}O}$	1.601	169.3	1.927	350.3	327
t-$\mathrm{Bu_2Si{=}NSiBu}$-t_2Me•THF	1.596	174.3	1.902	347.7	306
(2,4,6-t-$\mathrm{Bu_3C_6H_2}$)N=SiPr-i_2•FLi$\mathrm{(THF)_3}$	1.619	160.6			307, 357
(2,4,6-t-$\mathrm{Bu_3C_6H_2}$)N=SiBu-tMe•FLi$\mathrm{(THF)_3}$	1.606	161.3	1.676	342.3	358
(t-$\mathrm{Bu_2PhSi}$)N=SiBu-t_2• FLi$\mathrm{(THF)_3}$	1.608[c]	176.3	1.692		357, 307
[(t-$\mathrm{Bu_2PhSi}$)N=SiBu-t_2F]$^-$[Li(TMEDA)]$_2^+$[a]	1.616[d]	169.7	1.654		357, 307
	1.618[e]	176.2	1.651		
[(t-$\mathrm{Bu_2MeSi}$)N=$\mathrm{SiBu_2FLi}$]$_2$	1.647[f]	148.9	1.699	349.5	307
[(t-$\mathrm{Bu_2SiF}$)N]$^-$[Li$\mathrm{(THF)_2}$]$^+$	1.636	176.7	1.659		359
			1.653		
[(t-$\mathrm{Bu_2SiF}$)N]$^-$[Li([12]-C-4)$_2$]$^+$	1.606	162.6	1.644		359
	1.630		1.637		
[t-$\mathrm{Bu_2Si{=}NSi}$-i-$\mathrm{Pr_2(OSiMe_3)FLi}$]$_2$	1.636	155.6	1.680		354
[$\mathrm{Ph_3Si{-}N{-}SiPh_3}$]$^-$ [Li([12]-C-4)$_2$]$^+$	1.633	154.9			360
[(2,4,6-t-$\mathrm{Bu_3C_6H_2N)_2SiBu}$-$t$]$^-$[Li([12]-C-4) THF]$^+$	1.594	161.9		360	347
	1.626	136.5			
$\mathrm{Cp_2Zr}$(η^2-t-BuN=$\mathrm{SiMe_2}$)$\mathrm{PMe_3}$	1.687	133.8	2.654[g]	336.5	350
$\mathrm{Cp_2Zr}$(η^2-t-BuN=$\mathrm{SiMe_2}$)CO	1.661	131.1	2.706	348.6	349

[a] Two molecules in the unit cell.
[b] Sum of the three angles around the silicon atom, excluding the D→ Si bond.
[c] d[(t-$\mathrm{Bu_2PhSi}$)−N] 1.652 Å.
[d] d[(t-$\mathrm{Bu_2PhSi}$)−N] 1.645 Å.
[e] d[(t-$\mathrm{Bu_2PhSi}$)−N] 1.640 Å.
[f] d[(t-$\mathrm{Bu_2MeSi}$)−N] 1.694 Å.
[g] ‘D’ = Zr.

E. Spectroscopy

1. NMR spectroscopy

The NMR spectroscopic chemical shifts of the silicon atoms in multiply bonded compounds serve as the best evidence for the existence of sp^2-hybridized silicon species. Data for known silanimine and related compounds are summarized in Table 18. The ^{29}Si resonances of the stable silanimines are significantly shifted to lower field (60−80 ppm) as compared to singly bonded Si−N compounds[303,307]. The ^{14}N chemical shift of the nitrogen atom in the stable silanimine t-$\mathrm{Bu_2Si{=}N{-}SiBu}$-$t_3$ confirms the existence of the Si=N bond with a shift of −230 ppm[303]. The coordination of donors lessens the double bond character and the ^{29}Si and ^{14}N resonances are found at higher field; e.g. for t-$\mathrm{Bu_2Si{=}N{-}SiBu}$-$t_3$•THF, $\delta^{29}\mathrm{Si} = 1.0$, $\delta^{14}\mathrm{N} = -330$ ppm[303]. Fluoride as donor gives rise to quite large Si−F coupling constants and thus the ‘fluoride adducts’ are best

TABLE 18. NMR spectroscopic data (δ in ppm) of silanimines and related compounds

Compound	δ^{29}Si	δ^{n}E	References
t-$Bu_2Si^a{=}NSi^bBu$-t_3	a: 78; b: -7.7	^{14}N: -230	303
t-$Bu_2Si^a{=}NSi^bBu$-t_3•Ph_2CO	a: 54.2; b: -9.6		303
t-$Bu_2Si^a{=}NSi^bBu$-t_3•THF	a: 1.0; b: -14.7	^{14}N: -330	303
t-$Bu_2Si^a{=}NSi^bBu$-t_3•MeTHF	a: 3.60; b: -14.57	^{14}N: -329.08	306
t-$Bu_2Si^a{=}NSi^bBu$-t_3•NMe_2Et	a: 18.1; b: -13.6		303
$Me_2Si^a{=}NSi^bBu$-t_3•THF	a: -1.51; b: -11.1	^{14}N: -330	300
$Me_2Si^a{=}NSi^bBu$-t_3•Et_2O	a: -1.51; b: -11.1		300
$Me_2Si^a{=}NSi^bBu$-t_3•NEt_3	a: -11.2; b: -11.1		300
$Me_2Si^a{=}NSi^bBu$-t_3•NMe_2Et	a: -8.85; b: -10.25		300
t-$Bu_2Si^aF{-}N{-}Si^bBu$-t_2Me •Li (TMEDA)	a: -2.27; b: -10.19	^{19}F: 11.29	307
i-$Pr_2Si^a{=}N{-}Si^bi$-$Pr_2(OSiMe_3)$ •$FLi(THF)_3$	a: -5.39; b: -24.28	^{19}F: 7.22 ^1J(F,Si) = 261 Hz	354
t-$Bu_2Si^aF{=}N{-}Si^bBu$-t_2Me •Li([12]-C-4)	a: -19.69; b: -17.83	^{19}F: 14.78	307
i-$Pr_2Si{=}N(2,4,6$-t-$Bu_3C_6H_2)$	60.3		307
t-$Bu_2Si{=}N(2,4,6$-t-$Bu_3C_6H_2)$	63.1		307, 305[a]
t-$Bu_2Si{=}N{-}SiPhBu$-t_2	80.4		307
$[(t$-$Bu_2SiF)_2N]^-[Li(THF)_2]^+$	-12.3	^{19}F: 11.7 ^1J(F,Si) = 272.5 Hz	359
$[(t$-$Bu_2SiF)_2N]^-[Li(TMEDA)]^+$	-12.0	^{19}F: 13.1 ^1J(F,Si) = 271.4 Hz	359
$[(t$-$Bu_2Bu_2SiF)_2N]^-[Li(12$-C-$4)_2]^+$	[c]	^{19}F: -22.5 ^1J(F,Si) = 295.2 Hz	359
$[(2,4,6$-t-$Bu_3C_6H_2)N]_2SiPh^-$ $Li(OEt)^+$	3.2		346
$[(2,4,6$-t-$Bu_3C_6H_2)N]_2SiPh^-Li^+$	7.0		346
$[(2,4,6$-t-$Bu_3C_6H_2)N]_2SiPh^-$ $Li([15]$-C-$5)^+$	-37.5		346
$[(2,4,6$-t-$Bu_3C_6H_2)N]_2SiCl^-$ K^+	-54.2		346[b]
$Cp_2Zr(\eta^2$-$Me_2Si{=}NBu$-$t)(CO)$	-69.9		349

[a] For further data on lithiated aminofluorosilanes see Reference 305.
[b] For further data on silaamidides see Reference 346.
[c] $\delta(^{29}$Si) not reported.

described as covalently bonded fluorosilanes[359]. The negative charge in silaamidides leads to strong shielding of the silicon atom, which resonates at -54.2 ppm[346].

2. IR and UV-Vis spectroscopy

IR and UV spectroscopy are the primary analytical tools for the identification of highly reactive species trapped in low temperature matrices. Along with calculations the assignment of vibrations and electronic transitions to various species is possible. Additional verification for IR assignments is obtained through isotopic labeling. The stretching vibration of the Si=N bond is found to be 1326 cm^{-1} for the stable compound t-$Bu_2Si{=}N{-}Sit$-Bu_3 (see Table 19)[303]. The silanimine $H_2Si{=}NH$, without bulky substituents, exhibits a $\nu_{Si=N}$ at 1097 cm^{-1}[326]. The Si=N bond is significantly weakened

TABLE 19. IR and UV spectroscopic data of silanimines and related compounds

Compound	IR [cm^{-1}]		UV-vis (nm)	References
t-Bu$_2$Si=N−SiBu-t_3	$\nu_{\mathrm{Si=N}}$	1326		303
[(2,4,6-t-Bu$_3$C$_6$H$_2$)N]$_2$SiR$^-$	ν_{as} (N−Si−N]$^-$ 1303–1284			346, 347
(Me$_3$Si)(N$_3$)Si=N−SiMe$_3$			274	343
Me$_3$Si−N=Si=N−SiMe$_3$			324	
t-Bu$_2$Si=N$_2$	2150 (tentative)		300 (tentative)	345
t-Bu$_2$Si=N=^{15}N/t-Bu$_2$Si=^{15}N=N	2110			
t-BuN=Si=NBu-t			240, 385 (5 : 1 ratio)	
Mes$_2$Si=N−Mes			296, 444	317
Me$_2$Si=N−SiMes$_2$Bu-t				
i-Pr$_2$Si=N−SiMes$_2$Bu-t				
PhNSi	ν_{as} (CNSi) 1530		ca 315	325
	ip ring stretch			
Ph^{15}NSi		1514		
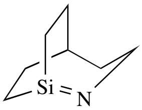	$\nu_{\mathrm{Si=N}}$ ^{15}N	1088 1077	397	321
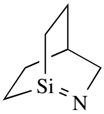	$\nu_{\mathrm{Si=N}}$ ^{15}N	1014 998	557	321
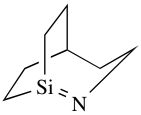	$\nu_{\mathrm{Si=N}}$ ^{15}N	1050 1042	406	321
HNSi	$\nu_{\mathrm{Si=N}}$	1202	250	328
HNSi•H$_2$	$\nu_{\mathrm{Si=N}}$1200; ν_{HH}	4178		
H$_2$Si=NH	$\nu_{\mathrm{Si=N}}$ 1097		240	
D$_2$Si=ND	$\nu_{\mathrm{Si=N}}$ 1063			
HSi≡N	$\nu_{\mathrm{Si\equiv N}}$ 1163		238, 258, 266, 350	
HSi≡N•H$_2$	$\nu_{\mathrm{Si\equiv N}}$ 1161; ν_{HH}	4164		
DSi≡N•D$_2$	$\nu_{\mathrm{Si\equiv N}}$ 1145			
Si≡N•D$_2$	$\nu_{\mathrm{Si\equiv N}}$ 1144; ν_{DD} 3010, 3005			
HNSi	IR emission: fundamental ν_1			336
	vibration-rotation			
	band (NH stretch) 3584			
Cp$_2$Zr(η^2-Me$_2$Si=NBu-t)(CO)	ν_{co} 1797			349
Cp$_2$Zr(η^2-Me$_2$Si=NBu-t)(CO)	ν_{co} 1756			

TABLE 20. Miscellaneous spectroscopic data of silaisocyanide

Compound	Method/Result	Reference
HNSi	mm wave spectroscopy/J: 6 → 7 rotational transition 266234.888 MHz	333
HNSi	HeI photoelectron spectroscopy/ionization potentials: 9.9, 9.9, 10.7 eV	316

by twisting. Thus, the incorporation into bicyclic systems gives rise to Si=N stretching vibrations at 1014–1088 cm^{-1}[321].

The parent silaisocyanide HNSi has a $\nu_{Si=N}$ of 1202 cm^{-1}[328], while the phenyl derivative PhNSi vibrates at the higher wavenumber of 1530 cm^{-1}[325]. The silanitrile HSiN has a stretching vibration at 1163 cm^{-1}, which indicates that the silicon–nitrogen bond is weaker in this isomer[328].

3. Miscellaneous

The theoretical analysis of the gas phase thermal fragmentation (flash pyrolysis with subsequent photoelectron spectroscopy) of trimethylsilyl azide combined with calculations of the ionization potentials has led to the conclusion that HNSi (calc. 10.18, 10.18, 10.71 eV; exptl. 9.9, 9.9, 10.7 eV) is formed[316].

The detection and identification of molecules in interstellar space is possible by millimeter wave spectroscopy. The independent synthesis and detection of such reactive species, e.g. by flash vaccuum thermolysis and mm wave spectroscopy, provides proof for their cosmochemical existence. The detection of the J: 6 → 7 rotational transition in the decomposition products of $t\text{-Bu}_2\text{HSi–NH(CH}_2\text{–C}\equiv\text{CH)}$ indicated the formation of HNSi (Table 20)[333].

F. Theoretical Studies

The interpretation and verification of analytical data, obtained especially for highly reactive species in the gas phase or matrix, is often possible only through the concomitant use of quantum chemical calculations. The listing of experimental data as above would be incomplete without at least mentioning the wealth of information available through theoretical methods. Thus interesting geometric and spectroscopic features have been included in the Table 21 which is sorted with respect to the systems studied. The geometries are always optimized at the indicated level. Details are given in the corresponding references.

In connection with the experimental data on silanimines (structures and NMR), it can generally be said that (a) donor addition lengthens the Si=N bond, (b) the bond order of silicon–nitrogen 'triply' bonded species is *ca* 2 and (c) the flexibility of the angle Si=N–R is greatest when R = silyl. Silyl-substituted O and N atoms (e.g. in disiloxanes and disilazanes) are known for the easy variability of the Si–E–Si angle. Computations preceding 1987 (not included in the table) on $H_2Si{=}NH$ by Truong and Gordon found a planar geometry with d(SiN) = 157.6 pm and a Si=N–H angle of 125.2°[373]. The *syn/anti* isomerization through inversion requires only 5.6 kcal mol^{-1}; the rotation around the Si–N bond needs 37.9 kcal mol^{-1}. The Si=N bond in the linear transition state is even shorter with 153.2 pm. Schleyer and Stout found similar results for $H_2Si{=}N{-}SiH_3$: d(SiN) = 154.9 pm, ∠Si=N–Si = 175.6°[374]. The angle flexibility at the silicon atom is also found for siladiimine, HN=Si=NH, where the conformational potential energy surface is very flat[377].

TABLE 21. Calculated data for various silicon-nitrogen species

Compound(s)/System(s)	Method(s)/Basis set(s)	Calculated properties	Reference
Silanimines			
$Me_2Si{=}NMe$	RHF/6-31G*	r(SiN) 1.551 pm	321
$Me_2Si{=}NMe$ (twisted to fit the 3 compds below)	ClS/DZ+d	UV-Vis	
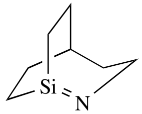	RHF/6-31G*	r(SiN) 1.592 Å	
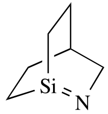	RHF/6-31G*	r(SiN) 1.596 Å	
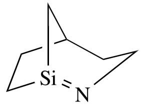	RHF/6-31G*	r(SiN) 1.600 Å	
$H_2Si{=}NH$	IGLOBII//HF/6-31G*	δ^{29}Si 52	361
	MP2/DZ+d	IR	
$H_2Si{=}NH$	RHF/3-21G*	r(SiN) 1.580 Å	316
$H_2Si{=}NMe$		r(SiN) 1.569 Å	
$MeHSi{=}NH$		r(SiN) 1.579 Å	
$H_3Si{-}N_3$	RHF/3-21G*	reaction pathways, ionization potentials	
$H_3Si{-}N_3$ and possible pyrolysis products	RHF/4-21G*		
[H_3, Si, N, O]	MP4/6-31G*//RHF/6-31G*; MP4/6-311G*//MP2/6-31G*	internal rotations MP2/6-31G*; $H_2SiN{-}OH$ d(SiN) 1.655 Å $(HO)HSi{=}NH$ r(SiN) 1.595 Å	362

(*continued overleaf*)

TABLE 21. (*continued*)

Compound(s)/System(s)	Method(s)/Basis set(s)	Calculated properties	Reference
$H_3SiN\mathbf{:} \rightarrow H_2Si{=}NH$	(U)HF/3-21G$^{(*)}$; (U)MP4/6-31G++G*//HF/3-21G*; RHF-CI	Curtius-type rearrangement reaction	320
[Si,N,H,F] system	BAC-MP4/6-31G**/(U)HF/6-31G*	thermochemistry, bond dissociation enthalpies	363
$H_nX{=}YH_m{-}ZH_2$ (X,Y = C,N,Si,P; Z = B,N)		rotational isomers; conjugation of double bonds	364
Si=N=Si systems			
$(H_3Si)_2N^-$	RHF/6-31+G*	r(SiN) 1.624 Å; αSiNSi 180°	307
		+25 kcal mol^{-1} for α SiNSi 120°	359
N=Si=N systems and isomers			
MeN=Si=NMe	MNDO	r(SiN) 1.51 Å, α NSiN 172°, α CSiN 153°, IR	345
	INDO/S	UV-Vis	
$Me_2Si{=}N_2$		r(SiN) 1.64 Å, α CSiC 128°, IR	
		UV-Vis	
cyclo-$(MeN)_2Si\mathbf{:}$		relative energies, UV-Vis	
cyclo-(MeSi−NMe=N)			
MeN=N−MeSi$\mathbf{:}$			
HN=Si=NH	RHF/6-31G*; MP4/6-31G**//MP2/6-31G*	RHF: r(SiN) 1.516 Å, α NSiN 180°	365
		MP2: r(SiN) 1.597 Å, α NSiN 156.9°	
		conformational PES^a very flat	
$HN{=}Si{=}CH_2$	RHF/6-31G*	r(SiN) 1.549 Å, α CSiN 172.3°	

Silanitrile and silaisocyanides			
PhSi≡N/PhN=Si**:**	INDO/S; MP2/6-31G*	UV-Vis; IR	325
$[HNSi]^{\bullet +}$ ($^1\Sigma^+$) $[HNSi]^{\bullet +}$ ($^2\Sigma^+$) ions	G1	PES^a	342
[HNSi], [DNSi]	MP2/6-31G*; MP2/D95**	IR	328
HNSi / DNSi	DFT method	PES^a, vibrational-rotational energies transition moments	366
HNSi		microwave transitions	336
PhSiN PhNSi	AM1; RHF/6-31G or 3-21G*; MP2/6-31G//RHF/6-31G or 3-21G*	3-21G*: r(SiN) 1.537 Å r(SiN) 1.534 Å	367
MeSiN MeNSi	RHF/6-31G**; MPn/6-31G**//RHF/6-31G**	6-31G**: r(SiN) 1.527 Å r(SiN) 1.530 Å $\Delta E = [E(\text{MeSiN})\text{-}E(\text{MeNSi})] = 48.3$ kcal mol^{-1}	
RNSi/RSiN R = F, Cl	MP4/6-311+G**//MP2(fu)//6-31G*; also in part: G2; QCISD(T)/6-311G**//QCISD/6-31G**; CASSCF//6-31G*; QCISD(T)/6-311G(2df,p)//QCISD/6-31G**	relative stabilities, energy barriers ΔE positive (22–76 kcal mol^{-1}) ⇒ RNSi more stable for R = H, Li, BeH, BH_2, CH_3, SiH_3, PH_2, SH $\Delta E = 10.5$ kcal mol^{-1} for R = NH_2; −0.5 kcal mol^{-1} for R = Cl ΔE negative ⇒ RSiN more stable for R = OH (6.5 kcal mol^{-1}); R = F (26.6 kcal mol^{-1}) Barrier heights: 22.7 kcal mol^{-1} for R = OH 29.4 kcal mol^{-1} for R = F	368

(*continued overleaf*)

TABLE 21. (*continued*)

HNSi	HF, MPn/various basis sets	interstellar production of HNSi from H_2NSi^+; HNSi proton affinity; IR	369
Metal compound			
$Cp_2Zr(\eta^2\text{-}Me_2Si{=}NBu\text{-}t)(CO)$	ZINDO	Zr−Si bond order 0.34	349
Ionic and radical systems			
$[HNSi]^{\bullet+}$ ($^2\Sigma^+$) ions	G1	PES[a]	342
$[HNSi]^{\bullet+}$ ($^1\Sigma^+$)			
$[HSi(O)NH]^-$, $[Si(O)NH_2]^-$, and 8 other related anionic isomer pairs	MP2/6-31+G**; MP4/6-311++G**	charge density, gas phase acidity	338
$[H_2,Si,N]^-$	MP2/6-31+G**	*trans*-$HSiNH^-$ r(SiN) 165.0 Å *cis*-$HSiNH^-$ 164.6° $[H_2SiN]^-$ 1.581 Å $[SiNH_2]^-$ 1.764 Å IR	336
H_2SiN^+	MPn (n = 2,3,4), CCSDT, CASSCF, Cl, MCSCF/6-311++G**	r(SiN) 1.772–1.794 Å; rotational constants IR; electronic absorption	370
$[H_5,Si,N]^{\bullet+}$	(U)HF/6-31G**; (U)MP4/6-31+G(2df,p)//MP2/6-31G**	spin density; unimolecular rearrangements	371
$[SiNNH]^\bullet$ and isomers	ROHF, UHF, MCSCF/6 −31G*	rotational constants	372

[a] PES = potential energy surface.

G. GeN, SiP and SiAs Multiply Bonded Species and Related Compounds

Germanimines, $R_2Ge{=}NR'$ have been studied in parallel to silanimines by Wiberg's group. Their formation is achieved by salt elimination via germaethenes, which are trapped with azides to yield the [3 + 2] cycloadducts, the germadihydrotriazoles[308]. Germanimines may be thermally liberated from the latter and their reactivity can then be studied[351]. Another storage form are the germadihydrotetrazoles, obtained from germanimines and azides[310].

Ando and coworkers used a different approach to bis(germanimines): the reaction of bis[bis(trimethylsilyl)methyl]germylene with diazidosilanes gave in the first step *N*-(azidosilyl) germanimines, which reacted with a second equivalent of germylene to give bis(germanimines)[375]. The X-ray structures of two such compounds were determined r(Ge=N): 1.704 Å.

The chemistry of Si=P and Si=As compounds has been well reviewed by Bickelhaupt[378,379] and by Driess[376,377]. A short overview is, however, given.

A transient phosphasilene **827**, which was generated from 1,2-phosphasiletane **826**, was first reported in 1979 (equation 286)[380]. Just recently, this cycloreversion reaction was used to produce the phosphasilene in the gas phase and to prove its existence by high resolution mass spectrometry and photoelectron spectroscopy[381]. Higher temperatures are needed for the decomposition of the diphosphadisiletane **828** to generate **829**. The first ionization potentials are listed (equation 287).

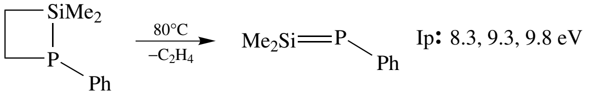

(826) **(827)** (286)

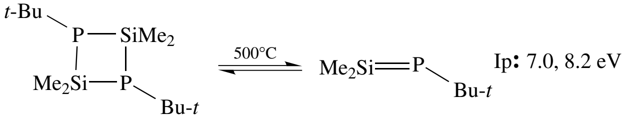

(828) **(829)** (287)

The most common route to phosphasilenes is by salt elimination from lithium(fluorosilyl)phosphanylides. Examples of transient to moderately stable species are t-$Bu_2Si{=}PBu$-t **830**, which could be observed by ^{31}P NMR spectroscopy[382], and t-$Bu_2Si{=}P(SiBu$-$t_3)$ **831** whose existence could only be proved by trapping reactions[383].

The first synthesis of a crystalline phosphasilene **832** was achieved by a two-step reaction of t-Bu_3SiCl with four equivalents of SupPHLi (Sup = 2,4,6-t-$Bu_3C_6H_2$) and Ph_2PCl[384,385] via the diphosphasila-allyl salt **833**[386], a remarkable conjugated sila-π system (equation 288). The Si=P bond length in **832** is 2.094 Å and the silicon atom is pyramidalized (Σ <= 356.7°). The $^1J_{P=Si}$ of **832** is remarkably high with 203 Hz.

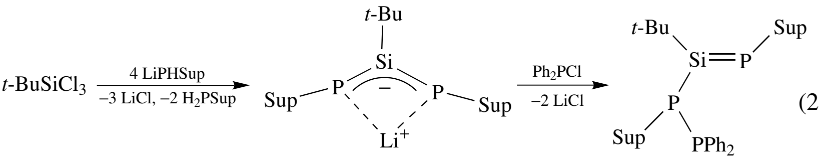

(833) **(832)** (288)

Bickelhaupt published an improved route for the synthesis of phosphasilenes **836** in a one-pot reaction via the dilithiated phosphine **835** obtained from the primary phosphine **834** (equation 289). The drawback is that the substituent at phosphorous may not be smaller than the supermesityl (Sup) group[387].

$$\underset{(\mathbf{834})}{R^1PH_2} \xrightarrow[-2\ C_4H_{10}]{2\ n\text{-BuLi}} \underset{(\mathbf{835})}{R^1PLi_2} \xrightarrow[-2\ LiCl]{R^2R^3SiCl_2} \underset{(\mathbf{836})}{R^1P{=}SiR^2R^3} \qquad (289)$$

The concept of the stabilization of unsaturated silicon centres by coordination has been applied in the synthesis of phosphasilene **837**[388].

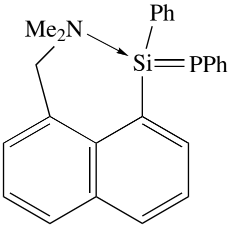

(837)

Phosphasilene **832** is rather labile in solution, and thus derivatives with silyl groups at phosphorous were synthesized and proved to be more stable[389,390]. The reaction of the silyl phosphines **838** with n-BuLi gave the lithiated species **839**, which eliminated LiF upon heating in solution to 60–80 °C and thus liberated the phosphasilenes **840** (equation 290).

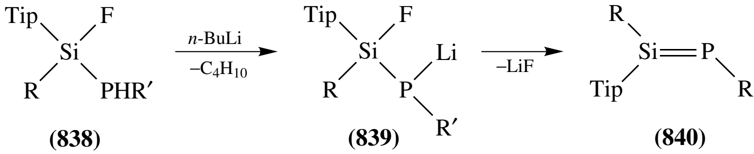

(838) **(839)** **(840)** (290)

R = Tip, t-Bu
R′ = silyl, germyl
Tip = (2,4,6-i-$Pr_3C_6H_2$)

For **840** with R = t-Bu and R′ = Si(Pr-i)$_3$ an X-ray structure could be obtained[381]. The Si=P bond length is 2.062 Å and the silicon atom has a trigonal planar geometry. The NMR chemical shifts of the phosphorous nuclei in **840** are found in the region of −30 to 28 ppm; the ^{29}Si resonances are mainly around 170 ppm. The $^1J_{\text{Si=P}}$ is found to be 150 to 160 Hz[389,390].

The attempt to stabilize transients in the formation reaction of phosphasilenes by transition metal centres directly bound to the precursors was not successful[392]. The metal substituent was either cleaved or behaved like a ‘normal’ substituent, as is shown for the synthesis of phosphasilene **842** from **841** (equation 291). The NMR parameters for **842** are as expected: δ^{29}Si = 201 ppm, $^1J_{P=Si} = 163$ Hz; δ^{31}P = 57 ppm.

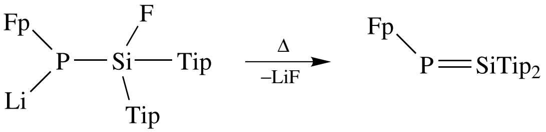

(291)

(841) **(842)**

Fp = Cp(CO)$_2$Fe

The synthesis of arsasilenes followed the same route as that employed for phosphasilenes[390,391,393]. Heating solutions of the precursors **843** to 60 °C gave the arsasilenes **844** (equation 292).

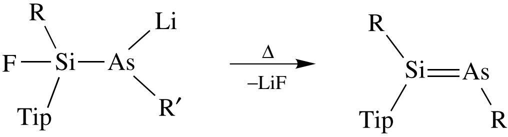

(292)

(843) **(844)**

R = Tip, *t*-Bu
R′ = silyl

The ^{29}Si NMR shift is found in the region from 180 to 190 ppm, with the exception of 228.8 ppm for R = *t*-Bu, R′ = Si(*i*-Pr)$_3$. The X-ray structure of the latter derivative was determined and the Si=As bond length was found to be 2.164 Å (Si–As = 2.363 Å). The silicon atom is trigonal planar.

Phospha- and arsasilenes undergo $[2+n]$ cycloadditions ($n = 1$–4), thermal decomposition, and reaction with P$_4$, sulphur and tellurium. In order to avoid excessive redundancy the interested reader should consult the two reviews by Driess on this subject[376,377]. A number of theoretical treatments on unsaturated silicon phosphorous compounds, apart from those cited in the above-mentioned reviews, has been published[394–398].

V. ACKNOWLEDGEMENTS

The authors express their gratitude to Professors M. Kira, R. West, R. Okazaki and to Dr M. Karni, who have kindly provided us with manuscripts prior to publication. We thank also Mr D. Parker from the Open University in Milton Keynes for reading Section IV and Mrs U. Kätel for assistance. The authors are particularly grateful to Prof. Zvi Rappoport. The Hebrew University of Jerusalem, for carefully reading the manuscript.

N.A. is especially indebted to his previous and present coworkers, who contributed to the research in the Berlin and Munich groups in the field of silene chemistry: M. Backer, R. Gleixner, B. Goetze, M. Grasmann, Dr C.-R. Heikenwälder, Dr B. Herrschaft, Dr M. Kersten, Dr M. Päch, Dr E. Penzenstadler, Dr R. Probst, Dr C. Seidenschwarz, U. Steinberger, Dr C. Wagner, Dr A. Weingartner, Dr A. Wolff and Dr W. Ziche. T. M. thanks the Fonds der Chemischen Industrie for a Liebig Scholarship.

VI. REFERENCES

1. L. E. Gusel'nikov and M. C. Flowers, *J. Chem. Soc., Chem. Commun.*, 864 (1967).
2. M. C. Flowers and L. E. Gusel'nikov, *J. Chem. Soc. (B)*, 419 (1968).
3. A. G. Brook, S. C. Nyburg, F. Abdesaken, B. Gutekunst, G. Gutekunst, R. K. M. R. Kallury, Y. C. Poon, Y.-M. Chang and W. Wong-Ng, *J. Am. Chem. Soc.*, **104**, 5667 (1982).
4. N. Wiberg, G. Wagner, J. Riede and G. Müller, *Organometallics*, **6**, 32 (1987).
5. G. E. Miracle, J. L. Ball, D. R. Powell and R. West, *J. Am. Chem. Soc.*, **115**, 11598 (1993).
6. N. Tokitoh, K. Wakita, R. Okazaki, S. Nagase, P. v. R. Schleyer and H. Jiao, *J. Am. Chem. Soc.*, **119**, 6951 (1997).
7. J. Michl and G. Raabe, *Chem. Rev.*, **85**, 419 (1985).
8. G. Raabe and J. Michl, in *The Chemistry of Organic Silicon Compounds*, Vol. 1 (Eds. S. Patai and Z. Rappoport), Wiley, Chichester, 1989.
9. G. A. Brook and M. A. Brook, *Adv. Organomet. Chem.*, **39**, 71 (1995).
10. (a) K. K. Baldridge, J. A. Boatz, S. Koseki and M. S. Gordon, *Ann. Rev. Phys. Chem.*, **38**, 211 (1987).
    (b) R. S. Grev, *Adv. Organomet. Chem.*, **33**, 125 (1991).
11. Y. Apeloig, in *The Chemistry of Organic Silicon Compounds* (Eds. S. Patai and Z. Rappoport), Wiley, Chichester, 1989.
12. M. Karni and Y. Apeloig, *Chem. Rev.*, to appear.
13. M. Steinmetz, *Chem. Rev.*, **95**, 1527 (1995).
14. P. P. Gaspar, D. Holten, S. Konieczny and J. Y. Corey, *Acc. Chem. Res.*, **20**, 329 (1987).
15. T. J. Barton, G. Marquardt and J. A. Kilgour, *J. Organomet. Chem.*, **85**, 317 (1975).
16. (a) N. S. Nametkin, N. N. Dolgopolov and L. E. Gusel'nikov, *J. Organomet. Chem.*, **169**, 165 (1979).
    (b) M. S. Gordon, T. J. Barton and H. Nakano, *J. Am. Chem. Soc.*, **119**, 11966 (1997).
17. J. Grobe and N. Auner, *J. Organomet. Chem.*, **197**, 13 (1980).
18. A. M. Fenton, P. Jackson, F. T. Lawrence and I. M. T. Davidson, *J. Chem. Soc., Chem. Commun.*, 806 (1982).
19. J. Pola, E. A. Volnina and L. E. Gusel'nikov, *J. Organomet. Chem.*, **391**, 275 (1990).
20. R. T. Conlin, M. Namavari, J. S. Chickos and R. Walsh, *Organometallics*, **8**, 168 (1989).
21. I. M. T. Davidson, R. Laupert, P. Potzinger and S. Basu, *Ber. Bunsenges. Phys. Chem.*, **83**, 1282 (1979).
22. R. T. Conlin and Y.-W. Kwak, *J. Am. Chem. Soc.*, **108**, 834 (1986).
23. M. Steinmetz and H. Bai, *Organometallics*, **8**, 1112 (1989).
24. A. Kumar, R. K. Vatsa, R. D. Saini, J. P. Mittal, J. Pola and S. Dhanya, *J. Chem. Soc., Faraday Trans.*, **92**, 179 (1996).
25. R. K. Vatsa, A. Kumar, P. D. Naik, H. P. Upadhyaya, U. B. Pavanaja, R. D. Saini, J. P. Mittal and J. Pola, *Chem. Phys. Lett.*, **255**, 129 (1996).
26. J. Grobe and N. Auner, *Z. Anorg. Allg. Chem.,* **459**, 15 (1979).
27. (a) N. Auner, Abstracts of the XI-th International Symposium on Organosilicon Chemistry, Montpellier, France (1996) OB20.
    (b) N. Auner, J. Grobe, H. Rathmann and T. Müller, to appear.
28. G. Mihm, H. P. Reisenauer and G. Maier, *Angew. Chem., Int. Ed. Engl.*, **20**, 597 (1981).
29. G. Mihm, H. P. Reisenauer and G. Maier, *Chem. Ber.*, **117**, 2351 (1984).
30. H. Bock, B. Soulouki, G. Maier, G. Mihm and P. Rosmus, *Angew. Chem., Int. Ed. Engl.*, **20**, 598 (1981).
31. S. Bailleux, M. Bogey, J. Breidung, H. Bürger, R. Fajgar, Y. Liu, J. Pola, M. Senzlober and W. Thiel, *Angew. Chem., Int. Ed. Engl.*, **35**, 2513 (1996).
32. M. Bogey, H. Bürger, R. Fajgar, Y. Liu, J. Pola, M. Senzlober and S. Bailleux, Abstracts of the XI-th International Symposium on Organosilicon Chemistry, Montpellier, France (1996) PA13-14.
33. S. Bailleux, M. Bogey, J. Demaison, H. Bürger, M. Senzlober, J. Breidung, W. Thiel, R. Fajgar and J. Pola, *J. Chem. Phys.*, **106**, 10016 (1997).
34. W. Leigh, C. Bradaric, C. Kerst and J.-A. Banisch, *Organometallics*, **15**, 2246 (1996).
35. (a) W. J. Leigh, C. Bradaric and G. W. Sluggett, *J. Am. Chem. Soc.*, **115**, 5332 (1993).
    (b) C. J. Bradaric and W. J. Leigh, *J. Am. Chem. Soc.*, **118**, 8971 (1996).
36. V. Volkova, L. Gusel'nikov, E. Volnina, and E. Buravtseva, *Organometallics*, **13**, 4661 (1994).
37. R. T. Conlin and K. L. Bobbitt, *Organometallics*, **6**, 1406 (1987).

38. A. G. Brook, S. C. Nyburg, W. F. Reynolds, Y. C. Poon, Y.-M. Chang and J.-S. Lee. *J. Am. Chem. Soc.*, **101**, 6750 (1979).
39. D. Bravo-Zhivotovskii, V. Braude, A. Stanger, M. Kapon and Y. Apeloig, *Organometallics*, **11**, 2326 (1992).
40. N. Auner, I. M. T. Davidson, S. Ijadi-Maghsoodi and F. T. Lawrence, *Organometallics*, **5**, 431 (1986).
41. I. Jung, D. Pae, B. Yoo, M. Lee and P. Jones, *Organometallics*, **8**, 2017 (1989).
42. B. Yoo, M. Lee and I. Jung, *Organometallics*, **11**, 1626 (1992).
43. K.-T. Kang, N. Inamoto and R. Okazaki, *Tetrahedron Lett.*, **22**, 235 (1981).
44. A. Naka, M. Hayashi, S. Okazaki and M. Ishikawa, *Organometallics*, **13**, 4994 (1994).
45. M. Ishikawa, H. Sakamoto and T. Tabuchi, *Organometallics*, **10**, 3173 (1991).
46. M. Ishikawa, A. Naka and S. Okazaki, in *Progress in Organosilicon Chemistry* (Eds. B. Marciniec and J. Chojnowski), Gordon and Breach, Basel, 1995, p. 309.
47. M. Ishikawa, S. Okazaki, A. Naka and H. Sakamoto, *Organometallics*, **11**, 4135 (1992).
48. M. Ishikawa, A. Naka and J. Ohshita, *Organometallics*, **12**, 4987 (1993).
49. M. Ishikawa, A. Naka, S. Okazaki and H. Sakamoto, *Organometallics*, **12**, 87 (1993).
50. M. Ishikawa, S. Okazaki, A. Naka, A. Tachibana, S. Kawauchi and T. Yamabe, *Organometallics*, **14**, 114 (1995).
51. A. Naka, M. Hayashi, S. Okazaki, A. Kunai and M. Ishikawa, *Organometallics*, **15**, 1101 (1996).
52. A. Fanta, D. DeYoung, J. Belzner and R. West, *Organometallics*, **10**, 346 (1991).
53. K. Kabeta, D. Powell, J. Hanson and R. West, *Organometallics*, **10**, 827 (1991).
54. R. Conlin and M. Namavari, *J. Am. Chem. Soc.*, **110**, 3689 (1988).
55. M. Steinmetz, B. Udayakumar and M. Gordon, *Organometallics*, **8**, 530 (1989).
56. L. K. Revelle and E. Block, *J. Am. Chem. Soc.*, **100**, 1630 (1978).
57. N. Auner, I. M. T. Davidson and S. Ijadi-Maghsoodi, *Organometallics*, **4**, 2210 (1985).
58. K. W. Egger and P. Vitins, *J. Am. Chem. Soc.*, **96**, 2714 (1974).
59. N. Wiberg, K. Schurz, G. Müller and J. Riede, *Angew. Chem., Int. Ed. Engl.*, **27**, 935 (1988).
60. N. Wiberg, G. Preiner, K. Schurz and G. Fischer, *Z. Naturforsch.*, **43b**, 1468 (1988).
61. N. Wiberg, G. Preiner, G. Wagner, H. Köpf and G. Fischer, *Z. Naturforsch.*, **42b**, 1055 (1987).
62. N. Wiberg, G. Preiner, G. Wagner and H. Köpf, *Z. Naturforsch.*, **42b**, 1062 (1987).
63. N. Wiberg and M. Link, *Chem. Ber.*, **128**, 1231 (1995).
64. N. Wiberg and M. Link, *Chem. Ber.*, **128**, 1241 (1995).
65. N. Wiberg and G. Wagner, *Chem. Ber.*, **119**, 1455 (1986).
66. N. Wiberg and G. Wagner, *Chem. Ber.*, **119**, 1467 (1986).
67. N. Wiberg, H.-S. Hwang-Park, H.-W. Lerner and S. Dick, *Chem. Ber.*, **129**, 471 (1996).
68. P. R. Jones and T. Bates, *J. Am. Chem. Soc.*, **109**, 913 (1987).
69. B. R. Yoo, M. E. Lee and I. N. Jung, *J. Organomet. Chem.*, **410**, 33 (1991).
70. I. Jung, B. Yoo, M. Lee and P. Jones, *Organometallics*, **10**, 2529 (1991).
71. N. Wiberg, in *Organosilicon Chemistry II—From Molecules to Materials* (Eds. N. Auner and J. Weis), VCH Verlag, Weinheim, **1996**, p. 367.
72. N. Wiberg, G. Preiner, O. Schieda and G. Fischer, *Chem. Ber.*, **114**, 3505 (1981).
73. N. Wiberg, G. Preiner, O. Schieda and G. Fischer, *Chem. Ber.*, **114**, 3518 (1981).
74. N. Wiberg, G. Preiner, O. Schieda and G. Fischer, *Chem. Ber.*, **122**, 409 (1989).
75. N. Wiberg, G. Fischer and K. Schurz, *Chem. Ber.*, **120**, 1605 (1987).
76. N. Wiberg, K. Schurz and G. Fischer, *Chem. Ber.*, **119**, 3498 (1986).
77. N. Wiberg, T. Passler and K. Polborn, *J. Organomet. Chem.*, **531**, 47 (1997).
78. N. Wiberg, C. Finger, T. Passler, S. Wagner and K. Polborn, *Z. Naturforsch.*, **51b**, 1744 (1996).
79. P. R. Jones, T. F. O. Lim and R. A. Pierce, *J. Am. Chem. Soc.*, **102**, 4970 (1980).
80. N. Auner, in *Organosilicon Chemistry—From Molecules to Materials* (Eds. N. Auner and J. Weis), VCH Verlag, Weinheim, 1994, p. 103.
81. N. Auner, *Z. Anorg. Allg. Chem.*, **558**, 55 (1988).
82. G. Delpon-Lacaze and C. Couret, *J. Organomet. Chem.*, **480**, C14 (1994).
83. N. Wiberg, G. Wagner, G. Reber, J. Riede and G. Müller, *Organometallics*, **6**, 35 (1987).
84. N. Wiberg, K.-S. Joo and K. Polborn, *Chem. Ber.*, **126**, 67 (1993).
85. N. Wiberg and H. Köpf, *J. Organomet. Chem.*, **315**, 9 (1986).
86. A. G. Brook, J. W. Harris, J. Lennon and M. El Sheikh, *J. Am. Chem. Soc.*, **101**, 83 (1979).
87. A. G. Brook, F. Abdesaken, B. Gutekunst, G. Gutekunst and R. K. M. R. Kallury, *J. Chem. Soc. Chem. Commun.*, 191 (1981).

88. R. T. Conlin, P. F. McGarry, J. C. Scaiano and S. Zhang, *Organometallics*, **11**, 2317 (1992).
89. K. M. Baines and A. G. Brook, *Organometallics*, **6**, 692 (1987).
90. K. M. Baines, A. G. Brook, R. R. Ford, P. D. Lickiss, A. K. Saxena, W. J. Chatterton, J. F. Sawyer and B. A. Behnam, *Organometallics*, **8**, 693 (1989).
91. A. G. Brook, F. Abdesaken, G. Gutekunst and N. Plavac, *Organometallics*, **1**, 994 (1982).
92. A. G. Brook, R. K. M. R. Kallury and Y. C. Poon, *Organometallics*, **1**, 987 (1982).
93. P. Lassacher, A. G. Brook and A. J. Lough, *Organometallics*, **14**, 4359 (1995).
94. A. G. Brook, A. Baumegger and A. J. Lough, *Organometallics*, **11**, 310 (1992).
95. A. G. Brook, A. Baumegger and A. J. Lough, *Organometallics*, **11**, 3088 (1992).
96. A. G. Brook, K. D. Safa, P. D. Lickiss and K. M. Baines, *J. Am. Chem. Soc.*, **107**, 4338 (1985).
97. N. Wiberg and H. Köpf, *Chem. Ber.*, **120**, 653 (1987).
98. J. Ohshita, H. Hasebe, Y. Masaoka and M. Ishikawa, *Organometallics*, **13**, 1064 (1994).
99. M. Ishikawa, S. Matsui, A. Naka and J. Ohshita, *Organometallics*, **15**, 3836 (1996).
100. A. G. Brook, A. Ionkin and A. J. Lough, *Organometallics*, **15**, 1275 (1996).
101. H. Oehme and R. Wustrack, *Z. Anorg. Allg. Chem.*, **552**, 215 (1987).
102. R. Wustrack and H. Oehme, *J. Organomet. Chem.*, **352**, 95 (191988).
103. H. Oehme, R. Wustrack, A. Heine, G. M. Sheldrick and D. Stalke, *J. Organomet. Chem.*, **452**, 33 (1993).
104. C. Krempner and H. Oehme, *J. Organomet. Chem.*, **464**, C7 (1994).
105. F. Luderer, H. Reinke and H. Oehme, *J. Organomet. Chem.*, **510**, 181 (1996).
106. C. Wendler and H. Oehme, *Z. Anorg. Allg. Chem.*, **622**, 801 (1996).
107. C. Krempner, H. Reinke and H. Oehme, *Chem. Ber.*, **128**, 143 (1995).
108. C. Krempner, H. Reinke and H. Oehme, *Chem. Ber.*, **128**, 1083 (1995).
109. F. Luderer, H. Reinke and H. Oehme, *Chem. Ber.*, **129**, 15 (1996).
110. C. Krempner, D. Hoffmann, H. Oehme and R. Kempe, *Organometallics*, **16**, 1828 (1997).
111. Y. Apeloig, M. Bendikov, M. Yuzefovich, M. Nakash, D. Bravo-Zhivotovskii, D. Bläser and R. Boese, *J. Am. Chem. Soc.*, **118**, 12228 (1996).
112. J. Ohshita, Y. Masaoka and M. Ishikawa, *Organometallics*, **10**, 3775 (1991).
113. J. Ohshita, Y. Masaoka, M. Ishikawa and T. Takeuchi, *Organometallics*, **12**, 876 (1993).
114. J. Ogasawara, K. Sakamoto and M. Kira, *30th Organo-silicon Symposium*, London, Ontario, Canada, May 1997, Abstr. P53.
115. D. Hoffmann, H. Reinke and H. Oehme, *J. Organomet. Chem.* **526**, 185 (1996).
116. A. G. Brook, P. Chiu, J. McClenaghnan and A. J. Lough, *Organometallics*, **10**, 3292 (1991).
117. C. Krempner, H. Reinke and H. Oehme, *Angew. Chem., Int. Ed. Engl.*, **33**, 1615 (1994).
118. D. Hoffmann, H. Reinke and H. Oehme, *Z. Naturforsch.*, **51b** 371 (1996).
119. K. Sakamoto. J. Ogasawara, H. Sakurai and M. Kira, *J. Am Chem. Soc.*, **119**, 3405 (1997).
120. J. Ohshita, Y. Masaoka, S. Masaoka, M. Ishikawa, A. Tachibana, T. Yano and T. Yamabe, *J. Organomet. Chem.*, **473**, 15 (1994).
121. J. Ohshita, S. Masaoka, Y. Masaoka, H. Hasebe, M. Ishikawa, A. Tachinaba, T. Yano and T. Yamabe, *Organometallics*, **15**, 3136 (1996).
122. I. S. Biltueva, D. A. Bravo-Zhivotovskii, I. D. Kalikhman, V. Y. Vitkovskii, S. G. Shevchenko, N. S. Vyazankin and M. G. Voronkov, *J. Organomet. Chem.*, **368**, 163 (1989).
123. J. Ohshita, S. Masaoka, Y. Morimoto and M. Ishikawa, *Organometallics*, **16**, 910 (1997).
124. M. Ishikawa, T. Fuchikami, T. Sugaya and M. Kumada, *J. Am. Chem. Soc.*, **97**, 5923 (1975).
125. M. Ishikawa and M. Kumada, *Adv. Organomet. Chem.*, **19**, 51 (1981).
126. K. Nate, M. Ishikawa, H. Ni, H. Watanabe and Y. Saheki, *Organometallics*, **6**, 1673 (1987).
127. M. Ishikawa, K. Watanabe, H. Sakamoto and A. Kunai, *J. Organomet. Chem.*, **455**, 61 (1993).
128. M. Ishikawa, H. Sakamoto and F. Kanetani, *Organometallics*, **8**, 2767 (1989).
129. M. Ishikawa, Y. Nishimura and H. Sakamoto, *Organometallics*, **10**, 2701 (1991).
130. M. Ishikawa, K. Watanabe, H. Sakamoto and A. Kunai, *J. Organomet. Chem.*, **435**, 249 (1992).
131. J. Ohshita, H. Ohsaki, M. Ishikawa, A. Tachibana, Y. Kurosaki and T. Yamabe, *Organometallics*, **10**, 880 (1991).
132. J. Ohshita, H. Ohsaki, M. Ishikawa, A. Tachibana, Y. Kurosaki, T. Yamabe, T. Tsukihara, K. Kiso, and Y. Takahashi, *Organometallics*, **10**, 2685 (1991).
133. M. Ishikawa, Y. Nishimura and H. Sakamoto, *Organometallics*, **10**, 2701 (1991).
134. K. Takaki, H. Sakamoto, Y. Nishimura, Y. Sugihara and M. Ishikawa, *Organometallics*, **10**, 888 (1991).
135. G. W. Sluggett and W. J. Leigh, *J. Am. Chem. Soc.*, **114**, 1195 (1992).

136. G. W. Sluggett, and W. J. Leigh, *Organometallics*, **13**, 1005 (1994).
137. W. J. Leigh and G. W. Sluggett, *Organometallics*, **13**, 269 (1994).
138. M. Kira, T. Miyazawa, H. Sugiyama, M. Yamaguchi and H. Sakurai, *J. Am. Chem. Soc.*, **115**, 3116 (1993).
139. G. W. Sluggett and W. J. Leigh, *Organometallics*, **11**, 3731 (1992).
140. W. J. Leigh and G. W. Sluggett, *J. Am. Chem. Soc.*, **115**, 7531 (1993).
141. M. Steinmetz and C. Yu. *J. Org. Chem.*, **57**, 3107 (1992).
142. M. Steinmetz and Q. Chen, *J. Chem. Soc., Chem. Commun.*, 133 (1995).
143. M. Kira, T. Maruyama and H. Sakurai, *J. Am. Chem. Soc.*, **113**, 3986 (1991).
144. H. Sakurai, H. Sugiyama and M. Kira, *J. Phys. Chem.*, **94**, 1837 (1990).
145. (a) J. Braddock-Wilking, M. Y. Chiang and P. P. Gaspar, *Organometallics*, **12**, 197 (1993).
(b) D. Pae, M. Xiao, M. Chiang and P. P. Gaspar, *J. Am. Chem. Soc.*, **113**, 1281 (1991).
146. H. F. Schaefer III, *Acc. Chem. Res.*, **15**, 283 (1982).
147. B. T. Luke, J. A. Pople, M.-B. Krogh-Jespersen, Y. Apeloig, M. Karni, J. Chandrasekhar and P. v. R. Schleyer, *J. Am. Chem. Soc.*, **108**, 270 (1986).
148. C. F. Melius and M. D. Allendorf, *J. Phys. Chem.*, **96**, 428 (1992).
149. H. M. Frey, B. P. Mason, R. Walsh and R. Becerra, *J. Chem. Soc., Faraday Trans.*, **89**, 411 (1993).
150. S. K. Shin, K. K. Irikura, J. L. Beauchamp and W. A. Goddard, *J. Am. Chem. Soc.*, **110**, 24 (1988).
151. R. S. Grev, G. E. Scuseria, A. C. Scheiner, H. F. Schaefer III and M. S. Gordon, *J. Am. Chem. Soc.*, **110**, 7337 (1988).
152. T. Kudo and S. Nagase, *J. Chem. Soc., Chem. Commun.*, 141 (1984).
153. H. Vancik, G. Raabe, M. J. Michalczyk, R. West and J. Michl *J. Am. Chem. Soc.*, **107**, 4097 (1985).
154. C. A. Arrington, K. A. Klingensmith, R. West and J. Michl, *J. Am. Chem. Soc.*, **106**, 525 (1984).
155. T. J. Drahnak, J. Michl and R. West, *J. Am. Chem. Soc.*, **103**, 1845 (1981).
156. G. Raabe, H. Vancik, R. West and J. Michl, *J. Am. Chem. Soc.*, **108**, 671 (1986).
157. C.-C. Chang, J. Kolc, M. E. Jung, J. A. Lowe and O. L. Chapman, *J. Am. Chem. Soc.*, **98**, 7846 (1976).
158. H.-P. Reisenauer, G. Mihm and G. Maier, *Angew. Chem., Int. Ed. Engl.*, **21**, 854 (1982).
159. V. N. Khabashesku, V. Balaji, S. E. Boganov, O. M. Nefedov and J. Michl, *J. Am. Chem. Soc.*, **116**, 320 (1994).
160. P. P. Gaspar, R.-J. Hwang and W. C. Eckelman, *J. Chem. Soc., Chem. Commun.*, 242 (1974).
161. M. J. Fink, D. B. Puranik and M. P. Johnson, *J. Am. Chem. Soc.*, **110**, 1315 (1988).
162. D. B. Puranik and M. J. Fink, *J. Am. Chem. Soc.*, **111**, 5951 (1989).
163. M. J. Fink, in *Frontiers of Organosilicon Chemistry* (Eds. A. R. Bassindale and P. P. Gaspar), Royal Society of Chemistry, Cambridge, 1991, p. 285.
164. A. Sekiguchi and W. Ando, *Organometallics*, **6**, 1857 (1987).
165. A. Sekiguchi, T. Sato and W. Ando, *Organometallics*, **6**, 2337 (1987).
166. G. Maas and A. Fronda, *J. Organomet. Chem.*, **398**, 229 (1990).
167. M. Fronda and G. Maas, *Angew. Chem., Int. Ed. Engl.*, **28**, 1663 (1989).
168. W. Ando, M. Sugiyama, T. Suzuki, C. Kato, Y. Arakawa and Y. Kabe, *J. Organomet. Chem.*, **499**, 99 (1995).
169. W. Ando, H. Yoshida, K. Kurishima and M. Sugiyama, *J. Am. Chem. Soc.*, **113**, 7790 (1991).
170. G. Märkl and W. Schlosser, *Tetrahedron Lett.*, **29**, 467 (1988).
171. N. Wiberg and S. Vasisht, *Angew. Chem., Int. Ed. Engl.*, **30**, 93 (1991).
172. N. Wiberg and S. Wagner, *Z. Naturforsch.*, **51b**, 838 (1996).
173. N. Wiberg and H. S. Hwangpark, *J. Organomet. Chem.*, **519**, 107 (1996).
174. N. Wiberg, H. S. Hwangpark, P. Mikulcik and G. Müller, *J. Organomet, Chem.*, **511**, 239 (1996).
175. M. Chaubon, J. Escudié, H. Ranaivonjatovo and J. Satgé, *J. Chem. Soc., Dalton Trans.*, **6**, 893 (1996).
176. N. Wiberg and S. Wagner, *Z. Naturforsch.*, **51b**, 629 (1996).
177. M. Takahashi, J. Ogasawara, K. Sakamoto, M. Kira and T. Veszpremi, submitted.
178. W. Ziche, N. Auner and P. Kiprof, *J. Am. Chem. Soc.*, **114**, 4910 (1992).
179. W. Ziche, N. Auner and J. Behm, *Organometallics*, **11**, 3805 (1992).
180. K. M. Baines and A. G. Brook, *Adv. Organomet. Chem.*, **25**, 1 (1986).
181. A. G. Brook and H.-J. Wessely, *Organometallics*, **4**, 1487 (1985).

182. U. Klingebiel, S. Pohlmann and L. Skoda, *J. Organomet. Chem.*, **291**, 277 (1985).
183. R. T. Zhang, S. Conlin, M. Namavari, K. L. Bobbitt and M. J. Fink, *Organometallics*, **8**, 571 (1989).
184. M. Ishikawa, D. Kovar, T. Fuchikami, K. Nishimura, M. Kumada, T. Higuchi and S. Miyamoto, *J. Am. Chem. Soc.*, **103**, 2324 (1981).
185. M. Ishikawa and S. Matsuzawa, *J. Chem. Soc., Chem. Commun.*, 588 (1985).
186. E. T. Seidl, R. S. Grev and H. F. Schaefer III, *J. Am. Chem. Soc.*, **114**, 3643 (1992).
187. F. Bernardi, A. Bottoni, M. Olivucci, M. A. Robb and A. Venturino, *J. Am. Chem. Soc.*, **115**, 3322 (1993).
188. F. Bernardi, A. Bottoni, M. Olivucci, A. Venturini and M. A. Robb, *J. Chem. Soc., Faraday Trans.*, **90**, 1617 (1994).
189. W. A. Howard, G. L. McPherson, M. J. Fink and J. R. Gee, *J. Am. Chem. Soc.*, **113**, 5461 (1991).
190. D. B. Puranik, M. P. Johnson and M. J. Fink, *J. Chem. Soc., Chem. Commun.*, 706 (1989).
191. D. Bravo-Zhivotovskii, personal communication to T. M., 1995.
192. M. Nishimura, K. Ishikawa, H. Ochial and M. Kum, *J. Organomet. Chem.*, **236**, 7 (1982).
193. M. Ishikawa, M. Kikuchi, H. Watanabe, H. Sakamoto and A. Kunai, *J. Organomet. Chem.*, **443**, C3 (1993).
194. M. Ishikawa, M. Kikuchi, A. Kunai, T. Takeuchi, T. Tsukihara and M. Kido, *Organometallics*, **12**, 3474 (1993).
195. G. Maas, K. Schneider and W. Ando, *J. Chem. Soc., Chem. Commun.*, 72 (1988).
196. K. Schneider, B. Daucher, A. Fronda and G. Maas, *Chem. Ber.*, **123**, 589 (1990).
197. N. Wiberg, G. Wagner, G. Müller and J. Riede, *J. Organomet. Chem.*, **271**, 381 (1984).
198. W. J. Leigh and G. W. Sluggett, *J. Am. Chem. Soc.*, **116**, 10468 (1994).
199. N. Auner, *Z. Anorg. Allg. Chem.*, **558**, 87 (1988).
200. C. Krempner, Ph. D. Thesis, University of Rostock, Rostock, FRG, 1996.
201. N. Wiberg, M. Link and G. Fischer, *Chem. Ber.*, **122**, 409 (1989).
202. A. MacMillan and A. G. Brook, *J. Organomet. Chem.*, **341**, C9 (1988).
203. N. Wiberg, G. Fischer and S. Wagner, *Chem. Ber.*, **124**, 769 (1991).
204. N. Wiberg, S. Wagner and G. Fischer, *Chem. Ber.*, **124**, 1981 (1991).
205. N. Auner, C. Seidenschwarz and N. Sewald, *Organometallics*, **11**, 1137 (1992).
206. N. Auner, W. Ziche and E. Herdtweck, *J. Organomet. Chem.*, **426**, 1 (1992).
207. N. Auner, *J. Organomet. Chem.*, **336**, 83 (1987).
208. N. Auner, J. Grobe, T. Schäfer, B. Krebs and M. Dartmann, *J. Organomet. Chem.*, **363**, 7 (1989).
209. N. Auner, C. Seidenschwarz and E. Herdtweck, *Angew. Chem., Int. Ed. Engl.*, **30**, 1151 (1991).
210. N. Auner, C.-R. Heikenwälder and C. Wagner, *Organometallics*, **12**, 4135 (1993).
211. W. Ziche, C. Seidenschwarz, N. Auner, E. Herdtweck and N. Sewald, *Angew. Chem., Int. Ed. Engl.*, **33**, 77 (1994).
212. N. Sewald, W. Ziche, A. Wolff and N. Auner, *Organometallics*, **12**, 4123 (1993).
213. N. Auner and A. Wolff, *Chem. Ber.*, **126**, 575 (1993).
214. N. Auner, C. Seidenschwarz, N. Sewald and E. Herdtweck, *Angew. Chem., Int. Ed. Engl.*, **30**, 444 (1991).
215. N. Auner and A. Wolff, *Organometallics*, submitted.
216. N. Auner and C. Seidenschwarz, *Z. Naturforsch.*, **45b**, 909 (1990).
217. N. Auner, A. W. Weingartner and G. Bertrand, *Chem. Ber.*, **126**, 581 (1993).
218. N. Auner and C.-R. Heikenwälder, *Organometallics*, submitted.
219. C.-R. Heikenwälder and N. Auner, in *Organosilicon Chemistry II—From Molecules to Materials* (Eds. N. Auner and J. Weis), VCH Verlag, Weinheim, 1996, p. 399.
220. N. Auner and C.-R. Heikenwälder, *Z. Naturforsch.*, **52b**, 500 (1997).
221. C.-R. Heikenwälder and N. Auner, in *Organosilicon Chemistry III —From Molecules to Materials* (Eds. N. Auner and J. Weis), VCH Verlag, Weinheim, 1997, p. 101.
222. W. Ziche, N. Sewald, C. Seidenschwarz, E. Herdtweck, V. Popkova and N. Auner, *Organometallics*, submitted.
223. J. Grobe, H. Schröder and N. Auner, *Z. Naturforsch.*, **45b**, 785 (1990).
224. N. Auner, C.-R. Heikenwälder and W. Ziche, *Chem. Ber.*, **126**, 2177 (1993).
225. N. Auner and E. Penzenstadler, *Z. Naturforsch.*, **47b**, 217 (1992).
226. N. Auner and E. Penzenstadler, *Z. Naturforsch.*, **47b**, 795 (1992).
227. N. Auner and E. Penzenstadler, *Z. Naturforsch.*, **47b**, 805 (1992).

228. N. Auner, E. Penzenstadler and E. Herdtweck, *Z. Naturforsch.*, **47b**, 1377 (1992).
229. N. Auner, A. W. Weingartner and E. Herdtweck, *Z. Naturforsch.*, **48b**, 318 (1993).
230. N. Auner, *J. Organomet. Chem.*, **377**, 175 (1989).
231. N. Auner and R. Gleixner, *J. Organometal. Chem.*, **393**, 33 (1990).
232. B. Goetze, B. Herrschaft and N. Auner, *Chem. Eur. J.*, **3**, 948 (1997).
233. W. Ziche, N. Auner and J. Behm, *Organometallics*, **11**, 2494 (1992).
234. N. Auner, C. Wagner and W. Ziche, *Z. Naturforsch.*, **49b**, 831 (1994).
235. A. G. Brook, W. J. Chatterton, J. F. Sawyer, D. W. Hughes and K. Vorspohl, *Organometallics*, **6**, 1246 (1987).
236. A. G. Brook, Y. Kun Kong, A. K. Saxena and J. F. Sawyer, *Organometallics*, **7**, 2245 (1988).
237. A. G. Brook, A. K. Saxena and J. F. Sawyer, *Organometallics*, **8**, 850 (1989).
238. (a) M. T. Nguyen, H. Vansweevelt, A. De Neef and L. G. Vanquickborne, *J. Org. Chem.*, **59**, 8015 (1994).
    (b) A. G. Brook, in *Heteroatom Chemistry* (Ed. E. Block), VCH verlag, Weinheim, **1990**, p. 105.
239. A. G. Brook, R. Kumarathasan and A. J. Lough, *Organometallics*, **13**, 424 (1994).
240. A. G. Brook, K. Vorspohl, R. R. Ford, M. Hesse and W. J. Chatterton, *Organometallics*, **6**, 2128 (1987).
241. D. Bravo-Zhivotovskii, Y. Apeloig, Y. Ovchinnikov, V. Igonin and Y. T. Struchkov, *J. Organomet. Chem.*, **446**, 123 (1993).
242. S. M. Bachrach and A. Streitwieser, *J. Am. Chem. Soc.*, **107**, 1186 (1985).
243. G. Märkl and M. Horn, *Tetrahedron Lett.* **14**, 1477 (1983).
244. A. G. Brook, S. S. Hu, W. J. Chatterton and A. J. Lough, *Organometallics*, **10**, 2752 (1991).
245. A. G. Brook, S. S. Hu, A. K. Saxena and A. J. Lough, *Organometallics*, **10**, 2758 (1991).
246. (a) Y. Apeloig, and M. Karni, *J. Am. Chem. Soc.*, **106**, 6676 (1984).
    (b) V. Braude, Ph. D. Thesis, Technion, Haifa, Israel, 1993.
247. A. G. Brook, R. Kumarathasan and W. Chatterton, *Organometallics*, **12**, 4085 (1993).
248. A. G. Brook, W. J. Chatterton and R. Kumarathasan, *Organometallics*, **12**, 3666 (1993).
249. N. Toltl and W. Leigh, *Organometallics*, **15**, 2554 (1996).
250. R. Conlin and M. Namavari, *J. Organomet. Chem.*, **376**, 259 (1989).
251. J. Ohshita, H. Niwa and M. Ishikawa, *Organometallics*, **15**, 4632 (1996).
252. W. Sander and M. Trommer, *Chem. Ber.*, **125**, 2813 (1992).
253. M. Trommer, W. Sander and A. Patyk, *J. Am. Chem. Soc.*, **115**, 1175 (1993).
254. V. V. Volkova, V. G. Avakyan, N. S. Nametkin and L. E. Gusel'nikov, *J. Organomet. Chem.*, **201**, 137 (1980).
255. O. M. Nefedov, A. K. Maltsev, V. N. Khabashesku and V. A. Korolev, *J. Organomet. Chem.*, **201**, 123 (1980).
256. G. Mihm, H. P. Reisenauer, D. Littmann and G. Maier, *Chem. Ber.*, **117**, 2369 (1984).
257. J. Chen, P. J. Hajduk, J. D. Keen, C. Chuang, T. Emilsson and H. S. Gutowsky, *J. Am. Chem. Soc.*, **113**, 4747 (1991).
258. J. Chen, P. J. Hajduk, J. D. Keen, T. Emilsson and H. S. Gutowsky, *J. Am. Chem. Soc.*, **111**, 1901 (1989).
259. M. Trommer, G. E. Miracle, D. R. Powell and R. West, *Organometallics*, in press (1997).
260. H. Sohn, U. Bankwitz, J. Calabrese, Y. Apeloig, T. Müller and R. West, *J. Am. Chem. Soc.*, **117**, 11608 (1995).
261. T. D. Tilley, G. P. A. Yap, A. L. Rheingold and W. P. Freeman, *Angew. Chem., Int. Ed. Engl.*, **35**, 976 (1996).
262. T. D. Tilley, L. M. Liable-Sands, A. L. Rheingold and W. P. Freeman, *J. Am. Chem. Soc.*, **118**, 10457 (1996).
263. R. Gutowsky, L. K. Montgomery and P. G. Mahaffy, *J. Am. Chem. Soc.*, **102**, 2854 (1980).
264. J.-P. Malrieu and G. Trinquier, *J. Am. Chem. Soc.*, **109**, 5303 (1987).
265. P. Boudjouk, S. Castellino and J-H. Hong, *Organometallics*, **13**, 3387 (1994).
266. R. West, H. Sohn, Y. Apeloig and T. Müller, in *Organosilicon Chemistry III—From Molecules to Materials* (Eds. N. Auner and J. Weis) VCH Verlag, Weinheim, 1997, p. 144.
267. P. v. R. Schleyer, F. Hampel and B. Goldfuss, *Organometallics*, **15**, 1755 (1996).
268. N. Wiberg, G. Wagner and G. Müller, *Angew. Chem., Int. Ed. Engl.*, **24**, 229 (1985).
269. R. Okazaki and R. West, *Adv. Organomet. Chem.*, **39**, 232 (1995).
270. J. D. Cavalieri, J. J. Buffy, C. Fry, K. W. Zilm, J. C. Duchamp, M. Kira, T. Iwamoto, T. Müller, Y. Apeloig and R. West, *J. Am. Chem. Soc.*, **119**, 4972 (1997).

271. G. E. Miracle, J. L. Ball, S. R. Bielmeier, D. R. Powell and R. West, in *Progress in Organosilicon Chemistry* (Eds. B. Mariciniec and J. Chojnowski) Gordon and Breach, Basel, 1995, pp. 83–100.
272. K. Wakitu, N. Tokitoh, R. Okazaki and S. Nagase, 30th Organosilicon Symposium, London, Ontario. Canada, May 1997, Abstr. P-52.
273. P. R. Jones and M. E. Lee, *J. Organomet. Chem.*, **271**, 299 (1984).
274. W. Schlosser and G. Märkl, *Angew. Chem., Int. Ed. Engl.*, **27**, 963 (1988).
275. R. Withnall and L. Andrews, *J. Phys. Chem.*, **92**, 594 (1988).
276. G. D. Josland, R. A. Lewis, A. Morris and J. M. Dyke, *J. Phys. Chem.*, **86**, 2913 (1982).
277. W. Ando and A. Sekiguchi, *Chem. Lett.*, 2025 (1986).
278. C. Kerst, C. W. Rogers, R. Ruffolo and W. Leigh, *J. Am. Chem. Soc.*, **119**, 466 (1997).
279. G. Mihm, H. P. Reisenauer and G. Maier, *Angew. Chem., Int. Ed. Engl.*, **19**, 52 (1980).
280. G. Mihm, H. P. Reisenauer and G. Maier, *Chem. Ber.*, **115**, 801 (1982).
281. G. Mihm, R. O. W. Baumgärtner, H. P. Reisenauer and G. Maier, *Chem. Ber.*, **117**, 2337 (1984).
282. K. Schöttler, H. P. Reisenauer and G. Maier, *Tetrahedron Lett.*, **26**, 4079 (1985).
283. O. L. Chapman, G. T. Burns, T. J. Barton and C. L. Kreil, *J. Am. Chem. Soc.*, **102**, 841 (1980).
284. C. Allison and T. McMahon, *J. Am. Chem. Soc.*, **112**, 1672 (1990).
285. (a) T. Müller and W. Ziche, unpublished results.
    (b) G. Maier, H. Pacl and H. P. Reisenauer, *Angew. Chem., Int. Ed. Engl.*, **34**, 1439 (1995).
286. J. Pacansky, N. Honjou and M. Yoshimine, *J. Am. Chem. Soc.*, **111**, 4198 (1989).
287. M. Ishikawa, H. Sugisawa, T. Fuchikami, M. Kumada, T. Yamabe, H. Kawakami, K. Fukui, Y. Ueki and H. Shizuka, *J. Am. Chem. Soc.*, **104**, 2872 (1982).
288. M. Ishikawa, H. Sugisawa, M. Kumada, T. Higichi, K. Matsui, K. Hirotsu and J. Iyoda, *Organometallics*, **2**, 174 (1983).
289. M. Ishikawa, T. Horio, Y. Yuzuriha and A. Kunai, *J. Organomet, Chem.*, **402**, C20 (1991).
290. M. Ishikawa, T. Horio, Y. Yuzuriha, A. Kunai, T. Tsukihara and H. Naitou, *Organometallics*, **11**, 597 (1992).
291. J. Ohshita, Y. Isomure and M. Ishikawa, *Organometallics*, **8**, 2050 (1989).
292. S. Landor, *The Chemistry of Allenes*, Academic Press, London, 1982.
293. K. Krogh-Jespersen, *J. Comput. Chem.*, **3**, 571 (1982).
294. G. Manuel, P. Mazerolles and G. Bertrand, *Tetrahedron*, **34**, 1951 (1978).
295. M. Urbanova, E. A. Volnina, L. E. Gusel'nikov, Z. Bastl and J. Pola, *J. Organomet. Chem.*, **509**, 73 (1996).
296. (a) M. Jakoubková, R. Fajgar, J. Tláskal and J. Pola, *J. Organomet. Chem.*, **466**, 29 (1994) and references cited there.
    (b) A. Sekiguchi, S. S. Ziegler, R. West and J. Michl, *J. Am. Chem. Soc.*, **108**, 4241 (1986).
    (c) A. Sekiguchi, G. R. Gillette and R. West, *Organometallics*, **7**, 1226 (1988).
297. (a) M. T. Nguyen, D. Sengupta and L. G. Vanquickenborne, *Chem. Phys. Lett.*, **244**, 83 (1995).
    (b) R. Stegmann and G. Frenking, *J. Comput. Chem.*, **17**, 781 (1996).
    (c) Y. Apeloig and M. Karni, *Organometallics*, **16**, 310 (1997).
298. (a) M. Izuha, S. Yamamoto and S. Saito, *J. Chem. Phys.*, **105**, 4923 (1996).
    (b) D. G. Leopold and A. A. Bengali, unpublished results, cited in C. D. Sherill and H. F. Schaefer III, *J. Phys. Chem.*, **99**, 1949 (1995).
    For mass spectroscopic evidence for $H_2C{=}Si\colon$ see
    (c) R. Srinivas, D. Sülzle and H. Schwarz *J. Am. Chem. Soc.*, **113**, 52 (1991).
    (d) R. Damrauer, C. H. DePuy, S. E. Barlow and S. Gronert, *J. Am. Chem. Soc.*, **110**, 2005 (1988).
299. (a) *Silicon Nitrogen Compounds in Gmelin Handbook of Inorganic Chemistry* (Ed. F. Schröder) 8th ed., Springer Verlag, Berlin, 1989.
    (b) I. Hemme and U. Klingebiel, *Adv. Organomet. Chem.*, **39**, 159 (1995).
300. N. Wiberg and K. Schurz, *J. Organomet. Chem.*, **341**, 145 (1988).
301. N. Wiberg, K. Schurz, G. Reber and G. Müller, *J. Chem. Soc., Chem. Commun.*, 591 (1986).
302. N. Wiberg, K. Schurz and G. Fischer, *Angew. Chem., Int. Ed. Engl.*, **24**, 1053 (1985).
303. N. Wiberg and K. Schurz, *Chem. Ber.*, **121**, 581 (1988).
304. M. Hesse and U. Klingebiel, *Angew. Chem., Int. Ed. Engl.*, **25**, 649 (1986).
305. D. Stalke, N. Keweloh, U. Klingebiel, M. Noltemeyer and G. M. Sheldrick, *Z. Naturforsch.*, **42b**, 1237 (1987).
306. S. Walter, U. Klingebiel and D. Schmidt-Bäse, *J. Organomet. Chem.*, **412**, 319 (1991).

307. D. Grosskopf, L. Marcus, U. Klingebiel and M. Noltemeyer, *Phosphorus, Sulfur, Silicon Relat. Elem.*, **97**, 113 (1994).
308. N. Wiberg, P. Karampatses and C.-K. Kim, *Chem. Ber.*, **120**, 1203 (1987).
309. N. Wiberg and G. Preiner, *Angew. Chem., Int. Ed. Engl.*, **17**, 362 (1978).
310. N. Wiberg, P. Karampatses and Ch.-K. Kim, *Chem. Ber.*, **120**, 1213 (1987).
311. K. Tamao, Y. Nakagawa and Y. Ito, *J. Am. Chem. Soc.*, **114**, 218 (1992).
312. A. Weingartner, W. Ziche and N. Auner, in *Organosilicon Chemistry: From Molecules to Materials* (Eds. N. Auner and J. Weis), VCH, Weinheim, 1994, p. 115.
313. M. Letulle, A. Systermans, J.-L. Ripoll and P. Guenot, *J. Organomet. Chem.*, **484**, 89 (1994).
314. S. Cradock and J. F. Ogilive, *J. Chem. Soc., Chem. Commun.*, 364 (1966).
315. H. Bock and R. Dammel, *Angew. Chem., Int. Ed. Engl.*, **24**, 111 (1985).
316. C. Guimon and G. Pfister-Guillouzo, *Organometallics*, **6**, 1387 (1987).
317. S. S. Zigler, L. M. Johnson and R. West, *J. Organomet. Chem.*, **341**, 187 (1988).
318. R. Abramovich and E. Kyba, *J. Am. Chem. Soc.*, **93**, 1537 (1971).
319. E. Kyba and R. Abramovich, *J. Am. Chem. Soc.*, **102**, 735 (1980).
320. M. T. Nguyen, M. Faul and N. J. Fitzpatrick, *J. Chem. Soc., Perkin Trans. 2*, 1289 (1987).
321. J. G. Radziszewski, P. Kaszynski, D. Littmann, V. Balaji, B. A. Hess and J. Michl, *J. Am. Chem. Soc.*, **115**, 8401 (1993).
322. M. Elseikh and L. Sommer, *J. Organomet. Chem.*, **186**, 301 (1980).
323. W. Jevons, *Proc. R. Soc. London, Ser. A*, **89**, 187 (1913).
324. R. S. Mulliken, *Phys. Rev.*, **26**, 319 (1925).
325. S. Saito, Y. Endo and E. Hirota, *J. Chem. Phys.*, **78**, 6447 (1983).
326. J. G. Radziszewski, D. Littmann, V. Balaji, L. Fabry, G. Gross and J. Michl, *Organometallics*, **12**, 4816 (1993).
327. G. Reber, J. Riede, N. Wiberg, K. Schurz and G. Müller, *Z. Naturforsch.*, **44**, 786 (1989).
328. G. Maier and J. Glatthaar, *Angew. Chem., Int. Ed. Engl.*, **33**, 473 (1994).
329. G. Maier, J. Glatthaar and H. Reisenauer, *Chem. Ber.*, **122**, 2403 (1989).
330. G. Maier and J. Glatthaar, in *Organosilicon Chemistry: From Molecules to Materials* (Eds. N. Auner and J. Weis), VCH, Weinheim, 1994, p. 131.
331. T. J. Barton and S. Bain, *Organometallics*, **7**, 528 (1988).
332. J.-M. Denis, P. Guenot, M. Letulle, B. Pellerin and J.-L. Ripoll, *Chem. Ber.*, **125**, 1397 (1992).
333. A. Chive, V. Lefevre, A. Systermans, J.-L. Ripoll, M. Bogey and A. Walters, *Phosphorus, Sulfur, Silicon*, **91**, 281 (1994).
334. M. Weidenbruch, B. Brand-Roth, S. Pohl and W. Saak, *J. Organomet. Chem.*, **379**, 217 (1989).
335. M. Denk and R. West, *Pure Appl Chem.* **68**, 785 (1996).
336. M. Elhanine, R. Farrenq and G. Guelachvili, *J. Chem. Phys.*, **94**, 2529 (1991).
337. R. Damrauer, M. Krempp and R. A. J. O'Hair, *J. Am. Chem. Soc.*, **115**, 1998 (1993).
338. J. A. Hankin, M. Krempp and R. Damrauer, *Organometallics*, **14**, 2652 (1995).
339. D. K. Bohme, *Int. J. Mass Spectrom. Ion Processes*, **100**, 719 (1990).
340. D. K. Bohme, *Chem. Rev.*, **92**, 1487 (1992).
341. S. Wlodek, C. F. Rodriguez, M. H. Lien, A. C. Hopkinson and D. K. Bohme, *Chem. Phys. Lett.*, **143**, 385 (1988).
342. N. Goldberg, M. Iraqi, J. Hrušák and H. Schwarz, *Int. J. Mass Spectrom. Ion Processes*, **125**, 267 (1993).
343. S. S. Zigler, K. M. Welsh and R. West, *J. Am. Chem. Soc.*, **109**, 4392 (1987).
344. W. Ando, H. Tsumaki and M. Ikeno, *J. Chem. Soc., Chem. Commun.*, 597 (1981).
345. K. M. Welsh, J. Michl and R. West, *J. Am. Chem. Soc.*, **110**, 6689 (1988).
346. G. E. Underiner and R. West. *Angew. Chem., Int. Ed. Engl.*, **29**, 529 (1990).
347. G. E. Underiner, R. Tan, D. Powell and R. West, *J. Am. Chem. Soc.*, **113**, 8437 (1991).
348. L. J. Procopio, P. J. Carroll and D. H. Berry, *Organometallics*, **12**, 3087 (1993).
349. L. J. Procopio, P. J. Carroll and D. H. Berry, *Polyhedron*, **14**, 45 (1995).
350. L. J. Procopio, P. J. Carroll and D. H. Berry, *J. Am. Chem. Soc.*, **113**, 1870 (1991).
351. N. Wiberg, G. Preiner, P. Karampatses, C.-K. Kim and K. Schurz, *Chem. Ber.*, **120**, 1357 (1987).
352. N. Wiberg, E. Kühnel, K. Schurz, H. Borrmann and A. Simon, *Z. Naturforsch.*, **43**, 1075 (1988).
353. D. Grosskopf, U. Klingebiel, T. Belgardt and M. Noltemeyer, *Phosphorus, Sulfur, Silicon*, **91**, 241 (1994).
354. S. Walter, U. Klingebiel and M. Noltemeyer, *Chem. Ber.*, **125**, 783 (1992).
355. S. Vollbrecht, U. Klingebiel and D. Schmidt-Bäse, *Z. Naturforsch.*, **46**, 709 (1991).

356. N. Wiberg, G. Preiner and K. Schurz, *Chem. Ber.*, **121**, 1407 (1988).
357. R. Boese and U. Klingebiel, *J. Organomet. Chem.*, **315**, C17 (1986).
358. D. Stalke, U. Piper, S. Vollbrecht and U. Klingebiel, *Z. Naturforsch.*, **45b**, 1513 (1990).
359. U. Pieper, S. Walter, U. Klingebiel and D. Stalke, *Angew. Chem., Int. Ed. Engl.*, **29**, 209 (1990).
360. H. Chen, R. A. Bartlett, H. V. R. Dias, M. M. Olmstead and P. P. Power, *J. Am. Chem. Soc.*, **111**, 4338 (1989).
361. M. Driess and R. Janoschek, *J. Mol. Structure (Theochem)*, **119**, 129 (1994).
362. P. Marshall, *Chem. Phys. Lett.*, **201**, 493 (1993).
363. C. F. Melius and P. Ho, *J. Phys. Chem.*, **95**, 1410 (1991).
364. A. Korkin, *Int. J. Quantum Chem.*, **38**, 245 (1990).
365. M. S. Gordon, M. W. Schmidt and S. Koseki, *Inorg. Chem.*, **28**, 2161 (1989).
366. D. P. Chong, D. Papousek, Y.-T. Chen and P. Jensen, *J. Chem. Phys.*, **98**, 1352 (1992).
367. M. S. El-Shall, *Chem. Phys. Lett.*, **159**, 21 (1989).
368. Y. Apeloig and K. Albrecht, *J. Am. Chem. Soc.*, **117**, 7263 (1995).
369. J. R. Flores and J. Largo-Cabrerizo, *J. Mol. Structure (Theochem)*, **52**, 17 (1989).
370. O. Parisel, M. Hanus and Y. Ellinger, *J. Chem. Phys.*, **104**, 1979 (1996).
371. M. Sana, M. Decrem, G. Levroy, M. T. Nguyen and L. G. Vanquickenborne, *J. Chem. Soc., Faraday Trans.*, **90**, 3505 (1994).
372. K. Fan and S. lwata, *Chem. Phys. Lett.*, **195**, 475 (1992).
373. T. N. Truong and M. S. Gordon, *J. Am. Chem. Soc.*, **108**, 1775 (1986).
374. P. v. R. Schleyer and P. D. Stout, *J. Chem. Soc., Chem. Commun.*, 1373 (1986).
375. W. Ando, T. Ohtaki and Y. Kabe, *Organometallics*, **13**, 434 (1994).
376. M. Driess, *Coord. Chem. Rev.*, **145**, 1 (1995).
377. M. Driess, *Adv. Organomet Chem.*, **39**, 183 (1995).
378. C. Smit and F. Bickelhaupt, *Phosphorus, Sulfur, Silicon*, **30**, 357 (1987).
379. Y. v. d. Winkel, H. Bastiaans and F. Bickelhaupt, *Phosphorus, Sulfur, Silicon*, **49–50**, 333 (1990).
380. C. Couret, J. Escudié, J. Satgé, J. Andriamizaka and B. Saint-Roch *J. Organomet. Chem.*, **182**, 9 (1979).
381. V. Lefevre, J. Ripoll, Y. Dat, S. Joanteguy, V. Metail, A. Chrostowskasenio and G. Pfistergui-llouzo, *Organometallics*, **16**, 1635 (1997).
382. U. Klingebiel, R. Boese, D. Bläser and M. Andrianarison, *Z. Naturforsch.*, **44b**, 265 (1989).
383. N. Wiberg and H. Schuster, *Chem. Ber.*, **124**, 93 (1991).
384. H. Bender, E. Klein, E. Niecke, M. Nieger and H. Ranaivonjatovo, in *Organosilicon Chemistry From Molecules to Materials* (Eds. N. Auner and J. Weis), VCH, Weinheim, 1994, p. 143.
385. H. Bender, E. Niecke and M. Nieger, *J. Am. Chem. Soc.*, **115**, 3314 (1993).
386. E. Niecke, E. Klein and M. Nieger, *Angew. Chem., Int. Ed. Engl.* **28**, 751 (1989).
387. Y. v. d. Winkel, H. Bastiaans and F. Bickelhaupt, *J. Organomet. Chem.*, **405**, 183 (1991).
388. R. Corriu, G. Lanneau and C. Priou, *Angew. Chem., Int. Ed. Engl.*, **30**, 1130 (1991).
389. M. Driess, *Angew. Chem., Int. Ed. Engl.*, **30**, 1022 (1991).
390. M. Driess, H. Pritzkow, S. Rell and U. Winkler, *Organometallics*, **15**, 1845 (1996).
391. M. Driess, S. Rell and H. Pritzkow, *J. Chem. Soc., Chem. Commun.*, 253 (1995).
392. M. Driess, H. Pritzkow and U. Winkler, *J. Organomet. Chem.*, **529**, 313 (1997).
393. M. Driess and H. Pritzkow, *Angew. Chem., Int. Ed. Engl.*, **31**, 316 (1992).
394. A. Baboul and H. Schlegel, *J. Am. Chem. Soc.*, **118**, 8444 (1996).
395. M. Nguyen, A. Vankeer and L. Vanquickenborne, *J. Organomet. Chem.*, **529**, 3 (1997).
396. W. Schoeller and T. Busch, *Chem. Ber.*, **125**, 1319 (1992).
397. W. Schoeller and T. Busch, *J. Chem. Soc., Chem. Commun.*, 234 (1989).
398. W. Schoeller, J. Strutwolf, U. Tubbesing and C. Begemann, *J. Phys. Chem.*, **99**, 2329 (1995).

CHAPTER 17

Recent advances in the chemistry of silicon–heteroatom multiple bonds

NORIHIRO TOKITOH and RENJI OKAZAKI

Department of Chemistry, Graduate School of Science, The University of Tokyo,
7-3-1 Hongo, Bunkyo-ku, Tokyo 113, Japan
Fax: +81-3-5800-6899

I. INTRODUCTION

A. Multiple Bonds to Silicon

For the past decades, it was considered that double-bond compounds of heavier main-group elements would be neither stable nor synthetically accessible because of their weak $p\pi-p\pi$ bonding (the so-called 'double-bond rule'). However, since the isolation of the first stable doubly-bonded compounds containing heavier group 14 or 15 elements such as silene (Si=C)[1], disilene (Si=Si)[2] and diphosphene (P=P)[3], remarkable progress has been made in the chemistry of unsaturated compounds of these elements, especially in the field of group 14 metals[4]. Thus far, as for the chemistry of multiply-bonded compounds to silicon, the syntheses and characterization of stable iminosilanes (Si=N)[5], phosphasilenes (Si=P)[6] and their heavier congeners[7] have been reported in addition to those of a variety of stable silenes and disilenes[8]. In most cases, these novel low-coordinate silicon compounds were synthesized and isolated by taking advantage of kinetic stabilization with bulky substituents, i.e. steric protection. With this stabilization method the highly reactive molecules can be isolated with only small electronic perturbation, and hence one can reveal the intrinsic nature of the newly obtained multiple bonds which will be of great importance for the investigation of their non-stabilized, transient analogues.

On the other hand, the chemistry of doubly-bonded compounds between silicon and group 16 elements (chalcogen atoms) has been less explored due to their much higher reactivity than that of the above-mentioned silicon-containing multiple bonds to group 14 and 15 elements. This results from the fact that bulky substituents for steric protection can be introduced only on the silicon atom and hence their oligomerization cannot be efficiently suppressed. Although thermodynamically stabilized silanethione (Si=S) and silaneselone (Si=Se)[9] have been reported, they are considerably perturbed by intramolecular coordination of a nitrogen substituent in the neighborhood of the double bond. Only recently was the first kinetically stabilized silicon–chalcogen doubly-bonded compound i.e. a stable silanethione with a new steric protection system, been successfully isolated[10].

Since several excellent reviews on the chemistry of multiple bonds to silicon [see the chapter written by G. Raabe and J. Michl in a previous volume of this series (1989)[4e]] and also the reviews in *Advances in Organometallic Chemistry*, Vol. 39 (1995) (e.g. 'The Chemistry of Silenes' by A. G. Brook and M. A. Brook[8a], 'Iminosilanes and Related Compounds — Synthesis and Reactions' by I. Hemme and U. Klingebiel[5d], 'Silicon–Phosphorus and Silicon–Arsenic Multiple Bonds' by M. Driess[7c] and 'Chemistry of Stable Disilenes' by R. Okazaki and R. West[8b]) have appeared in recent years and as some parts of this chapter will be discussed in detail in related chapters of this book (e.g. 'Silenes and Iminosilanes' by N. Auner and coworkers[11] and 'Recent Advances in the Chemistry of Disilenes' by H. Sakurai[12]), we will concentrate our attention in this chapter on the chemistry of silicon–chalcogen doubly-bonded compounds.

B. Theoretical Calculations

1. Silanones and silanethiones

In 1986, Nagase and coworkers reported a theoretical study of silanethione ($H_2Si{=}S$, **1**) in the ground, excited and protonated states together with a comparison with silanone ($H_2Si{=}O$, **2**) and the parent carbonyl system ($H_2C{=}O$, **3**) using *ab initio* calculations including polarization functions and electron correlation[13]. Scheme 1 shows unimolecular reactions pertinent to the stability of $H_2Si{=}S$ and Figure 1 shows the equilibrium structures on the ground singlet potential energy surface of H_2SiS species and a related silanethiol (H_3SiSH) obtained at the HF/6-31G* level of theory. Similar theoretical calculations for species on the $H_2S{=}O$ ground state potential surface are shown in Figure 2[14].

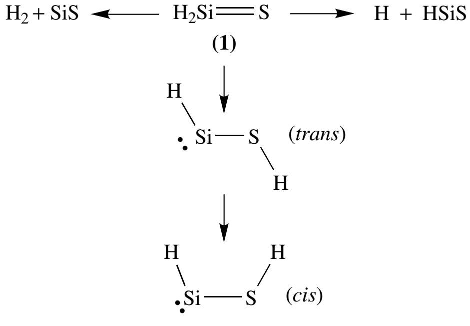

SCHEME 1

The equilibrium structure of $H_2Si{=}S$ is calculated to be planar with C_{2v} symmetry, as in the case of $H_2C{=}O$ and $H_2Si{=}O$. The Si–S bond length in **1** (1.936 Å) is by 0.438 and 0.752 Å longer than the Si–O and C–O bond lengths in **2** and **3**, respectively,

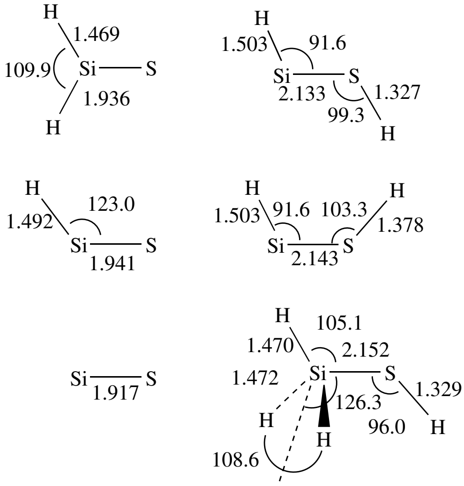

FIGURE 1. Equilibrium structures (in Å and deg) at the HF/6-31G* level

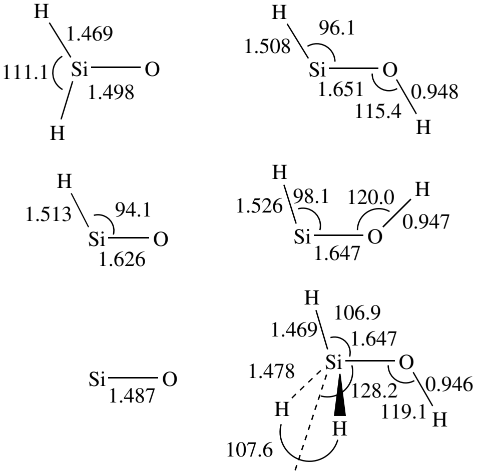

FIGURE 2. Equilibrium structures (in Å and deg) at the HF/6-31G* level

but it is by 0.216 Å shorter than the Si−S single bond length in H_3Si-SH (2.152 Å), indicating that a real π-bond exists between the Si and S atoms. The bond length shortening of 10% from H_3Si-SH to $H_2Si=S$ is comparable to that of 9% from H_3Si-OH to $H_2Si=O$, but it is smaller than the 15% shortening found on going from H_3C-OH to $H_2C=O$. A smaller shortening of silicon-containing π-bonds is found in the ethene analogues: 14% ($H_2C=CH_2$), 10% ($H_2Si=CH_2$) and 9% ($H_2Si=SiH_2$). According to the calculations, $H_2Si=S$ is found to be kinetically stable toward unimolecular dissociations such as $H_2Si=S \rightarrow H_2 + SiS$, $H_2Si=S \rightarrow H + HSiS$ and isomerization, i.e. $H_2Si=S \rightarrow H(HS)Si\!:$, as in the cases of **2** and **3**. For example, the barrier for the 1,2-H shift in $H_2Si=S$ to $H(HS)Si\!:$ is 54.8 kcal mol^{-1}, suggesting that **1** is kinetically stable to unimolecular isomerization and is expected to be isolable. Furthermore, it is found that $H_2Si=S$ is theremodynamically more stable than $H_2Si=O$. In an attempt to assess the strength of the silicon−sulfur double bond, they compared the calculated hydrogenation energies of **1, 2** and **3** at the MP3/6-31G**//6-31G* level. Using these calculated hydrogenation energies, the π-bond energies E_π(Si=S), E_π(Si=O) and E_π(C=O) are estimated to be 42, 33 and 63 kcal mol^{-1}, respectively. The calculated vibrational frequencies of $H_2Si=X$ (**1** and **2**) at the HF/6-31G* level were calculated to be 682 and 1203 cm^{-1} for the SiS and SiO stretching vibrations of **1** and **2**, respectively. The calculated proton affinities of **1, 2** and **3** were also reported and they are given in Table 1. The zero-point energy corrected MP3/6-31G**//6-31G* proton-affinity value of 174.7 kcal mol^{-1} for $H_2C=O$ agrees well with the experimental value of 171.7 kcal mol^{-1}.

The proton affinities increase in the order of **3** (174.7 kcal mol^{-1}) <**1** (190.5 kcal mol^{-1}) <**2** (208.3 kcal mol^{-1}). This was explained in terms of the predominance of the electrostatic over charge transfer interactions, thus the charge separations in the double bonds increase in the order of: $H_2C^{+0.2}-O^{-0.4}$ < $H_2Si^{+0.7}-S^{-0.4}$ < $H_2Si^{+1.0}-O^{-0.7}$, while the energy of the frontier n orbital levels rise in the order **3** (−11.8 eV) ≈ **2** (−11.9 eV) <**1** (−9.8 eV)[13]. The most important result of this theoretical study was the conclusion that silicon is significantly less reluctant to form double bonds with sulfur than with oxygen. Thus according to these calculations

TABLE 1. Calculated proton affinities (kcal mol^{-1}) of $H_2Si{=}S$ (**1**), $H_2Si{=}O$ (**2**) and $H_2C{=}O$ (**3**) at various theoretical levels[a]

Level of theory	$H_2Si{=}S$ (**1**)	$H_2Si{=}O$ (**2**)	$H_2C{=}O$ (**3**)
HF/6-31G*	192.6	215.6	182.0
HF/6-31G**	195.4	220.6	186.6
MP2/6-31G**	193.1	209.4	180.3
MP3/6-31G**	196.1	215.7	183.2
MP3/6-31G** + ZPC[b]	190.5	208.3	174.7

[a] All calculations used the HF/6-31G* optimized structures.

[b] Zero-point energy corrected calculations.

silanethiones are expected to be more stable and less reactive than the corresponding silanones[13]. The authors concluded that the major obstacle to the successful isolation of silanethiones is their relatively high reactivity.

2. Other double bonds to silicon

The π-bond strengths of double bonds to silicon were studied theoretically by Gordon and coworkers (in 1987)[15] and by Schleyer and coworkers (in 1988)[16]. In the former paper, all possible π-bonds between the elements C, N, O, Si, P and S were considered and the π-bond strengths were estimated by calculating the *cis–trans* rotation barriers (where possible) and by hydrogenation energies. The ability of these elements to form strong π-bonds was found to be in the order: $O > N \approx C \gg S > P > Si$. They reported the computed bond lengths and vibrational stretching frequencies for singly- and doubly-bonded compounds of all the possible combinations of these elements[15]. Schleyer and coworkers evaluated the π-bond energies (E_π) for the doubly-bonded systems $H_2Y{=}XH_n$ (Y = C, Si; X = B, C, N, O, Al, Si, P, S) employing the MP4SDTQ/6-31G*//6-31G* + ZPE level of theory. The difference between the energy of two single bonds, X−Y, and the corresponding double bond, X=Y, was calculated by means of isodesmic equations. E_π is given by subtraction of this difference from the dissociation energies of the single bonded X=Y system. Si=X bonds were found to have significantly lower E_π energies than the corresponding C=X bonds. For C=X and Si=X, the π-bond energies correlate with the electronegativities of X with different lines for second- and third-row substituents. Families of linear correlations are also observed between E_π and the Y=X bond lengths. Schleyer and coworkers criticized alternative procedures for estimating π-bond energies (such as rotation barriers and diradical components)[16].

3. Miscellaneous

The vertical electronic spectrum of silanethione ($H_2Si{=}S$; **1**) was investigated by using a multi-reference CI method and an expanded AO basis set including 4s and 4p Rydberg functions[17]. The equilibrium geometry of the X^1A_1 ($\sigma^2\pi^2n^2$) ground state was determined at the calculated MP2 level. The excited states studied include all those generated through single excitations from the σ, π and n MOs into the vertical π^*, σ^* and 4s, 4p Rydberg species. The lowest-lying states are $^3(n\pi^*)$ and $^3(\pi\pi^*)$, in the range from 2.72 to 4.55 eV above the ground state. Four allowed transitions lie in the energy range from 4.55 to 6.15 eV, namely $^1A_1(\pi\pi^*)$, $^1B_2(n\sigma^*)$, $^2B_1(\sigma\pi^*)$ and $^1B_2(n4s)$. The 0–0 origin for the strong absorption $X^1A_1 \rightarrow {}^1A_1(\pi\pi^*)$ is expected near 3.0 eV. Excitations into σ^* lie below transitions into the first 4s Rydberg species. The adiabatic ionization potentials (in eV) are 9.08 (X^2B_2, $n \rightarrow \infty$) and 9.84 ($^2B_1$, $n \rightarrow \infty$). The ground state of H_2SiS is highly polar, with a dipole moment of about 3.18 D ($H_2Si^+S^-$). A comparison of the vertical spectrum of H_2SiS with those of H_2CO, H_2CS and H_2SiO indicates a general stabilization of the valence electronic transitions relative to those of Rydberg character as C is replaced by Si.

II. DOUBLE BONDS BETWEEN SILICON AND GROUP 16 ELEMENTS

A. Introduction

Great advances have been made in recent years in studies of multiple bonding to silicon, and by 1990 we witnessed a wealth of excellent work on the isolation of stable compounds having Si double bonds where X belongs to group 14 or 15, i.e. silenes ($R_2Si{=}CR_2$)[1,8a,11], disilenes ($R_2Si{=}SiR_2$)[2,8b,12], silanimines ($R_2Si{=}NR$)[5,11] and phosphasilenes ($R_2Si{=}PR$)[6]. The kinetic stability of all these compounds depended on the presence of four or at least three bulky substituents [e.g. mesityl (Mes = 2,4,6-trimethylphenyl), 2,4,6-triisopropylphenyl (Tip), 2,4,6-tri-*t*-butylphenyl, *t*-butyl, adamantyl, trialkylsilyl, etc.). In contrast to these doubly-bonded species between silicon and group 14 or 15 elements which can be sterically protected by bulky substituents from both ends of the double bond, no kinetically stabilized silanones and silanethiones have been isolated, except in rigid matrices, until the recent successful isolation of a stable silanethione Tbt(Tip)Si=S {**4;** Tbt = 2,4,6-tris[bis(trimethylsilyl)methyl]phenyl}[10]. Since only the silicon atom can be sterically protected by substituents in the cases of silanones and silanethiones, the conventional steric protection groups such as those mentioned above are not large enough to prevent their oligomerization.

Although stable silanones are still unknown at this time, there have recently been several interesting reports on the chemistry of doubly-bonded compounds between silicon and chalcogen atoms. In the following sections, the new findings since 1987 on the generation method and some properties of these silicon–chalcogen doubly-bonded compounds are summarized separately for each chalcogen atom, together with some important reports which were not discussed in the previous reviews[4a,b,c].

B. Silicon–Oxygen Double Bonds (Silanones)

Evidence for the formation of silanones depends on two types of experiments. In the first, silanones are generated as unstable intermediates in reactions, and their formation is inferred from the isolation of trapping products with suitable substrates. The second approach is based on their generation in a low temperature matrix and their characterization by infrared spectroscopy which reveals $\nu_{(Si=O)}$ at *ca* 1200 cm^{-1}. These two groups of experiments are described below.

1. Formation from hydrosilanes

When a mixture of methylsilane (or dimethylsilane) deposited with ozone in an argon matrix at 17 K was photolyzed, the corresponding silanone, MeHSi=O (or $Me_2Si{=}O$), was generated and characterized by their infrared spectra. In the case of the parent silane, H_3SiH, a similar photolytic reaction with ozone in an Ar matrix led to the identification of SiO, $H_2Si{=}O$ (**2**), (HO)HSi=O (silanoic acid) and $(HO)_2Si{=}O$ (silicic acid)[18].

In 1989, Corriu and workers reported the thermal decomposition (85 °C) of the silyl formate **6**, having a remote stabilizing amino group, which was prepared by the insertion reaction of the corresponding pentacoordinated functional silane **5** with CO_2, into formaldehyde and the transient silanone **7** (Scheme 2)[9]. Silanone **7** was found to be trapped with $(Me_2SiO)_3(D_3)$ to give the eight-membered ring compound **8**, while it underwent ready trimerization leading to the formation of **9** in the absence of a trapping reagent.

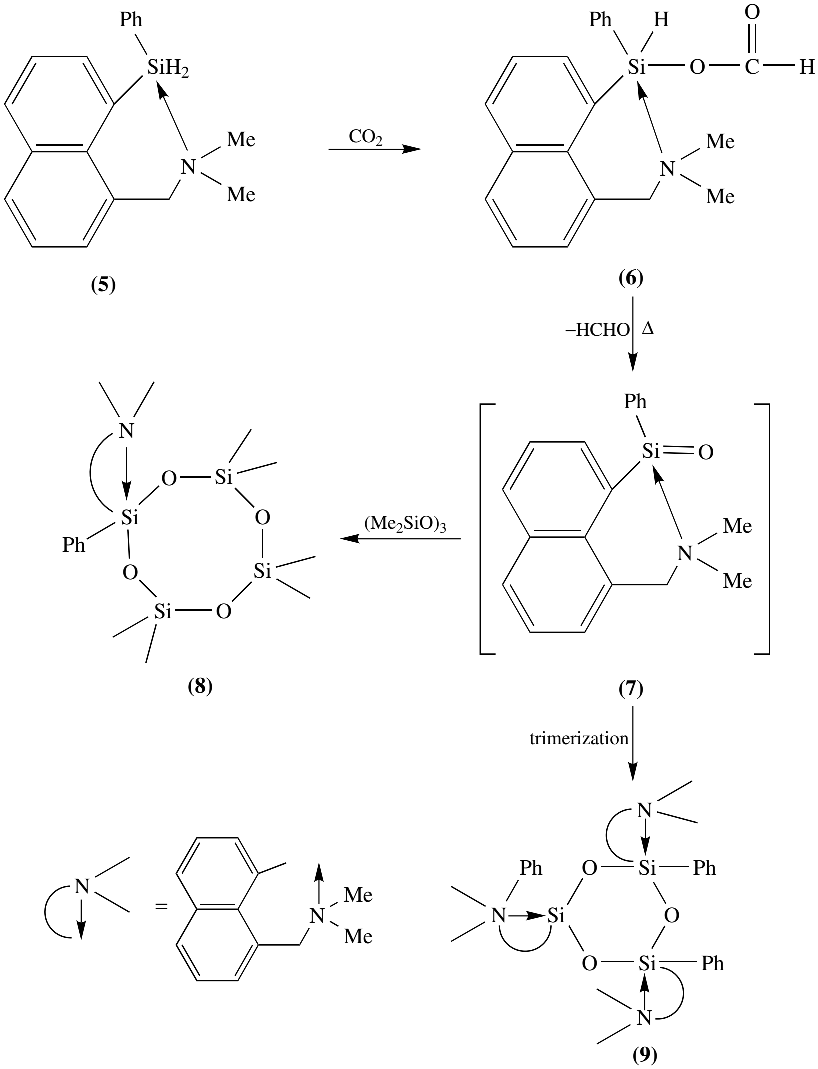

SCHEME 2

2. Formation from cyclic silyl ethers

The silanones $(CH_3)_2Si{=}O$ **(10)** and $(CD_3)_2Si{=}O$ **(11)** have been generated by vacuum pyrolysis of the corresponding 6-oxa-3-silabicyclo[3.1.0]hexanes **12** (Scheme 3)[19−21].

The Diels–Alder adduct **13** of silapyranes with maleic anhydride was also used as an alternative precursor for **10** (Scheme 3)[19]. In the pyrolysis of **12**, a 2-siloxetane intermediate **14** was proposed as a transient precursor leading to dimethylsilanone **10** (or **11**)[19–21].

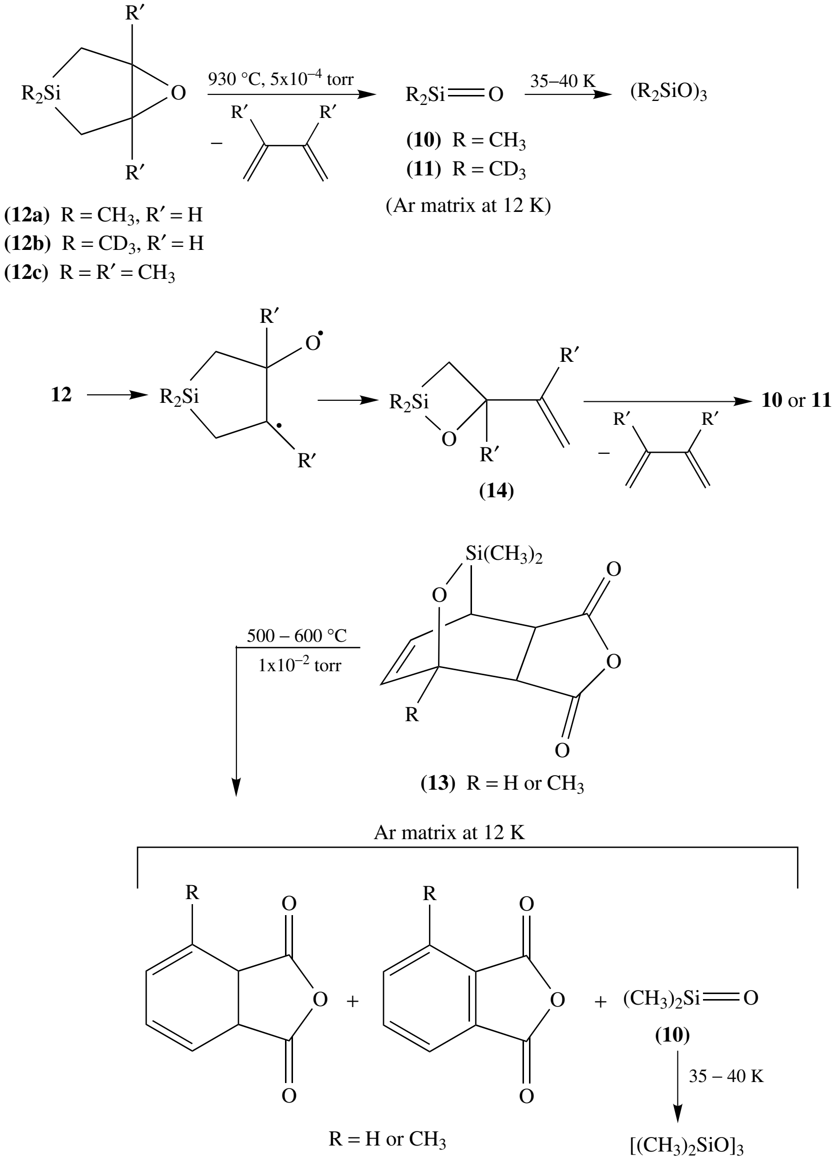

SCHEME 3

Silanones **10** and **11** have also been trapped in argon matrices at 12 K and they were studied by IR spectroscopy[19]. Using the dependence of the spectra on temperature and pressure in the pyrolysis zone or in warming-up experiments (to 35−40 K) the following vibrational bands of silanones have been revealed: 1244, 1240, 1210, 822, 798, 770, 657 cm^{-1} for **10**; 1215, 1032, 1007, 995, 712, 685, 674 cm^{-1} for **11**. The limits of thermal (*ca* 850 °C) and kinetic (5×10^{-4} torr) stability of dimethylsilanone were determined. By comparison of the measured and calculated frequencies the band at 1210 cm^{-1} in **10** (1215 cm^{-1} in **11**) was assigned to the Si=O stretching vibration. The calculated force constant (8.32 mdyn/Å) and bond order (1.45) of the Si=O bond have been presented as evidence for a significant double-bond character in dimethylsilanone.

The tricyclic silyl ether **13** (R = H) also undergoes photochemical fragmentation into dimethylsilanone **10** as shown in Scheme 4[22]. Of the two possible fragmentation mechanisms, the decomposition via a bicyclic intermediate **15** (path B) was preferred by the authors, based on the observed reaction products.

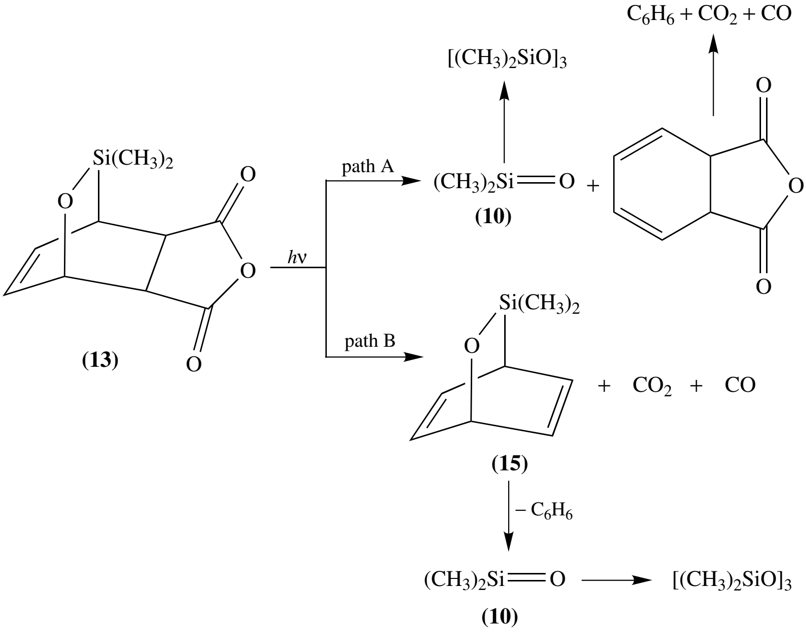

SCHEME 4

3. Formation from allyloxysilane derivatives

It is well known that thermal decomposition of allyl-substituted silanes proceeds by retro-ene reaction with formation of transient species having a Si=C bond, such as silabenzene, silatoluene and dimethylsilaethylene[4b,e]. The kinetic data on the gas-phase pyrolysis of a similar allyloxysilane derivative, (1,1-dimethylallyloxy)dimethylsilane **(16)**, and the results on thermolysis of allyloxydimethylsilane **(17)** in a flow system both indicate the participation of an intermediate silanone, $(CH_3)_2Si{=}O$ **(10)**, as shown in Scheme 5[23].

Allyl(allyloxy)dimethylsilane **(18)** was also proposed by Barton and coworkers as being the source of **10** in gas-phase pyrolysis[24]. It has been suggested that the generation of **10** by pyrolysis of **18** results from consecutive loss of two allyl radicals. 1,5-Hexadiene and cyclosiloxanes **19** (D_3) and **20** (D_4) were the final pyrolysis products of **18** (Scheme 6).

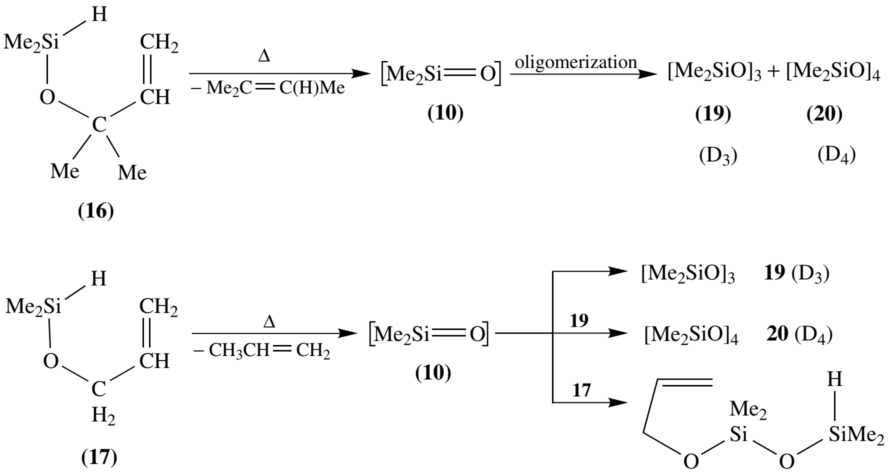

SCHEME 5

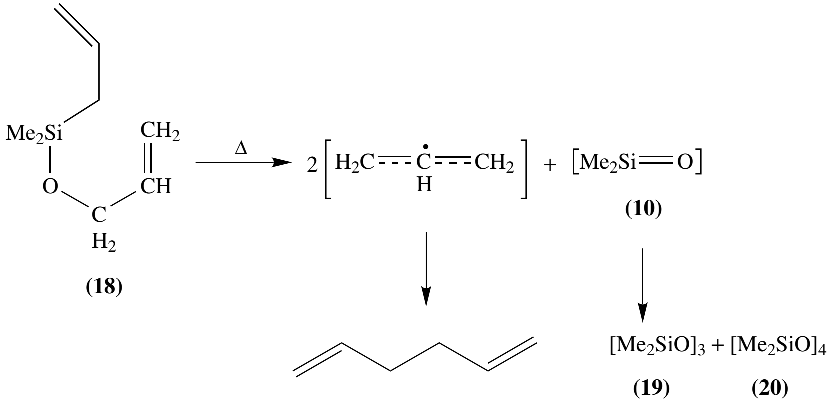

SCHEME 6

In 1989, Nefedov and coworkers have reinvestigated the thermolysis of the above-mentioned allyloxysilane derivatives **16**–**18** and of 2,2,6-trimethyl-2-silapyrane **(21)** using vacuum pyrolysis and matrix isolation techniques[23]. IR spectroscopic studies on the products isolated in the matrices enabled them to probe directly the intermediacy of **10** in these reactions and to discuss its thermal stability. Only in the case of allyloxydimethylsilane **(17)** did they find direct spectroscopic evidence for the formation of **10** by observation of its most intense band at 798 cm^{-1} in the matrix IR spectrum of the pyrolysis products. In all other cases silanone **10** was not detected and it was assumed that it is thermally unstable, undergoing fragmentation into SiO and CH_3 radicals as shown in Schemes 7, 8 and 9 (the species actually observed in the matrix are indicated). In this paper, Nefedov and coworkers have reaffirmed the thermal and kinetic stability of dimethylsilanone **10** in the gas phase, which they had previously described[19].

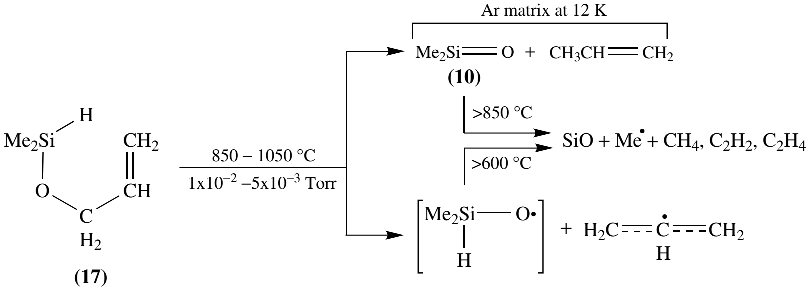

SCHEME 7

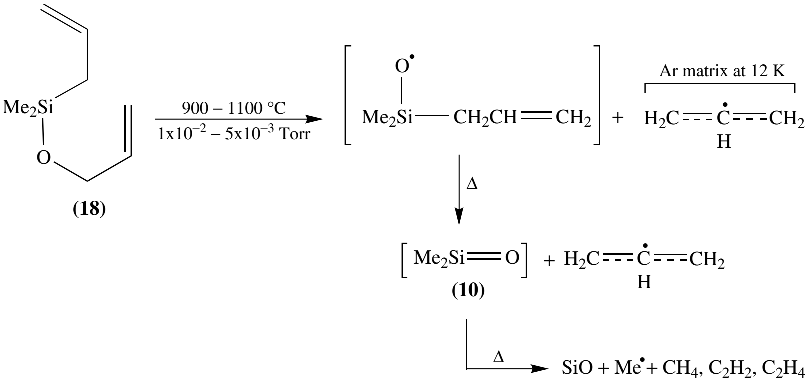

SCHEME 8

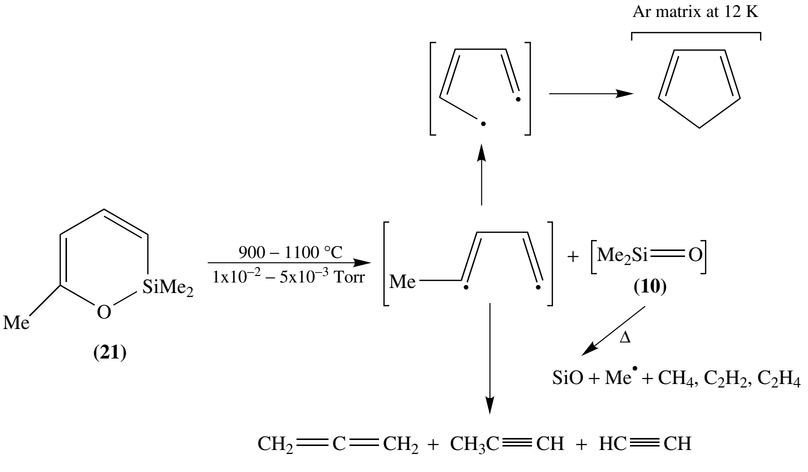

SCHEME 9

4. Formation from silanol derivatives

Eaborn and Stanczyk deduced from kinetic data that under basic conditions silanone **10** can be formed by loss of a proton and a carbanion R^- from the silanols **22** (R = *m*-$ClC_6H_4CH_2$ or PhC≡C) (Scheme 10)[25].

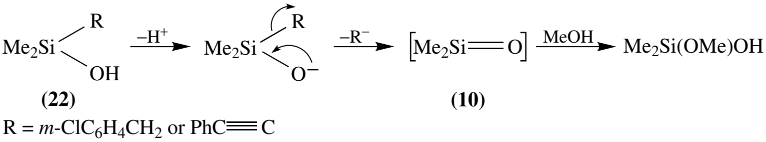

SCHEME 10

Although attempted dehydration of di-*t*-butylsilanediol into di-*t*-butylsilanone gave instead 1,1,3,3-tetra-*t*-butyl-1,3-dihydroxydisiloxane, a similar approach using di-*t*-butylsilanol **(23)** was found to be useful to generate an anion radical of silanone. Thus, while irradiation of a mixture of **23** and di-*t*-butyl peroxide in *t*-butyl alcohol resulted in the observation of an ESR spectrum of the corresponding di-*t*-butylhydroxysilyl radical **(24)**, the photolysis of a solution of **23** in di-*t*-butyl peroxide and *t*-butyl alcohol containing also potassium *t*-butoxide (in excess with respect to the silanol) gave an ESR spectrum assignable to the di-*t*-butylsilanone radical anion **(25)**, which is probably formed principally via the silanolate anion **26** (Scheme 11)[26]. The magnitude of the hyperfine coupling to ^{29}Si in the ESR spectrum of **25** shows that the radical anion is pyramidal at silicon. This approach seems to be particularly promising for the preparation of anion radicals of silanones since silanols are more acidic than the corresponding alcohols (e.g. Me_3SiOH compared with Me_3COH or Ph_3SiOH compared with Ph_3COH)[27] and alkoxy radicals abstract hydrogen from a Si−H bond more readily than from a C−H bond[28].

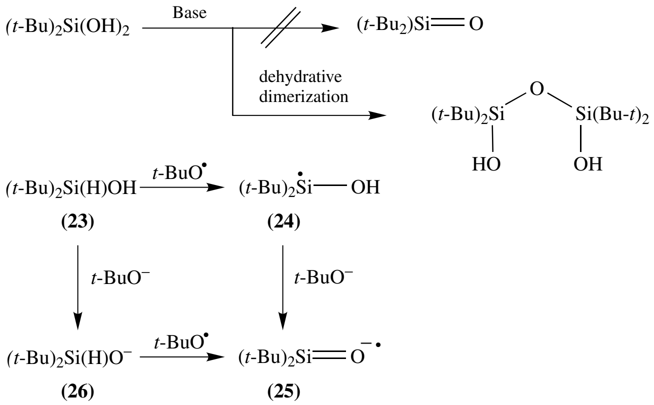

SCHEME 11

Most recently, Milstein and coworkers reported a new type of homogeneous catalytic reaction that generates silanones from secondary silanols under extremely mild conditions. The platinum complex (dmpe)Pt(Me)OTf) **(27)** (dmpe = $Me_2PCH_2CH_2PMe_2$, OTf = OSO_2CF_3 was treated with an equimolar amount of the silanol, (*i*-$Pr)_2SiH(OH)$ **(28)**, in acetone to yield a new dimeric hydrido-bridged complex **29** and the trimer **30** of diisopropylsilanone, **31** (Scheme 12)[29].

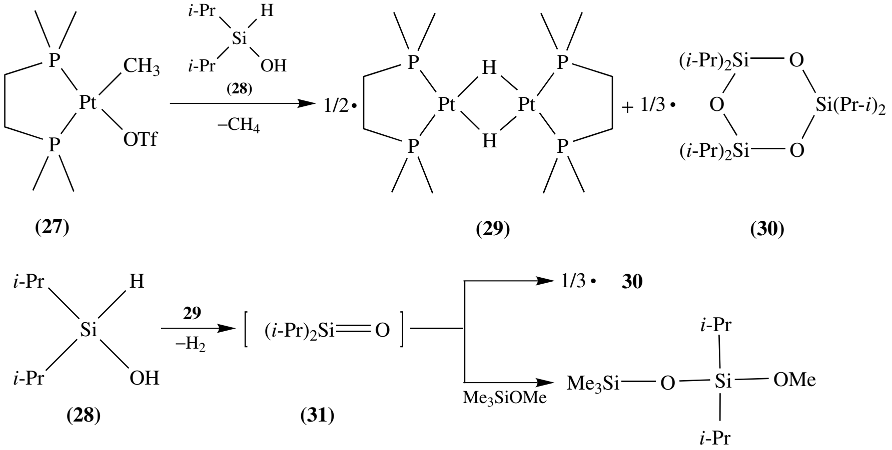

SCHEME 12

The generation of methane in the reaction was evidenced by the ^{1}H NMR spectrum of the reaction mixture. It was also shown that the newly obtained complex **29** reacts catalytically with silanol **28** to give the trimer **30** (presumably from trimerization of **31**) with the evolution of hydrogen gas. In the presence of Me_3SiOMe the same reaction resulted in the formation of an insertion product of the intermediate silanone **31** as shown in the lower part of Scheme 12. The proposed catalytic cycle for the dehydrogenation of **28** with **29** is shown in Scheme 13. It should be noted, however, that spectroscopic evidence for the proposed silanones was not presented.

Although no intermediates except for **29** are detected by NMR with **28** as a substrate, the use of bulkier di-*t*-butylsilanol **32** as a starting material allowed the authors to isolate and fully characterize by spectroscopy and X-ray crystallography the corresponding platinum–silanol complex **33**, which strongly suggested the intermediacy of **33** in this catalytic reaction as shown in Scheme 13. This reaction is formally analogous to (although mechanistically different from) the well-known catalytic dehydrogenation of alcohols[30] that leads to ketones.

5. Formation from silylenes

The oxidation of silylenes (silandiyls) by oxygen transfer reagents such as dimethyl sulfoxide[31], tertiary amine *N*-oxides[31] or epoxides[32] in the presence of trapping agents usually yields products, whose formation may be explained in terms of the capture of initially generated silanones. In those cases oligomerization products are usually obtained in the absence of trapping reagents, although in low yields. As mentioned in the previous reviews, unstable silanones are frequently postulated as intermediates in these reactions, but the involvement of free silanones in these oxidation reactions is still questionable[4e]. On the other hand, when silylenes are treated with oxidants such as N_2O[33] or O_2[34] in argon matrices, the formation of silanones as the oxidation products of silylenes was unambiguously demonstrated by IR spectroscopy.

Most recently, Belzner and coworkers reported a new type of oxygen transfer reaction from isocyanates to bis[2-(dimethylaminomethyl)phenyl]silylene (**35**)[35], which was thermally generated from the corresponding cyclotrisilane **34**[36], and they were able to obtain some convincing results that support the involvement of silanone **36** as an intermediate[37].

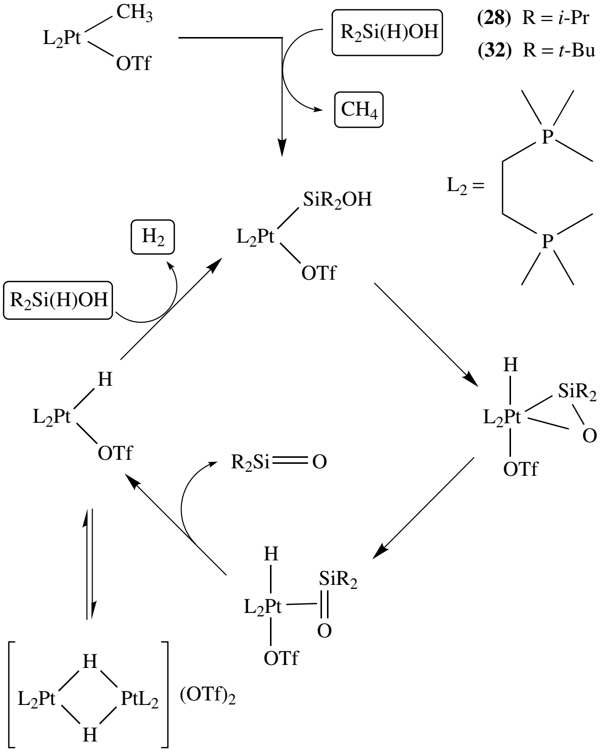

SCHEME 13

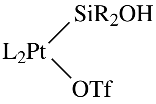

(33) R = *t*-Bu

When a toluene solution of a mixture of cyclotrisilane **34** and cyclohexyl isocyanate (or *t*-butyl isocyante) was heated at 70 °C, cyclic di- and trisiloxanes **37** and **38**, i.e. the cyclic dimer and trimer of the silanone **36**, were obtained together with the corresponding isonitrile RN=C. The formation of **37** as well as **38** was completely suppressed in the presence of hexamethylcyclotrisiloxane (**19**; D_3); instead, quantitative conversion of **35** into **39**, the formal insertion product of the silanone **36** into the Si−O bond of D_3, occurred (Scheme 14). Since neither cyclodisiloxane **37** nor cyclotrisiloxane **38** reacted with D_3 under the reaction conditions, the possibility that **37** or **38** is the precursor of **39** was ruled out. Whereas the oxidation of **35** with cyclohexyl and *t*-butyl isocyanates proceeded with exclusive formation of **37** and **38** (as the silicon-containing compounds) the reaction of **35** with phenyl isocyanate resulted in the formation of **37** in low yield. Furthermore, in this case the presence of D_3 did not totally suppress the formation of **37**. According to the authors, these results indicate that the oxidation of **35** with cyclohexyl and *t*-butyl isocyanates appears to use other reaction channels than that with phenyl isocyanate.

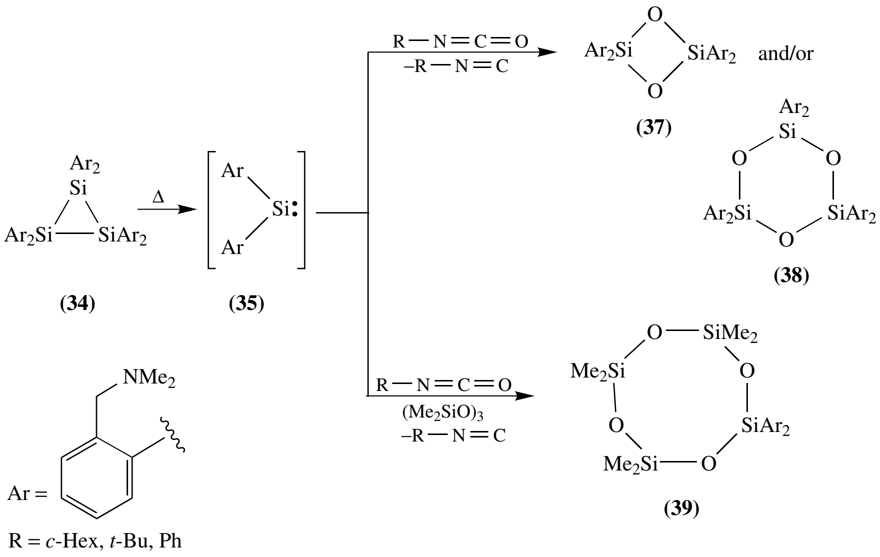

SCHEME 14

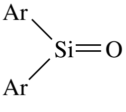

(36)

The reaction of **34** with isocyanates thus takes a different course from the photolysis of hexa-*t*-butylcyclotrisilane in the presence of tri-*t*-butylsilyl isocyanate, which was reported by Weidenbruch and coworkers to yield the five-membered ring product **40** (Scheme 15)[38].

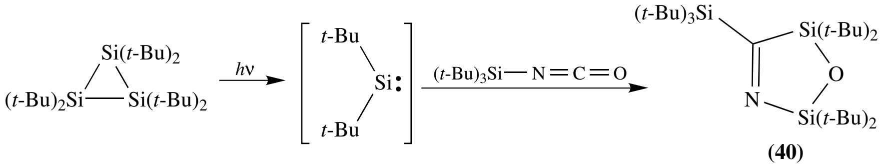

SCHEME 15

The formation of the cyclic siloxanes **37** and **38** from cyclotrisilane **34** and isocyanates is most likely explained by the oligomerization of an intermediate silanone **36**. This is further supported by the fact that the product ratio in this reaction is considerably affected by the concentration of the starting material. A high concentration of **36** favors trimerization to **38**, whereas in dilute solutions the dimerization product **37** is formed preferentially. The latter reaction is surprising in view of the fact that only one silanone bearing a very bulky 2,4,6-triisopropylphenyl substituent was reported to undergo dimerization[39]; less hindered silanones are known to form cyclic trimers and tetramers[4e,40]. The reason for this different behavior might be due to the fact that silanone **36** is electronically stabilized by intramolecular coordination with the nitrogen functionalities, which was confirmed by the X-ray structural analysis of the cyclic dimer **37**. The authors proposed various pathways to silanone **36** as a crucial intermediate in the oxidation of silylene **35** by isocyanates as shown in Scheme 16.

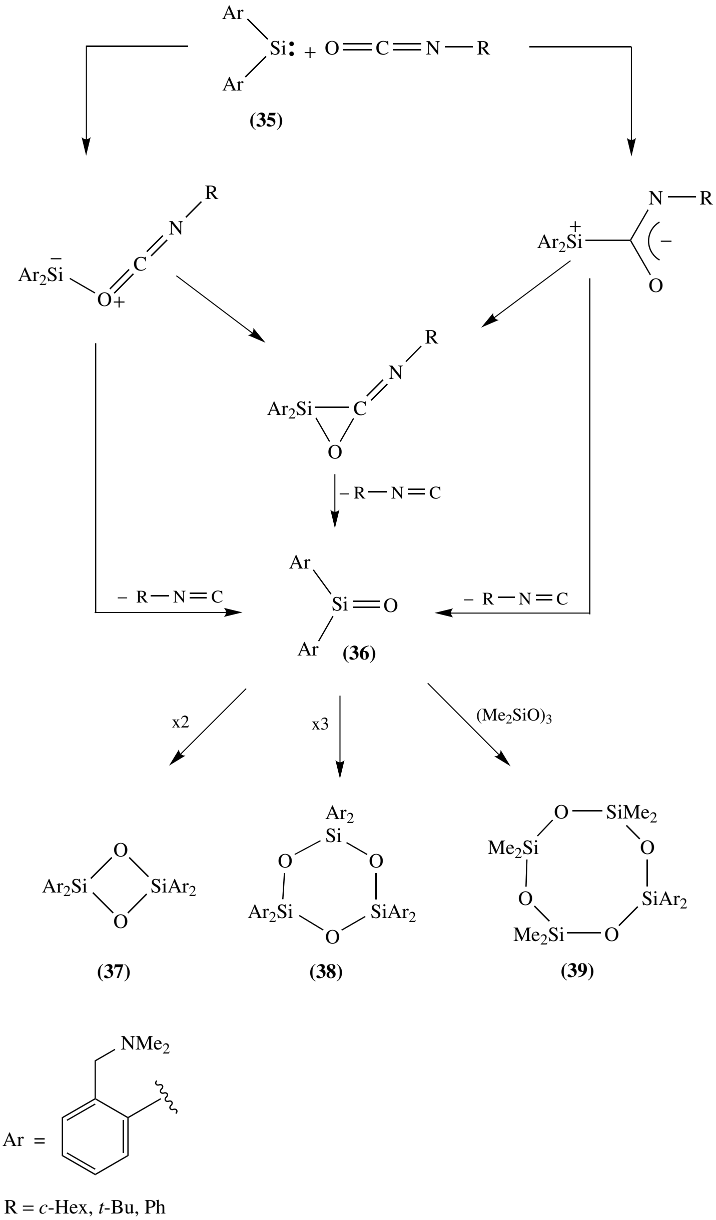

SCHEME 16

Oxygen transfer reactions were also examined by Jutzi and coworkers[41] for the nucleophilic decamethylsilicocene **41**. Silicocene **41** reacts with carbon dioxide under mild conditions to give two types of products, **46** and **47**, depending on the solvent used, as shown in Scheme 17.

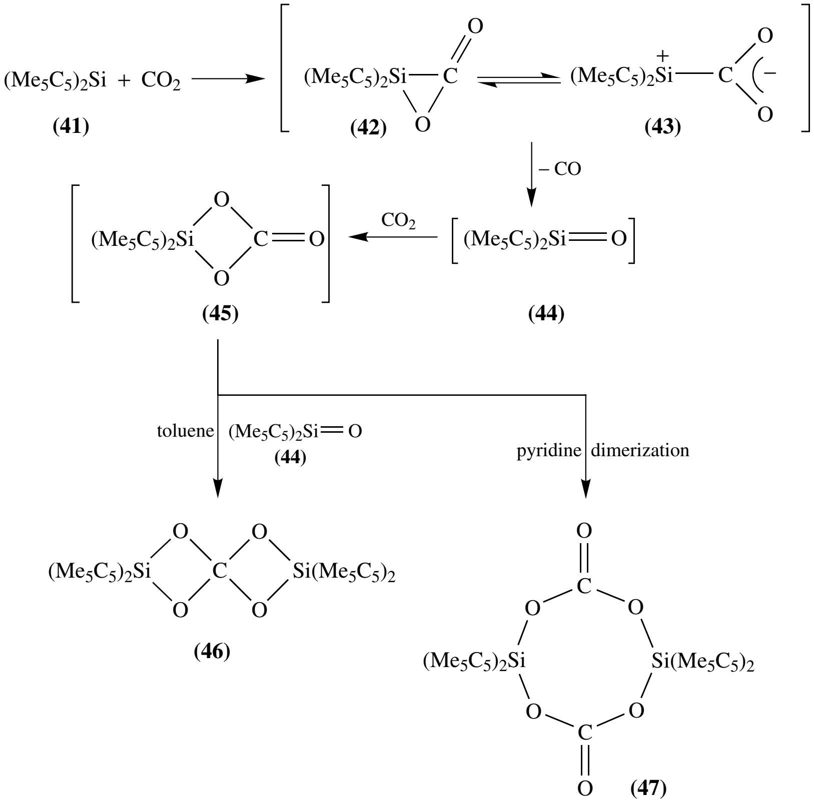

SCHEME 17

In these reactions the formal oxidation state of the silicon atom changes from +2 in **41** to +4 in the final products, and hapticity of the pentamethylcyclopentadienyl ligands changes from η^5 to η^1. The authors propose that the first intermediate is a highly reactive [2 + 1] cycloaddition product **42** or its ring-opened isomer **43**, which easily loses carbon monoxide to give the silanone intermediate **44**. The silanone **44** is not stable under the reaction conditions and is transformed by excess CO_2 to the [2+2] cycloaddition product **45**. In toluene as solvent, **45** reacts with the silanone **44** present in the reaction mixture to give the final product **46** in a further [2+2] cycloaddition step. In pyridine as solvent, the intermediate silanone **44** is deactivated by coordination to the solvent, and hence **45** does not react with **44** but forms the dimerization product after ring-opening of one of the Si–O bonds. The intermediacy of the silanone **44** was further supported by trapping reactions. In the presence of *t*-butyl methyl ketone or acetone, the addition products **48** or **49** were formed as expected if the silanone **44** undergoes an ene-type reaction[42] (Scheme 18).

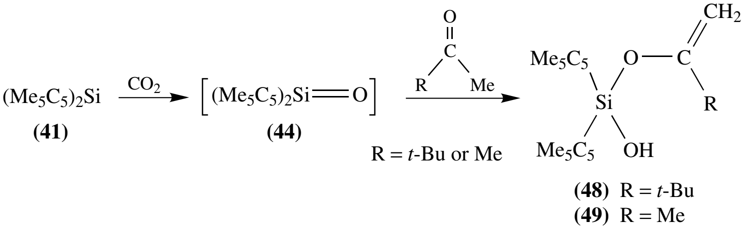

SCHEME 18

6. Formation from silenes and silicon–heteroatom double-bond compounds

Although silenes were long believed to undergo [2 + 2] cycloaddition reaction with carbonyl compounds to form the four-membered 2-siloxetane rings, only the products of retro-cleavage of the siloxetane ring, i.e. an alkene and oligomers of a silanone $R_2Si{=}O$ (presumed to be formed from individual silanone product molecules), were observed in most cases (Scheme 19)[4e,43].

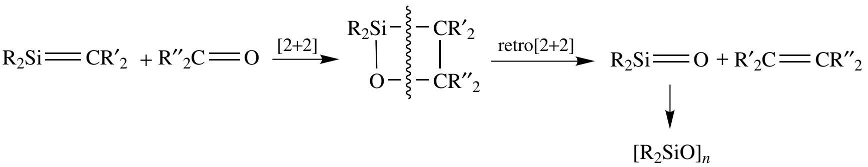

SCHEME 19

Bachrach and Streitwieser studied theoretically at the SCF level the cycloaddition of formaldehyde to the parent silanone ($H_2Si{=}O$)[44]. They found that the [2+2] cycloaddition reaction to form siloxetane is exothermic by about 80 kcal mol^{-1}, but that the further fragmentation of the siloxetane to ethylene and silanone is endothermic by *ca* 50 kcal mol^{-1}, an energy which is too large to be consistent with a spontaneous unimolecular retro-[2+2] cycloreversion process. Therefore, a free silanone is probably not involved as an intermediate in the thermal decomposition of a siloxetane, and bimolecular reactions between two siloxetanes are an energetically more feasible way to account for the experimentally obtained alkenes and silanone oligomers. This theoretical suggestion was experimentally supported by Brook and coworkers by a kinetic investigation of the thermolysis of a stable siloxetane obtained from $(Me_3Si)_2Si{=}C(OSiMe_3)(Ad\text{-}1)$ and benzophenone[45].

The reaction of a silene with molecular oxygen followed by the retro-[2+2] cylcoreversion with oxygen–oxygen bond cleavage seems to be another promising way to generate a silanone. The pyrolysis of 1,1-dimethylsilacylcobutane **(50)**, which would lead to the formation of the unstable 1,1-dimethylsilene **(51)**, gave in the presence of oxygen several oligomers of dimethylsilanone **10** among the products, indicating according to the authors the intermediacy of **10**, which was produced by a retro-[2 + 2] reaction of the dioxasiletane **52** (Scheme 20)[46]. The reaction of the stable silene $(Me_3Si)_2Si{=}C(OSiMe_3)(Ad\text{-}1)$ **(53)** with oxygen was also examined and it was found to give a carboxylic acid silyl ester **(55)** and a cyclic trimer **(56)** of the silanone $(Me_3Si)_2Si{=}O$ **(54)** (Scheme 21)[47]. The mechanism of these reactions has not been fully investigated.

Driess and Pritzkow have recently succeeded in the synthesis and isolation of a stable silicon–arsenic double-bond compound **(57)**, the first stable arsasilene (arsanilidenesilane)[7a]. The arsasilene **57** was found to undergo a ready [2 + 2],

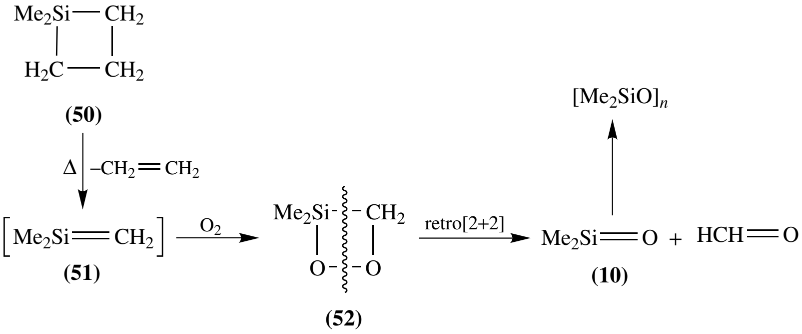

SCHEME 20

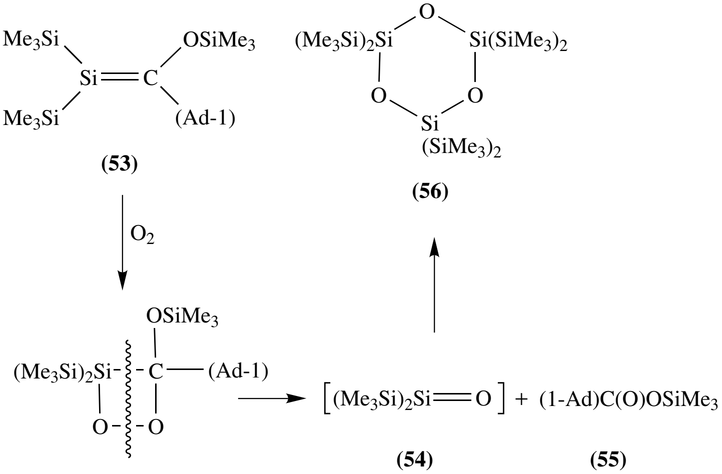

SCHEME 21

cycloaddition reaction with benzophenone to give the four-membered ring product **58** as a stable crystalline compound. As in the case of above-mentioned siloxetanes, the arsenic-containing siloxetane **58** was found to decompose thermally under drastic conditions (160 °C, 10 h) to give the cyclic dimer **(62)** of a silanone, $Tip_2Si{=}O$ **(59)**, together with the arsaalkenes **60** and **61** (Scheme 22)[7a].

As previously mentioned (see Section II.B.5), the formation of the dioxadisiletane **62** should be noted as the first example of a dimerization of a silanone, in contrast to the common trimerization or tetramerization of less hindered silanones. This metathetical reaction of arsasilene **57** with benzophenone represents a new approach to arsaalkenes via arsasilenes by means of a pseudo-Wittig reaction. More recently, Driess and coworkers reported the similar sila-Wittig-type reaction via the phosphorus analogue **64** of the above-mentioned arsenic-containing siloxetane **58**[48]. Thus, the [2 + 2] cycloadduct **(64)** of phosphasilene **(63)** with benzophenone afforded, upon heating at 160 °C for 2 days, the dioxadisiletane **62** along with two phosphaalkenes **65** and **66**, suggesting the intermediacy of silanone **59** (Scheme 22)[48].

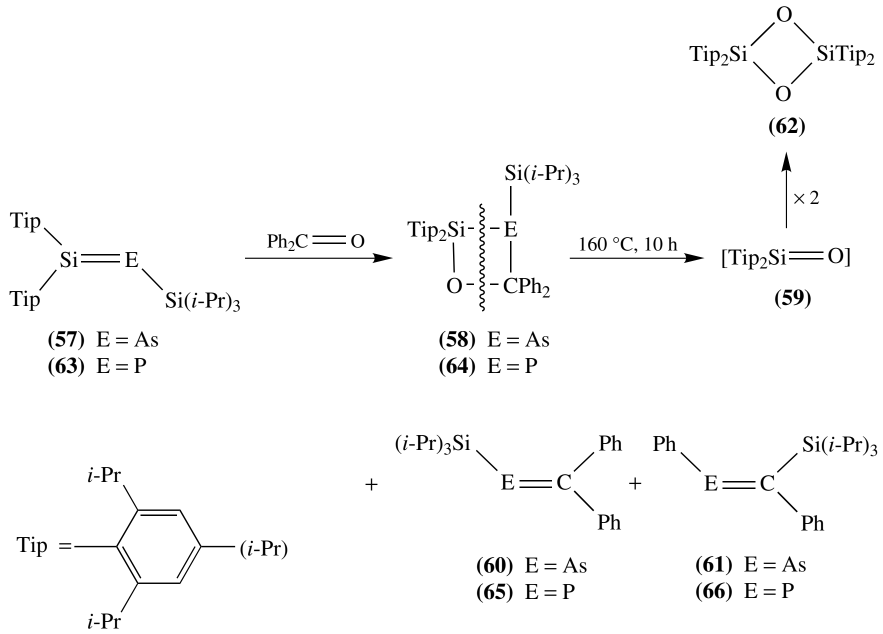

SCHEME 22

Kudo and Nagase have reported a theoretical *ab initio* investigation at both HF/3-21G and HF/6-31G* on the potential energy surface for the dimerization of $H_2Si{=}O$ **(2)**, revealing that this reaction proceeds with no barrier to yield the cyclic dimer $(H_2SiO)_2$ by a stepwise formation of two new bonds[49]. They have also discussed the structures and stability of the cyclic trimer $(H_2SiO)_3$ and tetramer $(H_2SiO)_4$, and calculated that the disproportionation for the reaction $3(H_2SiO)_2 \rightarrow 2(H_2SiO)_3$ is exothermic by $-110\ \mathrm{kcal\,mol^{-1}}$ at HF/6-31G*//3-21G. This very high negative value clearly favors the trimer over the dimer. Furthermore, the insertion of $H_2Si{=}O$ into the Si−O bond of the dimer $(H_2SiO)_2$, i.e. $(H_2SiO)_2 + H_2Si{=}O \rightarrow (H_2SiO)_3$, is calculated to be exothermic by $117.3\ \mathrm{kcal\,mol^{-1}}$ (HF/6-31G*//3-21G). These high exothermicities suggest that the ring expansion proceeds rapidly with no significant barrier. Similar calculations revealed that the energy released upon going from $4(H_2SiO)_3$ to $3(H_2SiO)_4$ is $74.2\ \mathrm{kcal\,mol^{-1}}$ (HF/3-21G level). This energy is by $88.1\ \mathrm{kcal\,mol^{-1}}$ smaller than that for $3(H_2SiO)_2 \rightarrow 2(H_2SiO)_3$, suggesting that the formation of the tetramer is less favorable than the formation of the trimer. However, tetramerization is likely to occur readily, as expected from the fact that the reactions $(H_2SiO)_3 + H_2Si{=}O \rightarrow (H_2SiO)_4$ and $(H_2SiO)_2 + (H_2SiO)_2 \rightarrow (H_2SiO)_4$ are calculated to be exothermic by 120.8 and $132.9\ \mathrm{kcal\,mol^{-1}}$, respectively, at the HF/3-21G level. To the extent that the difference in the exothermicities is meaningful, the tetramer may be produced more favorably by the reaction of two dimers than by the insertion of $H_2Si{=}O$ into the Si−O bond of the trimer[49]. The electronically stabilized silanone **7** (see also Section II.B.1) was postulated as an intermediate in the oxidation by air of the corresponding silanethione **67** (the synthesis of which will be described in the following section) (Scheme 23)[9]. The fast oxidation of **67** resulted in the formation of the same cyclic trimer **9** as previously mentioned.

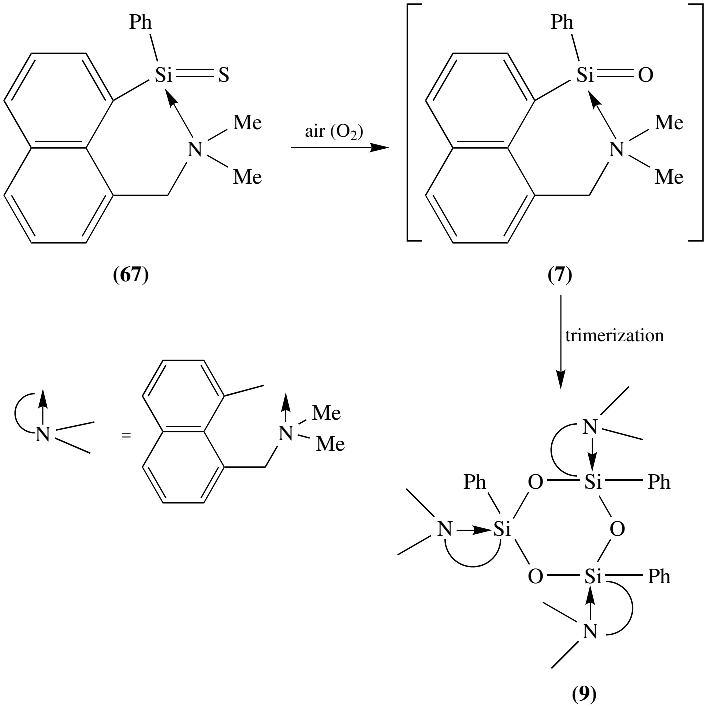

SCHEME 23

C. Silicon–Sulfur Double Bonds (Silanethiones)

Among the silicon–chalcogen double-bond compounds, the silicon–sulfur doubly-bonded compounds (silanethiones) are considered to be easier to synthesize, since it has been predicted by the theoretical calculations that a silicon–sulfur double bond is thermodynamically and kinetically more stable than a silicon–oxygen double bond (silanone)[13,14]. According to the calculations, the lower polarization of $Si{=}S$ compared to $Si{=}O$ should lead to a lower reactivity of $Si{=}S$. In addition, $H_2Si{=}S$ (**1**) is calculated to be by 8.9 kcal mol^{-1} more stable than its divalent isomer, H(HS)Si**:**, whereas $H_2Si{=}O$ (**2**) is by 2.4 kcal mol^{-1} less stable than H(HO)Si**:**.

As described in the preceding reviews on this field, most of the early work on silicon–sulfur doubly-bonded compounds was restricted to simple dialkylsilanethiones, which are all transient in solution or in the gas phase[4]. However, in contrast to the successful matrix isolation and spectroscopic identification of dimethylsilanone **10**[23], no spectroscopic detection of transient dialkylsilanethiones in matrices has been reported up to now, although the matrix isolation of $Cl_2Si{=}S$[50] and $Cl(H)Si{=}S$[51], the silicon analogues of thiophosgene and thioformyl chloride, has been reported.

In recent years, however, impressive progress has been made in the field of silicon– sulfur double-bond chemistry; the first examples of kinetically stabilized and electronically stabilized silanethiones were successfully synthesized and fully characterized by spectroscopic and X-ray crystallographic data[9,10]. These results together with the theoretical studies have revealed the intrinsic nature of this unique double bond to silicon.

The following sections review recent progress in the chemistry of silanethiones.

1. Formation from hydrosilanes

In 1980, Weidenbruch and coworkers reported the formation of 1,1,3,3-tetraalkyl-1,3,2,4-disiladithietanes **70**, i.e. the formal head-to-tail dimers of dialkylsilanethiones **69**, in the copyrolysis of the corresponding 1,1,2,2-tetraalkyldisilanes **68** with elemental sulfur (Scheme 24)[52]. Minor isolated products in these reactions were 1,1,3-trialkyl-1,3,2,4-disiladithietanes **71**, the formation of which was interpreted in terms of the elimination of R_3SiH from the substrates leading to the generation of R(H)Si**:** under the reaction conditions used (Scheme 24). The reaction of R(H)Si**:** with sulfur, followed by the [2 + 2] cycloaddition of the resulting R(H)Si=S **72** with the major intermediate $R_2Si{=}S$ **69** gives rise to the unusual minor reaction products **71** (Scheme 24).

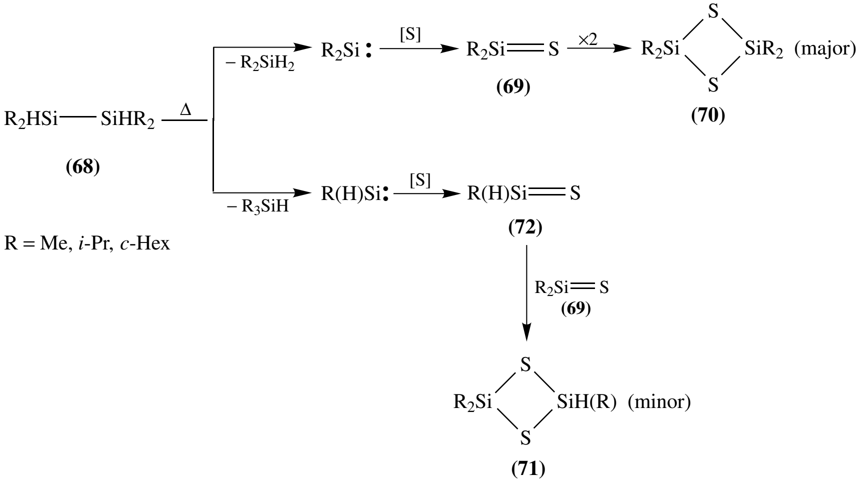

SCHEME 24

In 1989, Corriu and coworkers reported the first synthesis of an isolable silanethione **67** (although internally coordinated) by the reactions of the pentacoordinated functionalized silane **5** (see also Section II.B.1) with carbon disulfide or elemental sulfur (Scheme 25)[9].

In contrast to the fast trimerization of the silanone **7** having the same ligands, silanethione **67** was found to be relatively long-lived in solution ($t_{1/2}$: 3d in $CDCl_3$ at 25 °C) as a monomeric species, though extreme precautions must be taken to avoid exposure to minute amounts of air. Silanethione **67** shows a ^{29}Si chemical shift at $\delta + 22.3$ ppm, suggesting a strong intramolecular coordination with the nitrogen atom. The coordinated silanethione **67** showed unexpectedly low reactivity toward electrophiles and nucleophiles. Thus phosphanes, phosphites, ketones, epoxides, methyl iodide and hydrogen chloride are unreactive, as are alkoxysilanes, siloxanes and hydrosilanes. Only when **67** was treated with a large excess of methanol was the corresponding dimethoxysilane **73** produced (Scheme 26). Hydrolysis and oxidation lead to the silanone trimer **9**.

Crystallographic structural analysis of the coordinated silanethione was established with the more bulky silanethione **74** having a 1-naphthyl group replacing the phenyl group in **67**[9]. Figure 3 shows a schematic drawing of the molecular structure of **74** with some selected bond lengths.

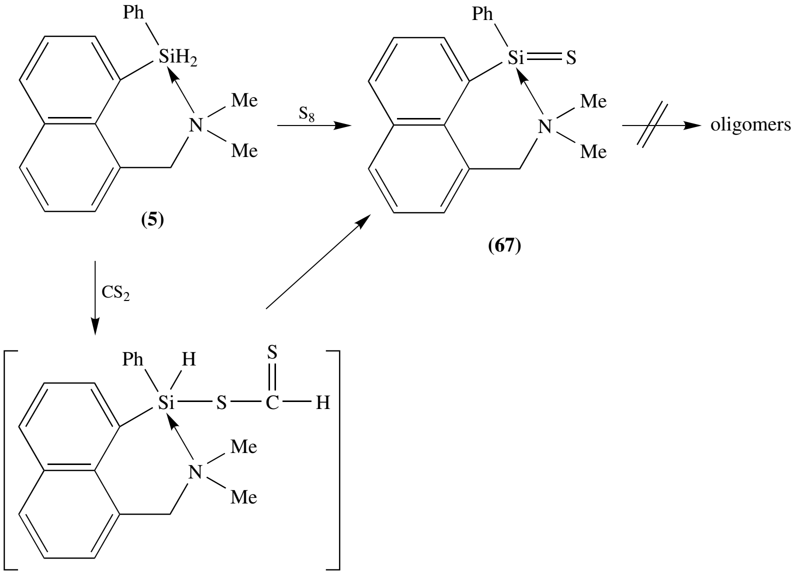

SCHEME 25

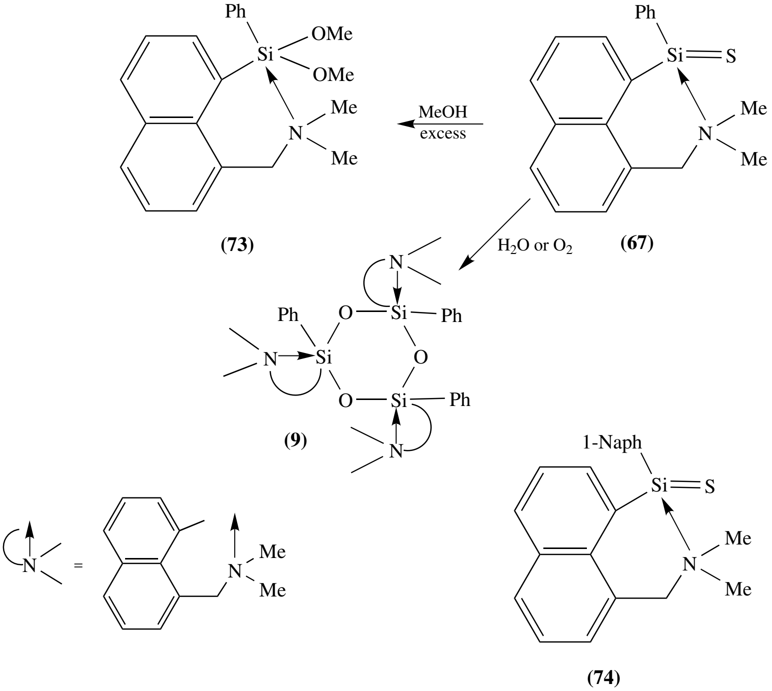

SCHEME 26

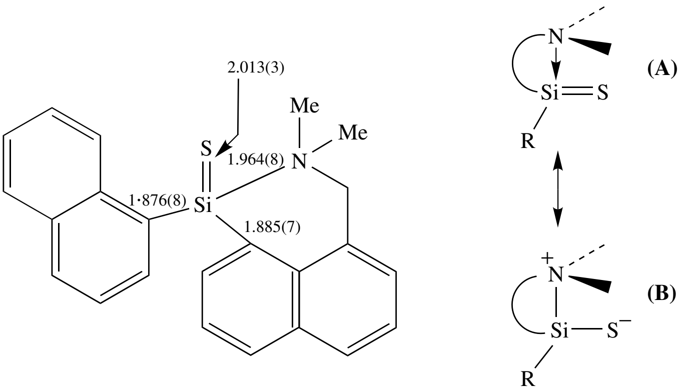

FIGURE 3. Molecular structure of silanethione **74** with selected bond lengths (Å)[9]

Although the Si−S bond (2.013 Å) in **74** is shorter than a typical Si−S single bond (2.13–2.16 Å)[53] suggesting its double-bond character to some extent, it is still 0.07 Å longer than the calculated value for the parent silanethione $H_2Si=S$ (**1**) (Section I.B.1). The Si−N distance (1.964 Å), which is only slightly longer than a Si−N σ bond (1.79 Å), supports a very strong coordination of the nitrogen atom of the dimethylaminomethyl group to the central silicon atom, which in turn makes the silathiocarbonyl unit of **74** considerably deviating from the ideal trigonal planar geometry around silicon; i.e. the sum of the angles around the central silicon atom is 344.9°. The authors concluded that the resonance betaine structure **B** (see Figure 3) contributes strongly to the electronic structure of the internally coordinated silanethiones **67** and **74**[9].

2. Formation from diaminosilanes

Corriu and coworkers also described an alternative synthetic method for internally coordinated silanethiones starting from pentacoordinated diaminosilanes. As shown in Scheme 27, the pentacoordinated diaminosilanes **75** are allowed to react with sulfur-containing heterocumulenes such as carbon disulfide or phenyl isothiocyanate to give the corresponding insertion products **76**, which undergoes thermal decomposition to produce the corresponding silanethiones **67**, **77** and **78**[54].

The silanethiones generated by these reactions were not isolated but their characteristic ^{29}Si NMR chemical shifts were reported to be +22.3, +34.2 and +41.1 ppm ($CDCl_3$) for **67**, **77** and **78**, respectively. The ^{29}Si chemical shift values of **77** and **78** are similar to those observed for **67** and **74** and therefore are indicative of their intramolecularly coordinated betaine structure.

3. Formation from silylenes

In analogy to silanone **36**, the reaction of the silylene, bis[2-(dimethylaminomethyl)phenyl]silanediyl (**35**), with phenyl isothiocyanate was examined (see Section II.B.5)[37]. In this reaction the expected silanethione **79** was obtained as a single product (Scheme 28), even in the presence of D_3 no insertion product of **79** into a Si−O bond of D_3 was observed, as shown by mass spectrometry and elemental analysis.

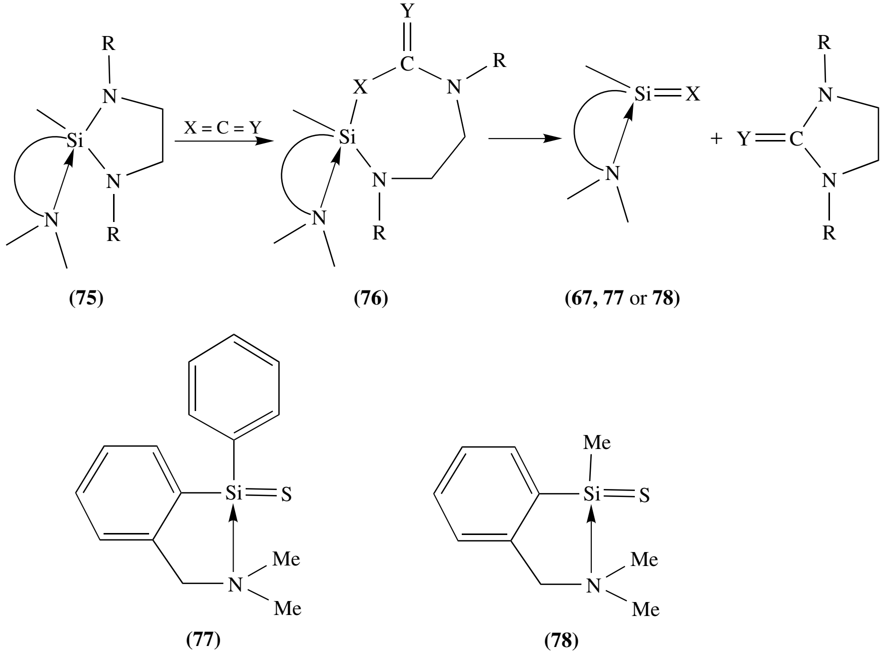

SCHEME 27

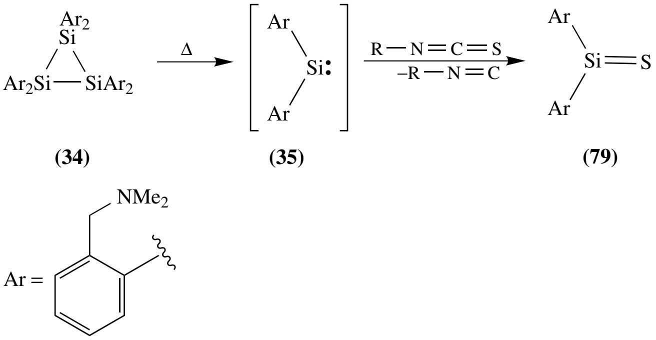

SCHEME 28

Silanethione **79** showed a characteristic ^{29}Si NMR chemical shift at $\delta - 21.0$, which is apparently upfield shifted from that reported recently for the noncoordinated silanethione **4** ($\delta + 166.56$ ppm), and is also at a significantly higher field than those of the tetracoordinated silanethiones **67**, **77** and **78** mentioned above. Accordingly, the silicon center of **79** is assumed to be pentacoordinated due to its intramolecular interaction with the two available terminal amino groups attached to the aryl substituents. This type of twofold coordination of the nucleophilic side arm of the 2-(dimethylaminomethyl)phenyl substituent to a coordinatively unsaturated silicon center has been shown to be also effective in thermodynamically stabilizing silicenium ions[55]. Although it was reported that silanethione **79** can be isolated as a white powder [mp 215 °C (dec)], there was no description of its reactivity or crystallographic structural analysis.

In analogy to the reaction of decamethylsilicocene **41** with carbon dioxide leading to the generation of intermediary silanone **44,** silicocene **41** was allowed to react with carbon oxysulfide under very mild conditions (−78 °C/toluene) to give the corresponding 1,3,2,4-dithiadisiletane derivative **81**, a formal head-to-tail [2 + 2] cycloaddition reaction product of the initially formed silanethione **80** (Scheme 29)^{41b}.

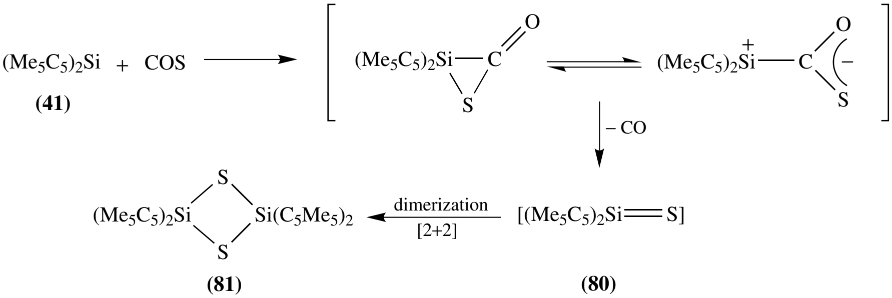

SCHEME 29

Silanethione **80** was also postulated as an intermediate in the reaction of silicocene **41** with isothiocyanates (room temperature/toluene/16 h for methyl isothiocyanate and 65 °C/toluene/5 h for phenyl isothiocyanate), which resulted in the formation of the corresponding intermolecular [2 + 2] cycloadducts (**82** and **83**) of **80** with the isothiocyanates (Scheme 30)^{41a,b}. Under even more drastic conditions (100 °C/toluene/20 h), the reaction of **41** with phenyl isothiocyanate gave the five-membered heterocycles **84**, which is most likely produced by a second attack of the silicocene **41** on the initially formed [2 + 2] cycloadduct **83** (Scheme 30).

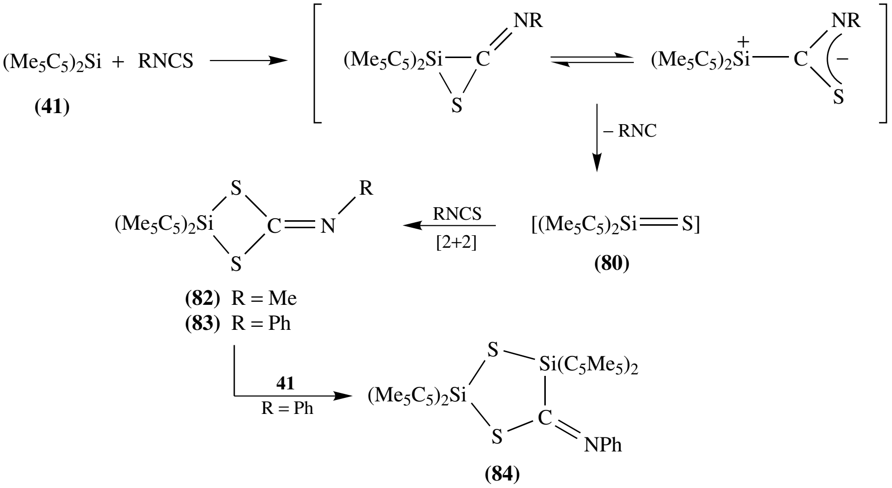

SCHEME 30

In contrast, the reaction of silicocene **41** with carbon disulfide did not give the reaction products derived from the expected silanethione **80**; instead a surprising multistep reaction product **89** was isolated (Scheme 31)[41b]. In the preliminary communication[41a], the authors misinterpreted the structure of this reaction product as being a simple dimer **90** of the initial intermediate, thiasiliranethione **85**, but the X-ray crystallographic analysis later revealed that **89** is the actual product, as shown in Scheme 31[41b].

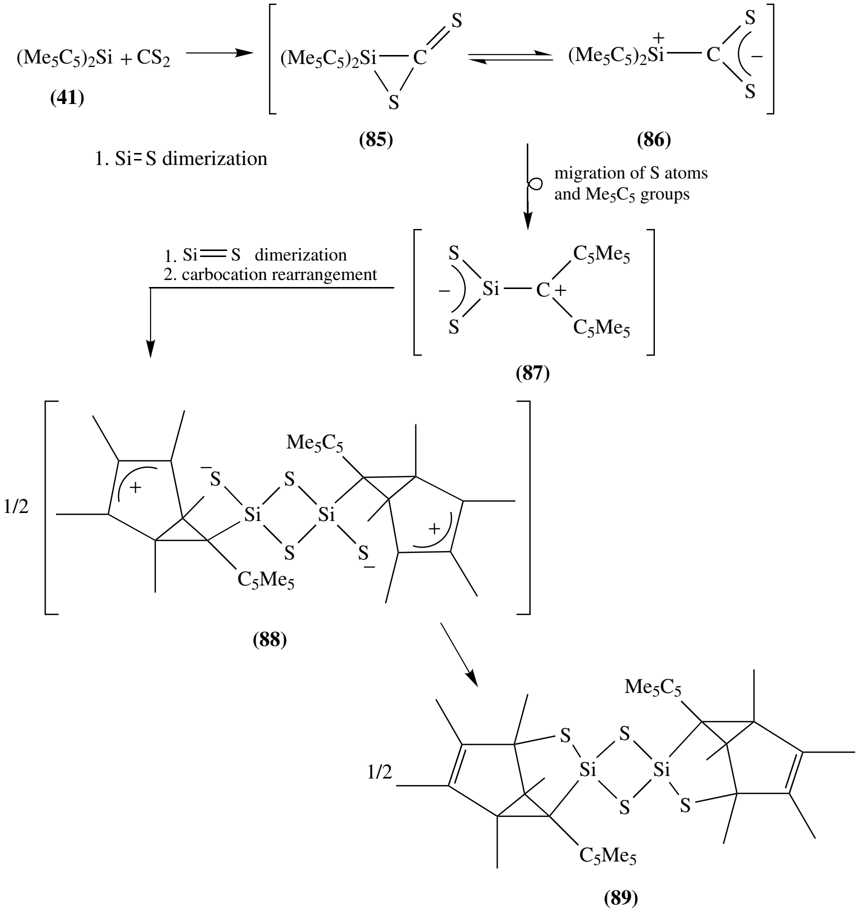

SCHEME 31

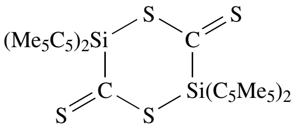

(90)

4. Formation from silicon-containing cyclic polysulfides

In order to synthesize a stable silanethione, it is important to choose a proper precursor and a suitable methodology, since it can be anticipated that the desired silanethione might be extremely reactive toward atmospheric oxygen and moisture to allow its purification by chromatography. Recently, the first kinetically stabilized silanethione **4** has been successfully synthesized and isolated by taking advantage of a new and efficient steric protection group, 2,4,6-tris[bis(trimethylsilyl)methyl]phenyl[10] (denoted as Tbt group in this chapter). The strategy for synthesizing this stable silanethione **4** is based on the simple desulfurization by a phosphine reagent of the corresponding silicon-containing cyclic polysulfides. Thus, a hexane solution of Tbt- and Tip-substituted tetrathiasilolane **91**[56], which was prepared by the reaction of the dibromosilane **92** with lithium naphthalenide followed by treatment with elemental sulfur, was refluxed in the presence of 3 molar equivalents of triphenylphosphine to produce quantitatively the silanethione **4** together with triphenylphosphine sulfide (Scheme 32). Since triphenylphosphine sulfide is almost insoluble in hexane, silanethione **4** was easily separated from the reaction mixture by filtration of the precipitated phosphine sulfide and was purified by recrystallization from hexane under argon atmosphere in a glovebox, yielding a yellow crystalline compound.

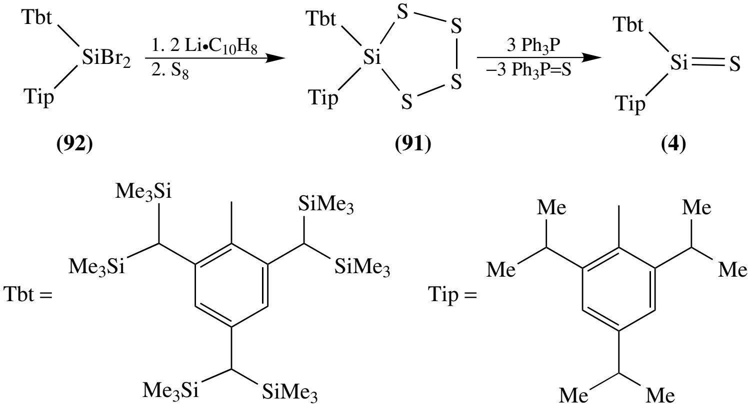

SCHEME 32

Silanethione **4** was characterized by ^{1}H, ^{13}C and ^{29}Si NMR, as well as by Raman and UV-vis spectroscopy. The ^{29}Si NMR chemical shift of **4** (δ 166.56 ppm/C_6D_6) for the silathiocarbonyl unit is significantly downfield shifted from those of the coordinatively stabilized silanethiones, **67, 77, 78**[54] and **79**[37], mentioned in the previous sections, clearly indicating the genuine Si=S double-bond nature of **4** without any intra- or intermolecular coordination. The UV-Vis spectrum of **4** exhibited an absorption maximum at 396 nm which was assigned to the n–π^* transition. The Raman spectrum of **4** in the solid state showed an absorption at 724 cm^{-1} attributable to the Si=S stretching; density functional calculations for $H_2Si{=}S$ **(1)** at the B3LYP/TZ (d,Z) level led to a Si=S stretching frequency of 723 cm^{-1} (see also Section I.B.1). The molecular structure of **4** was successfully solved by X-ray crystallographic analysis and the ORTEP and schematic drawings of the molecular structure of **4** are shown in Figure 4.

The silathiocarbonyl unit of **4** has a completely trigonal planar geometry, the sum of the bond angles around the central silicon atom being 359.9°. The dihedral angles between the trigonal plane and the two aryl planes are 41.8° for the Tbt ring and 67.8°

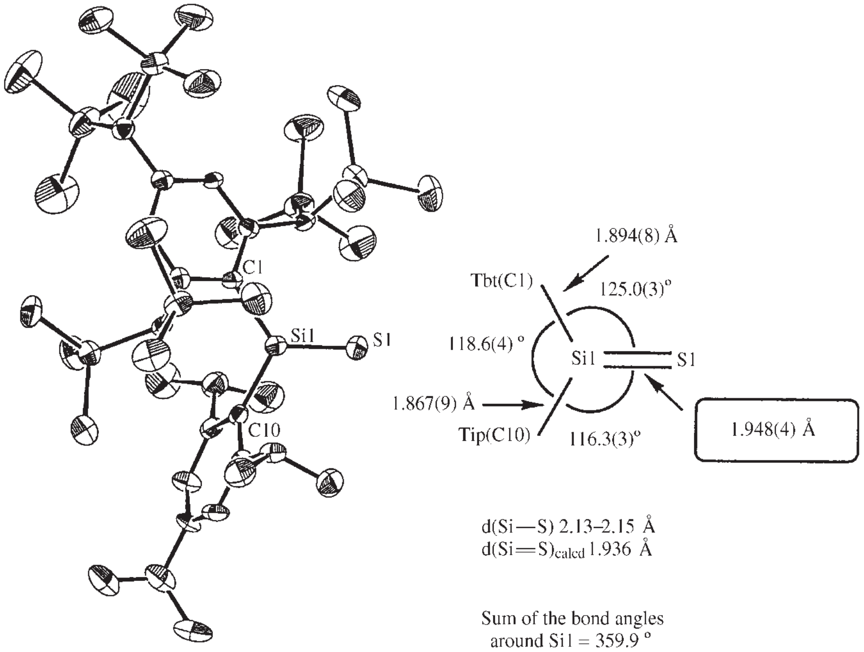

FIGURE 4. Molecular structure of silanethione **4** with selected bond lengths (Å) and angles (deg)[10]. Reprinted with permission from Ref. 10. Copyright (1994) American Chemical Society

for the Tip ring. The silicon–sulfur double-bond length is 1.948(4) Å, which is about 0.2 Å shorter than typical Si–S single-bond lengths[53] (*ca* 9% shortening) and significantly shorter than that reported for Corriu's silanethione **74** [2.013(3) Å][9]. These results support unambiguously a double-bond character between silicon and sulfur (a 'pure' silanethione nature) in compound **4**.

Though silanethione **4** is thermally very stable (up to its melting point of 185–189 °C), it has high chemical reactivity toward various reagents (Scheme 33). Methanol reacts instantaneously with **4** at room temperature to afford the expected addition product **93** (53%). Reactions of **4** with phenyl isothiocyanate and mesitonitrile oxide at room temperature resulted in the rapid formation of the [2 + 2] and [2 + 3] cycloadducts **94** (63%) and **95** (54%), respectively[10]. In contrast, 2,3-dimethyl-1,3-butadiene was very reluctant to react with **4**. The yellow color due to **4** did not disappear even upon heating a hexane solution of **4** and the diene in a sealed tube up to 150 °C. The reaction finally proceeded at 180 °C to give after 3 h the expected [2 + 4] cycloadduct **96** in 74% yield[10,57]. The formation of the [2 + 4] cycloadduct **96** from **4** demonstrates that the silanethione has a considerable extent of ene character like its carbon analogs such as thioketones and thioaldehydes, which are known to have high reactivities in Diels–Alder reactions[58]. It is surprising that silanethione **4** shows these high reactivities in spite of the extremely severe steric congestion around the Si=S group.

The synthesis of **4** makes it possible to compare the electronic spectra (n → π^*) of a series of $R^1R^2M{=}S$ (M = C[59], Si[10], Ge[60], Sn[61]) compounds. In Table 2 are listed the observed spectra of these compounds along with the calculated spectra (at the CIS/DZ+d level) for the corresponding parent molecules $H_2M{=}S$ (M = C, Si, Ge, Sn). The data in

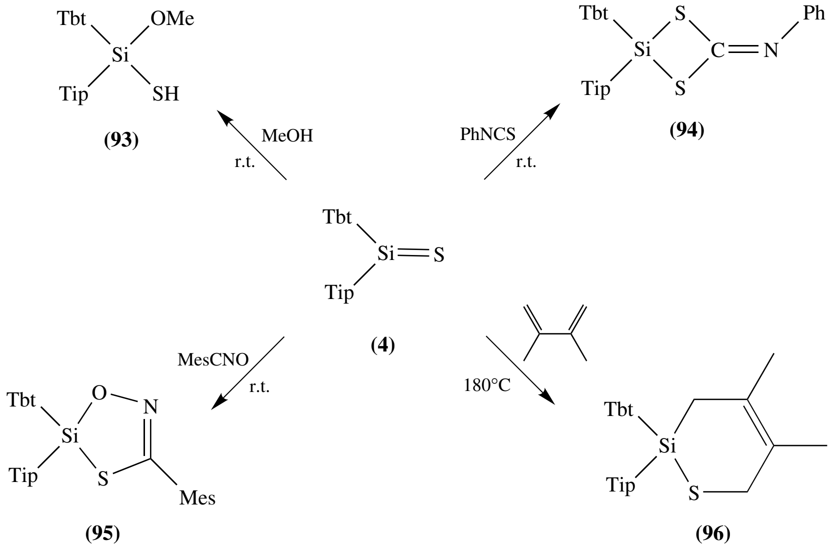

SCHEME 33

Table 2 show interesting change in the observed λ_{max} as a function of M; λ_{max} is significantly blue-shifted on going from thioaldehyde **97** to silanethione **4**, whereas λ_{max} values for **4**, germanethione **98** and stannanethione **99** are red-shifted when the atomic number of the group 14 element is increased. This trend is also found in the calculated values for $H_2M{=}S$ (M = C, Si, Ge, Sn). Since the calculated $\Delta\epsilon_{n\pi^*}$ values increase continuously from $H_2Sn{=}S$ to $H_2C{=}S$, the long-wavelength absorption for $H_2C{=}S$ (and hence for **97**) most likely results from a large repulsion integral ($J_{n\pi^*}$) for the carbon–sulfur double bond (as in the case of $H_2C{=}O$ vs $H_2Si{=}O$[62]), which causes λ_{max} to be longer than that expected from the HOMO–LUMO gap[10].

The less hindered tetrathiasilolane, Tbt(Mes)SiS_4 **(100)**, was also desulfurized with triphenylphosphine (3 equiv.) in hexane at −78 °C to give a yellow-colored solution[63],

TABLE 2. Electronic spectra ($n \rightarrow \pi^*$) of doubly-bonded compounds between group 14 elements and sulfur

Observed[a]		Calculated[e]		
compound	λ_{max} (nm)	compound	λ_{max} (nm)	$\Delta\epsilon_{n\pi^*}$ (eV)[f]
Tbt(H)C=S **(97)**	587[b]	$H_2C{=}S$	458	10.81
Tbt(Tip)Si=S **(4)**	396	$H_2Si{=}S$	345	10.39
Tbt(Tip)Ge=S **(98)**	450[c]	$H_2Ge{=}S$	363	9.97
Tbt(Tip)Sn=S **(99)**	473[d]	$H_2Sn{=}S$	380	9.30

[a] In hexane.
[b] Reference 59.
[c] Reference 60.
[d] Reference 61.
[e] At CIS/DZ + d.
[f] $\epsilon_{LUMO(\pi^*)} - \epsilon_{HOMO(n)}$.

suggesting in analogy with the desulfurization of **91** the generation of the corresponding silanethione **101** (Scheme 34). The yellow color of the solution disappeared on warming the solution to room temperature, resulting in the exclusive formation of *cis*-1,3,2,4-dithiadisiletane **102**, the stereospecific [2 + 2] cycloaddition product of silanethione **101**. Although the silanethione **101** could not be isolated and it rapidly dimerized at room temperature to dithiadisiletane **102**, the formation of the silanethione **101** is strongly supported by the isolation of the expected trapping products with various trapping reagents such as methanol, phenyl isothiocyanate and mesitonitrile oxide, i.e. **103, 104** and **105**, respectively, as shown in Scheme 34.

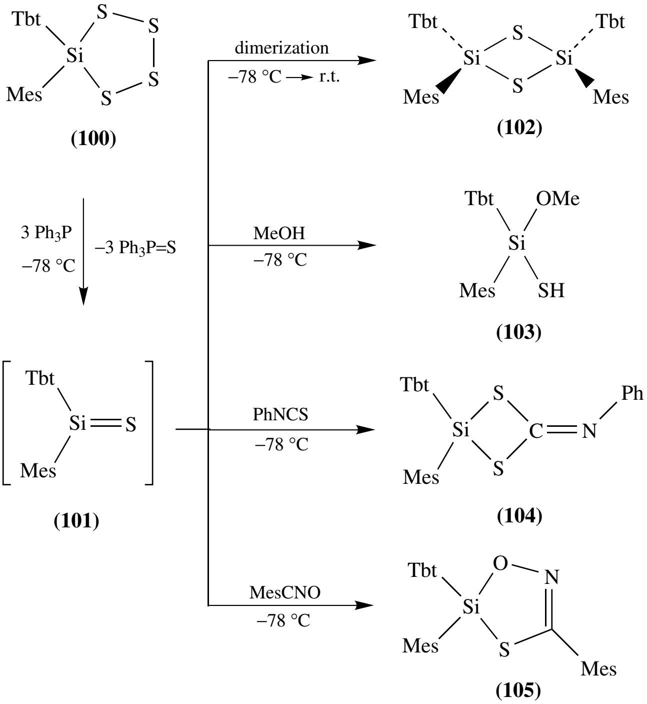

SCHEME 34

The synthetic strategy for the preparation of the stable silanethione **4** based on the desulfurization of the corresponding overcrowded tetrathiasilolane described above was found to be applicable to the syntheses of the other species having double bonds between group 14 and group 16 elements, such as thioaldehydes[59], selenoaldehydes[64], gemanethiones[60], germaneselones[65], stannanethiones[61], stannaneselones[66] and plumbanethiones[67] as shown in Scheme 35. The only exceptions are the germanetellones[68] which were synthesized by the reaction or a germylene with elemental tellurium. All the germanium–chalcogen double-bond compounds were isolated as stable crystalline compounds and were fully characterized by spectroscopic data and by X-ray structural analysis. All of them showed a substantial bond shortening of the Ge=X double bond compared to a Ge−X single bond by *ca* 8–9% and a completely planar trigonal geometry, as in the case of the silanethione **4**.

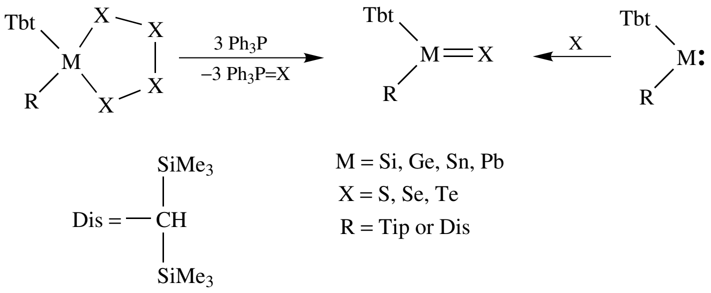

SCHEME 35

5. Formation from a disilene

As a new approach to a silanethione, West and coworkers reported the photolysis of a sterically crowded 1,2,3-thiadisiletane derivative **106** derived from the [2 + 2] cycloaddition reaction of tetramesityldisilene with thiobenzophenone[69]. Crystal structural analysis revealed that **106** has abnormally long Si−Si (2.443 Å) and Si−S (2.177 Å) distances and a highly distorted four-membered ring with a dihedral angle of 45.6° between the Si(1)−Si(2)−C and Si(1)−S−C planes. As shown in Scheme 36, photolysis of this strained silacyclic compound **106** in the presence of ethanol afforded two products, dimesityl(diphenylmethyl)ethoxysilane **(107)** and dimesitylethoxysilanethiol **(108)**. In the absence of ethanol, photolysis of **106** resulted in the formation of a silene, 1,1-dimesityl-2,2-diphenylsilene **(109)**, together with an oligomer of dimesitylsilanethione **110** (**111**; for this compound the authors proposed a dimer or a trimer structure).

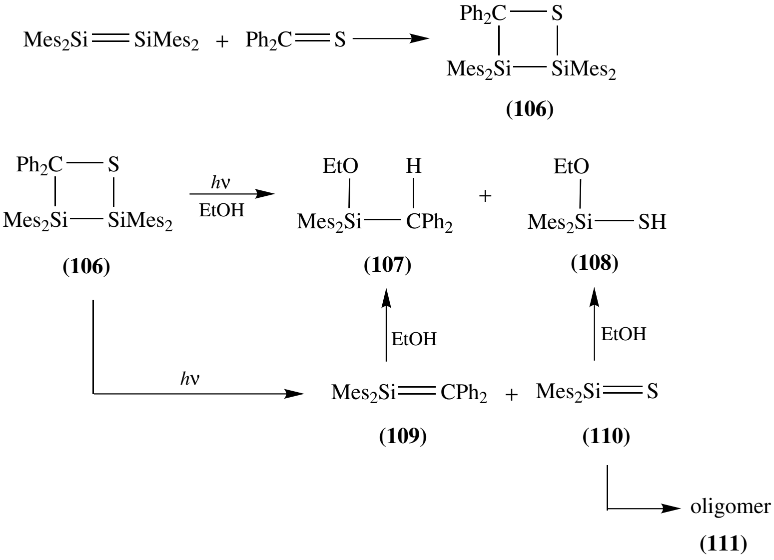

SCHEME 36

These results are most likely interpreted in terms of the photochemical cycloreversion of the thiadisiletane **106** leading to the formation of the silene **109** and silanethione **110**, though both of them were not isolated.

6. Formation from thioketenes

As in the case of extrusion of dimethylsilanone, $Me_2Si{=}O$ **(10)**, in the thermolysis of certain silaketenes[70], a similar type of silanethione ($Me_2Si{=}S$; **112**) extrusion was postulated in the flash vacuum pyrolysis of bis(trimethylsilyl)thioketene **(113)** and (dimethylsilyl)(trimethylsilyl)thioketene **(121)** as shown in Schemes 37 and 38[71]. In both cases, the formation of all the reaction products (compounds **115–120** for the pyrolysis of **113** shown in Scheme 37 and compounds **118, 120, 123** and **124** for the pyrolysis of **121** shown in Scheme 38) can be mechanistically rationalized by processes each initiated by isomerization of the starting thioketenes via a 1,2-shift of a trimethylsilyl group to the corresponding α-thioketocarbenes **114** and **122**. Under the pyrolytic reaction conditions used (700 or 768 °C) the intermediate silanethione **112** underwent ready oligomerization to give its dimer **120** and/or trimer **124**.

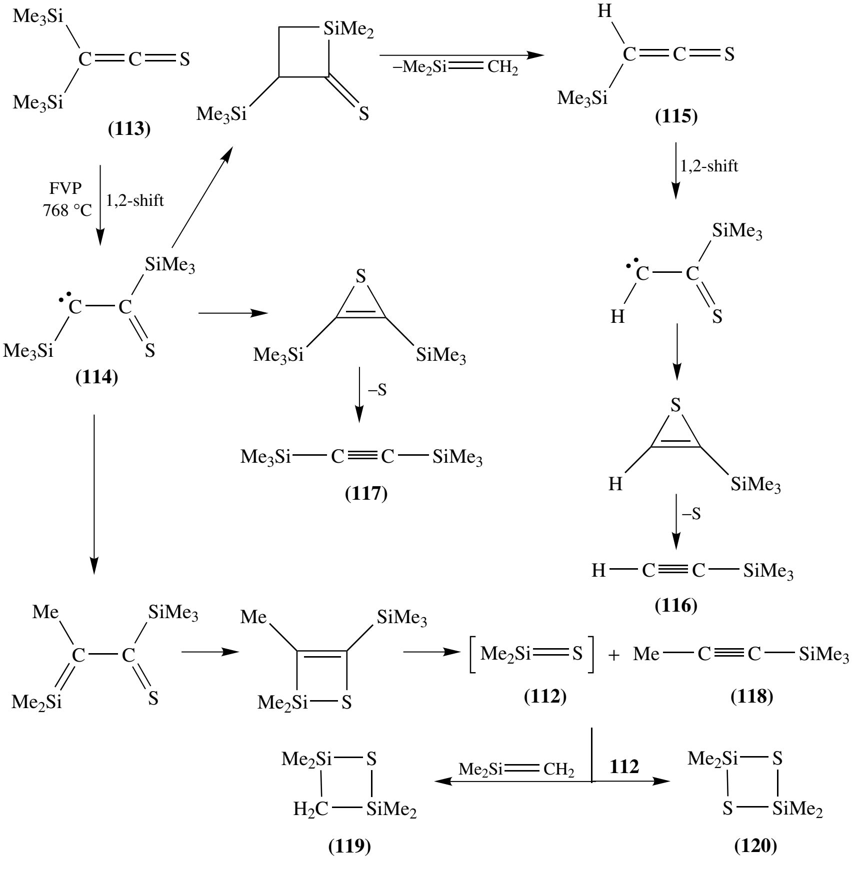

SCHEME 37

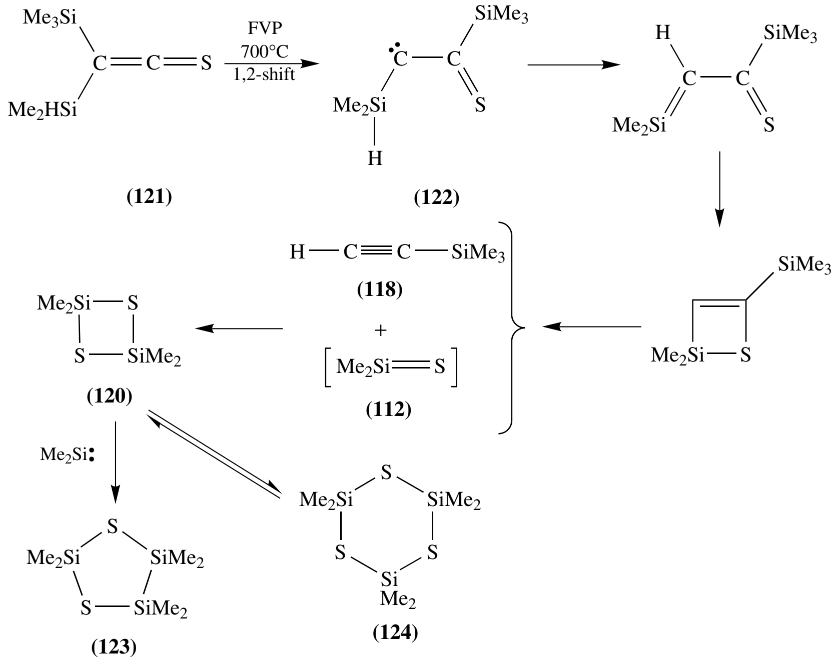

SCHEME 38

7. Matrix isolation of SiS_2, $Cl(H)Si{=}S$ and $Cl_2Si{=}S$

SiS_2 **(125)**[72], Cl(H)Si=S **(126)**[51] and $Cl_2Si{=}S$ **(127)**[50] were prepared and isolated in low temperature matrices. The properties of these species are of interest as the silicon analogues of carbon disulfide (CS_2), thioformyl chloride [S=C(H)Cl] and thiophosgene ($S{=}CCl_2$), which are well-known thiocarbonyl compounds.

Molecular SiS_2 **(125)** was generated in a solid argon matrix by a reaction of SiS with S atoms. The antisymmetric stretching vibration $\nu_{as}(SiS)$ is observed at 918 cm^{-1}. Bonding and structure properties (force constants from experimentally observed frequencies and results from *ab initio* SCF calculations) of SiS_2 were compared with those of similar molecules: CO, CS, CO_2, COS, CS_2, SiO, SiS, SiO_2 and SiOS[72].

Molecular Cl(H)Si=S **(126)** was also formed in an argon matrix in a photochemically induced reaction of SiS with HCl. From the isotopic splittings (H/D and $^{35}Cl/^{37}Cl$) of the IR absorptions the C_s structure of the species with silicon as the central atom is deduced. By a normal coordinate analysis a value of 4.83 mdyn $Å^{-1}$ is obtained for the SiS force constant, a value which was confirmed by *ab initio* SCF calculations of the IR spectrum[51].

Under similar reaction conditions, $Cl_2Si{=}S$ **(127)** was formed in a matrix reaction between SiS and Cl_2. The formation of **127** was also concluded from some isotopic shifts in the IR spectra. The force constant of the Si−S bond in **127** has a value of 4.9 mdyn $Å^{-1}$[50].

Schnöckel and coworkers have also calculated at SCF level, the molecular structures and charge distributions for $H_2S{=}S$ **(1)**, Cl(H)Si=S **(126)** and $Cl_2Si{=}S$ **(127)** as well as those of $Cl_2Si{=}O$ **(128)**, the oxygen analogue of **127**, and the results are presented in Figure 5.

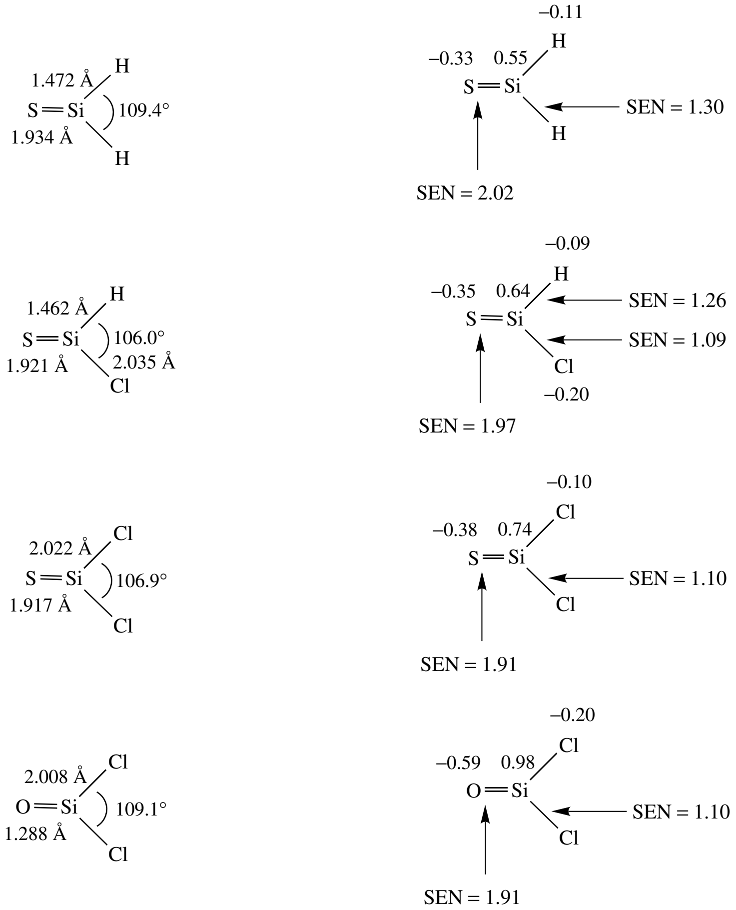

FIGURE 5. Molecular structures and charge distributions calculated at the SCF level for $H_2Si{=}S$ (**1**), $ClHSi{=}S$ (**126**), $Cl_2Si{=}S$ (**127**) and $Cl_2Si{=}O$ (**128**). SEN = shared electron numbers. See: C. Ehahardt and R. Ahlrichs, *Theor. Chim. Acta*, **68**, 231 (1985)

D. Silicon–Selenium and Silicon–Tellurium Double Bonds (Silaneselones and Silanetellones)

As can be seen in the previous sections of this chapter, remarkable progress has been made in the chemistry of silanones and silanethiones, but still very little is known on the chemistry of their heavier chalcogen analogues, i.e. silaneselones and silanetellones. Thus, up to now, no report has appeared on the preparation or the spectroscopic detection of a silanetellone, and only limited information is available on silaneselones.

1. Transient silaneselones

For the generation of silaneselones, Boudjouk and Thompson have described the photochemical and thermal fragmentations of cyclosilaselenanes[73]. Thus, several cyclodisiladiselenanes and cyclotrisilatriselenanes, $(R_2SiSe)_n$ (**129**–**134**; $n = 2, 3$), were generated from Na_2Se and the corresponding R_2SiCl_2 (Scheme 39)[74]. The properties of the cyclosilaselenanes are found to depend on the groups attached to silicon. Thus, while alkyl-substituted systems [e.g. **129** and **130** (R = Me) and **131** and **132** (R = Et) are thermally unstable air-sensitive yellow oils, the silyl-substituted one **134** ($R = SiMe_3$) was isolated as green crystals stable to air for several days.

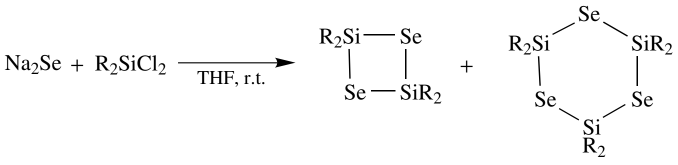

R = Me	**(129)** 6%	**(130)** 35%
R = Et	**(131)** 40%	**(132)** 30%
R = Ph	–	**(133)** 40%
$R = SiMe_3$	**(134)** 35%	–

SCHEME 39

The above-mentioned cyclosilaselenanes generate the corresponding silaneselones, $R_2Si{=}Se$ (**135**), both thermally and photochemically when R = Me, Et and $n = 3$ but only thermally when R = Me, Et and $n = 2$ (Scheme 40). The silaneselones **135** are easily trapped with hexamethylcyclotrisiloxane (D_3) to give the corresponding insertion product **136**.

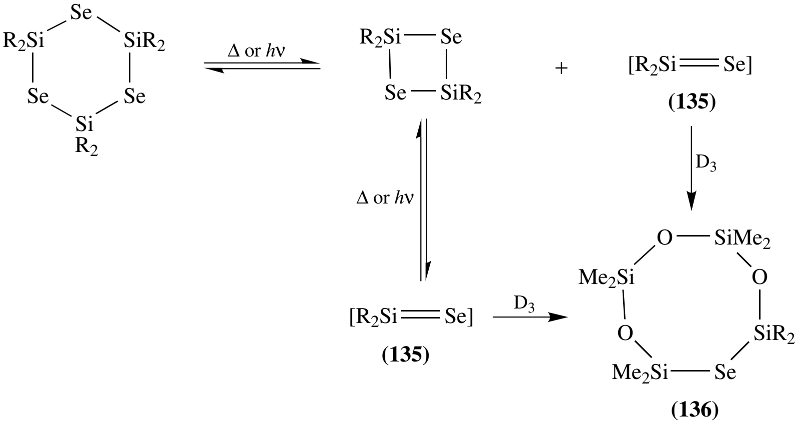

SCHEME 40

In the case of R = Ph only the six-membered ring product **133** was available as the precursor, and upon thermolysis it gave a modest yield of an insertion reaction product of $Ph_2Si{=}Se$ to D_3, but a complex mixture resulted upon photolysis. On the other hand, the trimethylsilyl substituted cyclodisiladiselenane **134** was found to be stable toward ring fragmentation either on thermolysis (250 °C for 5 days in a sealed tube) or on photolysis[73b].

2. Silaneselone derived from silicocene

In 1989 Jutzi and coworkers reported the reaction of decamethylsilicocene **41** with tri-*n*-butylphosphine selenide in benzene at room temperature leading to almost quantitative formation of 1,3,2,4-diselenadisiletane derivative **138**, a head-to-tail [2 + 2] cycloaddition reaction product of the initially formed silaneselone **137**[75]. The intermediacy of silaneselone **137** was supported by the fact that the reaction in the presence of 2,3-dimethyl-1,3-butadiene resulted in the formation of the corresponding [2+4] cycloaddition reaction product **139** (Scheme 41). As in the cases of silanone **44** and silanethione **80**, the ligands on silicon undergo a haptotropic rearrangement from η^5-C_5Me_5 in **41** to η^1-C_5Me_5 in **138** or **139**. Apparently, silaneselone **137** is not kinetically stable enough to be isolated under normal conditions.

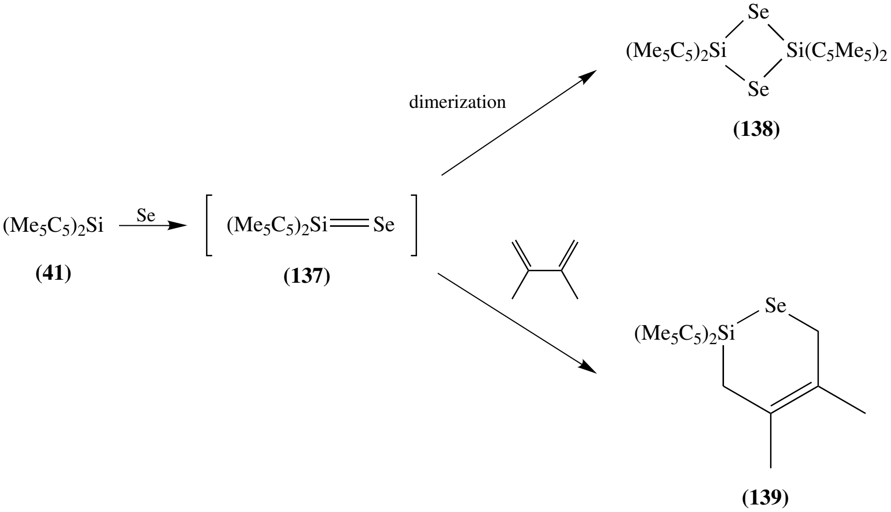

SCHEME 41

3. Thermodynamically stabilized silaneselone

Corriu and coworkers found that the reaction of the pentacoordinated functionalized silane **6** (see also Sections II.B.1 and II.C.1) with elemental selenium leads to a stable silaneselone **140**, which is stabilized by intramolecular coordination of the nitrogen-containing substituent to the doubly-bonded silicon (Scheme 42)[9]. Although the structure of **140** was supported by ^{29}Si and ^{13}C NMR and MS spectra, including a downfield ^{29}Si chemical shift ($\delta = +29.4$) and a high coupling constant with ^{77}Se ($J_{SeSi} = 257$ Hz), neither the crystallographical structure analysis nor the reactivity of this isolable Si=Se compound has been reported.

4. Sterically protected silaneselone stable in solution

In analogy to the case of stable silanethione **4**, kinetic stabilization of a silaneselone by the large Tbt group was examined (see Section II.C.3). Since the synthesis and isolation of the cyclic polyselenides Tbt(R)SiSe$_4$ (R = Mes or Tip) were unsuccessful, probably due to their lower stabilities than those of the corresponding tetrathiasilolanes such as **91**

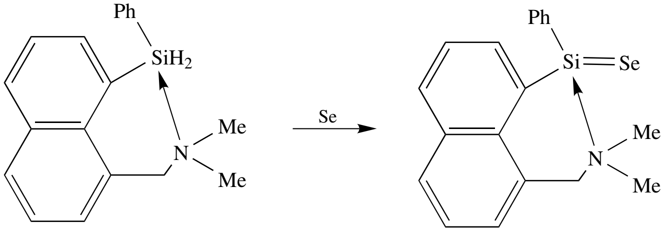

(6) **(140)**

SCHEME 42

and **100**, the direct selenation of the sterically hindered diarylsilylene Tbt(Dip)Si**:** (**142**; Dip = 2,6-diisopropylphenyl) was examined. Thus, the bicyclic silirane derivative **(141)** bearing Tbt and Dip groups on the silicon atom was treated with elemental selenium to afford a red solution, suggesting the formation of the corresponding silaneselone **143** (Scheme 43)[76].

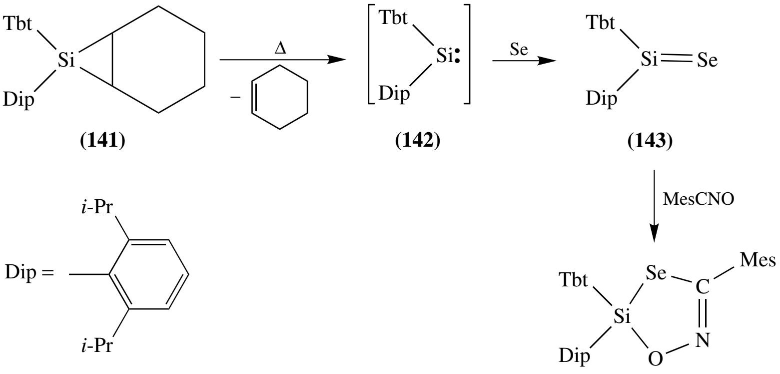

(141) **(142)** **(143)** **(144)**

SCHEME 43

The formation of silaneselone **143** was supported by the trapping reaction with mesitonitrile oxide leading to the expected corresponding cycloadduct **144** as well as by the observation of a remarkable downfield ^{29}Si chemical shift ($\delta_{\mathrm{Si}} = 174$ ppm) indicative of the Si=Se double bond of **143**.

III. OUTLOOK FOR THE CHEMISTRY OF SILICON−HETEROATOM MULTIPLE BONDS

As mentioned in this chapter, in recent years much progress has been made in the chemistry of silicon−chalcogen multiple bonds. For silicon−sulfur doubly-bonded compounds, we have now several isolated examples, both kinetically stabilized and thermodynamically stabilized. Furthermore, there have been reports of the synthesis and characterization of stable compounds with silicon−nitrogen double bonds (i.e. silanimines or iminosilanes) as well as their heavier group 15 element analogues such as phosphasilenes and arsasilenes.

In view of the recent investigations it seems that kinetic stabilization with bulky substituent(s) (steric protection) of silicon–heteroatom double bonds is superior to their thermodynamic stabilization [e.g. by mesomeric effects or intramolecular coordination of heteroatom-containing substituent(s) or metal complexation to the silicon–heteroatom π-bond]. Although except for the Si=S double bond (silanethiones) other silicon–chalcogen atom doubly-bonded species still remain a challenging and fascinating target for isolation and characterization, the remarkable progress in molecular design and steric protection will make it possible in the future, so we believe, to reveal the interesting bond character of these novel silicon-containing π-bond systems.

IV. REFERENCES

1. A. G. Brook, F. Abdesaken, B. Gutekunst, G. Gutekunst and R. K. Kallury, *J. Chem. Soc., Chem. Commun.*, 191 (1981).
2. R. West, M. J. Fink and J. Michl, *Science*, **214**, 1343 (1981).
3. M. Yoshifuji, I. Shima, N. Inamoto, K. Hirotsu and T. Higuchi, *J. Am. Chem. Soc.*, **103**, 4587 (1981).
4. (a) L. E. Gusel'nikov and N. S. Nametkin, *Chem. Rev.*, **79**, 529 (1979).
   (b) G. Raabe and J. Michl, *Chem. Rev.*, **85**, 419 (1985).
   (c) A. G. Brook and K. M. Bains, *Adv. Organomet. Chem.*, **25**, 1 (1986).
   (d) R. West, *Angew. Chem., Int. Ed. Engl.*, **26**, 1201 (1987).
   (e) G. Raabe and J. Michl, in *The Chemistry of Organic Silicon Compounds, Part 2* (Eds. S. Patai and Z. Rappoport), Wiley, New York, 1989, p. 1015.
   (f) J. Barrau, J. Escudié and J. Satgé, *Chem. Rev.*, **90**, 283 (1990).
   (g) T. Tsumuraya, S. A. Batcheller and S. Masamune, *Angew. Chem., Int. Ed. Engl.*, **30**, 902 (1991).
5. (a) N. Wiberg, K. Schurz and G. Fischer, *Angew. Chem., Int. Ed. Engl.*, **24**, 1053 (1985).
   (b) N. Wiberg, K. Schurz, G. Reber and G. Müller, *J. Chem. Soc., Chem. Commun.*, 591 (1986).
   (c) M. Hesse and U. Klingebiel, *Angew. Chem., Int. Ed. Engl.*, **25**, 649 (1986).
   (d) For a review on the synthesis and reactions of iminosilanes and related compounds see I. Hemme and U. Klingebiel, *Adv. Organomet. Chem.*, **39**, 159 (1996).
6. (a) C. N. Smit and F. Bickelhaupt, *Organometallics*, **6**, 1156 (1987).
   (b) Y. van den Winkel, H. M. M. Bastiaans and F. Bickelhaupt, *J. Organomet. Chem.*, **405**, 183 (1991).
   (c) M. Driess, *Angew. Chem., Int. Ed. Engl.*, **30**, 102 (1991).
7. (a) M. Driess and H. Pritzkow, *Angew. Chem., Int. Ed. Engl.*, **31**, 316 (1992).
   (b) For a review on stable doubly-bonded compounds of germanium and tin see K. M. Baines and W. G. Stibbs, *Adv. Organomet. Chem.*, **39**, 275 (1996).
   (c) For a review on silicon–phosphorus and silicon–arsenic multiple bonds see M. Driess, *Adv. Organomet. Chem.*, **39**, 193 (1996).
8. For recent reviews see
   (a) A. G. Brook and M. A. Brook (The Chemistry of Silenes), *Adv. Organomet. Chem.*, **39**, 71 (1996).
   (b) R. Okazaki and R. West (Chemistry of Stable Disilenes), *Adv. Organomet. Chem.*, **39**, 232 (1996).
9. P. Arya, J. Boyer, F. Carré, R. Corriu, G. Lanneau, J. Lapasset, M. Perrot and C. Priou, *Angew. Chem., Int. Ed. Engl.*, **28**, 1016 (1989).
10. H. Suzuki, N. Tokitoh, S. Nagase and R. Okazaki, *J. Am. Chem. Soc.*, **116**, 11578 (1994).
11. N. Auner, Chapter 16 in this volume.
12. H. Sakurai, Chapter 15 in this volume.
13. T. Kudo and S. Nagase, *Organometallics*, **5**, 1207 (1986).
14. T. Kudo and S. Nagase, *J. Phys. Chem.*, **88**, 2833 (1984).
15. M. W. Schmidt, P. N. Truong and M. S. Gordon, *J. Am. Chem. Soc.*, **109**, 5217 (1987).
16. P. v. R. Schleyer and D. Kost, *J. Am. Chem. Soc.*, **110**, 2105 (1988).
17. P. J. Bruna and F. Grein, *Chem. Phys.*, **165**, 265 (1992).
18. R. Withnall and L. Andrews, *J. Am. Chem. Soc.*, **107**, 2567 (1985).

19. V. N. Khabashesku, Z. A. Kerzina, E. G. Baskir, A. K. Maltsev and O. M. Nefedov, *J. Organomet. Chem.*, **347**, 277 (1988).
20. G. Manuel, G. Bertrand, W. P. Weber and S. A. Kazoura, *Organometallics*, **3**, 1340 (1984).
21. I. M. T. Davidson, A. Fenton, G. Manuel and G. Bertrand, *Organometallics*, **4**, 1324 (1985).
22. G. Hussmann, W. D. Wulff and T. J. Barton, *J. Am. Chem. Soc.*, **105**, 1263 (1983).
23. V. N. Khabashesku, Z. A. Kerzina, E. G. Baskir, A. K. Maltsev and O. M. Nefedov, *J. Organomet. Chem.*, **364**, 301 (1989).
24. T. J. Barton, Contribution to International Symposium of Orgaonsilicon Reactive Intermediates, Sendai, Japan, September 1984.
25. C. Eaborn and W. A. Stanczyk, *J. Chem. Soc., Perkin Trans. 2*, 2099 (1984).
26. A. G. Davies and A. G. Neville, *J. Organomet. Chem.*, **436**, 255 (1992).
27. R. West and R. H. Baney, *J. Am. Chem. Soc.*, **81**, 6145 (1959).
28. C. Chatgilialoglu, K. U. Ingold, J. C. Scaiano and H. Woynar, *J. Am. Chem. Soc.*, **103**, 3231 (1981).
29. R. Goikhman, M. Aizenberg, L. J. W. Shimon and D. Milstein, *J. Am. Chem. Soc.*, **118**, 10894 (1996).
30. T. Matsubara and Y. Saito, *J. Mol. Catal.*, **92**, 1 (1994) and references cited therein.
31. H. S. D. Soysa, H. Okinoshima and W. P. Weber, *J. Organomet. Chem.*, **133**, C-17 (1977).
32. (a) W. F. Gore and T. J. Barton, *J. Organomet. Chem.*, **199**, 33 (1980).
    (b) D. Tzeng and W. P. Weber, *J. Am. Chem. Soc.*, **102**, 1451 (1980).
    (c) W. Ando, M. Ikeno and Y. Hamada, *J. Chem. Soc., Chem. Commun.*, 621 (1981).
33. C. A. Arrington, R. West and J. Michl, *J. Am. Chem. Soc.*, **105**, 6176 (1983).
34. A. Patyk, W. Sander, J. Gauss and D. Cremer, *Angew. Chem., Int. Ed. Engl.*, **28**, 898 (1989).
35. (a) J. Belzner and H. Ihmels, *Tetrahedron Lett.*, **34**, 6541 (1993).
    (b) J. Belzner, H. Ihmels, B. O. Kneisel, R. O. Gould and R. Herbst-Irmer, *Organometallics*, **14**, 305 (1995).
    (c) R. Corriu, G. Laneau, C. Priou, F. Soulairol, N. Auner, R. Probst, R. Conlin and C. Tan, *J. Organomet. Chem.*, **466**, 55 (1994).
36. J. Belzner, *J. Organomet. Chem.*, **430**, C51 (1992).
37. J. Belzner, H. Ihmels, B. O. Kneisel and R. Herbst-Irmer, *Chem. Ber.*, **129**, 125 (1996).
38. M. Weidenbruch, B. Flintjer, S. Pohl and W. Saak, *Angew. Chem. Int. Ed. Engl.*, **28**, 95 (1989).
39. M. Driess and H. Prizkow, *Angew. Chem., Int. Ed. Engl.*, **31**, 316 (1992).
40. N. Wiberg, G. Preiner and K. Schurz, *Chem. Ber.*, **121**, 1407 (1988).
41. (a) P. Jutzi and A. Möhrke, *Angew. Chem. Int. Ed. Engl.*, **28**, 762 (1989).
    (b) P. Jutzi, D. Eikenberg, A. Möhrke, B. Neumann and H.-G. Stammler, *Organometallics*, **15**, 753 (1996).
42. N. Wiberg, G. Preiner and G. Wagner, *Z. Naturforsch. B*, **B426**, 1062 (1987).
43. (a) C. M. Golino, R. D. Bush, P. On and L. H. Sommer, *J. Am. Chem. Soc.*, **97**, 1957 (1975).
    (b) W. Ando, A. Sekiguchi and T. Migita, *J. Am. Chem. Soc.*, **97**, 7159 (1975).
    (c) W. Ando, M. Ikeno and A. Sekiguchi, *J. Am. Chem. Soc.*, **99**, 6447 (1977).
44. S. Bachrach and A. Streitwieser, Jr., *J. Am. Chem. Soc.*, **107**, 1186 (1985).
45. A. G. Brook, W. J. Chatterton, J. F. Sawyer, D. W. Hughes and K. Vorspohl, *Organometallics*, **6**, 1246 (1987).
46. I. M. T. Davidson, C. E. Dean and F. T. Lawrence, *J. Chem. Soc., Chem. Commun.*, 52 (1981).
47. A. G. Brook, S. C. Niburg, F. Abdesaken, B. Gutekunst, G. Gutekunst, R. K. M. R. Kallury, Y. C. Poon, Y.-M. Chang and W. Wong-Ng, *J. Am. Chem. Soc.*, **104**, 5667 (1982).
48. M. Driess, H. Pritzkow, S. Rell and U. Winkler, *Organometallics*, **15**, 1845 (1996).
49. T. Kudo and S. Nagase, *J. Am. Chem. Soc.*, **107**, 2589 (1985).
50. H. Schnöckel, H. J. Göcke and R. Köppe, *Z. Anorg. Allg. Chem.*, **578**, 159 (1989).
51. R. Köppe and H. Schnöckel, *Z. Anorg. Allg. Chem.*, **607**, 41 (1992).
52. M. Weidenbruch, A. Schäfer and R. Rankers, *J. Organomet. Chem.*, **195**, 171 (1980).
53. W. S. Sheldrick, in *The Chemistry of Organic Silicon Compounds, Part 1*, (Eds. S. Patai and Z. Rappoport), Wiley, New York, 1989, pp. 227–304. See also R. K. Sibao, N. L. Keder and H. Eckert, *Inorg. Chem.*, **29**, 4163 (1990).
54. R. J. P. Corriu, G. F. Laneau and V. D. Mehta, *J. Organomet. Chem.*, **419**, 9 (1991).
55. J. Beltzner, D. Schär, B. O. Kneisel and R. Herbst-Irmer, *Organometallics*, **14**, 1840 (1995).
56. N. Tokitoh, H. Suzuki, T. Matsumoto, Y. Matsuhashi, R. Okazaki and M. Goto, *J. Am. Chem. Soc.*, **113**, 7047 (1991).

57. N. Tokitoh, H. Suzuki and R. Okazaki, *Xth International Symposium on Organosilicon Chemistry*, Poznan, Poland, Abstract O-62, 1993, p. 110.
58. (a) W. J. Middleton, *J. Org. Chem.*, **30**, 1390 (1965).
    (b) A. Schönberg and B. König, *Chem. Ber.*, **101**, 725 (1968).
    (c) Y. Ohnishi, Y. Akasaki and A. Ohno, *Bull. Chem. Soc. Jpn.*, **46**, 3307 (1973).
    (d) J. E. Baldwin and R. C. G. Lopez, *Tetrahedron*, **39**, 1487 (1983).
    (e) G. W. Kirby, A. W. Lochead and G. N. Sheldrake, *J. Chem. Soc., Chem. Commun.*, 922 (1984).
    (f) G. A. Krafft and P. T. Meinke, *Tetrahedron Lett.*, **26**, 1947 (1985).
    (g) E. Vedejs, T. H. Eberlein, D. J. Mazur, C. K. McClure, D. A. Penny, R. Ruggeri, E. Schwartz, J. S. Stults, D. L. Varie, R. G. Wilde and S. Wittenberger, *J. Org. Chem.*, **51**, 1556 (1986).
    (h) M. Segi, T. Nakajima, S. Suga, S. Murai, A. Ogawa and N. Sonoda, *J. Am. Chem. Soc.*, **110**, 1976 (1988).
59. (a) N. Tokitoh, N. Takeda and R. Okazkai, *J. Am. Chem. Soc.*, **116**, 7907 (1994).
    (b) N. Takeda, N. Tokitoh and R. Okazaki, *Chem. Eur. J.*, **3**, 62 (1997).
60. N. Tokitoh, T. Matsumoto, K. Manmaru and R. Okazaki, *J. Am. Chem. Soc.*, **115**, 8855 (1993).
61. N. Tokitoh, M. Saito and R. Okazaki, *J. Am. Chem. Soc.*, **115**, 2065 (1993).
62. T. Kudo and S. Nagase, *Chem. Phys. Lett.*, **128**, 507 (1986).
63. H. Suzuki, Ph. D. Thesis, The University of Tokyo (1994); H. Suzuki, N. Tokitoh, R. Okazaki, M. Goto and S. Nagase, submitted to *J. Am. Chem. Soc*.
64. N. Takeda, N. Tokitoh and R. Okazaki, *Angew. Chem., Int. Ed. Engl.*, **35**, 660 (1996).
65. T. Matsumoto, N. Tokitoh and R. Okazaki, *Angew. Chem., Int. Ed. Engl.*, **33**, 2316 (1994).
66. (a) Y. Matsuhashi, N. Tokitoh and R. Okazaki, *Organometallics*, **12**, 2573 (1993).
    (b) M. Saito, N. Tokitoh and R. Okazaki, *J. Organomet. Chem.*, **499**, 43 (1995).
67. N. Tokitoh and R. Okazaki, *Main Group Chemistry News*, **3**, 4 (1995).
68. (a) N. Tokitoh, T. Matsumoto and R. Okazaki, *The IVth International Conference on Heteroatom Chemistry*, Seoul, Korea, Abstract OB-11, 1995, p. 54.
    (b) N. Tokitoh, T. Matsumoto and R. Okazaki, *The VIIIth International Conference on the Organometallic Chemistry of Germanium, Tin and Lead*, Sendai, Japan, Abstract O10, 1995, p. 36.
69. K. Kabeta, D. R. Powel, J. Hanson and R. West, *Organometallics*, **10**, 827 (1991).
70. T. J. Barton and B. L. Groh, *J. Am. Chem. Soc.*, **107**, 7221 (1985).
71. T. J. Barton and G. C. Paul, *J. Am. Chem. Soc.*, **109**, 5292 (1987).
72. H. Schnöckel and R. Köppe, *J. Am. Chem. Soc.*, **111**, 4583 (1989).
73. (a) D. P. Thompson and P. Boudjouk, *J. Chem. Soc., Chem. Commun.*, 1466 (1987).
    (b) P. Boudjouk, S. R. Bahr and D. P. Thompson, *Organometallics*, **10**, 778 (1991).
74. D. P. Thompson and P. Boudjouk, *J. Org. Chem.*, **53**, 2109 (1988).
75. P. Jutzi, A. Möhrke, A. Müller and H. Bögge, *Angew. Chem., Int. Ed. Engl.*, **28**, 1518 (1989).
76. T. Sadahiro, N. Tokitoh and R. Okazaki, unpublished results.

CHAPTER 18

Gas-phase ion chemistry of silicon-containing molecules[†]

NORMAN GOLDBERG[‡] and HELMUT SCHWARZ

Institut für Organische Chemie der Technischen Universität Berlin, Straße des 17. Juni 135, D-10623 Berlin, Germany

---

[†] This article is dedicated to Saul Patai.

[‡] *Present address:* Cornell University, Department of Chemistry, Baker Laboratory, Ithaca, NY 14853-1301, USA.

I. INTRODUCTION

The chemistry of silicon compounds has experienced tremendous research activities over the last decades, and researchers originally driven to find analogies between carbon and its higher homologue have had to realize that in many cases the differences between these elements far outweigh the similarities. The diversity of silicon chemistry and depth of penetration into other research areas can easily be seen by taking a look at the contributions to this compendium. One of the research fields that has contributed a great deal to our current understanding of the chemistry of this main-group element is that of mass spectrometry. Not only do some of the many mass-spectrometric techniques allow us to obtain thermochemical data on small charged and neutral silicon-containing species, but we can also obtain insight into intrinsic properties of this intriguing element. The absence of numerous perturbing effects which are common in liquids or solids is one of the main advantages of gas-phase studies.

The aim of this review is to give the reader an overview of the progress to date in the field. A detailed account by Schwarz[1a] on the ‘Positive and Negative Ion Chemistry of Silicon in the Gas Phase’ appeared in this series in 1989 as well as an exhaustive review by Bock and Solouki on ‘Organosilicon Radical Cations’[1b], and the present manuscript is intended to cover the literature that has appeared since the publication of this work until early 1996. A brief discussion of thermochemistry will be given in Section II. Section III gives a detailed account of the advances made in the exploration of ion–molecule reactions of atomic silicon-containing ions. Here in particular the reactions of neutral silicon-containing molecules with main-group and transition-metal ions, as well as the reactions of atomic silicon cations with neutral molecules will be reported. Section IV covers the field of small multiply bonded silicon species — ionic as well as neutral, as explored by mass-spectrometric techniques. The employment of methods such as neutralization–reionization mass spectrometry (NRMS) has allowed for the generation and detection of neutral highly reactive species by mass spectrometric techniques, and a number of such studies have been carried out. Section V will report on current advances in the investigations of rearrangements of silicon-containing ions as explored by mass spectrometric techniques. The generation and investigation of doubly charged cationic and anionic silicon ions will be mentioned in Section VI.

II. THERMOCHEMISTRY

There have been numerous experimental as well as theoretical studies dealing with the structural and thermochemical properties of cationic silicon hydrides, $Si_nH_m^{+\bullet}$, and a detailed discussion of these species would certainly exceed the limited space available. We will therefore confine ourselves to the discussion of only a few exemplary cases. For further information on Si-ion thermochemistry the reader is referred to several reviews on the experimental[2–4] as well as computational[5] determination of thermodynamic properties of silicon-containing ions.

A. Cationic Silicon Hydrides

The properties of ionized monosilane, $SiH_4^{+\bullet}$, have been reevaluated by Berkowitz and coworkers[6]. In agreement with earlier studies[2,7] it was found that ionized monosilane,

$SiH_4^{+\bullet}$, is a very unstable species. Generation of $SiH_4^{+\bullet}$ was accomplished by Photoionization Mass Spectrometry (PIMS) and only observed within a very narrow energy range. The original discrepancy between earlier Photoelectron Spectroscopic (PES) measurements which had obtained a value of 11.60 eV for the adiabatic ionization energy and the more recent PIMS measurements (appearance potential of $SiH_4^{+\bullet} = 11.00 \pm 0.02$ eV) could be explained by theoretical calculations which reveal that the $SiH_4^{+\bullet}$ cation undergoes a strong Jahn-Teller distortion[8–10]. The ground state of $SiH_4^{+\bullet}$ possesses a D_{4h} symmetry, **1**, whereas the tetrahedral $SiH_4^{+\bullet}$ ion **2** lies 7.1 kcal mol^{-1} higher in energy[8].

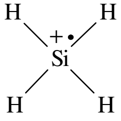

(1)

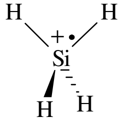

(2)

Thus the overlap between the vibrational wave functions of the tetrahedral **2** and Jahn-Teller distorted **1** is very small (weak Franck–Condon factors), and the small onset signal in the original PES measurement was simply overlooked in the significantly less sensitive PES experiments (as compared with PIMS).

Further support for the instability of $SiH_4^{+\bullet}$ comes from studies of the charge transfer reactions of a variety of small ions with SiH_4[11]. Although almost resonant charge transfer was achieved in the reaction of SiH_4 with $Xe^{+\bullet}$ ($\Delta IE = 0.08 \pm 0.21$ eV), no $SiH_4^{+\bullet}$ cations were observed in these guided-ion beam studies.

SiH_3^+ ions are easily formed in the reactions of noble gas cations and other small ions with SiH_4 via dissociative charge transfer (equation 1)[11].

$$X^{+\bullet} + SiH_4 \longrightarrow SiH_3^+ + X + H^\bullet \ (X = He, Ne, Ar) \qquad (1)$$

The appearance potential of SiH_3^+ formed from SiH_4 has been measured at 12.086 eV via PIMS[6].

The silylene cation, $SiH_2^{+\bullet}$ has been studied in a number of experimental setups[12,13]. As indicated by MO calculations, the species possesses a C_{2v} structure[8–10,14–16]. The heat of formation of $SiH_2^{+\bullet}$ has been determined as 12.06 eV[11]. This ion is one of the main products found upon ionization of SiH_4. Besides generation via electron ionization (EI), SiH^+ can be generated in the dissociative charge transfer reaction of SiH_4 with small ions[11].

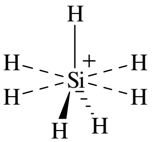

(3)

An interesting study on the hypervalent silanium ions SiH_7^+ has been carried out by Cao and coworkers[17]. These authors measured the infrared spectrum of **3** by vibrational predissociation spectroscopy. The ions were generated from a SiH_4/H_2 mixture in a high-pressure glow discharge source. A structure corresponding to a $H_2{-}SiH_3^+{-}H_2$

complex was assigned to this species. These findings are rather interesting in view of the fact that the hypervalent CH_7^+ congener is believed to possess a structure corresponding to a CH_5^+ complexed with a H_2 spectator molecule.

B. Substituted Silicenium Ions

While silicenium ions are still a rather elusive species in the solid state or in solution[18], their generation in the gas phase represents no major difficulties and their properties have been studied in great detail. In fact, the wealth of data that has been accumulated does not allow for a full treatment of all the results in this short section. Rather, we will confine ourselves to the discussion of a number of the more prominent examples here. Further details will also be discussed in Sections III and IV.

The methyl-substituted silicenium ions $SiMe_3^+$, $SiMe_2H^+$ and $SiMeH_2^+$ have been investigated by a number of groups. A particularly interesting study has been carried out by Shin and Beauchamp[19]. In this work the authors measured the hydride affinities of the Me_xSiH_{3-x} cations and compared these values with those of the carbon analogues. The results clearly indicate that the corresponding silyl-substituted ions are significantly more stable than the carbon species (when H^- is used as a reference base). The heats of formation for the silicenium ions $SiMeH_2^+$, $SiMe_2H^+$ and $SiMe_3^+$ (calculated from these hydride affinities) were determined to be 204, 172 and 147 kcal mol^{-1}, respectively, as compared to values of 215, 192 and 166 kcal mol^{-1} for $CMeH_2^+$, CMe_2H^+ and CMe_3^+. The apparent smaller stabilization of silicenium ions by successive methyl substitution can be explained by a smaller hyperconjugative interaction between the carbon−hydrogen σ bonds in the Si−C species due to the longer Si−C bond distance and the larger size of the empty Si 3p orbital, as compared with the C−C bond distance and the C 2p orbital. The relative stabilities of the MR_3^+ ions were shown to be strongly dependent on the reference anion that is used. When F^- or Cl^- are employed the $SiMe_3^+$ ion is significantly less stable than the CMe_3^+ cation. The higher affinity of silicenium ions for bases such as halogens or OH^- readily explains the fact that such species are not observed in the condensed phase[20].

The thermal-induced dissociation of tetraethylsilyl cations, $SiEt_4^{+\bullet}$, has been reported by Lin and Dunbar[21]. This technique which makes use of the blackbody background radiation field for the dissociation of a weakly bound cluster[22] allows for the study of weakly bound clusters with dissociation energies in the range of 0.5 to 1 eV. Thus, by measuring the rate constants for the loss of an ethyl radical from $SiEt_4^{+\bullet}$, a heat of formation of 131.7 ± 2 kcal mol^{-1} was derived for the $SiEt_3^+$ ion.

The thermochemistry of small SiX_n^+ cations, where X = F and Cl and $n = 1$–4, has been evaluated by Armentrout and coworkers[23–29]. ΔH_f° of SiF_3^+ was found to be −29.3 kcal mol^{-1}, while the value for the chlorine-analogue $SiCl_3^+$ is 99.8 kcal mol^{-1}. This difference reflects the exceptional thermodynamic stability of the Si−F bond. The significant differences in measured bond dissociation energies (BDE) when going from SiF_4^+ to SiF_3^+[27] (0.84 ± 0.16 eV and 6.29 ± 0.10 eV, respectively) can be explained by an enhancement of the s-orbital character in the lone-pair orbitals[30].

The resonance stabilization of the sila-allyl ion, $H_2C{=}CHSiH_2^+$, as compared to its other homologues, $H_2C{=}CHXH_2^+$ (C, Ge, Sn, Pb), has been studied theoretically by Gobbi and Frenking[31]. On the basis of *ab initio* calculations (MP2 level of theory), they predict that the resonance interaction decreases from 37.8 kcal mol^{-1} to 14.1 kcal mol^{-1} when going from the allyl cation to the sila-allyl species. The authors conclude in this study that in contrast to the allyl cations, the heavier analogues experience a significantly reduced stabilization by π-conjugative interactions.

C. Anionic Silicon Species

The thermochemistry of silicon-containing anions has very recently been compiled in an excellent review by Damrauer and Hankin[4], as well as in an earlier work by Damrauer[3]. In these reviews the authors give a detailed introduction into the experimental techniques as well as the cycles used to obtain thermodynamic data from negative-ion gas-phase chemistry. We will therefore confine ourselves here to the discussion of a few exemplary cases, and for a more detailed overview the reader is referred to the above-mentioned publications and the literature cited therein.

The formation and thermochemical properties of pentacoordinate silicon hydride anions, $SiH_{5-n}X_n^-$, have been reported by Squires and coworkers[32,33]. These ions can be generated via the addition of nucleophilic anions to silanes or, in the case of SiH_5^-[34,35], via hydride transfer from alkyl silicon hydride anions to SiH_4 in flowing afterglow experiments. It is interesting to note that Squires and coworkers observed hydride–deuteride exchange in the reaction of n-$BuSiH_4^-$ and SiD_4 of all four hydrogen atoms in the hydride anion. The hydride affinity ordering[36] of various alkylsilanes was determined from bracketing experiments, and was found to decrease with increasing alkyl substitution. However, the differences between the various alkylsilanes were found to be smaller than 2 kcal mol^{-1}. The absolute hydride affinity for SiH_4 was determined to lie between 19 and 20 kcal mol^{-1}.

The fact that α-silyl substitution leads to a significant stabilization of carbanionic species is well-known and has been exploited in synthetic chemistry. On the other hand, silyl anions themselves are in general much more stable than their carbon analogues. The stabilization of carbanions by silyl substituents in the α position has been measured by Brauman and coworkers[37]. The anions were generated via nucleophilic displacement reactions (equation 2) of a silyl group with F^-[38] (see also Section III.B).

$$F^- + (Me_3Si)_3SiH \longrightarrow (Me_3Si)_2SiH^- + Me_3SiF \tag{2}$$

The electron affinities of a number of α-silyl substituted silyl and carbon radicals were determined in photodetachment experiments and confirmed by data obtained from *ab initio* calculations. The authors conclude in this study that the stabilization a carbanion experiences through α-silyl substitution is approximately 14–20 kcal mol^{-1} per silyl group; that of a silyl anion is approximately 6–14 kcal mol^{-1}. The larger stabilization in the carbanionic systems is readily explained by stronger hyperconjugation of the anionic carbon center with the silyl groups as compared to that of the silyl anion with a silyl group.

Interestingly, theoretical studies[39] indicate that substituted silane radical anions $RSiH_3^{-\bullet}$ are stabilized more by second-row substituents than by first-row substituents. This increased stabilization was explained by the difference in the diffuseness of first- and second-row elements and thus a better overlap of the larger second-row orbitals with the anionic center.

III. ION–MOLECULE REACTIONS OF SILICON-CONTAINING MOLECULES

The field of ion–molecule reactions has profited immensely from the introduction of new techniques in mass spectrometry such as Fourier Transform Ion-Cyclotron Resonance Mass Spectrometry (FT-ICR) and Selected-Ion Flow Tube methods (SIFT). Several accounts of the progress in the field of ion–molecule reactions involving silicon-containing molecules have been published. For review articles the reader is referred elsewhere[1,3,4,40–51] A detailed compilation of the kinetic data for bimolecular ion-molecule reactions of positive silicon ions has been published by Anicich[52].

A. Reactions of Transition-metal Ions with Silicon-containing Molecules

As already mentioned, due to progress on the experimental side the last decade has seen tremendous research efforts in the area of ion–molecule reactions, and especially, the reactions of metal cations with neutral organic molecules have received a great deal of interest[53]. In particular, the possibilities of studying biomimetic effects and obtaining data about the intrinsic properties of unligated ('bare') metal ions in mass spectrometric experiments have prompted intense research activities.

Although not as numerous and detailed as the studies of organic molecules with metal cations, there have been a number of experiments reported which deal with the reactions of silanes and metal cations. Kickel and Armentrout have studied the reactions of *all* first-row d metals with monosilane, SiH_4, and the data gathered in these guided ion beam studies have been used to evaluate the thermochemistry of the metal–silicon bond in $M{-}SiH_x{}^+$ ions[54–57]. The authors analyzed the kinetic energy dependence found for the reactions of the metal cations with SiH_4 to obtain the bond energies for the metal–silicon bond in the $M{-}SiH_x{}^+$ ions ($x = 0{-}3$) (Table 1). The nature of the metal–silicon double bonds in these cationic $M{=}SiH_2{}^+$ complexes has been analyzed by *ab initio* (FORS-MCSCF) calculations[58,59].

Geribaldi and coworkers have examined the oligomerization of SiH_4 with the rare earth ions Sc^+, Y^+ and Lu^+[60,61a]. In these FT-ICR studies, clustering of up to seven silane molecules around a metal ion was observed. In the additions of silane molecules to the metal center, the excess energy of the initial complex was found to be dissipated via sequential H_2 loss, thus giving rise to $MSi_nH_{2n}{}^+$ ions among various other products (equation 3).

$$M^+ \ (M = Sc,\ Y,\ Lu) + n SiH_4 \longrightarrow M(SiH_2)_n{}^+ + n H_2 \qquad (3)$$

The reactions of the cations Fe^+, Co^+ and Ni^+ with cyclic silanes have been investigated in two separate ICR studies[62,63]. Bjarnason and Arnason reacted 1,3,5-trisilacyclohexane with bare and Cp-ligated metal ions. The authors observed the dehydrogenation of up to six hydrogen atoms from the trisilacyclohexane (equation 4) which led them to postulate a benzenoid structure **4** for the new metal-ligated $Si_3C_3H_6$ ligand. Further support for this structural assignment came from labeling studies and collisional induced dissociation (CID) experiments. Upon collisional activation the $(Cp)M{-}Si_3C_3H_6{}^+$ ions were found to lose an intact $Si_3C_3H_6$ unit as a main dissociation product, thus regenerating the $(Cp)M^+$ cations.

$$(Cp)M^+ + c\text{-}C_3Si_3H_{12} \longrightarrow (Cp)M{-}Si_3C_3H_6{}^+ + 3H_2 \ (M = Fe,\ Co,\ Ni) \qquad (4)$$

Similar experiments have been carried out with the monosilyl substituted cyclohexane, C_5SiH_{12}[63]. Reactions of the silane with Fe^+, Co^+ and Ni^+ in this case, however, did not lead to dehydrogenation, but instead to mainly ethene elimination. Labeling studies indicated a reaction mechanism as depicted in equation 5. Initially, insertion of the metal

TABLE 1. Experimental bond energies (D) at 0 K in eV[54–57]

D(eV)	Sc	Ti	V	Cr	Mn	Fe	Co	Ni	Cu	Zn
$D(M{-}Si^+)$	2.51	2.54	2.37	2.10	>0.87	2.87	3.03	3.38	2.65	2.84
$D(M{-}SiH^+)$	2.33	2.30	2.09	1.02	—	2.63	2.29	2.39	2.55	3.37
$D(M{-}SiH_2{}^+)$	2.17	2.17	2.02	0.99	0.43	1.88	2.66	2.66	2.39	1.65
$D(M{-}SiH_3{}^+)$	1.76	1.69	1.54	0.78	—	1.90	1.96	1.91	1.00	3.11

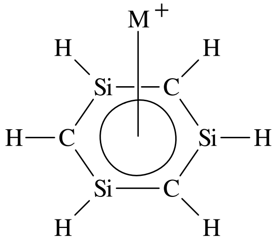

(4)

ion into the weak Si−C bond is believed to take place forming the metallacycle **5**, which subsequently can eliminate an ethene molecule.

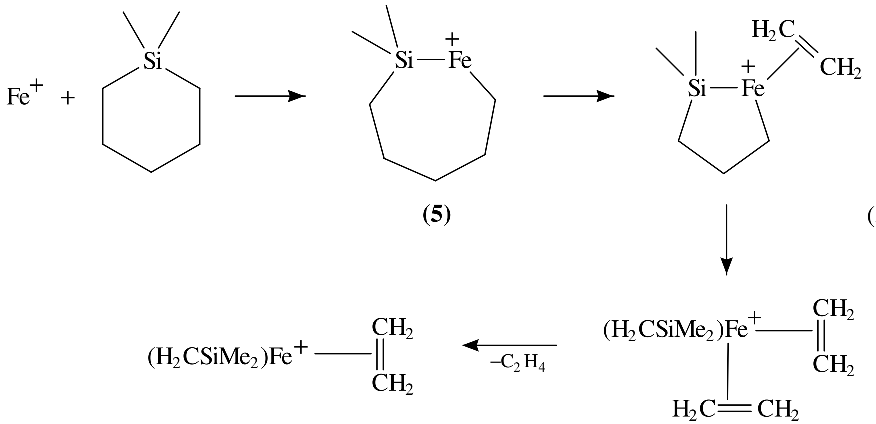

(5)

The enhanced tendency of the monosilacyclohexane to expel an ethene molecule and the fact that no ring cleavage was observed in the case of the trisilacyclohexane was tentatively explained by the lack of a stable leaving group in the latter case. In fact, the much smaller thermodynamic stability of the $H_2Si{=}CH_2$ leaving group seems to strengthen this argument.

Jacobson and coworkers[64,65] have recently investigated the reactions of Fe^+ with a variety of organosilanes. They reported compelling evidence for the formation of cationic iron−silylene, FeSiRR′, as well as iron−silene complexes, Fe−RR′Si=CR″R‴ (R^n = alkyl, H), which can be produced independently by reacting Fe^+ with different organosilicon molecules. Thus, reaction of Fe^+ with **6** can give rise to two different insertion products **7** and **8**, which form the metal−silene complex **10** via formation of the π-bonded species **9** and subsequent loss of an ethene molecule (equation 6). Whether the metal atom inserts into the thermodynamically weak Si−C bond or into the strained C1−C2 bond of the ring could not be distinguished on the basis of isotopic labeling studies; however, on the grounds that the silicon−carbon bond is considerably weaker than the C−C bond, insertion into a C−C bond seems less likely. Reaction of bare Fe^+ with dimethylsilane and ethenylsilanes (equation 7), on the other hand, was found to result in the formation of the isomeric iron−silylene complexes. The proposed mechanism for this reaction involves insertion into the Si−H bond giving **11**, as shown in path 7a, or into the vinylic C−Si bond giving **12** (path 7b). Subsequent formation of the silylene complex **13** can then proceed via ethene elimination following either an α- or β-H shift.

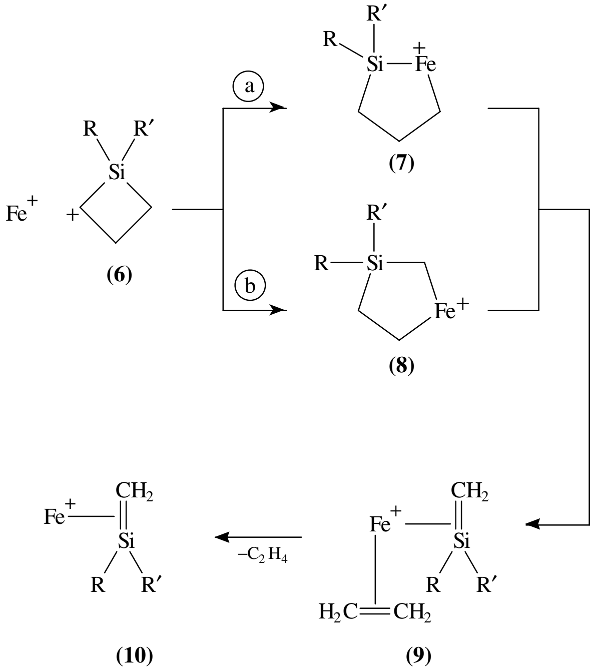

(6)

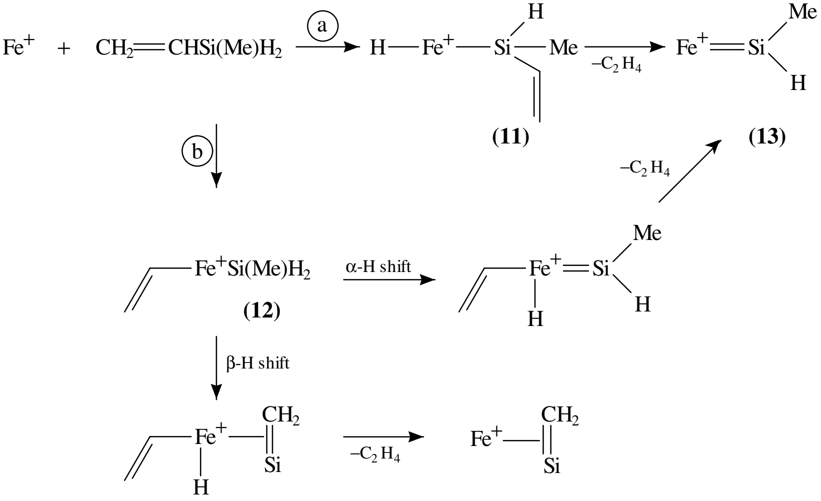

(7)

Data obtained from collision-induced dissociation experiments did not allow for a distinction of the isomeric metal–silene and–silylene species; however, structure-specific ion–molecule reactions of the complexes with labeled ethene were used to clearly differentiate between the metal silene and the silylene. In this intriguing study, Jacobson and coworkers also bracketed the bond dissociation energies of the isomeric ions.

They found that the dissociation energy for the silylene $Fe{-}Si(Me)H^+$ lies between 56 and 78 kcal mol^{-1}, and that of the silene isomer $Fe{-}H_2Si{=}CH_2{}^+$ between 55 and 70 kcal mol^{-1}. The similarity of the two energy ranges once again demonstrates the relative lability of the metal–silylene bond and suggests a potential stabilization of molecules which contain silicon, π-bonded to transition metals.

Replacement of CO in $FeCO^+$ by small silanes was observed to lead to strongly bound σ-complexes (equation 8)[66]. On the basis of simple displacement reactions it was concluded that the silane–metal ions actually correspond to the non-inserted species **14** (for $x = 0$) rather than the inserted isomer **15**. The binding energies of the metal–silane bond were observed to increase in the order of $Me_2SiH_2 > Me_3SiH > MeSiH_3 > Me_4Si > SiH_4$. The actual energies were found to lie in the range 39.9 ± 1.4 kcal mol^{-1} for D^o $Fe^+{-}SiMe_2H_2$ and 31.3 ± 1.8 kcal mol^{-1} for D^o $[Fe^+{-}SiH_4]$—values almost twice as high as those reported for simple alkanes (e.g. $D^o[\text{Fe–propane}] = 19 \pm 2$ kcal mol^{-1})[67]. The interesting trends in bond strength upon methyl substitution were tentatively explained by an interplay between polarizability of the silanes and σ-donation/σ^*-back donation features in these adducts.

$$Fe(CO)^+ + H_{4-x}SiMe_x \ (x = 0\text{–}4) \longrightarrow FeH_{4-x}SiMe_x{}^+ + CO \qquad (8)$$

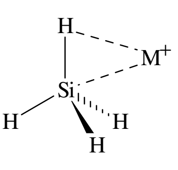
(14)

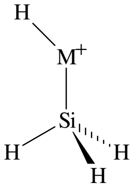
(15)

An interesting example for a methide transfer was observed in the reaction of Fe^+ and Co^+ cations with bis(trimethylsilyl)amine **(16)** and bis(trimethylsilyl)methane **(17)**[68]. The complexes of these molecules with the metal cations unimolecularly lose a neutral MCH_3 species (equation 9). Such processes had hitherto only been observed for the reactions of atomic Cu^+ with organic molecules. In these cases the formation of the strongly bound $CuCH_3$ species[69] (formally a d^{10} compound) compensates for the endothermicity of the carbenium ion formation. The observation of methide transfer from a trimethylsilyl group thus reflects the enhanced intrinsic stability of silicenium ions as compared with their carbon analogues (see Section II).

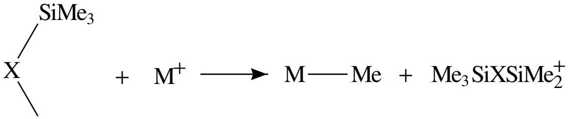

$$X(SiMe_3)_2 + M^+ \longrightarrow M{-}Me + Me_3SiXSiMe_2^+ \qquad (9)$$

(16) X = NH
(17) X = CH_2

The reactions of Fe^+ cations with a number of bis(trimethylsilyl) substituted amines and alkanes have been studied by Karrass and Schwarz[70]. Specific labeling studies indicate that the unimolecular decomposition of the ion–molecule complex proceeds via two possible intermediates, i.e. **18** or **19**. Both intermediates, however, require a β-methyl shift to be operative, in order to explain the experimentally observed loss of a neutral ethane molecule, which was found to occur from **20** (equation 10).

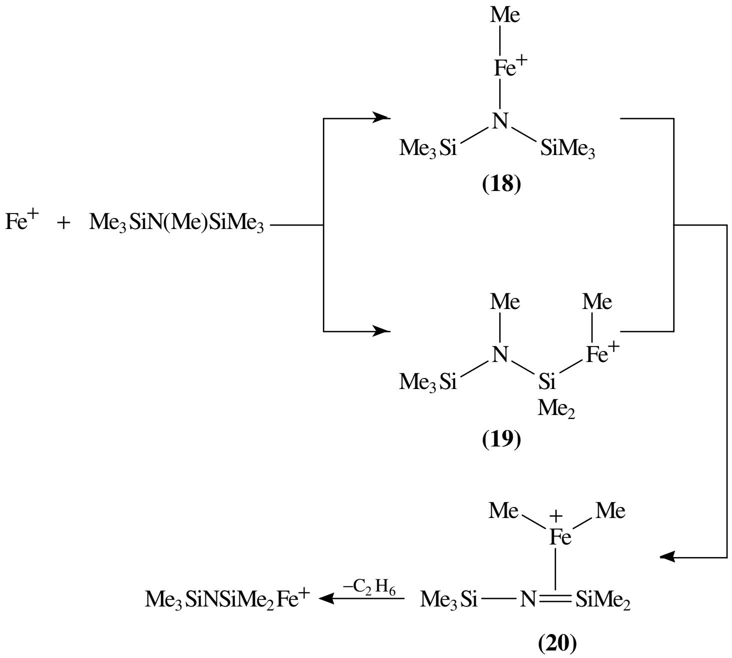

(10)

The mechanism of the C−H and C−C bond activation of bare Fe^+ with n-heptyltrimethylsilane has been elucidated with the help of extensive labeling studies[71]. The system was found to display a rather rich chemistry. Loss of neutral tetramethylsilane from the ion–molecule complex (equation 11) was explained by an initial insertion of the metal ion into the C1−C2 bond to form **21**, and a subsequent β-H shift giving rise to the iron–hydride complex **22**. This ion can then lose a tetramethylsilane molecule via reductive elimination.

The observed competitive loss of ethene in this system, together with labeling studies, point to an extensive skeletal rearrangement of the heptyl chain prior to the dissociation.

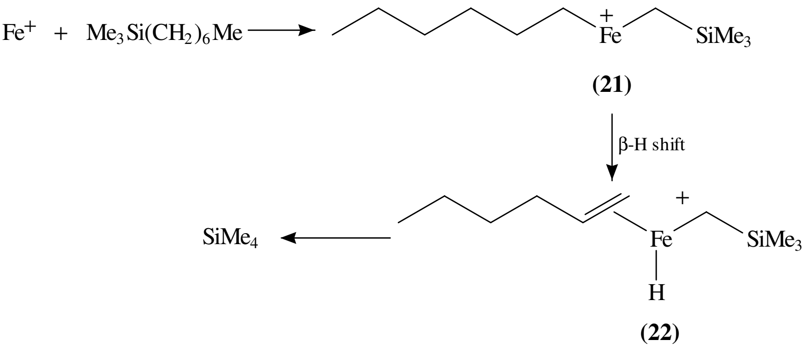

(11)

Interestingly, the closely related but now bifunctional system of the Fe^+ complex with 7-trimethylsilyl heptanenitrile displays a significantly different reactivity[72a]. No C−C bond activation was observed in the unimolecular decay of this ion−molecule complex, and the exclusive loss of an H_2 molecule was explained by the operation of a metal−ion mediated cooperative effect of the two functional groups. A suggested reaction mechanism involves an 'anchoring' of the metal cation in an end-on mode to the nitrogen atom of the nitrile group[53] and the loss of H_2 via an initial formation of a site-specific, silyl directed C−H bond activation (cf **23a**). A β-H shift can then give rise to the iron−dihydride complex **23b** and subsequent formation of H_2 via reductive elimination (equation 12). The fact that the hydrogen atoms were found to stem exclusively from the C6 and C7 positions of the methylene chain further supported this reaction mechanism as the postulated intermediate **23a** should gain some stabilization through the silicon atom in the β-position.

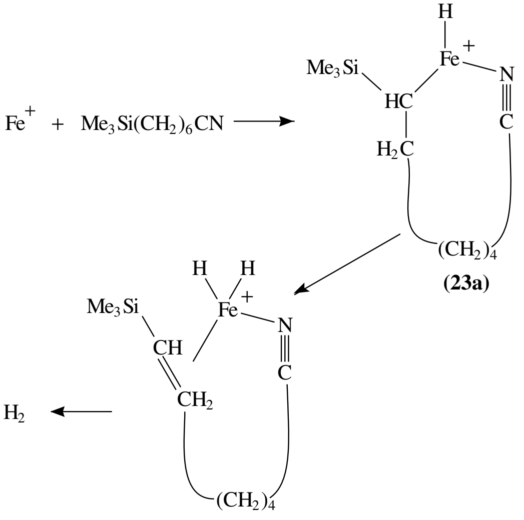

(23a)

(23b)

(12)

Recently the unprecedented example of stereoselective C−Si bond activation in ω-silyl-substituted alkane nitriles by 'bare' $C_o{}^+$ cations has been reported by Hornung and coworkers[72b]. Very little is known of the gas-phase reactions of anionic metal complexes with silanes. In fact there seems to be only one such study which has been carried out by McDonald and coworkers[73]. In this work the reaction of the metal−carbonyl anions $Fe(CO)_n{}^-$ ($n = 2, 3$) and $Mn(CO)_n{}^-$ ($n = 3, 4$) with trimethylsilane and SiH_4 have been examined. The reactions of $Fe(CO)_3{}^-$ and $Mn(CO)_4{}^-$ anions exclusively formed the corresponding adduct ions via an oxidative insertion into the Si−H bonds of the silanes. The 13- and 14-electron ions $Fe(CO)_2{}^-$ and $Mn(CO)_3{}^-$ were observed to form dehydrogenation products $(CO)_xM(\eta^2-CH_2{=}SiMe_2)^-$ besides simple adduct formation with trimethylsilane. The reaction of these metal carbonyl anions with SiH_4 afforded the dehydrogenation products $(CO)_2Fe(H)(SiH)^-$ and $(CO)_3Mn(H)(SiH)^-$.

B. Use of Silicon Compounds as Precursors for the Generation of Elusive Carbanions

The utility of the 'DePuy fluoride-induced desilylation reaction'[38] for the regioselective generation of gas-phase carbanions from trimethylsilyl compounds (equation 13) has been exploited by Squires and coworkers in a number of very elegant flowing-afterglow studies[74–78]. The driving force for this reaction is the formation of the extremely strong bond between silicon and fluorine, and Squires and colleagues have further pioneered this technique for the generation of a number of distonic anions. In these studies they used a second fluoride-induced desilylation reaction between the trimethylsilyl-containing anions and F_2 to generate biradical anions. This subsequent reaction allowed the generation of such elusive species as the trimethylenemethane anion **25**[76], via formation of anion **24b** (equation 14) from **24a.** The photoelectron spectrum of **25** generated via desilylation has thus recently been obtained and the electron affinity, as well as the singlet–triplet splitting of the neutral trimethylenemethane ($^3A_2'-^1A_1 = 16.1$ kcal mol^{-1}), have been determined from these data[79].

$$R{-}SiMe_3 + F^- \longrightarrow R^- + FSiMe_3 \tag{13}$$

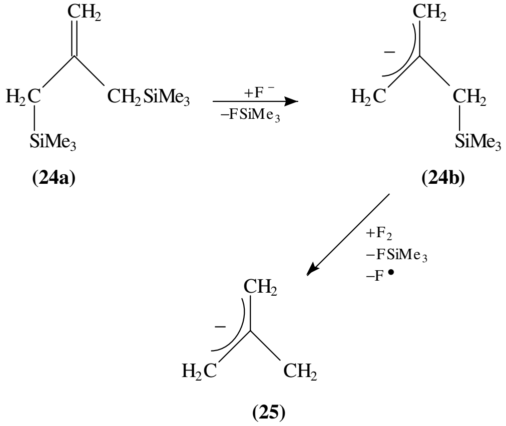

(14)

There is still a significant interest in the generation of such anions as a straightforward synthesis of these ions would allow the measurement of fundamental properties such as the acid–base character of neutral diradicals[80], their electron affinities and, most importantly, the singlet–triplet gaps of the diradical species[81,82]. Thus Squires and coworkers employed the desilylation reaction for the regioselective generation of chlorophenyl anions from the *meta*- and *para*-trimethylsilyl-substituted chlorobenzenes (**26** and **27**) (equation 15). Subsequent collision-induced dissociation of anions **28** and **29** gave rise to the *meta* **(30)** and *para* isomers **(31)**[76] of the elusive *ortho*-benzyne **(32)**[83]. Upon measuring the threshold for the dissociation reactions, the heats of formation for the neutral cyclic C_6H_4 isomers could thus be experimentally determined for the first time ($\Delta H^\circ_{298} = 122.0 \pm 3.1$; 137.3 ± 3.3 and 106.6 ± 3.0 kcal mol^{-1} for **30**, **31** and **32**, respectively)[78].

The desilylation procedure has furthermore been employed in the targeted synthesis of a number of enolate anions. In these intriguing flowing-afterglow studies the enolate anions were generated regioselectively by desilylation of the corresponding trimethylsilyl enol ethers with fluoride anions (equation 16)[74,75]. The rate coefficients measured for methanol-catalyzed tautomerization of the corresponding enolate anions were employed to derive the equilibrium ratios of the corresponding tautomers.

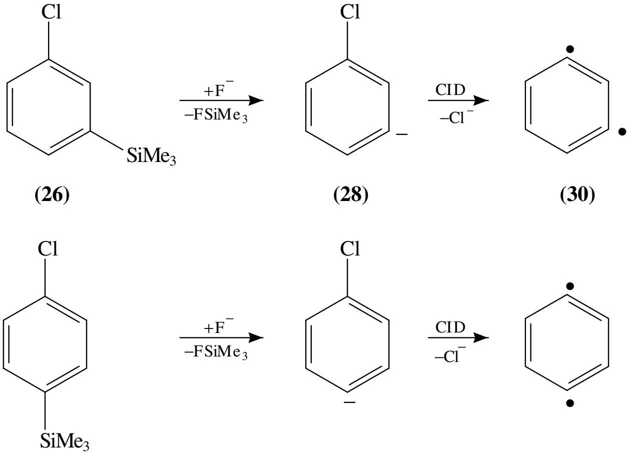

(26) **(28)** **(30)**

(27) **(29)** **(31)**

(15)

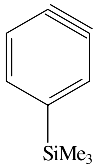

(32)

$$\mathrm{RR'C{=}CR''O{-}SiMe_3 + F^- \longrightarrow RR'C{=}CR''O^- + Me_3SiF}$$

$$\mathrm{R = R' = R'' = alkyl} \qquad (16)$$

C. Reactions of Atomic Silicon Cations with Neutral Molecules

The amount of literature which has accumulated over the last few years concerning the subject of ion–molecule reactions of silicon cations with neutral molecules is tremendous. In a review of the various reactions of $Si^{+\bullet}$ with neutral molecules published in 1990, Böhme[44] lists almost 100 reactions studied by selected-ion flow tube (SIFT) techniques alone[84,85]. In the meantime, this list will have grown to even larger dimensions and we can therefore only confine ourselves to the description of a few exemplary cases[45,50].

One of the reactions which has received special attention is the oxidation of $Si^{+\bullet}$ by oxygen-containing molecules. Thus the reaction of $Si^{+\bullet}$ in its ^2P ground state[86] with N_2O has been shown to give rise to $SiO^{+\bullet}$ which, in subsequent reactions with N_2O, has been reported to lead to the formation of the highly oxidized $SiO_4{}^{+\bullet}$ cation (equation 17)[87,88].

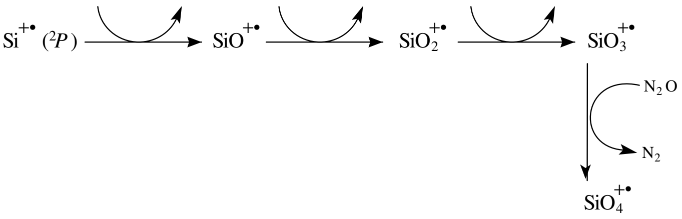

$$\mathrm{Si^{+\bullet}\,(^2\mathit{P}) \xrightarrow[\;]{N_2O \;\; N_2} SiO^{+\bullet} \xrightarrow[\;]{N_2O \;\; N_2} SiO_2^{+\bullet} \xrightarrow[\;]{N_2O \;\; N_2} SiO_3^{+\bullet} \xrightarrow[\;]{N_2O \;\; N_2} SiO_4^{+\bullet}} \qquad (17)$$

A subsequent ICR study of the reaction of $Si^{+\bullet}$ with N_2O has been carried out by Stöckigt and coworkers[89] in order to examine the structures of these polyoxides. Although the formation of a $SiO_4{}^{+\bullet}$ cation under ICR conditions was not observed, the $SiO_3{}^{+\bullet}$ ion was obtained in high abundance. Ligand displacement reactions and *ab initio* calculations (MP4/SDTQ) were used to elucidate the structure of this intriguing oxide. The studies suggest that **33** possesses a D_{3h} symmetrical $^4A_1'$ ground state. However, it should be noted that the $[Si,O_3]^{+\bullet}$ potential energy surface is probably rather flat and conversion to several other minima such as **34** and **35** is easily achieved. These quartet states which are ion–dipole complexes of $SiO^{+\bullet}$ and O_2 were calculated to be only 5.0 and 2.0 kcal mol^{-1} less stable than **33**.

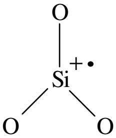

(33)

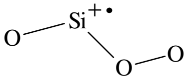

(34)

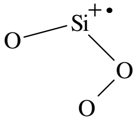

(35)

The reactions of $Si^{+\bullet}$ with small silanes have been examined in a number of experimental and theoretical studies. One of the reasons for the particular interest in these systems is due to a desire to understand plasma processes which are employed for the growth of silicon surfaces. Armentrout and coworkers studied the reactions of $Si^{+\bullet}$ with small silanes and hydrocarbons[24,90–92], and the data obtained have been used to evaluate the thermochemistry of a number of small organosilicon species (see also Section II). Thus the reactions of $Si^{+\bullet}$ (^2P) with methane[90] and ethane[91] have been investigated by guided ion beam techniques. The initial reaction step was found to correspond to an insertion into the covalent bonds of the hydrocarbon molecule. In the reaction of $Si^{+\bullet}$ with ethane, insertion into the C−C bond is exothermic by 65 kcal mol^{-1}. Thus, most products in this reaction evolve through an insertion into the C−C bond. However, a number of low-energy products that have been observed in this reaction, such as SiH^+ and $SiH_2{}^{+\bullet}$, cannot evolve directly via this reaction mechanism, and it was proposed that a relatively facile interconversion of silyl cations via a silacyclopropanium ion may take place.

There have been a number of theoretical studies describing the thermochemistry and structural properties of $SiC_nH_m{}^+$ cations. Ketvirtis and coworkers[93–95] investigated several small organosilicon cations by means of *ab initio* molecular orbital calculations, and found that, in general, the isomers which contain Si atoms that have no hydrogens bonded to them are considerably more stable than other isomers. This certainly is a consequence of the significantly weaker Si−H bond strength as compared to that of C−H bonds.

The association reactions of $Si^{+\bullet}$ (^2P) with acetylene and benzene have been measured by Glosik and coworkers[96], who found that the rate coefficients for these reactions have strong negative-temperature dependencies. These observations were rationalized in terms of a negative entropy change in the reactions.

D. Reactions of Silicon-containing Ions with Neutral Molecules

So-called clustering reactions of $SiH_n{}^+$ ions ($n = 0$–3) with silanes and other small molecules have attracted considerable interest. In particular, the reaction sequences which might lead to the formation of large-sized clusters have received attention, as these processes are thought to be involved in undesirable dust-formation which occurs during silicon-film depositions from silane plasmas and vapors[97–99]. Thus, Mandich and Reents have thoroughly studied the ion–molecule reactions of SiD_n^+ ions ($n = 0$–3) and Si_n^+ clusters ($n = 2$–7) with SiD_4[100–105]. These experimental studies were published together with companion papers by Raghavachari[106–109] in which quantum mechanical calculations (MP4/6-31G** level of theory) on the mechanisms of the clustering reactions were reported. The primary reaction pathway for the reactions of the SiD_n^+ ions was found to correspond to an insertion of the ion into a Si–D bond of SiD_4 and a subsequent D_2 loss from the ion–molecule complex (equation 18).

$$SiD_n{}^+ + SiD_4 \longrightarrow Si_2D_{n+2}{}^+ + D_2 \qquad (18)$$

The clustering reactions of the SiD_n^+ ions with SiD_4 were observed to stop at rather small cluster sizes, all leading to energetic bottlenecks. Addition of three SiD_2 units to SiD^+ gave rise to a $Si_4D_7^+$ ion[103] which, according to the theoretical calculations[108], corresponds to the highly stable silacyclobutyl cation. Further reactions of this ion were found to be endothermic.

The interesting nonclassical C_{2v}-symmeterical structure **36** was predicted to be the ground state structure for the $S_3H_7^+$ cation (and its deuterated analogue) which was calculated to correspond to the ground state of the potential energy surface[107]. This ion was obtained upon sequential SiH_2 addition to SiH_3^+ and its high stability was used to explain the inertness of $Si_3H_7^+$ in an SiH_4 atmosphere[102]. The termination of the clustering reactions of SiH_3^+ with SiH_4 was suggested to be due to the formation of this isomer. Thus it was concluded that clustering of silane in ion–molecule reactions reaches unreactive structures which contain less than six silicon atoms.

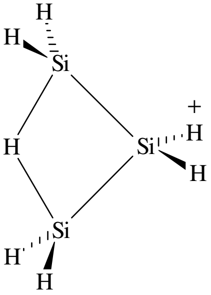

(36)

The clustering reactions of SiD_n^+ ($n = 0$–3) and $Si_2D_n^+$ ($n = 0$–6) cations with deuterated disilane, Si_2D_6, have been measured in a FTMS study[110]. The dominant pathway for these reactions was found to correspond to silylene transfer and SiD_4 elimination. The overall reactivity of disilane compared to monosilane was found to be higher, and this was explained by the fact that the silicon–silicon bond in disilane is considerably weaker (76 kcal mol^{-1}) than the Si–H bond of SiH_4 (88 kcal mol^{-1})[111]. Thus the insertion of $Si^{+\bullet}$ into the Si–Si bond was calculated to be 17 kcal mol^{-1} more favorable than $Si^{+\bullet}$ insertion into the Si–H bond of SiH_4[106,112].

Mandich and Reents[104] succeeded in observing the first reaction sequence which in fact leads to large-sized clusters in silane plasmas. They introduced a small amount of water along with the silane atmosphere and obtained clusters with masses of 650 amu and larger. Interestingly, the SiD^+ cation was found to correspond to the only SiD_x^+ cation which leads to the formation of a number of highly specific species. Among other clusters, the perdeuterated $Si_3D_7^+$ ion (**36**-D_7) is observed which then gives rise to the larger clusters upon reaction with D_2O and subsequent addition of a silylene unit from SiD_4 (equation 19).

$$\begin{aligned} Si_3D_7{}^+ + D_2O &\longrightarrow Si_3D_7O^+ + D_2 \\ Si_3D_7O^+ + n SiD_4 &\longrightarrow Si_{3+n}D_{7+2n}O^+ + nD_2 \end{aligned} \tag{19}$$

A number of other groups have investigated the clustering reactions of small cation silicon species with silanes and other small molecules. The ion–molecule reactions occurring between $SiH_x{}^+$ ($x = 0–3$) cations and neutral ammonia, as well as the reactions between $NH_x{}^+$ cations and SiH_4 were studied by FTMS[113,114]. The main channel for the reaction between $SiH_x{}^+$ ions and NH_3 was found to correspond to the elimination–addition reaction, well-known for silanes (equation 20), which formally corresponds to the transfer of a nitrene-unit (NH)[113].

$$SiH_x{}^+ + NH_3 \longrightarrow SiH_{x+1}N^+ + H_2 \tag{20}$$

Gal and coworkers[114] observed the formation of ionic clusters with up to five silicon and nitrogen atoms upon ionization of silane/ammonia mixtures. Again, the silylene and nitrene transfers via addition–elimination reactions were found to be the most important pathways leading to the formation of larger clusters (equation 21). However, it was concluded in these studies that chain propagation leading to the formation of large-sized clusters was not possible in these systems.

$$\begin{aligned} Si_xN_yH_n{}^+ + SiH_4 &\longrightarrow Si_{x+1}N_yH_{n+2} + H_2 \\ Si_xN_yH_n{}^+ + NH_3 &\longrightarrow Si_xN_{y+1}H_{n+1} + H_2 \end{aligned} \tag{21}$$

The ion–molecule reactions that occur in mixtures of SiH_4 and PH_3 have recently been described[115]. As in the aforementioned cases, the main reaction channels for the formation of larger-sized clusters from $SiH_n{}^+$ cations ($n = 0–3$) and PH_3, and from the reactions of $PH_x{}^+$ cations ($n = 0–3$) with SiH_4, correspond to the addition of the neutral molecule and dissipation of the excess energy via loss of a hydrogen molecule. It was concluded in this study that the nucleation of mixed silicon–phosphorous ions was favored upon ionization of mixtures that contain a large excess of SiH_4.

Experiments similar to those described above have been performed by Operti and coworkers[116–118] who investigated the gas-phase ion–molecule reactions taking place in silane/germane mixtures and their methyl derivatives. For the GeH_4/SiH_4 mixtures, the formation of mixed germanium and silicon-containing ions $GeSiH_n{}^+$ ($n = 2–5$) was observed. Ionization of SiH_3Me/GeH_4 mixtures was found to give rise to a number of ions containing the C, Si and Ge atoms.

Lim and Lampe[119] have studied the ion–molecule reactions in mixtures of SiH_4 and CO. During the course of these studies the authors observed that the intermediate $CSiH^+$ ion readily protonates CO and proposed that this reaction (equation 22) might be a possible source for the neutral SiC molecule in interstellar space.

$$CSiH^+ + CO \longrightarrow HCO^+ + SiC \tag{22}$$

The structure of ionic silicon clusters, the mixed silicon–carbon species and their reactions with neutral molecules have been investigated by a number of experimental[151,120–133] and theoretical groups[134–137]. Ion–molecule reactions of the silicon clusters have also been thoroughly studied by Jarrold and coworkers[51]. These authors reported for the reactions of larger silicon clusters with neutral molecules a simple association reaction (chemisorption); e.g. $Si_n{}^+$ reacts with C_2H_4 according to equation 23.

$$Si_n{}^+ + nC_2H_4 \longrightarrow Si_n(C_2H_4)_n{}^+ \tag{23}$$

Magic numbers for the stability of the clusters, and large variations in reactivity with respect to the number of silicon atoms per ionic cluster unit have not been observed in these experiments. The only cluster ion that displays some unique behavior was found to be $Si_{13}{}^{+\bullet}$. This cluster has been shown to be particularly unreactive in its ion–molecule reactions with O_2, H_2O and C_2H_4. As initially suggested in theoretical studies[138,139], the low reactivity of $Si_{13}{}^{+\bullet}$ was believed to be related to its proposed icosahedral structures (13, 19 and 23 atoms are magic numbers for an icosahedral packing sequence). However, recent Carr–Parrinello calculations by Andreoni and coworkers[140] show that the icosahedral structure corresponds to a high-energy isomer for the $Si_{13}{}^{+\bullet}$ cation.

The chemistry of mixed carbon- and silicon-containing cluster ions has been studied by several groups[128–133,141]. Parent reported the rate constants for the reactions of $SiC_n{}^+$ ($n = 2$–8) and $Si_2C_n{}^+$ ($n \leqslant 6$) with acetylene[130]. In this study an interesting exchange of carbon atoms upon reaction of ^{13}C-labeled $Si_2{}^{13}C_n{}^+$ clusters was observed (equation 24).

$$\begin{aligned} Si_2{}^{13}C_n{}^+ + {}^{12}C_2H_2 &\longrightarrow Si_2{}^{13}C_{n-1}{}^{12}C^+ + {}^{13}C^{12}CH_2 \\ &\longrightarrow Si_2{}^{13}C_{n-2}{}^{12}C_2{}^+ + {}^{13}C_2H_2 \end{aligned} \tag{24}$$

Interestingly, this carbon exchange was not observed in the reactions of acetylene with cluster ions which contain only one silicon atom. On the basis of the exchange reactions and CID experiments, it was concluded that the mixed clusters possess linear chain-like geometries. These findings were later confirmed by theoretical calculations of the $[Si_2, C_2]^+$ surface [RHF/CCSD(T) and UB3LYP-level of theory][137] which established that the linear $Si{=}C{=}C{=}Si^{+\bullet}$ cation does indeed correspond to the energetically most favorable structure. Very recently Negishi and coworkers[133] measured the reactions of cationic as well as anionic silicon–carbon clusters, $SiC_n{}^{+/-}$ ($n = 1$–6) with O_2. For all the cations, only the O atom adducts were observed in these experiments. The anion $SiC_2{}^-$ was found to form the oxygen adduct, SiC_2O^-, whereas the larger $SiC_n{}^-$ species did not react with O_2.

New reactions of neutral molecules with the trimethylsilyl ion, Me_3Si^+, have been studied by several groups. The Me_3Si^+ ion has been demonstrated to readily undergo radiative association reactions[48] (equation 25) with a number of bases[48,142,143]. In these reactions the initial complexation energy gained and stored in the ion–molecule complex is dissipated by emission of photons. It was concluded that the efficiency of these association reactions increased with increasing bond dissociation energy and higher number of degrees of freedom in the adducts.

$$SiMe_3{}^+ + B \longrightarrow [BSiMe_3{}^+]^* \longrightarrow BSiMe_3{}^+ + h\nu \tag{25}$$

The gas-phase affinities of primary, secondary and tertiary alkyl amines towards Me_3Si^+ were determined in a high-pressure mass spectrometer. The Me_3Si^+ affinities were found to increase linearly with the proton affinities of the amines. In these measurements trialkyl amines were found to undergo only very slow associations with Me_3Si^+ ions, which was explained by steric effects. The proton affinities of trimethylsilylamines which have been measured in these studies demonstrated again that the ability of an α-silicon to stabilize a positive charge on nitrogen is somewhat smaller than that at a carbon atom.

The aromatic silylation of benzene and substituted benzenes by Me_3Si^+ have been studied by several groups. In a high-pressure mass-spectrometric study, Stone and Stone[144] investigated the nature of the bonding in the adduct ions. They determined that the entropy value for the association of Me_3Si^+ with toluene (33.6±2.0 cal K^{-1} mol^{-1}) is significantly smaller than that of Me_3C^+ (54.6 ± 0.8 cal K^{-1} mol^{-1}). On the basis of these values the authors argue that the Me_3Si^+ ion in its toluene adduct must have considerable rotational freedom and is likely to correspond to a loose complex rather than to an arenium ion, or the energy difference between these two structures must be very small.

The ion–molecule reactions of Me_3Si^+ have been employed to distinguish between the *cis*- and *trans*- isomers of 1,2-cyclopentanediol[145]. The formation of a $[Me_3SiOH_2]^+$ cation (equation 26, top) was found to be indicative for a *cis*-structure of the reacted diol **37.** Thus the formation of the $[Me_3SiOH_2]^+$ cation from the adduct **38** proceeds without a barrier, whereas the production of this ion from the *trans*-diol **39** via adduct **40** (equation 26, bottom) was shown to be an endothermic process which possesses a translational energy onset. These studies are the first to use the reactivity of the Me_3Si^+ ion as a probe of the stereochemistry of the reacted neutrals in a mass spectrometer.

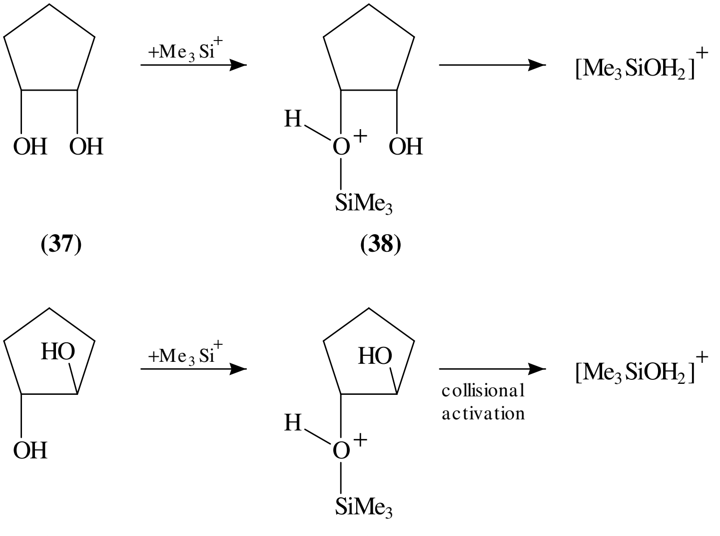

(37) **(38)**

(26)

(39) **(40)**

IV. GENERATION AND CHARACTERIZATION OF SMALL MULTIPLY BONDED SILICON-CONTAINING IONS AND THEIR NEUTRAL COUNTERPARTS

Over the past years a number of small silicon-containing ions have been structurally characterized by collisional-activation mass spectrometry. These ions have been used as precursors for the generation of their neutral counterparts via Neutralization–Reionization Mass Spectrometry (NRMS)[146–152]. To a large extent the interest in small elusive silicon-containing molecules is due to the role which these species have been postulated to play as intermediates and building blocks in the genesis of interstellar matter[46,85]. In particular, the different conceivable pathways which lead from atomic silicon cations to the formation of neutral silicon-containing molecules have been studied intensely[43–46,153]. A second driving force for the elucidation of the gas-phase chemistry of small silicon-containing ions and neutrals is the increasing importance of silicon-etching technologies[154]. These processes are known to lead to a large variety of ionic as well as neutral molecules and a better understanding of their chemistry is highly desirable.

A. Small SiC_xH_y Cations with Si−C Multiple Bonds and Their Neutral Counterparts

There has been particular interest in the chemistry of small organosilicon ions and their neutral counterparts for a number of reasons: (i) Small SiC_xH_y molecules are well suited to draw analogies between the structural chemistry of silicon and carbon — or to state differences. (ii) The chemistry of small silicon compounds is viewed as fundamental in astrophysics and astrochemistry, and a large number of cationic and neutral SiR_x molecules have been detected in interstellar and circumstellar matter.

The $SiCH_x^+$ ($x = 1$–3) (**41**–**43**) cations have been generated upon electron ionization (EI) of H_3SiCH_2Cl[155]. Collisional activation mass spectrometry (CA-MS) confirms that the hydrogen atoms reside on the carbon atom rather than on silicon in these ions — findings which are in keeping with the results from *ab initio* calculations[156].

$$HC{\equiv}Si^{+} \qquad H_2C{\equiv}Si^{+\bullet} \qquad H_3C{-}Si^{+}$$

(41) **(42)** **(43)**

Subsequent NR experiments[155] proved for the first time that the corresponding neutral counterparts of cations **41**–**43** are viable species in the gas phase.

EI of $Si(CH_3)_4$ yields ions of $[H_4,C,Si]^{+\bullet}$ and $[H_6,C_2,Si]^{+\bullet}$ compositions[157]. These ions have been previously observed in ion–molecule reactions of $Si^{+\bullet}$ with alkanes[90,91,158]. CA-mass spectrometry was used to establish that these ions correspond to the silylenes **44** and **45**.

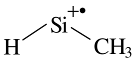

(44)

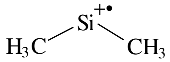

(45)

These findings are in agreement with the results of earlier theoretical results[158] which had predicted the cationic silylene **(44)** to correspond to the global minimum on the $[H_4,C,Si]^{+\bullet}$ surface. MP4 6-31G* calculations predicted the silaethene isomer $H_2CSiH_2^{+\bullet}$ to lie only 6.7 kcal mol^{-1} above the silylene, yet separated by a substantial barrier of 42.6 kcal mol^{-1}. The successful generation and characterization of the corresponding neutral silylenes $HSiCH_3$ and H_3CSiCH_3 by NRMS was in accordance with the results of earlier matrix-isolation experiments[159–163] which had shown that the silylene isomers of these molecules are energetically favored over the silaethene species.

Schwarz and coworkers[164,165] have been successful in characterizing several cationic silicon-acetylides $Si(C{\equiv}C)_nH^+$ ($n = 1$–3) (**46**–**48**) and their neutral counterparts via NRMS. Common to these and related species is the absence of (weak) Si−H bonds.

$$^{+}Si{-}C{\equiv}C{-}H \qquad ^{+}Si{-}C{\equiv}C{-}C{\equiv}C{-}H$$

(46) **(47)**

$$^{+}Si{-}C{\equiv}C{-}C{\equiv}C{-}C{\equiv}C{-}H$$

(48)

The SiC_2H^+ cations were generated by electron impact ionization of $(H_3C)_3SiC{\equiv}CH$. In agreement with *ab initio* data[166] which predict the Si-protonated C_2SiH^+ to be

94 kcal mol^{-1} less stable than the corresponding C-protonated molecule, a connectivity corresponding to a SiC_2H^+ ion was established via CA experiments. The neutral $SiC_2H^\bullet$ radical was successfully generated upon neutralization of the cationic precursor **(46)**. As suggested by theory[167] the linear acetylene, $SiC_2H^\bullet$ is approximately 4.5 kcal mol^{-1} more stable than the cyclic isomer and 70 kcal mol^{-1} energetically favored over the silylene radical.

The higher acetylene radicals $SiC_4H^\bullet$ and $SiC_6H^\bullet$ have received some experimental interest as these acetylenes are believed to play an important role in the interstellar genesis of silicon carbides (equation 27)[168,169].

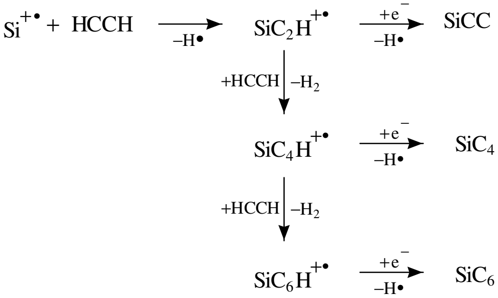

(27)

The cationic SiC_4H^+ and SiC_6H^+ molecules have been generated upon electron bombardment of phenylsilane. CA experiments indicate that, as in the case of the smaller homologue **46**, the hydrogen atom resides on the terminal carbon atom in these species. The successful neutralization of these ionic species by electron capture is believed to have some interesting implications for the proposed interstellar genesis of silicon–carbide species SiC_n as the experiments indicate that these acetylene molecules are stable species (at least on the μsec time-scale); of course, due to the different energetics neutralization of SiC_xH^+ under NR conditions does not necessarily lead to detachment of a hydrogen atom.

Another example which clearly demonstrates the advantageous interplay between different experimental techniques and state-of-the-art *ab initio* methods is that of the ionic and neutral 3-silacyclopropenylidene **(49)** and its isomers **50–53**[170].

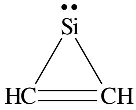

(49)

$H_2C{=}C{=}Si{:}$

(50)

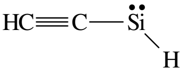

(51)

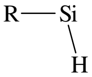

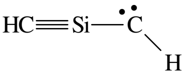

(52)

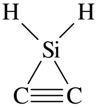

(53)

In the ion-source EI spectrum of $ClSi(CH_3)_3$, ions of the formal composition $[H_2,C_2,Si]^{+\bullet}$ have been observed[171]. Collisional activation experiments performed with these ions indicated that they possess a cyclic structure **49**[170]. The successful neutralization of this ion demonstrates nicely the stability of the corresponding cyclic silylene, and NRMS experiments could in fact distinguish this isomer from other conceivable species, such as **52** or **53**. These results were supported by *ab initio* MO calculations[172,173] which predicted the singlet isomer **51** to correspond to the energetically most stable species on the $[H_2,C_2,Si]$ hypersurface. Surprising experimental results on this system have been reported recently by Maier and coworkers[174,175] who also found the cyclic silacyclopropyne **(53)** to be a stable species under matrix isolation conditions[176,177].

The reactivity exhibited by silicon cations π-bonded to arenes such as benzene **(54)** and naphthalene[178] **(55)** has been demonstrated to be significantly different from that of atomic silicon ions[153,178]. In this context the parent system $Si{-}C_6H_6{}^{+\bullet}$ generated by co-ionization of $SiMe_4$ and benzene, has been studied by CA and NRMS methods[179]. The π-complex, **54** is readily distinguishable from the inserted σ-bonded silylene $PhSiH^{+\bullet}$ **(56)** by mass spectrometric means. Theoretical results[179] (MP2/6-31G**) reveal the cationic $Si{-}C_6H_6{}^{+\bullet}$ to prefer a C_s structure rather than the silicon being bonded on the center of the C_6 axis. This latter structure was found to correspond to a transition state. The isomeric phenylsilylene cation **(56)** was found to lie 5.5 kcal mol^{-1} higher in energy, thus indicating that in fact the ionic chemistry of silicon π-bonded to polyaromatic hydrocarbons (PAHs) represents an important alternative to conventional ion–molecule chemistry of atomic $Si^{+\bullet}$. A third isomer — the inserted seven-membered ring structure **57** — was located 30.8 kcal mol^{-1} above the π-bonded species **54**.

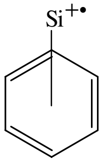

(54)

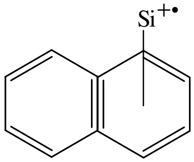

(55)

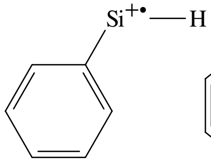

(56)

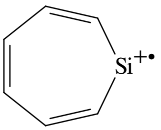

(57)

The ion $\cdot CH_2OSi^+$ is an interesting species in its own right as it provides the first direct proof for the existence of a distonic ion[180,181] which incorporates a silicon atom[182]. It can be generated via electron-impact ionization of tetramethoxysilane[183]. The genesis of this distonic ion presumably takes place via a sequence of unimolecular hydrogen and formaldehyde losses — a metastable behavior that has been observed previously in methoxy-substituted silane cations[184]. Neutralization of $^\bullet CH_2OSi^+$ leads to the stable $^\bullet CH_2OSi^\bullet$ diradical which, in accordance with *ab initio* calculations (MP2/6-31G**), corresponds to a local minimum on the $[H_2,C,O,Si]$ hypersurface[184].

B. Nitrogen- and Oxygen-containing Silicon Ions and Their Neutral Counterparts

Several new oxygen- and nitrogen-containing silicon ions have been studied (Table 2) and the stability of their neutral counterparts has been probed by NRMS experiments[148,151,152]. In view of the emerging insight into the remarkable differences between the π-bonding ability of carbon and silicon, the structural and energetic properties of small unsaturated silicon-containing ions has become the subject of considerable scrutiny. A further understanding of the chemistry of small oxygen-containing silicon radicals and molecules of the type H_xSiO_y is also desirable as these species are known to be relevant to the combustion chemistry taking place in silane–oxygen flames[185–188].

TABLE 2. Oxygen- and nitrogen-containing neutral molecules with silicon as studied by neutralization–reionization mass spectrometry

$Si_xO_yH_z$	$HSiO^{35}$, $HOSi^{193}$, H_2SiO^{194}, $HSiOH^{194}$, H_2SiOH^{194}, $H_3SiO_4{}^{194}$, Si_2O^{195}, c-$Si_2O_2{}^{196}$
$Si_xN_yH_z$	$HNSi^{197}$, H_2NSi^{198}, Si_2N^{195}, Si_3N^{199}

For recent theoretical studies of such species, see elsewhere[189–191]. It was found to be particularly useful to corroborate these experimental findings by theoretical studies dealing with the structures and thermochemistry of the observed molecules. Table 2 gives an overview of the species studied so far.

The careful reader will encounter a structural pattern exhibited by all these low-valent silicon species. Whereas the preferred bonding of silicon to other main group elements in these ions and neutral molecules can no longer be deduced on the grounds of simple 'Lewis-structure type reasoning' — as it is so successfully employed for the lower homologue carbon — the higher homologue silicon prefers to form cyclic or bridged 'nonclassical' structures[192]. This is presumably a consequence of the far more diffuse p orbitals of this element as compared with carbon, which not only leads to significantly weaker π-type interactions but also to much less 'directionality' in its bonding. Thus the successful thinking in terms of sp hybridizations for carbon molecules cannot be stringently applied to silicon!

Protonation of silicon monoxide can in principle give rise to two different isomers: the O-protonated $SiOH^+$ and the silicon-protonated form $HSiO^+$. $SiOH^+$ is formed upon reaction of water with silicon cations[200] and is believed to play a key role in the depletion mechanism of atomic silicon in the earth's ionosphere[50]. Theory (MP4) predicts the two cationic isomers to be separated by a substantial barrier of 91.5 kcal mol^{-1} (with respect to the formation of $HSiO^+$ from $SiOH^+$)[193]. The neutral counterpart $SiOH^\bullet$ has been generated in a NR experiment from the cationic precursor (equation 28)[193,201] (accessible via electron impact ionization of tetramethoxysilane). Neutral $HSiO^\bullet$ — in line with theoretical predictions[202,203] — was successfully generated via Charge-Reversal NRMS (CR-NRMS) of anionic $HSiO^{-}$[204] (equation 29).

$$SiOH^+ \longrightarrow SiOH^\bullet \longrightarrow SiOH^+ \tag{28}$$

$$HSiO^- \longrightarrow HSiO^\bullet \longrightarrow HSiO^+ \tag{29}$$

According to the computational studies, a species with $HSiO^\bullet$ connectivity forms the global minimum on both the neutral and cationic [H,O,Si] potential energy surfaces. The barrier for the 1,2-hydrogen shift generating $HSiO^\bullet$ from $HOSi^\bullet$ was estimated to be 35.9 kcal mol^{-1} above $HOSi^\bullet$; the latter represents the global minimum, lying 6.4 kcal mol^{-1} below $HSiO^\bullet$. This is an ordering of stability similar to that found on the cationic surface where $HOSi^+$ corresponds to the global minimum[204,205], and these findings once again underline the significant differences between carbon and its higher homologue silicon: on the neutral as well as ionic [H,C,O] surface[205] the order of stabilities is reversed, compared to that of [H,O,Si].

Among the other silicon-containing molecules and ions of the composition [Si,O,H_x], Srinivas and coworkers have characterized the ions $HSiOH^{+\bullet}$, $H_2SiO^{+\bullet}$, H_2SiOH^+ and H_3SiO^+ as well as their neutral counterparts in collision experiments[194]. The neutral and cationic H_xSiO species ($x = 2,3$) were generated by neutralization and charge-reversal experiments which employed the anionic counterparts as precursor molecules. The $H_2SiO^{-\bullet}$ and H_3SiO^- anions[206] can be readily obtained in the reaction of $O^{-\bullet}$ with phenylsilane according to equations 30 and 31.

$$O^{-\bullet} + C_6H_5SiH_3 \longrightarrow H_2SiO^{-\bullet} + C_6H_6 \qquad (30)$$

$$O^{-\bullet}(OH^-) + C_6H_5SiH_3 \longrightarrow H_3SiO^- + C_6H_5 \cdot (C_6H_6) \qquad (31)$$

The cations $HSiOH^{+\bullet}$ and H_2SiOH^+ were generated by electron ionization of tetramethoxysilane. As demonstrated by these NRMS experiments, all four species HSiOH, H_2SiO, $H_2SiOH^\bullet$ and $H_3SiO^\bullet$ are accessible, stable molecules in the gas phase (for matrix isolation studies on silanone, H_2SiO, and hydroxysilylene, HSiOH, see elsewhere)[207–209]. These findings are in line with earlier computational studies on the neutral and cationic $[H_n,O,Si]$ potential energy surfaces ($n = 2,3$) which had predicted high barriers for the interconversion of these isomers[209–212].

Two different silicon–oxygen cluster ions $Si_xO_y{}^{+\bullet}$ have been characterized by Schwarz and coworkers in the gas phase[195,196]. These clusters may be viewed as the simplest prototypes for the interaction of oxygen at silicon surfaces[210] and thus their structures are of particular interest. The ion $Si_2O^{+\bullet}$ can be generated via electron ionization of disilyl ether, $H_3SiOSiH_3$. The $Si_2O^{+\bullet}$ ion has been successfully neutralized and its dissociation pattern was found to agree well with the theoretically predicted energetics for Si_2O by Boldyrev and Simons[211]. According to the theoretical calculations[211,212], the global minimum structure for Si_2O corresponds to a C_{2v} symmetric species **58** with a $^1A_1$ ground state, with the neutral isomer **59** being 27 kcal mol^{-1} less stable than **58**. While an unambiguous differentiation between a cyclic and an open structure in these collision experiments was not possible, recourse to the *ab initio* data very much suggests that neutral Si_2O as well as its cationic counterpart possess a cyclic structure[213].

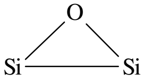

(58)

Si—O—Si

(59)

The $Si_2O_2{}^{+\bullet}$ cation has been generated upon ionizing a mixture of disilyl ether and N_2O under chemical ionization conditions[196]. The genesis of this interesting ion most likely proceeds via loss of the hydrogen atoms from $H_3SiOSiH_3$ upon electron impact, thus giving rise to $Si_2O^{+\bullet}$ which is subsequently oxidized in an ion–molecule reaction with N_2O (equation 32).

$$\begin{aligned} H_3SiOSiH_3 + e^- &\longrightarrow Si_2O^{+\bullet} + 3H_2 + 2e^- \\ Si_2O^{+\bullet} + N_2O &\longrightarrow Si_2O_2{}^{+\bullet} + N_2 \end{aligned} \qquad (32)$$

These results from collisional activation experiments have been augmented by *ab initio* calculations [MP2/6-311 G(df) CCSD(T) level] on the neutral and cationic $[Si_2,O_2]$ surface[196,214]. The theoretical results point to the existence of three low-lying cationic isomers **60**, **61** and **62**.

Isomer **60** was calculated to be 27.5 kcal mol^{-1} and 20.9 kcal mol^{-1} more stable than **61** and **62**, respectively. The relative abundances of fragment ions in the CA mass spectra reflected the predicted energetics for the dissociation processes. While CA mass spectrometry does not allow for a distinction of cyclic versus noncyclic isomers, the fact that the CA mass spectrum contained an $Si_2{}^{+\bullet}$ and $SiO_2{}^{+\bullet}$ ion leads to the exclusion of isomers **61** and **62**. On the neutral $[Si_2, O_2]$ surface[215] only two energetically low-lying

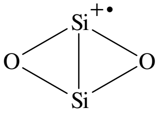

(60)

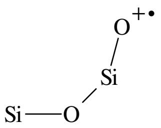

(61)

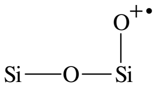

(62)

isomers (**63** and **64**) were located by the *ab initio* calculations. Isomer **63** possesses a D_{2h} symmetry and bond lengths rather similar to **60**, while **64** was found to constitute a monocyclic ring with an externally bound oxygen atom. In line with these calculations, neutralization of the $[Si_2,O_2]^{+\bullet}$ ion was found to lead to a strong signal for the survivor ions, indicating rather favorable Franck–Condon factors[216–218] for the electron-transfer processes — a finding that is expected to be valid for geometrically similar species. Thus the combined experimental as well as theoretical work, revealing that neutral Si_2O_2 forms a cyclic structure, once again point to the differences between carbon and silicon chemistry. While Si_2O_2 can be readily generated from its ionic precursor, the C_2O_2 molecule which has been theoretically predicted to correspond to a linear structure, O=C=C=O, still remains elusive despite numerous experimental attempts[219].

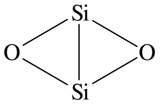

(63)

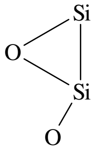

(64)

Among multiple-bond-containing silicon compounds, neutral HNSi holds a special place. The [H,N,Si] potential energy surface and several possible N- and Si-substituted isomers have formed the subject of several experimental[220–225] and theoretical investigations[226–228]. In a recent experimental and theoretical study, the ionic as well as the neutral [H,N,Si] surfaces were explored[197]. Ionization of a mixture of iodosilane and NH_3 gives rise to $[H,N,Si]^{+\bullet}$ cations, which according to CA experiments exist in an N-protonated **(65)** rather than the isomeric Si-protonated form **(66)**.

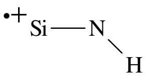

(65)

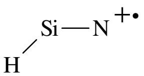

(66)

Ab initio MO calculations (GAUSSIAN-1) predict isomer **65** to correspond to the global minimum on the $[H,N,Si]^{+\bullet}$ surface; isomer **66** was calculated to be 42.5 kcal mol^{-1} less stable. The barrier for the 1,2-hydrogen shift was calculated to be 8 kcal mol^{-1} above **66**. Neutral HNSi **(67)** has been successfully generated from ionic **65** and, according to the calculations, exists in a singlet state $(^1\Sigma^+)$. Isomer **68** also prefers a singlet electronic ground state (65 kcal mol^{-1} higher than **67**) with a barrier for formation of **68** from **67** of 78 kcal mol^{-1}[224].

Again it is interesting to note the apparent differences between carbon and its higher homologue: HCN corresponds to the global minimum on the neutral [H,C,N] surface[229];

$Si{-}N{-}H$ **(67)** $H{-}Si{-}N$ **(68)**

thus, the order of stability is reversed upon silicon substitution. In this context Apeloig and Albrecht[228] have carried out instructive studies on the R−SiN ⇆ SiN−R isomerization and the dependence of the stabilities of the two possible isomers upon the substituent R. They found that substitution of R by a more electronegative ligand such as F or OH leads to a preference for the silanitrile structure over the N-substituted isomer. An experimental verification of these intriguing findings still remains to be done.

The N-protonated form of HNSi, the H_2NSi^+ cation **69** and its possible isomers have been studied extensively by theoretical methods[230–234]. Böhme[47] suggested that the ion **69**, which is formed upon reaction of silicon cations with ammonia and subsequent dissociation of **69** upon electron capture (equation 33)[235], is of prime importance for the formation of Si−N bonded species such as **67** in the chemistry of interstellar matter.

$$\begin{aligned} Si^{+\bullet}(^2P) + NH_3 &\longrightarrow SiNH_2{}^+ + H^\bullet \\ SiNH_2{}^+ + e^- &\longrightarrow SiNH + H^\bullet \end{aligned} \tag{33}$$

Thus, $SiNH_2{}^+$ has been proposed to give rise to neutral HNSi **(67)** upon neutralization via dissociative recombination. Electron bombardment of trisilylamine (or a mixture of iodosilane and ammonia) leads to the formation of $[Si,N,H_2]^+$ cations, which according to collision experiments can be assigned a H_2NSi^+ structure **(69)**[198]. Thus, the preferred site of protonation of the silaisonitrile molecule HNSi is the nitrogen atom. Theoretical calculations on the ionic $[H_2,N,Si]^+$ surface and all possible dissociation channels carried out in the same study indicate that the $^1A_1$ state of **69** corresponds to the most stable isomer. The isomers **70** ($^1A'$) and **71** ($^3A_2$) are predicted to lie respectively 50.3 and 116.7 kcal mol^{-1} higher in energy than **69**.

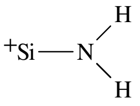
(69)

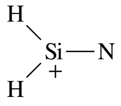
(70)

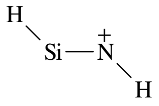
(71)

Neutralization of **69** was found to give rise to a stable $H_2NSi^\bullet$ radical **72**. The other possible isomers **73** and **74** were computationally estimated to be 21.8 and 45.8 kcal mol^{-1} less stable than **72**. However, significant barriers for the possible interconversion of the neutral isomers, found in these calculations, indicate that in principle isomers **73** and **74** should also be viable species.

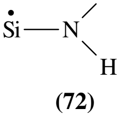
(72)

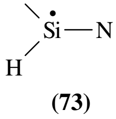
(73)

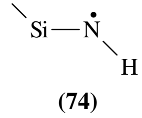
(74)

The Si_2N^+ cluster molecule has been generated upon ionization of trisilylamine[195]. Theory [QCISD(T)/6-311+G*][199] predicts a linear $D_{\infty h}$ structure for the cationic as well as the neutral $NSiN^\bullet$ radical **(75)**. The linear species was found to correspond to the global minimum on both the neutral and cationic potential energy surfaces and, in line with the theoretical predictions, NSiN$^\bullet$ has been identified in NRMS experiments[195]. According to the theoretical and recent spectroscopic measurements[35] NSiN$^\bullet$ possesses a linear structure **(75)** and a $^2\Pi_g$ ground electronic state.

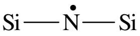

(75)

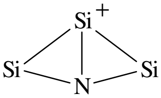

(76)

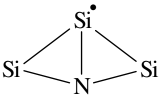

(77)

Electron ionization of trisilylamine was also found to give rise to the ionic cluster molecule Si_3N^+[199]. As indicated by *ab initio* calculations[198] [MP2(full)/6-311 +G*] on the ionic $[N, Si_3]^+$ surface, the ground state structure of the Si_3N^+ cluster corresponds to a C_{2v} symmetric species **(76)** with the nitrogen atom being bound to all three silicon atoms. The calculated dissociation energies for **76** were found to agree well with the relative abundances obtained in CA experiments. Neutralization of the ionic precursor **76** demonstrated the viability of the $Si_3N^\bullet$ radical in the gas phase. For this neutral species, the computational results predict a ground state $^2A_2$ structure **(77)** possessing C_{2v} symmetry with a geometry that is very similar to that of cation **76**.

It can be concluded from these studies on small silicon clusters which are bound to main-group elements, that the tendency of silicon to form significantly stronger σ-bonds with first-row main-group elements leads to the formation of cyclic 'nonclassical' structures, unknown in carbon chemistry. For carbon, the ability to form strong π-bonding interactions and the more pronounced directionality of its σ-bonding orbitals do not allow for an observation of such cyclic clusters as ground state species; it preferably forms linear clusters.

V. REARRANGEMENTS OF ORGANOSILICON IONS

A. Cationic Rearrangements

The unimolecular dissociation of Me_3Si^+ **(78)** has been studied experimentally[236]. As indicated by CAD studies and isotopic exchange reactions, ion **78** readily interconverts upon excitation to isomer **79** (equation 34). The reaction mechanism for this interesting interconversion has been proposed to proceed via a concerted 1,2-hydrogen/1,2-methyl migration. This dyotropic rearrangement[237] corresponds to a thermally allowed $[\sigma_s{}^2+\sigma_s{}^2]$ process[238]. In a similar fashion the ethene elimination from **78** was proposed to proceed via a dyotropic multicenter reaction mechanism (equation 35).

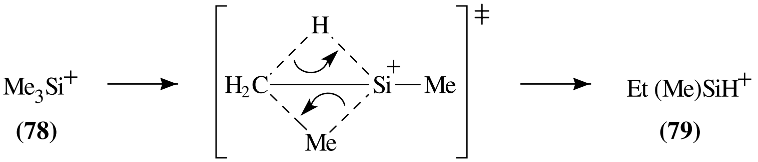

(34)

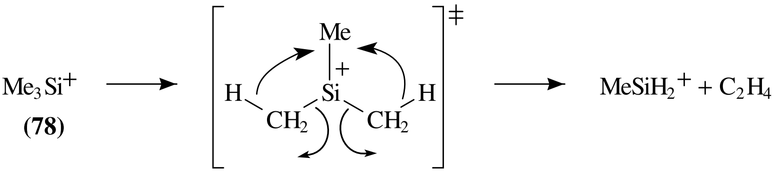

(35)

Excited ions of **78** were found to exchange an ethene molecule for the isotopomer C_2D_4, which lends further support to this hypothesis.

Bakhtiar and coworkers also studied the isomerization of $SiMe_2R^+$ **(80)** to $SiHEtR^+$ **(81)** upon collisional activation[239]. As already described for the trimethylsilyl cation, this isomerization seems to proceed via a concerted $[\sigma_s{}^2 + \sigma_s{}^2]$ process (equation 36).

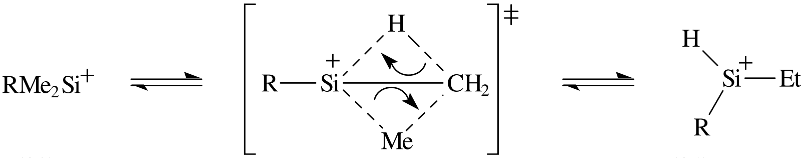

(36)

(80) **(81)**

The rearrangements preceding the dissociation of α-silyl substituted carbenium ions have been investigated earlier by Drewello and coworkers[240]. In this study, extensive isotopic labeling has been successfully employed to demonstrate that the metastable MeC^+HSiMe_3 ions **(82)** rapidly undergo 1,2-methyl migrations prior to dissociation to C_2H_4 and $SiMe_3{}^+$ with an almost complete exchange of the four methyl groups (equation 37). These findings are in line with earlier *ab initio* molecular orbital calculations[236] which predict that the ion $Me_2CH{-}Si^+Me_2$ **(83)** is approximately 28 kcal mol^{-1} more stable than the corresponding carbenium ion **82**. Thus the 1,2-methyl migration giving rise to **83** is a highly exothermic process. For the slow 1,2-hydrogen shift a kinetic isotope effect k_H/k_D of 2.5 was observed. In this study also a similarly rapid exchange of methyl groups was reported for the trimethylsilyl isopropyl carbenium ion, $Me_3SiC^+Me_2$.

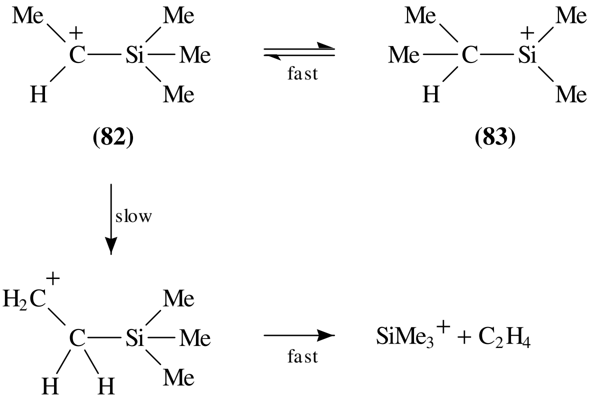

(82) **(83)**

(37)

The migratory aptitude of hydrogen, alkyl and phenyl groups in the silicon analogue of the Wagner–Meerwein rearrangement (migration from a silicon center to a carbenium ion) has been studied by Bakhtiar and coworkers[241]. The corresponding α-silyl-substituted carbenium ion **84** was generated by chloride elimination from the α-chloroalkylsilane and the nascent ions were found to undergo rearrangement to the thermodynamically favored silicenium ions upon 1,2-migration from silicon to carbon. The rearrangement of the ion $PhMeSiHCH_2{}^+$ allowed for a direct comparison of the competitive migrations of a phenyl, methyl and hydrogen (equation 38). The authors found that 94% of the obtained silicenium ions resulted from phenyl migration, the other 6% corresponded to a hydrogen migration and no methyl migration was observed.

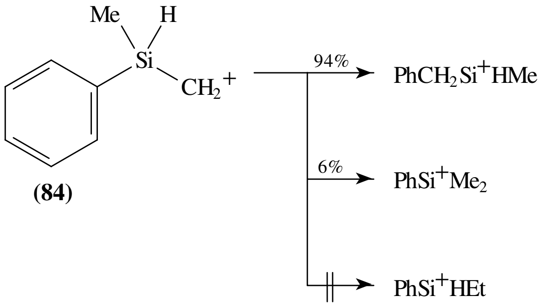

(84)

(38)

As an explanation for the preferred aryl migration, delocalization of the charge into the ring in the bridged transition state (leading to a phenonium ion) was invoked. It was concluded that the corresponding α-silylcarbenium ions as well as the silicenium ions may be important intermediates in the solvolytic rearrangements of α-functionalized silanes. These findings have been questioned by a recent theoretical study of Cho[242], who argues that the α-silylcarbenium ions do not correspond to energy minima on the PES and that the rate-determining step for the migration is really the departure of the Cl^- ion. On the basis of MP2/6-31G* calculations, the Cl^- dissociation and silicenium ion formation is predicted to correspond to a single process and thus Cho concludes that the differences in dissociation energies of the chloroalkylsilanes are responsible for the migratory tendencies. Further experimental as well as theoretical studies are needed to settle this point.

The phenylsilyl cation $C_6H_5SiH_2{}^+$ **(85)** and its interconversion to other possible isomers such as the silacylcoheptatrienyl cation **(86)** have attracted considerable experimental as well as theoretical interest in view of the possible similarities or differences of the well-known benzyl and cycloheptatrienyl cations[243] and their silicon analogues. Thus, Beauchamp and coworkers[244,245] have found that electron ionization of phenylsilane gives rise to both isomers **85** and **86**, which do not interconvert at room temperature and can be readily distinguished by their ion–molecule reactions.

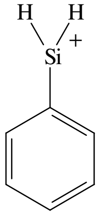

(85)

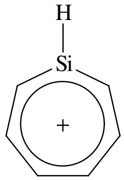

(86)

Recent theoretical results by Nicolaides and Radom[246], who employed isodesmic and isogyric reactions for an accurate determination of the heats of formation of both ions at the G2 level of theory, suggest that the silabenzyl cation **85** is more stable than the silatropylium ion **86** by approximately 40 kcal mol^{-1}. For the corresponding $[C_7,H_7]^+$ surface, they found a reverse ordering, here the tropylium ion is 29 kcal mol^{-1} more stable than the benzyl cation. These findings presumably reflect the well-documented inability of silicon to form π-bonds with significant strength.

Tajima, Okada and coworkers[247] reported the unimolecular metastable decompositions of alkoxysilanes in a number of recent studies[184,248,249]. These authors found significant differences in the ion fragmentation characteristics between the silanes and their carbon analogues. Thus, for example, the principal fragmentation process of ionized diethoxydimethylsilane was found to correspond to a consecutive loss of ethylene and aldehyde molecules from the silicenium ion formed by loss of an ethoxy radical. In contrast, the carbon analogue acetone diethyl acetal does not exhibit a significant loss of aldehyde molecules in its metastable ion mass spectrum.

B. Anionic Rearrangements

Bowie's group has investigated a number of rearrangements of sila anions. The authors reported the unimolecular chemistry of deprotonated α-alkoxyvinyltrimethylsilane[250]. Interestingly, these ions were found to lose a ketene molecule upon excitation via collisional activation. This unexpected behavior points to the fact that ions such as **87** rearrange via a methyl migration (equation 39) for which two different pathways are conceivable. The methyl either migrates to the silicon of an incipient dimethylsilene ($Me_2Si{=}CH_2$) (39a), or to the methylene carbon (39b). Charge reversal spectra indicate that the anions formed in this rearrangement possess a structure **88** and thus pathway 39b seems to be favored.

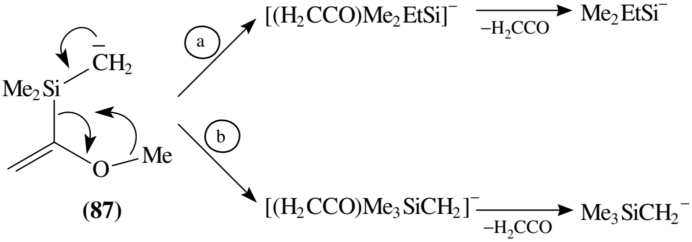

(87)

(39)

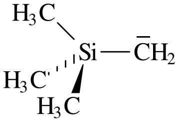

(88)

The rearrangements preceding collisional excitation of trimethylsilyl-substituted alkoxides, ketones or carboxylic acids carrying anions have been investigated[251]. Most of the products obtained correspond to a species in which a Si−O bond has been formed. Thus, for example, all species $Me_3Si(CH_2)_nO^-$ ions ($n = 2$–5), e.g. **89** where $n = 3$, were found to react via an intramolecular S_N2 reaction (equation 40) by an attack of the O^- at the silicon center and a subsequent formation of a fivefold coordinated intermediate **(90)**, which then reacts further to give the final products such as Me_3SiO^- and **91**.

Another interesting case of migration of a methoxide to a neutral silicon center has been reported by Krempp and Damrauer[252]. These authors reported that silanamide anions, H_3SiNH^- **(92)**, react with methyl formate to form the neutral methyl silyl ether and the formamide anion (equation 41). The thermodynamic driving force for this reaction as well as the above-mentioned rearrangements are most likely the formation of the strong Si−O bond in the silyl ether.

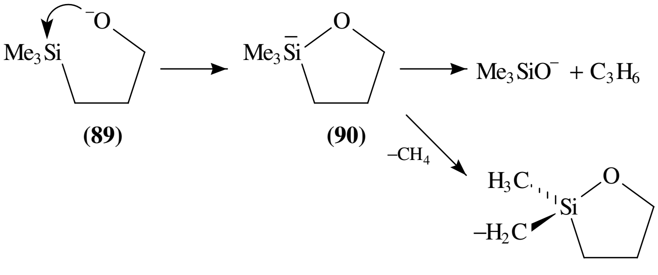

(89) **(90)** **(91)**

(40)

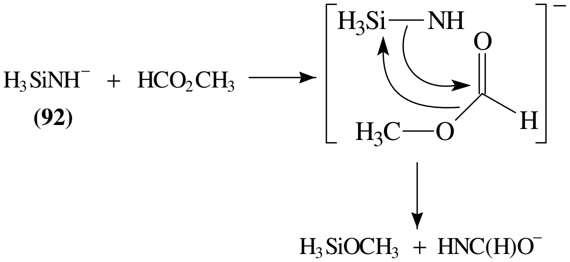

(92)

(41)

O'Hair and coworkers[253] have investigated the gas-phase chemistry of siloxide and silamide ions in flowing afterglow experiments. The reaction of siloxide anions, H_3SiO^- (as well as substituted analogues), with CS_2 was found to lead to the exclusive formation of COS and the corresponding H_3SiS^- anion (equation 42). As suggested by *ab initio* calculations carried out in the same study, the reaction quite likely proceeds via a fivefold coordinated cyclic transition state **(93)**.

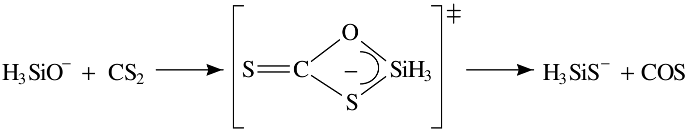

(93)

(42)

VI. DOUBLY CHARGED IONS

Although a large number of doubly charged cations can be observed in a typical mass spectrum of organo-silicon compounds[254–262], there have been relatively few recent studies dealing with these species. In general it must be noted that silicon-containing dications are far more stable than their carbon analogues due to the more electropositive character of silicon.

Schwarz and coworkers[258] have been successful in generating the diatomic dication SiF^{2+} by charge-stripping mass spectrometry (equation 43)[259–262].

$$SiF^+ \ [E_{\text{kin}} = 8\,\text{keV}] + O_2 \longrightarrow SiF^{2+} + O_2{}^* + e^- \qquad (43)$$

The theoretically predicted existence of SiF^{2+}[263] could be confirmed in these experiments. In addition, the vertical ionization energy ($MF^+ \rightarrow MF^{2+} + e^-$) of SiF^+ was calculated using single- and multi-reference configuration interaction methods. The experimental value of 21.7 eV mirrored the theoretically obtained values. An explanation for the stability of this diatomic dication may be seen in the extraordinary strength of the covalent silicon−fluoride bond (see Section III.C).

A number of small dications such as Si_2O^{2+}[195], Si_2N^{2+}[195], Si_3N^{2+}[199] have been observed in the CA mass spectra of their corresponding monocations. However, the ionization energies of the monocations have not been determined and no theoretical results are available on these interesting species as yet.

There are still very few examples of small stable doubly charged negative ions that have been characterized in the gas phase[264−266]. The main reason for the instability of dianions is certainly the strong electron−electron repulsion, causing species which possess two spatially close additional electrons to autodetach the second electron rather than form a stable system. In view of this, it is interesting to find that Sommerfeld, Scheller and Cederbaum[267] have recently proposed a number of small $Si_mO_n{}^{2-}$ clusters which should be stable with respect to electron detachment. In their theoretical study (DZ/SDCI level of theory) the authors predict that the smallest system which should be stable with respect to vertical electron loss (and hence to possess a finite lifetime) is the D_{2d} symmetrical cluster **94**, the silicon analogue of the oxalate dianion, $O_2CCO_2{}^{2-}$.

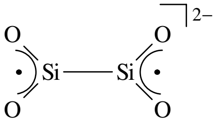

(94)

Interestingly, the authors find that the silicon-containing dianions are more stable with respect to electron detachment and dissociation than their corresponding carbon analogues. The predominantly covalent and stronger bonding in the silicon−oxygen clusters has been invoked as an explanation for this behavior. In a continuation of their search for small stable dianionic systems, these authors theoretically investigated the structures and stabilities of several $Si_2O_5{}^{2-}$ isomers[268]. They predict that the dianions **95**−**97** could be stable species with respect to dissociation into $SiO_3{}^-$ and $SiO_2{}^-$. With respect to possible electron autodetachment only **97** is found to lie in an unstable energy regime, and **95** as well as **96** might be further candidates for stable dianionic systems. The experimental verification of this theoretical work should be a challenging task.

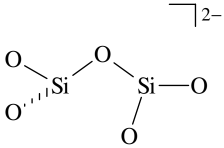

(95)

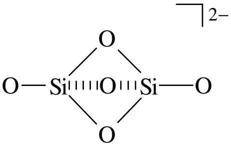

(96)

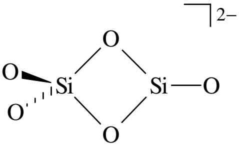

(97)

VII. ACKNOWLEDGMENTS

N.G. warmly thanks Professor Roald Hoffmann, Cornell University, for his kind hospitality and support whilst he worked on this review. He also thanks Alison for her invaluable help. The authors are grateful to many colleagues, in particular Professors P. B. Armentrout, D. K. Böhme, J. H. Bowie, R. Damrauer, D. B. Jacobson, R. Squires and F. Turecek, for providing them with re- and preprints of current results obtained in their laboratories. Financial support by the Deutsche Forschungsgemeinschaft (DFG) (research grant to N.G.) and the Fonds der Chemischen Industrie is gratefully acknowledged.

VIII. REFERENCES

1. (a) H. Schwarz, in *The Chemistry of Organic Silicon Compounds* (Eds. S. Patai and Z. Rappoport), Chap. 7, Wiley, Chichester, 1989, pp. 445–510; (b) H. Bock and B. Solouki, *Chem. Rev.*, **95**, 1161 (1995).
2. J. Berkowitz, *Acc. Chem. Res.*, **22**, 413 (1989).
3. R. Damrauer, in *Advances in Silicon Chemistry* (Ed. G. L. Larson), Vol. 2, JAI Press, Greenwich, Conn., 1993, p. 91.
4. R. Damrauer and J. A. Hankin, *Chem. Rev.*, **95**, 1137 (1995).
5. M. S. Gordon, J. S. Francisco and H. B. Schlegel, in *Advances in Silicon Chemistry* (Ed. G. L. Larson), Vol. 2, JAI Press, Greenwhich, Conn., 1993, p. 137.
6. J. Berkowitz, J. P. Greene, H. Cho and B. Ruscic, *J. Chem. Phys.*, **86**, 1235 (1987).
7. K. Börlin, T. Heinis and M. Jungen, *J. Chem. Phys.*, **103**, 93 (1985).
8. J. A. Pople and L. A. Curtiss, *J. Phys. Chem.*, **91**, 155 (1987).
9. J. A. Pople, B. T. Luke, M. J. Frisch and J. S. Binkley, *J. Phys. Chem.*, **89**, 2198 (1985).
10. J. A. Pople and L. A. Curtiss, *J. Phys. Chem.*, **91**, 3637 (1987).
11. E. R. Fisher and P. B. Armentrout, *J. Chem. Phys.*, **93**, 4858 (1990).
12. D. I. Hall, A. P. Levick, P. J. Sarre, C. J. Whitham, A. A. Alijah and G. Duxbury, *J. Chem. Soc., Faraday Trans. 2*, **89**, 177 (1993).
13. B. H. Boo and P. B. Armentrout, *J. Am. Chem. Soc.*, **109**, 3549 (1987).
14. P. J. Bruna, G. Hirsch, R. J. Buenker and S. D. Peyerimhoff, in *Molecular Ions* (Eds. J. Berkowitz and K.-O. Groeneveld), Chap. 4, Plenum Press, New York, 1993, p. 309.
15. S. P. Mort, N. A. Jennings, G. G. Balint-Kurti and D. M. Hirst, *J. Chem. Phys.*, **101**, 10576 (1994).
16. C. Bauer, D. M. Hirst, D. I. Hall, P. J. Sarre and P. Rosmus, *J. Chem. Soc., Faraday Trans. 2*, **90**, 517 (1994).
17. Y. Cao, J.-H. Choi, B.-M. Haas, M. S. Johnson and M. Okumura, *J. Phys. Chem.*, **97**, 5215 (1993).
18. J. B. Lambert, L. Kania and S. Zhang, *Chem. Rev.*, **95**, 1191 (1995).
19. S. K. Shin and J. L. Beauchamp, *J. Am. Chem. Soc.*, **111**, 900 (1989).
20. G. A. Olah and Y. K. Mo, *J. Am. Chem. Soc.*, **93**, 4942 (1971).
21. C.-Y. Lin and R. C. Dunbar, *J. Phys. Chem.*, **100**, 655 (1996).
22. D. S. Tonner, D. Thölmann and T. B. McMahon, *Chem. Phys. Lett.*, **233**, 324 (1995).
23. M. E. Weber and P. B. Armentrout, *J. Chem. Phys.*, **90**, 2213 (1989).
24. M. E. Weber and P. B. Armentrout, *J. Phys. Chem.*, **93**, 1596 (1989).
25. E. R. Fisher and P. B. Armentrout, *Chem. Phys. Lett.*, **179**, 435 (1991).
26. E. R. Fisher and P. B. Armentrout, *J. Phys. Chem.*, **95**, 4765 (1991).
27. E. R. Fisher, B. L. Kickel and P. B. Armentrout, *J. Phys. Chem.*, **97**, 10204 (1993).
28. B. L. Kickel, E. R. Fisher and P. B. Armentrout, *J. Phys. Chem.*, **97**, 10198 (1993).
29. B. L. Kickel, J. B. Griffin and P. B. Armentrout, *Z. Phys. D*, **24**, 101 (1992).
30. J. Walsh, *Acc. Chem. Res.*, **14**, 246 (1981).
31. A. Gobbi and G. Frenking, *J. Am. Chem. Soc.*, **116**, 9287 (1994).
32. D. J. Hajdasz, Y. Ho and R. R. Squires, *J. Am. Chem. Soc.*, **116**, 10751 (1994).
33. Pentacoordinated anionic silicon adducts had earlier been demonstrated to be intermediates in anionic gas-phase reactions: G. Angelini, C. E. Johnson and J. I. Brauman, *Int. J. Mass Spectrom. Ion Proc.*, **109**, 1 (1991).
34. For theoretical calculations on SiH_5^-, see: A. E. Reed and P. v. R. Schleyer, *Chem. Phys. Lett.*, **133**, 533 (1987).
35. A theoretical study on the pseudorotation in $SiH_{5-n}X_n{}^-$ (X = F, Cl) anions has been reported: T. L. Windus, M. S. Gordon, L. P. Davis and L. W. Burggraf, *J. Am. Chem. Soc.*, **116**, 3568 (1994).
36. R. R. Squires, in *Structure/Reactivity and Thermochemistry of Ions* (Eds. P. Ausloos and S. G. Lias), Reidel, Dordrecht, 1987, p. 177.
37. E. A. Brinkman, S. Berger and J. I. Brauman, *J. Am. Chem. Soc.*, **116**, 8304 (1994).

38. C. H. DePuy, V. M. Bierbaum, L. A. Flippin, J. J. Grabowski, G. K. King, R. J. Schmitt and S. A. Sullivan, *J. Am. Chem. Soc.*, **101**, 6443 (1979).
39. R. Yoshimura and T. Tada, *J. Phys. Chem.*, **97**, 845 (1993).
40. J. H. Bowie, *Mass Spectrom. Rev.*, **3**, 1 (1984).
41. A. Oppenstein and F. W. Lampe, *Rev. Chem. Intermed.*, **6**, 275 (1986).
42. C. H. DePuy, R. Damrauer, J. H. Bowie and J. C. Sheldon, *Acc. Chem. Res.*, **20**, 127 (1987).
43. D. K. Böhme, S. Wlodek and A. Fox, in *Rate Coefficients in Astrochemistry* (Eds. T. J. Millar and D. A. Williams), Kluwer Academic Publisher, Amsterdam, 1988, p. 193.
44. For an excellent earlier review on the chemistry of atomic silicon ions, see: D. K. Böhme, *Int. J. Mass Spectrom. Ion Proc.*, **100**, 719 (1990).
45. D. K. Böhme, in *Chemistry and Spectroscopy of Interstellar Molecules* (Eds. D. K. Böhme, E. Herbst, N. Kaifu and S. Saito), Chap. 3, University of Tokyo Press, Tokyo, 1992, p. 155.
46. D. K. Böhme, *Chem. Rev.*, **92**, 1487 (1992).
47. D. K. Böhme, *Adv. Gas-Phase Ion Chem.*, **1**, 225 (1992).
48. R. C. Dunbar, in *Unimolecular and Bimolecular Ion–Molecule Reaction Dynamics* (Eds. C.-Y. Ng, T. Baer and I. Powis), Wiley, Chichester, 1994.
49. J. M. Farrar and J. Saunders (Eds.), *Techniques for the Study of Ion–Molecule Reactions*, Vol. 20 in Techniques of Chemistry, Wiley, New York, 1988.
50. For a review of the chemistry of silicon in interstellar clouds, see: E. Herbst, T. J. Millar, S. Wlodek and D. K. Böhme, *Astron. Astrophys.*, **222**, 205 (1989).
51. For an excellent review on the structures and properties of Si-cluster ions, see: M. Jarrold, in *Cluster Ions* (Eds. C.-Y. Ng, T. Baer and I. Powis), Chap. 3, Wiley, Chichester, 1993, p. 165.
52. V. G. Anicich, *J. Phys. Chem. Ref. Data*, **22**, 1993 (1993).
53. For details on the reaction of transition-metal cations with organic molecules, see: K. Eller and H. Schwarz, *Chem. Rev.*, **91**, 1121 (1991).
54. B. L. Kickel and P. B. Armentrout, *J. Am. Chem. Soc.*, **116**, 10742 (1994).
55. B. L. Kickel and P. B. Armentrout, *J. Phys. Chem.*, **99**, 2024 (1995).
56. B. L. Kickel and P. B. Armentrout, *J. Am. Chem. Soc.*, **117**, 764 (1995).
57. B. L. Kickel and P. B. Armentrout, *J. Am. Chem. Soc.*, **117**, 4057 (1995).
58. T. R. Cundari and M. S. Gordon, *J. Phys. Chem.*, **96**, 631 (1992).
59. For a recent analysis of the nature of the metal–silicon bond in neutral transition-metal complexes, see: H. Jacobsen and T. Ziegler, *Inorg. Chem.*, **35**, 775 (1996).
60. M. Decouzon, J.-F. Gal, S. Geribaldi, M. Rouillard and J.-M. Sturla, *Rapid Commun. Mass Spectrom*, **3**, 298 (1989).
61. (a) M. Azzaro, S. Breton, M. Decouzon and S. Geribaldi, *Rapid Commun. Mass Spectrom*, **6**, 306 (1992), (b) For the reactions of atomic W^+ with SiH_4, see: A. Ferhati, T. B. MacMahon and G. Ohannesian *J. Am. Chem. Soc.*, **188**, 5997 (1996).
62. A. Bjarnason and I. Arnason, *Angew. Chem., Int. Ed. Engl.*, **31**, 12 (1992).
63. A. Bjarnason, I. Arnason and D. P. Ridge, *Org. Mass Spectrom.*, **28**, 989 (1993).
64. D. B. Jacobson and R. Bakhtiar, *J. Am. Chem. Soc.*, **115**, 10830 (1993).
65. (a) R. Bakhtiar, C. M. Holznagel and D. B. Jacobson, *J. Am. Chem. Soc.*, **115**, 345 (1993), (b) For a theoretical study of the interaction of Fe^+ with silene, see: J. Moc and M. S. Gordon, *J. Am. Chem. Soc.*, **16**, 27 (1997).
66. R. Bakhtiar and D. B. Jacobson, *Organometallics*, **12**, 2876 (1993).
67. R. H. Schultz and P. B. Armentrout, *J. Am. Chem. Soc.*, **113**, 729 (1991).
68. S. Karrass and H. Schwarz, *Int. J. Mass Spectrom. Ion Proc.*, **98**, R1 (1990).
69. For the observation of methide transfer in the reactions of Cu^+ with alcohols, see: D. A. Weil and C. L. Wilkins, *J. Am. Chem. Soc.*, **107**, 7316 (1985).
70. S. Karrass and H. Schwarz, *Organometallics*, **9**, 2409 (1990).
71. (a) A. Hässelbarth, T. Prüsse and H. Schwarz, *Chem. Ber.*, **123**, 213 (1990), (b) G. Hornung, D. Schröder and H. Schwarz, *J. Am. Chem. Soc.*, **119**, 2273 (1997).
72. A. Hässelbarth, T. Prüsse and H. Schwarz, *Chem. Ber.*, **123**, 209 (1990).
73. R. N. McDonald, M. T. Jones and A. K. Chowdhury, *Organometallics*, **11**, 356 (1992).
74. M. D. Brickhouse, L. J. Chyall, L. S. Sunderlin and R. R. Squires, *Rapid Commun. Mass Spectrom*, **7**, 383 (1993).
75. L. J. Chyall, M. D. Brickhouse, M. E. Schnute and R. R. Squires, *J. Am. Chem. Soc.*, **116**, 8681 (1994).
76. P. G. Wenthold, J. Hu and R. R. Squires, *J. Am. Chem. Soc.*, **116**, 6961 (1994).

77. P. G. Wenthold and R. R. Squires, *J. Am. Chem. Soc.*, **116**, 11890 (1994).
78. P. G. Wenthold and R. R. Squires, *J. Am. Chem. Soc.*, **116**, 6401 (1994).
79. P. G. Wenthold, J. Hu, R. R. Squires and W. C. Lineberger, *J. Am. Chem. Soc.*, **118**, 475 (1996).
80. Y. Guo and J. J. Grabowski, *J. Am. Chem. Soc.*, **113**, 5923 (1991).
81. D. G. Leopold, A. E. S. Miller and W. C. Lineberger, *J. Am. Chem. Soc.*, **108**, 1379 (1986).
82. K. M. Ervin and W. C. Lineberger, in *Advances in Gas Phase Ion Chemistry* (Eds. N. G. Adams and L. M. Babcock), Vol. 1, JAI Press, Greenwich, CT, 1993.
83. J. Lee and J. J. Grabowski, *Chem. Rev.*, **92**, 1611 (1992).
84. A. B. Raksit and D. K. Böhme, *Int. J. Mass Spectrom. Ion Phys.*, **55**, 69 (1983).
85. D. Smith, *Chem. Rev.*, **92**, 1473 (1992).
86. S. Wlodek, A. Fox and D. K. Böhme, *J. Am. Chem. Soc.*, **109**, 6663 (1987).
87. W. R. Creasy, A. O'Keefe and J. R. McDonald, *J. Phys. Chem.*, **91**, 2848 (1987).
88. S. Wlodek and D. K. Böhme, *J. Chem. Soc., Faraday Trans. 2*, **85**, 1643 (1989).
89. D. Stöckigt, N. Goldberg, J. Hrušák, D. Sülzle and H. Schwarz, *J. Am. Chem. Soc.*, **116**, 8300 (1994).
90. B. H. Boo, J. L. Elkind and P. B. Armentrout, *J. Am. Chem. Soc.*, **112**, 2083 (1990).
91. B. H. Boo and P. B. Armentrout, *J. Am. Chem. Soc.*, **113**, 6401 (1991).
92. B. L. Kickel, E. R. Fisher and P. B. Armentrout, *J. Phys. Chem.*, **96**, 2603 (1992).
93. A. E. Ketvirtis, D. K. Böhme and A. C. Hopkinson, *J. Phys. Chem.*, **98**, 13225 (1994).
94. A. E. Ketvirtis, D. K. Böhme and A. C. Hopkinson, *J. Phys. Chem.*, **99**, 16121 (1995).
95. A. E. Ketvirtis, D. K. Böhme and A. C. Hopkinson, *Organometallics*, **14**, 347 (1995).
96. J. Glosik, P. Zakouril, V. Skalsky and W. Lindinger, *Int. J. Mass Spectrom. Ion Proc.*, **149/150**, 499 (1995).
97. S. M. Sze, (Ed.), *VLSI Technology*, McGraw-Hill, New York, 1983.
98. M. J. Kushner, *J. Appl. Phys.*, **63**, 2532 (1991).
99. L. Boufendi, A. Bouchoule, A. Plain, J. P. Blondeau and C. Laure, *Appl. Phys. Lett.*, **60**, 169 (1992).
100. M. L. Mandich, W. D. Reents and M. F. Jarrold, *J. Chem. Phys.*, **88**, 1703 (1988).
101. M. L. Mandich and W. D. Reents, *J. Chem. Phys.*, **90**, 3121 (1989).
102. M. L. Mandich, W. D. Reents and K. D. Kolenbrander, *J. Chem. Phys.*, **92**, 437 (1990).
103. M. L. Mandich and W. D. Reents, *J. Chem. Phys.*, **95**, 7360 (1991).
104. M. L. Mandich and W. D. Reents, *J. Chem. Phys.*, **96**, 4233 (1992).
105. W. D. Reents and M. L. Mandich, *J. Chem. Phys.*, **96**, 4429 (1992).
106. K. Raghavachari, *J. Chem. Phys.*, **88**, 1688 (1988).
107. K. Raghavachari, *J. Chem. Phys.*, **92**, 452 (1990).
108. K. Raghavachari, *J. Chem. Phys.*, **95**, 7373 (1991).
109. K. Raghavachari, *J. Phys. Chem.*, **96**, 4440 (1992).
110. W. D. Reents, M. L. Mandich and C. R. C. Wang, *J. Chem. Phys.*, **97**, 7226 (1992).
111. L. A. Curtiss, K. Raghavachari, P. W. Deutsch and J. A. Pople, *J. Chem. Phys.*, **95**, 2433 (1991).
112. M. A. Al-Laham and K. Raghavachari, *J. Chem. Phys.*, **95**, 2560 (1991).
113. I. Haller, *J. Phys. Chem.*, **94**, 4135 (1990).
114. J.-F. Gal, R. Grover, P.-C. Maria, L. Operti, R. Rabezzana, G.-A. Vaglio and P. Volpe, *J. Phys. Chem.*, **98**, 11978 (1994).
115. P. Antoniotti, L. Operti, R. Rabezzana, G. V. Vaglio, P. Volpe, J.-F. Gal, R. Grover and P.-C. Maria, *J. Phys. Chem.*, **100**, 155 (1996).
116. L. Operti, M. Splendore, G. A. Vaglio and P. Volpe, *Organometallics*, **12**, 4516 (1993).
117. L. Operti, M. Splendore, G. A. Vaglio and P. Volpe, *Organometallics*, **12**, 4509 (1993).
118. L. Operti, M. Splendore, G. A. Vaglio and P. Volpe, *Spectrochim. Acta*, **49A**, 1213 (1993).
119. K. P. Lim and F. W. Lampe, *Int. J. Mass Spectrom. Ion Proc.*, **101**, 245 (1990).
120. U. Ray and M. F. Jarrold, *J. Chem. Phys.*, **93**, 5709 (1990).
121. M. F. Jarrold, J. E. Bower and K. M. Creegan, *J. Chem. Phys.*, **90**, 3615 (1989).
122. K. M. Creegan and M. F. Jarrold, *J. Am. Chem. Soc.*, **112**, 3768 (1990).
123. S. Maruyama, L. R. Anderson and R. E. Smalley, *J. Chem. Phys.*, **93**, 5349 (1990).
124. M. F. Jarrold and V. A. Constant, *Phys. Rev. Lett.*, **67**, 2994 (1991).
125. J. M. Alford, R. T. Laaksonen and R. E. Smalley, *J. Chem. Phys.*, **94**, 2618 (1991).
126. M. F. Jarrold and E. C. Honea, *J. Am. Chem. Soc.*, **114**, 459 (1992).
127. M. F. Jarrold and J. E. Bower, *J. Chem. Phys.*, **96**, 9180 (1992).
128. D. Consalvo, A. Mele, D. Stranges, A. Giardini-Guidoni and R. Teghil, *Int. J. Mass Spectrom. Ion Proc.*, **91**, 319 (1989).

129. R. J. Tench, M. Balooch, L. Bernadez, M. J. Allen and W. J. Siekhaus, *J. Vac. Sci. Technol. B*, **9**, 820 (1991).
130. D. C. Parent, *Int. J. Mass Spectrom. Ion Proc.*, **116**, 257 (1992).
131. P. F. Greenwood, G. D. Willett and M. A. Wilson, *Org. Mass Spectrom.*, **28**, 831 (1993).
132. A. Nakajima, T. Takuwa, N. Nakao, M. Gomei, R. Kishi, S. Iwata and K. Kaya, *J. Chem. Phys.*, **103**, 2050 (1995).
133. Y. Negishi, A. Kimura, N. Kobayashi, H. Shiromura, Y. Achiba and N. Watanabe, *J. Chem. Phys.*, **103**, 9963 (1995).
134. K. Raghavachari, *Z. Phys. D*, **12**, 61 (1989).
135. K. Raghavachari and C. M. Rohlfing, *J. Chem. Phys.*, **89**, 2219 (1989).
136. C. H. Patterson and R. P. Messmer, *Phys. Rev. B*, **42**, 9241 (1990).
137. I. S. Ignatyev and H. F. Schaefer. III, *J. Chem. Phys.*, **103**, 7025 (1995).
138. J. R. Chelikowsky and J. C. Phillips, *Phys. Rev. Lett.*, **63**, 1653 (1989).
139. J. R. Chelikowsky and J. C. Phillips, *Phys. Rev. B*, **41**, 5735 (1990).
140. U. Rothlisberger, W. Andreoni and P. Giannozi, *J. Chem. Phys.*, **96**, 1248 (1992).
141. D. C. Parent, *Int. J. Mass Spectrom. Ion Proc.*, **138**, 307 (1994).
142. Y. Lin, D. P. Ridge and B. Munson, *Org. Mass Spectrom.*, **26**, 550 (1991).
143. R. C. Dunbar, in *Radiative Association Workshop in Fundamentals of Gas-Phase Ion Chemistry*, (Eds. K. R. Jennings), *NATO ASI Series, Ser. C*, Kluwer, Dordrecht, 1991.
144. J. M. Stone and J. A. Stone, *Int. J. Mass Spectrom. Ion Proc.*, **109**, 247 (1991).
145. W. J. Meyerhoffer and M. M. Bursey, *Org. Mass Spectrom.*, **24**, 246 (1989).
146. J. K. Terlouw and H. Schwarz, *Angew. Chem., Int. Ed. Engl.*, **26**, 805 (1987).
147. F. W. McLafferty, *Science*, **247**, 925 (1990).
148. F. W. McLafferty, *Int. J. Mass Spectrom. Ion Proc.*, **118/119**, 221 (1992).
149. J. L. Holmes, *Mass Spectrom. Rev.*, **11**, 53 (1989).
150. F. Turecek, *Org. Mass Spectrom.*, **27**, 1087 (1992).
151. N. Goldberg and H. Schwarz, *Acc. Chem. Res.*, **27**, 347 (1994).
152. D. V. Zagorevskii and J. L. Holmes, *Mass Spectrom. Rev.*, **13**, 133 (1994).
153. D. K. Böhme, S. Wlodek and H. Wincel, *Astrophys. J.*, **342**, L91 (1989).
154. M. J. J. Kushner, *J. Appl. Phys.*, **63**, 2532 (1988).
155. R. Srinivas, D. Sülzle and H. Schwarz, *J. Am. Chem. Soc.*, **113**, 52 (1991).
156. B. T. Luke, J. A. Pople, M. Krogh-Jespersen, Y. Apeloig, M. Karni, J. Chandrashekhar and P. v. R. Schleyer, *J. Am. Chem. Soc.*, **108**, 270 (1986).
157. R. Srinivas, D. K. Böhme and H. Schwarz, *J. Phys. Chem.*, **97**, 13643 (1993).
158. S. Wlodek, A. Fox and D. K. Böhme, *J. Am. Chem. Soc.*, **113**, 4461 (1991).
159. P. Rosmus, H. Bock, B. Solouki, G. Maier and G. Rihm, *Angew. Chem., Int. Ed. Engl.*, **20**, 598 (1981).
160. G. Maier, G. Rihm and H. P. Reisenauer, *Chem. Ber.*, **117**, 2351 (1984).
161. G. Maier, G. Rihm, H. P. Reisenauer and D. Littmann, *Chem. Ber.*, **117**, 2369 (1984).
162. N. Auner and J. Grobe, *Z. anorg. allg. Chem.*, **459**, 15 (1979).
163. J. E. Baggott, M. A. Blitz, H. M. Frey, P. D. Lightfoot and R. Walsh, *Chem. Phys. Lett.*, **135**, 39 (1987).
164. R. Srinivas, D. Sülzle and H. Schwarz, *Chem. Phys. Lett.*, **175**, 575 (1990).
165. M. Iraqi and H. Schwarz, *Chem. Phys. Lett.*, **205**, 183 (1993).
166. J. R. Flores, A. Largo-Cabrerizo and J. Largo-Cabrerizo, *J. Mol. Struct. THEOCHEM*, **148**, 33 (1986).
167. J. Largo-Cabrerizo and J. R. Flores, *Chem. Phys. Lett.*, **90**, 147 (1988).
168. A. E. Glassgold and G. A. Manson, *The Chemistry and Spectroscopy of Interstellar Molecules*, Univ. of Tokyo Press, Tokyo, 1992, p 261.
169. K. P. Lim and F. W. Lampe, *Int. J. Mass Spectrom. Ion Proc.*, **101**, 245 (1991).
170. R. Srinivas, D. Sülzle, T. Weiske and H. Schwarz, *Int. J. Mass Spectrom. Ion Proc.*, **107**, 369 (1991).
171. W. R. Creasy and S. W. McElvany, *Surface Sci.*, **201**, 59 (1988).
172. G. Frenking, R. B. Remington and H. Schaefer III, *J. Am. Chem. Soc.*, **108**, 2169 (1986).
173. M.-D. Su, R. D. Amos and N. C. Handy, *J. Am. Chem. Soc.*, **112**, 1499 (1990).
174. G. Maier, H. P. Reisenauer and H. Pacl, *Angew. Chem., Int. Ed. Engl.*, **33**, 1248 (1994).
175. G. Maier, H. Pacl, H. P. Reisenauer, A. Meudt and R. Janoschek, *J. Am. Chem. Soc.*, **117**, 12712 (1995).

176. W. Sander, *Angew. Chem., Int. Ed. Engl.*, **33**, 1455 (1994).
177. An account on matrix-isolation spectroscopy of low-coordinated silicon atoms has recently been published in: V. K. Korolev, in *Advances in Physical Organic Chemistry* (Ed. D. Bethell), Vol. 30, Academic Press, London, 1995, p. 1.
178. D. K. Böhme, S. Wlodek and H. Wincel, *J. Am. Chem. Soc.*, **113**, 6396 (1991).
179. R. Srinivas, J. Hrušák, D. Sülzle, D. K. Böhme and H. Schwarz, *J. Am. Chem. Soc.*, **114**, 2803 (1992).
180. Radical ions are termed 'distonic' if they possess spatially separated charge and radical centers. For a definition and an excellent review, see: B. F. Yates, W. J. Bouma and L. Radom, *J. Am. Chem. Soc.*, **106**, 5805 (1984).
181. S. Hammerum, *Mass Spectrom. Rev.*, **7**, 123 (1988).
182. For a theoretical work on the stability of silicon-based distonic ions, see: K. Pius and J. Chandrasekhar, *Int. J. Mass Spectrom. Ion Proc.*, **87**, R15 (1989).
183. R. Srinivas, D. K. Böhme, J. Hrušák, D. Schröder and H. Schwarz, *J. Am. Chem. Soc.*, **114**, 1939 (1992).
184. S. Tajima, H. Ida, S. Tobita, F. Okada, E. Tabei and S. Mori, *Org. Mass Spectrom.*, **25**, 441 (1990).
185. O. Horie, R. Taege, B. Reimann, N. L. Arthur and P. Potzinger, *J. Phys. Chem.*, **95**, 4393 (1991).
186. M. Koshi, A. Myoshi and H. Matsui, *J. Phys. Chem.*, **95**, 9869 (1991).
187. S. Koda, *Prog. Energy Combust. Sci.*, **18**, 513 (1992).
188. L. Ding and P. Marshall, *J. Chem. Phys.*, **98**, 8545 (1993).
189. M. R. Zacharia and W. Tsang, *J. Phys. Chem.*, **99**, 5308 (1995).
190. C. L. Darling and H. B. Schlegel, *J. Phys. Chem.*, **97**, 8207 (1993).
191. D. J. Lucas, L. A. Curtiss and J. A. Pople, *J. Chem. Phys.*, **99**, 6697 (1993).
192. For a discussion and references of 'Polymorphism in the Heavier Analogues of the Ethyl Cation', see, for example: G. Trinquier, *J. Am. Chem. Soc.*, **114**, 6807 (1992).
193. R. Srinivas, D. Sülzle, W. Koch, C. H. DePuy and H. Schwarz, *J. Am. Chem. Soc.*, **113**, 5970 (1991).
194. R. Srinivas, D. K. Böhme, D. Sülzle and H. Schwarz, *J. Phys. Chem.*, **95**, 9836 (1991).
195. M. Iraqi, N. Goldberg and H. Schwarz, *J. Phys. Chem.*, **97**, 11371 (1993).
196. N. Goldberg, M. Iraqi, W. Koch and H. Schwarz, *Chem. Phys. Lett.*, **225**, 404 (1994).
197. N. Goldberg, M. Iraqi, J. Hrušák and H. Schwarz, *Int. J. Mass Spectrom. Ion Proc.*, **125**, 267 (1993).
198. N. Goldberg, J. Hrušák, M. Iraqi and H. Schwarz, *J. Phys. Chem.*, **97**, 10687 (1993).
199. N. Goldberg, M. Iraqi and H. Schwarz, *J. Chem. Phys.*, **101**, 2871 (1994).
200. S. Wlodek, D. K. Böhme and E. Herbst, *Mon. Not. Astron. Soc.*, **242**, 674 (1990).
201. For earlier reports on the matrix isolation of this species, see: R. J. VanZee, P. F. Ferrante and W. Weltner, *J. Chem. Phys.*, **83**, 6181 (1985).
202. G. Frenking and H. F. Schaefer, III, *J. Chem. Phys.*, **82**, 4584 (1985).
203. Y. Xie and H. F. Schaefer, III, *J. Chem. Phys.*, **93**, 1196 (1990).
204. S. Gronert, R. A. O'Hair, S. Prodnuk, D. Sülzle, R. Damrauer and C. H. DePuy, *J. Am. Chem. Soc.*, **112**, 997 (1990).
205. A. Fox, S. Wlodek, A. C. Hopkinson, M. H. Lien, M. Sylvain, C. Rodriguez and D. K. Böhme, *J. Phys. Chem.*, **93**, 1549 (1989) and references cited therein.
206. For a computational study of the silanol anion, H_3SiO^-, see: J. N. Nicholas and M. Feyereisen, *J. Chem. Phys.*, **103**, 8031 (1995).
207. R. Withnall and L. Andrews, *J. Phys. Chem.*, **89**, 3261 (1985).
208. R. J. Glinski, J. L. Gole and D. A. Dixon, *J. Am. Chem. Soc.*, **107**, 5891 (1985).
209. Z. K. Ismail, R. H. Hauge, L. Fredin, J. W. Kauffmann and J. L. Margrave, *J. Chem. Phys.*, **77**, 1617 (1982).
210. C.-M. Chiang, B. R. Zegarski and L. H. Dubois, *J. Phys. Chem.*, **97**, 6984 (1993).
211. A. I. Boldyrev and J. Simons, *J. Phys. Chem.*, **97**, 5875 (1993).
212. For an earlier theoretical study of Si_2O, see: R. L. DeKock, B. F. Yates and H. F. Schaefer III, *Inorg. Chem.*, **28**, 1680 (1989).
213. For earlier results from matrix spectroscopic studies which assigned a linear SiSiO structure to the triplet state of this molecule, see: R. J. VanZee, R. F. Ferrante and W. Weltner, *Chem. Phys. Lett.*, **139**, 426 (1987).
214. For previous calculations on Si_2O_2, see: L. C. Snyder and K. Raghavachari, *J. Chem. Phys.*, **80**, 5076 (1984).

215. For earlier results from matrix isolation experiments, see: H. Schnöckel, T. Mehner, H. S. Plitt and S. Schnuck, *J. Am. Chem. Soc.*, **111**, 4578 (1989) and references cited therein.
216. P. Fournier, J. Appell, F. C. Fehsenfeld and J. Durup, *J. Phys. B*, **5**, L58 (1972).
217. F. C. Fehsenfeld, J. Appell, P. Fournier and J. Durup, *J. Phys. B*, **6**, L268 (1973).
218. J. C. Lorquet, B. Leyh-Nihaut and F. W. McLafferty, *Int. J. Mass Spectrom. Ion Proc.*, **100**, 465 (1990).
219. For attempts to generate this long-sought-after triplet species and reasons why this molecule has still not been unequivocally identified, see: D. Sülzle, T. Weiske and H. Schwarz, *Int. J. Mass Spectrom. Ion Proc.*, **125**, 75 (1993).
220. The phenyl-substituted isomer PhNSi has been characterized by photoelectron spectroscopy some time ago: H. Bock and R. Dammel, *Angew. Chem.*, **97**, 128 (1985).
221. J. F. Ogilvie and S. Cradock, *J. Chem. Soc., Chem. Commun.*, 364 (1966).
222. M. Bogey, C. Demuynck, J. L. Destombes and A. Walters, *Astron. Astrophys.*, **244**, L47 (1991).
223. M. Elhanine, R. Farrenq and G. Guelachvili, *J. Chem. Phys.*, **94**, 2529 (1991).
224. For a recent report on the characterization of HSiN via photoisomerization of HNSi, see: G. Maier and J. Glatthaar, *Angew. Chem., Int. Ed. Engl.*, **33**, 473 (1994).
225. J. G. Radziszewski, D. Littmann, V. Balaji, L. Fabry, G. Gross and J. Michl, *Organometallics*, **12**, 4816 (1993).
226. R. Preuss, R. J. Buenker and S. D. Peyerimhoff, *J. Mol. Struct. THEOCHEM*, **49**, 171 (1978).
227. M. S. El-Shall, *Chem. Phys. Lett.*, **159**, 21 (1989).
228. Y. Apeloig and K. Albrecht, *J. Am. Chem. Soc.*, **117**, 7263 (1995).
229. For experimental work on R−CN and CN−R compounds, see: C. Rüchardt, M. Meier, K. Haaf, J. Pakusch and W. K. L. Wo, *Angew. Chem., Int. Ed. Engl.*, **103**, 907 (1991) and references cited therein.
230. J. R. Flores and J. Largo-Cabrerizo, *Chem. Phys. Lett.*, **142**, 159 (1987).
231. J. R. Flores and J. Largo-Cabrerizo, *J. Mol. Struct. THEOCHEM*, **183**, 17 (1989).
232. J. R. Flores, F. G. Crespo and J. Largo-Cabrerizo, *Chem. Phys. Lett.*, **147**, 84 (1988).
233. C. F. Melius and P. Ho, *J. Phys. Chem.*, **95**, 1410 (1991).
234. O. Parisel, M. Hanus and Y. Ellinger, *J. Chem. Phys.*, **100**, 2926 (1996).
235. For a recent theoretical investigation of this ion−molecule reaction, see: J. R. Flores, P. Redondo and S. Azpeleta, *Chem. Phys. Lett.*, **240**, 193 (1995).
236. Y. Apeloig, M. Karni, A. Stanger, H. Schwarz and T. Drewello, *J. Chem. Soc., Chem. Commun.*, 989 (1987).
237. M. T. Reetz, *Adv. Organomet. Chem.*, **16**, 33 (1977).
238. R. B. Woodward and R. Hoffmann, *The Conservation of Orbital Symmetry*, Academic Press, New York, 1970.
239. R. Bakhtiar, C. M. Holznagel and D. B. Jacobson, *Organometallics*, **12**, 621 (1993).
240. T. Drewello, P. C. Burgers, W. Zummack, Y. Apeloig and H. Schwarz, *Organometallics*, **9**, 1161 (1990).
241. R. Bakhtiar, C. M. Holznagel and D. B. Jacobson, *J. Am. Chem. Soc.*, **114**, 3227 (1992).
242. S. G. Cho, *J. Organomet. Chem.*, **510**, 25 (1996).
243. For a review on this interesting topic of gas-phase ion chemistry, see: C. Lifshitz, *Acc. Chem. Res.*, **27**, 138 (1994).
244. S. Murthy, Y. Nagano and J. L. Beauchamp, *J. Am. Chem. Soc.*, **114**, 3573 (1992).
245. Y. Nagano, S. Murthy and J. L. Beauchamp, *J. Am. Chem. Soc.*, **115**, 10805 (1993).
246. A. Nicolaides and L. Radom, *J. Am. Chem. Soc.*, **116**, 9769 (1994).
247. E. Tabei, S. Mori, F. Okada, S. Tajima, K. Ogino, H. Tanabe and S. Tobita, *Org. Mass Spectrom.*, **28**, 412 (1993).
248. S. Tobita, S. Tajima and F. Okada, *Org. Mass Spectrom.*, **24**, 373 (1989).
249. S. Tobita, S. Tajima, F. Okada, S. Mori, E. Tabei and M. Umemura, *Org. Mass Spectrom.*, **25**, 39 (1990).
250. P. C. H. Eichinger and J. H. Bowie, *Rapid Commun. Mass Spectrom.*, **5**, 629 (1991).
251. K. M. Downard, J. H. Bowie and R. N. Hayes, *Aust. J. Chem.*, **43**, 511 (1990).
252. M. Krempp and R. Damrauer, *Organometallics*, **14**, 170 (1995).
253. R. A. J. O'Hair, J. C. Sheldon, J. H. Bowie, R. Damrauer and C. H. DePuy, *Aust. J. Chem.*, **42**, 489 (1989).
254. H. Schwarz, *Pure Appl. Chem.*, **61**, 685 (1989).
255. K. Lammertsma, P. v. R. Schleyer and H. Schwarz, *Angew. Chem., Int. Ed. Engl.*, **28**, 1321 (1989).

256. L. M. Roth and B. S. Freiser, *Mass Spectrom. Rev.*, **10**, 303 (1991).
257. D. Matur, *Phys. Rep.*, **225**, 193 (1993).
258. C. Heinemann, D. Schröder and H. Schwarz, *J. Phys. Chem.*, **99**, 16195 (1995).
259. T. Ast, C. J. Proctor, C.J. Porter and J. H. Beynon, *Int. J. Mass Spectrom. Ion Phys.*, **40**, 111 (1981).
260. C. J. Procter, C. J. Porter, T. Ast and J. H. Beynon, *Int. J. Mass Spectrom. Ion Phys.*, **41**, 251 (1982).
261. C. J. Porter, C. J. Procter, T. Ast and J. H. Beynon, *Int. J. Mass Spectrom. Ion Phys.*, **41**, 265 (1982).
262. M. Rabrenovic, T. Ast and J. H. Beynon, *Int. J. Mass Spectrom. Ion Proc.*, **61**, 31 (1984).
263. M. Kolbuszewski and J. S. Wright, *J. Phys. Chem.*, **99**, 16196 (1995).
264. K. Leiter, W. Ritter, A. Stamatovic and T. D. Mark, *Int. J. Mass Spectrom. Ion Proc.*, **68**, 341 (1986).
265. W. P. M. Maas and N. M. M. Nibbering, *Int. J. Mass Spectrom. Ion Proc.*, **88**, 257 (1989).
266. S. N. Schauer, P. Williams and R. N. Compton, *Phys. Rev. Lett.*, **65**, 625 (1990).
267. T. Sommerfeld, M. K. Scheller and L. S. Cederbaum, *J. Chem. Phys.*, **103**, 1057 (1995).
268. T. Sommerfeld, M. K. Scheller and L. S. Cederbaum, *J. Chem. Phys.*, **104**, 1464 (1996).

CHAPTER 19

Matrix isolation studies of silicon compounds

GÜNTHER MAIER, ANDREAS MEUDT, JÖRG JUNG and HARALD PACL

Institut für Organische Chemie der Justus-Liebig-Universität Giessen, Heinrich-Buff-Ring 58, D-35392 Giessen, Federal Republic of Germany

---

I. INTRODUCTION

A. Motivation

Though numerous molecules involving tetravalent silicon atoms singly bonded to first- and second-row elements are known, the chemistry of compounds containing the element in 'unusual' low-valent bonding situations is a relatively young area of research. Some exotic representations like the very first compound of multiply bonded silicon, the SiN radical, were identified as early as 1925[1]. Nevertheless, countless investigations indicating the nonaccessibility of π-systems[2] of silicon and other third period elements resulted in the formulation of the classical double-bond rule, which predicted high reactivity for such compounds[1]. After some reports[3,4] on 'successful' syntheses, all of which failed to stand up to scrutiny, the existence of transient species with silicon–silicon multiple bond systems was first demonstrated convincingly as late as 1969 by the pyrolysis of 1,2-disila-4-cyclohexenes yielding disilenes, whose intermediate existence was demonstrated indirectly[5]. In the same decade, 1,1-dimethylsilaethene as the first silene was generated by pyrolysis of the appropriate silacyclobutane[6–8].

Novel highly reactive substances are often first proposed as transient intermediates, then later isolated in noble gas or hydrocarbon matrices at very low temperatures[9] and still later obtained as stable species in the form of highly substituted derivatives. The second step in this classic historical pattern, namely the matrix isolation of reactive intermediates, is mostly concentrated on the study of the prototype systems unadulterated by substituent effects. This area has become a field of especially fruitful interaction between experiment and theory, which allows the unequivocal identification of the often long sought-after substances. A good example for the development described above is the fate of silylenes. Soon following the proposal of these species as fleeting intermediates, some organic derivatives could be matrix-isolated starting in 1979 by photolytic decomposition of suitable precursors[10]. These investigations finally smoothened the way for the isolation of a destillable silylene which survives even heating in toluene solution to 150 °C for many months[11].

The matrix technique allowed even the isolation of compounds with silicon–nitrogen triple bonds such as HSiN and HNSi[12].

These isolations of highly reactive prototype systems are important for our understanding of chemical bonding.

B. Coverage

This survey covers the matrix isolation and spectroscopic analysis of a variety of molecules containing doubly and triply bonded silicon, strained silacycles and silylenes. In most cases, the matrix-isolated substances and their photoproducts were identified by IR and UV spectroscopy and the comparison of experimental with calculated spectra using quantum mechanical methods. The explosive growth of this field of organic chemistry is well documented by numerous reviews, for example the excellent article of Raabe and Michl[1] on 'Multiple Bonds to Silicon' and the review about 'Silylenes' by Gaspar[13] which serve as a basis for this review. Publications which appeared prior to the two cited reviews are only mentioned here if necessary in the context of the discussion. Our literature research relying on computerized search services in *Chemical Abstracts* extends to the end of 1995. Maybe we have failed to reach completeness in finding all relevant articles covering the present subject. If this is the case we apologize to both the readers and the authors.

It was impossible to avoid a certain amount of overlap between the sections of this review, especially because of the easy conversion of substituted silylenes into species with multiply bonded silicon and vice versa. But we tried to reduce duplications of this type as far as possible.

II. SILICON–CARBON MULTIPLE BONDS

A. Silenes

The chemistry of silenes presents an especially well-investigated area of organosilicon chemistry. Despite their high reactivity and tendency to dimerize, more than 150 different silenes were the subject of a large number of experiments[14]. The isolation of a crystalline silene — indefinitely stable at room temperature in the absence of air — represented a breakthrough in the chemistry of silicon π-systems[15]. In the meantime, a two-digit number of such stable silenes is known[1], crowned by the recent isolation of the first stable 1-silaallene[16].

The parent silaethylene **2** could be matrix-isolated by our group in 1981[17] by pyrolysis of the bicyclic system **1** (equation 1). Later, a new entry into this system was found by photolysis of methyldiazidosilane **3**[18] (equation 1). This simplest representative **2** shows already most aspects of the chemistry of the whole class of silenes, e.g. the photoisomerizability into the corresponding silylene (see Section VIII).

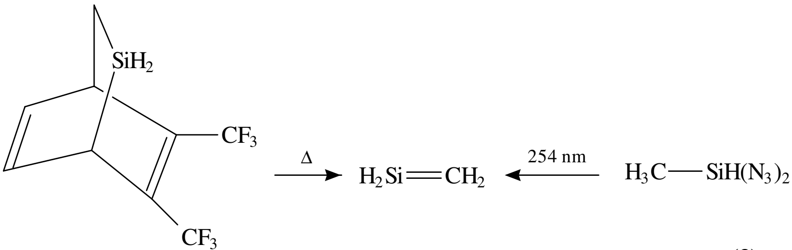

(1)

(1) **(2)** **(3)**

TABLE 1. Substituent effects on the UV maxima of silenes

Silene	λ_{max} (nm)	Literature
$H_2Si{=}CH_2$	258	20
$D_2Si{=}CH_2$	259	20
$Cl_2Si{=}CH_2$	246	20
$(Me_3Si)_2Si{=}C(OSiMe_3)$ (R)	*ca* 340	21
R = *t*-Bu, CEt$_3$, Ad-1		22
$Me_2Si{=}CHMe$	255	19
$Me_2Si{=}CH(SiMe_3)$	265	19
$Me_2Si{=}CMe(SiMe_3)$	274	19
$Me_2Si{=}C(SiMe_3)_2$	278	19
$Me_2Si{=}CPh(CO_2Me)$	280	19
$Me_2Si{=}C(SiMe_3)$(CO Ad-1p)	284	19
$Me_2Si{=}C(SiMe_3)(CO_2Et)$	293	19

In the last decade, the interest in this area focussed on the spectroscopic properties of silenes and their intermolecular reactions in matrices.

Before that time, little was known about their UV spectra. Ando and coworkers extended our knowledge about this facet of organosilicon chemistry by photolysis of silyldiazomethanes **4** in 3-methylpentane at 77 K yielding the expected silenes **5**[19] (equation 2). The measured UV spectra together with previous results are summarized in Table 1.

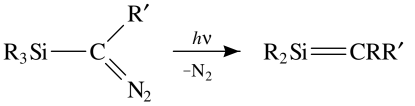

$$R_3Si{-}C(R')({=}N_2) \xrightarrow[-N_2]{h\nu} R_2Si{=}CRR' \qquad (2)$$

(4) **(5)**

The UV absorptions of the tri- or tetrasubstituted silenes are red-shifted compared to the parent silene **2** (λ = 258 nm) but occur at shorter wavelengths than in the highly substituted silenes of Brook (λ = *ca* 340 nm). The introduction of trimethylsilyl groups on the carbon atoms results in slight red-shifts just as the conjugation of the silene system with carbonyl groups.

Sander and coworkers studied intermolecular reactions of methylsilenes in argon matrices[23]. 1,1-Dimethylsilene **(7)** was generated by photolysis of precursor **6** in quantitative yield (equation 3). Warming to 35 K resulted in dimerization of silene **7** to the corresponding disilacyclobutane **8**. This kind of silene dimerization leading to the formation of 1,3-disilacyclobutane was originally one of the structural proofs for the parent silene **2**[20].

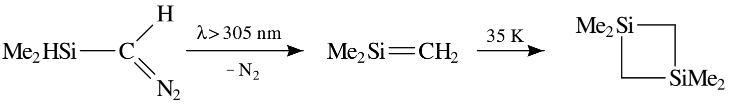

(3)

(6) **(7)** **(8)**

Photolysis of **6** in a formaldehyde-doped argon matrix (0.6%) yielded also silene **7** as the major product but also minor quantities of other products. Warming of the matrix to 30–35 K allowed the direct spectroscopic observation of the reaction between **7** and formaldehyde. The intensity of the IR absorptions of these compounds disappeared to a large extent, and in addition to **8** a new product, which could be identified as the siloxycarbene **10** was observed. This compound was stable under the reaction conditions (equation 4). Siloxycarbenes were frequently postulated[24–26] as fleeting intermediates in the photolysis of acylsilanes, but up to now only in one other case observed spectroscopically[27].

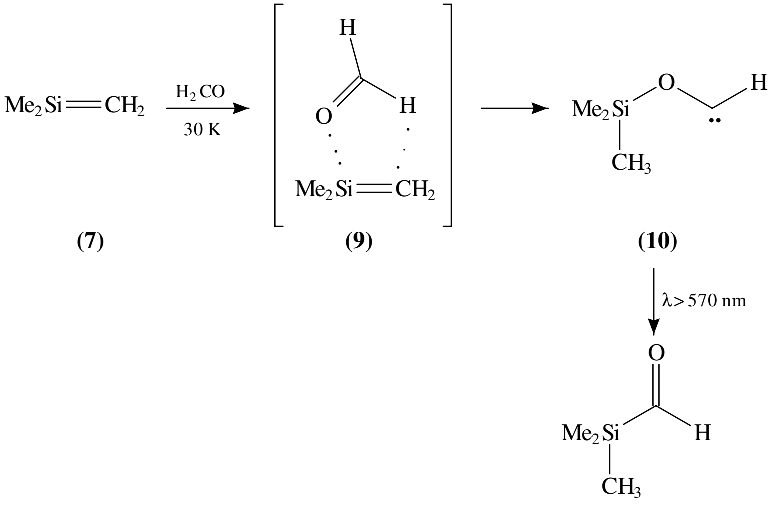

(7) **(9)** **(10)** **(11)**

(4)

Intermediate **10** turned out to be easily photoisomerizable yielding the stable acylsilane **11**. According to CCSD(T)/6-31G(d,p)//MP2/6-31G(d,p) calculations[23] carbene **10** originates from the initial complex **9**.

2-Silapropene **12** reacted much faster under analogous conditions with formaldehyde giving the expected 1,2-siloxetane, whereas 2-methyl-2-sila-2-butene **13** proved to be unreactive. Obviously the reactivity of silenes against H_2CO decreases with increasing degree of methyl substitution. Another interesting aspect of this reaction is the high kinetic isotope effect which totally inhibits the reaction even of silapropene **12** with D_2CO.

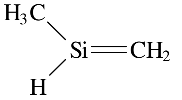

(12)

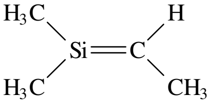

(13)

The same authors investigated the photochemical and thermal oxidation of 2-silapropene **12**, silaisobutene **7** and 1,1,2-trimethylsilene **13** in O_2-doped argon matrices (equation 5)[28]. These silenes are easily photooxidized in matrices containing more than 1% O_2, but only trimethylsilene **13** exhibits thermal reactivity toward oxygen at temperatures as low as 20–40 K.

The photochemical reactivity goes up with increasing number of methyl groups at the double bond and decreasing ionization potential[28]. Key intermediates in both the photochemical and the thermal oxidation of silenes **12**, **7** and **13** are the siladioxetanes **14**. These species are labile even in low-temperature matrices and could not be identified spectroscopically. Evidence for their formation comes from the observed oxidation products such as complexes **15** between silanones and formaldehyde and formylsilanols **16**.

The complexes **15** were identified by comparison of *ab initio* calculated and observed IR spectra[28]. They show the expected red-shifts of $\nu_{C=O}$ and $\nu_{Si=O}$.

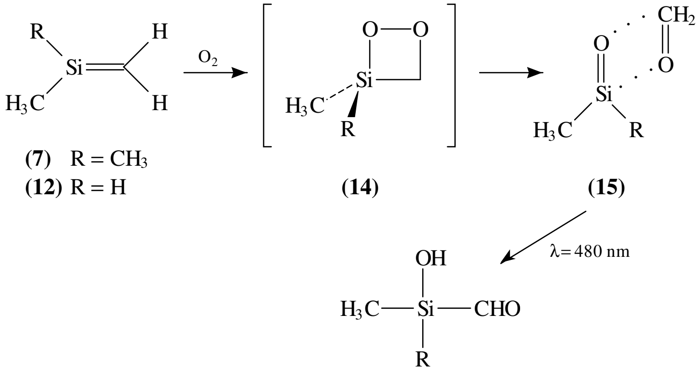

(7) R = CH_3
(12) R = H
(14)
(15)
(16)

(5)

An additional oxidation pathway is observed for **13** with a methyl group at the C-atom of the silene moiety. Here, the primary adduct of **13** and $^3O_2$ under photolytic conditions, i.e. triplet diradical **17**, can either ring-close to give the corresponding dioxetane (the dioxetane is not stable under the photolytic conditions required to induce the photooxidation, and therefore cannot be observed) leading to products derived from it, or produce dimethylvinylsilyl hydroperoxide **(18)** via H-abstraction from a methyl group (equation 6).

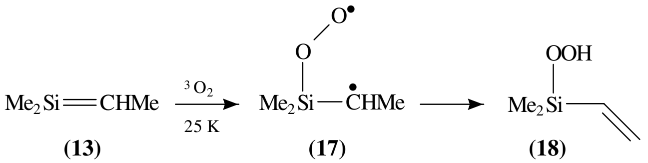

(13) **(17)** **(18)**

(6)

B. Silynes

No experimental evidence concerning compounds with silicon–carbon triple bonds is known, so that experimental efforts should be concentrated on the search for these fascinating species. 2-Silaallenes and 2-silaketenes, which also would contain a sp-hybridized silicon atom, could not be isolated up to now and remain a challenge of organosilicon chemistry (for 1-silaallene and for silylene–CO complexes cf Section VIII).

C. Silaaromatics

Theoretical studies have shown that the resonance energy of silabenzene should be 2/3 that of benzene[29]. Even though other isomers of C_5H_6Si such as Dewar silabenzene may be competitive in stability, silabenzene appears to have all the attributes expected for an analogue of benzene. Nevertheless, silaaromatics were for a long time thought to be elusive molecules despite the relative stability of similar heteroatomic derivatives of benzene such as phosphabenzene, arsabenzene and stibabenzene[30].

The first unambiguous evidence for the existence of a substituted silabenzene was reported by Barton and coworkers in 1978[31,32]. The pyrolysis of precursor **19** in the presence of perfluoro-2-butyne yielded adduct **21** and copyrolysis of **19** and MeOH(D) gave methoxysilane **22**[33], strongly suggesting the intermediate existence of silatoluene **20** (equation 7). In the absence of trapping agents, vacuum flow pyrolysis of silacyclohexadiene **19** resulted in the Diels–Alder dimer **23** of silatoluene **20** rather than the predicted[34] [2 + 2] dimer. The deposition of the products of neat pyrolysis of **19** together with argon on a spectroscopic window at low temperatures allowed the direct observation of silatoluene **20** whose UV spectrum ($\lambda_{max} = 310$ nm) showed the expected[29,34] bathochromic shift compared to the spectrum of benzene. The position of the band and its well-resolved vibrational structure are in good agreement with the prediction that silabenzene should be an aromatic system. Silatoluene **20** was stable to UV irradiation but vanished upon warming of the matrix producing a polymer, which was not characterized[33].

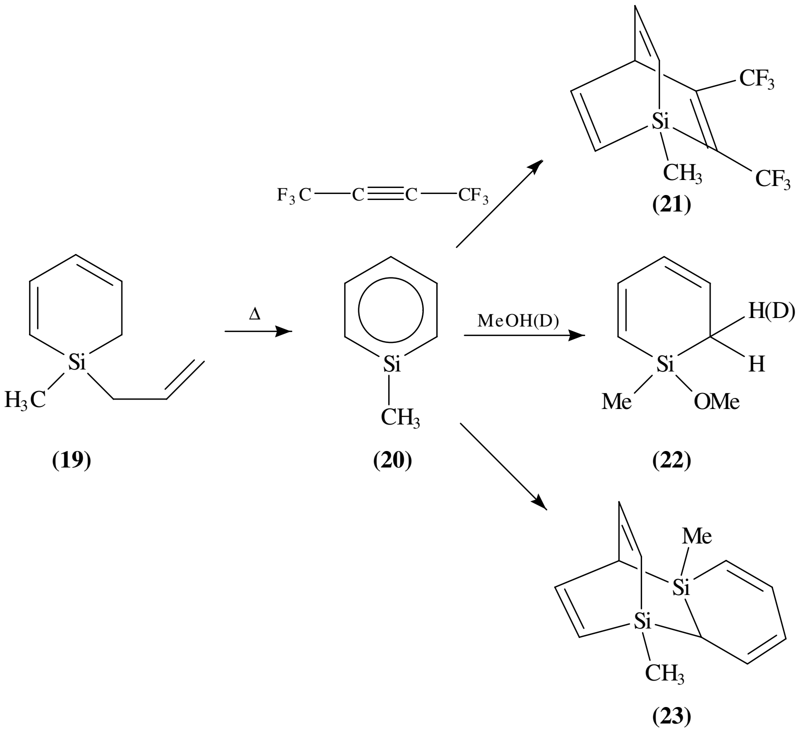

(7)

The parent silabenzene **24** was first matrix-isolated by our group in 1980[35] by pyrolysis of precursors **25** and **26**, which yield the expected silabenzene by retro-ene fragmentation. Later, it could be shown that in analogy to carbon chemistry the hydrogen elimination from silacyclohexadiene **27** also gives the silaaromatic **24**[36]. This reaction is allowed by the Woodward–Hoffmann rules. In accordance with the Woodward–Hoffmann rules, it could be demonstrated that silabenzene **24** is not accessible by pyrolysis of the conjugated silacyclohexadiene **28** (equation 8).

Silabenzene **24** reveals a characteristic Si–H stretching vibration at 2217 cm^{-1}, as expected for hydrogen attached to a sp^2-hybridized silicon atom. Compound **24** shows a typical benzene-type UV spectrum with absorptions at $\lambda = 217$, 272 and 320 nm, which fit into the series of the already known donor-substituted heterobenzenes[30]. An additional structural proof was the partially reversible photochemical conversion of **24** into Dewar silabenzene **29** whose Si−H stretching vibration is shifted to 2142 cm^{-1}, as expected for a hydrogen connected to a sp^3-hybridized silicon atom. Silabenzene **24** survived warming of the matrix to a temperature of 37 K, which allows intermolecular reactions. At still higher temperatures (80 K) the absorptions of **24** disappeared completely.

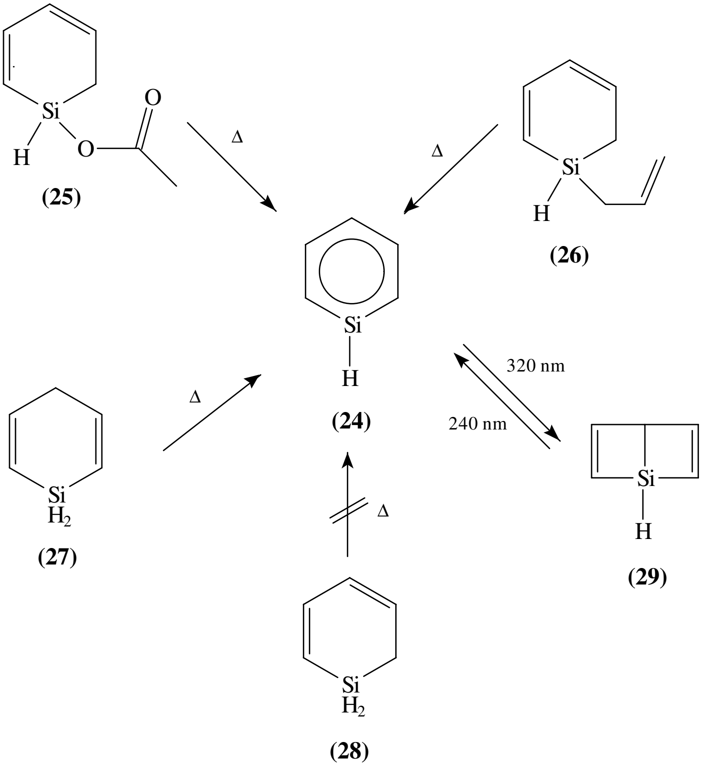

(8)

The properties of silabenzene **24** resemble strongly those of silatoluene **20** described above not only in the UV spectra, but also in the measured PE spectra[37−40]. In conclusion, one has to note that both species are best considered as symmetry-distorted delocalized 6π-electron systems in conformity with the above-mentioned calculations[40].

After the successful preparation of silabenzene **24** by hydrogen elimination from **27**, it was tempting to try to generate 1,4-disilabenzene **31** by pyrolysis of the easily accessible disilacyclohexadiene **30**[41] (equation 9).

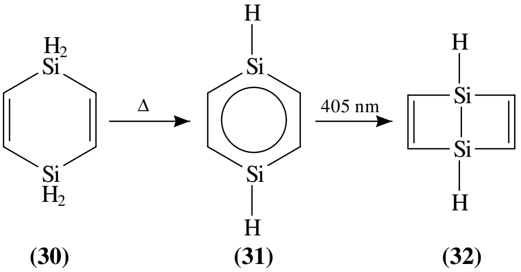

(9)

The dehydrogenation of **30** turned out to be more difficult than the analogous conversion of **27** to **24**. The IR spectrum of the matrix-isolated products showed only one absorption at 1273 cm^{-1}, which disappeared upon irradiation with $\lambda = 405$ nm probably yielding Dewar disilabenzene **32**. The UV spectrum proved to be of higher diagnostic value. 1,4-Disilabenzene **31** shows a typical heterobenzene electronic spectrum with absorptions at $\lambda = 408$, 340 and 275 nm displaying another bathochromic shift compared to silabenzene **24**.

No experimental data are available for derivatives of 1,2- or 1,3-disilabenzenes[42]. The same is true for the even more fascinating hexasilabenzene[43].

According to theoretical investigations[44,45] the reason for the high reactivity of silabenzenes is the polar SiC double bond. Silabenzenes bearing large substituents should be kinetically more stable than the parent system and could allow possibly the synthesis of isolable derivatives. As outlined in the other sections of this review, the strategy of kinetic stabilization by introducing bulky substituents led to a variety of silicon-element π-bond systems stable up to room temperature. Another way to stabilize the heterobenzene should be the benzoannelation of the central ring. This idea was the motivation for the preparation of 9-silaanthracenes by pyrolytic[46] and photolytic[47] methods. Older procedures, such as in the elimination of a hydrogen halide from suitable dihydro precursors, gave only dimeric or polymeric material[48]. Similarly, a thermolytic approach which had been developed for phosphorus and arsenic rings was unsuccessful when applied to silicon-containing educt molecules[49]. A breakthrough was achieved by pyrolysis of **33** (R = Ph), which gives the substituted 9-silaanthracene **34** (R = Ph) by elimination of benzene[46] (equation 10).

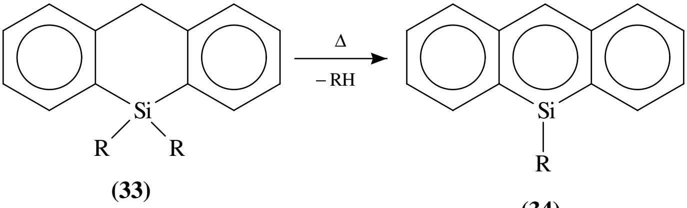

(33) **(34)** (10)

Evidence for the formation of **34** (R = Ph) was provided by neutralization reionization mass spectrometry and more directly by the matrix isolation and spectroscopic investigations on **34** (R = Ph) in an argon matrix at 12 K. The UV spectrum of **34** (R = Ph) exhibits characteristic bands at $\lambda = 364$, 386, 404, 420, 440, 470 and 502 nm, resembling those of the electronic spectrum of anthracene, but with the expected bathochromic shifts. If one irradiates into the maximum at $\lambda = 502$ nm, all bands shown in the spectrum disappear completely within 5 minutes. The vanishing of these characteristic bands can again be explained by the photoisomerization of silaanthracene **34** (R = Ph) to the corresponding Dewar valence isomer.

In the same way pyrolysis of unsubstituted dihydrosilaanthracene **33** (R = H) formed the parent silaanthracene **34** (R = H), which likewise could be photoisomerized into the corresponding Dewar silaanthracenes[46].

Silaanthracenes turned out to be also available by the 254 nm photolysis of the appropriate dihydrosilaanthracenes in rigid hydrocarbon glass at 77 K[47].

In summary, the benzoannelation of the central silabenzene ring is not enough to stabilize compounds of this type to a high extent. They still proved to be very thermolabile. Even phenyl substitution as in **34** (R = Ph) does not furnish sufficient steric protection for isolation outside of an argon matrix.

The sterically overcrowded silabenzenes **36** and **38** were generated by pyrolysis of the appropriate precursors **35** and **37** (equations 11a and 11b, respectively) and isolated in an argon matrix[50].

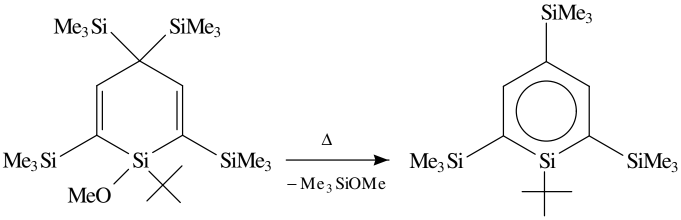

(35) **(36)**

(11a)

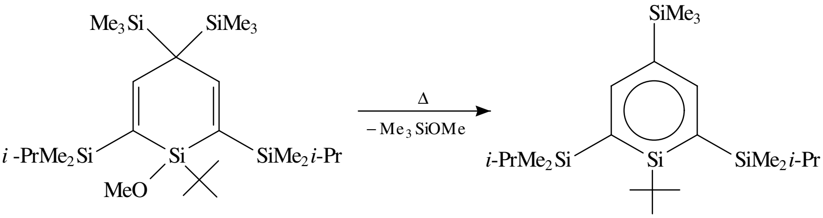

(37) **(38)**

(11b)

The silaaromatics **36** and **38** reveal in the observed UV spectra an additional bathochromic shift compared to silabenzene **24**. Both, **36** and **38**, disappear in an irreversible process upon irradiation with $\lambda = 290-420$ nm, probably due to the formation of the corresponding Dewar silabenzenes. The kinetically stabilized silaaromatics **36** and **38** turned out to be stable up to 90 K even without an argon cage, but decomposed unspecifically at higher temperatures.

In 1988, Märkl and Schlosser[51] reported the synthesis of the substituted silabenzene **40** by irradiation of the diazo compound **39**, which was found to be stable in solution up to 170 K (equation 12).

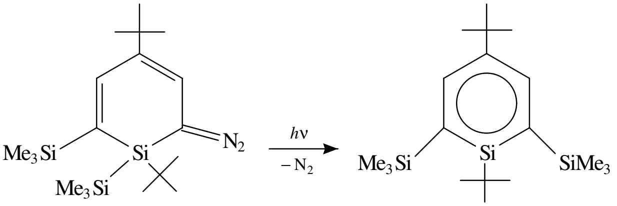

(39) **(40)**

(12)

Nevertheless, the synthesis of the first silabenzene stable up to room temperature remains a challenging problem.

D. Silaantiaromatics

Whereas the isomeric hydrocarbon skeletons cyclobutadiene and tetrahedrane have been the object of many investigations[52], little is known about the analogous silacyclobutadienes and silatetrahedranes. *Ab initio* calculations carried out by Gordon and coworkers[53,54] show that the most stable species among the cyclic C_3SiH_4 species should be 2-methylsilacyclopropenylidene, followed by other silylenic species which might be suitable precursors for unsubstituted silacyclobutadiene. Silacyclobutadiene is almost 60 kcal mol^{-1} less stable than methylsilacyclopropenylidene as a consequence of its calculated large antiaromatic destabilization energy. Silatetrahedrane lies 32 kcal mol^{-1} higher in energy than silacyclobutadiene[53,54].

Attempts to generate silacyclobutadienes through the thermal rearrangements of cyclopropenyl silylenes in solution proved to be unsuccessful[55], in contrast to the known similar rearrangements of cyclopropenyl carbenes[52,56,57] and nitrenes[58].

Our group tried to observe the formation of silacyclobutadienes via a photochemical pathway[59–61]. Photolysis of cyclopropenyl silanes **41 a–l** in hydrocarbon matrices at 77 K could produce the corresponding silylenes **42**, which should be suitable silacyclobutadiene precursors (equation 13). In only two cases **(41a,d)**, the photolysis produced the expected silylenes **42**, but it was not possible to initiate their photochemical conversion into the desired silacyclobutadienes **43**.

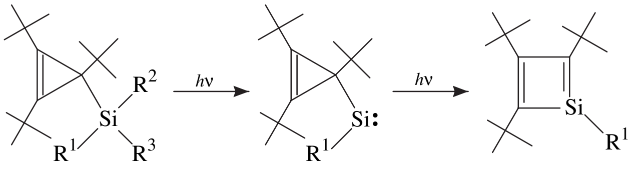

(41) **(42)** **(43)**

a	SiMe$_3$	SiMe$_3$	SiMe$_3$
b	Ph	SiMe$_3$	SiMe$_3$
c	*t*-Bu	SiMe$_3$	SiMe$_3$
d	SiMe$_3$	SiMe$_3$	SiPhMe$_2$
e	*t*-Bu	SiMe$_3$	SiPhMe$_2$
f	SiMe$_3$	SiPhMe$_2$	SiPhMe$_2$
g	*t*-Bu	SiPhMe$_2$	SiPhMe$_2$
h	*t*-Bu	I	I
i	SiMe$_3$	N$_3$	N$_3$
j	Ph	N$_3$	N$_3$
k	Mes	N$_3$	N$_3$
l	*t*-Bu	N$_3$	N$_3$

(13)

Irradiation of compound **41e** in solution yields a yellow species to which we tentatively assign structure **45** (equation 14). The radical character of **45** is supported by EPR spectroscopy and trapping experiments. The formation of cyclobutenyl radical **45** can be explained by homolytic cleavage of the Si–SiMe$_2$Ph bond in **41e** and rearrangement of the resulting primary product **44**.

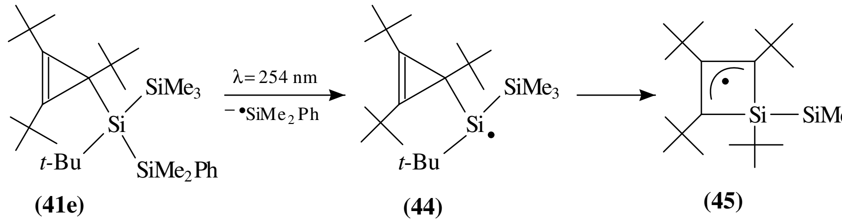

(14)

In this context it is astonishing that Fink and Purani succeeded (1987) in observing a photochemical rearrangement of a cyclopropenyl silylene of the same type to give the corresponding silacyclobutadiene[55]. The 254-nm photolysis of cyclopropenyltrisilane **46** (Ar = Mes) in a 3-methylpentane glass yielded the yellow mesityl(1,2,3-tri-*tert*-butylcyclopropenyl)silylene (**47**, Ar = Mes), which could be trapped in the presence of ethanol to give the corresponding ethoxysilane **48** (equation 15).

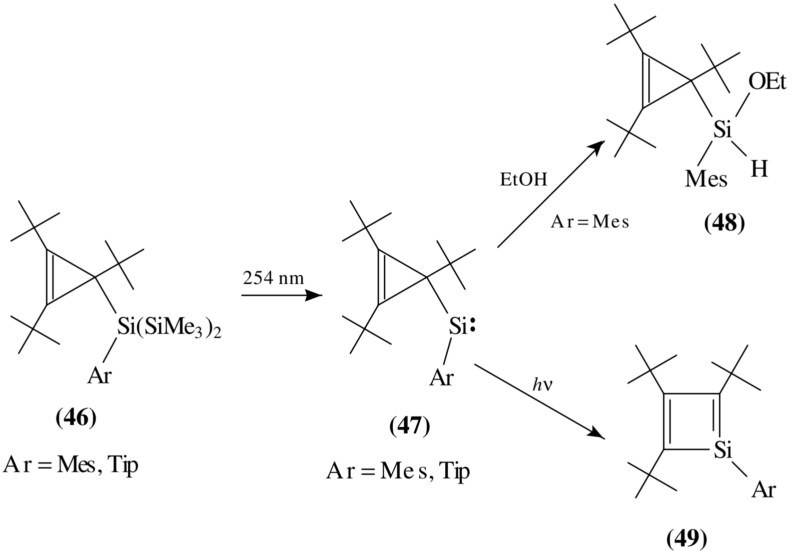

(15)

Irradiation of silylene **47** (Ar = Mes) with visible light resulted in the vanishing of the silylene absorption bands and the formation of a new species, which could be identified as the first example of a silacyclobutadiene **49** (Ar = Mes). Trapping of **49** (Ar = Mes) with methoxytrimethylsilane or ethanol yielded the expected products **50** and **51** in a completely stereospecific *syn* addition (equation 16). This result is in good agreement with reports by Jones and coworkers about *syn* additions of these reagents to simpler acyclic silenes[62,63] (equation 16).

Subsequent warming of matrix-isolated **49** (Ar = Mes) to room temperature results in the formation of a dimer[64,65]. As could be shown by EPR spectrometry and product analysis, triplet diradical **52** (Ar = Mes) seems to be the first product which can be detected during annealing of the matrix[65] (equation 17).

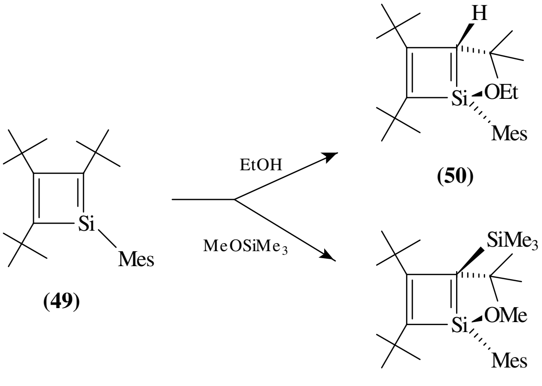

(49) (50) (51)

(16)

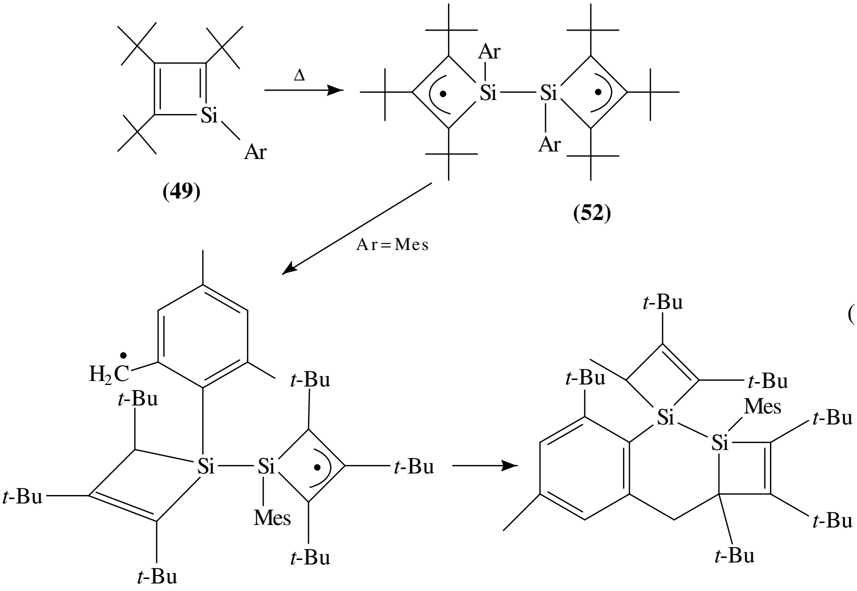

(49) (52) (53) (54)

(17)

The dimerization of **49** (Ar = Mes) yields compound **54**, whose X-ray crystal structure could be determined[64], via diradicals **52** and **53**. This reaction may be considered as a special case of silene dimerization. Although the typical course of silene dimerization leads to head-to-tail adducts (cf Section II.A), highly substituted analogues often give the head-to-head isomer. Brook and Baines have proposed that many of these dimerizations also proceed via initial formation of a Si−Si bond to give 1,4-diradicals which, in some cases, isomerize by intramolecular hydrogen abstractions[66,67].

Diradical **52** (Ar = Mes) and the corresponding 2,4,6-triisopropylphenyl substituted **52** (Ar = Tip), which is available in the same manner starting from trisilane **46** (Ar = Tip), were the first directly observed diradicals of this type.

III. SILICON–SILICON MULTIPLE BONDS

If the field of silicon–silicon multiple bond systems is compared with corresponding organic molecules, it becomes clear that there are still large gaps. For example, even the parent disilene $H_2Si{=}SiH_2$ could not be isolated up to now, in spite of the fact that its intermediate existence was strongly supported by copyrolysis of trisilane **55** and 1,3-butadiene as early as 1975[68] in which the trapping products **56**, **57** and **58** of SiH_2, disilene and its isomer silylsilylene, respectively, were found (equation 18).

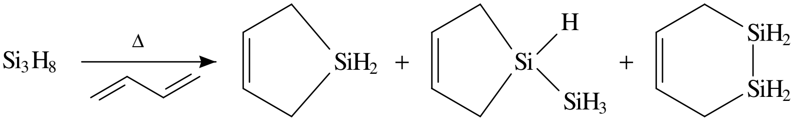

(18)

(55) **(56)** **(57)** **(58)**

Our group has been interested for quite some time in the matrix isolation of disilene, the prototype molecule for Si,Si π-systems. We have synthesized a great variety of precursors and used different methods of energy transfer, but none of the precursors or methods turned out to be suitable[69–73]. We think that only new, unconventional methods can bring the breakthrough in the isolation of this long sought-after molecule. Our own attempts are briefly summarized below.

Disilene and its isomer silylsilylene were neither available by standard vacuum flash pyrolysis of precursors **59**–**63**, nor by the more elaborate method of pulsed flash pyrolysis of **60**–**63**, a pulsed discharge in mixtures of argon and mono- and disilane[74] or by the matrix photolysis of educts **59**–**66** using various light sources (Hg lamps, excimer laser)[69,70,72], the microwave discharge in disilane **66** or the cocondensation of silicon atoms with SiH_4.

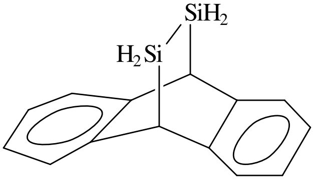

(59)

$Me_3Si{-}Si_2H_5$

(60)

$HI_2Si{-}SiH_3$

(61)

$IH_2Si{-}SiH_2I$

(62)

$PhH_2Si{-}SiH_3$

(63)

$PhMe_2Si{-}Si_2H_5$

(64)

$H_3Si{-}SiH(SiMe_3)_2$

(65)

$H_3Si{-}SiH_3$

(66)

Silyldisilene, which could be photoisomerizable into the likewise unknown cyclotrisilane, has also not yet been observed[69].

The only study in the field of matrix-isolated compounds containing silicon–silicon multiple bonds in the last decade exhibiting new aspects concerns the photolysis of cyclotetrasilanes, which shows a remarkable dependence of the reaction course on molecular structure[75]. It is known that the photolysis of peralkylcyclotetrasilanes leads to ring contraction[76–80]. However, steady-state photolysis of planar persilylcyclotetrasilanes **67** in hydrocarbon glass at 77 K gave rise to the corresponding disilenes **68**, identified by their UV spectra[75]. On the contrary, peralkylcyclotetrasilanes **69** having bent structures were photostable under these conditions, but reacted upon laser flash photolysis in solution at higher temperatures under ring contraction yielding the corresponding silylenes and cyclotrisilanes (equation 19)[75].

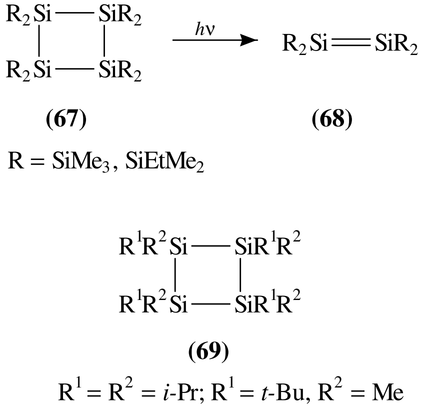

(67) **(68)**

R = SiMe$_3$, SiEtMe$_2$

(19)

(69)

R^1 = R^2 = *i*-Pr; R^1 = *t*-Bu, R^2 = Me

Tetrasilyldisilenes of type **68** have been the focus of much attention in the last years from an experimental[81,82] and theoretical[83,84] point of view. According to the latter, silyl-substituted disilenes should have significantly increased bond dissociation energies and are therefore interesting synthetic targets. Furthermore, silyl substituents are predicted to favor planar arrangement around the silicon–silicon double bond, a prediction which so far has not been supported experimentally[81,82]. It is tempting to try the photoisomerization of such persilylated disilenes to the corresponding silylenes by 1,2-silyl migration because the resulting highly substituted disilylsilylenes could be the first silylenes with a triplet ground state[85].

In analogy to the above-mentioned parent disilene, no compounds containing silicon–silicon triple bonds have so far been found. Even their intermediacy could not be proved unequivocally. Two isomers of Si_2H_2, namely **70** and **71**, were detected in a low pressure, low power plasma in a mixture of SiH_4 and argon by the measurement of their millimeter and submillimeter wave rotational spectrum[86,87]. Both compounds have no acetylene-type silicon–silicon triple bonds, in agreement with the predictions of theoretical studies[86,87].

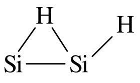

(70)

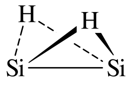

(71)

Recently, we were able to matrix-isolate a species which we also tentatively assume to be the energetically lowest-lying isomer on the H_2Si_2 energy hypersurface, namely compound **71**. The matrix-isolated products of pulsed flash pyrolysis of 1,1,1-trimethyltetrasilane **72**, originally believed to be a suitable cyclotrisilane precursor, reveal the absorptions of trimethylsilane and monosilane together with a band at 1093 cm^{-1}, which by comparison with the calculated IR spectrum (BLYP/6-31G*: strongest absorption at 1081 cm^{-1}; all other vibrations were calculated with much weaker intensities) can tentatively be assigned to the butterfly molecule **71** (equation 20)[69].

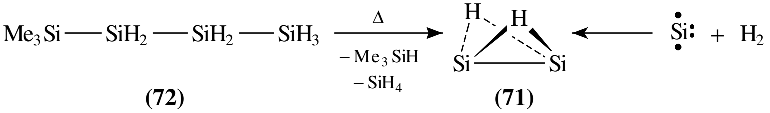

(72) **(71)** (20)

The same compound **71** was also formed together with monosilane in the evaporation and matrix-isolation of pure silicon (equation 20; for the origin of hydrogen cf Section VIII)[73]. This observation can be taken as a further support for structure **71**. By pyrolysis of a partially deuteriated tetrasilane precursor, $HDSi_2$ and D_2Si_2 were matrix-isolated showing the expected isotopic shifts ($HDSi_2$: 1061 cm^{-1} {BLYP/6-31G*: 1044}; D_2Si_2: 785 {784})[69].

Despite these successes, a compound containing a silicon–silicon triple bond is still lacking.

IV. SILICON–NITROGEN MULTIPLE BONDS

A. Silanimines, Silanitriles and Silaisonitriles

Compounds containing silicon–nitrogen multiple bonds have been investigated intensively in recent years[1]. The first silanimine, that is stable at room temperature, was synthesized in 1986[88]. Other sterically hindered silanimines were observed in matrices and glasses after irradiation of the corresponding azidosilane precursors[89–91].

In accordance with these results, Maier and Glatthaar showed that azidomethylsilane **(73)** and its deuteriated analogue azido(dideuterio)methylsilane [D_2]-**73** eliminate nitrogen upon irradiation with $\lambda = 254$ nm in an argon matrix[18]. The first observable product after nitrogen elimination is silanimine **74** which, based on the comparison of the experimental and calculated IR wavenumbers, should have the (*E*) configuration (equation 21). During further irradiation a second H-shift occurs yielding aminosilylene **75** (UV: $\lambda_{max} = 330$ nm). Additional isomerization can be achieved after the exposition of **75** to longer wavelengths. The resulting aminosilene **76** (UV: $\lambda_{max} = 256$ nm) reacts upon irradiation with shorter wavelengths to regenerate **75**.

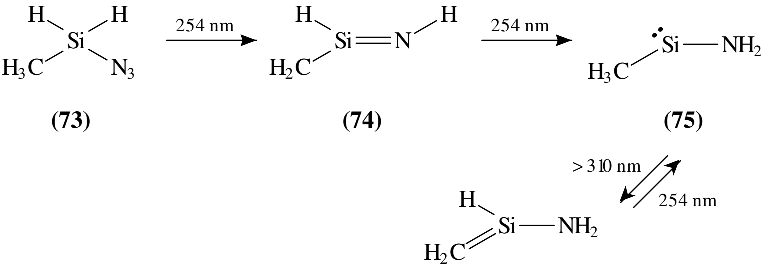

(73) **(74)** **(75)** (21)

(76)

Triazidophenylsilane is a good photochemical precursor for the preparation of phenylsilaisonitrile and presumably phenylsilanitrile[92,93]. Analogously triazidomethylsilane **(77)** should produce the methylated series upon irradiation. But the photochemistry of matrix-isolated **77** in argon turned out to be complex. The final product of the photofragmentation of **77** is isonitrile **80** (equation 22)[18]. **80** was identified by its IR spectrum. The same is true for methylsilaisonitrile **(79)**, which is a migration product of the assumed silanitrile intermediate **78**, that should be initially formed from **77**. A threefold 1,3 H-shift in **79** gives **80**, a molecule which also could be generated by photoisomerization of the long known[94] silylnitrile **(81)**. This was shown by irradiation of independently synthesized unmarked and perdeuteriated silylnitrile **(81)** in an argon matrix with the same wavelength[18]. In both cases the corresponding silylisonitrile **80** was formed. Furthermore, the irradiation of silanimine **74** ($\lambda = 254$ nm) under the same conditions yields traces of **80**, which are formed in addition to the main product **75** (equation 21)[18].

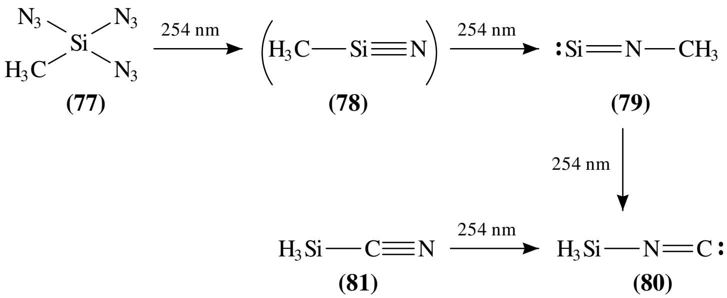

(22)

The photochemical behavior of the parent azidosilane **(82)** is also rather complex. Early investigations showed that **82** is converted into silaisonitrile **(87)** upon irradiation in an argon matrix[95]. Surprisingly, a dehydrogenation takes place and no H_3SiN isomer could be observed. Later reinvestigations of **82** by Maier, Glatthaar and Reisenauer led to new important findings[96]. Depending on the wavelength of the irradiating light four different products **83**, **85**, **86** and **87** are formed (equation 23). Firstly, irradiation of **82** with $\lambda = 254$ nm yields aminosilylene **(85)** (UV: $\lambda_{max} = 330$ nm; SiN stretching vibration: 866 cm^{-1}). Secondly, if **82** is irradiated with 222 nm light of a $KrCl_2$ excimer laser, the main product is the well-known[95] silaisonitrile **(87)**[12]. In contrast to earlier investigations[95] silanimine **(86)** (UV: $\lambda_{max} = 240$ nm; SiN stretching vibration: 1097 cm^{-1}) could be identified as an intermediate of the reaction **82** → **87**[12]. Lastly, if the 193 nm emission of an ArF excimer laser is used, an IR spectrum can be registered which indicates that in this case the newly formed compound is silanitrile **(83)** (UV: $\lambda_{max} = 350$ nm; SiN stretching vibration: 1162 cm^{-1})[12]. Silanitrile **(83)** is a species with a formal silicon–nitrogen triple bond. An additional structural proof is the fact that **83** looses its hydrogen atom upon prolonged irradiation and the long known[97] SiN molecule **84** remains as the final product.

In addition to these observations some more interconversions are worth noting, which for reasons of clearness were not included in equation 23. Aminosilylene **(85)** can be photoisomerized into silanimine **(86)** and vice versa[12]. The transition state for such an isomerization has been calculated[98]. The same is true for the dehydrogenated species **83** and **87**[12]. Irradiation of **87** with $\lambda = 254$ nm results in the formation of **85** after hydrogen recapture[96]. Thus hydrogen does not escape the argon cage except that the matrix has been tempered. Warm-up results in diffusion of the reagents. Moreover, there is also a direct spectroscopic proof that both **87** and **83** can associate with the eliminated hydrogen molecule[12]. The complexes with the 'disturbed' hydrogen molecule were identified by their infrared features at around 4170 cm^{-1} (HH stretching vibration, forbidden for undisturbed hydrogen).

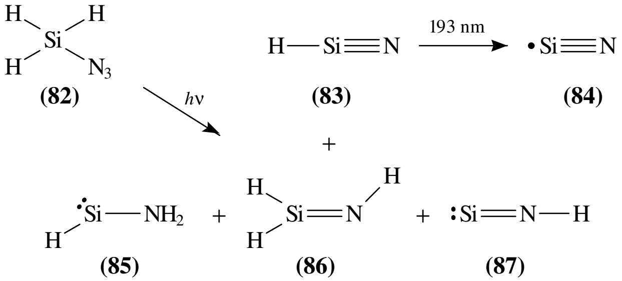

(23)

Due to the observed isotopic shifts the matrix experiments with deuteriated azidosilane $[D_3]$-**82**[12] support the described results. According to calculations (cf reference 6 in Reference 12), it is not surprising that the energy-rich silylnitrene, H_3SiN, was not observed upon the photolysis of **82**.

B. Silanediimines and Diazosilanes

Silanediimines are compounds which contain a digonal, sp-hybridized silicon atom. In 1987 *N*,*N*-bis(trimethylsilyl)silanediimine, the first silanediimine, was observed in a low temperature glass[1,99].

By using the same method, namely the photolysis of the sterically hindered diazidosilane **88**, a second silanediimine with a new substitution pattern [di-*tert*-butyl instead of bis(trimethylsilyl) substituents] was likewise accessible[100]. In solid argon as well as in glassy 3-methylpentane diazidosilane **88** is partially converted into silanediimine **89** (λ_{max} = 385 nm) upon irradiation (equation 24). Diimine **89** is the minor product of the photolysis of **88** and was identified by UV spectroscopy and results of chemical trapping experiments. The major product of the irradiation of **88** is di-*tert*-butylsilylene **(91)**, which undergoes a subsequent photochemical insertion to give silacyclopropane **92**. Silylene **91** is formed in at least two steps. The authors observed a small amount of a photochemical precursor to **91** with a UV band at λ_{max} = 300 nm and an IR band at 2150 cm^{-1}. Furthermore, ^{15}N-labelling proved that this species still contains nitrogen. The unknown substance was tentatively assigned as di-*tert*-butyldiazosilane **(90)**. If this assignment is correct, **90** is the first example of a diazosilane (for N_2Si cf Section VIII.D.3.b).

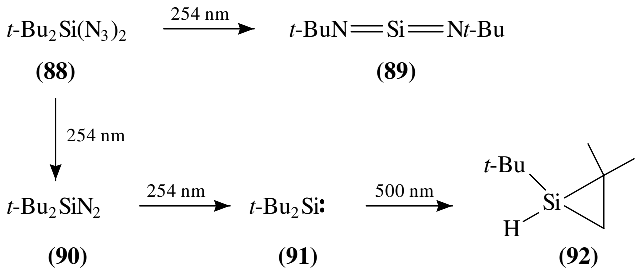

(24)

V. SILICON–OXYGEN MULTIPLE BONDS

A. Silanones, Silacarbonates and Silacarboxylic Esters

Up to 1986 several silanones have been matrix-isolated and their IR spectra were recorded[1]. Most of these silanones are accessible by intermolecular reactions in the matrix which take place under specific conditions, that allow the diffusion of the reagents.

As could be shown by Whithnall and Andrews, dimethylsilanone **(97)** is formed when dimethylsilane **(93)** and ozone **(94)** are codeposited and irradiated in solid argon at 14–17 K (equation 25)[101]. Beside **97**, methylsilanone[102] is generated as well.

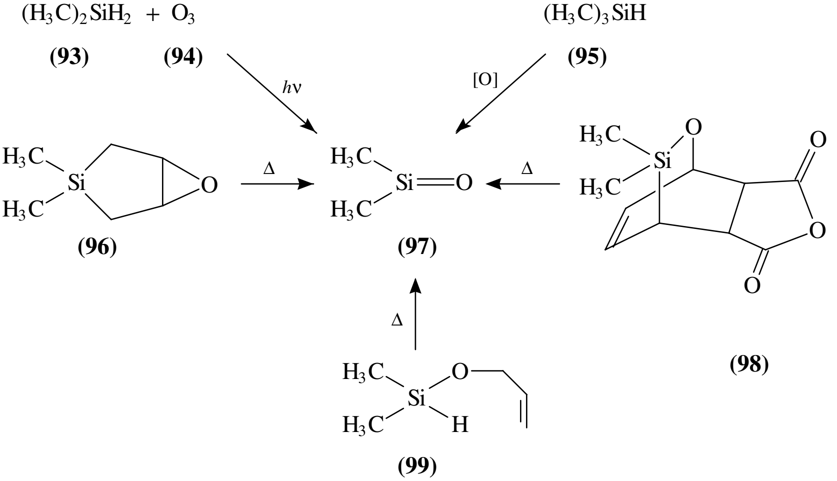

(25)

The use of methylsilane in this procedure results in the formation of methylsilanone and the parent silaformaldehyde H_2SiO[101,103]. The relative yields of the products show that H_2 elimination (Si–H instead of Si–C bond cleavage) is favored in both cases. Notwithstanding the behavior of methylsilane and dimethylsilane, a trimethylsilane/ozone mixture presumably gives $H_2C{=}Si(OH)CH_3$, the enol isomer of **97** (Si–C cleavage), when irradiated in the region $290\ \text{nm} < \lambda < 1000\ \text{nm}$[101]. However, full mercury arc irradiation of the trimethylsilane/ozone mixture produces the keto isomer, silanone **97**[101].

Dimethylsilanone **(97)** is also formed in the oxygenation of **95** with oxygen atoms generated by a microwave discharge of an Ar/O_2 stream and subsequent matrix isolation of the reaction products[101].

Pyrolytic fragmentations of other suitable precursors also lead to dimethylsilanone **(97)**. For example, 6-oxa-3-silabicyclo[3.1.0]hexane **96** is reported to be split into **97** and 1,3-butadiene upon pyrolysis[104]. Other possible routes to **97** consist in the pyrolysis of (allyloxy)dimethylsilane **(99)**[105] or Diels–Alder adduct **98**[104]. Matrix-isolated **97** gives its trimer hexamethylcyclotrisiloxane when the matrix is warmed up to 35–40 K. The SiO stretching vibration of **97** was found at $1210\ \text{cm}^{-1}$. This frequency fits the calculated force constant and bond order and has to be considered as evidence for significant double bonding in **97**[104]. Octamethylcyclotetrasiloxane, allyl(allyloxy)dimethylsilane and 2,2,6-trimethyl-2-silapyrane failed as precursors for **97** and only the SiO molecule (cf Section V.B) and CH_3 radicals were found on the matrix holder[105].

Using the corresponding derivatives of epoxide **96**, D_6-dimethylsilanone ([D_6]-**97**)[104], diphenylsilanone and silacarbonic acid dimethyl ester[106] were matrix-isolated and studied by IR spectroscopy.

Examples of matrix-isolated silacarboxylic esters are scarce. Only the argon matrix photolysis of dimethoxysilylene **(100)** (cf Section VIII.E.2) results in the formation of infrared bands and a UV maximum ($\lambda_{max} = 232$ nm) which are consistent with structure **101** (equation 26)[107,108].

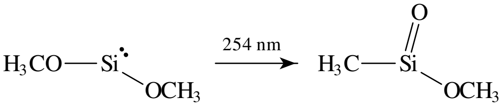

(100) **(101)** (26)

B. Silicon Oxides and Related Compounds

In principle this section can be divided into two parts. The first one deals with the matrix isolation of various silicon oxides whereas reactions of such oxides with metal atoms are presented in the second part.

Cocondensation in solid argon of SiO and oxygen atoms, generated by a microwave discharge, yields SiO_2[109]. SiO, $(SiO)_2$ and $(SiO)_3$ are well-known species[110,111] and can be obtained when molecular oxygen is passed over heated silicon (at about 1500 K)[112].

More recently, Schnöckel and coworkers reexamined the structure of dimeric SiO[113]. Using the method described above $(SiO)_2$ was generated and condensed together with an excess of argon on a liquid-helium-cooled copper surface. The IR spectra of the matrix-isolated species and their ^{29}Si and ^{18}O isotopomers are in good agreement with a planar cyclic structure of D_{2h} symmetry. The trimer $(SiO)_3$ has also a planar cyclic structure (D_{3h} symmetry)[113,114].

The reaction $M + SiO \rightarrow MSiO$ can be carried out with various metals. For that purpose the metal atoms are cocondensed with monomeric SiO onto an argon matrix holder. The identification of the reaction products is based on both their IR spectra and isotopic shifts.

In the case of sodium or potassium atoms[115] the SiO stretching vibration of the reaction product is detected at around 1020 cm^{-1} (uncoordinated SiO: 1226 cm^{-1}). Together with the observed isotopic splittings, the formation of an ionic species $M^+(SiO)^-$ seems reasonable, this species is very likely to have a strongly bent structure[114].

Less pronounced charge transfer to SiO and side-on coordination takes place in AgSiO (SiO stretching vibration in solid argon: 1163 cm^{-1})[116]. Ag_2SiO is probably a side product formed in the cocondensation of silver atoms with monomeric SiO[116]. The structure of AgSiO has been confirmed by hydrocarbon matrix electron magnetic resonance studies[117]. In addition to AgSiO the authors also observed $AgSi_2O_2$, $AgSi_3O_3$ and $AgSi_nO_n$ [derived from polymeric $(SiO)_n$] after the reaction of silver atoms with SiO in an adamantane matrix at 77 K.

In contrast to the results described above, experiments with palladium atoms and SiO lead to a different behavior. It is clear that PdSiO is formed, but compared with monomeric SiO the corresponding stretching vibration of PdSiO is shifted to higher wavenumbers (1246 cm^{-1} in solid argon)[118]. With the aid of a normal coordinate analysis involving different isotopomers, a linear structure of PdSiO is deduced. Bonding in PdSiO is similar to that in typical transition metal carbonyl complexes.

VI. SILICON–SULFUR MULTIPLE BONDS

Following the 'classical' double-bond rule, multiple bonds between silicon and sulfur, both elements of the third period, should be very difficult to obtain. Except for SiS[119,120], SiOS[121] and a sterically hindered silanethione[122] no compounds with silicon–sulfur multiple bonds have been isolated[1].

Recently, Schnöckel and Köppe generated SiS_2 in solid argon[120]. The authors cocondensed SiS with COS and, during irradiation of this mixture, the IR bands of SiS_2 appeared. In consideration of the formed CO it was concluded that sulfur atoms have been produced from COS which subsequently react with the SiS molecule to give SiS_2. Another possible but unsatisfying access (the observed spectra were not of comparable quality with those discussed above) to molecular SiS_2 consists in the vaporization of solid SiS_2 and matrix isolation of the products[120].

$S{=}SiCl_2$ was found in a photochemically induced argon matrix reaction between monomeric SiS and Cl_2[123]. With COS cocondensed $SiCl_2$ yields $S{=}SiCl_2$ after irradiation as well[123]. Later, S=Si(H)Cl was accessible via the photoreaction of SiS and HCl under argon matrix conditions[124]. The use of DCl instead of HCl confirmed the structural assignment for this species (C_s symmetry). $S{=}SiCl_2$ and S=Si(H)Cl have nearly the same values of the SiS force constants as the SiS multiple bonds in SiS and SiS_2[124].

AgSiS can be prepared by reaction of silver atoms with molecular SiS. Studies of AgSiS in both hydrocarbon matrices (electron paramagnetic resonance study)[125] and solid argon[126] demand a triangular structure with a Ag–S bond (similar to the structure of AgSiO; cf Section V.B).

VII. STRAINED SILACYCLES

A. Silacyclopropyne and Other C_2H_2Si Isomers

Maier and coworkers achieved the isolation of silacyclopropyne (**106**), a C_2H_2Si isomer, by irradiation ($\lambda = 254$ nm) of the matrix-isolated C_2H_2Si isomers 1-silacyclopropenylidene (**104**) or ethynylsilylene (**103**)[127–129]. The best access to the C_2H_2Si potential energy surface is offered by pulsed flash pyrolysis of 2-ethynyl-1,1,1-trimethyldisilane (**102**). Using this procedure apart from trimethylsilane only 1-silacyclopropenylidene (**104**), which is the most stable C_2H_2Si isomer[130–133] and possibly plays a role in the chemistry of interstellar clouds (like the cyclic C_2Si molecule **107**), could be isolated in an argon matrix and was identified by its IR spectrum. Trapping experiments make it likely that ethynylsilylene (**103**) is formed from **102** in the first step, but under the conditions of the pulsed flash pyrolysis a rearrangement immediately takes place resulting in the formation of 1-silacyclopropenylidene (**104**), which after leaving the hot zone can be isolated in solid argon (equation 27)[128]. In contrast, the high-vacuum flash pyrolysis of **102** followed by the direct condensation of the reaction products onto a spectroscopic window at 10 K remained unsuccessful; no C_2H_2Si isomer was obtained[127–129].

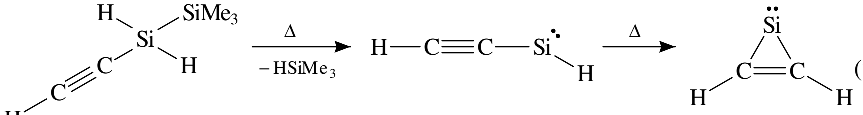

(27)

(102) **(103)** **(104)**

A particle whose connectivities are indicative of structure **104** has earlier been detected by neutralization–reionization mass spectrometry[134]. Furthermore, 1-silacyclopropenylidene (**104**) was recently identified by microwave spectroscopy[135]. 1-Silacyclopropenylidene (**104**) ($\lambda_{max} = 286$ nm[136]; a delocalized three-center π-bond orbital[128]) generated from **102** and matrix-isolated is transformed into ethynylsilylene

(103) upon irradiation with $\lambda = 313$ nm (equation 28)[127–129]. 2-Ethynyl-1,1,3,3-tetramethyl-1, 3-diphenyltrisilane, too, can be used as a photochemical precursor for **103** and other C_2H_2Si isomers (irradiation with $\lambda = 254$ nm). But the IR spectra measured in these experiments were not of comparable quality to those obtained after pyrolysis of 2-ethynyl-1,1,1-trimethyldisilane **(102)**[136].

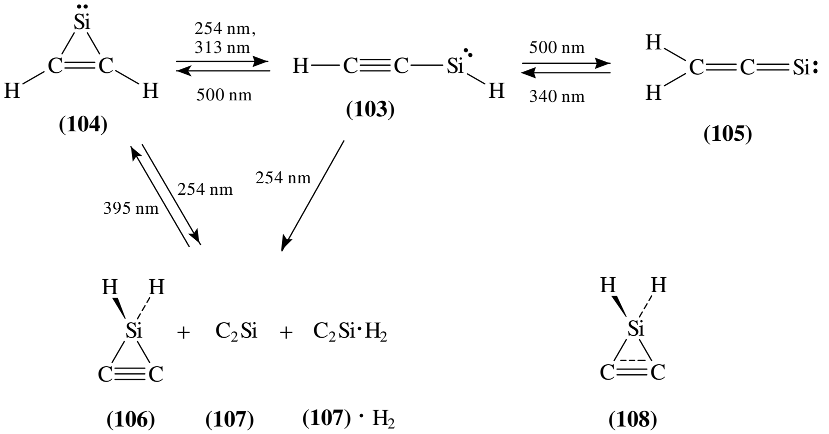

(28)

Ethynylsilylene **(103)** ($\lambda_{max} = 500$ nm[136]; calculated: $\lambda_{max} = 520$ nm[137]) isomerizes into 1-silacyclopropenylidene **(104)** and vinylidenesilylene **(105)** when irradiated with $\lambda = 500$ nm[127–129]. Vinylidenesilylene **(105)** shows two weak infrared bands and a UV absorption with vibrational fine structure ($\lambda = 340$, 325 and 310 nm[136]). Irradiation into this absorption leads back to ethynylsilylene **(103)** (equation 28)[127–129].

Irradiation of **104** with $\lambda = 254$ nm (as with $\lambda = 313$ nm) yields **103** as the first photoproduct. However, upon longer irradiation, silacyclopropyne **(106)** as well as the well-known[138–142] cyclic C_2Si molecule **107** (cf reference 128 for the electronic structure of **107**) and its adduct, $C_2Si{\cdot}H_2$ (**107**·H_2), can be detected[127–129]. Additional experiments with the corresponding ^{13}C and D isotopomers are in good agreement with the assigned structures. The structural assignment of silacyclopropyne **(106)**, which is the first example of a 'formal' cyclopropyne[143], is based on comparison of the experimental and calculated IR spectroscopic data. The CC stretching vibration of **106** was observed at 1769.8 cm^{-1}. Experiments with the corresponding ^{13}C and D isotopomers again support the cyclopropyne structure[128]. Upon long-wavelength irradiation ($\lambda > 395$ nm) **106** and **107**·H_2 are retransformed into **104**. Therefore these species have to be isomers.

In order to understand the unique bonding situation in silacyclopropyne **(106)** detailed *ab initio* calculations have been carried out[128]. It was found that the Lewis structure **108**, where the dashed line indicates an electron pair which occupies a CC nonbonding orbital, is the best possible compromise to describe the electronic structure of **106** correctly. Silacyclopropyne **(106)** is best considered as a closed-shell singlet diradical but with only one 'nonbonding' orbital. The energies (AU) and symmetries of the HOMO and LUMO describing the unique bonding situation in **106** are shown in Figure 1. The most striking feature of the canonical orbitals is the fact that the CC-σ' orbital (A_1) is the HOMO and lies higher in energy by 0.01 AU than the CC-π orbital. The occupation numbers of HOMO and LUMO were found to be $(A_1)^{1.913}$ $(B_2)^{0.095}$ [CASSCF (8.8)/6-31G(d,p)].

Quite recently, Maier and coworkers discovered another possible route to the C_2H_2Si potential energy surface[144]. Cocondensation of silicon atoms and acetylene onto an argon

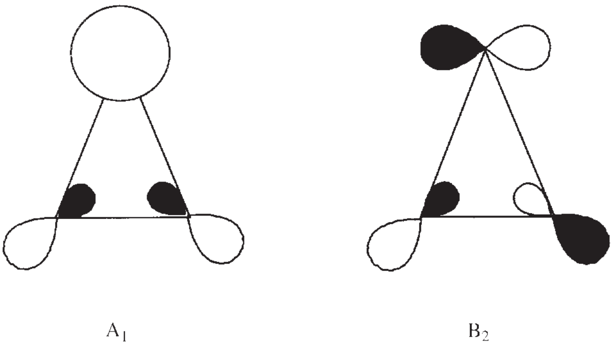

FIGURE 1. Schematic representation of HOMO and LUMO of **106** (C_{2v}) discussed in the text. Symmetries and orbital energies (AU): A_1 (CC-σ'. HOMO) -0.389, B_2 (CC-σ'^*, LUMO) 0.005.[MP2/6-311G(d,p)]

matrix holder results in the formation of 1-silacyclopropenylidene **(104)** as well (cf Section VIII.B.5) and again all the photoreactions shown in equation 28 can be carried out.

B. Silacyclopropenes

Tetramethylsilacyclopropene, the first silacyclopropene derivative, was prepared in 1976[145]. With the help of the matrix-isolation techniques, attempts were made to synthesize the parent silacyclopropene **(114)**. Experiments with this goal culminated in the isolation of 1, 1-dimethylsilacyclopropene **(110)** in solid argon[146]. Sander and coworkers showed that **110** is accessible by photolysis of the corresponding bis(diazomethyl)silane **(109)** (equation 29). After subsequent irradiation with shorter wavelengths, isomerization into the photostable ethynyldimethylsilane **(111)** takes place.

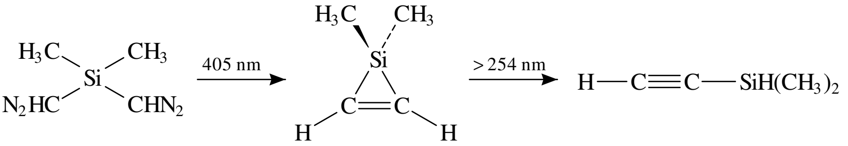

(109) **(110)** **(111)** (29)

Later on, Maier and coworkers succeeded in the synthesis of the unsubstituted silacyclopropene **(114)**[147]. Once more (cf Section VII.A) a precursor molecule was used which fragments into trimethylsilane and the corresponding silylene. Trapping experiments show that 1,1,1-trimethyl-2-vinyldisilane **(112)** (upon pyrolysis) gives vinylsilylene **(113)** in the first step (for **113** also cf Section VIII.B). However, only small amounts of this species were isolated on the matrix holder[136,144] because an isomerization into both silacyclopropene **(114)**, which according to calculations contains a localized π-bond orbital[128], and ethynylsilane **(115)**[148] occurs (equation 30). The latter two products were identified with the aid of their infrared spectra (CC stretching vibration of **114**: 1467.2 cm^{-1}). The same experiment carried out with 2,2-dideuterio-1,1,1-trimethyl-2-vinyldisilane ([D_2]-**112**) gives evidence for either a 1-silaallene **(161)** or a 1-silacyclopropylidene **(160)** participation (compare equations 44 and 45) in the discussed process **113** $\rightarrow$ **114** + **115**[136,147]. In accordance with the photochemical behavior of **110**, parent silacyclopropene **(114)** is transformed into the photostable ethynylsilane **(115)** upon irradiation with λ = 254 nm under argon matrix conditions.

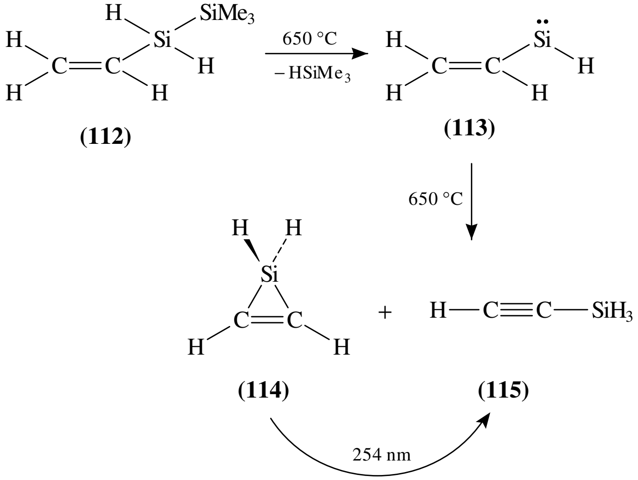

(112) **(113)** **(114)** **(115)** (30)

Attempts to generate the parent silacyclopropane from 2-ethyl-1,1,1-trimethyldisilane in an analogous manner failed[69] (for an example of a matrix-isolated silacyclopropane cf **92**, Section IV.B).

VIII. SILYLENES

Whereas the analogous carbenes easily isomerize wherever possible to compounds containing doubly bonded carbon atoms even under the conditions of matrix isolation, silylenes are almost as stable as the corresponding substances with doubly bonded silicon atoms. For example, methyl- and silylsilylene lie just 4 and 8 kcal mol^{-1} above silaethene and disilene, whereas the difference between ethene and methylcarbene is as high as 70 kcal mol^{-1} [149–151] As a consequence, silylenes are often key intermediates on the way to other highly reactive silicon compounds discussed above.

Furthermore, all known silylenes are singlets in their ground states. According to calculations, the singlet ground state of the parent compound $:SiH_2$ lies 21 kcal mol^{-1} lower than the first triplet state[152]. In the carbon analogue the situation is reversed. The first singlet state is calculated to lie 9 kcal mol^{-1} above its triplet ground state[152,153], in agreement with experimental data[154,155].

Several factors were mentioned as explanation for this important feature[156]. In addition to pairing energy and electrostatic effects, the small extent of s,p mixing in silicon seems to play an important role[156]. The last factor is manifested not only in the large stabilization of the singlet state but also in the bond angle of $:SiH_2$, calculated to be as small as 93.4 °[157]. This is a consequence of the relatively large difference of the sizes of the 3s and 3p orbitals compared with the difference between 2s and 2p[158].

According to *ab initio* calculations[85], to have triplet ground state silylenes it is necessary to enlarge the RSiR′ angle of substituted silylenes to more than 141° in the case of carbon substituted silylenes and to more than 115° for silyl substituted silylenes. However, even bis(1-adamantyl)silylene with its sterically very demanding substituents led only to trapping products of the singlet species[159]. Hence the generation of a triplet ground state silylene remains one of the most challenging goals in silylene chemistry.

A. Unsubstituted Silylene

The matrix isolation and spectroscopic examination of $:SiH_2$, the parent compound of the entire class, was reported twice. In 1970, Milligan and Jacox[160] photolyzed mono- and disilane and found new absorptions that they assigned to $:SiH_2$. But as mentioned by Margrave and coworkers[161], this assignment is erroneous and the observed bands are due to the formation of the $\cdot SiH_3$ radical. The same authors were able to generate silylene by the cocondensation reaction of silicon atoms with molecular hydrogen. Caused by the uptake of another hydrogen molecule, silane was obtained as a by-product (equation 31).

$$:\underset{\cdot}{\dot{Si}} \xrightarrow{H_2} :SiH_2 \xrightarrow{H_2} SiH_4 \qquad (31)$$

The observed IR spectrum agrees well with that expected for $:SiH_2$. Four bands were registered, three of them fundamentals and one an overtone. Furthermore, the assignment is supported by deuterium labelling.

On the other hand, up to now we were not able to generate $:SiH_2$ from a 'chemical' precursor. Despite the fact that Ring and coworkers could obtain trapping products of $:SiH_2$ (among others, see equation 18) in the copyrolysis of trisilane and 1,3-butadiene[68], we failed in matrix isolation of silylene generated by pyrolysis of di- or trisilane[69]. Obviously, silylenes bearing hydrogen atoms at the low-valent silicon center are too reactive to pass a pyrolysis tube.

B. Carbon Substituted Silylenes

1. Silylenes by photoisomerization of silenes

a. Methylsilylene. The photochemical interconversion of silylenes and silenes is an important link between these two classes of compounds. It was first established by Maier and coworkers[162], who irradiated the parent silene with light at the wavelength of $\lambda = 254$ nm and obtained methylsilylene (equation 32). The reaction is reversible by using 320 nm light.

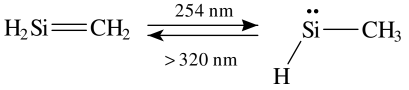

(30) **(116)**

(32)

As discussed later, the location of the UV-maximum of silylene **116** strongly depends on the matrix material. So irradiation of **30** in solid argon results in the growing of an absorption with $\lambda_{max} = 480$ nm, whereas $\lambda_{max} = 330$ nm is found if nitrogen is used instead[162]. This large hypsochromic shift of 150 nm is caused by complexation of methylsilylene with nitrogen[73b].

b. Dimethylsilylene. Although long assumed to be intermediates in several reactions, no carbon substituted silylene was directly observed for many years. In 1979 Michl, West and Drahnak[10] detected a broad UV absorption band ($\lambda_{max} = 453$ nm) after photolysis of dodecamethylcyclohexasilane **(117)** in 3-methylpentane. This band was assigned to dimethylsilylene **(118)**. Many different approaches to this intermediate, either photochemically or pyrolytically[163], were examined in the following years. They are shown in equation 33 in order to give a survey on the methods known to generate silylenes.

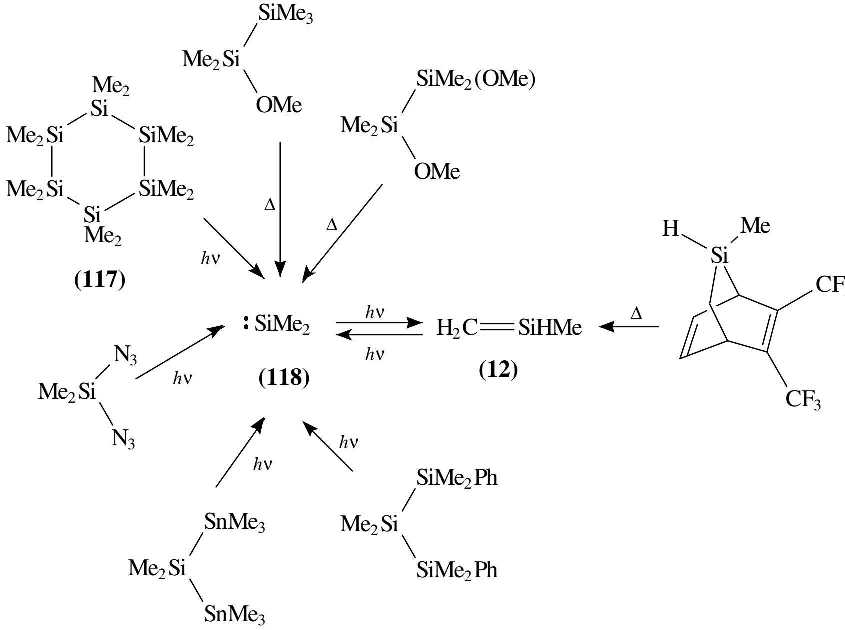

(33)

As in the case of methysilylene **(116)**, dimethylsilylene **(118)**, is accessible by irradiation of 2-silapropene **(12)** at $\lambda = 254$ nm. If light of a longer wavelength is used, the reaction is reversible again[162], which serves as an important structure proof for both species.

Dimethylsilylene **(118)** is one of the best examined silylenes. Not only IR and UV spectra are known[163,164], but also bimolecular reactions of the matrix-isolated compound, leading to new, highly reactive species. Arrington and coworkers[165] as well as West and Pearsall[166] reacted matrix-isolated dimethylsilylene **(118)** with carbon monoxide (equation 34). The resulting adduct **(119)** absorbs at about 340 nm, thus showing a blue-shift of more than 100 nm compared with the free silylene **(118)**. According to *ab initio* calculations[167], the structure of **119** is most likely pyramidal. The same result was obtained for the parent compound H_2SiCO. The planar silaketene-like isomer is the transition state between two pyramidal structures lying 18 kcal mol^{-1} above the pyramidal species[167].

The reaction of **118** with oxygen in an O_2 doped argon matrix yielded dioxasilirane **120**, identified by its vibrational spectrum[108] (equation 34).

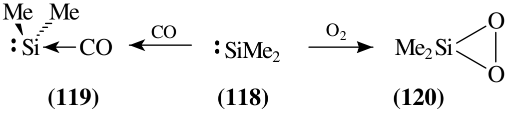

(34)

2. Silylenes by photolysis of oligosilanes

As mentioned above, the photolysis of cyclopolysilanes was the earliest method for the generation of silylenes in matrices. Indeed, such extrusions from oligosilanes were used for the generation of most silylenes known so far[10,137,163,168–175] (equation 35).

$$(RR'Si)_n \xrightarrow[\lambda = 254\ \text{nm}]{h\nu} RR'Si\colon + (RR'Si)_{n-1}$$

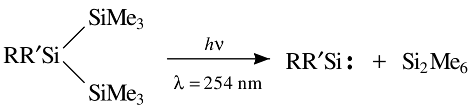

$$RR'Si(SiMe_3)_2 \xrightarrow[\lambda = 254\ \text{nm}]{h\nu} RR'Si\colon + Si_2Me_6 \qquad (35)$$

The effect of substituents on the properties and structure of silylenes was analyzed in detail by Apeloig and Karni on the basis of *ab initio* calculations[137].

In principle, two kinds of substituent effects can be distinguished. The first effect is steric; widening of the RSiR′ angle results in a bathochromic shift. This becomes evident if the phenyl substituents in diphenylsilylene are gradually replaced by more bulky mesityl groups. Whereas Ph_2Si: absorbs at 495 nm, MesPhSi: (Mes = 2,4,6-trimethylphenyl) has its UV maximum at 530 nm and Mes_2Si: at 577 nm[169]. These results agree nicely with theoretical predictions[85,176].

The second type of effects are electronic ones, which can further be divided into inductive and conjugative effects.

Inductive Effects: Electronegative substituents increase the n(Si) → 3p(Si) transition energy and thus induce a blue-shift. The opposite is true for electropositive substituents.

Conjugative Effects: Ligands acting as n-donors generally cause blue-shifts[107,137,171]. However, the n-donor does not have to be a real substituent at the subvalent silicon atom. Lewis bases which are matrix-isolated along with the silylene also induce blue-shifts by the formation of adducts. This was shown for phosphines, sulfides, amines, alcohols, ethers[177] and carbon monoxide[166]. As mentioned above, in the case of methylsilylene even the use of N_2 as the matrix material instead of argon led to a blue-shift of 150 nm[162].

A second possible conjugative interaction is that with a π-system. In contrast to n-donors, π-donors result in red-shifts, which is best understood qualitatively as a consequence of the presence of π^*-orbitals in these substituents[137]. As is the case in the examples above, also for π-donors the experimental data fit well with the theoretically predicted values[137]. So species **121**, **122** and **123**, accessible by photolysis of the appropriate trisilanes[174], absorb at 436, 475 and 505 nm.

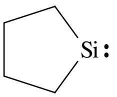

(121)

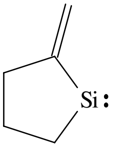

(122)

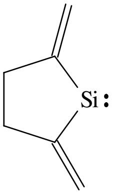

(123)

Frequently, UV absorptions of the respective silylenes are not the only observed absorptions from 3-methylpentane matrix experiments. Since the corresponding disilenes are often formed upon annealing of the matrix, their spectra can be registered as well[169].

As in the case of dimethylsilylene **(118)**, for the dimesityl compound **(124)** not only the spectral features are known but also its reaction with molecular oxygen[178] (equation 36). Surprisingly this reaction, performed by photochemical generation of **124** in an oxygen matrix, yielded silanone-*O*-oxide **125** and not the dioxasilirane as with **118**.

$$\mathrm{Mes_2Si\!:} \xrightarrow{O_2} \mathrm{Mes_2Si{=}\overset{+}{O}{-}\bar{O}} \qquad (36)$$

(124) **(125)**

3. Silylenes by photolysis of diazides

A third photochemical access to silylenes, beside the isomerization of silenes and the photolysis of tri- or cyclopolysilanes, is the irradiation of geminal diazidosilanes, which under nitrogen loss often gives the corresponding divalent silicon species. However, silanimines are frequent by-products[164] or in some cases even the only products (Section IV).

A silylene which can be generated in this way is, beside the methyl (Section II.A, equation 1) and dimethyl species, bis(*t*-butyl)silylene **(91)**[100]. Its chemistry was already discussed in Section IV.A (equation 24). A second silylene, indirectly accessible from the corresponding diazide **126**, is the silacyclopentadiene isomer **130**[179] (equation 37). Remarkably, in the photolysis of **126** as well as in the the pyrolysis of spirosilane **128** (a second access), silacyclopentadiene **127** is the first spectroscopically detectable substance. Upon irradiation with broad-band UV light (260–390 nm) silylene **130** is formed along with traces of its silene isomers **129** and **131**. The latter were formed in larger amounts upon irradiation with light of an appropriate wavelength. For the compounds **127, 129, 130** and **131** IR as well as UV spectra were recorded. The structural assignment of silole **(127)** and the silylenic compound **130** is unambiguous, whereas the distinction between the isomeric **129** and **131** is based solely on mechanistic arguments. A tetramethylated analogue of **128** was also examined, leading to the 3,4-dimethylsilole in the primary step and showing the same behavior as the parent compound[179].

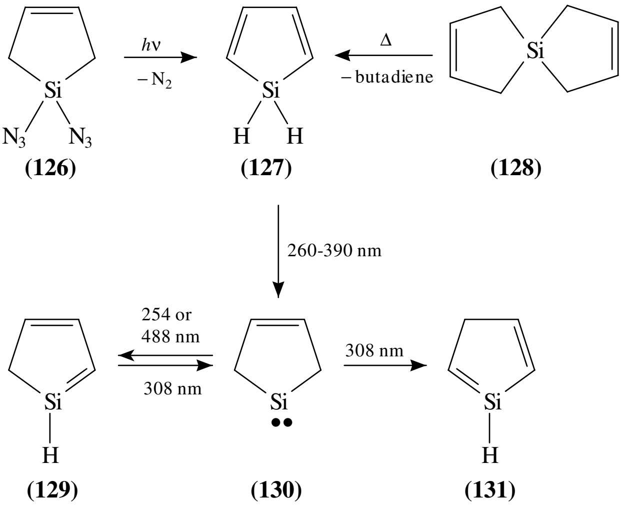

(126) **(127)** **(128)**

(37)

(129) **(130)** **(131)**

4. Silylenes by trimethylsilane extrusion

A relatively long known access to silylenes is the thermolysis of disilanes[13], used for preparative purposes[180] as well as for matrix-isolation studies of silylenes[107]. In our group this method was recently used in the generation of C_2H_2Si isomers. Trimethylsilane was extruded from 2-ethynyl-1,1,1-trimethyldisilane (**102**) pyrolytically, and silacyclopropenylidene (**104**) was the first species detectable after subsequent trapping in solid argon, as discussed in detail in Section VII.A (equations 27 and 28).

a. C_3H_4Si isomers. In the meantime this successful access to silylenes was extended to other hypersurfaces. The formal addition of a methylene unit to **102** leads to compounds that should yield C_3H_4Si species upon pyrolysis. Some of these intermediates are remarkable, e.g. the parent silacyclobutadiene (**132**), for which only mass spectroscopic indications are available[181], and even more for the unsubstituted silatetrahedrane (**133**).

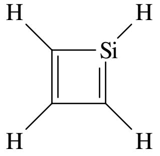

(132)

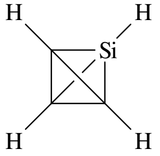

(133)

It was not expected that one could trap one of these target molecules directly from the pyrolysis of one of the appropriate precursors. But it was hoped to succeed in generating one of these compounds by photochemical conversion of the silylenes expected as primary products upon pyrolysis. So all stable open-chain precursors that should lead to C_3H_4Si isomers upon pyrolytic extrusion of trimethylsilane were prepared and examined[182,183]. The first precursor, propynyldisilane **134**, behaved completely analogous to the ethynyl compound **102** (equation 38). After pyrolysis, the methyl substituted silacyclopropenylidene **135** was matrix-isolated, representing the global minimum of the C_3H_4Si hypersurface, as is the case for the unsubstituted analogue (equations 27 and 28). Irradiation with light of an appropriate wavelength yielded propynylsilylene (**136**) and ethynylmethylsilylene (**138**) lying 14 and 16 kcal mol^{-1} (BLYP/6-31G*) above the global minimum, respectively. The given energy values derive from calculations at the BLYP/6-31G* level of theory and are corrected by zero-point vibrational energies[182]. Silylene **138** is also pyrolytically accessible from precursor **137**. An additional band was registered in this experiment that was later recognized to be the most intense absorption of silacyclobutenylidene **139**.

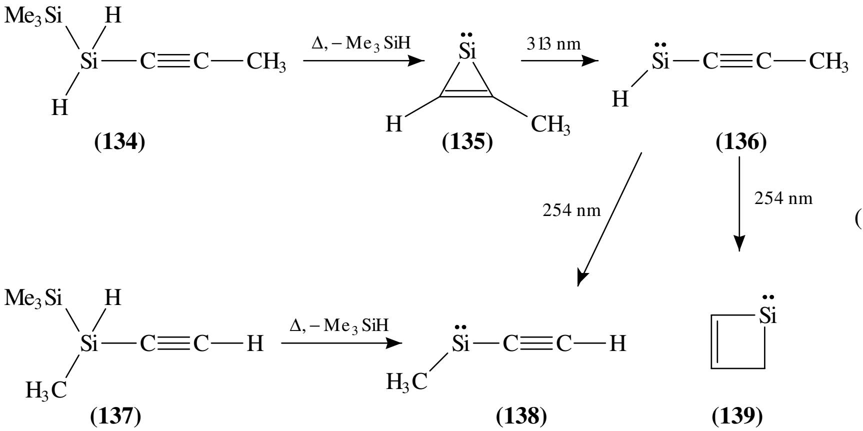

(38)

The two remaining stable open-chain isomers of **134** and **137**, propargyldisilane **140** and allenyldisilane **142**, yielded upon photolysis the cyclic silylene **139** as the first detectable product (equation 39). **139** lies only 5 kcal mol^{-1} above the global minimum **135** and was hoped to undergo a 1,2 H shift to silacyclobutadiene (45 kcal mol^{-1} above **135**) upon irradiation. Depending on the wavelength of the light used in the photolysis, silabutadienylidene **143** (13 kcal mol^{-1} above **135**) or allenylsilylene **(141)** (19 kcal mol^{-1} above **135**) was formed, i.e. ring opening occurred in all cases. Further irradiation led to **138**, therefore being an important link between the two described series. In all cases and irrespective of the wavelength of the used light, no silacyclobutadiene or silatetrahedrane could be observed in the photolysis experiments.

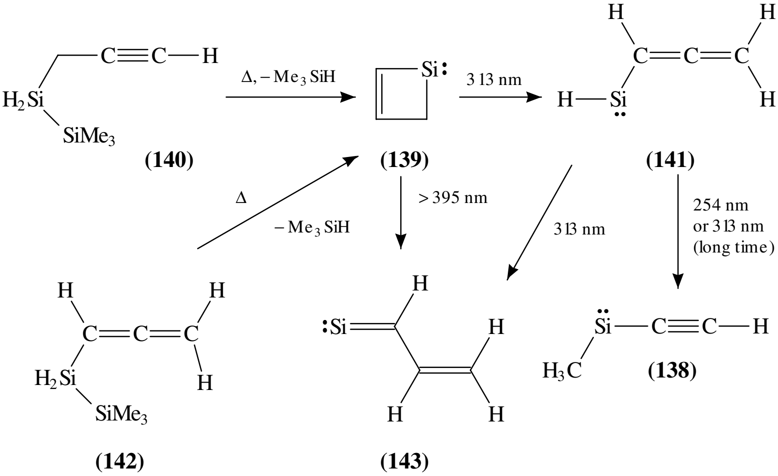

(39)

b. $C_2H_4Si_2$ isomers. If one saturated carbon atom in precursors **134, 137** and **140** is formally substituted by a silicon atom, compounds **144**, **147** and **148** are formed, all being appropriate precursors for $C_2H_4Si_2$ species[182,69] (equation 40). This hypersurface contains, among others, two disilacyclobutadienes which are of even more interest than the monosilicon analogue[184]. As in the examples above, trimethylsilane was extruded upon pyrolysis and in all cases the silyl substituted silacyclopropenylidene **145** was the first species detectable in solid argon. Silylene **145**, the global minimum of the hypersurface according to our calculations at the BLYP/6-31G* level of theory, and the open-chain compound **146**, lying 12 kcal mol^{-1} above **145**, could be interconverted photochemically.

c. C_4H_2Si isomers. A further target in our recent investigations on silylenes was the C_4H_2Si hypersurface[69]. **149** is an appropriate precursor using the reliable extrusion of trimethylsilane (equation 41). The pyrolysis of **149** yielded diethynylsilylene **(150)** as the primary product, being interconvertible with butadiynylsilylene **(153)** upon irradiation with light of appropriate wavelengths. In addition, some bands that do not belong to silylene **150** appeared after the pyrolysis and are assigned to the substituted silacyclopropenylidene **151**, which represents again the global minimum on the C_4H_3Si hypersurface according to our calculations at the BLYP/6-31G* level of theory (corrected by zero-point vibrational energies). Like **150** (13 kcal mol^{-1} above **151**), **151** is photochemically interconvertible with silylene **153** (22 kcal mol^{-1} above **151**). The structural assignments were confirmed by preparing the perdeuteriated and ^{13}C-labelled isotopomeres of these reactive intermediates.

Another entry to the C_4H_2Si hypersurface was found in the pyrolysis of triethynylsilane **(152)** (equation 41).

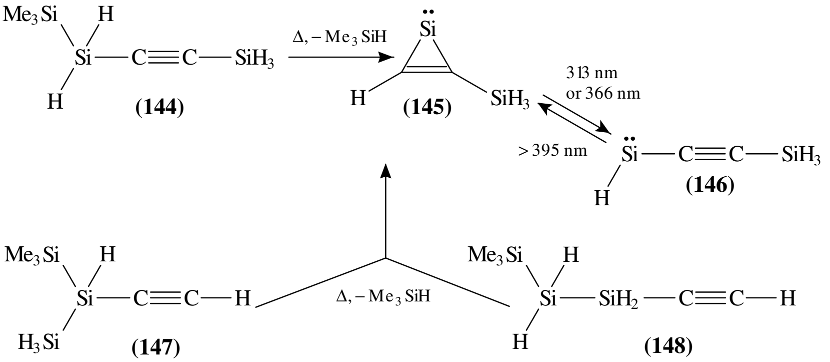

(40)

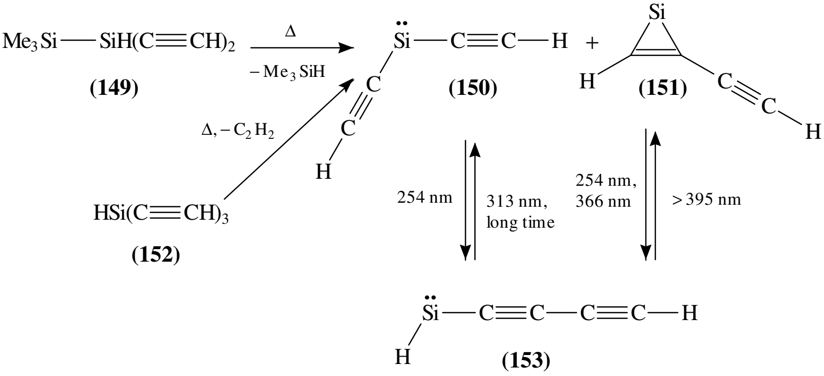

(41)

If the behavior of the related precursors **102**, **144**, **137** and **149** is compared (equation 42), it is remarkable that the two former yield the silacyclopropenylidenes **104** and **145** as the first detectable species, whereas the fragmentation of the methyl substituted compound **137** stops at the open-chain silylene **138**. In the case of the diethynyl precursor **149** both products (**150** and **151**) are observed.

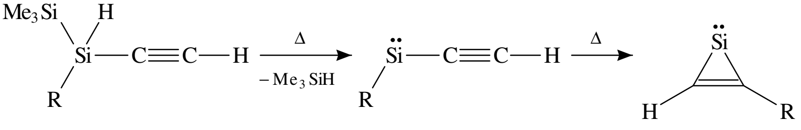

(42)

$R = H$	**(102)**	[$R = H$	**(103)**]	$R = H$	**(104)**
$R = SiH_3$	**(144)**	[$R = SiH_3$	**(146)**]	$R = SiH_3$	**(145)**
$R = CH_3$	**(137)**	$R = CH_3$	**(138)**	[$R = CH_3$	**(135)**]
$R = C_2H$	**(149)**	$R = C_2H$	**(150)**	$R = C_2H$	**(151)**

Since, as could be shown by trapping experiments with 2,3-dimethylbutadiene, the primary products upon trimethylsilane extrusion are always the expected open-chain silylenes, the formation of the cyclic compounds must arise from a rearrangement reaction. Whether really a one-step process with a transition state of type **155** occurs as indicated in equation 43, or whether the reaction pathway from **154** to **156** involves intermediates, cannot be decided here. But obviously, the more facile the migration of the group R from the silicon to the carbon atom, the more cyclic silylene **156** is formed. In addition to the migration tendency of the group R, there is another factor that could determine the product distribution, namely the sensitivity of the initially formed open-chain silylene **154**. So it is known that silylenes with a hydrogen atom at the subvalent silicon center are generally too sensitive to pass through a pyrolysis tube[69].

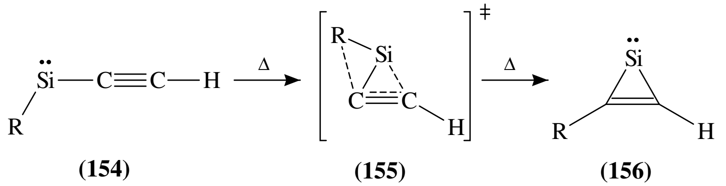

(43)

The observed product distributions reflect the influence of both factors. In the parent compound **102** and in the silyl substituted **104**, the initially formed open-chain silylenes **103** and **146** are relatively sensitive and the migration tendency of the group R is quite large, and therefore the silacyclopropenylidenes **104** and **145** are found. In contrast, the methyl and the ethynyl compound **138** and **150** are stable enough to pass the pyrolysis tube and both can be matrix-isolated upon pyrolysis of the appropriate precursors **137** and **149**. Due to the small migration tendencies of the methyl and the ethynyl group, the rearrangement product **135** is not found at all and **151** is detected only in relatively minor amounts.

Another transformation that should be discussed here briefly is the photochemical conversion of silylenes bearing a hydrogen atom and a substituted ethynyl function at the subvalent silicon center, i.e. **158**. If R is methyl (equation 38) or ethynyl (equation 41), irradiation with 254 nm light results in an exchange of the R group and the hydrogen atom. This can be rationalized in several ways (equation 44). Firstly, a series of two 1,3 shifts with either a silylenic **(159)** or a carbenic **(157)** intermediate is able to explain the formation of **154**. However, silylenes are much more stable than the isomeric carbenes and therefore a 1,3 R shift as the initial step is highly unlikely. A second possible pathway from **158** to **154** involves the cyclic intermediate **156**. At this time, it is not possible to differentiate between these possibilities.

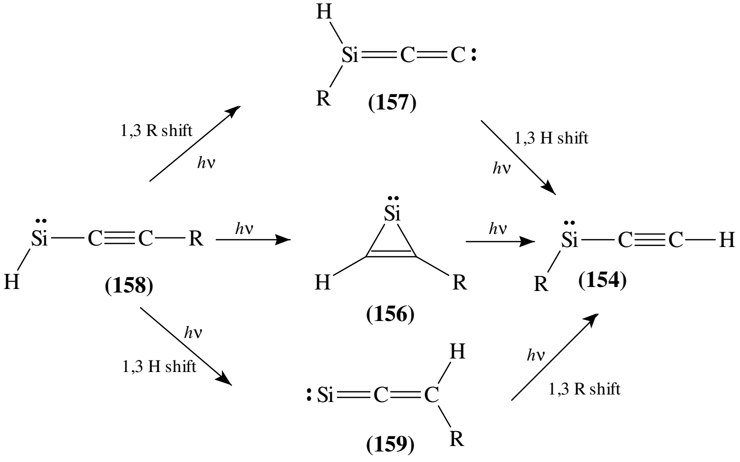

(44)

All compounds of compositions C_3H_4Si, $C_2H_4Si_2$ and C_4H_2Si discussed above were identified by comparison of their calculated and experimental vibrational spectra, some by their UV bands as well. These results are new examples for silylene–silylene interconversions, a class of reactions first observed recently in the related C_2H_2Si system (Section VII.B).

5. Silylenes by cocondensation reactions

All methods used for the generation of silylenes discussed so far are based on the fragmentation of 'chemical' precursors yielding the subvalent silicon compounds upon photolysis or pyrolysis. Hitherto, the formation of an organic silylene was never performed otherwise. For 'inorganic' silylenes like $:SiH_2$[161] or silicon–carbon clusters[185–187], the cocondensation of silicon atoms and the respective element is a long known procedure. Recently we were able to extend this method to 'organic' silylenes. For example, the cocondensation of silicon atoms with acetylene yields silacyclopropenylidene[73], a compound well known from the pyrolysis of 1,1,1-trimethyl-2-ethynyldisilane **(102)** (Section VII.A).

a. C_2H_4Si isomers. In the case of C_2H_4Si isomers the pyrolysis of the 'chemical' precursor 1,1,1-trimethyl-2-vinyldisilane **(112)** and the cocondensation of silicon atoms with ethylene led to complementary results[144]. Whereas silacyclopropene **(114)** and ethynylsilane **(115)** are the first species detectable in solid argon after pyrolysis of disilane **112** (Section VII.B), silacyclopropylidene **(160)** is the primary product in the cocondensation reaction (equation 45). In the subsequent photoisomerizations of silylene **160** three hydrogen atoms migrate consecutively to the silicon atom, resulting in the formation of ethynylsilane **(115)** as the final product, which represents the global minimum of this hypersurface. However, the assignment of 1-silaallene **(161)** has to be made with some caution since the agreement between the observed and calculated vibrational spectra is not as good as for all the other species. Remarkably, ethynylsilane **(115)** is the only link between the C_2H_4Si species generated in the pyrolysis of 1,1,1-trimethyl-2-vinyldisilane **(112)** and the reaction between silicon and ethene.

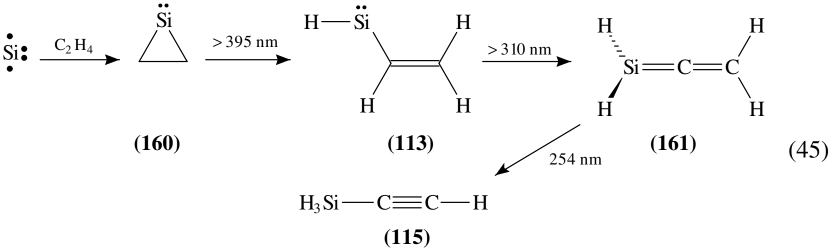

(45)

b. Silicon–carbon clusters. Further subjects to be discussed in this section are silicon–carbon clusters, since some exhibit silylenic structures. Besides the long known C_2Si[139], three other species consisting only of silicon and carbon were isolated in noble gas matrices. All are accessible by cocondensation of silicon and carbon atoms in suitable relative amounts. Firstly, CSi_2 **(164)** was examined by Margrave and coworkers[188] who assigned two absorptions (1188.9 and 658.2 cm^{-1}) to the species discussed. According to calculations, CSi_2 should not be a linear **(162)** but a bent molecule **(164)** with an angle of about 120° at the central carbon atom[189]. The system was reinvestigated later by Presilla-Márquez and Graham[185] who confirmed the assignment of the stronger absorption (1188.9 cm^{-1}), but showed that the less intense absorption is not due to CSi_2. Instead, they observed two additional weak vibrations at 1354.8 and 839.5 cm^{-1} that belong to this species.

Presilla-Márquez and coworkers also investigated the tetra-atomic silicon–carbon clusters C_2Si_2[186] and CSi_3[187]. According to calculations, a rhombic **(167)**[186] or a rhomboidal **(166)**[190] ground state geometry, respectively, is predicted for both. In the case of C_2Si_2 the vibrations of this species **(167)** are observed in solid argon along with others, that are tentatively assigned to the distorted trapezoidal isomer **165** and the linear compound **163**. The latter is predicted to lie 8 kcal mol^{-1} above the ground state **(167)** whereas **165** has an intermediate position[186]. For CSi_3 only the most stable species **(166)** was observed in matrix-isolation experiments, and five of the six fundamental modes could be assigned[187]. Interestingly, one of these vibrations, at 658.2 cm^{-1}, was originally assigned to CSi_2 by Margrave and coworkers[188].

$:\mathrm{Si}{=}\mathrm{C}{=}\mathrm{Si}:$ $:\mathrm{Si}{=}\mathrm{C}{=}\mathrm{C}{=}\mathrm{Si}:$

(162) **(163)**

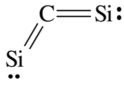

(164)

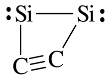

(165)

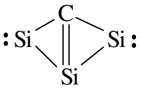

(166)

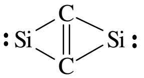

(167)

C. Silicon Substituted Silylenes

1. Silylenes with one silyl substituent

Silicon substituted silylenes attract the chemists' interest for a special reason. According to *ab initio* calculations[85,137,176], substituents acting as σ-donors should induce a relatively large red-shift of the UV maximum or, in other words, the n(Si) → 3p(Si) transition energy should be relatively small. Therefore these species are potential candidates for the long-sought triplet ground state silylenes, especially if this electronic effect is supported by a steric one. Nevertheless, reports on the matrix isolation of silicon substituted silylenes are comparatively scarce.

West and coworkers reported the generation of several silylenes[169] by photolysis of the corresponding trisilanes, among them (trimethylsilyl)mesitylsilylene **(168b)**. Surprisingly an absorption maximum at 368 nm is reported there for **168b**, which would indicate an unexpected blue-shift compared to dimethyl- (453 nm) or dimesitylsilylene (577 nm). This result was reexamined twice in the following years. In 1993 Kira, Maruyama and Sakurai prepared several (trimethylsilyl)- and (trimethylgermyl)arylsilylenes from the corresponding trisilanes in glassy 3-methylpentane[173]. In this paper a maximum at 760 nm is given for compound **168b**, being in much better agreement with the calculations[137] than the value reported first. However, this is the highest value feasible with aryl(trimethylsilyl)silylenes **(168)** since this system can avoid additional sterical pressure by a twist around the Si–C bond, i.e. the coplanarity between the p orbitals of the phenyl ring and the divalent silicon atom will not be maintained. So substitution of the *ortho* hydrogen atoms of the phenyl substituent in **168a** (660 nm for the unsubstituted phenyl derivative) leads to a bathochromic shift of 100 nm (760 nm for the mesityl compound), whereas replacement of the mesityl groups in 2,6-position by the more bulky ethyl or isopropyl substituents does not result in a further bathochromic shift, as might be expected. Actually these compounds absorb at shorter wavelengths, namely both (**168c** and **168d**) at 570 nm.

The formal substitution of the silicon atom in the trimethylsilyl group by a germanium atom yields silylenes that absorb approximately at the same wavelengths, but shifted hypsochromically by about 30 nm.

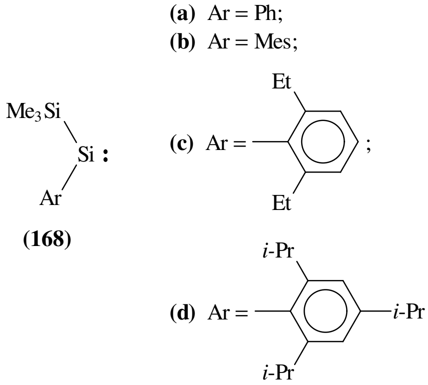

(168)

In 1995, Conlin and coworkers also reinvestigated the aryl(trimethylsilyl)silylenes **(168)** in organic glasses[172]. The value reported for λ_{max} of the mesityl compound **168b**, namely 776 nm, is approximately the same as given in the paper by Kira and coworkers. Again, no compound with an even stronger bathochromic shift could be generated. In addition, the absorption at 372 nm appearing together with that at 776 nm upon photolysis of the corresponding trisilane is tentatively assigned to the corresponding disilene, resulting from the dimerization product of **168b**. This result might explain the erroneous early assignment[169] of the 368 nm absorption to the silylene. Trapping experiments with 2,3-dimethylbutadiene and triethylsilane were also performed, confirming the appearance of the assumed silylenes[172].

2. Silylenes with two silyl substituents

As pointed out above, silyl substitution is evidently a promising strategy on the way to triplet ground state silylenes. The next consequent step is the investigation of silylenes carrying two silyl substituents. The first experiments concerning this subject were performed by Apeloig and coworkers[171]. The photolysis of 1,2-disilacyclobutane **169** (equation 46) yielded a deep violet solution with an absorption maximum higher than 750 nm (the calculated value is 886 nm[171]). Trapping products of silylene **170** as well as of disilene **171** and butadiene were isolated, too. It was not reported if the observed silylene is a ground-state singlet or triplet.

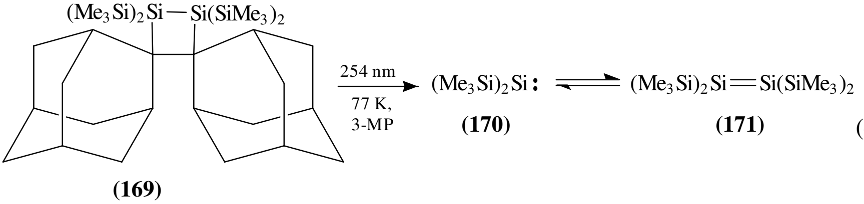

(169) **(170)** **(171)** (46)

Even though no triplet ground-state silylene could be isolated so far, silyl or germyl substitution is a promising strategy for this challenging goal. It remains to be seen if additional substitution of the methyl substituents in bis(trimethylsilyl)silylene by more bulky groups will result in the formation of the desired compounds. Nevertheless, the replacement of one methyl group by a *t*-butyl or of two by *i*-propyl groups does not seem to be sufficient for the generation of triplet ground-state silylenes, since trapping products of the intermediates generated upon photolysis of the appropriate cyclotrisilanes **172a** and **172b** in solution in the presence of *cis*- or *trans*-butene indicate singlet species[191]. In matrix-isolation experiments the precursors turned out to be photostable[191].

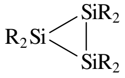

(a) R = Me(*i*-Pr)$_2$Si
(b) R = (*t*-Bu)Me$_2$Si

(172)

D. Nitrogen Substituted Silylenes

1. Silylenes by photolysis of oligosilanes

The first investigations dealing with nitrogen substituted silylenes were performed by West and coworkers in glassy 3-methylpentane with the corresponding trisilanes as precursors[169]. A strong hypsochromic shift is predicted for silylenes with substituents acting as n-donors[137,171] and this was actually found in the examples examined. Compared with mesitylmethylsilylene (λ_{max} = 496 nm) the nitrogen substituted species **173** (405 nm) and **174** (404 nm) exhibit a blue-shift of about 100 nm[169].

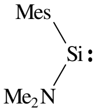

(173)

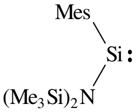

(174)

2. Silylenes by photolysis of diazides

Maier and coworkers were able to isolate the parent aminosilylene **(85)** in solid argon[96]. As already described in Section IV.A (equation 22), this species, representing the global minimum of the H$_3$NSi-hypersurface, was accessible by irradiation of silylazide and it was characterized by its vibrational and electronic spectrum. The latter shows three absorptions at 208, 220 and 348 nm. The structure was also confirmed by deuterium labelling.

Veith and coworkers examined the photochemistry of the highly substituted diazidosilane **175**[192]. The actual synthetic target was the preparation of a stable silylene like **176**. This silylene is expected to be isolable, since the homologous germanium **(177a)**, tin **(177b)** and lead compounds **(177c)** are accessible species and stable at room temperature[193,194]. The photolysis of **175** in benzene yielded only polymeric products in addition to the expected amount of nitrogen. However, if the photolysis of **175** is not carried out in benzene at room temperature but in solid argon, the expected silylene is formed (equation 47), as could be confirmed by comparison of the vibrational spectra with that of the homologues **177a** and **177b**.

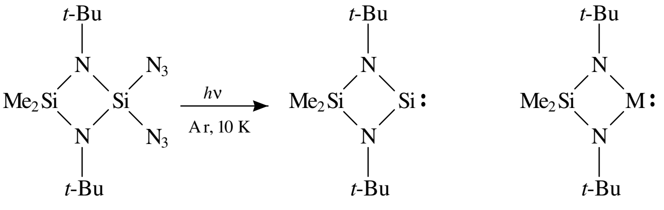

(175) **(176)** **(177)**

(a) M = Ge
(b) M = Sn
(c) M = Pb

(47)

3. Silylenes by cocondensation reactions

a. CHNSi isomers. The cocondensation reaction of silicon atoms and hydrogen cyanide was examined by Maier and coworkers[144]. In contrast to the reaction of ethene or acetylene with silicon atoms, not the π-system serves as a Lewis base, but the nitrogen lone pair, resulting in the formation of **178** as the primary product (equation 48). Irradiation of **178** yields, depending on the wavelength, either the azasilacyclopropenylidene **179** or the isocyanosilylene **181**, the latter being convertible to a species that most likely is the SiNC radical **(180)**. The identity of all CHNSi isomers was confirmed by their IR spectra[144].

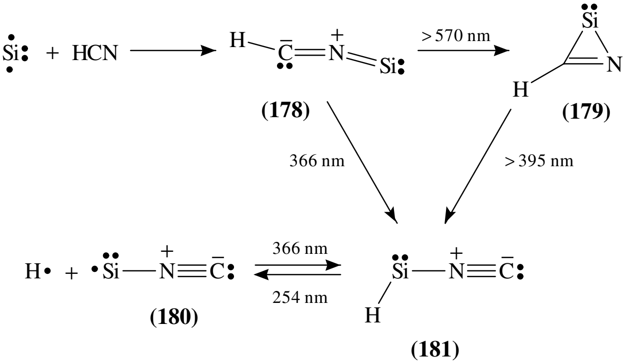

(48)

b. SiN₂ isomers. The hydrogen cyanide used in the reaction described above might be seen as an acetylene with one CH group replaced by the isoelectronic nitrogen atom. So the next consequent step is the replacement of the remaining CH group, leading to molecular nitrogen. In our cocondensation experiments of silicon atoms and N_2[73a] the already known linear :SiNN **(182)**[195] was the primary product (equation 49). As in the case of hydrogen cyanide, the nitrogen lone pair serves as a Lewis base and not the π-system. Upon irradiation cyclic SiN_2 **(183)** was formed. It is necessary to use nitrogen as the matrix material in these experiments (mixtures of argon and nitrogen fail). Again, both SiN_2 isomers were identified by their IR spectra[73]. The same sequence **182** → **183** could be observed when either diazidosilane or tetraazidosilane was irradiated in a nitrogen matrix[73b].

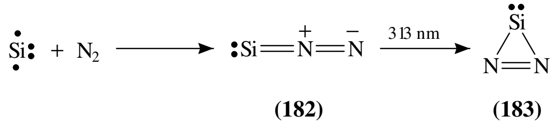

(49)

In all, the cocondensation with silicon atoms is a useful tool for the generation of silylenes. Sometimes, the same species are obtained as with 'chemical' precursors and sometimes new, otherwise not accessible compounds can be observed. So both methods nicely complement one another.

E. Oxygen Substituted Silylenes

1. Silylenes by photolysis of oligosilanes

The first isolation of an oxygen substituted silylene was reported by West and coworkers[169]. The generation of (*t*-butoxy)mesitylsilylene, (*t*-BuO)MesSi:, upon photolysis of the corresponding trisilane in 3-methylpentane was described[169]. As expected for a n-donor substituted silylene[137], the UV absorption (396 nm) is blue-shifted by more than 100 nm compared with (*t*-butyl)mesitylsilylene (505 nm). In a further study by the same group the UV absorptions of five additional silylenes of the general structures RO(Mes)Si: were reported[168]. Remarkably, the silylenes with bulky substituents at the oxygen atom (R = mesityl and 2,6-diisopropylphenyl) show UV spectra that vary with matrix viscosity. Conformational changes are proposed as explanation.

2. Silylenes by pyrolysis of suitable precursors

Maier and coworkers were able to generate silylenes that carry two oxygen substituents at the divalent silicon atom[107]. The dimethoxy compound **185a** was accessible from two totally different precursors upon pyrolysis, namely the silepine derivative **184a** and the disilane **186a** (equation 50). The structural assignment was confirmed by IR and UV spectra, the latter showing an absorption at 243 nm, which was in good agreement with the expected value[107]. In addition, a weak band was observed at 340 nm that was assigned to methoxysilylene **(187)**. Its formation is plausible if an intramolecular CH insertion of the initially formed dimethoxysilylene **(185a)** with subsequent formaldehyde elimination is considered. This interpretation is supported by the appearance of the aldehyde in the matrix. Methoxymethylsilylene **(185b)** is also accessible from the analogous precursors **184b** and **186b**. Again, **185b** was characterized by its vibrational and electronic spectra, the latter showing an absorption at 355 nm. Furthermore, the pyrolysis of $Si_2(Oi\text{-}Pr)_6$ yielded the expected diisopropoxysilylene, showing UV absorption at 247 nm.

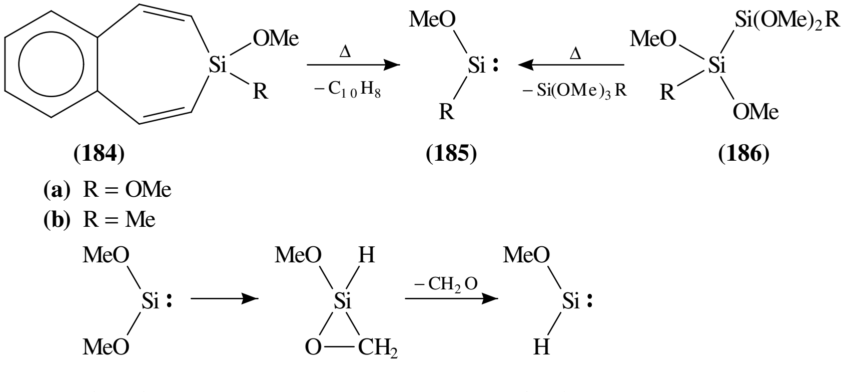

(50)

3. Silylenes by cocondensation reactions

The parent system, (HO)HSi:, was investigated by Margrave and coworkers[196]. In the cocondensation of silicon atoms and water, a complex was initially formed that spontaneously rearranged to hydroxysilylene. Photolysis led to loss of the hydrogen atoms and thus SiO was formed.

F. Halogen Substituted Silylenes

The members of this 'inorganic' subclass of silylenes were matrix-isolated much earlier than their 'organic' counterparts. Dihalosilylenes are accessible in several ways.

The dichloro compound was first generated upon photolysis of dichlorosilane by Milligan and Jacox[197]. In addition, all dihalosilylenes except of the diiodo compound are accessible from the reaction of the respective silicon tetrahalide with silicon at high temperatures[198,199]. A more recent approach to a halogen substituted silylene is the cocondensation of hydrogen fluoride with silicon atoms, yielding fluorosilylene[200].

In 1989, the reaction of difluoro- and dichlorosilylene **(188)** with molecular oxygen was investigated by Sander and coworkers[201]. The thermolysis of the corresponding hexahalodisilanes was used as access to the corresponding silylenes, which were isolated in pure oxygen or oxygen doped argon matrices. In contrast to dimethylsilylene **118**[108], the reaction of **188** with O_2 occurred only upon irradiation. The cyclic structure of compounds **189** was confirmed by isotope labelling (equation 51).

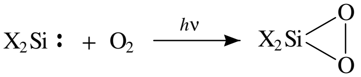

(51)

(188) **(189)**

X = F, Cl

IX. REFERENCES

1. G. Raabe and J. Michl, in *The Chemistry of Organic Silicon Compounds* (Eds. S. Patai and Z. Rappoport), Part 2, Wiley, Chichester, 1989.
2. P. Jutzi, *Chem. Unserer Zeit*, **15**, 149 (1981).
3. I. Pierre, *Justus Liebigs Ann. Chem.*, **69**, 73 (1849).
4. W. Schlenk and J. Renning, *Justus Liebigs Ann. Chem.*, **394**, 221(1912).
5. G. J. D. Peddle, D. N. Roark, A. M. Good and S. G. McGeachin, *J. Am. Chem. Soc.*, **91**, 2807 (1969).
6. N. S. Nametkin, V. M. Vdovin, L. E. Gusel'nikov and V. I. Zav'yalov, *Izv. Akad. Nauk SSSR, Ser. Khim.*, 584 (1966) *Chem. Absr.*, **65**, 5478e (1966).
7. L. E. Gusel'nikov and M. C. Flowers, *J. Chem. Soc., Chem. Commun.*, 864 (1967).
8. L. E. Gusel'nikov and M. C. Flowers, *J. Chem. Soc. (B)*, 419 (1968).
9. For a review about this topic, see M. J. Almond and A. J. Downs, in *Advances in Spectroscopy* (Vol. 17): *Spectroscopy of Matrix Isolated Species* (Eds. R. J. H. Clark and R. E. Hester), Wiley, Chichester, 1989.
10. T. J. Drahnak, J. Michl and R. West, *J. Am. Chem. Soc.*, **101**, 5427 (1979).
11. M. Denk, R. Lennon, R. Hayashi, R. West, A. V. Belyakov, H. P. Verne, A. Haaland, M. Wagner and N. Metzler, *J. Am. Chem. Soc.*, **116**, 2691 (1994).
12. G. Maier and J. Glatthaar, *Angew. Chem.*, **106**, 486 (1994); *Angew. Chem., Int. Ed. Engl.*, **33**, 473 (1994).
13. P. P. Gaspar, in *Reactive Intermediates* (Eds. M. Jones Jr. and R. A. Moss), Vol. 3, Wiley, New York, 1985, p. 333.
14. A. G. Brook and K. M. Baines, *Adv. Organomet. Chem.*, **25**, 1 (1986).
15. A. G. Brook, F. Abdesaken, B. Gutekunst, G. Gutekunst and R. K. Kallury, *J. Chem. Soc., Chem. Commun.*, 191 (1981).
16. G. E. Miracle, J. L. Ball, D. R. Powell and R. West, *J. Am. Chem. Soc.*, **115**, 11598 (1993).
17. G. Maier, G. Mihm and H. P. Reisenauer, *Angew. Chem.*, **93**, 615 (1981).
18. G. Maier and J. Glatthaar, in *Organosilicon Chemistry—From Molecules to Materials* (Eds. N. Auner and J. Weis), VCH, Weinheim, 1994, p. 131.
19. A. Sekiguchi and W. Ando, *Chem. Lett.*, 2025 (1986).
20. G. Maier, G. Mihm and H. P. Reisenauer, *Angew. Chem., Int. Ed. Engl.*, **20**, 597 (1981).
21. A. G. Brook, J. W. Harris, J. Lennon and M. El Sheikh, *J. Am. Chem. Soc.*, **101**, 83 (1979).
22. A. G. Brook, S. C. Nyburg, F. Abdesaken, B. Gutekunst, G. Gutekunst, R. K. M. R. Kallury, Y. C. Poon, Y.-M. Chang and W. Wong-Ng, *J. Am. Chem. Soc.*, **104**, 5667 (1982).
23. M. Trommer, W. Sander, C.-H. Ottoson and D. Cremer, *Angew. Chem.*, **107**, 999 (1995).
24. J. M. Duff and A. G. Brook, *Can. J. Chem.*, **51**, 2869 (1973).
25. R. A. Bourque, P. D. Davis and J. C. Dalton, *J. Am. Chem. Soc.*, **103**, 697 (1981).

26. H. M. Perrin, W. R. White and M. S. Platz, *Tetrahedron Lett.*, **32**, 4443 (1991).
27. M. Guth, Doctoral Dissertation, Universität Bochum, 1993.
28. M. Trommer, W. Sander and A. Patyk, *J. Am. Chem. Soc.*, **115**, 11775 (1993).
29. H. B. Schlegel, B. Coleman and M. Jones Jr., *J. Am. Chem. Soc.*, **100**, 6499 (1978).
30. A. J. Ashe III., R. R. Sharp and J. W. Tolan, *J. Am. Chem. Soc.*, **98**, 5451 (1976).
31. T. J. Barton and D. Banasiak, *J. Am. Chem. Soc.*, **99**, 5199 (1977).
32. T. J. Barton and G. T. Burns, *J. Am. Chem. Soc.*, **100**, 5246 (1978).
33. C. L. Kreil, O. L. Chapman, G. T. Burns and T. J. Barton, *J. Am. Chem. Soc.*, **102**, 841 (1980).
34. M. J. S. Dewar, D. H. Lo and C. A. Ramsden, *J. Am. Chem. Soc.*, **97**, 1311 (1975).
35. G. Maier, G. Mihm and H. P. Reisenauer, *Angew. Chem.*, **92**, 58 (1980).
36. G. Maier, G. Mihm and H. P. Reisenauer, *Chem. Ber.*, **115**, 801 (1982).
37. H. Bock, B. Solouki and G. Maier, *J. Organomet. Chem.*, **271**, 145 (1984).
38. G. Maier, G. Mihm, R. O. W. Baumgärtner and H. P. Reisenauer, *Chem. Ber.*, **117**, 2337 (1984).
39. J. N. Murrell, H. W. Kroto and M. F. Guest, *J. Chem. Soc., Chem. Commun.*, 619 (1977).
40. M. S. Gordon and J. A. Pople, *J. Am. Chem. Soc.*, **103**, 2945 (1981).
41. G. Maier, K. Schöttler and H. P. Reisenauer, *Tetrahedron Lett.*, **26**, 4079 (1985).
42. For a theoretical study see: K. K. Baldridge and M. S. Gordon, *J. Organomet. Chem.*, **271**, 369 (1984).
43. For theoretical studies, see A. Sax and R. Janoschek, *Angew. Chem., Int. Ed. Engl.*, **25**, 651 (1986); Z. Slanina, *J. Mol. Struct. (Theochem.)*, **65**, 143 (1990).
44. J. Chandrasekhar and P. v. R. Schleyer, *J. Organomet. Chem.*, **298**, 51 (1985).
45. K. K. Baldridge and M. S. Gordon, *Organometallics*, **7**, 144 (1988).
46. Y. van den Winkel, B. L. M. van Baar, F. Bickelhaupt, W. Kulik, C. Sierakowski and G. Maier, *Chem. Ber.*, **124**, 185 (1991).
47. H. Hiratsuka, M. Tanaka, T. Okutsu, M. Oba and K. Nishiyama, *J. Chem. Soc., Chem. Commun.*, 215 (1995).
48. See, for example, Reference 46 and references cited therein.
49. Y. van den Winkel, O. S. Akkerman and F. Bickelhaupt, *Main Group Metal Chem.*, **11**, 91 (1988).
50. P. Jutzi, M. Meyer, H. P. Reisenauer and G. Maier, *Chem. Ber.*, **122**, 1227 (1989).
51. G. Märkl and W. Schlosser, *Angew. Chem.*, **100**, 1009 (1988).
52. G. Maier, *Angew. Chem., Int. Ed. Engl.*, **27**, 309 (1988).
53. M. S. Gordon, *J. Chem. Soc., Chem. Commun.*, 1131 (1980).
54. G. W. Schriver, M. J. Fink and M. S. Gordon, *Organometallics*, **6**, 1977 (1987).
55. M. J. Fink and D. Puranik, *Organometallics*, **6**, 1809 (1987).
56. T. Bally and S. Masamune, *Tetrahedron*, **36**, 343 (1980).
57. G. Maier, *Pure Appl. Chem.*, **58**, 95 (1986).
58. U.-J. Vogelbacher, M. Regitz and R. Mynott, *Angew. Chem., Int. Ed. Engl.*, **25**, 842 (1986).
59. G. Maier and A. Kratt, unpublished results.
60. P Lingelbach, Doctoral Dissertation, Universität Giessen, Germany, 1989.
61. A. Schick, Doctoral Dissertation, Universität Giessen, Germany, 1992.
62. P. R. Jones, T. F. Bates, A. F. Cowley and A. M. Arif, *J. Am. Chem. Soc.*, **108**, 3123 (1986).
63. P. R. Jones and T. F. Bates, *J. Am. Chem. Soc.*, **109**, 913 (1987).
64. D. B. Puranik, M. P. Johnson and M. J. Fink, *J. Chem. Soc., Chem. Commun.*, 706 (1989).
65. J. R. Gee, W. A. Howard, G. L. McPherson and M. J. Fink, *J. Am. Chem. Soc.*, **113**, 5461 (1991).
66. A. G. Brook and K. M. Baines, *Adv. Organomet. Chem.*, **25**, 1 (1986).
67. K. M. Baines and A. G. Brook, *Organometallics*, **6**, 692 (1987).
68. A. J. Vanderwielen, M. A. Ring and H. E. O'Neal, *J. Am. Chem. Soc.*, **97**, 993 (1975).
69. A. Meudt, Doctoral Dissertation, Universität Giessen, Germany, 1996.
70. H. Büttner, Doctoral Dissertation, Universität Giessen, Germany, 1993.
71. U. Wessolek-Kraus, Doctoral Dissertation, Universität Giessen, Germany, 1988.
72. D. Littmann, Doctoral Dissertation, Universität Giessen, Germany, 1985.
73. (a) G. Maier, H. P. Reisenauer and H. Egenolf, unpublished results.
    (b) G. Maier and J. Glatthaur, unpublished results.
74. A. Thoma, B. E. Wurfel, R. Schlachter, G. M. Lask and V. E. Bondybey, *J. Phys. Chem.*, **96**, 7231 (1992).
75. H. Shizuka, K. Murata, Y. Arai, K. Tonokura, H. Tanaka, H. Matsumoto, Y. Nagai, G. Gillette and R. West, *J. Chem. Soc. Faraday Trans. I*, **85**, 2369 (1989).

76. B. J. Helmer and R. West, *Organometallics*, **1**, 1458 (1982).
77. C. W. Carlson and R. West, *Organometallics*, **2**, 1792 (1983).
78. H. Watanabe, Y. Kongo and Y. Nagai, *J. Chem. Soc., Chem. Commun.*, 66 (1984).
79. H. Watanabe, T. Okawa, M. Kato and Y. Nagai, *J. Chem. Soc., Chem. Commun.*, 781 (1983)
80. H. Watanabe, Y. Kongo, M. Kato, H. Kuwabara, T. Okawa and Y. Nagai, *Bull. Chem. Soc. Jpn.*, **57**, 3019 (1984).
81. M. Kira, T. Maruyama, C. Kabuto, K. Ebata and H. Sakurai, *Angew. Chem.*, **106**, 1575 (1994).
82. S. Masamune, Y. Eriyama and T. Kawase, *Angew. Chem.*, **99**, 601 (1987); *Angew. Chem., Int. Ed. Engl.*, **26**, 584 (1987).
83. M. Karni and Y. Apeloig, *J. Am. Chem. Soc.*, **112**, 8589 (1990).
84. C. Liang and L. C. Allen, *J. Am. Chem. Soc.*, **112**, 1039 (1990).
85. R. S. Grev, H. F. Schaefer III and P. P. Gaspar, *J. Am. Chem. Soc.*, **113**, 5638 (1991).
86. M. Bogey, H. Bolvin, C. Demuynck and J. L. Destombes, *Phys. Rev. Lett.*, **66**, 413 (1991).
87. M. Cordonnier, M. Bogey, C. Demuynck and J.-L. Destombes, *J. Chem. Phys.*, **97**, 7984 (1992).
88. N. Wiberg, K. Schurz, G. Reber and G. Müller, *J. Chem. Soc., Chem. Commun.*, 591 (1986).
89. A. Sekiguchi, W. Ando and K. Honda, *Chem. Lett.*, 1029 (1986).
90. S. S. Zigler, R. West and J. Michl, *Chem. Lett.*, 1024 (1986).
91. R. West, S. S. Zigler, J. Michl and G. Gross, presented at the 19th Organosilicon Symposium, Louisiana State University, Baton Rouge, LA, April 26–27, 1985.
92. H. Bock and R. Dammel, *Angew. Chem.*, **97**, 128 (1985); *Angew. Chem., Int. Ed. Engl.*, **24**, 111 (1985).
93. G. Gross, J. Michl and R. West, presented at the 19th Organosilicon Symposium, Lousiana State University, Baton Rouge, LA, April 26–27, 1985.
94. A. G. MacDiarmid, *J. Inorg. Nucl. Chem*, **2**, 88 (1956).
95. J. F. Ogilvie and S. Cradock, *J. Chem. Soc., Chem. Commun.*, 364 (1966).
96. G. Maier, J. Glatthaar and H. P. Reisenauer, *Chem. Ber.*, **122**, 2403 (1989).
97. R. S. Mulliken, *Phys. Rev.*, **26**, 319 (1925).
98. N. T. Truong and M. S. Gordon, *J. Am. Chem. Soc.*, **108**, 1775 (1986).
99. S. S. Zigler, K. M. Welsh and R. West, *J. Am. Chem. Soc.*, **109**, 4392 (1987).
100. K. M. Welsh, J. Michl and R. West, *J. Am. Chem. Soc.*, **110**, 6689 (1988).
101. R. Whithnall and L. Andrews, *J. Phys. Chem.*, **92**, 594 (1988).
102. R. Whithnall and L. Andrews, *J. Am. Chem. Soc.*, **108**, 8118 (1986).
103. R. Whithnall and L. Andrews, *J. Phys. Chem.*, **89**, 3261 (1985).
104. V. N. Khabashesku, Z. A. Kerzina, E. G. Baskir, A. K. Maltsev and O. M. Nefedov, *J. Organomet. Chem.*, **347**, 277 (1988).
105. V. N. Khabashesku, Z. A. Kerzina, A. K. Maltsev and O. M. Nefedov, *J. Organomet. Chem.*, **364**, 301 (1989).
106. V. N. Khabashesku, Z. A. Kerzina and O. M. Nefedov, *Izv. Akad. Nauk SSSR, Ser. Khim.*, **9**, 2187 (1988).
107. G. Maier, H. P. Reisenauer, K. Schöttler and U. Wessolek-Kraus, *J. Organomet. Chem.*, **366**, 25 (1989).
108. A. Patyk, W. Sander, J. Gauss and D. Cremer, *Angew. Chem.*, **101**, 920 (1989); *Angew. Chem., Int. Ed. Engl.*, **28**, 898 (1989).
109. H. Schnöckel, *Angew. Chem.*, **90**, 638 (1978); *Angew. Chem., Int. Ed. Engl.*, **17**, 616 (1978).
110. J. S. Anderson and J. S. Ogden, *J. Chem. Phys.*, **51**, 4189 (1969).
111. J. W. Hastie, R. H. Hauge and J. L. Margrave, *Inorg. Chim. Acta*, **3**, 601 (1969).
112. H. Schnöckel, *Z. Anorg. Allg. Chem.*, **460**, 37 (1980).
113. H. Schnöckel, T. Mehner, H. S. Plitt and S. Schunck, *J. Am. Chem. Soc.*, **111**, 4578 (1989).
114. H. Schnöckel and R. Köppe, in *Organosilicon Chemistry—From Molecules to Materials* (Eds. N. Auner and J. Weis), VCH, Weinheim, 1994, p. 147.
115. R. Köppe and H. Schnöckel, *Heteroatom Chem.*, **3**, 329 (1992).
116. T. Mehner, H. Schnöckel, M. J. Almond and A. J. Downs, *J. Chem. Soc., Chem. Commun.*, 117 (1988).
117. J. H. B. Chenier, J. A. Howard, H. A. Joly, B. Mile and P. L. Timms, *J. Chem. Soc., Chem. Commun.*, 581 (1990).
118. T. Mehner, R. Köppe and H. Schnöckel, *Angew. Chem.*, **104**, 653 (1992); *Angew. Chem., Int. Ed. Engl.*, **31**, 638 (1992).
119. R. M. Atkins and P. L. Timms, *Spectrochim. Acta*, **33A**, 853 (1977).

120. H. Schnöckel and R. Köppe, *J. Am. Chem. Soc.*, **111**, 4583 (1989).
121. H. Schnöckel, *Angew. Chem.*, **92**, 310 (1980); *Angew. Chem., Int. Ed. Engl.*, **19**, 323 (1980).
122. H. Suzuki, N. Tokitoh, S. Nagase and R. Okazaki, *J. Am. Chem. Soc.*, **116**, 11578 (1994).
123. H. Schnöckel, H. J. Göcke and R. Köppe, *Z. Anorg. Allg. Chem.*, **578**, 159 (1989).
124. R. Köppe and H. Schnöckel, *Z. Anorg. Allg. Chem.*, **607**, 41 (1992).
125. J. A. Howard, R. Jones, J. S. Tse, M. Tomietto, P. L. Timms and A. J. Seeley, *J. Chem. Phys.*, **96**, 9144 (1992).
126. R. Köppe, H. Schnöckel, F. X. Gadea, J. C. Barthelat and C. Jouany, *Heteroatom Chem.*, **3**, 333 (1992).
127. G. Maier, H. P. Reisenauer and H. Pacl, *Angew. Chem.*, **106**, 1347 (1994); *Angew. Chem., Int. Ed. Engl.*, **33**, 1248 (1994).
128. G. Maier, H. Pacl, H. P. Reisenauer, A. Meudt and R. Janoschek, *J. Am. Chem. Soc.*, **117**, 12712 (1995).
129. G. Maier, H. P. Reisenauer and H. Pacl, in *Organosilicon Chemistry II—From Molecules to Materials* (Eds. N. Auner and J. Weis), VCH, Weinheim, 1996, p. 303.
130. G. Frenking, R. B. Remington and H. F. Schaefer III, *J. Am. Chem. Soc.*, **108**, 2169 (1986).
131. G. Vacek, B. T. Colgrove and H. F. Schaefer III, *J. Am. Chem. Soc.*, **113**, 3192 (1991).
132. D. L. Cooper, *Astrophys. J.*, **354**, 229 (1990).
133. M.-D. Su, R. D. Amos and N. C. Handy, *J. Am. Chem. Soc.*, **112**, 1499 (1990).
134. R. Srinivas, D. Sülzle, T. Weiske and H. Schwarz, *Int. J. Mass Spectrom. Ion Processes*, **107**, 369 (1991).
135. M. Izuha, S. Yamamoto and S. Saito, *Can. J. Phys.*, **72**, 1206 (1994).
136. H. Pacl, Doctoral Dissertation, Universität Giessen, Germany, 1995.
137. Y. Apeloig, M. Karni, R. West and K. Welsh, *J. Am. Chem. Soc.*, **116**, 9719 (1994).
138. B. Kleman, *Astrophys. J.*, **33**, 473 (1956).
139. W. Weltner Jr. and D. McLeod Jr., *J. Chem. Phys.*, **41**, 235 (1964).
140. R. A. Shepherd and W. R. M. Graham, *J. Chem. Phys.*, **88**, 3399 (1988).
141. R. A. Shepherd and W. R. M. Graham, *J. Chem. Phys.*, **82**, 4788 (1985).
142. J. D. Presilla-Márquez, W. R. M. Graham and R. A. Shepherd, *J. Chem. Phys.*, **93**, 5424 (1990).
143. W. Sander, *Angew. Chem.*, **106**, 1522 (1994); *Angew. Chem., Int. Ed. Engl.*, **33**, 1455 (1994).
144. G. Maier, H. P. Reisenauer and H. Egenolf, presented at the III. Münchener Silicontage, Ludwig-Maximilians-Universität, München, April 1–2, 1996; in *Organosilicon chemistry III—From Molecules to Materials* (Eds. N. Auner and J. Weis), VCH, Weinheim, 1997, to appear.
145. R. T. Conlin and P. P. Gaspar, *J. Am. Chem. Soc.*, **98**, 3715 (1976).
146. M. Trommer, W. Sander and C. Marquard, *Angew. Chem.*, **106**, 816 (1994); *Angew. Chem., Int. Ed. Engl.*, **33**, 766 (1994).
147. G. Maier, H. Pacl and H. P. Reisenauer, *Angew. Chem.*, **107**, 1627 (1995); *Angew. Chem., Int. Ed. Engl.*, **34**, 1439 (1995).
148. E. A. V. Ebsworth and S. G. Frankiss, *J. Chem. Soc.*, 661 (1963).
149. B. T. Luke, J. A. Pople, M.-B. Krogh-Jespersen, Y. Apeloig, J. Chandrashekar, M. J. Karni and P. v. R. Schleyer, *J. Am. Chem. Soc.*, **108**, 270 (1986).
150. R. S. Grev, G. E. Scuseria, A. C. Scheiner, H. F. Schaefer III and M. S. Gordon, *J. Am. Chem. Soc.*, **110**, 7337 (1988).
151. J. A. Boatz and M. S. Gordon, *J. Phys. Chem.*, **94**, 7331 (1990).
152. K. Balasubramanian and A. D. McLean, *J. Chem. Phys.*, **85**, 5117 (1986).
153. H.-J. Werner and E.-A. Reinsch, *J. Chem. Phys.*, **76**, 3144 (1982).
154. J. Berkowitz, J. P. Greene, H. Cho and B. Ruscic, *J. Chem. Phys.*, **86**, 1235 (1987).
155. T. J. Sears and P. R. Bunker, *J. Chem. Phys.*, **79**, 5265 (1983).
156. M. Denk, R. West, R. Hayashi, Y. Apeloig, R. Pauncz and M. Karni, in *Organosilicon Chemistry II—From Molecules to Materials* (Eds. N. Auner and J. Weis), VCH, Weinheim, 1996, pp. 251–261.
157. B. T. Luke, J. A. Pople, M.-B. Krogh-Jespersen, Y. Apeloig, J. Chandrashekar and P.v.R. Schleyer, *J. Am. Chem. Soc.*, **108**, 260 (1986).
158. R. Janoschek, *Chem. Unserer Zeit*, **21**, 128 (1988).
159. D. H. Pae, M. Xiao, M. Y. Chiang and P. P. Gaspar, *J. Am. Chem. Soc.*, **113**, 1281 (1991).
160. D. E. Milligan and M. E. Jacox, *J. Chem. Phys.*, **52**, 2594 (1970).
161. L. Fredin, R. H. Hauge, Z. H. Kafafi and J. L. Margrave, *J. Chem. Phys.*, **82**, 3542 (1985).
162. G. Maier, G. Mihm, H. P. Reisenauer and D. Littmann, *Chem. Ber.*, **117**, 2369 (1984).

163. H. Vancik, G. Raabe, M. J. Michalczyk, R. West and J. Michl, *J. Am. Chem. Soc.*, **107**, 4097 (1985).
164. G. Raabe, H. Vancik, R. West and J. Michl, *J. Am. Chem. Soc.*, **108**, 671 (1986).
165. C. A. Arrington, J. T. Petty, S. E. Payne and W. C. K. Haskins, *J. Am. Chem. Soc.*, **110**, 6240 (1988).
166. M.-A. Pearsall and R. West, *J. Am. Chem. Soc.*, **110**, 7228 (1988).
167. T. P. Hamilton and H. F. Schaefer III, *J. Chem. Phys.*, **90**, 1031 (1989).
168. G. R. Gillette, G. Noren and R. West, *Organometallics*, **9**, 2925 (1990).
169. M. J. Michalczyk, M. J. Fink, D. J. De Young, C. W. Carlson, K. M. Welsh, R. West and J. Michl, *Silicon, Germanium, Tin Lead Compd.*, **9**, 75 (1986).
170. A. Sekiguchi, K. Hagiwara and W. Ando, *Chem. Lett.*, 209 (1987).
171. Y. Apeloig, M. Karni and T. Müller, in *Organosilicon Chemistry II—From Molecules to Materials* (Eds. N. Auner and J. Weis), VCH, Weinheim, 1996, pp. 263–288.
172. S. G. Bott, P. Marshall, P. E. Wagenseller, Y. Wang and R. T. Conlin, *J. Organomet. Chem.*, **499**, 11 (1995).
173. M. Kira, T. Maruyama and H. Sakurai, *Chem. Lett.*, 1345 (1993).
174. M. Kira, T. Maruyama and H. Sakurai, *Tetrahedron Lett.*, **33**, 243 (1992).
175. T. J. Drahnak, J. Michl and R. West, *J. Am. Chem. Soc.*, **103**, 1845 (1981).
176. Y. Apeloig and M. Karni, *J. Chem. Soc., Chem. Commun.*, 1048 (1985).
177. G. R. Gilette, G. H. Noren and R. West, *Organometallics*, **8**, 487 (1989).
178. T. Akasaka, S. Nagase, A. Yabe and W. Ando, *J. Am. Chem. Soc.*, **110**, 6270 (1988).
179. V. N. Khabashesku, V. Balaji, S. E. Boganov, O. M. Nefedov and J. Michl, *J. Am. Chem. Soc.*, **116**, 320 (1994)
180. G. Maier, K. Schöttler and H. P. Reisenauer, *Tetrahedron Lett.*, **26**, 4079 (1985).
181. T. M. Gentle and E. L. Muetterties, *J. Am. Chem. Soc.*, **105**, 304 (1983).
182. G. Maier, H. P. Reisenauer, J. Jung, A. Meudt and H. Pacl, presented at the III. Münchener Silicontage, Ludwig-Maximilians-Universität, München, April 1–2, 1996; in *Organosilicon chemistry III—From Molecules to Materials* (Eds. N. Auner and J. Weis), VCH, Weinheim, 1997, to appear.
183. J. Jung, Doctoral Dissertation, Universität Giessen, Germany, 1996.
184. T. A. Holme, M. S. Gordon, S. Yabushita and M. W. Schmidt, *Organomet.*, **3**, 583 (1984).
185. J. D. Presilla-Márquez and W. R. M. Graham, *J. Chem. Phys.*, **95**, 5612 (1991).
186. J. D. Presilla-Márquez, S. C. Gay, C. M. L. Rittby and W. R. M. Graham, *J. Chem. Phys.*, **102**, 6354 (1995).
187. J. D. Presilla-Márquez and W. R. M. Graham, *J. Chem. Phys.*, **96**, 6509 (1992).
188. Z. H. Kafafi, R. H. Hauge, L. Fredin and J. L. Margrave, *J. Phys. Chem.*, **87**, 797 (1983).
189. C. M. L. Rittby, *J. Chem. Phys.*, **95**, 5609 (1991).
190. C. M. L. Rittby, *J. Chem. Phys.*, **96**, 6768, (1992).
191. M. Kira and H. Sakurai, *Kagaku (Kyoto)*, **49**, 876 (1994) *Chem. Abstr.*, **122**, 56065e (1995).
192. M. Veith, E. Werle, R. Lisowsky, R. Köppe and H. Schnöckel, *Chem. Ber.*, **125**, 1375 (1992).
193. M. Veith, M. Grosser and V. Huch, *Z. Anorg. Allg. Chem.*, **513**, 89 (1984).
194. M. Veith, *Angew. Chem.*, **87**, 287 (1975).
195. R. R. Lembke, R. F. Ferrante and W. Weltner Jr., *J. Am. Chem. Soc.*, **99**, 416 (1977).
196. Z. K. Ismail, R. H. Hauge, L. Fredin, J. W. Kauffman and J. L. Margrave, *J. Chem. Phys.*, **77**, 1617 (1982).
197. D. E. Milligan and M. E. Jacox, *J. Chem. Phys*, **49**, 1938 (1968).
198. J. W. Hastie, R. H. Hauge and J. L. Margrave, *J. Am. Chem. Soc.*, **91**, 2536 (1969).
199. G. Maass, R. H. Hauge and J. L. Margrave, *Z. Anorg. Allg. Chem.*, **392**, 295 (1972).
200. Z. K. Ismail, L. Fredin, R. H. Hauge and J. L. Margrave, *J. Chem. Phys.*, **77**, 1626 (1982).
201. A. Patyk, W. Sander, J. Gauss and D. Cremer, *Chem. Ber.*, **123**, 89 (1990).

CHAPTER **20**

Electrochemistry of organosilicon compounds

TOSHIO FUCHIGAMI

Department of Electrochemistry, Tokyo Institute of Technology, Midori-ku, Yokohama 226, Japan
Fax: 81-45-921-1089; e-mail: fuchi@echem.titech.ac.jp

I. INTRODUCTION

Organosilicon compounds are readily available and fairly stable compared with other organometallic compounds. Over the past two decades, organosilicon chemistry has grown rapidly and nowadays organosilicon compounds are widely utilized not only as various functional materials, but also as valuable organic synthetic reagents owing to their unique chemical and physical properties. There has been a remarkable growth in electrochemistry of organosilicon compounds since the last decade. This is mainly due to the following unique electrochemical and chemical properties: (1) A silyl substituent increases the HOMO energy level of π-electron systems and heteroatoms at the β-position and promotes anodic oxidation, (2) a silyl substituent decreases the LUMO energy level of π-electron systems at the α-position and enhances cathodic reduction, (3) a silyl group is an excellent cationic leaving group ('super proton') particularly when cationic intermediates are generated at the β-position and (4) a silyl group stabilizes α-anions and consequently enhances their generation.

This review covers the recent remarkable advances in the electrochemistry of organosilicon compounds, although the emphasis herein is mainly on the electrochemical reactions rather than on electrochemical mechanistic details. Only few reviews dealing with organosilicon electrochemistry have been published so far[1,2].

II. ANODIC OXIDATION OF ORGANOSILICON COMPOUNDS

A. Alkylsilanes

Similarly to the low chemical reactivity of (simple) alkylsilanes devoid of functional groups, the electrochemical reactivity of simple alkylsilanes is quite low. Klingler and Kochi measured the oxidation potentials of tetraalkyl derivatives of group-14-metal compounds by using cyclic voltammetry[3]. These compounds exhibit an irreversible anodic peak in acetonitrile. The oxidation potential (E_p) decreases in the order of Si>Ge>Sn>Pb as illustrated in Table 1. This order is the same as that of the gas-phase ionization potentials (I_p). The absence of steric effects on the correlation of E_p with I_p indicates that the electron transfer should take place by an outer-sphere mechanism. Since tetraalkylsilane has an extremely high oxidation potential (>2.5 V), it is generally difficult to oxidize such alkylsilanes anodically.

However, interestingly, the oxidation potential of tetraalkylsilanes decreases considerably in the presence of fluoride ions[4]. For example, a cathodic shift from 2.6 V to 2.3 V vs Ag/AgNO$_3$ was observed in the oxidation potential of phenyltrimethylsilane in the presence of Et$_4$NF·3HF. This suggests that one-electron transfer from alkylsilanes is assisted by fluoride ions.

The constant potential anodic oxidation of tetraalkylsilanes in the presence of fluoride ions provides the corresponding fluorosilanes derived from cleavage of the C−Si bond[4].

TABLE 1. Oxidation potentials (E_p) and ionization potentials (I_p) of aliphatic group-14-metal compounds

Substrate	E_p (V vs SSCE)[a]	I_p (eV)
Et$_4$Si	2.56	9.78
Et$_4$Ge	2.24	9.41
Et$_4$Sn	1.76	8.93
Et$_4$Pb	1.26	8.13

[a] Saturated NaCl-SCE.

TABLE 2. Anodic oxidation of organosilicon compounds in the presence of fluoride ions

Substrate	Product yield (%)
$PhSiMe_3$	$PhSiMe_2F$ (80), CH_4, C_2H_6
$PhCH_2SiMe_3$	Me_3SiF (50), PhCHO
$PhCH_2SiEt_3$	Et_3SiF (70), PhCHO

The proposed intermediate is the pentacoordinate silyl radical, which eliminates the most stable alkyl radical to give the corresponding fluorosilane (equation 1 and Table 2).

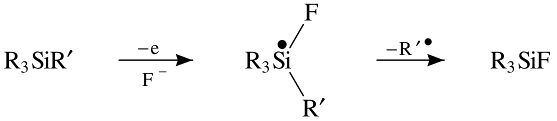

$$R_3SiR' \xrightarrow[F^-]{-e} R_3\overset{\bullet}{Si}(F)(R') \xrightarrow{-R'^{\bullet}} R_3SiF \qquad (1)$$

The anodic oxidation of silyl-substituted tetrahedranes was studied by cyclic voltammetry[5]. Tri-*t*-butyl(trimethylsilyl)tetrahedrane is oxidized more easily compared with tetra-*t*-butyltetrahedrane owing to the σ-donating silyl group (equation 2).

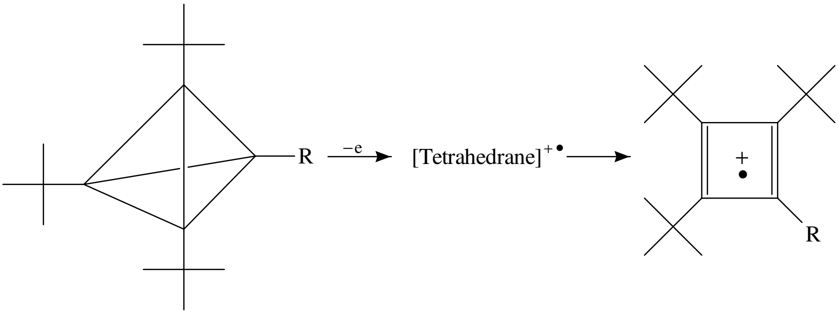

(2)

R = *t*-Bu : $E_p{}^{ox}$, +0.50 V vs SCE
R = Me_3Si : $E_p{}^{ox}$, +0.40 V vs SCE

B. Arylsilanes

Anodic oxidation of arylsilanes is slightly easier than that of alkylsilanes. The oxidation potential (E_p) of tetraphenylsilane was reported to be 2.1 V (vs Ag/Ag^+ in 0.01 M $LiClO_4/MeCN$)[6]. The cation radicals of aromatic silanes anodically generated in anhydrous CH_2Cl_2 in the presence of activated alumina are generally stable. However, in the presence of residual water, a black deposit, mainly consisting of conjugated aromatic polymers, was formed during electrolysis (equation 3)[6].

$$Ph_4Si \xrightarrow{-e} Ph_4Si^{+\bullet} \longrightarrow Ph_3Si^+ + Ph^{\bullet} \longrightarrow \text{polymer} \qquad (3)$$

Anodic oxidation of α-trimethylsilylated thiophene derivatives in nitrobenzene results in desilylation and formation of polythiophenes (equation 4), which have higher conductivity than those prepared from unsilylated thiophenes[7−9]. The silyl group increases the regioselectivity of carbon−carbon bond formation since the silyl group is an excellent cationic leaving group.

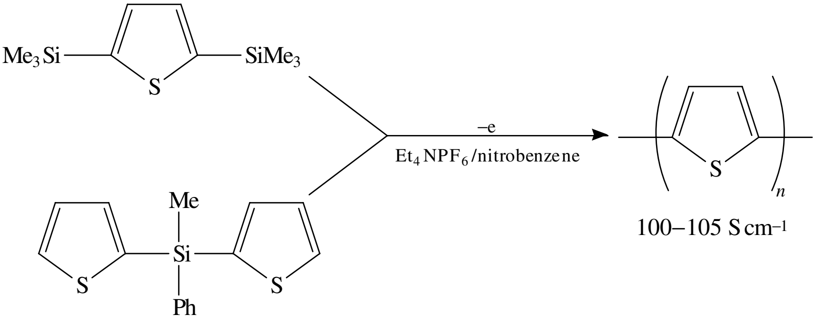

(4)

In contrast, anodic oxidation of tetra-2-(β'-methylterthienyl)silane provides polythiophene without desilylation[9]. The polymer has a 3D electroactive π-conjugated system (equation 5).

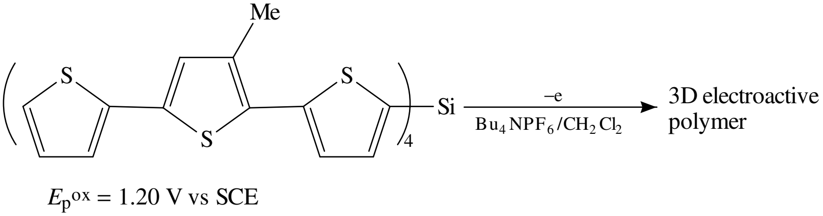

(5)

C. Benzylsilanes, Allylsilanes and Related Compounds

Benzylsilanes and allylsilanes are easily oxidized anodically compared with alkylsilanes and arylsilanes. Benzylsilanes exhibit irreversible cyclic voltammetric waves. It is notable that their oxidation potentials (E_p) are markedly less positive than those of the unsilylated parent compounds owing to the σ–π interaction (Table 3)[10a]. It is interesting that α-trimethylsilylation of xylenes markedly decreases their oxidation potential while additional α'-trimethylsilylation makes a little change (Table 3). It has also been reported that a σ, σ-interacting system (the neighboring C—Si bonds) in addition to a σ–π interaction caused a significant decrease of the oxidation potentials[10b].

Fuchigami and coworkers and Yoshida and coworkers independently found that anodic oxidation of benzylsilanes in the presence of nucleophiles such as alcohols and carboxylic acids resulted in a selective cleavage of the C—Si bond and the oxygen nucleophiles were introduced exclusively into the benzylic position (equation 6)[11–13]. In the absence of nucleophiles, the benzylsilane itself plays a role of a nucleophile and benzyl(trimethylsilylmethyl)benzene is formed (equation 7)[11,12].

Anodic oxidation of α, α'-bis(trimethylsilyl)xylenes in alcohols provides the corresponding monoalkoxylated products solely. Among α, α'-bis(trimethylsilyl)-*o*-, -*m*- and -*p*-xylenes, the *p*-xylene derivative gave the best yields of alkoxylated products as shown in equation 8[10].

Allylsilanes are also easily oxidized compared with nonsilylated olefines, as shown in Table 4[13].

TABLE 3. Oxidation potentials (E_p) of benzylsilanes and their unsilylated parent compounds[7]

Substrate	E_p[a]	Substrate	E_p[a]
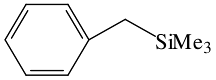	1.38	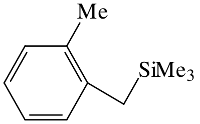	1.18
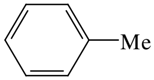	1.98	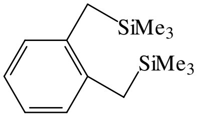	1.13
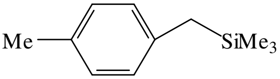	1.17	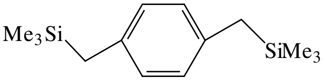	1.06
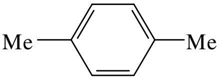	1.70	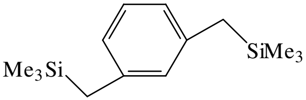	1.12

[a] V vs Ag/AgNO$_3$(sat).

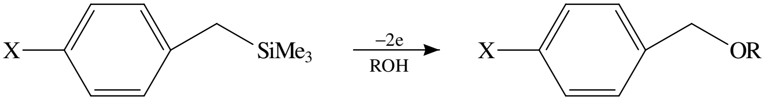

X = H, R = Me (91%)
X = SiMe$_3$, R = Me (100%)
X = Cl, R = Me (72%)
X = H, R = 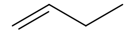 (34%)
X = H, R = CF$_3$CO (24%)

(6)

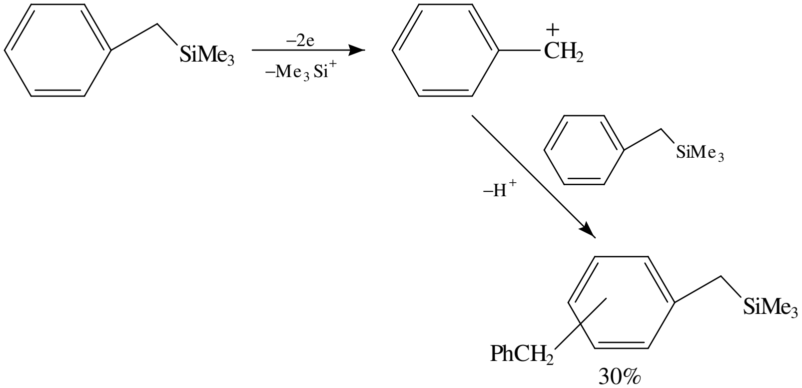

30%

(7)

TABLE 4. Oxidation potentials (E_p) of allylsilanes and olefins[10]

Substrate	E_p (V vs Ag/AgCl)
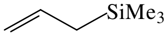	1.65
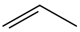	2.0
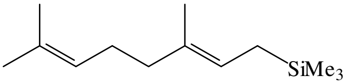	1.30
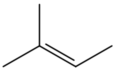	1.85

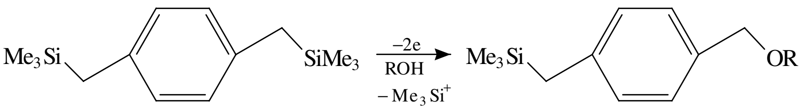

R = Me (67%)

R = CF_3CH_2 (50%)

R = 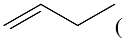 (50%)

R = Cl 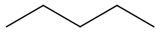 (48%)

(8)

Anodic oxidation of allylsilanes in the presence of nucleophiles results in replacement of a trimethylsilyl group by a nucleophile which is introduced into the allylic carbon. Various oxygen and nitrogen nucleophiles such as alcohols, water, caboxylic acids, *p*-toluenesulfonic acid, carbamates or a sulfonamide can be employed in this reaction (equations 9–11)[11–13].

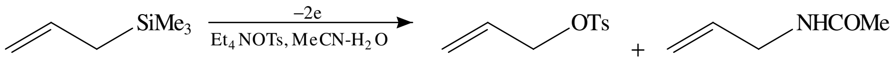

20% 15% (9)

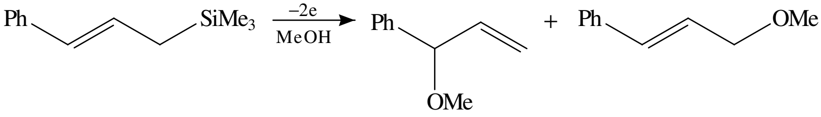

76% (2:1)

(10)

It should be noted that in the case of geranyltrimethylsilane, the carbon–carbon double bond of the allylsilane moiety is oxidized selectively to give two regioisomeric products (equation 11)[13]. This is due to the electron-donating effect of the β-silyl group. Since a methoxylated silane was formed in the anodic oxidation of an allylsilane as shown in equation 12, the reaction mechanism can be illustrated as in equation 13[13].

In contrast to the case of allylsilanes, anodic oxidation of disubstituted olefins provides in general four regioisomeric products because all the allylic carbon–hydrogen bonds can be cleaved. In the case of allylsilane, the cleavage of a C–Si bond takes place preferentially since a C—Si bond is more easily cleaved than a C—H one (equation 14), whereas allylsilanes usually act as nucleophiles; in this reaction the allylsilane works as a strong electrophile. Thus, the electrochemical reaction is an excellent method for *'oxidizable umpolung'* of allylsilanes.

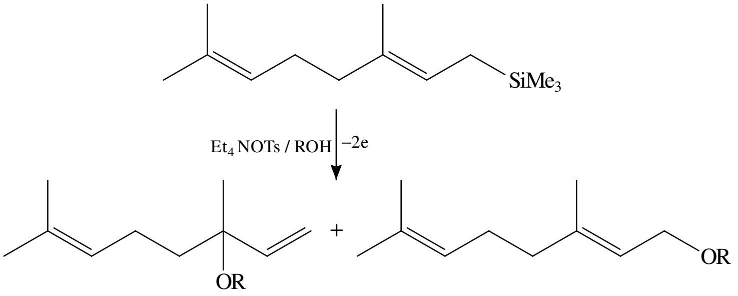

(11)

R = Me, 69% (68 : 32)
R = H, 62% (60 : 40)
R = Ac, 26% (63 : 27)

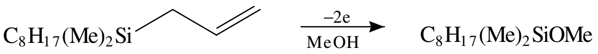

(12)

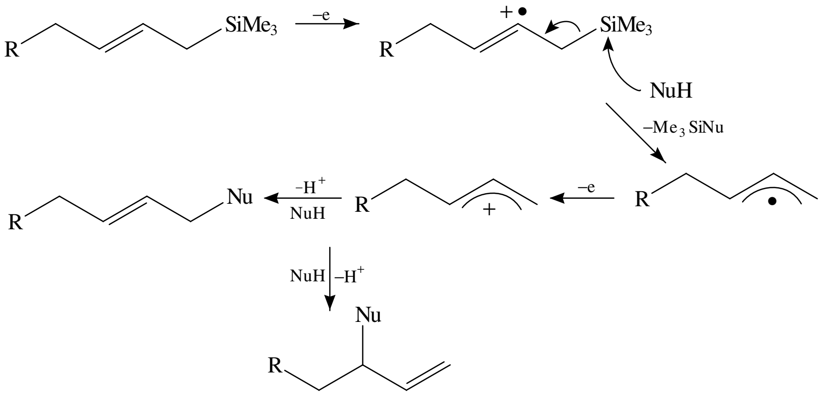

Nu = R′O, OH, R′NHCO$_2$Me, R′COO, TsO, MeCN (13)

Chemical[14] and photochemical[15] oxidizable umpolung of allylsilanes has been reported and a similar mechanism was proposed.

1-Silyl-1,3-dienes undergo anodic methoxylation in methanol to give 1,4-addition products with an allylsilane structure as intermediates. Therefore, they are further oxidized to give 1,1,4-trimethoxy-2-butene derivatives as the final products. The products are easily hydrolyzed to provide the corresponding γ-methoxy-α, β-unsaturated aldehydes. Since 1-trimethylsilyl-1,3-dienes are readily prepared by the reaction of the anion of 1,3-bis(trimethylsilyl)propene with aldehydes or ketones, 1,3-bis(trimethylsilyl)propene offers α, β-formylvinyl anion equivalent for the reaction with carbonyl compounds (equation 15)[16].

Anodic oxidation of a mixture of allylsilane and cyclic 1,3-diketones in the presence or absence of oxygen provides cyclic peroxides (equation 16) and dihydrofuran (equation 17) derivatives, respectively[17,18]. In these reactions, the cyclic diketones are discharged to generate radical intermediates, which are trapped with allylsilane as shown. In the former case, a catalytic amount of electricity (0.043 F/mol) is enough to complete the reactions[17].

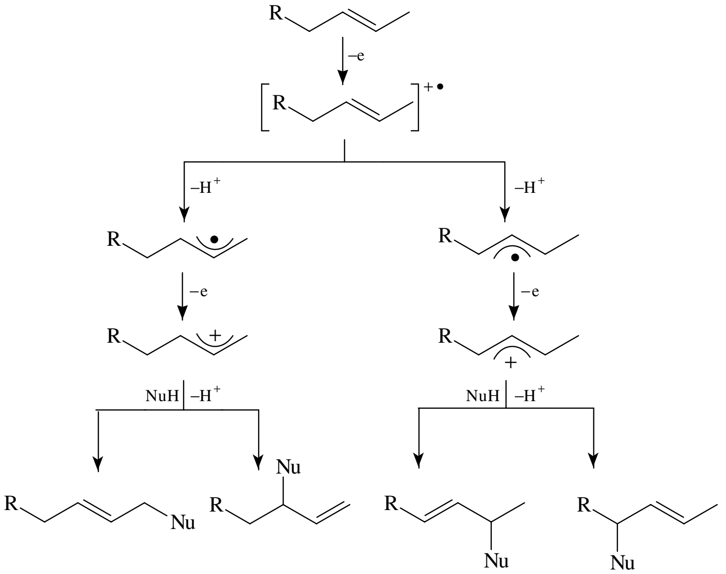

(14)

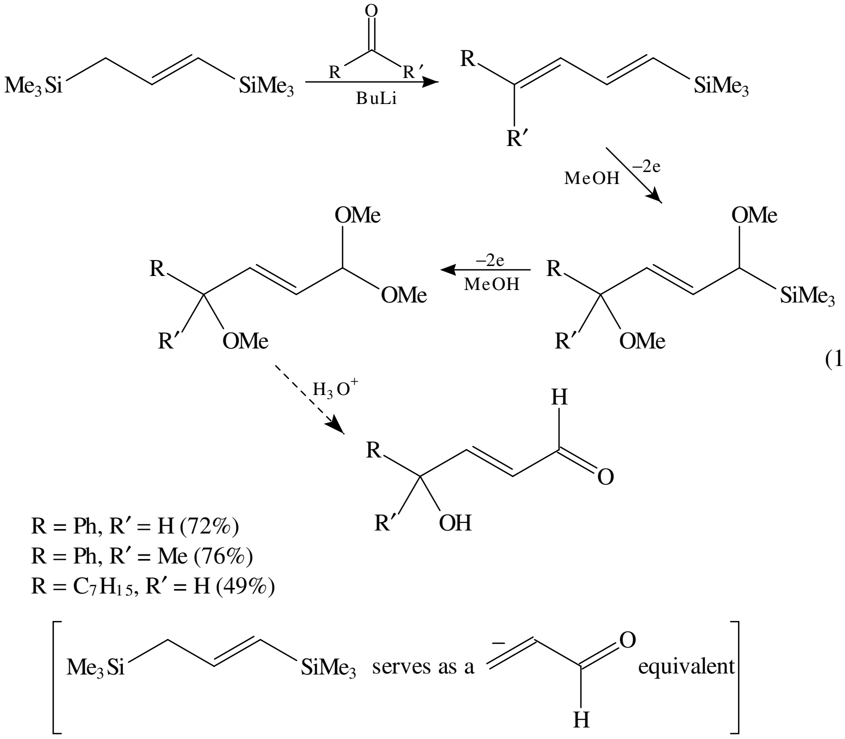

(15)

R = Ph, R′ = H (72%)
R = Ph, R′ = Me (76%)
R = C_7H_{15}, R′ = H (49%)

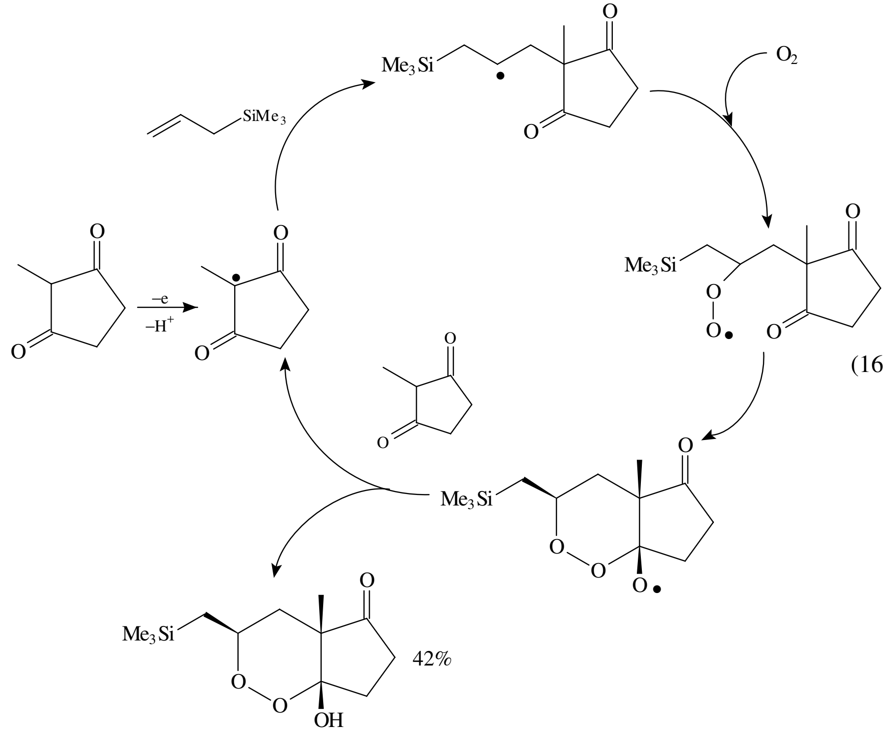

(16)

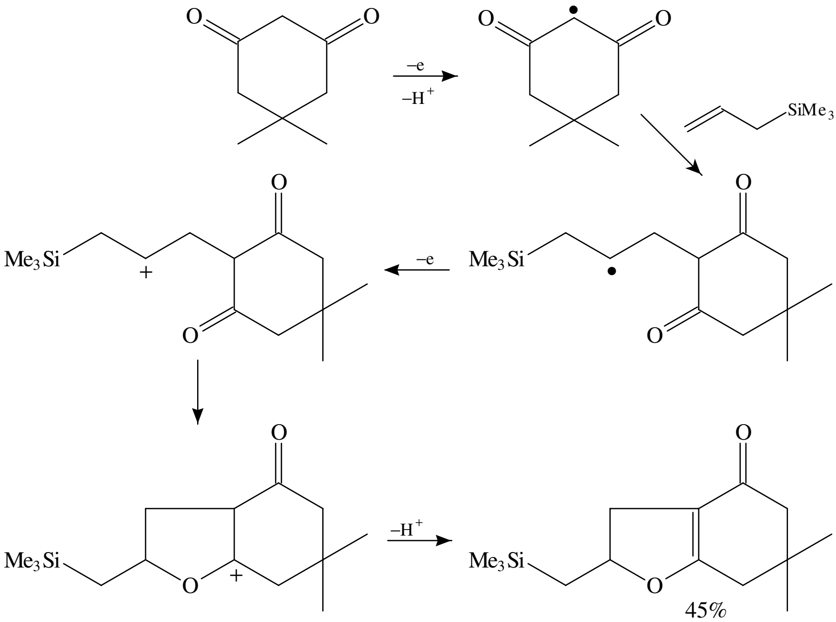

(17)

Intramolecular anodic olefin coupling reactions involving allyl- (equation 18) and vinylsilanes (equation 19) can lead to good yields of quaternary carbons with control of the relative stereochemistry[19,20]. This is the first example of an electrochemical reaction that makes use of a temporary silicon tether.

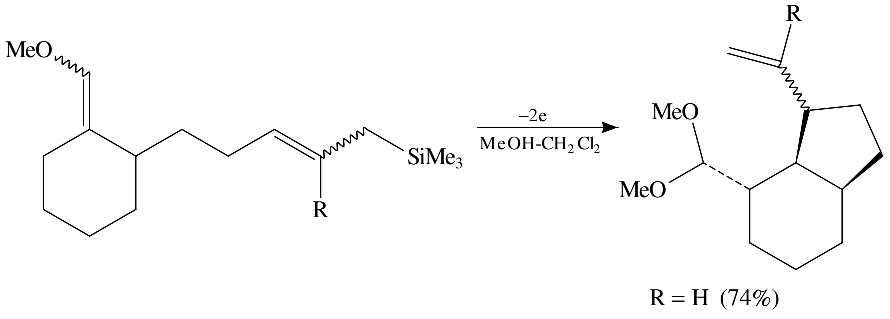

(18)

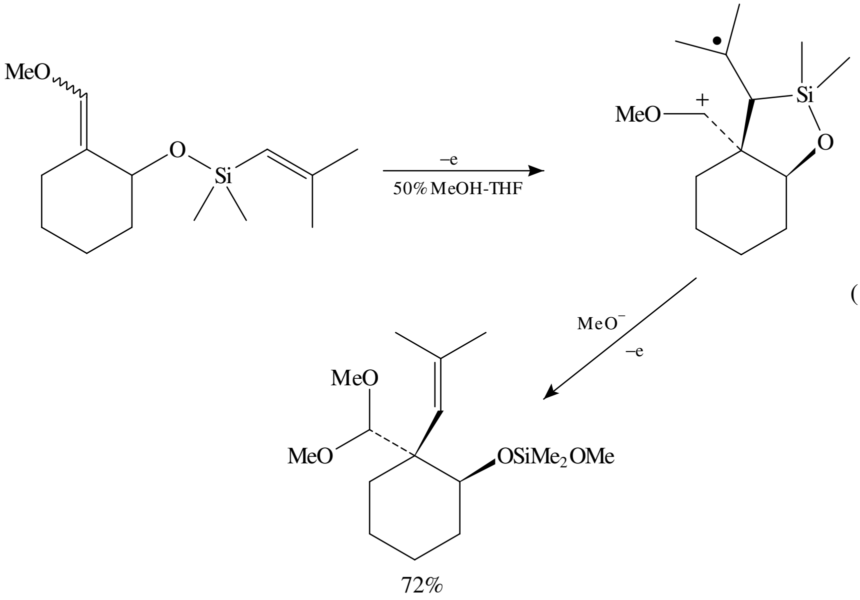

(19)

D. Organosilicon Compounds Bearing Heteroatoms

Anodic oxidation of organosilicon compounds bearing heteroatoms and its synthetic applications have been studied intensively. The oxidation potentials of organosilicon compounds bearing nitrogen, sulfur and phosphorus atoms at the α-, β- and γ-positions were shown in Table 5[12,21–23]. It should be noted that the silyl group α to the heteroatom decreases appreciably the oxidation potential.

Organosilicon compounds bearing heteroatoms generally undergo anodic substitutions with the elimination of a silyl group in a manner similar to that observed for benzylsilanes and allylsilanes as shown in equation 20.

TABLE 5. Oxidation potentials ($E_{p/2}$) of amines, sulfides and phosphines bearing a trimethylsilyl group[12,21–23]

Substrate	$E_{p/2}$ (V vs SCE)	Substrate	$E_{p/2}$ (V vs SCE)
$PhNHCH_2CMe_3$	0.60[21]	PhSMe	1.05[b,12]
$PhNHCH_2SiMe_3$	0.44[21]	$PhSCH_2SiMe_3$	1.15[21] (0.92)[b,12]
$PhNH(CH_2)_2SiMe_3$	0.60[21]	$PhS(CH_2)_2SiMe_3$	1.26[21]
$Ph(CH_2)_2\underset{\substack{\vert \\ Me}}{N}COOMe$	1.95[a,22]	$PhS(CH_2)_3SiMe_3$	1.28[21]
		$PhS(CH_2)_7Me$	1.35[a,23]
$Ph(CH_2)_2\underset{\substack{\vert \\ SiMe_3}}{N}COOMe$	1.45[a,22]	$PhCH(SiMe_3)(CH_2)_6Me$	1.25[a,23]
$Ph_2PCH_2SiMe_3$	0.63[21]	$MeSCH_2Ph$	1.25[b,12]
$Ph_2P(CH_2)_2SiMe_3$	0.88[21]	$MeSCH(SiMe_3)Ph$	0.99[b,12]

[a] E_p vs Ag/AgCl.

[b] E_p vs Ag/AgNO$_3$ (sat).

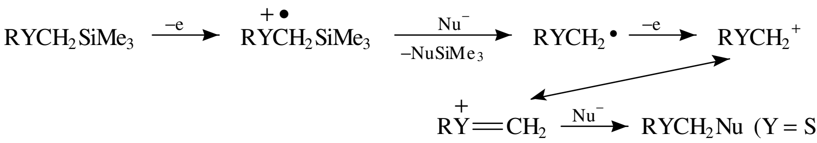

(20)

1. Organosilicon compounds bearing sulfur

Anodic oxidation of α-thiomethylsilanes in alcohols provides the α-alkoxylated sulfides selectively[23–25]. In this case, neither formation of sulfoxide nor C−S bond cleavage take place. Generally, anodic alkoxylation of sulfides is quite difficult except for sulfides carrying strong electron-withdrawing groups such as α-cyano[26] and α-(trifluoromethyl)[27,28]. Since the silyl group is a much better cationic leaving group than a proton, the alkoxylation proceeds selectively.

It is notable that allyloxylation can also be performed in relatively good yields (Table 6) although allyl alcohols are easily oxidized anodically[12]. The allyloxylated sulfides thus obtained are easily converted into the corresponding β, γ-unsaturated ketones by a [2,3] Wittig rearrangement using bases as shown in equation 21. Anodic desilylation/carboxylation of α-thiomethylsilanes also takes place similarly as shown in an example in Table 6.

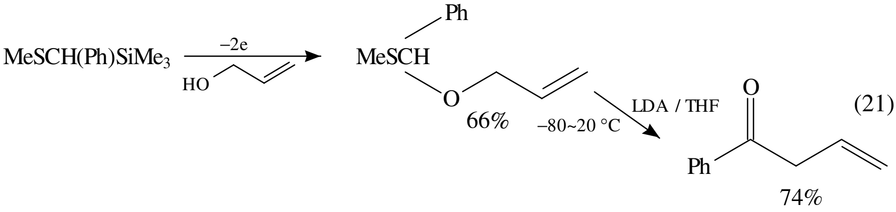

(21)

TABLE 6. Anodic oxidation of α-thiomethylsilanes in the presence of alcohols and carboxylic acid

$$R^1SCH(R^2)SiMe_3 \xrightarrow[Et_4NOTs/YOH\text{-}MeCN]{-2e} R^1SCH(R^2)OY$$

Substrate		YOH	Product yield (%)
R^1	R^2		
Ph	H	MeOH[a]	66
		EtOH	65
		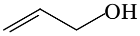	59
		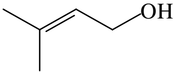	58
Me	Ph	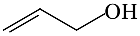	66
		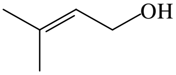	77
Ph	H	AcOH	66
Ph	H	$MeCH_2OH$	61

[a] Without MeCN.

On the other hand, when about 4 F mol^{-1} of electricity is passed in the anodic oxidation of α-thiomethylsilanes, both desilylation and desulfurization take place to give the corresponding acetals in good yields as follows. Since acetals are easily hydrolyzed to aldehydes, such an α-thiomethylsilane is a synthon of a formyl anion (equation 22).

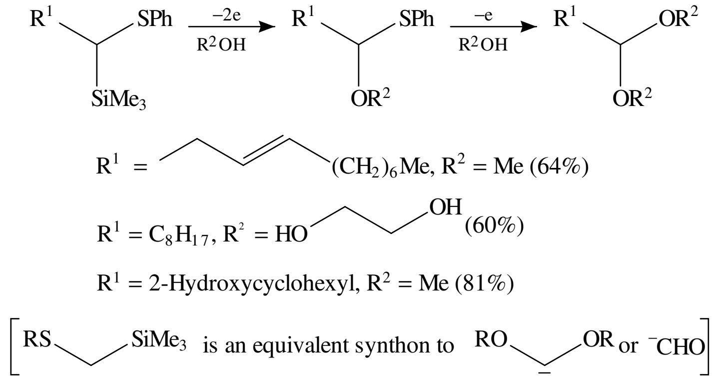

(22)

Furthermore, sulfides bearing two silyl groups can also be oxidized anodically in methanol to provide the corresponding esters as shown in equation 23[21,22]. Therefore, the α, α-disilylated sulfide provides a synthon of the anion of $^{-}C(CO)OMe$.

Indirect anodic oxidation of α-phenylthiomethylsilane in an alcohol using Ni^{2+}/Ni^{3+}-cyclam mediator also provides α-alkoxylated sulfides, although the turnover of the mediator is low (equation 24)[29].

It is interesting that anodic oxidation of 2-silyl-1,3-dithianes at a platinum anode provides the corresponding acylsilanes (equation 25)[30]. In this case, only a C−S bond cleavage takes place selectively and the C−Si bond is not cleaved. It is noted that this anodic transformation can be easily applied to the synthesis of α, β-unsaturated acylsilanes. The reactions are affected by the anode material used. A glassy carbon anode gives poor yields of acylsilanes.

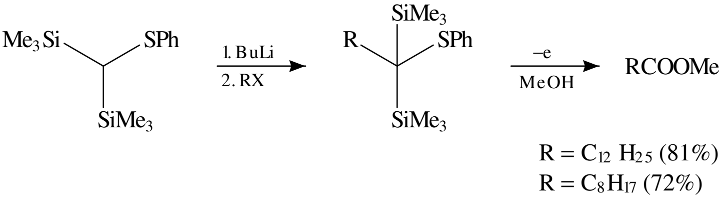

(23)

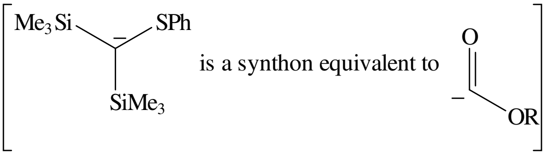

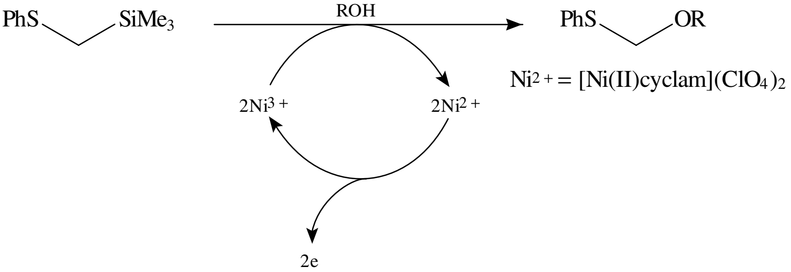

(24)

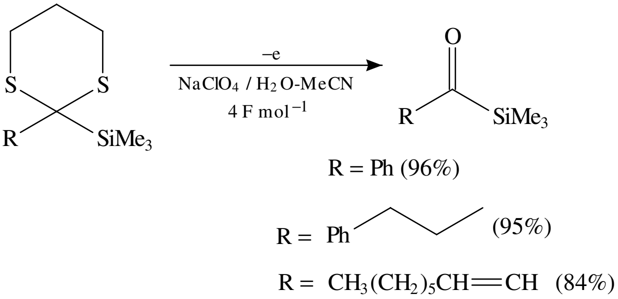

(25)

2. Organosilicon compounds bearing nitrogen

Introduction of a silyl group at the position α to the nitrogen decreases the oxidation potentials of organonitrogen compounds by at most 0.3 V (Table 7)[31]. β- and γ-silyl groups do not cause a significant decrease in the oxidation potential. The introduction of a silyl group directly on the amino nitrogen atom does not decrease the oxidation potentials of amines.

α-Silylcarbamates have much lower oxidation potentials of 0.5 V compared with the unsilylated carbamates (Table 5)[22].

TABLE 7. Oxidation potentials (E_p) of aminosilanes

Substrate	E_p (V vs SCE)	Reference
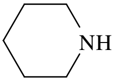	0.95	28
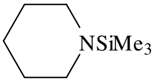	1.0	28
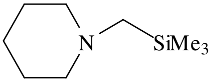	0.65	28
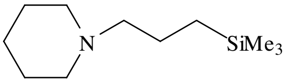	0.88	28
$(HOCH_2CH_2)_3N$	0.90	29
$(Me_3SiOCH_2CH_2)_3N$	0.92	29
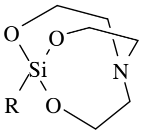 R = H	1.70	29
R = Me	1.43	29
$C_9H_{19}C(=NNHTs)H$	1.72[a]	30
$C_9H_{19}C(=NNHTs)SiMe_3$	1.43[a]	30

[a] E_d vs Ag/AgCl (decomposition potential determined by rotating-disk electrode voltammetry).

In sharp contrast to the cases of α-silylamines and α-silylcarbamates, silatranes have higher oxidation potentials than unsilylated triethanolamine and open-chain tris(trimethylsiloxyethyl)amine (Table 7)[32]. Transannular interaction between nitrogen and silicon atoms leads to the strong transmission of electron density from the nitrogen to silicon atom via donor–acceptor bonding. Considering the nitrogen as a site of anodic oxidation, such intramolecular charge transfer should result in higher oxidation potentials of the silatranes compared with those of unsilylated amines and open-chain silylated amines, where donor–acceptor interactions are excluded.

Anodic oxidation of *N*-benzyl-*N*-(α-silylmethyl)carbamate provides α-methoxylated product as a single regioisomer (equation 26), while the unsilylated parent carbamate gives a mixture of regioisomeric products (equation 27). Thus, the introduction of a silyl group can control completely the regiochemistry of the anodic methoxylation and can also activate the nitrogen atom toward anodic oxidation.

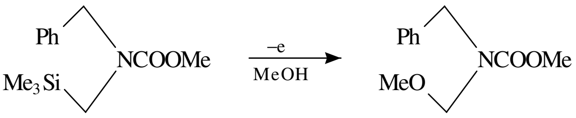

97%

(26)

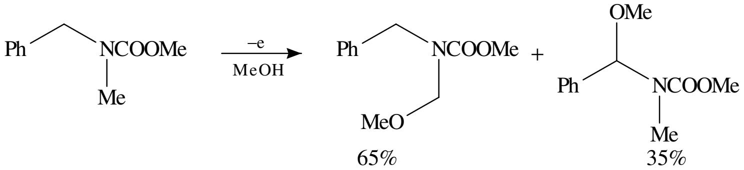

(27)

Anodic oxidation of 4-silylazetidin-2-ones in the presence of fluoride ions provides 4-fluoroazetidin-2-ones in high yields[33]. This fluorination is completely regioselective. Even in the case of the *N*-benzyl derivative, a fluorine atom is selectively introduced into the C-4 position of the β-lactam ring (equation 28). In contrast, unsilylated azetidin-2-ones give no fluorinated product.

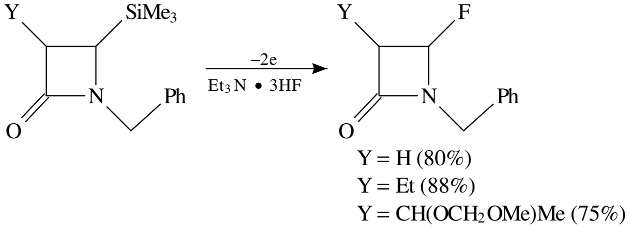

(28)

Electrochemical properties of tosylhydrazones of acylsilanes were also investigated. A decrease in the oxidation potential of tosylhydrazones caused by silylation is much smaller than that for carbonyl compounds (see Tables 7 and Section II.E., Table 9). Anodic oxidation of tosylhydrazones of acylsilanes provides the corresponding nitriles with consumption of a catalytic amount of electricity (equation 29)[34].

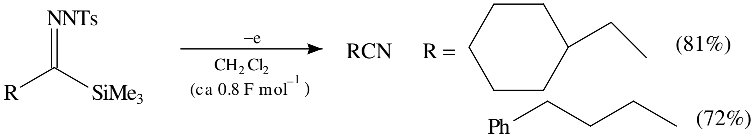

(29)

3. Organosilicon compounds bearing phosphorus

Trimethylsilyl phosphites can be anodically oxidized in the presence of arenes to form arylphosphonates (equation 30)[35].

$$(EtO)_2POSiMe_3 \xrightarrow{-e} (EtO)_2\overset{+\bullet}{P}OSiMe_3 \xrightarrow[\text{Ph—H}]{-e} (EtO)_2P(O)Ph \qquad (30)$$

4. Organosilicon compounds bearing oxygen

Although anodic oxidation of aliphatic ethers is generally difficult, the ethers bearing a silyl group at a position α to the oxygen atom can be oxidized rather easily. As shown in Table 8, α-silyl substitution causes significant decrease in the oxidation potential of ethers and alcohols[36,37]. The magnitude of the silicon effect is much greater than that for organo nitrogen and sulfur compounds. This is in accord with the better overlap of the nonbonding p orbital of oxygen with the C−Si σ orbital than that of the orbitals of nitrogen and sulfur.

TABLE 8. Oxidation potentials (E_p) of silylated ethers and related compounds

Substrate	E_p (V vs Ag/AgCl)	Substrate	E_p (V vs Ag/AgCl)
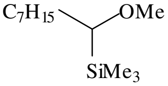	1.72	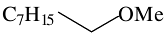	>2.5
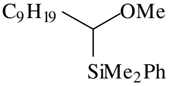	1.60	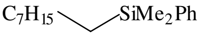	2.25
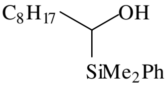	1.70	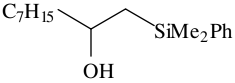	2.26

It is quite interesting that such a silicon effect depends strongly on the geometry of the molecule. Yoshida and coworkers found a linear correlation on plotting the oxidation potentials of α-silylated ethers, where the rotation around the C—O bond is restricted, against the HOMO energy–torsion angle (Si—C—O—C) curve obtained by MO calculation[36].

Anodic oxidation of α-silyl ethers in methanol provides acetals. Even a silylated allyl ether gives the corresponding acetals in good yield (equation 31)[2].

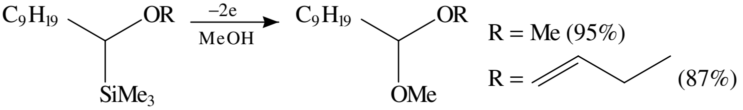

(31)

This electrochemical method can be widely applicable as shown in equation 32[25,38]. It is noted that anodic oxidation in dichloromethane containing water provides the aldehyde directly under neutral conditions. Thus, the methoxy(trimethylsilyl)methyl anion is an equivalent to the formyl anion[25,38].

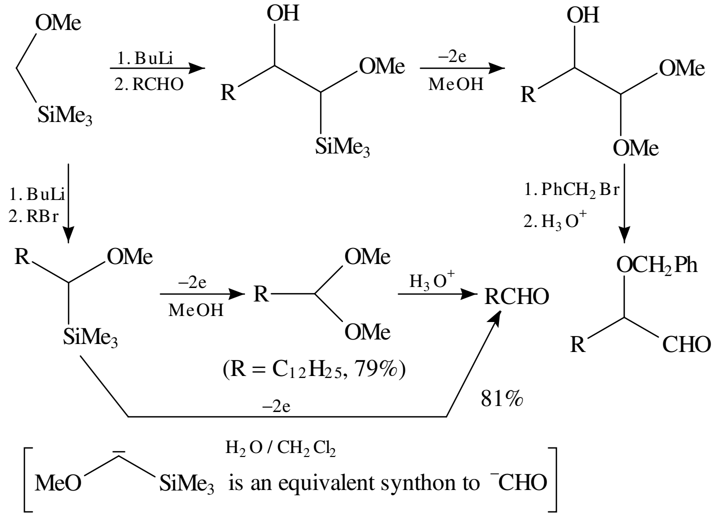

(32)

The anodic oxidation of ethers bearing two α-silyl groups is also useful. As shown in equation 33, the anion of methoxybis(trimethylsilyl)methane can be utilized as a synthon of the anion of the alkoxycarbonyl group.

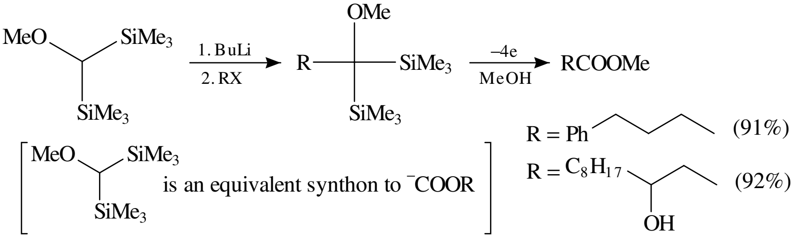

(33)

This methodology is also applicable to the synthesis of γ-lactones[25] and enantiomers or diastereomers of straight-chain 1,2-polyols[39].

Anodic oxidation of α-silyl ethers in the presence of nitrogen nucleophiles such as sulfonamides and carbamates provides N,O-acatals (equations 34 and 35)[2].

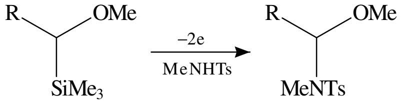

(34)

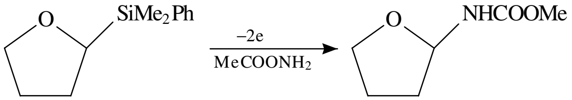

(35)

E. Acylsilanes

Anodic oxidation of aliphatic aldehydes and ketones is generally difficult because their oxidation potentials are very high (>2.5 V). However, silylation at the carbonyl carbon causes a marked decrease in the oxidation potential as shown in Table 9[33,40]. This silicon effect is much smaller in the case of aromatic carbonyl analogues[40]. The silicon effect is attributed to the rise of the HOMO level by the interaction between the C−Si σ orbital and the nonbonding p orbital of the carbonyl oxygen, which in turn favors the electron transfer.

Anodic oxidation of acylsilane in the presence of various nucleophiles provides the corresponding ester, acid and carbamate as shown in equation 36[41].

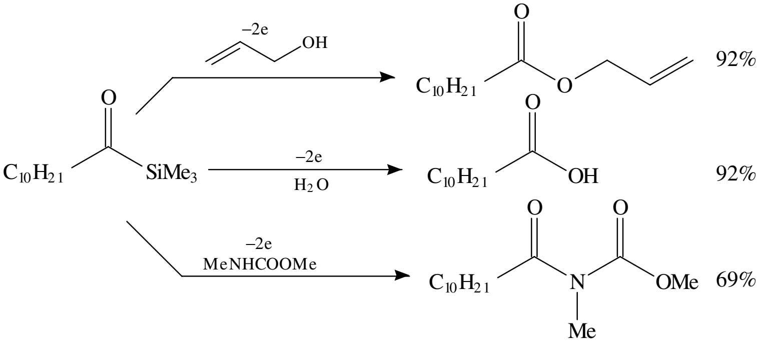

(36)

TABLE 9. Oxidation potentials (E_p) of acylsilanes and related compounds[30,37]

Substrate	E_p (V vs Ag/AgCl)	Substrate	E_p (V vs Ag/AgCl)
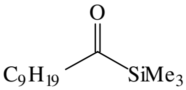 $C_9H_{19}COSiMe_3$	1.45	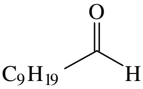 $C_9H_{19}CHO$	>2.5
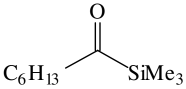 $C_6H_{13}COSiMe_3$	1.70	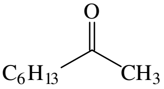 $C_6H_{13}COCH_3$	>2.5
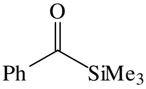 $PhCOSiMe_3$	1.88	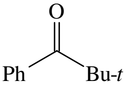 $PhCOBu\text{-}t$	1.96

F. Silyl Enol Ethers and Related Compounds

Since silyl enol ethers have a silyl group β to the π-system, anodic oxidation of silyl enol ethers takes place easily. In fact, anodic oxidation of silyl enol ethers proceeds smoothly to provide the homo-coupling products, 1,4-diketones (equations 37 and 38)[42]. This dimerization of the initially generated cation radical intermediate is more likely than the reaction of acyl cations formed by two electron oxidation of unreacted silyl enol ethers in these anodic reactions.

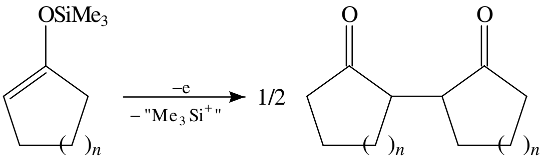

(37)

$n = 1(66\%)$
$n = 2\ (58\%)$

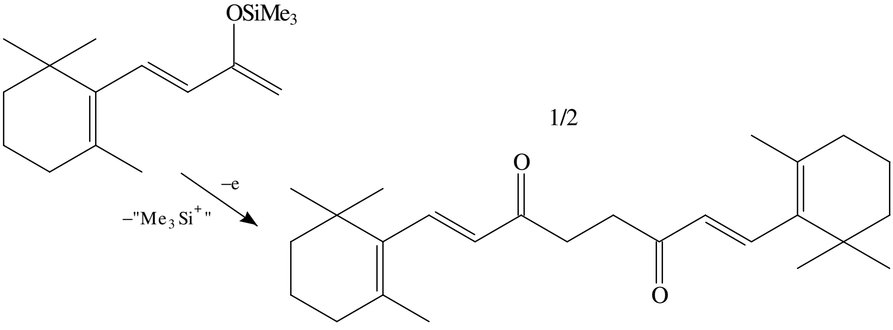

64% (38)

TABLE 10. Oxidation potentials (E_p) of trimethylsiloxyarenes

Substrate	E_p (V vs SCE)
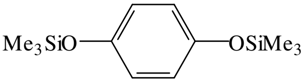	1.10
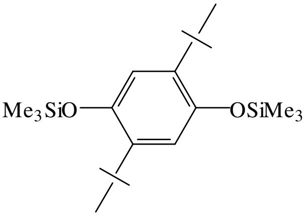	1.05
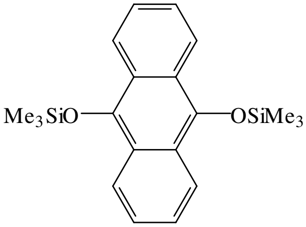	0.78
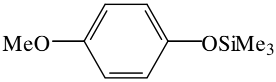	1.14

On the other hand, indirect anodic oxidation of cyclic silyl enol ethers in the presence of iodide ions gives α-iodocyclic ketones (equation 39)[43].

Anodic oxidation of hydroquinone disilyl ethers also takes place easily at around 1 V vs SCE, as shown in Table 10[44]. It was proposed that an initial one-electron oxidation generates a cation radical which decomposes by a Si—O bond cleavage to form quinones (equation 40)[44].

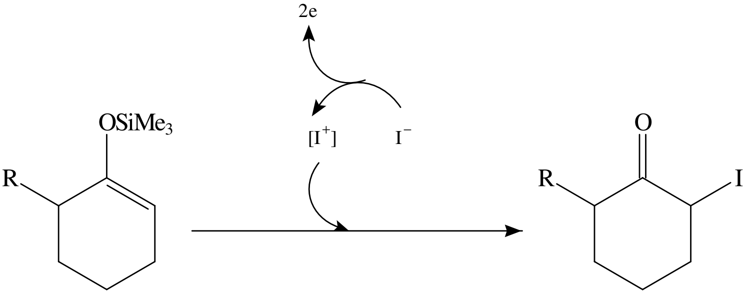

R = C_5H_{11} (97%)

(39)

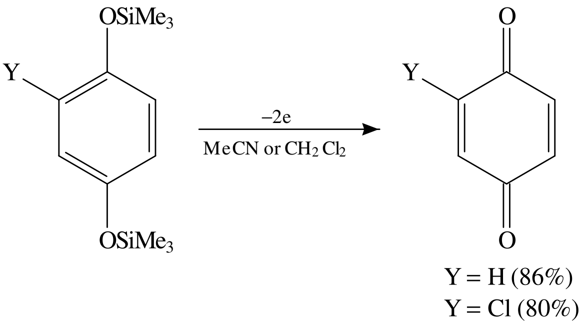

(40)

It is interesting that α-alkoxycarbonylcycloalkanones are formed from fused silyloxycarbonylcyclopropanes by anodic oxidation in methanol or ethanol in the presence of $Fe(NO_3)_3$ (equation 41)[45].

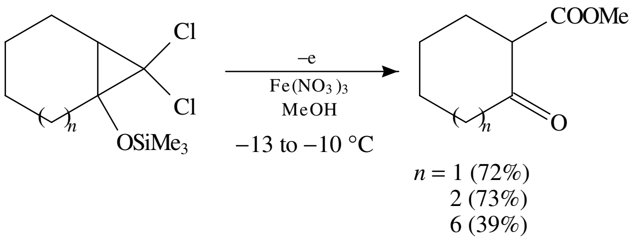

(41)

G. Carboxylic Acid Bearing a β-Trimethylsilyl Group

Anodic oxidation of carboxylic acids bearing a trimethylsilyl group on the β-position gives exclusively terminal olefins in rather good yields. The reaction seems to proceed via a carbocation intermediate formed by the oxidative elimination of CO_2 (equation 42)[46].

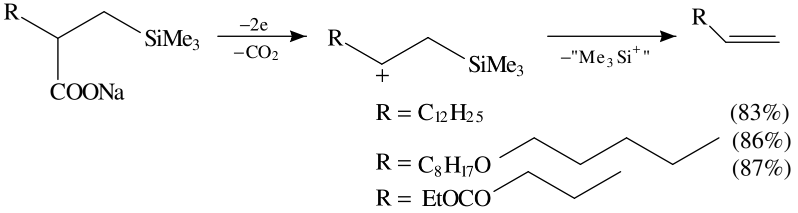

(42)

This method is applicable to the efficient synthesis of 2,5-norbornadiene, which can be obtained in low yield by anodic decarboxylation of 5-norbornene-2,3-dicarboxylic acid (equation 43)[47].

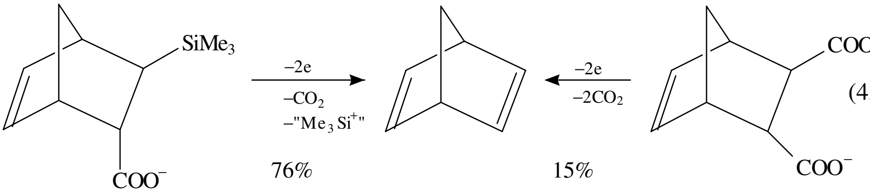

(43)

H. Organosilicon Compounds Having Si−Si Bonds and Related Compounds

The reactivity of the metal−metal bond of group-14-dimetals, such as the Si−Si bond, has attracted much interest in comparison with that of a carbon−carbon double bond. Table 11 shows oxidation potentials of group-14-dimetals[48].

The oxidation potential decreases in the order: Si−Si ∼ Si−Ge>Ge−Ge>Si−Sn> Ge−Sn >Sn−Sn in accord with the ionization potential (I_p) of the corresponding dimetal. Anodic generation of silicenium ions from disilanes was also reported. The reduction potentials of silicenium ions were determined by cyclic voltammetry of neutral precursor disilanes[49]. The reduction potential shifted to the negative direction as the center element changed from C to Ge as shown in equation 44.

$$\mathrm{Ph_3E{-}EMe_3} \xrightarrow[\mathrm{Bu_4NClO_4\,/\,MeCN}]{-2e} [\mathrm{Ph_3E^+}] + [\mathrm{Me_3E^+}] \tag{44}$$

$$\begin{array}{ll} \mathrm{E = Si}:\ E_{p/2}^{ox}\ 1.29\ \mathrm{V} & E_{p/2}^{red}\ [\mathrm{Ph_3Si^+}] = -0.3\ \mathrm{V\ vs\ Fc/Fc^+} \\ \mathrm{E = Ge}:\ E_{p/2}^{ox}\ 1.16\ \mathrm{V} & E_{p/2}^{red}\ [\mathrm{Ph_3Ge^+}] = -0.69\ \mathrm{V\ vs\ Fc/Fc^+} \\ & E_{p/2}^{red}\ [\mathrm{Ph_3C^+}] = -0.04\ \mathrm{V\ vs\ Fc/Fc^+} \end{array}$$

Table 12 shows oxidation potentials ($E_{1/2}$) of a series of permethylpolysilanes determined by a.c. polarography or cyclic voltammetry[50,51]. The $E_{1/2}$ values decrease as the chain length increases. This reflects the HOMO energy levels of these permethylpolysilanes[52].

Cyclic peralkylsilanes exhibit unique behavior which distinguishes these compounds from saturated catenates of carbon. In some ways, the properties of the cyclosilanes resemble these of poly-unsaturated or aromatic hydrocarbons. As shown in Table 12, five-membered permethyl cyclic silane shows a higher oxidation potential compared with the linear analog[51,53].

TABLE 11. Oxidation potentials of group-14-dimetals

Substrate	E_p (V vs Ag/AgCl)
$Me_3SiSiMe_3$	1.76
$Me_3SiGeMe_3$	1.76
$Me_3GeGeMe_3$	1.70
$Me_3SiSnMe_3$	1.60
$Me_3GeSnMe_3$	1.44
$Me_3SnSnMe_3$	1.28

TABLE 12. Lowest oxidation potentials ($E_{1/2}$) of permethylpolysilanes

Substrate	$E_{1/2}$ (V vs SCE)	Reference
$Me(SiMe_2)_2Me$	1.88[a]	50
$Me(SiMe_2)_3Me$	1.52[a]	50
$Me(SiMe_2)_4Me$	1.33[a]	50
$Me(SiMe_2)_5Me$	1.18[a]	50
$Me(SiMe_2)_6Me$	1.08[a]	50
$(Me_2Si)_5$	1.35[b]	51
$(Ph_2Si)_5$	1.50[b]	51

[a] Determined by a.c. polarography.

[b] Determined by cyclic voltammetry.

Becker and coworkers have studied intensively anodic behavior of cyclic polysilanes[53–55]. Oxidation potentials of cyclic polysilanes are affected by the counter anions of the supporting electrolytes. For example, in the presence of ClO_4^-, the first oxidation potential (E_p) of $[t\text{-Bu(Me)Si}]_4$ is significantly lower compared with other electrolytes such as BF_4^- and HSO_4^- (1.05 V, 1.15 V, 1.25 V vs Ag/AgCl, respectively)[54].

On controlled potential oxidation, cyclic peralkylsilanes undergo ring opening followed by further Si−Si bond cleavage and reaction with BF_4^- to form α, ω-difluorosilanes as the major products (equation 45)[53].

$$(Pr_2Si)_5 \xrightarrow[Et_4NBF_4/CH_2Cl_2MeCN]{-e} F(Pr_2Si)_nF \qquad (45)$$

+1.25 V vs Ag/AgCl
pulse electrolysis

$n =$ 2 (54%)
3 (30%)
4 (10%)

On the other hand, when this anodic oxidation was carried out in the presence of ClO_4^- or AcO^- salts instead of BF_4^-, it led to both oxygen insertion and ring-opening processes, to form mainly cyclic and linear siloxanes (equation 46). The ratio of these products greatly depends both on the amount of electricity passed and on the presence of oxygen[55].

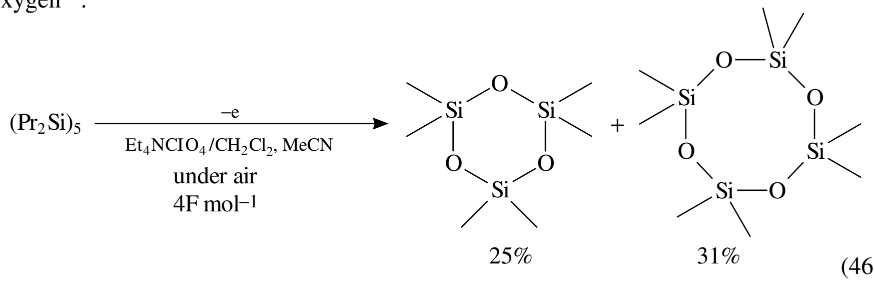

(46)

$+(n\text{-Pr})_2[(n\text{-Pr})_2Si]_4O_3$ 18%
+ other types of cyclic siloxanes

The mechanism given in equation 47 has been proposed for this reaction. The initially formed cation radical reacts with molecular oxygen to generate an intermediate, which may couple with a neutral cyclic silane to form species **A**. The intermediate **A** decomposes to the final product **B** and its cation radical $\mathbf{B}^{+\bullet}$, which could also be generated by direct anodic oxidation of the siloxane **B**. A further oxygen insertion step could take place via intermediate $\mathbf{C}^{+\bullet}$[54].

Disilenes undergo irreversible anodic oxidation at much less positive potentials, as shown in Table 13[56]. The oxidation potentials for these compounds are similar, indicating that the HOMO of each species lies at approximately the same energy level.

I. Hydrosilanes

The electrochemical properties of hydrosilanes were also examined and the hydrosilanes were found to be electrode active. Dimethylphenylsilane and methyldiphenylsilane show irreversible peaks at 2.2 and 2.1 V vs SCE, respectively, in their cyclic voltammograms measured by a glassy carbon in $LiClO_4$/MeCN[57].

TABLE 13. Oxidation potentials (E_p) of disilenes

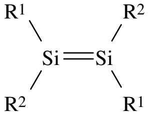

Substrate		E_p (V)[a]
R^1	R^2	
Mes[b]	Mes	+0.38
Xyl[c]	Xyl	+0.47
Tbp[d]	Tbp	+0.48
Mes	*t*-Bu	+0.54
Mes	Ad[e]	+0.36

[a] vs Fc/Fc$^+$.

[b] Mes = 2,4,6-trimethylphenyl.

[c] Xyl = 2,4-dimethylphenyl.

[d] Tbp = 4-*tert*-butyl-2,6-dimethylphenyl.

[e] Ad = 1-adamantyl.

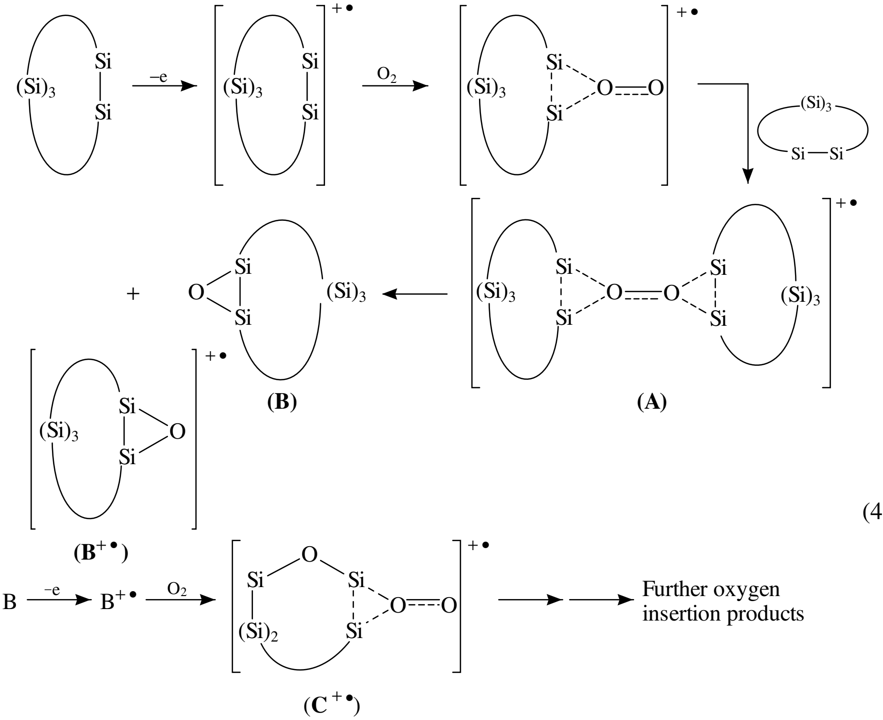

(47)

Anodic oxidation of dimethylphenylsilane in the presence of $CuCl_2$ or CuCl using platinum electrodes provides chlorodimethylphenylsilane in high yield (>90%), while similar electrolysis in the presence of BF_4^- affords fluorodimethylphenylsilane (equation 48)[57].

TABLE 14. Electrochemical polymerization of hydrosilanes

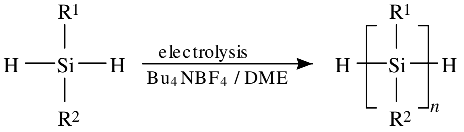

$$\mathrm{H{-}Si(R^1)(R^2){-}H} \xrightarrow[\mathrm{Bu_4NBF_4\,/\,DME}]{\text{electrolysis}} \mathrm{H{-}[Si(R^1)(R^2)]_n{-}H}$$

Monomer		Electricity ($\mathrm{F\,mol^{-1}}$)	Yield (%)	mol wt[a]	
R^1	R^2			M_w	M_w/M_n
Ph	Me	2.0	60	477	1.05
Ph	H	3.0	32	640	1.42
Hex	H	3.0	70	1240	1.09

[a] GPC vs polystyrene.

When a copper anode is used instead of platinum, the resulting chlorosilane is subsequently reduced to a Si−Si coupling product in a one-pot reaction (equation 49)[57]. Interestingly, when a mixture of hydrosilane and chlorosilane is electrolyzed using a copper anode and a platinum cathode, a Si−Si coupling product is obtained in 64% yield on the basis of the sum of both reagents used. Thus, the paired electrolysis of hydrosilane on the anode and chlorosilane on the cathode proceeds to give disilane (equation 50)[57].

$$\mathrm{Me_2PhSiH} \xrightarrow[\mathrm{CuCl\ or\ CuCl_2}]{-2e,\ -\mathrm{H^+}} \underset{>90\%}{\mathrm{Me_2PhSiCl}} \xrightarrow[\substack{-\mathrm{Cl^-} \\ \text{(halogen exchange)}}]{\mathrm{BF_4}^-} \underset{90\%}{\mathrm{Me_2PhSiF}} \qquad (48)$$

$$\mathrm{Me_2PhSiH} \xrightarrow[\mathrm{Cl^-}]{-2e,\ -\mathrm{H^+}} [\mathrm{Me_2PhSiCl}] \xrightarrow[\text{Cu anode}]{e} 1/2\,\mathrm{Me_2PhSiSiPhMe_2} \qquad (49)$$

$$\begin{aligned} &\text{at anode} && \mathrm{MePh_2SiH + Cl^- - 2e \longrightarrow MePh_2SiCl + H^+} \\ & && \mathrm{MePh_2SiCl + e \longrightarrow 1/2\,(MePh_2Si)_2} \\ &\text{at cathode} && \mathrm{H^+ + e \longrightarrow 1/2\,H_2} \end{aligned} \qquad (50)$$

Di- and trihydrosilanes are also active on the anode[58,59]. For example, methylphenylsilane, phenylsilane and hexylsilane have their decomposition oxidation potentials at +0.6−+0.7 V vs Ag/AgCl in TBAF/MeCN[59]. Constant current anodic oxidation of these hydrosilanes at platinum electrodes in an undivided cell provide linear polysilanes as shown in Table 14[59]. In the polymerization, silyl radical cations generated by the one-electron oxidation on the anode might attack another monomer to form a Si−Si bond needed for the propagation while reductive generation of hydrogen gas is occurring on the cathode. Although the molecular weight of the polymer formed is limited, this method does not require any sacrificial electrodes, which are necessary for electroreductive polymerization of chlorosilanes (see Section III.D.1).

J. Heterocycles Containing a Si Atom

Anodic oxidation of phenothiasilane and phenazasiline provides the corresponding neutral and oxidized polymers, respectively (equation 51)[60].

N-Trimethylsilylpyrrole is anodically oxidized at a higher oxidation potential (E_p: +0.55 V vs Fc/Fc$^+$) than simple unsilylated pyrrole (E_p: +0.47 V)[61]. This is due to the steric effect of the electrode. *N*-Trimethylsilylpyrrole is electrochemically polymerized to an electroconductive polymer (equation 52). The polymer has good film producibility and conductivity as high as that for polypyrrole[61].

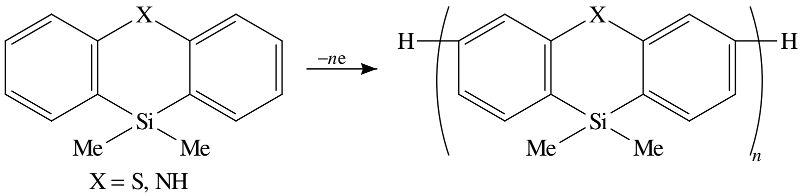

(51)

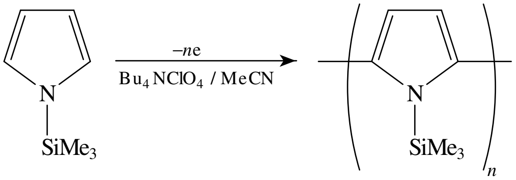

(52)

III. CATHODIC REDUCTION OF ORGANOSILICON COMPOUNDS

A. Arylsilanes

Owing to a dπ–pπ effect due to unoccupied silicon 3d orbitals, arylsilanes are reduced at less negative potentials compared with the corresponding unsilylated aromatic compounds. As shown in Table 15, a trimethylsilyl group decreases the reduction potential $E_{1/2}$ of naphthalenes while a *t*-butyl group increases $E_{1/2}$. An additional silyl substitution causes further anodic shift of the cathodic potential[62–64]. Although monosilylation of naphthalene causes a decrease in $E_{1/2}$, the addition of a second and third silicon atom to the chain (Me_5Si_2, Me_7Si_3) does not change $E_{1/2}$ any more[65].

The reduction potentials of *o*-, *m*- and *p*-nitrophenylsilanes are also less negative by 20–40 mV compared to that of unsilylated nitrobenzene[66].

The polarographic study of 1,4-bis(trimethylsilyl)benzene and its polyphenyl derivatives suggests that the first one-electron reduction wave is reversible[67].

TABLE 15. Reduction potential of silyl-substituted aromatics[62,63]

Substrate	Substituents	$E_{1/2}$ (V vs Ag/AgCl)[a]
Naphthalene	none	−2.58
	1-$SiMe_3$	−2.52
	2-$SiMe_3$	−2.57
	1,4-$(SiMe_3)_2$	−2.38
	2,6-$(SiMe_3)_2$	−2.44
	1-*t*-Bu	−2.64
	1,4-(*t*-Bu)$_2$	−2.67
Biphenyl	none	−2.05[b]
	4-$SiMe_3$	−2.03[b]
	4,4′-$(SiMe_3)_2$	−1.94[b]
	4-*t*-Bu	−2.10[b]

[a] Determined by polarography in Bu_4NI/DMF.

[b] vs $Ag/AgNO_3$ (sat. in DMF)

TABLE 16. Reduction potentials of cyclooctatetraene derivatives[a]

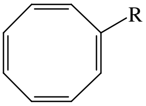

Substrate R	$E^1{}_{1/2}$ (V vs SCE)	$E^2{}_{1/2}$ (V vs SCE)
H	−1.61	−1.92
$SiMe_3$	−1.64	−1.82
t-Bu	−1.88	−2.00

[a] Determined by linear sweep voltammetry in HMPA.

Cathodic reduction of arylsilanes in methylamine using LiCl as a supporting electrolyte in an undivided cell gives 1,4-cyclohexadiene derivatives. The reaction seems to proceed in a manner similar to the Birch-type reduction. The cathodic reduction in a divided cell provides desilylation products (equation 53)[68].

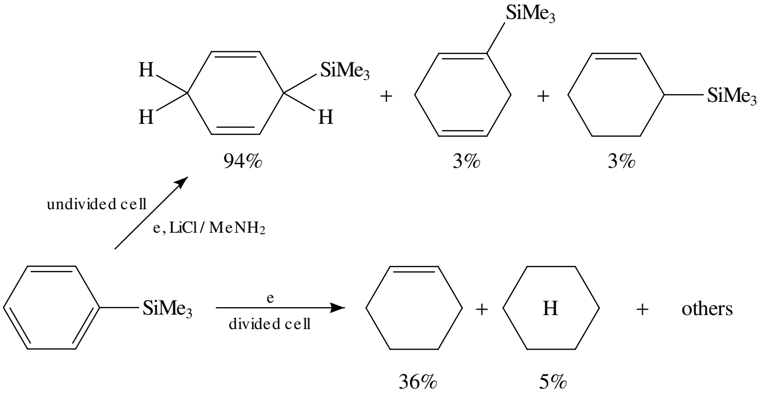

(53)

Linear sweep voltammetry of silylated cyclooctatetraene shows that silylation decreases the first reduction potential but increases the second one (Table 16). The effect on the second reduction potential seems to be due to the stabilization of the dianion by the dπ−pπ electron-withdrawing effect of the silyl group[69].

B. Acylsilanes

Cathodic reduction potentials of acylsilanes have been determined by polarography in Et_4NI/DMF[70] or by cyclic voltammetry in Et_4NClO_4/MeCN using a glassy carbon cathode[40] as shown in Table 17.

Controlled potential cathodic reduction of benzoylsilane provides benzyl as a main product[40]. Two possible mechanisms are illustrated in equation 54.

C. Polysilanes

One characteristic of Si−Si bonds is the low energy level of the LUMO. The LUMO levels also decrease with increasing chain length of polysilanes.

TABLE 17. Cathodic reduction potentials of acylsilanes and related compounds[40,70]

Substrate	$E_{1/2}$ (V vs Hg pool)	
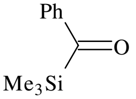	−1.30	(−1.98)[a]
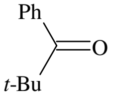	−1.58	
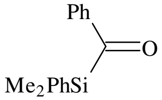	—	(−1.80)[a]
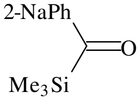	−1.17	
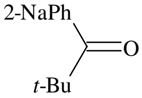	−1.32	

[a] E_p (V vs Ag/AgCl) determined by cyclic voltammetry[40].

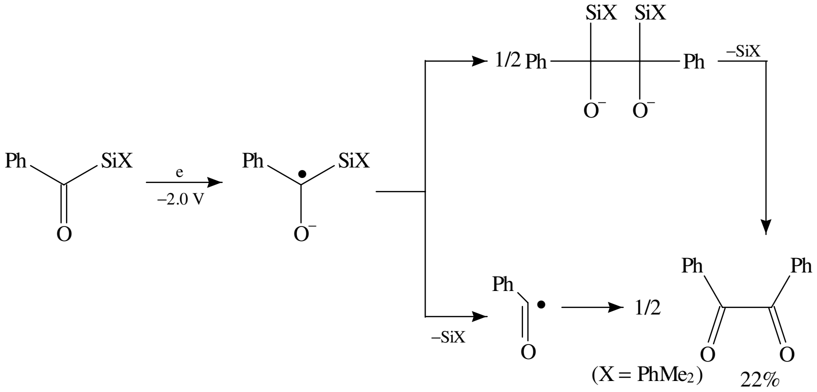

(54)

Reduction of cyclic polysilanes is possible. Permethylcyclopolysilanes can be reduced chemically and electrochemically at low temperatures to form anion radicals. Interestingly, permethylcyclopolysilanes, $(Me_2Si)_n$, where $n = 5, 6$ and 7, give only $(Me_2Si)_5{}^-$ upon reduction with alkali metal while $(Me_2Si)_5$ and $(Me_2Si)_6$ give the corresponding anion radicals, respectively, upon electrochemical reduction[71]. Electrochemical reduction of $(Me_2Si)_6$ in HMPA provides $Me_{11}Si_6{}^-$, which is a stable and useful intermediate that can be derivatized with a variety of electrophiles[72].

TABLE 18. Reduction potentials (E_p) of disilenes

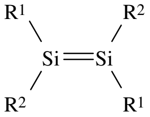

Substrate		E_p (V)[a]
R^1	R^2	
Mes[b]	Mes	−2.12
Xyl[c]	Xyl	−2.03
Tbp[d]	Tbp	−2.20
Mes	*t*-Bu	−2.66
Mes	Ad[e]	−2.64

[a] vs Fc/Fc$^+$.

[b] Mes = 2,4,6-trimethylphenyl.

[c] Xyl = 2,4-dimethylphenyl.

[d] Tbp = 4-*tert*-butyl-2,6-dimethylphenyl.

[e] Ad = 1-adamantyl.

Cathodic reduction of 1,1,1-trimethyl-2,2,2-triphenyldisilane under constant current in MeCN provides triphenylsilane quantitatively (equation 55). The reaction involves an electrochemically initiated chain reaction[73]. The source of oxygen in $(Me_3Si)_2O$ may be the residual water in acetonitrile.

$$Ph_3Si{-}SiMe_3 \xrightarrow[\text{MeCN}]{\text{e}} \underset{\text{quant.}}{Ph_3SiH} + (Me_3Si)_2O \tag{55}$$

Cathodic reduction potentials of disilenes were determined by cyclic voltammetry[56]. As shown in Table 18, tetraaryldisilenes are reduced at less negative potentials than dialkyldiaryl derivatives. This is in sharp contrast to the fact that anodic oxidation potentials are similar for both types of these disilanes (see Table 13).

D. Halosilanes

1. Cathodic reduction of halosilanes

Dessy and coworkers first studied cathodic behavior of halosilanes using polarography, constant potential electrolysis and triangular voltammetry[74]. They confirmed the formation of Ph_3SiH in the reduction of Ph_3SiCl in DME using a mercury cathode at −3.1 V vs $AgClO_4$/Ag (−2.5 V vs SCE). The cathodic reduction of Ph_2SiCl_2 at −1.3 V vs SCE under the same conditions gave Ph_2SiH_2.

On the other hand, Hengge and colleagues first showed the possibility of the Si−Si coupling through cathodic reduction of various mono- and disilanes in DME using a platinum cathode and a mercury or lead anode without control of the applied potential[75,76]. In this case, the mercury and lead anodes work as a *'sacrificial anode'*.

Allred and coworkers investigated cathodic reduction of Me_3SiCl at a platinum cathode in MeCN[77]. They pointed out that the Si−Si bond formation was affected by the supporting electrolytes. Namely, Bu_4NCl was effective while Bu_4NClO_4 gave only siloxane.

Corriu and colleagues also re-examined the cathodic reduction of halosilanes in anhydrous DME. They found that Ph_3SiCl and Me_3SiCl gave the corresponding disilanes in reasonable yields (equation 56). In this case, a large amount of siloxanes was also formed[78].

$$R_3SiCl \xrightarrow[\substack{-2.6\text{ V vs SCE}\\ \text{Hg cathode}}]{e} 1/2\ R_3Si{-}SiR_3 \qquad \begin{array}{l} \\ R = Ph\ (42\%) \\ R = Me\ (28\%) \end{array} \tag{56}$$

Generally, it is quite difficult to determine the precise reduction potentials of halosilanes because halosilanes such as Me_3SiCl are readily hydrolyzed during the measurement. Corriu and coworkers determined the precise reduction potential of Ph_3SiCl in anhydrous 0.1 M TBAP/DME using polarography[79]. Thus, Ph_3SiCl showed a one-electron single irreversible cathodic peak ($E_{1/2}$: -2.4 V vs SCE), which was not affected by addition of phenol[80]. Therefore, generation of Ph_3Si radical species was suggested in this case.

Umezawa, Fuchigami, Nonaka and coworkers found that organodichloromonosilanes such as Ph_2SiCl_2, $PhMeSiCl_2$ and Me_2SiCl_2 could be electroreductively polymerized by using a platinum cathode in Bu_4NBF_4/DME to give the corresponding oxygen-free organopolysilanes in 43, 40 and 26% yields, respectively (equation 57)[81].

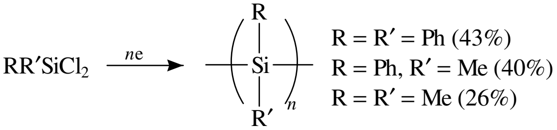

$$RR'SiCl_2 \xrightarrow{ne} \left(-\overset{R}{\underset{R'}{Si}}- \right)_n \qquad \begin{array}{l} R = R' = Ph\ (43\%) \\ R = Ph,\ R' = Me\ (40\%) \\ R = R' = Me\ (26\%) \end{array} \tag{57}$$

They also found that the yield of oxygen-free polysilane increased markedly by electrolysis of a 1 : 1 mixture of Me_2SiCl_2 and Ph_3SiCl[82]. Because Ph_3SiCl has a less negative reduction potential than that of Me_2SiCl_2[81], the bulkier Ph_3SiCl is reduced to the corresponding silyl anion which nucleophilically attacks Me_2SiCl_2 (equation 58, route a). This is desirable and the resulting [Ph_3Si $(Me_2Si)_nCl$] is more easily reduced than Me_2SiCl_2. This may improve the yield of oxygen-free polysilanes if the polymerization is then initiated by the reduction of Ph_3SiCl at a less negative potential than the reduction potential of Me_2SiCl_2 itself.

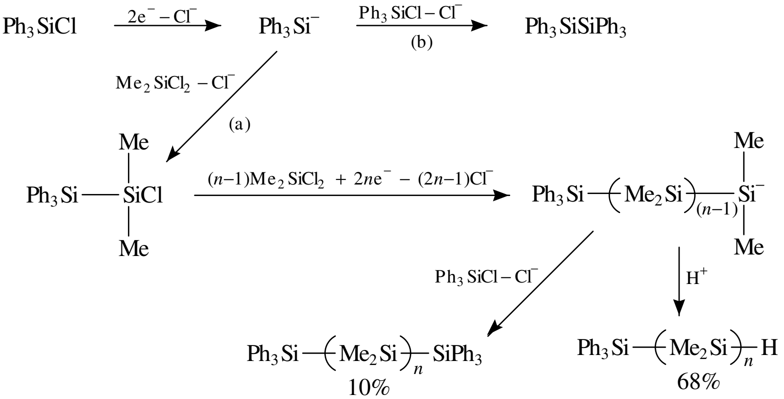

(58)

Recently, three research groups found almost independently that reactive metal anodes such as Al, Hg, Cu, Ag and Mg electrodes were highly effective for Si−Si bond formation from halosilanes even in an undivided cell.

Umezawa, Nonaka and coworkers demonstrated efficient electroreductive polymerization of Me_2SiCl_2 by using polarity-alternated electrolysis with sacrificial aluminum

TABLE 19. Cathodic Si−Si coupling of chlorosilanes

Chlorosilanes		Ratio B/A	Cathode	Anode	Electrolyte[a]	Product (Yield %)	Reference
A	B						
Me_3SiCl			Mg	Mg	A	$Me_3SiSiMe_3$ (82)	87
$Me_2PhSiCl$			Mg	Mg	A	$Me_2PhSiSiPhMe_2$ (92)	87
$Me_2PhSiCl$			Pt	Hg	B	$Me_2PhSiSiPhMe_2$ (84)	85
$Me_2PhSiCl$			Mg	Mg	B	$Me_2PhSiSiPhMe_2$ (50)	88
$Me_2PhSiCl$			Mg	Mg	C	$Me_2PhSiSiPhMe_2$ (75)	88
$MePh_2SiCl$			Mg	Mg	A	$MePh_2SiSiPh_2Me$ (77)	87
$MePh_2SiCl$			Cu	Cu	B	$MePh_2SiSiPh_2Me$ (83)	86
$MePh_2SiCl$			Pt	Hg	B	$MePh_2SiSiPh_2Me$ (89)	85
$MePh_2SiCl$			Pt	Al	B	$MePh_2SiSiPh_2Me$ (40)	85
Ph_3SiCl			Mg	Mg	A	$Ph_3SiSiPh_3$ (85)	87
$MePh_2SiCl$	Me_3SiCl	2.2	Pt	Hg	B	$MePh_2SiSiMe_3$ (94)	85
$MePh_2SiCl$	Me_3SiCl	2.6	Cu	Cu	B	$MePh_2SiSiMe_3$ (83)	86
$MePhSiCl_2$	Me_3SiCl	10.3	Cu	Cu	B	$Me_3Si\text{-}SiPMe\text{-}SiMe_3$ (61)	86
						$Me_3Si(SiPhMe)_2SiMe_3$ (23)	86
$MePhSiCl_2$	$Me_3Si\text{-}SiMe_2Cl$	4	Cu	Cu	B	$Me_3Si{-}SiMe_2{-}SiMePh{-}Me_2Si{-}SiMe_3$ (79)	86

[a] A=$LiClO_4$/THF, B=Bu_4NClO_4/DME, C=Bu_4NClO_4/THF.

electrodes (equation 59)[83].

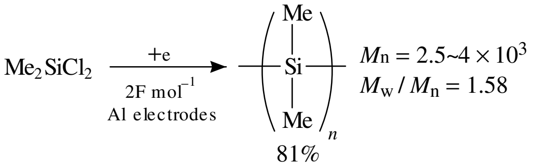

(59)

Bordeau and coworkers also reported that cathodic reduction of Me_2SiCl_2 without solvent using a sacrificial aluminum anode and a stainless steel cathode in an undivided cell produces polydimethylsilane with a very high current efficiency[84].

Kunai, Ishikawa and coworkers found that cathodic Si−Si coupling took place efficiently by using a mercury or silver anode and a platinum cathode in DME[85]. They also showed that disilanes, trisilanes, tetrasilanes and pentasilanes were readily obtained in high yields by use of copper nets as the cathode and anode[86].

On the other hand, Shono, Kashimura and coworkers found that alternating the polarity of Mg electrodes in $LiClO_4$/THF is quite effective for the formation of Si−Si bonds (Table 19)[87,88]. This method was successfully applied to the preparation of polysilanes. Sonication resulted in a marked increase in the yields of polysilanes as shown in Table 20[87,88]. Under higher concentration of dichlorosilane, polysilane of higher molecular weight was obtained.

The electroreduction of dichlorosilane also gave a polysilane in low yield, although its molecular weight is much higher than that of the polymer prepared by the reduction with Na (equation 60)[87]. Under similar conditions, ladder polysilanes were also formed (equation 61)[88].

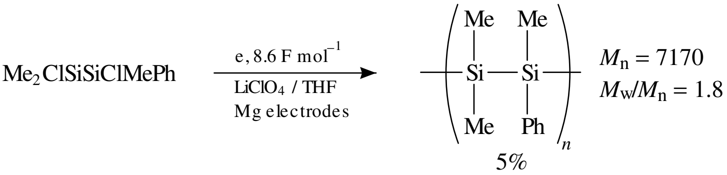

(60)

TABLE 20. Cathodic formation of polysilanes[88]

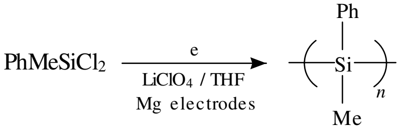

Dichlorosilane Concentration(M)	Electricity (F mol^{-1})	Yield (%)	M_n	M_w/M_n	Mg electrode	
					Sonication	Alternation
0.33	4	43	5200	1.5	○	○
0.33	4	17	3900	1.4	×	○
0.33	4	7	4000	1.4	○	×
0.67	4	79	9900	2.1	○	○
6.3	2.2	43	18000	2.1	○	○
12	0.5	8	31000	1.8	○	○

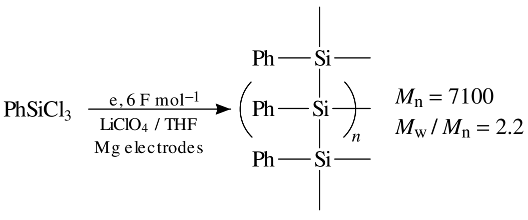

$$\mathrm{PhSiCl_3} \xrightarrow[\text{LiClO}_4\text{ / THF, Mg electrodes}]{\text{e, 6 F mol}^{-1}} (\mathrm{PhSi})_n \qquad M_n = 7100,\ M_w/M_n = 2.2 \tag{61}$$

71%

Polycarbosilanes have also attracted much interest as starting material for silicon carbide fiber production. Reactive metal such as Mg[88], Cu[86,89,90] and Al[91] electrodes have been shown to be highly effective for electrochemical synthesis of polycarbosilanes, as shown in Table 21.

The alternating magnesium electrode system is also applicable to the Si−Ge[92] or Si−Sn[93] bond formation (equations 62–64).

$$\underset{(1\,:\,3)}{\mathrm{R_2PhSiCl + Me_3GeCl}} \xrightarrow[3\mathrm{F\,mol^{-1}}]{2e} \underset{\substack{\mathrm{R = Ph\ (60\%)}\\ \mathrm{R = Me\ (52\%)}}}{\mathrm{R_2PhSiGeMe_3}} + \underset{(30\ \%)}{\mathrm{(Me_3Ge)_2}} \tag{62}$$

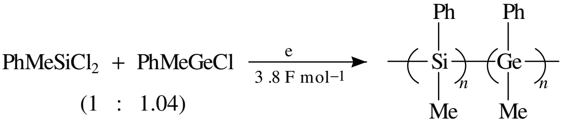

$$\underset{(1\ :\ 1.04)}{\mathrm{PhMeSiCl_2 + PhMeGeCl}} \xrightarrow{\substack{e\\ 3.8\ \mathrm{F\,mol^{-1}}}} -\!\left(\mathrm{SiPhMe}\right)_n\!\left(\mathrm{GePhMe}\right)_n\!- \tag{63}$$

33% (Ge content 33%)
$M_n = 20600$

$$\underset{(10\,:\,1)}{\mathrm{Me_3SiCl + Me_3SnCl}} \xrightarrow[6\mathrm{F\,mol^{-1}}]{2e} \underset{50\%}{\mathrm{Me_3SiSnMe_3}} + \underset{41\%}{\mathrm{(Me_3Sn)_2}} \tag{64}$$

Recently, Hengge and coworkers reported that the use of a silicon carbide and a hydrogen electrode instead of sacrificial anodes was effective for the electrochemical coupling of halosilanes without formation of metal chlorides (equation 65)[94].

$$\mathrm{Me_3SiCl} \xrightarrow[\substack{\mathrm{Et_4NBF_4/THF\text{–}HMPA\ (1{:}1)}\\ \text{Fe cathode}}]{e} \mathrm{Me_3SiSiMe_3} \tag{65}$$

SiC anode (65%)
Hydrogen anode (73%)

Cathodic formation of disilane from bulky dichlorosilane was reported as shown in equation 66[95]. However, this reaction seems to be difficult to reproduce.

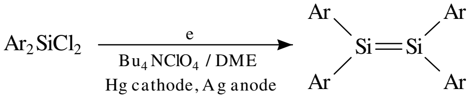

(66)

Ar = Mesityl (20 %)

2. Cathodic reduction of halomethylsilanes

Since silicon stabilizes an α-carbanion by d π–p π interaction, silicon should promote electron transfer to a carbon−halogen bond which generates the α-carbanion. In fact,

TABLE 21. Electrosynthesis of polycarbosilanes

Substrate	Conditions		Electricity (F/mol)	Yield (%)	M_n	M_w/M_n	Reference
Concentration(M)	Anode	Electrolyte					
ClPhMeSi 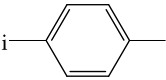 SiPhMeCl(0.27)	Mg	$LiClO_4$/THF	8.0	73	9450	1.88	88
ClPhMeSi 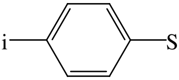 SiPhMeCl(0.24)	Cu	Bu_4NBPh_4/DME	6.7	27	3900[a]	2.1	90
ClPhMeSi 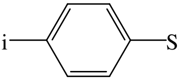 SiPhMeCl(0.24)	Cu	Bu_4NBPh_4/DME	3.1	19	6100[a]	3.4	90
ClMeEtSi 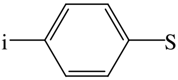 SiEtMeCl (0.27)	Mg	$LiClO_4$/THF	8.0	50	8570	1.61	88
$ClPhMeSiCH_2CH_2SiPhMeCl$ (0.14)	Cu	Bu_4NBPh_4/DME	3.5	13	61000[a]	16	89
$ClPhMeSiCH_2CH_2SiPhMeCl$ (0.12)	Cu	Bu_4NBPh_4/DME	12.4	17	120000[a]	8.0	89
$ClMe_2SiCH_2CH_2SiMe_2Cl$ (0.18)	Al	Bu_4NCl/THF	2.0	68	2500	—	91

[a] M_w.

TABLE 22. Reduction potentials of (iodomethyl)silanes and related compounds[96]

Substrate	$E_{1/2}$ (V vs SCE)
Et_3SiCH_2I	-1.54^a
$CF_3(CH_2)_2SiMe_2CH_2I$	-1.33^a
$PhSiMe_2CH_2I$	-1.43^a
p-$FC_6H_4SiMe_2CH_2I$	-1.40^a
MeI	-1.63^b

[a] 0.09 M KCl/75% alcohol.

[b] 0.05 M Et_4NBr/75% dioxane–water.

(iodomethyl) trialkylsilanes were shown by polarographic study to be reduced at less negative potentials compared with unsilylated simple iodoalkanes, as shown in Table 22[96].

Cathodic reduction of (chloromethyl)dimethylchlorosilane using an aluminum anode provided polycarbosilanes besides a large amount of di- and trisilacyclic compounds (equation 67)[97]. On the other hand, the electrolysis in the presence of Me_2SiCl_2 gave bis(dimethylchlorosilyl)methane, a useful polycarbosilane precursor (equation 68)[97]. Similarly, polycarbosilanes were prepared from dichlorocarbosilanes using sacrificial aluminum electrodes in DME (equation 69)[91].

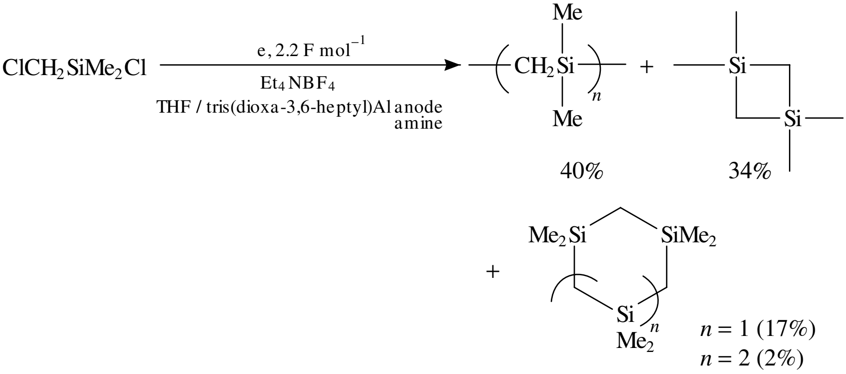

(67)

$$ClCH_2SiMe_2Cl + Me_2SiCl_2 \xrightarrow[\text{Al anode}]{\text{e, 2.2 F mol}^{-1}} \underset{60\%}{ClMe_2SiCH_2SiMe_2Cl} \qquad (68)$$

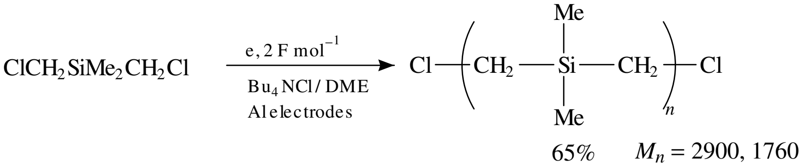

$$ClCH_2SiMe_2CH_2Cl \xrightarrow[\text{Bu}_4\text{NCl / DME, Al electrodes}]{\text{e, 2 F mol}^{-1}} Cl\left(CH_2-\underset{Me}{\overset{Me}{Si}}-CH_2\right)_n Cl \qquad (69)$$

$65\% \quad M_n = 2900, 1760$

3. Utilization as electrophiles

Since a carbon–halogen bond is more easily reduced than a silicon–halogen bond, cathodic reduction of organic halides such as allyl, benzyl, aryl and vinyl halides in the presence of a halosilane provides the corresponding organosilicon compounds. This is a convenient method for the introduction of a silyl group into organic molecules and a mechanism involving a cathodically generated carbanion intermediate is suggested.

The cathodic reduction of benzyl chlorides in the presence of a chlorosilane using a divided cell provides the corresponding benzylsilanes while the electrolysis in an undivided cell gives chlorinated benzylsilanes (equations 70–71)[98]. Similarly, vinyl halides provide the corresponding vinylsilanes as stereoisometic mixtures (equation 72)[99,100].

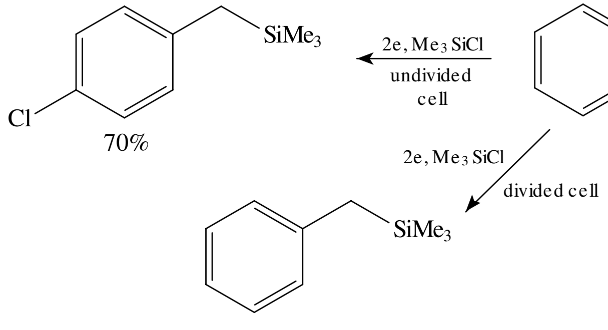

(70)

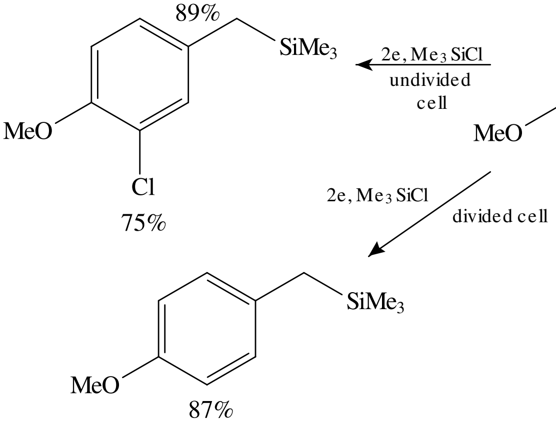

(71)

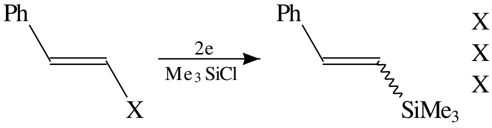

X = I, 51% (*E*/*Z* = 57/43)
X = Br, 23% (*E*/*Z* = 68/32)
X = Cl, 11% (*E*/*Z* = 78/22)

(72)

The regioselectivity of the reaction of allylic halides depends on the nature of the halosilanes: trimethylsilyl and dimethylphenylsilyl groups are introduced at the less substituted end of the allyl group, whereas the dimethylsilyl group is introduced at both ends of the allyl group (equation 73)[99,100]. This method is also highly chemoselective as demonstrated by selective monosilylation of *p*-bromoiodobenzene and *p*-bromocinnamyl chloride (equations 74 and 75). Whereas the electroreductive silylation of organic halides is efficient, this method cannot however, be applied to alkyl halides and aryl chlorides. Moreover, as already mentioned, benzene ring chlorination takes place simultaneously in the electrosynthesis of benzylsilanes in an undivided cell (equations 70 and 71).

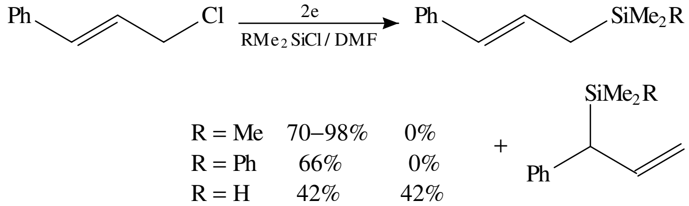

(73)

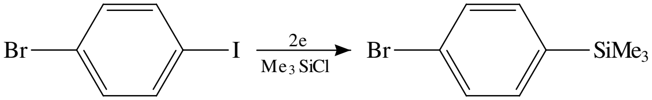

60%

(74)

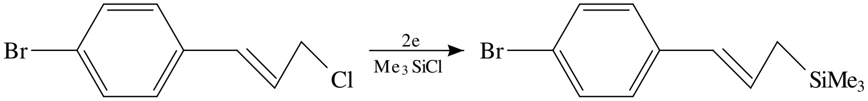

49%

(75)

Reactive metal anodes are quite effective in reactions of aryl chlorides in the presence of a large excess of chlorotrimethylsilane in an undivided cell using a sacrificial aluminum anode in THF/HMPA (4 : 1) which provide the corresponding aryltrimethylsilanes (equations 76 and 77)[101,102]. This method does not require any diaphragms since oxidation of the aluminum anode takes place predominantly as the anodic reaction (equation 76). When excess amount of electricity is passed, *trans*-tris(trimethylsilyl)chlorohexa-1,3-dienes are formed predominantly (equation 78).

$$\begin{aligned} &\text{at cathode :} \quad && \text{Ar--X} + 2e \longrightarrow \text{Ar}^- + \text{X}^- \\ & && \text{Ar}^- + \text{Me}_3\text{SiCl} \longrightarrow \text{ArSiMe}_3 + \text{Cl}^- \qquad (76) \\ &\text{at anode :} && 2/3\,\text{Al} - 2e \longrightarrow 2/3\,\text{Al}^{3+} \end{aligned}$$

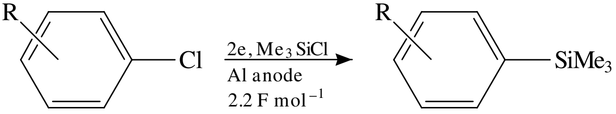

(77)

R = H (84%) ; *o* -Me (72%) ; *m*-Me (80%) ; *p*-Me (70%)

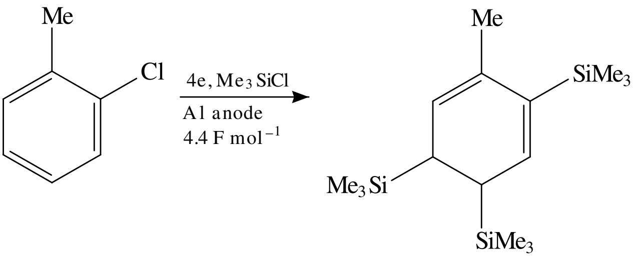

(78)

84% (*trans*/*cis* = 92/8)

Cathodic trimethylsilylation of simple arenes such as benzene and toluene is also possible by this method and gives bis(trimethylsilyl)cyclohexa-1,4-dienes[103]. 1-Methoxy-3,6-bis(trimethylsilyl)cyclohexa-1,4-diene, formed in equation 79, is a useful precursor to ketoprofen.

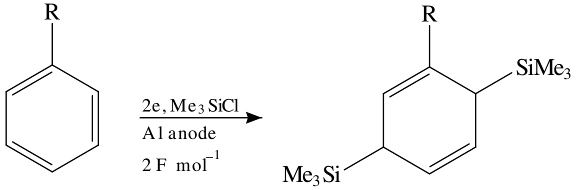

(79)

R = H, 62% (*trans*/*cis* = 7 : 3)
R = Me, 58% (*trans* only)
R = MeO, 70% (single isomer)

Polysilylation of *o*-dichlorobenzene was also successfully carried out similarly to provide mono-, di-, tetra- and hexasilylated products in fairly good yields, respectively, depending on the amount of electricity passed. This is a useful route to silylated cyclo-C_6 products (equation 80)[104]. Similarly, selective electrochemical mono- and polysilylation of halothiophenes was performed (equation 81)[105].

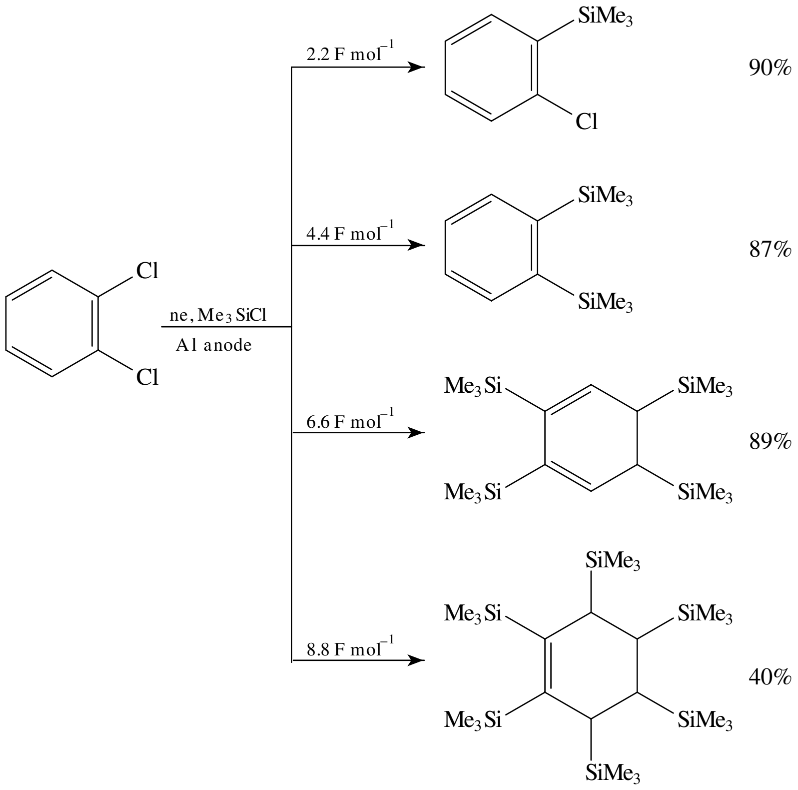

(80)

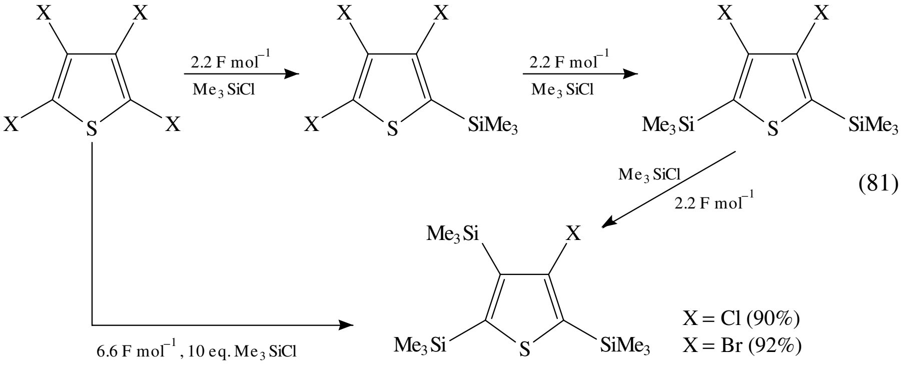

(81)

Selective electrochemical silylation of polychloromethane (equation 82)[106] and benzal chloride (equation 83)[107] is also possible using zinc and magnesium as a sacrificial anode.

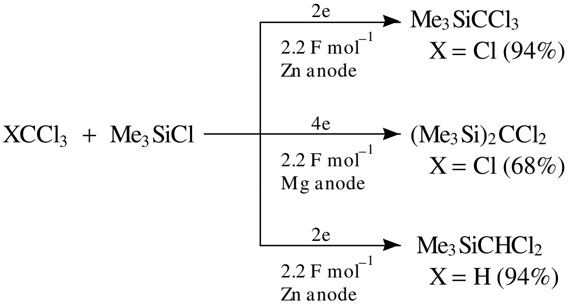

(82)

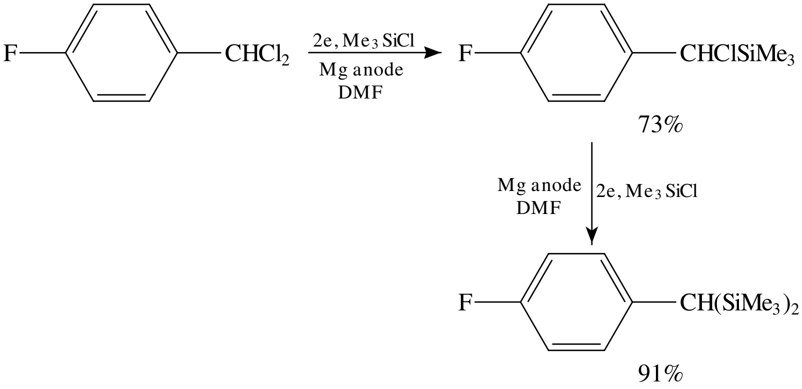

(83)

(Trifluoromethyl)trimethylsilane is a highly useful trifluoromethylating reagent. Efficient electrochemical trimethylsilylation of bromotrifluoromethane has been developed (equation 84)[108].

$$\mathrm{CF_3Br} + \mathrm{Me_3SiCl} \xrightarrow[\substack{\text{PhOMe/HMPA} \\ \text{Al anode}}]{2e} \underset{73\%}{\mathrm{F_3CSiMe_3}} \qquad (84)$$

Trifluoromethylbenzene is also trimethylsilylated electrochemically to provide α, α-difluoro-α-(trimethylsilyl)toluene (equation 85)[109].

$$\mathrm{PhCF_3 + Me_3SiCl} \xrightarrow[\substack{\text{PhOMe/HMPA} \\ \text{Al anode}}]{2e} \underset{70\%}{\mathrm{PhCF_2SiMe_3}} \tag{85}$$

Recently, selective electrochemical trimethylsilylation of tetrachlorocyclopropene has been achieved to provide 1-(trimethylsilyl)trichlorocyclopropene, which has been converted into hexakis(trimethylsilyl)-3,3′-bicyclopropenyl upon successive electrolysis (equation 86)[110–112].

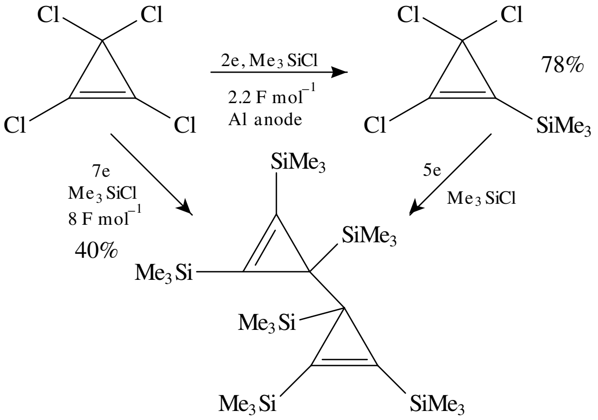

(86)

Electrochemical synthesis of various cyclic alkylsilanes has been performed similarly[113]. It should be noted that 5-silaspiro[4,4]nonane is formed despite the high probability of polymer formation due to the high functionality of the silicon. Such high selectivity in the electrochemical ring closure seems to be due to the orientating effect of an electrode in the course of an irreversible reduction of a carbon−halogen bond in the monosilylated intermediate (equations 87 and 88).

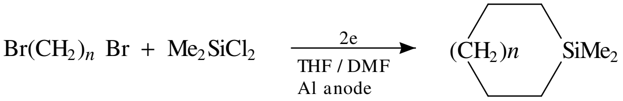

$n = 2$ (0%)
$= 3$ (18%)
$= 4$ (91%)
$= 5$ (68%)
$= 6$ (57%)

(87)

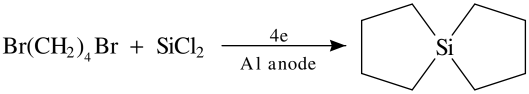

24%

(88)

Various activated olefins can also be employed instead of organic halide for the formation of a carbon−silicon bond. Thus, cathodic reduction of α,β-unsaturated esters, nitriles and ketones in the presence of chlorotrimethylsilane using a sacrificial magnesium anode provides the corresponding β-trimethylsilyl compounds (equation 89)[114].

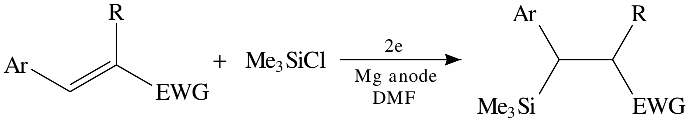

(89)

Ar = Ph, R = H, EWG = CO_2Et (66%)
Ar = p-ClC_6H_4, R = H, EWG = CO_2Et (70%)
Ar = Ph, R = EWG = CO_2Et (77%)
Ar = Ph, R = H, EWG = CN (70%)
Ar = Ph, R = H, EWG = Ac (68%)

Similar electroreductive silylation of a series of unsaturated nitrogen compounds such as trimethylsilyl cyanide, cyanamide or isocyanide, bis(trimethylsilyl)carbodiimide and trimethylsilyl isocyanate provide precursors of bis(trimethylsilyl)methylamine, which is useful for organic synthesis (equations 90 and 91)[115]. This electrochemical method is a safer and more economical process compared with the chemical process using an alkali metal such as lithium.

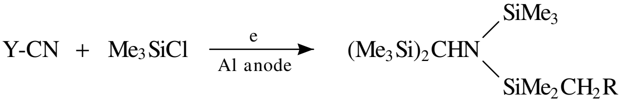

$$\text{Y-CN} + \text{Me}_3\text{SiCl} \xrightarrow[\text{Al anode}]{\text{e}} (\text{Me}_3\text{Si})_2\text{CHN}(\text{SiMe}_3)(\text{SiMe}_2\text{CH}_2\text{R}) \qquad (90)$$

Y = Me_3Si, 78% (R = H/Me_3Si = 5/95)
Y = Me_2N, 65% (R = H/Me_3Si = 25/75)

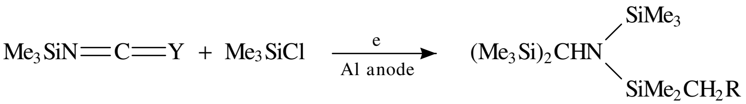

$$\text{Me}_3\text{SiN{=}C{=}Y} + \text{Me}_3\text{SiCl} \xrightarrow[\text{Al anode}]{\text{e}} (\text{Me}_3\text{Si})_2\text{CHN}(\text{SiMe}_3)(\text{SiMe}_2\text{CH}_2\text{R}) \qquad (91)$$

Y = O, 56% (R = H/Me_3Si = 12/88)
Y = $NSiMe_3$, 75% (R = H/Me_3Si = 10/90)

N,N-Disilylenamines of acylsilanes, which are excellent precursors for α-(trimethylsilyl)alkylamine, can be prepared electrochemically using a similar procedure (equation 92)[116].

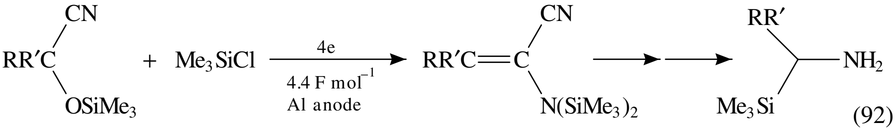

(92)

R = H, R′ = Et, 75% (E/Z = 88/12)
R = Me, R′ = n-Pr, 82% (E/Z = 58/42)
R = R′ = c-C_6H_{11}, 75%

Cathodic reduction of acylimidazoles in the presence of chlorotrimethylsilane gives the corresponding acylsilanes in satisfactory yields (equation 93)[117]. Acylsilanes having a functional group such as an alkoxycarbonyl or a chlorine are also synthesized effectively.

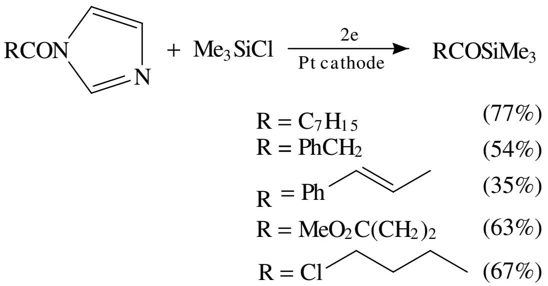

(93)

Cathodically induced silylation of unsaturated compounds such as phenylacetylene, styrene and cyclohexene has also been reported (equations 94 and 95)[118,119]. Since chlorotrimethylsilane is reduced at a less negative potential ($E_{1/2} = -1.95$ V vs Hg pool) compared with phenylacetylene ($E_{1/2} = -2.05$ V vs Hg pool), cathodic reduction of chlorotrimethylsilane to generate a silyl anion is possible in the presence of phenylacetylene.

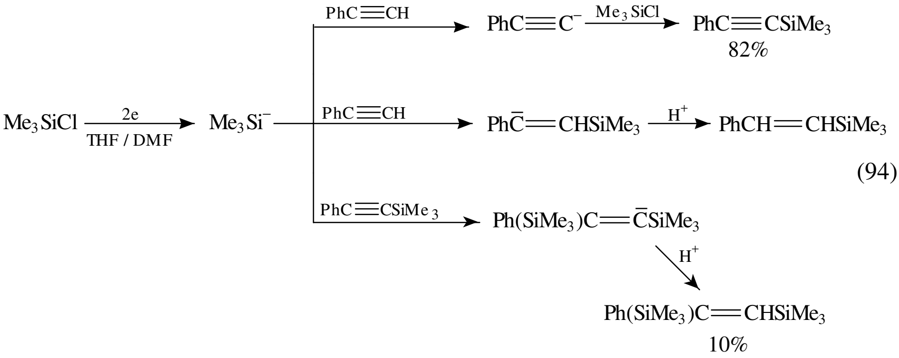

(94)

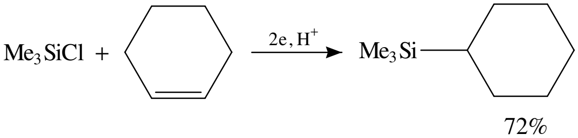

(95)

Cathodic reduction of dichlorosilanes in the presence of 2,3-dimethyl-1,3-butadiene provides cyclic silyl compounds (equation 96)[120].

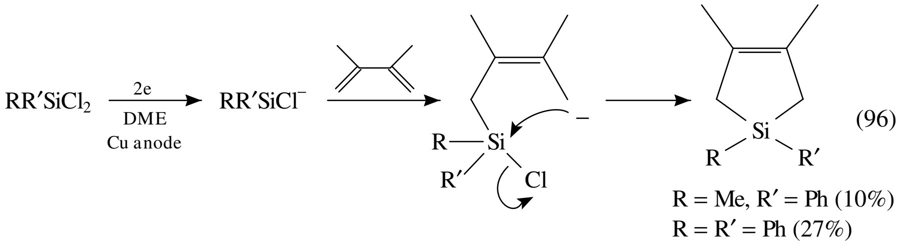

(96)

It is quite interesting that cathodic intra- and intermolecular coupling of a ketone with a vinylsilane (equations 97 and 98) takes place by using a carbon fiber cathode[121]. The carbon fiber cathode is essential for these reactions.

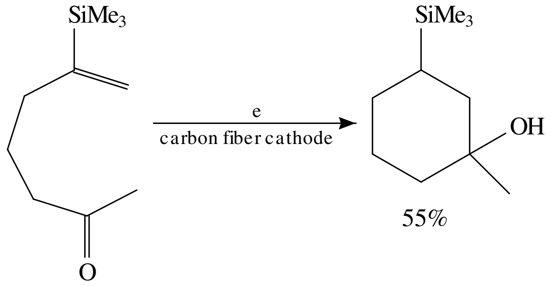

(97)

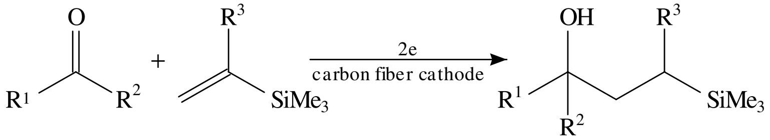

(98)

R^1 = Me, R^2 = *n*-Pr, R^3 = Me (75%)
R^1 = Me, R^2 = *n*-Hex, R^3 = H (72%)

Chlorotrimethylsilane (CTMS) has been shown to promote various cathodic hydrocoupling reactions. Thus, cathodic reduction of a mixture of carbonyl compounds and activated olefins[122] or imines[123] in the presence of CTMS provides carbon–carbon crossed-coupling products efficiently. The cathodic reduction of aromatic esters and an amide to produce aldehydes was also promoted in the presence of CTMS[124].

N-Methyl *o*-phthalimide and *o*-phthalic anhydride undergo cathodic trimethylsilylation to give monomeric and dimeric products, respectively (equation 99)[125].

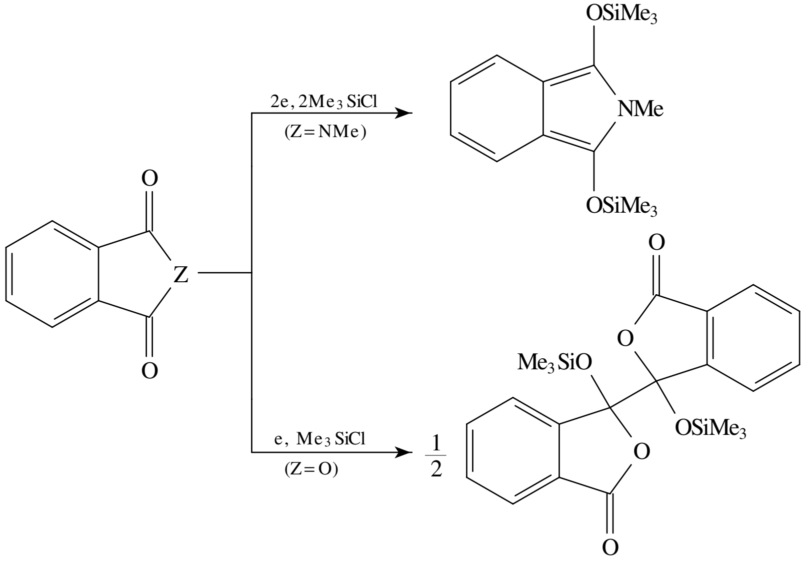

(99)

Quite recently, stereoselective electrochemical synthesis of silyl enol ethers using a sacrificial magnesium anode was reported, as shown in equation 100[126].

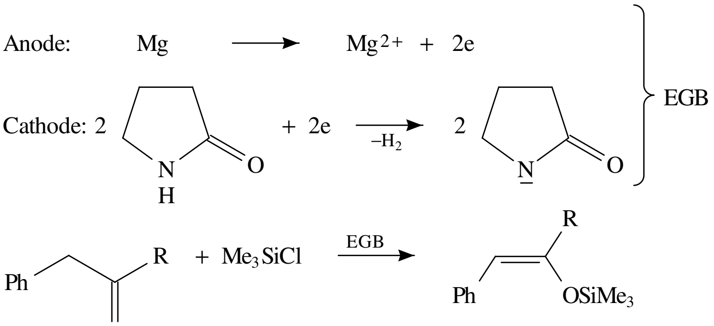

(100)

R = Ph, 90% (*Z* only)
R = Me, 100% (*Z*/*E* = 95/5)

E. Hydrosilanes

Cathodic reduction of triphenylhydrosilane in Bu_4NBF_4/MeCN provided triphenylfluorosilane besides a large amount of siloxane. Whereas radical species are likely, the reaction mechanism is still unclear[127].

It is interesting that electrocatalyzed reduction of carbonyl compounds to alcohols takes place by using trialkoxysilanes (equation 101)[128].

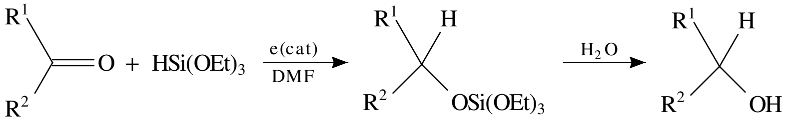

(101)

R^1 = Ph, R^2 = H (80%)
R^1 = Ph, R^2 = *t*-Bu (69%)

IV. ACKNOWLEDGMENT

The author wishes to thank Professors James Y. Becker of Ben-Gurion University and Tsutomu Nonaka of Tokyo Institute of Technology for encouraging him to write this chapter. Last but not least, he is grateful to Miss Motoko Miyazaki, his graduate student, who assisted in preparing the manuscript.

V. REFERENCES

1. E. M. Geniès and F. El Omar, *Electrochim. Acta*, **28**, 541 (1983).
2. J. Yoshida, in *Topics in Current Chemistry, Vol. 170, Electrochemistry V* (Ed. E. Steckhan), Springer-Verlag, Berlin, 1994, pp. 39–81.
3. R. J. Klingler and J. K. Kochi, *J. Am. Chem. Soc.*, **102**, 4790 (1980).
4. I. Y. Alyev, I. N. Rozhkov and I. L. Knunyants, *Tetrahedron Lett.*, 2469 (1976).
5. B. Hong, M. A. Fox, G. Maier and C. Hermann, *Tetrahedron Lett.*, **37**, 583 (1996).
6. E. M. Geniès and F. El Omar, *Electrochim. Acta*, **28**, 547 (1983).
7. M. Lemaire, W. Büchner, R. Garreau, H. A. Hoa, A. Guy and J. Roncali, *J. Electroanal. Chem.*, **312**, 277 (1991).
8. H. Masuda, Y. Taniki and K. Kaeriyama, *J. Polym. Sci., Part A*, **30**, 1667 (1992).

9. J. Roncali, C. Thobie-Gautier, H. Brisset, J. -F. Favart and A. Guy, *J. Electroanal. Chem.*, **381**, 257 (1995).
10. (a) T. Koizumi, T. Fuchigami and T. Nonaka, *Electrochim. Acta*, **33**, 1635 (1988).
    (b) K. Nishiwaki and J. Yoshida, *Chem. Lett.*, 787 (1996).
11. T. Koizumi, T. Fuchigami and T. Nonaka, *Chem. Express*, **1**, 355 (1986).
12. T. Koizumi, T. Fuchigami and T. Nonaka, *Bull. Chem. Soc. Jpn.*, **62**, 219 (1989).
13. J. Yoshida, T. Murata and S. Isoe, *Tetrahedron Lett.*, **27**, 3373 (1986).
14. (a) M. Ochiai, M. Arimoto and E. Fujita, *Tetrahedron Lett.*, **22**, 4491 (1981).
    (b) T. Fuchigami and K. Yamamoto, *Chem. Lett.*, 937 (1996).
15. K. Ohga and P. S. Mariano, *J. Am. Chem. Soc.*, **104**, 617 (1982).
16. J. Yoshida, T. Murata and S. Isoe, *Tetrahedron Lett.*, **28**, 211 (1987).
17. J. Yoshida, K. Sakaguchi and S. Isoe, *Tetrahedron Lett.*, **28**, 667 (1987).
18. J. Yoshida, K. Sakaguchi and S. Isoe, *Tetrahedron Lett.*, **27**, 6075 (1986).
19. K. D. Moeller, C. M. Hudson and L. V. Tinao-Wooldridge, *J. Org. Chem.*, **58**, 3478 (1993).
20. C. M. Hudson and K. D. Moeller, *J. Am. Chem. Soc.*, **116**, 3347 (1994).
21. B. E. Cooper and W. J. Owen, *J. Organometal. Chem.*, **29**, 33 (1971).
22. J. Yoshida and S. Isoe, *Tetrahedron Lett.*, **28**, 6621 (1987).
23. J. Yoshida and S. Isoe, *Chem. Lett.*, 631 (1987).
24. T. Koizumi, T. Fuchigami and T. Nonaka, *Chem. Lett.*, 1095 (1987).
25. J. Yoshida, S. Matsunaga, T. Murata and S. Isoe, *Tetrahedron*, **47**, 615 (1991).
26. M. Kimura, K. Koie, S. Matsubara, Y. Sawaki and H. Iwamura, *J. Chem. Soc., Chem. Commun.*, 122 (1987).
27. T. Fuchigami, Y. Nakagawa and T. Nonaka, *Tetrahedron Lett.*, **27**, 3869 (1986).
28. T. Fuchigami, K. Yamamoto and Y. Nakagawa, *J. Org. Chem.*, **56**, 137 (1991).
29. T. Takiguchi and T. Nonaka, *Chem. Lett.*, 1217 (1987).
30. K. Suda, J. Watanabe and T. Takanami, *Tetrahedron Lett.*, **33**, 1355 (1992).
31. K. Broka, J. Stradins, I. Sleiksa and E. Lukevics, *Latv. J. Chem.*, **5**, 575 (1992).
32. K. Broka, J. Stradins, V. Glezer, and G. Zelcans and E. Lukevics, *J. Electroanal. Chem.*, **351**, 199 (1993).
33. K. Suda, K. Hotoda, M. Aoyagi and T. Takanami, *J. Chem. Soc., Perkin Trans. 1*, 1327 (1995).
34. J. Yoshida, M. Itoh, S. Matsunaga and S. Isoe, *J. Org. Chem.*, **57**, 4877 (1992).
35. A. S. Romakhin, Yu. A. Babkin, E. V. Nikitin and Yu. M. Kargin, *Zh. Obshch. Khim.*, **58**, 13 (1988); *Chem. Abstr.*, **109**, 100628y (1988).
36. J. Yoshida, T. Maekawa, T. Murata, S. Matsunaga and S. Isoe, *J. Am. Chem. Soc.*, **112**, 1962 (1990).
37. J. Yoshida, H. Tsujishima, K. Nakano and S. Isoe, *Inorg. Chim. Acta*, **220**, 129 (1994).
38. J. Yoshida, S. Matsunaga and S. Isoe, *Tetrahedron Lett.*, **30**, 219 (1989).
39. J. Yoshida, T. Maekawa, Y. Morita and S. Isoe, *J. Org. Chem.*, **57**, 1321 (1992).
40. K. Mochida, S. Okui, K. Ichikawa, O. Kanakubo, T. Tsuchiya and K. Yamamoto, *Chem. Lett.*, 805 (1986).
41. J. Yoshida, S. Matsunaga and S. Isoe, *Tetrahedron Lett.*, **30**, 5293 (1989).
42. H. J. Schäfer, *Angew. Chem., Int. Ed. Engl.*, **20**, 911 (1981).
43. S. Torii, T. Inokuchi, S. Mishima and T. Kobayashi, *J. Org. Chem.*, **45**, 2731 (1980).
44. R. F. Stewart and L. L. Miller, *J. Am. Chem. Soc.*, **102**, 4999 (1980).
45. S. Torii, T. Okamoto and N. Ueno, *J. Chem. Soc., Chem. Commun.*, 293 (1978).
46. T. Shono, H. Ohmizu and N. Kise, *Chem. Lett.*, 1517 (1980).
47. D. Hermeling and H. J. Schäfer, *Angew. Chem., Int. Ed. Engl.*, **23**, 233 (1984).
48. K. Mochida, A. Itani, M. Yokoyama, T. Tsuchiya, S. D. Worley and J. K. Kochi, *Bull. Chem. Soc. Jpn.*, **58**, 2149 (1985).
49. M. Okano and K. Mochida, *Chem. Lett.*, 819 (1991).
50. W. G. Boberski and A. L. Allred, *J. Organometal. Chem.*, **88**, 65 (1975).
51. A. Diaz and R. D. Miller, *J. Electrochem. Soc.*, **132**, 834 (1985).
52. M. Okano and K. Mochida, *Chem. Lett.*, 701 (1990).
53. J. Y. Becker and E. Shakkour, *Tetrahedron Lett.*, **33**, 5633 (1992).
54. Z.-R. Zhang, J. Y. Becker and R. West, *Electrochem. Acta*, in press.
55. J. Y. Becker, M.-Q. Shien and R. West, *Electrochim. Acta*, **40**, 2775 (1995).
56. B. D. Shepherd and R. West, *Chem. Lett.*, 183 (1988).
57. A. Kunai, T. Kawakami, E. Toyoda, T. Sakurai and M. Ishikawa, *Chem. Lett.*, 1945 (1993).

58. Y. Kimata, H. Suzuki, S. Satoh and A. Kuriyama, *Chem. Lett.*, 1163 (1994).
59. Y. Kimata, H. Suzuki, S. Satoh and A. Kuriyama, *Organometallics*, **14**, 2506 (1995).
60. G. Casalbore-Miceli, G. Beggiato, N. Camaioni, L. Favaretto, D. Pietropaolo and G. Poggi, *Ann. Chim.*, **82**, 161 (1992).
61. M. Okano A. Toda and K. Mochida, *Bull. Chem. Soc. Jpn.*, **63**, 1716 (1990).
62. A. G. Evans, B. Jerome and N. H. Rees, *J. Chem. Soc., Perkin Trans. 2*, 447 (1973).
63. M. D. Curtis and A. L. Allred, *J. Am. Chem. Soc.*, **87**, 2554 (1965).
64. F. Correa-Duran, A. L. Allred, D. E. Glover and D. E. Smith, *J. Organometal. Chem.*, **49**, 353 (1973).
65. C. G. Pitt, R. N. Carey and E. C. Toren, Jr., *J. Am. Chem. Soc.*, **94**, 2554 (1972).
66. H. Watanabe, M. Aoki, H. Matsumoto, Y. Nagai and T. Sato, *Bull. Chem. Soc. Jpn.*, **50**, 1019 (1977).
67. A. L. Allred and L. W. Bush, *J. Am. Chem. Soc.*, **90**, 2554 (1968).
68. C. Eaborn, R. A. Jackson and R. Pearce, *J. Chem. Soc., Perkin Trans. 1*, 2055 (1973).
69. L. A. Paquette, C. D. Wright, III, S. G. Traynor, D. L. Taggart and G. D. Ewing, *Tetrahedron*, **32**, 1885 (1976).
70. H. Bock, H. Alt and H. Seidl, *J. Am. Chem. Soc.*, **91**, 355 (1969).
71. E. Carberry, R. West and E. Glass, *J. Am. Chem. Soc.*, **91**, 5446 (1969).
72. A. L. Allred, R. T. Smart and D. A. Van Beek, Jr., *Organometallics*, **11**, 4225 (1992).
73. M. Okano and K. Mochida, *Denki Kagaku*, **61**, 772 (1993); *Chem. Abstr.*, **119**, 203519z (1993).
74. R. E. Dessy, W. Kitching and T. Chivers, *J. Am. Chem. Soc.*, **88**, 453 (1966).
75. E. Hengge and G. Litscher, *Angew. Chem., Int. Ed. Engl.*, **15**, 370 (1976).
76. E. Hengge and H. Firgo, *J. Organometal. Chem.*, **212**, 155 (1981).
77. A. L. Allred, C. Bradley and T. H. Newman, *J. Am. Chem. Soc.*, **100**, 5081 (1978).
78. R. J. P. Corriu, G. Dabosi and M. Martineau, *J. Organometal. Chem.*, **186**, 19 (1980).
79. R. J. P. Corriu, G. Dabosi and M. Martineau, *J. Chem. Soc., Chem. Commun.*, 457 (1979).
80. R. J. P. Corriu, G. Dabosi and M. Martineau, *J. Organometal. Chem.*, **222**, 195 (1981).
81. M. Umezawa, M. Takeda, H. Ichikawa, T. Ishikawa, T. Koizumi, T. Fuchigami and T. Nonaka, *Electrochim. Acta*, **35**, 1867 (1990).
82. M. Umezawa, M. Takeda, H. Ichikawa, T. Ishikawa, T. Koizumi and T. Nonaka, *Electrochim. Acta*, **36**, 621 (1991).
83. M. Umezawa, H. Ichikawa, T. Ishikawa and T. Nonaka, *Denki Kagaku*, **59**, 421 (1991); *Chem. Abstr.*, **115**, 265356v (1991).
84. M. Bordeau, C. Brain, M. -P. Léger-Lambert and J. Dunodués, *J. Chem. Soc., Chem. Commun.*, 1476 (1991).
85. A. Kunai, T. Kawakami, E. Toyoda and M. Ishikawa, *Organometallics*, **10**, 893 (1991).
86. A. Kunai, T. Kawakami, E. Toyoda and M. Ishikawa, *Organometallics*, **10**, 2001 (1991).
87. T. Shono, S. Kashimura, M. Ishifune and R. Nishida, *J. Chem. Soc., Chem. Commun.*, 1160 (1990).
88. T. Shono, *Kino Zairyo*, **12**, 15 (1992); *Chem. Abstr.*, **117**, 7964 (1992).
89. A. Kunai, E. Toyoda, T. Kawakami and M. Ishikawa, *Organometallics*, **11**, 2899 (1992).
90. A. Kunai, E. Toyoda, T. Kawakami and M. Ishikawa, *Electrochim. Acta*, **39**, 2089 (1994).
91. M. Umezawa, M. Kojima, H. Ichikawa, T. Ishikawa and T. Nonaka, *Electrochim. Acta*, **38**, 529 (1993).
92. T. Shono, S. Kashimura and H. Murase, *J. Chem. Soc., Chem. Commun.*, 896 (1992).
93. T. Ishiwata, T. Nonaka, and M. Umezawa, *Chem. Lett.*, 1631 (1994).
94. Ch. Jammegg, S. Graschy and E. Hengge, *Organometallics*, **13**, 2397 (1994).
95. P. Boudjouk, B. -H. Han and K. R. Anderson, *J. Am. Chem. Soc.*, **104**, 4992 (1982).
96. S. G. Mairanovski, V. A. Ponomarenko, N. V. Barashkova, and A. D. Snegova, *Dokl. Akad. Nauk SSSR*, **134**, 387 (1960); *Chem. Abstr.*, **55**, 16221g (1961); S. G. Mairanovski, V. A. Ponomarenko, N. V. Barashkova and M. A. Kadina, *Izv. Akad. Nauk SSSR, Ser. Khim.*, 1951 (1964); *Chem. Abstr.*, **62**, 6378c (1965).
97. M. Bordeau, C. Biran, P. Pons, M. -P. Léger and J. Dunoguès, *J. Organomet. Chem.*, **382**, C21 (1990).
98. T. Shono, Y. Matsumura, S. Katoh and N. Kise, *Chem. Lett.*, 463 (1985).
99. J. Yoshida, K. Muraki, H. Funahashi and N. Kawabata, *J. Organomet. Chem.*, **284**, C33 (1985).
100. J. Yoshida, K. Muraki, H. Funahashi and N. Kawabata, *J. Org. Chem.*, **51**, 3996 (1986).
101. P. Pons, C. Biran, M. Bordeau, J. Dunoguès, S. Sibille and J. Perichon, *J. Organomet. Chem.*, **321**, C27 (1987).

102. M. Bordeau, C. Biran, P. Pons, M. -P. Léger-Lambert and J. Dunoguès, *J. Org. Chem.*, **57**, 4705 (1992).
103. C. Biran, M. Bordeau, F. Serein-Spirau, M. -P. Léger-Lambert and J. Dunoguès, *Synth. Commun.*, **23**, 1727 (1993).
104. D. Deffieux, M. Bordeau, C. Biran and J. Dunoguès, *Organometallics*, **13**, 2415 (1994).
105. D. Deffieux, D. Bonafoux, M. Bordeau, C. Biran and J. Dunoguès, *Organometallics*, **15**, 2041 (1996).
106. P. Pons, C. Biran, M. Bordeau and J. Dunoguès, *J. Organomet. Chem.*, **358**, 31 (1988).
107. A. J. Fry and J. Touster, *J. Org. Chem.*, **54**, 4829 (1989).
108. G. K. S. Prakash, D. Deffieux, A. K. Yudin and G. A. Olah, *Synlett*, 1057 (1994).
109. M. Bordeau, D. Deffieux, M. -P. Léger-Lambert, C. Biran and J. Dunoguès, Fr. Demande FR 2,681,866 (Cl. C07F7/12); *Chem. Abstr.*, **119**, 72833x (1993).
110. G. K. S. Prakash, S. Quaiser, H. A. Buchholz, J. Casanova and G. A. Olah, *Synlett*, 113 (1994).
111. G. K. S. Prakash, H. A. Buchholz, D. Deffieux and G. A. Olah, *Synlett*, 819 (1994).
112. G. K. S. Prakash, H. A. Buchholz, D. Deffieux and G. A. Olah, *J. Org. Chem.*, **59**, 7532 (1994).
113. V. Jouikov and V. Krasnov, *J. Organomet. Chem.*, **498**, 213 (1995).
114. T. Ohno, H. Nakahiro, K. Sanemitsu, T. Hirashima and I. Nishiguchi, *Tetrahedron Lett.*, **33**, 5515 (1992).
115. S. Grelier, T. Constantieux, D. Deffieux, M. Bordeau, J. Dunoguès, J. -P. Picard, C. Palomo and J. M. Aizpurua, *Organometallics*, **13**, 3711 (1994).
116. T. Constantieux and J. -P. Picard, *Organometallics*, **15**, 1604 (1996).
117. N. Kise, H. Kaneko, N. Uemoto and J. Yoshida, *Tetrahedron Lett.*, **36**, 8839 (1995).
118. V. Jouikov and L. Grigorieva, *Electrochim. Acta*, **41**, 469 (1996).
119. V. Jouikov and G. Salaheev, *Electrochim. Acta*, **41**, 2623 (1996).
120. A. Kunai, T. Ueda, E. Toyoda and M. Ishikawa, *Bull. Chem. Soc. Jpn.*, **67**, 287 (1994).
121. T. Shono, in *Organic Synthesis in Japan, Past, Present, and Future* (Ed. R. Noyori), Tokyo Kagaku Dozin, Tokyo, 1992, pp. 389–392.
122. T. Shono, H. Ohmizu, S. Kawakami and H. Sugiyama, *Tetrahedron Lett.*, **21**, 5029 (1980).
123. T. Shono, N. Kise, N. Kunimi and R. Nomura, *Chem. Lett.*, 2191 (1991).
124. P. -R. Goetz-Schatowitz, G. Struth, J. Voss and G. Wiegand, *J. Prakt. Chem.*, **335**, 230 (1993).
125. T. Troll and G. W. Ollmann, *Tetrahedron Lett.*, **22**, 3497 (1981).
126. D. Bonafoux, M. Bordeau, C. Biran and J. Dunoguès, *J. Organomet. Chem.*, **493**, 27 (1995).
127. M. Okano and K. Mochida, *Bull. Chem. Soc. Jpn.*, **64**, 1381 (1991).
128. M. Kimura, H. Yamagishi and Y. Sawaki, *Denki Kagaku*, **62**, 1119 (1994); *Chem. Abstr.*, **122**, 117417v (1995).

CHAPTER 21

The photochemistry of organosilicon compounds

A. G. BROOK

Lash Miller Chemical Laboratories, University of Toronto, Toronto M5S 3H6, Canada

---

I. INTRODUCTION

The dramatic increases in the breadth and scope of the field of organosilicon chemistry in recent years have been significantly influenced by the application of photochemical techniques to the studies. Thus the photolyses of organosilicon compounds, particularly in matrices, have allowed the creation, detection, characterization and, in some cases, isolation of unstable reaction intermediates such as silenes, silylenes and disilenes. In some cases photochemical methods have led to the formation of stable, isolable silenes and disilenes, species previously considered to be unobtainable. Increasingly, the applications of photochemistry have become more sophisticated, with greater concern for mechanistic and theoretical details, particularly for polysilane systems, where considerable industrial interest is found, because of the unusual photochemical behavior often displayed, which can be applied to photoresists, semiconductors and related applications. As well, in the last 3–5 years, considerable effort has been expended in studying cophotolyses of mixtures of an organosilicon compound with a co-reactant (usually an unsaturated compound) because of the recognition that the products formed (which frequently lack the original silyl group) are structures of synthetic interest, not readily prepared by other routes.

The present review mainly deals with publications from 1989 to early 1996, with some key earlier references as background. The photochemistry of organosilicon compounds has been reviewed previously, most recently in a detailed article by Steinmetz in 1995[1]. An earlier review was written by Brook in 1989[2], annual reviews have been published[3] and much material including photochemical studies can be found in general reviews of organosilicon chemistry[4–6]. Other specialized reviews will be noted in the appropriate sections of the text.

The chemistry reviewed herein is organized into the following main categories.

1. Compounds containing only one silicon atom (or, in a few cases, where there is more than one silicon atom but where they are separated from each other by carbon atoms and so behave as a single silicon atom) where the photochemistry observed normally involves cleavage (usually homolytically) of a carbon–silicon bond.

2. Compounds with two or more silicon atoms directly attached to one another, subdivided into sections based first on the number of silicon atoms and then on the carbon functionality attached to the silicon atoms. Frequently, but not exclusively, the main photochemical behavior involves homolysis of a silicon–silicon bond yielding silyl radicals, but in some cases silylenes result directly from the photochemistry. The resulting compounds are frequently the products of a molecular rearrangement.

3. Compounds in which one or more silicon atom(s) is (are) directly attached to a carbonyl group (acylsilanes) or to a diazo group (silyldiazoalkanes) where the main chromophore is the carbofunctional group but where the silicon atom, being strongly coupled, becomes involved in the reaction pathway. Radicals, siloxycarbenes or silenes may result from the acylsilanes, and silylcarbenes result from the silyldiazoalkanes, each of which shows interesting and unusual behavior.

4. Routes to the reactive species silenes, silylenes and disilenes, and the photochemical changes which they themselves undergo.

5. Other photochemical studies, including cases where compounds contain one or more silicon atoms but where the major chemical behavior observed may not involve a bond to silicon. Thus silicon may be used as a ‘tether’ to locate a pair of reacting functional groups in some desirable geometry, or an arylsilyl group may be an ‘antenna’ for radiation to promote reactivity at another site in the molecule. Also in this category are many cophotolyses involving an organosilicon compound and an unsaturated co-reactant, leading frequently to complex structures of synthetic interest. Thus these sections might have been titled ‘New Synthetic Routes Applying the Photochemistry of Organosilicon Compounds’.

Within these main categories a number of subdivisions will generally be found, usually based on the nature of the groups attached to silicon. The emphasis in the subject matter is chiefly in terms of the chemical transformations effected by the radiation, and little emphasis is placed on the photochemical mechanisms involved, which are dealt with in an accompanying chapter of this treatise[7]. Also, the photochemistry of high molecular weight polysilane polymers, or of polymers containing silicon as part of the backbone of the molecules, is not dealt with in this chapter, but some relevant material will be found in other chapters in this volume.

As a background for what is to follow it is useful to make some general comments about the photochemical behavior of organosilicon compounds. The photolysis of simple organosilicon compounds generally leads to homolysis of a bond to silicon leading to silyl and alkyl radicals which subsequently react in conventional ways including hydrogen abstraction, disproportionation, coupling etc. Generally, short-wavelength radiation is required, and the reactions are not very chemically interesting, at least from the synthetic point of view, because of the multiplicity of compounds formed. However, when there are unsaturated groups present in the molecule, or present in the photolysis mixture, interesting transformations may occur, as the following sections will illustrate.

Organosilicon compounds are very susceptible to photochemical rearrangements. This is because di-, tri- and polysilanes absorb at much longer wavelengths than their all-carbon analogs. This is particularly true for compounds in which a chromophore is directly attached to a silicon atom, as in vinylsilanes, acylsilanes and silyldiazoalkanes. Many simple organosilicon compounds also undergo interesting photochemical rearrangements. 1,2-Photochemical rearrangements of a silyl group from carbon to oxygen are well known with acylsilanes, and 1,2-carbon-to-carbon rearrangements are commonly found in ring-opening reactions of silylcyclopropenes and related species as will be seen below. 1,3-Photochemical rearrangements of a silyl group from carbon to carbon are commonly observed with allyl- and propargyl silanes, or with vinyl- or alkynyldisilanes, or from silicon to oxygen with polysilylacylsilanes. The ease of migration of silicon has been attributed in part to the β-silicon effect[8] whereby silicon stabilizes radical or cationic sites in a β-relationship as a result of hyperconjugative interactions, and to the inherent tendency of silicon to migrate, which has been shown to be much greater than that of hydrogen or alkyl groups in many circumstances[9].

II. COMPOUNDS CONTAINING A SINGLE SILICON ATOM

A. Acyclic Compounds

1. Photochemical rearrangements of organosilicon compounds

A few studies involving photochemical rearrangements of relatively simple organosilicon compounds have recently been reported.

Sakurai and coworkers[10] observed several years ago that benzyltrimethylsilane underwent a photochemical carbon-to-carbon 1,3-silyl migration and more recently[11] observed that allylsilanes such as **1** underwent clean 1,3-silyl rearrangements with inversion of configuration at a silicon stereocenter yielding the isomeric compound **2** as shown in equation 1, when photolyzed at 254 nm. The observed stereochemistry is contrary to the predictions of the Woodward–Hoffmann rules. Similar anti-Woodward–Hoffmann behavior had also been observed in the related thermal rearrangements of β-ketosilanes which occurred with retention of configuration at a chiral silicon stereocenter[12]. A related photochemical 1,3-silyl rearrangement of a vinylpolysilane is described below in Section IV.B.

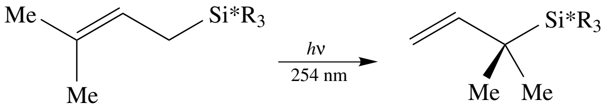

(1)

(1) **(2)**

Si*R$_3$ = SiMePh(1-Np)

Silyl-substituted cyclopropenes have been observed to rearrange photochemically giving high yields of allenes. A typical example is shown in equation 2 where the silylcyclopropene **3** apparently ring-opened to the carbene **4** which, following 1,2-silyl migration, led to the allene **5**[13].

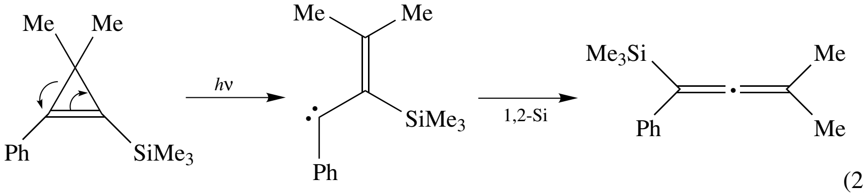

(2)

(3) **(4)** **(5)**

2. Laser-induced reactions involving small organosilicon compounds

In recent years the application of laser techniques has become an important tool in the study of the kinetics of relatively simple reactive organosilicon species (silylenes, silenes etc.). Gaspar and coworkers have reviewed the use of laser techniques to study the generation and reactions of silylenes[14].

Pola and coworkers have employed lasers, frequently using sulfur hexafluoride as a sensitizer, to generate silicon-containing reactive intermediates which polymerize under the reaction conditions, yielding high molecular weight materials of potential interest. Thus laser photolysis of 1-methyl-1-vinyl-1-silacyclobutane **6** gave rise to 2-silaisoprene **7** and ethylene following first-order kinetics. The reactions of siladiene **7** with tetrafluoroethylene to give 1,1-difluoro-2-methyl-2-silabutadiene **8**, were investigated, as was the subsequent polymerization of **8**, as shown in equation 3. The reactions of the siladiene **7** with hexafluoroacetone were also studied[15].

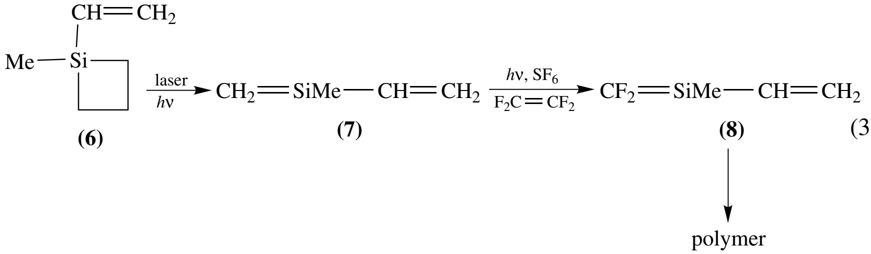

(6) **(7)** **(8)** (3)

In another study several simple silenes $RR'Si{=}CH_2$ (R, R′ = Me, Vinyl etc.) were formed by laser-powered pyrolysis and were found to form linear polymers, in contrast to the usual behavior of silenes which yield cyclodimers when formed by conventional thermolysis techniques[16]. Reactions of the silenes in the presence of several monomers such as vinyl acetate, allyl methyl ether and methyl acrylate were also studied. Laser-induced decomposition of silacyclobutane and 1,3-disilacyclobutane gave rise to silenes and other oxygen-sensitive deposits[17,18].

3. Miscellaneous organosilicon compounds

The photochemical behavior of numerous organic compounds containing one (or several separated) silicon atoms have been reported in recent years. A few interesting examples are mentioned below.

Pannell and coworkers[18b] prepared the novel compound **9** which contains the four group 14 elements in the order C–Si–Ge–Sn. On photolysis, the products isolated, **10** and **11**, indicate the elimination of dimethylgermylene and elimination of dimethylstannylene, respectively, from the starting material, while **12** indicates radical cleavage of the Ge–Sn bond followed by hydrogen abstraction of the resulting germyl radical, and **13** appears to have been derived from radical dimerization, as shown in Scheme 1. Compound **13** itself suffered further photolysis with loss of dimethylgermylene leading to **14**.

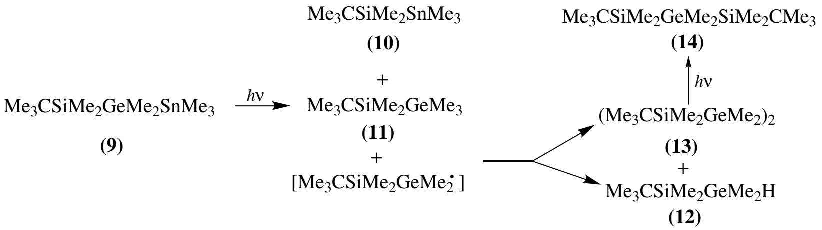

SCHEME 1

Hexakis(trimethylsilyl)benzene, **15**, a severely sterically hindered compound which exists in a chair conformation to minimize steric strain, when photolyzed at >300 nm is quantitatively converted to the Dewar benzene isomer **16**[19] or, in part, to the bis(cyclopropenyl) species **17** at 254 nm as shown in Scheme 2[20]. Compound **15** was thermally converted to the bis-allene **18**.

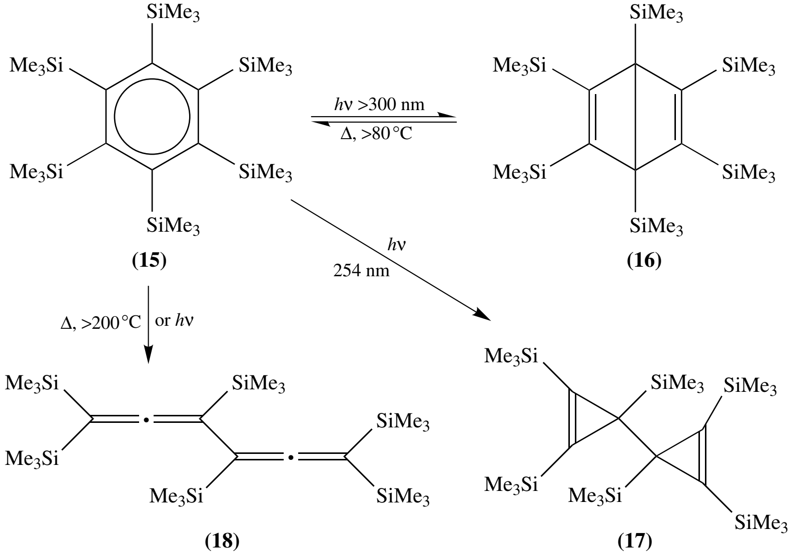

SCHEME 2

B. Cyclic Compounds Containing One Silicon Atom

1. Silacyclopropanes and silacyclopropenes

Silacyclopropanes are commonly formed from the reactions of alkenes with silylenes, which themselves are commonly prepared by photolysis of linear trisilanes (see Section VII). When photolyzed, silacyclopropanes are known to give rise to silylenes or, under other conditions, to undergo 1,3-shifts[2]. Boudjouk and coworkers have prepared a number of silylenes with various substituents on both the carbon and silicon atoms[21], and have shown that significant differences in photochemical behavior are obtained depending on the steric bulk of the substituents. For example, as shown in Scheme 3, the 1,1-di(*t*-butyl)-2,3-dimethylsilirane **19** readily forms di(*tert*-butyl)silylene **20** as does the monomethyl compound **21**, but the unmethylated silirane **22** fails to form the silylene when photolyzed. The differences in behavior were due, it was suggested, to varying degrees of steric strain between the groups on carbon and the groups on silicon[22]. The formation of silylenes from dialkylsiliranes is also discussed in Section VII.

Silacyclopropenes are commonly formed from the addition of a silylene to an alkyne, or in some cases as the result of photolysis of an alkynyldisilane (see Section III.C). Substituted silacyclopropenes have been shown to undergo both 1,2- or 1,3-shifts when photolyzed, yielding silyl-substituted allenes or alkynes, respectively[2]. More complex behavior was observed with methylenesilacyclopropenes such as **23**[23] which ring-opened to a diene, as shown in Scheme 4.

The unusual siladigermacyclopropane **24** on photolysis was observed to decompose to the silagermene **25** and the germylene **26**[24], as shown in equation 4. See Section IV.C.1

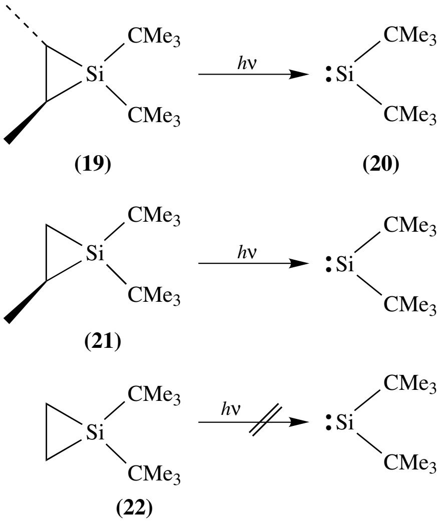

SCHEME 3

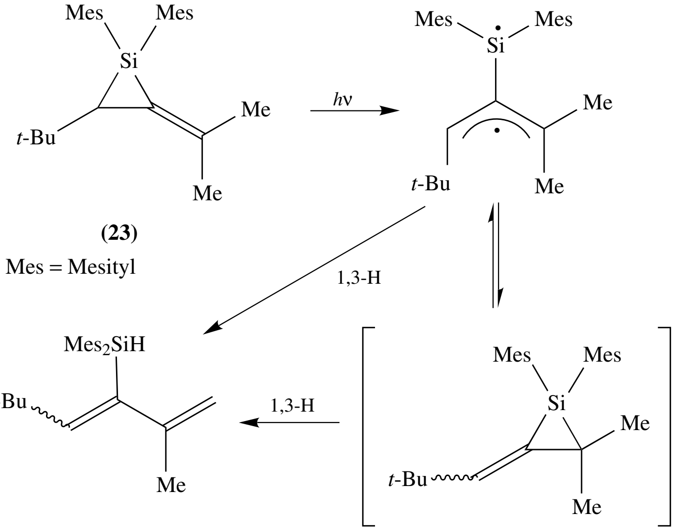

SCHEME 4

for the behavior of the related trisilacyclopropane.

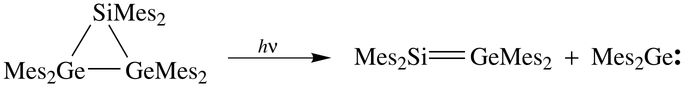

(24) **(25)** **(26)** (4)

2. Silicon in four-membered rings

A detailed study of the photolysis of the relatively simple silacyclobutane **27** was made by Steinmetz and Bai[25a]. When photolyzed at 185 nm in pentane containing methanol, not only was the initial *Z* isomer converted to an *E*,*Z* mixture (indicative of ring opening and reclosure), but also three ring-opened products, **28**, **29** and **30**, were obtained. Two of these seem clearly to be as the result of methanol addition to the intermediary silenes **31** and **32**, and both the silenes and product **30** were logically explained as arising from intramolecular hydrogen abstraction of diradical intermediates **33** and **34**, arising from the photochemical cleavage of a ring silicon−carbon bond, as shown in Scheme 5. The formation of *cis*- and *trans*-butene and propene in the course of the photolysis were explained as being derived from further cleavage of the intermediary diradicals.

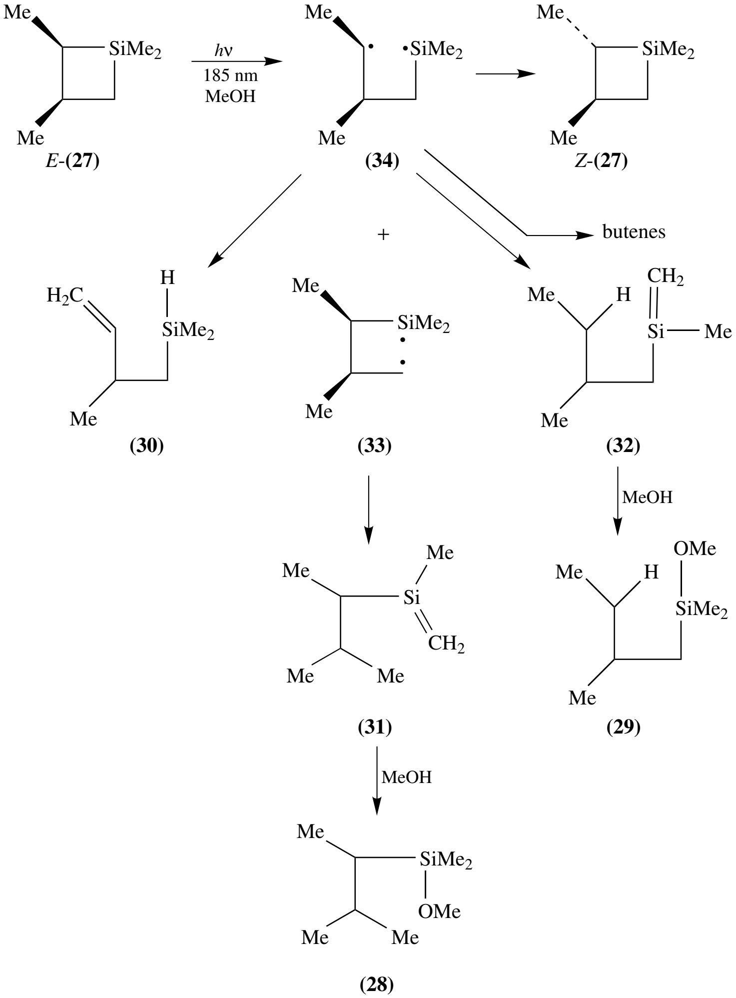

SCHEME 5

The photolysis and flash photolysis of 1,1-diphenyl-1-silacyclobutane has been reinvestigated and much new detail about the reactions of 1,1-diphenylsilene with alcohols and other nucleophiles are reported[25b].

The photolysis and flash photolysis of 1,1-dimethyl-1-sila-2-phenylcyclobut-2-ene, **35**, in the inert solvent cyclohexane have been studied by Conlin, Fink and coworkers[26]. The reaction yielded the siladiene **36**, as shown in equation 5; the kinetics of its reversion to the precursor silacyclobutene **35** were also studied.

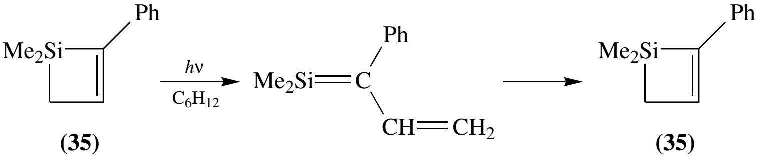

(5)

Steinmetz and coworkers[27] further investigated the behavior of the related 1,1-dimethyl-1-silacyclobut-2-ene and observed that fragmentation to acetylene and dimethylsilene occurred in addition to electrocyclic ring opening. These two studies are probably the most detailed investigations of siladienes to date.

In a related study Jones and coworkers photolyzed the 1,3-disilacyclobutane **37** and observed that a single diastereomer gave rise to a mixture of products[28]. They suggested that ring cleavage to a diradical **38** occurred which could ring-close to either the starting material or the isomer **39**, or the diradical could dissociate to two molecules of silene **40**, or disproportionate to the alkene **41**, which is photochemically convertible to its isomer **42**, as shown in Scheme 6. These products were proposed based on the structure of their trapping products when the photolysis was carried out in methanol. Attempts to trap the diradical with excess tributyltin hydride failed.

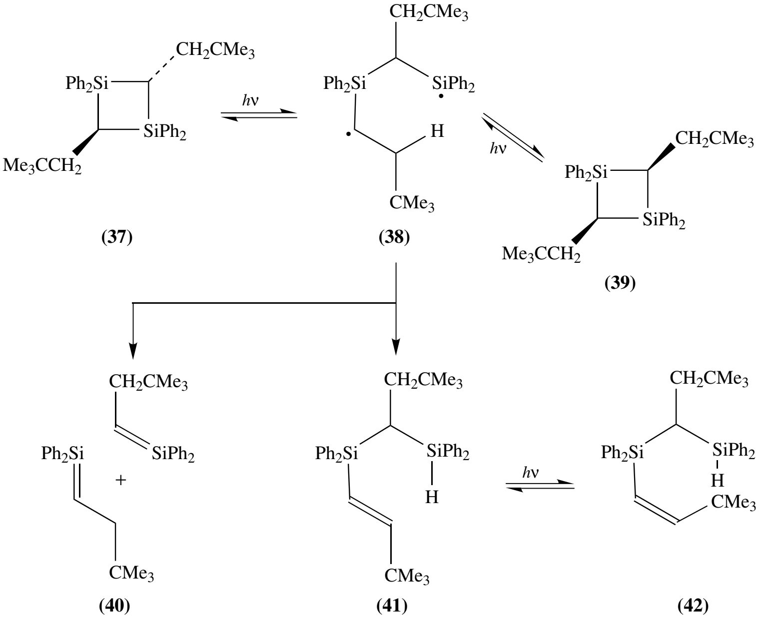

SCHEME 6

Ando and coworkers have recently described the photolysis of the novel 2,4,5,6-tetrathia-1,3-disilabicyclo[2.1.1]pentane, **43**[29]. As shown in Scheme 7, when **43** was photolyzed in the presence of 6 equivalents of trimethylphosphine, sulfur was extruded and the new compound **44** was formed quantitatively. However, when **43** was photolyzed with 10 equivalents of triphenylphosphine, both **44** and the 1,3-disila-2,4-dithiacyclobutane **45** were formed.

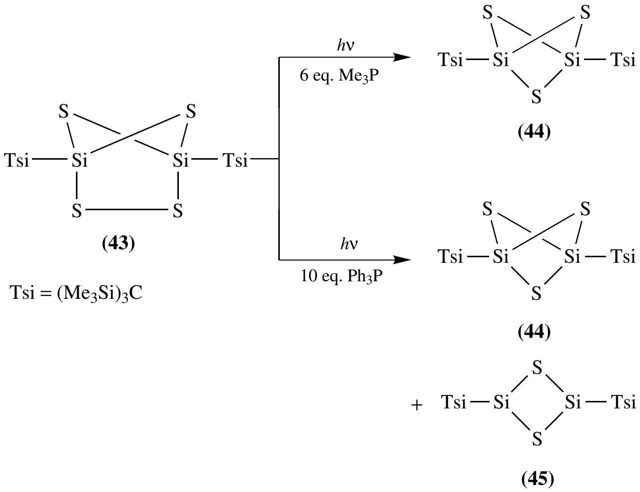

SCHEME 7

3. Other silacycloalkanes

The photolysis at 214 nm of a bridgehead silanorbornene **46** in alcohols has recently been reported by Steinmetz and Chen who proposed that a 1,3-Si to C migration occurred leading to the cyclic silene **47**, which then reacted with the alcohol to give the final product **48**[30]. The reactions are summarized in equation 6.

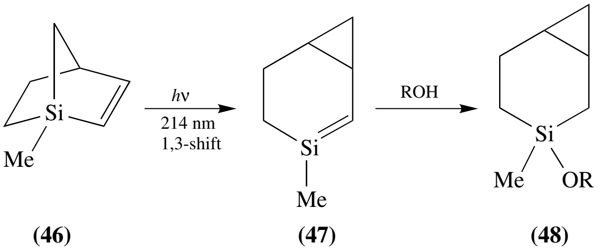

(6)

Jones and coworkers observed an interesting rearrangement of a 9,10-bridged dihydroanthracene **49** which on photolysis led, via a diradical **50**, to a mixture of the siladiene **51** and the eight-membered ring silene **52**, as judged by the products of methanol trapping. In addition, the methanol adduct **53** of the diradical was isolated[31]. This is the first example of a silicon–carbon double bond in an eight-membered ring. The reactions are shown in Scheme 8.

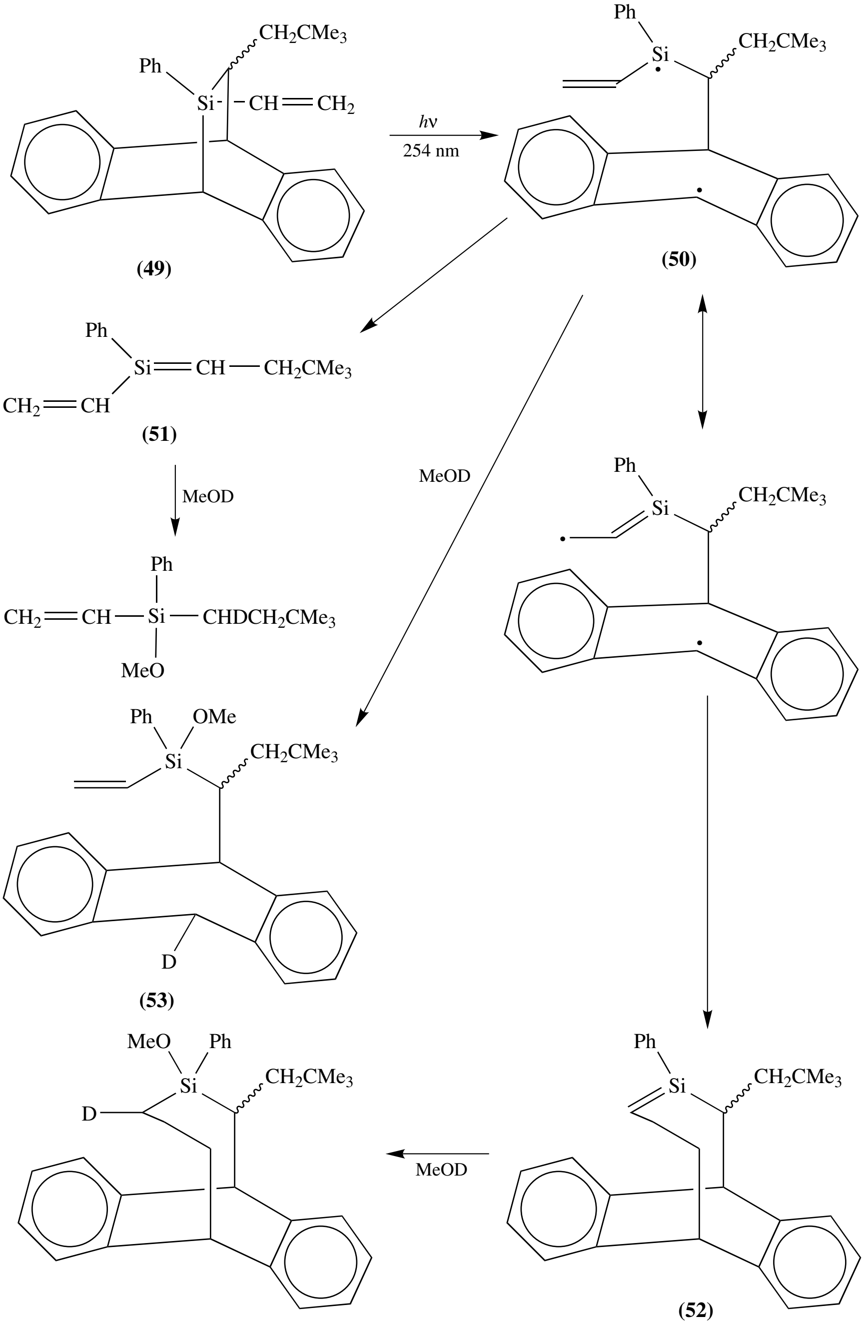

Ph
CH$_2$CMe$_3$
Si
CH═CH$_2$
(49)
hν
254 nm
(50)
(51)
CH$_2$═CH
Si═CH—CH$_2$CMe$_3$
MeOD
CH$_2$═CH—Si—CHDCH$_2$CMe$_3$
MeO
OMe
D
(53)
MeO
(52)

SCHEME 8

The mechanism of photochemical decomposition of the silyl-bridged naphthalene **54** was studied by Nefedov and coworkers using the CIDNP ^{1}H technique[32]. It was suggested that initially an excited diradical **55** was formed, which subsequently decomposed irreversibly to dimethylsilylene and polarized tetraphenylnaphthalene (equation 7). Other studies interpreting the UV absorptions during the photolysis of **54** have been reported[33]. See Section VII for other reactions leading to silylenes.

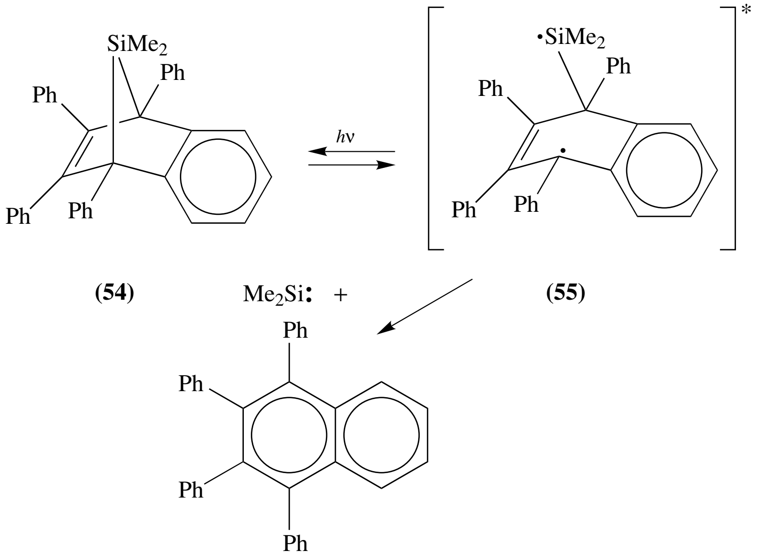

(54) **(55)** (7)

Compound **54** was also utilized as a photochemical source of dimethylsilylene to prepare the unusually substituted silirene **56**[34] as shown in equation 8.

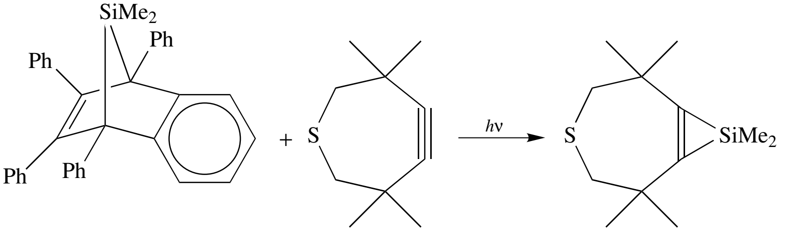

(8)

(54) **(56)**

Several detailed studies by Steinmetz and coworkers[35–37] have concerned the photolysis, in the presence of alcohols or other trapping reagents, of cyclic unsaturated compounds containing one or two silicon atoms in the ring. Thus photolysis of the 1,4-disilacyclohept-2-ene **57** gave products of intramolecular rearrangement, **58**, ring opening, **59**, and evidence, based on the structure of a dimer and of a trapping product, that the initial *cis* isomer, **57**, was converted in part to the *trans* geometric isomer **60**. A β-silylcarbocationic intermediate was proposed, as shown in Scheme 9, to account for the rearrangement products isolated. Formation of the *trans* disilacycloheptene reflects the flexibility and decreased ring strain present when silicon atoms replace carbon in medium-sized rings.

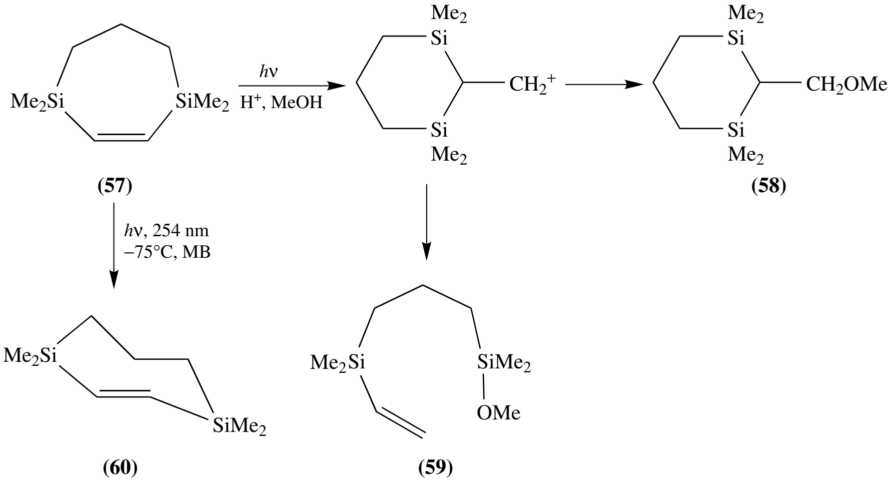

SCHEME 9

The simpler 1-silacyclopent-3-ene **61** gave evidence, based on the reaction products identified, both for silylene extrusion, trapped as **62** by deuteriomethanol, as well as for a 1,3-Si shift to a silirane intermediate **63** which ring-opened during reaction with the alcohol present yielding **64** (Scheme 10). In contrast, the 1-silacyclopent-2-ene **65** on photolysis in alcohols gave products best accounted for by protonation of the silacyclopentene α to silicon to form a β-silyl cation **66**, which then reacted with alcohol either at carbon β to silicon to give **67** or at silicon to give the product **68**. However, photolysis in the presence of Me$_3$SiOMe or acetone suggested that a silene intermediate **69** was formed as a result of a 1,3-C shift, and trapping led to **70** and **71**, respectively (Scheme 10). This photochemical behavior is very different from that observed for the analogous homocyclic cyclopentenes, demonstrating that the presence of the silicon atom had a significant influence on the course of the reaction.

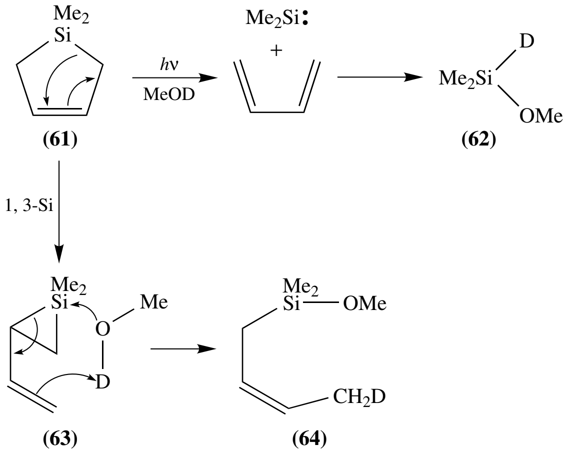

SCHEME 10. (*continued*)

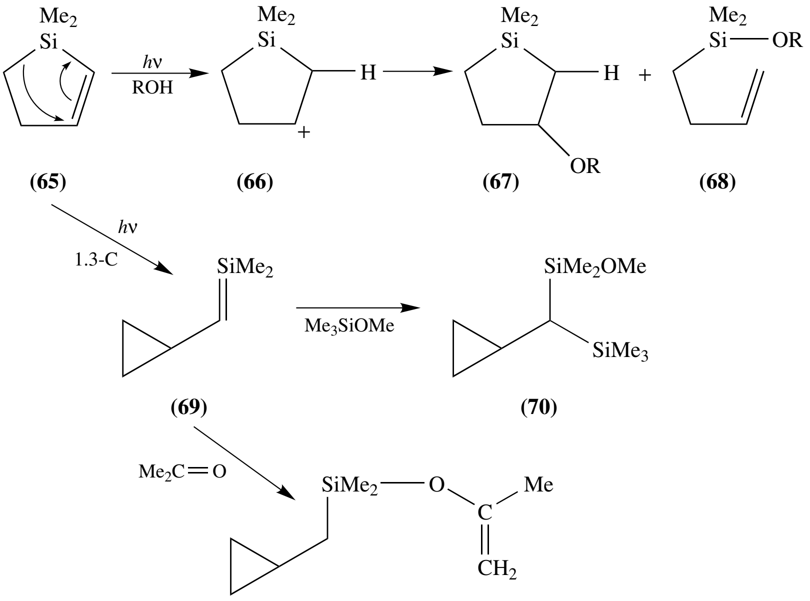

(65) **(66)** **(67)** **(68)**

(69) **(70)**

(71)

SCHEME 10. (*continued*)

4. Silaaromatics

Photochemical methods have been used in the past to prepare a variety of rather unstable silaaromatic compounds. The photolyses of cyclic unsaturated silyldiazo compounds, which yield silabenzenes and/or silafulvenes, are described in Section VI.

The flash photolysis of several 9,10-dihydrosilaanthracene derivatives **72** in argon matrices led to the detection of 9-silaanthracenes, **73**, characterized by their UV spectra[38] (equation 9).

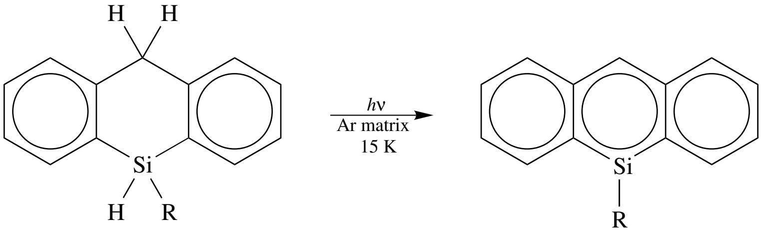

(9)

(72) **(73)**

R = H, Me, Ph

West and coworkers[39] used a 9,10-disilacyclohexadienyl-bridged anthracene **74** to synthesize a permethyl-1,4-disilabenzene, **75**, as shown in equation 10, and to study its reactions.

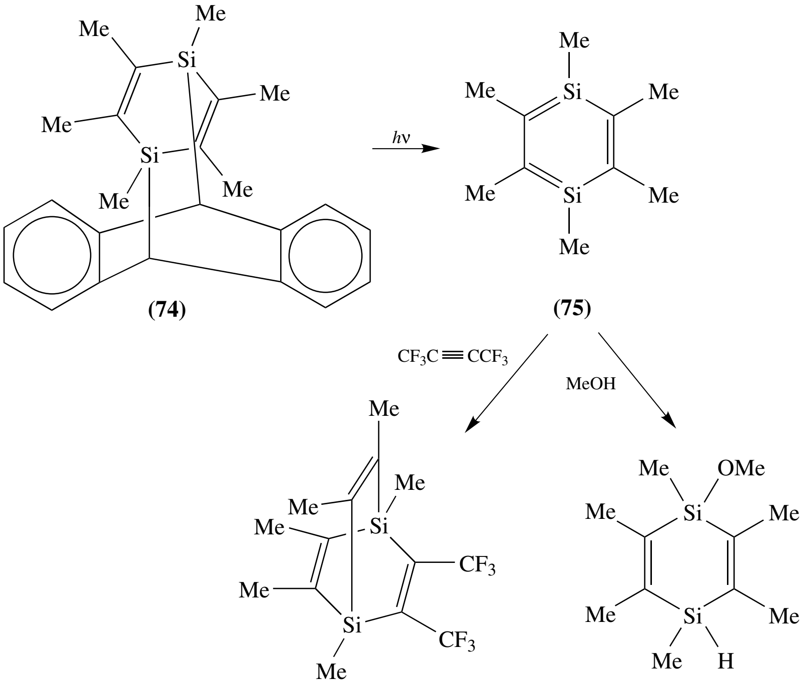

(10)

III. COMPOUNDS CONTAINING TWO SILICON ATOMS. DISILANES

A. Introduction

The photochemistry of disilanes has been investigated for several decades. Photolysis yielding two silyl radicals was recognized early on as one of the common modes of reaction. Studies of $Ph_3Si{-}SiPh_2Me$ or its trideuteriomethyl analog **76**, by Boudjouk and coworkers[40], indicated the homolysis of the silicon–silicon bond to a pair of radicals which subsequently disproportionated, yielding the silene **77** (equation 11). This provided some of the early evidence for the existence of the silicon–carbon double bond.

$$\underset{\textbf{(76)}}{Ph_3Si{-}SiPh_2CD_3} \xrightarrow{h\nu} Ph_3Si\bullet + \bullet SiPh_2CD_3 \longrightarrow Ph_3SiD + \underset{\textbf{(77)}}{Ph_2Si{=}CD_2} \qquad (11)$$

Subsequent studies by Sakurai and coworkers of the photolysis of disilyl-bridged aromatic compound **78**, indicated that two interesting (not necessarily independent) processes were occurring, namely elimination of the disilyl group as a disilene, **79**, another reactive intermediate of silicon chemistry, and secondly, Si–C homolysis to a diradical **80**, which overall underwent a 1,2-silyl shift yielding the isomeric disilyl-bridged compound **81**[41,42] (Scheme 11).

Further investigation of the photolysis of disilanes has been carried out in recent years in which 1,2-silyl and 1,3-silyl shifts were frequently observed. Some of these studies are reported below in sections based on the nature of the group(s) to which the disilyl group is attached.

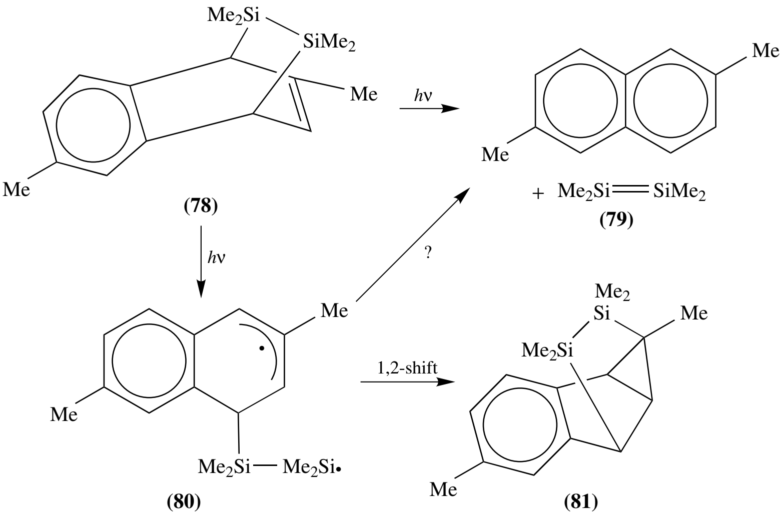

SCHEME 11

B. Vinyldisilanes

Earlier studies of the photolysis of vinyldisilanes **82**[43] clearly established the tendency of 1,3-silyl migrations to occur, leading to silenes **83** (equation 12).

$$\underset{\textbf{(82)}}{CH_2{=}CHSiR_2SiMe_3} \xrightarrow{h\nu} \underset{\textbf{(83)}}{Me_3SiCH_2CH{=}SiR_2} \qquad (12)$$

Sakurai and coworkers[44] took advantage of this rearrangement to prepare from the cyclic divinyldisilane **84** the cyclic silene **85**, in order to investigate the stereochemistry of alcohol addition to a silicon–carbon double bond. Diastereomeric products resulting from both *cis* and *trans* addition to the double bond were formed, whose proportions depended on the concentration of the alcohol in the system. A mechanism accounting for the results proposed that initial coordination of an alcohol molecule to the sp^2-hybridized silicon atom of the silene gave the complex **86**, which either underwent intramolecular proton transfer (path a) yielding the *cis* adduct **87** or else was protonated by a second molecule of alcohol located on the opposite side of the plane of the ring (intermolecular proton transfer, path b) yielding the *trans* product **88** as shown in Scheme 12. The mechanism satisfactorily accounts for several observations on the stereochemistry of alcohol addition to a variety of silenes. A further elaboration is reported in Section III.D.

Conlin and Bobbitt used 1,2-divinyl-tetramethyldisilane **89** to generate a simple silene **90** used to explore competing [2 + 2] and [2 + 4] cycloaddition reactions with butadiene (see Scheme 13), where the *E*-**91** and *Z*-**91** isomers of the [2 + 2] adduct predominated over the [2 + 4] cycloadduct **92**[45].

1,1-Divinyl-tetramethyldisilane similarly rearranged to the analogous silene $CH_2{=}CHMeSi{=}CHCH_2SiMe_3$, which showed a UV absorption maximum at 336 nm in 3-MP (3-methylpentane) glass at 77 K[46,47].

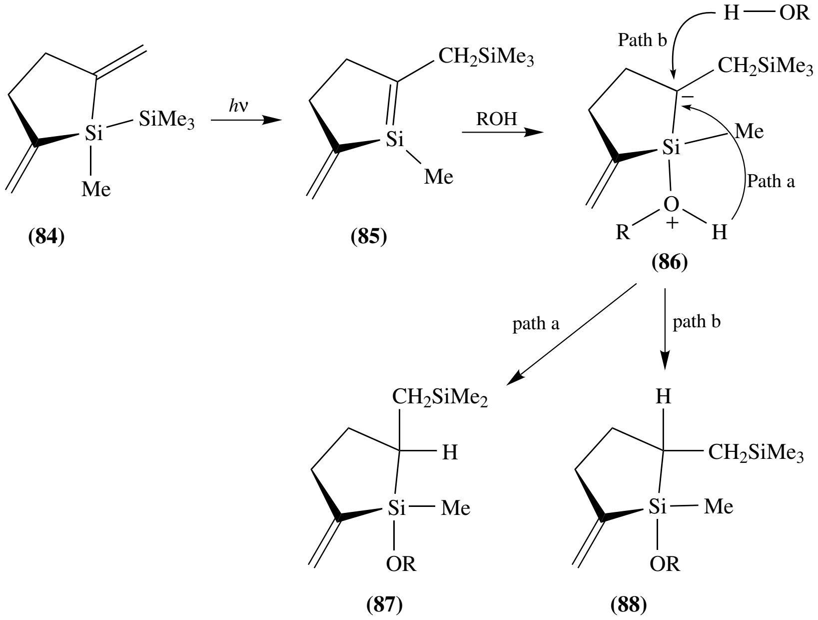

SCHEME 12

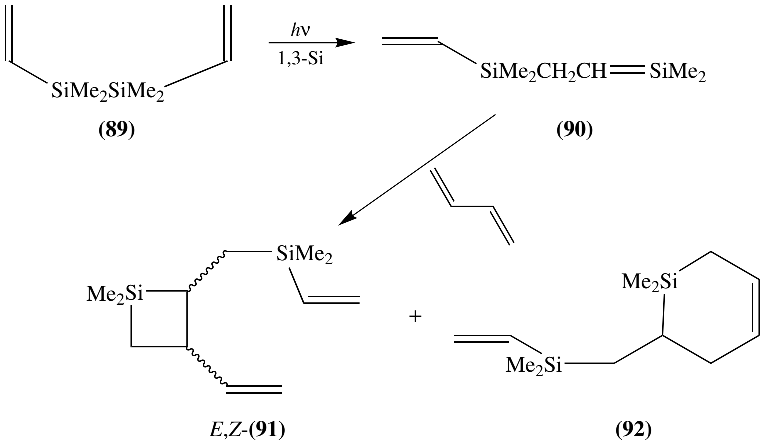

SCHEME 13

C. Alkynyldisilanes

Relatively simple alkynyldisilanes, **93**, have been observed to undergo both 1,2- and 1,3-silyl migrations during photolysis leading to silacyclopropenes **94** and silaallenes **95**, respectively[2] (equation 13).

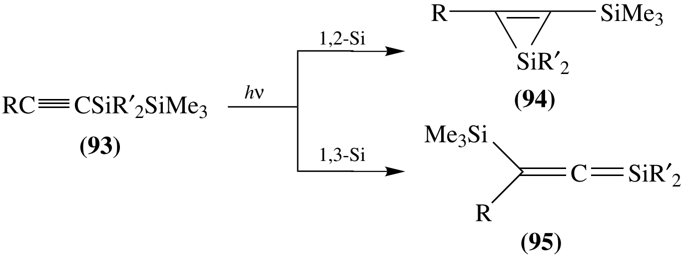

(13)

Recently, detailed mechanistic studies have been made of the photolysis of 1-aryl-4-(pentamethyldisilanyl)-1,3-butadiynes **96** in various solvents. Photolyses in the presence of methanol led to the isomeric products **97** and **98**, derived from solvolytic ring opening of the initially formed silacyclopropene, **99**, resulting in turn from 1,2-silyl migration[48], while photolyses in acetone led to the products **100** and **101** arising from two-atom insertion into the three-membered ring[49] (Scheme 14).

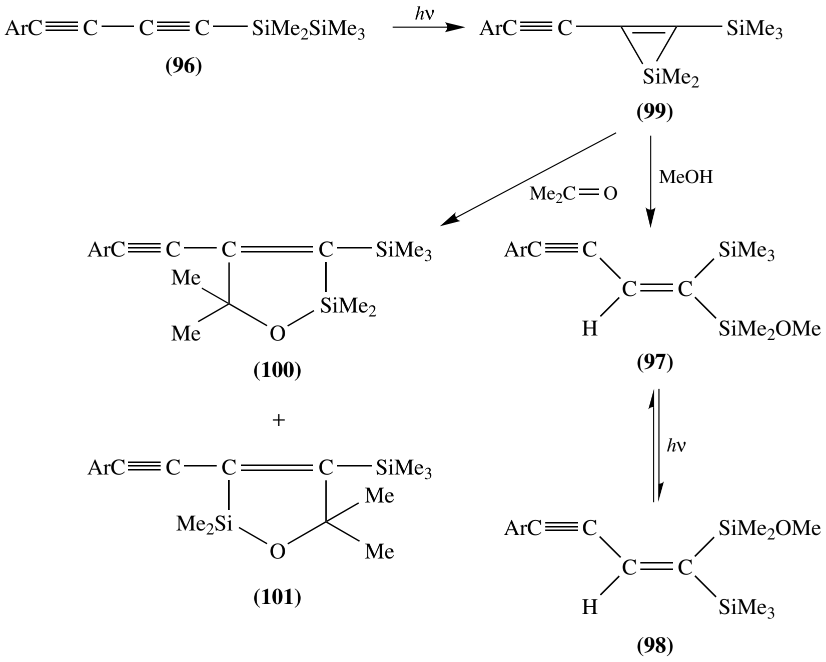

SCHEME 14

The palladium chloride-(PPh$_3$)$_2$ catalyzed photoisomerization of a disilylbutadiyne **102** has recently been described. It was shown that isomerization of the diyne initially led to the substituted silacyclopropene **103**, which subsequently dimerized to three isomers of 1,4-disilacyclohexadiene **104**, (equation 14). A mechanism was proposed.

The photochemistry of 1,4-bis(pentamethyldisilanyl)butadiyne in the presence of methanol, acetone and acetaldehyde has also been investigated[50].

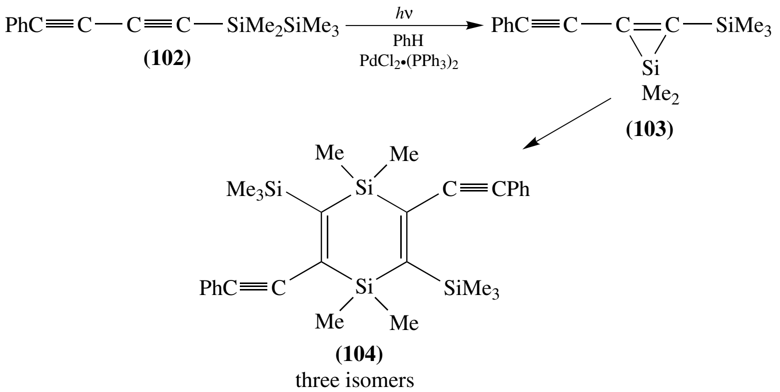

(14)

D. Aryldisilanes

The much studied photochemistry of aryldisilanes carried out in earlier years has been reviewed[51,52]. Cleavage of the silicon–silicon bond of the disilyl moiety is always involved, but various other reactions have been observed depending on the structure of the disilane and the conditions employed. Thus cleavage to a pair of silyl radicals, path a of Scheme 15, is normally observed, and their subsequent disproportionation to a silene and silane, path b, is often observed. There is evidence that the formation of this latter pair of compounds may also occur by a concerted process directly from the photoexcited aryldisilane (path c). Probably the most common photoreaction is a 1,3-silyl shift onto the aromatic ring to form a silatriene, **105**, path d, which may proceed via radical recombination[52]. A very minor process, observed occasionally, is the extrusion of a silylene from the molecule (path e), as shown in Scheme 15.

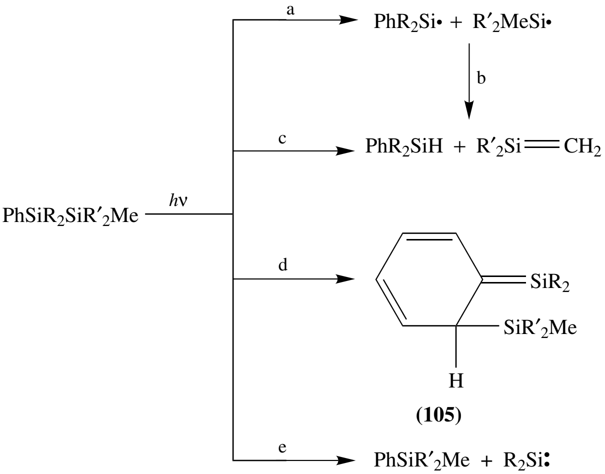

SCHEME 15

Much additional information has been accumulated on these systems in recent years. On the one hand Ishikawa and Sakamoto investigated tolyl-**106** and xylylpentamethyldisilanes and found that the main reaction involved the 1,3-shift of a trimethylsilyl group to the ring to yield the silatriene **107**, provided that an *ortho* position on the aromatic ring was vacant[53]. An example is shown in equation 15, where the silatriene was trapped as the adduct **108** by an ene reaction with isobutene.

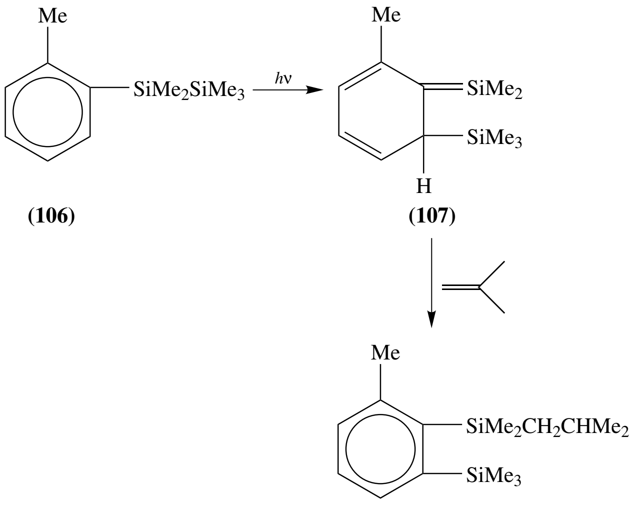

(106) **(107)** **(108)**

(15)

The same behavior was observed for bis(pentamethyldisilyl)-substituted aromatics[54] and for more complex systems such as $Me_3Si(SiMe_2C_6H_4\text{-}p\text{-}SiMe_2)_nSiMe_3$ ($n = 2, 3, 4$)[55], as confirmed by the structures of the products obtained by trapping of the intermediate silatrienes with isobutene or other reliable trapping reagents.

With 2-naphthyl systems **109**, 1,3-silyl migration to the 1-position on the ring was observed[56] since trapping by MeOD gave the product **110**, indicating the intermediacy of an arylsiladiene **111** (equation 16).

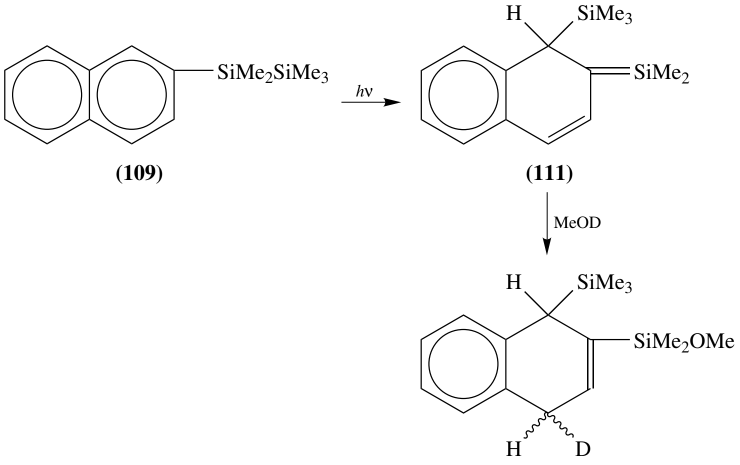

(109) **(111)** **(110)**

(16)

1-Naphthyldisilanes **112** were shown[57], after reinterpretation of earlier results, to undergo Si−Si bond cleavage with migration of a silyl group to the 8-position of the naphthyl ring to give the bis-silyl adduct **113**, the overall 1,4-rearrangement almost certainly being the result of homolytic cleavage, followed by homolytic aromatic substitution via the postulated intermediate **114**. Most conventional silene traps failed to detect the presence of a silene, but when 1,4-bis(pentamethyldisilyl)naphthalene **115** was photolyzed in MeOD a novel dimethylsilylene bridged species **116** was isolated in about 50% yield (Scheme 16).

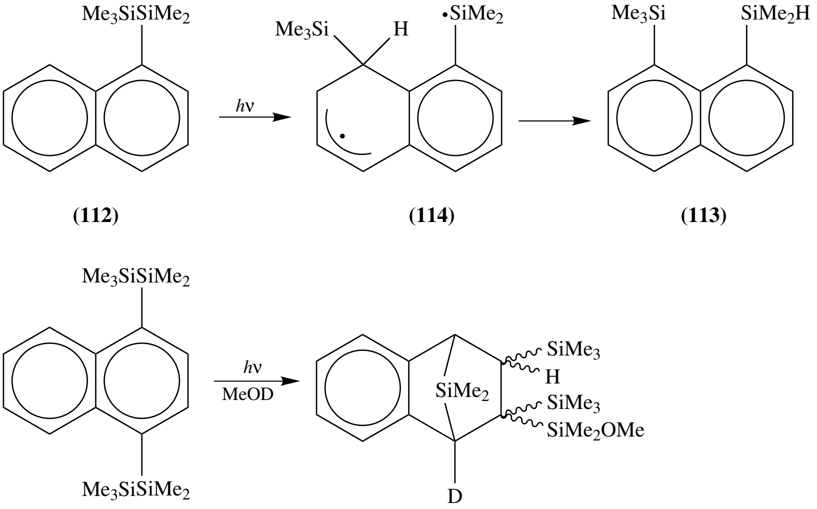

(112) **(114)** **(113)**

(115) **(116)**

SCHEME 16

Homolytic cleavage of the Si−Si bond, followed by homolytic aromatic substitution, was also invoked to explain the photochemical reactions of 1,1-di(1-naphthyl)- **117**, and 1,2-di(1-naphthyl)-tetramethyldisilane **118**[58] which yielded **119** and **120**, respectively, as the main reaction products (Scheme 17). A minor reaction pathway of the latter disilane involved dimethylsilylene expulsion.

Very recently Sluggett and Leigh have reinvestigated the photochemistry of several aryldisilanes having either methyl or phenyl groups on the disilane side chain. Both direct photolysis as well as laser flash photolysis produced a wealth of new information including fluorescence data for the disilanes, absorption maxima of silene and silyl radical transients, rate constants of quenching processes by a variety of quenching reagents (particularly those used to trap intermediary silatrienes), deuterium isotope effects for the reactions of the silatrienes with water, etc.[59−62]. These studies have contributed to the further understanding of the behavior, the mechanism of formation and the mechanisms of reaction with trapping agents such as alcohols, acetone, dimethylbutadiene and oxygen, of the silatriene intermediates formed in these reactions.

The more recent studies showed that methylpentaphenyldisilane, **121**, on photolysis formed the silatriene **122** in low yield by a 1,3-silyl migration, in addition to forming the silene **123**[59]. Flash photolysis of phenylpentamethyldisilane, **124**, for comparative purposes, formed the silatriene **125**, λ_{max} 420, $\tau = 5$ μs, in isooctane with no evidence for formation of the silene $PhMeSi{=}CH_2$. The silatrienes were readily quenched either by

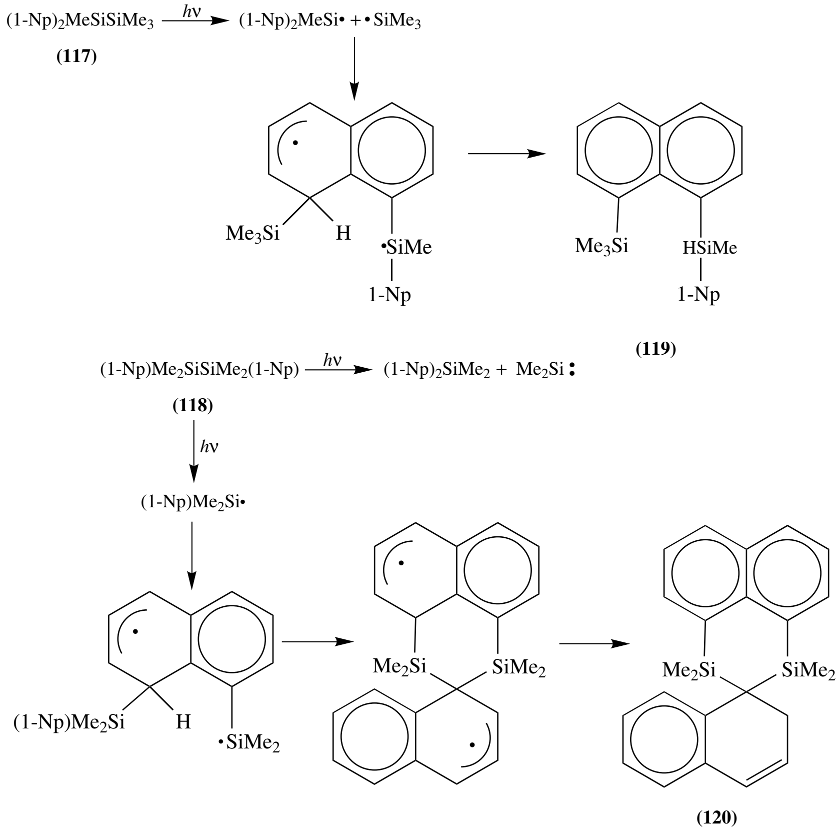

SCHEME 17

reagents which add in a 1,2 manner across the ends of the Si=C bond, or by reagents which react through an ene mechanism as shown in Scheme 18[59]. It was suggested that bulky groups like phenyl, attached to the silicon atoms, tended to hinder silatriene formation, relative to the formation of the simple silene $RR'Si=CH_2$. Consistent with this view was the observation that direct (or laser flash) photolysis of 1,2-di(*t*-butyl)-1,1,2,2-tetraphenyldisilane in chloroform exclusively yielded the silyl radical $(t\text{-Bu})Ph_2Si\bullet$, which was captured as silyl chloride in 95% chemical yield with a quantum efficiency of 0.64. The bimolecular rate constants for reactions of the radicals with a variety of reagents were determined[60]. While hexaphenyldisilane is known to mainly yield $Ph_3Si\bullet$ radicals on photolysis[63] it was suggested, based on absorption measurements, that the related silatriene was also formed, but only in low yield[60].

Re-examination of the photolyses of the family of aryldisilanes $PhRR'Si-SiMe_3$ ($R,R' = Me, Ph$) in solution containing acetone was found to give not only the previously observed products believed to be derived from an ene reaction between the silatriene and acetone, **126**[51], but in addition, and not previously observed, the $[2+2]$ siloxetanes, **127**, were detected and isolated, as were the silyl enol ethers **128** derived from the simple silene **129** formed by elimination of trimethylsilane[61], as shown in Scheme 19. The biradical **130** was proposed as an intermediate for some of the reactions involving acetone. Rate

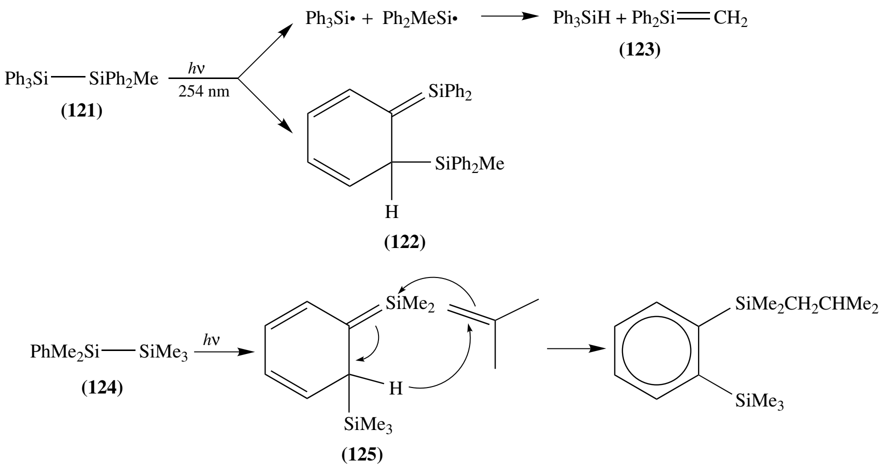

SCHEME 18

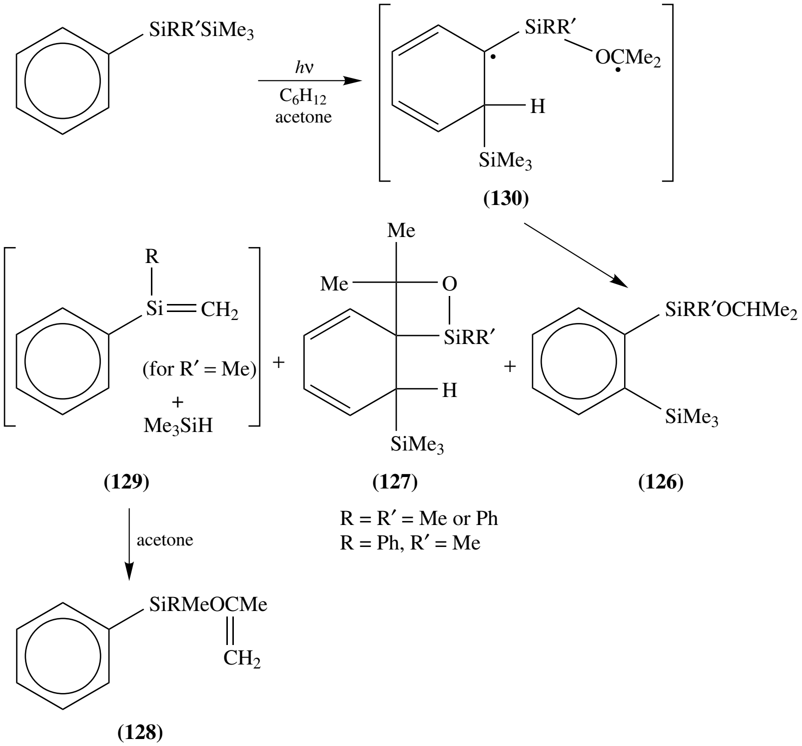

SCHEME 19

constants for the trapping of the silatrienes with several reagents, 2,3-dimethylbutadiene, methoxytrimethylsilane, oxygen and carbon tetrachloride, were also measured.

In earlier studies of the reactions of some of the silatrienes, e.g. **132**, derived from the photolysis of *p*-tolylpentamethyldisilane, **131**, with alcohols, it was reported[51], as shown in equation 17, that only the 1,4- adduct **133** and the 1,6-adduct **134** were formed, and there was no evidence that the 1,2-adduct **135** was formed. The absence of **135** was always difficult to rationalize.

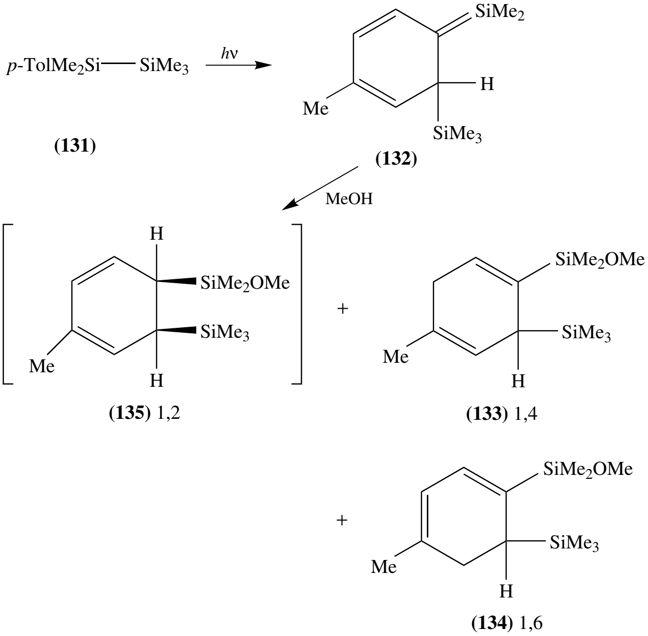

(17)

More recent studies by Leigh and Suggett[62] using phenylpentamethyldisilane and other aryldisilanes showed (Scheme 20) that the 1,2-methanol adduct **138** was indeed formed along with the 1,4-adduct **139** and the 1,6-adduct **140**, indicating that the behavior of the silatriene **136** (and its analogs) was consistent with the assigned structure as containing a silicon−carbon double bond. Much rate data were also presented.

Also arising from these important studies was further evidence about the mechanism of the addition of alcohols to silenes, and the silatriene **136** in particular, as illustrated in Scheme 20. In a minor revision of the Sakurai mechanism[44] it was suggested that the reaction was initiated by rapid reversible nucleophilic attack of the alcohol oxygen atom at the sp^2-hybridized silicon atom of the double bond (involving rate constants k_1 and k_{-1}) to form an alcohol−silene complex **137**. This is followed by either intramolecular (intracomplex) proton transfer (rate constant k_2) leading to the 1,2-adduct **138** or by an intermolecular proton transfer from the complex to further molecules of alcohol leading to **138** and its isomers **139** and **140**. The relative rates of these processes were shown to be affected by the nucleophilicities of the alcohol, its concentration and the nature of the groups on the sp^2-hybridized silicon atom of the silene.

Kira and Tikurs[64] observed an interesting variation of the 1,3-silyl rearrangement of aryldisilanes since, during the photolysis of pentafluorinated aryldisilanes such as **141**, in addition to the 1,3-silyl migration to the 2-position of the ring forming the silatriene **142**, a

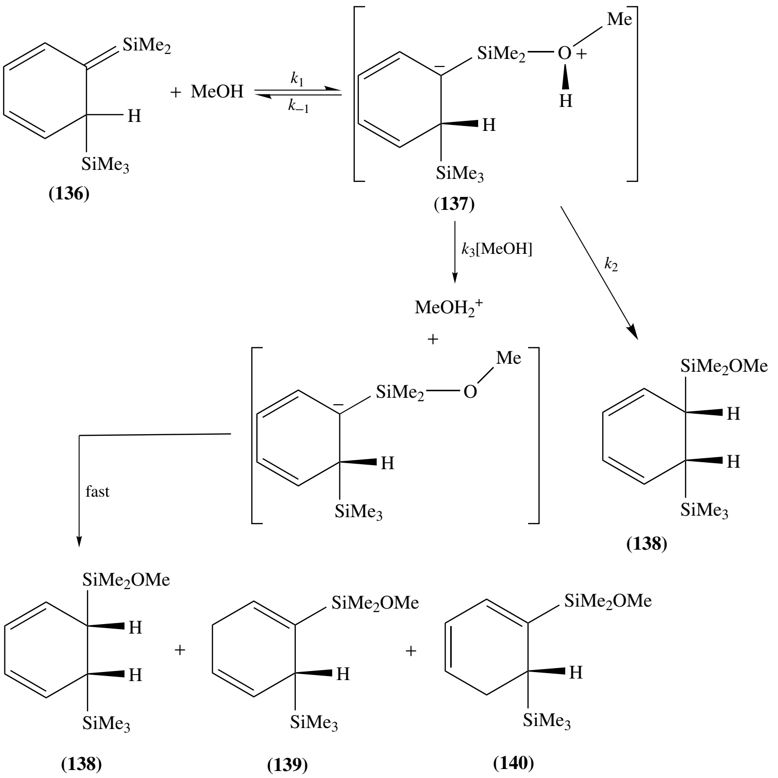

SCHEME 20

reverse 1,3-fluorine migration from the aromatic ring to silicon occurred yielding the product **143** as well as the product of alcohol addition when alcohol was present (Scheme 21). Similar behavior was found with a 2,6-difluorophenyldisilane as was observed with the pentafluoro compound (Scheme 21), but not with a 2,6-dichlorophenyldisilane.

Braddock-Wilking and Gaspar studied the photolysis of mesityl-substituted disilanes such as $Mes_2MeSiSiMeMes_2$, which was found to form $Mes_2MeSi\bullet$ radicals which disproportionated into the silene $Mes_2Si{=}CH_2$ and Mes_2MeSiH in an inert solvent. There was also evidence that these products were formed in part directly during the photolysis[65].

Mochida and coworkers observed that photolysis of 2-furylpentamethyldisilane also yielded silyl radicals on photolysis, the radicals being trapped as silyl chlorides by reaction with CCl_4[66].

Recently, several studies have been made of the photolysis of disilanes or polysilanes in the presence of an electron-deficient alkene using a photosensitizer (such as phenanthrene) and acetonitrile as solvent. These conditions result in the addition of silyl groups to one end of the alkene double bond and hydrogen to the other end (equation 18) and evidently involve the reaction of the radical anions of the electron-deficient silene with silyl radicals[67] (see also Section VIII.A).

$$\begin{aligned}\mathrm{PhCH{=}C(CN)_2 + Me_3SiSiMe_2Ar} &\xrightarrow[\substack{\text{phenanthrene}\\ \mathrm{CH_3CN}}]{h\nu} \mathrm{Ph(Me_3Si)CHCH(CN)_2}\\ &\qquad + \mathrm{Ph(ArMe_2Si)CHCH(CN)_2} \qquad (18)\end{aligned}$$

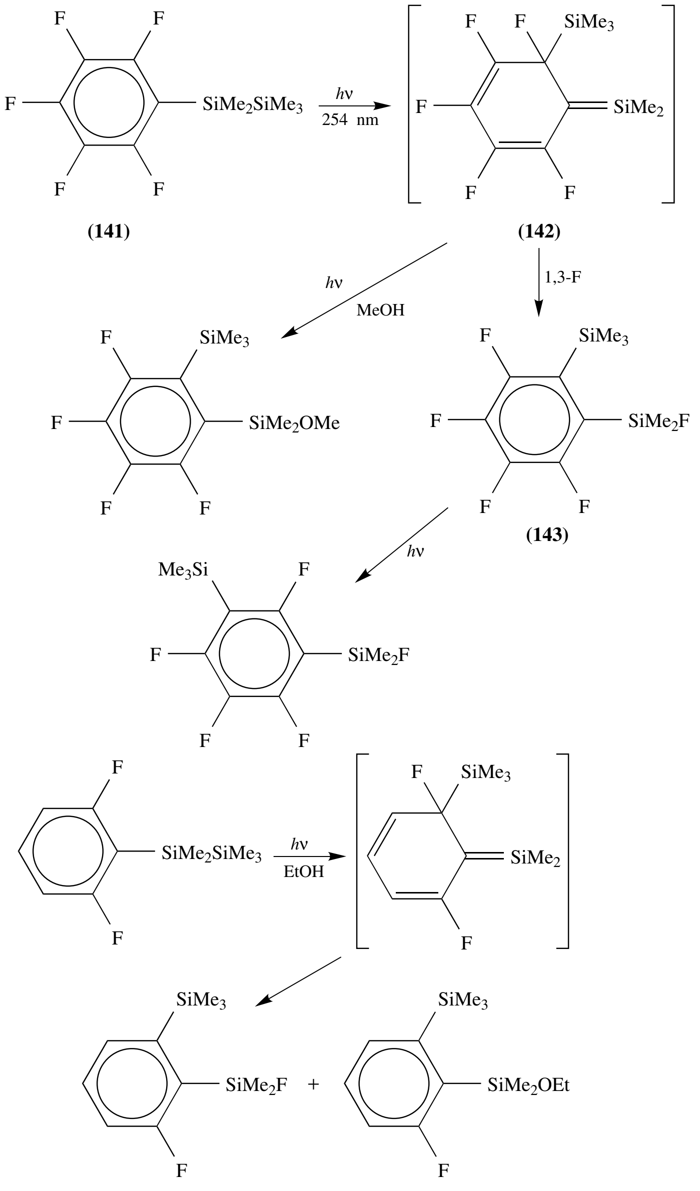

SCHEME 21

The photolysis of the benzodisilacyclobutane **144** was studied[68]. It was postulated that homolysis to the diradical **145** occurred which then disproportionated intramolecularly leading to the silene **146**, that was trapped by *t*-butyl alcohol. An unusual dimer **147** was also formed, postulated by the authors to be derived by head-to-head coupling of the silene to give the diradical **148**, which then abstracted hydrogen. However, intermolecular coupling of two molecules of the diradical to give **149**, followed by hydrogen abstraction, is perhaps a more reasonable explanation, as shown in Scheme 22.

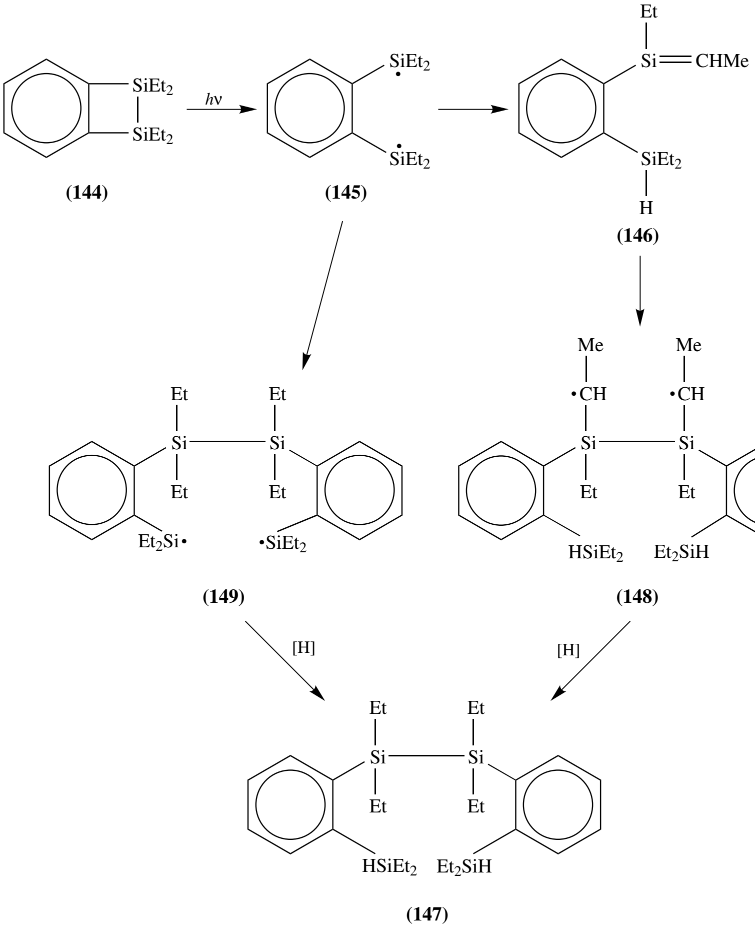

SCHEME 22

E. Arylvinyldisilanes

When a disilane contains both an aryl and a vinyl group as in **150** (or a substituted vinyl such as dihydropyranyl), the possibility exists that during photolysis 1,3-silyl migration to either or both groups may occur. Two studies[69,70] of model compounds clearly established that 1,3-silyl shifts to both the vinyl and phenyl groups generally occurred, which produced isomeric silene intermediates **151** and **152** that could be trapped subsequently by a variety of trapping agents (methanol, acetone, isobutene, 2,3-dimethylbutadiene). An example with acetone is given in Scheme 23. In most cases migration to the vinyl group was favored over migration to the phenyl group (where the usual silatriene was produced), but the extent of migration (based on the yields of trapped products) depended on both the structure of the starting material and the nature of the trapping agent.

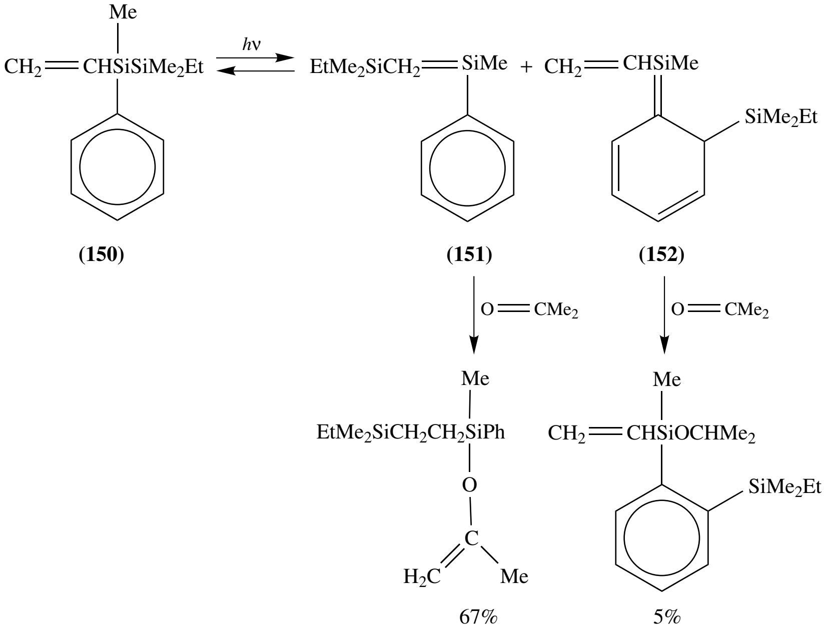

SCHEME 23

F. Transition Metal-substituted Disilanes and Related Compounds

In recent years considerable study has been made of the photochemical behavior of a number of di- or polysilanes which are bonded to a transition metal. Typical compounds are shown below.

$\eta^5 - [(C_5H_5)Fe(CO)_2](SiR_2)_nSiR_3$

$\eta^5 - [(C_5H_5)M(CO)_3](SiR_2)_nSiR_3 \quad M = Cr, Mo, W$

$\eta^5 - [(C_9H_7)Fe(CO)_2](SiR_2)_nSiR_3$

$\eta^5 - [(C_5R_5)M(CO)_2](SiR_2)_nSiR_3 \quad M = Fe, Ru, Os$

A review of the chemistry of these species has recently appeared[71]. These readily made compounds undergo interesting photochemistry, which includes silylene expulsion and/or scrambling of R groups within the disilyl group. An example involving $FpSiMe_2SiPh_3$, **153** $\{Fp = \eta^5 - [(C_5H_5)Fe(CO)_2]\}$ is shown in Scheme 24.

As shown, the process is believed to involve reversible elimination of a CO ligand followed by a 1,2-silyl migration to the Fe atom leading to **154**, which can undergo R group scrambling to **155** and **156** due to 1,3-alkyl or 1,3-aryl group migrations from Si to Si. Each of the three metal–silylene complexes can lose a silylene and regain CO, leading to the observed product mixture of **157**, **158** and **159**.

Support for this mechanism has been obtained from isolation of stabilized silylene intermediates[72], isotope labeling experiments[73] and low temperature studies[74]. Electron-donating groups on a phenyl group attached to silicon stabilize the intermediate $(\eta^5 - C_5H_5)FeCO(=SiMeAr)SiMe_3$[75].

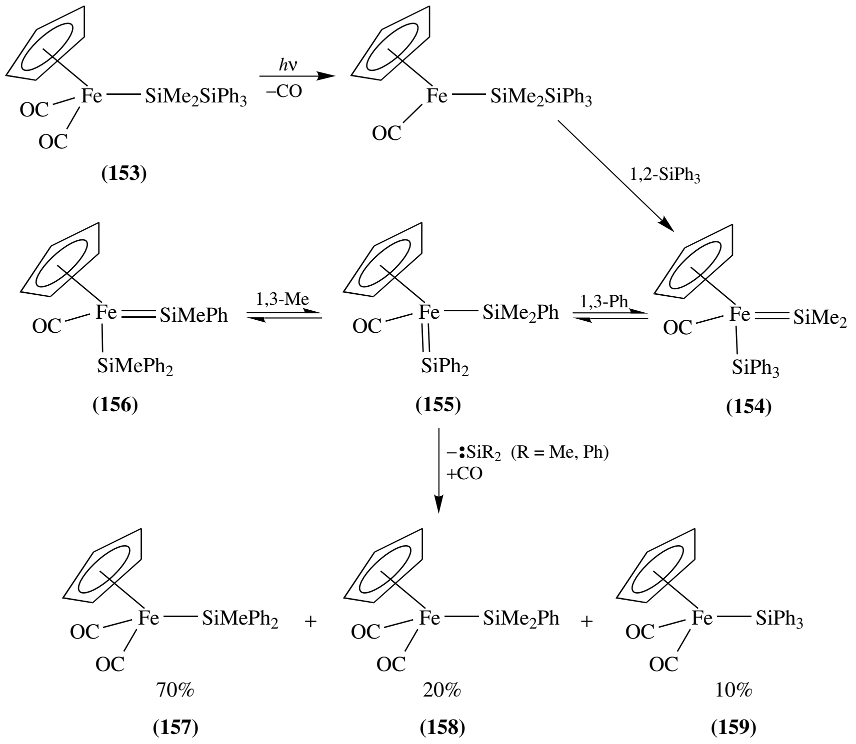

SCHEME 24

With trisilyl systems, e.g. $\eta^5 - [(C_5H_5)Fe(CO)_2](Si_3Me_6R)$, R = Me, Ph, studies have shown that isomerization occurs prior to loss of the silylene :SiMeR[76], while tetrasilyl systems primarily isomerize with little loss of silylene groups[77].

In contrast to the above, indenyl compounds such as **160**, with a silyl, disilyl or trisilyl group attached to the metal atom, fail to undergo loss of a silylene on photolysis, and simply rearrange to products such as **161**, as shown by the example given in equation **19**. The locations of aryl groups present in the silyl side chain become scrambled during photolysis[78].

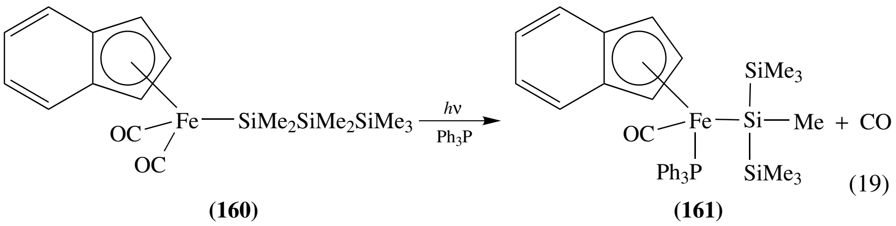

(19)

Whereas photolysis of cyclohexasilanes usually results in silylene elimination and the successive formation of cyclopentasilanes and cyclotetrasilanes[79], attachment of the Fp group to the ring as in **162** results in rearrangement to a silyl-substituted cyclopentasilane, **163**, revealing that the presence of the transition metal alters the chemistry of these systems in a major way (equation 20).

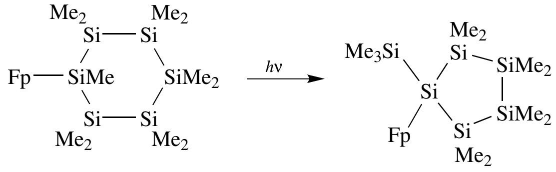

(20)

(162) **(163)**

Fp = η^5-[$C_5H_5Fe(CO)_2$]

When a methylene or dimethylgermyl group intervenes between the transition metal and the silyl group, as in **164**, photolysis results in rearrangement to **165**, which appears, for the methylene case, to involve the intermediacy of a metal–silene complex (Scheme 25).

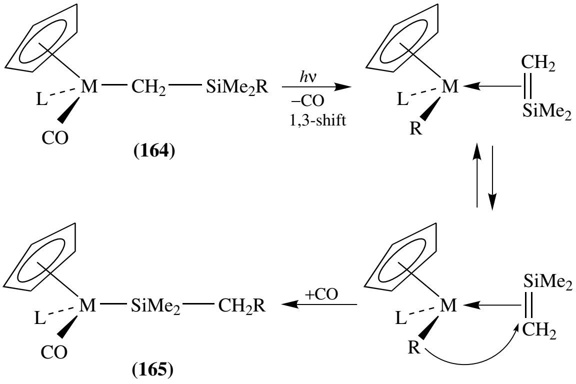

R = Me_3Si, $Me_3SiSiMe_2$, etc.
M = Fe, W
L = CO or another ligand

SCHEME 25

While the germanium-containing tungsten complex **166** rearranged to **167** on photolysis, the isomeric species **168** directly eliminated the silene $Me_2Si{=}CH_2$ yielding **169** (Scheme 26)[80].

The related system $FpSiMe_2GeMe_2Fp$, **170**, and other group 14 analogs have also been studied[81]. The initially formed products **171** involved only bridging GeMeR groups, but on extended photolysis further carbon monoxide was lost leading to isomeric species **172** involving both bridging $GeMe_2$ and $SiMe_2$ groups (Scheme 27).

G. Cyclic Disilanes and Related Species

The photochemistry of a number of cyclic systems containing a two- or three-silicon atom segment has been investigated. Sakurai and coworkers[82] showed that photolysis of the two atom-bridged biphenyl **173** led to formation of the silafluorene **174** and dimethylsilylene. Subsequently it was shown that the three atom-bridged biphenyl **175** led, via the diradical **176**, to the two-atom bridged **173** and dimethylsilylene, which was trapped with 2,3-dimethylbutadiene. An alternate reaction pathway led to silafluorene

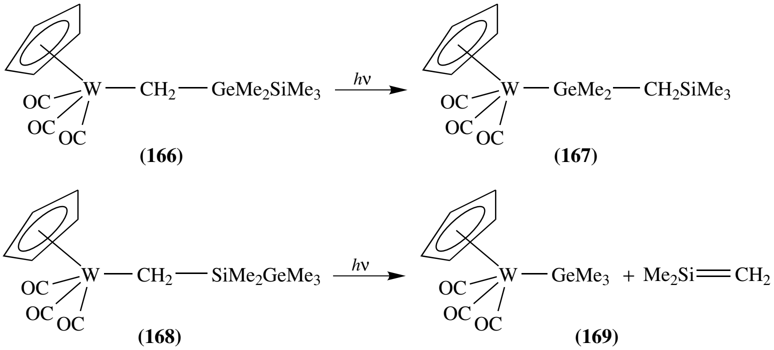

SCHEME 26

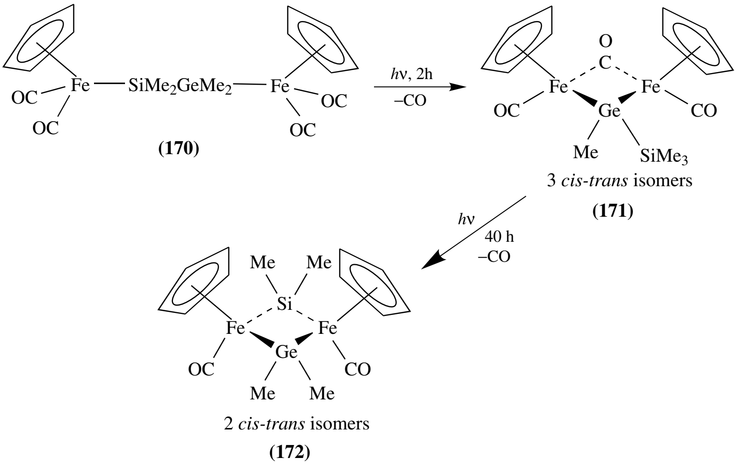

SCHEME 27

174 and tetramethyldisilene, which was also trapped. Convincing evidence that the reaction proceeded by a diradical pathway was obtained through photolysis in the presence of carbon tetrachloride, when the diradical centers were trapped as chlorosilanes (Scheme 28).

The photolysis of silicon-bridged dihydroaromatic compounds has been utilized to prepare reactive organosilicon species such as disilenes. Thus, photolysis of the

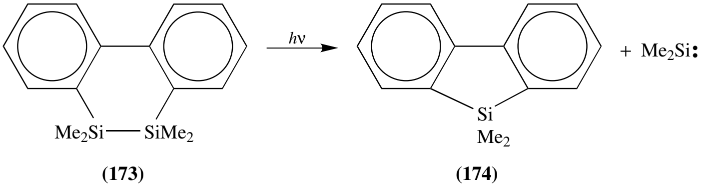

SCHEME 28

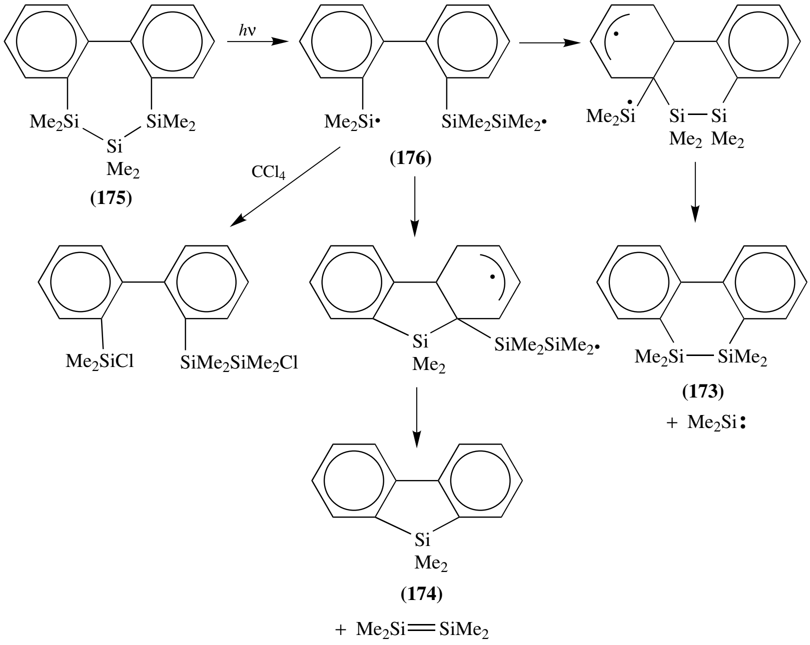

SCHEME 28. (*Continued*)

typical disilyl-bridged compound **177** was shown to yield tetra (*t*-butyl)disilene, **178** (equation 21).

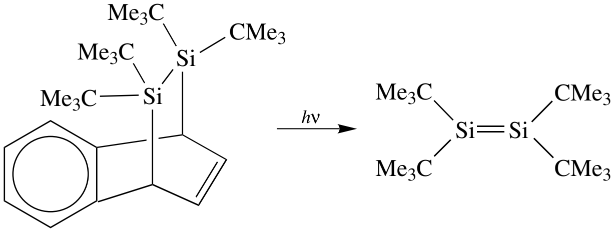

(177) **(178)**

(21)

West and coworkers studied the photolysis of several adducts of disilenes with ketones, i.e. 1,2-disiloxetanes[83]. Based on the products obtained when the photolysis was carried out in ethanol as a trapping agent, it appears that the heterocyclic disiloxetane **179** decomposed to the silanone **180** and the silene **181**, each trapped by ethanol to give the adducts **182** and **183**, respectively (Scheme 29). In the absence of a trapping agent the silene photochemically rearranged to **184**. A related 1,2-disilathietane **185** showed similar behavior (Scheme 29)[84].

Peralkylcyclodisilagermanes and peralkylgermadisilaoxetanes on photolysis at 254 nm were observed to yield predominantly the corresponding disilene and disiloxirane, respectively, in addition to the dialkylgermylene[85].

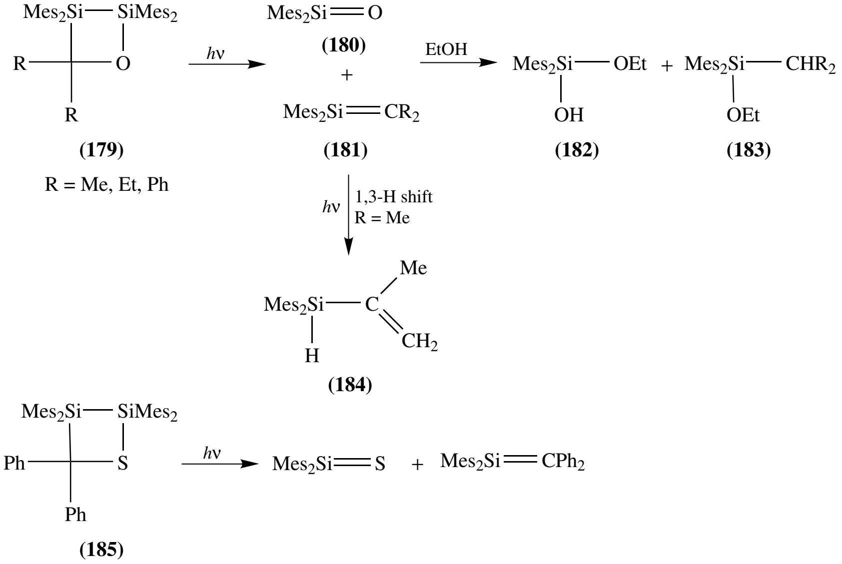

SCHEME 29

IV. TRI-, TETRA- AND POLYSILANES

A. Introduction

As a result of several decades of research it is now known that a polysilane of three or more contiguous silicon atoms is susceptible to reaction by one or more of several pathways when photolyzed, each associated with cleavage of a silicon–silicon bond. The two most common processes observed are the homolysis of a silicon–silicon bond to yield a pair of silyl radicals, and the elimination of a silicon atom from the chain in the form of a silylene. As discussed in Section VII, the use of trisilanes, particularly where the central silicon atom bears aryl groups, has become an important route for the preparation of a wide variety of diarylsilylenes, Ar_2Si:, many of which have been captured in glasses at low temperature, or have been allowed to dimerize to disilenes by warming.

B. Acyclic Polysilanes

Understanding of the behavior of tri-, tetra- or polysilanes during photolysis has been actively pursued in recent years, in part because of the potential application of the polysilanes as photoresists, and for other industrial applications. In addition to the reactions mentioned above, other reactions have now been recognized as occurring in the course of photolysis. These are summarized below.

The photolysis of polysilanes generally results in one or more of the following reaction pathways being followed, as illustrated in Scheme 30, where ch represents a segment of polysilane chain. Most common is the formation of a pair of silyl radicals, path **a**. When there are aryl groups on the silicon radical centers and particularly when a methyl group is one of the R groups on one of the silicon radical centers, it is found that these readily disproportionate to a silane −SiH, and a silene, Si=C, path **b**. However, in some cases it appears that the same products also can arise directly during the photolysis, path **c**. Also, a silylene R_2Si: is commonly extruded from the polysilane chain, path **d**. Finally, it was recently observed that persistent silyl radicals were produced during photolysis, apparently resulting from an internal 1,2-rearrangement of an R group to yield a shortened chain and a silylsilylene, path **e**. As a result of rearrangement of the silylsilylene to a disilene, a known facile process, followed by addition of a silyl radical produced by path **a** at the less hindered end of the silicon–silicon double bond, a highly hindered silyl radical **186** is produced, and recent studies have established the structure of this species[86,87]. Similar processes have subsequently been shown to occur in oligosilanes with as few as three silicon atoms[88].

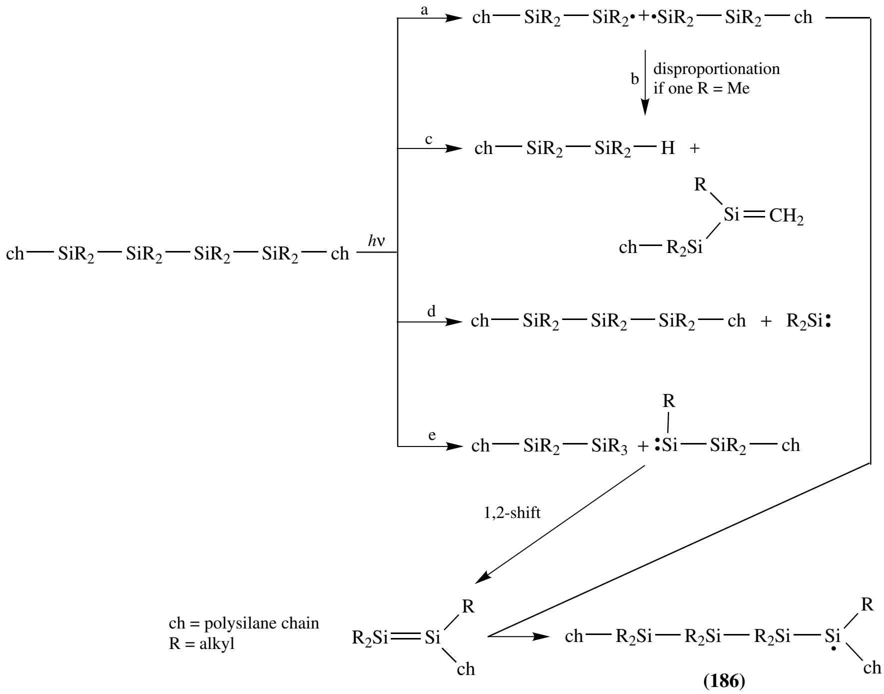

SCHEME 30

As an example of the application of these processes to a simple trisilane, the compound **187** was studied[88] where three of the five processes described above were detected on the basis of product analysis (Scheme 31). In this example no persistent silyl radical was observed because of the lack of steric crowding, but the products observed clearly indicate that processes **a**, **c** and **d** were being followed.

Other recent examples[89–92] of the photolysis of trisilanes to prepare silylenes as precursors to disilenes will be found in Section VII.

Conlin and coworkers photolyzed vinyltris(trimethylsilyl)silane **188** in the presence of a variety of trapping reagents such as butadiene, substituted butadienes or silanes and observed products derived from intermediate silenes **189** (formed by rearrangement) or from silylenes **190** resulting from elimination of hexamethyldisilane[93]. In some cases complex mixtures of products which could have been derived from intermediate silyl radicals were also observed. The reaction products formed from the silene and the silylene in the presence of butadiene, **191** and **192** respectively, are shown in Scheme 32.

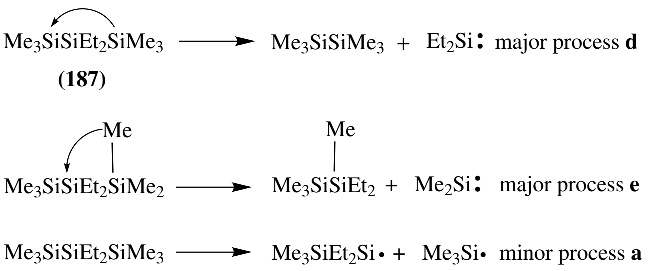

SCHEME 31

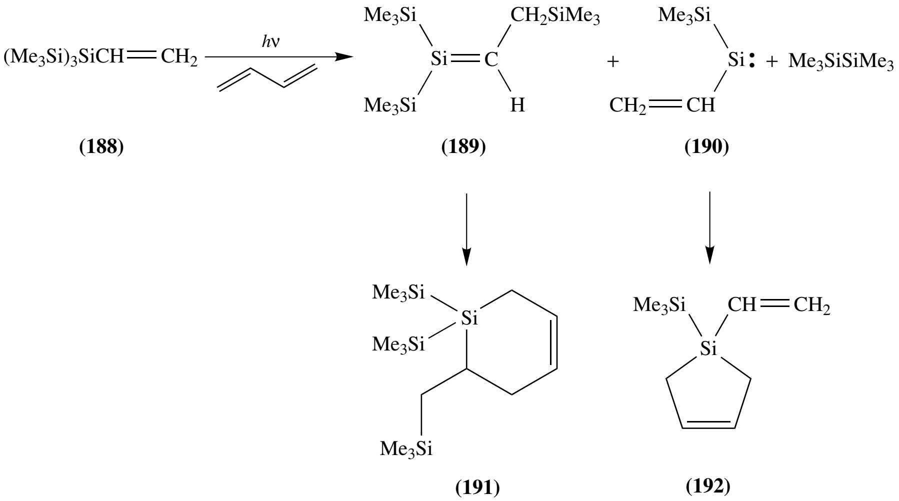

SCHEME 32

C. Cyclic Polysilanes

1. Homocyclic systems

The photolysis of a number of homocyclic silanes with various sized rings has been investigated in recent years: much of this material appears in a recent review by Hengge and Janoschek[94]. It is well known that the photolysis of dodecamethylcyclohexasilane leads to loss of dimethylsilylene, Me_2Si:, with the successive formation of the cyclopenta- and cyclotetrasilanes. This reaction constitutes a useful way to generate the silylene for various purposes. Further photolysis generally leads to complete degradation of the ring system.

The photolytic behavior of the cyclotetrasilanes depends on the structure of the molecule and, more particularly, on the shape of the ring. When silyl groups (Me_3Si or $EtMe_2Si$) are the substituents on the ring, the ring adopts a planar configuration, and photolysis in methylcyclohexane leads to the silyl-substituted disilenes. Alternatively, it was found that when isopropyl groups occupied all eight sites on the cyclotetrasilane ring, or where one methyl and one *t*-butyl group were attached to each silicon atom of the ring, the cyclotetrasilane ring was bent, and photolysis resulted in silylene expulsion and the formation of a cyclotrisilane. Details of the absorption processes are discussed in the original paper[95].

Photolysis at 300 nm of one of the stereoisomers of methyl(*t*-butyl)cyclotetrasilane $(Me(t\text{-}Bu)Si)_4$ resulted in the formation of an equilibrium mixture of all four possible stereoisomers indicating cleavage of a ring silicon–silicon bond to a diradical, followed by reclosure. Silylenes, which could be trapped, were also formed during the process[96] and low yields of linear trisilanes were also obtained.

Trisilacyclopropanes are also quite susceptible to photolysis, yielding disilenes $R_2Si{=}SiR_2$ and silylenes $R_2Si\colon$ (equation 22). A review of their behavior has recently appeared[97]. When the substituents on the ring silicon atoms were aromatic (e.g. Ar = 2,6-dimethylphenyl, 2,6-diethylphenyl or mesityl) the silylenes formed on photolysis dimerized, giving nearly quantitative yields of disilenes. On the other hand, when alkyl groups were attached to the ring silicon atoms, it was suggested that the disilenes and silylenes were formed in a cage, and as a result the silylene tended not to dimerize. With suitable added trapping reagents it was common to find products derived from both the expected disilene and the silylene[98].

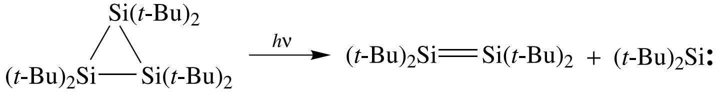

(22)

In a few special cases, as shown in Scheme 33, both the di(*t*-butyl)silylene **193** and the tetra(*t*-butyl) disilene **194** reacted with the same molecule of trapping agent on photolysis[99].

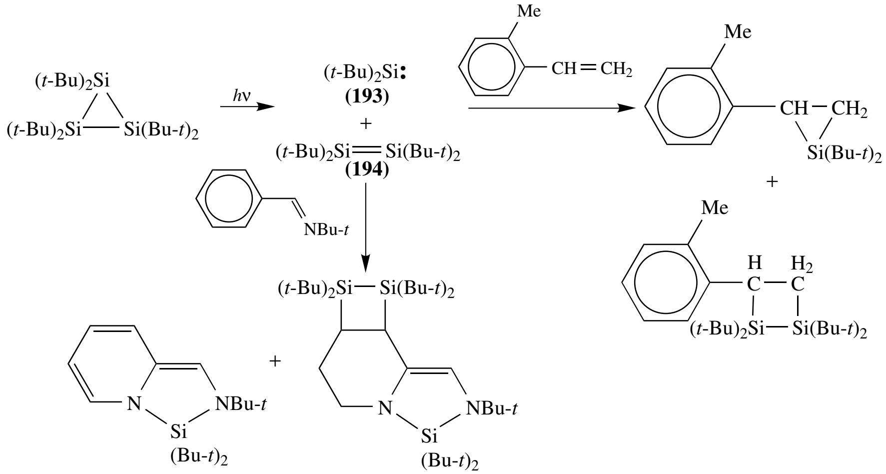

SCHEME 33

Several classes of polycyclic polysilanes, such as the octasilacubanes and the hexasilaprismanes, have been synthesized[100], but little is known about the photochemical behavior of the silacubanes which appear to be stable toward ultraviolet radiation. The silaprismanes, such as **195**, on the other hand, were observed to rearrange to the Dewar benzene isomer **196**, using 340–380 nm radiation[101]. The Dewar benzene reverted to the silaprismane if irradiated with radiation of wavelength longer than 460 nm (equation 23).

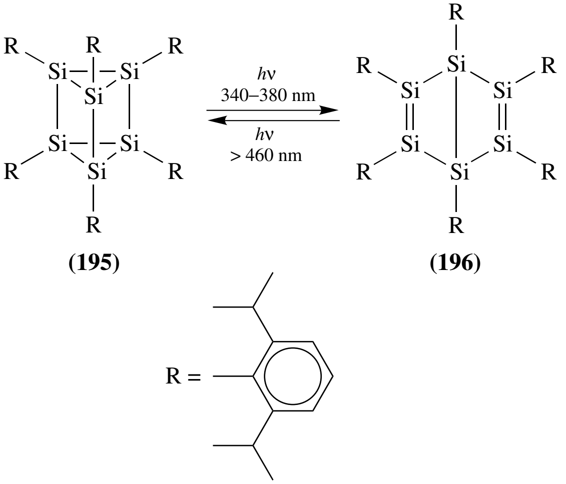

(195) **(196)**

(23)

2. Heterocyclic tri-, tetra- and polysilanes

Watanabe and coworkers synthesized several four-membered rings containing three silicon atoms and a heteroatom, either germanium or oxygen, and studied their photochemistry. Thus photolysis of the germatrisilacyclobutane **197** led to the extrusion of the germylene and, it was suggested, the diradical **198**, which cyclized to the trisilacyclopropane **199**. The latter either was trapped with oxygen as a mono- **200** or dioxa compound, **201**, or itself was photolyzed to yield the silylene and the expected disilene[102,103] (Scheme 34).

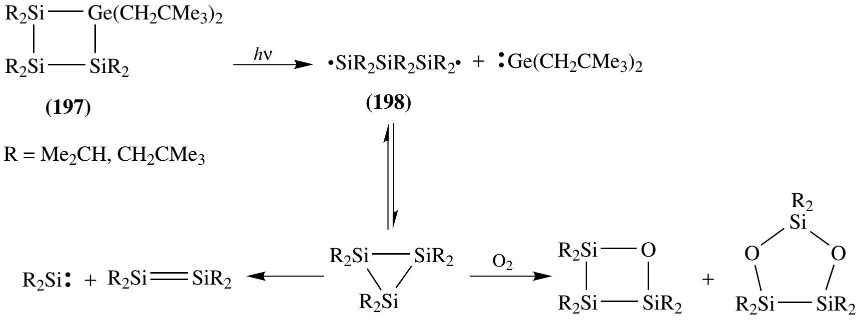

(197) **(198)** **(199)** **(200)** **(201)**

SCHEME 34

The photochemistry of the above oxatrisilacyclobutane **200** (R = CH_2CMe_3) was also investigated. Photolysis resulted in the extrusion of a silylene and the formation of a diradical **202**, which in the presence of cyclohexane afforded the dihydride **203** or in its absence cyclized to the disilaoxirane **204**, as shown in Scheme 35. If the photolysis was done in ethanol, the silylene was trapped, and ring opening of the oxirane occurred at both the Si—O bond and the Si—Si bond, the expected ethanol adducts **205** and **206** being obtained. In addition, the ring of the initial oxatrisilacyclobutane opened in ethanol to give the product **207**. It is of interest to note that there was no evidence that the oxatrisilacyclobutane underwent retro-cleavage to a disilene and silanone, under the photolytic conditions.

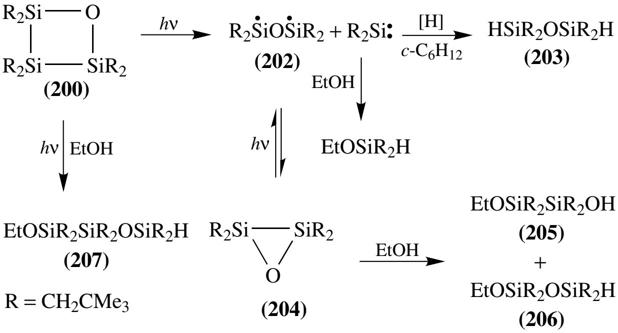

SCHEME 35

The preparations and photolyses of the tetrasilagermacyclopentanes **208** have recently been described[104]. The photolysis of **208** in cyclohexane gave the products **209** and **210**, and in the presence of dimethylbutadiene both the germacyclopentene **211** and the silacyclopentene **212** were formed. Thus it appeared that both a germylene (Ph_2Ge:) and a silylene ((*i*-Pr)$_2$Si: or (*t*- BuCH$_2$)$_2$Si:)) were extruded during the photolyses, as shown in Scheme 36.

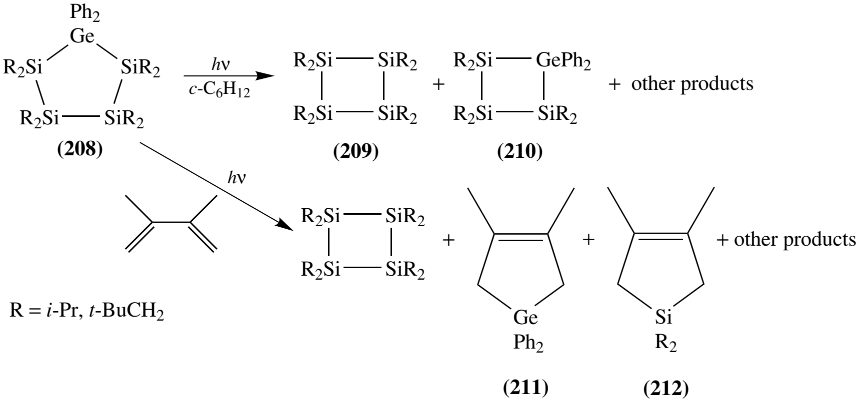

SCHEME 36

V. ACYLSILANE PHOTOCHEMISTRY

A. Simple Acylsilanes

As described in more detail in an earlier review[2] simple acylsilanes, R_3SiCOR', undergo two types of reaction when photolyzed. One involves the rapid reversible 1,2-silyl shift from carbon to oxygen of the carbonyl group leading to a siloxycarbene which can be trapped, particularly by alcohols. A slower competing reaction which becomes more prominent in less polar solvents is homolysis leading to a silyl radical and an acyl radical. In carbon tetrachloride (or other halogenated solvents) the silyl radical is efficiently trapped as the chlorosilane. In both reactions, if the silicon atom is a stereocenter, retention of configuration is largely preserved[105,106]. In hydrocarbon solvents, the silyl radical usually reacts with a hydrocarbon radical derived by decarbonylation of the acyl radical. In some cases disilanes are also produced. These reactions are summarized in Scheme 37.

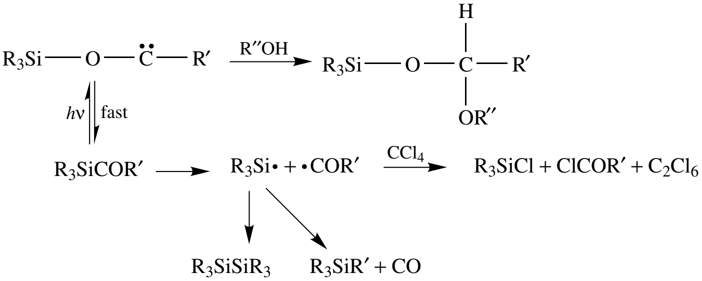

SCHEME 37

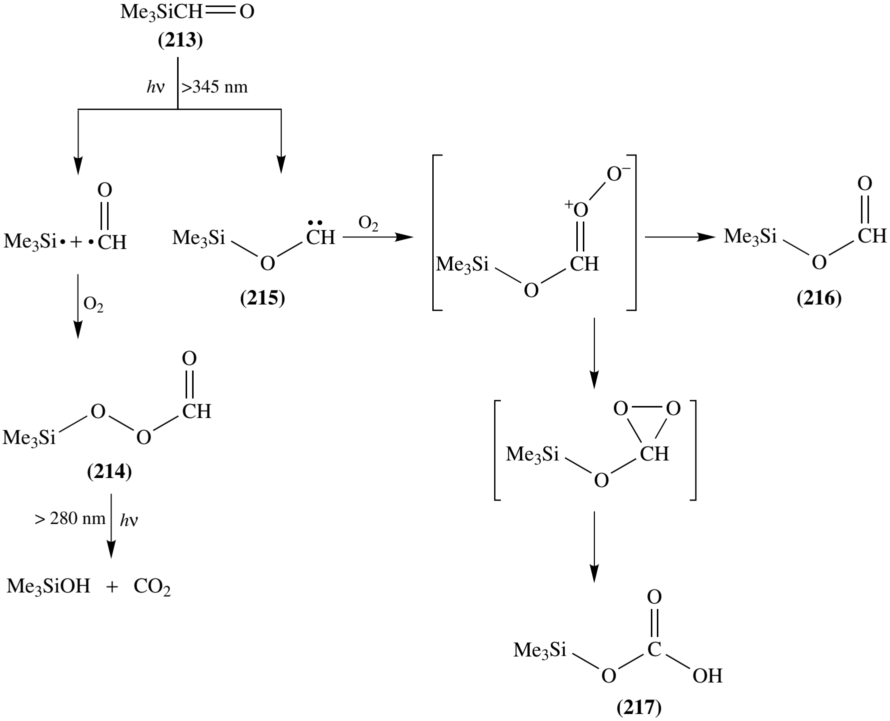

SCHEME 38

The photolyses and photooxidations of formyl-, acetyl-, and benzoyltrimethylsilane in argon or O_2 doped argon matrices have recently been reported[107]. The results are explained in terms of both Norrish type 1 cleavage to silyl and acyl radicals as well as 1,2-silyl shifts resulting in short-lived siloxycarbenes. The major product from photolysis of the formylsilane **213** in the presence of oxygen is trimethylsilyl peroxyformate, **214**, which if photolyzed at >280 nm yields trimethylsilanol and carbon dioxide. The component of the reaction proceeding via the siloxycarbene **215** apparently led to formation of trimethylsilyl formate, **216**, and trimethylsilyl carbonate, **217** (Scheme 38). These proposals were supported by isotopic labeling studies.

Photolysis of the acetylsilane **218** at 10 K in the absence of oxygen was said to yield initially the s-*Z* vinyloxysilane **219** which slowly isomerized to the s-*E* conformer **220**, or more rapidly at 45 K as shown in equation 24.

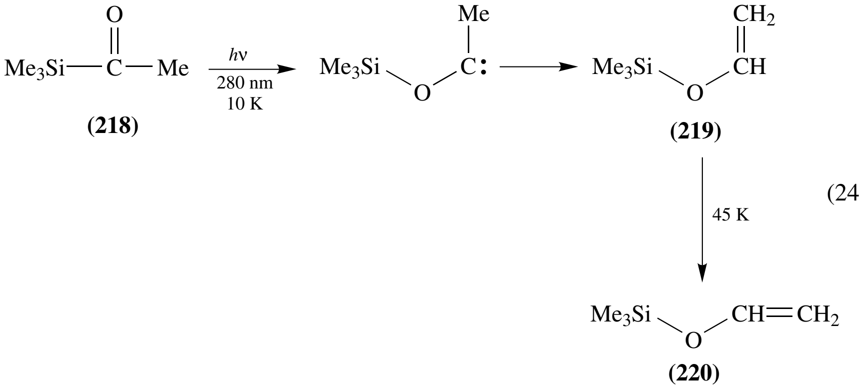

(24)

In the presence of oxygen, products analogous to those shown in Scheme 38 were formed.

Photolysis of benzoyltrimethylsilane at 10 K in the absence of oxygen showed no changes in the IR spectrum of the matrix after several hours. In the presence of oxygen a variety of products was identified including trimethylsilyl benzoate and the main product trimethylsilyl perbenzoate.

B. Acyldisilanes

Since the previous review[2] a further study of the photolysis of several acyldisilanes has been reported[108]. Like previously described di- or polysilylacylsilanes, the disilane **221** on photolysis underwent a 1,3-shift of a trimethylsilyl group from silicon to oxygen, yielding the silene **222** which could be trapped as the methanol adduct **223** if the photolysis was done in methanol. In no case was the possible 1,2-shift of the disilyl group from carbon to oxygen to yield a disilyloxycarbene observed, suggesting that the 1,3-shift is a much lower-energy pathway. In inert solvents, there was NMR evidence that the silene underwent reversible head-to-head dimerization to yield **224**. However, an unusual dimeric species, **225**, not previously observed in these photolyses, was also obtained as a major product, apparently derived from the reaction of the silene with the carbonyl group of unphotolyzed acyldisilane, a type of reaction recently shown to be possible (see below). In addition there was some product **226** derived from radical cleavage of the Si−Si bond followed by decarbonylation and recombination (Scheme 39).

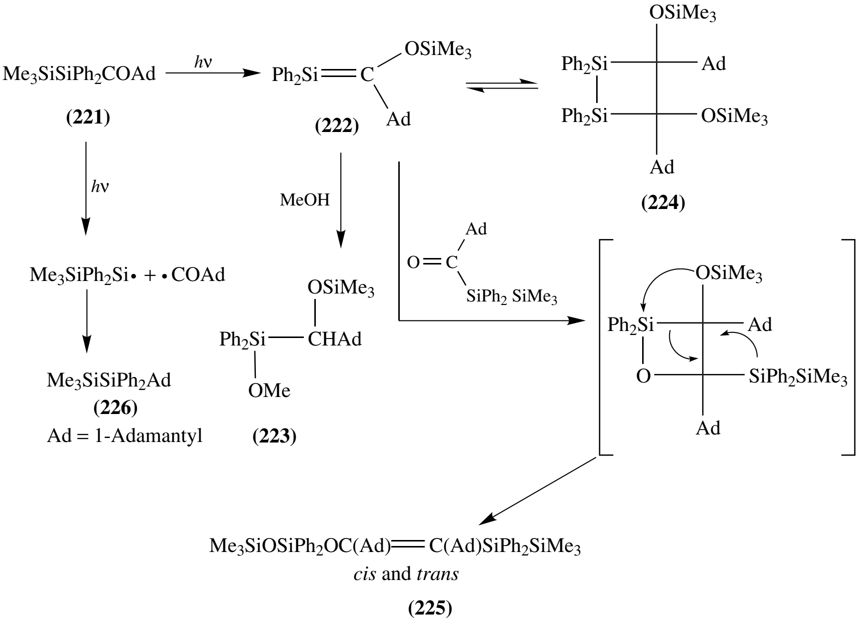

SCHEME 39

The analogous dimesitylacyldisilane **227** showed somewhat different behavior[108]. The silene **228** initially formed by photolysis apparently underwent a subsequent photochemically induced 1,2-trimethylsiloxy shift from carbon to silicon (a previously observed reaction[109]) leading to a silylcarbene **229**, which then inserted into the benzylic C−H bond of the *ortho*-methyl group of one of the mesityl groups to give the silaindane **230**. There were also products **231** and **232** derived from dimerization of each of the radicals produced by Norrish type 1 cleavage of the acyldisilane and, as well, when the photolysis was carried out in methanol, a product **233** derived by methanol trapping of an intermediary disilyloxycarbene **234** was observed (Scheme 40). While there were precedents known for each of these reactions, the mixture of products observed was derived from an unusual combination of these known photochemical processes.

C. Acylpolysilanes

The photolysis of acylpolysilanes has been extensively used as a route for the preparation of silenes, both transient and long-lived. Research to 1989 has been reviewed[2].

When photolyzed in inert solvents, the most common behavior of a polysilylacylsilane such as **235**, with three trimethylsilyl groups on silicon, is for a 1,3-shift of a silyl group from the central silicon atom to the carbonyl oxygen to occur, leading to the formation of a silene **236** bearing a trimethylsiloxy group on the carbon atom of the Si=C bond. (1,2-Shifts of the polysilyl group to oxygen, which would lead to a siloxycarbene, have never been observed in these polysilyl systems.) Silenes such as **236** may be stable if the attached groups are sufficiently bulky, as when groups like adamantyl or mesityl are attached to the carbon atom of the Si=C bond. Otherwise, the silenes dimerize in a head-to-head manner, probably via a diradical **237** leading either to 1,2-disilacyclobutanes,

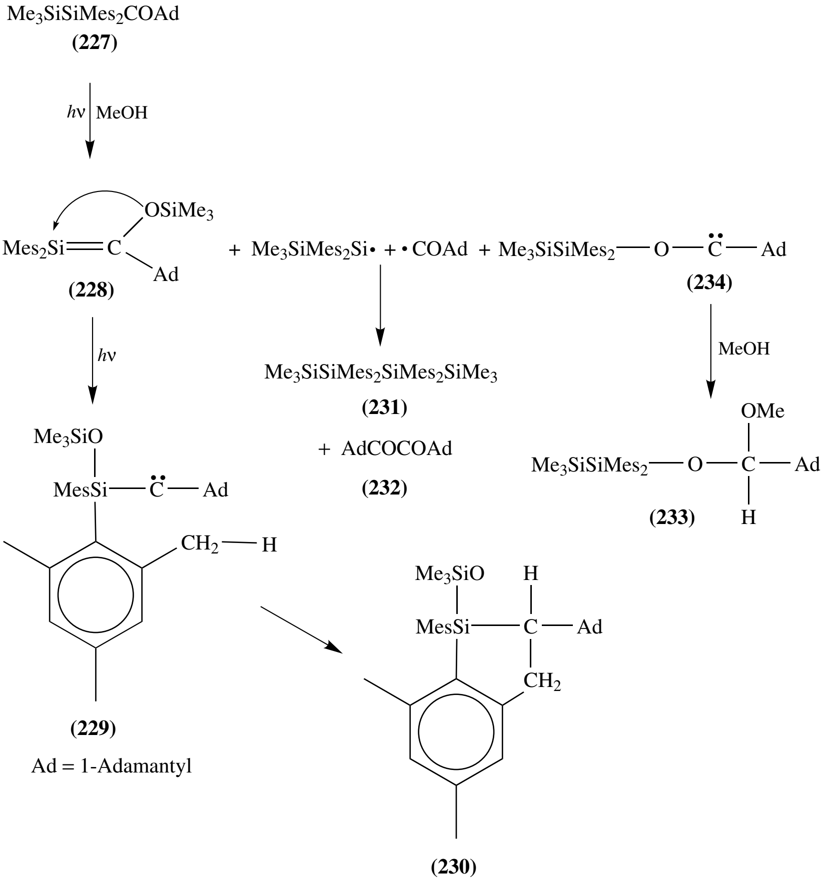

SCHEME 40

238, or to acyclic disilanes such as **239** if R′ has appropriately located hydrogen alpha to the original carbonyl–carbon atom. These acyclic dimers could be formed either by the 1,4-diradical **237** undergoing disproportionation, or by an ene reaction between two silene molecules as illustrated in Scheme 41.

Conlin and coworkers studied the silene $(Me_3Si)_2Si{=}C(OSiMe_3)$ Me using laser flash photolysis, and while much was learned about some details of its reactions, it was not possible to establish unambiguously the mechanism by which dimerization occurred[110].

The reactions of the silenes formed by photolysis of polysilylacylsilanes with a wide variety of reagents, e.g. alkenes[111] alkynes[112], dienes[111], carbonyl compounds[113], α,β-unsaturated carbonyl compounds[114,115], isonitriles[116,117], Grignard reagents[118], imines[119], sulfur[120], selenium[120], acylsilanes[121] and a silylketene[122], have been studied using two methods in most cases. On the one hand, the relatively stable and long-lived silenes were prepared by photolysis and then the reagent was added in the dark. Alternatively, a mixture of the polysilylacylsilane and reagent were co-photolyzed. In all cases the experimental results were virtually identical, indicating that the reaction of the silene with the reagent was a non-photochemical process.

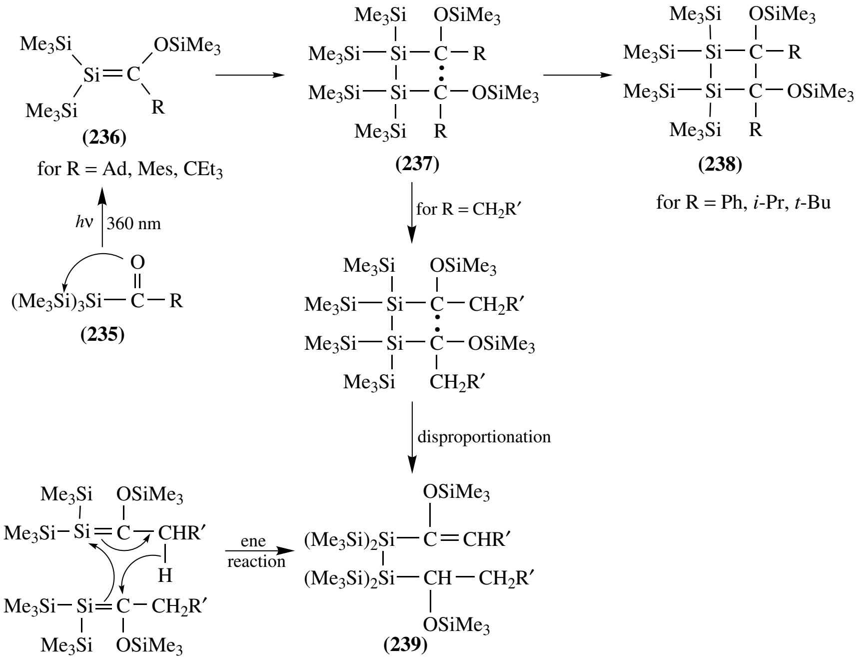

SCHEME 41

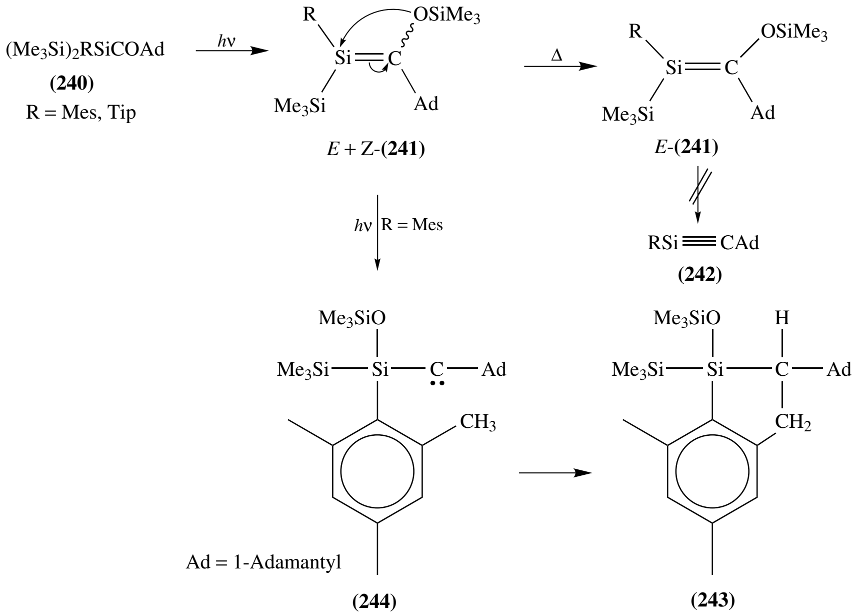

SCHEME 42

Polysilylacylsilanes with the structure $(Me_3Si)_2RSiCOAd$ (R = *t*-Bu, Ph, Mes, Tip) have also shown interesting behavior. In each case a 1,3-shift of a trimethylsilyl group occurred leading to a silene. When R = Mes[112] or Tip (= 2,4,6-tri-isopropylphenyl)[123] photolysis of **240** led to mixtures of the *E*- and *Z*-isomers of the silene **241** (Scheme 42) which were stable at room temperature, although at elevated temperatures they slowly decomposed, leading initially to essentially pure *E*-**241** without evidence for $E \rightleftharpoons Z$ interconversion, and ultimately to fragmentation, without any evidence that a silyne **242** was formed by loss of hexamethyldisiloxane from the silene. Prolonged photolysis gave rise primarily to silaindanes **243** resulting from a photochemical rearrangement of the silene by migration of the trimethylsiloxy group from carbon to silicon, followed by insertion of the carbene **244** into the benzylic C−H bond of the mesityl group. When R = *t*-Bu or Ph there was also evidence that the initially formed silene itself underwent photochemical rearrangement (see Section VIII)[109].

Photolysis of α,β-unsaturated acylpolysilanes of the general structure $(Me_3Si)_3SiCOCR{=}CR'_2$ failed to yield significant amounts of the isomeric siladienes, and gave instead products derived from the Norrish type 1 cleavage of the acylsilane into the radicals $(Me_3Si)_3Si\bullet$ and $\bullet COCR{=}CR'_2$[124].

VI. SILYLDIAZOALKANES AND SILYLCARBENES

The photolysis of silyldiazoalkanes, species which are much stabler than their all-carbon analogs, leads to the formation of silylcarbenes. The subsequent behavior of the silylcarbenes depends greatly on the nature of the groups attached to the diazo-carbon atom, as well as to the silicon atom. Early results have been reviewed[2]. In Scheme 43 several representative reactions are listed.

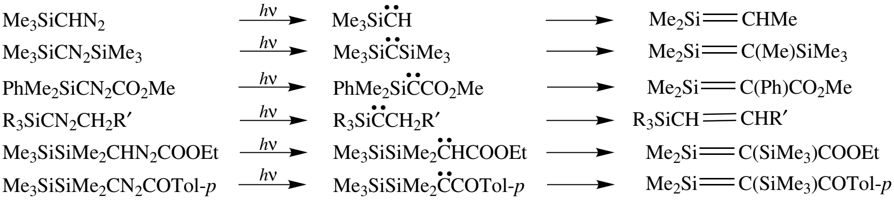

$$Me_3SiCHN_2 \xrightarrow{h\nu} Me_3Si\ddot{C}H \longrightarrow Me_2Si{=}CHMe$$
$$Me_3SiCN_2SiMe_3 \xrightarrow{h\nu} Me_3Si\ddot{C}SiMe_3 \longrightarrow Me_2Si{=}C(Me)SiMe_3$$
$$PhMe_2SiCN_2CO_2Me \xrightarrow{h\nu} PhMe_2Si\ddot{C}CO_2Me \longrightarrow Me_2Si{=}C(Ph)CO_2Me$$
$$R_3SiCN_2CH_2R' \xrightarrow{h\nu} R_3Si\ddot{C}CH_2R' \longrightarrow R_3SiCH{=}CHR'$$
$$Me_3SiSiMe_2CHN_2COOEt \xrightarrow{h\nu} Me_3SiSiMe_2\ddot{C}HCOOEt \longrightarrow Me_2Si{=}C(SiMe_3)COOEt$$
$$Me_3SiSiMe_2CN_2COTol\text{-}p \xrightarrow{h\nu} Me_3SiSiMe_2\ddot{C}COTol\text{-}p \longrightarrow Me_2Si{=}C(SiMe_3)COTol\text{-}p$$

SCHEME 43

The first three examples illustrate that facile migration of Me[125,126] or Ph[125] from silicon to the carbene carbon atom can occur giving rise to silenes, while the fourth example[127] illustrates that hydrogen, if adjacent to the carbene carbon, migrates in preference to a group on silicon, forming an alkene. On the other hand, as illustrated by the last two examples[126,128], migration of a trimethylsilyl group from silicon to the carbene carbon was found to occur easily and cleanly. Many silenes have been prepared by photolysis of the silyldiazoalkanes at low temperature in glasses, allowing the determination of their UV absorption maxima[125,126,129].

More recently, more complex systems have been studied by the groups of Ando[129] and Maas[128,130,131]. As illustrated in Scheme 44, photolysis of the acyldisilyldiazoalkanes **245** yielded successively the disilylcarbene **246**, and then the acylsilene **247** which underwent a variety of rearrangements depending on the R group present. Intramolecular electrocyclic ring closure to give **248** occurred when bulky groups like *t*-Bu and 1-adamantyl were present, while smaller groups (Me, *i*-Pr) led to products of intermolecular dimerization, **249**. In addition, 1,3-migration of the R group from C to Si led to ketenes **250**.

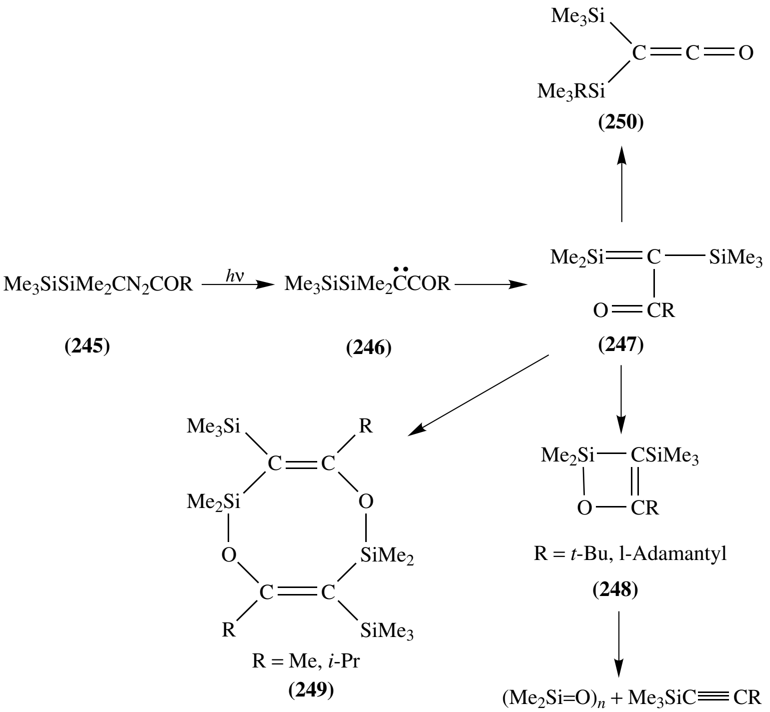

SCHEME 44

The photolysis of dimethylsilyldiazomethane **251** in an argon matrix at 10 K (Scheme 45) was shown by Sander and coworkers to lead to the diazirine **252** and, via the carbene **253** and a 1,2-H shift, to dimethylsilene **254**, used to study the thermal reaction of the silene with formaldehyde[132].

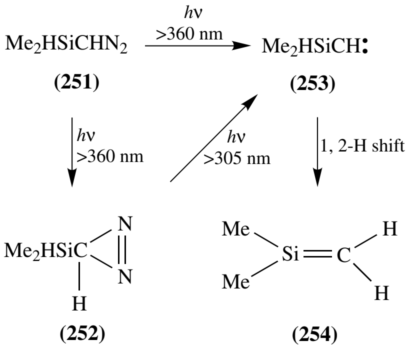

SCHEME 45

Sander and coworkers have recently studied the photolysis of 2,2-dimethyl-2-sila-1,3-bis(diazo)propane **255**[133]. When photolyzed at >305 nm in ethanol or EPA (2 : 5 : 5

EtOH:isopentane:Et_2O) glasses at 77 K, four products **256**, **257**, **258** and **259** were obtained in overall >95% yield. The major product **256** was shown by isotopic labeling studies to have been derived from the silirene **260** formed by intramolecular coupling of the bis-carbene **261**, and pathways for the formation of the other products were proposed. The photolysis of the bis-diazo compound **255** was studied in detail at 405 nm and it was found that the diazirine **262** was formed: this on photolysis at 305 nm also gave **260** on the pathway to **256**. The chemistry is shown in Scheme 46.

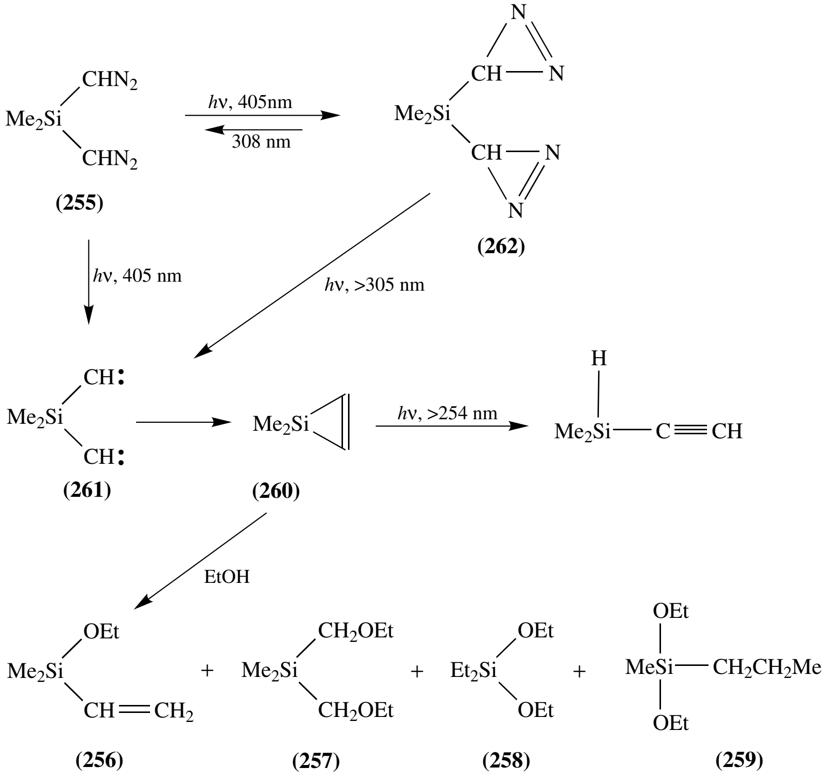

SCHEME 46

The silylcarbene $:CHSi(OMe)_3$ was generated by low-temperature photolysis at 345 nm of the related diazomethane, and was characterized. Photolysis of the silyldiazomethane at 280 nm in the cold led to 1,1-dimethoxy-1-sila-2-oxetane, arising from insertion of the carbene into one of the methoxy groups[134].

Ando and coworkers have described unusual photochemical behavior of a bis-diazo compound **263** which on photolysis gave rise to a bis-silene **264**[135]. In inert solvents this spontaneously underwent two modes of reaction, 'criss-cross' (head-to-tail) addition and 'parallel' (head-to-head) addition, leading to bridged disilacyclobutanes **265** and **266** (Scheme 47).

In a subsequent paper[136] further studies of these and other bis(diazo) compounds having two, three, or four $SiMe_2$ groups between the two diazo groups were described. In contrast to the photolyses in inert solvents, where products of intramolecular [2 + 2]

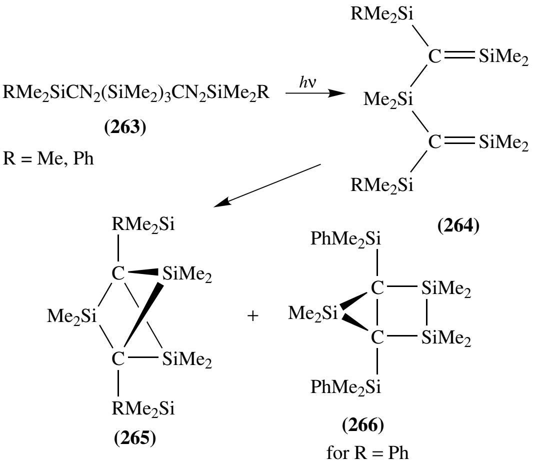

SCHEME 47

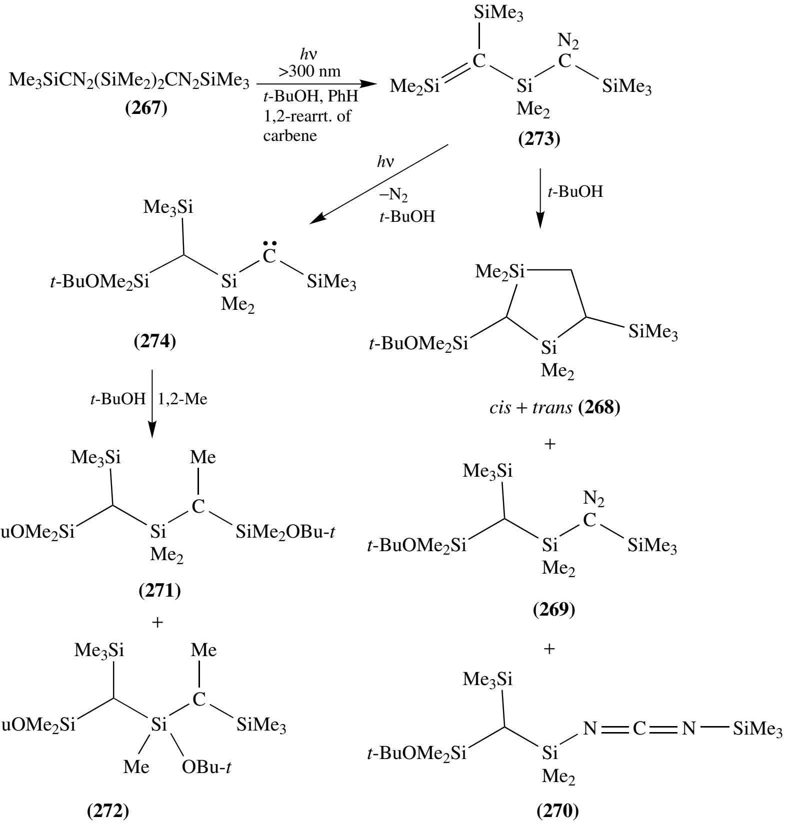

SCHEME 48

cyclization were obtained, when compound **267**, as an example, was photolyzed in *t*-butyl alcohol five structurally different products, **268**–**272**, derived from several different intermediates, were identified (Scheme 48). Thus the carbene formed from initial photolysis, followed by a 1,2-silyl migration of the internal Me_2Si-terminated group, led to the silene **273**, which reacted with one mole of the alcohol in different ways yielding **268**, **269**, and **270**. Alternatively, further photolysis apparently led to a carbene, **274**, which then underwent a 1,2-Me shift prior to reacting with the alcohol, leading to **271**, and **272**.

As another example, photolysis in inert solvents of compound **275**, where four $SiMe_2$ groups bridged the two diazo functions, led to the bis-silene **276**, which reacted by either head-to-head or head-to-tail pathways resulting in the formation of the bicyclic compounds **277** and **278**, respectively. Alternatively, [2 + 3] cycloaddition gave the intermediate **279** which led to the formation of the bicycloadduct **280** (Scheme 49).

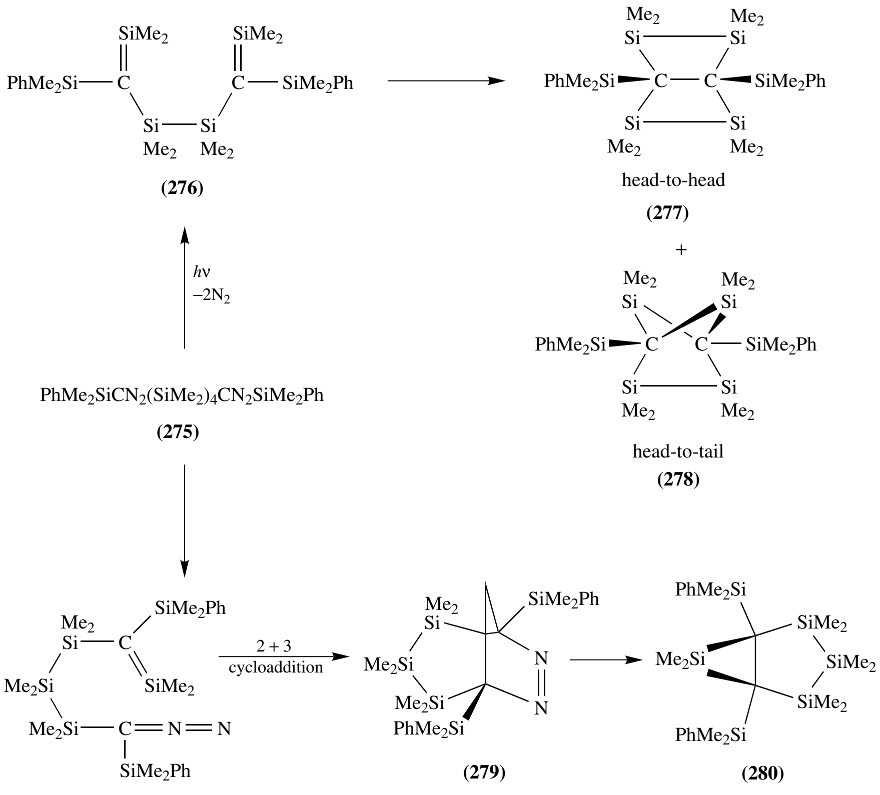

SCHEME 49

The photolyses of several transition metal-substituted silyldiazoalkanes have recently been described[137,138]. As indicated by the examples given in Scheme 50, the silyldiazoalkane **281** initially formed the carbene **282**, which underwent a phosphine 1,2-rearrangement from the transition metal to the carbene–carbon yielding the ylide **283**, which subsequently dimerized to form the product **284**. The related nickel compound also gave a dimer when photolyzed (Scheme 50).

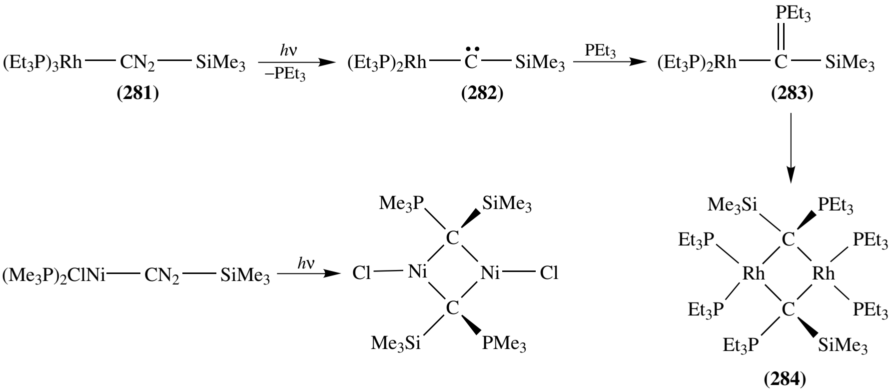

SCHEME 50

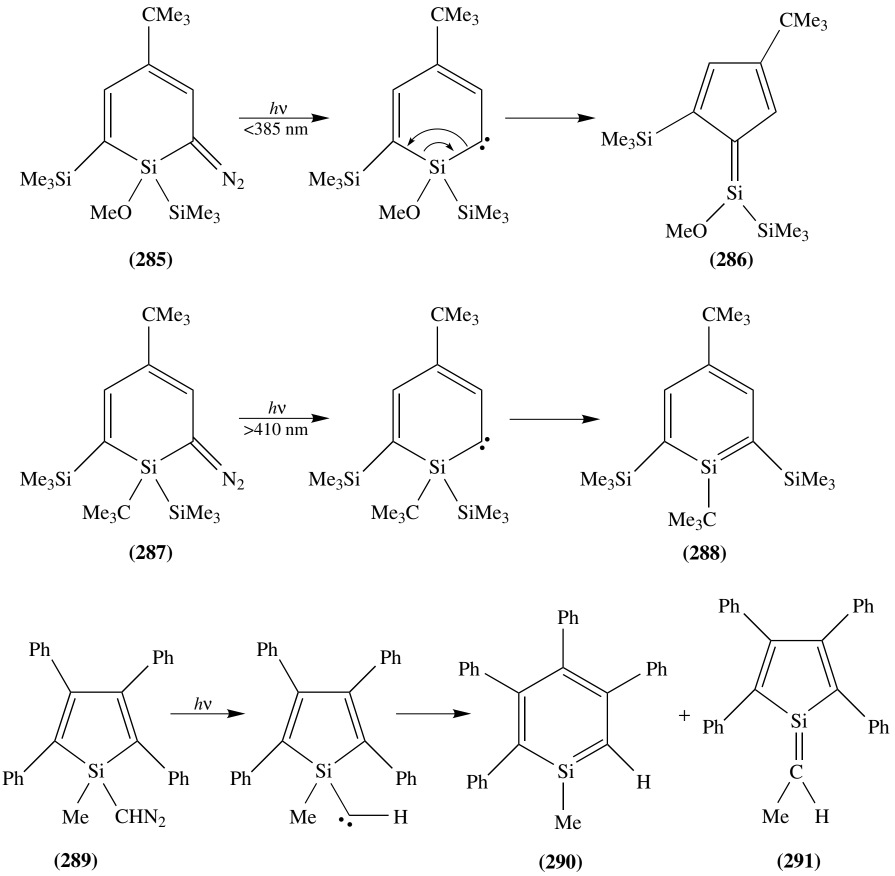

SCHEME 51

The photolysis of unsaturated cyclic silyldiazoalkanes has also been employed as a route to several silaaromatic compounds such as silabenzenes and silafulvenes. Märkl and coworkers showed that the diazo compound **285** was converted on photolysis at <385 nm to the silafulvene **286**[139] and that photolysis of the diazo compound **287** led to the silabenzene **288**[140]. Each of the processes involved a 1,2-shift of a group from silicon to carbon. Earlier, Ando and coworkers[141] had shown that photolysis of the silacyclopentadienyldiazomethane **289** led to the formation of both a silabenzene **290** and a silafulvene **291** (Scheme 51).

These silaaromatics are not stable, although one example described by Märkl and coworkers was sufficiently stable at −100 °C to be characterized by ^{29}Si NMR spectroscopy[140].

VII. PHOTOCHEMICAL ROUTES TO SILENES, SILYLENES AND DISILENES

Some of the reactions given in the sections above are important routes to reactive organosilicon intermediates such as silenes and silylenes, and because of their tendency to dimerize readily, to disilenes, the latter being formed when matrix-isolated silylenes are warmed up. It appears worthwhile to summarize some of the more useful reactions leading to silenes and silylenes, and their subsequent behaviors. The topics of silylenes[97,142] and disilenes[97,142,143] have recently been reviewed.

Simple silenes are probably most easily and gently generated by the photolysis of silyldiazoalkanes, often done in low-temperature matrices, since the subsequent 1,2-rearrangement that the initially formed silylcarbene undergoes on warming is normally a clean reaction. More stable silenes are best prepared by the photolysis of polysilylacylsilanes as was described in Section V.C, although further rearrangements may occur, as will be described below, depending on the substituents on the Si=C bond, and the length of photolysis. The chemistry of silenes has recently been reviewed[144].

Silylenes are produced by several photochemical routes. Dimethylsilylene, Me_2Si:, is produced during the photolysis at 254 nm of dodecamethylcyclohexasilane, $(Me_2Si)_6$, but the cyclopentasilane and lower homologues are by-products of this approach, which

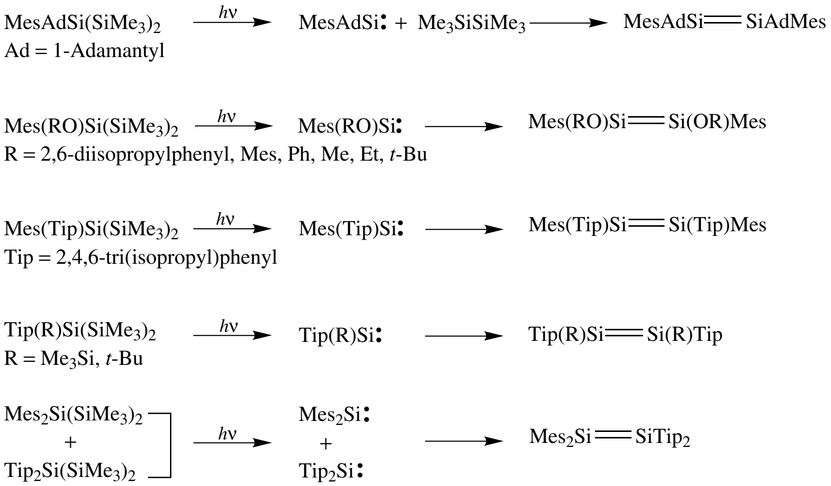

SCHEME 52

may be inconvenient. Fink and coworkers have recently shown that when $(Me_2Si)_6$ was photolyzed in a molecular beam using a pulsed supersonic jet, a single photolysis photon was capable of producing the silylene Me_2Si: in contrast to the behavior of other common silylene precursors such as $PhMe(SiMe_3)_2$ or $PhSi(SiMe_3)_3$, where a single photon removed only a single Me_3Si group[145]. The conventional photolysis of the latter two compounds, and the photolysis of linear trisilanes, particularly those such as $Me_3Si{-}SiAr_2{-}SiMe_3$, where the groups on the central silicon atom are aromatic (e.g. Ph, Mes, Tip etc.), is a very convenient source of silylenes for synthetic and other related purposes by trapping in the cold, or for disilene formation by dimerization at higher temperatures. Several examples of disilenes formed from silylenes by this route are shown in Scheme 52[146–148].

When the R groups on the central silicon atom of the trisilanes are aliphatic, e.g. as in $PhMe_2Si{-}SiR_2{-}SiMe_2Ph$ [R = *t*-Bu, 1-Adamantyl (Ad)], photolysis does not give rise to much silylene[149,150]. However, dialkyl-substituted silylenes, e.g. Ad_2Si:, are readily available by the photolysis of dialkylsiliranes **292**[150,151] or by the photolysis of the reasonably readily available cyclotrisilanes such as **293** (Scheme 53)[97,142]. These photochemically generated singlets add with considerable stereospecificity to alkenes yielding siliranes, the loss of complete stereospecificity being attributed to photochemical ring opening and reclosure of the silirane ring.

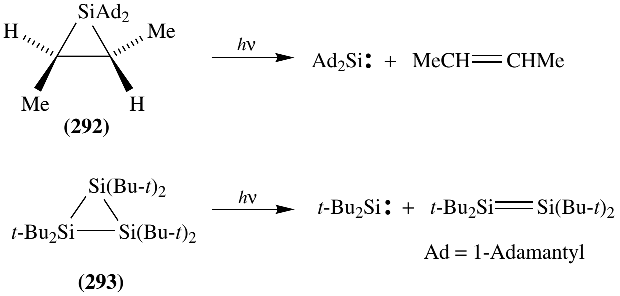

SCHEME 53

Cyclotrisilanes are easily converted to a mixture of silylene and disilene. Reactions of the silylene $(t\text{-}Bu)_2Si$: and the disilene $t\text{-}Bu_2Si{=}Si(Bu\text{-}t)_2$ produced by photolysis of the cyclotrisilane **293** with cyclopentadiene, furan, and thiophene have been reported recently[152], as were their reactions with 2,2′-bipyridyl, pyridine-aldimine and ketoimines[153].

Bobbitt and Gaspar have described preparations of Me_2Si:, PhMeSi: and Ph_2Si:, as well as the kinetics and products formed from their reactions with butadiene[154].

Three unusual and interesting examples of silylene formation from photolyses are shown in Scheme 54. In the first, Fink and coworkers[155] photolyzed the trisilane **294** at 254 nm and produced the relatively stable silylene **295**. This on further photolysis gave rise to the sterically crowded silacyclobutadiene **296** which was trapped with several reagents. In the second example Michl and coworkers[156] photolyzed the matrix-isolated bis-azide **297** to form the cyclic silylene **298**, and this on further photolysis at selected wavelengths, using matrices and low temperatures, isomerized to the silacyclopentadienes **299** and **300** and finally to the 1-sila-2,4-cyclopentadiene **301**. Finally, Sakurai and coworkers[157] were able to convert the trisilane **302** to the cyclic divinylsilylene **303**.

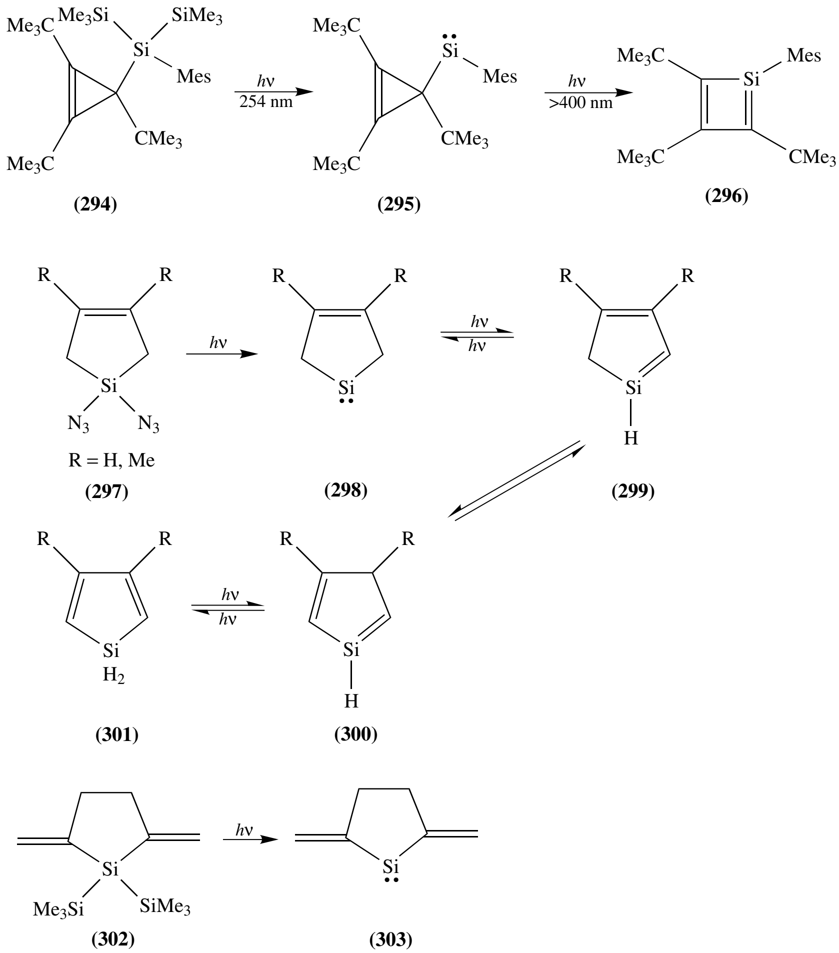

SCHEME 54

VIII. PHOTOCHEMICAL REARRANGEMENTS OF SILENES, SILYLENES AND DISILENES

Knowledge concerning the photochemistry of silenes, silylenes or disilenes is somewhat limited, largely because they are usually reactive transient species difficult to handle. However, a number of interesting and important observations have been made which are reported below.

A. Photolysis of Silenes

The earlier controversy about whether silene–silylene interconversions could occur was settled by studies of West, Michl and coworkers[158]. They generated dimethylsilylene $Me_2Si\mathbf{:}$ from several precursors in glasses at temperatures from 10 to 77 K and characterized it by its UV and IR spectra. This yellow species was bleached by irradiation with visible light to form colorless methylsilene, $MeHSi{=}CH_2$, which was also characterized spectroscopically. Its irradiation at 248 nm reconverted it back to dimethylsilylene (equation 25).

$$Me_2Si\colon \underset{\underset{248\ \text{nm}}{h\nu}}{\overset{\overset{h\nu}{>400\ \text{nm}}}{\rightleftharpoons}} MeSiH{=}CH_2 \qquad (25)$$

Photochemical rearrangements of more complex silenes have also been observed. Thus the *t*-butylsilene **304**, (generated photochemically from its acylsilane precursor, as shown by trapping reactions), when further photolyzed at wavelengths >360 nm, rearranged via an intermediary silene **305** to an isomeric dimethylsilene **306**, as shown by the X-ray crystal structure of its anticipated head-to-head dimer **307**[109]. It was suggested that **306** was the result of a 1,2-carbon-to-silicon migration of the trimethylsiloxy group and a 1,2-silicon-to-carbon migration of the trimethylsilyl group of **304**, giving **305**, both previously observed rearrangements, followed by a 1,3-silicon-to-silicon methyl shift. Originally it was suggested, since attempts to trap an intermediate silylcarbene **308** failed, that the above transformation might be a dyotropic process, but subsequent studies (see below) indicated that the silylcarbene **308** was probably formed as an intermediate, at least in some cases (Scheme 55). Closely related behavior was also observed for an analog of **304** with Ph instead of *t*-Bu.

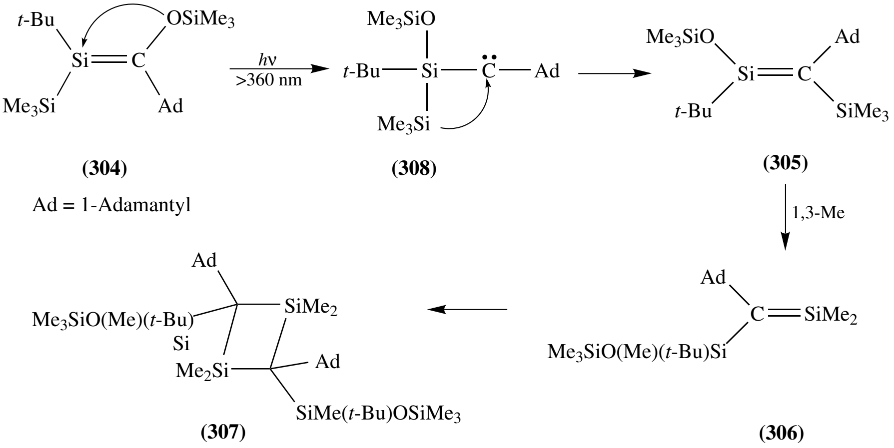

SCHEME 55

When the mesityl analog **309** of **304** was photolyzed with >360 nm radiation, the major product was a diastereomeric pair of silaindanes **310**, due to the two stereocenters present. Their formation was explained as involving the above-described 1,2-trimethylsiloxy shift to give the silylcarbene **311**, which then inserted into the benzylic C−H bond of the methyl group of mesityl (instead of undergoing a 1,2-trimethylsilyl group shift as in Scheme 55); see Scheme 56. Based on this finding it seems reasonable to suggest that the two groups involved in the silene-to-silene **304** → **305** rearrangement rearrange sequentially rather than simultaneously.

In another example West and coworkers photolyzed the stable silaallene **312** which led to the product **313** (Scheme 57). Nominally, this corresponds to an addition of a benzylic C−H bond across the ends of the Si=C bond of the silaallene[159].

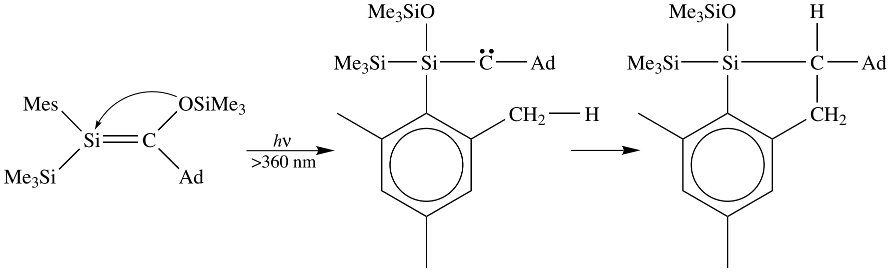

(309) **(311)** **(310)**

SCHEME 56

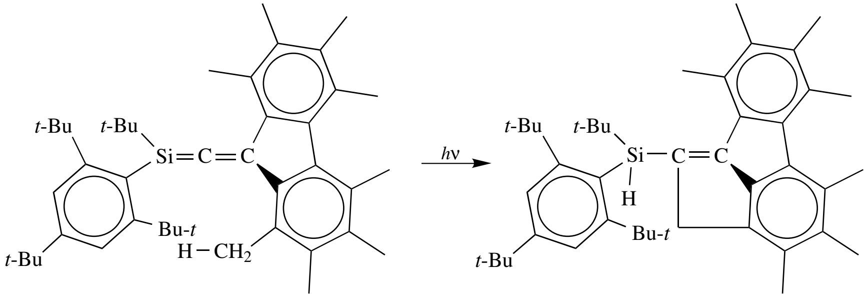

(312) **(313)**

SCHEME 57

A recent study of the photolysis of simple diazoalkanes **314** or diazirines **315**, compounds known to lead to the formation of silenes under inert conditions, led, in oxygen-doped argon matrices, via the silene **316** to the siladioxirane **317**. While previously postulated as an intermediate in silene oxidations, this is important experimental evidence for this intermediate. Continued photolysis of the system led to a compound identified as the silanone–formaldehyde complex **318**, which on further irradiation led to the silanol–aldehyde **319**. The latter compound itself underwent further photochemical oxidation leading to the silanediol **320**[160]. The reactions are summarized in Scheme 58. Detailed infrared studies, including the use of isotopes, and calculations, were used to establish the structures of the compounds.

B. Photolysis of Silylenes

When di(*t*-butyl)silylene **321**, generated in a 3-methylpentane glass at 77 K or in an argon matrix at 10 K by photolysis of a precursor bis-azide, was irradiated with 500-nm light, intramolecular C−H insertion occurred yielding the silacyclopropane **322** (equation 26)[161].

Maier and coworkers have found that pulsed flash pyrolysis of an acetylenic disilane **323** gave rise to the acetylenic silylene **324**, which subsequently rearranged to the cyclic silylene 1-silacyclopropenylidene **325**[162]. Irradiation of this cyclic silylene resulted in its isomerization to the isomeric acetylenic silylene **324**, which itself could be photochemically converted to the allenic silylene **326**. As well, both **324** and **325** were said to isomerize on photolysis to the unusual silacycloalkyne **327**, which was characterized

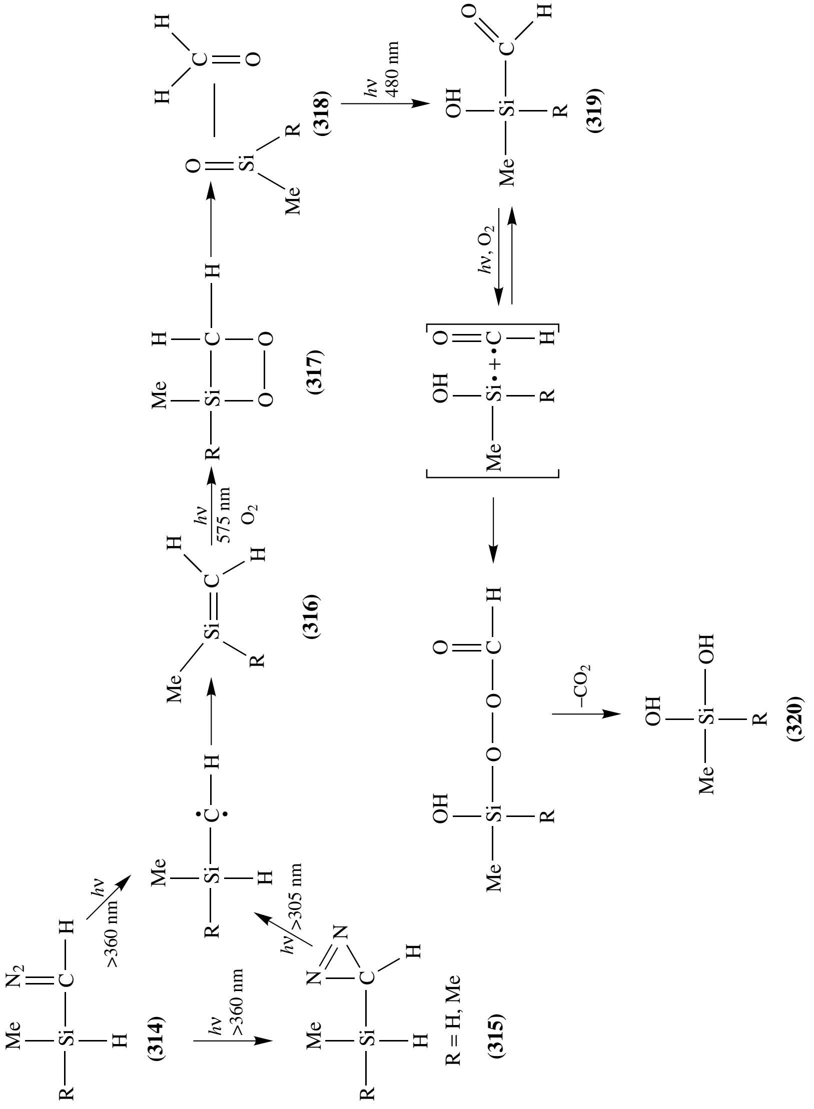
(314)
hν >360 nm
(315)
R = H, Me
hν >305 nm
(316)
hν 575 nm O2
(317)
(318)
hν 480 nm
(319)
hν, O2
−CO2
(320)

SCHEME 58

spectroscopically (Scheme 59).

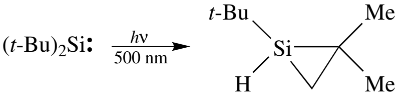

(321) **(322)**

(26)

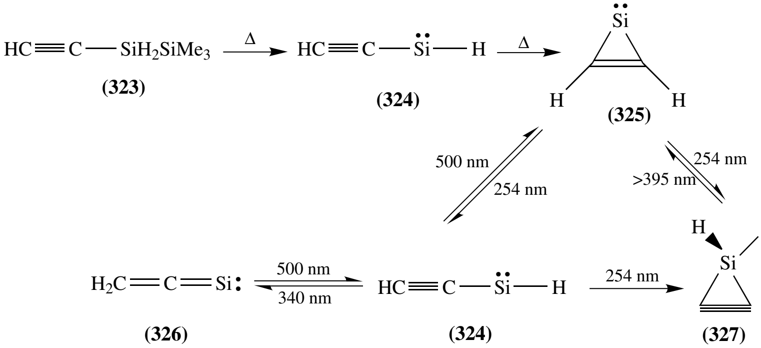

SCHEME 59

C. Photolysis of Disilenes

Among the limited studies of the photochemistry of disilenes, it has been reported that photolysis of tetramesityldisilene, **328**, at 254 nm in pentane gave rise to the dihydrido compound **329** (equation 27), probably as a result of the radical character of the excited state[163].

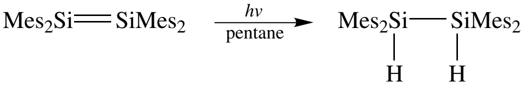

$$\mathrm{Mes_2Si{=}SiMes_2} \xrightarrow[\text{pentane}]{h\nu} \mathrm{Mes_2Si(H){-}Si(H)Mes_2} \qquad (27)$$

(328) **(329)**

The *trans* isomers of two disilenes were observed to undergo photoisomerization to mixtures enriched in the *cis* isomers when irradiated at either 254 or 350 nm (equation 28), and the kinetics of the thermal *cis–trans* isomerization have been determined[164].

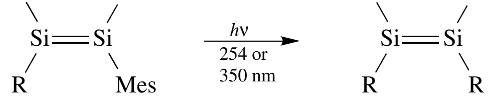

(28)

R = t-Bu or $N(SiMe_3)_2$

In other studies, the photochemical rearrangements of disilenes with the general structures $A_2Si{=}SiB_2 \rightleftharpoons ABSi{=}SiAB$ were observed[165]. This was believed to be a dyotropic process.

There is now significant evidence that highly sterically hindered disilenes readily dissociate to the related silylenes, which then undergo their characteristic reactions[166].

An example where this was effected either thermally or photochemically is given in equation 29[167].

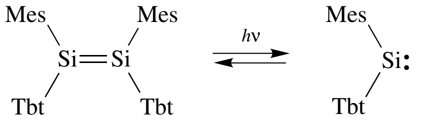

(29)

Tbt = 2,4,6-tris[bis(trimethylsilyl)methyl]phenyl

IX. OTHER PHOTOLYSES LEADING TO MULTIPLY BONDED SILICON

The photolysis of various cyclic compounds containing silicon atoms in the ring have been found to lead to the formation of transient intermediates containing multiple bonds to silicon. For example, Boudjouk and coworkers observed that photolysis of the trisilatriselenacyclohexane **330** gave rise to the silaselenone **331**, captured as the insertion product into the ring of D_3, yielding the product **332**[168] (equation 30).

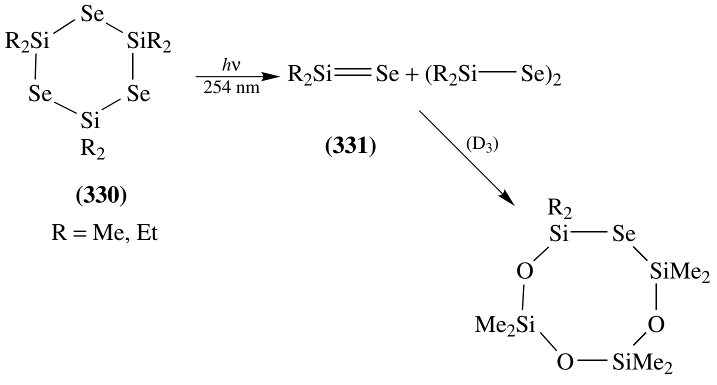

(330)

R = Me, Et

(331)

(332)

(30)

The photolysis of the phenylsilyltriazide **333** in a matrix indicated, based on UV and infrared absorption spectral data, the formation of compound **334**, the first example of an isolated compound containing a triple bond to silicon[169]. Further irradiation (or thermolysis) of **334** led to an isomer, **335**, believed to be the analog of an isonitrile. Both these compounds were characterized spectroscopically, and were trapped with *t*-butyl alcohol (equation 31).

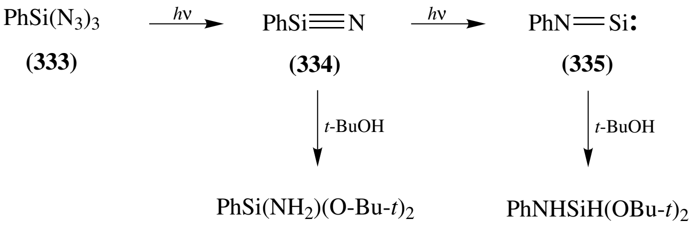

(333) **(334)** **(335)**

(31)

X. PHOTOLYSIS OF MISCELLANEOUS COMPOUNDS

A. Photochemically-induced Electron Transfer Involving Organosilicon Compounds

In the past few years many publications have appeared in which a variety of classes of organosilicon compound have been photolyzed in the presence of aromatic cyano compounds. In many cases the photolyses resulted in substitution of a ring cyano group by the hydrocarbon portion R of the organosilicon compound employed, $RSiMe_3$, and mechanistic evidence[170], which will not be discussed here, suggested that single-electron transfers were being effected, leading to the loss of the silyl group as a cation radical. Many of these reactions could be of synthetic importance to organic chemists, and some examples are shown below.

Nakadaira and coworkers[171] described the reaction of 6-trimethylsilylhex-1-ene with 1,2,4,5-tetracyanobenzene in which both the cyclic adduct **336** and the acyclic product **337** were formed (equation 32), and other workers further investigated the mechanistic details of this and related alkylations[172].

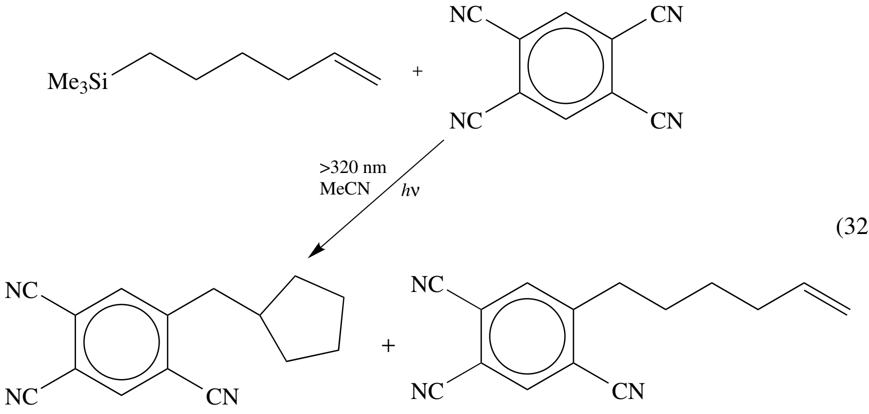

(336) **(337)**

(32)

Closely related studies by Mizuno and coworkers[173] involved the photolysis of dicyanobenzenes with allylsilanes where, as shown by the two examples in equation 33, a cyano group was replaced by an allyl group.

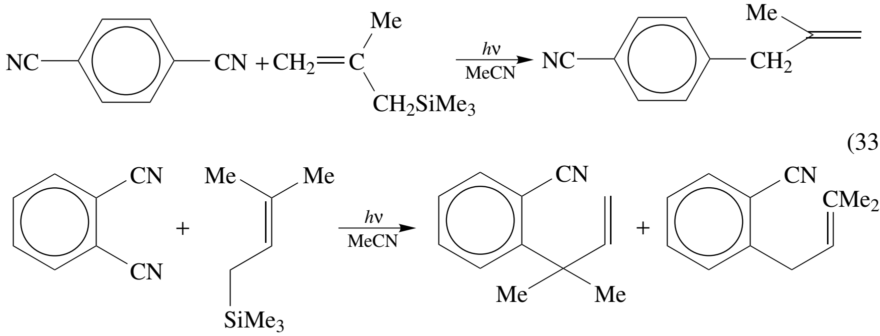

(33)

More recently Mizuno and coworkers studied the photoallylation of various cyanonaphthalenes with allyltrimethylsilane, using added phenanthrene which, in some cases, facilitated the formation of the benzotricyclic compound **338**, as shown in equation 34[174].

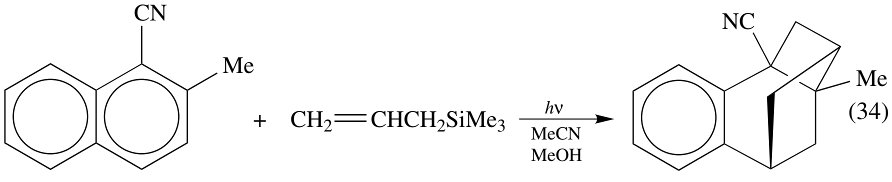

(338)

A number of aromatic dicarboxylate esters were also found to undergo allylation with loss of the silyl group when photolyzed in the presence of allyltrimethylsilane in acetonitrile-methanol[175]. As illustrated in equation 35 the naphthalene dicarboxylate **339** evidently underwent allylation, but then subsequently underwent photochemical [2 + 2] cycloaddition to give the polycyclic product **340**; in other cases the reaction stopped after allylation.

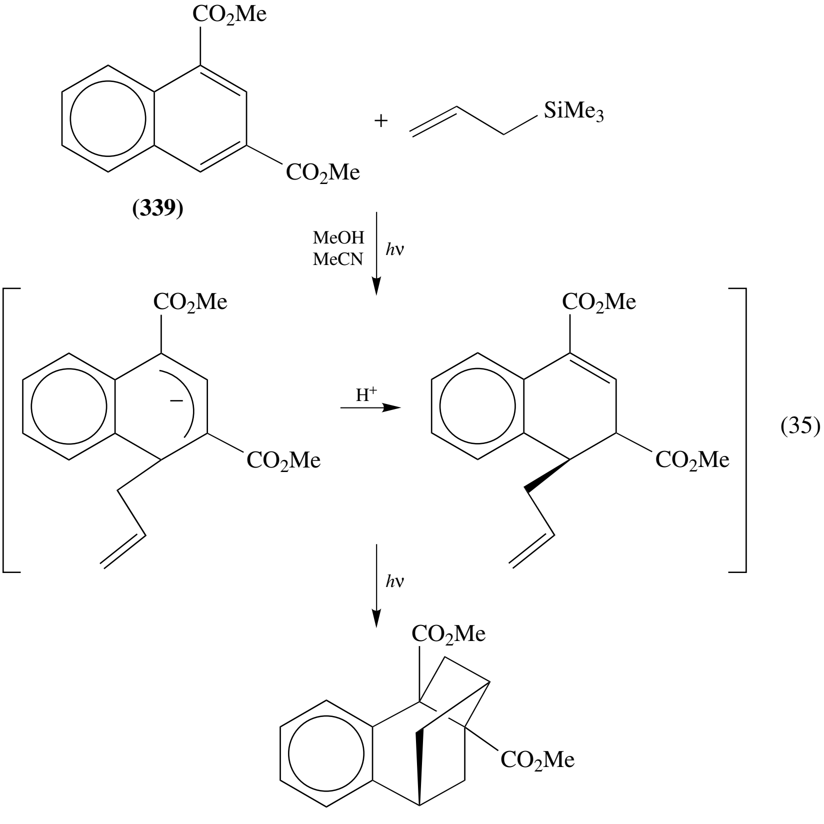

(340)

10-Methylacridinium ion also underwent allylation using allyltrimethylsilanes under photochemical conditions (equation 36)[176].

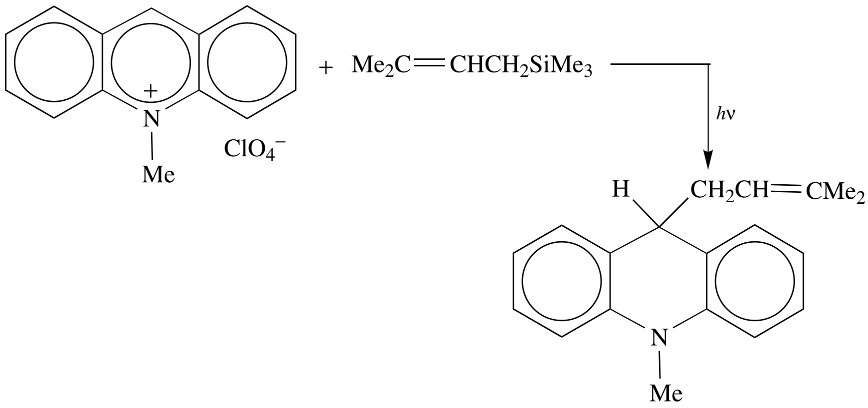

(36)

It was also shown that under somewhat different experimental conditions benzyl- and related silanes added to the ring of aryl nitriles, as exemplified in equation 37[177].

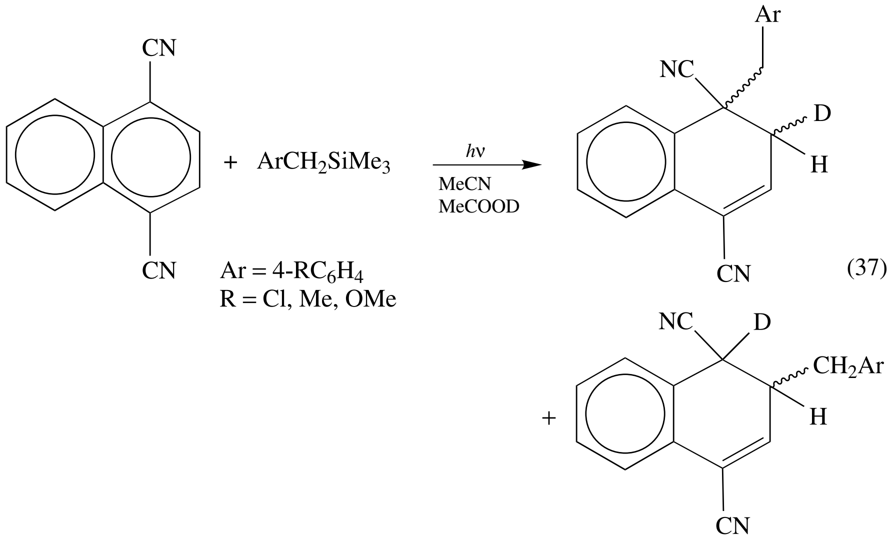

(37)

Modification of these procedures by using only catalytic amounts of the cyano compound dicyanonaphthalene (DCN) allowed the cyclization of silyl enol ethers to bicyclic compounds in good yield (equation 38)[178].

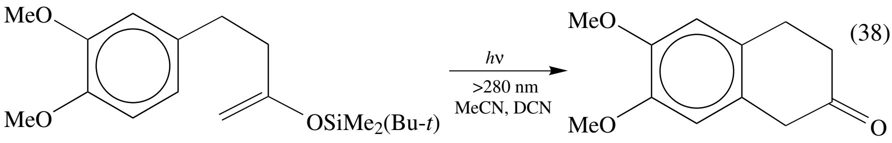

(38)

Ketene silyl acetals underwent photoaddition involving single electron transfer with electron-deficient alkenes and sensitizers such as phenanthrene (phen)[179]. Two examples of the types of products, which were formed regioselectively, are illustrated in Scheme 60.

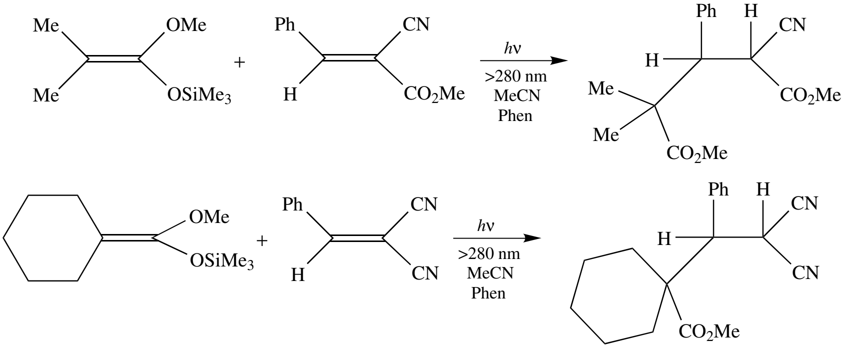

SCHEME 60

Detailed studies of the photochemistry of the (*p*-cyanophenyl)vinyldisilane **341** in methanol gave rise to products with the structures **342** and **343**, believed to be the result of both charge transfer and silyl radical involvement (equation 39)[180].

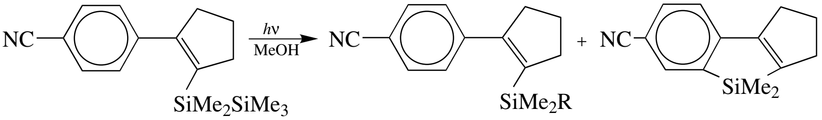

(341) **(342)** **(343)**

R = H, Me, OMe

(39)

The photolysis of silanorbornadienes such as **344** sensitized by dicyanoanthracene (DCA) induced electron transfer and led to rearrangement affording the products **345**, **346**, and anthracene[181] (equation 40).

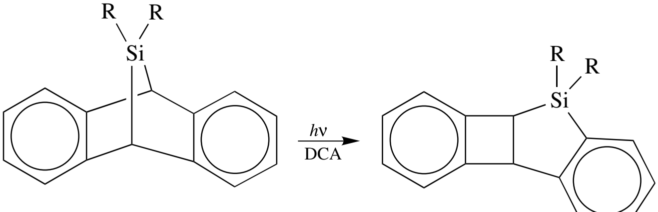

(344)

R = Mes

(345)

(40)

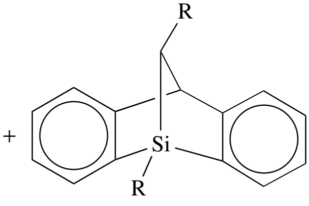

(346)

Silyl carbamates have recently been shown to undergo photoinduced electron transfer with substituted alkenes, in the presence of catalytic amounts of dicyanoanthracene and biphenyl (BP), to yield more complex carbamates[182]. Two examples which illustrate the complex structures created in good yield are shown in Scheme 61.

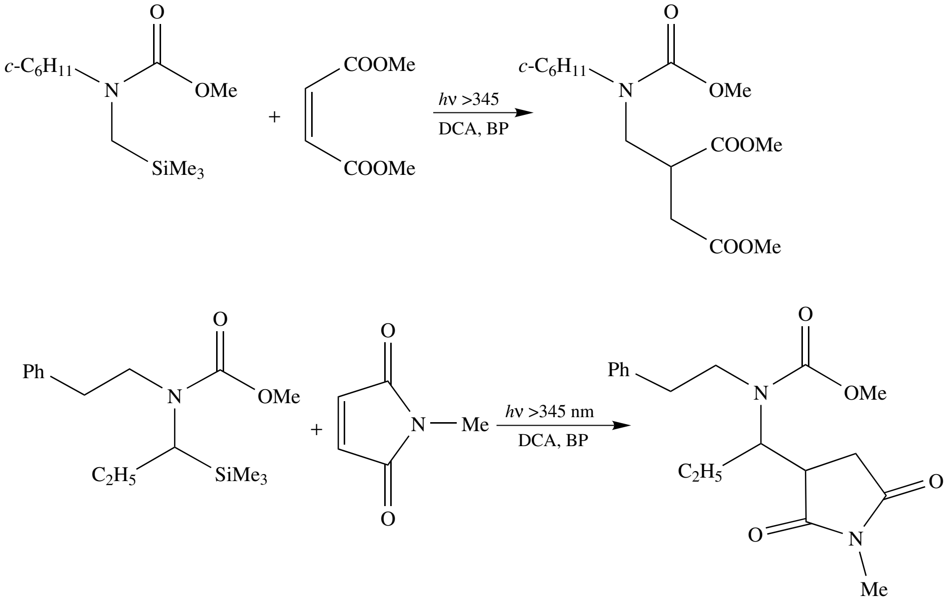

SCHEME 61

The photolysis of *N*-silylmethylphthalimides, **347**, in the presence of various reagents has been shown to give rise to products effectively derived from azomethine ylides **348**, which subsequently reacted with the reagents present[183]. The reactions are of potential synthetic use. Some examples, which involve a 1,4-silyl migration from carbon to oxygen, followed by reaction with the added reagent, are illustrated in Scheme 62. Other phthalimido compounds were also investigated. Among the mechanisms discussed was the possibility that single electron transfer was involved.

B. Miscellaneous Photolyses of Organosilicon Compounds Where Bonds to Si are Not Directly Involved

A number of photolyses of compounds containing a silicon atom have been studied in which the bonds to the silicon atom are not directly involved in the photolysis, but where the changes effected are potentially of synthetic interest. In many cases the presence of the silyl group may have an influence on the regiochemistry of the reaction, or an activating influence on an adjacent functional group. It is difficult to categorize these reactions, and thus they will simply be listed in an arbitrary order.

The Norrish type 1 cleavage of cyclic ketones has been found to be strongly influenced by the presence of a silyl group β to the carbonyl group, where the acyl radical intermediate was believed to be stabilized by the β effect[184]. For example, as shown in equation 41 with the ketone **349**, C_1-C_2 cleavage led to the diradical **350**, and thence to the products **351**

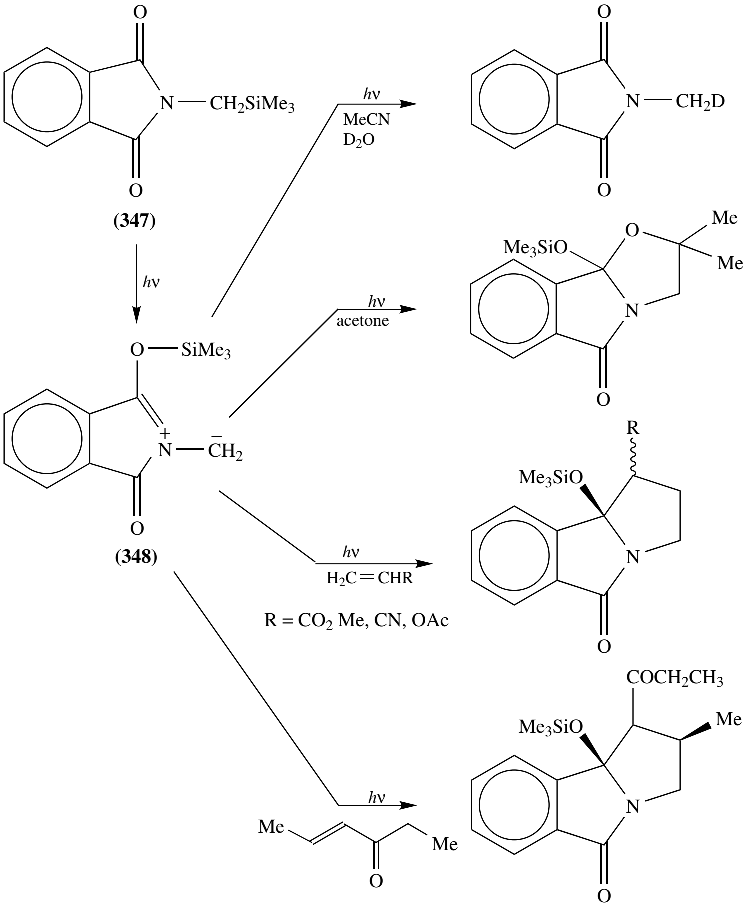

SCHEME 62

and **352**, whereas C_1-C_6 cleavage was known to be the major pathway occurring from the photolysis of the corresponding methylcyclohexanone. Not only was the regiospecificity much higher, but the rates of the reactions were enhanced when the silyl group was present.

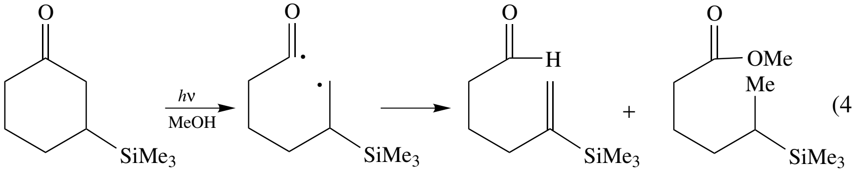

(349) **(350)** **(351)** **(352)** (41)

The sensitized photochemically-induced [2 + 2] cycloadditions of silyl enol ethers with acrylonitrile or methyl acrylate have been found, because of the regiospecificity of the reactions, to be a useful route for the preparation of functionalized eight-membered rings. Thus Suginome and coworkers[185] showed, for example, that the trimethylsilyl enol ether of *β*-tetralone **353** underwent regiospecific *syn* addition with acrylonitrile to give the tricyclic ring compound **354** which, after removal of the silyl group, could be converted to the benzocyclooctanone **355** (Scheme 63).

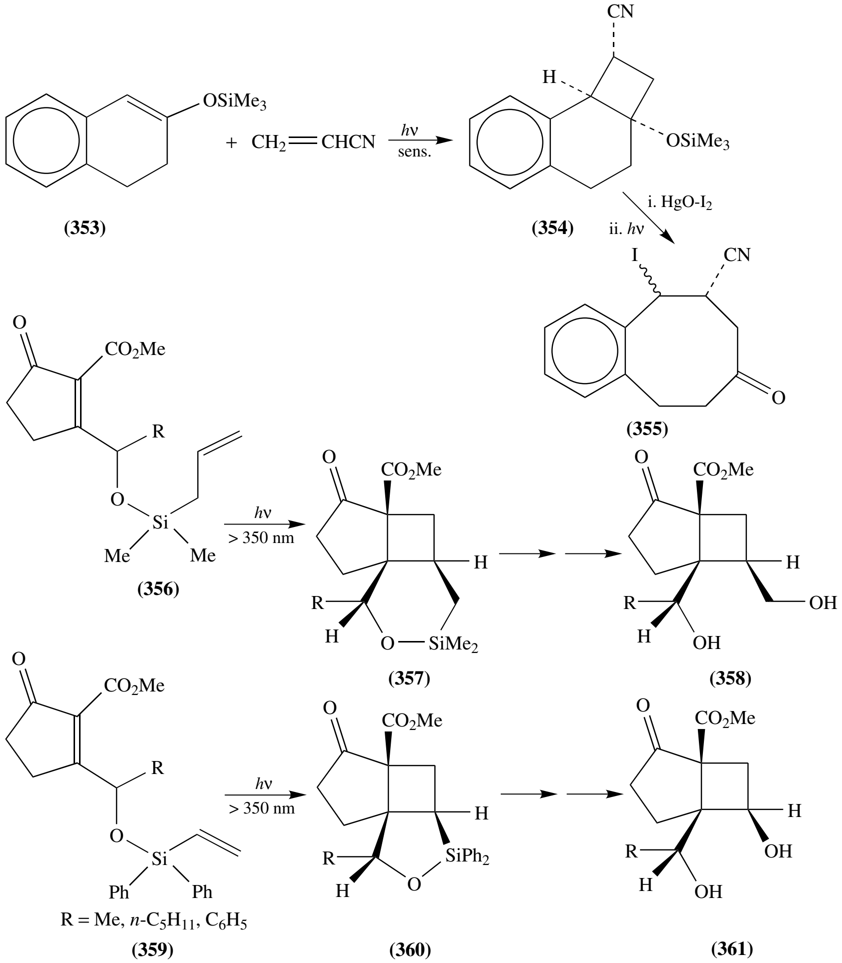

SCHEME 63

Closely related studies by Crimmins and Guise[186], also shown in Scheme 63, described the photochemical ring closure of the allyl silyl ether **356**, leading by virtue of the siloxane tether to the tricyclic species **357**, which after removal of the silyl group gave the bicyclic compound **358**. Also, the vinyl silyl ether **359** photochemically closed to compound **360**, which after removal of the silyl group led to the bicyclic species **361** (Scheme 63). These compounds were prepared with complete regiospecificity and high stereospecificity.

Photocycloadditions of silyl enol ethers **362** with aromatic aldehydes **363** have been used to prepare substituted oxiranes with high diastereoselectivities favoring the isomer

364 relative to other isomers such as **365**[187]. Hydrogenolysis of the ring with loss of the silyl group gave the vicinal diols **366**, useful for further synthetic elaboration (Scheme 64).

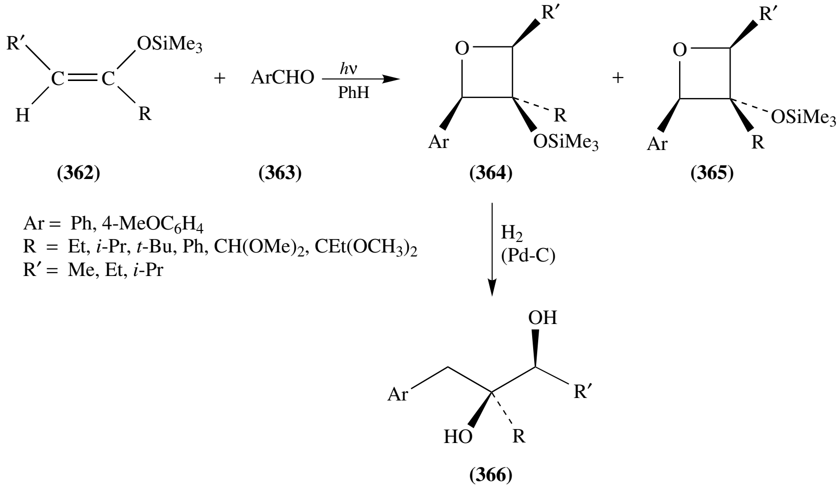

Ar = Ph, 4-$MeOC_6H_4$
R = Et, *i*-Pr, *t*-Bu, Ph, $CH(OMe)_2$, $CEt(OCH_3)_2$
R′ = Me, Et, *i*-Pr

SCHEME 64

Pirrung and Lee[188] have developed protecting groups, (hydroxystyryl)dimethylsilyl and (hydroxystyryl)di-isopropylsilyl, for primary and secondary alcohols which can be removed conveniently by irradiation with 254-nm light in a polar solvent such as acetonitrile. An example, the protected menthol silyl ether **367**, when photolyzed, gave menthol, **368**, and also yielded the heterocycle **369**. In nonpolar solvents, photolysis resulted in a 1,5-shift of hydrogen or deuterium to presumably give **370** followed by a 1,5-shift of the dimethylalkoxysilyl group giving the isomerized product **371** (Scheme 65).

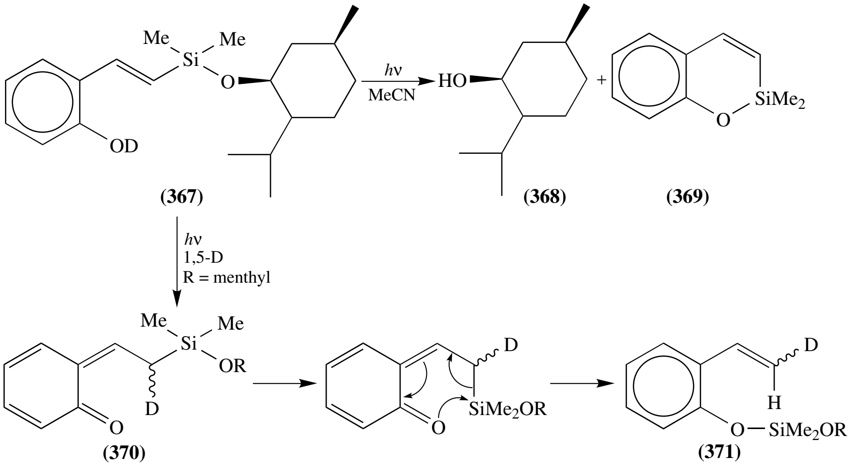

SCHEME 65

In a related vein ‘antenna’ chromophores have been developed for the self-sensitized photoreduction of ketones using isopropyl alcohol as a mild reducing agent[189]. One of the most effective chromophores for reduction of the model ketone 4-hydroxycyclohexanone was found to be the dimethylphenylsilyl group, as illustrated in equation 42.

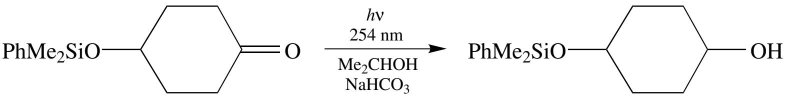

(42)

The synthesis of heterocycles containing both silicon and sulfur in the ring from linear thiols have recently been described by Kirpichenko and coworkers[190] (Scheme 66).

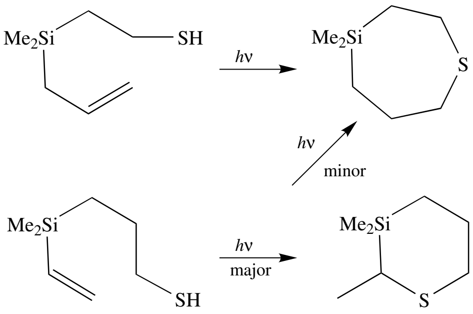

SCHEME 66

Photochemical [2 + 2] ring closures have been used to synthesize cyclophanes and related polycyclic ring systems containing silicon in the ring using triplet sensitizers such as benzophenone or dicyanonaphthalene[191] as shown in Scheme 67. The photochemistry of simpler allylsilanes was also investigated, as shown in the scheme[192]. In these reactions the silyl group and its substituents acted as tethers which controlled the orientation of the two carbon–carbon double bonds involved in the photocyclization.

Similarly, the bis(allyl)disiloxane **372** when photolyzed underwent [2 + 2] cycloaddition to yield the compound **373** as the sole product, the disiloxane linkage acting as a tether to assist in the orientation of the carbon–carbon double bonds involved in the cycloaddition[193]. The product had the all-*trans* structure (equation 43).

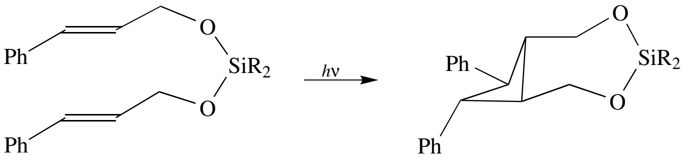

(372) **(373)**

R = Me, Ph

(43)

The photodimerization of a silylalkynylbenzene to cyclooctatetraenes has been reported by West and coworkers[194]. It was proposed that this occurred via intermolecular [2 + 2] dimerization followed by ring opening to the cyclooctatetraene (equation 44).

As illustrated in equation 45, Ando and coworkers photolyzed the cyclic trisilacycloheptene **374** at 254 nm to give the remarkably stable *trans* isomer **375** in modest

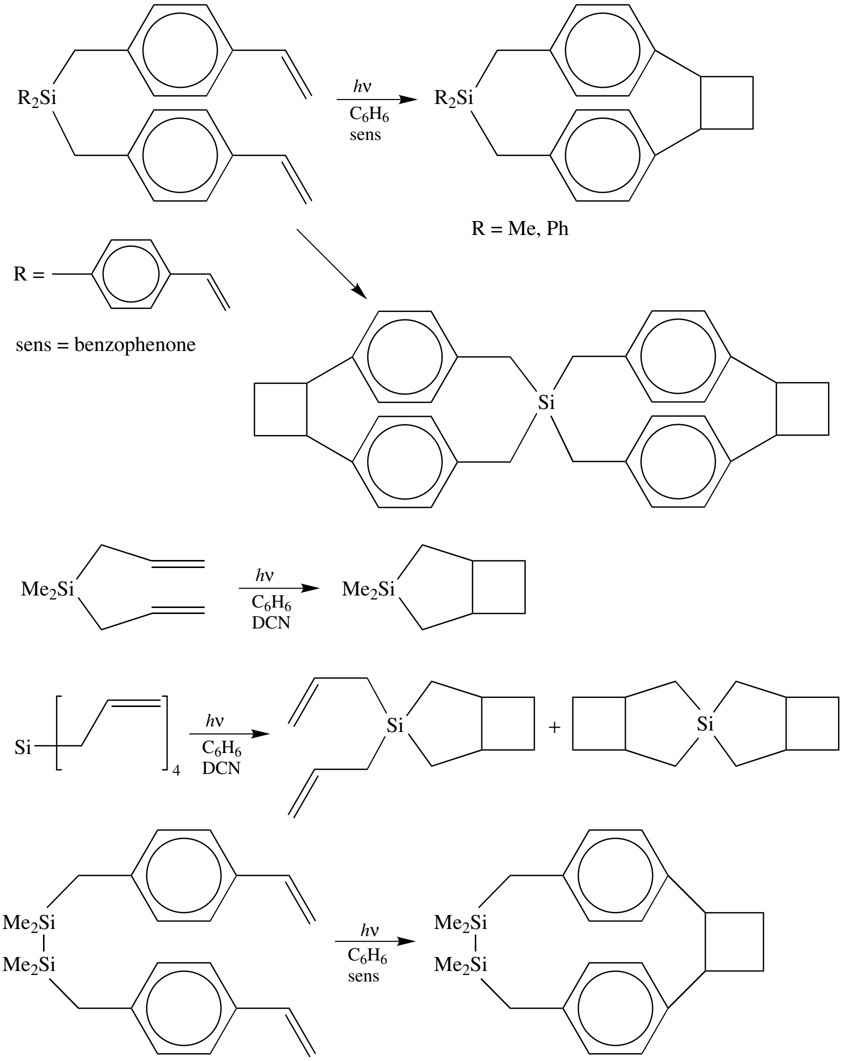

DCN = 1,4-Dicyanonaphthalene

SCHEME 67

yield: the X-ray structure was obtained[195]. This is another case where silicon atoms in a seven-membered ring permit enough flexibility to allow the formation of *trans* geometry.

An interesting study of rhodium complexes of 1,3-divinyldisiloxanes and disilazanes has recently been reported in which the nature and geometry of the complex can be altered photochemically[196]. The rhodium atom binds to both vinyl groups of a single disiloxane or disilazane molecule in either a *cis* or *trans* manner, **376** and **377**, or the rhodium bonds to two disiloxane or disilazane molecules, again in a *cis* or *trans* relationship, **378** and **379**, as shown in Scheme 68.

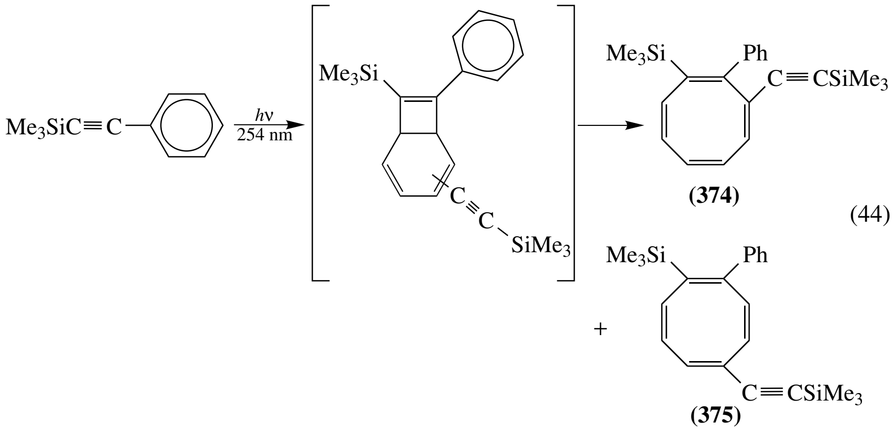

(44)

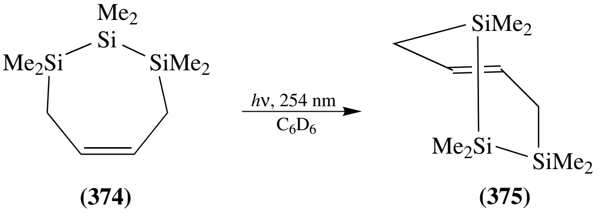

(45)

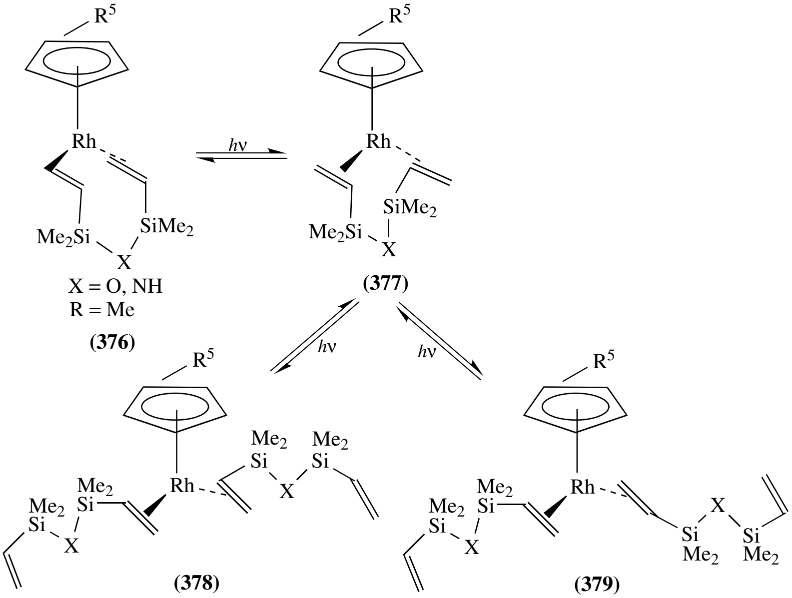

SCHEME 68

The photoionization of benzylic alcohols leading to carbocations has recently been reported[197]. Taking advantage of the stabilization provided by the β-silicon effect, flash photolysis of **380** in trifluoroethanol gave rise to the fluorenyl cation **381** which was characterized spectroscopically (equation 46).

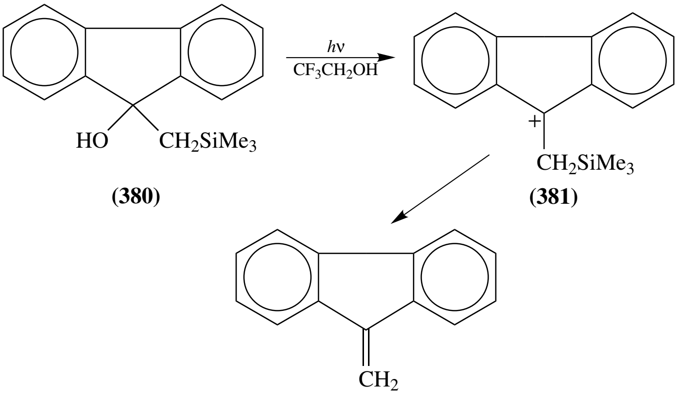

(380) **(381)** (46)

C. Cophotolyses of Various Organosilicon Compounds with Fullerenes

In the past few years a number of unusual photochemical reactions of fullerenes with a variety of types of organosilicon compounds have been described. It seems most useful to report these studies under a single heading, rather than in the sections corresponding to the particular type of organosilicon compound involved.

Ando and coworkers found that the silylene Dip_2Si**:** **382** (Dip = 2,6-di-*i*-propylphenyl), formed on photolysis of the trisilane **382** in the presence of C_{60}, gave an adduct assigned the structure of the silacyclopropane **384** which evidently arose from addition of the silylene across the C=C between two six-membered rings of the fullerene[198]. A segment of the structure of **384** is shown in equation 47.

$$C_{60} + Dip_2Si(SiMe_3)_2 \xrightarrow{h\nu} [Dip_2Si\colon] \xrightarrow{C_{60}} Dip_2SiC_{60} =$$

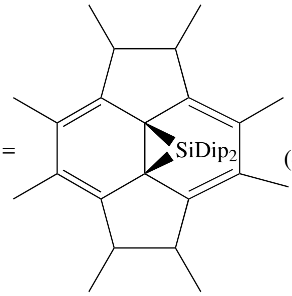

(382) **(383)** **(384)** (47)

Photolysis of a mixture of C_{60} with the disilacyclopropane **385** led to ring opening by cleavage of the Si−Si bond, and addition of the silyl ends to the ends of one of the fullerene double bonds of a six-membered ring giving the adduct **386**[199]. When the fullerene was photolyzed with the disilacyclobutane **387** it was suggested that an initial adduct **388** was formed which then rearranged to the final product **389**, obtained in good yield[200]. Finally, when photolyzed with the tetrasilacyclobutanes two types of adduct, **390** and **391**, were obtained[201] (Scheme 69).

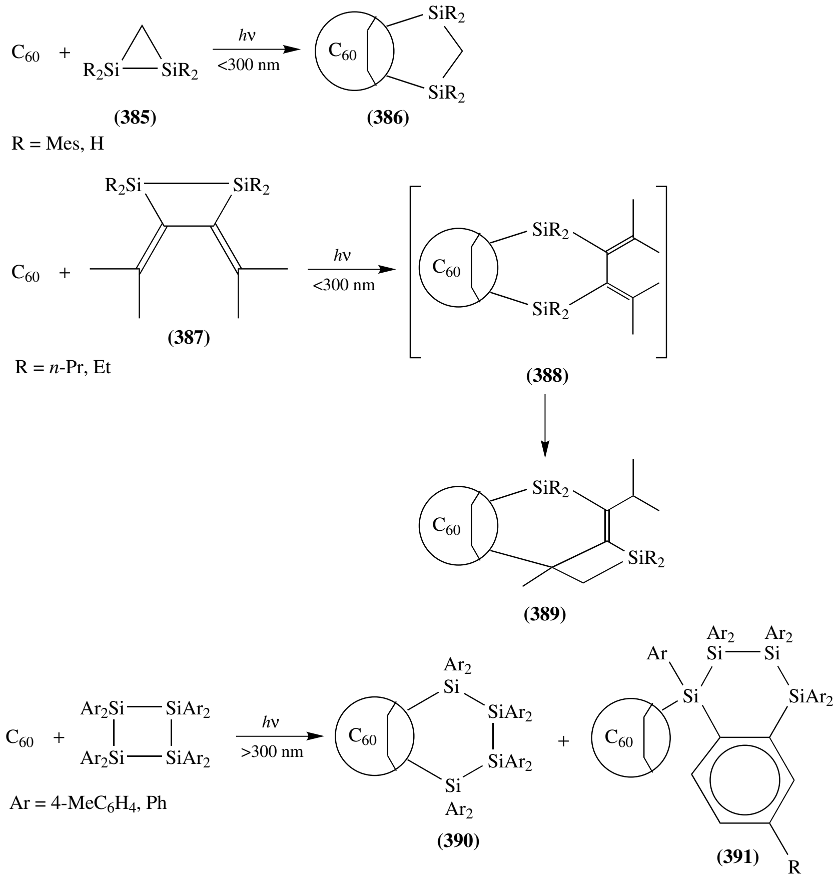

SCHEME 69

More recently, the same research group showed that the same silylene, $Dip_2Si:$, added in a similar manner to the C_{70} fullerene to yield the related silacyclopropane[202].

The dimetallofullerenes $La_2@C_{80}$[203], $La_2@C_{82}$[204] and $Sc_2@C_{84}$[203] reacted similarly with 1,1,2,2-tetramesityl-1,2-disilirane (or other tetraaryldisiliranes) to form the adducts $La_2@C_{80}(Mes_2Si)_2CH_2$, $La_2@C_{82}(Mes_2Si)_2CH_2$ and $Sc_2@C_{84}(Mes_2Si)_2CH_2$, characterized spectroscopically, each of which was believed to contain a 1,3-disilapropylene bridge across the ends of a bond of one of the six-membered rings of the original fullerene.

C_{60} also reacts with silyl ketene acetals when photolyzed with a high-pressure mercury arc. The reaction, illustrated in equation 48, leads to functionalization of the fullerene as an ester, and is said to involve single electron transfer[205].

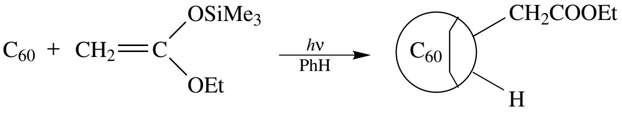

(48)

XI. ADDENDUM

Since this chapter was completed at the end of May 1996, several additional papers involving the photolysis of organosilicon compounds have appeared in the literature, or were presented at the XI International Organosilicon Conference held in Montpellier, France from 1 September to 7th September 1996. Some of these new results are described below, using the original subdivisions of the chapter to aid in their proper location.

III. D. Aryldisilanes

Results of the photolysis of both a *meso* and a *racemic* diastereomer of the 1,2-diphenyldisilane **392** indicated that the reaction leading to the silene **393**, followed by its ene reaction with an alkene leading to the adduct **394**, was a diastereospecific process[206]. A concerted mechanism, illustrated in equation 49 for one isomer of the disilane, was proposed to account for the results: such results would not be expected of a process involving silyl radical intermediates, which had been proposed earlier as intermediates in the photolysis of disilanes.

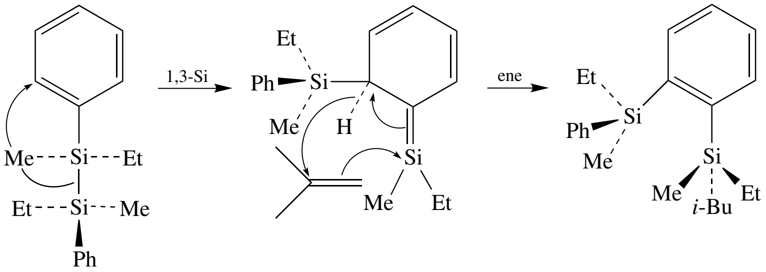

(49)

(392) (*R*,*R*) **(393)** (*E*) (*S*,*S*) **(394)** (*R*,*R*)

Further studies of the photolysis of aryldisilanes in which stable siloxetanes were obtained have been reported by Totyl and Leigh[207].

III. G. Cyclic Disilanes and Related Species

Barton and coworkers have described the interesting rearrangements under photochemical, thermal and Pd-catalyzed conditions of the eight-membered ring **395** which contains both a disilane and alkynyl groups as shown in equation 50[208].

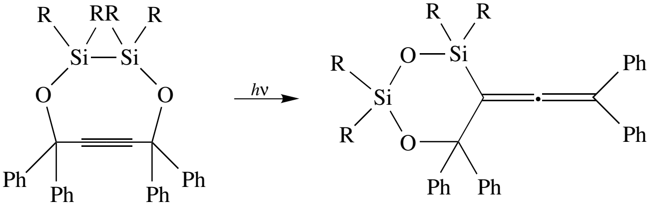

(50)

(395)

IV. B. Acyclic Polysilanes

Photolyses of some highly silyl-substituted disilanes were found to result in exclusively Si−Si homolysis leading to stable silyl radicals, studied by ESR techniques, as shown in equation 51[209].

$$(Et_nMe_{3-n}Si)_3Si{-}Si(SiMe_{3-n}Et_n)_3 \longrightarrow (Et_nMe_{3-n}Si)_3Si\bullet \qquad (51)$$

IV. C. 1. Homocyclic Systems

Kira and coworkers recently described the preparation of the first cyclic disilene, **396**[210]. On photolysis at 420 nm 1,2-silyl rearrangement occurred to yield the bicyclic[1.1.0] system, **397** (equation 52), which on standing in the dark reverted to the relatively stabler disilene.

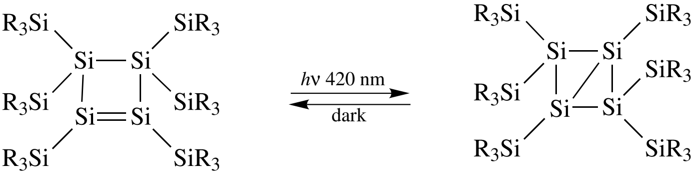

(52)

(396) **(397)**

The chemistry of octasilacubanes continues to be investigated. Ring-opening halogenation[211] has been described, as has a photochemical oxidation using DMSO as the oxygen source in which an oxygen is inserted into one or two ring Si—Si bonds, as shown in equation 53[212].

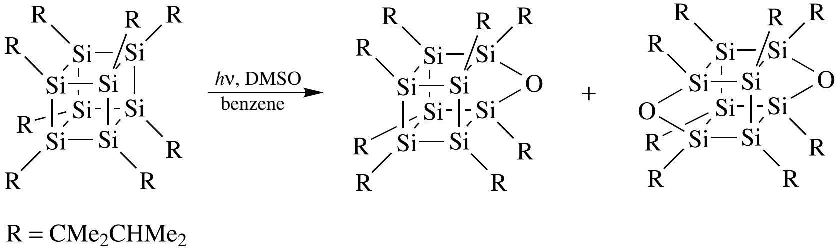

(53)

VII. PHOTOCHEMICAL ROUTES TO SILENES, SILYLENES AND DISILENES

Further reactions of the silylene t-Bu_2Si**:** produced by photolysis of hexa-t-butylcyclotrisilane with alkenes and cycloalkenes have recently been described[213].

X. A. Photochemically-Induced Electron Transfer Involving Organosilicon Compounds

Tamao and coworkers[214–216] recently demonstrated that several π-conjugated systems containing silole (1-silacyclopenta-2,4-diene) rings are capable of emitting visible light under the influence of electric charge and may be useful in molecular electronics. Structures **398**–**400** of some of the polymers are given.

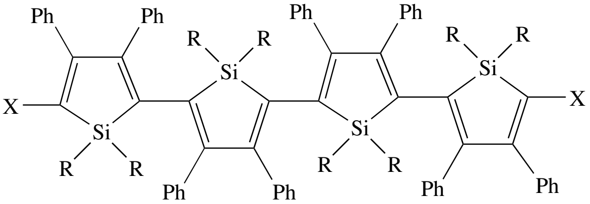

(398), X = Br, R = Me

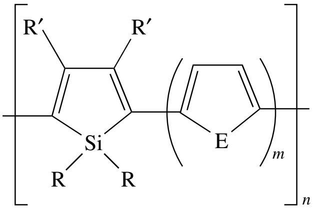

(399)
E = S, NMe

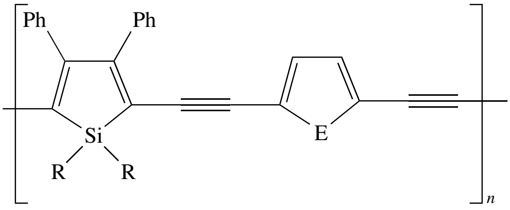

(400)
E = S, NMe, CH═CH, CH═N

XII. SUMMARY

It should be very evident from the above survey that the field of organosilicon chemistry, and in particular the photochemistry of organosilicon compounds, is a very active area of research. The field is of increasing interest not only to chemists whose primary interest lies with the silicon aspect of the subject, but increasingly it is also of interest to organic chemists because of the synthetically novel and useful products of photolysis which can be obtained, and to photochemists where the field presents a wealth of different types of reaction, few of which have been studied mechanistically. It seems certain that there will continue to be great activity in the field of organosilicon chemistry in the near future.

XIII. REFERENCES

1. M. G. Steinmetz, *Chem. Rev.*, **95**, 1527 (1995).
2. A. G. Brook, in *The Chemistry of Organosilicon Compounds* (Eds. S. Patai and Z. Rappoport), Chap 15, Wiley, Chichester, 1989, p. 965.
3. S. T. Reid, *Spec. Period. Rep.: Photochem.*, **22**, 360 (1991); **23**, 350 (1992); **24**, 350 (1993).
4. A. G. Brook and K. M. Baines, *Adv. Organomet. Chem.*, **25**, 1 (1986).
5. G. Raabe and J. Michl, *Chem. Rev.*, **85**, 419 (1985).
6. G. Raabe and J. Michl, in *The Chemistry of Organosilicon Compounds* (Eds. S. Patai and Z. Rappoport), Chap. 17, Wiley, Chischester, 1989, p. 1015.
7. M. Kira and T. Miyazawa, Chap. 22 in this volume.
8. E. W. Colvin, in *Silicon in Organic Synthesis*, Chap. 3, Butterworths, London, 1981, p. 15.
9. R. Walsh, S. Untiedt, M. Stuhlmeier and A. de Meijere, *Chem. Ber.*, **122**, 637 (1989).
10. M. Kira, H. Yoshida and H. Sakurai, *J. Am. Chem. Soc.*, **107**, 7767 (1985).
11. M. Kira, T. Taki and H. Sakurai, *J. Org. Chem.*, **54**, 5647 (1989).
12. A. G. Brook, D. M. MacRae and W. W. Limburg, *J. Am. Chem. Soc.*, **89**, 5493 (1967).
13. A. Padwa, K. E. Krumpe, L. W. Terry and M. W. Wannamaker, *J. Org. Chem.*, **54**, 1635 (1989).
14. P. P. Gaspar, D. Holten, S. Konieczny and J. Y. Corey, *Acc. Chem. Res.*, **20**, 329 (1987).
15. J. Pola, E. A. Volnina and L. E. Gusel'nikov, *J. Organomet. Chem.*, **391**, 275 (1990).
16. J. Pola, D. Cukanova, M. Minarik, A. Lycka and J. Tlaskal, *J. Organomet. Chem.*, **426**, 23 (1992).

17. Z. Bastl, H. Burger, R. Fajgar, D. Pokorna, J. Pola, M. Senzlober, J. Subrt and M. Urbanova, *Appl. Organomet. Chem.*, **10**, 83 (1996).
18. (a) S. Dhanya, A. Kumar, R. K. Vatsa, R. K. Saini, J. P. Mittal and J. Pola, *J. Chem. Soc., Faraday. Trans.*, **92**, 179 (1996).
    (b) H. K. Sharma, F. Cervantes-Lee, L. Párkányi and K. H. Pannell, *Organometallics*, **15**, 429 (1996).
19. H. Sakurai, K. Ebata, K. Kabuto and A. Sekiguchi, *J. Am. Chem. Soc.*, **112**, 1799 (1990).
20. K. Sakamoto, T. Saeki and H. Sakurai, *Chem. Lett.*, 1675 (1993).
21. P. Boudjouk, U. Samaraweera, R. Sooriyakakumaran, J. Chrusciel and K. R. Anderson, *Angew. Chem., Int. Ed. Engl.*, **27**, 1355 (1988).
22. P. Boudjouk, E. Black and R. Kumarathasan, *Organometallics*, **10**, 2095 (1991).
23. H. Saso, W. Ando and K. Ueno, *Tetrahedron*, **45**, 1929 (1989).
24. K. M. Baines and J. A. Cooke, *Organometallics*, **11**, 3487 (1992).
25. (a) M. G. Steinmetz and H. Bai, *Organometallics*, **8**, 1112 (1989).
    (b) W. J. Leigh, C. J. Bradaric, C. Kerst and J.-A. H. Babisch, *Organometallics*, **15**, 2246 (1996).
26. R. T. Conlin, S. Zhang, M. Namavari, K. L. Bobbitt and M. J. Fink, *Organometallics*, **8**, 571 (1989).
27. M. G. Steinmetz, B. S. Udayakumar and M. S. Gordon, *Organometallics*, **8**, 530 (1989).
28. I. N. Jung, D. H. Pae, B. R. Yoo, M. E. Lee and P. R. Jones, *Organometallics*, **8**, 2017 (1989).
29. N. Choi, K. Asano and W. Ando, *Organometallics*, **14**, 3146 (1995).
30. M. G. Steinmetz and Q. Chen, *J. Chem. Soc., Chem. Commun.*, 133 (1995).
31. I. N. Jung, B. R. Yoo, M. E. Lee and P. R. Jones, *Organometallics*, **10**, 2529 (1991).
32. O. M. Nefedov, S. P. Kolesnikov, M. P. Egorov, A. M. Gal'minas and M. B. Ezhova, in *Proc. IXth Int. Symp. Organosilicon Chem.* (Eds. A. R. Bassindale and P. P. Gaspar), Royal. Soc. Chem., Cambridge, UK, 1990, p. 145.
33. A. Sekiguchi, I. Maruki, K. Ebata, C. Kabuto and H. Sakurai, *J. Chem Soc., Chem. Commun.*, 341 (1991).
34. O. M. Nefedov, M. P. Egorov, S. P. Kolesnikov, A. M. Gal'minas, Y. T. Struchkov, M. Y. Antipin and S. V. Sereda *Izv. Akad. Nauk. SSSR, Ser. Khim.*, 1693 (1986); *Chem. Abstr.*, **106**, 196487b (1987).
35. M. G. Steinmetz, K. J. Seguin, B. S. Udayakumar and J. S. Behnke, *J. Am. Chem. Soc.*, **112**, 6601 (1990).
36. M. G. Steinmetz and C. Yu, *Organometallics*, **11**, 2686 (1992).
37. M. G. Steinmetz and C. Yu, *J. Org. Chem.*, **57**, 3107 (1992).
38. H. Hiratsuka, M. Tanaka, T. Okutsu, M. Oba and K. Nishiyama, *J. Chem. Soc., Chem. Commun.*, 215 (1995).
39. K. M. Welsh, J. D. Rich, R. West and J. Michl, *J. Organomet. Chem.*, **325**, 105 (1987).
40. P. Boudjouk, J. R. Roberts, C. M. Golino and L. H. Sommer, *J. Am. Chem. Soc.*, **94**, 7926 (1972).
41. Y. Nakadaira, T. Otsuka and H. Sakurai, *Tetrahedron Lett.*, **22**, 2417 (1981).
42. Y. Nakadaira, T. Otsuka and H. Sakurai, *Tetrahedron Lett.*, **22**, 2421 (1981).
43. M. Ishikawa and M. Kumada, *Adv. Organomet. Chem.*, **19**, 51 (1981).
44. M. Kira, T. Maruyama and H. Sakurai, *J. Am. Chem. Soc.*, **113**, 3986 (1991).
45. R. T. Conlin and K. L. Bobbitt, *Organometallics*, **6**, 1406 (1987).
46. W. J. Leigh, G. W. Sluggett, P. Venneri, M. Ezhova, M. S. K. Dhurjati and R. T. Conlin, *Abstr. XXVIII Organosilicon Symposium*, Gainesville, Fla., March 1995, A20.
47. M. B. Ezhova and R. T. Conlin, *Abstr. XXVII Organosilicon Symposium*, Troy, NY, March 1994, A-8.
48. J. H. Kwon, S. T. Lee, S. C. Shim and M. Hoshino, *J. Org. Chem.*, **59**, 1108 (1994).
49. S. C. Shim and S. T. Lee, *J. Chem. Soc., Perkin Trans. 2*, 1979 (1994).
50. S. T. Lee, E. K. Baek and S. C. Shim, *Organometallics*, **15**, 2182 (1996).
51. M. Ishikawa, T. Fuchikami and M. Kumada, *J. Organomet. Chem.*, **118**, 155 (1976).
52. H. Sakurai, *J. Organomet. Chem.*, **200**, 261 (1980).
53. M. Ishikawa and H. Sakamoto, *J. Organomet. Chem.*, **414**, 1 (1991).
54. M. Ishikawa, H. Sakamoto, F. Kanetani and A. Minato, *Organometallics*, **8**, 2767 (1989).
55. M. Ishikawa, K. Watanabe, H. Sakamoto and A. Kunai, *J. Organomet. Chem.*, **455**, 61 (1993).
56. J. Ohshita, H. Ohsaki, M. Ishikawa, A. Tachibani, Y. Kurosaki, T. Yamabe, T. Tsukihara, K. Takahashi and Y. Kiso, *Organometallics*, **10**, 2685 (1991).

57. J. Ohshita, H. Ohsaki, M. Ishikawa, A. Tochibana, Y. Kurosaki, T. Yamabe and A. Minato, *Organometallics*, **10**, 880 (1991).
58. J. Ohshita, H. Ohsaki and M. Ishikawa, *Organometallics*, **10**, 2695 (1991).
59. G. W. Sluggett and W. J. Leigh, *J. Am. Chem. Soc.*, **114**, 1195 (1992).
60. G. W. Sluggett and W. J. Leigh, *Organometallics*, **11**, 3731 (1992).
61. W. J. Leigh and G. W. Sluggett, *Organometallics*, **13**, 269 (1994).
62. W. J. Leigh and G. W. Sluggett, *J. Am. Chem. Soc.*, **116**, 10468 (1994).
63. O. Ito, K. Hoteiya, A. Watanabe and M. Matsuda, *Bull. Chem. Soc. Jpn.*, **64**, 962 (1991).
64. M. Kira and S. Tikurs, *Chem. Lett.*, 1459 (1994).
65. J. Braddock-Wilking and P. P. Gaspar, *Abstr. IXth International Symposium on Organosilicon Chemistry*, Edinburgh, Scotland, July 1990, B.25.
66. K. Mochida, K. Kimijima, M. Wakasa and H. Hayashi, *Abstr. Xth International Symposium on Organosilicon Chemistry*, Poznan, Poland, Aug. 1993, P-107.
67. K. Mizuno, K. Nakanishi, J.-i. Chosa and Y. Otsuji, *J. Organomet. Chem.*, **473**, 35 (1994).
68. H. Sakamoto and M. Ishikawa, *Organometallics*, **11**, 2580 (1992).
69. K. Takaki, H. Sakamoto, Y. Nishimura, Y. Sugihara and M. Ishikawa, *Organometallics*, **10**, 888 (1991).
70. M. Ishikawa, Y. Nishimura and H. Sakamoto, *Organometallics*, **10**, 2701 (1991).
71. H. K. Sharma and K. H. Pannell, *Chem. Rev.*, **95**, 1351 (1995).
72. H. Tobita, K. Ueno, M. Shimoi and H. Ogino, *J. Am. Chem. Soc.*, **112**, 3415 (1990).
73. H. Tobita, K. Ueno and H. Ogino, *Bull. Chem. Soc. Jpn.*, **61**, 2797 (1988).
74. A. Haynes, M. W. George, M. T. Haward, M. Poliakoff, J. J. Turner, N. M. Boag and M. Green, *J. Am. Chem. Soc.*, **113**, 2011 (1991).
75. K. L. Jones and K. H. Pannell, *J. Am. Chem. Soc.*, **115**, 11336 (1993).
76. C. Hernandez, H. K. Sharma and K. H. Pannell, *J. Organomet. Chem.*, **462**, 259 (1993).
77. K. H. Pannell, L.-J. Wong and J. M. Rozell, *Organometallics*, **8**, 550 (1989).
78. Z. Zheng, R. Sanchez and K. H. Pannell, *Organometallics*, **14**, 2605 (1995).
79. M. Kumada, *J. Organomet. Chem.*, **100**, 127 (1975).
80. H. Sharma and K. H. Pannell, *Organometallics*, **12**, 3979 (1993).
81. H. Sharma and K. H. Pannell, *Organometallics*, **13**, 4946 (1994).
82. M. Kira, K. Sakamoto and H. Sakurai, *J. Am. Chem. Soc.*, **106**, 7469 (1984).
83. A. D. Fanta, D. J. DeYoung, J. Belzner and R. West, *Organometallics*, **10**, 3466 (1991).
84. K. Kabeta, D. R. Powell, J. Hanson and R. West, *Organometallics*, **10**, 827 (1991).
85. H. Suzuki, K. Okabe, S. Uchida, H. Watanabe and M. Goto, *J. Organomet. Chem.*, **509**, 177 (1996).
86. A. J. McKinley, T. Karatsu, G. M. Wallraff, R. D. Miller, R. Sooriyakumaran and J. Michl, *Organometallics*, **7**, 2567 (1988).
87. A. J. McKinley, T. Karatsu, G. M. Wallraff, D. P. Thompson, R. D. Miller and J. Michl, *J. Am. Chem. Soc.*, **113**, 2003 (1991).
88. I. M. T. Davidson, J. Michl and T. Simpson, *Organometallics*, **10**, 842 (1991).
89. B. D. Shepherd, D. R. Powell and R. West, *Organometallics*, **8**, 2664 (1989).
90. G. R. Gillette, G. Noren and R. West, *Organometallics*, **9**, 2925 (1990).
91. R. S. Archibald, Y. Van den Winkel, A. J. Millevolte, J. M. Desper and R. West, *Organometallics*, **11**, 3276 (1992).
92. R. S. Alexander, Y. von den Winkel, D. R. Powell and R. West, *J. Organomet. Chem.*, **446**, 67 (1993).
93. S. Zhang, M. B. Ezhova and R. T. Conlin, *Organometallics*, **14**, 1471 (1995).
94. E. Hengge and R. Janoschek, *Chem. Rev.*, **95**, 1495 (1995).
95. H. Shizuka, K. Murata, Y. Arai, K. Tonokura, H. Tanake, H. Matsumoto, Y. Nagai, G. Gillette and R. West, *J. Chem. Soc., Faraday Trans. 1*, **85**, 2369 (1989).
96. B. J. Helmer and R. West, *Organometallics*, **1**, 1458 (1982).
97. M. Weidenbruch, *Chem. Rev.*, **95**, 1479 (1995).
98. M. Weidenbruch, E. Kroke, H. Marsmann, S. Pohl and W. Saak, *J. Chem. Soc., Chem. Commun.*, 1233 (1994).
99. M. Weidenbruch, H. Piel, A. Lesch, K. Peters and H. G. Von Schnering, *J. Organomet. Chem.*, **454**, 35 (1993).
100. A. Sekiguchi and H. Sakurai, *Adv. Organomet. Chem.*, **37**, 1 (1995)
101. A. Sekiguchi, T. Yatabe, C. Kabuto and H. Sakurai, *J. Am. Chem. Soc.*, **115**, 5853 (1993).

102. H. Suzuki, K. Okabe, R. Kato, N. Sato, Y. Fukuda and H. Watanabe, *J. Chem. Soc., Chem. Commun.*, 1298 (1991).
103. H. Suzuki, K. Okabe, R. Kato, N. Sato, Y. Fukuda, H. Watanabe and M. Goto, *Organometallics*, **12**, 4833 (1993).
104. H. Suzuki, N. Kenmoto, K. Tanaka, H. Watanabe and M. Goto, *Chem. Lett.*, 811 (1995).
105. A. G. Brook and J. M. Duff, *J. Am. Chem. Soc.*, **89**, 454, (1967).
106. A. G. Brook and J. M. Duff, *J. Am. Chem. Soc.*, **91**, 2118 (1969).
107. M. Trommer and W. Sander, *Organometallics*, **15**, 189 (1996).
108. A. G. Brook, A. Baumegger and A. J. Lough, *Organometallics*, **11**, 310 (1992).
109. K. M. Baines, A. G. Brook, R. R. Ford, P. D. Lickiss, A. K. Saxena, W. J. Chatterton, J. Sawyer and B. A. Behnam, *Organometallics*, **8**, 693 (1989).
110. S. Zhang, R. T. Conlin, P. F. McGarry and J. C. Scaiano, *Organometallics*, **11**, 2317 (1992).
111. A. G. Brook, K. Vorspohl, R. R. Ford, M. Hesse and W. J. Chatterton, *Organometallics*, **6**, 2128 (1987).
112. A. G. Brook, A. Baumegger and A. J. Lough, *Organometallics*, **11**, 3088 (1992).
113. A. G. Brook, W. J. Chatterton, J. F. Sawyer, D. W. Hughes and K. Vorspohl, *Organometallics*, **6**, 1246 (1987).
114. A. G. Brook, S. S. Hu, W. J. Chatterton and A. J. Lough, *Organometallics*, **10**, 2752 (1991).
115. A. G. Brook, S. S. Hu, A. K. Saxena and A. J. Lough, *Organometallics*, **10**, 2758 (1991).
116. A. G. Brook, K. Y. Kong, A. K. Saxena and J. F. Sawyer, *Organometallics*, **7**, 2245 (1988).
117. A. G. Brook, A. K. Saxena and J. F. Sawyer, *Organometallics*, **8**, 850 (1989).
118. A. G. Brook, P. Chiu, J. McClenaghnan and A. J. Lough, *Organometallics*, **10**, 3292 (1991).
119. A. G. Brook, W. J. Chatterton and R. Kumarathasan, *Organometallics*, **12**, 3666 (1993).
120. A. G. Brook, R. Kumarathasan and A. J. Lough, *Organometallics*, **13**, 424 (1994).
121. A. G. Brook, R. Kumarathasan and W. J. Chatterton, *Organometallics*, **12**, 4085 (1993).
122. A. G. Brook and A. Baumegger, *J. Organomet. Chem.*, **446**, C9 (1993).
123. P. Lassacher, A. G. Brook and A. J. Lough, *Organometallics*, **14**, 4359 (1995).
124. A. G. Brook, A. Ionkin and A. J. Lough, *Organometallics*, **15**, 1275 (1996).
125. A. Sekiguchi and W. Ando, *Chem. Lett.*, 2025 (1986).
126. A. Sekiguchi and W. Ando, *Organometallics*, **6**, 1857 (1987).
127. A. G. Brook and P. F. Jones, *Can. J. Chem.*, **49**, 1841 (1971).
128. K. Schneider, B. Daucher, A. Fronda and G. Maas, *Chem. Ber.*, **123**, 589 (1990).
129. A. Sekiguchi, T. Sato and W. Ando, *Organometallics*, **6**, 2337 (1987).
130. G. Maas, K. Schneider and W. Ando, *J. Chem. Soc., Chem. Commun.*, 72 (1988).
131. G. Maas, M. Alt, K. Schneider and A. Fronda, *Chem. Ber.*, **124**, 1295 (1991).
132. M. Trommer, W. Sander, C.-H. Ottoson and D. Cremer, *Angew. Chem., Int. Ed. Engl.*, **34**, 929 (1995).
133. M. Trommer, W. Sander and C. Marquand, *Angew. Chem., Int. Ed. Engl.*, **33**, 766 (1994).
134. M. Trommer and W. Sander, *Organometallics*, **15**, 736 (1996).
135. W. Ando, H. Yoshida, K. Kurishima and M. Sugiyama, *J. Am. Chem. Soc.*, **113**, 7790 (1991).
136. W. Ando, M. Sugiyama, T. Suzuki, C. Kato, Y. Arakawa and Y. Kabe, *J. Organomet. Chem.*, **499**, 99 (1995).
137. M. J. Menu, H. König, M. Dartiguenave, Y. Dartiguenave and H. F. Klein, *J. Am. Chem. Soc.*, **112**, 5351 (1990).
138. E. Deydier, M. J. Menu, M. Dartiguenave, Y. Dartiguenave, M. Simard, A. L. Beauchamp, J. C. Brewer and H. B. Gray, *Organometallics*, **15**, 1166 (1996).
139. G. Märkl, W. Schlosser and W. S. Sheldrick, *Tetrahedron Lett.*, **29**, 467 (1988).
140. G. Märkl and W. Schlosser, *Angew. Chem., Int. Ed. Engl.*, **27**, 963 (1988).
141. A. Sekiguchi, H. Tanikawa and W. Ando, *Organometallics*, **4**, 584 (1985).
142. M. Weidenbruch, *Coord. Chem. Rev.*, **130**, 275 (1994).
143. R. Okazaki and R. West, *Adv. Organomet. Chem.*, **39**, 232 (1996).
144. A. G. Brook and M. A. Brook, *Adv. Organomet. Chem.*, **39**, 71 (1996).
145. Y. Huang, M. Sulkes and M. J. Fink, *J. Organomet. Chem.*, **499**, 1 (1995).
146. M. Ishikawa, N. Nakagawa, M. Ishiguro, F. Ohi and M. Kumada, *J. Organomet. Chem.*, **152**, 155 (1978).
147. M. J. Michalczyk, M. J. Fink, D. J. De Young, C. W. Carlson, K. M. Walsh, R. West and J. Michl, *Silicon, Germanium, Tin and Lead Compd.*, **9**, 75 (1986).
148. R. S. Archibald, Y. van den Winkel, D. R. Powell and R. West, *J. Organomet. Chem.*, **446**, 67 (1993).

149. J. Hockemayer, Diploma Thesis, University of Oldenburg, 1990.

150. D. H. Pae, M. Xiao, M. Y. Chiang and P. P. Gaspar, *J. Am. Chem. Soc.*, **113**, 1281 (1991).

151. P. Boudjouk, E. Black and R. Kumarathasan, *Organometallics*, **10**, 2095 (1991).

152. E. Kroke, M. Weidenbruch, W. Saak, S. Pohl and H. Marsmann, *Organometallics*, **14**, 5695 (1995).

153. M. Weidenbruch, H. Piel, A. Lesch, K. Peters and H. G. von Schnering, *J. Organomet. Chem.*, **454**, 35 (1993).

154. K. L. Bobbitt and P. P. Gaspar, *J. Organomet. Chem.*, **499**, 17 (1995).

155. M. J. Fink, D. B. Puranic and M. P. Johnson, *J. Am. Chem. Soc.*, **110**, 1315 (1988).

156. V. N. Khabashesku, V. Balaji, S. E. Boganov, O. M. Nefedov and J. Michl, *J. Am. Chem. Soc.*, **116**, 320 (1994).

157. M. Kira, T. Maruyama and H. Sakurai, *Tetrahedron Lett.*, **33**, 243 (1992).

158. A. Vancik, G. Raabe, M. J. Michalczyk, R. West and J. Michl, *J. Am. Chem. Soc.*, **107**, 4097 (1985).

159. G. E. Miracle, J. L. Ball, D. R. Powell and R. West, *J. Am. Chem. Soc.*, **115**, 11598 (1993).

160. M. Trommer, W. Sander and A. Patyk, *J. Am. Chem. Soc.*, **115**, 11775 (1993).

161. K. M. Welsh, J. Michl and R. West, *J. Am. Chem. Soc.*, **110**, 6689 (1988).

162. G. Maier, H. Pacl, H. P. Reisenauer, A. Meudt and R. Janoschek, *J. Am. Chem. Soc.*, **117**, 12712 (1995).

163. M. J. Fink, D. J. DeYoung and R. West, *J. Am. Chem. Soc.*, **105**, 1070 (1983).

164. M. J. Michalczyk, R. West and J. Michl, *Organometallics*, **4**, 826 (1985).

165. H. B. Yokelson, D. A. Siegel, A. J. Millevolte, J. Maxma and R. West, *Organometallics*, **9**, 1005 (1990).

166. H. Suzuki, N. Tokitoh and R. Okazaki, *Bull. Chem. Soc. Jpn.*, **68**, 2471 (1995).

167. N. Tokitoh, H. Suzuki and R. Okazaki, *Abstr. Xth International Organosilicon Symposium*, Poznan, Poland, 1993, O-62.

168. P. Boudjouk, S. R. Bahr and D. P. Thompson, *Organometallics*, **10**, 778 (1991), *Tetrahedron Lett.*, **33**, 243 (1992).

169. J. G. Radziszewski, D. Littmann, V. Balaji, L. Fabry, G. Gross and J. Michl, *Organometallics*, **12**, 4816 (1993).

170. Mechanisms for many of these reactions will be found in the original article, and also in: M. Kira and T. Miyazaw Chap. 22 in this volume.

171. Y. Nakadaira, S. Kyushin and M. Ohashi, *Abstr. IX International Symposium on Organosilicon Chemistry*, Edinburgh, Scotland, July 1990, 1.12.

172. M. Fagnoni, M. Mella and A. Albini, *Tetrahedron*, **50**, 6401 (1994).

173. K. Nakanishi, K. Mizuno and Y. Otsuji, *Bull. Chem. Soc. Jpn.*, **66**, 2371 (1993)

174. T. Nishiyama, K. Mizuno, Y. Otsuji and H. Inoue, *Tetrahedron*, **51**, 6695 (1995).

175. Y. Kubo, T. Todani, T. Inoue, H. Ando and T. Fujiwara, *Bull. Chem. Soc. Jpn.*, **66**, 541 (1993).

176. S. Fukuzumi, M. Fujita and J. Otera, *J. Chem. Soc., Chem. Commun.*, 1536 (1993).

177. T. Tamai, K. Mizuno, I. Hashida and Y. Otsuji, *Bull. Chem. Soc. Jpn.*, **66**, 3747 (1993).

178. G. Pandey, A. Krishna, K. Girija and M. Karthikeyan, *Tetrahedron Lett.*, **34**, 6631 (1993).

179. K. Mizuno, N. Takahashi, T. Nishiyama and H. Inoue, *Tetrahedron Lett.*, **36**, 7463 (1995).

180. M. G. Steinmetz, C. Yu and L. Li, *J. Am. Chem. Soc.*, **116**, 932 (1994).

181. M. Kako, S. Kakuma, K. Hatakenaka, Y. Nakadaira, M. Yasui and F. Iwasaki, *Tetrahedron Lett.*, **36**, 6293 (1995).

182. E. Meggers, E. Steckhan and S. Blechert, *Angew. Chem., Int. Ed. Engl.*, **34**, 2137 (1995).

183. U. C. Yoon, D. U. Kim, Y. S. Choi, Y.-J. Lee, H. L. Ammon and P. S. Marino, *J. Am. Chem. Soc.*, **117**, 2698 (1995).

184. J. R. Hwu, B. A. Gilbert, L. C. Lin and B. R. Liaw, *J. Chem. Soc., Chem. Commun.*, 161 (1990).

185. H. Suginome, T. Takeda, M. Itoh, Y. Nakayama and K. Kobayashi, *J. Chem. Soc., Perkin Trans. 1*, 49 (1995).

186. M. T. Crimmins and L. E. Guise, *Tetrahedron Lett.*, **35**, 1657 (1994).

187. T. Bach, *Tetrahedron Lett.*, **35**, 5845 (1994).

188. M. C. Pirrung and Y. R. Lee, *J. Org. Chem.*, **58**, 6961 (1993).

189. Z.-Z. Wu and H. Morrison, *Photochem. Photobiol.*, **50**, 525 (1989).

190. S. V. Kirpichenko, L. L. Olstikova, E. N. Suslova and M. G. Voronkov, *Tetrahedron Lett.*, **34**, 3889 (1993).

191. K. Nakanishi, K. Mizuno and Y. Otsuji, *J. Chem. Soc., Perkin Trans. 1*, 3362 (1990).

192. K. Nakanishi, K. Mizuno and Y. Otsuji, *J. Chem. Soc., Chem. Commun.*, 90 (1991).
193. S. A. Fleming and S. C. Ward, *Tetrahedron Lett.*, **33**, 1013 (1992).
194. R. S. Archibald, D. Chinnery, A. Fanta and R. West, *Organometallics*, **10**, 3769 (1991).
195. T. Shimizu, K. Shimizu and W. Ando, *J. Am. Chem. Soc.*, **113**, 354 (1991).
196. S. S. D. Brown, S. N. Heaton, M. H. Moore, R. N. Perutz and G. Wilson, *Organometallics*, **15**, 1392 (1996).
197. C. S. Q. Lew, R. A. McClelland, L. J. Johnston and N. P. Schepp, *J. Chem. Soc., Perkin Trans. 2*, 395 (1994).
198. T. Akasaka, W. Ando, K. Kobayashi and S. Nagase, *J. Am. Chem. Soc.*, **115**, 1605 (1993).
199. T. Akasaka, W. Ando, K. Kobayashi and S. Nagase, *J. Am. Chem. Soc.*, **115**, 10366 (1993).
200. T. Kusakawa, Y. Kabe, T. Erata, B. Nestler and W. Ando, *Organometallics*, **13**, 4186 (1994).
201. T. Kusukawa, Y. Kabe and W. Ando, *Organometallics*, **14**, 2142 (1995).
202. T. Akasaka, E. Mitsuhida, W. Ando, K. Kobayashi and S. Nagase, *J. Chem. Soc., Chem. Commun.*, 1529 (1995).
203. T. Akasaka, S. Nagase, K. Kobayashi, T. Suzuki, T. Kato, K. Kikuchi, Y. Achiba, K. Yamamoto, H. Funasaki and T. Takahashi, *Angew. Chem., Int. Ed. Engl.*, **34**, 2139 (1995).
204. T. Akasaka, T. Kato, K. Kobayashi, S. Nagase, K. Yamamoto, H. Funasaki and T. Takahashi, *Nature*, **374**, 600 (1995).
205. K. Mikami and S. Matsumoto, *Synlett.*, 229 (1995).
206. J. Ohshita, H. Niwa, M. Ishikawa, T. Yamabe, T. Yoshii and K. Nakamura, *J. Am. Chem. Soc.*, **118**, 6853 (1996).
207. N. P. Totyl and W. J. Leigh, *Organometallics*, **15**, 2554 (1996).
208. T. J. Barton, Z. Ma and S. Ijadi-Maghsoodi, *Abstr. XI International Symposium on Organosilicon Chemistry*, Montpellier, France, September 1–7, 1996, OB15.
209. S. Kyushin, T. Betsuyaku and H. Matsumoto, *Abstr. XI International Symposium on Organosilicon Chemistry*, Montpellier, France, September 1–7, 1996, PC12.
210. T. Iwamoto, C. Kabuto, and M. Kira, *Abstr. XI International Symposium on Organosilicon Chemistry*, Montpellier, France, September 1–7, 1996, PA99.
211. M. Unno and H. Matsumoto, *Organometallics*, **13**, *4663* (1994); **14**, 4004 (1995).
212. M. Unno, T. Yokota and H. Matsumoto, *Abstr. XI International Syposium on Organosilicon Chemistry*, Montpellier, France, September 1–7, 1996, OD2.
213. E. Kroke, S. Willms, M. Weidenbruch, W. Saak, S. Pohl and H. Marsmann, *Tetrahedron Lett.*, **37**, 3675 (1996).
214. K. Tamao, *Abstr. XI International Symposium on Organosilicon Chemistry*, Montpellier, France, September 1–7, 1996, LA10.
215. K. Tamao, S. Yamaguchi and M. Shiro, *J. Am. Chem. Soc.*, **116**, 11715 (1994).
216. K. Tamao, S. Yamaguchi, Y. Ito, Y. Matsuzaki, T. Yamabe, M. Fukushima and S. More, *Macromolecules*, **28**, 8668 (1995).

CHAPTER 22

Mechanistic aspects of the photochemistry of organosilicon compounds

MITSUO KIRA

Department of Chemistry, Graduate School of Science, Tohoku University, Aoba-ku, Sendai 980-77, Japan

and

TAKASHI MIYAZAWA

Photodynamics Research Center, The Institute of Physical and Chemical Research, (RIKEN), 19-1399, Koeji, Nagamachi, Aoba-ku, Sendai 980, Japan

---

I. INTRODUCTION

The photochemistry of organosilicon compounds has been extensively studied, since many types of interesting reactive intermediates such as silylenes, silenes, disilenes and silyl radicals as well as highly strained organosilicon molecules, which are usually very difficult to prepare by other methods, have been created via photochemical reactions. Organosilicon compounds possessing unique photochemical and photophysical properties such as thermochromism, photochromism, photoconductivity, nonlinear optical properties and so on would be expected as modules for future optoelectronic devices. Recent advances in the photochemistry of organosilicon compounds have been thoroughly reviewed by Brook[1,2] and Steinmetz[3], including analysis of the photochemical intermediates and their fates.

A complete mechanism of a photochemical reaction of a molecule should require the knowledge of (1) the electronic structure of the excited states attained by absorption of light, (2) the photophysical events arising from the excited states such as emission, internal conversion, radiationless transition, intersystem crossing, quenching and energy transfer, (3) the photochemical events originating from the excited state such as bond breaking, rearrangement, electron transfer and intermolecular reactions and (4) the dynamics of the photophysical and photochemical events. In this respect, very few studies of the mechanistic aspects of organosilicon photochemistry have been reported so far. The detailed mechanistic photochemistry will be delineated by future generations of organosilicon chemists. In this chapter, only selected topics will be discussed, in cases where the electronic structures of excited states and their responsibility for photoreactions have been investigated.

II. OLIGOSILANES AND POLYSILANES

A. Introduction

Polysilane high polymers possessing fully saturated all-silicon backbone have attracted remarkable attention recently because of their unique optoelectronic properties and their importance in possible applications as photoresists, photoconductors, polymerization initiators, nonlinear optical materials etc. A number of review articles have been published on this topic[4–9]. The studies in this field have stimulated both experimental and theoretical chemists to elaborate on understanding the excited state nature of polysilanes and oligosilanes and of their mechanistic photochemistry.

B. Excited State Nature of Peralkyloligosilanes

Historically, the unique electronic properties of linear peralkyloligosilanes[4] were first reported by Gilman and coworkers[10,11] who reported the electronic spectra of permethyloligosilanes, $Me(SiMe_2)_nMe$ ($n \geqslant 2$), which exhibited electronic transitions in the ultraviolet region. The properties of open-chain and cyclic oligosilanes have been reviewed[12,13]. The absorption maxima shift to the red on increasing the number of silicon atoms in the chain[10,11,14]. Table 1 records the reported UV absorption maxima for linear permethyloligosilanes.

Whereas the finding by Gilman and coworkers was the first recognition of the so-called σ-conjugation in polysilanes, the origin of the red shift of the absorption maxima on increasing the silicon chain length was the subject of controversial discussions. Thus, Pitt and coworkers ascribed it first to lowering of the LUMO of permethyloligosilanes, which was represented by the linear combination of the unoccupied orbitals localized on individual $-SiMe_2-$ groups[15]. On the other hand, a Russian group[16] and later also Pitt and coworkers[17,18] assigned the electronic transitions to $\sigma \rightarrow \sigma^*$ transitions and treated the transition energies by using the Sandorfy C method[19], which was originally used to describe σ conjugation in alkane chains[20]. Thus, the Hamiltonian is of the Hückel type, with a strongly negative vicinal resonance integral β_{vic} and a more weakly negative geminal resonance integral β_{gem} as shown in Figure 1. This type of σ conjugation results

TABLE 1. UV absorption maxima of permethyloligosilanes $Me(Me_2Si)_nMe$ in hydrocarbon solvents at room temperature[a]

n	λ_{max} (ϵ)
2	197 (8500)
3	215 (9000)
4	235 (14700)
5	250 (18400)
6	260 (21100)
7	266.5 (23000)
8	272.5 (38000)
10	279 (42700)
12	285 (43000)[b]
16	293 (68000)[c]
18	291 (44300)[b]
24	293 (45500)[b]

[a] Unless otherwise noted, data were taken from Reference 12.

[b] From Reference 14.

[c] From Reference 45.

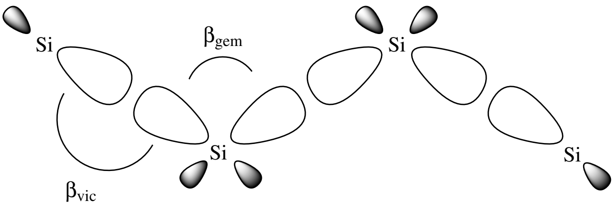

(a) Sandorfy C method

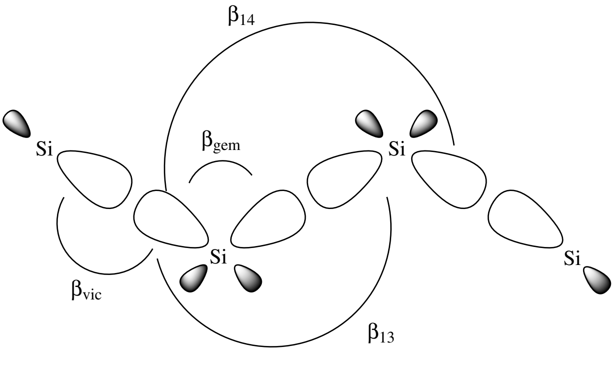

(b) Ladder C method

FIGURE 1. Schematic representation of the interactions between sp^3(Si) hybrid orbitals in linear oligosilanes. (a) Reprinted by permission of The Royal Society of Chemistry, from Reference 33; (b) Reprinted with permission from Reference 17. Copyright 1970 American Chemical Society

in both raising the HOMO levels and lowering the LUMO levels in oligosilanes and explains the red shift of the absorption maxima on increasing the chain length. The existence of the high-lying HOMO in linear and cyclic peralkyloligosilanes is evident from photoelectron[21−23] and charge-transfer[24,25] spectroscopy, and from ESR spectroscopy of the corresponding radical cations[26−28], and that of the low-lying LUMO is evident by ESR of the corresponding radical anions[29−31].

Recently, a deeper understanding of the excited state nature of the oligosilanes has been obtained. In relation to the remarkable thermochromism observed in peralkylpolysilanes (*vide infra*), the dependence of the electronic spectra of peralkyloligosilanes on the conformations of the silicon backbone has been investigated in detail. Plitt and Michl have investigated UV and IR spectra of permethyltetrasilane[32], the shortest peralkylated silicon chain expected to show conformational isomerism in the backbone, in Xe and Ar matrices. The UV spectrum shows a weak peak at 206 nm and a strong peak at 228 nm, the origin of which was first ascribed to the *gauche* and *anti* conformers of permethyltetrasilane, respectively, on the basis of a correlation of the peaks in the IR and UV spectra; irradiation using 206 nm light destroys the *gauche* peaks and 229 nm light destroys the *trans* peaks in the IR spectrum. The simple Sandorfy C model[19] cannot explain the conformational dependence. Michl and coworkers have refined the model and proposed the ladder C model[32,33] where 1,3- and 1,4- orbital interactions are considered and the dihedral angle (θ) dependence is incorporated in the resonance integrals β_{14}, which are -0.40 eV at $\theta = 90°$ and $+0.75$ eV at $\theta = 165°$; $\alpha = -2.63$ eV, $\beta_{\text{vic}} = -3.32$ eV, $\beta_{\text{gem}} = -0.62$ eV and $\beta_{13} = 0$ eV, which were determined also using nonlinear least-squares optimization of the resonance integrals (Figure 1)[33]. The calculated λ_{max} for *gauche* and *anti* tetrasilane are 209 and 230 nm, respectively, being in good accord with the two observed band maxima for permethyltetrasilane. The calculations reproduce the chain-length dependence of the energies of the intense $\sigma \rightarrow \sigma^*$ transitions of permethylated oligosilanes and their conformational dependence[33]. However, the optimized β_{14} for the *gauche* geometry is unexpectedly more negative than that for the *anti* geometry having better orbital overlap. On the basis of recent *ab initio* MO calculations and more detailed selective irradiation experiments, the explanation has been somewhat modified[34]. Thus, the *ab initio* MO calculations for decamethyltetrasilane have shown an interesting conformational dependence on the ground-state potential surface. Six conformational minima whose energies lie within 1 kcal mol^{-1} of each other and whose dihedral angles are near ±162 (*anti*), ±91 (*ortho*) and ±53° (*gauche*) have been found. This can be contrasted with the situation in both *n*-butane and *n*-tetrasilane, which have only three minima at 180 (*anti*) and ±60° (*gauche*). The IR spectral peaks previously assigned to the *gauche* conformer of permethyltetrasilane should be taken as those of overlapping contributions from two conformers, *gauche* and *ortho* (Figure 2).

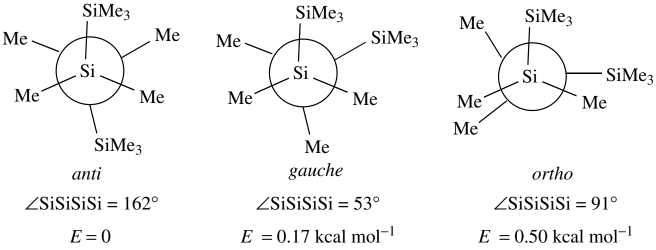

FIGURE 2. Newman projections and energies of the MP2/6-31G* calculated geometries of the *anti, gauche* and *ortho* conformers of permethyltetrasilane

The highest occupied and lowest unoccupied molecular orbitals of *anti*-tetrasilane are shown schematically in Figure 3. The calculations predict that one-photon allowed transitions to two *B* states and two-photon allowed transitions to two *A* states for permethyltetrasilane are in the UV region. The two *B* states are of the $\sigma\sigma^*$ and $\sigma\pi^*$ types, the transitions to which are "strongly allowed" and "weakly allowed", respectively. The $\sigma\sigma^*$ state is the lower state at the *anti* geometry (dihedral angle = 180°), while the $\sigma\pi^*$ state at the *cis* geometry (dihedral angle = 0°) is the consequence of an avoided crossing between the two lowest *B* states (Figure 4). Thus, at the *anti* geometry the transition to the $1B$ ($\sigma\sigma^*$) state is intense and the transition to the $2B$ ($\sigma\pi^*$) state is very weak. At the *twisted* (i.e. *gauche* and *ortho*) geometries, symmetry is lower and both transitions into *B* states are predicted to have fairly high intensities due to the mixing of the $\sigma\pi^*$ and

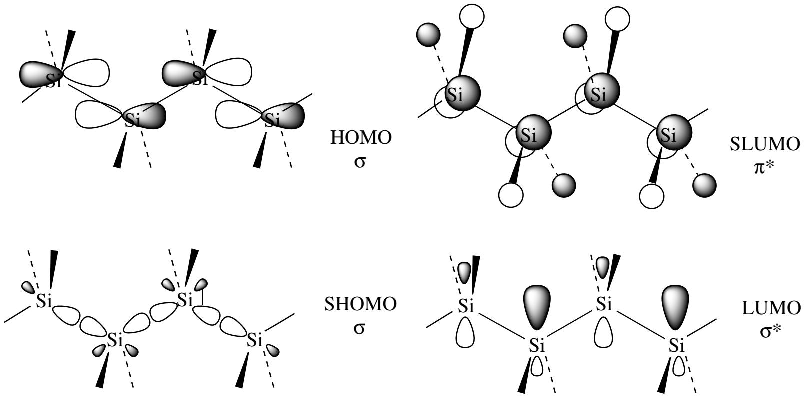

FIGURE 3. Schematic representation of the highest occupied and lowest unoccupied molecular orbitals of tetrasilane. Reproduced by permission of Elsevier Science Ltd from Ref. 35

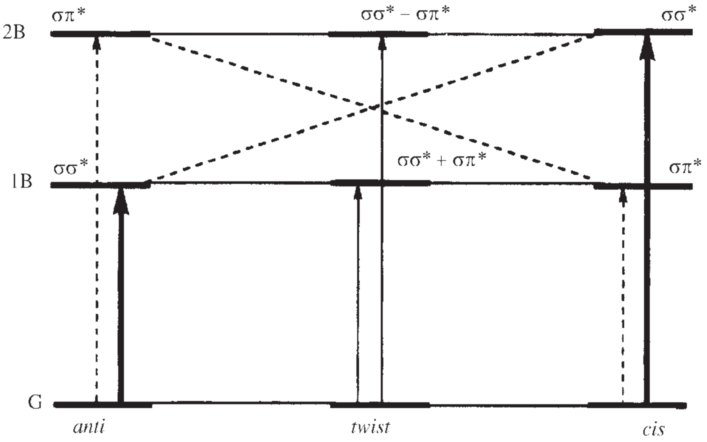

FIGURE 4. Schematic representation of the correlation diagram of *B* states among *anti, twist* and *cis* geometries of tetrasilane: ⟶, allowed transition; →, partially allowed transition; ----►, forbidden transition

$\sigma\sigma^*$ *B* configurations. Because of the strongly avoided crossing, the energies of both the lower and upper *B* states are nearly independent of the twist angle, while the intensity is conformation-sensitive. Thus, the weak peak at 206 nm and the strong peak at 228 nm in the UV spectrum of decamethyltetrasilane have now been assigned to intense transitions to the $2B$ $(\sigma\sigma^* - \sigma\pi^*)$ states of the *twisted* conformers and to a mixture of an intense transition to the $1B$ $(\sigma\sigma^*)$ state of the *anti* conformer and weak transitions to the $1B$ $(\sigma\sigma^* + \sigma\pi^*)$ states of the *twisted* conformers, respectively.

Instead of the ladder C model, the ladder H model, where the electrons of the bonds to substituents in addition to those in the backbone are considered, is suggested to be essential for drawing even the simplest picture of σ conjugation[35]. The *A* states are also of a $\sigma\sigma^*$ and a $\sigma\pi^*$ type, and are calculated to undergo a similar avoided crossing. In view of their very low calculated absorption cross sections, they could be detected only by two-photon absorption spectroscopy.

A number of semiempirical[36–40] and *ab initio* MO[35,41] calculations have been carried out for singlet excited states of polysilanes and oligosilanes. *Ab initio* MO calculations have been performed for the excited singlet states of the linear oligosilanes Si_nH_{2n+2}, $n = 2$–5, at SCF-CI levels with several basis sets, in order to establish their nature as a function of chain length[35]. The results suggest that the lowest $\sigma\pi^*$ $(\sigma_{SiSi} \rightarrow \pi^*{}_{SiH})$ excited state lies below the first $\sigma\sigma^*$ $(\sigma_{SiSi} \rightarrow \sigma^*{}_{SiSi})$ state in the shortest few oligosilanes, and that the order of the states changes as the number of silicon atoms in the chain increases. Rydberg states are expected to dominate the low energy region of the spectra of oligosilanes shorter than Si_6H_{14}; for longer-chain oligosilanes, all Rydberg excitations will be higher in energy than the lowest valence excitations. The lowest excited state with a large two-photon absorption cross section is well represented by the SHOMO → LUMO $(\sigma_{SiSi} \rightarrow \sigma^*{}_{SiSi})$ configuration and has essentially no doubly excited [$\mathrm{HOMO}^2 \rightarrow \mathrm{LUMO}^2$ $(\sigma_{SiSi}{}^2 \rightarrow \sigma^*{}_{SiSi}{}^2)$ configuration] character. The alkyl substitution at the central silicon of trisilane lowers the $\sigma\sigma^*$ excitation energy, primarily by destabilizing the highest σ_{SiSi} orbital by hyperconjugative interaction with the substituents.

Absorption and emission properties of permethylhexasilane have been investigated in detail[42]. While a hexane solution of Si_6Me_{14} exhibits a strong absorption band at 260 nm at room temperature, the band becomes much narrower ($\Delta\nu = 1400$ cm^{-1}) with a red shift of 640 cm^{-1} in a 3-methylpentane glass at 77 K. Whereas the hexasilane was very weakly fluorescent ($\phi_f < 10^{-4}$) at room temperature in solution, an intense but very broad fluorescence band ($\phi_f = 0.45$, $\Delta\nu = 5350$ cm^{-1}) with a large Stokes shift (9400 cm^{-1}) was observed in a 77 K glass matrix, being independent of the excitation energy. The absorption band is assigned quite reasonably to a $\sigma \rightarrow \sigma^*$ (HOMO–LUMO) excitation. On the other hand, the origin of the fluorescence has been ascribed to the emission from a less strongly allowed and Franck–Condon forbidden excited state lying somewhat lower in energy than the strongly allowed $\sigma\sigma^*$ state that dominates the absorption spectrum, on the basis of the large Stokes shift, the broad fluorescence bandwidth and the temperature effects; the transition from the ground state to the emitting state is masked and hard to see in ordinary absorption spectra. Permethylated tetrasilane and pentasilane exhibit similar broad fluorescence bands with large Stokes shifts as permethylhexasilane in argon matrices. As the Si chain becomes shorter, the emission becomes weaker and its peak red-shifts slightly. Unusually, permethylheptasilane shows a broad fluorescence band with a large Stokes shift in solution at room temperature, but a very slightly Stokes-shifted sharp band at 77 K, similarly to linear long-chain peralkyloligosilanes and polysilanes[43]. In order to explain the anomalous emitting state for short-chain oligosilanes, two models, a self-trapped exciton state, where the excitation is localized in a small fraction of the total segment length, and a $\sigma\pi^*$ state, which is calculated to lie below the lowest $\sigma\sigma^*$ state in the short oligosilane chains, were proposed by Hochstrasser and coworkers[44] and by Sun and Michl[42], respectively. Sun and Michl have excluded the latter assignment and given evidence for the self-trapped exciton model. Michl and coworkers have proposed that the emission is due to a nonvertical excited state with a single greatly stretched SiSi bond[43].

As a model for polysilane high polymers, photophysics of linear permethylhexadecasilane (n-$Si_{16}Me_{34}$) which showed similar behavior to linear polysilane polymers have been investigated in detail[45]. At room temperature in dilute hexane solution, the UV spectrum of $Si_{16}Me_{34}$ showed a band maximum at 293 nm (ϵ 68,000) with a bandwidth at a half-maximum ($\Delta\nu$) of 6200 cm^{-1}, while the maximum was red shifted and had a narrower bandwidth (λ_{max} 312 nm, $\Delta\nu$ 1400 cm^{-1}) in 3-methylpentane glass at 77 K. A broad Gaussian-like fluorescence band appeared at 327 nm ($\Delta\nu = 1500$ cm^{-1}) at room temperature in solution. The fluorescence quantum yield depends strongly on the excitation energies. Thus, it was about 0.07 at excitation wavelengths (λ_{ex}) shorter than the absorption maximum and 0.63 at the red edge of the absorption spectrum ($\lambda_{ex} = 325$ nm). The fluorescence decay of $Si_{16}Me_{34}$ is essentially independent of the excitation energy and the monitored emission frequency ($\tau_F = 179 \pm 20$ ps). The absorption and emission spectra of $Si_{16}Me_{34}$ at low temperature solutions and glass are quite different from those in solution at room temperature and depend strongly on the concentration of the sample and also on its thermal history. In dilute 3-methylpentane glass ($c \leqslant 1.6 \times 10^{-7}$ M) at 77 K, two overlapping absorption maxima at 312 and 315 nm are observed but the band is quite narrow. While the fluorescence and the excitation spectra depend strongly on the excitation and the monitored emission energies, respectively, even in the region of $\lambda_{ex} < \lambda_{max}$, a fluorescence spectrum excited at λ_{max} (312 nm) showed two peaks at 320 nm and 315 nm. The combination of absorption, fluorescence and fluorescence excitation spectra suggests the existence of the following three distinct conformers with low energy states in addition to a large number of others: a species responsible for the 315 nm absorption shoulder and the 320 nm emission peak, a species responsible for the fluorescence peak at 315 nm, and a nonfluorescent species responsible for the absorption peak at 312 nm. The ϕ_f value of the dilute sample was *ca* 0.5, being essentially independent of the excitation wavelengths. Rapidly cooled more concentrated 4.7×10^{-6} M solution of $Si_{16}Me_{34}$ showed an additional fluorescence band at 321 nm assignable to the oligosilane dimer or to more highly aggregated clusters. The quantum yield of the cluster emission is about 0.06. Slow cooling of the concentrated $Si_{16}Me_{34}$ solution allows the clusters to develop further into microcrystals, which give the same absorption and emission spectra as that of the solid film at 77 K. The phenomena have been understood by a segment model proposed for long-chain polysilane high polymers (Section II.C). Thus, the excitation of $Si_{16}Me_{34}$ using $\lambda_{ex} < \lambda_{max}$ generates initially excited short segments, which transfer the energy to the emitting long segments. At low temperatures, they are also generated through adiabatic excited-state conformational changes that extend the length of a particular excited short segment at the expense of its neighbors, presumably producing primarily the all-*trans* conformer, as suggested by the constant ϕ_f, irrespective of the excitation wavelength. The actual value of ϕ_f is 6 times lower for $Si_{16}Me_{34}$ than for the model polymer $[SiMePr]_x$ at $\lambda_{ex} < \lambda_{max}$, suggesting that adiabatic generation of long-segment chromophores by conformational change is less efficient than energy transfer along the backbone of a polymer; there are many molecules having only short segments in the hexadecasilane and the excited short segments will undergo dark processes such as intersystem crossing, internal conversion or photochemical reactions.

C. Excited State Nature of Peralkylpolysilane High Polymers

Linear-chain polysilanes have been found to show unusual optical properties[4–9]. At room temperatures in hydrocarbon solution, linear peralkylpolysilanes having more than

50 silicon atoms in a chain, such as $[SiBu_2]_n$, $[SiHex_2]_n$, $[SiOctyl_2]_n$, etc., exhibit an intense absorption band at *ca* 315 nm and a strong fluorescence peak at *ca* 340 nm. Upon cooling below *ca* $-30\,^\circ$C, the absorption and emission bands become much narrower and shift to about 350 nm, with a very small Stokes shift. The temperature dependence of the absorption spectra is discontinuous; in a very narrow temperature range upon cooling, one absorption band disappears and a new band grows at a longer wavelength. Primarily on the basis of its long-axis polarization, this strong absorption has been assigned to a $\sigma \rightarrow \sigma^*$ transition. It was first proposed that this transformation is due to a coil-to-rod transition[46]. However, rigid-rod-like conformations of macromolecules in solution require either a stiff main-chain structure, particular interaction forces within the chain such as hydrogen bonding, or very strong steric constraints; neither of these requirements is substantially fulfilled for these peralkylpolysilanes. Light scattering experiments[47,48] have shown that aggregation of the polysilane chains is associated with the thermochromism even at concentrations below 10^{-4} M. The remarkable thermochromism would be associated with an aggregation of long, approximately all-*trans* chain segments, intramolecular and/or intermolecular, depending on concentration. Since thermochromism occurs even at low concentrations of polymers, the aggregation should be cooperative with the formation of all-*trans* chain segments.

Using the segment model[5,38,49–51], the photophysical properties of the high-temperature solution form can be understood if the polymer chain behaves as a string of fairly localized, loosely coupled chromophores represented by approximately planar all-*trans* chain segments, separated by one or more stronger (e.g. *gauche*) twists. The $\sigma \rightarrow \sigma^*$ excitation energy of a segment decreases rapidly as a function of its length at first, and reaches a limiting value when the segment contains approximately a dozen silicon atoms. After initial light absorption, the chromophores undergo fluorescence, intersystem crossing and energy transfer from the shorter segments to longer ones, as well as photochemical transformations from both the singlet and triplet excited states. The origin of the inhomogeneous broadening of the room-temperature solution spectra of polysilanes is ascribed to the following three intramolecular causes in addition to the usual solvent effects: a distribution of chain segment lengths, a distribution of deviations from exact planarity within a segment and a distribution of alkyl side-chain conformations. At low temperatures, almost all the segment lengths are presumably so large that a variation in their length has only a very small effect on the excitation energy, so that the first source of inhomogeneous broadening is much less important, the absorption band is much narrower and the optical inhomogeneity is dominated by random disorder within the segments. Whereas a number of band structure calculations have been performed for linear polysilanes[52–58], the interband transition is of limited relevance for the relatively short segments in room-temperature solutions. In these excited segments, the hole and the excited electron are necessarily localized in the same small region of space.

An alternative view of the polysilane structure is depicted using the worm-like model as proposed for poly(diacetylene)s[59], where the linear chain has a large number of small twists without sharp twists playing a special role[60–62]. In this model, a Gaussian distribution of site energies and/or exchange interactions and the coherence of the excitation is terminated by any of the numerous usual random deviations from perfect symmetry.

A two-photon allowed absorption of poly(dihexylsilane) has been observed at 0.9 eV above the one-photon excitation[63–65], in contrast to the two-photon absorption of linear polyenes, which is about 0.5 eV below the intense one-photon absorption. Absorption spectra and the dynamics of other high-lying excited states of the polysilane have been investigated by means of femtosecond time-resolved excited-state absorption spectroscopy[66].

D. Mechanistic Aspects of Photochemistry of Peralkyloligosilanes and Polysilanes

There are two types of basic photoreactions of peralkyloligosilanes and polysilanes:

(1) Homolytic cleavage of a silicon–silicon bond

$$R_3SiSiR'_3 \xrightarrow{h\nu} R_3Si^\bullet + {}^\bullet SiR'_3 \qquad (1)$$

(2) Silylene extrusion

$$R_3SiSiR'_2SiR''_3 \xrightarrow{h\nu} R'_2Si\colon + R_3SiSiR''_3 \qquad (2)$$

A prototypical oligosilane, hexamethyldisilane, reacts upon irradiation of 147 nm light without any trapping reagent to give trimethylsilyl radicals[67]. Recombination and redistribution reactions of the trimethylsilyl radicals give back the starting hexamethyldisilane as well as 1,1-dimethylsilaethene plus trimethylsilane, respectively[68–70] (equation 3).

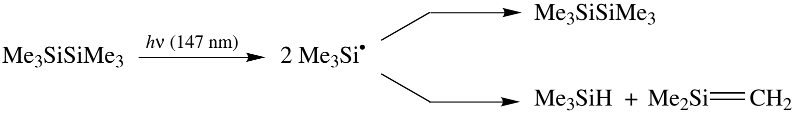

$$Me_3SiSiMe_3 \xrightarrow{h\nu\ (147\ nm)} 2\ Me_3Si^\bullet \begin{cases} \longrightarrow Me_3SiSiMe_3 \\ \longrightarrow Me_3SiH + Me_2Si{=}CH_2 \end{cases} \qquad (3)$$

Photolysis of permethyloligosilanes [Me(Me$_2$Si)$_n$Me, $n = 4–8$] in cyclohexane solution with a 254 nm light have been investigated and found to finally give $Me_3SiSiMe_2SiMe_3$ and $Me_3SiSiMe_2SiMe_2H$ as the sole volatile products[71,72]. These results are well understood when the reactions via two competitive reaction pathways of equations 1 and 2 are taken into account. Photolysis of several branched permethyloligosilanes gives a similar result[71–73]. Photolysis of cyclic oligosilanes like dodecamethylcyclohexasilane[74,75] affords predominantly the corresponding dialkylsilylenes accompanied by ring contraction. Although simple peralkyltrisilanes do not react any more on irradiation with a 254 nm light, irradiation of 1,2,3-trisilacycloheptane derivatives extrudes the central silicon atom as a silylene[76,77].

Much attention has been focused on the detailed mechanism of silylene extrusion from oligosilanes. The following three possible pathways (A-C, equations 4–7) should be first taken into account.

Path A (Stepwise SiSi Bond Cleavages)

$$R_3Si{-}SiR'_2{-}SiR''_3 \xrightarrow{h\nu} R_3Si{-}SiR'^{\bullet}_2 + {}^\bullet SiR''_3 \qquad (4)$$

$$R_3Si{-}SiR'^{\bullet}_2 \xrightarrow{\Delta} R_3Si^\bullet + \colon SiR'_2 \qquad (5)$$

Path B (Concerted Silylene Extrusion)

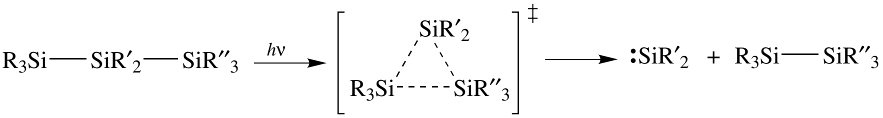

$$R_3Si{-}SiR'_2{-}SiR''_3 \xrightarrow{h\nu} \left[R_3Si\cdots SiR''_3 \ (\text{bridged by } SiR'_2) \right]^{\ddagger} \longrightarrow \colon SiR'_2 + R_3Si{-}SiR''_3 \qquad (6)$$

Path C (Simultaneous Two SiSi Bond Cleavages)

$$R_3Si{-}SiR'_2{-}SiR''_3 \xrightarrow{h\nu} R_3Si^\bullet + \colon SiR'_2 + {}^\bullet SiR''_3 \qquad (7)$$

Since photon energies are insufficient for simultaneous cleavage of two SiSi bonds to afford two silyl radicals and a silylene, Path C is an unlikely mechanism. The stepwise mechanism (Path A) could also be excluded because thermal α-elimination from pentamethyldisilanyl radical (i.e. equation 5) does not occur at room temperature[78]. The concertedness of the photochemical silylene extrusion from a peralkyltrisilane is corroborated by the high stereoselectivity. Thus, irradiation of *E*- and *Z*-1,3-diphenyl-1,2,2,3-tetramethyl-1,2,3-trisilacycloheptane gave, respectively, *E*- and *Z*-1,2-diphenyl-1,2-dimethyl-1,2-disilacyclohexane, in a highly stereospecific manner, together with dimethylsilylene[77] (equations 8 and 9).

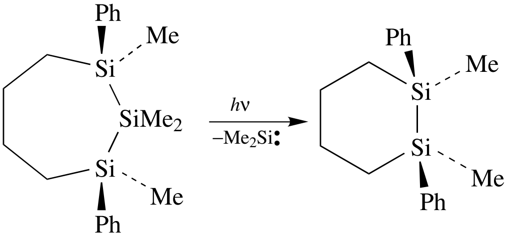

(8)

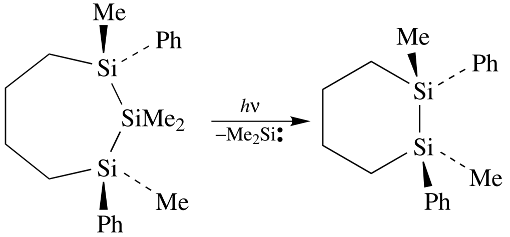

(9)

Several authors have discussed the nature of the excited states responsible for the photochemical silylene extrusion from a trisilane. On the basis of the Woodward–Hoffmann rules, Ramsey concluded that the long-wavelength transition is a $\sigma \rightarrow \sigma^*$ transition and the reaction occurs from the $\sigma\sigma^*$ state[79]. A modified correlation diagram was presented using the energy levels calculated by a pseudopotential method[41]. Bock and coworkers have suggested that Rydberg states can play a role in the photochemical silylene extrusion[80]. The potential energy surface of the S_1 state of 2-methyltrisilane has been studied by using MC-SCF and multireference MP2 methods[81]. These calculations have shown that the avoided crossing first located by Michl and coworkers[42,45] turns out to be points of real crossing when full geometry optimization is performed; two elementary processes, homolysis to produce a silyl radical pair (equation 4; 1st step of Path A) and silylene extrusion (Path B, equation 6) can occur through the (n-2)-dimensional conical intersections between the excited S_1 and the ground S_0 states. Fragmentation to two silyl radicals can be achieved in this way and not only through an intersystem crossing between the S_1 and T_1 repulsive states, as suggested by Michl and Balaji[82].

The photochemical behavior of linear peralkylpolysilane high polymers is also understood by invoking the two basic processes, i.e. homolytic cleavage of the SiSi bond and silylene extrusion[83]. In addition, Michl and coworkers[84] have pointed out another pathway, which implies the initial formation of the polysilanylsilylene (equation 10) followed by silylsilylene-to-disilene rearrangement (equation 11). Addition of a silyl radical generated by the SiSi bond cleavage to the disilene give finally a rather stable silyl radical (equation 11).

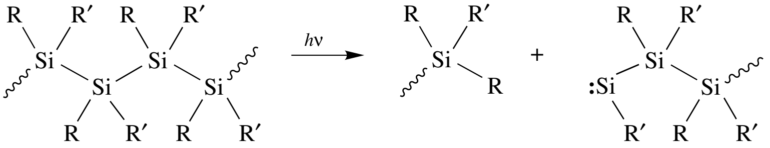

(10)

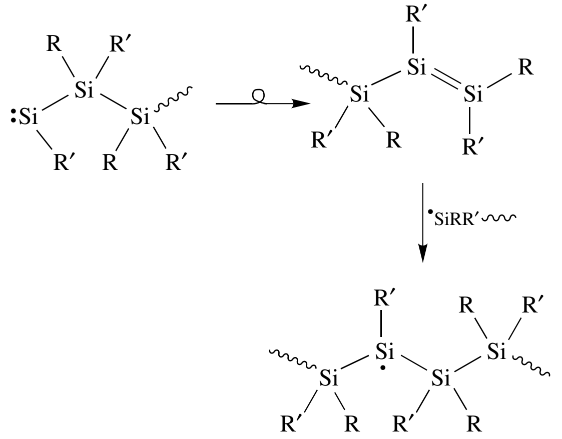

(11)

The silylene extrusion should occur from the high polymer, because $Et_3SiSiBu_2H$ appears with no induction period when poly(dibutylsilane) is irradiated in the presence of excess Et_3SiH. Hence the possibility that R_2Si**:** is produced only from a very short photodegradated silicon chain and not from the high polymer is ruled out[84]. The quantum yield of $Et_3SiSiBu_2H$ decreases as the irradiation wavelength increases and falls to zero above 300 nm, while the polymer absorption band at 315 nm still disappears rapidly and persistent ESR signals are observed[85,86]. Michl and coworkers[84] concluded that silylene production and radical formation occur as two distinct processes, and that the thermal fragmentation of polysilanyl radicals with a sequential loss of a single silylene unit does not occur at room temperature, this being in accord with the result for pentamethyldisilanyl radical[78].

III. ARYLPOLYSILANES

A. Photophysics of Aryldisilanes

In 1964, Sakurai and Kumada[87], Gilman and coworkers[88] and Hague and Prince[89] reported independently that aryl- and vinyl-substituted polysilanes showed appreciable

TABLE 2. ^1L_a absorption maxima of silylbenzenes[87]

Compound	λ_{max} (nm) (ϵ)
PhH	204 (7900)
$PhSiMe_3$	211 (10600)
$PhSiMe_2SiMe_3$	230 (11200)
$PhSiMe_2SiMe_2SiMe_3$	240 (15400)

red shift of the absorption maxima of the corresponding monosilanes (Table 2). Although these and related works[90-98] constitute the first recognition of the conjugation between a silicon–silicon bond and a π system, these conjugating properties were first rationalized in terms of d–π^* interaction in the excited state. Later, the $\sigma - \pi$ conjugation between a silicon–silicon σ orbital and a pπ orbital was taken as the origin of the unique electronic properties, on the basis of the results of the charge-transfer (CT)[99-102] and photoelectron spectroscopic studies of aryldisilanes[103], and the remarkable stereoelectronic effects[104,105] on the absorption spectra. In this model, the high-lying HOMO of an aryl–SiSi system is represented mainly by the linear combination of the σ(SiSi) orbital and the HOMO of the component aromatic π system (Figure 5), while the contribution of the σ(SiSi) orbital in the aryl–SiSi HOMO depends on the HOMO level of the aromatic π system[101] as well as the dihedral angle between an SiSi σ bond and a pπ orbital of the π system[104,105]. The ^1L_a absorption at 230 nm (ϵ *ca* 10000) of phenylpentamethyldisilane (**1a**) has a strong intramolecular charge-transfer [σ(SiSi) $\rightarrow$ π^*] nature. In accord with this model, no characteristic band at around 230 nm is observed for the cyclic aryldisilane **2a**, where a SiSi σ bond is in the nodal plane of the π system, while an intense absorption maximum is observed for a cyclic aryldisilane **3a**[104,105].

In 1981, Shizuka and coworkers reported unusual dual fluorescence phenomena of aryldisilanes[106-111]. Thus, in addition to a regular $\pi\pi^*$ (LE, locally excited) emission band from an aromatic π system, a broad band has been observed at a longer wavelength, which is assigned to the emission from a CT excited state ([(2$\pi\pi^*$, 3dπ(Si)] state). In the πd model, the disilanyl group and the aromatic π system are assumed to work as an electron acceptor and an electron donor, respectively. Contrary to the argument by Shizuka and coworkers, Sakurai, Sugiyama and Kira have proposed the intramolecular $\sigma\pi^*$ charge-transfer model[112], in which the disilanyl group and the aromatic π system work as an electron donor and an electron acceptor, respectively, on the basis of a study of substituent and solvent effects on the dual fluorescence of phenylpentamethyldisilane; most distinguishably, the wavelengths of the CT emission band are found to be longer on increasing electron-accepting ability of the substituents.

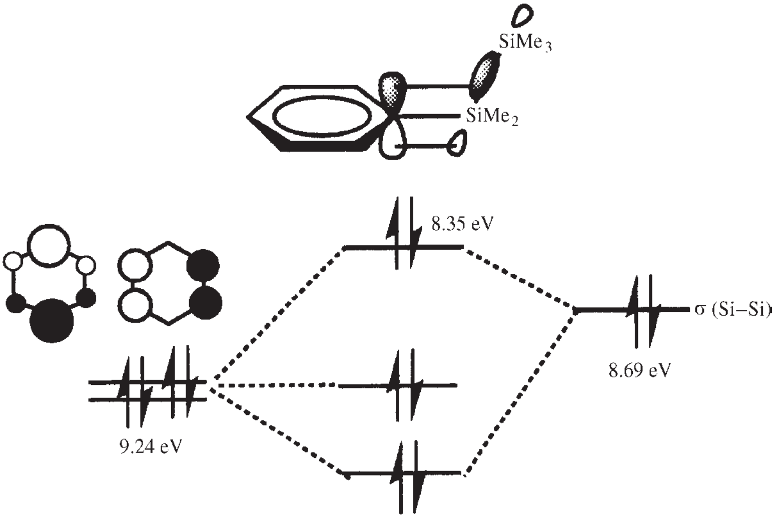

FIGURE 5. Schematic representation of σ(SiSi)–π conjugation. Modified from Reference 103

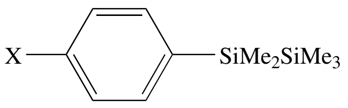

(1)

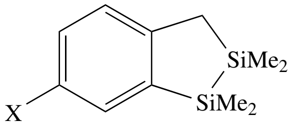

(2)

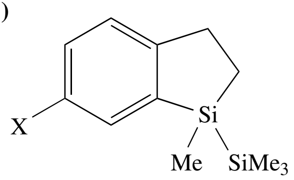

(3)

(a) X = H; **(b)** X = CF_3

Dual fluorescence is now a well-documented phenomenon since the discovery by Lippert and coworkers of the dual fluorescence in (*p*-dimethylamino)benzonitrile (DMABN) in dilute polar solvents[113–115]. Many spectroscopic, thermodynamic and quantum-chemical studies have been devoted to these systems and reviewed recently by Rettig[116a] and by Bhalfacharyya and Chowdury[116b] Grabowski and coworkers have proposed that the charge separation in an $\mathrm{n}\pi^*$ intramolecular charge-transfer (ICT) system such as DMABN is attained in a twisted conformation[117], where the two π moieties involved in the charge transfer, the donor and the acceptor, are orbitally decoupled, nearly perpendicular to each other. This led to the terminology of 'twisted intramolecular charge transfer' (TICT) states. However, since CT emission of TICT compounds is not observed in nonpolar solvents, it is obvious that solvation by polar solvents also plays a certain role in the formation of a CT excited state, in addition to internal twisting motion. Such outer contributions for charge separation in $n\pi^*$ ICT systems make the arguments complex and controversial. Since several aryldisilanes exhibit CT emission even in a nonpolar solvent, aryldisilanes may occupy an important position in attempts to understand the intramolecular stabilization of CT excited states. Very recently, (*p*-cyanophenyl)pentamethyldisilane (**1c**), which bears one of the strongest electron-accepting π systems in the molecule, has been found to show ICT emission even in an isolated jet-cooled condition[118].

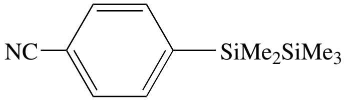

(1c)

In order to explain the stabilization of the CT excited state even in a nonpolar solvent, the orthogonal intramolecular charge-transfer (OICT) mechanism, which is a conceptually similar term to the TICT mechanism but is used to stress the orbital orthogonality rather than the twisting of the molecular frame, has been proposed. The OICT mechanism for the CT fluorescence of aryldisilanes in nonpolar solvents was supported by the remarkable dependence of the fluorescence spectra on the dihedral angle between a benzene $\mathrm{p}\pi$

orbital and an SiSi σ bond in an aryldisilane[105,112]. Thus, 6-(trifluoromethyl)-1,1,2,2-tetramethyl-1,2-disilaindane (**2b**), where the σ–π overlap is less effective but the CT excited state is well stabilized, showed the typical CT emission, while no intense CT absorption was observed because of forbiddenness of the overlap. On the other hand, 6-(trifluoromethyl)-1-methyl-1-(trimethylsilyl)-1-silaindane (**3b**), which is rigidly held in the perpendicular conformation, showed intense and sharp LE emission but lacked the CT emission. [5-(Trifluoromethyl)-2-methylphenyl]pentamethyldisilane (**1b**) revealed both intense CT absorption and CT fluorescence. The fact that the absorption spectrum of **1b** resembles that of **3b**, while the fluorescence spectrum of **1b** is similar to that of **2b**, is in good agreement with the OICT mechanism for the CT fluorescence of **1b**; the absorption occurs at the preferred conformation **A** and then the OICT state would be formed at the conformation **B** via a dynamic relaxation with internal rotation about the C(aryl)–Si bond (Figure 6). A free jet spectroscopic study on phenylpentamethyldisilane and related compounds also indicated that the most favorable conformation at the ground state is a perpendicular one, which has large overlap between σ (Si–Si) and π orbitals of the aromatic ring[119].

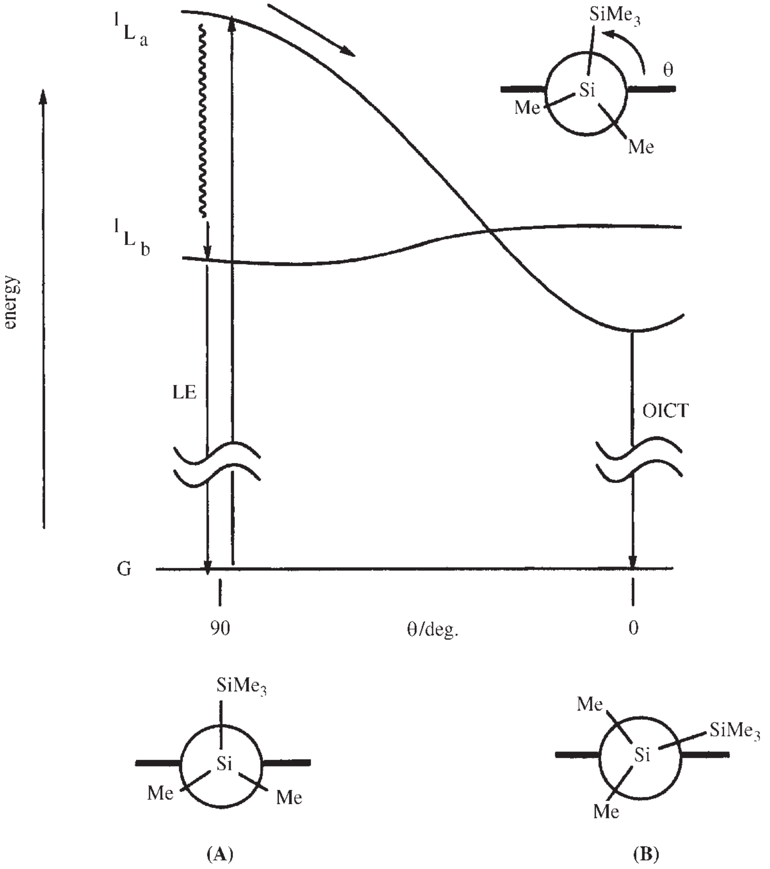

FIGURE 6. Schematic potential surfaces for the OICT mechanism in **1b**. Modified from Reference 105

Contrary to the OICT mechanism, Shizuka and coworkers have concluded that the charge separation does not require internal rotation, on the basis of the very short rise time of the CT band of phenylpentamethyldisilane (<10 ps)[120] in comparison with that of DMABN. However, the rise time may not be a decisive criterion of whether internal rotation is required or not, since the rise time depends not only on the amplitude of the structural change but also on other factors such as the rotational barrier around the pertinent bond[121].

Horn and coworkers have concluded that the $\sigma\pi^*$ charge-transfer model is suitable for explaining the CT fluorescence spectra of (phenylethynyl)pentamethyldisilanes[122].

B. Mechanistic Aspects of Photoreactions of Aryldisilanes

Much attention has been focused on the photochemistry of aryldisilanes[72,123,124], since they generate interesting reactive silicon species such as silylenes, silenes and silyl radicals, as has been shown by chemical trapping. The photolysis of phenyldisilanes in the presence of alcohols gives rise to four types of reaction as shown in Scheme 1: (1) formation of a silaethene via elimination of a hydrosilane (type 1)[125], (2) formation of a silatriene via 1,3-silyl migration (type 2)[126–147], (3) elimination of a silylene (type 3)[148–150] and (4) nucleophilic cleavage of a SiSi bond in the excited state (type 4)[151–153]. The detailed analysis of the steady-state photolysis of (*p*-trifluoromethylphenyl)pentamethyldisilane **1b**[105] in the presence of alcohols revealed the nature of the excited states responsible for the photoreactions; the 1,3-silyl migration occurs from LE, while the direct alcoholysis of the aryldisilane takes place mainly from the OICT state.

The kinetic profile for the photophysical and photochemical processes of *p*-(trifluoromethylphenyl)pentamethyldisilane **(1b)** in alcohol–hexane mixtures is represented schematically in Figure 7. Whereas the nature of the excited states of aryldisilanes varies significantly depending on the electronic nature of the aromatic π system, the mechanistic profile shown in Figure 7 would be generally adopted to the photoreactions of aryldisilanes. In contrast to this, Shizuka and coworkers[120] have proposed that 1,3-silyl migration occurs from the πd-type ICT state of phenyldisilanes, on the basis of the time-resolved emission studies of aryldisilanes.

One of the interesting mechanistic problems in photoreactions of phenyldisilanes is whether the 1,3-silyl migration giving a silatriene derivative occurs concertedly, or via the recombination of an intimate silyl radical pair generated by the homolytic cleavage of the SiSi bond in the LE excited state. While Ishikawa and coworkers first suggested a concerted 1,3-migration[133], Sakurai and coworkers have noted that the type 1–type 3 photoreactions of aryldisilanes in nonpolar solvents are all explained by an initially formed silyl radical pair, on the basis of the ESR evidence for the formation of silyl radicals during the photolysis of aryldisilanes[148]. Shizuka and coworkers[120] have shown that the formation of the silatriene from phenylpentamethyldisilane occurs very rapidly, i.e. within *ca* 30 ps, and supported the concerted mechanism. Quite recently, Ohshita, Ishikawa and coworkers have reported the diastereospecific formation of the corresponding silatriene in the photolysis of *meso*- and *dl*-1,2-diethyl-1,2-dimethyl-1,2-diphenyldisilanes (cf **4**) in the presence of olefins to give **5** and carbonyl compounds (equation 12) as more direct evidence for the concerted mechanism[141].

Leigh and Sluggett have demonstrated that the photolysis of 1,1,1-trimethylsilyltriphenylsilane **(6)** gives the rearranged silatriene largely via a singlet excited state of **6** and free silyl radicals are formed via the triplet state[144–146]. Irradiation of **6** and acetone in cyclohexane in the presence of chloroform as a silyl radical trap gives mainly the ene adducts of a silatriene, while a similar irradiation in acetonitrile affords

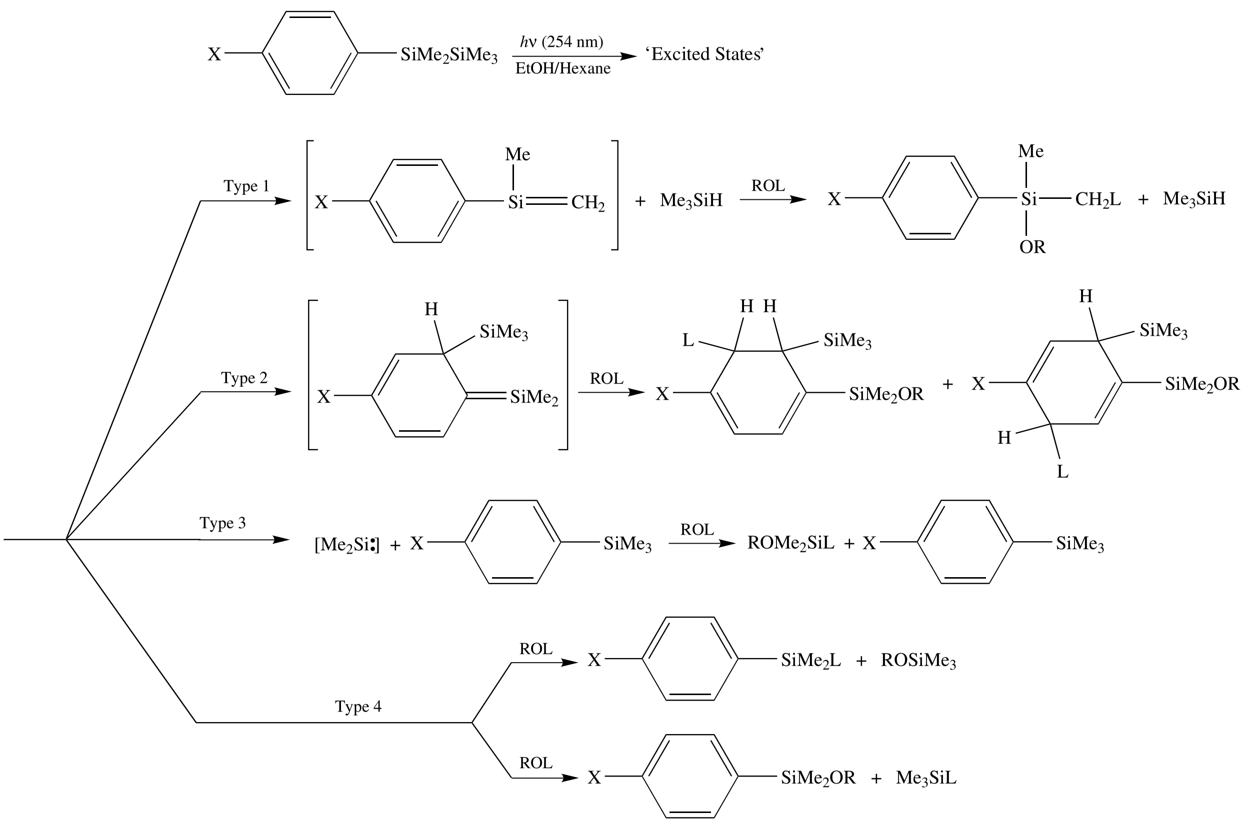

L = H or D

SCHEME 1. Modified from Reference 105

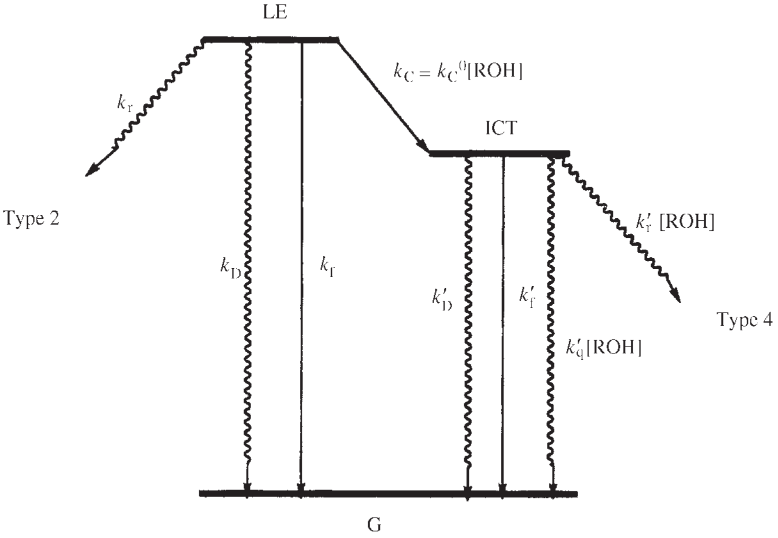

FIGURE 7. Kinetic profile for photophysical and photochemical processes of a phenylpentamethyldisilane in alcohol–hexane mixtures: k_f, k'_f = fluorescence rates; k_D, k'_D = radiationless decay rates; k'_q = rate for CT quenching; k_r, k'_r = reaction rates for 1,3-silyl migration and reaction with alcohol, respectively; k_C = formation rates of ICT state from LE. Modified from Reference 105

triphenylchlorosilane and trimethylchlorosilane as the major products (Scheme 2). Large solvent effects on the relative yields of silatriene- and radical-derived products are ascribed to an intersystem crossing which is enhanced in polar solvents.

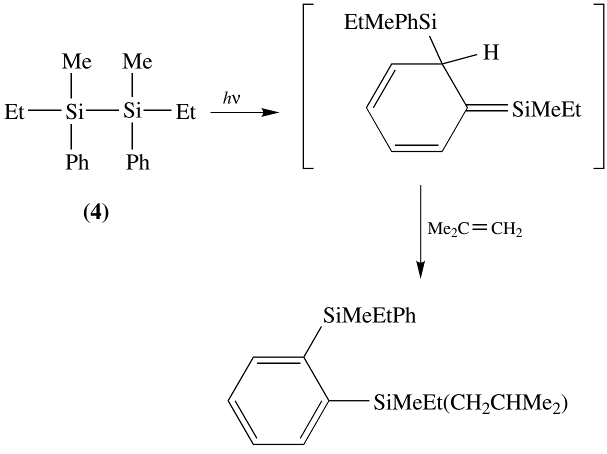

(4)

(5)

(12)

(*S,S*)- and (*R,R*)-**4** ⟶ (*S,S*)- and (*R,R*)-**5**

meso-**4** ⟶ (*S,R*)- and (*R,S*)-**5**

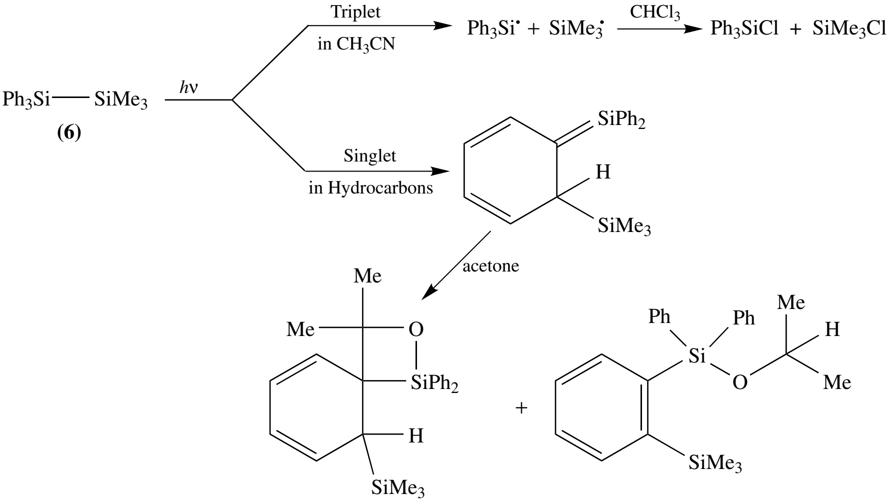

SCHEME 2

In relation to the reactions of CT excited states of aryldisilanes, photochemistry of LE and ICT states of the rigid, *p*-cyano-substituted styryldisilane **7** was investigated by Steinmetz and coworkers[154]. Although no 1,3-silyl shift is observed in this sytem, **7** affords a major product attributable to addition of alcohol across the Si−Si bond in the CT state. The roles of LE and CT states in the formation of additional minor products of silylene extrusion and homolytic Si−Si cleavage have also been elucidated.

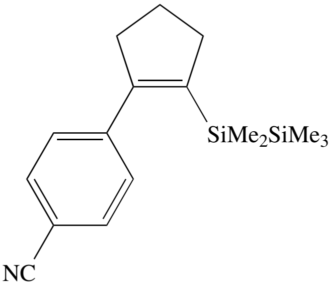

(7)

C. Photochemistry of Aryltrisilanes

Whereas 2,2-diphenylhexamethyltrisilane **(8)** is a well-known photochemical precursor of diphenylsilylene[72,155,156], a 1,3-silyl migration is usually a major side reaction in solution at room temperature. In the presence of excess ethanol, the irradiation of **8** in hexane gives **9** via diphenylsilylene extrusion and **10** (an isomeric mixture) via 1,3-silyl migration in 50 and 37%, respectively (Scheme 3)[157]. Since the product ratio does not depend on the solvent polarity, both reactions, silylene extrusion and 1,3-silyl migration, do not occur via the ICT state but via the nonpolar excited state[158]. However, the excited states responsible for these two pathways are suggested to be different from each other by the nonresonant two-photon (NRTP) method, where the highly selective silylene extrusion was observed[157]. Thus, irradiation of a hexane solution of **8** with pulsed 532 nm laser light at room temperature gives **9** and **10** in 80 and 13% yields, respectively, in the presence of ethanol, although **8** shows no absorption at wavelengths longer than 300 nm. The product yields increased in proportion to the square of the laser intensity, being indicative of the simultaneous two-photon nature of the reaction[158].

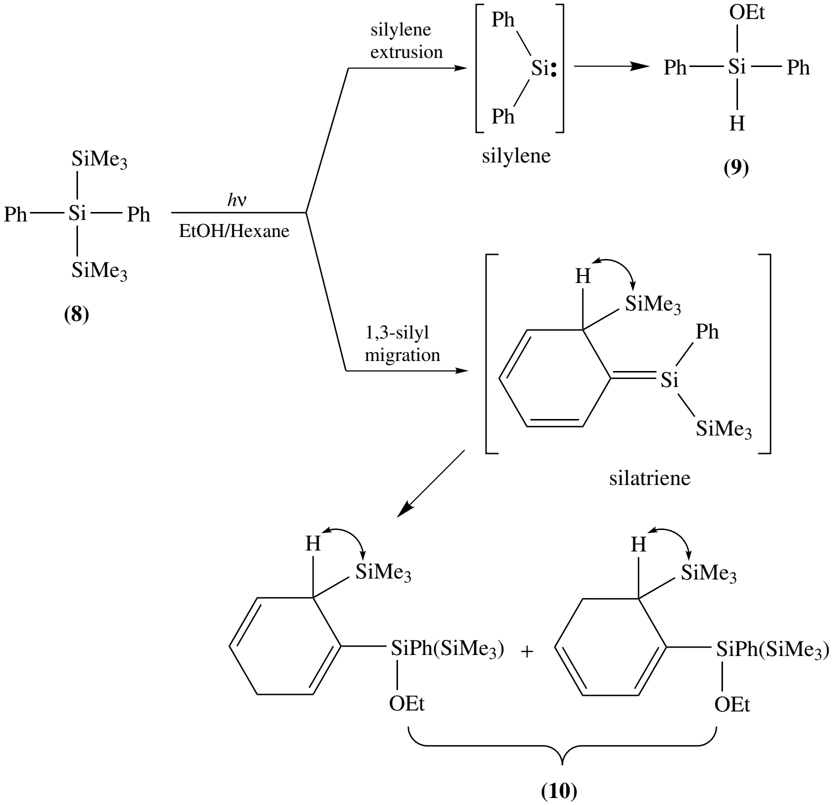

SCHEME 3. Modified from Ref. 157

IV. SILYLENES

The electronic structure of silylenes has been discussed in depth since the first matrix isolation of dimethylsilylene by West and coworkers[159], who observed that dimethylsilylene produced by the irradiation of dodecamethylcyclohexasilane in an argon matrix at 10 K or in a 3-methylpentane glass matrix at 77 K showed a characteristic absorption maximum at 450 nm. All the silylenes investigated so far are known to be ground state singlets and the absorption due to the excitation of a lone-pair electron to the vacant pπ orbital of the silylene (equation 13) is observed in the UV-VIS region[159–170]. The absorption maxima depend strongly on the electronic and steric effects of the substituents. Absorption maxima of various silylenes observed in hydrocarbon matrices at 77 K are shown in Table 3.

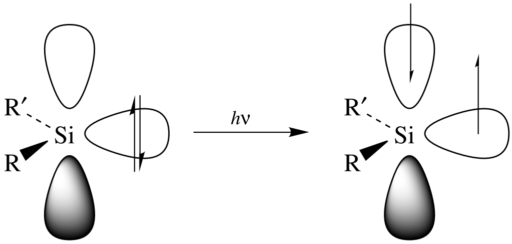

(13)

Electronically, the substituent effects can be discussed in terms of their inductive and conjugative effects. Electronegative substituents increase the transition energy (ΔE), as well as the singlet–triplet gap, and thus induce blue shifts. This can be understood in terms of Bent's rule[171–173] by the effect that such substitutents have on the hybridization and energy of the n(Si) orbital. Introduction of electropositive trialkylsilyl and trialkylgermyl substituents on the silylene causes quite large red shifts of n(Si)–3p(Si) absorption; typically, Mes(Me$_3$Si)Si: has its λ_{max} at 760 nm[168–170]. Conjugation between the substituent and the empty 3p(Si) orbital in the ground-state singlet and/or with the half-filled orbitals in the first excited state can have a strong effect on the electronic spectrum of silylenes. Large blue shifts are caused by introduction of n donors such as OR and NR$_2$[162,174], because n donors stabilize the singlet ground state by conjugation with the empty 3p(Si) orbital, while the excited state is actually destabilized by these substituents (Figure 8a). The ethynyl, vinyl and phenyl substituents are all much weaker π donors than OR and NR$_2$, so the stabilization and thus the blue shift resulting from π conjugation are expected to be smaller. However, these unsaturated substituents actually produce red shifts relative

TABLE 3. n(Si)→3p(Si) absorption maxima of substituted silylenes (RR′Si:) in hydrocarbon matrices at 77 K

R	R′	λ_{max} (nm)	References
CH$_3$	CH$_3$	453	159, 163
CH$_3$	Ph	490	163
CH$_3$	Mesityl	495	163
CH$_3$	C≡CSiMe$_3$	473	176
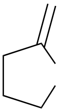		475	166
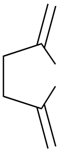		505	166
Mesityl	OPh	400	162
N(Pr-*i*)$_2$	N(Pr-*i*)$_2$	335	174
Ph	SiMe$_3$	660	169
Mesityl	SiMe$_3$	760	169

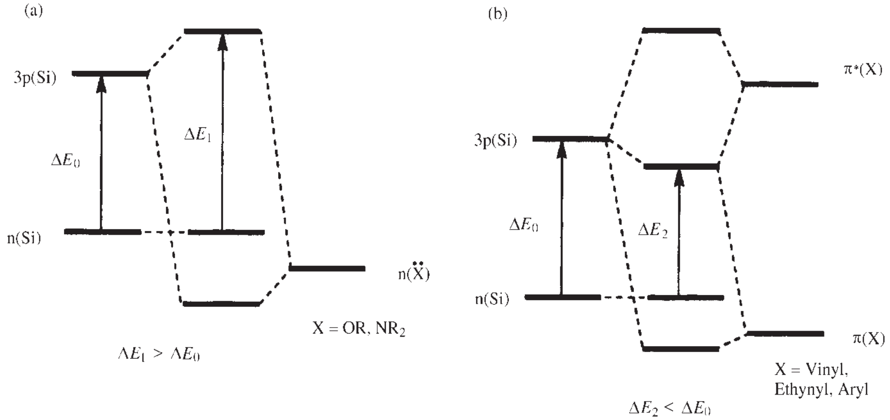

FIGURE 8. Schematic orbital interaction diagram for silylenes having (a) n donors and (b) π groups as substituents. ΔE_0, ΔE_1 and ΔE_2 denote the vertical excitation energies in the parent, an n-donor-substituted and a π-substituted silylenes, respectively. Modified from Reference 176

to Me_2Si[163,166,167]. The different behavior of n donors such as OR and a π group such as vinyl is best understood qualitatively as resulting from the presence of a π^* orbital in the unsaturated substituents. According to simple frontier molecular orbital (FMO) theory, the relatively high-lying 3p(Si) orbital can interact more effectively with the low-lying π^* orbital than with the bonding π orbital of the substituents, reducing the n(Si)−3p(Si) energy gap, as displayed schematically in Figure 8b[163,167,175]. Steric effects can affect the apex angle at silicon and thus cause a red shift or a blue shift, depending on whether the angle increases or is reduced.

Substituent effects on the transition energy of silylene have been investigated systematically by *ab initio* MO calculations and good agreement between the calculations and experiment has been attained[175,176].

A number of experimental[177–181] and theoretical studies[182,183] have anticipated formation of silylene–base complexes during reactions of silylenes with oxygen-, sulfur-, nitrogen- and phosphorus-containing compounds. A number of silylene–base complexes have been actually observed in low-temperature glass matrices[167,184–188]. The absorption maxima of silylenes were shifted significantly to the blue by the complexation. The origin of this is ascribed to a weak bonding interaction between the vacant 3p(Si) orbital in a silylene and an n orbital in a base, which raise the LUMO level.

Whereas much effort has been devoted to the search for triplet silylenes in the ground and excited states both experimentally[189–194] and theoretically[195,196], no successful result has been reported so far. Introduction of two bulky trialkylsilyl substituents to a silylene is predicted to lead to a ground state triplet[196].

Irradiation of dimethylsilylene at 450 nm gives the corresponding silaethene, which is reconverted back to dimethylsilylene upon irradiation with 248 nm light (equation 14)[197,198]. The interesting photochemical conversion from silylene to silene in low-temperature matrices has been investigated with polarized light[198]; the 1,2-hydrogen migration has never been discussed on the basis of the excited-state nature of the silylene.

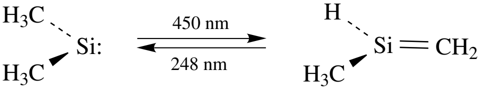

(14)

V. SUMMARY

Photochemically induced electron-transfer reactions involving electron-donating organosilicon compounds such as oligosilanes, polysilanes, allylic and benzylic silanes have attracted much attention in recent years[2,3]. While these reactions are synthetically interesting, we have not dealt with them in this chapter, because most of the reactions can be understood as due to the behavior of the corresponding radical cations generated by the electron transfer in the environment.

Many interesting photoreactions of organosilicon compounds have been reported without thinking about the nature of the excited states responsible for the photoreactions. Among them, the following reactions are involved: (1) photochemical 1,3-silyl migration in allylic silanes[199,200], (2) photolysis of 1,1-diphenylsilacyclobutane forming diphenylsilaethene[201–203], (3) photochemical rearrangement of disilanyl-iron complexes[204,205], (4) photochemical dissociation of disilene to silylene[206], (5) photochemical isomerization from a tetrasilacyclobutene to a tetrasilabicyclo[1.1.0]-butane[207] and so on. Elucidation of the detailed mechanism of these basic organosilicon photoreactions is required not only for the well-balanced development of the basic organosilicon chemistry, but also for future application of organosilicon substances as optoelectronic materials.

VI. ACKNOWLEDGMENT

The authors wish to thank Miss M. Kodaka, Mrs H. Kano and Mr U. Kwon for their assistance in the preparation of the manuscript.

VII. REFERENCES

1. A. G. Brook, in *The Chemistry of Organosilicon Compounds* (Eds. S. Patai and Z. Rappoport) Part 2, Chap. 15, Wiley, Chichester, 1989, p. 965.
2. A. G. Brook, Chap. 21 in this volume.
3. M. G. Steinmetz, *Chem. Rev.*, **95**, 1527 (1995).
4. R. D. Miller and J. Michl, *Chem. Rev.*, **89**, 1359 (1989).
5. J. Michl, J. W. Downing, T. Karatsu, A. J. McKinley, G. Poggi, G. M. Wallraff, R. Sooriyakumaran and R. D. Miller, *Pure Appl. Chem.*, **60**, 959 (1988).
6. J. M. Zeigler, *Synth. Met.*, **28**, C581 (1989).
7. R. West, *J. Organomet. Chem.*, **300**, 327 (1986).
8. R. West, in *The Chemistry of Organosilicon Compounds* (Eds. S. Patai and Z. Rappoport), Part 2, Chap. 19, Wiley, Chichester, 1989, p. 1207.
9. R. West and P. P. Gaspar, Chapter 43 in this volume.
10. H. Gilman, W. H. Atwell and G. L. Schwebke, *Chem. Ind. (London)*, 1063 (1964).
11. H. Gilman, W. H. Atwell and G. L. Schwebke, *J. Organomet. Chem.*, **2**, 369 (1964).
12. M. Kumada and K. Tamao, *Adv. Organomet. Chem.*, **6**, 19 (1968).
13. R. West, in *Comprehensive Organometallic Chemistry* (Eds. G. Wilkinson, F. G. A. Stone and E. W. Abel), Vol. 12, Pergamon, Oxford, 1982, p. 365.
14. W. G. Boberski and A. L. Allred, *J. Organomet. Chem.*, **88**, 65 (1975).
15. C. G. Pitt, L. L. Jones and B. G. Ramsey, *J. Am. Chem. Soc.*, **89**, 5471 (1967).
16. P. P. Shorygin, V. A. Petakhov, O. M. Nefedov, S. P. Kolesnikov and V. I. Shiryaev, *Theor. i Eksperim. Khim. Akad. Nauk Ukr. SSR*, **2**, 190 (1966); *Chem. Abstr.*, **65**, 14660f (1966).
17. C. G. Pitt, M. M. Bursey and P. F. Rogerson, *J. Am. Chem. Soc.*, **92**, 519 (1970).
18. B. G. Ramsey, *Electronic Transitions in Organometalloids*, Academic Press, New York, 1968.
19. C. Sandorfy, *Can. J. Chem.*, **33**, 1337 (1955).
20. K. Fukui, K. Kato and T. Yonezawa, *Bull. Chem. Soc. Jpn.*, **33**, 1197 (1960).
21. H. Bock and W. Ensslin, *Angew. Chem., Int. Ed. Engl.*, **10**, 404 (1971).
22. H. Bock, W. Ensslin, F. Fehér and R. Freund, *J. Am. Chem. Soc.*, **98**, 668 (1976).

23. H. Bock and B. Solouki, in *The Chemistry of Organosilicon Compounds* (Eds. S. Patai and Z. Rappoport), Chap. 9. Vol. 1, Wiley, Chichester, 1989, p. 555.
24. V. F. Traven and R. West, *J. Am. Chem. Soc.*, **95**, 6824 (1973).
25. H. Sakurai, M. Kira and T. Uchida, *J. Am. Chem. Soc.*, **95**, 6826 (1973).
26. H. Bock, W. Kaim, M. Kira and R. West, *J. Am. Chem. Soc.*, **101**, 7667 (1979).
27. T. Shida, H. Kubodera and Y. Egawa, *Chem. Phys. Lett.*, **79**, 179 (1981).
28. J. T. Wang and F. Williams, *J. Chem. Soc., Chem. Commun.*, 666 (1981).
29. R. West and E. Carberry, *Science*, **189**, 179 (1975).
30. E. Carberry, R. West and G. E. Glass, *J. Am. Chem. Soc.*, **91**, 5446 (1969).
31. R. West and E. S. Kean, *J. Organomet. Chem.*, **96**, 323 (1975).
32. H. S. Plitt and J. Michl, *Chem. Phys. Lett.*, **198**, 400 (1992).
33. H. S. Plitt, J. W. Downing, M. K. Raymond, V. Balaji and J. Michl, *J. Chem. Soc., Faraday Trans.*, **90**, 1653 (1994).
34. B. Albinsson, H. Teramae, J. W. Downing and J. Michl, *Chem. Eur. J.*, **2**, 529 (1996).
35. V. Balaji and J. Michl, *Polyhedron*, **10**, 1265 (1991).
36. R. W. Bigelow, *Chem. Phys. Lett.*, **126**, 63 (1986).
37. R. W. Bigelow, *Organometallics*, **5**, 1502 (1986).
38. K. A. Klingensmith, J. W. Downing, R. D. Miller and J. Michl, *J. Am. Chem. Soc.*, **108**, 7438 (1986).
39. Z. G. Soos and G. W. Hayden, *Chem. Phys.*, **143**, 199 (1990).
40. Z. G. Soos, G. W. Hayden and P. C. M. McWilliams, *Polym. Prepr.*, **31**, 286 (1990).
41. E. A. Halevi, G. Winkelhofer, M. Meisl and R. Janoschek, *J. Organomet. Chem.*, **294**, 151 (1985).
42. Y.-P. Sun and J. Michl, *J. Am. Chem. Soc.*, **114**, 8186 (1992).
43. H. S. Plitt, V. Balaji and J. Michl, *Chem. Phys. Lett.*, **213**, 158 (1993).
44. J. R. G. Thorne, S. A. Williams, R. M. Hochstrasser and P. J. Fagan, *Chem. Phys.*, **157**, 401 (1991).
45. Y.-P. Sun, Y. Hamada, L.-M. Huang, J. Maxka, J.-S. Hsiao, R. West and J. Michl, *J. Am. Chem. Soc.*, **114**, 6301 (1992).
46. L. A. Harrah and J. M. Zeigler, *J. Polym. Sci., Polym. Lett. Ed.*, **23**, 209 (1985).
47. P. M. Cotts, R. D. Miller, P. T. Trefonas, III, R. West and G. N. Fickes, *Macromolecules*, **20**, 1046 (1987).
48. P. Shukla, P. M. Cotts, R. D. Miller, T. P. Russell, B. A. Smith, G. M. Wallraff, M. Baier and P. Thiyagarajan, *Macromolecules*, **24**, 5606 (1991).
49. Y.-P. Sun, R. D. Miller, R. Sooriyakumaran and J. Michl, *J. Inorg. Organomet. Polym.*, **1**, 3 (1991).
50. Y.-P. Sun, G. M. Wallraff, R. D. Miller and J. Michl, *J. Photochem. Photobiol. A: Chem.*, **62**, 333 (1991).
51. R. D. Miller, G. M. Wallraff, M. Baier, P. M. Cotts, P. Shukla, T. P. Russell, F. C. De Schryver and D. Declercq, *J. Inorg. Organomet. Polym.*, **1**, 505 (1991).
52. K. Takeda, N. Matsumoto and M. Fukuchi, *Phys. Rev. B*, **30**, 5871 (1984).
53. K. Takeda, M. Fujino, K. Seki and H. Inokuchi, *Phys. Rev. B*, **36**, 8129 (1987).
54. K. Takeda, H. Teramae and N. Matsumoto, *J. Am. Chem. Soc.*, **108**, 8186 (1986).
55. H. Teramae, T. Yamabe and A. Imamura, *Theoret. Chim. Acta (Berl.)*, **64**, 1 (1983).
56. J. W. Mintmire, *Phys. Rev. B*, **39**, 13350 (1989).
57. K. Takeda and N. Matsumoto, *J. Phys. C*, **18**, 6121 (1985).
58. H. Teramae and K. Takeda, *J. Am. Chem. Soc.*, **111**, 1281 (1989).
59. G. Wenz, M. A. Müller, M. Schmidt and G. Wegner, *Macromolecules*, **17**, 837 (1984).
60. A. Tilgner, H. P. Trommsdorf, J. M. Zeigler and R. M. Hochstrasser, *J. Lumin.*, **45**, 373 (1990).
61. A. Tilgner, H. P. Trommsdorf, J. M. Zeigler and R. M. Hochstrasser, *J. Inorg. Organomet. Polym.*, **1**, 343 (1991).
62. A. Tilgner, H. P. Trommsdorf, J. M. Zeigler and R. M. Hochstrasser, *J. Chem. Phys.*, **96**, 781 (1992).
63. J. R. G. Thorne, Y. Ohsako, J. M. Zeigler and R. M. Hochstrasser, *Chem. Phys. Lett.*, **162**, 455 (1989).
64. Y. Moritomo, Y. Tokura, H. Tachibana, Y. Kawabata and R. D. Miller, *Phys. Rev. B*, **43**, 14746 (1991).
65. H. Tachibana, Y. Kawabata, S. Koshihara and Y. Tokura, *Solid State Commun.*, **75**, 5 (1990).

66. J. R. G. Thorne, S. T. Repinec, S. A. Abrash, J. M. Zeigler and R. M. Hochstrasser, *Chem. Phys.*, **146**, 315 (1990).
67. P. Boudjouk and R. D. Koob, *J. Am. Chem. Soc.*, **97**, 6595 (1975).
68. S. K. Tokach and R. D. Koob, *J. Am. Chem. Soc.*, **102**, 376 (1980).
69. B. J. Cornett, K. Y. Choo and P. P. Gaspar, *J. Am. Chem. Soc.*, **102**, 377 (1980).
70. L. Gammie, I. Safarik, O. P. Strausz, R. Roberge and C. Sandorfy, *J. Am. Chem. Soc.*, **102**, 378 (1980).
71. M. Ishikawa, T. Takaoka and M. Kumada, *J. Organomet. Chem.*, **42**, 333 (1972).
72. M. Ishikawa and M. Kumada, *Adv. Organomet. Chem.*, **19**, 51 (1981).
73. I. M. T. Davidson, J. Michl and T. Simpson, *Organometallics*, **10**, 842 (1991).
74. M. Ishikawa and M. Kumada, *J. Chem. Soc., Chem. Commun.*, 612 (1970).
75. M. Ishikawa and M. Kumada, *J. Organomet. Chem.*, **42**, 325 (1972).
76. H. Sakurai, Y. Kobayashi and Y. Nakadaira, *J. Am. Chem. Soc.*, **93**, 5272 (1971).
77. H. Sakurai, Y. Kobayashi and Y. Nakadaira, *J. Am. Chem. Soc.*, **96**, 2656 (1974).
78. J. A. Hawari, D. Griller, W. P. Weber and P. P. Gaspar, *J. Organomet. Chem.*, **326**, 335 (1987).
79. B. G. Ramsey, *J. Organomet. Chem.*, **67**, C67 (1974).
80. H. Bock, K. Wittel, M. Veith and N. Wiberg, *J. Am. Chem. Soc.*, **98**, 109 (1976).
81. A. Venturini, T. Vreven, F. Bernardi, M. Olivucci and M. A. Robb, *Organometallics*, **14**, 4953 (1995).
82. J. Michl and V. Balaji, in *Computational Advances in Organic Chemistry: Molecular Structure and Reactivity* (Eds. C. Ogretir and I. G. Csizmadia), Kluwer Academic Publishers, Dordrecht, 1991, p. 323.
83. P. Trefonas, III, R. West and R. D. Miller, *J. Am. Chem. Soc.*, **107**, 2737 (1985).
84. T. Karatsu, R. D. Miller, R. Sooriyakumaran and J. Michl, *J. Am. Chem. Soc.*, **111**, 1140 (1989).
85. A. J. McKinley, T. Karatsu, G. M. Wallraff, R. D. Miller, R. Sooriyakumaran and J. Michl, *Organometallics*, **7**, 2567 (1988).
86. A. J. McKinley, T. Karatsu, G. M. Wallraff, D. P. Thompson, R. D. Miller and J. Michl, *J. Am. Chem. Soc.*, **113**, 2003 (1991).
87. H. Sakurai and M. Kumada, *Bull. Chem. Soc. Jpn.*, **37**, 1894 (1964).
88. H. Gilman, W. H. Atwell and G. L. Schwebke, *J. Organomet. Chem.* **2**, 369 (1964).
89. D. N. Hague and R. H. Prince, *Chem. Ind. (London)*, 1492 (1964).
90. H. Sakurai, H. Yamamori and M. Kumada, *Bull. Chem. Soc. Jpn.*, **38**, 2024 (1965).
91. H. Sakurai, K. Tominaga and M. Kumada, *Bull. Chem. Soc. Jpn.*, **39**, 1279 (1966).
92. H. Sakurai, H. Yamamori and M. Kumada, *J. Chem. Soc., Chem. Commun.*, 198 (1965).
93. H. Sakurai, M. Ichinose, M. Kira and T. G. Traylor, *Chem. Lett.*, 1383 (1984).
94. H. Gilman and W. H. Atwell, *J. Organomet. Chem.*, **4**, 176 (1965).
95. H. Gilman, W. H. Atwell, P. K. Sen and C. L. Smith, *J. Organomet. Chem.*, **4**, 163 (1965).
96. H. Gilman and P. J. Morris, *J. Organomet. Chem.*, **6**, 102 (1966).
97. C. G. Pitt, *J. Am. Chem. Soc.*, **91**, 6613 (1969).
98. C. G. Pitt, *J. Chem. Soc., Chem. Commun.*, 816 (1971).
99. H. Bock and H. Alt, *J. Am. Chem. Soc.*, **92**, 1569 (1970).
100. C. G. Pitt, R. N. Carey and E. C. Toren, Jr., *J. Am. Chem. Soc.*, **94**, 3806 (1972).
101. H. Sakurai and M. Kira, *J. Am. Chem. Soc.*, **96**, 791 (1974).
102. H. Sakurai and M. Kira, *J. Am. Chem. Soc.*, **97**, 4879 (1975).
103. C. G. Pitt and H. Bock, *J. Chem. Soc., Chem. Commun.*, 28 (1972).
104. H. Sakurai, S. Tasaka and M. Kira, *J. Am. Chem. Soc.*, **94,** 9285 (1972).
105. M. Kira, T. Miyazawa, H. Sugiyama, M. Yamaguchi and H. Sakurai, *J. Am. Chem. Soc.*, **115**, 3116 (1993).
106. H. Shizuka, H. Obuchi, M. Ishikawa and M. Kumada, *J. Chem. Soc., Chem. Commun.*, 405 (1981).
107. H. Shizuka, Y. Sato, M. Ishikawa and M. Kumada, *J. Chem. Soc., Chem. Commun.*, 439 (1982).
108. H. Shizuka, Y. Sato, Y. Ueki, M. Ishikawa and M. Kumada, *J. Chem. Soc., Faraday Trans. 1*, **80**, 341 (1984).
109. H. Shizuka, H. Obuchi, M. Ishikawa and M. Kumada, *J. Chem. Soc., Faraday Trans. 1*, **80**, 383 (1984).
110. H. Hiratsuka, Y. Mori, M. Ishikawa, K. Okazaki and H. Shizuka, *J. Chem. Soc., Faraday Trans. 2*, **81**, 1665 (1984).
111. H. Shizuka, *Pure Appl. Chem.*, **65**, 1635 (1993).

112. H. Sakurai, H. Sugiyama and M. Kira, *J. Phys. Chem.*, **94**, 1837 (1990).
113. E. Lippert, W. Lüder, F. Moll, W. Nägele, H. Boos, H. Prigge and I. Seibold-Blankenstein, *Angew. Chem.*, **73**, 695 (1961).
114. E. Z. Lippert, *Z. Naturforsch*, **10a**, 541 (1955).
115. E. Lippert, W. Lüder and H. Boos, in *Advances in Molecular Spectroscopy* (Ed. A. Magnani), Pergamon Press, Oxford, 1962, p. 443.
116. (a) W. Rettig, *Angew. Chem., Int. Ed. Engl.*, **25**, 971 (1986).
     (b) K. Bhalfacharyya and M. Chowdhury, *Chem. Rev.*, **93**, 507 (1993).
117. K. Rotkiewicz, K. H. Grellmann and Z. R. Grabowski, *Chem. Phys. Lett.*, **19**, 315 (1973).
118. Y. Tajima, H. Ishikawa, T. Miyazawa, N. Mikami and M. Kira, *J. Am. Chem. Soc.*, **118**, in press (1997).
119. M. Kira, T. Miyazawa, N. Mikami and H. Sakurai, *Organometallics*, **10**, 3793 (1991).
120. H. Shizuka, K. Okazaki, M. Tanaka, M. Ishikawa, M. Sumitani and K. Yoshihara, *Chem. Phys. Lett.*, **113**, 89 (1985).
121. K. B. Eisenthal, in *Ultrashort Laser Pulses* (Ed. W. Kaiser), Springer-Verlag, Berlin, 1988, p. 319 and references cited therein.
122. K. A. Horn, R. B. Grossman, J. R. G. Thorne and A. A. Whitenack, *J. Am. Chem. Soc.*, **111**, 4809 (1989).
123. H. Sakurai, *J. Organomet. Chem.*, **200**, 261 (1980).
124. B. Coleman and M. Jones, Jr., *Rev. Chem. Intermediates*, **4**, 297 (1989).
125. P. Boudjouk, J. R. Roberts, C. M. Golino and L. H. Sommer, *J. Am. Chem. Soc.*, **94**, 7926 (1972).
126. M. Ishikawa, *Pure Appl. Chem.*, **50**, 11 (1978).
127. M. Ishikawa, T. Fuchikami, T. Sugaya and M. Kumada, *J. Am. Chem. Soc.*, **97**, 5923 (1975).
128. M. Ishikawa, T. Fuchikami and M. Kumada, *J. Organomet. Chem.*, **118**, 139 (1976).
129. M. Ishikawa, T. Fuchikami and M. Kumada, *J. Organomet. Chem.*, **118**, 155 (1976).
130. M. Ishikawa, T. Fuchikami and M. Kumada, *Tetrahedron Lett.*, 1299 (1976).
131. M. Ishikawa, T. Fuchikami and M. Kumada, *J. Organomet. Chem.*, **133**, 19 (1977).
132. M. Ishikawa, T. Fuchikami and M. Kumada, *J. Organomet. Chem.*, **162**, 223 (1978).
133. M. Ishikawa, M. Oda, N. Miyoshi, L. Fabry, M. Kumada, T. Yamabe, K. Akagi and K. Fukui, *J. Am. Chem. Soc.*, **101**, 4612 (1979).
134. M. Ishikawa, M. Oda, K. Nishimura and M. Kumada, *Bull. Chem. Soc. Jpn.*, **56**, 2795 (1983).
135. J. Ohshita, H. Ohsaki, M. Ishikawa, A. Tachibana, Y. Kurosaki, T. Yamabe and A. Minato, *Organometallics*, **10**, 880 (1991).
136. K. Takaki, H. Sakamoto, Y. Nishimura, Y. Sugihara and M. Ishikawa, *Organometallics*, **10**, 888 (1991).
137. J. Ohshita, H. Ohsaki, H. Takahashi, M. Ishikawa, A. Tachibana, Y. Kurosaki, T. Yamabe, T. Tsukihara, K. Takahashi and Y. Kiso, *Organometallics*, **10**, 2685 (1991).
138. J. Ohshita, H. Ohsaki and M. Ishikawa, *Organometallics*, **10**, 2695 (1991).
139. M. Ishikawa, Y. Nishimura and H. Sakamoto, *Organometallics*, **10**, 2701 (1991).
140. M. Ishikawa, M. Kikuchi, A. Kunai, T. Takeuchi, T. Tsukihara and M. Kido, *Organometallics*, **12**, 3474 (1993).
141. J. Ohshita, H. Niwa, M. Ishikawa, T. Yamabe, T. Yoshii and K. Nakamura, *J. Am. Chem. Soc.*, **118**, 6853 (1996).
142. G. W. Sluggett and W. J. Leigh, *Organometallics*, **11**, 3731 (1992).
143. G. W. Sluggett and W. J. Leigh, *J. Am. Chem. Soc.*, **114**, 1195 (1992).
144. W. J. Leigh and G. W. Sluggett, *J. Am. Chem. Soc.*, **115**, 7531 (1993).
145. W. J. Leigh and G. W. Sluggett, *Organometallics*, **13**, 269 (1994).
146. G. W. Sluggett and W. J. Leigh, *Organometallics*, **13**, 1005 (1994).
147. J. Braddock-Wilking, M. Y. Chiang and P. P. Gaspar, *Organometallics*, **12**, 197 (1993).
148. H. Sakurai, Y. Nakadaira, M. Kira, H. Sugiyama, K. Yoshida and T. Takiguchi, *J. Organomet. Chem.*, **184**, C36 (1980).
149. M. Kira, K. Sakamoto and H. Sakurai, *J. Am. Chem. Soc.*, **105**, 7469 (1983).
150. H. Sakurai, K. Sakamoto and M. Kira, *Chem. Lett.*, 1213 (1984).
151. H. Sakurai, in *Silicon Chemistry* (Eds. J. Y. Corey, E. Y. Corey and P. P. Gaspar), Chap. 16, Ellis Horwood, Chichester, 1988.
152. H. Okinoshima and W. P. Weber, *J. Organomet. Chem.*, **149**, 279 (1978).
153. S.-S. Hu and W. P. Weber, *J. Organomet. Chem.*, **369**, 155 (1989).

154. M. G. Steinmetz, C. Yu and L. Li, *J. Am. Chem. Soc.*, **116**, 932 (1994).
155. M. Ishikawa and M. Kumada, *J. Organomet. Chem.*, **81**, C3 (1974).
156. M. Ishikawa, K.-I. Nakagawa, M. Ishiguro, F. Ohi and M. Kumada, *J. Organomet. Chem.*, **201**, 151 (1980).
157. M. Kira, T. Miyazawa, S. Koshihara, Y. Segawa and H. Sakurai, *Chem. Lett.*, 3 (1995).
158. T. Miyazawa, H. Sakurai and M. Kira, unpublished results.
159. T. J. Drahnak, J. Michl and R. West, *J. Am. Chem. Soc.*, **101**, 5427 (1979).
160. G. Maier, G. Mihm, H. P. Reisenhauer and D. Littman, *Chem. Ber.*, **117**, 2369 (1984).
161. B. J. Helmer and R. West, *Organometallics*, **1**, 1463 (1982).
162. M. J. Fink, M. J. Michalczyk, K. J. Haller, R. West and J. Michl, *Organometallics*, **3**, 793 (1984).
163. M. J. Michalczyk, M. J. Fink, D. J. De Young, C. W. Carlson, K. M. Welsh, R. West and J. Michl, *Silicon, Germanium, Tin, Lead Compd.*, **9**, 75 (1986).
164. R. West, *Pure Appl. Chem.*, **56**, 163 (1984).
165. R. West, M. J. Fink and J. Michl, *Science*, **214**, 1343 (1981).
166. M. Kira, T. Maruyama and H. Sakurai, *Tetrahedron Lett.*, **33**, 243 (1992).
167. M. Kira, T. Maruyama and H. Sakurai, *Heteroatom Chem.*, **5**, 305 (1994).
168. T. Maruyama, M. Kira and H. Sakurai, XXV Silicon Symposium, Los Angeles, April 1992, paper 72P.
169. M. Kira, T. Maruyama and H. Sakurai, *Chem. Lett.*, 1345 (1993).
170. K. E. Banks, Y. Wang and R. T. Conlin, XXV Silicon Symposium, Los Angeles, April 1992, paper 7.
171. H. A. Bent, *J. Chem. Educ.*, **37**, 616 (1960).
172. H. A. Bent, *J. Chem. Phys.*, **33**, 1258 (1960).
173. H. A. Bent, *Chem. Rev.*, **61**, 275 (1961).
174. S. Tsutsui, K. Sakamoto and M. Kira, to appear.
175. Y. Apeloig, M. Karni, R. West and K. Welsh, *J. Am. Chem. Soc.*, **116**, 9719 (1994).
176. Y. Apeloig and M. Karni, *J. Chem. Soc., Chem. Commun.*, 1018 (1985).
177. D. Seyferth and T. F. O. Lim, *J. Am. Chem. Soc.*, **100**, 7074 (1978).
178. K. P. Steele and W. P. Weber, *J. Am. Chem. Soc.*, **102**, 6095 (1980).
179. T.-Y. Y. Gu and W. P. Weber, *J. Am. Chem. Soc.*, **102**, 1641 (1980).
180. D. Tzeng and W. P. Weber, *J. Am. Chem. Soc.*, **102**, 1451 (1980).
181. A. Chihi and W. P. Weber, *Inorg. Chem.*, **20**, 2822 (1981).
182. K. Raghavachari, J. Chandrasekhar and M. J. Frisch, *J. Am. Chem. Soc.*, **104**, 3779 (1982).
183. K. Raghavachari, J. Chandrasekhar, M. S. Gordon and K. J. Dykema, *J. Am. Chem. Soc.*, **106**, 5853 (1984).
184. G. R. Gillette, G. H. Noren and R. West, *Organometallics*, **6**, 2617 (1987).
185. G. R. Gillette, G. H. Noren and R. West, *Organometallics*, **8**, 487 (1989).
186. M.-A. Pearsall and R. West, *J. Am. Chem. Soc.*, **110**, 7228 (1988).
187. W. Ando, K. Hagiwara and A. Sekiguchi, *Organometallics*, **6**, 2270 (1987).
188. W. Ando, A. Sekiguchi, K. Hagiwara, A. Sakakibara and H. Yoshida, *Organometallics*, **7**, 558 (1988).
189. W. Ando, M. Fujita. H. Yoshida and A. Sekiguchi, *J. Am. Chem. Soc.*, **110**, 3310 (1988).
190. S. Zhang and R. T. Conlin, *J. Am. Chem. Soc.*, **113**, 4272 (1991).
191. S. Zhang, P. E. Wagenseller and R. T. Conlin, *J. Am. Chem. Soc.*, **113**, 4278 (1991).
192. P. Boudjouk, U. Samaraweera, R. Sooriyakumaran, J. Chrusciel and K. R. Anderson, *Angew. Chem., Int. Ed. Engl.*, **27**, 1355 (1988).
193. P. Boudjouk, E. Black and R. Kumarathasan, *Organometallics*, **10**, 2095 (1991).
194. D. H. Pae, M. Xiao, M. Y. Chiang and P. P. Gaspar, *J. Am. Chem. Soc.*, **113**, 1281 (1991).
195. Y. Apeloig, in *The Chemistry of Organosilicon Compounds* (Eds. S. Patai and Z. Rappoport), Vol. 1, Chap. 2. Chichester, 1989, p. 57.
196. R. S. Grev, H. F. Schaefer, III and P. P. Gaspar, *J. Am. Chem. Soc.*, **113**, 5638 (1991).
197. H. P. Reisenauer, G. Mihm and G. Maier, *Angew. Chem., Int. Ed. Engl.*, **21**, 854 (1982).
198. C. A. Arrignton, K. A. Klingensmith, R. West and J. Michl, *J. Am. Chem. Soc.*, **106**, 525 (1984).
199. M. Ishikawa, K.-I. Nakagawa, M. Ishiguro, F. Ohi and M. Kumada, *J. Organomet. Chem.*, **152**, 155 (1978).
200. M. Kira, T. Taki and H. Sakurai, *J. Org. Chem.*, **54**, 5647 (1989).
201. P. Boudjouk and L. H. Sommer, *J. Chem. Soc., Chem. Commun.*, 54 (1973).

202. W. J. Leigh, C. J. Bradaric and G. W. Sluggett, *J. Am. Chem. Soc.*, **115**, 5332 (1993).
203. W. J. Leigh and C. J. Bradaric, *J. Am. Chem. Soc.*, **118**, 8971 (1996).
204. H. Tobita, K. Ueno and H. Ogino, *Bull. Chem. Soc. Jpn.*, **61**, 2797 (1988).
205. H. K. Scharma and K. H. Pannell, *Chem. Rev.*, **95**, 1351 (1995) and references cited therein.
206. H. Suzuki, N. Tokitoh and R. Okazaki, *Bull. Chem. Soc. Jpn.*, **68**, 2471 (1995).
207. M. Kira, T. Iwamoto and C. Kabuto, *J. Am. Chem. Soc.*, **118**, 10303 (1996).

CHAPTER 23

Hypervalent silicon compounds

DANIEL KOST and INNA KALIKHMAN

Department of Chemistry, Ben-Gurion University of the Negev, Beer Sheva 84105, Israel
Fax: +972-7-647-2943; e-mail: kostd@bgumail.bgu.ac.il

I. INTRODUCTION

Hypervalent silicon compounds have generated much interest in recent years. This is evident from the numerous papers published every year on this topic, and from the extensive reviews which have appeared in recent years[1−7]. In this review we have attempted to cover only the most recent (five year) literature. Only for subjects for which we felt that the new work would not be fully appreciated without the previous reports did we include earlier citations, or for those subjects which in our judgment, were not sufficiently covered in earlier reviews.

The most recent comprehensive review focused primarily on the reactivity aspects of hypervalent silicon complexes[6], while the latest review covers only silicon–oxygen coordination[7]. The present chapter focuses on synthesis and structure, silicon-29 NMR spectroscopy, and on the nonrigidity of hypervalent silicon compounds and the resulting kinetic and stereochemical studies.

II. PENTACOORDINATE ANIONIC SILICON COMPOUNDS

A. Fluorosilicates

1. Monosilicates

Penta- and hexacoordinate silicate anions containing four and five fluorine atoms have been known for about 30 years, and were first reviewed by Müller ($[RSiF_4]^-$, $[RSiF_5]^{2-}$, $[R_2SiF_4]^{2-}$)[8]. More recently pentacoordinate complexes with fewer fluorine atoms have been reported[9−18] ($[R_2SiF_3]^-$, as well as the following $[R_3SiF_2]^-$ silicates: $[Ph_3SiF_2]^-$[11], $[1\text{-NaphPh}_2SiF_2]^-$[12], and $[Me_3SiF_2]^-$)[15]. The general synthetic route to organofluorosilicates involves the reaction of an organofluorosilane with a fluoride donor, such as alkali metal fluoride, ammonium fluoride or tetraalkyl ammonium fluoride, in protic or aprotic solvents[8−16]. The resulting anionic complexes are usually highly hygroscopic and proved difficult to study in detail. A significant improvement was introduced by Damrauer and coworkers, who prepared the anionic silicates with potassium counter ions in the presence of crown ethers[11]. These products proved to be nonhygroscopic, and hence much easier to study.

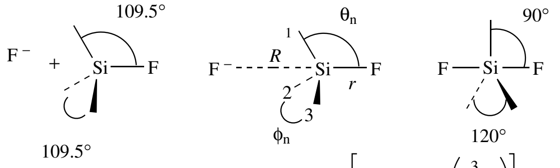

$$\text{(a) Pentacoordination character (\% TBPa)} = \frac{\left[109.5^\circ - \frac{1}{3}\left(\sum_{n=1}^{3}\theta_n\right)\right]}{(109.5^\circ - 90^\circ)} \times 100$$

$$\text{(b) Pentacoordination character (\% TBPa)} = \frac{\left[120^\circ - \frac{1}{3}\left(\sum_{n=1}^{3}\phi_n\right)\right]}{(120^\circ - 109.5^\circ)} \times 100$$

FIGURE 1. Methods for calculating the percent TBP character for fluorosilicates: (a) based on angle θ_n; (b) calculated from angle ϕ_n

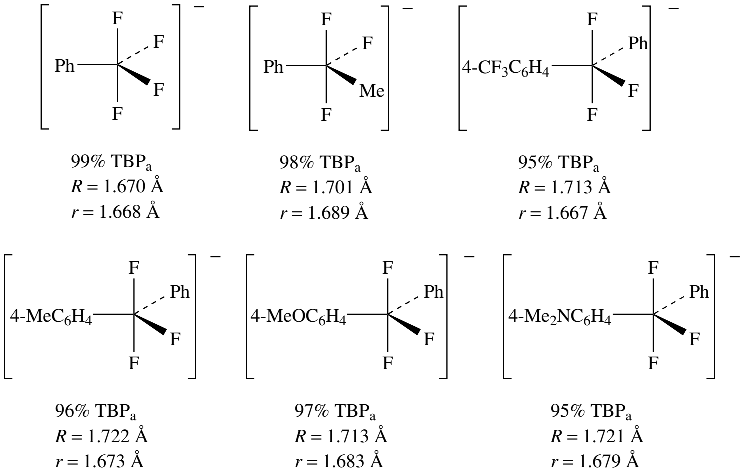

FIGURE 2. Percent TBP character for fluorosilicates where TBP_a, R and r are defined in Figure 1 (adapted from Reference 17a)

The geometries of most pentacoordinate fluorosilicates are nearly ideal trigonal bipyramids (TBP) (i.e. the bond angles correspond closely to those of an ideal TBP), with fluorines occupying the apical positions[3,4,10–14,18]. Tamao and coworkers, following an approach developed by Bürgi and Dunitz[19], calculated the TBP character of some fluorosilicates in terms of the correspondence of bond angles to those present in an ideal TBP (Figure 1)[17]. For unconstrained pentacoordinate silicates the TBP percentage was found to be between 95 and 99% (Figure 2). Even in cases of severe steric requirements of the carbon ligands attached to silicon ($[Mes_2SiF_3][K(18\text{-crown-6})]$[14] and $[2,4,6\text{-}t\text{-}Bu_3C_6H_2SiF_4][K(18\text{-crown-6})]$)[13a], no significant distortion of the basic TBP geometry has been observed. An exception has been reported, in which a fluorine occupies an equatorial position while one of the apical positions is occupied by carbon (**1**)[20]. This is obviously due to the steric strain in the five-membered ring, which can only accommodate the 90° angle between apical and equatorial ligands, rather than the 120° required by two equatorial positions, if a second fluorine were to occupy the apical position.

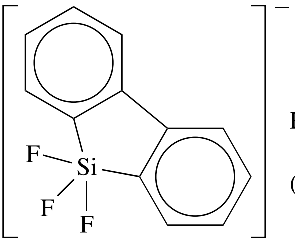

K^+(18-c-6)

(18-c-6) ≡ (18-crown-6)

(1)

TABLE 1. ^{29}Si NMR spectroscopic data for diorganotrifluorosilicates and organotetrafluorosilicates

Anion	Temperature (°C)	$\delta^{29}Si$ (ppm)	$J(\mathrm{Si{-}F}_{ax})$ (Hz)	$J(\mathrm{Si{-}F}_{eq})$ (Hz)	References
c-$(CH_2)_4SiF_3$	−68.7	−63.84	255		13b
c-$(CH_2)_5SiF_3$	−98.2	−76.97	254	213	13b
$MePhSiF_3$	−120	−86.89	250	212	13b
$(2\text{-Tol})_2SiF_3$	−92	−91.60	255	218	13b
$(Mes)_2SiF_3$	−70	−92.52	262	219	13b
t-$BuPhSiF_3$	−88.2	−94.52	268	222	13b
Ph_2SiF_3	−107.2	−106.4	252	204	13b
2,2′-$BiPhSiF_3$[a]	−58.2	−91.47	259	220	13b
2,2′-$BiBzSiF_3$[a]	−88.2	−105.9	245	206	13b
4-TolPhSiF_3	25	−109.71	237.74		18
$(4\text{-MeOC}_6H_4)PhSiF_3$	25	−110.04	237.82		18
$(4\text{-CF}_3C_6H_4)PhSiF_3$	25	−110.44	239.73		18
n-$PrSiF_4$	−78.2	−110.8	225		13a
$F_4SiCH_2CH_2SiF_4$	−98.2	−109.9	227		13a
t-$BuSiF_4$	−58.2	−114.8	237		13a
c-$C_6H_{11}SiF_4$	−68.7	−114.7	232		13a
$BzSiF_4$	−98.2	−116.4	218		13a
$PhSiF_4$	−58.2	−125.9	210		13a
4-TolSiF_4	−62.3	−126.1	209		13a
3-TolSiF_4	−58.2	−124.3	214		13a
2-TolSiF_4	−58.2	−121.9	216		13a
$(4\text{-ClC}_6H_4)SiF_4$	−58.3	−125.2	213		13a
$MesSiF_4$	21.0	−120.1	219		13a
c-$(CH_2)_4SiF(o\text{-}O_2C_6H_4)$	25	−52.1	324		20
c-$(CH_2)_5SiF(o\text{-}O_2C_6H_4)$	25	−68.37	250		20

[a] BiPh = biphenyl; BiBz = bibenzyl

^{29}Si chemical shift has become a powerful diagnostic tool for the silicon coordination number[21]. ^{29}Si chemical shifts and Si−F coupling constants for various fluorosilicates have been collected in Table 1. On average, $\delta(^{29}Si)$ for $[RSiF_4]^-$ are 51 ppm upfield from the corresponding $RSiF_3$ (average $\delta = -126$ ppm), whereas $[R_2SiF_3]^-$ (average $\delta = -90$ ppm) are shifted on average 71 ppm upfield from their silane analogs.

Ligand–site exchange is found in all of the fluorosilicates, and monitored primarily by ^{19}F NMR spectroscopy[6,11,13]. The exchange between equatorial and apical positions is very rapid in the case of $[RSiF_4]^-$ silicates[13a] and leads to the observation of only one average signal for all fluorine atoms in the ^{19}F NMR spectrum, at temperatures as low as can be practically reached in the solvents used. Steric crowding in $[2,4,6\text{-}t\text{-}Bu_3C_6H_2SiF_4][K(18\text{-crown-6})]$ has been reported to slow down this exchange, to the extent that separate apical and equatorial fluorines can be seen at low temperature (205 K), as well as their eventual coalescence at higher temperature (270 K, $\Delta G^{\ddagger} = 12.8\ \text{kcal mol}^{-1}$)[11,13a]. The rate of fluorine–site exchange diminishes with the decrease in the number of fluorine atoms. Thus, in trifluorosilicates the isochrony of apical and equatorial fluorine ligands can be removed and the exchange effectively 'frozen', relative to the NMR time scale, with activation barriers ranging between 9–14 kcal mol^{-1}[13b]. By contrast, in difluorosilicates no fluorine–site exchange is observed even at elevated temperatures, as a result of the higher stability of complexes with fluorine atoms in apical positions: replacement of an apical fluorine by a carbon ligand is too costly in terms of energy, and is not observed[11a].

The convenient range of exchange barriers found in trifluorosilicates permitted a more detailed polar substituent effect study[6,18]. A series of diaryltrifluorosilicates with different substituents on one of the phenyl groups **(2)** were prepared, and the free energy barriers for fluorine exchange were measured. The barriers were found to decrease linearly with the electron-withdrawing power of the substituent, as expressed by the σ^+ substituent constant, with a reaction constant $\rho = +2.0$[18]. This result is consistent with the general observation (mentioned above) that the barrier for fluorine interconversion decreases with increasing number of fluorine ligands.

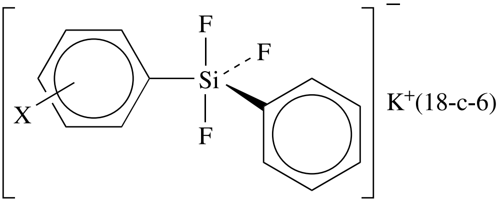

(**2a**) X = 4-CF_3; (**2b**) X = 4-Cl; (**2c**) X = H; (**2d**) X = 4-Me;
(**2e**) X = 4-OMe; (**2f**) X = 4-NMe_2; (**2g**) X = 4-SiF_2Ph;
(**2h**) X = 3-SiF_2Ph

An interesting case of simultaneous exchange of two fluorides has been reported recently[22]. In compounds **2g** and **2h** there is one tetra- and one pentacoordinate silicon. Fluoride transfer from the pentacoordinate silicate to the silane was found to be intermolecular, with a large negative entropy of activation. It was concluded that exchange takes place simultaneously between two complexes, through a cyclophane-like transition state (equation 1).

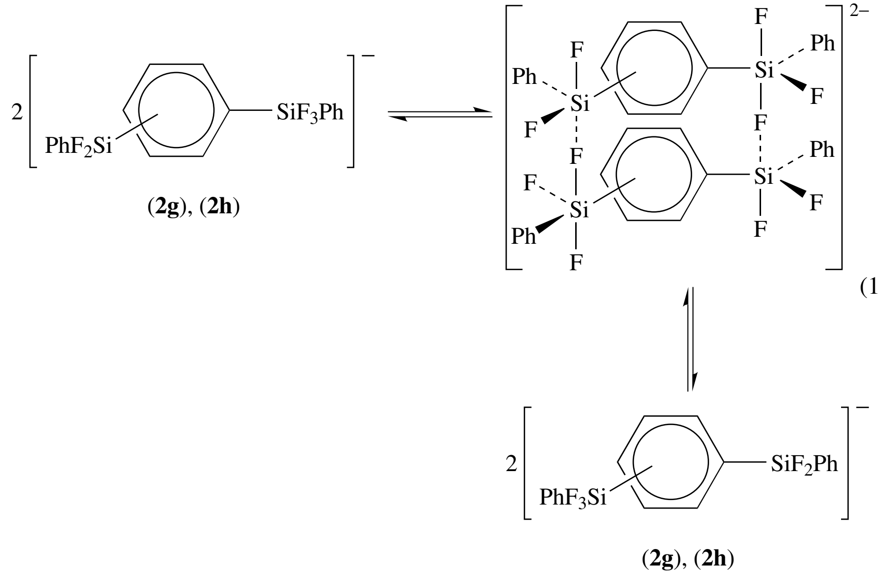

(1)

The reactivity of perfluorophenyltetrafluorosilicates ($M^+[C_6F_5SiF_4]^-$, M = K, Cs, Me_4N) toward electrophiles has been studied recently[23]. These compounds were found to be highly reactive in the presence of Br_2, ICN, IF_5, XeF_2, $NOBF_4$ which cause immediate C−Si bond cleavage (equation 2).

$$Me_4N^+[C_6F_5SiF_4]^- + Br_2 \xrightarrow{\text{Diglyme}} C_6F_5Br + Me_4N^+Br^- + SiF_4 \qquad (2)$$

2. Fluorosilicates with intramolecular exchange of ‘bridged’ fluorine

An interesting case of fluorine atom bridging between two silicon centers has been reported in fluorosilicates[17]. Compounds **3** and **4**, formally possessing one penta- and one tetracoordinate silicon each, were prepared by reacting KF and 18-crown-6 with the corresponding bis-silanes. The crystal structures show that a central fluorine bridges between the two silicon atoms such that both silicons are essentially pentacoordinate with a distorted TBP geometry. The bridging fluorine and another fluorine on each silicon occupy the apical positions. The bridging fluorine is not symmetrically positioned between the silicons in any of the complexes, not even in **3a**, in which the ligands on the two silicon atoms are equivalent. The authors compared the Si−F bond lengths and calculated the percent TBP in the bridged complexes according to Figure 1. The results given in Table 2 confirm the basic TBP character of the bis silicates, although significant deviations are observed relative to the unconstrained monosilicates.

The bis-silicates **3** and **4** provide an elegant model for the gradual change in geometry from tetrahedral to TBP, associated with the S_N2 reaction on silicon. A linear correlation was found between the calculated percent TBP and the $Si-F_{br}$ (bridging fluorine) and $Si-F_a$ (apical fluorine) bond lengths, as might be expected along the S_N2 reaction coordinate. The change of $Si-F_{br}$ bond length is much greater than that of $Si-F_a$[17].

^{29}Si NMR chemical shifts and Si−F coupling constants were used for a structural analysis of the bis-complexes in solution. At 20 °C all complexes show rapid exchange

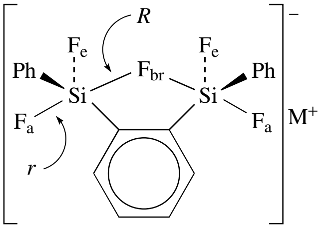

(**3a**)

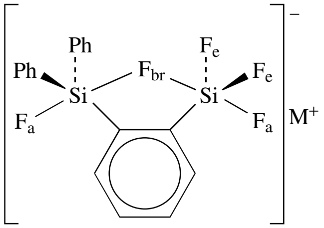

(**3b**)

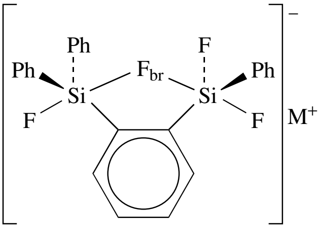

$M^+ = K^+$ (18-c-6)

(**4**)

TABLE 2. Bond lengths, % TBP and deviations (ΔSi)^a in **3** and **4**[17a]

	Anion of **3a**		Anion of **3b**		Anion of **4**	
Position	Si2	Si1	Si2	Si1	Si2	Si1
Si−F$_{ap}$ (Å)						
R	2.065	1.898	2.369	1.700	2.090	1.805
r	1.638	1.657	1.639	1.667	1.672	1.669
Si−F$_{eq}$ (Å)	1.601	1.616		1.598		1.624
Si−C$_{eq}$ (Å)	1.871	1.879	1.870 1.878		1.860 1.887	1.889
ΔSi (Å)	0.205	0.131	0.314	0.040	0.207	0.078
%TBP	66	78	50	93	68	88

[a] Displacement of the central Si from the plane defined by the three equatorial ligands.

of fluorine sites. Three significant features were noted: (1) Both silicons give rise to one sextet, indicating the equivalence and fast exchange of all fluorines. (2) The ^{29}Si chemical shift for **3a** (−90.03 ppm) is intermediate between similar tetra- (Ph_2SiF_2, −29.00 ppm) and pentacoordinate ($[Ph_2SiF_3]^-$, −109.55 ppm) compounds. The closer resemblence of $\delta(^{29}Si)$ to the pentacoordinate complex is consistent with the average calculated TBP character for **3a** of 66 and 78%, respectively, obtained from the solid state structure. (3) The Si−F coupling constant in **3a** (134.74 Hz) is much smaller than in either tetra- [^1J(Si−F) = 291 Hz] or pentacoordinate [^1J(Si−F) = 238 Hz] structures. It can be obtained as an average (130 Hz) of two tetracoordinate fluorines (2 × 291 Hz), three pentacoordinate (3 × 238 Hz) and five distant fluorines representing ^4J(Si−F) between silicon and the fluorines attached to the neighboring silicon (5 × 0 Hz). This supports rapid exchange between tetra- and pentacoordinate silicons[17].

(a) F_{br} – exchange

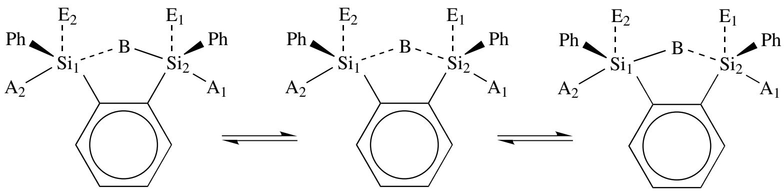

(b) Flipping

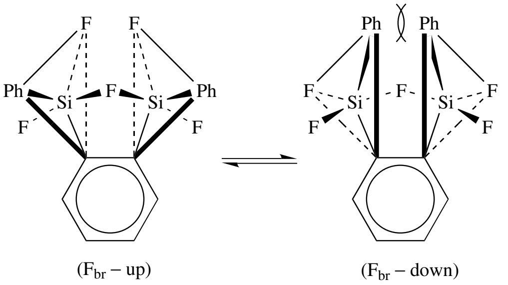

(c) Si—C rotation

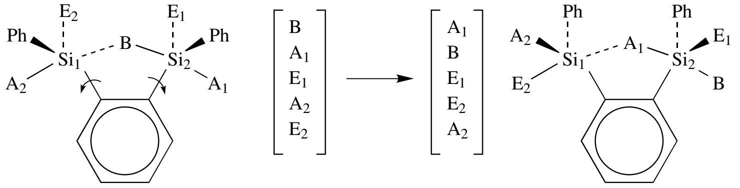

(d) Pseudorotation

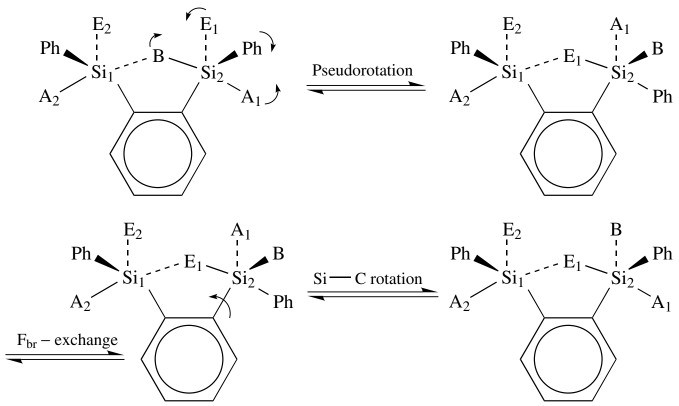

FIGURE 3. Stereodynamics of **3a:** four distinct rate processes were observed[17a]; F_{br}, F_a and F_e are abbreviated B, A and E, respectively

The variable-temperature ^{19}F NMR spectra of **3** and **4** were carefully analyzed and interpreted in terms of four different rate processes (Figure 3). For **3a** the fastest rate process was the exchange between penta- and tetracoordinate silicon, i.e. the interchange of bond lengths between the bridging fluorine and each silicon atom ($F_{br}{-}Si_1 \leftrightarrows F_{br}{-}Si_2$, process a in Figure 3). The spectra were consistent with symmetrical silicon complexes down to the lowest temperature measured, −90 °C. While this result does not distinguish a truly symmetrical structure from a rapidly interconverting one, the fact that significantly different $F_{br}{-}Si_1$ and $F_{br}{-}Si_2$ bond lengths were found in the crystal structure analysis (Table 2) strongly supports rapid dynamic equilibration in solution.

The second process to become apparent at the NMR time scale as the temperature is raised (Figure 3, process b), is the 'flipping' of the bridging fluorine from one side of the aromatic plane to the other, with 'puckering' of the five-membered heterocycle. This results in interconversion and coalescence of signals due to two diastereomeric conformations, in which the phenyl rings are close or farther away from each other. Further warming of the sample resulted in asymmetric coalescence of signals due to apical and equatorial fluorines, and this was interpreted in terms of fast rotation about the Si−C bonds. Finally, at −16 °C, all the fluorines were completely scrambled, indicating rapid Berry-type pseudorotation. The coalescence temperature for this process falls within the range of known barriers for pseudorotation in $Ph_2SiF_3^-$ and similar silicates[13b,18].

Recently, the intensity of fluoride binding in **3** and **4** was estimated using fluoride-transfer equilibrium reactions[17c]. Surprisingly, no exchange at the NMR time scale was found between the bis-silane [1,2-$(PhSiF_2)_2C_6H_4$] and **3a**. The equilibrium in this reaction was substantially shifted to the bis-silicate **(3a)** side, and did not permit measurement of K_{eq}. The relative fluoride-binding strength was therefore estimated from the equilibrium reactions shown in Figure 4, for which K_{eq} lies within the measureable range. It is interesting to note that the 'Lewis acidity' toward fluorine of the *ortho*-bis-silanes increases sharply with increasing number of fluorine atoms attached to silicon, i.e. the bridging fluoride is bound more strongly in the more highly fluorinated complexes. The resulting fluoride ion binding constants are shown in Figure 4[17c].

Recently, a case of fluorine exchange among *three* silicon sites has been reported by Corriu and coworkers[24]: when 1,1,3,3,5,5-hexafluoro-1,3,5-trisilacyclohexane was treated with KF[18-crown-6], a fluoride was incorporated into the molecule to produce **5**. The crystal structure of **5** showed that the additional F is closer to one of the Si atoms than to the others. In solution, however, the three silicons were equivalent and gave rise to a sharp singlet at room temperature. The chemical shift for this signal ($\delta^{29}Si = -25.56$ ppm) was intermediate between those for tetracoordinate and purely pentacoordinate analogous compounds. When the temperature was lowered down to 183 K the silicons remained equivalent, however the signal was split to an octet, due to coupling to seven equivalent and hence rapidly exchanging fluorine ligands. Interestingly, the solid state ^{29}Si NMR spectrum of **5** indicated rapid exchange even in the solid, since a broad Si singlet was observed[24].

Another case of bridging was also reported recently in a neutral poly-silicon complex, and is discussed in the section on neutral pentacoordinate complexes (Section III.C.2).

A different class of bis-silicate complexes has also been termed 'bridged'[25], or also 'dinuclear λ^5Si, λ^5Si′-silicon complexes' (see Section II.B.3). These are bis-pentacoordinate silicon anions, connected to each other by a carbon chain or aromatic ring (**6**[13a], **7**[26], **8**[27]). Unlike the previous bridged complexes, in which the bridging atom was directly involved in coordination at silicon, in the present cases the bridges merely connect two silicate anions by covalent bonding.

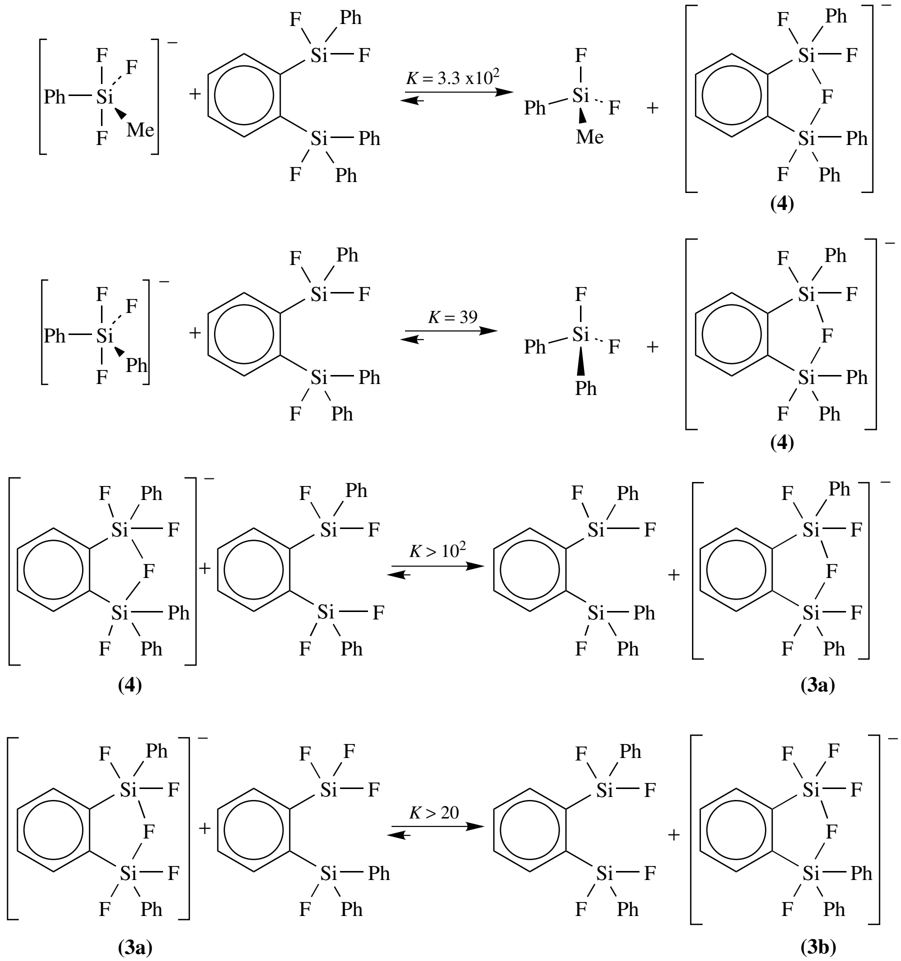

FIGURE 4. Fluoride binding estimated by intermolecular fluoride exchange equilibrium constants[17c]

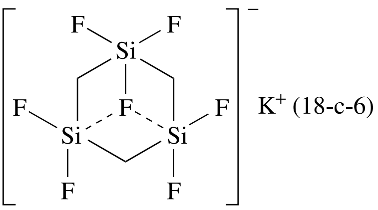

(**5**)

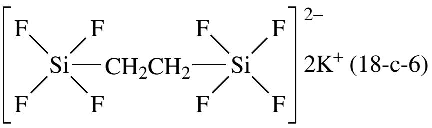

(**6**)

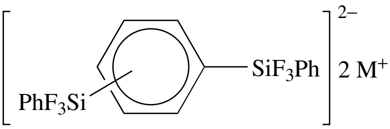

(**7a**) *para*-isomer; (**7b**) *meta*-isomer
M = K^+ (18-c-6), *n*-Bu_4N^+

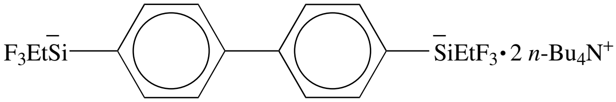

(**8**)

3. Zwitterionic fluorosilicates

A new direction in the chemistry of hypervalent silicon compounds has recently been developed by Tacke and coworkers: the chemistry of zwitterionic organosilicates[28−31]. In these compounds the silicon is formally negative, with a cationic nitrogen attached to it by an alkyl chain. One of the groups of products of this general class is the pentacoordinate zwitterionic fluorosilicates[31].

The synthesis is accomplished by HF treatment of (aminoalkyl)polyalkoxysilanes and involves the substitution of alkoxy groups by fluorines (equations 3 and 4)[29].

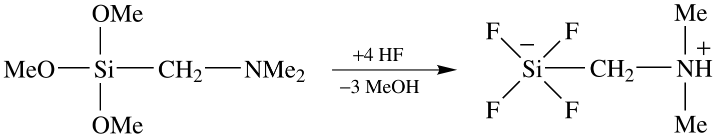

(3)

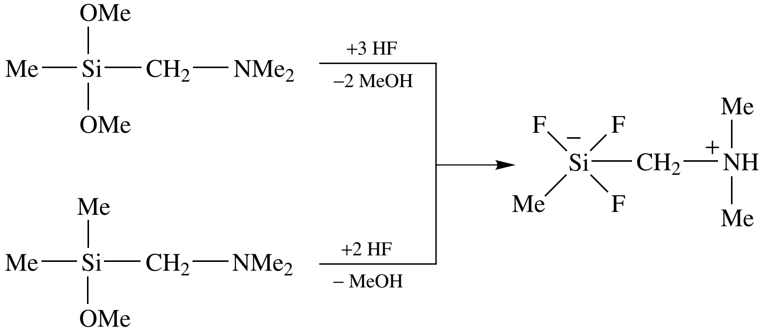

(4)

By this method also the zwitterionic silicates **9**–**15** were obtained

The geometry at silicon in these compounds is TBP, like in anionic and neutral pentacoordinate silicon complexes. A typical crystal structure is shown in Figure 5 for compound **9**. This structure apparently also exists in solution (CD_3CN), as the ^{29}Si chemical shift for **9** in this solvent (−122.9 ppm) compares well with the solid state CP-MAS shift of −121.0 pm[28,31].

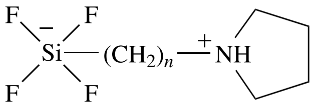

(**9**) $n = 1$
(**10**) $n = 2$

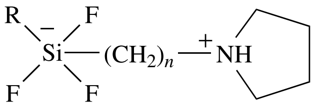

(**11**) R = Me
(**12**) R = Ph
(**13**) R = *t*-Bu

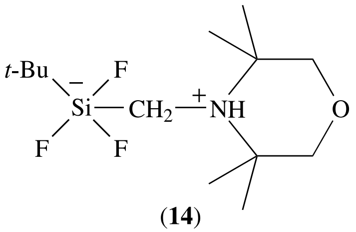

(**14**)

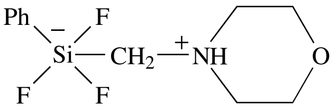

(**14a**)

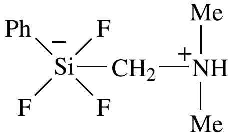

(**15**)

An interesting reaction found in zwitterionic fluorosilicates is their transformation from acyclic to monocyclic complexes (equation 5), with oxygens replacing fluorine ligands[30a].

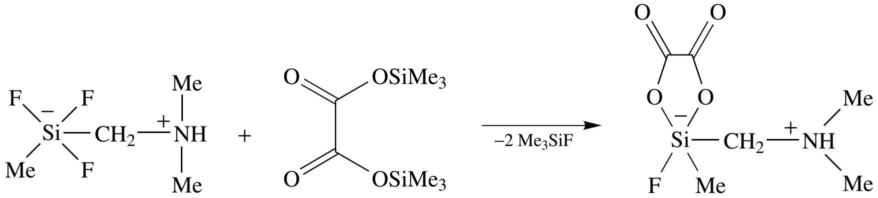

(5)

The zwitterionic trifluorosilicate **14** shows two ligand exchange processes in the ^{19}F NMR spectra[30b]. The first ($\Delta H^{\ddagger} = 9.8$ kcal mol^{-1}) involves interchange of the two axial fluoro ligands, in what must be a rotation of the piperidiniomethyl group around the Si−C bond. The other process ($\Delta H^{\ddagger} = 10.6$ kcal mol^{-1}) averages all three fluoro ligands and was assigned to pseudorotation. The DNMR results were simulated and studied further by high-level *ab initio* SCF-MO calculations of model compounds, $F_4\overset{-}{Si}CH_2\overset{+}{N}H_3$ and $Me\overset{-}{Si}F_3CH_2\overset{+}{N}H_3$. The stationary points (ground and transition states) along the two reaction coordinates: pseudorotation and Si−C bond rotation, were calculated. The calculated barriers for the two processes for the first model were found to be of comparable magnitudes: 5.0 and 5.8 kcal mol^{-1}. For the second (trifluoro) model the calculations resulted in a clear torsional reaction coordinate, with a barrier $\Delta H^{\ddagger}$ of 6.1 kcal mol^{-1}.

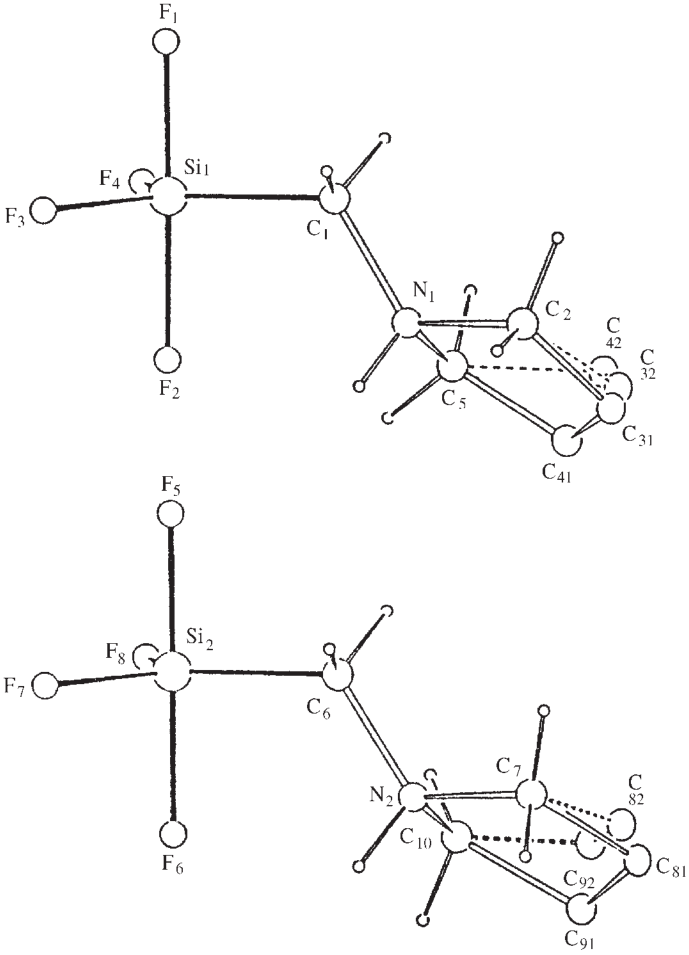

FIGURE 5. X-ray crystallographic structure of **9** (zwitterionic fluorosilicate). Reproduced from Reference 31a by permission of VCH Verlagsgesellschaft

For the exchange of all five ligand atoms bound to silicon two alternative pathways were calculated with six local minima, and comparable activation enthalpies[30b].

B. Pentacoordinate Spirosilicate Anions

1. Spirosilicates

Apart from fluoro ligands at hypervalent silicon complexes, also oxo and aza ligands are known to support penta- and hexacoordination in silicon compounds[1-8]. Among the various pentacoordinate oxo complexes, those with bidentate ligands (1,2-diols, aliphatic or aromatic, as well as α-hydroxycarboxylic acids) are most readily prepared, and are thermodynamically more stable than their acyclic analogs[32]. Two bidentate oxo ligands at the silicon center form a complex with a spiro arrangement around silicon.

Several synthetic pathways for the preparation of spirosilicates have been reported:

(1) From a tri- or tetraalkoxysilane by the reaction with 1,2-diols (catechols and glycols) in the presence of a tertiary amine (for example, equation 6)[32b].

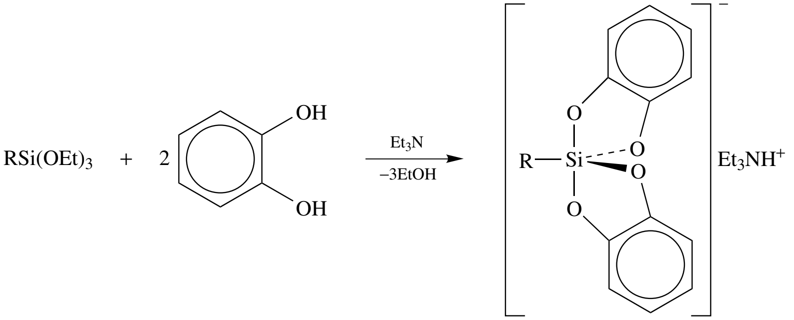

(6)

(2) Likewise, catechol reacts with a triaminosilane (equation 7)[33].

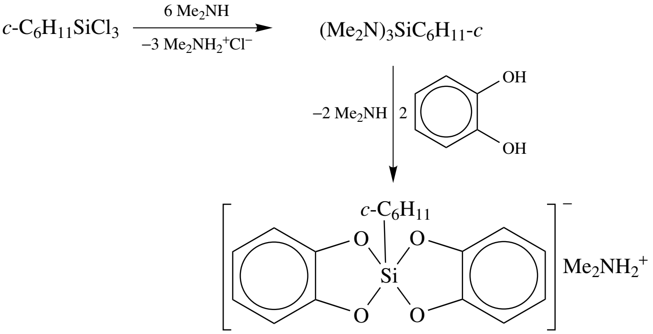

(7)

(3) By the coordination of an anion to a spirosilane, either in the presence of a tertiary amine (equation 8), or with potassium alkoxide in the presence of 18-crown-6 (equation 9)[34].

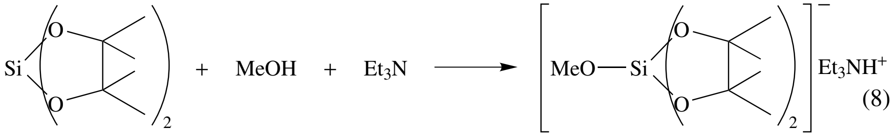

(8)

$$\mathrm{Si(OCMe_2CMe_2O)_2 + K^+OR^- + 18\text{-}c\text{-}6 \longrightarrow [(OCMe_2CMe_2O)_2SiOR]\,[K(18\text{-}c\text{-}6)]} \qquad (9)$$

$R = \mathrm{Et}, i\text{-}\mathrm{Pr}$

(4) The reaction of polyalkoxysilicate anion with pinacol (equation 10). When catechol was used instead of pinacol, a hexacoordinate spirosilicate was formed.

$$\mathrm{[Si(OR)_5]\,[K(18\text{-}c\text{-}6)] + 2HOCMe_2CMe_2OH \longrightarrow [(Me_4C_2O_2)_2SiOR]\,[K(18\text{-}c\text{-}6)] + 4ROH} \qquad (10)$$

$R = \mathrm{Et}, i\text{-}\mathrm{Pr}$

(5) The dilithio derivatives of catechol and hexafluorocumyl alcohol react with organotrichlorosilanes to give spirosilicates (equations 11 and 12)[34,35].

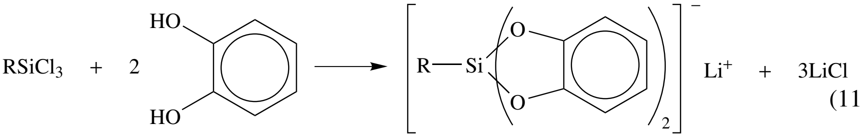

(11)

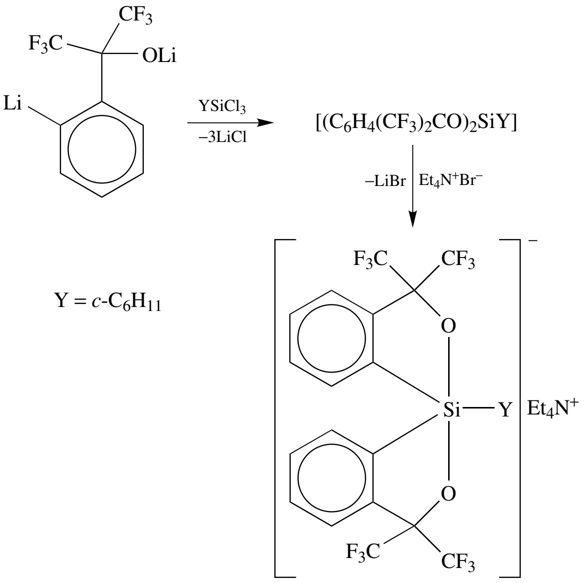

(12)

(6) The most intriguing synthetic approach is the conversion of inorganic silica to spirosilicate by the reaction with a 1,2-diol and alkali hydroxide (equation 13)[36].

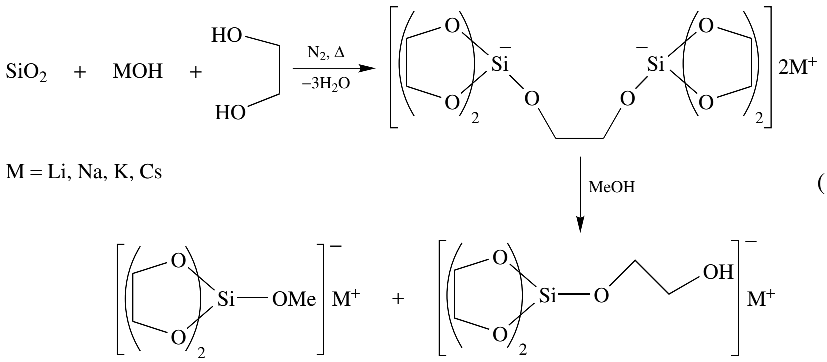

(13)

The structures of spirosilicates were found to range between TBP and square pyramid (SP), depending on the electronegativities of the ligands and the possible formation of hydrogen bonds with the counter ions[4]. Highly electronegative monodentate ligands such as fluoro, or electronegative substituents attached to the bidentate ligand (such as in tetrachlorocatechol), drive the structure toward SP geometry. The same effect results also from hydrogen bonding to the counter ion, such as Et_3NH^+, as opposed to a more TBP-like structure in the presence of K^+(18-crown-6) without hydrogen bonds. The geometries, based on X-ray structure determinations, were analyzed in terms of the percent deviation from TBP toward the SP geometry. Great structural variation was reported, between 9% deviation from ideal TBP to a nearly perfect SP, with a calculated 97% deviation from TBP. This structural variation parallels the progress along the Berry pseudorotation reaction coordinate (in which SP is the assumed transition state), and supports the facility of such a transformation.

More complete discussions with comprehensive compilations of published results were reviewed previously, and are hence omitted from this chapter[3–7].

Anionic five-coordinated silicates have been prepared also with oxygen-containing six- and seven-membered chelate rings **(16–18)**, using suitable aromatic diols, 1,8-dihydroxynaphthalene and 2,2′-dihydroxybiphenyl, respectively[37]. However, spirosilicates

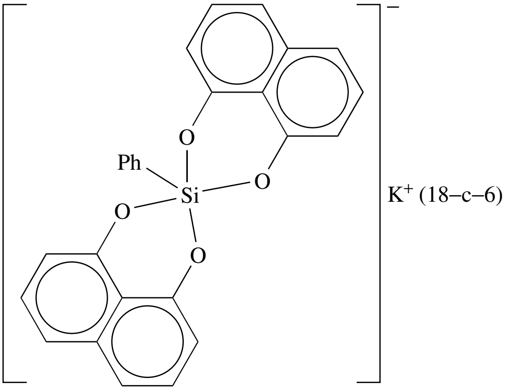

(**16**)

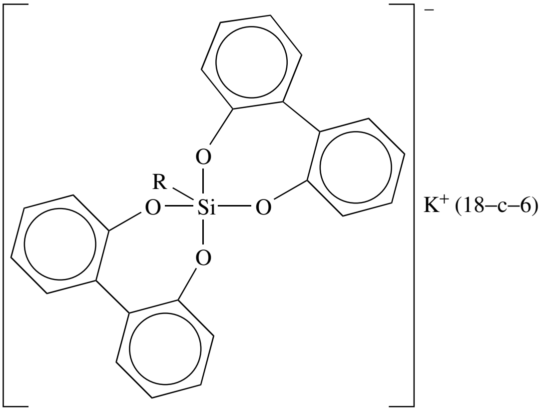

(**17**) R = OBu-*t*
(**18**) R = F

17 and **18**, with the seven-membered chelate ring, were found to be relatively unstable, and slowly decomposed in solution to tetracoordinate silanes and the free or anionic diols[37].

The geometry of **16** around silicon, as revealed by X-ray crystallography, was found similar to that of **19**, the five-membered-ring analog, i.e. both have nearly the same percent distortion from TBP to SP (32.5% and 29.5%, respectively)[4,37].

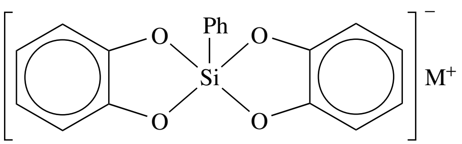

(**19**) M = Me_4N
(**21**) M = Et_3NH
(**22**) M = K(18-c-6)

Interesting structural information about the TBP–SP problem can be obtained from bis-(bidentate ligand)silicates with *unsymmetrically* substituted catechols as ligands[38]. These compounds can, in principle, have five different geometries, shown schematically in Figure 6. However, since single isomers are found in the solution NMR spectra (^1H, ^{13}C and ^{29}Si) for the complexes derived from symmetrical catechols, it was concluded that no TBP $\rightleftharpoons$ SP isomerism can be seen[38]. In all the unsymmetrical complexes only two isomers could be observed in the different NMR spectra, suggesting that either the SP geometry is the actual structure, or that the two *trans* TBP isomers are rapidly interconverting, presumably through the very close SP transition state or intermediate.

Intermolecular ligand exchange in a solution of two symmetrical complexes **22** and **30** (see Table 3 for structures) produced a mixed complex, with two different catechol ligands, as was evident from the appearance of a new signal in the ^{29}Si and ^1H and ^{13}C NMR spectra. When two complexes of unsymmetrical catechols, **20** and **28**, were mixed in solution, two new signals due to the mixed complex were observed. In this case two *trans* and two *cis* isomers are possible in the TBP geometry, and yet only two isomers were observed. Again, this can either be interpreted in terms of an SP structure, with only two possible isomers, or in terms of a large difference in thermodynamic stability of the

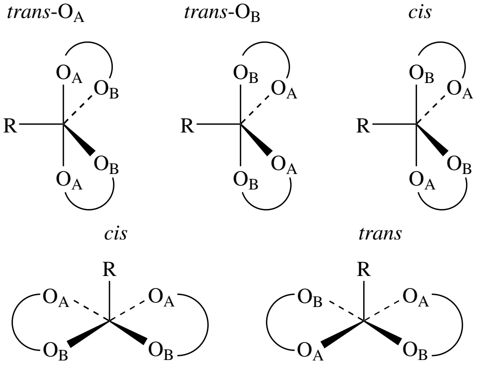

FIGURE 6. Geometrical isomers of pentacoordinate bis(bidentate ligand)silicon complexes

solution isomers preventing the observation of the minor isomers; or it may be interpreted in terms of fast interconversion between the *trans* isomers and between the *cis* isomers, respectively, in a TBP structure[38].

A compilation of ^{29}Si chemical shifts for bis-spirosilicates and related acyclic oxosilicates is given in Table 3. It can be seen that δ^{29}Si is primarily dependent on the monodentate ligand attached directly to silicon, in a manner similar to that found in neutral silanes[40].

No simple correlation can be found between the solid state calculated percent (TBP → SP) deviation and the ^{29}Si chemical shifts in solution. Table 4 demonstrates this analysis for complexes sharing the same ligand environment at silicon, four oxygens and a phenyl group: the crystal structures of four closely related spirosilicates (**19**, **21**, **49**, **50**) were

TABLE 3. ^{29}Si chemical shift in spirosilicates

Number	Compound	$\delta^{29}Si$ (ppm)	References
20	$\{[3,5\text{-}(t\text{-Bu})_2{-}C_6H_2O_2]_2SiPh\}^-\ [K(18\text{-c-}6)]^+$	−88.06,−87.31	38
21	$[(C_6H_4O_2)_2SiPh]^-[NEt_3H]^+$	−87.53	38
22	$[(C_6H_4O_2)_2SiPh]^-[K(18\text{-c-}6)]^+$	−87.51	38
23	$[(2,3\text{-}C_{10}H_6O_2)_2SiPh]^-[NBu_4]^+$	−87.14	38
24	$[(2,3\text{-}C_{10}H_6O_2)_2SiPh]^-[NEt_3H]^+$	−87.11	38
25	$[(4\text{-}t\text{-Bu}{-}C_6H_3O_2)_2SiPh]^-[K(18\text{-c-}6)]^+$	−87.07	38
26	$[(Br_4{-}C_6O_2)_2SiPh]^-[K(18\text{-c-}6)]^+$	−86.03	38
27	$[(4\text{-CHO}{-}C_6H_3O_2)_2SiPh]^-[K(18\text{-c-}6)]^+$	−85.12	38
28	$[(3\text{-CHO}{-}C_6H_3O_2)_2SiPh]^-[K(18\text{-c-}6)]^+$	−85.12,−84.90	38
29	$[(4,5\text{-}Cl_2{-}C_6H_2O_2)_2SiPh]^-[K(18\text{-c-}6)]^+$	−84.23	38
30	$[(Cl_4{-}C_6O_2)_2SiPh]^-[K(18\text{-c-}6)]^+$	−83.94	38
31	$[(4\text{-}NO_2{-}C_6H_3O_2)_2SiPh]^-[NEt_3H]^+$	−83.41	38
32	$[(2,3\text{-}C_{10}H_6O_2)_2Si{-}Pr\text{-}n]^-[K(18\text{-c-}6)]^+$	−74.83	38
33	$[(C_6H_4O_2)_2SiEt]^-[K(18\text{-c-}6)]^+$	−74.77	38
34	$[(C_6H_4O_2)_2SiMe]^-[K(18\text{-c-}6)]^+$	−74.32	38
35	$[(2,3\text{-}C_{10}H_6O_2)_2SiEt]^-[K(18\text{-c-}6)]^+$	−74.13	38
36	$[(4\text{-CHO}{-}C_6H_3O_2)_2SiMe]^-[K(18\text{-c-}6)]^+$	−71.45,−71.33	38
37	$[(4\text{-}NO_2{-}C_6H_3O_2)_2SiMe]^-[K(18\text{-c-}6)]^+$	−69.41,−69.25	38
38	$[(4\text{-}NO_2{-}C_6H_3O_2)_2SiEt]^-[K(18\text{-c-}6)]^+$	−68.88,−68.77	38
39	$[(3,5\text{-}(NO_2)_2{-}C_6H_2O_2)_2SiMe]^-[NEt_3H]^+$	−67.19,−65.33	38
40	$[(4,5\text{-}(NO_2)_2{-}C_6H_2O_2)_2SiMe]^-[NEt_3H]^+$	−66.81	38
41	$[(2,3\text{-}C_{10}H_6O_2)_2SiMe]^-[NEt_3H]^+$	−73.68	38
16	$[(1,8\text{-}C_{10}H_6O_2)_2SiPh]^-[K(18\text{-c-}6)]^+$	−132.35	37
42	$[(MeO)_4SiPh]^-[K(18\text{-c-}6)]^+$	−112.4	34
43	$[(EtO)_4SiPh]^-[K(18\text{-c-}6)]^+$	−117.3	34
44	$[(CF_3CH_2O)_4SiPh]^-[K(18\text{-c-}6)]^+$	−120.1	34
45	$[(EtO)_5Si]^-[K(18\text{-c-}6)]^+$	−131.1	34
46	$[(4\text{-Me}{-}C_6H_3O)_4SiPh]^-[K(18\text{-c-}6)]^+$	−129.7	34
47	$[(MeO)_3SiPh_2]^-[K(18\text{-c-}6)]^+$	−100.2	39
48	$[(MeO)_4SiPh]^-[K(18\text{-c-}6)]^+$	−114.1	39
51g	$[(1,2\text{-}C_6H_4C(CF_3)_2O)_2SiCN]^-[NEt_4]^+$	−91.54	41

TABLE 4. Comparison of solution ^{29}Si chemical shifts and percent deviation (TBP → SP) for tetraoxosilicates

Anion	%(TBP → SP)	Compounds (cation)	References	$\delta^{29}Si$ (ppm)	Compounds (Cation)	References
$(C_6H_4O_2)_2SiPh$	29.5	**19** (Me_4N)	42	−87.51	**22** (K,18-c-6)	38
$(C_6H_4O_2)_2SiPh$	59.4	**21** (Et_3NH)	43	−87.10	**21** (Et_3NH)	40
$(C_6Cl_4O_2)_2SiPh$	89.8	**49** (Et_4N)	44	−83.94	**30** (K,18-c-6)	38
$(2,3\text{-}C_{10}H_6O_2)_2SiPh$	97.6	**50** (C_5H_6N)	45	−87.14	**23** (Bu_4N)	38
$(2,3\text{-}C_{10}H_6O_2)_2SiPh$	97.6	**50** (C_5H_6N)	45	−87.11	**24** (Et_3NH)	38
$(1,8\text{-}C_{10}H_6O_2)_2SiPh$	32.5	**16** (K,18-c-6)	37	−132.35	**16** (K,18-c-6)	37

determined, and the corresponding percent deviations from TBP geometries were reported. These differ substantially among the four, while the δ^{29}Si are nearly equal (for the same or analogous complexes differing only in the counter ion), with a relatively small downfield shift in the octachloro complex **30**. This comparison may indicate that δ^{29}Si does not depend on the geometry of the pentacoordinate complex, or, alternatively, one could assume that the substantially different geometries are characteristic of the solid state, and that in solution all of these complexes have essentially the same geometry around silicon, and hence similar chemical shifts.

Conversely, the spirosilicates **16**[37] and **19**[42] (Table 4), having five- and six-membered chelate rings, respectively, are reported to have essentially the same degree of deviation from TBP toward SP structure in the crystal (32.5 and 29.5%, respectively), while their ^{29}Si chemical shifts (**22** is taken as an analog of **19**) are dramatically different (−132.35 and −87.51 ppm, respectively)[37,38,42]. No explanation has been offered for this difference. The ^{29}Si chemical shift in **16** compares favorably with shifts measured in acyclic oxosilicates, **46** and **43**[34,39] (Table 3). It is tempting to conclude that steric strain has a profound effect on δ^{29}Si: the values measured in the strain-free acyclic compounds are nearly equal to that found in **16**, with six-membered chelate rings, while in **22**, with its five-membered rings, the chemical shift is substantially different. However, this leads to the conclusion that six-membered chelate rings are less strained, and hence more stable, than five-membered rings, a result not entirely consistent with known pentacoordinate silicon chemistry.

The percentage TBP → SP character measured in the solid state shows no correlation with the ligand-exchange barriers measured in solution[35b]. The barriers for interchange of CF_3 groups in compounds **51** decreased linearly with increasing electron-withdrawing power (σ^* substituent constant) of the ligand Y. On the other hand, the distortion from TBP structure (relative to SP) was determined for two of the complexes, **51d** and **51f**[35b]. These data are presented in Table 5. Clearly, the large difference in activation barriers is not reflected in a parallel difference in the ground state structure[35b].

2. Zwitterionic organospirosilicates

A new class of pentacoordinate zwitterionic silicates **(52–70)** has been developed and reported by Tacke and his coworkers[28–31,46–52] (cf Section II.A.3). These are generally high melting crystalline solids, which are almost insoluble in nonpolar organic solvents, and only slightly soluble in polar solvents.

The general method for the preparation of this class of compounds involves exchange of alkoxy groups in a trialkoxy(aminoalkyl)silane with bidentate ligands, such as catechols

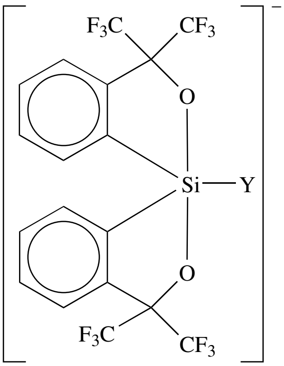

(**51a**) Y = *n*-Bu
(**51b**) Y = PhMeCH
(**51c**) Y = 4-MeOC$_6$H$_4$
(**51d**) Y = F
(**51e**) Y = 3-CF$_3$C$_6$H$_4$
(**51f**) Y = Ph
(**51g**) Y = CN

TABLE 5. Comparison of ligand-exchange barriers with percent (TBP → SP) deviation in the crystal for spirosilicates **51**[35b]

Compound	Y	% (TBP → SP)	$\Delta G^{\ddagger}$ (kcal mol^{-1})
51d	F	23.9	17.5
51f	Ph	27.4	26.0

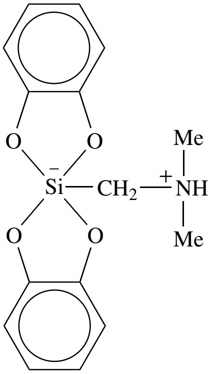

(**52**)[46]

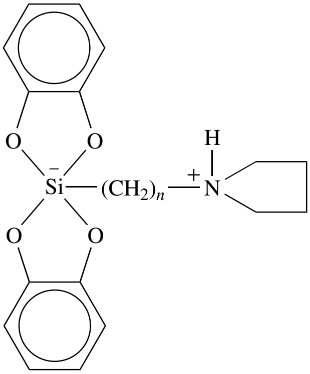

(**53**) $n = 1$[28]
(**54**) $n = 2$[28]
(**55**) $n = 3$[28]

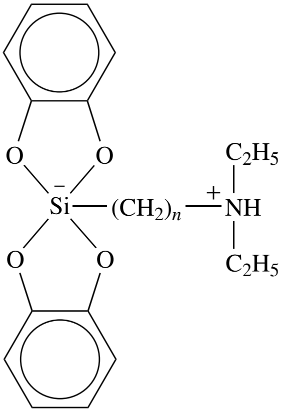

(**56**)[28]

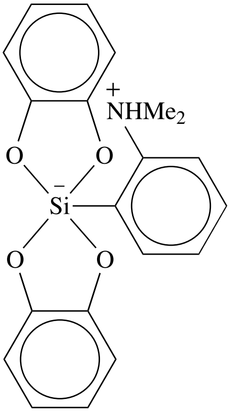

(**57**)[46]

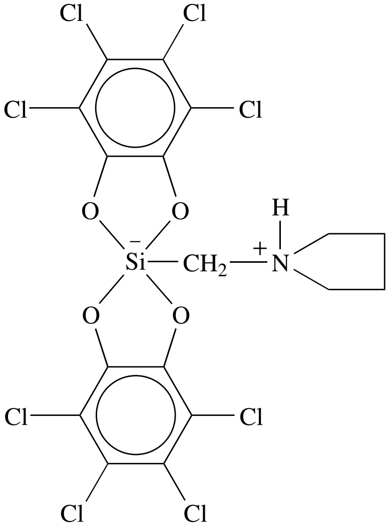

(**58**)[29]

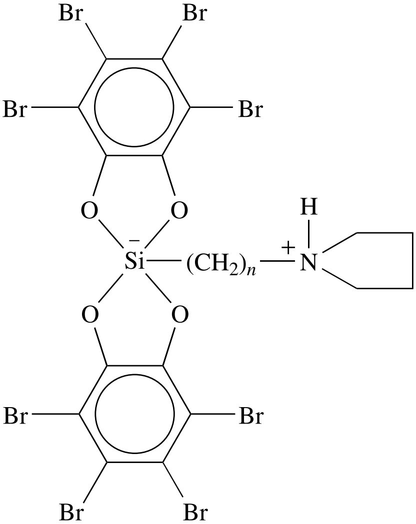

(**59**) $n = 1$[46]

(**60**) $n = 2$[47]

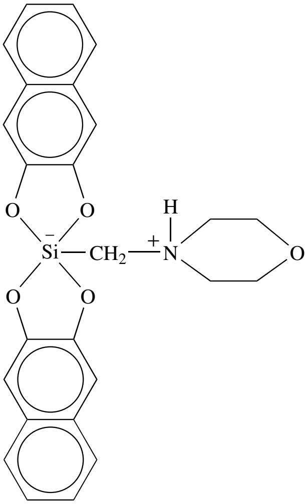

(**61**)[47]

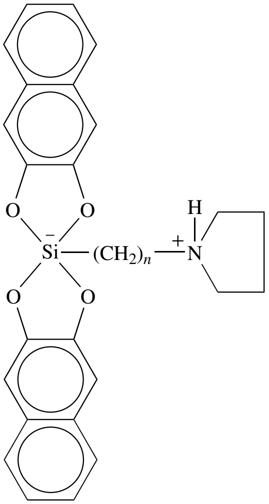

(**62**) $n = 1$[47]

(**63**) $n = 2$[46]

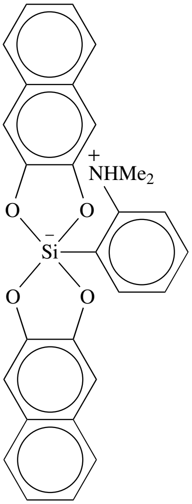

(**64**)[28]

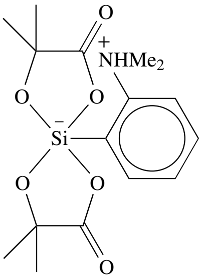

(**65**) R = H[49]

(**66**) R = Me[49]

(**67**) R = Ph[49]

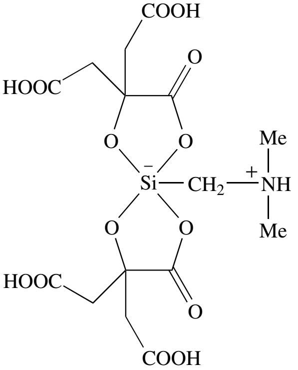

(**68**)[50]

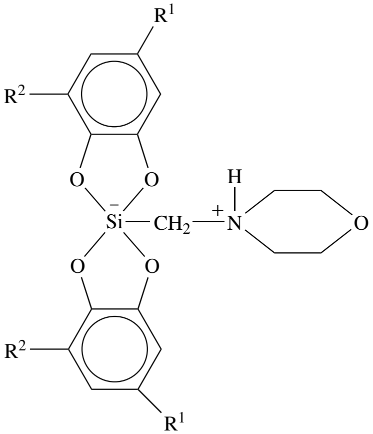

(**69**) $R^1 = NO_2$, $R_2 = H$[51]

(**70**) $R^1 = R^2 = t$-Bu[51]

and similar aromatic diols, as well as glycolic acid and its derivatives, as shown, for example, in equation 14.

Another synthesis, which is less general but of great interset, is the cleavage of Si−C bonds and displacement of alkyl or aryl groups, in addition to alkoxy groups, from alkyldialkoxy(aminoalkyl)silanes or dialkylalkoxy(aminoalkyl)silanes with appropriate 1,2-diols (equation 15)[46]. The cleavage of Si−C bonds even in silanes with only one alkoxy group attached to silicon, seems to indicate a particular stability of these complexes relative to anionic pentacoordinate spirosilicates. The latter are not formed from analogous silanes which do not contain the amino group, since no Si−C cleavage takes place in the absence of the amino group[28].

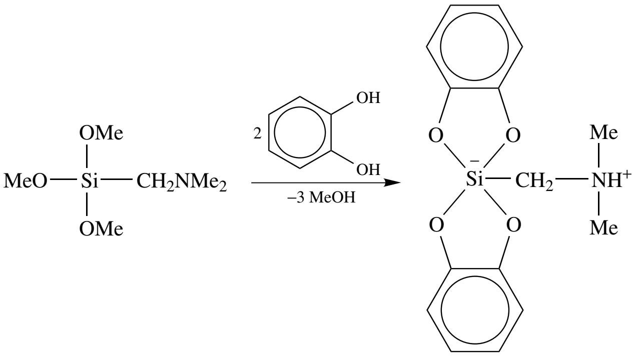

(52)

(14)

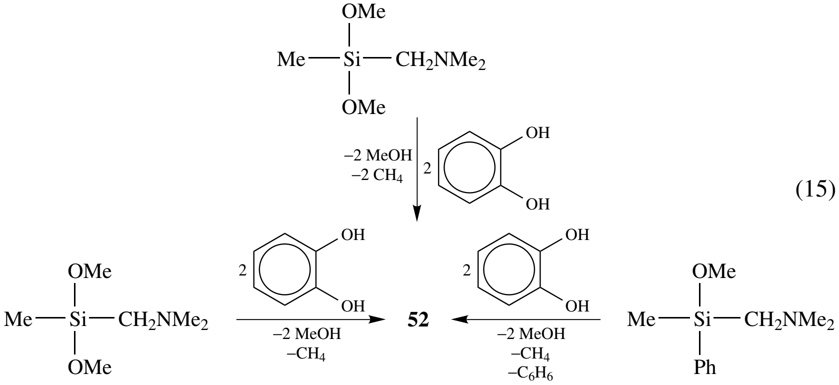

(15)

In contrast to the syntheses described above, leading to zwitterionic complexes based on the (SiO_4C) ligand framework, a direct synthesis of SiO_5-based zwitterions has also been reported: simultaneous reaction of one equivalent of 2-(dimethylamino)ethanol and two equivalents of glycolic acid or 2,2-diphenylglycolic acid with tetramethoxysilane afforded the zwitterionic bis-glycolatosilicates **71** and **72** (equation 16)[30].

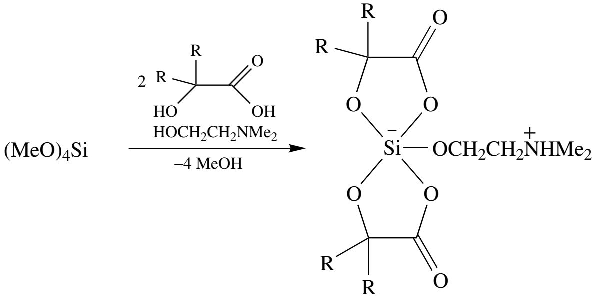

(16)

(**71**) R = H
(**72**) R = Ph

Unusual selectivities have sometimes been observed in the displacement reactions leading to zwitterions: equation 17 shows a case of ‘inverse selectivity’, in which the aminoalkyl group is displaced, rather than the phenyl, leading to an anionic spirosilicate[28].

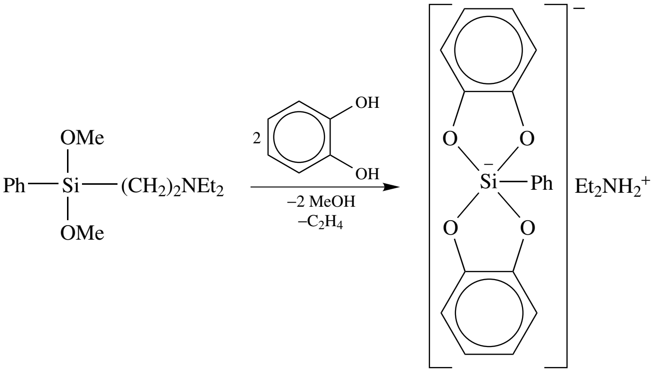

(17)

The preparation of similar zwitterionic silicates based on glycolic acid was also reported by Erchak and coworkers[53,54].

The crystal structures of several members of the zwitterionic complex family were determined. Like in the anionic spirosilicates, the structures were found to vary continuously between TBP and SP, with Si−O bond lengths essentially equal to those in anionic analogs. More than one crystalline modification was found for some of the zwitterions, and even those (even for the same complex!) were substantially different in molecular geometry: for **60** the percent deviation from TBP → SP was calculated to be 34.9% in the monoclinic crystal, 70.0% in the orthorombic, 86.2% in the crystalline hydrate and 96.3% in another crystal form of the monohydrate[46,47]. These results were interpreted in terms of variation in hydrogen bonds in the different crystal modifications. In the hydrates

TABLE 6. Comparison of solid state vs solution ^{29}Si chemical shifts for several zwitterionic complexes

Compound	δ^{29}Si (ppm) CP-MAS	δ^{29}Si (ppm) DMSO	References
59•MeCN	−84.8	−123.0	46
65	−91.8	−94.4	49
66	−103.2	−103.5	49
67	−102.6		49
62•MeCN	−84.9	−87.0	48
68•H_2O	−95.3	−97.3	50
63•MeCN	−81.6	−76.6	46
60a[a]	−73.5	−79.1	47
60b[a]	−79.7		47
60•H_2O	−80.8		47
57	−84.8	−85.9	46
61a[b]	−89.1	−85.3	47
61b[b]	−85.1	−85.3	47
61•MeCN	−85.5	−85.3	47
61•Me_2CO	−85.3	−85.3	47
61•$MeNO_2$	−83.6	−85.3	47

[a] Two solvent free crystallographic modifications of **60**.
[b] Two solvent free crystallographic modifications of **61**.

hydrogen bonding was intermolecular, and in the nonhydrate crystals the hydrogen bonds were intramolecular, between the NH and one of the chelate ring oxygens. The O••H—N and O—H••O distance requirements for hydrogen bonding promote substantial molecular distortions in the solid state. This suggests that the percent deviation from TBP might be a property characteristic of the crystal form, which may not necessarily reflect the molecular structure in solution.

The ^{29}Si CP-MAS solid state NMR spectra of the crystal modifications of **60** and its hydrate were found to depend on the crystal structure, as shown in Table 6. In fact, the chemical shift difference between the pure (anhydrous) crystalline modifications was used to demonstrate the kinetic transformation in the solid state of one crystal structure to the other (Figure 7)[47].

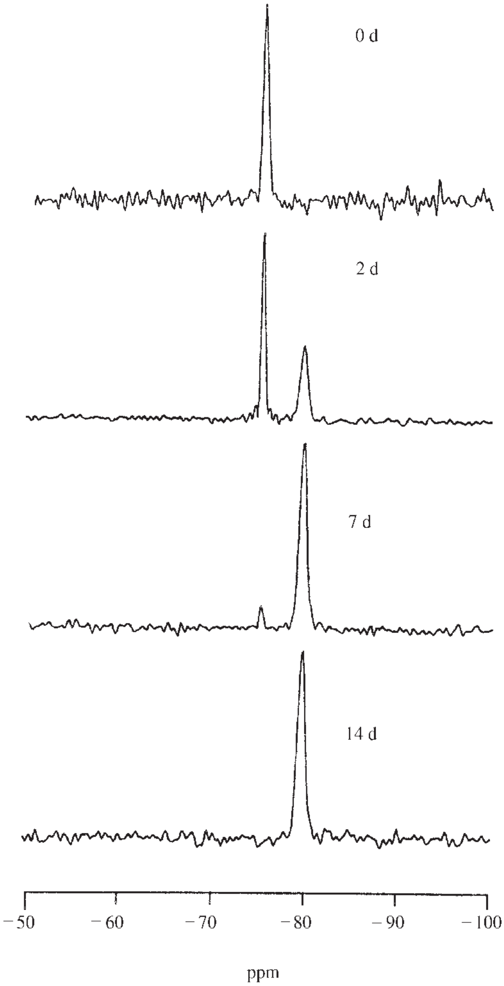

FIGURE 7. CP-MAS ^{29}Si NMR spectra of crystalline **60** at 150 °C showing the transformation of one crystal form to another (d = day). Reproduced from Reference 47 by permission of Hüthig Fachverlage

Table 6 lists comparisons of solid state vs solution ^{29}Si chemical shifts for several other zwitterionic complexes. In general the values obtained in solution agree quite well with those in the solid state, with one notable exception: for **59** dissolved in DMSO-d$_6$ δ^{29}Si is shifted 38.2 ppm upfield relative to the solid state[46].

In the simple symmetrical bis-catecholatosilicates the NMR spectra provided no information on possible exchange phenomena, suggesting that intramolecular ligand exchange, leading to enantiomer interconversion, was rapid on the NMR time scale. Even in cases of unsymmetrical glycolate ligands, such as in **65–67**, the NMR evidence showed a single isomer in solution, indicating fast exchange between the possible isomers[49]. However, when unsymmetrical catecholate ligands were used **(69, 70)**, the NMR at room temperature (in DMSO-d$_6$ solution) showed doubling of the signals as a result of slow exchange of diastereomers, with an activation free energy of 16.7 kcal mol^{-1} for **69** and 17.2 kcal mol^{-1} for **70**[51].

To interpret these dynamic NMR observations, high level *ab initio* SCF-MO calculations were carried out for a model anion, **73**[52]. The ground state geometry was confirmed to be an almost ideal TBP (Figure 8, **a**, C_2 symmetry), with two pathways leading from it to

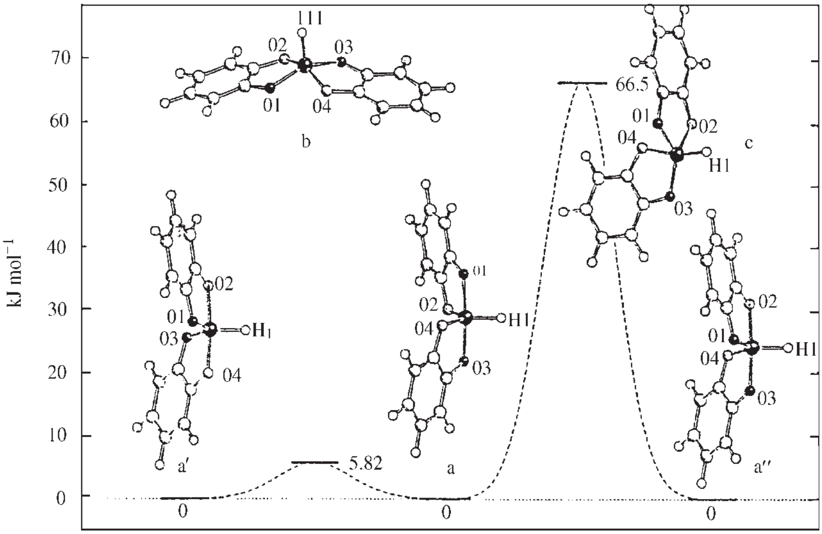

FIGURE 8. Calculated structures (RHF, using an optimized SVP basis set)[52] of **73** and illustration of the different ligand-exchange processes of this anion. **a** = **a**′ = **a**″ = ground state TBP, **b** = SP transition state, **c** = TBP transition state. Reproduced from Reference 52 by permission of VCH Verlagsgesellschaft

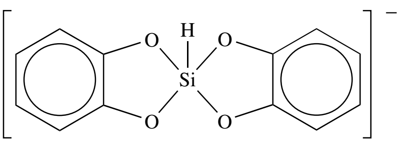

(73)

the diastereomeric TBP geometries, **a**' and **a**" (due to the lack of symmetry of the bidentate ligands). The first exchange mechanism is the Berry pseudorotation using the hydrogen as the pivot atom. This process has a very low activation barrier (1.39 kcal mol^{-1}), and it affects exchange of *both* cyclic ligands such that axial and equatorial positions interchange. Obviously this low barrier is very rapid at the NMR time scale at any temperature studied, and cannot be observed by dynamic NMR. This has also been suggested as the reason for the different geometries observed for various molecules of this family in the solid state: since the potential energy difference between the TBP and SP geometries is so small (the latter being the transition state for pseudorotation, **b** in Figure 8), packing forces associated with the crystallization of each molecule may effect the observed changes.

The second isomerization process in this class of molecules involves two consecutive Berry-type pseudorotations with oxygen as the pivot atoms (Figure 8). This pathway requires a substantially higher activation energy (calculated: 15.9 kcal mol^{-1}), because at the transition state (Figure 8, **c**), one of the bidentate ligands occupies equatorial positions, associated with significant strain. It was therefore concluded that this latter process, which 'rotates' one of the bidentate ligands (i.e. interchanges the equatorial with the axial oxygens for that ligand), is the process actually observed by dynamic NMR spectroscopy[51].

Similar calculations were conducted also for the analogous glycolate complexes, using the hydrido complex **74** as model (Figure 9)[30a]. The calculations confirmed the ground state structure (**I**) established for similar compounds in the solid state. The diastereomeric TBP structures **II** and **III**, as well as the distorted SP structures **IV** and **V**, were calculated

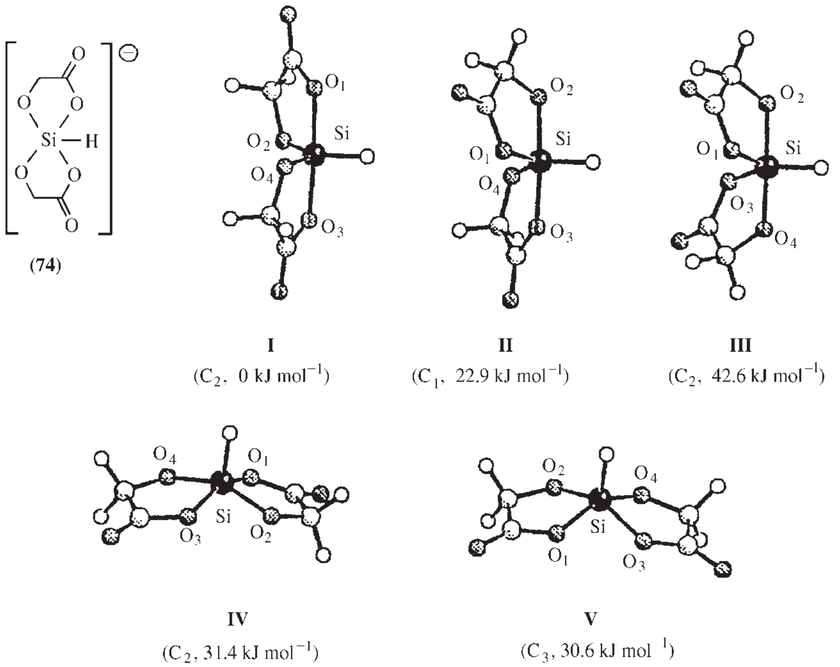

I
(C$_2$, 0 kJ mol^{-1})

II
(C$_1$, 22.9 kJ mol^{-1})

III
(C$_2$, 42.6 kJ mol^{-1})

IV
(C$_2$, 31.4 kJ mol^{-1})

V
(C$_3$, 30.6 kJ mol ^{1})

FIGURE 9. Calculated structures and relative energies (RHF, using an optimized SVP basis set, for the isomers **I**–**V** of the anion **74**. Reproduced from Reference 30a by permission of VCH Verlagsgesellschaft

to be substantially higher in energy than **I**, in agreement with the observation of only one structure in solution, without exchange phenomena[29,49].

Intermolecular ligand exchange has been reported in bis-catecholates as well as in bis-glycolate complexes (equations 18[29] and 19[49], respectively). This was observed after 24 h by the appearance of NMR signals for the mixed complex (**76** and **77** respectively) in the ^{1}H, ^{13}C and ^{29}Si spectra, as well as by FAB MS experiments. A statistical distribution of the three compounds was evident from the 1 : 2 : 1 triplet found in the ^{29}Si spectrum.

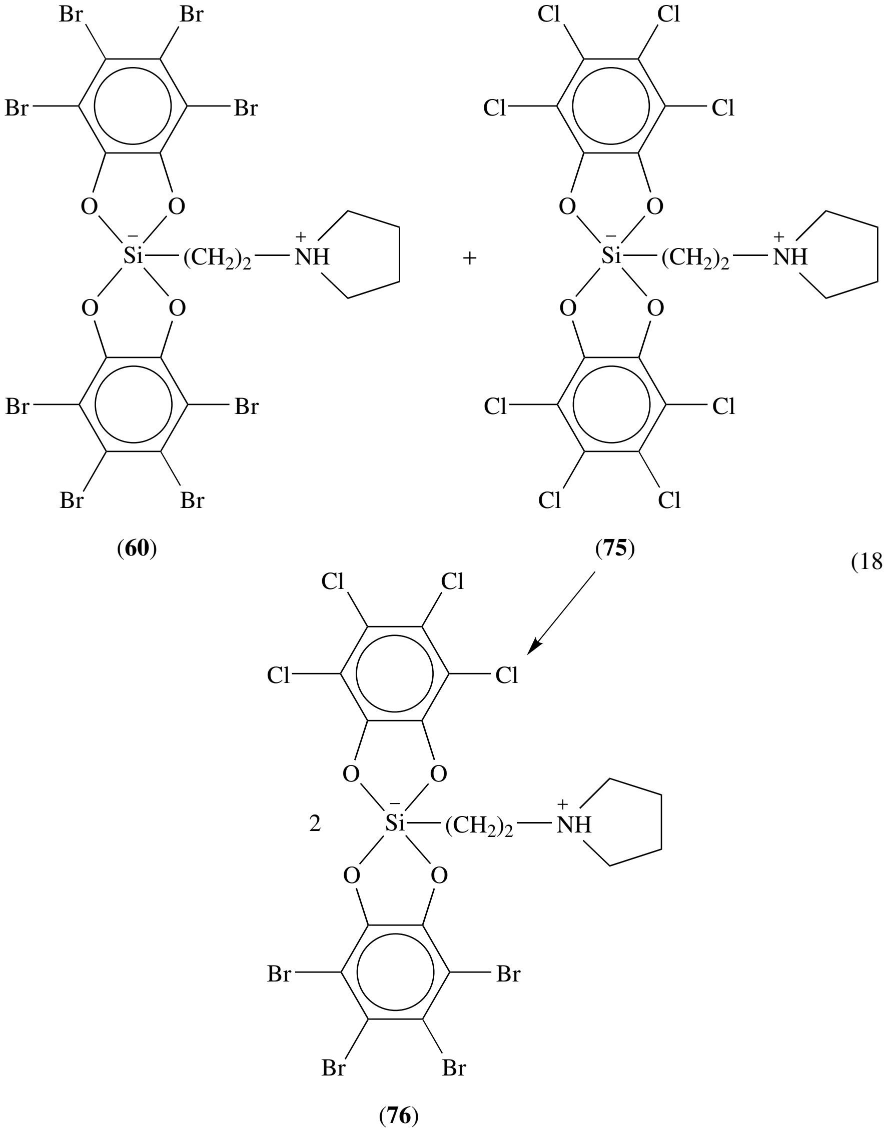

(**60**) (**75**) (18)

(**76**)

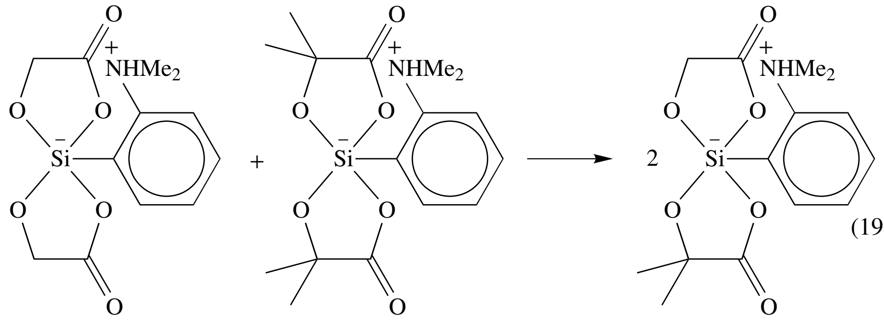

(**65**) (**66**) (**77**)

(19)

3. Polynuclear spirosilicates

A new class of pentacoordinate spirosilicate compounds with two silicon centers connected through a carbon bridge has been reported by several groups[25,55]. The reaction of bridged bis-(trialkoxysilyl)-arylene or -alkylene with catechol in the presence of triethylamine (TEA) yielded arylene- (alkylene) bridged bis(bis-spirocyclic)silicates **78–83**[25] and **84**[55] (equation 20). The crystal structure of **78** was determined, and the geometry was found to conform to a slightly distorted TBP[25].

$(EtO)_3Si—X—Si(OEt)_3$

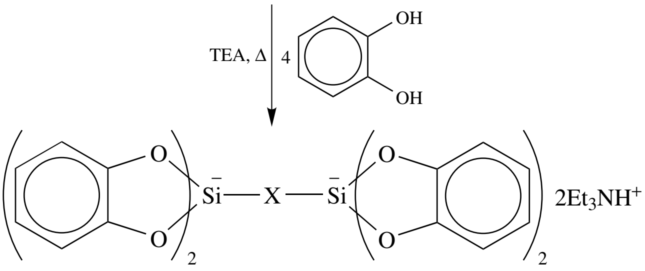

(**78** – **84**)

(20)

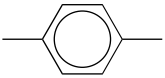

(**78**) X =

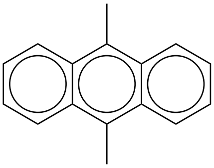

(**81**) X =

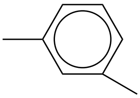

(**79**) X =

(**82**) X = $—(CH_2)_2—$ (**83**) X = $—(CH_2)_6—$

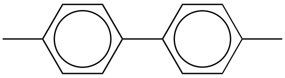

(**80**) X =

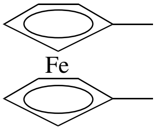

(**84**) X =

A bridged bis-spirosilicate with an ethylenedioxy bridge **(85)** (i.e. based on the SiO_5 ligand framework) was prepared directly from inorganic silica and ethylene glycol in the presence of potassium hydroxide (equation 13)[36].

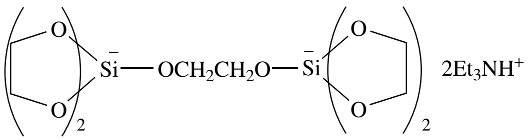

(**85**)

Erchak and coworkers obtained the bridged bis-silicate **86** based on glycolic acid as the spiro-forming chelate. The synthesis is shown in equation 21[56].

$$(EtO)_3SiH + CH_2{=\!=}CHSi(OEt)_3 \longrightarrow (EtO)_3SiCH_2Si(OEt)_3 \xrightarrow[NEt_3]{+2HOCH_2COOH}$$

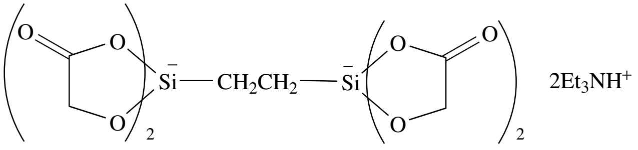

(21)

(86)

Dinuclear zwitterionic spirosilicates were also synthesized and characterized by Tacke and coworkers (equations 22 and 23)[30,57]. These differ from previous dinuclear silicates in that they are bis-zwitterionic. The bridge in **87** is through the covalent bonding of a 1,4-(dimethylene)piperazine, whereas in equation 23 a double bridge is formed by two tetradentate ligand molecules, tartaric acid. The crystal structure of **87** proved that the product was the *meso* compound, with opposite configurations at the silicon centers[57a]. When the reaction in equation 23 was run with optically active (*R*,*R*)-(+)-tartaric acid the first optically active zwitterionic bis-silicate (**88**) was obtained[57b].

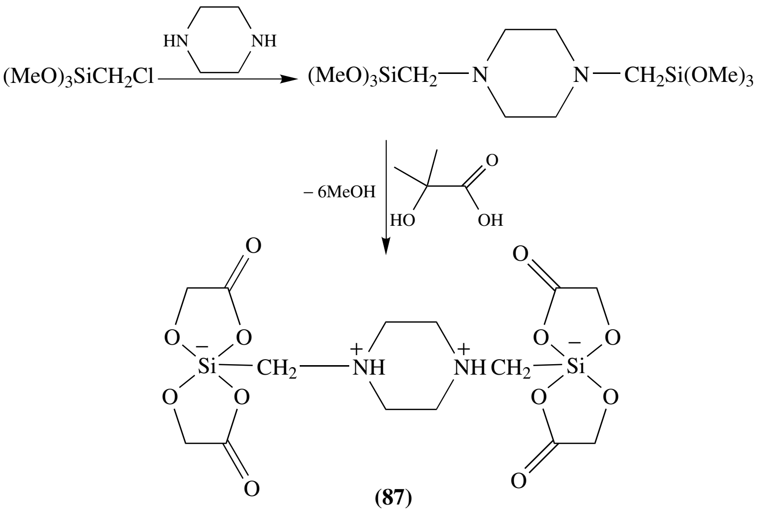

(22)

(87)

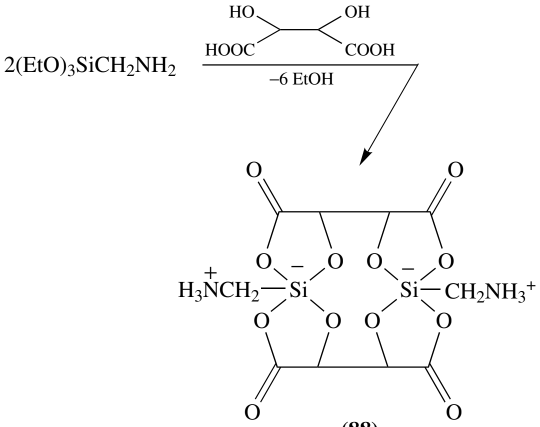

(88)

(23)

The ^{29}Si chemical shifts for dinuclear pentacoordinate silicates have been compiled in Table 7.

The reaction of 1,2,4,5-tetrahydroxybenzene with phenyltriethoxysilane was reported to yield polysiliconates, with pentacoordinate silicon in a spirocyclic arrangement as part of the polymer chain (equation 24)[58a].

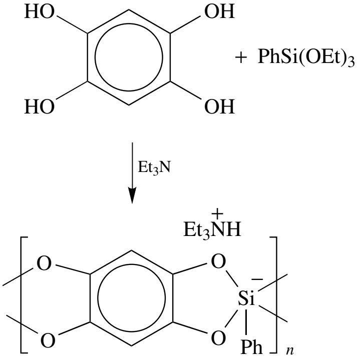

(24)

TABLE 7. ^{29}Si chemical shifts for dinuclear Si,Si′ complexes

Compound	δ^{29}Si (ppm)	References
78	−87.0	25
79	−86.7	25
80	−87.4	25
81	−81.7	25
82	−73.7	25
83	−71.9	25
84	−78.63	55
85	−103.1	36
88	−91.7	58

Similar condensation of phenyltriethoxysilane with a spirocatechol yielded the first macrocyclic tetrasiliconate, a tetraanion containing four pentavalent silicons (equation 24a)[58b]. NMR evidence showed that only one *meso*-stereomer (C_{2h} symmetry) was formed in solution out of the four possible diastereomers. The ^{29}Si chemical shifts of the two unique silicons in DMSO-d$_6$ solution were −86.3 and −86.9 ppm, respectively, consistent with a pentacoordinate silicate anion.

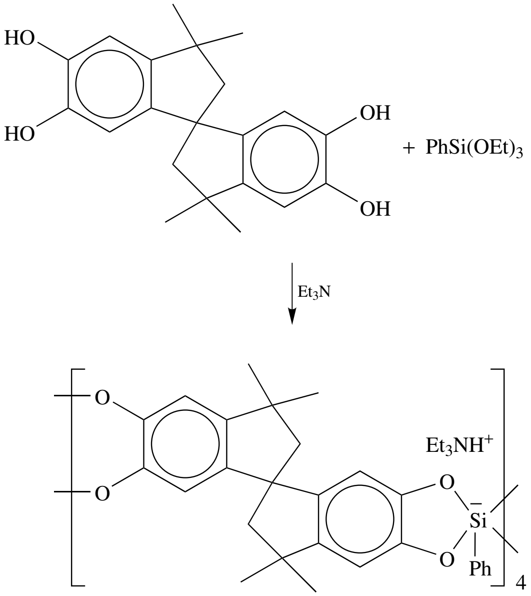

(24a)

C. Hydridosilicates

1. Alkoxyhydridosilicates

Hydrido- and dihydridosilicates have been prepared and studied by Corriu and coworkers[59–62]. The subject was reviewed in 1993[6], and will only be outlined briefly here for completeness.

Hydridosilicates are readily formed by the reaction of trialkoxysilanes with alkali-metal alkoxides[60] (equation 25). The results are best when potassium alkoxides are used.

$$\mathrm{HSi(OR)_3} + \mathrm{ROK} \xrightarrow[\text{room temp.}]{\text{THF or DME}} [\mathrm{HSi(OR)_4}]\mathrm{K}$$

$$\mathrm{R} = \mathrm{Me, Et,}\ n\text{-Bu},\ i\text{-Pr, Ph} \qquad (25)$$

When trialkoxysilanes are reacted with alkali metal hydrides, mixtures of mono- and dihydrosilicates are obtained (equation 25a)[59,61]. The results of this reaction depend strongly upon several factors: the size of the alkoxy group, the solvent, and in particular whether the hydride is used in the presence of 18-crown-6 or not (Table 8). The Table shows that as the bulk of the alkoxy group increases, the ratio of monohydrido to dihydrido products increases. Use of 18-crown-6 makes the reaction less selective, in the sense that both products are obtained, while without the crown ether quantitative yields of the monohydrido complexes are obtained (for the same alkoxy group).

$$HSi(OR)_3 \xrightarrow{KH} K[H_2Si(OR)_3] + K[HSi(OR)_4] \qquad (25a)$$

^{29}Si chemical shifts in anionic mono- and dihydrosilicates move to higher fields, relative to the analogous hydridosilanes, as is expected for pentacoordinate silicates. Also, the one-bond coupling constant $^1J(^1H-^{29}Si)$ is reduced relative to the precursor hydrosilanes, as is expected due to the decrease in the s-character at the Si−H bond[59]. The ^{29}Si chemical shifts and $^1J(^1H-^{29}Si)$ for some of the hydrido and dihydrido silicates are collected in Table 9. Results which disagree with those mentioned above concerning $^1J(^1H-^{29}Si)$ were communicated recently: for some pentacoordinate complexes the one-bond coupling constant $^1J(^1H-^{29}Si)$ *increased* relative to the precursor tetracoordinate silane: thus, for $MeHSi(OTf)_2$, $^1J(^1H-^{29}Si) = 306$ Hz, while for the silicate anion $MeHSi(OTf)_3^-$, $^1J(^1H-^{29}Si) = 351$ Hz[63].

The ^{29}Si and ^{1}H chemical shifts of the dihydridosilicates indicate some dynamic behavior[61]. For the silicates $K[H_2Si(OR)_3]$ with less bulky alkoxy groups (methoxy, ethoxy) the ^{29}Si signal was a triplet, proving the equivalence of the two hydrogens. This might be the result of either of two reasons: fast exchange between hydrido groups, or the occupation of equivalent, equatorial positions by both hydrogens. In the more bulky alkoxides, R = *i*-propyl and *s*-butyl, in benzene-d$_6$ or toluene-d$_8$ solutions, the Si signal appeared as a doublet of doublets, as a result of the anisochrony (i.e. chemical shift nonequivalence) of the hydrido groups [$J(Si-H_1)$ = 222–227 Hz, $J(Si-H_2)$ = 192–195 Hz, hydride exchange barrier at 363 K for the dihydrido–triisopropoxy complex in toluene-d$_8$: 16.3 kcal mol^{-1}]. In solutions of the more strongly solvating THF or DME, as well as in the presence of 18-crown-6, the hydrogens became equivalent

TABLE 8. Effect of reaction conditions on product distribution (equation 25)[61].

Run	$HSi(OR)_3$	Solvent	Reaction time (h)	% $K[H_2Si(OR)_3]$	% $K[HSi(OR)_4]$
1	$HSi(OMe)_3$	THF	2	0	100
2	$HSi(OEt)_3$	THF	6	40	60
3	$HSi(OEt)_3$	THF	24	0	100
4	$HSi(OEt)_3$	THF (18-c-6)	26	55	45
5	$HSi(OEt)_3$	DME	2	0	100
6	$HSi(OBu\text{-}n)_3$	THF	4	50	50
7	$HSi(OPr\text{-}i)_3$	THF	6	100	0
8	$HSi(OPh)_3$	THF	2	0	100
9	$HSi(OPh)_3$	THF (18-c-6)	2	15	85

TABLE 9. ^{29}Si NMR data for $HSi(OR)_3$ and related hydridosilicates[60]

R	$HSi(OR)_3$		$[HSi(OR)_4]K$		$[H_2Si(OR)_3]K$	
	δ (ppm)	J_{Si-H} (Hz)	δ (ppm)	J_{Si-H} (Hz)	δ (ppm)	J_{Si-H} (Hz)
Me	−62.6	290	−82.5	223		
Et	−59.6	285	−86.2	218	−81.8	218
n-Bu	−59.2	286	−86.1	219	−80.8	215
i-Pr	−63.4	285	−90.5	215	−87.1	213
Ph	−71.3	320	−112.6	296		
s-Bu	−62.6	282			−85.6	222, 194

in the *i*-propoxy silicate. These observations were interpreted as follows: (a) the rate of exchange between hydrido groups decreases with increasing steric bulk of the alkoxy group; (b) the rate also depends on the metal–ion complexation by the solvent and, in poorly solvating solvents, the K^+ is solvated by coordination to the three alkoxy oxygens, forcing one hydrido group to an axial position as depicted in **89**. The results suggest an interplay between the tendency of electronegative ligands to occupy axial positions in TBP complexes, against the steric bulk which dictates a preference for the equatorial position. The available results do not conclusively distinguish between a kinetic or thermodynamic effect in this series of dihydridosilicates: the effect of solvent and steric bulk may either be on the rate of exchange, or alternatively on the equilibrium distribution between equatorial and axial positions.

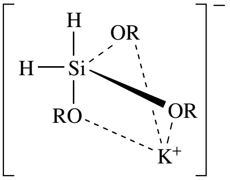

(89)

2. Gas-phase chemistry of hydridosilicates

The formation and properties of alkylhydridosilicates in the gas phase under conditions of flowing afterglow were reported by several authors[64,65] and were recently reviewed[66,67]. Some aspects of this topic are discussed below.

Direct addition of H^- and other nucleophilic anions to primary, secondary and tertiary alkylsilanes formed pentacoordinate silicate anions (equation 26). Interestingly, the parent silicate, SiH_5^-, could not be prepared in this way from silane and hydride[65,68]. SiH_5^- was prepared from alkylhydridosilicates by a hydride transfer reaction (equation 27). The reducing activity of alkylhydridosilicates toward various substrates via hydride transfer in the gas phase was discussed in detail in a previous review[67].

$$RSiH_3 + H^- \longrightarrow RSiH_4^- \tag{26}$$

$$R = n\text{-pentyl}, n\text{-Bu}, \text{Et}$$

$$RSiH_4^- + SiH_4 \longrightarrow SiH_5^- + RSiH_3 \tag{27}$$

Fluxional behavior was demonstrated for pentacoordinate alkylhydridosilicates in the gas phase, by the reaction of deuterium-labeled alkylsilicate with carbon dioxide[65]. The monodeuteriated silicate was first obtained in the flow tube by D^- addition to a neutral alkylsilane, followed by H^-/D^- transfer to CO_2 (equation 28). A statistical distribution of HCO_2^-/DCO_2^- (3 : 1 ratio) indicated complete scrambling of the hydrogens and deuterium in the silicate, presumably by a Berry pseudorotation mechanism.

$$n\text{-}C_5H_{11}SiH_3 \xrightarrow{D^-} n\text{-}C_5H_{11}SiH_3D^- \xrightarrow{CO_2} \underset{(3\,:\,1)}{HCO_2^- + DCO_2^-} \tag{28}$$

3. Computational studies of hydridosilicates

Numerous high-level theoretical computations of the SiH_5^- anion and SiH_5 neutral species have been reported[69–73]. In contrast to the carbon analog, SiH_5^- is a stable ground state structure with respect to decomposition to SiH_4 and H^-. SiH_5^- has a TBP geometry. The binding energy of the hydride to SiH_4 was calculated to be 16–22 kcal mol^{-1}[69,70]. The silicon anion is stable relative to the neutral species, while in the carbon analogs the opposite is calculated to be true[71a]. However, decomposition of SiH_5^- to SiH_3^- and H_2 is exothermic[65], with a substantial activation barrier which suggests that observation of the pentacoordinate anion should be possible under mild conditions. The question of inversion or retention of configuration at silicon in silanes upon nucleophilic displacement via pentacoordinate species was studied carefully by several groups, and was reviewed by Apeloig[74]. The following brief discussion relates only to recent theoretical calculations relevant to hypervalent hydridosilicates.

It was shown at the MP4/6-31++G** level of theory that the TBP $SiH_3F_2^-$ anion is 9.27 kcal mol^{-1} more stable when both fluorine atoms are at axial positions, relative to the species with one axial and one equatorial fluorine[73]. However, it was pointed out that at higher levels of theory the latter structure may not be a stable species, judging from the calculations of Gordon and coworkers on the SiH_4F^- ion, in which the TBP structure with an equatorial fluorine was not a minimum on the potential energy surface[72a].

Gordon and coworkers have conducted a detailed high-level computational analysis of the Berry pseudorotation mechanism in the series of hydridosilicates SiH_nX_{5-n}, where $X = F$, Cl, and compared their results with previous studies[71b–71d]. For the tetrahydridosilicates SiH_4F^- and SiH_4Cl^- they report substantially distorted pseudorotation pathways: the TBP structures with equatorial F or Cl are unstable, and the square-pyramidal structures with basal electronegative substituents, presumed to be transition states for the Berry process, were also unstable. For the more highly substituted silicates of this series the behavior was closer to expectation, based on a Berry pseudorotation model. Their major conclusions are as follows[72b]: (1) The higher the substitution at silicon (smaller n), the more closely the potential energy surface resembles an idealized Berry pseudorotation model. (2) The simple electronegativity model proposed by Willhite and Spialter[72c] is generally supported by the high level calculations. (3) In systems of the type SiX_5^-, the Si−X bond lengths follow the trend: $\text{Si–X}_{\text{axial}} > \text{Si–X}_{\text{apical}} > \text{Si–X}_{\text{basal}} > \text{Si–X}_{\text{equatorial}}$ where the first and last values relate to the TBP and the others to the square-pyramidal structures. (4) The Si−H bonds are consistently longer in the fluoro systems than in the analogous chloro systems. This was attributed to the stronger bonding of F to silicon relative to Cl, causing in turn 'loosening' of the SiH bonds. (5) Most of the structures were found to lie below the X^- dissociation limits.

The possibility of ligand substitution reactions in pentacoordinate silicates $SiH_3F_2^-$ and $SiH_2F_3^-$ via hexacoordinate intermediates was studied by Fujimoto, Arita and Tamao[73]. Attack on each of these silicates by F^- or hydride produced qualitatively similar reaction pathways, leading to stable hexacoordinate intermediates, without significant breaking of the bond between silicon and the leaving group. It was concluded that a nonconcerted displacement mechanism via a hexacoordinate intermediate is likely.

III. PENTACOORDINATE NEUTRAL SILICON COMPLEXES

A. Chelates with Nitrogen–Silicon Coordination

1. Synthesis

The most widely studied compounds possessing N → Si coordination are silatranes, azasilatranes and their analogs[75]. This family of chelates warrants a separate discussion, which can be found elsewhere[75].

Stable N–Si coordinated complexes generally contain a chelate ring with a covalent bond to silicon on one side, and a dative N → Si bond on the other. Only few such bidentate ligand types have been used, and the resulting families of related chelates are depicted in structures **90–100**[76–95].

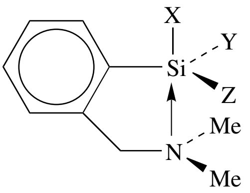

(90a) X = Y = F, Z = Me
(90b) X = Y = H, Z = 1-Naph
(90c) X = Y = Cl, Z = 2-$C_6H_4CH_2NMe_2$
(90d) X = Y = Cl, Z = 2-$C_6H_4CH_2NH^+Me_2$
(90e) X = Cl, Y = H, Z = Me
(90f) X = Y = Z = F
(90g) X = Y = Z = OEt
(90h) X = Me, Y = Z = OEt
(90i) X = Y = Z = Me
(90j) X = Y = Cl, Z = Ph
(90k) X = Y = H, Z = 2-$C_6H_4CH_2NMe_2$
(90l) X = Cl, Y = H, Z = 2-$C_6H_4CH_2NMe_2$
(90m) X = Y = OEt, Z = 2-$C_6H_4CH_2NMe_2$
(90n) X = Y = Z = Cl
(90o) X = Y = Z = H
(90p) X = Y = Cl, Z = 2–$C_6H_4CH_2NMe_2$
(90q) X = Cl, Y = CH$=$CH$_2$, Z = 2-$C_6H_4CH_2NMe_2$

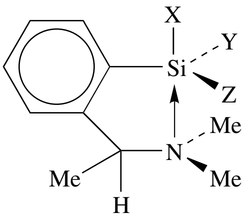

(91a) X = F, Y = Ph, Z = Me
(91b) X = Y = F, Z = Me
(91c) X = Y = Z = F
(91d) X = Y = Z = OEt
(91e) X = Cl, Y = Z = H

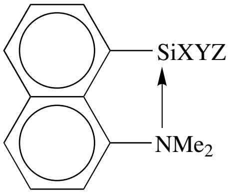

(92a) X = Y = Z = F
(92b) X, Y = $OCMe_2CMe_2O$, Z = H
(92c) X = Ph, Y = Z = H
(92d) X = Ph, Y = Z = OMe
(92e) X = Y = Z = H

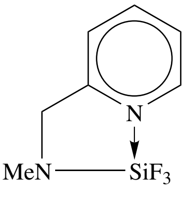

(93)

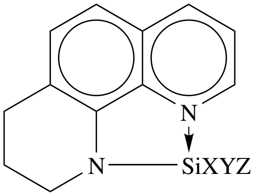

(94a) X = Y = Z = Me
(94b) X = Cl, Y = Z = Me
(94c) X = Y = Cl, Z = Me
(94d) X = Y = Z = Cl

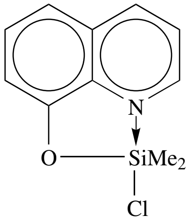

(95)

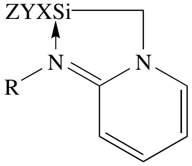

(96a) R = 2-Pyr, X = Cl, Y = Z = Me
(96b) R = 2-Pyr, X = Y = Z = Cl
(96c) R = H, X = Cl, Y = Z = Me

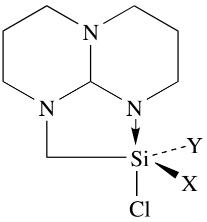

(97a) X = Y = Me
(97b) X = Cl, Y = Me
(97c) X = Y = Cl

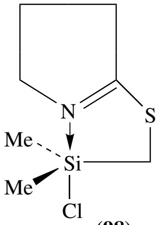

(98)

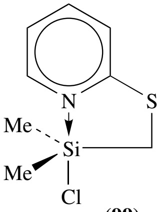

(99)

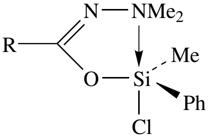

(100a) R = Me
(100b) R = $PhCH_2$
(100c) R = PhMeCH
(100d) R = Ph
(100e) R = 4-MeC_6H_4
(100f) R = 4-$O_2NC_6H_4$
(100g) R = 3,5-$(NO_2)_2C_6H_3$
(100h) R = CF_3

Neutral pentacoordinate N→Si complexes have been prepared by several methods[6]. The most extensively used method consists of reacting a lithio derivative of an aromatic amine with a tetracoordinated functionalized silane (compounds **90–92**)[76–84] such that a new covalent Si–C bond is formed, and the amino group is now in a geometrically favored position to form a chelate ring by coordinating to silicon. The selective metalation by butyllithium is facilitated by the presence of the neighboring amino group, which directs the proton abstraction to a nearby position (*ortho* position in the case of anilines or benzylamine, 8-position in the case of 1-dimethylaminonaphthalene) presumably through interaction with the lithium ion. Sometimes butyllithium is used to remove a proton from nitrogen **(93,94)**[85–87] or oxygen **(95)**[88], in a similar manner, followed by reaction with the polyhalosilane. Several different substituted silane types were reacted with the lithio amines: di- or trihydridosilanes, di-, tri- or tetraalkoxysilanes[76–78] and sometimes also polychlorosilanes[80–82]. The initial complexes can further be transformed to the desired products by substitution with a variety of reagents[76,84]. A selection of the transformations which were used in one particular case is shown in Figure 10. In addition, the alkoxy complexes can be reduced by $LiAlH_4$ back to the corresponding hydrido complexes. Instead of *N*-chlorosuccinimide (NCLS) used in Figure 10, PCl_5 has also been used for the replacement of hydrido by chloro ligands[76]. A variety of transformations leading to differently substituted pentacoordinate complexes has been reported by various groups[76–88].

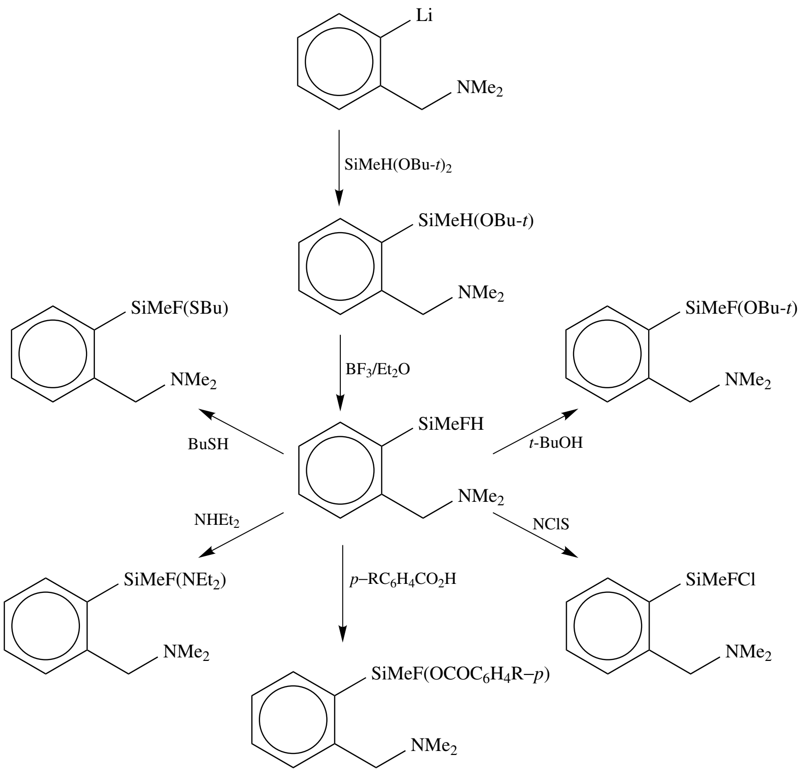

FIGURE 10. Synthetic pathways for some neutral pentacoordinate silicon chelates[76]

A second method for the preparation of neutral pentacoordinate complexes consists of an exchange reaction between chloromethylchlorosilanes (ClCH$_2$SiMe$_n$Cl$_{3-n}$, n = 0–2) and N-trimethylsilylated compounds, as shown for example in equation 29[89]. The compounds of types **96–99** were prepared by this method[89–93]. The same reagent was used extensively for the synthesis of O→Si complexes, and this is discussed in more detail in the corresponding section (III.B.1).

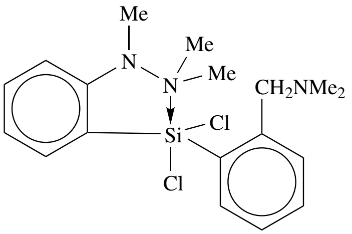

(101)

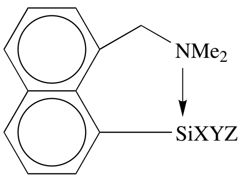

(102a) X = Ph, Y = Me, Z = H
(102b) X = Ph, Y = Z = H
(102c) X = Ph, Y = Z = F

Another route to pentacoordinate N→Si complexes **(100)** consists of the substitution of an O-trimethylsilyl group of O-silylated hydrazides by a halogenated silyl group, capable of coordinating to nitrogen (equation 30)[94,95]. The O-trimethylsilylated precursor molecules are prepared from various hydrazides by reaction with trimethylchlorosilane or other silylation reagents[98].

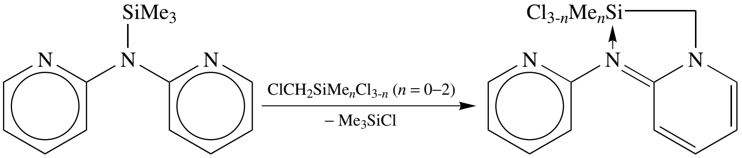

(29)

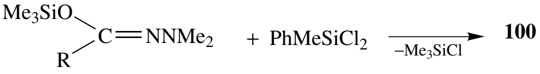

$$\mathrm{Me_3SiO}(\mathrm{R})\mathrm{C{=}NNMe_2} + \mathrm{PhMeSiCl_2} \xrightarrow[-\mathrm{Me_3SiCl}]{} \mathbf{100} \qquad (30)$$

2. Structure

a. Crystallographic data. Numerous X-ray crystallographic structures for pentacoordinate silicon complexes have been reported in recent years. All of the reported complexes had essentially TBP structures, with slight distortions. In Table 10 we have collected some of the crystallographic data pertinent to the TBP structures: the bond lengths of silicon to the two apical ligands and, where available, the displacement (Δ) of the silicon atom from the central plane defined by the three equatorial ligands. Several common structural features can be extracted from Table 10 and from the associated literature, as summarized below:

TABLE 10. X-ray data for (N−Si) chelates.

Compound	X	Y	Z	Si−N (Å)	Si−X (Å)	Δ^a (Å)	References
90a	F	F	Me	2.356	1.627	−0.24	83
90b	H	H	$C_{10}H_7$	2.44	1.47		79
90c	Cl	Cl	$PhCH_2NMe_2$	2.291	2.181		81
90d	Cl	Cl	$PhCH_2N^+HMe_2$	2.163	2.210		81
92a	F	F	F	2.318, 2.287	1.612, 1.612		77
92b	$OCMe_2CMe_2O$		H	2.339	1.678	−0.03	78
92c	Ph	H	H	2.584	1.787		99
93	F	F	F	1.974	1.621		85
94a	Me	Me	Me	2.689	1.897		86
94b	Cl	Me	Me	2.028	2.269	−0.135	87
94c	Cl	Cl	Me	2.027	2.207		87
94d	Cl	Cl	Cl	1.984	2.150		87
96a	Cl	Me	Me	1.898	2.598	0.167	89
96b	Cl	Cl	Cl	1.901	2.238	0.01	89
96c	Cl	Me	Me	1.766, 1.777	3.908, 4.111		90
97	Cl	Me	Me	1.852	2.679	0.166	91
98	Cl	Me	Me	1.945	2.423	0.05	85
100d	Cl	Ph	Me	2.264	2.192		87
101	Cl	Cl	$PhCH_2NMe_2$	2.564	2.118		96
102a	Ph	Me	H	2.660	1.910		99

[a] Deviation of Si atom from equatorial plane toward Cl is negative, toward N is positive.

(1) In general, pentacoordinate silicon complexes have a five-membered chelate cycle. Few exceptions are known with larger (six-membered, **102**)[99] and smaller (four-membered **103**[97a], **104**[97b]) chelate cycles.

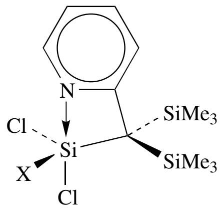

(103)

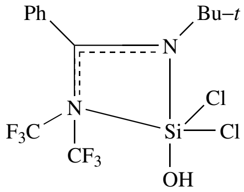

(104)

(2) The dative bond to nitrogen generally occupies an axial position, with one of the electronegative ligands (F, Cl, O, N) in position *trans* to it. If only one electronegative element is attached to silicon, it always occupies the *trans* position to the dative bond. If more than one electronegative ligand is present, the ligand in the apical position relative to the dative bond is determined by the apicophilicity of the ligand, which follows the order: Cl, OCOR $>$ F $\sim$ SR $>$ OR, NR_2 $>$ aryl $>$ alkyl $>$ H[4,77]. The apicophilicity is the aptitude of a ligand to occupy the apical position and support the *trans* coordination[4]. It depends on both the electronegativity of the ligand and the polarizability of its bond to silicon.

(3) An approximate inverse relationship is found between the bond lengths of the opposing axial ligands. For example, the Si−N and Si−Cl axial bonds may be compared in the series of complexes **96c, 96a, 98** and **94b** (Table 10). Along this series the Si−Cl bonds shorten from 3.908 to 2.269 Å, while the coordinative Si−N bonds lengthen from 1.766 to 2.028 Å. This behavior roughly represents a concept of 'constant total bonding' in the two axial bonds to silicon. It agrees well with the hypervalency theory, first developed by Musher[100] and further discussed by Pestunovitch and coworkers[101,102], according to which the axial ligands are bound to the p_z orbital of silicon in a three-center four-electron MO system. This approach is particularly compatible with the observation of a pronounced effect of the two axial ligands on each other and on the overall stability of the hypervalent complex, and the lack of a significant similar effect of the equatorial ligands.

Furthermore, the inverse variation in length of the axial bonds to silicon may be viewed as a representation of different points along a hypothetical reaction coordinate of a bimolecular nucleophilic substitution (S_N2) reaction at silicon[4,6,86,103,104]. The progress along this reaction coordinate is reflected in a decrease in the donor−silicon distance, and a parallel increase in the Si−leaving group distance. Another (related) parameter which may serve as a probe for the progress of the nucleophilic substitution reaction is the Δ value shown in Table 10, which is the deviation of the silicon atom from the central (equatorial) plane. Indeed, examination of the Δ values for **96a, 98** and **94b** (Table 10), which have the same equatorial ligands, shows a variation from positive (0.167 Å) through zero (0.05 Å) to negative (−0.135 Å), respectively, as a function of the change in apical ligand opposite the coordination bond to nitrogen. Thus, depending on the position along the reaction coordinate, the silicon geometry has retained or inverted its initial configuration.

(4) An effect of equatorial substituents on the complex strengths has been noted[87,102]: the more electronegative substituents at equatorial positions tend to shorten the axial bonds. This effect is rather small, but apparently significant. For example, compounds **94b, 94c** and **94d** (Table 10) differ only in the number of equatorial chloro groups (0, 1 and 2, respectively); as a result, *both* of the axial bonds decrease in length: Si−Cl, 2.269, 2.207 and 2.150 Å, respectively, and Si−N, 2.028, 2.027 and 1.984 Å, respectively[87].

The equatorial bonds (in an ideal TBP geometry, when $\Delta = 0$) are orthogonal to the three-center MOs associated with the axial ligands, and bond shortening is presumably caused by inductive charge withdrawal from silicon, and a resulting stronger attraction between the latter and the axial ligands.

(5) In complexes where two nitrogen ligands are available for coordination, the more nucleophilic or stronger base will preferentially coordinate to silicon[96]. In **101** (Table 10), a dimethylamino group and a hydrazino nitrogen compete on the coordination site to silicon. The evidence shows that only the hydrazino group is effectively coordinated. However, if both nitrogens are part of hydrazino groups and hence more nucleophilic (as in the symmetrical **105**), *both* are coordinated to silicon and form a hexacoordinate complex[96]. That this is the result of nucleophilic strengths of the ligands, and not from the symmetry, is evident from the symmetric complex **90c**, in which the ligands are dimethylamino groups, and only one nitrogen is coordinated in the solid state and forms a pentacoordinate chelate[80–82].

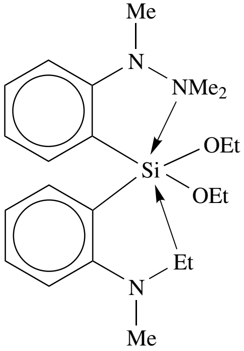

(105)

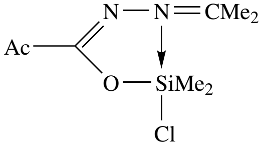

(106)

Another manifestation of the different strength of coordination as a function of the ligand–nitrogen nucleophilicity may be seen in the comparison of complexes **100d** and **106**. Although no crystal structures are available for these compounds, the strength of coordination can be evaluated indirectly by looking at the ^{29}Si chemical shifts: the more upfield shifted silicon resonance represents a more highly coordinated pentacoordinate complex. Indeed, δ^{29}Si was measured for the two complexes, -30.6 and -41.8 ppm, respectively. Thus, the stronger amino base (*iso*-propylidenehydrazide) in **106** coordinates more strongly to silicon than the dimethylhydrazino group in **100d**[105].

(6) Finally, an interesting effect on axial bond lengths was found upon protonation of an adjacent (not coordinated) amino nitrogen[81,82]. Substantial changes in axial bond lengths were observed in **90c** (in the solid state) when the hydrochloride salt was crystallized and its structure determined by X-ray crystallography: the axial Si–Cl distance increased slightly (from 2.18 to 2.22 Å in **90d**), while the dative N–Si bond decreased in length (from 2.29 to 2.16 Å). The interpretation offered by the authors was that protonation of the uncoordinated nitrogen causes some increase in the electronegativity of silicon which, in turn, strengthens the coordination to nitrogen and hence shortens the N→Si bond. Increase of the N→Si coordination is accompanied by a parallel decrease in the Si–Cl bond strength (increasing length), in line with the 'constant total bonding' concept discussed earlier.

b. ^{29}Si NMR spectroscopy. Upon coordination of silanes to form pentacoordinate complexes, substantial upfield shifts of the ^{29}Si resonances in the ^{29}Si NMR spectra are observed. However, only in chelates, in which the overall charge on the molecule does not change upon complexation, can an exact contribution of the coordination to the ^{29}Si chemical shift be evaluated. This is accomplished by taking the difference ($\Delta\delta$) between δ^{29}Si(complex) and δ^{29}Si(silane), where both have the same chemical environment around silicon, except that in the complex an additional coordination to a neutral atom is present. $\Delta\delta$ is commonly referred to as the 'coordinative shift', and serves as a measure for the extent of coordination[79,81,88].

TABLE 11. ^{29}Si chemical shifts (δ) and coordinative chemical shifts ($\Delta\delta$) for (N−Si) chelates at 300 K.

Compound	X	Y	Z	δ^{29}Si (ppm)	$\Delta\delta$ (ppm)	References
90f	F	F	F	−102.27	−29.41	79
90a	Me	F	F	−36.13	−27.55	79
90b	H	H	1-Naph	−47.25	−11.62	79
90g	OEt	OEt	OEt	−57.17	0.59	79
90h	Me	OEt	OEt	−18.19	−0.25	79
90i	Me	Me	Me	−4.89	−0.78	79
90j	Cl	Cl	Ph	−27.5	−33.8	81
90c	Cl	Cl	2-$C_6H_4CH_2NMe_2$	−30.1	−36.4	96
90k	H	H	2-$C_6H_4CH_2NMe_2$	−45.0	−11.2	96
90l	Cl	H	2-$C_6H_4CH_2NMe_2$	−54.2	−48.8	81
90m	OEt	OEt	2-$C_6H_4CH_2NMe_2$	−35.6	−1.1	96
90n	Cl	Cl	Cl	−58.2	−57.4	81
90o	H	H	H	−71.5	−11.7	81
90p	Cl	Cl	$CH{=}CH_2$	−38.7	−42.5	81
90q	Cl	$CH{=}CH_2$	2-$C_6H_4CH_2NMe_2$	−27.7	−22.4	81
92c	Ph	H	H	−44.1	−8.47	79
92a	F	F	F	−96.0		79
92d	Ph	OMe	OMe	−38.16	−10.56	79
102a	H	Me	Ph	−25.84	−6.03	79
102b	H	H	Ph	−55.52	−19.89	79
94a	Me	Me	Me	−1.5		88
94b	Cl	Me	Me	−53.6	−48.2	88
94c	Cl	Cl	Me	−75.9	−70.9	88
94d	Cl	Cl	Cl	−125.2	−71.2	88
95	Cl	Me	Me	−21.0	−35.1	88
96a	Cl	Me	Me	6.4		89
97a	Cl	Me	Me	17.1		91
97b	Cl	Cl	Me	−19.3		91
97c	Cl	Cl	Cl	−81.9		91
100a	Cl	Ph	Me	−30.6		95
101a	Cl	Cl	2-$C_6H_4CH_2NMe_2$	−31.0	−37.1	96
101b	OEt	OEt	2-$C_6H_4CH_2NMe_2$	−42.1	−7.6	96
101c	H	H	2-$C_6H_4CH_2NMe_2$	−43.8	−10.0	96
103	Cl	Cl	Me	−30.9	−15.5	97

Table 11 lists various N$\rightarrow$Si pentacoordinate complexes and their respective ^{29}Si chemical shifts and coordinative shifts. When the latter are near zero, complexation is minimal or nonexistent. Conversely, a large $\Delta\delta$ value represents a substantial effect of coordination, and may be taken to mean a stronger complex. For example, compounds with three alkoxy ligands attached to silicon **(90g)** have very small $\Delta\delta$ values, and are considered barely coordinated. On the other hand, comparison of **90c, 90a, 90b** and **92c** shows a gradual decrease in $\Delta\delta$ (-36.4, -27.6, -11.6 and -8.5 ppm, respectively), with a concomitant increase in coordinative N$\rightarrow$Si distances (2.291, 2.356, 2.44 and 2.584 Å, respectively). Thus, in a qualitative manner the two criteria for coordination strength, dative bond length and coordinative shift, seem to agree.

Another interesting observation in connection with ^{29}Si chemical shifts of chelates is their pronounced temperature dependence[1,83,89,91]. In general, at lower temperatures the ^{29}Si signals are further shifted to high field, suggesting stronger complexation. The upfield shift at low temperatures has been interpreted in two ways: (a) a shift of the equilibrium between tetra- and pentacoordination toward the latter, or (b) a shorter dative bond length, in an essentially pentacoordinated system[106–108]. It appears that the available evidence is insufficient to clearly distinguish between these two options, and the question remains open.

In some cases the changes observed in ^{29}Si chemical shifts upon changing the temperature are *opposite* to those described above. For example, in complex **96a** the ^{29}Si chemical shift at 80 °C is -6.2 ppm, while at -80 °C it is shifted *downfield* to $+18.4$ ppm[89]. This was interpreted by Kummer and coworkers by reference to the equilibrium shown in equation 31: in the general case the equilibrium reaction which responds to changes in temperature is the interconversion I $\rightleftharpoons$ II, in which the coordination number increases as the temperature decreases; in the special case of **96a**, however, the opposite is true: the N$-$Si bond is relatively strong at high temperatures (1.898 Å at RT), and becomes even stronger at low temperature causing ionization of the Si$-$Cl bond and formation of the tetracoordinate species III[89,91]. The change in temperature is associated in this case with the equilibrium II $\rightleftharpoons$ III, and not I $\rightleftharpoons$ II.

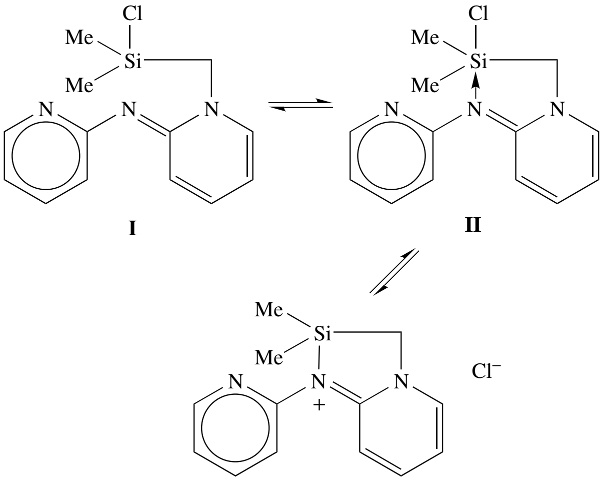

(31)

III

(96a)

Nitrogen-coordinated pentacoordinate complexes have been used as stereoselective reducing agents in the preparation of *erythro*-(*meso*)-1,2-diols from diketones and α-hydroxyketones[109]. The reducing agent was the (1-naphthylamino-8)trihydridosilane **92e**. After formation of the dioxo chelate from the diketone (equation 32), the diol was obtained from the pentacoordinate silicon complex by reduction with $LiAlH_4$. ^{29}Si NMR spectroscopy was used for the product-ratio analysis in this reaction, which was found to yield primarily the *erythro* diols.

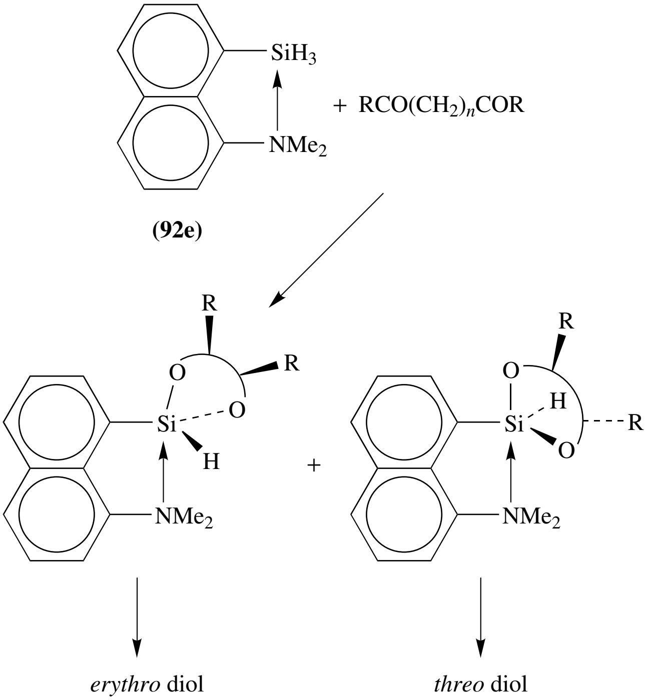
(92e)

(32)

3. Stereodynamics

Ligand exchange phenomena in neutral Si−N complexes differ from those in silicates; not only pseudorotation, as in the latter, but also N−Si cleavage was found to take place in this system[2,5,6,103]. The question of 'regular' (nondissociative) vs 'irregular' (dissociative) mechanism of ligand site exchange was studied extensively[76,77,83]. The two mechanisms can be distinguished by reference to the coordination number: in the 'regular' mechanism the coordination number of silicon remains five throughout the process, i.e. no bond cleavage takes place. In the 'irregular' mechanism the exchange involves reduction in the coordination from five to four at an intermediate stage. This problem was discussed in review articles[5,6].

In many studies the diastereotopic N-methyl groups of a dimethylamino ligand were found to be convenient for monitoring and mechanistic elucidation of the exchange processes[2,5,6,76,77]. However, the stereodynamics of the N-methyl groups alone is insufficient for the exact assignment of the exchange mechanism: for example, in series **92** *both* pseudorotation *and* Si−N cleavage bring about coalescence of the N-methyl groups, and hence the two mechanisms are indistinguishable[77,110]. Coalescence of the silicon ligand signals in these compounds can also lead to mechanistic information, but again it is insufficient by itself. In **92a**, for example, the process rendering the axial fluoro group equivalent to the two equatorial fluorines can be monitored, and should measure the same barrier as the N-methyl coalescence. However, the three fluorines may become equivalent either by Si−N cleavage, followed by rotation about the Si−C and reclosure of the dative bond, or they may equilibrate by pseudorotation.

Exact assignment of either mechanism was possible only by taking advantage of an additional structural feature: (a) If in addition to a chiral silicon atom a second chiral center was present in the molecule (**91a**, or **91b** in which one fluorine is axial and the other equatorial, as well as **100c**). In these cases two diastereomers can be seen in the NMR spectra, in each of which the N-methyl groups are diastereotopic and nonequivalent under conditions of slow exchange[76,95,111]. Two different coalescence phenomena were observed in **91b**, as a result of pseudorotation at silicon and Si−N cleavage[111]. (b) If a chiral neighboring carbon is present, while the ligands at silicon are fluorines or other NMR-active groups and are observed directly, even though silicon may not be chiral. This situation is found, for example, in **91c**: there are no diastereomers in this compound, but pseudorotation can be observed by the equilibration of the axial and equatorial fluoro groups, while Si−N bond cleavage renders the N-methyl groups equivalent[111]. (c) The third structure type allowing, in principle, assignment of pseudorotation and Si−N cleavage is a system containing a chiral silicon and a prochiral group elsewhere, such as in **90e**[76]. Coalescence of the N-methyl groups represents Si−N cleavage, while coalescence of the benzylic methylene protons results from rapid inversion of configuration at the silicon center.

By applying these three methods, Corriu was able to demonstrate the existence of both processes (pseudorotation and Si−N cleavage) in several complexes of type **90–91**, with a chiral or prochiral neighboring carbon[76,77,110,111]. This enabled a discussion of the factors affecting the barriers for Si−N bond cleavage. The barriers ranged between 7.6 (in **91d**) to 16.7 kcal mol^{-1} (in **91e**), as a function of the ligands on silicon, and were taken as measures for the strength of coordination. The following order of ligands was established, corresponding to the relative strength of coordination: Cl, OAc $>$ F, SR $>$ OR, NR$_2$ $>$ aryl $>$ alkyl $>$ H. This order is essentially the same as that of the apicophilicity series[76,77].

Another related effect of ligands on the barrier is due to the number of similar electronegative ligands. In Table 12 are listed the free energy barriers of three complexes differing in the number of fluoro ligands. As expected, the greater total electronegative substitution on silicon effects stronger coordination of nitrogen, and hence results in higher barriers for cleavage of the Si−N coordination bond. This effect parallels the observation discussed earlier (Section III.A.2.a), in which increasing the number of chloro ligands resulted in shorter Si−N distances in the solid state.

TABLE 12. Barriers for pseudorotation and Si−N cleavage in neutral pentacoordinate complexes

Compound	X	Y	Z	$\Delta G^{\ddagger}$ pseudorotation (kcal mol^{-1})	$\Delta G^{\ddagger}$ Si−N cleavage (kcal mol^{-1})	References
91e	F	Me	Ph	$>$17	10	76
91f	F	F	Me	9.4	11.8	77, 111
91g	F	F	F	13.1	15.8	77, 111
100c	Cl	Ph	Me	18.7	11.4	95

The relationship between complex strengths and the silicon–nitrogen cleavage barriers has recently also been reported in another study[95]. Compounds **100a–100h** were prepared from $MePhSiCl_2$ and trimethylsilylated hydrazides according to equation 30, and their barriers for N-methyl exchange were studied by NMR spectroscopy. In order to unambiguously assign the observed barriers to either pseudorotation or Si–N cleavage, **100c**, possessing two chiral centers, at silicon and carbon, was studied. Both barriers for pseudorotation (18.7 kcal mol^{-1}) and Si–N cleavage (11.4 kcal mol^{-1}) were measured for **100c**, by monitoring the coalescence spectra for the N-methyl groups, and the equilibration of diastereomers caused by epimerization at the silicon center: coalescence of the initial four N-methyl signals to two without concomitant coalescence of signal pairs due to the two diastereomers must result from Si–N cleavage. Conversely, coalescence of signal pairs associated with equilibration of diastereomers is a result of epimerization of the silicon center via pseudorotation.

The single activation barriers determined for each of the rest of the series **(100)** were near or below the lower of the two barriers in **100c**, and it was concluded by analogy that all of the barriers represented Si–N cleavage. A linear correlation was found between the Si–N cleavage barriers and the ^{29}Si chemical shifts of the corresponding complexes (Figure 11). The correlation was interpreted as two manifestations of the coordination strength, as a function of the R substituent: the higher Si–N cleavage barriers represent

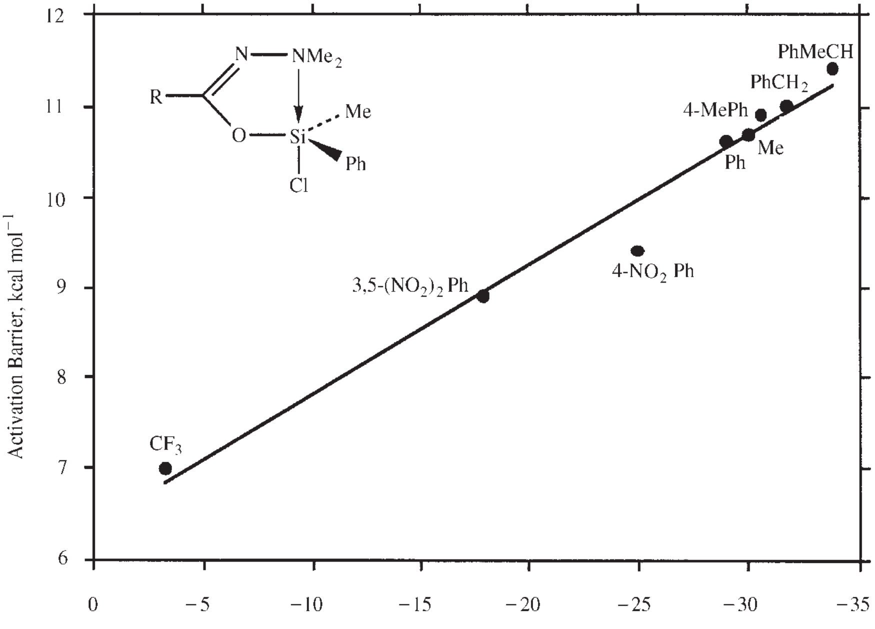

FIGURE 11. Correlation of activation barriers for Si–N cleavage and ^{29}Si chemical shifts (at 300 K) for complexes **100a–100h**[95]

stronger coordination which, in turn, are associated with ^{29}Si chemical shifts more characteristic of pentacoordination, i.e. at higher fields. This conclusion was further supported by a correlation found between ^{29}Si and ^{15}N NMR chemical shifts (taken as 'coordinative shifts': the differences between shifts of penta- and corresponding tetracoordinate silanes, Figure 12)[95].

The parameters affecting the barriers for pseudorotation are more subtle and not completely clear. Corriu has pointed out the existence of two different pseudorotation processes[77]: one which involves only two steps and exchanges between axial and equatorial ligands in $LSiRX_2$-type chelates. The other process is a complete inversion of configuration at silicon, brought about by at least five consecutive pseudorotation steps (Figure 13). This latter process involves a substantially high activation barrier, because it requires that at an intermediate step the chelate be connected in a diequatorial position associated with considerable ring strain (the 90° angle is replaced by 120°). Several barriers of the first type were measured and those ranged (for difluoro or dichloro complexes) between 9 and 12 kcal mol^{-1}[77]. For the trifluoro complex **91c** the barrier was higher, 13.1 kcal mol^{-1}. No explanation was offered for this difference in barriers, despite the conclusion that they represent similar processes: the exchange of axial and equatorial fluorines by the two-step pseudorotation. The barrier for the five-step pseudorotation cannot be measured without a second chiral center(in addition to silicon) in the molecule[76,77].

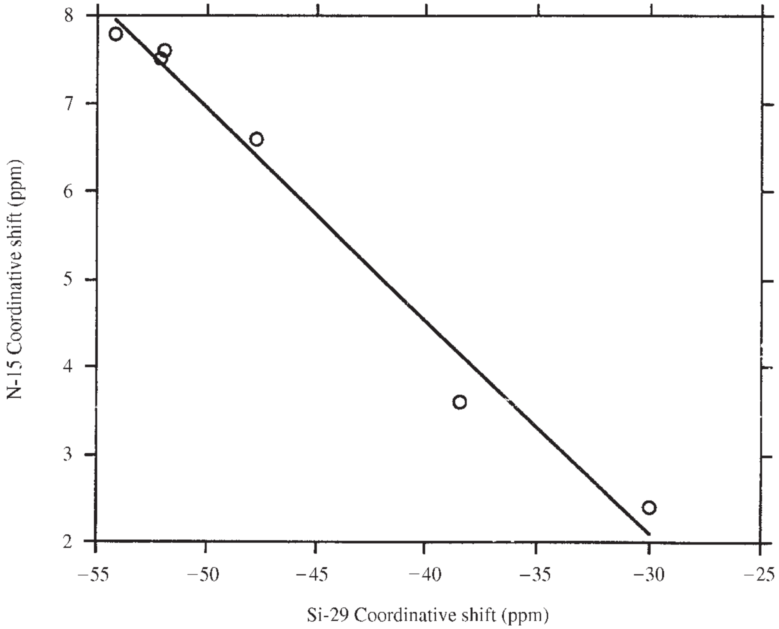

FIGURE 12. ^{15}N NMR coordinative chemical shifts as a function of corresponding ^{29}Si shifts for compounds **100**[95]

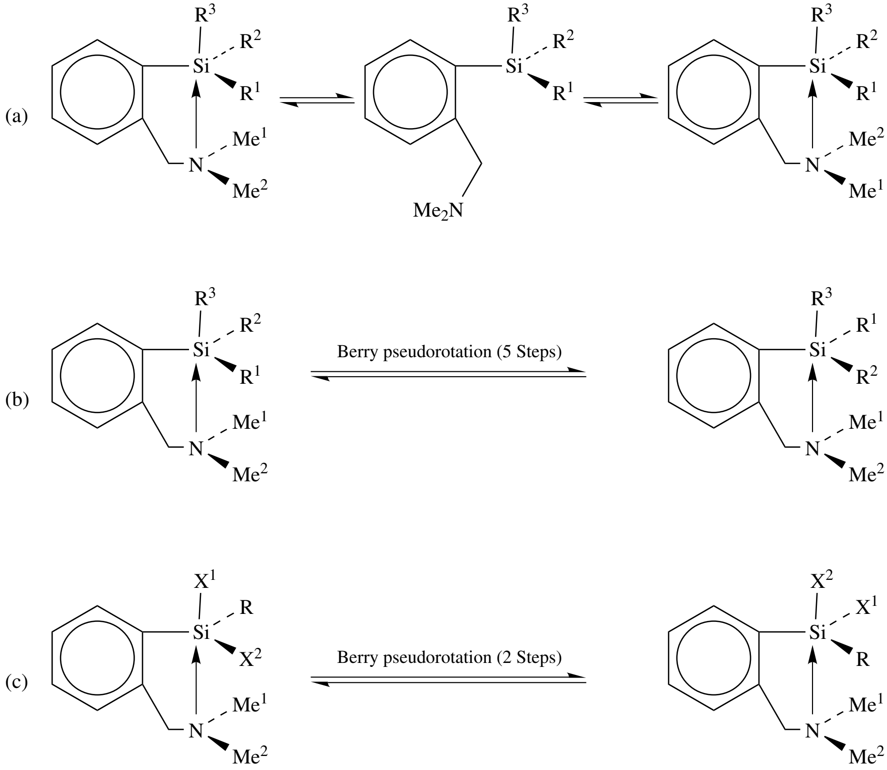

FIGURE 13. Ligand–site exchange mechanisms in **90**: (a) 'irregular' N-methyl exchange via Si–N cleavage; (b) inversion of configuration at silicon through a five-step pseudorotation; (c) exchange of X (fluoro) ligands on silicon without epimerization through a two-step pseudorotation

The barrier for inversion of configuration at silicon was, however, reported recently in a different type of complex, **100c**, in which the chelate cycle is apparently more flexible than in **91a**[76] and allows for the transformation through a 120° angle[95]. The barrier (18.7 kcal mol^{-1}) for pseudorotation (epimerization) was determined from the coalescence of signal pairs of the two diastereomers. Indeed, this barrier is substantially higher than those measured for the two-step pseudorotation, as might have been expected.

An interesting case of ligand exchange through a 'flip-flop' (intramolecular displacement) mechanism was described by Auner and Zybill and coworkers[112,113]. Complex **90c** was shown to be pentacoordinate in the ground state by a crystallographic study (Si–N1 = 2.291 Å while Si–N2 = 4.93 Å)[112], as well as in solution (δ^{29}Si ranged between −30 ppm at room temperature to −54.5 ppm at −70.1 °C)[113]. In solution, the evidence showed equivalence of the two dimethylamino groups and methylene groups, as a result of rapid intramolecular displacement of each other through a hexacoordinate transition state. Two possible transition states of this type could be invoked, **a** and **b** (Figure 14), which *both* have C_2 symmetry and hence retain the configuration at silicon. It was concluded that this process proceeded with retention of configuration at silicon, which caused the two geminal protons in each of the methylene groups to remain diastereotopic.

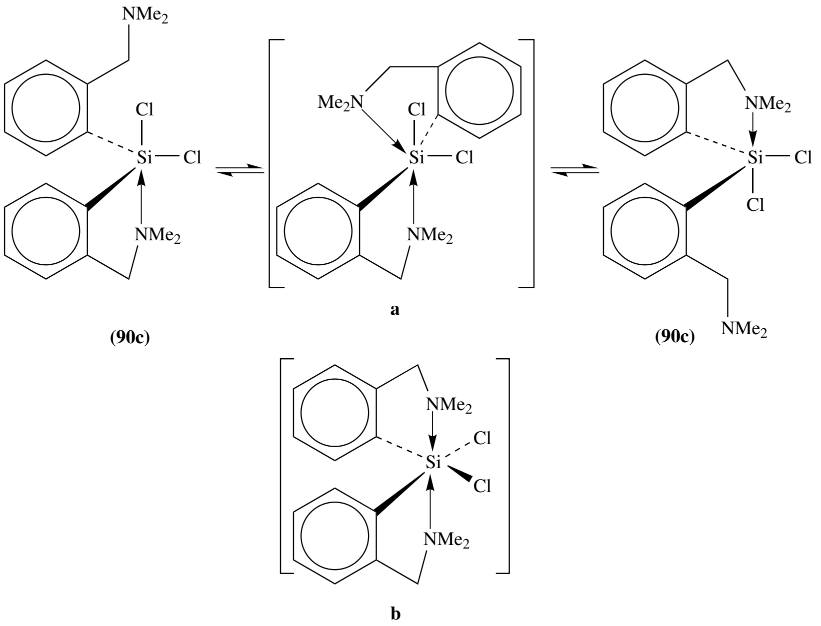

FIGURE 14. Exchange of (dimethylamino)methyl groups in **90c** through hexacoordinate transition states, **a** or **b**[113]

4. Intramolecular Lewis-base-stabilized low-valency silanes

In an attempt to stabilize low-valent silicon compounds, a class of compounds was studied in which N → Si coordination served to stabilize a double bond between silicon and either sulfur[114,115] phosphorus[116], nitrogen[116], oxygen[114,115,117] or a transition metal[113,118–121] (e.g. **107**). In these compounds the silicon is formally pentavalent, though it is coordinated to only four atoms. This topic belongs more appropriately to the chapter on silylenes, and is summarized here briefly for the sake of completeness.

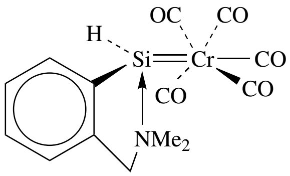

(107)

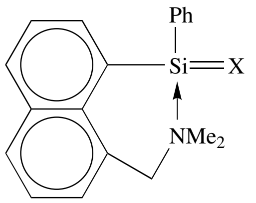

(108) X = O
(109) X = S
(110) X = NBu-*t*
(111) X = PPh
(112) X = $Fe(CO)_4$
(113) X = $Mn(MeCp)(CO)_2$

Intramolecular base-stabilization of low valency silicon compounds was first reported by Corriu's group in 1988[117]. The reaction of a dihydrido chelate **102b** with CO_2 gave the silyl formate which, upon heating, was shown to yield the transient silanone **108** which spontaneously trimerized by opening the Si=O double bonds (equation 33). Subsequently a stable silanethione **(109)** was isolated from the reaction of CS_2 and **102b**, and an analog containing a 1-naphthyl instead of the phenyl substituent was characterized by X-ray crystallography[114]. The Si−N distance was short (1.96 Å, relative to the common 2.3–2.5 Å) indicating very strong coordination. Several analogous silanethiones with different ligands at silicon were prepared[115].

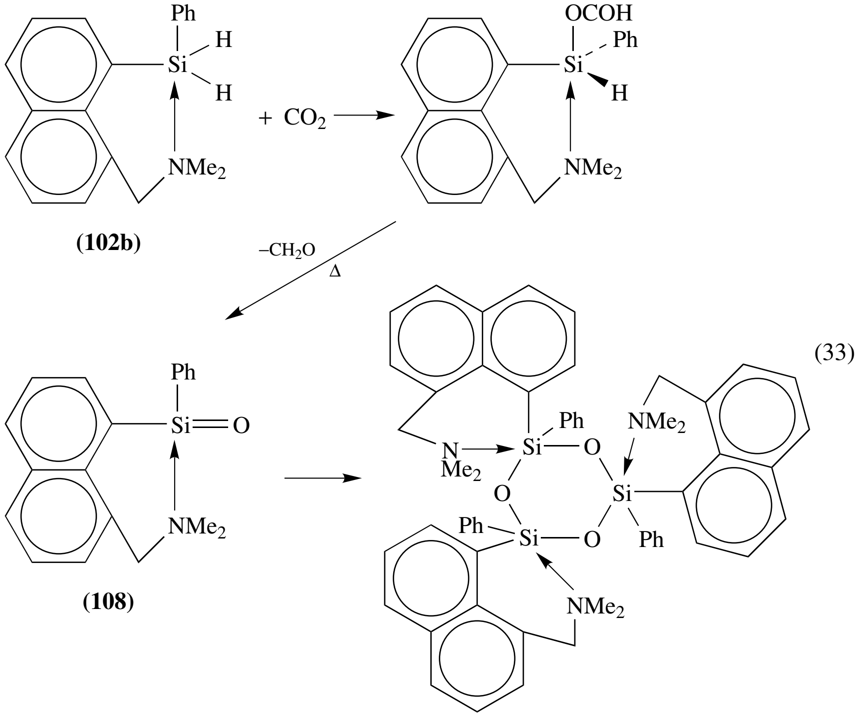

(33)

The reaction of **102c** with the lithium derivative of *t*-butylamine replaced both fluorines and resulted in the silaneimine **110**[116]. A similar reaction with $PhPLi_2$ yielded *syn* and *anti* diastereomers of **111**, observable in the ^{31}P and ^{29}Si NMR spectra[116]. The presence of the stereomers is indicative of a double bond in **111**; however, the ^{29}Si chemical shift (−2.7 and −6.4 ppm for each diastereomer, respectively) is in disagreement with previously reported base free silaphosphenes (150–200 ppm)[122], and suggests that the structure is in fact zwitterionic (with positive charge on nitrogen and negative charge on phosphorus). Likewise, the one-bond couplings ($^1J_{PSi} = 9.2$ in **102c** and 24.1 Hz in **111**) are in very poor agreement with the previously reported large coupling of 130–150 Hz in base free silaphosphenes[122].

Finally, **102b** reacted readily with $Fe(CO)_5$ to yield the remarkably stable **112**, and with cyclopentadienylmanganesetricarbonyl to yield **113** with double bonds between silicon and the metal[116]. Analogous aryl(dimethylaminomethyl)dihydrosilanes reacted with other transition metal carbonyls in the presence of light and yielded analogous doubly bonded, pentavalent silanes[118–120]. Like in **109** (see above), the Si−N distance in transition-metal silicon complexes was relatively short (1.99 Å in **114**[113] and 1.96 Å in an iron complex[120]) indicating substantial coordination and 'Lewis base stabilization' of the double bonds.

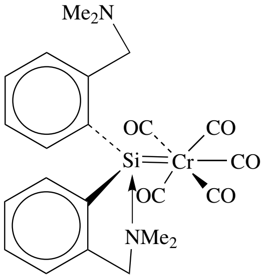

(114)

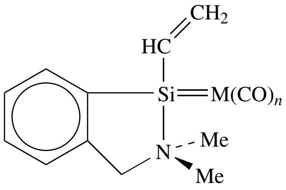

(115a) $M = Fe, n = 4$
(115b) $M = Cr, n = 5$

The analogous complex of chromium **(114)**, obtained from **90c** and $Na_2Cr(CO)_5$, showed a 'flip-flop' intramolecular displacement reaction of the two dimethylamino ligands by each other, like **90c** itself[112,113]. This dynamic exchange was observable by the variable-temperature NMR spectra, which gradually changed from a slow exchange (on the NMR time scale) of dimethylamino groups to fast exchange with no discrimination between the two ligand groups, and finally at 58 °C the benzyl-methylene protons also became equivalent. The ^{29}Si chemical shift changed *downfield* with increasing temperature, an observation which was explained as evidence that coordination of *both* dimethylamino groups was no longer significant[113].

The silicon−metal doubly bonded compounds can further react to yield desired derivatives. Recently, vinyl magnesium bromide was reported to react with chloro complexes containing chromium or iron double bonds to silicon, to yield the 1-metalla-2-sila-1,3-diene compounds (**115**, equation 34), which can potentially be used to functionalize silicon polymers in a desired fashion[121].

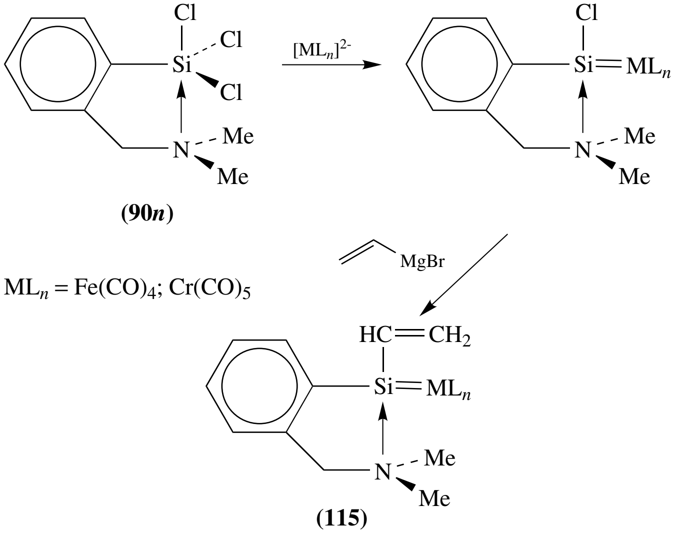

(90*n*)

$ML_n = Fe(CO)_4; Cr(CO)_5$

(115)

(34)

Attempts to stabilize a sila-ylide (hypercoordinated silylene) by intramolecular Lewis-base coordination did not result in sufficiently stable compounds for actual isolation. Formation of the sila-ylide was demonstrated by trapping with 2,3-dimethylbutadiene[123].

B. Chelates with Oxygen–Silicon Coordination

1. Synthesis

a. Amide-type (O—Si) complexes. The reaction of dimethyl(chloromethyl)chlorosilane ($ClCH_2SiMe_2Cl$, **116**) with N- or O-trimethylsilyl-amides[124–127], -lactames[128–130], -ureas[131], -acetylacetamide[132–134], 1,1-dimethyl-2-acylhydrazines[135–137] and 2-oxypyridines[104,138] afforded oxygen–silicon pentacoordinate complexes **117–125**[139].

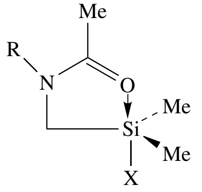

(117a) R = CH_2SiMe_2Cl, X = Cl
(117b) R = Me, X = Cl
(117c) R = Ph, X = Cl
(117d) R = 4-$MeOC_6H_4$, X = Cl
(117e) R = 4-ClC_6H_4, X = Cl
(117f) R = 4-BrC_6H_4, X = Cl
(117g) R = 4-$CF_3C_6H_4$, X = Cl
(117h) R = 4-$NO_2C_6H_4$, X = Cl
(117i) R = CH_2SiMe_2F, X = F
(117j) R = CH_2SiMe_2F, X = Cl

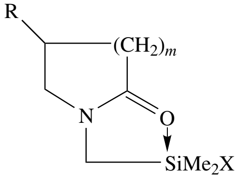

(118a) X = F, m = 1, R = H
(118b) X = Cl, m = 2, R = H
(118c) X = Br, m = 2, R = H
(118d) X = I, m = 2, R = H
(118e) X = Cl, m = 3, R = H
(118f) X = Cl, m = 1, R = Ph
(118g) X = F, m = 2, R = H
(118h) X = OPh, m = 1, R = H
(118i) X = OCOPh, m = 1, R = H
(118j) X = OC_6F_5, m = 3, R = H
(118k) X = OSO_2CF_3, m = 2, R = H
(118l) X = $OCOCF_3$, m = 1, R = Ph

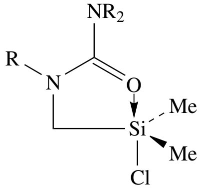

(119) R = Alk

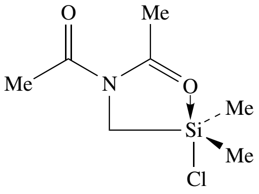

(120a) X = Cl
(120b) X = Br
(120c) X = I
(120d) X = OCOMe
(120e) X = $OCOCF_3$

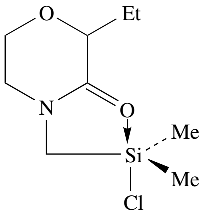

(121)

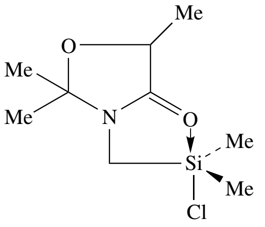

(122)

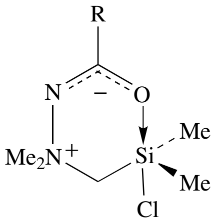

(123a) R = 4-MeOC$_6$H$_4$
(123b) R = CF$_3$
(123c) R = Me
(123d) R = Ph

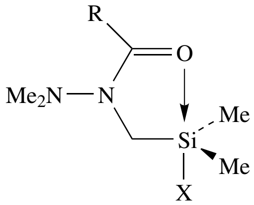

(124a) R = 4-MeOC$_6$H$_4$
(124b) R = CF$_3$
(124c) R = Me
(124d) R = Ph

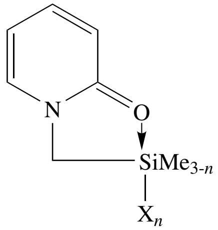

(125a) n = 1, X = Cl
(125b) n = 1, X = Br
(125c) n = 2, X = Cl

The reaction was shown, by NMR monitoring, to proceed in several steps (Figure 15)[140]. Initially, *trans*-silylation takes place resulting in replacement of the Me$_3$Si group by Me$_2$SiCH$_2$Cl **(126)**. This intermediate was identified at low temperature (−60 to −80 °C), but was completely converted at −30 to −20 °C by an internal alkylation to **128**, or by a tautomerization to **127**. Under mild conditions (−20 °C) **128** is the main product obtained by kinetic control. At higher temperatures the final O→Si coordinated complex **(117, 118)** is observed, which may result either from a Chapman-like rearrangement[141] of **128**, or by N-alkylation of the O-silylated intermediate **127**, followed by migration of chloride to silicon.

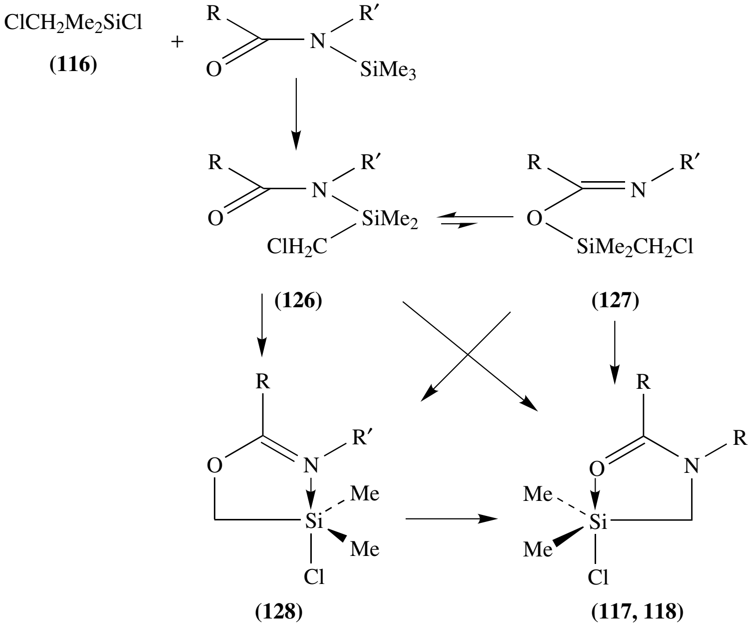

FIGURE 15. Reaction of **116** with trimethylsilylated amides

This reaction pathway appears to be general for a variety of amide-containing complexes; thus, for example, in the case of *N*,*N*-dialkyl-*N′*-(trimethylsilyl)urea the initial chloromethylsilylated intermediate is stable up to 200 °C and is isolated in the reaction together with the final complex **119**[131].

An interesting case of regioselectivity was observed in this synthesis when *O*-trimethylsilyl-1,1-dimethyl-2-acylhydrazines **(129)** reacted with **116**[135–137]. Depending on the stereochemistry at the double bond of **129** (*E* or *Z*), either the six- **(123)** or the five-membered chelate **(124)** was obtained (equations 35 and 36). Both products were stable at ambient temperature. However, heating **123** to its melting point temperature for a short period of time resulted in its irreversible transformation to **124**, in analogy to the Wawsonek rearrangement of ylides[142]. For **124** with R = Ar, CF_3 the only known synthetic route for the five-membered chelate is through this rearrangement.

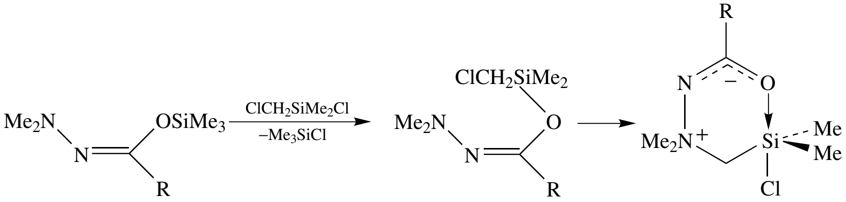

(129–*Z*) **(123)** (35)

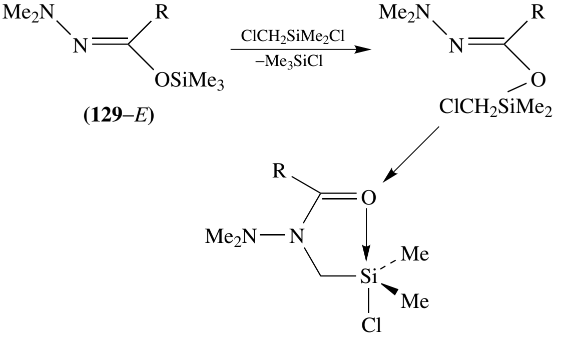

(129–*E*) (36)

(124)

Substitution of the chloro ligand on silicon for other groups X was accomplished (for analogous complexes **117, 118** and **120**) by the appropriate trimethylsilanes, where X = I, Br, F, OCOR, and OR[129,132,139,143]. The fluoro derivative **117i** was also prepared by treatment of the chloro complex **(117a)** with SbF_3[144]. The same substitution was also obtained by direct reaction of trimethylsilylated amides or lactams with the appropriate XCH_2SiMe_2Y[126,127,144].

A single-pot synthesis for complexes **117, 118** consists of reacting amides with a 1 : 3 mixture of hexamethyldisilazane and **116**[145]. It was suggested that this reaction also proceeds in two consecutive steps as in Figure 15, but without the need to isolate intermediate products.

b. Amide-type bis-(O–Si) complexes. The reaction of **116** with *O*,*O′*-bis(trimethylsilyl)-1,2-diacetylhydrazine forms molecules with two (O–Si) chelates having a $ClSi(C)_3O$ coordination framework (equation 37)[146,147]. The reaction proceeds in several steps, which could be monitored by multinuclear NMR spectroscopy. The product obtained spontaneously is the tetravalent silane **130**. However, when heat (80 °C) and excess **116** are applied the major product is the bis-complex **131a**. The latter was converted by methanolysis to the dimethoxy compound **131b**, which upon treatment with BF_3 was converted to the difluoro **(131c)** complex. From the ^{29}Si chemical shifts of these complexes it was concluded that the O→Si coordination decreased in the order **131a** > **131c** > **131b**. Compounds **131** are chiral due to restricted rotation about the N−N bond and a nonplanar ground state conformation. They are the first examples of substances with two (O−Si) chelated pentacoordinate silicon atoms in one molecule[147].

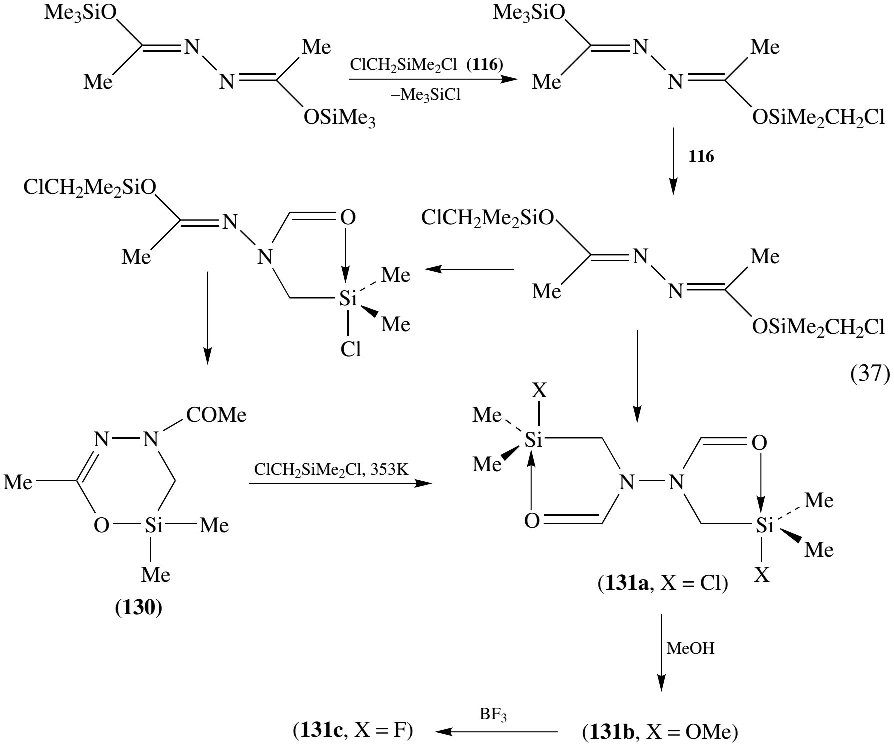

(37)

Bis-(O−Si) chelates containing two amide groups (**132a** and **133**) have also been prepared by similar reactions from **116** and the cyclic diamides **134** and **135**, respectively (equations 38 and 39)[148,149]. **132a** was converted to the ditriflate complex **132b** by trimethylsilyl triflate. Surprisingly, despite the very similar environments near the two silicon atoms in **133**, the ^{29}Si chemical shifts were substantially different, indicating different O → Si coordination strengths.

c. Other (O−Si) complexes. Other than amide-containing (O−Si) complexes, several complexes have been prepared with other oxygen functionalities[150]. These include triamidophosphate **(136)**[151], (aroyloxymethyl)trifluorosilane **(137)**[152] and sulfoxide **(138)**[153]. **136** was prepared by the reaction of **116** with the lithiated derivative of triamidophosphate (equation 40)[151].

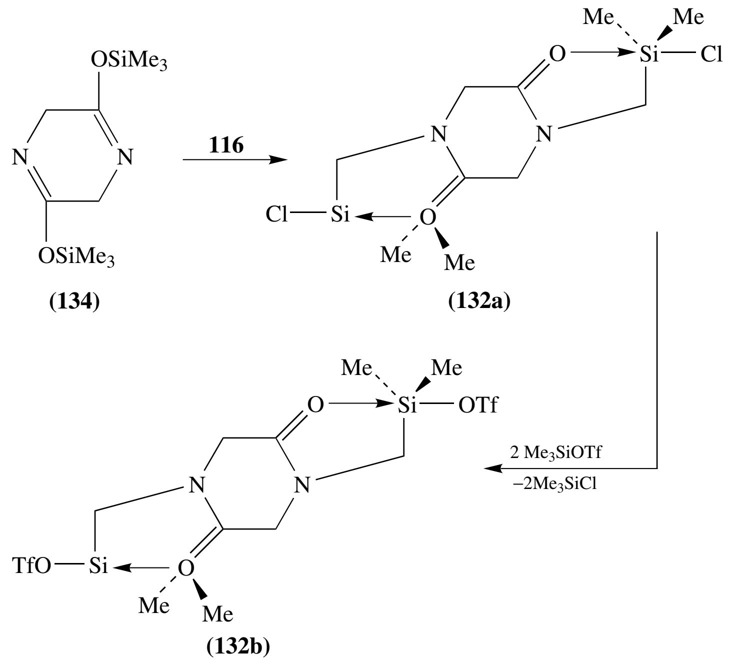

(134) **(132a)**

(132b)

(38)

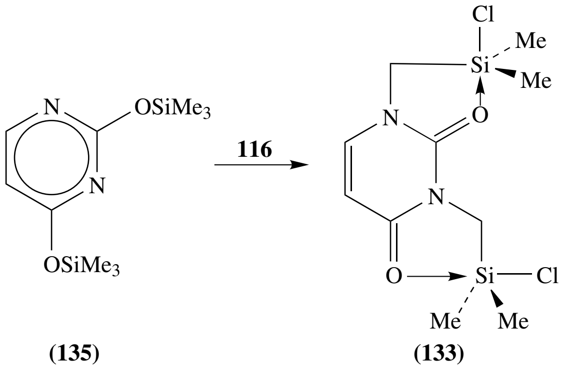

(135) **(133)**

(39)

$$(\mathrm{Et_2N})_2\mathrm{P(O)NHBu}\text{-}t + \mathrm{BuLi} \longrightarrow (\mathrm{Et_2N})_2\mathrm{P(O)N(Li)Bu}\text{-}t$$

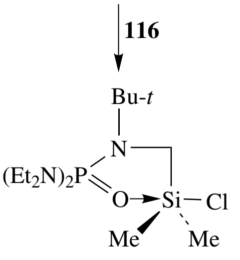

(136)

(40)

The ester-containing **137** were obtained from aroyloxymethyltriethoxysilanes with HF or SF_4 (equation 41)[152].

$$4\text{–}RC_6H_4COOCH_2Si(OR)_3 + HF\ (\text{or } SF_4) \longrightarrow$$

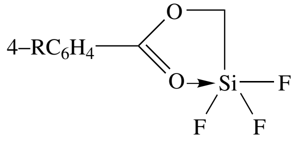

(41)

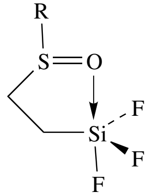

(137a) R = MeO
(137b) R = H
(137c) R = NO_2

(138a) R = Me
(138b) R = Et
(138c) R = $PhCH_2$

The sulfoxide complexes **138a–c** were prepared by oxidation of the corresponding sulfides with hydrogen peroxide[153].

2. *Crystal structures*

The X-ray crystallographic structures of a number of O–Si complexes were described in the literature and reviewed[139,154,155]. In general, all of these complexes have a near TBP geometry. Most of these complexes have a five-membered chelate ring, with one exception, **123**, having a six-membered ring[105,139]. Some of the crystallographic data are collected in Table 13.

Some interesting features emerge from examination of the data in Table 13:

(a) A general phenomenon common to all of the complexes in Table 13 is the observation that shortening of the dative Si–O distance is accompanied by a parallel relative lengthening of the Si–X distance, where X is the apical ligand.

(b) When compounds containing an acyclic amide function **(117)** are compared with those with a lactam ring (**118b**, six-membered lactam) which otherwise have equivalent ligand frameworks at silicon, the effect of the lactam ring is to somewhat increase the Si–O distance, i.e. the coordination is weaker. In the presence of a lactam, the ring size has a small effect on coordination: for the five-membered lactam **118f** the Si–O distance was determined as 2.050 Å. the six- and seven-membered lactam systems have nearly the same Si–O bond length (**118b**, 1.954 and **118e**, 1.950 Å, respectively), significantly shorter than for **118f**. Introduction of an oxygen atom to the lactam ring has a profound effect on coordination: the Si–O distance in **122** is 2.450 Å, compared to 2.050 Å in **118f**.

(c) The Si–O bond length is dramatically effected by the type of halogen in the apical position: for **118a–118d** the respective change of ligand from F to I is accompanied by a large decrease in Si–O bond length from 2.316 to 1.749 Å[156,157]. The last value is essentially that of a covalent Si–O bond. Clearly the strength of coordination is not promoted by the electronegativity of the halogen (although electronegativity formally increases the acceptor properties of silicon) but by the apicophilicity of the element, which follows the opposite order. A similar trend in Si–O distances is found in series **120** (Table 13)[105,139], although they are slightly longer than in the corresponding **118** analogs, presumably because the second carbonyl reduces the nucleophilicity of the lactam oxygen.

TABLE 13. Crystallographic data for (O−Si) chelates

Compound	*m*	X	Si−O (Å)	Si−X (Å)	Δ^a (Å)	References
117a		Cl	1.918	2.348	0.029	124
118a	1	F	2.395	1.652	0.286	156
118b	2	Cl	1.954	2.307	0.058	156
118c	2	Br	1.800	3.122	−0.218	156
118d	2	I	1.749	3.734	−0.348	157
118e	3	Cl	1.950	2.315	0.055	156
118f	1	Cl	2.050	2.284		162
118g	2	F	2.316−2.461	1.630−1.665	0.238−0.305	158
118h	1	OPh	2.367	1.711		159
118i	1	OC(O)Ph	2.228	1.778		159
118j	3	OC_6F_5	2.078	1.787		159
118k	2	OSO_2CF_3	1.753	2.785		159
120a		Cl	2.077	2.229	0.131	160
120b		Br	1.978	2.467	0.052	105, 161
120c		I	1.830	3.03	−0.09	105, 161
122		Cl	2.450, 2.425	2.154, 2.148	0.251, 0.251	162
121		Cl	2.021	2.282	0.082	163
123a		Cl	1.788	2.624	−0.178	164
123b		Cl	1.879	2.432	−0.078	165
124d		Cl	1.975	2.294	0.077	105, 161
131a		Cl	2.142	2.223	0.19	105, 161
136		Cl	1.840	2.438	−0.073	151

[a] Deviation of the silicon atom from the equatorial plane; positive Δ indicates deviation toward X.

(d) When the ligand element in the apical position is oxygen (as in **118h, 118i** in Table 13, in the general complex framework $O-Si(C)_3-O$), the coordination, as represented by the Si−O bond length, is weaker than for Cl, Br or I ligand, in accord with the rules of apicophilicity. When comparison is made between the different oxygen ligands, the dative Si−O distance *decreases* as the electron-withdrawing power of the group attached to oxygen increases **(118h−118j)**, until in **118k**, with the powerful electronegative triflate group, the dative bond is so short that it essentially is a covalent bond, while the triflate group becomes a coordinated anion. The X-ray evidence also shows a similar change in coordination from $O\rightarrow Si-X$ to $O-Si\leftarrow X$ in **118c, 118d** and **120c**, in which the apical ligand is a bromo or iodo group. A similar exchange of the coordinating atom was observed for a chloro ligand in a particular series of chelates, **123**, with a $OSi(C)_3Cl$ framework[164,165]. The Si−O and Si−Cl bond lengths (Table 13) clearly show that oxygen is attached to silicon by a nearly covalent bond, while chloride is coordinated. This obviously is a result of the greater donor ability of oxygen in the zwitterionic six-membered hydrazide ring. A second case of reversal of the coordinating O and Cl ligands is found in **136**[151], from the corresponding Si−O and Si−Cl bond lengths in Table 13.

(e) An important structural parameter in Table 13 is Δ, the deviation of the silicon from the plane defined by the three equatorial ligands. This parameter is closely related to the mutual changes in axial bond lengths discussed above, and has been referred to in connection with a model for the S_N2 reaction coordinate[139,156,161,166,167]. The silicon generally deviates towards the more covalently-bonded ligand, and away from the dative ligand. For similar complexes **(118a–118d)**, in which only the axial halogen is changed, Δ is positive for the F, near zero for $X = Cl$, and negative for Br, I. In terms of the reaction coordinate for substitution at silicon, this means that the former ($X = F$) represents an early step in the reaction, before the tetrahedral silicon configuration has inverted (Figure 16). $X = Cl$ represents a symmetrical, nearly TBP midway state (resembling the transition state for displacement at a central carbon analog) for the reaction. For the heavier halogens the progress of the reaction is more advanced: the oxygen nucleophile has already essentially displaced the halogen, which remains weakly coordinated, and the pyramidal (Walden) inversion of the silicon center is almost complete. This description of the progress along a hypothetical reaction coordinate obtained from a collection of crystal structures follows a Bürgi–Dunitz-type analysis[19,168,169].

From an analysis of the crystal structures of 18 compounds of the type $O{-}Si(C)_3{-}Cl$ the sum of Si–Cl and Si–O bond orders was shown to be roughly constant (ranging between 1.172 and 1.230)[167], while the deviations of the Si–Cl and Si–O distances from the standard tetracoordinate values (Δl_{Si-Cl}, Δl_{Si-O}, respectively) related to each other as a hyperbola (i.e. $\Delta l_{Si-Cl} \bullet \Delta l_{Si-O} = \text{constant}$)[139,167]

3. ^{29}Si NMR

Like in the other types of pentacoordinate complexes, the ^{29}Si NMR signal in O–Si chelates is shifted to high field relative to its tetracoordinate analogs (Tables 14 and 15). Therefore the difference between the ^{29}Si chemical shifts of penta- vs. tetracoordinate silanes (the 'coordinative shift') serves as a measure for the extent of coordination (Table 15). It can be seen from the data in Table 14 that in series **117** the silicon signal is shifted downfield as the electron-withdrawing power of the *para*-substituent on the aromatic ring increases, resulting in weaker coordination[170]. This information can also be seen in the ^{14}N chemical shifts, and to a lesser extent in the carbonyl–^{13}C shifts listed in Table 14. Similar trends in the coordinative ^{29}Si shifts as well as in the carbonyl ^{13}C- and ^{17}O-chemical shifts for complexes of type **118** were reported by Pestunovich and coworkers[139].

It is of interest to compare the variation in the ^{29}Si chemical shifts with the corresponding Si–O dative-bond lengths and associated Si–Cl bond lengths in the solid state in compounds sharing the same coordinative center: $OSi(C)_3Cl$ (Table 16). Clearly all three parameters show similar trends in the series from **131a** to **123b**: high field shielding is associated with shorter Si–O and longer Si–Cl distances. The only exception to the general trend is **123a**, in which Si–O appears to be covalent and chloride coordinated, with a corresponding reversal in the deviation of silicon from the central plane of the TBP ($\Delta < 0$, Table 13, cf Section III.B.2).

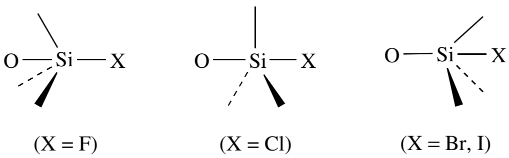

FIGURE 16. Simulated S_N2 reaction coordinate: the variation of Δ as a function of X in **118**

TABLE 14. ^{14}N and ^{29}Si NMR chemical shifts for $MeCONR(CH_2Si(CH_3)_2Cl)$ (**117**)[170]

Compound	R	$\delta^{14}N$ (ppm)	$\delta^{13}\underline{C}O$ (ppm)	$\delta^{29}Si$ (ppm)
117b	Me	−252	173.2	−37.6
117c	Ph	−235	173.8	−34.1
117d	4-$MeOC_6H_4$	−234	173.6	−34.0
117e	4-ClC_6H_4	−245	173.3	−30.7
117f	4-BrC_6H_4	−240	173.2	−31.1
117g	4-$CF_3C_6H_4$	−250	173.2	−29.0
117h	4-$O_2NC_6H_4$	−250	173.0	−26.9

TABLE 15. ^{29}Si chemical shifts (δ) and coordinative shifts ($\Delta\delta$) for (O−Si) chelates

Compound	*m*	R	X	$\delta^{29}Si$ (ppm)	$\Delta\delta$ (ppm)	References
118a	1		F	14.2	−9.4	139
118b	2		Cl	−38.5	−62.2	139
118c	2		Br	−22.6	−40.3	139
118e	3		Cl	−35.0	−59.3	139
118g	2		F	−19.6	−44.4	139
118f	1	Ph	Cl	−5.7	−30.0	139
118l	1	Ph	$OCOCF_3$	−14.3		139
120a			Cl	−24.2	−47.7	133
120b			Br	−29.1	−48.0	133
120c			I	−14.9	−15.6	133
123a		MeOPh	Cl	−17.4	−40.4	137
123b		CF_3	Cl	−42.9	−65.9	137
123c		Me	Cl	−33.5	−56.5	137
123d		Ph	Cl	−20.8	−43.8	137
124a		MeOPh	Cl	−36.3	−59.3	137
124b		CF_3	Cl	11.9	−12.1	137
124c		Me	Cl	−35.9	−58.9	137
124d		Ph	Cl	−34.1	−57.1	137
131a			Cl	−8.8	−31.8	147
131b			MeO	9.1		147
131c			F	4.1		147
133			Cl	−8.9, 13.3		149
137a		MeO	F	−96.3		152
137b		H	F	−94.8		152
137c		NO_2	F	−90.9		152
138a		Me	F	−86.4		153
138b		Et	F	−85.7		153
138c		$PhCH_2$	F	−83.6		153
125a	1		Cl	−39.0		171
125b	1		Br	−19.0		171
125c	2		Cl	−52.4		138
125d	3		Cl	−77.7		138

TABLE 16. ^{29}Si chemical shifts and Si—O, Si—Cl bond lengths in complexes with $OSiC_3Cl$ ligand framework

Compound	δ^{29}Si (ppm)	References	Si—O (Å)	Si—Cl (Å)	References
131a	−8.8	147	2.142	2.223	105,161
120a	−24.2	133	2.077	2.229	160
124d	−34.1	137	1.975	2.294	105,161
118b	−38.5	139	1.954	2.307	156
118e	−35.0	139	1.950	2.315	156
117a	−42.0	138	1.918	2.348	124
123a	−42.9	137	1.879	2.432	165
123b	−17.4	137	1.788	2.624	164

A similar manifestation of the effects of coordination upon chemical shifts, and the sudden changes in trend associated with reversal of the coordinating ligand (and the change of sign of the measured deviation Δ) can be seen in Figure 17. The figure depicts a reasonable linear correlation between the NMR chemical shifts of silicon and the corresponding Si—O dative bond lengths, as obtained from crystallographic data. As long as oxygen is coordinated to silicon (and the deviation Δ of silicon from the equatorial plane is positive) the correlation holds. For those compounds in which Δ is negative, and hence the halogen is the dative ligand, the points are totally off the linear correlation[105].

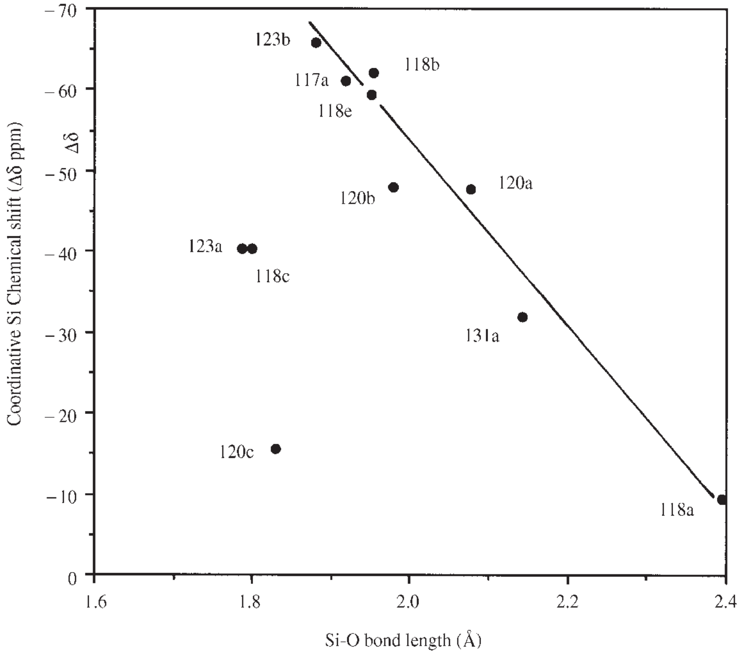

FIGURE 17. Correlation of coordinative ^{29}Si chemical shifts ($\Delta\delta$) for Si—O pentacoordinate chelates with the Si—O dative bond length[105]

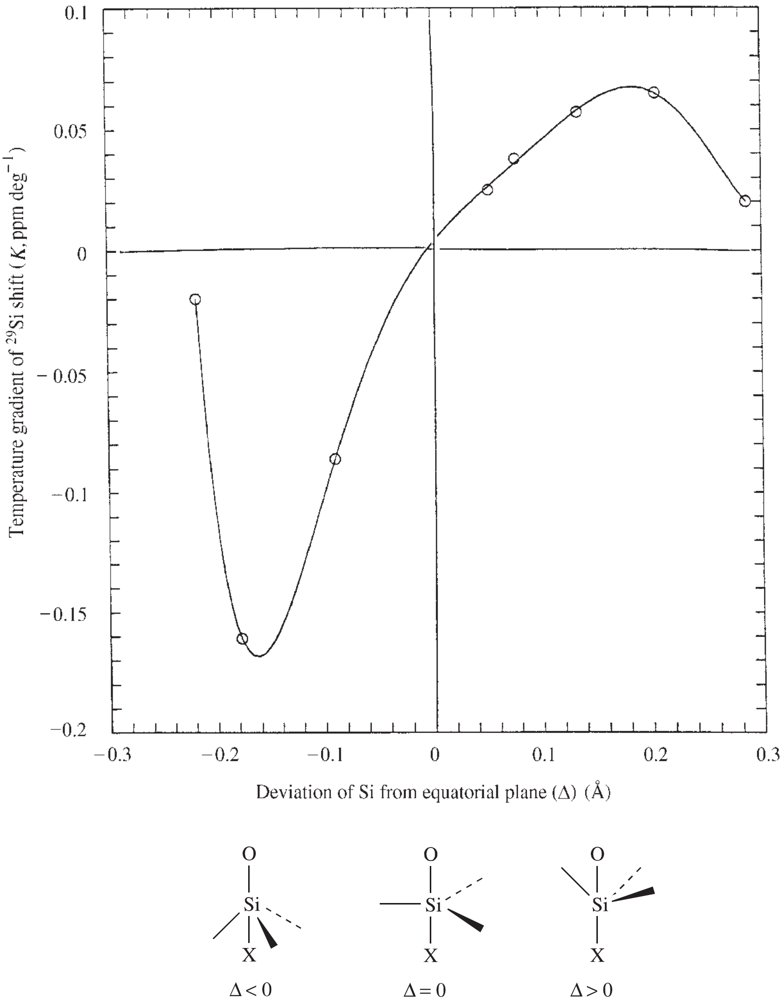

FIGURE 18. The temperature gradient of the ^{29}Si chemical shift in Si—O chelate complexes (in solution) plotted against the deviation (Δ) of silicon from the equatorial plane (in the solid state). The gradient K is expressed as: $K = (\delta^{29}\text{Si}_{T_1} - \delta^{29}\text{Si}_{T_2})/(T_1 - T_2)$

Another criterion for assessing coordination is the temperature dependence of the ^{29}Si chemical shift. In most pentacoordinate complexes the ^{29}Si signal shifts to higher field as the temperature is lowered. This has often been attributed to more intense coordination at lower temperature[139,171]. However, the *extent* to which δ^{29}Si changes with temperature differs among different compounds[137]. It was found that the temperature gradient K of the Si chemical shift is related to the deviation of silicon (Δ parameter) obtained from the crystal structure in a series of compounds sharing similar ligand frameworks at the silicon, $\text{OSi(C)}_3\text{X}$[105,139]. The function describing this relationship is shown in Figure 18[105]. The temperature gradient is positive for as long as Δ is positive, i.e. as long as the coordination is to oxygen. At large deviations from planarity (large positive Δ), the geometry at silicon is essentially tetrahedral, and coordination is negligible. At this region no significant temperature dependence of the chemical shift is found. At intermediate Δ values the gradient goes through a maximum, at which point the chemical shift shows the strongest temperature dependence: lowering the temperature for these molecules is most effective in increasing coordination.

When silicon lies in the equatorial plane ($\Delta = 0$), the coordination is strongest and δ^{29}Si does not significantly depend on the temperature (i.e. $K = 0$)[139]. Negative temperature gradients are found for those complexes in which $\Delta < 0$, i.e. in which halogen is coordinated to silicon[89–91,105,137,171]. The function plotted in Figure 18 provides yet another means of mapping the hypothetical progress along the reaction coordinate of a nucleophilic substitution at silicon, using solution (rather than solid state) data: complexes in which the gradient is positive lie on one side of the reaction coordinate, those with negative gradients are advanced toward the products and chelates with negligible temperature gradient represent the TBP intermediate at the midpoint of the reaction coordinate.

The question of mapping the reaction coordinate by observing changes in chemical shifts has also been addressed by Bassindale[104,138]. By varying the ligands and substituents on a pyridone chelate **(125)**, it was possible to follow changes in coordination along the reaction coordinate described by equation 42. This was done by observing the changes in ^{13}C and ^{29}Si NMR chemical shifts as a function of structural modifications in **125**. The ^{13}C shifts were compared against the corresponding shifts of two standard compounds, **139** and **140**, which represent models for the two extreme points along the reaction shown in equation 42. From the relative location of the pyridone-ring ^{13}C chemical shifts of differently substituted chelates between **139** and **140**, the extent of Si−O bond making was assessed (Figure 19). From the variation of ^{29}Si chemical shift between the extremes of tetracoordinate silicon to fully pentacoordinated silicon, it was possible to obtain a map of nucleophilic substitution at silicon for some 25 compounds (Figure 20)[104,138]. The advantage of this method is that it is based completely on solution data, as opposed to the Dunitz–Bürgi[19,168,169] approach which compares crystal data.

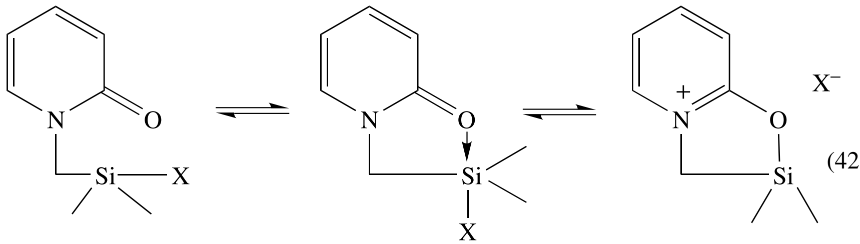

(125)

(42)

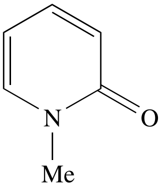

(139)

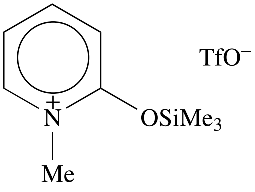

(140)

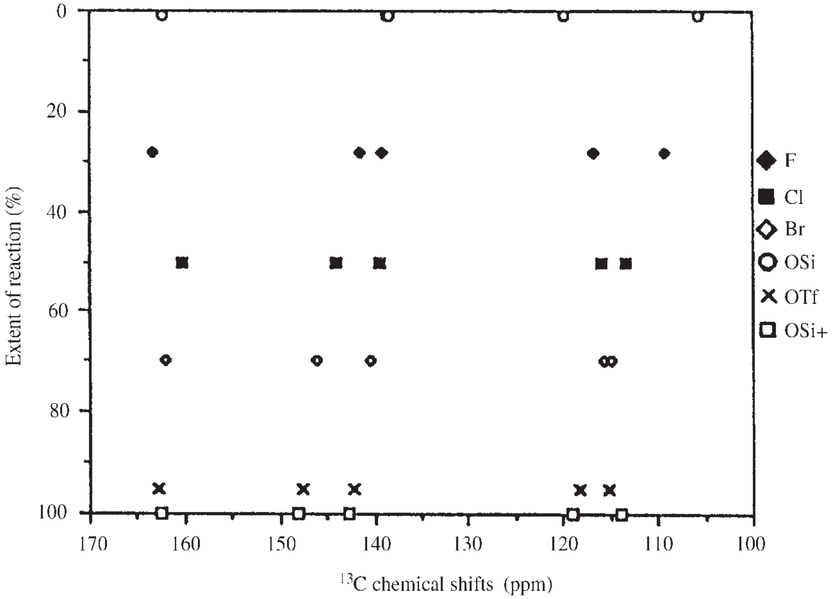

FIGURE 19. Variation of ^{13}C chemical shifts with the extent of Si–O bond making in pyridone complexes **125**[104,138]. Reproduced from Reference 138 by permission of The Royal Society of Chemistry

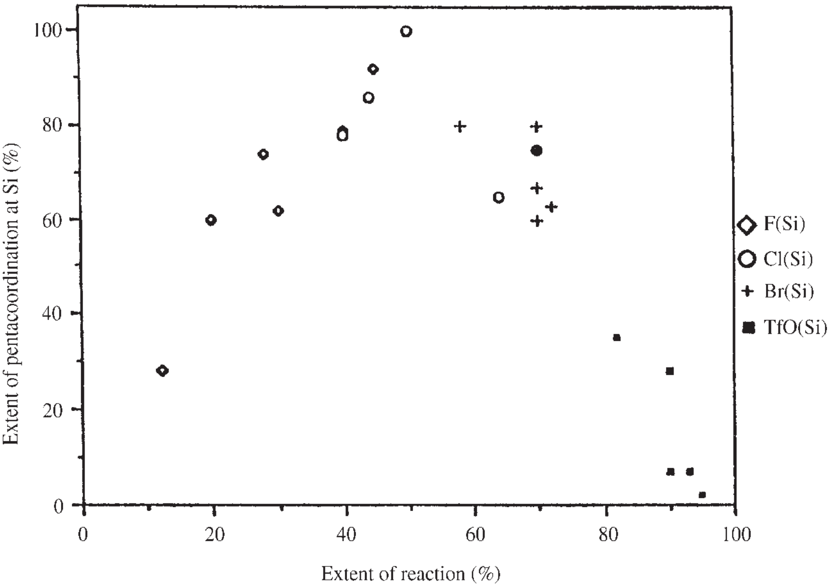

FIGURE 20. A map representing the progress along a reaction coordinate for nucleophilic substitution at silicon in solution, for a series of substituted silylpyridones. Derived from ^{29}Si and ^{13}C chemical shifts[104,138]. Reproduced from Reference 138 by permission of The Royal Society of Chemistry

The above analysis was based on data measured for a collection of silicon complexes. In a recent different approach a gradual change could be observed from $O \rightarrow SiCl$ to $OSi \leftarrow Cl$ coordination in a single compound (**125a**, X = Cl), as the temperature was changed[171]. Figure 21 shows the temperature dependence of the ^{29}Si chemical shift for **125a** over a 180 °C range. Within this range the temperature gradient changes from positive to negative, in accord with a gradual increase of pentacoordinate character when the temperature is first lowered from 100 °C, until a maximum coordination is reached and the gradient is zero at about 10 °C, followed by a decrease in coordination with decreasing temperature after the midpoint has been reached and the coordinating ligand has switched. Figure 21 may also be viewed as a plot of the progress along the S_N2 reaction coordinate[171].

In an approach similar to Bassindale's[138], Kummer and Abdel Halim also probed the variation of ^{29}Si chemical shifts as a function of ^{13}C shifts of the pyridone-ring carbons, but using a single compound (**125b**, X = Br) and modifying the temperature, solvent and concentration[171]. These measurements were also interpreted in terms of various extents of progress along the reaction coordinate of equation 42.

4. Ligand exchange

Unlike in the Si−N complexes, where ligand exchange is conveniently followed by coalescence of the N-methyl groups, in Si−O complexes only the ligands on silicon enable monitoring of the exchange processes. In **118f** and **118l** the presence of a chiral carbon atom in the lactam ring makes the Si-methyl groups diastereotopic. Their coalescence was used to obtain ligand exchange barriers resulting from either pseudorotation or Si−O bond cleavage: 11 and 14 kcal mol^{-1}, respectively[139]. Reference to Table 15 reveals the ^{29}Si chemical shifts for **118f** and **118l**, −5.7 and −14.3 ppm, respectively. In analogy to the linear correlation found between ^{29}Si chemical shifts and Si−N cleavage barriers (cf Figure 11) we tend to conclude that the barriers in **118f** and **118l** are Si−O cleavage barriers.

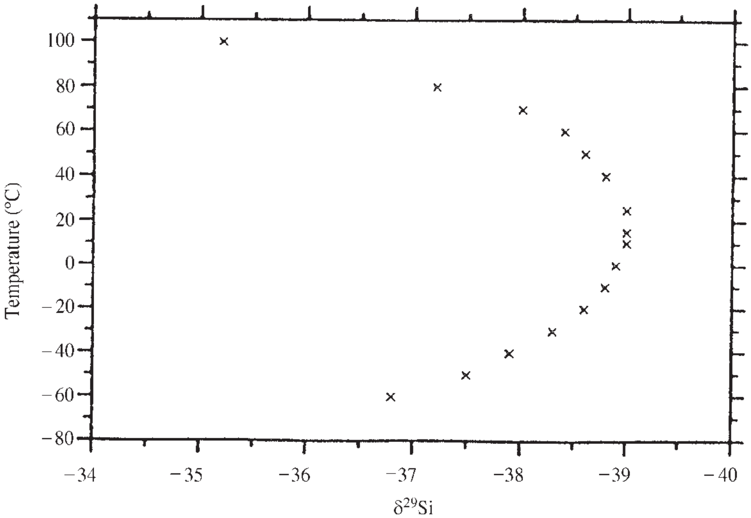

FIGURE 21. Temperature dependence of the ^{29}Si chemical shift for **125a** in $CDCl_3$. Reproduced from Reference 171 by permission of Hüthig Fachverlage

Other cases of diastereotopicity of ligand groups due to the presence of adjacent chirality are found in **138** (chiral sulfoxide) and **141** (chiral carbon). The chirality renders both equatorial fluorine ligands diastereotopic at the slow exchange temperature (*ca* 170 K)[150,153]. Exchange phenomena were measured also in **131**, in which the diasteretopicity of geminal methylene protons and Si−methyl groups results from the N−N chiral axis and the substantial activation barrier for rotation about the N−N bond[147]. Coalescence was measured for the Si−methyls at 70−75 °C, but the nonequivalence of the CH_2 protons was retained. This meant that rotation about the N−N bond was still slow at this temperature, and that exchange of Si−methyls resulted from inversion of configuration at the silicon atoms, either by pseudorotation, or by Si−O cleavage, followed by rotation and reclosure, or by intermolecular exchange. Further evidence indicated that intermolecular exchange was predominant: in **131c**, in which the Si−methyls are coupled to the F-ligand, coalescence of the methyls (two doublets) occurred simultaneously with the collapse of ^{19}F−(Si)−$^{13}CH_3$ coupling (singlet). Furthermore, in a mixture of **131a** and **131b** no individual coalescence of Si−methyl groups could be observed, but rather a simultaneous exchange in both compounds, in accord with scrambling of all methyl groups due to intermolecular exchange[147].

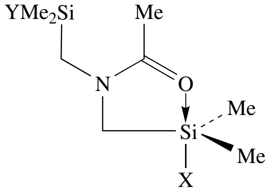

(117a) X = Y = Cl
(117i) X = Y = F
(117j) X = Cl, Y = F

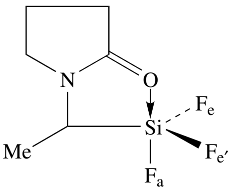

(141)

Intermolecular ligand exchange was reported also for **117a**, in which the chloro ligand in the O−Si−Cl fragment is replaced by *N*-methylimidazole more rapidly than the other chlorine, attached to the tetracoordinate silicon[144]. Interestingly, in the difluoro analog **117i** only the fluorine atom attached to the tetracoordinate silicon is replaced, whereas the coordinated fluoro group is retained. Admixture of the two chelates, **117a** and **117i**, resulted in regiospecific exchange to the mixed chelate **117j**. These experiments confirm the greater apicophilicity of chlorine vs. fluorine.

117c was shown to exist in CD_2Cl_2 solution in two different pentacoordinated forms, both by ^{29}Si and ^{1}H NMR spectroscopy[172]. At low temperature (185 K in the ^{1}H NMR spectrum) the Si−methyl groups gave two singlets, as did the ^{29}Si signal. This was attributed to the formation of an oligomeric complex: dimer, trimer or larger, in addition to the monomeric chelate, based on the change in relative signal intensities as a function of concentration.

Amide bond rotation barriers were measured in compounds of series **117** in $CDCl_3$ solutions, by measuring the coalescence of two unequal singlets for the Si−methyl groups observed at low temperature[170]. Amide rotation in these compounds (**117c−117h**) is associated with cleavage of the Si−O coordination. The barriers ranged between 13.3-16.9 kcal mol^{-1}, and the population of the open N−C rotamer ranged from 0.5 to 11%, as a function of the *para* substituent on the N-phenyl group. In other solvents (toluene, dichloromethane and THF) no splitting of the Si−methyl signals was observed and the barriers could not be measured[170].

TABLE 17. Bond lengths, ^{29}Si chemical shifts and their temperature gradients [$K = (\delta^{29}\text{Si}_{T_1} - \delta^{29}\text{Si}_{T_2})/(T_1 - T_2)$], and ligand exchange barriers in **120**[133]

Compound	X	Si−O (Å)	δ^{29}Si (ppm)	K (ppm deg^{-1})	δ^{13}CO (ppm)	$\Delta G^{\ddagger}$ (kcal mol^{-1})
120a	Cl	2.077	−24.2	0.07	175.8	8.3
120b	Br	1.978	−29.1	0.04	176.8	9.3
120c	I	1.830	−14.9	−0.11	177.1	10.6
120d	$OCOCH_3$		−11.3	0.11	174.1	7.8
120e	$OCOCF_3$		−30.1	0.04	175.9	9.2

In imide structures **120** the coordination of oxygen to silicon is switched between the two oxygens (equation 43). This was observed for the first time in **120a**, in which both ^{13}C and ^{1}H NMR C−methyl and carbonyl signals split at low temperatures[133]. The barriers for this exchange process depended on the apical ligand X in a manner which roughly follows the order of apicophilicity, and was inversely related to the Si−O distances (Table 17). These observations strongly suggest that the process represents Si−O cleavage rather than rate-determining amide rotation. Interestingly, the correlation of ^{29}Si chemical shifts with activation barriers breaks down for iodine **(120c)**. This can be rationalized with reference to the temperature gradient of δ^{29}Si, K, shown in Table 17. For **120c** the temperature gradient is opposite to all other complexes. As discussed earlier (Figure 18, Section III.B.3) this is related to the change from O → Si to I → Si coordination.

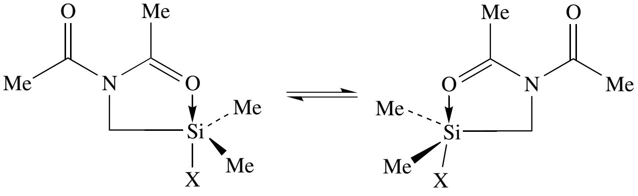

(43)

(120)

Similar amide-switching phenomena were reported in other compounds **(142, 143)**. X-ray crystallography for **143** showed that only one amide-oxygen was coordinated to silicon (Si−O distance: 1.992 Å)[173]. However, in solution the two amide-moieties were NMR-equivalent and could not be resolved down to −65 °C in toluene-d_8 solution[173].

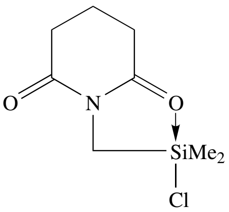

(142)

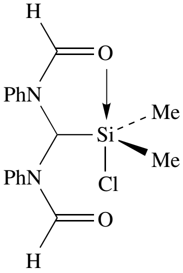

(143)

C. Other Neutral Pentacoordinate Silicon Compounds

1. Sulfur coordination

Sulfur to silicon coordination was achieved in a series of eight-membered cyclic silanes, **144** and **145**[174,175]. The complexes were prepared from aromatic diols by reaction with $SiCl_4$ **(144)**, Me_2SiCl_2, $MePhSiCl_2$, Ph_2SiCl_2, $Ph(CH_2{=}CH)SiCl_2$ and c-$(CH_2)_4SiCl_2$ **(145a–145g)**. The silanes were found by crystal analyses to deviate from tetrahedral geometry toward TBP structure, with sulfur coordination to silicon, except in **145b**, where the eight-membered chelate ring is in the chair conformation. Table 18 summarizes some of the crystallographic and NMR data for these compounds. Judging from the change in the ^{29}Si chemical shift of **144** and **145** relative to the tetracoordinate carbon analogs **(146, 147)**, the extent of pentacoordination is not very large (*ca* 7 ppm upfield shift). This conclusion is supported by the calculated TBP character of the complexes, which is as low as 35–54%. The changes measured in the Si–S distances were discussed in terms of conformational changes in the macrocycles[174].

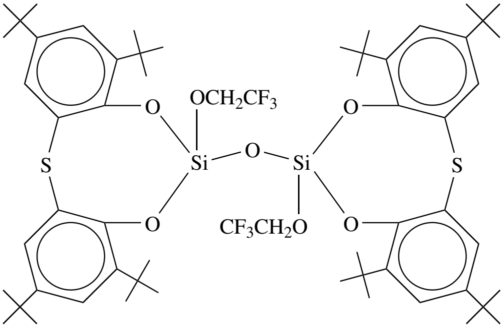

(144)

Several analogs of **145** were prepared in which the sulfur atom is oxidized to S=O **(148)**[176a] and to SO_2 **(149)**[176b]. All the sulfinyl compounds **(148)** have the macrocycle in a chair conformation, and hence there is no S–Si coordination[176a]. In the sulfonyl analogs, however, one of the oxygens is coordinated to silicon, as long as the phenyl-*ortho* positions are occupied by *t*-butyl groups[176b].

TABLE 18. Comparison of Si–S bond parameters and ^{29}Si chemical shifts for cyclic silanes[174]

Compound	Si–S (Si–C) (Å)	% TBP[a]	δ^{29}Si (ppm) ($CDCl_3$)	δ^{29}Si (ppm) (solid)
144	3.04	50.6		−107.84
	3.11	46.5		−99.35
145	3.292	35.8	−13.22	
	3.280	36.5		
146	3.074	48.6	−13.51	
147	2.978	54.2	−1.62	−6.55
148	(3.418)		−5.62	
149	(3.100)		5.44	5.88

[a] Percent geometrical displacement from a tetrahedron to a trigonal bipyramid.

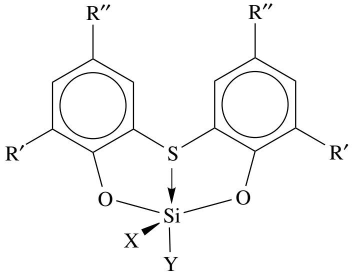

(145)

(**a**) X = Y = R′ = R″ = Me
(**b**) X = Y = Ph, R′ = R″ = Me
(**c**) X = Y = Me, R′ = *t*-Bu, R″ = Me
(**d**) X = Ph, Y = CH=CH$_2$, R′ = *t*-Bu, R″ = Me
(**e**) X Y = (CH$_2$)$_4$, R′ = R″ = *t*-Bu
(**f**) X = Me, Y = Ph, R′ = R″ = *t*-Bu
(**g**) X = Y = Ph, R′ = R″ = *t*-Bu

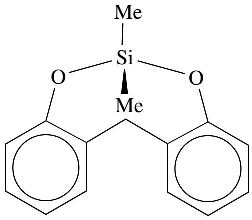

(146)

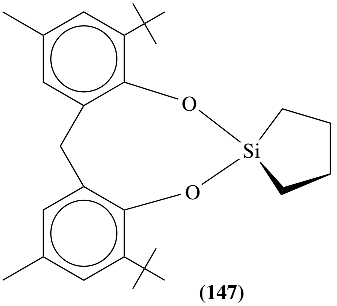

(147)

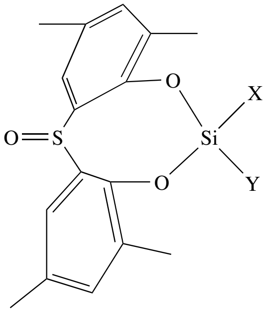

(148)

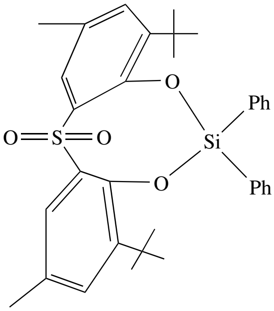

(149)

a, X = Y = Me
b, X = Ph ; Y = Me
c, X = Y = Ph

2. Fluorine coordination: degenerate fluorine migration in a 'Merry-Go-Round' type mechanism

An elegant example of neutral pentacoordinate silicon complexes was reported by Sakurai and coworkers[177]: the hexakis(fluorodimethylsilyl)benzene **(150)** was shown by X-ray crystallography to have nearly TBP silicon centers, arranged in a gear-meshed structure (Figure 22). The Si−F distances (1.68 and 2.39 Å) are not equal, but are typical of SiF bonds (covalent and dative, respectively) in pentacoordinate complexes [i.e. longer than a regular Si−F bond in a silane (1.50 Å) and shorter than the sum of van der Waals radii (2.63 Å), respectively]. All the F−Si−F angles were near 180° (average 176°), as required by a pentacoordinate TBP structure.

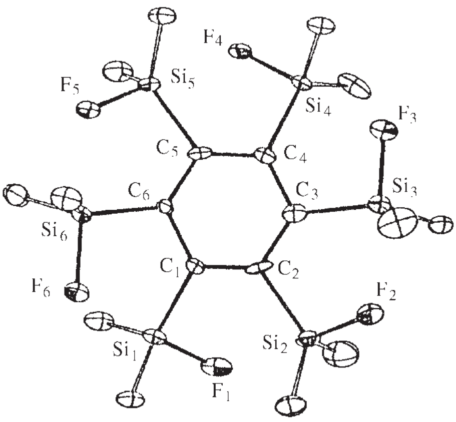

FIGURE 22. An X-ray crystallographic structure of **150**. Reprinted with permission from Reference 177. Copyright 1994 American Chemical Society

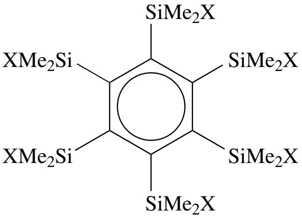

(150) X = F
(151) X = OMe

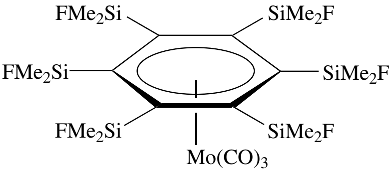

(152)

In solution the bridging fluorines are rapidly transferred between adjacent silicons, such that the ^{29}Si spectrum features a triplet due to two equivalent fluorines ($^{1}J_{\mathrm{Si-F}} =$ 127 Hz). This triplet did not change to a doublet of doublets at the low-temperature limit in toluene-d$_8$ solution, and hence 'freezing out' of the fluorine transfer between vicinal silicons could not be achieved. When the temperature was raised, all six fluorines became equivalent, causing the silicon resonance to be a septet ($^{1}J_{\mathrm{Si-F}} = 43$ Hz), presumably due to exchange by correlated rotation[178] of the silicon substituents about the Si−benzene bonds. This rotational process was stopped when a molybdenum complex was formed **(152)**, presumably as a result of increased steric hindrance for rotation.

It was shown that a $D_{6\mathrm{h}}$ symmetric structure for **150** required a 1.88 Å long Si−F bond, and was not possible due to the substantially shorter Si−F bonds (1.68 Å). For this purpose the hexamethoxy analog **(151)** was prepared and studied, and indeed, with the longer (1.88 Å) Si−O bonds, a perfect $D_{6\mathrm{h}}$ structure was obtained in a single crystal study[177].

IV. CATIONIC PENTACOORDINATE COMPLEXES

Trivalent silyl cations in the gas phase[179] and coordinated silyl cations in condensed phase were described in recent reviews and papers[180–182].

The first few pentacoordinate cationic silicon complexes **(153–155)** were discussed in an earlier review[2]. The first two were described as trivalent silicenium ions stabilized by *inter*molecular coordination[183,184], while **155** is an intramolecular silicenium ion[21a]. Since then, a few other compounds were reported. Oxidation of the dihydrido-hexacoordinate chelate **156** by the addition of excess iodine produced **157**[185]. The X-ray structure of **157** showed a slightly distorted TBP for the cation, with a well separated (Si–I distance 5.036 Å) I_8^{-2} anion for every two cations. The nitrogens are in the apical positions, and both Si–N distances (2.08 and 2.06 Å) are longer than covalent bonds but well within the coordination distance.

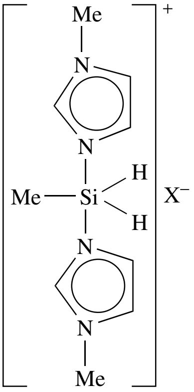

(153)

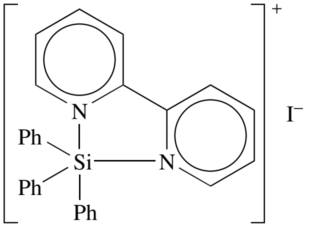

(154)

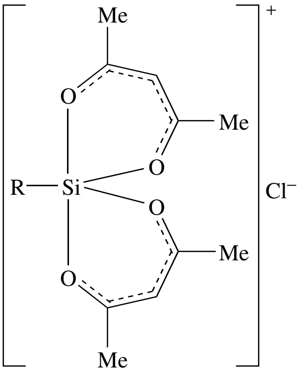

(155)

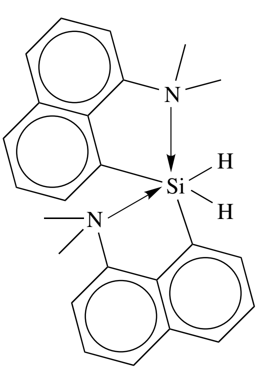

(156)

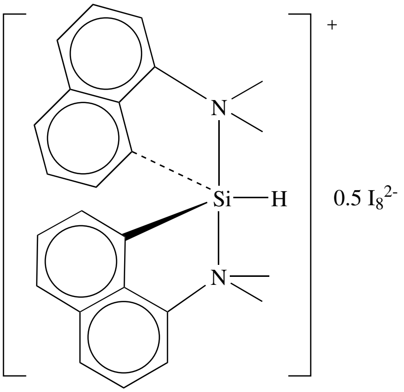

(157)

Reaction of the dihydrido complex **158** with a variety of reagents (equation 44) led to abstraction of a hydride and formation of the symmetrically dicoordinated cations **159a–159e**[186a], differing in the counter anion. **159c** was also prepared by a different route: from the 2,6-bis(dimethylaminomethyl)phenyl lithium and phenyldichlorosilane. The ionic character of these complexes was unequivocally demonstrated by conductivity studies. Other cationic complexes **(160, 161)** were similarly prepared from the trihydrido and monohydrido precursors[186a].

The NMR in $CDCl_3$ solution suggested the equivalence of the dimethylamino groups, in analogy to the solid state. This was later disputed in a similar compound, **161b**[187]. In this compound the low temperature ^1H and ^{13}C NMR spectra showed splitting of the N-methyl and CH_2 signals, suggesting that only one dimethylamino group was coordinated, and that rapid exchange of the two occurred at higher temperatures, i.e. that in solution the silicon was, in fact, tetracoordinate. This complex was reported to be remarkably air-stable, and to dissolve in protic solvents[187].

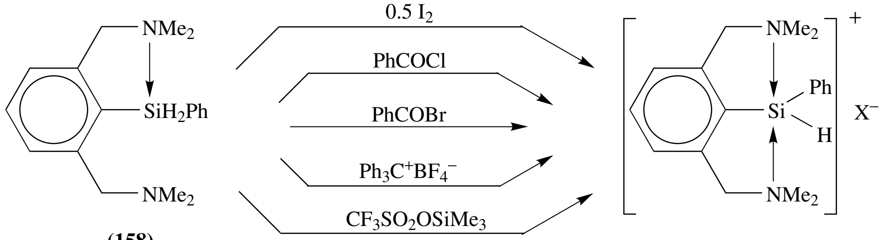

(158)

(159a) X = I
(159b) X = Br
(159c) X = Cl (44)
(159d) X = BF_4
(159e) X = CF_3SO_3

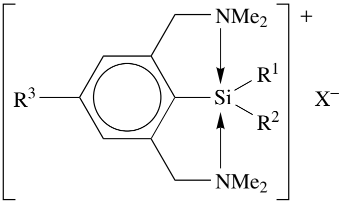

(160a) $R^1 = R^2 = R^3 = H$, X = I
(160b) $R^1 = R^3 = H$, $R^2 = X = Cl$
(161a) $R^1 = R^2 = Me$, $R^3 = H$, X = CF_3SO_3
(161b) $R^1 = R^2 = Me$, $R^3 = t$-Bu, X = Cl
(162a) $R^1 = Ph$; $R^2 = Me$, $R^3 = H$; X = Cl
(162b) $R^1 = Ph$; $R^2 = Me$, $R^3 = H$; X = I
(162c) $R^1 = Ph$; $R^2 = Me$, $R^3 = H$, X = $[3,5\text{-}(CF_3)_2C_6H_3]_4B$
(162d) $R^1 = Ph$; $R^2 = Me$, $R^3 = H$, X = BPh_4

A further contribution to this controversy has recently been added by Corriu's group, showing that, depending on the counter anion and solvent, each of the penta and tetracoordinate structures **(162)** can predominate, and in one particular case **(162d)** both were shown to coexist in nearly equal concentrations[186b].

Two additional cationic complexes were recently reported, **163** and **164**, prepared by the reaction of trimethylsilyl triflate with bis[2-((dimethylamino)methyl)phenyl]silane **(165)** and [2-((dimethylamino)methyl)phenyl]phenylsilane **(166)**, respectively[188]. The X-ray crystallographic structure of **163** clearly showed a cationic complex with a distant triflate anion. By contrast, in **164** the anion is directly coordinated to silicon (Si−O distance 1.951 Å), as is the apical dimethylamino-nitrogen (Si−N distance 2.052 Å). The structure is very near a TBP, and may be viewed as a doubly-coordinated silicenium ion, or a tight ion-pair[188].

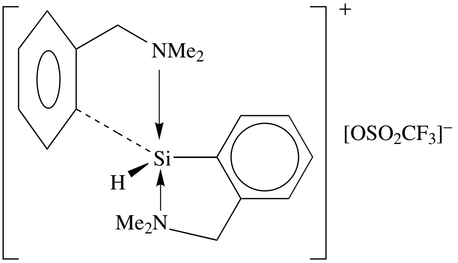

(163)

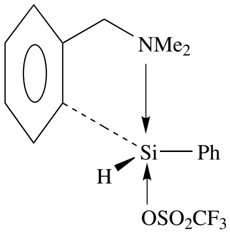

(164)

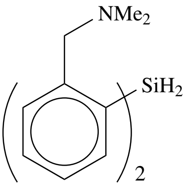

(165)

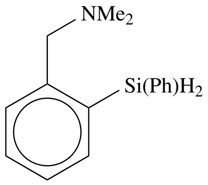

(166)

Table 19 presents ^{29}Si chemical shifts and Si−H coupling constants for some of the cationic pentacoordinate silicon complexes and for some of their precursors. No clear trend can be seen for the ^{29}Si chemical shifts of these compounds: some are shifted downfield and others upfield, relative to their pentacoordinated neutral precursors. However, a trend seems to emerge from the one-bond Si−H coupling constants: in the cationic pentacoordinate complexes ^1J(Si−H) is generally greater than for neutral pentacoordinate complexes. This is possibly the result of the greater s-character in the Si−H bonds, in the doubly coordinated (sp^2-hybridized) silicenium cations[185,186].

A formally pentavalent cationic silicenium complex, with intramolecular base-stabilization, is the silylene-iron **167**, with a Fe=Si double bond. The crystal structure of **167** shows that silicon is essentially tetrahedral in this compound, and the solution ^{29}Si chemical shift is $\delta = 118.3$ ppm, compatible with the double bond character rather than with pentacoordination at silicon[189].

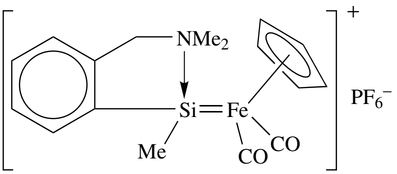

(167)

TABLE 19. ^{29}Si NMR data for cationic complexes and their neutral precursors

Complex	Counter anion	δ^{29}Si (ppm)	J(Si−H) (Hz)	References
157	0.5 I_8^-	−43.5	290	185
158		−51.5	200	186a
159a	I^-	−29.7	280	186a
160a	I^-	−46.4	265	186a
160b	Cl^-	−40.3	334	186a
161a	$CF_3SO_3^-$	−4.1		186a
161b	Cl^-	6.57		187
162a	Cl^-	−7.0		186b
162b	I^-	−8.0		186b
162c	$[3,5\text{-}(CF_3)_2C_6H_3]_4B^-$	−15.0		186b
162d	Ph_4B^-	−8.5, −14.5		186b
163		−51.6	272	188
164	$CF_3SO_3^-$	−56.2	294	188
165		−45.0	216	188
166		−43.3	208	188

V. HEXACOORDINATE IONIC SILICON COMPOUNDS

The main methods for the synthesis of hexacoordinate silicon compounds are similar to those for pentacoordinate complexes and were outlined in a recent review[6]. These methods include: (a) addition of nucleophiles (neutral or anionic) to tetracoordinate silanes; (b) intermolecular or intramolecular coordination to an organosilane; (c) substitution of a bidentate ligand in a tetrafunctional silane. The following discussion focuses mainly on new complexes, reported since the recent reviews[6,7] were published.

A. Fluorosilicates

The first studies of fluorosilicates were reported by Müller[8,32a] and by Kumada and coworkers[190], and later reviewed by Voronkov[9a], Gel'mbol'dt,[9b] Corriu[6] and their coworkers. More recently some interesting hexacoordinate fluorosilicates were reported by Corriu and coworkers[191,192] and by Tacke and Mühleisen[193].

Hexacoordinate fluorosilicates were obtained from neutral pentacoordinate complexes by addition of K[18-crown-6]F[191,192]. In this way compounds **168–173** were prepared from their pentacoordinate precursors. These compounds, in addition to being fluorosilicates, contain in each chelate ring a dative Si−N bond.

An X-ray crystallographic study for **170** revealed a slightly distorted octahedral geometry, as is expected for hexacoordination[191]. The four Si−F bonds in this compound are essentially equal in length, while the Si−N distance (2.213 Å) is shorter than that found in the neutral pentacoordinate precursor (2.318 Å), or in a previously reported neutral hexacoordinate difluorosilane, **174** (2.59, 2.81 Å)[194]. The position of silicon in **170** is 0.16 Å displaced from the mean plane defined by carbon and three fluorine ligands, away from the coordinated nitrogen[191].

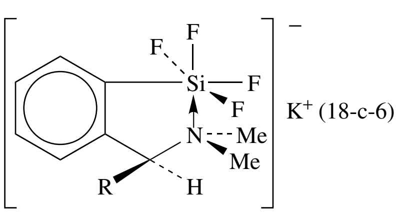

(168) R = H
(169) R = Me

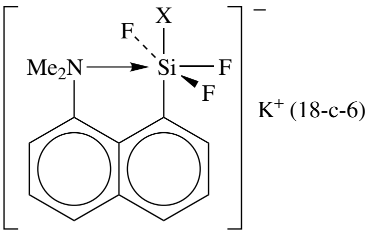

(170) X = F
(171) X = Ph

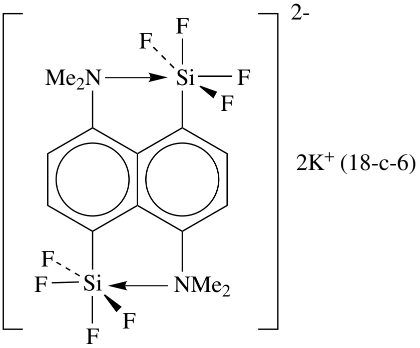

(172)

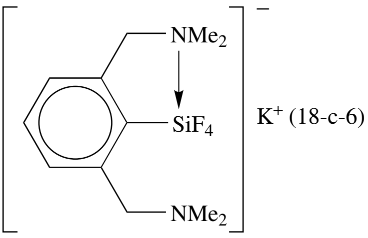

(173)

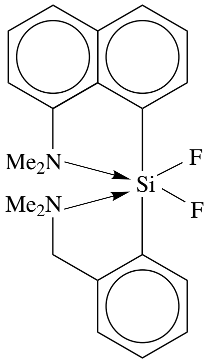

(174)

The ^{29}Si NMR (Table 20) supports a hexacoordinate structure in solution which is similar to that in the solid state. δ^{29}Si for the hexacoordinate fluorosilicates is *ca* 50 ppm shifted upfield relative to the pentacoordinate precursors. The multiplicity of the ^{29}Si resonances indicates the nonequivalence of fluorine ligands at low temperatures (between 25 and −60 °C). These become equivalent as the temperature is raised, such that a symmetrical ^{29}Si multiplet is observed.

TABLE 20. ^{29}Si NMR data and ligand exchange barriers (determined by ^{19}F NMR) for hexacoordinated anionic silicates

Compound	Temp (°C)	δ (ppm) (multiplicity)	J(Si−F)^{a} (Hz)	$\Delta G_{F}^{\ddagger}$ (kcal mol^{-1})	References
168	+25	−160.1(quint.)	197.1	11	191
	−60	−161.6 (ddt)	218.4(SiX$_2$),186.7(SiY),147.6(SiZ)		
169	+25	−159.9(quint.)	193.1	11	191
	−40	−161.1(dt)	219.0(SiX$_2$),184.0(SiY),146.3(SiZ)		
170	+25	−156.3(ddt)	223(SiX$_2$),181.2(SiY),149.8(SiZ)	15	191
171	+25	−137.0(dt)	246.2(SiX$_2$),196.7(SiY)	15	191
172	+25	−154.5(ddt)	225.3(SiX$_2$),184.0(SiY),117.6(SiZ)		191
173	+25	−161.0(quint.)	197.1		192
	−90	−162.6(ddt)	217.5(SiX$_2$),191.2(SiY),142.5(SiZ)		

[a] X, Y and Z refer to non-equivalent fluorine atoms at slow exchange conditions.

Measurement of the temperature dependence of ^{19}F NMR spectra for **169** revealed two distinguishable coalescence phenomena: the averaging of diastereotopic fluorine signals in the ^{19}F spectrum, and the coalescence of the N-methyl groups[191]. The latter process can only result from Si−N cleavage, followed by rotation about the C−N bond and reclosure of the chelate ring. During this process the fluorines can become equivalent. However, the exchange and coalescence of fluorines occurs with a lower activation barrier than the N-methyl exchange (14 kcal mol^{-1}, measured by ^{1}H NMR), and hence it was concluded that fluorine exchange is a regular, nondissociative reaction of the Bailar[195a] or Ray–Dutt (RD)[195b] type. The presence of a chiral group is necessary for the observation and measurement of the two barriers. This was not possible for the other compounds, **168, 170–172**[191].

Complex **173** is unique in that it has a tridentate ligand[192]. It can serve as a model for nucleophilic substitution on hexacoordinate silicon. The NMR provides evidence that only one of the dimethylamino groups is coordinated: both ^{29}Si chemical shift and the ^{1}J(Si−F) are in accord with those of **168**, in which only one nitrogen ligand is present. However, at room temperature the ^{1}H NMR spectrum of **173** shows a sharp singlet for all 12 N-methyl protons, indicating fast exchange. Also, the fluorine ligands are equivalent at this temperature. At low temperature, the N-methyl singlet splits in two, and the ^{19}F signal splits to three signals, providing evidence for a dynamic equilibration of the two dimethylamino groups via a heptacoordinate C_{2v} transition state, **173a**, in which the fluorines are equivalent.

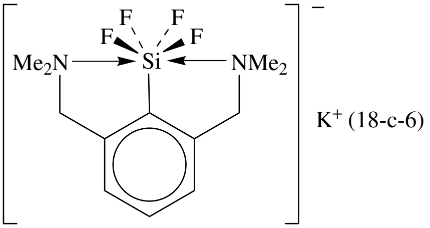

(173a)

A zwitterionic hexacoordinate pentafluorosilicate **(175)** was recently reported by Tacke[193]. **175** was prepared in the same manner as pentacoordinate zwitterionic complexes (cf Section II.A.3), as shown in equation 45. The crystal structure of **175** showed that one water molecule is present for each molecule, and that the structure is dominated by N−H••F and O−H••F hydrogen bonds. The Si−C bond length (1.943–1.946 Å) is distinctly longer than in the corresponding pentacoordinate zwitterion **(9)**, while the Si−F bonds (1.685–1.740 Å) are comparable to those in the pentacoordinate analog. The solid state ^{29}Si NMR of **175** is also compatible with hexacoordination, with $\delta^{29}\text{Si} = -177.2$ ppm.

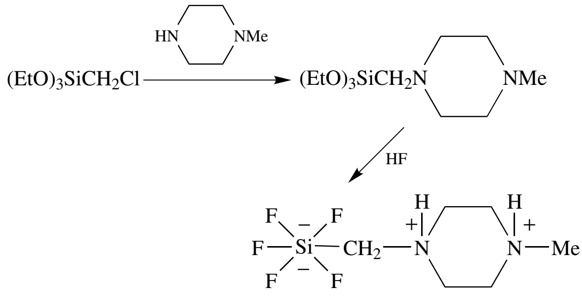

(45)

(175)

B. Ionic (O−Si) Chelates

The first ionic hexacoordinate complexes, silicon-tris-acetylacetonate cations **(176)**, were reported as early as 1903 by Dilthey[196a] and Rosenheim and coworkers[196b]. Subsequently many other *β*-diketonate complexes were studied[197–199], and the subject was extensively reviewed[7,200] and will not be discussed further here.

A rather similar class of compounds is the group of tris-catecholato anionic complexes, **176a**. These may be obtained by the reactions of catechol and base with either silica (SiO_2), $Si(OR)_4$, $[SiF_6]^{2-}2M^+$ or $SiCl_4$[6,7,201a]. The reaction with silica provides a direct route from an inorganic silicon source to organometallic compounds. This has further been developed to a general and efficient synthesis of organosilanes, using **176a** as intermediate[201b].

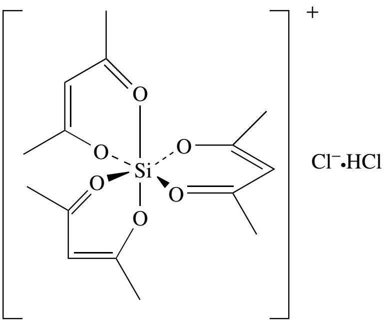

(176)

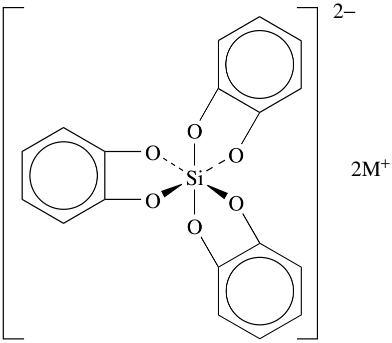

(176a)

Tris-catecholate complexes were prepared from symmetrically and unsymmetrically substituted catechols (LH_2): 4-chlorocatechol, 4,5-dichlorocatechol, 4-nitrocatechol, 3,4-dinitrocatechol and 4,5-dinitrocatechol[202]. All of these complexes are prepared in aqueous solution and are water-stable, down to *ca* pH 4. The ^1H NMR signals for the free and complexed catechol moieties are well separated, and enable the determination of formation constants for each of the complexes, according to equation 46, where L is the catechol dianion.

$$3LH_2 + Si(OH)_4 \leftrightarrows SiL_3{}^{2-} + 4H_2O + 2H^+ \tag{46}$$

When differently substituted tris-catecholato complexes are mixed in solution they undergo intermolecular ligand exchange, resulting in mixed complexes. Thus the water solution of tris-catecholato and tris-4-nitrocatecholato complexes shows in the ^{29}Si NMR spectrum the signals for all four permutations of tris-ligand complexes. However, solution of the same complexes (as triethylammonium salts) in DMSO did not show signs of ligand exchange after 24 h. As expected, the unsymmetrically substituted catechols give rise to two isomeric complexes: facial and meridional, differing in the relative orientations of

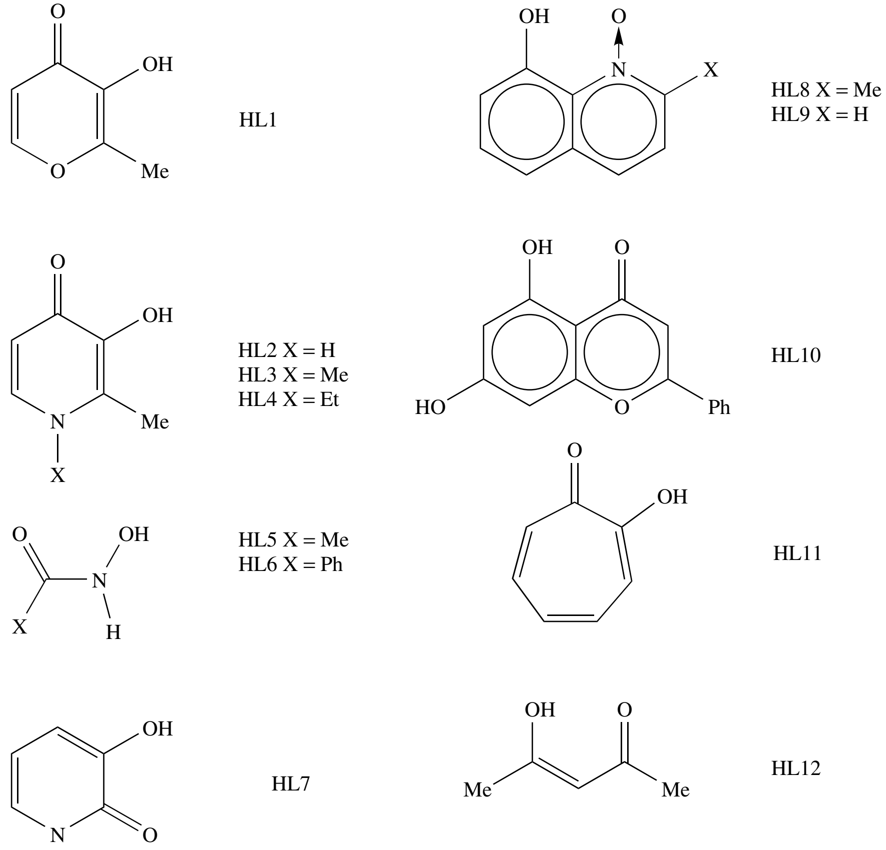

FIGURE 23. Ligand molecules used in hexacoordinate cationic complexes[203]

the nonequivalent oxygens of each catechol unit. The isomers were observed in the ^{1}H NMR spectra[202].

Evans has also reported on the preparation of similar water-soluble hexa-oxosilicon complexes, in which the overall charge is positive[203,204]. Two synthetic methods were used, reacting the bidentate ligands with either $SiCl_4$ or $Si(OEt)_4$. The latter method was reported to be generally preferred. The ligands used are shown in Figure 23[203]. The ^{29}Si chemical shifts of these complexes (Table 21) were analyzed: a substantial effect of chelate-ring size on δ^{29}Si was found (−130 to −150 ppm for the five- vs −190 to −200 ppm for the six-membered chelate rings)[21a,203]. By contrast to this large effect, the nature of the coordinating oxygens, the nature of the counter anion and the overall charge of the complex had little or no effect on δ^{29}Si.

An interesting observation for one group of ligands (L2–L4 in Figure 23) is the fact that they can etch glass at a significant rate, to form the hexacoordinate complex $SiL_3{}^{+}Cl^{-}$ from a dilute acid solution[204].

C. Bis-catecholato Complexes with N−Si Coordination

A few ionic bis-catecholato N-coordinated complexes **177–181** have been reported[192,205–207]. Crystallographic studies of **177, 180** and **181** showed all three to have a near-octahedral geometry, with Si−O bond lengths very similar to those in the tris-catecholato complexes, and typical Si−N dative bond lengths of 2.157, 2.085 and 2.173 Å, respectively. The ^{29}Si chemical shifts for **177–181**, which are in line with hexacoordination, are listed in Table 22.

Variable-temperature ^{1}H NMR spectra were measured for **177** and **178** in CD_2Cl_2 solutions[205]. In the former the N-methyl groups and the methylene protons appeared as sharp singlets down to the lowest attainable temperature, while in **178**, with two chiral centers, signals due to only one diastereomer could be observed, and the initially diastereotopic N-methyls (due to the chiral carbon center) coalesced with an activation barrier of 10.25 kcal mol^{-1}[205]. This is evidence that inversion of configuration at silicon is rapid relative to the NMR time scale at the low temperatures used in the measurements and that the barrier measured for **178** is associated with Si−N bond cleavage.

TABLE 21. ^{29}Si chemical shifts for ionic hexacoordinate complexes (in DMSO)[203]

Complex[a]	δ^{29}Si (ppm)	Complex[a]	δ^{29}Si (ppm)
$[Si(L1)_3]^{+}[Cl]^{-}$	−134.9,−134.4	$[Si(L6)_3]^{+}[CF_3SO_3]^{-}$	−138.7
$[Si(L1)_3]^{+}[CF_3SO_3]^{-}$	−134.9,−134.4	$[Si(L7)_3]^{+}[CF_3SO_3]^{-}$	−141.6
$[Si(L2)_3]^{+}[CF_3SO_3]^{-}$	−136.4	$[Si(L8)_3]^{+}[CF_3SO_3]^{-}$	−192.3,−192.7
$[Si(L3)_3]^{+}[HSO_4]^{-}$	−135.3	$[Si(L8)_3]^{+}[Cl]^{-}$	−192.3,−192.7
$[Si(L3)_3]^{+}[cam]^{-}$	−135.3	$[Si(L9)_3]^{+}[CF_3SO_3]^{-}$	−193.4,−193.8
$[Si(L3)_3]^{+}[CF_3SO_3]^{-}$	−135.5	$Si(L10)_3]^{+}[Cl]^{-}$	−193.1
$[Si(L3)_3]^{+}[Cl]^{-}$	−135.5	$[Si(catecholato)_3]^{2-}[(Et_3NH)_2]^{2+}$	−139.3
$[Si(L3)_3]^{+}[CF_3CO_2]^{-}$	−135.3	$[Si(catecholata)_3]^{2-}[K_2]^{2+}$	−140.3
$[Si(L4)_3]^{+}[HSO_4]^{-}$	−135.4	$[Si(L11)_3]^{+}[Cl]^{-}$	−140.7
$[Si(L4)_3]^{+}[Cl]^{-}$	−135.5	$[Si(L11)_3]^{+}[SbF_6]^{-}$	−139.4
$[Si(L5)_3]^{+}[CF_3SO_3]^{-}$	−137.7	$[Si(L12)_3]^{+}[ZnCl_3]^{-}$	−193.7

[a] For the identity of L see Figure 23, $[cam]^{-}$ – 10-camphorsulfonate anion.

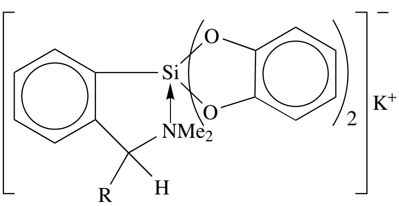

(177) R = H
(178) R = Me

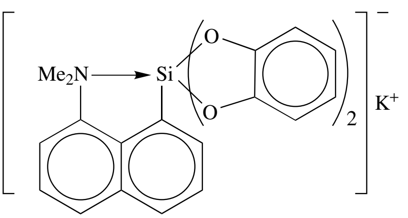

179)

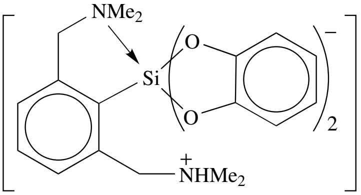

(180)

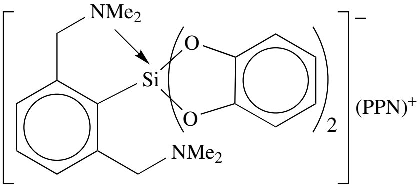

(181)

$PPN^+ = Ph_3P{=}\overset{+}{N}{=}PPh_3$

TABLE 22. ^{29}Si chemical shifts for bis-catecholato silicon complexes with N−Si coordination (CD_2Cl_2)

Compound	δ^{29}Si (ppm)	References
177	−121.1	205
178	−199.88	205
179	−124.5	206
180	−134.9[a]	207
181	−127.2[a]	207

[a] Solid state.

Complex **181**, with its two dimethylamino groups, is octahedral in the solid state with one dative and one loose dimethylamino nitrogens. In solution the NMR evidence shows rapid displacement of one dimethylamino ligand by the other, their NMR resonances being equivalent at 295 K. At 183 K, however, the methyls of one of the NMe_2 groups are diastereotopic, while the other group shows a singlet. At this temperature also both methylene groups give rise to AB quartets, as a result of the chirality at silicon[192]. Such internal nucleophilic substitution has been observed previously in pentacoordinate complexes, but it is the first report of dynamic internal substitution in hexacoordinate complexes.

VI. NEUTRAL HEXACOORDINATE SILICON COMPLEXES

A. Intramolecular Coordination

1. Synthetic methods

Relatively few ligand types have been used for the formation of neutral hexacoordinate silicon complexes, resulting in several complex types **182**–**193**[208–218]. Acetylacetonato (acac) chelates [**182**, $(acac)_2SiXY$] were prepared directly from the reaction of

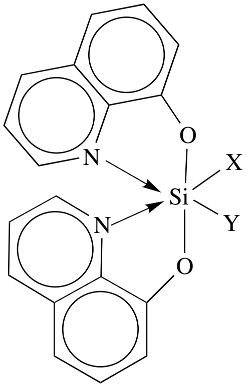

(183a) X = Cl, Y = Me
(183b) X = Y = Ph

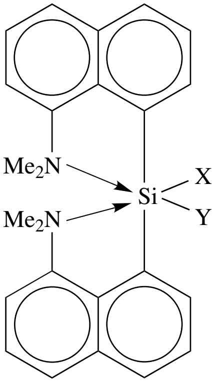

(184a) X = H, Y = F
(184b) X = Y = H
(184c) XY = 1,2-$O_2C_6H_4$
(184d) X = Y = C≡CH
(184e) X = Y = Cl
(184f) X = H, Y = OMe
(184g) X = H, Y = Me
(184h) X = Me, Y = Ph
(184i) X = Y = F

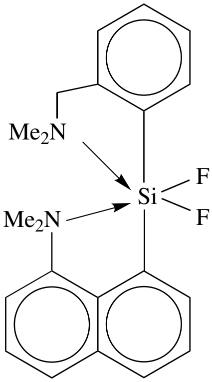

(185)

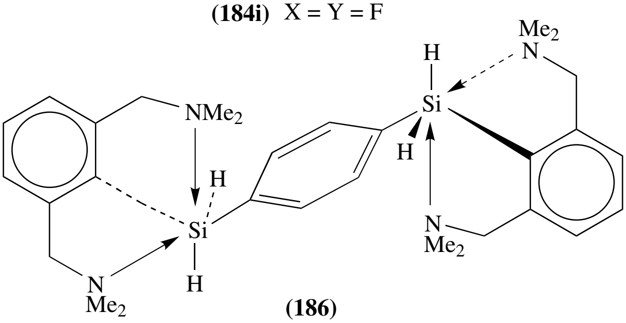

(186)

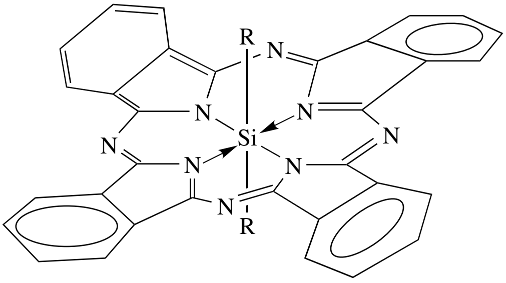

(187) R = alkyl, Ar, Cl

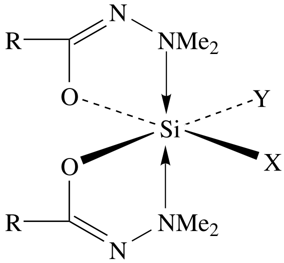

(188a–f) R = Me
(189a–f) R = Ph
(190a–f) R = CF_3
(191a–f) R = $PhCH_2$
(192a–f) R = PhMeCH

(a) X = Cl, Y = Me
(b) X = Cl, Y = Ph
(c) X = Cl, Y = H
(d) X = Y = Cl
(e) X = F, Y = Ph
(f) X = Y = F

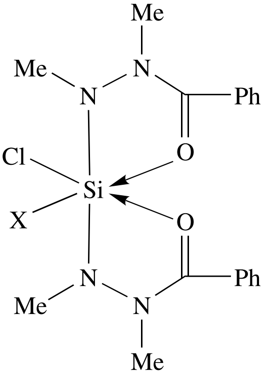

(193a) X = Ph
(193b) X = Cl

acetylacetone with a polyhalosilanes[197,198,200]. These earlier compounds were described in detail and reviewed previously[6,7]. The other types of complexes **(183–193)** were obtained by three main synthetic methods: (a) Reaction of the lithio-derivative of a bidentate ligand with a polyhalo- or polyalkoxy-silane (compounds **183–187**; equation 47[209]). (b) Exchange reaction of a trimethylsilylated derivative of the bidentate ligand with a polyhalosilane (compounds **188–193**; equation 48)[210–212]. (c) Modification of hexacoordinate complexes obtained by (a) or (b): an example of many synthetic transformations of a dihydro complex to other hexacoordinate complexes was presented by Corriu and coworkers, and is shown in Figure 24[213]. Interestingly, chloro ligands are reactive toward nucleophiles, while fluoro ligands are not effected by nucleophiles under similar conditions[206] (Figure 25; cf also work by Bassindale and Borbaruah[144]).

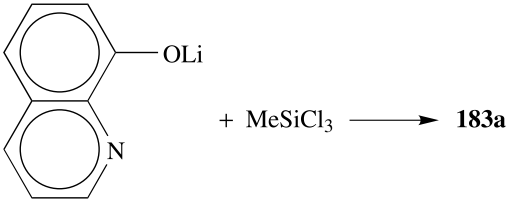

(47)

$$2Me_2NN{=}C(Me)OSiMe_3 \xrightarrow[-2Me_3SiCl]{XSiCl_3} \mathbf{188} \tag{48}$$

The synthetic route (c) was recently utilized to prepare unsaturated monomers containing the hexacoordinate silicon unit, followed by polymerization to form novel polymers with hexacoordinate silicon in the polymer chain (equation 49)[214]. The ^{29}Si chemical shift measured in the polymer solution (*ca* −60 ppm) is very similar to that of the monomer (−63.8 ppm), and is evidence for hexacoordination in the polymer solution.

Method (b), in which ligand exchange between silanes takes place, has been used to obtain both N→Si (equation 48)[210,211] and O→Si complexes (equation 50)[212], depending on the site of trimethylsilylation in the ligand molecule.

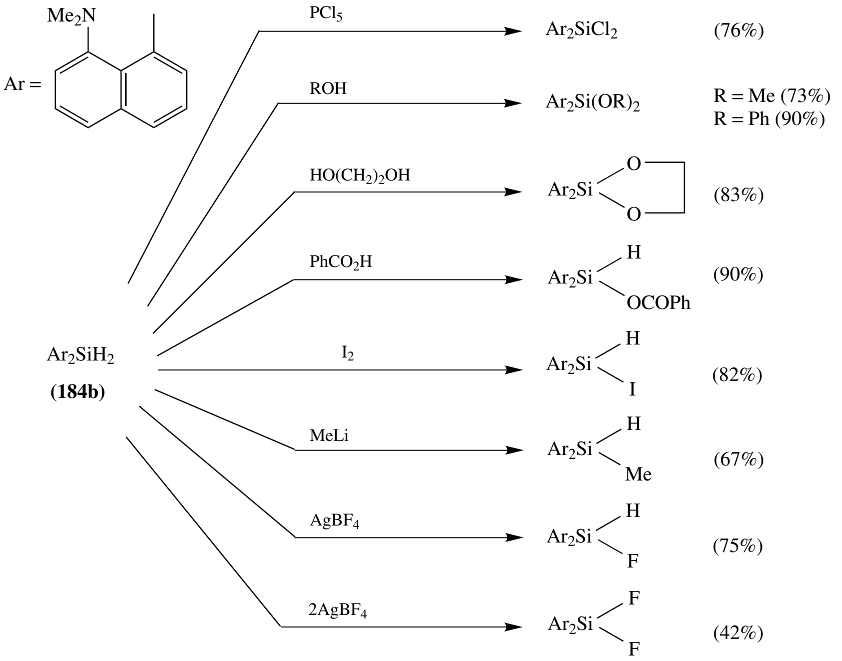

FIGURE 24. Reactivity of **184b**[6,213]

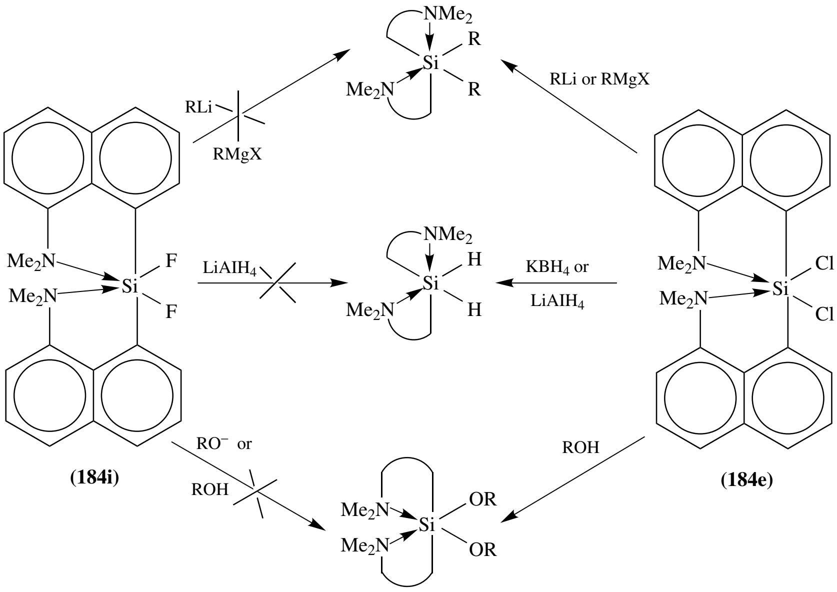

FIGURE 25. Different reactivities of the dichloro **(184e)** vs the difluoro **(184i)** complexes

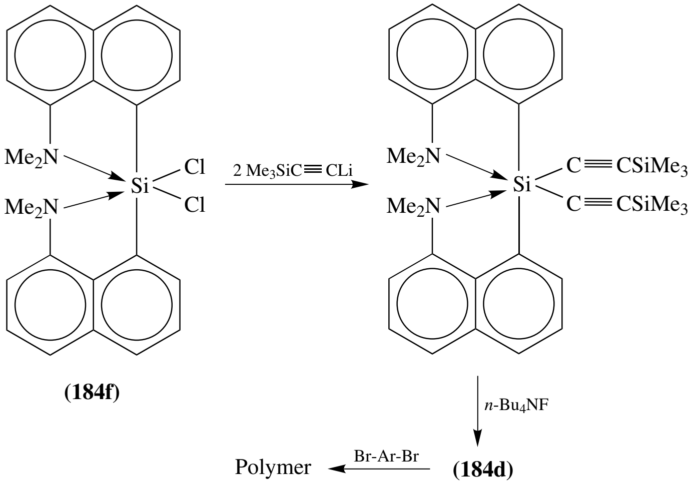

(49)

$$2Me_3SiN(Me)N(Me)COPh \xrightarrow[-2\ Me_3SiCl]{XSiCl_3} \mathbf{189} \qquad (50)$$

186 is an example of a special compound which is both a dinuclear complex and is prepared with a tridentate chelating ligand, in analogy to the synthesis labeled (a)[215].

2. Structure

The X-ray crystallographic studies of neutral and anionic hexacoordinate bischelates show that the pair of monodentate ligands prefer the *cis* orientation with respect to each other[209]. In general, the electronegative ligands occupy *trans* positions relative to the dative ligands. However, exceptions have been reported: **189a** has the two dative N−Si bonds *trans* to each other, despite the presence of the more electronegative O and Cl ligands[216]. Remarkably, hexacoordinate complexes with the same ligand environment, SiO_2N_2CCl **(183)**, were found with the oxygens in *trans* position[209].

Geometrically unrestricted hexacoordinate complexes are generally octahedral, as, for example, the anionic $SiF_6{}^{-}$[219]. However, intramolecular neutral hexacoordinate complexes contain one or two chelate rings, which may impose strain on the complex and modify the geometry. As a consequence, complexes can have more or less distorted octahedral geometries, depending on the ligands. Thus, while X-ray structure determinations for **183** and **189a**[209,216] (Table 23) show that the complexes have near-regular octahedron geometry, in the more constrained complexes **184–186**[194,206,215] the silicon atom largely maintains its basic tetrahedral geometry, with the two dative ligands loosely coordinated opposite two of the tetrahedron faces. This structure was termed 'bicapped tetrahedron'[194]. The features characteristic of this type of complexes are the substantially longer Si−N distances, *ca* 2.5–2.8 Å, relative to the octahedral complexes with 2.0–2.1 Å. The Si−N distances in the bicapped tetrahedral complexes are, nevertheless, shorter than the sum of van der Waals radii. Unlike octahedral complexes, in which the ^{29}Si signal is shifted *ca* 70–80 ppm upfield relative to analogous tetracoordinate complexes[21a,40,211], in the bicapped tetrahedral complexes the ^{29}Si coordinative shift (relative to tetracoordinate analogs) is negligible or very small (Table 24).

TABLE 23. X-ray structural data for neutral hexacoordinate (N−Si) chelate complexes

Complex	X	Y	Si−N (Å)	Si−X or Si−Y, (Å)	Geometry	References
183	Cl	Me	2.014	2.17(Cl)	octahedron	209
			2.016	1.94(C)		
184a	F	H	2.680	1.628(F)	bicapped	194
			2.646	1.550(H)	tetrahedron	
184b	H	H	2.610	1.44	bicapped	194
			2.800	1.54	tetrahedron	
184c	OCH_2	OCH_2	2.560	1.74	bicapped	206
			2.640	1.72	tetrahedron	
184d	C≡CH	C≡CH	2.836	1.840	bicapped	214
			2.789	1.851	tetrahedron	
185	F	F	2.770	1.617	bicapped	194
			2.594	1.603	tetrahedron	
186	H	Ph	3.008	1.44(H)	bicapped	215
			2.681	1.883(C)	tetrahedron	
189a	Cl	Me	2.036	2.197(Cl)	octahedron	216
			2.015	2.089(C)		

TABLE 24. Comparison of ^{29}Si NMR data for hexa- and tetracoordinate silicon compounds

Compound	X	Y	δ^{29}Si (ppm) ($J_{\text{Si−X}}$, Hz)	Tetracoordinate model	δ^{29}Si (ppm) ($J_{\text{Si−X}}$, Hz)	References
184a	H	F	−37.3 (285.4)			217
184b	H	H	−41.1 (216.4)	$(1\text{-Np})_2SiH_2$	−38.7 (197.7)	217
184d	C≡CH	C≡CH	−63.8	$Ph_2Si(C{\equiv}CH)_2$	−48.2	214
184e	Cl	Cl	−33.6			213
184i	F	F	−61.4 (276.9)	Ph_2SiF_2	−29.1 (302.7)	213
185a	F	F	−52.8 (273.0)	Ph_2SiF_2	−29.1 (302.7)	194
186	H	H	−51.3 (194.0)	Ph_2SiH_2	−33.8	215
188a	Me	Cl	−121.0	$MeClSi(OSiMe_3)_2$	−46.2	211
188b	Ph	Cl	−128.8			221
188c	H	Cl	−137.7 (341.8)	$HClSi(O-)_2$	−64.8 (381)	211
188d	Cl	Cl	−147.2			211
188e	Ph	F	−148.6 (272.9)	$PhFSi(O-)_2$		222
188f	F	F	−160.7 (202.0)			213
193a	Me	Cl	−78.9			212
193b	Cl	Cl	−100.1			212

It is interesting to note that in **186** the two N-dimethylamino ligands are in *cis* positions relative to each other, despite the fact that hydrogens, and no electronegative ligands, are in the apical positions, and the likely expectation that the aromatic-ring planarity would prefer the *trans* arrangement[215].

Like ^{29}Si chemical shifts, also the Si−H coupling constants are sensitive to the hybridization at silicon, and not only to the formal coordination number. The increase in coordination number is normally associated with a decrease in ^{29}Si−^{1}H coupling constants (and ^{29}Si−^{19}F coupling as well), due to rehybridization at silicon and the associated decrease in the Si−H (or Si−F) s-character. However, since in the bicapped-tetrahedral complexes there is essentially no change in hybridization at silicon, the coupling constants do not change significantly. To the extent that Si−H coupling constants do change, they have the *opposite* trend, since the weakly coordinated ligands add electron density to the Si−H bonds[217].

Chemical shifts for the hexacoordinate complexes behave differently relative to pentacoordinate complexes. Firstly, no significant temperature dependence of chemical shifts was observed for hexacoordinate complexes[211,215], in contrast to pentacoordinate complexes. Comparison of ^{29}Si chemical shifts for the hexacoordinate octahedral complexes reveals a trend as a function of monodentate ligand electronegativity[211,220]. Thus ^{29}Si resonance in octahedral complexes seems to shift uniformly upfield as the monodentate ligands are more electronegative (−128.8 ppm in **188b** with X = Ph and Y = Cl, and −148.6 ppm in **188e** in which X = Ph and Y = F, i.e. F replaced Cl; likewise we find −137.7 ppm in **188c** with X = H and Y = Cl, and −147.2 ppm in **188d** where X = Y = Cl). This is in contrast to pentacoordinate complexes, in which the chemical shift responds to the *apicophilicity* of the ligands and not to electronegativity[4,77].

3. Stereodynamics

Neutral hexacoordinate silicon complexes can undergo a variety of ligand exchange reactions, which are observable by NMR spectroscopy. These may include intermolecular exchange via an increase in the coordination number (i.e. nucleophilic substitution) or a decrease in coordination of silicon (i.e. dissociation). Alternatively, ligand exchange can be intramolecular and nondissociative, in analogy to pseudorotation in pentacoordinate silicon compounds[211,217]. Such internal ligand permutations have been described as twists of one triangular face of the octahedral skeleton with respect to the opposite face, in what are generally termed Bailar[195a] and Ray–Dutt[195b] twists. The richness of possible exchange mechanisms makes it difficult to determine with certainty in each case which mechanism actually takes place, and considerable work has been published on the stereodynamic behavior of hexacoordinate neutral complexes.

At least three different ligand exchange mechanisms, which operate simultaneously, have been reported in a series of complexes, **188–192**[211,222]. The slowest of the exchange processes is intermolecular, and is effective at the laboratory time scale, i.e. exchange takes place within minutes to several hours. It consists of exchange of the electronegative ligands from a silane to the hexacoordinate complex (equation 51), in a selective manner: Y replaces any X which is positioned to its right in the following priority list: Cl > H > Ph > Me[220]. The exact mechanism and scope of this reaction have not yet been reported.

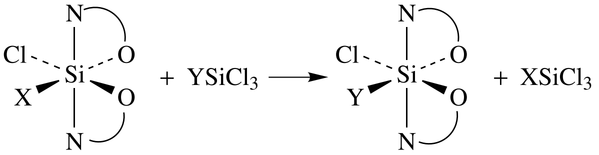

(51)

(188 – 192)

In addition, **188–192** undergo two rate processes at the NMR time scale, which have been studied in more detail[211,220]. All of these compounds appear as a single diastereomer in solution, despite the existence, in principle, of six geometrical arrangements for each of the complexes. Since the diastereomer present in solution is chiral, the four N-methyl groups are unique and give rise to four singlets in the NMR spectra at the slow exchange limit temperature. These coalesce, as the temperature is raised, in two distinct steps: first to two singlets, with one activation barrier, and at slightly higher temperature to a singlet, with another barrier. The barriers were independent of concentration, within a tenfold concentration range, indicating intramolecular exchange for both processes. The lower of the two rate processes was shown to involve exchange of the two chelate rings: in **188a**, for example, the initial coalescence of N-methyl signals from four to two was accompanied by a simultaneous exchange of the C-methyl groups, residing on different chelate cycles.

The ligand exchange barriers were found to depend substantially on the solvent. For **189b** the exchange barriers were studied in several solvents (Table 25). The apolar solvents (benzene-d$_6$, toluene-d$_8$ and CCl_4) displayed the highest barriers; the π-acceptor solvents (nitrobenzene-d$_5$, acetone-d$_6$) had barriers lower by *ca* 2 kcal mol^{-1}, while the hydrogen-bond donors chloroform-d and dichloromethane-d$_2$, as well as the strong acceptor nitromethane-d$_3$, gave the lowest barriers. This suggested that the solvent attaches to the dimethylamino nitrogens and weakens the Si–N coordination.

Additional evidence for the relationship of barriers with the Si–N coordination strength came from the observation of a linear correlation between barriers and the corresponding ^{29}Si chemical shifts (Figure 26). Both the barriers and the ^{29}Si chemical shifts are effected by the strengths of coordination.

These results (solvent and chemical shift dependence of the barriers) suggested that the exchange process observed involves Si–N cleavage. However, evidence for an intramolecular exchange process was recently obtained from ^{15}N NMR spectroscopy[221,222], through direct observation of ^{15}N–(Si)–^{1}H coupling *across the dative bond* [**188c**, ^2J(N–Si–H) = 11.5 Hz; **189c**, ^2J(N–Si–H) = 12.9 Hz; **190c**, ^2J(N–Si–H) = 13.0 Hz]. The persistence of ^2J(N–Si–H) up to 355 K in **188c–190c** is evidence that intermolecular ligand exchange does not occur at the time scale at which N-methyl exchange is rapid[221].

TABLE 25. Solvent effect on activation free energies for exchange of NMe groups in **189b**[211]

Solvent	$\Delta G_1^\ddagger$ (kcal mol^{-1})	$\Delta G_2^\ddagger$ (kcal mol^{-1})
CCl_4	16.4	16.9
$C_6D_5CD_3$	15.8	16.4
C_6D_6	16.3	16.7
C_4Cl_6	16.6	16.9
C_5D_5N	13.9	16.1
$C_6D_5NO_2$	13.2	16.2
$(CD_3)_2CO$	13.8	15.0
CD_2Cl_2	10.6	15.0
CD_3NO_2	10.6	16.0

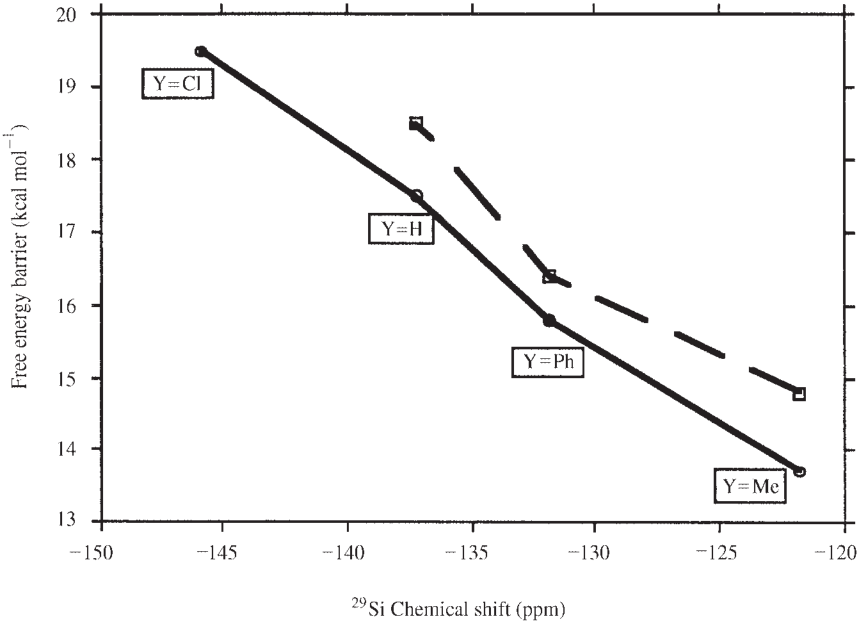

FIGURE 26. Activation free energies for two exchange barriers in **189a–189d** as a function of the ^{29}Si chemical shift[211]

Direct evidence was also obtained that no Si–F dissociation takes place in **188e** during the exchange process of N-methyl groups[222]: The one-bond ^{19}F–^{29}Si coupling constant (273 Hz) persisted essentially unchanged upon heating up to 350 K, at which N-methyl coalescence had occurred. By analogy it was also concluded that in the Si–Cl complexes no dissociation took place, in view of very similar behavior. It was thus shown that both of the observed ligand exchange processes are nondissociative.

Since only one diastereomer was observed in solution, any exchange process must be a topomerization, i.e. an exchange of diastereotopic groups within the original, unchanged diastereomer. Neither of the common exchange mechanisms (Bailar and RD twists) can account for a direct topomerization. However, it was argued that if a series of consecutive Bailar and/or RD twists were to occur and effect an overall topomerization in several steps, it would be difficult to justify two distinct exchange barriers in all of the compounds. The proposed exchange mechanism which seemed to account best for all of the observations in this series **(188–192)** was a 1,2-shift of adjacent ligands via a bicapped-tetrahedron-like transition state or intermediate. The two processes of this kind are the exchange of Cl and Y, and of the two chelate oxygens, labeled (Cl, Y)- and (O, O)-exchange, respectively (Figure 27). The former is a true topomerization, while the second converts the complex to its enantiomer. The arguments put forth in support of this mechanism are: (a) It offers two distinct and yet closely related exchange processes with slightly different activation barriers. (b) The process involves elongation of the dative bonds (up to 32%, according to one analysis)[223], which explains both the solvent dependence and the correlation of barriers with ^{29}Si chemical shifts, without Si–N cleavage. (c) The two processes generate the observed spectral changes and coalescence phenomena: examination of the processes showed that (Cl, Y)-exchange effects equilibration and coalescence of signals of the two chelate rings, while (O, O)-shift exchanges the chelate rings and in addition inverts the configuration at silicon. (d) The reports by Corriu and coworkers of hexacoordinate complexes which have the bicapped-tetrahedron geometry *in the ground state*[194,214] make such a structure a very reasonable intermediate or low-energy transition state.

The distinction between the two 1,2-shift mechanisms (i.e. the assignment of each to the lower and higher energy processes) was achieved by the study of the chiral complex **192b**, made of the optically pure (*R*) ligand[221,222]. The solution of **192b** contains two diastereomers, *RRR* and *RSR*, differing in configuration at the silicon atom. Since the (Cl, Ph)-exchange is a topomerization, and does not effect epimerization at silicon, no interchange of the two diastereomers is involved. On the other hand, the (O, O)-exchange epimerizes the silicon configuration, and constitutes the exchange: *RRR* $\rightleftharpoons$ *RSR*. It follows that the former exchange is only *within* each diastereomer, whereas the latter is *between* the diastereomers. A 2D-NOESY and Saturation-Transfer experiment at low temperature clearly revealed that the first (low activation) process interchanges signals belonging to the same diastereomer only, i.e. the low-activation process was identified as (Cl, Ph)-exchange[222].

Another series of neutral hexacoordinate complexes for which exchange reactions have been studied is the group of bis-(8-dimethylamino-1-naphthyl)silanes **184**, whose structure in the solid corresponded to a bicapped tetrahedron[194,217]. The nonsymmetrically substituted **184a** and **184f** are chiral and give rise to four N-methyl signals, which coalesce to two signals. The fact that the geminal N-methyl groups remained diastereotopic is evidence that the observed process was a nondissociative (regular) exchange involving epimerization at silicon: Si−N cleavage would have permitted rotation about the N−Ph bond and exchange of geminal methyls, and was ruled out[217]. The intramolecular exchange was attributed to one of the twist mechanisms: Bailar, RD or Springers–Sievers[217]. Table 26 lists the free energies of activation measured in these compounds for N-methyl exchange.

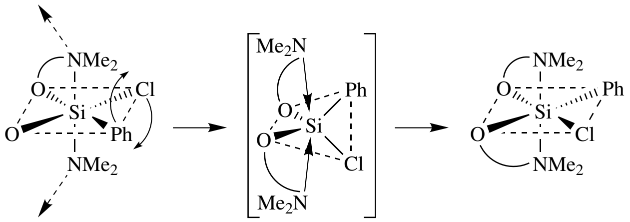

'Bicapped Tetrahedron'
(Ph-Cl) 1,2-shift

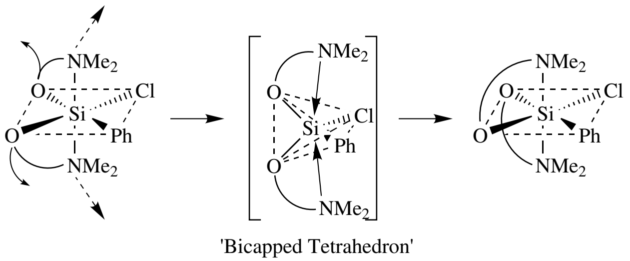

'Bicapped Tetrahedron'
(O,O) 1,2-shift

FIGURE 27. 1,2-shift mechanism of topomerization via 'bicapped tetrahedron' intermediate or transition state: upper part, (Ph, Cl)-interchange; lower part, (O, O)-interchange[211]

TABLE 26. Free energies of activation for isomerization of hexacoordinate compounds (at 300 K)[217]

Compound	X	Y	$\Delta G^{\ddagger}$ (kcal mol^{-1})
184a	H	F	14.7
184f	H	OMe	15.2
184g	H	Me	9.3
184h	Me	Ph	12.7

When the monodentate ligands in **184** are equivalent, the molecule has a C_2 symmetry axis and the chelate rings are homotopic and equivalent. As a result the four N-methyl groups give rise to two singlets. In **184c** the coalescence of the N-methyl signals to a singlet was observed, and the barrier for exchange was determined as 20.5 kcal mol^{-1}. It was not possible, however, to determine whether the barrier was due to Si−N dative bond cleavage or to a nondissociative isomerization of ligands around silicon[206].

The DNMR study of **186** revealed, as expected, the equivalence of the two silicon complexes, as well as the equivalence, at room temperature, of all the methyl groups and methylene protons, respectively[215]. When the temperature was lowered, the geminal methyls and the geminal protons became diastereotopic, while the two (dimethylamino)methyl groups attached to each aromatic ring remained equivalent. Over this temperature range the Si−H protons also remained isochronous *(chemical shift equivalent)*. To rationalize this NMR behavior, the authors offered two alternative explanations: either that in solution the predominant conformation was as in the crystal, i.e. with the dimethylamino groups in *cis* positions and the Si−H protons in *cis* positions, with a rapid Bailar-type twist rendering the Si−H and the (dimethylamino)methyl groups equivalent, respectively. Alternatively, the conformation with C_s symmetry depicted in **186a** is predominant in solution, which *a priori* renders the two Si−H and two (dimethylamino)methyl groups equivalent[215]

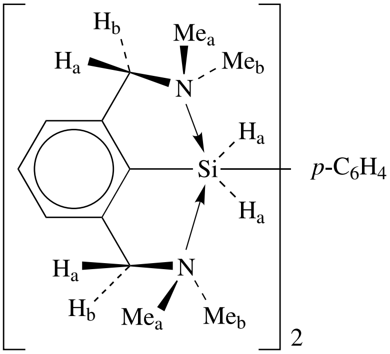

(186a)

At lower temperatures the methylene protons and the N-methyl groups decoalesced in two distinct rate processes: $\Delta G^{*}{}_{\mathrm{Me}} = 8.4$ kcal mol^{-1}; $\Delta G^{*}_{\mathrm{CH_2}} = 11.5$ kcal mol^{-1}. This was interpreted by the authors as Si−N dissociation leading to N-methyl exchange, with a concomitant rotation about the Si-aromatic bond (with a slightly higher barrier) to account for the exchange of geminal methylene protons[215].

B. Intermolecular Coordination

Polyhalosilanes form neutral intermolecular hexacoordinate complexes with donor molecules such as pyridine, triethylamine, 2,2′-bipyridine and 1,10-phenanthroline. This topic has recently been reviewed[6]. It was demonstrated that electronegative substituents on the silicon are essential for the formation of intermolecular complexes. Thus, while $SiCl_4$ and $Cl_2CHSiCl_3$ react with 1,10-phenanthroline and with 2,2′-bipyridine to form hexacoordinate chelates, $MeSiCl_3$ does not react[224,225]. For completion we discuss here a few examples, and compare some of the properties of intermolecular complexes with those of the intramolecular complexes.

An interesting example of an intermolecular complex is the trisilicon complex **194**, in which only the central silicon is coordinated to the bidentate donor molecule[225]. The structure is a regular octahedron, with two tetrahedral termini. The silicon nitrogen bonds are rather short (2.012 and 1.991 Å), and are comparable to those of octahedral intramolecular complexes (Table 23). **194** permits a comparison of Si−Cl bonds in a tetrahedral silicon moiety (2.03 to 2.07 Å) with Si−Cl bonds *trans* to the dative bond in a hexacoordinate silicon (2.39 and 2.21 Å). As expected, the latter are substatntially longer than the regular covalent bonds.

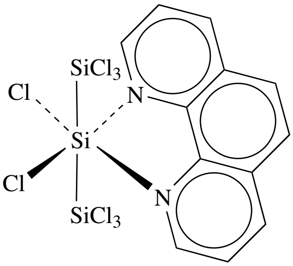

(194)

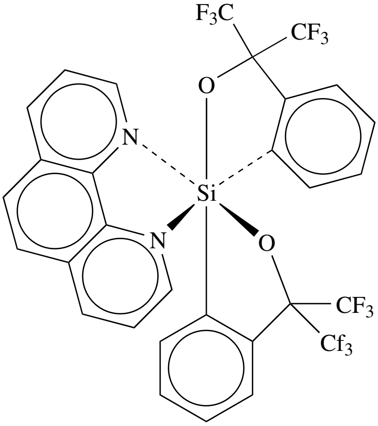

(195a)

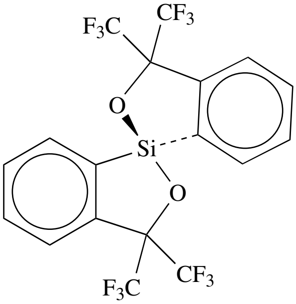

(195b)

A stereodynamic study in an intermolecular complex, **195a**, was reported by Farnham and Whitney[226]. **195a** undergoes intermolecular exchange, which is observed in the ^{19}F NMR spectrum by warming a mixture of **195a** and **195b**. The equilibrium reaction between **195b**, the donor molecule and **195a** provided the mechanism for both the exchange between diastereomers of **195a**, as well as for enantiomerization (exchange of CF_3 groups within **195a**).

A crystallographic structure was reported for an oxygen-coordinated intermolecular complex, $[Si(catecholato)_2]$•2THF **(196)**[201a]. Interestingly, the two catechol ligands in **196** are coplanar ($Si-O_{cat}$ = 1.719, 1.727 Å), while the THF molecules occupy *trans* positions ($Si-O_{THF}$ = 1.930 Å)

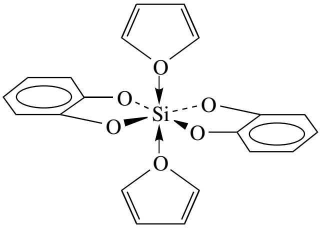

(**196**)

VII. COMPLEXES WITH HIGHER COORDINATION NUMBERS

A few examples have been reported in which presumably silicon has a coordination number greater than six[227–229]. All of the hepta- and octa-coordinated silicon complexes for which single-crystal X-ray diffraction structures were obtained have a basic tetrahedral geometry, with three or four distantly coordinated ligand groups positioned against faces of the tetrahedron, in analogy to the bicapped tetrahedron structure mentioned earlier (Section VI.A.2).

The first reported synthesis of a heptacoordinate complex of silicon **(197)** was accomplished by the reaction of $HSiCl_3$ with 2-lithio-(dimethylaminomethyl)-benzene[227]. The crystal structure was determined later and confirmed the 'tricapped tetrahedron' geometry[81,82]. Replacement of the hydrido ligand by chloro **(198)** led to the formation of a tetracoordinate silane without any dative bonds, apparently due to the steric bulk associated with the chloro ligand[81].

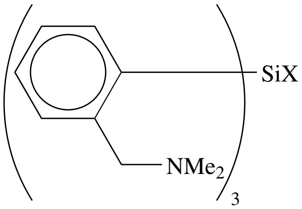

(**197**) X = H
(**198**) X = Cl
(**199**) X = F

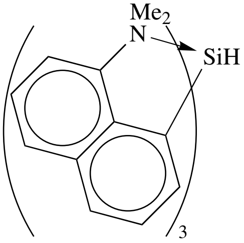

(**200**)

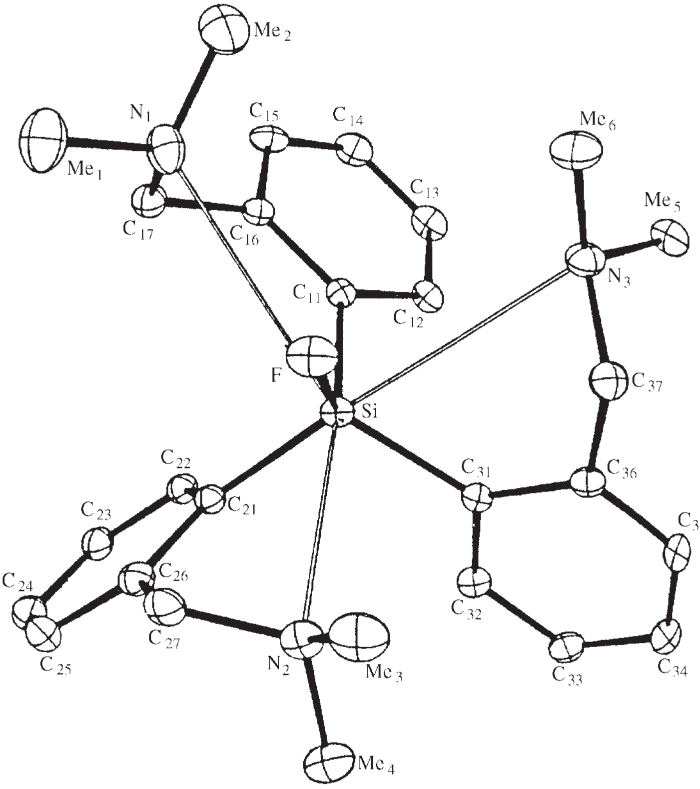

FIGURE 28. Crystallographic structure of the heptacoordinate complex **199**. Reprinted with permission from Reference 228. Copyright 1994 American Chemical Society.

The analogous fluoro compound **(199)** was shown to have heptacoordination[228]. Interestingly, the X-ray crystal structure of **199** (Figure 28) showed that neither of the three nitrogens is coordinated in *trans* position to the Si−F bond, and all three are opposite the Si−C bonds. This was rationalized in terms of the least steric hindrance for approach of the ligand groups from the fluoro side, or, more precisely, from the normals to the triangular faces of the tetrahedron skeleton which have the fluorine in one corner.

A different synthesis of a heptacoordinate silicon complex **(200)** is shown in equation 52. The resulting complex had the same basic tricapped-tetrahedron structure (Figure 29)[228].

Formal octacoordination ('4 + 4')[229] in a silicon complex was recently demonstrated by Corriu's group, who prepared **201** (equation 53). The Si−N distances (Table 27) are long relative to those common in penta- and hexacoordinate compounds, but are in the same range as those found in the heptacoordinate compounds discussed here. Also, the geometry resembles the heptacoordinate complexes, in that it is basically a tetrahedron with dimethylamino donor groups pointing toward the center, in what may be termed a 'tetracapped tetrahedron'.

A similar tetracapped tetrahedral geometry was recently found by X-ray crystallography in bis[2,4,6-tris(trifluoromethyl)phenyl]-fluorosilane **(202)**[230] and -difluorosilane **(203)**[231],

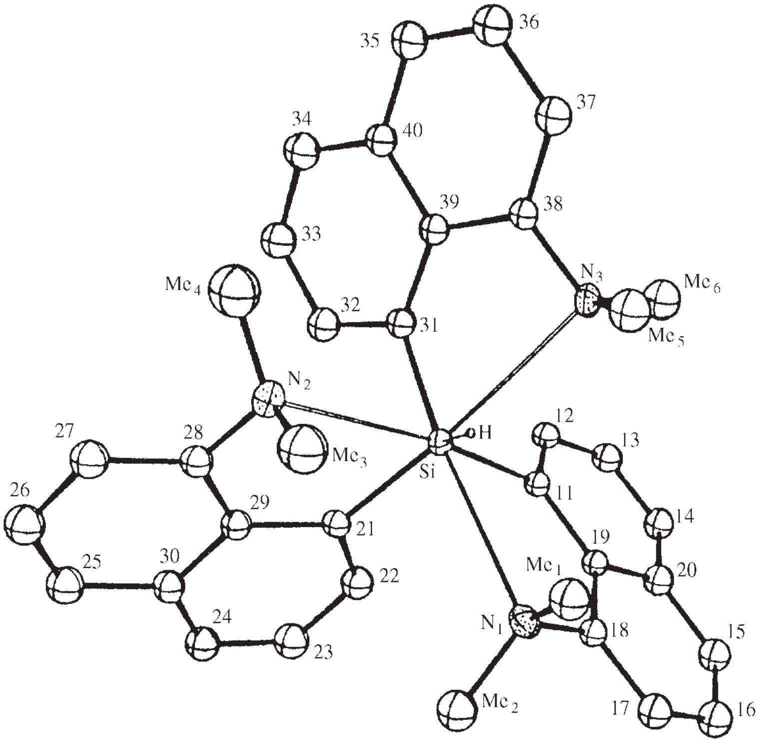

FIGURE 29. X-ray crystallographic structure of **200**. Reprinted with permission from Reference 228, Copyright 1994 American Chemical Society

in which one fluorine atom from each of the *ortho* CF_3 groups is coordinated to silicon.

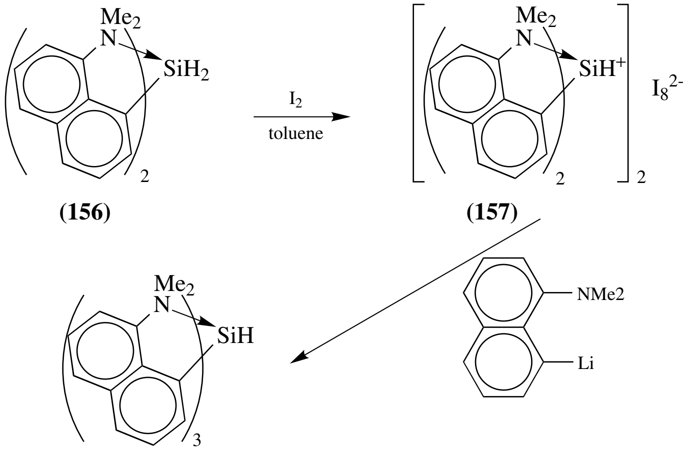

(156) **(157)**

(52)

(200)

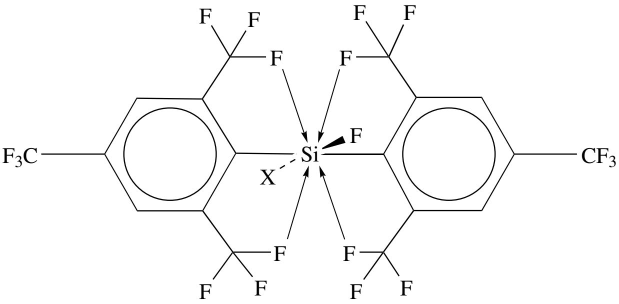

(202) X = H
(203) X = F

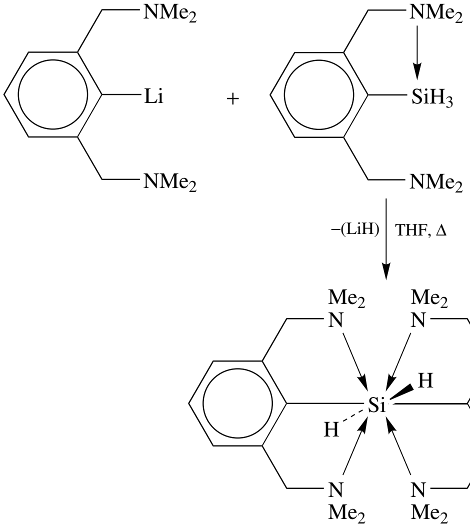

(53)

(**201**)

Table 27 lists the ^{29}Si chemical shifts for the high coordination complexes. Triphenylsilane serves as a tetracoordinate model for the complexes **197** and **200**, for comparison. It can be seen that the increased coordination in the latter complexes effects a small upfield shift, much smaller than is normally observed upon going from tetra- to penta- (Table 11, Section III.A.2.b) and hexacoordination (Table 24, Section VI.A.2). This is in accord with the crystallographic results, which show that no significant change in hybridization takes place in these compounds, in contrast to TBP and octahedral complexes.

In line with this result, also the one-bond Si−H coupling constants respond differently to hepta- and octacoordination than to TBP and octahedral geometries (Table 27). While in the latter the change in coordination brings about a decrease in the Si−H s-character, with consequent decrease in ^{1}J(Si−H), in the *higher* coordinated compounds described in this section there is no significant change in s-character, and the only effect is some addition of electron density to the silicon due to donation from the ligands resulting in *increased* ^{1}J(Si−H).

TABLE 27. X-ray crystallographic and ^{29}Si NMR data for hepta- and octacoordinate silicon complexes and tetravalent model compounds

Compound	Si−N (Å)			δ^{29}Si (ppm) ($J_{\text{Si-H}}$, Hz)	References
197	3.006	3.039	2.997	−34.9(226.4)	81, 82
	2.981	3.009	3.043		
199	3.489	3.004	3.307	−9.86	228
200	2.882	2.876	2.928	−25.86(284.0)	228
201	3.117	2.895		−61.6(213.0)	229
Ph_3SiH				−21.1(205.1)	40
Ph_2SiH_2				−33.8(200.0)	40

The ^{1}H NMR specrum of **201** showed all four dimethylamino groups to be equivalent, an indication of rapid exchange between them. This presumably occurs by rapid displacement of one group by the other.

Finally, a group of hypercoordinated silicon compounds, the decamethyl silicocenes, in which the formal silicon coordination number is ten, is worthy of mention in connection with this chapter. These analogs of ferrocene have been studied extensively[232], and are described in detail in Jutzi's chapter in this volume.

VIII. ADDENDUM

Since the major parts of this chapter were written in July 1996, a number of papers dealing with hypervalent silicon compounds were published[233−251]. In this late addendum we have tried to cite all the recent relevant publications and give a very brief account of their content. The following citations have been arranged in the order of the most relevant sections in this chapter.

For Section I

Crystal structures of hypervalent silicon complexes were discussed in detail and reviewed by Lukevics and Pudova[233].

For Section II

An equilibrium reaction between a pentaorganosilicate complex (**204**) and its tetracoordinate precursor **205** and methyllithium was observed using ^{29}Si NMR spectroscopy at low temperature[234].

A novel fluoro-bridged complex, pentafluoro-1,4-disilacyclohexane anion (**206**), was reported to undergo unusual intramolecular fluoride ion exchange between two silicon atoms, synchronized with a ring inversion process[235].

A new mass spectrometric technique, triple quadrupole detection, was employed to study 1,1-dimethyl-1-fluorosilacyclobutane anion, a pentacoordinate silicate[236].

A theoretical comparison between the structures and properties of cyclic pentacoordinate anionic pentaoxysilicates and phosphoranes is described[237]. The results are compared with NMR and X-ray crystallographic data.

The preparation of a novel neutral zwitterionic λ^5-spirosilicate and its characterization was reported[238].

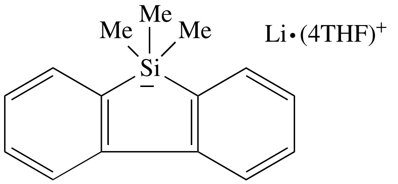

(**204**)

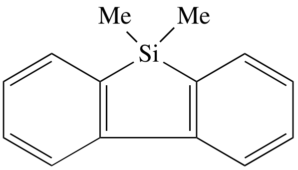

(**205**)

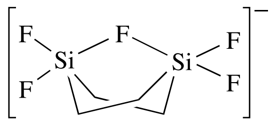

(206)

For Section III

New neutral pentacoordinate silicon complexes with a dative O→Si bond **(207, 208)** have been prepared and studied. The NMR spectral data and crystal structures were reported[239].

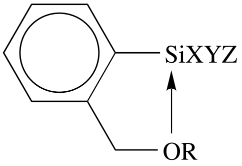

(207a) X = Y = Z = F, R = Me
(207b) X = Y = Z = F, R = $CHMe_2$
(208) X = H, Y = Ph, Z = OSO_2CF_3, R = Me

Pentacoordinate O→Si complexes analogous to series **117** with the chiral (R = 1-phenylethyl) ligand were prepared, with various electronegative ligands, (**117k–117n**, X = F, Cl, Br, $OCHMe_2$, respectively). Their stereochemical nonrigidity was studied by variable-temperature ^{29}Si NMR spectroscopy[240].

A study of the solvolytic and thermolytic reactions of a series of heterocyclic pentacoordinate silicon complexes was described[241].

A novel (3,3) sigmatropic rearrangement of a hexacoordinate allyl–silicon complex (neutral tetraoxyspirosilicate) to a pentacoordinate complex was recently described[242]. The allyl group migrates from silicon to the α-carbon of a tropolone ligand[242].

Trapping of an intermediate silylene by reaction with diphenylacetylene to form a pseudo-pentacoordinate silole **(209)** was reported[243]. The silylene was obtained by a Ni(0)-catalyzed degradation of **92f** (X = $SiPh_3$, Y = Me, Z = H)[243].

For Section IV

A full discussion of earlier preliminary results[186] (discussed in this review) has now appeared[244].

A high-level theoretical investigation of the structure of the experimentally studied compound **160a** and some of its analogs is described[245]. The question of solvation of a silicenium cation is addressed and **160a** served as a model[245].

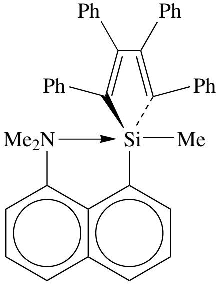

(209)

For Section V

Treatment of tetracoordinated silanes by the NCS^- anion afforded some new pentacoordinate anionic spirobicyclic siliconates $[(C_6H_4O_2)_2SiNCS]^-M^+$ with various M^+ counter cations[246], as well as some hexacoordinate dianions $[(C_6H_4O_2)_2Si(NCS)_2]^{-2}$.

3-Picoline was found to react in chloroform solution with bis(dichlorosilyl)amine to form two hexacoordinate silicon complexes: the ionic $[H_2Si(3\text{-}MeC_5H_4N)_4]^{2+}\cdot 2Cl^-$ and a neutral $H_2Si(3\text{-}MeC_5H_4N)_2Cl_2$. These complexes are in equilibrium with each other in chloroform solution. The crystal structure of the ionic complex was reported[247].

For Section VI

Karsch and coworkers report the formation of new penta- **(210)** and hexacoordinate **(211)** complexes with novel bidentate phosphorus-donor ligands[248–250]. The phosphorus ligands form four-membered chelate rings (siladiphosphacyclobutane). Interestingly, the crystal structure of **210** indicates a near-square pyramid[248]. The hexacoordinate complexes were found to have the *cis* geometry when the monodentate ligands are methyl groups[250], and *trans* geometry for dichloro complexes[249] (i.e. the monodentate ligands adopt either the *trans* or the *cis* geometry). For **211c** both *cis* and *trans* isomers were obtained, and the former rearranged spontaneously to the latter at room temperature[249].

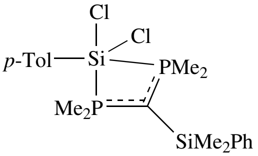

(210)

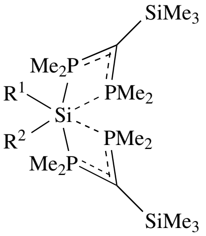

(211a) $R^1R^2 = -(CH_2)_3$

(211b) $R^1 = R^2 = Me$

(211c) $R^1 = R^2 = Cl$

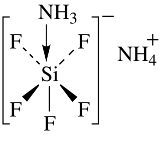

(212)

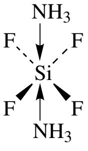

(213)

The reaction of silicon powder with NH_4HF_2 at 400 °C in a sealed ampoule afforded single crystals of the hexacoordinate complexes **(212)** and **(213)**. The crystallographic analyses of both compounds showed near-octahedral arrangements, with the NH_3 groups of the latter compound in *trans* positions[251].

IX. REFERENCES

1. S. N. Tandura, M. G. Voronkov and N. V. Alekseev, *Top. Curr. Chem.*, **131**, 99 (1986).
2. R. J. P. Corriu and J. C. Young, in *The Chemistry of Organic Silicon Compounds* (Eds. S. Patai and Z. Rappoport), Wiley, Chichester, 1989, pp. 1241–1288.
3. W. S. Sheldrick, in *The Chemistry of Organic Silicon Compounds* (Eds. S. Patai and Z. Rappoport), Wiley, Chichester, 1989, pp. 227–304.
4. (a) R. R. Holmes, *Chem. Rev.*, **90**, 17 (1990).
   (b) R. R. Holmes, *Chem. Rev.*, **96**, 927 (1996).
5. R. J. P. Corriu, *J. Organomet. Chem.*, **400**, 81 (1990).
6. C. Chuit, R. J. P. Corriu, C. Reye and J. C. Young, *Chem. Rev.*, **93**, 1371 (1993).
7. C. Y. Wong and J. D. Woollins, *Coord. Chem. Rev.*, **130**, 175 (1994).
8. (a) R. Müller, *Organomet. Chem. Rev.*, **1**, 359 (1966).
   (b) R. Müller, *Z. Chem.*, **24**, 41 (1984).
9. Reviews:
   (a) M. G. Voronkov and L. I. Gubanova, *Main Group Metal Chem.*, **10**, 209 (1987).
   (b) V. O. Gel'mbol'dt and A. A. Ennan, *Usp. Khim.*, **58**, 626 (1989); *Chem. Abstr.*, **111**, 174159g (1989).
10. (a) D. Schomburg, *J. Organomet. Chem.*, **221**, 137 (1981).
    (b) D. Schomburg and R. Krebs, *Inorg. Chem.*, **23**, 1378 (1984).
11. (a) R. Damrauer and S. E. Danahey, *Organometallics*, **5**, 1490 (1986).
    (b) R. Damrauer, B. O'Connell, S. E. Danahey and R. Simon, *Organometallics*, **8**, 1167 (1989).
12. J. J. Harland, J. S. Payne, R. O. Day and R. R. Holmes, *Inorg. Chem.*, **26**, 760 (1987).
13. (a) S. E. Johnson, R. O. Day and R. R. Holmes, *Inorg. Chem.*, **28**, 3182 (1989).
    (b) S. E. Johnson, J. S. Payne, R. O. Day, J. M. Holmes and R. R. Holmes, *Inorg. Chem.*, **28**, 3190 (1989).
14. S. E. Johnson, J. A. Deiters, R. O. Day and R. R. Holmes, *J. Am. Chem. Soc.*, **111**, 3250 (1989).
15. F. Scherbaum, B. Huber, G. Muller and H. Schmidbaur, *Angew. Chem., Int. Ed. Engl.*, **27**, 1542 (1988).
16. F. Klanberg and E. L. Muetterties, *Inorg. Chem.*, **7**, 155 (1968).
17. (a) K. Tamao, T. Hayashi and Y. Ito, *Organometallics*, **11**, 2099 (1992).
    (b) K. Tamao, T. Hayashi, Y. Ito and M. Shiro, *J. Am. Chem. Soc.*, **112**, 2422 (1990).
    (c) K. Tamao, T. Hayashi and Y. Ito, *J. Organomet. Chem.*, **506**, 85 (1996).
18. K. Tamao, T. Hayashi, Y. Ito and M. Shiro, *Organometallics*, **11**, 182 (1992).
19. H. B. Bürgi and J. Dunitz, *Acc. Chem. Res.*, **16**, 153 (1983).
20. (a) R. O. Day, C. Sreelatha, J. A. Deiters, S. E. Johnson, J. M. Holmes, L. Howe and R. R. Holmes, *Organometallics*, **10**, 1758 (1991).
    (b) R. O. Day, C. Sreelatha, J. A. Deiters, S. E. Johnson, J. M. Holmes, L. Howe and R. R. Holmes, *Phosphorus, Sulfur Silicon Relat. Elem.*, **100**, 87 (1995).
21. (a) J. A. Cella, J. D. Cargioli and E. A. Williams, *J. Organomet. Chem.*, **186**, 13 (1980).
    (b) V. F. Sidorkin, V. A. Pestunovich and M. G. Voronkov, *Magn. Res. Chem.*, **23**, 491 (1985).
22. M. Kira, T. Hoshi and H. Sakurai, *Chem. Lett.*, 807 (1995).
23. H. J. Frohn and V. V. Bardin, *J. Organomet. Chem.*, **501**, 155 (1995).
24. D. Brondani, F. H. Carre, R. J. P. Corriu, J. J. E. Moreau and M. Wong Chi Man, *Angew. Chem., Int. Ed. Engl.*, **35**, 324 (1996).
25. D. A. Loy, J. H. Small and K. J. Shea, *Organometallics*, **12**, 1484 (1993).
26. M. Kira, T. Hoshi, C. Kabuto and H. Sakurai, *Chem. Lett.*, 1859 (1993).
27. R. O'Dell, *Tetrahedron Lett.*, **36**, 5723 (1995).
28. R. Tacke, J. Becht, A. Lopez-Mras and G. Sperlich, *J. Organomet. Chem.*, **446**, 1 (1993).
29. R. Tacke, J. Becht, O. Dannappel, M. Kropfgans, A. Lopez-Mras, M. Mühleisen and J. Sperlich, in *Progress in Organosilicon Chemistry* (Eds. B. Marciniec and J. Chojnowski), Gordon and Breach, Basel, 1995, pp. 55–68.

30. (a) R. Tacke, O. Dannappel and M. Mühleisen, in *Organosilicon Chemistry II* (Eds. N. Auner and J. Weis), VCH, Weinheim, 1996, pp. 427–446.
    (b) R. Tacke, J. Becht, O. Dannappel, R. Ahlrichs, U. Schneider, W. S. Sheldrick, J. Hahn and F. Kiesgen, *Organometallics*, **15**, 2060 (1996).
31. (a) R. Tacke, J. Becht, G. Mattern and W. F. Kuhs, *Chem. Ber.*, **125**, 2015 (1992).
    (b) R. Tacke, A. Lopez-Mras, J. Becht and W. S. Sheldrick, *Z. Anorg. Allg. Chem.*, **619**, 1012 (1993).
32. For early discussions of this topic see:
    (a) R. Müller and L. Heinrich, *Chem. Ber.*, **94**, 1943 (1961).
    (b) C. L. Frye, *J. Am. Chem. Soc.*, **86**, 3170 (1964).
    (c) C. L. Frye, *J. Am. Chem. Soc.*, **92**, 1205 (1970).
    (d) D. Shomburg, *Z. Naturforsch.*, **37B**, 195 (1982).
33. J. J. Harland, R. O. Day, J. F. Vollano, A. C. Sau and R. R. Holmes *J. Am. Chem. Soc.*, **103**, 5269 (1981).
34. K. C. Kumara Swamy, V. Chandrasekhar, J. J. Harland, J. M. Holmes, R. O. Day and R. R. Holmes, *J. Am. Chem. Soc.*, **112**, 2341 (1990).
35. (a) E. F. Perozzi and J. C. Martin, *J. Am. Chem. Soc.*, **101**, 1591 (1979).
    (b) W. H. Stevenson III, S. Wilson, J. C. Martin and W. B. Farnham, *J. Am. Chem. Soc.*, **107**, 6340 (1985).
36. R. M. Laine, K. Y. Blohowiak, T. R. Robinson, M. L. Hoppe, P. Nardi, J. Kampf and J. Uhm, *Nature*, **353**, 642 (1991).
37. (a) K. C. Kumara Swamy, Channareddy Sreelatha, R. O. Day, J. Holmes and R. R. Holmes, *Inorg. Chem.*, **30**, 3126 (1991).
    (b) K. C. Kumara Swamy, Channareddy Sreelatha, R. O. Day, J. Holmes and R. R. Holmes, *Phosphorus, Sulfur Silicon Relat. Elem.*, **100**, 107 (1995).
38. D. F. Evans, A. M. Z. Slawin, D. J. Williams, C. Y. Wong and J. D. Woollins, *J. Chem. Soc., Dalton Trans.*, 2383 (1992).
39. J. L. Brefort, R. J. P. Corriu, C. Guerin, B. J. L. Henner and W. W. C. Wong Chi Man, *Organometallics*, **9**, 2080 (1990).
40. H. Marsmann, *Nucl. Magn. Reson.*, **17**, 65, (1981).
41. D. A. Dixon, W. R. Hertler, D. B. Chase, W. B. Farnham and F. Davidson, *Inorg. Chem.*, **27**, 4012 (1988).
42. F. P. Boer, J. J. Flynn and J. W. Turley, *J. Am. Chem. Soc.*, **90**, 6973 (1968).
43. R. R. Holmes, R. O. Day, V. Chandrasekhar and J. M. Holmes, *Inorg. Chem.*, **24**, 2009, 2016 (1985).
44. R. R. Holmes, R. O. Day, J. J. Harland, A. C. Sau and J. M. Holmes, *Organometallics*, **3**, 341 (1984).
45. R. R. Holmes, R. O. Day, J. J. Harland and J. M. Holmes, *Organometallics*, **3**, 347 (1984).
46. R. Tacke, A. Lopez-Mras, J. Sperlich, C. Strohmann, W. Kuhs, G. Mattern and A. Sebald, *Chem. Ber.*, **126**, 851 (1993).
47. R. Tacke, M. Mühleisen, A. Lopez-Mras and W. S. Sheldrick, *Z. Anorg. Allg. Chem.*, **621**, 779 (1995).
48. R. Tacke, J. Sperlich, C. Strohmann and G. Mattern, *Chem. Ber.*, **124**, 1491 (1991).
49. R. Tacke, A. Lopez-Mras and P. G. Jones, *Organometallics*, **13**, 1617 (1994).
50. M. Mühleisen and R. Tacke, *Chem. Ber.*, **127**, 1615 (1994).
51. M. Mühleisen and R. Tacke, in *Organosilicon Chemistry II* (Eds. N. Auner and J. Weis), VCH, Weinheim, 1996, pp. 447–452.
52. O. Dannappel and R. Tacke, in *Organosilicon Chemistry II* (Eds. N. Auner and J. Weis), VCH, Weinheim, 1996, pp. 453–458.
53. (a) N. Erchak, A. Kemme and G. Ancens, *Xth International Symposium on Organosilicon Chemistry*, August 15–20, 1993, Poznan, Poland. Abstract, **P - 35**, p. 159.
    (b) N. Erchak, *Xth International Symposium on Organosilicon Chemistry*, August 15–20, 1993, Poznan, Poland. Abstract, **O - 29**, p. 77.
54. (a) N. P. Erchak, Doct. Dissertation Latvian Inst. of Organic Synthesis, Riga 1990.
    (b) N. P. Erchak, G. A. Ancens, A. A. Kemme and E. J. Lukevics, *XI International Symp. on Organosilicon Chemistry*, Montpellier, France 1996, p. PA60.
55. G. Cerveau, C. Chuit, E. Colomer, R. J. P. Corriu and C. Reye, *Organometallics*, **9**, 2415 (1990).
56. N. Erchak, G. Ancens and V. Ryabova, *Xth International Symposium on Organosilicon Chemistry*, August 15–20, 1993, Poznan, Poland. Abstract, **P - 179**, p. 299.

57. (a) M. Mühleisen and R. Tacke., *Organometallics*, **13**, 3740 (1994).
(b) R. Tacke, M. Mühleisen and P. G. Jones, *Angew. Chem., Int. Ed. Engl.*, **33**, 1186 (1994).
58. (a) K. J. Shea, D. A. Loy and J. H. Small, *Chem. Mater.*, **4**, 255 (1992).
(b) J. H. Small, D. J. McCord, J. Greaves and K. J. Shea, *J. Am. Chem. Soc.*, **117**, 11588 (1995).
59. B. Becker, R. J. P. Corriu, C. Guerin, B. Henner and Q. Wang, *J. Organomet. Chem.*, **368**, C25 (1989).
60. R. J. P. Corriu, C. Guerin, B. Henner and Q. Wang, *Organometallics*, **10**, 2297 (1991).
61. R. J. P. Corriu, C. Guerin, B. J. L. Henner and Q. Wang, *Organometallics*, **10**, 3574 (1991).
62. R. J. P. Corriu, C. Guerin, B. J. L. Henner and Q. Wang, *J. Organomet. Chem.*, **439**, C1 (1992).
63. A. R. Bassindale and J. Jiang, *J. Organomet. Chem.*, **446**, C3 (1993).
64. R. Damrauer, L. W. Burggrae, L. P. Davis and M. S. Gordon, *J. Am. Chem. Soc.*, **110**, 6601 (1988).
65. D. J. Hajdasz, Y. Ho and R. R. Squires, *J. Am. Chem. Soc.*, **116**, 10751 (1994).
66. C. H. DePuy, R. Damrauer, J. H. Bowie and J. C. Sheldon, *Acc. Chem. Res.*, **20**, 127 (1987).
67. (a) R. Damrauer, *Adv. Silicon Chem.*, **2**, 91 (1993).
(b) R. Damrauer and J. A. Hankin, *Chem. Rev.*, **95**, 1137 (1995).
68. J. D. Payzant, K. Tanaka, L. D. Betowski and D. K. Bohme, *J. Am. Chem. Soc.*, **98**, 894 (1976).
69. A. E. Reed and P. v. R. Schleyer, *Chem. Phys. Lett.*, **133**, 533 (1987).
70. A. I. Boldyrev and J. Simons, *J. Chem. Phys.*, **99**, 4628 (1993).
71. (a) M. T. Carroll, M. S. Gordon and T. L. Windus, *Inorg. Chem.*, **31**, 825 (1992).
(b) M. S. Gordon, L. P. Davis, L. W. Burggraf and R. J. Damrauer, *J. Am. Chem. Soc.*, **108**, 7889 (1986).
(c) L. P. Davis, L. W. Burggraf and M. S. Gordon, *J. Am. Chem. Soc.*, **110**, 3056 (1988).
(d) M. S. Gordon, T. L. Windus, L. W. Burggraf and L. P. Davis, *J. Am. Chem. Soc.*, **112**, 7167 (1990).
72. (a) T. L. Windus, M. S. Gordon, L. W. Burggraf and L. P. Davis, *J. Am. Chem. Soc.*, **113**, 4356 (1991).
(b) T. L. Windus, M. S. Gordon, L. P. Davis and L. W. Burggraff, *J. Am. Chem. Soc.*, **116**, 3568 (1994).
(c) D. L. Willhite and L. Spialter, *J. Am. Chem. Soc.*, **95**, 2100 (1973).
73. H. Fujimoto, N. Arita and K. Tamao, *Organometallics*, **11**, 3035 (1992).
74. Y. Apeloig, in *The Chemistry of Organic Silicon Compounds* (Eds. S. Patai and Z. Rappoport), Wiley, Chichester, 1989, pp. 57–226.
75. (a) J. G. Verkade, *Coord. Chem. Rev.*, **137**, 233 (1994) and references cited therein.
(b) M. G. Voronkov, *Top. Curr. Chem.*, **84**, 77 (1979).
(c) M. G. Voronkov, V. P. Baryshok, L. P. Petukhov, V. I. Rachlin, R. G. Mirskov and V. A. Pestunovich, *J. Organomet. Chem.*, **358**, 39 (1988).
(d) E. Kupce, E. Liepins, A. Lapsina, G. Zelcans and E. Lukevics *J. Organomet. Chem.*, **333**, 1 (1987).
(e) J. J. H. Edema, R. Libbers, A. Ridder and R. M. Kellogg, *J. Organomet. Chem.*, **464**, 127 (1994).
76. R. J. P. Corriu, A. Kpoton, M. Poirier, G. Royo, A. de Saxce and J. C. Young, *J. Organomet. Chem.*, **395**, 1 (1990).
77. F. Carre, R. J. P. Corriu, A. Kpoton, M. Poirier, G. Royo, J. C. Young and C. Belin, *J. Organomet. Chem.*, **470**, 43 (1994).
78. F. H. Carre, R. J. P. Corriu, G. F. Lanneau and Z. Yu, *Organometallics*, **10**, 1236 (1991).
79. J. Boyer, C. Breliere, F. Carre, R. J. P. Corriu, A. Kpoton, M. Poirier, G. Royo and J. C. Young, *J. Chem. Soc., Dalton Trans.*, 43 (1989).
80. N. Auner, R. Probst, C. Heikenwalder, E. Herdtweck, S. Gamper and G. Müller, *Z. Naturforsch.*, **48b**, 1625 (1993).
81. N. Auner, R. Probst, F. Hahn and E. Herdtweck, *J. Organomet. Chem.*, **459**, 25 (1993).
82. N. Auner, *J. Prakt. Chem.*, **337**, 79 (1995).
83. G. Klebe, *J. Organomet. Chem.*, **332**, 35 (1987).
84. H. Lang, E. Meichel, M. Weinmann and M. Melter in *Organosilicon Chemistry III* (Eds. N. Auner and J. Weis), VCH, Weinheim, in press.
85. G. Klebe, M. Nix and K. Hensen, *Chem. Ber.*, **117**, 797 (1984).
86. G. Klebe, *J. Organomet. Chem.*, **293**, 147 (1985).
87. G. Klebe, J. W. Bats and K. Hensen, *J. Chem. Soc., Dalton Trans.*, 1 (1985).

88. G. Klebe, K. Hensen and J. von Jouanne, *J. Organomet. Chem.*, **258**, 137 (1983).
89. D. Kummer, S. C. Chaudhry, J. Seifert, B. Deppisch and G. Mattern, *J. Organomet. Chem.*, **382**, 345 (1990).
90. D. Kummer, S. H. Abdel Halim, W. Kuhs and G. Mattern, *Z. Anorg. Allg. Chem.*, **614**, 73 (1992).
91. D. Kummer, S. H. Abdel Halim, W. Kuhs and G. Mattern, *J. Organomet. Chem.*, **446**, 51 (1993).
92. (a) M. G. Voronkov, A. I. Albanov, A. E. Pestunovich, V. N. Sergeev, S. V. Pestunovich, I. I. Kandror and Yu. I. Baukov, *Metalloorg. Khim.*, **1**, 1435 (1988); *Chem. Abstr.*, **112**, 77288p (1990).

    (b) A. A. Macharashvili, Yu. E. Ovchinnikov, Yu. T. Struchkov, V. N. Sergeev, S. V. Pestunovich and Yu. I. Baukov, *Izv. Akad. Nauk SSSR, Ser. Khim.*, 189 (1993); *Russ, Chem. Bull.*, **42**, 173 (1993).
93. A. R. Bassindale, S. G. Glynn, J. Jiang, D. J. Parker, R. Turtle, P. G. Taylor and S. S. D. Brown, in *Organosilicon Chemistry II* (Eds. N. Auner and J. Weis), VCH, Weinheim, 1996, pp. 411–426.
94. I. D. Kalikhman, B. A. Gostevskii, O. B. Bannikova, M. G. Voronkov and V. A. Pestunovich, *Metalloorg. Khim.*, **2**, 205 (1989); *Chem. Abstr.*, **112**, 77291j (1990).
95. (a) I. Kalikhman, S. Krivonos, A. Ellern and D. Kost, *Organometallics*, **15**, 5073 (1996).

    (b) I. D. Kalikhman and D. Kost, in *Organosilicon Chemistry III* (Eds. N. Auner and J. Weis), VCH, Weinheim, 1997, pp. 446–451.
96. J. Belzner and D. Schar, in *Organosilicon Chemistry II* (Eds. N. Auner and J. Weis), VCH, Weinheim, 1996, pp. 459–465.
97. (a) T. van den Ancker, B. S. Jolly, M. F. Lappert, C. L. Raston, B. W. Skelton and A. H. White, *J. Chem. Soc., Chem. Commun.*, 1006 (1990).

    (b) H. H. Karsch, F. Bienlein, A. Sladek, M. Heckel and K. Burger, *J. Am. Chem. Soc.*, **117**, 5160 (1995).
98. A. B. Kalinin, E. T. Apasov, S. B. Bugaeva, S. L. Yoffe and B. A. Tartakovskii, *Izv. Akad. Nauk SSSR, Ser. Khim.*, 1413 (1983); *Chem. Abstr.*, **99**, 175871f (1983).
99. C. Breliere, F. Carre, R. J. P. Corriu, M. Poirier and G. Royo, *Organometallics*, **5**, 388 (1986).
100. J. I. Musher, *Angew. Chem., Int. Ed. Engl.*, **8**, 54 (1969).
101. V. F. Sidorkin, V. A. Pestunovich and M. G. Voronkov, *Dokl. Akad. Nauk SSSR*, **235**, 1363 (1977); *Chem. Abstr.*, **87**, 173187Z (1977).
102. V. A. Pestunovich, V. F. Sidorkin and M. G. Voronkov, in *Progress in Organosilicon Chemistry* (Eds. B. Marciniec and J. Chojnowski), Gordon and Breach, Basel, 1995, pp. 69–82.
103. A. R. Bassindale, P. G. Taylor, in *The Chemistry of Organic Silicon Compounds* (Eds. S. Patai and Z. Rappoport), Wiley, Chichester, 1989, pp. 839–892.
104. A. R. Bassindale, in *Progress in Organosilicon Chemistry* (Eds. B. Marciniec and J. Chojnowski), Gordon and Breach, Basel, 1995, pp. 191–208.
105. I. D. Kalikhman, Dissertation, Institute of Organic Chemistry, Sib. Div. Acad. Science SSSR, Irkutsk, 1989.
106. B. J. Helmer, R. West, R. J. P. Corriu, M. Poirier, G. Royo and A. de Saxce, *J. Organomet. Chem.*, **251**, 295 (1983).
107. V. A. Pestunovich, B. Z. Shterenberg, E. T. Lippmaa, M. Ja. Miagi, M. J. Alla, S. N. Tandura, V. P. Baryshok, L. P. Petukhov and M. G. Voronkov, *Dokl. Akad. Nauk SSSR*, **258**, 1410 (1981); *Chem. Abstr.*, **95**, 186219t (1981).
108. V. A. Pestunovich, B. Z. Shterenberg, S. N Tandura, V. P. Baryshok, E. I. Brodskaya, N. G. Komalenkova and M. G. Voronkov, *Dokl. Akad. Nauk SSSR*, **264, 632** (1982); *Chem. Abstr.*, **97**, 144918f (1982).
109. R. J. P. Corriu, G. F. Lanneau and Z. Yu, *Tetrahedron*, **49**, 9019 (1993).
110. R. J. P. Corriu, M. Mazhar, M. Poirier and G. Royo, *J. Organomet. Chem.*, **306**, C5 (1986).
111. R. J. P. Corriu, A. Kpoton, M. Poirier, G. Royo and J. Y. Corey, *J. Organomet. Chem.*, **277**, C25 (1984).
112. R. Probst, C. Leis, S. Gamper, E. Herdtweck, C. Zybill and N. Auner, *Angew. Chem., Int. Ed. Engl.*, **30**, 1132 (1991).
113. H. Handwerker, C. Leis, R. Probst, P. Bissinger, A. Grohmann, P. Kiprof, E. Herdtweck, J. Blumel, N. Auner and C. Zybill, *Organometallics*, **12**, 2162 (1993).
114. P. Arya, J. Boyer, F. Carre, R. Corriu, G. Lanneau, J. Lapasset, M. Perrot and C. Priou, *Angew. Chem., Int. Ed. Engl.*, **28**, 1016 (1989).

115. R. J. P. Corriu, G. F. Lanneau and V. D. Mehta, *J. Organomet. Chem.*, **419**, 9 (1991).
116. R. Corriu, G. Lanneau and C. Priou, *Angew. Chem., Int. Ed. Engl.*, **30**, 1030 (1991).
117. P. Arya, J. Boyer, R. J. P. Corriu, G.F. Lanneau and M. Perrot, *J. Organomet. Chem.*, **346**, C11 (1988).
118. R. J. P. Corriu, B. P. S. Chauhan and G. F. Lanneau, *Organometallics*, **14**, 1646 (1995).
119. R. J. P. Corriu, G. F. Lanneau and B. P. S. Chauhan, *Organometallics*, **12**, 2001 (1993).
120. B. P. S. Chauhan, R. J. P. Corriu, G. F. Lanneau, C. Priou, N. Auner, H. Handwerker and E. Herdtweck, *Organometallics*, **14**, 1657 (1995).
121. (a) M. Weinmann, H. Lang, O. Walter and M. Buchner, in *Organosilicon Chemistry II* (Eds. N. Auner and J. Weis), VCH Weinheim, 1996, pp. 569–574.
  (b) H. Lang, M. Weinmann, W. Frosch, M. Buchner and B. Schiemenz, *Chem. Commun.*, 1299 (1996).
122. C. N. Smit and F. Bickelhaupt, *Organometallics*, **6**, 1156 (1987).
123. (a) K. Tamao, K. Nagata, M. Asahara, A. Kawachi, Y. Ito and M. Shiro, *J. Am. Chem. Soc.*, **117**, 11592 (1995).
  (b) R. J. P. Corriu, G. F. Lanneau, C. Priou, F. Soulairol, N. Auner, R. Probst, R. Conlin and C. Tan, *J. Organomet. Chem.*, **466**, 55 (1994).
124. K. D. Onan, A. T. McPhail, C. H. Yoder and R. W. Hillyard, *J. Chem. Soc., Chem. Commun.*, 209 (1978).
125. R. W. Hillyard, C. M. Ryan and C. H. Yoder, *J. Organomet. Chem.*, **153**, 369 (1978).
126. C. H. Yoder, C. M. Ryan, G. F. Martin and P. S. Ho, *J. Organomet. Chem.*, **190**, 1 (1980).
127. C. H. Yoder, J. A. Gullinane and G. F. Martin, *J. Organomet. Chem.*, **210**, 289 (1981).
128. V. A. Pestunovich, A. I. Albanov, M. F. Larin, M. G. Voronkov, E. P. Kramarova and Yu. I. Baukov, *Izv. Akad. Nauk SSSR, Ser. Khim.*, 2178 (1980); *Chem. Abstr.*, **94**, 29677c (1981).
129. A. I. Albanov, Yu. I. Baukov, M. G. Voronkov, E. P. Kramarova, M. F. Larin and V. A. Pestunovich, *Zh. Obshch. Khim.*, **53**, 246 (1983); *Chem. Abstr.*, **98**, 215656c (1983).
130. Yu. I. Baukov, E. P. Kramarova, A. G. Shipov, G. I. Oleneva, O.B. Artamkina, A. I. Albanov, M. G. Voronkov and V. A. Pestunovich, *Zh. Obshch. Khim.*, **59**, 127 (1989); *Chem. Abstr.*, **112**, 56003b (1990).
131. M. G. Voronkov, A. E. Pestunovich, A. I. Albanov, N. N. Vlasova and V. A. Pestunovich, *Izv. Akad. Nauk SSSR, Ser. Khim.*, 2841 (1989); *Chem. Abstr.*, **113**, 6424q (1990).
132. L. I. Belousova, B. A. Gostevskii, I. D. Kalikhman, O. A. Vyazankina, O. B. Bannikova, N. S. Vyazankin and V. A. Pestunovich, *Zh. Obshch. Khim.*, **58**, 407 (1988); *Chem. Abstr.*, **110**, 114908 x (1989).
133. I. D. Kalikhman, O. B. Bannikova, L. I. Belousova, B. A. Gostevskii, E. Liepinsh, O. A. Vyazankina and N. S. Vyazankin, *Metalloorg. Khim.*, **1**, 683 (1988); *Chem. Abstr.*, **111**, 57840 p (1989).
134. I. D. Kalikhman, O. B. Bannikova, B. A. Gostevskii, O. A. Vyazankina, N. S. Vyazankin and V. A. Pestunovich, *Izv. Akad. Nauk SSSR, Ser. Khim.*, 1688 (1985); *Chem. Abstr.*, **104**, 148977k (1986).
135. I. D. Kalikhman, O. B. Bannikova, L. P. Petuchov, V. A. Pestunovich and M. G. Voronkov, *Dokl. Akad. Nauk SSSR*, **287**, 870 (1986); *Chem. Abstr.*, **106**, 50289d (1987).
136. I. D. Kalikhman, O. B. Bannikova, B. A. Gostevskii, L. I. Volkova, O. A. Vyazankina, N. S. Vyazankin, T. G. Yushmanova, V. A. Lopirev, M. G. Voronkov and V. A. Pestunovich, *Izv. Akad. Nauk SSSR, Ser. Khim.*, 459 (1987); *Chem. Abstr.*, **108**, 94627h (1988).
137. I. D. Kalikhman, V. A. Pestunovich, B. A. Gostevskii, O. B. Bannikova and M. G. Voronkov, *J. Organomet. Chem.*, **338**, 169 (1988).
138. A. R. Bassindale and M. Borbaruah, *J. Chem. Soc., Chem. Commun.*, 1499, 1501 (1991).
139. M. G. Voronkov, V. A. Pestunovich and Yu. I. Baukov, *Organomet. Chem. USSR*, **4**, 593 (1991); *Chem. Abstr.*, **116**, 41503y (1992).
140. I. D. Kalikhman, A. I. Albanov, O. B. Bannikova, L. I. Belousova, M. G. Voronkov, V. A. Pestunovich, A. G. Shipov, E. P. Kramarova and Yu. I. Baukov, *J. Organomet. Chem.*, **361**, 147 (1989).
141. R. Roger and D. G. Nielson, *Chem. Rev.*, **61**, 179 (1961).
142. S. Wawsonek and E. Yeakey, *J. Am. Chem. Soc.*, **82**, 5718 (1960).
143. O. B. Artamkina, E. P. Kramarova, A. G. Shipov, Yu. I. Baukov, A. A. Macharashvili, Yu. E. Ovchinnikov and Yu. T. Struchkov, *Zh. Obshch. Khim.*, **63**, 2289 (1993); *Chem. Abstr.*, **121**, 255881x (1994).

144. A. R. Bassindale and M. Borbaruah, *J. Chem. Soc., Chem. Commun.*, 352 (1993).

145. (a) A. G. Shipov, E. P. Kramarova and Yu. I. Baukov, *Zh. Obshch. Khim.*, **64**, 1220 (1994); *Chem. Abstr.*, **122,** 314629s (1995).
(b) E. P. Kramarova, V. V. Negrebezkii, A. G. Shipov and Yu. I. Baukov, *Zh. Obshch. Khim.*, **64**, 1222 (1994); *Chem. Abstr.*, **122**, 314630k (1995).

146. I. D. Kalikhman, O. B. Bannikova, B. A. Gostevskii, M. G. Voronkov and V. A. Pestunovich, *Izv. Akad. Nauk SSSR, Ser. Khim.*, 492 (1989); *Chem. Abstr.*, **112**, 35947x (1990).

147. I. D. Kalikhman, B. A. Gostevskii, O. B. Bannikova, M. G. Voronkov and V. A. Pestunovich, *J. Organomet. Chem.*, **376**, 249 (1989).

148. A. G. Shipov, O. B. Artamkina, E. P. Kramarova, G. I. Oleneva and Yu. I. Baukov, *Zh. Obshch. Khim.*, **61**, 1914 (1991); *Chem. Abstr.*, **116**, 106355y (1992).

149. O. B. Bannikova, B. A. Gostevskii and I. D. Kalikhman, *Abstracts of VII Conference for Chemistry, Technology and Utility of Organosilicon Compounds*, SSSR, Irkutsk, 1990, p. 59.

150. M. G. Voronkov, V. A. Pestunovich and Yu. L. Frolov, *Advances in Organosilicon Chemistry* (Ed. M.G. Voronkov), Mir Publishers, Moscow, 1985, pp. 54–68.

151. A. I. Albanov, N. M. Kudiakov, V. A. Pestunovich, M. G. Voronkov, A. A. Macharashvili, V. E. Shklover and Yu. T. Struchkov, *Metalloorg. Khim.*, **4**, 1228 (1991); *Chem. Abstr.*, **116**, 83789b (1992).

152. A. I. Albanov, L. I. Gubanova, M. F. Larin, V. A. Pestunovich and M. G. Voronkov, *J. Organomet. Chem.*, **244**, 5 (1983).

153. V. A. Pestunovich, M. F. Larin, M. S. Sorokin, A. I. Albanov and M.G. Voronkov, *J. Organomet. Chem.*, **280**, C17 (1985).

154. V. E. Shklover, Yu. T. Struchkov and M. G. Voronkov, *Russ. Chem. Rev.*, **58**, 211 (1989).

155. M. Yu. Antipin, *Russ. Chem. Rev.*, **59**, 1052 (1990).

156. A. A. Macharashvili, V. E. Shklover, Yu. T. Struchkov, G. I. Oleneva, E. P. Kramarova, A. G. Shipov and Yu. I. Baukov, *J. Chem. Soc., Chem. Commun.*, 683 (1988).

157. A. A. Macharashvili, V. E. Shklover, Yu. T. Struchkov, Yu. I. Baukov, E. P. Kramarova and G. I. Oleneva, *J. Organomet. Chem.*, **327**, 167 (1987).

158. A. A. Macharashvili, V. E. Shklover, N. Yu. Chernikova, M. Yu. Antipin, Yu. T. Struchkov, Yu. I. Baukov, G. I. Oleneva, E. P. Kramarova and A. G. Shipov, *J. Organomet. Chem.*, **359**, 13 (1989).

159. Yu. E. Ovchinnikov, A. A. Macharashvili, Yu. T. Struchkov, A. G. Shipov and Yu. I. Baukov, *J. Struct. Chem.*, **35**, 91 (1994).

160. A. A. Macharashvili, V. E. Shklover, Yu. T. Struchkov, M. G. Voronkov, B. A. Gostevskii, I. D. Kalikhman, O. B. Bannikova and V. A. Pestunovich, *Metalloorg. Khim.*, **1**, 1131 (1988); *Chem. Abstr.*, **110**, 135298 p (1989).

161. A. A. Macharashvili, Dissertation, Institute of Organometallic Chemistry, Acad. Science SSSR, Moscow, 1990.

162. O. B. Artamkina, E. P. Kramarova, A. G. Shipov, Yu. I. Baukov, A. A. Macharashvili, Yu. E. Ovhinnikov and Yu. T. Struchkov, *Zh. Obshch. Khim.*, **64**, 263 (1994); *Chem. Abstr.*, **121**, 255882y (1994).

163. N. A. Orlova, A. G. Shipov, Yu. I. Baukov, A. O. Mozzhukhin, M. Yu. Antipin and Yu. T. Struchkov, *Metalloorg. Khim.*, **5**, 666 (1992); *Chem. Abstr.*, **117**, 251439d (1992).

164. A. A. Macharashvili, V. E. Shklover, Yu. T. Struchkov, B. A. Gostevskii, I. D. Kalikhman, O. B. Bannikova, M. G. Voronkov and V. A. Pestunovich, *J. Organomet. Chem.*, **356**, 23 (1988).

165. A. A. Macharashvili, V. E. Shklover, Yu. T. Struchkov, M. G. Voronkov, B. A. Gostevskii, I. D. Kalikhman, O. B. Bannikova and V. A. Pestunovich, *J. Organomet. Chem.*, **340**, 23 (1988).

166. A. O. Mozzhukhin, Yu. Antipin, Yu. T. Struchkov, A. G. Shipov, E. P. Kramarova and Yu. I. Baukov, *Metalloorg. Khim.*, **5**, 906 (1992); *Chem. Abstr.*, **118**, 102109q (1993).

167. A. O. Mozzhukhin, Yu. Antipin, Yu. T. Struchkov, A. G. Shipov, E. P. Kamarova and Yu. I. Baukov, *Metalloorg. Khim.*, **5**, 917 (1992); *Chem. Abstr.*, **118**, 80993u (1993).

168. H. B. Bürgi, *Angew. Chem., Int. Ed. Engl.*, **14**, 460 (1975).

169. J. D. Dunitz, *X-ray Analysis and Structure of Organic Molecules*, Cornell University Press, Ithaca, 1979.

170. C. H. Yoder, W. D. Smith, B. L. Buckwalter, C. D. Schaeffer, Jr., K. J. Sullivan and M. F. Lehman, *J. Organomet. Chem.*, **492**, 129 (1995).

171. D. Kummer and S. H. Abdel Halim, *Z. Anorg. Allg. Chem.*, **622**, 57 (1996).

172. V. V. Negrebetsky, V. V. Negrebetsky, A. G. Shipov, E. P. Kramarova and Y. I. Baukov, *J. Organomet. Chem.*, **496**, 103 (1995).

173. J. C. Otter, C. L. Adamson, C. H. Yoder and A. L. Rheingold, *Organometallics*, **9**, 1557 (1990).
174. (a) T. K. Prakasha, S. Srinivasan, A. Chandrasekaran, R. O. Day and R. R. Holmes, *J. Am. Chem. Soc.*, **117**, 10003 (1995).
    (b) N. V. Timosheva, T. K. Prakasha, A. Chandrasekaran, R. O. Day and R. R. Holmes, *Inorg. Chem.*, **35**, 3614 (1996).
175. (a) R. O. Day, T. K. Prakasha, R. R. Holmes and H. Eckert, *Phosphorus, Sulfur Silicon Relat. Elem.*, **100**, 211 (1995).
    (b) R. O. Day, T. K. Prakasha, R.R . Holmes and H. Eckert, *Organometallics*, **13**, 1285 (1994).
176. (a) A. Chandrasekaran, R. O. Day and R. R. Holmes, *Organometallics*, **15**, 3182 (1996).
    (b) A. Chandrasekaran, R. O. Day and R. R. Holmes, *Organometallics*, **15**, 3189 (1996).
177. K. Ebata, T. Inada, C. Kabuto and H. Sakurai, *J. Am. Chem. Soc.*, **116**, 3595 (1994).
178. I. I. Schuster, W. Weissensteiner and K. Mislow, *J. Am. Chem. Soc.*, **108**, 6661 (1986).
179. H. Schwarz, in *The Chemistry of Organic Silicon Compounds* (Eds. S. Patai and Z. Rappoport), Wiley, Chichester, 1989, pp. 445–510.
180. J. B. Lambert, L. Kania and S. Zhang, *Chem. Rev.*, **95**, 1191 (1995).
181. J. B. Lambert, S. Zhang and S. M. Ciro, *Organometallics*, **13**, 2430 (1994).
182. G. A. Olah, L. Heiliger, X. Y. Li and G. K. S. Prakash, *J. Am. Chem. Soc.*, **112**, 5991 (1990).
183. A. R. Bassindale and T. Stout, *J. Chem. Soc., Chem. Commun.*, 1387 (1984).
184. J. Y. Corey and R. West, *J. Am. Chem. Soc.*, **85**, 4034 (1963).
185. (a) C. Breliere, F. Carre, R. J. P. Corriu and M. Wong Chi Man, *J. Chem. Soc., Chem. Commun.*, 2333 (1994).
    (b) M. Chauhan, C. Chuit, R. J. P. Corriu and C. Reye, *Tetrahedron Lett.*, **37**, 845 (1996).
186. (a) C. Chuit, R. J. P. Corriu, A. Mehdi and C. Reye, *Angew. Chem., Int. Ed. Engl.*, **32**, 1311 (1993).
    (b) M. Chauhan, C. Chuit, R. J. P. Corriu and C. Reye, *Tetrahedron Lett.*, **37**, 845 (1996).
187. V. A. Benin, J. C. Martin and M. R. Willcott, *Tetrahedron Lett.*, **35**, 2133 (1994).
188. J. Belzner, D. Schär, B. O. Kneisel and R. Herbst-Irmer, *Organometallics*, **14**, 1840 (1995).
189. H. Kobayashi, K. Ueno and H. Ogino, *Organometallics*, **14**, 5490 (1995).
190. K. Tamao, J. Toshida, H. Yamamoto, T. Kakui, H. Yatsumoto, M. Takahashi, A. Kurita, M. Murata and M. Kumada, *Organometallics*, **1**, 355 (1982).
191. C. Breliere, F. Carre, R. J. P. Corriu, W. E. Douglas, M. Poirier, G. Royo and M. Wong Chi Man, *Organometalics*, **11**, 1586 (1992).
192. F. Carre, C. Chuit, R. J. P. Corriu, A. Fanta, A. Mehdi and C. Reye, *Organometallics*, **14**, 194 (1995).
193. R. Tacke and M. Mühleisen, *Angew. Chem., Int. Ed. Engl.*, **33**, 1359 (1994).
194. C. Breliere, F. Carre, R. J. P. Corriu, M. Poirier, G. Royo and J. Zwecker, *Organometallics*, **8**, 1831 (1989).
195. (a) J. C. Bailar, *J. Inorg. Nucl. Chem.*, **8**, 165 (1958).
    (b) P. Ray and N. K. Dutt, *J. Ind. Chem. Soc.*, **20**, 81 (1943).
196. (a) W. Dilthey, *Chem. Ber.*, **36**, 923 (1903).
    (b) A. Rosenheim, W. Loewenstamm and L. Singer, *Chem Ber.*, **36**, 1833 (1903).
197. R. West, *J. Am. Chem. Soc.*, **80**, 3246 (1958).
198. N. Serpone and K. A. Hersh, *J. Organomet. Chem.*, **84**, 177 (1975).
199. T. Shimizutani and Y. Yoshikawa, *Inorg. Chem.*, **30**, 3236 (1991).
200. R. M. Pike, *Coord. Chem. Rev.*, **2**, 163 (1967).
201. (a) F. E. Hahn, M. Keck and K. N. Raymond, *Inorg. Chem.*, **34**, 1402 (1995).
    (b) A. Boudin, G. Cerveau, C. Chuit, R. J. P. Corriu and C. Reye, *Organometallics*, **7**, 1165 (1988).
202. D. F. Evans, J. Parr and E. N. Coker, *Polyhedron*, **9**, 813 (1990).
203. D. F. Evans and C. Y. Wong, *Polyhedron*, **10**, 1131 (1991).
204. D. F. Evans, J. Parr and C. Y. Wong, *Polyhedron*, **11**, 567 (1992).
205. F. Carre, G. Cerveau, C. Chuit, R. J. P. Corriu and C. Reye, *Angew. Chem., Int. Ed. Engl.*, **28**, 489 (1989).
206. F. Carre, G. Cerveau, C. Chuit, R. J. P. Corriu and C. Reye, *New J. Chem.*, **16**, 63 (1992).
207. (a) F. Carre, C. Chuit, R. J. P. Corriu, A. Mehdi and C. Reye, *J. Organomet. Chem.*, **446**, C6 (1993).
    (b) C. Chuit, R. J. P. Corriu, A. Mehdi and C. Reye, *Chem. Eur. J.*, **2**, 342 (1996) [*Angew. Chem., Int. Ed. Engl.*, **35**, 342 (1996)].

208. K. M. Taba and W. V. Dahlhoff, *J. Organomet. Chem.*, **280**, 27 (1985).
209. G. Klebe and D. Tran Qui, *Acta Crystallogr.*, **C40**, 476 (1984).
210. I. D. Kalikhman, B. A. Gostevskii, O. B. Bannikova, M. G. Voronkov and V. A. Pestunovich, *Metalloorg. Khim.*, **2**, 937 (1989); *Chem. Abstr.*, **112**, 118926r (1990).
211. (a) I. Kalikhman and D. Kost, *J. Chem. Soc., Chem. Commun.*, 1253 (1995).
(b) D. Kost, I. Kalikhman and M. Raban, *J. Am. Chem. Soc.*, **117**, 11512 (1995).
212. I. D. Kalikhman, B. A. Gostevskii, O. B. Bannikova, M. G. Voronkov and V. A. Pestunovich, *Metalloorg. Khim.*, **2**, 704 (1989); *Chem. Abstr.*, **112**, 139113p (1990).
213. C. Breliere, R. J. P. Corriu, G. Royo, W. W. C. Wong Chi Man and J. Zwecker, *Organometallics*, **9**, 2633 (1990).
214. K. Boyer-Elma, F. H. Carre, R. J. P. Corriu and W. E. Douglas, *J. Chem. Soc., Chem. Commun.*, 725 (1995).
215. F. Carre, C. Chuit, R. J. P. Corriu, A. Mehdi and C. Reye, *Organometallics*, **14**, 2754 (1995).
216. A. O. Mozzhukhin, M. Yu. Antipin, Yu. T. Struchkov, B. A. Gostevskii, I. D. Kalikhman, V. A. Pestunovich and M. G. Voronkov, *Metalloorg. Khim.*, **5**, 658 (1992); *Chem. Abstr.*, **117**, 234095w (1992).
217. C. Breliere, R. J. P. Corriu, G. Royo and J. Zwecker, *Organometallics*, **8**, 1834 (1989).
218. (a) K. Tamao, M. Akita, H. Kato and M. Kumada, *J. Organomet. Chem.*, **341**, 165 (1988).
(b) K. M. Kane, F. R. Lemke and J. L. Petersen, *Inorg. Chem.*, **34**, 4085 (1995).
219. J. A. A. Ketelaar, *Z. Kristallogr.*, **92**, 155 (1935).
220. D. Kost and I. Kalikhman, *Bull. Magn. Reson.*, **17**, 108 (1995).
221. I. Kalikhman, S. Krivonos, D. Stalke, T. Kottke and D. Kost, *Organometallics*, **16**, 3255 (1997).
222. D. Kost, S. Krivonos and I. Kalikhman, in *Organosilicon Chemistry III* (Eds. N. Auner and J. Weis), VCH, Weinheim, 1997, pp. 435–445.
223. A. Rodger and B. F. G. Johnson, *Inorg. Chem.*, **27**, 3061 (1988).
224. D. Kummer, S. C. Chaudhry, T. Debaerdemaeker and U. Thewalt, *Chem. Ber.*, **123**, 945 (1990).
225. D. Kummer, S. C. Chaudhry, W. Depmeier and G. Mattern, *Chem. Ber.*, **123**, 2241 (1990).
226. W. B. Farnham and J. F. Whitney, *J. Am. Chem. Soc.*, **106**, 3992 (1984).
227. C. Breliere, F. Carre, R. J. P. Corriu and G. Royo, *Organometallics*, **7**, 1006 (1988).
228. C. Breliere, F. Carre, R. J. P. Corriu, G. Royo, M. Wong Chi Man and J. Lapasset, *Organometallics*, **13**, 307 (1994).
229. F. Carre, C. Chuit, R. J. P. Corriu, A. Mehdi and C. Reye, *Angew. Chem., Int. Ed. Engl.*, **10**, 1097 (1994).
230. J. Braddock-Wilking, M. Schieser, L. Brammer, J. Huhmann and R. Shaltout, *J. Organomet. Chem.*, **499**, 89 (1995).
231. J. -K. Buijink, M. Noltemeyer and E. T. Edelmann, *J. Fluorine Chem.*, **61**, 51 (1993).
232. (a) P. Jutzi, D. Eikenberg, E. A. Bunte, A. Mohrke, B. Neumann and H. G. Stammler, *Organometallics*, **15**, 1930 (1996).
(b) P. Jutzi, U. Holtmann, D. Kanne, C. Kruger, R. Blom, R. Gleiter and I. Hyla-Kryspin, *Chem. Ber.*, **122**, 1629 (1989).
233. E. Lukevics and O. A. Pudova, *Khimiya Geterotsiklicheskikh Soedin.*, 1605 (1996). *Chem. Abstr.*, **126**, 157528w (1997).
234. A. H. J. F. de Keijzer, F. J. J. de Kanter, M. Schakel, R. F. Schmitz and G. W. Klumpp, *Angew. Chem., Int. Ed. Engl.*, **35**, 1127 (1996).
235. T. Hoshi, M. Takahashi and M. Kira, *Chem. Lett.*, 683 (1996).
236. R. Damrauer and J. A. Hankin, *J. Organomet. Chem.*, **521**, 93 (1996).
237. J. A. Deiters and R. R. Holmes, *Organometallics*, **15**, 3944 (1996).
238. M. Veith and A. Rammo, *J. Organomet. Chem.*, **521**, 429 (1996).
239. A. Mix, U. H. Berlekamp, H. -G. Stammler, B. Neumann and P. Jutzi, *J. Organomet. Chem.*, **521**, 177 (1996).
240. V. V. Negrebetsky, A. G. Shipov, E. P. Kramarova, V. V. Negrebetsky and Yu. I. Baukov, *J. Organomet. Chem.*, **530**, 1 (1997).
241. D. Kummer, S. H. Abdel Halim and M. F. El-Shahat, *Z. Anorg. Allg. Chem.*, **622**, 1701 (1996).
242. M. Kira, L. Cheng Zhang, C. Kabuto and H. Sakurai, *Organometallics*, **15**, 5335 (1996).
243. K. Tamao, M. Asahara and A. Kawachi, *J. Organomet. Chem.*, **521**, 325 (1996).
244. M. Chauhan, C. Chuit, R. J. P. Corriu, A. Mehdi and C. Reye, *Organometallics*, **15**, 4326 (1996).
245. C. -H. Ottosson and D. Cremer, *Organometallics*, **15**, 5309 (1996).
246. S. P. Narula, R. Shankar and Meenu, *Proc. Indian Acad. Sci., Chem. Sci.*, **108**, 123 (1996).

247. H. Fleischer, K. Hensen and T. Stumpf, *Chem. Ber.*, **129**, 765 (1996).

248. H. H. Karsch, R. Richter and E. Witt, *J. Organomet. Chem.*, **521**, 185 (1996).

249. H. H. Karsch, B. Deubelly, U. Keller, O. Steigelmann, J. Lachmann and G. Muller, *Chem. Ber.*, **129**, 671 (1996).

250. H. H. Karsch, B. Deubelly, U. Keller, F. Bienlein, R. Richter, P. Bissinger, M. Heckel and G. Muller, *Chem. Ber.*, **129**, 759 (1996).

251. C. Plitzko and G. Meyer, *Z. Anorg. Allg. Chem.*, **622**, 1646 (1996).

CHAPTER 24

Silatranes and their tricyclic analogs

VADIM PESTUNOVICH, SVETLANA KIRPICHENKO and MIKHAIL VORONKOV

Irkutsk Institute of Chemistry, Siberian Branch of the Russian Academy of Sciences,
1 Favorsky St, 664033, Irkutsk, Russia
Fax: +7 3952 356046; e-mail: vadim@irioch.irk.ru

I. GENERAL INTRODUCTION

Since the first preparation[1], determination of the unusual structure[1−3] and the sensational discovery of amazing biological activity[2] of silatranes, 2,8,9-trioxa-5-aza-1-silatricyclo[3.3.3.0$^{1.5}$]undecanes (**1**), they became a fascinating class of pentacoordinate organosilicon compounds. Several hundreds of Si-substituted silatranes bearing H, organyl, organoxy, thioorganyl, acyloxy, halogen, pseudohalogen and other groups as substituent X have been synthesized and studied. Numerous C-substituted (mono- and poly-substituted at positions 3, 4, 7 and 10) silatranes and silatrane analogs with partly or completely modified tripodal ligands at the silicon atom are also known. Some of them are shown in Scheme 1, which demonstrates the formal methods of the transformation of silatranes to related compounds by replacing the oxygen atom or a methylene group(s) of the parent compound by another group(s).

The main features of the silatranes and their analogs are predetermined by their cage structure with a nearly trigonal-bipyramidal (TBP) silicon and an *in*-oriented nitrogen involved in the transannular Si←N bonding. The simplicity of the synthesis and relatively high stability of silatranes and their analogs together with a wide diversity of their substituent X and the tricyclic skeleton character made it possible to use them for detailed studies of some intriguing problems of the chemistry of hypervalent silicon compounds. These are the bonding model, the mutual influence of substituents at the TBP silicon and the structural, spectral and chemical manifestations of the silicon hypervalency as well as modelling of the pathway of the S_N2 substitution at the tetrahedral Si.

To explain the great interest in silatranes in recent decades one should bear in mind two points. First, for a long time silatranes remained the only accessible class of neutral derivatives of pentacoordinated silicon. Second, the specific physiological action of many silatranes refuted the traditional opinion that organosilicon compounds do not differ much

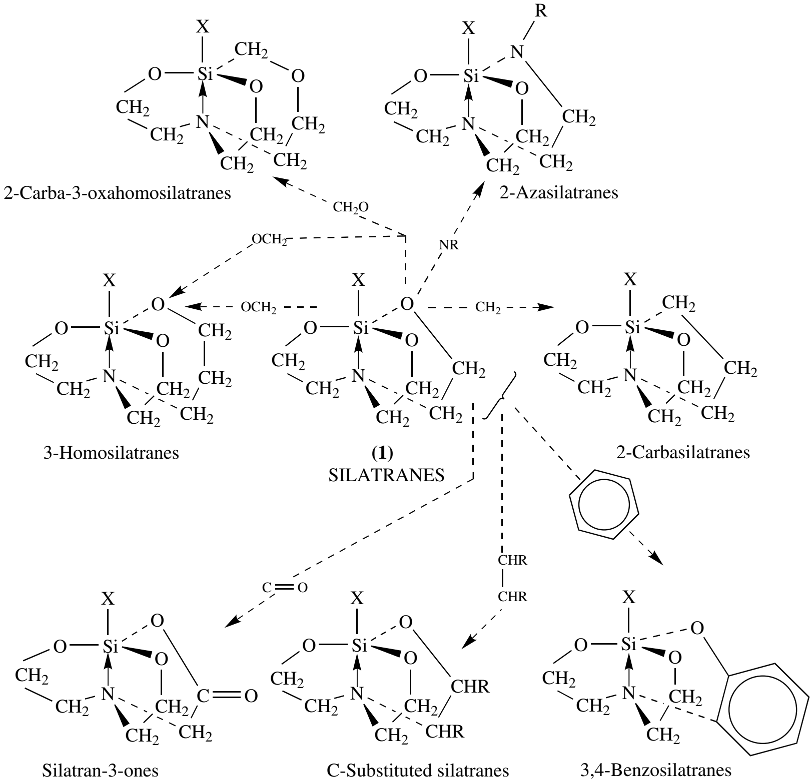

SCHEME 1. Silatranes and some of their analogs.

in biological activity from their organic precursors or analogs. That is why the results of their investigation stimulated an extensive development of the chemistry of hypervalent organosilicon compounds and bioorganosilicon chemistry.

The aim of the present chapter is to give a short review of the present knowledge concerning synthesis, structure and reactivity of silatranes and their analogs. By 1997 several hundred publications on these themes appeared from the research groups of Corriu, Frye, Hencsei, Lukevics, Verkade, Voronkov and others. These publications include several books[4–7] and reviews[2,8–19]. In some recent reviews[20–31] the structure and reactivity of silatranes and their analogs are compared with those of other hypervalent organosilicon compounds and atrane derivatives of nonmetallic main group elements. To avoid superfluous details we shall refer to these earlier publications.

II. SILATRANES

A. Methods of Synthesis

1. Introduction

The most common and convenient methods for the preparation of a variety of Si- and C-substituted silatranes are the reactions of trifunctional silanes with tris(2-hydroxyalkyl)amines (equation 1). Halo, alkoxy, acyloxy and dialkylamino groups can serve as functional substituents at silicon.

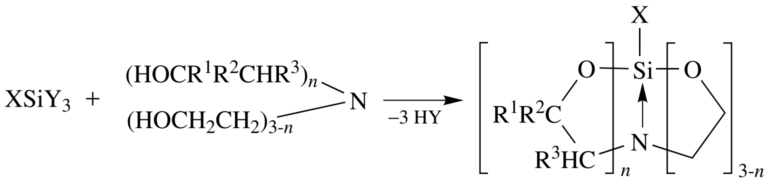

(1)

It should be emphasized that these reactions involving two trifunctional reagents afford monomeric compounds in high yields instead of polymeric products. There is no question that the driving force of these reactions which generate the tricyclic silatrane skeleton is the formation of the transannular Si←N bond.

2. Formation from organyltrialkoxysilanes

As an organosilicon component for the reaction shown in equation 1, trialkoxysilanes are used predominantly since these are widely available. The transetherification of phenyltriethoxysilane and tetraethoxysilane with triethanolamine [tris(2-hydroxyethyl)amine, THEA] in the presence of the basic catalyst has led to the first silatranes (equation 2)[1,32].

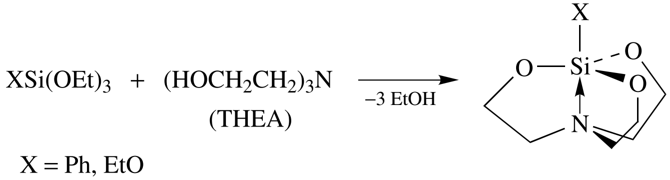

(2)

Similar transformations can be used with a wide range of organyltrialkoxysilanes, so that a large number of silatranes can be prepared with yields of up to 95%. Examples include 1-hydrosilatrane[1], 1-alkyl-[1,33], 1-cyclopropyl-[34–36], 1-[(cycloalkyl)alkyl]-[37], 1-alkenyl-[1,38–40], 1-alkynyl-[38,41], 1-aralkyl-[1,33,38] and 1-arylsilatranes[1,33,42–44].

The exchange reactions of organyltrialkoxysilanes with THEA mostly require heating of the components in an appropriate inert solvent (benzene, toluene, xylene, anisole, chloroform, methanol, ethanol etc.) for a long time. However, in some cases the reactions can be carried out at room temperature or, if necessary, with cooling. The transetherification rates and silatrane yields increase in the presence of an alkali metal hydroxide or alkoxide as a basic catalyst.

According to equation 2, disilatranylalkanes can be obtained from THEA and the corresponding bis(triethoxysilyl)alkanes (equation 3)[45]. For example, heating (up to 220 °C) of 1,2-bis(triethoxysilyl)ethane ($n = 2$) with THEA in the presence of KOH leads to the corresponding 1,2-disilatranylethane in 43% yield[45]. A significant yield decrease (to 24%) of this compound is observed when the reaction occurs without catalyst under reflux in xylene even for a longer time (70 h)[46]. Attempts to obtain disilatranylmethane ($n = 1$) failed because of unfavorable steric effects[47]. However, germatranylmethylsilatrane, $N(CH_2CH_2O)_3GeCH_2Si(OCH_2CH_2)_3N$, is formed in moderate yield (30%) under the same conditions[47]. It is of interest that 1-triorganylsilylmethylsilatranes, $R_3SiCH_2Si(OCH_2CH_2)_3N$, are obtained from 1-chloromethylsilatrane in good yields[48].

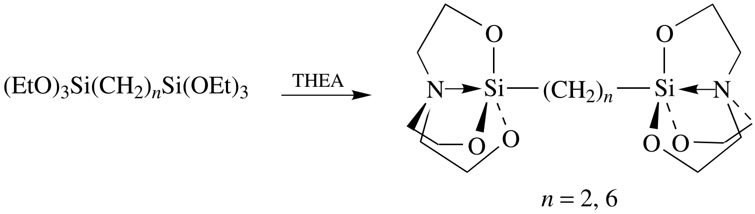

(3)

Starting from heteryltrialkoxysilanes and THEA, 1-heterylsilatranes can be synthesized in high yield (60–90%) (equation 4)[49–51]. As a catalyst, KOH or NaOH are suitable. However, cleavage of the Si–C bond and formation of 1-ethoxysilatrane are observed when 2-furyl- or 5-methyl-2-furyltriethoxysilanes react with THEA in the presence of KOH[50]. Use of H_2PtCl_6 as a catalyst favors transetherification of the two triethoxysilanes as shown by the increased silatrane yields[50].

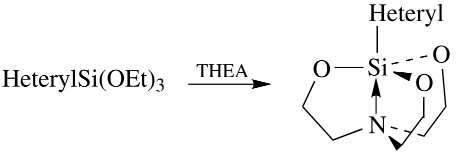

Heteryl	R	Ref.
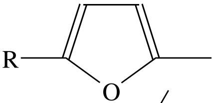	H, Me	50
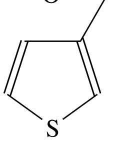		50
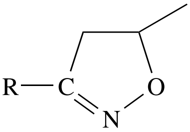	Me, Ph	51
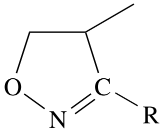	Me, Ph	51

(4)

Use of triethanolamine derivatives allows various substituents to be introduced into the silatrane ring, as illustrated in equations 5–7[52–58].

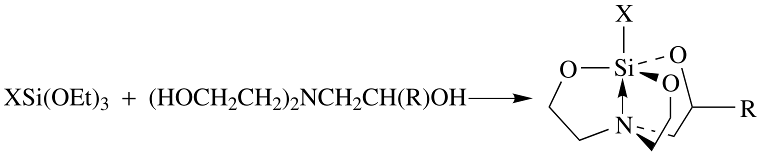

X	R	Yield, %	Ref.
Me	Me		1
Ph	Me		1
Me	Ph	70	52
Ph	Vinyl	75	52
Ph	$ClCH_2$	45	52

(5)

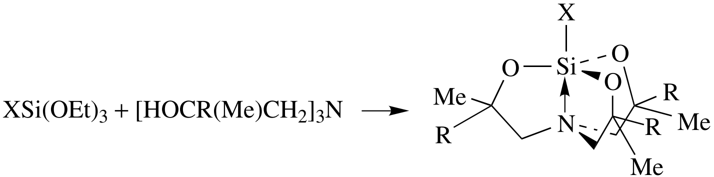

X	R	Ref.
Vinyl	H	53
Ph	H	54
$4\text{-}MeC_6H_4$	H	55
Ph	Me	58

(6)

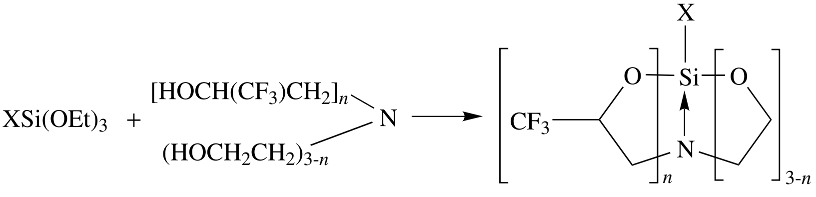

(7)

X = Me, Ph, $ClCH_2$, MeCHCl, $Cl(CH_2)_4$, etc., $n = 1–3$[57]

Organyltriethoxysilanes react with racemic[59] or optically active triethanolamine derivatives[60,61] to afford 4-substituted 1-organylsilatranes (equation 8).

The reaction of equation 8 can proceed without a catalyst. However, the reaction rates and product yields increase in the presence of sodium methoxide[59]. 4,4-Dimethyl substituted silatranes are formed in a similar way[62].

$$XSi(OR)_3 + [(HOCH_2CH_2)_2NCHR'CH_2OH \longrightarrow \qquad (8)$$

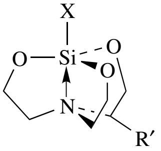

X	R	R′	Ref.
Me	Et	Et	59
Vinyl	Et	Et	59
Ph	Et	Et	59
Ph	Me	Me	61
Ph	Me	*i*-Pr	61
S-(+)-4-ClC_6H_4	Et	Et	60

Reaction 2 can also be applied to the synthesis of a number of 1-alkoxy-[1,53,61] and 1-aryloxysilatranes[33,63] as illustrated by equations 9[61] and 10[33,63].

$$(MeO)_4Si + (HOCH_2CH_2)_2NCH(R)CH_2OH \longrightarrow MeOSi(OCH_2CH_2)_2(OCH_2CHR)N \qquad (9)$$

$R = H, Me, i\text{-}Pr$

$$4\text{-}YC_6H_4OSi(OEt)_3 \xrightarrow{THEA} 4\text{-}YC_6H_4OSi(OCH_2CH_2)_3N \qquad (10)$$

$Y = Cl^{33,63}, Br^{33}, O_2N^{63}$

Higher 1-organoxysilatranes can conveniently be obtained by treatment of lower tetraalkoxysilanes with a mixture of THEA and an appropriate hydroxyl-containing compound in high or almost quantitative yields (equation 11)[33,64–66]. An organoxy–alkoxy exchange easily occurs when the formed, low boiling alcohol (MeOH or EtOH) is immediately removed from the reaction mixture by distillation. In some cases, e.g., with bulky alcohols, the use of KOH as a catalyst can be helpful[64].

$$ROH + (R'O)_4Si + THEA \longrightarrow ROSi(OCH_2CH_2)_3N \qquad (11)$$

$R = Alk, cyclo\text{-}Alk, ArCH_2^{64}, Ar^{33,65,66}; R' = MeO, EtO$

The classical way shown in equation 2 was used to prepare silatranes having a labile exocyclic S–Si bond (equation 12)[67] or a pseudohalogen function at the silicon (equation 13)[68].

$$RSSi(OMe)_3 + THEA \xrightarrow{THF} RSSi(OCH_2CH_2)_3N \qquad (12)$$

$R = HCl \cdot H_2NCH_2CHR'$ [$R' = H$ (83%), Me (67%)]

$$SCNSi(OEt)_3 + THEA \xrightarrow{CH_2Cl_2} \underset{84\%}{SCNSi(OCH_2CH_2)_3N} \qquad (13)$$

Organyltrialkoxysilanes can be converted to the corresponding silatranes by a one-pot reaction with bis(2-hydroxyalkyl)amines and epoxides[52,69]. According to Frye and coworkers[69] the procedure involves *in situ* formation of trialkanolamine. For instance, treatment of phenyltrimethoxysilane with diethanolamine and styrene oxide affords 1,3-diphenylsilatrane in good yield (equation 14)[69].

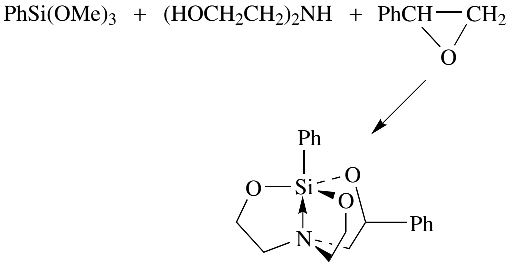

(14)

Reaction 2 is a very helpful synthetic route to various substituted carbofunctional silatranes, $Y(CH_2)_nSi(OCHRCH_2)_3N$, where Y = Hal^{70-77}, $CF_3{}^{56,73}$, $HO^{78,79}$; $R'O^{80-82}$, $R'COO^{83,84}$, $HS^{85,86}$, $R'S^{87-89}$, $R'C(O)S^{90}$, SCN^{91}, $R'Se^{92}$, R'_2N (R = $H^{53,93-95}$, R′ = Alk or $Ar^{55,96-101}$), $R'CON(R')^{99,102-107}$, $R'CSN(R')^{102,107}$, $(R'O)_2P(O)^{108,109}$, etc., n = 1–3. Preparation of several main types of these compounds is illustrated by the examples in equations 15–21.

$$R_FCH_2CH_2Si(OR)_3 \xrightarrow{\text{THEA, R}'\text{OM, }\Delta} R_FCH_2CH_2Si(OCH_2CH_2)_3N \tag{15}$$

$R_F = FCH_2, CF_3$, R = Me, Et, R′ = H, M = K; R′ = Et, M = Na^{56}

$$Me_3SiO(CH_2)_3Si(OEt)_3 \xrightarrow{\text{THEA, MeOH}} \underset{95\%^{78}}{HO(CH_2)_3Si(OCH_2CH_2)_3N} \tag{16}$$

$$H(CF_2)_nCH_2OCH_2Si(OEt)_3 \xrightarrow{\text{THEA, RT}} H(CF_2)_nCH_2OCH_2Si(OCH_2CH_2)_3N \tag{17}$$

$n = 2$ (80%)
$n = 12$ (94%)
$n = 16$ (96%)[82]

$$ArZ(CH_2)_nSi(OR)_3 \xrightarrow{\text{THEA, RT}} ArZ(CH_2)_nSi(OCH_2CH_2)_3N \tag{18}$$

Ar = C_6F_5, $n = 3$, Z = O (100%)[81], Z = S (97%)[89]; Ar = Ph, Z = Se, $n = 1, 2^{92}$

$$MeOOC(CH_2)_nN(Me)CH_2Si(OR)_3 \xrightarrow{\text{THEA}} MeOOC(CH_2)_nN(Me)CH_2Si(OCH_2CH_2)_3N \tag{19}$$

$n = 1, 2^{100}$

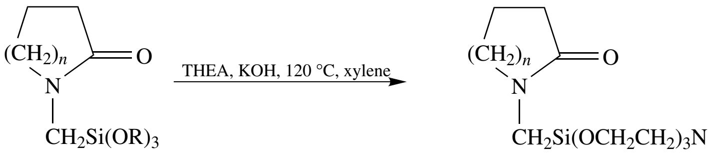

$n = 1–3^{106}$

(20)

$$(RO)_2P(X)Y(CH_2)_nSi(OR')_3 \xrightarrow{\text{THEA, KOH, xylene}} (RO)_2P(X)Y(CH_2)_nSi(OCH_2CH_2)_3N \qquad (21)$$

$X = O, S, Y = NH, n = 3;$

$X = Y = S, n = 1$[108, 109]

As catalysts in the above reactions, alkali metal hydroxides or alkoxides are used (equations 15, 19–21).

However, in some cases the use of a basic catalyst can result in cleavage of the Si—C bond[59,76]. For example, treatment of dichloromethyltriethoxysilane with trialkanolamine in the presence of sodium methoxide affords the corresponding 1-ethoxysilatrane in 84% yield (equation 22). The target 1-dichloromethyl-4-ethylsilatrane (96%) is formed in the absence of a catalyst[59].

$$Cl_2CHSi(OEt)_3 + (HOCH_2CH_2)_2N(CHEtCH_2OH)$$

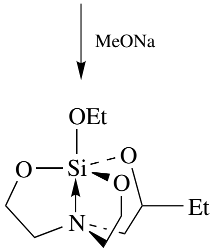

(22)

The reaction given in equation 2 cannot be applied for the preparation of 1-(2′-haloethyl)silatranes because of β-elimination leading to cleavage of the Si—C bond (equation 23)[76].

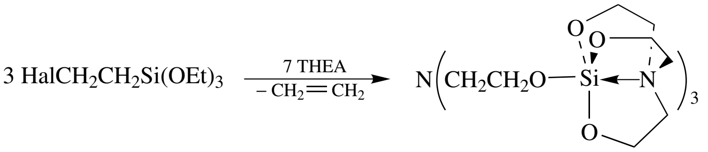

(23)

$$+$$

$$3(HOCH_2CH_2)_3N \cdot HHal$$

Treatment of chloromethyl- or 3-chloropropyltriethoxysilanes with L-*N*,*N*-bis(2-hydroxyethyl)serine or -threonine in the presence of a catalytic amount of pyridine at 70–80 °C gave a novel class of silatranes, (4*S*)-silatrane-4-carboxylic acids (equation 24)[110,111].

Reaction 24 does not occur with the protonated amine (i.e. with the zwitterionic form of the dihydroxyethylated amino acid) in the absence of pyridine. It seems most likely that the catalytic role of pyridine involves release of the lone-pair electrons of the nitrogen atom, that facilitates the formation of the transannular Si←N bond and, consequently, the silatrane ring[110].

A variety of 1-(heteroarylalkyl)silatranes can be obtained from heteroarylalkyltrialkoxysilanes and THEA according to equation 2[50,112–114]. For instance, 2-(benzoxazolylthiomethyl)trimethoxysilane reacts with THEA at room temperature to give the corresponding silatrane in high (86%) yield. 1-(2′-Benzothiazolythiomethyl)- and 1-(2′-benzimidazolylthiomethyl)-silatranes are obtained in a similar manner (equation 25)[112].

$$\mathrm{Cl(CH_2)}_n\mathrm{Si(OEt)_3} + \mathrm{(HOCH_2CH_2)_2NCH(COOH)CH(R)OH}$$

R = H, Me, $n = 1,3$

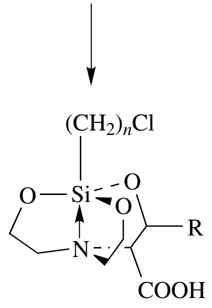

(24)

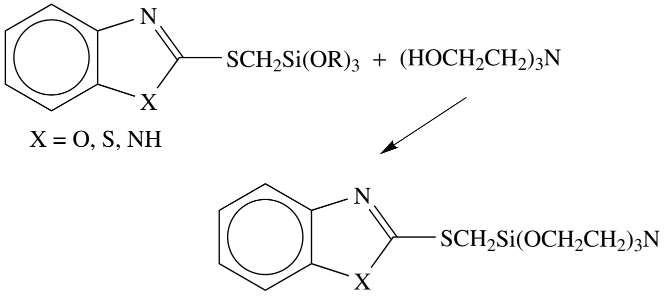

(25)

It should be noted that the stronger (shorter) is the formed transannular Si←N bond, the easier are the above transetherification reactions. For example, $2\text{-}\mathrm{O_2NC_6H_4Si(OEt)_3}$ reacts exothermally and rapidly at room temperature, $\mathrm{PhSi(OMe)_3}$ requires heating for the reaction to proceed with a reasonable rate and conversion of $4\text{-}\mathrm{Me_2NC_6H_4Si(OMe)_3}$ occurs under more drastic conditions[69]. In line with these qualitative observations, the Si←N bond lengths for 1-(2′-nitrophenyl)silatrane and 1-phenylsilatrane were found to be 2.116 Å[115] and 2.193 Å[3], respectively. The reaction rates between organyltrialkoxysilanes $\mathrm{RSi(OEt)_3}$ and THEA are enhanced by the electron-withdrawing effect of the substituents in the order: $\mathrm{Cl_2CH} > \mathrm{ClCH_2} > \mathrm{Me}$[116]. The strength of the Si←N bond decreases in the same sequence[117].

3. Formation from organyltriacetoxysilanes

By using organyltriacetoxysilanes, which are considerably more reactive than organyltrialkoxysilanes, it is possible to obtain the corresponding silatranes by the reaction shown in equation 1 in almost quantitative yields. This method has some advantages, namely mild reaction conditions, no need for a catalyst and convenient isolation of pure products. For example, 1-alkyl- or 1-alkenylsilatranes are formed by treatment of alkyl- or alkenyltriacetoxysilanes with tris(2-hydroxyalkyl)amines in chloroform at 0 °C (equation 26)[37,118,119].

$$\mathrm{XSi(OCOCH_3)_3 + (HOCHRCH_2)_3N \longrightarrow XSi(OCHRCH_2)_3N + 3CH_3COOH} \tag{26}$$

X = Me, Et, n-Pr, n-Bu, n-Oct, Vin, All, etc., R = H[37,118]; X = Vin, R = Me[119]

By comparison, 1-allylsilatrane is prepared in a lower yield (86%) when a mixture of allyltrimethoxysilane and THEA is heated at 75 °C for 4 h in the presence of NaOH[39].

A modified version of this procedure (equation 26) is a one-pot reaction involving conversion of organyltrichlorosilanes into the corresponding organyltriacetoxysilanes without their isolation, followed by treatment with THEA in chloroform at 0 °C (equation 27)[118].

$$\mathrm{MeSiCl_3 + (CH_3CO)_2O + (HOCH_2CH_2)_3N \longrightarrow \underset{70\%}{MeSi(OCH_2CH_2)_3N}} \qquad (27)$$

4. Formation from organylhalosilanes

A potentially more direct route to 1-organylsilatranes as compared with the conversion of organylalkoxysilanes (or organyltriacetoxysilanes) is the reaction of organyltrichlorosilanes with tris(2-hydroxyalkyl)amines or their hydrochlorides (equation 28)[13,62]. Thus, 1-chloromethyl-3-(2′,2′,2′-trifluoroethyl)silatrane is obtained in 69% yield from chloromethyltrichlorosilane and the corresponding trialkanolamine at 10–15 °C[62].

$$\mathrm{ClCH_2SiCl_3 + [HOCH(CH_2CF_3)CH_2](HOCH_2CH_2)_2N}$$

$$\Big\downarrow\ -3\mathrm{HCl}$$

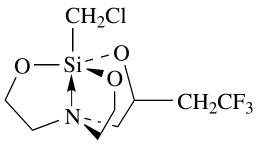

(28)

However, with vinyl- or phenyltrichlorosilanes, the protolytic cleavage of the Si–C bond becomes the main process, leading to the formation of 1-chlorosilatrane or its C-derivatives[62].

This problem can be resolved by the use of silylated tris(2-hydroxyalkyl)amines. For example, 1-vinyl- or 1-phenylsilatranes are prepared from the corresponding organyltrichlorosilanes and tris(2-trimethylsiloxyethyl)amine (equation 29). Pure products are easily isolated in good yield (80 and 83%, respectively)[120].

$$\mathrm{XSiCl_3 + (Me_3SiOCH_2CH_2)_3N \longrightarrow XSi(OCH_2CH_2)_3N + 3Me_3SiCl} \qquad (29)$$

$$\mathrm{X = Vin, Ph}$$

Analogously, 1-hydrosilatrane (X = H)[121] and some 1-organylsilatranes, including carbofunctional derivatives [X = $\mathrm{ClCH_2}$, $\mathrm{Cl(CH_2)_3}$, $\mathrm{NC(CH_2)_2}$], can be synthesized in high yields[120].

With a slight modification of equation 29, 1-allylsilatrane can be obtained in 96% yield (equation 30). Reaction occurs at room temperature in pentane solution[37].

$$\mathrm{H_2C{=}CHCH_2SiCl_3 + (Et_3SnOCH_2CH_2)_3N}$$

$$\Big\downarrow \qquad (30)$$

$$\mathrm{H_2C{=}CHCH_2Si(OCH_2CH_2)_3N + 3Et_3SnCl}$$

Treatment of tris(2-trimethylsiloxyethyl)amine with organyltrifluorosilanes in an aprotic solvent (benzene, *o*-xylene) results in the corresponding 1-organylsilatranes, as shown in equation 31[69,122,123].

$$\mathrm{RCOO(CH_2)}_n\mathrm{SiF_3} + \mathrm{(Me_3SiOCH_2CH_2)_3N} \xrightarrow[-3\,\mathrm{Me_3SiF}]{\mathrm{C_6H_6},\ \Delta} \mathrm{RCOO(CH_2)}_n\mathrm{Si(OCH_2CH_2)_3N} \tag{31}$$

$\mathrm{R = CF_3, C_3F_7, C_4F_9}, n = 3$[122]; R = Ph, $n = 2$[123]

Tris(2-trimethylsiloxyethyl)amine is also a useful reagent for the preparation of 1-chlorosilatrane (equation 32)[121] including those labelled with ^{15}N[124].

$$\mathrm{SiCl_4 + (Me_3SiOCH_2CH_2)_3N} \xrightarrow{\text{hexane, }-10\,^{\circ}\mathrm{C}} \underset{95\%}{\mathrm{ClSi(OCH_2CH_2)_3N}} + \mathrm{3Me_3SiCl} \tag{32}$$

Tetrabromosilane reacts with THEA in $\mathrm{CHCl_3}$ at $-10\,^{\circ}$C to afford 1-bromosilatrane in 31% yield (equation 33)[121].

$$\mathrm{SiBr_4 + (HOCH_2CH_2)_3N \longrightarrow BrSi(OCH_2CH_2)_3N} \tag{33}$$

5. Formation from organyltris(dialkylamino)silanes

An alternative synthetic route to silatranes is the reaction of organyltris(dialkylamino)silanes with tris(2-hydroxyalkyl)amines[52,125]. Examples are given in equation 34[52].

$$\mathrm{XSi(NMe_2)_3 + (HOCH_2CH_2)_2NCH_2CH(Ph)OH} \xrightarrow{\Delta} \mathrm{XSi(OCH_2CH_2)_2(OCHPhCH_2)N} \tag{34}$$

X = Me (55%), Et (35%), Ph (50%), Bz (20%)

6. Formation from organylsilanes

The hydrocondensation reaction of organylsilanes and triethanolamine affords the corresponding 1-organylsilatranes (equation 35). Transition metal compounds can be used as catalysts[126]. However, the method has a limited synthetic utility because of the high cost of the initial silanes.

$$\mathrm{XSiH_3 + (HOCH_2CH_2)_3N \longrightarrow XSi(OCH_2CH_2)_3N + 3H_2} \tag{35}$$

X = Me, *n*-octyl, Ph, Bz, etc

7. Miscellaneous preparations

The exothermic uncatalyzed reaction of THEA with the tris(*O*,*O*-dialkylphosphito)organylsilanes having 3 Si—OP bonds is shown in equation 36[127].

$$\mathrm{XSi[OP(OEt)_2]_3 + (HOCH_2CH_2)_3N \longrightarrow XSi(OCH_2CH_2)_3N} \tag{36}$$

X = Me (60%), Ph (63%), $\mathrm{ClCH_2}$ (70%)

The cleavage of the Si—O—Si moiety of polyorganylsilsesquioxanes (equation 37), polyorganylsiloxanols (equation 38) or polyorganylhydrosiloxanes (equation 39) by tris(2-hydroxyalkyl)amines results in the corresponding 1-organylsilatranes in 80–90% yields.

The reactions occur in a boiling solvent (toluene, xylene) in the presence of KOH[69,128]. This method can be preferably applied when the initial compounds are more available than organyltrialkoxysilanes.

$$1/n(XSiO_{1.5})_n \xrightarrow{\text{THEA}} XSi(OCH_2CH_2)_3N + H_2O \qquad (37)$$

$$1/n[XSiO_{1.5-n}(OH)_{2n}]_m \xrightarrow{\text{THEA}} XSi(OCH_2CH_2)_3N + (1.5 + m)H_2O \qquad (38)$$

$$1/n(XSiHO)_n \xrightarrow{\text{THEA}} XSi(OCH_2CH_2)_3N + H_2O + H_2 \qquad (39)$$

X = alkyl, alkenyl, aryl

A very elegant reaction is the synthesis of 1-hydrosilatrane and its C-substituted derivatives via readily available boratranes. Aprotic conditions exclude side processes involving the Si−H bond, so that the desired silatranes are formed in high yields (60–95%)[59,129–132]. For example, triethoxysilane reacts with 4-ethylboratrane in xylene in the presence of magnesium propoxide to give 1-hydro-4-ethylsilatrane (92%) (equation 40)[59]. Aluminium alkoxides[129] or aluminum chloride[130–132] are also used as catalysts. The reaction rate decreases sharply in the absence of catalysts. Attempts to prepare 1-(2′-chloroethyl)silatrane by this mild method failed[59].

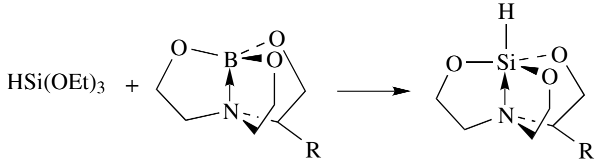

(40)

R = Et

In some cases, cleavage of a sensitive Si−C bond allows one to use bifunctional diorganylsilanes[133,134] and even tetraorganylsilanes[135] for the preparation of silatranes. Thus, 1-phenylsilatrane is formed in 80% yield from diphenyldimethoxysilane and THEA in the presence of sodium methoxide at 250 °C (equation 41)[133].

$$Ph_2Si(OMe)_2 + (HOCH_2CH_2)_3N \longrightarrow PhSi(OCH_2CH_2)_3N \qquad (41)$$

A versatile approach to 1-heteroarylsilatranes is the cleavage reaction of tetraheteroarylsilanes (equation 42) which are hydrolytically and thermally stable compounds. The latter are more easily available compared with trifunctional heteroarylsilanes. The reaction is effectively catalyzed by CsF[135].

$$X_4Si + (HOCH_2CH_2)_3N \longrightarrow XSi(OCH_2CH_2)_3N \qquad (42)$$

X =

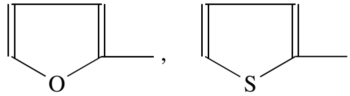

In summary, the procedures described in equations 2, 26, 28 and 34 are fairly efficient and versatile for the synthesis of a large number of silatranes. This is clearly illustrated in the preparation of 1-methylsilatrane (equation 43). However, it should be noted that only equation 2 can be considered as a truly general route to this class of compounds.

$$\mathrm{MeSiY_3 + (HOCH_2CH_2)_3N \longrightarrow MeSi(OCH_2CH_2)_3N} \qquad (43)$$

Y	Solvent	t (°C)	Cat.	Yield (%)	Ref.
OR	benzene	70	KOH	high	136
$OCOCH_3$	$CDCl_3$	0		95	118
Cl	DMF	140–150		77	120
NEt_2	xylene	135		88	125

B. Structure and Physical Properties

1. Molecular structure

Transannular interaction between the silicon and the nitrogen atoms in Si- and C-substituted silatranes is strongly proved by numerous X-ray studies[5–7,13–15,18–22,29]. Table 1 provides structural parameters for a large fraction of the approximately 60 crystallographically determined structures of 1-substituted silatranes which are mainly collected in a recent review[29].

The X-ray data demonstrate that silatranes exist in an *endo* form in which the nitrogen lone pair is oriented toward the silicon. The silicon has a distorted trigonal-bipyramidal (TBP) structure with nearly equatorial disposition of three oxygen atoms and an axial location of the nitrogen and the substituent X. The X−Si←N angle of 174°–179° is close to ideal for the TBP structure value of 180°. The valence O−Si−O and X−Si−O angles vary from 116° to 120° and from 75° to 90°, respectively. The mean length of the equatorial Si−O bonds is about 1.66 Å, compared to 1.65 Å in alkoxysilanes. The Si←N bond distance in crystals of most silatranes is in the range 1.965–2.240 Å and the difference Fourier synthesis shows a high peak of electron density at the region of the transannular bond[154,157]. This bond is considerably shorter than the sum of the van der Waals radii (3.54 Å) but certainly longer than a usual single Si−N bond of 1.7–1.8 Å. The X−Si bond in silatranes is also longer (by 0.02–0.10 Å) than that in related tetrahedral silicon compounds. The mutual weakening of the axial X−Si and Si←N bonds, first noted by Parkanyi and coworkers[158], is very important for understanding the bonding nature in silatranes. Recent investigations show that a visible shortening of the Si←N bond upon π-coordination of transition metals to the phenyl group of 1-phenylsilatrane accompanies a regular elongation of the Si−C bond in complexes[159–161].

As a rule, the Si←N bond length in silatranes decreases on increasing the electron-withdrawing effect of the substituent X (Table 1). The longest Si←N bond (2.89 Å[156]) is found for the silatranylplatinum complex **39**, which should be classified as a 'quasi-silatrane'[27]. The transannular bond of 2.007 Å in 1-isothiocyanatosilatrane **29**[68] is the shortest reported so far in neutral silatranes. In silatranyl oxonium salts **36** the Si←N bond is a record short value, 1.965 Å[150]. However, despite a lower electronegativity of the substituent X, a shorter transannular bond is observed for 1-chlorosilatrane **38** (2.023 Å[155]) than in 1-fluorosilatrane **37** (2.042 Å[154]).

The strengthening of the Si←N bond is accompanied by a reduction in the XSiO angles and an increase in the nitrogen pyramidalization. These are reflected in the corresponding decrease in the deviation of the silicon atom from the plane of the equatorial oxygen atoms (Δ_{Si}) and increase in the deviation of the nitrogen atom from the plane of the neighboring

TABLE 1. Structural parameters for Si-substituted silatranes

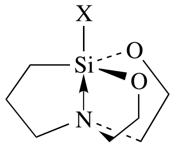

Compound	X	d(N−Si) (Å)	d(X−Si) (Å)	d(Si−O) (Å) (mean)	N−Si−X (°)	N−Si−O (°) (mean)	Δ_{Si} (Å)[a]	Δ_N (Å)[b]	Ref.
2	Me	2.175(4)	1.870(6)	1.670(4)	179.4(2)	82.7	0.211	0.379	137
3	Et	2.214(8)	1.881(10)	1.658	178.7(1)	82.0	0.229	0.342	29
4	Cyclopropyl	2.228(9)	1.94(1)	1.664(8)	176.0(7)	81.7	0.24	0.35	34
5	2-Chlorocyclopropyl	2.150(3)	1.877(4)	1.664(3)	187.7(2)	83.2	0.2		35
6	Cyclopropylmethyl	2.149(4)	1.874(5)	1.659(4)	177.2(2)	83.1	0.2		37
7	$H_2N(CH_2)_2NH(CH_2)_3$	2.165(2)	1.875(2)	1.666	179.1(1)	82.7	0.210(1)	0.383(3)	138
8	$HO(CH_2)_3$	2.173(2)	1.869(2)	1.665(1)	179.4(2)	82.7	0.21(1)	0.372(3)	69
9	$HS(CH_2)_3$	2.177(4)	1.872(4)	1.652(4)	178.6(5)	81.7	0.21	0.37	139
10	$Cl(CH_2)_3$	2.181(7)	1.875(8)	1.662	178.2(6)	83.2	0.199	0.368	140
11	2-(1-Silatranyl)ethyl	2.230(5)	1.874(6)	1.650(5)	177.5(2)	81.6	0.24		46
12	$H(O)CCH_2$	2.108(6)	1.914(8)	1.660(5)	179.4(3)	86.0			141
13	$MePhSi(H)CH_2$[c]	2.208(9)	1.864(10)	1.638(8)			0.222(3)		49
		2.240(9)	1.869(10)	1.642(7)			0.241(3)		
14	$MePhSi(OH)CH_2$	2.214(9)	1.864(16)	1.655(10)			0.222(3)		49
15	$PhCOOCH_2$	2.112(7)	1.954(5)	1.661(7)	174.0(1)	78.5	0.16	0.36	142
16	$ClCH_2$	2.120(8)	1.912(11)	1.676	176.4(4)	84.4	0.163(3)	0.385(8)	143
17	$I^-Me_2S^+CH_2$	2.046(2)	1.930(3)	1.667(2)	179.1(1)	86.0	0.115	0.396	144
18	$I^-Me_3N^+CH_2$	2.080(13)	1.915(15)	1.662(11)	175.7(6)	85.1	0.13	0.41	145
19	Cl_2CH	2.062	1.937		176.4	85.7	0.12	0.38	17
20	$CH_2{=}CH$	2.150(6)	1.880(8)	1.664(5)	178.72(25)	83.2	0.20	0.40	146

(*continued overleaf*)

TABLE 1. *(continued)*

Compound	X	*d*(N−Si) (Å)	*d*(X−Si) (Å)	*d*(Si−O) (Å) (mean)	N−Si−X (°)	N−Si−O (°) (mean)	Δ_{Si} (Å)[a]	Δ_N (Å)[b]	Ref.
21	Ph(α)	2.193(5)	1.882(6)	1.656(5)	177.90(22)	82.9	0.204	0.34	3
22	Ph(β)	2.156(4)	1.908(5)	1.657(5)	177.04(29)	83.3	0.195	0.379	147
23	Ph(γ)	2.132(4)	1.894(5)	1.656(4)	179.0(2)	83.7	0.183	0.39	148
24	4-MeC_6H_4	2.171(1)	1.887(1)	1.656	178.8(1)	82.9	0.204	0.366	149
25	3-$O_2NC_6H_4$	2.116(8)	1.904(9)	1.656(6)	177.4(3)	84.1	0.17	0.39	115
26	2-Furyl	2.112(5)	1.894(6)	1.656(6)	177.2(2)	85.0	0.144	0.387	29
27	3-Furyl	2.130(9)	1.892(11)	1.675	177.7(4)	84.0	0.175	0.384	29
28	2-Thienyl	2.133(9)	1.905(11)	1.666	177.2(4)	84.4	0.162	0.360	29
29	SCN	2.007(3)	1.888(3)	1.639(3)	179.5(1)	87.6(2)			68
30	EtO	2.152	1.658	1.648			0.179		150
31	*t*-BuO	2.189(4)	1.659(4)	1.650(4)	179.4	83.0	0.201	0.371	151
32	4-MeC_6H_4O	2.107(2)	1.677(2)	1.649(2)	174.7(2)	84.7	0.154	0.372	152
33	3-ClC_6H_4O	2.079(2)	1.690(2)	1.656	176.5(2)	85.3	0.14	0.40	42
34	$Co_3(CO)_9CO$	2.010(5)	1.677(2)	1.649(2)	178.9(2)	86.2			153
35	EtO••$HOOCCF_3$	2.050	1.710	1.652			0.102		150
36	$BF_4{}^-Me_2O^+$	1.965	1.830	1.642			0.017		150
37	F	2.042(1)	2.042(1)	1.645(2)	179.7(1)	85.9	0.117	0.390	154
38	Cl	2.022(9)	2.022(9)	1.649	179.8(3)	86.7	0.095	0.396	155
39	$Cl(PhMe_2P)_2Pt$	2.89(1)	2.292(4)	1.649(9)	176.7	71.2	0.53	0.07	156

[a] Δ_{Si} = the deviation of the Si atom from the plane of the equatorial oxygen atoms.

[b] Δ_N = the deviation of the N atom from the plane of the neighboring carbon atoms.

[c] Two independent molecules in the unit cell.

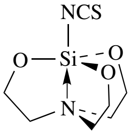

(29)

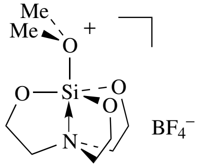

(36)

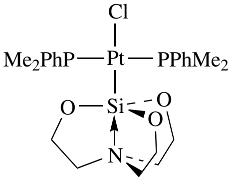

(39)

carbon atoms (Δ_N). Numerous relationships between these geometrical parameters and correlations of the Si←N bond distance with the inductive σ_I and σ^* constants and the electronegativity of the substituent X were found. These regularities were discussed recently in some reviews[17–22]. A general similarity between self-consistent change in the geometry of the silicon polyhedron upon strengthening of the Si←N bond within the silatrane series and the molecular deformation in the course of the intramolecular S_N2 substitution reaction at a tetrahedral silicon atom was found[162,163] by the Bürgi–Dunitz method of structural correlation[164]. In particular, it was demonstrated that with a successive increase in the order of the Si←N bond, the X–Si bond order is reduced[163]. The constancy of the total order of the axial bonds in silatranes is one of the fundamental properties of these and other compounds of a TBP silicon[28,165].

The cage skeleton of most silatranes possesses an approximate threefold (C_3) symmetry and in its five-membered (N–Si) chelate rings the carbon atoms in the α-position to the nitrogen deviate from the plane formed by the other atoms[15,29] (Scheme 2). The partial disordered structure observed for some silatranes may be regarded as a frozen state of the dynamic flapping of the α-C atoms in the crystals[15].

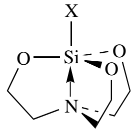

(1)

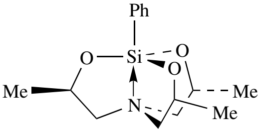

(40)

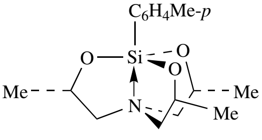

(41)

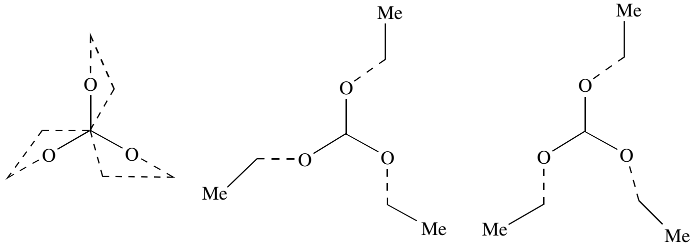

SCHEME 2. Schematic representation of silatrane moieties of compounds **1**, **40** and **41** as viewed along the X–Si←N axis.

In 3,7,10-trimethylsilatranes the β-carbons are on the flaps of their ring envelopes and the methyl groups occupy a pseudo-equatorial position in the five-membered rings[149,166,167]. Therefore, in contrast with the symmetric isomer **40** of 1-phenyl-3,7,10-trimethylsilatrane[166], the asymmetric isomer **41** of 1-(p-tolyl)-3,7,10-trimethylsilatrane[149] has a skeleton in which the 'flap'-atoms C(3) and C(7) lie on the same side of the ring planes while C(10) is on the opposite side (Scheme 2). The Si−N bond in 3,7,10-trimethylsilatranes seems to be slightly longer in their more strained asymmetric isomer[167].

Both steric interaction between the carbon substituents and the strong electron-withdrawing effect of the carboxylic acid group decrease the donor ability of the nitrogen and hence the strength of the Si←N bond in 1-organyl-3-methylsilatrane-4-carboxylic acids **42**[110,111,168].

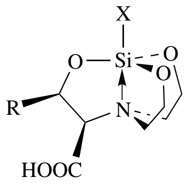

(42)

X	R	d(SiN) (Å)	Ref.
Vinyl	H	2.169	110
$ClCH_2$	Me	2.136	111
$Cl(CH_2)_3$	H[a]	2.176 and 2.208	168
$Cl(CH_2)_3$	Me[a]	2.198 and 2.244	111

[a] Two independent molecules.

It should be noted that, unlike many pentacoordinated organosilicates and organosilanes[24,25,165], silatranes are extremely ineffective in participating in a hexacoordinated structure. The silicon atom appears to be pentacoordinate[44,103,104,142] even in silatranes **15**, **43**−**45** bearing a carbofunctional substituent X having a very high (O−Si)- or (N−Si)-chelating ability[24,25,165]. This could be ascribed to a high energetic cost for the cage deformation under the flank side approach of the donor to the silicon.

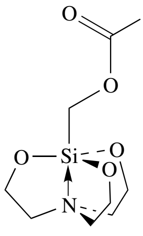

(15)[142]

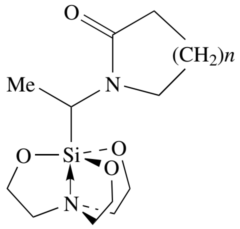

$n = 1$ **(43)**[104]
$n = 2$ **(44)**[103]

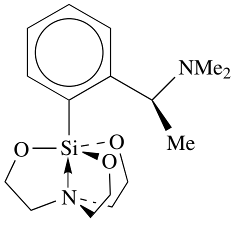

(45)[44]

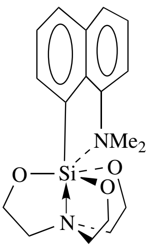

(46)[44]

A single hexacoordinated silatrane **46** possessing a very weak additional Si←NMe$_2$ bond (2.952 Å) was obtained recently by Corriu and coworkers[44]. The hexacoordination in **46** is most likely due to the rigid geometry of its 8-dimethylaminonaphthyl group. The reluctance of silicon to become hexacoordinated in the silatrane structure is its special characteristic feature which, as will be shown below (Section II.C), predetermines the low reactivity of silafunctional silatranes toward nucleophiles.

The X-ray data demonstrate that the equatorial oxygen of silatranes bearing acidic OH or COOH groups in the substituent X or the cage can be involved in the intermolecular or intramolecular hydrogen bonding[29]. The formation of a hydrogen bond leads to a visible lengthening of the protonated Si−O bond. Judging by some spectral data (Section II.B.8) and the structures of the hydrogen bonded complex **35**[150] and the oxonium salt **36**[150], the axial oxygen in 1-alkoxysilatranes is more basic than the equatorial oxygens.

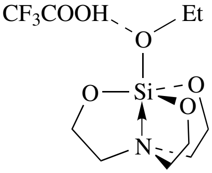

(35)

Mutual weakening of the axial bonds in silatranes predetermines the unprecedented difference between the Si←N bond lengths in the crystal and in the gas phase. Electron diffraction studies of 1-methylsilatrane **(2)**[169] and 1-fluorosilatrane **(37)**[170] found that in the vapors their transannular bond is 0.28 Å longer and the X−Si bonds are somewhat shorter than those in their crystals.

2. Bonding model

The first model of the bonding in silatranes invoked an sp^{3}d hybridization of the silicon atom[2,3,69]. However, this theoretical scheme was of very limited analytical value for understanding the silatrane properties. Moreover, many experimental and quantum chemical data ruled out the valence role of d orbitals in molecules of main group elements[171,172]. In 1977 the Musher model of hypervalency[173] was modified with reference to the Group 14 elements and used for a qualitative analysis of the structural trends in silatranes[12,13,174].

This model implies that the TBP silicon could use its sp^2 orbitals for the bonding with the equatorial oxygen atoms, whereas its p$_z$ orbital could be involved in the interaction with an appropriate orbital of the axial substituent X and a lone electron pair of the donor nitrogen atom. These generate three usual, two-center bonds in the equatorial SiO$_3$ fragment and a hypervalent, three-center four-electron (3c4e) bond in the axial moiety XSiN. The simplest MO diagram of a 3c4e bond may be represented by three molecular orbitals, bonding (b), nonbonding (nb) and antibonding (ab) (Scheme 3).

The nonbonding orbital should have a node in a region of the weakest, Si←N component of a hypervalent X−Si←N bond. This explains a typical distortion of a TBP configuration of the silicon in silatrane and its displacement from the equatorial plane toward the substituent X.

Analysis of the MO diagram of the 3c4e bond shows that the charge transfer from the nitrogen atom to the substituent X should be less than unity. Since the axial and

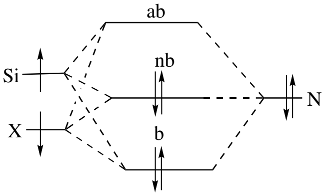

SCHEME 3. The simplest MO diagram of a 3c4e bonding in silatranes

equatorial bonds are practically orthogonal, the proposed model predicts a predominant *trans* effect of the axial substituent X. By use of the second-order perturbation theory, both the X−Si and Si←N components of hypervalent X−Si←N bond were shown to be mutually weakened in comparison with the usual two-center bonds. The corresponding analytical equations describing the energy of the axial bonding predetermine (at the energetic level) a constancy of the total order of the X−Si and Si←N bonds in silatranes. According to the 3c4e model, the degree of the Si←N bonding is determined not only by the electronegativity of the substituent X but also by the strength of the X−Si bond. Displacement of the substituent X by a more electronegative or a better leaving group should increase the energy (decrease the length) of the Si←N component of the X−Si←N bond. In molecules with the same $XSiO_3N$ coordination center, a variation in the Si←N bond length (strength) should be accompanied by a change in the opposite direction in the corresponding descriptions of the X−Si bond. Due to a strong influence of the substituent X on the Si←N bond length and a charge transfer in the axial moieties, the values of inductive and resonance effects of the silatranyl group cannot be constant within a series of silatranes. Finally, the 3c4e model predicts that the introduction of a less electronegative substituent in the equatorial sites of silicon TBP should decrease the central atom bonding with both axial substituents.

This model and its consequences appear to be a very constructive and useful concept for a consistent analysis of the physical and chemical properties of silatranes and other organic compounds of TBP silicon[20,24,27,28].

3. Quantum mechanical studies

Despite the extensive experimental evidence for the silicon pentacoordination in silatranes, for a long time there were doubts concerning the true reasons of the *endo* configuration of these molecules (see literature cited elsewhere[12,13]). In particular, it was suggested that this geometry is not realized due to a transannular Si←N bonding, but primarily owing to steric factors typical for medium-ring bicyclic nitrogen compounds[175] which push the nitrogen atom inside the molecular cage. A weak dipole–dipole interaction of the nitrogen lone electron pair with a tetrahedral silicon atom and its neighboring atoms was also considered as a stabilizing factor of the *endo* structure of silatranes.

Calculations of the strain energies of the *endo* and *exo* forms of the 1-methyl-, 1-fluoro- and 1-chlorosilatranes carried out by the methods of molecular mechanics found these assumptions to be unsound[176–180]. Even with an additional consideration of the intramolecular electrostatic interactions[177–179], employment of the usual force field for tetracoordinate silicon led to potential functions of the *endo*–*exo* isomers (equation 44) with a deeper minimum corresponding to the *exo* form **47**, with *out*-orientation of the nitrogen.

However, it was difficult to exclude a hypothetical *exo* form at least as a minor component in solution or in the gas phase. Since the chemical and physical properties of the *exo* and *endo* forms should differ sharply, their relative thermodynamic and kinetic stability as well as the nature of the bonding in silatranes constitute a major concern in silatrane chemistry.

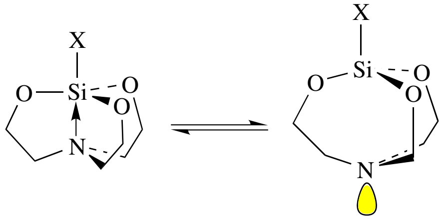

(1) **(47)**

(44)

The energetic preference of the *endo* form was demonstrated by the first quantum chemical calculations of silatranes performed on 1-hydro- and 1-fluorosilatranes[12,181]. These calculations employed the CNDO/2 semiempirical method with spd basis set and geometries of the *endo* and *exo* forms corresponding to those obtained for 1-methylsilatrane by modified molecular mechanics method. The energy of the Si←N coordinative bonding was found to be about 20–25 kcal mol^{-1} and to be the main contributor to stabilization of the *endo* structure of silatranes.

Subsequent theoretical calculations confirmed the important role of the Si←N interaction in the formation of the silatrane structure. A significant Si←N bond order was determined at the CNDO/2 level using the experimental solid state geometries of silatranes[182–185]. Thus, the Wiberg indexes of this bond in the crystalline α, β and γ modifications of 1-phenylsilatrane were estimated to be 0.35–0.39 and 0.15–0.18 within the spd and sp basis sets, respectively[182]. It was shown that a transannular Si←N bonding decreases the bond order of the Ph−Si bond. Together with a significant bond order of the Si←N bond in 1-methylsilatrane, detected by CNDO/2[186] and MNDO[187] calculations using sp basis set, these data confirmed the validity of the 3c4e bonding model.

The first semiempirical studies of the potential functions of silatranes revealed that their Si←N bond could be very easily deformed by crystal packing and solvation forces[188a]. Direct MINDO/3 and MNDO calculations demonstrated a significant shortening of the equilibrium, gas phase Si←N distance due to the contribution of the solute–solvent interaction energy (within the Onsager reaction field model[188b]) to the total energy of 1-methyl- and 1-fluorosilatranes[188a].

The first *ab initio* calculations on silatranes proved that only a small amount of energy (a few kcal mol^{-1}) is required to decrease the Si←N bond length from the gas-phase to the solid-state value. The single point computations were carried out by using the 3-21G* basis set for two Si←N 'bond-stretch' isomers of 1-methylsilatrane[189], using the solid-state and an approximate gas-phase geometry, and with the 6-31G* basis for 1-hydroxysilatrane with geometries optimized by the AM1 method[190]. According to the Bader electron density analysis, the Si←N bond critical point should still exist even in the gas-phase 1-hydroxysilatrane structure[190].

AM1 and PM3 computation on 1-methyl-[191], 1-fluoro-[180], 1-chloro-[192] and 1-isothiocyanatosilatranes[68] using full geometry optimization confirmed the small energy cost for a shortening of the Si←N bond in silatranes. The potential profiles of these molecules were shown to be very flat in the 2.00–3.60 Å range of the Si←N distance, with two distinct minima related to the *endo* and *exo* forms. Both parametrizations found the *endo* structure to be the more stable in the case of 1-isothiocyanato- and 1-halosilatranes, where the equilibrium Si←N distances are shorter than in 1-methylsilatrane. Both semiempirical methods overestimate the Si$\leftarrow$N bond lengths (by 0.11–0.21 Å) with respect to the experimentally observed gas-phase values. Frequency analysis predicts that a separate Si$\leftarrow$N vibration frequency should not exist. For 1-methylsilatrane, the Si$\leftarrow$N stretching vibration (in the region of 280 cm^{-1}) should be combined with the C−N (at about 450 cm^{-1}), Si−O and Si−C (at about 720 cm^{-1}) vibrations[191] whereas for 1-chlorosilatrane a combined Cl−Si$\leftarrow$N vibration should appear at 364 cm^{-1}[192].

In contrast to the semiempirical results, full optimization of the molecular geometry of 1-fluorosilatrane by restricted Hartree–Fock (RHF) calculations using the 3-21G, 3-21G* and 6-31G* basis sets did not find evidence for the existence of an *endo* minimum on the energy hypersurface[193]. Since the *exo* form was never found experimentally, the *ab initio* results support the view of the exclusive existence of silatranes in the *endo* form. As for the equilibrium Si$\leftarrow$N distance, the *ab initio* calculations using polarized basis sets overestimated its value (2.556 Å) even more than the AM1 and PM3 methods.

Nearly the same energy profile and Si$\leftarrow$N bond length (2.534 Å) of 1-fluorosilatrane were computed by Gordon's group[194] at the RHF/6-31G* level. The use of the extended, 6-31G*EXT basis (two sets of d functions on Si, O, F and N atoms and a diffuse sp shell situated on the same atoms) changed the geometry and decreased the equilibrium Si$\leftarrow$N distance by 0.117 Å. However, adding a set of f functions on silicon and all adjacent atoms to this basis set (to produce a 6-31G*EXT+f basis set) led to an apparently large change in the geometry but cancelled 0.08 Å of the shorting achieved in the Si$\leftarrow$N distance.

Inclusion of single point MP2 treatment of electron correlation along the SCF 6-31G* potential curve shifted its minimum by about 0.15 Å and brought the computed Si$\leftarrow$N bond length (2.29 Å) into extremely close agreement with the experimental gas-phase value[194]. Boggs and coworkers[195] found just the same effect of electron correlation on the equilibrium Si$\leftarrow$N bond length of 1-fluorosilatrane by MP2 calculation using the 6-31G* basis set for Si, N, F and O and the 6-31G basis set for C and H at MNDO optimized structures. However, since both latter numerical results[194,195] did not include a full geometry optimization at the MP2 level, they should be viewed with some caution.

Gordon and coworkers performed a quantitative study of the effect of solvation on the molecular geometry of 1-fluorosilatrane[194] using the Onsager reaction field cavity model[188a]. The solute phase Si$\leftarrow$N bond length in 1-fluorosilatrane was predicted to be 2.104 Å, a very close value to the known solid state X-ray distance. The energy of solvation and the amount of energy gained by reoptimizing geometry with such a drastic shortening of the Si−N distance were found to be about 10.5 and 4.1 kcal mol^{-1} respectively.

The results of semiempirical and *ab initio* calculations are consistent with the general tendency toward strengthening of the Si$\leftarrow$N bond on increasing the electronegativity of the substituent X. However, the experimentally observed shortening of the Si$\leftarrow$N bond in 1-chlorosilatrane as compared with that in 1-fluorosilatrane was reproduced successfully only by the PM3 method[180,192,194]. Comparison of the semiempirical results show that the PM3 and MNDO equilibrium geometries of silatranes are generally closer to the experimental data, whereas the AM1 method gives a more reliable picture of charge distribution and orbital energies[193,196].

Calculations of the potential functions governing the Si$\leftarrow$N bond stretching motion made it possible to trace regularities in the variation of the atomic charges and stereoelectronic and orbital structure of silatranes with the change in the coordination number of the silicon atom and the degree of the Si$\leftarrow$N bonding[180,188,191,192,196]. It was found that the main changes in atomic charges upon variation in the Si$\leftarrow$N bond length occur on the O, N and X atoms, rather than on silicon. The values of atomic charges and the signs of their gradients are naturally very sensitive to the computation method.

Previous semiempirical computations of silatranes and some other pentacoordinated organosilicon species found either increase or decrease in the negative silicon charge under pentacoordination, depending on the method and the basis set used[12]. However, the view of a higher positive charge on the pentacoordinate silicon as compared with the tetracoordinate state is widely accepted[184]. Results of *ab initio* 6-31G* calculations on 1-fluorosilatrane[12] demonstrate a definite decrease in the positive charge on silicon, an increase in the negative charge on nitrogen and an elongation of the F−Si and Si−O bonds with a shortening of the Si−N distance. These changes enlarge the values of the dipole moment and the Si←N bond order. The latter value is not negligible in the equilibrium geometry despite the large Si−N distance.

Ab initio study of structural trends[194] led to the conclusion that the dative bonding model rather than the 3c4e model could describe the character of the X−Si←N bonding in silatranes. Within the dative model, which represents a limiting extreme of the basic MO diagram (Scheme 3), the primary interaction includes the formation of bonding and antibonding orbitals between X and Si. The nitrogen lone pair remains essentially unaffected during the molecular formation and the only Si−N binding is provided by a small dative interaction. The model predicts a very weak Si←N bond, a small electron transfer in the axial moiety and an ordinary covalent character of the X−Si bond. In agreement with this prediction, the RHF/6-31G*EXT analysis of the Boys localized orbitals of 1-fluorosilatrane show only slight bonding of the nitrogen lone pair with the silicon atom[194]. Moreover, the RHF/6-31G* calculations found that the X−Si bond in silatranes with X = H, F and Cl is somewhat shorter than in the model trisilanols $XSi(OH)_3$.

However, these arguments call for additional study. The dihedral angles at the Si−O bonds for the model molecules appeared to differ strongly from those in silatranes[197]. The conformation of these trisilanols allows an effective interaction of the oxygen lone pairs with the geminal σ^*-Si−X orbital. This is why the difference in the calculated X−Si bond distances in the molecules compared testifies to a different nature of their anomeric effects[198] rather than to the preference of the dative bonding model for silatranes. Indeed, trisilanols with X = H_3Si, Me, H_2P, HS, H_2N and HO having nearly the same dihedral angles as in silatranes were shown to have a shorter X−Si bond than that in related silatranes[194]. Together with the well known general tendency for the X−Si bond lengthening upon strengthening of the Si←N bond, these results suggest that the bonding in silatranes is closer to the 3c4e picture.

4. Thermochemical data

The enthalpies of combustion and sublimation were determined[199–203] for a number of 1-organyl- and 1-organoxysilatranes. These data made it possible to calculate the enthalpies of formation and atomization of silatranes as well as an energy correction term ($E_{\text{cycl}} - E_{\text{Si}\leftarrow\text{N}} = 7.2\text{–}11.7\ \text{kcal}\,\text{mol}^{-1}$) combining strain energy and dative bond strength. The $E_{\text{Si-N}}$ values were estimated to be 13–22 $\text{kcal}\,\text{mol}^{-1}$ on the basis of various experimental spectroscopic and kinetic data[204]. Using the correction terms derived from the thermochemical data, the lower limit of the strain energies of most simple silatranes appears to be close to 15 $\text{kcal}\,\text{mol}^{-1}$, a value known in bicyclo[3.3.3]undecane (manxane)[205]. The thermochemical data indicate also that the enthalpy of formation of the silatranyl group varies only slightly, its value being $186.4 \pm 1.7\ \text{kcal}\,\text{mol}^{-1}$[203].

5. Dipole moments

The high polarity of silatranes is one of the most convincing pieces of evidence for the Si←N bonding in silatranes in solution. Their dipole moments (μ) lie in the range

5–11 D, while the influence of the Si and C substituents and the medium on the μ values has been discussed in detail in previous reviews[1,5,6,12,13,28].

By use of the X-ray data and the method of bond moments, the contribution of the Si←N bond to the molecular dipole moment of 1-organylsilatranes was calculated to be 1.5–3.1 D[12,206]. These values correspond to a transfer of approximately 0.2e from the nitrogen to the silicon atom. Use of the known empirical relationship (equation 45) between the heat of formation of the donor–acceptor (DA) bond (ΔH_{DA}) in DA complexes, the dipole moment (μ_{DA}) and the inverse value of the length of the DA bond (d_{DA}) made it possible to estimate $-\Delta H_{\text{Si}\leftarrow\text{N}}$ values of 5–15 kcal mol^{-1}[207]. Electron-withdrawing substituents increase the dipole moment and energy of the Si←N bond.

$$\Delta H_{\text{DA}} = -7.47\mu_{\text{DA}} d_{\text{DA}}^{-1} \tag{45}$$

Within a series of 1-alkylsilatranes, the magnitude of the alkyl group has a negligible effect on the μ value of the molecule[208]. The increase in temperature causes only slight and irregular changes in the dipole moments. This seems to be unexpected, since the IR and NMR data indicate an elongation of the Si←N bond on heating of silatrane solutes (Section II.B.9) and *ab initio* and semiempirical studies predict a decrease in the μ value with the increase in the Si–N interatomic distance.

6. Photoelectron spectra

X-ray photoelectron spectroscopic (ESCA) studies[209–211] found a correlation between the N_{1s} and Si_{2p} binding energies in silatranes, thus providing evidence for a strong Si←N interaction in these molecules. In 1982 an analysis of the Si–K_α chemical shifts in the X-ray fluorescent spectra argued in favor of a higher positive charge on the silicon atom in silatranes than in related Si-substituted triethoxysilanes[212]. Meanwhile, results of previous X-ray fluorescent studies of silatranes suggested that the Si←N bond formation reduced the effective positive charge on the silicon[213,214].

Despite some inconsistencies in the experimental data and their interpretation, the PE spectroscopy studies of silatranes led to some common conclusions[196,215–218]. For most silatranes the IP_1^v is associated with the nitrogen lone pair orbital which involves at least some Si character. The IP_1^v values (9–10 eV) are sensitive to the substituent X and generally increase with strengthening of the Si←N bond. They exceed not only the IP_1^v value of the model compound manxine **48** (7.05 eV)[219], which also has near-planar nitrogen atom, but even the IP_1^v value of triethanolamine (8.7 eV)[215] and tris(2-trimethylsiloxyethyl)amine (7.94 eV)[217], which possess usual, tetrahedral nitrogen. These observations are regarded as a manifestation of the bonding effects in silatranes[215,217].

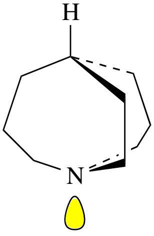

(48)

In silatranes which do not have more easily ionizing groups in the substituent X, the IP_1^v was attributed to the Si←N sigma bond orbital[218] or to a MO localized to a great extent on the axial X−Si←N fragment[196]. The first assignment was based on the *ab initio* STO-3G calculations of silatranes with X = Me, $ClCH_2$, Vinyl, F and Cl using common skeleton geometry based on the solid state structure of 1-methylsilatrane. It was shown, however, that the 3-21G* IP_1^v (assuming the validity of Koopmans' theorem) of the latter compound changes from 10.14 eV for the solid state structure to 9.87 eV for the gas phase structure[189]. The second assignment was based on analysis of the dynamic orbital-correlation diagrams and the results of MNDO and AM1 calculations. It was noted that the increase in IP_1^v on shortening of the Si←N bond is caused by the corresponding increase in the nitrogen atom pyramidality[196], whereas the higher IP_1^v in silatranes relative to those in model compounds can be explained by a probable interaction between the nitrogen lone pair and the antibonding σ^* MOs of the neighboring C−C−O fragments in the former molecules[216,217]. All these results demonstrate that the problems of MO structure and PE spectroscopy of silatranes are still open.

7. Ultraviolet spectra

The ultraviolet absorption spectra of silatranes display only an edge of the n-σ^* band ($\lambda_{max} < 190$ nm)[216,220,221]. A hypsochromic shift of this band relative to that observed in the spectra of triethylamine (204 nm), triethanolamine and its tris-TMS derivative (195–196 nm) confirms the Si←N bonding in silatranes. The CNDO/S study of the electronic excited states of 1-methyl- and 1-vinylsilatranes had shown that their UV spectra are determined by two transitions corresponding to charge transfer from the highest occupied molecular orbital, which is localized on the Si←N, Si−C, Si−O and C−O bonds[222]. Despite a high polarity of 1-arylsilatranes (X = Ph, C_6F_5), the solvent effect on their UV absorption and fluorescence spectra was shown to be only slightly higher than that for the corresponding aryltriethoxysilanes[223]. A silicon pentacoordination does not affect the absorption bands of the aromatic groups in the spectra of 1-aryloxysilatranes[224]. UV absorption spectra of charge-transfer complexes of silatranes [X = Ph, $FC_6H_4CH_2$[54] and $RS(CH_2)_n$[225] where R = Alk, Bz, Allyl and $n = 1, 2$] and the corresponding trialkoxysilanes with TCNE revealed a higher electron-releasing ability of the silatranyl group. The aromatic substituent and the sulfur were shown to be the electron-donor centers in these complexes.

8. Vibrational spectra

The main features of the IR and Raman spectra of silatranes were reviewed at the beginning of the 1980s[12,13]. There were two hypotheses concerning the manifestation of the Si←N bond vibrations in the spectra. The first presumed that this stretching vibration is in the range 568–590 cm^{-1} since the corresponding absorption band has not been observed in the spectra of the related model compounds, triethanolamine and trialkoxysilanes $XSi(OAlk)_3$. According to the second hypothesis, bands detected in this range should be assigned to the skeleton vibrations of silatranes, whereas the Si←N vibration should be observed in the region of 340–390 cm^{-1}. The main arguments in favor of the latter were obtained from study of the $^{15}N/^{14}N$ isotopic effect in the IR spectra of silatranes[207].

Since then a number of new results on IR and Raman spectra of silatranes and computation of the force field of their vibrations were published[33,226–232]. Most of them, together with results of frequency analyses based on semiempirical calculations[191,192], show that no pure Si$\leftarrow$N vibration frequency exists. Thus, calculations of vibration spectra of 1-hydrosilatrane revealed that at least two completely symmetric vibrations of silatrane molecules should include the Si$\leftarrow$N vibration. One of these vibrations is predicted to be at 590 cm^{-1} and to combine with the δ(SiOC)[230] or ν(CCN)[228] vibrations. Another should be displayed in a lower frequency region, combining with δ(CCO)[230] at 450 cm^{-1} or ν(SiO)[228] at 350 cm^{-1}. By normal coordinate analysis for A$_1$-type vibrations of 1-methylsilatrane, the f(Si$\leftarrow$N) force constant was estimated to be 0.70×10^{-6} cm^{-2} based on Billes' tensor method. A band at 348 cm^{-1} was attributed to the combined vibration of the silatrane cage including 35% ν(Si$\leftarrow$N) + 27% ν(C$-$C) + 20% ν(C$-$O) + 6% ν(O$-$C$-$C)[231]. The calculated ν(Si$\leftarrow$N) values were found to be nearly the same for both the gas-phase and solid-state geometries of 1-methylsilatrane. This agrees with an experimentally observed indifference of the corresponding Raman band to melting or dissolving of the crystal, which should be accompanied by lengthening of the Si$\leftarrow$N bond[227]. At the same time, in a series of silatranes the Raman ν(Si$\leftarrow$N) wavenumbers depend on the substituent X changing from 348 cm^{-1} (X = H) to 398 cm^{-1} (X = F) as shown below[227].

X:	H	Me	$H_2N(CH_2)_3$	EtO	F
ν(Si$\leftarrow$N), cm^{-1}:	348	354	354	366	398

It was shown that introduction of methyl groups in the 3, 7, 10 positions of silatranes shifts the band of skeleton vibration from 560–590 cm^{-1} to 440 cm^{-1}[229].

The bathochromic shift of the ν(Si$-$H), ν_{as}(Si$-$C) and ν(Si$-$Hal) frequencies of 1-hydro-, 1-alkyl- and 1-halosilatranes as compared with those in the IR spectra of triethoxysilanes indicates a weakening of the X$-$Si bond in silatranes[2,13,69].

A striking sensitivity of silatranes to the physical environment was first detected by the observations of a very strong effect of the phase and solvent on the ν(Si$-$H) value in the spectra of 1-hydrosilatrane[69,233a] and its 3,7,10-trimethyl and 3,7,10-tris(trifluoromethyl) derivatives[233a]. For example, the ν(Si$-$H) of solid 1-hydrosilatrane is higher by 83 cm^{-1} than in its solution in CCl_4. It was suggested[233a] that a decrease in the ν(Si$-$H) frequency upon dissolving these compounds in solvent of decreasing polarity is provided by the weakening of the Si$\leftarrow$N bond. Subsequent electron diffraction investigation of the gas-phase geometry of 1-methyl-[169] and 1-fluorosilatranes[170] and multinuclear NMR studies of the influence of the physical environment on silatrane structure (see the next section) corroborated this conclusion. Interestingly, a large decrease (of about 80 cm^{-1}) in the ν(Si$-$H) frequency of C-substituted 1-hydrosilatranes in $CC1_4$ was recently found[233b] under a pressure of 1 kbar.

Spectroscopic studies of hydrogen bond formation between silatranes and such proton donors as phenol and methanol revealed enhanced basicity of silatranes relative to the corresponding organyltriethoxysilanes[150,216,217,221,234]. Analysis of the solvent effects on the spectroscopic basicity of these compounds showed that the oxygen atoms (equatorial in 1-organylsilatranes and axial in 1-alkoxysilatranes) rather than the nitrogen are the proton acceptor centers[216,217,221,234]. A higher basicity of these atoms in silatranes and also in O-trimethylsilylated 2-aminoalkanols was explained by a peculiarity of through-bond interactions in compounds containing the Si$-$O$-$C$-$C$-$N fragment[216,217]. Recently it was shown, however, that the origin of the observed difference in basicity of silatranes and triethoxysilanes could be due to a difference between the anomeric effects in the molecules[198].

9. NMR spectra

The results of the NMR studies of silatranes gave one of the first unambiguous pieces of evidence for the existence of the transannular Si←N bonding in silatrane solutions[2,12,13]. Moreover, extensive NMR investigations of silatranes revealed a number of reliable spectral indications for the silicon pentacoordination and earlier unknown spectral and structural regularities which appeared to be typical for most organic derivatives of the TBP silicon[20,28].

a. ^1H NMR spectra. The NCH_2 and OCH_2 protons of the three identical cage rings of silatranes give deceptively simple AA′MM′ spectra of two triplets[13,20,235–237]. Chemical equivalence of the geminal protons of both the N- and O-methylene groups is observed even at a very low temperature. This indicates a high flexibility of the unsubstituted silatrane skeleton and a fast rate (on the NMR time scale) of the degenerate transitions between enantiomeric conformers (equation 46). There are two viewpoints concerning the mechanism of epimerization of these conformers. The first suggests a synchronous conversion of all the three rings of the silatrane cage[238], whereas the second proposes their non-correlated successive flips[239].

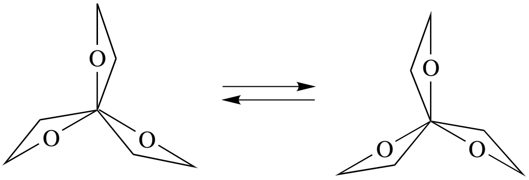

(46)

The ^3J(HH) coupling constants are within the narrow range of 5.75–5.97 Hz and tend to increase on increasing the value of Taft polar substituent constants[236]. This was explained[236] by a decrease in the dihedral angles HCCH on shortening the Si←N bond. Precise determination of ^3J(HH) in the skeleton of some silatranes[237] made it possible to estimate the NCCO torsion angles, which appeared to be comparable to the solid-state angles. This means that in solution the silatrane molecules have a Si←N bond and a conformation similar to that in the solid state.

An increased preference for a *trans* location of the vicinal oxygens in the 2-methoxyethoxy fragment of 1-(2′-methoxyethoxy)silatrane as compared with tetrakis(2-methoxyethoxy)silane was found[237] by analysis of their vicinal $^1H-^1H$ coupling constants using a modified Karplus equation. Enhanced electrostatic repulsion between these heteroatoms reflects the electron donation from nitrogen via silicon to the axial ligand in the former compound.

^1H NMR studies of 3-methylsilatranes[238], 4-organylsilatranes[61] and diastereomeric 3,7-dimethyl- and 3,7,10-trimethylsilatranes[238,239] revealed conformational rigidity of their substituted five-membered rings and the equatorial position of the C-substituent. It was shown that for most 3,7-dimethyl- and 3,7,10-trimethylsilatranes the diastereomer distributions are nearly statistical, indicating a kinetic control of the reactions leading to the formation of the silatrane cage[238].

The X−Si←N bonding and the corresponding transfer of electron density in silatranes are well reflected in the values of their ^1H NMR chemical shifts[13,20,235,236]. Thus, the shielding of the substituent X protons in 1-organylsilatranes is higher than in the model tetracoordinate compounds, organyltriethoxysilanes $XSi(OEt)_3$, whereas the NCH_2 protons in silatranes are less shielded than in triethanolamine and its tris-TMS ether. A change in the nature of the substituent X has approximately the same influence on the chemical shifts of both OCH_2 and NCH_2 groups of most silatranes (Table 2). In onium salts of 1-aminomethyl- and 1-organylthiomethylsilatranes the substituent X strongly affects the OCH_2 proton chemical shifts. For 1-alkylsilatranes, their 1′- and 3′-functionally substituted derivatives and 1-alkenylsilatranes, the chemical shift of the cage protons correlate with the lengths of the Si←N bond (in crystals) and the inductive substituent constants σ^{*235}. Within a wider set of silatranes including 1-aryl-, 1-organoxy- and 1-halo derivatives, the δ values are correlated by a dual-substituent parameter equation, using the polar and resonance (σ_I and $\sigma_R{}^0$ or F and R) constants of the substituent X[235].

Due to strong intermolecular dipole–dipole interactions, the ^1H NMR chemical shifts of silatranes vary with concentration and solvent[235,240]. For example, the NCH_2 protons are more shielded (by 0.8–1.2 ppm) in benzene than in $CDCl_3$ solution. The shifts induced by the aromatic solvent are linearly correlated with the dipole moments of the silatranes[240].

Multiple quantum NMR study found an increase in the $^3J(^{29}Si{-}O{-}C{-}^1H)$ coupling constants in the cage moiety of silatranes as compared with those in triethoxysilanes $XSi(OEt)_3$[241]. In contrast, the $^{29}Si{-}^1H$ coupling across one[242,243], two[241] or three[241] bonds in the axial fragment of 1-hydro-, 1-organyl- and 1-ethoxysilatranes appeared to be lower than those in the model compounds. The $^1J(^{13}C{-}^1H)$ coupling constant in 1-methylsilatrane (115.6 Hz) is also lower than in $MeSi(OEt)_3$ (118.9 Hz)[243]. These data reflect the corresponding changes in the bond order and s-character of silicon bonds upon variation of silicon coordination numbers. Very small influence of the substituent X on the $^1J(^3C{-}^1H)$[236,244], $^2J(^{15}N{-}^1H)$[245] and $^3J(^{15}N{-}^1H)$[245] couplings in the cage moiety were found for silatranes.

b. ^{13}C NMR spectra. The ^{13}C chemical shifts for the silatrane cage are practically insensitive to the nature of substituent X and are within a narrow range of δ 51–52 ppm for NCH_2 and 57–58 ppm for the OCH_2 carbons[20,183,236,246,247]. The NCH_2 carbons of silatranes are more shielded than those in THEA (δ 57.2), probably due to a strong 1,5-interaction between the hydrogen atoms in the $N(CH_2)_3$ silatrane moiety and the nearly ammonium character of its nitrogen[20,236]. Despite the electron transfer via the X–Si←N bonding, the α-^{13}C chemical shift of the organyl group of 1-organylsilatranes is

TABLE 2. ^1H, ^{15}N and ^{29}Si NMR chemical shifts of silatranes (**1**) in $CDCl_3$ solutions (sol) and in powders (cryst)[235,255,256,260,263,266]

Compd	X	$\delta(NCH_2)$	$\delta(OCH_2)$	δ_{Si}(sol)	δ_{Si}(cryst)	δ_N(sol)	δ_N(cryst)
49	H	2.87	3.83	−83.6	−85.8[b]	−354.4	−351.6
2	Me	2.81	3.78	−64.4	−70.8	−359.4	−355.6
16	$ClCH_2$	2.89	3.86	−79.9	−81.9	−354.1	−351.9
19	Cl_2CH	2.96	3.93	−87.6	−89.4	−351.8	−349.2
20	Vinyl	2.85	3.83	−81.1	−83.4[b]	−356.8	−353.9[b]
21	Ph	2.92	3.91	−80.2	−82.9	−356.3	−353.6
30	EtO	2.84	3.84	−94.7	−96.0	−353.3	−350.1
37	F	2.95	3.91	−100.5	−101.5	−349.3	−348.3[b]
38	Cl	3.01	3.97	−85.8[a]	−85.2[b]	−348.8	−348.1[b]
50	Br	3.04	4.01	−88.8		−348.0	
51	I	3.08	4.04	−98.6		−346.9	

[a] Datum taken from Reference 236.

[b] Data taken from Reference 254.

downfield relative to that of the corresponding organyltriethoxysilanes[20,183,236,242,246,247]. Perhaps it results from a weakening of the C_α−Si bond in silatranes due to reduction in the average excitation energy of the occupied molecular orbitals of the α-carbon atom. Within Karplus–Pople theory[248], an inverse value of this energy term together with charge characteristics govern the local paramagnetic term of the ^{13}C shielding constant. There is a linear correlation between the α-^{13}C chemical shifts of 1-alkylsilatranes with those of the terminal carbon of related alkanes[236], but the changes in this chemical shift induced by the silatranyl group are not constant and they increase with the strength of the Si←N bond.

A strong electron-releasing effect of the silatranyl group is displayed in the upfield shift of the β- and p-^{13}C signals of the vinyl, ethynyl, and phenyl groups of silatranes relative to those of the parent triethoxysilanes[244,246,248]. By use of the linear correlations between the ^{13}C chemical shifts of the aromatic carbons and the σ_1, σ_R, $\sigma_R{}^0$, $\sigma_R{}^+$ and $\sigma_R{}^-$ substituent constants in mono-substituted benzenes, the values of these constants for the silatranyl group were determined from the NMR data for 1-phenylsilatrane[249]. The nature of the substituent R (Me, $ClCH_2$, Vinyl and Ph) at C3 in 1-phenyl-3-substituted silatranes does not affect the ^{13}C chemical shifts of the phenyl group[250].

^{13}C NMR spectroscopy was used for structural studies of silatranyl derivatives of some monosaccharides[251], silatranylmethyl esters of substituted benzoic acids[252], diastereomeric 3,7,10-trimethyl-substituted 1-chloromethylsilatranes[253], several 1-organyl-4-ethylsilatranes[59] and 1-organyl-4,4-dimethylsilatranes[62].

In line with these solution-phase ^{13}C NMR results, the isotropic solid-state ^{13}C NMR chemical shifts of the cage carbons of silatranes appeared to be nearly independent on the Si←N bond length[254].

The absolute values of the $^1J(^{29}\mathrm{Si}-^{13}\mathrm{C})$ coupling constants for silatranes are greater than for the corresponding triethoxysilanes[124,236,242,244]. The $^1J(^{15}\mathrm{N}-^{13}\mathrm{C})$ coupling in silatranes decreases on increasing the electron-withdrawing ability of the substituent X and the polarity of the medium[124].

c. ^{29}Si NMR spectra. Within a series of silatranes, the influence of the substituent X on the solution ^{29}Si NMR chemical shifts is nearly the same as in triethoxysilanes[236,255] (Table 2). Only the enhanced ^{29}Si shielding constants of the former compounds by 11–25 ppm clarifies the pentacoordination state of their silicon atom[236,242,246,255,256]. However, the difference in the ^{29}Si chemical shifts between a silatrane and related triethoxysilane ($\Delta\delta_{Si}$) is not a direct measure of the Si←N bond strength in a silatrane[255]. Thus, despite a shorter Si←N bond, the absolute value of $\Delta\delta_{Si}$ for 1-fluorosilatrane is greater than for 1-methylsilatrane[255].

Straightforward interpretation of these peculiarities of the ^{29}Si NMR of silatranes is as yet difficult. It was suggested that a higher positive charge at the silicon in silatranes than in triethoxysilanes, together with the well known chemical shift–effective charge relationship could explain the upfield shift in the ^{29}Si NMR spectra of silatranes[212]. On the other hand, use of the Flygare approach[257] to the calculation of the diamagnetic and paramagnetic molecular terms in the average magnetic shielding of the heavy nuclei revealed a diamagnetic origin of the high-field shift in the silatrane spectra[258]. The calculated difference in the diamagnetic components of the ^{29}Si nuclear shielding constant between silatranes and the related triethoxysilanes appears to be practically insensitive to the nature of the substituent X. The difference in the corresponding paramagnetic terms increases with the strengthening of the Si←N bond in silatranes. These regularities are responsible for the observed trends in the variation of the $\Delta\delta_{Si}$. It should be added that a recent study of solid-state NMR spectra of silatranes found a very strong influence of the substituent X and the Si←N bonding on the principal elements of the ^{29}Si chemical shift powder patterns of Si-substituted silatranes[254]. Unfortunately, the combination of these effects is too difficult to be easily interpreted.

The ^{29}Si chemical shifts of silatranes depend on whether it is in the crystal or in solution, on the medium and the temperature[243,259,260]. The greatest ^{29}Si shielding is observed in powder silatrane patterns[254,260]. Dissolution of silatranes and decrease in the polarity, polarizability and acidity of the solvent, as well as heating of a solute result in a downfield shift of their ^{29}Si signal[243,259,260]. It indicates once more that the Si←N bond is very deformable and sensitive to the influence of the physical environment[188]. The weaker the Si←N bond in a silatrane crystal, the higher the solvent and temperature effects on the ^{29}Si chemical shift[243]. That is why the latter effects were proposed to be used for a fast estimation of the related strength of the Si←N bond within a series of these compounds[261]. Despite its simplicity, this method proved to be rather reliable and after some modifications it was successfully applied to numerous (N−Si)− and (O−Si)chelate compounds[28,165,262].

3,7,10-Substitution induces small and nonadditive changes in the ^{29}Si chemical shifts of silatranes. High-field shifts of 1–2.5 ppm were observed for the 3-Me, 3-$ClCH_2$, 3-Vinyl and 3-Ph substituted silatranes[57,238,262] but downfield shifts of 2.7 ppm were found for the 3-CF_3 derivatives[57]. In the spectra of diastereomeric 3,7-dimethyl- and 3,7,10-trimethylsilatranes, symmetric isomers show more shielded signals than asymmetric isomers[238], due to a stronger transannular bonding in the former isomers.

d. ^{15}N NMR spectra. The ^{15}N chemical shifts (Table 2) were shown to be a direct measure of the transannular interaction in Si-substituted silatranes. Indeed, their solid-state[254,263] and gas-phase[263] ^{15}N NMR chemical shifts correlate linearly with the Si←N bond lengths determined in the corresponding phase by the X-ray or electron diffraction method (Figure 1). Changes in the isotropic ^{15}N chemical shift are primarily due to changes in the value of the $\delta_\perp$ diagonal element of the ^{15}N chemical shift tensor for powder

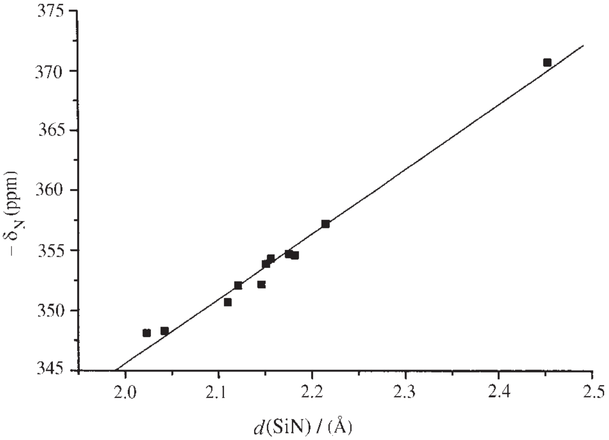

FIGURE 1. Correlation between the ^{15}N chemical shift and the Si←N bond length of powder and gaseous Si-substituted silatranes

patterns[254]. This element, which from local symmetry considerations lies in a plane perpendicular to the Si−N internuclear axis, increases on strengthening the Si←N bond. The observation agrees with the prediction based on Karplus-Pople theory of chemical shifts[248] and the simple 3c4e model of the X−Si← N bonding in silatranes[28,174,254].

Solution-phase ^{15}N NMR chemical shifts which are intermediate between those in the solid state and the gas phase depend on both the substituent X and the solvent. For a series of patterns in the same medium, the ^{15}N chemical shifts of most silatranes vary linearly with the σ^* polar constants of the substituent X[245,264,265]. 1-Halosilatranes are the exception and their ^{15}N shielding constants do not decrease on increasing the $-I$ effect of the halogen but on increasing its atomic number[266]. This is in agreement with the X-ray detection of a shorter Si←N bond in 1-chlorosilatrane[155] than in 1-fluorosilatrane[154].

The solvent effect on the δ_N values of silatrane was shown[243,259,263,267] to be described by equations 47 and 48, which reflect linear solvation energy relationships.

$$\delta_{\mathrm{N}} = A + yY + pP + eE \tag{47}$$

$$\delta_{\mathrm{N}} = A + s(\pi^* - d\delta) + a\alpha \tag{48}$$

In these equations the Palm−Koppel[268] or Taft−Kamlet[269] solvatochromic parameters are a measure of the polarity (Y or π^*), the polarizability (P or δ) and the acidity (E or α) of a solvent. The larger these solvent properties, the lower the ^{15}N shielding of the silatrane molecules. Interestingly, in the polar DMSO and in H_2O solutions the δ_{N} and δ_{Si} values are very close to those in the powder patterns[243,260,263]. On the other hand, the δ_N value of −370.6 (±1.8) predicted for 1-methylsilatrane in the gas phase by equation 48 is the same as that observed experimentally (−370.7)[251]. A change of the solvent and the temperature affects the ^{15}N and ^{29}Si shielding constants in the opposite directions. Linear correlations between the corresponding changes in the δ_{N} and δ_{Si} values were found for some silatranes[243,259,263]. These indicate the same origin of the solvent effect on the shielding of the donor and acceptor centers in silatranes. It is a change in the Si←N bonding and hence in the corresponding structure reorganization of the silatrane under a variation of physical environments. Solution-phase NMR data imply bond distances which are intermediate between those in the solid state and the gas phase[263]. The amazing softness of the Si←N bond was rationalized by theoretical analysis and semiempirical[188a] and *ab initio* computations[194] of the solvent effect on the silatrane geometry.

According to the Onsager model[188b], the dipole of the neutral spherical cavity solute embedded in a continuum dielectric induces a dipole within the dielectric. The induced dipole, in turn, changes the dipole of the solute and then both dipoles are iterated to self-consistency. The energy of the interaction E_{solv} is represented by equation 49

$$E_{\mathrm{solv}} = -\tfrac{1}{2}R\bullet\mu \tag{49}$$

where the induced dipole R depends on the dielectric constant of the solvent (ϵ), the radius of the cavity containing the solute (a_0), the gas-phase dipole (μ_0) of the solute and its polarizability (α) according to equation 50:

$$R = g\mu, \quad g = 2(\epsilon - 1)/(2\epsilon + 1)a_0{}^3, \quad \mu = \mu_0(1 + \alpha g) \tag{50}$$

It is clear that for a given cavity size the energy of solvent−solute interaction will increase on increasing the solvent dielectric constant and the solute dipole. In the case of silatranes, the dipole moment increases when the Si←N bond length decreases and the X−Si bond length increases. Hence, enlarging the dipole under the influence of a solvent will result in a corresponding shortening of the easily compressed Si←N bond. As a result, increasing the solute dipole will increase the interaction with the solvent, providing in turn an additional driving force for a further decrease in the Si−N distance.

Indeed, theoretical analysis (using the harmonic approximation) of the potential function of the deformation of the hypervalent X−Si←N bond of silatranes in solution leads[188a] to equations 51 and 52

$$\Delta d_{\mathrm{SiN}} = -2\mu_{\mathrm{e}}(1+\alpha R)^2(\partial\mu_0/\partial d_{\mathrm{SiN}}\bullet k_{\mathrm{SiN}}{}^{-1} - \partial\mu_0/\partial d_{\mathrm{XSi}}\bullet k_{\mathrm{XSiN}}\bullet k_{\mathrm{XSi}}{}^{-1}\bullet k_{\mathrm{SiN}}{}^{-1}) \qquad (51)$$

$$\Delta d_{\mathrm{XSi}} = -2\mu_{\mathrm{e}}(1+\alpha R)^2(\partial\mu_0/\partial d_{\mathrm{XSi}}\bullet k_{\mathrm{XSi}}{}^{-1} - \partial\mu_0/\partial d_{\mathrm{SiN}}\bullet k_{\mathrm{XSiN}}\bullet k_{\mathrm{XSi}}{}^{-1}\bullet k_{\mathrm{SiN}}{}^{-1}) \qquad (52)$$

which reflect the changes in the length of the Si←N and X−Si bonds (Δd_i) in going of these compounds from the gas phase to the solution. Here μ_{e} is a dipole moment of the isolated molecule at the equilibrium values of the X−Si←N bond and k_i is the force constant of the i-th bond. It could be seen that the absolute Δd_i values should increase on increasing solvent polarity and the sensitivity of the μ_0 to the hypervalent bond deformation. The sign of the Δd_i is determined by the sign of the $\partial\mu_0/\partial d_i$ derivatives. Semiempirical and *ab initio* calculations on silatranes showed that the latter terms are negative for the Si←N bond and positive for the X−Si bonds. Thus, in polar medium, silatranes should have a shorter Si←N bond and a longer X−Si bond than those in a less polar solvent or in the gas phase. The same regularities should be also observed on cooling the solution due to a known increase in the solvent polarity at a lower temperature.

These results enabled one to employ the solution-phase ^{15}N NMR chemical shifts for estimating of the length of the Si←N bond in solute silatrane patterns[28,263,266,270]. This approach made use of equation 53, which was derived from the corresponding solid-state and gas-phase data[263]:

$$d(\mathrm{SiN}) = -4.30 - 1.82 \times 10^{-2}\delta_{\mathrm{N}} \qquad (53)$$

Table 3 illustrates some examples of such estimations taken from References 28, 263 and 264.

In line with the hypervalent bonding model[174], these data show that 1-iodosilatrane should have one of the shortest Si←N bonds and hence a very weak I−Si bond. This explains why this compound possesses high reactivity as an electrophile (Section II.C).

TABLE 3. Estimated values of the Si←N bond length in solute silatrane patterns

X in **1**	Solvent	d(SiN) (Å)	X in **1**	Solvent	d(SiN) (Å)
Me	(crystal)	2.17[a]	$ClCH_2$	DMSO	2.13
Me	DMSO	2.19	$ClCH_2$	C_6H_5Cl	2.18
Me	$MeNO_2$	2.21	Cl_2CH	DMSO	2.10
Me	CH_2Cl_2	2.23	Cl_2CH	C_6H_5Cl	2.13
Me	C_6H_5Cl	2.27	MeO	DMSO	2.11
Me	CCl_4	2.31	MeO	C_6H_5Cl	2.13
Me	(vapour)	2.45[b]	F	CH_2Cl_2	2.06
H	(crystal)	2.11	Cl	CH_2Cl_2	2.05
H	DMSO	2.14	Br	CH_2Cl_2	2.03
H	C_6H_5Cl	2.19	I	CH_2Cl_2	2.01

[a] X-ray data[137]

[b] ED data[169].

The $^1J(^{29}Si-^{15}N)$ spin–spin coupling constants in silatranes are 0.2–3.4 Hz and increase with the increased strength of the Si←N bond caused by the substituent X and by solvent effects[124,245,270–272]. However, the nonlinear character of the dependence of $^1J(^{29}Si-^{15}N)$ on the Si←N bond length makes the use of these coupling constants as a measure of a transannular interaction in silatranes too difficult[124,270,272].

e. Other NMR studies. ^{19}F NMR chemical shifts of 1-(*p*-fluorophenyl)silatrane[273] and *m*- and *p*-fluoro-substituted 1-benzylsilatrane[54] were used for estimation of the inductive and resonance effects of silatranyl and silatranylmethyl groups. Observation of a lower $^1J(^{19}F-^{29}Si)$ coupling in 1-fluoro-3,7,10-trimethylsilatrane (131.2 Hz) than in the model $FSi(OEt)_3$ (199.1 Hz) was one of the first pieces of evidence for a reduction in the bond order in axial moieties of silatranes[242]. Very unusual long-range coupling, formally $^8J(^{19}F-^{19}F)$, was found for the asymmetrical diastereomers of 3,7-bis- and 3,7,10-tris(trifluoromethyl)silatranes[57,274]. This through-space coupling reflects a relatively close contact between the corresponding ^{19}F nuclei in these molecules.

The ^{17}O NMR chemical shifts of the equatorial oxygens in silatranes were found to be nearly the same as in related triethoxysilanes[275]. However, the signal of the axial oxygen in 1-ethoxysilatrane is downfield shifted as compared with $Si(OEt)_4$. This shift indicates an electron transfer via a hypervalent X—Si←N bond in the silatranes.

10. Electronic effects of the silatranyl group

The silatranyl group was shown to be a stronger σ-donor than the trialkoxysilyl and even trimethylsilyl groups (Table 4). The Taft inductive constant σ^* of the silatranyl group was derived for the first time from ^{35}Cl NQR frequencies of 1-dichloromethyl- and 1-(1′-chlorovinyl)silatranes by the use of linear relations between $\nu(^{35}Cl)$ and $\sigma_X{}^*$ values for the $CHCl_2X$ and $H_2C{=}CClX$ derivatives[276]. The corresponding relationships between spectroscopic or potentiometric basicity and the $\sigma_X{}^*$ values for a number of mono-substituted acetylenes, organonitriles and N-substituted piperidines were used to estimate the Taft inductive constants of silatranylalkyl and related triethoxysilylalkyl groups[277]. The ^{13}C and ^{19}F NMR chemical shifts of aromatic moieties in the spectra of silatranes with X = Ph and $4\text{-}FC_6H_4CH_2$ were employed to estimate the values of inductive and resonance constants σ_I and $\sigma_R{}^0$ of silatranyl[249] and silatranylmethyl[54] groups. The $\sigma_R{}^0$ value of the silatranyl group was also determined by the methods of Katritzky from the integral intensities of the corresponding IR bands of 1-vinyl-, 1-ethynyl- and 1-phenylsilatranes[277]. The $\sigma_p{}^+$ value of silatranyl (−0.40) and silatranylmethyl (−0.48) groups were estimated from the frequencies of the charge-transfer band of the corresponding $XC_6H_5{\bullet}TCNE$ (TCNE = tetracyanoethylene) complexes which are determined by the ability of the group X to release electrons to the ring[54].

It was assumed that the π-acceptor effect of the silicon influences the $\nu(^{35}Cl)$ values of 1-dichloromethyl- and 1-(1′-chlorovinyl)silatranes and the spectroscopic basicity of 1-ethynylsilatrane. Hence, the value $\sigma^* = -3.49$ derived from ^{13}C NMR data is regarded to be more reliable. This value demonstrates a super electron-releasing effect of the silatranyl group. There is a good correlation between the obtained σ^* values and the IP values of the nitrogen atom of the piperidine fragment in a series of compounds $C_5H_{10}N(CH_2)_nX$ with $X = Si(OCH_2CH_2)_3N$ and $Si(OEt)_3$ for $n = 1, 3$[278].

Interestingly, the inductive effect of the $N(CH_2CH_2O)_3Si(CH_2)_n$ groups decreases upon increasing the number of methylene groups ($n = 0–3$) fivefold faster than that of the $(RO)_3Si(CH_2)_n$ group[277]. From our point of view, this means that the σ-donor ability

TABLE 4. Inductive and resonance σ constants of the silatranyl and silatranylalkyl groups

Group	σ^*	σ_I	$\sigma_R{}^0$	Method	Reference
$N(CH_2CH_2O)_3Si$	-1.2			^{35}Cl NQR	276
$N(CH_2CH_2O)_3Si$	-3.49^a	-0.56	0.02	^{13}C NMR	249
$N(CH_2CHRO)_3Si$	-1.24		0.02–0.10	IR	277
$N(CH_2CH_2O)_3SiCH_2$	-2.24^a	-0.36	-0.21	^{19}F NMR	273
$N(CH_2CH_2O)_3SiCH_2CH_2$	-1.48			IR	277
$N(CH_2CH_2O)_3SiCH_2CH_2CH_2$	-0.32			Potentiometry	277

[a] Estimated[277] by the relationship $\sigma^* = 6.3\ \sigma_I$.

of the silatranyl moiety within $N(CH_2CH_2O)_3Si(CH_2)_n$ groups is not constant and it decreases on increasing n. The reason for this is very clear: the closer the silatranyl group is to the electronegative reaction (indicator) center, the stronger is the SiN bonding and hence the higher the electron-releasing effect of the silatranyl group.

11. Electrochemical studies

Owing to the silicon hypervalency and the cage structure, silatranes are of considerable interest from the standpoint of molecular electrochemistry. However, little work has been devoted to electrochemistry of silatranes[279–281].

The very strong electron-releasing effect of the silatranyl group causes a significant reduction in the redox potential corresponding to the reversible Fe^{II}/Fe^{III} transition of 1-silatranyl-1′-(trimethoxysilyl)ferrocene **52** ($\Delta E_{1/2} = -0.19$ V) and 1,1′-bis(silatranyl)ferrocene **53** ($\Delta E_{1/2} = -0.47$ V) with respect to that of ferrocene ($E_{1/2} = +0.40$ V)[279].

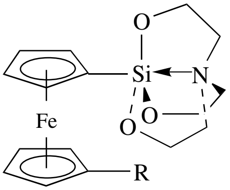

(52) R = $Si(OMe)_3$
(53) R = $Si(OCH_2CH_2)_3N$

Electrochemical oxidation of silatranes in carefully dried MeCN on a glassy carbon electrode was shown[280,281] to be a diffusional process which proceeds with one-electron transfer. At room temperature electrooxidation is reversible at scan rates below 100 mV s^{-1} and is partially reversible at higher scan rates (200, 500 mV s^{-1}) but becomes reversible at low temperatures ($< -10\,°C$). It was suggested that the primary products are cation radicals **54** of relatively low stability in which the distance between the silicon and nitrogen atom is higher than in the parent molecules (equation 54).

$$XSi(OCH_2CH_2)_3N - e^- \rightleftarrows \underset{\mathbf{(54)}}{[XSi(OCH_2CH_2)_3N]^{+\bullet}} \qquad (54)$$

TABLE 5. Electrochemical oxidation peak potentials (E_p, V) of Si-substituted silatranes (**1**)[280,281]

X	E_p	X	E_p	X	E_p
H	1.70	Ph	1.55	3-Thienyl	1.55
Me	1.43	4-ClC_6H_4	1.60	HC≡C	1.80
Et	1.42	2-Furyl	1.45	MeO	1.53
$ClCH_2$	1.85	3-Furyl	1.60	EtO	1.53
Vinyl	1.52	2-Thienyl	1.60	Cl	no oxidation

Silatranes undergo oxidation at higher potentials than the model compounds containing ordinary nitrogen and silicon atoms. The values of the electrochemical oxidation peak potentials (E_p) of silatranes are in the range 1.42–1.85 V (Table 5) whereas the E_p values of triethanolamine and its tris-O-TMS derivative are 0.90 and 0.92 V, respectively. There are pronounced effects of the substituent X on the oxidation potentials of silatranes and good correlations between their E_p values and the NMR parameters (^{15}N chemical shifts and $^{29}Si-^{15}N$ spin–spin coupling constants). The values of E_p increase on increasing the strength of the Si←N bond in the silatrane. It is very significant that for 1-chlorosilatrane no oxidation peak is observed in the accessible range. These results indicate the decisive role of the Si←N bonding on the electrooxidation of silatranes.

In wet acetonitrile electrochemical oxidation of silatranes becomes a multielectron, completely irreversible process. Participation of H_2O molecules in the electrochemical reaction leads to a product of a total hydrolysis of the silatrane molecule, i.e. to $Si(OH)_4$[281].

12. Mass spectra

The common features of the electron-impact (EI) mass spectra of Si- and C-substituted silatranes have been reviewed[6,13]. As a rule, the intensity of the molecular ion in the spectra is very low and the fragmentation proceeds via a cleavage of the X−Si bond or one of the silatrane rings depending on the nature of the Si and C substituents[6,13,110,282–292].

The EI mass-spectroscopic fragmentation pattern was analyzed recently[285] within the well-known organic mass-spectroscopy concept of the preferential localization of a positive charge. It was assumed that if the silatrane molecules would not have the Si←N bond in the gas phase, the primary cation-radicals $M^{+\bullet}$ (**55**) with the positively charged nitrogen atom should behave as the molecular ions of usual 2-aminoalkoxysilyl compounds and be transformed predominantly to the fragment ions $[M - RCHO]^+$, **A** (Scheme 4, path *i*). Homolytic cleavages of the X−Si and Si−O bonds in the molecular ions (Scheme 4, paths *ii* and *iii*), leading to the formation of the silatranyl cation **B** and bicyclic cation **C**, should be less probable. On the other hand, if the molecular ions $M^{+\bullet}$ were to have a structure **56**, with a pentacoordinate silicon, the formation of ions **A** should become less probable as compared with the formation of cations **B** and **C** (equation 55).

In the spectra of most silatranes the $[M - RCHO]^+$ ions are not observed or their peaks have a very low intensity (<5% of the full electron current), whereas the dependence of the intensity of the silatranyl ion peak on the substituent X differs from that expected for a tetracoordinate silicon species (Table 6). Introduction of methyl or phenyl groups into the silatrane rings increases the probability of elimination of the $OCHRCH_2$ (R = Me, Ph) fragment, whereas introduction of trifluoromethyl groups stabilizes the $[M - X]^+$ ions. Hence, the regularities observed in the fragmentation of silatranes are consistent with the existence of the Si←N bond in silatranes in the gas phase and with the stability of this bond to electron impact[285]. Interestingly, the analysis of the fragmentation products of

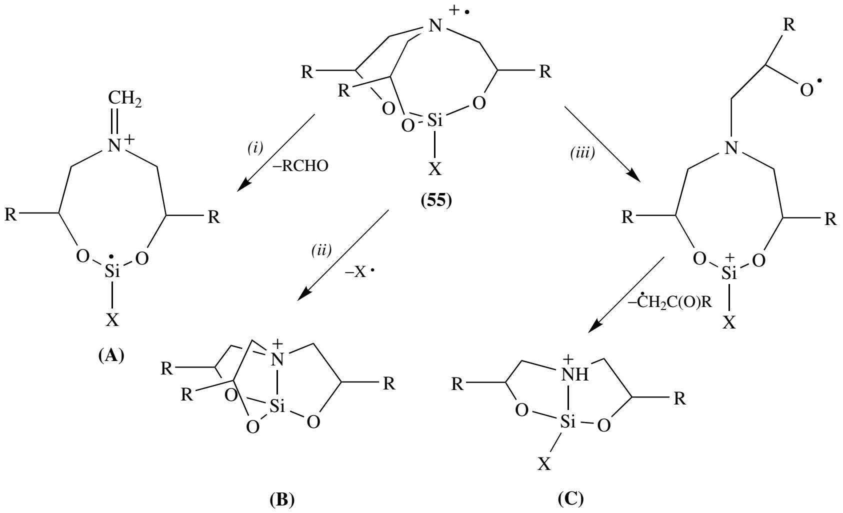

SCHEME 4

germatranes has demonstrated the absence of the Ge←N transannular bond in the gas phase[292].

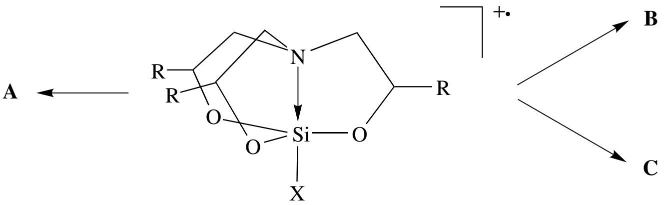

(56)

(55)

TABLE 6. Intensity (% of the total ion current) of the primary fragment ions **A**, **B** and **C** in the mass spectra of Si-substituted silatranes and 3,7,10-trimethylsilatranes[295]

X in **56**	R	**A**	**B**	**C**	X in **56**	R	**A**	**B**	**C**
HC≡C	H	3.8	2.2	11	Cl	Me	13	13	2.7
PhC≡C	H	4.5	4.1	4.1	Br	H	0.6	33	8.2
F	H	2.4	4.6	10	Vinyl	H		73	2.8
F	Me	14	0.6	3.6	Ph	H		80	
EtO	H	1	51	7.9	Ph	Me	2.5	46	6
EtO	Me	5.3	43		H	H	5.6	17	16
t-BuO	H		64	11	Me	H	2.2	19	22
PhO	H		66		Me	Me	6.1	14	5.1
4-$O_2NC_6H_4O$	H		20		Et	H	3.8	42	3.3
2-$O_2NC_6H_4O$	H		35		*n*-Pen	H		86	
3-$O_2NC_6H_4O$	H		66		$ClCH_2$	H	0.7	56	3
Cl	H	2.1	19	35	$ClCH_2$	Me	1.8	82	

The additional characteristic ions in the EI mass spectra of 1-substituted silatrane-4-carboxylic acids **42** were shown to arise from the loss of a carboxyl group ($[M - COOH]^+$ or, in the case of 3-methyl-substituted compounds, $[M - CO_2]^+$ peaks) and from a ring rupture ($[SiC_4H_{10}O_2N]^+$)[110].

In chemical ionization (CI) mass spectra of 1-phenyl- and 1-heteroarylsilatranes[289,210] (X = 2-furyl, 3-furyl, furfuryl, 2-thienyl and 3-thienyl) employing NH_3 as the carrier gas, the main peak corresponds to the adduct ion $[(M - X)NH_3]^+$.

Due to the Si←N interaction in silatranes, the protonated molecular ions MH^+ are usually less abundant than the molecular ions $M^{+\bullet}$. Further decomposition of both types of ions involves a loss of the substituent X and a subsequent adduct ion formation.

The fast atom bombardment (FAB) mass spectra of 1-organylsilatranes are also characterized by the most intensive $[M - X]^+$ ion peaks[286,288–291]. As a rule, the intensity of their molecular ion peaks is weak, whereas the content of the quasi-molecular MH^+ ions varies from large for 1-alkyl (and 1-alkoxy) derivatives to small for 1-phenyl- and 1-heteroarylsilatranes. An interesting peculiarity of Si- and C-substituted silatranes is the formation of the $[M - H]^+$ ions which are rather rare in FAB spectra[289–291]. In FAB spectra of some silatranes intense peaks of the protonated molecular ion of triethanolamine, $(HOCH_2CH_2)_3NH^+$, were observed. This was ascribed to the alleged reaction of silatrane hydrolysis, caused by the argon atom bombardment[286,288–291].

For silatranes containing alkyl and aryl substituents at the skeleton carbons, additional fragmentation paths were found under FAB. They lead to formation of $[MH - OCHR'CH_2]^+$ and $[MH - OCH_2CR_2]^+$ ions as products of side chain elimination from the MH^+ ions. An α-cleavage with elimination of benzaldehyde molecule from the molecular ions was observed in the spectra of 1-methyl- and 1-benzyl-3,7-diphenylsilatranes[291].

Characteristic features of the FAB spectra of silatranes are also maintained in the spectra of 1-phenyl-2-azasilatrane and 1-phenyl-3,7-dimethyl-10,11-benzosilatrane[291]. However, in the former compound only the nitrogen-containing half cycle is destroyed to form ions $[MH - CH_2NH]^+$ with m/z 222 and $[MH - C_2H_2NH]^+$ with m/z 208.

C. Chemical Properties

1. Introduction

Both the hypervalent bonding of the silicon and the cage skeleton structure provide some special characteristics to the chemical behavior of silatranes. First, in contrast with four-coordinate analogs and many pentacoordinate organosilicon compounds, silatranes display low activity in nucleophilic substitution reactions at the silicon. The *in*-oriented nitrogen atom appears to be inert toward electrophiles such as MeI[13] and tetracyanoethylene[293]. The strong electron-releasing effect combined with the large bulk of the silatranyl group affect the reactivity of the exocyclic groups of these compounds.

2. Hydrolysis

Owing to the transannular bonding, silatranes are relatively stable to atmospheric moisture, and their hydrolysis and solvolysis are considerably slower than those of the corresponding trialkoxysilanes[13]. Compounds with a relatively short Si←N bond, e.g. 1-fluoro- and 1-chlorosilatranes, can be recrystallized from alcoholic solvents[69], whereas 1-isothiocyanatosilatrane is recovered unchanged from refluxing methanol or ethanol even after 24 h[68]. Some silatranes were found to remain unchanged even in the presence of 0.1 N $HClO_4$ in glacial acetic acid for a long time[69].

Kinetic studies show that hydrolysis of 1-organyl- and 1-alkoxysilatranes in neutral aqueous solutions is a first-order reaction catalyzed by the formed tris(2-hydroxyalkyl)amine[13,294]. As a rule, electron release and steric effects of the substituent X hinder the reaction. However, the hydrolytic stability of 1-methylsilatrane is just below that of 1-chloromethylsilatrane[294]. Successive introduction of methyl groups into the 3, 7 and 10 sites of the silatrane skeleton[13,294] and substitution with ethyl group on C-4[59] retard sharply the hydrolysis rate. It was proposed[294] that nucleophilic attack at silicon by water proceeds via formation of the four-centered intermediate **57** (equation 56).

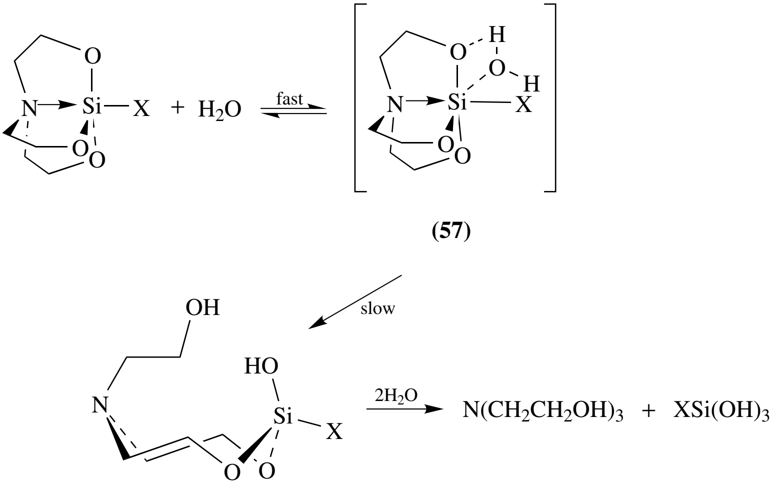

(57)

(56)

The S_N2-Si mechanism of neutral hydrolysis and the parallel operation of the S_N2-Si and S_N1-Si mechanisms in base-catalyzed hydrolysis of 1-aryloxysilatranes in aqueous solutions and in media of different polarity were proposed[295–297]. The contribution of the S_N1-Si pathway in the latter process was presumed to vary from 0 to 60%, depending on the conditions[297].

The hydrolysis rate of 1-organylsilatranes in acidic medium is much higher than in neutral media[13]. The reaction was found to be of first order in both silatrane and acid[13,298]. For 1-arylsilatranes, electron-releasing substituents in the aromatic ring increase, and electron-withdrawing groups decrease the hydrolysis rate. On the basis of these data and the study of the solvent isotope effect, it was suggested that the rate-determining step involves protonation of the nitrogen with concerted breaking of the transannular bond and a subsequent rapid hydrolytic cleavage of the Si−O bonds[298]. However, a more recent investigation of the acid-catalyzed hydrolysis of 1-aryloxysilatranes assumed that a cleavage of the protonated Si−O bond is the rate-determining stage[295].

Substitution of the cage with the methyl groups increases the solvolytic stability of the silatranes[13,58,298]. The symmetric isomer **40** of 1-phenyl-3,7,10-trimethylsilatrane shows little reaction in acetic acid containing 5% water after 90 h, whereas the half-life of the asymmetric isomer **40a** is about 2–3 h. The half-live of 1-phenyl-3,3,7,7,10,10-hexamethylsilatrane **58** bearing the sterically hindered oxygen atoms is at least one year[58]!

The difference between the solvolysis rate of diastereomers **40** and **40a** made it possible to purify and isolate the former isomer by partial hydrolysis of their mixture[58b]. A similar approach allowed earlier[24] the separation and purification (up to 99.9%) of both isomers of some 1-organyl-3,7,10-trimethylsilatranes. This was performed by partial

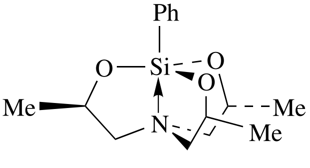

(40)

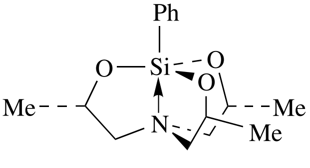

(40a)

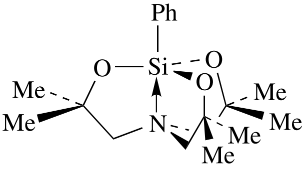

(58)

titrations of their benzene solutions by a saturated solution of dry HCl in C_6H_6 with subsequent isolation of the symmetric and asymmetric isomers from the filtrate and precipitate, respectively.

The problems concerning the ability of the silatrane's nitrogen to be protonated by acid under the solvolysis conditions in organic media are far from being resolved. There are some reports about the preparation of silatrane hydrochlorides, $XSi(OCH_2CH_2)_3N{\bullet}HCl$, by bubbling dry HCl through a benzene solution of silatranes[62,299] or by exposing solid 1-methylsilatrane to a stream of dry HCl[300]. However, IR spectra show that the products obtained by these methods are not the same. Moreover, multinuclear NMR study proved that two rather than one molecule of HCl are involved in the interaction with silatranes in organic media[301] (equation 57). The exchange between the reagents and the product in the reversible reaction 57 was shown to be fast on the NMR time-scale. Molecular mechanics and semiempirical study, including analysis of the map of the electrostatic potential of silatrane molecules, predicted kinetic and thermodynamic preference for a proton attack on the oxygen[302].

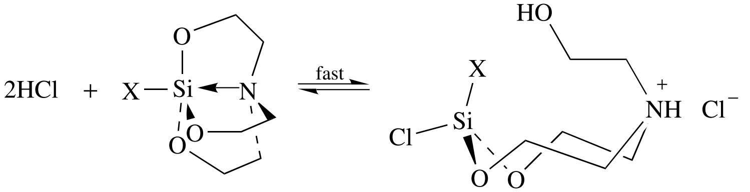

(57)

Taking into account the high electrophilicity of the cage oxygen atoms in silatranes, the weakening of the Si−O bond and the strengthening of the Si←N bond under H-bonding (see Section II.B), these results suggest that protonation of the nitrogen occurs only after the Si−O bond fission. This is corroborated by the extreme resistance of 1-phenyl-3,3,7,7,10,10-hexamethylsilatrane (**58**) to solvolysis[58b].

On the other hand, IR data suggested that some silatrane-4-carboxylic acids might be present in solution as an equilibrium mixture of the acid **(42)** and the salt **(42a)** forms (equation 58). These results, combined with the stability of the protonated equatorial Si−O bond of these acids in their crystals, was regarded as favoring the primary protonation of the axial nitrogen under acidic hydrolysis of silatranes[110,111,168].

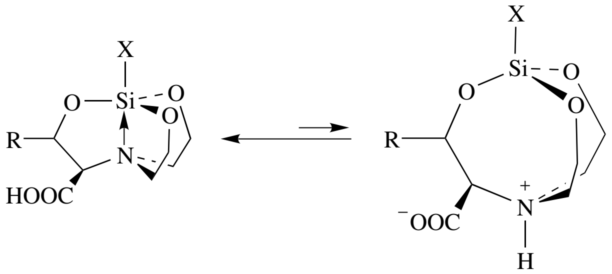

(42) **(42a)**

(58)

3. 1-Hydrosilatranes

1-Hydrosilatrane **(49)** and its 3,7,10-trimethyl derivative **(49a)** can be converted to the corresponding 1-halosilatranes by treatment with halogens (equation 59)[69,129,303], anhydrous HX (X = Cl, Br) (equation 60)[69] or the appropriate *N*-halosuccinimide in a chloroform solution (equation 61)[69]. In reactions 59–61 triethylamine can be used as an acceptor of HX[303]. Attempts to prepare an iodo derivative by the procedure of reaction 61 using *N*-iodosuccinimide were unsuccessful[69].

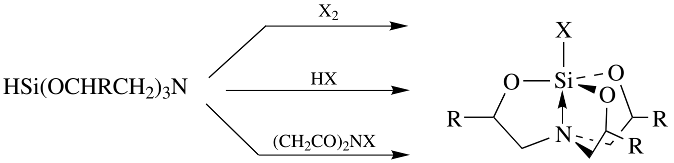

(59)

(60)

(61)

(49) R = H
(49a) R = Me

(38) X = Cl, R = H
(38a) X = Cl, R = Me
(50) X = Br, R = H
(50a) X = Br, R = Me

It is remarkable that tetracoordinate silanes such as Et_3SiH are not involved in related reactions. The higher reactivity of the 1-hydrosilatranes arises from the enhanced hydridic character of the Si–H bond in the silatrane[69].

1-Hydrosilatrane **(49)** reacts readily with alcohols and phenols in boiling xylene (equation 62). The process is catalyzed by sodium alkoxides or phenoxides[304]. As the acidity of the phenols decreases, the dehydrocondensation rate increases. An opposite tendency is observed for nucleophilic substitution by alkoxide ions. In this case the steric effect of the bulky alcohol plays a more important role than the electronic effect in governing the reaction rate.

$$\mathbf{49} + \mathrm{ROH} \longrightarrow \mathrm{ROSi(OCH_2CH_2)_3N} + \mathrm{H_2} \tag{62}$$

$$\mathrm{R} = \mathrm{Me}, n\text{-Bu}, i\text{-Bu}, t\text{-Bu}, \mathrm{Ph}, 4\text{-MeC}_6\mathrm{H}_4, 4\text{-MeOC}_6\mathrm{H}_4, 4\text{-ClC}_6\mathrm{H}_4, \mathrm{C}_6\mathrm{F}_5, \text{etc}$$

It should be mentioned that the reaction shown in equation 62 does not proceed in the presence of H_2PtCl_6[304]. However, the platinum catalyst is very effective in obtaining alkoxy derivatives from both tetracoordinate triorganosilanes[305,306] and silatrane having an H−Si−CH$_2$ moiety (equation 63)[49].

$$\mathrm{MePh(H)SiCH_2Si(OCH_2CH_2)_3N} \xrightarrow{\mathrm{ROH/H_2PtCl_6}} \mathrm{MePh(RO)SiCH_2Si(OCH_2CH_2)_3N} \qquad (63)$$
$$\mathrm{R = Me\ (95\%),\ Et\ (90\%),\ \mathit{i}\text{-}Pr\ (77\%),\ \mathit{t}\text{-}Bu\ (95\%)}$$

Treatment of a twofold excess of 1-hydrosilatrane **(49)** with alkanediols results in the corresponding bis(silatranyloxy)alkanes in a quantitative yield (equation 64)[307].

$$\underset{\mathbf{(49)}}{\mathrm{2HSi(OCH_2CH_2)_3N}} + \mathrm{HOROH} \xrightarrow[-\,2\mathrm{H_2}]{} \mathrm{N(CH_2CH_2O)_3SiOROSi(OCH_2CH_2)_3N} \qquad (64)$$
$$\mathrm{R} = \!-\!(\mathrm{CH_2})_n\!-\ (n = 2\text{–}6),\ -\mathrm{CH_2CHMe}-,\ \mathrm{CH_2CH_2OCH_2CH_2}-$$

Reactions of **49** with carboxylic acids take place in the presence of ZnCl$_2$ to give 1-acyloxysilatranes in 40–80% yields (equation 65)[13].

Weakening of the Si−H bond favors radical reactions of **49** with a variety of organohalides and some reactive organic compounds. Thus, polyhalomethanes CH$_2$Cl$_2$, CHCl$_3$ and CHBr$_3$ are reduced by **49** in the presence of organic peroxides (equation 66)[308].

$$\mathbf{49} + \mathrm{RCOOH} \longrightarrow \mathrm{RCOOSi(OCH_2CH_2)_3N} \qquad (65)$$
$$\mathrm{R = Me,\ Et,\ Ph,\ 3\text{-}C_5H_4N,\ 2\text{-}C_4H_3O}$$

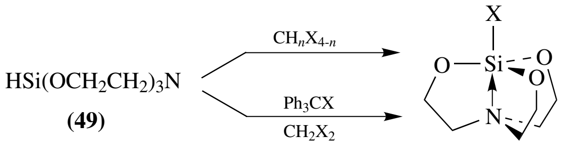

(66)

(67)

(38) X = Cl
(50) X = Br

A similar reaction of **49** with triphenylmethyl halides in the appropriate methylene halide affords the corresponding 1-halosilatranes (equation 67). The reaction rate increases in going from chloro- to bromomethanes ($k = 1.56 \times 10^{-3}\ \mathrm{M^{-1}\,s^{-1}}$ at 24 °C and $2.94 \times 10^{-3}\ \mathrm{M^{-1}\,s^{-1}}$ at 20 °C for the Cl and Br derivatives, respectively)[308].

A much lower reaction rate of 1-hydrosilatrane compared with triorganylsilanes seems to be due to the steric bulk of the silatranyl group that hinders a side attack at the silicon by the Ph$_3$C$^+$X$^-$ ion pair[308].

According to EPR data, reaction 67 proceeds via a homolytic pathway in nonpolar solvents.

The use of iodo derivatives CH$_2$I$_2$ or CHI$_3$ in reaction 66 results only in polymeric products[308]. However, 1-iodosilatrane **(51)** can be obtained in almost quantitative yield from 1-hydrosilatrane **(49)** and perfluoroalkyl iodides under UV irradiation (equation 68)[309].

$$\underset{\mathbf{(49)}}{\mathrm{HSi(OCH_2CH_2)_3N}} + \mathrm{R_FI} \xrightarrow{h\nu} \underset{\mathbf{(51)}}{\mathrm{ISi(OCH_2CH_2)_3N}} + \mathrm{R_FH} \qquad (68)$$
$$\mathrm{R_F = CF_3,\ C_3F_7,\ C_6F_{13}}$$

Silatrane **(49)** reduces benzyl bromide, benzoyl chloride, azoxybenzene, nitrobenzene and some carbonyl compounds under rather drastic conditions (140–250 °C); see equations 69–72[131].

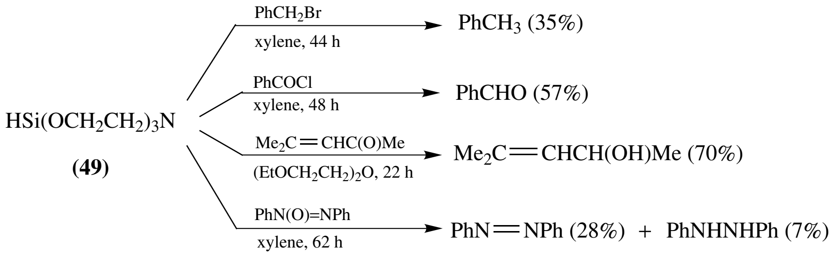

$$HSi(OCH_2CH_2)_3N \; \mathbf{(49)} \xrightarrow[\text{xylene, 44 h}]{PhCH_2Br} PhCH_3 \; (35\%) \qquad (69)$$

$$\xrightarrow[\text{xylene, 48 h}]{PhCOCl} PhCHO \; (57\%) \qquad (70)$$

$$\xrightarrow[(EtOCH_2CH_2)_2O, \text{ 22 h}]{Me_2C{=}CHC(O)Me} Me_2C{=}CHCH(OH)Me \; (70\%) \qquad (71)$$

$$\xrightarrow[\text{xylene, 62 h}]{PhN(O){=}NPh} PhN{=}NPh \; (28\%) + PhNHNHPh \; (7\%) \qquad (72)$$

Both **49** and trialkylsilanes undergo exchange reactions with trimethylhalosilanes in the presence of quinoline to give 1-halosilatranes (equation 73)[16]. It is likely that steric hindrance is responsible for the lack of addition of 1-hydrosilatrane **(49)** to the multiple bond of monosubstituted alkenes and acetylenes in the presence of H_2PtCl_6 or under UV irradiation[129,310].

$$\mathbf{49} + Me_3SiX \longrightarrow XSi(OCH_2CH_2)_3N + Me_3SiH \qquad (73)$$

$$\mathbf{(38)}\ X = Cl$$

$$\mathbf{(50)}\ X = Br$$

Silatrane **(49)** reacts with *n*-butyllithium and with Grignard reagents to give tri-*n*-butyl or triarylsilane even with a deficiency of the organometallic reagent (equation 74)[311].

$$\underset{\mathbf{(49)}}{HSi(OCH_2CH_2)_3N} + RM \longrightarrow R_3SiH + R_4Si \qquad (74)$$

$$R = n\text{-Bu, Ph}$$

$$M = Li, MgBr$$

The initial rate-determining nucleophilic attack at the silicon involves cleavage of the silicon–oxygen bond. The reaction selectivity is dependent on the nucleophilic reagent. Thus, a mixture of n-Bu_3SiH (90%) and n-Bu_4Si (10%) is obtained when 3.2 molar equivalents of n-BuLi are used in the reaction, i.e. cleavage of the equatorial Si—O bonds occurs more readily than that of the apical Si—H bond. With PhLi, the prevailing tetrasubstitution reaction results in Ph_4Si (68% yield). At the same time, a slower reaction of **49** with a Grignard reagent leads to the formation of only R_3SiH in high yield (80–95%)[311].

4. 1-Halosilatranes

The halosilatranes are the most interesting members of the silatrane family because of their general unreactivity, except for 1-iodosilatrane. In contrast to chlorotriorganyl- and chlorotrialkoxysilanes, 1-chlorosilatrane **(38)** does not participate in nucleophilic substitution reactions at silicon. The low reactivity of **38** was explained to be a consequence of its unusual geometry. Indeed, a backside attack is forbidden due to its cage structure and a side attack is disfavored since it demands a high energy for deformation of the skeleton upon formation of the hexacoordinate intermediate.

The reaction of **38** with *n*-BuLi followed by reduction with $LiAlH_4$ gave tri-*n*-butylsilane as the major product even when an excess of *n*-BuLi was used (equation 75).

$$\underset{\textbf{(38)}}{\mathrm{ClSi(OCH_2CH_2)_3N}} + n\text{-BuLi} \longrightarrow n\text{-Bu}_3\text{SiCl} \xrightarrow{\mathrm{LiAlH_4}} n\text{-Bu}_3\text{SiH} \qquad (75)$$

It was concluded that the initial substitution involved cleavage of an Si−O bond rather than the Cl−Si bond as is usually observed with chloroalkoxysilanes[311]. Since oxygen is more electronegative than chlorine, it is reasonable to suggest that reaction 75 occurs via intermediate **59**.

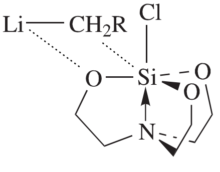

(59)

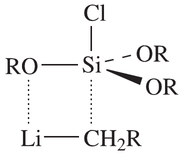

(60)

Weakening of the LiO−Si bond and nucleophilic attack of RCH_2^- on silicon results in generating a six-coordination site. In similar reactions with tetracoordinate $ClSi(OR)_3$ compounds, any such weakening of the LiO−Si bond would be dominated by weakening of the Si−Cl link in a linear 3c4e MO system in **60**[312].

1-Fluorosilatrane **(37)** is formed by treatment of **38** with potassium fluoride in HMPA (equation 76)[16].

$$\underset{\textbf{(38)}}{\mathrm{ClSi(OCH_2CH_2)_3N}} + \mathrm{KF} \longrightarrow \underset{\textbf{(37)}}{\mathrm{FSi(OCH_2CH_2)_3N}} \qquad (76)$$

1-Bromosilatrane **(50)** can be involved in electrophilic displacement reactions with silver compounds[26,27] to give products **21**, **37**, **61** and **62** (equations 77–80).

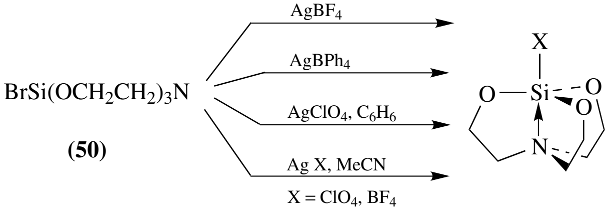

(37) X = F (77)

(21) X = Ph (78)

(61) X = $OClO_3$ (79)

(62) X = $N{\equiv}CMe^+$ (80)

Silatrane **50** reacts with substituted benzoic acids in the presence of pyridine to afford the corresponding 1-acyloxysilatranes (equation 81)[313,314]

$$\textbf{50} + \mathrm{XC_6H_4COOH} \longrightarrow \mathrm{XC_6H_4COOSi(OCH_2CH_2)_3N} \qquad (81)$$

X = 4-F, 4-Cl, 4-Br, 4-I, 4-MeO, 4-O_2N, 3-F, 3-Br, 2-MeO, etc.

If the precursor is 1-bromosilatrane **(50)**, the reaction shown in equation 75 occurs in a similar manner[311].

The oxidation reaction of 1-bromosilatrane **(50)** or its 3,7,10-trimethyl derivative **(50a)** and tin dibromide leads to the formation of adduct/solvent complexes **63a,b** (equation 82). Acetonitrile, DMF or methanol are used as the solvent[315].

$$\underset{\textbf{(50,50a)}}{BrSi(OCHRCH_2)_3N} + SnBr_2 \xrightarrow{\text{solv.}} \underset{\textbf{(63,63a)}}{Br_3SnSi(OCHRCH_2)_3N \cdot (solv)} \qquad (82)$$

$$\textbf{50/63} \quad R = H$$
$$\textbf{50a/63a} \ R = Me$$

1-Iodosilatrane **(51)** can behave as a powerful electrophilic reagent with respect to various classes of organic and organometallic compounds. For example, **51** can be involved in cleavage reactions of the C–O or Si–O bonds of a variety of organic and organosilicon compounds to give the corresponding silatrane derivatives as shown by equations 83–88[309,316].

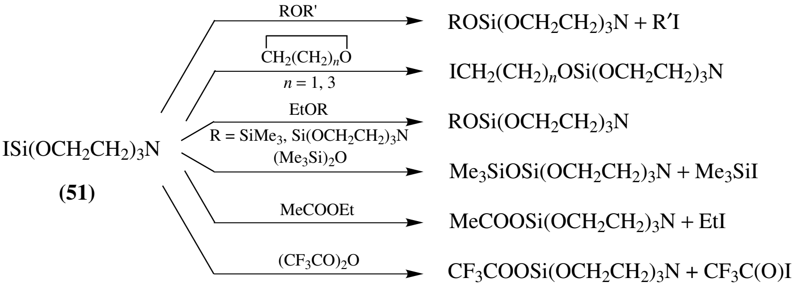

$$\underset{\textbf{(51)}}{ISi(OCH_2CH_2)_3N} \xrightarrow{ROR'} ROSi(OCH_2CH_2)_3N + R'I \qquad (83)$$

$$\xrightarrow[n = 1, 3]{\overline{CH_2(CH_2)_nO}} ICH_2(CH_2)_nOSi(OCH_2CH_2)_3N \qquad (84)$$

$$\xrightarrow[R = SiMe_3,\ Si(OCH_2CH_2)_3N]{EtOR} ROSi(OCH_2CH_2)_3N \qquad (85)$$

$$\xrightarrow{(Me_3Si)_2O} Me_3SiOSi(OCH_2CH_2)_3N + Me_3SiI \qquad (86)$$

$$\xrightarrow{MeCOOEt} MeCOOSi(OCH_2CH_2)_3N + EtI \qquad (87)$$

$$\xrightarrow{(CF_3CO)_2O} CF_3COOSi(OCH_2CH_2)_3N + CF_3C(O)I \qquad (88)$$

Compared to **51**, the reaction of THF with iodotrimethylsilane requires a more prolonged time and takes place at a higher temperature (60 °C)[317].

1-Iodosilatrane **(51)** readily adds to acetaldehyde to give 1-(1′-iodoethoxy)silatrane (**64**) (equation 89)[19].

$$\textbf{51} + MeCH{=}O \longrightarrow \underset{\textbf{(64)}}{MeCH(I)OSi(OCH_2CH_2)_3N} \qquad (89)$$

Compound **51** can be converted to 1-alkoxysilatranes by treatment with alcohols or alkali metal alkoxides[316] (equation 90).

$$\textbf{51} + ROM \longrightarrow ROSi(OCH_2CH_2)_3N + MI \qquad (90)$$
$$R = Me,\ M = H, Na;\ R = Me_3C,\ M = H, K;\ R = \text{1-adamantyl},\ M = H$$

It is remarkable that alkyl iodides and trimethylsilanol are formed by treatment of alcohols with iodotrimethylsilane[318].

The conversions described in equations 83–90 can be carried out *'in situ'* or *'in statu nascendi'*, when 1-iodosilatrane **(51)** is prepared from 1-allylsilatrane and C_3F_7I[319].

The reaction of **51** with alkali thiolates or thiols without a HI acceptor yields silatranes having a S–Si bond (equation 91)[320].

$$\textbf{51} + RSM \longrightarrow RSSi(OCH_2CH_2)_3N + MI \qquad (91)$$
$$R = Et,\ M = H, Na;\ R = Me_3C,\ Ph,\ 4\text{-}MeC_6H_4,\ M = H$$

Silatrane **51** reacts with acetylenes having an electron-withdrawing substituent to give 1-alkynylsilatranes (equation 92). No reaction takes place with butylacetylene[321].

$$\mathbf{51} + \mathrm{RC{\equiv}CH} \longrightarrow \mathrm{RC{\equiv}CSi(OCH_2CH_2)_3N + HI} \qquad \mathrm{R = Vinyl, Ph} \tag{92}$$

1-Organylsilatranes or 1-chlorosilatrane are obtained from 1-iodosilatrane **(51)** and appropriate organomercury compounds in $CHCl_3$ (equation 93)[322].

$$\mathbf{51} + \mathrm{RR'\,Hg} \longrightarrow \mathrm{RSi(OCH_2CH_2)_3N + R'\,HgI} \qquad \mathrm{R = R' = Et, Ph;\ R = Cl,\ R' = Et} \tag{93}$$

This reaction allowed one to prepare the first of the spin-labeled silatranes, (1′-oxy-2′,2′,6′,6′-tetramethyl-3′,4′-dehydropiperidinyl-4′)silatrane[323].

The Si–N(CS) bond of tetracoordinate silicon compounds is very sensitive towards alcoholysis[324]. By contrast, 1-isothiocyanatosilatrane **(29)** reacts with methanol only in the presence of a strong base such as biguanidine (B) to afford 1-methoxysilatrane **(65)** (equation 94)[68].

$$\underset{\mathbf{(29)}}{\mathrm{SCNSi(OCH_2CH_2)_3N}} + \mathrm{MeOH} \xrightarrow{\mathrm{B,\ CH_2Cl_2,\ RT}} \underset{\mathbf{(65)}}{\mathrm{MeOSi(OCH_2CH_2)_3N}} + \mathrm{B{\cdot}HNCS} \tag{94}$$

The reactions of **29** with secondary amines such as piperidine and diethylamine and with Lewis acids (including hard, soft and borderline acids in Pearson's sense) afford 1 : 1 adducts[68].

5. 1-Hydroxysilatrane

1-Hydroxysilatrane **(66)** can undergo nucleophilic displacement at silicon. For example, it reacts with acetyl chloride (in the presence of Et_3N) or with acetic acid/acetic anhydride to yield unstable 1-acetoxysilatrane **67** (equation 95)[69]. 1-Trimethylsiloxysilatrane **(68)** was obtained by treatment of **66** with chlorotrimethylsilane (equation 96)[69]. The reaction of **66** with diphenylchlorophosphine in THF led to the substitution product **69** in 37% yield. When treated with sulfur the latter compound was converted to the corresponding thio derivative **70** (equation 97)[325].

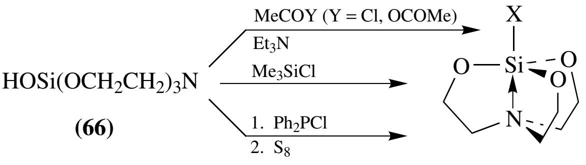

$HOSi(OCH_2CH_2)_3N$

(66)

(67) $X = MeCOO$ (95)

(68) $X = Me_3SiO$ (96)

(69) $X = Ph_2PO$

(70) $X = Ph_2P(S)O$ (97)

6. 1-Alkoxysilatranes

1-Fluorosilatrane **(37)** or its 3,7,10-trimethyl derivative **(37a)** are formed by the reaction of the corresponding 1-ethoxysilatranes **(30, 30a)** with concentrated HF in *i*-propanol at room temperature[69,154] or with KHF_2 at 200–240 °C[16] (equation 98).

$$\mathrm{EtOSi(OCHRCH_2)_3N} \xrightarrow{\text{HF or KHF}_2} \mathrm{FSi(OCHRCH_2)_3N} \qquad (98)$$

(30, 30a) **(37, 37a)**

30/37 R = H (25%)

30a/37a R = Me (73%)

Silatrane **(30)** can be readily converted via alcoholysis or acidolysis reactions to the corresponding organoxy or acyloxy compounds. A variety of higher alcohols[53], glycols[53], phenols[326], alkanolamines[327] and carboxylic acids[69,83] can be used as appropriate hydroxylic reagents (equation 99).

$$\mathrm{EtOSi(OCH_2CH_2)_3N + ROH \longrightarrow ROSi(OCH_2CH_2)_3N} \qquad (99)$$

R = Alk, Ar, $Me_2NCH_2CH_2$, R′CO (R′ = Me, Ph), 2-furyl, 2-pyridinyl, 2-thienyl, etc.

Alcoholysis of 1-alkoxysilatranes proceeds more slowly than that of tetraalkoxysilanes due to the bulk of the silatranyl group. The exchange rate falls with the decreasing acidity of the hydroxylic compound, suggesting an initial protonation of the EtO oxygen. Therefore, a Lewis acid catalyst such as $Zn(OAc)_2$ is required for effective silanolysis (reaction 99, $R = Ph_3Si$)[69].

The high-temperature reaction of **30** with THEA leads to tris-(2-silatranyloxyethyl)amine **71** (equation 100). The latter is a very useful precursor for the preparation of 1-hydroxysilatrane **(66)**[69].

$$\mathbf{30} + \mathrm{(HOCH_2CH_2)_3N \longrightarrow N[CH_2CH_2OSi(OCH_2CH_2)_3N]_3} \qquad (100)$$

(71)

Silatranes **(72** and **72a)** with an exocyclic S−Si bond are formed by treatment of 1-methoxysilatrane **(65)** with compounds having an HS function (equation 101)[67].

$$\mathrm{MeOSi(OCH_2CH_2)_3N + RSH \xrightarrow{\text{THF or PhH, }\Delta} RSSi(OCH_2CH_2)_3N + MeOH} \qquad (101)$$

(65) **(72, 72a)**

R = HCl• H_2NCH_2CHR'

(72) R′ = H (83%)

(72a) R′ = Me (67%)

7. 1-Alkyl-, 1-aralkyl- and 1-arylsilatranes

1-Alkyl- and 1-aralkylsilatranes are converted to the corresponding tetraorganylsilanes in high yields (70–92%) by treatment with an excess of n-BuLi (equation 102)[311].

$$\mathrm{RSi(OCH_2CH_2)_3N} + n\text{-BuLi} \longrightarrow n\text{-Bu}_3\mathrm{SiR} \qquad (102)$$

$R = n$-Bu, Bz, $Ph(CH_2)_2$

1-Arylsilatranes are reduced by lithium aluminum hydride in ether to the corresponding arylsilanes (equation 103). The reaction does not take place in the case of 1-aralkylsilatranes[311].

$$\mathrm{RSi(OCH_2CH_2)_3N + LiAlH_4 \longrightarrow RSiH_3} \qquad (103)$$

R = Ph (32%), 1-Naph (65%), $Ph(CH_2)_2$ (0%)

The apical Si—C bond of 1-organylsilatranes is very sensitive to direct electrophilic attack. As a consequence, alkyl or aryl bromide are formed by treatment of 1-organylsilatranes or the corresponding organyltrialkoxysilanes with *N*-bromosuccinimide (NBS) (equation 104)[328].

$$\mathrm{RSi(OCH_2CH_2)_3N + NBS \longrightarrow RBr} \tag{104}$$

$$\mathrm{R = Alk, Ph, 4\text{-}MeC_6H_4, 4\text{-}ClC_6H_4, 4\text{-}MeOC_6H_4}$$

The reaction of 1-organylsilatranes with 3-chloroperbenzoic acid (*m*-ClPBA) in methanol or dichlorometane affords primary alcohols or phenols due to the cleavage of C—Si bond (equation 105)[328].

$$\mathrm{RSi(OCH_2CH_2)_3N \xrightarrow{\textit{m}\text{-ClPBA}} ROH} \tag{105}$$

$$\mathrm{R = Alk, Ph, 4\text{-}MeC_6H_4, 4\text{-}ClC_6H_4, 4\text{-}MeOC_6H_4}$$

The Si—C bond in 1-organylsilatranes is easily cleaved by bromine or iodine chloride even at −50 °C (equation 106)[329]. This route is observed in CH_2Cl_2 or $CHCl_3$ as a solvent. By using diethyl ether–bromine, THF–bromine or dioxane–bromine adducts, a mixture of 1-halo- and 1-haloalkoxysilatranes is formed. For example, the reaction of 1-phenylsilatrane **(21)** with dioxane-bromine results in 1-bromosilatrane **(50)** and 1-[2′-(2″-bromoethoxy)ethoxy]silatrane **(73)** in 39% and 12% yield, respectively (equation 107)[329].

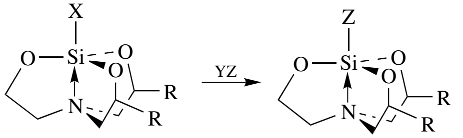

Y = Br, I, Z = Cl (106)

(2) X = Me, R = H
(2a) X = Me, R = Me
(20) X = Vin, R = H
(21) X = Ph, R = H

(38) Z = Cl, R = H
(38a) Z = Cl, R = Me
(50) Z = Br, R = H

$$\underset{\textbf{(21)}}{\mathrm{PhSi(OCH_2CH_2)_3N}} \xrightarrow{\text{dioxane}\bullet\mathrm{Br_2}} \mathbf{50} + \underset{\textbf{(73)}}{\mathrm{Br(CH_2)_2O(CH_2)_2OSi(OCH_2CH_2)_3N}} + \mathrm{PhBr} \tag{107}$$

Treatment of 1-organylsilatranes with mercury(II) salts in protic or aprotic media gives the corresponding organomercury compound and the substituted silatrane (equation 108)[132,330].

$$\mathrm{XSi(OCH_2CH_2)_3N + HgY_2 \longrightarrow XHgY + YSi(OCH_2CH_2)_3N} \tag{108}$$

$$\mathrm{Y = Cl, I, CH_3COO}$$

The relative reaction rates depend on both the steric and electronic effects of the substituent X and decrease in the order Vinyl, Ph, 4-ClC_6H_4 > Me > Et, *n*-Pr > $ClCH_2$, Cl_2CH, EtO[132]. The parent organyltrialkoxysilanes are essentially inert under similar conditions[331].

Reactions of 1-organylsilatranes with a metal fluoride[332] or heavy metal salts in aqueous solutions containing fluoride ions yield the corresponding organometallic compounds[332–334]. For example, triorganyllead fluorides are formed by treatment of 1-organylsilatranes with a mixture of lead tetraacetate/ammonium fluoride in water (equation 109)[333].

$$\begin{array}{c} 3XSi(OCH_2CH_2)_3N + Pb(OAc)_4 + NH_4F + 6H_2O \\ \downarrow \\ X_3PbF + 3\,SiO_2 + 3[HOCH_2CH_2)_3NH]OAc + NH_4OAc \end{array} \tag{109}$$

X = Me, Vinyl, Ph

8. 1-Alkenylsilatranes

1-Alkenylsilatranes can undergo a variety of useful addition reactions involving carbon-centered or heteroatom-centered species. For instance, 1-vinylsilatrane **(20)** reacts regioselectively with polyhaloalkanes to afford the corresponding terminal adducts **(74)** and **(75)** in high yields of 78–100% (equations 110 and 111)[335,336].

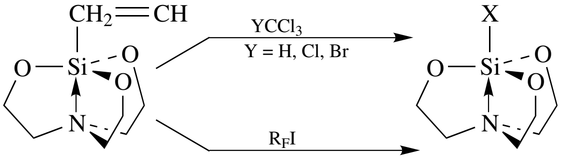

(20)

(74) $X = Cl_3CCH_2CHY$ (110)

(75) $X = R_FCH_2CHI$ (111)

The reactions occur in the presence of peroxides or under UV irradiation. Under the same conditions, 1-allylsilatrane **(76)** is converted to 1-halosilatrane arising from a thermally unstable adduct **(77a–c)** by a β-cleavage (equation 112)[319]. The reaction provides a simple and successful route to 1-halosilatranes, which are easily isolated in quantitative yields.

$$\mathbf{76} + RX \longrightarrow \underset{\mathbf{(77a\text{-}c)}}{RCH_2CHXCH_2Si(OCH_2CH_2)_3N} \xrightarrow[-RCH_2CH:CH_2]{} XSi(OCH_2CH_2)_3N \tag{112}$$

(a) $R = CCl_3,\ X = Cl$
(b) $R = CCl_3,\ X = Br$
(c) $R = C_3F_7,\ X = I$

The addition of methyl trichloroacetate to **20** is initiated by benzoyl peroxide or $Fe(CO)_5$ (equation 113). In the latter case, conducting the nucleophile-assisted reaction in an aprotic solvent (HMPA or MeCN) results in a higher yield of the adduct[337].

$$\mathbf{20} + CCl_3COOCH_3 \xrightarrow{(PhCOO)_2} \underset{\mathbf{(78)}}{CH_3OOCCCl_2CH_2CHClSi(OCH_2CH_2)_3N} \tag{113}$$

Silatrane **(20)** reacts with nitrile oxides to afford **79** and **80** in a ratio depending on the method for the *in situ* preparation of the initial oxides (equation 114)[338].

The photochemical thiylation of 1-vinyl- **(20)**, 1-allyl- **(76)** and 1-allyl-3,7,10-trimethylsilatranes **(76a)** by alkanethiols gives the terminal adducts in high yield of 90% (equation 115)[339].

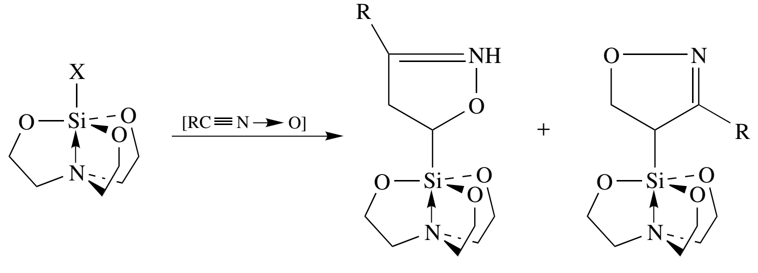

(20) **(79)** **(80)**

(114)

$$CH_2{=}CH(CH_2)_nSi(OCHRCH_2)_3N + R'SH \longrightarrow R'S(CH_2)_{n+2}Si(OCHRCH_2)_3N \qquad (115)$$

$$R = H, Me, R' = Alk, n = 0, 1$$

1-Vinyl- and 1-allylsilatranes react at comparable rates, as is evident from the competitive addition of *tert*-butanethiol (R′ = *t*-Bu). However, in a similar reaction 1-alkenylsilatranes display higher reactivity compared with the corresponding alkenyltrialkoxysilanes. For example, **76** is about 2.7 times more reactive than allyltrimethoxysilane. It is likely that the increase in the electron density of the C=C bond by the strong −*I* effect of the silatranyl group facilitates the addition of alkanethiyl radicals[339].

The reaction of 1-allylsilatrane **(76)** with *O*,*O*-diethyldithiophosphoric acid in $CHCl_3$ at room temperature gave *O*,*O*-diethyl *S*-(silatran-1-yl)dithiophosphate **(81)** in low yield (15%) instead of the terminal adduct (equation 116)[109].

$$\mathbf{76} + (EtO)_2P(S)SH \xrightarrow{CHCl_3} \underset{\mathbf{(81)}}{(EtO)_2P(S)SSi(OCH_2CH_2)_3N} \qquad (116)$$

Addition products are obtained from 1-vinylsilatranes **(20, 20a)** and compounds with a P—H moiety, i.e. dialkyl phosphites (equation 117) and diarylphosphines (equation 118)[340].

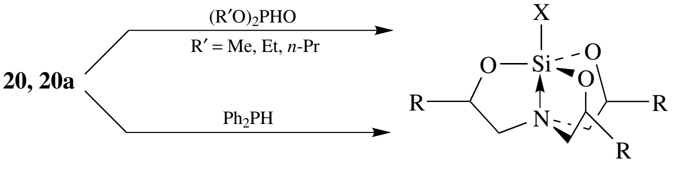

(117)

(118)

(82) X = $(R'O)_2POCH_2CH_2$, R = H

(82a) X = $(R'O)_2POCH_2CH_2$, R = Me

(83) X = $Ph_2PCH_2CH_2$, R = H

(83a) X = $Ph_2PCH_2CH_2$, R = Me

With **20**, reaction 117 occurs more rapidly in the presence of sodium alkoxide than under UV irradiation. In the latter case, no addition takes place at all when di(*n*-propyl) phosphite is the precursor. Under similar conditions the terminal adduct is produced from **20a** and di(*n*-propyl) phosphite in high yield (68%) due to the rate acceleration by the methyl ring substituents.

Silatrane **(20)** displays a similar reactivity toward organolithium reagents[311] as the corresponding tetracoordinate organylsilanes[341]. Thus, addition of *n*-BuLi to the C=C bond of **20** occurs with a simultaneous substitution of the Si−O bonds, while *t*-BuLi is added to the C=C bond at −78 °C without attack on the silatrane ring (equation 119).

$$\begin{array}{lll} \mathbf{20} \xrightarrow{\text{RLi}} & \text{RCH}_2\text{CH}_2\text{Si(OCH}_2\text{CH}_2)_3\text{N} \;+ & \text{RCH}_2\text{CH}_2\text{SiR}_3 \\ & \text{R} = n\text{-Bu},\ t\text{-Bu} & \text{R} = n\text{-Bu} \end{array} \qquad (119)$$

In contrast to **20**, no addition to the double bond occurs in the case of 1-allylsilatrane **(76)**; only the cleavage product of the Si−O bonds, i.e. $CH_2{=}CHCH_2SiBu\text{-}n_3$, is formed[311].

1-Alkenylsilatranes can add triorganylsilanes or -germanes to give the corresponding β-adducts (equation 120)[342–344]. The reaction is catalyzed by H_2PtCl_6[342,343] or $RhAcac(CO)_2$[344]. The addition of R_3SnH proceeds in a similar manner without any catalyst[344].

$$\text{CH}_2{=}\text{CH(CH}_2)_n\text{Si(OCH}_2\text{CH}_2)_3\text{N} + \text{R}_3\text{MH} \longrightarrow \text{R}_3\text{M(CH}_2)_{n+2}\text{Si(OCH}_2\text{CH}_2)_3\text{N}$$

$$\begin{array}{l} \text{M} = \text{Si},\ n = 0,\quad \text{R} = \text{Et, EtO}^{344},\ \text{R}_3 = \text{Me}_m(\text{2-Furyl})_{3-m},\ m = 0\text{–}2^{342,343}; \\ \text{M} = \text{Ge},\ n = 0, 1,\ \text{R} = \text{Et}^{344}; \\ \text{M} = \text{Sn},\ n = 0, 1,\ \text{R} = \text{Bu}^{344} \end{array} \qquad (120)$$

Treatment of 1-vinyl- **(20)** or 1-allylsilatrane **(76)** and their 3,7,10-trimethyl derivatives **(20a, 76a)** with $CH_2N_2/Pd(OAc)_2$ in ether affords the corresponding 1-cyclopropyl- and 1-cyclopropylmethylsilatranes (80–100%), respectively (equation 121)[37,345].

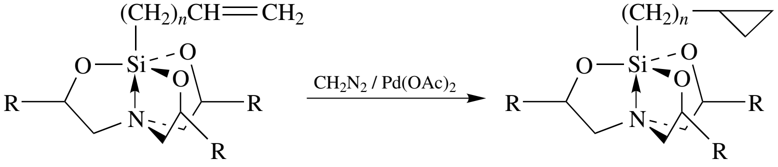

(121)

(84) R = H, $n = 0$
(84a) R = Me, $n = 0$
(85) R = H, $n = 1$
(85a) R = Me, $n = 1$

Under the same conditions, vinyltriethoxysilane reacts readily with diazomethane to yield the corresponding 1,3-cycloadduct, i.e. 3-triethoxysilyl-1-pyrazoline[345]. In contrast to 1-allylsilatrane, the degree of conversion of allyltriethoxysilane to the corresponding silyl-substituted cyclopropane is rather low (15%)[37].

1-Alkenylsilatranes can react with a variety of electrophiles to give products of substitution or addition. In the latter case, the adducts can undergo subsequent elimination, either thermally or by treatment with a good nucleophile toward silicon, resulting in an overall substitution. Thus, the addition of various derivatives of sulfenyl chlorides to

1-alkenylsilatranes occurs easily even at low temperature (−50 °C) (equations 122)[346,347].

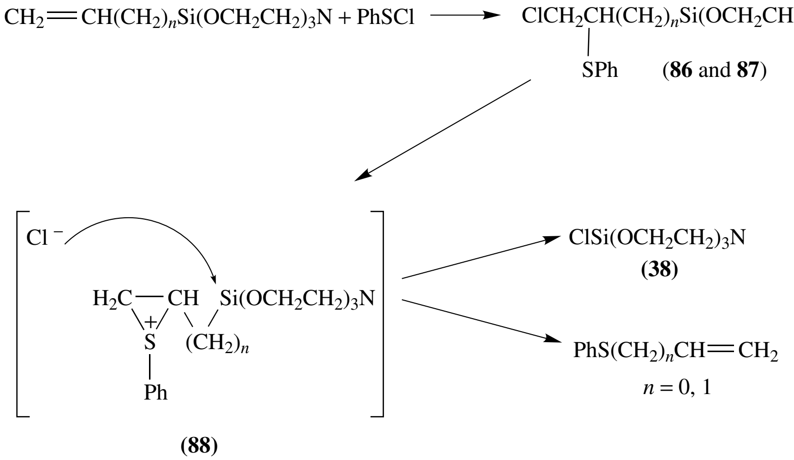

(122)

However, the thermal stability of the adducts depends on the nature of the sulfenyl chloride and on the structure of the alkenyl group. For instance, 1-chlorosilatrane **(38)** and alkenyl phenyl sulfides are formed by treatment of **20** or **76** with phenylsulfenyl chloride (equation 122). It is likely that the initial adducts (**86** and **87**), which are unstable at −10 °C, undergo elimination reaction via the formation of an episulfonium intermediate **(88)**, followed by nucleophilic attack of Cl^- at silicon. In contrast, the adducts from phenylsulfenyl chloride and trialkylalkenylsilanes are thermally stable and decompose by strong bases[348]. The larger electron-donating ability of the silatranyl group compared with the trialkylsilyl group is most probably responsible for these differences in stability.

The adducts from **20** and *O*,*O*-dialkylphosphoryl- or dialkylthiophosphorylsulfenyl chlorides are unstable at room temperature. Their transformations proceed in two directions as illustrated by equation 123[346,347].

The reaction course is determined by the heteroatom X. Since the migration of the silatranyl group to the oxygen of the phosphoryl group in the episulfonium intermediate is more preferable than that to sulfur, the a/b ratio is 3 : 2 and 6 : 1 for X = O and S, respectively. Similar sequences are likely to be involved in the reaction with 1-allylsilatranes[346].

A facile reaction between 1-alkenylsilatranes and *N*,*N*-dichloroarylsulfonamides in chloroform at room temperature results in almost quantitative yields of the adducts. Depending on the ratio of the starting reagents, the addition may involve one or both chlorine atoms of the dichloroamide (equations 124a and b)[349].

Silatranes **20** and **20a** are readily converted to α,β-epoxy derivatives **89** and **89a** (83–96% yield) by treatment with *m*-chloroperbenzoic acid in dichloromethane at room temperature (equation 125)[141,350]. Only polymeric products are obtained from 1-allylsilatrane **(76)** under the same conditions[350].

Electrophilic reactions of **20** and **20a** with *N*-bromosuccinimide in excess of water at room temperature lead to the stable adducts (**90** and **90a**, respectively) in 80% yields (equation 126)[119,351].

Similarly to allylsilanes[352], 1-allysilatrane **(76)** reacts with carbonyl compounds such as aldehydes, ketones or esters. Thus, treatment of **76** with aldehydes in the presence of $TiCl_4$ followed by hydrolysis afforded γ,δ-unsaturated alcohols (equation 127). Allyl transfer is also catalyzed by other Lewis acids, such as $AlCl_3$ or $BF_3{-}OEt_2$, but the alcohol yields are usually lower[39].

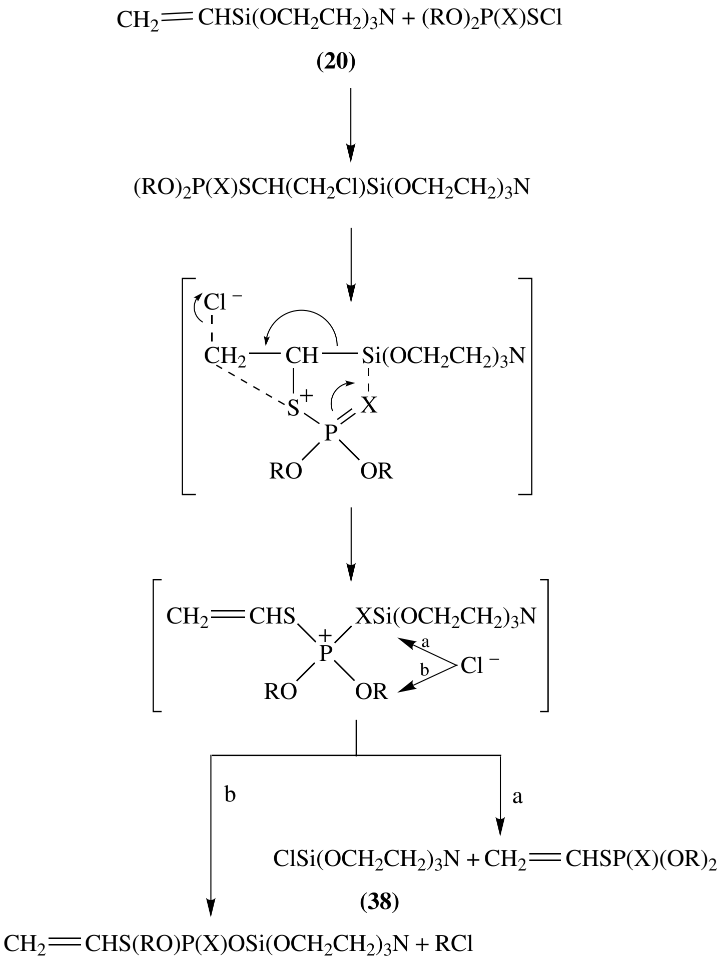

X = O, S

(123)

$$\textbf{20} + ArSO_2NCl_2 \longrightarrow ArSO_2NClCH_2CHClSi(OCH_2CH_2)_3N \qquad (124a)$$

$$\textbf{20} + ArSO_2NCl_2 \longrightarrow ArSO_2N[CH_2CHClSi(OCH_2CH_2)_3N]_2 \qquad (124b)$$

Ar = Ph, 4-ClC_6H_4, 4-MeC_6H_4

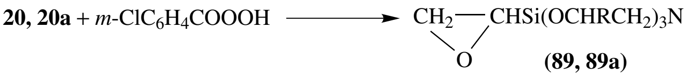

(89, 89a)

(125)

20/89 R = H
20a/89a R = Me

$$\mathbf{20, 20a} \xrightarrow{NBS/H_2O} \underset{\mathbf{(90,\ 90a)}}{HOCH_2CHBrSi(OCHRCH_2)_3N} \qquad (126)$$

20/90 R = H

20a/90a R = Me

$$\mathbf{76} + PhCH_2CH_2CHO \xrightarrow{cat.} PhCH_2CH_2CH(OH)CH_2CH{=}CH_2 \qquad (127)$$

cat. = $TiCl_4$ (96%); $AlCl_3$(83%); BF_3–OEt_2 (52%)

Allyl transfer does not take place with **76** under nucleophilic conditions[39]. By contrast, the reactions of allylsilanes with carbonyl compounds are activated by fluoride ion[353].

Diels–Alder cycloadditions between **20** or **76** and cyclopentadiene or hexachlorocyclopentadiene occur at 170–180 °C. The adduct **(91)** is a mixture of *exo*- and *endo*-isomers in a 3 : 1 ratio (equation 128)[354,355].

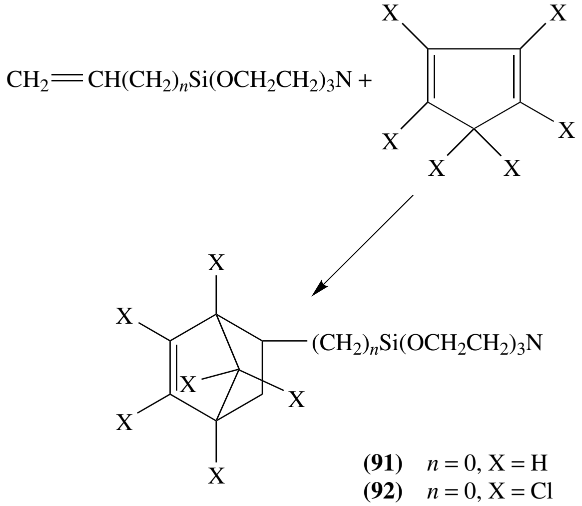

(128)

(91) $n = 0$, X = H
(92) $n = 0$, X = Cl
(92a) $n = 1$, X = Cl

Both 1-(butadien-1′,3′-yl)silatrane **(93)** and -trialkoxysilane can react by a Diels–Alder-type reaction with tetracyanoethylene (TCNE) or maleic anhydride (MA) to give the corresponding adducts (equations 129 and 130). However, a higher temperature is required for effective conversion of trialkoxysilane[355].

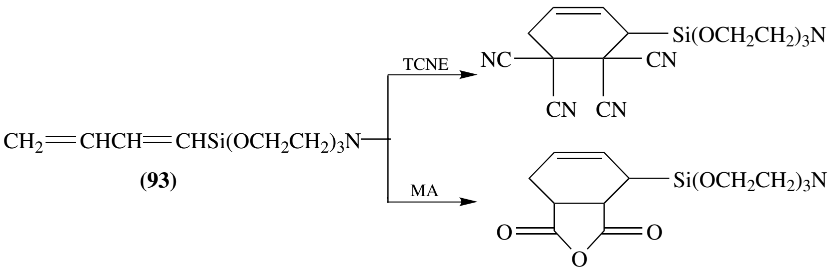

(93)

(129)

(130)

9. Carbofunctional silatranes

Generally, carbofunctional silatranes behave in a remarkably similar manner to the corresponding trialkoxysilanes. The reactivity differences may arise from the stereoelectronic influence of the silatranyl group.

1-(Haloalkyl)silatranes can react with a variety of heteronucleophiles. Thus, 1-chloromethylsilatrane **(16)** reacts with sodium or potassium alkoxides to afford 1-alkoxy-2-carba-3-oxahomosilatranes **(94)** instead of 1-alkoxymethylsilatranes. The ring enlargement proceeds via initial cleavage of a Si−O bond by alkoxide ion, followed by intramolecular nucleophilic substitution (equation 131)[356].

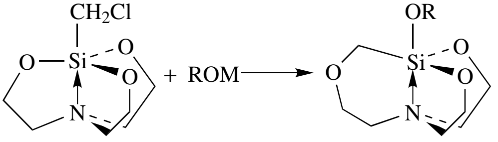

(16) R = Me (54%) **(94)**
R = Et (40%)
M = K, Na

(131)

Cleavage of the Si−C bond to give **96** occurs when 1-iodomethylsilatrane **(95)** is treated with dimethylethanolamine at 150 °C (equation 132)[327]. A related reaction also occurs with tetracoordinated halomethyltriorganylsilanes[357].

$$\underset{\textbf{(95)}}{ICH_2Si(OCH_2CH_2)_3N} + Me_2NCH_2CH_2OH \longrightarrow \underset{\textbf{(96)}}{Me_2N(CH_2)_2OSi(OCH_2CH_2)_3N} \qquad (132)$$

1-(Haloalkyl)silatranes react with alkali mercaptides or alkali salts of thiolcarboxylic acids to give **97** (equation 133)[88], with primary or secondary amines to give **98** (equation 134)[99,358] and with potassium diethyldithiophosphate to give **99** (equation 135)[109]. In the latter case no conversion of 1-chloromethyl- or 1-iodomethylsilatrane is observed under the same conditions[109]. The Arbuzov reaction is used to transform 1-(haloalkyl)silatranes into the corresponding dialkyl phosphonate derivatives **100** (equation 136)[359].

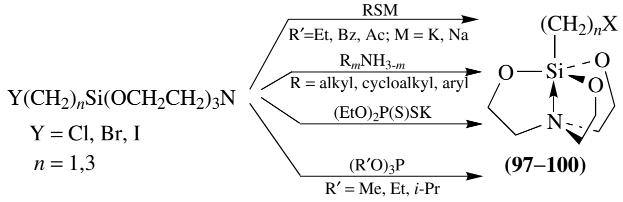

(97) $X = RS$ (133)
(98) $X = R_mNH_{2\text{-}m}$ (134)
(99) $X = (EtO)_2P(S)S$ (135)
(100) $X = (R'O)_2P(O)$ (136)

In the reactions in equations 133–136 the chloro derivatives were found to be considerably less reactive than the bromo- and iodoalkylsilatranes. It should be noted that chloro–halogen exchange does not occur when **16** is treated with NaI[72], NaBr, KBr, $AlBr_3$ or PBr_3[71]. However, NaI reacts easily with chloromethyltrialkoxysilanes[74].

A variety of onium salts **(101–103)** are formed by reaction of 1-(iodomethyl)silatrane with tertiary amines[358], triorganylphosphines[360] or diorganylchalcogenides (equation 137)[92,361,362].

$$ICH_2Si(OCH_2CH_2)_3N + B \longrightarrow [BCH_2Si(OCH_2CH_2)_3N]I \qquad (137)$$

(95)

(101) $B = R_3N$

(102) $B = R_3P$

(103) $B = R_2Y$ (Y = S, Te, Se)

The rearrangement of silatranyloxiranes (**89** and **89a**) to silatranylacetaldehydes (**104** and **104a**) occurs at 100–110 °C in the presence of triethyltin bromide as a catalyst (equation 138)[327].

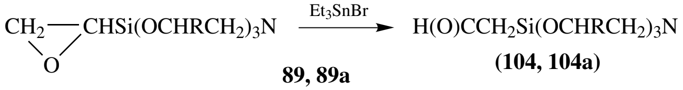

89, 89a **(104, 104a)** (138)

89/104 R = H

89a / 104 R = Me

2-Silatranylacetaldehyde **(104)** is also formed in a very high yield (98%) by heating 2-silatranyl-2-bromoethanol **(90)** with a small excess of triethylmethoxystannane (equation 139)[119].

$$HOCH_2CHBrSi(OCH_2CH_2)_3N \xrightarrow{Et_3SnOMe} H(O)CCH_2Si(OCH_2CH_2)_3N \qquad (139)$$

(90) **(104)**

Under similar conditions, 2-trialkylsilyl-2-bromoethanols are converted to a mixture of three isomers, e.g. trialkylsilyloxiranes (20–30%), trialkylvinyloxysilanes (10%) and trialkylsilylacetaldehydes (60–70%). The latter are unstable and easily rearrange at 180–190 °C to trialkylvinyloxysilanes[363,364]. In contrast, silatranylacetaldehyde **104** does not rearrange at 200 °C after prolonged heating (4 h)[119], probably due to the bulky silatranyl group.

1-(3′-Aminopropyl)silatranes **(105 and 105a)** react with halogen-containing compounds including acyl chlorides (equations 140 and 141)[96,99,365,366] and with aldehydes (equation 142)[366,367] to give the corresponding derivatives **(106–108)**.

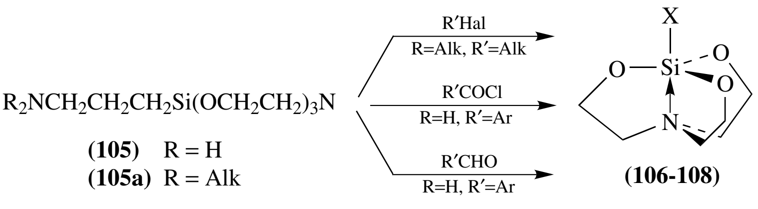

(105) R = H
(105a) R = Alk

(106-108)

(140)

(141)

(142)

(106) $X = Hal[R_2R'N(CH_2)_3]$

(107) $X = R'CO(R)N(CH_2)_3$

(108) $X = R'CH{=}N(CH_2)_3$

The cyclic adduct **109** is obtained from **105** and divinyl sulfoxide (equation 143)[368,369].

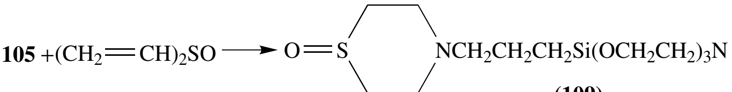

(109) (143)

Relative to organic and organosilicon sulfides, 1-(organylthioalkyl)silatranes **(110–112)** show an enhanced tendency for the formation of a variety of onium salts[361]. Due to the very strong $-I$ effect of the silatranyl group, 1-(organothiomethyl)silatranes **(110)** are very reactive toward organic iodides [including iodomethyltrimethylsilane and 1-iodomethylsilatrane] and toward bromides and even toward organic chlorides giving the sulfonium salts **113** (equation 144).

$$\underset{\textbf{(110)}}{\mathrm{RSCH_2Si(OCH_2CH_2)_3N}} + \mathrm{R'X} \longrightarrow \underset{\textbf{(113)}}{[\mathrm{RR'S^+CH_2Si(OCH_2CH_2)_3N}]\mathrm{X^-}} \qquad (144)$$

$R = Me, Et, n\text{-}Bu, t\text{-}Bu, Bz, 4\text{-}MeC_6H_4$

$R' = Me, i\text{-}Pr, All, HOCH_2CH_2, PhC(O)CH_2, Me_3SiCH_2$, etc.

$X = I, Br, Cl$

At higher temperature (130–140 °C) the reaction of bulky bis(silatran-1-ylmethyl)sulfide with 1-iodomethylsilatrane results in the formation of $S^+[CH_2Si(OCH_2CH_2)_3N]_3I^-$, having three pentacoordinate silicon atoms.

1-(Organylthioalkyl)silatranes $RS(CH_2)_nSi(OCH_2CH_2)_3N$ (**111**, $n = 2$; **112**, $n = 3$) react with alkyl iodides more slowly than **110**. The β-sulfonium salts are stable only in nonpolar solvents, whereas they undergo β-cleavage in polar solutions[361].

Hydrogen peroxide (30 or 80%) oxidizes 1-(organylthioalkyl)silatranes (**110** and **111**) in chloroform to the corresponding sulfoxides **114a** and **115a** (at 0–10 °C) or sulfones **114b** and **115b** (at 60 °C) (equation 145)[370].

$$\underset{\textbf{(110, 111)}}{\mathrm{RS(CH_2)_{\mathit{n}}Si(OCH_2CH_2)_3N}} + \mathrm{H_2O_2} \xrightarrow{\mathrm{CHCl_3}} \underset{\textbf{(114a,b, 115a)}}{\mathrm{RS(O)_{\mathit{m}}(CH_2)_{\mathit{n}}Si(OCH_2CH_2)_3N}} \qquad (145)$$

110/114a/114b $R = Me, Et, Bz, Ph, N(CH_2CH_2O)_3SiCH_2, n = 1$

111/115a $R = Me, Et, n = 2$

(**a**) $m = 1$, (**b**) $m = 2$

The reactivity diminishes in going from thiomethyl to thioethyl derivatives. Thus, 1-(phenylthiomethyl)silatrane is oxidized by 80% H_2O_2 to the corresponding sulfoxide whereas 1-(phenylthioethyl)silatrane is unreactive even under more drastic conditions.

The oxidation of (silatranylmethyl)phenylselenide **(116)** with 30% hydrogen peroxide in ethanol affords the corresponding selenoxide **(117a)** in 91% yield (equation 146). The selenone **117b** is formed by using 70% H_2O_2[92]. Unstable selenoxide is obtained from (2-silatranylethyl)phenyl selenide under the same conditions[92].

$$\underset{\textbf{(116)}}{\mathrm{PhSeCH_2Si(OCH_2CH_2)_3N}} + \mathrm{H_2O_2} \longrightarrow \underset{\textbf{(117a,b)}}{\mathrm{PhSe(O)_{\mathit{n}}CH_2Si(OCH_2CH_2)_3N}} \qquad (146)$$

(**a**) $n = 1$ and (**b**) $n = 2$

The high nucleophilicity of sulfur in $MeSOCH_2Si(OCH_2CH_2)_3N$ favors a more facile reaction with MeI (equation 147)[370] compared with DMSO[371]. Selenoxides can also be involved in the reaction in equation 147[92].

$$\mathrm{RZ(O)CH_2Si(OCH_2CH_2)_3N} + \mathrm{MeI} \longrightarrow [\mathrm{MeRZ(O)CH_2Si(OCH_2CH_2)_3N}]\mathrm{I} \qquad (147)$$

$R = Me, Z = S$

$R = Ph, Z = Se$

Treatment of 1-(mercaptoalkyl)silatranes with organomercury acetate in chloroform affords the corresponding mercury derivatives in 80–85% yield (equation 148). A related reaction with diorganylmercury results in lower product yields[372].

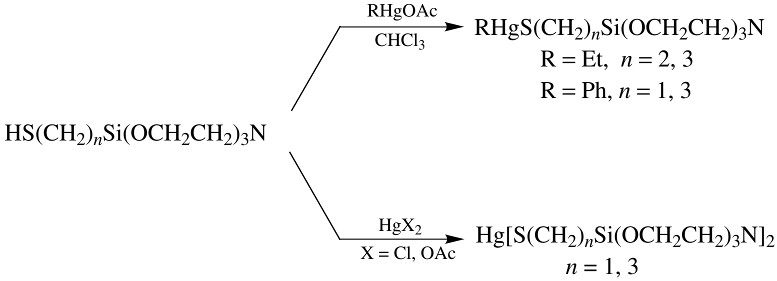

$$HS(CH_2)_nSi(OCH_2CH_2)_3N \xrightarrow[CHCl_3]{RHgOAc} RHgS(CH_2)_nSi(OCH_2CH_2)_3N \qquad (148)$$

$R = Et,\ n = 2, 3$

$R = Ph,\ n = 1, 3$

$$HS(CH_2)_nSi(OCH_2CH_2)_3N \xrightarrow[X = Cl,\ OAc]{HgX_2} Hg[S(CH_2)_nSi(OCH_2CH_2)_3N]_2 \qquad (149)$$

$n = 1, 3$

Bis(silatran-1-ylalkylthio)mercuranes are obtained from 1-(mercaptoalkyl)silatranes with mercury salts (equation 149)[372].

10. Silatranyl arene and cyclohexadiene complexes

1-Phenylsilatranes can act as π-coordinating ligand for transition metals[159–161,330,373–377]. Thus, the reactions of 1-phenylsilatrane with $M(CO)_6$ where $M = Cr$[159] and W[161] and with $[Mn(CO)_5]ClO_4$[373] afford the corresponding π-coordinated η^6-phenylsilatrane complexes **118**, **119** and **120a** (equations 150a and b).

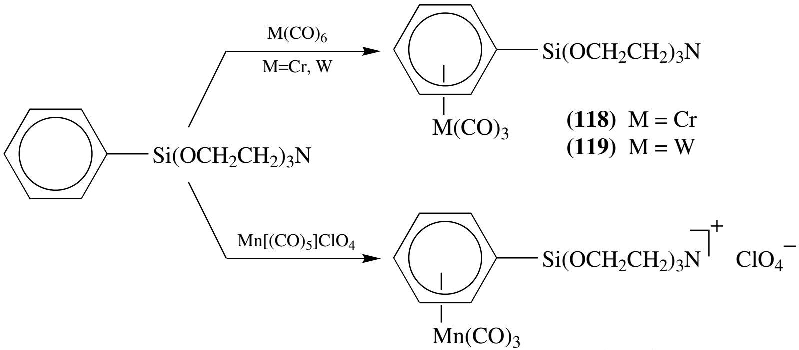

(150a)

(118) M = Cr

(119) M = W

(150b)

(120a)

These stable-in-air compounds are versatile precursors for the preparation of a wide range of new complexes. For example, manganese complex **120a** is easily transformed into $[\eta^6\text{-phenylsilatrane})Mn(CO)_2P(OMe)_3]ClO_4$ **(120b)** via a photochemical reaction with $P(OMe)_3$[374].

With $NaBH_4$ and some carbanions, complexes **120a** and **120b** and similar manganese complexes of 4′-substituted 1-arylsilatranes **(120c–g)** undergo a highly regioselective nucleophilic addition reaction (equation 151) yielding mainly one of the isomeric η^5-cyclohexadienylsilatrane complexes **(121–123a–g)**[160,373–375].

Treatment of complex **124** (which was obtained from **120a** via reaction 151) with $NOBF_4$ result in displacement of the carbonyl group to give the product **125**

(equation 152)[330].

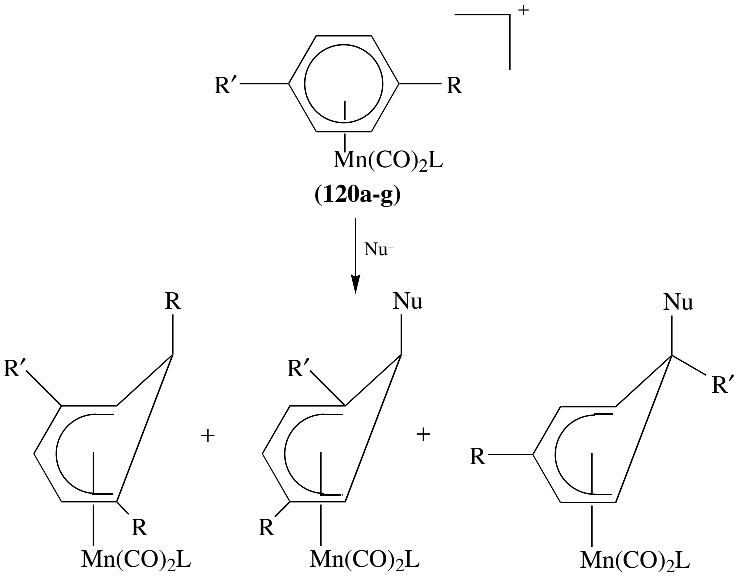

(120a-g)

(121a-g) **(122a-g)** **(123a-g)**

(151)

$R = Si(OCH_2CH_2)_3N$
(a) R′ = H, L = CO
(b) R′ = H, L = $P(OMe)_3$
(c) R′ = Me, L = CO
(d) R′ = *t*-Bu, L = CO
(e) R′ = Cl, L = CO
(f) R′ = MeO, L = CO
(g) R′ = H_2N, L = CO

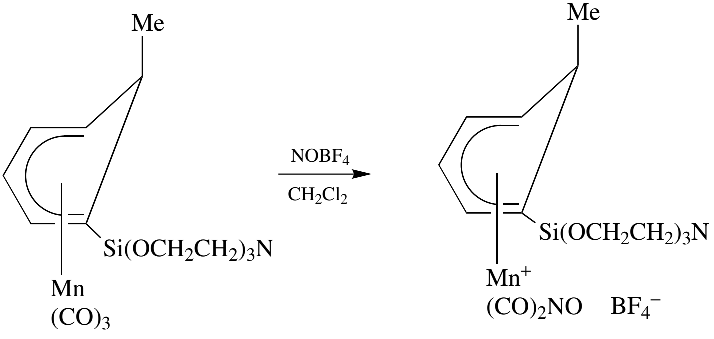

(152)

(124) **(125)**

The addition reactions of hydride and several kinds of carbon nucleophiles to **125** provide an easy synthetic route to some new silatranyl η^4-cyclohexadienyl complexes, such as **126a** and **126b** (equation 153)[330]. Demetalation of **126a** and **126b** with Me_3NO in refluxing benzene is a very versatile route to 1-(cyclohexadienyl)silatranes **127a** and **127b** (equation 154)[330,376]. Compounds **127a** and **127b** can be transformed to the η^4- and η^5-(silatranylcyclohexadienyl)iron complexes by treatment with $Fe_2(CO)_9$[377].

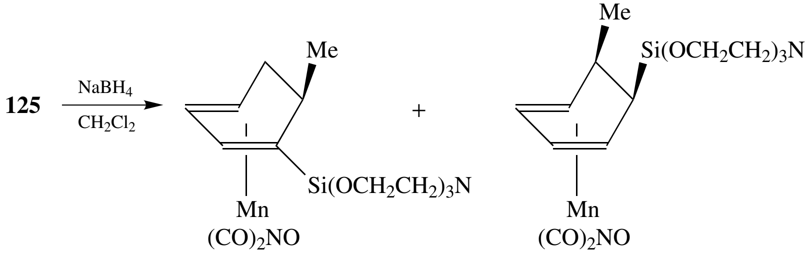

(153)

(126a) **(126b)**

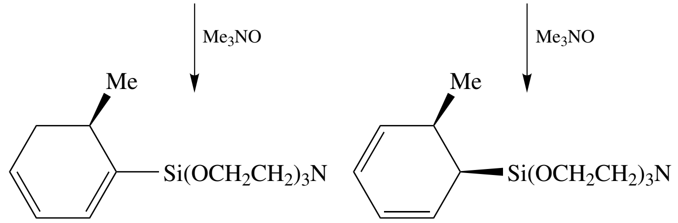

(154)

(127a) **(127b)**

III. SILATRANE ANALOGS

A. 3-Homosilatranes

The general method for the formation of 1-organyl-2,9,10-trioxa-6-aza-1-silatricyclo[4.3.3.$0^{1,6}$]dodecanes (1-organyl-3-homosilatranes) having an enlarged ring system is the transetherification reaction of a trifunctional silane with 3-hydroxypropyl-bis(2-hydroxyalkyl)amine in boiling toluene or xylene (equation 155)[326,378]. When Y = OR′, KOH is used as a catalyst. The yields of the desired compounds are excellent (70–90%)[326,378].

$$XSiY_3 + (HOCH_2CH_2CH_2)(HOCHRCH_2)_2N \longrightarrow$$

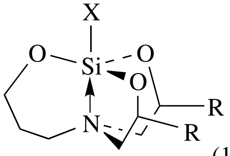

X = Me, Vinyl, Ar, $ClCH_2$
Y = OR′, NMe_2
R = H, Me

(155)

Treatment of tetramethoxy- or tetraethoxysilane with phenol and trialkanolamine affords 1-phenoxyhomosilatrane (equation 156)[326].

1-Aryloxyhomosilatranes can also be obtained from 1-alkoxyhomosilatranes and the appropriate phenols (equation 157)[326]. However, reaction 156 proceeds at a higher rate.

$Si(OR)_4$ + PhOH + $(HOCH_2CH_2CH_2)(HOCHMeCH_2)_2N$

R = Me, Et

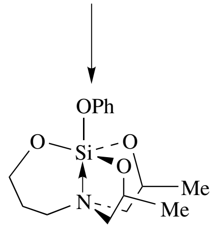

(156)

$$ROSi(OCH_2CH_2CH_2)(OCHMeCH_2)_2N \xrightarrow{ArOH} ArOSi(OCH_2CH_2CH_2)(OCHMeCH_2)_2N \qquad (157)$$

R = Me, Et; Ar = Ph, 1-Naph

Attempts to prepare a stable cage structure from organyltrialkoxysilanes and (2-hydroxyethyl)bis(3-hydroxypropyl)-[326] or tris(3-hydroxypropyl)amines[69,326] yielded only macromolecular products. It is not surprising since the strong transannular bonding contributes to the shape of the silatrane cage (see Section II.A.2). Meanwhile, insertion of an additional methylene group into the silatrane framework was shown by some physical methods to weaken the Si←N bond in 3-homosilatranes compared with the parent silatrane analogs[6,13].

The Si←N bond length was measured by X-ray method to be 2.291 Å in 1-chloromethyl-3-homosilatrane[379] and 2.43 and 2.49 Å in two independent molecules of 1-phenyl-7-methyl-3-homosilatrane[6]. Elongation of this bond relative to that observed in the corresponding silatranes is by 0.2–0.3 Å and it may be explained by an increase in the strain energy of the skeleton in 3-homosilatranes: a six-membered chelate ring is obviously more strained than a five-membered ring. The relative weakness of the Si←N bond is accompanied by a small shortening of the apical C−Si bond. Since the silicon electronegativity in 3-homosilatranes and silatranes is nearly the same, these distinctions between their axial X−Si←N moieties agree with the prediction by the 3c4e bonding model[174].

Dipole moment studies[207,378,380] found a lower dipole moment of the Si←N bond in 3-homosilatranes (1–2 D) than in silatranes (1.5–3.1 D). The enthalpy of formation of this bond was estimated to be 3–11 $\mathrm{kcal\,mol^{-1}}$ depending on the substituent X and on the method of the bond dipole calculation[207]. The observation of an absorption band at 570–600 $\mathrm{cm^{-1}}$ in the IR spectra suggests a tricyclic structure of 3-homosilatranes in solution[378].

The general trends of the influence of the substituent X on the ^{1}H[239,378], ^{13}C[250], ^{15}N[250] and ^{29}Si[250,261] NMR chemical shifts of 3-homosilatranes are close to those found for silatranes. However, there are some definite spectral indications for a weakening of the Si←N bond in the former molecules[250,261,378].

In the EI mass spectra of 1-organyl-3-homosilatranes[286] the $[M - X]^+$ ion (m/z = 188) is generally the most abundant. The FAB spectra of these compounds contain a very intensive peak of protonated 3-[*N*,*N*-bis(2′-hydroxyethyl)]aminopropanol (m/z 164) together with peaks of the very characteristic MH^+ and $[M - X]^+$ ions[286]. A decrease in the intensity ratio of the latter peak (m/z 188) to that at m/z 164 upon increasing the total irradiation time indicates that the ring rupture is a FAB-induced reaction.

B. Silatranones

1-Organylsilatran-3-ones (2,8,9-trioxa-5-aza-1-silatricyclo[3.3.3.0$^{1.5}$]undecan-3-ones) can be prepared from organyltrialkoxysilanes and *N*,*N*-bis(2-hydroxyethyl)aminoacetic acid in the appropriate boiling solvent (DMF/C_6H_6, DMSO/C_6H_6) in the presence of KOH (equation 158). The yields are 30–75%[381].

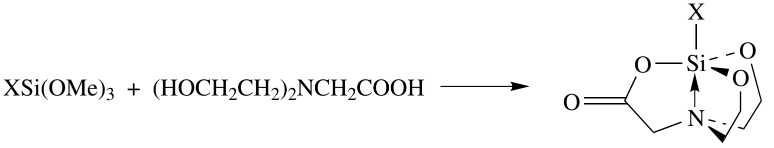

(158)

X = Alk, Vin, Ar

A slight modification of the synthesis involves the application of silylated amino acids which are more soluble in organic solvents (equation 159). In this case reactions occur rapidly (0.5–1 h) at lower temperatures (40–50 °C, DMF) to give the corresponding silatranones **(128–134)** in good yields. 1-Methylsilatrane-3,7,10-trione **(134)** was isolated as a complex with DMF[382].

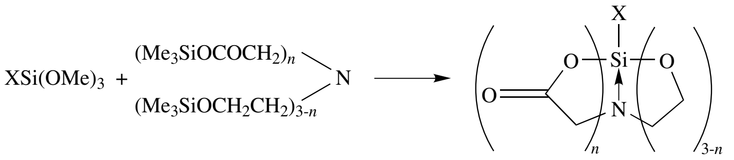

(159)

	X	*n*	Yield (%)
(128)	$ClCH_2$	1	63
(129)	MeO	1	32
(130)	Me	2	69
(131)	Et	2	70
(132)	Ph	2	70
(133)	$ClCH_2$	2	70
(134)	Me	3	83

Organyltriacetoxysilanes can be converted almost quantitatively to 1-organylsilatrane-3,7,10-triones **(134–142)** by heating with aminotriacetic acid at 90–100 °C (equation 160)[383].

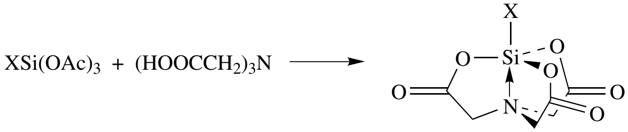

(160)

(134) X = Me
(135) X = H
(136) X = Et
(137) X = $ClCH_2$
(138) X = Vin
(139) X = All
(140) X = HC≡C
(141) X = Ph
(142) X = $EtSCH_2CH_2$

1-Substituted silatrane-3,7,10-triones **143–147** are formed in high yield (80–95%) from tetrachlorosilane or organyloxytrichlorosilanes and tris(trialkylstannyl) esters of aminotriacetic acid (equation 161). CCl_4, pentane or petroleum ether can be used as a solvent. Tetraethoxy- and tetraacetoxysilanes are ineffective under the same conditions[384].

$$XSiCl_3 + (Me_3SnOOCCH_2)_3N \xrightarrow{\qquad} XSi(OCOCH_2)_3N \tag{161}$$

	X	Yield (%)
(143)	Cl	96
(144)	MeO	90
(145)	EtO	83
(146)	PhO	95
(147)	MeCOO	72

Monosilatranones are rather stable to hydrolysis and alcoholysis. Thus, *N*,*N*-bis(2-hydroxyethyl)aminoacetic acid is formed in only 50% yield when 1-(3′-trifluoromethylphenyl)silatran-3-one) **(148)** is treated with H_2O/THF at room temperature for 7 h. **148** (80%) is recovered from a MeOH/THF mixture upon prolonged (9 h) heating[381].

X-ray studies revealed a shortening of the Si←N bond in 1-organylsilatran-3-ones and 1-methylsilatrane-3,7-dione relative to the corresponding silatranes[385–390] (Scheme 5). This shortening was attributed to a higher effective electronegativity of the silicon which, in accordance with a 3c4e model of silicon bonding[174], should provide (and provides) the strengthening of both components of the hypervalent X—Si←N bond. An elongation of the Si—O(CO) bond is the second peculiarity of silatranones. The influence of the substituent X on the molecular structure of these compounds seems to be similar to that found for silatranes.

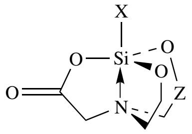

Compound	X	Z	d(SiN) (Å)	Reference
149	Me	CH_2	2.134	385
128	$ClCH_2$	CH_2	2.085	386
150	$Cl(CH_2)_3$	CH_2	2.149	387
151	Ph[a]	CH_2	2.126, 2.111	388
152	4-FC_6H_4	CH_2	2.129	389
148	3-$CF_3C_6H_4$	CH_2	2.106	389
130	Me	C=O	2.146	390

[a]Two independent molecules

SCHEME 5. Bond lengths in 1-organylsilatran-3-ones

The prochirality of the silicon and nitrogen atoms in silatran-3-ones makes the geminal protons of both unsubstituted OCH_2CH_2N fragments anisochronic in the ^1H NMR spectra[239,247,381]. The same reason leads to a nonequivalence of the geminal protons of the $OC(O)CH_2N$ groups in silatrane-3,7-diones[247]. Subsequent replacement of the OCH_2 groups in the silatrane skeleton by the OC(O) moieties increases the chemical shifts of all protons[247]. For the silatrane-3,7,10-triones the resonance of the NCH_2 protons was found to be in the range 3.8–4.1 δ (in DMSO) and to be slightly less sensitive to the substituent effect than in the silatrane spectra[383,391]. It was noted that silatrane-3,7,10-triones are able to form 1 : 1 complexes with DMSO and DMF, in which the silicon atom is hexacoordinated[247]. The Si←N bonding in silatranones is displayed in upfield and downfield shifts of their ^{29}Si and ^{15}N NMR signals relative to those observed for model compounds[247].

The values of $^{1}J(^{29}Si^{15}N)$ in 1-methyl-substituted silatran-3-one (0.9 Hz) and silatrane-3,7,10-trione (8.2 Hz) indicate an increase in the Si←N bond strength with increase in the number of carbonyl groups in the silatranones[247]. From the relationship between the $^{1}J(^{29}Si^{15}N)$ and d(SiN) values in silatranes and their analogs, the lengths of the transannular bond in 1-methyl- **(134)** and 1-chloromethylsilatrane-3,7,10-triones **(137)** were estimated to be 2.05 and 2.01 Å, respectively[124]. The silatranonyl groups were shown to be less electron-releasing than the silatranyl group. Their σ_I constants derived from the ^{13}C NMR spectra of 1-phenylsilatranones are −0.08, 0.04 and 0.04 for mono-, di- and tricarbonyl-substituted groups, respectively[247].

In IR spectra of 1-organylsilatrane-3,7,10-triones **(134–142)** the complex skeleton and Si←N bond vibrations are displayed at 550–570 cm^{-1}[383]. The frequency of the stretching vibration of their carbonyl groups, ν(C=O), is higher than that observed for triacetoxysilanes. A Si←N bonding in 1-hydrosilatrane-3,7,10-trione **(135)** is confirmed by a low-frequency shift of the ν(SiH) band (2234 cm^{-1}) relative to that at 2290 cm^{-1} for $HSi(OOCCH_3)_3$, triacetoxysilane.

The mass spectra of 1-alkyl- and 1-arylsilatran-3-ones differ from those of silatranes: their most intensive peak is ascribed to $[M - CO_2]^+$ ions, formed perhaps owing to a weakening of the Si−OC(O) bonds[287]. Two pathways, with a primary breaking of the X−Si bond and a splitting of the CO_2, are found for the fragmentation of silatrane-3,7,10-triones[391].

C. Carbasilatranes

2-Carbasilatranes (1-organyl-2,8-dioxa-5-aza-1-silatricyclo[3.3.3.0$^{1.5}$]undecanes) are derived formally from silatranes by substituting one equatorial oxygen atom with a CH_2 group. 1-Alkyl- and 1-alkoxy-2-carbasilatranes **(153–154)** and their 7,10-dimethyl derivative **(154a)** were obtained from organyl(3-aminopropyl)diethoxysilanes[392,393] or 3-aminopropyltriethoxysilane[69,392] and oxiranes (equation 162).

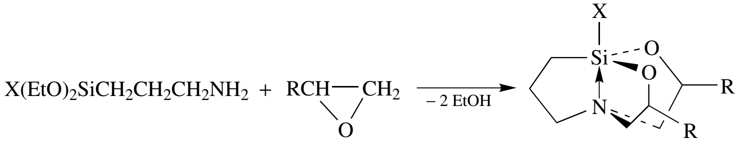

(162)

(153) X = Me, R = H
(154) X = EtO, R = H
(154a) X = EtO, R = Me

An alternative route to 1-organyl-2-carbasilatranes involves the reaction of organyl(3-chloropropyl)dialkoxysilanes with diethanolamine[393–396]. For example, phenyl(3-chloropropyl)dimethoxysilane is converted to **155** (38%) by treatment with diethanolamine in xylene (equation 163). Triethylamine acts as an HCl acceptor[394].

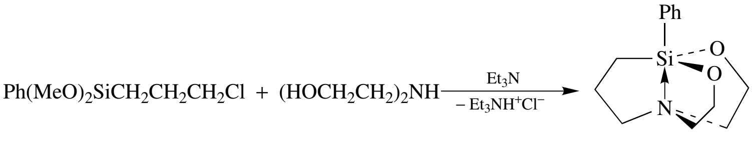

(163)

(155)

Owing to the introduction of the carbon atom into the equatorial site, the effective electronegativity of silicon in 2-carbasilatranes is lower than in silatranes. For this case, the 3c4e bonding model predicts a weakening of both axial X−Si and Si←N bonds of the hypervalent silicon[12,174]. Available X-ray data for 2-carbasilatranes confirmed it as shown below:

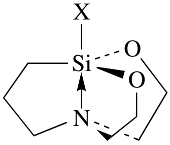

Compound	X	d(SiN) (Å)	d(XSi) (Å)	Δ_{Si} (Å)[b]	Reference
153	Me	2.336(4)	1.898(5)	0.29	397
155	Ph	2.291(1)	1.897(1)	0.27	395
156	4-MeC_6H_4[a]	2.311(2) 2.269(3)	1.892(3) 1.905(3)	0.24	166
157	MeO	2.223(5)	1.672(4)	0.23	396

[a] Two independent molecules.

[b] Δ_{Si} is the deviation of the TBP Si atom from the equatorial plane.

The NMR spectra of Si-substituted 2-carbasilatranes reveal a smaller effect of the substituent X on the ^1H chemical shifts of their cage framework relative to that in silatranes[6,12,13]. Diastereotopy of the geminal protons and a high conformational flexibility of the chelate aminoethoxy rings in 1-methyl-2-carbasilatrane **(153)** were detected by ^1H NMR study[239]. ^{29}Si NMR study of powder[260] and solute[261] patterns found a high sensitivity of the transannular bond in 2-carbasilatranes to the physical environment. Peculiarities of the solution-phase ^{13}C, ^{15}N and ^{29}Si NMR chemical shifts suggest that the transannular bonding in 2-carbasilatranes is weaker than in the related silatranes and 3-homosilatranes[250,261].

The most intensive peak in the mass spectra of 1-methyl- and 1-phenyl-2-carbasilatranes corresponds to the $[M - X]^+$ ion ($m/z = 172$) whereas for 1-alkoxy-2-carbasilatranes a cleavage of the skeleton yields the $[M - C_2H_5]^+$ ions as the major ions[287].

The ability of the silicon atom to extend its coordination number even when it is bonded to three or four carbon atoms was demonstrated by the preparation and structural studies of 2,8,9-tricarbasilatranes **158**–**160**[398–400].

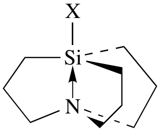

(158) X = Me
(159) X = Cl
(160) X = $OSi(CH_2CH_2CH_2)_3N$

1-Methyl-2,8,9-tricarbasilatrane **(158)** was obtained in 14% yield via the reaction of methyltrichlorosilane with a Grignard reagent (equation 164)[399].

$$MeSiCl_3 + (ClMgCH_2CH_2CH_2)_3N \xrightarrow{THF/C_6H_6} \mathbf{158} \tag{164}$$

The Me−Si bond in **158** was found to be easily cleaved by dimethyldichlorostannane to give 1-chloro-2,8,9-tricarbasilatrane **(159)** in almost quantitative yield (equation 165)[398,399].

$$\mathbf{158} + Me_2SnCl_2 \longrightarrow \underset{\mathbf{(159)}}{ClSi(CH_2CH_2CH_2)_3N} \tag{165}$$

The hydrolysis of **159** in benzene in the presence of triethylamine affords the oxygen-bridged bis(tricarbasilatrane) in 89% yield (equation 166)[400].

$$\mathbf{159} + H_2O \xrightarrow{Et_3N} \underset{\mathbf{(160)}}{N(CH_2CH_2CH_2)_3SiOSi(CH_2CH_2CH_2)_3N} \tag{166}$$

The typical upfield shift of the ^{29}Si NMR signals of tricarbasilatranes relative to those for the corresponding derivatives of triethylsilane provides strong evidence for a transannular Si←N bonding even in the solution state[398–400]. Temperature dependence of the ^{1}H NMR spectra detects a fast ring flip of their skeleton and a possible strengthening of the Si←N bond on cooling of the solutions[398–400].

According to X-ray study, the Si←N bond distance (2.477 Å) and the degree of pyramidality of the silicon and nitrogen atoms in compound **160** are rather close to those in silatranes[400]. The steric repulsion between the two cages provides a linear arrangement of the Si−O−Si group. The Si−O bond (1.631 Å) is no longer than in usual siloxanes. This surprising behavior of the apical bond was ascribed to compensation of its expected lengthening by the well-known decrease in Si−O distance on increasing the Si−O−Si angle.

Recent *ab initio* calculations of a wide series of Si-substituted 2,8,9-tricarbasilatranes (X = H, Me, H_2N, HO, F, H_3Si, H_2P, HS and Cl) found a single minimum corresponding to the *endo* form on the potential energy coordinate of the Si←N bond deformation[194]. The transannular bond was shown to be very soft and sensitive to the medium. The substituent effect on this bond length and mutual weakness of the axial bonds of the TBP silicon are well described by the 3c4e bonding model.

D. Benzosilatranes

The first monobenzosilatrane, 1-phenylbenzosilatrane **(161)**, was synthesized in good yield by treatment of phenyltrimethoxysilane with 2-aminophenol and ethylene oxide (equation 167)[69].

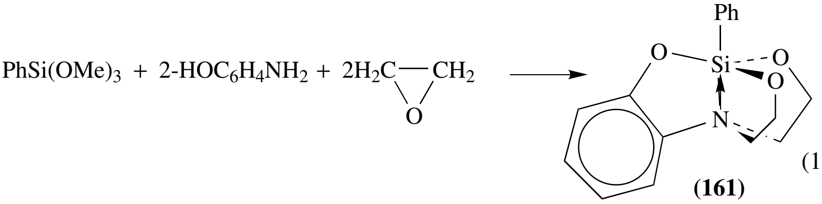

(167)

(161)

An extension of this method allows one to obtain 1-organyl-3,7-dimethyl-10,11-benzosilatranes from the corresponding organyltrialkoxysilanes (equation 168)[401].

A standard synthesis of 1-organyltribenzosilatranes is the reaction of a trifunctional silane with tris(2-hydroxyphenyl)amine (equation 169)[402].

Tris(2-hydroxyphenyl)amine reacts with organyltrichlorosilanes, e.g. phenyltrichlorosilane, more slowly and at higher temperature than with the acetoxy derivative[402].

The striking contrast between these two reagents was explained by the operation of different mechanisms for the processes. The reaction of tris(2-hydroxyphenyl)amine with acetoxysilane may involve simultaneous nucleophilic attack at the silicon and electrophilic attack upon the leaving acetoxy group via a six-membered transition state. Similar reactions with alkoxy- or chlorosilanes are likely to occur via a disfavored four-membered strained transition state[402].

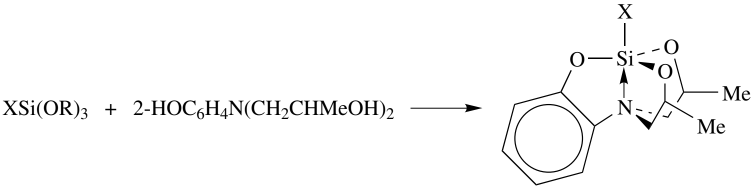

$$\mathrm{XSi(OR)_3} + \mathrm{2\text{-}HOC_6H_4N(CH_2CHMeOH)_2} \longrightarrow$$

(168)

	X	Yield (%)
(162)	Ph	50
(163)	$ClCH_2$	86
(164)	Cl_2CH	42
(165)	CH_3CHCl	74
(166)	$Cl(CH_2)_3$	73

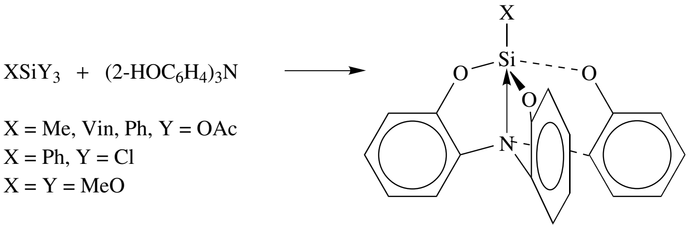

$$\mathrm{XSiY_3} + \mathrm{(2\text{-}HOC_6H_4)_3N} \longrightarrow$$

X = Me, Vin, Ph, Y = OAc
X = Ph, Y = Cl
X = Y = MeO

(169)

X	Y	Solvent	T (°C)	Yield (%)
Ph	OAc	CCl_4	75	89
Ph	Cl	CCl_4	75	0
Ph	Cl	Bu_2O	140	74

Nevertheless, more accessible organyltrichlorosilanes are good reagents for the preparation of various organyltribenzosilatranes[403], including *o*-substituted derivatives[404,405]. Tribenzosilatrane **(167)** having four alkyl chains was obtained in 52% yield from *n*-octyltrichlorosilane and tris(2-hydroxy-4-dodecylphenyl)amine by reaction 169[404,405]. This compound was designed for fabricating a new type of material where the overall global shape could facilitate the formation of cubic symmetry mesophases.

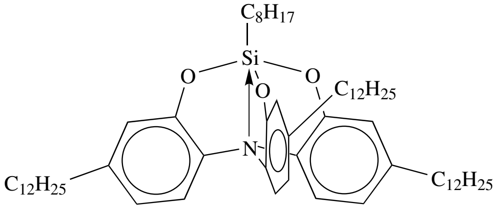

(167)

The reactions of tris(2-hydroxyphenyl)amine with trichloro-, trimethoxy- or triacetoxysilanes in boiling toluene afford the corresponding Si-substituted derivatives instead of 1-hydrotribenzosilatrane (equation 170)[402]. As evident from this reaction, the H−Si bond of 1-hydrotribenzosilatrane is very sensitive to electrophilic attack.

$$HSiX_3 + 3\,(2\text{-}HOC_6H_4)_3N \xrightarrow[-3\,HX]{} [HSi(OC_6H_4)_3N] \xrightarrow{+\,HX} XSi(OC_6H_4)_3N \qquad (170)$$

$$X = Cl, MeO, AcO$$

1-Acetoxytribenzosilatrane undergoes hydrolysis to the corresponding disiloxane **(168)** when treated with moist solvents or with H_2O in acetonitrile solution (equation 171)[402].

$$AcOSi(OC_6H_4)_3N + H_2O \longrightarrow \underset{\textbf{(168)}}{N(C_6H_4O)_3SiOSi(OC_6H_4)_3N} \qquad (171)$$

It was suggested that the rate-determining step of the acid-catalyzed hydrolysis of tribenzosilatranes $XSi(OC_6H_4)_3N$ (X = Me, Ph, $4\text{-}MeC_6H_4$) involves a rapid protonation of an oxygen atom, followed by cleavage of the Si−O bond[406].

Solvolysis of 1-chloro- or 1-acetoxytribenzosilatranes with methanol or phenol yields the methoxy or phenoxy derivatives (equation 172)[402].

$$XSi(OC_6H_4)_3N + ROH \longrightarrow ROSi(OC_6H_4)_3N \qquad (172)$$

$$X = AcO,\ R = Me$$
$$X = Cl,\ \ R = Ph$$

Unlike the reaction of 1-ethoxysilatrane with CF_3COOH, which results in the hydrogen-bonded adduct, 1-ethoxytribenzosilatrane is converted to disiloxane **168** under the same conditions (equation 173)[27].

$$2\,EtOSi(OC_6H_4)_3N \xrightarrow{2CF_3COOH} \textbf{168} + 2\,CF_3COOEt + H_2O \qquad (173)$$

X-ray studies show that substitution of the ethylene bridge for the *o*-phenylene group in the silatrane framework leads to an essential lengthening of the Si←N bond in Si-substituted 3,7-dimethylbenzosilatranes and tribenzosilatranes compared to that in silatranes[17] (Scheme 6). However, the delayed neutralization of an acidic titrant observed for 1-phenylbenzosilatrane[69] and the very low basicity of the nitrogen in tribenzosilatranes[402] imply a transannular bonding in solution.

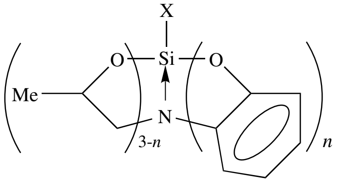

X	n	d(SiN) (Å)	d(XSi) (Å)	Δ_{Si} (Å)[b]	Reference
$ClCH_2$[a]	1	2.177	1.887	0.19	17
		2.185	1.883	0.21	
Ph	1	2.193	1.887	0.21	17
$ClCH_2$	3	2.256	1.864		17
Ph	3	2.344	1.853	0.29	121

[a] Two independent molecules.

[b] Δ_{Si} is the deviation of the TBP Si atom from the equatorial plane

SCHEME 6. Bond lengths in benzosilatranes

^{29}Si NMR chemical shifts of 1-ethoxytribenzosilatrane and the oxygen-bridged bis(tribenzosilatrane) were observed in a region which is typical for five-coordinate compounds[27]. A weaker spectroscopic basicity of the axial oxygen in the former compound as compared with that in related silatrane was found by comparing the O−H stretching frequency of phenol in CCl_4 solutions of these compounds[27]. This result is a strong indication of reduced transannular bonding in the tribenzosilatranes.

In the FAB mass spectra of 1-phenyl-3,7-dimethyl-10,11-benzosilatrane, the most intensive peak corresponds to the $[M - X]^+$ ion[291].

E. Triazasilatranes

2,8,9-Triazasilatranes (2,5,8,9-tetraaza-1-silatricyclo[3.3.3.0^{1,5}]undecanes) are very promising analogs of silatranes. Variation of the substituent at the silicon and the equatorial nitrogen atoms provides important changes in the structure and properties of these molecules. Since reactions of triazasilatranes could potentially proceed not only by participation of the silicon atom and its substituent but also by the equatorial nitrogens and their substituents and even by the axial nitrogen as well, their chemistry should be more diverse than the chemistry of silatranes. Many volatile triazasilatranes, primarily 1-aminotriazasilatranes containing five nitrogens in the immediate proximity of silicon, are candidates for the molecular organic chemical vapor deposition (MOCVD) of silicon nitride[26,27].

1-Organyl-2,8,9-triazasilatranes can be obtained from organyltris(dialkylamino)silanes and tris(2-aminoethyl)amines (equation 174)[407,408a]. The use of a solvent[312] or catalytic amounts of Me_3SiCl or $(NH_4)_2SO_4$[409] increases the yields of products **169–178**[312].

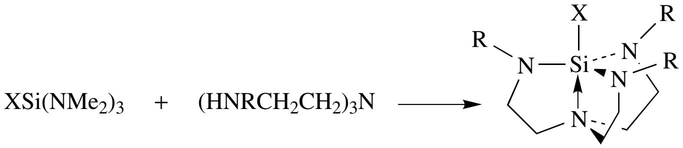

(174)

	X	R	Yield (%)	Reference
(169)	H	H	72–84	408a, 409
(170)	H	Me	54	409
(171)	H	Me_3Si	61	409
(172)	Me	H	∼100	408a
(173)	Et	H	∼100	408a
(174)	Vin	H	∼100	408a
(175)	Ph	H	∼100	408a,b
(176)	EtO	H	84	409
(177)	EtO	Me	58	409
(178)	PhO	H	34	409

This approach is unsuitable for the preparation of 1-chlorotriazasilatrane due to the formation of polymeric mixtures[409]. However, 1-hydrotriazasilatrane **(169)** can be converted into the 1-chloro derivative **179** by treatment with CCl_4 (equation 175)[312,409]. Considerable lowering of the yield and increase in the reaction rate are observed in the presence of a catalytic amount of a bis(phosphine)platinum or -palladium dichloride[312,409].

169 or **170**

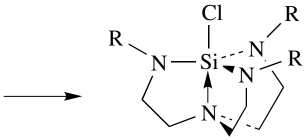

(175)

169/179: R = H
170/180: R = Me

(179, 180)

A similar type of transformation of 1-hydro-2,8,9-trimethyl-2,8,9-triazasilatrane **(170)** occurs by using *N*-chlorosuccinimide as a chlorinating agent (equation 175)[312].

Triazasilatranes **179** and **180** react with various nucleophiles such as organometallic reagents (equation 176), metal alkoxides (equation 177) and amides (equations 178 and 179) to give the substitution products **172**, **181–184** as well as hydride transfer products **169**, **170** . The relative ratios of these products depend on stereoelectronic factors, the nature of the nucleophilic reagents and the reaction conditions[312]. Thus, the reaction of triazasilatrane **180** with *n*-butyllithium affords **181a**, which is the product of substitution, while only 1-hydrotriazasilatrane **(170)** is formed from **180** and *tert*-butyllithium in a hydride transfer process.

179 or **180** + R′Li

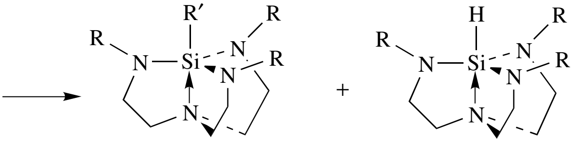

(172, 181–184) R = H
(172a, 181a–184a) R = Me

(169, 170)

(176)

	R′	Yield (%)		R′	Yield (%)
(172)	Me	26	**(172a)**	Me	0
(181)	*n*-Bu	14	**(181a)**	*n*-Bu	95
(182)	*s*-Bu	<10	**(182a)**	*s*-Bu	0
(183)	*t*-Bu	<10	**(183a)**	*t*-Bu	0
(184)	Ph	<10	**(184a)**	Ph	96

179 or **180** + R′OM

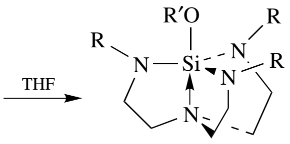

(177)

R′	R	M	Yield (%)
Me	H	Na	85
Me	Me	Na	85
Et	Me	Na	81
i-Pr	Me	Li	80
t-Bu	Me	Li	86

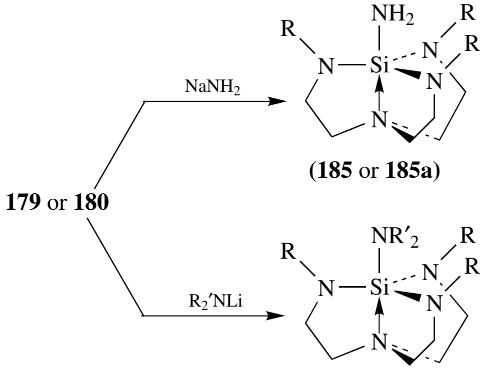

(178)

(185 or 185a)

(179)

(186 – 189) R = H
(186a – 189a) R = Me

	R′	Yield (%)		R′	Yield (%)
(186)	Me	60	**(186a)**	Me	41
(187)	Et	19	**(187a)**	Et	25
(188)	*i*-Pr	0	**(188a)**	*i*-Pr	30
(189)	Me$_3$Si	50	**(189a)**	Me$_3$Si	88

It should be noted that similar nucleophilic chloride substitution reactions in the tetracoordinate compound ClSi(NMe$_2$)$_3$ occur only at higher temperatures over prolonged reaction times[312].

In contrast to **179**, the reaction of **180** with C$_6$F$_5$Li affords not only the expected compound **190**, but also the fluoride transfer product **191** and the tetrafluorobenzene insertion product **192** in 1 : 2 : 1 ratio (equation 180)[312].

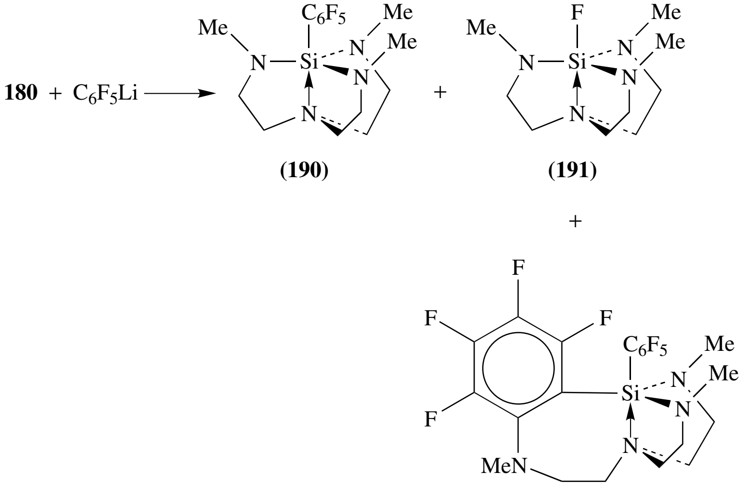

(190)

(191)

(180)

(192)

Silylation of the NH groups of triazasilatranes is effected by chlorosilanes in a benzene solution in the presence of Et_3N as an HCl acceptor[409,410]. The degree of substitution depends on the nature of the triazasilatrane and the chlorosilane (equation 181). In most cases disubstitution is the main process.

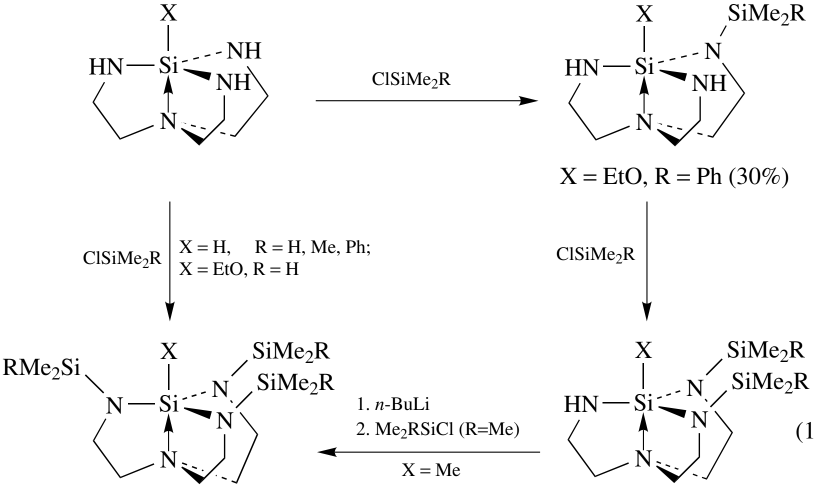

(181)

X	R	Yield (%)
Me	Me	
EtO	Me	74
EtO	Ph	45

The reaction of 1-ethoxytriazasilatrane **(193)** with diphenylchlorophosphine leads to N,N′-bis(diphenylphosphino)triazasilatrane **(195)** via the spectroscopically detected monosubstituted intermediate **194** (equation 182)[411].

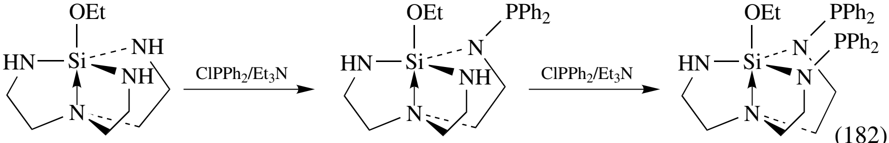

(193) **(194)** **(195)** (182)

Triazasilatrane **195** behaves as a bidentate (P,P′) or a tridentate (P,P′,O) ligand to form chelate complexes with transition metal compounds[411]. On reaction with sulfur or methyl iodide, compound **195** is converted into the corresponding derivatives **196** and **197** (equations 183 and 184)[411].

The greatly increased steric repulsion between the axial and the bulky equatorial groups in trisilylated 1-methyltriazasilatrane **(198)** leads to a significant weakening of the transannular Si←N bond. The $Si-N_{ax}$ distance in **198** is the longest ever recorded in a triazasilatrane (2.775 Å)[410]. It makes the N_{ax} atom sufficiently basic to react with CF_3SO_3Me, forming the cationic species **199** in which the silicon atom is tetracoordinated

(equation 185)[410].

(195)

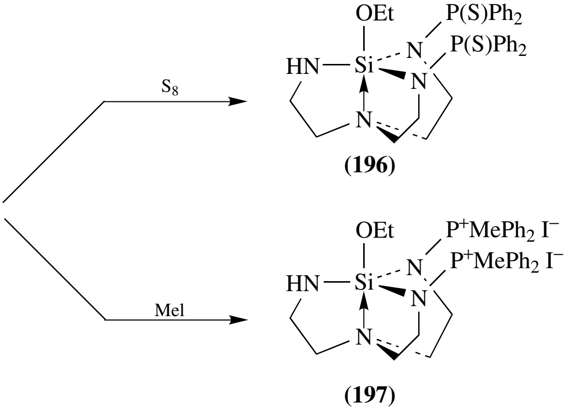

(196)

(197)

(183)

(184)

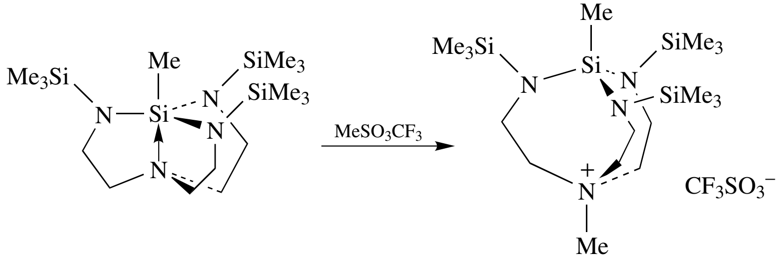

(198) **(199)**

(185)

It seemed tempting to involve the N_{eq} atom in triazasilatranes in the quaternization reactions owing to its greater basicity compared with that of O_{eq} in silatranes. However, protonation of 1-hydrotriazasilatrane **(169)** by CF_3SO_3H or strong electrophiles such as CF_3SO_3Me or $CF_3SO_3SiMe_3$ results in cleavage of the atrane cage[412]. The successful synthesis of **200** and **201** the first stable models of incipient proton-assisted equatorial bond cleavage of five-coordinate intermediates was carried out by the following procedure. Nucleophilic attack of N_{eq} of the triazasilatrane on the silicon of the weakly electrophilic Me_3SiN_3 or Me_3SiSCN affords silylated products **171**, **202** and **203** and free acids, HN_3 or HSCN, respectively. The latter acids form with **169** the salts **200** and **201**, containing equatorially protonated cations (equation 186)[412,413].

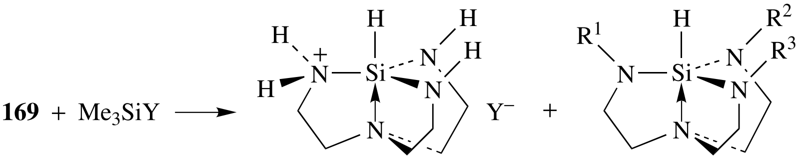

(186)

(200) Y = N_3
(201) Y = SCN

(171) $R^1 = R^2 = R^3 = SiMe_3$
(202) $R^1 = H$, $R^2 = R^3 = SiMe_3$
(203) $R^1 = R^2 = H$, $R^3 = SiMe_3$

Presumably, the Si−H bond in the cationic species points toward one of the ammonium protons, thus favoring an easy hydrogen elimination by their thermolysis (equation 187)[413].

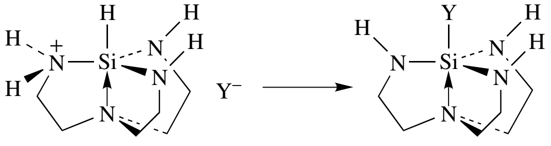

(200) Y = N_3 **(204)** Y = N_3

(201) Y = SCN **(205)** Y = SCN

(187)

Triazasilatranes are hydrolytically less stable than silatranes[408a,414]. However, it is of interest that 1-aminotriazasilatrane **(185)** is stable to solvolysis by EtOH in C_6D_6 at room temperature[312]. Methanolysis of triazasilatranes **169**, **172** and **176** at room temperature does not proceed by an initial displacement of an axial substituent but by attack on the tricyclic structure to afford tris(2-aminoethyl)amine and the corresponding trimethoxysilanes (equation 188)[414].

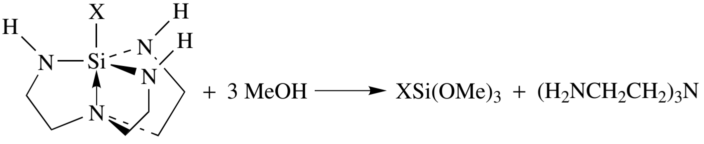

(188)

(169) X = H

(172) X = Me

(176) X = EtO

The rate and pathway of the methanolysis appear to depend strongly on the steric and electronic effects of the equatorial substituents. Because of the steric hindrance at the pentacoordinate silicon induced by N_{eq} substitution in N-silylated triazasilatranes, nucleophiles can attack their four-coordinate silicon atoms (equation 189)[414].

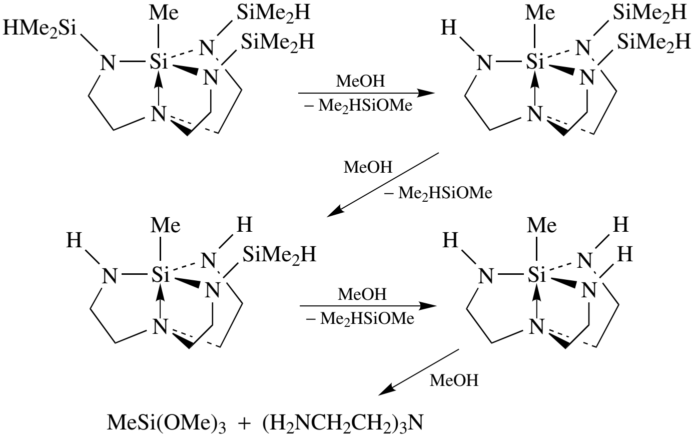

(189)

On the other hand, the greatly weakened transannular bond in trisilylated 1-methyltriazasilatrane derivative **198** makes quite comparable solvolytic reactivity of the endocyclic and exocyclic $N_{eq}{-}Si$ bonds. In this case cleavage of the cage structure can proceed by solvolytic displacement of the exocyclic silyl substituent, so that monocyclic intermediates **206** and **207** were observed in the stepwise opening of the tricyclic structure (equation 190)[414].

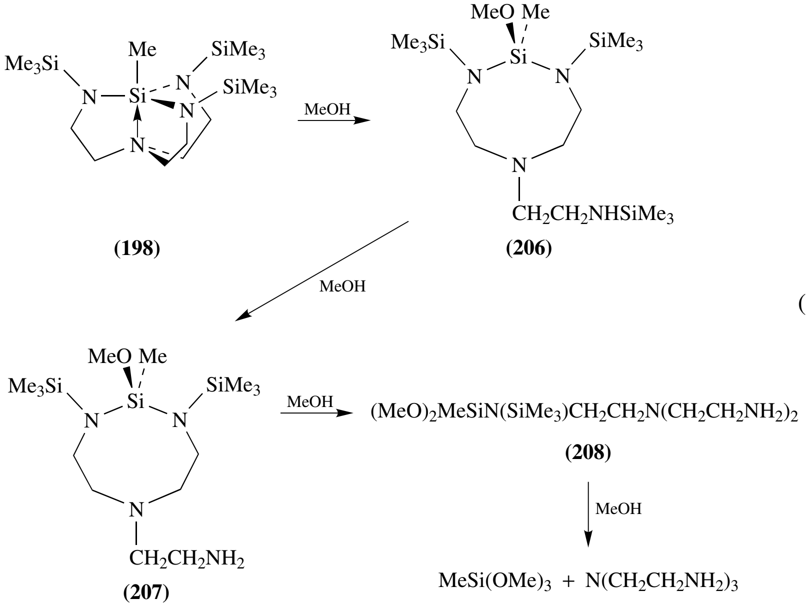

(190)

The reaction of 1-methyltriazasilatrane **(172)** with triethanolamine results in the formation of 1-methylsilatrane **(2)** (equation 191)[415].

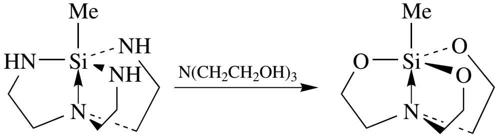

(172) **(2)**

(191)

1-Hydrotriazasilatrane **(169)** easily undergoes dehydrocyclodimerization to give the dehydrocyclodimer **209** in high yield, 77–95% (equation 192). The reaction can occur on heating to 200 °C or at a low temperature (−35 °C) in the presence of $NaNH_2$[416].

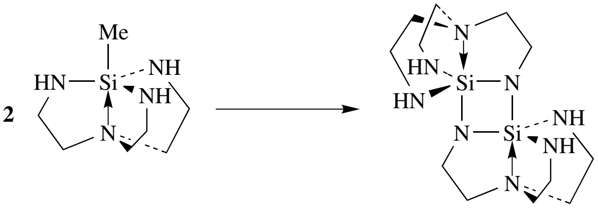

(169) **(209)**

(192)

TABLE 7. ^{29}Si and ^{15}N NMR chemical shifts of triazasilatranes $XSi(NHCH_2CH_2)_3N$ in $CDCl_3$[418]

X	$\delta(^{29}Si)$	$\Delta\delta(^{29}Si)$	$\delta(^{15}NC_3)$	$\delta(^{15}NH)$
H	−82.3	−47.5	−346.8	−350.1
Me	−68.3	−45.0	−354.5	−352.8
Vinyl	−79.2	−46.6	−352.8	−354.0
Ph	−77.2	−44.2	−352.2	−354.1

^{1}H and ^{29}Si NMR studies suggest a stronger Si←N bonding in triazasilatranes bearing the unsubstituted N_{eq} atoms than in silatranes[408a,417]. Similar to other compounds of pentacoordinate silicon, these triazasilatranes are characterized by a higher shielding of the ^{29}Si nuclei than that in the model compounds of tetracoordinate silicon, $XSi(NHPr)_3$. The corresponding ^{29}Si NMR coordination shift $\Delta\delta(^{29}Si)$ is almost twice as large as that in silatranes and is close to −46 ppm (Table 7). As in the spectra of silatranes, the ^{15}N NMR signals for the apical cage nitrogen are shifted downfield on increasing the acceptor ability of the substituent X, i.e. on strengthening the Si←N bond[418].

Reduction of the *s* character of the axial X−Si bond causes a decrease in the one-bond and two-bond $^{29}Si-^{1}H$ and $^{29}Si-^{13}C$ coupling in triazasilatranes relative to the model compounds[417,418]. In the IR spectra the ν(SiH) frequency of 1-hydrotriazasilatrane **(169)** is lower than that for $HSi(NHAlk)_3$ (2115 cm^{-1}). The solvent effect on ν(SiH) in the IR spectra of **169** is weaker than for 1-hydrosilatrane. The $^1J(^{29}Si^1H)$ and ν(SiH) values decrease with increasing solvent polarity as shown below[418].

Solvent	C_6D_{12}	$CDCl_3$	CD_3COCD_3	DMSO-d_6	Nujol
$^1J(^{29}Si^1H)$ (Hz)	178.4	176.6	175.1	171.6	
ν(SiH) (cm^{-1})	1995	1995	1988	1980	1980

Apparently, this is a result of lengthening of the Si−H bond upon strengthening of the Si←N bond in polar media.

As a rule, the ^{29}Si shielding in 2,8,9-triazasilatranes decreases with substitution of the hydrogen on the equatorial NH functions by Me[312], SiR_3[414] or PPh_2[411] groups. For 1-diethylamino-2,8,9-trimethyltriazasilatrane, the ^{29}Si shielding falls about 38 ppm[312]. In the 2,8,9-tris-TMS derivative of 1-hydrotriazasilatrane the corresponding downfield ^{29}Si chemical shift is about 13 ppm, whereas in 1-ethoxytriazasilatrane bearing three Me_2HSi groups at the N_{eq} atoms this shift is 24 ppm[414]. This indicates a strong weakening of the Si←N bond owing to steric crowding by bulky substituents attached to both the silicon and the equatorial nitrogen atoms[312,409,411,414]. However, 2,8,9-trimethyltriazasilatranes, $XSi(NMeCH_2CH_2)_3N$, with relatively small electronegative groups X (Cl, MeO, H_2N and Me) are characterized by upfield shifts relative to their unsubstituted analogs[312]. This phenomenon was explained by stretching of the X−Si bond and hence strengthening of the Si←N bond upon steric congestion.

Investigations carried out by Verkade and coworkers show that the ^{29}Si shielding of most 1-substituted triazasilatranes are sensitive to the phase and temperature[312,409,411,414]. In this respect triazasilatranes resemble silatranes. *Ab initio* calculations predict that the differences between the gas phase and the solution or solid state geometries of triazasilatranes should be rather less than in the case of silatranes[194].The lower sensitivity of

TABLE 8. Si←N bond distances in triazasilatranes 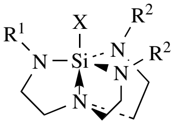 , and their salts

Compound	X	R^1	R^2	d(SiN) (Å)	Reference
169	H	H	H	2.109	409
169 (in **210**)	H	H	H	2.080	412
200 (in **210**)	H	H, H^+	H	2.087	412
201a	H	H, H^+	Me_3Si	2.062	413
198	Me	Me_3Si	Me_3Si	2.775	410
175	Ph	H	H	2.132	408b
209	(N)	(Si)	H	2.139	416
177	EtO	Me	Me	2.135	409
196	EtO	H	$Ph_2P(S)$	2.214	411
191	F	Me	Me	2.034	312

the triazasilatrane structure to the physical environment could be explained by a stronger Si←N bonding and lower polarity of the molecules. The optimized length of the Si←N bond in triazasilatranes was found to be much shorter (by 0.3 Å) than in related silatranes. The dipole moments of triazasilatranes (3–4 D) are considerably lower than those of silatranes[408a].

Available X-ray data demonstrate great changes in the Si←N bond distance, d(SiN), in triazasilatranes on variation in the electronic and steric effects of the substituents at the silicon and equatorial nitrogens (Table 8). The shortest Si←N bond was found to be in 1-fluoro-2,8,9-trimethyltriazasilatrane **(191)**, possessing the very electronegative fluorine at the silicon atom. Lengthening of this bond in **196** as compared with **177** and an extremely long Si←N bond distance in **198** reveal a strong destabilizing repulsion between the substituents at Si and N_{eq} on the transannular bonding. A comparison of the d(SiN) values in 1-hydrotriazasilatrane **(169)** and in salt **201a** confirms the expectation from the 3c4e bonding model of strengthening the Si←N bond upon protonation of an equatorial nitrogen. An opposite relation between the corresponding bond lengths in the parent molecule **169** and cation **200** was observed for compound **210**, formed when **169** and **200** were cocrystallized. This could be explained by the differences in the packing of the lattices of **169**, **201a** and **210**.

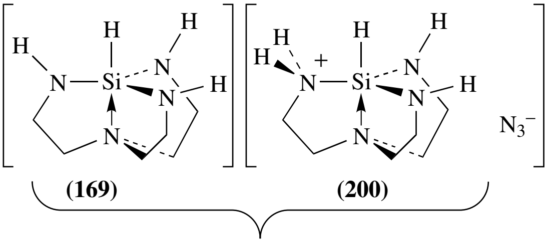

(210)

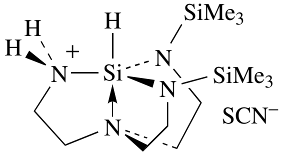

(201a)

Data listed in Tables 1 and 7 show that the Si←N bond lengths in triazasilatranes with $R^1 = R^2 =$ H or Me are nearly the same, or just shorter than in the related silatrane. At the same time, the X−Si bonds in the former compounds are definitely longer than in silatranes. For triazasilatranes **175**, **177** and **191**, the corresponding elongations are 0.02−0.04 Å. Consequently, it is difficult to judge from these facts in which class of the compared compounds the total energy of the hypervalent (3c4e) X−Si←N bond is higher. The 3c4e bonding model predicts that this bond should be stronger in silatranes, where the silicon atom is surrounded by more electronegative equatorial substituents[12,28,174].

The value of the inductive substituent constant σ_I for the triazasilatranyl group (−0.38) was estimated from ^{13}C NMR data for 1-phenyltriazasilatrane[418] and indicates that the triazasilatranyl group is a stronger electron-releasing substituent compared with $Si(NMe_2)_3$ or $Si(OEt)_3$ groups ($\sigma_I = -0.03$[418] and −0.13[249], respectively). However, the donor ability of the triazasilatranyl group is lower than that of the silatranyl group ($\sigma_I = -0.54$[13,20,249]).

Mass spectra measured under EI conditions were shown to reflect the expected order of X−Si energy in triazasilatranes: F−Si > O−Si > N−Si > C−Si[312]. For the 1-alkyl derivatives, the cage cation moiety is generally the base peak.

F. Miscellaneous

There are some kinds of silatrane analogs whose chemistry and structure were not studied enough. Some data concerning their preparation and properties are discussed below.

The reaction of phenyltris(dimethylamino)silane with bis(2-hydroxyethyl)(2-aminoethyl)amine affords 1-phenyl-2-azasilatrane **(210)** in a small yield (equation 193)[291]. The compound is very unstable to moisture.

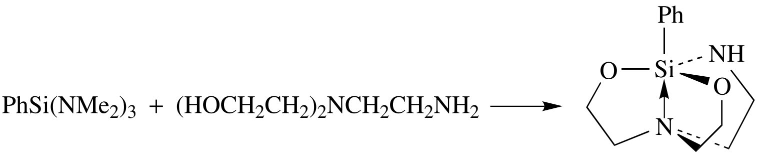
$PhSi(NMe_2)_3 + (HOCH_2CH_2)_2NCH_2CH_2NH_2 \longrightarrow$

(193)

(210)

Characteristic features of the FAB spectrum of **210** resemble those mentioned for silatranes[291]. However, in **210** only the nitrogen-containing half-cycle is destroyed to form ions $[MH - CH_2NH]^+$ with m/z 222 and $[MH - C_2H_2NH]^+$ with m/z 208.

1-Methyl-2-azasilatran-3-ones **(211a** and **211b)** are prepared from methyltrichlorosilane and silylated derivatives of amides of *N*,*N*-bis(2-hydroxyethyl)aminoacetic acid (equation 194)[419].

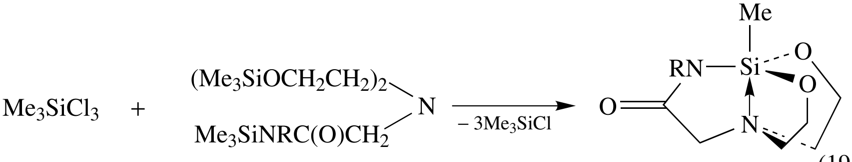

(194)

(211a) R = H (70%)
(211b) R = Me (80%)

The reactions of 1,2,2-trifunctional disilanes with triethanolamine, using the 'Dilution principle', result in the formation of compounds **212–214** (equation 195)[420] which are the silyl analogs of 2-carba-3-oxahomosilatranes **(94)**.

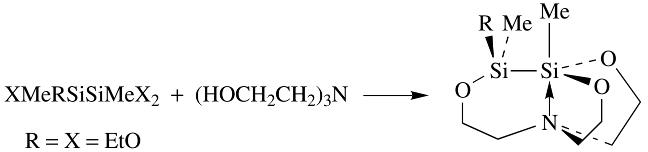

$XMeRSiSiMeX_2 + (HOCH_2CH_2)_3N \longrightarrow$ (195)

$R = X = EtO$
$R = Me,\ X = Me_2N$
$R = Ph,\ X = Me_2N$

(212) $R = EtO$
(213) $R = Me$
(214) $R = Ph$

The structures of these compounds were determined by ^1H NMR spectroscopy and X-ray diffraction. They demonstrate the preference of five- over six-membered chelating rings. The length of the Si←N bond in **213** is 2.768 Å[420].

1-Substituted 2,8,9-trithiasilatranes can be synthesized by the reactions of tris(2-mercaptoethyl)amine with tris(diethylamino)silane derivatives. Examples are given in equation 196[27,421] and equation 197[422].

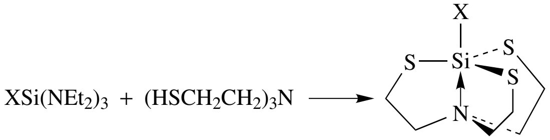

$XSi(NEt_2)_3 + (HSCH_2CH_2)_3N \longrightarrow$ (196)

$X = H, Me, Ph, EtO$

$$\begin{array}{l} Si(NEt_2)_4 + (HSCH_2CH_2)_3N \xrightarrow{THF} Et_2NSi(SCH_2CH_2)_3N \xrightarrow{X-H} XSi(SCH_2CH_2)_3N \\ \qquad\qquad\qquad\qquad\qquad\qquad\qquad\qquad\qquad\qquad\qquad \downarrow HCl \\ \qquad\qquad\qquad\qquad\qquad\qquad\qquad\qquad\qquad\qquad XSi(SCH_2CH_2)_3N{\cdot}HCl \end{array} \tag{197}$$

$X = HCl{\cdot}H_2NCH_2CH_2S$ (55%), $2HCl{\cdot}H_2N(CH_2)_3NHCH_2CH_2S$ (68%)

Pentacoordination of the silicon atom in some 2,8,9-trithiasilatranes was proved by ^{29}Si NMR spectroscopy[27].

IV. ACKNOWLEDGMENTS

The authors wish to thank all our colleagues who have been involved in the chemistry of silatranes and whose names have been cited in the text. We are indebted to Elena Belogolova, Yuri Danilevich, Gennadij Dolgushin, Natal'ya Lazareva, Antonina Pestunovich, Elena Petrova and Nina Semenova for assistance with the preparation of the manuscript. We are also grateful to the RFBR for a grant (96-03-32718).

V. REFERENCES

1. C. L. Frye, G. E. Vogel and J. A. Hall, *J. Am. Chem. Soc.*, **83,** 996 (1961).
2. M. G. Voronkov, *Pure Appl. Chem.*, **13**, 35 (1966).
3. J. W. Turley and F. P. Boer, *J. Am. Chem. Soc.*, **90**, 4026 (1968).

4. (a) M. G. Voronkov, G. I. Zelchan and E. Ya. Lukevit. *Kremnij and Zhizn'*, Zinatne, Riga, 1971.
(b) M. G. Voronkov, G. I. Zelcian and E. Ya. Lukevit, *Siliciul si Viata*, Editura Stiintifica, Bucuresti, 1974.
(c) M. G. Voronkov, G. I. Zelchan and E. Lukevitz, *Silicium und Leben*, Akademie-Verlag, Berlin, 1975.
5. M. G. Voronkov and V. M. Dyakov, *Silatrany*, Nauka, Novosibirsk, 1978.
6. I. S. Birgele, A. A. Kemme, E. L. Kupcè, E. E. Liepins, I. B. Mazeika and V. D. Shatz, *Kremnijorganicheskie Proizvodnye aminospirtov* (Ed. E. Lukevics), Zinatne, Riga, 1987.
7. (a) E. Lukevics, O. A. Pudova and R. Sturkovich, *Molekulyarnaya Struktura Kremnijorganicheskikh Soedinenij*, Zinatne, Riga, 1988.
(b) E. Lukevics, O. A. Pudova and R. Sturkovich, *Molecular Structure of Organosilicon Compounds*, Ellis Horwood, Chichester, 1989.
8. M. G. Voronkov, *Pure Appl. Chem.*, **19**, 399 (1969).
9. M. G. Voronkov, in *XXIVth International Congress of Pure and Applied Chemistry*, Butterworths, London, **4**, 45 (1973).
10. M. G. Voronkov, in *Biochemistry of Silicon and Related Problems* (Eds. G. Bendz and I. Lundqvist), Plenum Press, New York–London, 1978, pp. 395–433.
11. M. G. Voronkov, *Top. Curr. Chem.*, **84**, 77 (1979).
12. V. F. Sidorkin, V. A. Pestunovich and M. G. Voronkov, *Usp. Khim.*, **49**, 789 (1980); *Russ. Chem. Rev. (Engl. Transl.)*, **49**, 414 (1980).
13. M. G. Voronkov, V. M. Dyakov and S. V. Kirpichenko, *J. Organomet. Chem.*, **233**, 1 (1982).
14. P. Hencsei and L. Parkanyi, *Kém. Közl.*, **61**, 319 (1984); *Chem. Abstr.*, **103**, 105019m (1985).
15. P. Hencsei and L. Parkanyi, *Rev. Silicon, Germanium, Tin, Lead Compd.*, **8**, 191 (1985).
16. M. G. Voronkov, V. P. Baryshok, L. P. Petukhov, V. I. Rakhlin, R. G. Mirskov and V. A. Pestunovich, *J. Organomet. Chem.*, **358**, 39 (1988).
17. A. Greenberg and G. Wu, *Struct. Chem.*, **1**, 79 (1990).
18. P. Hencsei, *Struct. Chem.*, **2**, 21 (1991).
19. L. Parkanyi, P. Hencsei and L. Nyulaszi, *J. Mol. Struct.*, **377**, 37 (1996).
20. S. N. Tandura, M. G. Voronkov and N. V. Alekseev, *Top. Curr. Chem.*, **131**, 99 (1986).
21. V. E. Shklover, Yu. T. Struchkov and M. G. Voronkov, *Main Group Metal Chem.*, **11**, 109 (1988).
22. V. E. Shklover, Yu. T. Struchkov and M. G. Voronkov, *Usp. Khim.*, **58**, 353 (1989); *Russ. Chem. Rev. (Engl. Transl.)*, **58**, 211 (1989).
23. R. J. P. Corriu, *J. Organomet. Chem.*, **400**, 81 (1990).
24. M. G. Voronkov, *Izv. Akad. Nauk SSSR, Ser. Khim.*, 2664 (1991); *Bull. Acad. Sci. USSR, Div. Chem. Sci. (Engl. Transl).*, **40**, 2319 (1991).
25. C. Chuit, R. J. P. Corriu, C. Reye and J. C. Young, *Chem. Rev.*, **93**, 1371 (1993).
26. J. G. Verkade, *Acc. Chem. Res.*, **26**, 483 (1993).
27. J. G. Verkade, *Coord. Chem. Rev.*, **137**, 233 (1994).
28. V. A. Pestunovich, V. F. Sidorkin and M. G. Voronkov, in *Progress in Organosilicon Chemistry* (Eds. B. Marciniec and J. Chojnowski). Gordon and Breach, New York., 1995, pp. 9–82.
29. E. Lukevics and O. A. Pudova, *Khim. Geterotsikl. Soed.*, 1605 (1996); *Chem. Heterocycl. Compd. (Eng. Transl.)*, **32**, 1381 (1996).
30. W. S. Sheldrick, in *The Chemistry of Organic Silicon Compounds*, Part 1 (Eds. S. Patai and Z. Rappoport), Wiley, Chichester, 1989, pp. 227–303.
31. R. J. P. Corriu and J. C. Young, in *The Chemistry of Organic Silicon Compounds*, Part 2 (Eds. S. Patai and Z. Rappoport), Wiley, Chichester, 1989, pp. 1241–1288.
32. A. B. Finestone, US Patent 2953545 (Westinghouse Electric Corp.), 1960; *Chem. Abstr.*, **55**, 4045i (1961).
33. P. Hencsei, L. Bihatsi, I. Kovacz, E. Szalay, E. B. Karsai, A. Szollosy and M. Gal, *Acta Chim. Acad. Sci. Hung.*, **112**, 261 (1983).
34. S. N. Gurkova, A. I. Gusev, N. V. Alekseev and M. A. Ignatenko, *Zh. Strukt. Khim.*, **29 (2)**, 203 (1988); *J. Struct. Chem. (Engl. Transl.)*, **29**, 345 (1988).
35. S. N. Gurkova, A. I. Gusev, N. V. Alekseev and M. A. Ignatenko, *Metalloorg. Khim.*, **1**, 1251 (1988); *Organomet. Chem. USSR (Engl. Transl.)*, **1**, 684 (1988).
36. K. V. Pavlov, N. A. Viktorov and V. F. Mironov, *Izv. Akad. Nauk, Ser. Khim.*, 756 (1993); *Russ. Chem. Bull. (Engl. Transl.)*, **42**, 723 (1993).
37. G. S. Zaitseva, S. S. Karlov, A. V. Churakov, E. V. Avtomonov, J. Lorberth and D. Hertel, *J. Organomet Chem.*, **523**, 221 (1996).

38. M. G. Voronkov, O. G. Yarosh, L. V. Shchukina, E. O. Tsetlina, S. N. Tandura and I. M. Korotaeva, *Zh. Obshch. Khim.*, **49**, 614 (1979); *Chem. Abstr.*, **91**, 39563q (1979).
39. G. Cereveau, C. Chuit, R. J. P. Corriu and C. Reye, *J. Organomet. Chem.*, **328**, C17 (1987).
40. M. G. Voronkov, O. G. Yarosh, Z. G. Ivanova, V. K. Roman and A. I. Albanov, *Izv. Akad. Nauk. SSSR, Ser. Khim.*, 1403 (1987); *Bull. Acad. Sci. USSR, Div. Chem. Sci. (Engl. Transl.)*, **36**, 1297 (1987).
41. M. G. Voronkov, O. G. Yarosh, L. V. Shchukina and E. E. Kuznetsova, *Izv. Akad. Nauk SSSR, Ser. Khim.*, 2611 (1984); *Bull. Acad. Sci. USSR, Div. Chem. Sci. (Engl. Transl.)*, **33**, 2391 (1984).
42. L. Parkanyi, P. Hencsei and L. Bihatsi, *J. Organomet. Chem.*, **232**, 315 (1982).
43. L. Bihatsi and P. Hencsei, *Magy. Kem. Foly.*, **87**, 137 (1981); *Chem. Abstr.*, **95**, 169078d (1981).
44. F. Carre, G. Cerveau, C. Chuit, R. J. P. Corriu, N. K. Nayyar and C. Reye, *Organometallics*, **9**, 1989 (1990).
45. L. Birkofer and K. Grafen, *J. Organomet. Chem.*, **299**, 143 (1986).
46. Yu. E. Ovchinnikov, T. G. Kovyazina, V. E. Shklover, Yu. T. Struchkov, V. M. Kopylov and M. G. Voronkov, *Dokl. Akad. Nauk SSSR*, **297**, 108 (1987); *Dokl. Chem. (Engl. Transl.)*, **297**, 474 (1987).
47. T. K. Gar, N. Yu. Khromova, V. M. Nosova and V. F. Mironov, *Zh. Obshch. Khim.*, **50**, 1764 (1980); *J. Gen. Chem. USSR (Engl. Transl.)*, **50**, 1433 (1980).
48. (a) V. Gevorgyan, L. Borisova and E. Lukevics, *J. Organomet. Chem.*, **418**, C21 (1991).
    (b) V. Gevorgyan, L. Borisova, A. Vjater, J. Popelis, S. Belyakov and E. Lukevics, *J. Organomet. Chem.*, **482**, 73 (1994).
49. E. Lukevics, O. A. Pudova, J. Popelis and N. P. Erchak, *Zh. Obshch. Khim.*, **51**, 369 (1981); *J. Gen. Chem. USSR (Engl. Transl.)*, **51**, 300 (1981).
50. E. Lukevics and M. M. Ignatovich, *Khim. Geterotsikl. Soed.*, 725 (1992); *Chem. Heterocycl. Compd. (Engl. Transl.),* **28**, 603 (1992).
51. E. Lukevics, V. Dirnens, A. Kemme and J. Popelis, *J. Organomet. Chem.*, **521**, 235 (1996).
52. E. Lukevics, G. Zelchans, T. J. Barton, A. Lapsina and I. Judeika, *Latv. PSR Zina. Akad. Vestis, Khim. Ser.*, 747 (1978); *Chem. Abstr.*, **90**, 137894x (1979).
53. C. M. Samour, US Patent 3118921 (Kendall Co.), 1964; *Chem. Abstr.*, **60**, 10715h (1964).
54. A. Daneshrad, C. Eaborn and D. R. M. Walton, *J. Organomet. Chem.*, **85**, 35 (1975).
55. I. Kovacs, L. Bihatsi and P. Hencsei, *Magy. Kem. Lapja*, **40**, 562 (1985); *Chem. Abstr.*, **106**, 18660g (1987).
56. M. G. Voronkov, V. M. D'yakov, O. N. Florensova, V. P. Baryshok, I. G. Kuznetsov and V. Chvalovsky, *Collect. Czech. Chem. Commun.*, **42**, 480 (1977).
57. M. G. Voronkov, V. P. Baryshok, S. N. Tandura, V. Yu. Vitkovskii, V. M. D'yakov and V. A. Pestunovich, *Zh. Obshch. Khim.*, **48**, 2238 (1978); *Chem. Abstr.*, **90**, 104051s (1979).
58. (a) C. L. Frye and R. D. Streu, *Main Group Metal. Chem.*, **16**, 211 (1993).
    (b) C. L. Frye and R. D. Streu, *Main Group Metal. Chem.*, **16**, 217 (1993).
59. V. P. Baryshok, S. N. Tandura, G. A. Kuznetsova and M. G. Voronkov, *Metalloorg. Khim.*, **4**, 1150 (1991); *Organomet. Chem. USSR (Engl. Transl.)*, **4**, 568 (1991).
60. Y. Yang and C. Yin, *Gaodeng Xuexiao Huaxue Xuebo*, **7**, 430 (1986); *Chem. Abstr.*, **107**, 217703u (1987).
61. M. Tasaka, M. Hirotsu, M. Kojima, S. Utsuno and Y. Yoshikawa, *Inorg. Chem.*, **35**, 6981 (1996).
62. M. G. Voronkov, V. P. Baryshok and G. A. Kuznetsova, *Zh. Obshch. Khim.*, **66**, 1943 (1996); *Russ. J. Gen. Chem.*, **66**, 1889 (1996).
63. P. Hencsei and L. Bihatsi, *Period. Polytech., Chem. Eng.*, **26**, 35 (1982); *Chem. Abstr.*, **97**, 38992r (1982).
64. M. G. Voronkov and G. I. Zelchans, *Khim. Geterotsikl. Soed.*, 210 (1965); *Chem. Abstr.*, **63**, 9936b (1965).
65. M. G. Voronkov, I. B. Mazeika and G. I. Zelchans, *Khim. Geterotsikl. Soed.*, 58 (1965); *Chem. Abstr.*, **63**, 5506e (1965).
66. M. G. Voronkov and G. I. Zelchans, *Khim. Geterotsikl. Soed.*, 511 (1966); *Chem. Abstr.*, **66**, 85780q (1967).
67. J. Satge, G. Rima, M. Fatome, H. Sentenac-Roumanou and C. Lion, *Eur. J. Med. Chem.*, **24**, 48 (1989).
68. S. P. Narula, R. Shankar, M. Kumar, R. K. Vhandra and C. Janaik, *Inorg. Chem.*, **36**, 1268 (1997).
69. C. L. Frye, G. A. Vincent and W. A. Finzel, *J. Am. Chem. Soc.*, **93**, 6805 (1971).

70. M. G. Voronkov, V. M. D'yakov and V. P. Baryshok, *Zh. Obshch. Khim.*, **43**, 444 (1973); *Chem. Abstr.*, **79**, 5384u (1973).
71. M. G. Voronkov, V. M. D'yakov and L. I. Gubanova, *Izv. Akad. Nauk SSSR, Ser. Khim.*, 657 (1974); *Chem. Abstr.*, **81**, 13585s (1974).
72. M. G. Voronkov, V. M. D'yakov, Yu. A. Lukina, G. A. Samsonova and N. M. Kudyakov, *Izv. Akad. Nauk SSSR, Ser. Khim.*, 2794 (1974); *Chem. Abstr.*, **82**, 140247d (1975).
73. M. G. Voronkov, V. M. D'yakov and O. N. Florensova, *Zh. Obshch. Khim.*, **45**, 1902 (1975); *Chem. Abstr.*, **83**, 206365v (1975).
74. M. G. Voronkov, V. M. D'yakov, G. A. Samsonova, Yu. A. Lukina and N. M. Kudyakov, *Zh. Obshch. Khim.*, **45**, 2010 (1975); *Chem. Abstr.*, **84**, 17471m (1976).
75. M. G. Voronkov, V. M. D'yakov and V. P. Baryshok, *Zh. Obshch. Khim.*, **45**, 1650 (1975); *Chem. Abstr.*, **83**, 193426p (1975).
76. M. G. Voronkov, V. M. D'yakov and V. P. Baryshok, *Zh. Obshch. Khim.*, **47**, 797 (1977); *Chem. Abstr.*, **87**, 85075x (1977).
77. M. G. Voronkov, N. F. Lazareva, V. P. Baryshok, V. I. Dymchenko and N. A. Nedolya, *Izv. Akad. Nauk SSSR, Ser. Khim.*, 740 (1989); *Bull. Acad. Sci. USSR, Div. Chem. Sci. (Engl. Transl.)*, **38**, 666 (1989).
78. P. Hencsei, L. Parkanyi, V. Fulop, V. P. Baryshok, M. G. Voronkov and G. A. Kuznetsova, *J. Organomet. Chem.*, **346**, 315 (1988).
79. V. P. Baryshok, E. I. Brodskaya, N. F. Lazareva, G. A. Kuznetsova and M. G. Voronkov, *Metalloorg. Khim.*, **5**, 1136 (1992); *Organomet. Chem. USSR (Engl. Transl.)*, **5**, 555 (1992).
80. M. G. Voronkov, V. M. D'yakov, M. S. Sorokin, S. N. Tandura and N. F. Chernov, *Zh. Obshch. Khim.*, **45**, 1901 (1975); *Chem. Abstr.*, **83**, 206363t (1975).
81. M. G. Voronkov, N. F. Chernov, O. N. Florensova, V. P. Baryshok, E. E. Kuznetsova, T. I. Malkova, T. A. Pushechkina and L. I. Tokareva, *Zh. Obshch. Khim.*, **54**, 2017 (1984); *J. Gen. Chem. USSR (Engl. Transl.)*, **54**, 1800 (1984).
82. M. G. Voronkov, N. F. Chernov and E. O. Fedorova, *Zh. Org. Khim.*, **30**, 1263 (1994); *Russ. J. Org. Chem. (Engl. Transl.)*, **30**, 1328 (1994).
83. J. Wang, Q. Xie, R. Liao, J. Li and X. Lin, *Youji Huaxue*, 199 (1987); *Chem. Abstr.*, **108**, 150548x (1988).
84. M. G. Voronkov, V. M. D'yakov and L. I. Gubanova, *Zh. Obshch. Khim.*, **45**, 1905 (1975); *Chem. Abstr.*, **83**, 206369z (1975).
85. K. N. Grundy, J. D. Crabtree and A. E. Johnson, Brit. Patent 1243629 (Fiberglass Ltd.), 1968; South Afr. Patent 6806969, 1970; *Chem. Abstr.*, **73**, 121219u (1970).
86. M. G. Voronkov, M. S. Sorokin, V. M. D'yakov, F. P. Kletsko and N. N. Vlasova, *Zh. Obshch. Khim.*, **45**, 1649 (1975); *Chem. Abstr.*, **83**, 179196g (1975).
87. M. G. Voronkov, M. S. Sorokin and V. M. D'yakov, *Zh. Obshch. Khim.*, **45**, 1904 (1975); *Chem. Abstr.*, **83**, 206368y (1975).
88. M. G. Voronkov, M. S. Sorokin and V. M. D'yakov, *Zh. Obshch. Khim.*, **49**, 605 (1979); *Chem. Abstr.*, **91**, 57093r (1979).
89. N. F. Chernov, S. V. Shilin, O. N. Florensova, E. O. Novikova and M. G. Voronkov, *Zh. Obshch. Khim.*, **62**, 1300 (1992); *J. Gen. Chem. USSR (Engl. Transl.)*, **62**, 1069 (1992).
90. M. G. Voronkov, M. S. Sorokin, F. P. Kletsko, V. M. D'yakov, N. N. Vlasova and S. N. Tandura, *Zh. Obshch. Khim.*, **45**, 1395 (1975); *Chem. Abstr.*, **83**, 131674y (1975).
91. M. G. Voronkov, M. S. Sorokin and V. M. D'yakov, *Zh. Obshch. Khim.*, **45**, 1394 (1975); *Chem. Abstr.*, **83**, 131673h (1975).
92. M. G. Voronkov and M. S. Sorokin, *Zh. Obshch. Khim.*, **56**, 1818 (1986); *J. Gen. Chem. USSR (Engl. Transl.)*, **56**, 1608 (1986).
93. M. G. Voronkov, V. P. Baryshok, N. F. Lazareva, V. V. Saraev, T. I. Vakul'skaya, P. Hencsei and I. Kovacs, *J. Organomet. Chem.*, **368**, 155 (1989).
94. V. D. Sheludyakov and N. S. Fedotov, *Andrianovskie Chteniya*, Abstracts, Moscow, 1995, p. 2.75.
95. J.-M. Lin, L. Fang and W.-T. Huang, *Synth. React. Inorg. Met.- Org. Chem.*, **25**, 1467 (1995).
96. E. J. Lukevics, L. I. Libert and M. G. Voronkov, *Latv. PSR Zinat. Akad. Vestis, Khim. Ser.*, 451 (1972); *Chem. Abstr.*, **77**, 152270r (1972).
97. J. Lukasiak, A. Radecky and Z. Jamrogiewicz, *Rocz. Chem.*, **47**, 1975 (1973); *Chem. Abstr.*, **80**, 83126w (1974).
98. E. Lukevics, R. Ya. Moskovich, E. Liepins and I. S. Yankovskaya, *Zh. Obshch. Khim.*, **46**, 604 (1976); *Chem. Abstr.*, **85**, 21526w (1976).

99. G. Wu, K. Lu and Y. Wu, *Huaxue Togbao, Chemistry*, 10 (1983); *Chem. Abstr.*, **99**, 105333h (1983).
100. N. F. Lazareva, V. P. Baryshok and M. G. Voronkov, *Izv. Akad. Nauk, Ser. Khim.*, 341 (1995); *Russ. Chem. Bull. (Engl. Transl.)*, **44**, 333 (1995).
101. K. Lu and T. Wang, *Huaxue Togbao, Chemistry*, 30 (1995); *Chem. Abstr.*, **124**, 87120q (1996).
102. M. G. Voronkov, A. E. Pestunovich, E. I. Kositsyna, B. Z. Shterenberg, T. A. Pushechkina and N. N. Vlasova, *Z. Chem.*, **23**, 248 (1983).
103. V. E. Shklover, Yu. E. Ovchinnikov, Yu. T. Struchkov, V. M. Kopylov, T. G. Kovyazina and M. G. Voronkov, *Dokl. Akad. Nauk SSSR*, **284**, 131 (1985); *Chem. Abstr.*, **105**, 226714j (1986).
104. Yu. E. Ovchinnikov, V. E. Shklover, Yu. T. Struchkov, V. M. Kopylov, T. G. Kovyazina and M. G. Voronkov, *Zh. Strukt. Khim.*, **27(2)**, 133 (1986); *J. Struct. Chem. (Engl. Transl.)*, **27**, 287 (1986).
105. M. G. Voronkov, V. P. Baryshok, N. F. Lazareva, G. A. Kuznetsova, E. I. Brodskaya, V. V. Belyaeva, A. I. Albanov and L. S. Romanenko, *Metalloorg. Khim.*, **5**, 1323 (1992); *Organomet. Chem. USSR (Engl. Transl.)*, **5**, 648 (1992).
106. E. P. Kramarova, A. G. Shipov and Yu. I. Baukov, *Zh. Obshch. Khim.*, **62**, 2559 (1992); *J. Gen. Chem. USSR (Engl. Transl.)*, **62**, 2113 (1992).
107. M. G. Voronkov, N. N. Vlasova and L. I. Belousova, *Zh. Obshch. Khim.*, **65**, 270 (1995); *Chem. Abstr.*, **123**, 228269p (1995).
108. M. G. Voronkov, N. M. Kudyakov and A. I. Albanov, *Zh. Obshch. Khim.*, **56**, 1094 (1986); *J. Gen. Chem. USSR (Engl. Transl.)*, **56**, 962 (1986).
109. M. G. Voronkov, N. M. Kudyakov and A. I. Albanov, *Izv. Akad. Nauk SSSR, Ser. Khim.*, 1882 (1987); *Bull. Acad. Sci. USSR, Div. Chem. Sci. (Engl. Transl.)*, **36**, 1745 (1987).
110. R. Zhuo, Z.-R. Lu and J. Liao, *J. Organomet. Chem.*, **446**, 107 (1993).
111. Z.-R. Lu, R.-X. Zhuo, L.-R. Shen, X.-D. Zhang and L.-F. Shen, *J. Organomet. Chem.*, **489**, C38 (1995).
112. M. G. Voronkov, N. F. Chernov, O. M. Trofimova and T. N. Aksamentova, *Izv. Akad. Nauk, Ser. Khim.*, 1965 (1993); *Russ. Chem. Bull. (Engl. Transl.)*, **42**, 1883 (1993).
113. M. G. Voronkov, N. F. Chernov, O. M. Trofimova, Yu. E. Ovchinnikov, Yu. T. Struchkov and G. A. Gavrilova, *Izv. Akad. Nauk, Ser. Khim.*, 758 (1993); *Russ. Chem. Bull. (Engl. Transl.)*, **42**, 725 (1993).
114. M. G. Voronkov, V. P. Baryshok, N. F. Lazareva and G. G. Efremova, *Izv. Akad. Nauk, Ser. Khim.*, 384 (1995); *Russ Chem. Bull. (Engl. Transl.)*, **44**, 375 (1995).
115. J. W. Turley and F. P. Boer, *J. Am. Chem. Soc.*, **91**, 4129 (1969).
116. G. Wu and K. Lu, *Youji Huaxue, Org. Chem.*, 109 (1982); *Chem. Abstr.* **97**, 55882x (1982).
117. G. Wu, K. Lu and Y. Wu, in *Fundam. Res. Organomet. Chem., Proc. China–Japan–U.S. Trilateral Semin Organomet. Chem. Peking, June 1980* (Eds. M. Tsutsui, Y. I. Tshui and Y. Huang), van Nostrand Reinhold, New York, 1982, pp. 737–742; *Chem. Abstr.*, **98**, 4601t (1983).
118. M. Nasim, A. K. Saxena, I. P. Pal and L. M. Pande, *Synth. React. Inorg. Met.-Org. Chem.*, **17**, 1003 (1987).
119. M. Nasim, L. I. Livantsova, D. P. Krul'ko, G. S. Zaitseva, J. Lorberth and M. Otto, *J. Organomet. Chem.*, **402**, 313 (1991).
120. M. G. Voronkov, G. A. Kuznetsova and V. P. Baryshok, *Zh. Obshch. Khim.*, **53**, 1682 (1983); *J. Gen. Chem. USSR (Engl. Transl.)*, **53**, 1512 (1983).
121. S. N. Adamovich, V. Yu. Prokopyev, V. I. Rakhlin, R. G. Mirskov and M. G. Voronkov, *Synth. React. Inorg. Met.-Org. Chem.*, **21**, 1261 (1991).
122. M. G. Voronkov, V. M. D'yakov, E. E. Kuznetsova, O. N. Florensova, G. S. Dolgushina, G. V. Kozlova and V. B. Pukhnarevich, *Khim.-Pharm. Zh.*, **18**, 811 (1984); *Pharm. Chem. J. (Engl. Transl.)*, **18**, 467 (1984).
123. M. G. Voronkov, L. I. Gubanova, Yu. L. Frolov, N. F. Chernov, G. A. Gavrilova and N. N. Chipanina, *J. Organomet. Chem.*, **271**, 169 (1984).
124. E. Kupce, E. Liepins, A. Lapsina, I. Urtane, G. Zelchans and E. Lukevics, *J. Organomet. Chem.*, **279**, 343 (1985).
125. E. Lukevics, L. I. Libert and M. G. Voronkov, *Zh. Obshch. Khim.*, **38**, 1838 (1968); *Chem. Abstr.*, **70**, 11742q (1969).
126. H. Sakurai and A. Shirohata, Japan Kokai (Ajinomoto Co., Inc), 7831689, 1978; *Chem. Abstr.*, **89**, 43759j (1978).
127. G. I. Orlov, V. M. D'yakov, T. A. Tandura, E. F. Bugerenko and E. A. Chernyshov, *Zh. Obshch. Khim.*, **56**, 2653 (1986); *J. Gen. Chem. USSR (Engl. Transl.)*, **56**, 2349 (1986).

128. M. G. Voronkov and G. I. Zelchans, *Khim. Geterotsikl. Soed.*, 51 (1965); *Chem. Abstr.*, **63**, 5670d (1965).
129. G. I. Zelchans and M. G. Voronkov, *Khim. Geterotsikl. Soed.*, 371 (1967); *Chem. Abstr.*, **67**, 108112k (1967).
130. S. Cradock, E. A. V. Ebsworth and I. B. Muiry, *J. Chem. Soc., Dalton Trans.*, 25 (1975).
131. M. T. Attar-Bashi, C. Eaborn, J. Vencel and D. R. M. Walton, *J. Organomet. Chem.*, **117**, C87 (1976).
132. J. N. Dirk, J. M. Bellama and N. Ben-Zvi, *J. Organomet. Chem.*, **296**, 315 (1985).
133. I. P. Urtane, G. I. Zelchans, E. E. Liepin'sh, E. L. Kupche and E. Lukevits, *Zh. Obshch. Khim.*, **57**, 1110 (1987); *J. Gen. Chem. USSR (Engl. Transl.)*, **57**, 991 (1987).
134. M. G. Voronkov, V. P. Baryshok, G. A. Kuznetsova, V. Yu. Vitkovskii and A. G. Gorshkov, *Metalloorg. Khim.*, **3**, 181 (1990); *Organomet. Chem. USSR (Engl. Transl.)*, **3**, 99 (1990).
135. V. Gevorgyan, L. Borisova and E. Lukevics, *J. Organomet. Chem.*, **527**, 295 (1996).
136. P. Hencsei, Gy. Zsombok, L. Bihatsi and J. Nagy, *Period. Polytech., Chem. Eng.*, **23**, 185 (1979).
137. L. Párkányi, L. Bihatsi and P. Hencsei, *Cryst. Struct. Commun.*, **7**, 435 (1978).
138. P. Hencsey, L. Párkányi and I. Kovacs, *Khim. Geterotsikl. Soed.*, 1600 (1996); *Chem. Heterocycl. Compd.*, **32**, 1376 (1996).
139. P. Hencsei, I. Kovacs and V. Fülöp, *J. Organomet. Chem.*, **377**, 19 (1989).
140. A. A. Kemme, Ya. Ya. Bleidelis, V. M. D'yakov and M. G. Voronkov, *Izv. Akad. Nauk SSSR, Ser. Khim.*, 2400 (1976); *Chem. Abstr.*, **86**, 71739j (1977).
141. M. Nasim, V. S. Petrosyan, G. S. Zaitseva, J. Lorberth, S. Wocadlo and W. Massa, *J. Organomet. Chem.*, **441**, 27 (1992).
142. E. A. Zelbst, V. E. Shklover, Yu. T. Struchkov, A. A. Kashaev, M. P. Demidov, L. I. Gubanova and M. G. Voronkov, *Dokl. Akad. Nauk SSSR*, **260**, 107 (1981); *Dokl. Phys. Chem. (Engl. Transl.)*, **260**, 403 (1981).
143. A. A. Kemme, Ya. Ya. Bleidelis, V. M. D'yakov and M. G. Voronkov, *Zh. Strukt. Khim.*, **16**, 914 (1975); *Chem. Abstr.*, **84**, 82847c (1976).
144. V. E. Shklover, Yu. T. Struchkov, M. S. Sorokin and M. G. Voronkov, *Dokl. Akad. Nauk SSSR*, **274**, 615 (1984); *Dokl. Phys. Chem. (Engl. Transl.)*, **274**, 36 (1984).
145. M. P. Demidov, V. E. Shklover, Yu. L. Frolov, Yu. A. Lukina, V. M. D'yakov, Yu. T. Struchkov and M. G. Voronkov, *Zh. Strukt. Khim.*, **32(1)**, 177 (1991); *J. Struct. Chem. (Engl. Transl.)*, **32**, 154 (1991).
146. S. Wang and C. Hu, *K'o Hsueh T'ung Pao*, **26**, 603 (1981); *Chem. Abstr.*, **95**, 53095c (1981).
147. L. Párkányi, K. Simon and J. Nagy, *Acta Crystallogr.*, **30B**, 2328 (1974).
148. L. Párkányi, J. Nagy and K. Simon, *J. Organomet. Chem.*, **101**, 11 (1975).
149. L. Párkányi, P. Hencsei, L. Bihátsi, I. Kovacs and A. Szöllösy, *Polyhedron*, **4**, 243 (1985).
150. R. J. Garant, L. M. Daniels, S. K. Das, M. N. Janakiraman, R. A. Jacobson and J. G. Verkade, *J. Am. Chem. Soc.*, **113**, 5728 (1991).
151. A. A. Macharashvili, V. E. Shklover, Yu. T. Struchkov, V. P. Baryshok and M. G. Voronkov, *Dokl. Akad. Nauk SSSR*, **297**, 1123 (1987); *Chem. Abstr.*, **108**, 122284q (1988).
152. I. Kovacs, P. Hencsei and L. Párkányi, *Period. Polytech., Chem. Eng.*, **31**, 155 (1987).
153. M. W. Kim, D. S. Uh, S. Kim and Y. Do, *Inorg. Chem.*, **32**, 5883 (1993).
154. L. Párkányi, P. Hencsei, L. Bihátsi and T. Müller, *J. Organomet. Chem.*, **269**, 1 (1984).
155. A. A. Kemme, Ya. Ya. Bleidelis, V. A. Pestunovich, V. P. Baryshok and M. G. Voronkov, *Dokl. Akad. Nauk SSSR*, **243**, 688 (1978); *Chem. Abstr.*, **90**, 86560a (1979).
156. (a) C. Eaborn, K. J. Odell, A. Pidcock and G. R. Scollary, *J. Chem. Soc., Chem. Commun.*, 317 (1976).
     (b) G. R. Scollary, *Aust. J. Chem.*, **30**, 1007 (1977).
157. Yu. E. Ovchinnikov, Yu. T. Struchkov, N. F. Chernov, O. M. Trofimova and M. G. Voronkov, *Dokl. Akad. Nauk*, **328**, 330 (1993); *Chem. Abstr.*, **119**, 37830x (1993).
158. L. Parkanyi, K. Simon and J. Nagy, *J. Organomet. Chem.*, **101**, 11 (1975).
159. T.-M. Chung, Y. A. Lee, Y. K. Chung and I. N. Jung, *Organometallics*, **9**, 1976 (1990).
160. A.-S. Oh, Y. K. Chung and S. Kim, *Organometallics*, **11**, 1394 (1992).
161. J.-S. Lee, Y. K. Chung, D. Whang and K. Kim, *J. Organomet. Chem.*, **445**, 49 (1993).
162. M. J. Barrow, E. A. V. Ebsworth and M. M. Harding, *J. Chem. Soc., Dalton Trans.*, 1838 (1980).
163. V. A. Pestunovich, V. F. Sidorkin, O. B. Dogaev and M. G. Voronkov, *Dokl. Akad. Nauk SSSR*, **251**, 1140 (1980); *Chem. Abstr.*, **93**, 203827f (1980).
164. H. B. Bürgi and J. D. Dunitz, *Acc. Chem. Res.*, **16**, 153 (1983).

165. M. G. Voronkov, V. A. Pestunovich and Yu. A. Baukov, *Metalloorg. Khim.*, **4**, 1210 (1991); *Organomet. Chem. USSR (Engl. Transl.)*, **4**, 593 (1991).
166. L. Parkanyi, V. Fülöp. P. Hencsei and I. Kovacs. *J. Organomet. Chem.*, **418**, 173 (1991).
167. J. Wang, F. Maio, K. Lu, Y. Wu, G. Wu and S. Dou, *Jiegou Huaxue*, **5**(2), 78 (1986); *Chem. Abstr.*, **106**, 224889s (1987).
168. Z.-R. Lu, R.-X. Zhuo, L.-R. Shen and B.-S. Luo, *Main Group Metal Chem.*, **17**, 377 (1994).
169. Q. Shen and R. I. Hilderbrandt, *J. Mol. Struct.*, **64**, 257, (1980).
170. G. Forgacs, M. Kolonits and I. Hargittai, *Struct. Chem.*, **1**, 245 (1990).
171. Y. Apeloig, in *The Chemistry of Organic Silicon Compounds*, Part 1 (Eds. S. Patai and Z. Rappoport), Wiley, Chichester, 1989, pp. 57–225.
172. E. Magnusson, *J. Am. Chem. Soc.*, **112**, 7940 (1990).
173. J. I. Musher, *Angew. Chem., Int. Ed. Engl.*, **8**, 54 (1969).
174. V. F. Sidorkin, V. A. Pestunovich and M. G. Voronkov, *Dokl. Akad. Nauk SSSR*, **235**, 1363 (1977); *Dokl. Phys. Chem. (Engl. Transl.)*, **235**, 850 (1977).
175. R. W. Alder, *Tetrahedron*, **46**, 683 (1990).
176. M. G. Voronkov, V. V. Keiko, V. F. Sidorkin, V. A. Pestunovich and G. I. Zelchan, *Khim. Geterotsikl. Soed.*, 613 (1974); *Chem. Abstr.*, **81**, 119809h (1974).
177. M. G. Voronkov, V. F. Sidorkin, V. A. Shagun, V. A. Pestunovich and G. I. Zelchan, *Khim. Geterotsikl. Soed.*, 715 (1975); *Chem. Abstr.*, **83**, 96248r (1975).
178. M. G. Voronkov, V. F. Sidorkin, V. A. Shagun, V. A. Pestunovich and G. I. Zelchan, *Khim. Geterotsikl. Soed.*, 1347 (1976); *Chem. Abstr.*, **86**, 89065w (1977).
179. G. K. Balakhchi, V. V. Keiko, V. F. Sidorkin, V. A. Pestunovich and M. G. Voronkov, *Dokl. Akad. Nauk SSSR*, **275**, 393 (1984); *Chem. Abstr.*, **101**, 72816x (1984).
180. G. I. Csonka and P. Hencsei, *J. Organometal. Chem.*, **446**, 99 (1993).
181. V. F. Sidorkin, V. A. Pestunovich, V. A. Shagun and M. G. Voronkov, *Dokl. Akad. Nauk SSSR*, **233**, 386 (1977); *Dokl. Phys. Chem. (Engl. Transl.)*, **233**, 160 (1977).
182. P. Hencsei and G. Csonka, *Acta Chim. Acad. Sci. Hung.*, **106**, 285 (1981).
183. J.-C. Zhu, H.-J. Wu, C. S. Li, G. I. Martin, P.-C. Chen, G.-L. Wu and Z.-G. Lai, *J. Chim. Phys. Phys.-Chim. Biol.*, 407 (1984).
184. Yu. L. Frolov, S. G. Shevchenko and M. G. Voronkov, *J. Organomet. Chem.*, **292**, 159 (1985).
185. A. K. Kozyrev, R. G. Kutlubaev, N. P. Erchak and E. Lukevits, *Khim. Geterotsikl. Soed.*, 1314 (1989); *Chem. Heterocycl. Compd. (Engl. Transl.)*, **25**, 1096 (1989).
186. Zh. E. Grabovskaya, N. M. Klimenko and G. N. Kartsev, *Zh. Strukt. Khim.* **28(6)**, 34 (1987); *J. Struct. Chem. (Engl. Transl.)*, **28**, 840 (1987).
187. G. N. Kartsev, N. M. Klimenko, Zh. E. Grabovskaya and G. M. Chaban, *Zh. Strukt. Khim.* **29(6)**, 126 (1988); *J. Struct. Chem. (Engl. Transl.)*, **29**, 931 (1988).
188. (a) V. F. Sidorkin, G. K. Balakhchi, M. G. Voronkov and V. A. Pestunovich, *Dokl. Akad. Nauk SSSR*, **296**, 113 (1987); *Dokl. Phys. Chem. (Engl. Transl.)*, **296**, 400 (1987).
 (b) L. Onsager, *J. Am. Chem. Soc.*, **58**, 1486 (1936).
189. A. Greenberg, C. Plant and C. A. Venanzi, *J. Mol. Struct. (Theochem)*, **234**, 291 (1991).
190. M. S. Gordon, M. T. Carroll, J. H. Jensen, L. P. Davis, L. W. Burggraf and R. M. Guidry, *Organometallics*, **10**, 2657 (1991).
191. G. I. Csonka and P. Hencsei, *J. Mol. Struct. (Theochem)*, **283**, 251 (1993).
192. G. I. Csonka and P. Hencsei, *J. Organomet. Chem.*, **454**, 15 (1993).
193. G. I. Csonka and P. Hencsei, *J. Comput. Chem.*, **15**, 385 (1994).
194. M. W. Schmidt, T. L. Windus and M. S. Gordon, *J. Am. Chem. Soc.*, **117**, 7480 (1995).
195. J. E. Boggs, Ch. Peng, V. A. Pestunovich and V. F. Sidorkin, *J. Mol. Struct. (Theochem)*, **357**, 67 (1995).
196. V. F. Sidorkin and G. K. Balakhchi, *Struct. Chem.*, **5**, 187 (1994).
197. M. W. Schmidt, private communication.
198. V. F. Sidorkin, V. A. Shagun and V. A. Pestunovich, *Izv. Russ. Akad. Nauk, Ser. Khim.*, in press.
199. V. A. Klyuchnikov, G. N. Shvetz, M. S. Sorokin and M. G. Voronkov, *Dokl. Akad. Nauk SSSR.*, **282**, 1174 (1985); *Chem. Abstr.*, **103**, 167173r (1985).
200. M. G. Voronkov, V. A. Klyuchnikov, T. F. Danilova, A. N. Korchagina, V. P. Baryshok and L. M. Landa, *Izv. Akad. Nauk SSSR, Ser. Khim.*, 1970 (1986); *Bull. Acad. Sci. USSR, Div. Chem. Sci. (Engl. Transl.)*, **35**, 1789 (1986).
201. M. G. Voronkov, V. A. Klyuchnikov, A. N. Korchagina T. F. Danilova, G. N. Shvets, V. P. Baryshok and V. M. D'yakov, *Izv. Akad. Nauk SSSR, Ser. Khim.*, 1976 (1986); *Bull. Acad. Sci. USSR, Div. Chem. Sci. (Engl. Transl.)*, **35** 1795 (1986).

202. M. G. Voronkov, V. P. Baryshok, V. A. Klyuchnikov, A. N. Korchagina and K. L. Pepekin, *J. Organomet. Chem.*, **359**, 169 (1989).
203. M. G. Voronkov, M. S. Sorokin, V. A. Klyuchnikov, G. N. Shvetz and V. I. Pepekin, *J. Organomet. Chem.*, **359**, 301 (1989).
204. E. I. Brodskaya and M. G. Voronkov, *Izv. Akad. Nauk SSSR, Ser. Khim.*, 1694 (1986); *Bull. Acad. Sci. USSR Div. Chem. Sci. (Engl. Transl.)*, **35**, 1545 (1986).
205. W. Parker, W. V. Steele, W. Stirling and I. Watt, *J. Chem. Thermodyn.*, **7**, 795 (1975).
206. P. Hencsei, G. Csonka, G. Zsombok and E. Gergö, *Period. Polytech. Chem. Eng.*, **27**, 263 (1983).
207. I. S. Birgele, I. B. Mazheika, E. E. Liepin'sh and E. Lukevits, *Zh. Obshch. Khim.*, **50**, 882 (1980); *J. Gen. Chem. USSR (Engl. Transl.)*, **50**, 711 (1980).
208. P. Hencsei, L. Ambrus, R. Farkas, L. Morvai, L. Szakacs and M. Gal, *Acta Chim. Acad, Sci. Hung.*, **126**, 145 (1989).
209. R. C. Gray and D. M. Hercules, *Inorg. Chem.*, **16**, 1426 (1977).
210. D. Wang, G. Wu, S. Li and C. Chen, *Fenzi Kexue Yu Huaxue Yanjiu*, **3(3)**, 35 (1983); *Chem. Abstr.*, **100**, 121162w (1984).
211. D. Wang, D. Zhang, K. Lu, Y. Wu and G. Wu, *Sci. Sin., Ser. B*, **26**, 9 (1983).
212. S. G. Shevchenko, V. P. Elin, G. N. Dolenko, V. P. Baryshok, V. P. Feshin, Yu. L. Frolov, L. N. Mazalov and M. G. Voronkov, *Zh. Strukt. Khim.*, **23**, 43 (1982); *J. Struct. Chem. (Engl. Transl.)*, **23**, 360 (1982).
213. A. P. Zemlyanov, A. T. Shuvaev, V. V. Krivitskii and M. G. Voronkov, *Izv. Akad. Nauk SSSR, Ser. Fiz.*, **36**, 255 (1972); *Chem. Abstr.*, **77**, 11885h (1972)
214. T. Shuvaev, A. P. Zemlyanov, Yu. V. Kolodyazhnyi, O. A. Osipov, V. N. Eliseev and M. M. Morgunova, *Zh. Strukt. Khim.*, **15**, 433 (1974); *Chem. Abstr.*, **81**, 63003w (1974).
215. S. Gradock, E. A. V. Ebsworth and J. B. Muire, *J. Chem. Soc., Dalton Trans.*, 25 (1975).
216. M. G. Voronkov, E. I. Brodskaya, V. V. Belyaeva, D. D. Chuvashov, D. D. Toryashinova, A. F. Ermikov and V. P. Baryshok, *J. Organomet. Chem.*, **311**, 9 (1986).
217. E. I. Brodskaya, M. G. Voronkov, D. D. Toryashinova, V. P. Baryshok, G. V. Ratovski, D. D. Chuvashov and V. G. Efremov, *J. Organomet. Chem.*, **336**, 49 (1987).
218. J. B. Peel and D. Wang, *J. Chem. Soc., Dalton Trans.*, 1963 (1988).
219. D. H. Aue, H. M. Webb and M. T. Bowers, *J. Am. Chem. Soc.*, **97**, 4136 (1975).
220. V. A. Petukhov, L. V. Gudovich, G. Zelchans and M. G. Voronkov, *Khim. Geterotsikl. Soed.*, 968 (1969); *Chem. Abstr.*, **72**, 105542t (1970).
221. M. G. Voronkov, E. I. Brodskaya, N. M. Deriglazov, V. P. Baryshok and V. V. Belyaeva, *J. Organomet. Chem.*, **225**, 193 (1982).
222. M. G. Voronkov, D. D. Chuvashov, G. V. Ratovski and E. I. Brodskaya, *Dokl. Akad. Nauk SSSR*, **292**, 384 (1987); *Chem. Abstr.*, **107**, 236819c (1987).
223. M. G. Voronkov, E. I. Brodskaya, V. V. Belyaeva and V. P. Baryshok, *Dokl. Akad. Nauk SSSR*, **261**, 1362 (1981); *Chem. Abstr.*, **96**, 142125a (1982).
224. M. G. Voronkov, Yu. L. Frolov, O. A. Zasyadko and I. S. Emel'yanov, *Dokl. Akad. Nauk SSSR*, **213**, 1315 (1973); *Chem. Abstr.*, **80**, 69917g (1974).
225. M. G. Voronkov, M. S. Sorokin, V. F. Traven', M. I. German and B. I. Stepanov, *Dokl. Akad. Nauk SSSR*, **243**, 926 (1978); *Chem. Abstr.*, **90**, 151165s (1979).
226. M. G. Voronkov, S. G. Shevchenko, E. I. Brodskaya, V. P. Baryshok, P. Reich, D. Kunat and Yu. L. Frolov, *Izv. Sib. Otd. Akad. Nauk SSSR, Ser. Khim.*, 135 (1981); *Chem. Abstr.*, **96**, 34361r (1982).
227. M. Imbenotte, G. Palavit and P. Legrand, *J. Raman Spectrosc.*, **14**, 135 (1983).
228. M. Imbenotte, G. Palavit, P. Legrand, J. P. Huvenne and G. I. Fleury, *J. Mol. Spectrosc.*, **102**, 40 (1983).
229. P. Hencsei, M. Gál and L. Bihátsi, *J. Mol. Struct.*, **114**, 391 (1984).
230. I. S. Ignat'ev, A. N. Lazarev, S. G. Shevchenko and V. P. Baryshok, *Izv. Akad. Nauk SSSR, Ser. Khim.*, 1526 (1986); *Bull. Acad. Sci. USSR, Div. Chem. Sci. (Engl. Transl.)*, **35**, 1375 (1986).
231. P. Hencsei and A. Sebestyen, *Acta Chim. Acad. Sci. Hung.*, **127**, 501 (1990).
232. J.-M. Lin, *Jiegou Huaxue*, **15**, 57 (1995); *Chem. Abstr.*, **124**, 232554r (1996).
233. (a) M. G. Voronkov, E. I. Brodskaya, P. Reich, S. G. Shevchenko, V. P. Baryshok and Yu. L. Frolov, *J. Organomet. Chem.*, **164**, 35 (1979).
     (b) M. G. Voronkov, E. I. Brodskaya, Yu. N. Udodov, Yu. M. Sapozhnikov and V. P. Baryshok, *Dokl. Akad. Nauk SSSR*, **313**, 1153 (1990); *Chem. Abstr.*, **114**, 102175a (1991).
234. M. G. Voronkov, E. I. Brodskaya, V. V. Belyaeva, V. P. Baryshok, M. S. Sorokin and O. G. Yarosh, *Dokl. Akad. Nauk SSSR*, **267**, 654 (1982); *Chem. Abstr.*, **98**, 160752y (1983).

235. S. N. Tandura, V. A. Pestunovich, G. I. Zelchan, V. P. Baryshok, Yu. A. Lukina, M. S. Sorokin and M. G. Voronkov, *Izv. Akad. Nauk SSSR, Ser. Khim.*, 295 (1981); *Bull. Acad. Sci. USSR, Div. Chem. Sci. (Engl. Transl.)*, **30**, 223 (1981).
236. J. M. Bellama, J. D. Nies and N. Ben-Zvi, *Magn. Reson. Chem.*, **24**, 748 (1986).
237. M. H. P. van Genderen and H. M. Buck, *Recl. Trav. Chim. Pays-Bas*, **106**, 449 (1987).
238. S. N. Tandura, V. A. Pestunovich, M. G. Voronkov, G. I. Zelchan, V. P. Baryshok and Yu. A. Lukina, *Dokl. Akad. Nauk SSSR*, **235**, 406 (1977); *Dokl. Phys. Chem. (Engl. Transl.)*, **235**, 688 (1977).
239. K. Kupce, E. Liepins and E. Lukevics, *Khim, Geterotsikl. Soed.*, **129** (1987); *Chem. Abstr.*, **108**, 56176c (1988).
240. E. E. Liepin'sh, I. S. Birgele, E. L. Kupche and E. Lukevits, *Zh. Obshch. Khim.*, **57**, 1723 (1987); *J. Gen. Chem. USSR (Engl. Transl.)*, **58**, 1537 (1987).
241. E. Liepins, I. Birgele, P. Tomsons and E. Lukevics, *Magn. Reson. Chem.*, **23**, 485 (1985).
242. V. A. Pestunovich, S. N. Tandura, M. G. Voronkov, V. P. Baryshok, G. I. Zelchan, V. I. Glukhikh, G. Engelhardt and M. Witanovsky, *Spectrosc. Lett.*, **11**, 339 (1978).
243. V. A. Pestunovich, S. N. Tandura, B. Z. Shterenberg, V. P. Baryshok and M. G. Voronkov, *Dokl. Akad. Nauk SSSR*, **253**, 400 (1980); *Chem. Abstr.*, **94**, 46558g (1981).
244. S. N. Tandura, Yu. A. Strelenko, M. G. Voronkov, N. V. Alekseev and O. G. Yarosh, *Dokl. Akad. Nauk SSSR*, **267**, 397 (1982); *Dokl. Phys. Chem. (Engl. Transl.)*, **267**, 421 (1982).
245. E. Liepins, I. Birgele, G. Zelchans and E. Lukevics. *Zh. Obshch. Khim.*, **49**, 1537 (1979); *Chem. Abstr.*, **91**, 210444c (1979).
246. R. K. Harris, J. Jones and S. Ng, *J. Magn. Reson.*, **30**, 521 (1978).
247. E. Kupce, E. Liepins, A. Lapsina, G. Zelchan and E. Lukevics, *J. Organomet. Chem.*, **251**, 15 (1983).
248. M. Karplus and J. A. Pople, *J. Chem. Phys.*, **38**, 2803 (1963).
249. M. G. Voronkov, V. I. Glukhikh, V. M. D'yakov, V. V. Keiko, G. A. Kuznetsova and O. G. Yarosh, *Dokl. Akad. Nauk SSSR*, **258**, 382 (1981); *Chem. Abstr.*, **95**, 114573f (1981).
250. E. E. Liepin'sh, I. S. Birgele, I. S. Solomennikova, A. F. Lapsinya, G. I. Zelchan and E. Lukevits, *Zh. Obshch. Chem.*, **50**, 2462 (1980); *J. Gen. Chem. USSR (Engl. Transl.)*, **50**, 1989 (1980).
251. J. Schraml, A. M. Krapivin, A. P. Luzin, V. M. Kilesso and V. A. Pestunovich, *Collect. Czech. Chem. Commun.*, **49**, 2897 (1984).
252. M. G. Voronkov, L. I. Gubanova, V. M. D'yakov, V. I. Glukhikh, N. G. Glukhikh and B. Shirchin, *Zh. Obshch. Khim.*, **55**, 1041 (1985); *J. Gen. Chem. USSR (Engl. Transl.)*, **55**, 928 (1985).
253. S. N. Tandura, M. G. Voronkov, A. V. Kisin, N. V. Alekseev, E. E. Shestakov, Z. A. Ovchinnikova and V. P. Baryshok, *Zh. Obshch. Chem.*, **54**, 2012 (1984); *J. Gen. Chem. USSR (Engl. Transl.)*, **54**, 1795 (1984).
254. H. Iwamija and G. E. Maciel, *J. Am. Chem. Soc.*, **115**, 6835 (1993).
255. V. A. Pestunovich, S. N. Tandura, M. G. Voronkov, G. Engelhardt, E. Lippmaa, T. Pehk, V. F. Sidorkin, G. I. Zelchan and V. P. Baryshok, *Dokl. Akad. Nauk SSSR*, **240**, 914 (1978); *Chem. Abstr.*, **89**, 107136p (1978).
256. P. Hencsei and H. C. Marsmann, *Acta Chim. Acad. Sci. Hung.*, **105**, 79 (1980).
257. W. H. Flygare, *Chem. Rev.*, **74**, 653 (1974).
258. V. F. Sidorkin, V. A. Pestunovich and M. G. Voronkov, *Magn. Reson. Chem.*, **23**, 491 (1985).
259. V. A. Pestunovich, S. N. Tandura, B. Z. Shterenberg, V. P. Baryshok and M. G. Voronkov. *Izv. Akad. Nauk SSSR, Ser. Khim.*, 2653 (1978); *Chem. Abstr.*, **90**, 86545r (1979).
260. M. Ya. Myagi, A. V. Samoson, E. T. Lippmaa, V. A. Pestunovich, S. N. Tandura, B. Z. Shterenberg and M. G. Voronkov, *Dokl. Akad. Nauk SSSR*, **252**, 140 (1980); *Chem. Abstr.*, **93**, 238047r (1980).
261. V. A. Pestunovich, B. Z. Shterenberg, S. N. Tandura, G. I. Zelchan, V. P. Baryshok, I. I. Solomennikova, I. P. Urtane, E. Lukevics and M. G. Voronkov, *Izv. Akad. Nauk SSSR, Ser. Khim.*, 467 (1981); *Chem. Abstr.*, **95**, 79412d (1981).
262. D. Kost and I. D. Kalikhman, Chapter 23 in this book.
263. V. A. Pestunovich B. Z. Shterenberg, E. T. Lippmaa, M. Ya. Myagi, M. A. Alla, V. P. Baryshok, L. P. Petukhov and M. G. Voronkov, *Dokl. Akad. Nauk SSSR*, **258**, 1410 (1981); *Dokl. Phys. Chem. (Engl. Transl.)*, **258**, 587 (1981).
264. V. A. Pestunovich, S. N. Tandura, B. Z. Shterenberg, V. P. Baryshok and M. G. Voronkov, *Izv. Akad. Nauk SSSR, Ser. Khim.*, 2159 (1979); *Chem. Abstr.*, **92**, 75393p (1980).
265. J.-C. Zhu, X.-Y. Sun, H.-J. Wu, L.-J. Jiang, B.-Q. Chen and G.-L. Wu, *Acta Chim. Sin. (Engl. Ed.)*, **44** 140 (1986).

266. V. A. Pestunovich, B. Z. Shterenberg, L. P. Petukhov, V. I. Rakhlin, V. P. Baryshok, R. G. Mirskov and M. G. Voronkov, *Izv. Akad. Nauk SSSR, Ser. Khim.*, 1935 (1985); *Bull. Acad. Sci. USSR, Div. Chem. Sci. (Engl. Transl.)*, **34**, 1790 (1985).
267. R. W. Taft and M. J. Kamlet, *Org. Magn. Reson.*, **14**, 485 (1980).
268. I. A. Koppel and V. A. Palm, in *Advances in Linear Free Energy Relationships* (Eds. N. B. Chapman and J. Shorter), Plenum Press, London, 1972, pp. 203–280.
269. J. Kamlet, J. L. M. Abboud and R. W. Taft, *Prog. Phys. Org. Chem.*, **13**, 485 (1981).
270. E. L. Kupche and E. Lukevits, *Khim. Geterotsikl. Soed.*, 701 (1989); *Chem. Heterocycl. Compd. (Engl. Transl.)*, **25**, 586 (1989).
271. V. A. Pestunovich, B. Z. Shterenberg, M. G. Voronkov, M. Ya. Myagi and A. V. Samoson, *Izv. Akad. Nauk SSSR, Ser. Khim.*, 1435 (1982); *Bull. Acad. Sci. USSR, Div. Chem. Sci. (Engl. Transl.)*, **31**, 1284 (1982).
272. E. Kupce and E. Lukevics, *J. Organomet. Chem.*, **358**, 67 (1988).
273. J. Lipowitz, *J. Am. Chem. Soc.*, **94**, 1582 (1972).
274. S. N. Tandura, V. A. Pestunovich, V. I. Glukhikh, V. P. Baryshok and M. G. Voronkov, *Spectrosc. Lett.*, **10**, 163 (1977).
275. E. E. Liepinsh, I. A. Zitsmane, G. I. Zelchan and E. Lukevits, *Zh. Obshch. Khim.*, **53**, 245 (1983); *J. Gen. Chem. USSR (Engl. Transl.)*, **53**, 215 (1983).
276. M. G. Voronkov, V. P. Feshin, V. M. D'yakov, L. S. Romanenko, V. P. Baryshok and M. V. Sigalov, *Dokl. Akad. Nauk SSSR*, **223**, 1133 (1975); *Chem. Abstr.*, **84**, 3940b (1976).
277. M. G. Voronkov, E. I. Brodskaya, V. V. Belyaeva, T. V. Kashik, V. P. Baryshok and O. G. Yarosh, *Zh. Obshch. Khim.*, **56**, 621 (1986); *J. Gen. Chem. USSR (Engl. Transl.)*, **56**, 550 (1986).
278. E. I. Brodskaya, M. G. Voronkov, V. V. Belyaeva, V. P. Baryshok and N. F. Lazareva, *Zh. Obshch. Khim.*, **63**, 2252 (1993); *Russ. J. Gen. Chem. (Engl. Transl.)*, **63**, 1564 (1993).
279. G. Cerveau, C. Chuit, E. Colomer, R. J. P. Corriu and C. Reyé, *Organometallics*, **9**, 2415 (1990).
280. K. A. Broka, V. T. Glezer, Ya. P. Stradyn' and G. I. Zelchan, *Zh. Obshch. Chem.*, **61**, 1374 (1991); *J. Gen. Chem. USSR (Engl. Transl.)*, **61**, 1252 (1991).
281. K. Broka, J. Stradinš, V. Glezer, G. Zelčans and E. Lukevics, *J. Electroanal. Chem.*, **351**, 199 (1993).
282. T. Müller, P. Hencsei and L. Bihatsi, *Period. Polytech., Chem. Eng.*, **25**, 181 (1981).
283. Yu. W. Fang, S.-W. Hu, G.-L. Wu and M.-S. Xu, *Acta Chim. Sin. (Engl. Ed.)*, **41**, 630 (1983).
284. I. B. Mazheika, A. P. Gaukhman, I. I. Solomennikova, A. F. Lapsinya, G. I. Zelchan and E. Ya. Lukevits, *Zh. Obshch. Khim.*, **54**, 117 (1984); *J. Gen. Chem. USSR (Engl. Transl.)*, **54**, 103 (1984).
285. V. N. Bochkarev, A. E. Chernyshov, V. Yu. Vitkovskii and M. G. Voronkov, *Zh. Obshch. Khim.*, **55**, 1354 (1985); *J. Gen. Chem. USSR (Engl. Transl.)*, **55**, 1209 (1985).
286. L. Yan, W. Chai, G. Wang, G. Wu, K. Lu and Y. Luo, *Org. Mass Spectrom.*, **22**, 279 (1987).
287. P. Hencsei, I. Kovacs, I. Bihatsi, E. B. Karsai, T. Müller and P. Miklos, *Period. Polytech., Chem. Eng.*, **33**, 1 (1989).
288. M. G. Voronkov, V. P. Baryshok, N. F. Lazareva, V. V. Saraev, T. I. Vakul'skaya, P. Hencsei and I. Kovacs, *J. Organomet. Chem.*, **368**, 155 (1989).
289. S. Rozite, I. Mazeika, A. Gaukhman, N. P. Erchak, L. M. Ignatovich and E. Lukevics, *Metalloorg. Khim.*, **2**, 1389 (1989); *Organomet. Chem. USSR (Engl. Transl.)*, **2**, 736 (1989).
290. S. Rozite, I. Mazeika, A. Gaukhman, N. P. Erchak, L. M. Ignatovich and E. Lukevics, *J. Organomet. Chem.*, **384**, 257 (1990).
291. I. Mazeika, S. Grinberga, A. P. Gaukhman, G. I. Zelchan and E. Lukevics, *J. Organomet. Chem.*, **426**, 41 (1992).
292. A. E. Chernyshev and V. N. Bochkarev, *Zh. Obshch. Khim.*, **57**, 154 (1987); *Chem. Abstr.*, **108**, 56230r (1988).
293. V. A. Pestunovich, L. P. Petukhov, T. I. Vakul'skaya, V. P. Baryshok, V. K. Turchaninov, Yu. L. Frolov and M. G. Voronkov, *Izv. Akad. Nauk SSSR, Ser. Khim.*, 1470 (1978); *Chem. Abstr.*, **89**, 89839p (1978).
294. M. G. Voronkov, D.-S. D. Toryashinova, V. P. Baryshok, B. A. Shainyan and E. I. Brodskaya, *Izv. Akad. Nauk SSSR, Ser. Khim.*, 2673 (1984); *Bull. Acad. Nauk USSR, Div. Chem. Sci. (Engl. Transl.)*, **33**, 2447 (1984).
295. J. Lukasiak and Z. Jamrodgiewicz, *Acta Chim. Acad. Sci. Hung.*, **105**, 19 (1980).
296. J. Lukasiak and Z. Jamrodgiewicz, *Acta Chim. Acad. Sci. Hung.*, **115**, 167 (1984).
297. J. Lukasiak and Z. Jamrodgiewicz, *Acta Chim. Acad. Sci. Hung.*, **123**, 99 (1986).

298. A. Daneshrad, C. Eaborn, R. Eidensshink and D. R. M. Walton, *J. Organomet. Chem.*, **90**, 139 (1975).
299. M. G. Voronkov, S. G. Shevchenko, E. I. Brodskaya, Yu. L. Frolov, V. P. Baryshok, N. M. Deriglazov, E. S. Deriglazova and V. M. D'yakov, *Dokl. Akad. Nauk SSSR*, **230**, 627 (1976); *Chem. Abstr.*, **86**, 111751r (1977).
300. M. Imbenotte, G. Palavit and P. Legrand, *J. Raman Spectrosc.*, **15**, 293 (1984).
301. V. A. Pestunovich, L. P. Petukhov, B. Z. Shterenberg and M. G. Voronkov, *Izv. Akad. Nauk SSSR, Ser. Khim.*, 2169 (1981); *Bull. Acad. Nauk Sci., Div. Chem. Sci. (Engl. Transl.)*, **30**, 1784 (1981).
302. L. P. Kuzmenko, M. G. Voronkov, V. V. Keiko and V. A. Pestunovich, *Zh. Obshch. Khim.*, **53**, 105 (1983); *Chem. Abstr.*, **98**, 126217t (1983).
303. M. G. Voronkov, G. I. Zelchan, G. F. Tsybulya and P. G. Volfson, USSR Patent 299510, 1971; *Chem. Abstr.*, **75**, 63951 (1975j).
304. M. G. Voronkov and G. I. Zelchan, *Khim. Geterotsikl. Soed.*, 43 (1969); *Chem. Abstr.*, **71**, 3363x (1969).
305. G. H. Barnes and G. W. Schweitzer, US Patent 2967171 (Dow Corning Corp.), 1961; *Chem. Abstr.*, **55**, 9281e (1961).
306. R. J. Boyer, R. J. P. Corriu, R. Perz and C. Reye, *J. Organomet. Chem.*, **148**, C1 (1978).
307. M. G. Voronkov, G. I. Zelchan, G. F. Tsybulya and L. P. Urtane, *Khim. Geterotsikl. Soed.*, 756 (1975); *Chem. Abstr.*, **83**, 164146s (1975).
308. M. G. Voronkov, L. P. Petukhov, T. I. Vakul'skaya, V. P. Baryshok, S. N. Tandura and V. A. Pestunovich, *Izv. Akad. Nauk SSSR, Ser. Khim.*, 1665 (1979); *Chem. Abstr.*, **91**, 211391v (1979).
309. M. G. Voronkov, L. P. Petukhov, V. I. Rakhlin, V. P. Baryshok, B. Z. Shterenberg, R. G. Mirskov and V. A. Pestunovich, *Izv. Akad. Nauk SSSR, Ser. Khim.*, 2412 (1981); *Bull. Acad. Sci. USSR, Div. Chem. Sci. (Engl. Transl.)*, **30**, 1991 (1981).
310. M. G. Voronkov, V. I. Rakhlin, S. N. Adamovich, L. P. Petukhov and R. G. Mirskov, *Izv. Akad. Nauk SSSR, Ser. Khim.*, 899 (1986); *Bull. Acad. Sci. USSR, Div, Chem. Sci. (Engl. Transl.)*, **35**, 819 (1986).
311. G. Cerveau, C. Chuit, R. J. P. Corriu, N. K. Nayyar and C. Reye, *J. Organomet. Chem.*, **389**, 159 (1990).
312. Y. Wan and J. G. Verkade, *J. Am. Chem. Soc.*, **117**, 141 (1995).
313. J. Wang, Q. Xie, R. Liao, J. Li and X. Lin, *Youji Huaxue*, **4**, 285 (1987); *Chem. Abstr.*, **108**, 94532y (1988).
314. J. Wang, Q. Xie, R. Liao, J. Li and X. Lin, *Chem. J. Chin. Univ.*, **9**, 466 (1988).
315. M. W. Kim, D. S. Un, H. C. Shin, J. Kim and Y. Do, *J. Korean Chem. Soc.*, **38**, 241 (1994); *Chem. Abstr.*, **121**, 49020n (1994).
316. V. A. Pestunovich, L. P. Petukhov, V. I. Rakhlin, B. Z. Shterenberg, R. G. Mirskov and M. G. Voronkov, *Dokl. Akad. Nauk SSSR*, **263**, 904 (1982); *Dokl. Phys. Chem. (Engl. Transl.)*, **263**, 128 (1982).
317. M. G. Voronkov, V. G. Komarov, A. I. Albanov, I. M. Korotaeva and E. I. Dubinskaya, *Izv. Akad. Nauk SSSR, Ser. Khim.*, 1415 (1978); *Chem. Abstr.*, **89**, 109712x (1978).
318. A. H. Schmidt, *Aldrichimica Acta*, **14**, 31 (1981).
319. M. G. Voronkov, L. P. Petukhov, V. I. Rakhlin, B. Z. Shterenberg, S. H. Hangazheev, R. G. Mirskov and V. A. Pestunovich, USSR Patent 1031181, 1985; *Chem. Abstr.*, **104**, 6017y (1986).
320. M. G. Voronkov, V. I. Rakhlin, L. P. Petukhov, R. G. Mirskov, B. Z. Shterenberg and V. A. Pestunovich, *Zh. Obshch. Khim.*, **54**, 2398 (1984); *J. Gen. Chem. USSR (Engl. Transl.)*, **54**, 2144 (1984).
321. M. G. Voronkov, L. P. Petukhov, V. I. Rakhlin, B. Z. Shterenberg, R. G. Mirskov, S. N. Adamovich and V. A. Pestunovich, *Zh. Obshch. Khim.*, **56**, 964 (1986); *J. Gen. Chem. USSR (Engl. Transl.)*, **56**, 849 (1986).
322. M. G. Voronkov, V. A. Pestunovich, L. P. Petukhov and V. I. Rakhlin, *Izv. Akad. Nauk SSSR, Ser. Khim.*, 699 (1983); *Bull. Acad. Sci. USSR, Div. Chem. Sci. (Engl. Transl.)*, **32**, 637 (1983).
323. L. P. Petukhov, E. V. Bakhareva, V. A. Pestunovich, A. B. Shapiro, P. I. Dmitriev and M. G. Voronkov, *Khim.-Pharm. Zh.*, **20**, 979 (1986); *Pharm. Chem. J. (Engl. Transl.)*, **20**, 562 (1986).
324. C. Eaborn, *J. Chem. Soc.*, 3077 (1950).
325. D. S. Uh, Y. Do, J. H. Lee and H. Suh, *Main Group Metal Chem.*, **16**, 131 (1993); *Chem. Abstr.*, **120**, 270557u (1994).

326. E. Lukevics, I. I. Solomennikova and G. Zelchans, *Zh. Obshch. Khim.*, **46**, 134 (1976); *Chem. Abstr.*, **84**, 150696e (1976).
327. M. G. Voronkov, Yu. A. Lukina, V. M. D'yakov and M. V. Sigalov, *Zh. Obshch. Khim.*, **53**, 803 (1983); *J. Gen. Chem. USSR (Engl. Transl.)*, **53**, 703 (1983).
328. A. Hosomi, S. Iijima and H. Sakurai, *Chem. Lett.*, 243 (1981).
329. M. G. Voronkov, V. P. Baryshok and N. F. Lazareva, *Izv. Akad. Nauk, Ser. Khim.*, 2075 (1996); *Russ. Chem. Bull. (Engl. Transl.)*, **45**, 1970 (1996).
330. S. S. Lee, E. Jeong and Y. K. Chung, *J. Organomet. Chem.*, **483**, 115 (1994).
331. M. G. Voronkov, N. F. Chernov and T. A. Dekina, *Dokl. Akad. Nauk SSSR*, **230**, 853 (1976); *Chem. Abstr.*, **86**, 16767s (1977).
332. R. Müller, *Organomet. Chem. Rev.*, **1**, 359 (1966).
333. R. Müller and H. J. Frey, *Z. Anorg. Allg. Chem.*, **368**, 113 (1969).
334. R. Müller and C. Dathe, *J. prakt. Chem.*, **22**, 232 (1963).
335. M. G. Voronkov, L. P. Petukhov, S. N. Adamovich, V. P. Baryshok, V. I. Rakhlin and B. Z. Shterenberg, *Izv. Akad. Nauk SSSR, Ser. Khim.*, 204 (1987); *Bull. Acad. Sci. USSR, Div. Chem. Sci. (Engl. Transl.)*, **36**, 182 (1987).
336. M. G. Voronkov, V. P. Baryshok, E. E. Kuznetsova, I. M. Remez and L. E. Deev, *Khim.-Farm. Zh.*, 44 (1991); *Pharm. Chem. J. (Engl. Transl.)*, **25**, 405 (1991).
337. A. A. Kamyshova, M. Nasim, G. S. Zaitseva and A. B. Terent'ev, *Metalloorg. Khim.*, **4**, 459 (1991); *Organomet. Chem. USSR (Engl. Transl.)*, **4**, 222 (1991).
338. E. Lukevics, V. Dirnens, N. Pokrovska, J. Popelis and A. Kemme, *Main Group Metal Chem.*, **18**, 337 (1995).
339. M. G. Voronkov and M. S. Sorokin, *Zh. Obshch. Khim.*, **54**, 2020 (1984); *J. Gen. Chem. USSR (Engl. Transl.)*, **54**, 1803 (1984).
340. M. G. Voronkov, N. M. Kudyakov and A. I. Albanov, *Zh. Obshch. Khim.*, **49**, 1525 (1979); *Chem. Abstr.*, **91**, 175431x (1979).
341. E. W. Colvin, *Silicon in Organic Synthesis*, Chap. 4, Butterworth, London, 1981, pp. 21–29.
342. E. Lukevics and N. P. Erchak, *Latv. PSR Zinat. Akad. Vestis, Khim. Ser.*, 250 (1975); *Chem. Abstr.*, **83**, 79323c (1975).
343. E. Lukevics and N. P. Erchak, *Zh. Obshch. Khim.*, **47**, 809 (1977); *Chem. Abstr.*, **87**, 53422s (1977).
344. M. G. Voronkov, S. N. Adamovich, N. M. Kudyakov, S. Yu. Khramtsova, V. I. Rakhlin and R. G. Mirskov, *Izv. Akad. Nauk SSSR, Ser. Khim.*, 488 (1986); *Bull. Acad. Sci. USSR, Div. Chem. Sci. (Engl. Transl.)*, **35**, 451 (1986).
345. M. Nasim, V. S. Petrosyan and G. S. Zaitseva, *J. Organomet. Chem.*, **430**, 269 (1992).
346. G. A. Kutyrev, A. A. Kapura, M. S. Sorokin, R. A. Cherkasov, M. G. Voronkov and A. N. Pudovik, *Dokl. Akad. Nauk SSSR*, **275**, 1104 (1984); *Dokl. Phys. Chem. (Engl. Transl.)*, **275**, 141 (1984).
347. G. A. Kutyrev, A. A. Kapura, M. S. Sorokin, R. A. Cherkasov, M. G. Voronkov and A. N. Pudovik, *Zh. Obshch. Khim.*, **55**, 1030 (1985); *J. Gen. Chem. USSR (Engl. Transl.)*, **55**, 918 (1985).
348. F. Cooke, R. Moerek, J. Schwindeman and F. Magnus, *J. Org. Chem.*, **45**, 1046 (1980).
349. S. N. Adamovich, V. Yu. Prokopyev, V. I. Rakhlin, R. G. Mirskov, B. Z. Shterenberg and M. G. Voronkov, *Izv. Akad. Nauk SSSR, Ser. Khim.*, 2839 (1989); *Bull. Acad. Sci. USSR, Div. Chem. Sci. (Engl. Transl.)*, **38**, 2603 (1989).
350. M. G. Voronkov, S. N. Adamovich, V. I. Rakhlin and R. G. Mirskov, *Zh. Obshch. Khim.*, **57**, 1661 (1987); *J. Gen. Chem. USSR (Engl. Transl.)*, **57**, 1481 (1987).
351. M. Nasim, L. I. Livantsova, A. V. Kisin, G. S. Zaitseva and V. S. Petrosyan, *Metalloorg. Khim.*, **3**, 949 (1990); *Organomet. Chem. USSR (Engl. Transl.)*, **3**, 486 (1990).
352. A. Hosomi and H. Sakurai, *Tetrahedron Lett.*, 1295 (1976).
353. T. K. Sarkar and N. H. Andersen, *Tetrahedron Lett.*, 3513 (1978).
354. M. G. Voronkov, S. N. Adamovich, V. I. Rakhlin, R. G. Mirskov and M. V. Sigalov, *Izv. Akad. Nauk SSSR, Ser. Khim.*, 2792 (1984); *Bull. Acad. Sci. USSR, Div. Chem. Sci. (Engl. Transl.)*, **33**, 2558 (1984).
355. M. G. Voronkov, S. N. Adamovich, V. I. Rakhlin and R. G. Mirskov, *Zh. Obshch. Khim.*, **54**, 475 (1984); *J. Gen. Chem. USSR (Engl. Transl.)*, **54**, 425 (1984).
356. M. V. Kilesso, V. I. Kopkov, A. S. Shashkov and B. N. Stepanenko, *Izv. Akad. Nauk SSSR, Ser. Khim.*, 1404 (1986); *Bull. Acad. Sci. USSR, Div. Chem. Sci. (Engl. Transl.)*, **35**, 1276 (1986).
357. J. E. Noll, J. L. Speier and B. F. Daubert, *J. Am. Chem. Soc.*, **73**, 3867 (1951).

358. M. G. Voronkov, Yu. A. Lukina, V. M. D'yakov, Yu. L. Frolov and S. N. Tandura, *Zh. Obshch. Khim.*, **52**, 349 (1982); *J. Gen. Chem. USSR (Engl. Transl.)*, **52**, 301 (1982).
359. M. G. Voronkov, V. M. D'yakov, G. A. Samsonova, N. M. Kudyakov, Yu. A. Lukina and E. K. Vugmeister, *Izv. Akad. Nauk SSSR, Ser. Khim.*, 2059 (1975); *Chem. Abstr.*, **84**, 17475r (1976).
360. V. M. D'yakov, N. I. Liptuga, G. A. Samsonova, Yu. A. Lukina, M. G. Voronkov and A. V. Kirsanov, USSR Patent 572466, 1976; *Chem. Abstr.*, **87**, 167538q (1977).
361. M. G. Voronkov and M. S. Sorokin, *Zh. Obshch. Khim.*, **49**, 2671 (1979); *Chem. Abstr.*, **92**, 164026p (1980).
362. M. G. Voronkov and M. S. Sorokin, *Zh. Obshch. Khim.*, **59**, 590 (1989); *J. Gen. Chem. USSR (Engl. Transl.)*, **59**, 522 (1989).
363. G. S. Zaitseva, A. I. Chernyavskii, Yu. I. Baukov and I. F. Lutsenko, *Zh. Obshch. Khim.*, **46**, 843 (1976); *Chem. Abstr.*, **85**, 46806a (1976).
364. L. Birkofer and W. Quittmann, *Chem. Ber.*, **118**, 2874 (1985).
365. V. E. Udre and E. J. Lukevits, *Khim. Geterotsikl. Soed.*, 493 (1973); *Chem. Heterocycl. Compd. (Engl. Transl.)*, **9**, 454 (1973).
366. E. Lukevics, A. Lapsina, G. Zelchans, A. Dauvarte and A. Zidermane, *Latv. PSR Zinat. Akad. Vestis, Khim. Ser.*, 338 (1978); *Chem. Abstr.*, **89**, 129581g (1978).
367. F. Ye, X. Luo and R. Zhuo, *Huaxue Shiji*, **17**, 186 (1995); *Chem. Abstr.*, **124**, 8886t (1996).
368. M. G. Voronkov, V. M. D'yakov, G. G. Efremova, G. A. Kuznetsova, N. K. Gusarova, S. V. Amosova and B. A. Trofimov, USSR Patent 722913, 1978; *Chem. Abstr.*, **93**, 114696g (1980).
369. M. G. Voronkov, A. E. Pestunovich, N. N. Vlasova, T. V. Kashik, T. I. Nikiforova, A. I. Albanov, Yu. N. Pozhidaev and S. V. Amosova, *Zh. Obshch. Khim.*, **63**, 869 (1993); *Russ. J. Gen. Chem. (Engl. Transl.)*, **63**, 609 (1993).
370. M. G. Voronkov and M. S. Sorokin, *Zh. Obshch. Khim.*, **56**, 1098 (1986); *J. Gen. Chem. USSR (Engl. Transl.)*, **56**, 962 (1986).
371. S. G. Smith and S. Winstein, *Tetrahedron*, **3**, 317 (1958).
372. N. F. Chernov, O. N. Florensova and M. G. Voronkov, *Metalloorg. Khim.*, **2**, 902 (1989); *Organomet. Chem. USSR (Engl. Transl.)*, **2**, 472 (1989).
373. Y. A. Lee, Y. K. Chung, Y. Kim and J. H. Jeong, *Organometallics*, **9**, 2851 (1990).
374. Y. A. Lee, Y. K. Chung, Y. Kim, J. H. Jeong, G. Chung and D. Lee, *Organometallics*, **10**, 3707 (1991).
375. S. S. Lee, J.-S. Lee and Y. K. Chung, *Organometallics*, **12**, 4640 (1993).
376. T.-Y. Lee, Y. K. Kang, Y. K. Chung, R. D. Pike and D. A. Sweigardt, *Inorg. Chim. Acta*, **214**, 125 (1993).
377. S. S. Lee, I. S. Lee and Y. K. Chung, *Organometallics*, **15**, 5428 (1996).
378. E. Lukevics, I. I. Solomennikova, G. I. Zelchans, I. A. Judeika, E. E. Liepins, I. S. Yankovskaya and I. B. Mazeika, *Zh. Obshch. Khim.*, **47**, 105 (1977); *Chem. Abstr.*, **86**, 171535h (1977).
379. A. Kemme, J. Bleidelis, I. Solomennikova, G. Zelchan and E. Lukevics, *J. Chem. Soc., Chem. Commun.*, 1041 (1976).
380. I. S. Jankovska, I. I. Solomennikova, I. Mazeika, G. Zelchans and E. Lukevics, *Latv. PSR Zinat. Akad. Vestis., Khim. Ser.*, 366 (1975); *Chem. Abstr.*, **83**, 96199j (1975).
381. E. Popowski, DDR Patent 106389, 1974; *Chem. Abstr.*, **81**, 169626s (1974); E. Popowski, M. Michalik and H. Kelling, *J. Organomet. Chem.*, **88**, 157 (1975).
382. G. I. Zelchan, A. F. Lapsinya and E. Lukevits, *Zh. Obshch. Khim.*, **53**, 465 (1983); *J. Gen. Chem. USSR (Engl. Transl.)*, **53**, 409 (1983).
383. M. G. Voronkov, S. V. Basenko, R. G. Mirskov, T. D. Toryashinova and E. I. Brodskaya, *Dokl. Akad. Nauk SSSR*, **268**, 102 (1982); *Dokl. Chem. (Engl. Transl.)*, **268**, 1 (1983).
384. M. G. Voronkov, S. V. Basenko, R. G. Mirskov, V. Yu. Vitkovskii and T. D. Toryashinova, *Zh. Obshch. Khim.*, **53**, 944 (1983); *J. Gen. Chem. USSR (Engl. Transl.)*, **53**, 832 (1983).
385. V. Fulop, A. Kalman, P. Hencsei, G. Csonka and I. Kovacs, *Acta Crystallogr.*, **C47**, 720 (1988).
386. J. Dai, J. Zhang, Y. Wu and G. Wu, *Jiegou Huaxue*, **2(3)**, 207 (1983); *Chem. Abstr.*, **101**, 141415e (1984).
387. J. Dai, J. Zhang and Y. Wu, *Jiegou Huaxue*, **2(2)**, 107 (1983); *Chem. Abstr.*, **100**, 94789x (1984).
388. L. Parkanyi, P. Hencsei, G. Csonka and I. Kovacs, *J. Organomet. Chem.*, **329**, 305 (1987).
389. L. Parkanyi, P. Hencsei and E. Popowski, *J. Organomet. Chem.*, **197**, 275 (1980).
390. A. Kemme, J. Bleidelis, A. F. Lapsina, M. Fleisher, G. I. Zelchans and E. Lukevics, *Latv. PSR Zinat. Akad. Vestis, Khim. Ser.*, 242 (1985); *Chem. Abstr.*, **103**, 87961f (1985).

391. M. G. Voronkov, V. Yu. Vitkovskii, S. N. Tandura, N. V. Alekseev, S. V. Basenko and R. G. Mirskov, *Izv. Akad. Nauk SSSR, Ser. Khim.*, 2696 (1982); *Bull. Acad. Sci. USSR, Div. Chem. Sci. (Engl. Transl.)* **31**, 2384 (1982).
392. E. L. Morehouse, US Patent 3032576 (Union Carbide Corp.), 1962; *Chem. Abstr.*, **57**, 9881h (1962).
393. E. Lukevics, L. I. Libert and M. G. Voronkov, *Zh. Obshch. Khim.*, **39**, 1784 (1969); *Chem. Abstr.*, **71**, 124571x (1969).
394. E. Lukevics, L. I. Libert and M. G. Voronkov, USSR Patent 1213588 (1969); *Chem. Abstr.*, **71**, 3465g (1969).
395. P. Hencsei, I. Kovacs and L. Parkanyi, *J. Organomet. Chem.*, **293**, 185 (1985).
396. A. Kemme, J. Bleidelis, G. Zelchans, I. Urtane and E. Lukevics, *Zh. Strukt. Khim.*, **18(2)**, 343 (1977); *J. Struct. Chem. (Engl. Transl.)*, **18**, 268 (1977); *Chem. Abstr.*, **87**, 68452a (1977).
397. F. P. Boer and J. W. Turley, *J. Am. Chem. Soc.*, **91**, 4134 (1969).
398. K. Jurkschat, C. Mugge, J. Schmidt and A. Tzschach, *J. Organomet. Chem.*, **287**, C1 (1985).
399. K. Jurkschat, A. Tzschach, J. Meunier-Piret and M. van Meersche, *J. Organomet. Chem.*, **317**, 145 (1986).
400. A. Tzschach and K. Jurkschat, *Pure Appl. Chem.*, **58**, 639 (1986).
401. M. G. Voronkov, V. P. Baryshok and V. M. D'yakov, *Zh. Obshch. Khim.*, **46**, 1188 (1976); *Chem. Abstr.*, **85**, 46810x (1976).
402. C. L. Frye, G. A. Vincent and G. L. Hauschildt, *J. Am. Chem. Soc.*, **88**, 2727 (1966).
403. M. A. Paz-Sandoval, C. Fernandez-Vincent, G. Uribe and R. Contreras, *Polyhedron*, **7**, 679 (1988).
404. C. Soulie, P. Bassoul and J. Simon, *J. Chem. Soc., Chem. Commun.*, 114 (1993).
405. C. Soulie and J. Simon, *New J. Chem.*, **17**, 267 (1993).
406. R. E. Timms, *J. Chem. Soc. (A)*, 1969 (1971).
407. G. E. Le Grow, US Patent 3576026 (Dow Corning Corp.), 1971; *Chem. Abstr.*, **75**, 37252h (1972).
408. (a) E. Lukevits, G. I. Zelchan, I. I. Solomennikova, E. E. Liepin'sh, I. S. Yankovskaya and I. B. Mazheika, *Zh. Obshch. Khim.*, **47**, 109 (1977); *J. Gen. Chem. USSR (Engl. Transl.)*, **47**, 98 (1977).
    (b) A. A. Macharashvili, V. E. Shklover, Yu. T. Struchkov, A. Lapsina, G. Zelcans and E. Lukevics, *J. Organomet. Chem.*, **349**, 23 (1988).
409. D. Gudat and J. G. Verkade, *Organometallics*, **8**, 2772 (1989).
410. D. Gudat, L. M. Daniels and J. G. Verkade, *J. Am. Chem. Soc.*, **111**, 8520 (1989).
411. D. Gudat, L. M. Daniels and J. G. Verkade, *Organometallics*, **9**, 1464 (1990).
412. J. Woning, L. M. Daniels and J. G. Verkade, *J. Am. Chem. Soc.*, **112**, 4601 (1990).
413. J. Woning and J. G. Verkade, *Organometallics*, **10**, 2259 (1991).
414. D. Gudat and J. G. Verkade, *Organometallics*, **9**, 2172 (1990).
415. J. Pinkas and J. G. Verkade, *Phosphorus, Sulfur, Silicon*, **93–94**, 333 (1994).
416. Y. Wan and J. G. Verkade, *Organometallics*, **15**, 5769 (1996).
417. S. N. Tandura, V. A. Pestunovich, M. G. Voronkov, G. I. Zelchans, I. I. Solomennikova and E. Lukevics, *Khim. Geterotsikl. Soed.*, 1063 (1977); *Chem. Abstr.*, **88**, 5715p (1978).
418. E. Kupce, E. Liepins, A. Lapsina, G. Zelchan and E. Lukevics, *J. Organomet. Chem.*, **333**, 1 (1987).
419. V. A. Pestunovich, N. F. Lazareva, O. B. Kozyreva, L. V. Klyba. G. A. Gavrilova and M. G. Voronkov, *Zh. Obshch. Khim.*, in press
420. J. Grobe, G. Henkel, B. Krebs and N. Voulgarakis, *Z. Naturforsch., B: Anorg. Chem., Org. Chem.*, **39B**, 341 (1984).
421. E. Lukevics, I. I. Solomennikova and G. I. Zelchans, USSR Patent 509049, 1974; *Bull. Izobret.*, No. 9, 217 (1977); *Chem. Abstr.*, **87**, 23483w (1977).
422. F. G. Rima, J. Satge, M. Fatome, J. D. Laval, H. Sentenac-Roumanou, C. Lion and M. Lazraq, *Eur. J. Med. Chem.*, **26**, 291 (1991).

CHAPTER 25

Tris(trimethylsilyl)silane in organic synthesis

C. CHATGILIALOGLU, C. FERRERI* and T. GIMISIS

I.Co.C.E.A., Consiglio Nazionale delle Ricerche, Via P. Gobetti 101, 40129 Bologna, Italy

I. INTRODUCTION

The synthetic application of free-radical reactions has increased dramatically within the last decade. Nowadays, radical reactions can often be found driving the key steps of multistep chemical synthesis oriented towards the construction of complex natural products[1]. Tributyltin hydride is the most commonly used reagent for the reduction of functional groups and formation of C−C bonds either inter- or intramolecularly (cyclization)[2,3]. However, it is well known that there are several problems associated with organotin compounds[4]. The main drawback consists of the incomplete removal of highly toxic tin by-products from the final material. For this reason, it is inappropriate to extend these reactions to industrial and medicinal chemistry. It is therefore of great importance to find new reagents which are suitable from a toxicological point of view and are analogous to organotin hydrides in their chemistry, so that the knowledge gained in the last thirty years in the field of free radicals can be further applied.

---

* On sabbatical leave. Permanent address: Dipartimento di Chimica Organica e Biologica, Università di Napoli 'Federico II', Via Mezzocannone 16, 80134 Napoli, Italy.

Ten years ago, one of us introduced tris(trimethylsilyl)silane, $(TMS)_3SiH$, as an alternative approach[5,6]. $(TMS)_3SiH$ has indeed quickly proven to be a valid alternative to tin hydride for the majority of its radical chain reactions, although in some cases the two reagents can complement each other[4,7]. Although the above considerations coupled with the ease of purification and lack of toxicity of $(TMS)_3SiH$ and its by-products should have rendered this reducing agent as the reagent of choice in radical reactions, tributyltin hydride still remains the reagent primarily used by synthetic chemists who decide to incorporate one or more radical steps in their synthetic schemes. Attempting to explain this fact by cost arguments is no longer valid, especially when one takes into account the effective loss of valuable products through exhausting purification procedures for the elimination of stubborn tributyltin residues. In our opinion the following two arguments can explain why $(TMS)_3SiH$ is still waiting to be fully recognized and widely used as radical-based reducing agent: (a) the fact that Bu_3SnH has long been established as a reliable radical reducing agent, supported by a vast literature which highlights its advantages and also clarifies its limitations; (b) more specifically, the fact that the slower hydrogen donation of $(TMS)_3SiH$ is considered in many cases a disadvantage for its use in radical chemistry. It is also worth emphasizing that there is a growth of cases where the two reagents behave differently.

It is not our purpose to review the entire chemistry of $(TMS)_3SiH$. Rather, this survey reflects the scientific interest of our group and deals mainly with the recent literature on the application of $(TMS)_3SiH$ in organic synthesis. We do not also wish to discuss further the differences between the silicon and tin hydrides, although some salient features of the two reagents will be included. In order to help those readers who are not familiar with radical chemistry, we discuss below some general aspects of radical chain reactions as well as the abilities of group 14 hydrides, particularly silanes, to donate hydrogen atom.

A. General Aspects of Radical Chain Reactions

The majority of radical reactions of interest to synthetic chemists are chain processes[2,3]. Scheme 1 represents the simple reduction of an organic halide by silicon hydride as an example of a chain process. Thus, $R'_3Si^\bullet$ radicals, generated by some initiation processes, undergo a series of propagation steps generating 'fresh' radicals. The chain reactions are terminated by radical combination or disproportionation. In order to have an efficient chain process, the rate of chain-transfer steps must be higher than that of chain-termination steps. The following observations: (i) the termination rate constants in liquid phase are controlled by diffusion (i.e. 10^{10} M^{-1} s^{-1}), (ii) radical concentrations in chain reactions are about 10^{-7}–10^{-8} M (depending upon the reaction conditions) and (iii) the concentration of reagents is generally between 0.05–0.5 M, indicating that the rate constants for the chain-transfer steps must be higher than 10^3 M^{-1} s^{-1}.

The free-radical construction of C−C bonds either inter- or intramolecularly using a hydride as mediator is of great importance in chemical synthesis. The propagation steps for the intermolecular version are shown in Scheme 2. For a successful outcome, it is important (i) that the $R'_3Si^\bullet$ radical reacts faster with RZ (the precursor of radical $R^\bullet$) than with the alkene and (ii) that the alkyl radical reacts faster with alkene (to form the adduct radical) than with the silane. In other words, for a synthetically useful radical chain reaction, the intermediates must be *disciplined*. Therefore, in a synthetic plan one is faced with the task of considering kinetic data or substituent influence on the selectivity of radicals. The reader should note that the hydrogen donation step controls the radical sequence and, often, the concentration of silane provides the variable by which the products distribution can be influenced.

Initiation steps:

$$R'_3SiH \xrightarrow[\text{Initiator}]{\text{Radical}} R'_3Si\bullet$$

Propagation steps:

$$R'_3Si\bullet + RX \longrightarrow R'_3SiX + R\bullet$$

$$R\bullet + R'_3SiH \longrightarrow RH + R'_3Si\bullet$$

Termination steps:

$$\left.\begin{array}{r} 2R'_3Si\bullet \longrightarrow \\ R\bullet + R'_3Si\bullet \longrightarrow \\ 2R\bullet \longrightarrow \end{array}\right\} \text{no radical products}$$

SCHEME 1

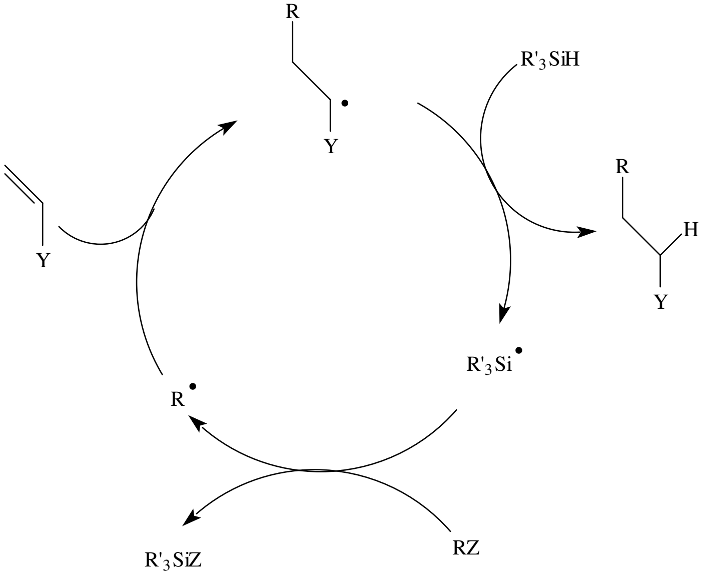

SCHEME 2

B. Hydrogen Donor Abilities of Silanes

We already mentioned that the majority of free-radical reactions applied in synthesis deal with Bu_3SnH. Occasionally, Bu_3GeH has been used as complement to Bu_3SnH. The corresponding silanes, i.e. trialkylsilanes, are not capable of donating hydrogen atom at a sufficient rate to propagate the chain. Rate constants for hydrogen abstraction from

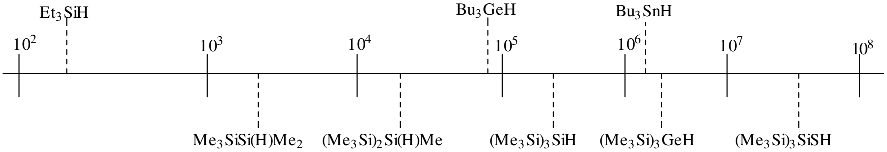

FIGURE 1. Rate constants for hydrogen abstraction (k, $M^{-1}\,s^{-1}$) from a variety of group 14 reducing agents by primary alkyl radicals at 25 °C

TABLE 1. Rate constants for the reaction of some radicals with $(TMS)_3SiH$

Radical	$\log A - E_a/\theta^a$	k_{SiH} ($M^{-1}\,s^{-1}$) at *ca* 27 °C	Reference
t-BuO$^•$		1.1×10^8	12
RCH$_2$$^•$	$8.9 - 4.5/\theta^b$	3.8×10^5	13
R$_2$CH$^•$	$8.3 - 4.3/\theta^b$	1.4×10^5	13
R$_3$C$^•$	$7.9 - 3.4/\theta^b$	2.6×10^5	13
Ph$^•$		$2.8 \times 10^{8^c}$	13,14
n-C$_7$F$_{15}$$^•$		$5.1 \times 10^{7^d}$	15
RC(O)$^•$	$8.2 - 5.4/\theta^{e,f}$	1.8×10^4	16

[a] Absolute rate expression, i.e. $\log k_{SiH} = \log A - E_a/\theta$, where $\theta = 2.3\ RT$ kcal mol^{-1}

[b] Depends on literature values for 5-hexenyl-type rearrangements.

[c] Depends on the rate constant for the cyclization of o-(allyloxy)phenyl radical.

[d] Depends on the rate constant for the addition of the radical to 1-hexene.

[e] Similar values are obtained for R being primary, secondary and tertiary.

[f] Depends on literature Arrhenius parameters for the decarbonylation of propanoyl radical in the gas phase.

a variety of group 14 hydrides by primary alkyl radicals at ambient temperature are reported on a reactivity scale in Figure 1. In the upper part of the diagram the reactivities of trialkyl-tin, -germanium and -silicon hydrides are shown[8–10].

Following the success of $(TMS)_3SiH$, other organosilanes capable of sustaining analogous radical chain reactions have been introduced. In the lower part of Figure 1 the reactivities of a variety of organosilanes towards primary alkyl radicals are reported. In conclusion, a reactivity scale that is useful in synthetic planning has been established. The rate constants cover a range of several orders of magnitude and therefore the hydrogen donating abilities of organosilanes can be modulated by substituents. A recent review by Chatgilialoglu provides in-depth coverage of this class of reactions[11].

Table 1 summarizes the kinetic data available for the reaction of $(TMS)_3SiH$ with a variety of radicals. It has been shown that the attacks of both t-BuO$^•$ and RCH$_2$$^•$ radicals on the Si−H bond and the methyl groups occur in about 95% and 5% of the cases, respectively[11]. The rate constants for the reaction of primary, secondary and tertiary alkyl radicals with $(TMS)_3SiH$ are very similar in the range of temperatures that are useful for chemical transformation in the liquid phase. This is due to compensation of entropic and enthalpic effects through this series of alkyl radicals.

II. AUTOXIDATION OF TRIS(TRIMETHYLSILYL)SILANE

This silane reacts spontaneously at ambient temperature with molecular oxygen to form siloxane as the sole product (equation 1).

$$(Me_3Si)_3SiH + O_2 \longrightarrow (Me_3SiO)_2Si(H)SiMe_3 \qquad (1)$$

Mechanistic studies based on labeling experiments[17] and kinetic studies[18] have indicated a chain reaction to occur in which the silyl radical adds to molecular oxygen to form the corresponding peroxyl species which undergoes a cascade of unimolecular reactions and, finally, abstracts hydrogen to give the observed product and regenerate $(TMS)_3Si^\bullet$ radical. The rate constant for the initiation step is found to be $5.1 \times 10^{-5}\ M^{-1}\ s^{-1}$ at 70 °C.

Two aspects of the autoxidation of $(TMS)_3SiH$ are of interest to synthetic chemists[19]: (i) for radical reactions having long chain length, traces of molecular oxygen can serve to initiate reactions, and therefore no additional radical initiator is needed, and (ii) the oxidized product does not interfere with radical reactions, and therefore the reagent can be used even if partially oxidized, taking into account the purity of the material. From GC analysis, the exact concentration of silane can be deduced.

III. REDUCTIONS

Tris(trimethylsilyl)silane is found to be an efficient reducing agent for a variety of functional groups. In particular, the reduction of halides, chalcogen groups, thiono esters and isocyanides are the most common ones. The efficiency of these reactions is also supported by available kinetic data. The rate constants for the reaction of $(TMS)_3Si^\bullet$ radicals with a variety of organic substrates are collected in Table 2.

Reduction of iodides and bromides is straightforward, and the reactions are complete after a short time. Two examples are given in equations 2 and 3[22,23]. The efficiency depends to a limited extent on the substituent; in alkyl bromides the rate constants decrease along the series benzyl > tertiary alkyl > secondary alkyl > primary alkyl > phenyl (see Table 2). $(TMS)_3SiH$ can be also used as a reagent for driving the reduction of iodides and bromides through a radical mechanism with sodium borohydride, the reductant that is consumed. In equation 4, 1-bromonaphthalene is treated with an excess of $NaBH_4$ (50 equiv) and a small amount of $(TMS)_3SiH$ (0.1 equiv), under photochemical initiation conditions, to give the reduced product in 88% yield[24].

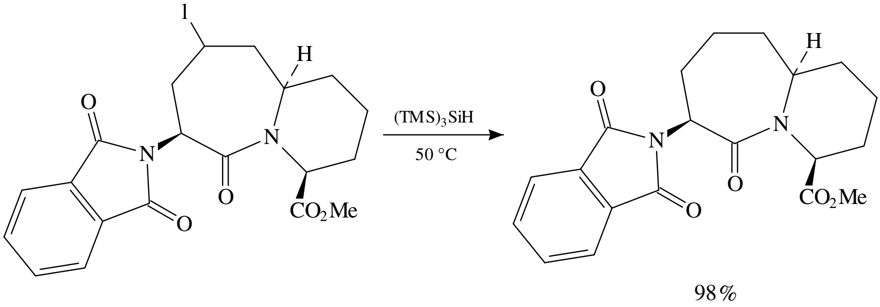

(2)

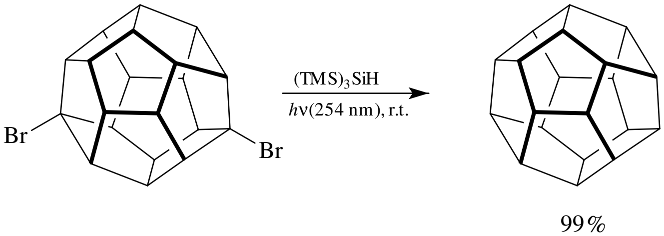

(3)

TABLE 2. Rate constants for the reaction of $(TMS)_3Si^{\bullet}$ radicals with some organic substrates at ambient temperature

Halides[a]	k ($M^{-1}\,s^{-1}$)	Others[c]	k ($M^{-1}\,s^{-1}$)
$CH_3(CH_2)_4Br$	2.0×10^7	n-$C_{10}H_{21}SPh$	$< 5 \times 10^6$
$CH_3CH_2CH(CH_3)Br$	4.6×10^7	n-$C_{10}H_{21}SePh$	9.6×10^7
$(CH_3)_3CBr$	1.2×10^8	n-$C_{12}H_{25}C(O)SePh$[b,d]	2×10^8
$PhCH_2Br$	9.6×10^8	c-$C_6H_{11}OC(S)SMe$	1.1×10^9
C_6H_5Br	4.6×10^6	c-$C_6H_{11}NC$	4.7×10^7
$CH_3(CH_2)_5C(CH_3)_2Cl$	4.0×10^5	$(CH_3)_3CNO_2$	1.2×10^7
$PhCH_2Cl$	4.6×10^6		
$CHCl_3$	6.8×10^6		
CCl_4	1.7×10^8		
n-$C_{12}H_{25}C(O)Cl$[b,d]	7×10^5		

[a] From Reference 20. [b] From Reference 16. [c] From Reference 21. [d] At 80 °C.

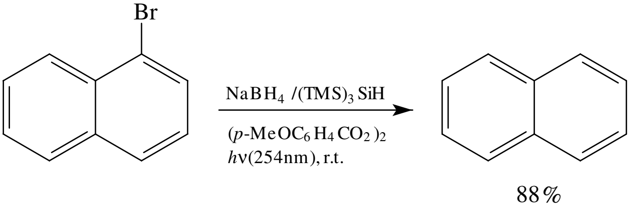

(4)

For tertiary, secondary and primary chlorides the reduction becomes increasingly difficult due to shorter chain lengths. On the other hand, the replacement of a chlorine atom by hydrogen in polychlorinated substrates is much easier. The reduction of the dichloride depicted in equation 5 represented the key step in the total synthesis of dactomelynes[25], natural products isolated from a marine organism. The use of $(TMS)_3SiH$ at room temperature allowed one to obtain in high yield and stereoselectively the monochloride ($\beta : \alpha = 13 : 1$), whereas other radical-based reducing systems failed. In this respect, the stereoselectivity in the reduction of *gem*-dichlorides by $(TMS)_3SiH$ and Bu_3SnH was previously reported[26] and showed that the silane has a stronger preference than tin to transfer a hydrogen atom from the less hindered side of the ring due to the different spatial shapes of the two reagents.

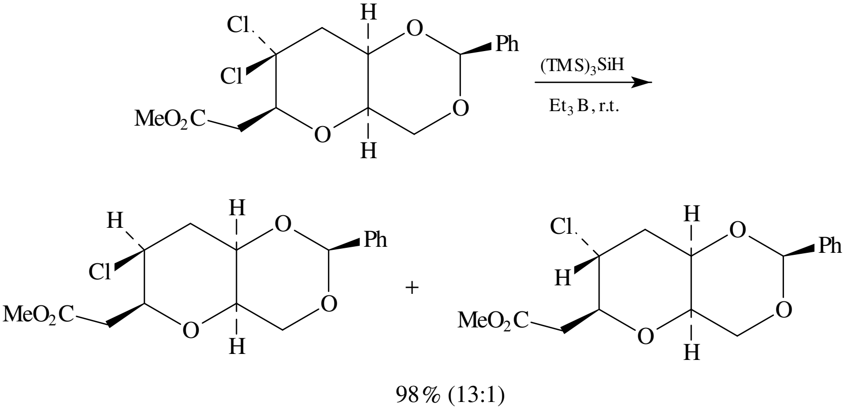

(5)

$(TMS)_3SiH$ does not react spontaneously with acid chlorides, in contrast with Bu_3SnH. Under free-radical conditions, the reaction of $(TMS)_3SiH$ with acid chlorides, RC(O)Cl, gives the corresponding aldehydes and/or the decarbonylation products depending on the nature of substituent R. The reduction of 1-adamantanecarbonyl chloride is shown in equation 6[27].

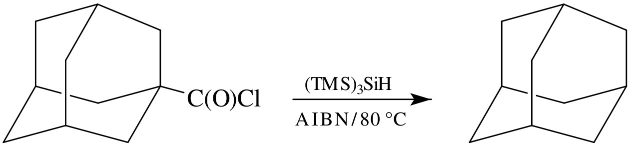

90%

(6)

Early data from product studies and kinetic measurements established that the reaction of $(TMS)_3Si^\bullet$ radical with phenyl alkyl sulfides is sluggish[21]. Nevertheless, it was reported soon after that efficient S_H2 cleavage of C−S bonds could be effected by $(TMS)_3SiH$ when the resulting carbon-centered radicals were further stabilized by an α-heteroatom[28,29]. Therefore, $(TMS)_3SiH$ can induce the efficient radical chain monoreduction of 1,3-dithiolane[28,30], 1,3-dithiane[28], 1,3-oxathiolane[29,30], 1,3-oxathiolanone[29,30] and 1,3-thiazolidine[29,30] derivatives. Three examples are outlined in equation 7. The $(TMS)_3Si$ group incorporated in the adducts could be conveniently deprotected with fluoride ions generating a thiolate anion which could be used for further synthetic transformations[31]. The reduction of chiral 1,3-thiazolidine derivatives (as 1 : 1 mixture of diastereoisomers) was used as a model for studying the stereoselectivity in the hydrogen abstraction of α-aminoalkyl radicals[32]. These intermediates abstract hydrogen giving different *anti*/*syn* ratios, depending on the substituents. An example is given in equation 8.

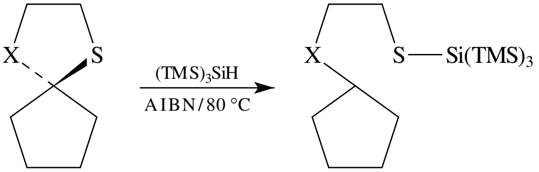

(7)

X = S 85%
X = O 84%
X = NC(O)OEt 79%

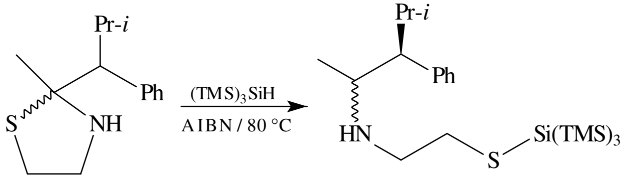

(8)

92% (*anti*:*syn* = 84:16)

Secondary alkyl selenides are reduced by $(TMS)_3SiH$ (equation 9), as expected in view of the affinity of silyl radicals for selenium-containing substrates (Table 2)[21]. Similarly to 1,3-dithiolanes and 1,3-dithianes, 5- and 6-membered selenoacetals can be monoreduced to the corresponding selenides in the presence of $(TMS)_3SiH$[33]. The silicon hydride approached from the less hindered equatorial position to give *trans*/*cis* ratios of 30/70 and 25/75 for the 5-membered (equation 10) and 6-membered selenoacetals, respectively, whereas Bu_3SnH transferred a hydride preferentially from the axial position.

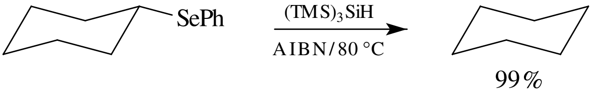

(9)

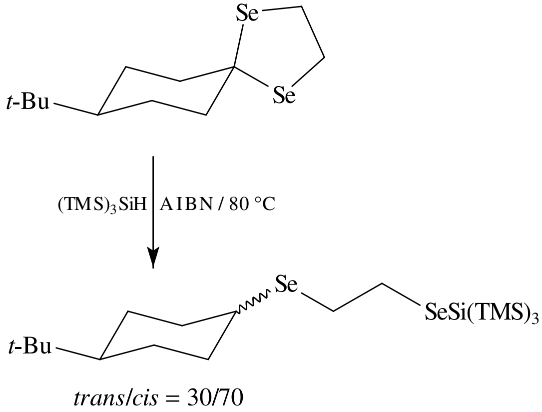

(10)

Phenyl selenoesters have been reported to undergo reduction to the corresponding aldehydes and/or alkanes in the presence of $(TMS)_3SiH$ under free-radical conditions[16]. The decrease of aldehyde formation through the primary, secondary and tertiary substituted series, under the same conditions, indicated that a decarbonylation of acyl radicals takes place. Equation 11 shows an example of a tertiary substituted substrate.

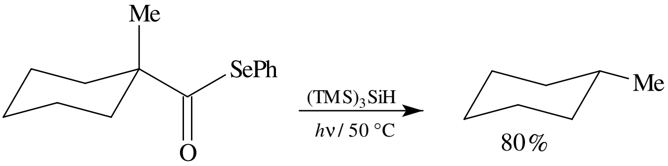

(11)

The removal of the hydroxy group has been achieved from an appropriate selenocarbonate by heating with $(TMS)_3SiH$ and AIBN in benzene. Equation 12 outlines a particular of a multistep synthesis of an alkaloid. The deoxygenation was achieved with 87% efficiency of the two steps[34].

In the above-described displacement reactions (S_H2) of sulfur and selenium containing compounds, the mechanism could either be a synchronous or a stepwise process (Scheme 3). Thus, in the S_H2 stepwise path an intermediate sulfuranyl or selenanyl radical is formed[35a], followed by α-cleavage. Based on competitive studies, a stepwise process was suggested to occur in the reaction of $(TMS)_3Si^\bullet$ radical with *n*-decyl phenyl selenide[21]. On the other hand, *ab initio* calculations favored the synchronous process and the same observations were explained in terms of an overall reversible reaction[35b].

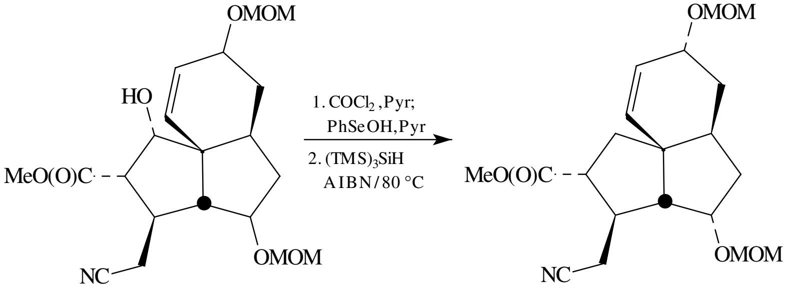

(12)

MOM = Methoxymethyl

87%

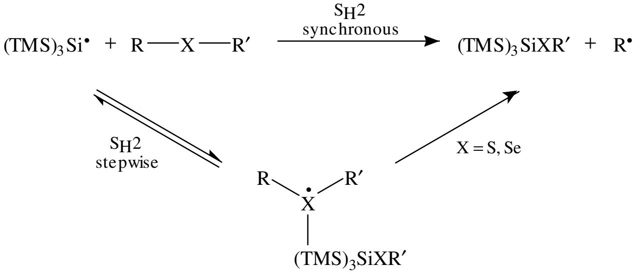

SCHEME 3

Another relevant reductive process which has been largely applied and studied in organic synthesis is the deoxygenation reaction, well known as the Barton–McCombie reaction. The reaction, shown in equation 13, involves thiocarbonyl derivatives, easily obtained from the alcohol, and a radical reducing agent which acts as hydrogen donor, in the presence of initiator and appropriate conditions. The use of silicon hydrides as radical-based reducing agents in the Barton–McCombie reaction and their comparison with Bu_3SnH has recently been reviewed by two of us[7]. Therefore, only examples of $(TMS)_3SiH$ that have appeared in the more recent literature will be discussed.

$$\text{ROH} \longrightarrow \text{ROC(S)X} \xrightarrow{(\text{TMS})_3\text{SiH}} \text{RH} \qquad (13)$$

An improved homolytic deoxygenation of amino acid derivatives has been reported[36]. The reaction with *O*-phenyl chlorothionocarbonate/DMAP afforded the phenoxythiocarbonyl derivative of a protected homoserine dimethylphosphonate (95% yield), followed by its treatment with the silane at 80 °C in toluene to give the deoxygenated product. Without purification, acid treatment by TFA and an aqueous extraction gave the final products in 72% yield (equation 14). Using the silane procedure a simplification of the work-up resulted, since the extraction with water was enough to separate the product from silyl and sulfur containing by-products.

The dideoxygenation of 1,6-anhydro-D-glucose with $(TMS)_3SiH$ has been described to yield the desired product in 86% yield (equation 15), whereas other radical-based reducing systems give much poorer yields[37]. Radical dideoxygenation was also useful to prove the structure of a stemodane ring system, achieved by other routes. The dithioimidazolyloxy compound in equation 16 was reduced in quantitative yield under normal experimental conditions[38].

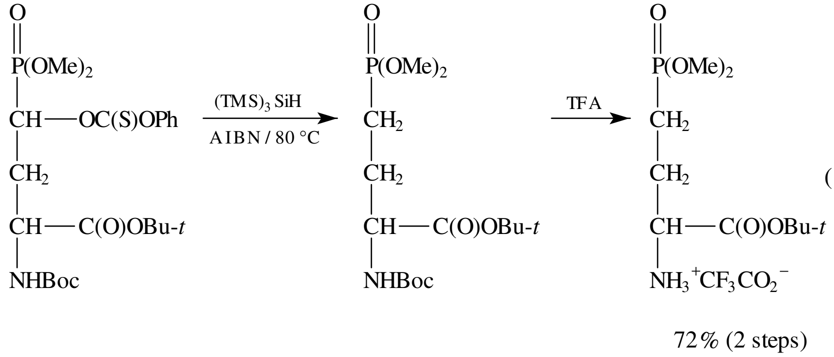

(14)

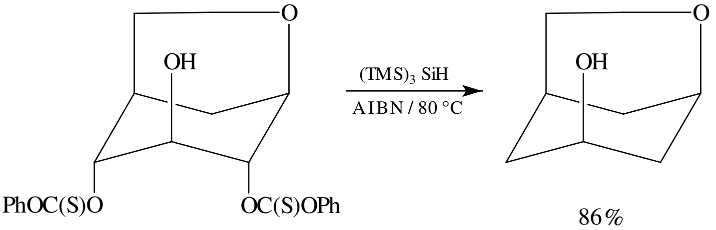

(15)

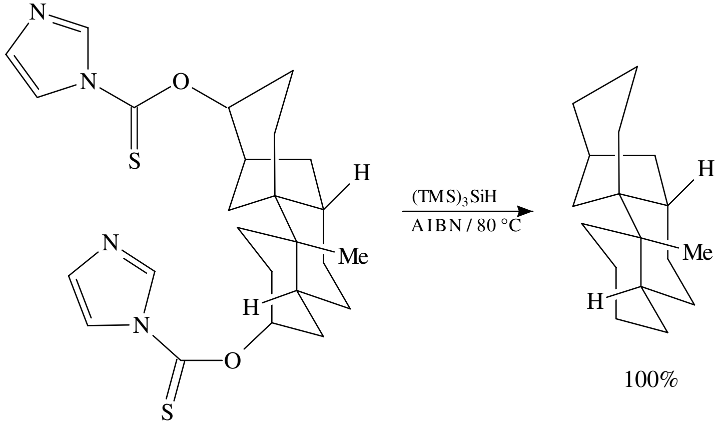

(16)

In order to study the structure–activity relationship of pharmaceutically active derivatives of baccatin III, radical-based deoxygenations were used to generate a systematic defunctionalization of the taxole core. When tris(trimethylsilyl)silane was used as reducing agent of the xanthate functionality (equation 17; yields based on the consumption of the starting material), a cascade of intramolecular rearrangements took place, due to the slower hydrogen donation of silane relative to tin hydrides[39].

It is worth adding that the usual starting derivatives for the deoxygenation of alcohols (i.e. X = SMe, OPh and imidazolyl in equation 13) have recently been extended to include thioxocarbamates (X = HNPh) with the same success[40]. The mechanism of the reduction of thionoesters by $(TMS)_3SiH$ is the following: $(TMS)_3Si^{\bullet}$ radical, initially generated by small amounts of AIBN, attacks the thiocarbonyl moiety to form in a reversible manner a radical intermediate that undergoes β-scission to form an alkyl radical. Hydrogen abstraction from the silane gives the alkane and $(TMS)_3Si^{\bullet}$ radical, thus completing the cycle of this chain reaction[7,21].

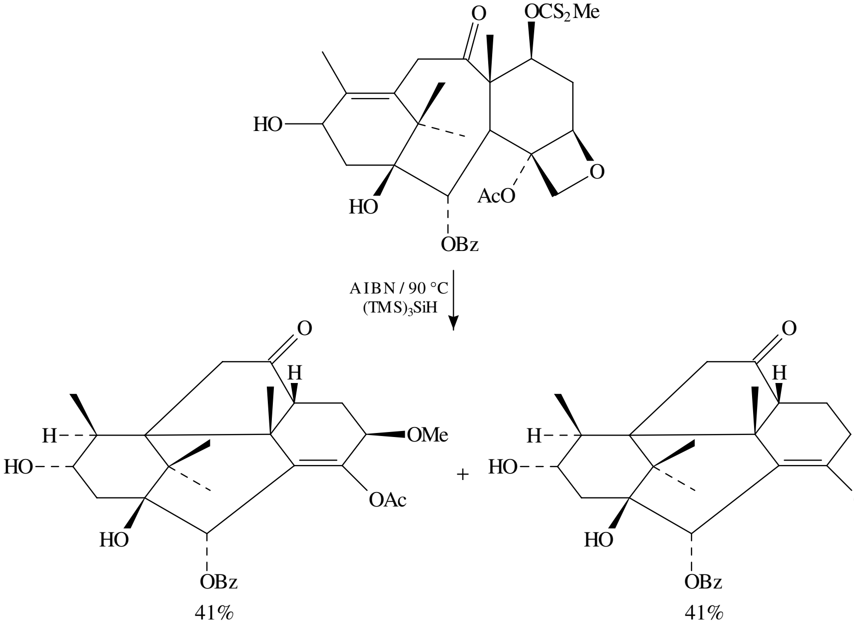

(17)

Isocyanides can be reduced to the corresponding hydrocarbon by $(TMS)_3SiH$. The reaction can be considered as the deamination of primary amines since isocyanides are obtained via formylation of amines and dehydration. The efficiency of the reduction is independent of the nature of the alkyl substituent. That is, primary, secondary and tertiary isocyanides at 80 °C gave the corresponding hydrocarbon in good yields[21]. An example is given in equation 18[4].

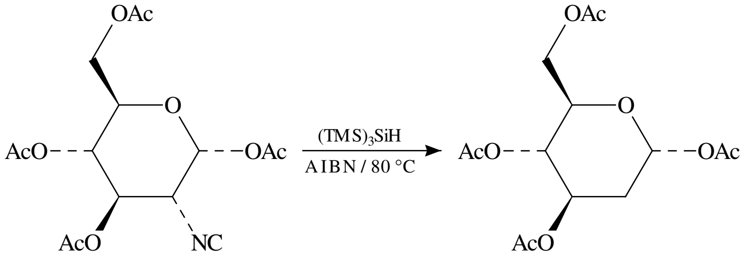

(18)

$(TMS)_3SiH$ is not able to reduce tertiary nitroalkanes to the corresponding hydrocarbons whereas tin hydrides are efficient in this process[41]. This 'anomalous' behavior is due to the fact that the nitroxide adducts formed by addition of $(TMS)_3Si^{\bullet}$ radical to the nitro compounds, i.e. $RN(O^{\bullet})OSi(TMS)_3$, fragment preferentially at the nitrogen–oxygen bond rather than at the carbon–nitrogen bond as in the analogous tin adduct (equation 19)[41a].

For the reactions of *N*-nitramines with $(TMS)_3SiH$ a similar behavior has also been observed, although in this case the corresponding *N*-nitrosoamines are obtained in *ca* 60% yield[41b].

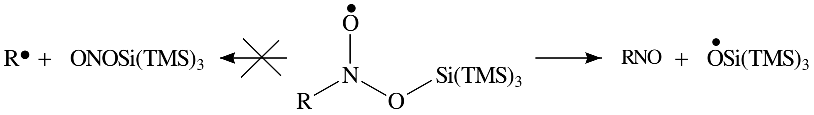

(19)

1-Methylquinolinium ion derivatives are reduced regioselectively to 1,4-dihydroquinones by $(TMS)_3SiH$ under photochemical conditions[42]. Mechanistic studies demonstrated that the reactions are initiated by photoinduced electron transfer from silane to the singlet excited states of 1-methylquinolinium ion derivatives to give the silane radical cation — quinolinyl radical pairs, followed by hydrogen transfer in the cage to yield 1,4-dihydroquinones and silicenium ion. The one-electron oxidation potential of $(TMS)_3SiH$ is 1.30 V[42].

It is worth pointing out that the replacement of a variety of functional groups by a hydrogen described so far is not only an efficient and straightforward process but the work-up is rather simple: the reaction mixtures can be concentrated by evaporation of the solvent and then flash-chromatographed to isolate the products. Furthermore, it has been shown that $(TMS)_3SiH$ and its silylated by-products are not toxic; this is very important for pharmaceutical application of the silane reagent, since the biological assays on the final compounds are not affected by the eventually remaining silylated materials[43]. It can be expected that in the future an increasing choice of $(TMS)_3SiH$ as reducing agent, especially in the field of natural products synthesis, will take place.

In this respect, some recent reports on the radical reduction of pharmaceutically relevant compounds showed the efficiency and effectiveness of this reagent. Here below we describe some examples in the field of nucleoside chemistry.

The deoxygenation of nucleosides has been well represented in the last few years for at least two main reasons: the radical deoxygenation in C-2′ can be used as simple conversion from ribonucleosides to deoxyribonucleosides to be incorporated in DNA oligomers, and many new potent anti-HIV and antiviral drugs having the 2′- or 3′-deoxy as well as 2′,3′-dideoxy nucleosides skeleton were recently introduced in therapy. Compared with other routes, the formation of thiocarbonyl derivatives of the alcoholic function on the sugar moiety and its subsequent radical reduction has appeared to provide the easiest access to these substrates, avoiding any other side reactions. 2′-Deoxyapio-*β*-D-furanosyl nucleosides were prepared by deoxygenation from the corresponding thiocarbonate derivatives (equation 20), and tested against HIV, Herpes simplex and other viruses[44]. Pharmaceutically important 2′-and/or 3′-deoxynucleosides were described in a patent[45] and the key step for the synthesis was achieved by treating the new and economically more convenient (cyanoethylthio) thiocarbonyl derivatives of nucleosides, instead of classical xanthates, with $(TMS)_3SiH$ under very mild conditions (equation 21). In the field of nucleosides mimic, *β*-2′-deoxypseudouridine[46] and *β*-2′-deoxyzebularine[47] were prepared by radical-based deoxygenation from the corresponding *β*-pseudouridine and *β*-zebularine using $(TMS)_3SiH$ as reducing agent.

Equations 22 and 23 show two examples of chloride and phenylseleno removal from the sugar moiety under normal radical conditions[48], whereas in equation 24 the removal of the tritylthio protecting group (TrS) on the base moiety has been accomplished in good yield[49]. On the other hand, starting from the bromide in equation 25 a novel type of a *β*-(acyloxy)alkyl radical rearrangement has been observed, which leads through the generation of a C-1′ radical species to the stereoselective preparation of an *α*-ribonucleoside[48].

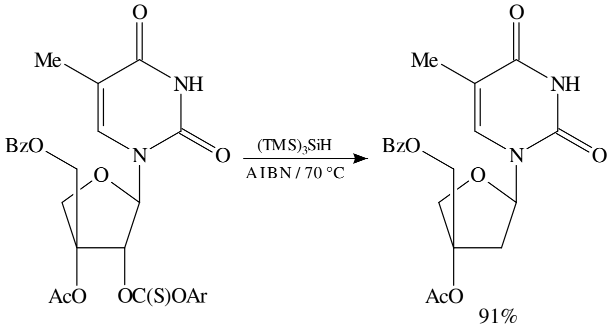
Me
NH
O
BzO
N
O
AcO
OC(S)OAr
(TMS)3SiH
AIBN / 70 °C
91%

(20)

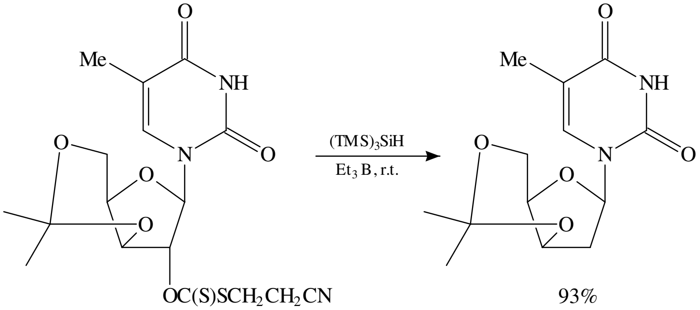
Me
NH
O
N
OC(S)SCH2CH2CN
(TMS)3SiH
Et3 B, r.t.
93%

(21)

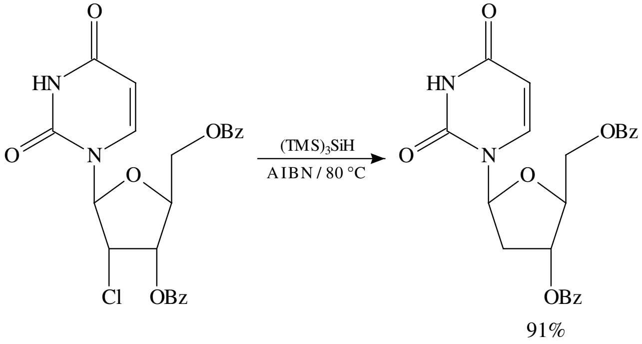
O
HN
N
OBz
Cl
(TMS)3SiH
AIBN / 80 °C
91%

(22)

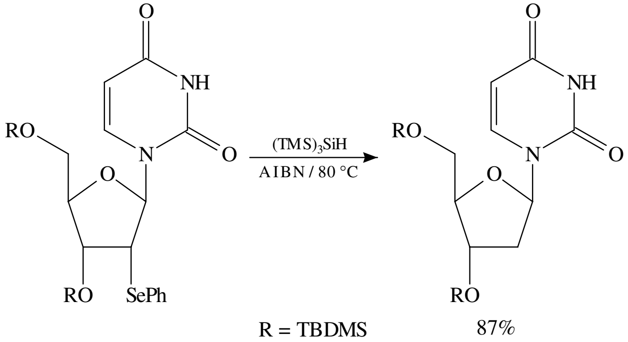
O
NH
RO
N
SePh
(TMS)3SiH
AIBN / 80 °C
R = TBDMS
87%

(23)

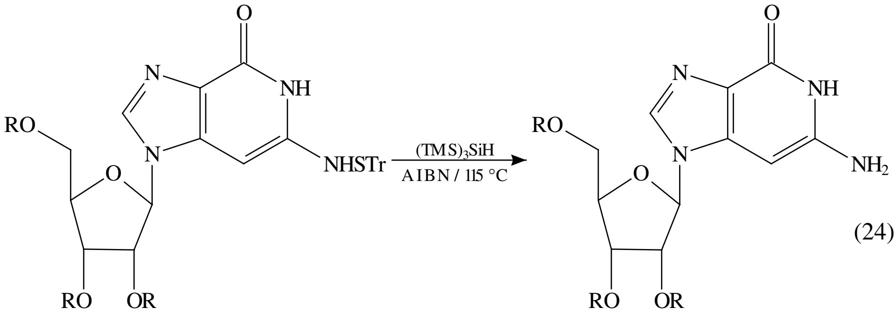

(24)

R = TBDMS 81%

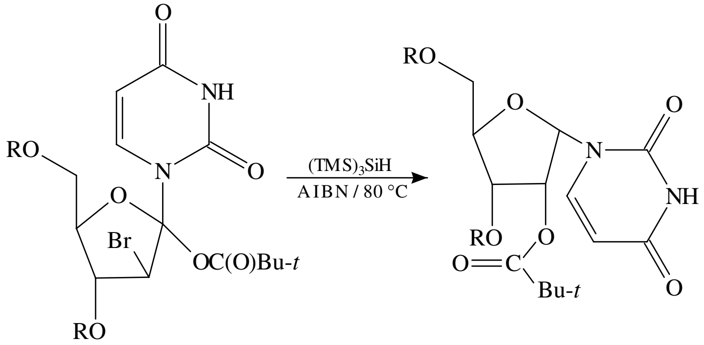

(25)

R = TBDMS 86%

IV. HYDROSILYLATIONS

$(TMS)_3SiH$ adds across the C=C and C=O double bonds of a variety of compounds under free-radical conditions. The propagation steps for these hydrosilylation processes are reported in equations 26 and 27. The available rate constants for the reaction of $(TMS)_3Si^\bullet$ radicals with some ketones and alkenes (equation 26) are collected in Table 3. In the ketone series, the rate constants decrease in the series of quinone > diaryl ketone > dialkyl ketone[50]. On the other hand, the rate constants for the addition of $(TMS)_3Si^\bullet$ radical to activated alkenes[21] are close to $10^8\ M^{-1}\,s^{-1}$.

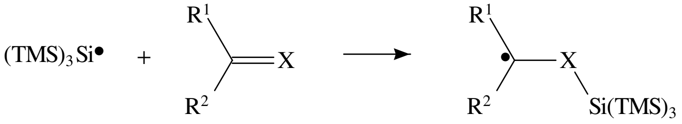

(26)

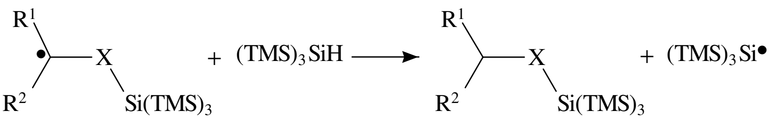

(27)

$X = O$ or CR^3R^4

The hydrosilylation of monosubstituted and *gem*-disubstituted olefins (equation 28 and 29) are efficient processes and have been shown to occur with high regioselectivity

TABLE 3. Rate constants at 20 °C for the reaction of $(TMS)_3Si^\bullet$ radicals with some ketones and alkenes

Substrate[a]	k ($M^{-1}\,s^{-1}$)
Duroquinone[a]	1.0×10^8
Fluorenone[a]	3.8×10^7
Acetone[a]	8.0×10^4
Styrene[b]	5.9×10^7
Acrylonitrile[b]	6.3×10^7
Ethyl acrylate[b]	9.7×10^7

[a] From reference 50. [b] From reference 21

(*anti*-Markovnikov) in the case of both electron-rich and electron-poor olefins[51]. For *cis* or *trans* disubstituted double bonds, hydrosilylation is still an efficient process, although it required slightly longer reaction times (equation 30) and an activating substituent[51]. No hydrosilylation product has been observed with 1,2-dialkyl- and 1,2-diaryl-substituted olefins, due to the reversible addition of $(TMS)_3Si^\bullet$ radical to the double bond[52].

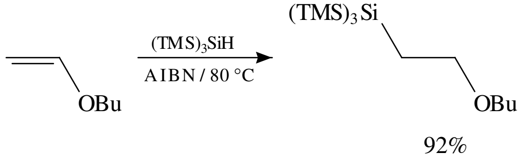

(28)

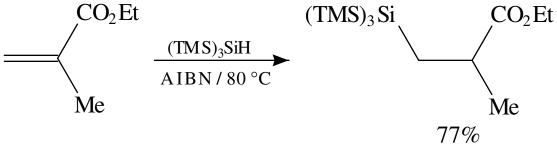

(29)

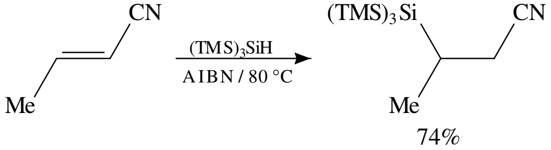

(30)

The above observation on the reversible addition of $(TMS)_3Si^\bullet$ radical to the double bonds is noteworthy from a synthetic point of view. The first consequence is that $(TMS)_3Si^\bullet$ radical is able to isomerize alkenes. That is, this radical adds to (*Z*)- or (*E*)-alkenes to form radical **1** or **2**, respectively (equation 31). Interconversion between the two radical adducts by rotation around the carbon–carbon bond, followed by β-scission, can then lead to the formation of either (*Z*)- or (*E*)-alkene, depending on the radical-alkene combination. For comparison, we report in Figure 2 the reaction profile for the interconversion of (*E*)-to (*Z*)-3-hexen-1-ol and *vice versa* by $(TMS)_3Si^\bullet$ and $Bu_3Sn^\bullet$ radicals, under identical experimental conditions. The choice of either $Bu_3Sn^\bullet$ or $(TMS)_3Si^\bullet$ radical does not influence the isomeric composition of the alkene after completion, i.e. $Z/E = 18/82$, although the equilibration of the two geometrical isomers is reached much faster with tin radicals. Therefore, care must be taken when the isomerization can occur *in situ*, while accomplishing other reactions[52–55]. A postisomerization process can be invoked in several reported cases where the two reagents behave differently (*vide infra*).

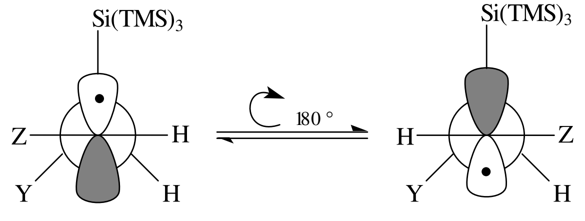

(1) **(2)**

(31)

Depending upon the choice of substrates, the hydrosilylation of alkenes can also be highly stereoselective. Two examples are given below. The reaction with methylmaleic anhydride proceeded regiospecifically to the less substituted side, but also diastereoselectively to afford the thermodynamically less stable *cis* isomer. The stereoselectivity decreased by increasing the reaction temperature, indicating the difference in enthalpy of activation for *syn* vs *anti* attack (equation 32). On the other hand, a complete stereocontrol has been achieved in the reaction with the α-chiral olefins (equation 33, R = Me)[56]. The observed stereoselectivity was rationalized in terms of steric and Felkin–Anh

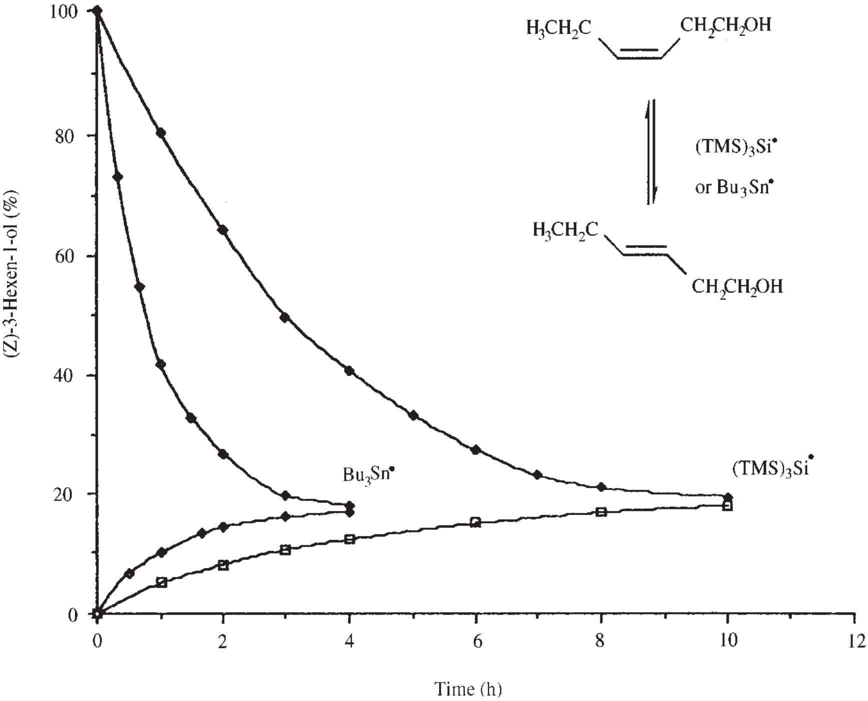

FIGURE 2. Isomerizations of *E*- and *Z*-3-hexen-1-ol. Conditions: 0.5 equiv of hydride and AIBN (5 mol%) at intervals of 2 h in refluxing benzene

stereoelectronic controls.

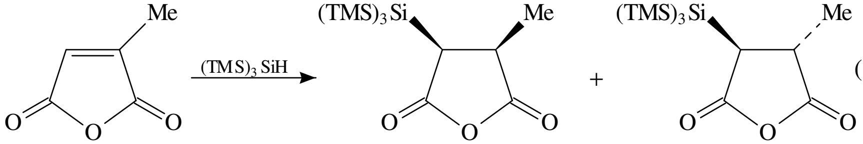

(32)

AIBN / 90°C 89% (16:1)

Et_3B, O_2/–15°C 60% (99:1)

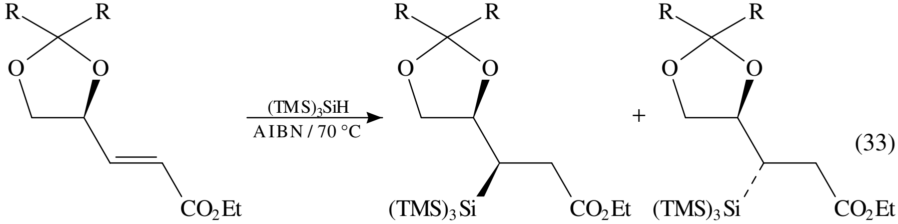

(33)

R = H 65% (85:15)

R = Me >95% (100:0)

Hydrosilylation of ketones with $(TMS)_3SiH$ were also examined[50,57] and resulted in generally good yields. For example, the reactions with cycloalkanones under normal conditions, i.e. AIBN/80 °C, gave the silylated products in high yields (>70%). With 4-*tert*-butylcyclohexanone, the products ratio *trans* : *cis* = 10 : 1 was obtained, indicating that axial attack by the intermediate α-silyloxy radical is favored[57]. By means of the addition of $(TMS)_3SiH$ to chiral ketones, the 1,2-stereoinduction in carbon-centered radicals bearing an α-silyloxy substituent has been studied[58]. An example is given in equation 34.

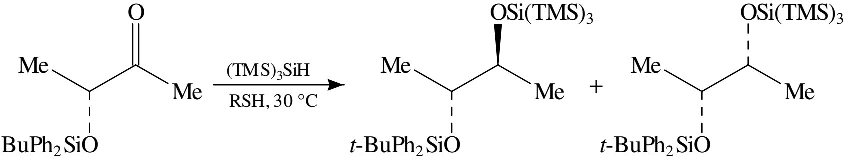

64% (1:4)

(34)

The addition of $(TMS)_3SiH$ to a number of mono and disubstituted acetylenes has also been studied[51,59]. The reaction gives $(TMS)_3Si$-substituted alkenes in good yields via a radical chain mechanism where the key intermediate is a vinyl radical. The reaction is highly regioselective (*anti*-Markovnikov) and can also show high *cis* or *trans* stereoselectivity depending on the nature of the substituents at the acetylenic moiety. Two examples are given in equations 35 and 36. Although the $(TMS)_3Si^\bullet$ has been proven to isomerize alkenes, the postisomerization of the hydrosilylation adduct could not be observed due to steric hindrance. The (*Z*)–(*E*) interconversion of $(TMS)_3Si$-substituted alkenes was achieved by using $Ph_3Ge^\bullet$ radical as an isomerizing agent[59]. The hydrodesilylation and bromodesilylation of adducts were performed in good yields and with retention of stereochemistry (equations 35 and 36)[51,59].

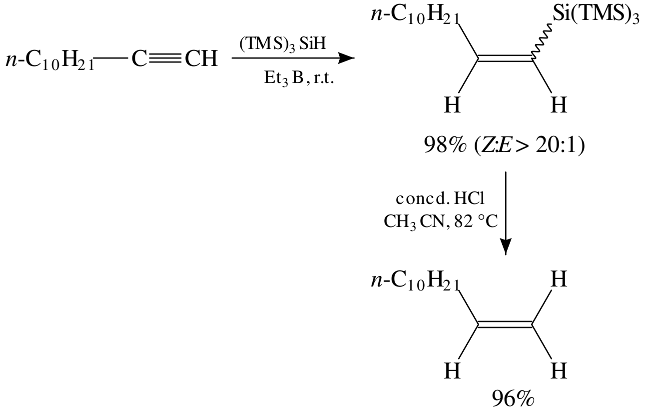

(35)

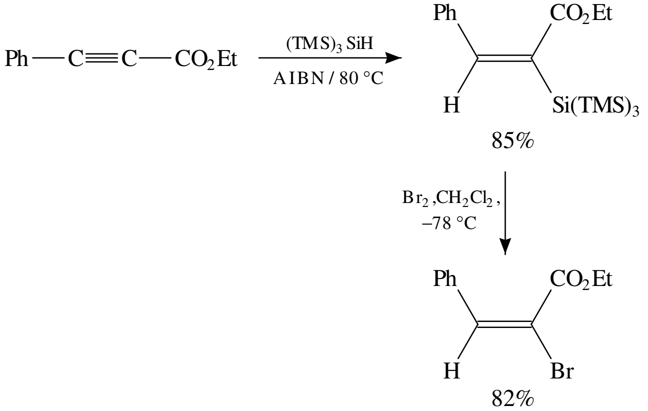

(36)

V. CONSECUTIVE RADICAL REACTIONS

The alkyl radical that is created by the initial atom (or group) abstraction by $(TMS)_3Si^\bullet$ radical or by addition of $(TMS)_3Si^\bullet$ to unsaturated bonds is often designed so that it can undergo a number of consecutive reactions. Care has to be taken in order to ensure that the effective rates of the consecutive radical reactions are higher than the rate of hydrogen abstraction from $(TMS)_3SiH$. Apart from standard synthetic planning based on known rate constants (see Sections I.A and I.B), this is usually effected either by controlling the concentration of the reducing agent present (slow addition by syringe-pump) or, in the case of intermolecular addition reactions, by adding a large excess of the radical acceptor. In both cases, however, tris(trimethylsilyl)silane is advantageous when compared with Bu_3SnH due to its lower hydrogen donation ability which provides the intermediate radical species the time to undergo the desired sequential reactions prior to reduction. In fact, in many cases direct addition of $(TMS)_3SiH$ often gives results comparable to the syringe-pump addition of Bu_3SnH. The purpose of the following paragraphs is to introduce $(TMS)_3SiH$ as a reliable radical mediator in the synthetic community, providing also some enlightenment on its advantages and disadvantages based on the updated work published on its use.

A. Initiation by Atom (or Group) Abstraction

The intermolecular C−C bond formation mediated by $(TMS)_3SiH$ has been the subject of several investigations. In the initial work, the reaction of cyclohexyl iodide or isocyanide with a variety of alkenes was tested in order to find out the similarities with tin reagents (equations 37 and 38)[60,61]. The propagation steps for these reactions are shown in Scheme 2 in Section I.A. It is worth pointing out that with iodides the reaction yields are comparable with those obtained by the tin method, whereas no C−C bond formation takes place when alkyl isocyanides are used together with Bu_3SnH in the presence of alkenes. Similarly, bishomolithocholic acid **(3)** was synthesized from the corresponding iodo derivative (equation 39)[62]. This analog of lithocholic acid with a modification of the side chain was synthesized together with others in order to study their inhibitory effects on glucuronosyl transferase activity in a colon-cancer cell line, thus attempting to identify structural features critical for the enzyme inhibition. The ease of isolation and purification of the product was in accord with the intended purpose of its synthesis, i.e. biological testing. The reactions of β- or γ-phenyl substituted α-methylenebutyrolactones with BuI in the presence of $(TMS)_3SiH$ afforded α, β- or α, γ-disubstituted lactones in good yield and with high diastereoselectivity (equation 40)[63]. With β- or γ-alkyl substituted substrates the same reaction was found to be less selective.

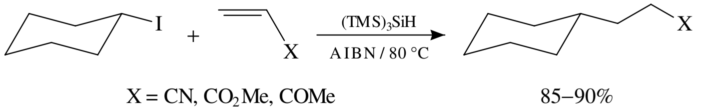

(37)

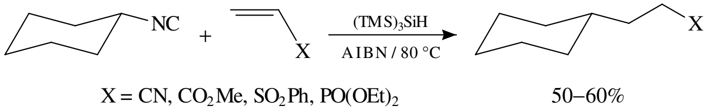

(38)

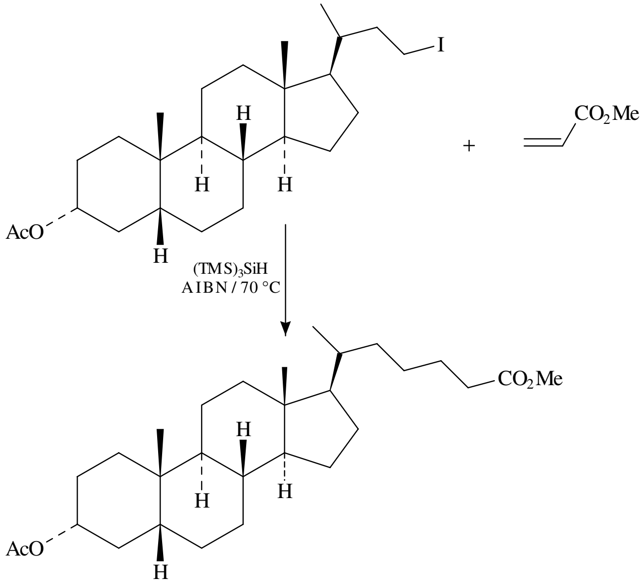

(3) 64%

(39)

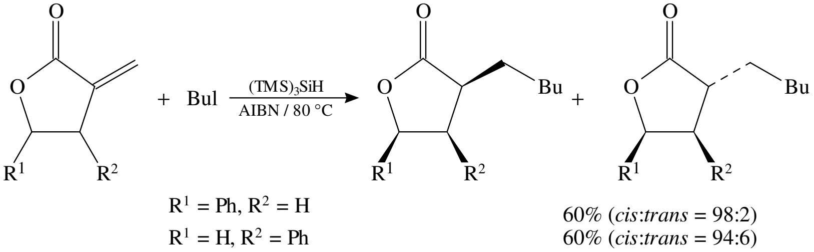

(40)

Radical allylation with 2-functionalized allyl phenyl sulfones has been performed by using $(TMS)_3SiH$ as radical mediator[64]. Yields varied from moderate to good depending on the nature of the starting materials. Two examples are given in equation 41. The reaction proceeded via addition of adamantyl radical to the double bond, giving rise to an intermediate that undergoes β-scission to form $PhSO_2^{\bullet}$ radical which abstracts hydrogen from the silane to regenerate the $(TMS)_3Si^{\bullet}$ radical.

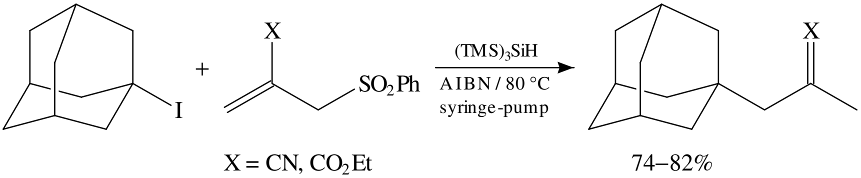

(41)

$(TMS)_3SiH$ has been used as mediator for the alkylation of heteroaromatic compounds by two independent groups[65,66]. Alkyl bromides or iodides treated with protonated heteroaromatic bases and $(TMS)_3SiH$ either under photochemical (irradiation with 400 W of visible light in CH_2Cl_2) or thermal (in the presence of 1–2 molar amounts of AIBN in benzene) conditions afforded the desired product in moderate to good yields. Two examples are given in equations 42 and 43. The presence of AIBN in at least stoichiometric quantity in this homolytic aromatic substitution reaction ensured rearomatization of the intermediate stabilized cyclohexadienyl-type radical, which can reach a stationary concentration suitable for intercepting an α-cyanoisopropyl radical, thus leading to the substitution product. At the same time, the electrophilicity of the α-cyanoisopropyl radical prevents it from adding to the protonated heteroaromatic base while completing the course of this nonchain process. It is worth pointing out that this method is the first report on the alkylation of heteroaromatic bases under nonoxidative conditions.

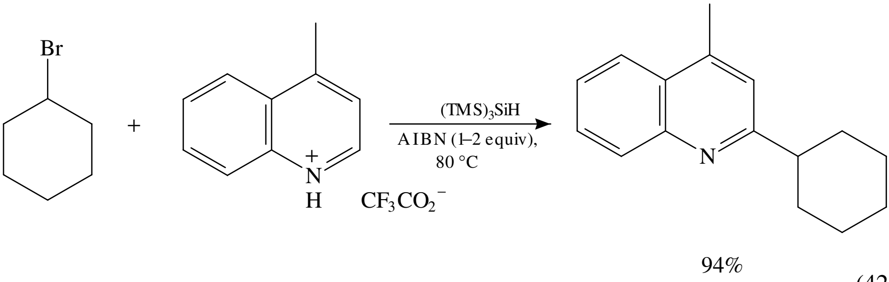

(42)

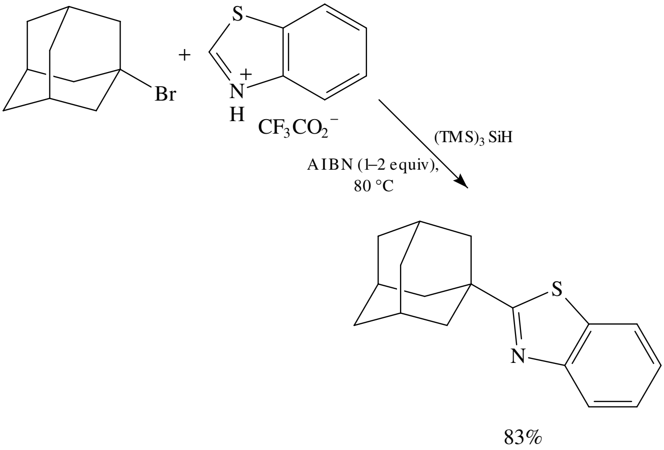

(43)

The full advantages of using a slow hydrogen donating reagent as $(TMS)_3SiH$ were perhaps best demonstrated in the free-radical carbonylation reactions developed by Ryu and Sonoda where the syringe-pump addition cannot be applied[67]. These radical chain reactions proceeded by formation of an alkyl radical which may be reduced to **4** or add onto carbon monoxide, generating an acyl radical intermediate which, in turn, can either abstract hydrogen from the reducing agent to give the corresponding aldehyde **5** (Scheme 4) or further react with electron-deficient olefins to lead, after reduction, to a formal double alkylation of carbon monoxide (equations 44 and 45)[68]. This three-component coupling reaction requires the generation of four highly disciplined radical species which have specific functions during the chain reaction. Employment of $(TMS)_3SiH$ in place of Bu_3SnH resulted in a multifaceted improvement of the reaction: (i) Since alkyl radicals abstract a hydrogen atom from $(TMS)_3SiH$ approximately ten times slower than from tin hydride (e.g. see Figure 1), $(TMS)_3SiH$ can mediate the carbonylation of free radicals at CO pressures lower than those needed for the tin hydride system (15 atm compared with 50, see Scheme 4). (ii) Similarly, the intermediate acyl radical abstracts hydrogen from $(TMS)_3SiH$ twenty times slower than from tin hydride[16]. This lead to an efficient three-component coupling reaction even in the presence of a stoichiometric amount of

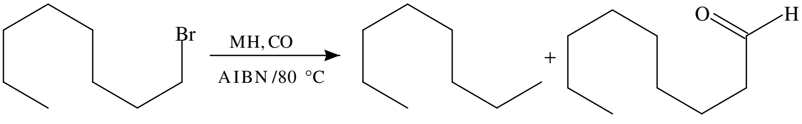

(**4**) (**5**)

MH	CO (atm)	**4** (%)	**5** (%)
$(TMS)_3SiH$	30	16	80
	15	29	65
Bu_3SnH	50	36	63
	15	49	38

SCHEME 4

the alkene, whereas in the presence of Bu_3SnH three to four equivalents of alkene are necessary for efficient coupling. (iii) Finally, since the rate of hydrogen abstraction from tributyltin hydride by vinyl radicals is about 100 times faster than by primary alkyl radicals, vinyl halides cannot participate in free radical carbonylations in the presence of Bu_3SnH but they did afford good yields of β'-substituted-α, β-enones in the presence of $(TMS)_3SiH$ (equation 45).

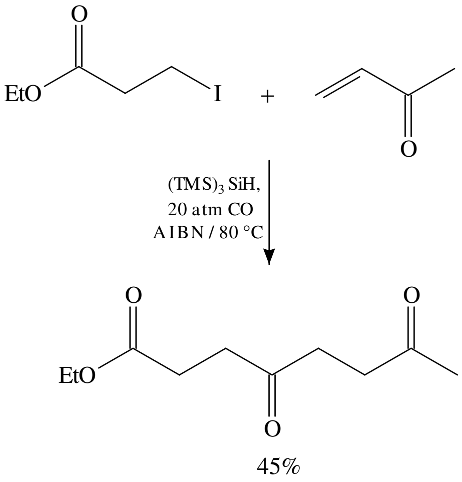

(44)

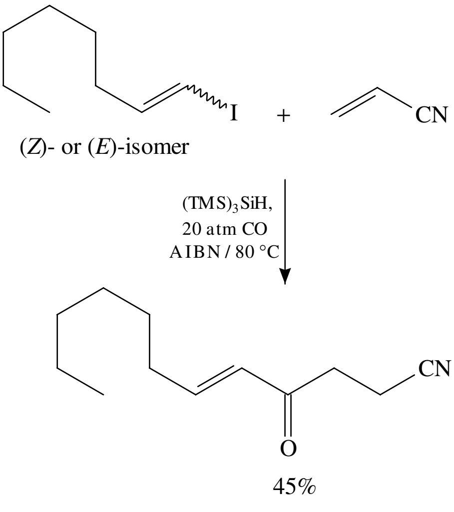

(45)

The field of macrocyclization reactions was recently augmented by the same group[69] with an $n + 1$ radical annulation which results in the incorporation of a CO molecule in the macrocycle. Thus, in the presence of highly diluted (0.005–0.01 M) $(TMS)_3SiH$, ω-iodoacrylates underwent efficient three-step radical chain reaction to generate 10- to 17-membered macrocycles in 28–78% yields, respectively (equation 46). It has also been shown that $(TMS)_3SiH$ mediates a 14-*endo-trig* macrocyclization in 55% yield as a key step feature in a concise synthesis of optically active (−)-zearalenone[70].

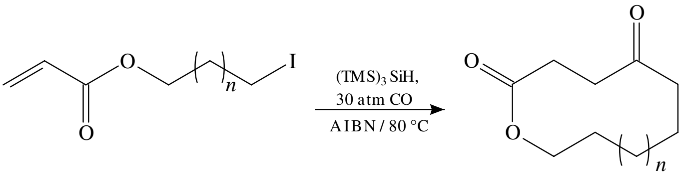

$n = 1,2,4,6,7,8$ 28–78%

(46)

The intramolecular C−C bond formation (or cyclization) mediated by $(TMS)_3SiH$ has been the subject of numerous publications. Scheme 5 presents the simplest and more popular type of 5-hexenyl radical cyclization. Thus, a 50 mmolar solution of 5-hexenyl bromide and silane (or tin hydride) lead to a 24 : 1 (or 6 : 1) ratio of cyclized versus uncyclized products[61]. Therefore, under the same conditions the silane gives higher yields of cyclization than the stannane.

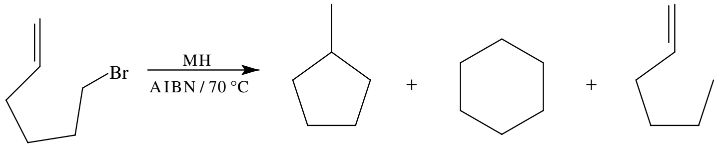

$(TMS)_3SiH$	93%	2%	4%
Bu_3SnH	83%	1.5%	15%

SCHEME 5

Tacamonine, an indole alkaloid of the *Iboga* type, isolated from *Tabernaemontana eglandulosa*, the root of which is used to treat snake bites in Zaire, bears structural similarity to the *Hunteria* alkaloids, eburnamonines, which possess vasodilator and hypotensive activities. Its synthesis in racemic and homochiral form was accomplished by incorporating a classic 6-*exo-trig* radical cyclization in the key step of the synthesis (Scheme 6)[71]. The radical precursor **6** was constructed in a 7-step synthesis by starting from racemic or chiral propane-1,3-diol. The radical cyclization of **6** produced the piperidinone in 72% yield as a diastereomeric mixture, which was then transformed into tacamonine.

Pattenden and coworkers have designed and performed a cascade of radical reactions towards the synthesis of angular triquinanes[72]. Irradiation of the refluxed benzene solution containing a 1 : 1 mixture of diastereomers of bromide **7** and $(TMS)_3SiH$ gave the corresponding triquinane oxime **8** as a 1 : 1 mixture of α- and β-methyl diastereomers in 38% yield.

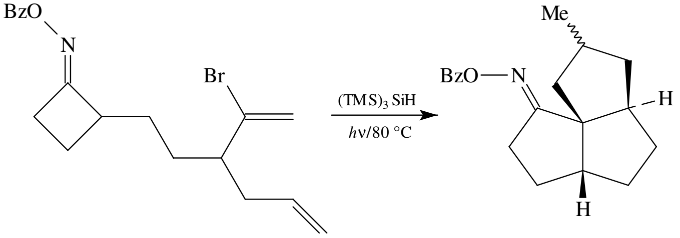

(7) **(8)** 38%

(47)

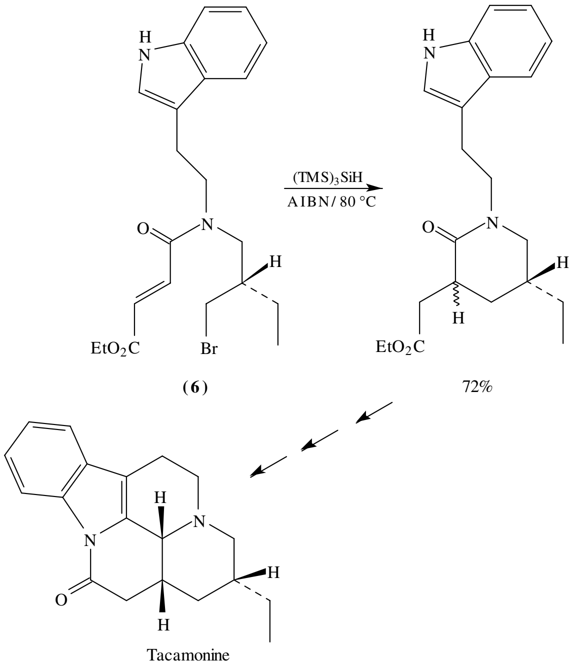

SCHEME 6

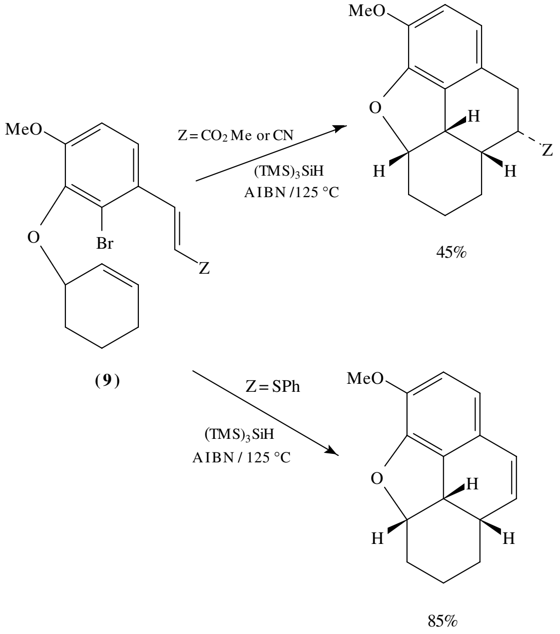

SCHEME 7

A tandem cyclization as key steps in the synthesis of morphine alkaloids has been projected and successfully performed[73]. Three examples are given in Scheme 7. Specifically, the initially formed aryl radical, generated by bromine abstraction from compound **9**, underwent a tandem cyclization to construct the desired carbocyclic skeleton. The product radicals either abstracted hydrogen from silane ($Z = CO_2Me$ or CN) or eliminated thiyl radical (Z = SPh). On the other hand, the planned tandem cyclization starting from the bromide **10**, toward the construction of indole alkaloids skeleton, gave an unexpected result (equation 48)[74a]. Mechanistic considerations for the formation of quinoline have been advanced. In model studies directed towards the synthesis of (±)-gelsemine[74b], 5-*exo-trig*-cyclization of an aryl radical, derived from the vinylogous urethane **11**, onto a methoxymethyl enol ether resulted in partial fragmentation of the intermediate radical species with expulsion of a methoxymethyl radical and generation of the ketone group (equation 49).

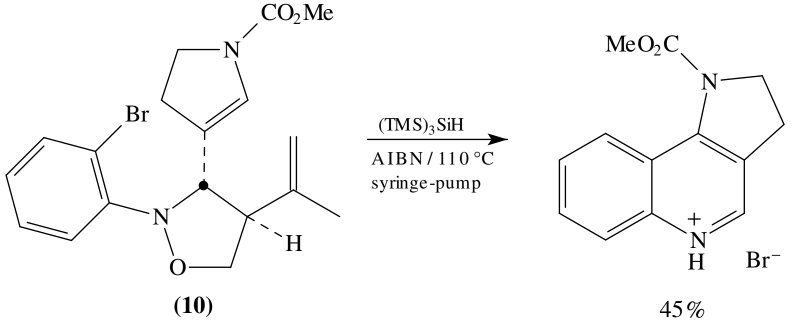

(48)

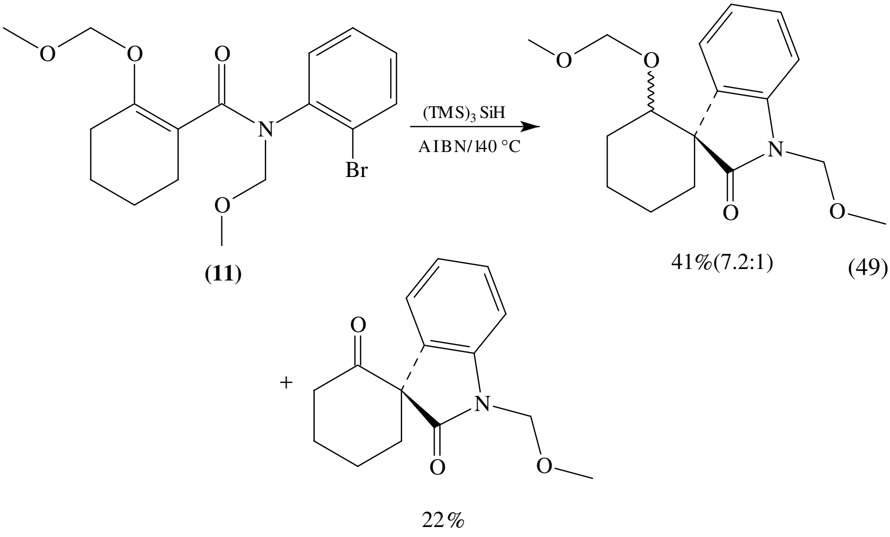

It is known that the geometries of the reactants play an important role in the regio- and stereochemical outcome of radical reactions since they are commonly involved in early transition states. Previous attempts to affect rotamer populations during the reaction included, among others, control of temperature and addition of a Lewis acid. It was recently reported[75] that organotin halides, common byproducts of radical reactions, act as Lewis acids and control the course of such reactions. An indicative example of this control is given in Scheme 8; the reaction of oxazolidinone **12** with $(TMS)_3SiH$ giving products **13** and/or **14** has been performed in the absence and in the presence of organotin halides. The results demonstrated that higher temperatures and weak Lewis acids were necessary not only for inducing the conformational change from the stable *anti-(s)-Z*-**12** to the *syn-(s)-Z*-**12** required for the radical cyclization reaction, but also for obtaining high diastereoselectivity.

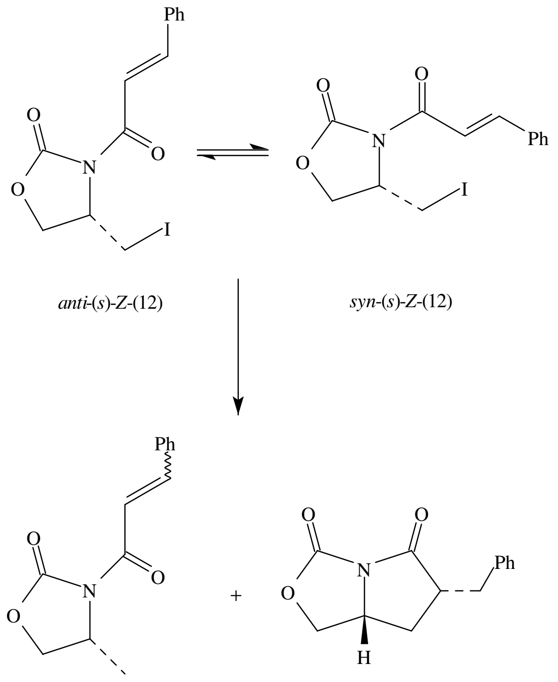

anti-(*s*)-*Z*-(12)

syn-(*s*)-*Z*-(12)

	(13) (E:Z)	**(14)** (de%)
$(TMS)_3SiH$, AIBN/80 °C	78 % (100:0)	13 % (87)
$(TMS)_3SiH$, *hv*/r.t.	72 % (71:29)	0 %
$(TMS)_3SiH$, Bu_3SnCl, AIBN/80 °C	0 %	87 % (>97)
$(TMS)_3SiH$, Bu_3SnCl, *hv*/ r.t.	60 % (60:40)	14 % (86)

SCHEME 8

An example in which primary alkylamines are used as alkyl radical precursors for cyclization is reported in equation 50[61], in which the initial transformation to isocyanide and subsequent reaction with $(TMS)_3SiH$ gave the desired products in 78% yield after workup.

The intermediate α-heterosubstituted carbon radicals generated by reaction of $(TMS)_3Si^•$ radical with 1,3-dithiane[28], or *N*-(ethoxycarbonyl)-1,3-thiazolidine[76] derivatives, can participate in consecutive intramolecular C—C bond formation reactions in the presence of proximate 1,2-disubstituted double bonds (equation 51). In the presence of terminal double bonds or in an attempted intermolecular addition of the intermediate radical species to electron-deficient olefins, hydrosilylation of the double bond by $(TMS)_3SiH$ competed with the reduction and prevented C−C bond formation.

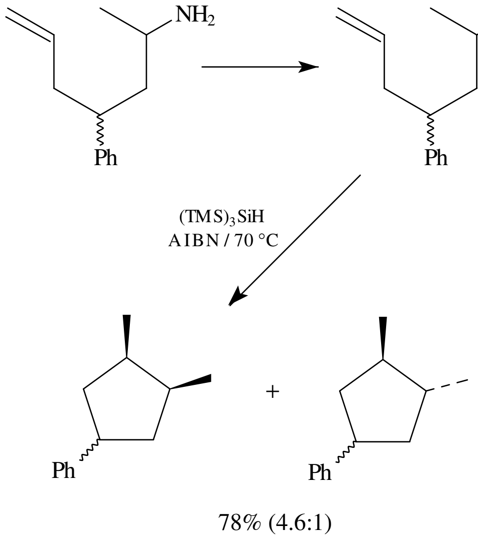

(50)

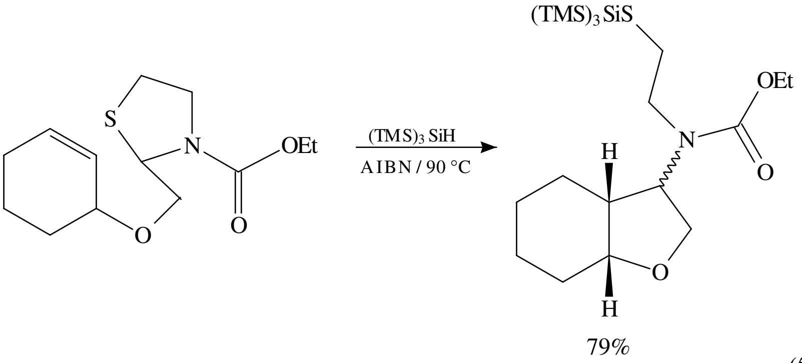

(51)

Free-radical cyclization of phenyl selenide **15** to indolizidinone **16** represented a key step in the total synthesis of (−)-slaframine (equation 52). The two pairs of diastereomers were first separated and then hydrolyzed to the corresponding alcohols in 76% overall yield[77]. $(TMS)_3SiH$-mediated acyl radical reactions from phenylseleno esters **17** have recently been utilized for the stereoselective synthesis of cyclic ethers[78]. In fact, the experimental conditions reported in equation 53 are particularly good for both improving *cis* diastereoselectivity and suppressing decarbonylation.

The cyclization of secondary alkyl radicals with α, β-alkynyl esters **18** proceeded with high stereoselectivity to give predominantly (Z)-exocyclic alkenes at low temperature upon reaction with $(TMS)_3SiH$ (equation 54)[79]. On the other hand, the formation of (E)-exocyclic alkenes predominated with Bu_3SnH, the E/Z ratio being 98 : 2 at 80 °C. It has been suggested that the main factor controlling the formation of these products is the ability of $(TMS)_3Si^\bullet$ and $Bu_3Sn^\bullet$ radicals to isomerize the product alkene. That is, the (E) ⇌ (Z) isomerization occurred under tin hydride reduction conditions whereas no such transformation was observed with $(TMS)_3SiH$. This class of reactions has also been extended to cyclization of difluoroalkyl radicals[80].

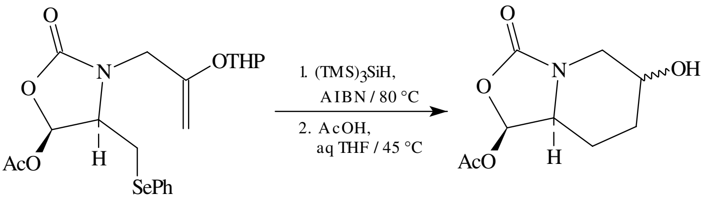

(52)

(15)

(16) 76% (α:β=7:1)

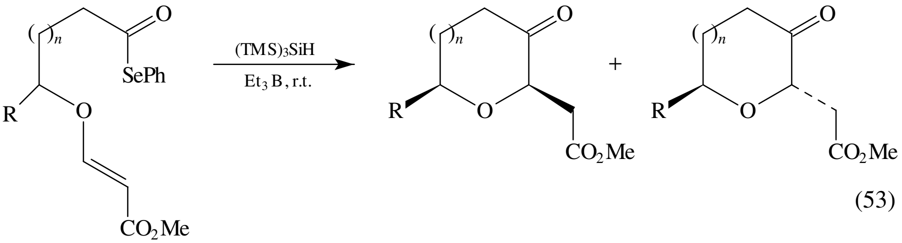

(53)

(17)
R = Me, Ph, *i*-Pr

$n = 1$ 94% (5.7:1)
$n = 2$ 90% (≥19:1)

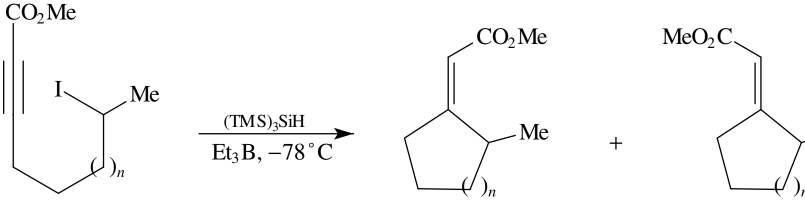

(54)

(18)

$n = 1$ 85% (Z:E = 11:89)
$n = 2$ 82% (Z:E = 9:91)

The radical cyclization of bromomethyldimethylsilyl propargyl ethers has recently been utilized by Malacria and coworkers[81,82] in order to generate precursors for the synthesis of the triquinane framework. In the first of these reports[81], reduction of the bromide **19** in the presence of $(TMS)_3SiH$ and subsequent treatment with MeLi produced the functionalized cyclopentanone precursor **20** as a single diastereomer (Scheme 9). The formation of **20** could be explained by a series of reactions, indicated in Scheme 9, involving a 5-*exo-trig* cyclization of the initial α-silylalkyl radical followed by a [1,5]-radical translocation of the generated σ-type vinyl radical onto the proximal acetal function and a final 5-*exo-trig* process. Stereoselective hydrogen abstraction, dependent on the steric bulkiness of the hydrogen donor, followed by MeLi induced opening of the Si−O bond afforded the final product. The introduction of different substituents on the skeleton, as in compound **21** resulted in a completely different reaction pattern (equation 55)[82].

In this case, the intermediate vinyl radical (cf Scheme 9) underwent a remarkable [1,5]-hydrogen abstraction from the non-activated C−H bond of the proximal isopropyl group. Furthermore, the resulting primary alkyl radical underwent a unique, stereoselective 5-*endo-trig* cyclization onto the adjacent double bond to generate a tertiary radical, which is a precursor of the highly substituted cyclopentanols **22** and **23**. The reaction with Bu_3SnH as radical mediator totally reversed the products ratio obtained in 88% yield, i.e. **22** : **23** = 19 : 81.

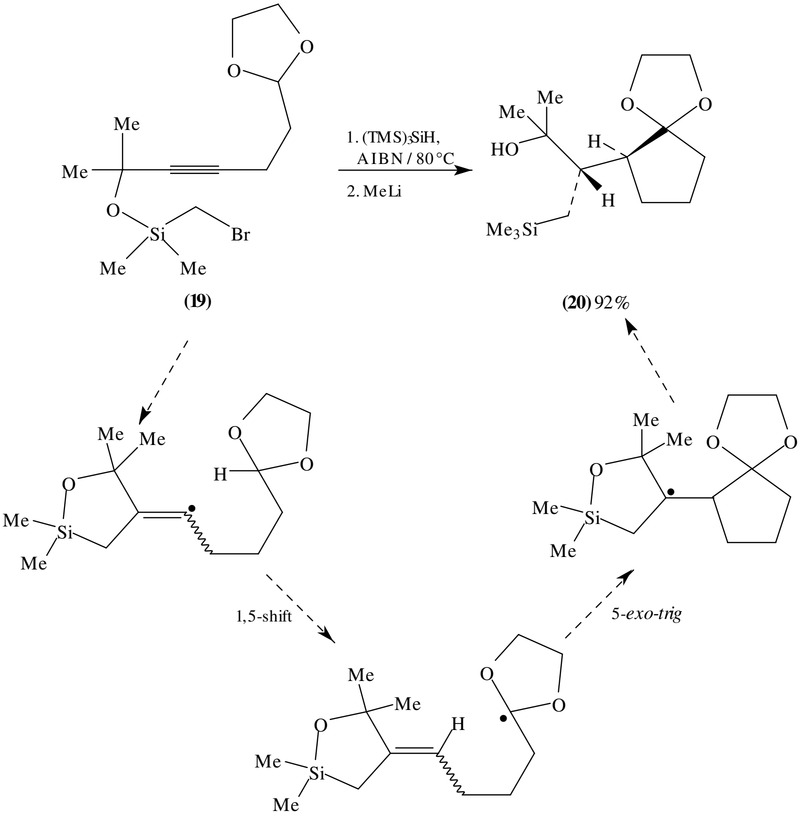

SCHEME 9

Interestingly, another example of a [1,5]-radical translocation coupled with an unusual 5-*endo-trig* radical cyclization was reported in a structurally different system (Scheme 10)[83]. In this case, the α-bromovinyl radical abstracted a hydrogen either from $(TMS)_3SiH$ to give vinyl bromide in 25% yield or from the anomeric position to generate the C-1′ radical which underwent an unusual 5-*endo-trig* cyclization onto the proximal double bond to generate an anomeric mixture of spironucleosides after bromine atom ejection.

The utilization of the azido group as radical acceptor in radical reactions shown in equation 56, has been tested by Kim and coworkers[84,85] using $(TMS)_3SiH$, which is relatively inert towards azides when compared to Bu_3SnH. Therefore, alkyl bromides and thionocarbonates can be used as precursors of radicals, generated by $(TMS)_3SiH$ which

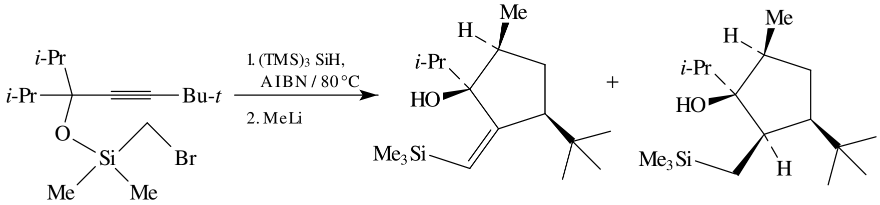

(21) **(22)** **(23)**

95% (90:10)

(55)

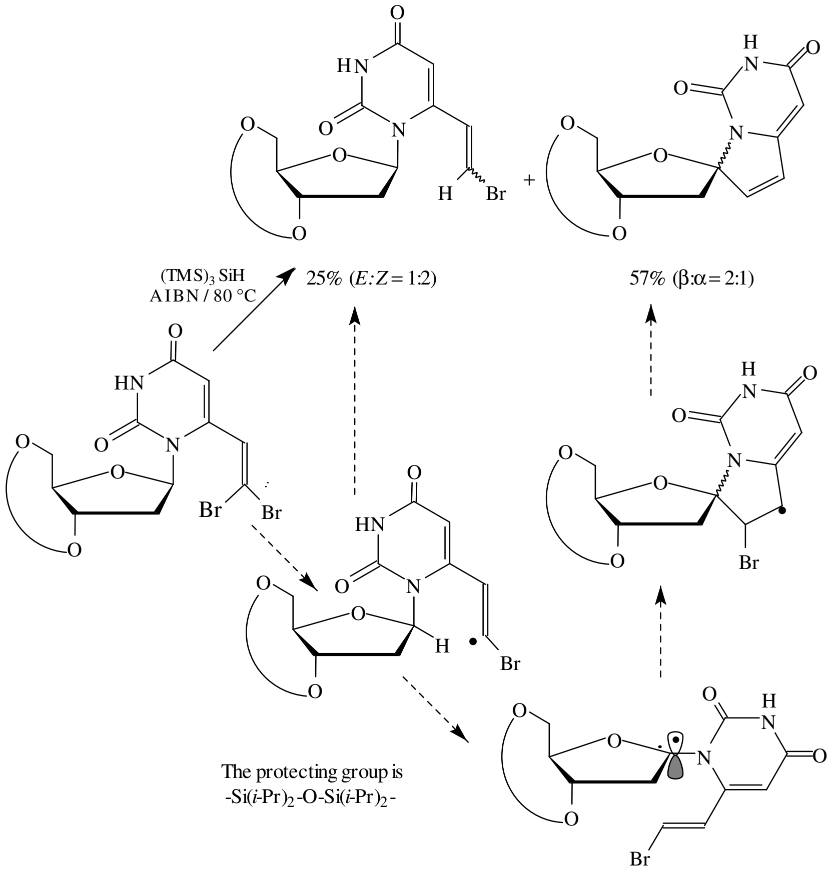

The protecting group is
-Si(i-Pr)$_2$-O-Si(i-Pr)$_2$-

SCHEME 10

in turn can cyclize onto suitably positioned azides to provide nitrogen heterocycles. An example is given in equation 57 where the amine product was tosylated before work-up. For comparison, in the presence of Bu_3SnH only alkyl iodides are reactive enough to be used for the same purpose. An analogous behavior of the azide group was observed by others[86] in a similar cascade of radical reactions.

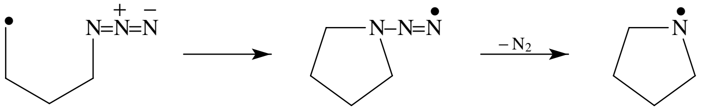

(56)

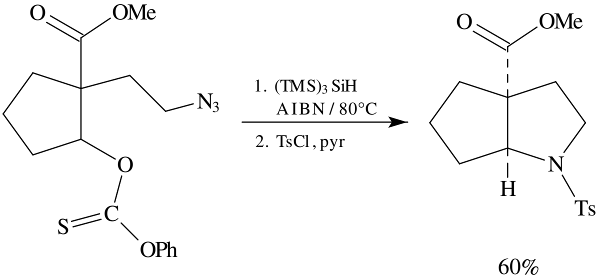

(57)

More recently, the radical cyclization onto azide groups pioneered by Kim was applied in the construction of the *B*/*E* spirocyclic junction found in the [6.5.6.5] *ABCE* ring system of indole alkaloids such as strychnine, the clinically used anticancer agents vincristine and vinblastine and, in particular, aspidospermine[87]. In model system studies, cyclization of the iodoazide **24**, prepared in 6 steps, in the presence of $(TMS)_3SiH$, produced the N−Si $(TMS)_3$ protected alkaloid **25**, that after washing with dilute acid afforded the amine **26** in 95% yield from **24** (equation 58). The formation of the liable $N-Si(TMS)_3$ bond was considered to arise from the reaction of the product amine **26** with the byproduct $(TMS)_3SiI$.

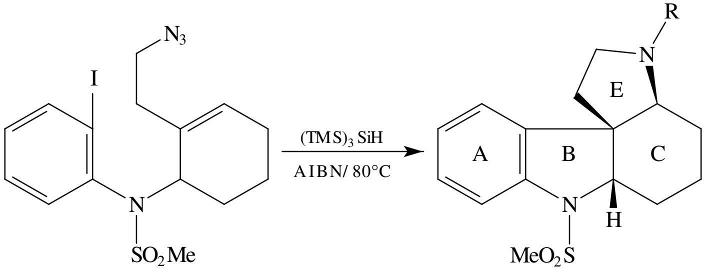

(58)

(24)

(25) R = $Si(TMS)_3$

(26) R = H, 95%

The different H-atom donor abilities of $(TMS)_3SiH$ and Bu_3SnH, which have been encountered many times, can also be useful to solve intriguing radical mechanisms, and an example of this was recently reported[88]. The outcome of the reaction of δ, ϵ-unsaturated acyl radicals has been the research subject of several groups and can be illustrated as in Scheme 11[89]. Based on the available kinetic data of secondary substituted acyl radicals with the two reagents [i.e. 1.1×10^6 and 7.2×10^4 $M^{-1}\,s^{-1}$ at 80 °C for Bu_3SnH and $(TMS)_3SiH$, respectively][16], of the decarbonylation of acyl radicals[16], and of different hydrogen donor abilities of $(TMS)_3SiH$ and Bu_3SnH towards alkyl radicals (Section I.B), it was possible to plan and perform kinetic experiments. In particular, the reactions of thionocarbonate **27** with $(TMS)_3SiH$ and of phenylseleno ester **28** with Bu_3SnH were informative on the rate constants of the possible transformations, thus clarifying the overall mechanism (Scheme 12)[88].

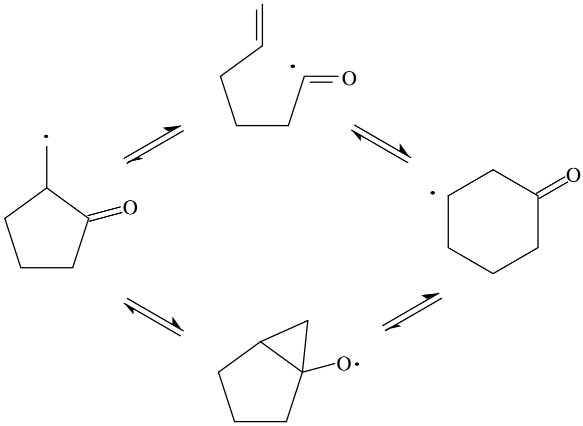

SCHEME 11

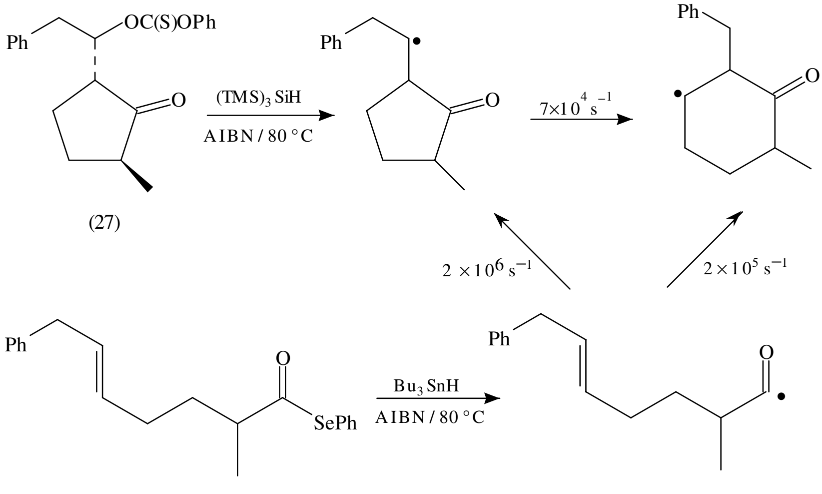

SCHEME 12

The reaction of iodide **29** with $(TMS)_3SiH$ under free radical conditions gave the products depicted in equation 59 in quantitative yield[90]. This procedure, which used a homolytic substitution at sulfur, has been proposed as versatile and alternative to phenylseleno esters for the generation of acyl radicals. In fact, the aryl radical formed by iodine abstraction rearranged with expulsion of the acyl radical and concomitant formation of dihydrobenzothiophene. Similarly, internal homolytic substitution of aryl radicals at selenium has been used for the preparation of selenophenes and benzoselenophenes[91]. Scheme 13 illustrates the reaction of iodides **30** with $(TMS)_3SiH$ to afford benzoselenophenes in good yield. The presence of $(TMS)_3SiI$ after the reduction induced dehydration of the intermediate 3-hydroxybenzoselenophenes, presumably through an intermediate silyl ether.

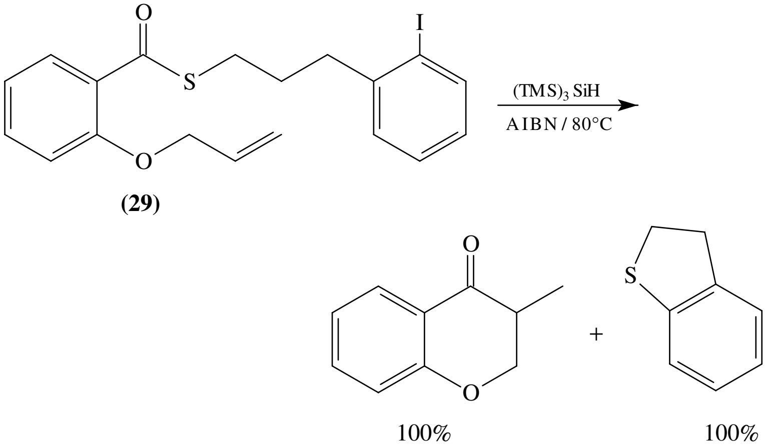

(29)

(59)

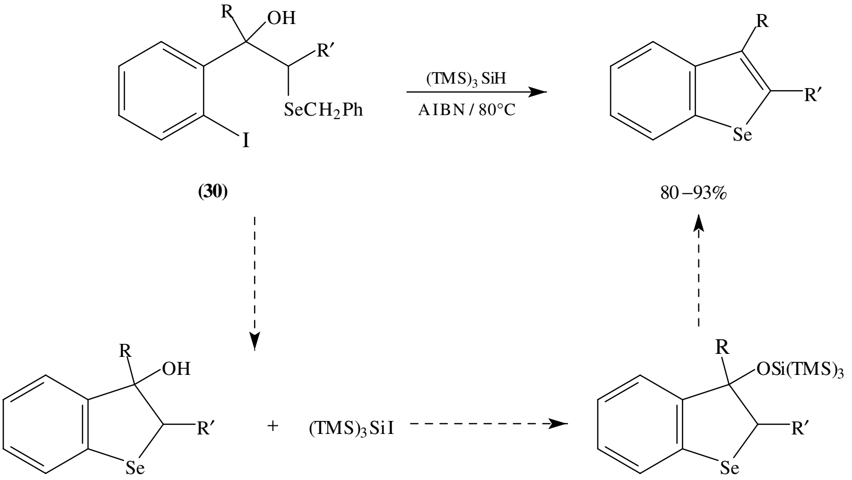

(30)

R = R′ = H; R = Me, R′ = H; R = Ph, R′ = H; R = H, R′ = Ph

SCHEME 13

Reflux of bromide **31** in benzene in the presence of small amounts of $(TMS)_3SiH$ and AIBN afforded the silabicycle **32** in 88% yield (equation 60)[92]. The key step for this transformation is the intramolecular homolytic substitution at the central silicon atom which occurred with a rate constant of 2.4×10^5 s^{-1} at 80 °C. The reaction has also been extended to the analogous vinyl bromide (equation 61)[93].

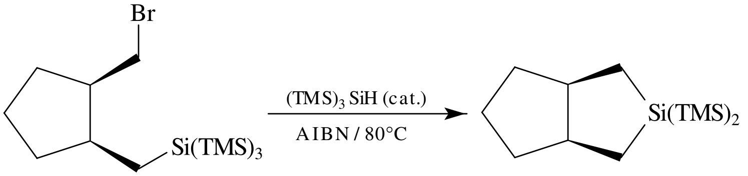

(60)

(31) **(32)** 88%

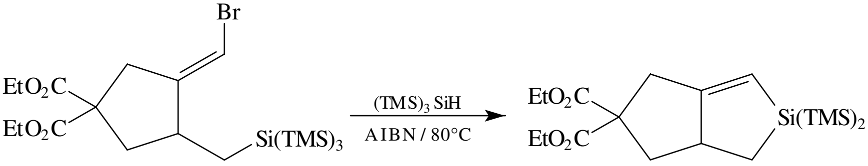

75%

(61)

B. Initiation by $(TMS)_3Si^•$ Radical Addition to Unsaturated Bonds

β-Silyl substituted carbon-centered radicals which are produced upon addition of $(TMS)_3Si^•$ to unsaturated bonds can participate in consecutive reactions. A simple example is given in equation 62 where the adduct of $(TMS)_3Si^•$ radical to β-pinene rearranged by opening the four-membered ring prior to H atom transfer[21]. Reactions of unsubstituted and 2-substituted allyl phenyl sulfides with $(TMS)_3SiH$ provided the corresponding allyl tris(trimethylsilyl)silanes in high yields (equation 63)[94]. That is, $(TMS)_3Si^•$ radical adds to the double bond giving rise to a radical intermediate that undergoes β-scission with ejection of thiyl radical. Hydrogen abstraction from the silane completes the cycle of these chain reactions. 2-Functionalized allyl tris(trimethylsilyl)silanes have been employed in the radical-based allylation reactions[95].

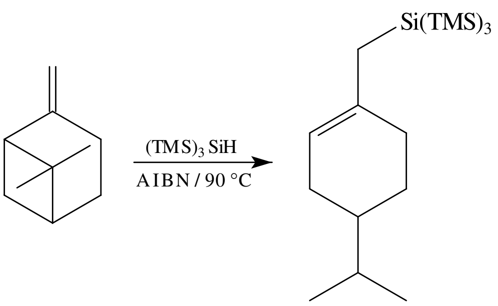

(62)

82%

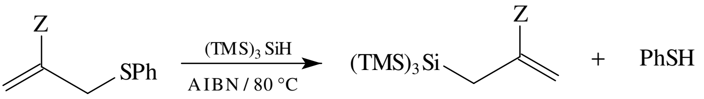

(63)

Z = H, Me, Cl, CN, CO_2Et

>80%

The product distribution of the (TMS)$_3$SiH addition to 1,6-dienes depends on the concentration of reducing agent. As an example, diallyl ether reacted with 1.2 equivalents of silane to give 63% yield of **33** in a *cis*:*trans* ratio of 3 : 1[21]. The same reaction performed by syringe-pump addition of the silicon reagent gave silabicycle **34** in 55% yield together with **33** in 15% yield (equation 64). The reaction mechanism for this reaction is analogous to that described earlier in equation 60[92].

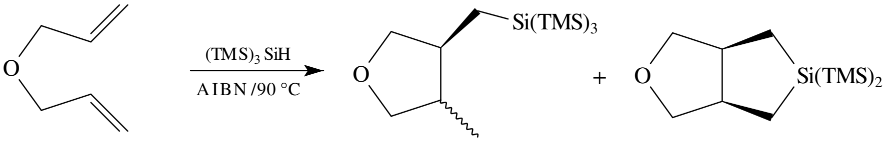

(33) **(34)**

(64)

Reaction of (TMS)$_3$SiH with *β*-alkenyloxyenones can follow either one or both of two different pathways depending on the substitution at the double bond[96a]. Specifically, in the case of loosely conjugated s-*cis* enone **35**, addition of silyl radical to the terminal double bond was accompanied by a 5-*exo-trig* radical cyclization leading to the diastereomeric cyclic products (equation 65). In the case of nonterminal double bonds such as in **36**, exclusive addition of the (TMS)$_3$Si$^•$ radical to the carbonyl was followed by a 5-*exo-trig* cyclization and hydrogen abstraction. In the presence of cyclohexenones or cyclopentenones and terminal double bonds, a combination of both chemistries was observed. Useful bicyclic ring systems are obtained by (TMS)$_3$Si$^•$ radical mediated fragmentation of strained alkene precursors[96b]. For example, the ketoalkene **37** reacted with 1.5 equivalents of silane to give 95% of hydrindanone **38** (equation 66).

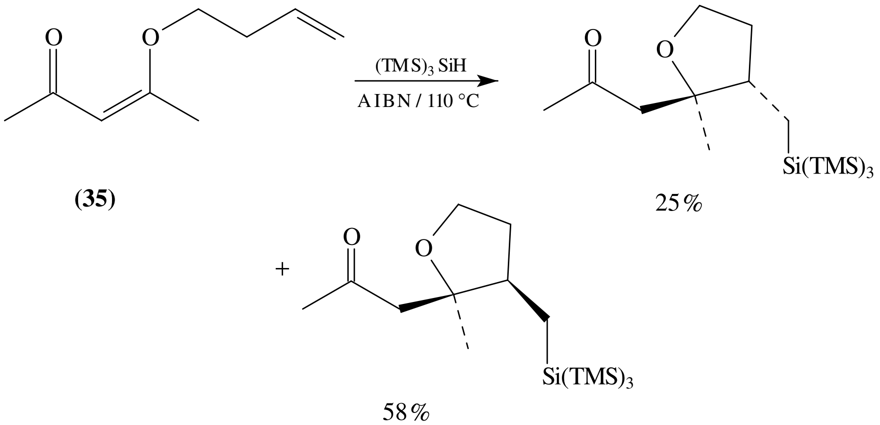

(35)

(65)

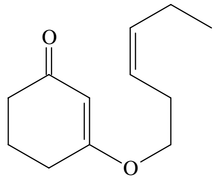

(36)

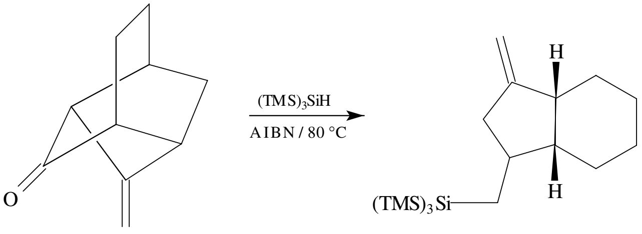

(37) (**38**, 95%)

(66)

The α-silyloxy alkyl radical generated by addition of $(TMS)_3Si^{\bullet}$ radical to the aldehyde moiety of **39** has been employed in radical cyclization onto β-aminoacrylates (equation 67)[97]; the *trans*-hydroxy ester and the lactone formed in a 2.4 : 1 ratio were the two products. An alternative route to N-heterocycles has been developed by Kim and coworkers[84,85] using the azido group as radical acceptor (cf equation 56). Two examples are given in equations 68 and 69. The carbon-centered radical, derived by addition of $(TMS)_3Si^{\bullet}$ radical to **40**, cyclized to the azido group to afford the desired product in good yields, independently of the ring size. On the other hand, the radical adduct arising from **41** underwent an opening of the cyclopropyl ring, with formation of **42** as intermediate, prior to the intramolecular addition to the azido group. After tosylation the final product was obtained in 61% yield.

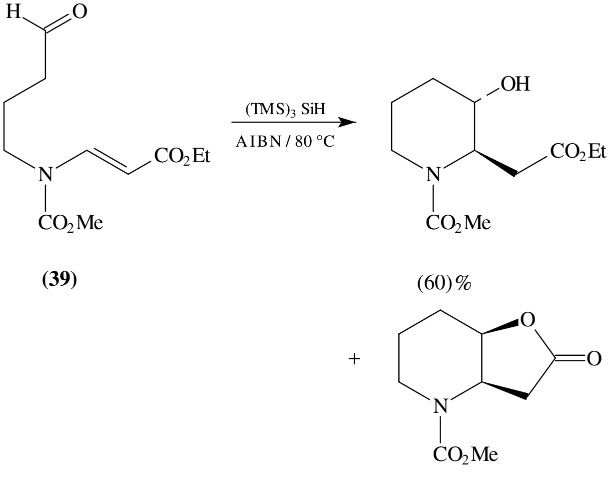

(39) (60)% (25)%

(67)

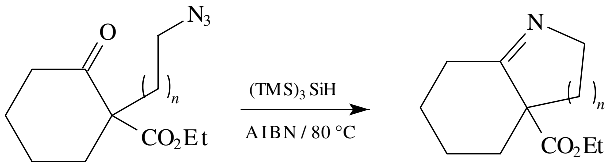

(40) $n = 1, 2$ 78%

(68)

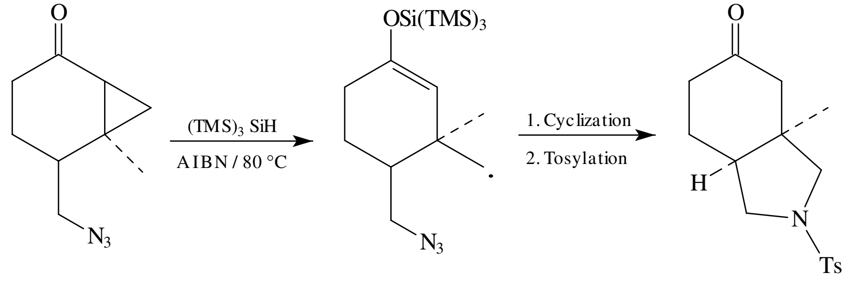

(41) **(42)** 61%

(69)

The addition of $(TMS)_3SiH$ to the 3-oxo-1,4-diene steroid-type derivative promoted C(9)−C(10) bond cleavage (equation 70)[98]. The removal of the silyl group was achieved by treatment with dilute aqueous hydrochloric acid at room temperature in 86% yield.

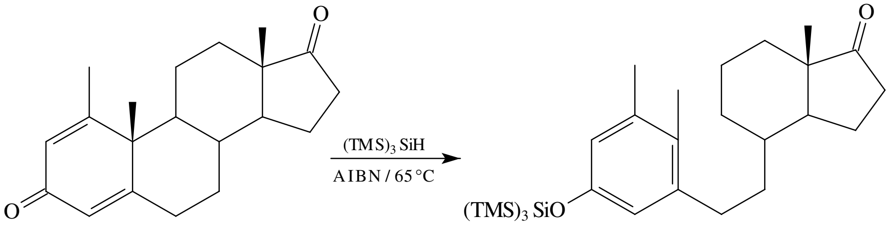

84%

(70)

Pattenden and Schulz have reported that treatment of the acetylene derivative **43** with $(TMS)_3SiH$ leads, in one pot, to the bicyclic compound **44** in 70% yield (equation 71)[99]. The proposed mechanism involves $(TMS)_3Si^{\bullet}$ radical addition to the triple bond to form a vinyl radical followed by a remarkable cascade of radical cyclization−fragmentation−transannulation−ring expansion and termination via ejection of the $(TMS)_3Si^{\bullet}$ radical to afford the bicyclic product.

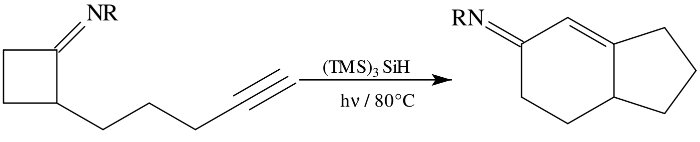

(71)

(**43**) R = OCH_2Ph (**44**) 70%

Treatment of isothiocyanide derivatives of glycine **45** or **46** with the silane under radical conditions afforded the corresponding pyroglutamates in good yields (equation 72)[100]. The expected products, derived from the cyclization of α-silylthio imidoyl radicals, hydrolyzed spontaneously during chromatography. α-Diazo ketones were found to react with $(TMS)_3SiH$ under free radical conditions to give α-silyl ketones (equation 73)[101]. Mechanistic evidence that the attack of $(TMS)_3Si^\bullet$ takes place at carbon rather than nitrogen, to give a diazenyl radical adduct which decomposes to α-silyl substituted radical and nitrogen, has been obtained. α-Silyl carbonyl compounds have also been obtained in moderate yields from the reaction of α-diazo esters with $(TMS)_3SiH$ in the presence of rhodium(II) complexes as catalysts (equation 74)[102]. This reaction was presumed to be mediated by transition metal carbenoid rather than by radical intermediates.

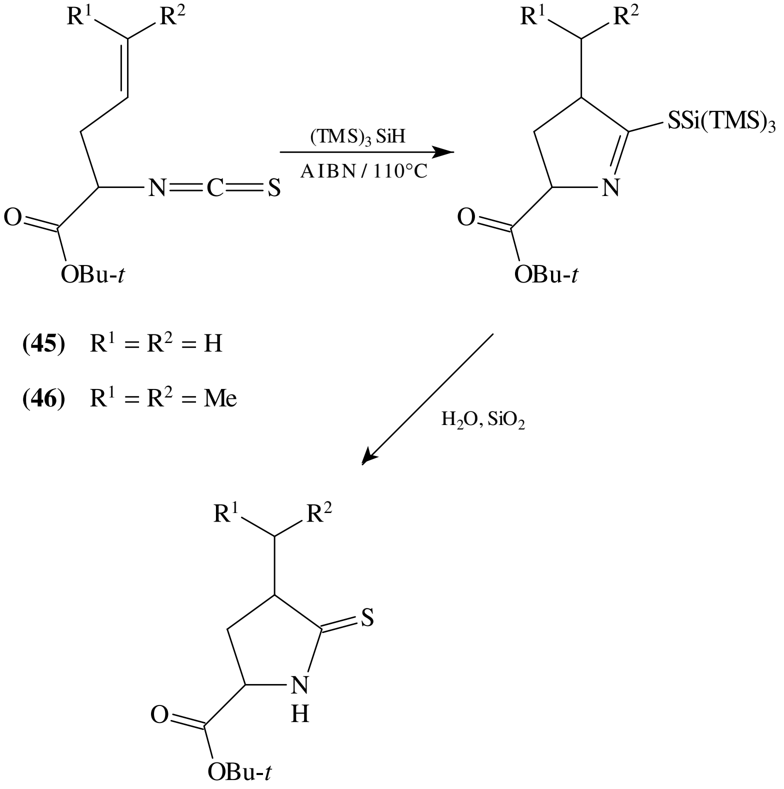

(45) $R^1 = R^2 = H$

(46) $R^1 = R^2 = Me$

93–96%

(72)

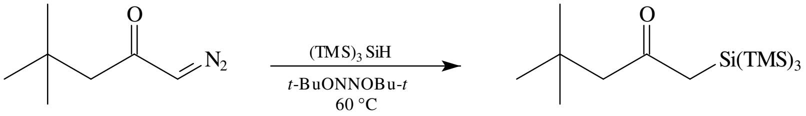

63%

(73)

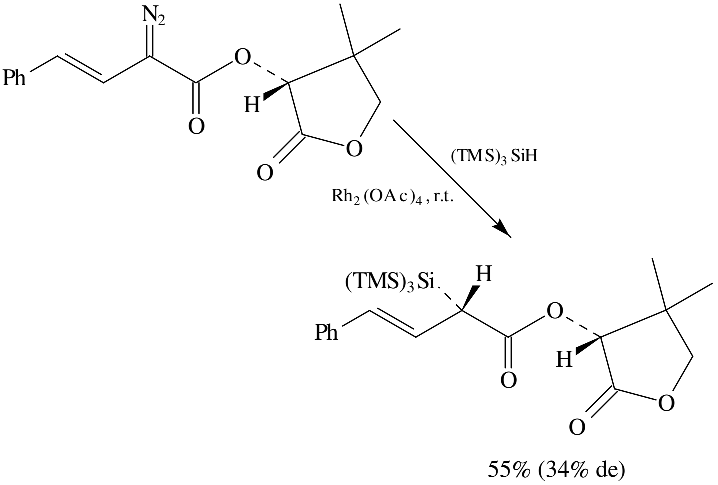

(74)

VI. REFERENCES

1. U. Koert, *Angew. Chem., Int. Ed. Engl.*, **35**, 405 (1996) and references cited therein.
2. For example, see:
   (a) W. B. Motherwell and D. Crich, *Free Radical Chain Reactions in Organic Synthesis*, Academic Press, London, 1992.
   (b) B. Giese, *Radicals in Organic Synthesis: Formation of Carbon–Carbon Bonds*, Pergamon Press, Oxford, 1986.
3. For example, see:
   (a) D. P. Curran, *Synthesis*, 417, 489 (1988).
   (b) C. P. Jasperse, D. P. Curran and T. L. Fevig, *Chem. Rev.*, **91**, 1237 (1991).
   (c) D. P. Curran in *Comprehensive Organic Synthesis* (Eds. B. M. Trost and I. Fleming), Vol. 4, Pergamon Press, Oxford, 1991, pp. 715–831.
4. C. Chatgilialoglu, *Acc. Chem. Res.*, **25**, 188 (1992) and references cited therein.
5. J. M. Kanabus-Kaminska, J. A. Hawari, D. Griller and C. Chatgilialoglu, *J. Am. Chem. Soc.*, **109**, 5267 (1987).
6. C. Chatgilialoglu, D. Griller and M. Lesage, *J. Org. Chem.*, **53**, 3641 (1988).
7. C. Chatgilialoglu and C. Ferreri, *Res. Chem. Intermed.*, **19**, 755 (1993).
8. C. Chatgilialoglu, K. U. Ingold and J. C. Scaiano, *J. Am. Chem. Soc.*, **103**, 7739 (1981).
9. C. Chatgilialoglu and M. Ballestri, *Organometallics*, **14**, 5017 (1995).
10. C. Chatgilialoglu, C. Ferreri and M. Lucarini, *J. Org. Chem.*, **58**, 249 (1993).
11. C. Chatgilialoglu, *Chem. Rev.*, **95**, 1229 (1995).
12. C. Chatgilialoglu and S. Rossini, *Bull. Soc. Chim. Fr.*, 298 (1988).
13. C. Chatgilialoglu, J. Dickhaut and B. Giese, *J. Org. Chem.*, **56**, 6399 (1991).
14. S. J. Garden, D. V. Avila, A. L. J. Beckwith, V. W. Bowry, K. U. Ingold and J. Lusztyk, *J. Org. Chem.*, **61**, 805 (1996).
15. X. X. Rong, H.-Q. Pan, W. R. Dolbier, Jr. and B. E. Smart, *J. Am. Chem. Soc.*, **116**, 4521 (1994).
16. C. Chatgilialoglu, C. Ferreri, M. Lucarini, P. Pedrielli and G. F. Pedulli, *Organometallics*, **14**, 2672 (1995).
17. C. Chatgilialoglu, A. Guarini, A. Guerrini and G. Seconi, *J. Org. Chem.*, **57**, 2208 (1992).
18. C. Chatgilialoglu, V. Timokhin, A. Zaborovskiy and A. Berlin, manuscript in preparation.
19. C. Chatgilialoglu, unpublished results.
20. C. Chatgilialoglu, D. Griller and M. Lesage, *J. Org. Chem.*, **54**, 2492 (1989).
21. M. Ballestri, C. Chatgilialoglu, K. B. Clark, D. Griller, B. Giese and B. Kopping, *J. Org. Chem.*, **56**, 678 (1991).
22. J. A. Robl, *Tetrahedron Lett.*, **35**, 393 (1994).
23. F. Wahl, J. Wörth and H. Prinzbach, *Angew. Chem., Int. Ed. Engl.*, **32**, 1722 (1993).

24. M. Lesage, C. Chatgilialoglu and D. Griller, *Tetrahedron Lett.*, **30**, 2733 (1989).
25. E. Lee, C. M. Park and J. S. Yun, *J. Am. Chem. Soc.*, **117**, 8017 (1995).
26. Y. Apeloig and M. Nakash, *J. Am. Chem. Soc.*, **116**, 10781 (1994).
27. M. Ballestri, C. Chatgilialoglu, N. Cardi and A. Sommazzi, *Tetrahedron Lett.*, **33**, 1787 (1992).
28. P. Arya, C. Samson, M. Lesage and D. Griller, *J. Org. Chem.*, **55**, 6248 (1990).
29. P. Arya, M. Lesage and D. D. M. Wayner, *Tetrahedron Lett.*, **32**, 2853 (1991).
30. M. Lesage and P. Arya, *Synlett*, 237 (1996).
31. P. Arya and D. D. M. Wayner, *Tetrahedron Lett.*, **32**, 6265 (1991).
32. D. P. Curran and S. Sun, *Tetrahedron Lett.*, **34**, 6181 (1993).
33. A. Krief, E. Badaoui and W. Dumont, *Tetrahedron Lett.*, **34**, 8517 (1993).
34. L. A. Paquette, D. Friedrich, E. Pinard, J. P. Williams, D. St. Laurent and B. A. Roden, *J. Am. Chem. Soc.*, **115**, 4377 (1993).
35. (a) C. Chatgilialoglu, in *The Chemistry of Sulphenic Acids and Their Derivatives* (Ed. S. Patai), Wiley, Chichester, 1990, pp. 549–569.
    (b) C. H. Schiesser and B. A. Smart, *Tetrahedron*, **51**, 6051 (1995).
36. J. W. Perich, *Synlett*, 595 (1992).
37. P. Boquel, C. Loustau Cazalet, Y. Chapleur, S. Samreth and F. Bellamy, *Tetrahedron Lett.*, **33**, 1997 (1992).
38. M. Toyota, T. Seishi, M. Yokoyama, K. Fukumoto and C. Kabuto, *Tetrahedron*, **50**, 1093 (1994).
39. S.-H. Chen, S. Huang, Q. Gao, J. Golik and V. Farina, *J. Org. Chem.*, **59**, 1475 (1994).
40. M. Oba and K. Nishiyama, *Tetrahedron*, **50**, 10193 (1994).
41. (a) M. Ballestri, C. Chatgilialoglu, M. Lucarini and G. F. Pedulli, *J. Org. Chem.*, **57**, 948 (1992).
    (b) C. Imrie, *J. Chem. Res. (S)*, 328 (1995).
42. S. Fukuzumi and S. Noura, *J. Chem. Soc., Chem. Commun.*, 287 (1994).
43. D. Schummer and G. Höfle, *Synlett*, 705 (1990).
44. F. Hammerschmidt, E. Öhler, J.-P. Polsterer, E. Zbiral, J. Balzarini and E. DeClercq, *Liebigs Ann.*, 551 (1995).
45. C. K. Chu and Y. Chen, US Patent 5,384,396, (1995); *Chem. Abstr.*, **122**, 265937 (1995).
46. J. R. Grierson, A. F. Shields, M. Zheng, S. M. Kozawa and J. H. Courter, *Nucl. Med. Biol.*, **22**, 671 (1995).
47. J. J. Barchi, Jr., A. Haces, V. E. Marquez and J. J. McCormack, *Nucleosides & Nucleotides*, **11**, 1781 (1992).
48. T. Gimisis, G. Ialongo, M. Zamboni and C. Chatgilialoglu, *Tetrahedron Lett.*, **36**, 6781 (1995).
49. M. Sekine and K. Seio, *J. Chem. Soc., Perkin Trans. 1*, 3087 (1993) and references cited therein.
50. A. Alberti and C. Chatgilialoglu, *Tetrahedron*, **46**, 3963 (1990).
51. B. Kopping, C. Chatgilialoglu, M. Zehnder and B. Giese, *J. Org. Chem.*, **57**, 3994 (1992).
52. C. Chatgilialoglu, M. Ballestri, C. Ferreri and D. Vecchi, *J. Org. Chem.*, **60**, 3826 (1995).
53. D. W. Johnson and A. Poulos, *Tetrahedron Lett.*, **33**, 2045 (1992).
54. C. Ferreri, M. Ballestri and C. Chatgilialoglu, *Tetrahedron Lett.*, **34**, 5147 (1993).
55. G. Emmer and S. Weber-Roth, *Tetrahedron*, **48**, 5861 (1992); corrigenda, *Tetrahedron*, **49**, 291 (1993).
56. W. Smadja, M. Zahouily and M. Malacria, *Tetrahedron Lett.*, **33**, 5511 (1992).
57. K. J. Kulicke and B. Giese, *Synlett*, 91 (1990).
58. (a) B. Giese, W. Damm, J. Dickhaut, F. Wetterich, S. Sun and D. P. Curran, *Tetrahedron Lett.*, **32**, 6097 (1991).
    (b) W. Damm, J. Dickhaut, F. Wetterich and B. Giese, *Tetrahedron Lett.*, **34**, 431 (1993).
    (c) B. Giese, M. Bulliard, J. Dickhaut, R. Halbach, C. Hassler, U. Hoffmann, B. Hinzen and M. Senn, *Synlett*, 116 (1995).
59. K. Miura, K. Oshima and K. Utimoto, *Bull. Chem. Soc. Jpn.*, **66**, 2356 (1993).
60. B. Giese, B. Kopping and C. Chatgilialoglu, *Tetrahedron Lett.*, **30**, 681 (1989).
61. C. Chatgilialoglu, B. Giese and B. Kopping, *Tetrahedron Lett.*, **31**, 6013 (1990).
62. H. Schneider, H. Fiander, K. A. Harrison, M. Watson, G. W. Burton and P. Arya, *Bioorg. Med. Chem. Lett.*, **6**, 637 (1996).
63. H. Urabe, K. Kobayashi and F. Sato, *J. Chem. Soc., Chem. Commun.*, 1043 (1995).
64. C. Chatgilialoglu, A. Alberti, M. Ballestri, D. Macciantelli and D. P. Curran, *Tetrahedron Lett.*, **37**, 6391 (1996).
65. F. Minisci, F. Fontana, G. Pianese and Y. M. Yan, *J. Org. Chem.*, **58**, 4207 (1993).

66. (a) H. Togo, K. Hayashi and M. Yokoyama, *Chem. Lett.*, 641 (1993).
    (b) H. Togo, K. Hayashi and M. Yokoyama, *Bull. Chem. Soc. Jpn.*, **67**, 2522 (1994).
67. For recent reviews on free-radical carbonylation, see:
    (a) I. Ryu, N. Sonoda and D. P. Curran, *Chem. Rev.*, **96**, 177 (1996).
    (b) I. Ryu and N. Sonoda, *Angew. Chem., Int. Ed. Engl.*, **35**, 1050 (1996).
68. I. Ryu, M. Hasegawa, A. Kurihara, A. Ogawa, S. Tsunoi and N. Sonoda, *Synlett*, 143 (1993).
69. I. Ryu, K. Nagahara, H. Yamazaki, S. Tsunoi and N. Sonoda, *Synlett*, 643 (1994).
70. S. A. Hitchcock and G. Pattenden, *J. Chem. Soc., Perkin Trans. 1*, 1323 (1992).
71. (a) M. Ihara, F. Setsu, M. Shohda, N. Taniguchi and K. Fukumoto, *Heterocycles*, **37**, 289 (1994).
    (b) M. Ihara, F. Setsu, M. Shohda, N. Taniguchi, Y. Tokunaga and K. Fukumoto, *J. Org. Chem.*, **59**, 5317 (1994).
72. G. J. Hollinworth, G. Pattenden and D. J. Schulz, *Aust. J. Chem.*, **48**, 381 (1995).
73. K. A. Parker and D. Fokas, *J. Org. Chem.*, **59**, 3927 and 3933 (1994).
74. (a) P. J. Parsons, C. S. Penkett, M. C. Cramp, R. I. West and E. S. Warren, *Tetrahedron*, **52**, 647 (1996).
    (b) D. J. Hart and D. Kuzmich, *J. Chin. Chem. Soc.*, **42**, 873 (1995).
75. M. P. Sibi and J. Ji, *J. Am. Chem. Soc.*, **118**, 3063, (1996).
76. P. Arya and D. D. M. Wayner, *Tetrahedron Lett.*, **32**, 6265 (1991).
77. S. Knapp and F. S. Gibson, *J. Org. Chem.*, **57**, 4802 (1992).
78. (a) P. A. Evans and J. D. Roseman, *J. Org. Chem.*, **61**, 2252 (1996).
    (b) P. A. Evans, J. D. Roseman and L. J. Garber, *J. Org. Chem.*, **61**, 4880 (1996).
79. T. B. Lowinger and L. Weiler, *J. Org. Chem.*, **57**, 6099 (1992).
80. L. A. Buttle and W. B. Motherwell, *Tetrahedron Lett.*, **35**, 3995 (1994).
81. (a) S. Bogen, M. Journet and M. Malacria, *Synlett*, 958 (1994).
    (b) L. Fensterbank, A.-L. Dhimane, E. Lacote, S. Boger and M. Malacria, *Tetrahedron*, **52**, 11405 (1996).
82. S. Bogen and M. Malacria, *J. Am. Chem. Soc.*, **118**, 3992 (1996).
83. T. Gimisis and C. Chatgilialoglu, *J. Org. Chem.*, **61**, 1908 (1996).
84. S. Kim, G. H. Joe and J. Y. Do, *J. Am. Chem. Soc.*, **116**, 5521 (1994).
85. S. Kim, *Pure Appl. Chem.*, **68**, 623 (1996).
86. M. Santagostino and J. D. Kilburn, *Tetrahedron Lett.*, **36**, 1365 (1995).
87. M. Kizil and J. A. Murphy, *J. Chem. Soc., Chem. Commun.*, 1409 (1995).
88. C. Chatgilialoglu, C. Ferreri and A. Sommazzi, *J. Am. Chem. Soc.*, **118**, 7223 (1996).
89. P. Dowd and W. Zhang, *Chem. Rev.*, **93**, 2091 (1993).
90. D. Crich and Q. Yao, *J. Org. Chem.*, **61**, 3566 (1996).
91. J. E. Lyons, C. H. Schiesser and K. Sutej, *J. Org. Chem.*, **58**, 5632 (1993).
92. K. J. Kulicke, C. Chatgilialoglu, B. Kopping and B. Giese, *Helv. Chim. Acta*, **75**, 935 (1992).
93. K. Miura, K. Oshima and K. Utimoto, *Bull. Chem. Soc. Jpn.*, **66**, 2348 (1993).
94. C. Chatgilialoglu, M. Ballestri, D. Vecchi and D. P. Curran, *Tetrahedron, Lett.*, **37**, 6383 (1996).
95. C. Chatgilialoglu, C. Ferreri, M. Ballestri and D. P. Curran, *Tetrahedron Lett.*, **37**, 6387 (1996).
96. (a) J. Cossy and L. Sallé, *Tetrahedron Lett.*, **36**, 7235 (1995).
    (b) C. Dufour, S. Iwasa, A. Fabré and V. H. Rawal, *Tetrahedron Lett.*, **37**, 7867 (1996).
97. E. Lee, T. S. Kang, B. J. Joo, J. S. Tae, K. S. Li and C. K. Chung, *Tetrahedron Lett.*, **36**, 417 (1995).
98. H. Künzer, G. Sauer and R. Wiechert, *Tetrahedron Lett.*, **32**, 7247 (1991).
99. G. Pattenden and D. J. Schulz, *Tetrahedron Lett.*, **34**, 6787 (1993).
100. M. D. Bachi, A. Balanov, N. Bar-Ner, E. Bosch, D. Denenmark and M. Mizhiritskii, *Pure Appl. Chem.*, **65**, 595 (1993).
101. H.-S. Dang and B. P. Roberts, *J. Chem. Soc., Perkin Trans. 1*, 769 (1996).
102. Y. Landais, D. Planchenault and V. Weber, *Tetrahedron Lett.*, **35**, 9549 (1994).

CHAPTER **26**

Recent advances in the direct process[†]

LARRY N. LEWIS

GE Corporate Research & Development Center, Schenectady, NY 12309, USA

[†] This review is dedicated to the memory of Alan Ritzer.

I. INTRODUCTION

The so-called ‘Direct Process’ is the industrial process for the synthesis of alkyl chlorosilanes. When the direct process produces methyl chlorosilanes the reaction is frequently called the Methyl Chlorosilane Process (MCS) (equation 1)[1]. Prior to the 1940s, alkyl chlorosilanes were primarily prepared via Grignard-like reactions. In 1940 Eugene Rochow of General Electric invented the direct process[2]. Rochow’s work, together with work by J. F. Hyde of Corning Glass (later Dow Corning)[3] led to the birth of the industrial silicones industry. Independently, Muller discovered an analog of the MCS reaction but his discovery was not well known in the West until later[4]. The history of the development of the Silicones Industry vis-a-vis the Direct Process is well documented in two excellent books on the subject[5,6].

$$\mathrm{Si} + \mathrm{MeCl} \xrightarrow[\substack{250-330\,^{\circ}\mathrm{C} \\ \text{fluidized bed}}]{\text{Cu + promoters}} \qquad (1)$$

Compound	%
Me_2SiCl_2(Di)	83–93
$MeSiCl_3$(Tri)	3–10
Me_4Si	0.01–0.5
Me_2SiHCl	0.01–0.5
$MeSiHCl_2$	0.1–1
Me_3SiCl	1–5
High boilers	1–5

From the 1940s through the 1970s, while the MCS reaction was practiced industrially on a large scale, it was frequently the source of frustrating irreproducibility. The major treatises on the subject of Direct Process failed to mention the importance of promoter elements in the catalyst[7–10]. In addition, the use of substrates other than MeCl was explored only occasionally. Finally, there were few successful attempts to understand the Direct Process on a fundamental level before 1980.

This review attempts to summarize the published literature and information in patents from the 1980s to the present. The effect of promoters will be discussed first because it was the understanding of their function which led to a quasi-second revolution in the area of the Direct Process. The second area discussed will be the effect of silicon morphology on selectivity and yield. The third area of this review will focus on mechanistic studies aimed at understanding the fundamental chemical and physical effects in the Direct Process. The fourth area of review will be the use of substrates other than MeCl in the Direct Process. Finally, a discussion will be presented on the recovery and use of by-products from MCS, previously considered waste products.

II. THE EFFECT OF PROMOTERS ON THE DIRECT PROCESS

A. Promoters in the MCS Reaction

Ward and coworkers at GE described the importance of both tin and zinc in the Direct Process[11,12]. They claimed that their work was the first reported description of the importance of these trace impurities. The Ward promoter work marked a benchmark in Direct Process literature because without controlling the levels of Sn, Zn and other promoters other effects are equivocal. The effect of zinc was known to some extent as early as 1949[4] but this knowledge was not clearly manifest in patents or publications on the subject. Fluidized and stirred bed reactors were used to show that trace quantities of Sn affect the MCS process profoundly and the effects of Sn and Zn were synergistic[11,12]. A catalyst system consisting of Cu, Zn and Sn was discovered which yielded 90% Di with nearly complete Si utilization. The trace elements in silicon used were (ppm): Fe (5600), Al (2700), Ti (850), Mn (200), Ca (160) and Ni (120) and the silicon was ball-milled to give particles with a surface area of 0.5 m^2 g^{-1}. Pure CuCl was used and the zinc added also contained (ppm): Pb (1700) and Cd (170). Pure tin and methyl chloride were employed in the experiments. The best rate and Tri/Di were obtained when element ratios were: Cu (5%), Zn (0.5%) and Sn (0.005%). When tin was $>$ 2200 an increase in residue occurred. Further work was done in the GE labs on the effect of tin and zinc[13,14].

Kim and Rethwisch further investigated the affect of tin and zinc on the MCS reaction[15]. Ball milling was used to grind copper and silicon and to impregnate the mixture with tin and zinc. When MeCl was passed over the balled milled mixtures, silanes began to form at 147 °C with a maximum production at 317–347 °C. When the catalyst consisted of only copper and zinc, MeCl decomposed without formation of silanes. However, when MeCl reacted with copper and tin, some Me_xSiCl_{4-x} was observed. Reacting MeCl with SiZnSn gave 64% $MeSiCl_3$. The addition of zinc to the MCS bed decreased the coking rate. Furthermore, surface chlorine was necessary for direct reaction; Zn and Sn promote its formation. Consistent with the synergism reported by Ward and coworkers, zinc was found not to increase the overall rate but increased the selectivity for methylated silanes. Tin increased the selectivity for chlorinated silanes. Tin and zinc together increased the rate of the MCS reaction.

Recently the effects of tin, zinc and antimony were studied in more detail leaving the frustrated researchers to state, ‘At present, no justified mechanistic explanation of the effect can be given, because of the total lack of information on nature, number and energetic distribution of the active sites of the catalyst system’.[16] Thus Lieske and coworkers report several important empirical observations[16]. In order to determine the effects of Zn, Sb and Sn, different combinations of silicon and copper catalyst were used: $CuCl_2/Si_{pure}$, $CuCl_2/Si_{tech}$, CuO/Si_{pure} and CuO/Si_{tech}. Zinc promoted the reaction of $CuCl_2/Si_{tech}$, CuO/Si_{pure} and CuO/Si_{tech} but not of $CuCl_2/Si_{pure}$, the latter was active without promoter. CuO/Si_{pure} and CuO/Si_{tech} were nearly inactive without promoters. With $CuCl_2/Si_{pure}$, antimony and tin caused higher activities than zinc but, with CuO/Si_{pure}, addition of Sn and Sb to the reaction did not reach the efficiency obtained with zinc. With $CuCl_2$, antimony promoted Si_{pure} and was more active than Si_{tech}, but with CuO, Si_{tech} was more active than Si_{pure}. Zinc appears to prevent detrimental effects of Si impurities and the authors note that zinc may catalyze formation of CuCl from Cu[17]. Additionally, zinc may help to remove the high oxygen content formed by using CuO[18]. No correlations were found between promoter and amount and size of Cu_3Si, nor was there a correlation between Cu_3Si amount and particle size *and* catalyst properties.

Since the discovery of the importance of some metal impurities on the rate and selectivity of the MCS reaction, several other combinations of promoter elements have appeared in the patent literature. One patent employs tin and/or antimony (they seem to be interchangeable) and zinc in combination with a lanthanide metal[19] (the promoter effects of barium and strontium have also been described[20]). In one case silicon (210 g) was preconditioned by reaction with MeCl (16 $L h^{-1}$) at 345 °C for 1 h, and then reacted at 315 °C for the duration of the reaction, in the presence of a catalyst consisting of CuCl (16.3 g), a bronze (0.38 g) containing 10% (by wt) tin, $ZnCl_2$ (1.60 g) and K_3LaCl_6 (1.69 g). The yields were: 93.6% Me_2SiCl_2, 2.8% $MeSiCl_3$ and 1.7% Me_3SiCl, with 58% conversion of silicon[19]. The relationship between zinc and antimony is also addressed in a Czech patent[21]. In the reaction of MeCl with Si–Cu substrate, replacing the catalytic mixture

TABLE 1. Percentage of silane products with Zn vs Sb in MCS

Promoter	Me_2SiCl_2	$MeSiCl_3$	Me_3SiCl	$MeHSiCl_2$
Sb	78	18	3	0.5
Zn	25	52	8	7

of $ZnCl_2$ with Sb shifted the product composition in favor of Me_2SiCl_2 as shown in Table 1.

A summary of the various metals used as promoters was prepared by Kanner and Lewis[1] and by Rethwisch and coworkers[22]. Zinc is claimed by Bayer workers as well to improve selectivity of the MCS reaction[23]. Further improvements in the use of zinc as a promoter are described wherein the zinc is in the form of a zinc salt of a weak acid having a pK_a of 3.50–10.25 (e.g. carbonic acid, carboxylic acids)[24].

Alkali metal salts are effective promoters in the direct process. Improved synthesis of Me_2SiCl_2 has been claimed in the presence of copper, tin and zinc and either KCl[25] or CsCl[26]. Alkali earth metals are also effective promoters. Beryllium, magnesium and calcium were claimed to improve the selectivity for Di in the MCS reaction. For example, a mixture of silicon (210 g), CuCl (16.4 g), $CaCl_2$ (1.244 g), $ZnCl_2$ (1.53 g) and bronze (2% Sn, 2.0 g) was pre-activated at 200 °C under nitrogen, whereupon MeCl was fed in at 16–27 $L\,h^{-1}$ at 330–345 °C for 15.5 h to give 55% conversion of Si and 86.7% selectivity to Me_2SiCl_2[27].

Phosphorus has been added to MCS beds and reported to improve selectivity for Di when tin and zinc are also present. Margaria and others describe the use of phosphorus as a promoter and cite a US patent where the benefits of phosphorus were realized as early as 1954[28]. Dow Corning workers describe the use of various phosphides such as copper phosphide to improve selectivity for Di[29]. Alternatively, phosphorus was introduced into an MCS bed by manufacturing silicon metal from quartz that was naturally high in phosphorus[30,31]. Apparently the use of any phosphorus compound that is not volatile, such as phosphides, leads to improved Di yield. Table 2 shows that use of phosphorus gave improved Di in the MCS reaction where copper, tin and zinc were also present as promoters[32]. Other workers have employed phosphorus as a promoter in volatile or gaseous form[33].

Other main group elements have been used as promoters in MCS beds containing copper, tin and zinc. Phosphorus and indium have been used in the MCS reaction. The reaction of silicon (40 g) with MeCl (2 bar) at 300 °C in the presence of Cu (3.2 g), ZnO (0.05 g), In (0.004 g) and P (0.056 g) gave 1.7% of Me_3SiCl, 0.017% mixture of $MeSiCl_3/Me_2SiCl_2$ and 3.7% of polysilanes[34]. Antimony, just below phosphorus in

TABLE 2. Effect of phosphorus on the MCS reaction

Sample	Analytical data on Si (in ppm)				% Di	Me/Me_2^a	Si conv (%)
	Al	Ca	Fe	P			
Conventional Si, no P	4100	5300	3200	0	81.6	0.11	77.8
Conventional Si, 14 ppm P	4500	1900	4900	14	84.6	0.08	80.7
Si refined with P	2170	250	2130	32	83.5	0.09	50
Si refined with P	2520	280	3620	33	84.6	0.08	59.9
Added tricalcium phosphate	2520	330	3560	148	90.5	0.04	82
Added tricalcium phosphate	2760	430	3450	69	88	0.06	79.4

[a] Me/Me_2 = wt% Me_2SiCl_3/wt% Me_2SiCl_2.

group V on the periodic table, also appears to be a promoter as well in the MCS reaction[35,36].

B. Use of Promoters to Improve the Yield of Si−H Containing Products

In 1975 van den Berg and coworkers reported on improved direct synthesis of methyldichlorosilane and dimethylchlorosilane[37]. The key elements of the van den Berg work were the use of hydrogen co-feed with the methyl chloride and the use of promoters. The paper is important because several important patents followed in its wake on improved methods for production of Si−H containing silanes and because it begins to address the use of promoters. The use of hydrogen was shown to improve the yield of $MeHSiCl_2$ (DH) and Me_2ClSiH (MH) vs reactions run without hydrogen. The authors concluded that metal halides, which are promoters for formation of Me_2SiCl_2, are not promoters for formation of DH and MH. Using a contact mass 'without promoter' gave higher per cent of MH and DH than experiments where either Ag, Cd, Zn or Al were added. Unfortunately, precise compositional analysis of the 'un-promoted' experiment was not discussed, leading one to wonder if promoters were present or not.

Both Dow Corning and the old Union Carbide silicones group were active in optimizing conditions for formation of MH and DH. Halm and Zapp of Dow Corning improved the method for making DH[38] by using both hydrogen and HCl as a co-feed with MeCl. By also employing silicon containing Al (0.22%), Ca (0.046%), Fe (0.34%) and by adding brass with tin and CuP alloy, improved yield of DH was obtained. In a control reaction (no HCl/H_2) the crude product contained Di (92.1%), $MeHSiCl_2$ (1.3%), Me_2HSiCl (0.3%) and Tri (4.1%), but with a feed that contained 1% H_2 and 1% HCl the crude product contained Di (76.1%), $MeHSiCl_2$ (12.1%), Me_2HSiCl (1.5%). If HCl is used without hydrogen, lower yield of DH is obtained[39].

The Union Carbide workers report a much higher overall yield of Si−H containing monomers if transition metal promoters are employed[40]. In one case, a high yield of MeH_2SiCl was obtained if a fluidized bed of CuCl, Si and MeCl also contained certain attributes, namely MeH_2SiCl yield improved if the silicon had 0.004–0.02% Ni and 0.002–0.01% Cr (Rh is also a promoter); $CaSi_2$ also helped. Poor results were obtained if the following were present: CuS_x, Cu_xP, Zn, Sn and Cd (last 3 lower selectivity for alkylhalosilanes). A fluidized bed run at 325 °C and which had HCl in the feed gave: Me_2SiHCl (7.4%), $MeSiHCl_2$ (21.5%), Me_3SiCl (2.9%), Tri (12%), Di (55%); total MeSiH 29%. When Ni was present the yield of MH was 16.2% and that of DH was 43.5%, with a total MeSiH of 60%. Earlier work showed the effectiveness of other metal promoters to increase SiH yield[41].

III. THE EFFECT OF SILICON, CATALYST AND PROMOTER MORPHOLOGY ON THE MCS REACTION

A. The Effect of Surface Area

The MCS reaction is a solid/gas reaction, so that it is natural that morphological effects of the solid components of the reaction should be important. Workers at Wacker defined a surface area parameter, QF, which relates the ratio of elongated to round structural forms[42]. MCS promoters controlled by employing Si particles for a given surface area defined the ratio QF as the ratio of the area portion of intermetallic phases at grain boundaries to the area portion of intermetallic phases in primary silicon[43]. These workers found that maximum Di was obtained for silicon particles having QF = 18–60. Furthermore, the rate was effected by QF, so that for CuO, ZnO, and Sn and Si with QF = 29.55, the rate of Di formation was 103.28 $mg\,m^{-2}\,min^{-1}$, but with Si with a QF value of 2.34 the rate was 50.70 $\mathrm{mg\,min^{-1}}$. The value of QF could be effected by variation of the range of solidification speed from atomization to extremely slow cooling. Atomized silicon has a QF value of 64.

B. The Effect of Silicon Size on the MCS Reaction

Dow Corning workers describe the improvements in the MCS reaction obtained by selecting a particular particle size distribution[44]. They found the best results when the particle size of the silicon was within a range of 1 to 85 microns. Specifically, the most effective silicon was when the particle size of the silicon had a mass distribution characterized by a 10th percentile of 2.1 to 6 microns, a 50th percentile of 12 to 25 microns and a 90th percentile of 35 to 45 microns. Bayer workers specify a silicon particle size distribution of 5–15 microns[45] in one case and 71 to 160 microns in another[46].

C. The Effect of Oxygen in Silicon Metal Used in the Direct Process

Considering the high oxophilicity of silicon, it is not surprising that oxygen has a negative effect on the MCS reaction. Careful research by workers from silicon manufacturer Elkem showed that oxygen in silicon varies from 0.02 to 1 weight percent[47]. There is a native oxide layer of 20 Å on silicon, which for a 50-micron particle contributes about 0.012 weight % oxygen to the total mass of the particle. Oxygen in the silicon is detrimental to its reactivity in the Direct Process. Oxygen is present as a small amount of SiO inclusions and present as oxides of Al_2O_3, CaO, SiO_2 and lesser amounts of MgO, K_2O and Na_2O. Slag in silicon in the Direct Process is detrimental due to the presence of aluminum as an oxide[48]. Also, slag particles accumulate and reduce reactivity because less silicon is available for reaction.

The results reported by Dubrous of silicon manufacturer Pechiney[49] apparently contradict the above work. Dubrous describes a process wherein the crushing and grinding steps of making silicon form an oxide layer and the presence of the oxide layer facilitates the manufacture of Di. When silicon containing Ca (0.08%), Al (0.21%) and Fe (0.39%) was crushed and powdered in the presence of 0.3% silicones under an atmosphere of Ar, it had a 1.2-nm-thick SiO_2 coating, and gave a conversion rate of MeCl in MCS of 88% and MeCl conversion 85%, vs 70 and 85%, respectively, for conventionally coated Si powder.

D. Preparation of Catalyst, Silicon and Promoters for Use in the MCS Reaction

As already discussed, the particle size and surface properties of silicon used in the MCS reaction are important. Several groups have reported improvements in the MCS reaction by different methods of physically combining silicon, copper catalyst and promoters. In Kim and Rethwisch's fundamental studies on activation energies in the MCS reaction (*vide infra*) copper and silicon were ball milled and then tin and zinc promoters were combined by ball milling or by impregnation[50]. Ball milling (specifically energy milling) was also used by SCM workers to prepare copper catalysts (<15 microns) for use in the silicon direct process[51].

More intricate treatment of silicon and copper was reported by Mui[52]. The Si/Cu contact mass was prepared by (1) treating Si particles with Cu catalyst vapor in a mechanical mixer, (2) mixing the Si particles with the Cu catalyst vapor, (3) contacting the vapor with the particles and (4) forming active Cu–Si alloys on the Si particles. The CuCl vapor was formed at 1200 °C and fed to silicon at 320 °C. This author claims that treating the contact mass in this way and by using zinc carbonate and tin oxide there was no induction period, and performance of this contact mass was comparable to that of contact masses with much higher Cu content.

It is possible that the improvements described above are due to pre-formation of silicon copper alloys, as claimed by Elattar[53]. Improved activity of MCS contact mass was obtained by forming a contact mass of particulate Si and Cu (16.9% metallic Cu, 45.5% Cu_2O, 36.9% CuO) by heating the mass in the presence of MeCl gas at 305 °C for a time sufficient to form active spots of Cu–Si alloy on the surface. The nature of these copper–silicon alloys may include those described by some former E. German workers who showed the importance of forming Cu_6Si and $CuSi_2$ among others[54].

E. The Effect of Copper Catalyst Preparation on the MCS Reaction

Several groups have investigated improvements in the MCS reaction wrought by improving the physical and chemical nature of the copper catalyst. SCM workers made an improved catalyst by grinding a charge of Cu(I) particulates with a small proportion of a hydroxide of group IV metals [e.g. Fe(III) oxide monohydrate][55]. The grind charge contained a major proportion of Cu and CuO and was subjected to high energy milling with concomitant crystal lattice distortion. The SCM workers additionally note the importance of copper catalyst size (average 20 microns) tin concentration (400–3000 ppm)[56].

Workers at Wacker employed a more chemical approach to producing and activating their copper catalyst. They added an aqueous solution of $CuCl_2$ to a suspension of iron particles (average particle size 60–70 microns). The catalyst was mixed with Si, $ZnCl_2$ and Zn powder to give a contact mass which was heated to 350 °C and treated with MeCl to give a product mixture containing 80.6% Di[57]. Another chemical process for formation of the copper catalyst was described by workers from Leuna-Werke A.-G where an aqueous $Cu(NO_3)_2$ was added to an aqueous solution of Na_2CO_3 at 40 °C until the resulting suspension was neutral. The product was filtered, washed and treated with oxalic acid and H_2O to bring the solution to a pH of <1. After 1 h stirring, additional oxalic acid was added, followed by stirring and drying at 200 °C to give a product showing 82% selectivity for Di in the MCS reaction[58]. These workers also employed copper salts of mono- and di-carboxylic acids[59] and copper hydroxide/copper carbonate precursors[60]. Published work by GE shows the use of copper oxide precursors for MCS[61].

While most published efforts aim toward maximum production of Di, one set of workers prepared a catalyst which selectively makes Tri. Workers from Wacker prepared a mixture containing SiO_2 powder (75 parts), Fe (75 parts), carbon black (60 parts) and Cu (18 parts) which was pelletized with H_2O, dried at 220 °C and heated at 1100 °C for 17 h[62]. The resulting solid was treated with MeCl at 200–350 °C under Ar to give a mixture containing $MeSiCl_3$ 80%, Me_2SiCl_2 5% and $SiCl_4$ 15 mol%.

F. The Effects of Intermetallics in the Contact Mass on the MCS Reaction

There has been extensive work devoted to correlating the effects of the various recipes described in this section with formation of specific reactive sites and intermetallics on silicon. A quite comprehensive study of this kind was reported by Laroze and others[63]. These authors point out that aluminum is an activator for the overall consumption of silicon in the MCS reaction; however, it does not stabilize Cu_3Si alloy because it increases the rate of alloy consumption by CuCl. Aluminum does not dissolve in the crystal lattice of silicon but is present as an intermetallic, e.g. Si_2Al_2Ca, $Si_8Al_6Fe_4Ca$, $Si_{2.4}FeAl$, Si_2Al_3Fe and $Si_7Al_8Fe_5$. The formation of these silicides and of Si_2FeTi and Si_2Ca is effected by cooling rates and annealing. The reaction of Si_2Al_2Ca with CuCl at 25 °C is violent, giving

Cu_3Si, Cu_5Si and Cu. At lower temperatures the only product is Cu. Intermetallics have an important effect on the direct process. For example, the activating effect of aluminum disappears when added as the quaternary alloy $Fe_4Si_8Al_6Ca$ but an increase in selectivity is noted when the ternary alloy is present. Aluminum added as the ternary alloy $Si_7Al_8Fe_5$, Al_3Si_2Fe and Al_2Si_2Ca favors activity but decreases selectivity.

The formation of intermetallics is clearly critical in the MCS reaction as further shown in recent work by Margaria and coworkers[28]. These inventors describe the harmful effects of the Si_2Al_2Ca ternary phase (must be below 0.3%). The ternary phase was limited during silicon refining by simultaneously regulating the range of Fe, Al and Ca impurities and setting the solidification rate. Silicon with 0.15% ternary phase gave a Di yield of 86.4% while silicon with no ternary phase gave a Di yield of 90.3%.

IV. SURFACE FUNDAMENTALS AND MECHANISTIC STUDIES OF THE MCS REACTION

Eugene Rochow himself wrote about the factors that led to the use of copper catalyst in the direct process. Rochow's knowledge of metallurgy certainly played a part in the discovery of the direct process but serendipity certainly contributed as well[64]! Details of the copper catalyzed MCS reaction at the molecular level are still not well understood over 50 years after its discovery. The most extensive investigations of the surface chemistry occurring during the direct process have been carried out by the Falconer group in Colorado[65–71]. They have used surface analyses to determine the changes that occur on a silicon surface under MCS conditions. Typical experiments were carried out on silicon wafers and characterized before and after exposure to MeCl reaction by X-ray photoelectron spectroscopy (XPS), Auger electron spectroscopy (AES), X-ray diffraction (XRD), scanning electron microscopy (SEM), electron disperssive spectroscopy (EDS) and optical microscopy.

Without zinc, silicon diffusion to the surface is slow under MCS conditions. Furthermore, when only tin is used as a promoter, no Cu is observed at the surface. Table 3 shows the elemental concentration under various conditions. Under MCS reaction conditions, when zinc was present silicon was not depleted from the subsurface, and when zinc was absent the subsurface was depleted in silicon. Zinc causes the rate of silicon diffusion and copper dispersion to increase. Zinc accumulates at grain boundaries and lowers the free energy of Cu_3Si. Tin and zinc appear to work synergistically but tin does not enhance silicon diffusion on its own. Tin does appear to lower the surface energy of silicon/copper.

Further surface studies have addressed the effect of different forms of copper as a catalyst in the direct process[65–69]. Analyzing Si(100) surfaces it was shown that the form of copper is critical for selectivity in the MCS reaction. The most effective combination was 82% Cu and 18% Cu_2O (neither worked very well alone). There was no correlation between the amount of Cu_3Si on the surface and rate or selectivity for the direct process.

TABLE 3. Auger analysis of Cu_3Si after reaction at 277 °C[71]

Promoter	Time (min)	Si[a]	Cu[a]	C[a]	Cl[a]	O[a]	Sn[a]
None	240	8	52	14	24	2	0
Sn	220	61	<0.5	20	12	7	0
Zn	210	23	39	23	11	3	0
Zn,Sn	250	40	15	24	9	9	3

[a] Atom %.

The orientation of Cu_3Si relative to the Si(100) face did correlate to rate and selectivity; a random orientation gave the best results. One study found that the reaction was inhibited by a SiO_2 layer[65] and a second study found no such inhibition[66]. SEM analysis of several surfaces after reaction with MeCl showed square reaction pits.

Lewis and coworkers have also made significant contributions to the understanding of the MCS reaction via the use of surface studies[72]. XPS and AES analysis of catalytically active surfaces showed that zinc causes a restructuring of the Cu_3Si surface. Additionally, zinc enrichment is enhanced by the addition of $SnCl_4$. Lead is a well known poison for the direct reaction and the Lewis group found that lead suppressed enrichment of the Cu_3Si surface in zinc and silicon.

A 1989 review of the literature by Clarke gave many examples which support the importance of copper–silicon rich phases near the surface during the MCS reaction[73]. Clarke noted that Cu_3Si (eta phase) forms above 880 °C but will form at 350 °C in the presence of chloride ion. Methyl chloride reacts with copper to form copper chloride which then serves as the chloride source needed for formation of the eta phase, thus explaining the shorter induction period obtained using copper chloride vs other copper catalysts. The mechanism of replacement of silicon from the surface is by diffusion of copper into the bulk silicon to reform a copper–silicon rich surface. Iron–silicon phases stabilize the eta phase and metal promoters catalyze chloride transfer, e.g. see equation 2. Silicon also reacts with $ZnCl_2$ and $AlCl_3$. Excess zinc causes unproductive decomposition of MeCl to give methane. Finally, Clarke presented data that ruled out the importance of methyl radicals in the MCS reaction.

$$CdCl_2 + Si \longrightarrow CdCl + SiCl \qquad (2)$$

More recent support has appeared for the importance of the copper–silicon rich phase on the silicon surface in the MCS reaction. Lieske and coworkers[74] showed that redispersion of the eta phase can be an element of the induction period of the MCS reaction and seems to be brought about by the reaction itself. The Cu–Si surface species, perhaps Cu–Si surface compounds or extremely small Cu–Si particles, seem to be of similar importance as X-ray detectable Cu–Si phases.

Finally, Rong and coworkers discuss the roll of surface oxygen on the MCS process[75]. Rong employed a lab-scale stirred bed reactor and then applied XPS to analyze the silicon samples before and after the reaction. The reactivity of silicon depended on the initial thickness of the native oxide on the silicon. After the reaction the surfaces of all of the samples were mostly covered with SiO_2. There was no observed correlation between the surface and bulk O content. XPS analysis showed the presence of Al, Ca and Ti impurities in some samples. Titanium on the surface appeared to increase the reactivity, whereas Ca decreased the selectivity of Di formation. Addition of ZnO to the silicon before CuCl improved reactivity and also decreased the induction period of the reaction. XPS studies of samples prepared in this manner exhibited a lower Zn surface concentration compared to the samples where CuCl, Si and ZnO were mixed together.

V. SILICON DIRECT PROCESS REACTIONS WITH REAGENTS OTHER THAN MeCl

A. Other Organic Halides

There are many examples of the direct reaction of silicon with ethyl chloride, vinyl chloride and chlorobenzene[1]. Vinyl and allylchlorosilanes[76] were first made via a direct process in 1945 as were phenylchlorosilanes[77]. Jung's group has recently extended the direct reaction of silicon with a variety of substrates including allyl chloride[78]. Silicon reacted with allyl chloride in a stirred reactor in the presence of HCl and a copper catalyst at 220–320 °C in a stirred reactor to make (allyl)Cl_2SiH as the major product and allyl$SiCl_3$ as the minor product. Unlike MeCl reactions cadmium was a good promoter and zinc was an inhibitor. Jung also published (in the Gelest Inc. product catalogue) a review of direct reactions between silicon and a variety of organic halides including methylene chloride, benzyl chlorides, etc. The reaction of α-(chloromethyl)silanes with silicon is shown in equation 3[79]. The reaction of α, α'-dichloro-*o*-xylene with silicon gives the silicon-containing ring product shown in equation 4[80].

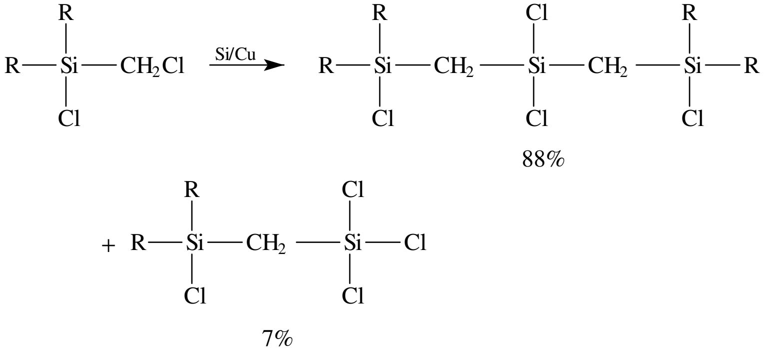

$$R_2ClSi{-}CH_2Cl \xrightarrow{Si/Cu} \underset{88\%}{R_2ClSi{-}CH_2{-}SiCl_2{-}CH_2{-}SiClR_2} + \underset{7\%}{R_2ClSi{-}CH_2{-}SiCl_3} \qquad (3)$$

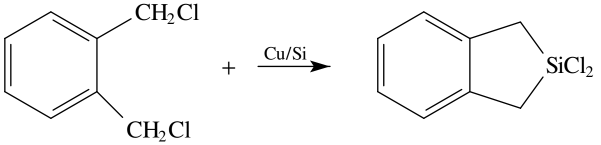

(4)

B. Reactions of Silicon with Alcohols

The first attempts at direct reaction of silicon with methanol and ethanol were reported shortly after the methylchlorosilane reaction was discovered[81]. Rochow and Newton continued their interest in the non-halogen direct process and in 1970 described the direct synthesis of $(MeO)_3SiH$ and $(MeO)_4Si$[82]. There has been much recent effort in the alcohol-based direct process. Okamoto and coworkers report high silicon conversions and selectivity for $(MeO)_3SiH$ by reaction of silicon and methanol in the presence of copper acetate and small amounts of thiophene[83]. Shiozawa and Okumura report similar results in a Japanese patent[84]. Earlier work by the Union Carbide group showed that greater than 80% selectivity for $(MeO)_3SiH$ was possible in the copper catalyzed reaction between methanol and silicon[85,86]. Unlike the methyl chloride reaction where tin is a promoter, tin had adverse effects on the reaction between methanol and silicon.

There are several groups working toward large-scale manufacture of alkoxysilanes via a direct process. Workers at Japan's Tonen Corporation report 84% silicon conversion and 96% selectivity for $(MeO)_3SiH$ by reacting pulverized silicon, $Cu(OMe)_2$ and methanol[87]. The silicon pulverization was carried out using an alumina vibrator mill under argon to make 150-micron particles. These workers also use silicon essentially free of iron. Mitsubishi workers report that the reaction of silicon with methanol and cuprous chloride in dodecyl benzene at 220 °C gave 69% $(MeO)_3SiH$[88]. The silicon was pretreated by grinding with stainless steel balls at −25 °C. Toa Gosei Chemical Industries in Japan also report a commercial methanol direct process[89]. The (former) Union Carbide silicones group also reported a method for commercialization of a methanol direct process[90]. The Union Carbide group employed a continuous reactor for the synthesis of $(MeO)_3SiH$ and they specified a silicon particle size <420 microns, 0.1 to 2.6 parts (based on silicon) of $Cu(OH)_2$ catalyst and the use of high boiling aromatic solvents. These workers again point out the adverse effects of tin in this reaction.

Some work has appeared discussing the mechanism of the alcohol-based direct process. A kinetic study by Suzuki and coworkers using a fixed bed reactor found that the rate of $(MeO)_3SiH$ formation from methanol, silicon and a copper catalyst was proportional to methanol pressure[91]. Preheating the reactants was found to have an important effect on the kinetics. Further XRD work by Suzuki and Ono linked the methyl chloride process to the methanol process[92]. Cuprous chloride and silicon powder were preheated at 350 °C for 3 h and then reacted with methanol (99 kPa, 270 °C) in a fixed bed reactor for 5 h to give $(MeO)_3SiH$ (98% selectivity, 82% silicon conversion). XRD analysis after reaction showed Cu_3Si formation had occurred. SEM analysis of silicon from the MCS process showed reaction pits. Likewise, Suzuki's group reports formation of pits on silicon after a methanol direct process[93]. The amount of reaction pits increased as silicon conversion increased. Pretreatment of the silicon is important for silicon conversion and selectivity to $(MeO)_3SiH$[94]. When the silicon was pretreated above 350 °C, 65% selectivity for $(MeO)_3SiH$ was obtained and surface analysis such as XRD showed Cu_3Si. When the silicon was pretreated at <280 °C the rate was higher, the selectivity for $(MeO)_3SiH$ increased to >98% and no Cu_3Si was observed.

A key report investigated a variety of substrates in their reaction with silicon in an effort to find evidence for silylene intermediates during the silicon direct process reaction. When silicon, copper and methanol were reacted as described above but in the presence of alkenes, alkyldimethoxysilanes and $(MeO)_3SiH$ were formed[95–97]. The use of allyl propyl ether instead of alkenes gave allyldimethoxysilane, with 38% selectivity. These results and the reaction of silicon with MeCl in the presence of butadiene to give silacyclopent-3-enes indicates intermediate formation of silylenes.

In some cases, the reaction of silicon and methanol has been optimized for formation of $(MeO)_4Si$. As discussed above, thiophene addition favored formation of $(MeO)_3SiH$. Both thiophene and propyl chloride poison copper; copper poisoning seems to favor formation of the trialkoxysilane. High-temperature pretreatment disfavors trialkoxysilane formation; copper is formed on the surface of the silicon during pretreatment at 450 °C[98]. Metallic Cu catalyzes dehydrogenation of alcohols and favors formation of $(RO)_4Si$. Workers from Tonen Corporation reported 50% conversion of silicon to make $(MeO)_4Si$ with 92% selectivity if silicon, methanol and $Cu(OMe)_2$ were pretreated (lower conversion and selectivity without pretreatment) and then reacted at 180 °C and 1 atmosphere[99].

C. Alternative Methods to Formation of $Si-CH_3$ Bonds

Newton and Rochow reported low (1–2%) yields of methylalkoxysilanes during the copper catalyzed reaction of silicon and methanol[82]. In 1988 a group from Lopata R&D Corporation reported a version of the silicon methanol direct reaction wherein they added metal formates such as potassium formate and employed about 100 psi H_2 (out of a total pressure of 900 psi). Under these conditions about 10% $MeSi(OMe)_3$ was produced (<0.1% when potassium formate was not present)[100]. These results represented one of the highest production of silicon-methyl containing products in the absence of halogen. Rochow has stated that the non-halogen based direct process was and continues to be one of the great challenges left for the silicon direct process[64]. In this author's opinion an even greater challenge is a direct process based on SiO_2!

Two groups have made minor breakthroughs in the non-halogen direct process. In 1978 Malek, Speier and coworkers reported the reaction between dimethyl ether and silicon[101]. Prior to their work there were some attempts to employ dimethyl ether as a substrate. Rochow and Zuckerman[102] disputed one claim[103]. Later Newton and Rochow discussed the difficulty of using dimethyl ether in a direct process[82]. Malek's and Speier's work showed that when silicon was reacted with MeOMe in the presence of metal catalysts and MeBr, 64.4% $Me_2Si(OMe)_2$ could be obtained. The silicon (150 g, 98%, 0.44% Fe, 0.26% Al, 0.058% Ca, 0.005% Sn, 0.04% Mn, 0.032% Ti, 0.051% V, 0.002% B, 0.014% Cr, 0.05% Zn and 0.002% Pb) was ground with steel balls to 2.7 microns for 16 h with Cu powder (12 g). One-hundred parts of silicon, 3.3 parts of copper, 0.3 part of iron, 0.43 part of aluminum and 0.13 part of calcium were combined in an autoclave and MeOMe and MeBr were added (mole ratio of Si:MeOMe:MeBr 100:350:1) and then heated for 20 h at 258 °C. While this process was not entirely halogen-free, it was the most successful ether silicon direct process to date.

Since the Malek and Speier work, Lewis and Kanner also reported a dimethyl ether direct process which was a great improvement over Malek's and Speier's because it employed a fluidized bed in place of an autoclave[104,105]. Lewis and Kanner found that silicon (200 g, 98.4%, 0.35% Al, 0.55% Fe), copper cement (5 g, Cu 22%, Cu_2O 50.4% and CuO 18.8%) and $ZnCO_3$ (0.5 g), when preheated in the presence of HCl at 300 °C after N_2 fluidization and then addition of MeCl (0.8 std $\mathrm{lit\,min^{-1}}$), after 8 h at 325 °C yielded Di (90%) and Tri (1%). If just MeOMe and HCl were added, no silicon products were obtained. If, however, the feed contained MeOMe (0.37 std $\mathrm{lit\,min^{-1}}$) and MeCl (0.54 std $\mathrm{lit\,min^{-1}}$), then 8% methylsiloxanes were obtained at atmospheric pressure. Using a fluidized bed and MeBr a product mixture containing Me_3SiOMe, $(Me_3Si)_2O$, $Me_2Si(OMe)_2$, $Me_3Si(OSiMe_2)_nMe$ ($n = 1$–4), $Me_3Si(OSiMe_2)_nSiMe_3$ ($n = 1$–4) and $(Me_2SiO)_n$ ($n = 3$–7) was obtained.

VI. RECOVERY AND USE OF BY-PRODUCTS FROM THE MCS REACTION

A. High Boiling Residues from the Direct Process

The MCS reaction is characterized by production of high boiling fractions and spent silicon solids enriched in various metals. Industry is continually improving their ability to minimize waste due to environmental and economic realities. In the 1980s workers from Bayer described a method to convert a complicated mixture into useful monomers. Their mixture was composed of approximately 14.7% low boilers ($SiMe_4$, 61.3%; Me_2SiHCl, 11.9%), 14.7% high boilers (Me_6Si_2, 18%; Me_5ClSi_2, 18.4%; $Me_2ClSiSiClMe_2$, 11.7%; $MeCl_2SiSiClMe_2$, 3.5%) and 68.6% $MeSiCl_3$. The Bayer mixture was combined with $AlCl_3$ and then heated to give a mixture where 80% of the product had a boiling point less than 80 °C and was composed of Me_2SiCl_2, 58.3%; Me_3SiCl, 5.2%; $MeSiCl_3$, 32.8% and $MeSiHCl_2$, 2.0%[106]. These workers also employed alumina and $SOCl_2$-containing catalysts[107]. An early but excellent discussion of the whole problem of waste recovery reactions from the MCS reaction was published by Calas, Dunogues, Deleris and Duffaut in 1982[108]. The disilane residue from the direct process can be converted into useful materials by disproportionation (equation 5), cleavage by HCl (equation 6), cleavage in the presence of H_2 (equation 7), cleavage of $Cl_3SiSiCl_3$ in the presence of organic halide RCl, such as MeCl or allyl chloride to give $Cl_3SiR + Cl_4Si$ catalyzed by Pd, Pt, Ni, and finally disilane addition to unsaturated molecules like acetylenes and dienes catalyzed by Pd.

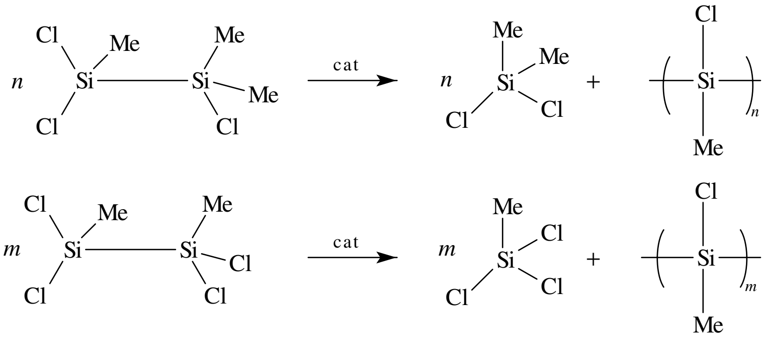

(5)

Cat = Bu_3N, Me_4NCl etc.; most efficient is $P(O)(NMe_2)_3$/(HMPA)

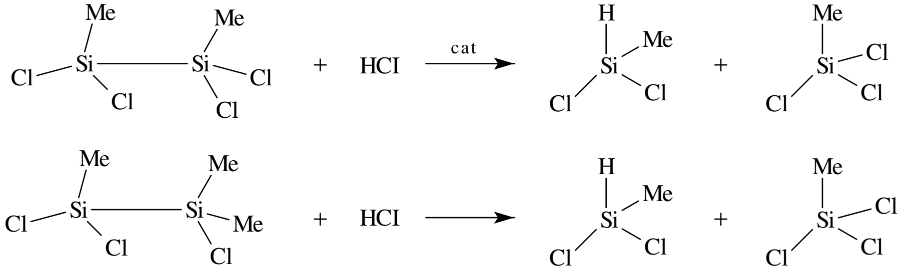

Cat = amines and amides

(6)

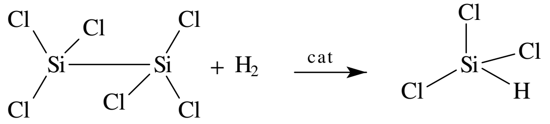

(7)

cat = Ni(0); others include Pd, Ru, etc.

Recently, there has been a lot of activity in the area of recovery of high boilers from the direct process. Dow Corning workers add Me_3SiCl to high boilers in the presence of H_2 and $AlCl_3$[109] or supported metal catalysts[110,111] to make 91% $Me_yH_zSiCl_{4-y-z}$, whereas workers from Chemiewerk Nuenchritz employ catalysts derived from alkyl amine-trialkoxysilane on an SiO_2 support[112]. Pachaly and Schinabeck from Wacker Chemie convert a mixture composed of 7% $Me_4Si_2Cl_2$, 46.5% $Me_3Cl_3Si_2$ and 46.5% $Me_2Cl_4Si_2$ into a mixture composed of 45% $MeCl_2SiH$, 28% $MeSiCl_3$ and 27% Me_2SiCl_2 in the presence of Bu_3N and HCl[113]. Similar results were obtained by Bokerman and coworkers using supported Pd and Cu catalysts[114].

B. Recycle of Solid Waste Products from the MCS Reaction

In order to maintain a steady-state concentration of bed metals during MCS production, metals are constantly blown out of the bed and replaced by fresh metals. The metal dust is separated from crude chlorosilane in devices called cyclones. Residual bed and cyclone dust represent a serious waste problem because of the high metal content of the waste. Workers from Wacker Chemie have described a method for leaching the metals from the solid waste with water/HCl. The leachate is then recovered and used as a catalyst for further MCS reaction. The precipitated silicon is fed back into the MCS reaction to obtain further silicon utilization and minimize land fill[115]. GE workers Webb, Ritzer and Neely successfully used 'spent contact mass' to catalyze the reaction of silicon with MeCl under MCS conditions to make Di and Tri[116]. Other work by the same researchers has focused on converting the pyrophoric, spent reactor contact mass (obtained from the reaction of metallic Si with MeCl under direct process conditions) into air-stable powder. The spent mass was thermally treated at 1100 °C for 3 min under nitrogen. The treated contact mass could then be used in the MCS reaction, for example it was placed in a stirred bed reactor exposed to flowing MeCl at 300 °C to give Di and Tri[117].

The late Alan Ritzer of GE wrote of the opportunities that environmental regulations present to silicone manufactures[118]. A major strategy of GE Silicones continues to be avoidance of landfilling and incineration and returning key materials back into commerce. Said Ritzer, 'Additional opportunities remain as overall silicon utilization still can be further improved'. Residue cleavage represents one method to create more Di and Tri. Mono and Tri redistribution (equation 8) represents yet another method to improve Di yield.

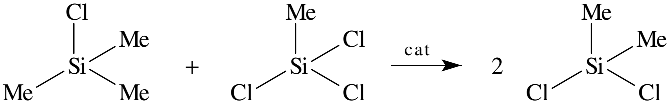

(8)

VII. ACKNOWLEDGMENTS

Help in preparing this review in the form of literature search and discussions is due to Caroline Warden and Bill Ward.

VIII. REFERENCES

1. B. Kanner and K. M. Lewis, in *Catalyzed Direct Reactions of Silicon* (Eds. K. M. Lewis and D. G. Rethwisch), Elsevier, Amsterdam, 1993, p. 1.
2. E. G. Rochow and W. Gilliam, *J. Am. Chem. Soc.*, **63**, 798 (1941).
3. J. F. Hyde and R. DeLong, *J. Am. Chem. Soc.*, **63**, 1194 (1941).
4. J. J. Zuckerman, *Adv. Inorg. Chem. Radiochem.*, **6**, 383 (1964) and references cited therein.
5. H. A. Liebhafsky, *Silicones Under the Monogram*, Wiley, New York, 1978.
6. E. L. Warrick, *Forty Years of Firsts*, McGraw-Hill, New York, 1990.
7. W. Noll, *Chemistry and Technology of Silicones*, Academic Press, New York, 1968.
8. A. Petrov, B. F. Mironov, V. A. Ponomarenko and E. A. Chernyshev, *Synthesis of Organosilicon Monomers*, Consultants Bureau, New York, 1976.
9. R. J. H. Voorhoeve, *Methylchlorosilanes: Precursors to Silicones*, Elsevier, New York, 1967.
10. W. Buechner, *Organometallic Reviews*, *5th Int. Symp. on Organosilicon Chem.* (Eds. D. Seyferth, A. G. Davies, E. O. Fischer, J. F. Normant and O. A. Keutov), Elsevier, Amsterdam, 1980, p. 409.
11. W. J. Ward, A. Ritzer, K. M. Carroll and J. W. Flock, *J. Catal.*, **100**, 240 (1986).
12. W. J. Ward, A Ritzer and J. W. Flock, U.S. Patent 4,500,724 (1985).
13. W. J. Ward, G. L. Gaines and A. Ritzer, Brit. Pat. Appl. GB 2119808, (1983) **100**, *Chem. Abstr.*, 103630 (1984).
14. W. J. Ward, G. L. Gaines and A. Ritzer, Ger. Offen. DE 3312775 (1983); *Chem. Abstr.*, **100**, 68521 (1984).
15. J. P. Kim and D. G. Rethwisch, *J. Catal.*, **134**, 168 (1992).

16. H. Lieske, U. Kretzshmar and R. Zimmermann in *Silicon Chem. Ind. II, 2nd Int. Cong.* (Eds. H. A. Oye, H. M. Rong, L. Nygaard, G. Schussler and J. Kr. Tuset), Trondheim, Norway, 1994, p. 147.
17. R. A. Turetskaya, K. A. Andrianov, I. V. Trofimova and E. A. Chernyshev, *Usp. Khim.*, **44**, 444 (1975); *Chem. Abstr*, **82**, 154580 (1975).
18. A. F. Hollemann and E. Wiberg, *Lehrbuch der Anorgaischen Chemie*, Walter de Gruyter, Berlin–New York, 1985, p. 1038.
19. J. L. Plagne, G. Godde and R. Cattoz, Eur. Pat. Appl. EP 470020 (1992); *Chem Abstr.*, **116**, 152011 (1992).
20. C. P. Homme, Fr. Demande FR 2577929 (1987); *Chem Abstr.*, **106**, 158883 (1987).
21. J. Mlynar, L. Dvorak and B. Kurka, Czech. CS 207859, (1983); *Chem. Abstr*, **101**, 192187 (1984).
22. L. D. Gasper-Galvin, D. G. Rethwisch, D. M. Sevenich and H. B. Friedrich, in *Catalyzed Direct Reactions of Silicon*, (Eds. K. M. Lewis and D. G. Rethwisch), Elsevier, Amsterdam, 1993, p. 279.
23. K. Feldner, B. Degen, G. Wagner and M. Schulze, Ger. Offen. DE 3823308 (1990); *Chem. Abstr.*, **112**, 179469 (1990).
24. E. Klar and A. Elattar, Eur. Pat. Appl. EP 304144 (1989); *Chem. Abstr.*, **110**, 213073 (1989).
25. C. Prud'Homme and G. Simon, Eur. Pat. 138679 (1985); *Chem. Abstr.*, **103**, 88071 (1989).
26. C. Prud'Homme and G. Simon, Eur. Pat. Appl. EP 138678 (1985); *Chem. Abstr.*, **103**, 88070 (1985).
27. C. Prud'Homme, Eur. Pat. Appl. EP194214 (1986); *Chem. Abstr.*, **105**, 209196 (1986).
28. T. Margaria, B. Degen, E. Licht and M. Schultze, World Patent, WO/95/01303 (1994).
29. R. L. Halm, A. B. Pierce and O. K. Wilding, U.S. Patent 4762940 (1990).
30. R. L. Halm and O. K. Wilding, U.S. Patent 4,946,978 (1990).
31. V. D. Dosaj, R. L. Halm and O. K. Wilding, U.S. Patent 4,898,960 (1990).
32. R. L. Halm and O. K. Wilding, U.S. Patent 5,059,343 (1991).
33. B. Degen, K. Feldner, H. J. Kaiser and M. Schulze, DE 3910665 (1990); U.S. Patent 5,059,706 (1991); *Chem. Abstr.*, **114**, 62348 (1991).
34. B. Degen, K. Felder, E. Licht and G. Wagner, Eur. Pat. Appl. EP 416406 (1991); also US 5,068,385 (1991); *Chem. Abstr.*, **114**, 164496 (1991).
35. W. Walkow, H. Lieske, G. Meier, A. Schenk, K. Dreier, W. Lambrecht, R. Thaetner, K. Ohl and R. Berk, Ger. (East) DD 265407 (1989); *Chem. Abstr.*, **111**, 154103 (1989).
36. G. N. Kozlova, E. S. Starodubtsev, L. M. Khananashvili, L. V. Gasanova and N. I. Tsomaya, *Soobshch. Akad. Nauk Gruz. SSR*, **117**, 329 (1985); *Chem. Abstr.*, **104**, 88657 (1986).
37. M. G. R. T. DeCooker, J. H. N. DeBruyn and P. J. Van Den Berg, *J. Organomet. Chem.*, **99**, 371 (1975).
38. R. L. Halm and R. H. Zapp, U.S. Patent 4,962,220 (1990).
39. R. L. Halm and R. H. Zapp, U.S. Patent 4,966,986 (1990).
40. K. M. Lewis, R. A. Cameron, J. M. Larnerd and B. Kanner, U.S. Patent 4,973,725 (1990).
41. K. M. Lewis, R. A. Cameron, J. M. Larnerd and B. Kanner, Eur. Pat. Appl. EP 348902 (1989); *Chem Abstr.*, **112**, 235609 (1990).
42. B. Pachaly, V. Frey and H. Strausberger, Ger Offen. DE 4303766 (1994); *Chem. Abstr.*, **122**, 58821 (1995).
43. B. Pachaly, in *Silicon Chem. Ind. II, 2nd Int. Cong.*, (Eds. H. A. Oye, H. M. Rong, L. Nygaard, G. Schussler and J. Kr. Tuset), Trondheim, Norway, 1994, p. 55.
44. S. K. Freeburne, R. L. Halm, J. P. Kohane and J. D. Wineland, U.S. Patent 5,312,948 (1994).
45. B. Degen, E. Licht, M. Schulze, G. Wagner and K.-P. Minuth, Eur. Pat. Appl. EP 617039, (1994); *Chem. Abstr.*, **121**, 280876 (1994).
46. K. Feldner, B. Degen, G. Wagner and M. Schulze, Ger. Offen. DE 3841417, (1990); *Chem. Abstr.*, **113**, 132505 (1990).
47. A. G. Forwald, H. M. Rong and G. C. Vogelaar, in *Silicon Chem. Ind. II, 2nd Int. Cong.* (Eds. H. A. Oye, F., H. M. Rong, L. Nygaard, G. Schussler and J. Kr. Tuset), Trondheim, Norway, 1994, p. 107.
48. G. Laroze, in *Silicon Chem. Ind. II, 2nd Int. Cong.* (Eds. H. A. Oye, H. M. Rong, L. Nygaard, G. Schussler and J. Kr. Tuset), Trondheim, Norway, 1994, p. 121.
49. F. Dubrous, Eur. Pat. Appl. EP 494837 (1992); *Chem. Abstr.*, **117**, 133933 (1992).
50. J. P. Kim and D. G. Rethwisch, *J. Catal.*, **134**, 168 (1992).

51. E. Klar, D. H. Hashiguchi and R. J. Dietrich, U.S. Patent 4,504,597 (1985).
52. J. Y. P. Mui, U.S. Patent 5,250,716 (1993).
53. A. A. Elattar, Eur. Pat. Appl. EP 440414 (1991); *Chem. Abstr.*, **115**, 208249 (1991).
54. M. Selenina, H. Lieske, G. Meier and U. Heinze, Ger. (East) DD 250534 (1987); *Chem. Abstr.*, **109**, 212781 (1988).
55. D. Hashiguchi, R. Dietrich and G. Schoepe, U.S. Patent 4,503,165 (1985).
56. D. Hashiguchi, E. Klar and R. Dietrich, U.S. Patent 4,520,130 (1985).
57. W. Streckel, H. Straussberger and B. Pachaly, Ger. Offen. DE 4142432 (1993); *Chem. Abstr.*, **120**, 54691 (1994).
58. R. Thaetner, K. Ohl, P. Birke, W. Koegler, H. Guenschel, H. Lieske, W. Walkow, G. Meier and J. Brumme, Ger. (East) DD 293507 (1991); *Chem. Abstr.*, **116**, 6739 (1992).
59. W. Walkow, H. Lieske, G. Meier, A. Schenk and U. Heinze, Ger. (East) DD 250536 (1987); *Chem. Abstr.*, **109**, 131214 (1988).
60. W. Walkow, H. Lieske, G. Meier and A. Schenk, Ger. (East) DD 250535 (1987); *Chem. Abstr.*, **108**, 204835 (1988).
61. A. Ritzer and H. Lapidot, U.S. Patent 4,450,282 (1984).
62. L. Roesch, G. Kratel and A. Stroh, Ger. Offen. DE3610267 (1987); *Chem. Abstr.*, **108**, 132044 (1988).
63. G. Laroze, J. L. Plagne, G. Weber and B. Gillot, in *Silicon for the Chemical Industry* (Eds. H. A. Øye and H. Rong), Geiranger, Norway, June 1992, p. 151.
64. E. G. Rochow, *Main Group Chemistry News*, **2**, 27 (1995).
65. S. Yilmaz, N. Floquet and J. L. Falconer, in *Silicon Chem. Ind. II, 2nd Int. Cong.* (Eds. H. A. Oye, H. M. Rong, L. Nygaard, G. Schussler and J. Kr. Tuset), Trondheim, Norway, 1994, p. 137.
66. N. Floquet, S. Yilmaz and J. L. Falconer, *J. Catal.*, **148**, 348 (1994).
67. K. A. Magrini, J. L. Falconer and B. E. Kohl, in *Catalyzed Direct Reactions of Silicon* (Eds. K. M. Lewis and D. G. Rethwisch), Elsevier, Amsterdam, 1993, p. 249.
68. T. C. Frank, K. B. Kester and J. L. Falconer, *J. Catal.*, **91**, 44 (1985).
69. J. L. Falconer and S. Yilmaz, in *Silicon Chem. Ind.* (Eds. H. A. Oeye and H. Rong), Norway Inst. Technol., Inst. Inorg. Chem., Trondheim, Norway, 1992, p. 99.
70. T. C. Frank, K. B. Kester and J. L. Falconer, *J. Catal.*, **95** 396 (1985).
71. S. J. Potochnik and J. L. Falconer, *J. Catal.*, **147**, 101 (1994).
72. K. M. Lewis, D. McLeod and B. Kanner, *Stud. Surf. Sci. Catal. 1987*, Vol. 38, Elsevier, Amsterdam, 1988, p. 415.
73. M. P. Clarke, *J. Organomet. Chem.*, **376**, 165 (1989).
74. H. Lieske, H. Fichtner, I. Grohmann, M. Selenina, W. Walkow and R. Zimmermann, in *Silicon Chem. Ind.* (Eds. H. A. Oeye and H. Rong), Norway Inst. Technol., Inst. Inorg. Chem., Trondheim, Norway, 1992, p. 111.
75. G. J. Hutchings, R. W. Joyner, M. R. H. Siddiqui and H. M. Rong, *Silicon Chem. Ind.* (Eds. H. A. Oeye and H. Rong), Norway Inst. Technol., Inst. Inorg. Chem., Trondheim, Norway, 1992, p. 85.
76. D. T. Hurd, *J. Am. Chem. Soc.*, **67**, 1813 (1945).
77. E. G. Rochow and W. F. Gilliam, *J. Am. Chem. Soc.*, **67**, 1772 (1945).
78. S. H. Yeon, B. W. Lee, S.-I. Kim and I. N. Jung, *Organometallics*, **12**, 4887 (1993).
79. I. N. Jung, G. H. Lee, S. H. Yeon and M. Y. Suk, *Bull. Korean Chem. Soc.*, **12**, 445 (1991).
80. I. N. Jung, S. H. Yeon and J. S. Han, *Bull. Korean Chem. Soc.*, **14**, 315 (1993).
81. E. G. Rochow, *J. Am. Chem. Soc.*, **70**, 2170 (1948).
82. W. E. Newton and E. G. Rochow, *Inorg. Chem.*, **9**, 1071 (1970).
83. M. Okamoto, N. Mimura, E. Suzuki and Y. Ono, *Catal. Lett.*, **33**, 421 (1995).
84. M. Shiozawa and Y. Okumura, Jpn. Kokai Tokkyo Koho JP 06306083 (1994); *Chem. Abstr.*, **123**, 199138 (1995).
85. F. D. Mendicino, U.S. Patent 4,727,173 (1988).
86. L. G. Moody, T. E. Childress, R. L. Pitrolo, J. S. Ritscher and R. P. Leichliter, U.S. Patent 4,999,446 (1991).
87. M. Shiozawa and Y. Okumura, Jpn. Kokai Tokkyo Koho JP 06271587 (1994); *Chem. Abstr.*, **122**, 106124 (1995).
88. K. Adachi, H. Kumoyama, Jpn Kokai Tokkyo Koho JP 06293776 (1994); *Chem. Abstr.*, **122**, 106125 (1995).
89. M. Harada and Y. Yoshinori, Ger. Offen DE 4415418 (1994); *Chem. Abstr.*, **122**, 81621 (1995).

90. J. S. Ritscher and T. E. Childress, U.S. Patent 5,084,590 (1992).
91. E. Suzuki, M. Okamoto and Y. Ono, *Chem. Lett.*, 199 (1991).
92. E. Suzuki and Y. Ono, *Chem. Lett.*, 47 (1990).
93. E. Suzuki, T. Kamata and Y. Ono, *Bull. Chem. Soc. Jpn.*, **64**, 3445 (1991).
94. M. Okamoto, M. Osaka, K. Yamamoto, E. Suzuki and Y. Ono, *J. Catal.*, **143**, 64 (1993).
95. Y. Ono, E. Suzuki and M. Okamoto, Jpn. Kokai Tokkyo Koho JP 06263769 (1994); *Chem. Abstr.*, **123**, 83719 (1995).
96. M. Okamoto, N. Watanabe, E. Suzuki and Y. Ono, *J. Organomet. Chem.*, **489**, C12 (1995).
97. Y. Ono, M. Okano, N. Watanabe and E. Suzuki, in *Silicon Chem. Ind. II, 2nd Int. Cong.* (Eds. H. A. Oye, H. M. Rong, L. Nygaard, G. Schussler and J. Kr. Tuset), Trondheim, Norway, 1994, p. 185.
98. M. Okamoto, K. Yamamoto, E. Suzuki and Y. Ono, *J. Catal.*, **147**, 15 (1994).
99. M. Shiozawa and Y. Okumura, Jpn. Kokai Tokkyo Koho JP 06009652 (1994); *Chem. Abstr.*, **121**, 109252 (1994).
100. J. O. Stoffer, J. F. Montle and N. L. D. Somasivi, U.S. Patent 4,778,010 (1988).
101. J. R. Malek, J. L. Speier and A. P. Wright, U.S. Patent 4,088,669 (1978).
102. E. G. Rochow and J. J. Zuckerman, PB 157357 NTIS. U.S. Dept of Commerce (1960).
103. S. Yamada and E. Yasunaga, Jp. Patent 286 (1951); *Chem. Abstr.*, **47**, 3334 (1953).
104. K. M. Lewis and B. Kanner, U.S. Patent 4,593,114 (1986).
105. K. M. Lewis and B. Kanner, Eur. Pat. Appl. EP 175282 (1986); *Chem. Abstr.*, **105**, 60753 (1986).
106. K. Feldner and W. Grape, Ger. Offen. DE 3410644 (1985); *Chem. Abstr.*, **104**, 19670 (1986).
107. K. Feldner and W. Grape, Ger. Offen. DE 3436381 (1986); *Chem. Abstr.*, **105**, 60755 (1986).
108. R. Calas, J. Dunogues, G. Deleris and N. Duffaut, *J. Organomet. Chem.*, **225**, 117 (1982).
109. S. P. Ferguson, R. F. Jarvis, B. M. Naasz, K. K. Oltmanns, G. L. Warrick and D. L. Whitely, U.S. Patent 5,430,168 (1995); *Chem. Abstr.*, **123**, 257007 (1995).
110. K. M. Chadwick, A. K. Dhaul, R. L. Halm and R. L. Johnson, U.S. Patent 5,326,896 (1994); *Chem. Abstr.*, **121**, 206,245 (1994).
111. K. M. Chadwick, A. K. Dhaul, R. L. Halm, R. G. Johnson and R. D. Steinmeyer, U.S. Patent 5,321,147 (1994); *Chem. Abstr.*, **121**, 109261 (1994).
112. J. Albrecht, R. Neumann and W. Geisler, Ger. Offen. DE 4323406 (1995); *Chem. Abstr.*, **122**, 265626 (1995).
113. B. Pachaly and A. Schinabeck, Eur. Pat. Appl. EP574912 (1993); *Chem. Abstr.*, **120**, 191988 (1994).
114. G. N. Bokerman, J. P. Cannady and A. E. Ogilvy, U.S. Patent 5,175,329 (1992); *Chem. Abstr.*, **118**, 191999 (1993).
115. B. Pachaly, H. Straussberger and W. Streckel, in *Silicon Chem. Ind. II, 2nd Int. Cong.* (Eds. H. A. Oye, H. M. Rong, L. Nygaard, G. Schussler and J. Kr. Tuset), Trondheim, Norway, 1994, p. 235.
116. S. W. Webb, A. Ritzer and J. D. Neely, U.S. Patent 5,243,061 (1993).
117. S. W. Webb, A. Ritzer and J. D. Neely, U.S. Patent 5,239,102 (1993).
118. A. Ritzer, in *Silicon Chem. Ind. II, 2nd Int. Cong.* (Eds. H. A. Oye, H. M. Rong, L. Nygaard, G. Schussler and J. Kr. Tuset), Trondheim, Norway, 1994, p. 241.

CHAPTER **27**

Acyl silanes

PHILIP C. BULMAN PAGE, MICHAEL J. McKENZIE, SUKHBINDER S. KLAIR and STEPHEN ROSENTHAL

Department of Chemistry, Loughborough University, Loughborough, Leicestershire LE11 3TU, UK
Fax: +44(0)1509 223926; e-mail: p.c.b.page@lboro.ac.uk

I. INTRODUCTION

Early work on acyl silanes, perhaps spurred by the green or yellow-green colour of simple examples, concentrated on spectroscopic properties, but in addition to their unusual spectroscopic behaviour, acyl silanes exhibit interesting chemistry. In general, they display rather poor stability towards basic conditions and light, but their sensitivity depends to a large degree upon structure and substitution; for example, α,β-unsaturated acyl silanes are relatively stable, while α-ketoacyl silanes are especially sensitive. The last ten to fifteen years have seen a steady increase in the level of investigation into the chemistry of acyl silanes, resulting both in valuable new reactions and in improved methods of synthesis of many types of acyl silanes[1]. This chapter is principally concerned with methods of synthesis of all types of acyl silanes together with the development of their chemistry since the first isolation in 1968. A simple descriptive spectroscopy section is included; readers are referred to publications cited in the text for a more thorough treatment of the structure and bonding aspects of acyl silane chemistry.

II. STRUCTURE AND SPECTROSCOPY OF ACYL SILANES

A. Infrared Spectroscopy

Acyl silanes exhibit interesting and unusual spectroscopic properties, and early work was stimulated by these observations[2–4]. Carbonyl stretching frequencies in their infrared absorption spectra are lower relative to those of simple ketones. For example, benzoyl trimethylsilane and acetyl trimethylsilane have carbonyl stretching frequencies at *ca* 1620 cm^{-1} and 1645 cm^{-1}, respectively, in their infrared spectra (Table 1, entries 6 and 7). This relative lowering of the carbonyl stretching frequency is usually explained as a consequence of an inductive effect: Polarization of the carbonyl group as a consequence of electron release from the silicon atom towards the carbonyl group weakens the C=O bond[5].

It is perhaps surprising that the position of the carbonyl group absorption of acyl silanes is not significantly altered by changing the type of group attached to the silicon atom, similar absorptions being observed for acyl, trimethyl, triphenyl and tris(p-substituted) phenyl silanes, the last showing a linear correlation of the C=O wavelength with Hammett substituent constants. Further, the position of acyl silane carbonyl absorptions is relatively independent of medium polarity, again unlike the behaviour of simple ketones, where carbonyl absorptions are shifted to lower frequency on increasing the polarity of the medium in which they are measured[6]. The proposed large σ-inductive effect is caused by the low electronegativity of silicon (1.8) relative to carbon (2.5), and by the larger mass

TABLE 1. Infrared C=O absorption of selected acyl metalloids and related compounds[a]

Entry	Compound	ν (M=C)	ν (M=Si)	ν (M=Ge)	ν (M=Sn)	Reference
1	Ph_3MCOMe		1645	1669	1670	5
2	Ph_3MCOPh	1692	1618	1629	1627	5,7
3	Ph_3MCH_2COPh	1698	1667	1661		5
4	$Ph_3MCH_2CH_2COPh$	1692	1692			5
5	$PhMe_2MCOPh$		1620			5,7
6	Me_3MCOPh	1675	1620	1629		5,7
7	Me_3MCOMe	1710	1645			5,7
8	$Me_3MCO(CH_2)_4Me$	1700	1640			7–9
9	$(Me_3MCOCH_2CH_2)_2$		1640			10
10	Me_3MCOCH_2Ph		1635	1660	1656	11
11	$Me_3MCOCHBr(CH_2)_3Me$		1645,1652			7,12
12	$Me_3MCOCH=CHMe$		1642	1644	1648	11
13	$Me_3MCOCH=CMe_2$		1640	1645	1640	11
14	$Me_3MCOCMe_3$		1636			5
15	$Me_3MCOMMe_3$		1556, 1570			13
16	$Ph_3MCOMPh_3$		1558 + 1592	1616		5
17	$Me_3MCOCOMe$		1713 + 1658			7,14
18	Me_3MCOCO_2Me		1660			15
19	$Me_3MCONEt_2$	1620	1560			16
20	$(Me_3Si)_3MCO_2H$		1630			17

[a] For additional examples, see References 18–26.

of silicon. Such differences in electronegativity, producing significant inductive release of electron density towards the carbonyl group, would be expected to lead to a decrease in the frequency, as is indeed the case[5,6].

The carbonyl groups of acyl silanes and acyl germanes display lower frequency absorptions than those of α-silyl ketones, which in turn absorb at lower frequencies than those of β-silyl ketones (Table 1, entries 2–4) a pattern consistent with inductive release of electrons. Indeed, β-silyl ketone carbonyl groups absorb at similar frequencies to their carbon analogues (Table 1, entry 4). The effect is weaker in the α-silyl ketones, where it must operate through an extra methylene group, and is not apparent at all in the β-silyl ketones, where it must operate through two methylene groups. The strong inductive release in acyl silanes appears to be approximately additive, as shown by the pink-coloured carbonyl bis(trimethylsilane), where the infrared stretching frequency is lowered by approximately 80 cm^{-1} compared with acetyl triphenylsilane (Table 1, entries 14 and 15)[5].

B. ^{1}H NMR Spectroscopy

Generally, protons attached to the α-carbon atoms of acyl silanes are somewhat deshielded relative to their carbon analogues (Table 2). Differences in magnetic anisotropy and electronegativity are no doubt responsible for this effect. It is interesting that α,β-unsaturated acyl silanes appear to be an exception (entry 12).

TABLE 2. ^1H chemical shifts (δ_H) at α-carbon atom of selected acyl metalloids

Entry	Compound	M=C	M=Si	M=Ge	M=Sn	Reference
1	$Me_3MCOC\underline{H}_2Ph$		3.77	3.73	3.80	11
2	Me_3MCOMe	2.07	2.18,2.20			5,7
3	Ph_3MCOMe	2.01	2.30	2.38		5
4	$t\text{-}BuMe_2MCOMe$		2.32			18
5	$Me_3MCOC\underline{H}_2(CH_2)_3Me$	2.33	2.50			7–9
6	$Me_3MCOC\underline{H}Et_2$		2.50			18
7	$Et_3MCOC\underline{H}_2Me$		2.60			19
8	$Me_3MCOC\underline{H}PhEt$		3.86			18
9	$Me_3MCOCOMe$		2.03			7,14
10	$Me_3MCOCOC\underline{H}_2Bu\text{-}n$		2.55			7
11	$Me_3MCOC\underline{H}BrBu\text{-}n$		4.39,4.33			7,12
12	$Me_3MCOC\underline{H}{=}CH_2$	6.88	6.28,6.38			7,14,20,27
13	$Me_3MCOC\underline{H}{=}CMe_2$		6.56	6.32	6.40	11

C. ^{13}C NMR Spectroscopy

The ^{13}C NMR signals of carbonyl groups in acyl silanes are dramatically shifted downfield in comparison to the analogous ketones (Table 3)[28,29]. The effect ranges from *ca* 25 to 100 ppm, and is approximately additive.

^{13}C NMR studies also expose some interesting features of acyl silane bonding. The carbonyl group carbon atom of an alkyl phenyl ketone displays a ^{13}C chemical shift similar

TABLE 3. ^{13}C carbonyl group chemical shifts (δ_c) of selected acyl silanes and related compounds[a]

Entry	Compound	M=Si	M=C	Reference
1	$Me_3MCOCMe_3$	249.0	215.1	29
2	Me_3MCOMe	244.3,247.6	210.4	29,30
3	Me_3MCOPh	233.6,237.5	207.8,209.1	29,30
4	$Me_3MCOCH{=}CH_2$	236.7,237.9		14,20
5	$t\text{-}BuMe_2COC{\equiv}CMe$	225.7		14
6	$Me_3MCOCHBr(CH_2)_4Me$	234.8		7
7	$Me_3MCOSiMe_3$	318.2,318.8	249.0	13,29
8	$Me_3M\underline{CO}CO(CH_2)_4Me$	235.1		7
9	$Me_3M\underline{CO}COPh$	220.4		7
10	Ph_3MCOMe	240.1		31
11	$(Me_3Si)_3MCOPh$	233.8		31
12	$(Me_3Si)_3MCOCMe_3$	244.6		31
13	Me_3MCOFc[b]	236.8		32
14	Ph_3MCOFc[b]	231.3		32
15	$PhMe_2MCOFc$[b]	234.7		32
16	$Ph_2MeMCOFc$[b]	232.9		32

[a] For additional examples see References 10,23 and 33.

[b] Fc = ferrocenyl.

to aliphatic analogues, but the difference between the two corresponding silicon species (e.g. $PhCOSiMe_3$ and $MeCOSiMe_3$) is somewhat more marked. For example, the carbonyl group carbon atom of benzoyl trimethylsilane has a ^{13}C NMR chemical shift *ca* 11–14 ppm upfield of that displayed by acetyl trimethylsilane (Table 3, entries 2 and 3). This effect could be ascribed to participation of resonance structures which could increase the shielding of the carbonyl group carbon atom by reducing the amount of positive charge, so positioning the chemical shift upfield relative to the aliphatic analogue, where such an effect could not operate.

D. ^{17}O NMR Spectroscopy

The oxygen atoms of acyl silanes resonate at higher chemical shifts than do those of the analogous carbon compounds (Table 4). The displacement to higher chemical shifts (i.e. downfield) of ^{17}O and ^{13}C carbonyl group signals in acyl silanes has been attributed to lowering of the HOMO–LUMO gap ΔE[34]. Partial reversal of this effect is possible by increasing the electron density in the α-carbon atom $p\pi$ orbitals (Table 4, entries 1 and 3); even though ΔE is smaller for the aryl derivative, the ^{17}O chemical shift of the alkyl derivative is the larger.

E. ^{29}Si NMR Spectroscopy

The ^{29}Si NMR properties of acyl silanes indicate that the acyl group has a moderate shielding effect upon the silicon atom, similar in magnitude to that observed in vinyltrimethylsilane (Table 5)[28]. As would be expected, the nature of the groups attached to the silicon moiety affects the chemical shift of the silicon atom.

F. Ultraviolet and Visible Spectroscopy

The unusual ultraviolet and visible spectroscopic characteristics of the simpler acyl silanes are perhaps their most immediately obvious feature: they are green in colour. Data for selected acyl silanes and other acyl metalloids are given in Table 6[36–41]. As for simple ketones, acyl silanes show absorptions due to $n-\pi^*$ and $\pi-\pi^*$ transitions. The $n-\pi^*$ transition in alkyl acyl silanes, however, occurs at *ca* 370 nm, a shift of about 100 nm to longer wavelength compared with the same transition in pinacolone, the analogous carbon compound (ν_{max} 279 nm), corresponding to a *ca* 25 $kcal\,mol^{-1}$ reduction in the $n-\pi^*$ transition energy. Comparison of the extinction coefficients of acetyl trimethylsilane and pinacolone ($\epsilon = 126$ and 21, respectively) shows that absorption for the acyl silane derivative is by far the more intense. The λ_{max} values for acyl silanes have been shown to be proportional to the degree of deshielding observed in the ^{17}O NMR spectra, which, in agreement with the Karplus–Pople equation, is *ca* four times larger than is the corresponding effect on the ^{13}C signal of the carbonyl carbon atom[42].

TABLE 4. ^{17}O chemical shifts (δ_o) of selected acyl silanes and related compounds[34]

Entry	Compound	M=Si	M=C
1	Me_3MCOMe	692	553
2	$Me_3MCOCMe_3$	659	550
3	Me_3MCOPh	671	554
4	$Me_3MCOC_6H_4Cl$-*p*	673	551

TABLE 5. ^{29}Si chemical shifts (δ_{Si}) of selected acyl silanes and related compounds[a]

Entry	Compound	δ_{Si}	Reference
1	$\mathrm{Me_3SiCOMe}$	−10.1	30
2	$\mathrm{Ph_3SiCOMe}$	−30.4	31
3	$\mathrm{(Me_3Si)_4}$	−135.5	31
4	$\mathrm{Ph_3SiCOPh}$	−28.3	31
5	$\mathrm{Et_3SiCOPh}$	−28.3	31
6	$\mathrm{Me_3SiCOPh}$	−7.4,−15.1	30,31
7	$\mathrm{Me_3SiCOSiMe_3}$	−14.4	13
8	$\mathrm{Me_3SiCH{=}CH_2}$	−7.6	35
9	$\mathrm{(Me_3Si)_3\underline{Si}CO{-}Ad}$[b]	−78.8	31
10	$\mathrm{(Me_3\underline{Si})_3SiCO{-}Ad}$[b]	11.5	31
11	$\mathrm{Ph(Me_3Si)_2\underline{Si}CO{-}Ad}$[b]	−44.75	26
12	$\mathrm{Ph(Me_3\underline{Si})_2SiCO{-}Ad}$[b]	−13.45	26
13	$\mathrm{(Me_3Si)_3\underline{Si}CO_2H}$	−73.84	17
14	$\mathrm{(Me_3\underline{Si})_3SiCO_2H}$	−6.15	17
15	$\mathrm{(Me_3Si)_3\underline{Si}CO_2Me}$	−74.45	17
16	$\mathrm{(Me_3\underline{Si})_3SiCO_2Me}$	−6.34	17
17	$\mathrm{Me_3SiCOFc}$[c]	−9.5	32
18	$\mathrm{Ph_3SiCOFc}$[c]	−30.9	32
19	$\mathrm{PhMe_2SiCOFc}$[c]	−16.5	32
20	$\mathrm{Ph_2MeSiCOFc}$[c]	−21.9	32

[a] For additional examples see References 23 and 25.

[b] Ad = 1-adamantyl.

[c] Fc = ferrocenyl.

TABLE 6. UV/Visible absorption of selected acyl metalloids and related compounds[a]

Entry	Compound	$n \rightarrow \pi^*$ [λ_{max}/nm (ε)]	$\pi \rightarrow \pi^*$	Reference
1	$\mathrm{Me_3CCOMe}$	278 (15)		5
2	$\mathrm{Me_3SiCOMe}$	372 (126)		5
3	$\mathrm{Et_3GeCOMe}$	365 (173)		5
4	$\mathrm{Me_3SiCO(CH_2)_4Me}$	367 (129)		8
5	$\mathrm{Me_3SiCOCHBr(CH_2)_4Me}$	374 (142)		7
6	$\mathrm{Ph_3CCOPh}$	329 (299)	251 (11 600)	5
7	$\mathrm{Ph_3SiCOPh}$	424 (292)	257 (16 200)	5
8	$\mathrm{Ph_3GeCOPh}$	417 (210)	254 (16 200)	5
9	$\mathrm{Ph_3SnCOPh}$	435		5
10	$\mathrm{Me_3SiCOPh}$	425 (127)	250 (14 500)	5,7
11	$\mathrm{Me_3GeCOPh}$	412 (120)	252 (10 700)	5
12	$\mathrm{Me_3SiCOCH{=}CHMe}$	424 (98)	224 (10 300)	7,11
13	$\mathrm{Me_3GeCOCH{=}CHMe}$	416 (109)	258 (11 300)	11
14	$\mathrm{Me_3SnCOCH{=}CHMe}$	432	258	11
15	$\mathrm{Me_3SiCOC(Me){=}CH_2}$	425 (77)	222 (5 900)	20
16	$\mathrm{Me_3SiCOC{\equiv}CMe}$	420 (170)	227 (7 450)	14
17	$\mathrm{Me_3SiCOCO_2Me}$	455 (100)	227 (254)	15
18	$\mathrm{Me_3SiCOCO_2Et}$	455 (97)	230 (388)	15
19	$\mathrm{PhMe_2SiCOCO_2Me}$	455 (213)	279 (620)	15
20	$\mathrm{Me_3SiCOCOMe}$	535 (99)		14
21	$\mathrm{Me_3SiCOCOPh}$	518 (117)	275 (6 500)	7
22	$\mathrm{Me_3SiCONEt_2}$	264 (270)		16

For additional data see References 26 and 33.

Considerable fine structure is often observed in the ultraviolet/visible spectra of acyl silanes, usually consisting of three main bands, sometimes with two additional shoulders at lower wavelengths[5]. This vibrational structure persists in polar solvents, an effect which is not commonly observed in ketones, and is not well understood. In α,β-unsaturated acyl silanes, and in aryl acyl silanes, which can be lime green in colour, the $n-\pi^*$ transition occurs around 420 nm again shifted to longer wavelength by about 100 nm compared with the analogous carbon compounds. In α-carboxyacyl silanes, which are usually yellow, the transition occurs at around 455 nm, and in the deep crimson α-ketoacyl silanes at *ca* 520 nm; carbonyl bis(trimethylsilane) is also pink in colour.

The $\pi-\pi^*$ transition of the carbonyl group in aryl acyl silanes produces an intense absorption band at around 250–260 nm, and the position and extinction coefficient of this transition are largely independent of the nature of the substituents on the silyl group. As would be expected for conjugated carbonyl group transitions, small red shifts are observed in polar solvents.

A third absorption is usually observed at approximately 185–195 nm. For acyl silanes with aromatic substituents, this may be ascribed to a primary arene band or could arise from a second $\pi-\pi^*$ transition, but for other acyl silanes, this transition (at 195 nm, $\epsilon = 4200$ for acetyl trimethylsilane) is presumably the latter. In general, however, the nature of the groups attached to the silicon atom (other than the acyl group) has little effect on the energies of the $n-\pi^*$ and $\pi-\pi^*$ transitions[5].

Several acyl metalloids, including acetyl trimethylsilane and acetyl trimethylgermane, have also been studied by photoelectron spectroscopy[38], and various *ab initio* and semiempirical calculations have been carried out[38,39].

G. X-ray Diffraction Studies

In 1968, Chieh and Trotter reported the single-crystal X-ray analysis of acetyl triphenylsilane[43]. The acetyl group and the three phenyl groups were found to be located tetrahedrally around the silicon atom. The silicon–carbonyl group bond length is considerably elongated, at 1.926 Å; generally, silicon–carbon single bonds fall in the range 1.85–1.90 Å. Trotter ascribes this lengthening of the silicon–carbonyl group bond to a contribution to the structure not only of canonical forms with single C—O bonds, which contribute to the structure of ordinary ketones, but also to a canonical form in which there is no formal bond between the metalloid atom and the acetyl carbon atom. This structure was considered possible as a contributing resonance form because of the considerable differences in electronegativity between silicon and carbon[43,44]. The silicon–phenyl group bond lengths were found to be more typical, at 1.864 Å, and the carbonyl bond length, which one might expect to be abnormally long, reflecting the unusually long wavelength carbonyl group absorption and the enhanced basicity, was found to be 1.21 Å, approximately the same as that found in simple ketones.

More recently, Sharma has completed single-crystal X-ray analyses of four ferrocenyl acyl silanes[32]. In line with the earlier observations, the silicon–carbonyl group bond lengths were significantly elongated, at 1.935 Å. However, they also observed some elongation of the carbonyl bond length. In all four examples, which vary only in the substituents at silicon, the carbonyl bond length was 1.230 Å, somewhat longer than that reported for acetyl ferrocene (1.220 Å)[45], and significantly longer than in the Trotter structure. The Si—C—O bond angle in acetyl triphenylsilane was approximately the theoretical value of 120°, but was compressed, at 115.7°, in the ferrocenyl triphenyl acyl silane.

The structure of acetyl triphenylgermane is very similar to its silicon analogue[44], and shows a lengthening of the germanium–carbonyl group bond length by 0.066 Å over that of the germanium–phenyl group bond. The acetyl triphenylgermane molecule was represented by Trotter with formal C=O double and C−Ge single bonds, and with partial negative charge at oxygen and partial positive charge at germanium, a structure said to represent both the basicity of the ketone oxygen atom and the long germanium−carbonyl carbon bond[43].

III. SYNTHESIS OF ACYL SILANES

A. Simple Acyl Silanes

1. Formyl silanes

Formyl silanes remain rare in the literature, due no doubt to their instability. They are in general thermally stable, but are extremely sensitive to air, spontaneously igniting or decomposing violently upon exposure to atmospheric oxygen. Following several years of speculation[5,46], Ireland and Norbeck achieved strong evidence for the formation of formyl trimethylsilane using a trap with a Wittig reagent following Swern oxidation[47] of trimethylsilyl methanol (*vide infra*, Section III.A.5)[48]. Formyl trimethylsilane was subsequently identified by Tilley using NMR spectroscopy as the product of reaction of the zirconium η^2-sila-acyl complex $(\eta^5\text{-}C_5H_5)_2Zr(\eta^2\text{-}COSiMe_3)Cl$ **(1)** with hydrochloric acid[49], and has recently been prepared by *in situ* reaction of 1,1-dimethylsilene with formaldehyde; the formyl silane rearranged quantitatively to 2,2-dimethyl-2-silapropanal within a few minutes (Scheme 1)[50]. Tilley was later able to prepare, isolate and characterize the first stable formyl silane, formyl tris(trimethylsilyl)silane, from the zirconium η^2-sila-acyl complex **(2)**[51] by treatment with anhydrous hydrogen chloride at −78 °C in toluene solution. Formyl tris(trimethylsilyl)silane was stable under an inert atmosphere and showed typical carbonyl group reactivity. More recently, the stable greenish-yellow formyl triisopropylsilane was isolated in 91% yield by hydrolysis of the dimethyl acetal, prepared from the dithiane derivative by transacetalization mediated by mercury salts[52a], an approach also used by Silverman in a preparation, from the corresponding dioxolane, of formyl *t*-butyldimethylsilane, which was converted *in situ* into the 2,4-dinitrophenylhydrazone derivative in 70% overall yield[52b]. Katritzky has trapped formyl silanes *in situ* as their 2,4-dinitrophenylhydrazone derivatives by hydrolysis of trialkylsilyl benzotriazolyl carbazolyl methanes in the presence of the hydrazine (Scheme 2)[53]. Formyl silanes prepared *in situ* have been used to produce α,β-acetylenic acyl silanes by lithium acetylide addition and Swern oxidation[54]. Triphenylsilyl bis(cyclopentadienyl) zirconium chloride undergoes carbonyl insertion under carbon monoxide pressure to give an acyl zirconium species which, when treated with anhydrous hydrogen chloride in a benzene matrix at −196 °C and warmed to room temperature, produces formyl triphenylsilane (*vide infra*, Section III.A.3)[55].

2. Hydrolysis of acetals

The most general approach to the synthesis of acyl silanes is based on hydrolysis of 2-silyl-1,3-dithioacetals, first investigated for 1,3-dithiane derivatives by Brook[56] and Corey[57] in the late 1960s (Scheme 3). Oxathioacetals and protected hemithioacetals have also been used, and some formyl silanes have been isolated by hydrolysis of dioxa-acetals (*vide supra*).

The major disadvantage of the dithiane approach lies in the final deprotection step; the ease and success of hydrolysis of the 2-silyl-1,3-dithiane with retention of the silicon group is highly dependent upon the dithiane 2-substituent and on the size of the groups attached to silicon, production of the corresponding aldehyde often accounting

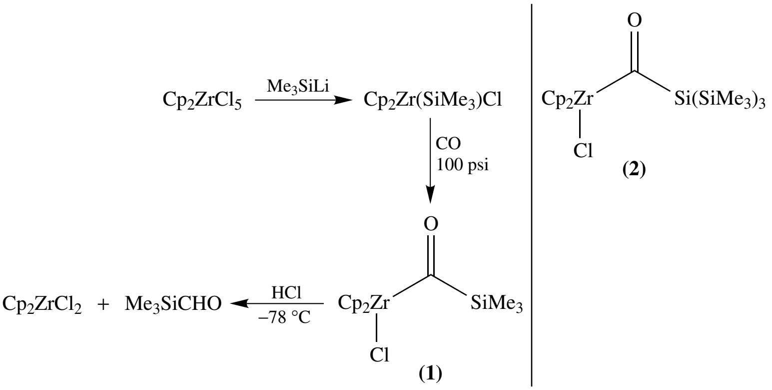

SCHEME 1

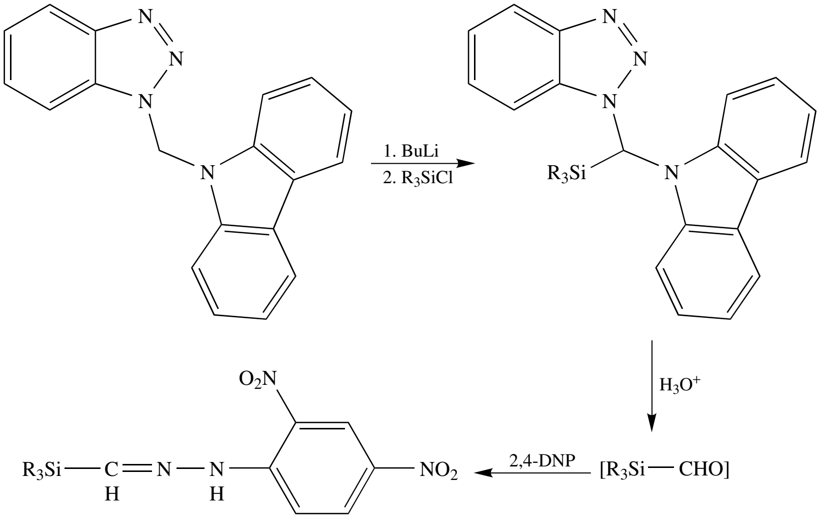

SCHEME 2

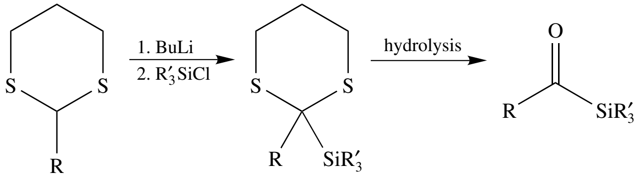

SCHEME 3

for 10–100% of the product mixture. In general, the larger these groups are, the more successful is the final deprotection step. Early methods of hydrolysis involved the use of mercury(II) salts, for example in one synthesis of thienamycin[58], and, although this process has been improved by the use of such reagents as chloramine T hydrate[59–62], this step still remains a significant problem in some cases[7], although anodic oxidation appears to be particularly successful[63]. A number of interesting acyl silanes including chiral[64] and cyclic[60] examples have been prepared using the dithiane method.

A number of more readily hydrolysed acetals have been investigated, including lithio bis(methylthio) methanes[65] and methoxy phenylthio trialkylsilyl methane **(3)**, which acts as an α-silyl acyl anion equivalent[66]. This route (Scheme 4) is successful for a wide range of aliphatic electrophiles and is even successful in conjugate addition to enones[67].

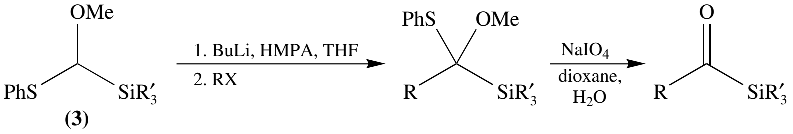

SCHEME 4

O-Trimethylsilyl hemithioacetal **(4)**, an example of a group of acetals which are very readily hydrolysed[68], is an intermediate in the synthesis of carbonyl bis(trimethylsilane). The unstable sulphoxide species **(5)**, prepared as shown in Scheme 5, undergoes a sila-Pummerer rearrangement to give the intermediate hemithioacetal **(4)**[69], which in turn reacts with the Pummerer intermediate to give a 1 : 1 mixture of carbonyl bis(trimethylsilane) and a dimethyl thioacetal. In a related reaction, the sila-Pummerer rearrangement of bis(trimethylsilyl) phenylseleninyl phenyl methane has been used to prepare benzoyl trimethylsilane in 46% yield[70].

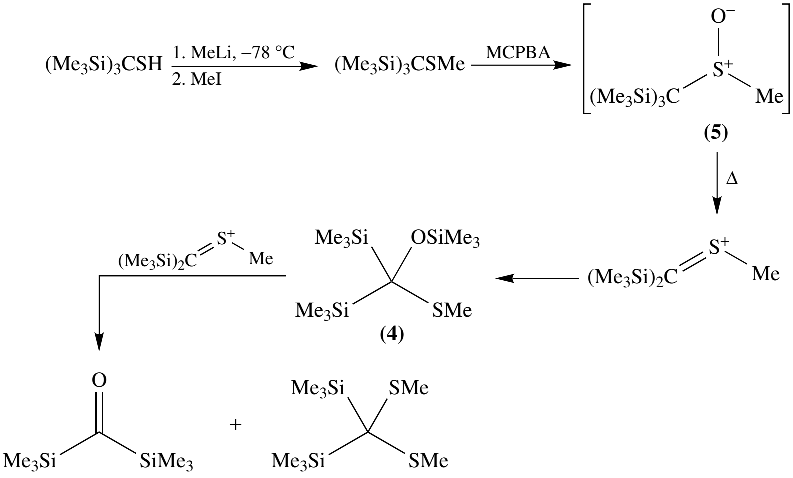

SCHEME 5

3. Silyl metallic species

One of the very earliest syntheses of an acyl silane involved the reaction of benzoyl chloride with triphenylsilyl potassium at low temperature (Scheme 6)[2]. The very low yield of benzoyl triphenylsilane (6%) obtained, and the similar yields of acetyl triphenylsilane obtained from the reactions of silyl lithium reagents with acetyl chloride[71], demonstrate that this is not a useful method for the synthesis of simple acyl silanes. It is, however, successful for the preparation of acyl tris(trimethylsilyl)silanes and some derivatives[24,31,72,73]. Tris(trimethylsilyl) and alkyl bis(trimethylsilyl)silyl lithium reagents react cleanly with acyl chlorides, typically at 0 °C, to give the corresponding acyl silanes in up to *ca* 85% yields. The tris(trimethylsilyl)silyl ('sisyl') lithium reagent is prepared by deprotonation of tris(trimethylsilyl)silane using an alkyl lithium reagent. The related alkyl bis(trimethylsilyl)silyl lithium species have been prepared by several methods (Scheme 7)[26]. The silyl lithium reagents, which are yellow to orange to brown in colour, can be remarkably stable; for example, phenyl bis(trimethylsilyl)silyl lithium forms a recrystallizable pale yellow solid 'ate' complex with THF with the stoichiometry $Ph(Me_3Si)_2SiLi\cdot 3THF$. Tris(trimethylsilyl)silyl lithium, which also forms an 'ate' complex with three molecules of THF, reacts with carbon dioxide to give the interesting crystalline tris(trimethylsilyl)silane carboxylic acid after acidic work-up, in 85% yield[17]. The methyl ester and several silyl esters were prepared from this acid by conventional means[28]. Phenyldimethylsilyl lithium reacts rapidly with some methyl esters at −110 °C and with amides at −78 °C to give acyl silanes smoothly. Use of other esters can lead to further addition of silyl lithium species to give disilyl carbinols; these materials may, however, be converted into acyl silanes with loss of one silyl moiety by oxidation with pyridinium dichromate[74].

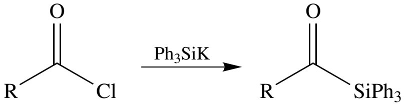

SCHEME 6

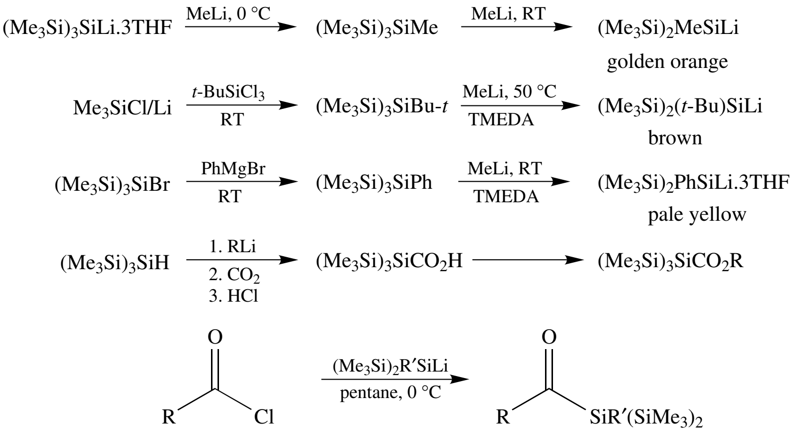

SCHEME 7

Less reactive silyl metal species such as lithium bis(triphenylsilyl) cuprate react with a variety of acyl chlorides to give the corresponding acyl silanes in moderate to good yields[75]. Dilithium bis(trimethylsilyl) cyanocuprate is particularly effective for the preparation of sterically hindered acyl silanes (Scheme 8), and appears to provide a good general preparative method[10]. Other higher-order lithium silyl cuprate species have more recently been shown to be effective in combination with the use of thiolesters as electrophiles[76].

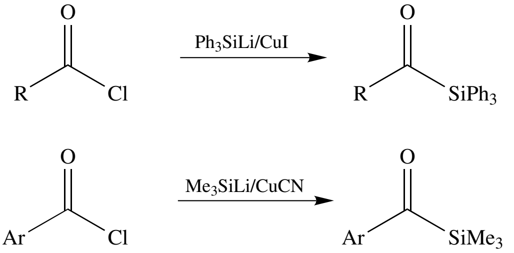

Ar = Ph, 3-MeC_6H_4, 4-$MeOC_6H_4$, 2,4,6-$Me_3C_6H_2$, 2-Furyl
R = Me, Et, *t*-Bu

SCHEME 8

The low ionic character of the aluminium–silicon bond has been cleverly utilized to develop a very mild, general and effective synthesis of acyl silanes, successful for aliphatic, aromatic, heteroaromatic, α-alkoxy, α-amino and even α-chiral and α-cyclopropyl acyl silanes[77]. Acyl chlorides are treated with lithium tetrakis(trimethylsilyl)aluminium or lithium methyl tris(trimethylsilyl) aluminium in the presence of copper(I) cyanide as catalyst to give the acyl silanes in excellent yields after work-up[77]. Later improvements include the use of 2-pyridinethiolesters in place of acyl halides, allowing preparation of acyl silanes in just a few minutes in very high yields indeed (Scheme 9)[80], and the use of bis(dimethylphenylsilyl) copper lithium[78] and a dimethylphenylsilyl zinc cuprate species[79,80] as nucleophiles.

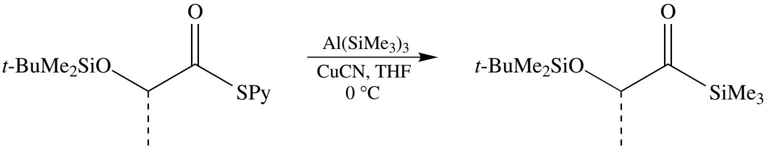

SCHEME 9

Triphenylsilyl zirconium and hafnium derivatives have been prepared from the silyl lithium species. Triphenylsilyl bis(cyclopentadienyl) zirconium chloride undergoes carbonyl insertion under pressure of carbon monoxide (100 psi) to give the corresponding acyl zirconium species which, upon treatment with anhydrous hydrogen chloride in a benzene matrix at $-196\,^{\circ}$C and warming to room temperature, gives rise to formyl triphenylsilane[55].

4. Palladium-catalysed coupling

Many aromatic and heteroaromatic acyl silanes have been prepared by transition metal catalysed coupling (e.g. Scheme 10)[23,81]. This is a very successful approach for most aromatic substrates, including furyl, thienyl, pyrryl and electron-deficient aryl acyl silanes, which can otherwise be difficult to prepare.

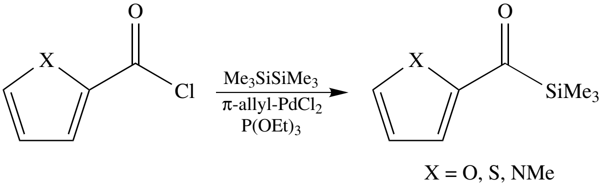

SCHEME 10

Palladium-mediated addition of silyl stannane reagents to alkynyl ethers has been employed for the synthesis of aliphatic acyl silanes in very good yields via the intermediate α-alkoxy-β-stannyl vinyl silanes (enol ethers of acyl silanes)[82]. In a second palladium-catalysed step, the vinyl stannane moiety could be coupled to suitable halides before hydrolysis to the acyl silanes with trifluoroacetic acid (Scheme 11).

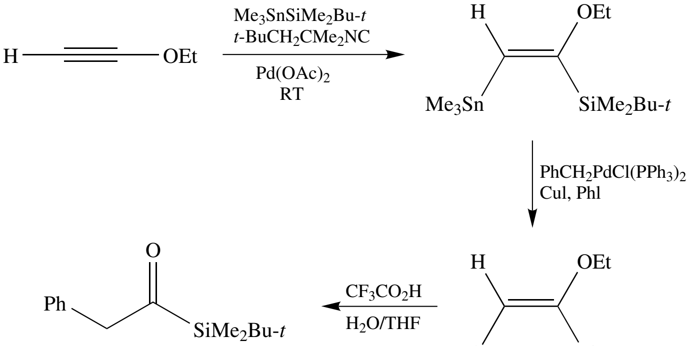

SCHEME 11

5. Oxidation reactions

The oxidation of secondary alcohols to ketones by any of a wide variety of oxidizing agents is a standard reaction, and it might therefore be supposed that the corresponding oxidation of α-hydroxy silanes would be effective for acyl silane preparation[5]. This approach is, however, commonly less than straightforward. A number of oxidizing systems have been examined[83], but the most satisfactory method for oxidation of α-hydroxy silanes to acyl silanes remains the Swern procedure[47,48,54], as used recently to prepare a series of acyl triisopropylsilanes as shown in Scheme 12, where the α-hydroxy silanes were produced by nucleophilic ring cleavage of triisopropylsilyl oxirane[84].

Use of chromic acid-based oxidation reagents often results in silicon–carbon bond cleavage (Scheme 13)[5], although such an oxidation has been used to produce α-cyclopropyl acyl silanes (*vide infra*, Section III.E)[85]. In an interesting development, this handicap of ready silicon–carbon bond cleavage during oxidation of α-hydroxy silanes has been cleverly utilized in an acyl silane synthesis by incorporation of two silicon moieties in the substrate (Scheme 14).

Several benzoyl silanes have been generated in good yields from the corresponding α,α-dibromobenzyl silanes by treatment with the oxidant silver acetate in acetone–ethanol–water mixture[4], or by simple hydrolysis with silica gel[86]. Indeed, the

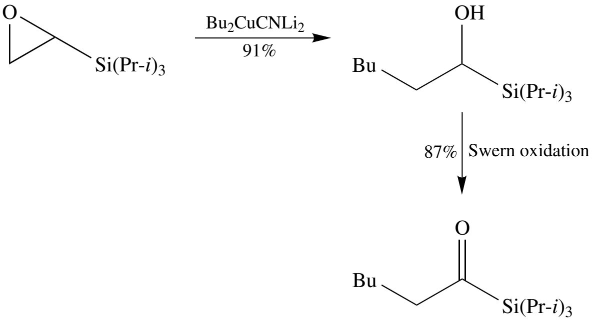

SCHEME 12

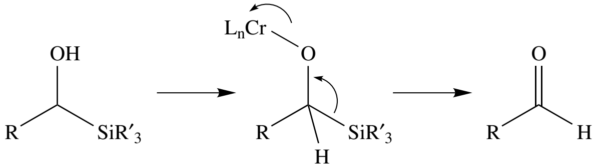

SCHEME 13

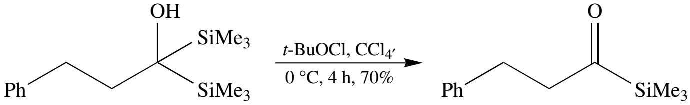

SCHEME 14

very first synthesis of an acyl silane was achieved using this method[4], and Brook has even prepared the diacyl silane **6** in this way[4], but the process is of course restricted to systems where geminal dihalides can easily be procured. Several unusual cyclic acyl silanes such as **7** have also been prepared using this approach[87].

A number of acyl silanes have been isolated from the photosensitized oxygenation of silyl diazo compounds using *meso*-tetraphenylporphine (TPP) as the sensitizer (Scheme 15)[15]. This synthesis is most useful for aromatic acyl silanes and the yellow α-carboxyacyl silanes, but it is not of general applicability, isolation difficulties commonly being encountered in the synthesis of aliphatic and other acyl silanes, resulting in poor overall yields.

A much more general method for acyl silane synthesis involving silyl diazo intermediates is illustrated in Scheme 16[88]. The lithiated derivative of trimethylsilyl diazomethane reacts smoothly with alkyl halides in THF solution to give α-trimethylsilyl diazoalkanes in good yields. Oxidative cleavage of the diazo moiety is effected using 3-chloroperbenzoic acid in benzene solution, to give access to a wide variety of acyl silanes in yields of up to 71%. A phosphate buffer (pH 7.6) is used to prevent side reactions. Aromatic acyl silanes clearly cannot be prepared by this chemistry since an aromatic nucleophilic substitution reaction would be required.

Several aromatic acyl silanes and the fascinating but unstable pink carbonyl bis(trimethylsilane) have been prepared in reasonably good yields by the oxidation of phosphonium ylids (Scheme 17)[13].

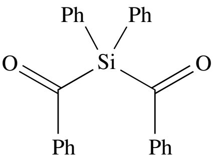

(6)

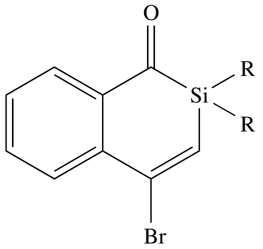

(7)

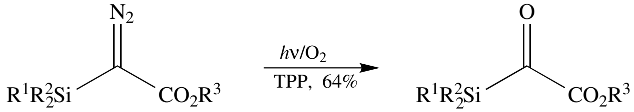

SCHEME 15

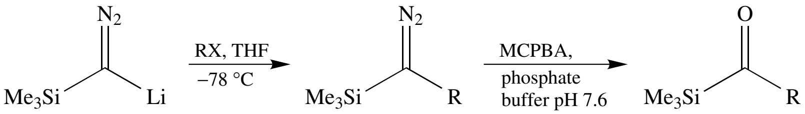

SCHEME 16

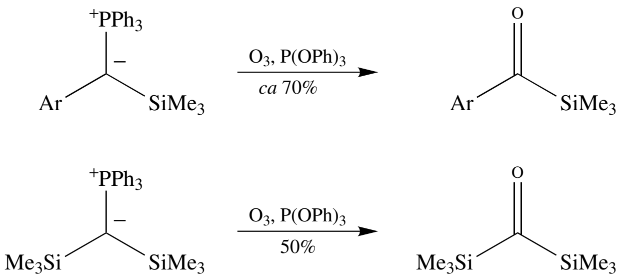

SCHEME 17

6. Hydroboration–oxidation of alkynyl silanes

Hydroboration–oxidation of alkynyl silanes is an excellent general method for synthesis of substituted acyl silanes from readily available starting materials[89,90]. Although the system as originally studied gave only moderate yields, the sequence was later modified by Zweifel and Miller to produce a superior and high-yielding one-pot synthesis of alkyl acyl silanes (Scheme 18), limited only by the reduced yields obtained from very bulky substrates[8]. The use of alkaline peroxide in the oxidation step must be avoided as the acyl silane product is converted into silyl ester by this reagent. It is the opinion of the present authors that this method remains the best general procedure for the preparation of simple aliphatic acyl silanes; aryl acyl silanes obviously cannot be prepared in this way.

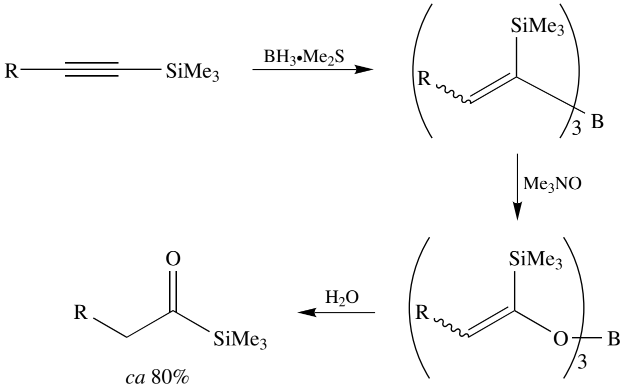

SCHEME 18

7. Rearrangement of silyloxy carbenes

Acyl silanes have been obtained by the pyrolytic rearrangement of silyloxy carbenes derived from α-keto silyl esters (Scheme 19)[91]. The pyrolysis takes place in high yield for aroyl silanes, but is less effective for other substrates.

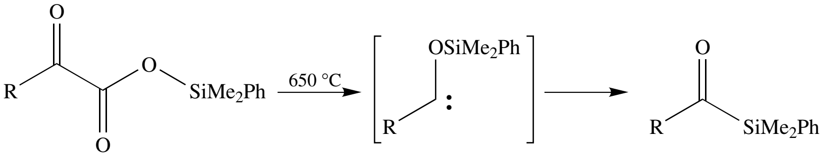

SCHEME 19

8. Preparation from enol ethers

Trialkylsilyl enol ethers of acyl silanes have been prepared using a variety of routes and can be excellent precursors to acyl silanes through simple hydrolysis.

Acyl imidazoles take part in a silyl acyloin reaction to give the corresponding silyl enol ethers in moderate yields. A possible mechanism is outlined in Scheme 20[92]. The silyl enol ethers could be hydrolysed to acyl silanes by treatment with acid.

Lithium alkoxides of bis(trimethylsilyl) carbinols react with benzophenone to produce silyl enol ethers of acyl silanes in good yields[93]. The alcohols were prepared in reasonable yields by hydrolysis of the bis(trimethylsilyl) carbinol silyl ethers[94,95], which in turn were produced from the corresponding esters using another silyl acyloin reaction, which itself, ironically, proceeds through an acyl silane intermediate (Scheme 21)[94].

Picard has reported more direct approaches to acyl silanes and to their silyl enol ethers by reductive silylation of substituted benzoates and of α,β-dihalo-α,β-unsaturated acyl chlorides, respectively, using a similar reagent mixture of trimethylchlorosilane, magnesium and HMPA[96].

A much more general synthesis of these silyl enol ethers, however, is based on the reductive cleavage of the carbon–sulphur bond of the silyl enol ether of a thiolester using sodium metal and chlorotrimethylsilane, once again in a silyl acyloin reaction (Scheme 22)[97,98].

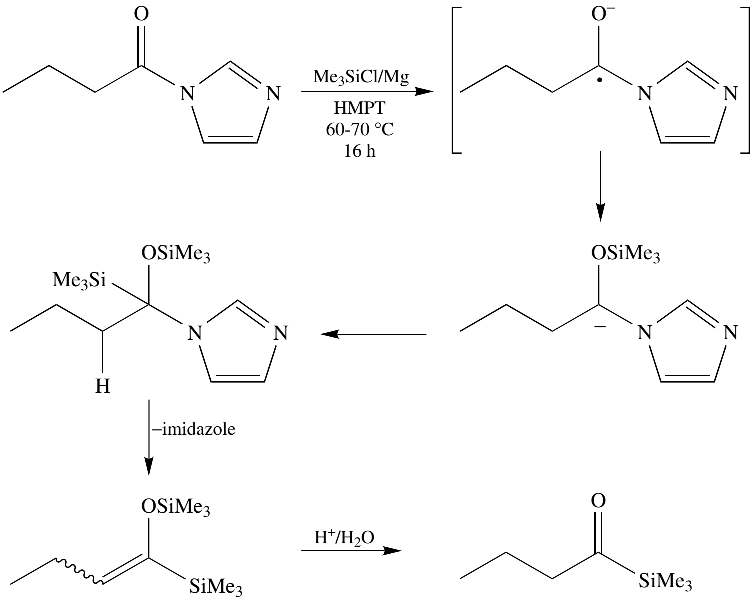

SCHEME 20

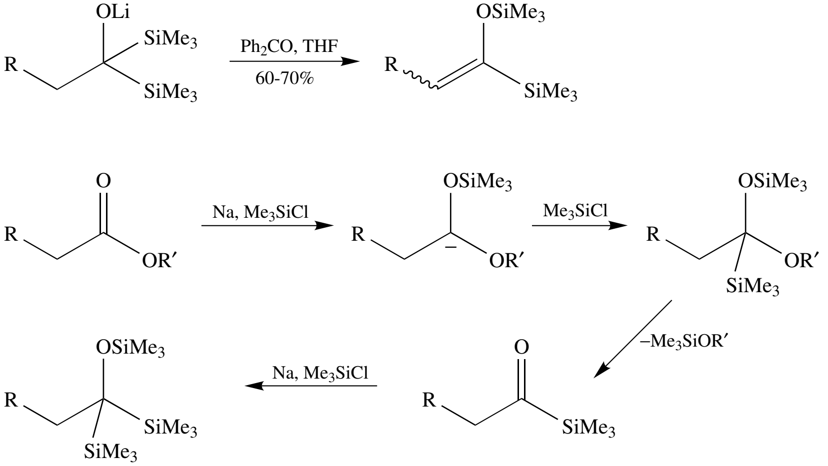

SCHEME 21

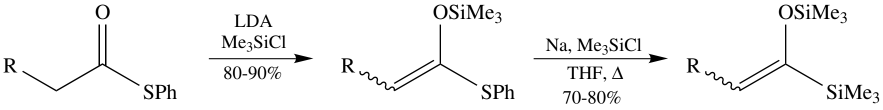

SCHEME 22

A further efficient preparation of these silyl enol ethers proceeds through an intramolecular 1,2-silicon shift in an α-silyl acyl lithium substrate **(8)**, prepared from an α-lithiosilane (Scheme 23)[99]. This method appears very simple to carry out, and produces the silyl enol ethers in good yields with high isomeric purity (usually, E isomer $>$ 90% of mixture).

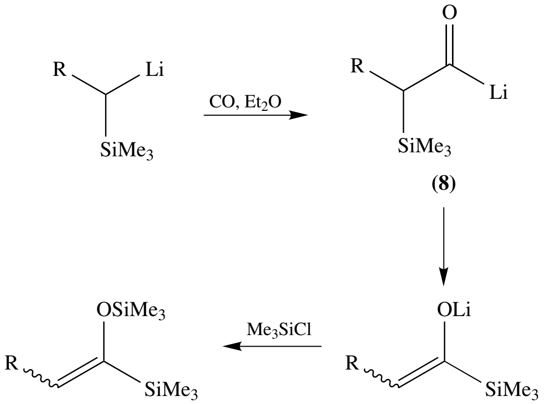

SCHEME 23

In a rather more unusual process, presumably involving tellurium–lithium exchange, acyl tellurides may be converted into silyl enol ethers of acyl silanes by treatment with butyl lithium and trimethylchlorosilane. In this procedure it is the Z isomer which is the predominant product (Scheme 24)[100].

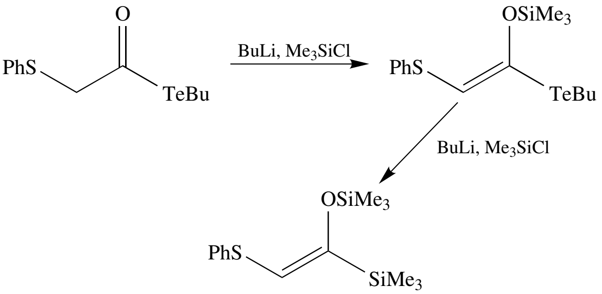

SCHEME 24

Another metal–metal exchange procedure involves tin–lithium exchange in 1-silyloxy vinyl stannanes (silyl enol ethers of acyl stannanes) induced by butyl lithium. The resulting lithio species suffers migration of the silicon moiety from oxygen to carbon to generate the lithium enolates of acyl silanes, which were shown to undergo enolate alkylation and aldol reaction, so producing new, functionalized acyl silanes (Scheme 25)[101].

A number of silyl enol ethers of acyl silanes have been produced from alkenes by subjection to 50 atmospheres of carbon monoxide in the presence of 0.1 equivalents of trialkylsilane and 2 mol% of an iridium catalyst (Scheme 26)[102]. Hydrolysis to the acyl silanes was achieved using hydrochloric acid–acetone.

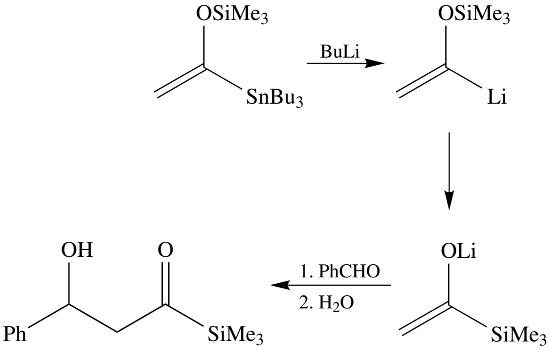

SCHEME 25

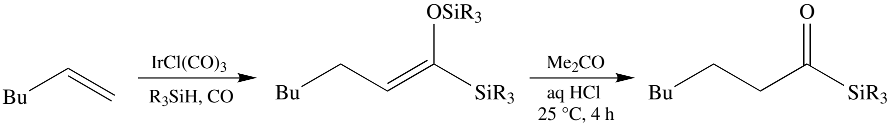

SCHEME 26

Methyl enol ethers of acyl silanes have been prepared in good yield by the silylation of vinyl lithium reagents derived from methyl enol ethers[103]. Indeed, perhaps the simplest preparation of a methyl enol ether of an acyl silane results from addition of α-methoxyvinyl lithium to chlorotrimethylsilane. Acid hydrolysis gave acetyl trimethylsilane in *ca* 80% yield[104]. A similar reaction has been carried out with phenyl methyl *t*-butyl chlorosilane. Again, acid hydrolysis gave the acyl silane, which is of course chiral at silicon[64].

In another simple procedure, deprotonation of methoxy bis(trimethylsilyl)methane with butyl lithium and addition of the resulting anion to aldehydes induces Peterson elimination (Scheme 27). The product methyl enol ethers could be hydrolysed to the parent acyl silanes with hydrochloric acid–THF or could be treated with electrophiles such as N-halosuccinimides to give α-haloacyl silanes[105]. Alternatively, treatment with phenyl selenenyl chloride, oxidation at selenium and selenoxide elimination afforded α,β-unsaturated acyl silanes.

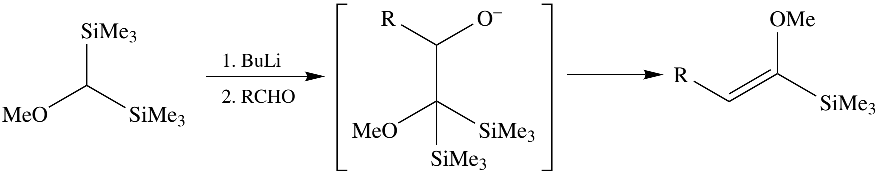

SCHEME 27

Ethyl enol ethers of acyl silanes have been prepared by the palladium-mediated addition of silyl stannanes to alkynyl ethers. Hydrolysis using trifluoroacetic acid gave very high yields of acyl silanes (*vide supra*, Section III.A.4)[82].

9. Silylation of acyl metallic species

Perhaps the most direct method of synthesizing an acyl silane is by reaction of an acyl lithium, prepared by carbonylation of an alkyl lithium at $-110\,^{\circ}\mathrm{C}$, with a silicon electrophile, illustrated in Scheme 28[106,107]. Although this method is successful for a variety of alkyl acyl silanes in moderate yields, low temperatures must be used, and the method is not suitable for aryl acyl silanes.

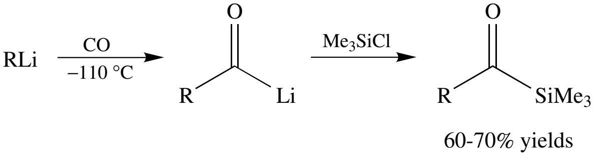

SCHEME 28

Several acyl silanes have been prepared by the silylation of metalloaldimines followed by hydrolysis (Scheme 29)[108,109]. One limitation of this scheme is the ready decomposition of the aldimine to give aldehyde in addition to acyl silane in approximately equal amounts.

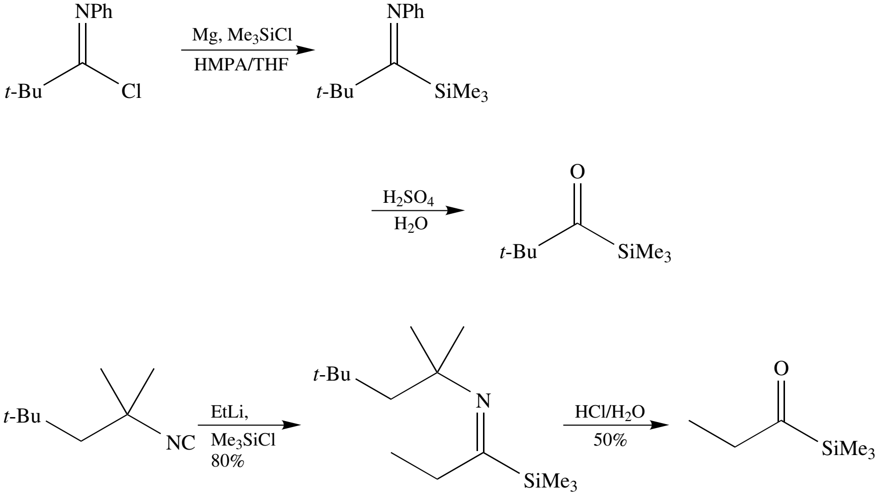

SCHEME 29

N,*N*-Diethylcarbamoyl trimethylsilane has been prepared by the reaction of bis(trimethylsilyl) sulphide with bis(*N*,*N*-diethylcarbamoyl) mercury (Scheme 30)[16]. Silylation of the carbamoyl cuprate reagent derived from a lithium amide, by addition of copper(I) cyanide and subsequent exposure to carbon monoxide (1 atm), is also effective[75,110]. Poor to moderate yields of carbamoyl silanes may be isolated by treatment of lithium silylamides with carbon monoxide and methyl iodide, in a reaction sequence involving a nitrogen to carbon silyl shift in an intramolecular silylation (Scheme 31)[111].

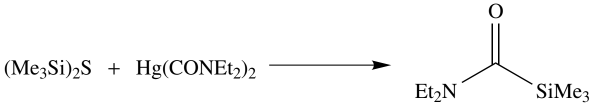

SCHEME 30

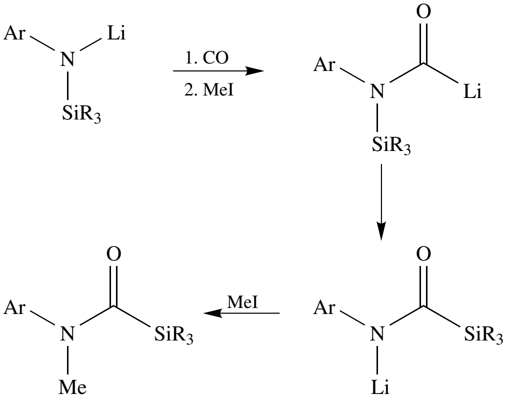

SCHEME 31

10. Non-racemic acyl silanes

A number of acyl trimethyl silanes chiral at the α- or β-carbon atom have been prepared in non-racemic form. Chiral α-alkoxy and α-silyloxy acyl silanes have been generated in very high yields by oxidative rearrangement of enantiomerically pure silyl epoxides, induced by dimethyl sulphoxide and silyl triflates (Scheme 32)[112].

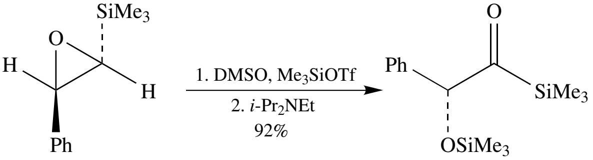

SCHEME 32

Chiral β-amino acyl silanes have been prepared through the addition of 2-lithio-2-trimethylsilyl-1,3-dithiane to enantiomerically pure *N*-tosylaziridines followed by mercury-mediated thioacetal hydrolysis[113].

Enantioselective Claisen rearrangement of allyl (α-trimethylsilyl)vinyl ethers in the presence of aluminium binaphthol derivatives gives β-chiral γ, δ-unsaturated acyl silanes with good ee (Scheme 33)[114].

B. α-Haloacyl Silanes

The most direct procedure for the synthesis of α-haloacyl silanes is electrophilic halogenation of enolates or enol ethers of acyl silanes. This has been achieved with the silyl enol ethers using bromine at low temperatures, but the reaction suffers from the general

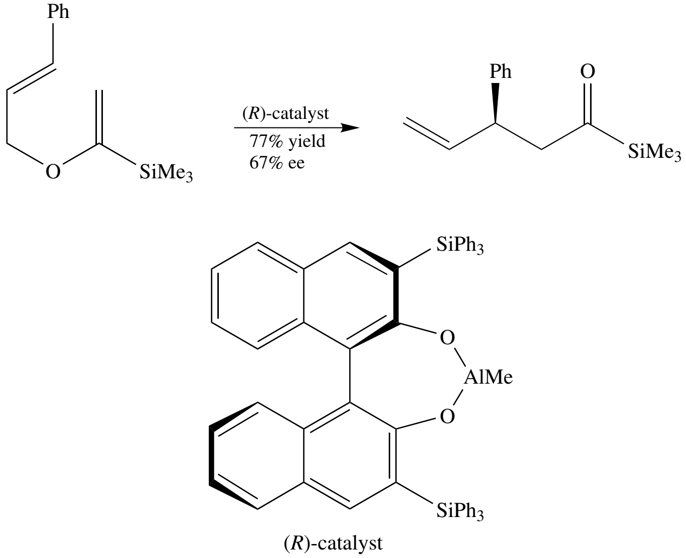

SCHEME 33

sensitivity of both the starting materials and the products[12,115]. Alkyl enol ethers of acyl *t*-butyldimethylsilanes, prepared by deprotonation and silylation of vinyl ethers[103], are also successful substrates[105,116]. α-Iodoacyl silanes were prepared by the same authors by treatment of α-bromoacyl silanes with sodium iodide in acetone.

Bis(trimethylsilyl)carbinols have been reported to react with *N*-bromosuccinimide in carbon tetrachloride to give the corresponding α-haloacyl silanes in moderate yields (Scheme 34)[115].

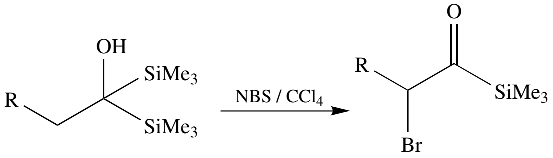

SCHEME 34

Perhaps the best general method to date for preparing α-haloacyl silanes involves bromination of silyl enol borinates **(9)** at 0 °C, a reaction which proceeds in good yield and involves no sensitive intermediates. This route offers a most convenient one-pot synthesis of α-haloacyl silanes from readily available starting materials, as the intermediate enol borinates are very easily prepared from silyl acetylenes (Scheme 35)[7,117,118].

α-Bromoacyl silanes may be isolated in variable yields by bromination–rearrangement of 1-phenylsulphonyl-1-trimethylsilyl oxiranes induced by magnesium bromide etherate (Scheme 36)[119,120]. The process appears to be rather sensitive towards the reaction conditions used, and can give rise to a number of by-products. In a recently-reported related rearrangement, 1-halo-1-trimethylsilyl oxiranes are converted into α-haloacyl silanes upon exposure to Lewis acids, generally in high yields[121].

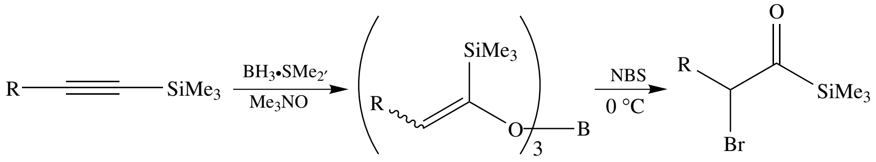

(9)

50-60% overall

SCHEME 35

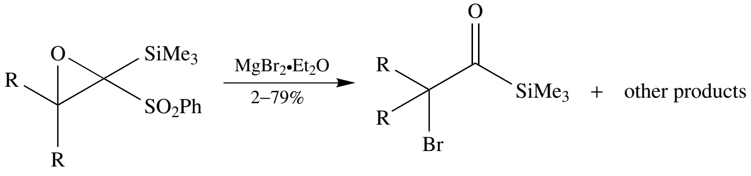

SCHEME 36

The pale yellow crystalline trifluoroacetyl triphenylsilane and a number of other perfluoroalkyl acyl triphenylsilanes have been prepared by simple acylation of triphenylsilyl lithium with perfluoroalkyl anhydrides[122].

C. α-Ketoacyl Silanes

α-Ketoacyl silanes have a deep rich crimson colour and are particularly sensitive to light, often requiring purification by chromatography at −78 °C, preferably in the dark. They were first isolated in 1982 using allene methodology as shown in Scheme 37[14], although the yellow α-carboxyacyl silanes were already known at that time (*vide supra*, Section III.A.4)[15]. Thus, lithiation of allene **(10)** with butyl lithium at −78 °C and subsequent reaction with a chlorosilane, followed by oxidative work-up with *m*-chloroperbenzoic acid, provided the unstable α-ketoacyl silanes in moderate yields, presumably via the epoxides[123].

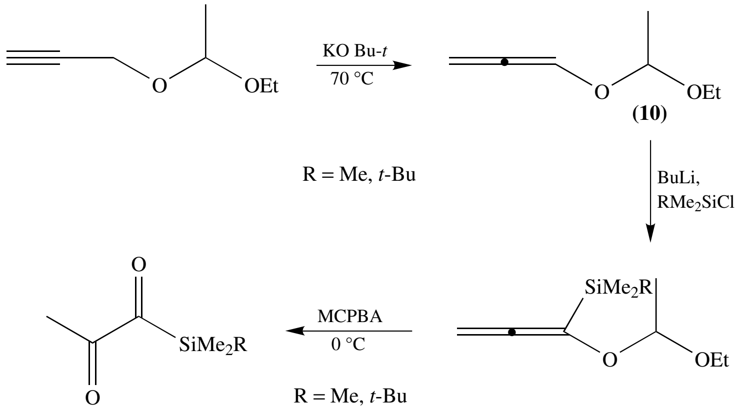

SCHEME 37

A much more general and very simple synthesis requiring a minimum of laboratory manipulation uses a Swern oxidation of the corresponding diols to give the α-ketoacyl silanes directly in useful yields (Scheme 38)[7,124]. Purification in this case was accomplished in the dark, by chromatography at −78 °C or by distillation. α-Ketoacyl silanes appear to be intermediates in the oxidation of silyl acetylenes to α-ketoesters by osmium tetroxide[125], and indeed have been isolated from the oxidation of silyl acetylenes by dimethyl dioxirane[126].

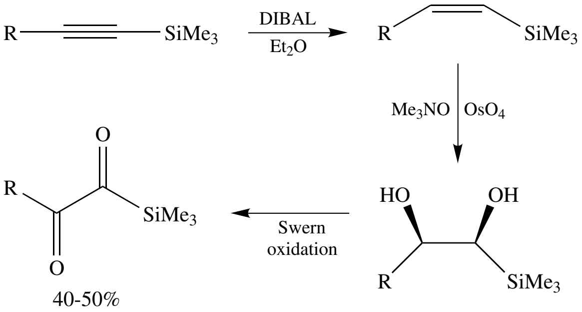

SCHEME 38

D. α,β-Unsaturated Acyl Silanes

α,β-Unsaturated acyl silanes, which are yellow or yellow-green in colour, are generally less sensitive than those types of acyl silane discussed above and have been prepared through a number of different approaches.

1. Hydroboration–oxidation of enynes

α,β-Unsaturated acyl silanes have been prepared by hydroboration methodology, similar to that used in the synthesis of aliphatic acyl silanes (*vide supra*) (Scheme 39)[89]. This synthesis is effective, but suffers from the relative difficulty of synthesis of the necessary functionalized enynes.

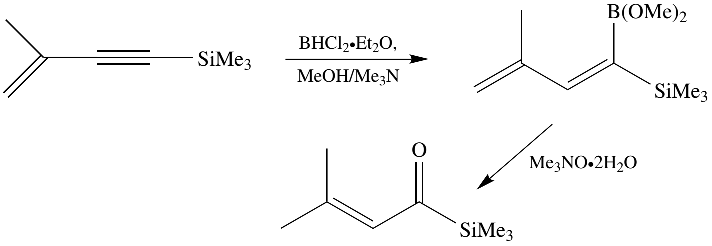

SCHEME 39

2. Oxidation of allylic carbinols

An excellent synthesis of α,β-unsaturated acyl silanes from allyl silyl ethers is shown in Scheme 40[20]. This simple two-step procedure hinges on the Wittig rearrangement[127,128], and is successful on a large scale. The metallation of allyl silyl ethers generates a rapidly interconverting mixture of two organometallic species, **11** and **12**. Although alkylation of this mixture of organometallic derivatives generally proceeds at the C-3 position via **11**, hard electrophiles such as protons react predominantly at the oxygen atom of the alkoxide intermediates **(12)**, leading to α-hydroxy allyl silanes **(13)**. Swern oxidation leads to α,β-unsaturated acyl silanes.

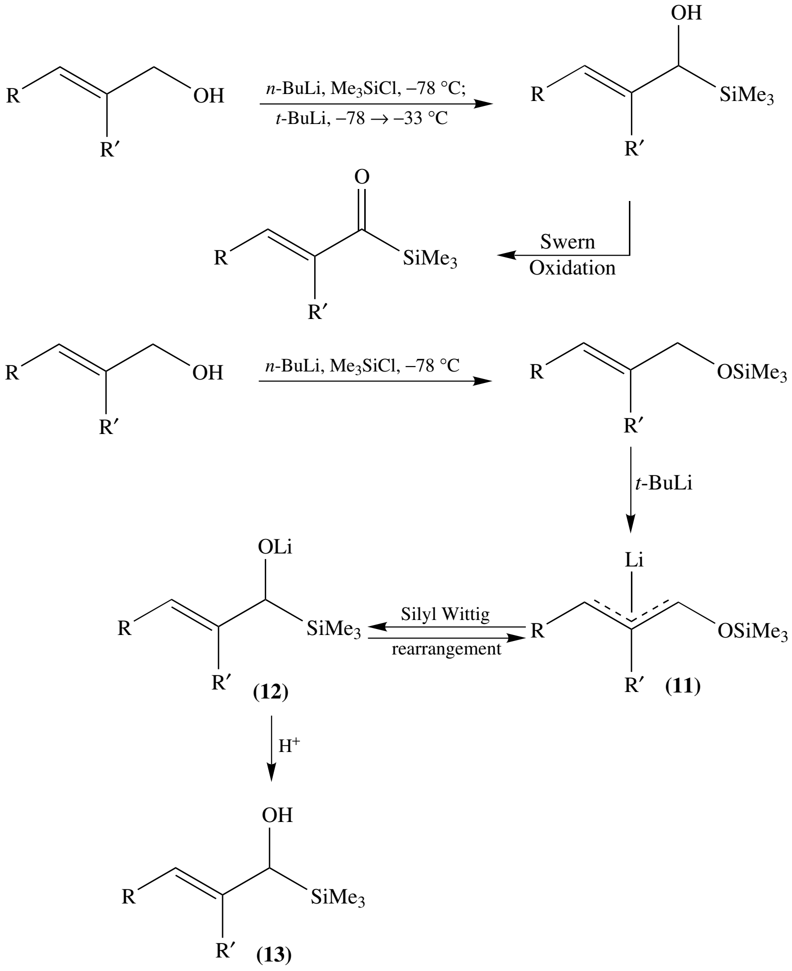

SCHEME 40

3. Preparation from enol ethers of acyl silanes

A number of α,β-unsaturated acyl silanes have been prepared from silyl enol ethers of acyl silanes (Scheme 41)[129]. Addition of phenyl sulphenyl chloride to the silyl enol ether with subsequent elimination of chlorotrimethylsilane gives the α-(phenylthio)acyl silane. Oxidation to the sulphoxide followed by *in situ* elimination of benzenesulphenic acid produces the α,β-unsaturated acyl silane in good yield. A similar sequence has been carried out with the corresponding methyl enol ethers[105].

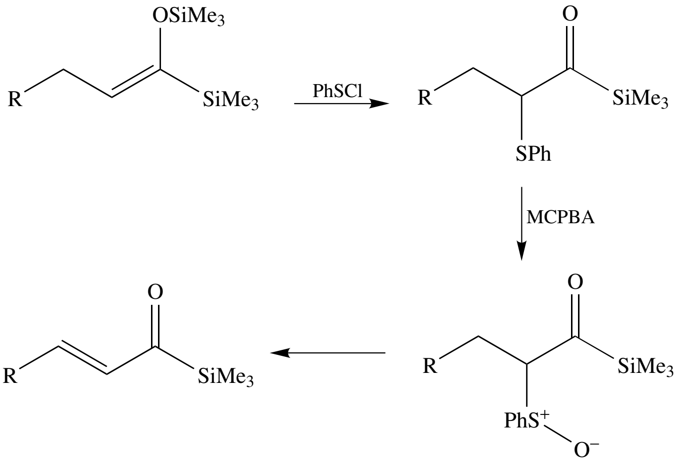

SCHEME 41

One of the simplest methods for preparation of an α,β-unsaturated acyl silane is by hydrolysis of a 1-alkoxy-1-trimethylsilylbutadiene, the conjugated dienol ether of α,β-unsaturated acyl silane, prepared by deprotonation and alkylation of the 1-alkoxydiene (Scheme 42)[11]. This method is generally limited in application to simple substrates, presumably due to the complexity of preparation of more highly functionalized 1-alkoxydienes.

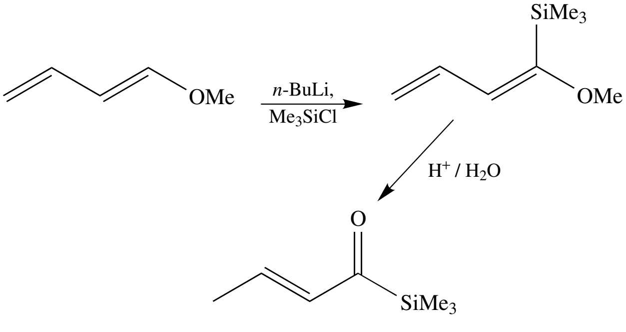

60-70% yields

SCHEME 42

The most versatile synthesis of α,β-unsaturated acyl silanes involves the use of allene methodology, developed by a number of groups[14,22]. Deprotonation and silylation of allenyl ethers followed by hydrolysis gives rise directly to α,β-unsaturated acyl silanes via their enol ethers, 1-alkoxy-1-trimethylsilylallenes (Scheme 43). Indeed, the first example of an α,β-unsaturated acyl silane was prepared by such a route[22a], as was the first example of an allenic acyl silane (from a 1-trimethylsilyl-1-trimethylsilyloxy-1,2,3-alkatriene)[22b].

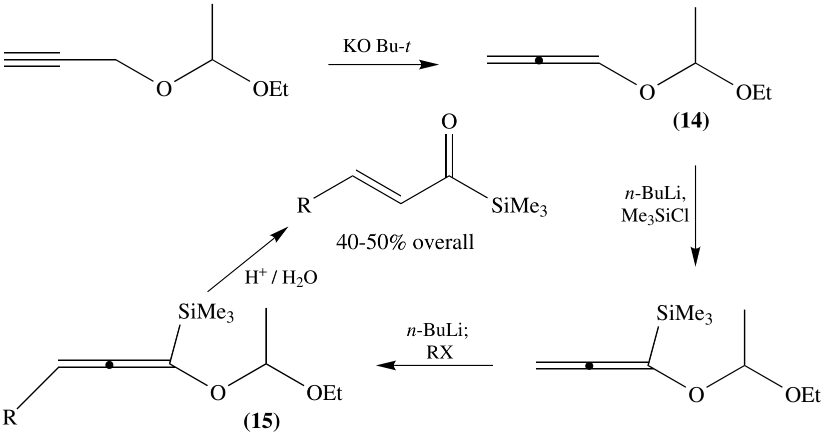

SCHEME 43

Reich uses ethoxyethyl propargyl ether as precursor to the allenyl ether **(14)**, because the relatively large and polar protecting group gives it much better handling characteristics than simpler analogues[14]. The resulting 1-alkoxy-1-trimethylsilylallene may be further deprotonated and functionalized at the C-3 terminus to give the substituted derivatives **(15)** for hydrolysis to 3-substituted α,β-unsaturated acyl silanes. The 1-trimethylsilyl-1-alkoxyallenes **(15)** are also excellent precursors to α-halo and α-selenenyl α,β-unsaturated acyl silanes (Scheme 44)[14].

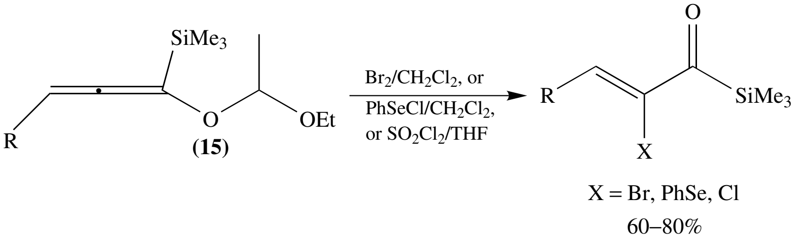

SCHEME 44

In a further development of this approach, the synthesis of α,β-acetylenic acyl silanes has been achieved as shown in Scheme 45[14]. Oxidation of the 3-selenenyl allenyl ethers **(16)** with *m*-chloroperbenzoic acid at $-78\,^\circ$C gave the corresponding unstable selenoxides, which underwent *in situ* [2,3] sigmatropic shift producing acetals **(17)**. Loss of selenenyl ester on work-up gave the α,β-acetylenic acyl silanes in *ca* 50% yields.

1-Alkoxy-1-trimethylsilylallenes also undergo a Lewis acid-induced rearrangement to give 2-substituted α,β-unsaturated acyl silanes in reasonable yields (Scheme 46)[130]. The related 1-methylthio-1-trialkylsilylallenes undergo Lewis acid-induced aldol and Mukaiyama reactions to produce 2-alkoxyalkylated α,β-unsaturated acyl silanes (Scheme 47)[131].

Lewis acid-mediated addition of (phenylthio)trimethylsilane to acryloyl silane takes place to give 1,3-bis(phenylthio)-1-trimethylsilylprop-1-ene **(18)**. This compound may be deprotonated with *t*-butyl lithium at the β-position and alkylated to give a range

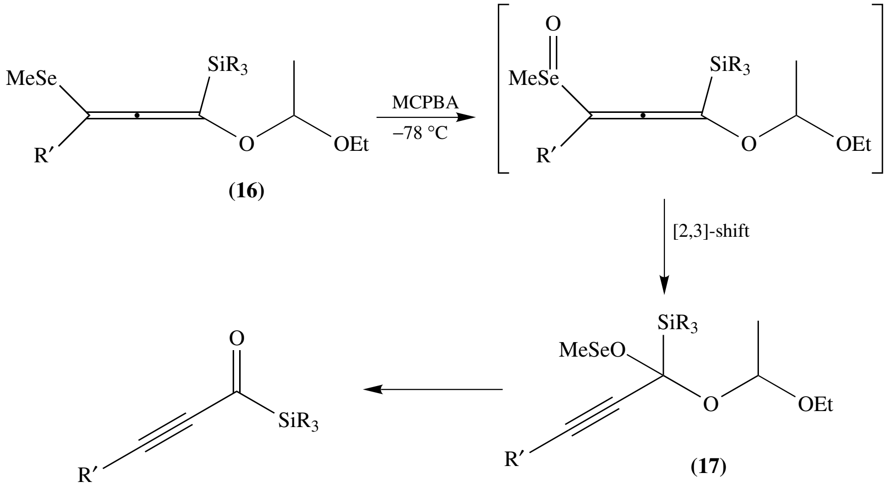

SCHEME 45

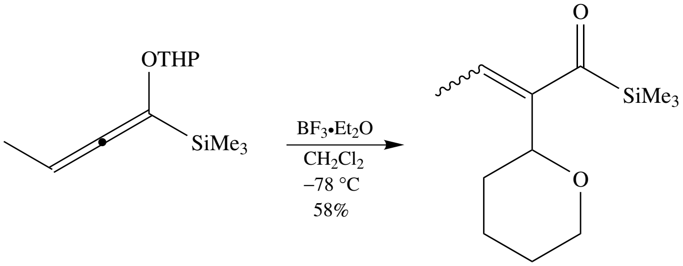

SCHEME 46

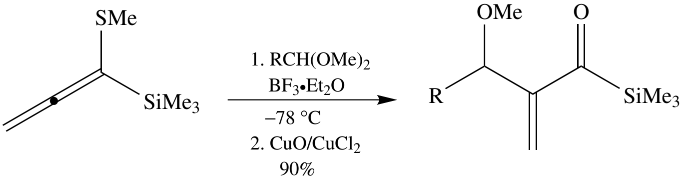

SCHEME 47

of substituted derivatives, which may be converted into β-substituted α,β-unsaturated acyl silanes by hydrolysis–elimination with mercuric chloride in aqueous acetonitrile (Scheme 48) (*vide infra*, Section IV.D)[132]. It should be noted that the β-substituent has here been introduced as an electrophile, complementing other methods of preparation of β-substituted α,β-unsaturated acyl silanes.

α,β-Unsaturated acyl silanes have been prepared in a stereospecific manner from α-trimethylsilylacyl trimethylsilanes by an interesting aldol-Peterson reaction sequence via intermediate **19** (Scheme 49)[133,134].

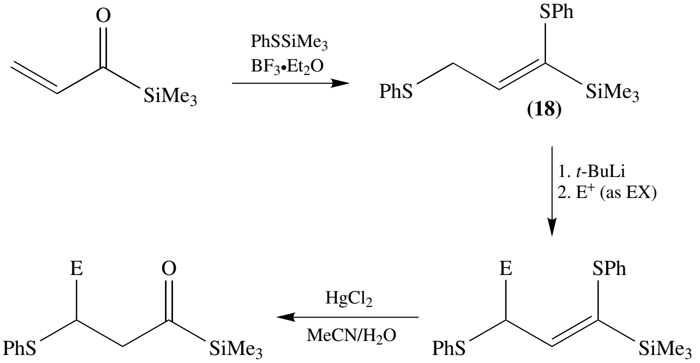

e.g. EX = BuI, MeOCOCl, $CH_2{=}CHCH_2Br$

SCHEME 48

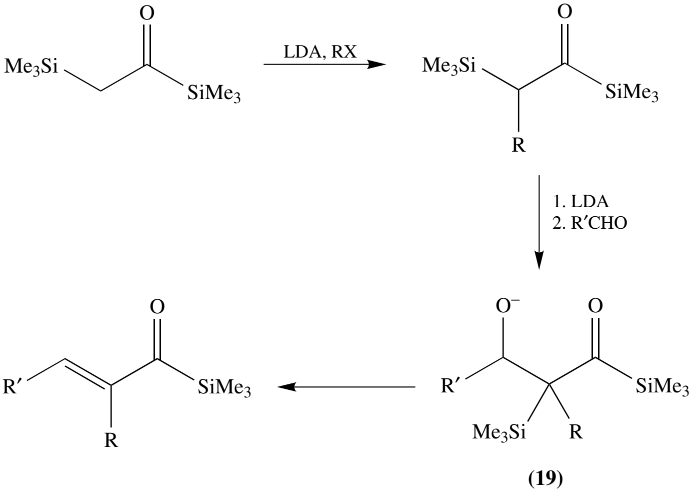

SCHEME 49

Photochemically-induced addition of bromotrichloromethane to 1-ethoxy-1-trimethylsilylethene, the ethyl enol ether of acetyl trimethylsilane, generates a 1 : 1 adduct which provides 3,3-dichloropropenoyl trimethylsilane **(20)** on solvolysis. Treatment of this material with lithium alkyl cyanocuprates resulted in addition–elimination to give the *E*-isomers of the 3-substituted α,β-unsaturated acyl silane products (Scheme 50)[135].

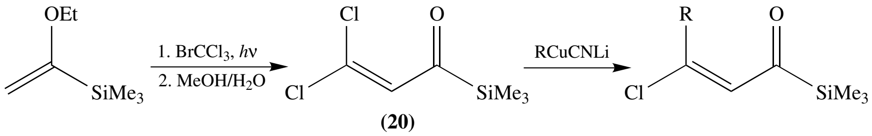

SCHEME 50

4. Preparation from *α,β*-alkynyl acyl silanes

α,β-Acetylenic acyl triphenylsilanes have been used by the Degl'Innocenti group as precursors of *α,β*-unsaturated and other acyl silanes[136]. Several reaction types have been utilized. Simple conjugate addition of lithium dialkyl cuprates is successful and proceeds in good to excellent yields[137]. Conjugate addition of heteroatomic nucleophiles is also successful[138], including the addition of a tin nucleophile to give 3-(tributylstannyl)propenoyl triphenylsilane. This last example is interesting because it allows subsequent palladium-catalysed coupling to produce structurally more complex *α,β*-unsaturated acyl silanes, for example with extended conjugation (Scheme 51)[139]. The *β*-iodo derivative has been similarly used[140].

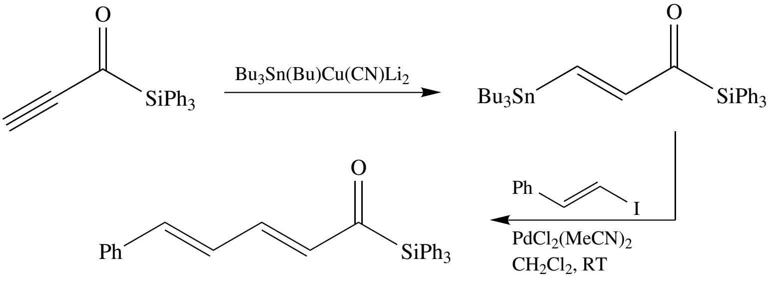

SCHEME 51

5. Miscellaneous methods

A limited number of functionalized acyl silanes have been prepared by the use of 1,3-dithiane methodology as described above[46,141], but this route is unfavourable for the synthesis of *α,β*-unsaturated acyl silanes[20]. Several *β*-hydroxy acyl silanes have, however, been produced in high yields using this chemistry; acid-catalysed elimination of water from these compounds does give *α,β*-unsaturated acyl silanes, and Swern oxidation gives *β*-ketoacyl silanes (Scheme 52)[142]. Analogous acetylenic 1,3-dioxanes have been used as precursors to *α,β*-acetylenic acyl silanes[143], as have formyl silanes (*vide supra*, Section III.A.1)[54].

Nowick and Danheiser have employed the Horner–Emmons reaction of *α*-phosphonoacyl silanes to prepare *α,β*-unsaturated acyl silanes in 54–97% yields[116]. The *α*-phosphonoacetyl silane intermediate (**21**), prepared from *α*-iodoacetyl *t*-butyldimethylsilane through the Arbuzov reaction, undergoes enolate alkylation, for example using potassium *t*-butoxide and methyl iodide; the alkylated products also underwent Horner–Emmons reaction (Scheme 53).

Isomerization of a *β*-trimethylsilylpropargyl alcohol to give the *α,β*-unsaturated acyl silane via the intermediate enol form, the 1-hydroxy-1-trimethylsilylallene, occurs upon treatment with tetrabutylammonium per-rhenate and *p*-toluenesulphonic acid[144]. While several examples of the isomerization reaction are given, only one is able to give an acyl silane product.

In an interesting and unusual reaction, Paquette and Maynard have shown that peracid oxidation of 1,2-disilyl-3,3-dimethylcyclopropene gives rise to an *α*-silyl-*α,β*-unsaturated acyl silane, through rearrangement of the intermediate epoxycyclopropane. Further treatment with peracid gave the *α*-epoxy acyl silane (Scheme 54)[145].

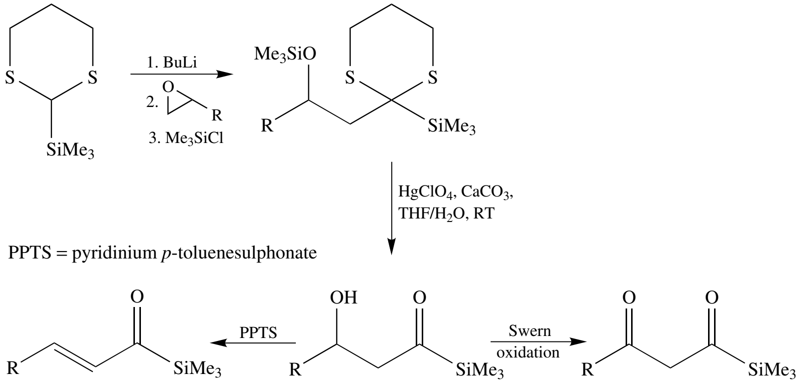

PPTS = pyridinium *p*-toluenesulphonate

SCHEME 52

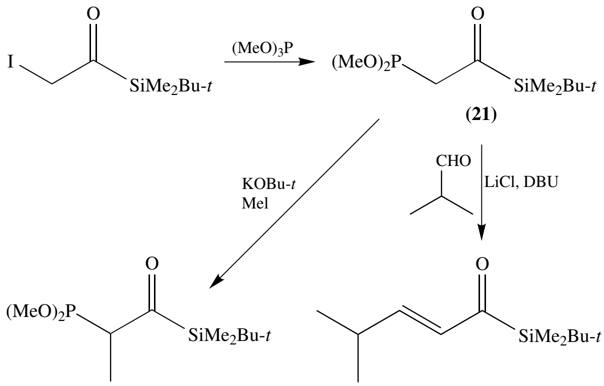

SCHEME 53

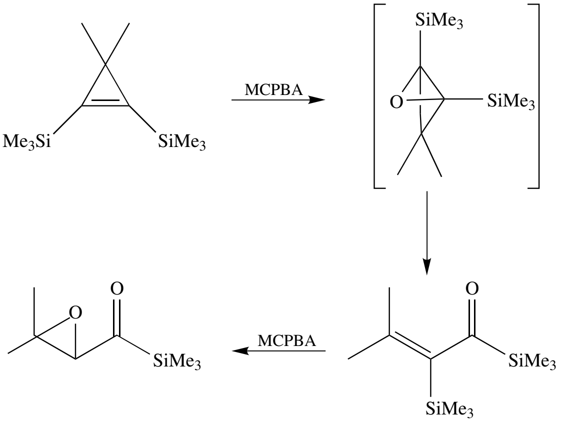

SCHEME 54

E. α-Cyclopropyl and α-Epoxyacyl Silanes

The first α-cyclopropyl acyl silanes to be isolated were generated by treatment of α,β-unsaturated acyl silanes with diazomethane, followed by vapour-phase pyrolysis of the intermediate pyrazoline derivatives (*vide infra*, Section IV.D)[141]. They suffer acid-induced cleavage or rearrangement under more mild conditions than do their carbon analogues[146].

Wittig rearrangement of allyl silyl ethers, followed by Simmons–Smith cyclopropanation and Collins oxidation, produces α-cyclopropyl acyl silanes, e.g. **22**, in 10–85% yields (Scheme 55)[85].

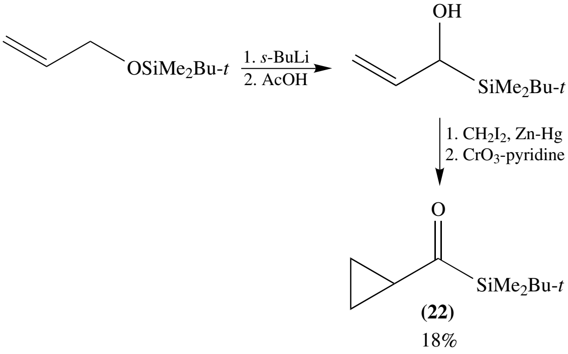

SCHEME 55

Nakajima has shown that α-cyclopropyl acyl silane **(23)** results from reaction of 1-trimethylsilyl cyclopropyl lithium with dichloromethyl methyl ether at low temperature in THF solution, in a reaction said to involve a carbene intermediate and a 1,2-silicon shift (Scheme 56)[147].

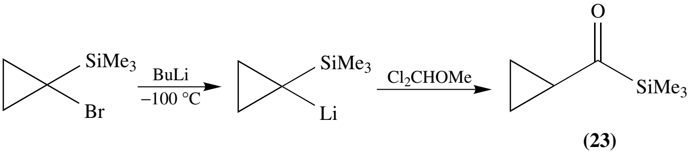

SCHEME 56

One general method for acyl silane synthesis particularly successful for α-cyclopropyl examples (and even an α-cyclobutyl example) involves treatment of acid chlorides with lithium tetrakis(trimethylsilyl) aluminum or lithium methyl tris(trimethylsilyl) aluminium and cuprous cyanide (*vide supra*, Section III.A.3)[77]. For example, cyclopropyl acyl silane **(23)** was obtained in 89% yield by this process. Improved procedures use lithium *t*-butyldimethylsilyl cuprate[78] and a dimethylphenylsilyl zinc cuprate species[79,80] as reagents.

Nowick and Danheiser[148] have explored α-cyclopropyl acyl silane generation from α-haloacyl silanes through McCoy reactions (Scheme 57) and via sulphur ylids (Scheme 58). Ylid species such as **24** were found to be stable in aprotic solvents in the presence of lithium salts, and were used for the cyclopropanation of α,β-unsaturated aldehydes.

α-Epoxy acyl silanes may be prepared by simple epoxidation of α,β-unsaturated acyl silanes[145].

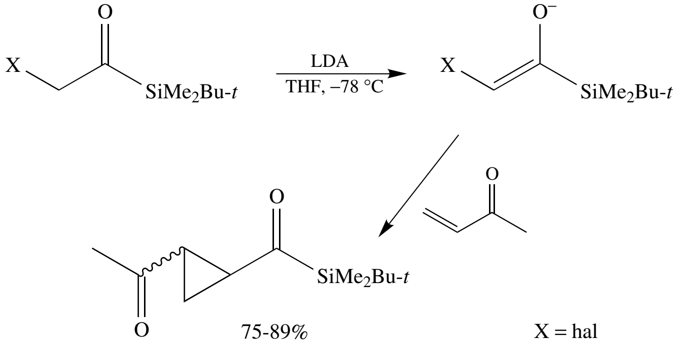

SCHEME 57

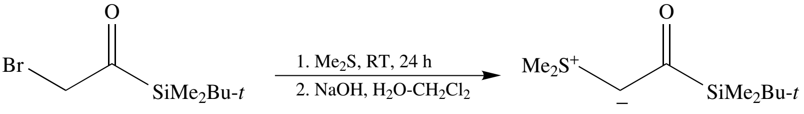

(24)

SCHEME 58

IV. REACTIONS OF ACYL SILANES

A. General Reactivity

Acyl silanes, although sensitive to light and to basic media, behave as typical ketones when treated with a wide variety of reagents. Some examples are shown in Scheme 59[5,149–152].

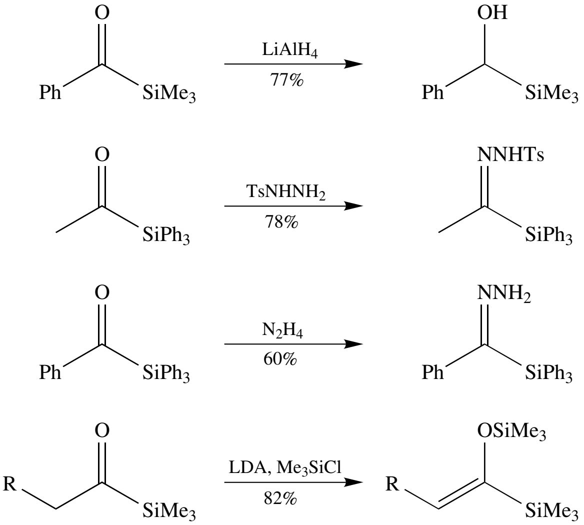

SCHEME 59

Acyl silanes often, however, exhibit abnormal behaviour, for example involving rearrangements leading to silicon–oxygen bond formation, especially when treated with nucleophilic reagents[5,61,149,150].

1. Nucleophilic addition

Acyl silanes are extremely sensitive towards nucleophiles and nucleophilic bases[1,5]; for example, alcoholic solutions of benzoyl triphenylsilane containing a trace of aqueous hydroxide ion rapidly produce triphenylsilanol and benzaldehyde[1,5]. Three reasonable mechanisms may be conceived for this reaction (Scheme 60): S_N2 displacement at the silicon atom (path A); nucleophilic attack at the carbonyl carbon atom followed by Brook rearrangement, initially to give a hemiacetal (path B); and nucleophilic attack at the silicon atom to form a pentacoordinate silicon anionic intermediate, followed by migration of the nucleophile to the carbonyl group and subsequent Brook rearrangement (path C).

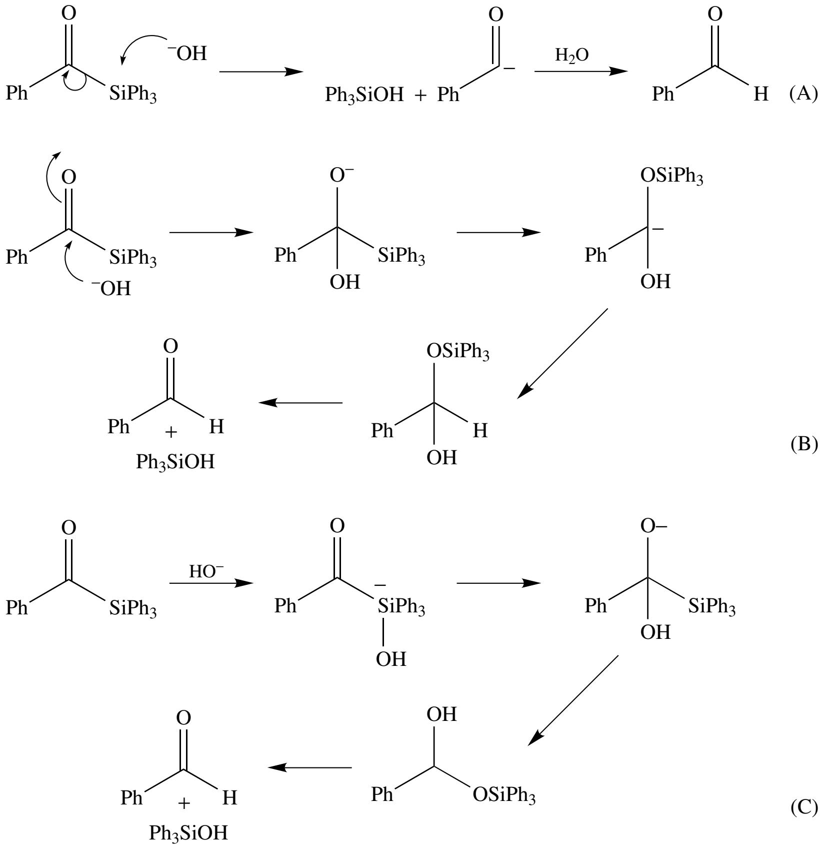

SCHEME 60

The 1,2-migration of a silicon moiety to the oxygen anion of a carbon–oxygen single bond produced by nucleophilic addition to a carbonyl group (Brook rearrangement)[1,5,153,154] is a very common pathway by which acyl silanes react when treated with nucleophiles, the major driving force presumably being formation of the strong Si−O bond. In seminal work, Brook has shown by using various enantiomerically pure acyl silanes, chiral at silicon, that this rearrangement usually occurs with retention of configuration at the silicon atom (*vide infra*)[153]. The stereochemical course of the Brook rearrangement and that of a multitude of other reactions involving nucleophilic additions to silicon atoms can be accounted for if a pentacovalent trigonal bipyramidal silicon intermediate is involved in the substitution process[154b,155]. In the simplest case, inversion of configuration is observed when the intermediate is both formed (**25** → **26**) and undergoes decomposition (**26** → **27**) without pseudorotation taking place (Scheme 61). The base-mediated solvolysis of acyl silanes has been studied in detail by Ricci who, following various kinetic measurements, have suggested that the probable reaction pathway involves direct attack of hydroxide ion at the carbonyl group (Scheme 60, Path B), the rate-determining step being the migration of the trialkylsilyl group from carbon to oxygen[156].

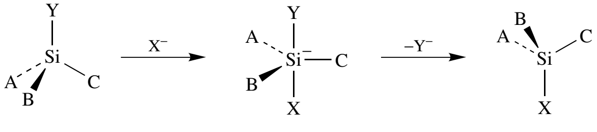

(25) **(26)** **(27)**

SCHEME 61

The reaction of acyl silanes with alkoxide ions has been studied in great detail (Scheme 62)[157,158]. Again, the reaction pathway may be rationalized by invoking a nucleophilic attack by alkoxide ion at the silicon atom of the ketone, giving a pentacoordinate silicon anionic species which can suffer 1,2-migration of an alkyl group from the silicon atom to the carbonyl carbon atom to give the alkoxide ion. This intermediate then undergoes a Brook rearrangement to give the unsymmetrical dialkoxysilane **(28)** after protonation, which is usually the major product. Other reaction products, such as the alcohol **(29)** and the dialkoxysilane **(30)**, arise from a transetherification reaction between the alkoxide ion and the unsymmetrical dialkoxysilane **(28)**. A competing reaction, formally corresponding to nucleophilic displacement of the acyl group from the silicon atom, is also observed. This displacement reaction becomes favoured over rearrangement as the polarity of the solvent system increases[5,159].

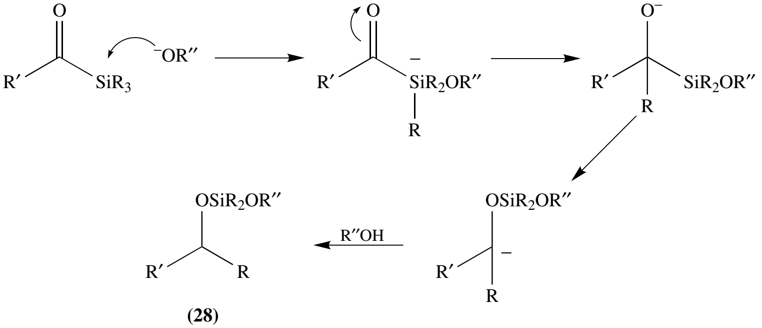

(28)

SCHEME 62

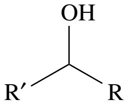

(29)

$SiR_2(OR'')_2$

(30)

Later elegant work by Brook using *t*-butoxide ion and enantiomerically pure acyl silanes led him to suggest that the cleavage products arise from direct attack of the *t*-butoxide ion at the carbonyl group followed by Brook rearrangement[58]. The evidence for this proposal is outlined in Scheme 63 for (*R*)-acetyl 1-naphthyl phenyl methyl silane **(31)**. Should cleavage arise via pentacoordinate anion **32**, without pseudorotation, through attack at silicon, then the (*S*)-*t*-butoxy silane **(33)** would be formed with overall inversion of configuration at silicon relative to starting material. Reduction of **33** would lead, with retention of configuration, to (*R*)-(+)-1-naphthyl phenyl methyl silane (**34**, path B), although experiments have shown that, under the reaction conditions employed by Brook, this reduction is at best very slow. Such rearrangements of alkyl acyl silanes have indeed been observed upon treatment with fluoride ion, giving rearranged secondary alcohols upon desilylation[154b,160].

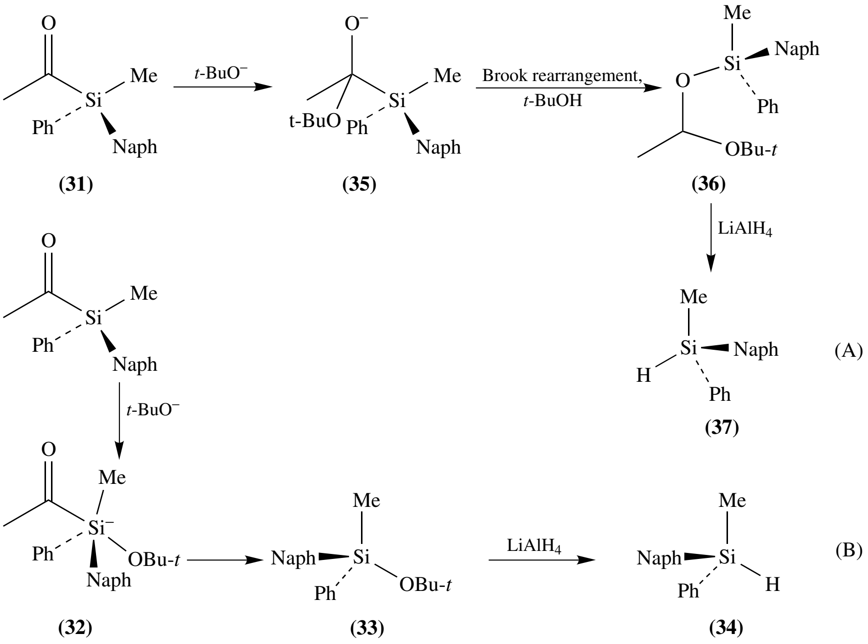

Naph = 1-naphthyl

SCHEME 63

Conversely, were nucleophilic attack of the alkoxide ion to occur at the carbonyl group of **31**, then the species formed **(35)** should undergo Brook rearrangement to **36** with retention of configuration at silicon (Path A). Reduction of **36** with lithium aluminium hydride would then produce (*S*)-(−)-1-naphthyl phenyl methyl silane **(37)**.

When the reaction was carried out, only the (*S*)-(−)-silane **37** was isolated from the reduction products of the reaction mixture, leading Brook to suggest that cleavage occurred through nucleophilic attack of the alkoxide ion at the carbonyl group (Path A). No *t*-butoxysilane was detected among the reduction products. Brook does not discuss the possibility of pseudorotation of **32**, which could lead to (*R*)-*t*-butoxysilane **33** being formed, with overall retention of configuration at the silicon atom, as observed (see Scheme 61). However, the fact that no *t*-butoxysilane was isolated from the reduction products strongly suggests that cleavage does indeed arise through path A. There is in addition the possibility of migration of the *t*-butoxide group from the silicon atom to the carbonyl carbon atom, a sequence which cannot be disproved by these experiments. Such a migration of the *t*-butoxide moiety in **32** seems unlikely, however, as it requires the strong silicon–oxygen bond to be broken[10,75].

In contrast, the carbonyl groups of acyl silanes undergo nucleophilic addition by hydride and by reactive carbon nucleophiles such as Grignard and organolithium reagents to give α-hydroxysilanes. For example, propargyl magnesium, zinc and zinc–copper species add efficiently to aryl and alkyl acyl silanes[161,162], as do allyl magnesium and zinc species, in a reaction used in prostaglandin synthesis[161]. Sila-β-ionone **38**, an intermediate in sila-vitamin A synthesis, has been prepared by addition of an acetylenic Grignard reagent to a cyclic acyl silane[163]. Even Reformatsky reactions are known, although subsequent Brook rearrangement and elimination of trialkylsilanolate, to give alkenes, was observed in some cases (Scheme 64)[164].

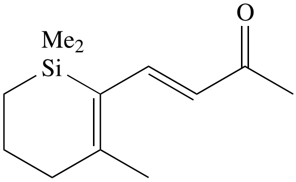

(38)

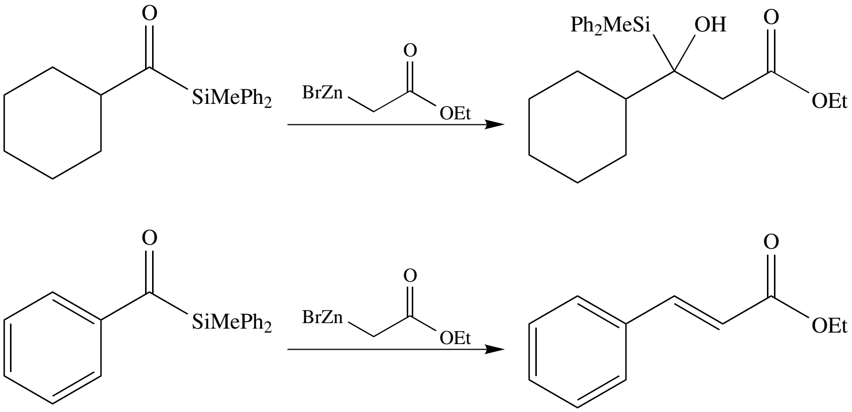

SCHEME 64

Acyl silanes have been used as synthetic equivalents of sterically-hindered aldehydes[165]. Treatment of several aldehydes, including **39** and **40**, with 3-methylpenta-2,4-dienyl lithium gave rise to a mixture of regioisomers. However, when the corresponding acyl silanes **41** and **42** were used, only the conjugated isomers were formed (Scheme 65); selectivity was similar to that observed in the reaction of sterically-hindered ketone **43**. The α-hydroxysilane adducts were readily desilylated with potassium hydride to give the corresponding alcohols, presumably through the Brook rearrangement. Adduct **44** underwent a highly diastereoselective intramolecular Diels–Alder reaction to give alcohol **45** after desilylation without loss of stereochemical integrity (Scheme 66). The authors comment that acyl silanes provide higher overall yields than aldehydes in these reactions as they are less prone to self-condensation and are also superior substrates in that the bulky silyl group may be used for stereocontrol of subsequent reactions.

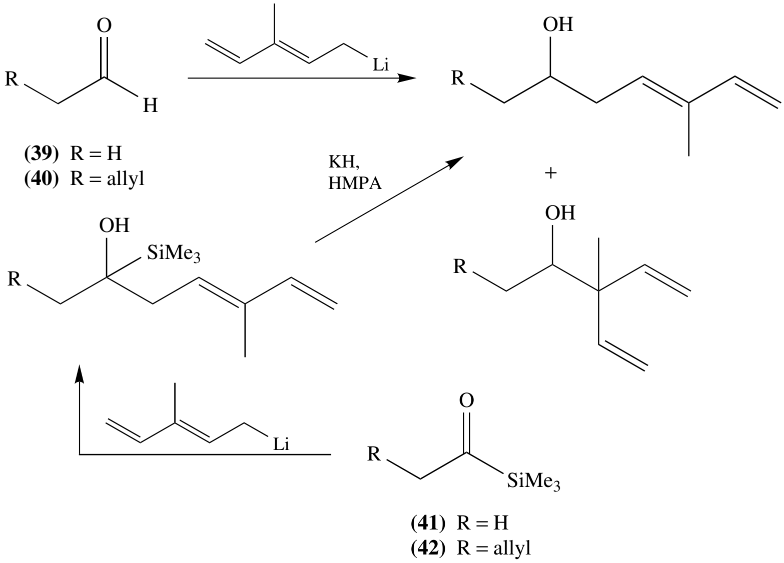

SCHEME 65

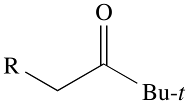

(43)

Kuwajima has used acyl silanes as homoenolate equivalents (Scheme 67)[18,166]. Addition of vinyl Grignard reagents give intermediates which subsequently undergo Brook rearrangement to give the homoenolates **46**. Compounds **46** can undergo a further, irreversible, 1,4-silyl group migration, producing the enolates of β-trimethylsilyl ketones **47**, a side-reaction which may be partially suppressed by keeping the temperature low, by using larger alkyl groups attached to the silicon atom, and by using magnesium

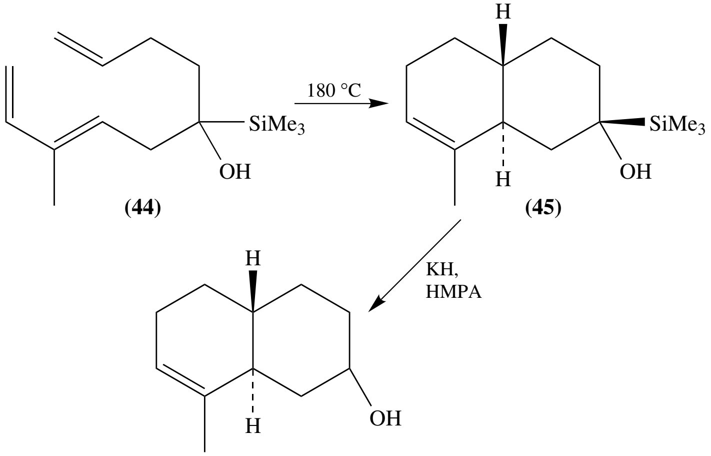

SCHEME 66

instead of lithium enolates. The difference observed between the magnesium and lithium homoenolates may be due to a reduction in the propensity for attack at the silicon atom to form **47**, as a result of the less ionic character of the carbon–magnesium bond. Kuwajima was able to form cuprate reagents from homoenolates **46** by use of copper trimethylsilyl acetylide. The reagents effect various conjugate addition reactions with enones to provide 1,6-dicarbonyl compounds or their equivalents in good overall yields (Scheme 68).

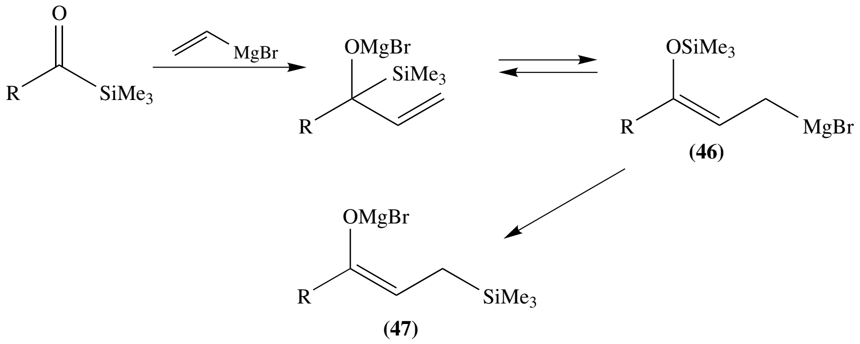

SCHEME 67

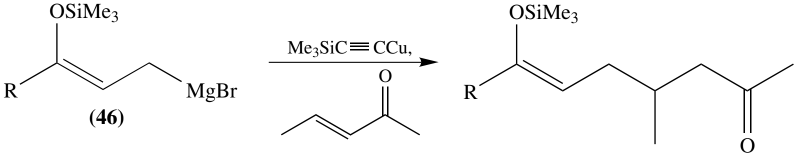

SCHEME 68

The steric bulk of the silyl group in some acyl silanes allows enantioselective reduction of the carbonyl group by asymmetric reducing agents including the Itsuno reagent[167] [a 2 : 1 complex of borane and (*S*)-2-amino-3-methyl-1,1-diphenylbutan-1-ol][168] and di-isopinocampheyl chloroborane/(+)-α-pinene[169,170], often in better than 95% ee. The resulting α-hydroxy silanes could be converted via their acetates into secondary alcohols of high enantiomeric purity by a thermally-induced stereospecific migration of a substituent from silicon to carbon, followed by oxidative desilylation (Scheme 69)[170,171]. This reduction has been used in a synthesis of (+)-sesbanimide[172]. In a derivative process, treatment of acyl silanes with di-isopinocampheyl allyl borane results in enantioselective formation of allylated α-hydroxy silanes, in some cases in high ee[173].

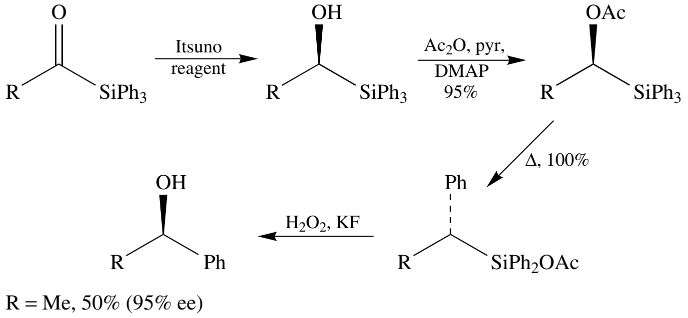

SCHEME 69

Recently, several acyl silanes chiral at silicon have been prepared and shown to undergo diastereoselective addition to the carbonyl groups by hydride, Grignard and organolithium reagents through chelated transition states[174–176]. High diastereoselectivities were observed in some examples, particularly where an alkoxymethyl group was present on the silicon atom (Scheme 70).

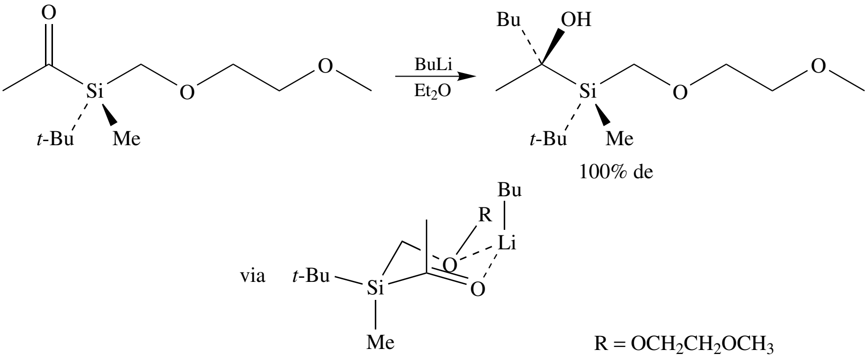

SCHEME 70

Acyl silanes containing chiral centres at the α- and/or β-carbon atoms have also been shown to undergo highly stereoselective addition of organolithium and Grignard reagents, and of various allyl tin and allyl silane reagents in the presence of Lewis acids (Scheme 71). The resulting α-hydroxy silanes, formed in up to 98% yield and with diastereoselectivities up to >100:1, can be protiodesilylated with >99% retention of configuration[177–179].

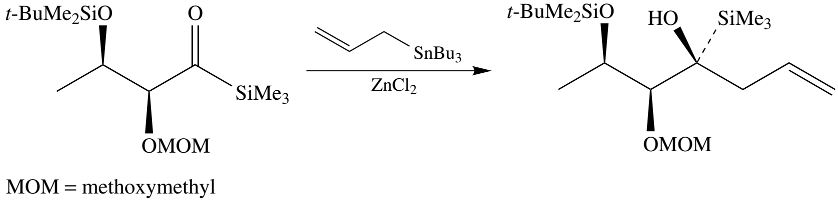

SCHEME 71

Upon treatment with organolithium reagents, α-(phenylthio)acyl silanes give silyl enol ethers with very high *erythro* stereoselectivities (Scheme 72),[180] rationalized by invoking a Felkin–Anh transition state[181]. The alcohols rearrange by a Brook-type migration with concerted expulsion of the phenylthiolate leaving group; because of the stereoelectronic demands of the reaction, the silyl group approaches eclipsing with a hydrogen atom during the reaction pathway leading to carbon to oxygen migration in the major diastereoisomer **48**, but with a benzyl moiety during the reaction pathway leading to the minor, less reactive diastereoisomer **49**.

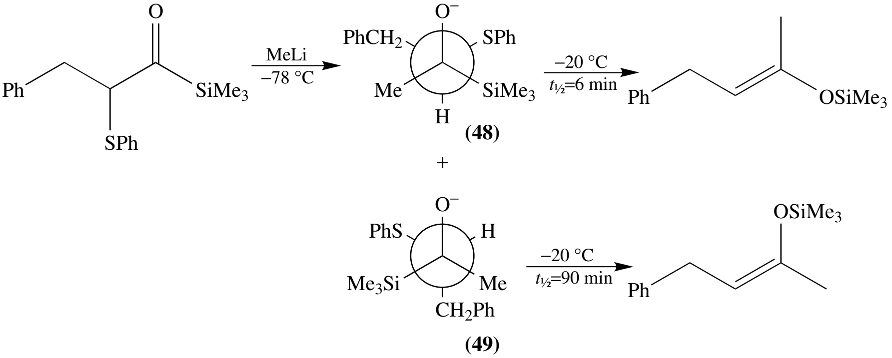

SCHEME 72

Acyl silanes can display disparate behaviour when treated with carbon nucleophiles, even of related types[5,61,149]. For example, when aroyl silanes were treated with a Wittig reagent, none of the expected alkenes was obtained, and the only reaction products isolated were silyl enol ether and triphenylphosphine (Scheme 73)[182,183]. When alkanoyl silanes were treated with Wittig reagents, however, only the normal olefinated vinyl silane products were isolated (Scheme 74)[182–184]. Under soluble lithium salt conditions, *Z*-vinyl silanes were produced with very high selectivities; the reaction was used to prepare a pheromone component **(50)** of the sweet potato leaf folder moth (Scheme 75)[183].

The pattern of results suggest that, if the substituent at the acyl group is alkyl, and hence relatively carbanion-destabilizing, rearrangement is inhibited relative to the alternative 'normal' Wittig reaction pathway; when the substituent is aromatic, however, and therefore capable of stabilizing incipient carbanion formation as the silicon–carbon bond

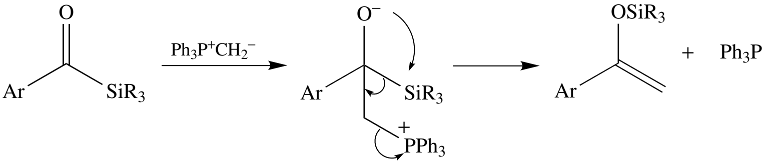

SCHEME 73

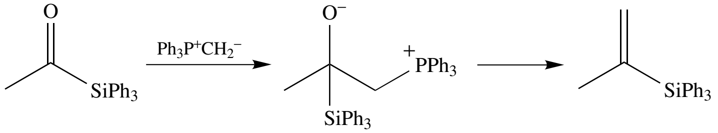

SCHEME 74

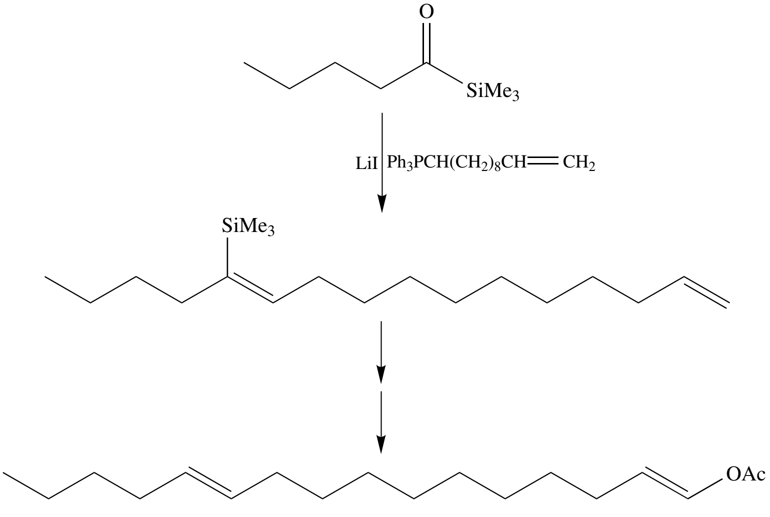

(50)

SCHEME 75

cleaves, rearrangement occurs readily, and the silyl ether product is predominant. Diazomethane reacts in a similar manner[5]. An alkyl acyl silane has been shown to react as a normal ketone with dimethyl titanocene, giving the methylenated vinyl silane product in 65% yield[185].

Sulphur ylids also react with acyl silanes by two different, competing pathways, to give either silyl enol ethers, formed under salt-free conditions, or β-ketosilanes, formed in the presence of soluble inorganic salts (Scheme 76)[186].

In an interesting transformation, reaction of benzoyl trimethylsilane with lithium enolates derived from various methyl ketones gives rise to 1,2-cyclopropanediols, predominantly with the *cis* configuration, in good yields (Scheme 77). The reaction, which proceeds through addition, Brook rearrangement and cyclization, is also successful with α,β-unsaturated acyl silanes (*vide infra*, Section IV.D)[187].

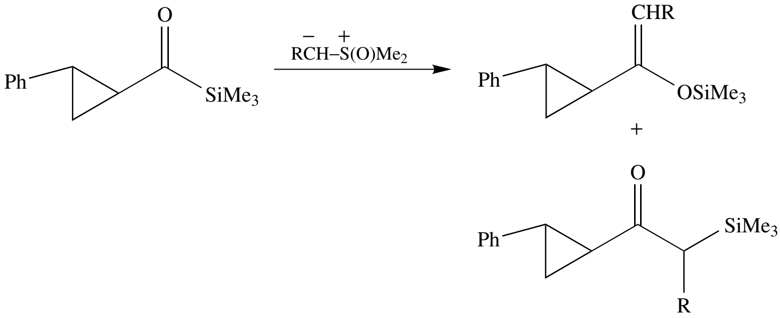

SCHEME 76

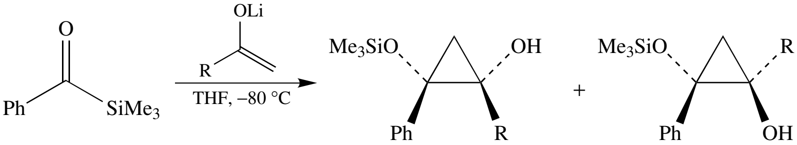

SCHEME 77

Fluoride ion-catalysed addition of trifluoromethyltrimethylsilane to acyl silanes occurs to give 1,1-difluoro-2-trimethylsilyloxyalkenes (silyl enol ethers of difluoromethyl ketones), through nucleophilic addition of trifluoromethyl anion, Brook rearrangement and loss of fluoride. These compounds could be isolated when tetrabutylammonium difluorotriphenylstannate was used as a catalyst; use of tetrabutylammonium fluoride gave the product corresponding to subsequent aldol reaction with the difluoromethyl ketone (Scheme 78)[188].

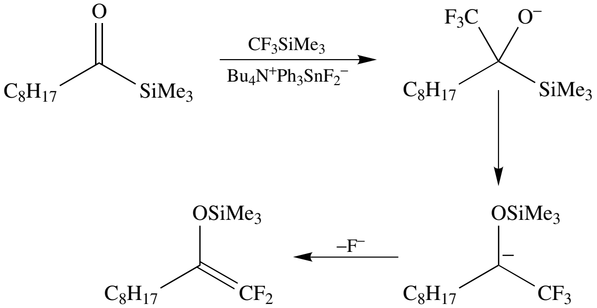

SCHEME 78

A Japanese group have reported an unusual reaction, mediated by lanthanide metals, involving the deoxygenative acylation of diaryl ketones with aryl acyl silanes, to give 1,1-diaryl acetophenones (Scheme 79)[189].

Treatment of α-cyclopropyl acyl silanes with sulphuric or triflic acids results in rearrangements to give cyclobutanones and 2-silyl-4,5-dihydrofurans, respectively, in processes formally involving intramolecular nucleophilic attack at the acyl silane moiety (Scheme 80)[190].

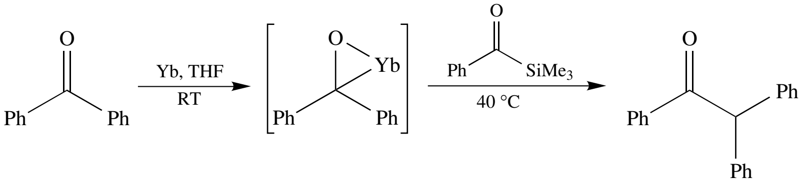

SCHEME 79

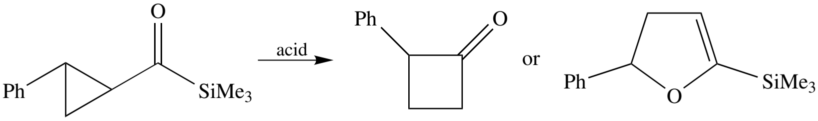

SCHEME 80

2. Acyl silanes as acyl anion precursors

Several aromatic and heterocyclic acyl trimethylsilanes have been used as acyl anion equivalents by treatment with fluoride ion (Scheme 81, path a)[23,133,154b,160,191,192]. Provided that the acyl substituent is electron-withdrawing, and that there are no aryl substituents on the silicon atom, acyl anions can be trapped by various electrophiles in moderate to good yields; indeed, acyl anions and pentacoordinate silicon anionic species have both been detected in gas-phase reactions of acyl silanes with fluoride ion[193].

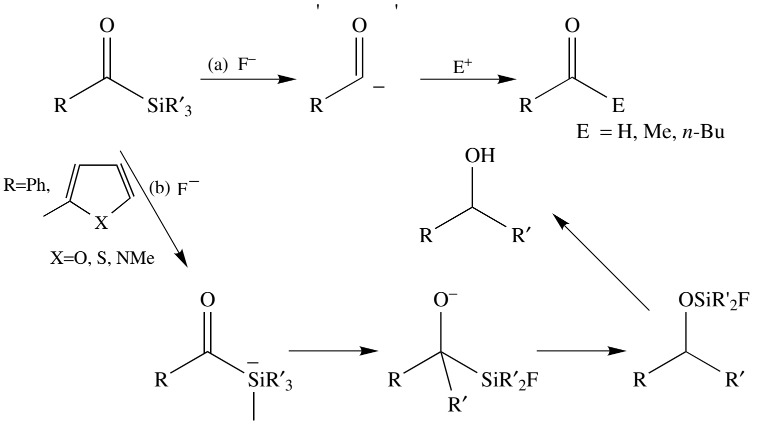

(51)

SCHEME 81

An alternative rearrangement pathway may be observed when the silicon atom bears aryl substituents or when simple alkanoyl trialkylsilanes are used. This pathway is similar to one suggested, but not observed, by Brook for reaction of acyl silanes with alkoxide ions[157,158]. Addition of fluoride ion to silicon induces a migration to the carbonyl carbon atom of one of the groups attached to the silicon atom, to give **51**, followed by a Brook-type rearrangement, giving a rearranged alcohol after protic work-up (Scheme 81, path b)[154b,160]. The acyl anion reaction pathway may only be observed for these substrates at higher temperatures in the presence of acid. Both pathways may proceed via a pentacoordinate silicon anionic species as a common intermediate.

Remarkably, carbonyl bis(trimethylsilane) can act as a source of the CO^{2-} dianion in the presence of fluoride ion (Scheme 82)[13].

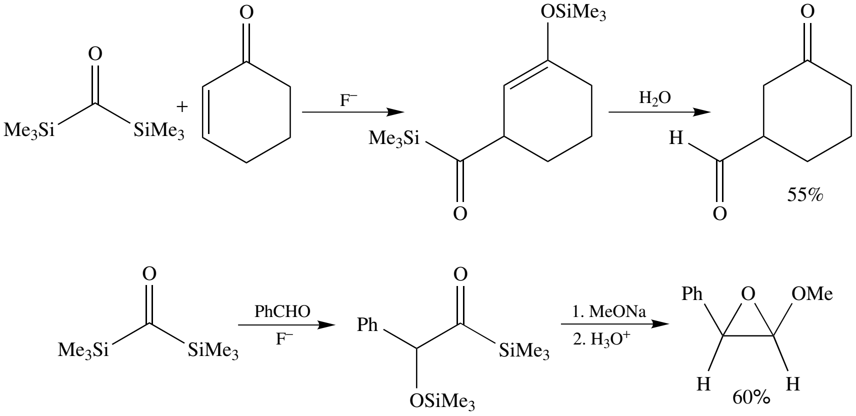

SCHEME 82

3. Cyclization reactions

A number of types of cyclization reaction have been reported in which the reactivity of the acyl silane grouping is a factor in the transformation. These are discussed below.

Molander and Siedem have reported the reaction of 1-methoxy-1,3-bis(trimethylsilyloxy)-buta-1,3-diene, the bis(trimethylsilyl) enol ether of methyl acetoacetate, with 1,4- and 1,5-dicarbonyl species under the influence of trimethylsilyl triflate. Two regioisomeric oxabicyclo[3.2.1]octane products are formed (Scheme 83)[194]. Use of 4- or 5-ketoacyl silanes as the dicarbonyl species can result in a reversal of the sense of regioselectivity.

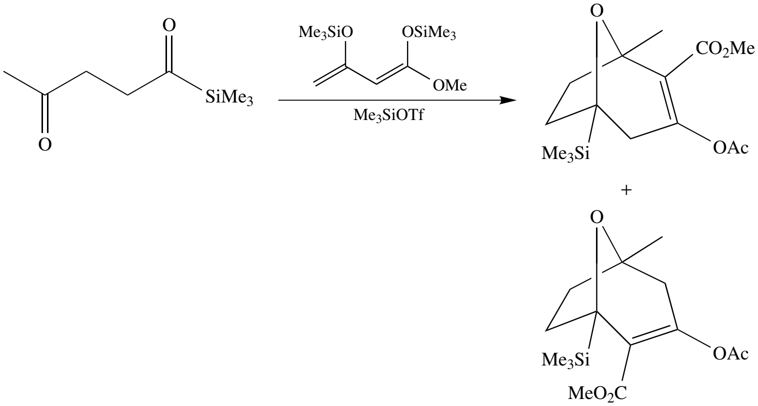

SCHEME 83

Heating 4- and 5-bromoacyl silanes at 100 °C in a polar aprotic solvent induces cyclization through the enol forms to give 2-silyldihydrofurans and 2-silyldihydropyrans, respectively[195]. Similar transformation of 4- to 7-halothioacyl silanes, prepared from the corresponding haloacyl silanes by reaction with hydrogen sulphide, but induced by sodium hydroxide, gave the 2-silylated sulphur heterocycles in excellent yields (Scheme 84)[196]. Intermolecular enolate reactions of acyl silanes are also known (*vide infra*, Section IV.A.6).

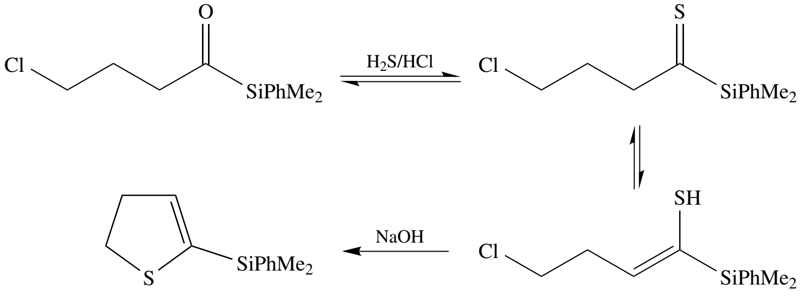

SCHEME 84

5- and 6-haloacyl silanes also undergo radical-mediated cyclization with Brook-type migration of the silyl radical moiety to give the cyclized silyloxy radical intermediates[197], which may in turn undergo further reaction in a tandem process, for example to form spiro or fused bicyclic products (Scheme 85)[198,199]. The acyl silane unit is thus acting as a formal geminal diradical species. An interesting development of this reaction includes a stannyl group at the halo- (or xanthate-) bearing carbon atom, cyclization of an α-stannyl radical then resulting in formation of an α-stannylated silyloxy radical, from which the stannyl unit is lost, providing a regiospecific synthesis of cyclic silyl enol ethers (Scheme 86)[200].

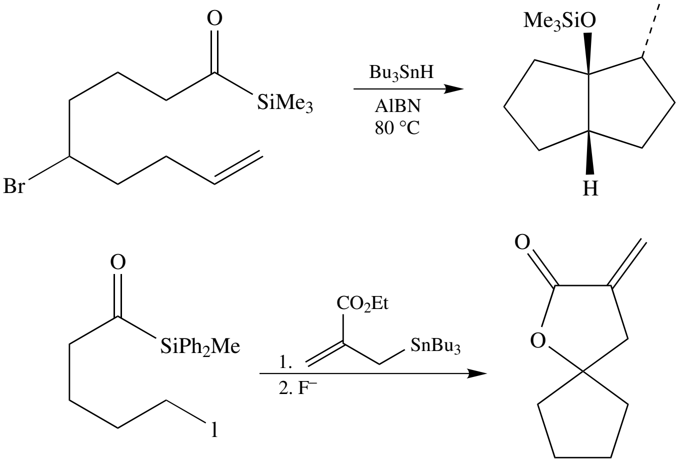

SCHEME 85

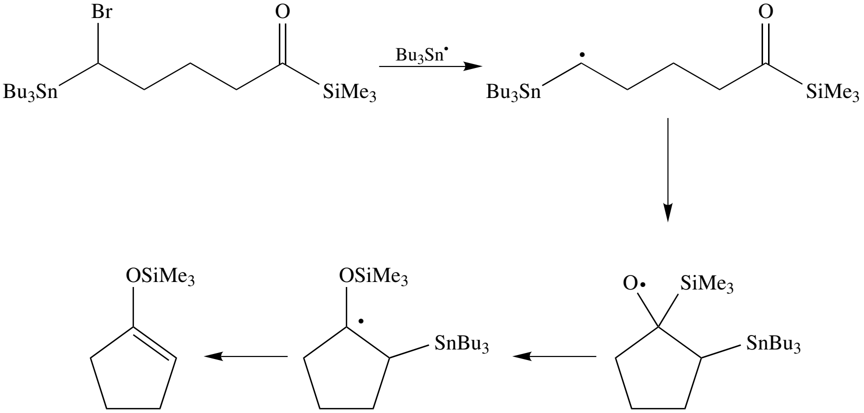

SCHEME 86

Cycloaddition reactions of acyl silanes appear to be rare, but Brook has shown that α-silyloxy bis(trimethylsilyl)silenes **(52)**, generated photochemically from acyl tris(trimethylsilyl)silanes (*vide infra*, Section IV.A.4), undergo [2 + 2] and [4 + 2] cycloaddition reactions with ketones, and [4 + 2] cycloaddition reactions with less bulky acyl silanes, as illustrated in Scheme 87[17,24,26,72,73,201]. They do not, however, react with their parent acyl tris(trimethylsilyl)silanes.

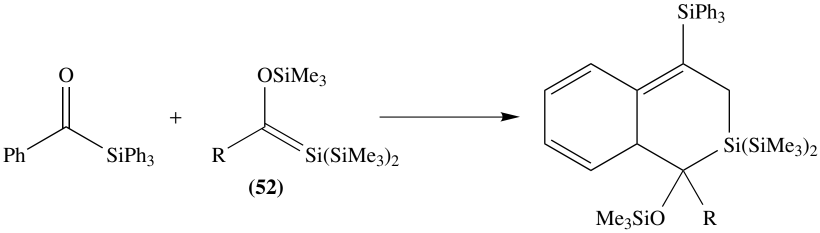

SCHEME 87

4. Photochemistry

Acyl silanes display a range of behaviour upon irradiation, depending upon their structure and the reaction conditions. The interesting photochemistry displayed by acyl silanes has been attributed to the low-energy n → π^* carbonyl group transition.

Brook has shown that a wide variety of acyl tris(trimethylsilyl)silanes and acyl alkyl bis(trimethylsilyl)silanes undergo clean 1,3-rearrangements of silyl groups from silicon to oxygen to give α-silyloxy silenes upon irradiation, in an analogue of photoenolization (Scheme 88). Many of the silenes are remarkably stable and even recrystallizable[17,24,26,72,73]. They may undergo head-to-head or head-to-tail [2 + 2] dimerization to give 1,2- or 1,3-disilacyclobutanes, dependent upon the nature of the alkyl groups present[26], and, while α-silyloxy bis(trimethylsilyl)silenes **(52)** do not cycloadd to their parent acyl tris(trimethylsilyl)silanes, they do cycloadd to less bulky acyl silanes (Scheme 87)[202]. The structures of several 1,3-disilacyclobutanes have been determined by X-ray crystallography[201].

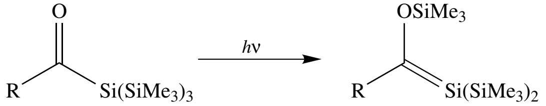

SCHEME 88

Acyl silanes react readily in alcoholic solution upon near-visible irradiation[203]. In the absence of base, the reaction process involves cleavage of the acyl–silicon bond to give a silyl ether and an acetal. Silanol and aldehyde may also be isolated. The proposed mechanism, suggested following experiments involving an enantiomerically pure acyl silane, is shown in Scheme 89[5]. Although also proceeding through a carbene intermediate, quite distinct from this process is the near-quantitative formation of mixed acetal which occurs upon irradiation of an alcoholic solution of an acyl silane in the presence of traces of base (typically pyridine)[5]. In this case, the acetal is formed by the photochemical generation of a silyloxycarbene from the acyl silane, which then inserts into the O—H bond of a solvent molecule (Scheme 90). Dalton has examined the kinetics of the latter reaction and have confirmed that acetal formation occurs exclusively through reaction of alcohol with an intermediate presumed to be the silyloxycarbene, generated from the acyl silane T1 state[204].

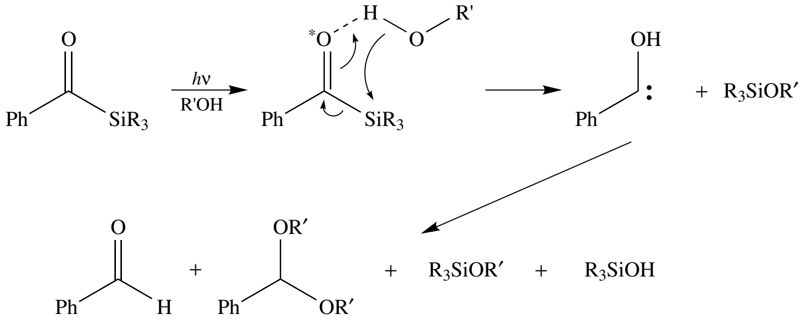

SCHEME 89

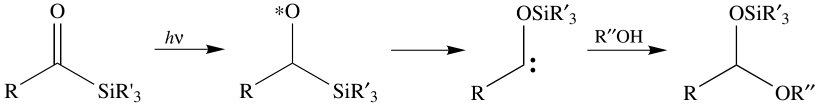

SCHEME 90

Silyloxycarbenes are also formed on heating acyl silanes; intramolecular C—H bond insertion may then occur, as illustrated in Scheme 91[205]. Such an intramolecular insertion reaction of a silyloxycarbene generated from *ortho*-tolyl acyl trimethylsilane has been investigated as a potential route to benzocyclobutenols (Scheme 92)[206]. The unstable benzocyclobutenol silyl ether (**53**), however, underwent ring opening and further rearrangement as shown, to give the aldehyde **54** in good yield.

2-(Diphenylsila)cyclohexanone, an unusual cyclic acyl silane, has been found to undergo photo-oxidation promoted by ambient light to produce the silicon-containing lactone **55**. 1,1-Diphenylsilacyclohexanone was stable in the presence of oxygen in the

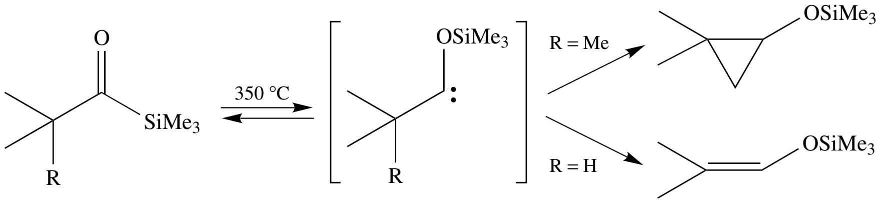

SCHEME 91

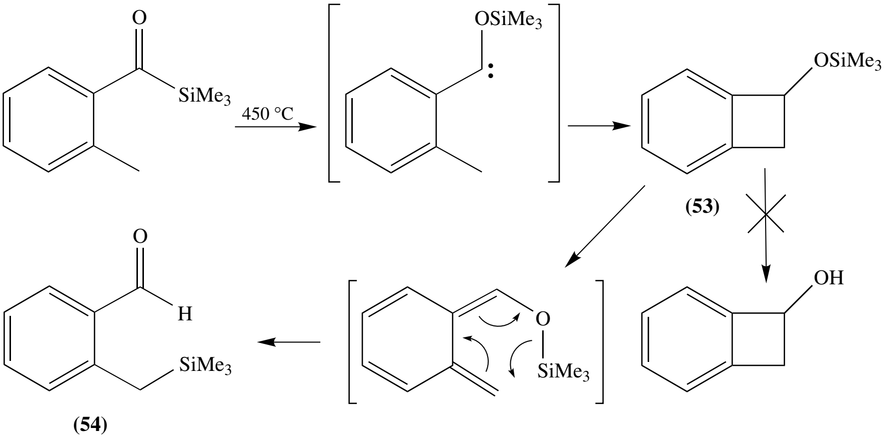

SCHEME 92

absence of light over long periods; subsequent investigations have demonstrated that this photo-oxidation is typical of other alkyl acyl silanes, but that aryl acyl silanes are inert[5]. The lactone **55** was hydrolysed to give a δ-(hydroxysilyl) carboxylic acid (Scheme 93)[5,60].

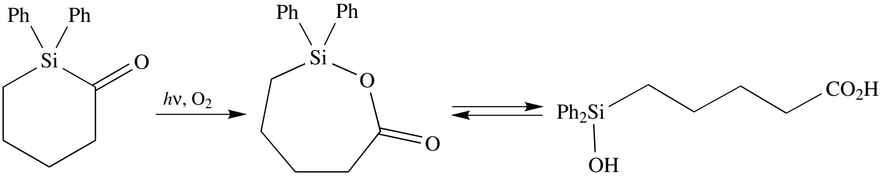

(55)

SCHEME 93

The terpene-derived acyl silane **56** undergoes a Norrish type II cleavage reaction as the major pathway upon n $\rightarrow$ π^* excitation, involving hydrogen abstraction and fragmentation to give an acetyl silane and a diene as the major products (Scheme 94)[33]. The corresponding ketone **(57)** behaves in an analogous manner. Acyl silane **56** also displays typical photochemical behaviour, undergoing rearrangement to the silyloxycarbene **58**. Insertion of **58** into the O−H bond of the enol **59** led to compound **60** among others (Scheme 95). The silyloxycarbene **58** therefore reacts through intermolecular insertion into the O−H bond rather than by insertion into a neighbouring C−H bond or intramolecular addition to a carbon−carbon double bond.

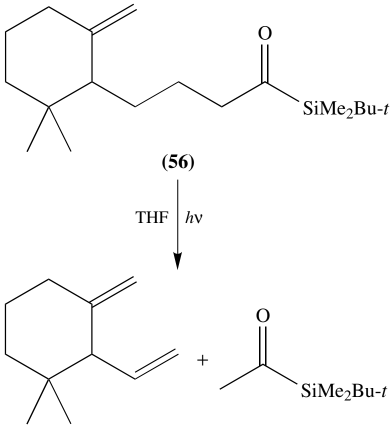

SCHEME 94

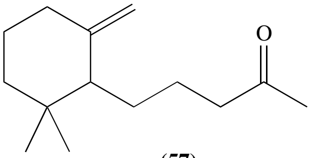

(57)

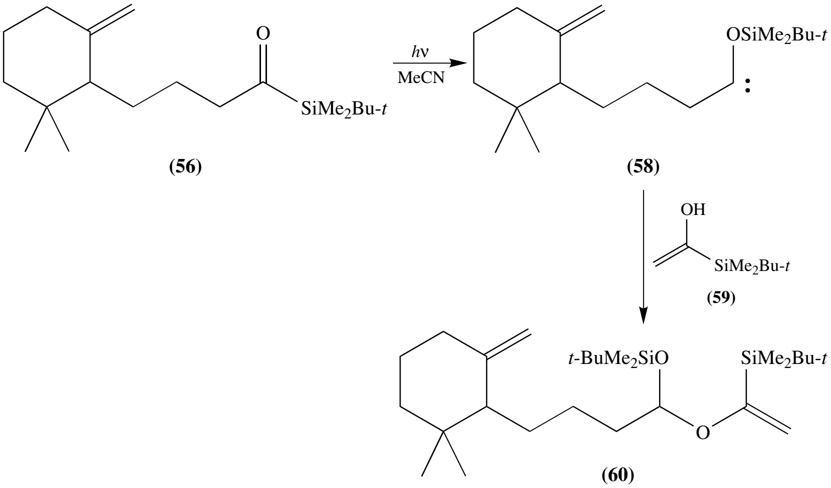

SCHEME 95

In a further unusual process, irradiation of α,β-epoxyacyl silanes in acetonitrile induces cleavage to give a silylketene species and a ketone, with quantitative conversion[207]. The initial step of the mechanism is presumably analogous to the α-(C—O) bond cleavage of α,β-epoxymethyl ketones (Scheme 96).

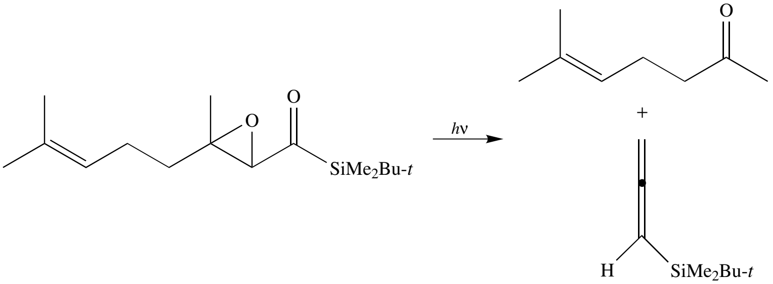

SCHEME 96

5. Biotransformations

A number of reductive biotransformations of acyl silanes into α-hydroxy silanes have appeared recently. Acetyl dimethylphenylsilane is converted into (*R*)-(1-hydroxyethyl) dimethylphenylsilane by plant cell suspension cultures of *Symphytum officinale* L. and *Ruta graveolens* L. in low yields but in 81% ee and 6% ee, respectively[208]. Silanol and disiloxane were observed as by-products. Microbial reduction of racemic acetyl *t*-butyldimethylsilane has been achieved using *Trigonopsis variabilis* (DSM 70714) and *Corynebacterium dioxydans* (ATCC 21766) on a 10- gramme scale with > 96% ee in each case and in up to 78% yield[209a]. Recently, *Saccharomyces cerevisiae* (DHWS 3), a commercially available form of bakers' yeast, has been shown to reduce acetyl dimethylphenylsilane, again to (*R*)-(1-hydroxyethyl) dimethylphenylsilane, in 40% yield and >99.5% ee[209b].

6. Miscellaneous

Intramolecular alkylation of the enol forms of 4- and 5-bromoacyl silanes has been observed upon heating at 100 °C in a polar aprotic solvent, inducing cyclization to give 2-silyldihydrofurans and 2-silyldihydropyrans, respectively[195]. Similar transformation of the thiono analogues, 4- to 7-halothioacyl silanes, induced by sodium hydroxide, gave the 2-silylated sulphur heterocycles in excellent yields (*vide supra* Section IV.A.4)[196].

Enolates or enol ethers derived from acyl silanes have been used by several groups as reagents for stereoselective aldol condensations[19,210,211]. Acyl silanes, treated with LDA followed by aldehydes, give aldol products in up to > 20 : 1 selectivity in favour of the *syn* products (Scheme 97)[19]; increasing steric bulk around the silicon atom appears to give increased selectivities. Product mixtures were analysed as the carboxylic acids. A similar scheme using acyl silanes chiral at silicon, however, gave an anomalous reaction resulting from aldol reaction as desired followed by Cannizaro-type hydride transfer processes (Scheme 98)[211].

Silyl enol ethers of acyl silanes have been used in Lewis acid-mediated Mukaiyama reactions with acetals. Treatment of the resulting β-alkoxy acyl silanes with tetrabutylammonium hydroxide or tetrabutylammonium fluoride gave the corresponding α,β-unsaturated aldehydes (Scheme 99)[210].

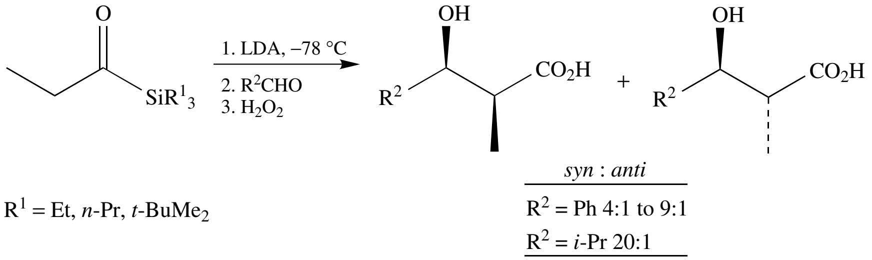

SCHEME 97

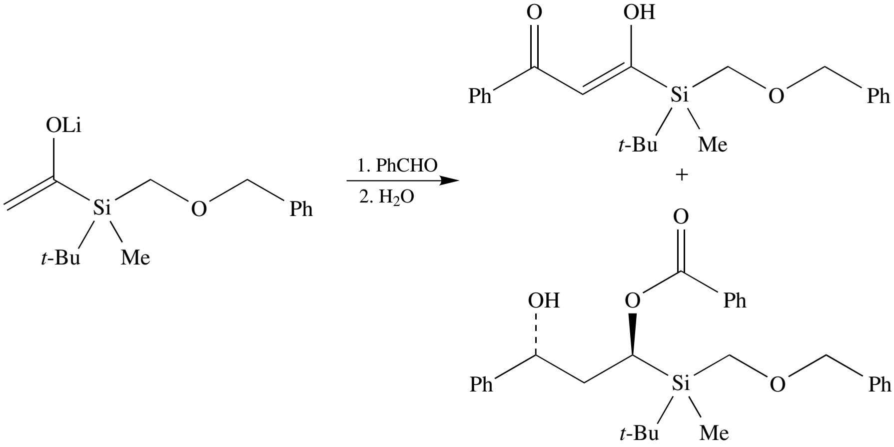

SCHEME 98

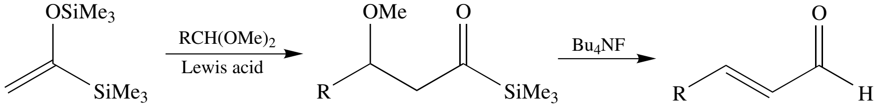

SCHEME 99

Reductive cleavage of the carbon−silicon bond of acyl silanes, including α-alkoxy and α,β-dialkoxy derivatives, to give aldehydes may be accomplished by palladium-catalysed hydrogenolysis at ambient temperature and pressure[212].

The electrochemical oxidation of acyl silanes has been investigated, giving rise to esters and amides when carried out in the presence of alcohols and amines. The oxidation potentials of acyl silanes proved to be much lower than those of the corresponding ketones[213].

Bis(trimethylsilyl) sulphide reacts with acyl silanes in the presence of a cobalt chloride catalyst to afford the corresponding thiocarbonyl derivatives, thioacyl silanes (Scheme 100)[214]. The reaction is mild and proceeds in good yields. It is also applicable to aldehydes. Thioacyl silanes have been prepared from the corresponding haloacyl silanes by reaction with hydrogen sulphide (*vide supra*, Section IV.A.3)[196].

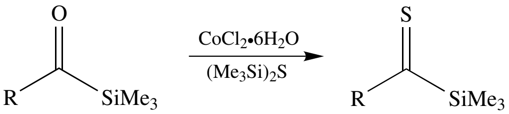

SCHEME 100

Acyl silanes react with ytterbium by two different pathways, depending upon structure. Aroyl silanes undergo reductive coupling to produce diaryl acetylenes, while alkanoyl silanes give the product of carbonyl group reduction (Scheme 101)[215]. Benzoyl silanes react with benzylmanganese pentacarbonyl to give *ortho*-metallated tetracarbonyl manganese complexes, which could be desilylated to give the previously inaccessible benzaldehyde complex[216].

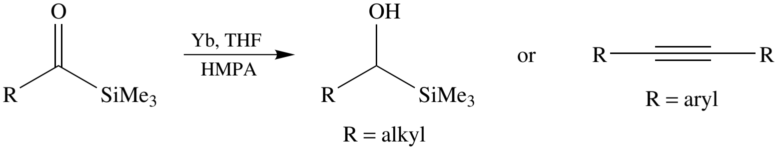

SCHEME 101

B. α-Haloacyl Silanes

α-Chloroacyl silanes react with Grignard reagents by initial addition to the carbonyl group as expected, followed not by Brook rearrangement, but by 1,2-migration of silicon with expulsion of halide ion to afford α-silyl ketones (Scheme 102)[12,151,152]. α-Haloacyl silanes therefore behave as α-trimethylsilyl acylium ion **(61)** equivalents in this reaction. The 1,2-rearrangement may be accelerated compared with the lithium analogue by the more polar character of the oxygen−magnesium bond[217,218].

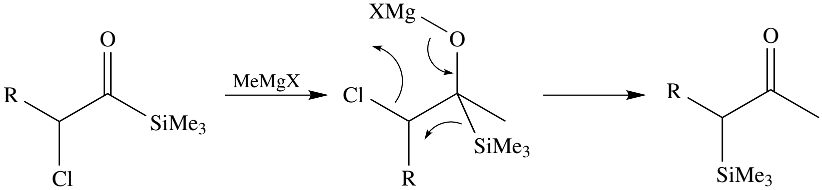

SCHEME 102

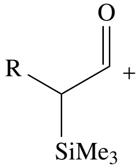

(61)

Further addition of the Grignard reagent can take place to give β-hydroxy silanes with high diastereoselectivity (Scheme 103)[12,165]. The hydroxy silanes can of course undergo subsequent stereocontrolled acid or base catalysed elimination of trialkylsilanol to give alkenes.

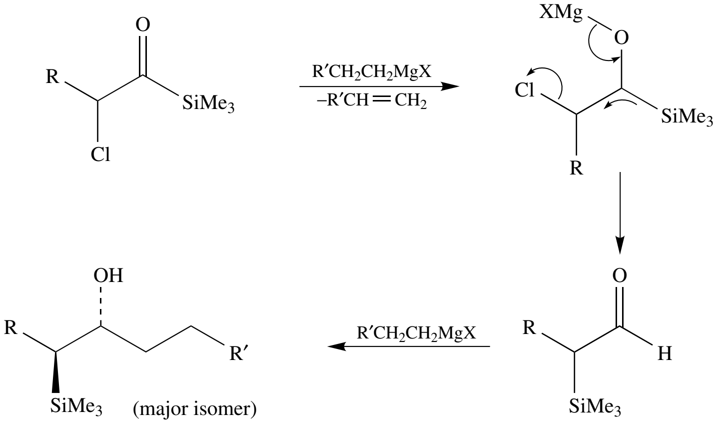

SCHEME 103

Similar reactions of α-haloacyl silanes take place with enolates (Scheme 104)[219].

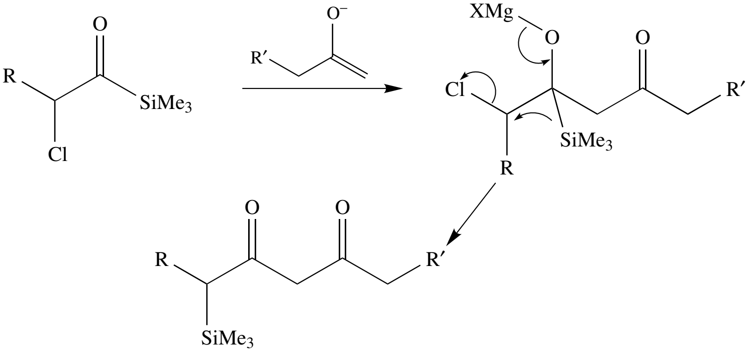

SCHEME 104

It is fascinating that a completely different reaction pathway takes over for trifluoroacetyl silanes. In this case, initial addition of Grignard reagent, in THF solution, to the carbonyl group of the acyl silane is followed by Brook rearrangement, as might be expected from general patterns of acyl silane reactivity. Elimination of fluoride ion then occurs to give 1-silyloxy-2,2-difluoroalkenes (silyl enol ethers of difluoromethyl ketones)[220,221]. The same type of intermediates and subsequent reaction are of course seen in the addition of trifluoromethyl anion to alkanoyl silanes (*vide supra*, Section IV.A.1)[188]. The reaction was applied to a synthesis of a fluorinated brassinosteroid. Similar reaction of vinyl magnesium bromide with trifluoroacetyl triphenylsilane gives rise to 1,1-difluoro-2-triphenylsilyloxybuta-1,3-diene (**62**, Scheme 105) which has been used in a number of [4 + 2] and [2 + 2] cycloadditions[222].

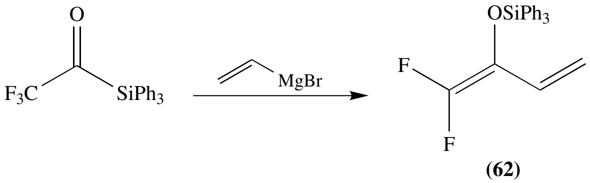

(62)

SCHEME 105

The related Brook rearrangement of α-halo-α,β-unsaturated acyl silanes produces silyloxy allenes **(63)**, from which several sesquiterpenes have been synthesized (Scheme 106)[21]. Silyloxy allenes may also be prepared by the alkylation of silyloxy allenyl lithium reagents; the acyl silane route is, however, less sensitive to solvent effects and other experimental parameters. An outline of the synthesis of dehydrofukinone **(64)**, which elegantly exemplifies this methodology, appears in Scheme 107.

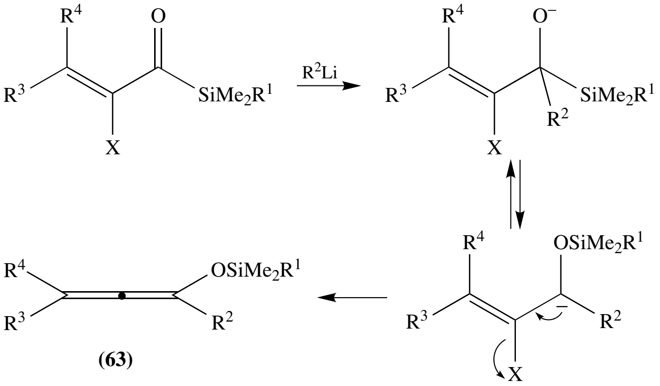

(63)

SCHEME 106

α-Phosphonoacyl silanes, which may be prepared from α-iodoacyl silanes through the Arbuzov reaction, undergo enolate alkylation, and are precursors of α,β-unsaturated acyl silanes through the Horner–Emmons reaction (*vide supra*)[116]; α-haloacyl silanes are also precursors of cyclopropyl acyl silanes through conversion into sulphur ylids and through McCoy reactions (*vide supra*)[146].

C. α-Ketoacyl Silanes

α-Ketoacyl silanes are a deep rich red in colour and are especially sensitive to light, often necessitating purification and handling in a darkened room. Very little chemistry of these interesting materials has been reported, although they are implicated as intermediates in the oxidation of trimethylsilyl acetylenes with osmium tetroxide to give α-ketoesters (Scheme 108)[7,125].

D. α,β-Unsaturated Acyl Silanes

A good deal of chemistry of α,β-unsaturated acyl silanes has been published, perhaps reflecting their added stability over other types of acyl silane. Much of this chemistry

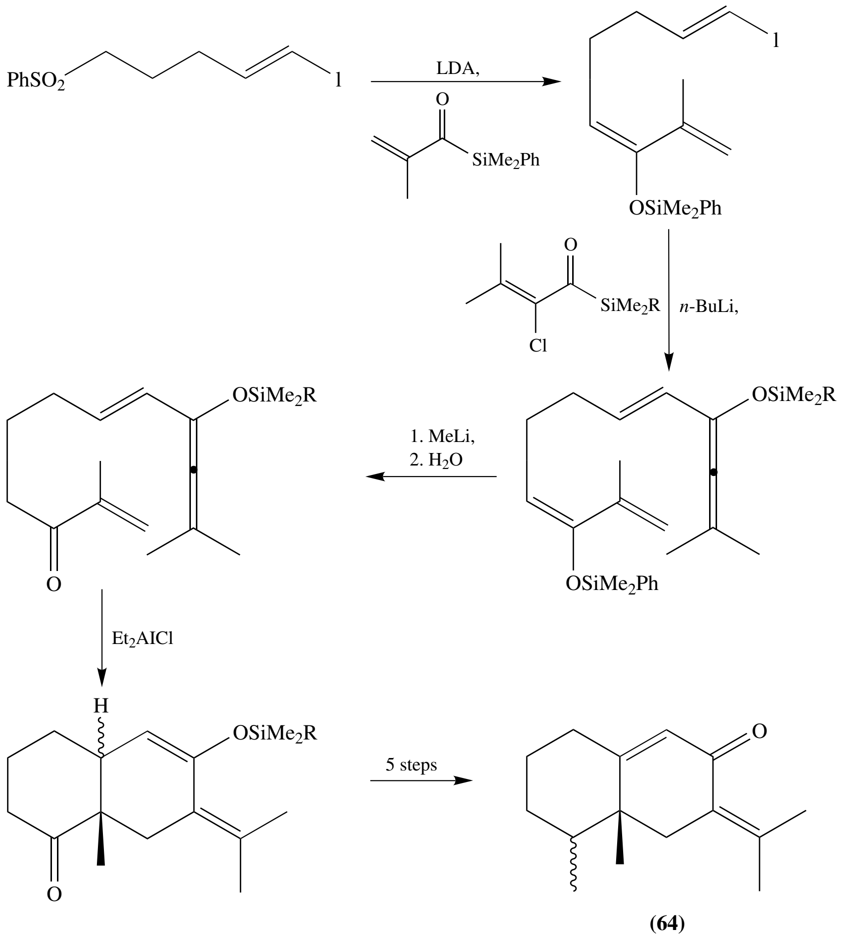

(64)

SCHEME 107

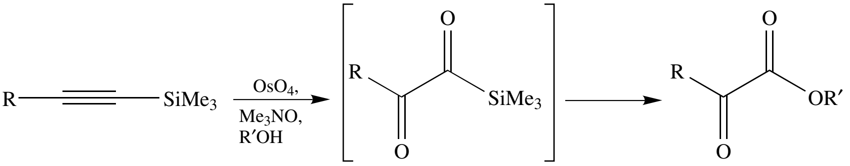

SCHEME 108

involves conjugate addition or cycloaddition involving the carbon–carbon double bond. In one exception, reaction of lithium enolates derived from various methyl ketones with but-2-enoyl *t*-butyldimethylsilane gives rise to *cis* vinyl 1,2-cyclopropanediols through addition to the carbonyl group, Brook rearrangement and cyclization, as well as to the conjugate addition products (Scheme 109). The reaction is also successful with simple aroyl silanes (*vide supra*, Section IV.A.1)[187]. Wittig reactions have also been carried out with the carbonyl group of α,β-unsaturated acyl silanes. Desilylation gives the E-alkene, in contrast to the Wittig reaction of the related aldehydes[137].

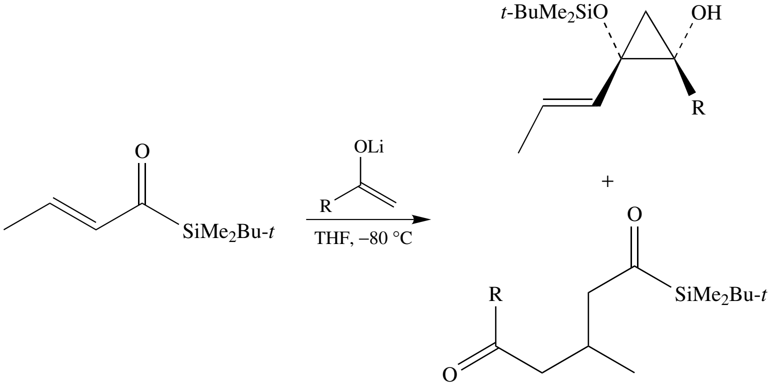

SCHEME 109

α,β-Unsaturated acyl silanes are oxidized to carboxylic acids by alkaline hydrogen peroxide[133], and can therefore be regarded as α,β-unsaturated carboxylic acid equivalents. They have been so used in Lewis acid-mediated conjugate allylation reactions with allyl silane derivatives (Scheme 110)[62,116,141]. The acyl silanes are highly reactive, and the authors suggest that they are much more electrophilic than the corresponding carboxylic acids and esters due to the net destabilizing effect of trialkylsilyl groups on developing α-carbocationic centres in the reaction intermediates[30].

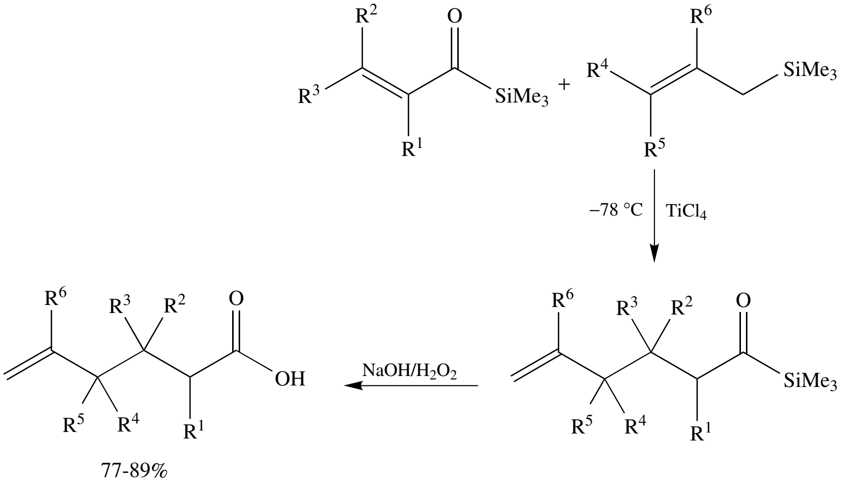

SCHEME 110

The Degl'Innocenti group has published a number of reactions of α,β-acetylenic acyl silanes, mostly involving initial conjugate addition to give α,β-unsaturated acyl silanes with a range of substituents[136]. For example, reaction with dialkyl, diaryl and divinyl lithium cuprates provides β-substituted α,β-unsaturated acyl silanes in high yields[137]. Heteroatomic β-substituents, including β-halo, β-amino, β-thio and β-azido groupings, may be introduced by the use of heterosubstituted trimethylsilanes as reagents[138,140]. Conjugate addition of a tributyltin unit has also been carried out, using a lithium tributylstannyl cuprate species[139].

3-Iodopropenoyl triphenylsilane takes part in palladium-catalysed coupling with alkyl tin derivatives to give β-substituted α,β-unsaturated acyl silanes, normally with the *E* configuration[140]. In a nicely complementary process, 3-(tributylstannyl)prop-2-enoyl triphenylsilane takes part in palladium-catalysed coupling with vinyl iodides (*vide supra*, Section III.D.4)[139]. Interestingly, the compound is also capable of acting as a nucleophile at the 2-position.

3,3-Dichloropropenoyl trimethylsilane, prepared by photochemically induced addition of bromotrichloromethane to the ethyl enol ether of acetyl trimethylsilane, undergoes completely regioselective addition–elimination upon treatment with lithium cyanocuprate reagents, giving the *E*-3-chloroalk-2-enoyl silane products (*vide supra*, Section III.D.3)[135].

Some β-heteroatom substituted α,β-unsaturated acyl silanes react with methyl ketone enolates in a stepwise stereoselective cyclopentannelation process, formally a [3 + 2] annelation, which may proceed through aldol reaction followed by Brook rearrangement and cyclization (Scheme 111)[223].

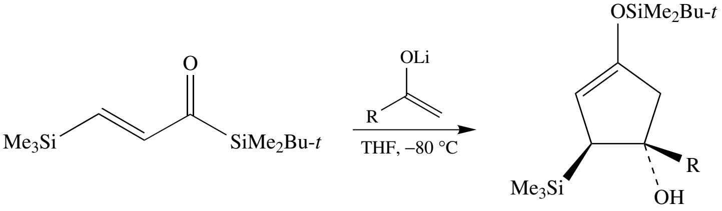

SCHEME 111

α,β-Unsaturated acyl silanes also combine with allenyl silanes in the presence of $TiCl_4$ in [3 + 2] and [3 + 3] annelations to give five- and six-membered carbocycles (Scheme 112)[141]. It is particularly interesting that the course of these reactions may be controlled to produce either five- or six-membered rings as desired by manipulating the trialkylsilyl group, the reaction temperature and the nature of the acyl group. Following regiospecific electrophilic substitution at C-3 of the allenyl silane, cyclization of a rearranged vinyl cationic intermediate (**65**) provides the cyclopentene **66**. If R^1 is alkyl, R_3Si is trimethylsilyl, and the reaction is carried out at elevated temperature, cyclopentene **66** can undergo a ring expansion to give the six-membered carbocyclic cation **67**, which undergoes a second 1,2-cationic shift of the trimethylsilyl moiety to produce the cyclohexenone **68**. This transformation can be prevented by employing the less mobile *t*-butyldimethylsilyl acyl silanes, by maintaining the reaction temperature below −78 °C and by minimizing the reaction time.

The first recorded cyclopropyl acyl silane (**69**) was generated by vapour phase pyrolysis of a pyrazoline derived from α,β-unsaturated acyl silane by 1,3-dipolar cycloaddition of diazomethane (*vide supra*, Section III.E)[141]. Exposure of **69** to titanium tetrachloride induced ring expansion to give the cyclobutanone in 75% yield (Scheme 113).

The Diels–Alder reactivity of α,β-acetylenic and α,β-unsaturated acyl silanes is comparable to that of the related methyl ketones, and such reactions have been used to prepare other α,β-unsaturated acyl silanes. For example, the α,β-acetylenic acyl silanes

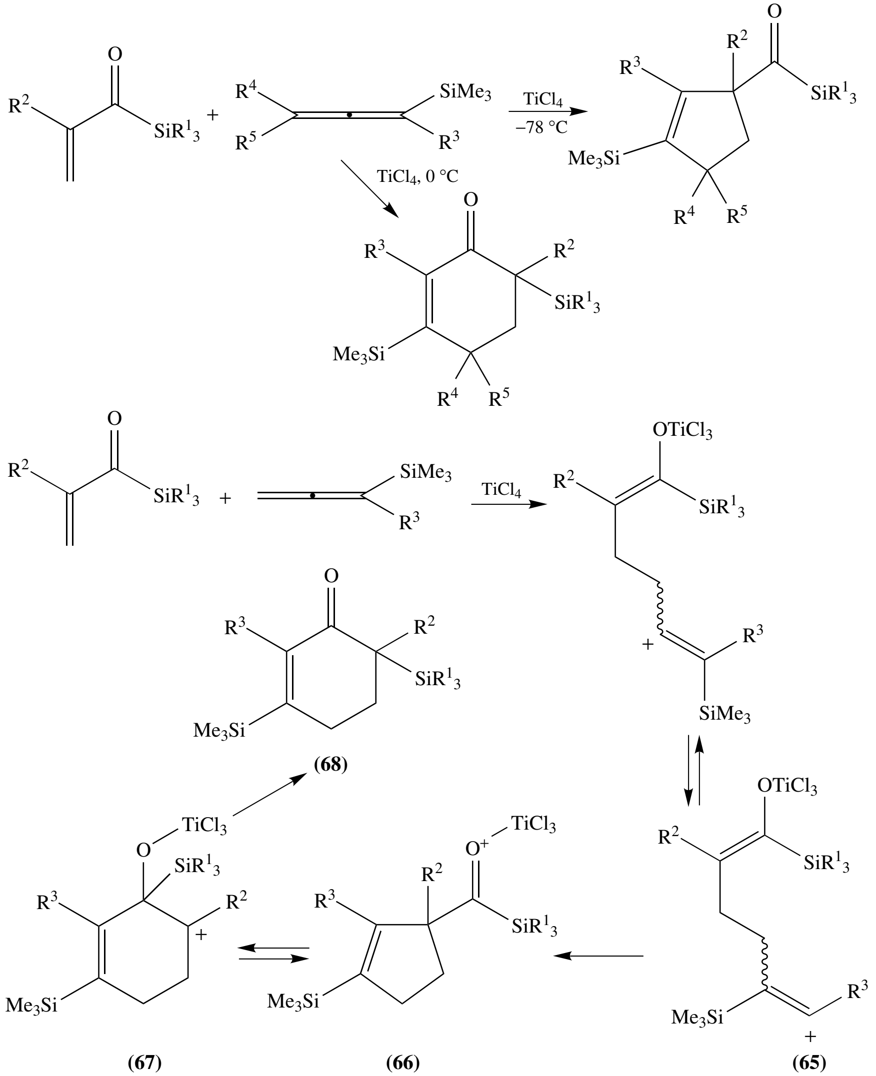

SCHEME 112

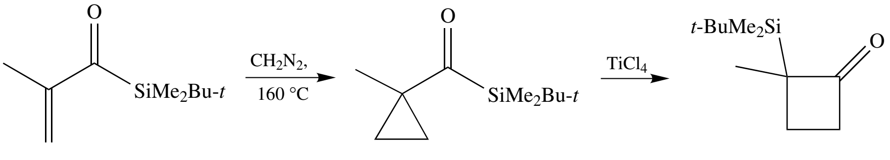

SCHEME 113

70 and **71** react with 2,3-dimethylbuta-1,3-diene and 4-phenyloxazole to give **72** and **73**, respectively, under conditions similar to those appropriate for conventional acetylenic dienophiles (Scheme 114)[14]. Diels–Alder reactions of propenoyl trimethylsilane with thioketones take place at room temperature in ethereal solution to give 6-trimethylsilyl-(4*H*)-dihydro-1,3-oxathiins **74** (Scheme 115)[224].

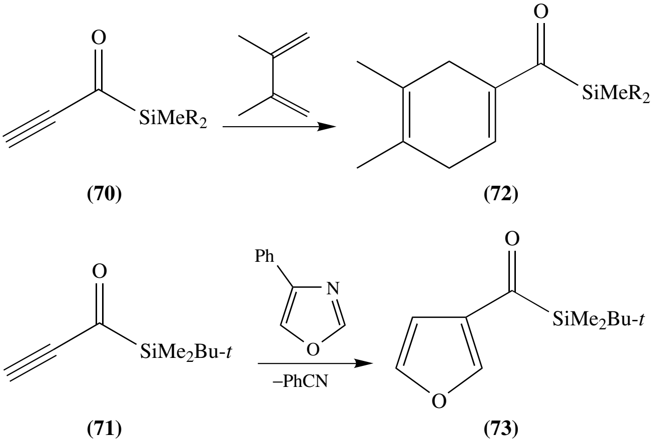

SCHEME 114

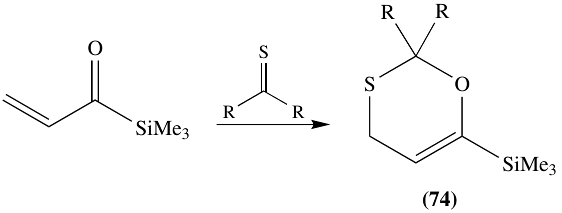

SCHEME 115

The [4 + 2] cycloaddition of α-phenylselenopropenoyl trimethylsilane **(75)** with 2,3-dimethylbuta-1,3-diene is unusual in that a significant portion of product mixture consists of the hetero-Diels–Alder dihydropyran adduct **76**. The phenylselenenyl substituent appears to be responsible for this unusual pattern of reactivity, since propenoyl trimethylsilane gives only the expected regioisomer (**77**, X = H) (Scheme 116)[14]. α-Selenenyl substituted α,β-unsaturated acyl silanes such as **75** were used to prepare a series of substituted dienes in excellent yields through the addition of α-sulphinyl carbanions, Brook rearrangement and expulsion of sulphinate, in a reaction pathway recognisably more typical of acyl silanes (Scheme 117).

Phenylthiotrimethylsilane adds to propenoyl trimethylsilane under the influence of Lewis acid to give 1,3-bis(phenylthio)-1-trimethylsilylprop-1-ene **(18)**. This enol thioether may be deprotonated with *t*-butyl lithium and alkylated with any of a large range of electrophiles. Subsequent hydrolysis–elimination with mercuric chloride in aqueous acetonitrile provides β-substituted α,β-unsaturated acyl silanes (*vide supra*, Section III.D.3)[132]. It should be noted that, in this transformation, the β-substituent has

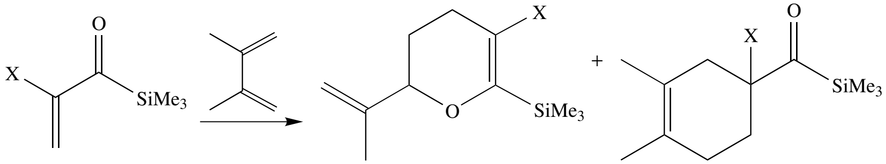

(75) **(76)** **(77)**

X = PhSe X = PhSe, 15:85

SCHEME 116

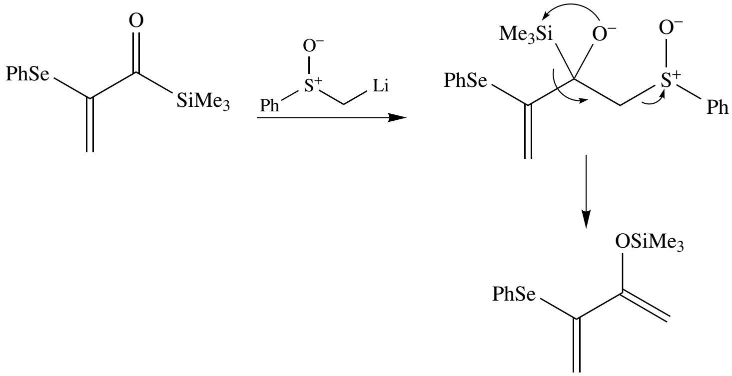

SCHEME 117

been introduced as an electrophile, complementing other methods of preparation of β-substituted α,β-unsaturated acyl silanes.

Acyl tri-isopropylsilanes containing alkene or alkyne functionality undergo smooth hydrozirconation with Schwartz' reagent, in contrast to the corresponding aldehydes, which also suffer addition to the carbonyl group (Scheme 118)[225].

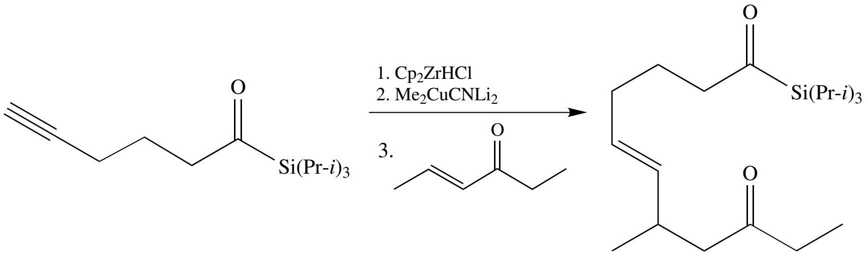

SCHEME 118

Gibson née Thomas, and Tustin have reported the formation of a number of iron carbonyl complexes of α,β-unsaturated acyl silanes[226]. Propenoyl trimethylsilane did not give a stable complex, but the iron tricarbonyl complexes of cinnamoyl silanes were very stable.

V. CONCLUSION

The last few years have seen a continued expansion in acyl silane chemistry, both in synthetic methods and in reactivity. There can now be no doubt that the difficulties encountered in preparing and isolating acyl silanes in the early investigations have been quite surmounted. While acyl silanes have been used merely as alternative carboxylic acid derivatives, they have also become synthetic intermediates in their own right, as some reactions particular to acyl silanes, such as the Brook rearrangement, have been used to great effect as synthetic processes. It can surely be expected that the synthesis of acyl silanes of all types will continue to become more sophisticated, and that, as functionalized acyl silanes become more accessible, these interesting materials will continue to find new uses in organic chemistry for a diverse range of purposes.

VI. REFERENCES

1. A. Ricci and A. Degl'Innocenti, *Synthesis*, 647 (1989); P. C. B. Page, S. S. Klair and S. Rosenthal, *Chem. Soc. Rev.*, **19**, 147 (1990); P. F. Cirillo and J. S. Panek, *Org. Prep. Proced. Int.*, **24**, 555 (1992).
2. A. G. Brook, *J. Am. Chem. Soc.*, **79**, 4373 (1957); A. G. Brook, M. A. Quigley, G. J. D. Peddle, N. V. Schwartz and C. M. Warner, *J. Am. Chem. Soc.*, **82**, 5102 (1960).
3. V. Bazant, V. Chvalovsky and J. Rathousky, *Organosilicon Compounds*, Academic Press, New York, 1965; V. Chvalovsky, *Handbook or Organosilicon Compounds —Advances Since 1961*, Marcel Dekker, New York, 1974.
4. A. G. Brook and R. J. Mauris, *J. Am. Chem. Soc.*, **79**, 971 (1957); A. G. Brook and G. J. D. Peddle, *Can. J. Chem.*, **41**, 2351 (1963).
5. A. G. Brook *Adv. Organomet. Chem.*, **7**, 96 (1968).
6. A. G. Brook, R. Kiviskik and G. E. Le Grow, *Can. J. Chem.*, **43**, 1175 (1965).
7. P. C. B. Page and S. Rosenthal, *Tetrahedron*, **46**, 2573 (1990); P. C. B. Page and S. Rosenthal, unpublished data.
8. G. Zweifel and J. A. Miller, *Synthesis*, 288 (1981).
9. C. Heathcock and J. Lampe, *J. Org. Chem.*, **48**, 4330 (1983).
10. A. Capperucci, A. Degl'Innocenti, C. Faggi, A. Ricci, P. Dembech and G. Seconi, *J. Org. Chem.*, **53**, 3612 (1988).
11. J. A. Soderquist and A. Hassner, *J. Am. Chem. Soc.*, **102**, 1577 (1980); D. I. Gasking and G. H. Whitham, *J. Chem. Soc., Perkin Trans. 1*, 409 (1985).
12. I. Kuwajima, T. Sato, K. Matsumoto and T. Abe, *Bull. Chem. Soc. Jpn.*, **57**, 2167 (1984); T. Sato, T. Abe and I. Kuwajima, *Tetrahedron Lett.*, 259 (1978).
13. A. Ricci, M. Fiorenza, A. Degl'Innocenti, G. Seconi, P. Dembech, K. Witzgall and H. J. Bestmann, *Angew. Chem., Int. Ed. Engl.*, **24**, 1068 (1985).
14. H. J. Reich, M. J. Kelly, R. E. Olson and R. C. Holtan, *Tetrahedron*, **39**, 949 (1983); H. J. Reich and M. J. Kelly, *J. Am. Chem. Soc.*, **104**, 1119 (1982).
15. A. Sekiguchi, Y. Kabe and W. Ando, *Tetrahedron Lett.*, 871 (1979).
16. G. J. D. Peddle and R. W. Walsingham, *J. Chem., Soc., Chem. Commun.*, 462 (1969).
17. A. G. Brook and L. Yau, *J. Organomet. Chem.*, **271**, 9 (1984).
18. I. Kuwajima and J. Enda, *J. Am. Chem. Soc.*, **107**, 5495 (1985).
19. D. Schinzer, *Synthesis*, 179 (1989).
20. R. L. Danheiser, D. M. Fink, K. Okano, Y.-M. Tsai and S. W. Szczepanski, *J. Org. Chem.*, **50**, 5393 (1985).
21. H. J. Reich, E. K. Eisenhart, R. E. Olson and M. J. Kelly, *J. Am. Chem. Soc.*, **108**, 7791 (1986); H. J. Reich and E. K. Eisenhart, *J. Org. Chem.*, **49**, 5282 (1984).
22. (a) R. Mantione and Y. Leroux, *Tetrahedron Lett.*, 591 (1971).
    (b) R. G. Visser, L. Brandsma and H. J. T. Bos, *Tetrahedron Lett.*, **22**, 2827 (1981).
    (c) K. J. H. Kruithof and G. W. Klumpp, *Tetrahedron Lett.*, **23**, 3101 (1982).
    (d) J. C. Clinet and G. Linstrumelle, *Tetrahedron Lett.*, **21**, 3987 (1980).
23. A. Ricci, A. Degl'Innocenti, S. Chimichi, M. Fiorenza, G. Rossini and H. J. Bestmann, *J. Org. Chem.*, **50**, 130 (1985).

24. A. G. Brook, J. W. Harris, J. Lennon and M. El Sheikh, *J. Am. Chem. Soc.*, **101**, 83 (1979); A. G. Brook, S. C. Nyburg, W. F. Reynolds, Y. C. Poon, Y.-M. Chang, J.-S. Lee and J.-P. Picard, *J. Am. Chem. Soc.*, **101**, 6750 (1979); A. G. Brook, S. C. Nyburg, F. Abdesaken, B. Gutekunst, G. Gutekunst, R. K. M. R. Kallury, Y. C. Poon, Y.-M. Chang and W. Wong-Ng, *J. Am. Chem. Soc.*, **104**, 5667 (1982).
25. A. G. Brook, F. Abdesaken and H. Sollradl, *J. Organomet. Chem.*, **299**, 9 (1986).
26. K. M. Baines, A. G. Brook, R. R. Ford, P. D. Lickiss, A. K. Saxena, W. J. Chatterton, J. F. Sawyer and B. A. Benham, *Organometallics*, **8**, 693 (1989).
27. I. Naito, A. Kanishita and T. Yonenitsu, *Bull. Chem. Soc. Jpn.*, **49**, 339 (1976).
28. E. M. Dexheimer, G. L. Buell and C. le Croix, *Spectrosc. Lett.*, **11**, 751 (1978).
29. F. Bernardi, L. Lunazzi, A. Ricci, G. Seconi and G. Tonachini, *Tetrahedron*, **42**, 3607 (1986).
30. G. A. Olah, A. L. Berrier, L. D. Field and G. K. Surya Prakash, *J. Am. Chem. Soc.*, **104**, 1349 (1982).
31. A. G. Brook, F. Abdesaken, G. Gutekunst and N. Plavac, *Organometallics*, **1**, 994 (1982).
32. H. K. Sharma, S. P. Vincenti, R. Vicari, F. Cervantes and K. H. Pannel, *Organometallics*, **9**, 2109 (1990).
33. B. Frei and M. E. Scheller, *Helv. Chim. Acta*, **67**, 1734 (1984).
34. S. Chimichi and C. Mealli, *J. Mol. Struct.*, **271**, 133 (1992).
35. E. Lippmaa, M. Magi, V. Chvalovsky and J. Schraml, *Collect. Czech. Chem. Comm.*, **42**, 318 (1977).
36. R. West, *J. Organomet. Chem.*, **3**, 314 (1965).
37. D. F. Harnish and R. West, *Inorg. Chem.*, **2**, 1082 (1963).
38. B. G. Ramsey, A. G. Brook, A. R. Bassindale and H. Bock, *J. Organomet. Chem.*, **74**, C41 (1974); F. Agolini, S. Klemenko, I. G. Csizmadia and K. Yates, *Spectrochim. Acta*, **24A**, 169 (1968).
39. E. B. Nadler, Z. Rappoport, D. Arad and Y. Apeloig, *J. Am. Chem. Soc.*, **109**, 7873 (1987).
40. L. E. Orgel, in *Volatile Silicon Compounds* (Ed. E. A. V. Ebsworth), Pergamon Press, Oxford, 1963, p. 81.
41. K. Yates and F. Agolini, *Can. J. Chem.*, **44**, 2229 (1966).
42. H. Dahn, P. Péchy and H. J. Bestmann, *J. Chem. Soc., Perkin Trans. 2*, 1497 (1993).
43. P. C. Chieh and J. Trotter, *J. Chem. Soc.*, 1778 (1969).
44. R. W. Harrison and J. Trotter, *J. Chem. Soc.*, 258 (1968).
45. Q. Liu, Y. Hu, J. Huang and F. Li, *Huaxue Xuabao*, **2**, 68 (1986); *Chem. Abstr.*, **104**, 234791b (1986).
46. L. H. Sommer, D. L. Bailey, G. M. Goldberg, C. E. Buck, T. S. Bye, F. J. Evans and F. C. Whitmore, *J. Am. Chem. Soc.*, **76**, 1613 (1954).
47. A. J. Mancuso, D. S. Brownfain and D. Swern, *J. Org. Chem.*, **44**, 4148 (1979).
48. R. E. Ireland and D. W. Norbeck, *J. Org. Chem.*, **50**, 2198 (1985).
49. B. K. Campion, J. Falk and T. D. Tilley, *J. Am. Chem. Soc.*, **109**, 2049 (1987).
50. W. Sander, M. Trommer, C. H. Ottoson and D. Cremer, *Angew. Chem., Int. Ed. Engl.*, **34**, 929 (1995).
51. F. H. Elsner, H.-G. Woo and T. D. Tilley, *J. Am. Chem. Soc.*, **110**, 313 (1988).
52. (a) J. A. Soderquist and E. I. Miranda, *J. Am. Chem. Soc.*, **114**, 10078 (1992).
    (b) R. B. Silverman, X. Lu and G. M. Banik, *J. Org. Chem.*, **57**, 6617 (1992).
53. A. R. Katritzky, Z. Yang and Q. Hong, *J. Org. Chem.*, **59**, 5097 (1994).
54. R. J. Linderman and Y. Suhr, *J. Org. Chem.*, **53**, 1569 (1988).
55. H. Woo, W. P. Freeman and T. D. Tilley, *Organometallics*, **11**, 2198 (1992).
56. A. G. Brook, J. M. Duff, P. F. Jones and N. R. Davis, *J. Am. Chem. Soc.*, **89**, 4431 (1967).
57. E. J. Corey, D. Seebach and R. Freedman, *J. Am. Chem. Soc.*, **89**, 434 (1967).
58. T. N. Salzmann, R. W. Ratcliffe, B. G. Christensen and F. A. Bouffard, *J. Am. Chem. Soc.*, **102**, 6163 (1980).
59. D. W. Emerson and H. Wynberg, *Tetrahedron Lett.*, 3445 (1971); M. E. Scheller, G. Iwasaki and B. Frei, *Helv. Chim. Acta*, **69**, 1378 (1986).
60. A. G. Brook and H. W. Kucera, *J. Organomet. Chem.*, **87**, 263 (1975).
61. H. J. Reich, J. J. Rusek and R. E. Olson, *J. Am. Chem. Soc.*, **101**, 2225 (1979).
62. R. L. Danheiser and D. M. Fink, *Tetrahedron Lett.*, **26**, 2509 (1985).
63. K. Suda, J. Watanabe and T. Takanami, *Tetrahedron Lett.*, **33**, 1355 (1992).
64. R. Tacke, K. Fritsche, A. Tafel and F. Wuttke, *J. Organomet. Chem.*, **388**, 47 (1990).

65. R. Burstinghaus and D. Seebach, *Chem. Ber.*, **110**, 841 (1977).
66. T. Mandai, M. Yamaguchi, Y. Nakayama, J. Otera and M. Kawada, *Tetrahedron Lett.*, **26**, 2675 (1985).
67. J. Otera, Y. Niibo and H. Nozaki, *Tetrahedron Lett.*, **33**, 3655 (1992).
68. A. Ricci, A. Degl'Innocenti, M. Ancillotti, G. Seconi and P. Dembech, *Tetrahedron Lett.*, **26**, 5985 (1985).
69. D. J. Ager, *Chem. Soc. Rev.*, **11**, 493 (1982).
70. H. J. Reich and S. K. Shah, *J. Org. Chem.*, **42**, 1773 (1977).
71. D. Wittenberg and H. Gilman, *J. Am. Chem. Soc.*, **80**, 4529 (1958).
72. A. G. Brook and K. M. Baines, *Adv. Organomet. Chem.*, **25**, 1 (1986).
73. G. Raabe and J. Michl in *Chem. Rev.*, **85**, 419 (1985); *The Chemistry of Organic Silicon Compounds*, S. Patai and Z. Rappoport, (Eds.), Wiley-Interscience, New York, 1989.
74. I. Fleming and U. Ghosh, *J. Chem. Soc., Perkin Trans. 1*, 257 (1994).
75. N. Duffaut, J. Dunogues, C. Biran, R. Calas and J. Gerval, *J. Organomet. Chem.*, **161**, C23 (1978).
76. A. Degl'Innocenti, *Synlett*, 937 (1993).
77. J. Kang, J. H. Lee, K. S. Kim, J. U. Jeong and C. Pyun, *Tetrahedron Lett.*, **28**, 3261 (1987).
78. M. Nakada, S. Nakamura, S. Kobayashi and M. Ohno, *Tetrahedron Lett.*, **32**, 4929 (1991).
79. B. F. Bonini, F. Busi, R. C. de Laet, G. Mazzanti, J.-W. J. Thuring, P. Zani and B. Zwanenburg, *J. Chem. Soc., Perkin Trans. 1*, 1011 (1993).
80. B. F. Bonini, M. Comes-Franchini, G. Mazzanti, U. Passamonti, A. Ricci and P. Zani, *Synthesis*, 92 (1995).
81. K. Yamamoto, S. Suzuki and J. Tsuji, *Tetrahedron Lett.*, **21**, 1653 (1980).
82. M. Murakami, A. Hideki, N. Takizawa and Y. Ito, *Organometallics*, **12**, 4223 (1993).
83. A. G. Brook and J. Pierce, *J. Organomet. Chem.*, **30**, 2566 (1965).
84. B. H. Lipshutz, C. Lindsley, R. Susfalk and T. Gross, *Tetrahedron Lett.*, **35**, 8999 (1994).
85. M. E. Scheller and B. Frei, *Helv. Chim. Acta*, **69**, 44 (1986).
86. A. Degl'Innocenti, D. R. M. Walton, G. Seconi, G. Pirazzini and A. Ricci, *Tetrahedron Lett.*, **21**, 3927 (1980).
87. R. Corriu and J. Masse, *J. Organomet. Chem.*, **22**, 321 (1970).
88. T. Aoyama and T. Shioiri, *Tetrahedron Lett.*, **27**, 2005 (1986).
89. A. Hassner and J. Soderquist, *J. Organomet. Chem.*, **131**, C1 (1977).
90. G. Zweifel and S. J. Bäcklund, *J. Am. Chem. Soc.*, **99**, 3184 (1977).
91. A. G. Brook, J. W. Harris and A. R. Bassindale, *J. Organomet. Chem.*, **99**, 379 (1975).
92. P. Bourgeois, J. Dunogues, N. Duffaut and P. Lapouyade, *J. Organomet. Chem.*, **80**, C25 (1974).
93. I. Kuwajima, M. Arai and T. Sato, *J. Am. Chem. Soc.*, **99**, 4181 (1977).
94. I. Kuwajima, N. Minami, T. Abe and T. Sato, *Bull. Chem. Soc. Jpn.*, **51**, 2391 (1978).
95. I. Kuwajima, T. Sato, N. Minami and T. Abe, *Tetrahedron Lett.*, 1591 (1976).
96. J.-P. Picard, R. Calas, J. Dunogues and N. Duffaut, *J. Organomet. Chem.*, **26**, 183 (1971); J.-P. Picard, R. Calas, J. Dunogues, N. Duffaut, J. Gerval and P. Lapouyade, *J. Org. Chem.*, **44**, 420 (1979); J.-P. Picard, A. Ekouya, J. Dunogues, N. Duffaut and R. Calas, *J. Organomet. Chem.*, **93**, 51 (1975); P. Bourgeois, *J. Organomet. Chem.*, **76**, C1 (1972).
97. I. Kuwajima, M. Kato and T. Sato, *J. Chem. Soc., Chem. Commun.*, 478 (1978).
98. T. Cohen and J. R. Matz, *J. Am. Chem. Soc.*, **102**, 6900 (1980).
99. S. Murai, I. Ryu, J. Iriguchi and N. Sonoda, *J. Am. Chem. Soc.*, **106**, 2440 (1984).
100. T. Inoue, N. Kambe, I. Ryu and N. Sonoda, *J. Org. Chem.*, **59**, 8209 (1994).
101. J. B. Verlhac, H. Kwon and M. Pereyre, *J. Organomet. Chem.*, **437**, C13 (1992).
102. N. Chatani, S. Ikeda, K. Ohe and S. Murai, *J. Am. Chem. Soc.*, **114**, 9710 (1992).
103. J. A. Soderquist and G. J.-H. Hsu, *Organometallics*, **1**, 830 (1982); E. M. Dexheimer and L. Spialter, *J. Organomet. Chem.*, **107**, 229 (1976).
104. J. A. Soderquist, *Org. Synth.*, **68**, 25 (1990).
105. J. Yoshida, S. Matsunaga, Y. Ishichi, T. Maekawa and S. Isoe, *J. Org. Chem.*, **56**, 1307 (1991).
106. D. Seyferth and R. M. Weinstein, *J. Am. Chem. Soc.*, **104**, 5534 (1982).
107. D. Seyferth and R. C. Hui, *Organometallics*, **3**, 327 (1984).
108. P. Bourgeois, *J. Organomet. Chem.*, **76**, C1 (1974).
109. G. E. Niznik, W. H. Morrison and H. M. Walborsky, *J. Org. Chem.*, **39**, 600 (1974).
110. A. Orita, K. Ohe and S. Murai, *J. Organomet. Chem.*, **474**, 23 (1994).
111. A. Orita, K. Ohe and S. Murai, *Organometallics*, **13**, 1533 (1994).

112. P. Raubo and J. Wicha, *J. Org. Chem.*, **59**, 4355 (1994).
113. H. M. I. Osborn, J. B. Sweeney and B. Howson, *Synlett*, 675 (1993).
114. K. Maruoko and H. Yamamoto, *Synlett*, 793 (1991); K. Maruoko, H. Banno and H. Yamamoto, *Tetrahedron: Asymmetry*, **2**, 647 (1991).
115. I. Kuwajima, T. Abe and N. Minami, *Chem. Lett.*, 993 (1976).
116. J. S. Nowick and R. L. Danheiser, *J. Org. Chem.*, **54**, 2798 (1989).
117. P. C. B. Page and S. Rosenthal, *Tetrahedron Lett.*, **27**, 5421 (1986).
118. J. Hooz and J. N. Bridson, *Can. J. Chem.*, **50**, 2387 (1972).
119. C. T. Hewkin and R. F. W. Jackson, *Tetrahedron Lett.*, **31**, 1877 (1990).
120. C. T. Hewkin and R. F. W. Jackson, *J. Chem. Soc., Perkin Trans. 1*, 3103 (1991); M. Ashwell, W. Clegg and R. F. W. Jackson, *J. Chem. Soc., Perkin Trans. 1*, 897 (1991).
121. Y. Horiuchi, M. Taniguchi, K. Oshima and K. Utimoto, *Tetrahedron Lett.*, **36**, 5353 (1995).
122. F. Jin, B. Jiang and Y. Xu, *Tetrahedron Lett.*, **33**, 1221 (1992).
123. S. Hoff, L. Brandsma and J. F. Arens, *Recl. Trav. Chim. Pays-Bas*, **87**, 916 (1968).
124. P. C. B. Page and S. Rosenthal, *Tetrahedron Lett.*, **27**, 2527 (1986).
125. P. C. B. Page and S. Rosenthal, *Tetrahedron Lett.*, **27**, 1947 (1986).
126. R. W. Murray and M. Singh, *J. Org. Chem.*, **58**, 5076 (1993).
127. W. C. Still and T. L. Macdonald, *J. Am. Chem. Soc.*, **96**, 5561 (1974).
128. A. Wright and R. West, *J. Am. Chem. Soc.*, **96**, 3214 (1974).
129. N. Minami, T. Abe and I. Kuwajima, *J. Organomet. Chem.*, **145**, C1 (1978).
130. A. Ricci, A. Degl'Innocenti, A. Capperucci, C. Faggi, G. Seconi and L. Favaretto, *Synlett*, 471 (1990).
131. K. Narasaka and T. Shibata, *Bull. Chem. Soc. Jpn.*, **65**, 2825 (1992).
132. A. Degl'Innocenti, P. Uliva, A. Capperucci, G. Reginato, A. Mordini and A. Ricci, *Synlett*, 883 (1992).
133. J. A. Miller and G. Zweifel, *J. Am. Chem. Soc.*, **103**, 6217 (1981).
134. D. J. Ager, *Synthesis*, 384 (1984).
135. R. F. Cunico and C. Zhang, *Tetrahedron Lett.*, **33**, 6751 (1992).
136. A. Degl'Innocenti, A. Ricci, G. Reginato and G. Seconi, *Pure Appl. Chem.*, **64**, 439 (1992).
137. A. Degl'Innocenti, E. Stucchi, A. Capperucci, A. Mordini, G. Reginato and A. Ricci, *Synlett*, 329 (1992).
138. A. Degl'Innocenti, A. Capperucci, G. Reginato, A. Mordini and A. Ricci, *Tetrahedron Lett.*, **33**, 1507 (1992).
139. A. Degl'Innocenti, E. Stucchi, A. Capperucci, A. Mordini, G. Reginato and A. Ricci, *Synlett*, 332 (1992).
140. A. Degl'Innocenti, A. Capperucci, L. Bartoletti, A. Mordini and G. Reginato, *Tetrahedron Lett.*, **35**, 2081 (1994).
141. R. L. Danheiser and D. M. Fink, *Tetrahedron Lett.*, **26**, 2513 (1985).
142. R. Plantier-Royon and C. Portella, *Synlett*, 527 (1994).
143. K. J. H. Kruithof, R. F. Schmitz and G. W. Klumpp, *J. Chem. Soc., Chem. Commun.*, 239 (1983); K. J. H. Kruithof, R. F. Schmitz and G. W. Klumpp, *Tetrahedron*, **39**, 3073 (1983).
144. K. Narasaka, H. Kusama and Y. Hayashi, *Tetrahedron*, **48**, 2059 (1992).
145. L. A. Paquette and G. D. Maynard, *J. Org. Chem.*, **56**, 5480 (1991).
146. T. Nakajima, H. Miyaji, M. Segi and S. Suga, *Chem. Lett.*, 181 (1986).
147. T. Nakajima, H. Miyaji, M. Segi and S. Suga, *Chem. Lett.*, 177 (1986).
148. J. S. Nowick and R. L. Danheiser, *Tetrahedron*, **44**, 4113 (1988).
149. I. Fleming, in *Comprehensive Organic Chemistry*, Vol. 3 (Ed. N. Jones), Pergamon Press, Oxford, 1979, p. 647.
150. P. D. Magnus, T. Sarkar and S. Dujuric, in *Comprehensive Organometallic Chemistry*, Vol. 7, Pergamon Press, Oxford, 1982, p. 631.
151. E. W. Colvin, *Silicon in Organic Synthesis*, Butterworths, London, 1981.
152. E. W. Colvin, *Silicon Reagents in Organic Synthesis*, Academic Press, London, 1988.
153. A. G. Brook, *Acc. Chem. Res.*, **7**, 77 (1974).
154. (a) I. Fleming, in *Comprehensive Organic Chemistry*, Vol. 3 (Ed. N. Jones), Pergamon Press, Oxford, 1979, p. 554.
    (b) P. C. B. Page and S. Rosenthal, *J. Chem. Res. (S)*, **10**, 302 (1990).
155. R. J. P. Corriu and C. Guerin, *Adv. Organomet. Chem.*, **20**, 265 (1982).
156. D. Rietropaolo, A. Ricci, M. Taddei and M. Fiorenza, *J. Organomet. Chem.*, **197**, 7 (1980).

157. A. G. Brook and N. V. Schwartz, *J. Org. Chem.*, **27**, 2311 (1962).
158. A. G. Brook, W. Limburg and T. S. D. Vandersar, *Can. J. Chem.*, **56**, 2758 (1978).
159. E. D. Hughes and C. K. Ingold, *J. Chem. Soc.*, 244 (1935).
160. P. C. B. Page, S. Rosenthal and R. V. Williams, *Tetrahedron Lett.*, **28**, 4455 (1987).
161. A. Yanagisawa, S. Habaue and H. Yamamoto, *Tetrahedron*, **48**, 1969 (1992).
162. M. R. Burns and J. K. Coward, *J. Org. Chem.*, **58**, 529 (1993).
163. R. Munsted and U. Wannagat, *J. Organomet. Chem.*, **322**, 11 (1987); R. Munsted and U. Wannagat, *Monatsh. Chem.*, **116**, 693 (1985).
164. A. Fürstner, G. Kollegger and H. Weidmann, *J. Organomet. Chem.*, **414**, 295 (1991).
165. S. R. Wilson, M. S. Hague and R. N. Misra, *J. Org. Chem.*, **47**, 747 (1982).
166. I. Kuwajima, T. Matsutani and J. Enda, *Tetrahedron Lett.*, **25**, 5307 (1984).
167. J. D. Buynak, J. B. Strickland, T. Hurd and A. Phan, *J. Chem. Soc., Chem. Commun.*, 89 (1989).
168. S. Itsuno, M. Nakano, K. Miyazaki, H. Masuda, K. Ito, A. Hirao and S. Nakahama, *J. Chem. Soc., Perkin Trans. 1*, 2039 (1985).
169. J. A. Soderquist, C. L. Anderson, E. I. Miranda and I. Rivera, *Tetrahedron Lett.*, **31**, 4677 (1990).
170. J. D. Buynak, J. B. Strickland, G. W. Lamb, D. Khasnis, S. Modi, D. Williams and H. Zhang, *J. Org. Chem.*, **56**, 7076 (1991).
171. A. R. Bassindale, A. G. Brook, P. F. Jones and J. M. Lennon, *Can. J. Chem.*, **53**, 332 (1975).
172. P. F. Cirillo and J. S. Panek, *J. Org. Chem.*, **59**, 3055 (1994).
173. J. D. Buynak, B. Geng, S. Uang and J. B. Strickland, *Tetrahedron Lett.*, **35**, 985 (1994).
174. B. F. Bonini, S. Masiero, G. Mazzanti and P. Zani, *Tetrahedron Lett.*, **32**, 6801 (1991).
175. A. Chapeaurouge and S. Bienz, *Helv. Chim. Acta*, **76**, 1876 (1993).
176. S. Bienz and A. Chapeaurouge, *Helv. Chim. Acta*, **74**, 1477 (1991).
177. M. Nakada, Y. Urano, K. Susumu and M. Ohno, *J. Am. Chem. Soc.*, **110**, 4826 (1988).
178. M. Nakada, Y. Urano, S. Kobayashi and M. Ohno, *Tetrahedron Lett.*, **35**, 741 (1994).
179. P. F. Cirillo and J. S. Panek, *J. Org. Chem.*, **55**, 6071 (1990).
180. H. J. Reich, R. C. Holtan and S. L. Borkowsky, *J. Org. Chem.*, **52**, 312 (1987).
181. M. Cherest, H. Felkin and N. Prudent, *Tetrahedron Lett.*, 2199 (1968); N. T. Anh and O. Eisenstein, *Nouv. J. Chim.*, **1**, 61 (1977); A. S. Cieplak, *J. Am. Chem. Soc.*, **103**, 4540 (1981).
182. A. G. Brook and S. A. Fieldhouse, *J. Organomet. Chem.*, **10**, 235 (1967).
183. J. A. Soderquist and C. L. Anderson, *Tetrahedron Lett.*, **29**, 2425 (1988); J. A. Soderquist and C. L. Anderson, *Tetrahedron Lett.*, **29**, 2777 (1988).
184. C. L. Anderson, J. A. Soderquist and G. W. Kabalka, *Tetrahedron Lett.*, **33**, 6915 (1992).
185. N. A. Petasis and S.-P. Lu, *Tetrahedron Lett.*, **36**, 2393 (1995).
186. T. Nakajima, M. Segi, F. Sugimoto, R. Hioki, S. Yokota and K. Miyashita, *Tetrahedron*, **49**, 8343 (1993).
187. K. Takeda, J. Nakatani, H. Nakamura, K. Sako, E. Yoshii and K. Yamaguchi, *Synlett*, 841 (1993).
188. T. Brigaud, P. Doussot and C. Portella, *J. Chem. Soc., Chem. Commun.*, 2117 (1994).
189. Y. Taniguchi, A. Nagafuji, Y. Makioka, K. Takaki and Y. Fujiwara, *Tetrahedron Lett.*, **35**, 6897 (1994).
190. T. Nakajima, M. Segi, T. Mituoka, Y. Fukute, M. Honda and K. Naitou, *Tetrahedron Lett.*, **36**, 1667 (1995).
191. C. H. Heathcock and D. Schinzer, *Tetrahedron Lett.*, **22**, 1881 (1981).
192. A. Degl'Innocenti, S. Pike, D. R. M. Walton, G. Seconi, A. Ricci and M. Fiorenza, *J. Chem. Soc., Chem. Commun.*, 1201 (1980).
193. C. H. DePuy, V. M. Bierbaum, R. Damrauer and J. A. Soderquist, *J. Am. Chem. Soc.*, **107**, 3385 (1985).
194. G. A. Molander and C. S. Siedem, *J. Org. Chem.*, **60**, 130 (1995).
195. Y.-M. Tsai, H.-C. Nieh and C.-D. Chemg, *J. Org. Chem.*, **57**, 7010 (1992).
196. B. F. Bonini, M. Comes-Franchini, G. Mazzanti, A. Ricci, L. Rosa-Fauzza and P. Zani, *Tetrahedron Lett.*, **35**, 9227 (1994).
197. J. M. Harris, I. MacInnes, J. C. Walton and B. Maillard, *J. Organomet. Chem.*, **403**, 25 (1991).
198. Y.-M. Tsai, K.-H. Tang and W.-J. Jiaang, *Tetrahedron Lett.*, **34**, 1303 (1993).
199. D. P. Curran, W.-J. Jiaang, M. Palovich and Y.-M. Tsai, *Synlett*, 403 (1993).
200. Y.-M. Tsai and S.-Y. Chang, *J. Chem. Soc., Chem. Commun.*, 981 (1995).
201. K. M. Baines, A. G. Brook, P. D. Lickiss and J. F. Sawyer, *Organometallics*, **8**, 709 (1989).
202. A. G. Brook, R. Kumarathasan and W. Chatterton, *Organometallics*, **12**, 4085 (1993).
203. A. G. Brook and J. M. Duff, *J. Am. Chem. Soc.*, **89**, 454 (1967).

204. R. A. Bourque, P. D. Davis and J. C. Dalton, *J. Am. Chem. Soc.*, **103**, 697 (1981).
205. A. R. Bassindale, A. G. Brook and J. Harris, *J. Organomet. Chem.*, **90**, C6 (1975).
206. C. Shih and J. S. Swenton, *J. Org. Chem.*, **47**, 2668 (1982).
207. M. E. Scheller and B. Frei, *Helv. Chim. Acta*, **75**, 69 (1992).
208. R. Tacke, S. A. Wagner, S. Brakmann, F. Wüttke, U. Eilert, L. Fischer and C. Syldatk, *J. Organomet. Chem.*, **458**, 13 (1993).
209. (a) R. Tacke, S. Brakmann, F. Wüttke, J. Fooladi, C. Syldatk and D. Schomburg, *J. Organomet. Chem.*, **403**, 29 (1991).
(b) L. Fischer, S. A. Wagner and R. Tacke, *Appl. Microbiol. Biotechnol.*, **42**, 671 (1995).
210. T. Sato, M. Arai and I. Kuwajima, *J. Am. Chem. Soc.*, **99**, 5827 (1977).
211. P. Huber, V. Enev, A. Linden and S. Bienz, *Tetrahedron*, **51**, 3749 (1995).
212. P. F. Cirillo and J. S. Panek, *Tetrahedron Lett.*, **32**, 457 (1991).
213. J. Yoshida, M. Itoh, S. Matsunaga and S. Isoe, *J. Org. Chem.*, **57**, 4877 (1992).
214. A. Ricci, A. Degl'Innocenti, A. Capperucci and G. Reginato, *J. Org. Chem.*, **54**, 19 (1989).
215. Y. Taniguchi, N. Fujii, Y. Makioka, K. Takaki and Y. Fujiwara, *Chem. Lett.*, 1165 (1993).
216. R. C. Cambie, L. C. M. Mui, P. S. Rutledge and P. D. Woodgate, *J. Organomet. Chem.*, **464**, 171 (1994).
217. N. de Kimpe, P. Sulmon and N. Schamp, *Angew. Chem., Int. Ed. Engl.*, **24**, 881 (1985).
218. D. J. Cram and F. A. Abd Elhafez, *J. Am. Chem. Soc.*, **74**, 5828 (1952).
219. I. Kuwajima and K. Matsumoto, *Tetrahedron Lett.*, 4095 (1979).
220. F. Jin, Y. Xu and W. Huang, *J. Chem. Soc., Perkin Trans. 1*, 795 (1993).
221. F. Jin, B. Jiang and Y. Xu, *Tetrahedron Lett.*, **33**, 1221 (1992).
222. F. Jin, Y. Xu and W. Huang, *J. Chem. Soc., Chem. Commun.*, 814 (1993).
223. K. Takeda, M. Fujisawa, T. Makino and E. Yoshii, *J. Am. Chem. Soc.*, **115**, 9351 (1993).
224. B. F. Bonini, S. Masiero, G. Mazzanti and P. Zani, *Tetrahedron Lett.*, **32**, 2971 (1991).
225. B. Lipshutz, C. Lindsley and A. Bhandari, *Tetrahedron Lett.*, **35**, 4669 (1994).
226. S. E. Thomas and G. J. Tustin, *Tetrahedron*, **48**, 7629 (1992).

CHAPTER **28**

Recent synthetic applications of organosilicon reagents

ERNEST W. COLVIN

Department of Chemistry, University of Glasgow, Glasgow G12 8QQ, UK

I. INTRODUCTION

It is the purpose of this chapter to review selectively the advances in the synthetic applications of organosilicon compounds, excluding those organosilanes covered in other chapters. Since the publication of *The Chemistry of Organic Silicon Compounds*, two monographs[1,2] and several reviews[3–5] have been published, as have three conference proceedings[6–8] and a ‘symposium-in-print’[9].

II. TRIALKYLSILYL HALIDES

The chemistry of iodotrimethylsilane (TMSI) has been reviewed[10].

The role of chlorotrimethylsilane (TMSCl) in accelerating organocuprate conjugate additions[11] continues to arouse much discussion. It has been proposed that TMSCl acts as a Lewis acid in complexing the enone. However, high level *ab initio* calculations have shown that such complexation is only a weak dipole–dipole interaction, and cannot be responsible for the rate acceleration. The most recent suggestion[12] proposes two fundamentally different modes of action. With the powerful silylating conditions of TMS-Cl/HMPA, direct silylation of the initially formed π-complex **1** can occur. Under relatively weak silylating conditions, i.e. TMSCl alone, the rate of cuprate addition can be enhanced by conversion of the π-complex into a tetravalent copper species **2** which then undergoes reductive elimination to **3**, the transition state for this elimination being stabilized by the complexation which places silicon β to copper (equation 1).

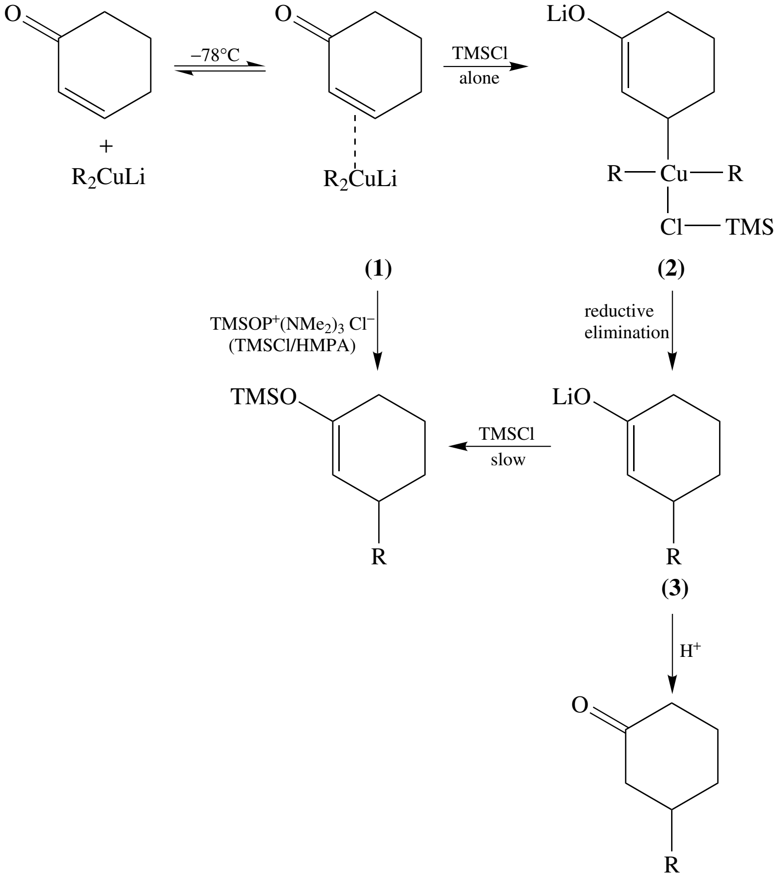

(1)

An RCu(LiI)/TMSI combination[13] promotes conjugate addition to α,β-unsaturated ketones, leading directly to TMS enol ethers from a presumed organocopper–enone π-complex, thus ruling out significant amounts of enolate as an intermediate on the reaction pathway (equation 2). However, these results do not allow discrimination between an α-cuprio ketone or a β-silyl copper species.

Activation by TMSCl has also been applied to the allylstannane allylation of aldimines[14], the copper-catalysed conjugate addition of organoaluminium reagents[15] to enones, and in the uncatalysed conjugate addition of organozincs[16] in THF/N-methylpyrrolidone. Its involvement in the conjugate addition of stabilized organolithiums[17] results in yield and selectivity enhancement.

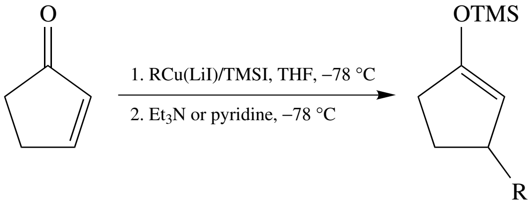

(2)

NMR spectroscopic experiments on the role of TMSCl in lithium dialkylamide deprotonations have shown[18] that LDA and TMSCl react at −78 °C to generate enough LiCl to be responsible for the stereoselectivities normally observed, i.e. hindered amide bases are not fully compatible with TMSCl at −78 °C. This does not apply when TBDMSCl or TBDPSCl is used; in such cases, it is probably necessary to add externally prepared LiCl to enhance stereoselectivity.

Motherwell and Roberts' dicarbonyl coupling reaction[19] can be improved by substituting 1,2-bis(chlorodimethylsilyl)ethane for TMSCl. The intermediate organozinc carbenoids can be trapped with alkenes to produce cyclopropanes, as exemplified in the intramolecular case in equation 3.

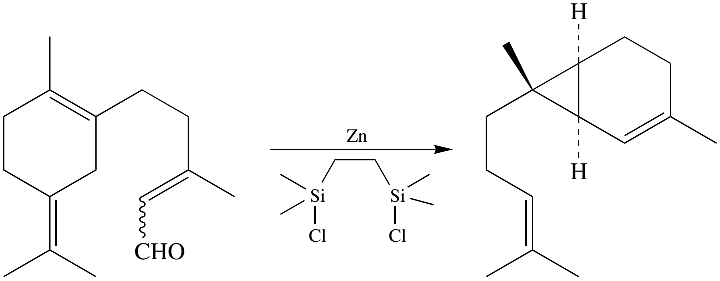

(3)

TMSCl serves as an efficient chlorinating agent[20] in the presence of a catalytic amount of selenium dioxide for a wide variety of alcohols; the reagent system TMSCl/DMSO converts primary and tertiary alcohols into the corresponding chlorides, probably by S_N2 and S_N1 pathways, respectively, although no stereochemical detail was given[21]. Allylic acetates can be converted into allylic bromides using TMSBr with ZnI_2 as catalyst, with the regiochemistry being controlled by the relative stabilities of the product alkenes[22].

The combination of TMSCl and $NaNO_2$ converts anilines efficiently into the corresponding aryl chlorides[23]; use of TMSBr or TMSI gives the corresponding bromides or iodides, respectively. $AlCl_3$ catalysed aromatic nitration[24] can be performed using TMSCl/$NaNO_3$.

TMSCl is essential as a promoter in a low-valent vanadium-catalysed reductive cyclotrimerization[25] of aliphatic aldehydes, producing 1,3-dioxolanes (equation 4). It is also an essential component in the zinc-induced intramolecular imine cross coupling[26] of diarylidene sulphamides; subsequent cleavage provides a route to unsymmetrical 1,2-diaryl-1,2-diaminoethanes (equation 5). It acts as an activating agent in the samarium-promoted cyclopropanation[27] of allylic and α-allenic alcohols.

A synthesis of 1-β-methylcarbapenems has been described[28] in which TMSCl acts both as a Lewis acid in accelerating the Dieckmann-type cyclization and as a trapping agent for the initially liberated thiolate anion (equation 6).

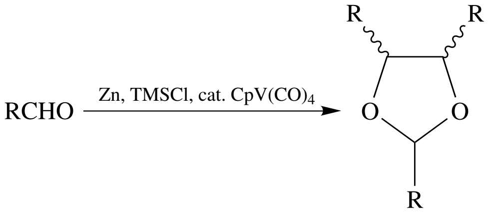

(4)

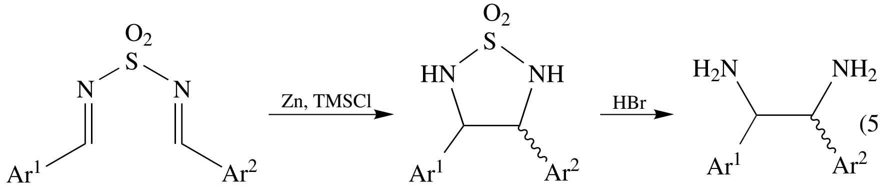

(5)

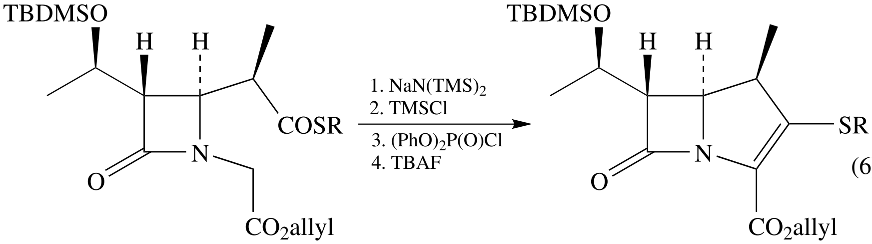

(6)

III. TRIALKYLSILYL CYANIDES

The chemistry of TMSCN has been reviewed[29].

α,β-Unsaturated ketones undergo regioselective addition[30] with TMSCN to give 1,4-adducts in the presence of strongly acidic montmorillonite or 1,2-adducts when strongly basic CaO or MgO is employed. Dibutyltin and diphenyltin dichloride are effective catalysts[31] for the addition of TMSCN to aldehydes and unactivated ketones; with an α,β-unsaturated aldehyde, exclusive 1,2-addition was observed.

A key step in a synthesis[32] of 18-*O*-methyl mycalamide B involved the conjugate addition of TBDMSCN, with TBDMSOTf catalysis, to give a dihydropyranone; this proceeded with very high 1,3-asymmetric induction (equation 7).

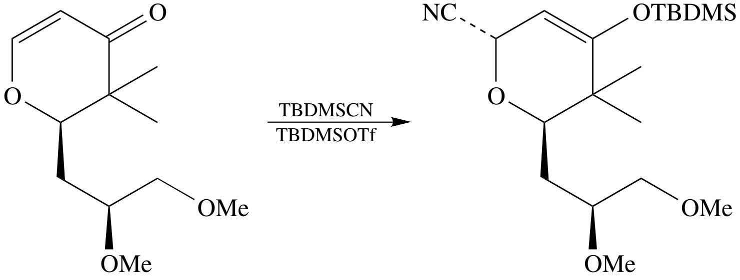

(7)

Di-isobutylaluminium hydride reduction[33] of aldehyde-derived *O*-TBDMS cyanohydrins, followed by hydrolysis with a tartaric acid buffer, gives the corresponding *O*-protected 2-hydroxyaldehydes. Related methodology has been employed in a diastereoselective synthesis[34] of a potential precursor of taxol®.

Enantioselective TMS cyanohydrin formation with aldehydes can be achieved using a variety of chirally-modified titanium catalytic systems; chiral modifiers include Schiff bases[35], including salen ligands[36] and sulphoximines[37]. A chirally-modified yttrium complex[38] has been employed for the same purpose (equation 8); here, the chiral modifier was a ferrocene-derived 1,3-diketone. This general area has been reviewed recently[39].

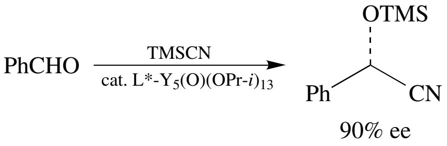

(8)

There have been further reports[40,41] on the Lewis acid induced opening of epoxides with TMSCN to produce *β*-trimethylsilyloxy nitriles.

Full details[42] have been published on the conversion of enynes into iminocyclopentenes using a titanium precatalyst in the presence of BuLi and TESCN (equation 9); the resulting iminocyclopentenes can be hydrolysed to cyclopentenones or reduced to allylic silylamines. In a related protocol[43], the tandem insertion of TMSCN and alkenes, alkynes, ketones or isocyanates into zirconacyclo-pentanes or -pentenes leads to cyclopentylamines carrying an *α*-alkyl, -alkenyl, -1-hydroxyalkyl or -carboxamide substituent, respectively (equation 9).

TMSCN has been employed (equation 10) in an efficient conversion[44] of 1-tetralones into the less readily available 2-tetralones via the derived unsaturated nitriles.

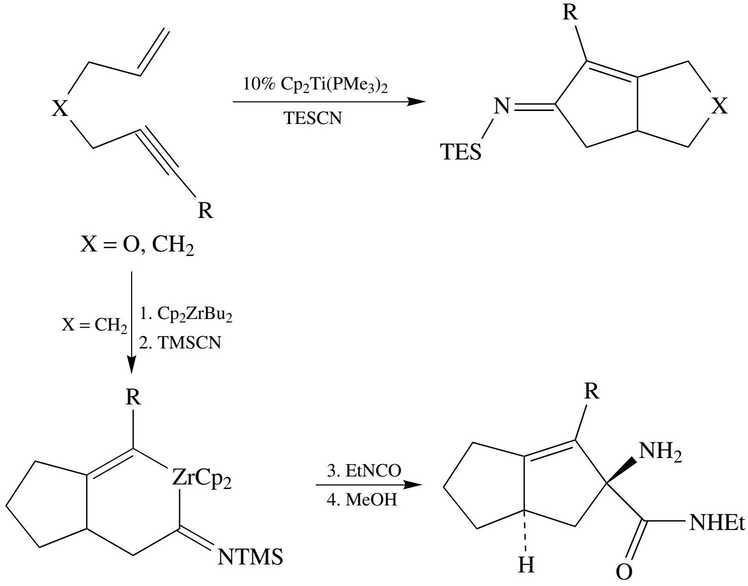

(9)

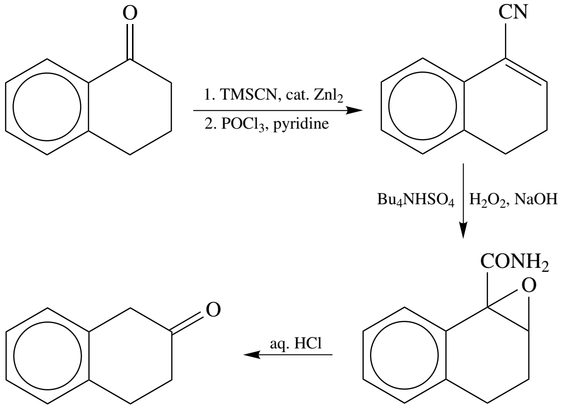

(10)

IV. TRIALKYLSILYL AZIDES

Both samarium iodide and ytterbium triisopropoxide catalyse the ring opening[45] of epoxides by TMS-azide; in the latter case, due to an acidic work-up, the products are isolated as vicinal azido alcohols.

Full details on this ring opening[46] under titanium tetraisopropoxide or aluminium triisopropoxide catalysis have been published. Using chirally modified titanium catalysts, cyclohexene oxide provides[47] *trans*-2-azidocyclohexanol in up to 63% ee.

More recently, Jacobsen and coworkers have found that epoxides undergo a highly enantioselective ring-opening with TMS-azide when catalysed by (salen)Cr(III) complexes such as (*S*,*S*)-**4**[48]. This asymmetric ring opening shows a second-order rate dependence on catalyst concentration[49]. Applications of the process have included kinetic resolution of terminal epoxides[50], an efficient synthesis[51] of (*R*)-4-(trimethylsilyloxy)cyclopent-2-enone, the dynamic kinetic resolution (equation 11) of epichlorohydrin[52], an enantioselective route[53] to carbocyclic nucleoside analogues and a formal synthesis[54] (equation 12) of the protein kinase inhibitor **5**.

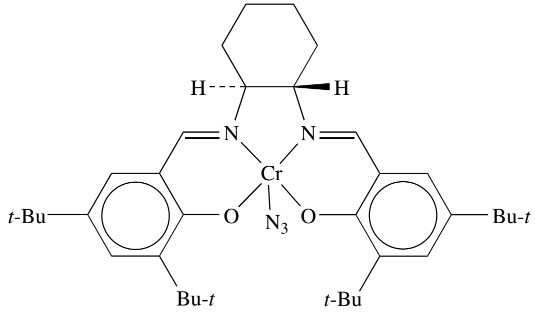

(*S*,*S*)-(**4**)

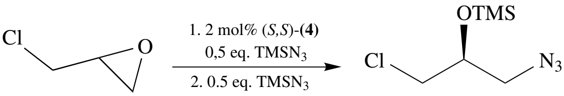

76%, 97% ee

(11)

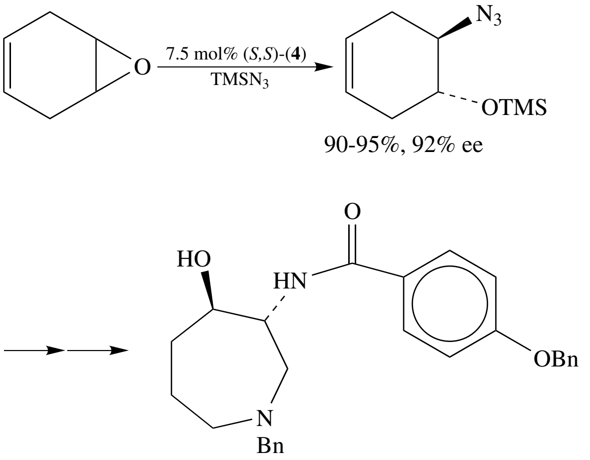

(12)

(5)

Magnus and coworkers have published full details[55] on the direct α- or β-azido functionalization of triisopropylsilyl (TIPS) enol ethers using an iodosylbenzene–TMS-azide combination (equation 13); the α-pathway, favoured at $-78\,^{\circ}$C, is an azide radical addition process, whereas the β-pathway, favoured at -15 to $-20\,^{\circ}$C, involves ionic dehydrogenation. Attempts to extend the β-functionalization to other TMSX derivatives failed.

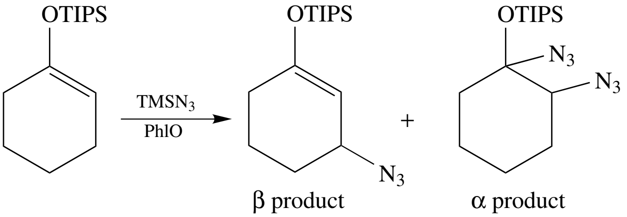

(13)

A novel approach to the synthesis of lactams has been reported[56] which involves reaction of such enol ethers with TMS-azide to give (triisopropylsilyl)azidohydrins, which then undergo a photoinduced Schmidt rearrangement (equation 14).

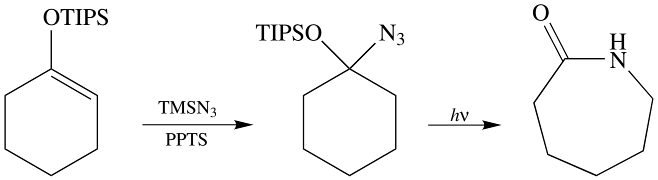

(14)

PPTS = Pyridinium *p*-toluenesulfonate

The reagent system TMS-azide/triflic acid performs efficient amination[57] of arenes, while the combination of TMS-azide and *N*-bromosuccinimide with Nafion-H® transforms alkenes into β-bromoalkyl azides[58]. On the other hand, the combination of TMS-azide and chromium trioxide converts alkenes into α-azidoketones[59] and aldehydes into acyl azides[60].

Alkyl halides can be converted into alkyl azides with inversion of configuration[61] using TMS-azide in the presence of TBAF.

V. ALKYL SILYL ETHERS

The protection of alcohols as silyl ethers has been reviewed[62], as have the relative stabilities of the different trialkylsilyl groups[63]. Their stability under alcohol oxidation conditions and their oxidative deprotection have been discussed[64]. Methods for selective deprotection of the various silyl ethers have been the subject of an excellent review[65].

The merits of TIPS ether protection have been reviewed[66], with emphasis on those reactions where the incremental structural difference between TIPS and other commonly used trialkylsilyl groups leads to results quite different from those obtained with TMS or TBDMS ethers.

The 'temporary silicon connection', pioneered by Stork,[67a] and based on the protocol of temporarily bringing two reaction partners together by means of an eventually removable silicon atom, often as silyl ethers, has been surveyed[67b]. This concept, i.e. that of converting an intermolecular reaction into its intramolecular equivalent, has proven a very valuable synthetic strategy for various types of reactions.

The selective cleavage of the *N*-*t*-butoxycarbonyl group in the presence of TBDMS (*t*-butyldimethylsilyl) (selective only when the protected alcohol was phenolic) or TBDPS (*tert*-butyldiphenylsilyl) (completely selective) ethers can be achieved[68] using a saturated solution of HCl in ethyl acetate.

Primary TBDMS ethers can be cleaved selectively[69] in the presence of THP ethers and ketals using ceric ammonium nitrate in methanol. Both phenolic[70] and aliphatic[71] TBDMS ethers undergo cleavage when exposed to catalytic amounts of $PdCl_2(MeCN)_2$; in the latter case, and with longer exposure, this also results in oxidation to the corresponding aldehyde or ketone, if the alcohol was primary or secondary, respectively. This cleavage and oxidation can be performed selectively in the presence of TIPS, TBDPS and benzyl ethers (equation 15).

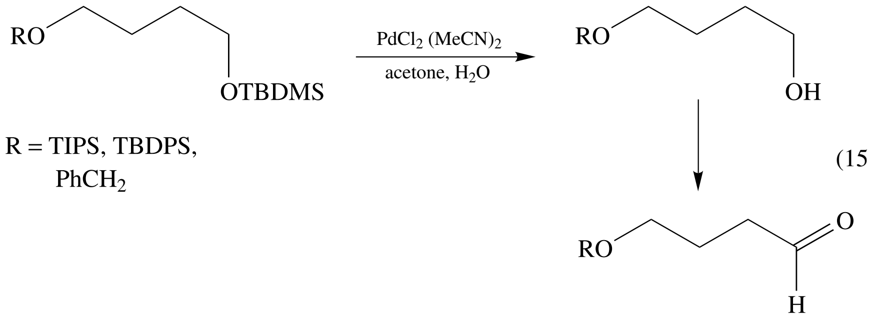

(15)

Two closely related methods for the direct transformation of THP ethers into TBDMS ethers, using TBDMSOTf and a tertiary amine base, have been disclosed[72,73]. This reagent system has been reported[74] to perform the same transformation on *t*-butyl and *t*-amyl ethers. In a similar vein[75], *p*-methoxybenzyl ethers are converted directly into the corresponding silyl ethers using TMSOTf and triethylamine.

A new alcohol and phenol protective group, the 1-[(2-trimethylsilyl)ethoxy]ethyl moiety, readily introduced using 2-(trimethylsilyl)ethyl vinyl ether and catalytic pyridinium *p*-toluenesulfonate (PPTS), has been described[76]. Cleavage is achieved under near-neutral conditions using TBAF monohydrate (equation 16).

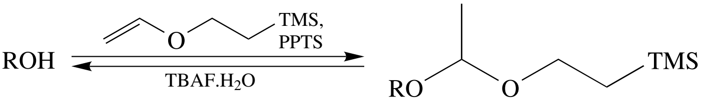

(16)

VI. (TRIHALOMETHYL)TRIALKYLSILANES

Full details[77] have been provided for the optimized preparation of (trifluoromethyl)trimethylsilane (Ruppert's Reagent[78]). It acts as a nucleophilic trifluoromethide equivalent, normally under fluoride ion initiation, reacting readily with a variety of carbonyl electrophiles and related species[79].

It adds (equation 17) to α-amino acid derived oxazolidin-5-ones giving, after acid hydrolysis, protected α-amino trifluoromethyl ketones[80], which are of interest as serine protease inhibitors.

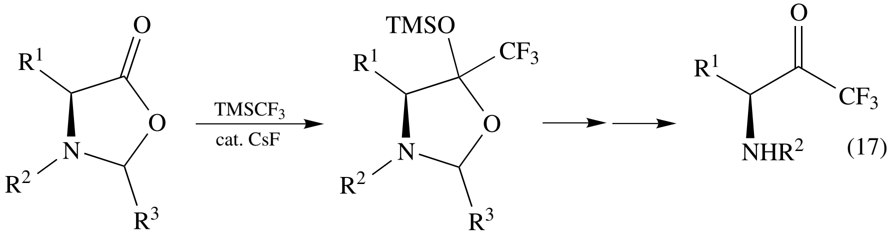

(17)

(Trifluoromethyl)tributyl tin, prepared from (trifluoromethyl)trimethylsilane and bis(tributyltin) oxide, has been reported[81] to react with disilyl sulphides to give the corresponding (trifluoromethyl)di- and (trifluoromethyl)trialkylsilanes.

The preparation and reactions of a range of mixed (trihalomethyl)trimethylsilanes have been described[82].

VII. TRIMETHYLSILYLDIAZOMETHANE

The chemistry of TMS-diazomethane has been reviewed[83].

The reaction between lithio TMS-diazomethane and carbonyl compounds, which generates alkylidenecarbenes, has been studied further. Aliphatic ketones give cyclopentene derivatives[84], while aldehydes and aryl alkyl ketones give alkynes[85]. The diazoalkene intermediates from aliphatic ketones can be trapped with diisopropylamine, producing aldehyde enamines and thus a method[86] for the one-carbon homologation of ketones to aldehydes (equation 18).

Lithio TMS-diazomethane reacts with ketenimines to produce 4-TMS-1,2,3-triazoles or 4-amino-3-TMS-pyrazoles[87,88], depending on the keteneimine substitution pattern.

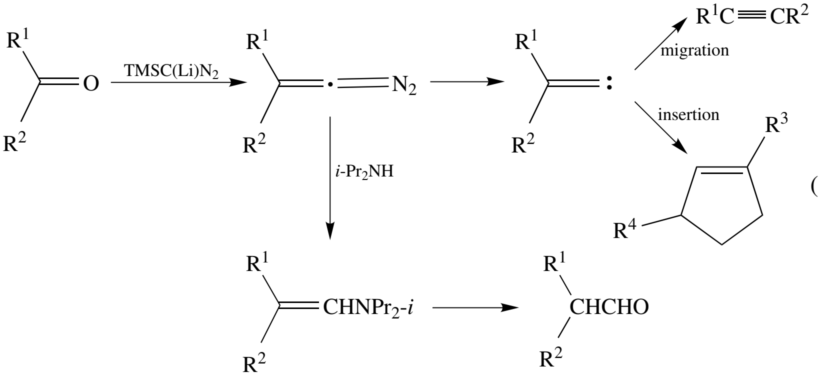

(18)

VIII. TRIALKYLSILYL TRIFLUOROMETHANESULPHONATES

The preparation and utility of trialkylsilyl perfluoroalkanesulphonates have been reviewed[89].

Trimethylsilyl fluorosulphonate, generated by *in situ* reaction of fluorosulphonic acid with either tetramethylsilane or allyltrimethylsilane, has been proposed[90] as a cheaper alternative to TMSOTf.

The combination of TMSOTf, dimethyl sulphide and 1,2-bis(trimethylsilyloxy)ethane provides a method[91] for the selective dioxolanation of ketones in the presence of aldehydes, via intermediate protection of the aldehyde as its silyloxysulphonium salt (equation 19).

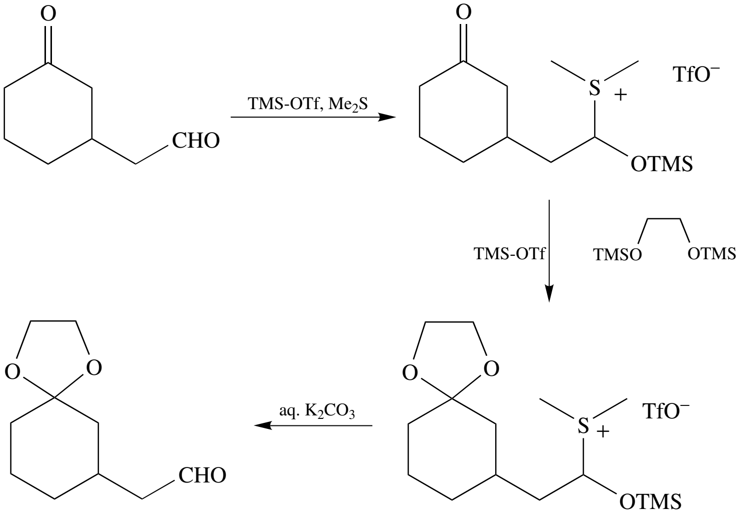

(19)

Dimethoxyamine reacts with simple alkenes in the presence of TMS-OTf to produce *N*-methoxyaziridines in good yield[92]; cyclic ketones react in a Beckmann-type process to yield *N*-methoxylactams (equation 20).

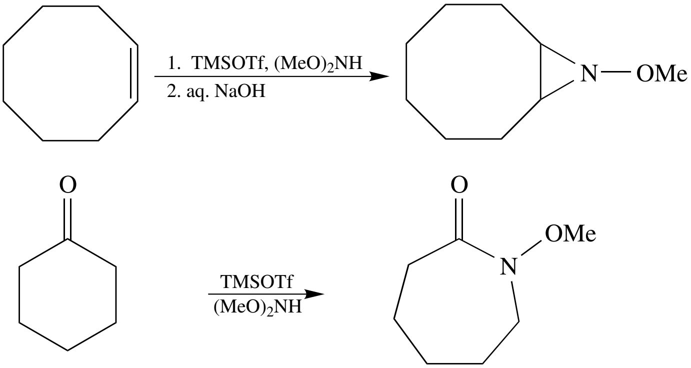

(20)

The aluminoxy acetal intermediates in ester reduction using DIBALH can be trapped with either TMSOTf[93] or TMS imidazole[94] to give monosilyl acetals (equation 21).

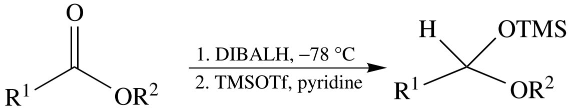

(21)

Ring-opening[95] of tetrahydrofuran with TBDMS-$Mn(CO)_5$, generated *in situ* from TBDMSOTf and $NaMn(CO)_5$, proved a key step (equation 22) in the synthesis of spiroketal lactones, precursors of certain insect pheromones.

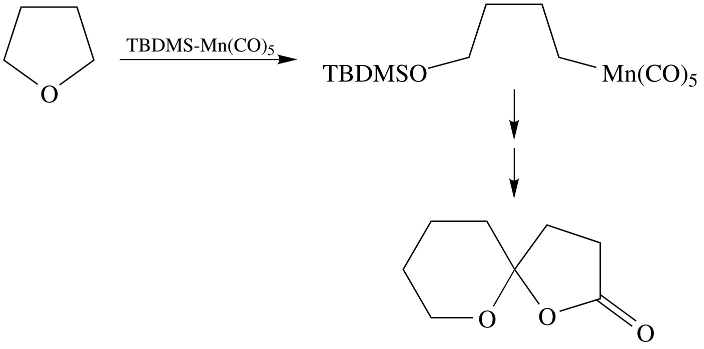

(22)

IX. THIO- AND SELENOSILANES

The preparation and reactions of organosilathianes and other mixed silicon–sulphur compounds have been reviewed[96,97].

Full details[98] have been published on the use of hexamethyldisilathiane in the generation of thioaldehydes and thioketones, which can be trapped *in situ* (equation 23). The corresponding selenium reagent has been employed[99] in the generation of selenoaldehydes.

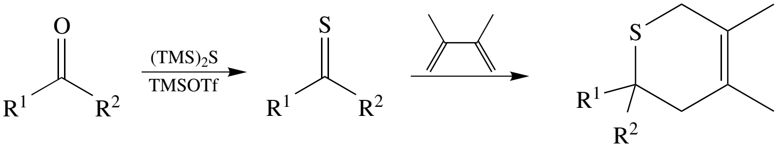

(23)

Triphenylsilanethiol, a white crystalline solid, has been recommended[100] for the ring-opening of epoxides to β-hydroxymercaptans or β-dihydroxysulphides, depending on the choice of base (equation 24).

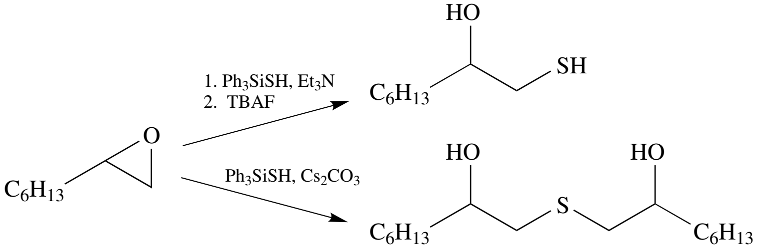

(24)

Nucleophilic bis-*O*-demethylation of dimethoxybenzenes in one flask is often difficult. It can, however, be achieved by use of sodium TMS thiolate in 1,3-dimethyl-2-imidazolidinone (DMEU) at high temperature in a sealed tube[101]. The same reagent system converts nitriles into primary thioamides at or slightly above room temperature in varying yields[102].

The TMSOTf catalysed reaction of (phenylthio)trimethylsilane with aldehydes to give hemithioacetals has been employed in a stereocontrolled route to polyols, via the 1,3-diol synthon shown (equation 25)[103].

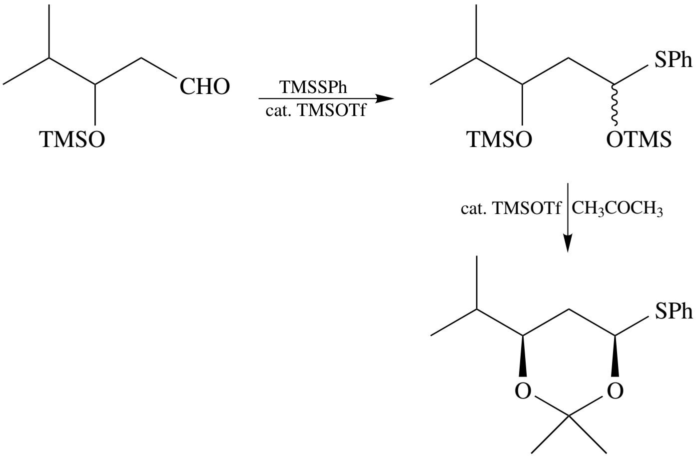

(25)

TMS isoselenocyanate, $Me_3SiNCSe$, prepared *in situ* from TMSCl and excess KSeCN, shows remarkable chemoselectivity[104] in the transformation of carbonyl compounds into

O-TMS cyanohydrins. Aliphatic aldehydes react smoothly, aromatic and α,β-unsaturated aldehydes react very slowly, with ketones being unreactive.

X. α,β-EPOXYSILANES

The preparation and applications of α,β-epoxysilane α-anions have been described in detail[105], as have the preparation and applications of α,β-epoxysilanes themselves[106].

α,β-Epoxysilanes undergo nucleophilic ring-opening with a regioselectivity normally, but not exclusively, due to α-attack. The question of whether this nucleophilic ring-opening involves prior coordination of the nucleophile with silicon has been addressed further. It has been concluded[107] that whether or not pentacoordinate intermediates are involved, they do not appear to be on the product-determining pathway.

A careful re-investigation[108] of the ring-opening reactions of (triphenylsilyl)ethylene oxide by Grignard reagents with added $MgBr_2$ has shown them to be analogous to that of the trimethylsilyl analogues. The observed regiochemistry can be explained by an initial magnesium halide induced rearrangement to (triphenylsilyl)ethanal followed by reaction with the Grignard reagent (equation 26), and not by direct β-attack.

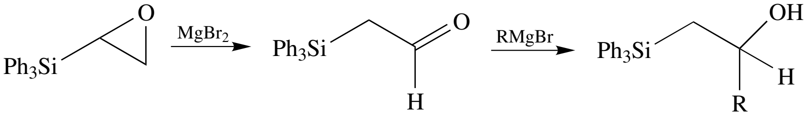

(26)

ϵ-Hydroxy-α,β-epoxysilanes undergo a regioselective intramolecular ring-opening[109]. The regioselectivity is highly dependent[110] on the configuration of the hydroxy epoxysilanes, with the *anti* diastereomers yielding tetrahydropyrans by α-attack and the *syn* stereoisomers leading to tetrahydrofurans by β-attack (equation 27).

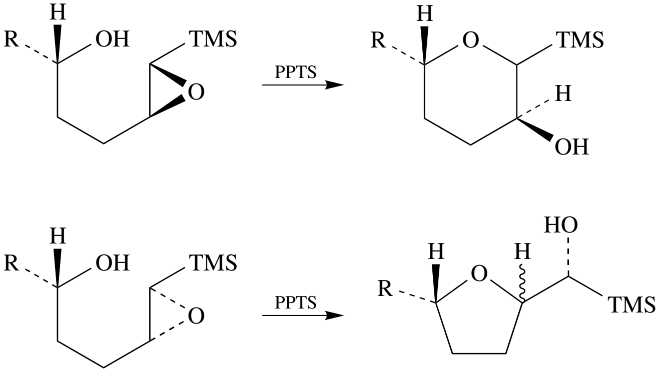

(27)

α,β-Epoxytriphenylsilanes undergo β-opening[111] when reacted with anions of hindered sulphones. The more usual selective α-opening[112] can be seen in the silica gel catalysed reaction of α,β-epoxytrimethylsilanes with benzenethiol; the products lead to α-hydroxyaldehydes after sila-Pummerer rearrangement and hydrolysis.

Sharpless kinetic resolution of γ-trimethylsilyl allylic alcohols can be highly efficient; in the case shown (equation 28), the epoxyalcohol and the remaining allylic alcohol were both formed in greater than 99% ee. Further synthetic applications of the product chiral epoxysilanes have been reviewed[113]. The preparation of several optically active α,β-epoxysilanes from the corresponding chiral diols has been described[114].

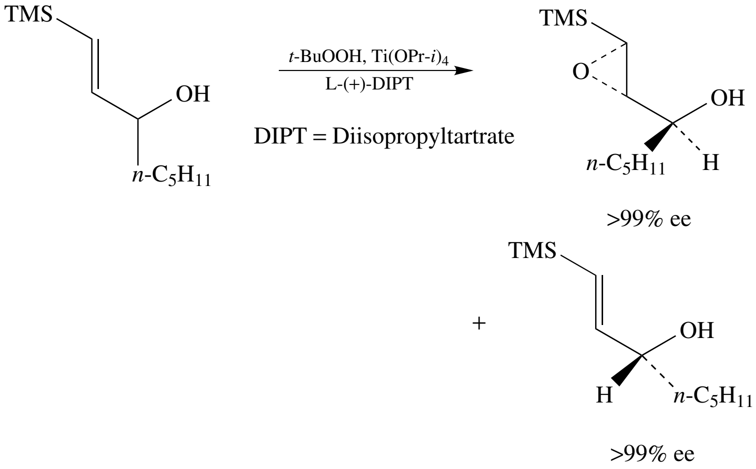

(28)

α,β-Epoxydisilanes undergo an acid-catalysed rearrangement[115] to acylsilanes. On the other hand, on treatment with LDA, simple epoxydisilanes rearrange (equation 29) to vinylsilane silanols[116].

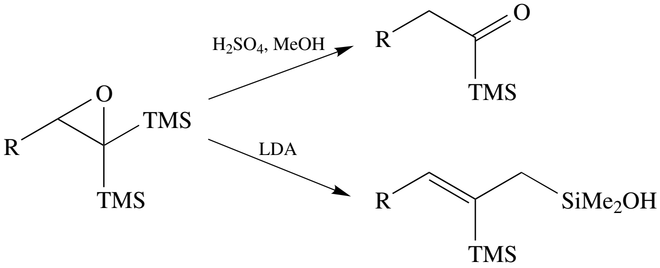

(29)

α-Halo-α,β-epoxysilanes rearrange in the presence of metal salts such as ZnCl$_2$ to produce α-haloacylsilanes[117]. Chiral β-vinyl-α,β-epoxysilanes undergo a Pd(0)-catalysed rearrangement to α-silyl-β,γ-unsaturated aldehydes[118] in high yield and with high stereoselectivity.

XI. Si—C OXIDATIVE CLEAVAGE

Oxidative cleavage of the carbon–silicon bond has been the subject of a recent and comprehensive review[119], in which emphasis has been placed on the compatibility of the oxidation conditions with various functional groups, with the inclusion of very useful compatibility tables.

A limitation on the use of the phenyldimethylsilyl group as a masked hydroxyl group is that treatment with acidic or electrophilic reagents is required to instal the necessary heteroatom prior to oxidative cleavage. Many of these reagents are incompatible with the presence of an alkene, although Fleming has shown[120] that the 2-methylbut-2-enyl(diphenyl)silyl group can be converted to the alcohol in the presence of certain types of alkenes (equation 30).

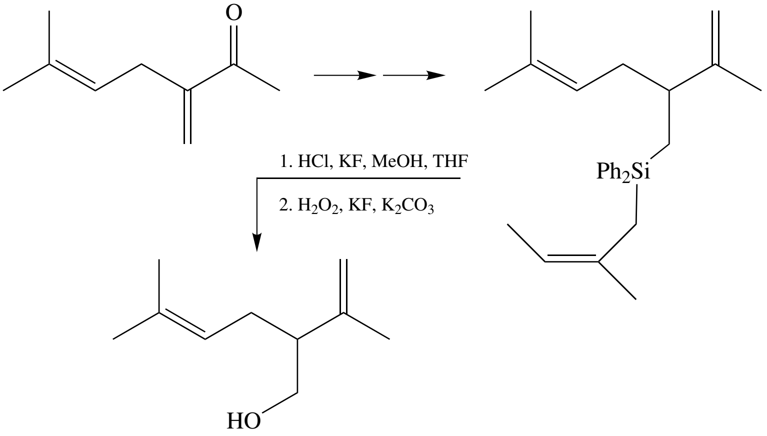

(30)

Recently, two completely different methods which are compatible with an alkene have been used successfully. The first of these involves[121] prior Birch reduction of the phenyl group to a cyclohexadiene. Subsequent treatment with fluoride ion and basic hydrogen peroxide then completes the overall cleavage (equation 31).

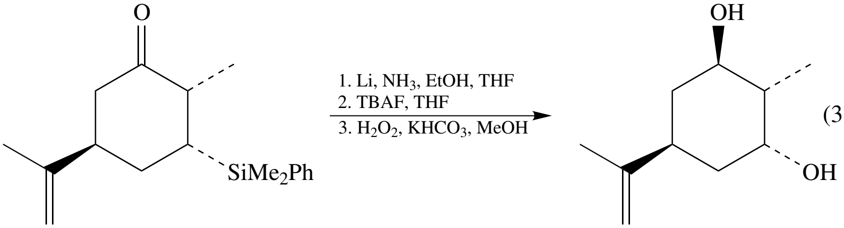

(31)

The second method[122] uses a polar aprotic medium, such as DMF or *N*-methylpyrrolidone, a strong base, such as CsOH or KH, and *t*-BuOOH to facilitate nucleophilic attack at silicon; sometimes, the presence of fluoride ion is advantageous. This protocol also cleaves sterically hindered alkoxysilanes. It provided a key step (equation 32) in a total synthesis[123] of (±)-lupinine.

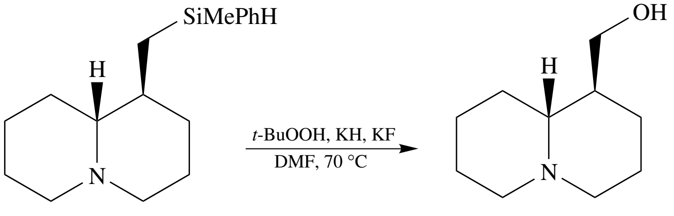

(32)

The Grignard reagent from (1-chloroethyl)dimethylphenylsilane, prepared in turn by α-methylation of (chloromethyl)dimethylphenylsilane, acts as a hydroxyethylating reagent after oxidative cleavage; its use can be seen in a stereoselective synthesis[124] of lincosamine, the sugar component of the antibiotic lincomycin.

XII. MISCELLANEOUS

The ability of silicon substituents to direct or control certain types of reactions, mainly fragmentation processes, has been reviewed[125].

Use of the urea-hydrogen peroxide complex and *N*,*N*′-bis(TMS) urea provides an improved method[126] for the preparation of bis(TMS) peroxide, TMSOOTMS. In the presence of Fe(III)(picolinic acid)$_3$, bis(TMS) peroxide carries out selective oxidation of alkanes to ketones by a non-radical mechanism. The Fe(III)−Fe(IV) manifold is believed to be responsible[127]. On the other hand, using $FeCl_2$ in pyridine, alkyl chlorides are formed through a radical mechanism. Here, the Fe(II)−Fe(IV) manifold has been proposed[128].

Selective inter- and intra-molecular oxidation reactions using α-silyloxyalkyl hydroperoxides have been reviewed[129].

Finally, an efficient method[130] for the synthesis of Mosher's acid has been reported; this involves the addition of TMS trichloroacetate to 1,1,1-trifluoroacetophenone followed by hydrolysis.

XIII. REFERENCES

1. E. W. Colvin, in *Silicon Reagents in Organic Synthesis*, Academic Press, London, 1988; updated and reprinted 1990.
2. S. E. Thomas, in *Organic Synthesis. The Roles of Boron and Silicon*, Oxford University Press, Oxford, 1991.
3. E. W. Colvin, in *Chemistry of the Metal−Carbon Bond*, Vol. 4 (Ed. F. R. Hartley), Wiley, Chichester, 1987, pp. 539−621.
4. E. W. Colvin, in *Comprehensive Organometallic Chemistry II*, Vol. 11 (Ed. A. McKillop), Elsevier, Oxford, 1995, pp. 313−354.
5. M. Wills and E. W. Colvin, in *Comprehensive Organic Functional Group Transformations*, Vol. 2 (Ed. S. V. Ley), Elsevier, Oxford, 1995, pp. 513−547.
6. E. R. Corey, J. Y. Corey and P. P. Gaspar (Eds.) *Silicon Chemistry*, Ellis Horwood, Chichester, 1988.
7. D. Schinzer (Ed.) *Selectivities in Lewis Acid Promoted Reactions*, Kluwer Academic Publishers, Dordrecht, 1989.
8. A. R. Bassindale and P. P. Gaspar (Eds.) *Frontiers of Organosilicon Chemistry*, The Royal Society of Chemistry, Cambridge, 1991.
9. I. Fleming (Ed.) *Organosilicon Chemistry in Organic Synthesis*, in *Tetrahedron*, **44**, 3761 (1988).
10. G. A. Olah, G. K. Surya Prakash and R. Krishnamurti, in *Advances in Silicon Chemistry*, Vol. 1 (Ed. G. L. Larson), Jai Press, London and Greenwich, Connecticut, 1991, pp. 1−64.
11. E. Nakamura, *Synlett*, 539 (1991).
12. S. H. Bertz, G. Miao, B. E. Rossiter and J. P. Snyder, *J. Am. Chem. Soc.*, **117**, 11023 (1995).
13. M. Eriksson, A. Johansson, M. Nilsson and T. Olsson, *J. Am. Chem. Soc.*, **118**, 10904 (1996).
14. D.-K. Wang, L.-X. Dai and X.-L. Hou, *Tetrahedron Lett.*, **36**, 8649 (1995).
15. J. Kabbara, S. Flemming, K. Nickisch, H. Neh and J. Westermann, *Tetrahedron Lett.*, **35**, 8591 (1994).
16. Ch. Kishan Reddy, A. Devasagayaraj and P. Knochel, *Tetrahedron Lett.*, **37**, 4495 (1996).
17. H. Liu and T. Cohen, *Tetrahedron Lett.*, **36**, 8925 (1995).
18. B. H. Lipshutz, M. R. Wood and C. W. Lindsley, *Tetrahedron Lett.*, **36**, 4385 (1995); see also D. C. Harrowven and H. S. Poon, *Tetrahedron Lett.*, **37**, 4281 (1996).
19. W. B. Motherwell and L. R. Roberts, *Tetrahedron Lett.*, **36**, 1121 (1995).
20. J. G. Lee and K. K. Kang, *J. Org. Chem.*, **53**, 3634 (1988).
21. D. C. Snyder, *J. Org. Chem.*, **60**, 2638 (1995).
22. H. H. Seltzman, M. A. Moody and M. K. Begum, *Tetrahedron Lett.*, **33**, 3443 (1992).
23. J. G. Lee and H. T. Cha, *Tetrahedron Lett.*, **33**, 3167 (1992).
24. G. A. Olah, P. Ramaiah, G. Sandford, A. Orlinkov and G. K. Surya Prakash, *Synthesis*, 468 (1994).
25. T. Hirao, T. Hasegawa, Y. Muguruma and I. Ikeda, *J. Org. Chem.*, **61**, 366 (1996).
26. S. V. Pansare and M. G. Malusare, *Tetrahedron Lett.*, **37**, 2859 (1996).

27. M. Lautens and Y. Ren, *J. Org. Chem.*, **61**, 2210 (1996).
28. M. Seki, K. Kondo and T. Iwasaki, *Synlett*, 315 (1995).
29. J. K. Rasmussen, S. M. Heilman and L. Krepski, in *Advances in Silicon Chemistry*, Vol. 1 (Ed. G. L. Larson), Jai Press, London and Greenwich, Connecticut, 1991, pp. 65–187.
30. K. Higuchi, M. Onaka and Y. Izumi, *J. Chem. Soc., Chem. Commun.*, 1035 (1991).
31. J. K. Whitesell and R. Apodaca, *Tetrahedron Lett.*, **37**, 2525 (1996).
32. P. Kocienski, P. Raubo, J. K. Davis, F. T. Boyle, D. E. Davies and A. Richter, *J. Chem. Soc., Perkin Trans. 1*, 1797 (1996).
33. N. Adjé, F. Vogeleisen and D. Uguen, *Tetrahedron Lett.*, **37**, 5893 (1996).
34. B. Muller, F. Delaloge, M. den Hartog, J.-P. Férézou, A. Pancrazi, J. Prunet, J.-Y. Lallemand, A. Neuman and T. Prangé, *Tetrahedron Lett.*, **37**, 3313 (1996).
35. M. Hayashi, T. Inoue, Y. Miyamoto and N. Ogune, *Tetrahedron*, **50**, 4385 (1994) and references cited therein.
36. W. D. Pan, X. M. Feng, L. Z. Gong, W. H. Hu, Z. Li, A. Q. Mi and Y. Z. Jiang, *Synlett*, 337 (1996).
37. C. Bolm and P. Müller, *Tetrahedron Lett.*, **36**, 1625 (1995) and references cited therein.
38. A. Abiko and G. Wang, *J. Org. Chem.*, **61**, 2264 (1996).
39. M. North, *Synlett*, 807 (1993).
40. M. Hayashi, M. Tamura and N. Oguni, *Synlett*, 663 (1992) and references cited therein.
41. P. Van de Weghe and J. Collin, *Tetrahedron Lett.*, **36**, 1649 (1995).
42. F. A. Hicks, S. C. Berk and S. L. Buchwald, *J. Org. Chem.*, **61**, 2713 (1996).
43. G. D. Probert, R. J. Whitby and S. J. Coote, *Tetrahedron Lett.*, **36**, 4113 (1995).
44. D. C. Pryde, S. S. Henry and A. I. Meyers, *Tetrahedron Lett.*, **37**, 3243 (1996).
45. M. Meguro, N. Asao and Y. Yamamoto, *J. Chem. Soc., Chem. Commun.*, 1021 (1995).
46. K. I. Sutowardoyo, M. Emziane, P. Lhoste and D. Sinou, *Tetrahedron*, **47**, 1435 (1991).
47. M. Hayashi, K. Kohmura and N. Oguni, *Synlett*, 774 (1991).
48. L. E. Martínez, J. L. Leighton, D. H. Carsten and E. N. Jacobsen, *J. Am. Chem. Soc.*, **117**, 5897 (1995).
49. K. B. Hansen, J. L. Leighton and E. N. Jacobsen, *J. Am. Chem. Soc.*, **118**, 10924 (1996).
50. J. F. Larrow, S. E. Schaus and E. N. Jacobsen, *J. Am. Chem. Soc.*, **118**, 7420 (1996).
51. J. L. Leighton and E. N. Jacobsen, *J. Org. Chem.*, **61**, 389 (1996).
52. S. E. Schaus and E. N. Jacobsen, *Tetrahedron Lett.*, **37**, 7937 (1996).
53. L. E. Martínez, W. A. Nugent and E. N. Jacobsen, *J. Org. Chem.*, **61**, 7963 (1996).
54. M. H. Wu and E. N. Jacobsen, *Tetrahedron Lett.*, **38**, 1693 (1997).
55. P. Magnus, J. Lacour, P. A. Evans, M. B. Roe and C. Hulme, *J. Am. Chem. Soc.*, **118**, 3406 (1996).
56. P. A. Evans and D. P. Modi, *J. Org. Chem.*, **60**, 6662 (1995).
57. G. A. Olah and T. D. Ernst, *J. Org. Chem.*, **54**, 1203 (1989).
58. G. A. Olah, Q. Wang, X.-Y. Li and G. K. Surya Prakash, *Synlett*, 774 (1991).
59. M. V. R. Reddy, R. Kumareswaran and Y. D. Vankar, *Tetrahedron Lett.*, **36**, 6751 (1995).
60. J. G. Lee and K. H. Kwak, *Tetrahedron Lett.*, **33**, 3165 (1992).
61. M. Ito, K. Koyakumaru, T. Ohta and H. Takaya, *Synthesis*, 376 (1995).
62. T. W. Greene and P. G. M. Wuts, *Protective Groups in Organic Synthesis*, 2nd ed., Wiley, Chichester, 1991.
63. G. Simchen and J. Heberle, *Silylating Agents*, 2nd ed., Fluka Chemie AG, Buchs, Switzerland, 1995.
64. J. Muzart, *Synthesis*, 11 (1993)
65. T. D. Nelson and R. D. Crouch, *Synthesis*, 1031 (1996).
66. C. Rücker, *Chem. Rev.*, **95**, 1009 (1995).
67. (a) G. Stork, T. Y. Chan and G. A. Breault, *J. Am. Chem. Soc.*, **114**, 7578 (1992) and references therein.
    (b) M. Bols and T. Skrydstrup, *Chem. Rev.*, **95**, 1253 (1995).
68. F. Cavelier and C. Enjalbal, *Tetrahedron Lett.*, **37**, 5131 (1996).
69. A. DattaGupta, R. Singh and V. K. Singh, *Synlett*, 69 (1996).
70. N. S. Wilson and B. A. Keay, *Tetrahedron Lett.*, **37**, 153 (1996).
71. N. S. Wilson and B. A. Keay, *J. Org. Chem.*, **61**, 2918 (1996).
72. S. Kim and I. S. Kee, *Tetrahedron Lett.*, **31**, 2899 (1990).
73. T. Oriyama, K. Yatabe, S. Sugawara, Y. Machiguchi and G. Koga, *Synlett*, 523 (1996).

74. X. Franck, B. Figadère and A. Cavé, *Tetrahedron Lett.*, **36**, 711 (1995).
75. T. Oriyama, K. Yatabe and Y. Kawada, *Synlett*, 45 (1995).
76. J. Wu, B. K. Shull and M. Koreeda, *Tetrahedron Lett.*, **37**, 3647 (1996).
77. P. Ramaiah, R. Krishnamurti and G. K. Surya Prakash, *Org. Synth.*, **72**, 232 (1993).
78. I. Ruppert, K. Schlich and W. Volbach, *Tetrahedron Lett.*, **25**, 2195 (1984).
79. G. K. Surya Prakash, in *Synthetic Fluorine Chemistry* (Ed. G. A. Olah, R. D. Chambers and G. K. Surya Prakash), Wiley, New York, 1992.
80. M. W. Walter, R. M. Adlington, J. E. Baldwin, J. Chuhan and C. J. Schofield, *Tetrahedron Lett.*, **36**, 7761 (1995).
81. G. K. Surya Prakash, A. K. Yudin, D. Deffieux and G. A. Olah, *Synlett*, 151 (1996).
82. A. K. Yudin, G. K. Surya Prakash, D. Deffieux, M. Bradley, R. Bau and G. A. Olah, *J. Am. Chem. Soc.*, **119**, 1572 (1997).
83. T. Shioiri and T. Aoyama, in *Advances in the Use of Synthons in Organic Chemistry*, Vol. 1 (Ed. A. Dondoni), Jai Press, London and Greenwich, Connecticut, 1993, p. 51; R. Anderson and S. B. Anderson, in *Advances in Silicon Chemistry*, Vol. 1 (Ed. G. L. Larson), Jai Press, London and Greenwich, Connecticut, 1991, pp. 303–325.
84. S. Ohira, K. Okai and T. Moritani, *J. Chem. Soc., Chem. Commun.*, 721 (1992).
85. K. Miwa, T. Aoyama and T. Shioiri, *Synlett*, 107 (1994).
86. K. Miwa, T. Aoyama and T. Shioiri, *Synlett*, 109 (1994).
87. T. Aoyama, S. Katsuta and T. Shioiri, *Heterocycles*, **28**, 133 (1989).
88. T. Aoyama, T. Nakano, K. Marumo, Y. Uno and T. Shioiri, *Synthesis*, 1163 (1991).
89. G. Simchen in *Advances in Silicon Chemistry*, Vol. 1 (Ed. G. L. Larson), Jai Press, Greenwich, Connecticut, 1991, pp. 189–301.
90. B. H. Lipshutz, J. Burgess-Henry and G. P. Roth, *Tetrahedron Lett.*, **34**, 995 (1993).
91. S. Kim, Y. G. Kim, and D. Kim, *Tetrahedron Lett.*, **33**, 2565 (1992).
92. E. Vedejs and H. Sano, *Tetrahedron Lett.*, **33**, 3261 (1992).
93. K. Shibata, N. Tokitoh and R. Okazaki, *Tetrahedron Lett.*, **34**, 1491 (1993).
94. R. Polt, M. A. Peterson and L. DeYoung, *J. Org. Chem.*, **57**, 5469 (1992).
95. P. DeShong and P. J. Rybczynski, *J. Org. Chem.*, **56**, 3207 (1991).
96. M. D. Mizhiritskii and V. O. Reikhsfel'd, *Russ. Chem. Rev. (Engl. Transl.)*, **57**, 447 (1988)
97. E. Block and M. Aslam, *Tetrahedron*, **44**, 281 (1988).
98. A. Capperucci, A. Degl'Innocenti, A. Ricci, A. Mordini and G. Reginato, *J. Org. Chem.*, **56**, 7323 (1991); A. Degl'Innocenti, A. Capperucci, A. Mordini, G. Reginato, A. Ricci and F. Cerreta, *Tetrahedron Lett.*, **34**, 873 (1993).
99. M. Segi, T. Nakajima, S. Suga, S. Murai, I. Ryu, A. Ogawa and N. Sonoda, *J. Am. Chem. Soc.*, **110**, 1976 (1988); for another silicon-based route to these reactive species, see G. A. Krafft and P. T. Meinke, *J. Am. Chem. Soc.*, **108**, 1314 (1986).
100. J. Brittain and Y. Gareau, *Tetrahedron Lett.*, **34**, 3363 (1993).
101. J. R. Hwu and S.-C. Tsay, *J. Org. Chem.*, **55**, 5987 (1990).
102. P.-Y. Lin, W.-S. Ku and M.-J. Shiao, *Synthesis*, 1219 (1992).
103. S. D. Rychnovsky, *J. Org. Chem.*, **54**, 4982 (1989).
104. K. Sukata, *J. Org. Chem.*, **54**, 2015 (1989).
105. G. A. Molander and K. Mautner, *J. Org. Chem.*, **54**, 4042 (1989); G. A. Molander and K. Mautner, *Pure Appl. Chem.*, **62**, 707 (1990).
106. P. F. Hudrlik and A. M. Hudrlik, in *Advances in Silicon Chemistry*, Vol. 2 (Ed. G. L. Larson), Jai Press, Greenwich, Connecticut, 1993, pp. 1–89.
107. P. F. Hudrlik, D. Ma, R. S. Bhamidipati and A. M. Hudrlik, *J. Org. Chem.*, **61**, 8655 (1996).
108. P. F. Hudrlik, M. E. Ahmed, R. R. Roberts and A. M. Hudrlik, *J. Org. Chem.*, **61**, 4395 (1996).
109. H. Flörke and E. Schaumann, *Synthesis*, 647 (1996).
110. G. Adiwidjaja, H. Flörke, A. Kirschning and E. Schaumann, *Tetrahedron Lett.*, **36**, 8771 (1995).
111. P. Jankowski and J. Wicha, *J. Chem. Soc., Chem. Commun.*, 802 (1992).
112. P. Raubo and J. Wicha, *Synlett*, 25 (1993).
113. F. Sato and Y. Kobayashi, *Synlett*, 849 (1992).
114. A. R. Bassindale, P. G. Taylor and Y. Xu, *Tetrahedron Lett.*, **37**, 555 (1996).
115. D. M. Hodgson and P. J. Comina, *Chem. Commun.*, 755 (1996).
116. D. M. Hodgson and P. J. Comina, *Tetrahedron Lett.*, **37**, 5613 (1996).
117. Y. Horiuchi, M. Taniguchi, K. Oshima and K. Utimoto, *Tetrahedron Lett.*, **36**, 5353 (1995).
118. F. Gilloir and M. Malacria, *Tetrahedron Lett.*, **33**, 3859 (1992).

119. G. R. Jones and Y. Landais, *Tetrahedron*, **52**, 7599 (1996).
120. I. Fleming and S. B. D. Winter, *Tetrahedron Lett.*, **34**, 7287 (1993); I. Fleming and D. Lee, *Tetrahedron Lett.*, **37**, 6929 (1996).
121. D. F. Taber, L. Yet and R. S. Bhamidipati, *Tetrahedron Lett.*, **36**, 351 (1995); D. F. Taber, R. S. Bhamidipati and L. Yet, *J. Org. Chem.*, **60**, 5537 (1995); D. F. Taber, R. S. Bhamidipati and L. Yet, *J. Org. Chem.*, **61**, 1554 (1996); R. Angelaud and Y. Landais, *J. Org. Chem.*, **61**, 5202 (1996).
122. J. H. Smitrovich and K. A. Woerpel, *J. Org. Chem.*, **61**, 6044 (1996).
123. G. A. Molander and P. J. Nichols, *J. Org. Chem.*, **61**, 6040 (1996).
124. F. L. van Delft, M. de Kort, G. A. van der Marel and J. H. van Boom, *J. Org. Chem.*, **61**, 1883 (1996).
125. J. R. Hwu and H. V. Patel, *Synlett*, 989 (1995).
126. W. P. Jackson, *Synlett*, 536 (1990).
127. D. H. R. Barton and B. M. Chabot, *Tetrahedron*, **53**, 487 (1997).
128. D. H. R. Barton and B. M. Chabot, *Tetrahedron*, **53**, 511 (1997).
129. R. Nagata and I. Saito, *Synlett*, 291 (1990).
130. Y. Goldberg and H. Alper, *J. Org. Chem.*, **57**, 3731 (1992).

CHAPTER 29

Recent advances in the hydrosilylation and related reactions

IWAO OJIMA, ZHAOYANG LI and JIAWANG ZHU

Department of Chemistry, State University of New York at Stony Brook, Stony Brook, New York 11794-3400, USA

I. INTRODUCTION

Hydrosilylation, especially of carbon–carbon multiple bonds, is one of the most important reactions in organosilicon chemistry, and thus the reaction has been studied extensively for half a century. Even after five decades of research, it is apparent that interest in this process has been continuing and even increasing in the last several years rather than fading, judging from the number of publications. The reaction is used for the industrial production of organosilicon compounds such as adhesives, binders and coupling agents. In research laboratories, hydrosilylation is a very convenient and efficient method for the syntheses of a variety of organosilicon compounds not only for the study of organosilicon chemistry, but also for silicon-based polymers and dendrimers for new materials. The hydrosilylation of various functional groups catalyzed by transition metal complexes or promoted by radical initiators provides facile routes to various organosilicon reagents and synthetic intermediates in organic syntheses as well as a unique method for the selective reduction of carbon–heteroatom bonds. Catalytic asymmetric hydrosilylation applied to organic syntheses has been substantially advanced[1–3]. New reactions related to hydrosilylation have been discovered and developed such as silylcarbonylation, silylformylation and silylcarbocyclization, which are useful in organic syntheses.

This chapter will summarize the recent advances in hydrosilylation and related reactions catalyzed by transition metal complexes since this subject was reviewed in *The Chemistry of Organic Silicon Compounds* in 1989 that covered the advances till the end of 1986[3].

II. HYDROSILYLATION OF ALKENES

A. Simple and Functionalized Alkenes

1. By Group VIII transition metal catalysts

Platinum and rhodium catalysts have been the most frequently used catalysts among all the metal-based catalysts for the hydrosilylation of alkenes to date. In particular, a variety of rhodium catalysts have been extensively studied[3–6], while the development of other Group VIII transition metal catalysts such as those of palladium and ruthenium continues. In general, the hydrosilylation of an alkene gives the corresponding silylalkanes with varying regioselectivity (equation 1).

$$R^1CH{=}CHR^2 + HSiR_3 \xrightarrow{\text{catalyst}} R^1\,(R^3{}_3Si)CHCH_2R^2 + R^1CH_2CHR^2(SiR_3) \qquad (1)$$

Little attention has been paid to the hydrosilylation reactions using monosilane, SiH_4, for synthetic purposes, mainly because of its limited availability and difficulty in handling. However, SiH_4 has recently emerged as a new raw material in the organosilicon industry in connection with the recent development of polysilicon and amorphous silicon products[7]. Thus, the hydrosilylation of alkenes with SiH_4 may provide a direct and practical route to trihydroalkylsilanes. A preliminary study on the reactions of 1-hexene with SiH_4 catalyzed by Group VIII transition metal and metal complexes at 80 °C and 10 atm for 3 h shows that the reaction gives a mixture of $H_3Si(C_6H_{13}\text{-}n)$ (major) and $H_2Si(C_6H_{13}\text{-}n)_2$ (minor)[7]. The most active catalyst so far examined is $Pt(PPh_3)_4$ which gives $H_3Si(C_6H_{13}\text{-}n)$ in 37.4% yield and $H_2Si(C_6H_{13}\text{-}n)_2$ in 4.7% yield. The relative catalytic activity decreases in the order $Pt(PPh_3)_4 > Rh/C > PtCl_2(PPh_3)_2 > Pt/C \gg NiCl_2(PPh_3)_2$. The reaction of 1,5-hexadiene with SiH_4 using Pt and Rh catalysts affords two major products, H_3Si(5-hexenyl)SiH_3 and silacycloheptane in 1:1 – 4:1 ratio accompanied by a small amount of H_2Si(5-hexenyl)$_2$ in 8–38% total yield[7]. The product ratio is mainly dependent on the catalyst species used.

The reactions of styrene, α-methylstyrene and methyl methacrylate (equation 2) with $HSiEt_3$ and $HSiPh_3$ catalyzed by $PtCl_2$, $PtCl_2(PhCN)_2$ or $PtCl_2(PhCN)_2PR_3$ give the linear hydrosilylation products predominantly[8]. The activity and selectivity of these catalysts are dependent on the nature of the phosphine ligand as well as the Pt/ligand ratio. The use of chelating bidentate diphosphine ligands results in the loss of catalytic activity.

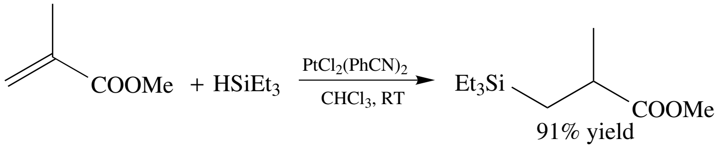

(2)

The reactions of enamides (**1**) and *N*-vinylureas (**2**) with $HSiMe_2Ph$ catalyzed by $Rh_2(OAc)_4$ give the corresponding 1-silylalkylamides (**3**) and 1-silylalkylureas (**4**) in 38–93% isolated yields with complete regio- and site selectivity (equations 3–5)[9]. The directing effect of the carbonyl oxygen illustrated for the key intermediate **5** is proposed to account for the remarkable regioselectivity. In fact, the reaction of vinyl acetate that can take a similar chelate structure also gives 1-silylethyl acetate **6** as the major product in 61% isolated yield[9]. Other rhodium catalysts, $[Rh(CO)_2Cl]_2$, $HRh(PPh_3)_3$, $Rh(acac)_3$, $[Rh(COD)Cl]_2$ and $RhCl(PPh_3)_3$, are found to be much less active.

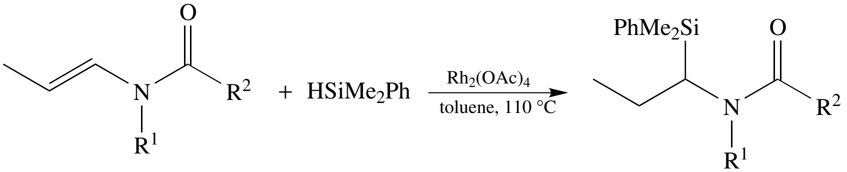

(**1**) (**3**) (3)

$R^1 = CH_2Ph$, H, Me; R^2 = Me, NMe_2

Remarkable effects of non-vicinal, proximate polar groups on the reaction rates are disclosed in the hydrosilylation of substituted bicyclo[2.2.1]hept-5-enes (**8**) catalyzed by $Pt[(CH_2{=}CHSiMe_2)_2O]_2$ (Karstedt's catalyst)[10,11] or $PtCl_4$ (equation 6)[12]. *Endo*-2,3-dicarboxylic *N*-phenylimide **8c** does not react at all and the reaction of *endo*-2,3-dicarboxylic anhydride **8a** is unusually slow. On the contrary, the reaction of *exo*-imide

8d or *exo*-anhydride **8b** is very fast, completing in 30 min or less under the same conditions, while *endo*-ether **8h** reacts normally (equation 6) (Table 1). These results clearly indicate that extremely strong field effects of the electron-deficient imide and anhydride groups are operative in these reactions[12]. Also, the nature of hydrosilane exerts marked influence on the reaction rate, i.e., the reactivity of hydrosilanes is in the order: $HSiMe_2Cl \sim HSiMe_2Ph > HSiMeCl_2 \gg HSiMe_3 \sim HSiCl_3$[12].

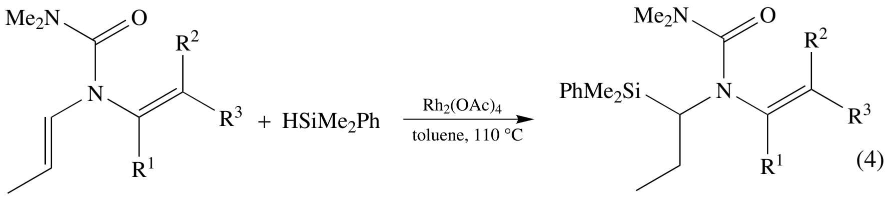

(4)

(2) **(4)**

a: $R^1 = R^2 = R^3 = H$; **b:** $R^1 = H$, $R^2 = Me$, $R^3 = Et$; **c:** $R^1 = Me$, $R^2 = H$, $R^3 = Me$;
d: $R^1, R^3 = (CH_2)_4$, $R^2 = Me$

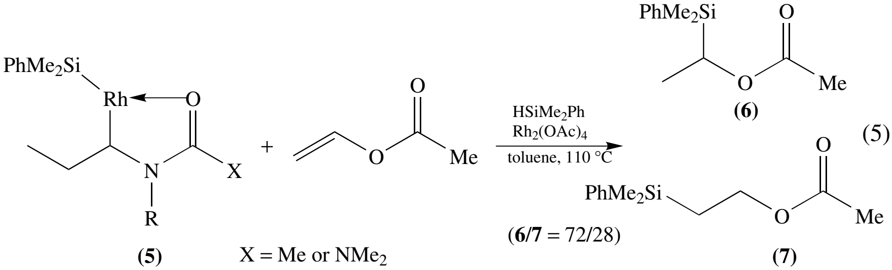

(5)

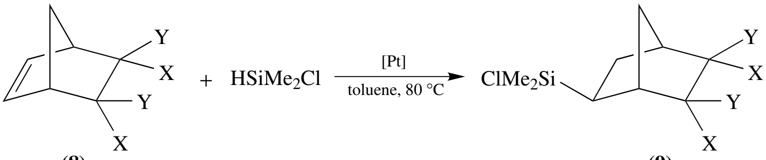

(6)

(8) **(9)**

$[Pt] = Pt[(CH_2{=}CHSiMe_2)O]_2$ (Karstedt's catalyst) or $PtCl_4$

TABLE 1. Hydrosilylation of norbornene derivatives

X,X	Y,Y	Yield (%)	Time (h)
8a CO−O−CO	H,H	95	48
8b H,H	CO−O−CO	99	<0.5
8c CO−N(Ph)−CO	H,H	0	48
8d H,H	CO−N(Ph)−CO	99	0.5
8e CO_2Me,CO_2Me	H,H	99	2
8f H, CO_2Me	H,CO_2Me	99	0.5
8g H,H	CO_2Me,CO_2Me	99	1
8h CH_2OCH_2	H,H	99	<0.5
8i H,H	H,H	99	<0.5

Hydrosilylation of divinyl ether has been applied for the synthesis of silacyclopentane **12** using Speier's catalyst (Scheme 1)[13]. One of the two carbon–carbon double bonds was hydrosilylated first with a dialkyl(ethoxy)silane, giving silylethyl vinyl ether **10** in 53–59% yield, which was reduced with $LiAlH_4$ to hydrosilane **11**. The intramolecular hydrosilylation of **11** affords silacyclopentane **12** in moderate yields (Scheme 1). The reaction with $HSiEt_2(OEt)$ gives **12a** exclusively in 45% yield, while silacyclohexane **13b** is formed as the minor product when $HSiMe_2(OEt)$ is used as the hydrosilane (**12b/13b** = 2.3/1; 50% total yield)[13]. Other intramolecular hydrosilylation reactions useful in organic syntheses will be discussed in the section II.C. (*vide infra*).

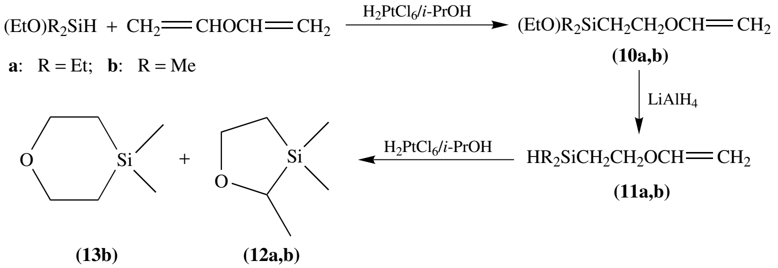

SCHEME 1

The reactions of styrene, 4-chlorostyrene, 4-methoxystyrene, and methyl acrylate with 1,2-bis(dimethylsilyl)benzene (**14**) catalyzed by $Pt(CH_2{=}CH_2)(PPh_3)_2$ give the corresponding "dehydrogenative double silylation" products **15** in good to high yields (equation 7)[14]. When dimethyl maleate is employed, benzo-1,4-disilacyclohexene **16** (R^1 = R^2 = CO_2Me) is obtained as the major product (**15/16** = 22/78) (equation 7). In the reactions of 1-alkenes, i.e., ethylene and 1-octene, the formation of monosilylated products is also observed (13–57% yield). On the basis of the fact that no deuterium is incorporated into the products when 1,2-dideuterio-1,2-bis(dimethylsilyl)benzene is used, disilyl-Pt metallacycle **17** is proposed to be the key intermediate of this process (equation 7).

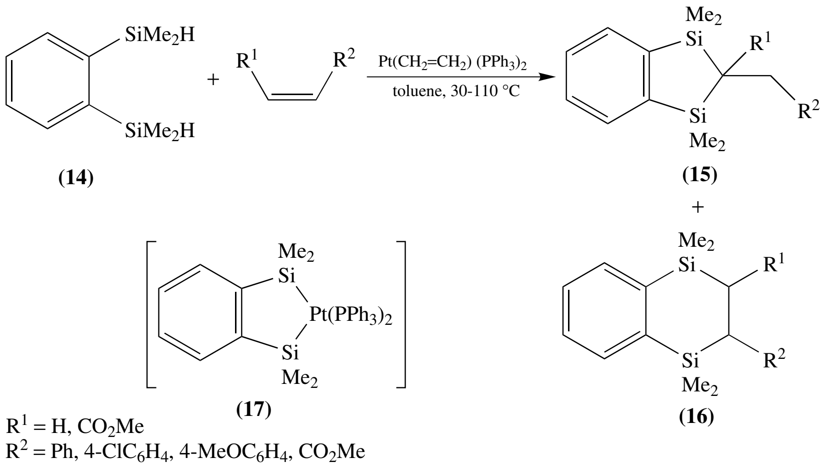

(7)

The reaction of 3,3-dimethyl-1-butene or styrene with 1,2-bis(dimethylsilyl)ethane catalyzed by $RhCl(PPh_3)_3$ gives only linear monosilylation product, $RCH_2CH_2SiMe_2(CH_2)_2SiMe_2(H)$, in high yield, i.e., there is a stark difference in reactivity of the Si–H moiety between 1,2-bis(dimethylsilyl)ethane and $RCH_2CH_2SiMe_2(CH_2)_2SiMe_2(H)$ toward hydrosilylation[15]. Although clear enhancement of reaction rate is not observed in the reaction of alkenes, marked rate enhancement in comparison with normal trialkylsilanes is exhibited in the reactions of alkynes and ketones (*vide infra*)[15].

The isocyanide complexes of platinum, $PtCl_2(C{\equiv}N\text{-}C_6H_3Me_2\text{-}2,6)_2$, show modest catalytic activity for the hydrosilylation of α-methylstyrene with $HSiMe_2Ph$. The corresponding Ni-isocyanide complex shows a low catalytic activity and the Pd-isocyanide complex is inactive[16]. The platinum complex of bidentate 2,2′-bis(isocyano)-1,1-binaphthyl (DIBN), $Pt_2Cl_4(DIBN)_2$, is more active than those of PPh_3 or the monodentate isocyanide complexes[16]. However, $PtCl_2(C{\equiv}N\text{-}C_6H_3Me_2\text{-}2,6)_2$ is an excellent catalyst for the hydrosilylation of 5-hexen-2-one (0.034 mol % catalyst, 25 °C, 3 h), giving 6-silyl-2-hexanone **18** in 98% yield (equation 8)[16]. Under the same reaction conditions, $Pt_2Cl_4(DIBN)_2$ is also highly active (74% yield), but $PtCl_2(PPh_3)_2$ gives only a trace amount of **18**. The isocyanide complexes of rhodium, $RhCl(C{\equiv}N\text{-}C_6H_3Me_2\text{-}2,6)_3$ and $[RhCl(DIBN)_2]_n$, are excellent catalysts for this reaction (96–99% yield), whereas $RhCl(PPh_3)_3$ is much less active affording **18** in only 5% yield.

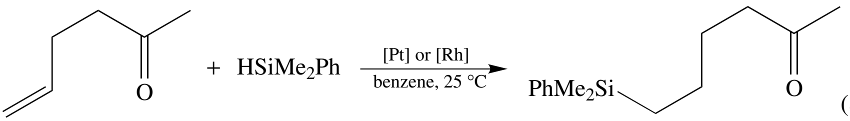

(8)

(18)

$[Pt] = PtCl_2(CN\text{-}C_6H_3Me_2\text{-}2.6), Pt_2Cl_4(DIBN)_2$
$[Rh] = RhCl(CN\text{-}C_6H_3Me_2\text{-}2.6)_3, [RhCl(DIBN)_2]_n$

The reaction of styrene with H_2SiPh_2 catalyzed by $RhCl(PPh_3)_3$ in THF at ambient temperature is shown to give the linear monohydrosilylation product, $Ph_2HSiCH_2CH_2Ph$, in 77–89% isolated yield, accompanied by $Ph_2HSi(CH{=}CHPh)$ or $PhCH_2CH_3$ (1–7%). The observed linear selectivity as well as product selectivity is substantially better than that of the reaction using $HSiEt_3$ as the hydrosilane[17].

Palladium complexes with bis(diphenylphosphino)methane (dpm), $Pd_2(dpm)_3$, $PdCl_2(dpm)$, $Pd_2Cl_2(\mu\text{-dpm})_2$, and $Pd_2Cl_2(\mu\text{-S})(\mu\text{-dpm})_2$, are found to catalyze the hydrosilylation of 1-hexene, styrene, and vinyltrichlorosilane with $HSiCl_3$ at 120 °C without solvent, giving branched products, i.e., 2-silylhexane, 1-silylethylbenzene, and 1,1-disilylethane, respectively, in moderate to high yields[18]. A similar regioselectivity is observed in the reactions of styrene and 1-hexene with $HSiCl_3$ catalyzed by $PdCl_2(PhCN)_2$ and $Pd(acac)_2$, while opposite regioselectivity predominates when $HSiMeCl_2$ or $HSiEtCl_2$ is employed[19].

Rh-phosphite clusters, $[\{HRh\{P(OR)_3\}_2]_3$ (R = Me, 2-MeC_6H_4) and $[RhCl\{P(OR)_3\}_2]_2$ (R = Me, 2-MeC_6H_4) serve as moderate catalysts effecting the hydrosilylation of 2,3-dimethylbutadiene with $HSiEt_3$ or $HSi(OEt)_3$, yielding a mixture of 1,2- (minor) and 1,4-adduct (major)[20]. The reaction of 1-octene is sluggish with $HSi(OEt)_3$.

With regard to a possible cluster catalysis of $Ru_3(CO)_{12}$, the kinetic study of the hydrosilylation of 1-octene with $HSi(OEt)_3$ in the presence of $Ru_3(CO)_{12}$ at 70 °C in benzene shows that the cluster catalysis is indeed involved, especially during the first 11 min of the reaction[21]. However, the lower nuclearity species becomes predominant as the reaction proceeds. The $Ru_3(CO)_{12}$-catalyzed hydrosilylation of allyl chloride with $HSi(OMe)_3$ gives 3-chloropropyltrimethoxysilane, a useful silane coupling agent, in good yield[22].

2. By metallic and colloidal metal catalysts

Since the intermediacy of metal colloids in Pt-catalyzed hydrosilylation reactions was strongly indicated by Lewis in 1986[23], the use of colloidal metals as catalysts for hydrosilylation has been actively investigated[24–27]. It appears to be recognized to date that the ostensibly homogeneous catalysis of many platinum group metals goes through colloidal intermediates in hydrosilylation reactions. The platinum group metal colloids can be prepared through direct reaction of metal halide salts with excess $HSiMe_2(OEt)$ (equation 9)[28].

$$\underset{\text{(excess)}}{HSiMe_2(OEt)} + MCl_x + D_4^{vi} \longrightarrow H_2 + \text{Si products} + M_{colloid} \tag{9}$$

$$M = Pt(\text{no } D_4^{vi}), Rh, Ru, Ir, Os, Pd$$

$$D_4^{vi} = [Me(CH_2{=}CH)Si-O]_4$$

Relative catalytic activity of these metal colloids in the hydrosilylation of vinyltrimethylsilane with $HSi(C_6H_{13}\text{-}n)_3$ and $HSi(OEt)_3$ (25 ppm of catalyst at ambient temperature) is determined to be in the order $Pt > Rh > Ru \sim Ir \gg Os$, and Pd-colloid does not show any activity[29]. The catalytic activity depends on the nature of the hydrosilane used, i.e., Ru, Ir, and Os show almost negligible activity with $HSi(C_6H_{13}\text{-}n)_3$, while Ru and Ir display much higher activity, equivalent to Rh, with $HSi(OEt)_3$.

However, Pt-colloid is found to be less active than Rh-colloid when a dihydrosilane or a trihydrosilane is used. Recently, "silahydrocarbon", $Me(n\text{-}C_{10}H_{21})Si(C_8H_{17}\text{-}n)_2$, is attracting research interest as a hydraulic fluid in a wide temperature range, and the double hydrosilylation of 1-octene with $H_2SiMe(n\text{-}C_{10}H_{21})$ is an apparently efficient synthetic route to this compound. The reaction catalyzed by Karstedt's Pt catalyst that is shown to be a precursor of Pt-colloid at 80 °C is very sluggish, giving a mixture of the starting dihydrosilane (35.1%), monohydrosilylation product, $Me(n\text{-}C_{10}H_{21})Si(C_8H_{17}\text{-}n)H$ (58.7%), and $Me(n\text{-}C_{10}H_{21})Si(C_8H_{17}\text{-}n)_2$ (6.2%) after 1 h, while the same reaction catalyzed by Rh-colloid affords $Me(n\text{-}C_{10}H_{21})Si(C_8H_{17}\text{-}n)_2$ in 99.8% yield after 1 h[29]. Accordingly, the relative reaction rate is determined using H_2SiEt_2, $HSiEt_3$, $H_3Si(C_6H_{13}\text{-}n)$, and $HSi(C_6H_{13}\text{-}n)_3$ in the reaction of vinyltrimethylsilane catalyzed by Pt-colloid and Rh-colloid. The results are noteworthy in that the order of the reactivity of hydrosilanes is $H_3SiR > H_2SiR_2 > HSiR_3$ for the Rh-catalyst, whereas the order is $HSiR_3 > H_2SiR_2 > H_3SiR$ for the Pt-catalyst. This rather unusual phenomenon observed for the Pt-catalyst can be ascribed to the poisoning of the active Pt species by H_2SiR_2 and H_3SiR[29].

The attempted syntheses of tetraalkylsilanes through the triple hydrosilylation of monoalkylsilanes with 1-alkenes catalyzed by commercially available platinum catalysts, e.g., Pt/C, $PtCl_2(PPh_3)_2$, $PtCl_2(CH_3CN)_2$, $H_2PtCl_6{\cdot}6H_2O$, and PtO_2 suffer from a low reactivity of monoalkylsilanes[24]. However, oxygen-activated $H_2PtCl_6{\cdot}6H_2O$, and PtO_2 (purging the reaction system by air) catalysts are found to promote the desired triple hydrosilylation of $H_3SiC_6H_{13}\text{-}n$ with 1-octene or 1-decene to give the corresponding tetraalkylsilanes exclusively[24]. The active species in this system is considered to be colloidal Pt(0)[24].

A mechanistic study on the Pt-colloid catalyzed hydrosilylation by Lewis has revealed that molecular oxygen, i.e., dioxygen, serves as the crucial cocatalyst[30]. It is proposed that the catalytically active Pt-colloid, $Pt_x^0(O{-}O)$ **19** (a yellow color in the reaction mixture), is formed from Karstedt's catalyst by the action of a hydrosilane and molecular oxygen. Then, the active colloid **19** reacts with a hydrosilane to generate the non-classical hydrosilane-Pt complex **20**. Molecular oxygen plays two unique roles in these processes: (1) inhibition of the formation of large Pt-colloid (dark color or black) that has much reduced activity or is inactive, and (2) enhancement of electron deficiency of **20**, thus making it more susceptible to the nucleophilic attack of olefin. The proposed mechanism illustrated in Scheme 2[30] is in accordance with (i) the fact that the reaction stops when the catalytic system is depleted in oxygen, (ii) the dependence of the reaction rate on the electronic nature of substitutents of alkene substrates, i.e., the more electron-rich the alkene is, the faster is the reaction: The reaction rate decreases in the order $H_2C{=}CH_2 > CH_2{=}CF_2 > F_2C{=}CFCl > F_2C{=}CF_2$, (iii) $CH_2{=}CHSiMe_3$ reacts faster than $CH_2{=}CHSiCl_3$, (iv) $HSi(OEt)_3$ reacts faster than $HSiEt_3$. The substituent effects observed in the reactions of substituted styrenes, 4-X-$C_6H_4CH{=}CH_2$, with $HSiCl_2Me$, i.e., the rate decreases in the order (X =) Me > H > OMe > Cl, indicate the importance of σ induction effects and the lack of resonance effects of the substituents. The hydrosilane-Pt complex **20** reacts with nucleophiles other than alkenes. Thus, the reaction of **20** with an alcohol or water leads to the generation of molecular hydrogen and an alkoxysilane or silanol via a non-classical complex **22** (Scheme 2). Although the Lewis mechanism does not explain how an alkene reacts with **20** to form another non-classical complex **21** and then the hydrosilylation product, the classical Harrod-Chalk mechanism for a mononuclear Pt catalyst appears to be adopted for this part of the catalytic cycle (Scheme 2)[30].

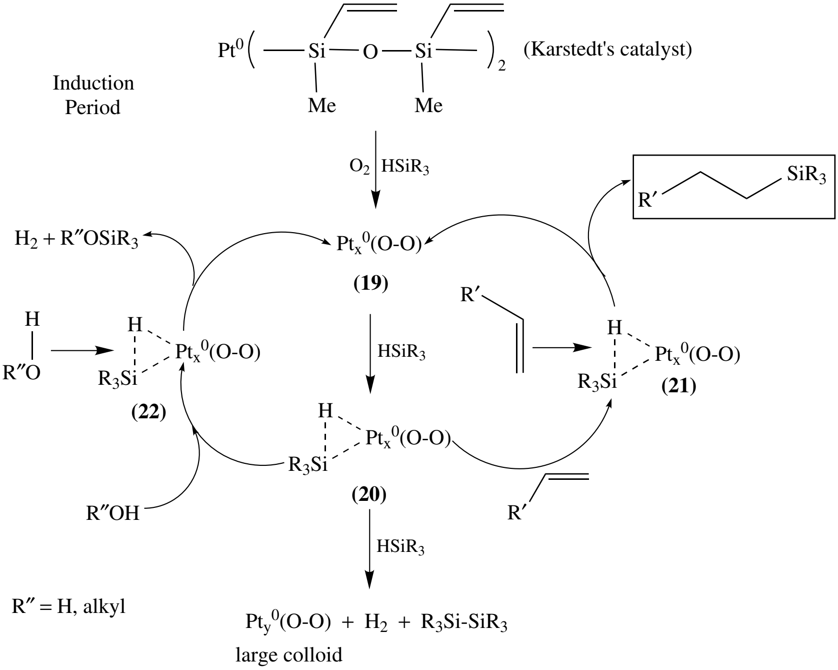

SCHEME 2

As described above, Karstedt's catalyst appears to be an excellent precursor for the generation of catalytically highly active Pt-colloid. Karstedt's catalyst can be prepared by reacting $H_2PtCl_6{\cdot}xH_2O$, K_2PtCl_4, $[Pt(CH_2{=}CH_2)Cl(\mu\text{-}Cl)]_2$, *cis*-$Pt(\eta^2\text{-}CH_2{=}CHPh)_2Cl_2$ or $Pt(COD)_2$ with excess $(CH_2{=}CHSiMe_2)_2O$[10,11,31,32]. However, the mechanism of

Pt(IV) or Pt(II) to Pt(0) reduction and the structure of Karstedt's catalyst needs to be clarified. The X-ray crystallographic structure of the Pt complex isolated from the reaction mixture of $H_2PtCl_6 \cdot xH_2O$ with excess $(CH_2{=}CHSiMe_2)_2O$ followed by neutralization with $NaHCO_3$ is determined to be $Pt_2[(CH_2{=}CHSiMe_2)_2O]_3$ **(23)**[32]. The NMR (^1H, ^{13}C, ^{29}Si and ^{195}Pt) studies of **23** with $(CH_2{=}CHSiMe_2)_2O$ and styrene in toluene-d_8 has disclosed equilibrium between **23** and other 16-electron Pt(0) complexes **24** and **25** (Scheme 3)[33].

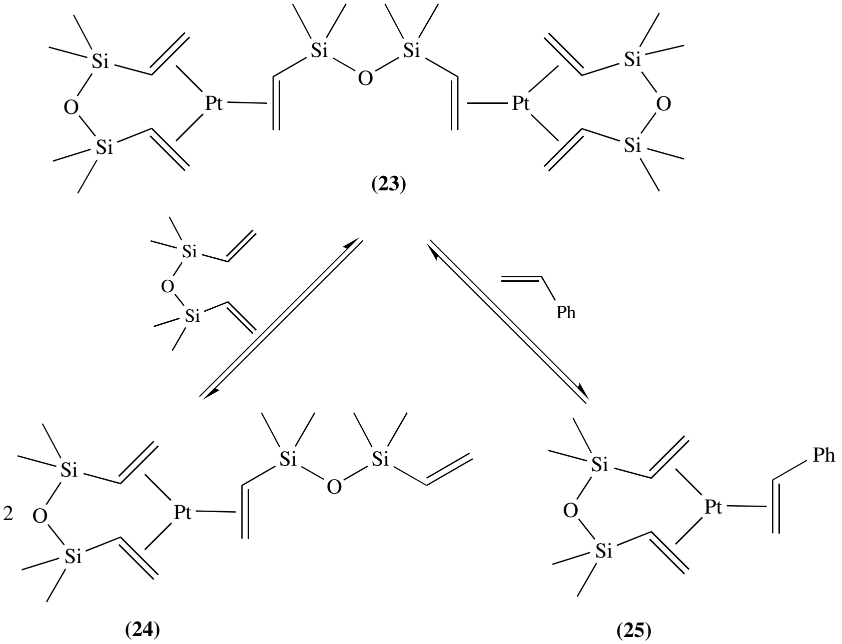

SCHEME 3

On the basis of the multinuclei NMR study and the fact that the reactions of Pt(IV) and Pt(II) chlorides with $(CH_2{=}CHSiMe_2)_2O$ yield polysiloxanes[31], vinyl chloride[31], 1,3-butadiene[32] and ethene[32], Lappert and coworkers have proposed a plausible mechanism illustrated in Scheme 4[33], which includes a rather unique vinyl–chlorine exchange (**26** → **27**) and reductive elimination of vinyl chloride (**28** → **29**). The homolytic fission of $Pt{-}CH{=}CH_2$ bond is also suggested. If a divinyl–Pt complex is formed by double vinyl–chlorine exchange, the observed formation of 1,3-butadiene can be explained as well. This study concludes that 16-electron species such as **24** and **25** are considered to be highly active catalytic species due to the availability of a vacant site for oxidative addition by a hydrosilane[33].

Highly active homogeneous Pt-catalysts are also shown to be generated by photoactivation of $Pt(acac)_2$, $Pt(ba)_2$ (ba = benzoylacetonate) $Pt(dbm)_2$ (dbm = dibenzoylmethanate) and $Pt(hfac)_2$ (hfac = hexafluoroacetylacetonate) in the presence of $HSiEt_3$ and/or $CH_2{=}CHSiEt_3$[34]. These photoactivated Pt catalysts promote the reaction of $CH_2{=}CHSiEt_3$ with $HSiEt_3$ efficiently, giving $Et_3SiCH_2CH_2SiEt_3$ in good to high yield. Once the active catalyst species is generated, the reactions proceed smoothly without

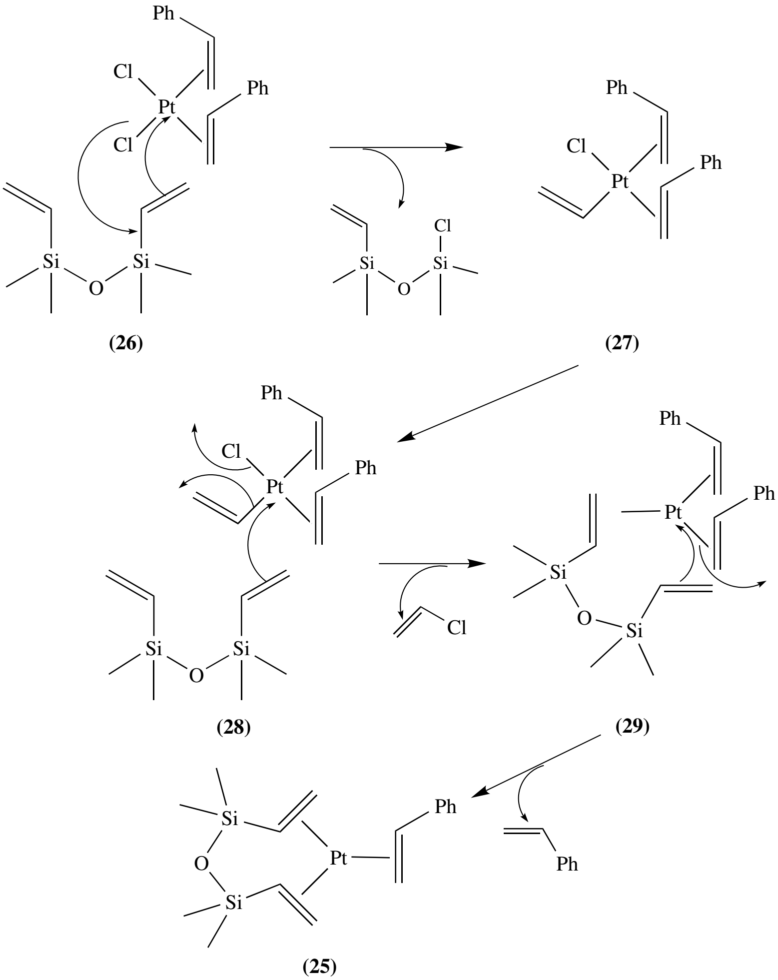

SCHEME 4

irradiation. The presence of oxygen prior to the photoactivation inhibits the generation of active catalyst species, but the addition of oxygen after the photoactivation does not affect the catalytic activity of the active species. In the absence of $HSiEt_3$ or $CH_2{=}CHSiEt_3$, only a less active heterogeneous Pt species is formed either photochemically or thermally. Thus, either $HSiEt_3$ or $CH_2{=}CHSiEt_3$ is essential for the generation of active homogeneous Pt catalyst species.

Highly dispersed metallic platinum catalysts prepared by treating mesitylene-solvated Pt atoms with solid supports such as carbon, graphite and γ-Al_2O_3 support are found to be active (Pt/hydrosilane = $1.1-4.9 \times 10^{-4}$ g-atom mol^{-1}) for the hydrosilylation of isoprene at 70 °C under neat conditions, giving a mixture of 4-silyl-2-methyl-2-butene (76–83%) and 4-silyl-2-methyl-1-butene (24–17%)[35]. The catalytic activity decreases in the order Pt/C > Pt/graphite $\gg$ Pt/Al_2O_3[35].

3. By Group IV metallocenes, lanthanides and other metal catalysts

Metallocenes of early-transition metals (Group IV) have recently been recognized as a new class of catalysts for the hydrosilylation of alkenes[36–39]. Metallocenes of Ti, Zr and Hf have been used mainly for the dehydrogenative coupling of hydrosilanes, especially dihydrosilanes to form polysilanes[39–42]. However, Cp_2MMe_2 (M = Ti, Zr) and $Cp_2M(Bu\text{-}n)_2$ (M = Ti, Zr, Hf) generated *in situ* from Cp_2MCl_2 and *n*-BuLi (2 equiv.) are found to be active catalysts for 1-alkenes[36–38]. The reaction of a 1-alkene, e.g. 1-hexene, 1-octene and vinyltrimethylsilane, with H_2SiPh_2 or $H_2SiMePh$ proceeds with complete regioselectivity, giving a 1-silylalkane in excellent yield accompanied by a small amount of an alkane via hydrogenation (equation 10)[37,38]. A small amount of a dehydrogenative silylation product, 1-silyl-1-alkene, is also formed in the reaction of styrene[37]. The reaction of 2-pentene with H_2SiPh_2 gives 1-$Ph_2(H)SiC_5H_{11}$-*n* in 85% yield[37]. The result clearly indicates rapid isomerization of the olefinic bond under the reaction conditions. When $HSiPh_3$ is used for styrene hydrosilylation, a 1:1 mixture of $Ph_3SiCH{=}CHPh$ and PhEt is formed, i.e. no hydrosilylation product is obtained[37]. The relative reactivity of hydrosilanes decreases in the order $H_3SiPh > H_2SiPh_2 \sim H_2SiMePh > H_2SiEt_2 \gg HSiPh_3$[37]. The relative catalytic activity of metallocenes decreases in the order $Cp_2ZrCl_2/2\ n\text{-BuLi} > Cp_2TiCl_2/2\ n\text{-BuLi} > Cp_2ZrMe_2 \gg Cp_2HfCl_2/2\ n\text{-BuLi}$[37]. Cycloalkenes and substituted alkenes are much less reactive, promoting the dehydrogenative coupling of hydrosilanes[37,38]. These catalysts do not show any activity in the hydrosilylation of phenylacetylene, benzaldehyde and acetophenone[37].

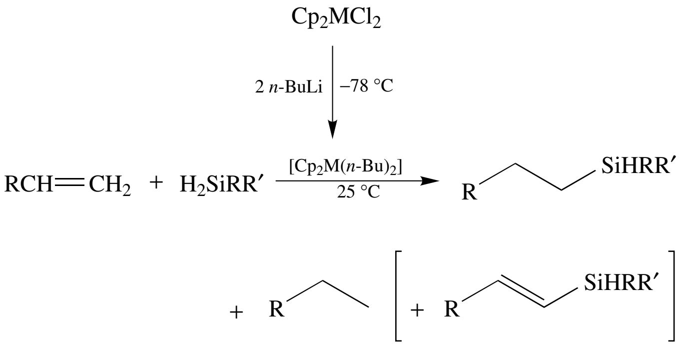

(10)

Lanthanum (La) and lanthanide metals neodymium (Nd), samarium (Sm) and lutetium (Lu) as well as yttrium (Y) with pentamethylcyclopentadienyl (η^5-Me_5C_5 = Cp*) and a silicon-bridged bis(tetramethylcyclopentadienyl) (Me_4C_5-$SiMe_2$-C_5Me_4 = $Me_2SiCp''_2$) ligand have been proved to be excellent and unique hydrosilylation catalysts which exhibit distinctive features in comparison with traditional Group VIII late-transition metal catalysts[43–45].

The hydrosilylation of vinylarenes including styrene catalyzed by $Cp^*_2LnCH(SiMe_3)_2$ (Ln = La, Nd, Sm, Lu) or $Me_2SiCp''_2SmCH_2(SiMe_3)_2$ with H_3SiPh gives the corresponding 1-silylethylarenes **30** with complete regioselectivity (equation 11)[43] in sharp contrast to the reactions promoted by traditional Group VIII transition metal catalysts which favor the formation of 2-silylethylarenes (*vide supra*). The relative catalytic activity of these complexes in the reaction of styrene decreases in the order $Me_2SiCp_2''SmCH(SiMe_3)_2 \gg Cp^*_2LaCH(SiMe_3)_2 > Cp^*_2NdCH(SiMe_3)_2 > Cp^*_2SmCH(SiMe_3)_2 \gg Cp^*_2LuCH(SiMe_3)_2$[43]. The observed unique regioselectivity can be ascribed to the formation of η^n-benzylic metal species **(31)** through interaction of the electrophilic lanthanide metal center with the arene π-system. The active catalyst species of these complexes are very likely to be the hydride complexes, Cp^*_2LnH and $Me_2SiCp''_2LnH$, that are formed via reductive cleavage of a $Ln-CH(SiMe_3)_2$ bond by the action of H_3SiPh[43].

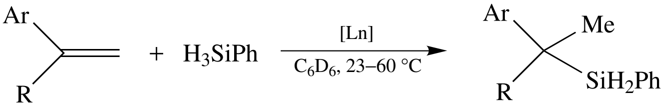

(30)

(11)

$[Ln] = Cp^*_2LnCH(SiMe_3)_2$ or $Me_2SiCp''_2SmCH(SiMe_3)_2$

(a) Ar = Ph, R = H; **(b)** Ar = 4-$MeOC_6H_4$, R = H; **(c)** Ar = 4-FC_6H_4, R = H;
(d) Ar = 2-$MeOC_6H_4$, R = H; **(e)** Ar = Ph, R = Me; **(f)** Ar = Ph, R = Et;
(g) Ar = R = Ph; **(h)** Ar = 2-Np, R = H

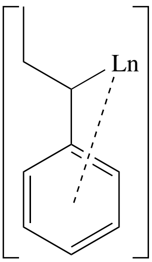

(31)

The reversed regioselectivity is also observed in the reaction of 1-hexene with H_3SiPh catalyzed by $Me_2Cp''_2SmCH(SiMe_3)_2$, which affords 2-silylhexane as the major product (⩽76% regioselectivity)[43]. However, the reactions of sterically more demanding 1-alkenes, cyclohexylethene and 2-ethyl-1-butene, with H_3SiPh catalyzed by $Me_2Cp''_2SmCH(SiMe_3)_2$, afford linear products, $PhH_2Si-CH_2CH_2(C_6H_{11}$-*c*) (96% yield) and $PhH_2Si-CH_2CH(C_2H_5)_2$ (98% yield), exclusively[43]. Exclusive formation of 1-silylalkanes is also observed in the reactions of 1-decene with H_3SiPh, $H_3SiC_6H_{13}$-*n* and $H_2SiMePh$ catalyzed by Cp^*_2Nd-R [R = $CH(SiMe_3)_2$, H, Cl] at 80 °C[44]. The reactions of isoprene, 1,5-cyclohexadienes, and 1,6-heptadiene with H_3SiPh are also effected by $Cp^*_2Nd-CH(SiMe_3)_2$[46]. The reaction of isoprene gives a mixture of 1,4-addition products in which (*E*)-1-silyl-2-methyl-2-butene is the major (63%) product. The reactions of 1,5- and 1,6-dienes give silylmethylcyclopentane (84% yield) and 1-silylmethyl-2-methylcyclopentane (54%), respectively, as the major products.

Highly regio- and site-selective hydrosilylation of 1-alkenes (equation 12) and nonconjugated alkadienes (Table 2) with H_3SiPh can be achieved using $Cp^*_2YCH(SiMe_3)_2$ as the catalyst in benzene at ambient temperature[45]. It appears that this catalyst is sterically very demanding so that it reacts with the terminal olefinic bond exclusively, delivering the silicon moiety to the terminal carbon. The active catalyst species is most likely to be

$Cp^*{}_2YH$ in the same manner as the lanthanide catalysts mentioned above.

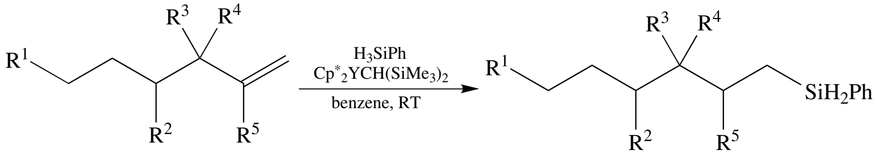

(a) $R^1 = n\text{-}C_4H_9$, $R^2 = R^3 = R^4 = R^5 = H$ (95%) (12)
(b) $R^1 = R^2 = H$, $R^3 = R^4 = Me$, $R^5 = H$ (94%)
(c) $R^1 = H$, $R^2 = Me$, $R^3 = R^4 = H$, $R^5 = Me$ (56%)
(d) $R^1 = Cl$, $R^2 = R^3 = R^4 = R^5 = H$ (85%)
(e) $R^1 = OCH_2Ph$, $R^2 = R^3 = R^4 = R^5 = H$ (90%)
(f) $R^1 = OTBDMS$, $R^2 = R^3 = R^4 = R^5 = H$ (83%)

The hydrosilylation of acrylates with chlorohydrosilanes using Group VIII transition metal catalysts has been shown to yield either a mixture of 3-silylpropanoate and 2-silylpropanoate (Pt[47,48]) or 2-silylpropanoate selectively (Ni[49], Rh[50]). However, a binary catalyst system, Cu_2O–TMEDA (TMEDA $= N, N, N', N'$-tetramethylethylenediamine), is found to promote the exclusive β-addition of $HSiCl_3$, $HSiCl_2Me$ and $HSiCl_2Ph$, giving the corresponding 3-silylpropanoates **32** exclusively in 93–99% yields (equation 13)[51]. A variety of copper salts other than Cu_2O which include CuCl, CuBr, $CuCl_2$, $CuBr_2$, CuCN, CuO, $(CuO)_2{\bullet}Cr_2O_3$ can also effect the reaction. It is proposed that TMEDA

TABLE 2. Hydrosilylation of nonconjugated dienes with $PhSiH_3$ catalyzed by $Cp^*_2YCH(SiMe_3)_2$

Substrate	Product	Yield (%)
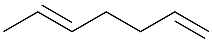	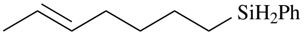	96
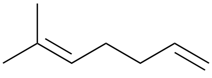	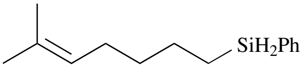	94
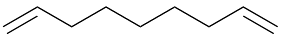	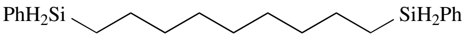	96
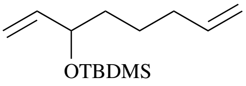	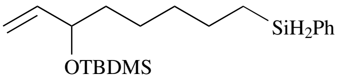	54
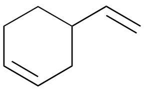	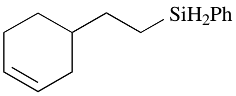	97

reacts with $HSiCl_2R$ to generate a hydrosilane–amine complex, $[TMEDA\text{-}H]^+RCl_2Si^-$, that undergoes conjugate addition to an acrylate, but the role of the copper salt is not clear at present.

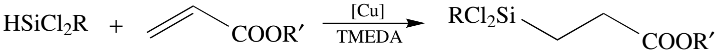

(R = Cl, Me, Ph; R′ = Me, Et)

(32)

(13)

The β-addition of chlorohydrosilanes to acrylonitrile, yielding 3-silylpropanenitrile **33**, can be effected by different promoters[3], and $CuCl/NBu_3/TMEDA$[52] or a copper salt–isocyanide[53] combination is known to be a good catalyst for a long time. Ultrasound is found to accelerate the reaction catalyzed by Cu_2O–TMEDA at ambient temperature, but the reaction also proceeds effectively under reflux (equation 14)[54]. The relative reactivity of chlorohydrosilanes in this catalyst system decreases in the order $HSiCl_3 >$ $HSiCl_2Ph \sim HSiCl_2Me \gg HSiClPh_2$, and $HSiClMe_2$ does not show any reactivity.

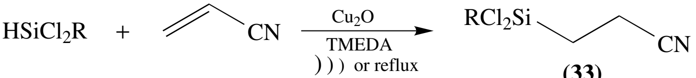

R = Cl, Me, Ph
))) = ultrasound

(33)

(14)

A manganese(0) carbonyl complex, $Mn_2(CO)_{10}$, is found to be a fairly active catalyst for the reaction of 1-hexene with $HSiEt_3$ or $HSi(OEt)_3$ in toluene or THF at 40 °C[55]. Kinetic study suggests that $HMn(CO)_5$ is the catalytically active species.

The reaction of triethoxyvinylsilane, $CH_2{=}CHSi(OEt)_3$, with $HSi(OEt)_3$ catalyzed by $Ni(acac)_2$ gives a complex mixture of products, arising from dehydrogenative silylation, hydrogenation, disproportionation, and dimerization besides the normal hydrosilylation product, $(EtO)_3SiCH_2CH_2Si(OEt)_3$[56]. The dimerization product is a mixture of $(EtO)_3Si(CH_2)_4Si(OEt)_3$ and $(EtO)_3SiCH(Me)(CH_2)_2Si(OEt)_3$. A possible mechanism that can accommodate the formation of these products is proposed, which includes key intermediates such as $(EtO)_3Si(CH_2)_2Ni{-}CH[Si(OEt)_3]CH_2Si(OEt)_3$ and $Ni[(CH_2)_2Si(OEt)_3]$[56].

The photocatalytic hydrosilylation of 1,3-dienes in the presence of $Cr(CO)_6$ is known to proceed smoothly at ambient temperature to give (*Z*)-1,4-addition product(s) exclusively. A detailed follow-up study[57] on the reactions of 1,3-butadiene, 2,3-dimethyl-1,3-butadiene and isoprene with $HSiEt_3$ confirmed the previously reported results using $HSiMe_3$ except for a higher regioselectivity for the reaction of isoprene, i.e. (*Z*)-$Et_3SiCH_2C(Me){=}CHMe/Et_3SiCH_2CH{=}CMe_2 = 72/28$ (60/40 for $HSiMe_3$). However, the minor product (3% isolated yield; the major product **34** is isolated in 86% yield) in the reaction of 1,3-pentadiene is found to be (*E*)-product **35**[57] instead of the previously reported (*Z*)-product (for $HSiMe_3$-reaction[58,59]). The reaction of 2-methyl-1,3-pentadiene affords one regioisomeric product, (*Z*)-$Et_3SiCH_2C(Me){=}CHEt$, exclusively, but in only 14% isolated yield (equation 15)[57]. The reactions of 1,3-cyclohexadiene and 1,4-cyclohexadiene both give a mixture of 3-silyl-1-cyclohexene **36** and 1-silyl-1-cyclohexene **37** (**36/37** = 86/14, 84% yield from 1,3-hexadiene; **36/37** = 88/12, 23% yield from 1,4-hexadiene) (equation 16)[57]. In the latter case, only a low conversion of 1,4-hexadiene is observed, and it is apparent that the isomerization of 1,4-cyclohexadiene to 1,3-cyclohexadiene takes place prior to hydrosilylation. Detailed mechanistic study shows intermediacy of $Cr(CO)_4(\eta^4\text{-1,3-diene})$ and $Cr(CO)_3(H)(SiEt_3)(1,3\text{-diene})$ complexes, and deuterium labeling experiments unambiguously indicate that a π-allylic silyl chromium species, (η^3-enyl)$Cr(CO)_3(SiEt_3)$, arising from the insertion of 1,3-diene into the H−Cr bond, is the key intermediate in this catalytic cycle[57].

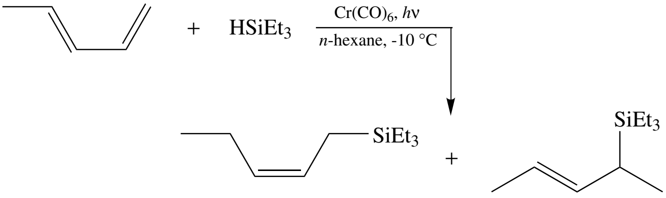

(34) **(35)**

(25:1)

(15)

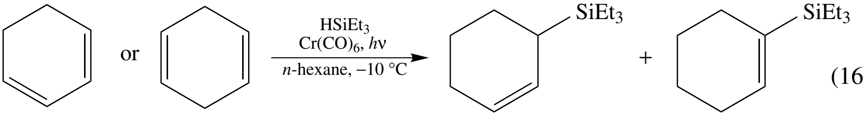

(36) **(37)**

(16)

4. By immobilized catalysts

The development of Group VIII transition metals immobilized on inorganic or polymer support continues to be an active area in the hydrosilylation reaction, mainly because of easy separation and recycling capability of these catalysts[60−65].

Rhodium(I) complexes immobilized on silica using 3-(3-silylpropyl)-2,4-pentanedionato ligands **(38)** show good activity in the hydrosilylation of 1-octene with $HSi(OEt)_3$ at 100 °C[60]. The immobilized Rh catalysts are prepared by (i) reaction of $(EtO)_3Si(CH_2)_3C(COMe)_2Rh(CO)_2$ with untreated silica (Catalyst A), (ii) reaction of $Rh(acac)(CO)_2$ (acac = acetylacetonato = 2,4-pentanedionato) with silica modified by $[(EtO)_3Si(CH_2)_3C(COMe)_2]^-$ prior to the complexation (Catalyst B), (iii) reaction of $[Rh(CO)_2Cl]_2$ with a polycondensate of $[(EtO)_3Si(CH_2)_3C(COMe)_2]^-$, $Si(OEt)_4$ and water (Catalyst C) and (iv) sol-gel processing of $(EtO)_3Si(CH_2)_3C(COMe)_2Rh(CO)_2$ and $Si(OEt)_4$ (Catalyst D). The Catalysts A and B show *ca* three times better activity than their homogeneous counterparts, while the Catalyst D exhibits only low activity and the Catalyst C is inactive[60].

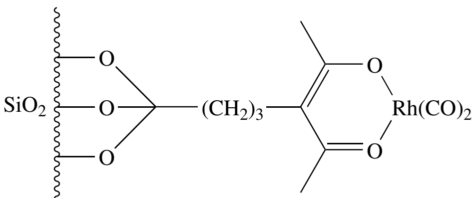

(38)

In a manner similar to the four methods mentioned above, rhodium complex catalysts immobilized on silica modified by $2\text{-}(MeO)_3Si(CH_2)_2C_5H_4N$ and $(MeO)_3Si(CH_2)_3OCOCMe{=}CH_2$ using $[Rh(CO)_2Cl]_2$ as the precursor are prepared[61]. These immobilized pyridine−Rh complexes are shown to be active catalysts in the hydrosilylation of 1-octene, and claimed to be more efficient than their homogeneous counterparts[61].

Polyamide-supported Rh, Pd, Pt and Ru complex catalysts are shown to be active in the hydrosilylation of 2-methyl-1,3-pentadiene and isoprene with $HSiMe_2Ph$ and $HSi(OEt)_3$[63,64]. The catalysts are prepared by immobilizing $[Rh(CO)_2Cl]_2$, $PdCl_2(PhCN)_2$, $PtCl_2(PhCN)_2$ and $RuCl_2(bipy)_2$ on the polyamide supports **39a,b** and **40a,b** that have relatively uniform distribution of micropores with voids from 1.0 to 3.0 nm. The reaction of 2-methyl-1,3-pentadiene catalyzed by these polyamide-supported catalyst ([M]–P) gives a mixture of 1,4-addition product **41** and 1,2-addition product **42** regioselectively, i.e. the silyl group is exclusively delivered to the C-1 of the diene (equation 17). It is noteworthy that $HSiMe_2Ph$ favors 1,4-addition (51–95%) while $HSi(OEt)_3$ does 1,2-addition (75–85%) in the reactions using the Pd, Pt and Ru catalysts. However, the Rh-catalyzed reactions favor 1,4-addition regardless of the hydrosilane used (85–95%). The reactions of isoprene promoted by the Pd, Pt and Ru catalysts follow the same 1,4/1,2 selectivity pattern depending on the hydrosilane used although two regioisomers are formed for both 1,4-addition **(43a,b)** and 1,2-addition **(44a,b)** processes for this substrate (equation 18). In contrast, the Rh-catalyzed reaction gives only (*Z*)-**43a** as the 1,4-adduct (86–95%) regardless of the hydrosilane used although the 1,2-addition product was a mixture of **44a** and **44b**. These polyamide-immobilized metal catalysts exhibit virtually the same regio- and stereoselectivity as those observed for their homogeneous counterparts. This fact indicates a good match of the dimensions of the key intermediates in the catalytic process to those of the polymer micropores. The Rh complexes with the polyamide supports **40a** and **40b** are found to show highest selectivities among the catalysts examined, and are proved to be extremely stable, keeping the same activity even after six runs[64].

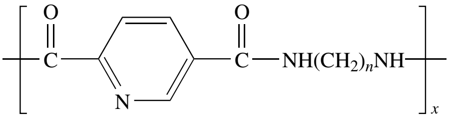

Support **39a:** $n = 2$
Support **39b:** $n = 6$

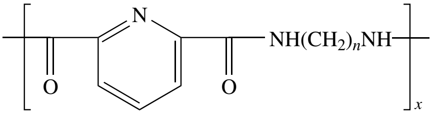

Support **40a:** $n = 2$
Support **40b:** $n = 6$

(17)

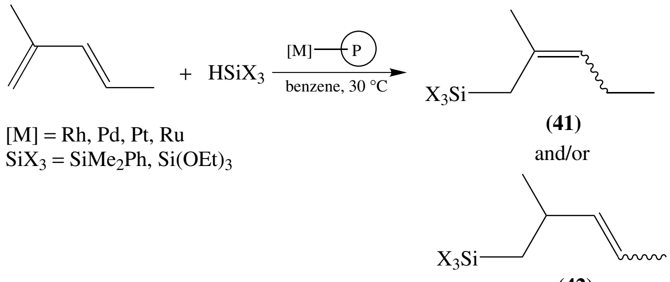

(41)

(42)

[M] = Rh, Pd, Pt, Ru
$SiX_3 = SiMe_2Ph, Si(OEt)_3$

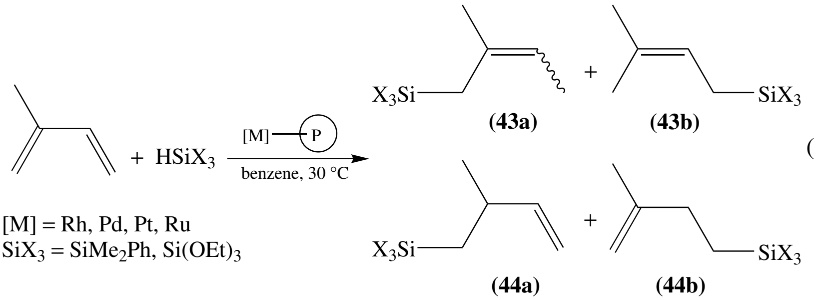

[M] = Rh, Pd, Pt, Ru
SiX_3 = $SiMe_2Ph$, $Si(OEt)_3$

(18)

Platinum complexes of ferrocenes attached to cross-linked polystyrene support **45** are shown to be highly active in the hydrosilylation of styrene and 1-hexene with $HSiCl_3$, giving linear products, 2-silylethylbenzene and 1-silylhexane, respectively, in excellent yields with complete regioselectivity[65]. These catalysts can be recycled without appreciable loss of activity. However, the absence of any ligand effects on the selectivity and activity indicates that catalytically active metallic Pt is generated in these systems[65]. The corresponding palladium complexes are also active in the hydrosilylation of styrene with $HSiCl_3$ at 70–90 °C (0.1 mol% of the catalyst for 24–48 h), giving 1-silylethylbenzene in excellent yields with 95–100% regioselectivity[65]. These Pd catalysts possess, however, only a low catalytic activity for the reaction of 1-hexene.

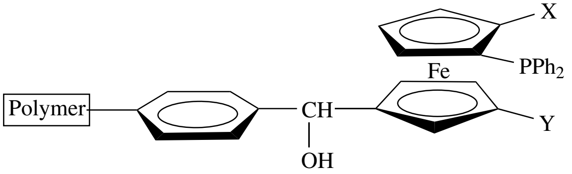

X = H or $CHMe(NMe_2)$
Y = H or PPh_2

(45)

5. *By radical initiators*

The hydrosilylation of alkenes with $HSiCl_3$ and $HSiCl_2Me$ under free-radical conditions using UV irradiation or organic peroxides was studied in the early years since the discovery of the reaction. However, Speier's catalyst and other transition metal catalysts have been almost exclusively used for the reaction afterwards. It has been shown that trialkylsilyl radicals are extremely reactive species for addition to carbon–carbon multiple bonds, but the hydrosilylation of alkenes with trialkylsilanes under free-radical conditions, e.g. $(t\text{-BuO})_2$ as the initiator, is limited to nonpolymerizable alkenes. Tris(trimethylsilyl)silane, $HSi(SiMe_3)_3$ (TTMSS), however, is found to have a very low Si–H dissociation energy (11 $kcal\,mol^{-1}$)[66], which is even lower than that of trialkylsilanes. This unique hydrosilane, TTMSS, undergoes smooth addition to simple and functionalized alkenes **46** in the presence of azobis(isobutyronitrile) (AIBN) at 80–90 °C in toluene to give the corresponding hydrosilylation products **47** in high yields (equation 19)[66–68].

The reaction clearly includes carbon-centered radical, which can account for the observed skeletal rearrangement in the reaction of β-pinene (equation 20) and extremely high stereoselectivity in the reactions of methylmaleic anhydride (equation 21) and a methylfumarate (equation 22) using Et_3B/O_2 as the initiator at −15 °C [The reactions using AIBN at 90 °C give the isomer ratios of 16 : 1 **(48a:48b)** and 12 : 1

(49a:49b), respectively].

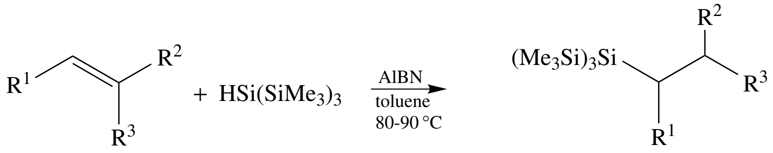

(46) **(47)** (19)

(a) $R^1 = R^2 = H$, $R^3 = (CH_2)_7CH_3$, Ph, CN, CO_2Me, COMe, OBu, OAc, $P(O)(OEt)_2$ or SPh

(b) $R^1 = H$, $R^2 = Me$, $R^3 =$ Ph or CO_2Me

(c) $R^1 = Me$, $R^2 =$ CN or CO_2Et, $R^3 = H$

(d) $R^1 = R^2 = CO_2Et$, $R^3 = H$

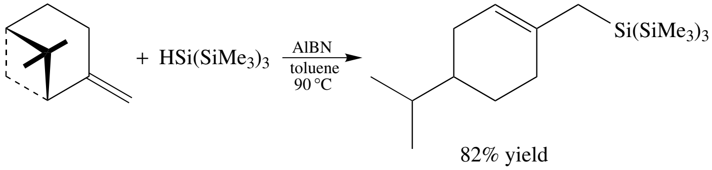

82% yield (20)

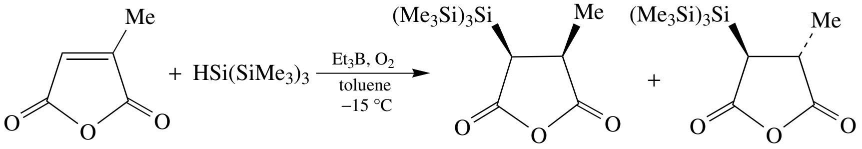

(48a) (99 : 1) **(48b)** (21)

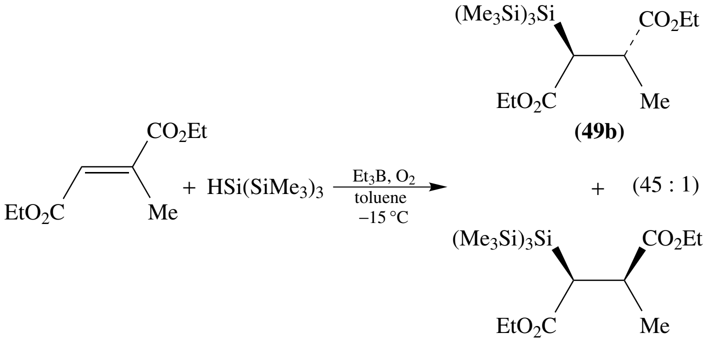

(49b) (45 : 1) **(49a)** (22)

B. Mechanism of Alkene Hydrosilylation

When the hydrosilylation reactions were reviewed in this series and published in 1989[3], the 'Chalk–Harrod mechanism'[69] (Scheme 5) was apparently the most widely accepted mechanism for the alkene hydrosilylation, with minor exceptions of photocatalyzed reactions using $Fe(CO)_5$, $M_3(CO)_{12}$ (M = Fe, Ru, Os) and $R_3SiCo(CO)_4$[59,70,71]. However, extensive mechanistic studies recently conducted have revealed that there are many catalyst systems which do not follow the Chalk–Harrod mechanism.

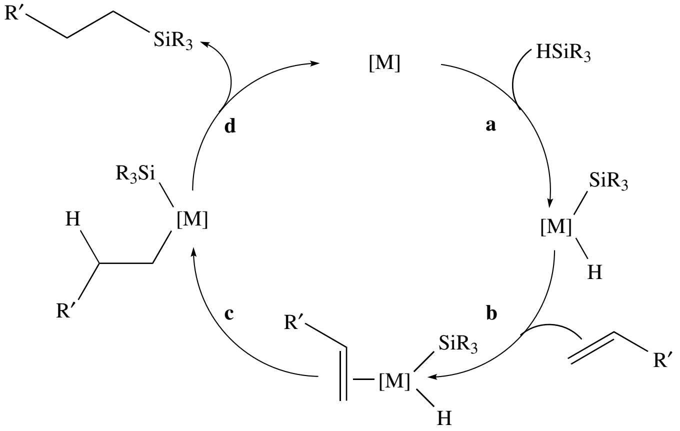

SCHEME 5. Chalk–Harrod mechanism

The hydrosilylation of alkenes often yields silylalkenes through dehydrogenative silylation (*vide infra*) and an alkane by hydrogenation besides normal hydrosilylation product, silylalkane[3]. Since the Chalk–Harrod mechanism cannot accommodate these products, mechanisms including the initial insertion of an alkene to the [M]–Si bond rather than the [M]–H bond (i.e. 'silyl migration pathway'[72]), followed by β-hydride elimination, forming a silylalkene and the subsequent hydrogenation of the alkene by $[M](H)_2$ species generated, were proposed as a part of or as a competing pathway in the hydrosilylation process[59,73–80]. Another important point is the fact that a facile reductive elimination of a silylalkane from an alkyl–[M]–SiR_3 species, which is one of the key steps in the Chalk–Harrod mechanism (step **d** in Scheme 5), is not well-established or precedented in stoichiometric reactions.

The first convincing results for the occurrence of the 'silyl migration pathway' were presented by Seitz and Wrighton in the photochemical reaction of $Et_3SiCo(CO)_4$ with ethene[81]. On the basis of FTIR and ^1H NMR studies monitoring the reaction, the mechanism illustrated in Scheme 6 is proposed, in which the steps (a)–(c), (f) and (g) are confirmed[81]. For the steps (d) and (e), $MeCo(CO)_4$ is used as a model complex and subjected to the reaction with $HSiMe_3$. The reaction gives CH_4 (detected by ^1H NMR) and $Me_3SiCo(CO)_4$ (by FTIR) as the products and the formation of $SiMe_4$ is not observed (equation 23)[81]. Although the formation of a trace amount of $SiMe_4$ cannot be completely ruled out, it is evident that the reductive elimination of alkane is predominant over that of silylalkane (step **e** in Scheme 6), which strongly supports the 'silyl migration pathway'.

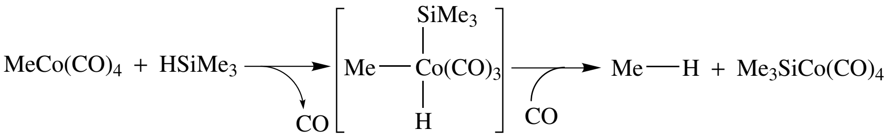

$$\mathrm{MeCo(CO)_4 + HSiMe_3} \xrightarrow[\mathrm{CO}]{} \left[\mathrm{Me{-}\overset{\displaystyle SiMe_3}{\underset{\displaystyle H}{Co(CO)_3}}}\right] \xrightarrow[\mathrm{CO}]{} \mathrm{Me{-}H + Me_3SiCo(CO)_4} \qquad (23)$$

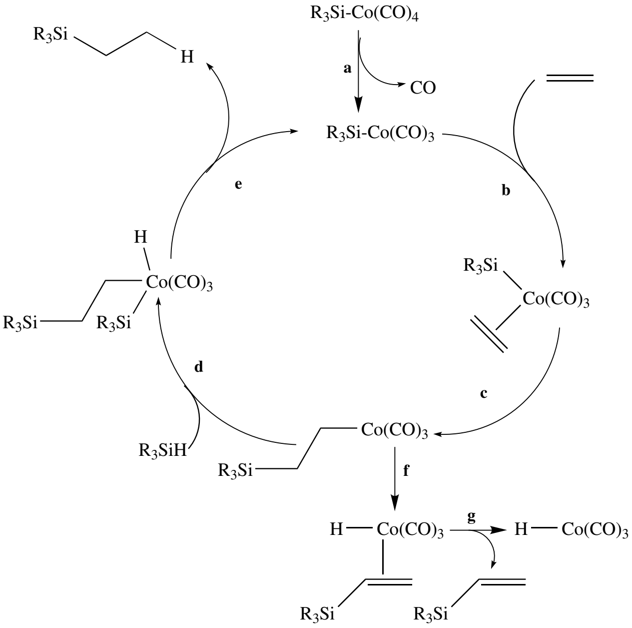

SCHEME 6. Seitz–Wrighton mechanism

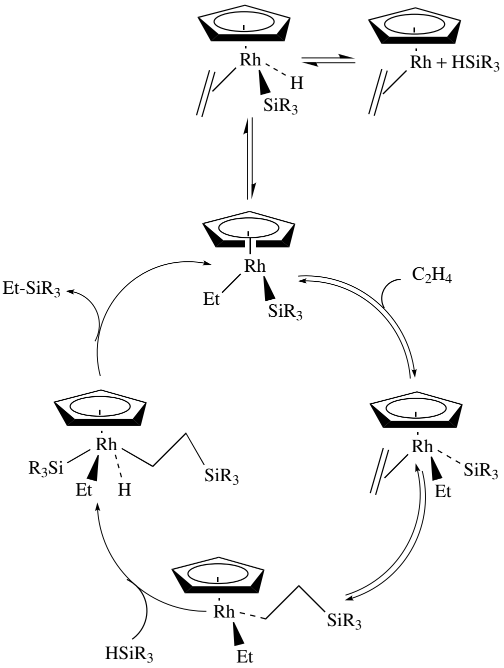

SCHEME 7. Two-silicon cycle by Duckett and Perutz

A detailed mechanistic study on the hydrosilylation of ethene with $HSiR_3$ (R = Et, *i*-Pr, *sec*-Bu, Me) catalyzed by (η^5-C_5H_5)Rh(CH_2=CH_2)(SiR_3)H has demonstrated on the basis of deuterium labeling experiments and a series of control experiments[82] that the Chalk–Harrod mechanism is not operative in this catalyst system. The 'two-silicon cycle' mechanism (another 'silyl migration pathway') including a Rh(V) intermediate is proposed by Duckett and Perutz for this catalysis (Scheme 7)[82]. The integrity of the original ethene (or ethyl) group is proved to be retained. The proposed mechanism is essentially the same as the Seitz–Wrighton mechanism (*vide supra*) if the CpRh–Et moiety is replaced by $Co(CO)_3$ in the catalytic cycle. A possible involvement of Rh(V) species has been proposed by Maitlis and coworkers as well[74,83].

Direct evidence for the 'silyl migration pathway' was presented by Brookhart and Grant in the hydrosilylation of 1-hexene catalyzed by a cobalt(III) complex[72]. The detailed mechanistic study was conducted on the reaction using $[Cp^*Co\{P(OMe)_3\}CH_2CH_2{-}\mu{-}H]^+$ $[BAr_4]^-$ (Ar = 3, 5-$CF_3C_6H_3$) **(50)** as the catalyst precursor based on the spectroscopic detection of catalyst species in a 'working' catalytic cycle, kinetics, deuterium labeling techniques and a convincing mechanism including the silyl migration step to form the secondary alkyl–Co complex with agostic hydrogen (μ-H) (step **c**) and the unexpected isomerization of **53** to the primary alkyl–Co complex with a μ-H **54** as the 'turnover-limiting step' (step **d**) (Scheme 8)[72]. This unique isomerization process is elucidated by a labeling experiment using $DSiEt_3$, which shows almost exclusive incorporation of deuterium at the C-6 position to yield $Et_3Si(CH_2)_5CH_2D$ (>95% based on ^{13}C NMR analysis) (equation 24)[72]. This labeling experiment clearly indicates that the isomerization to **54** takes place prior to the reaction of **53** (or any other possible intermediates involved in

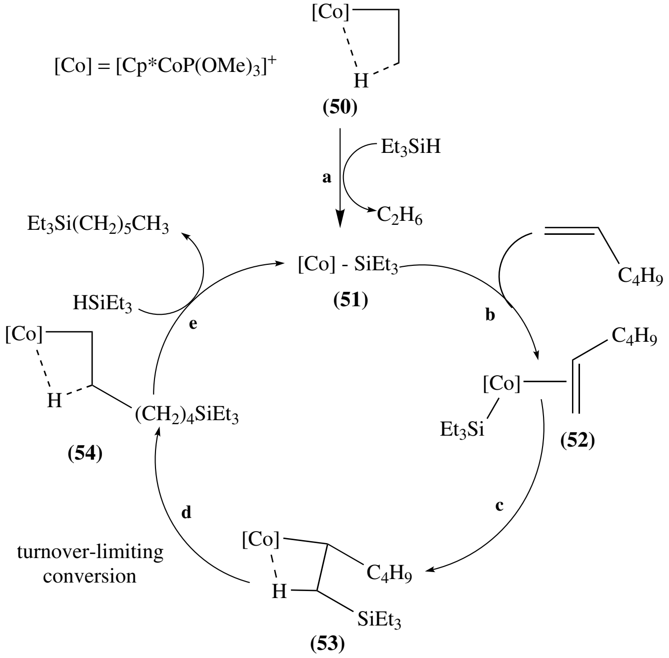

SCHEME 8. Brookhart–Grant mechanism

the isomerization) with $HSiEt_3$ (step **e**). For the final H-shift or reductive elimination step (step **e**), a σ-bond metathesis mechanism either via concerted fashion or via η^2-$HSiEt_3$ coordination to the electrophilic Co(III) metal center is strongly suggested[72] rather than the one including classical oxidative addition of $HSiEt_3$ to form a cationic Co(V) intermediate like the Rh(V) species proposed by Duckett and Perutz[82] (*vide supra*).

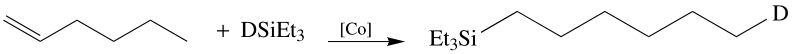

(24)

$[Co] = [Cp^*Co(P(OMe)_3)CH_2CH_2\text{-}\mu\text{-}H]^+$ **(50)**

In the hydrosilylation of alkenes catalyzed by Group IV metallocene complexes, $Cp_2MCl_2/2BuLi(M = Zr, Hf, Ti)$[37,38] (*vide supra*), the 'olefin-first' mechanism including σ-bond metathesis of η^2-alkene-MCp_2 and $HSiR_3$ is proposed by Kesti and Waymouth (Scheme 9)[37]. After the formation of β-silylalkyl—M—H species **56** via σ-bond metathesis

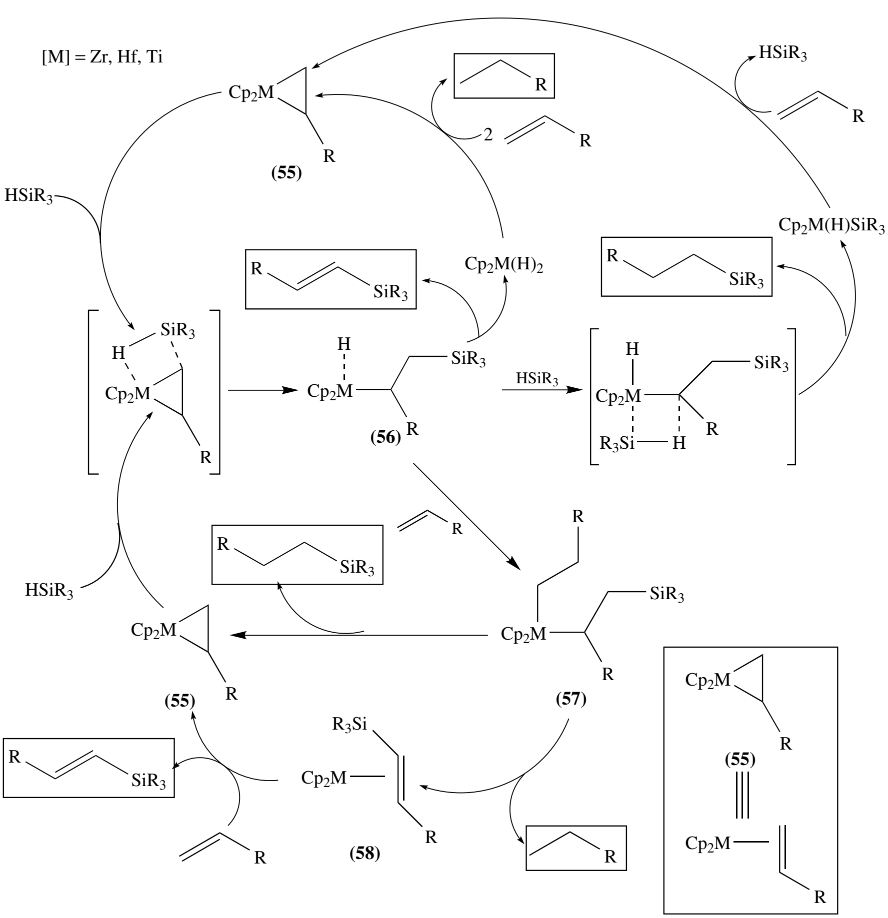

SCHEME 9. Kesti–Waymouth's 'olefin-first' mechanism

of **55**, another σ-bond metathesis of **56** with $HSiR_3$ yields silylalkane (hydrosilylation product) and $Cp_2M(H)SiR_3$, while the β-hydride elimination of **56** gives alkenylsilane (dehydrogenative silylation product) and $Cp_2M(H)_2$. It appears that the $Cp_2M(H)SiR_3$ is not stable[37] and thus an alkene molecule can readily replace the silyl hydride moiety to regenerate η^2-alkene-MCp_2 species **55**. Also, $Cp_2M(H)_2$ can react with alkene molecules to yield alkane and **55**. In this way, the 'olefin first' catalyst cycle completes. Alternatively, **55** reacts with another alkane molecule to form dialkyl-M species **57**, which undergoes a combination of β-hydride elimination and hydride shift to form either η^2-silylalkene-M complex **58** and alkane (hydrogenation product) or η^2-alkene-M complex **55** and silylalkane (hydrosilylation product) (Scheme 9)[37]. The latter mechanism has close precedents in the Rh and Ru catalyzed reactions proposed by Maitlis and coworkers[74] and Ojima and coworkers[80]. Consequently, the most characteristic feature in the Group IV metallocene catalyzed reaction is σ-bond metathesis processes which are not very common in the Group VIII metal-catalyzed reactions.

The Chalk–Harrod type mechanism is proposed to be operative in the reaction of ethene with $HSiMe_3$, $HSiEt_3$ and $HSiPh_3$ catalyzed by an early–late heterobimetallic complex, $Cp_2Ta(CH_2)_2Ir(CO)_2$[84,85]. The proposed catalytic cycle is very similar to the one shown in Scheme 5, wherein [M] is $Cp_2Ta(CH_2)_2Ir(CO)$, except for the dissociation of CO at the oxidative addition of $HSiR_3$ and the coordination of CO at the reductive elimination of $EtSiR_3$[84]. This catalyst, however, only promotes the hydrosilylation of ethene, and higher alkenes are isomerized[84].

The hydrosilylation of alkenes catalyzed by organolanthanide complexes, $Cp^*{}_2LnCH(SiMe_3)_2$ (Ln = La, Nd, Sm, Lu) and $Me_2SiCp''{}_2SmCH(SiMe_3)_2$ ($Me_2SiCp''{}_2 = Me_4C_5-SiMe_2-C_5Me_4$)[43], or the organoyttrium complex, $Cp^*{}_2YCH(SiMe_3)_2$[45], is proposed to proceed via the Chalk–Harrod type mechanism except for the inclusion of σ-bond metathesis (steps **b** and **e**) instead of a classical oxidative addition–reductive elimination process (Scheme 10). The organolanthanide complex-catalyzed reactions of

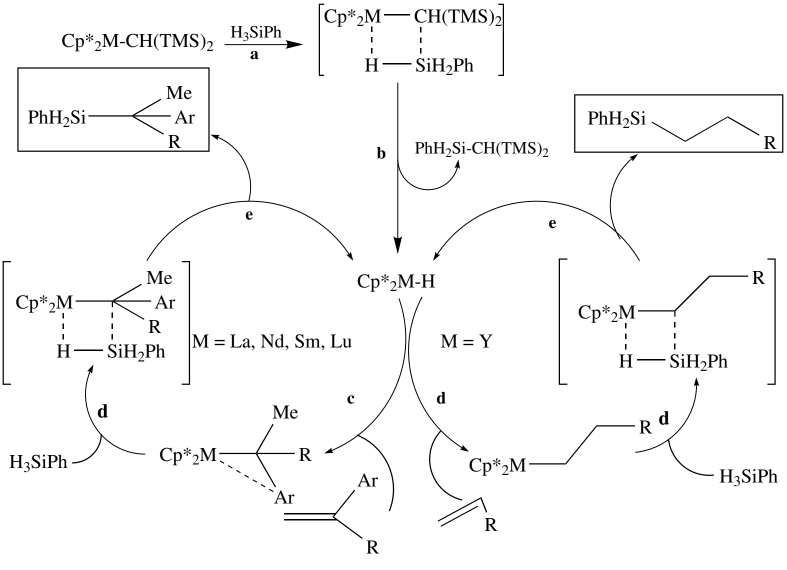

SCHEME 10. Proposed mechanism for organolanthanide or yttrium-catalyzed reaction

vinylarenes with H_3SiPh give the branched hydrosilylation products exclusively via η^n-benzylic metal species **31** (*vide supra*). In the absence of such an arene–Ln interaction, i.e. normal 1-alkenes including 2-alkyl-1-alkenes, these lanthanide catalysts afford 1-silylalkenes except for the reaction of 1-hexene catalyzed by sterically less demanding $Me_2SiCp''_2SmCH(SiMe_3)_2$[43] (*vide supra*). Exclusive formation of 1-silylalkanes with or without functional groups is observed in the $Cp^*_2YCH(SiMe_3)_2$-catalyzed reactions[45] (*vide supra*). The observed extremely high terminal selectivity can be ascribed to the substantial steric demands as well as the electrophilic nature of the bulky Cp^*_2M moiety in the olefin insertion to the M–H bond (step **c**)[45].

C. Intramolecular Hydrosilylation of Alkenes

Intramolecular hydrosilylations of functionalized alkenes followed by hydrogen peroxide oxidation provide powerful methods for organic syntheses[86–88]. The reactions of allylic *O*-dimethylsilyl ethers **59** promoted by platinum catalysts, e.g. Karstedt's catalyst and $Pt(PPh_3)_2(CH_2{=}CH_2)$, or rhodium catalysts, e.g. Rh(acac)(COD) and $[RhCl(CH_2{=}CH_2)_2]_2$, proceed via 5-*endo* cyclization to give oxasilacyclopentanes **60** with a couple of exceptions in which siloxatanes **61** are formed (Scheme 11)[87,89].

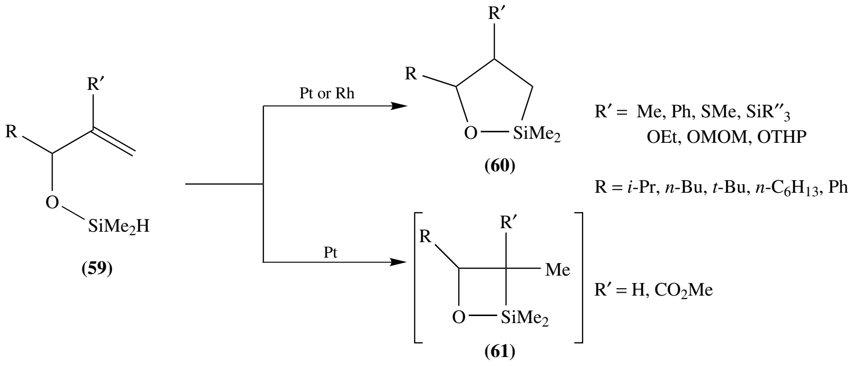

SCHEME 11. Intramolecular hydrosilylation of *O*-silylallylic alcohols **59**

When silyloxy enol ethers (**59:** R′ = EtO, MOMO, THPO) are used as the substrates, the reactions proceed with excellent *syn*-selectivity ($syn/anti = 14/1 \sim> 99/1$)[87]. The resulting oxasilacyclopentanes **60** are subjected to the Tamao oxidation after the removal of the catalyst to afford the corresponding triol derivatives **62** in good to high overall yields. For example, the reaction of 3-(2-furyl)-3-HMe_2SiO-2-OTHP-1-propene (**59a:** R = 2-furyl; R′ = OTHP), prepared from 3-(2-furyl)-2-OTHP-1-propene and $(HMe_2Si)_2NH$, using Karstedt's catalyst, followed by the Tamao oxidation gives the 2-*O*-THP-triol **62a** in 90% isolated yield with >99/1 *syn/anti* ratio (equation 25)[87]. As an application of the process yielding **62**, the stereoselective syntheses of enantiopure pentitols, D-arabinitol and xylitol as their pantaacetates have been achieved in just 4 steps from an enantiopure glyceraldehyde ketal[87].

Remarkable dependence of the regioselectivity on the catalyst species employed is observed in the intramolecular hydrosilylation of allylic *N*-dimethylsilylamines **63**, i.e. the Rh-catalyzed reactions proceed via 5-*endo* cyclization to give 1-aza-2-silacyclopentanes **64** whereas the Pt-catalyzed reactions yield 1-aza-2-silacyclobutanes **65** via 4-*exo* cyclization (Scheme 12)[89,90].

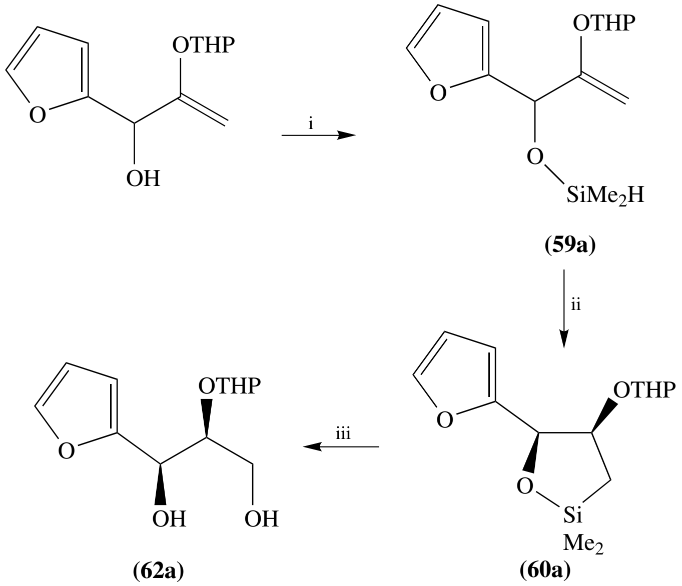

(25)

(i) $(HMe_2Si)_2NH$, RT, then *in vacuo*;

(ii) (a) [Pt] = $Pt[(CH_2{=}CHSiMe_2)_2O]_2$ in toluene, 60°C, (b) $EDTA^{2-}.2Na^+$, hexane;

(iii) 30% H_2O_2, 15% KOH, MeOH/THF, RT

The 4-*exo* cyclization of open-chain substrates **63** proceeds in *trans*-fashion with moderate to excellent selectivity (*trans/cis* = 77/23 ∼> 99/1)[90]. The *trans* selectivity is dependent on the substitution pattern of R^2, R^3 and R^4. The reactions giving *trans*-1-aza-2-silacyclobutanes **65** have been applied to the stereoselective syntheses of *syn*-amino alcohols **66** via the Tamao oxidation as exemplified by the reaction of **63d** (R = HMe_2Si), affording **66d** (76% overall yield in 4 steps, *syn/anti* = > 99/1) via **65d** (*trans/cis* = > 99/1) in equation 26[90]. In the case of 3-*N*-disilylamino-1-cyclohexene **63f** (R = HMe_2Si), however, *cis*-1-aza-2-silacyclobutane **65f** is formed exclusively, that is converted to *cis*-2-amino-1-cyclohexanol **(66f)** (equation 27)[90].

Detailed mechanistic study on these intramolecular hydrosilylation of allylic *O*-silyl ethers **59** and allylic *N*-silylamines **63** using deuterium labeling techniques shows that 5-*endo* cyclization giving **60** or **64** proceeds via a Chalk–Harrod type hydrometalation catalytic cycle, while 4-*exo* cyclization process yielding **61** or **65** includes a Seitz–Wrighton type silylmetalation mechanism[89].

In a similar manner, 1-cyclopentene-3-carboxylic acid **(67a)** and *N*-*t*-Boc-(*S*)-3,4-didehydroproline **(67b)** can be transformed to methyl *cis*-2-hydroxycyclopentane-1-carboxylate **(70a)** and methyl (3*R*, 2*S*)-*N*-*t*-Boc-3-hydroxyprolinate **(70b)** in 67% and 76% overall yields (4 steps), respectively (equation 28)[91].

Intramolecular hydrosilylation of *O*-dimethylsilylalkenoate **71**, promoted by Karstedt's catalyst, provides an efficient route to *cis*-4-methyl-5-substituted-γ-lactone **73** (*cis/trans* = 76/24–98/2) in 21–87% yield (equation 29)[92]. The reaction proceeds through 5-*endo* cyclization exclusively. The stereoselectivity of the reaction is highly

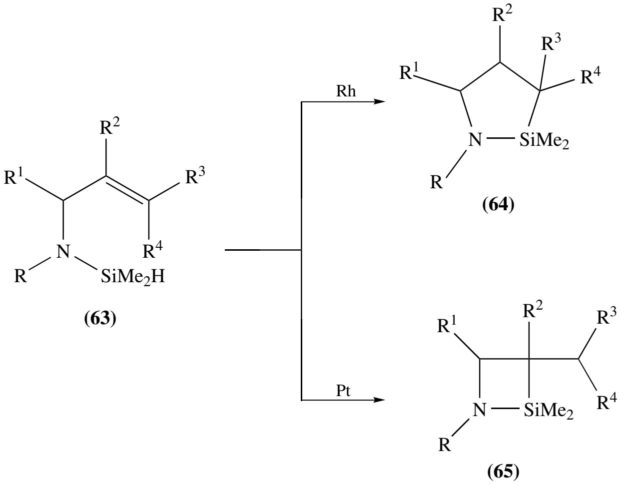

[Rh] = [RhCl($CH_2{=}CH_2$)$_2$]$_2$ or RhCl(PPh_3)$_3$
[Pt] = Pt[($CH_2{=}CHSiMe_2$)$_2$O]$_2$

R = HMe_2Si, *t*-$BuMe_2Si$, $PhCH_2$
(a) $R^1 = R^2 = R^3 = R^4 = H$
(b) R^1 = *i*-Pr, $R^2 = R^3 = R^4 = H$
(c) R^1 = Ph, $R^2 = R^3 = R^4 = H$
(d) R^1 = Ph, R^2 = H, $R^3 = R^4$ = Me
(e) R^1 = Ph, R^2 = Me, $R^3 = R^4 = H$
(f) R^1R^4 = —(CH_2)$_3$—, $R^2 = R^3 = H$

SCHEME 12. Intramolecular hydrosilylation of *N*-silylallylic amines **63**

dependent on the size of the substituent R, while it is much less sensitive to the substituent on silicon. For bulkier R, stereoselectivity increases, but yield decreases. The $A^{1,2}$ strain can account for the observed *cis*-selectivity[92].

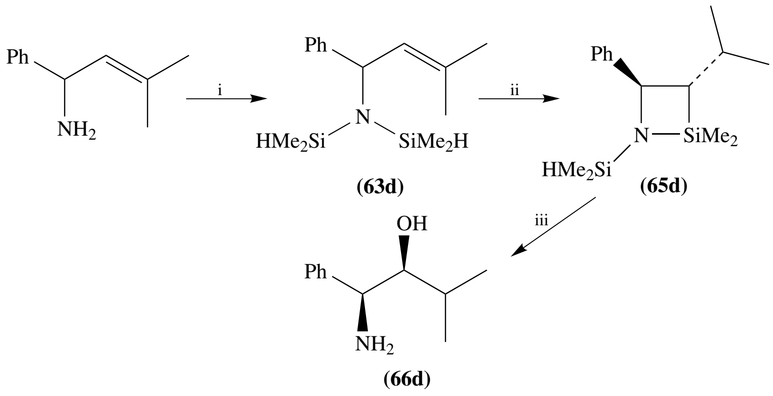

(26)

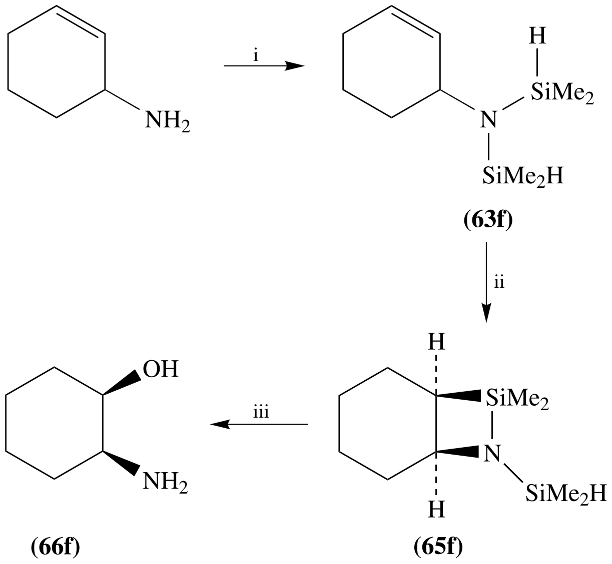

(27)

(i) n–BuLi, then HMe_2SiCl (twice); (ii) (a) [Pt] =

$Pt[(CH_2{=}CHSiMe_2)_2O]_2$ in toluene, 60 °C

(b) $EDTA^{2-}.2Na^+$, hexane; (iii) 30% H_2O_2, 15% KOH, MeOH/THF, RT

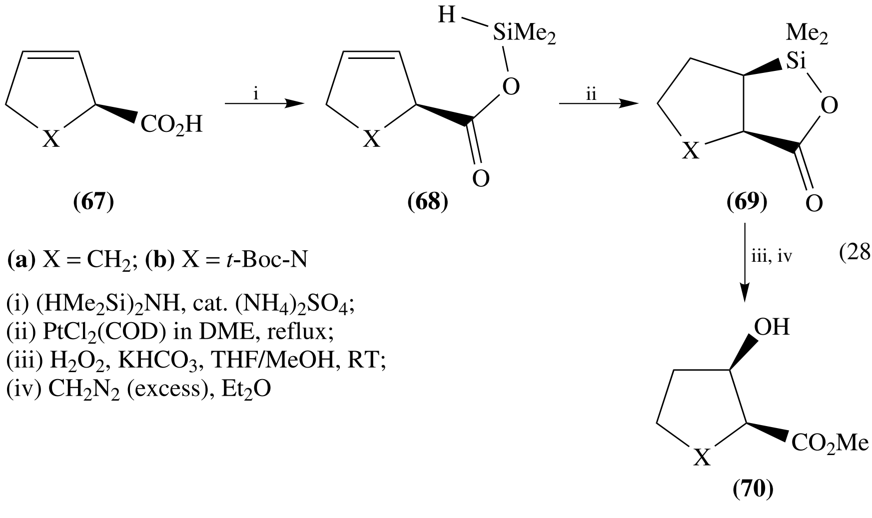

(28)

(**a**) X = CH_2; (**b**) X = t-Boc-N

(i) $(HMe_2Si)_2NH$, cat. $(NH_4)_2SO_4$;
(ii) $PtCl_2(COD)$ in DME, reflux;
(iii) H_2O_2, $KHCO_3$, THF/MeOH, RT;
(iv) CH_2N_2 (excess), Et_2O

In the reaction of $HMe_2SiOCMe_2CH{=}CH_2$ using Karstedt's catalyst in pentane at ambient temperature, an eight-membered ring product **75** is formed (35% yield) besides the normal 5-*endo* cyclization product **74** (35% yield) (equation 30)[93].

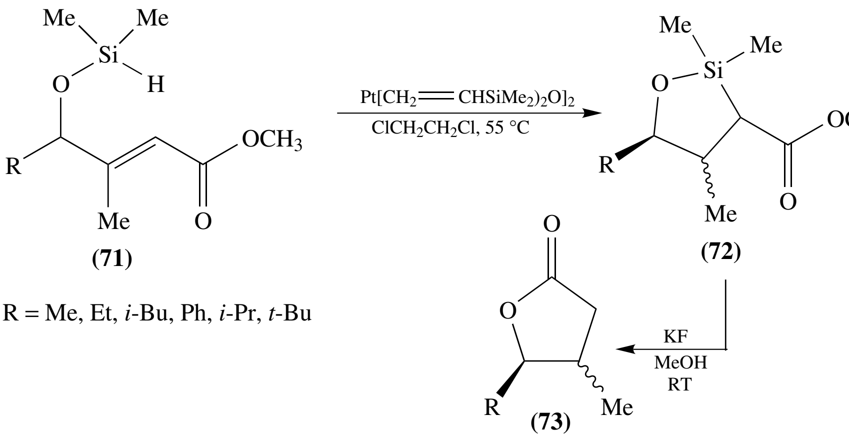

(71) **(72)** **(73)**

R = Me, Et, *i*-Bu, Ph, *i*-Pr, *t*-Bu

(29)

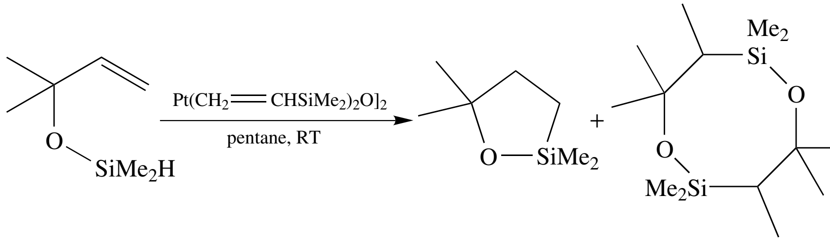

(74) **(75)**

(30)

A combination of dehydrogenative silylation and the subsequent intramolecular hydrosilylation of allylic alcohols with H_2SiPh_2 and $H_2SiMePh$ catalyzed by Cp_2TiMe_2 or racemic (EBTHI)$TiMe_2$ [EBTHI = ethylene-1,2-bis(η^5-4,5,6,7-tetrahydroindenyl)] gives the desired 5-*endo* cyclization product **60** in up to 75% yield together with a rather complex mixture of redistribution and hydrogenation products[94].

Applications of the intramolecular hydrosilylation to catalytic asymmetric synthesis will be discussed in Section V (*vide infra*).

D. Other Reactions Associated with Alkene Hydrosilylation

Dehydrogenative silylation of alkenes is often observed as a side reaction of hydrosilylation (*vide supra*). However, this reaction becomes a predominant or exclusive process depending on the nature of the catalysts used as well as substrates[3,79,80,95–99].

Exclusive formation of silylstyrenes **76** is achieved when the reactions of styrene and 4-substituted styrenes with $HSiEt_3$ are catalyzed by $Fe_3(CO)_{12}$ or $Fe_2(CO)_9$[100]. Other iron-triad metal carbonyl clusters, $Ru_3(CO)_{12}$ and $Os_3(CO)_{12}$, are also highly active catalysts, but a trace amount of hydrosilylation product **77** is detected in the Ru-catalyzed reactions and the Os-catalyzed reactions are accompanied by 3–12% of **77** (equation 31)[100]. Mononuclear iron carbonyl, $Fe(CO)_5$, is found to be inactive in this reaction[100].

1,5-Hexadiene is also found to undergo extremely selective dehydrogenative silylation in the presence of a catalytic amount of $RhCl(PPh_3)_3$ at the terminal olefin moiety to give (*E*)-1-silyl-1,5-hexadiene **78** in excellent yields (equation 32)[101]. In order for this reaction to be highly selective, excess 1,5-hexadiene should be used, i.e. a mixture of **78** and the usual hydrosilylation product is obtained when an equal amount or excess hydrosilane is used. The reaction with $HSiEt_2Me$ proceeds with >98% stereoselectivity, giving (*E*)-**78** in 90% yield, which is accompanied by 9% of an olefin-isomerization product, 1-silyl-1,4-diene **79**. The reaction using $HSi(OEt)_3$ gives **78** in 99% yield (no side product is detected), but stereoselectivity is somewhat decreased ($E/Z = 92/8$). Other Rh-catalysts, e.g. $Rh_6(CO)_{16}$, $RhCl(CO)(PPh_3)_3$, $HRh(CO)(PPh_3)_3$, $RhCl_3 \cdot 3H_2O$ and $Rh_2(OAc)_2$, show good activities in the reaction of 1,5-hexadiene with $HSiEt_2Me$. The results using other 1,5-dienes are exemplified in Table 3[101]. It is noteworthy that only 1,5-dienes yield dehydrogenative silylation products cleanly, i.e. the reactions of 1,4-dienes and 1,6-dienes under the same conditions suffer from the extensive occurrence of hydrosilylation and double-bond isomerization[101].

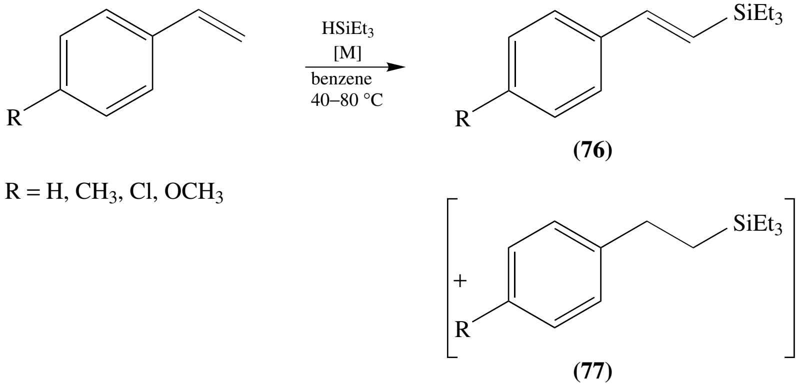

(76)

(77)

R = H, CH_3, Cl, OCH_3

[M] = $Fe_2(CO)_9$, $Fe_3(CO)_{12}$, $Ru_3(CO)_{12}$, $Os_3(CO)_{12}$

(31)

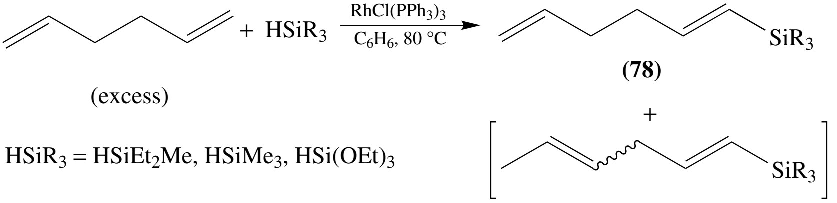

(78)

(excess)

$HSiR_3$ = $HSiEt_2Me$, $HSiMe_3$, $HSi(OEt)_3$

(79) $E/Z = 1/1$

(32)

The formation of allylsilanes **80** is found to take place in the reaction of alkenes with $HSiEt_3$ catalyzed by $Rh_2(pfb)_4$ (pfb = perfluorobutanoate) when the hydrosilane is added to a mixture of an alkene with the catalyst in CH_2Cl_2 (equation 33)[102]. The reactions of simple 1-alkenes, e.g. 1-hexene, 1-octene and 1-decene, give 31–34% of **80**, 3–6% of **81** and 61–66% of **82**, while a highly selective allylsilane formation [91% of **80** (*E/Z* = > 50/1), 1% of **81** and 8% of **82**] is observed in the reaction of 3-phenyl-1-propene (R = Ph). 1-Silylalkene **81** (R = *n*-BuO) is formed as the predominant product (61%) together with **80** (12%) and **82** (27%) when 3-(*n*-butoxy)-1-propene is employed. Since the reaction should generate molecular hydrogen, substantial hydrogenation of the alkene substrate is also observed during the reaction. It should be noted that usual $Rh_2(pfb)_4$-catalyzed hydrosilylation of these 1-alkenes proceeds with 95–98% selectivity when the

TABLE 3. Dehydrogenative silylation with $HSiEt_2Me$ of 1,5-dienes

1,5-Diene	Product	Yield (%) (*E*/*Z* at C-1)	Side product (%)
 (*E*/*Z* = 11/1)	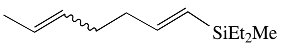	85 (*E*/*Z* at C_5 = 11/1)	7
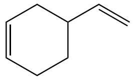	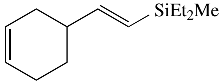	90	9
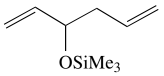	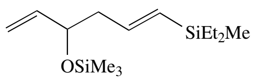	44	trace
	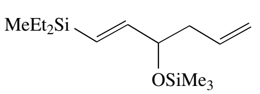	49	

alkene is added to a mixture of the Rh-catalyst and $HSiEt_3$[102].

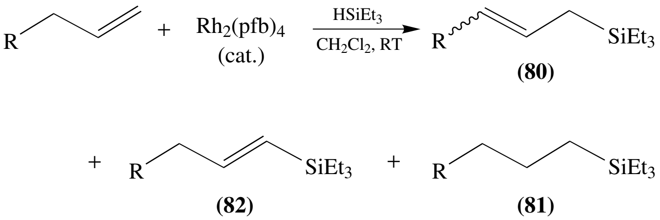

(33)

When a Si−C bond has substantial strain, the addition of hydrosilane to such a Si−C σ-bond takes place. The hydrosilylations of 1,3-disilacyclobutanes, *cis*-**83** and *trans*-**83**, catalyzed by $Pt(PPh_3)_2Cl_2$, proceed stereospecifically to give trisilanes, *meso*-**84** and *dl*-**84**, respectively, in quantitative yields (equations 34 and 35)[103].

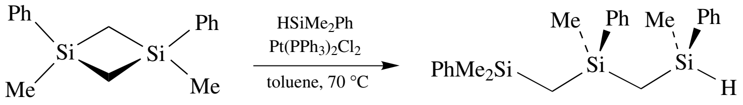

(34)

cis-**(83)** *meso*-**(84)**

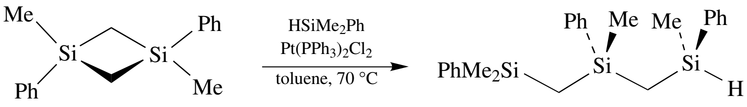

(35)

trans-**(83)** *dl*-**(84)**

III. HYDROSILYLATION OF ALKYNES

The hydrosilylation of alkynes provides a direct route to a variety of alkenylsilanes that serve as important intermediates for cross-linking silicones as well as versatile reagents in organic syntheses. This reaction appears to have been attracting increasing attention among synthetic chemists. The hydrosilylation of alkynes catalyzed by transition metal complexes including clusters proceeds, in general, more smoothly than that of alkenes, and terminal alkynes are much more reactive than internal alkynes[104]. Platinum, especially Speier's catalyst, rhodium and other Group VIII transition metals and their complexes are commonly used as catalysts. The reaction of a 1-alkyne, $R-C\equiv CH$, with a hydrosilane, $HSiX_3$, possibly gives three products, i.e. (E)-$R-CH=CH-SiX_3$, (Z)-$R-CH=CH-SiX_3$ and $R(X_3Si)C=CH_2$ (equation 36). Accordingly, the stereoselectivity and the regioselectivity of the reaction are important issues in this reaction.

$$RC\equiv CH + HSiX_3 \xrightarrow{\text{catalyst}} (E)\text{-and/or }(Z)\text{-}RCH=CHSiX_3 + R(X_3Si)C=CH_2 \qquad (36)$$

A. Simple Alkynes

1. By platinum catalysts

Speier's catalyst (H_2PtCl_6/i-PrOH), the most commonly used catalyst in the hydrosilylation of alkenes (*vide supra*), can be used for the reaction of alkynes[3]. A related potassium salt K_2PtCl_6, however, does not show appreciable catalytic activity. A number of quaternary ammonium, phosphonium and arsonium hexachloroplatinates are shown to be highly active catalysts for the hydrosilylation of phenylacetylene with different hydrosilanes, giving a mixture of (E)-β-silylstyrene (40–95%) and α-silylstyrene (60–65%) in excellent yields under neat conditions (0.1 mol% Pt catalyst) at 80 °C (equation 37)[105]. The complexes with highly lipophilic cations such as $(n\text{-}Bu_4N)_2PtCl_6$, $[(n\text{-}C_8H_{17})_4N]_2PtCl_6$ and $[(n\text{-}C_{18}H_{37})_4N]_2PtCl_6$ are found to be the most active catalysts among the hexachloroplatinates examined. A phase transfer agent, n-Bu_4NHSO_4, and a crown ether, 18-crown-6, are found to activate K_2PtCl_6 by solubilizing $PtCl_6{}^{2-}$ ion[105]. The results clearly show that the counter cation plays an important role in this catalytic process.

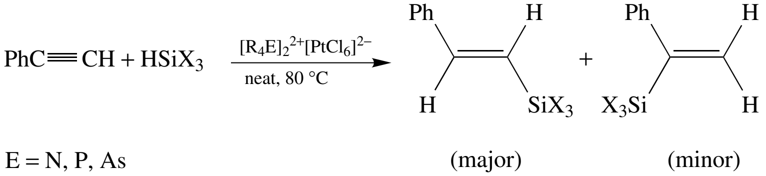

(37)

A quaternary phosphonium hexachloroplatinate bound to the Merrifield resin is also an effective hydrosilylation catalyst which can be used repeatedly without appreciable loss of activity.[105]

Highly dispersed metallic platinum systems prepared by treating mesitylene-solvated Pt atoms with solid supports, carbon, graphite and γ-Al_2O_3 provide highly active catalysts (Pt/hydrosilane $= 2.3 \times 10^{-4}$–5.8×10^{-5} g-atom mol^{-1}) for the hydrosilylation of 1-hexyne and 2-hexyne at 25–70 °C under neat conditions[35]. Although the regioselectivity achieved by these catalysts is similar to that by H_2PtCl_6, the specific catalytic activity is superior to that of the homogeneous system. The observed high specific activity can be attributed to the high dispersion and small particle size of platinum metal in these systems, i.e. *ca* 20 Å for Pt/Al_2O_3, *ca* 15 Å for Pt/graphite and too small to detect for Pt/C: Pt/C is the most active among the three systems. The catalysts are claimed to be recyclable for several times without loss of activity[35].

2. By rhodium catalysts

The hydrosilylation of 1-alkynes catalyzed by rhodium complexes proceeds predominantly in an *anti*-fashion, giving thermodynamically unfavorable (*Z*)-alkenylsilanes as the major product (up to 99%)[3,106–108]. For example, the hydrosilylation of 1-hexyne with $HSiEt_3$ catalyzed by $RhCl(PPh_3)$, $Rh_4(CO)_{12}$, $Rh_2Co_2(CO)_{12}$ and $RhCo_3(CO)_{12}$ in toluene gives (*Z*)-1-silylhexene **85** as the major product (79–98%), (*E*)-1-silyl-1-hexene **86** (1–10%) and 2-silyl-1-hexene **87** (1–14%), in which the product ratio depends on the reaction conditions (*vide infra*) (equation 38) (see also Section III.B).

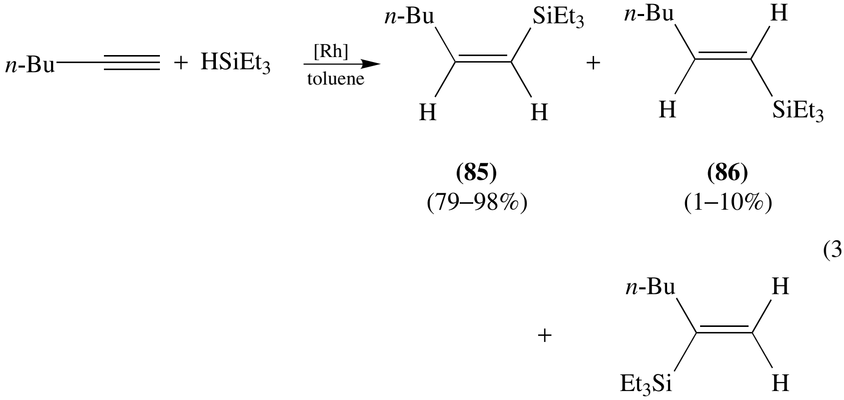

(85) (79–98%)

(86) (1–10%)

(38)

(87) (1–14%)

[Rh] = $RhCl(PPh_3)_3$, $Rh_4(CO)_{12}$, $Rh_2Co_2(CO)_{12}$, $RhCo_3(CO)_{12}$

Other neutral rhodium complex catalysts such as $[Rh(COD)Cl]_2$, $HRh(CO)(PPh_3)_3$ and $HRh(PPh_3)_4$ also give (*Z*)-1-silyl-1-hexene **85** as the predominant product when the reactions are run in benzene[109]. However, it has recently been shown that the *Z*- or *E*-stereoselectivity of the Rh-catalyzed reactions can be effectively controlled by a proper combination of solvent and ligand[109,110]. For example, the reaction of 1-hexyne with $HSiEt_3$ catalyzed by $[Rh(COD)Cl]_2$ in DMF gives (*Z*)-1-silyl-1-hexene **85** with 97% selectivity, whereas the same reaction catalyzed by $[Rh(COD)Cl]_2/2PPh_3$ in MeCN affords (*E*)-1-silyl-1-hexene **86** with 97% selectivity (equation 39)[109]. Similar results are obtained for $RhCl(PPh_3)_3$-catalyzed reactions. Solvents such as benzene, acetone, THF, CH_2Cl_2, EtOH, DMF and NEt_3 favor the formation of the (*Z*)-product, while MeCN and *n*-PrCN promote the (*E*)-product formation. Triphenylphosphine is necessary to generate the selective catalyst species in MeCN. Based on these results, a cationic rhodium(I) species, $[Rh(COD)(PPh_3)_2]^+$, is proposed to be the active species that promotes highly selective *cis*-addition of $HSiEt_3$ to a 1-alkyne[109]. In fact, a cationic phosphine-Rh(I) complex, $[Rh(COD)_2]BF_4/2PPh_3$ is proved to be an excellent catalyst for the formation of (*E*)-1-triethylsilyl-1-alkenes, regardless of the solvent employed (equation 39)[109].

Although Rh and Rh–Co carbonyl clusters such as $Rh_4(CO)_{12}$, $Rh_2Co_2(CO)_{12}$ and $RhCo_3(CO)_{12}$ are highly efficient catalysts promoting the *trans*-addition of hydrosilanes to 1-alkynes[106,107] (*vide supra*), dimeric phosphite–Rh(I) complexes, $[RhCl\{P(OAr)_3\}_2]_2$ (Ar = 2-MeC_6H_4, 2-*t*-BuC_6H_4, 2,6-$Me_2C_6H_3$), effect the *cis*-addition of $HSiEt_3$ to 1-hexyne, yielding (*E*)-product **86** exclusively in moderate to high yield[20]. The bulkiness of the phosphite ligand is crucial for highly selective *cis*-addition. Thus, the corresponding

$P(OMe)_3$ complex gives a 55 : 45 mixture of **86** and **85**[20].

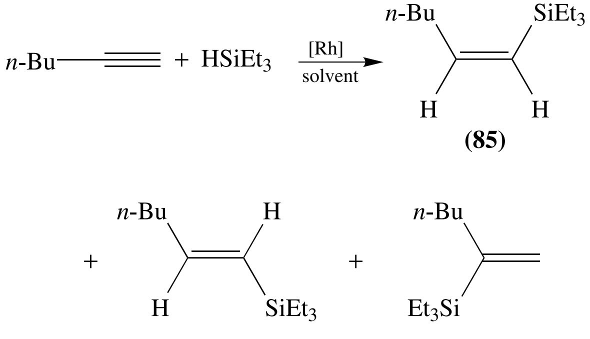

(39)

[Rh]	Solvent	**85**	**86**	**87**
$[Rh(COD)Cl]_2$	DMF	97%	1%	2%
$[Rh(COD)Cl]_2$	EtOH	94	4	2
$[Rh(COD)Cl]_2$	MeCN	36	33	31
$[Rh(COD)Cl]_2/2PPh_3$	MeCN	2	97	1
$[Rh(COD)_2]BF_4/2PPh_3$	MeCN	2	95	3
$[Rh(COD)_2]BF_4/2PPh_3$	EtOH	5	95	0
$[Rh(COD)_2]BF_4/2PPh_3$	Acetone	1	99	0

A dinuclear Rh(II) complex, $Rh_2(pfb)_4$ (pfb = perfluorobutanoate), effectively catalyzes the hydrosilylation of 1-alkynes to give (*Z*)-1-silyl-1-alkenes as the major product when a trialkylsilane is added to the mixture of a 1-alkyne and the catalyst in CH_2Cl_2[111]. However, the reverse addition, i.e. addition of the 1-alkyne to the mixture of the hydrosilane and the catalyst, affords an allylic silane in place of the silylalkenes in high yield (*vide infra*)[111].

A rhodium(III) complex of Troger's base (TB), $TB{\bullet}2RhCl_3$ **(88)**, prepared by treating $RhCl_3$ with TB is an active catalyst, promoting the hydrosilylation of 1-alkynes, giving a mixture of (*Z*)-1-silyl-1-alkene (29–95%), (*E*)-1-silylalkene (5–95%), and 2-silyl-1-alkene (5–20%)[112]. The regio- and stereoselectivity as well as total yield depend on the nature of 1-alkyne and hydrosilane used. The best result is obtained in the reaction of phenylacetylene with $HSiCl_3$ or $HSiMe_2Ph$, giving (*Z*)-β-silylstyrene (equation 40)[112]. The use of bulky hydrosilanes such as $HSiMe_2Bu$-*t* and $HSi(Pr\text{-}i)_3$ dramatically changes the selectivity, yielding a mixture of (*E*)-β-silylstyrene (80–95%) and α-silylstyrene (20–25%)[112].

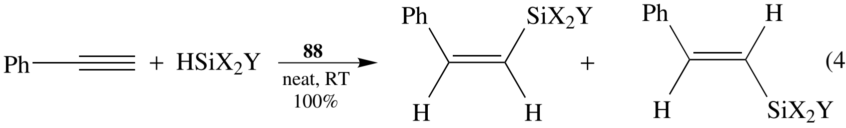

(40)

Z (95%) *E* (5%)

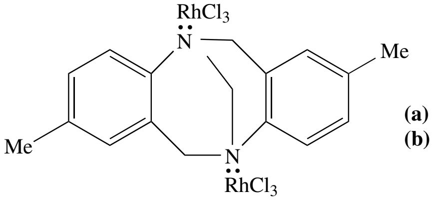

(a) X = Y = Cl
(b) X = Me, Y = Ph

(88)

Although Wilkinson's catalyst, $RhCl(PPh_3)_3$, usually promotes the *trans*-addition of hydrosilanes to 1-alkynes (*vide supra*), the reactions of 1-alkynes bearing bulky substituents such as *tert*-butyl and cyclohexyl give predominantly (*E*)-1-silyl-1-alkenes via *cis*-addition together with 1-alkynylsilanes via dehydrogenative silylation (*vide infra*)[113]. The use of H_3SiPh in the reaction of phenylacetylene also affords (*E*)-$PhCH{=}CHSiH_2Ph$ exclusively[17].

Rhodium complexes with 1,3-bis(di-*tert*-butylphosphino)methane (dtbpm), [(dtbpm) $RhCl]_2/PPh_3$ **(89)**, (dtbpm)$RhSi(OEt)_3(PMe_3)$ **(90)** and (dtbpm)$RhMe(PMe_3)$ **(91)** are found to be effective catalysts for the hydrosilylation of an internal alkyne, 2-butyne, with $HSi(OEt)_3$ at ambient temperature without solvent to yield (*E*)-2-triethoxysilyl-2-butene with complete stereoselectivity in quantitative yield using a proper concentration of the catalysts, i.e. $\geqslant 0.05$ mol% for **89**, >0.4 mol% for **90** and **91**[114]. When the reaction is carried out at lower catalyst concentrations, i.e. 0.1 mol% for **90** or **91**, (*Z*)-product is formed via *trans*-addition in 7–13% yield.

3. By iridium, ruthenium, osmium and other catalysts

Iridium complexes with a unique oxygen donor ligand, $C[P(O)Ph_2]_3^-$(triso), such as $IrH_2(triso)(SiMePh_2)_2$, $Ir(triso)(COE)_2$ (COE = cyclooctene) and $Ir(triso)(C_2H_4)_2$ are excellent catalysts for the hydrosilylation of 1-alkynes (equation 41)[115,116]. These triso-Ir complex catalysts are extremely chemo-, regio- and stereoselective in that only 1-alkenes, except for *t*-$BuC{\equiv}CH$ and $HC{\equiv}CCO_2Me$, are hydrosilylated via *trans*-addition, giving (*Z*)-1-triethylsilyl-1-alkenes with extremely high stereoselectivity ($Z/E \leqslant 190/1$). Internal alkynes, e.g. 3-hexyne, diphenylacetylene and dimethyl acetylenedicarboxylate, are totally unreactive and the reaction of methyl propynoate only gives trimethyl benzene-1,3,5-tricarboxylate via trimerization in trace amount[115].

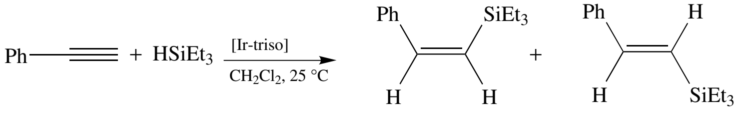

(41)

(128 : 1)

[Ir-triso] = $IrH_2(triso)(SiMePh_2)_2$, $Ir(triso)(COE)_2$, $Ir(triso)C_2H_4)_2$

Other iridium complexes, such as $IrH_2(SiEt_3)(COD)(AsPh_3)$ (COD = 1, 5-cyclooctadiene)[117], $[Ir(OMe)(COD)]_2/2PPh_3$ (or $AsPh_3$)[117], $[IrH(H_2O)(bq)(PPh_3)_2]SbF_6$ (bq = 7, 8-benzoquinolinato)[113], $[Ir(COD)(\eta^2\text{-}(i\text{-}Pr)_2PCH_2CH_2NMe_2)]BF_4$, $[Ir(TFB)(\eta^2\text{-}(i\text{-}Pr)_2PCH_2CH_2OMe)]BF_4$ (TFB = tetrafluorobenzobarrelene)[118], $Ir(C{\equiv}CPh)(CO)_2(PCy_3)$ (Cy = cyclohexyl), $Ir(C{\equiv}CPh)(TFB)(PCy_3)$[119], are also found to be active catalysts for the hydrosilylation of phenylacetylene and 1-hexyne, giving a mixture of (*Z*)- and (*E*)-$RCH{=}CHSiX_3$, $R(X_3Si)C{=}CH_2$, $RC{\equiv}CSiX_3$, and $RCH{=}CH_2$. The products ratio is highly dependent on the reaction conditions. The reactions catalyzed by $[IrH(H_2O)(bq)(PPh_3)_2]SbF_6$ give (*Z*)-$RCH{=}CHSiX_3$ with excellent selectivity comparable to that achieved by using the Ir(triso) complexes[113].

A ruthenium complex with triisopropylphosphine, $HRuCl(CO)[P(Pr\text{-}i)_3]_2$, is a highly efficient catalyst for the hydrosilylation of phenylacetylene with $HSiEt_3$ (1.0 equiv.) in $ClCH_2CH_2Cl$ at 60 °C, yielding (*Z*)-$PhCH{=}CHSiEt_3$ via *trans*-addition with 100% selectivity in quantitative yield[120]. The corresponding osmium complex, $HOsCl(CO)[P(Pr\text{-}i)_3]_2$, is an active catalyst as well[121]. The Os-catalyzed reaction using one equivalent of $HSiEt_3$ to the alkene gives (*Z*)-$PhCH{=}CHSiEt_3$ with high selectivity ($\leqslant$98%), whereas the (*E*)-product is formed selectively ($\leqslant$99%) when excess $HSiEt_3$ is used[121]. Ruthenium complexes **92a**, **93a**, and **94a** as well as osmium complexes **92b**, **93b**, and **94b** are also found to be active catalysts for the hydrosilylation of phenylacetylene with $HSiEt_3$ under the same conditions[122]. The reactions catalyzed by the ruthenium complexes give (*Z*)-$PhCH{=}CHSiEt_3$ with 91–96% selectivity, while the osmium catalysts are less selective (62–70%)[122].

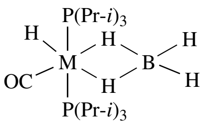

(92)

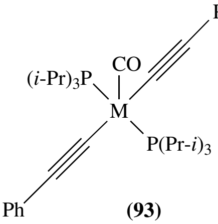

(93)

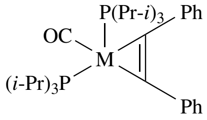

(94)

(**a**) M = Ru, (**b**) M = Os

Nickel(0) complexes with trialkylphosphine or trialkylphosphite ligands with lower linear alkyl groups (C_1–C_4) can catalyze the hydrosilylation of phenylacetylene with $HSiPh_3$ to afford (*E*)-$PhCH{=}CHSiPh_3$ in good yield[123]. The ligand/Ni ratio of 2 as well as the $HSiPh_3/PhC{\equiv}CH$ ratio of 2 is essential to promote the hydrosilylation selectively, suppressing the trimerization of phenylacetylene[123].

An organoyttrium complex, $Cp^*{}_2YCH_3(THF)$ (Cp^* = pentamethylcyclopentadienyl), is found to be an excellent catalyst for regioselective hydrosilylation of functionalized unsymmetrical internal alkynes with H_3SiPh. The reactions are carried out in cyclohexane at 40–90°C for 24–48 h to give single isomers when one of the alkyl substituents of the acetylene moiety is primary and the other secondary or tertiary[124]. No stereoisomers are formed, i.e. complete *cis*-addition. The regioselectivity drops naturally when both substituents of the acetylene moiety are primary. Nevertheless, good selectivity is observed for 2-alkynes such as 2-nonyne (2-Si/3-Si = 4.1–7.3) and 5-methyl-2-heptyne (2-Si/3-Si = 7.3). Thus, $Cp^*{}_2YCH_3(THF)$ or its precursor, $Cp^*{}_2YCH(TMS)_2$, appears to be the most regioselective catalyst for the internal alkynes to date. Examples are shown in equation 42 and Table 4.

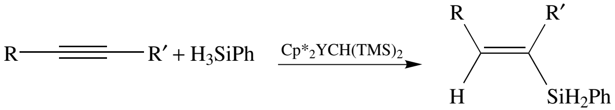

(95) **(96)** (42)

(**a**) R = cyclohexyl, R′ = Me 74%
(**b**) R = *sec*-Bu, R′ = *n*-pentyl 93%

TABLE 4. Selective hydrosilylation of alkynes with H_3SiPh, catalyzed by $Cp^*{}_2YCH_3(THF)$

Substrate	Product	Yield (%)
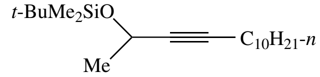	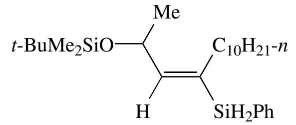	89
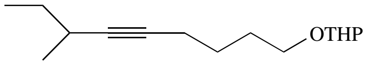	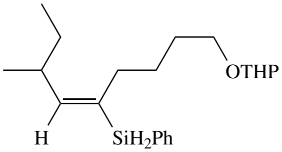	89
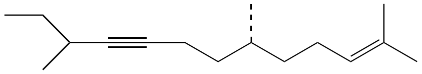	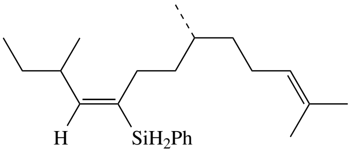	80

4. By radical initiators

Although the hydrosilylation of alkynes under free-radical conditions using UV irradiation or organic peroxides was studied in 1940s and 1950s[4,125,126], the reactions promoted by transition metal catalysts took over the main stream of research and development afterwards[3,4]. As discussed in Section II. A.5, tris(trimethylsilyl)silane, $HSi(SiMe_3)_3$ (TTMSS), is found to undergo smooth addition to simple and functionalized alkenes in the presence of a radical initiator to give the corresponding hydrosilylation products in high yields[66–68] (*vide supra*). TTMSS also participates in hydrosilylation of alkynes in the presence of AIBN (80–90 °C) or BEt_3/O_2 (0–70 °C). The stereochemistry of the reaction follows usual radical addition to 1-alkynes, i.e. *trans*-addition, yielding the (*Z*)-product[3]. The Z/E selectivity is dependent on the reaction conditions as well as the steric and electronic nature of the substituents of alkyne. The reactions of 1-alkynes using BEt_3/O_2 as the initiator at lower temperatures (0–25 °C) favor the formation of the (*Z*)-product **97** ($Z/E = 95/5–99/1$; the Z/E ratio of the same reaction with AIBN at 80–90 °C ranges from 51/49 to 92/8) (equation 43). A mixture of *Z*- and *E*-products, **98** and **99**, are formed in the reactions of 2-substituted phenylacetylenes, PhC≡CX, with variable Z/E ratios (45/55–92/8) depending on the conditions and the substituent X (equation 44): The reactions using AIBN at 80–90 °C give either no or a very low selectivity. The reactions of *t*-BuC≡CH and $PhC{\equiv}CCO_2Et$ yield the corresponding (*E*)-products exclusively, regardless of the conditions.

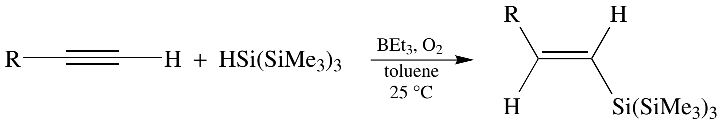

(43)

(97)

R = *n*-Bu, *n*-C_6H_{13}, Ph, CO_2Et

$Z/E = 95/5–99/1$

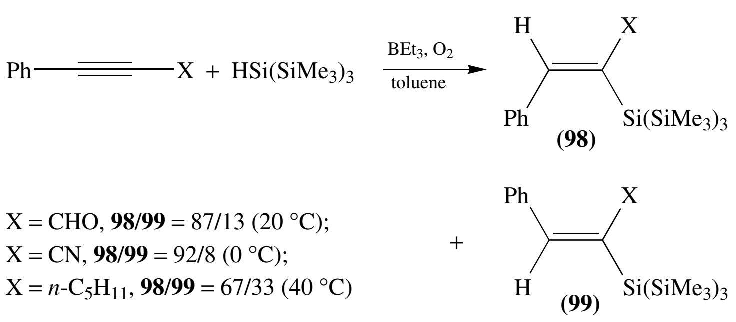

X = CHO, **98/99** = 87/13 (20 °C);
X = CN, **98/99** = 92/8 (0 °C);
X = n-C_5H_{11}, **98/99** = 67/33 (40 °C)

(44)

B. Mechanism of the Stereoselective Hydrosilylation of 1-Alkynes

It has been shown that the stereochemistry of the hydrosilylation of 1-alkynes giving 1-silyl-1-alkenes depends on the catalysts or promoters used. For example, the reactions under radical conditions give the *cis*-product predominantly via *trans*-addition[3,66], while the platinum-catalyzed reactions afford the *trans*-product via exclusive *cis*-addition[3]. In the reactions catalyzed by rhodium complexes, thermodynamically unfavorable *cis*-1-silyl-1-alkenes are formed via apparent *trans*-addition as the major or almost exclusive product. Since the *trans*-addition of $HSiEt_3$ to 1-alkynes catalyzed by $RhCl(PPh_3)_3$ was first reported in 1974[108], there have been controversy and dispute on the mechanism of this mysterious *trans*-addition that is very rare in transition-metal-catalyzed addition reactions to alkynes[3]. Recently, iridium[115,116] and ruthenium[120] complexes were also found to give the *cis*-product with extremely high selectivity (*vide supra*).

The mystery of the unusual *trans*-addition has been resolved by essentially the same two mechanisms proposed by Ojima and Crabtree and their coworkers for the rhodium- and iridium-catalyzed reactions, respectively[106,115]. The integrated mechanism is shown in Scheme 13. The most significant feature of the Ojima–Crabtree mechanism is the exclusive insertion of 1-alkyne into the Si–metal bond, i.e. not to the H–metal bond, forming (Z)-silylethenyl-[M] intermediate **101**. Because of severe steric repulsion between the two bulky groups, i.e. R_3Si and [M], in **101**, it isomerizes to thermodynamically more favorable (E)-silylethenyl-[M] intermediate **103** via either zwitterionic carbene species **102a** (proposed for the Rh-catalyzed process)[106] or metallacyclopropene species **102b** (proposed for the Ir-catalyzed process)[113,115,116]. Coordination of a hydrosilane molecule to **103** promotes the reductive elimination of (Z)-product **105**, regenerating **100**. Since the reductive elimination is the rate-determining step, (Z)-product **105** is formed as the kinetic product. The isomerization of **101** (intramolecular process) competes with the reductive elimination of **104** (intermolecular bimolecular process). Thus, the concentration of reactants exerts a marked influence on the Z/E selectivity, i.e. low concentrations favor the (Z)-product formation[106]. Also, highly reactive hydrosilanes bearing electron-withdrawing groups, e.g. $HSi(OMe)_3$, $HSiMe_2Cl$ and $HSiMeCl_2$, predominantly (65–98%) give (E)-product **104**, whereas $HSiEt_3$, $HSiEt_2Me$ and $HSiMe_2Ph$ afford (Z)-product **105** as the major product (57–99%)[106]. The bulkiness of the R group has a strong influence on the Z/E selectivity, i.e. when 1-alkynes bearing bulky R groups are used, e.g. c-$C_6H_{11}C{\equiv}CH$ and t-$BuC{\equiv}CH$, the reaction yields (E)-product selectively (89–100%)[113]. It has not been elucidated which of the two species **102a** and **102b** is the intermediate of the unique isomerization of **101** to **103**. A zwitterionic carbene intermediate similar to **102a** was proposed by Brady and Nile[127,106], and the rearrangement of η^1-ethenyl-[M] to η^2-[M] species was shown by Green and coworkers[128,115].

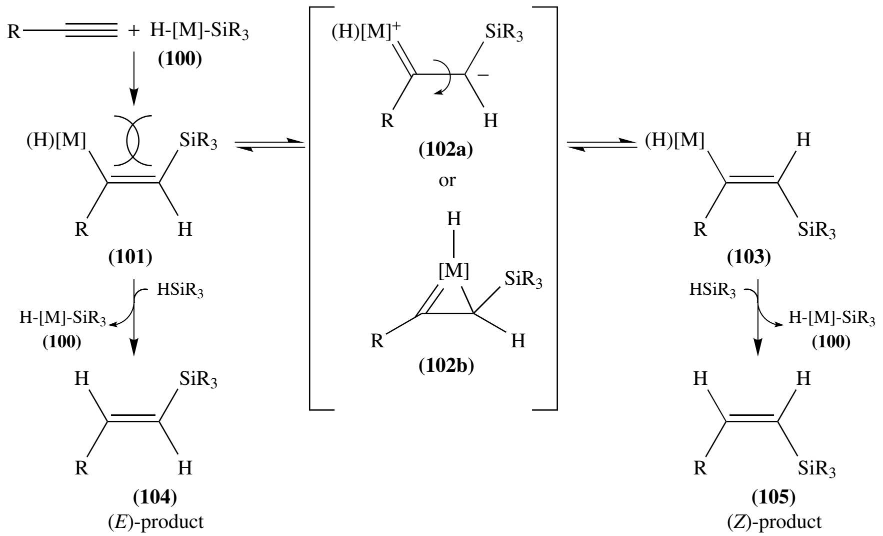

SCHEME 13. The Ojima–Crabtree mechanism for stereoselective hydrosilylation of 1-alkynes

The Ojima–Crabtree mechanism is applicable to the selective formation of (Z)-PhCH=CHSiEt$_3$ (exclusive for Ru; 60–98% for Os) in the reaction of PhC≡CH with HSiEt$_3$ catalyzed by HRuCl(CO)(P(Pr$^i_3$)$_2$[120,122], HOsCl(CO)(P(Pr$^i_3$)$_2$[121], IrH$_2$(SiEt$_3$)(TFB)(PR$_3$) (R = Ph, Cy, i-Pr)[129], [Ir(COD)(η^2–^{i}Pr$_2$PCH$_2$CH$_2$OMe)]BF$_4$[118] and Ir(C≡CPh)L$_2$PCy$_3$ (L = 2 CO or TFB)[119]. (Z)- and (E)-β-ethenyl–Rh complexes **107** have indeed been isolated from the reaction of (dtbpm)Rh[Si(OEt)$_3$](PMe$_3$) **(106)** with dimethyl acetylenedicarboxylate, and their structures identified by ^{31}P NMR analysis (equation 45)[114]. The reaction of 2-butyne with HSi(OEt)$_3$ catalyzed by (dtbpm)Rh[Si(OEt)$_3$](PPMe$_3$) gives (E)-MeCH=C(Me)Si(OEt)$_3$ as the predominant product[114], which is consistent with the previously reported (E)-product formation with reactive HSi(OEt)$_3$ through the path **101** → **104** in Scheme 13.

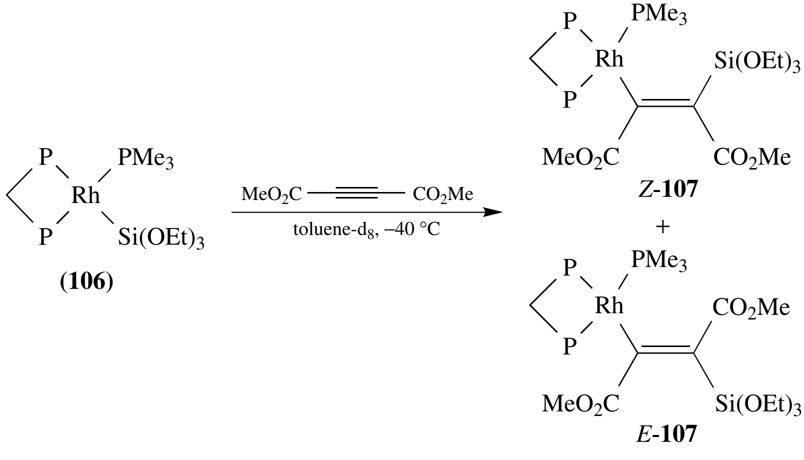

(45)

C. Intramolecular Hydrosilylation of Alkynes

The hydrosilylation of disilylalkyne $HMe_2Si[CH_2]_nSiMe_2C{\equiv}CR$ (**108b–e**: R = H or Ph, $n = 2$ or 3) catalyzed by H_2PtCl_6 proceeds via 5-*exo*-dig or 6-*exo*-dig cyclization to give *exo*-cyclic disilylalkene **109** exclusively except for the case of **108c** ($n = 3$, R = H) in which a minor (21%) amount of 6-*endo*-dig cyclization product **110c** is formed (equation 46)[130]. However, no reaction takes place for **108a** ($n = 1$, R = H)[130].

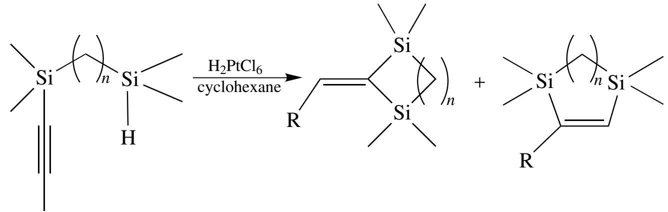

(108) **(109)** **(110)**

(46)

	Yield (%)	**109**	**110**
(a) $n = 1$, R = H	0	0	0
(b) $n = 2$, R = H	58	100	0
(c) $n = 3$, R = H	71	79	21
(d) $n = 2$, R = Ph	42	100	0
(e) $n = 3$, R = Ph	60	100	0

In a similar manner, the reaction of 5-dimethylsilyl-1-hexyne (**111**) catalyzed by H_2PtCl_6 affords 5-*exo*-dig cyclization product **112** exclusively (equation 47)[130].

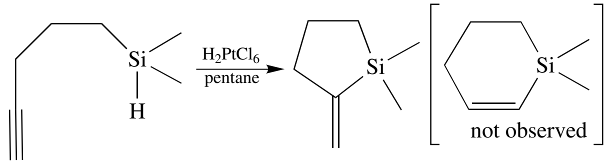

(111) **(112)**

(47)

Intramolecular hydrosilylation of ω-dimethylsiloxyalkynes such as **114**, readily derived from alkynol **113**, provides a convenient method for the regioselective functionalization of internal alkynes in combination with the Tamao oxidation and other transformations. An example of such a process giving **117** via **115** and **116** is illustrated in Scheme 14[87].

D. Bis-TMS-ethyne and Bis-TMS-butadiyne

The reaction of bis(trimethylsilyl)ethyne **(118)** with a high boiling hydrosilane, $HSiMe_2C_6H_{13}$-*n*, promoted by Karstedt's catalyst affords normal *cis*-addition product **119** in good yield under nitrogen at 90 °C. However, significant amounts of disilylethynes **120** and **121** are unexpectedly formed when the reaction is carried out under dry air and at 130–150 °C (Scheme 15)[131]. The observed scrambling of silyl groups suggests that the hydrosilylation trisilylethene product[119] is not stable under those conditions and undergoes *trans*-elimination of a $HSiMe_3$ forming **120**, followed by the addition of $HSiMe_2C_6H_{13}$-*n* and elimination of $HSiMe_3$ to yield **121**[132].

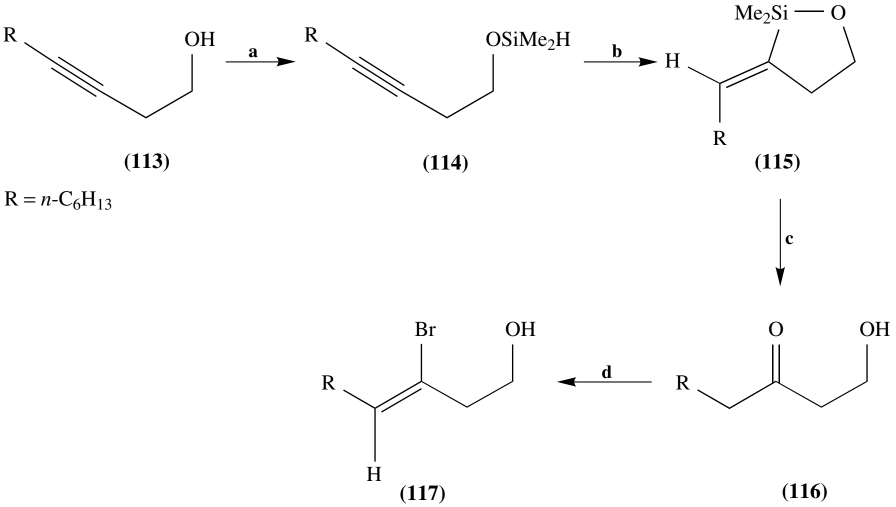

a. $(HMe_2Si)_2NH$;
b. $H_2PtCl_6.H_2O$ (0.1 mol%) / CH_2Cl_2 / room temp. / 0.5 h;
c. 30%H_2O_2 / KF / $KHCO_3$ / MeOH / THF/ 30 °C / overnight
d. (1) Br_2 / 0 °C; (2) KHF_2 / MeOH / room temp. / overnight.

SCHEME 14

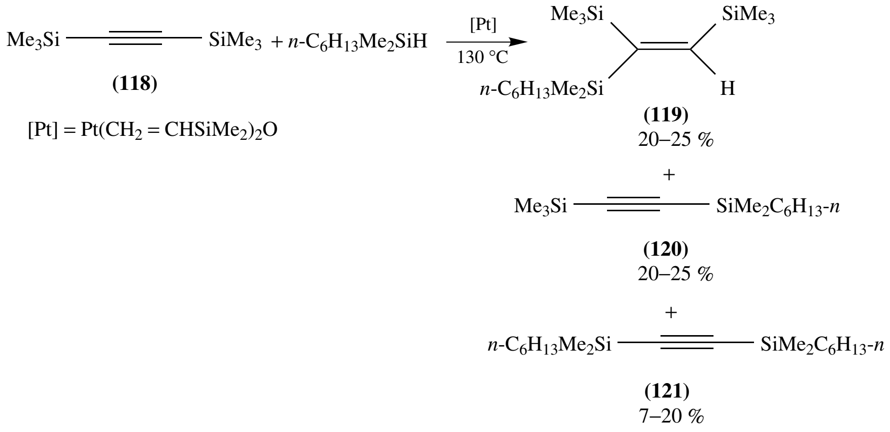

SCHEME 15

The hydrosilylation of 1,4-bis(trimethylsilyl)butadiyne **(122)** with $HSiMeCl_2$ in the presence of Speier's catalyst at 80 °C followed by methylation gives 1,1,3,4-tetrakis(trimethylsilyl)-1,3-butadiene **(123)** as the sole product in 54% yield (equation 48)[133]. However, the reactions using $HSiMe_2Ph$ at 50–60 °C afford trisilylbutenyne **124a** (70%) and allene **125a** (10%) (equation 49)[133]. The allene **125b** can be obtained exclusively when the reaction is carried out with $HSiMe_3$ using $Pt(PPh_3)_4$ as the catalyst at 90 °C for 12 h (**124b**, 1%; **125b**, 94%). When the reaction is stopped at 1 h, butenyne **124b** is formed as the major product (**124b**, 69%; **125b**, 2%). Thus, this is clearly a stepwise reaction process. The $RhCl(PPh_3)_3$-catalyzed reactions with different hydrosilanes give **124** and/or **125** with varying ratios depending on the hydrosilane used, e.g. the reaction with $HSiMe_3$ gives **125b** exclusively in 90% yield, while the reaction with H_2SiPh_2 affords **124c** as the sole product in 49% yield[133]. The reactions with $HSiEt_3$ catalyzed by palladium complexes, $PdCl_2(PPh_3)_2$ and $Pd(PPh_3)_4$, give **124d** selectively in low yields (8–18%)[133].

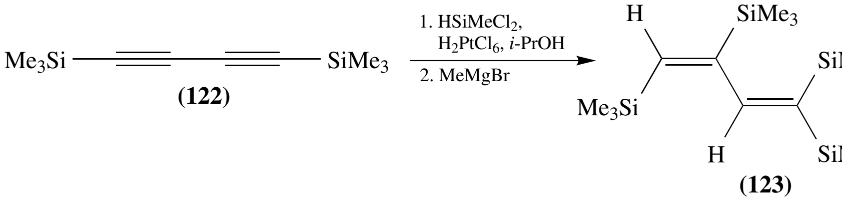

(48)

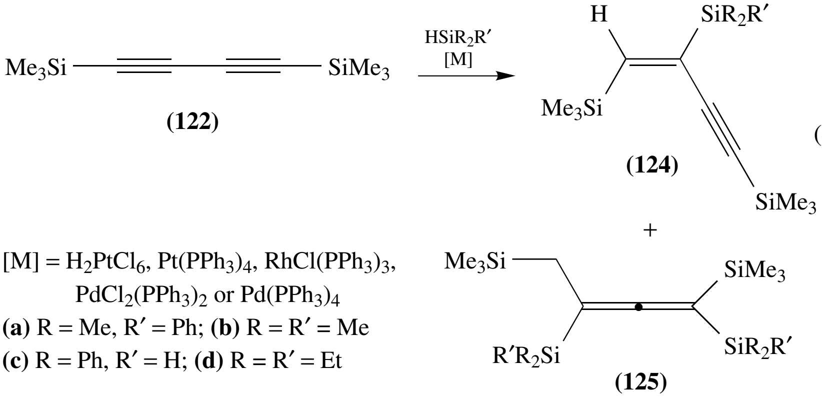

(49)

$[M] = H_2PtCl_6, Pt(PPh_3)_4, RhCl(PPh_3)_3,$
$PdCl_2(PPh_3)_2$ or $Pd(PPh_3)_4$
(**a**) R = Me, R′ = Ph; (**b**) R = R′ = Me
(**c**) R = Ph, R′ = H; (**d**) R = R′ = Et

E. Functionalized Alkynes

The hydrosilylation of propargylic alcohols should provide the most straightforward route to (*E*)-γ-silylallylic alcohols, which are useful building blocks in organic syntheses. However, the reactions promoted by commonly used Speier's catalyst were found to be nonselective, giving an almost 1 : 1 mixture of γ- and β-silylallylic alcohols[134]. Thus, catalyst systems that can achieve high regio- and stereoselectivity are necessary for this reaction to be synthetically useful.

The reaction of propargyl alcohol with $HSiMe_2Ph$ or $HSiPh_3$ catalyzed by a phosphine–Pt(0) complex, $(t\text{-}Bu_3P)Pt(NBE)_2$ (NBE = norbornene) or $(t\text{-}Bu_3P)Pt(CH_2{=}CH)_2Si(OMe)_2$, gives the desired (*E*)-γ-silylallyl alcohols **126** with excellent regioselectivity ($\gamma/\beta > 19/1$) in high yields (equation 50)[135]. No dehydrogenative silylation takes place with the hydroxyl group under the reaction conditions so that no protection is necessary. When a similar Pt(0) catalyst, $(Cy_3P)Pt(CH_2{=}CH_2)_2$, is employed, the γ/β-regioselectivity drops to 5.3 with $HSiMe_2Ph$, 3.1 with $HSiBu_3$ and 1.2 with $HSiPh_3$[135].

A cationic rhodium complex, $[Rh(COD)_2]BF_4{\bullet}2PPh_3$, is a highly efficient catalyst for this reaction, which gives (*E*)-γ-triethylsilylallyl alcohol **(127)** with complete γ-selectivity and >99% *E*-selectivity (equation 51)[136,137].

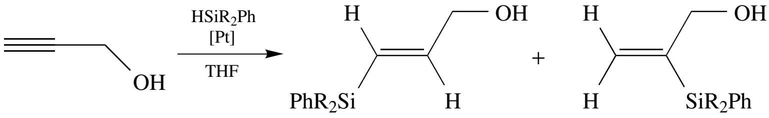

(126) > 95% > 5% (50)

[Pt] = (t-Bu$_3$P)Pt(NBE)$_2$ or (t-Bu$_3$P)Pt(CH$_2$═CH)$_2$Si(OMe)$_2$
R = Me, Ph

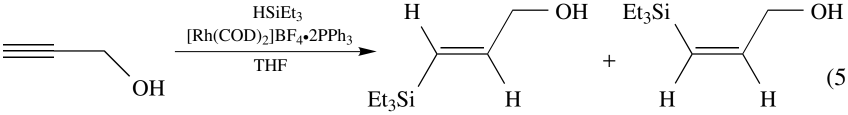

(51)

(127) >99% >1%

α-Substituted *γ*-silylallylic alcohols can be converted to functionalized chiral allylsilanes through Claisen rearrangement, which are useful intermediates in stereoselective organic syntheses. Accordingly, the highly regio- and stereoselective hydrosilylation of *sec*-propargylic alcohols has a particular synthetic interest for this purpose.

Among the phosphine–Pt(0) complex catalysts mentioned above, (Cy$_3$P)Pt(CH$_2$=CH$_2$)$_2$ exhibits the best results for the reaction of but-1-yn-3-ol with HSiPh$_3$, giving (*E*)-Ph$_3$SiCH=CH-CH(Me)OH with >95% *γ*-selectivity in 94% yield[135]. In a similar manner, the reactions of other *sec*-propargyl alcohols **128** with HSiMe$_2$Ph catalyzed by (Cy$_3$P)Pt(CH$_2$=CH$_2$)$_2$ give the corresponding (*E*)-*γ*-triethylsilylallyllic alcohols **129** with >95% *γ*-selectivity in high yields (equation 52)[135]. The reaction of a *tert*-propargyl alcohol, 3-methylbut-1-yn-3-ol, with HSiMe$_2$Ph catalyzed by (Cy$_3$P)Pt(CH$_2$=CH$_2$)$_2$ afforded (*E*)-PhMe$_2$SiCH=CH-CMe$_2$OH with >95% *γ*-selectivity in 98% yield[135]. However, the reaction of *γ*-alkylpropargyl alcohols **131** under the same conditions proceeds with almost no or very low regioselectivity giving a mixture of **132** and **133** (equation 53)[135].

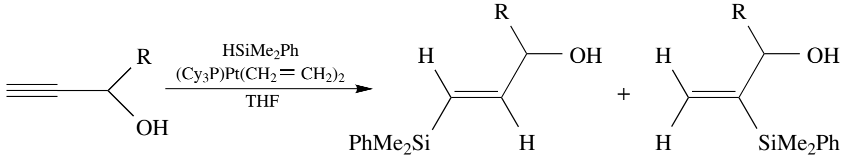

(128) **(129)** >95% **(130)** >5% (52)

R = n-C$_5$H$_{11}$, PhCH$_2$OCH$_2$

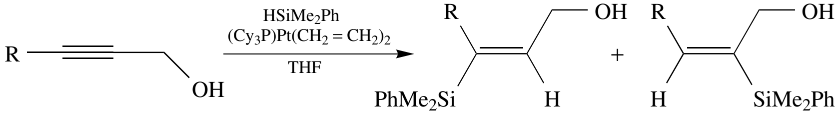

(131) **(132)** **(133)**

(a) R = Me 91% 1.1 : 1
(b) R = n-C$_5$H$_{11}$ 99% 2.1 : 1 (53)

The use of $[Rh(COD)_2]BF_4{\bullet}2PPh_3$ as the catalyst appears to be a better choice for this type of reaction. Thus, the reactions of *sec*- and *tert*-propargylic alcohols **134** with $HSiEt_3$ promoted by this rhodium catalyst system provide the desired (*E*)-γ-silylallyllic alcohols **135** with 100% γ-selectivity and virtually complete stereoselectivity ($E/Z => 99/1$) in excellent yields (equation 54)[136,137].

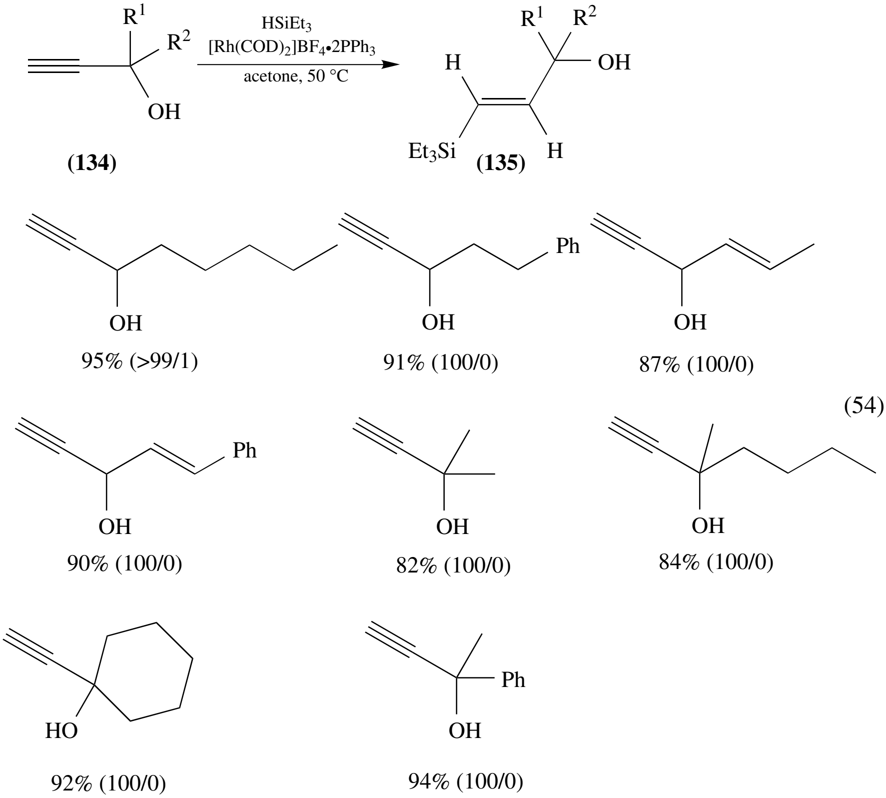

(134) **(135)**

(54)

The hydrosilylation of 3-butyn-1-ol, i.e. homopropargyl alcohol, with $HSiMe_2Ph$ catalyzed by $(Cy_3P)Pt(CH_2{=}CH_2)_2$ gives a 4.2 : 1 mixture of (*E*)-4-silyl- and (*E*)-3-silyl-3-buten-1-ols[135], whereas the cationic rhodium complex-catalyzed reaction with $HSiEt_3$ affords (*E*)-4-triethylsilyl-3-buten-1-ol **(136)** exclusively in 97% yield (equation 55)[136].

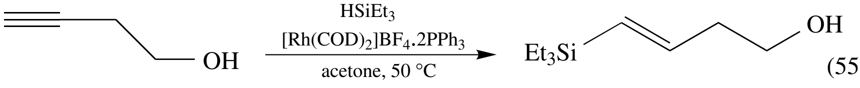

(55)

(136)

97%

In a similar manner, the cationic Rh-catalyzed reaction of 4-pentynol **(137)** with $HSiEt_3$ gives (*E*)-5-triethylsilyl-4-penten-1-ol **(138)** with excellent selectivity (equation 56)[136].

The tandem hydrosilylation–isomerization process of *sec*-propargyl alcohols **140** provides an easy access to β-silylketones **142** via silylallylic alcohols **141** (equation 57)[136].

The reaction of methyl 3-butynoate **(143)** with $HSiMe_2Ph$ catalyzed by $(Cy_3P)Pt(CH_2{=}CH_2)_2$ gives a mixture of 4-silyl- and 3-silyl-3-butenoates, **144** and **145**, respectively in 71% yield (equation 58)[135].

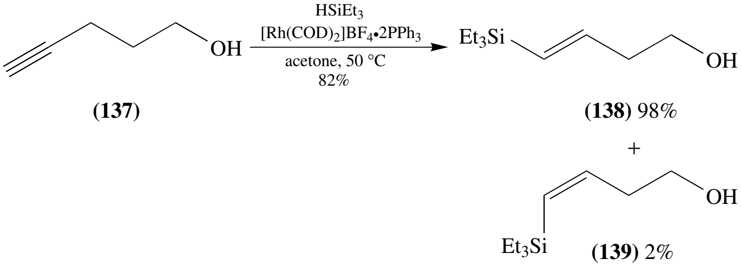

(56)

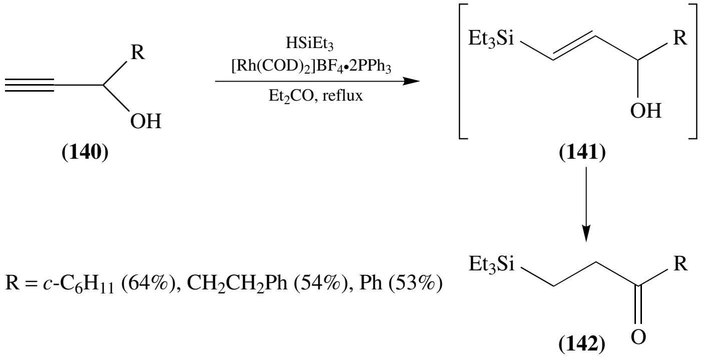

(57)

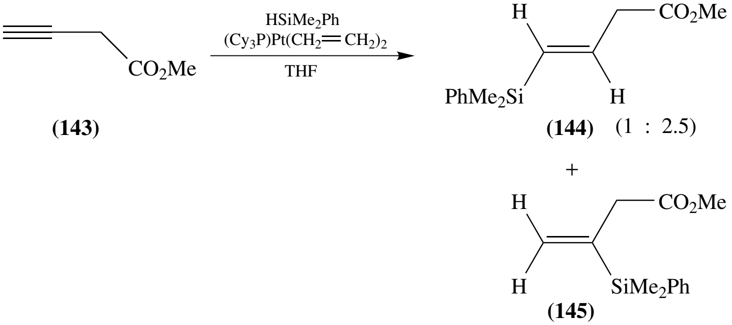

(58)

The reactions of phenylacetylene, 2-(ethynyl)thiophene, 2-(propargyl)thiophene, methyl propynoate, propargyl alcohol, propargyl methyl ether, $HC{\equiv}C\text{-}CH_2NR_2$ [$NR_2 = NEt_2$, $N(CH_2)_4$, $N(CH_2)_5$, $N(CH_2)_6$] with $HSiMe_2(4\text{-}XC_6H_4)$ (X = H, Me, F, Cl, Br and NMe_2) and $HSiMe_2$(2-thienyl) catalyzed by $H_2PtCl_6{\bullet}6H_2O$, $RhCl(PPh_3)_3$, $H_2OsCl_6{\bullet}6H_2O$ and $Co_2(CO)_8$ give a mixture of *trans*-1-silyl-1-alkene and 2-silyl-1-alkene (50/50–94/6 ratio)[134]. The relative activity of the catalysts in the reaction of *N*-propargylpiperidine with $HSiMe_2$(2-thienyl) decreases in the order $H_2PtCl_6{\bullet}6H_2O > RhCl(PPh_3)_3 \gg H_2OsCl_6{\bullet}6H_2O \gg Co_2(CO)_8$. The total yield of the hydrosilylation products in the reactions of $HC{\equiv}C{-}Y$ with $HSiMe_2$(2-thienyl) catalyzed by $H_2PtCl_6{\bullet}6H_2O$ at 50 °C decreases in the order $CO_2Me \sim$ 2-thienylmethyl $\geqslant HOCH_2 > Ph > MeOCH_2 >$

2-thienyl > R_2NCH_2. The amount of the *trans*-1-silyl-1-alkene decreases in the order R_2NCH_2 > 2-thienylmethyl ⩾ Ph > $MeOCH_2$ > $HOCH_2$ > CO_2Me > 2-thienyl. The effect of the *para*-substituent X of $HSiMe_2(4\text{-}XC_6H_4)$ on regioselectivity (1-silyl/2-silyl) is rather minor, i.e. 94/6 (Me_2N)−88/12 (Me, H).

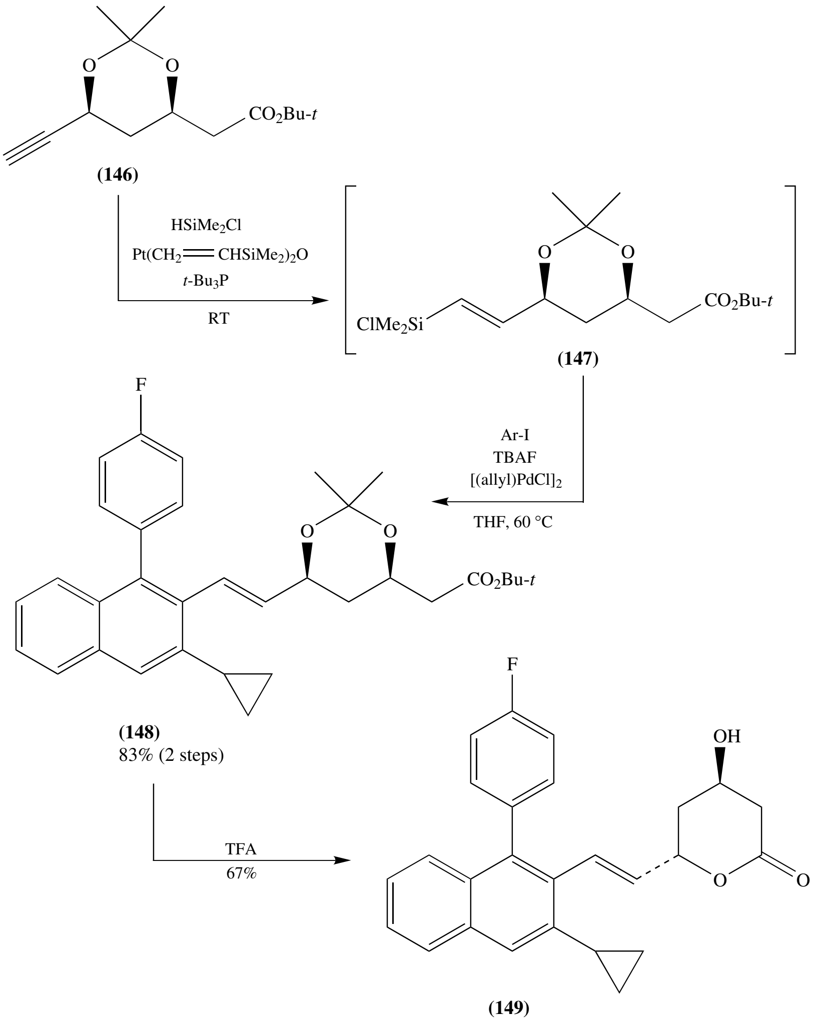

SCHEME 16

The hydrosilylation−cross-coupling process has been applied to the synthesis of the key intermediate to an HMG-CoA reductase inhibitor (Scheme 16)[138,139]. This one-pot process consists of the Pt-catalyzed hydrosilylation of **146**, giving (*E*)-product **147** and its regioisomer, followed by the Pd-catalyzed cross-coupling with 2-cyclopropyl-4-(4-fluorophenyl)quinolin-3-yl iodide (ArI), affording **148** in 83% isolated yield (2 steps). The key intermediate **148** thus obtained is treated with CF_3CO_2H to give the target inhibitor molecule **149**.

F. Other Reactions Associated with Alkyne Hydrosilylation

As described above, $Rh_2(pfb)_4$ and H_2PtCl_6 effectively catalyze the hydrosilylation of 1-alkynes to give (*Z*)-1-silyl-1-alkenes and (*E*)-1-silyl-1-alkenes, respectively, as the major products. However, the exclusive formation of allylic silane **150** (68–73% yield; as a mixture of *E* and *Z* isomers) is observed when the order of the addition of reactants is reversed, i.e. slowly adding 1-alkyne to the solution of excess hydrosilane (2 equiv.) in CH_2Cl_2 at 25 °C over a period of 1 h (equation 59)[111]. The results imply that two different catalyst species, one for hydrosilylation and the other for the formation of allylic silane, are generated just by changing the order of the addition[111].

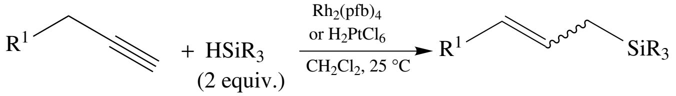

(slow addn.) **(150)** (59)

$HSiR_3 = HSiEt_3, HSiMe_2Bu\text{-}t$

$R^1 = n\text{-}C_5H_{11}, n\text{-}C_3H_7, MeO, PhCH_2O$

Although iridium complexes such as $IrH_2(SiEt_3)(COD)(AsPh_3)$ (COD = 1, 5-cyclooctadiene)[117], $[Ir(OMe)(COD)]_2/2PPh_3$ (or $AsPh_3$)[117], $[IrH(H_2O)(bq)(PPh_3)_2]SbF_6$[113], $[Ir(COD)(\eta^2\text{-}(i\text{-}Pr)_2PCH_2CH_2NMe_2)]BF_4$, $[Ir(TFB)(\eta^2\text{-}(i\text{-}Pr)_2PCH_2CH_2OMe)]BF_4$[118], $Ir(C{\equiv}CPh)(CO)_2(PCy_3)$ and $Ir(C{\equiv}CPh)(TFB)(PCy_3)$[119] are active catalysts for the hydrosilylation of 1-alkynes (see Section III.A.3), the dehydrogenative silylation of 1-alkynes is also promoted by these catalysts to give 1-silylalkynes **151** (equation 60)[113,117–119]. This reaction can become the major pathway ($\leqslant$84%) in some cases, especially in the presence of excess 1-alkyne that acts as the hydrogen acceptor.

$$\mathrm{R{-}C{\equiv}C{-}H} + \mathrm{HSiR_3'} \xrightarrow{[\mathrm{Ir}]} \mathrm{R{-}C{\equiv}C{-}SiR_3'} + \mathrm{RHC{=}CHSiR_3'} \qquad (60)$$

Two different mechanisms have been proposed for this dehydrogenative silylation process. The first mechanism proposed by Oro, Esteruelas and coworkers includes the oxidative addition of 1-alkyne to the Ir–Si bond, followed by the reductive elimination of **151** (equation 61)[117,118]. The proposed mechanism is supported by the identification of $[IrH(C{\equiv}CPh)(\eta^2\text{-}(i\text{-}Pr)_2PCH_2CH_2OMe)]BF_4$ in stoichiometric as well as catalytic conditions by $^{31}P\{^1H\}$ NMR analyses[118]. The other mechanism proposed by Jun and Crabtree includes the insertion of 1-alkyne into the Ir–Si bond, followed by isomerization and β-hydride elimination (equation 62)[113], which is consistent with the mechanism proposed for the highly selective formation of (*Z*)-1-silyl-1-alkenes (see Section III.B)[115].

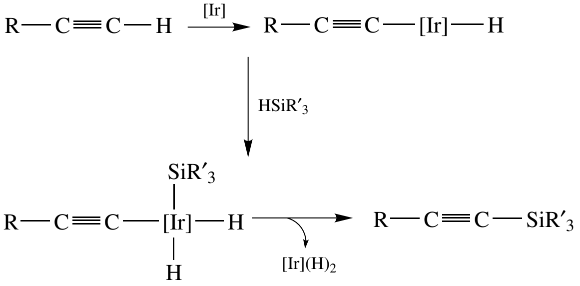

$$\begin{tikzcd}[column sep=small] \mathrm{R{-}C{\equiv}C{-}H} \arrow[r, "{[\mathrm{Ir}]}"] & \mathrm{R{-}C{\equiv}C{-}[Ir]{-}H} \arrow[d, "\mathrm{HSiR'_3}"] & \\ & \mathrm{R{-}C{\equiv}C{-}\overset{\displaystyle SiR'_3}{\underset{\displaystyle H}{[Ir]}}{-}H} \arrow[r, "", "{[\mathrm{Ir}](\mathrm{H})_2}"'] & \mathrm{R{-}C{\equiv}C{-}SiR'_3} \end{tikzcd} \qquad (61)$$

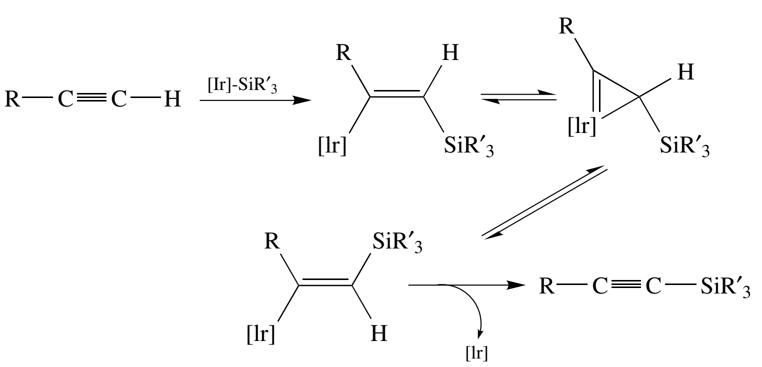

(62)

IV. HYDROSILYLATION OF CARBONYL AND RELATED COMPOUNDS

Hydrosilylation of various carbonyl compounds, enones and related functional groups catalyzed by Group VIII transition metal complexes, especially phosphine–rhodium complexes, have been extensively studied[1,3], and the reactions continue to serve as useful methods in organic syntheses.

Rhodium carbonyl clusters such as $Rh_4(CO)_{12}$, $Rh_2Co_2(CO)_{12}$ and $RhCo_3(CO)_{12}$ are found to be highly active catalysts for the hydrosilylation of cyclohexenones[140]. The reaction of cyclohexenone with $HSiMe_2Ph$ catalyzed by these Rh and Co–Rh carbonyl clusters proceeds smoothly at ambient temperature to give the 1,4-addition product (cyclohex-1-en-1-yloxy)dimethylphenylsilane exclusively. On the other hand, the reaction with H_2SiPh_2 proceeds at −35 °C to give the 1,2-addition product (cyclohex-2-en-1-yloxy)diphenylsilane exclusively. Kinetic study shows that the clusters $Rh_4(CO)_{12}$ and $Rh_2Co_2(CO)_{12}$ possess more than one order of magnitude higher catalytic activity than that of $RhCl(PPh_3)_3$. Rhodium phosphite clusters, $[HRh\{P(OR)_3\}_2]_3$ (R = Me, $2\text{-}MeC_6H_4$) and $[RhCl\{P(OR)_3\}_2]_2$ (R = Me, $2\text{-}MeC_6H_4$), are shown to be moderately active catalysts in the hydrosilylation of cyclohexenone and mesityl oxide (1,4-addition) with $HSiEt_3$[20].

Stereoselectivity of the hydrosilylation of cyclic ketones catalyzed by $RhCl(PPh_3)_3$ has been shown to depend on the bulkiness as well as electronic nature of the hydrosilane used[3,141–143]. A systematic study of the reaction of 2- and 4-alkylcyclohexanones (alkyl = Me, Pr-*i*, Bu-*t* and Ph) with H_2SiPh_2 catalyzed by $RhCl(PPh_3)_3$ shows that *cis*-1-siloxy-2-alkylcyclohexane is the predominant product in the reactions of 2-alkylcyclohexanone, while *trans*-isomer is formed as the major product in the reaction of 4-alkylcyclohexanone[144]. The results support the previously proposed mechanism for the reaction, involving the insertion of the carbonyl group into the Rh–Si bond[3].

Unusual rate enhancement is observed in the mono-hydrosilylation of ketones with organosilanes bearing two Si–H groups at appropriate distances, **152–156**, catalyzed by $RhCl(PPh_3)_3$[15,145,146]. Other 1,ω-bis(dimethylsilyl)alkanes, $HMe_2SiCH_2SiMe_2H$, $HMe_2Si(CH_2)_4SiMe_2H$, do not show such an enhancement. It is noteworthy that the second hydrosilylation does not have any particular rate enhancement. The reactions of acetone with **152** and **153** are 50 and 120 times faster than that with $HSiMe_2Et$, $HSiMe_2Ph$, $HMe_2SiCH_2SiMe_2H$ or $HMe_2Si(CH_2)_4SiMe_2H$. It should be noted that in the reaction of an α, β-unsaturated ketone, 4-methyl-3-penten-2-one, with **152**, the 1,4-addition product is obtained exclusively although the reaction is as fast as that with H_2SiPh_2 which exclusively gives 1,2-adduct[15]. Mechanistic study has revealed that disilyl–Rh(V) trihydride **157** arising from the double oxidative addition of **152–156** to

$RhCl(PPh_3)_3$ is very likely to be the active catalyst species (Scheme 17)[145]. Although detailed understanding of this unique rate enhancement needs further investigation, the mechanism proposed by Nagashima, Itoh and coworkers[145] has indicated intriguing new possibilities for the mechanism of $RhCl(PPh_3)_3$-catalyzed hydrosilylation of carbonyl compounds and other substrates. (For the proposed mechanisms including Rh(V) species in alkene hydrosilylation, see Section II.B.)

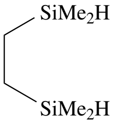

(152)

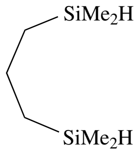

(153)

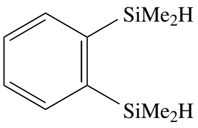

(154)

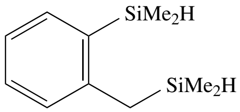

(155)

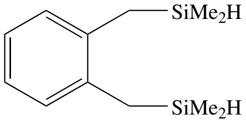

(156)

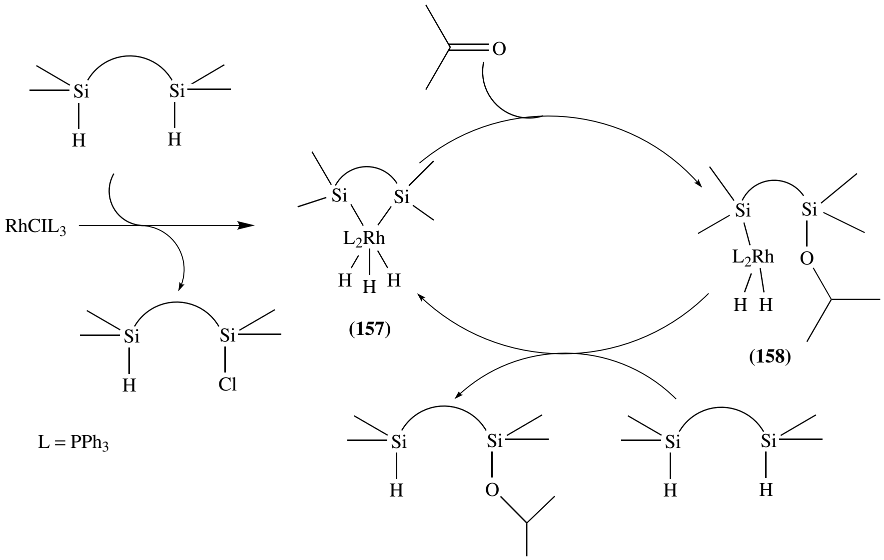

SCHEME 17

The hydrosilylation of cyclopentadienylorganoiron acyl complexes **159** with dihydrosilanes such as H_2SiEt_2, H_2SiPh_2 and $H_2SiPhMe$, catalyzed by $RhCl(PPh_3)_3$, proceeds smoothly at ambient temperature to give α-siloxyalkyliron complexes **160** in 50–91% yields (equation 63)[147]. Dihydrosilane is the silane of choice for the hydrosilylation of **159** since monohydrosilanes do not show reactivity, while trihydrosilanes reduce the acyl group to the corresponding alkyl group[147]. Manganese carbonyl acetyl complexes $(L)(CO)_4Mn{-}COCH_3$ (**161**, L = CO, PPh_3) are also found to catalyze this reaction efficiently[148].

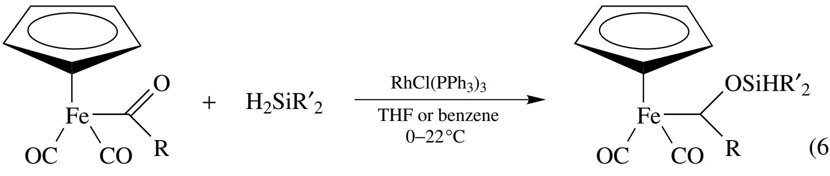

(63)

(159) **(160)**

R = Me, Et, Pr-*i*, Bu-*i*
$SiR'_2 = SiEt_2, SiPh_2, SiMePh$

The manganese complex **161** is also found to be an excellent catalyst for the reduction of esters to ethers in high yields using H_3SiPh (equations 64 and 65)[149].

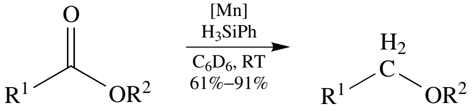

(64)

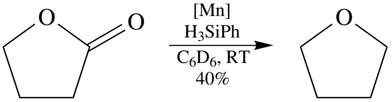

(65)

$[Mn] = (Ph_3P)(CO)_4Mn\text{-}COCH_3$ **(161)**

The 1,4-addition of hydrosilanes to α, β-unsaturated esters affords the corresponding silyl ketene acetals that are versatile reagents in organic syntheses. Accordingly, this reaction has been studied extensively using phosphine–rhodium complexes and Speier's catalyst[3,48,50,150,151]. However, the reaction is often accompanied by a small amount of inseparable 1,2-adduct and/or 3,4-adduct[50]. The hydrosilylation of methacrylates **162** with excess $HSiMe_3$ using $RhCl_3{\bullet}6H_2O$ as the catalyst provides an improved route to *O*-TMS-*O*-substituted dimethylketene acetals **163** with excellent product selectivity in high yields (equation 66)[152].

The hydrosilylation of α, β-unsaturated carbonyl compound **164** gives either silyl enol ether **165** via 1,4-addition or *O*-silylallylic alcohol **166** via 1,2-addition, which are desilylated to afford saturated carbonyl compound **167** or allylic alcohol **168** (Scheme 18). Wilkinson's complex, $RhCl(PPh_3)_3$, and Speier's catalyst, $H_2PtCl_6{\bullet}2H_2O/i\text{-}PrOH$, are most commonly used for the 1,4-addition of monohydrosilanes, whereas the combination of $RhCl(PPh_3)_3$ and a dihydrosilane or a trihydrosilane is used exclusively for the 1,2-addition process[3]. The marked dependence of 1,4/1,2-selectivity on the nature of the hydrosilane used was first reported by Ojima and coworkers in 1972 for the $RhCl(PPh_3)_3$-catalyzed reactions[153], and this rather unique dependence of regioselectivity on the nature of hydrosilanes has been proved to be general for phosphine–rhodium complex catalysts and other catalysts[3]. A mechanism that can account for the observed results has been proposed by Ojima and Kogure[154], which includes 1-siloxy-σ-allylic Rh(III)(H) species (for 1,2-addition) as well as 3-siloxy-σ-allylic Rh(III)H species (for 1,4-addition).

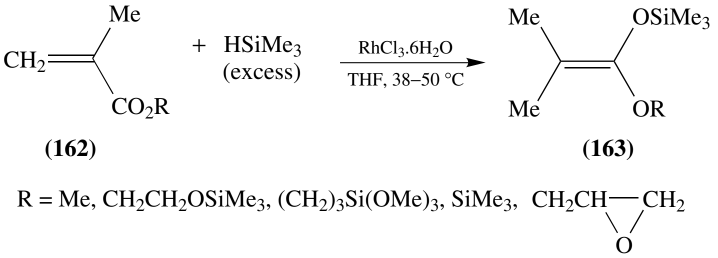

(162) **(163)** (66)

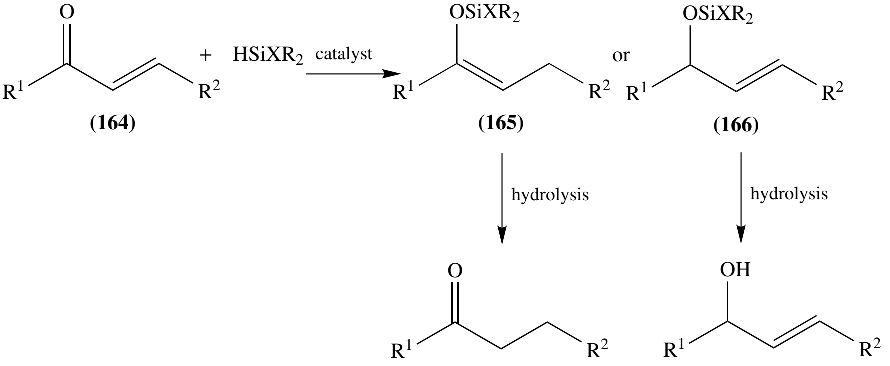

(164) **(165)** **(166)**

$SiXR_2 = SiEt_3$, $Si(Pr\text{-}n)_3$, $SiMe_2Ph$, $SiHEt_2$, $SiHPh_2$ **(167)** **(168)**

SCHEME 18

Hydridorhodium(I) complex, $HRh(PPh_3)_4$, is shown to be another efficient catalyst for the 1,2-addition of H_2SiPh_2 to enones giving the corresponding *O*-diphenylsilylallylic alcohols in high yields[155]. The reaction is highly chemoselective, thus an isolated double bond is unaffected (equation 67)[155]. In the reaction of a diketone **171**, the nonconjugated ketone moiety is selectively reduced (equation 68)[155]. The reactions of α, β-unsaturated ketones, esters and lactones with dimethylphenylsilane and other monohydrosilanes exclusively give 1,4-addition products in high yields (equations 69 and 70)[155].

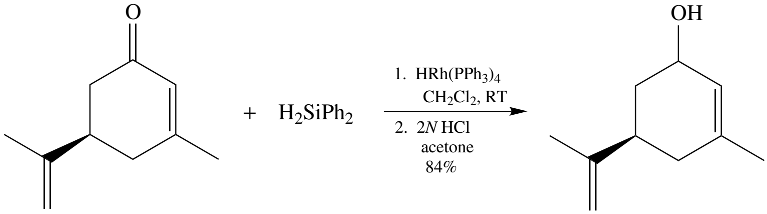

(67)

(**169**) **(170)**
(*syn/anti* = 65:35)

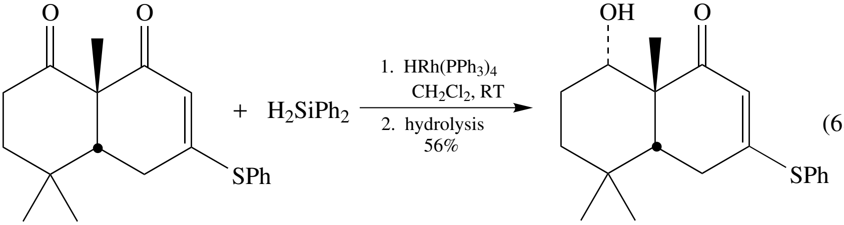

(171) **(172)**

(68)

(69)

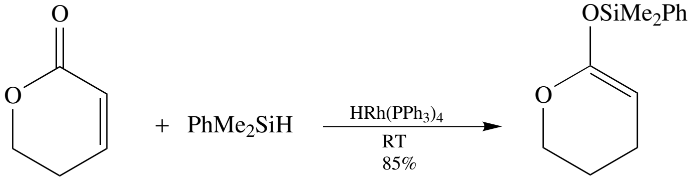

(70)

On the basis of the observed kinetic isotope effect ($k_H/k_D = 2$) in the reaction of acetophenone with $HSiMe_2Ph$ and $DSiMe_2Ph$ catalyzed by $HRh(PPh_3)_4$, Zheng and Chan[155] proposed a variation of the Ojima–Kogure mechanism[154], in which a ketone molecule coordinates to silicon rather than rhodium to form alkoxysilyl–Rh(III)H species **(173)** (Scheme 19). This unique mechanism needs further investigation. Nagashima, Itoh and coworkers invoke a possible double oxidative addition of H_2SiPh_2 to $RhCl(PPh_3)_3$ in a manner similar to the one shown in Scheme 17[145].

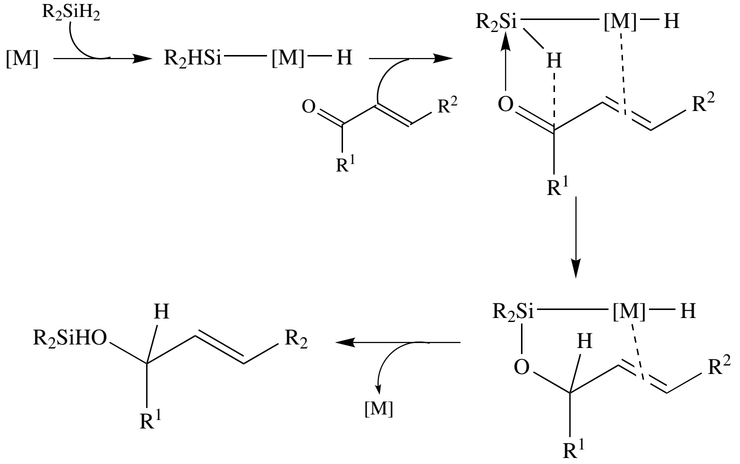

(173)

SCHEME 19

The Rh−isocyanide complex, $RhCl(C{\equiv}N{-}C_6H_3Me_2\text{-}2,6)_3$, is a highly active catalyst for the hydrosilylation of α,β-unsaturated ketones with $HSiMe_2Ph$, giving 1,4-adducts in nearly quantitative yields[16]. This catalyst is more active than $RhCl(PPh_3)_3$ for the reactions of α,β-unsaturated ketones, acetophenone and 5-hexen-2-one with $HSiMe_2Ph$ under the same conditions, but less active for the reaction of 2-butanone. The corresponding Pt−isocyanide as well as Pd−isocyanide complexes are inactive for the reaction of 2-butanone. However, Pt-isocyanide complexes, $PtCl_2(C{\equiv}N{-}C_6H_3Me_2\text{-}2,6)_2$ and $Pt_2Cl_4(DIBN)_2$ (DIBN $= 2,2'$-isocyano-1,1-binaphthyl), show high activity for the reaction of 5-hexen-2-one. Rhodium complex with DIBN, $[RhCl(DIBN)_2]_n$, is an excellent catalyst (99% yield) for this reaction, while $RhCl(PPh_3)_3$ (5% yield) and $PtCl_2(PPh_3)_2$ (trace) are poor catalysts.

While $Mo(CO)_6$ is only a modest hydrosilylation catalyst[156], oxadiene complexes of molybdenum and tungsten, $M(CO)_2(oxadiene)_2$ (oxadiene = pulegone, pinocarvone and (*E*)-5-methyl-3-hexen-2-one), exhibit good catalytic activity for the hydrosilylation of α,β-unsaturated ketones and aldehydes with H_3SiPh[157]. Although the 1,4/1,2-selectivity for the reactions of α,β-unsaturated ketones is low to modest at best with one exception for the reaction of pinocarvone catalyzed by $Mo(CO)_2(pinocarvone)_2$ which undergoes 1,4-addition with 92% selectivity, the reactions of α,β-unsaturated aldehydes proceed via 1,2-addition exclusively[157].

Bis(η^5-cyclopentadienyl)diphenyltitanium, Cp_2TiPh_2, is found to be an active catalyst for the hydrosilylation of ketones with H_2SiPh_2, $H_2SiMePh$ at 120 °C[158].

Completely regioselective 1,6-hydrosilylation of dimethyl *cis,cis*-muconate **174** with $HSiMe_2Ph$, $DSiMe_2Ph$ or $HSiEt_2Me$ is observed using $RhCl(PPh_3)_3$ as the catalyst (equation 71)[159]. However, the reaction of *trans,trans*-muconate **175** under the same conditions gives only a 3,4-adduct, and that of *trans,cis*-muconate results in a complicated mixture of adducts[159].

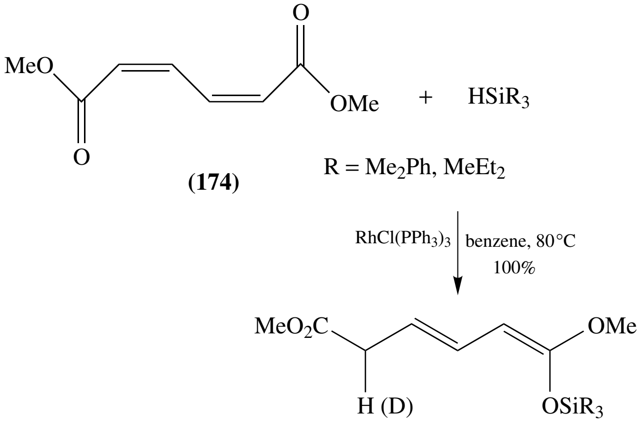

(174)

(71)

Selective reduction of 2,2,4,4-tetramethyl-1,3-cyclobutanedione through hydrosilylation catalyzed by $RhCl(PPh_3)_3$ or $[Rh(COD)Cl]_2$ with various phosphine ligands gives the corresponding hydroxycyclobutanone ($H_2Si(Pr\text{-}i)_2$, $RhCl(PPh_3)_3$, 100%) or dihydroxycyclobutane (H_2SiPh_2, dppp-Rh, 100%, *syn/anti* $= 7/3$)[160].

Hydrosilylation of carbonyl compounds catalyzed by fluoride salts such as CsF and KF, originally developed by Corriu and coworkers[161−165], has been modified to homogeneous systems and found applications in organic syntheses as an efficient and selective reduction method.

Fujita and Hiyama have developed a homogeneous fluoride ion catalyst system consisting of tetrabutylammonium fluoride (TBAF) or tris(diethylamino)sulfonium difluorotrimethylsilicate (TASF) in hexamethylphosphoric triamide (HMPA), which can promote and complete the hydrosilylation of aldehydes and ketones at room temperature or lower temperatures within one hour in most cases (equation 72)[166–169]. The relative reactivity of hydrosilanes decreases in the order: $H_2SiPh_2 \gg HSiMe_2Ph > HSiMePh_2 > HSiPh_3$, and $HSiEt_3$ can be used for the reaction as well[166]. For solvents, HMPA and 1,3-dimethyl-3,4,5,6-tetrahydro-2(1*H*)-pyrimidinone (DMPU) are the best, while DMF is less effective, THF and CH_2Cl_2 are nonpractical[166].

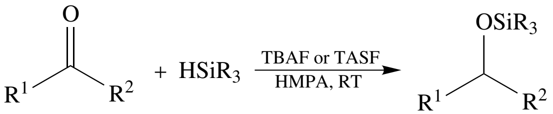

(72)

On the basis of a significant isotope effect ($k_H/k_D = 1.5$) when using $HSiMe_2Ph$ and $DSiMe_2Ph$, the hydride transfer from hexavalent silicate species $[HSiR_3F(HMPA)]^-$ to the carbonyl functionality is proposed to be the rate-determining step of this reaction[166,170].

The hydrosilane/TBAF in HMPA is a powerful reagent for the *threo*-selective reduction of α-oxy and α-amino ketones **176** at 0 °C or room temperature, giving the corresponding alcohols **177** with excellent diastereoselectivity (*threo*/*erythro* = 84/16 → 99/1) in high yields (equation 73)[166]. This reagent is also effective for the stereoselective reduction of α-methyl-β-keto amides **178** to *threo*-β-hydroxy amides **179** with excellent selectivity (*threo*/*erythro* = 98/2 → 99/1) in 86–98% yields as long as R is an aromatic group (equation 74). When R is *tert*-butyl, the *threo/erythro* ratio becomes 91/9, and the reversal of selectivity is observed when R is ethyl (*threo*/*erythro* = 23/77) or isopropyl (*threo*/*erythro* = 25/75).

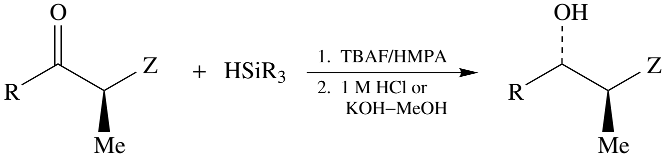

(73)

(176) **(177)**

R = Ph, Bu, PhCH=CH; Z = OAc, OBz, OEE, OBu-*t*, OTHP, NMe_2

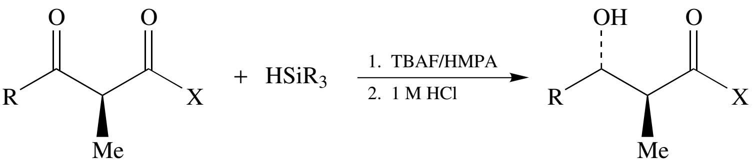

(74)

(178) **(179)**

R = Ph, 4-ClC_6H_4, 4-$MeOC_6H_4$, *t*-Bu; X = NEt_2, pyrrolidinyl, piperidinyl

When 18-crown-6 is used for the hydrosilane/CsF system, the hydrosilylation of aromatic aldehydes and ketones proceeds smoothly in CH_2Cl_2 under phase-transfer conditions at room temperature[171,172]. The isolation of the products in this $HSiMe_2Ph/CsF/18$-crown-6 system is claimed to be much easier than that in the $HSiMe_2Ph$/TBAF/HMPA system.

Strong acids, e.g. CF_3CO_2H[173,174] and CF_3SO_3H,[175,176], as well as Lewis acids, e.g. $BF_3{\bullet}OEt_2$[177,178], are well known to promote the reduction of carbonyl compounds with hydrosilanes. It has recently been shown that the same catalytic mechanism is operating in the Lewis acid (Et_3SiClO_4)—and Brønsted acid ($HClO_4$)—catalyzed reactions of carbonyl compounds with $HSiEt_3$[179]. The hydrosilane/solid base combination, i.e. $HSi(OEt)_3$/hydroxyapatite [HAp = $Ca_{10}(PO_4)_6(OH)_2$] or CaO, is found to be very effective for the hydrosilylation of a variety of aldehydes and ketones in heptane at 90 °C[176,180]. The reactions of α, β-unsaturated aldehydes and ketones by this combination give the corresponding *O*-silyl allylic alcohols exclusively via 1,2-addition[176]. The reactions of carbonyl compounds using hydrosilane/solid acid combinations, e.g. $HSiEt_3/Fe^{3+}$-ion exchanged montmorillonite, give deoxygenated products, i.e. hydrocarbons from aldehydes and ketones, or symmetrical ethers $(R^1R^2CH)_2O$ from $R^1R^2C{=}O$[176].

Intramolecular hydrosilylation of β-(hydrosilyloxy)ketone **181**, readily prepared from β-hydroxyketone **180**, catalyzed by $SnCl_4$, $MgBr_2{\bullet}OEt_2$, $ZnBr_2$, $ZnCl_2$, CF_3CO_2H, TBAF or $RhCl(PPh_3)_3$, gives *anti*-**182** as the predominant product. The stereoselectivity depends on the bulkiness of R^1–R^3 as well as the catalyst used. An excellent selectivity (*anti*/*syn* = 120/1) is achieved in the reaction of 2,6-dimethylhepta-3,5-dione (R^1–R^3 = *i*-Pr) using $SnCl_4$ as the catalyst at −80 °C, giving the *anti*-diol **183** in 67% overall isolated yield (Scheme 20)[181].

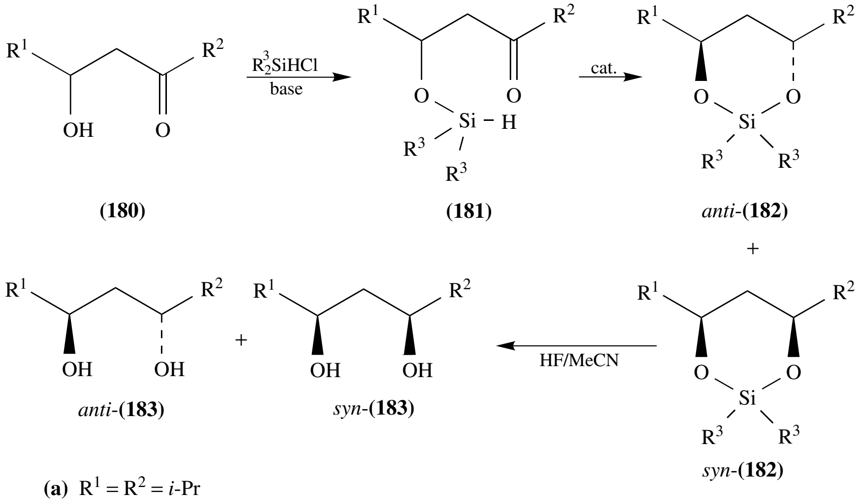

(a) $R^1 = R^2 =$ *i*-Pr

(b) $R^1 = R^2 =$ *n*-Bu

(c) $R^1 =$ *i*-Pr, $R^2 =$ Me

(d) $R^1 =$ Me, $R^2 =$ *i*-Pr

$R^3 =$ *i*-Pr or Me

SCHEME 20

Intramolecular hydrosilylation of β-(hydrosiloxy)alkanoate **184** catalyzed by TBAF in CH_2Cl_2 at 0 °C, followed by Lewis acid-catalyzed allylation with allyltrimethylsilane in

CH_2Cl_2, gives *anti*-**186** in high yield with the *anti/syn* ratio up to 23/1 ($R^1 = n$-Bu, R^2 = Me, Lewis acid = $TfOH_2{}^+B(OTf)_4{}^-$ at −50 °C) (equation 75)[182,183].

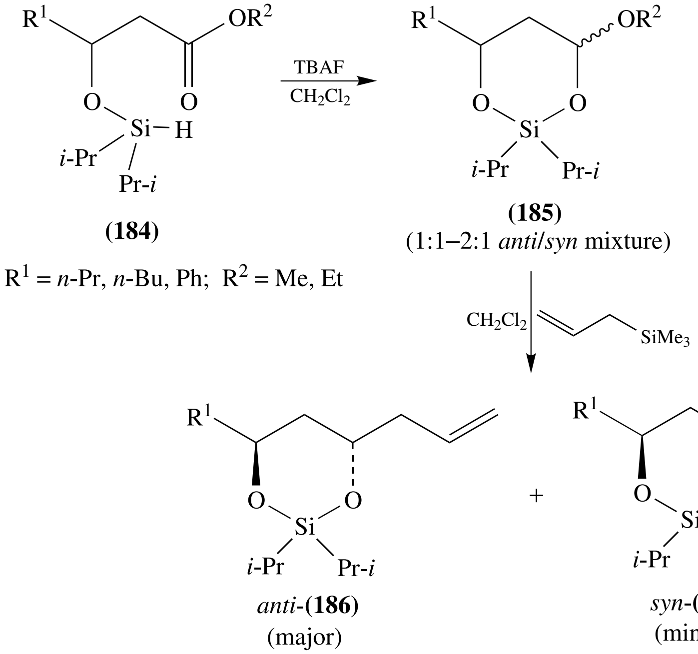

(184)

$R^1 = n$-Pr, n-Bu, Ph; R^2 = Me, Et

(185)
(1:1–2:1 *anti/syn* mixture)

(75)

anti-**(186)**
(major)

syn-**(186)**
(minor)

The combination of polymethylhydrosiloxane (PMHS) and catalytic amounts of TBAF (1 mol%) and $Cp_2Ti(OC_6H_4Cl\text{-}4)_2$ (2 mol%) provides an efficient and convenient method for the partial reduction of lactones **187** to lactols **189** via hydrosilylation and subsequent hydrolysis of the resulting *O*-silyllactols **188** (equation 76)[184].

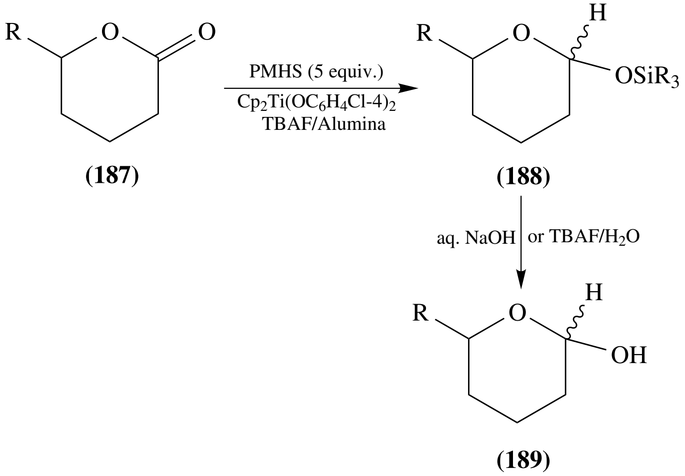

(187)

(188)

(76)

(189)

While hydrosilylation of imines is known to be effected by rhodium catalysts[3], nickel catalysts prepared *in situ* from $Ni(OAc)_2 \cdot 4H_2O$ and thiosemicarbazones are also found to promote the reactions of *N*-substituted imines with $HSiEt_3$ in dry DMSO at 35 °C, giving the corresponding secondary amines in excellent yields after basic work-up (equation 77)[185].

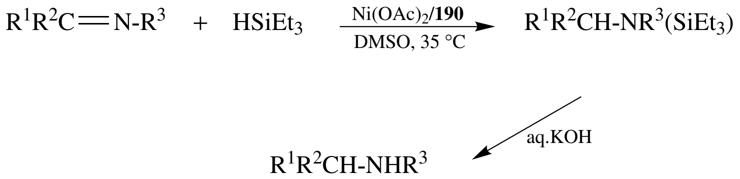

(77)

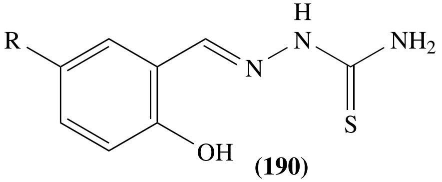

(190)

R = H, NaO_3S, *t*-octyl

Cobalt carbonyl-catalyzed hydrosilylation of aromatic nitriles with $HSiMe_3$ proceeds smoothly at 60 °C and ambient pressure of carbon monoxide in toluene to give *N*, *N*-bis-TMS-amines **191** in moderate to excellent yields (equation 78)[186]. Reactions of aliphatic nitriles require 100 °C, except for cyclopropanenitrile, to give **191** in 87–100% yields. The reaction of butanenitrile gives a mixture of **191** (R = *n*-Bu) (44%) and *N*, *N*-bis-TMS-enanime $CH_3CH_2CH{=}CHN(SiMe_3)_2$ (20%). The reactions of α, β-unsaturated nitriles bearing substituent(s) at the α- and/or β-position(s) give *N*, *N*-bis-TMS-enamines **192** (*Z*/*E* mixture) as the major products accompanied by *N*, *N*-bis-TMS-allylic amines **193** and/or saturated *N*, *N*-bis-TMS-amines **194** (equation 79)[186].

$$RC{\equiv}N \; + \; HSiMe_3 \xrightarrow[\text{toluene, 60–100 °C}]{\substack{Co_2(CO)_8 \\ \text{CO (1 atm)}}} RCH_2N(SiMe_3)_2 \qquad (78)$$

(191)

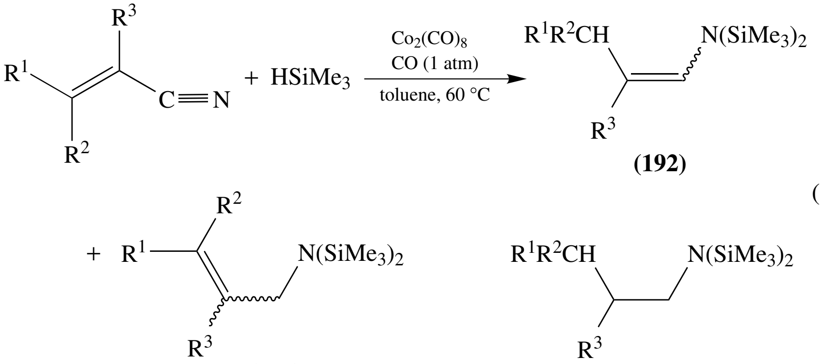

(192)

(79)

(193) **(194)**

V. ASYMMETRIC HYDROSILYLATION

Asymmetric hydrosilylation of prochiral carbonyl compounds, imines, alkenes and 1,3-dienes has been extensively studied and continues to be one of the most important subjects in the hydrosilylation reactions. This topic has been reviewed at each stage of its development as a useful synthetic method based on asymmetric catalytic processes[1,3,187–189]. In the last decade, however, substantial progress has been made in the efficiency of this reaction. Accordingly, this section summarizes the recent advances in this reaction.

A. Of Prochiral Ketones, Imines and Imine *N*-Oxides

Asymmetric hydrosilylation of prochiral ketones continues to be the most popular reaction to examine the efficacy of new chiral ligands or chiral catalyst systems. This asymmetric catalytic process gives enantiomerically enriched secondary alcohols after facile desilylation of the resulting silyl ethers (equation 80).

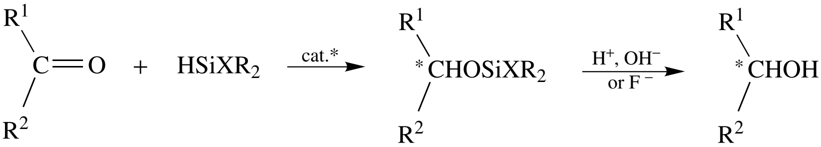

$$R^1R^2C{=}O + HSiXR_2 \xrightarrow{\text{cat.*}} R^1R^2\,{}^{*}CHOSiXR_2 \xrightarrow[\text{or } F^-]{H^+,\ OH^-} R^1R^2\,{}^{*}CHOH \qquad (80)$$

A variety of newer chiral ligands has been emerging for traditional rhodium catalyst systems[190–223] as well as other transition metal catalyst systems including iridium[209,213], cobalt[224] and titanium complexes[225,226]. Chiral ligands for Rh(I) or Rh(III) catalysts that have been shown to realize high to excellent asymmetric induction ($\geqslant$80% ee) and were not included in *The Chemistry of Organic Silicon Compounds*[3] are summarized in Figure 1. Figure 1 also includes a chiral titanocene catalyst precursor that has exhibited excellent enantioselectivity. Representative results using transition metal catalysts with these chiral ligands as well as the chiral titanocene catalyst precursor are listed in Table 5.

As Figure 1 shows, the most characteristic feature in the development of the newer chiral ligands for Rh-catalysts in the last decade is the emergence of highly efficient bidentate dinitrogen ligands as well as tridentate trinitrogen ligands bearing oxazoline moieties in place of chiral diphosphines and chiral pyridylthiazolidines that were extensively used in 1970s and mid-1980s, respectively[3]. Chiral bis(1-phosphinoethylferrocenyl) (TRAP, **206**)[207] and bis(1-aminoethylferrocenyl)dichalcogenide (**208**)[211] ligands can be pointed out as new developments. Highly effective chiral P−N ligands have also been developed[208,209]. It is worth mentioning that the success of the chiral C_2-symmetrical bis(oxazolinyl)pyridine ligands[190–192,194], pybox **195** and **196**, developed by Nishiyama and coworkers, has stimulated the development of a new series of chiral N−N and P−N ligands. It should also be noted that the chiral Rh-catalyst precursors with pybox[190–192], pymox[190] or bipymox[193] are Rh(III) complexes which are reduced to Rh(I) species by H_2SiPh_2 in the presence of $AgBF_4$.

Another important development is chiral titanocene catalyst using **203** as the catalyst precursor[225]. The (*R*, *R*)-(EBTHI)Ti(OR)$_2$ (**203**) is proposed to generate the active catalyst species, '(*R*, *R*)-(EBTHI)TiH', upon reaction with *n*-BuLi (2 equivalents) and polymethylhydrosiloxane (PMHS). This chiral Ti-catalyst system is highly efficient for the reactions of aromatic alkyl ketones achieving >90% ee in many cases. In sharp contrast to this, only 24% ee is obtained for the reaction of cyclohexyl methyl ketones. However, the reaction of cyclohexen-1-yl methyl ketone achieved 85–90% ee. Thus, it is extremely important for this chiral Ti-catalyst to have a π-system to be effective.

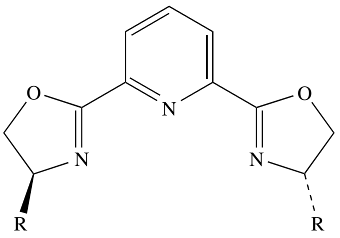

(*S,S*)-pybox **(195)**

(a) ip-pybox (R = *i*-Pr)
(b) sb-pybox (R = *s*-Bu)
(c) tb-pybox (R = *t*-Bu)

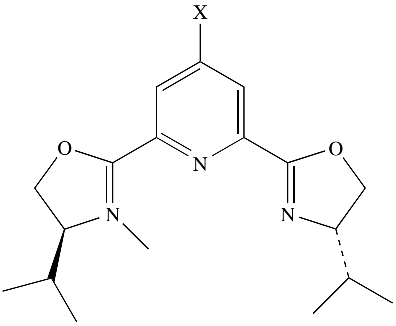

(*S,S*)-4-X-ip-pybox **(196)**

(a) $X = Cl$
(b) $X = MeO$
(c) $X = Me_2N$

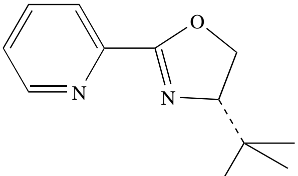

(*S*)-tb-pymox **(197)**

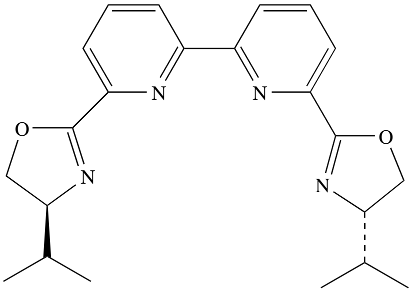

bipymox-(*S,S*)-Pr-*i* **(198)**

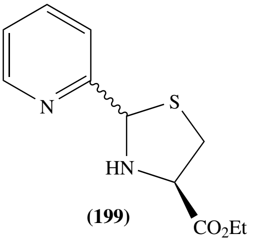

(199)

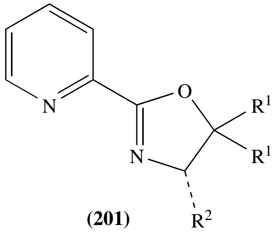

(201)

(a) $R^1 = H, R^2 = t\text{-Bu}$
(b) $R^1 = Ph, R^2 = CH_2Ph$
(c) $R^1 = Ph, R^2 = i\text{-Pr}$
(d) $R^1 = Ph, R^2 = i\text{-Bu}$
(e) $R^1 = Ph, R^2 = (S)\text{-}s\text{-Bu}$

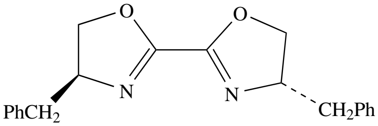

(200)

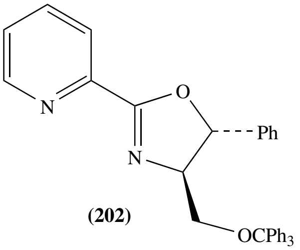

(202)

FIGURE 1

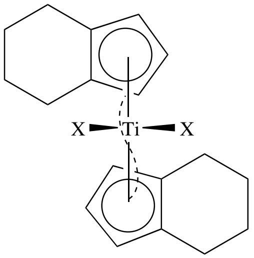

(*R*,*R*)-(EBTHI)TiX$_2$ **(203)**

X$_2$ = (*R*,*R*)-1, 1′-binaphthyl-2, 2′-diolate

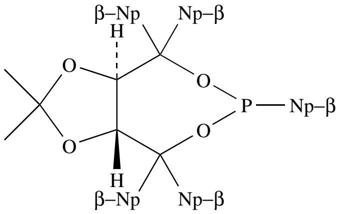

(204)

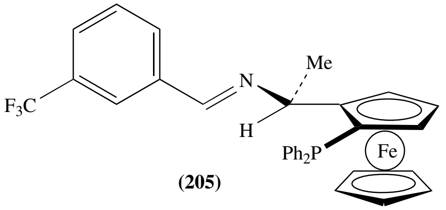

(205)

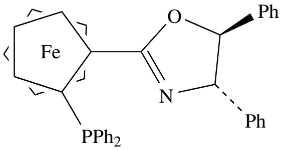

(*S*,*S*,*S*)-DIPOF **(207)**

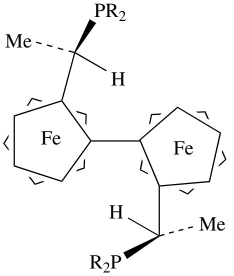

(206)

(a) R = *n*-Pr; (*R*,*R*)-(*S*,*S*)-*n*-PrTRAP
(b) R = *n*-Bu; (*R*,*R*)-(*S*,*S*)-*n*-BuTRAP
(c) R = Et; (*R*,*R*)-(*S*,*S*)-EtTRAP

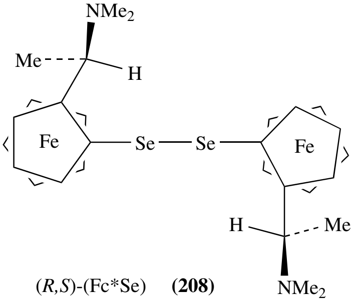

(*R*,*S*)-(Fc*Se) **(208)**

FIGURE 1. (*continued*)

As Table 5 indicates, alkyl aryl ketones are the best substrates for this reaction. This has also been the case for the previously developed chiral ligand systems. Nevertheless, there have been substantial improvements in enantioselectivity for the reactions of alkenyl methyl ketones and alkyl methyl ketones, using Rh-catalysts with chiral ligands **195a**[191], **206b**[207], and **207**[209].

A curious reversal of configuration is observed when Ir-catalyst is used instead of Rh-catalyst for the same chiral ligand[209,213]. For example, the asymmetric hydrosilylation followed by desilylation of acetophenone catalyzed by **207**/[Rh(COD)Cl]$_2$ gives (*R*)-1-phenylethanol with 91% ee, while the same reaction catalyzed by **207**/[Ir(COD)Cl]$_2$ yields (*S*)-alcohol with 96% ee (Scheme 21). The rationale for this remarkable reversal in the direction of asymmetric induction has not been given clearly, but either a change

TABLE 5. Typical results on the asymmetric reduction of prochiral ketones via hydrosilylation

Prochiral ketone	Hydro-silane	Catalyst	Temp. (°C) Solvent	Product	% ee	Reference
PhCOMe	H_2SiPh_2	**195a**/Rh(III) $AgBF_4$	0 THF	PhMeCHOH (*S*)	94	191
PhCOMe	H_2SiPh_2	**195b**/Rh(III) $AgBF_4$	−5 THF	PhMeCHOH (*S*)	91	191
PhCOMe	H_2SiPh_2	**195c**/Rh(III) $AgBF_4$	0 THF	PhMeCHOH (*S*)	83	191
PhCOMe	H_2SiPh_2	**196a**/Rh(III) $AgBF_4$	−5 THF	PhMeCHOH (*S*)	94	192
PhCOMe	H_2SiPh_2	**196b**/Rh(III) $AgBF_4$	10 THF	PhMeCHOH (*S*)	93	192
PhCOMe	H_2SiPh_2	**196c**/Rh(III) $AgBF_4$	20 THF	PhMeCHOH (*S*)	90	192
PhCOMe	H_2SiPh_2	**197**/Rh(I)	−5 THF	PhMeCHOH (*R*)	91	192
PhCOMe	H_2SiPh_2	**198**/Rh(III) $AgBF_4$	5 THF	PhMeCHOH (*S*)	90	193
PhCOMe	H_2SiPh_2	**198**/Rh(III) $AgBF_4$	0 → 20 CCl_4	PhMeCHOH (*R*)	83	195
PhCOMe	H_2SiPh_2	**198**/Rh(III) $AgBF_4$	0 → 20 CCl_4	PhMeCHOH (*R*)	89	195
PhCOMe	H_2SiPh_2	**198**/Rh(III) $AgBF_4$	0 → 20 CCl_4	PhMeCHOH (*R*)	81	195
PhCOMe	H_2SiPh_2	**198**/Rh(III) $AgBF_4$	0 → 20 CCl_4	PhMeCHOH (*R*)	82	195
PhCOMe	H_2SiPh_2	**199**/Rh(I)	0 → 20 neat	PhMeCHOH (*R*)	86	203
PhCOMe	H_2SiPh_2	**200**/Rh(I)	0 CCl_4	PhMeCHOH (*R*)	84	227
PhCOMe	H_2SiPh_2	**201a**/Rh(I)	0 → 20 CCl_4	PhMeCHOH (*R*)	83	201
PhCOMe	$H_2SiPhNp$-α	**202**/Rh(I)	0 neat	PhMeCHOH (*R*)	84	223
PhCOMe	PMHS[a]	**203** *n*-BuLi PMHS[a]	room temp. benzene	PhMeCHOH (*R*)	97	225
PhCOMe	H_2SiPh_2	**204**/Rh(I)	0 → 20 CCl_4	PhMeCHOH (*R*)	84	212
PhCOMe	H_2SiPh_2	**205**/Rh(I)	20 THF	PhMeCHOH (*S*)	90	208
PhCOMe	H_2SiPh_2	**206a**/Rh(I)	−40 THF	PhMeCHOH (*S*)	92	207
PhCOMe	H_2SiPh_2	**206b**/Rh(I)	−40 THF	PhMeCHOH (*S*)	92	207

TABLE 5. (*continued*)

Prochiral ketone	Hydro-silane	Catalyst	Temp. (°C) Solvent	Product	% ee	Reference
PhCOMe	H_2SiPh_2	**207**/Rh(I)	25 Et_2O	PhMeCHOH (*R*)	91	209
PhCOMe	H_2SiPh_2	**208**/Rh(I)	0 THF	PhMeCHOH (*R*)	85	211
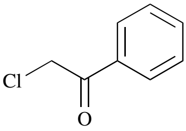	H_2SiPh_2	**208**/Rh(I)	0 THF	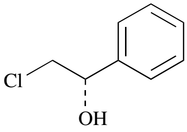	88	210, 211
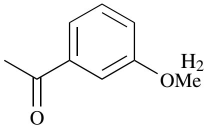	H_2SiPh_2	**200**/Rh(I)	0 → 20 neat	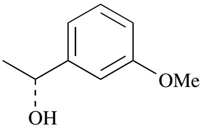	93	203
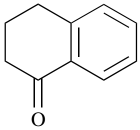	H_2SiPh_2	**195a**/Rh(III) $AgBF_4$	0 THF	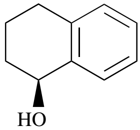	99	191
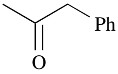	H_2SiPh_2	**196a**/Rh(III) $AgBF_4$	−5 THF	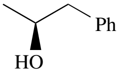	80	192
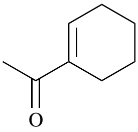	PMHS[a]	**203**/*n*-BuLi PMHS[a]	room temp. benzene	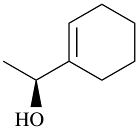	85–90	225
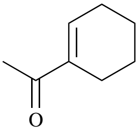	H_2SiPh_2	**206b**/Rh(I)	−40 THF	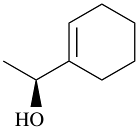	95	207
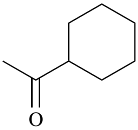	H_2SiPh_2	**206b**/Rh(I)	−40 THF	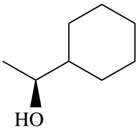	80	207
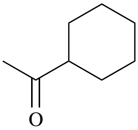	H_2SiPh_2	**207**/Rh(I)	25 Et_2O	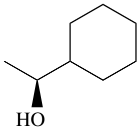	89	209

(*continued overleaf*)

TABLE 5. (*continued*)

Prochiral ketone	Hydro-silane	Catalyst	Temp. (°C) Solvent	Product	% ee	Reference
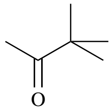	H_2SiPh_2	f 207/Rh(I)	25 Et_2O	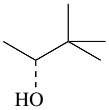	87	209
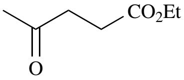	H_2SiPh_2	**195a**/Rh(III) $AgBF_4$	0 THF	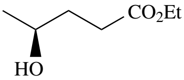	95	191
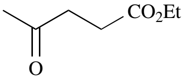	H_2SiPh_2	**206c**/Rh(I)	room temp. THF	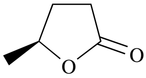	88	206
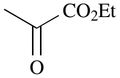	H_2SiPh_2	**206c**/Rh(I)	room temp. THF	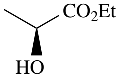	80	206
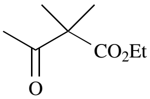	H_2SiPh_2	**206c**/Rh(I)	room temp. THF	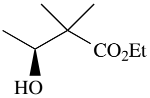	93	206

[a] PMHS = polymethylhydrosiloxane.

in the mechanism or catalyst geometry may account for the phenomenon. An intriguing possibility of the C−H activation of the Me_2N group by Ir(I), but not by Rh(I), is invoked by Faller and Chase[213].

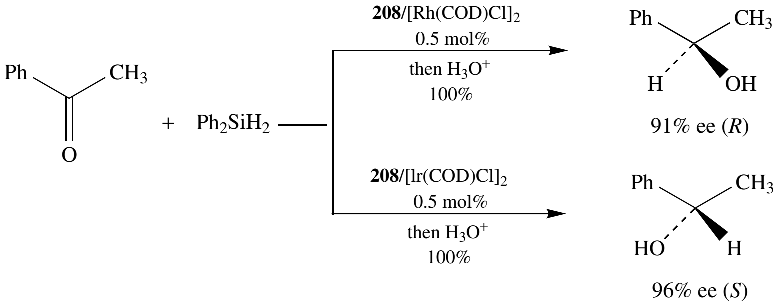

SCHEME 21

Reversal of configuration is also observed when a polystyrene-bound **201**-type pyridyloxazolidine–Rh(I) complex is used as the catalyst for the reaction of acetophenone with H_2SiPh_2 and recycled. This catalyst shows only marginal enantioselectivity (11–27% ee) for (*S*)-product formation, while it gives (*R*)-product with 92.5% ee after recycling 9 times, although the chemical yield drops to only 15% under the same reaction conditions. Change in the active catalyst species during recycling is suggested[196].

In comparison with the asymmetric hydrosilylation of prochiral ketones, the reaction of prochiral imines has been more challenging in achieving good enantioselectivity[3] (equation 81). For example, the reaction of PhMeC=NPh with H_2SiPh_2 catalyzed by **208**/$[Rh(COD)Cl]_2$ in ether gives PhMeCH−NHPh with 53% ee but in only 28% yield after 140 h[211]. The reaction of 2-methylquinoxaline with H_2SiPh_2 catalyzed by (+)-DIOP−Rh(H) complex prepared from $[Rh(CO)_2Cl]_2$, (+)-DIOP and KBH_4 in ethanol gives (*S*)-2-methyltetrahydroquinoxaline with 19% ee[228]. When the sodium amide of (*R*)-2,2′-diamino-1,1′-binaphthyl is used as the chiral ligand for this reaction, (*R*)-product with 36% ee is obtained[228].

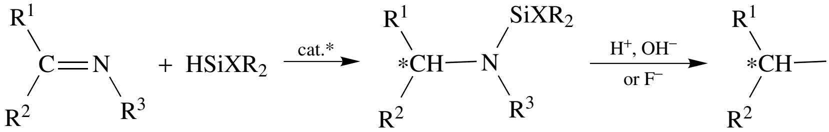

$$R^1R^2C{=}NR^3 + HSiXR_2 \xrightarrow{\text{cat.*}} R^1R^2{*}CH{-}N(SiXR_2)R^3 \xrightarrow[\text{or } F^-]{H^+,\ OH^-} R^1R^2{*}CH{-}NHR^3 \qquad (81)$$

A breakthrough for this reaction has just been achieved by Buchwald and coworkers using (*S*,*S*)-(EBTHI)TiF_2 as a precatalyst[229]. The active catalyst species '(EBTHI)Ti−H' (*vide supra*) is generated by treating (*S*,*S*)-(EBTHI)TiF_2 with H_3SiPh in the presence of a small amount of methanol and pyrrolidine in THF. This chiral catalyst system can achieve >90% ee for the reactions of various imines. The reaction is proposed to include σ-bond metathesis (see Section IIB) for the cleavage of Ti−N bond with $H{-}SiH_2Ph$. Representative results are listed in Table 6[229].

TABLE 6. Asymmetric reduction of prochiral imines via hydrosilylation catalyzed by (*S*,*S*)-(EBTHI)Ti complex[a] in THF

Prochiral imine	Hydrosilane	Temp. (°C)	Product	% ee
PhMeC=NMe	H_3SiPh	35	(*S*)-PhMeCH-NHMe	99
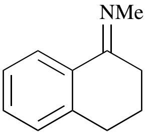	H_3SiPh	room temp.	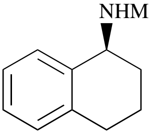	96
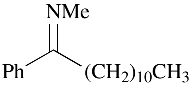	H_3SiPh	50	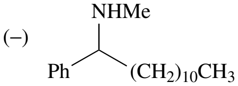	95
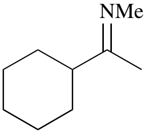	H_3SiPh	room temp.	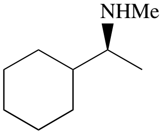	93
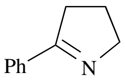	H_3SiPh	room temp.	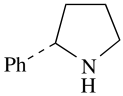	99

[a] Catalyst amount = 0.02−1 mol%.

Asymmetric hydrosilylation of prochiral imine *N*-oxides (nitrones) **(209–211)** catalyzed by $Ru_2Cl_4[(S)\text{-}(-)\text{-tolbinap}]_2(NEt_3)$ with H_2SiPh_2 gives the corresponding *N*,*N*-disubstituted hydroxylamines **(212–214)** with high enantiomeric purity (equations 82–84)[230].

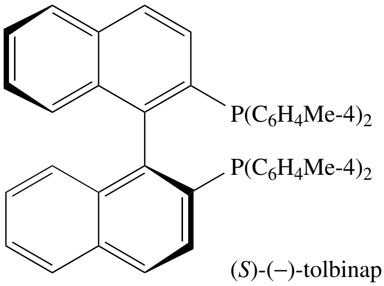

(*S*)-(−)-tolbinap (82)

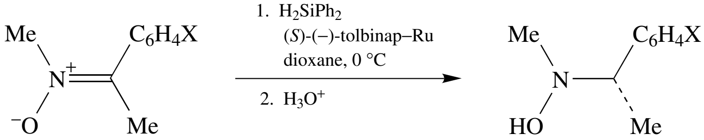

(209) **(212)**

X = H, 4-Cl, 4-F, 3-Cl

83-86% ee

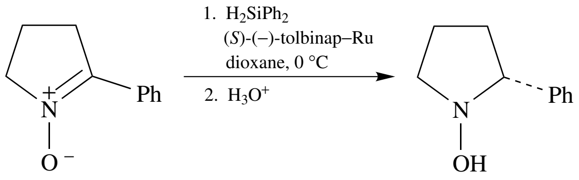

(83)

(210) **(213)** 69% ee

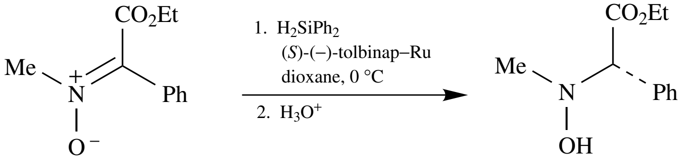

(84)

(211) **(214)** 91% ee

Asymmetric intramolecular hydrosilylation of α-dimethylsiloxyketones **(216)**, which are prepared from α-hydroxyketones **215**, catalyzed by $[(S,S)\text{-R-DuPHOS)Rh(COD)}]^+CF_3{}^-SO_3{}^-$, **(219)** proceeds smoothly at 20–25 °C to give siladioxolanes **217**. Desilylation of **217** affords 1,2-diols **218** with 65–93% ee in good yields (Scheme 22)[231]. The best result (93% ee) is obtained for the reaction of α-hydroxyacetone using (*S*, *S*)-*i*-Pr-DuPHOS-Rh^+ as the catalyst. The same reactions using (*S*,*S*)-Chiraphos and (*S*)-binap give **218** ($R' = Me$) with 46 and 20% ee, respectively.

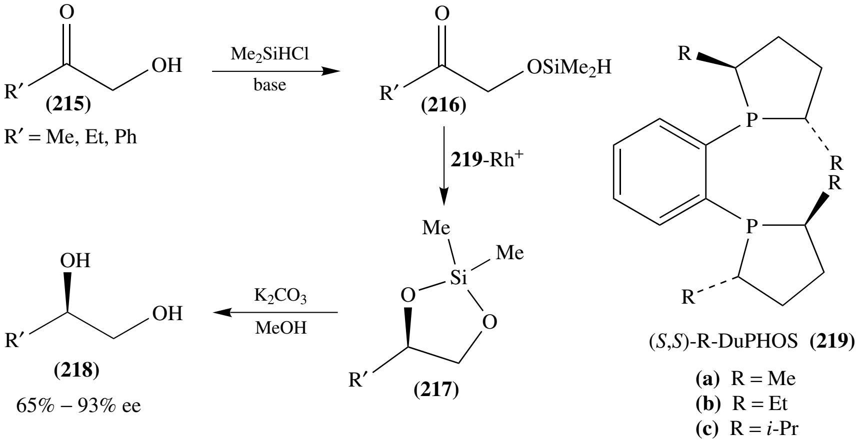

SCHEME 22

Asymmetric synthesis of chiral tertiary hydrosilanes can be realized by means of catalytic asymmetric hydrosilylations of ketones with dihydrosilanes $H_2SiR^1R^2$ ($R^1 \neq R^2$). The asymmetric hydrosilylation of a ketone with such a dihydrosilane gives a silyl ether possessing a chiral silicon center, which is readily converted to the corresponding chiral tertiary hydrosilane by reaction with a Grignard reagent. The reactions of $H_2SiPh(Np\text{-}\alpha)$ with 3-pentanone, propiophenone and (−)-menthone using (+)-DIOP−Rh complex as the catalyst, followed by reaction with MeMgBr or EtMgBr, gave $HSi^{*}RPh(Np\text{-}\alpha)$ with 46, 36 and 82% ee, respectively[3,232–236]. The same reactions (R = Me) using (*R*)-Cybinap as the chiral ligand improved the enantiomeric purity of the resulting (*R*)-HSiMePh(Np-α) **(220)** with up to >99% ee (equation 85)[237]. Chiral ligands, binap, tolbinap (*vide supra*) and *p*-MeObinap are also effective, but the best results are achieved with Cybinap. It should be noted that the absolute configuration of the product obtained with (*R*)-Cybinap is opposite to those with (*R*)-binap, tolbinap and *p*-MeObinap[237].

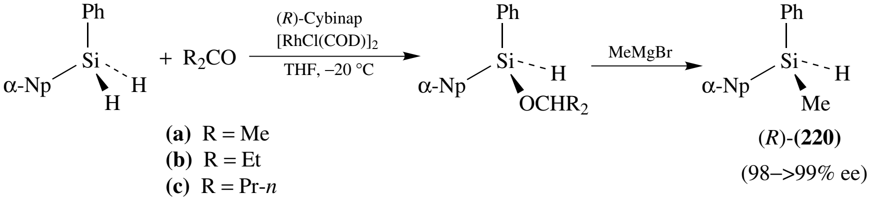

(85)

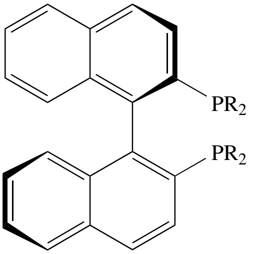

R = H, (*R*)-binap
R = cyclohexyl, (*R*)-Cybinap
R = 4-MeOC$_6$H$_4$, (*R*)-*p*-MeObinap

B. Of Alkenes and 1,3-Dienes

Asymmetric hydrosilylation of prochiral alkenes has been one of the most challenging reactions to achieve high enantioselectivity[3]. A significant breakthrough for this process, however, was brought about by Uozumi and Hayashi in 1991 using a unique chiral monophosphine ligand MOP **(221)**[238–240]. The hydrosilylation of 1-alkenes with $HSiCl_3$ catalyzed by (*S*)-MOP/$[PdCl(\eta^3\text{-}C_3H_5)]_2$ gives the corresponding 2-trichlorosilylalkanes **(222)** with 91–97% ee [all *R*-products except for the case of $Ph(CH_2)_2CH(SiCl_3)CH_3$ (*S*)] as the predominant product in excellent yields (equation 86) accompanied by a small amount of 1-trichlorosilylalkanes **(222′)**. Since **222** is readily converted to the corresponding secondary alcohols via Tamao oxidation, this process provides an efficient method for the asymmetric synthesis of 2-alkanols **(223)** with high enantiopurity from 1-alkenes (equation 86). The regioselectivity of this reaction using MOP as the chiral ligand is quite unexpected since it is well known that the hydrosilylation of 1-alkenes catalyzed by Pt, Rh and Ni complexes proceeds in an *anti*-Markovnikov manner, yielding 1-silylalkanes selectively (see Section II). The regioselectivity is good to high (**222**/**222′** = 80/20–94/6) for linear 1-alkenes, but a bulky substituent such as cyclohexyl substantially decreases the selectivity, i.e. **222**/**222′** = 66/34 for $c\text{-}C_6H_{11}CH{=}CH_2$, without affecting enantioselectivity (96% ee).

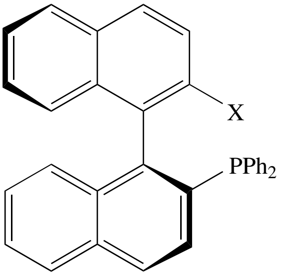

(*S*)-MOP **(221)**

X = MeO (MeO–MOP); OPr-*i* (*i*-PrO-MOP);
OCH_2Ph (BnO–MOP); Et (Et–MOP)

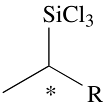

(222)

+

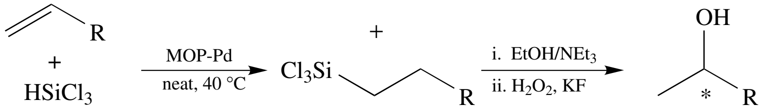

(222′) **(223)** (86)

R = $n\text{-}C_4H_9$, $n\text{-}C_6H_{13}$, $n\text{-}C_{10}H_{21}$, CH_2CH_2Ph, $c\text{-}C_6H_{11}$

Norbornene (**224**, $n = 1$, X = H), 5,6-bis(*endo*-carbomethoxy)norbornene (**224**, $n = 1$, X = CO_2Me), bicyclo[2.2.2]oct-2-ene (**224**, $n = 2$, X = H) and norbornadiene **(227)** are excellent substrates for the MOP–Pd-catalyzed asymmetric hydrosilylation, giving *exo*-products exclusively, which are readily transformed to the corresponding *exo*-alcohols **(226, 228b)** with 92–96% ee in excellent yields (equations 87 and 88)[241]. *exo*-2-Trichlorosilylnorbornane (**225**, $n = 1$, X = H) can also be transformed to *endo*-2-bromonorbornane in 81% yield by reacting with KF and NBS[241]. The reaction of norbornadiene **(227)** with 2.5 equivalents of $HSiCl_3$ gives double hydrosilylation product **229a** with >99% ee and excellent regioselectivity (e.g. 2,5-/2,6- product = 18/1), which is converted to the corresponding diol **229b** and diacetate **229c** (equation 88)[241].

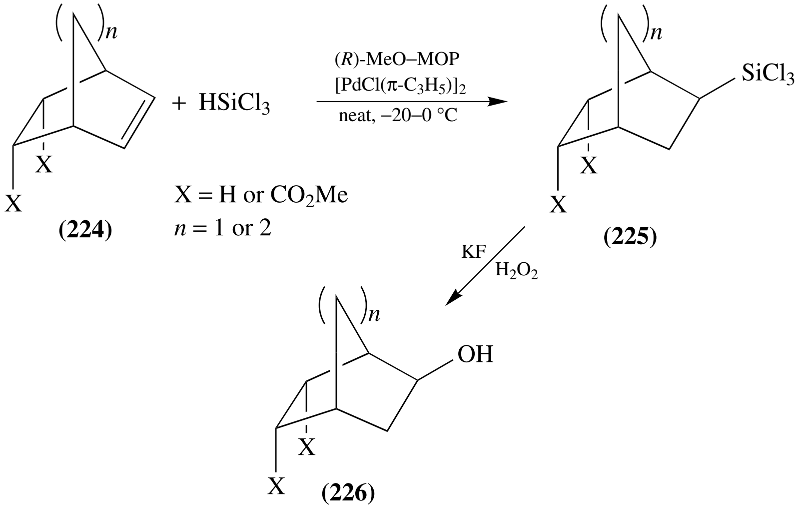

X = H or CO_2Me
n = 1 or 2

(87)

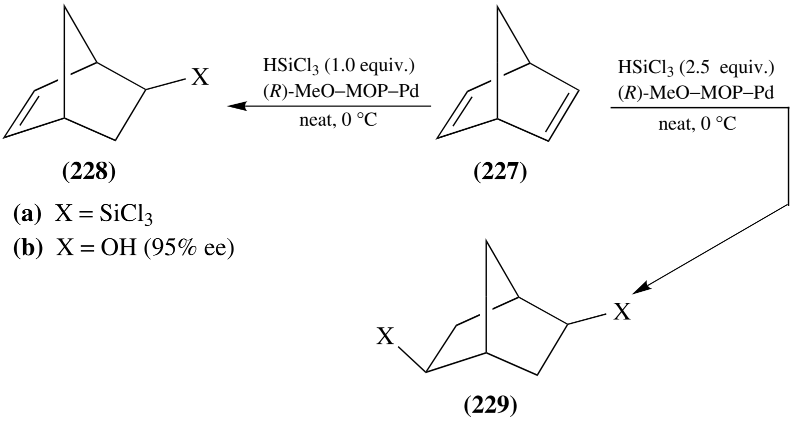

(228)
(a) X = $SiCl_3$
(b) X = OH (95% ee)

(88)

(229)
(a) X = $SiCl_3$
(b) X = OH
(c) X = OAc (>99% ee)

In a similar manner, the reactions of dihydrofurans **230** and **231** with $HSiCl_3$ catalyzed by (*R*)-MeO-MOP give 3- and 4-trichlorosilyltetrahydrofurans **232** (with *S* absolute configuration) and **233** (whose configuration was not determined) with 95% ee and 82% ee, respectively (equations 89 and 90)[242].

In a similar manner, the reactions of 5,6-disubstituted 7-oxabicyclo[2.2.1]hept-2-enes **(234)** with $HSiCl_3$ catalyzed by (*R*)-MeO–MOP–Pd give the corresponding *exo*-2-trichlorosilyl-7-oxabicyclo[2.2.1]heptanes **(235)** exclusively with excellent enantiopurity (Z = CO_2Me, 20 °C, 95% ee; Z = CH_2OCH_3, −20 °C, 90% ee) (equation 91), which are converted to *exo*-2-hydroxy-7-oxabicyclo[2.2.1]heptanes **(236)** and their esters and carbamates via Tamao oxidation and the subsequent esterification[242]. A trimethylsilyl derivative of **235** (Z = CH_2OCH_3) is further reacted with MeCOBr to afford 1-bromo-2,3-di(methoxymethyl)-4-acetoxy-5-TMS-cyclohexane stereospecifically in 81% yield[242].

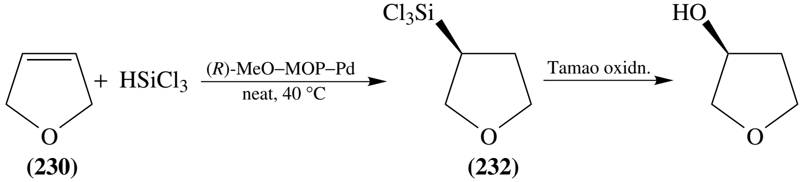

(89)

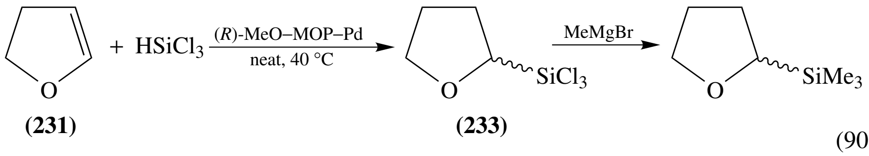

(90)

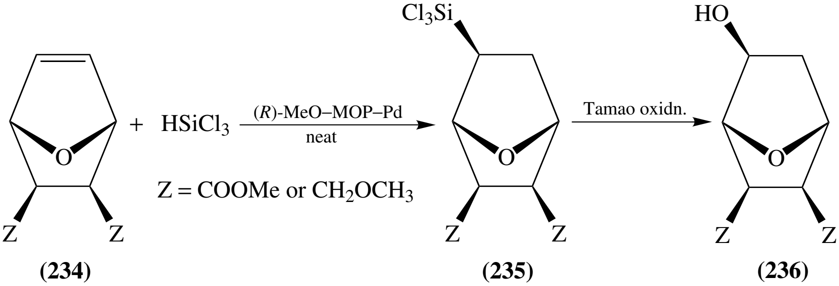

(91)

Although the MOP ligands induce excellent enantioselectivity in the asymmetric hydrosilylation of 1-alkenes, norbornenes and dihydrofurans as described above, the reaction of styrene catalyzed by (*R*)-MeO–MOP–Pd under the same conditions, i.e. neat at 0 °C, gives Ph(Me)CH$SiCl_3$ with only 14% ee[243]. The enantioselectivity can be improved up to 71% ee by using benzene as the solvent at 5 °C[243,244], and the reactions of indene and other 1-arylalkenes catalyzed by MeO–MOP–Rh can achieve 80–85% ee[244]. Other MOP ligands (*vide supra*) or sulfonylaminoalkylphosphines cannot achieve higher enantioselectivity[243,245]. However, a simpler MOP ligand, (*S*)-H–MOP (MOP, X = H, *vide supra*), is found to achieve 89–96% ee in the reactions of styrene and styrene derivatives giving **237** and then **238** (equation 92)[243].

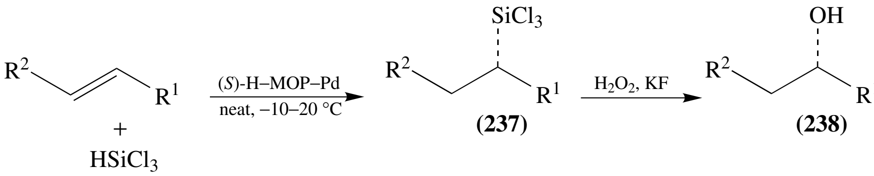

$R^1 = H, 4\text{-}MeC_6H_4, 4\text{-}CF_3C_6H_4, 3\text{-}ClC_6H_4$ (92)

$R^2 = Me, n\text{-}Bu$

Asymmetric hydrosilylation of styrene with $HSiCl_3$ catalyzed by a palladium complex of a chiral ferrocenylphosphine attached to cross-linked polystyrene support at 70 °C gives $PhMeC^*HSiCl_3$ in quantitative yield with only 15.2% ee[65].

Chiral lanthanide catalysts, (*R*)- and (*S*)-$Me_2Si(Me_4Cp)[(-)\text{-menthylCp}]SmCH(SiMe_3)_2$, are effective for the asymmetric hydrosilylation of 2-phenyl-1-butene with H_3SiPh, giving (*R*)- and (*S*)-2-phenyl-2-silylbutanes with 68 and 65% ee, respectively (Scheme 23)[43].

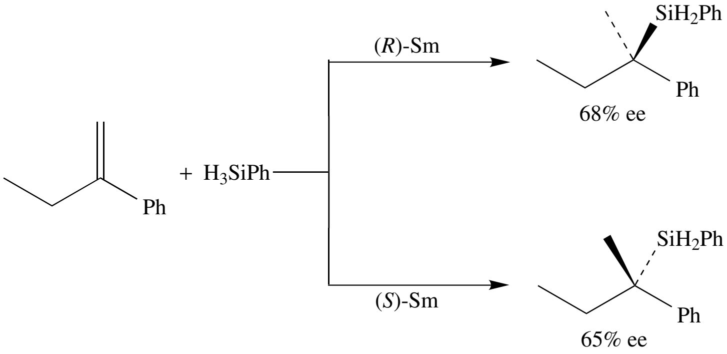

Sm = $Me_2Si(Me_4Cp)[(-)\text{-menthylCp}]SmCH(SiMe_3)_2$

SCHEME 23

Asymmetric hydrosilylation of cyclopentadiene with $HSiCl_3$ catalyzed by a Pd complex of (*S*)-(*R*)-ferrocenylphosphine (**240**, Rf = C_3F_7) proceeds in a 1,4-manner to give 3-silyl-1-cyclopentene (**239**, X = Cl) with up to 60% ee (*R*) (equation 93)[246]. The same reaction using (*S*)-2-(*N*-methanesulfonylamino)-3-methyl-1-diphenylphosphinobutane **(241)** and $HSiMeCl_2$ yields **239** (X = Me) with up to 71% ee (*S*) (equation 93)[245]. In a similar manner, the reaction of 1,3-cyclohexadiene with $HSiF_2Ph$ catalyzed by (*R*)-(*S*)-1-diphenylphosphino-2-(1-acetoxyethyl)ferrocene (PPF−OAc) affords (*S*)-3-silyl-1-cyclohexene **(242)** with 77% ee (equation 94)[247].

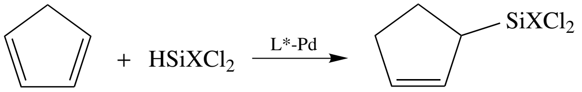

(93)

X = Cl or Me
L* = **240** or **241**

(239)

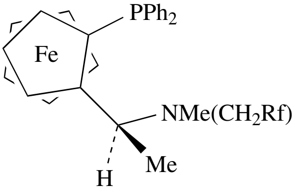

(240)

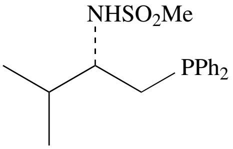

(241)

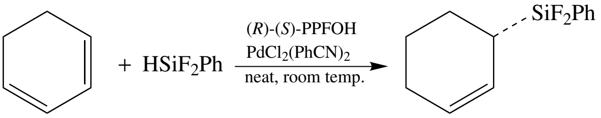

(242)

(94)

Asymmetric hydrosilylation of linear 1,3-alkadienes **(243)** also proceeds in a 1,4-manner with high regioselectivity to give the corresponding allylic silanes **244** (equation 95). The enantioselectivity of this reaction is 37–66% ee using $HSiCl_3$ and Pd-complexes of chiral ferrocenylphosphines **240** (Rf = C_3F_7 or C_8F_{17}) as the catalyst at 30–80 °C[246]. The reactions of 1,3-pentadiene (**243**, R = Me), 1,3-hexadiene (**243**, R = Et) and 1-phenyl-1,3-butadiene (**243**, R = Ph) with $HSiF_2Ph$ catalyzed by (*R*)-(*S*)-PPFA–Pd (PPFA = *N*, *N*-dimethyl-1-[2-(diphenylphosphino)ferrocenyl]ethylamine) at room temperature give the corresponding (*Z*)-allylic silanes with 69% ee[247]. The reactions of 1-phenyl-1,3-butadiene (**243**, R = Ph) with phenylhalosilanes, $HSiPh_nX_{3-n}$ (X = F or Cl), catalyzed by Pd-complexes with (*R*)-OH–MOP (X = OH) at 20 °C yield (*S*)-(*Z*)-1-phenyl-1-silyl-2-butene (**244**, R = Ph) with 17–66% ee, while the reactions with (*R*)-(TBS)–MOP (X = $OSiMe_2Bu$-*t*) yield (*R*)-(*Z*)-1-phenyl-1-silyl-2-butene (**244**, R = Ph) with 9–56% ee[248].

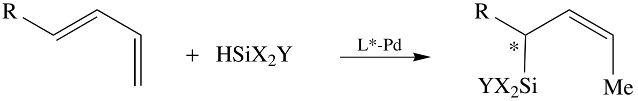

(243) **(244)** (95)

R = Me, Et, *n*-Pr, *c*-C_6H_{11}, Ph, *o*-FC_6F_4
X, Y = Ph, F, or Cl (X≠Y)

C. Intramolecular Reactions

Catalytic asymmetric intramolecular hydrosilylation of dialkyl- and diarylsilyl ethers of bis(2-propenyl)methanol **(245)** catalyzed by (*R*, *R*)-DIOP–Rh or (*R*)-binap–Rh complex, followed by Tamao oxidation, gives (2*S*, 3*R*)-2-methyl-4-pentene–1,3-diol **(247)** with 71–93% ee and excellent *syn* selectivity (*syn*/*anti* = 95/5– > 99/1) (equation 96)[249]. The enantioselectivity of this reaction depends on the bulkiness of the silyl moiety, i.e. the bulkier the substituent, the higher is the enantiopurity of the product, except for the case of 2-MeC_6H_4: R = Me, 80% ee (binap–Rh); R = Ph, 83% ee (DIOP–Rh); R = 2-MeC_6H_4, 4% ee (DIOP–Rh); R = 3-MeC_6H_4, 87% ee (DIOP–Rh); R = 3,5-$Me_2C_6H_3$, 93% ee (DIOP–Rh). This methodology is successfully applied to the asymmetric synthesis of versatile polyoxygenated synthetic intermediate **249** (equation 97)[249].

Asymmetric intramolecular hydrosilylation of allylic hydrosilyl ethers **(251)** catalyzed by (*S*)-binap–Rh^+ complex gives the corresponding oxasilacyclopentanes **(252)** with moderate to excellent enantiomeric purity (equations 98)[250–252]. The bulkiness of the hydrosilyl group exerts a marked influence on enantioselectivity, i.e. silacyclohexyl **(251)** and silacyclopentyl (**253**, equation 99) give much better selectivity than Ph_2HSi–, *i*-Pr_2HSi– and Me_2HSi– groups[250]. (*S*)-Binap is superior to (*S*, *S*)-Chiraphos as the chiral ligand for this reaction[250]. An alkenylsilane **255** is also employed as the substrate, affording **256** with 60% ee using (*S*, *S*)-Chiraphos as the ligand (equation 100)[250]. Possible mechanisms for asymmetric induction and catalytic cycles are proposed[251,253]. The products of these reactions can be transformed to enantiomerically enriched diols via Tamao oxidation[250].

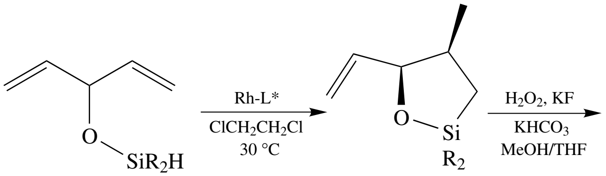

(245) **(246)** **(247)** (96)

Rh-L* = [RhCl(CH$_2$=CH$_2$)]$_2$ + (*R,R*)-DIOP or (*R*)-binap

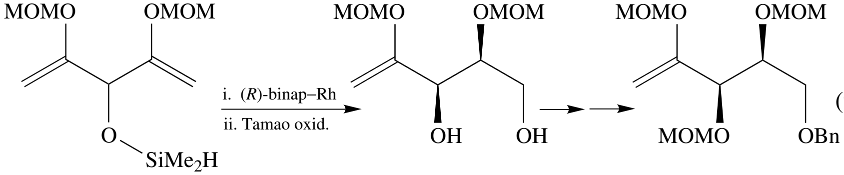

(248) **(249)** **(250)** (97)

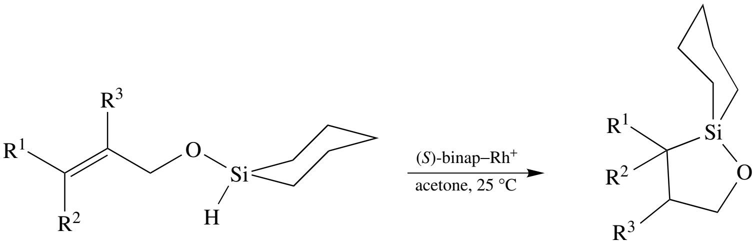

(251) **(252)** (98)

R^1 = Ph, 3,4-(MeO)$_2$C$_6$H$_3$ or 2-Np; R^2 = R^3 = H: 94–97% ee (*R*)
R^1 = R^3 = H, R^2 = Ph: 96% ee (*R*)
R^1 = Ph; R^2 = H; R^3 = Ph or Me: 88–90% ee [(*R,R*) for R^3 = Me]
R^1 = CO$_2$Me; R^2 = R^3 = H: 78% ee
R^1 = R^2 = H; R^3 = Me: 41% ee
R^1 = R^2 = H; R^3 = *t*-Bu, PhCO or (MeO)Me$_2$C; 95–96% ee
R^1 = R^2 = H; R^3 = CO$_2$Et, CO$_2$Pr-*i*, CO$_2$Bu-*t* or SiMe$_3$: 69–87% ee (CH$_2$Cl$_2$ as solvent)

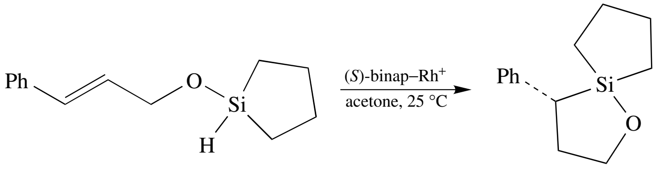

(253) **(254)** 97% ee (99)

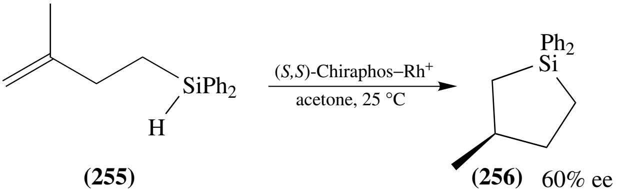

(255) **(256)** (100)

VI. SYNTHESES OF SILICON-CONTAINING DENDRIMERS AND POLYMERS USING HYDROSILYLATION

A. Silicon-containing Dendrimers

Catalytic hydrosilylation provides a convenient route to silicon-containing dendrimers. Combinations of hydrosilylation with allylation, ethenylation and ethynylation provide powerful protocols for the rapid and efficient syntheses of carbosilane dendrimers. The allylation of $SiCl_4$ with allylmagnesium bromide in ether gives tetraallylsilane (G0). The hydrosilylation of tetraallylsilane (G0) using $HSiCl_3$ and Speier's catalyst or Karstedt's catalyst (*vide supra*) affords the first generation dendrimer **257** (G1-Cl) in quantitative yield (Scheme 24)[254]. The reaction of **257** (G1-Cl) with excess allylmagnesium bromide in ether gives another first generation dendrimer **258** (G1) (Scheme 24). The repetition of the hydrosilylation–allylation cycle then produces second generation (36 allyl end-groups), third generation (108 allyl end–groups), fourth generation (324 allyl end-groups) and fifth generation (972 allyl end-groups) dendrimers in excellent yields[254]. These dendrimers are characterized by ^{1}H, ^{13}C, ^{29}Si NMR, gel-permeation chromatography (GPC) and elemental analyses. In a similar manner, carbosilane dendrimers bearing 64 and 96 allyl end-groups are also synthesized[255,256].

The hydrosilylations of tetraallylsilane with $HSiMe_2Cl$ and $HSiMeCl_2$ in the presence of Karstedt's catalyst (*vide supra*) gives versatile dendrimer units bearing reactive Si–Cl bonds, **259** (G1-Cl) and **260** (G1-Cl_2), respectively (Scheme 25)[257]. The bis-allylation of **260** (G1-Cl_2) with allyl Grignard reagent followed by hydrosilylation with $HSiMe_2Cl$ using Karstedt's catalyst affords (via **261**) dendrimer **262** that possesses 8 reacting Si–Cl bonds (Scheme 25). The reaction of **262** (G2-Cl) with ferrocenylethylamine in the presence of NEt_3 yields dendrimer **263** (Scheme 26)[257]. In a similar manner, the reaction of **259** (G1-Cl) with ferrocenylethylamine gives a dendrimer bearing four ferrocene units[257]. The reactions of **259** (G1-Cl) and **262** (G2-Cl) with ferrocenyllithium in THF at 0 °C afford the corresponding starburst macromolecules bearing 4 and 8 ferrocene unites, respectively[257]. Each of these compounds shows a single reversible oxidation wave in cyclic voltammetry. Differential pulse voltammetry measurements display only one wave, indicating that oxidation of all ferrocene units takes place at the same potential, i.e. the ferrocene units are essentially noninteracting redox centers. The dendrimers with 8 ferrocene units undergo oxidative precipitation, producing a coated film on the Pt electrode surface when oxidized to the polycation in THF[257].

The hydrosilylation–allylation protocol is applicable to the syntheses of dendritic polyols[258,259]. The hydroboration–oxidation of G0–G3 dendrimers prepared in accordance with the synthetic routes shown in Scheme 24 give the corresponding dendritic polyols, G0-OH–G3-OH, which are characterized by ^{1}H NMR and MALDI–TOF analyses[258]. Further modifications of the dendritic polyols with cholesteryl chloroformate yield unique dendrimers possessing 12, 36 and 108 cholesteryl units, providing the first examples of flexible dendrimers substituted with rigid mesogenic units that are expected to have unusual liquid crystalline properties[259]. The second generation polyol dendrimer **264**

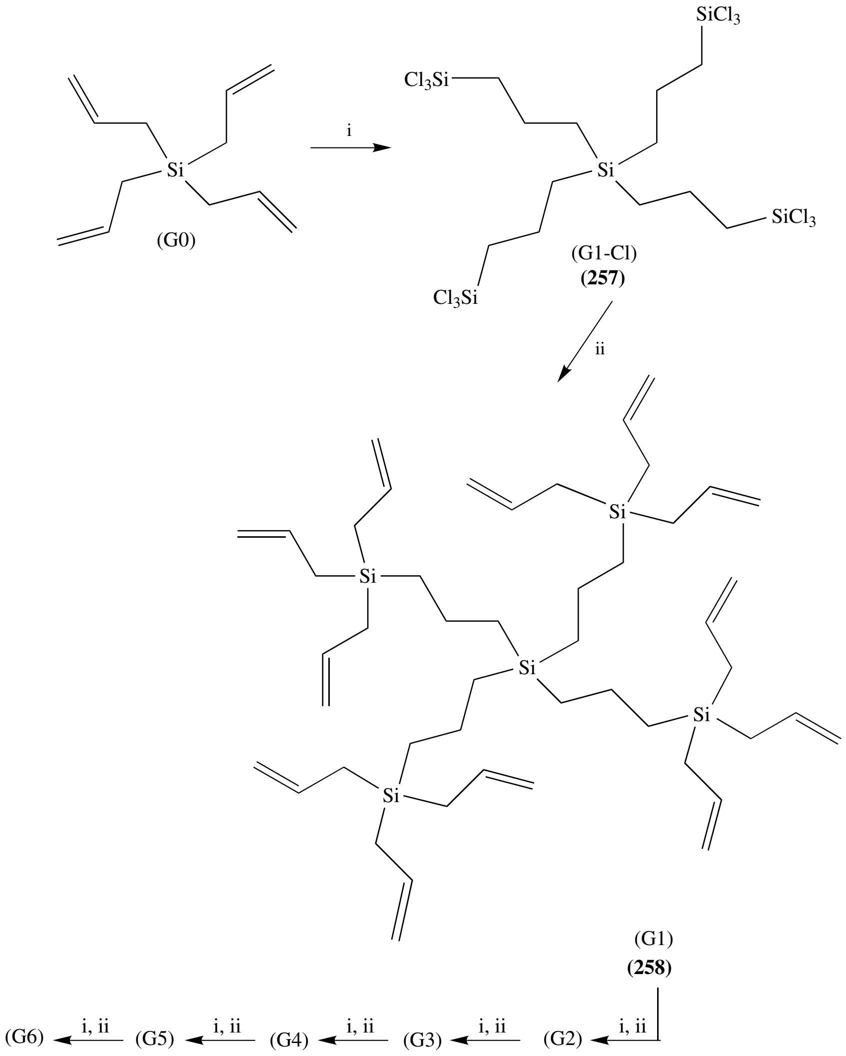

i. $HSiCl_3$, [Pt]; ii. $CH_2{=\!=}CHCH_2MgBr$, Et_2O

SCHEME 24

(G2-OH) and cholesteryl dendrimer **265** (G2-DLCP) (DLCP = dendritic liquid crystalline polymer) are shown in Scheme 27 as examples.

In a similar manner, the hydrosilylation-ethenylation cycle starting from tetraethenylsilane (G0) in THF yields up to fourth generation dendrimers[254,260,261]. This protocol is combined with reduction of the $SiCl_3$ moieties by $LiAlH_4$ to afford starburst dendrimers bearing up to 324 Si−H bonds at its periphery[262]. The structure of the second generation dendrimer **267** (G2-H) is characterized by X-ray crystallography[262]. The synthesis of **267** is shown in Scheme 28 as an example.

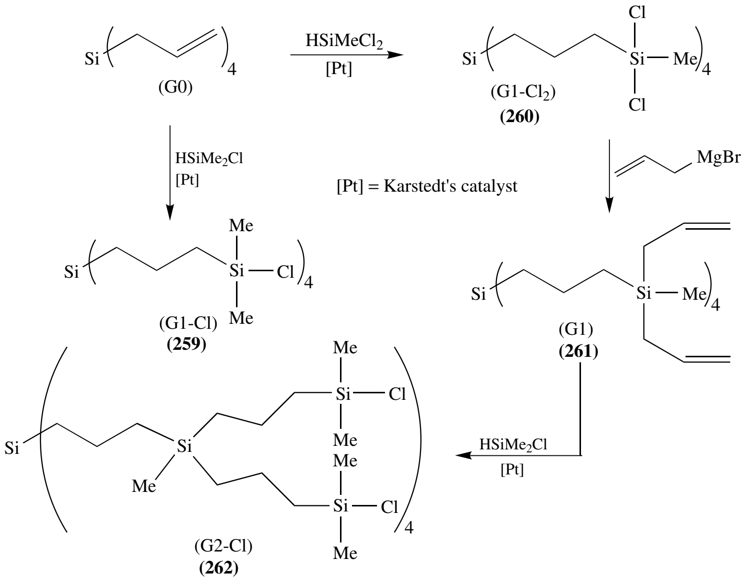

SCHEME 25

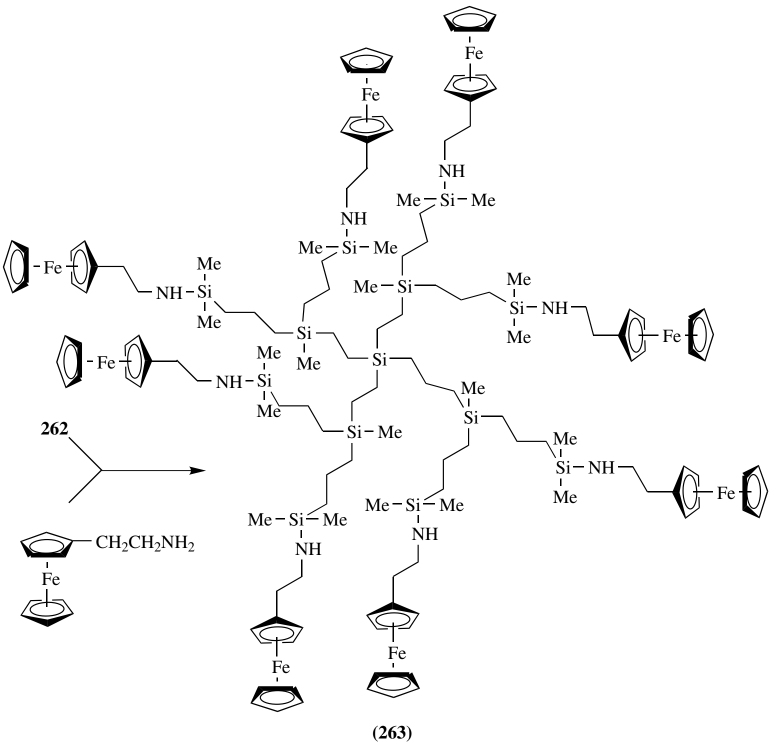

SCHEME 26

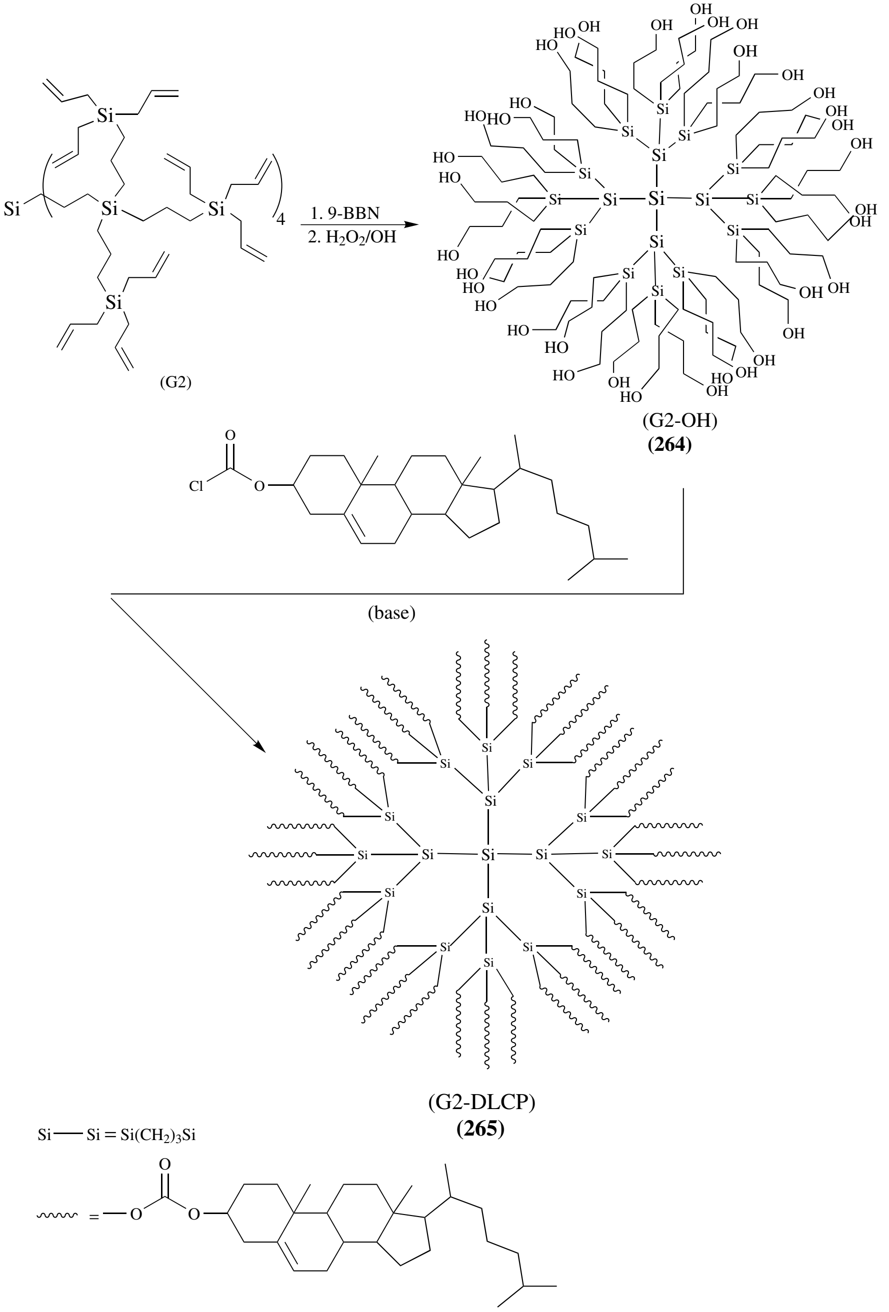

SCHEME 27

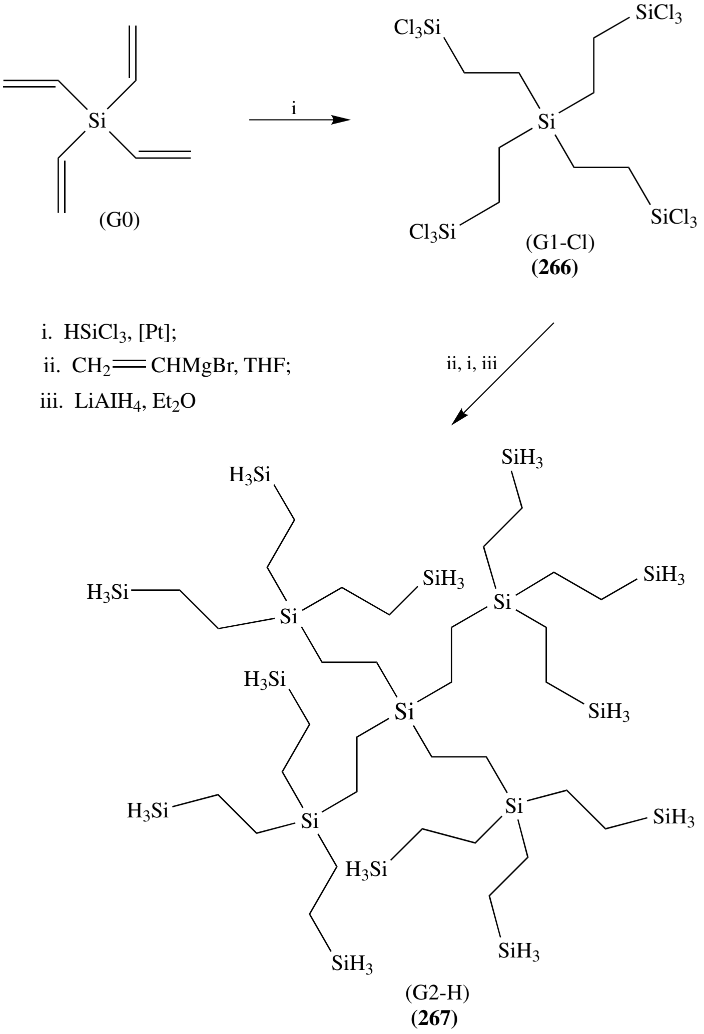

SCHEME 28

A combination of hydrosilylation–ethynylation and hydrosilylation–reduction is successfully applied to the syntheses of carbosilane dendrimers bearing 4, 8 and 12 end-ethynyl groups as well as their $Co_2(CO)_6$ complexes[263]. The synthesis of a second generation dendrimer **268** possessing twelve $Co_2(CO)_6(HC{\equiv}C-)$ units is shown in Scheme 29 as an example. The structure of **268** is confirmed by X-ray crystallographic analysis[263].

Hyper-branched starburst poly(siloxysilane) polymers are synthesized through hydrosilylation–polymerization of $CH_2{=}CHSi(OSiMe_2H)_3$ **(269)** and $HSi(OSiMe_2CH{=}CH_2)_3$ **(270)**. The polymer from **269** has Si−H moieties on the surface of the dendrimer, while that arising from **270** possesses vinyl groups on the outer sphere[264].

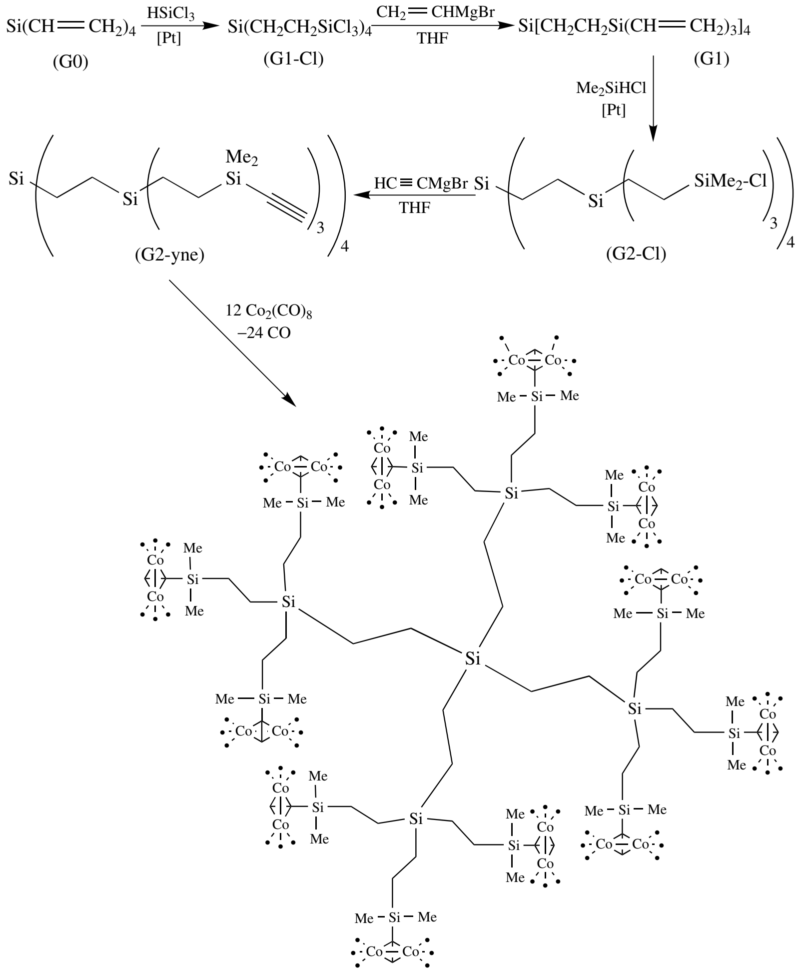

(268)

SCHEME 29

Siloxane-based dendritic hindered amine light stabilizers (HALS) such as **271** are synthesized through hydrosilylation of methacrylates containing hindered amines with polyhydrosiloxanes (equation 101)[265].

B. Silicon-containing Polymers

Hydrosilylation of 4-vinylcyclohex-1-ene-1,2-oxide, glycidyl ether, 1,5-hexadiene-5,6-oxide, etc. with $HSiMe_2O(SiMe_2O)_nSiMe_2H$ ($n = 0$–2), 1,4-$HSiMe_2{-}C_6H_4{-}SiMe_2H$, 1,4-$HSiMe_2{-}C_6H_4{-}O{-}C_6H_4{-}SiMe_2H$, etc. catalyzed by $RhCl(PPh_3)_3$ gives mono-hydrosilylation products in excellent selectivity[266–268]. The second hydrosilylation of the mono-hydrosilylation products with epoxyalkenes different from those used in the initial reaction provides ambifunctional silicon-containing epoxy monomers[268]. When the second hydrosilylation employs $CH_2{=}CHSi(OMe)_3$, the reaction gives monomers bearing epoxy and trialkoxysilane moieties[269]. The photopolymerization of these monomers has been studied[269]. In a similar manner, polysiloxanes bearing 1-propenyl ether groups are synthesized through highly chemoselective Pt-hydrosilylation of 1-allyloxy-4-(1-propenyloxy)butane with various hydrosiloxanes, and converted to thin films by photopolymerization[270].

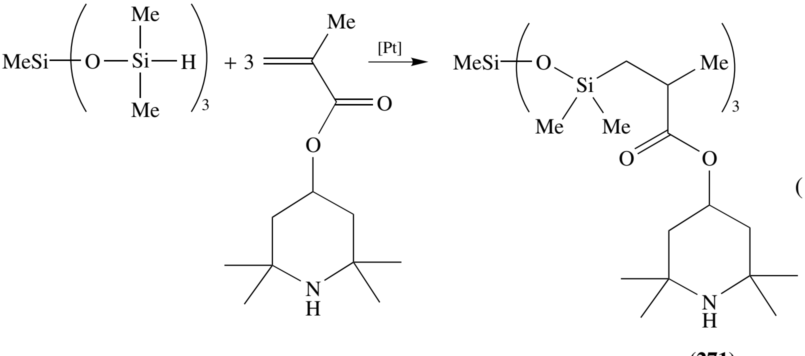

(101)

(271)

The simultaneous hydrosilylation and ring-opening polymerization process provides a powerful method for the construction of a variety of novel polymer networks including comb, block and graft polymers, e.g. **272** (equation 102)[271].

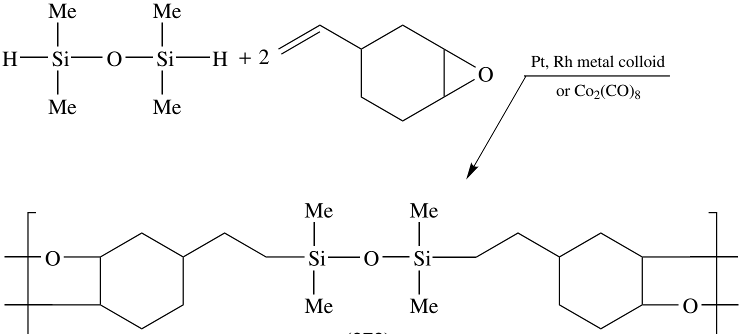

(102)

(272)

Hydrosilylation–polymerization provides a new approach to the syntheses of macromonomers such as poly(arylene-silylethylene) and poly(aralkylene-silylethylene) **(274)** that possess reactive ethenyl and SiH termini for further manipulations through self-polyaddition of **273** promoted by Speier's catalyst (equation 103)[272].

The hydrosilylation–polymerization of 1,3-diethenyltetramethyldisiloxane **(276)** with 1,3-dihydrotetramethyldisiloxane **(275)** proceeds smoothly in the presence of Karstedt's catalyst to give high molecular weight poly[(1,1,3,3-tetramethyldisiloxanyl)ethylene] **(277)** (equation 104)[273,274].

In a similar manner, the hydrosilylation–polymerization of 'diallyl bisphenol A' **(278)** with **275** in the presence of a platinum catalyst affords polymer **279** that possesses a relatively high glass transition temperature for siloxane polymers ($T_g = 28$–$34\,^\circ C$) and good thermal stability (equation 105)[275].

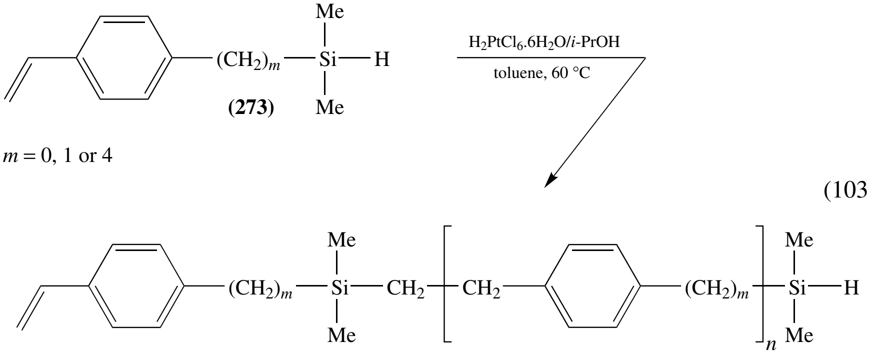

(273)

$m = 0, 1$ or 4

(103)

(274)

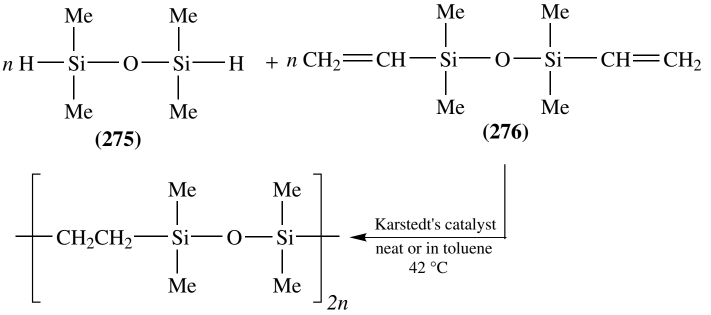

(275) **(276)**

(104)

(277)

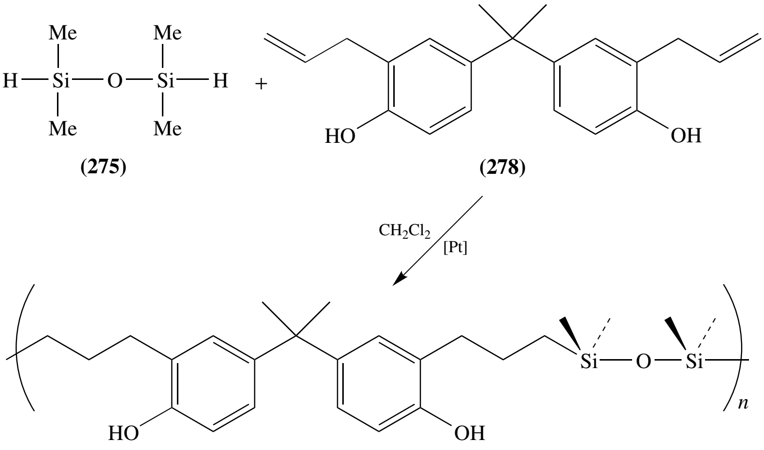

(275) **(278)**

(105)

(279)

Novel thermoset nonlinear optical (NLO) polymers **283** and **284** are synthesized through the hydrosilylation of NLO chromophores such as **281** and **282** and dicyclopentadiene with tetramethylcyclotetrasiloxane **280** (Scheme 30)[276,277]. Typical NLO chromophores **281a** and **282a** are shown below. The resultant NLO materials exhibit excellent nonlinear optical and thermal properties.

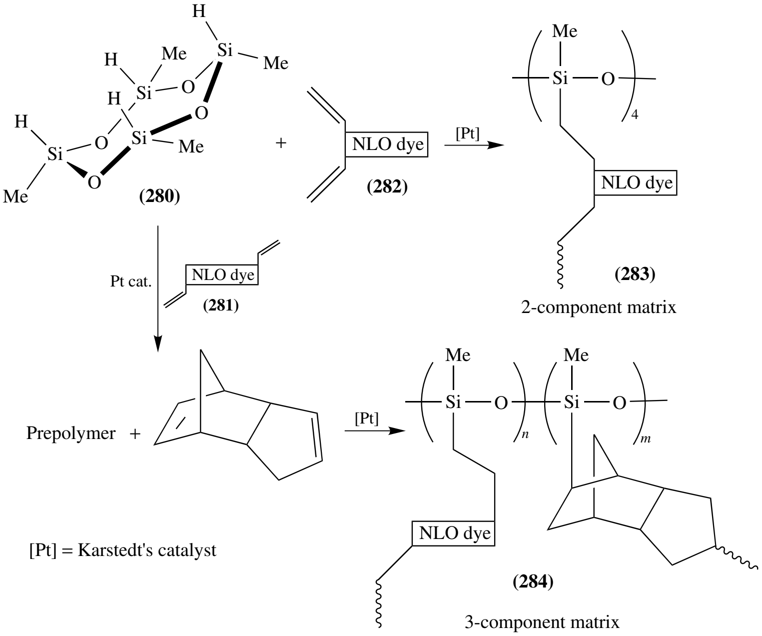

SCHEME 30

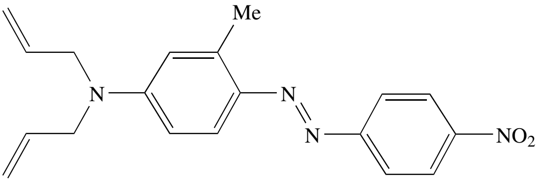

(281a)

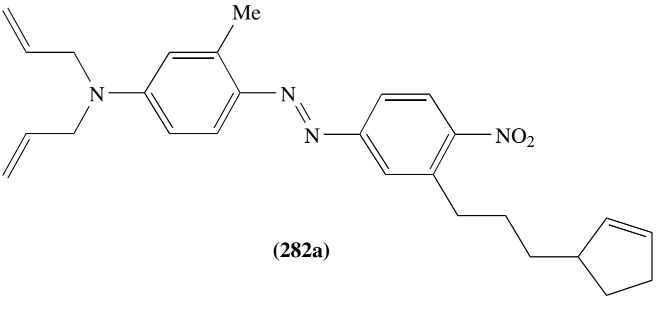

(282a)

Ethynylsilanes **285** undergo self-polymerization via hydrosilylation catalyzed by H_2PtCl_6 in THF to give high molecular weight polymers **286** (equation 106)[278]. The reaction of diethylethynylsilane (**285c**) requires 160 °C to proceed, but yields the highest molecular weight polymer **286c**.

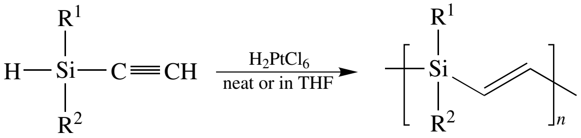

(285) **(286)** (106)

(a) $R^1 = R^2 = Me$; 50°C; $M_w = 85{,}000$ (neat); 30,380 (THF)

(b) $R^1 = Me$, $R^2 = Ph$; 65°C; $M_w = 30{,}000$ (neat), 11,400 (THF)

(c) $R^1 = R^2 = Et$; 160°C; $M_w = 110{,}700$ (neat)

A new functionalized polysiloxane bearing crown ether moieties in the main chain as well as its platinum complex are prepared from 3,19-dihydroxy-1-thia-5,8,11,14,17-pentaoxacycloicosane through ether formation with ω-chloroundecene, followed by hydrosilylation with triethoxysilane, copolymerization with octamethylcyclotetrasiloxane and reaction with potassium chloroplatinate[279].

Polysiloxane-fluoro copolymers with low dielectric constants are prepared through hydrosilylation of 1,3,5-$[CH_2{=}CHCH_2OC(CF_3)_2]_3C_6H_3$ with polymethylhydrosiloxane catalyzed by Cp_2PtCl_2[280].

Hydrosilylation was also applied to the preparation of thiophene-terminated dimethylsiloxane macromonomer, which is used for the synthesis of thiophene–dimethylsiloxane graft copolymers by oxidative polymerization[281]. Polycarbosilanes have been prepared by hydrosilylation–polymerization of 1,4-bis(ethenylmethylphenylsilyl)benzene with 1,4-bis(methylphenylsilyl)benzene in various ratios[282].

A combination of anionic ring-opening of 1-methyl- or 1-phenyl-1-silacyclobutane (**287**) and the Pt-catalyzed graft hydrosilylation of the resulting carbosilane polymer **288** with functionalized alkenes gives poly(1-silacyclobutane) graft polymers (**289**) possessing functionalized alkyl pendant groups on silicon (equation 107)[283]. The same type of functionalized polycarbosilanes **290** can be synthesized in one step through the simultaneous Pt-catalyzed ring-opening polymerization and hydrosilylation of 1-phenyl-1-silacyclobutane (**287**, R = Ph) with functionalized alkenes (equation 108)[284].

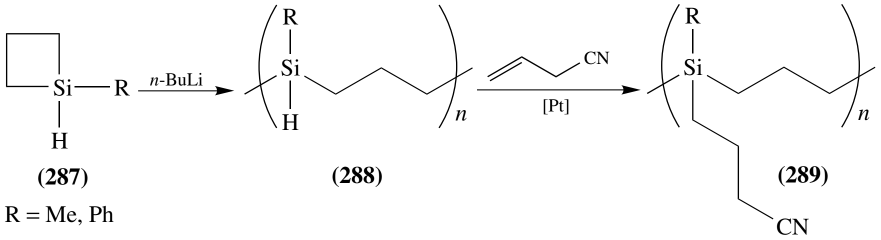

(287) **(288)** **(289)**

R = Me, Ph

(107)

Exclusive polymerization of phenylacetylene takes place, unexpectedly, under hydrosilylation conditions in the presence of a zwitterionic Rh(I) complex, $[Rh(COD)]^+BPh_4^-$, and $HSiEt_3$ to give all-*cis*-poly(phenylacetylene)[285].

A platinum(II) complex-catalyzed hydrosilylation provides a convenient route to polysiloxane macrocycles **291** (equation 109)[286].

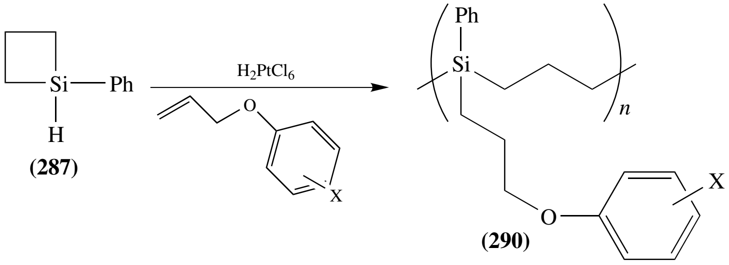

(108)

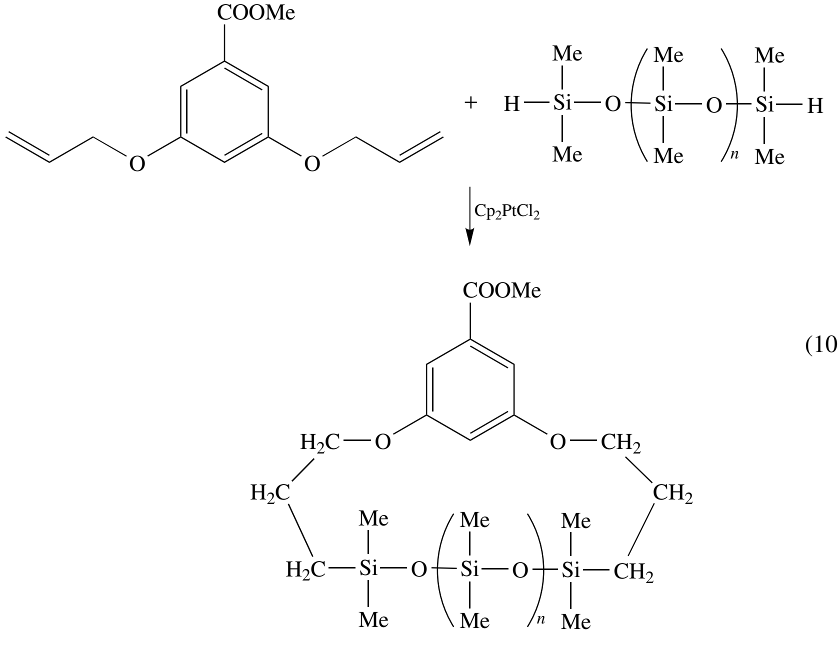

(109)

(291)

C. Modification of Polymers by Hydrosilylation

α, ω-Bifunctional fluorine-containing polysiloxanes **293** are prepared through hydrosilylation of 3,3,4,4,5,5,5-heptafluoro-1-pentene with functionalized polysiloxane **292** bearing Si−H moieties catalyzed by H_2PtCl_6 (equation 110)[287]. This modification increased the glass transition temperature by *ca* 40 °C as compared to the parent polysiloxanes.

Perfluoroalkyl-containing hydrosilanes, $Rf(CH_2)_{n+2}SiMe_2H$, for the syntheses of fluorosilicone-containing polybutadienes, are prepared through the Pt-catalyzed hydrosilylation of $Rf(CH_2)_nCH{=}CH_2$ with $HSiClMe_2$[288]. In a similar manner, (fluoroalkyl)chlorosilanes, $Rf(CH_2)_nSiR^1R^2Cl$ and $R^1R^2ClSi(CH_2)_2(CF_2)_3(CH_2)_2SiR^1R^2Cl$, and tetra(fluoroalkyl)silanes, $[Rf(CH_2)_3]_3Si(CH_2)_nRf$, are prepared via hydrosilylation of

Rf-containing alkene units[289].

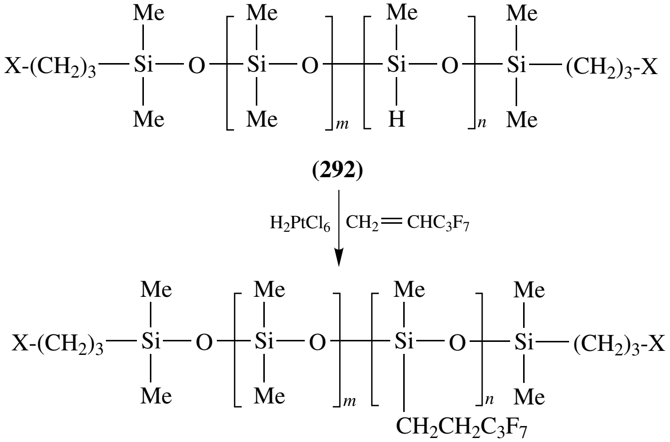

(292)

(293)

(110)

X = CF$_3$ CONH, H$_2$N,
HOCH$_2$, HO$_2$C

Chemical modifications of copoly[methylsilylene(alkylene)/1,4-phenylene] bearing Si−H moieties as well as poly(methylhydrosiloxane) are readily performed through Pt-catalyzed graft hydrosilylation with functionalized allyl ethers, 3-cyano-1-propene, and allyl carbamates in a manner similar to the process shown in equation 107 (*vide supra*)[290,291].

Free radical hydrosilylation of poly(phenylsilanes) **(294)** with alkenes, aldehydes or ketones promoted by 2,2′-azo(bisisobutyronitrile) (AIBN) provides functional polysilanes **(295)** possessing a variety of properties (equation 111)[292].

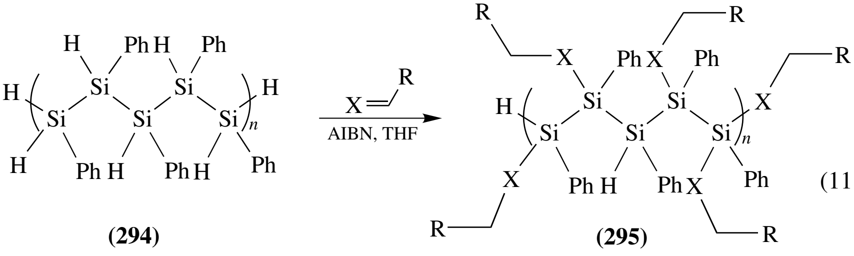

(294)

(295)

(111)

X = CH$_2$, O

RCH$_2$X− = C$_5$H$_{11}$O$_9$, C$_6$H$_{13}$, cyclo-C$_6$H$_{10}$O, MeOCO(CH$_2$)$_3$,
HO(CH$_2$)$_5$, HOCO(CH$_2$)$_4$, Me$_2$N(CH$_2$)$_5$

Platinum-catalyzed hydrosilylation is applicable for the crosslinking of copoly(methylsilylene/1,4-phenylene/methylvinylsilylene), yielding a thermoset material[293].

Regioselective hydrosilylation of poly[(dimethylsilylene)but-1,3-diyne] **(296a)** with HSiEt$_3$ using Rh$_6$(CO)$_{16}$ as the catalyst at 40 °C gives poly[2-(triethylsilyl)(dimethylsilylene)but-1-en-3-yne-1,4-diyl][294]. In a similar manner, the reactions of poly[(silylene) but-1,3-diynes] **(296)** with 1,4-bis(methylphenylsilyl)benzene **(297)** catalyzed by $Rh_6(CO)_{16}$ in benzene or THF yields branched silicon-containing polymers **298** with high molecular weights up to 424,000 in 49–79% yields (Scheme 31)[294,295].

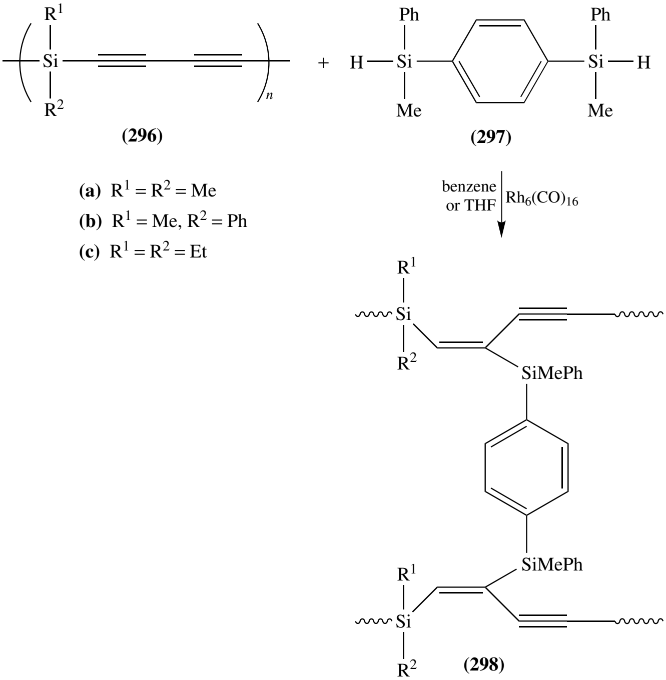

(a) $R^1 = R^2 = Me$

(b) $R^1 = Me, R^2 = Ph$

(c) $R^1 = R^2 = Et$

SCHEME 31

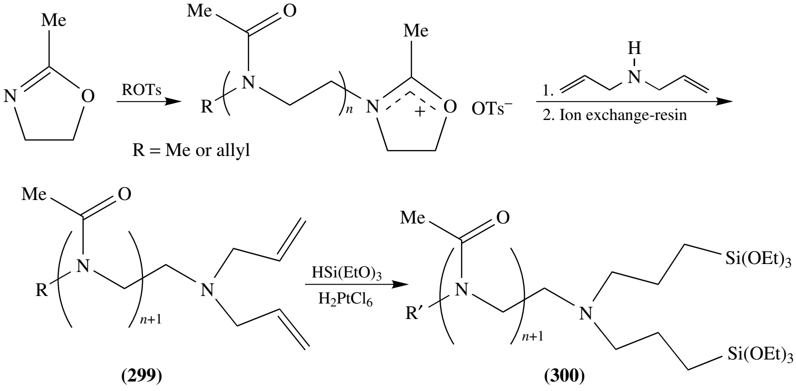

$R' = Me$ or $(EtO)_3Si(CH_2)_3$

SCHEME 32

Triethoxysilyl-terminated polyoxazolines **(300)** are prepared by the hydrosilylation of allyl-terminated polyoxazolines **(299)**, obtained via ring-opening polymerization of 2-methyloxazoline, catalyzed by H_2PtCl_6 (Scheme 32)[296]. Polyoxazolines **300** and related polymers are useful for the syntheses of organic–inorganic polymer hybrid using the 'sol-gel' method.

Hydrosilylations of buckminsterfullerene (C_{60}) with a poly(hydrosiloxane) **(301)** or $H(SiMe_2O)_3SiMe_2H$ in the presence of Karstedt's catalyst (*vide supra*) proceed smoothly at 29 °C to give the corresponding (1 : 1) C_{60}-polysiloxanes **(302)** with molecular weights of 5000 and 4000, respectively (equation 112)[297].

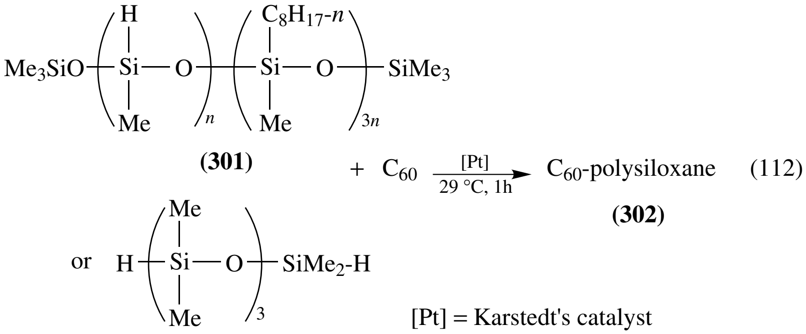

(301)

(302)

(112)

[Pt] = Karstedt's catalyst

Hydrosilylation of polybutadienes bearing olefinic bonds in the backbone or as pendant groups with $HSiMe_xCl_{3-x}$ ($x = 0{-}2$) in the presence of H_2PtCl_6 provides an efficient method for the syntheses of functional polymers[298]. In a similar manner, high molecular weight ($M_W = 10,000{-}543,000$) styrene–butadiene block copolymers can be modified by hydrosilylation with pentamethyldisiloxane, heptamethyltrisiloxane and bis(trimethylsiloxy)methylsilane using Karstedt's catalyst[299]. Silicone acrylates are also synthesized through hydrosilylation of polyacryloyloxy functional monomers with copolymers of dimethyl and hydromethylsiloxanes[300]. Platinum-catalyzed hydrosilylation is also applied to the modification of vinyl-functionalized silica with $HSiMe_2$-terminated silicones, eventually leading to the formation of colloidal polymer-grafted silica[301].

VII. SILYLCARBONYLATION AND SILYLCARBOCYCLIZATION REACTIONS

A. Silylcarbonylation Reactions

The silylcarbonylation of alkenes catalyzed by $Co_2(CO)_8$ giving homologous silyl enol ethers was reported by Murai and coworkers in 1977 as a silicon version of hydroformylation of alkenes, and developed as a unique synthetic method[302–304]. Although other catalysts such as $RhCl(PPh_3)_3$, $Ru_3(CO)_{12}$ and $[HRu_3(CO)_{11}]^-$ [305] can also effect the reaction, $Co_2(CO)_8$ and its PPh_3 or $P(Bu\text{-}n)_3$ complex are the best catalysts[306]. The cobalt-catalyzed silylcarbonylation of alkenes exhibits strikingly similar features to those of hydroformylations in terms of the effects of CO pressure, phosphine ligands, reactant ratios and reaction temperature on the reaction rate and product distribution[307]. The $Co_2(CO)_8$-catalyzed reactions of oxygen-containing substrates with $HSiR_3$–CO combination have also been found to provide unique and useful organic transformations, e.g. (i) silylformylations of cyclic ethers and aldehydes, (ii) 1,2-siloxyvinylation of THF, (iii) siloxymethylations of aldehydes, esters, cyclobutanones, THF, cyclic ethers[308], glycosyl acetates[309], benzylic esters, cyclic orthoesters[310], acetals and aromatic aldehydes.

The earlier development of these reactions were covered by a couple of reviews[3,306,311]. Recent developments include Rh, Ir and Ru complex catalysts in place of $Co_2(CO)_8$.

Iridium carbonyl complexes, $[Ir(CO)_3Cl]_n$ and $Ir_4(CO)_{12}$, are found to be effective catalysts for the regioselective silylcarbonylation of ethene, norbornene and 1-alkenes with and without functional groups using $HSiEt_2Me$ as the hydrosilane, affording the corresponding silyl ethers of acylsilanes **(303)** as an E/Z mixture in moderate to high yields (equation 113)[312]. Many functional groups such as acetal, ether, nitrile and epoxide are tolerated in this reaction, which makes a sharp contrast to the $Co_2(CO)_8$-catalyzed reactions. Acid hydrolysis of **303** readily provide acylsilanes in quantitative yields (equation 113)[312]. Although the mechanism of this reaction is not fully understood, it is clear that the process does not include an acylsilane as the intermediate based on a control experiment, and thus the intermediacy of a siloxycarbyne complex ($Ir{\equiv}C{-}OSiR_3$) is suggested[312].

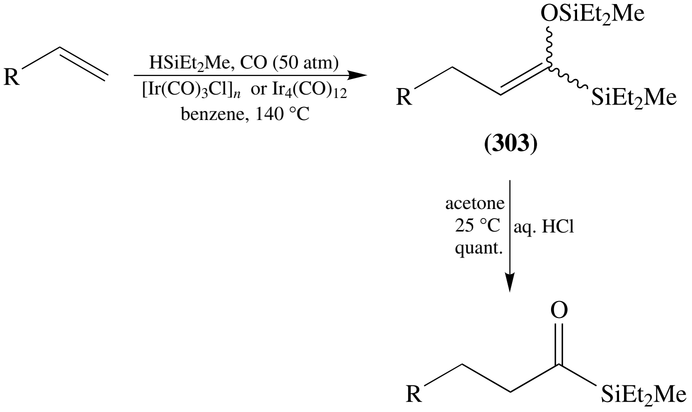

(303)

(304)

(113)

R = H, *n*-Bu, *t*-Bu, cyclohexyl, Ph, *n*-BuO, Me_3Si, *n*-$BuOCH_2$, Me_3SiCH_2, Me_3SiOCH_2, $(EtO)_2CH$, $NCCH_2$, glycidylmethyl

Regioselective silylcarbonylation of enamines **(305)** with $HSiEt_2Me$ is promoted by $[Rh(CO)_2Cl]_2$, giving α-(siloxymethylene)amines **(306)** as a E/Z mixture (E/Z = 51/49–84/16) in modest to high yields, which are readily hydrolyzed to afford α-siloxyketones **(307)** (equation 114)[313]. Enamines of morpholine give much better results than those of diethylamine or benzyl(methyl)amine in this reaction.

Although the $Co_2(CO)_8$-catalyzed ring-opening silylformylation of epoxides gives β-siloxyaldehydes, the products tend to undergo further reactions such as formylation, hydrosilylation and dehydrogenative silylation under the reaction conditions (140 °C and 50 atm of CO)[306,314]. In order to suppress such secondary reactions, the use of excess epoxide as compared to a hydrosilane is necessary, which is an apparent shortcoming of the process. The use of $[RhCl(CO)_2]_2$ and 1-methylpyrazole in place of $Co_2(CO)_8$ is found to circumvent this problem[315,316]. Thus, the reactions of a variety of epoxides with $HSiMe_2Ph$ catalyzed by $[Rh(CO)_2Cl]_2$ in the presence of 1-methylpyrazole (0.4 equivalents to the epoxide) at 50 °C and 50 atm of CO give β-siloxyaldehydes in good yields (equations 115–117)[315]. The reaction is stereospecific, yielding *anti*- and *syn*-products from *cis*- and *trans*-2-butene oxides, respectively (equations 116 and 117).

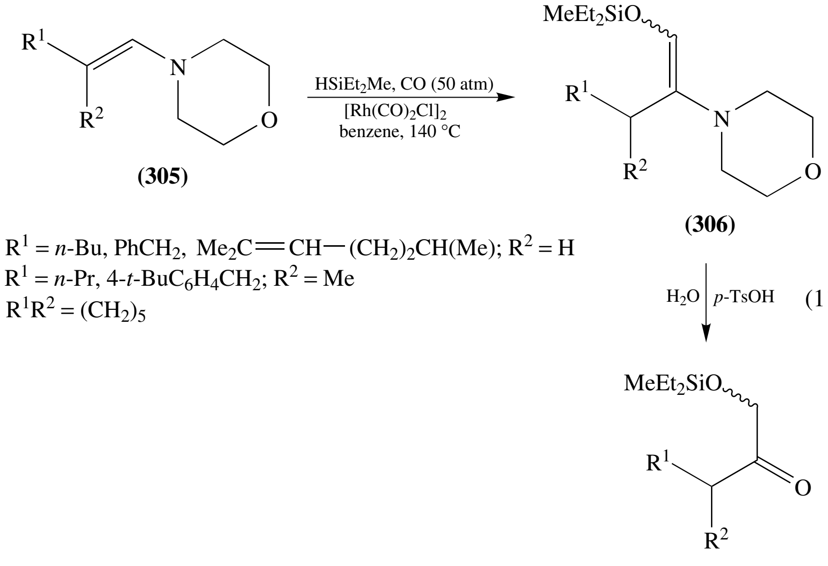

(305)

(306)

(307)

$R^1 = n$-Bu, $PhCH_2$, $Me_2C{=}CH{-}(CH_2)_2CH(Me)$; $R^2 = H$
$R^1 = n$-Pr, 4-t-$BuC_6H_4CH_2$; $R^2 = Me$
$R^1R^2 = (CH_2)_5$

(114)

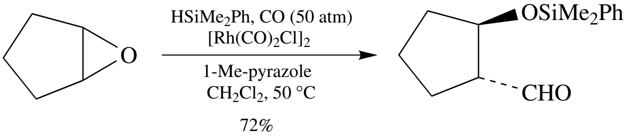

(115)

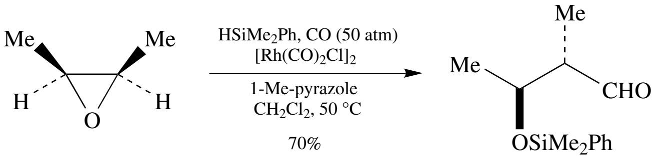

(116)

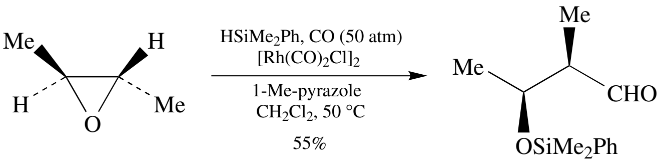

(117)

The Rh-catalyzed reactions of *N*,*N*-aminals with $HSiEt_2Me$ and CO (50 atm) at 140 °C in benzene give unique siloxymethylation or ring-expansion products, e.g. **308–310** (equations 118–120)[317]. Incorporation of two CO molecules and rearrangement of the dimethylamino group take place in the reaction of *N*, *N*, *N*′, *N*′-tetramethylmethylenediamine (equation 119)[317].

The reaction of *N*,*O*-acetal **311** in the presence of NEt_3 under the same conditions gives ring-opening siloxymethylation product **312** arising from exclusive C−O cleavage (equation 121)[317]. No reaction takes place with *O*, *O*-acetals under these conditions[317].

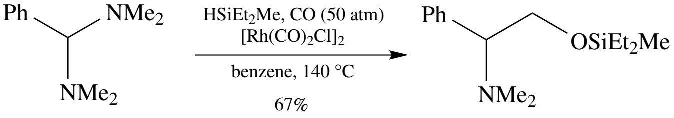

(308)

(118)

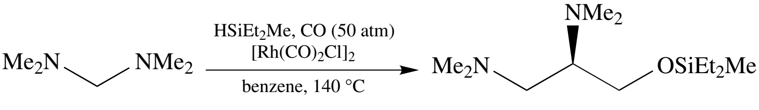

(309)

(119)

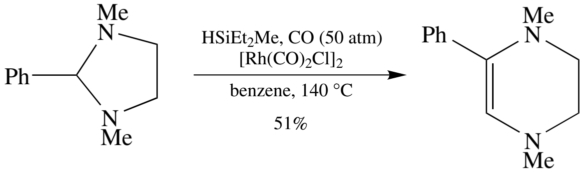

(310)

(120)

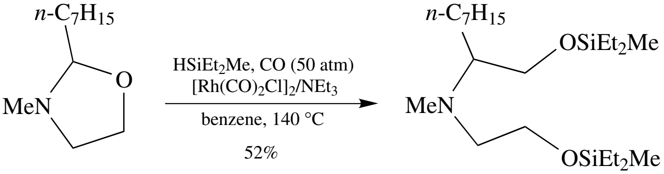

(311) **(312)**

(121)

Although the silylformylation of alkanals is effected by $Co_2(CO)_8-PPh_3$ catalyst at 100 °C and 50 atm of CO, $[Rh(COD)Cl]_2$ and $[Rh(CO)_2Cl]_2$ are found to catalyze the reaction using $HSiMe_2Ph$ as the hydrosilane under much milder conditions, i.e. at room temperature and 17 atm of CO, to give homologous α-siloxyalkanals **(313)** in 50–90% yields (equation 122)[318,319]. When 1-phenylpropanal is used as a substrate, *syn*-aldehyde **314** is formed as the predominant product (equation 123)[319]. A double silylformylation of benzaldehyde takes place to yield *syn*-2,3-disiloxy-3-phenylpropanal **(315)** when excess hydrosilane is used (equation 124)[319]. The attempted silylformylation of ketones results in the formation of silyl enol ethers, and no reaction takes place with imines[319].

Silylformylation of 1-alkynes giving (*Z*)-2-formyl-1-silyl-1-alkenes **(316)** was discovered independently by Matsuda and coworkers[320] and Ojima and coworkers[321–323] using $Rh_4(CO)_{12}/NEt_3$ and $Rh_2Co_2(CO)_{12}$, respectively, as the catalysts, and first reported by Matsuda in 1989[320] (equation 125). The reactions of 1-alkynes, internal alkynes and functionalized alkynes with $HSiMe_2Ph$ are effected by $Rh_4(CO)_{12}$ in the presence of NEt_3 at 100 °C and 10–30 atm of CO in benzene[320]. The reaction is extremely regioselective for 1-alkynes, but a mixture of regioisomers is formed for internal alkynes, and the stereoselectivity is highly dependent on the structure of alkyne ($Z/E = 0/100-100/0$). Functional groups such as hydroxyl, olefin, trimethylsilyl and ester are tolerated in this reaction. The reactions of alkynoates, $PhC{\equiv}CCO_2Me$ and $MeC{\equiv}CCO_2Me$, give (*Z*)-3-formyl-2-silyl-2-propenoates exclusively (equation 126).

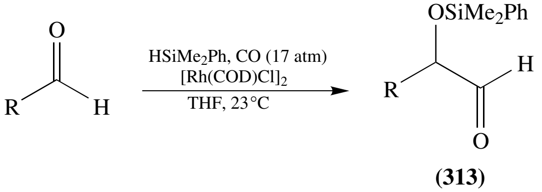

(122)

R = Ph, 4-BrC_6H_4, 4-$Me_2NC_6H_4$, 4-$Me_3SiOC_6H_4$,
4-$Me_3SiC{\equiv}CC_6H_4$, 4-$AcOC_6H_4$, $PhCH_2$, ferrocenyl, 2-furyl, 2-thienyl,
1-methylpyrrol-2-yl, *n*-Pr, *i*-Pr,$Me_2C{=}CH(CH_2)_2CH(Me)$

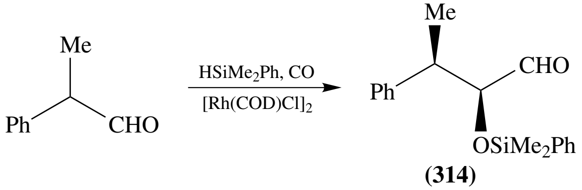

(123)

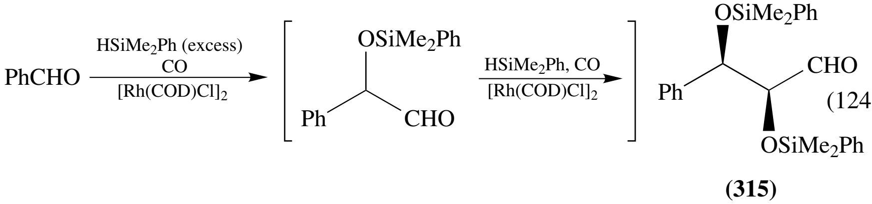

(124)

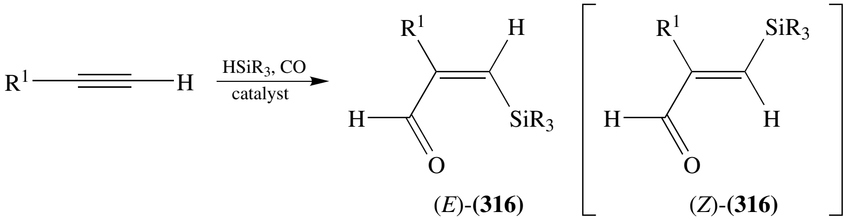

(125)

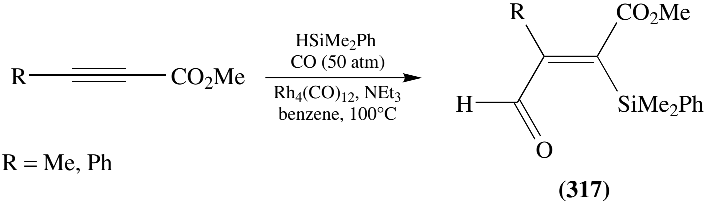

(126)

The reactions of 1-alkynes with $HSiMe_2Ph$ catalyzed by $Rh_2Co_2(CO)_{12}$ proceed at 25 °C and ambient pressure of CO in toluene, yielding (*Z*)-2-formyl-1-silyl-1-alkenes

(316) with complete regio- and stereoselectivity[107,323,324]. When $HSiMe_2Et$, $HSiEt_3$ and $HSi(OMe)_3$ are used, substantial amounts of hydrosilylation products are formed. The hydrosilylation can be effectively suppressed by increasing the CO pressure to 10 atm[323,324]. Phenyl-containing hydrosilanes, $HSiMe_2Ph$, $HSiMePh_2$ and $HSiPh_3$, are all very reactive and selective for this reaction[324]. In spite of the increasing bulkiness, $HSiMePh_2$ and $HSiPh_3$ give the silylformylation products with 1-hexyne in 97% and 98% isolated yields, respectively, in the reactions at 25 °C and ambient pressure of CO (equation 125)[324]. The activities of different catalysts (0.2 mol% per Rh metal) in the reaction of 1-hexyne with $HSiMe_2Ph$ at ambient temperature and pressure are found to be in the order[324]: $Rh(CN\text{-}Bu\text{-}t)_4Co(CO)_4$ (99%) > $Rh(acac)(CO)_2$ (97%) > $Rh_2Co_2(CO)_{12}$ (92.5%) > $Rh_4(CO)_{12}$ (90%) $\gg$ $RhCl(PPh_3)_3$ (0%)–$Co_2(CO)_8$ (0%), i.e. $RhCl(PPh_3)_3$ and $Co_2(CO)_8$ are inactive. Besides the functional groups listed above, allylic ether and nitrile functionalities are found to be tolerated[324]. Possible mechanisms of silylformylation catalyzed by $Rh_2Co_2(CO)_{12}$ were proposed, which unveiled the presence of $(R_3Si)_2Rh(CO)_nCo(CO)_4$ ($n = 2$ or 3) and $RhCo(n\text{-}BuC{\equiv}CH)(CO)_5$ as key active catalyst species for the reaction, invoking the occurrence of unique homogeneous bimetallic catalysis[107,323].

In addition to these Rh and Rh–Co mixed metal complexes, $Rh_2(pfb)_4$ (pfb = perfluorobutanoate) is found to be a highly active catalyst, i.e. the reactions proceed smoothly at 0 °C and ambient pressure of CO in CH_2Cl_2 with complete regioselectivity and high stereoselectivity ($Z/E = 10/1{-}40/1$) (equation 125)[325,326]. When electron-deficient alkynes, $HC{\equiv}CCOMe$ and $HC{\equiv}CCO_2Me$, are used for the $Rh_2(pfb)_4$-catalyzed reaction with $HSiEt_3$ under ambient CO, cyclotrimerization of these alkynes takes place exclusively yielding substituted benzenes. The alkyne cyclotrimerization can be circumvented by using 10 atm of CO, but the yields of the silylformylation products for these alkynes are only 20–24% and almost 1 : 1 mixtures of *E*- and *Z*-isomers **318** are formed (equation 127)[326].

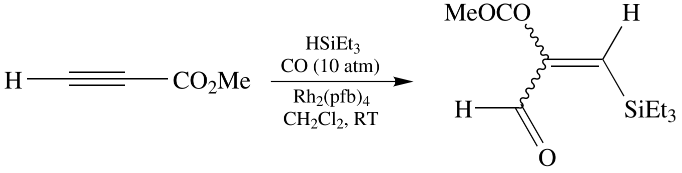

(127)

(318)

Zwitterionic rhodium(I) complex, $Rh^+(COD)(\eta^6\text{-}C_6H_5BPh_3)^-$, is also found to be an efficient catalyst for the silylformylation of 1-alkynes at 40 °C and 40 atm of CO in CH_2Cl_2 (equation 125) although no reaction occurs with internal alkynes[327]. However, 'silylhydroformylation' takes place when the reaction is carried out under hydroformylation conditions, i.e. in the presence of CO and H_2 ($CO/H_2 = 1/1$), to give (*E*)-2-silylmethyl-2-alkenals **(319)** in 54–92% isolated yields (equation 128). The intermediacy of π-allenyl–Rh species is proposed to account for the formation of **319**[327]. When 4-acetoxy-1-butyne and 4-(*p*-tosyloxy)-1-butyne are used as the substrates, saturated silylhydroformylation products are obtained[327].

Although the silylformylation of aldehydes is catalyzed by $[Rh(COD)Cl]_2$ or $[Rh(CO)_2Cl]_2$, no secondary silylformylation of β-silylenals **(316–318)** takes place, probably due to the electronic nature of the aldehyde functionality conjugated to olefin moiety (*vide supra*). Direct comparison of the reactivity of acetylene and aldehyde functionalities is performed using alkynals[328]. The reactions of 5-hexyn-1-al, 6-heptyn-1-al and 7-octyn-1-al with different hydrosilanes catalyzed by Rh or Rh–Co complexes at

25 °C and 10 atm of CO give the corresponding (*Z*)-2-(silylmethylene)-1,ω-dialdehydes **(320)** exclusively in good to excellent isolated yields (equation 129), i.e. the reaction takes place at the acetylene moiety with complete chemoselectivity[328]. In the case of 5-hexyn-1-al, the reaction using Rh(CN-Bu-*t*)$_4$Co(CO)$_4$ or $Rh_2Co_2(CO)_{12}$ under ambient pressure of CO yields a unique silylcarbocyclization product (*vide infra*).

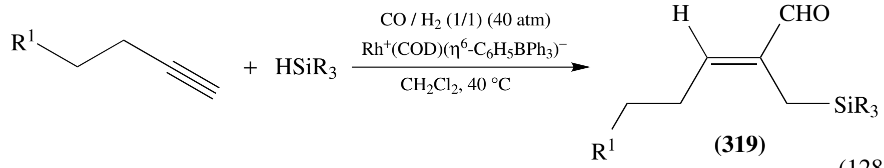

(319)

(128)

R^1 = Et, Ph, $ClCH_2$
R = $PhMe_2Si$, Et_3Si, Ph_3Si

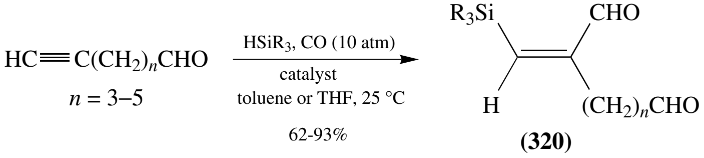

(320)

(129)

R_3Si = $PhMe_2Si$, Ph_2MeSi, Ph_3Si, Et_3Si, *t*-$BuMe_2Si$

Catalyst = Rh(acac)$(CO)_2$, Rh(CN-Bu-*t*)$_4$Co(CO)$_4$, $Rh_2Co_2(CO)_{12}$,
$Rh_4(CO)_{12}$, $[Rh(NBD)_2]BF_4$, $[Rh(NBD)Cl]_2$, $[Rh(COD)Cl]_2$

The reactions of α-substituted or α,α-disubstituted propargyl alcohols and propargylamines under silylformylation conditions using $Rh_4(CO)_{12}$ and NEt_3 or DBU afford the corresponding α-silylmethylene-β-lactones **(321)**[329] and α-silylmethylene-β-lactams **(322)**[330], respectively, in high yields (equation 130). In the absence of base, the reaction tends to give a normal silylformylation product. The use of bulky hydrosilane such as $HSiMe_2Bu$-*t* favors the cyclization process[329].

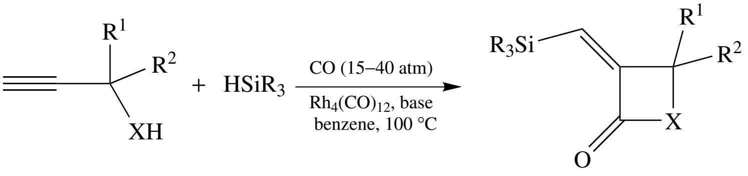

(130)

(321) X = O
(322) X = *N*-*p*-tosyl

R_3Si = $PhMe_2Si$, *t*-$BuMe_2Si$

R^1 = H, Me, *i*-Bu; R^2 = H, Me; $R^1R^2 = -(CH_2)_n-$ ($n = 4$–6)

In a similar manner, the reaction of 1-propargyltetrahydroisoquinoline **(323)** and (*R*)-2-(3-butynyl)pyrrolidine **(325)** with $HSiMe_2Ph$ yields (*E*)-8-silylmethylene-4,5-benzo-9-indolizidinone **(324)** and (*R*)-3-(silylmethylene)-2-indolizidinone **(326)** in 65% and 43%

isolated yields, respectively (equations 131 and 132)[331].

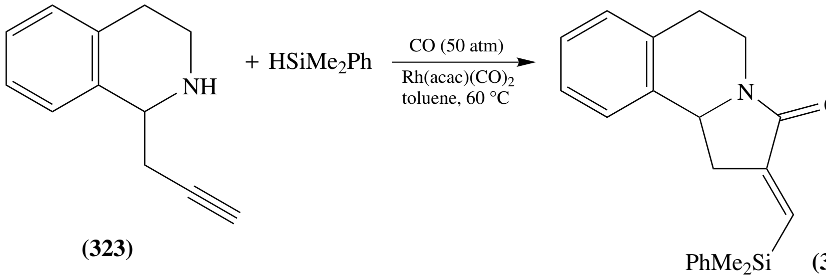

(323) **(324)** (131)

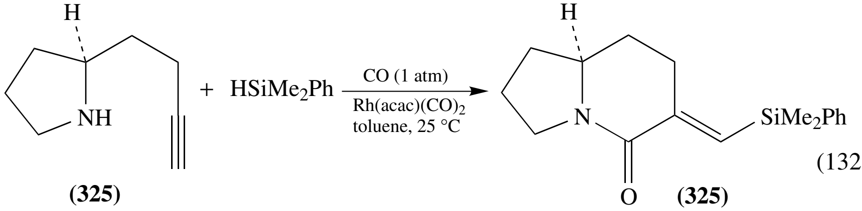

(325) **(325)** (132)

The reactions of N-alkyl and N,N-dialkylpropargylamines with 2 equivalents of $HSiMe_2Ph$ catalyzed by $Rh_4(CO)_{12}$ give 2-silylmethyl-2-enals **(327)** in 40–94% yields via formal silylformylation of allenes generated *in situ* (equation 133)[332].

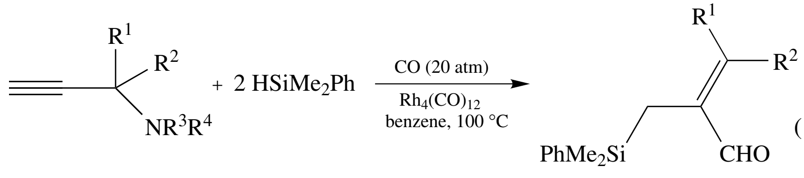

(133)

R^1, R^2 = H, Me; R^3, R^4 = Me, CH_2Ph

(327)
+
$[Me_2PhSiNR^3R^4]$

Although the regioselectivity for the silylformylation of 1-alkynes is excellent, that of internal alkynes is low except for 2-alkynoates (*vide supra*). Also, in the reactions of 1-alkynes, the silyl group is always delivered to the terminal position and the formyl to the C-2 position, thus it is impossible to synthesize 3-silyl-2-alkenals, which requires opposite regioselectivity. Intramolecular directed reactions can circumvent these limitations and expand the scope of the silylformylation of alkynes.

The reactions of ω-hydrosilylalkynes **(328)** catalyzed by $Rh_4(CO)_{12}/NEt_3$ or $Rh^+(COD)(\eta^6\text{-}C_6H_5BPh_3)^-$ give 2-(1-formyl-1-alkylene)-1-silacycloalkanes **(329)** through 5- or 6-*exo*-trig cyclization in moderate to high yields (equation 134)[333].

In a similar manner, the reactions of ω-hydrodimethylsiloxyalkynes **(330)** catalyzed by Rh or Rh−Co complexes at 60–70 °C and 10 atm of CO afforded 5- or 6-*exo* cyclization products **(331)** (equation 135)[334]. When Rh(CN-Bu-*i*)$_4$Co(CO)$_4$ is used as the catalyst, **331** is formed in 89–99% yield. This reaction is applicable to cyclic systems **332**, giving

333 in quantitative yields (equation 136)[334].

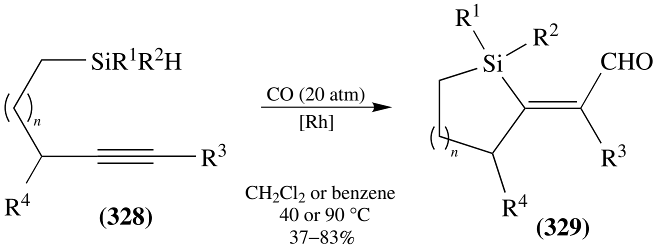

(134)

$n = 1,2$

R^1 = Me, Ph; R^2 = Me, Ph; R^3 = H, Et, *n*-Bu, Ph; R^4 = H or Me

[Rh] = $Rh^+(COD)(\eta^6\text{-}C_6H_5BPh_3)^-$ or $Rh_4(CO)_{12}$, Et_3N

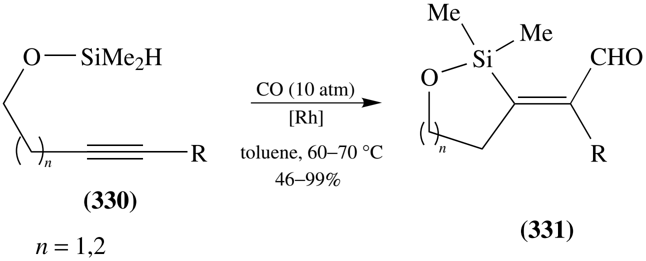

(135)

$n = 1,2$

R = H, Et, *n*-Bu

[Rh] = (*t*-BuNC)$_4$RhCo(CO)$_4$, $Rh_2Co_2(CO)_{12}$, $Rh(acac)(CO)_2$, $Rh_4(CO)_{12}$-Et_3N

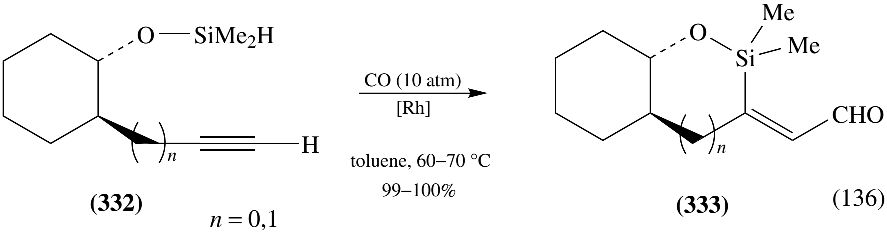

(136)

[Rh] = (*t*-Bu-NC)$_4$RhCo(CO)$_4$, $Rh_2Co_2(CO)_{12}$, $Rh(acac)(CO)_2$

Silylformylation is successfully applied to the syntheses of pyrrolizidine alkaloids, (±)-isoretronecanol and (±)-trachelanthamidine, from 5-ethynyl-2-pyrrolidinone **(334)** via *β*-silylenal **335** in combination with amidocarbonylation (Scheme 33)[324,335].

B. Silylcarbocyclization and Related Reactions

In contrast to the reactions catalyzed by Group VIII transition metal complexes (see Section II.A.1), the hydrosilylation of 1,5- or 1,6-dienes with H_3SiPh catalyzed by $Cp_2{}^*NdCH(SiMe_3)_2$ results in the formation of (silylmethyl)cyclopentanes **(336)** via 5-*exo* carbocyclization (equation 137)[46].

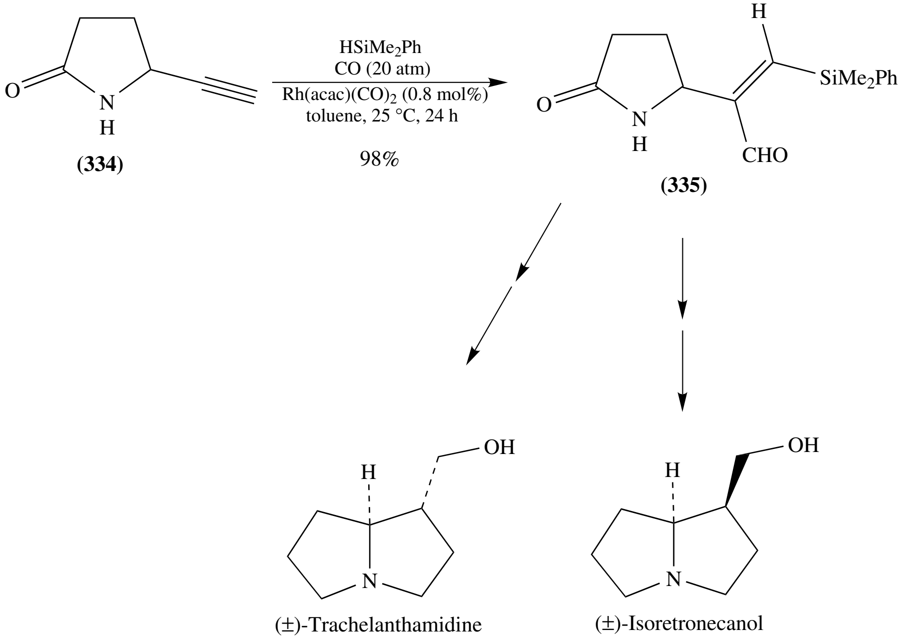

SCHEME 33

Reactions of 1,6-enynes **337** and **340** with $HSiMe_2Ph$ catalyzed by Rh or Rh−Co complexes such as $Rh(acac)(CO)_2$, $Rh_4(CO)_{12}$, $Rh_2Co_2(CO)_{12}$ or Rh(CN-Bu-*t*)$_4$Co(CO)$_4$ give 5-*exo*-trig silylcarbocyclization (SiCaC) to 3-*exo*-silylmethylene-4-methyltetrahydrofuran **(338)** and its pyrrolidine counterpart **(341)**, respectively, in high yields (equations 138 and 139)[336]. The reaction of **337** under CO atmosphere also gives **338** accompanied by a small amount of CO−SiCaC product **339** (9%) (equation 138). The reaction of **340** requires ambient CO atmosphere, i.e. no reaction takes place under N_2[336].

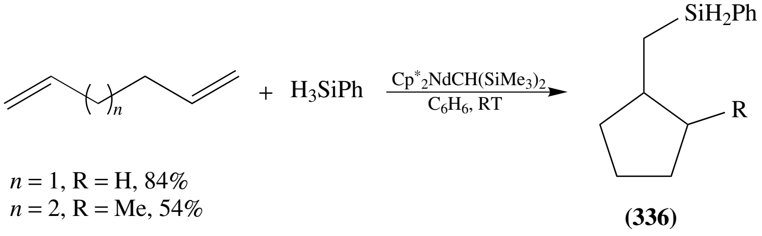

n = 1, R = H, 84%
n = 2, R = Me, 54%

(137)

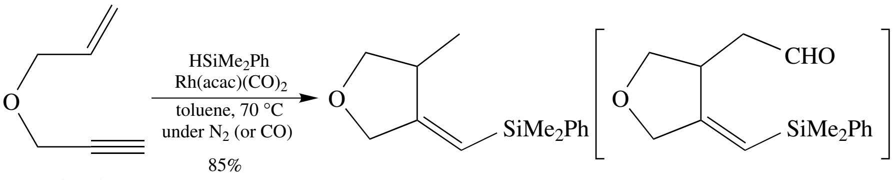

(138)

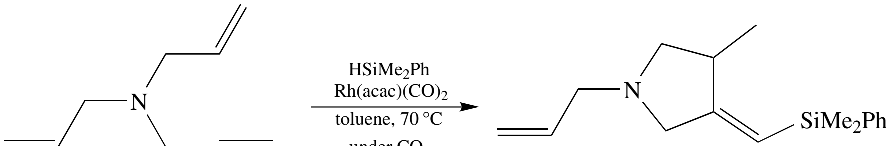

(139)

(340) **(341)**

In the reaction of 1,6-enyne **342**, either SiCaC product **343** (98% yield) or CO−SiCaC product **344** (84% yield) can be obtained selectively just by changing reaction conditions, including the addition of $P(OPh)_3$ to the catalyst (Scheme 34)[337]. The SiCaC reaction also takes place with 5-hexyn-1-al **(345)** using $HSiEt_3$ under ambient CO atmosphere to give *exo*-(silylmethylene)cyclopentanol **(346)** in high yield (equation 140) through extremely chemoselective silylmetallation of the acetylene moiety[328].

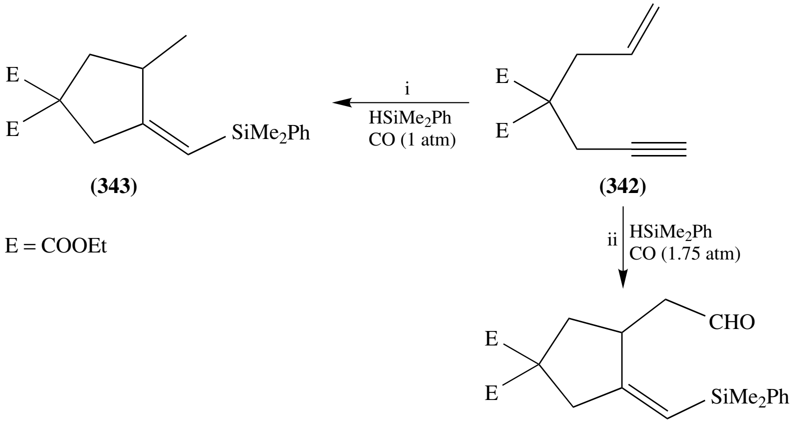

(343) **(342)** **(344)**

E = COOEt

(i) $Rh(acac)(CO)_2$, 80°C, 0.5 M **342** in hexane: **343/344** = 10/1, 98%.
(ii) $Rh(acac)(CO)_2$, 50°C, 0.2 M **342** in toluene: **343/344** = 0/100, 84%.

SCHEME 34

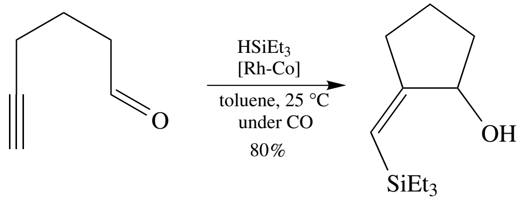

(140)

(345) **(346)**

$[Rh\text{-}Co] = Rh_2Co_2(CO)_{12}$ or $Rh(CN\text{-}Bu\text{-}t)_4Co(CO)_4$

Possible mechanisms of these SiCaC reactions have been proposed, which include β-silylethenyl−metal species (metal = Rh_n or Rh−Co) as a key intermediate, which is trapped by an alkene or an aldehyde moiety[336,337]. The CO−SiCaC reaction further includes CO insertion after the carbocyclization[336,337].

Reactions of 1,6-diynes with $HSiMe_2Bu$-*t* catalyzed by $Rh_2Co_2(CO)_{12}$[338], $Rh(acac)(CO)_2$[338] or $Rh_4(CO)_{12}$[339] give 2-silylbicyclo[3.3.0]octen-3-ones through silylcarbo*bi*cyclization including the trapping of *β*-silylethenyl-metal species mentioned above with another acetylene moiety (first carbocyclization) followed by CO insertion and the second carbocyclization.

The reaction of diethyl dipropargylmalonate **(347)**, with $HSiMe_2Bu$-*t* catalyzed by $Rh_2Co_2(CO)_{12}$ or $Rh(acac)(CO)_2$ at 50 °C and 15−50 atm of CO affords 2-silylbicyclo[3.3.0]oct-$\Delta^{1,5}$-en-3-one **(348)** in excellent yield, which is readily isomerized to bicyclo[3.3.0]oct-1-en-3-one **(349)** (equation 141). The reactions of other 1,6-diynes including benzyldipropargylamine proceed in the same manner, but a mixture of **348**-type and **349**-type products is formed in some cases[338].

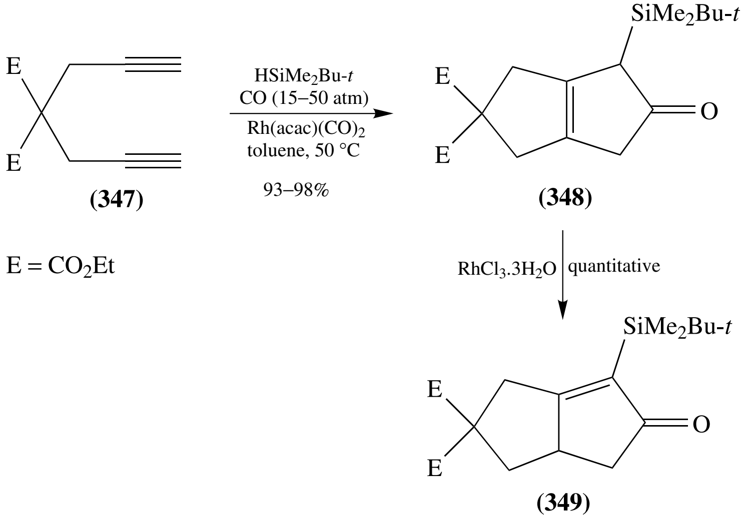

(141)

The $Rh_4(CO)_{12}$-catalyzed reactions of 1,6-diynes at 95 °C and 20 atm of CO in benzene or acetonitrile are less selective than those catalyzed by $Rh_2Co_2(CO)_{12}$ or $Rh(acac)(CO)_2$, and a different type of silylcarbobicyclization product, azabicyclo[3.3.0]octadienone **(351)**, is formed in addition to **349**-type product **(352)** when benzyldipropargylamines **(350)** are used (equation 142)[339]. The formation of a small amount (5%) of the bicyclic pyrrole of **351**-type with *N*-tosyl group is also observed besides **348**-type (18%) and **349**-type (51%) products in the reaction of *N*-tosyldipropargylamine[339].

Another type of bicyclo[3.3.0]octadienone formation is observed in the reactions of 4,4-*gem*-disubstituted 1,6-heptadiynes **(353)** with $HSiMe_2Bu$-*t* catalyzed by $Rh(acac)(CO)_2$ or $Rh_2Co_2(CO)_{12}$ under forced conditions, i.e. at 120 °C and 50 atm of CO, affording 7,7-disubstituted bicyclo[3.3.0]octa-1,5-dien-3-ones **(354)** in 71−95% isolated yields (equation 143)[340,341].

Cascade silylcarbocyclization of (*E*)- or (*Z*)-dodec-6-ene-1,11-diyne **(355)** with $HSiMe_2Ph$ catalyzed by $Rh(acac)(CO)_2$ gives the bis(*exo*-methylenecyclopentyl) **(356)** with complete stereospecificity (equation 144)[342]. The reaction of dodec-1,6,11-triyne **(357)** under the same conditions affords a 3 : 1 mixture of **358** and **359** in 75% yield (equation 145)[343,344].

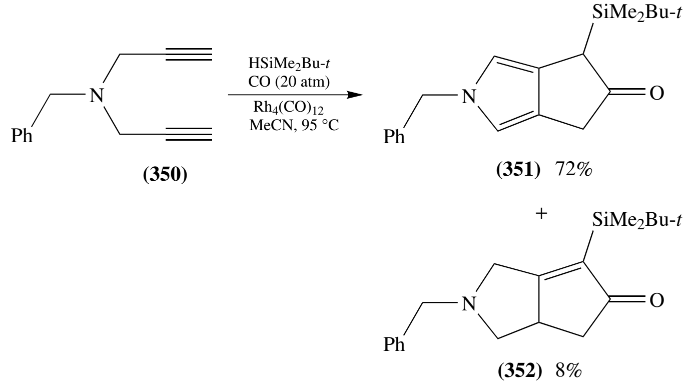

(350) **(351)** 72% **(352)** 8%

(142)

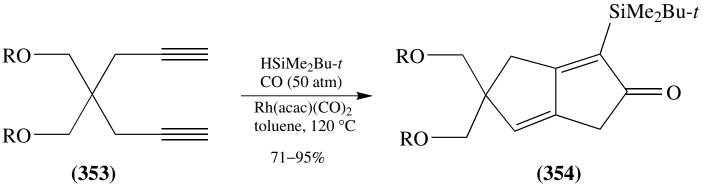

(353) **(354)**

(143)

R = H, *t*-$BuMe_2Si$, (i-$Pr)_3Si$, Ac

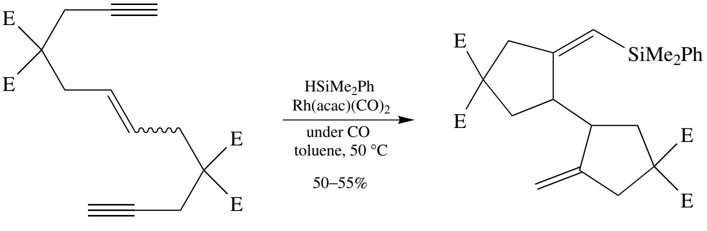

(355) **(356)**

(144)

E = CO_2Et

Formal silylcarbocyclization of 1,7-diynes such as **360** and **362** catalyzed by $Ni(acac)_2$/DIBAL (DIBAL = i-Bu_2AlH) gives the corresponding vicinal *exo*-dimethylenecyclohexanes (equations 146 and 147)[345].

Novel carbonylative carbocyclizations of 1,6-diynes promoted by $Ru_3(CO)_{12}$/P(hex-*c*)$_3$ in the presence of $HSiMe_2Bu$-*t* give bicyclic *o*-catechol derivatives by incorporating two carbon monoxide molecules as the 1,2-dioxyethenyl moiety (equations 148 and 149)[346]. This reaction is tolerant of functional groups such as ester, ketone, ether and amide. The disilylated product **366** is formed through dehydrogenative silylation of the initially formed mono-silyl product **365** under the reaction conditions.

The proposed catalytic cycle for this unique process includes (i) oxidative addition of a hydrosilane to [Ru−CO] species to form (R_3Si)(H)Ru complex **369**, (ii) silyl migration to generate siloxycarbyne−Ru species **370**, (iii) carbyne reaction with CO to form metallacyclopropanone **371**, (iv) hydride shift to generate oxyacetylene−Ru complex **372** and

(v) carbocyclization to form *o*-catechol derivative **373** and regenerate active [Ru−CO] species (Scheme 35)[346].

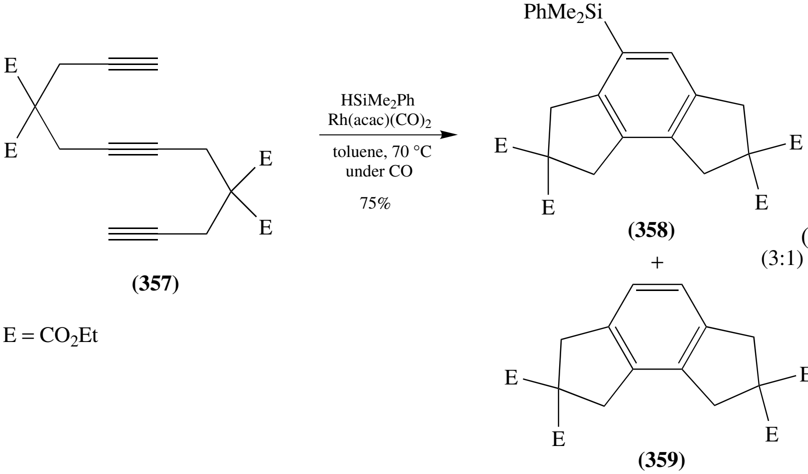

(145)

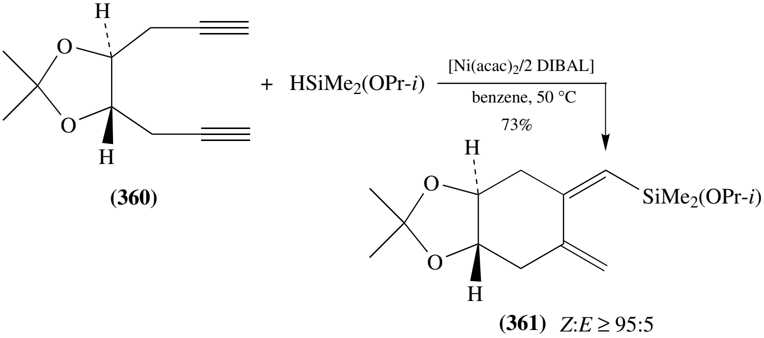

(146)

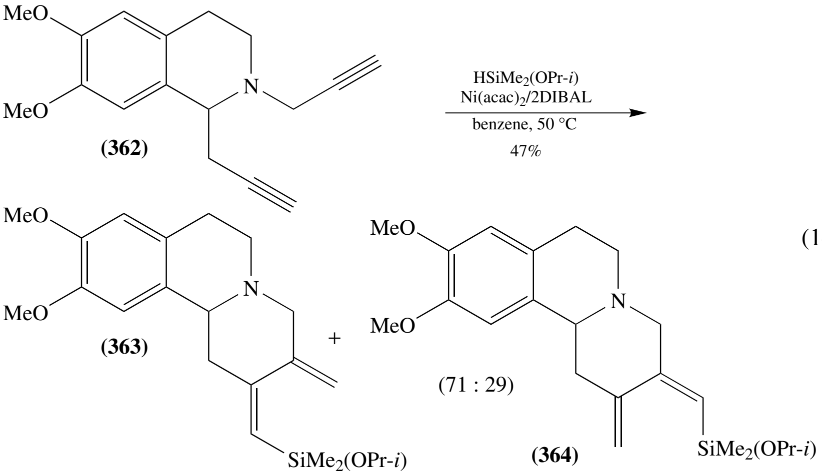

(147)

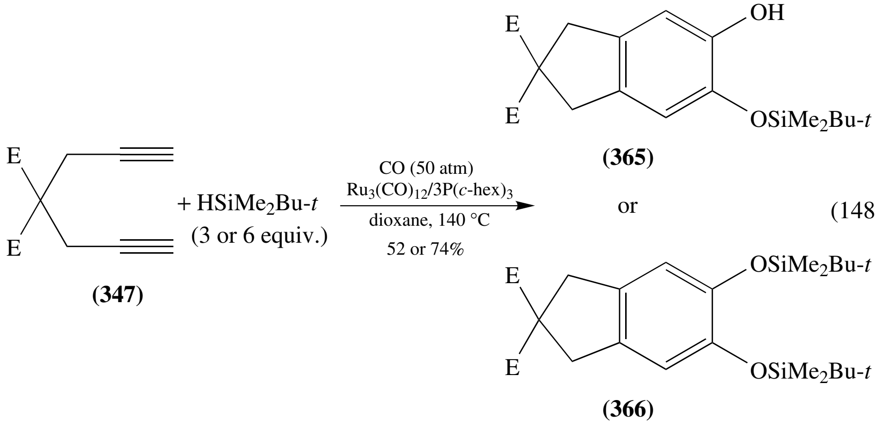

(148)

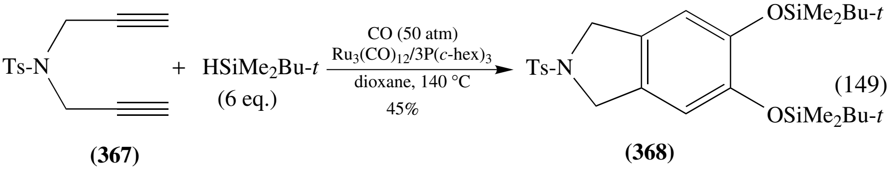

(149)

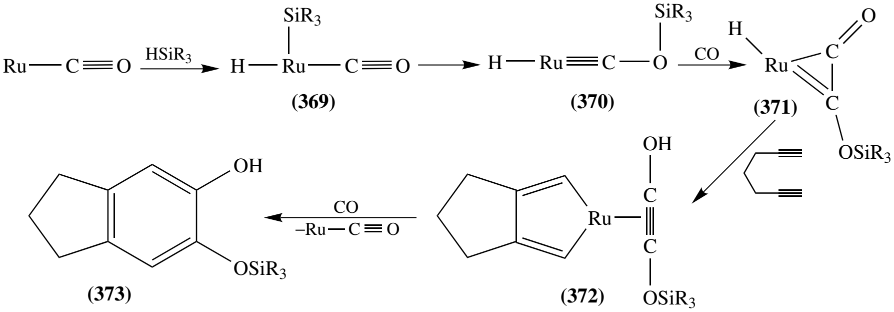

SCHEME 35

VIII. REFERENCES

1. H. Brunner, H. Nishiyama and K. Itoh, in *Catalytic Asymmetric Synthesis* (Ed. I. Ojima), VCH Publ., New York, 1993, pp. 303–322.
2. R. Noyori, *Asymmetric Catalysis in Organic Synthesis*, Wiley, New York, 1994.
3. I. Ojima, in *The Chemistry of Organic Silicon Compounds* (Eds. S. Patai and Z. Rappoport), Wiley, New York 1989, pp. 1479–1526.
4. J. L. Speier, *Adv. Organomet. Chem.*, **17**, 407 (1979).
5. T. Hiyama and T. Kusumoto, in *Comprehensive Organic Synthesis* (Ed. B. M. Trost), Pergamon Press, Oxford, 1991, p. 763.
6. B. Marcinec and J. Gulinski, *J. Organomet. Chem.*, **446**, 15 (1993).
7. M. Itoh, K. Iwata, R. Takeuchi and M. Kobayashi, *J. Organomet. Chem.*, **420**, C5 (1991).
8. R. Skoda-Foldes, L. Kollar and B. Heil, *J. Organomet. Chem.*, **366**, 275 (1989).

9. T. Murai, T. Oda, F. Kimura, H. Onishi, T. Kanda and S. Kato, *J. Chem. Soc., Chem. Commun.*, 2143 (1994).
10. B. Karstedt, *U.S. Patent*, 3,775,452 (1973); *Chem. Abstr.*, **90**, 16134j (1973).
11. D. N. Willing, *U.S. Patent*, 3,419,593 (1968); *Chem. Abstr.*, **75**, 2123z (1968).
12. V. J. Eddy and J. E. Hallgren, *J. Org. Chem.*, **52**, 1903 (1987).
13. M. G. Voronkov, S. V. Kirpichenko, V. V. Keiko and A. I. Albanov, *J. Organomet. Chem.*, **427**, 289 (1992).
14. M. Tanaka, Y. Uchimaru and H. J. Lautenschlager, *J. Organomet. Chem.*, **428**, 1 (1992).
15. H. Nagashima, K. Tatebe, T. Ishibashi, J. Sakakibara and K. Itoh, *Organometallics*, **8**, 2495 (1989).
16. T. Hagiwara, K. Taya, Y. Yamamoto and H. Yamazaki, *J. Mol. Catal.*, **54**, 165 (1989).
17. J. B. Baruah, K. Osakada and T. Yamamoto, *J. Mol. Catal. A: Chem.*, **101**, 17 (1995).
18. J. Gulinski and B. R. James, *J. Mol. Catal.*, **72**, 167 (1992).
19. L. I. Kopylova, V. B. Pukhnarevich, V. S. Tkach and M. G. Voronkov, *Zh. Obshch. Khim.*, **63**, 1294 (1993); *Chem. Abstr.*, **120**, 134613s (1993).
20. J. M. Chance and T. A. Nile, *J. Mol. Catal.*, **42**, 91 (1987).
21. H. S. Hilal, S. Khalaf and W. Jondi, *J. Organomet. Chem.*, **452**, 167 (1993).
22. M. Tanaka, T. Hayashi and Z.-Y. Mi, *J. Mol. Catal.*, **81**, 207 (1993).
23. L. N. Lewis and N. Lewis, *J. Am. Chem. Soc.*, **108**, 7228 (1986).
24. A. Onopchenko and E. T. Sabourin, *J. Org. Chem.*, **52**, 4118 (1987).
25. K. A. Brown-Wensley, *Organometallics*, **6**, 1590 (1987).
26. W. C. Trogler, *J. Chem. Educ.*, **65**, 294 (1988).
27. A. L. Prignano and W. C. Trogler, *J. Am. Chem. Soc.*, **109**, 3586 (1987).
28. L. N. Lewis and N. Lewis, *Chem. Mater.*, **1**, 106 (1989).
29. L. N. Lewis and R. J. Uriarte, *Organometallics*, **9**, 621 (1990).
30. L. N. Lewis, *J. Am. Chem. Soc.*, **112**, 5998 (1990).
31. G. Chandra, P. Y. Lo, P. B. Hitchcock and M. F. Lappert, *Organometallics*, **6**, 191 (1987).
32. P. B. Hitchcock, M. F. Lappert and N. J. W. Warhurst, *Angew. Chem., Int. Ed. Eng.*, **30**, 438 (1991).
33. M. F. Lappert and F. P. A. Scott, *J. Organomet. Chem.*, **492**, C11 (1995).
34. F. D. Lewis and G. D. Salvi, *Inorg. Chem.*, **34**, 3182 (1995).
35. C. Polizzi, A. M. Caporusso, G. Vitulli, P. Salvadori and M. Pasero, *J. Mol. Catal.*, **91**, 83 (1994).
36. M. R. Kesti, M. Abdulrahman and R. M. Waymouth, *J. Organomet. Chem.*, **417**, C12 (1991).
37. M. R. Kesti and R. M. Waymouth, *Organometallics*, **11**, 1095 (1992).
38. J. Y. Corey and X. H. Zhu, *Organometallics*, **11**, 672 (1992).
39. J. F. Harrod and S. S. Yun, *Organometallics*, **6**, 1381 (1987).
40. J. Y. Corey, X.-H. Zhu, T. C. Bedard and L. D. Lange, *Organometallics*, **10**, 924 (1991).
41. J. F. Harrod in *Organometallic and Inorganic Polymers* (Eds. H. R. Zeldin, H. R. Allcock and K. J. Wynne), American Chemical Society, Washignton, D. C., 1988, p. 89.
42. J. F. Harrod, *Polym. Prepr.*, **28**, 403 (1987).
43. P.-W. Fu, L. Brard, Y. Li and T. B. Marks, *J. Am. Chem. Soc.*, **117**, 7157 (1995).
44. T. Sakakura, H. Lautenschlager and M. Tanaka, *J. Chem. Soc., Chem. Commun.*, 40 (1991).
45. G. A. Molander and M. Julius, *J. Org. Chem.*, **57**, 6347 (1992).
46. S. Onozawa, T. Sakakura and M. Tanaka, *Tetrahedron Lett.*, **35**, 8177 (1994).
47. J. L. Speier, J. A. Webster, and G. H. Barens, *J. Am. Chem. Soc.*, **79**, 974 (1957).
48. E. Yoshii, Y. Kobayashi, T. Koizumi and T. Oribe, *Chem. Pharm. Bull.*, **22**, 2767 (1974).
49. Y. Kiso, M. Kumada, K. Tamao and M. Umeno, *J. Organometal. Chem.*, **50**, 297 (1973).
50. I. Ojima, M. Kumagai and Y. Nagai, *J. Organometal. Chem.*, **111**, 43 (1976).
51. P. Boudjouk, S. Kloos and A. B. Rajkumar, *J. Organomet. Chem.*, **443**, C41 (1993).
52. B. A. Bluestein, *J. Am. Chem. Soc.*, **83**, 1000 (1961).
53. P. Svoboda and J. Hetflejs, *Collect. Czech. Chem. Commun.*, **38**, 3834 (1973).
54. A. B. Rajkumar and P. Boudjouk, *Organometallics*, **8**, 549 (1989).
55. H. S. Hilal, M. Abu-Eid, M. Al-Subu and S. Khalaf, *J. Mol. Catal.*, **39**, 1 (1987).
56. B. Marciniec, H. Maciejewski and J. Mirecki, *J. Organomet. Chem.*, **418**, 61 (1991).
57. W. Abdelqader, D. Chmielewski, F.-W. Grevels, S. Oezkar and N. B. Peynircioglu, *Organometallics*, **15**, 604 (1996).
58. M. A. Wrighton and M. S. Schroeder, *J. Am. Chem. Soc.*, **96**, 6235 (1974).

59. M. A. Schroeder and M. S. Wrighton, *J. Organometal. Chem.*, **128**, 345 (1977).
60. M. Capka and M. Czakoova, *J. Mol. Catal.*, **74**, 335 (1992).
61. M. Capka, M. Czakoova and U. Schubert, *Appl. Organomet. Chem.*, **7**, 369 (1993).
62. M. Capka, M. Czakoova, J. Hjortkjaer and U. Schubert, *React. Kinet. Catal. Lett.*, **50**, 71 (1993).
63. Z. M. Michalska, B. Ostaszewski, K. Strzelec, R. Kwiatkowski and A. Wlochowicz, *React. Polym.*, **23**, 85 (1994).
64. Z. M. Michalska, B. Ostaszewski and K. Strzelec, *J. Organomet. Chem.*, **496**, 19 (1995).
65. W. R. Cullen and N. F. Han, *J. Organometal. Chem.*, **333**, 269 (1987).
66. B. Kopping, C. Chatgilialoglu, M. Zehnder and B. Giese, *J. Org. Chem.*, **57**, 3994 (1992).
67. C. Chatgilialoglu, *Acc. Chem. Res.*, **25**, 188 (1992).
68. M. Ballestri, C. Chatgilialoglu, K. B. Clark, D. Griller, B. Kopping and B. Giese, *J. Org. Chem.*, **56**, 678 (1991).
69. A. J. Chalk and J. F. Harrod, *J. Am. Chem. Soc.*, **87**, 16 (1965).
70. C. L. Reichel and M. S. Wrighton, *Inorg. Chem.*, **19**, 3858 (1980).
71. C. L. Randolph and M. S. Wrighton, *J. Am. Chem. Soc.*, **108**, 3366 (1986).
72. M. Brookhart and B. E. Grant, *J. Am. Chem. Soc.*, **115**, 2151 (1993).
73. J. C. Mitchener and M. S. Wrighton, *J. Am. Chem. Soc.*, **103**, 975 (1981).
74. A. Millan, M.-J. Fernandez, P. Bentz and P. Maitlis, *J. Mol. Catal.*, **26**, 89 (1984).
75. A. Millan, E. Towns and P. Maitlis, *J. Chem. Soc., Chem. Commun.*, 673 (1981).
76. Y. Seki, K. Takeshita and K. Kawamoto, *J. Organometal. Chem.*, **369**, 117 (1989).
77. Y. Seki, K. Takeshita, K. Kawamoto, S. Murai and N. Sonoda, *J. Org. Chem.*, **52**, 4864 (1987).
78. A. Onopchenko, E. T. Sabourin and D. L. Beach, *J. Org. Chem.*, **49**, 3389 (1984).
79. A. Onopchenko, E. T. Sabourin and D. L. Beach, *J. Org. Chem.*, **48**, 5101 (1983).
80. I. Ojima, T. Fuchikami and M. Yatabe, *J. Organometal. Chem.*, **260**, 335 (1984).
81. F. Seitz and M. S. Wrighton, *Angew. Chem., Int. Ed. Engl.*, **27**, 289 (1988).
82. S. B. Duckett and R. N. Perutz, *Organometallics*, **11**, 90 (1992).
83. J. Ruiz, P. O. Bentz, B. E. Mann, C. M. Spencer, B. F. Taylor and P. M. Maitlis, *J. Chem. Soc., Dalton Trans.*, 2709 (1987).
84. M. J. Hostetler, M. D. Butts and R. G. Bergman, *Organometallics*, **12**, 65 (1993).
85. M. J. Hostetler and R. G. Bergman, *J. Am. Chem. Soc.*, **112**, 8621 (1990).
86. K. Tamao, T. Nakajima, R. Sumiya, H. Arai, N. Higuchi and Y. Ito, *J. Am. Chem. Soc.*, **108**, 6090 (1986).
87. K. Tamao, Y. Nakagawa, H. Arai, N. Higuchi and Y. Ito, *J. Am. Chem. Soc.*, **110**, 3712 (1988).
88. K. Tamao, *J. Syn. Org. Chem. Jpn.*, **46**, 861 (1988).
89. K. Tamao, Y. Nakagawa and Y. Ito, *Organometallics*, **12**, 2297 (1993).
90. K. Tamao, Y. Nakagawa and Y. Ito, *J. Org. Chem.*, **55**, 3438 (1990).
91. M. P. Sibi and J. W. Christensen, *Tetrahedron Lett.*, **36**, 6213 (1995).
92. S. E. Denmark and D. C. Forbes, *Tetrahedron Lett.*, **33**, 5037 (1992).
93. H. K. Chu and C. L. Frye, *J. Organomet. Chem.*, **446**, 183 (1993).
94. S. Xin and J. F. Harrod, *J. Organomet. Chem.*, **499**, 181 (1995).
95. A. N. Nesmeyanov, R. K. Freidlina, E. C. Chukovskaya, R. G. Petrova and A. B. Belyavsky, *Tetrahedron*, **17**, 61 (1962).
96. Y. Seki, K. Takeshita, K. Kawamoto, S. Murai and N. Sonoda, *Angew. Chem., Int. Ed. Engl.*, **19**, 928 (1980).
97. K. Takeshita, Y. Seki, K. Kawamoto, S. Murai and N. Sonoda, *J. Chem. Soc., Chem. Commun.*, 1193 (1983).
98. Y. Seki, K. Takeshita, K. Kawamoto, S. Murai and N. Sonoda, *J. Org. Chem.*, **51**, 3890 (1986).
99. K. Takeshita, Y. Seki, K. Kawamoto, S. Murai, and N. Sonoda, *J. Org. Chem.*, **52**, 4864 (1987).
100. F. Kakiuchi, Y. Tanaka, N. Chatani and S. Murai, *J. Organomet. Chem.*, **456**, 45 (1993).
101. F. Kakiuchi, K. Nogami, N. Chatani, Y. Seki and S. Murai, *Organometallics*, **12**, 4748 (1993).
102. M. P. Doyle, G. A. Devora, A. O. Nefedov and K. G. High, *Organometallics*, **11**, 549 (1992).
103. K. Hayakawa, M. Tachikawa, T. Suzuke, N. Choi and M. Murakami, *Tetrahedron Lett.*, **36**, 3181 (1995).
104. L. N. Lewis, K. G. Sy and P. E. Donahue, *J. Organomet. Chem.*, **427**, 165 (1992).
105. I. G. Iovel, Y. S. Goldberg, M. V. Shymanska and E. Lukevics, *Organometallics*, **6**, 1410 (1987).
106. I. Ojima, N. Clos, R. L. Donovan and P. Ingallina, *Organometallics*, **9**, 3127 (1990).
107. I. Ojima, R. J. Donovan, P. Ingallina and N. Clos, *J. Cluster Sci.*, **3**, 423 (1992).

108. I. Ojima, M. Kumagai and Y. Nagai, *J. Organometal. Chem.*, **66**, C14 (1974).
109. R. Takeuchi and N. Tanouchi, *J. Chem. Soc.*, *Perkin Trans. 1*, 2909 (1994).
110. R. Takeuchi and N. Tanouchi, *J. Chem. Soc., Chem. Commun.*, 1319 (1993).
111. M. P. Doyle, K. G. High, C. L. Nesloney, T. W. J. Layton and J. Lin, *Organometallics*, **10**, 1225 (1991).
112. Y. Goldberg and H. Alper, *Tetrahedron Lett.*, **36**, 369 (1995).
113. C.-H. Jun and R. H. Crabtree, *J. Organomet. Chem.*, **447**, 177 (1993).
114. P. Hofmann, C. Meier, W. Hiller, M. Heckel, J. Riede and M. U. Schmidt, *J. Organomet. Chem.*, **490**, 51 (1995).
115. R. S. Tanke and R. H. Crabtree, *J. Am. Chem. Soc.*, **112**, 7984 (1990).
116. R. S. Tanke and R. H. Crabtree, *J. Chem. Soc., Chem. Commun.*, 1056 (1990).
117. M. J. Fernandez, L. A. Oro and B. R. Mamzano, *J. Mol. Catal.*, **45**, 7 (1988).
118. M. A. Esteruelas, M. Oliván, L. A. Oro and J. I. Tolosa, *J. Organomet. Chem.*, **487**, 143 (1995).
119. M. A. Esteruelas, M. Oliván and L. A. Oro, *Organometallics*, **15**, 814 (1996).
120. M. A. Esteruelas, J. Herrero and L. A. Oro, *Organometallics*, **12**, 2377 (1993).
121. M. A. Esteruelas, L. A. Oro and C. Valero, *Organometallics*, **10**, 462 (1991).
122. M. A. Esteruelas, A. M. López, L. A. Oro and J. I. Tolosa, *J. Mol. Catal. A: Chem.*, **96**, 21 (1995).
123. T. Bartik, G. Nagy, P. Kvintovics and B. Happ, *J. Organomet. Chem.*, **453**, 29 (1993).
124. G. A. Molander and W. H. Retch, *Organometallics*, **14**, 4570 (1995).
125. R. A. Benkeser, *Pure Appl. Chem.*, **13**, 133 (1966).
126. L. H. Sommer, E. W. Pietrusza and F. C. Whitmore, *J. Am. Chem. Soc.*, **69**, 188 (1947).
127. K. A. Brady and T. A. Nile, *J. Organometal. Chem.*, **206**, 299 (1981).
128. S. R. Allen, R. G. Beevor, M. Green, N. C. Norman, A. G. Orpen and I. D. Williams, *J. Chem. Soc., Dalton Trans.*, 435 (1985).
129. M. A. Esteruelas, O. Nurnberg, M. Olivan, L. A. Oro and H. Werner, *Organometallics*, **12**, 3264 (1993).
130. M. G. Steinmetz and B. S. Udayakumar, *J. Organomet. Chem.*, **378**, 1 (1989).
131. T. Suzuki and P. Y. Lo, *J. Organomet. Chem.*, **396**, 299 (1990).
132. T. Suzuki and P. Y. Lo, *J. Organomet. Chem.*, **391**, 19 (1990).
133. T. Kusumoto, K. Ando and T. Hiyama, *Bull. Chem. Soc. Jpn.*, **65**, 1280 (1992).
134. E. Lukevics, R. Y. Sturkovich and O. A. Pudova, *J. Organomet. Chem.*, **292**, 151 (1985).
135. P. J. Murphy, J. L. Spencer and G. Procter, *Tetrahedron Lett.*, **31**, 1051 (1990).
136. R. Takeuchi, S. Nitta and D. Watanabe, *J. Org. Chem.*, **60**, 3045 (1995).
137. R. Takeuchi, S. Nitta and D. Watanabe, *J. Chem. Soc., Chem. Commun.*, 1777 (1994).
138. K. Takahashi, T. Minami, Y. Ohara and T. Hiyama, *Tetrahedron Lett.*, **34**, 8263 (1993).
139. K. Takahashi, T. Minami, Y. Ohara and T. Hiyama, *Bull. Chem. Soc. Jpn.*, **68**, 2649 (1995).
140. I. Ojima, R. J. Donovan and N. Clos, *Organometallics*, **10**, 3790 (1991).
141. M. F. Semmelhack and R. N. Misra, *J. Org. Chem.*, **47**, 2469 (1982).
142. J. Ishiyama, Y. Senda, I. Shinoda and S. Imaizumi, *Bull. Chem. Soc. Jpn.*, **52**, 2353 (1979).
143. I. Ojima, M. Nihonyanagi and Y. Nagai, *Bull. Chem. Soc. Jpn.*, **45**, 3722 (1972).
144. K. Felföldi, I. Kapocsi and M. Bartök, *J. Organomet. Chem.*, **362**, 411 (1989).
145. H. Nagashima, K. Tatebe, T. Ishibashi, A. Nakaoka, J. Sakakibara and K. Itoh, *Organometallics*, **14**, 2868 (1995).
146. H. Nagashima, K. Tatebe and K. Itoh, *J. Chem. Soc., Perkin Trans. 1*, 1707 (1989).
147. E. J. Crawford, P. K. Hanna and A. R. Cutler, *J. Am. Chem. Soc.*, **111**, 6891 (1989).
148. P. K. Hanna, B. T. Gregg and A. R. Cutler, *Organometallics*, **10**, 31 (1991).
149. Z. Mao, B. T. Gregg and A. R. Cutler, *J. Am. Chem. Soc.*, **117**, 10139 (1995).
150. B. Marciniec and J. Gulinski, *J. Organomet. Chem.*, **446**, 15 (1993).
151. J. E. Hill and T. A. Nile, *J. Organometal. Chem.*, **137**, 293 (1977).
152. A. Revis and T. K. Hilty, *J. Org. Chem.*, **55**, 2972 (1990).
153. I. Ojima, T. Kogure and Y. Nagai, *Tetrahedron Lett.*, 5035 (1972).
154. I. Ojima and T. Kogure, *Organometallics*, **1**, 1390 (1982).
155. G. Z. Zheng and T. H. Chan, *Organometallics*, **14**, 70 (1995).
156. E. Keinan and D. Perez, *J. Org. Chem.*, **52**, 2576 (1987).
157. T. Schmidt, *Tetrahedron Lett.*, **35**, 3513 (1994).
158. T. Nakano and Y. Nagai, *Chem. Lett.*, 481 (1988).
159. K. Yamamoto and T. Tabei, *J. Organomet. Chem.*, **427**, 165 (1992).

160. B. Töröek, K. Felföldi, A. Molnár and M. Bartók, *J. Organomet. Chem.*, **460**, 111 (1993).
161. J. Boyer, R. J. P. Corriu, R. Perz and C. Reye, *J. Organometal. Chem.*, **157**, 153 (1978).
162. J. Boyer, R. J. P. Corriu, R. Perz and C. Reye, *J. Organometal. Chem.*, **172**, 142 (1979).
163. C. Chuit, R. J. P. Corriu, R. Perz and C. Reye, *Tetrahedron*, **37**, 2165 (1981).
164. J. Boyer, R. J. P. Corriu, R. Perz, M. Poirier and C. Reye, *Synthesis*, 558 (1981).
165. R. J. P. Corriu, R. Perz and C. Reye, *Tetrahedron*, **39**, 999 (1983).
166. M. Fujita and T. Hiyama, *J. Org. Chem.*, **53**, 5405 (1988).
167. M. Fujita and T. Hiyama, *J. Am. Chem. Soc.*, **107**, 8294 (1985).
168. T. Hiyama, K. Kobayashi and M. Fujita, *Tetrahedron Lett.*, **25**, 4959 (1984).
169. M. Fujita and T. Hiyama, *J. Am. Chem. Soc.*, **106**, 4629 (1984).
170. M. Fujita and T. Hiyama, *Tetrahedron Lett.*, **28**, 2263 (1987).
171. Y. Goldberg, E. Abele, M. V. Shimanskaya and E. Lukevics, *J. Organomet. Chem.*, **372**, C9 (1989).
172. Y. Goldberg, K. Rubina, M. Shymanska and E. Lukevics, *Synth. Commun.*, **20**, 2439 (1990).
173. W. P. Weber, in *Silicon Reagents for Organic Synthesis*, Springer-Verlag, Berlin, 1983, pp. 273–287.
174. M. Fujita and T. Hiyama, *J. Org. Chem.*, **53**, 5415 (1988).
175. G. A. Olah, M. Arvanaghi and L. Ohannesian, *Synthesis*, 770 (1986).
176. M. Onaka, K. Higuchi, H. Nanami and Y. Izumi, *Bull. Chem. Soc. Jpn.*, **66**, 2638 (1993).
177. M. P. Doyle, C. T. West, S. J. Donnelly and C. C. McOsker, *J. Organometal. Chem.*, **117**, 129 (1976).
178. J. L. Fry, M. Orfanopoulos, M. G. Adlington, W. R. Dittman and S. B. Silverman, *J. Org. Chem.*, **43**, 374 (1978).
179. M. Fujita, S. Fukuzumi and J. Otera, *J. Mol. Catal.*, **85**, 143 (1993).
180. Y. Izumi, H. Nanami, K. Higuchi and M. Onaka, *Tetrahedron Lett.*, **32**, 4741 (1991).
181. S. Anwar and A. P. David, *Tetrahedron*, **44**, 3761 (1988).
182. A. P. Davis and S. C. Hegarty, *J. Am. Chem. Soc.*, **114**, 2745 (1992).
183. A. P. Davis and S. C. Hegarty, *J. Am. Chem. Soc.*, **114**, 8753 (1992).
184. X. Verdagnuer, S. C. Berk and S. L. Buchwald, *J. Am. Chem. Soc.*, **117**, 12641 (1995).
185. A. H. Vetter and A. Berkessel, *Synthesis*, 419 (1995).
186. T. Murai, T. Sakane and S. Kato, *J. Org. Chem.*, **55**, 449 (1990).
187. I. Ojima, in *Asymmetric Synthesis*, Vol. 5 (Ed. J. D. Morrison) Academic Press, New York, 1985, pp. 103–146.
188. I. Ojima, K. Yamamoto and M. Kumada, in *Aspects of Homogeneous Catalysis*, Vol. 3 (Ed. R. Ugo,) Reidel, Amsterdam, 1977, pp. 85–228.
189. H. Brunner, *Adv. Chem. Ser.*, **230**, 143 (1992).
190. H. Nishiyama, H. Sakaguchi, T. Nakamura, M. Horihata, M. Kondo and K. Itoh, *Organometallics*, **8**, 846 (1989).
191. H. Nishiyama, M. Kondo, T. Nakamura and K. Itoh, *Organometallics*, **10**, 500 (1991).
192. H. Nishiyama, S. Yamaguchi, M. Kondo and K. Itoh, *J. Org. Chem.*, **57**, 4306 (1992).
193. H. Nishiyama, S. Yamaguchi, S. B. Park and K. Itoh, *Tetrahedron: Asymmetry*, **4**, 143 (1993).
194. H. Nishiyama and K. Itoh, *J. Syn. Org. Chem. Jpn. (Yuki Gosei Kagaku Kyokaishi)*, **53**, 500 (1995).
195. H. Brunner and C. Henrichs, *Tetrahedron: Asymmetry*, **6**, 653 (1995).
196. H. Brunner and P. Brandl, *Z. Naturforsch.*, **47b**, 609 (1992).
197. H. Brunner and P. Brandl, *Tetrahedron: Asymmetry*, **2**, 919 (1991).
198. H. Brunner and C. Huber, *Z. Naturforsch.*, **46b**, 1145 (1991).
199. H. Brunner and P. Brandl, *J. Organomet. Chem.*, **390**, C81 (1990).
200. S. Gladiali, L. Pinna, G. Delogu, E. Graf and H. Brunner, *Tetrahedron: Asymmetry*, **1**, 937 (1990).
201. H. Brunner and U. Obermann, *Chem. Ber.*, **122**, 499 (1989).
202. G. Balavoine, J. C. Clinet and I. Lellouche, *Tetrahedron Lett.*, **30**, 5141 (1989).
203. H. Brunner and A. Kuerzinger, *J. Organomet. Chem.*, **346**, 413 (1988).
204. H. Brunner and H. Fisch, *J. Organomet. Chem.*, **335**, 15 (1987).
205. H. Brunner, U. Obermann and P. Wimmer, *J. Organometal. Chem.*, **316**, C1 (1986).
206. M. Sawamura, R. Kuwano, J. Shirai and Y. Ito, *Synlett*, 347 (1995).
207. M. Sawamura, R. Kuwano and Y. Ito, *Angew. Chem., Int. Ed. Engl.*, **33**, 111 (1994).
208. T. Hayashi, C. Hayashi and Y. Uozumi, *Tetrahedron: Asymmetry*, **6**, 2503 (1995).

209. Y. Nishibayashi, K. Segawa, K. Ohe and S. Uemura, *Organometallics*, **14**, 5486 (1995).
210. Y. Nishibayashi, J. D. Singh, K. Segawa, S. Fukuzawa and S. Uemura, *J. Chem. Soc., Chem. Commun.*, 1375 (1994).
211. Y. Nishibayashi, K. Segawa, J. D. Singh, S. Fuzukawa, K. Ohe and S. Uemura, *Organometallics*, **15**, 370 (1996).
212. J. Sakaki, W. B. Schweizer and D. Seebach, *Helv. Chim. Acta*, **76**, 2654 (1993).
213. J. W. Faller and K. J. Chase, *Organometallics*, **13**, 989 (1994).
214. A. Tillack, M. Michalik, D. Fenske and H. Goesmann, *J. Organomet. Chem.*, **482**, 85 (1994).
215. Y. Goldberg and H. Alper, *Tetrahedron: Asymmetry*, **3**, 1055 (1992).
216. M. E. Wright and S. A. Svejda, *Polyhedron*, **10**, 1061 (1991).
217. M. E. Wright, S. A. Svejda, M. J. Jin and M. A. Peterson, *Organometallics*, **9**, 136 (1990).
218. C. Botteghi, A. Schionato, G. Chelucci, H. Brunner, A. Küerzinger and U. Obermann, *J. Organomet. Chem.*, **370**, 17 (1989).
219. A. Kinting, H. J. Kreuzfeld and H. P. Abicht, *J. Organomet. Chem.*, **370**, 343 (1989).
220. W. R. Cullen and E. B. Wickenheiser, *J. Organomet. Chem.*, **370**, 141 (1989).
221. A. F. M. Mokhlesur Rahman and S. B. Wild, *J. Mol. Catal.*, **39**, 155 (1987).
222. V. A. Pavlov, E. Y. Zhorov, A. A. Voloboev and E. I. Klabunovskii, *J. Mol. Catal.*, **59**, 119 (1990).
223. Y. Vannoorenberghe and G. Buono, *Tetrahedron Lett.*, **29**, 3235 (1988).
224. H. Brunner and K. Amberger, *J. Organomet. Chem.*, **417**, C63 (1991).
225. M. B. Carter, B. Schiøtt, A. Gutiérrez and S. L. Buchwald, *J. Am. Chem. Soc.*, **116**, 11667 (1994).
226. R. L. Halterman, T. M. Ramsey and Z. Chen, *J. Org. Chem.*, **59**, 2642 (1994).
227. G. Helmchen, A. Krotz, K.-T. Ganz and D. Hansen, *Synlett*, 257 (1991).
228. S. Murata, T. Sugimoto and S. Matsuura, *Heterocycles*, **26**, 763 (1987).
229. X. Verdaguer, U. E. W. Lange, M. T. Reding and S. L. Buchwald, *J. Am. Chem. Soc.*, **118**, 6784 (1996).
230. S. Murahashi, S. Watanabe and T. Shiota, *J. Chem. Soc., Chem. Commun.*, 725 (1994).
231. M. J. Burk and E. Feaster, *Tetrahedron Lett.*, **33**, 2099 (1992).
232. R. J. P. Corriu and J. J. E. Moreau, *J. Organometal. Chem.*, **85**, 19 (1975).
233. R. J. P. Corriu and J. J. E. Moreau, *J. Organometal. Chem.*, **64**, C51 (1974).
234. T. Hayashi, K. Yamamoto and M. Kumada, *Tetrahedron Lett.*, 331 (1974).
235. R. J. P. Corriu and J. J. E. Moreau, *J. Organometal. Chem.*, **91**, C27 (1975).
236. R. J. P. Corriu and J. J. E. Moreau, *Nouv. J. Chim.*, **1**, 71 (1977).
237. T. Ohta, M. Ito, A. Tsuneto and H. Takaya, *J. Chem. Soc., Chem. Commun.*, 2525 (1994).
238. Y. Uozumi and T. Hayashi, *J. Am. Chem. Soc.*, **113**, 9887 (1991).
239. T. Hayashi and Y. Uozumi, *Pure Appl. Chem.*, **64**, 1911 (1992).
240. Y. Uozumi, K. Kitayama, T. Hayashi, K. Yanagi and E. Fukuyo, *Bull. Chem. Soc. Jpn.*, **68**, 713 (1995).
241. Y. Uozumi, S. Y. Lee and T. Hayashi, *Tetrahedron Lett.*, **33**, 7185 (1992).
242. Y. Uozumi and T. Hayashi, *Tetrahedron Lett.*, **34**, 2335 (1993).
243. K. Kitayama, Y. Uozumi and T. Hayashi, *J. Chem. Soc., Chem. Commun.*, 1533 (1995).
244. Y. Uozumi, K. Kitayama and T. Hayashi, *Tetrahedron: Asymmetry*, **4**, 2419 (1993).
245. T. Okada, T. Morimoto and K. Achiwa, *Chem. Lett.*, 999 (1990).
246. T. Hayashi, Y. Matsumoto, I. Morikawa and Y. Ito, *Tetrahedron: Asymmetry*, **1**, 151 (1990).
247. H. Ohmura, H. Matsuhashi, M. Yanaka, M. Kuroboshi, T. Hiyama, Y. Hatanaka and K.-I. Goda, *J. Organomet. Chem.*, **499**, 167 (1995).
248. Y. Hatanaka, K. Goda, F. Yamashita and T. Hiyama, *Tetrahedron Lett.*, **35**, 7981 (1994).
249. K. Tamao, T. Tohma, N. Inui, O. Nakayama and Y. Ito, *Tetrahedron Lett.*, **31**, 7333 (1990).
250. S. H. Bergens, P. Noheda, J. Whelan and B. Bosnich, *J. Am. Chem. Soc.*, **114**, 2121 (1992).
251. R. W. Barnhart, X. Wang, P. Noheda, S. H. Bergens, J. Whelan and B. Bosnich, *Tetrahedron*, **50**, 4335 (1994).
252. X. Wang and B. Bosnich, *Organometallics*, **13**, 4131 (1994).
253. S. H. Bergens, P. Noheda, H. Whelan and B. Bosnich, *J. Am. Chem. Soc.*, **114**, 2128 (1992).
254. A. W. van der Made and P. W. N. M. van Leeuwen, *J. Chem. Soc., Chem. Commun.*, 1400 (1992).
255. C. Kim, D.-D. Sung, D.-I. Chung, E. Park and E. Kang, *J. Korean Chem. Soc.*, **39**, 789 (1995).
256. C. Kim, E. Park and E. Kang, *J. Korean Chem. Soc.*, **39**, 799 (1995).

257. B. Alonso, I. Cuadrado, M. Moran and J. Losada, *J. Chem. Soc., Chem. Commun.*, 2575 (1994).
258. K. Lorenz, R. Mülhaupt, H. Frey, U. Rapp and F. J. Mayer-Posner, *Macromolecules*, **28**, 6657 (1995).
259. H. Frey, K. Lorenz and R. Muelhaupt, *Macromol. Symp.*, **102**, 19 (1996).
260. J. Roovers, P. M. Toporowski and L.-L. Zhou, *Polym. Prepr., Am. Chem. Soc., Div. Polym. Chem.*, **33**, 182 (1992).
261. L.-L. Zhou and J. Roovers, *Macromolecules*, **26**, 963 (1993).
262. D. Seyferth, D. Y. Son, A. L. Rheingold and R. L. Ostrander, *Organometallics*, **13**, 2682 (1994).
263. D. Seyferth, T. Kugita, A. L. Rheingold and G. P. A. Yap, *Organometallics*, **14**, 5362 (1995).
264. S. Rubinsztajn, *J. Inorg. Organomet. Polym.*, **4**, 61 (1994).
265. J. Pan, W. W. Y. Lau and C. S. Lee, *J. Polym. Sci., Part A: Polym. Chem.*, **32**, 997 (1994).
266. J. V. Crivello, D. Bi and M. Fan, *J. Polym. Sci., Part A: Polym. Chem.*, **31**, 2563 (1993).
267. J. V. Crivello, D. Bi and M. Fan, *J. Polym. Sci., Part A: Polym. Chem.*, **31**, 2729 (1993).
268. J. V. Crivello and D. Bi, *J. Polym. Sci., Part A: Polym. Chem.*, **31**, 3109 (1993).
269. J. V. Crivello and D. Bi, *J. Polym. Sci., Part A: Polym. Chem.*, **31**, 3121 (1993).
270. J. V. Crivello, B. Yang and W.-G. Kim, *J. Polym. Sci., Part A: Polym. Chem.*, **33**, 2415 (1995).
271. J. V. Crivello and M. Fan, *Macromol. Symp.*, **77**, 413 (1994).
272. S. Itsuno, D. Chao and K. Ito, *J. Polym. Sci., Part A: Polym. Chem.*, **31**, 287 (1993).
273. P. R. Dvornic and V. V. Gerov, *Macromolecules*, **27**, 1068 (1994).
274. P. R. Dvornic, V. V. Gerov and M. N. Govedarica, *Macromolecules*, **27**, 7575 (1994).
275. C. M. Lewis and L. J. Mathias, *Polym. Prepr., Am. Chem. Soc., Div. Polym. Chem.*, **34**, 491 (1993).
276. W. M. Gibbons, R. P. Grasso, M. K. O'Brein, P. J. Shannon and S. T. Sun, *Appl. Phys. Lett.*, **64**, 2628 (1994).
277. W. M. Gibbons, R. P. Grasso, M. K. O'Brien, P. J. Shannon and S. T. Sun, *Macromolecules*, **27**, 771 (1994).
278. Y. Pang, S. Ijadi-Magsoodi and T. J. Barton, *Macromolecules*, **26**, 5671 (1993).
279. Y. Chen, L. Hong and X. Lu, *Youji Huaxue*, **13**, 260 (1993); *Chem. Abstr.*, **119**, 2712286d (1993).
280. H. S. W. Hu, J. R. Griffith, L. J. Buckley and A. W. Snow, *ACS Symp. Ser.*, **614**, 369 (1995).
281. L. M. Pratt, M. Waugaman and I. M. Khan, *Polym. Prepr., Am. Chem. Soc., Div. Polym. Chem.*, **36**, 263 (1995).
282. M. Tsumura, T. Iwahara and T. Hirose, *Polym. J.*, **27**, 1048 (1995).
283. C. X. Liao and W. P. Weber, *Macromolecules*, **26**, 563 (1993).
284. J. Lu and W. P. Weber, *Bull. Soc. Chim. Fr.*, **132**, 255 (1995).
285. Y. Goldberg and H. Alper, *J. Chem. Soc., Chem. Commun.*, 1209 (1994).
286. X. Coqueret and G. Wegner, *Makromol. Chem.*, **193**, 2929 (1992).
287. Y. Chujo and J. E. Mcgrath, *J. Macromol. Sci., Pure Appl. Chem.*, **A32**, 29 (1995).
288. B. Améduri, B. Boutevin, M. Nouiri and M. Talbi, *J. Fluorine Chem.*, **74**, 191 (1995).
289. B. Boutevin, F. Guida-Pietrasanta, A. Ratsimihety and G. Caporiccio, *J. Fluorine Chem.*, **68**, 71 (1994).
290. J. M. Yu, D. Teyssie and S. Boileau, *J. Polym. Sci., Part A: Polym. Chem.*, **31**, 2373 (1993).
291. G. Wang, H. Guo and W. P. Weber, *Polym Prepr., Am. Chem. Soc., Div. Polym. Chem.*, **36**, 523 (1995).
292. Y.-L. Hsiao and R. M. Waymouth, *J. Am. Chem. Soc.*, **116**, 9779 (1994).
293. M. W. Chen, C. X. Liao and W. P. Weber, *J. Inorg. Organomet. Polym.*, **3**, 241 (1993).
294. M. Ishikawa, E. Toyoda, T. Horio and A. Kunai, *Organometallics*, **13**, 26 (1994).
295. A. Kundai, E. Toyoda, I. Nagamoto, T. Horio and M. Ishidawa, *Organometallics*, **15**, 75 (1996).
296. Y. Chujo, E. Khara, S. Kure and T. Saegusa, *Macromolecules*, **26**, 5681 (1993).
297. R. West, M. Miller, H. Takahashi, T. Gunji and K. Oka, *Polym. Prepr., Am. Chem. Soc., Div. Polym. Chem.*, **34**, 227 (1993).
298. A. Iraqi, S. Seth, C. A. Vincent, D. J. Cole-Hamilton, M. D. Watkinson, I. M. Graham and D. Jeffrey, *J. Mater. Chem.*, **2**, 1057 (1992).
299. A. H. Gabor, E. A. Lehner, G. Mao, L. A. Schneggenburger and C. K. Ober, *Polym. Prepr., Am. Chem. Soc., Div. Polym. Chem.*, **33**, 136 (1992).
300. B. J. Kokko, *J. Appl. Polym. Sci.*, **47**, 1309 (1993).
301. H. A. Ketelson, M. A. Brook and R. H. Pelton, *Polym. Adv. Technol.*, **6**, 335 (1995).
302. Y. Seki, A. Hidaka, S. Murai and N. Sonoda, *Angew. Chem., Int. Ed. Engl.*, **16**, 174 (1977).
303. Y. Seki, S. Murai, A. Hidaka and N. Sonoda, *Angew. Chem., Int. Ed. Engl.*, **16**, 881 (1977).

304. Y. Seki, A. Hidaka, S. Makino, S. Murai and N. Sonoda, *J. Organomet. Chem.*, **140**, 361 (1977).
305. G. Süss-Fink and J. Reiner, *J. Mol. Catal.*, **16**, 231 (1982).
306. S. Murai and N. Sonoda, *Angew. Chem., Int. Ed. Engl.*, **18**, 837 (1979).
307. Y. Seki and K. Kawamoto *J. Organomet. Chem.*, **403**, 73 (1991).
308. T. Murai, E. Yasui, S. Kato, Y. Hatayama, S. Suzuki, Y. Yamasaki, N. Sonoda, H. Kurosawa, Y. Kawasaki and S. Murai, *J. Am. Chem. Soc.*, **111**, 7938 (1989).
309. N. Chatani, T. Ikeda, T. Sano, N. Sonoda, H. Kurosawa, Y. Kawasaki and S. Murai, *J. Org. Chem.*, **53**, 3387 (1988).
310. N. Chatani, Y. Kajikawa, H. Nishimura and S. Murai, *Organometallics*, **10**, 21 (1991).
311. S. Murai and N. Sonoda, *J. Mol. Catal.*, **41**, 197 (1987).
312. N. Chatani, S. Ikeda, K. Ohe and S. Murai, *J. Am. Chem. Soc.*, **114**, 3710 (1992).
313. S. Ikeda, N. Chatani, Y. Kajikawa, K. Ohe and S. Murai, *J. Org. Chem.*, **57**, 2 (1992).
314. Y. Seki, S. Murai, I. Yamamoto and N. Sonoda, *Angew. Chem., Int. Ed. Engl.*, **16**, 789 (1977).
315. Y. Fukumoto, N. Chatani and S. Murai, *J. Org. Chem.*, **58**, 4187 (1993).
316. N. Chatani and S. Murai, *Synlett*, 415 (1996).
317. S. Ikeda, N. Chatani and S. Murai, *Organometallics*, **11**, 3494 (1992).
318. M. E. Wright and B. B. Cochran, *J. Am. Chem. Soc.*, **115**, 2059 (1993).
319. M. E. Wright and B. B. Cochran, *Organometallics*, **15**, 317 (1996).
320. I. Matsuda, A. Ogiso, S. Sato and Y. Izumi, *J. Am. Chem. Soc.*, **111**, 2332 (1989).
321. I. Ojima, *22nd Organosilicon Symposium, April 7–8, Philadelphia, PA, U.S.A., Abstracts*, Plenary 7 (1989).
322. P. Ingallina, N. Clos and I. Ojima, *23rd Organosilicon Symposium, April 20-21, Midland, MI, U.S.A., Abstracts*, G2 (1990).
323. I. Ojima, P. Ingallina, R. J. Donovan and N. Clos, *Organometallics*, **10**, 38 (1991).
324. I. Ojima, R. J. Donovan, M. Eguchi, W. R. Shay, P. Ingallina, A. Korda and Q. Zeng, *Tetrahedron*, **49**, 5431 (1993).
325. M. P. Doyle and M. S. Shanklin, *Organometallics*, **12**, 11 (1993).
326. M. P. Doyle and M. S. Shanklin, *Organometallics*, **13**, 1081 (1994).
327. J.-Q. Zhou, and H. Alper, *Organometallics*, **13**, 1586 (1994).
328. I. Ojima, M. Tzamarioudaki and C.-Y. Tsai, *J. Am. Chem. Soc.*, **116**, 3643 (1994).
329. I. Matsuda, A. Ogiso and S. Sato, *J. Am. Chem. Soc.*, **112**, 6120 (1990).
330. I. Matsuda, J. Sakakibara and H. Nagashima, *Tetrahedron Lett.*, **32**, 7431 (1991).
331. I. Ojima, D. Machnik, R. J. Donovan and O. Mneimne, *Inorg. Chim. Acta*, **251**, 299 (1996).
332. I. Matsuda, J. Sakakibara, H. Inoue and H. Nagashima, *Tetrahedron Lett.*, **33**, 5799 (1992).
333. F. Monteil, I. Matsuda and H. Alper, *J. Am. Chem. Soc.*, **117**, 4419 (1995).
334. I. Ojima, E. Vidal, M. Tzamariondaki and I. Matsuda, *J. Am. Chem. Soc.*, **117**, 6797 (1995).
335. M. Eguchi, Q. Zeng, A. Korda and I. Ojima, *Tetrahedron Lett.*, **34**, 915 (1993).
336. I. Ojima, R. J. Donovan and W. R. Shay, *J. Am. Chem. Soc.*, **114**, 6580 (1992).
337. I. Ojima, M. Tzamarioudaki, Z. Li and R. J. Donovan, *Chem. Rev.*, **96**, 635 (1996).
338. I. Ojima, D. A. Fracchiolla, R. J. Donovan and P. Banerji, *J. Org. Chem.*, **59**, 7594 (1994).
339. I. Matsuda, H. Ishibashi and N. Li, *Tetrahedron Lett.*, **36**, 241 (1995).
340. I. Ojima, D. A. F. Kass and J. Zhu, *Organometallics*, **15**, 5191 (1996).
341. D. A. Fracchiolla, C. S. Takeuchi, and I. Ojima, *Eighth IUPAC Symposium on Organometallic Chemistry directed toward Organic Syntheses (OMCOS), August 6–10, Santa Barbara, U.S.A., Abstracts*, 248 (1995).
342. I. Ojima, J. V. McCullagh and W. R. Shay, *J. Organometal. Chem.*, **521**, 421 (1996).
343. J. V. McCullagh and I. Ojima, *212th American Chemical Society National Meeing, Orlando, Florida, August 25–29, 1996; Abstracts*, ORGN 0013 (1996).
344. J. V. McCullagh and I. Ojima, *10th International Symposium on Homogeneous Catalysis, August 11–16, Princeton, New Jersey, U.S.A., Abstracts*, PP-B43 (1996).
345. K. Tamao, K. Kobayashi and Y. Ito, *J. Am. Chem. Soc.*, **111**, 6478 (1989).
346. N. Chatani, Y. Fukumoto, T. Ida and S. Murai, *J. Am. Chem. Soc.*, **115**, 11614 (1993).

CHAPTER **30**

Synthetic applications of allylsilanes and vinylsilanes

TIEN-YAU LUH and SHIUH-TZUNG LIU

Department of Chemistry, National Taiwan University, Taipei, Taiwan 106, Republic of China
Fax: +886-2-364-4971; e-mail: tyluh@ccms.ntu.edu.tw

I. INTRODUCTION

During the last three decades, an ever increasing number of silicon-based reagents and reactions has been discovered to provoke an enormous variety of fascinating transformations under mild conditions. It is the unique properties of the silicon element that renders these synthetic applications[1–6]. The use of allylsilanes and vinylsilanes in organic synthesis has been particularly attractive and the chemistry has been covered extensively in several excellent monographs[1–6] and numerous review articles[7–32]. This chapter summarizes recent developments of the synthetic applications of these silyl functionalities. Material covered in earlier reviews will not be repeated here. As in-depth discussions regarding the syntheses of allyl- and vinylsilanes can easily be found in these reviews[1–32], the syntheses of these organosilicon compounds are, in general, not included, unless the allyl- or vinylsilanes are used for the synthesis of other analogs. Literature dates up to early 1996, but comprehensive coverage has not been attempted. Personal prejudice and ignorance become factors dictating the selection or omission of various important works for which the authors assume full responsibility.

II. ELECTROPHILIC SUBSTITUTION OF C−Si BONDS

Substitution of the carbon–silicon bond in allyl- and vinylsilanes by an electrophile has served as a powerful tool in organic synthesis. Electrophiles ranging from proton, carbon and main group heteroatoms to certain transition metal species have been employed. A comprehensive review covers literature up to early 1989[19]. The directive effect of the silicon moiety and the mechanistic aspects of these substitution reactions have been discussed in detail[19,33]. Scheme 1 summarizes the typical reaction patterns for the displacement of C−Si bonds in allyl- and vinylsilanes by electrophiles E^+.

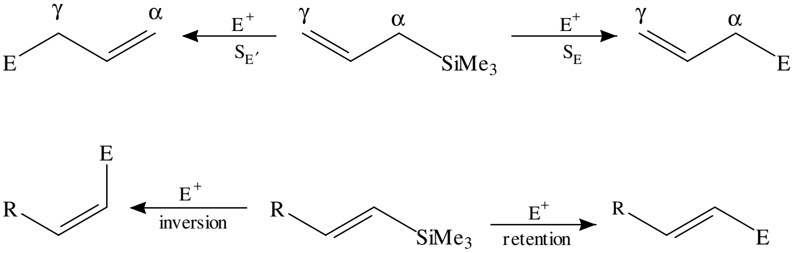

SCHEME 1

In the case of allylsilanes, most reactions occur via an $S_{E'}$ manner. In other words electrophile attacks selectively at the γ-position. This process is applied particularly when the silyl group has strongly electronegative substituent(s) and carbonyl electrophiles or the like are employed. A possible six-membered ring transition state has been suggested. The reaction is, in general, stereoselective. As can be seen in Section II.B.6, electrophiles derived from sterically hindered alkyl halides may attack preferentially at the α-position.

In the case of vinylsilanes, retention of configuration is usually observed, although inversion of configuration is also known. Depending on the relative reactivity of the electrophile, nucleophilic or Lewis acid catalysts are occasionally employed to facilitate the displacement reactions. The applications of these reactions in the synthesis of natural products have recently been reviewed[32]. Selected recent examples are presented here for illustration.

A. Substitution of C−Si Bond by an Electrophile Other than Carbon

1. Protodesilylation of allyl- and vinylsilanes

The proton serves as the simplest electrophile to displace the silyl group stereo- and regioselectively. Numerous conditions have been used for the electrophilic protodesilylation of allyl- and vinylsilanes[19]. (*E*)-vinyl sulfones **2** are prepared from the silylallylic sulfones **1** in the presence of protic acids in high yield (equation 1)[34]. Diastereoselective protodesilylation of allylsilane **3** gives **4** with excellent control of the geometry of the double bond exocyclic to the ring (equation 2)[35].

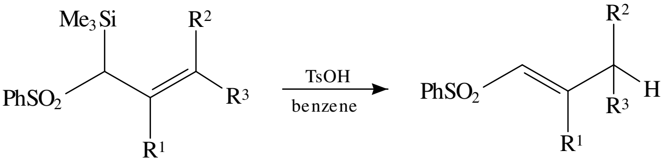

(1) **(2)**

(1)

$R^1 = H, Me; R^2, R^3 = H, Me; R^2R^3 = (CH_2)_5$

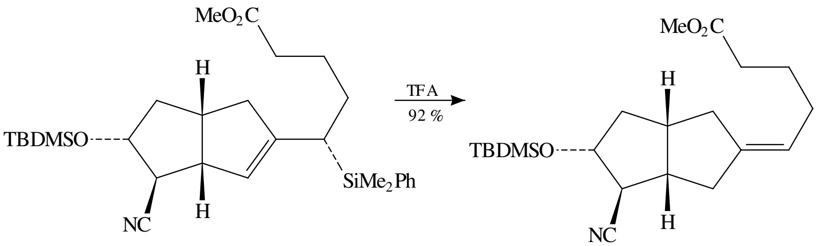

(3) **(4)**

(2)

Vinylsilanes can be desilylated stereoselectively upon treatment with iodine in water (equation 3)[36,37]. Under basic conditions, TBAF-mediated stereoselective desilylation proceeds smoothly[38]. Although desilylation of a vinylsilane can readily be achieved by treatment with hydroiodic acid, selective destannation is observed when a substrate contains both stannyl and silyl groups at the olefinic carbons (equation 4)[39].

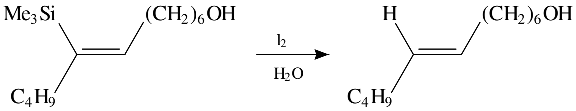

(3)

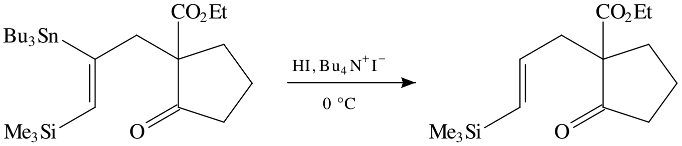

(4)

2. Halodesilylation of allyl- and vinylsilanes

Whereas an allylsilane can serve as an allyl anion synthon, the reaction of 1,3-bis(silyl)propene with electrophiles can afford the 1,3-disubstituted propene. Thus, treatment of a mixture of (*E*)- and (*Z*)-2-aryl-1,3-bis(trimethylsilyl)propenes **5** with 2 equivalents of NBS at −78 °C stereoselectively yields the corresponding (*Z*)-2-aryl-1,3-dibromopropene **6**. When 1 equivalent of NBS is employed, the monobromo product **7** is obtained (equation 5). The reactions apparently proceed via the pattern of sequential displacement of allylsilane moieties[40,41].

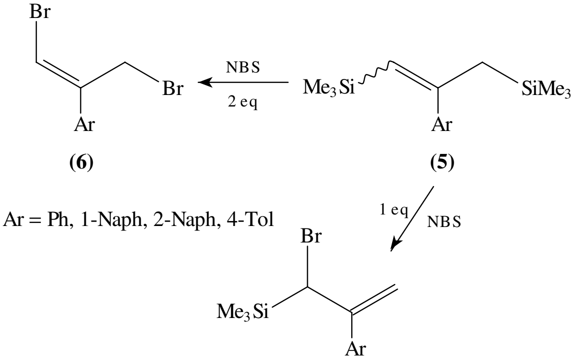

(7)

(5)

Reaction of **8** with chlorine followed by a brief exposure to KF in DMSO at 25 °C gives mycorrhizin in good yield with an inversion of stereochemistry (equation 6)[42–44].

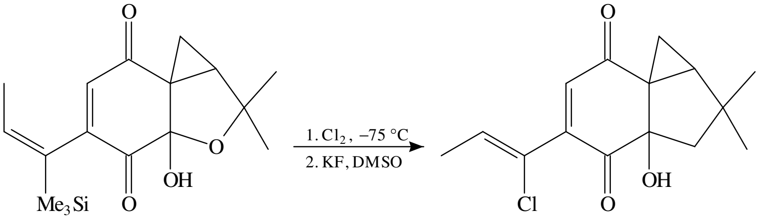

(6)

(8)

Iododesilylation of vinylsilanes gives regio- and stereoselectively the corresponding vinyl iodides. Depending on the nature of the iodination reagent and the reaction conditions, both retention and inversion of configuration take place[19,33,45]. When the reaction is carried out in DMF, HMPA or NMP solvent, the products predominantly, if not exclusively, retain their configurations[46]. The substituent on the silicon atom and its coordination state also determine the stereoselectivity of the halogenolysis of vinylsilanes. Retention of stereochemistry for vinylpentafluorosilicates is commonly found[46]. Electrophilic attack on hypervalent silicon species is suggested. More recently, IPy_2BF_4 has been found to be a useful reagent for the stereospecific iodine–silicon exchange in vinylsilanes[47]. Labile (*Z*)-vinyl(phenyl)iodonium salts **9** are synthesized from (*Z*)-vinylsilanes by the reaction with (diacetoxyiodo)benzene in the presence of $BF_3 \cdot Et_2O$[48].

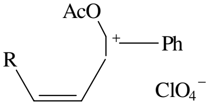

(9)

3. Other heteroatom electrophiles

Sulfonation of allylsilanes with SO_3 gives the corresponding trimethylsilyl allylsulfonates in excellent yields. The sultone intermediate **10** has been detected (equation 7)[49].

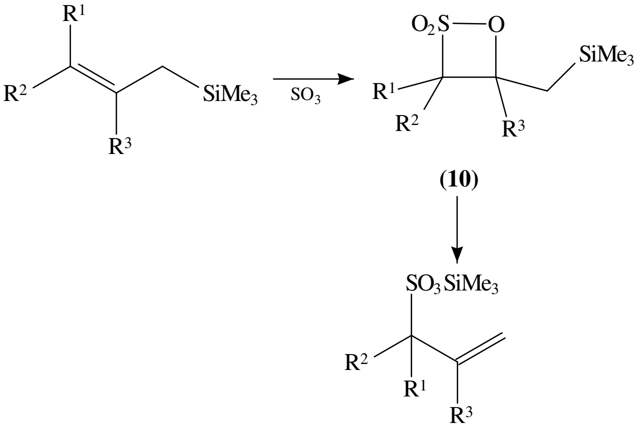

(10)

(7)

B. Substitution of C—Si Bond by a Carbon Electrophile

1. Reactions with acetals

Using liquid sulfur dioxide as a Lewis-acid solvent for the alkoxyalkylation and alkylation of allylsilanes has been investigated[50]. The reaction of acetals with allylsilanes results in the formation of homoallyl ethers **11** in excellent yields (equation 8).

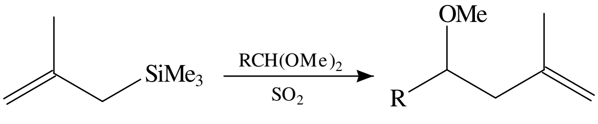

(11)

(8)

R = 1° Alk, Ph

The coupling reaction of allylsilane with the α-thiomethoxyacetal is catalyzed by TMSOTf[51]. TiCl$_4$-mediated reaction of α-bromoallylsilane **7** with 1,1-diethoxyethane leads to homoallylic ether **12** stereoselectively in excellent yield (equation 9)[40]. Under similar reaction conditions, double substitution of allylsilane to diketals **13** affords **14** in high diastereoselectivity (equation 10)[52].

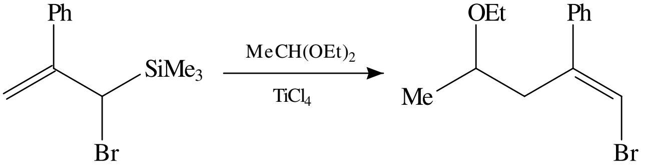

(7) **(12)**

(9)

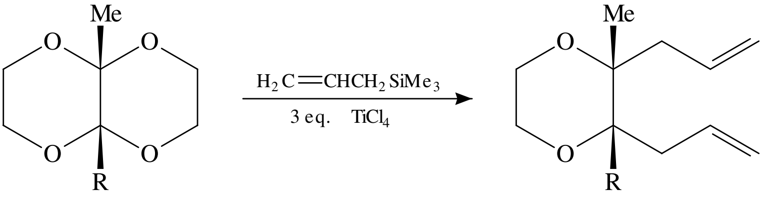

(13) **(14)**

(10)

R	*cis:trans*
Me	85 : 15
Et	90 : 10

BF$_3$ · OEt$_2$ has been shown to promote the reaction of **15** with allylsilanes to yield the corresponding 4-allylcyclobutenone **16**[53], which undergoes stereoselective thermal ring opening and subsequent intramolecular [2+2] cycloaddition[54] leading to **17** (equation 11).

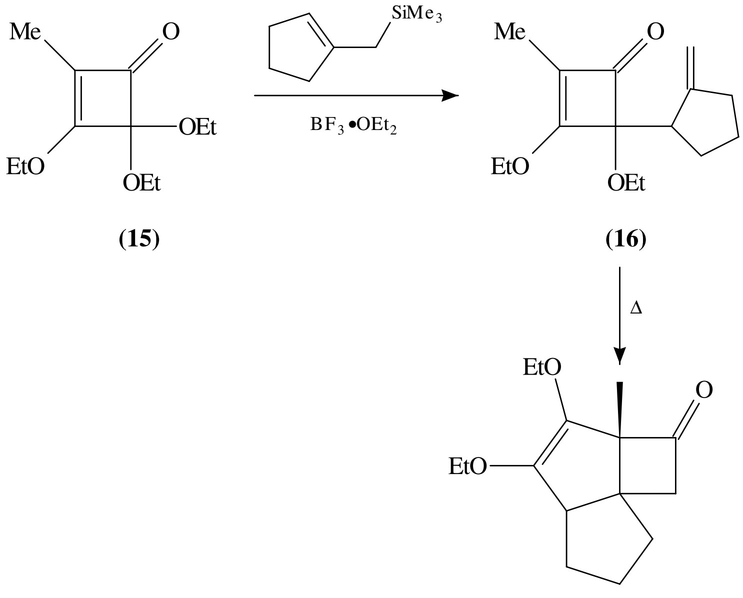

(15) **(16)** **(17)**

(11)

Neighboring methoxy group assisted asymmetric induction is demonstrated in the TMSOTf-catalyzed reaction of γ-alkoxy acetal **18** with allylsilane. A possible cyclic oxocarbenium ion intermediate **19** is proposed (equation 12)[55]. Siladioxanes **20** react with allylsilane in the presence of a catalytic amount of the Brønsted superacid $TfOH_2^+$ $B(OTf)_4^-$ to afford the allylated products **21** diastereoselectively (equation 13)[56,57].

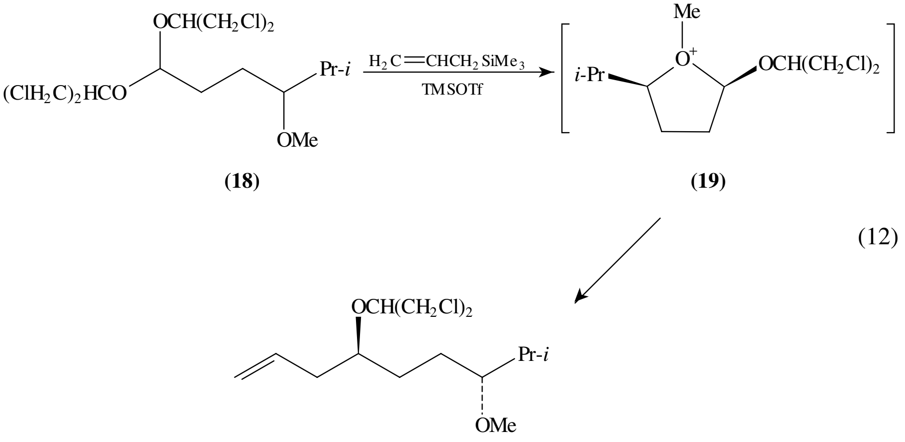

(18) **(19)**

(12)

anti : *syn* = 6 : 1

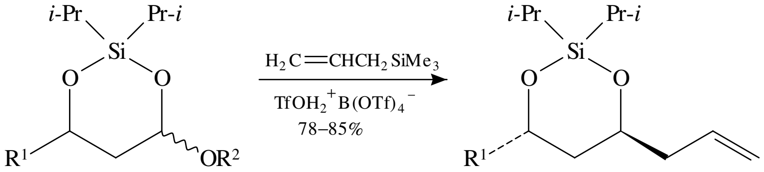

(13)

(20) **(21)**

R^1 = Pr, Bu, Ph
R^2 = Me, Et

anti : *syn* = 20–23 : 1

Optically active crotylsilane **22** functions as a chiral carbon nucleophile in TMSOTf-catalyzed reactions with acetals giving homoallylic ethers **23** in high diastereo- and enantioselectivities (equation 14)[58,59].

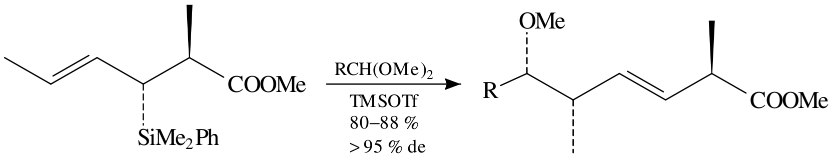

(14)

(22) **(23)**

R = $BnOCH_2$, $BnOCH_2CH_2$, Ar

(2-Siloxyallyl)silane **24**, acting as a synthetic equivalent of acetone α,α'-dianion, readily undergoes double alkylation (equation 15)[60]. An acid-catalyzed transacetalization-ring closure reaction occurs in the reaction of 6-hydroxy substituted allylsilanes **25** with acetals to afford the corresponding trisubstituted tetrahydropyrans in moderate to good yield with high diastereoselectivity (equation 16)[61].

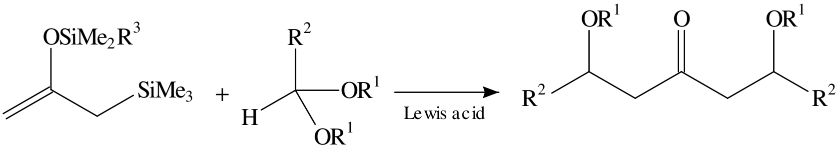

(24) (15)

R^1 = Me; R^2 = Alk, Ar, $BrCH_2$; R^3 = Me, *t*-Bu

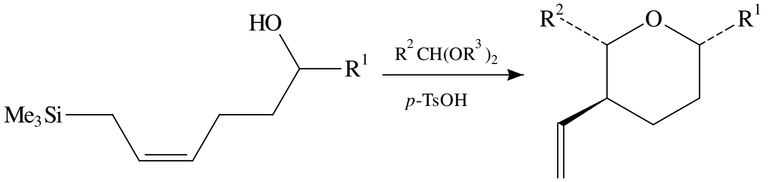

(16)

(25)

R^1 = Alk, Ph, $EtOOCH_2$; R^2 = Alk, $HC(CH_2)_2$, $MeOCH_2$; R^3 = Me, Et

Selenoacetals are found to be good electrophiles towards allylsilanes. Under $SnCl_4$ catalyzed conditions, selenoketals couple with allylsilane to produce the corresponding homoallyl selenides in moderate to good yield[62]. Reaction of allylsilanes with tris(phenylseleneno)methane or tris(phenylthio)methane in the presence of a Lewis acid furnishes the corresponding homoallylchalcogenoacetals **26** in moderate to good yields (equation 17)[63]. Thionium ion generated *in situ* from **27** leads to the corresponding coupling product (equation 18)[64].

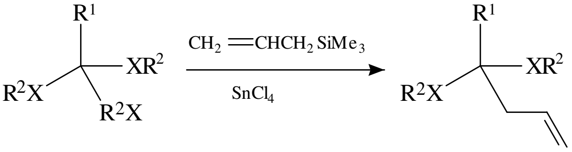

(17)

R^1 = Substituted allyl; X = S, Se

(26)

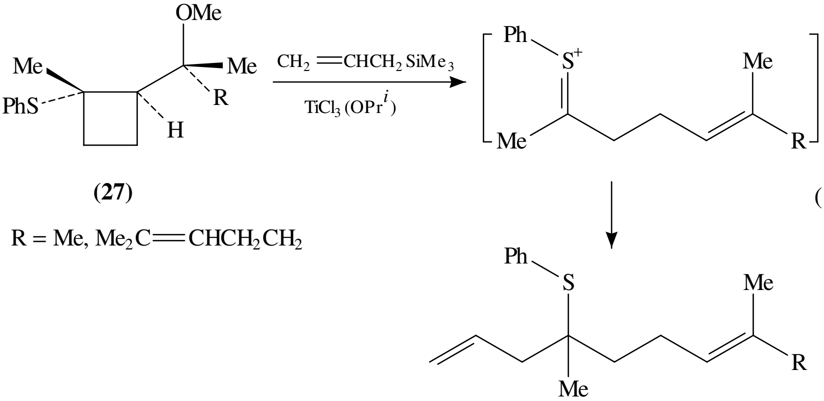

(27)

(18)

R = Me, $Me_2C{=}CHCH_2CH_2$

$Cp_2Ti(OTf)_2$ has been found to be an effective catalyst for the Sakurai–Hosomi reaction of allylsilanes with a variety of electrophiles[65].

2. Reactions with aldehydes and ketones

The reaction of allylsilanes with a carbonyl functionality has been continuously useful for the formation of carbon–carbon bonds. In the presence of a Lewis acid allylsilane, in general, undergoes $S_{E'}$ reaction with a carbonyl compound to afford the corresponding homoallylic alcohol[19,24,32]. The addition of allylsilane to carbonyl compounds catalyzed by the Brønsted acid $HN(SO_2F)_2$ gives the corresponding homoallylic alcohols in high yields[66]. It is interesting to note that cyclopentanone and acetophenone do not undergo addition reaction, whereas cyclohexanone and cyclododecanone give the corresponding homoallylic alcohols in excellent yields. Selective addition to aldehydes in the presence of α-tetralone or cyclopentanone can be achieved. Occasionally, ene reaction product has been found to be the major side product in these coupling reactions (*cf* Section V.F.1)[67]. $TiCl_4$-mediated reactions of **28** with aliphatic aldehydes afford 2,5-divinylhexane-1,6-diols in good yield with very high diastereoselectivity (equation 19)[68]. Fluoride ion promoted intramolecular cyclization of the allylsilanes **30** produced from anionic oxy-Cope rearrangement of 1,2-divinylcyclohexanols **29** leads to hydroazulenols with the *cis* ring fusion (equation 20)[69]. It is noteworthy that the Lewis acid catalyzed cyclization proceeds with high selectivity via an *anti* $S_{E'}$ pathway, which suggests that the silicon electrofuge is located away from the approaching electrophile regardless of the nature of Lewis acid or of the orientation of the double bond[70]. BF_3-catalyzed reactions of siloxy-substituted allylsilanes **31** with aldehydes give the corresponding unsaturated heterocycles **32** (equation 21)[71].

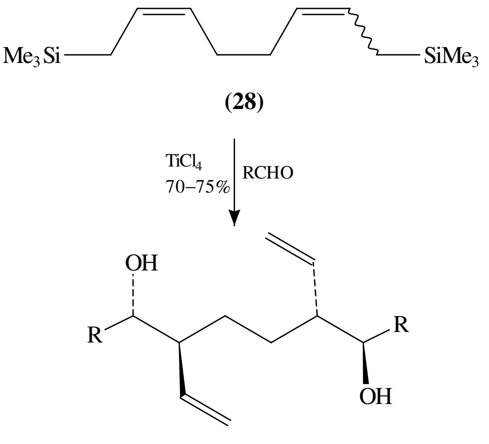

(28)

(19)

R = Ph, 4-$O_2NC_6H_4$, Alk

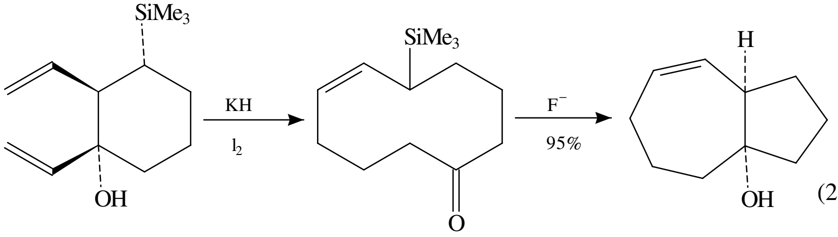

(29)

(30)

(20)

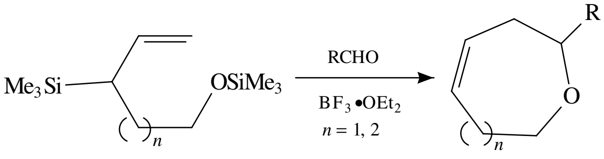

(31)

(32)

(21)

R = Me, Et, *i*-Pr, Ph

The nature of the Lewis acid catalyst has been found to play a pivotal role in the chemo- and stereoselectivities of the Sakurai–Hosomi reaction. For example, the reaction of **33**, which contains both allylsilane and allylstannane moieties, with benzaldehyde leads to the silyl-substituted homoallylic alcohol **34** in moderate yield when a mild Lewis acid such as Et_3Al is used. On the other hand, when $BF_3 \cdot OEt_2$ or fluoride ion is employed, the silyl group is displaced to give **35** (equation 22)[72]. Other strong Lewis acids such as $TiCl_4$, $SnCl_4$, $FeCl_3$, $MgBr_2$, $ZnCl_2$ and TMSOTf, however, give unsatisfactory results. As expected, the trimethylsilyl group is a much better leaving group than the diphenylmethylsilyl moiety in these $S_{E'}$ reactions.

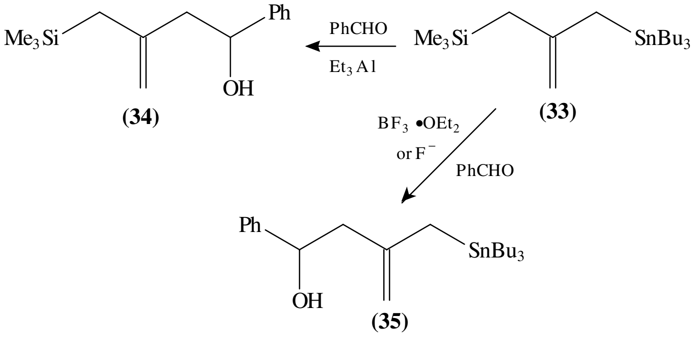

(22)

Carbamate and amide groups have been found to be stable under these coupling conditions[73]. In the presence of $TiCl_4$ or $SnCl_4$, chiral α-keto amides **36** react with allylsilane to produce, after hydrolysis, optically active tertiary alcohols **37** with extremely high optical selectivity (equation 23)[74]. The addition reaction appears to occur from the *Si* face of the carbonyl group. In a similar manner, a high degree of stereoselectivity is obtained from the reactions of *N*-Boc-α-amino aldehydes **38** with 2-substituted allylsilanes (equation 24)[75].

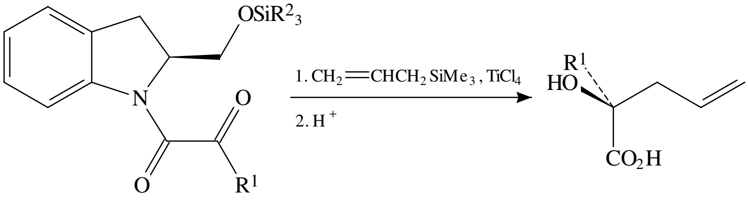

(23)

(37)

(36) R^1 = Me or Ph

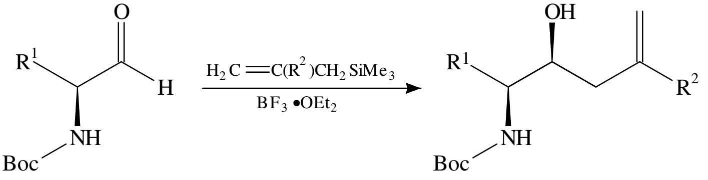

(24)

(38)

R^1 = 1° and 2° Alk; R^2 = *i*-Pr, $ClCH_2$, PhCH=CH

Parallel to an earlier work on the highly diastereoselective reactions of aliphatic aldehydes with allylsilane in the presence of **39**[76], treatment of methyl ketones under the same conditions yields the corresponding tertiary homoallylic ether with a diastereomeric excess of up to 90% (equation 25)[77].

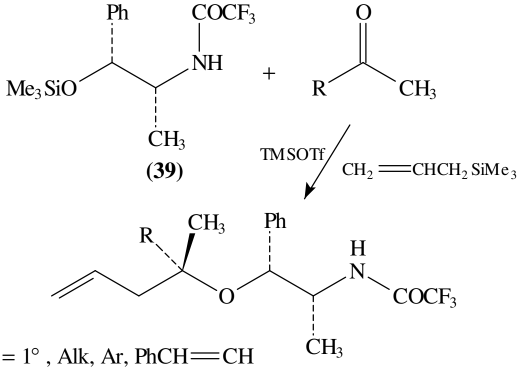

(25)

The reaction of (Z)-β-methylcrotylsilane with 2-benzyloxypropanal in the presence of chelative $SnCl_4$ gives the *anti*-homoallylic alcohol **40** diastereoselectively (equation 26)[78]. The use of chelative $TiCl_4$ versus nonchelative $BF_3 \cdot OEt_2$ Lewis acids also gives different stereoselectivity in the coupling of allylsilane with the aldehydes **41** (equation 27)[79].

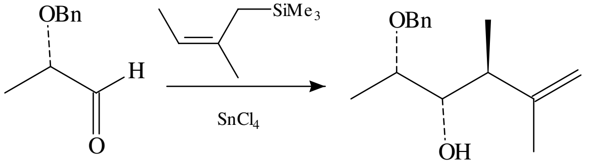

(26)

(40) *anti* : *syn* = 94 : 6

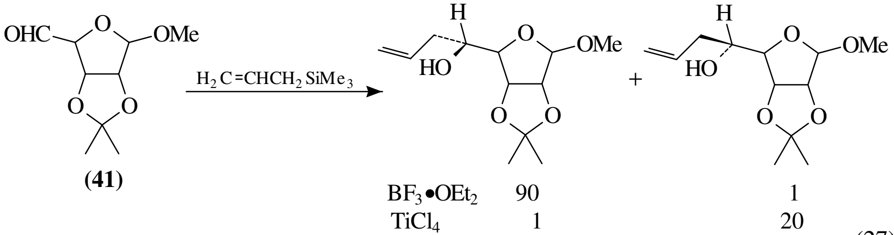

(27)

The addition of chiral (E)-crotylsilanes **42** to (S)-2-alkoxypropanal **43** has been investigated in detail[80]. When the (S)-silane **42** and **43a** are employed, nonchelating $BF_3 \cdot OEt_2$ promotes the addition reaction from the *Re* face of the aldehyde moiety to give *syn* homoallylic alcohol **44a** with excellent levels of Felkin induction. *Anti* homoallylic alcohol **45** is obtained with high levels of *anti*-Felkin selectivity from the *Si* face of the aldehyde group when a chelative Lewis acid such as $TiCl_4$ is employed (equation 28). Interestingly, both $TiCl_4$ and $BF_3 \cdot OEt_2$ mediated condensations of (R)-silane **42** with **43a** yield the same *syn* disposed crotylsilation product **46a** having *anti*-Felkin induction (equation 29). Reactions of sterically hindered **43b** with (S)-**42** yield **44b** predominantly (>30 : 1) in the presence of $TiCl_4$ or $BF_3 \cdot OEt_2$. In these cases, the bulky silicon group prevents the Lewis acid from chelate formation with the aldehyde. In a similar manner, treatment of (R)-**42** with **43b** affords **46b** as the major product no matter which catalyst ($TiCl_4$ or $BF_3{\cdot}OEt_2$) is used (equation 29). An open transition state model has been employed to rationalize the stereoselectivity (Scheme 2).

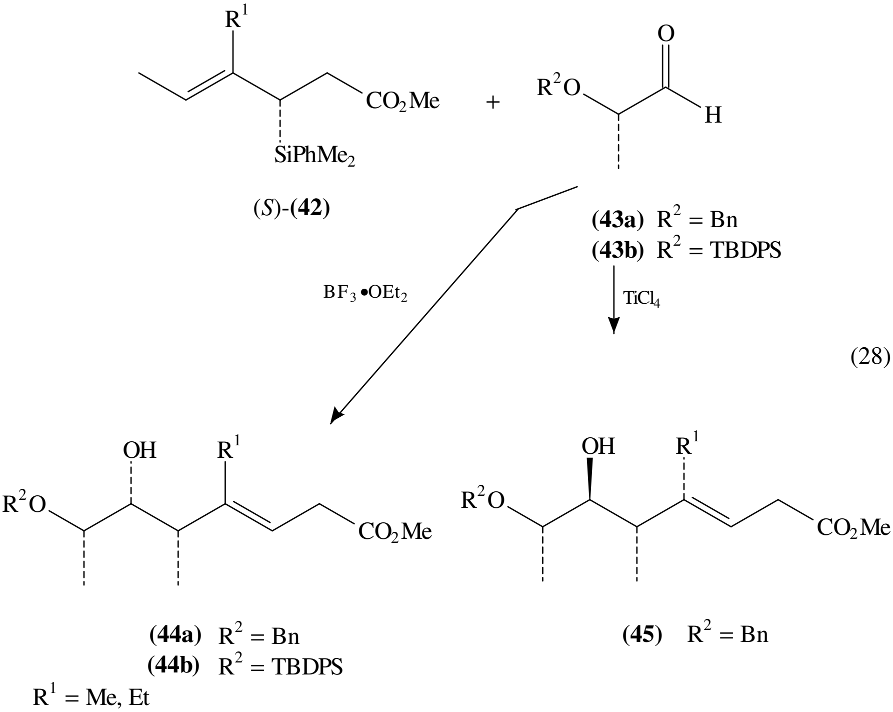

(28)

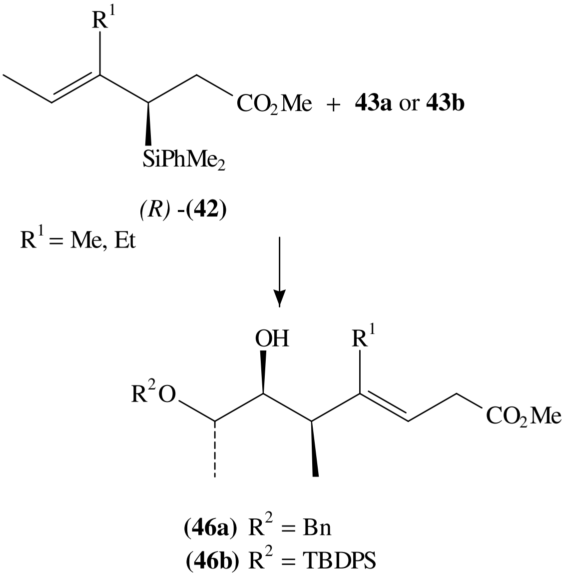

(29)

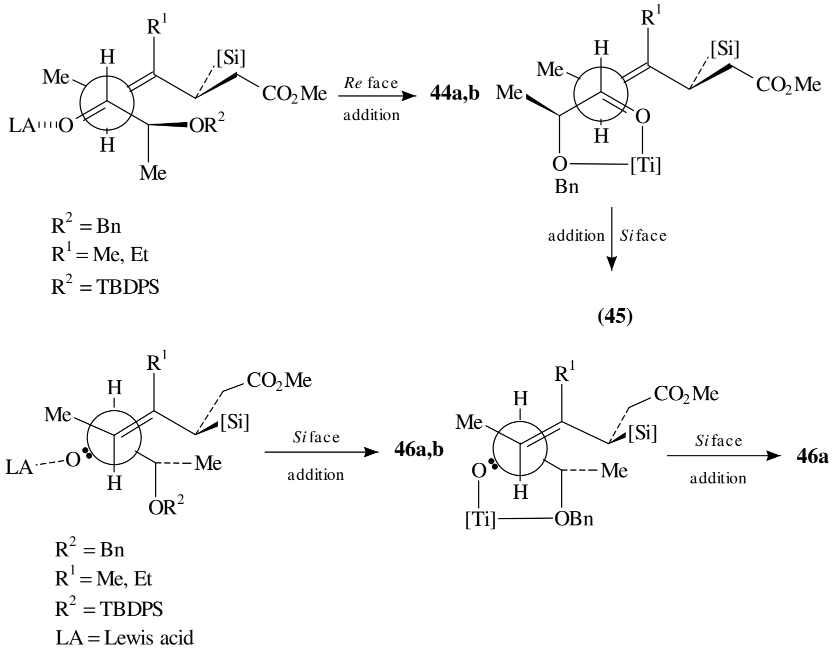

SCHEME 2

Treatment of chiral (*E*)-crotylsilanes **47** with **43a** in the presence of $BF_3 \cdot OEt_2$ gives tetrahydrofuran derivatives in good yield with 96% de. Interestingly, 1,2-silyl group migration competes favorably with elimination of the silyl group after condensation with **43a** (equation 30)[81].

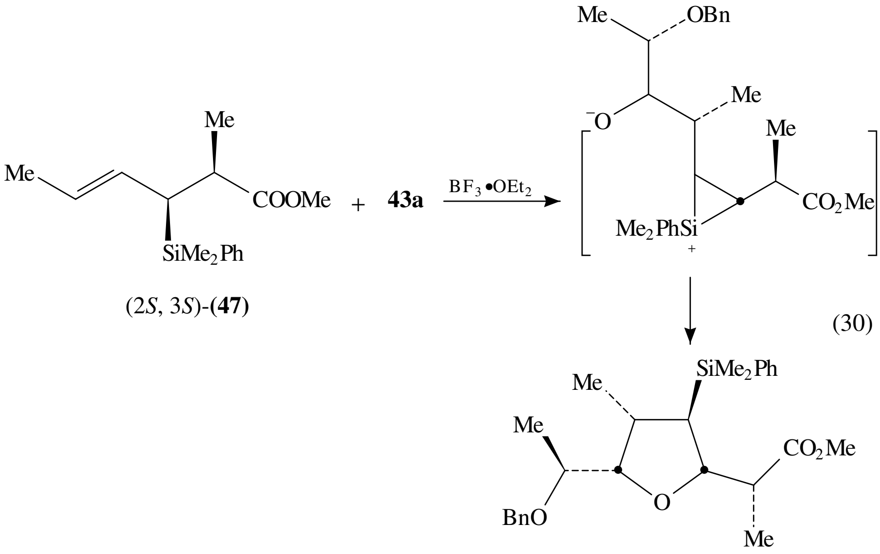

(2*S*, 3*S*)-**(47)**

(30)

The $TiCl_4$-induced three-component coupling reaction of an α-haloacylsilane, allylsilane and another carbonyl compound gives **48** in good yield. A silyl enol ether intermediate is suggested (equation 31)[82]. The reaction of a cyclopropyl ketone with allylsilane yields a mixture of skeletal rearranged products[83].

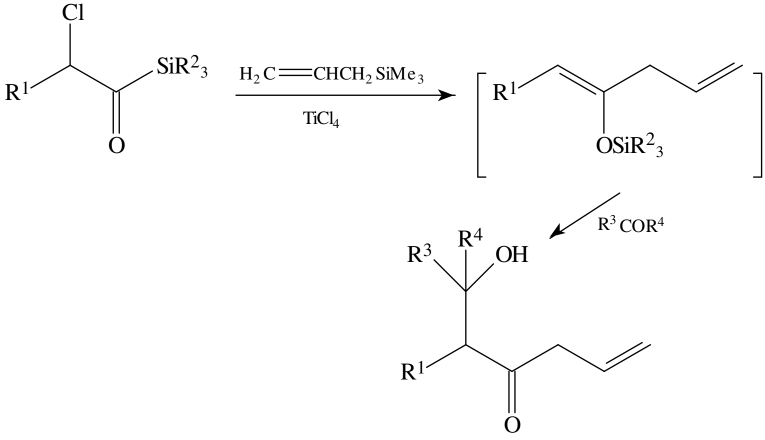

(31)

(48)

$R^1 = n\text{-}C_3H_7, n\text{-}C_6H_{13}$; R^2 = Me, *t*-Bu, Ph; R^3 = Me, Et, Ph; R^4 = H, Me

The TMSOTf-catalyzed reaction of allylsilane, a carbonyl compound and a trimethylsilyl ether gives the corresponding homoallylic ether (equation 32)[84]. Tetrahydropyran derivatives **49** are thus obtained conveniently (equation 33)[85–87]. The extension of this intramolecular reaction to vinylsilane derivatives also yields dihydropyran derivatives **50** (equation 34)[88]. Interestingly, two equivalents of the carbonyl compounds react with **51** in the presence of $BF_3 \cdot OEt_2$ catalyst to yield tetrahydropyran derivatives (equation 35). Presumably, an ene reaction may occur first[89]. The methodology consists of the coupling between a carbonyl compound and a silyl ether, containing a judiciously positioned allylsilane moiety. The oxonium cation initially formed is the key intermediate leading to these products.

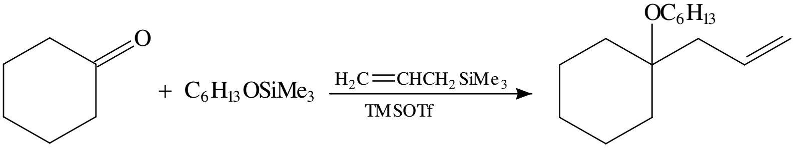

(32)

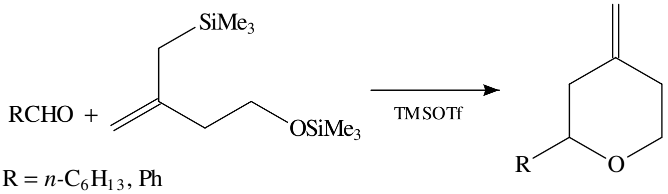

(33)

R = *n*-C_6H_{13}, Ph

(49)

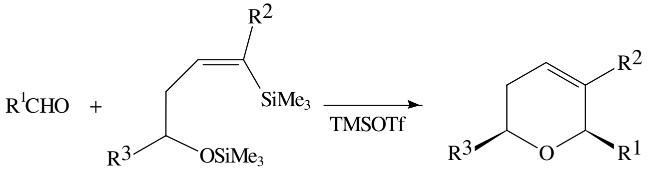

R^1 = 1° and 2° Alk, Ph; R^2, R^3 = H, Me

(50)

(34)

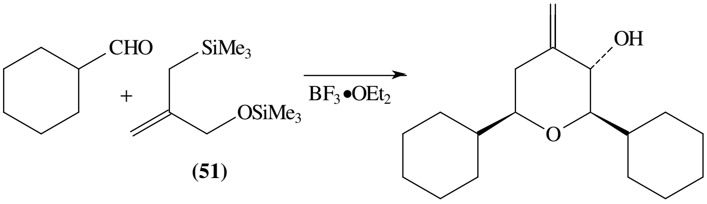

(51)

(35)

Structural variation at the silicon atom changes the reactivity and the selectivity. The reactions of pentacoordinated allylic silicates are remarkably different from their tetracoordinated allylic silane counterparts[90–95]. Extremely high regio- and stereospecificites in reactions with carbonyl compounds are well documented[20]. Thus, allylation of aldehydes with allyltrifluorosilane in the presence of catechol and triethylamine gives the corresponding homoallylic alcohols in a regiospecific manner. The pentacoordinated allylsilicate **52** is suggested as the key intermediate. Unlike reactions with tetracoordinated allylsilanes which occur via the acyclic $S_{E'}$ mechanism, the reactions of an aldehyde with **52** proceeds via a cyclic transition state **53** (equation 36)[90,91]. Similar reactions with α-hydroxyketones[92] and with β-functionalized α,β-unsaturated enones[93] give the corresponding homoallylic alcohols with excellent diastereoselectivity. $BF_3 \cdot OEt_2$-mediated condensation of allylalkoxysilane with aldehydes gives 2,4,6-trisubstituted tetrahydropyrans **54** (equation 37)[95].

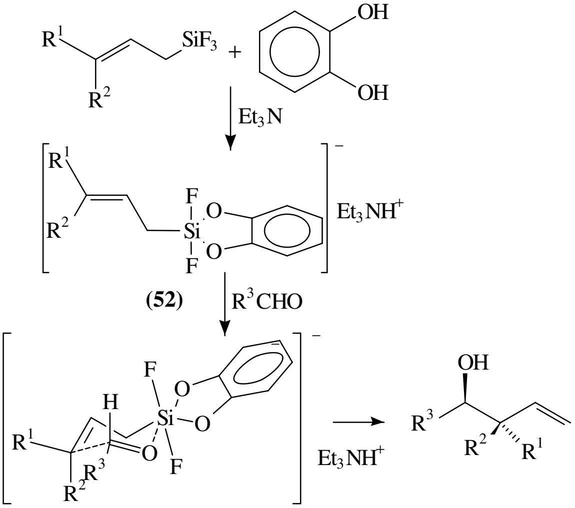

(52)

(53)

(36)

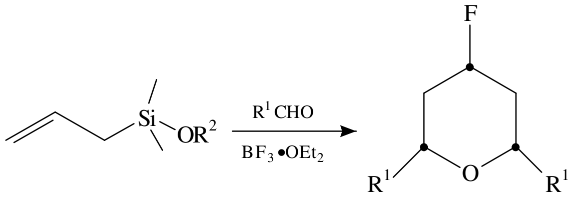

(54)

(37)

$R^1 = n\text{-}C_6H_{13}, n\text{-}C_8H_{17}$; $R^2O = (-)$-menthoxy

Allyltrichlorosilanes react regioselectively with aldehydes in the presence of an amide additive[96] to afford the corresponding homoallylic alcohols in high yields. The reaction can also be carried out in DMF without a catalyst (equation 38)[97,98]. It is noted that *syn* and *anti* homoallylic alcohols are obtained stereospecifically from (*Z*)- and (*E*)-crotyltrichlorosilanes, respectively. Again, a cyclic transition state similar to **53** is proposed. A one-pot synthesis of homoallylic alcohols from the reactions of allyl halides with trichlorosilane in the presence of triethylamine and copper(I) chloride followed by the addition of an aldehyde is achieved (equation 39)[99]. Allyltrichlorosilane is believed to be generated *in situ* under these conditions. The reactions of 1-chloro-2,4-pentadiene with aldehydes under the same conditions give **55** exclusively, which suggests that the incoming electrophile attacks at the γ position of the diene system (equation 40). This result further supports the early suggestions that the reaction may proceed via a cyclic transition state like **53**. It is noteworthy that 2,4-pentadienyltrimethylsilane reacts with aldehydes at the terminal position of the diene[100–102].

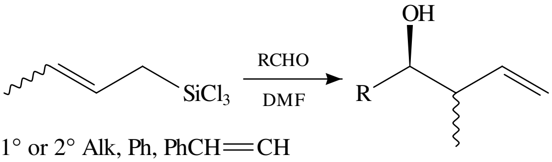

(38)

R = 1° or 2° Alk, Ph, PhCH=CH

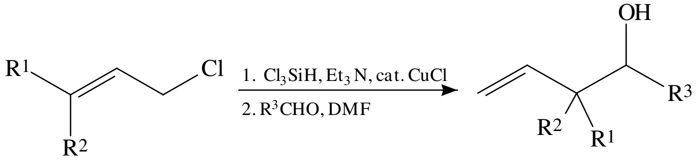

(39)

$R^1 = H, Me, Me_2C{=}CHCH_2$
$R^2 = H, Me$

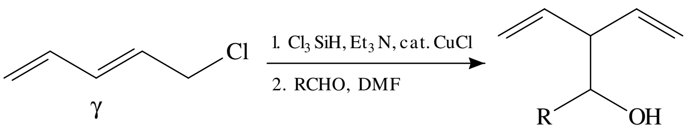

(55)

(40)

R = Ph, $PhCH_2CH_2$, PhCH=CH

It is well documented that strained 1-silacyclobutyl enol ethers undergo aldol reactions at a much accelerated rate compared to that of the acyclic counterpart[103,104]. Similar behavior has been observed in the reactions of the corresponding allylsilanes with aldehydes[105]. Thus, thermolyses of **56** with aldehydes give stereospecifically 1-silacyclobutyl ethers which are hydrolyzed under acidic conditions to yield the corresponding homoallylic alcohols (equation 41). Although ketones do not react under similar conditions, hydroxyketones **58** undergo coupling reactions with **57** to give diols **60** stereoselectively. The cyclic transition state **59** is suggested (equation 42).

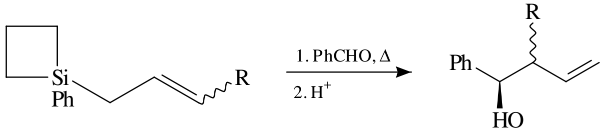

(41)

(56)
R = Ph, *n*-Pr

Z-(**56**) *syn* : *anti* = 5 : 95
E-(**56**) *syn* : *anti* = 95 : 5

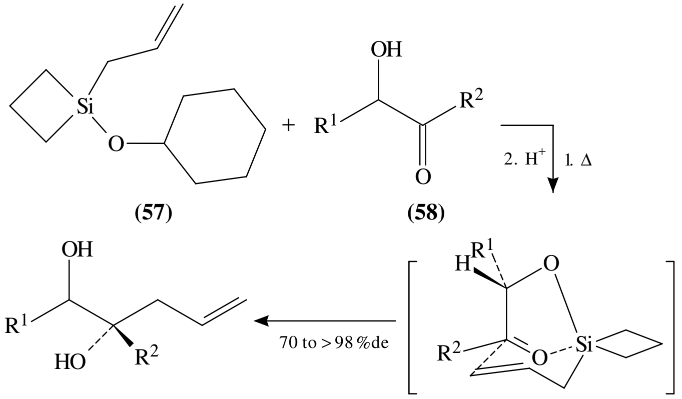

(42)

(57) **(58)** **(59)** **(60)**

R¹ = Ph, *n*-Bu
R² = Ph, Me
R¹ = Ph, *n*-Bu; R² = Ph, Me

3-Methylenesilacyclobutane **61** reacts with aldehydes thermally to give the cyclic siloxy adduct **62**[105]. In the presence of BF_3OEt_2, treatment of **61** with 1,4-dicarbonyl compounds yields the corresponding 8-oxabicyclo[3.2.1]octane skeleton **63** (equation 43)[106].

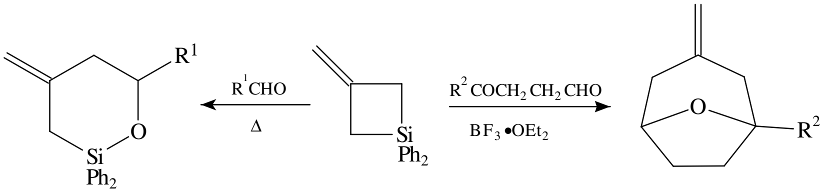

(43)

(62) **(61)** **(63)**

$R^1 = n\text{-}C_6H_{13}$, Ph; R^2 = Me, Ph

Cathodic coupling of ketones with **64** takes place regioselectively at the β-position to the silyl substituent to give **65** in good yields (equation 44). A radical anionic intermediate derived from the carbonyl compound is proposed[107].

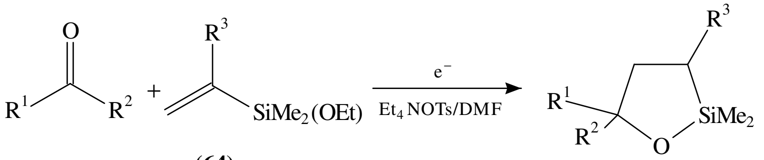

(44)

(64)

(65)

$R^1, R^2 = Alk ; R^3 = H, n\text{-}Pr$

3. Reactions with enones

Since allylsilane can be considered as a very soft nucleophile because of the involvement of $\sigma-\pi$ conjugation between the π-electrons of the double bond and the σ-electrons in the carbon–silicon bond, the addition of allylsilanes to α,β-unsaturated enone moiety occurs exclusively via 1,4-addition[19,20]. A typical Sakurai–Hosomi reaction is illustrated in the reaction of allylsilane **66** with enone **67** in the presence of $TiCl_4$ to give **68** which is used for the synthesis of a cyclic enediyne (equation 45)[108]. A similar reaction has been used for the synthesis of *ent*-herbasolide **70** from enone **69** (equation 46)[109]. Prenylsilane undergoes 1,4-addition with squaric acid chloride **71** followed by dechlorosilylation to give **72** as the predominant product (equation 47). Interestingly, other simple allylsilanes react in a 1,2-addition fashion to yield **73**[110].

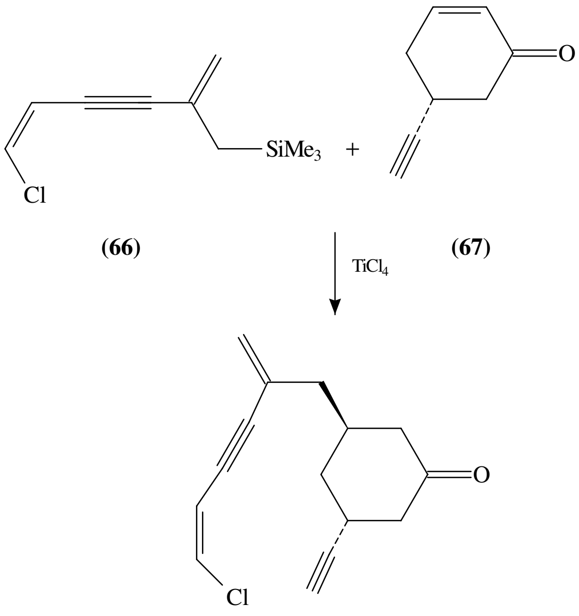

(66)

(67)

(45)

(68)

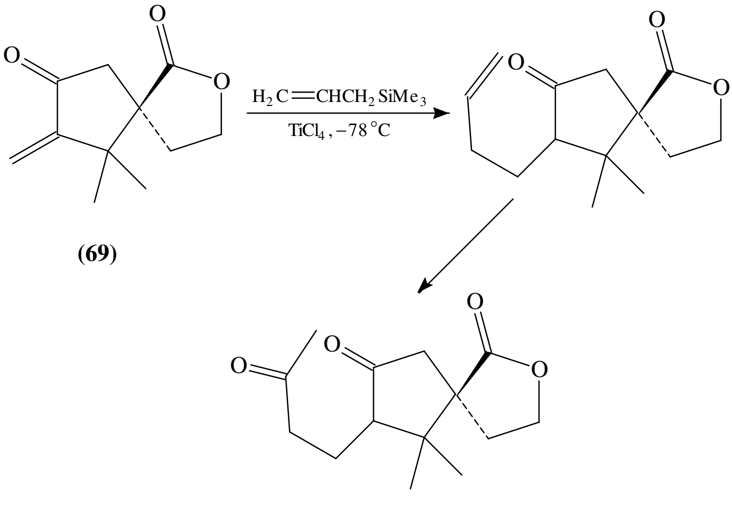

(69)

(70)

(46)

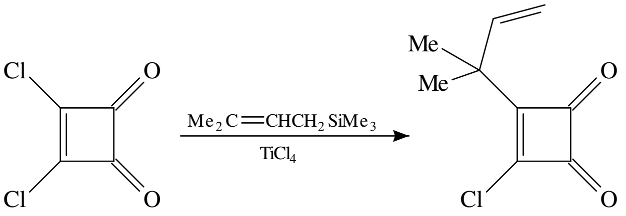

(71) **(72)**

(47)

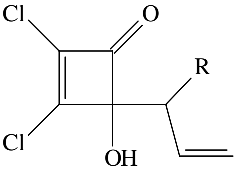

(73)

R = H or Me

Lewis acid-catalyzed stereoselective addition of crotylsilanes to chiral **74** has been studied in detail[111,112]. The presence of the chiral auxiliary at C_2 (e.g. *p*-tolylsulfinyl or menthoxy carbonyl group) induces the diastereofacially selective addition of cyclopentenones with crotylsilanes. Thus, (*E*)-crotylsilane favors the *erythro* product, whilst (*Z*)-isomer favors the *threo* product. High enantioselectivity is observed in both reactions (equation 48). In a similar manner, conjugated addition of allylsilane to **75** proceeds with high efficiency (equation 49)[113]. Interestingly, the yield and enantiomeric excess of the product is dependent on the amount of $TiCl_4$ used and the best selectivity

(94–96 %ee) is obtained with 0.8–0.95 equivalent of the Lewis acid catalyst.

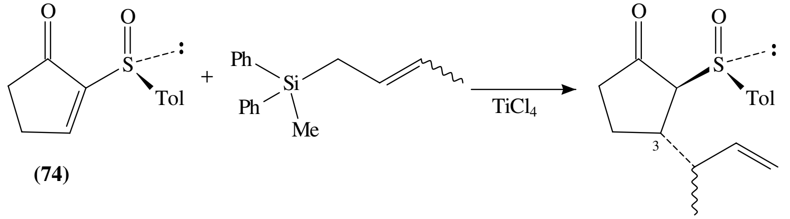

(74)

(48)

E *erythro* : *thero* = 9 : 1 3*S* : 3*R* = 99 : 1

Z *erythro* : *thero* = 1 : 14 3*S* : 3*R* = 99 : 1

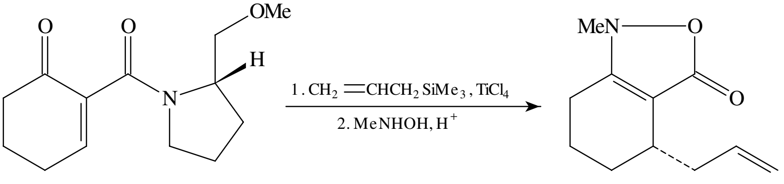

(75)

(49)

TMSOTf-mediated intramolecular cyclization of allylsilanes with alkylidene 1,3-dioxo moiety gives almost exclusively the *trans*-1,2-disubstituted cyclopentanes **76** in high yield (equation 50). Other Lewis acids or fluoride ion can also promote similar reactions[114]. In the presence of the chiral auxiliary, such intramolecular cyclization gives the corresponding *trans*-1,2-disubstituted cyclopentanes and cyclohexanes **77** (equation 51) in excellent enantioselectivity[115].

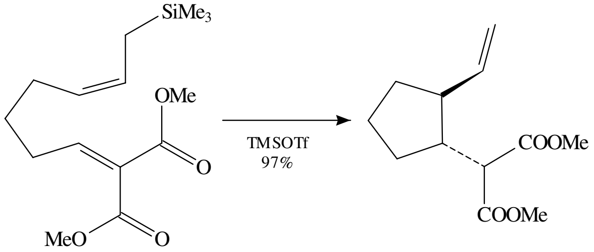

(76)

(50)

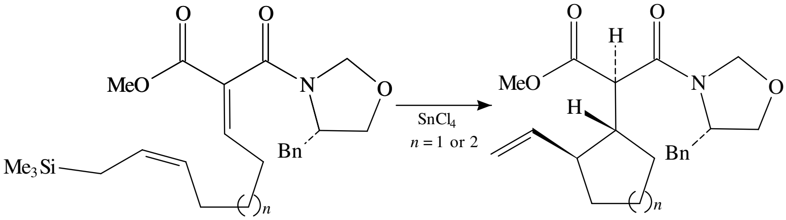

(77)

(51)

Intramolecular cyclization of allylsilane moiety with conjugated dienone groups occurs readily. Both S_E and $S_{E'}$ reactions are observed depending on the nature of the catalyst.

Amberlyst 15 and $EtAlCl_2$ catalysts give γ-substitution products **78** (equation 52) and **79** (equation 53)[116,117]. Fluoride ion, on the other hand, selectively promotes α-displacement reaction (giving e.g. **80**) (equation 53)[118].

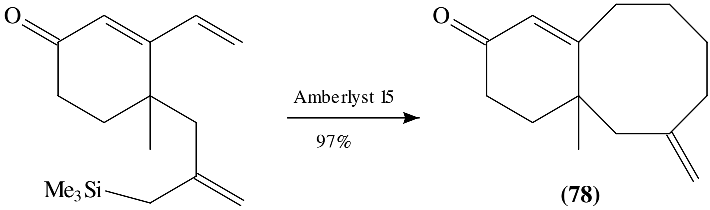

(52)

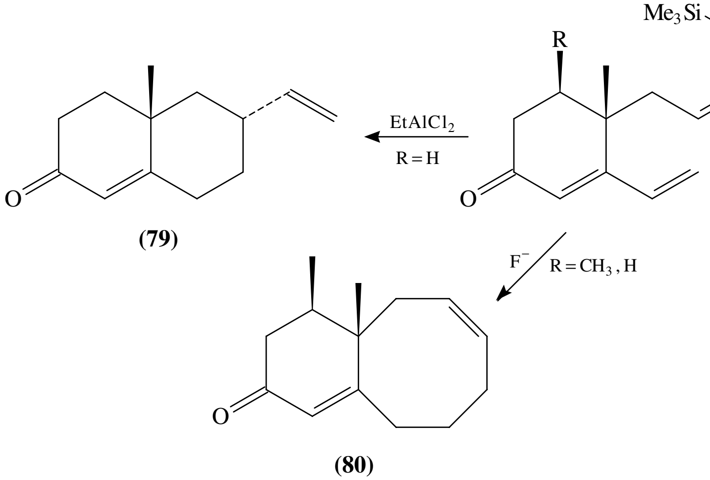

(53)

4. Reactions with iminium ions

In the presence of a Lewis acid or fluoride ion, imines react with allylsilane to yield the homoallylic amines with high stereoselectivity[119,120]. Thus, treatment of N-galactosylaldimine **81** with allylsilane in the presence of excess of $SnCl_4$ yields the corresponding allylated product **82** (equation 54). It is noted that aliphatic aldimines do not react under these conditions. Fluoride ion promoted crotylation of aldimines proceeds in a regiospecific and diasteroselective manner[121]. A pentacoordinate silicate moiety is involved in this reaction.

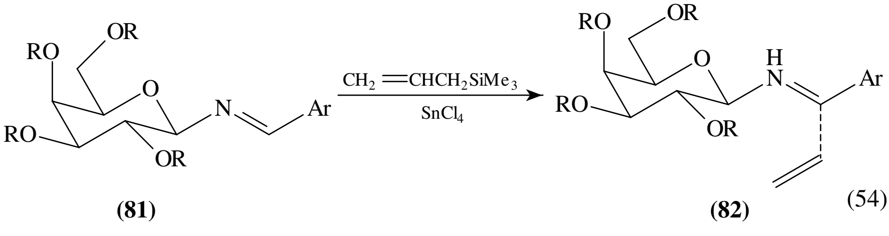

(54)

R = t-BuCO

Treatment of an α-acylaminal derivative **83** with allylsilanes in the presence of a Lewis acid or a Brønsted acid gives the corresponding condensation products (equation 55)[122–125]. The reaction can also proceed intramolecularly, e.g. in the formation of **84** and **85** (equations 56 and 57). A piperidine skeleton **86** can also be formed by such intramolecular cyclization (equation 58)[126].

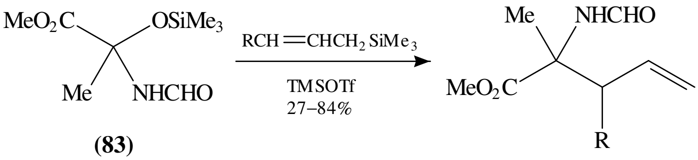

(83)

(55)

R = H, Alk

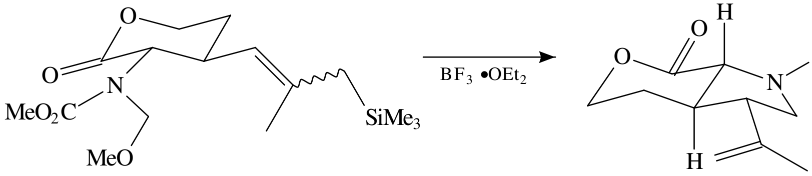

(56)

(84)

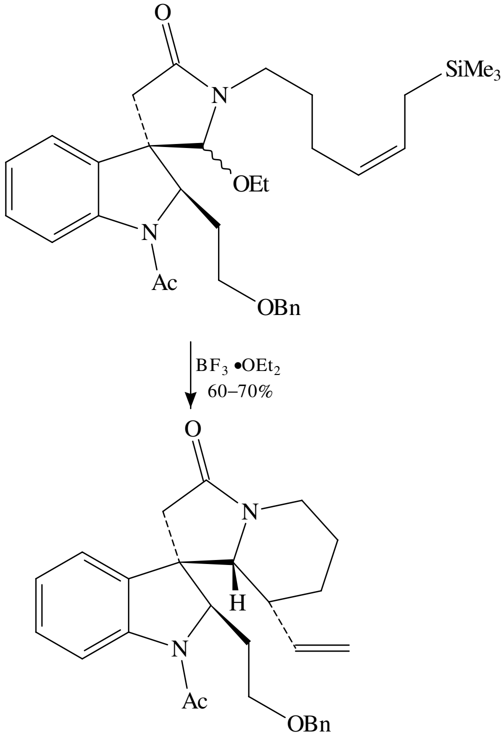

(57)

(85)

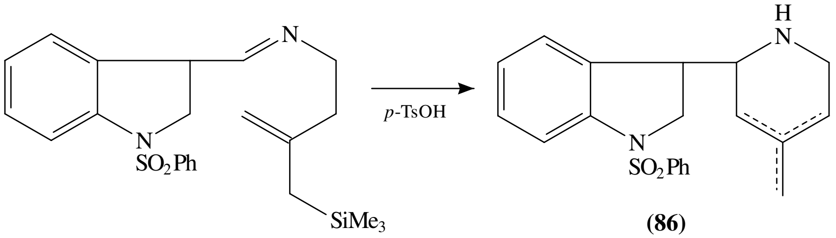

(86)

(58)

The reaction of 2,4-pentadienyltrimethylsilane with *N*-acyliminium ion generated *in situ* at −78 °C results in the formation of pentadienyl-substituted lactams **87** in good yield (equation 59). It is noted that the reaction temperature is an important factor for controlling the ϵ-regioselectivity. A mixture of ϵ- and γ-substitution products at the dienyl system is obtained when the reaction is carried out at 0 °C[127].

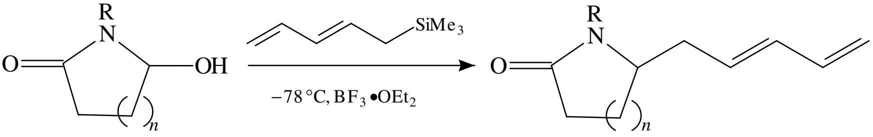

(87)

(59)

$R = PhCH_2, PhCH_2OCH_2, CH{=}CHCH_2$

In the presence of the $TiCl_4$ catalyst, δ-amino-substituted allylsilanes readily react with isobutyraldehyde to yield piperidine derivatives **88** (equation 60)[128]. Presumably, an iminium ion intermediate is formed and the Boc group is replaced under the reaction conditions. It is noteworthy that the regioselectivity is different when acid chloride in used as the electrophile (*cf* Section II.B.5).

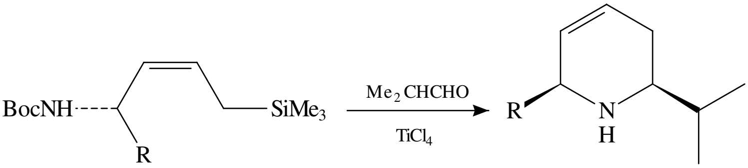

(88)

(60)

$R = Me, Me_2CHCH_2, Et(Me)CH$

The coupling reactions of imines with vinylsilanes serve as a key protocol for the synthesis of various alkaloids (equation 61 and 62)[129−132].

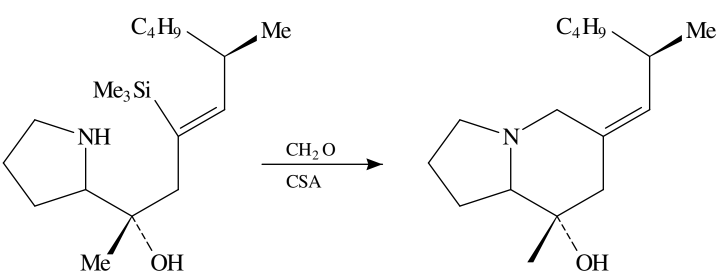

(61)

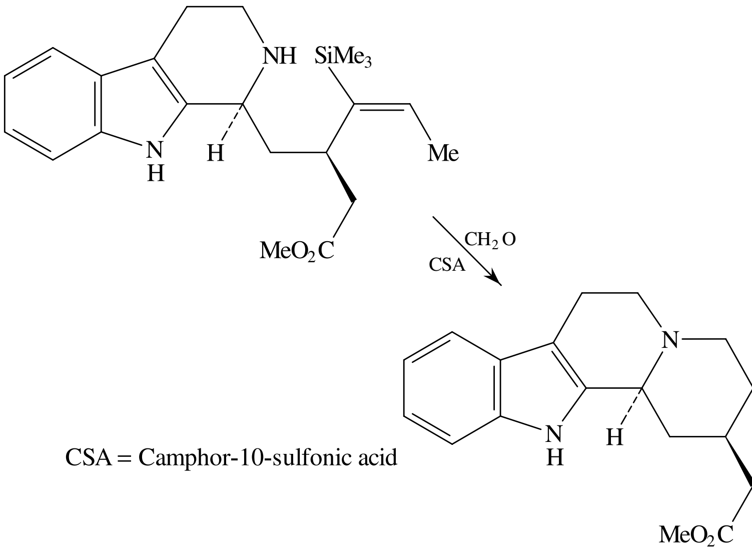

(62)

CSA = Camphor-10-sulfonic acid

Protonation of an imine also leads to the corresponding intramolecular cyclization product[133]. Acyliminium ion behaves similarly[134,135]. Representative examples are shown in equations 63–65.

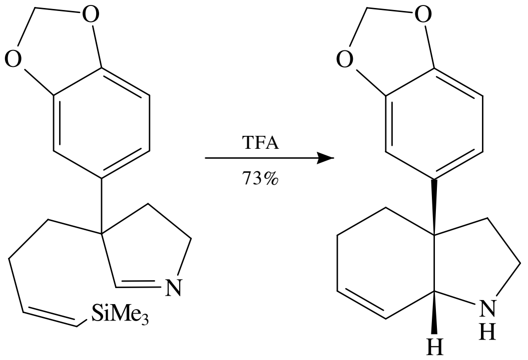

(63)

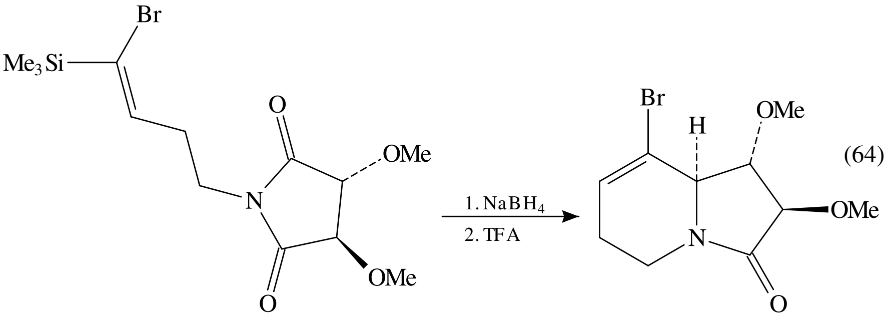

(64)

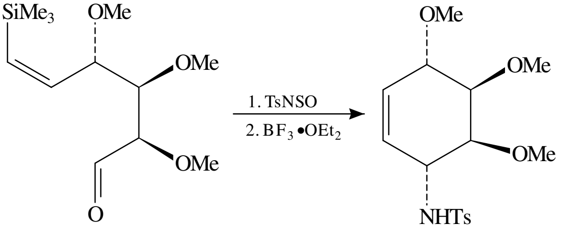

(65)

The iminium ion generated *in situ* from the oxazolidine in equation 66 undergoes cyclization with (*Z*)-vinylsilane satisfactorily. Attempts to cyclize the corresponding *E*-isomer are unsuccessful[136].

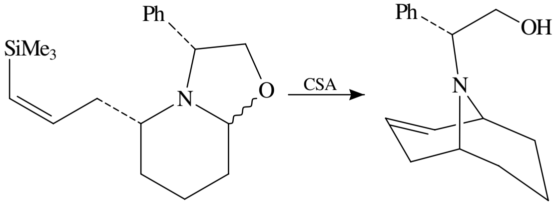

(66)

5. Reactions with acid chlorides

Treatment of **7** with acid chloride at −60 °C in the presence of $TiCl_4$ gives the corresponding coupling product **89** stereoselectively (equation 67)[40]. The reaction of aryl chloroformate with allylsilane in the presence of aluminum trichloride gives aryl 4-alkenoates **90** in excellent yield (equation 68)[137].

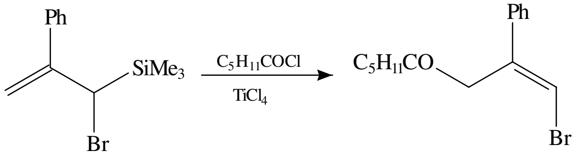

(7) **(89)**

(67)

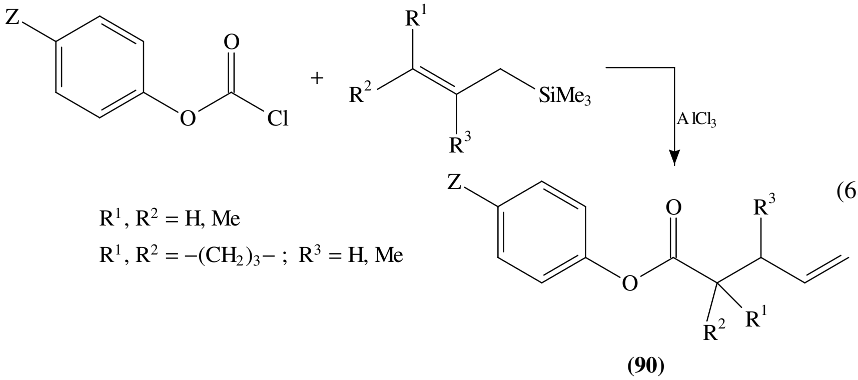

R^1, R^2 = H, Me

$R^1, R^2 = -(CH_2)_3-$; R^3 = H, Me

(90)

(68)

Depending on the nature of the substrate, treatment of acid chloride with δ-aminoallylsilane derivatives **91** gives different regioisomers. When R^1 is methyl or a primary alkyl group, a normal S'_E reaction takes place. When R^1 is the sterically hindered isopropyl group, direct displacement of the silyl group occurs (equation 69)[128]. Similar regioselectivity is observed when an aldehyde is employed as the electrophile (see Section II.B.6).

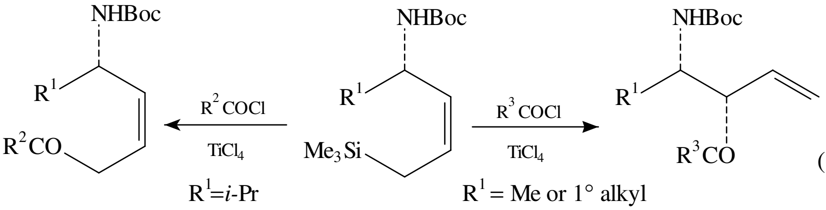

(69)

(91)

R^2 = Me, $PhCH_2$

R^3 = Me, $PhCH_2$, $n\text{-}C_6H_{13}$

Reactions of 2-stannyl-3-silylpropene with acid chlorides in the presence of Lewis acid afford vinylsilanes **92** via 1,2-silyl migration followed by destannylation (equation 70)[138].

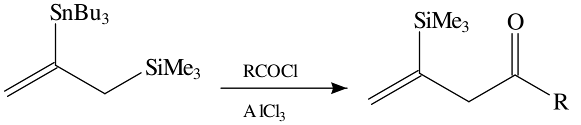

(70)

(92)

Lewis acid-mediated reactions of acid chlorides with vinylsilanes have demonstrated numerous fascinating transformations leading to carbon–carbon bond formation. The reactions can occur either intermolecularly or intramolecularly. Various key intermediates in the total syntheses of natural products are prepared by these coupling processes[28]. In the presence of Lewis acids, the reaction of vinylsilanes with chlorothiocarbonate gives α,β-unsaturated thiocarboxylates **93** in good yield (equation 71)[139]. The reactivity of the silyl substituent as an electrofugal group following electrophilic attack depends on the substituent on the silicon. Whereas trimethylsilyl is highly reactive, *tert*-butyldiphenylsilyl is much less reactive (equation 72)[140]. Sequential replacement of silyl groups with different acyl groups has been reported (equation 73)[141,142].

$$\mathrm{RCH{=}CHSiMe_3} \xrightarrow[\mathrm{AlCl_3,\,-60\,^\circ C}]{\mathrm{ClCOSEt}} \underset{\textbf{(93)}}{\mathrm{RCH{=}CHCOSEt}} \qquad (71)$$

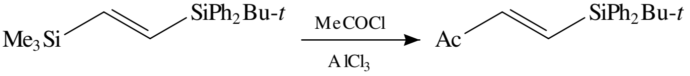

(72)

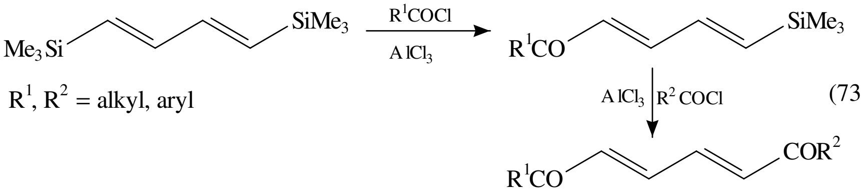

R^1, R^2 = alkyl, aryl

(73)

6. Reactions with alkyl halides and related electrophiles

S_E-Substitution has been found when α-bromoallylsilane **7** is treated with *tert*-alkyl chloride in the presence of $TiCl_4$ at −78 °C to give **94**[40]. The reaction with α-bromoethylbenzene under the same conditions yields the corresponding indane **96**. Apparently, the intermediate **95** may further undergo an intramolecular Friedel-Crafts reaction under these conditions (equation 74)

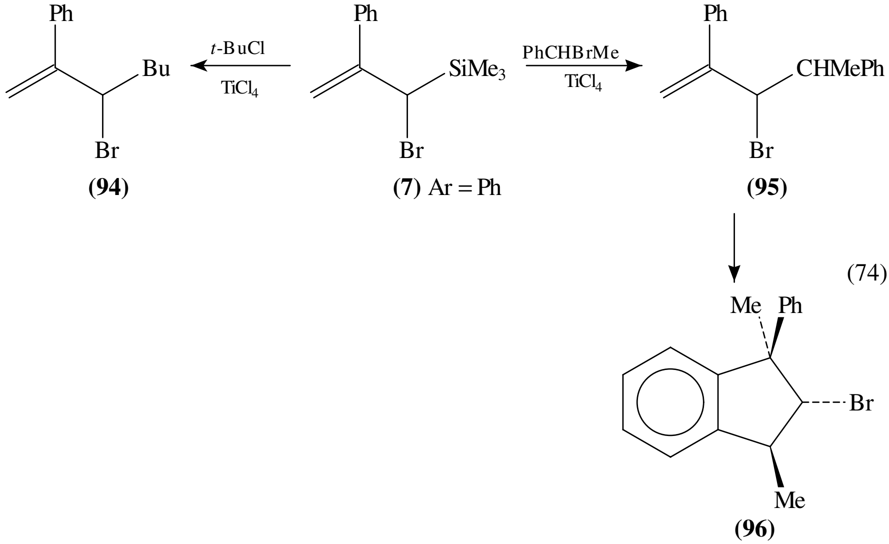

(94) **(7)** Ar = Ph **(95)**

(74)

(96)

Without a catalyst, tropylium ion reacts with allylsilanes regioselectively to give 7-alkylated cycloheptatriene **97** (equation 75)[143].

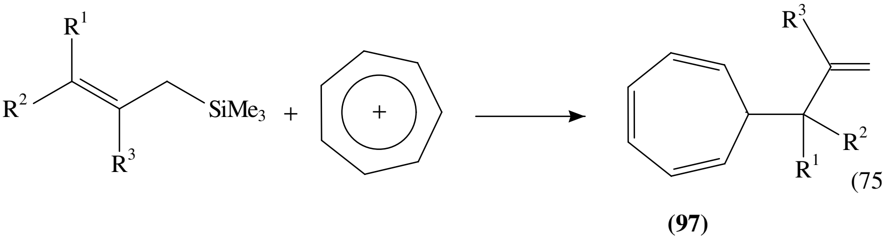

(75)

(97)

R^1 = H, Me; R^2 = H, Me; R^3 = H; $R^2R^3 = -(CH_2)_3-$

The intramolecular reaction of allylsilane with the tosylate moiety induced by fluoride ion is designed in the last step of the synthesis of (±)-norartemeseol **98** (equation 76)[144].

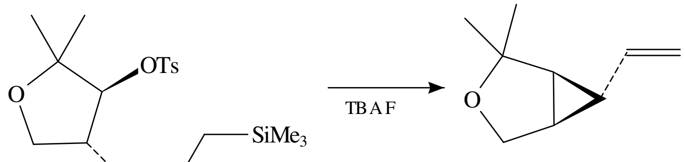

(98)

(76)

Benzylic silyl ethers couple with allylsilanes in the presence of trityl tetrakis [3,5-bis(trifluoromethyl)phenyl]borate (TFPB) catalyst leading to carbon–carbon bond formation (equation 77). The corresponding $ZnCl_2$-catalyzed reactions with an allyl silyl ether lead to a mixture of regioisomers[145,146].

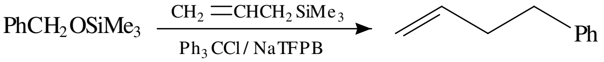

(77)

Difficulties have been found in the intermolecular coupling reactions of allylsilanes with epoxides other than the simplest ethylene oxide[19]. For example, reactions of allylsilane **99** with epichlorohydrins in the presence of $TiCl_4$ or $EtAlCl_2$ give chlorohydrins in moderate to good yields. However, treatment of epichlorohydrin with **99** furnishes the expected allylated chlorohydrin product **100** (equation 78)[147]. In the intramolecular addition of the allylsilane moiety to 2,3-epoxyether moiety of **101**, the ratio of 6- and 7-membered ring products is affected by the nature of the Lewis acid. When $BF_3 \cdot OEt_2$ is used, a mixture of **102** and **103** is obtained (equation 79). Interestingly, **102** is the exclusive product in the $TiCl_4$-catalyzed reaction[148].

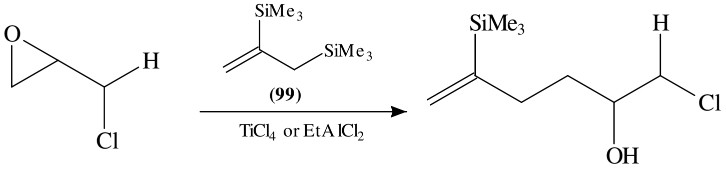

(100)

(78)

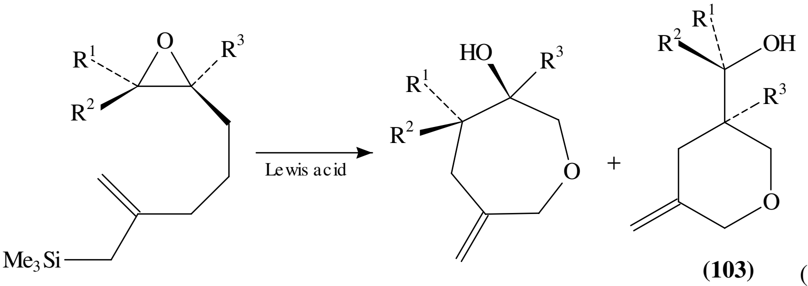

(101) **(102)** **(103)** (79)

R^1, R^2 = H, Me, n-Pr, $Me_2C{=}CHCH_2CH_2$; R^3 = H, Me

Lewis acid catalyzed intramolecular coupling of allylsilanes with aziridines serves as a useful route for the synthesis of carbocycles having the γ-amino olefin unit **104** (equation 80)[149]. However, this reaction does not occur in an intermolecular manner.

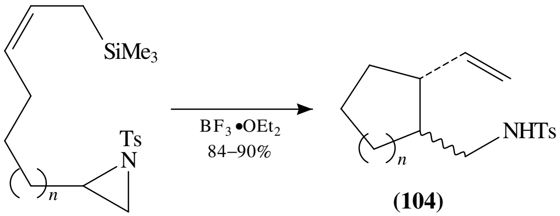

(104)

(80)

$n = 1,2$

trans : *cis* = 2.7 :1

7. Reactions with alkenes

Silyl enol ethers undergo cross-coupling with allylsilane in the presence of a Lewis acid. For example, an oxovanadium(V) complex can induce such condensation reactions (equation 81)[150].

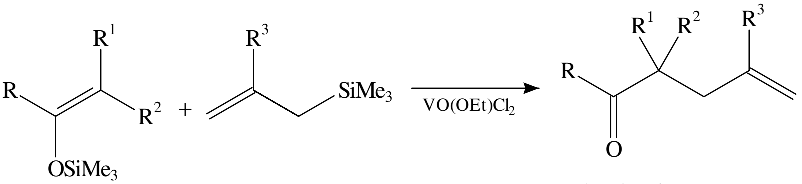

(81)

R, R^1, R^2, R^3 = H, alkyl, aryl

Treatment of **106** with silylated enediols **105** in the presence of TMSOTf gives the corresponding annulated bicyclic diols **107** (equation 82)[151]. A similar reaction with cyclobutenediol derivative **108** followed by oxidative cleavage of thus formed diol **109** yields a seven-membered ring product (equation 83).

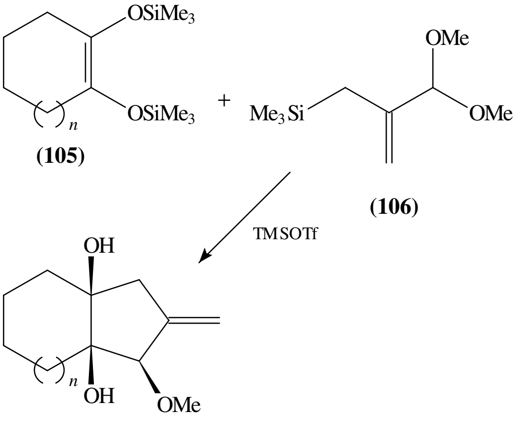

(105)

(106)

(107)

(82)

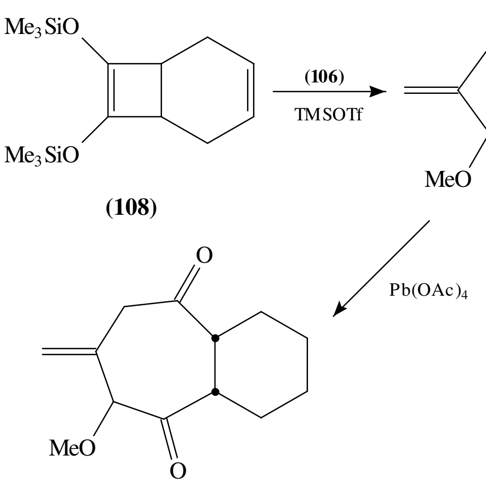

(108) **(109)**

(83)

Intramolecular anodic oxidation of allylsilane moiety with enol ether moiety gives the corresponding cyclized product **110** (equation 84)[152].

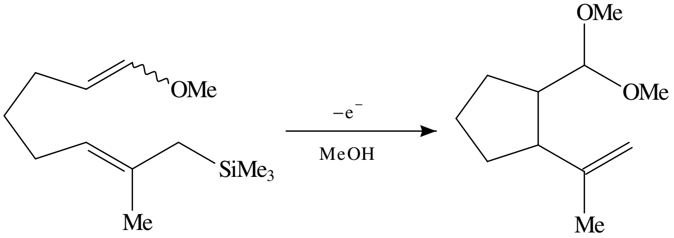

(110)

(84)

In the presence of the Lewis acid, the carbocation generated *in situ* can serve as an electrophile to replace, intramolecularly, the silyl substituent at the olefinic carbon[153–155]. The stereochemical requirements at the silyl substituent appear not to be important (equations 85–87).

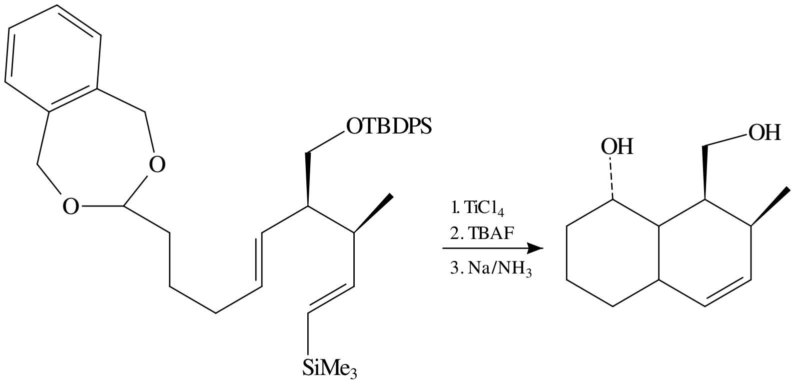

(85)

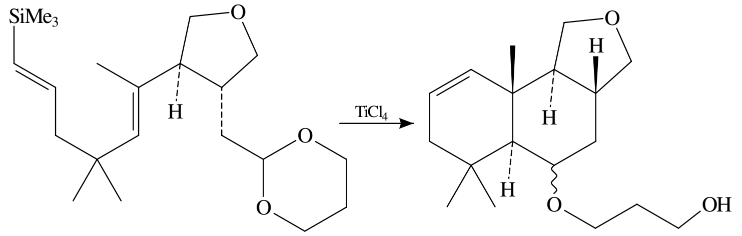

(86)

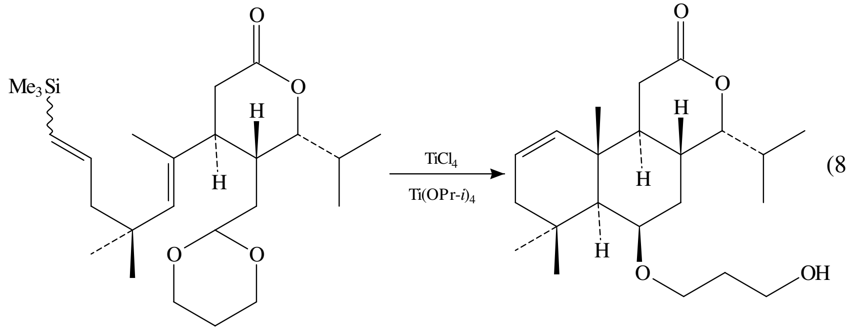

(87)

III. ORGANOMETALLIC REAGENTS PROMOTED C−Si CLEAVAGE REACTIONS

A. Coupling Reactions Involving the Cleavage of the Carbon−Silicon Bond

Transition-metal catalyzed cross-coupling reactions have been demonstrated to be an extremely powerful tool for the construction of carbon−carbon bonds in regio- and stereoselective manners. These metal catalysts enable the transmetallation of carbon−silicon bonds into other carbon−metal bonds from which further reactions can proceed, leading to carbon−carbon bond formation. The use of palladium catalyst[156] in the activation of the carbon−silicon bond is particularly noteworthy[31]; various important transformations have thus been developed. The presence of fluoride ions will make the reaction more facile, pentacoordinate organofluorosilicates being presumably formed under these conditions[157,158].

1. Heck reactions

Organosilicon compounds are versatile in the Heck reaction. The silyl moiety can serve as a halide-like leaving group and transfer the vinyl or aryl group to the olefin. Alternatively, it can serve as an organometallic acceptor and couple with the vinyl or aryl group from corresponding halides or triflates. In the latter case, the silyl group can be eliminated stereoselectively under the reaction conditions or a β-hydride elimination can occur readily to yield the corresponding silyl-substituted alkenes (Section V.C.2).

a. Silyl group as a halide-like leaving group. Both styryl and 1-alkenyl pentafluorosilicates **111** can undergo the Heck reaction in the presence of a stoichiometric quantity of palladium acetate[159]. A similar reaction with allyl chloride gives the corresponding 1,4-diene (equation 88). Apparently, the reaction may proceed via β-chloride elimination[159]. The Heck-type reaction can also be used for the coupling of (E)-β-(trimethylsilyl)styrene with methyl acrylate or related alkenes[160]. Under the carbon monoxide atmosphere, an α,β-unsaturated ester is obtained (equation 88)[159].

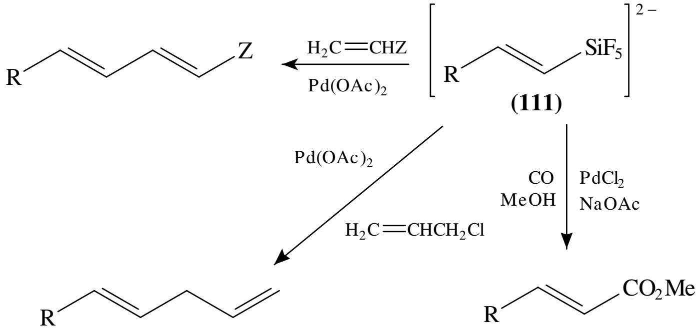

(111)

(88)

R = 1° or 3° Alk, Ph

b. Vinylsilanes as organometallic acceptors. Vinylsilanes have been used extensively as the acceptor for the arylpalladium intermediate generated *in situ* in the Heck reaction[161–168]. In the absence of a promoter, the reaction is generally nonselective. The desilylation product is a major side product if not the predominant product (Section V.C.2). Moreover, the addition reaction occasionally gives a mixture of regioisomers[163–165]. Nevertheless, when the silyl group at the olefinic carbon is displaced, an inversion of configuration is noted (equation 89)[163,168].

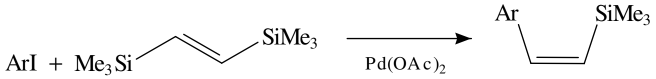

(89)

Ar = 1-Naph, 4-XC_6H_4(X = H, NO_2, MeO)

$(Et_2N)_3S^+$ $SiMe_3F_2^-$ (TASF) has been known to generate petacoordinate silicates. Thus, treatment of vinyl or aryl iodides with vinylsilanes in the presence of TASF and a catalytic amount of (η^3-$C_3H_5PdCl)_2$ affords the corresponding coupling products in good to excellent yield[169,170]. Retention of configuration is generally observed. This version of a silicon-based coupling reaction has provided a general and highly stereospecific route to 1,3-dienes **112** (equation 90) as well as alkenylarenes. The triflate leaving group can couple efficiently under similar conditions[171]. It is noteworthy that alkylfluorosilanes **113** also undergo this coupling reaction in satisfactory yield with retention of configuration (equation 91). Unlike the reactions of organotin compounds, lithium halide is not necessary for the reactions with silanes. Under a carbon monoxide atmosphere, carbonylative cross-coupling reactions have been found when an aryl halide is treated with an aryl- or an alkenylfluorosilane[172].

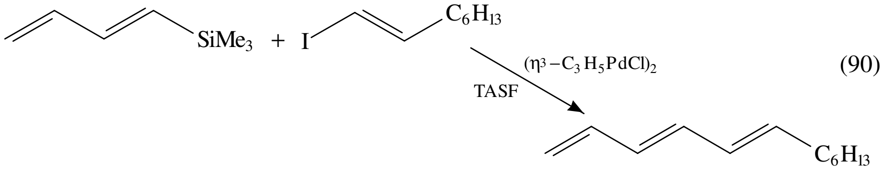

(90)

(112)

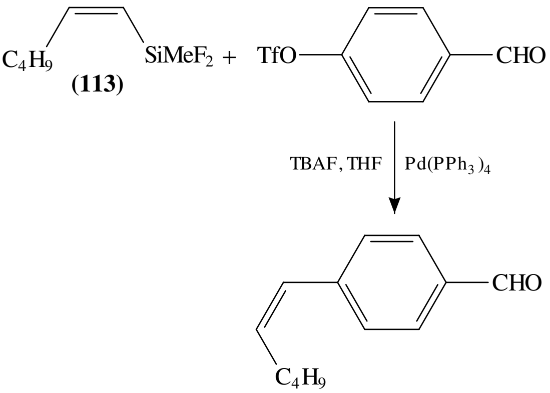

(91)

Cross-coupling reactions of alkenylsilicates **114** with aryl or vinyl halides or triflates are catalyzed by a palladium complex to give the corresponding alkenes (equation 92)[173].

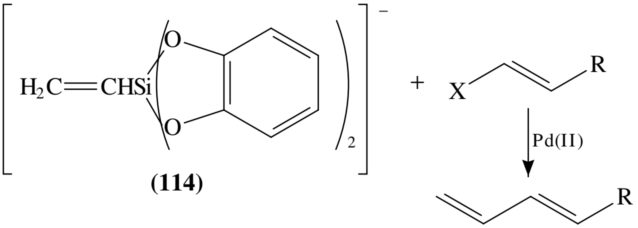

(92)

More recently, allylic carbonates **115** have been found to couple with alkenylfluorosilanes in the presence of a palladium catalyst to yield the corresponding 1,4-dienes (equation 93)[174]. The corresponding palladium-catalyzed reaction of allylsilane with allyl acetate **116** has been explored (equation 94)[175].

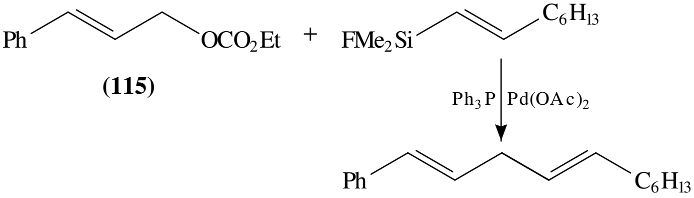

(93)

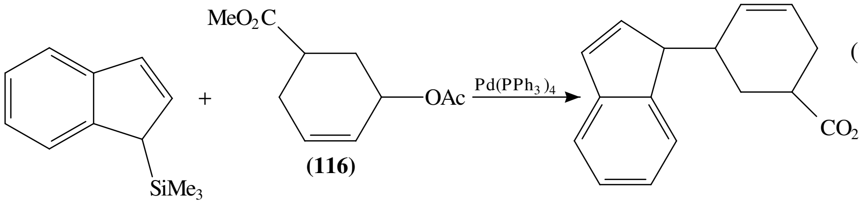

(94)

Use of the allylsilanes as the alkene components in the Heck reaction is illustrated in the palladium catalyzed γ-allylation of organic halides or triflate or acetate[176]. The reaction has been used for the synthesis of ibuprofen **117** (equation 95). Interestingly, the regioselectivity of such a coupling reaction is quite dependent on the phosphine ligands associated with the metal center. α-Selectivity is obtained by using good chelating bidentate ligands, whereas γ-selectivity is favored by mondentate ligands, as shown in the reaction of **118** (equation 96)[177].

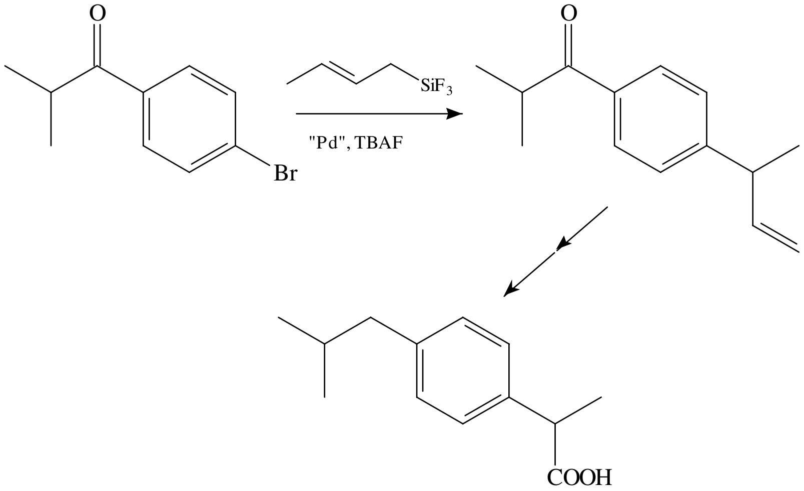

(117)

(95)

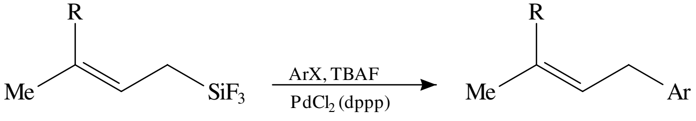

(96)

(118)

R = H, Me, 4-YC$_6$H$_4$ (Y = MeCO, CN, MeO, CO$_2$Me); X = Br, I, OTf

Chiral benzyl or allyl silanes **119** couple with aryl triflates to give the corresponding products having 58–99% enantioselectivities (equation 97)[176,178,179]. The selectivity appears to be very much dependent on the reaction conditions.

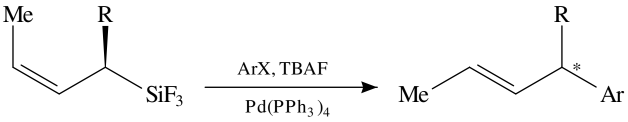

(97)

(119)

R = Me, Et; Ar = 1- and 2-Naph

Use of the allylsilanes as the alkene components in the Heck reaction is illustrated in the regioselective intramolecular cyclization of **120** (equation 98)[180]. In addition, a high enantioselectivity of 90 %ee is obtained when the chiral phosphine (*S*)-BINAP is employed. The propargylsilane analog undergoes a similar reaction[181].

2. Homocoupling reactions

In the presence of a stoichiometric amount of $PdCl_2$, styrylpentafluorosilicate (**111**, R = Ph) dimerizes to give (E,E)-1,4-diphenyl-1,3-butadiene in moderate yield (equation 99)[159]. Interestingly, the corresponding 1-alkenyl analogs give only trace amount of the dimers under the same conditions. A similar catalytic homocoupling reaction has been found when $(E)-\beta$-(trimethylsilyl)styrene is treated with $PdCl_2$[160,182]. Heteroatom substituents such as alkoxy groups or fluorine atoms on silicon in general facilitate the reaction[183]. Surprisingly, trifluorosilylethene, unlike the corresponding mono- or difluoro derivatives, does not undergo the cross-coupling reactions. Presumably, the hexacoordinated silicate species thus generated is unreactive toward coupling.

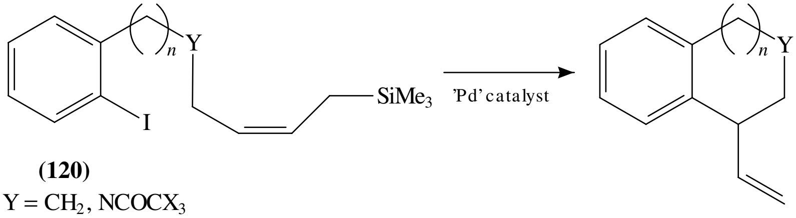

(98)

(120)
Y = CH_2, $NCOCX_3$

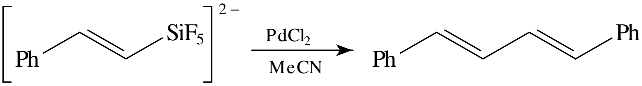

(99)

(111) R = Ph

3. Other coupling reactions

The reaction of **121** with LiCl in the presence of a catalytic amount of $LiPdCl_4$ and p-benzoquinone (p-$C_6H_4O_2$) and in acetone–acetic acid gives a mixture of two isomeric allylic chlorides **122a** and **122b** in a ratio of 3:1 (equation 100). Employment of the corresponding (Z)-allylsilane under the same conditions provides the same products but with opposite selectivity (**122a: 122b** = 1:3). This reaction demonstrates a Pd(II)-catalyzed intramolecular C–C bond formation by addition of an allylsilane to the coordinated diene leading to the highly stereoselective 1,4-*syn*-adduct[184].

B. Transmetallation

Allyl group transfer from silicon to bismuth takes place when allylsilanes are treated with triarylbismuth difluorides in the presence of $BF_3 \cdot OEt_2$ (equation 101). The resulting allylbismuthonium species **123** reacts readily with arenes and nucleophiles to give the corresponding allylated products[185]. Transformation of allyl group from silanes to other elements has been performed using $(NH_4)_2Ce(NO_3)_6$[186], $Tl(O_2CCF_3)_3$[187], $PhTe(O)O_2CCF_3$[188], $PhIO/BF_3 \cdot OEt_2$[189,190] and $Ti(OPr^i)$[191]

Vinylsilanes react with boron trichloride to give the corresponding borodesilylation products in good yield which, in turn, can be transformed into boronic esters **124** by alcoholysis (equation 102). The initial dichloroorganoborane products can be used directly in the Suzuki–Miyaura cross-coupling reaction[192]. Replacement of a carbon–silicon bond by a carbon–tin bond in fluorinated alkenes (e.g. **125**) can be achieved by the reaction of silanes with Bu_3SnCl and KF in DMF under mild conditions (equation 103)[193]. It is noteworthy that a vinylic iodine remains intact under these conditions.

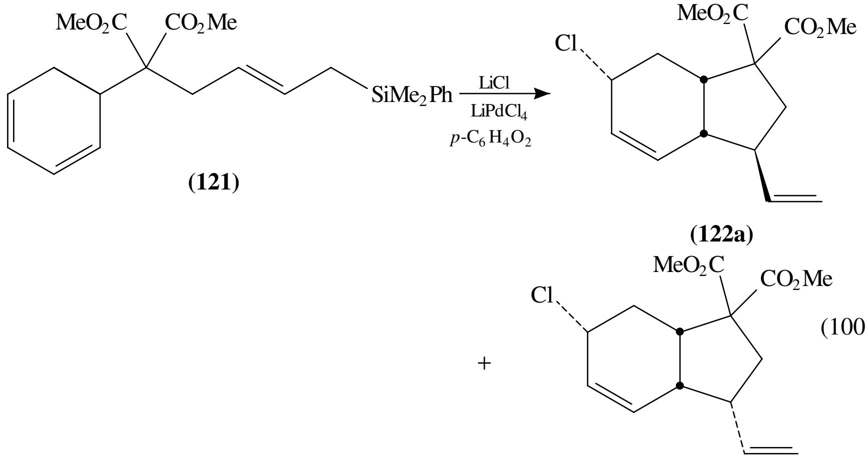

(121) **(122a)** **(122b)**

(100)

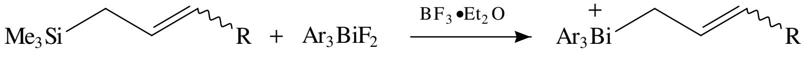

(123)

(101)

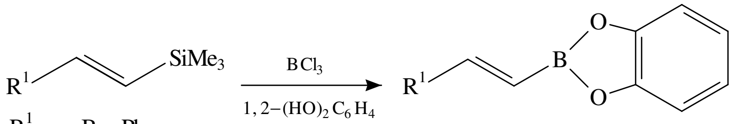

R^1 = n-Bu, Ph

(124)

(102)

$$R^1FC{=\!=}CFSiR^2_3 \xrightarrow[\text{rt to 80 °C}]{\text{KF, DMF, Bu}_3\text{SnCl}} R^1FC{=\!=}CFSnBu_3 \quad \textbf{(125)} \qquad (103)$$

R^1 = alkyl, aryl, F or I; R^2 = Me, Et

Disproportionation between vinylsilanes and monosubstituted alkenes catalyzed by ruthenium complex (equation 104) has been suggested to occur via a β-silyl group elimination. The intermediate silylruthenium complex, RuCl(CO)(PPh$_3$)$_2$(SiMe$_2$R^1), has been characterized by spectroscopic means[194].

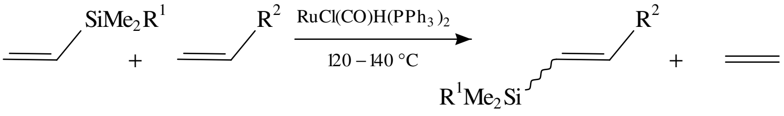

(104)

R^1 = Me, OEt; R^2 = Me$_3$Si, Me, Ph, CO$_2$Me, OBu-n

IV. MISCELLANEOUS C—Si CLEAVAGE REACTIONS

As discussed in Section II, allylsilane normally serves as a nucleophile which reacts with an electrophile. However, pentafluorosilicates occasionally behave like an electrophile in certain palladium-catalyzed reactions (Section III.A.1). It is interesting to note that $VO(EtO)Cl_2$ (*cf* Section II.B.7) has also been found to promote the coupling reaction of allylsilanes with β-dicarbonyl compounds to give the corresponding allylation product **126** (equation 105)[195].

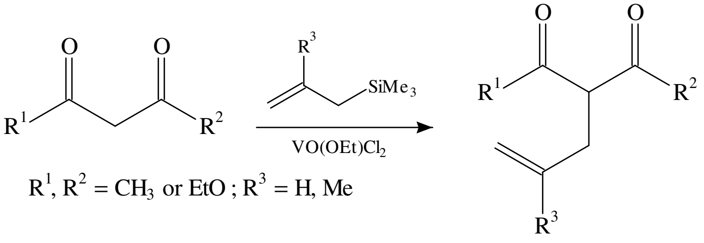

$R^1, R^2 = CH_3$ or EtO ; R^3 = H, Me

(126)

(105)

Allylic selenocyanates and thiocyanates are prepared from the reaction of allylsilanes with $KSeCN \cdot 2CuBr_2$ and $KSCN \cdot 2CuBr_2$, respectively. Both cyanoselenation and cyanothianation take place at the α-position of allylsilanes (equation 106). Presumably, the electrophile 'XCN' generated *in situ* is first added to the γ-position, followed by a [1,3]-migration[196]. Fluoride induced reactions of allylsilanes with thioketones yield the corresponding allyl sulfides[197]. Displacement via an S_E route is noted.

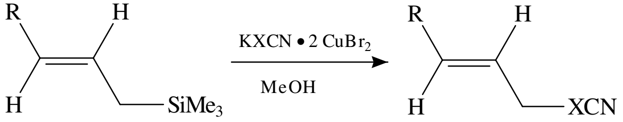

X = Se, S

R = H, Me, $SiMe_3$

(106)

Insertion of a bromocarbene unit into the Si−C bond has been observed in the reaction of **61** with CH_2Br_2 in the presence of LDA (equation 107)[105,106].

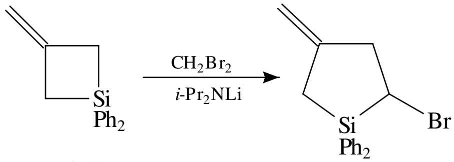

(61)

(107)

Upon treatment with $WCl_2(PMe_3)_4$ at 65 °C, vinylsilane can serve as a precursor of methylcarbyne complex **127**[198]. It is noteworthy that the C1 carbon is converted into the corresponding carbyne carbon. Under similar conditions, allylsilane gives the corresponding ethylcarbyne complex **128** (equation 108)[198].

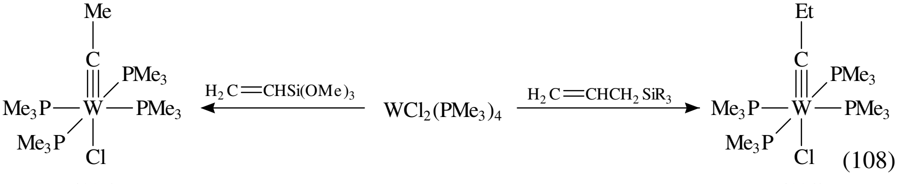

(108)

(127) **(128)**

Electrochemical oxidation of 1-(trimethylsilyl)dienes in MeOH affords **129** in moderate to satisfactory yield. It is worth noting that the reaction shows some diastereoselectivity (equation 109)[199].

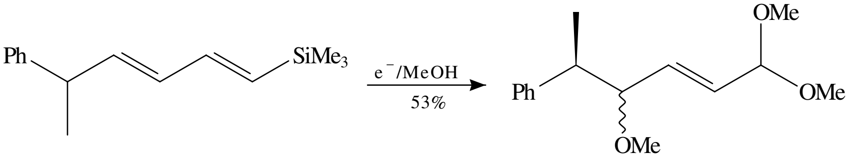

(129) (109)

syn : *anti* = 4 : 1

Although the elimination of saturated β-hydroxysilane giving olefin is well-documented, a similar reaction involving β-silylallylic alcohol normally gives a mixture of products. When NaH is employed in refluxing octane, allene **130** is obtained as the major product (equation 110)[200]. However, when the reaction is carried out in the presence of a catalytic amount of NaH in HMPA at room temperature, a 1,3-silyl group shift from carbon to oxygen occurs readily (e.g. to give **131**) (equation 111)[201].

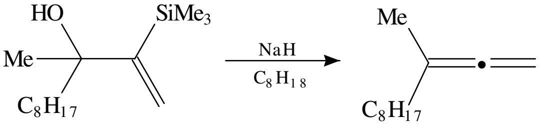

(110)

(130)

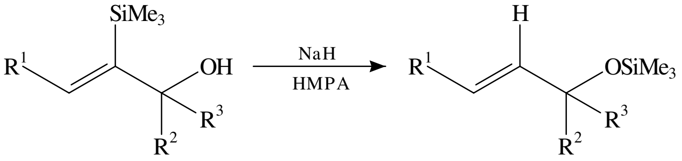

(111)

(131)

$R^1 = H$, *n*-Bu ; $R^2 = H$, Me ; $R^3 = H$, 1° Alk, Ph, $CH_2{=}CH$

Tris(trimethylsilyl)silyl radical is relatively stable and can therefore serve as a radical leaving group. This reaction has been extended to the radical-initiated allylation of organic halides[202,203]. Thus, thermolyses of bromides α to a carbonyl substituent **144** or of simple iodides with allyltris(silyl)silane in the presence of a radical initiator gives the corresponding allylation products (equation 112).

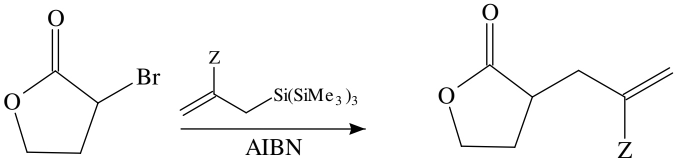

(112)

(144)

$Z = H$, Me, CN, CO_2Et

V. REACTIONS OF ALLYLSILANES AND VINYLSILANES WITHOUT CLEAVAGE OF THE C−Si BOND

A. Lewis Acid Catalyzed Addition of an Electrophile to the Double Bond

As described in Section II, Lewis acid catalyzed desilylative carbon−carbon bond formation with an electrophile has been shown to be very versatile in organic synthesis. Occasionally, depending on the nature of the substrates (e.g. the presence of appropriate functional groups), the carbon−silicon bond may remain intact. For example, treatment of **132** with a Lewis acid affords a mixture of cyclization products **133**−**135** (equation 113). The isolation of **133** indicates that the carbocation intermediate thus formed is trapped by the oxygen nucleophile before elimination of the silyl moiety occurs[204].

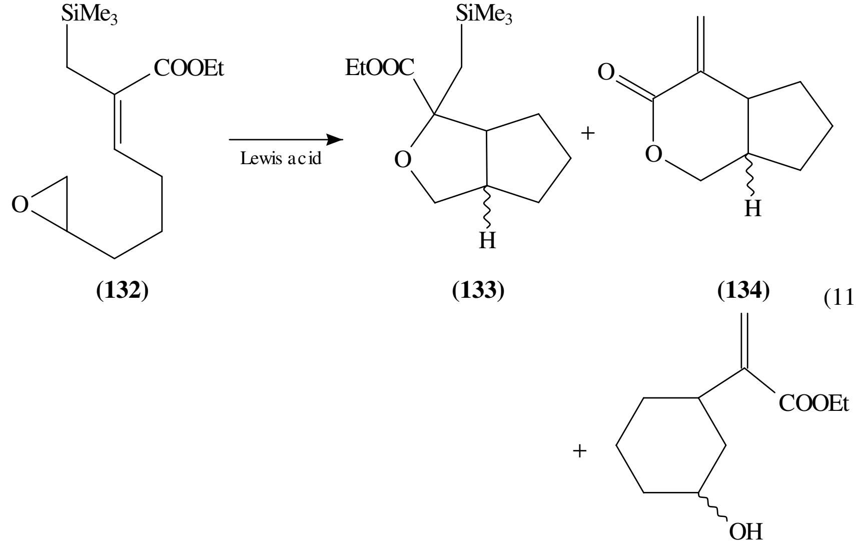

(132) **(133)** **(134)** (113)

(135)

$SnCl_4$-mediated intramolecular cyclization of vinylsilane **136** with the acetal moiety leads to the corresponding cyclization product **137** (equation 114). The electrophile apparently attacks at the *β*-carbon to the silyl substituent[205]. It is noteworthy that desilylation has been observed in the similar case of **138** when BCl_3 is employed as the Lewis acid catalyst (equation 115)[206].

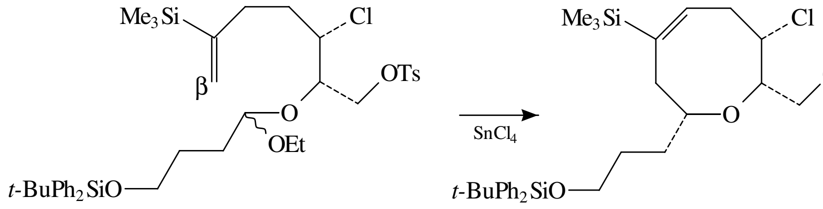

(114)

(136) **(137)**

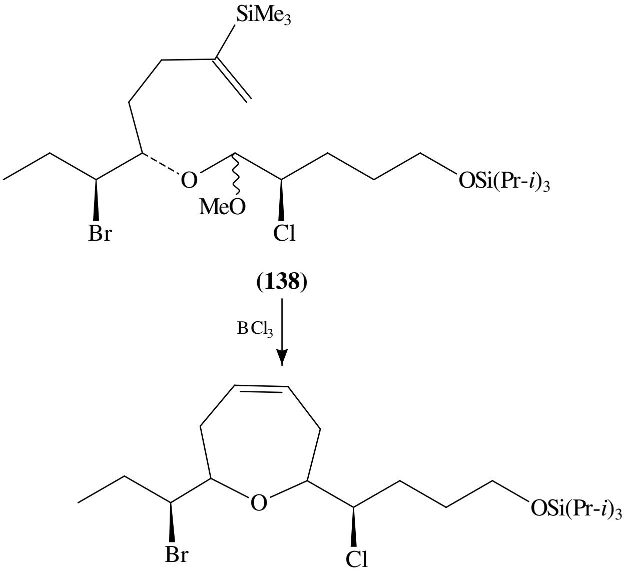

(138)

(115)

Silicon-directed stereoselective *syn* addition of the hydroxy group to the olefinic double bond occurs intramolecularly in a $TiCl_4$–or TsOH-catalyzed cyclization of vinylsilanes **139** bearing a hydroxy group[207]. The reaction gives mainly the *trans*-isomer (*trans* : *cis* = 80–90:20–10) (equation 116)[208]. It is noteworthy that no cyclization is observed in the absence of the silyl substituent under the same conditions.

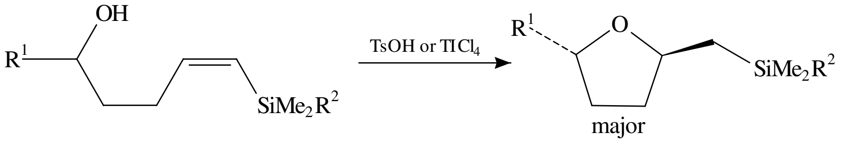

(139)

(116)

R^1 = *i*-Pr, *n*-C_6H_{13}, Ph; R^2 = H, Me, *t*-Bu, Ph

1-Trimethylsilylbutadiene **140** is treated with acetyl chloride at −80 °C to give the adducts, which are dehydrochlorinated to give **141** (equation 117)[209]. No carbon–silicon bond cleavage is observed.

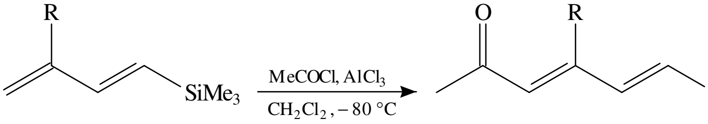

(117)

(140) **(141)**

R = Me, Et, *i*-Pr

Convenient procedures for the synthesis of β-nitrovinylsilanes **142** from vinylsilanes have been developed (equation 118)[210]. Similarly, nitration of allylsilane at the γ-position is achieved when a mixture of allylsilane, $NaNO_2$ and CAN in HOAc is treated ultrasonically (equation 119)[211].

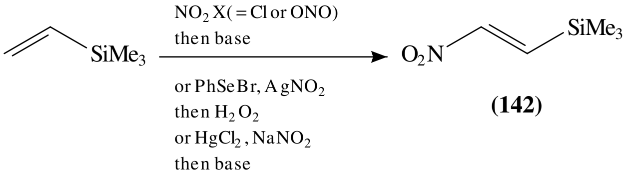

(142)

(118)

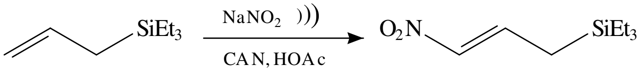

(119)

During the course of the acid-catalyzed hydrolysis of allylic acetal moiety, the vinylsilane moiety in **143** has been found to be stable (equation 120)[212].

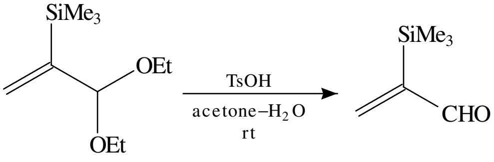

(120)

(143)

B. Radical Reactions

A three-component radical coupling reaction involving allylsilanes has been employed leading to **145** (equation 121)[213]. It is noteworthy that the corresponding carbon–silicon bond remains intact in this reaction.

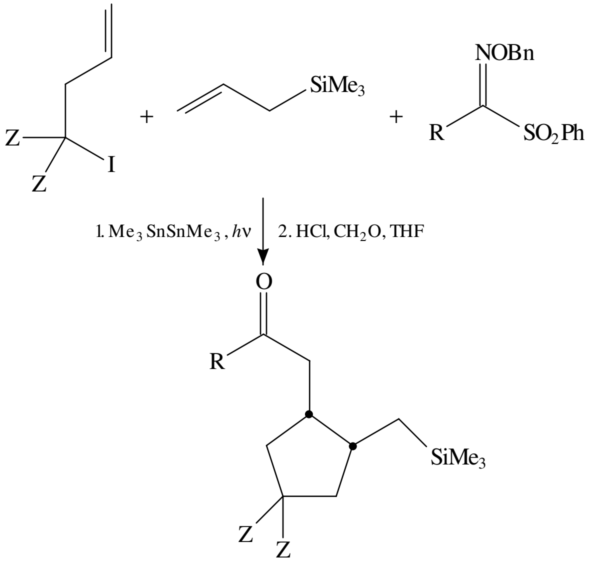

(121)

(145)

Intermolecular free-radical addition of iodoalkyl sulfones to vinylsilanes yields regioselectively the adduct **146** which can be further transformed to cyclopropene derivatives (equation 122)[214].

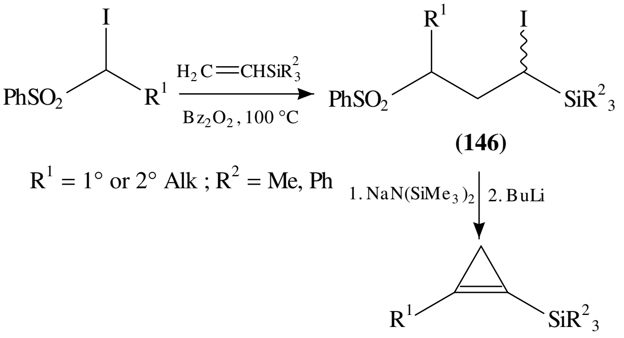

(146)

(122)

Treatment of a vinylsilane with ketones in the presence of 2 equivalents of MnO_2 and a drop of acetic acid at 140 °C in a sealed tube produces the corresponding adduct **147** in moderate to good yields (equation 123)[215].

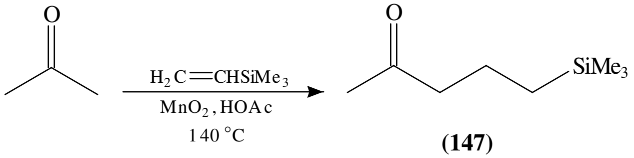

(147)

(123)

Intramolecular radical addition to vinylsilane moiety has been used for the synthesis of statine **148** (equation 124)[216] and the pyrrolizidine skeleton[217]. Tandem [2 + 1] radical cyclization of bromides **149** with Bu_3SnH is extremely sensitive to the nature of the substituent on the diene moiety. Bicyclo[3.1.0] skeleton **150** is obtained in the presence of the silyl substituent (equation 125). When the silyl substituent in **149** is replaced by a *t*-butyl group, the six-membered ring product **151** is obtained exclusively[218].

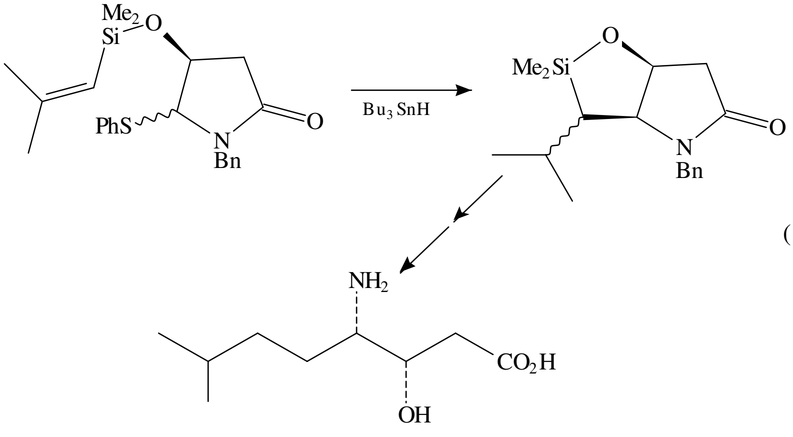

(148)

(124)

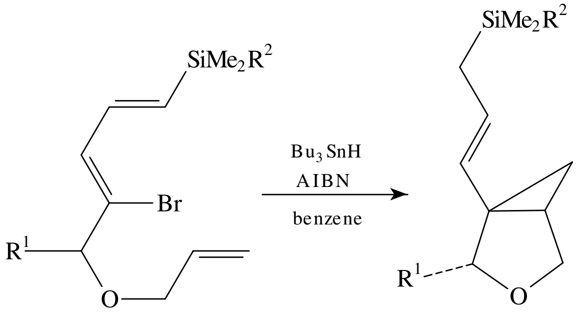

(125)

(149) **(150)**

R^1 = Me, n-C$_6$H$_{13}$, Ph; R^2 = Me, Ph

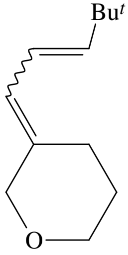

(151)

Decomposition of perfluoroalkyl peroxide in the presence of trimethoxyvinylsilane gives the corresponding oligomers **152** (equation 126)[219]

$$(R_FCO)_2O_2 + H_2C{=}CHSi(OMe)_3 \xrightarrow[30\,^{\circ}C]{} R_F[CH_2{-}CHSi(OMe)_3]_nR_F \qquad (126)$$

$R_F = C_3F_7C_3F_7OC(Me)F$
$n = 2,3$

(152)

C. Organometallic Reagents Promoted Reactions

1. Cross-coupling reactions

Allyl- and vinylsilanes having bromide or iodide substituents at the double bond undergo various kinds of cross-coupling reactions. For example, Stephens–Castro coupling of such halides gives polyunsaturated silanes **153** in good to excellent yields (equation 127)[220]. A hydroxy group can be tolerated under these conditions. The cross-coupling reactions of vinylsilane phosphate with organocuprate reagents give a single stereoisomer of substituted vinylsilanes **154** with retention of configuration (equation 128)[221]. Aryl, vinyl and alkynyl bromides undergo the efficient Suzuki–Miyaura coupling with **155** under basic conditions to produce the corresponding *trans*-styryl-, dienyl- (equation 129) and enynylsilanes in good to excellent yields[222,223]. It is also noteworthy that the carbon−silicon bond in allylsilanes remains intact under Stille coupling conditions[224].

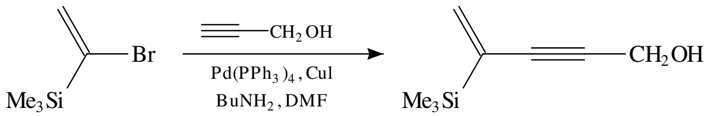

(127)

(153)

(128)

(154)

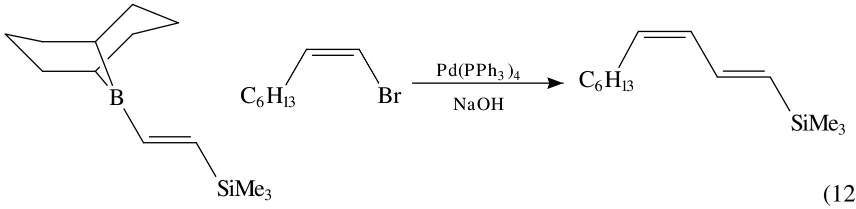

(155)

(129)

Organozinc reagent prepared from the 2-(trimethylsilyl)allyl bromide **156** and zinc react with alkynes or carbonyl compounds as well as nitriles to give the corresponding coupling products in moderate to good yields (equation 130)[225].

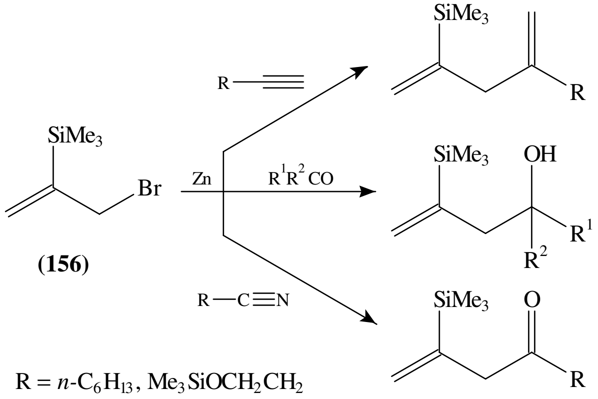

(156)

(130)

R = n-C_6H_{13}, $Me_3SiOCH_2CH_2$

R^1 = H, Me ; R^2 = Ph, PhCH(Me), n-C_6H_{13}

R = 1°Alk, c-C_6H_{11}, Ph

2. Heck reaction

As described in Section III.A.1, the silyl group in vinylsilanes is replaced under the Heck reaction conditions. Several procedures are known to enable the carbon−silicon bond to remain intact. Thus, under phase transfer conditions, arylation of vinylsilanes in the presence of $Pd(OAc)_2$ catalyst gives (*E*)-β-(trialkylsilyl)styrenes in excellent yield[226]. The addition of the Ag(I) salt[227,228] or Ph_3P[229] to the reaction mixture also suppresses the desilylation products (equation 131).

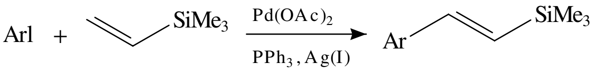

(131)

Aryl bromides or iodides react with di- or monochloro(vinyl)silanes or triethoxy(vinyl)silane in the presence of Et_3N and palladium catalyst to give β-arylvinylsilanes in moderate to excellent yields. In contrast to the simple silyl substituent, the presence of the electron-withdrawing group on silicon is essential to avoid the elimination of the silyl group. No silver ion is necessary in these examples[230]. The palladium-catalyzed reaction of aryldiazonium tetrafluoroborates with vinylsilanes gives a mixture of terminal and internal vinylsilanes together with styrenes[231].

3. Murai reaction

The ruthenium-catalyzed addition of the carbon–hydrogen bond at the *ortho* position of aromatic ketones or imines to vinylsilanes serves as an elegant method for the regioselective introduction of the carbon–carbon bond at the *ortho* position to the acyl substituent (e.g. **157**) (equation 132)[232–235]. When CF_3 and NMe_2 substituents are present at the *meta* position, the coupling takes place at the less congested position to give the 1:1 adduct as the sole product[236,237]. The reaction can also be extended to the activation of the olefinic C–H bond. α, β-Unsaturated carbonyl compounds behave similarly and give the corresponding coupling products **158** (equation 133)[238,239]. Alkynylsilanes can also be used to give the corresponding (*E*)-vinylsilanes **159** (equation 134)[240]. Aromatic imines behave similarly[241].

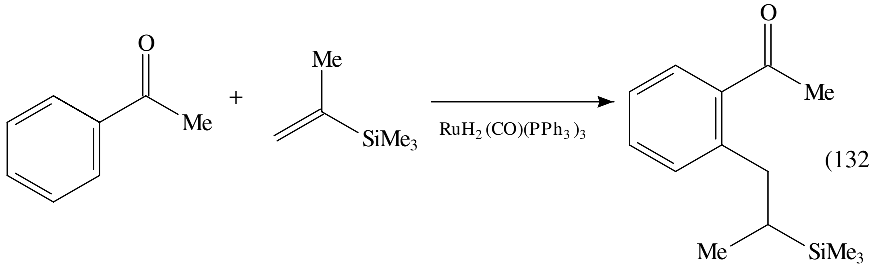

(132)

(157)

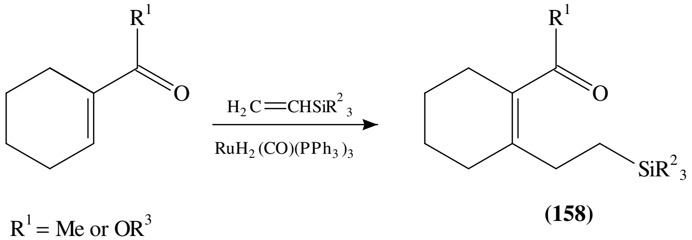

(133)

(158)

R^1 = Me or OR^3

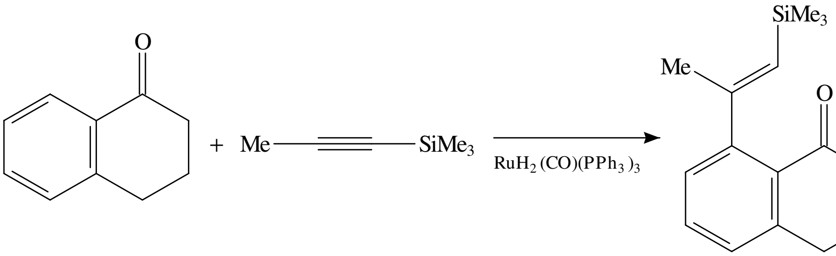

(159) (134)

This reaction can also be applied to achieve step-growth copolymerization of aromatic ketone with α,ω-dienes and to synthesize high molecular weight copolymers (equation 135)[242,243].

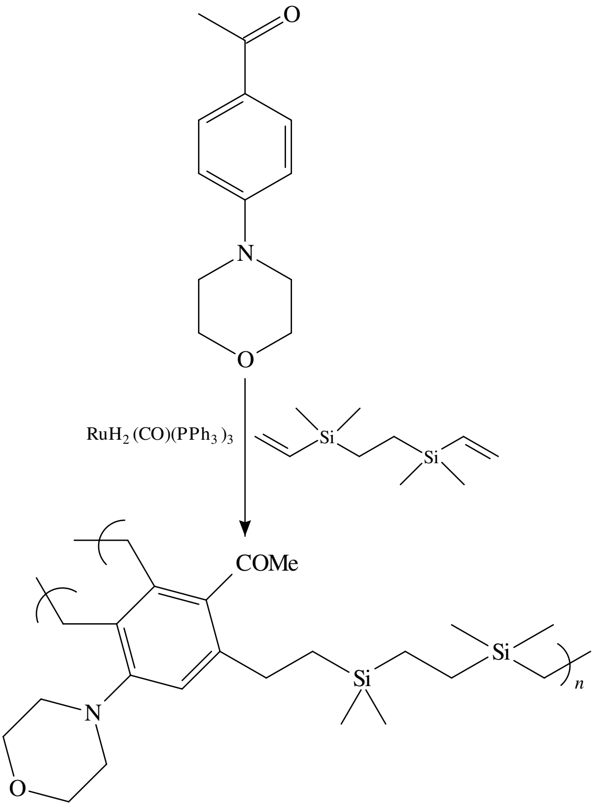

(135)

4. Carbonylation

The regioselectivity of carbonylation of vinylsilanes appears to depend on the nature of the catalysts. Thus, the $PdCl_2(PPh_3)_2$-catalyzed hydroesterification of vinylsilanes yields β-silylesters in high yields with high regioselectivity[244]. On the other hand, when $Co_2(CO)_8$ is used as the catalyst, α-silylesters are obtained predominantly (equation 136)[245].

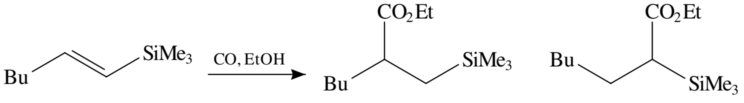

$PdCl_2(PPh_3)_2$	96	4
$Co_2(CO)_8$	0	100

(136)

It is interesting to note that hydroformylation of vinylsilanes catalyzed by a Co or a Pt catalyst gives β-silylaldehydes exclusively. A rhodium catalyst exhibits poor regioselectivity. However, in the presence of a large excess of Ph_3P, the regioselectivity improves to that of a normal aldehyde[246–248].

5. Metathesis

Metathesis of silacyclopent-3-ene **(160)** and diallylsilane using the Schrock molybdenum catalyst [$Mo(NC_6H_3$ *i*-Pr-2,6) $(CHCMe_2Ph)\{OCMe(CF_3)_2\}_2$] produces a mixture of disilacyclodeca-3,8-dienes **161** and silicon-containing polymers (equation 137)[249]. Under similar conditions, cross-metathesis reactions of allylsilane with π-substituted terminal olefins such as styrene, 1-phenyl-1,3-butadiene and acrylonitrile give substituted allylsilanes in excellent yields with very high selectivity. Employment of simple α-olefins in these reaction gives lower but still useful selectivities (equation 138)[250]. Ruthenium and tungsten chlorides also catalyze metathesis between vinylsilanes and α-olefins[251,252].

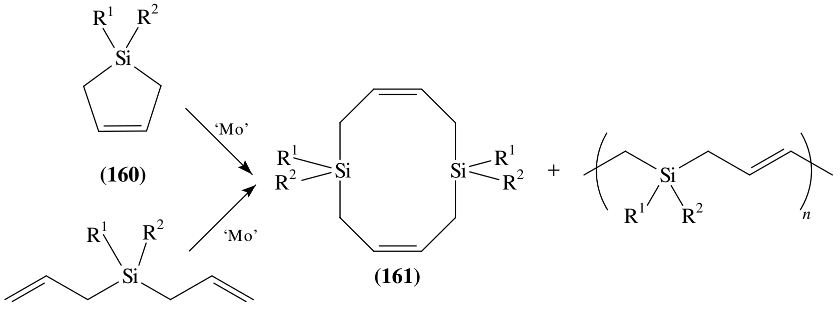

(160)

(161)

$R^1 = R^2 = Me, Ph$

(137)

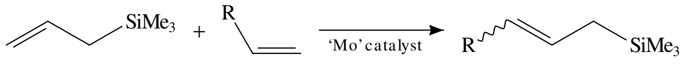

(138)

R = Ar, CN, $(CH_2)_2Br$, $(CH_2)_nOTBS$, $(CH_2)_nCN$

D. Oxidation Reactions

1. Epoxidation

Epoxidation of ω-hydroxy allylsilanes **162** with *t*-BuOOH in the presence of a catalytic amount of $VO(acac)_2$ in toluene gives the corresponding epoxide **163** with high *erythro*-

selectivity[253]. The resulting epoxide is treated with fluoride to yield the 1,3-diol species (equation 139). Epoxidation of allylsilane **164** with MCPBA at −20 °C gives **165** in extremely high diastereoselectivity, which is then converted into an allylic alcohol under acidic conditions (equation 140)[254].

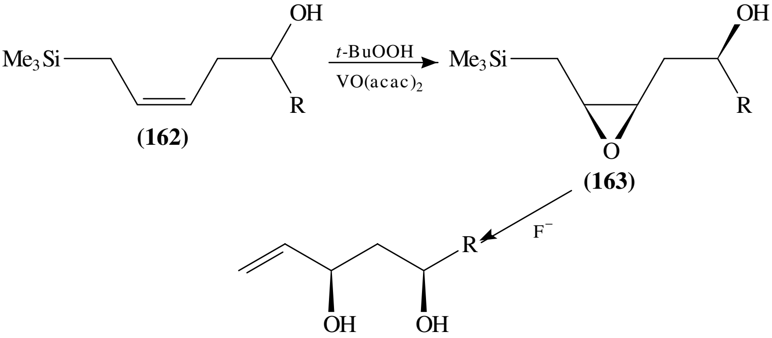

(139)

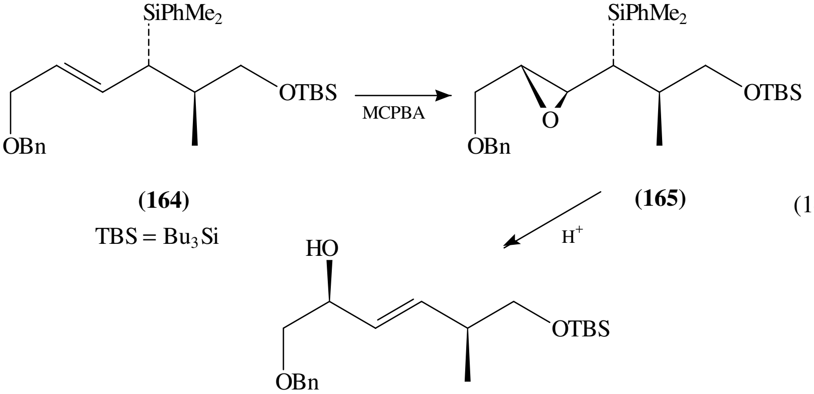

$TBS = Bu_3Si$

(140)

$TBS = Bu_3Si$

Dimethyldioxirane oxidizes acyclic vinylsilanes at room temperature to the corresponding epoxides **166** in excellent yield (equation 141)[255]. Allylic oxidation is found in appreciable amounts when cyclic vinylsilanes are used. It is interesting to note that simple alkenes react faster with dioxirane than vinylsilanes. The trend appears to be reversed when MCPBA is employed as the oxidant.

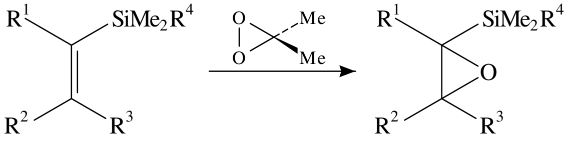

(141)

(166)

$R^1 = H, Me, Et; R^2 = H, 1°Alk; R^3 = H, Me; R^4 = Me, Ph$

Photooxygenation of vinylsilanes in the presence of $Ti(Pr\text{-}i)_4$ affords, regio- and diastereoselectively, the epoxy alcohols **167** in satisfactory yield (equation 142).

Cycloalkenones and α-silylcycloalkenones are obtained as by-products from these reactions[256].

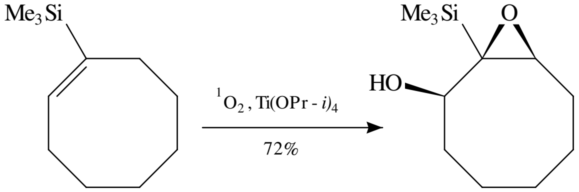

(167)

(142)

Epoxidation of vinylsilanes will lead to silyl epoxides, which can be transformed into the carbonyl compounds **168** and **169** upon treatment with acid (equations 143 and 144)[36,257,258]. Conversion of the vinylsilane **170** into methyl enol ether **171** has recently been reported (equation 145)[259].

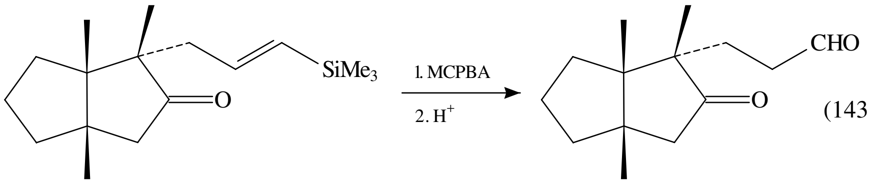

(168)

(143)

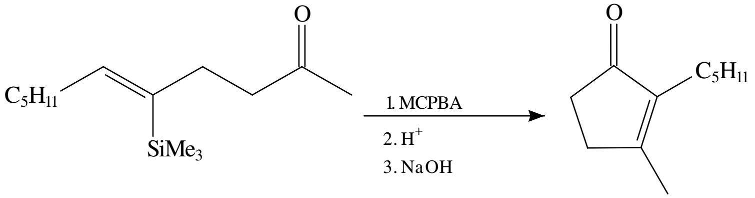

(169)

(144)

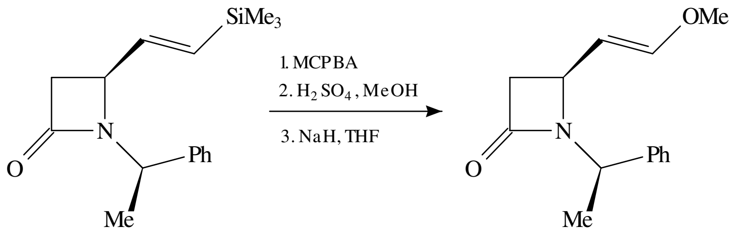

(170) **(171)**

(145)

As mentioned in Section II.B.5, the *tert*-butyldiphenylsilyl group attached to the olefinic carbon is a poor electrofugal group and hence does not leave easily in electrophilic substitution reactions[140]. On the other hand, the epoxide **172**, obtained from the corresponding vinylsilane having such a bulky silyl substituent, gives the carbonyl compound upon treatment with acid, with the silyl group remaining intact (equation 146)[260].

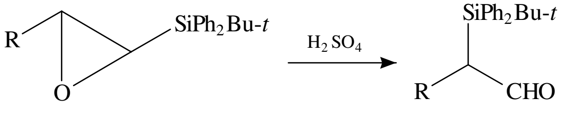

(146)

(172)

R = 1° Alk

Electro-initiated oxygenation of alkenylsilanes is found to proceed in the presence of thiophenol to give the corresponding α-(phenylthio)carbonyl compounds **173** regiospecifically (equation 147)[261]. Hydroxy and carbonyl functionalities remain intact under these conditions.

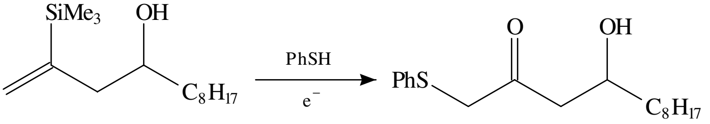

(147)

(173)

Treatment of vinylsilane epoxides with nucleophiles followed by acid promoted *anti*-elimination or base-promoted *syn* elimination gives the corresponding *Z*- or *E*-alkenes **174**, respectively (equation 148)[262,263]. A similar approach has been employed for the synthesis of *exo*-brevicomin **175** (equation 149)[264]. Allylsilanes are obtained stereoselectively under similar conditions when $Li_2Cu(CN)(CH_2SiMe_3)_2$ is employed as the nucleophile[265].

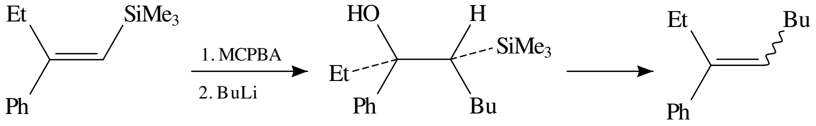

(148)

(174)

BF_3	(*Z*) 65%
KH	(*E*) 50%

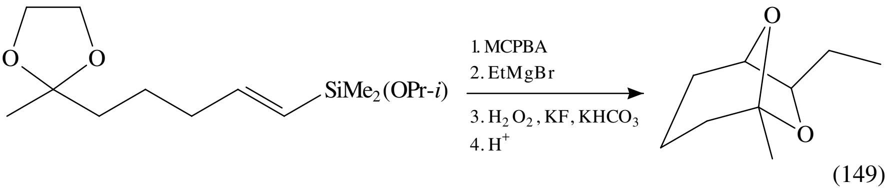

(149)

(175)

Addition of nitrene to allylsilane gives the corresponding aziridine intermediate **176** which undergoes a ring-opening process to give allylamine **177** as the major product (equation 150)[266,267]. Aziridination of β-trimethylsilylstyrene with the chiral 3-acetoxyaminoquinazolinone reagent[268] lead to aziridine **178** in high diastereoselectivity (equation 151)[269].

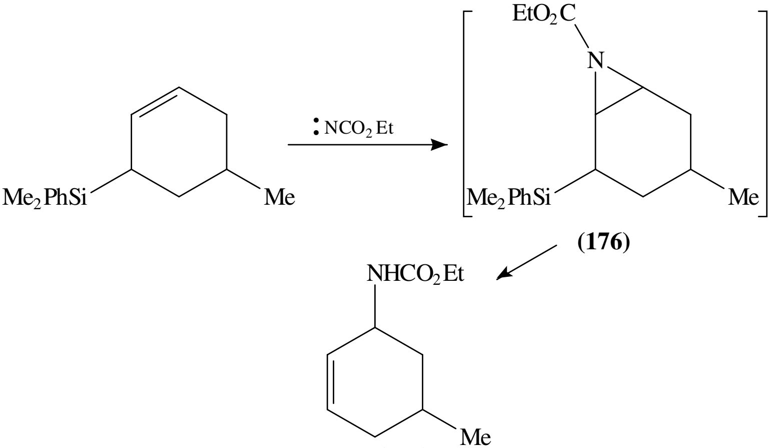

(176)

(177)

(150)

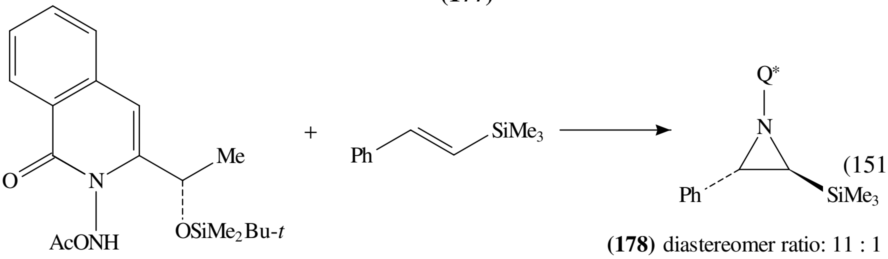

Q*NHOAc

(178) diastereomer ratio: 11 : 1

(151)

2. *OsO_4 oxidation*

Dihydroxylation of allylsilanes with OsO_4 has been investigated extensively. The reaction has been used for the synthesis of β-damascone **179** (equation 152)[270].

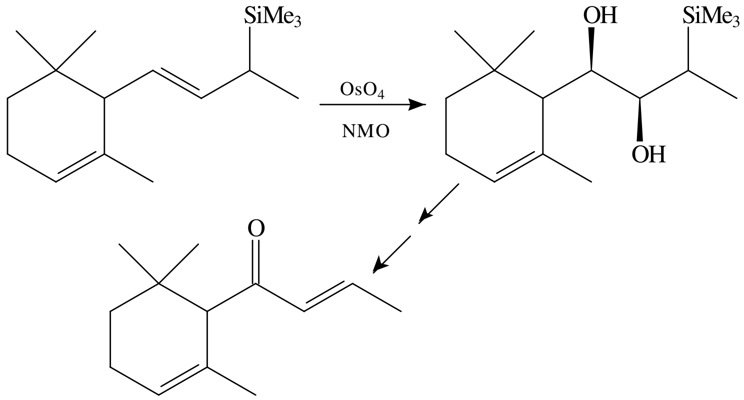

(179)

(152)

α-Hydroxycrotylsilane **180** undergoes diastereoselective bishydroxylation with OsO_4 to form 1,2-*anti*-1,2,3-triol **181** (equation 153)[271,272]. It is noted that by increasing the size of the silyl group, the *anti* selectivity improves.

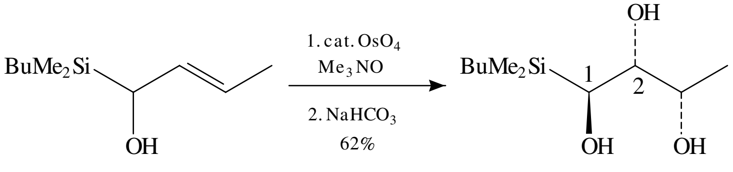

(153)

(180) **(181)** *anti* : *syn* = 120–147 : 1

Sharpless asymmetric dihydroxylation of simple allylsilanes yields the corresponding diols **182** with moderate enantioselectivity (equation 154)[273]. However, when **183** is treated under similar conditions, substituted γ-lactones **184a** and **184b** are obtained in high diastereo- and enantioselectivities (equation 155)[274–277].

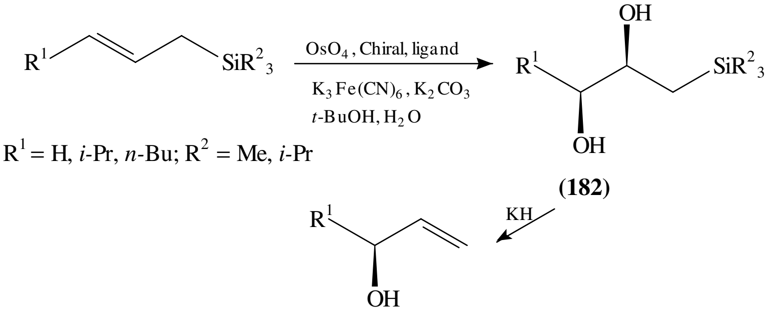

(154)

(182)

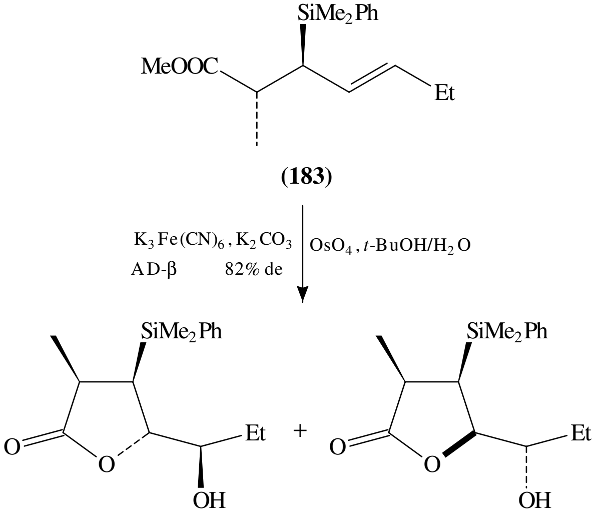

(183)

(155)

(184a) ee > 95% **(184b)** ee > 95%

3. Other oxidation reactions

Photooxygenation of vinylsilane in the presence of acetic anhydride and pyridine furnishes a convenient procedure for the synthesis of α-trimethylsilylenones **185** in moderate to good yields (equation 156)[278]. Dye-sensitized photooxidations of allylsilane with singlet oxygen produces a mixture of (*E*)- and (*Z*)-3-trimethyl-silylallyl hydroperoxides **186** (equation 157)[279].

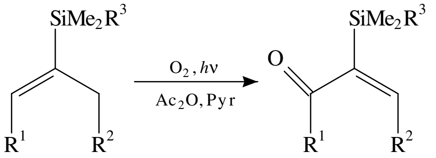

(156)

(185)

R^1 = Me, *n*-Bu; R^2 = H

R^{1}R^2 = (CH$_2$)$_n$, n = 2, 3; R^3 = Me, Ph

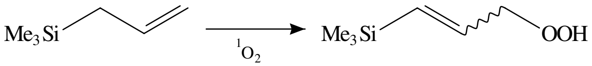

(186)

(157)

$E:Z = 22:78$

Various vinylsilanes are oxidized to the corresponding ketones **187** in excellent yield upon treatment with oxygen in the presence of Co(ecbo)$_2$ (ecbo = 2-ethoxycarbonyl-1,3-butanedionato) catalyst under neutral conditions (equation 158)[280].

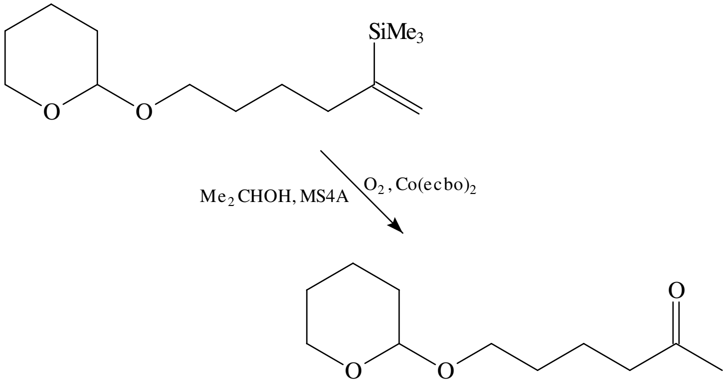

(158)

(187)

E. Cycloaddition Reactions

1. [2 + 1] Cycloaddition

The addition of a carbene unit to the double bond of silyl-substituted dienes has been executed. It is noteworthy that the addition reaction occurs at the double bond more remote from the silyl substituent. Further reactions of these cyclopropyl products **188** with AgBF$_4$

give the functionalized silyl-substituted dienes **189** in moderate yield (equation 159)[281]. In a similar manner, dichlorocyclopropane **190** is converted into the corresponding diene **191** by desilylation (equation 160)[282].

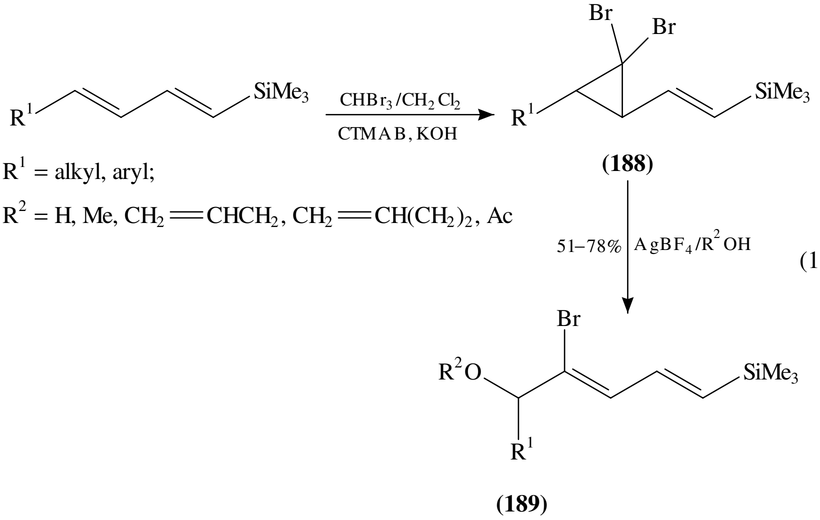

(159)

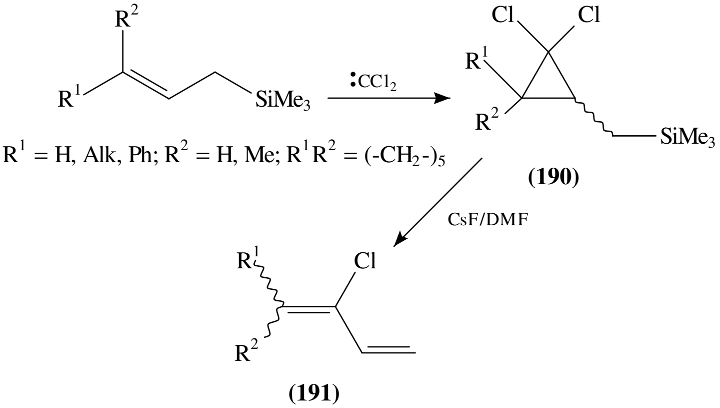

(160)

The Simmons–Smith reaction of chiral (*E*)-crotylsilane **192** produces **193**, which subsequently undergoes a ring-opening reaction followed by cyclization under acidic conditions to give **194** (equation 161)[283].

2. [2 + 2] Cycloaddition

The reaction of vinylsilane with dichloroketene gives **195** as the major product in 37% yield (equation 162). The minor product **196** decomposes during the course of chromatography on silica gel[284]. The regioselectivity of this reaction is in accord with frontier molecular orbital predictions.

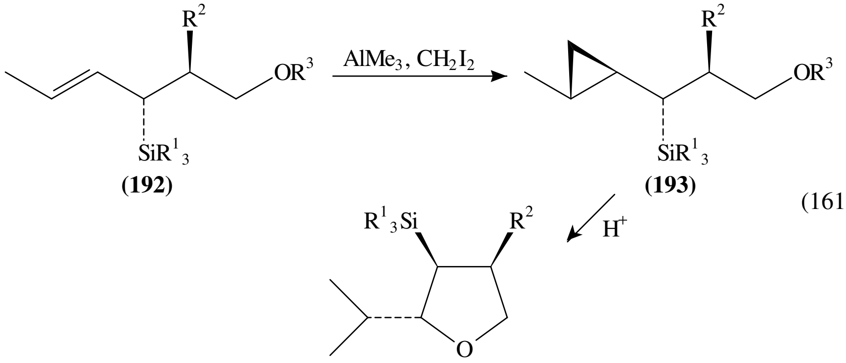

(192) **(193)** **(194)**

(161)

R^1 = H, Me, Bu; R^2 = H, *t*-BuPh$_2$Si

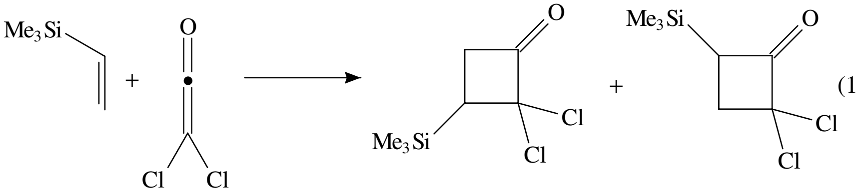

(195) **(196)**

(162)

In the cycloaddition of triisopropylallylsilane to α, β-unsaturated lactams **197**, cyclobutane adducts **198** have been found to be the kinetic products whereas the formation of cyclopentanes **199** is thermodynamically controlled[285]. Reactions of allenylmethylsilanes with activated unsaturated esters and nitriles (equation 163)[286] and allylsilanes with unsaturated esters[287] are other examples of using [2+2] cycloaddition to construct cyclobutane derivatives.

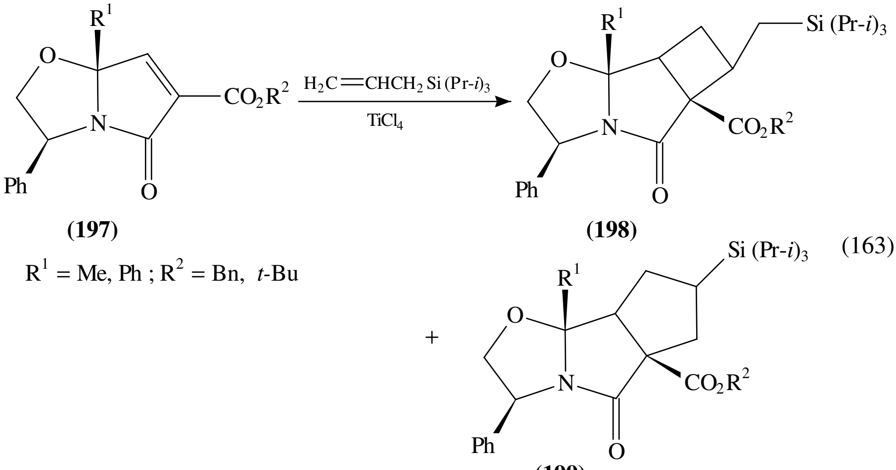

(197) **(198)** **(199)**

(163)

R^1 = Me, Ph ; R^2 = Bn, *t*-Bu

Lewis acids play a dominant role on the chemoselectivity of the cycloaddition of allylsilanes and 3-butyn-2-ones. $AlCl_3$ and $EtAlCl_2$ promote [2+2] cycloaddition predominantly, whereas $TiCl_4$-mediated reaction gives significant amount of the [3+2] adduct[288,289]. The reaction of 2,2-bis(trifluoromethyl)ethylene-1,1-dicarbonitrile with allylsilane without any Lewis acid catalysts yields the cyclobutane derivative via a nonconcerted fashion[290].

Photocycloaddition proceeds between allylsilane and *N*-methylphthalimide to yield a mixture of [2 + 2] and [4 + 2] adducts along with the allylated product[291]. Intramolecular cycloadditions of the vinylsilanes with the cyclopentenone moieties in **200** furnish good yields of cyclic products stereoselectively (equation 164)[292]. In the presence of 1,4-dicyanonaphthalene, diallylsilane **201** undergoes an intramolecular photocycloaddition reaction in an aromatic solvent to give a four-membered ring product (equation 165)[293].

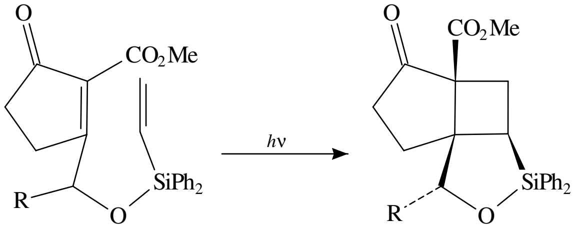

(164)

(200)

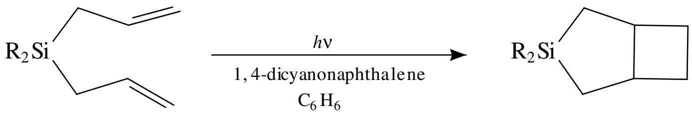

(165)

(201)

R = alkyl, aryl

$TiCl_4{}^-$ or $BF_3 \cdot OEt_2$-catalyzed addition of *N*-acylated aromatic aldimine to triisopropylallylsilane gives azetidine derivatives **202** (equation 166) accompanied by some allylated products[294]. Cycloaddition of allylsilanes and chlorosulfonyl isocyanate yields the silyl-substituted *β*-lactam **203**[295,296]. The presence of an electronegative substituent on the silicon will induce ring opening and fragmentation to yield allyl cyanides **204** (equation 167)[296].

Oxetanes **205** are produced with a high degree of stereoselectivity when an allylsilane with bulky substituents at the silicon center reacts with *α*-keto ester in the presence of $TiCl_4$ (equation 168). It is interesting to note that tetrahydrofuran derivatives are obtained at high temperature[297].

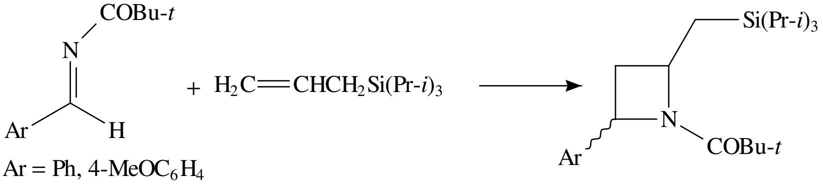

Ar = Ph, 4-MeOC$_6$H$_4$

(166)

(202)

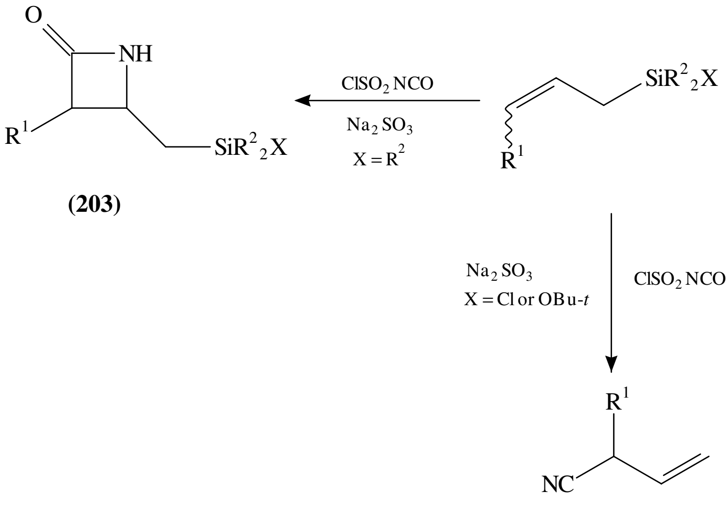

(203)

(204)

(167)

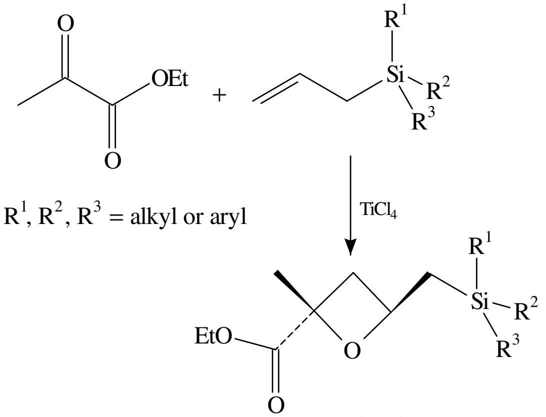

R^1, R^2, R^3 = alkyl or aryl

(205)

(168)

3. [3 + 2] Cycloaddition

In the presence of a Lewis acid, allylsilane can act as a three-carbon component and react with α,β-unsaturated ketones to yield cyclopentane derivatives **206** (equation 169)$^{298-310}$. The reaction is believed to involve a conjugate addition of allylsilane to the α, β-unsaturated system, resulting in the cationic intermediate followed by a 1,2-silyl shift and cyclization. The new stereogenic center generated through the cationic 1,2-silyl shift preserves a high degree of *anti* selectivity[309]. This outcome suggests that allylsilane is a synthetic equivalent for a 2-silyl substituted 1,3-dipole. In general, allylsilane with a sterically hindered silicon center is required for cycloaddition in order to suppress the Sakurai–Hosomi reaction. The silyl group can then be replaced by a Tamao oxidation[309]. High diastereoselectivities are obtained when chiral allylsilanes are employed in the [3 + 2] annulation with α, β-unsaturated carbonyl compounds as in the formation of **207** (equation 170)[303,304,310].

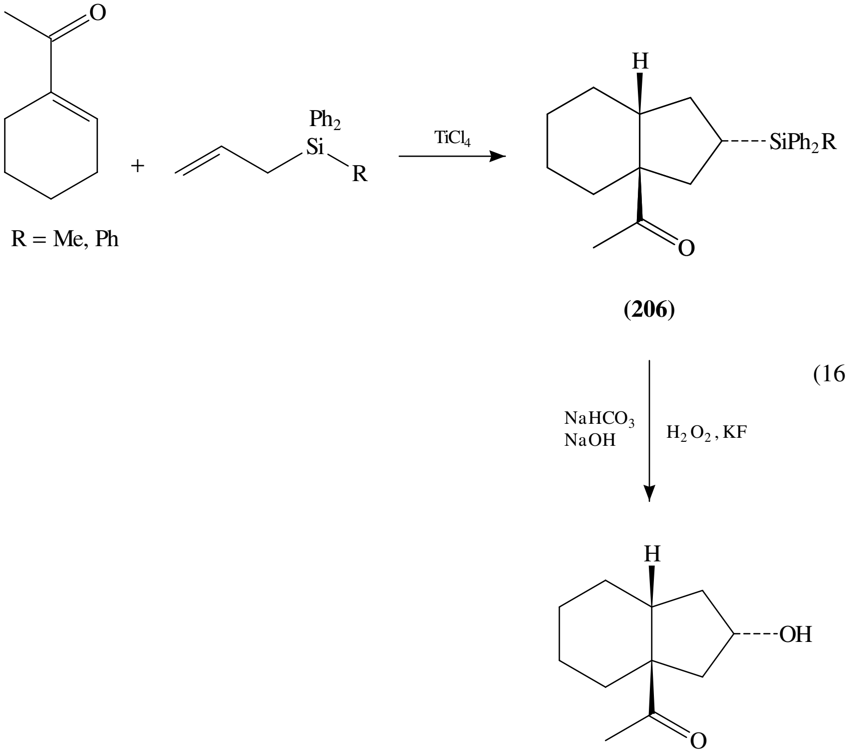

(206)

(169)

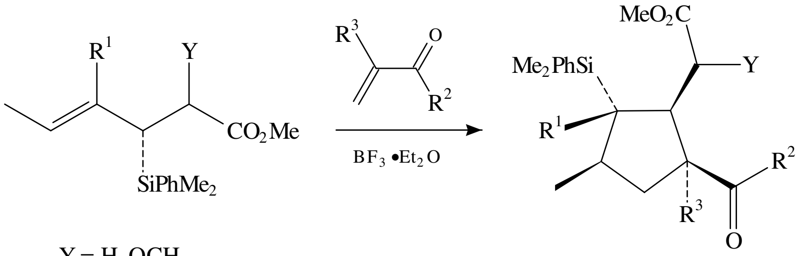

(170)

$Y = H, OCH_3$

$R^1 = R^3 = H, Me; R^2 = H, Me, Et$

(207)

The [3 + 2] annulation reaction can be extended to the synthesis of heterocycles. Thus, the reaction of crotylsilanes with *in situ*-generated imines produces, diastereoselectively, [3 + 2] adducts **208** at low temperature or homoallylic *N*-acylamines **209** at elevated temperature (equation 171)[311,312].

Another approach leading to pyrrolidine **210** via [3 + 2] cycloaddition is the reaction of *N*-protected α-amino aldehydes with allylsilanes in the presence of a catalytic amount of $BF_3 \cdot OEt_2$ (equation 172). No 1,2-silyl group migration occurs in these annulation processes[313].

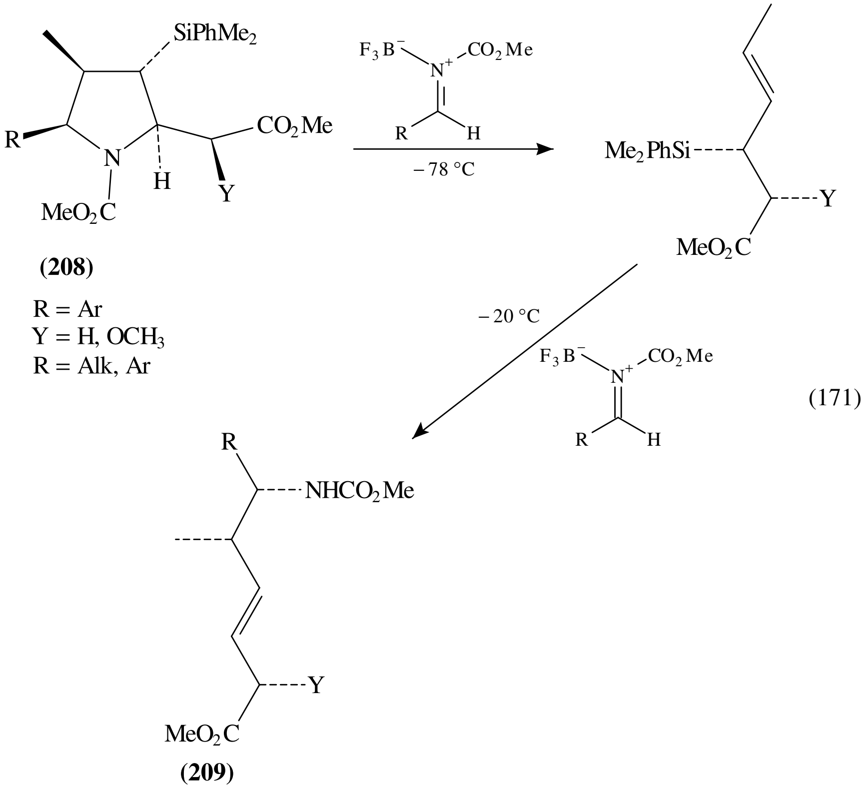

(208)

R = Ar
Y = H, OCH$_3$
R = Alk, Ar

(171)

(209)

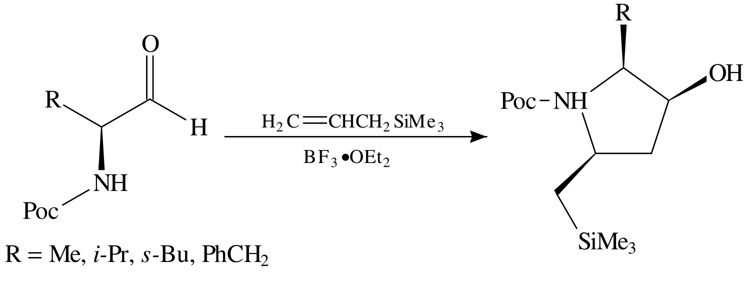

R = Me, *i*-Pr, *s*-Bu, PhCH$_2$

(172)

(210)

As for oxygen heterocycles, several reports involving the diastereoselective synthesis of highly substituted tetrahydrofuran derivatives have appeared. SnCl$_4$-mediated [3 + 2] cycloaddition of allylsilane with optically active α-ketoesters affords **211** with excellent diastereoselectivity (equation 173)[314–317].

When chiral allylsilanes are used for coupling with aldehydes, the diastereoselectivity of the reaction depends on the nature of the Lewis acid employed. Chelative SnCl$_4$-promoted reaction gives **212** whereas BF$_3$ · OEt$_2$ catalyzes the annulation reactions leading to **213** (equation 174)[315–317].

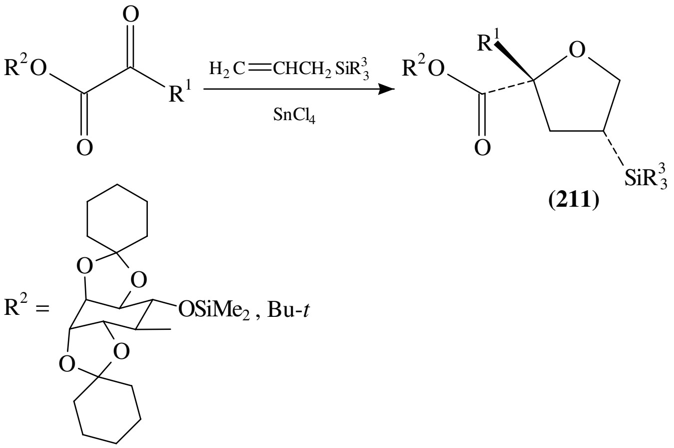

(211)

(173)

R^1 = Me, Ph; R^3_3 = Me$_3$, Me$_2$Ph, *t*-BuMe$_2$, *t*-BuPh$_2$

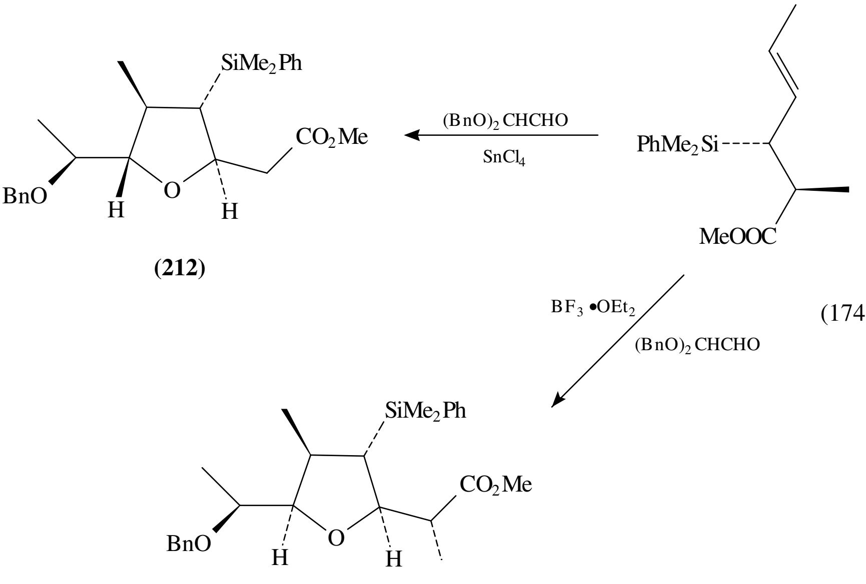

(212)

(174)

(213)

Formation of Δ^2-isoxazolines **214** can be achieved by the cycloaddition of allylsilanes to NOBF$_4$ in excellent diastereoselectivity (equation 175)[318].

4. [4 + 2] Cycloaddition

Silyl-substituted alkenes or dienes can undergo the Diels–Alder reaction[28]. The reactivity of these alkenes, however, is generally lower than those without silyl substituent. In addition, the degree of regioselectivity of the silyl group is evidently small. Only when both steric and electronic factors are in the same direction can a single adduct be obtained.

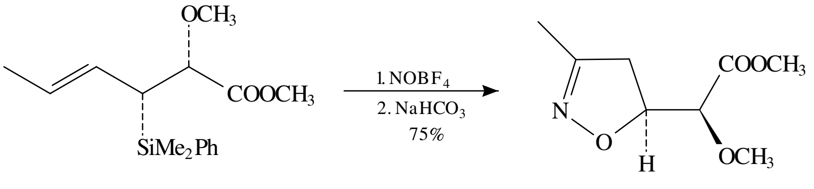

(175)

(214)

diastereomer ratio 40 : 1

a. Silyl-substituted alkenes as dienophiles. Intramolecular Diels–Alder reaction of a vinylsilane moiety with a diene group gives predominantly the corresponding bicyclic product **215** (equation 176). Several factors affect the stereoselectivity of this reaction. When $n = 1$, the bulky R^1 group on the silicon and the *trans* substituent group at C_3 appear to favor a *trans*-fused bicyclic skeleton. Poor selectivity, however, is observed when n is larger than $1^{319-321}$.

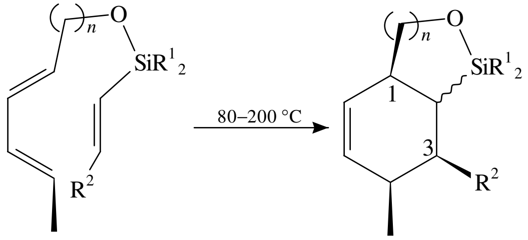

(176)

R = Me, Ph; R^2 = H, Ph

(215)

Vinylsilane reacts with **216** in the presence of $ZnCl_2$ and gives the corresponding Diels–Alder adduct stereoselectively in good yield (equation 177)[322].

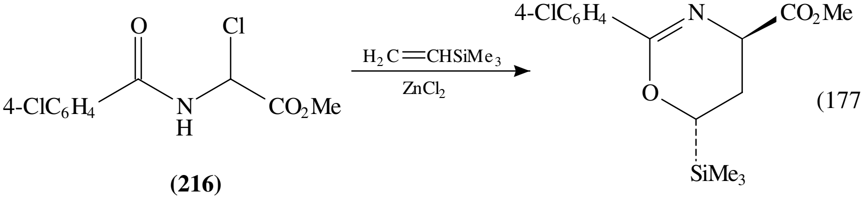

(216)

(177)

b. Silyl-substituted alkenes as dienes. The use of silyl-substituted dienes as dienes in the Diels–Alder reaction has been reviewed[26,27]. Only recent representative examples are summarized here. As the carbon–silicon bonds are readily converted into a number of other functionalities, silicon-tethered intramolecular Diels–Alder reactions have paved the way for the synthesis of functionalized cyclohexane derivatives **217–219** (equation 178–180)[28]. When the silicon atom is directly attached to the diene moiety, stereoselective cycloaddition has been achieved[323–325].

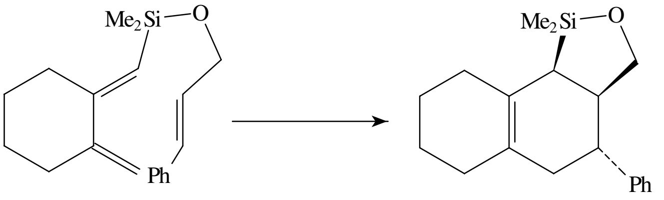

(217)

(178)

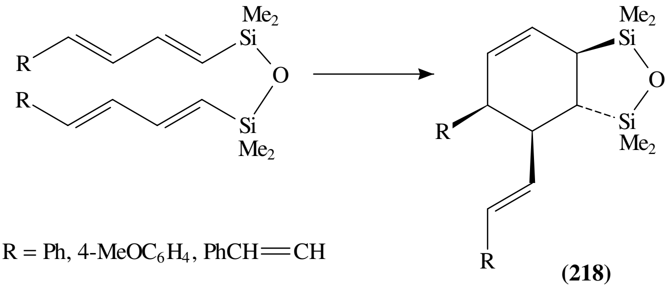

R = Ph, 4-MeOC$_6$H$_4$, PhCH=CH

(218)

(179)

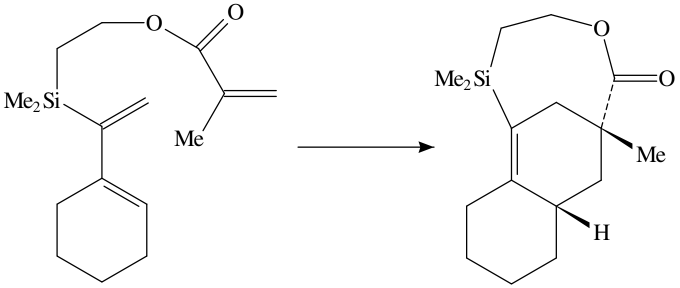

(219)

(180)

5. [5 + 2] Cycloaddition

A silicon-tethered [5+2] intramolecular cycloaddition of vinylsilane moiety to a pyrone ring to **220** has been executed in regio- and stereoselective manners (equation 181)[326].

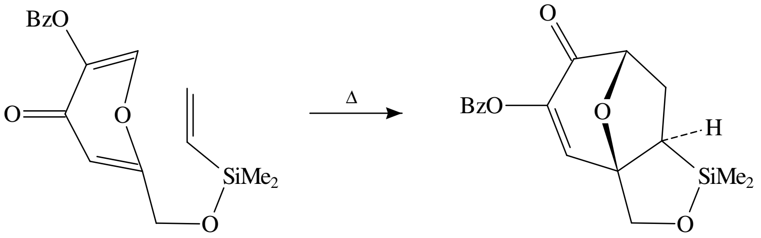

(220)

(181)

F. Rearrangements

1. Ene reaction

The ene reaction is the major side reaction in the Sakurai–Hosomi coupling reaction. Thus, treatment of **221** with carbonyl or with azo compounds in the presence of $TiCl_2(OPr\text{-}i)_2$ furnishes a mixture of ene-type product **222** and the Sakurai–Hosomi-type product **223** (equation 182)[327]. Allylsilylation of alkenes[328] and alkynes[329,330] proceeds regioselectively to give **224** (equation 183) and **225** (equation 184), respectively, when aluminum catalysts are used.

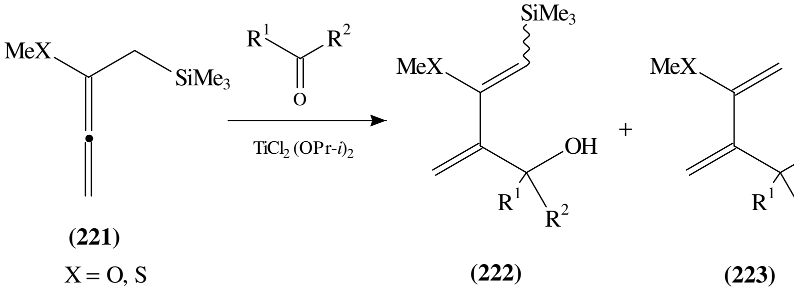

(221)

X = O, S

R^1 = Ar, CO_2Et ; R^2 = H, CO_2Et

(222) **(223)**

(182)

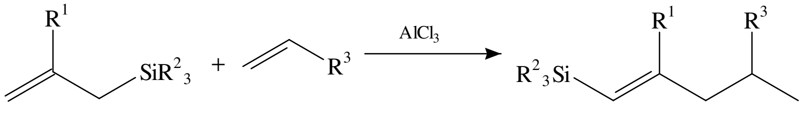

R^1 = H, Me; R^2 = Me, Ph; R^3 = *n*-Bu, *n*-C_6H_{13}, $PhCH_2$

(224)

(183)

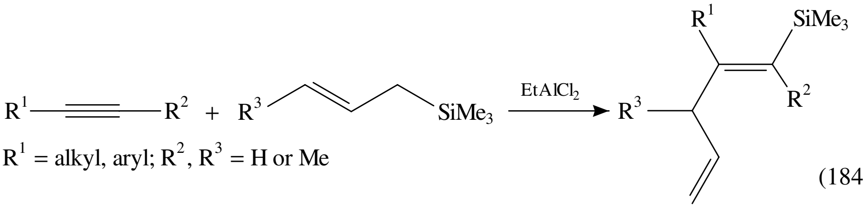

R^1 = alkyl, aryl; R^2, R^3 = H or Me

(184)

(225)

It is noteworthy that the ene product **227** is obtained exclusively when allylsilane **226** is treated with butynone in the presence of ZnI_2 catalyst and molecular sieve (ms) 4Å(equation 185)[331]. Methyl vinyl ketone behaves similarly. High enantioselectivity has been observed in product **228** when triphenylallylsilane is coupled with methyl glyoxylate in the presence of (*R*)-(BINOL)$TiCl_2$ catalyst (equation 186)[332]. In addition to [2 + 2] cycloaddition, TCNE undergoes a regiospecific ene reaction with γ-alkyl substituted allylsilanes to yield the substituted olefins **229** (equation 187)[333].

The presence of the silyl substituent at the olefinic carbon provides an important feature in the regio- and stereochemical control of the Lewis acid-catalyzed carbonyl-ene reactions which gives **230** (equation 188)[334]. The changeover of the olefinic stereoselectivity from *'trans'* to *'cis'* is observed (*cf* **231a**) (equation 189). when R is a silyl group[334]. Without a silyl group (R = H) *'trans'* product **231b** is obtained predominantly[334]. It is noteworthy that a *trans* selectivity is widely recognized for the ene reaction with alkenes without silyl group[335–339].

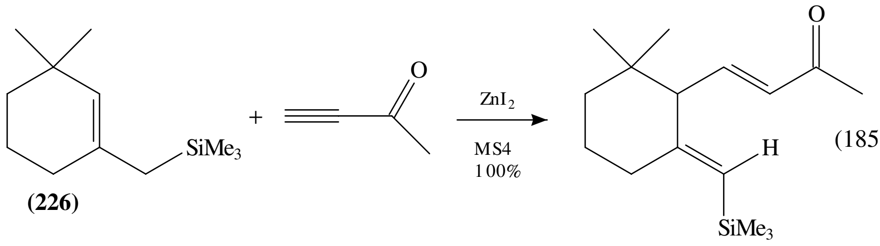

(226) **(227)**

(185)

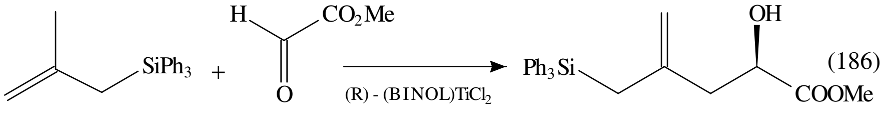

(186)

BINOL = 1,1′-Binaphthyl-2, 2′-diol

(228)

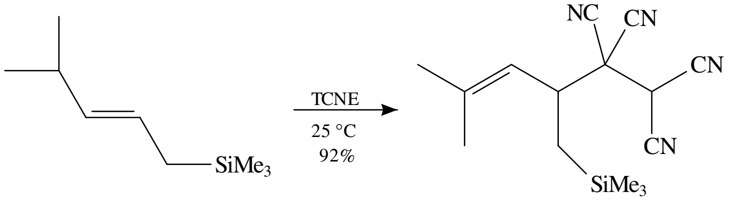

(187)

(229)

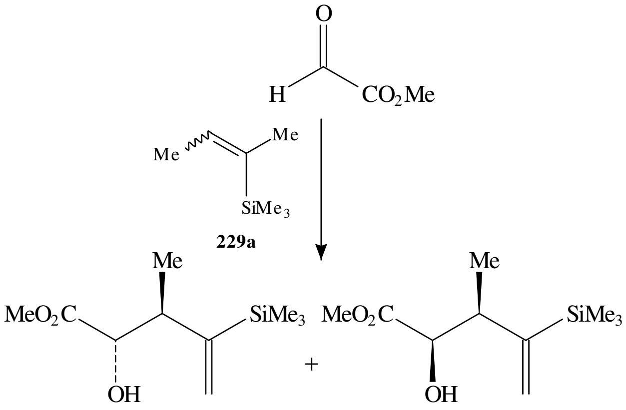

(188)

(230a) **(230b)**

	(230a)	(230b)
From *E* – **229a** :	7	93
From Z – **229a** :	98	2

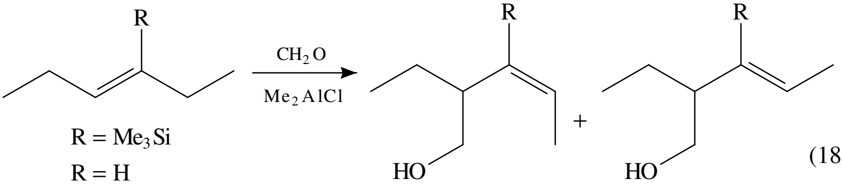

(189)

(231a) **(231b)**

98 : 2
15 : 85

Silicon-tethered intramolecular carbonyl-ene reactions of vinylsilanes have been shown to generate methylene silacyclohexanols **232** stereoselectively in good yield (equation 190)[340].

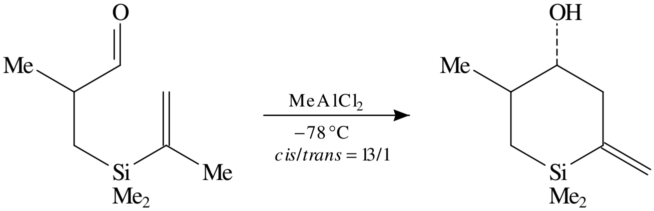

(190)

(232)

The ene reaction of *N*-methyltriazolinedione with vinylsilanes yields **233** (equation 191). Only hydrogen at the carbon geminal to the silyl group will be abstracted[340–342].

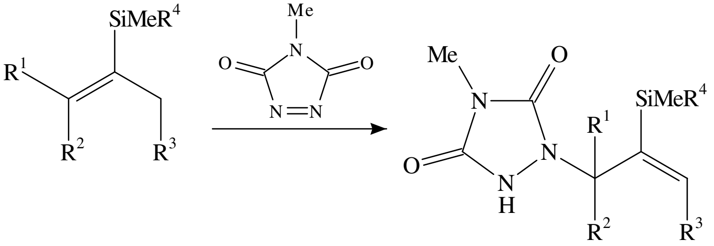

(191)

(233)

R^1 = H, Me, *n*-Bu; R^2, R^3 = H, Me; R^2R^3 = —$(CH_2)_3$—; R^4 = Me, Ph

2. Sigmatropic rearrangements

β-(Silyl)allylic ethers **234** readily undergo 2,3-Wittig rearrangement upon treatment with an amide base to give, after methylation, **235** (equation 192)[37,343]. Tandem Claisen-2,3-Wittig-oxy-Cope rearrangement has been observed when **236** is treated under similar conditions to give **238** (equation 193)[343].

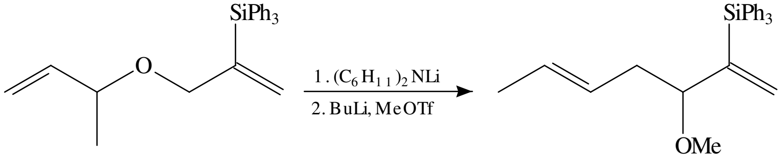

(234) **(235)**

(192)

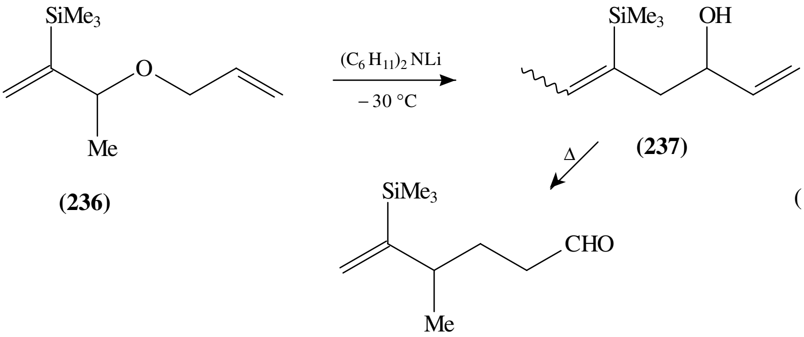

(236) **(237)** **(238)**

(193)

Claisen–Ireland rearrangement of **239** followed by DIBALH reduction gives a mixture of *syn* and *anti* isomers **240** (equation 194)[34−347]. In a similar manner, orthoester Claisen rearrangements of **241** give stereoselectively the corresponding chiral allylsilanes **242** (equation 195)[348].

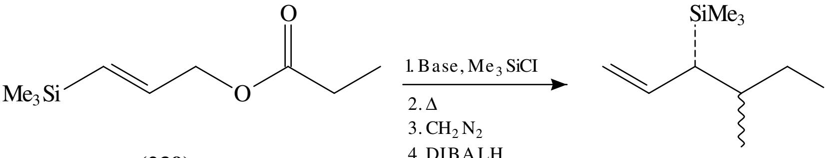

(239) **(240)**

(194)

Base	*syn/anti*
LDA	1/2
$LiH(SiMe_3)_2$/HMPA	4/1

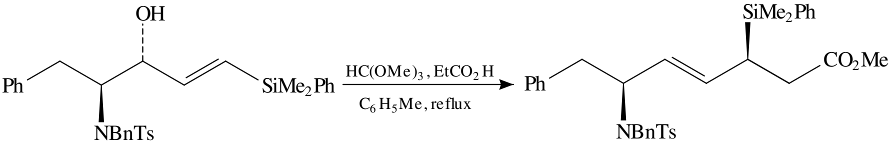

(195)

(241) **(242)**

3. Miscellaneous rearrangements

β-Silylallylic alcohols undergo rhodium-catalyzed double bond migration to give the corresponding α-silyl-substituted ketones in excellent yields[349]. Thermolysis of **243** gives the corresponding silacyclopentenes **244** (equation 196). The reaction may proceed via an olefin to a carbene isomerization[325,350,351].

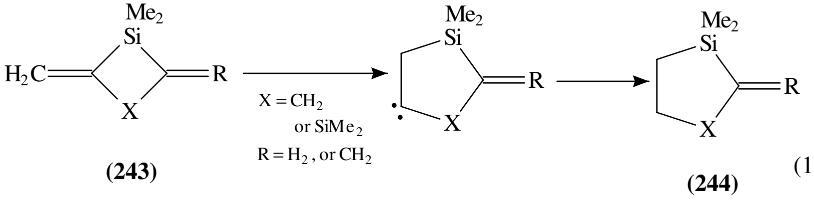

(243) **(244)** (196)

G. Other Reactions

The use of silylallyl anion in organic synthesis has been extensive[24,29]. The regio- and stereochemistry of these reactions can be controlled. For example, alkylation of the anion generated from the corresponding allylsilane with an electrophile E^+ takes place selectively at the γ-position due to steric hindrance (equation 197)[352].

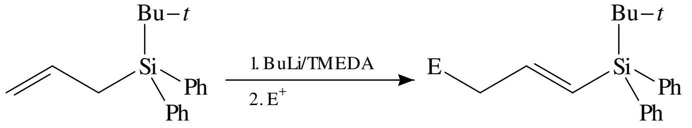

(197)

E = H, Me, 1° or 2° Alk, MeCH(OH), PhCH(OH)

3-Silyl-substituted allyl acetates react with $Fe_2(CO)_9$ under a CO atmosphere to give the corresponding η^2-$Fe(CO)_4$ complexes which are treated with a silyl enol ether in the presence of $BF_3 \cdot OEt_2$ to yield vinylsilanes **245** stereoselectively in moderate to good yields (equation 198). Allylstannane can also react under these conditions[353]. The silyl-substituted butadiene complex of tricarbonyliron is treated with acetyl chloride in the presence of $AlCl_3$ at 0 °C to give the Friedel–Crafts acylation products, dienone complexes, without desilylation[354,355].

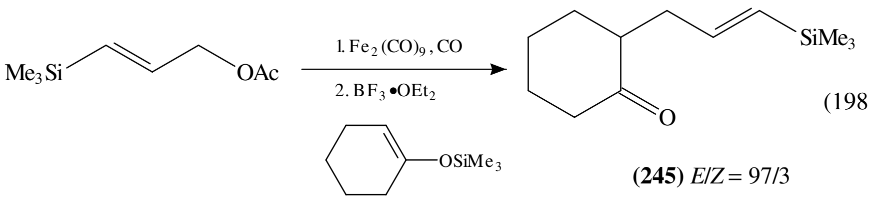

(198)

(245) *E*/*Z* = 97/3

Desulfonylation of β-silylvinyl sulfone **246** with Bu_3SnLi followed by treatment with aldehydes affords γ-hydroxyvinylsilanes **247** in good yields (equation 199)[356]. Reactions of trimethyl(2-nitrovinyl)silane with organometallic reagents give regioselectively the corresponding Michael adducts in excellent yields[357].

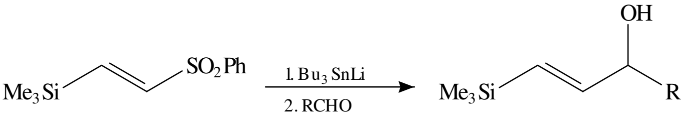

(246) **(247)**

(199)

R = 1° or 2° Alk

Hydroboration of **248** takes place at the terminal position which provides an approach to prepare ε-(trimethylsilyl)homogeraniol (equation 200)[358].

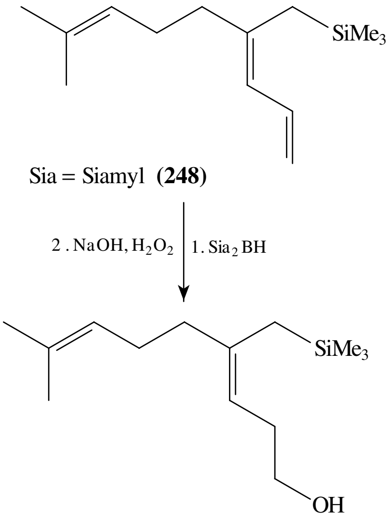

Sia = Siamyl (**248**)

(200)

The double bond in vinylsilanes can be hydrogenated under various catalytic conditions. Ni/Et_3SiH[359] and rhodium[360] catalysts have been used recently (equation 201).

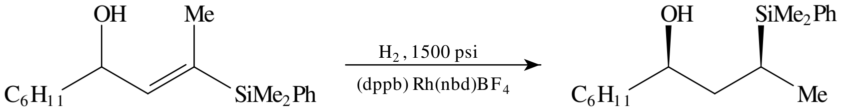

dppb = $Ph_2PCH_2(CH_2)_2CH_2PPh_2$
nbd = 2,5-Norbornadiene

(>500 : 1)

(201)

Vinylsilane works as an effective chain transfer agent in the Mo- or W-catalyzed polymerization of various substituted acetylenes. The molecular weight of the polymer can be controlled[361]. Perfluorovinylsilanes undergo fluoride ion promoted polymerization reaction[362]. The polymeric product which is insoluble in most of the solvents but HMPA at elevated temperature (200–230 °C) shows infrared absorption at 1630 cm^{-1} which indicates the presence of conjugated fluoroolefin moiety. Apparently some of the silyl groups have been eliminated during the polymerization process. The polymer forms metallic luster on the glass wall and shows a conductivity of $8.5 \times 10^{-9}\ \Omega^{-1}\ cm^{-1}$.

VI. REFERENCES

1. E. W. Colvin, *Silicon in Organic Synthesis*, Butterworth, London, 1981.
2. W. P. Weber, *Silicon Reagents for Organic Synthesis*, Springer-Verlag, New York, 1983.
3. H. Sakurai (Ed.), *Organosilicon and Bioorganosilicon Chemistry, Structure, Bonding, Reactivity and Synthetic Application*, Horwood, Chichester, 1985.
4. S. Pawlenko, *Organosilicon Chemistry*, Walter de Gruyter, Berlin, 1986.
5. E. W. Colvin, *Silicon Reagents in Organic Synthesis*, Academic Press, London, 1988.
6. S. Patai and Z. Rappoport (Eds.), *The Chemistry of Organic Silicon Compounds*, Parts 1 and 2, Wiley, Chichester, 1989.
7. T. H. Chan and I. Fleming, *Synthesis*, 761 (1979).
8. I. Fleming, in *Comprehensive Organic Chemistry*, Vol. 3 (Eds. D. H. R. Barton and W. D. Ollis), Chap. 13, Pergamon Press, Oxford, 1979.
9. H. Sakurai, *Pure Appl. Chem.*, **54**, 1 (1982).
10. P. D. Magnus, T. Sarkar and S. Djuric, in *Comprehensive Organometallic Chemistry*, Vol. 8 (Eds. G. Wilkinson, F. G. A. Stone and E. W. Abel), Chap. 48.4, Pergamon Press, New York, 1983.
11. Z. N. Parnes and G. I. Bolestova, *Synthesis*, 991 (1984).
12. H. Sakurai, *Pure Appl. Chem.*, **57**, 1759 (1985).
13. L. A. Paquette, *Chem. Rev.*, **86**, 733 (1986).
14. T. A. Blumenkopf and L. E. Overman, *Chem. Rev.*, **86**, 857 (1986).
15. D. Schinzer, *Synthesis*, 263 (1988).
16. A. Hosomi, *Acc. Chem. Res.*, **21**, 200 (1988).
17. G. Majetich, in *Organic Synthesis, Theory and Applications*, (Ed. T. Hudlicky), JAI Press, Greenwich, CT, 1989.
18. G. Majetich, in *Selectivities in Lewis Acid Promoted Reactions*, (Ed. D. Schinzer), Kluwer Academic Publishers, Dordrecht, 1989, p. 169.
19. I. Fleming, J. Dunoguès and R. Smithers, *Org. React.*, **37**, 57 (1989).
20. H. Sakurai, *Synlett*, 1 (1989).
21. D. J. Ager, *Org. React.*, **38**, 1 (1990).
22. T. K. Sarkar, *Synthesis*, 969 (1990).
23. J. S. Panek, in *Comprehensive Organic Synthesis*, Vol. 1 (Eds. B. M. Trost and I. Fleming), Pergamon Press, Oxford, 1991, p. 579.
24. T. H. Chan and D. Wang, *Chem. Rev.*, **92**, 995 (1992).
25. Y. Yamamoto and N. Asao, *Chem. Rev.*, **93**, 2207 (1993).
26. T. -Y. Luh and K. -T. Wong, *Synthesis*, 349 (1993).
27. M. D. Stadnichuk and T. I. Voropaeva, *Russ. Chem. Rev.*, **64**, 25 (1995).
28. M. Bols and T. Skrydstrup, *Chem. Rev.*, **95**, 1253 (1995).
29. T. H. Chan and D. Wang, *Chem. Rev.*, **95**, 1279 (1995).
30. C. E. Masse and J. S. Panek, *Chem. Rev.*, **95**, 1293 (1995).
31. K. A. Horn, *Chem. Rev.*, **95**, 1317 (1995).
32. E. Langkopf and D. Schinzer, *Chem. Rev.*, **95**, 1375 (1995).
33. A. R. Bassindale and P. G. Taylor, in Reference 6, Chap. 14.
34. R. L. Funk, J. Umstead-Daggett and K. M. Brummond, *Tetrahedron Lett.*, **34**, 2867 (1993).
35. I. Fleming and D. Higgins, *Tetrahedron Lett.*, **30**, 5777 (1989).
36. F. Sato, H. Watanabe, Y. Tanaka, T. Yamaji and M. Sato, *Tetrahedron Lett.*, **24**, 1041 (1983).
37. N. Kishi, H. Imma, K. Mikami and T. Nakai, *Synlett*, 189 (1992).
38. A. Degl'Innocenti, E. Stucchi, A. Capperucci, A. Mordini, G. Reginato and A. Ricci, *Synlett*, 329 (1992).
39. M. Mori, N. Watanabe, N. Kaneta and M. Shibasaki, *Chem. Lett.*, 1615 (1991).
40. W. -W. Weng and T. -Y. Luh, *J. Org. Chem.*, **57**, 2760 (1992).
41. E. Schaumann, A. Kirschning and F. Narjes, *J. Org. Chem.*, **56**, 717 (1991).
42. E. R. Koft and A. B. Smith, III, *J. Am. Chem. Soc.*, **104**, 2659 (1982).
43. A. B. Smith, III, Y. Yokoyama, D. M. Huryn and N. K. Dunlap, *Tetrahedron Lett.*, **28**, 3659 (1987).
44. A. B. Smith, III, Y. Yokoyama and N. K. Dunlap, *Tetrahedron Lett.*, **28**, 3663 (1987).
45. T. H. Chan and K. Koumaglo, *J. Organomet. Chem.*, **285**, 109 (1985).
46. K. Tamao, M. Akita, K. Maeda and M. Kumada, *J. Org. Chem.*, **52**, 1100 (1987).
47. J. Barluenga, L. J. Alverez-García and J. M. González, *Tetrahedron Lett.*, **36**, 2153 (1995).
48. M. Ochiai, K. Oshima and Y. Musaki, *J. Chem. Soc., Chem. Commun.*, 869 (1991).

49. H. Cerfontain, J. B. Kramer, R. M. Schonk and R. H. Bakker, *Recl. Trav. Chim. Pays-Bas*, **114**, 410 (1995).
50. H. Mayr, G. Gorath and B. Bauer, *Angew. Chem., Int. Ed. Engl.*, **33**, 788 (1994).
51. K. Saigo, K. Kudo, Y. Hashimoto, H. Kimoto and M. Hasegawa, *Chem. Lett.*, 941 (1990).
52. H. Pellissier and M. Santelli, *J. Chem. Soc., Chem. Commun.*, 607 (1995).
53. Y. Yamamoto, M. Ohno and S. Eguchi, *Chem. Lett.*, 525 (1995).
54. S. L. Xu, H. Xia and H. W. Moore, *J. Org. Chem.*, **56**, 6094 (1991).
55. G. A. Molander and J. P. Haar, Jr., *J. Am. Chem. Soc.*, **115**, 40 (1993).
56. A. P. Davis and S. C. Hegarty, *J. Am. Chem. Soc.*, **114**, 2745 (1992).
57. A. P. Davis and M. Jaspars, *J. Chem. Soc., Chem. Commun.*, 1176 (1990).
58. J. S. Panek and M. Yang, *J. Org. Chem.*, **56**, 5755 (1991).
59. J. S. Panek and M. Yang, *J. Am. Chem. Soc.*, **113**, 6594 (1991).
60. A. Hosomi, H. Hayashida and Y. Tominaga, *J. Org. Chem.*, **54**, 3254 (1989).
61. P. Mohr, *Tetrahedron Lett.*, **36**, 2453 (1995).
62. B. Hermans and L. Hevesi, *Tetrahedron Lett.*, **31**, 4363 (1990).
63. C. C. Silveira, G. L. Fiorin and A. L. Braga, *Tetrahedron Lett.*, **37**, 6085 (1996).
64. T. Fujiwara, T. Iwasaki, J. Miyagawa and T. Takeda, *Chem. Lett.*, 343 (1994).
65. T. K. Hollis, N. P. Robinson, J. Whelan and B. Bosnich, *Tetrahedron Lett.*, **34**, 4309 (1993).
66. G. Kaur, K. Manju and S. Trehan, *J. Chem. Soc., Chem. Commun.*, 581 (1996).
67. H. Monti and M. Féraud, *Synth. Commun.*, **26**, 1721 (1996).
68. H. Pellissier, L. Toupet and M. Santelli, *J. Org. Chem.*, **59**, 1709 (1994).
69. J. Li, T. Gallardo and J. B. White, *J. Org. Chem.*, **55**, 5426 (1990).
70. S. E. Denmark and N. G. Almstead, *J. Org. Chem.*, **59**, 5130 (1994).
71. B. Guyot, J. Pornet and L. Miginiac, *J. Organomet. Chem.*, **373**, 279 (1989).
72. G. Majetich, H. Nishidie and Y. Zhang, *J. Chem. Soc., Perkin Trans. 1*, 453 (1995).
73. M. Tsukazaki and V. Snieckus, *Tetrahedron Lett.*, **34**, 411 (1993).
74. Y. H. Kim and S. H. Kim, *Tetrahedron Lett.*, **36**, 6895 (1995).
75. F. D'Aniello, A. Mann, D. Mattii and M. Taddei, *J. Org. Chem.*, **59**, 3762 (1994).
76. L. F. Tietze, A. Dölle and K. Schiemann, *Angew. Chem., Int. Ed. Engl.*, **31**, 1372 (1992).
77. L. F. Tietze, K. Schiemann and C. Wegner, *J. Am. Chem. Soc.*, **117**, 5851 (1995).
78. K. Mikami, K. Kawamoto, T. -P. Loh and T. Nakai, *J. Chem. Soc., Chem. Commun.*, 1161 (1990).
79. S. Danishefsky and M. DeNinno, *Tetrahedron Lett.*, **26**, 823 (1985).
80. N. F. Jain, P. F. Cirillo, R. Pelletier and J. S. Panek, *Tetrahedron Lett.*, **36**, 8727 (1995).
81. J. S. Panek and M. Yang, *J. Am. Chem. Soc.*, **113**, 9868 (1991).
82. Y. Horiuchi, K. Oshima and K. Utimoto, *J. Org. Chem.*, **61**, 4483 (1996).
83. H. Monti, M. Afshari and G. Léandri, *J. Organomet. Chem.*, **486**, 69 (1995).
84. A. Mekhalfia and I. E. Markó, *Tetrahedron Lett.*, **32**, 4779 (1991).
85. A. Mekhalfia, I. E. Markó and H. Adams, *Tetrahedron Let.*, **32**, 4783 (1991).
86. I. E. Markó and A. Mekhalfia, *Tetrahedron Lett.*, **33**, 1799 (1992).
87. I. E. Markó, A. Mekhalfia, D. J. Bayston and H. Adams, *J. Org. Chem.*, **57**, 2211 (1992).
88. I. E. Markó and D. J. Bayston, *Tetrahedron*, **50**, 7141 (1994).
89. I. E. Markó and D. J. Bayston, *Tetrahedron Lett.*, **34**, 6595 (1993).
90. M. Kira, K. Sato and H. Sakurai, *J. Am. Chem. Soc.*, **112**, 257 (1990).
91. M. Kira, K. Sato, H. Sakurai, M. Hada, M. Izawa and J. Ushio, *Chem. Lett.*, 387 (1991).
92. K. Sato, M. Kira and H. Sakurai, *J. Am. Chem. Soc.*, **111**, 6429 (1989).
93. M. Kira, K. Sato, K. Sekimoto, R. Gewald and H. Sakurai, *Chem. Lett.*, 281 (1995).
94. A. Hosomi, S. Kohra, K. Ogata, T. Yanagi and T. Tominaga, *J. Org. Chem.*, **55**, 2415 (1990).
95. Z. Y. Wei, D. Wang, J. S. Li and T. H. Chan, *J. Org. Chem.*, **54**, 5768 (1989).
96. S. E. Denmark, D. M. Coe, N. E. Pratt and B. D. Griedel, *J. Org. Chem.*, **59**, 6161 (1994).
97. S. Kobayashi and K. Nishio, *Tetrahedron Lett.*, **34**, 3453 (1993).
98. S. Kobayashi and K. Nishio, *J. Org. Chem.*, **59**, 6620 (1994).
99. S. Kobayashi and K. Nishio, *Chem. Lett.*, 1773 (1994).
100. D. Seyferth, J. Pornet and R. M. Weinstein, *Organometallics*, **1**, 1651 (1982).
101. D. Seyferth and J. Pornet, *J. Org. Chem.*, **45**, 1722 (1980).
102. A. Hosomi, M. Saito and H. Sakurai, *Tetrahedron Lett.*, **21**, 3783 (1980).
103. A. G. Myers, S. E. Kephart and H. Chen, *J. Am. Chem. Soc.*, **114**, 7922 (1992).
104. S. E. Denmark, B. D. Griedel, D. M. Coe and M. E. Schnute, *J. Am. Chem. Soc.* **116**, 7026 (1994).

105. K. Matsumoto, K. Oshima and K. Utimoto, *J. Synth. Org. Chem. Jpn.*, **54**, 289 (1996).
106. K. Okada, K. Matsumoto, K. Oshima and K. Utimoto, *Tetrahedron Lett.*, **36**, 8067 (1995).
107. S. Kashimura, M. Ishifune, Y. Murai and T. Shono, *Chem. Lett.*, 309 (1996).
108. D. Schinzer and J. Kabbara, *Synlett*, 766 (1992).
109. T. -L. Ho and F. -S. Liang, *Chem. Commun.*, 1887 (1996).
110. M. Ohno, Y. Yamamoto and S. Eguchi, *J. Chem. Soc., Perkin Trans. 1*, 2272 (1991).
111. L. -R. Pan and T. Tokoroyama, *Chem. Lett.*, 1999 (1990).
112. L. -R. Pan and T. Tokoroyama, *Tetrahedron Lett.*, **33**, 1469 (1992).
113. A. G. Schultz and H. Lee, *Tetrahedron Lett.*, **33**, 4397 (1992).
114. L. F. Tietze and M. Ruther, *Chem. Ber.*, **123**, 1387 (1990).
115. L. F. Tietze and C. Schünke, *Angew. Chem., Int. Ed. Engl.*, **34**, 1731 (1995).
116. G. Majetich, K. Hull and R. Desmond, *Tetrahedron Lett.*, **26**, 2751 (1985).
117. D. Schinzer and K. Ringe, *Synlett*, 463 (1994).
118. G. Majetich, D. Lowery and V. Khetani, *Tetrahedron Lett.*, **31**, 51 (1990).
119. S. Laschat and H. Kunz, *J. Org. Chem.*, **56**, 5883 (1991).
120. S. Laschat and H. Kunz, *Synlett*, 51 (1990).
121. M. Kira, T. Hino and H. Sakurai, *Chem. Lett.*, 277 (1991).
122. E. C. Roos, H. Hiemstra, W. N. Speckamp, B. Kaptein, J. Kamphuis and H. E. Schoemaker, *Synlett*, 451 (1992).
123. H. H. Mooiweer, H. Hiemstra and W. N. Speckamp, *Tetrahedron*, **45**, 4627 (1989).
124. H. H. Mooiweer, H. Hiemstra and W. N. Speckamp, *Tetrahedron*, **47**, 3451 (1991).
125. J. Mittendorf, H. Hiemstra and W. N. Speckamp, *Tetrahedron*, **46**, 4049 (1990).
126. M. Rubiralta, A. Diez and D. Miguel, *Synth. Commun.*, **22**, 359 (1992).
127. J. M. Takacs and J. J. Weidner, *J. Org. Chem.*, **59**, 6480 (1994).
128. M. Franciotti, A. Mann, A. Mordini and M. Taddei, *Tetrahedron Lett.*, **34**, 1355 (1993).
129. L. E. Overman and K. L. Bell, *J. Am. Chem. Soc.*, **103**, 1851 (1981).
130. L. E. Overman and N. -H. Lin, *J. Org. Chem.*, **50**, 3670 (1985).
131. L. E. Overman, K. L. Bell and F. Ito, *J. Am. Chem. Soc.*, **106**, 4192 (1984).
132. L. E. Overman and A. L. Robichaud, *J. Am. Chem. Soc.*, **111**, 300 (1989).
133. L. E. Overman and R. M. Burk, *Tetrahedron Lett.*, **25**, 5739 (1984).
134. C. J. Flann and L. E. Overman, *J. Am. Chem. Soc.*, **109**, 6115 (1987).
135. M. C. McIntosh and S. M. Weinreb, *J. Org. Chem.*, **56**, 5010, (1991).
136. L. Vidal, J. Royer and H. -P. Husson, *Tetrahedron Lett.*, **36**, 2991 (1995).
137. G. A. Olah, D. S. Van Vliet, Q. Wang and G. K. Surya Prakash, *Synthesis*, 159 (1995).
138. K. -T. Kang, J. C. Lee and J. S. U, *Tetrahedron Lett.*, **33**, 4953 (1992).
139. E. Schaumann and B. Mergardt, *J. Chem. Soc., Perkin Trans. 1*, 1361 (1989).
140. A. Barbero, P. Cuadrodo, I. Fleming, A. M. González, F. J. Pulido and A. Sánchez, *J. Chem. Soc., Perkin Trans. 1*, 1525 (1995).
141. F. Babudri, V. Fiandanese, G. Marchese and F. Naso, *J. Chem. Soc., Chem. Commun.*, 237 (1991).
142. F. Babudri, V. Fiandanese and F. Naso, *J. Org. Chem.*, **56**, 6245 (1991).
143. G. Picotin and P. Miginiac, *Tetrahedron Lett.*, **29**, 5897 (1988).
144. A. Kirschning, F. Narjes and E. Schaumann, *Justus Liebigs Ann. Chem.*, 933 (1991).
145. M. Kira, T. Hino and H. Sakurai, *Chem. Lett.*, 555 (1992).
146. T. Yokozawa, K. Furuhashi and H. Natsume, *Tetrahedron Lett.*, **36**, 5243 (1995).
147. L. E. Overman and P. A. Renhowe, *J. Org. Chem.*, **59**, 4138 (1994).
148. G. A. Molander and S. W. Andrews, *J. Org. Chem.*, **54**, 3114 (1989).
149. S. C. Bergmeier and P. P. Seth, *Tetrahedron Lett.*, **36**, 3793 (1995).
150. T. Hirao, T. Fujii and Y. Ohshiro, *Tetrahedron*, **50**, 10207 (1994).
151. T. V. Lee, F. S. Roden and J. R. Porter, *J. Chem. Soc., Perkin Trans 1*, 2139 (1989).
152. C. M. Hudson, M. R. Marzabadi, K. D. Moeller and D. G. New, *J. Am. Chem. Soc.*, **113**, 7372 (1991).
153. S. D. Burke and D. N. Deaton, *Tetrahedron Lett.*, **32**, 4651 (1991).
154. S. D. Burke, K. Shankaran and M. J. Helber, *Tetrahedron Lett.*, **32**, 4655 (1991).
155. S. D. Burke, M. E. Kort, M. S. S. Strickland, H. M. Organ and L. A. Silks, III, *Tetrahedron Lett.*, **35**, 1503 (1994).
156. J. Tsuji, *Palladium Reagents and Catalysts*, Wiley, Chichester, 1995
157. R. J. P. Corriu, R. Perz and C. Reys, *Tetrahedron*, **39**, 999 (1983).

158. G. G. Furin, O. A. Vyazankina, B. A. Gostevsky and N. S. Vyazankin, *Tetrahedron*, **44**, 2675 (1988).
159. J. Yoshida, K. Tamao, H. Yamamoto, T. Kakui, T. Uchida and M. Kumada, *Organometallics*, **1**, 542 (1982).
160. W. P. Weber, R. A. Felix, A. K. Willard and K. E. Koenig, *Tetrahedron Lett.*, 4701 (1971).
161. A. Hallberg and C. Westerlund, *Chem. Lett.*, 1993 (1982).
162. N. M. Chistovalova, I. S. Akhrem, E. V. Reshetova and M. E. Vol'pin, *Izvest. Akad. Nauk SSR, Ser. Khim.*, 2342 (1984); *Chem. Abstr.*, **102**, 78961 (1985).
163. K. Kikukawa, K. Ikenaga, F. Wada and T. Matsuda, *Tetrahedron Lett.*, **25**, 5789 (1984).
164. K. Ikenaga, K. Kikukawa and T. Matsuda, *J. Org. Chem.*, **52**, 1276 (1987).
165. K. Kikukawa, K. Ikenaga, F. Wada and T. Matsuda, *Chem. Lett.*, 1337 (1983).
166. K. Ikenaga, K. Kikukawa and T. Matsuda, *J. Chem. Soc., Perkin Trans. 1*, 1959 (1986).
167. M. E. Garst and B. J. McBride, *J. Org. Chem.*, **54**, 249 (1989).
168. K. Karabelas and A. Hallberg, *J. Org. Chem.*, **54**, 1773 (1989).
169. Y. Hatanaka and T. Hiyama, *J. Org. Chem.*, **53**, 918 (1988).
170. Y. Hatanaka and T. Hiyama, *J. Org. Chem.*, **54**, 268 (1989).
171. Y. Hatanaka and T. Hiyama, *Tetrahedron Lett.*, **31**, 2719 (1990).
172. Y. Hatanaka and T. Hiyama, *Chem. Lett.*, 2049 (1989).
173. M. Hojo, C. Murakami, H. Aihara, E. -i. Komori, S. Kohra, Y. Tominaga and A. Hosomi, *Bull. Soc. Chem. Fr.*, **132**, 499 (1995).
174. H. Matsuhashi, Y. Hatanaka, M. Kuroboshi and T. Hiyama, *Tetrahedron Lett.*, **36**, 1539 (1995).
175. B. M. Trost and E. Keinan, *Tetrahedron Lett.*, **21**, 2595 (1980).
176. Y. Hatanaka, Y. Ebina and T. Hiyama, *J. Am. Chem. Soc.*, **113**, 7075 (1991).
177. Y. Hatanaka, K. -i. Goda and T. Hiyama, *Tetrahedron Lett.*, **35**, 6511 (1994).
178. Y. Hatanaka and T. Hiyama, *J. Am. Chem. Soc.*, **112**, 7793 (1990).
179. Y. Hatanaka, K. -i. Goda and T. Hiyama, *Tetrahedron Lett.*, **35**, 1279 (1994).
180. L. F. Tietze and R. Schimpf, *Angew. Chem., Int. Ed. Engl.*, **33**, 1089 (1994).
181. L. F. Tietze and R. Schimpf, *Chem. Ber.*, **127**, 2235 (1994).
182. G. D. Daves, Jr. and A. Hallberg, *Chem. Rev.*, **89**, 1433 (1989).
183. K. Tamao, K. Kobayashi and Y. Ito, *Tetrahedron Lett.*, **30**, 6051 (1989).
184. A. M. Castaño and J. -E. Bäckvall, *J. Am. Chem. Soc.*, **117**, 560 (1995).
185. Y. Matano, M. Yoshimune and H. Suzuki, *Tetrahedron Lett.*, **36**, 7475 (1995).
186. S. R. Wilson and C. E. Augelli-Szafran, *Tetrahedron*, **44**, 3983 (1988).
187. M. Ochiai, M. Arimoto and E. Fujita, *Tetrahedron Lett.*, **22**, 4491 (1981).
188. M. Ochiai, E. Fujita, M. Arimoto and H. Yamaguchi, *Chem. Pharm. Bull.*, **33**, 41 (1985).
189. K. Lee, D. Y. Kim and D. Y. Oh, *Tetrahedron Lett.*, **29**, 667 (1988).
190. N. X. Hu, Y. Aso, T. Otsubo and F. Ogura, *Tetrahedron Lett.*, **29**, 4949 (1988).
191. Y. Ikeda and H. Yamamoto, *Bull. Chem. Soc. Jpn.*, **59**, 657 (1986).
192. G. M. Farinola, V. Fiandanese, L. Mazzone and F. Naso, *J. Chem. Soc., Chem. Commun.*, 2523 (1995).
193. L. Xue, L. Lu, S. Pederson, Q. Liu, R. Narske and D. J. Burton, *Tetrahedron Lett.*, **37**, 1921 (1996).
194. Y. Wakatsuki,, H. Yamazaki, M. Nakano and Y. Yamamoto, *J. Chem. Soc., Chem. Commun.*, 703 (1991).
195. T. Hirao, M. Sakaguchi, T. Ishikawa and I. Ikeda, *Synth. Commun.*, **25**, 2579 (1995).
196. A. S. Guram, *Synlett*, 259 (1993).
197. A. Capperucci, M. C. Ferrara, A. Degl'Innocenti, B. F. Bonini, G. Mazzanti, P. Zani and A. Ricci, *Synlett*, 880 (1992).
198. L. M. Atagi, S. C. Critchlow and J. M. Mayer, *J. Am. Chem. Soc.*, **114**, 1483 (1992).
199. J.-i. Yoshida, T. Murata and S. Isoe, *Tetrahedron Lett.*, **28**, 211 (1987).
200. P. F. Hurdrlik, A. M. Kassim, E. L. O. Agwaramgbo, K. A. Doonquah, R. R. Roberts and A. M. Hudrlik, *Organometallics*, **12**, 2367 (1993).
201. F. Sato, Y. Tanaka and M. Sato, *J. Chem. Soc., Chem. Commun.*, 165 (1983).
202. M. Kosugi, H. Kurata, K. -i. Kawata and T. Migita, *Chem. Lett.*, 1327 (1991).
203. C. Chatgilialoglu, C. Ferreri, M. Ballestri and D. P. Curran, *Tetrahedron Lett.*, **37**, 6387 (1996).
204. K. Nishitani, Y. Harada, Y. Nakamura, K. Yokoo and K. Yamakawa, *Tetrahedron Lett.*, **35**, 7809 (1994).
205. L. E. Overman and A. S. Thompson, *J. Am. Chem. Soc.*, **110**, 2248 (1988).

206. D. Berger, L. E. Overman and P. A. Renhowe, *J. Am. Chem. Soc.*, **115**, 9305 (1993).
207. K. Miura, S. Okajima, T. Hondo and A. Hosomi, *Tetrahedron Lett.*, **36**, 1483 (1995).
208. K. Miura, T. Hondo, S. Okajima and A. Hosomi, *Tetrahedron Lett.*, **37**, 487 (1996).
209. J. -P. Pillot, J. Dunoguès and R. Calas, *J. Chem. Res. (S)*, 268 (1977).
210. R. F. Cunico, *Synth. Commun.*, **18**, 917 (1988).
211. J. R. Hwu, K. -L. Chen, S. Ananthan and H. V. Patel, *Organometallics*, **15**, 499 (1996).
212. H. Okumoto and J. Tsuji, *Synth. Commun.*, **12**, 1015 (1982).
213. S. Kim, I. Y. Lee, J. -Y. Yoon and D. H. Oh, *J. Am. Chem. Soc.*, **118**, 5138 (1996).
214. P. Jankowski, M. Masnuk and J. Wicha, *Synlett*, 866 (1995).
215. J. R. Hwu, B. -L. Chen and S. -S. Shiao, *J. Org. Chem.*, **60**, 2448 (1995).
216. W. -J. Koot, R. van Ginkel, M. Kranenburg, H. Hiemstra, S. Louwrier, M. J. Moolenaar and W. N. Speckamp, *Tetrahedron Lett.*, **32**, 401 (1991).
217. J. M. Dener and D. J. Hart, *Tetrahedron*, **44**, 7037 (1988).
218. W. -W. Weng and T. -Y. Luh, *J. Org. Chem.*, **58**, 5574 (1993).
219. H. Sawada and M. Nakayama, *J. Chem. Soc., Chem. Commun.*, 677 (1991).
220. J. Kabbara, C. Hoffmann and D. Schinzer, *Synthesis*, 299, (1995).
221. F. L. Koerwitz, G. B. Hammond and D. F. Wiemer, *J. Org. Chem.*, **54**, 743 (1989).
222. J. A. Soderquist and J. C. Colberg, *Tetrahedron Lett.*, **35**, 27 (1994).
223. J. A. Soderquist and G. León-Colón, *Tetrahedron Lett.*, **32**, 43 (1991).
224. K. -T. Kang, S. S. Kim and J. C. Lee, *Tetrahedron Lett.*, **32**, 4341 (1991).
225. P. Knochel and J. F. Normant, *Tetrahedron Lett.*, **25**, 4383 (1984).
226. N. M. Chistovalova, I. S. Akhrem, V. F. Sizoi, V. V. Bardin and M. E. Vol'pin, *Izvest. Akad. Nauk SSR, Ser. Khim.*, 1180 (1988); *Chem. Abstr.*, **110**, 95337 (1989).
227. K. Karabelas and A. Hallberg, *Tetrahedron Lett.*, **26**, 3131 (1985).
228. K. Karabelas and A. Hallberg, *J. Org. Chem.*, **51**, 5286 (1986).
229. K. Karabelas and A. Hallberg, *J. Org. Chem.*, **53**, 4909 (1988).
230. H. Yamashita, B. L. Roan and M. Tanaka, *Chem. Lett.*, 2175 (1990).
231. K. Kikukawa, K. Ikenaga, K. Kono, K. Toritani, F. Wada and T. Matsuda, *J. Organomet. Chem.*, **270**, 277 (1984).
232. S. Murai, F. Kakiuchi, S. Sekine, Y. Tanaka, A. Kamatani, M. Sonoda and N. Chatani, *Nature*, **369**, 529 (1993).
233. S. Murai, F. Kakiuchi, S. Sekine, Y. Tanaka, A. Kamatani, M. Sonoda and N. Chatani, *Pure Appl. Chem.*, **66**, 1527 (1994).
234. S. Murai, *J. Synth. Org. Chem. Jpn.*, **52**, 993 (1994).
235. F. Kakiuchi, S. Sekine, Y. Tanaka, A. Kamatani, M. Sonoda, N. Chatani and S. Murai, *Bull. Chem. Soc., Jpn.*, **68**, 62 (1995).
236. M. Sonoda, F. Kakiuchi, N. Chatani and S. Murai, *J. Organomet. Chem.*, **504**, 151 (1995).
237. M. Sonoda, F. Kakiuchi, A. Kamatani, N. Chatani and S. Murai, *Chem. Lett.*, 109 (1996).
238. B. M. Trost, K. Imi and I. W. Davies, *J. Am. Chem. Soc.*, **117**, 5371 (1995).
239. F. Kakiuchi, Y. Tanaka, T. Sato, N. Chatani and S. Murai, *Chem. Lett.*, 679 (1995).
240. F. Kakiuchi, Y. Yamamoto, N. Chatani and S. Murai, *Chem. Lett.*, 681 (1995).
241. F. Kakiuchi, M. Yamauchi, N. Chatani and S. Murai, *Chem. Lett.*, 111 (1996).
242. H. Guo, M. A. Tapsak and W. P. Weber, *Macromolecules*, **28**, 4714 (1995).
243. H. Guo, G. Wang, M. A. Tapsak and W. P. Weber, *Macromolecules*, **28**, 5686 (1995).
244. R. Takeuchi, N. Ishii and N. Sato, *J. Chem. Soc., Chem. Commun.*, 1247 (1991).
245. R. Takeuchi, N. Ishii, M. Sugiura and N. Sato, *J. Org. Chem.*, **57**, 4189 (1992).
246. R. Takeuchi and N. Sato, *J. Organomet. Chem.*, **393**, 1 (1990).
247. M. M. Doyle, W. R. Jackson and P. Perlmutter, *Tetrahedron Lett.*, **30**, 233 (1989).
248. C. M. Crudden and H. Alper, *J. Org. Chem.*, **59**, 3091 (1994).
249. J. A. Anhaus, W. Clegg, S. P. Collingwood and V. C. Gibson, *J. Chem. Soc., Chem. Commun.*, 1720 (1991).
250. W. E. Crowe, D. R. Goldberg and Z. J. Zhang, *Tetrahedron Lett.*, **37**, 2117 (1996).
251. Z. Foltynowicz and B. Marciniec, *J. Organomet. Chem.*, **376**, 15 (1989).
252. M. Berglund, C. Andersson and R. Larsson, *J. Organomet. Chem.*, **292**, C15 (1985).
253. P. Mohr, *Tetrahedron Lett.*, **33**, 2455 (1992).
254. P. J. Murphy and G. Procter, *Tetrahedron Lett.*, **31**, 1059 (1990).
255. W. Adam, F. Prichtl, M. J. Richter and A. K. Smerz, *Tetrahedron Lett.*, **36**, 4991 (1995).
256. W. Adam and M. Richter, *Tetrahedron Lett.*, **33**, 3461 (1992).

257. Y. -K. Han and L. A. Paquette, *J. Org. Chem.*, **44**, 3731 (1979).
258. L. A. Paquette, R. A. Galemmo, Jr., J. -C. Caille and R. S. Valpey, *J. Org. Chem.*, **51**, 686 (1986).
259. S. G. Davies, C. J. R. Hedgecock and J. M. McKenna, *Tetrahedron: Asymmetry*, **6**, 2507 (1995).
260. J. M. Muchowski, R. Naef and M. L. Maddox, *Tetrahedron Lett.*, **26**, 5375 (1985).
261. J. -i. Yoshida, S. Nakatani and S. Isoe, *J. Org. Chem.*, **54**, 5655 (1989).
262. S. -S. P. Chou, H. -L. Kuo, C. -J. Wang, C. -Y. Tsai and C. -M. Sun, *J. Org. Chem.*, **54**, 868 (1989).
263. Y. Ukaji, A. Yoshida and T. Fujisawa, *Chem. Lett.*, 157 (1990).
264. K. Tamao, E. Nakajo and Y. Ito, *J. Org. Chem.*, **52**, 4412 (1987).
265. J. A. Soderquist and B. Santiago, *Tetrahedron Lett.*, **30**, 5693 (1989).
266. M. A. Loreto, P. A. Tardella and D. Tofani, *Tetrahedron Lett.*, **36**, 8295 (1995).
267. S. Fioravanti, M. A. Loreto, L. Pellacani, S. Raimondi and P. A. Tardella, *Tetrahedron Lett.*, **34**, 4101 (1993).
268. R. S. Atkinson, M. J. Grimshire and B. J. Kelly, *Tetrahedron*, **45**, 2875 (1989).
269. R. S. Atkinson, M. P. Coogan and I. S. T. Lochrie, *Tetrahedron Lett.*, **37**, 5179 (1996).
270. E. Azzari, C. Faggi, N. Gelsomini and M. Taddei, *J. Org. Chem.*, **55**, 1106 (1990).
271. J. S. Panek and P. F. Cirillo, *J. Am. Chem. Soc.*, **112**, 4873 (1990).
272. P. F. Cirillo and J. S. Panek, *J. Org. Chem.*, **59**, 3055 (1994).
273. J. A. Soderquist, A. M. Rane and C. J. López, *Tetrahedron Lett.*, **34**, 1893 (1993).
274. R. A. Ward and G. Procter, *Tetrahedron*, **51**, 12821 (1995).
275. M. J. Daly, R. A. Ward, D. F. Thompson and G. Procter, *Tetrahedron*, **51**, 7545 (1995).
276. M. J. Daly and G. Procter, *Tetrahedron*, **51**, 7549 (1995).
277. R. W. Ward and G. Procter, *Tetrahedron Lett.*, **33**, 3363 (1992).
278. W. Adam and M. J. Richter, *Synthesis*, 176 (1994).
279. N. Shimizu, F. Shibata, S. Imazu and Y. Tsuno, *Chem. Lett.*, 1071 (1987).
280. K. Kato and T. Mukaiyama, *Chem. Lett.*, 2233 (1989).
281. W. -W. Weng and T. -Y. Luh, *J. Chem. Soc., Perkin Trans. 1*, 2687 (1993).
282. M. Mitani, Y. Kobayashi and K. Koyama, *J. Chem. Soc., Perkin Trans. 1*, 653 (1995).
283. J. S. Panek, R. M. Garbaccio and N. F. Jain, *Tetrahedron Lett.*, **35**, 6453 (1994).
284. R. L. Danheiser and H. Sard, *Tetrahedron Lett.*, **24**, 23 (1983).
285. G. P. Brengel, C. Rithner and A. I. Meyers, *J. Org. Chem.*, **59**, 5144 (1994).
286. M. Hojo, K. Tomita, Y. Hirohara and A. Hosomi, *Tetrahedron Lett.*, **34**, 8123 (1993).
287. H. -J. Knölker, G. Baum and R. Graf, *Angew. Chem., Int. Ed. Engl.*, **33**, 1612 (1994).
288. H. Monti, G. Audran, J. -P. Monti and G. Léandri, *Synlett*, 403 (1994).
289. H. Monti, G. Audran, G. Léandri and J. -P. Monti, *Tetrahedron Lett.*, **35**, 3073 (1994).
290. R. Huisgen and R. Brückner, *Tetrahedron Lett.*, **31**, 2553 (1990).
291. Y. Kubo, E. Taniguchi and T. Araki, *Heterocycles*, **29**, 1857 (1989).
292. M. T. Crimmins and L. E. Guise, *Tetrahedron Lett.*, **35**, 1657 (1994).
293. K. Nakanishi, K. Mizuno and Y. Otsuji, *J. Chem. Soc., Chem. Commun.*, 90 (1991).
294. T. Uyehara, M. Yuuki, H. Masaki, M. Matsumoto, M. Ueno and T. Sato, *Chem. Lett.*, 789 (1995).
295. E. W. Colvin and M. Monteith, *J. Chem. Soc., Chem. Commun.*, 1230 (1990).
296. C. Nativi, E. Perrotta, A. Ricci and M. Taddei, *Tetrahedron Lett.*, **32**, 2265 (1991).
297. T. Akiyama and M. Kirino, *Chem. Lett.*, 723 (1995).
298. H. -J. Knölker, P. G. Jones and J. -B. Pannek, *Synlett*, 429 (1990).
299. K. Ohkata, K. Ishimaru, Y. -g. Lee and K. -y. Akiba, *Chem. Lett.*, 1725 (1990).
300. Y. -G. Lee, K. Ishimaru, H. Iwasaki, K. Ohkata and K. -y. Akiba, *J. Org. Chem.*, **56**, 2058 (1991).
301. H. -J. Knölker, P. G. Jones, J. -B. Pannek and A. Weinkauf, *Synlett*, 147 (1991).
302. B. B. Snider and Q. Zhang, *J. Org. Chem.*, **56**, 4908 (1991).
303. R. L. Danheiser, B. R. Dixon and R. W. Gleason, *J. Org. Chem.*, **57**, 6094 (1992).
304. R. L. Danheiser, T. Takahashi, B. Bertók and B. R. Dixon, *Tetrahedron Lett.*, **34**, 3845 (1993).
305. H. -J. Knölker and R. Graf, *Tetrahedron Lett.*, **34**, 4765 (1993).
306. H. -J. Knölker, N. Foitzik, H. Goesmann and R. Graf, *Angew. Chem., Int. Ed. Engl.*, **32**, 1081 (1993).
307. M. -J. Wu and J. -Y. Yeh, *Tetrahedron*, **50**, 1073 (1994).
308. H. -J. Knölker and R. Graf, *Synlett*, 131 (1994).

309. H. -J. Knölker and G. Wanzl, *Synlett*, 378 (1995) and references cited therein.
310. J. S. Panek and N. F. Jain, *J. Org. Chem.*, **58**, 2345 (1993).
311. J. S. Panek and N. F. Jain, *J. Org. Chem.*, **59**, 2674 (1994).
312. A. Stahl, E. Steckhan and M. Nieger, *Tetrahedron Lett.*, **35**, 7371 (1994).
313. S. -i. Kiyooka, Y. Shiomi, H. Kira, Y. Kaneko and S. Tanimori, *J. Org. Chem.*, **59**, 1958 (1994).
314. T. Akiyama, T. Yasusa, K. Ishikawa and S. Ozaki, *Tetrahedron Lett.*, **35**, 8401 (1994).
315. T. Akiyama, K. Ishikawa and S. Ozaki, *Chem. Lett.*, 627 (1994).
316. J. S. Panek and R. Beresis, *J. Org. Chem.*, **58**, 809 (1993).
317. K. Shanmuganthan, L. G. French and B. L. Jensen, *Tetrahedron: Asymmetry*, **5**, 797 (1994).
318. J. S. Panek and R. T. Beresis, *J. Am. Chem. Soc.*, **115**, 7898 (1993).
319. G. Stork, T. -Y. Chan and G. A. Breault, *J. Am. Chem. Soc.*, **114**, 7578 (1992).
320. S. M. Sieburth and L. Fensterbank, *J. Org. Chem.*, **57**, 5279 (1992).
321. D. F. Taber, R. S. Bhamidipati and L. Yet, *J. Org. Chem.*, **60**, 5537 (1995).
322. S. Ebeling, D. Matthies and D. McCarthy, *Phosphorus, Sulfur and Silicon*, **60**, 265 (1991).
323. K. Tamao, K. Kobayashi and Y. Ito, *J. Am. Chem. Soc.*, **111**, 6478 (1989).
324. R. -M. Chen, W. W. Weng and T. -Y. Luh, *J. Org. Chem.*, **60**, 3272 (1995).
325. K. J. Shea, A. J. Staab and K. S. Zandi, *Tetrahedron Lett.*, **32**, 2715 (1991).
326. A. Rumbo, L. Castedo Mouriño and J. L. Mascareñas, *J. Org. Chem.*, **58**, 5585 (1993).
327. M. Hojo, C. Murakami, H. Aihara, K. Tomita, K. Miura and A. Hosomi, *J. Organomet. Chem.*, **499**, 155 (1995).
328. S. H. Yeon, B. W. Lee, B. R. Yoo, M. -Y. Suk and I. N. Jung, *Organometallics*, **14**, 2361 (1995).
329. S. H. Yeon, J. S. Han, E. Hong, Y. Do and I. N. Jung, *J. Organomet. Chem.*, **499**, 159 (1995).
330. N. Asao, E. Yoshikawa and Y. Yamamoto, *J. Org. Chem.*, **61**, 4874 (1996).
331. G. Audran, H. Monti, G. Léandri and J. -P. Monti, *Tetrahedron Lett.*, **34**, 3417 (1993).
332. K. Mikami and S. Matsukawa, *Tetrahedron Lett.*, **35**, 3133 (1994).
333. S. Imazu, N. Shimizu and Y. Tsuno, *Chem. Lett.*, 1845 (1990).
334. K. Mikami, T. -P. Loh and T. Nakai, *J. Am. Chem. Soc.*, **112**, 6737 (1990).
335. K. Mikami, M. Tarada, M. Shimizu and T. Nakai, *J. Synth. Org. Chem. Jpn.*, **48**, 292 (1990).
336. B. B. Snider, *Acc. Chem. Res.*, **13**, 426 (1980).
337. H. M. R. Hoffmann, *Angew. Chem., Int. Ed. Engl.*, **8**, 556 (1969).
338. J. K. Whitesell, *Acc. Chem. Res.*, **18**, 280 (1985).
339. J. Dubac and A. Laporterie, *Chem. Rev*, **87**, 319 (1987).
340. J. Robertson, G. O'Connor and D. S. Middleton, *Tetrahedron Lett.*, **37**, 3411 (1996).
341. W. Adam and M. Richter, *Chem. Ber.*, **125**, 243 (1992).
342. M. Orfanopoulos, Y. Elemes and M. Stratakis, *Tetrahedron Lett.*, **31**, 5775 (1978).
343. K. Mikami, N. Kishi and T. Nakai, *Chem. Lett*, 1643 (1982).
344. S. Marumoto and I. Kuwajima, *J. Am. Chem. Soc.*, **115**, 9021 (1993).
345. S. Marumoto and I. Kuwajima, *Chem. Lett.*, 1421 (1992).
346. M. A. Sparks and J. S. Panek, *J. Org. Chem.* **56**, 3431 (1991).
347. M. A. Sparks and J. S. Panek, *Tetrahedron Lett.*, **32**, 4085 (1991).
348. M. Heneghan and G. Procter, *Synlett*, 489 (1992).
349. R. Takeuchi, S. Nitta and D. Watanabe, *J. Org. Chem.*, **60**, 3045 (1995).
350. T. J. Barton, J. Lin, S. Ijadi-Maghsoodi, M. D. Power, X. Zhang, Z. Ma, H. Shimizu and M. S. Gordon, *J. Am. Chem. Soc.*, **117**, 11695 (1995).
351. R. H. Conlin, H. B. Huffaker and Y. -W. Kwak, *J. Am. Chem. Soc.*, **107**, 731 (1985).
352. F. J. Blanco, P. Cuadrado, A. M. González and F. J. Pulido, *Synthesis*, 42 (1996).
353. C. Gajda and J. R. Green, *Synlett*, 973 (1992).
354. M. Franck-Neumann, M. Sedrati and M. Mokhi, *J. Organomet. Chem.* **326**, 389 (1987).
355. M. Franck-Neumann, M. Sedrati and A. Abdali, *J. Organomet. Chem.* **339**, C9 (1988).
356. M. Ochiai, T. Ukita and E. Fujita, *Tetrahedron Lett.*, **24**, 4025 (1983).
357. T. Hayama, S. Tomoda, Y. Takeuchi and Y. Nomura, *Tetrahedron Lett.*, **24**, 2795 (1983).
358. P. V. Fish, *Synth. Commun.*, **26**, 433 (1996).
359. J. -P. Picard, J. Dunogues and A. Elyusufi, *Synth. Commun.*, **14**, 95 (1984).
360. M. Lautens, C. H. Zhang and C. M. Crudden, *Angew. Chem., Int. Ed. Engl.*, **31**, 232 (1992).
361. T. Masuda, H. Kouzai and T. Higashimura, *J. Chem. Soc., Chem. Commun.*, 252 (1991).
362. T. Hiyama, K. Nishide and M. Obayashi, *Chem. Lett.*, 1765 (1984).

CHAPTER 31

Chemistry of compounds with silicon–sulphur, silicon–selenium and silicon–tellurium bonds

D. A. ('FRED') ARMITAGE

Department of Chemistry, King's College London, Strand, London WC2R 2LS, UK

I. INTRODUCTION

Since 1990, several reviews have appeared covering silicon–chalcogen chemistry. These include the spectroscopic properties of silicon–sulphur compounds along with structural data[1]. The synthesis of metal–chalcogen clusters using $(Me_3Si)_2X$ (X = S, Se, Te), Me_3SiX^{-2}, $(Me_3Si)_3SiX^-$ are covered[3]. The only compound of this chapter to be included recently in *Inorganic Syntheses* is hexamethyldisilthiane, prepared by a method improving the yield of previous reports[4]. A report of the structures of $(PhSe)_4Si$ with

Si−S bond lengths of 212.3 and 212.9 pm) and $(PhSe)_4Si$ (Si−Se bond lengths are 227.2 and 227.4 pm) includes a comprehensive list of the structures of silicon−sulphur and silicon−selenium compounds. These suggest a decrease in the Si−S bond length from 216 pm to 212 pm as the number of Si−S bonds in the molecule increases[5].

II. THIOSILANES

Though there are no new routes to supercede the most convenient synthetic route to thiosilanes — thiolation of a halosilane — two new classes of thiosilanes have been prepared. Dialkyl (*S*-trimethylsilyl) tetrathiophosphates result from P_4S_{10} and alkylthiosilanes (equation 1). They react with $(EtO)_2CHR$ to give (1-alkoxy)alkyltetrathiophosphates and with $(EtS)_2CH_2$ and Et_2S_2 at 150 °C to give the alkylthiosilane (equation 2)[6].

$$P_4S_{10} + 8\,Me_3SiSR \longrightarrow 4\,Me_3SiSP(S)(SR)_2 + 2(Me_3Si)_2S \qquad (1)$$

$$R(EtO)HCSP(S)(SR)_2 \xleftarrow[-EtOSiMe_3]{(EtO)_2CHR} Me_3SiSP(S)(SR)_2 \xrightarrow[-Me_3SiSEt]{Et_2S_2} EtSSP(S)(SR)_2 \qquad (2)$$

Aliphatic thioketones result tautomerically pure from the reaction of H_2S with ketals in the presence of $ZnCl_2$. Deprotonation with LDA gives the enethiolate which can be silylated to form the silyl vinyl sulphide. These are fairly stable to traces of water but react with MeOH to give the enethiol (equation 3)[7].

$$\begin{tikzcd} R^1R^2HC{-}C(S)R^3 \arrow[r, "\text{i. LDA/THF}", "\text{ii. } Me_3SiCl"'] & R^1R^2C{=}C(R^3)SSiMe_3 \arrow[d, "MeOH"] \\ & R^1R^2C{=}C(R^3)SH \end{tikzcd}$$

(3)

In the case of $R^3 = MeS$, the reaction with imines in the presence of Lewis acid catalysts give the *syn* and *anti* β-amino dithioesters with *anti* selectivity (equation 4)[8].

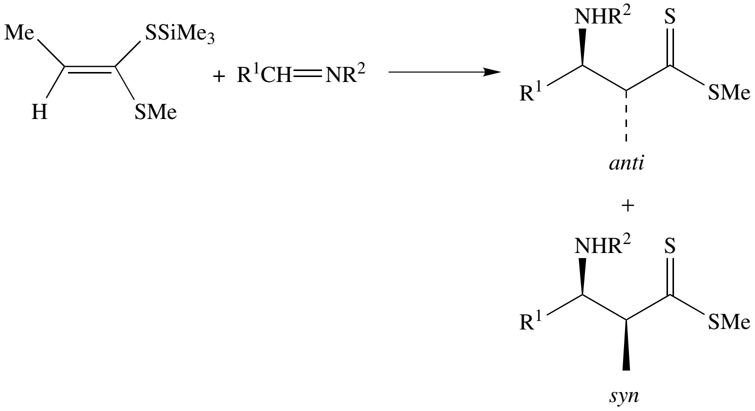

(4)

Monothioacetals have been prepared from alkyl and arylthiosilanes generated *in situ* from the thiol and silylimidazole in the presence of Me_3SiOTf as catalyst[9]. Yields are greater than 80%, and somewhat better than those obtained from the reaction of $PhSSiMe_3$

with aldehydes using silyl triflate as catalyst[10], or with acetals using dicyanoketene acetals as catalyst[11]. Monothioacetals can be reduced by Et_3SiH using $Me_3SiCl/InCl_3$ to give the monosulphide (**1**). The monosulphide also results from the reaction of a ketone and thiosilane (equation 5)[12].

$$\begin{tikzcd}
R^1R^2C(OSiMe_3)SR^3 + Et_3SiH \arrow[r, "Me_3SiCl/InCl_3"] & \underset{\mathbf{(1)}}{R^1R^2CHSR^3} \\
 & R^1R^2CO + R^3SiSiMe_3 \arrow[u, "Me_3SiCl/InCl_3", "Et_3SiH"']
\end{tikzcd} \tag{5}$$

With (*E*)-chalcone dimethyl acetal, in the presence of trityl perchlorate, $PhSSiMe_3$ adds to give the 1,3-disubstituted-1-propene as the major product (equation 6)[13].

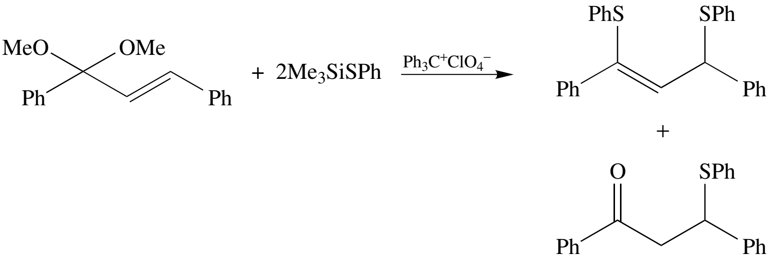

(6)

α-Silyl vinyl ketones react with $PhSSiMe_3$ in the presence of $Et_2O{\bullet}BF_3$ to give silylated bis(phenylthio)propene which serves as a silyl β-acyl carbanion equivalent, and readily substitutes position 3 with electrophiles (E^+) (equation 7)[14].

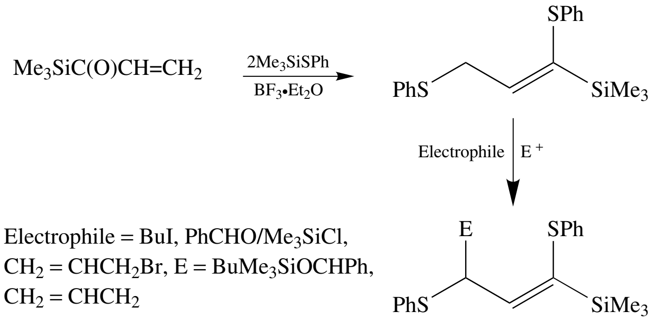

Electrophile = BuI, $PhCHO/Me_3SiCl$,
$CH_2 = CHCH_2Br$, E = $BuMe_3SiOCHPh$,
$CH_2 = CHCH_2$

(7)

i-$PrSSiMe_3$ catalyses the asymmetric allylation of aldehydes using (*S*)-BINOL–Ti(IV) complex (equation 8)[15].

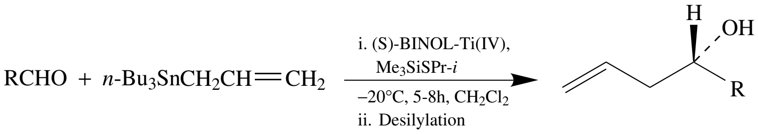

(8)

Thiosilanes provide the first step in the conversion of amino sugars aryl and alkylthio substituted 2-azido-2-deoxyhexopyranosyl building blocks for oligosaccharide synthesis[16]. 2-(2-Phenylthiocyclobutyl)oxirane and oxetane (**2**) undergo acid-catalyzed ring opening with $PhSSiMe_3$ to give the *gem*-phenylthio substituted allyl and homoallyl alcohol (equation 9)[17].

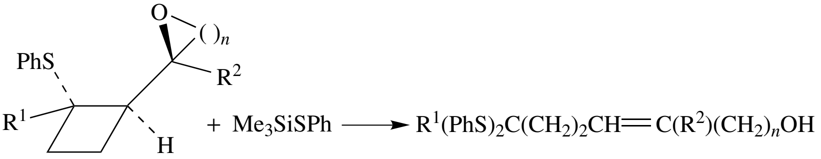

(9)

(2)

$n = 1,2$

Silicon is most important in the cycloaddition of alkynyl silyl sulphides to ynamines, the silyl shift giving the 4-silylcyclobut-2-enethione which, on S-methylation and desilylation, yields the cyclobutadiene (equation 10)[18].

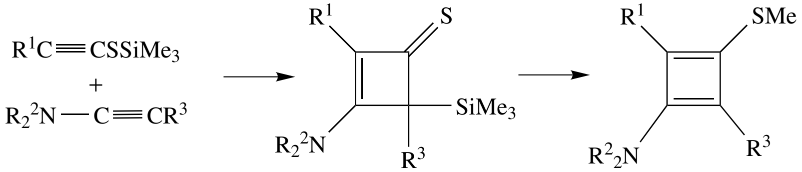

(10)

Reacting Ph_2SiH_2 with $Rh(SAr)(PMe_3)_3$ gives the complex *mer*-$RhH(SiHPh_2)SAr(PMe_3)_3$ (**3**) which isomerizes through SR transfer to silicon to give *fac*-$RhH_2(SiPh_2SAr)(PMe_3)_3$ with a Si—S bond length of 222.8 pm. Since the silyl group in **3** is *trans* to the thio group and the isomerization is intramolecular, it is suggested that *cis–trans* isomerization occurs prior to transfer (equation 11)[19].

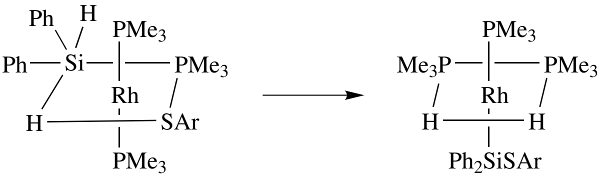

(3)

(11)

Rhodium(I) catalyses the dehydrogenative coupling of silanes with arene thiols. Thus Ar_2SiH_2 reacts with 1,3- and 1,4-benzene dithiols to give polymers with molecular weights in the range 1.5 to 7×10^3. In the presence of alkynes, arylthiolation of $PhSiH_3$ results in the formation of arylthio substituted styryl silanes $PhCH{=}CHSi(SAr)_2H$ in excellent yield[20]. The intermediacy of metal–silyl intermediates in such a reaction has been established through the reaction of $(EtS)_3SiH$ with Rh(I) and Ir(I)[21], while Me_3SiSNa substitutes $[Me_3Ru(Br)(N)]^-$ to give $[Ph_4P][Me_3Ru(N)SSiMe_3]$ which can be readily desilylated to give the monomeric sulphide and, with $[(Me_3SiCH_2)_2Os(N)Cl]_2$, couples to give the mixed sulphide with Ru—S—Os bridge with chlorosilane loss[22].

Bis(benzylthio)dimethylsilane readily undergoes a double rearrangement in the presence of 2 equivalents of *t*-BuLi in THF to give a mixture of the *meso*- and *d,l*-forms of the dithiol $[PhCH(SH)]_2SiMe_2$. It models dithiol bimetallic action of nitrogeneous substrates by the Mo-containing enzyme nitrogenase. The *meso* isomer reacts with $MoCl_5$ to give $Mo_2Cl_4[(PhCHS)_2SiMe_2]_3$ which complexes Me_2NNHPh[23].

The silyl substituted dithiol $(Me_3SiSCF_2)_2$, prepared from the sulphenyl chloride $ClSC_2F_4SCl$ **(4)** and $(Me_3Si)_2Hg$, reacts with the dichlorides $RECl_2$ (E = P, As) to give the heterocycle, the phosphorus derivative undergoing a Michaelis–Arbuzov rearrangement, but not the arsenic one (equation 12). These heterocycles also result directly from **(4)** and the bis-silyl phosphine or arsine[24].

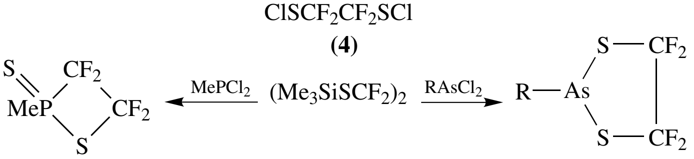

(12)

The hindered silyl chlorides $(Ar^*X)_3SiCl$ (X = S, Se) react with $AgClO_4$ to give a range of sulphides and selenides which are thought to result through the intermediacy of the silicenium ion which loses Ar^*X^+ and $(Ar^*X)_2Si$**:** (X = S) or $Ar^*X^\bullet$ (X = Se). With the thio derivative, the products are the disulphide **(5)**, sulphide **(6)** and arene (equation 13), while for the selenium chloride, diselenides and selenides dominate (equation 14)[25].

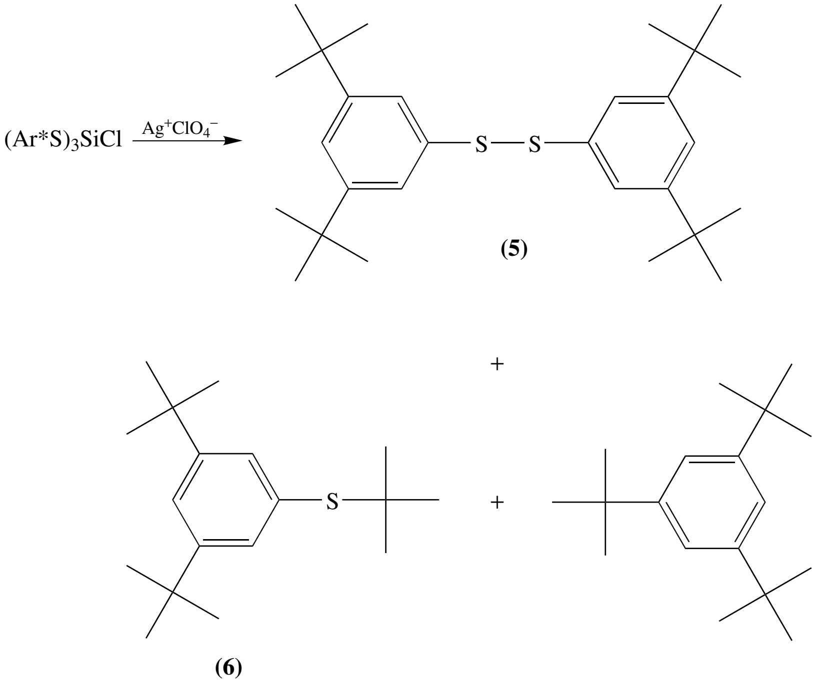

(13)

$Ar^* = 2,4,6\text{-}t\text{-}Bu_3C_6H_2$

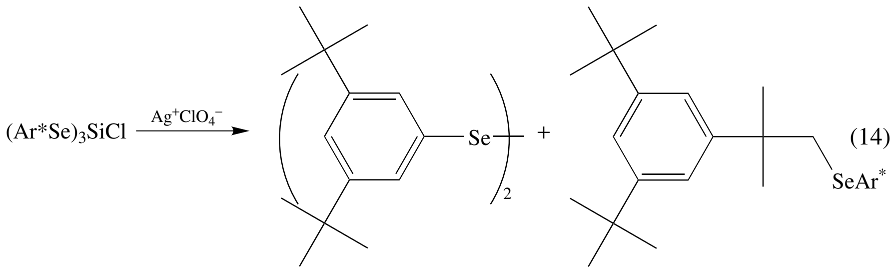

(14)

III. SILANE THIOLS AND POLYSULPHIDES

Triphenylsilane thiol, a white crystalline solid, attacks epoxides on warming in the presence of $Et_3N/MeOH$ on the less hindered side to give the β-hydroxymercaptans. In the presence of $CsCO_3$, however, the β-dihydroxysulphide results (equation 15 and 16)[26].

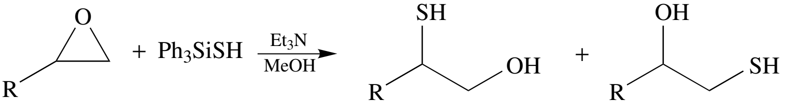

(15)

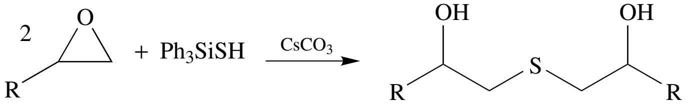

(16)

The triphenylsilylthiyl radical, generated from Ph_3SiSH in the presence of AIBN or photolytically, adds to olefins through *anti*-Markovnikov addition to give the H_2S adduct RCH_2CH_2SH on desilylation with trifluoroacetic acid[27].

The silanethiyl radical **(7)** generated from the silane thiol, which is prepared from the silane using first $CuCl_2$ and then LiSH, abstracts hydrogen enantioselectively from silicon in (±)-*trans*-2,5-dimethyl-1-phenyl-1-silacyclopentane, to bring about kinetic resolution of the latter. Such reactions are rare (equation 17)[28].

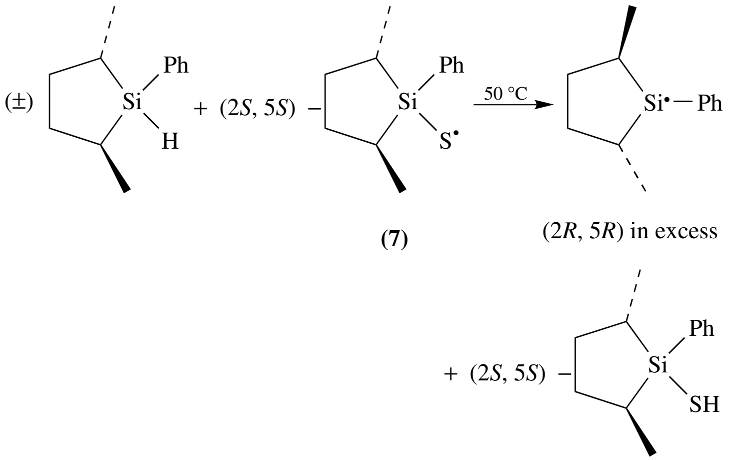

(17)

Ph_3SiSH can be S-halogenated using the *N*-halosuccinimide. The bromo and iodo derivatives decompose to release sulphur in polar solvents, but a structure determination of the bromo derivative shows the Si–S bond to be 216 pm, compared with 215 pm in the parent thiol. Surprisingly, the S–Br bond is 217 pm long[29].

Reacting Ph_3SiSNa with SCl_2 or S_2Cl_2 gives the bis-silyl tri- and tetra-sulphides. Both are thermally stable. The structure of the latter indicates a range of conformations present within the molecule involving *cis–cis*, *cis–trans* and *trans–trans* arrangements[30].

$(Me_3Si)_3SiSH$ results from the thiolation of $(Me_3Si)_3SiLi(THF)_3$ followed by protolysis[31]. It also results from the silane $(Me_3Si)_3SiH$ through chlorination with CCl_4, amination with NH_3 and then reaction with H_2S. It isomerizes in toluene at 80 °C in the presence of AIBN to give the silyl substituted silthiane (equation 18) through a 1,2-shift in 74% yield. At 85 °C, both compounds reduce terminal alkenyl bromides to the alkene or cycloalkane. With $(Me_3Si)_2Si(Me)SH$, the thiyl radical reduces terminal alkyl bromides to the alkene and likewise isomerizes to a silthiane (equation 19), while allylSSi$(SiMe_3)_3$ is less efficient than tin-substituted propenes in radical allylations[32].

$$(Me_3Si)_3SiSH \xrightarrow[\text{AIBN}]{80\,^{\circ}\text{C, toluene}} (Me_3Si)_2Si(H)SSiMe_3 \tag{18}$$

$$(Me_3Si)_2Si(Me)SH \xrightarrow[\text{initiator}]{80\,^{\circ}\text{C, benzene}} (Me_3Si)(Me)Si(H)SSiMe_3 \tag{19}$$

Reacting Me_2SiCl_2 with H_2S at -78 °C gives the silane dithiol as an unstable oil which shows ν_{S-H} stretching at 2500 cm^{-1}. The alkali metal derivatives of this dithiol result from the sulphide M_2S (M = Li, Na, K) and react with RI (R = Me, Et) to give the bis (alkylthio)silane and show ν_{Si-S} stretching frequencies at 400 and 447 cm^{-1}[33].

IV. LINEAR DISILTHIANES

Hexamethyldisilthiane can be conveniently prepared from Na_2S, freshly synthesized from the elements in THF with naphthalene, silylation with Me_3SiCl giving the silthiane in 90–95% yield[4]. 1,3-Diphenyldisilthiane results from H_2S, PhH_2SiCl and Et_3N in 83% yield, in contrast to the time-consuming *trans*-silylation of $(Me_3Si)_2S$ with $PhSiH_2Cl$ when only 40% yield could be obtained[34].

Electron diffraction studies of the three methylsilyl sulphides $(Me_nH_{3-n}Si)_2S$ (n = 1–3) show Si–S bond lengths of 214.1, 214.6 and 215.4 pm respectively, with SiSSi angles of 97.9°, 100.8° and 105.8°, hindrance indicating a steady increase without undue lengthening of the Si–S bonds[35].

The photoelectron spectra of $(Et_3Si)_2S$ and the silylalkyl sulphides $(Et_3Si(CH_2)_n)_2S$ ($n = 0$–3) support a greater silyl donor influence for $n = 0, 2$ than for $n = 1, 3$, while the charge transfer spectra show a first ionization potential greatest for $n = 0$[36].

While organic sulphides can be readily synthesized from silthiane and organic halides, diallyl sulphides result in good yield from the allyl alcohols in the presence of 1 equivalent of $Et_2O{\bullet}BF_3$. As the sodium salt, generated from NaH/$(Me_3Si)_2S$, it induces bis-O-demethylation of aryl methyl ethers through initial demethylation with Me_3SiSNa or NaH. The anion so formed can then react with $(Me_3Si)_2S$ to give the silylated phenol and Me_3SiS^- (Scheme 1)[37].

$(Me_3Si)_2S$ in the presence of Me_3SiOTf induces the rearrangement of bis[(Mes)methanoyl] bicyclo[2.2.1]hept-5-enes to 2-oxabicyclo[3.3.0]octa-3,7-dienes (equation 20)[38].

3-Oxo dithioic acids react with a combination of $(Me_3Si)_2S$ and *N*-chlorosuccinimide in the presence of imidazole to give oxidative ring closure to the 3*H*-1,2-dithiole-3-thiones (equation 21)[39].

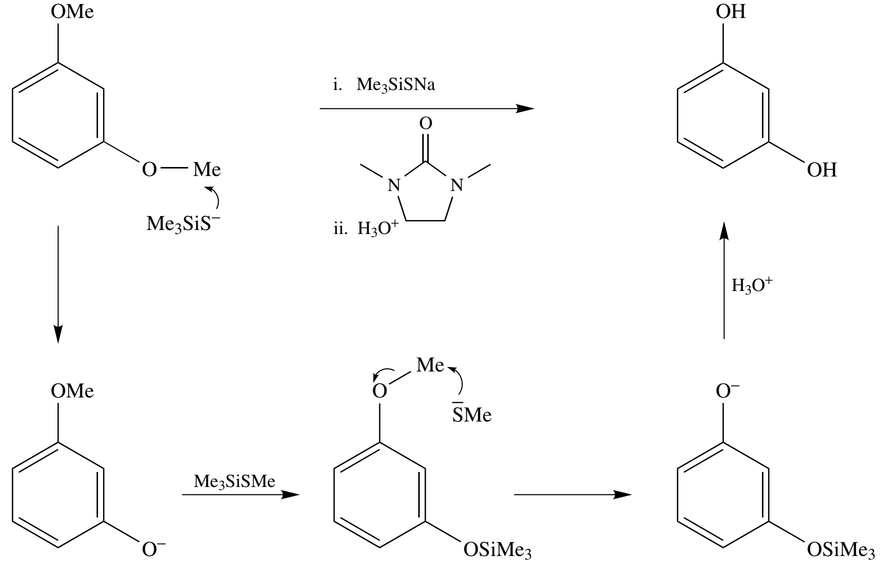

SCHEME 1

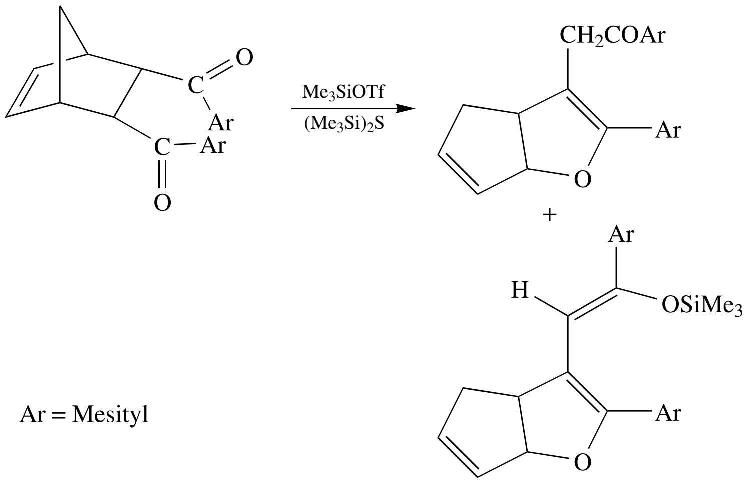

(20)

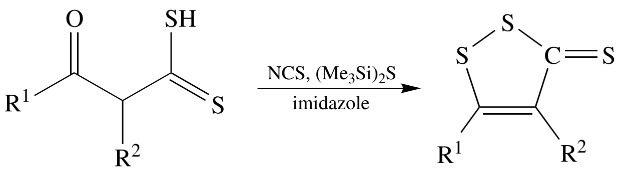

(21)

Hexamethyldisilthiane, despite its disgusting smell, has been extensively used in the conversion of carbonyl compounds to thiocarbonyls.

In the presence of $\mathrm{CoCl_2{\bullet}6H_2O}$, thioaldehydes can be generated from $\mathrm{(Me_3Si)_2S}$ and RCHO *in situ*, and form Diels–Alder adducts with cyclohexa-1,3-diene. Ketones react similarly in the presence of $\mathrm{Me_3SiOTf}$ to give the thioketone in good yield after 2 days. *o*-Azidohetarenecarboxaldehydes react with $\mathrm{(Me_3Si)_2S}$ to give the thioaldehyde in the presence of Co(II), and likewise adds dienes. In the presence of hydrochloric acid, however, intramolecular cyclization occurs to give the fused isothiazole, while with MeOH/HCl, the stable furan and thiophene *o*-aminothioaldehydes result (equation 22)[40].

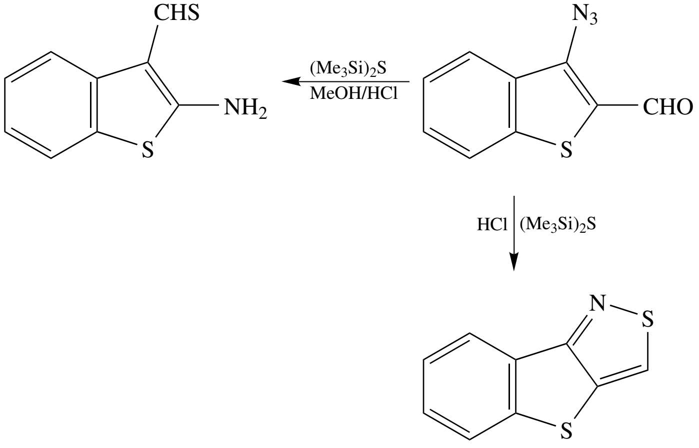

(22)

Electrophilic aromatic and heteroaromatic azides react with $\mathrm{(Me_3Si)_2S}$ to provide a route on methanolysis to the amine through $\mathrm{N_2}$ and S loss and the intermediacy of the silylthio triazane $\mathrm{ArNH{-}N{=}N{-}NSSiMe_3}$. Reaction times range from 1/2 to 6 h, and yields from 45 to 92%[41]. Peptides coupled to Kaiser's oxime ester resin can be cleaved using $\mathrm{(Me_3Si)_2S/Bu_4NF}$ to give the peptide C-terminal thioacids, which are useful for peptide fragment coupling[42]. Reductively condensing primary nitro compounds using $\mathrm{KH/(Me_3Si)_2S}$ provides a route to thiohydroxamic acids, which give nitriles on acidification (equation 23)[43].

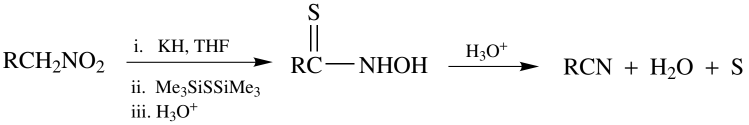

$$\mathrm{RCH_2NO_2} \xrightarrow[\text{ii. Me}_3\text{SiSSiMe}_3\ \ \text{iii. H}_3\text{O}^+]{\text{i. KH, THF}} \mathrm{R\overset{\overset{\displaystyle S}{\|}}{C}{-}NHOH} \xrightarrow{\mathrm{H_3O^+}} \mathrm{RCN + H_2O + S} \qquad (23)$$

Aryl nitriles with $\mathrm{(Me_3Si)_2S}$ in the presence of MeONa/1,3-dimethyl-2-imidazolidinone results in the conversion to primary thioamides, while amides and lactams yields the thio derivative using $\mathrm{(Me_3Si)_2S}$ and an oxophilic promoter such as $\mathrm{POCl_3}$, triphosgene or oxalyl chloride. Thus the intermediate $[\mathrm{ClRC{=}NR'R''}]^+\mathrm{Cl}^-$ reacts with the silthiane to give the thioamide (equation 24)[44].

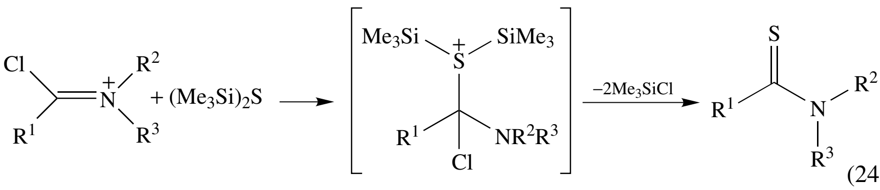

(24)

Gallium-chalcogen clusters $(Cp^*GaE)_4$ (E = S, Se) result from the reaction of $(Me_3Si)_2E$ with Cp^*GaCl_2, while the P−N heterocycle **(8)** can be thiolated at P(V) using $(Me_3Si)_2S$ (equation 25)[45].

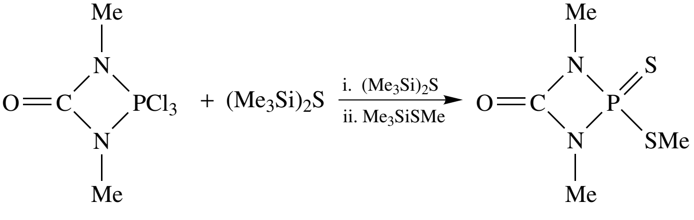

(25)

(8)

Molybdenum and tungsten chlorides react to give the thiochlorides $MoSCl_3$ and $WSCl_4$, $M(O)Cl_4$ (M = Mo, W) reacting to give the mixed derivatives $M(O)(S)Cl_2$[46]. Tungsten hexafluoride reacts similarly to give WSF_4 at room temperature, and MCl_5 (M = Nb, Ta) yield $MSCl_3$[47]. With $CpZrCl_3$, however, the zirconium sulphide cluster $Cp_6Zr_6S_9$ results, in which the Zr_6 octahedron surrounds a μ_6-S atom with μ_3-S covering each triangular face[48]. With the nickel and palladium salts $(R_3P)_2MCl_2$, the clusters $M_3S_2Cl_2(PPh_3)_4$ are formed and contain the triangular M_3 core with capping μ_3-S ligands[49].

Copper sulphide clusters result from the reaction of Cu(I) acetate and $(Me_3Si)_2S$, with Ph_2EtP and Et_3P giving $Cu_{12}S_6(phosphine)_8$, while with Ph_3P, $Cu_{20}S_{10}(PPh_3)_8$ results. With the more hindered phosphines i-Pr_2MeP and t-Bu_2MeP, the larger clusters $Cu_{24}S_{12}(PMePr\text{-}i_2)_{12}$, $Cu_{28}S_{14}(PMeBu\text{-}t_2)_{12}$ and $Cu_{50}S_{25}(PMeBu\text{-}t_2)_{16}$ are formed[50].

V. SILICON−SULPHUR DOUBLE BOND

Silane thiones have been shown to be formed as intermediates in a range of reactions, and either oligomerize or react with other suitable acceptors. Thus, pyrolysing the propargylthiosilane **9** at 600 °C gives the silanethione which dimerises, while in the presence of ketene at 800 °C the 4-membered ring **10** results. The latter decomposes at 900 °C to give silanone and thioketene (equation 26)[51].

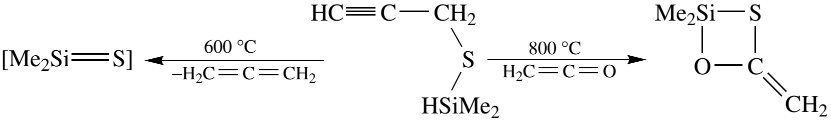

(26)

(9) **(10)**

The highly hindered dibromosilane $[2,4,6\text{-}\{(Me_3Si)_2CH\}_3C_6H_2](2,4,6\text{-}(i\text{-}Pr)_3C_6H_2)SiBr_2$ $[Tbt(Tip)SiBr_2]$ on reduction and reaction with elemental sulphur gives the tetrathiasilolane **11** as pale yellow crystals. In the presence of 3 moles of Ph_3P, the silane thione **12** results as yellow crystals (equation 27). The ^{29}Si NMR signal at 166.56 is downfield from that of Corriu's complexed silanethione **(13)** at 22.3, supporting a double bond, while the absorption maximum at 396 nm is assigned to the n−π^* transition and the Raman spectral peak at 724 cm^{-1} to the Si=S stretching frequency. The silathiacarbonyl unit shows trigonal planar geometry and the Si−S bond length of 194.8 pm, some 9% shorter than the single bond, supports a double bond and is shorter than Corriu's complexed silathione (201.3 pm)[52].

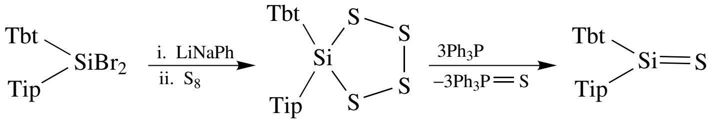

(11) **(12)** (27)

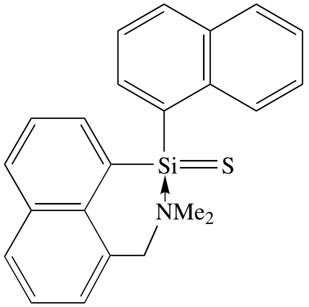

(13)

The structures of a range of organothio substituted silylene and silyl complexes of transition metals support a degree of Si−S multiple bonding. The Si−S bond lengths in $[Cp^*Ru(PMe_3)_2Si(o\text{-phen})STol\text{-}p]^{2+}$ and $Cp^*Ru(PMe_3)_2Si[Os(CO)_4]STol\text{-}p$ are 217.9 and 217.2 pm respectively, somewhat shorter than in $Cp^*Ru(PMe_3)_2RuSi(STol\text{-}p)_3$, implying some degree of π-bonding. This is also suggested for the short Si−S bonds of 209.2 and 207.4 pm in $(Cy_3P)_2(H)Pt{=}Si(SEt)_2]^+$, and therefore supporting some silylsulphonium resonance[53].

VI. CYCLIC SILTHIANES

Cyclotrisilthianes $(R_2SiS)_3$ have been prepared from Li_2S and R_2SiCl_2 (R = alkyl) in 70% yield with a view to using them as solid electrolytes for rechargeable batteries, and they also result in very good yield from the silyl triflate and H_2S in the presence of Et_3N[54]. The methyl derivative reacts with RLi to give the thiolate, which couples with a range of organic bromides to give the sulphide in good yield[55]. Reacting $(C_6F_5)_2SiH_2$ with sulphur or $(Me_3Si)_2S$ gives the cyclodisilthiane $[(C_6F_5)_2SiS]_2$[56]. The adamantane-like tricyclo$[3.3.1.1^{3,7}]$ tetrasilathiones $(RSi)_4S_6$ (R = Me, Et) result from reaction of sodium sulphide and $RSiCl_3$ in THF at room temperature for 1 day. The analogous selenium compounds result similarly[57].

The silicocene $Cp^*{}_2Si$**:** reacts with a range of heterocumulenes and it is pertinent to include CO_2 along with the sulphur ones COS, CS_2 and RNCS (R = Me, Ph) for completeness. CO_2 gives an adduct which loses CO to form the silanone, which then adds more CO_2 to give the $[2 + 2]$ cyclic adduct, the carbonate **14**. This dimerizes in pyridine through ring opening to give **15** and adds silanone $Cp^*{}_2Si{=}O$ in toluene through a further $[2 + 2]$ cycloaddition to give the orthocarbonate **16** (Scheme 2)[58].

With COS, CO loss on addition gives the silathione which dimerizes to the disiladithietane (cyclodisilthiane). With CS_2 however, the cyclodisilthiane **17** also results through carbocation rearrangement of the adduct without CS loss (Scheme 3).

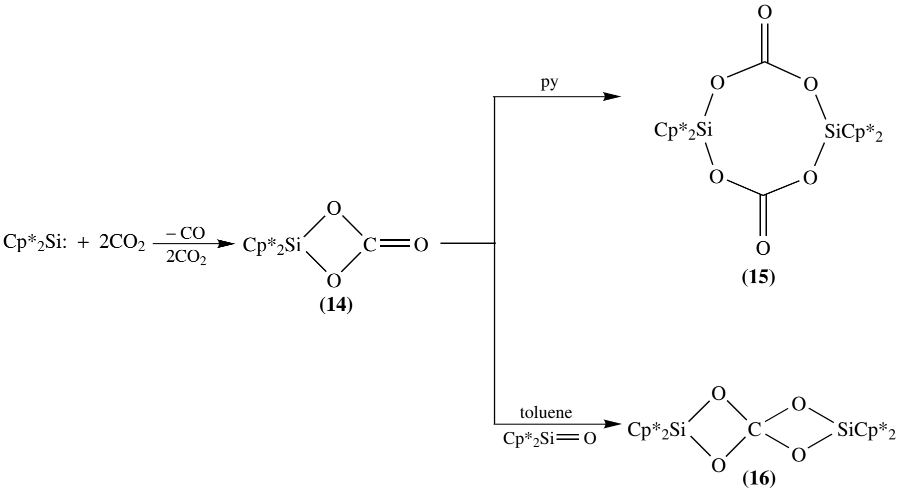

SCHEME 2

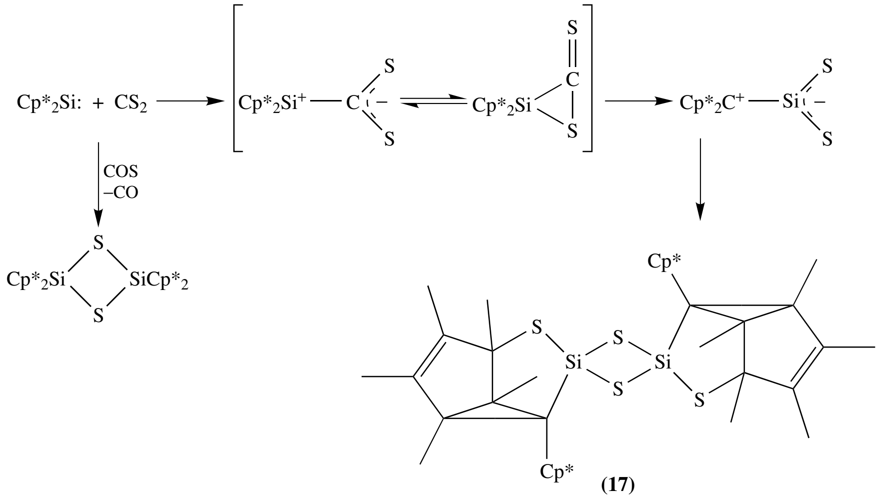

SCHEME 3

With RNCS, $Cp^*_2Si{=}S$ gives, together with isocyanide loss, further [2 + 2] addition of isothiocyanate leading to the dithiasilatane, while for R = Ph, further insertion of Cp^*_2Si**:** results in the formation of **18** (equation 28)[58].

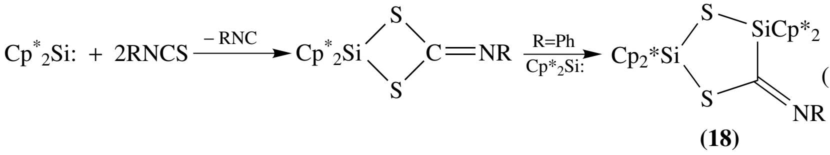

(28)

Reacting the hindered silane $(Me_3Si)_3CSiH_3$ ($TsiSiH_3$) with sulphur in Ph_2O at 200–210 °C gives the 2,3,5,6-tetrathia-1,4-disilabicyclo[2.1.1]hexane **(19)** in 6.1% yield as a crystalline solid, mp $\leqslant$330°. In decalin, however, the [3.2.1] and [2.2.1] homologues also result, while the [2.1.1] derivative **19** can be readily desulphurized photolytically in the presence of Ph_3P to give **20**, as can the higher homologues Scheme 4.

VII. MISCELLANEOUS SILICON−SULPHUR RINGS

Thiadisilacyclopropanes result from the reaction of disilenes with sulphur and episulphides. From the mechanistic standpoint, the reaction of $RR'Si{=}SiRR'$ is of great interest and the separation of the (*E*)- and (*Z*)-isomers (*trans* and *cis*) [$R = 2,4,6\text{-}(i\text{-}Pr)_3C_6H_2$, $R' = t\text{-}Bu$] has led to the separate addition of sulphur to each. This occurs within a minute to give *trans* and *cis*-isomers, respectively, the latter with slightly different Si−S bond lengths[60]. Propylene sulphide reacted similarly, and the reaction of $(t\text{-}Bu)_2Si{=}Si(Bu\text{-}t)_2$ with thiophene leads to sulphur abstraction with the formation of the thiadisilacyclopropane, with Si−S bonds of 217.1 pm, along with the 1,2-disilacyclohexa-3,5-diene and 2,6-disilabicyclo[3.1.0]hex-3-ene (equation 29)[61].

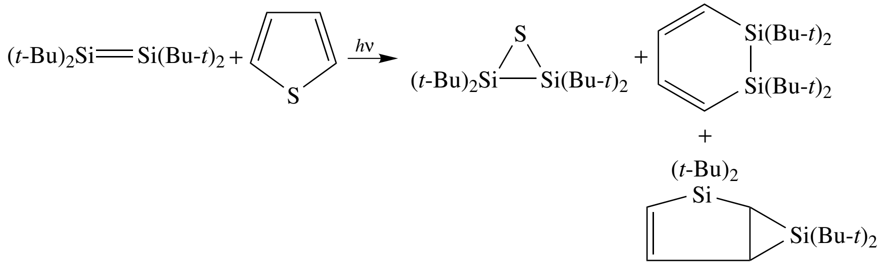

(29)

The stable silathiirane **21** results from the silene and elemental sulphur on photolysis. It has an Si−S bond of 212.9 pm, slightly longer than that found in the silathiirane formed from $Mes_2Si\colon$ addition to tetramethyl-2-indanethione[62]. In addition, the cyclodisilthiane results and can also be made from the disilabicyclo[1.1.1] pentane **(20)** on hydrolysis. It possesses Si−S bonds of length 217–219 pm (Scheme 4)[59].

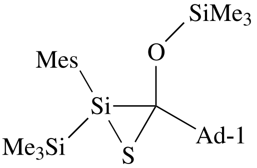

(21)

Mes = Mesityl, Ad = Adamntyl

Reacting tetramesityldisilene with PhHC=S gives the air-stable 1,2,3-disilathietane with a long Si−Si bond of 244.3 pm, longer than that in the oxetane. On photolysis in EtOH,

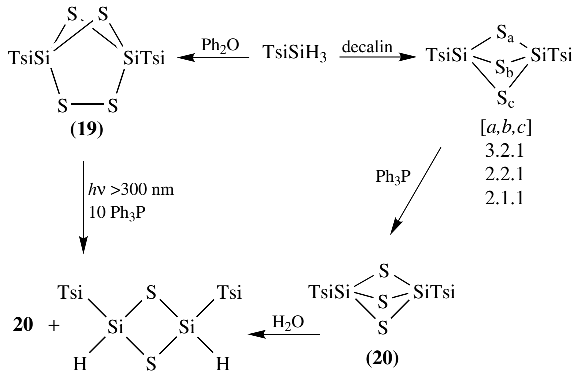

SCHEME 4

the ethoxysilane and silanethiol are formed (equation 30)[63].

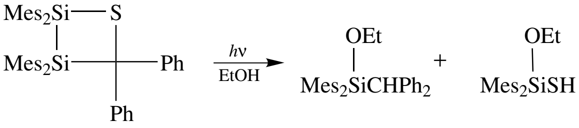

(30)

The first 1,2,4-thiadisiletane results from the reaction of carbon disulphide and the hindered silylene [2,4,6-$\{(Me_3Si)_2CH\}_3C_6H_2$]MesSi: (TbtMesSi:) formed from the *Z*-disilene precursor. The mechanism is thought to involve a skeletal rearrangement of the 3,3′-spirobi(1,2-thiasilirane) intermediate formed by silylene addition to each carbon-sulphur double bond (equation 31)[64].

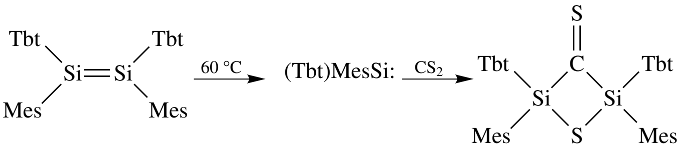

(31)

Coupling Na_2S with $ClMe_2SiCH_2GeMe_2Cl$ gives the 1,3,2-germasilathietane which slowly dimerizes on heating, with subsequent decomposition through silene and germathione formation to give 6-membered heterocycles containing the CSiSGe unit (equation 32)[65].

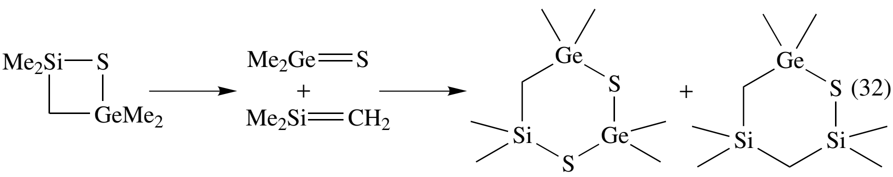

(32)

Stepwise insertion of sulphur into the silirane ring gives the 1,2-silathietane and siladithietane in 60% and 19% yield, respectively (equation 33). Pyrolysis of the

1,2-silathietane gives the cyclodisilthiane and the 2,4-dithia-1,3-disilacyclohexane[66].

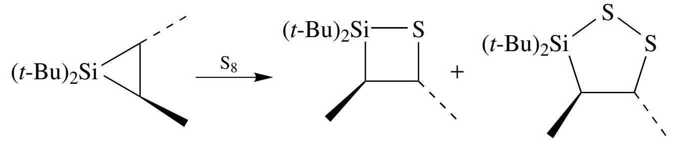

(33)

Similarly, ring expansion of fused ring siliranes also occurs stepwise with silabicyclo[3.1.0]hexane and silabicyclo[4.1.0]heptane (equation 34). With 1,1-dimethyl-1-silacyclobutane, sulphur insertion occurs to give the 1-thia-2-silacyclopentane in 72% yield[67].

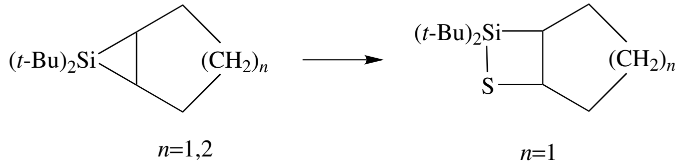

(34)

The structure of the 2,3-dithia-4-silabicyclo[4.3.0]nonane shows a Si−S bond length of 217.3 pm. The analogous selenium compound has a Si−Se bond length of 232.4 pm.

The dephenylation of $(t\text{-BuPh}_2\text{Si})_2$ using CF_3SO_3H, followed by thiolysis with H_2S gives the *meso*-dithiol in 67% yield. On lithiation and cyclization with a metallocene dichloride, the metallocycles react with a range of dichlorides to give chalcogeno substituted rings (equation 35)[68].

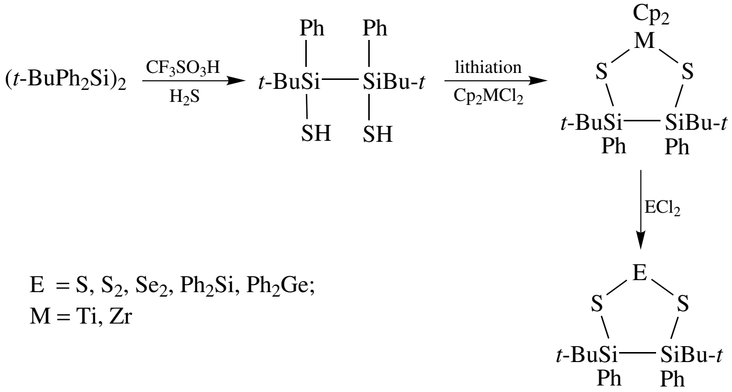

(35)

Phosphines attack the disilatrithiane ring to give the cyclodisilthiane predominantly as the *trans* isomer, with Si−S bonds of 214.9 pm, a little shorter than in the disilatrithiane (217–218 pm), while in the titanocene derivatives, they are 210–213 pm. Photolysing the 6-membered selenium heterocycle eliminates one atom of Se to give a 5-membered mixed chalcogeno derivative (equation 36). $(Me_2SiOTf)_2$ in the presence of H_2S/Et_3N, gives the 1,2,4,5-tetrasila-3,6-dithiacyclohexane in excellent yield[54b].

The 4-membered titanocycle **22** reacts with S_2Cl_2 to eliminate Cp_2TiCl_2 and give the sulphur-rich silatetrathialane as a colourless wax which decomposes above −20 °C

(equation 37)[69].

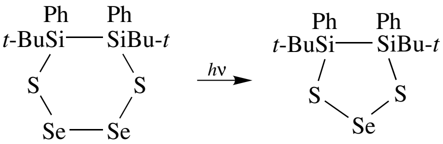

(36)

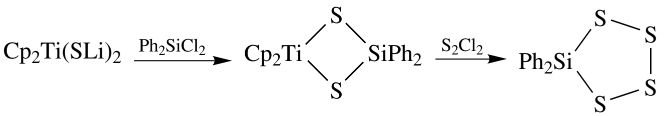

(22)

(37)

Heating $TbtPhSiH_2$ with sulphur at 280 °C gives **23** while the mesityl derivative gives TbtMesSi(SH)OH. However, the silatetrathialane **24** does form at 230 °C and the crystals have a distorted half-chair conformation and Si−S bonds of 216 and 222 pm[70]. It also results from the silylene and sulphur at 70 °C[71].

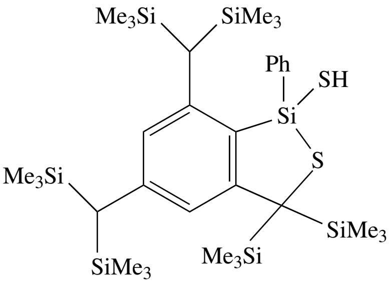

(23)

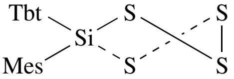

(24)

Condensing $EtB(Cl)C(Et){=}C(Me)SiMe_2Cl$ with LiSXSLi [$X = (CH_2)_n$, $n = 2–4$, *o*-phenylene] gives the heterocycles **25**. The structure of the *o*-phenylene derivative shows a Si−S bond length of 221.9 pm and a transannular donor S → B bond some 10 pm longer than that within the ring (equation 38)[72].

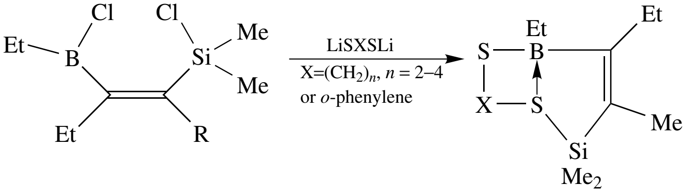

R=Me, $H_2C{=}C(Me)$

(25)

(38)

VIII. SELENOSILANES

There have been no recent, nor more efficient, general methods to prepare organoselenasilanes. However, $Mes^*SeSiMe_3$ results from Mes*SeLi in (Mes* = 2,4,6-$(t\text{-}Bu)_3C_6H_2$) in

94% yield, while i-$C_3F_7SeSiMe_3$ is formed from Me_3SiI and (i-$C_3F_7Se)_2Hg$ in 83% yield[73].

Monoselenoacetals can be conveniently synthesized from acetals using $Me_3SiSePh$ in the presence of a catalytic amount of Me_3SiOTf with yields in most cases in excess of 80%. With 2-methoxytetrahydropyrans, selenation is highly chemoselective. It gives no ring-opened product, in contrast to the selenation with i-$Bu_2AlSePh$ or n-$Bu_3SnSePh$. In addition, the reaction is tolerant to ether, halogen and ester groups[74]. Radical cyclization of ω-halogeno-1-alkenes and $PhSeSiPh_2Bu$-t leads to the $PhSeCH_2$-substituted cyclized product in yields of between 55 and 87% (equation 39)[75].

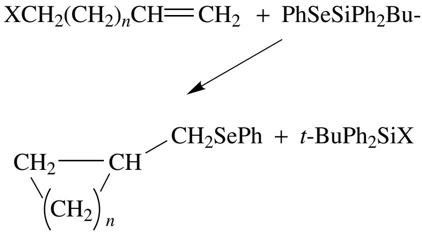

(39)

In the presence of XeF_2, $PhSeSiMeR_2$ readily adds to acetylenes to give the vicinal (E)-fluoroalkenyl selenides (equation 40), but only diphenyl ditelluride results using $PhTeSiMe_3$[76].

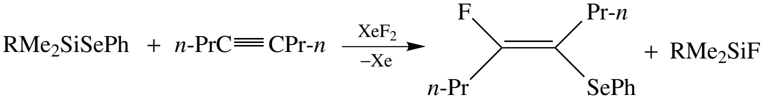

(40)

$Me_3SiSeMe$ reacts with both $(MeCN)WCl_4(NCl)$ and $[Ph_3PMe]^+[Cl_5W{=}NCl]^-$ to give N-selenenation without cleavage of the W−Cl bonds. However, condensing $(MePh_2P)_4WCl_2$ with $Me_3SiSePh$ in THF results in both Si−Se and C−Se cleavage by W−Cl to give $W_2Se_2(PPh_2Me)_2(SePh)_4$ with a W−W bond bridged by the selenide ions with each tungsten coordinated to one phosphine ligand as well as two selenolate ligands[77].

IX. BIS(SILYL)SELENIDES

Bis(phenysilyl)selenide results from freshly prepared K_2Se in 23% yield[33].

In the presence of $Et_2O{\bullet}BF_3$, $(Me_3Si)_2Se$ reacts with nitriles to give selenoamides while cyanates give the selenourea. Amides and tetramethylurea behave similarly, but the reaction with benzoates gives benzoin and 2,3,5,6-tetraphenyl-1,4-diselenin via selenoesters. These selenoesters can be trapped as conjugated diene cycloadducts (Scheme 5)[78].

A series of O-triorganosilyl selenocarboxylates $RC(Se)OSiR'_3$ result from the isomeric Se-triorganosilyl selenocarboxylates formed initially from $RC(O)Se^-M^+$ (M = Na, K) and R'_3SiCl. These O-silyl esters are thermally stable but isomerize in the mass spectrometer to Se-silyl derivatives. The carboxylates t-$BuMe_2SiOC(Se)Ar$ react readily with acyl halides to give selenoanhydrides, while a range of organometalloid chlorides cleave the Si−O bond to give the Se-metalloido selenocarboxylates (equation 41)[79].

An extensive range of transition metal selenide clusters result from $(Me_3Si)_2Se$ and a range of transition metal salts. $Cp'TiCl_3$ (Cp'= MeC_5H_4) reacts with $(Me_3Si)_2Se$ to give the cluster $Cp'_5Ti_5Se_6$, which possesses a distorted trigonal bipyramidal structure with

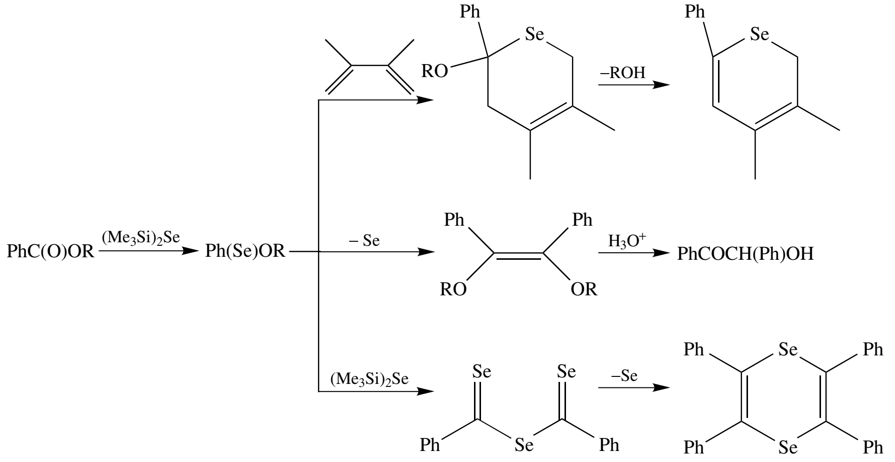

SCHEME 5

μ_3-Se ligands[80]. $CpVCl_2(PMe_3)$ reacts to give $V_6Se_8O(PMe_3)_6$ with oxygen within the octahedral V_6 cluster[48]. With $(Ph_2PCl)Cr(CO)_5$, Si$-$Se bond cleavage by P$-$Cl leads to three products $[(CO)_5CrPPh_2]_2Se$, $(CO)_5Cr[Ph_2P)_2Se]$ and $Se(PPh_2)_2Cr(CO)_4$, involving coordination of the $(Ph_2P)_2Se$ ligand, in each case through phosphorus[81].

$$t\text{-BuMe}_2\text{SiOC(Se)Ar} + \text{ArCOCl} \longrightarrow (\text{ArCO})_2\text{Se} \qquad \text{Ar} = \text{Ph}, p\text{-Ar} \tag{41}$$

Phosphine substituted nickel(II) chloride gives a range of clusters, the cluster size being determined by the subtle steric and electronic effects of the chelating phosphine. Thus $[(PhCH_2CH_2CH_2)_3P]_2NiCl_2$ (L_2NiCl_2) gives $Ni_4Se_3L_5$, while $(Et_2MeP)_2NiCl_2(L'_2NiCl_2)$ yields $Ni_5Se_4Cl_2L''_6$. With $(i\text{-}Pr_3P)_2NiCl_2(L''_2NiCl_2)$, however, two larger clusters $Ni_7Se_5L''_6$ and $Ni_8Se_6L''_4$ result, while with $(PhEt_2P)_2NiCl_2(L'''_2NiCl_2)$, $Ni_8Se_6L'''_6$ and $Ni_{21}Se_{14}L'''_{12}$ are formed. In the smaller clusters, the selenium atoms bridge but three metal atoms while, in the larger clusters, coordination to four metal atoms tends to dominate[82].

With $CpNi(PPh_3)_2SnCl_3$, the mixed Ni$-$Sn cluster $Cp_4(Ph_3P)_3Ni_5Sn_6Se_9$ results, in which a polycyclic Sn_6Se_9 cage encloses a central Cp_2Ni unit and coordinates three tin atoms to three $(Ph_3P)CpNi$ units. Each tin atom interacts with 3 selenium atoms[83].

With $[(PhCH_2CH_2)_3P]_2NiCl_2$, $(Me_3Si)_2Se$ gives the $Ni_3Se_2(SeSiMe_3)_2[P(CH_2CH_2Ph)_3]_4$ in which the μ_3-Se ligands cap the Ni_3 unit[84]. A similar Pd complex **26**, $Pd_3Se_2(SeSiMe_3)_2(PPh_3)_4$, results from $(Ph_3P)_2PdCl_2$, together with $[Ph_3PPdSe]_n$ (n = 5, 8). **26** reacts further with $CpCrCl_2(THF)$, and $MCl_2(PPh_3)_2$ (M = Ni, Pd) to give a range of chloro substituted Pd_n clusters with $n = 5$, 6, 7, 8[85].

Interest in copper selenide clusters is more recent, possibly because the clusters are even larger. Reacting copper(I) acetate with $(Me_3Si)_2Se$ and Ph_2PEt yields the solitary cluster $Cu_{12}Se_6(Ph_2EtP)_8$ as red crystals[50]. However, relatively small clusters tend to be the exception in the products produced by this route. Thus $t\text{-}Bu_2MeP$ leads to the two clusters $Cu_{31}Se_{15}(SeSiMe_3)(PMe(Bu\text{-}t)_2)_{12}$ and $Cu_{70}Se_{35}(PMe(Bu\text{-}t)_2)_{21}$ while Me_2PPh gives $Cu_{48}Se_{24}(PMe_2Ph)_{20}$. With copper(I) chloride, various size clusters result depending on the phosphine used. $i\text{-}Pr_3P$ gives $Cu_nSe_{15}(P(Pr\text{-}i)_3)_{12}$ (n = 29, 30), $t\text{-}Bu_3P$ gives $Cu_{36}Se_{18}(P(Bu\text{-}t)_3)_{12}$, while with $PhPEt_2$ and $n\text{-}BuP(Bu\text{-}t)_2$, $Cu_{44}Se_{22}(PEt_2Ph)_{18}$ and

$Cu_{44}Se_{22}(P(Bu\text{-}n)(Bu\text{-}t)_2)_{12}$ are formed, with each containing a deltahedron of 20 selenium atoms[86].

With Et_3P, a little $Cu_{20}Se_{13}(PEt_3)_{12}$ results but the major product is $Cu_{70}Se_{35}(PEt_3)_{22}$ and both are believed to be formed via a Cu_9 intermediate[87]. An even larger cluster results from copper(I) chloride and Ph_3P in THF, with $Cu_{146}Se_{73}(PPh_3)_{30}$ as the product with the selenium atoms arranged in layers of 21, 31 and 21 atoms, respectively, a similar layer structure being found in β-Cu_2Se[88].

The mononuclear mercury(II) derivatives result from 2,4,6-t-$Bu_3C_6H_2SeSiMe_3$ with $HgCl_2$[89], while with $PhSeSiMe_3$ and $Fe(CO)_4(HgCl)_2$, $Hg_{32}Se_{14}(SePh)_{36}$ results with a cubic space group. However, with $HgCl_2$, the trigonal polymorph results. With $CdCl_2(PPh_3)_2$, the analogous Cd compound results with a $Cd_{32}Se_{50}$ cage[90].

X. CYCLIC SELENIDES

The cyclic selenides $(R_2SiSe)_2$ or $(R_2SiSe)_3$ (R = Me, Et) result from Na_2Se and R_2SiCl_2 as thermally unstable oils, but $[Me_3Si)_2SiSe]_3$, a green crystalline solid, is more stable and, on heating with hexamethylcyclotrisiloxane, gives the silaseleninone insertion derivative[91]. There is no evidence for silylene extrusion from the Si–Se ring. In DMP, M_2E (E = Se, Te; M = Na, K) reacts with R_2SiX_2 to give the silicon — selenium rings[92], while with $RSiCl_3$, the adamantane-like cage derivatives **27** result[57].

Heating $TsiSiH_3$ with selenium at 150–160 °C in decalin containing DBU gives 8.4% yield of the 2,3,5,6-tetraselena-1,4-bicyclodisila[2.1.1] hexane **28**, which on irradiation loses selenium to give the bicyclo[1.1.1]pentane **29**[59]. This shows Si–Se bonds of 232 pm, a little longer than the normal length of 227 pm[93].

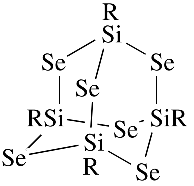

(27)

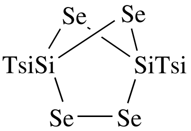

(28)

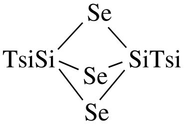

(29)

Tsi = $(Me_3Si)_3C$

Addition of selenium and tellurium to tetramesityldisilene gives the selenirane and tellurirane (equation 42), which continue the trend with the chalcogen derivatives of a steady increase of the Si–Si bond length in going from the oxirane to the tellurirane[94].

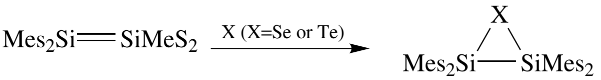

$$Mes_2Si{=\!=}SiMeS_2 \xrightarrow{X\ (X{=}Se\ or\ Te)} \overset{X}{Mes_2Si{-\!-}SiMes_2} \qquad (42)$$

Reacting the silene $Mes(Me_3Si)Si{=}C(OSiMe_3)Ad$-1 with selenium gives the silaselenirane with a 3-membered CSiSe ring, which shows no tendency to dimerize[62].

The silylene Tbt(Ph)Si**:** reacts with selenium to give the 6-membered heterocycle **30** through insertion of silylene, once the 5-membered derivative **31** has been formed

(equation 43)[71].

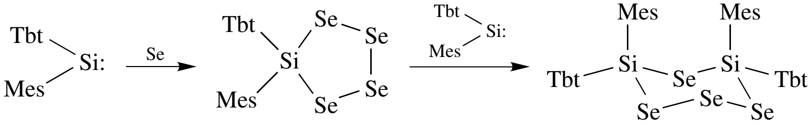

(43)

(31) **(30)**

XI. TRIS(TRIMETHYLSILYL)SILYL SELENIDE DERIVATIVES

Reacting $(Me_3Si)_3SiLi(THF)_3$ with selenium results in the insertion of selenium into the Si−Li bond to give the dimeric $(Me_3Si)_3SiSeLi(THF)_2$[31]. The DME (1,2-dimethoxyethane) derivative is similarly dimeric with Si−Se bonds of 227.5 pm and Si−Si bonds of 234 pm[95]. Protonation gives the selenenol, pK_a 8.3, which reacts with a range of amides and organo derivatives of p-block, d-block and f-block elements. In addition, $(Me_3Si)_3SiSeLi(THF)_2$ reacts with a range of chlorides of these elements to give the seleno derivatives.

Thus for the p-block elements, the range of products are summarized in equations 44–46 and Scheme 6[96].

$$M(NR_2)_3 + 3(Me_3Si)_3SiSeH \longrightarrow [(Me_3Si)_3SiSe]_3M \tag{44}$$

M = Al, Bi; R = Me_3Si; M = As, Sb; R = Me

$$Cp_3In + 3(Me_3Si)_3SiSeH \longrightarrow [(Me_3Si)_3SiSe]_3In \tag{45}$$

$$CpM + (Me_3Si)_3SiSeH \longrightarrow (Me_3Si)_3SiSeM \tag{46}$$

M = In, Te

$$\begin{tikzcd}
(THF)Et_2AlSeSi(SiMe_3)_3 & (Me_3Si)_3SiSeLi(THF)_2 \arrow[l, "Et_2AlCl"'] \arrow[r, "InCl_3"] \arrow[dl, "InCl"'] \arrow[dr, "PCl_3"] & (THF)In[SeSi(SiMe_3)_3]_3 \\
(Me_3Si)_3SiSeIn & & [(Me_3Si)_3SiSe]_3P
\end{tikzcd}$$

SCHEME 6

A similar range of derivatives of Ti, Zr and Hf result as indicated in Scheme 7, and of particular interest are the reactions of **32** with DMPM to give the 'A-frame'-like complexes **33** with disilyl selenide elimination[97].

The vanadium(III) complex **34** has a Si−Se bond length of 230.3 and, like the Ph_3Si derivative, reacts with styrene oxide, propylene sulphide and selenium or $Ph_3P{=}Se$, to give the vanadium(V) derivative (equation 47)[98].

Lanthanide(II) selenides result similarly from their THF amide complexes $[Me_3Si)_2N]_2Ln(THF)_2$ (Ln = Yb, Eu, Sm) with $(Me_3Si)_3SiSeH$ in Et_2O with excess TMEDA or DMPE. $Yb(SeSi(SiMe_3)_3]_2{\bullet}(TMEDA)_2$ shows the selenide ligands in a *trans* relationship while $[Eu[SeSi(SiMe_3)_3]_2(DMPE)_2\}_2\{\mu\text{-DMPE}\}$ crystallizes as ligand bridged dimers. The Yb derivative pyrolyses at 200 °C to give $[(Me_3Si)_3Si]_2Se$ and

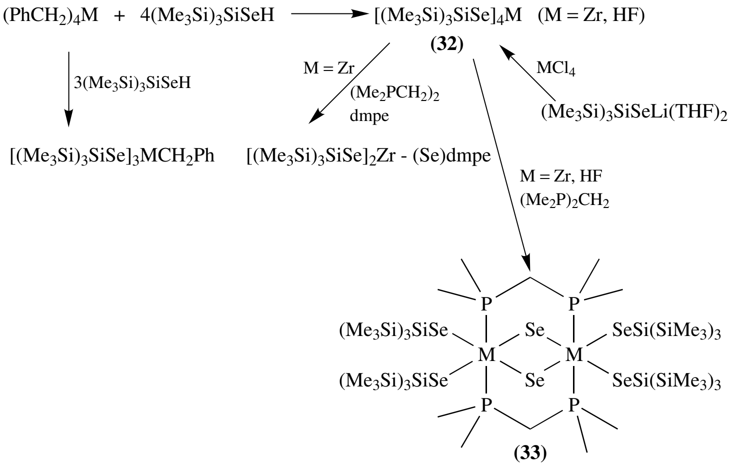

SCHEME 7

YbSe[99]. With $(Me_3Si)_2N]_3M$ (M = La, Ce) and $(Me_3Si)SiSeH$, 3-coordinate monomers result in toluene but the Y derivative occurs in solution as a selenium bridged dimer. The La, Sm and Yb(III) derivatives complex with 2 moles of THF[100].

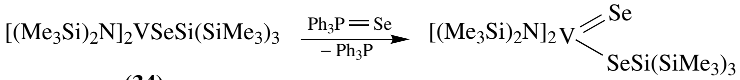

$$[(Me_3Si)_2N]_2VSeSi(SiMe_3)_3 \xrightarrow[-\,Ph_3P]{Ph_3P=Se} [(Me_3Si)_2N]_2V(=Se)SeSi(SiMe_3)_3 \qquad (47)$$

(34)

XII. TELLUROSILANES

Coupling sodium tellurocarboxylates with R'_3SiCl gives the unstable silyl derivative which isomerizes to the more thermodynamically stable $RC(Te)OSiR'_3$ through a facile rearrangement that can be readily followed by ^{13}C NMR spectroscopy. This contrasts with the reaction of alkali metal thiocarboxylates which give the O-silyl ester directly. There is no evidence for the S-silyl intermediate[101].

$Ph_3SiTeLi(THF)_3$ results from the $Ph_3SiLi(THF)_3$ and tellurium and reacts with CF_3CO_2H to give the tellurol, the structure of which indicates a Si−Te bond of 251.1 pm. It couples with Ph_3SiCl to give the disilyl telluride and gives Te derivatives of the group 4 metalocenes. $(t\text{-}BuC_5H_4)_2Zr(TeSiPh_3)_2$ reacts with *t*-butylpyridine to give the disilyl telluride and $[(t\text{-}BuC_5H_4)_2ZrTe]_2$, its formation supporting an intramolecular elimination of the disilyl telluride[102]. With $Cp'TiCl_3$ and $(Me_3Si)_2Te$, $Cp'_5Ti_5Te_6$ results while Cp'_2TiCl_2 gives $Cp'_4Ti_2Te_4$, the structure of which comprises a symmetrical chair conformation[80].

An extensive range of copper telluride clusters results from $(Me_3Si)_2Te$ and copper(I) chloride in Et_2O with a range of phosphines. With $i\text{-}Pr_3P(L)$ the small cluster $Cu_4Te_4[P(Pr\text{-}i_3]_4$ results along with $Cu_{23}Te_{13}L_{10}$ and $Cu_{29}Te_{16}L_{12}$, while with $Et_3P(L')$, $Cu_{16}Te_9L'_8$ results. With Et_2PPh (L''), $Cu_{16}Te_9L''_8$ and $Cu_{28}Te_{17}L''_{12}$ form and, for $(t\text{-}Bu)_3P$ (L^t) in Et_2O/THF, $Cu_{26}Te_{16}L^t{}_{10}$ is formed[103].

Both alkyl and aryl tellurosilanes act as a good source of RTe^- and Te^{2-} ligands, forming transition metal−tellurium clusters with cobalt(II) and copper(I) salts. The nuclearity of the cluster is determined primarily by the phosphine present, but also by the metal. Cobalt gives but one derivative, $Co_6Te_8(PPh_2(Pr\text{-}n))_6$, with each triangular face of the Co_6 octahedron bridged by Te ions, thereby supporting C−Te cleavage. With copper, however, the 4 derivatives $Cu_{11}(\mu_3\text{-Te(Bu-}n))_7(\mu_4\text{-Te(Bu-}n))_2(\mu_7\text{-Te})(PPh_3)_5$, $Cu_{18}(\mu_3\text{-Te(Bu-}n))_6Te_6(P(Pr\text{-}n)_3)_8$, $Cu_{58}Te_{32}(PPh_3)_{16}$ and $Cu_{23}Te_{13}(PEt_3)_{12}$ result, and again C−Te cleavage occurs[104].

XIII. TRIS(TRIMETHYLSILYL)SILYL TELLUROL DERIVATIVES

For the past few years, silicon–tellurium chemistry has been dominated by the use of $(Me_3Si)_3SiTe^-$ and its derivatives. $(Me_3Si)_3SiLi(THF)_3$ reacts at room temperature with tellurium in THF to give the lithium telluride as a THF complexed dimer $[(Me_3Si)_3SiTeLi(THF)]_2$ **(35)** with Si−Te bonds of 248 pm[31]. DME displaces THF to give the dimer with a planar Li_2Te_2 ring and the bulky $(Me_3Si)_3SiTe$ substituents *trans* to one another and Si−Te bonds of 250 pm[105]. In the presence of 12-crown-4, however, the ionic $[Li(12\text{-crown-}4)_2]^+[TeSi(SiMe_3)_3]^-$ results with the ions separated and an Si−Te distance of 246.8 pm[106].

Acidification of **(35)** gives the highly stable tellurol $(Me_3Si)_3SiTeH$ as an air-sensitive wax, with pK_a 7.3, which readily oxidizes to the ditelluride and gives base-free derivatives of the alkali metal with $(Me_3Si)_2NM$ (M = Li, Na) or KOBu-*t*[31].

Alkaline earth metal derivatives can also be prepared from the tellurol and $[Me_3Si)_2N]_2M(THF)_2$ (M = Ca, Sr, Ba) in hexane and crystallize from THF with 4 ligands (M = Ca, Sr) or 5 (M = Ba). The magnesium compound is prepared from Bu_2Mg and the tellurol as a THF complex of tetrahedral structure. The Mg derivative substitutes Cp_2MCl_2 to give the group IV tellurides[107].

A range of group 13 derivatives results from the tellurol and $[Me_3Si)_2N]_3Al$ and Cp_3 In, the Ga derivative from the lithium telluride and $GaCl_3$. They readily give complexes as does the In(I) derivative[96].

The gallium derivative $[(Me_3Si)_2CH]_2GaTeSi(SiMe_3)_3$ results from either metathetical exchange between the Li–telluride and gallium chloride, or from the digallane and ditelluride. It is monomeric and, with the $C_2Ga{-}TeSi$ unit lying in the mirror plane of the molecule, a short Ga−Te bond and high barrier to rotation suggests a π-interaction between Te and Ga[108].

The tin(II) and lead(II) tellurides result from the amide $M[N(SiMe_3)_2]_2$ and tellurol. The tin derivative is dimeric with the Sn_2Te_2 unit adopting a butterfly-like structure with the terminal tellurol groups *cis*[109]. The antimony and bismuth derivatives result from amides and the tellurol[96].

The zinc, cadmium and mercury derivatives result from the silyl amide and tellurol and, while the zinc and cadmium derivatives are dimeric in solution, the mercury derivative is a monomer. Vapour pressure molecular weight measurements indicate a decreasing tendency to dimerization with increasing atomic weight of the metal. The zinc derivative crystallizes with a planar telluride bridged Zn_2Te_2 unit, and give monomeric 4-coordinate complexes with pyridine and bipyridyl. The cadmium results in a 6-coordinate derivative $Cd[TeSi(SiMe_3)_3]_2(bipy)_2$ but 4-coordinate with dmpe[110].

$(Me_3Si)_3SiTeH$ demethylates Cp_2ZrMe_2 in a stepwise manner to give $Cp_2Zr[TeSi(SiMe_3)_3]_2$[111] while this and the Ti and Hf derivatives also result from the metallocene dichloride and the lithium telluride. The methyl tellurate $Cp_2Zr(Me)[TeSi(SiMe_3)_3]$ reacts with CO to give the η_2-acyl derivative. Addition of base to the titanium derivative $Cp_2Ti[TeSi(SiMe_3)_3]L$ (L = phosphine or isocyanide), which can be prepared directly from $(Cp_2TiCl)_2{\cdot}Cp_2Ti[TeSi(SiMe_3)_3]_2$, eliminates the ditelluride $[Me_3Si)_3SiTe]_2$ on coordination to CO, CO_2 or CS_2[112].

The lithium telluride substitutes $TiCl_3(THF)_3$ and $(PhCH_2)_4M$ react with the tellurol, the $[(Me_3Si)_3SiTe]_4M$ derivatives complexing with isocyanides or dmpe, the latter inducing decomposition to the disilyl telluride and metal telluride[97] (equation 48).

$$[(Me_3Si)_3SiTe]_4Mdmpe \xrightarrow[\substack{M{=}Zr,\ Hf \\ -[(Me_3Si)_3Si]_2Te}]{dmpe} [(Me_3Si)_3SiTe]_2(dmpe)_2M{=}Te \tag{48}$$

The vanadium(III) derivative $[(Me_3Si)_2N]_2VTeSi(SiMe_3)_3$ shows a Si−Te bond length of 252.7 pm, slightly longer than that in $[(Me_3Si)_2N]_2VTeSiPh_3$ (250.7 pm), and readily reacts with styrene oxide, propylene sulphide and elemental selenium or $Ph_3P{=}Se$ to give the vanadium(V) derivative. The sulphur derivative decomposes on heating to eliminate ditelluride and form the vanadium(III) sulphide bridged dimer[98].

Reacting $(Me_3Si)_3SiTeLi(THF)_2$ with $MCl_2(dmpe)$ (M = Cr, Mn, Fe) gives $M[TeSi(SiMe_3)_3]_2(dmpe)_2$, but $CoBr_2(PMe_3)_3$ gives $Co[TeSi(SiMe_3)_3](PMe_3)_3$ through disproportionation giving the ditelluride $[(Me_3Si)_3SiTe)_2$[113].

Tellurolysis of $[(Me_3Si)_2N]_2M$ with $(Me_3Si)_3SiTeH$ in the presence of base gives the 4-coordinate ditellurides, while the structures of the dmpe complexes of Mn(II) and Fe(II) show Si−Te bond lengths of 250 −252 pm, shorter than those in Fe(II) complexes (with values 253.7 −254.6 pm), while that in the Co(I) derivative was shorter than both at 249.4 pm.

Tellurolysis of $[(Me_3Si)_2N]_3M$ (M = La, Ce) gives the tritellurols, which complex dmpe but decompose at 20 °C to give the clusters $M_5Te_3[TeSi(SiMe_3)_3]_9$ through elimination of the disilyl telluride. The structures of these clusters indicate a Ce_3Te_3 ring capped by $Ce[TeSi(SiMe_3)_3]_3$ units, with terminal $(Me_3Si)_3SiTe$ units on the three Ce atoms. Pyrolysis at 600 °C gives M_2Te_3. These tellurols, like that of yttrium, complex with dmpe, while the europium derivative gives a 7-coordinate complex with dmpe bridging two $[(Me_3Si)_3SiTe]_2Eu(dmpe)_2$ units. The ytterbium complex $[(Me_3Si)_3SiTe]_2Yb$ (TMEDA) pyrolyses to the disilyl telluride and YbTe. The selenide behaves similarly [114].

XIV. REFERENCES

1. H.-G. Horn, *J. prakt. Chem.*, **334**, 201 (1992).
2. I. Dance and K. Fisher, *Prog. Inorg. Chem.*, **41**, 637 (1994).
3. J. Arnold, *Prog. Inorg. Chem.*, **43**, 353 (1995).
4. *Inorg. Synth.*, **29**, 30 (1992).
5. R. K. Sibao, N. L. Keder and H. Eckert, *Inorg. Chem.*, **29**, 4163 (1990).
6. I. S. Nizamov, V. A. Kuznetzov, E. S. Batyeva, V. A. Al'fonsov and A. N. Pudovik, *Phosphorus, Sulphur, Silicon*, **93**, 179 (1993); I. S. Nizamov, V. A. Kuznetzov and E. S. Batyeva, *Phosphorus, Sulphur, Silicon*, **90**, 249 (1994).
7. A.-M. Le Nocher and P. Metzner, *Tetrahedron Lett.*, **33**, 6151 (1992).
8. P. Beslin and P. Marion, *Tetrahedron Lett.*, **33**, 5339 (1992).
9. M. B. Sassaman, G. K. S. Prakash and G. A. Olah, *Synthesis*, 104 (1990).
10. A. Kusche, R. Hoffmann, I. Munster, P. Keiner and R. Bruckner, *Tetrahedron Lett.*, **32**, 467 (1991).
11. T. Miura and Y. Masaki, *Tetrahedron*, **51**, 10477 (1995).
12. T. Mukaiyama, T. Ohno, T. Nishimura, J. S. Han and S. Kobayashi, *Bull. Chem. Soc. Jpn.*, **64**, 2524 (1991).
13. T. Soga, H. Takenoshita, M. Yamada, J. S. Han and T. Mukaiyama, *Bull. Chem. Soc. Jpn.*, **64**, 1108 (1991).
14. A. Degl'Innocenti, P. Ulivi, A. Capperucci, G. Reginato, A. Mordini and A. Ricci, *Synlett*, 883 (1992).
15. C.-M. Yu, H.-S. Choi, W.-H. Jung and S.-S. Lee, *Tetrahedron Lett.*, **37**, 7095 (1996).

16. T. Buskas, P. J. Garegg, P. Konradsson and J.-L. Maloisel, *Tetrahedron: Asymmetry*, **5**, 2187 (1994).
17. Y. Lim and W. K. Lee, *Tetrahedron Lett.*, **36**, 8431 (1995).
18. M. Muller, W. R. Forster, A. Holst, A. J. Kingma, W. Schaumann and G. Adiwidjaja, *Chem. Eur. J.*, **2**, 949 (1996).
19. K. Osakada, K. Hataya and T. Yamamoto, *J. Chem. Soc., Chem. Commun.*, 2315 (1995).
20. J. B. Baruah, K. Osakada and T. Yamamoto, *Organometallics*, **15**, 456 (1996); J. B. Baruah, *Polyhedron*, **15**, 3709 (1996).
21. M. Aizenberg, R. Goikhman and D. Milstein, *Organometallics*, **15**, 1075 (1996).
22. H.-C. Liang and P. A. Shapley, *Organometallics*, **15**, 1331 (1996).
23. J. Zubieta, E. Block, G. Ofori-Okai and K. Tang, *Inorg. Chem.*, **29**, 4595 (1990).
24. H. W. Roesky and U. Otten, *J. Fluorine Chem.*, **46**, 433 (1990).
25. N. Tokitoh, T. Imakubo and R. Okazaki, *Tetrahedron Lett.*, **33**, 5819 (1992).
26. J. Brittain and Y. Gareau, *Tetrahedron Lett.*, **34**, 3363 (1993).
27. B. Hache and Y. Gareau, *Tetrahedron Lett.*, **35**, 1837 (1994).
28. H.-S. Dang and B. P. Roberts, *Tetrahedron Lett.*, **36**, 3731 (1995).
29. R. Minkowitz, A. Kornath and H. Preut, *Z. Anorg. Allg. Chem.*, **619**, 877 (1993).
30. R. Minkowitz, A. Kornath and H. Preut, *Z. Anorg. Allg. Chem.*, **620**, 981 (1994).
31. P. J. Bonasai, V. Christou and J. Arnold, *J. Am. Chem. Soc.*, **115**, 6777 (1993).
32. M. Ballestri, C. Chatgilialoglu and G. Seconi, *J. Organomet. Chem.*, **408**, C1 (1991); J. Daroszewski, J. Lusztyk, M. Degueil, C. Navarro and B. Maillard, *J. Chem. Soc., Chem. Commun.*, 586 (1991); D. P. Curran and B. Yoo, *Tetrahedron Lett.*, **33**, 6931 (1992).
33. G. Gattow and H.-P. Dewald, *Z. Anorg. Allg. Chem.*, **604**, 63 (1991).
34. N. W. Mirzel, A. Schier, H. Baruda and H. Schmidbaur, *Chem. Ber.*, **125**, 1053 (1992).
35. D. G. Anderson, G. A. Forsyth and D. W. H. Rankin, *J. Mol. Struct.*, **221**, 45 (1990); D. G. Anderson, V. A. Campbell, G. A. Forsyth and D. W. H. Rankin, *J. Chem. Soc., Dalton Trans.*, 2125 (1990).
36. G. N. Dolenko, M. G. Voronkov, V. P. Elin, E. V. Dolenko, T. O. Pavlova, M.Yu.Maroshina, V. V. Belova and T. I. Zhidkova, *J. Mol. Struct.*, **326**, 221 (1994); M.Yu.Maroshina, N. N. Vlasova and M. G. Voronkov, *J. Organomet. Chem.*, **406**, 279 (1991).
37. S.-C. Tsay, G. L. Yep, B.-L. Chen, L. C. Lin and J. R. Hwu, *Tetrahedron*, **49**, 8969 (1993); J. R. Hwu and S.-C. Tsay, *J. Org. Chem.*, **55**, 5987 (1990).
38. F. Freeman, J. D. Kim, M. Y. Lee and X. Wang, *Tetrahedron*, **52**, 5699 (1996).
39. T. J. Curphey and H. H. Joyner, *Tetrahedron Lett.*, **34**, 7231 (1993).
40. A. Capperucci, A. Degl'Innocenti, A. Ricci, A. Mordini and G. Reginato, *J. Org. Chem.*, **56**, 7323 (1991); A. Degl'Innocenti, A. Capperucci, A. Mordini, G. Reginato, A. Ricci and F. Cerreta, *Tetrahedron Lett.*, **34**, 873 (1993); A. Degl'Innocenti, M. Funicello, P. Scafato and P. Spagnolo, *Chem. Lett.*, 1873 (1994) and 147 (1995); A. Capperucci, A. Degl'Innocenti, M. Funicello, P. Scafato and P. Spagnolo, *Synthesis*, 1185 (1996).
41. A. Capperucci, A. Degl'Innocenti, M. Funicella, G. Mauriello, P. Scafato and P. Spagnolo, *J. Org. Chem.*, **60**, 2254 (1995).
42. A. W. Schabacher and T. L. Maynard, *Tetrahedron Lett.*, **34**, 1269 (1993).
43. J. R. Hwu and S.-C. Tsay, *Tetrahedron* **46**, 7413 (1990); S.-C. Tsay, P. Gani and J. R. Hwu, *J. Chem. Soc., Perkin Trans. 1*, 1493 (1991).
44. P.-Y. Lin, W.-S. Ku and M.-J. Shaio, *Synthesis*, 1219 (1992); D. C. Smith, S. W. Lee and P. L. Fuchs, *J. Org. Chem.*, **59**, 348 (1994).
45. S. Schulz, E. G. Gillan, J. L. Ross, L. M. Rogers, R. D. Rogers and A. R. Barron, *Organometallics*, **15**, 4880 (1996); J. Breker, U. Wermuth and R. Schmutzler, *Z. Naturforsch., Teil B*, **45**, 1398 (1990).
46. V. C. Gibson, T. P. Kee and A. Shaw, *Polyhedron*, **9**, 2293 (1990).
47. K. K. Banger, C. S. Blackman and A. K. Brisdon, *J. Chem. Soc., Dalton Trans.*, 2975 (1996); B. Siewek, G. Koellner, K. Ruhlandt-Senge, F. Schmock and U. Muller, *Z. Anorg. Allg. Chem.*, **593**, 160 (1991).
48. D. Fenske, A. Grissinger, M. Loos and J. Magull, *Z. Anorg. Allg. Chem.*, **598/9**, 121 (1991).
49. D. Fenske, H. Fleischer, H. Krautscheid and J. Magull, *Z. Naturforsch., Teil B*, **45**, 127 (1990).
50. S. Dehnen, A. Schafer, D. Fenske and R. Ahlrichs, *Angew. Chem., Int. Ed. Engl.*, **33**, 746 (1994); S. Dehnen and D. Fenske, *Chem. Eur. J.*, **2**, 1407 (1996).
51. V. Lefevre and J.-L. Ripoll, *Tetrahedron Lett.*, **37**, 7017 (1996).

52. H. Suzuki, N. Tokitoh, S. Nagase and R. Okazaki, *J. Am. Chem. Soc.*, **116**, 11578 (1994).
53. S. D. Grumbine, R. K. Chadha and T. D. Tilley, *J. Am. Chem. Soc.*, **114**, 1518 (1992); S. D. Grumbine, T. D. Tilley and A. L. Rheingold, *J. Am. Chem. Soc.*, **115**, 358 (1993); S. D. Grumbine, T. D. Tilley, F. P. Arnold and A. L. Rheingold, *J. Am. Chem. Soc.*, **115**, 7884 (1993).
54. (a) E. I. Band and S. T. Eberhart, US Patent 4,885,378; *Chem. Abstr.*, **112**, 179472m (1990). (b) W. Uhlig, *Z. Anorg. Allg. Chem.*, **588**, 133 (1990).
55. G. A. Kraus and B. Andersh, *Tetrahedron Lett.*, **32**, 2189 (1991).
56. H.-G. Horn and M. Probst, *Monatsh. Chem.*, **126**, 1169 (1995).
57. S. R. Bahr and P. Boudjouk, *Inorg. Chem.*, **31**, 712 (1992).
58. P. Jutzi, D. Eikenberg, A. Mohrke, B. Neumann and H.-G. Stammler, *Organometallics*, **15**, 753 (1996).
59. H. Yoshida, Y. Kabe and W. Ando, *Organometallics*, **10**, 27 (1991); H. Yoshida and W. Ando, *Phosphorus, Sulphur, Silicon*, **67**, 45 (1992); N. Choi, K. Asano and W. Ando, *Organometallics*, **14**, 3146 (1995); N. Choi, K. Asano, N. Sato and W. Ando, *J. Organomet. Chem.*, **516**, 155 (1996).
60. J. E. Magnette, D. R. Powell and R. West, *Organometallics*, **14**, 3551 (1995).
61. E. Kroke, M. Weidenbruch, W. Saak, S. Pohl and H. Marsmann, *Organometallics*, **14**, 5695 (1995).
62. A. G. Brook, R. Kumarathasan and A. J. Lough, *Organometallics*, **13**, 424 (1994).
63. K. Kabeta, D. R. Powell, J. Hanson and R. West, *Organometallics*, **10**, 827 (1991).
64. N. Tokitoh, H. Suzuki and R. Okazaki, *J. Chem. Soc., Chem. Commun.*, 125 (1996).
65. J. Barrau, N. Ben Hamida and J. Stage, *Synth. React. Inorg. Met.-Org. Chem.*, **20**, 1373 (1990).
66. P. Boudjouk and U. Samaraweera, *Organometallics*, **9**, 2205 (1990).
67. P. Boudjouk, E. Black, R. Kumarathasan, U. Samaraweera, S. Castellino, J. P. Oliver and J. W. Kampf, *Organometallics*, **13**, 3715 (1994).
68. N. Choi, S. Morino, S. Sugi and W. Ando, *Bull. Chem. Soc. Jpn.*, **69**, 1613 (1996).
69. J. Albertsen and R. Steudel, *J. Organomet. Chem.*, **424**, 153 (1992).
70. N. Tokitoh, M. Takahashi, T. Matsumoto, H. Suzuki, Y. Matsuhashi and R. Okazaki, *Phosphorus, Sulphur, Silicon*, **59**, 455 (1991); N. Tokitoh, H. Suzuki, T. Matsumoto, Y. Matsuhashi, R. Okazaki and M. Goto, *J. Am. Chem. Soc.*, **113**, 7047 (1991).
71. H. Suzuki, N. Tokitoh and R. Okazaki, *Bull. Chem. Soc. Jpn.*, **68**, 2481 (1995).
72. R. Koster, G. Seidel and R. Boese, *Chem. Ber.*, **123**, 2109 (1990).
73. W.-W. du Mont, S. Kubiniok, L. Lange, S. Pohl, W. Saak and I. Wagner, *Chem. Ber.*, **124**, 1315 (1991); A. Haas, C. Limberg and M. Spehr, *Chem. Ber*, **124**, 423 (1991).
74. M. Sakakibara, K. Katsumata, Y. Watanabe, T. Toru and Y. Ueno, *Synlett*, 965 (1992).
75. G. Pandey and K. S. S. P. Rao, *Angew. Chem., Int. Ed. Engl.*, **34**, 2669 (1995).
76. H. Poleschner, M. Heydenreich, K. Spindler and G. Haufe, *Synthesis*, 1043 (1994).
77. D. Fenske, A. Frankenau and K. Dehnicke, *Z. Naturforsch., Teil B*, **45**, 427 (1990); P. M. Boorman, H.-B. Kraatz and M. Parvez, *J. Chem. Soc., Dalton Trans.*, 3281 (1992).
78. K. Shimada, S. Hikage, Y. Takeishi and Y. Takikawa, *Chem. Lett.*, 1403 (1990); Y. Takikawa, H. Watanabe, R. Sasaki and K. Shimada, *Bull. Chem. Soc. Jpn.*, **67**, 876 (1994).
79. S. Kato, H. Kageyama, Y. Kawahara, T. Murai and H. Ishihara, *Chem. Ber.*, **125**, 417 (1992); H. Kageyama, K. Kido, S. Kato and T. Murai, *J. Chem. Soc., Perkin Trans. 1*, 1083 (1994).
80. D. Fenske and A. Gressinger, *Z. Naturforsch., Teil B*, **45**, 1309 (1990).
81. K. Merzweiler and H.-J. Kersten, *Z. Naturforsch., Teil B*, **46**, 1025 (1991).
82. D. Fenske, H. Krautscheid and M. Muller, *Angew. Chem., Int. Ed. Engl.*, **31**, 321 (1992).
83. K. Merzweiler and L. Weisse, *Z. Naturforsch., Teil B*, **46**, 695 (1991).
84. D. Fenske, H. Fleischer, H. Krautscheid and J. Magull, *Z. Naturforsch., Teil B*, **45**, 127 (1990).
85. D. Fenske, H. Fleischer, H. Krautscheid, J. Magull, C. Oliver and S. Weisgerber, *Z. Naturforsch., Teil B*, **46**, 1384 (1991).
86. D. Fenske, H. Krautscheid and S. Balter, *Angew. Chem., Int. Ed. Engl.*, **29**, 796 (1990); S. Dehnen and D. Fenske, *Angew. Chem., Int. Ed. Engl.*, **33**, 2287 (1994).
87. D. Fenske and H. Krautscheid, *Angew. Chem., Int. Ed. Engl.*, **29**, 1452 (1990).
88. H. Krautscheid, D. Fenske, G. Baum and M. Semmelmann, *Angew. Chem., Int. Ed. Engl.*, **32**, 1303 (1993).
89. I. Wagner and W.-W. du Mont, *J. Organomet. Chem.*, **395**, C23 (1990).
90. S. Behrens, M. Bettenhausen, A. C. Deveson, A. Eichhofer, D. Fenske, A. Lohde and U. Woggon, *Angew. Chem. Int., Ed. Engl.*, **35**, 2215 (1996).

91. P. Boudjouk, S. R. Bahr and D. P. Thompson, *Organometallics*, **10**, 778 (1991).
92. P. Boudjouk, *Polyhedron*, **10**, 1231 (1991).
93. H. Yoshida, Y. Takahara, T. Erata and W. Ando, *J. Am. Chem. Soc.*, **114**, 1098 (1992).
94. R. P.-K. Tan, G. R. Gillette, D. R. Powell and R. West, *Organometallics*, **10**, 546 (1991).
95. K. E. Flick, P. J. Bonasia, D. E. Gindelberger, J. E. B. Katari and D. Schwartz, *Acta Crystallogr.*, **C50**, 674 (1994).
96. S. P. Wuller, A. L. Seligson, G. P. Mitchell and J. Arnold, *Inorg. Chem.*, **34**, 4861 (1995).
97. C. P. Gerlach, V. Christou and J. Arnold, *Inorg. Chem.*, **35**, 2758 (1996).
98. C. P. Gerlach and J. Arnold, *Inorg. Chem.*, **35**, 5770 (1996).
99. D. R. Cary and J. Arnold, *Inorg. Chem.*, **33**, 1791 (1994).
100. D. R. Cary, G. E. Ball and J. Arnold, *J. Am. Chem. Soc.*, **117**, 3492 (1995).
101. S. Kato, H. Kageyama, T. Kanda, T. Murai and T. Kawamura, *Tetrahedron Lett.*, **31**, 3587 (1990).
102. D. E. Gindelberger and J. Arnold, *Organometallics*, **13**, 4462 (1994).
103. D. Fenske and J.-C. Steck, *Angew. Chem., Int. Ed. Engl.*, **32**, 238 (1993).
104. J. F. Corrigan, S. Balter and D. Fenske, *J. Chem. Soc., Dalton Trans.*, 729 (1996).
105. G. Becker, K. W. Klinkhammer, S. Lartiges, P. Bottcher and W. Poll, *Z. Anorg. Allg. Chem.*, **613**, 7 (1992).
106. P. J. Bonasia, D. E. Gindelberger, B. O. Dabbousi and J. Arnold, *J. Am. Chem. Soc.*, **114**, 5209 (1992).
107. G. Becker, K. W. Klinkhammer, W. Schwarz, M. Westerhausen and T. Hildenbrand, *Z. Naturforsch., Teil B*, **47**, 1225 (1992); D. E. Gindelberger and J. Arnold, *J. Am. Chem. Soc.*, **114**, 6242 (1992).
108. W. Uhl, M. Layh, G. Becker, K. W. Klinkhammer and T. Hildenbrand, *Chem. Ber.*, **125**, 1547 (1992).
109. A. L. Seligson and J. Arnold, *J. Am. Chem. Soc.*, **115**, 8214 (1993).
110. P. J. Bonasia and J. Arnold, *Inorg. Chem.*, **31**, 2508 (1992).
111. B. O. Dabbousi, P. J. Bonasai and J. Arnold, *J. Am. Chem. Soc.*, **113**, 3186 (1991).
112. V. Christou, S. P. Wuller and J. Arnold, *J. Am. Chem. Soc.*, **115**, 10545 (1993).
113. D. E. Gindelberger and J. Arnold, *Inorg. Chem.*, **32**, 5813 (1993).
114. D. R. Cary and J. Arnold, *J. Am. Chem. Soc.*, **115**, 2520 (1993).

CHAPTER 32

Cyclic polychalcogenide compounds with silicon

NAMI CHOI and WATARU ANDO

Department of Chemistry, University of Tsukuba, Tsukuba, Ibaraki 305, Japan
Fax: +81 298 53 6503

I. INTRODUCTION

The chemistry of silachalcogenides has been studied widely and reviewed extensively[1,2]. A variety of polycyclic silachalcogenides has been synthesized during the past decade. The structures of these species are strongly dependent upon the substituents. Recently, some facile syntheses of cyclic silachalcogenides have been reported[3–5]. In this chapter, the chemistry of cyclic silachalcogenides will be reviewed, mainly with respect to disilapolychalcogenides and silasquichalcogenides, although some reference will be made to cyclic siloxanes.

Another class of compounds that has attracted much interest are the sesquioxides and sesquichalcogenides of the type $(RE)_{2n}Y_{3n}$ $[(M_2Y_3)_n]$ (E = Si, Ge, Sn; Y = O, S, Se), due to their unique structural properties. These molecules have polyhedral cage-like structures analogous to those of bicyclo[1.1.1]pentane ($n = 1$) **(1)**, adamantane ($n = 2$)

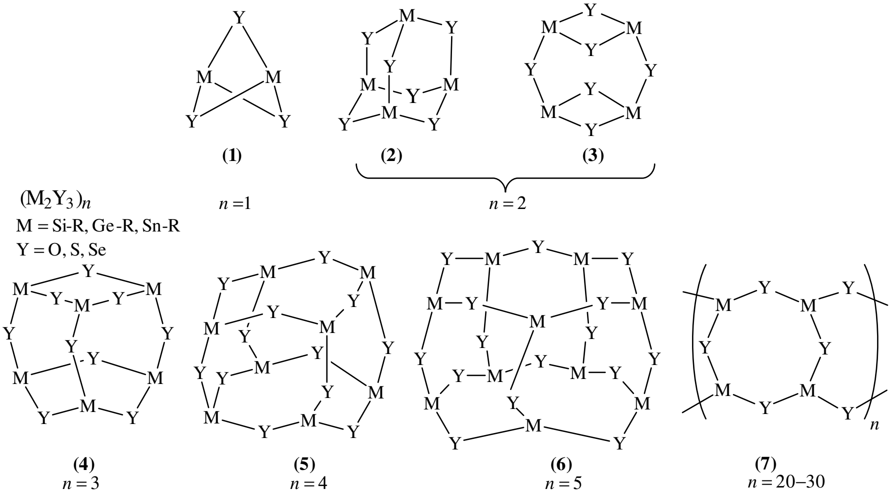

(1) $n = 1$

(2) **(3)** $n = 2$

(4) $n = 3$

(5) $n = 4$

(6) $n = 5$

(7) $n = 20–30$

FIGURE 1. Series of sesquichalcogenides

(2) or double-decker ($n = 2$) **(3)**, prismane ($n = 3$) **(4)**, cubane ($n = 4$) **(5)**, pentagonal prismane ($n = 5$) **(6)**, ladder ($n = 20-30$) **(7)** etc. (Figure 1). The isolated sesquisulfide and selenide (Y = S, Se) have been restricted to the adamantane-type structure **(2)** or the double-decker structure **(3)** while higher homologous molecules are known for the sesquioxide (**4**, M = Ge, Y = O; M = Si, Y = O)[6]. Although many silsesquioxanes have been reported, there is no example of an adamantane-type structure.

At an early stage in silicon chemistry, Kipping and coworkers proposed a propellane-type sesquioxide (**1**, M = Si, Y = O) as an intermediate in the hydrolysis of trichlorosilanes[7]. However, the synthesis of this attractive molecule has not been achieved despite much interest from both theoretical and practical chemists. Under the appropriate conditions, trihydro- and trihalosilanes react with elemental chalcogenides or chalcogen transfer reagents to give adamantane-type silachalcogenanes[8–11] and/or bicyclopolychalcogenasilanes[12], dependent upon the bulkiness of the substituents. The smallest silasesquichalcogenide has a 2,4,5-chacogena-1,3-disilabicyclo[1.1.1]pentane skeleton. The synthesis of the sulfur and selenium analogues has been achieved by kinetic stabilization[13–15].

II. MONOCYCLOSILACHALCOGENIDES

A. Introduction

Cyclic siloxanes are important precursors in the silicon industry, being formally dimers or trimers of silanone ($R_2Si{=}O$), a known intermediate. Cyclic siloxanes have been synthesized by four routes, the conventional methods being the condensation of silanediol or the hydrolysis of species such as halosilanes or aminosilanes (Scheme 1)[16–20]. Alternatively, oxidation of disilene by triplet oxygen (equation 1)[21–27] or oxidation of oxadisiliranes by singlet oxygen (equation 2)[28–31] may be utilized.

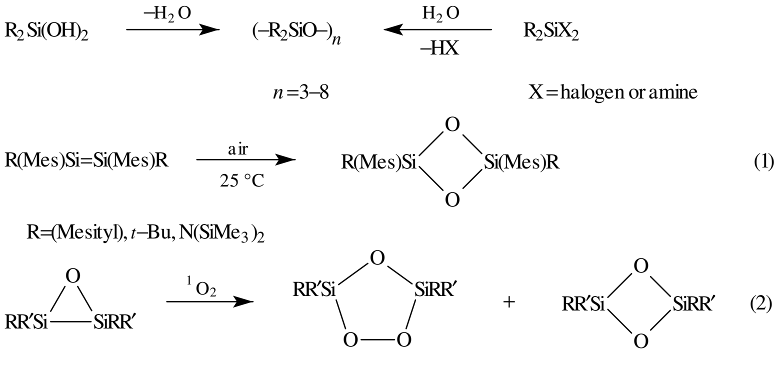

R = Mes, Dip, Dep; R′ = Mes, Dip, Dep, Det; Mes = 2,4,6-$Me_3C_6H_2$; Dip = 2,6-i-$Pr_2C_6H_3$;
Dep = 2,6-$Et_2C_6H_3$; Det = 4-t-Bu-2,6-$Et_2C_6H_2$

SCHEME 1

B. Cyclodisiloxanes and Cyclotrisiloxanes

Tetramesityldisiloxane [$(Mes_2SiO)_2$] **(8)** has been prepared by the reaction of tetramesityldisilene with atmospheric oxygen[22,24]. It has been reported that 1,2-cyclodisiloxane is

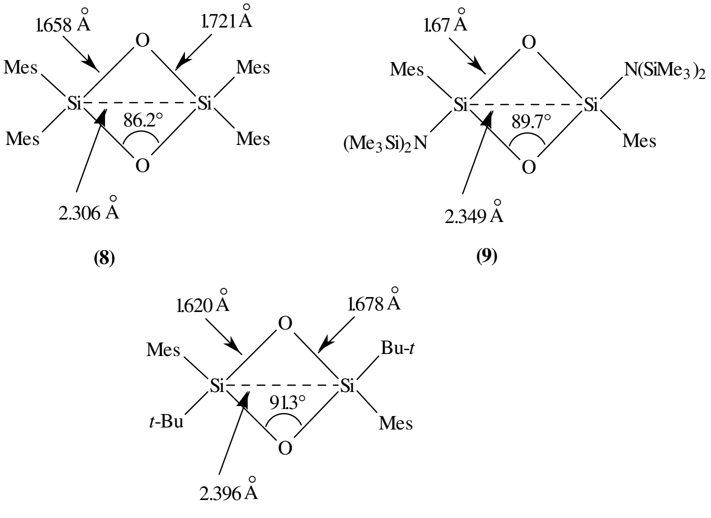

(8) **(9)**

(10)

FIGURE 2. Atomic distances (Å) and angles (deg) of cyclodisiloxanes

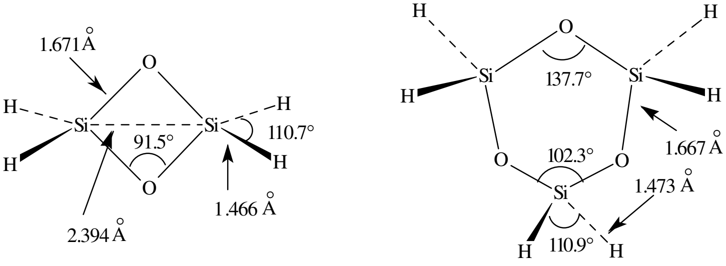

(11) **(12)**

FIGURE 3. Geometries of $(H_2SiO)_2$ and $(H_2SiO)_3$

stereospecifically isomerized to 1,3-cyclodisiloxane in both solution and the solid state[32]. Crystal structures of the 1,3-cyclodisiloxanes **8, 9** and **10**, differing only in their substituents, have been determined (Figure 2). The structure of tetramesitylcyclodisiloxane consists of roughly a square cyclodisiloxane ring orthogonal to a slightly distorted planar skeleton due to the steric hindrance between mesityl groups. The mesityl rings are diposed in a roughly helical fashion about this skeleton. Therefore, the cyclodisiloxane ring has two independent silicon—oxygen bond lengths. 1.658(4) and 1.721(4) Å. The Si−Si distance in **8** of 2.306 Å is shorter than the theoretical value (*vide infra*); this may be explained by the fact that the four-membered ring is not planar, but distorted with a O−Si−Si−O angle of 6°[25]. The Si−Si distance in **9** is slightly shorter than the calculated distance of $(H_2SiO)_2$ **(11)** 2.394 Å[33], and the HF/6-31G* value of 2.469 Å[34] in the cyclic dimer $(SiO)_2$. By comparison of the calculated distances in $(F_2SiO)_2$ (2.341 Å) and $(H_2SiO)_2$ (2.394 Å), it appears that the greater the charge separation (or ionic character) the shorter the Si−Si bond distance. Moreover, the HF/3-21G optimized structure of cyclic trimer $(H_2SiO)_3$ **(12)** (Figure 3) has D_{3h} symmetry with alternative silicon and oxygen atoms arranged in a planar six-membered ring[33]. The planarity of the Si_3O_3 ring has also been observed in the electron diffraction study of hexamethylcyclotrisiloxane $(Me_2SiO)_3$ **(13)**[35,36]. The Si−O−Si and O−Si−O angles of 137.7° and 102.3° in the trimer $(H_2SiO)_3$ are much larger than those in the dimer $(H_2SiO)_2$. The disproportionation energies for $3(H_2SiO)_2 \rightarrow 2(H_2SiO)_3$ are calculated to be -162.3 kcal mol^{-1} at the HF/3-21G level and -110.4 kcal mol^{-1} at the HF/6-31G*//3-21G level. These large negative values clearly favor the trimer over the dimer[33]. In contrast, the disproportionation energy for $3(H_2SiS)_2 \rightarrow 2(H_2SiS)_3$ is calculated to be much less negative (-30.3 kcal mol^{-1})[33].

C. Oxidation of Disiliranes with Molecular Oxygen

Photochemical reactions of silicon−silicon σ-bonds of disilirane **(14)** with molecular oxygen have been studied in three modes: charge transfer (CT), electron transfer (ET) and singlet oxygen. An oxygen-saturated acetonitrile solution of 1,1,2,2-tetramesityl-1,2-disilirane **(14a)** was irradiated to give 3,3,5,5-tetramesityl-1,2-dioxa-3,5-disilolane **(15a)** in 36% yield (equation 3). Similar results were obtained with 2,2,3,3-tetrakis(2,6-diisopropylphenyl)oxadisilirane **(14b)** and 2,2,3,3-tetrakis(2,6-diethylphenyl)oxadisilirane **(14c)** affording the corresponding 1,2,4-trioxa-3,5-disilolanes **(15b** and **15c)** (equation 3). The structure of **15c** is given in Figure 4[37]. The UV absorption spectrum of the disilirane **14a** in oxygen-saturated solvents such as methylene chloride or acetonitrile reveals a weak broad contact CT band with a maximum at 300 nm. Photolysis of **14a** in an oxygen matrix at 16 K resulted in smooth oxygenation, giving a new species with an intense IR band at 1078 cm^{-1}. When $^{18}O_2$ is employed, the IR band shifts by 39 cm^{-1} to a lower wave number. Upon subsequent warming of the matrix to temperatures higher than 50 K, the intense band at 1078 cm^{-1} disappeared and the oxygen matrix became cloudy[38]. Product analysis at room temperature showed the formation of **15a** and 1,2,4-oxadisiletane **16a.** The intense band at 1078 cm^{-1} is ascribable to the characteristic O−O stretching mode of the disilirane−oxygen adduct **17** in the triplet state. Accordingly, the silicon−silicon bond with its low ionization energy easily donates σ-electrons to the oxygen molecule, thereby forming a CT complex. A calculation of vibrational frequencies predicts that the O−O stretching frequency of **17** should be near 1083 cm^{-1} and should shift to 1026 cm^{-1} upon double ^{18}O substitution. Thus, the labile intermediate which is formed in CT photooxygenation of **14** can be represented by structure **17**.

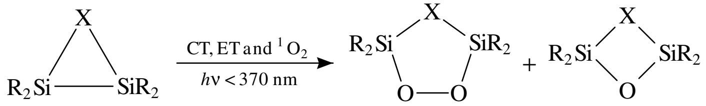

(14) **(15)** **(16)**

(a) R = Mes; X = CH_2
(b) R = Dip; X = O
(c) R = Dep; X = O
(d) R = Mes; X = O
(e) R = Xyl; X = O
(f) R = Mes; X = N-Ph

CT = hν (<370 nm)/O_2/C_6H_6 (3)
ET = hν (>400 nm)/O_2/DCA/CH_2Cl_2
or hν / MB/O_2/−78 °C/CH_2Cl_2
$^1O_2$ = hν/TPP/O_2/C_6H_6

(Dip = 2,6-i-$Pr_2C_6H_3$; Det:4-t-Bu-2,6-$Et_2C_6H_2$; Dep = 2,6-$Et_2C_6H_3$; Xyl = 2,6-$Me_2C_6H_3$)

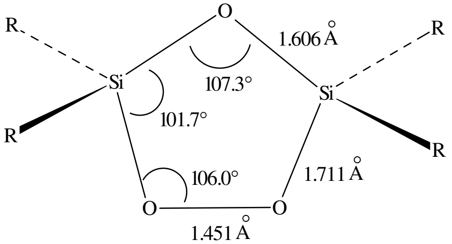

(15c)

FIGURE 4. X-ray structure analysis of **15c**

Irradiation of oxadisilirane **14c** in an acetonitrile–methylene chloride solvent mixture in the presence of 9,10-dicyanoanthracene (DCA) as the sensitizer with tungsten–halogen lamps under an oxygen flow resulted in the formation of **15c** in 69% yield[31]. In the absence of the sensitizer, no reaction occurred and **14c** was recovered quantitatively. A similar result was also obtained in the reaction of **14c** with $^3O_2$ in the presence of 10 mol% of tris(*p*-bromophenyl)aminium hexachloroantimonate $[(p\text{-BrC}_6H_4)_3N^+SbCl_6{}^-]$ as the single ET reagent, giving **15c** in 58% yield. The free-energy changes (ΔG) of -26.7 kcal mol^{-1} for electron transfer from **14a** to DCA and -23.0 kcal mol^{-1} in the case of **14c** are indicative of an exothermic ET. The DCA fluorescence was efficiently quenched by **14c** [$k_q = 1.12 \times 10^{10}$ (M s^{-1})]. The proposed mechanism for ET oxygenation of **14** is shown in Scheme 2. The initially formed radical cation $\mathbf{14}^{+\bullet}$ is attacked by either $O_2{}^{-\bullet}$ or $^3O_2$, directly giving **15** or $[[\mathbf{14}] \bullet O_2]^{+\bullet}$ as the intermediate (Scheme 2). In the

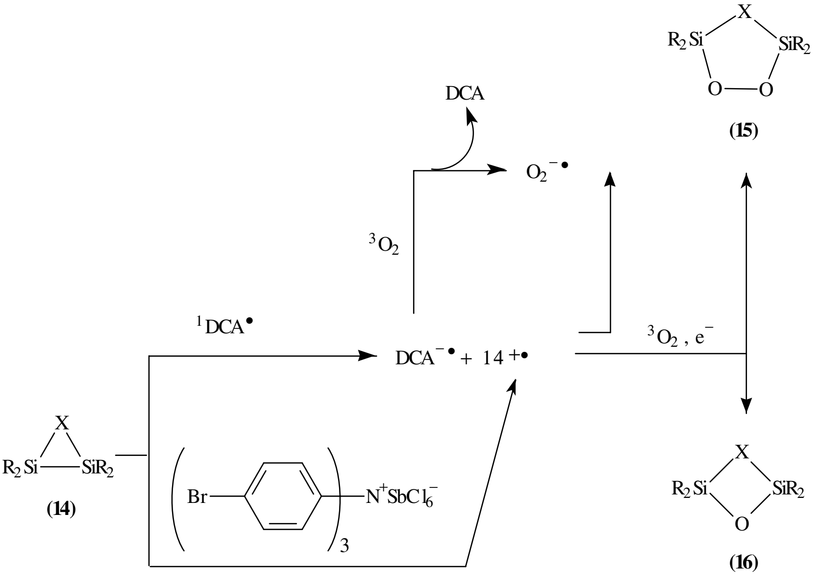

SCHEME 2

latter case, ET to $[[\mathbf{14}] \bullet O_2]^{+\bullet}$ affords **15**. It should be noted that participation of $O_2^{-\bullet}$ is excluded when $(p\text{-}BrC_6H_4)_3N^+SbCl_6^-$ is present.

Although singlet oxygen reacts with various electron-rich olefins and heteroatomic molecules, so far there have been no reports concerning direct reactions with σ-bonds. The photooxygenations of disiliranes **14b–f**, carried out in benzene with tetraphenylporphine (TPP) as the sensitizer, gave cyclic peroxides **15b–f** in 40–71% isolated yield with a small amount of monooxygenated products **16**[29–31,39]. The reactions were inhibited by addition of DABCO, a known $^1O_2$ quencher, whereas the addition of triphenylmethane, a free-radical scavenger, did not have any influence on the course of the reactions.

D. Stereochemistry and Azetidinium Imide Intermediate

DCA-sensitized photooxygenations of *cis*- and *trans*-**18** gave 68:32 and 41:59 mixtures of *cis*- and *trans*-**19**, respectively[31]. These results are in agreement with the formation of the open intermediate **17**, and the fact that rotation around the Si—O bonds is fairly competitive with the collapse to **19**. Similar results, i.e. nonstereospecific formation of *cis*- and *trans*-**19** with almost identical selectivity, were also observed in the contact CT oxygenation of *cis*- and *trans*-**19** with $(p\text{-}BrC_6H_4)_3N^+SbCl_6^-$ (Scheme 3 and Table 1). Moreover, stereochemical studies of singlet oxygenation were carried out. The TPP-sensitized photooxygenation of *trans*-**18** gave *trans*-**19** as the exclusive product in 84% yield. Similarly, photooxygenation of *cis*-**18** afforded only *cis*-**19** in 79% yield[31]. Clearly, the TPP-sensitized photooxygenations of *cis*- and *trans*-**18** proceed in a stereospecific manner, which is consistent with a peroxonium ion mechanism with **20** as the intermediate. A similar mechanism has been proposed for 1,2-dioxetane formation by $^1O_2$ (Scheme 4).

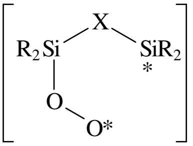

(17)

$* = \bullet$ or $+ / -$

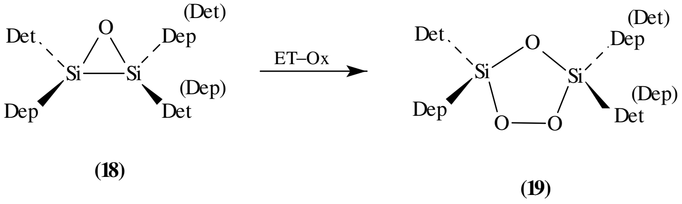

SCHEME 3. (For definition of Det and Dep, see equation 3)

4-Phenyl-1,2,4-triazoline-3,5-dione (PTAD) is a reagent which mimics the behavior of singlet oxygen. Thus it is capable of undergoing [2 + 2] and [2 + 4] cycloadditions, as well as ene reactions, and exhibits a similar reactivity toward azines and sulfides. Moreover, in most cases, similar mechanistic pathways have been proposed for both reagents, while in singlet-oxygen chemistry, the lifetime of intermediates is often too

TABLE 1

Substrate	Condition	Products and yields	
		19 (%)	*cis/trans*
cis-**18**	hν(λ > 400 nm)/O_2/DCA[a]/CH_2Cl_2	51	68/32
trans-**18**	hν(λ > 400 nm)/O_2/DCA[a]/CH_2Cl_2	35	41/59
cis-**18**	M.B.[b]/O_2/−78 °C/CH_2Cl_2	88	66/34
trans-**18**	M.B.[b]/O_2/−78 °C/CH_2Cl_2	95	42/58

[a] 9,10-Dicyanoanthracene.

[b] $(p\text{-}BrC_6H_4)_3N^+SbCl_6^-$; 10 mol%

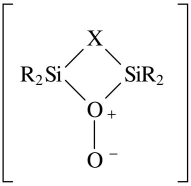

(20)

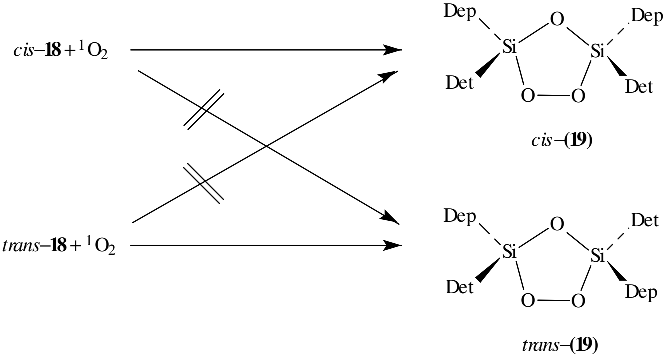

SCHEME 4

short to allow their direct detection. PTAD intermediates have a much longer lifetime and can be detected. Consequently, PTAD might be a useful reagent to obtain insight into the structure of reactive intermediates in the singlet oxygenation of disiliranes (**14** and **18**). As mentioned above, the results of addition reactions of singlet oxygen with strained silicon–silicon σ-bonds of disilirane derivatives (**14** and **18**) provide considerable evidence of peroxonium ion intermediates. This prompted us to investigate reactions of disiliranes with PTAD instead of singlet oxygen. Addition of PTAD to a $CHCl_3$ solution of 1,1,2,2-tetramesityldisilirane **14a** led to rapid disappearance of the red color of PTAD, and gave adduct **21** as colorless crystals in 38% isolated yield (69% yield in the crude reaction mixture as determined by ^1H NMR) (equation 4). The course of the reaction of PTAD with **14a** was monitored by ^1H, ^{13}C and ^{29}Si NMR spectroscopy at −78 °C. A series of new resonances in the ^{13}C NMR spectrum appeared at δ 157.29(s), 150.70(s), 143.73(s), 140.68(s), 141.39(s), 129.81(d), 129.62(d) 127.58(d), 126.48(d), 130.91(d), 129.32(d), 24.30(q), 23.61(q), 21.10(q) and 5.81(t) which gradually decreased at −55 °C, while those of **21** increased. The presence of two different carbonyl carbon resonances at δ 157.29 and 150.70 showed that the mirror plane orthogonal to the plane of the PTAD moiety is lost; similarly, the appearance of two signals for the diastereomeric methylene protons in the ^{1}H NMR spectra indicates a loss of symmetry. The 2D NMR and C−H COSY spectra imply the presence of a four-membered ring, as indicated by a comparison of the observed ^{13}C−^{1}H coupling constants with those of other cyclic disiletanes, thus the structure of the intermediate is best represented by the azetidinium structure **22**. The rate of disappearance of intermediate **22** has been measured by the integration of characteristic ^{1}H NMR signals at several temperatures; from these values an activation energy of 20.6 ± 2.0 kcal mol^{-1} required for the breakdown of **21** is calculated. A plausible rationale for these observations is that in the reaction of **14a** with PTAD, **22** is initially formed, which collapses to **21**, similar to the singlet oxygenation of **14a**. Meanwhile, comparable cycloadditions of cyclopropanes with PTAD have been reported. Roth and Martin[40] postulated the formation of a diradical intermediate in the reaction of PTAD with the strained central σ-bond of a bicyclo[2.1.0]pentane derivative. Nevertheless, although [$_\pi 2$ + $_\sigma 2$] additions have been a subject of continual interest, no direct observation of such intermediates has been reported so far. The above results provide not only proof of a peroxonium intermediate **(20)** in the singlet oxygenation of disiliranes, but also represent the first example of a direct observation of an intermediate in [$_\pi 2$ + $_\sigma 2$] addition.

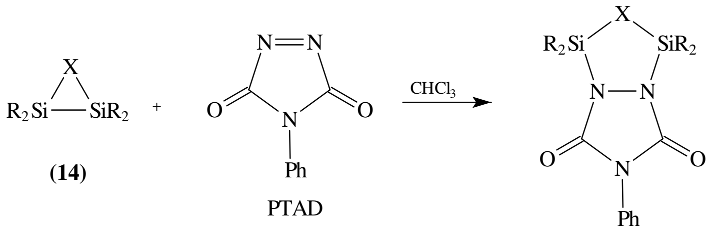

(14) PTAD **(21)** (4)

(a) R = Mes, X = CH$_2$
(b) R = Dip, X = O
(c) R = Dep, X = O

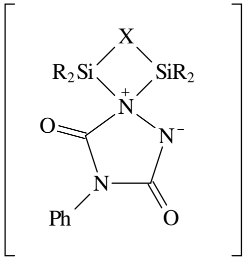

(22)

E. Cyclic Silathianes and Silaselenanes

1. Synthesis of cyclic silathianes and silaselenanes

Heterocycles containing group 14 elements[1,41−44] have received much attention in terms of both their chemistry and their use in material science. Cyclic silathianes were synthesized by the reaction of dihalosilanes or trihalosilanes with alkali sulfides or dihydrosilanes or trihydrosilanes with elemental sulfur (equation 5)[1,41b]. The facile syntheses of cyclosilachalcogenides by the reaction of halosilanes with alkali sulfides or selenides were reported by Thompson and Boudjouk (equation 6)[45]. Rauchfuss and coworkers[46,47] and Albertsen and Steudel[3] have reported the synthesis of silapolychalcogenides via silatitanacycles. Disilachalcogenides via disilatitanacycles and disilazirconacycles were reported[4,5]. Okazaki, Tokitoh and coworkers have devised a method to prepare silachalcogenanes bearing bulky groups (Scheme 5)[48–50].

$$\underset{M = \mathrm{Li, Na}}{M_2E + R_2SiCl_2} \xrightarrow[E = \mathrm{S, Se}]{} \underset{n = 2,3}{(R_2SiE)_n} \qquad (5)$$

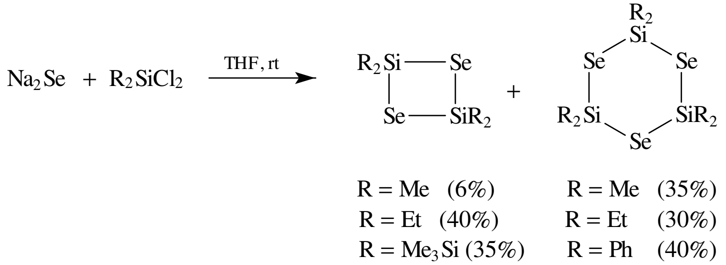

(6)

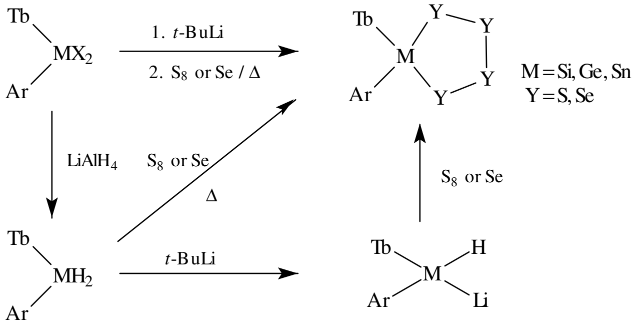

Tb = 2,4,6-Tris[bis(trimethylsilyl)methyl]phenyl
Ar = Mesityl or 2,4,6-Triisopropylphenyl

SCHEME 5

2. Syntheses of disilathianes via silametallacycles

The halides Ph_2SiCl_2, Ph_2GeBr_2 and Ph_2SnCl_2 react with Li_2S and $(\eta^5\text{-}C_5H_4R)_2TiCl_2$ (R = H, Me) to give the corresponding four-membered titanacycles $Cp_2TiS_2MPh_2$ (M = Si, Ge, Sn) (**23**) (equation 7). $Cp_2TiS_2SiPh_2$ (**23**) reacts with S_2Cl_2 to afford Ph_2SiS_4 (**24**) quantitatively (equation 8)[3]. Dimesityldichlorogermane reacted with 2 eq. of Li_2S and did not yield lithium germanedithiolate (**26**) but rather tetramesityl dithiadigermetane (**25**) (Scheme 6)[3]. On the other hand, dilithium dimesitylgermanedithiolate **26** was readily obtained by the treatment of a THF solution of $Mes_2Ge(SH)_2$ (**27**) with a THF solution of $LiBEt_3H$ at room temperature (equation 9). Successive addition of a THF solution of dichlorobis(η^5-cyclopentadienyl)titanium to $Mes_2Ge(SLi)_2$ (**26**) gave a germatitanacycle **28a** as a green crystalline solid in 70% yield (equations 9 and 10). Germazirconacycle **28b** was also obtained as a yellow solid in 90% yield in a similar manner. Germatitanacycle **28a** underwent ready substitution reaction at the titanocene moiety with S_2Cl_2 in CS_2 to give tetrathiagermolane **29** as a yellow oil in 53% yield (equation 11). When a toluene solution of **28b** and Ph_2GeCl_2 was refluxed for 20 hours, unsymmetric 1,3-dithia-2,4-digermetane **30** was prepared in 52% yield (equation 12).

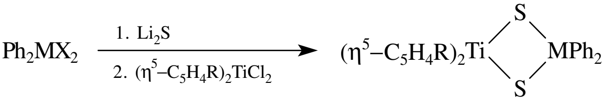

(7)

M = Si, Ge, Sn R = H, Me
X = Cl or Br

(23)

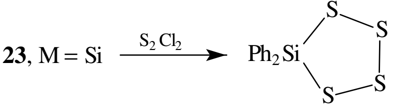

(8)

(24)

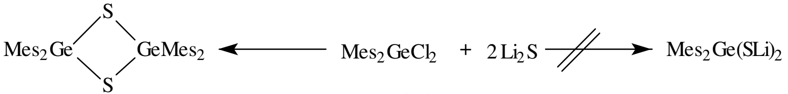

Mes = 2,4,6-trimethylphenyl

(25) **(26)**

SCHEME 6

$$Mes_2Ge(SH)_2 + 2\ LiBEt_3H \xrightarrow{\text{THF, rt}} \mathbf{26} \tag{9}$$

(27)

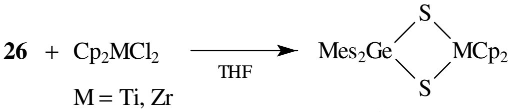

(10)

(28a) M = Ti
(28b) M = Zr

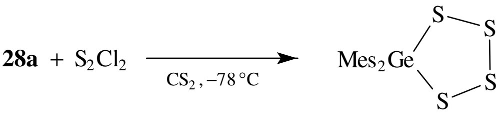

(11)

(29)

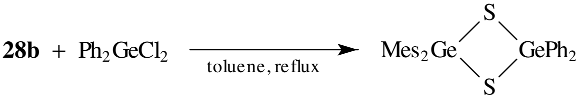

(12)

(30)

3. Syntheses of 1,4-dithia-2,3-disilametallacyclopentanes (32a and 32b)

Disilametallacyclopentanes, **32a** and **32b**, can be prepared from *meso*-1,2-di-*t*-butyl-1,2-diphenyldisilane-1,2-dithiol **(31)** in high yield (equations 13 and 14)[4,5]. Disilatitanacycle **32a** can be isolated as green crystals in 80% yield, and zirconacycle **32b** as a yellow crystalline solid in 90% yield. Disilatitanacycle **32a** is relatively stable toward moisture and air, but zirconacycle **32b** is unstable toward moisture and is air-sensitive.

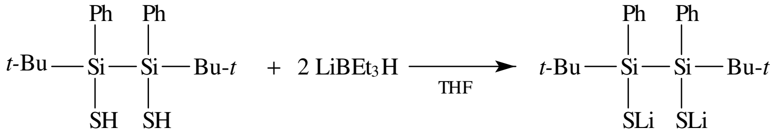

$$t\text{-Bu}-\underset{\text{SH}}{\overset{\text{Ph}}{\text{Si}}}-\underset{\text{SH}}{\overset{\text{Ph}}{\text{Si}}}-\text{Bu-}t + 2\,\text{LiBEt}_3\text{H} \xrightarrow[\text{THF}]{} t\text{-Bu}-\underset{\text{SLi}}{\overset{\text{Ph}}{\text{Si}}}-\underset{\text{SLi}}{\overset{\text{Ph}}{\text{Si}}}-\text{Bu-}t \qquad (13)$$

(31) *meso*

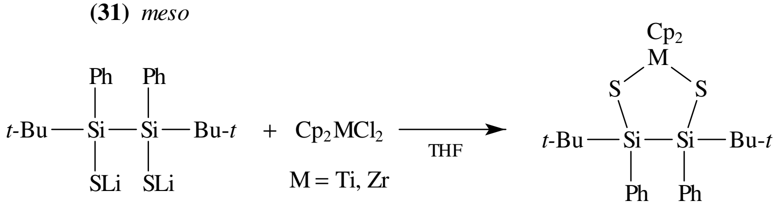

(14)

(32a) M = Ti
(32b) M = Zr

4. Reaction of disilametallacycle (32a and 32b) with various electrophiles

By using the disilametallacycles **32a** and **32b**, various disilaheterocycles are readily prepared under appropriate conditions, as shown in Scheme 7 and Table 2[4,5].

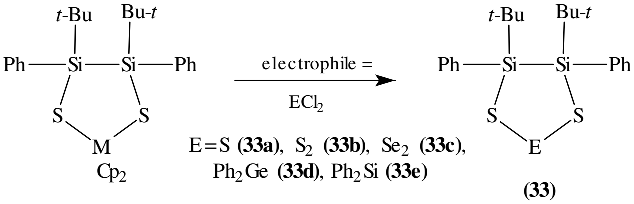

(32a) M = Ti
(32b) M = Zr

(33)

SCHEME 7

Although silyl-substituted sulfides are well known as sulfur-transfer reagents[51] by Si—S bond cleavage, the reaction of **32a** or **32b** with SCl_2 or S_2Cl_2 was performed on the site of Ti or Zr. The relative reactivity of the Ti—S and Si—S bonds in a four-membered TiS_2Si ring is explained by Rauchfuss and coworkers[47] as an example of frontier orbital control.

Treatment of disilametallacycles **32a** and **32b** with selenium monochloride at −78 °C affords the dithiadiselenadisilacyclohexane **33c** in 90–100% yield. Compound **33c** is stable at room temperature, but decomposes under irradiation, liberating selenium as a red precipitate to yield dithiaselenadisilacyclopentane. The reaction of **32a** with dichlorodiphenylgermane gives a corresponding dithiadisilagermacyclopentane

TABLE 2. Reactions of **32a** or **32b** with various electrophiles

Entry	Electrophile	Product	Solvent	Time (h)	Temp. (°C)	Yield (%)	
						32a	**32b**
1	SCl_2	**33a**	CS_2	0.5	−78	90	93
2	S_2Cl_2	**33b**	CS_2	0.5	−78	92	66
3	Se_2Cl_2	**33c**	CS_2	0.5	−78	90	quant.
4	Ph_2GeCl_2	**33d**	toluene	24	110	55	40
5	Ph_2SiCl_2	**33e**	xylene[a]	48	140	—	—

[a] Isomeric mixture.

derivative **33d.** On the other hand, the reaction of **32a** with halosilane to give dithiatrisilacyclopentane **33e** was unsuccessful, even under xylene reflux for 72 hours.

F. Reaction of Silathianes and Silaselenanes

1. Thermolysis or photolysis of cyclosilathianes and cyclosilaselenanes

Pyrolysis of cyclic silachalcogenides is a well-known route to reactive intermediates of the $R_2Si{=}X$ ($X = O, S, Se$) species (equation 15)[52]. $(Me_2SiSe)_3$ and $(Et_2SiSe)_3$ undergo ring transformation, photochemically and thermally, to form $(Me_2SiSe)_2$ and $(Et_2SiSe)_2$, respectively (equation 16)[53]. Photolysis or thermolysis of $(Me_2SiSe)_3$ or $(Me_2SiSe)_2$ in the presence of $(Me_2SiO)_3$ gives trioxatetrasilaselenocane derivative **(36)**, which is produced by trapping of silaneselone ($R_2Si{=}Se$, **35**) with $(Me_2SiO)_3$ (Schemes 8 and 9).

$$(R_2E-X)_n \xrightarrow{\Delta'} nR_2E = X$$

$$R = \text{alkyl, H, halogen; } E = Si, Ge; X = O, S, Se \tag{15}$$

$$2(R_2SiSe)_3 \longrightarrow 3(R_2SiSe)_2 \tag{16}$$

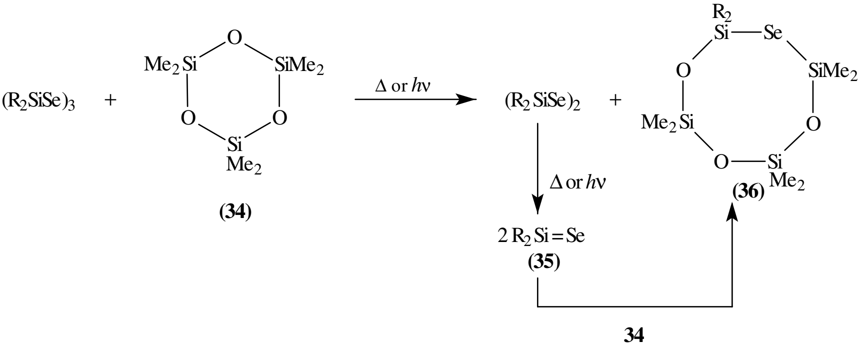

34

SCHEME 8

2. Dechalcogenation

Polychalcogenasilane is a good precursor of silanechalcogenone (equation 17)[48–51]. Desulfurization of polychalcogenadisilane **33a** and **33b** gives 1,3-cyclodisilathiane **(37)**.

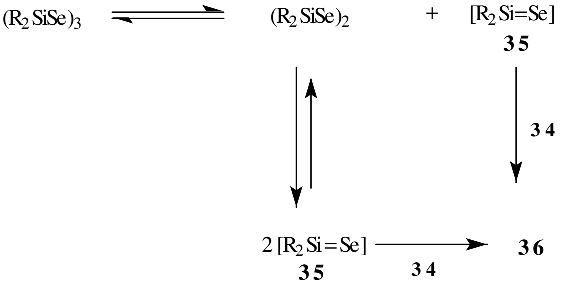

SCHEME 9

Desulfurization of **33a** by PPh_3 (1.1 eq.) gives 2,4-di-*t*-butyl-2,4-diphenyl-1,3-dithia-2,4-disilacyclobutane **37** containing *cis*- and *trans*-isomers (ratio: *cis*/*trans* = 1/9) without 1,2-dithia-3,4-disilacyclobutane **36**, as shown in Scheme 10. The desulfurization of **33a** by hexamethylphosphorous triamide at room temperature also gave similar results. A mixture of *cis*- and *trans*-isomers of **37** was also obtained from desulfurization of **33b** (*cis*). The formation of **37** suggests two plausible routes, as shown in Scheme 11. One possible route is an intramolecular rearrangement via an intermediate **36.** The stereospecific rearrangements of 1,2-dioxa-3,4-disilacyclobutanes to 1,3-dioxa-2,4-disilacyclobutanes are reported by West and coworkers[26]. Since this reaction is not stereospecific, the first route (a) is not likely. Another, more likely route is (b), which is the dimerization of thioxosilane derivative **39**.

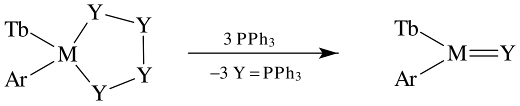

(17)

M = Si, Ge, Sn
Y = S, Se, Te
Tb = 2,4,6-$\{(Me_3Si)_2CH\}_3C_6H_2$
Ar = 2,4,6-$R_3C_6H_2$ (R=Me, *i*-Pr)

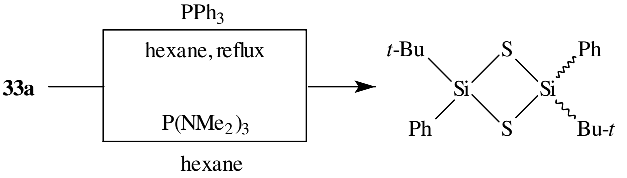

(37)

cis : *trans* = 1 : 9

SCHEME 10

G. Structures of Cyclic Silathianes

*1. Structures of dithiadisilatitanacycle **32a**, trithiadisilacyclopentane **33a** and cyclodisilathiane **37***

The titanacycle **32a** exhibits a half-chair conformation as depicted in Figure 5. The Ti−S bond lengths (2.430 Å and 2.437 Å) are within the normal range (2.42–2.45

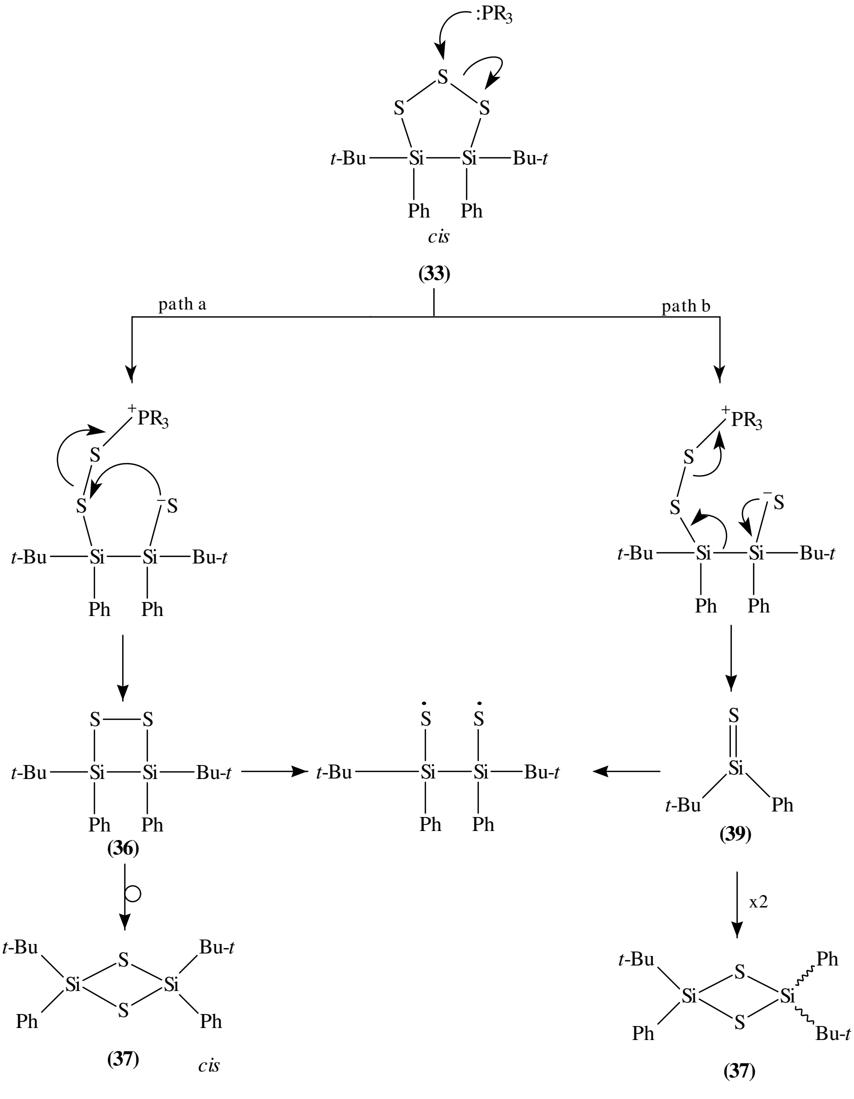

(a) 1, 4- Attack by the thiolate ion

(b) 1, 2- Attack by the thiolate ion

SCHEME 11

Å[46]), the Si−S bonds (2.13 Å) are slightly shortened (usually 2.16−2.17 Å)[46]. Interestingly, the Ti−S−Si bond angles (113.0° and 108.4°) are larger than those of other five-membered dithiatitanacycles [e.g. *o*-(−SC_6H_4S−)$TiCp_2$: 95.7−97.0°[54]; (−SCH=CHS−)$TiCp_2$: 94.2−95.0°[55]] and resemble those of acyclic derivatives [e.g. $Cp_2Ti(SPh)_2$: 113.6−115.5°[56]]. On the other hand, the S−Ti−S bond angle (93.9°) takes

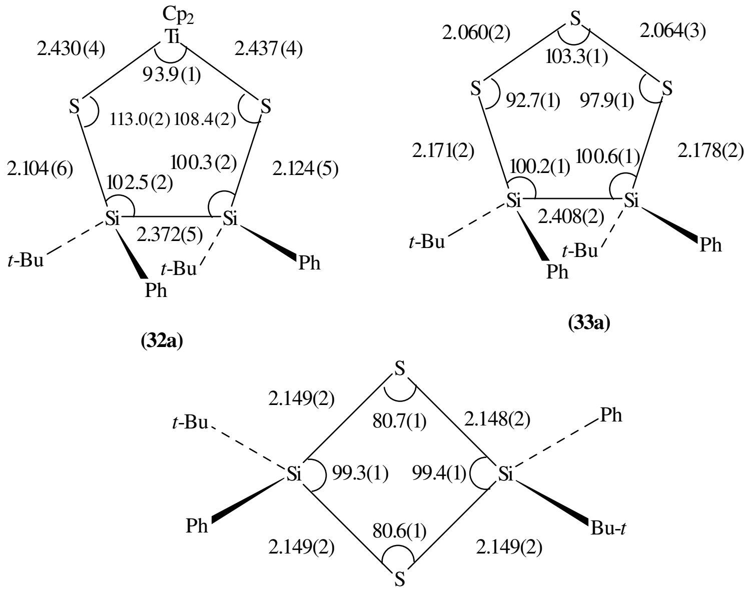

(32a)

(33a)

(37)

FIGURE 5. Bond distances and angles of **32a**, **33a** and **37**.

an intermediate value between five-membered titanacycles [e.g. *o*-($-SC_6H_4S-$)$TiCp_2$: 82.2°[54]; ($-SCH{=}CHS-$)$TiCp_2$: 83.2°[55]] and acyclic ones [e.g. $Cp_2Ti(SPh)_2$: 99.3°[56]]. The trithiadisilacyclopentane skeleton in compound **33a** has a half-chair conformation. The central four-membered ring of **37** was found to be completely planar (dihedral angle; S1$-$Si1$-$Si2$-$S2 $=$ 0.7°). The Si$-$S bond lengths [2.148(2)–2.149(2) Å] are within the normal range[46]. The Si$-$S$-$Si angles [80.64(6) and 80.66(6)°] are smaller than those of other cyclodisilathianes [e.g. tetramethylcyclodisilathiane 82.46(6)°[57]; tetra-*t*-butoxycyclodisilathiane 82.2(1)°[58]] and the S$-$Si$-$S angles [99.40(7) and 99.30(7)°] are larger than those of other cyclodisilathiane derivatives [97.54(7)[57] and 97.8(1)°[58]]. Nonbonding Si- - -Si and S- - -S distances are 2.78 and 3.28 Å, respectively, which are within the normal range of those of cyclodisilathianes $(R_2Si)_2S_2$ [Si- - -Si; R $=$ Me, 2.837(2)[57]; R $=$ Cl, 2.725(1)[59]; R $=$ Br, 2.741(6)[59] Å].

III. BICYCLOSILACHALCOGENIDES

A. Introduction

There has been considerable interest in the chemistry of group 4 propellanes **(40a)** and bicyclo[1.1.1]pentanes **(41b)** in view of the nature of the bridgehead bonds[60]. Pentasila[1.1.1]propellane has not been isolated as yet, although a derivative of bicyclo[1.1.1]pentasilane[61] has been synthesized. According to both calculations and experiments, M$-$M distances in [1.1.1]propellanes (M $=$ C, Si, Ge, Sn; Y $=$ CH_2, SiH_2, GeH_2, SnH_2) are much shorter than those in bicyclo[1.1.1]pentanes except for the

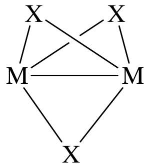

(40)

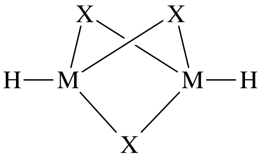

(41)

M = C, Si, Ge
X = CH_2, SiH_2, GeH_2, O, S, Se

TABLE 3. Calculated atomic distances (Å) and angles (deg) of disilabicyclo[1.1.1]pentane derivatives.^{a}

X	Atomic distance or angle	**40** (M = Si)	**41** (M = Si)
(a) SiH_2	Si_b- - -Si_b	2.719	2.915
	Si_p- - -Si_p	2.347	2.364
	Si_b−Si_p−Si_b	70.8	76.2
(b) O	Si- - -Si	2.089	2.060
	Si−O	1.714	1.698
	Si−O−Si	75.1	74.7
(c) S	Si- - -Si	2.347	2.363
	Si−S	2.171	2.176
	Si−S−Si	65.4	65.8
(d) Se	Si- - -Si	2.457	2.484
	Si−Se	2.340	2.339
	Si−Se−Si	63.3	64.1

^{a}Si_b denotes bridgehead Si, Si_p denotes peripheral Si.

tin analogue[60−74]. Theoretically, substitution of electronegative groups relative to silicon (e.g. O, CH_2) at the peripheral positions should stabilize the central M−M interaction for M = Si[72]. Therefore, the structures of [1.1.1]propellanes of the type M_2 X_3 [M = Si, Ge, Sn; Y = O, S, Se] **(40)** and the corresponding bicyclo[1.1.1]pentanes $H_2M_2X_3$ **(41)** are very similar. The calculated geometries of silicon analogues are shown in Table 3[70,73,74b]. According to theoretical studies, trioxadisilabicyclo[1.1.1]pentane **(41b)** is predicted to have a short distance between the bridgehead silicon atoms of only 2.060 Å[74a]; this is shorter than that of a silicon−silicon double bond. The corresponding distance in the sulfur analogue, trithiadisilabicyclo[1.1.1]pentane (**41c**), has been predicted to be 2.363 Å[74a], which corresponds to a Si−Si single bond. Trithiadisilabicyclo[1.1.1]pentane derivative and its selenium analogue were isolated by the introduction of the bulky substituent, tris(trimethylsilyl)methyl group, on the silicon atom[14,15]. The next section will describe the synthesis and reactivities of polychalcogenadisilabicyclo[*k*.*l*.*m*]alkanes.

B. Synthesis and Reactions

Chalcogenation of conventional substituted trihydrosilanes gives silachalcogenides having adamantane skeletons (see Section IV.B)[12−15,75]. Tris(trimethylsilyl)methylsilane ($TsiSiH_3$) (**42**, M = Si) reacts with elemental sulfur to give 2,4,5,6-tetrathiadisilabicyclo[2.1.1]hexane derivative (**43a**, 22% yield) along with $(TsiSi)_2S_5$ (**44a**, 12%) and $(TsiSi)_2S_6$ (**45a** 12%) as shown in equation 18 and Table 4. Bicyclosilathianes **43**−**45** (M=Si) are stable toward air and moisture. The structures of polythiadisilabicyclo[*k*.*l*.*m*]alkanes **43a, 44a** and **45a** are confirmed by X-ray structure analysis to be 2,4,5,6-tetrathia-1,3-disilabicyclo[2.1.1]hexane, 2,4,5,6,7-pentathia-1,3-disilabicyclo[2.2.1]heptane and 2,4,5,6,7,8-hexathia-1,3-disilabicyclo[3.2.1]octane, respectively. The reaction of $TsiGeH_3$ with elemental sulfur gave 2,4,5,6,7,8,9-heptathia-1,3-disilabicyclo[3.3.1]nonane **46a** along with **43a, 44a** and **45a** (equation 18 and Table 4). Trithiadisilabicyclo[1.1.1]pentanes **47a** can be synthesized by photolysis of tetrathiadisilabicyclo[2.1.1]hexane in the presence of trimethylphosphine or triphenylphosphine in 100% or 64% yield, respectively. Tetraselenadisilabicyclo[2.1.1]hexane can be prepared by the reaction of $TsiSiH_3$ with selenium/1,8-diazabicyclo[5.4.0]undec-7-ene. Triselena-1,3-disilabicyclo[1.1.1]pentane and its germanium analogue can be prepared in a similar manner (Scheme 12).

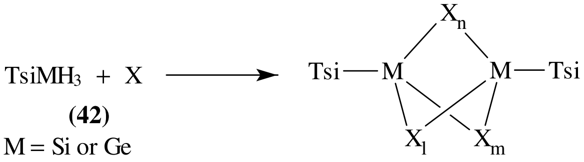

(42)

M = Si or Ge

$Tsi = C(SiMe_3)_3$ $X = S_8$ or Se

(43) – **(46)**

(a) M = Si; (b) M = Ge

$k+l+m = 4–7$

(18)

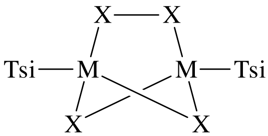

(43)

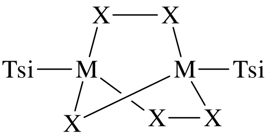

(44)

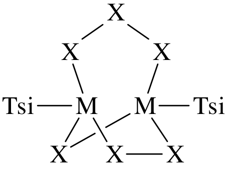

(45)

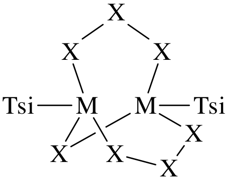

(46)

TABLE 4. Yield and reaction conditions in equation 18

M	X	Reaction conditions		Yield (%)			
				43	**44**	**45**	**46**
			[*k.l.m*]	[2.1.1]	[2.2.1]	[3.2.1]	[3.3.1]
Si	S_8	30 eq. decalin, 190–200 °C		22	12	12	—
	Se	10 eq. decalin, DBU 160 °C		19	—	—	—
Ge	S_8	30 eq. Ph_2O, 150–160 °C		8	8	26	9
	Se	10 eq. decalin, DBU 160 °C		19	12	27	—

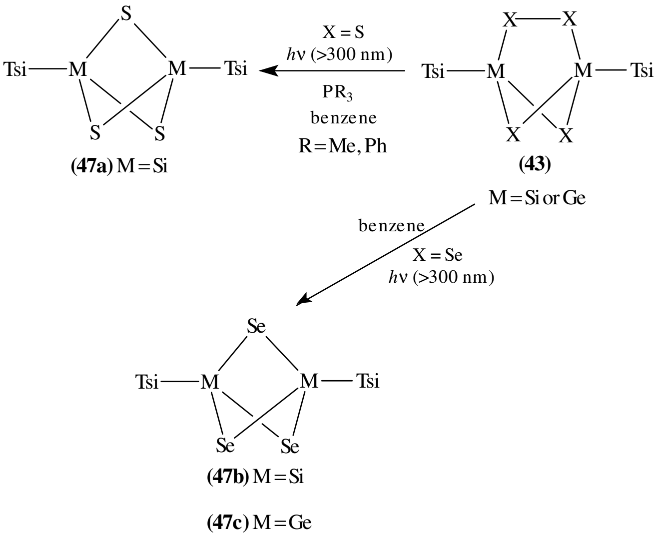

SCHEME 12

C. Structure

1. X-ray analysis of polythiadisilabicyclo[k.l.m]alkanes and polyselenadisilabicyclo[k.l.m]alkanes

The results of single-crystal X-ray diffraction analyses of polychalcogenadisilabicyclo-[*k.l.m*]alkanes are summarized in Figures 6 and 7 and Tables 5 and 6.

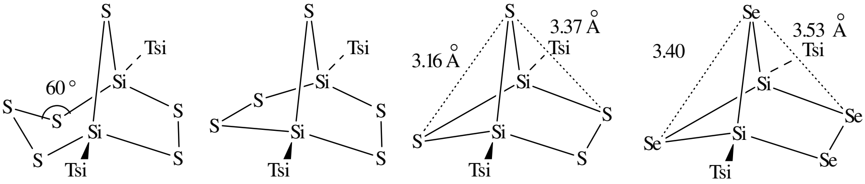

(45a) **(44a)** **(43a)** **(43b)**

FIGURE 6. Structures of polythiadisilabicyclo[*k.l.m*]alkanes

The five-membered ring in bicyclo[2.1.1]hexane skeleton is an envelope conformation, and torsion angles of Si−S−S−Si = 0.05–0.08°. The structure of **47a**[13] is in good agreement with the results of the quantum chemical calculation[73,74], which is reported by Gordon and coworkers as shown in Table 3. The bicyclo[1.1.1]pentane skeleton is constructed from three cyclobutanes (dihedral angles of each of the cyclobutanes are 120.40°, 119.75° and 118.85°, av. 120.0°). The nonbonding Si- - -Si distances of **44a, 43a** and **47a** are 3.00, 2.66 and 2.407 Å. The Si−S−Si angles of **44a, 43a** and **47a** are 89.2°, 75.9° (av.) and 67.08° (av.). Considering the common Si−S−Si angles (*ca* 82°)[76–79] in

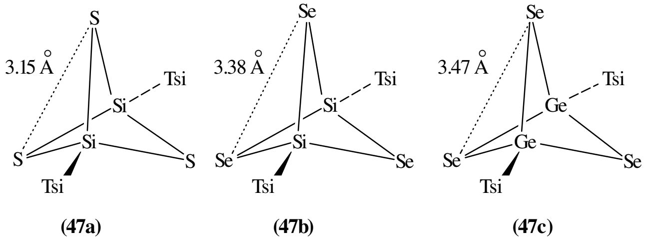

FIGURE 7. Structures of 2,4,5-trichalcogena-1,3-disila- and digerma-bicyclo[1.1.1]pentanes

TABLE 5. Atomic distances, angles and UV absorptions of **43a**, **43b**, **44a** and **45a**

X = S or Se	**43a**	**43b**	**44a**	**45a**
Si−X bond distance	2.160–2.180 Å	2.234–2.325 Å	2.128–2.168 Å	2.122–2.183 Å
Si- - -Si distance	2.66 Å	2.82 Å	3.00 Å	3.21 Å
S−S bond distance	2.096 Å	2.353 Å	2.035 Å	2.028, 2.073 Å
Si−X−Si angle	75.9°	74.8, 77.9°	89.2°	108.7°
X−Si−X angle	94.1, 102.2°	95.9, 100.9°	101.5–106.4°	102.5–109.3°
Si−X−X−Si torsion angle	0°	0°	11–19°	22°
UV λ_{max} (nm)	280 ($\varepsilon = 320$), 366 ($\varepsilon = 41$)	290 ($\varepsilon = 470$), 440 ($\varepsilon = 48$), 458 ($\varepsilon = 48$), 505 ($\varepsilon = 25$)	287 ($\varepsilon = 365$), 375 ($\varepsilon = 200$)	265 ($\varepsilon = 2200$), 350 ($\varepsilon = 340$)

TABLE 6. Atomic distances, angles and UV absorptions of **47a**, **47b** and **47c**

M = Si, Ge X = S, Se	**47a**	**47b**	**47c**
M−X bond distance	2.171–2.186 Å	2.316–2.327 Å	2.398–2.412 Å
M- - -M distance	2.407 Å	2.515 Å	2.672 Å
M−X−M angle	67.08°	65.54°	67.45°
X−M−X angle	91.76–92.87°	93.61°	92.15°
UV λ_{max} nm	257 ($\varepsilon = 210$), 290 ($\varepsilon = 38$)	300 ($\varepsilon = 300$), 366 ($\varepsilon = 33$)	265 ($\varepsilon = 4220$), 365 ($\varepsilon = 100$)

cyclodisilathianes, these Si−S−Si values of **43a** and **47a** are extremely sharp. Especially, in **47a** the acute Si−S−Si angles [66.88(3)°, 66.98(3)° and 67.27(4)°] can be regarded as angles of three-membered ring compounds rather than those of normal four-membered ring compounds. One of the features of **47a** is a very short S- - -S distance, 3.15 Å, which is within the sum of van der Waals radii of sulfur (3.70 Å). Interestingly, the bridgehead Si- - -Si distance of 2.407 Å lies within the range of common Si−Si single bond lengths (2.23–2.70 Å)[80], and is *ca* 0.1 Å shorter than that of its selenium analogue (2.515 Å)[15]. This value is very short relative to that of the cyclodisilathianes (2.78–2.83 Å)[76–79]. This unusual shortening of the Si- - -Si distance is caused by the difference in electronegativity between the peripheral sulfur atom and the bridgehead silicon atom. Actually, no such shortening is observed in the corresponding silicon analogue, bicyclo[1.1.1]pentasilane (Si- - -Si, 2.92 Å)[81]. The repulsion between sulfur atoms affects the shortening of the Si- - -Si distance of **47a.** Then the unusual short Si- - -Si distance is due to the geometrical factor, thus a tug-of-war between the three Si−S−Si and six S−Si−S angles occurs.

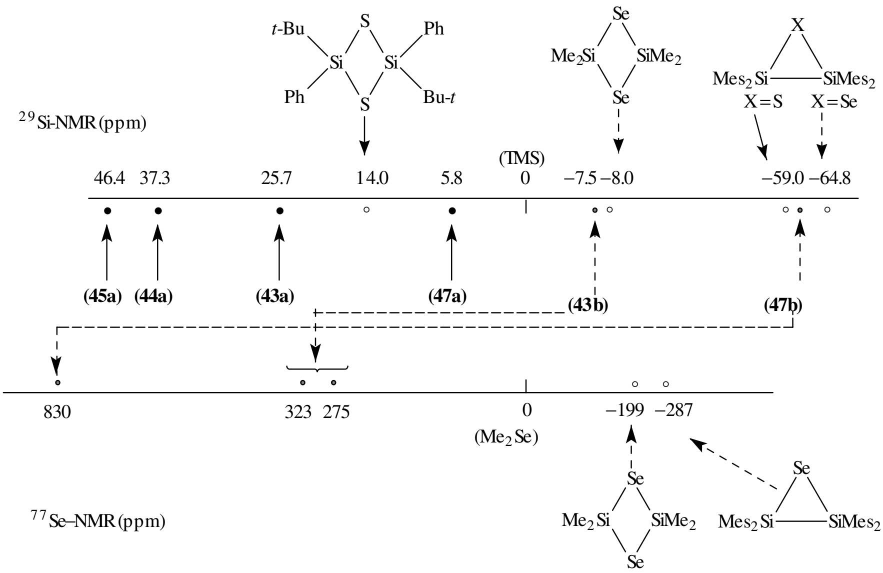

FIGURE 8. ^{77}Se and ^{29}Si-NMR data of cyclosilthianes and cyclosilselenane

D. Spectroscopic Data

1. NMR spectra of trithia- and triselena-disilabicyclo[1.1.1]pentanes

^{29}Si NMR chemical shift of the bridgehead silicons in **45a, 44a, 43a** and **47a** are 46.4, 37.3, 25.7 and 5.8 ppm, which are in the order of the strain of silathiane rings (Figure 8). On the other hand, the shifts of **43b**[14] and **47b**[15] are −7.5 and −59.0 ppm, respectively. The difference of the bridgehead silicons chemical shift between **47a** and **47b** is derived from the stereo-compression effect between the peripheral atoms[75].

2. UV spectra of polythiadisilabicyclo[k.l.m]alkanes

Although the absorption maximum of polysulfides in the UV-VIS spectrum is shifted to longer wavelengths with the number of sulfur atoms[82], that of cyclic polysulfides is shifted to shorter wavelengths with the number of ring atoms[83]. The smaller dihedral angle of cyclic polysulfides is responsible for the increase of the ring strain. Typical cyclic disulfides, tetramethylene disulfide and trimethylene disulfide have dihedral angles (C−S−S−C) of 60° and 27° and absorption maxima at 286 and 330 nm, respectively[83]. Interestingly, **43a** has a dihedral (Si−S−S−Si) angle of 0° and the absorption maximum is at 366 nm. Compound **44a** has also small dihedral angles of Si−S−S−Si, 11° and 19°, and absorption maximum at 375 nm. The longer wavelength of 375 nm in **44a** than in **43a** is due to the through-space interaction between the two intramolecular disulfides. A remarkable S- - -S interaction in **47a** was observed by the 290 nm maximum (ε 38) in the electronic spectrum. The following two reasons were invoked that the weak but definite absorption at 290 nm was assigned as originating from the S- - -S interaction in **47a**. Firstly, cyclodisilathiane **48** does not have a definite absorption around 290 nm. It suggests that the absorption of 290 nm in **47a** is not derived from the Si−S bond. Secondly, the selenium analogue **47b** displays an absorption band at 365 nm (ε 33)[14].

Moreover, **47c** also exhibits an absorption maximum in the same region (365 nm). It was concluded that the absorption at 365 nm was derived from Se- - -Se interaction[75].

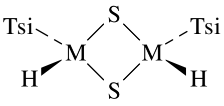

(48)

E. Reactions

1. Hydrolysis of trithiadisilabicyclo[1.1.1]pentane

Trithiadisilabicyclo[1.1.1]pentane **47a** is thermally quite stable (>300 °C) but is slowly hydrolyzed by moisture to provide 1,3-bis{tris(trimethylsilyl)methyl}-1-hydroxy-3-mercaptocyclodisilathiane **49**, which was further hydrolyzed to 1,3-bis{tris(trimethylsilyl)methyl}-1,3-dihydroxy-1,3-dimercaptosulfide **50** (equation 19)[13,14].

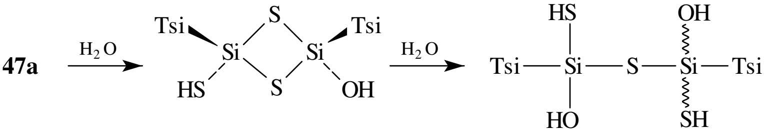

(49) **(50)** *dl* : *meso* = 1:1

(19)

2. Oxidation of trithiadisilabicyclo[1.1.1]pentane

Oxidation of trithiadisilabicyclo[1.1.1]pentane **47a** by 1 eq. of *m*-chloroperbenzoic acid (*m*-CPBA) gives 27% of the ring expansion product **51** and recovered **47a** in 37% yields, respectively (equation 20)[84]. By using 2 eq. of *m*-CPBA, **51** is obtained in 62% yield.

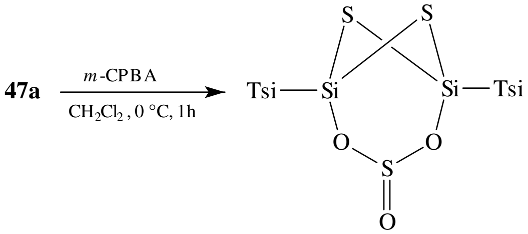

(51)

(20)

IV. TRICYCLOSILACHALCOGENIDES

A. Introduction

In the series of sesquichalcogenides containing group 14 elements, the structures of sesquisulfides and sesquiselenides are known to have adamantane **(2)** and double-decker **(3)** skeletons. On the other hand, sesquioxides have prismane **(4)** or cubane (**5**) skeletons. Neither adamantane nor double-decker type silsesquioxanes have been synthesized. These results are due to the M−X−M angles, i.e. the M−O−M angle is much larger than the M−S−M or M−Se−M angles. There are nor-adamantane

(52), bis-nor-adamantane (**53**), nor-double-decker **(54)** and bis-nor-double-decker (**55**) type cage compounds, which are derived from the removal of one or two chalcogen atoms from adamantane or double-decker type sesquichalcogenides (Scheme 13). In this section, adamantane and double-decker type sesquichalcogenides and their nor- and bis-nor derivatives are reviewed.

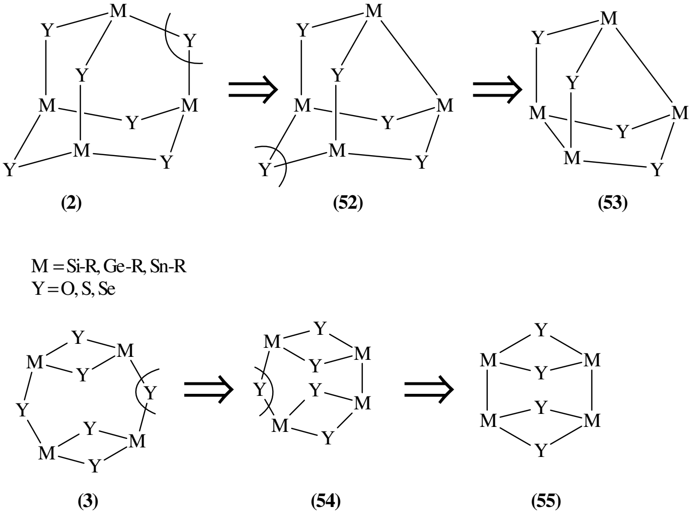

SCHEME 13

B. Synthesis and Reactions

1. Adamantane and double-decker type

Adamantane-type silathianes can be made by heating organosilanes with hydrogen sulfide or elemental sulfur. The tricyclic silathianes are also synthesized by the reaction of halosilanes with sulfurization reagents, e.g. Li_2S, Na_2S, $(Me_3Si)_2S$ and H_2S (Scheme 14). Phenyl or *t*-butyltrichlorosilane reacts with Na_2S to afford adamantane skeleton silsesquisulfides **(56)**. These bulky substituted trichlorosilanes do not react with H_2S/pyridine or $(NH_4)_2S_5$ (equation 21). On the contrary, halogermane or halostannane easily reacts with H_2S/pyridine or $(NH_4)_2S_5$ to afford **57** (equation 22). Silaselenides

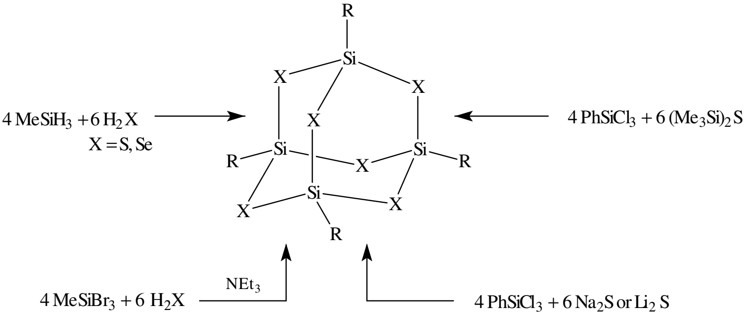

SCHEME 14

with adamantane skeleton **(58)** are also prepared by the reaction of methyl- or ethylsilane or halosilanes with H_2Se[8,85]. Adamantane-like structure silaselenanes are prepared by reaction of organochlorosilanes with Na_2Se in improved yields (equation 23)[86]. The double-decker structure silathiane is one of two reasonable isomers from these reactions. In 1996, the first example of double-decker type silsesquisulfide **(59)** was reported by Matsumoto and coworkers using the conventional method (equation 24)[87]. Both adamantane and double-decker type isomers can be made by sulfurization of halogermanes[88]. Treatment of *tert*-butyltrichlorogermane **(60a)** with H_2S/pyridine in refluxing benzene yields adamantane-type sesquisulfide **(61a)** of the stoichiometry $(t\text{-}BuGe)_4S_6$ in 67% yield. When this reaction is carried out at room temperature, two diastereomeric bis(germanethiols) (**62a**) are formed in 43% yield (Scheme 15). The latter thermally releases H_2S to afford **61a**[6]. Tetra(*t*-butylgermanium)sesquichlorosulfide and selenide are prepared by using 5/4 equivalents of Na_2Y (Y = S, Se) (equation 25)[89]. By using 1/2 equivalent of Li_2S, sesquisulfide having nor-adamantane skeleton **(64a)** is yielded along with **63a** (Scheme 15)[88].

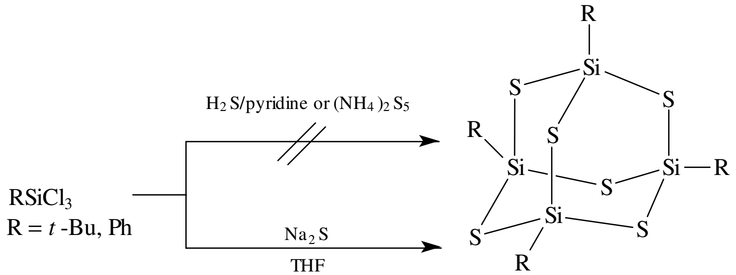

(56)

(21)

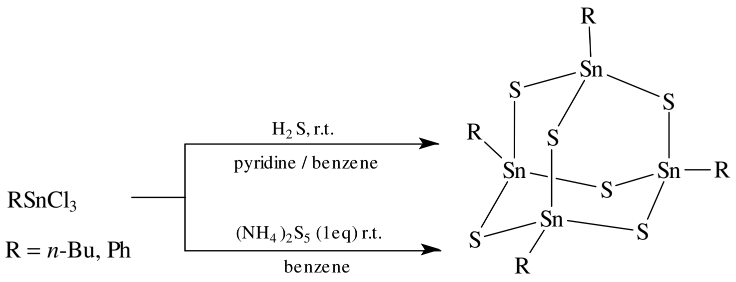

(57)

(22)

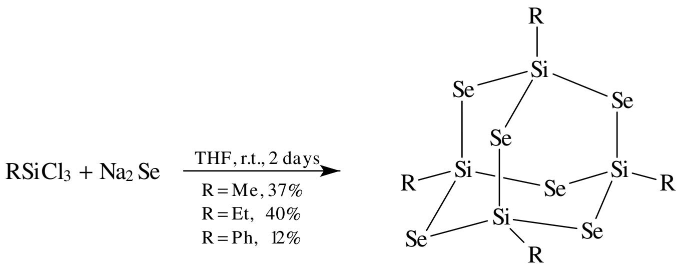

(58)

(23)

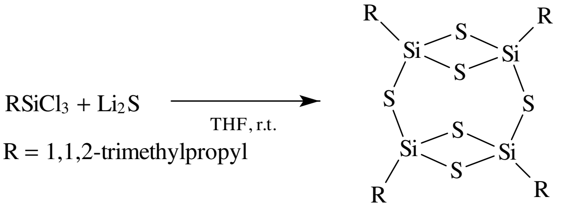

(59)

(24)

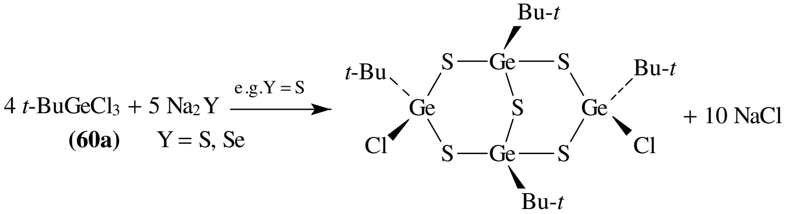

(63a)

(25)

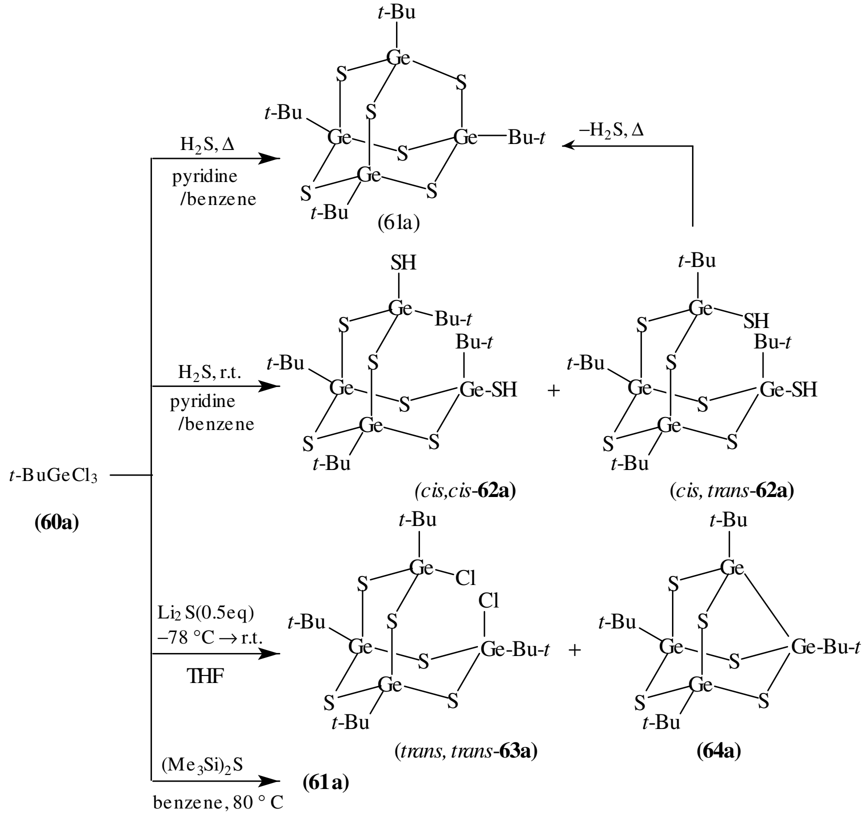

SCHEME 15

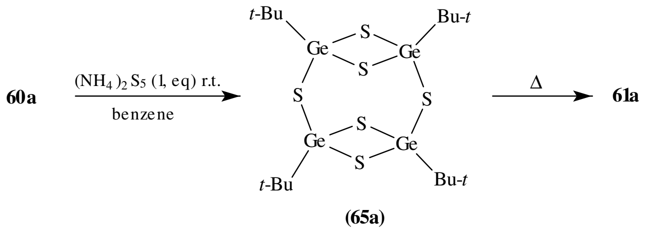

SCHEME 16

On the other hand, when ammonium pentasulfide is applied as the sulfur source, sesquisulfide **65a** is obtained in 30% yield (Scheme 16). Unfortunately, ^{1}H and ^{13}C NMR data of **65a** and **61a** cannot distinguish between the double-decker and adamantane-type structures. It is possible to distinguish both structures by Raman spectroscopy. Thus in the range of the Ge−S framework vibrations (200–650 cm^{-1}), the Raman spectrum of **65a** exhibits six bands, whereas that of **61a** only gives two bands. This observation does not only allow differentiation of the two isomers, but also reveals that the molecular symmetry of **65a** (D_{2h}) is lower than that of **61a** (T_d). Furthermore, the rearrangement of **65a** to **61a** was followed by Raman spectroscopy, i.e. five bands of **65a** vanished and simultaneously a strong band of **61a** appeared. According to X-ray analysis of the double-decker structure type **65a**, the molecule crystallographically possesses three orthogonal 2-fold axes. The Ge atoms and S atoms form two four-membered and two eight-membered rings which are mutually perpendicular; the four-membered rings are almost planar.

This unique formation of the double-decker structure is highly dependent on the correct choice of the substituents. When the reaction is performed with $MesGeCl_3$ (Mes = 2,4,6-trimethylphenyl) **(60b)** instead of *tert*-butyltrichlorogermane **(60a)**, only the adamantane-like sesquisulfide **(61b)** is formed (Scheme 17).

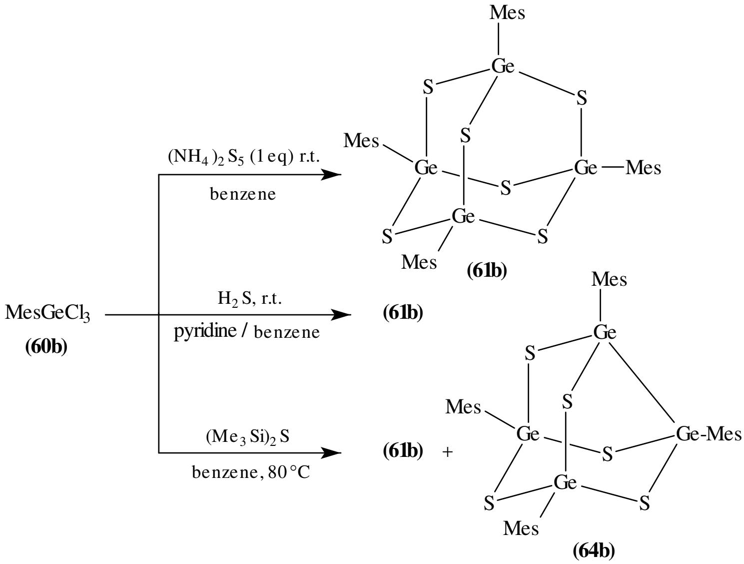

SCHEME 17

2. Nor- and bis-nor-adamantane type sesquichalcogenides

The reaction of tetrachlorodisilane with chalcogenation reagents is one of the synthetic methods to bis-nor-adamantane or double-decker type compounds. When a solution of di-*tert*-butyltetrachlorodisilane **66** in THF is refluxed together with one equivalent of lithium sulfide or stirred with lithium selenide at room temperature, the tetra(*tert*-butylsilicon)pentachalcogenides **67** and **68**, respectively, are formed (Scheme 18)^6. Each pentachalcogenide exhibits one resonance of a *tert*-butyl group in the ^{1}H and ^{13}C NMR spectra. Most likely, the bis-nor-adamantane derivatives **69** and **70** are initially formed. Insertion of a sulfur or selenium atom into one of the two strained Si−Si bonds would then lead to the observed products.

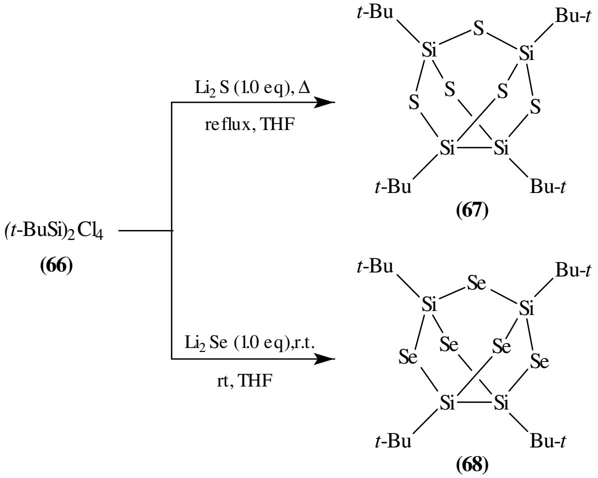

SCHEME 18

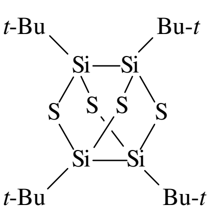

(69)

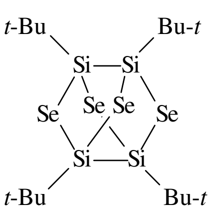

(70)

On the other hand, when di-*tert*-butyltetrachlorodigermane **(71)** is reacted with lithium sulfide at −78 °C, the corresponding bis-nor-adamantane **72** is formed along with pentasulfide **(64a)** (Scheme 19). Presumably, due to the long Ge−Ge bond distance, **72** is less strained than the silicon analogues **69** and **70**, and thus sulfur insertion is less favored.

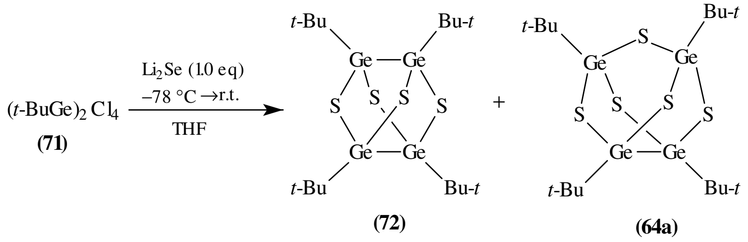

SCHEME 19

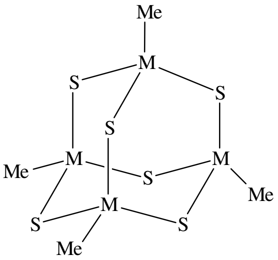

M	S—M—S (°)	M—S—M (°)	M—S (Å)
C	110.4	107.2	1.84
Si	111.8(2)	104.5(3)	2.129(2)
Ge	111.8(3)	104.6(2)	2.218(3)
Sn	111.3(6)	105.7(2)	2.392(3)

FIGURE 9. Bond distances and angles of adamantane-type sesquisulfides.

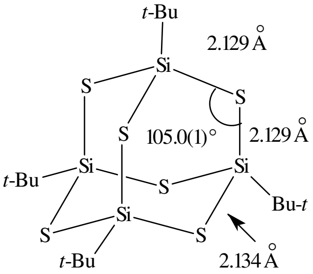

(56), R = *t*-Bu

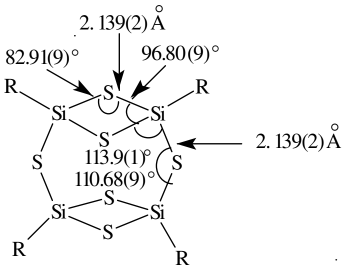

(59) R = 1,1,2-trimethylpropyl

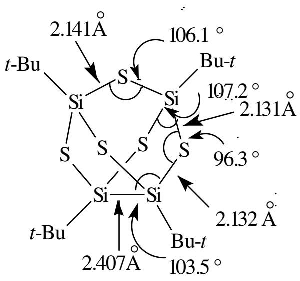

(67)

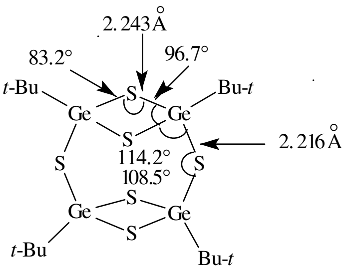

(65a)

FIGURE 10. Bond distances and angles of **56**, **59**, **67** and **65a**.

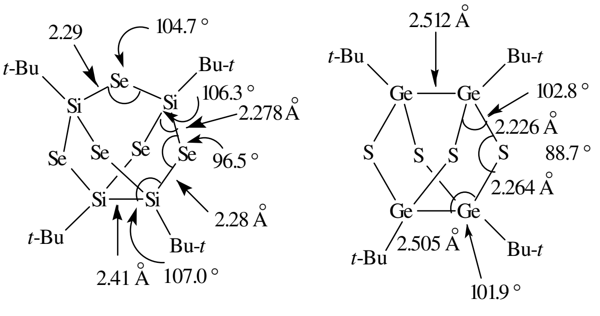

(68) **(72)**

FIGURE 10. Bond distances and angles of **68** and **72**

C. Structure

1. Adamantane and double-decker type sesquichalcogenides

Structures of adamantane and nor-adamantane type silsesquichalcogenides are shown in Figure 9[90] and Figure 10 along with those of adamantane, nor-adamantane, bis-nor-adamantane and double-decker type germasesquichalcogenides[6,86,88,91].

V. POLYCYCLOSILOXANES

A. Introduction

Organosilsesquioxanes $(RSiO_{1.5})_n$[92–94] are organometallic analogues of silicate anions $[Si_nO_{2.5}]^{n-}$. The silsesquioxanes were first prepared by hydrolysis of organotrichlorosilanes[95,96]. Recently, the yields of silsesquioxanes were much improved by a new synthetic method. In the past decade, the structures of organosilsesquioxanes were determined by X-ray structure analysis.

B. Synthesis and Reactions

1. Prismane and cubane type silsesquioxanes

Silsesquioxanes are reported as $(RSiO_{1.5})_n$ $(n \geqslant 4)$ where R is either H, Cl or any of a large number of organic groups[97–100]. The first silsesquioxane (O_h-$H_8Si_8O_{12}$; T_8) **(73)** was synthesized in 1959 by Müller, Köhne and Silwinski (<1% yield from $HSiCl_3$) and shown to be **73**[101]. In 1970 an improved synthesis of this compound (T_8) was reported by Frye and Collins [*ca* 13% yield from $HSi(OCH_3)_3$][98]. They also reported an unusual preparative procedure that yielded a mixture of hydridospherosiloxanes in highly variable yields (T10, 4%; T12, 43%; T14, 39%; T16, 14% by the treatment of $HSiCl_3$ with H_2SO_4 and successive hydrolysis). Day, Klemperer and coworkers reported the synthesis of O_h-$(CH_3O)_8Si_8O_{12}$ by the reaction of O_h-$Cl_8Si_8O_{12}$ with methyl nitrite in 45% yield (equation 26)[99]. Agaskar, Day and Klemperer reported in 1987 that a modification of Frye and Collins' procedure gave improved yields (>30%) and also described a purification protocol that yielded gram quantities of four pure hydridospherosiloxanes[102]. The structures of the compounds O_h-$H_8Si_8O_{12}$ **(73)**, D_{5h}-$H_{10}Si_{10}O_{15}$ **(74)**, D_{2d}-$H_{12}Si_{12}O_{18}$ and D_{3h}-$H_{14}Si_{14}O_{21}$, which were obtained in *ca* 0.5, 3.5, 3.5 and 0.5% yields, respectively, have been determined by X-ray analysis. They have reported a new synthetic procedure to give O_h-$H_8Si_8O_{12}$ **(73)** and D_{5h}-$H_{10}Si_{10}O_{15}$ **(74)** (*ca* 3.5 : 1) in *ca* 27.2% yield by treatment of $HSiCl_3$ with $FeCl_3-HCl-CH_3OH$[103,104].

$$[Si_8O_{12}]Cl_8 + 8CH_3ONO \xrightarrow{25\,°C} [Si_8O_{12}](OCH_3)_8 + 8\,NOCl \qquad (26)$$

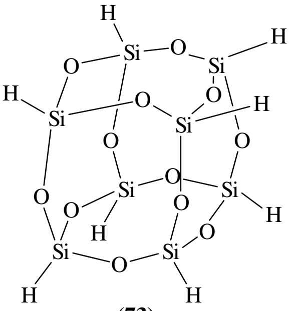

(73)

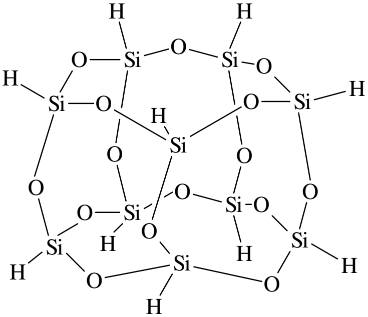

(74)

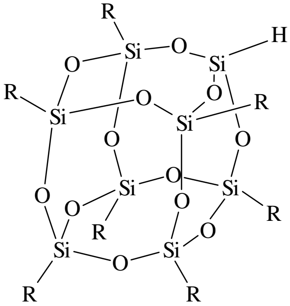

(75) R = $PhCH_2$

Silsesquioxane (**75**, R = $PhCH_2$) can be synthesized by the hydrolytic condensation of benzyltrichlorosilane in 95% ethanol in 24% yield[105]. Feher and coworkers reported the facile synthesis of O_h-$H(c$-$C_6H_{11})_7Si_8O_{12}$ **(77)** by the reaction of **76** with $HSiCl_3$ in Et_3N/Et_2O (equation 27)[106]. Matsumoto and coworkers reported the facile synthesis of octakis(silsesquioxane) [$(RSi)_8O_{12}$, R = *t*-$BuMe_2Si$] by the oxidation of octasilacubane[107].

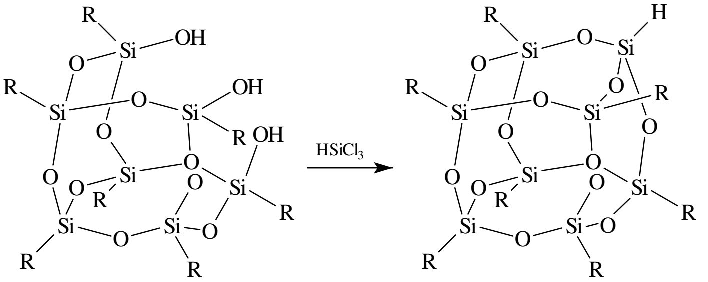

(27)

R = cyclohexyl

(76)

R = cyclohexyl

(77)

The synthesis of hexakis(cyclohexylsilsesquioxane) in 10% yield by the treatment of cyclohexyltrichlorosilane with water was first reported in 1965[108]. The X-ray structure of hexakis(cyclohexylsilsesquioxane) was determined by Molloy and coworkers in 1994[109]. The hexasilsesquioxanes **(80)** substituted by *t*-butyl or 1,1,2-trimethylpropyl groups are prepared by condensation of the corresponding silanetriol **(78)** or tetrahydroxysiloxane **(79)** using dicyclohexylcarbodiimide (DCC) as a dehydrating reagent in DMSO or DMF (Scheme 20)[110].

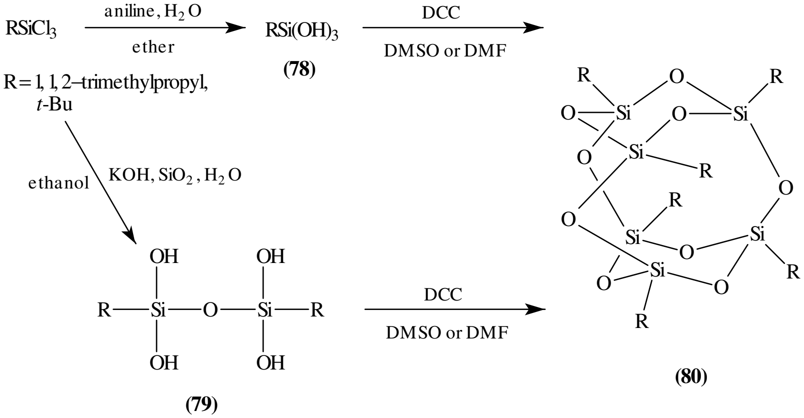

SCHEME 20

2. Transformation of functionalized spherosilicate

A hydridespherosiloxane, $H_{10}Si_{10}O_{15}$ **(74)**, can be easily converted to $[Si_{10}O_{25}](Si(CH_3)_2(CH{=}CH_2))_{10}$ by using the reagent $(CH_3)_3NO\cdot ClSi(CH_3)_2(CH{=}CH_2)$[111].

VI. REFERENCES

1. D. A. ('Fred') Armitage, in *The Chemistry of Organic Silicon Compounds*, Part 2 (Eds. S. Patai and Z. Rappoport); Chap. 23, Wiley, New York, 1989, pp. 1395–1414.
2. D. A. ('Fred') Armitage, in *The Silicon–Heteroatom Bond* (Eds. S. Patai and Z. Rappoport), Wiley, New York, 1991, Chap. 7, pp. 213–231; Chap. 8, pp. 233–243.
3. J. Albertsen and R. Steudel, *J. Organomet. Chem.*, **424**, 153 (1992).
4. N. Choi, S. Sugi and W. Ando, *Chem. Lett.*, 1395 (1994).
5. N. Choi, S. Morino, S. Sugi and W. Ando, *Bull. Chem. Soc. Jpn.*, **69**, 1613 (1996).
6. W. Ando, T. Kadowaki, A. Watanabe, N. Choi, Y. Kabe, T. Erata and T. Ishii, *Nippon Kagaku Kaishi*, 214 (1994); *Chem. Abstr.*, **121**, 205539w (1994).
7. (a) F. S. Kipping and R. Robinson, *J. Chem. Soc.*, **105**, 484 (1914).
   (b) F. S. Kipping, *J. Chem. Soc.*, **101**, 2108 (1912).
   (c) F. S. Kipping, *J. Chem. Soc.*, **101**, 2125 (1912).
8. J. A. Forstner and E. L. Muetterties, *Inorg. Chem.*, **5**, 552 (1966).
9. S. R. Bahr and Boudjouk, *Inorg. Chem.*, **30**, 712 (1991).
10. R. H. Benno and C. J. Fritchie, *J. Chem. Soc., Dalton Trans.*, 543 (1973).
11. H. Berwe and A. Haas, *Chem. Ber.*, **120**, 1175 (1987).
12. H. Yoshida, Y. Kabe and W. Ando, *Organometallics*, **10**, 27 (1991).
13. N. Choi, K. Asano and W. Ando, *Organometallics*, **14**, 3146 (1995).
14. N. Choi, K. Asano, N. Sato and W. Ando, *J. Organomet. Chem.*, **516**, 155 (1996).
15. H. Yoshida, Y. Takahara, T. Erata and W. Ando, *J. Am. Chem. Soc.*, **114**, 1098 (1992).

16. L. Birkofer and O. Stuhl, in *The Chemistry of Organic Silicon Compounds*, Part 1 (Eds. S. Patai and Z. Rappoport), Chap. 10, Wiley, New York, 1989, pp. 655–762.
17. N. G. Bokii, G. N. Zakharova and Yu. T. Z. Struchkov, *Z. Strukt. Khim.*, **13**, 291 (1972); *Chem. Abstr.*, **77**, 25794q (1972).
18. M. A. Hossain, M. D. Hursthouse and K. M. A. Malik, *Struct. Crystallogr. Cryst. Chem.*, **B35**, 522 (1979).
19. R. K. Harns, B. J. Kimber, M. D. Wood and A. Holt, *J. Organomet. Chem.*, **116**, 291 (1976).
20. G. Engelhardt, M. Magi and E. Lippmaa, *J. Organomet. Chem.*, **54**, 115 (1973).
21. R. West, M. J. Fink and J. Michl, *Science (Washington, D.C.)*, **214**, 1343 (1981).
22. M. J. Fink, D. J. De Young, R. West and J. Michl, *J. Am. Chem. Soc.*, **105**, 1070 (1983).
23. M. J. Fink, K. J. Haller, R. West and J. Michl, *J. Am. Chem. Soc.*, **106**, 823 (1984).
24. M. J. Michalczyk, R. West and J. Michl, *J. Chem. Soc., Chem. Commun.*, **22**, 1525, (1984).
25. M. J. Michalczyk, M. J. Fink, K. J. Haller, R. West and J. Michl, *Organometallics*, **5**, 531 (1986).
26. K. L. McKillop, G. R. Gillette, D. R. Powell and R. West, *J. Am. Chem. Soc.*, **114**, 5203 (1992).
27. N. Tokitoh, H. Suzuki and R. Okazaki, *J. Am. Chem. Soc.*, **115**, 10428 (1993).
28. W. Ando, in *Reviews on Heteroatom Chemistry*, Vol. 2 (Ed. S. Oae), MYU, Tokyo, 1994, pp. 121–142.
29. W. Ando, M. Kako, T. Akasaka, S. Nagase, T. Kawai, Y. Nagai and T. Sato, *Tetrahedron Lett.*, **30**, 6705 (1989).
30. W. Ando, M. Kako, T. Akasaka and Y. Kabe, *Tetrahedron Lett.,* **31**, 4117 (1990).
31. W. Ando, M. Kako, T. Akasaka and S. Nagase, *Organometallics*, **12**, 1514 (1993).
32. R. West, *Angew. Chem., Int. Ed. Engl.*, **26**, 1201 (1987).
33. T. Kudo and S. Nagase, *J. Am. Chem. Soc.*, **107**, 2589 (1985).
34. L. C. Snyder and K. Raghavachari, *J. Chem. Phys.*, **80**, 5076 (1984).
35. E. H. Aggarwal and S. H. Bauer, *J. Chem. Phys.*, **18**, 42 (1950).
36. (a) G. Peyronel, *Chim. Ind.*, **36**, 441 (1954).
    (b) G. Peyronel, *Atti Accad. Naz. Lincei, Cl. Sci. Fis., Mat. Nat. Rend.*, **16**, 231 (1954).
37. W. Ando, M. Kako and T. Akasaka, *Chem. Lett.*, 1679 (1993).
38. The annealing temperature, melting point and boiling point of Oxygen are 26, 54 and 90 K, respectively. M. Moskovits and G. A. Ozin, in *Cryochemistry* (Eds. M. Moskovits and G. A. Ozin), Wiley, New York, 1976, p. 24.
39. W. Ando (Ed.), *Singlet* O_2, CRC, Boca Raton, 1985.
40. (a) W. R. Roth and M. Martin, *Tetrahedron Lett.*, 4695 (1967).
    (b) W. R. Roth, F. G. Klarner, W. Grimme, H. G. Roser, R. Busch, B. Muskulus, R. Breuckmann, B. P. Scholz and H. W. Lennartz, *Chem. Ber.*, **116**, 2717 (1983).
41. (a) L. Birkofer and O. Stuhl, in *The Chemistry of Organic Silicon Compounds* (Eds. S. Patai and Z. Rappoport), Chap. 10, Wiley, New York, 1989, pp. 706–721.
    (b) D. A. Armitage ('Fred'), in *The Chemistry of Organic Silicon Compounds* (Eds. S. Patai and Z. Rappoport), Chap. 22, Wiley, New York, 1989, pp. 1363–1394.
42. J. X. McDermott, M. E. Wilson and G. M. Whitesides, *J. Am. Chem. Soc.*, **98**, 6529 (1976).
43. M. A. Chaudhari and F. G. A. Stone, *J. Chem. Soc. (A)*, 838 (1966).
44. D. Sen and U. N. Kantak, *Indian J. Chem.*, **9**, 254 (1971).
45. D. P. Thompson and P. Boudjouk, *J. Chem. Soc., Chem. Commun.*, 1466 (1987).
46. D. M. Giolando, T. B. Rauchfuss, A. L. Rheingold and S. R. Wilson, *Organometallics*, **6**, 667 (1987).
47. D. M. Giolando, T. B. Rauchfuss and G. M. Clark, *Inorg. Chem.*, **26**, 3080 (1987).
48. N. Tokitoh, H. Suzuki, T. Matsumoto, Y. Matsuhashi, R. Okazaki and M. Goto, *J. Am. Chem. Soc.*, **113**, 7047 (1991).
49. N. Tokitoh, M. Takahashi, T. Matsumoto, H. Suzuki, Y. Matsuhashi and R. Okazaki, *Phosphorous, Sulfur and Silicon*, **59**, 161 (1991).
50. N. Tokitoh, T. Matsumoto and R. Okazaki, *Tetrahedron Lett.*, **33**, 2531 (1992).
51. N. Yamazaki, S. Nakahama, K. Yamaguchi and T. Yamaguchi, *Chem. Lett.*, 1355 (1980).
52. For reviews on heavy atom analogues of ketones see:
    (a) J. C. Guziec, in *Organoselenium Chemistry* (Ed. D. Liotta), Wiley, New York, 1987, p. 237.
    (b) C. Raabe and J. Michl, *Chem. Rev.*, **85**, 419 (1985).
    (c) J. Stage, *Pure Appl. Chem.*, **56**, 137 (1984).
53. P. Boudjouk, *Polyhedron*, **10**, 1231 (1991).

54. V. A. Kutoglu, *Z. Anorg. Allg. Chem.*, **390**, 195 (1972).
55. V. A. Kutoglu, *Acta Crystallogr.*, **B29**, 2891 (1973).
56. E. G. Müller, J. L. Petersen and L. F. Dahl, *J. Organomet. Chem.*, **111**, 91 (1976).
57. W. E. v. Schklower, Y. Yu. T. Strutschkow, L. E. Guselnikow, W. W. Wolkowa and W. G. Awakyam, *Z. Anorg. Allg. Chem.*, **501**, 153 (1983).
58. K. Peters, D. Weber and H. G. von Schnering, *Z. Anorg. Allg. Chem.*, **519**, 134 (1984).
59. J. Peters, J. Mandt, M. Meyring and B. Krebs, *Z. Kristallogr.*, **156**, 90 (1981).
60. [1.1.1]propellanes, M=C.
    (a) K. B. Wiberg and F. H. Walker, *J. Am. Chem. Soc.*, **104**, 5239 (1982).
    (b) K. B. Wiberg, W. P. Dailey, F. H. Walker, S. T. Waddell, L. S. Crocker and M. D. Newton, *J. Am. Chem. Soc.*, **107**, 7247 (1985).
    (c) L. Hedberg and K. Hedberg, *J. Am. Chem. Soc.*, **107**, 7257 (1985).
    (d) E. Honegger, H. Huber, E. Heilbronner, W. P. Dailey and K. B. Wiberg, *J. Am. Chem. Soc.*, **107**, 7172 (1985).
    (e) J. Belzner, U. Bunz, K. Semmler, G. Szeimies, K. Opitz and A. D. Schlüter, *Chem. Ber.*, **122**, 397 (1989).
    (f) P. Seiler, *Helv. Chim. Acta*, **73**, 1574 (1990).
    M = Sn.
    (g) L. R. Sita and I. Kinoshita, *J. Am. Chem. Soc.*, **112**, 8839 (1990).
    (h) L. R. Sita and I. Kinoshita, *J. Am. Chem. Soc.*, **114**, 7024 (1992).
61. Y. Kabe, T. Kawase and J. Okada, *Angew. Chem., Int. Ed. Engl.*, **29**, 794 (1990).
62. W. D. Stohrer and R. Hoffmann, *J. Am. Chem. Soc.*, **94**, 779 (1972).
63. M. D. Newton and J. M. Schulman, *J. Am. Chem. Soc.*, **94**, 773 (1972).
64. J. E. Jackson and L. C. Allen, *J. Am. Chem. Soc.*, **106**, 591 (1984).
65. D. B. Kitchen, J. E. Jackson and L. C. Allen, *J. Am. Chem. Soc.*, **112**, 3408 (1990).
66. N. D. Epiotis, *J. Am. Chem. Soc.*, **106**, 3170 (1984).
67. R. F. W. Bader, T. T. Nguyen-Dang and Y. Tal, *Rep. Prog. Phys.*, **44**, 893 (1981).
68. P. v. R. Schleyer and R. Janoschek, *Angew. Chem., Int. Ed. Engl.*, **26**, 1267 (1987).
69. S. Nagase and T. Kudo, *Organometallics*, **6**, 2456 (1987).
70. S. Nagase, T. Kudo and T. Kurakake, *J. Chem. Soc., Chem. Commun.*, 1063 (1988).
71. S. Nagase and T. Kudo, *Organometallics*, **7**, 2534 (1988).
72. A. Streitwieser, *J. Chem. Soc., Chem. Commun.*, 1261 (1989).
73. M. S. Gordon, K. A. Nguyen and M. T. Carroll, *Polyhedron*, **10**, 1247 (1991).
74. (a) K. A. Nguyen, M. T. Carroll and M. S. Gordon, *J. Am. Chem. Soc.*, **113**, 7924 (1991).
    (b) S. Nagase, *Polyhedron*, **10**, 1299 (1991).
75. W. Ando, S. Watanabe and N. Choi, *J. Chem. Soc., Chem. Commun.*, 1683 (1995).
76. W. Wojnowski, K. Peters, D. Weber and H. G. v. Schnering, *Z. Anorg. Allg. Chem.*, **519**, 134 (1984).
77. W. E. v. Schklower, Y. T. Strutschkow, L. E. Guselnikow, W. W. Wolkowa and W. G. Awakyan, *Z. Anorg. Allg. Chem.*, **501**, 153 (1983).
78. J. Peters and B. Krebs, *Acta Crystallogr., Sect. B*, **B38**, 1270 (1982).
79. J. Peters, J. Mandt, M. Meyring and B. Krebs, *Z. Kristallogr.*, **156**, 90 (1981).
80. W. S. Sheldrick, in *The Chemistry of Organic Silicon Compounds*, Part 1 (Eds. S. Patai and Z. Rappoport), Chap. 3, Wiley, Chichester 1989, pp. 227–303.
81. The distances between the bridgehead silicon atoms were investigated by *ab initio* calculations and found to be 2.69–2.89 Å[60,68].
82. F. Serrano, *Rev. Fac.ciênc., Lisboa, 2a Sér.*, **B7**, 105 (1959–60); *Chem. Abstr.*, **55**, 20978h (1961).
83. M. S. Kharasch, W. Nundnberg and G. Mantell, *J. Org. Chem.*, **16**, 524 (1951).
84. N. Choi, K. Asano, S. Watanabe and W. Ando, *Phosphorous, Sulfur and Silicon* (1997), in press.
85. A. Hass, R. Hitze, C. Kruger and K. Angermund, *Z. Naturforsch.*, **39B**, 890 (1984).
86. P. Boudjouk, *Polyhedron*, **10**, 1231 (1991).
87. M. Unno, H. Shioyama and H. Matsumoto, *Phosphorous, Sulfur and Silicon*, (1997), in press.
88. W. Ando, T. Kadowaki and Y. Kabe, *Angew. Chem., Int. Ed. Engl.*, **31**, 59 (1992).
89. H. Puff, K. Braun, S. Franken, T. R. Kök and W. Schuh, *J. Organomet. Chem.*, **335**, 167 (1987).
90. J. C. J. Bart and J. J. Daly, *J. Chem. Soc., Dalton Trans.*, 2063 (1975).
91. W. Ando, N. Choi, S. Watanabe, K. Asano, T. Kadowaki, Y. Kabe and H. Yoshida, *Phosphorous, Sulfur and Silicon*, **93–94**, 51 (1994).

92. U. Dittmar, B. J. Hendan, U. Floerke and H. C. Marsmann, *J. Organomet. Chem.*, **489**, 185 (1995).
93. R. H. Baney, M. Itoh, A. Sakakibara and T. Suzuki, *Chem. Rev.*, **95**, 1409 (1995).
94. F. J. Feher, K. Rahimian, T. A. Budzichowski and Z. W. Ziller, *Organometallics*, **14**, 3920 (1995).
95. D. W. Scott, *J. Am. Chem. Soc.*, **68**, 356 (1946).
96. J. F. Brown, L. H. Vogt and P. I. Prescott, *J. Am. Chem. Soc.*, **86**, 1120 (1964).
97. M. G. Voronkov and V. I. Lavrent'yev, *Top. Curr. Chem.*, **102**, 199 (1982).
98. C. L. Frye and W. T. Collins, *J. Am. Chem. Soc.*, **92**, 5586 (1970).
99. V. W. Day, W. G. Klemperer, V. V. Mainz and D. M. Millar, *J. Am. Chem. Soc.*, **107**, 8262 (1985).
100. F. J. Feher and T. A. Budzichowski, *J. Organomet. Chem.*, **379**, 33 (1989).
101. R. Müller, F. Köhne and S. Silwinski, *J. Prakt. Chem.*, **9**, 71 (1959).
102. P. A. Agaskar, V. W. Day and W. G. Klemperer, *J. Am. Chem. Soc.*, **109**, 5554 (1987).
103. P. A. Agaskar, *Inorg. Chem.*, **29**, 1603 (1990).
104. P. A. Agaskar, *Inorg. Chem.*, **30**, 2707 (1991).
105. F. J. Feher and T. A. Budzichowski, *J. Organomet. Chem.*, **373**, 153 (1989).
106. F. J. Feher and K. J. Weller, *Organometallics*, **9**, 2638 (1990).
107. H. Matsumoto, K. Higuchi and M. Goto, *31st Symposium of Organometallic Chemistry*, Osaka, Japan, abstract (1986).
108. J. F. Brown and L. H. Vogt, *J. Am. Chem. Soc.*, **87**, 4313 (1965).
109. H. Behbehani, B. J. Brisdon, M. F. Mahon and K. C. Molloy, *J. Organomet. Chem.*, **469**, 19 (1994).
110. M. Unno, S. B. Alias, H. Saito and H. Matsumoto, *Organometallics*, **15**, 413 (1996).
111. P. A. Agaskar, *J. Am. Chem. Soc.*, **111**, 6858 (1989).

CHAPTER **33**

Organosilicon derivatives of fullerenes

WATARU ANDO and TAKAHIRO KUSUKAWA

Department of Chemistry, University of Tsukuba, Tsukuba, Ibaraki 305, Japan

I. INTRODUCTION

The fullerenes (C_{60}, C_{70} and higher molecular allotropes)[1a], discovered by Kroto, Smalley and coworkers in 1985[1b], represent the third form of carbon, following graphite and diamond. However, it was not until 1990, when Kräschmer, Huffman and coworkers[1c,1d]

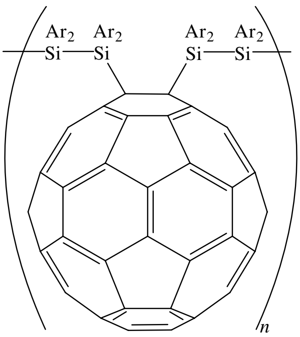

FIGURE 1. Fullerene-bonded polysilane

discovered the method of arc vaporization of graphite affording these marvelous new materials in macroscopic amounts, that the fullerene emerged from the realm of being a scientific curiosity. Since the isolation of C_{60} in preparatively useful quantities, the chemical functionalization of this new allotropic form of carbon has attracted much interest, and has led to fascinating results[1a,2–5]. In spite of a number of studies with different types of substrates, relatively few examples with silicon are known and this prompted recent investigations. One particular target which is attractive in view of its possible photoconductivity is a fullerene-bonded polysilane (Figure 1).

II. PHOTOCONDUCTIVITY OF FULLERENE-DOPED POLYSILANES

Polysilanes are a unique class of polymers with the backbone consisting entirely of tetrahedrally coordinated silicon atoms[6,7]. Because of the σ-conjugation, carrier transport along the silicon backbone is very efficient. The hole mobility of polysilanes, *ca* 10^{-4} cm^2 V^{-1} s^{-1}, is among the highest observed for polymers. Fullerenes are known to be good electron acceptors. In the presence of electron donors such as aromatic amines, weakly bonded charge-transfer complexes can be formed. Poly(methylphenylsilylene) (PMPS, **1** Scheme 1) can be doped with 1.6% by weight with C_{60}. As a result, its photoinduced discharge rate (a tungsten lamp, 50 mW cm^{-2}) is enhanced by an order of magnitude[8]. The same result is obtained when the samples are irradiated with monochromatic irradiation at 340 nm. However, in the shorter wavelength region (<350 nm), PMPS is a light absorber and the charge is generated by an electron transfer from an excited state of the polysilane to the fullerene. Extension of this approach to other polysilanes such as cyclohexylmethylpolysilane and dimethylpolysilane has been tried. However, no significant photoinduced discharge can be observed from these polysilanes. These results suggest that specific interaction exists between the fullerene and the phenyl group in PMPS which leads to the formation of a weakly bonded complex between them and enhances the transfer of an electron from PMPS to fullerene.

The photoinduced electron transfer between C_{60} and polysilane was investigated by laser flash photolysis[9]. The transient absorption spectra of the C_{60} triplet ($^3C_{60}{}^*$) **(2),** the C_{60} radical anion **(3)** and the poly(methylphenylsilylene) radical cation (**4**, M = Si) (Scheme 2) were observed in the region 600–1600 nm in a polar solvent.

Electron transfer from the germanium analog of **1**, $(PMePhGe)_n$, to photoexcited C_{60} in benzene–acetonitrile solution has also been investigated by 532 nm laser flash photolysis[10]. The transient absorption band at 730 nm which appears immediately after laser exposure is attributed to $^3C_{60}{}^*$ **(2)**. With the decay of $^3C_{60}{}^*$ **(2)**, the intensities of the

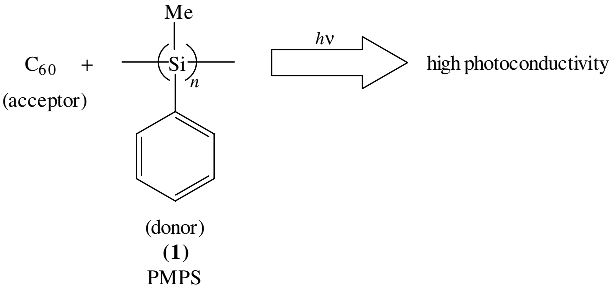

SCHEME 1. A Fullerene-doped polysilane photoconductor

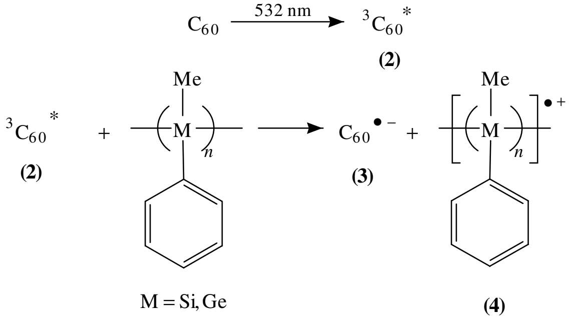

SCHEME 2. Photoinduced electron transfers from polysilane and polygermane to C_{60}

absorption bands increase in the region 900–1600 nm. The absorption band at 1030 nm is a characteristic band of the radical anion of C_{60} ($C_{60}{}^{\bullet -}$) (**3**). The broad absorption band extending from 1200 to 1600 nm may be attributed to the radical cation of $(\mathrm{PMePhGe})_n$, $(\mathrm{PPhMeGe}^{\bullet +})_n$ (**4**, M = Ge). Such radical ions generated by the electron transfer were not observed in neat benzene. $^3C_{60}{}^*$ is the only transient species observed by nanosecond laser flash photolysis in the nonpolar solvent benzene.

III. PHOTOCHEMICAL REACTIONS OF 2,2-DIARYLTRISILANE

A. Reaction of 2,2-Diaryltrisilane with C_{60}

Ando, Akasaka and coworkers have studied the reaction of 2,2-diaryltrisilane with C_{60}[11]. When 2,2-bis(2,6-diisopropylphenyl)hexamethyltrisilane (**5**) the silylene (**6**) precursor, was photolyzed with a low-pressure mercury lamp in a toluene solution of C_{60}, the color of the solution changed from purple to dark brown. Flash chromatography on silica gel furnished thermally stable **7** and **8** in 58% and 27% yields, respectively. Small amounts of **9** and **10** were also obtained (equation 1). It has been observed that the product composition of the silylene-addition reaction varies with the amount of the trisilane used. The fast atom bombardment (FAB) mass spectrometry of **7** displays a peak for adduct **7** at 1074–1070 as well as for C_{60} at 723–720 which arises from loss of diarylsilylene (**6**). The FAB mass spectra of the $C_{60}(\mathrm{Dip_2Si})_2$ (**8**), $C_{60}(\mathrm{Dip_2Si})_3$ (**9**) and $C_{60}(\mathrm{Dip_2Si})_4$ (**10**) adducts of C_{60} were reasonably analyzed. The UV-vis absorption spectra of **7** is virtually identical to that of C_{60} except for subtle differences in the 400–700 nm region (Figure 2). Adduct **7** exhibits a new band at 421 nm but lacks the C_{60} band at 406 nm.

Relative to C_{60}, adduct **7** shows stronger absorptions at 463 and 508 nm and weaker absorptions at 539 and 599 nm. The FAB mass, UV-vis spectra of **7** contain a number of unique features, but also suggest that this new fullerene retains the essential electronic and structural character of C_{60}.

$$\underset{\textbf{(5)}}{\mathrm{Dip_2Si(SiMe_3)_2}} \xrightarrow[-\mathrm{Me_3SiSiMe_3}]{h\nu} \underset{\textbf{(6)}}{[\mathrm{Dip_2Si{:}}]} \xrightarrow{C_{60}} \underset{\textbf{(7)}}{\mathrm{C_{60}Dip_2Si}} + \underset{\textbf{(8)}}{\mathrm{C_{60}(Dip_2Si)_2}} + \underset{\textbf{(9)}}{\mathrm{C_{60}(Dip_2Si)_3}} + \underset{\textbf{(10)}}{\mathrm{C_{60}(Dip_2Si)_4}} \qquad (1)$$

$$\mathrm{Dip} = 2,6\text{-}i\text{-}\mathrm{Pr_2C_6H_3}$$

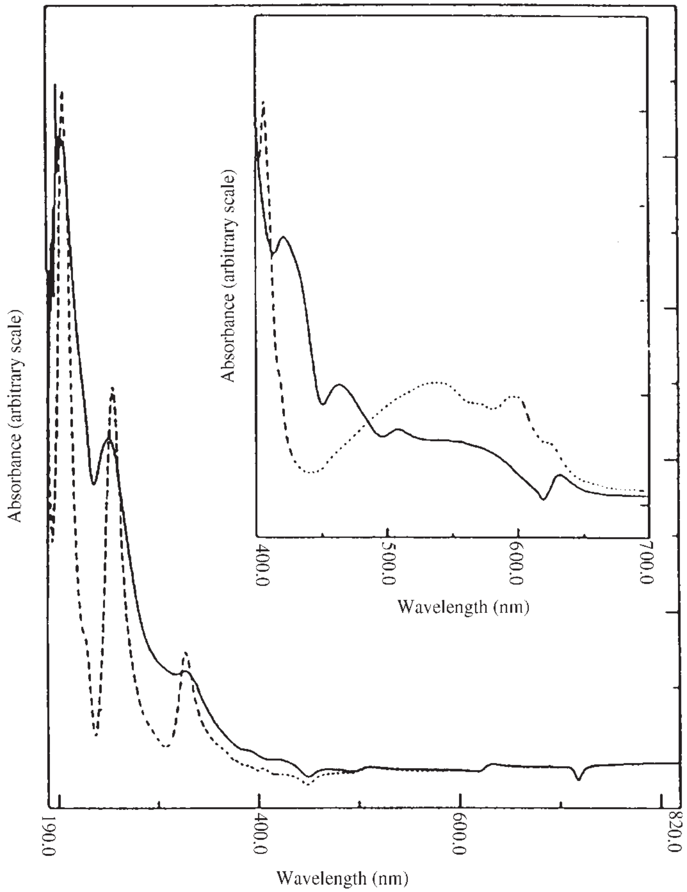

FIGURE 2. UV-vis spectra of C_{60} (- - - -) and **7** (———) from 190 to 829 nm in hexane Insert: Spectra of C_{60} (- - - -) and **7** (———) from 400 to 700 nm in toluene. Reprinted with permission from Ref. 11. Copyright 1993 American Chemical Society

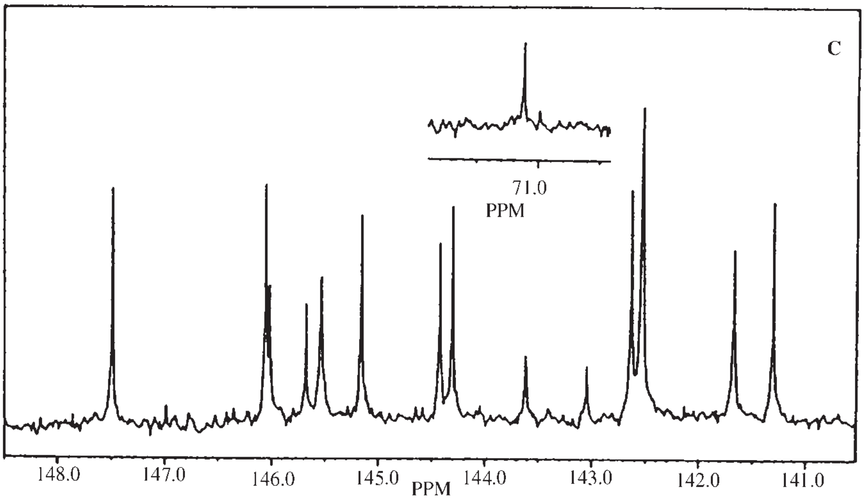

FIGURE 3. ^{13}C NMR spectrum of **7**. Reprinted with permission from Ref. 11. Copyright 1993 American Chemical Society

The possible structures of **7** are **7a** and **7b**. The silirane structure **7a**, of C_{2v} symmetry, is derived from the addition of the diarylsilylene across the reactive 1,2-junction. Silamethano[10]annulene **7b**, analogous to the structure proposed for Ph_2C_{61}, could arise via isomerization of **7a**. The ^{1}H NMR of **7** is consistent with the Dip_2Si adduct of C_{60}. The ^{13}C-NMR spectrum of **7** shows 17 signals for the C_{60} skeleton, of which four correspond to two carbons each and thirteen correspond to four carbon atoms each; one signal is at 71.12 ppm and the remainder between 140 and 150 ppm (Figure 3). This is the appropriate number and ratio of peak intensities for a C_{60} adduct of C_{2v} symmetry. The ^{13}C-NMR signal at 71.12 ppm strongly supports structure **7a** rather than **7b** (Scheme 3). The ^{29}Si-NMR spectrum of **7** shows a peak at −72.74 ppm which is also assigned to the silicon atom of **7a**. These data are fully consistent with the structural representation of **7a**.

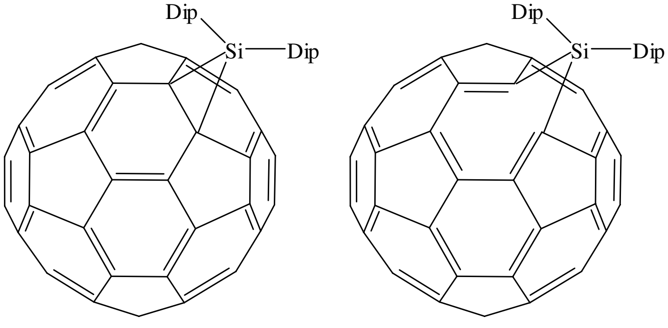

(7a) **(7b)**

SCHEME 3. Two possible structures of adduct **7**

Further support for structure **7a** is obtained by AM1 molecular orbital calculations performed on the reaction of C_{60} and silylenes (Ph_2Si**:**). These calculations show that Ph_2Si adds across the junction of two six-membered rings in C_{60} to give the 1,2-addition silirane analogous to **7a** with an exothermicity of 61.3 kcal mol^{-1}. The analog of **7b** was not located on the potential energy surface. Also, **7a** was 19.4 and 10.7 kcal mol^{-1} more stable than the 1,6-adducts **11a** and **11b**, respectively (Scheme 4).

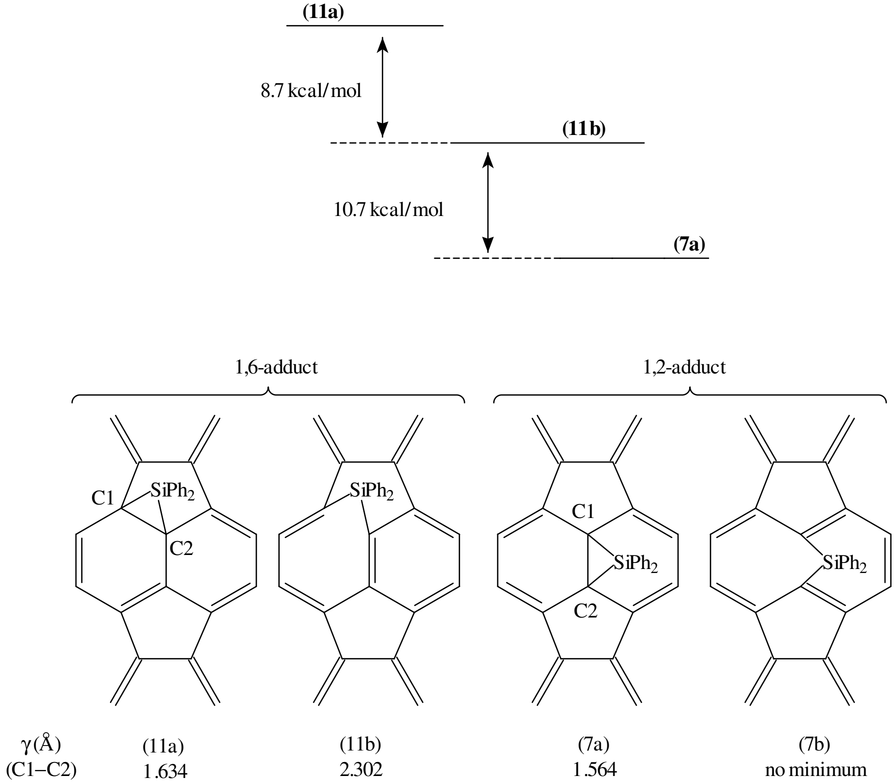

SCHEME 4. Relative energies and bond distances (C1–C2) of four isomers

Thus, we have shown that the addition of a diarylsilylene with C_{60} occurs in a facile manner analogous to the carbene addition[3] reported recently.

B. Reaction of 2,2-Diaryltrisilane with C_{70}

The silylene precursor, 2,2-bis(2,6-diisopropylphenyl)hexamethyltrisilane (**5**), was photolyzed with a low-pressure mercury lamp in a toluene solution of C_{70}[12]. The adduct **12** obtained (equation 2) contains two isomers of $(Dip)_2SiC_{70}$ (**12a** and **12b**) which were separated by flash chromatography on silica gel. FAB mass spectrometry of **12** displays a peak for adduct **12** at 1190–1194 as well as for C_{70} at 840–843 which arises from the loss of diarylsilylene. The UV-vis absorption spectra of **12** are virtually identical to those of C_{70} with bands at 333, 381 and 471 nm. AM1 molecular orbital calculations on the reaction of C_{70} with dihydrosilylene show that the 1,2-adduct is more stable than the 1,6-adduct. In the two adducts the silyl group is positioned differently with respect to the mirror planes of C_{70} such that they each correspond to a characteristic number of symmetry-independent carbons and protons (Table 1 and Figure 4).

$$\underset{(\mathbf{5})}{\mathrm{Dip_2Si(SiMe_3)_2}} \xrightarrow[-\mathrm{Me_3SiSiMe_3}]{h\nu} \underset{(\mathbf{6})}{[\mathrm{Dip_2Si:}]} \xrightarrow{C_{70}} \underset{(\mathbf{12})}{\mathrm{C_{70}Dip_2Si}} \qquad (2)$$

$\mathrm{Dip} = 2,6\text{-}i\text{-}\mathrm{Pr_2C_6H_3}$

The ^{1}H-NMR spectrum of **12a** displays four methyl signals at 1.59, 1.35, 1.21 and 0.93, and two methine signals at 3.81 and 3.60 ppm. Similarly, four methyl signals at 1.75, 1.47, 1.39 and 1.32, and two methine signals at 4.09 and 3.83 ppm are observed in the ^{1}H-NMR spectrum of **12b**. The ^{13}C-NMR spectrum of **12a** displays two signals at 78.51 and 66.77 ppm for the C_{70} skeleton which are attributed to the sp^3 fullerene carbons. From Table 1, **12a** and **12b** correspond to a=b and c=c addition products, respectively. The kinetically controlled regioselectivity observed for the addition of silylene **6** to C_{70} agrees qualitatively with the AM1 calculations on C_{70}. Products **12a** and **12b** are calculated to

TABLE 1. Number of independent protons and carbons in the 1,2-isomeric adducts of $(Dip)_2SiC_{70}$

Isomer	Symmetry	CH	CH_3	sp^3 Carbon on C_{70}
12a	C_s	2	4	2
12b	C_s	2	4	1
a,b-	C_s	2	4	2
c,c-	C_s	2	4	1
d,e-	C_1	4	8	2
e,e-	C_{2v}	1	1	1

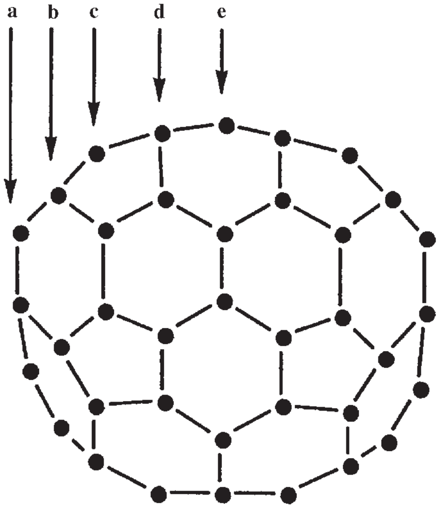

FIGURE 4. Structure of C_{70}

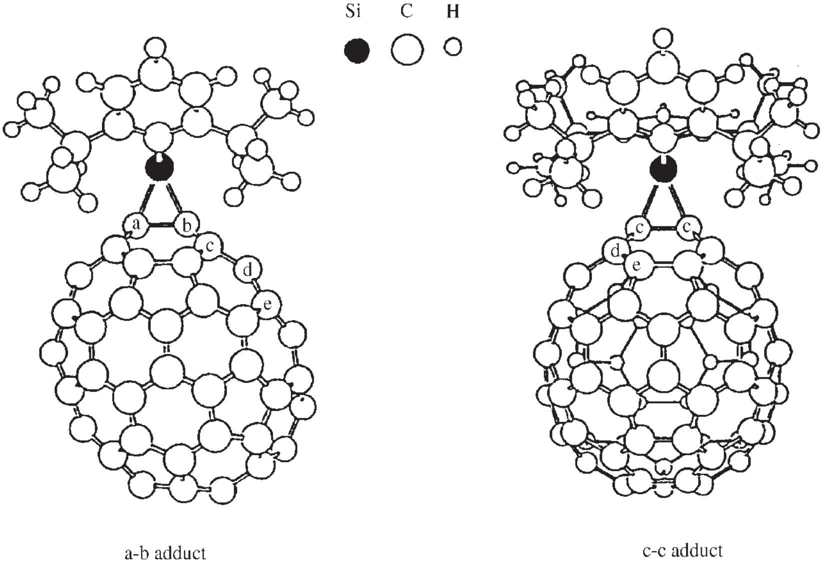

FIGURE 5. Optimized structures of **12a** (left) and **12b** (right) calculated by the AM1 method. Reproduced by permission of the Royal Society of Chemistry from Ref. 12

have almost the same energy; **12a** and **12b** are formed with an exothermicity of 46.3 and 46.4 kcal mol^{-1}. The LUMO electron densities fit very well with the product ratios of the adducts. The C_s structures of **12a** and **12b** obtained by full geometry optimization at the AM1 level are shown in Figure 5.

IV. PHOTOCHEMICAL AND THERMAL ADDITIONS OF CYCLOSILANES TO FULLERENES

A. Additions of Disilirane to C_{60}

C_{60} is a strong electron acceptor capable of taking on as many as six electrons and the photoexcited C_{60} is an even stronger acceptor than the C_{60} in the ground state. On the other hand, strained Si−Si bonds can act as the source of electrons which shows low oxidation potentials and high ionization potentials (Table 2).

Photochemical reaction of C_{60} with disilirane **(13)** was reported by Ando and coworkers[13]. Irradiation of a toluene solution of 1,1,2,2-tetramesityl-1,2-disilirane **(13)** and C_{60} with a high-pressure mercury lamp resulted in the formation of 1,1,3,3-tetramesityl-1,3-disilorane **(14)** in 82% yield with the complete consumption of C_{60} (equation 3). The UV-vis spectrum of **14** and the progress of its generation by irradiation are shown in Figure 6. FAB mass spectroscopy of **14** displays a peak at m/z 1270−1266 besides showing loss of **13** in the fragmentation. The ^{1}H-NMR spectrum of **14** displays six methyls and four *meta*-proton signals of mesityl groups. An AB quartet ($J = 13.0$ Hz) is displayed by two methylene protons at 3.61 and 2.38 ppm supporting a C_s symmetry for the molecules. The ^{13}C-NMR spectrum of **14** shows 32 signals for the C_{60} skeleton. Of these, 28 signals have a relative intensity of 2 and four signals have a relative intensity of 1: one of these signals appears at 73.36 ppm and the remainder between 130 and 150 ppm. These spectral data suggest a C_s symmetry for **14**.

TABLE 2. Oxidation potential and ionization potential of disilirane and digermirane

Substrate	E_{ox} (V) vs SCE[a]	I_p (eV)[b]
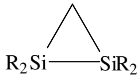	0.81 (R = Mes)	8.9 (R = H)
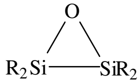	0.97 (R = Dep) 0.79 (R = Dip)	9.4 (R = H)
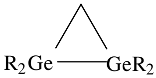	0.72 (R = Dep)	

[a] Measured by cyclic voltammetry at a platinum electrode in CH_2Cl_2 with 0.1 M n-Bu_4 $NClO_4$ as a supporting electrolyte.

[b] Calculated at the HF/6-31G* level.

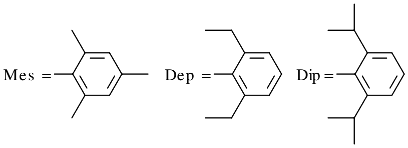

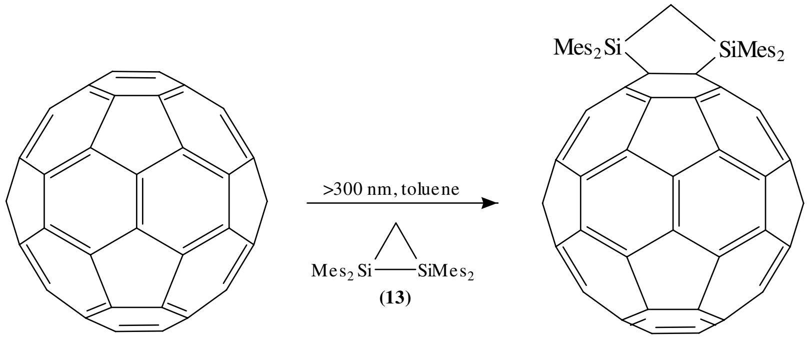

(3)

(14)

Symmetry arguments support the following possibilities for the structure of **14**: (i) addition at the 1,6-junction on the fullerene without free rotation of mesityl groups at 30 °C resulting in a 'frozen' (no ring inversion) single conformer in the envelope conformation, (ii) a 1,6-junction addition on the fullerene without free rotation of mesityl groups at 30 °C and (iii) a 1,2-ring junction addition on the C_{60} without free rotation of mesityl groups at 30 °C and with a 'frozen' conformer (no ring inversion) (Scheme 5).

To obtain further information on the structure of **14**, a variable-temperature ^{1}H-NMR measurement was carried out. Coalescence of the *para*-methyl signals at 2.06 and 1.96 ppm at 44 °C, reflecting a conformational change of the molecule, was observed with an activation free energy of $\Delta G^{\neq} = 17.0$ kcal mol^{-1}. The two pairs of four resonances of *meta*-protons between 6.7 and 6.3 ppm and mesityl *ortho*-methyl protons between 3.3 and 2.3 ppm also coalesce at 60 °C and 80 °C, respectively (Figure 7). $\Delta G^{\neq}$ for the coalescence of both the *meta*-protons and *ortho*-methyl groups at the coalescence

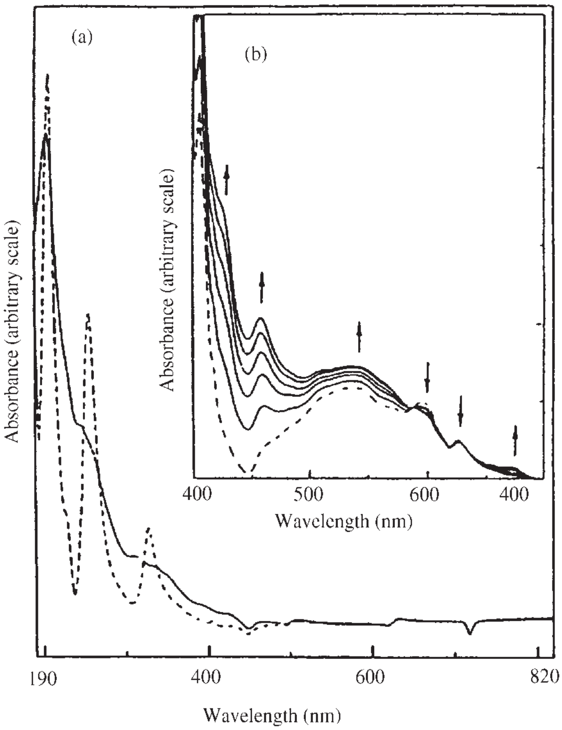

FIGURE 6. (a) UV-vis spectra of C_{60} (- - - -) and **14** (———) from 190 to 820 nm in hexane. (b) Time-dependent spectral changes of a toluene solution of C_{60} and **13** upon irradiation. Reprinted with permission from Ref. 13. Copyright 1993 American Chemical Society

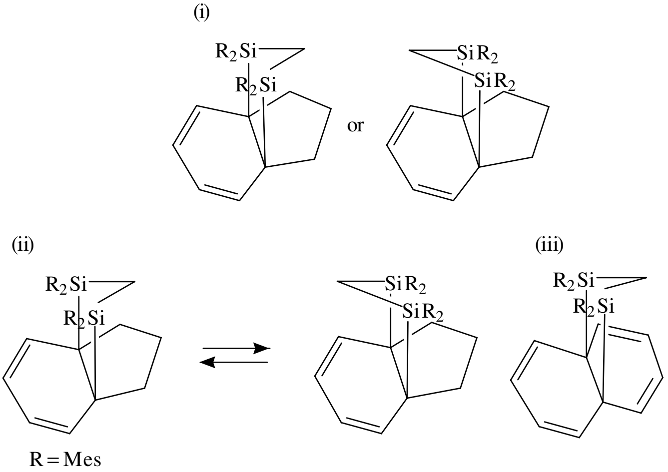

SCHEME 5. Schematic description of disilirane-C_{60} adduct

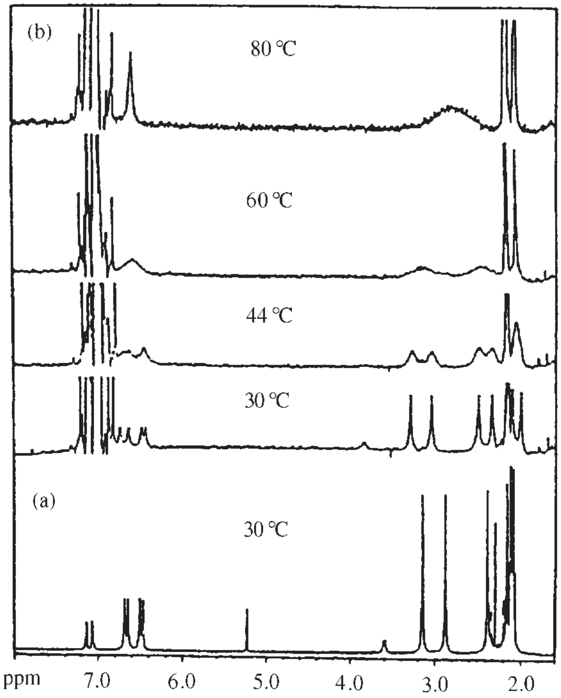

FIGURE 7. ^{1}H-NMR spectra of **14** (a) in CS_2/CD_2Cl_2 and (b) in $CD_3C_6D_5$ at different temperatures. Reprinted with permission from Ref. 13. Copyright 1993 American Chemical Society

temperature is 16.2 kcal mol^{-1}. These results reveal the equivalency of the methylene, methyl and aromatic protons at the coalescence temperature and support possibility (iii) in Scheme 5 as the structure of **14**.

B. Additions of Oxadisilirane to C_{60}

In contrast to the reaction of **13**, the oxadisilirane **(15)** reacts with C_{60} to give mixtures of the mono adducts, 1,2-envelope form **(16)** and the 1,4-twist form **(17)** in 17% yield, and bis-adducts in 39% yield (equation 4). The stabilities of the products were calculated

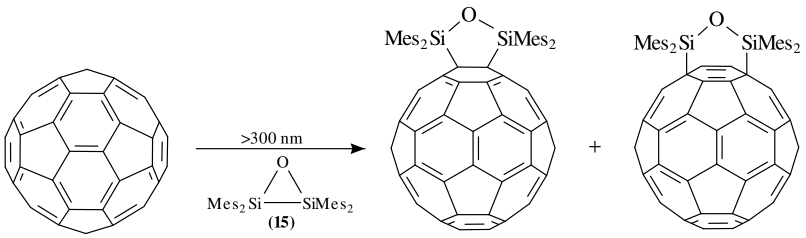

(4)

envelope form **(16)**

twist form **(17)**

TABLE 3. Relative energies ($kcal\,mol^{-1}$) of $C_{60}(Mes_2Si)_2O$ isomers

1,2-Addition		1,4-Addition		
envelope form	twist form	envelope form		twist form
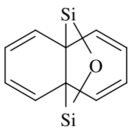	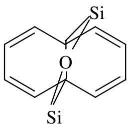	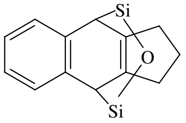	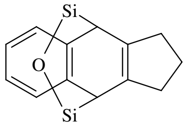	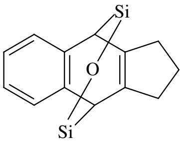
0.0(Cs)	8.7(C_2)	1.8(Cs)	2.7(Cs)	−2.9(C_1)

by semiempirical calculation and found to be fully consistent with the experimental results (Table 3). A photochemical and thermal rearrangement of the 1,2-adduct **(16)** to the 1,4-adduct **(17)** was also observed, as shown by the ^1H-NMR spectral changes with time (Figure 8)[14].

On the other hand, the digermirane **(18)** reacts with C_{60} to afford the 1,4-adduct (**19**, twist form) selectively[15]. The structure of the 1,4-adduct was confirmed by $^{13}C-^{13}C$ INADEQUATE (Incredible Natural Abundance Double Quantum Experiment) spectroscopy (equation 5). The rate of disappearance of C_{60} was suppressed by addition of diazabicyclo[2.2.2]octane and 1,2,4,5-tetramethoxybenzene. Furthermore, the reaction was completely inhibited by addition of rubrene as triplet quencher. One plausible rationale for these observations is that an exciplex intermediate may be responsible for formation of the products (Scheme 6).

C. Additions of Disilirane to C_{70}

Irradiation of a toluene solution of 1,1,2,2-tetramesityl-1,2-disilirane **(13)** and C_{70} with a high-pressure mercury lamp resulted in the formation of 1,1,3,3-tetramesityl-1,3-disilorane **(20)** in 85% yield with complete consumption of C_{70} (equation 6)[16]. FAB mass spectroscopy of **20** displays a peak at m/z 1390–1386. The ^1H-NMR spectrum of **20** displays six methyls and four *meta*-proton signals of the mesityl groups and a singlet for the methylene protons at 1.83 ppm. The ^{13}C-NMR spectrum of **20** shows 35 signals for the C_{70} skeleton: one at 60.61 ppm and the remainder between 128 and 160 ppm. The ^{29}Si-NMR spectrum of **20** shows a peak at −15.88 ppm. In the variable-temperature ^1H NMR, coalescence of the *meta*-protons was observed, with an activation free energy of $\Delta G^{\neq} = 18.1\ kcal\,mol^{-1}$. This result reveals the equivalency of aromatic protons above the coalescence temperature, indicative of (a) 1,2-addition across a 6,6-ring junction at the equatorial belt (e—e bond) or (b) 1,4-addition at the same position. The equatorial bonding structure for **20**, in which either 1,2-adduct **(20a)** or 1,4-adduct **(20b)** structures are conceivable, was confirmed by AM1 molecular orbital calculation (Figure 9).

D. Photochemical and Thermal Additions of Disilirane to Metallofullerene

A toluene solution of La@C_{82} and 1,1,2,2-tetramesityl-1,2-disilirane **(13)** was photoirradiated with a tungsten halogen lamp (cutoff <400 nm) (equation 7)[17]. The MALDITOF mass spectrum of the product shows the presence of La@$C_{82}(Mes_2Si)_2CH_2$ **(21)**. The EPR spectrum of the adduct **(21)** in 1,2,4-trichlorobenzene shows the presence of at least two species, presumably two positionally isomeric forms of the disilirane

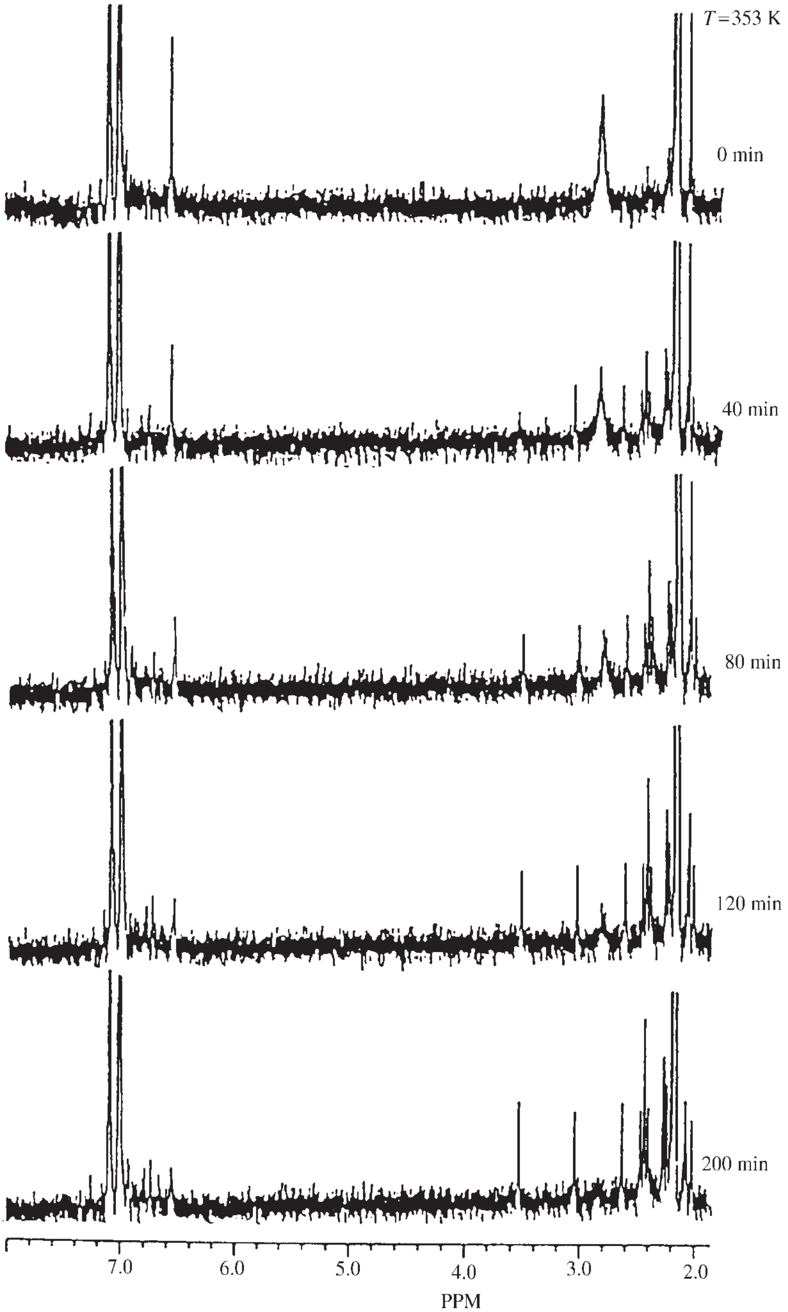

FIGURE 8. Thermal isomerization of 1,2-adduct **(16)** to 1,4-adduct **(17)**

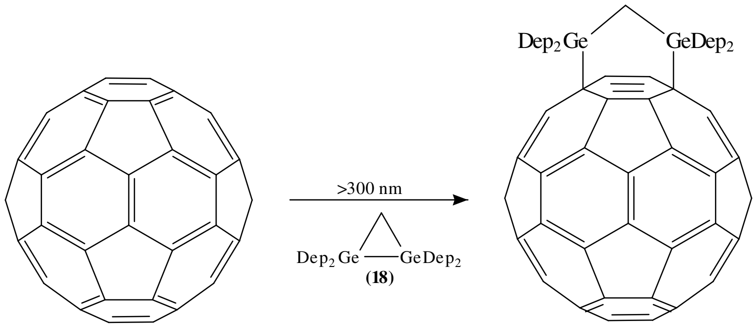

(5)

Dep = 2,6-$Et_2C_6H_3$

twist form

(19)

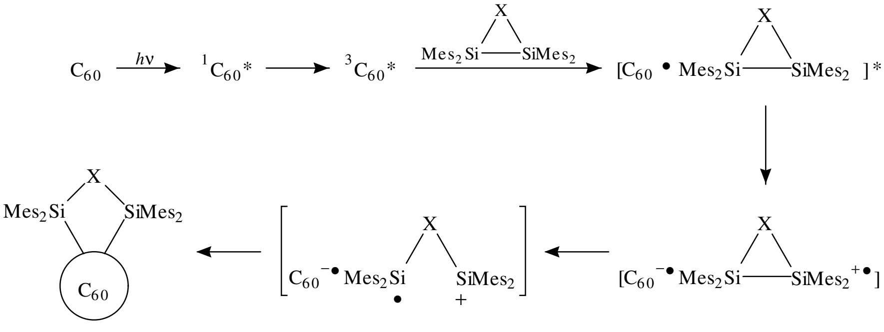

X = CH_2, O

SCHEME 6. A possible mechanism for the formation of bis-silylated fullerene

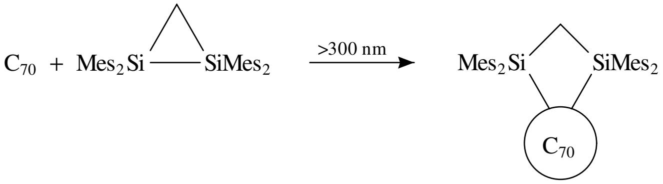

(6)

(13) **(20)**

derivative. La@C_{82} is also thermally reactive towards **13**; in a reaction at 80 °C for 10 h, formation of the adduct **21** was verified by means of mass and EPR spectroscopic studies. The high thermal reactivity of La@C_{82} towards **13** can be rationalized on the basis of its stronger electron donor and acceptor properties relative to C_{60} and C_{70}: *ab initio* calculations predict that while the ionization potential of La@C_{82} (6.19 eV) is much smaller than that of C_{60} (7.78 eV) or C_{70} (7.64 eV), its electron affinity is larger than either that of C_{60} (2.57 eV) or of C_{70} (2.69 eV). Gd@C_{82}[18], La_2@C_{80}[19] and Sc_2@C_{82}[19] are also thermally reactive with disilirane **13**. This can be rationalized on the basis of

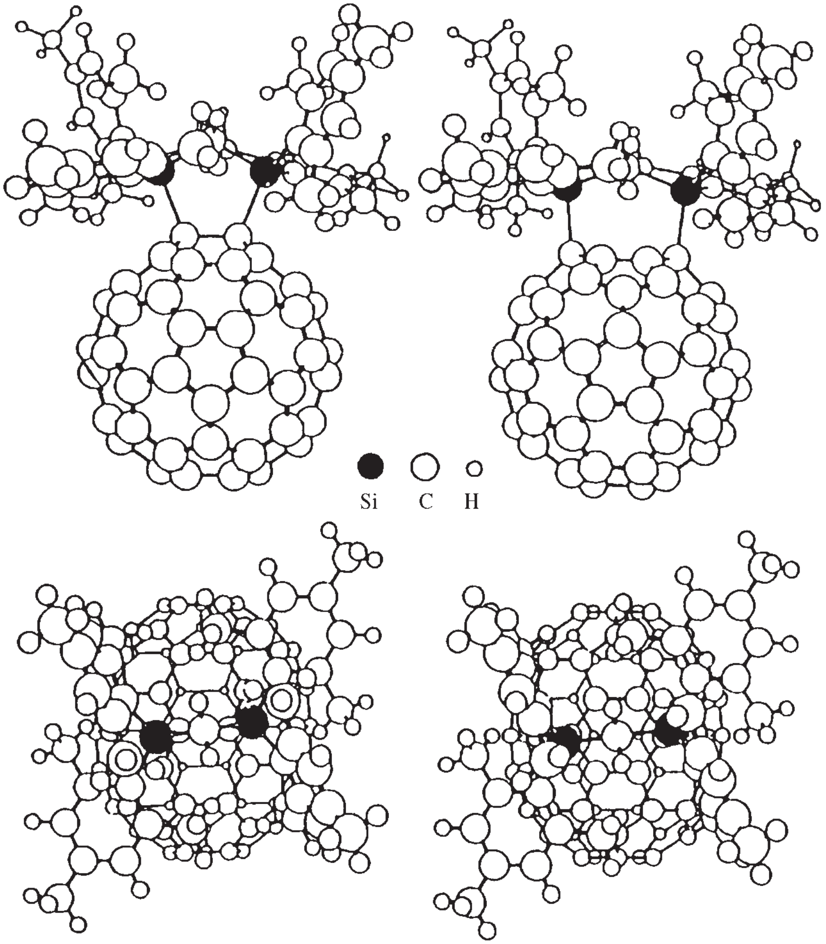

FIGURE 9. Two views of the optimized C_2 structures of **20a** (left) and **20b** (right) calculated with the AM1 method. Reprinted with permission from Ref. 16. Copyright 1994 American Chemical Society

their stronger electron donor acceptor reactivities.

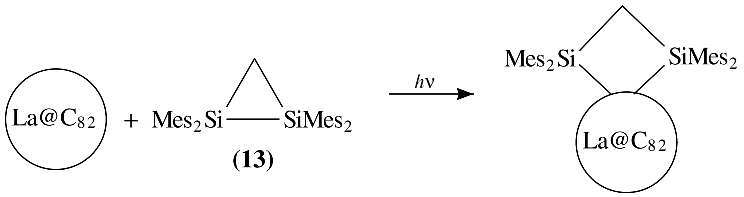

(13)

(21)

(7)

V. PHOTOCHEMICAL ADDITIONS OF POLYSILACYCLOBUTANES AND -BUTENE TO C_{60}

A. Additions of Benzodisilacyclobutene

The reaction of 3,4-benzo-1,2-disilacyclobutene **(22)** with C_{60} yields the corresponding disilacyclohexane derivative **(23)**[20]. Irradiation of a solution of disilacyclobutene **22** and C_{60} in toluene with a low-pressure mercury lamp (254 nm) afforded the brown adduct **23** in 14% yield (based on unreacted C_{60}) (equation 8). The FAB mass spectrum of **23** exhibits one peak at m/z 1024–1027 ($C_{78}H_{32}Si_2$, M^+, molecular cluster ion), as well as one for C_{60} at m/z 720–723. The ^{1}H-NMR spectrum of **23** showed a symmetrical spectrum with two diastereotopic isopropyl methyl protons, one isopropyl methine proton and a AA′BB′ pattern assigned to phenyl protons. The ^{13}C-NMR spectrum of **23** shows 17 signals for the C_{60} skeleton, of which four correspond to two carbon atoms each and 13 correspond to four carbon atoms each: one signal appears at 63.93 ppm and the remainder between 130 and 160 ppm (Scheme 7, Figure 10). This pattern is consistent

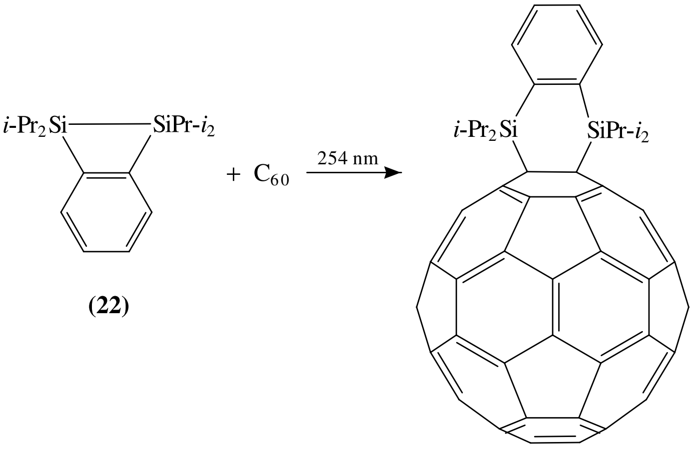

(22) **(23)** (8)

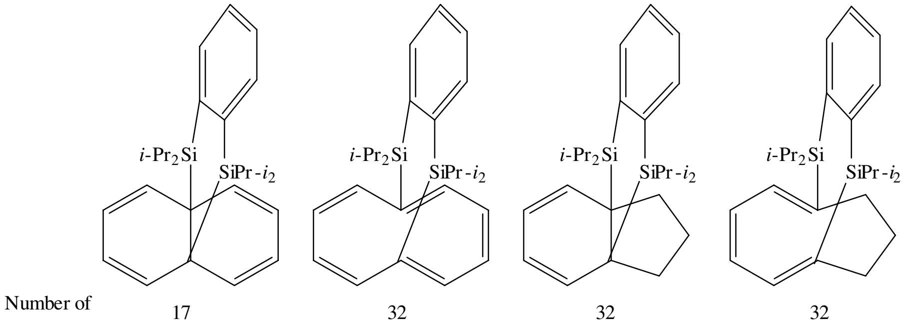

SCHEME 7. Schematic description of benzodisilacyclobutene-C_{60} adduct

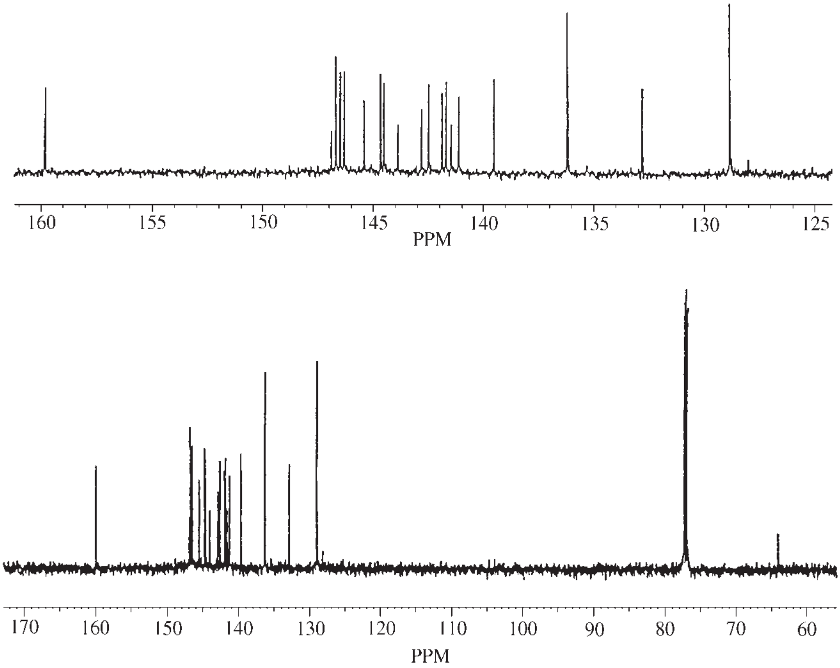

FIGURE 10. ^{13}C NMR spectrum (125 MHz, 1 : 1 CS_2-$CDCl_3$) of **23**. Reprinted by permission of Elsevier Science Ltd from Ref. 20

for a C_{60} adduct of **23**. Furthermore, the ^{13}C-NMR signal at 63.93 ppm strongly supports 1,2-addition. Adduct **23** did not form under the irradiation of a high-pressure mercury lamp (>300 nm), which indicates that the diradical formed by the initial Si−Si bond cleavage is trapped by C_{60} to afford adduct **23**.

B. Additions of Bis(alkylidene)disilacyclobutanes

The photochemical reaction of bis(alkylidene)disilacyclobutane (**24a** and **24b**) with C_{60} by a high-pressure mercury lamp (cutoff <300 nm) proceeds to afford the adducts **26a** (61%) and **26b** (52%) instead of **25**[21]. The formation of these products is a result of an unexpected rearrangement of the disilacyclobutane moiety (equation 9). The FAB mass spectrum of **26a** exhibits one peak at m/z 1056–1059 ($C_{80}H_{40}Si_2$, $M^{+}+1$ cluster), as well as one for C_{60} at m/z 720–723.

The C_{60} unit of **26a** displays 52 resonances in the ^{13}C-NMR spectrum which indicates the absence of any symmetry element in this molecule. One signal has a relative intensity of four, two signals have each a relative intensity of three and one signal has a relative intensity of two; thus the number of carbon atoms sums up to 60. While two fullerene carbon atoms resonate at 63.99 (C^i) and 77.50 (C^h) ppm, the other 50 signals appear in the region between 130–165 ppm. In the ^{1}H-NMR spectrum of **26a**, the four alkylidene methyl protons gave rise to new resonances; two isopropyl methyl protons H^a and $H^{a'}$, isopropyl methine proton H^b, one methyl proton H^g and methylene protons H^f and $H^{f'}$. These observations support the migration of an alkylidene methyl proton to an alkylidene quaternary carbon to form an isopropyl and a 1-propanyl-2-ylidene group. Analysis of the $^{13}C-^{1}H$ three-bond coupling as shown in structure **26** from the $^{13}C-^{1}H$ COLOC and HMBC (^{1}H-Detected Multiple-bond Heteronuclear Multiple Quantum Coherence Spectrum) NMR of **26a** allowed one to show that the isopropyl group (H^{a}, H^{b}) is connected to the olefinic carbon (C^{c}), whereas methyl (H^{g}) and methylene (H^{f}, $H^{f'}$) groups are bonded to another olefinic carbon (C^{d}) and fullerene carbon (C^{h}) through quaternary carbon (C^{e}) shown in **26a** and **26b** (Scheme 8).

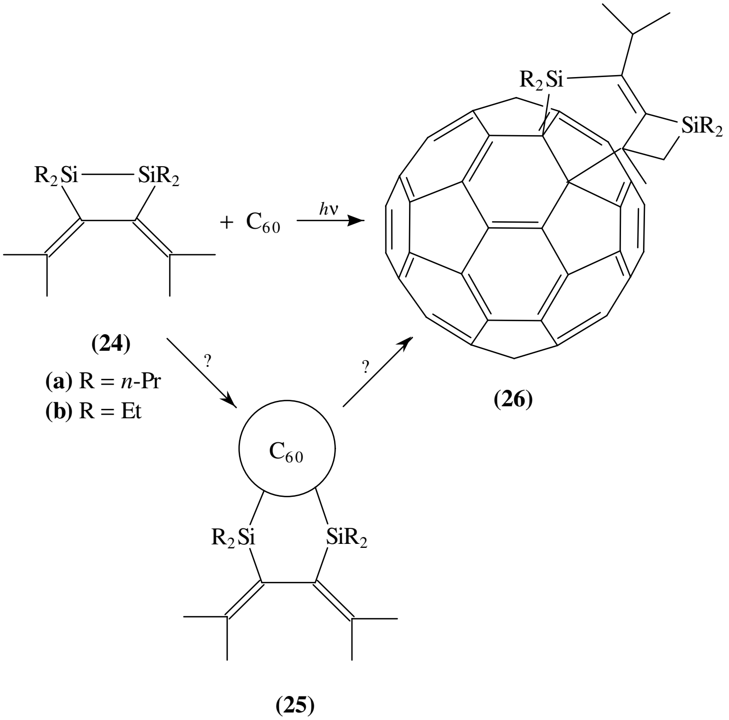

(24)

(a) R = *n*-Pr

(b) R = Et

(26)

(25)

(9)

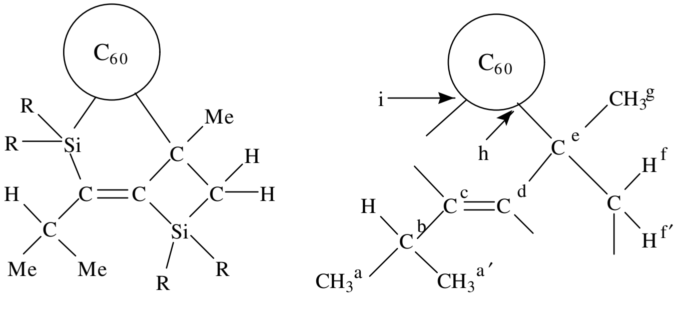

(26a) **(26c)**

SCHEME 8. Connectivities derived from $^{1}H-^{1}H$ and $^{1}H-^{13}C$ shift correlation experiments

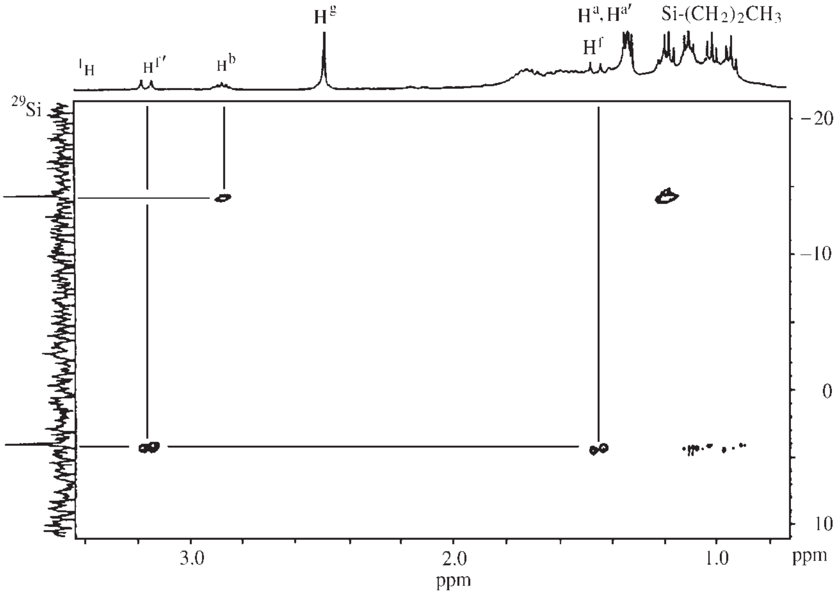

FIGURE 11. ^{29}Si-^{1}H HMBC NMR spectrum of **26a**. Reprinted with permission from Ref. 21. Copyright 1994 American Chemical Society

In order to narrow down the possibilities, Ando and coworkers[21] measured ^{29}Si−^{1}H HMBC spectra. The ^{29}Si-NMR spectrum of **26a** showed two peaks at 4.20 and −14.30 ppm. From the ^{29}Si−^{1}H HMBC spectrum of **26a** the silicon resonance at −14.30 ppm correlates with isopropyl methine proton (H^b) and the silicon resonance at 4.20 ppm correlates with the methylene protons (H^f, H$^{f'}$) (Figure 11). Furthermore, NOE enhancement of **26a** was observed for signals between isopropyl methyl and methine protons and the four Si-*n*-propyl methyl groups. Clearly this is only possible for structure **26a.** With regard to the addition pattern of the fullerene moiety, a 1,2-junction of the silabutene fragment is most probable. In this arrangement, two diastereomeric adducts are expected.

C. Additions of Cyclotetrasilanes and Cyclotetragermane

Photochemical reactions of cyclotetrasilane **27a** with C_{60} by irradiation of a solution of the reactants in toluene with a high-pressure mercury lamp (>300 nm) for 6 h yielded **28a** and **29a** in 13% and 46% yields, respectively (based on unreacted C_{60}) (equation 10)[22]. Similarly, the adducts **29b** and **29c** were obtained from the reaction of **27b** and **27c** in 87% and 41% yields, respectively, but **28b** and **28c** were not obtained.

The FAB mass spectrum of **28a** exhibits one peak at m/z 1560−1563 ($C_{116}H_{56}Si_4$, $M^+ + 1$, molecular cluster ion), as well as one for C_{60} at m/z 720−723. The ^{13}C-NMR spectrum of **28a** displays 38 signals for all quaternary carbons. The ^{1}H-NMR spectrum of **28a** displays 4 methyl signals and 4 pairs of AB quartets, supporting a C_s symmetry for the molecule. The ^{29}Si-NMR spectrum of **28a** shows two peaks at −22.25 and −11.34 ppm which are assigned to the silicon atoms of **28a**. Symmetry arguments support the following

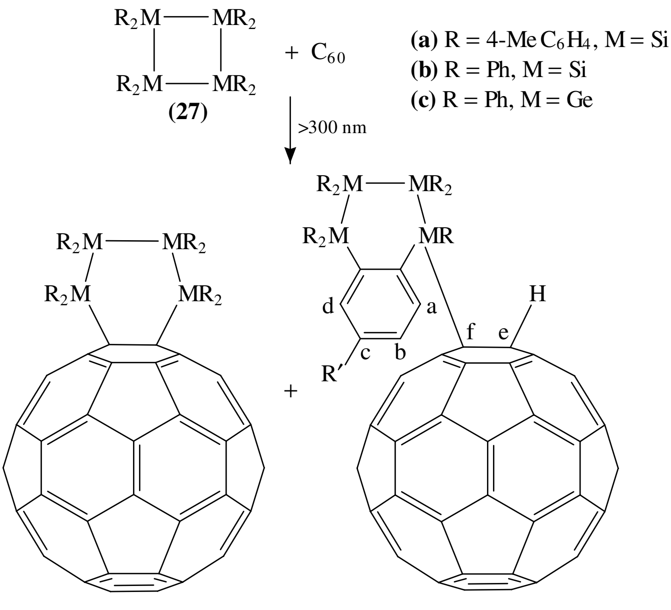

(27)

(a) $R = 4\text{-}MeC_6H_4$, M = Si
(b) R = Ph, M = Si
(c) R = Ph, M = Ge

(10)

(28) **(29)**

(a) $R = 4\text{-}MeC_6H_4$, $R' = Me$, M = Si
(b) R = Ph, $R' = H$, M = Si
(c) R = Ph, $R' = H$, M = Ge

possibilities: (i) a 1,6-junction or a 1,4-addition to the C_{60} with ring inversion (a frozen conformer with this addition mode would give 60 signals in the ^{13}C NMR for the C_{60} moiety) and (ii) a 1,2-junction on the C_{60} with a frozen conformer (no ring inversion) (Scheme 9). A chemical shift change of the *p*-tolyl groups, reflecting a conformational change of the molecule, was observed by variable-temperature ^1H-NMR measurement. Therefore, a 1,2-junction on the C_{60} moiety with a frozen conformer is the most probable structure for **28a**. The FAB mass spectrum of **29a** exhibits one peak at m/z 1560–1563 ($C_{116}H_{56}Si_4$, $M^+ + 1$, molecular cluster ion), as well as one for C_{60} at m/z 720–723. The ^{13}C-NMR spectrum of **29a** displays 64 signals for all quaternary carbon which indicates the absence of any symmetry element in this structures. One 4-methyl-*o*-phenylene group and other seven $4\text{-}MeC_6H_4$ groups appear in the ^1H, ^{13}C, $^1H-^1H$ COSY $^1H-^{13}C$ COSY experiments. The presence of one hydrogen connected to C_{60} is deduced from the appearance of one doublet at 60.35 (C^e) ppm in the ^{13}C NMR and one singlet at δ 6.91 (H^e) in the ^1H-NMR spectrum, respectively. The ^{29}Si-NMR spectrum shows four peaks at −44.83, −41.26, −24.30 and −12.66 ppm which are assigned to the silicon atoms of **29a**. The connectivities between these structural elements were determined by ^{29}Si-^1H HMBC experiment. It was shown that the silicon resonance at −12.66 ppm correlated with both H^a and H^e methine proton signals (Figure 12). The mechanistic pathway suggested for the formation of **28** and **29** was supported by control experiments; photochemical reaction (>300 nm) of **27b** in the presence of CCl_4 affords 1,4-dichloro-1,1,2,2,3,3,4,4-octaphenyltetrasilane **(30b)** and 1,3-dichloro-1,1,2,2,3,3-hexaphenyltrisilane **(31b)** in 37% and 31% yield, respectively. Under identical photolytic conditions, adduct **28a** did not convert to **29a** in a control experiment. These findings indicate that biradical **32** might be

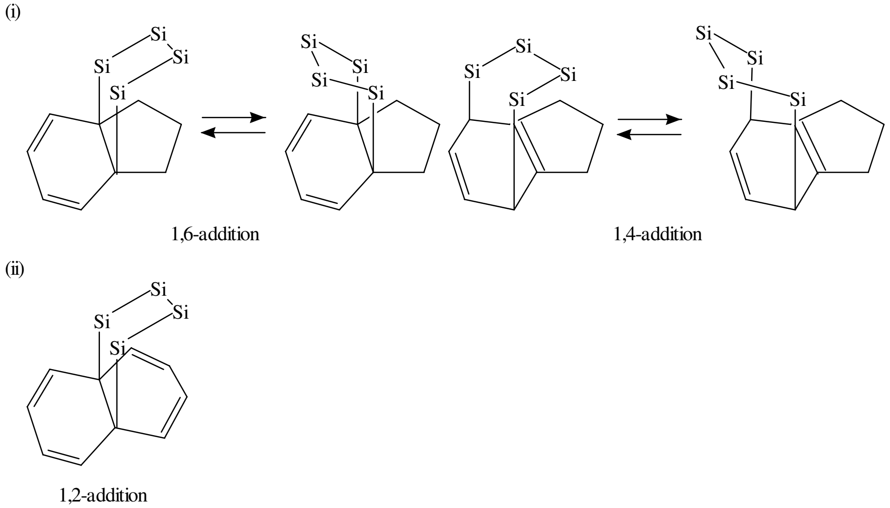

SCHEME 9. Schematic description of cyclotetrasilane-C_{60} adduct

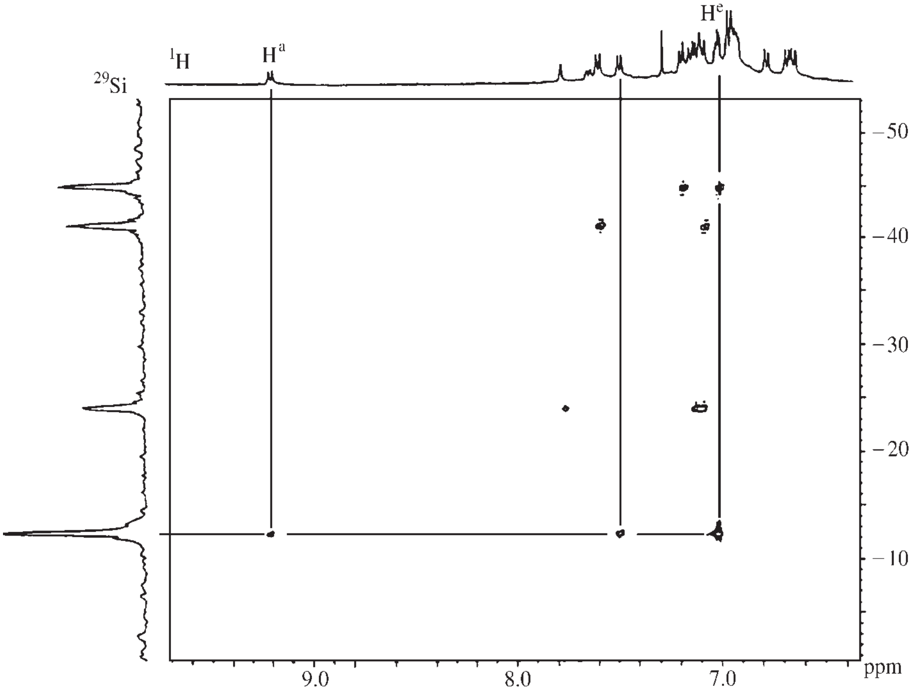

FIGURE 12. ^{29}Si-^{1}H HMBC NMR spectrum of **29a**. Reprinted with permission from Ref. 22. Copyright 1995 American Chemical Society

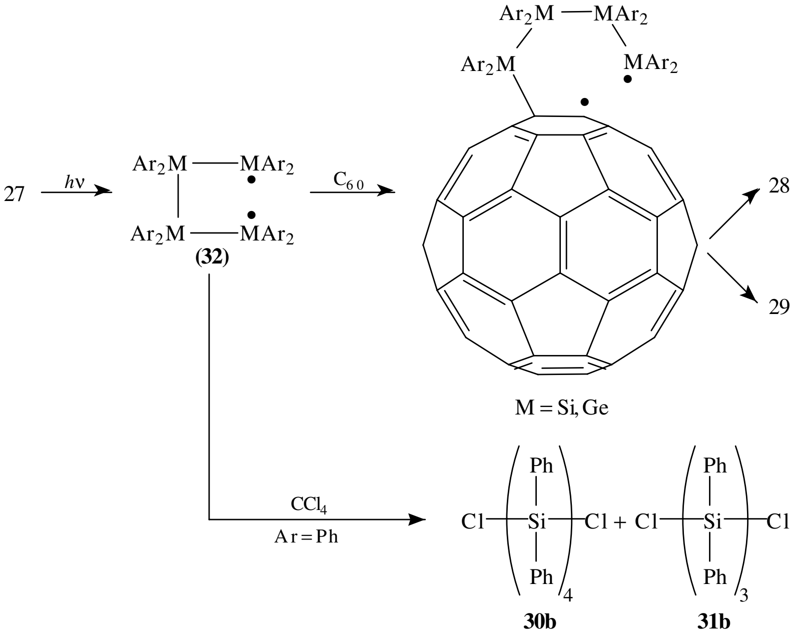

SCHEME 10. A possible mechanism for the formation of **28** and **29**

involved in the course of the reaction (Scheme 10).

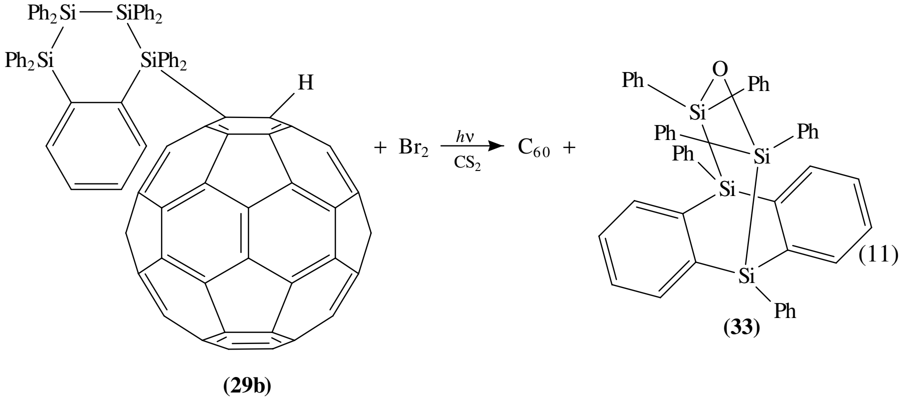

In the reaction of cyclotetragermane **27c**, products **28c** and **29c** were obtained in 43% and 37% yields, respectively, based on unreacted C_{60}. In order to examine the reactivity of fullerene-silicon derivatives, **29b** was irradiated with a carbon disulfide solution of bromine. Purification of the product by means of gel-permeation chromatography afforded C_{60} and **33** in 93% and 45% yields, respectively (equation 11)[23]. The structure of **33** was determined by X-ray crystallographic analysis (Figure 13). Adduct **33b** did not react with bromine in the dark, and therefore a bromine radical seems to participate in this reaction.

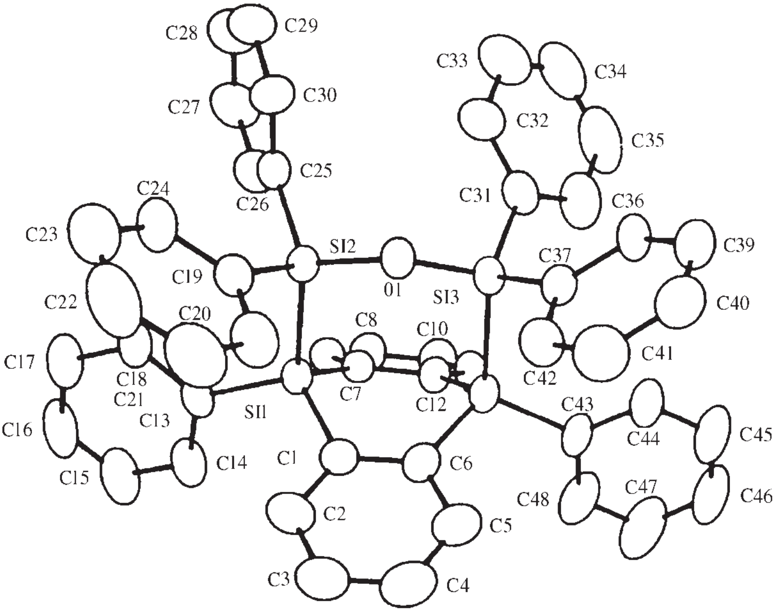

FIGURE 13. X-ray structure of **33**

VI. REACTIONS OF SILYLLITHIUM REAGENTS WITH C_{60}

Nucleophilic addition to C_{60} is among the most common reaction types in fullerene chemistry. The reactions of silyllithium reagents with C_{60} have been reported by Kusukawa and Ando (equation 12)[24]. Reactions of C_{60} with Ph_3SiLi have been unsuccessful and formation of a brown precipitate was observed at −78 °C; when the suspension was quenched with EtOH, only C_{60} was recovered. The analogous reaction with other silyllithium derivatives ($Me_2PhSiLi$, $MePh_2SiLi$, $Et_2PhSiLi$, $EtPh_2SiLi$) leads to similar results. On the other hand, diisopropylphenylsilyllithium **34a** reacted with C_{60} under these conditions to produce **35a** in 78% yield (based on unreacted C_{60}) upon quenching with EtOH (Table 4). The ^{13}C-NMR spectrum of **35a** displays 30 signals for the C_{60} carbons, supporting a C_s symmetry for the molecule. Similarly, diphenylisopropyl- and diphenyl-*t*-butyl-silyllithiums, **34b** and **34c**, react with C_{60} to give monoadducts **35b** and **35c**, respectively.

On the other hand, the reaction of tris(trimethylsilyl)silyllithium **34d** with equivalent amounts of C_{60} at −78 °C give bisadduct **36d** in 69% yield (based on unreacted C_{60}), and the monoadduct **35d** could not be detected. The FAB mass spectra of **36d** exhibit one peak at m/z 1215–1218 ($C_{78}H_{54}Si_8$, $M^+ + 1$, molecular cluster ion), as well as one for C_{60} at m/z 720–723. The ^{13}C-NMR spectrum of **36d** displays 29 signals for all quaternary carbons. Symmetry arguments support a 1,6-addition or 1,4-addition to the C_{60}; however, a 1,6-addition of the bulky substituent [$(TMS)_3Si$] is unfavorable. Modification **36d** crystallized in the triclinic space group $P - 1$, with two enantiomorphic molecules of **36d** and two CS_2 molecules in the unit cell, and the crystal structure of **36d** and selected bond angles are shown in Figure 14. The C−C bond lengths C(2)−C(12), C(9)−C(10), C(11)−C(28) and C(13)−C(30) are located within 1.363(7)–1.390(7) Å, which are close to the C−C double-bond length. The bond angles between fullerene C atoms, excluding the bonds in rings A and B, are 107.3(4)–109.2(4) deg in the pentagons and 118.3(4)–121.5(5) deg in the hexagons, values which are within the normal range. The lengths of the bond in the C_{60} skeleton, excluding the bonds in rings A and B, range from 1.371(7) to 1.474(8)Å (Figure 15). The structure of **36d** is a new type of addition mode to the C_{60}.

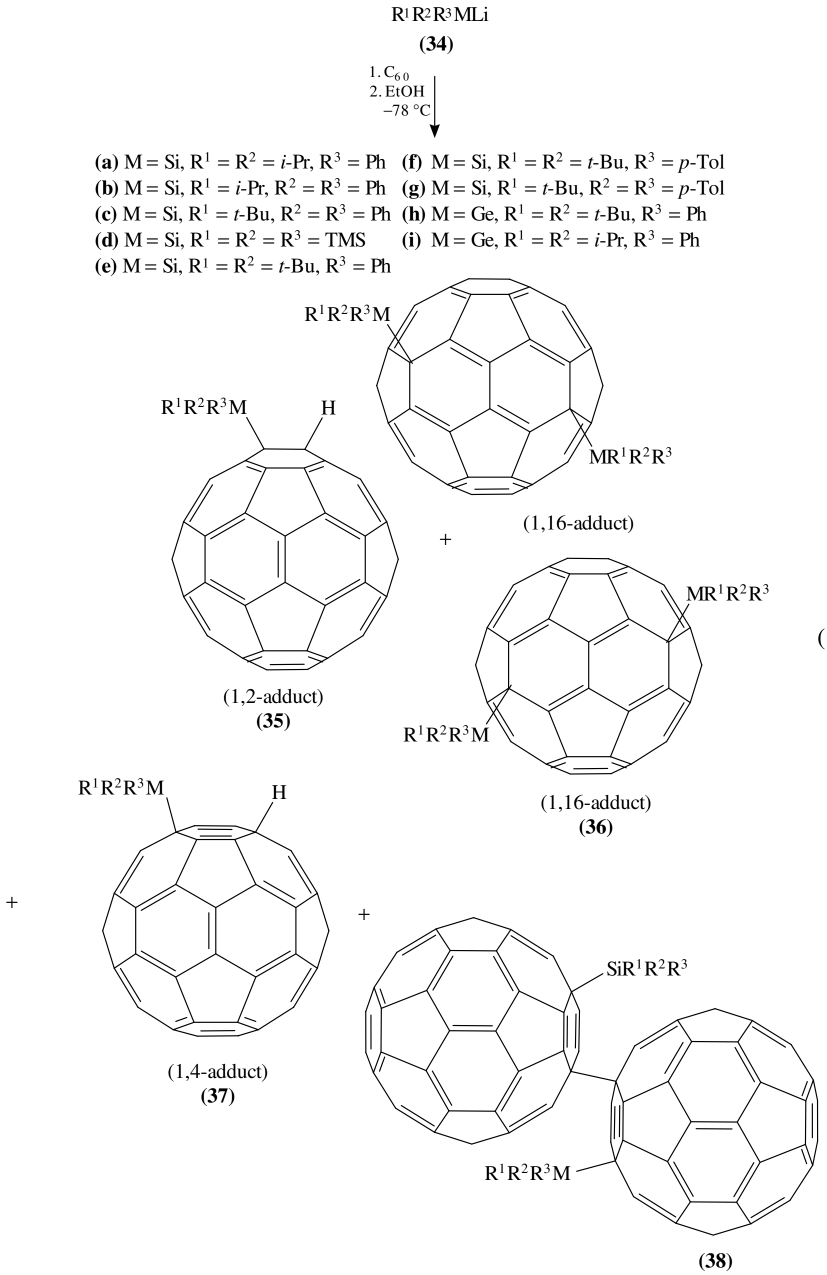

(a) M = Si, $R^1 = R^2 = i$-Pr, R^3 = Ph
(b) M = Si, $R^1 = i$-Pr, $R^2 = R^3$ = Ph
(c) M = Si, $R^1 = t$-Bu, $R^2 = R^3$ = Ph
(d) M = Si, $R^1 = R^2 = R^3$ = TMS
(e) M = Si, $R^1 = R^2 = t$-Bu, R^3 = Ph
(f) M = Si, $R^1 = R^2 = t$-Bu, $R^3 = p$-Tol
(g) M = Si, $R^1 = t$-Bu, $R^2 = R^3 = p$-Tol
(h) M = Ge, $R^1 = R^2 = t$-Bu, R^3 = Ph
(i) M = Ge, $R^1 = R^2 = i$-Pr, R^3 = Ph

(12)

TABLE 4. Reactions of silyllithium reagents with C_{60}

Silyllithium	Product and isolated yield (%)			
	35	**36**	**37**	**38**
34a	78			
34b	80			
34c	50	22		
34d		69		
34e		72		
34f	11	42	11	6
34g		29	19	7
34h		87		
34i	76			

Relative energies of the bis adducts ($[(TMS)_3Si]_2C_{60}$) calculated by the AM1 method (Scheme 11) are: 1,6 (1041.6 kcal mol^{-1}) >1,2 (1024.8 kcal mol^{-1}) >1,4 (987.5 kcal mol^{-1}) >1,16 or 1,29 (977.9 kcal mol^{-1}). Additions of two $(TMS)_3Si$ groups to the 1,2-and 1,4-positions are unfavourable because of steric hindrance. Therefore, the $(TMS)_3Si$ groups might be bonded to the 1,16 (or 1,29) positions. The UV-vis absorption spectrum of **35a**–**35c** shows absorption at 416–417 nm and 444–445 nm. On the other hand, bisadducts **36d** and **36e** show broad absorption at 520–600 nm.

Interestingly, silyllithium reagents substituted with aromatic electron-releasing groups (**34f)** and **34g**) gave **35** (1,2-adduct), **36** (1,16- and 1,29-adduct), **37** (1,4-adduct) and **38** (dimer at 1,4-position) which can be separated by gel permeation chromatography (GPC). The ^{13}C-NMR spectrum of **37f** displays 60 signals for all quaternary carbons.

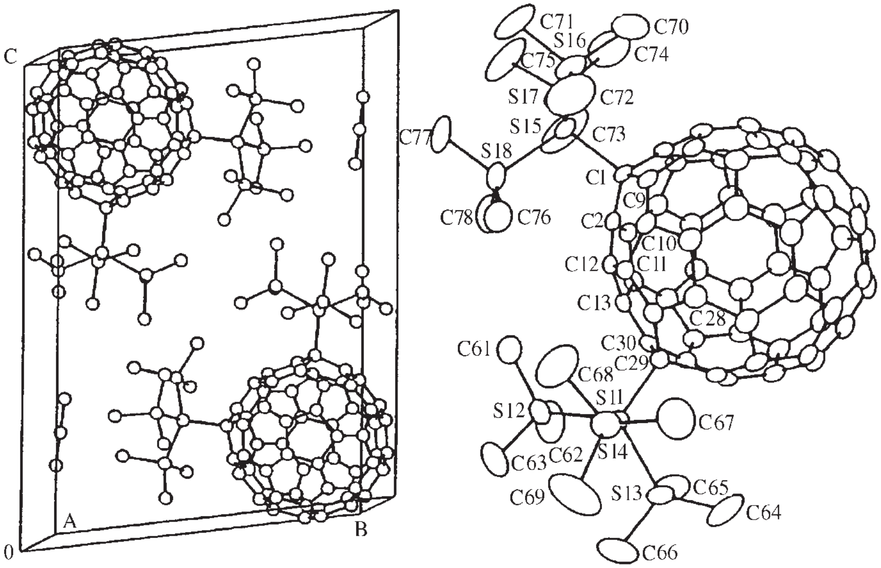

FIGURE 14. X-ray crystallographic characterization of **36d**·CS_2. Left: arrangement in the unit cell. Right: crystal structure of one of the two enantiomorphic molecules in the unit cell. The ellipsoids represent 50% probability. From Ref. 26

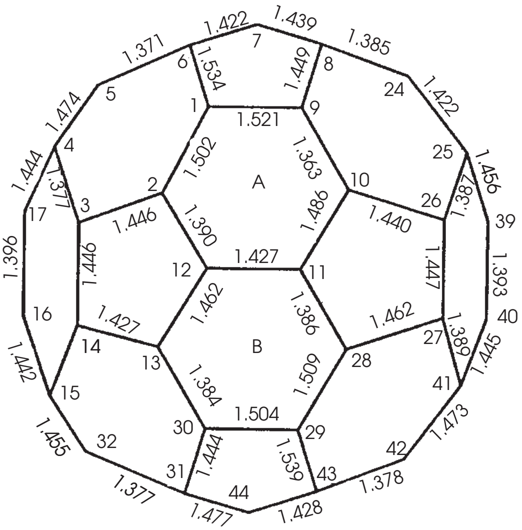

FIGURE 15. Details of bond lengths (Å) and selected bond angles (°) in **36d**: C(2)–C(1)–C(6) 121.9, C(2)–C(1)–C(10) 109.1, C(6)–C(1)–C(10) 117.3, C(1)–C(2)–C(3) 123.2, C(2)–C(3)–C(4) 110.2, C(3)–C(4)–C(5) 124.0, C(4)–C(5)–C(6) 120.6, C(1)–C(6)–C(5) 117.2, C(1)–C(6)–C(7) 122.0, C(5)–C(6)–C(7) 108.9, C(6)–C(7)–C(8) 123.3, C(7)–C(8)–C(9) 109.7, C(8)–C(9)–C(10) 124.3, C(1)–C(10)–C(9) 120.4. Reproduced by permission of VCH Verlagsgesellschaft mbH from Ref. 24

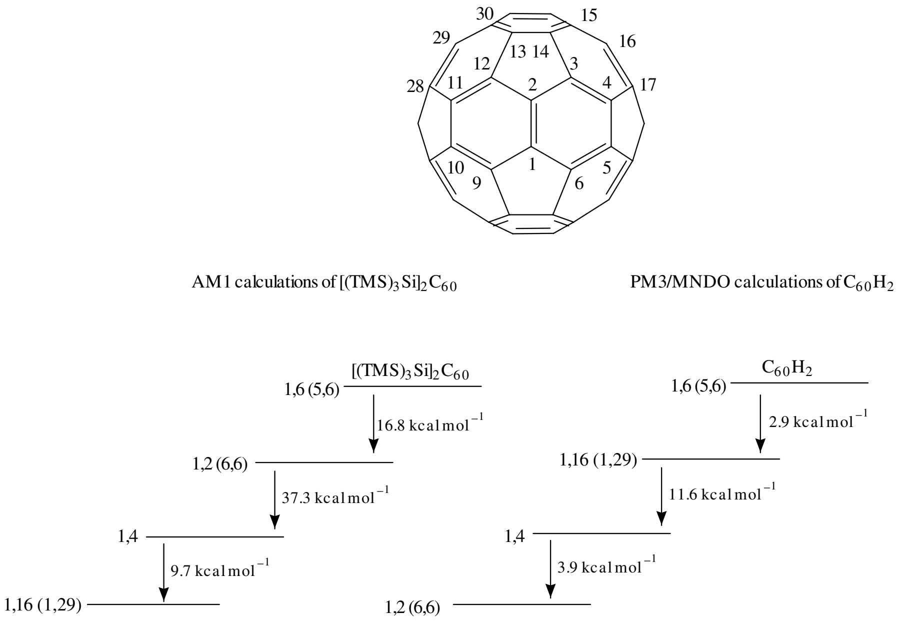

SCHEME 11. Relative energies of $[(TMS)_3Si]_2C_{60}$ and $C_{60}H_2$ isomers

TABLE 5. HOMO energies of hydrosilanes calculated by semiempirical methods

Hydrosilane	HOMO (eV)		Product formed
	PM3	AM1	
$(TMS)_3SiH$	−8.60	−9.24	
t-Bu_2(p-Tol)SiH	−9.01	−9.22	Bis-adduct
t-Bu(p-$Tol)_2SiH$	−9.02	−9.23	
t-Bu_2PhSiH	−9.16	−9.45	
t-$BuPh_2SiH$	−9.20	−9.49	
i-Pr_2PhSiH	−9.22	−9.50	Mono-adduct
i-$PrPh_2SiH$	−9.29	−9.52	
Et_2PhSiH	−9.30	−9.53	
$MePh_2SiH$	−9.34	−9.59	
Ph_3SiH	−9.36	−9.52	No reaction
Me_2PhSiH	−9.39	−9.62	
$EtPh_2SiH$	−9.41	−9.59	

One fullerene carbon resonates at 62.37 ppm whereas the signals of all other carbons appear in the region between δ 130 and 160 ppm. The partial structure of the fragment annulated to the C_{60} moiety can be derived from the NMR spectroscopic properties for **37f**. The presence of one hydrogen connected to C_{60} is deduced from the appearance of one doublet at 49.54 ppm in the ^{13}C-NMR spectrum and one singlet at 5.44 ppm in the ^{1}H-NMR spectrum, respectively. The ^{29}Si-NMR spectrum of **37f** shows one signal at 3.59 ppm. From these findings, a 1,4-ring junction is most probable for **37f**. The MALDI-TOF mass spectrum of **38f** exhibits one peak at m/z 1907 ($C_{150}H_{50}Si_2$, M^+, molecular cluster ion), as well as one peak for C_{60} at m/z 720. The ^{13}C-NMR spectrum of **38f** displays 60 signals for all quaternary carbons; two fullerene carbons resonate at 75.49 and 62.19 ppm and the signals of all other carbons appear in the region between 135 and 160 ppm. The ^{29}Si-NMR spectrum of **38f** shows one signal at 6.17 ppm, which is assigned to the silicon atoms of **38f**. Additionally, germyllithium compounds **34h** and **34i** also gave mono- and bis-adducts, selectively.

The reactivity difference of the silyllithium reagents raises some questions concerning the mechanism. To clarify the mechanistic pathway, it was examined by semiempirical calculations using hydrosilanes instead of silyllithium compounds (Table 5)[25]. As deduced from the HOMO energies of Table 5, electron-releasing substituents favor the formation of adducts **35** and **36**, which indicate that their formation should involve a radical reaction proceeding via electron transfer from the silyllithium to C_{60}.

In order to clarify the mechanistic pathway, the photochemical reactions of disilanes **39** with C_{60} were carried out and gave 1,16- and 1,29-adducts (equation 13, Table 6)

TABLE 6. Photochemical reactions of disilanes with C_{60}

Disilane	Product and isolated yield (%)	
	36	**40**
39c	56	
39e	62	
39g	54	
39i	43	24

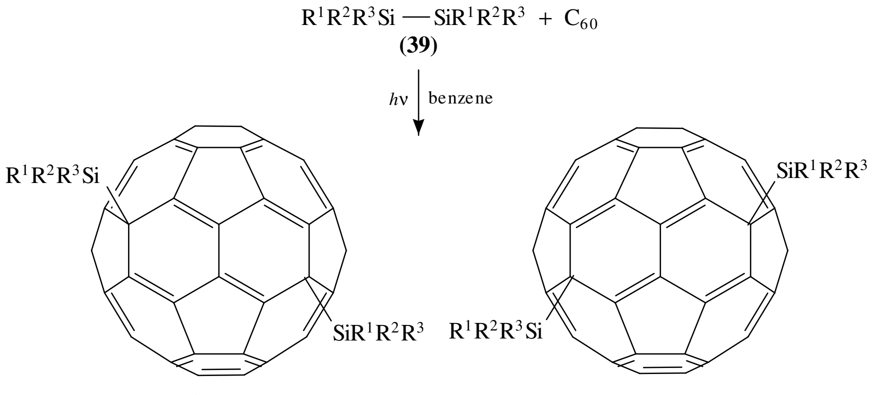

(1,16-adduct)

(1,29-adduct)
(36)

(13)

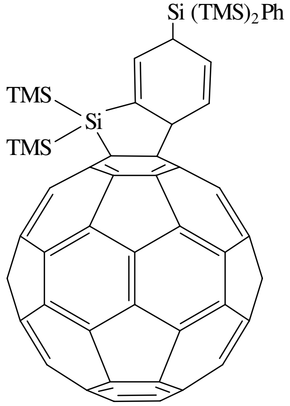

(40)

(c) $R^1 = t\text{-Bu}, R^2 = R^3 = \text{Ph}$
(e) $R^1 = R^2 = t\text{-Bu}, R^3 = \text{Ph}$
(g) $R^1 = t\text{-Bu}, R^2 = R^3 = p\text{-Tol}$
(k) $R^1 = \text{TMS}, R^2 = R^3 = \text{Ph}$

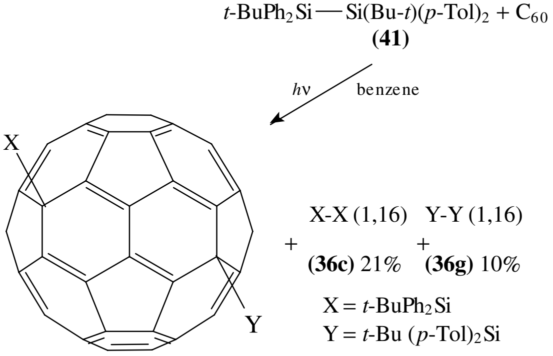

(1,16-adduct)
(42) 17%

+ X-X (1,16) **(36c)** 21% + Y-Y (1,16) **(36g)** 10%

$X = t\text{-BuPh}_2\text{Si}$
$Y = t\text{-Bu}\ (p\text{-Tol})_2\text{Si}$

(14)

in moderate yields; in the case of **39k**, rearranged product **40** was also obtained as a by-product, probably via a radical reaction. When unsymmetrical disilane **41** was reacted with C_{60}, bis-adducts **36c**, **36g** and **42** which should involve the additions of silyl radicals, were formed (equation 14).

VII. REACTIONS OF SILICON-SUBSTITUTED NUCLEOPHILES

A. Reactions of Silylmethyl Grignard Reagents

Addition reactions of Me_2YSiCH_2MgCl (**43**) to C_{60} provided two products, $HC_{60}CH_2SiYMe_2$ (**44**) and $[Me_2YSiCH_2]_2C_{60}$ (**45**) (Y = Me, H, CH=CH$_2$, Ph, OPr-*i*)[26] (equation 15). Selective preparation of either **44** or **45** was accomplished by a selection of the solvent. **44** is formed in THF, whereas **45** was produced in toluene. ^{13}C-NMR resonances of the C_{60} moiety of **44** consist of 30 carbons in the aromatic region and two carbons around 62 ppm (one CH and one quaternary carbon). However, ^{13}C-NMR resonances of **45** are compatible with 31 carbons in the aromatic region and one carbon at 54.90 ppm.

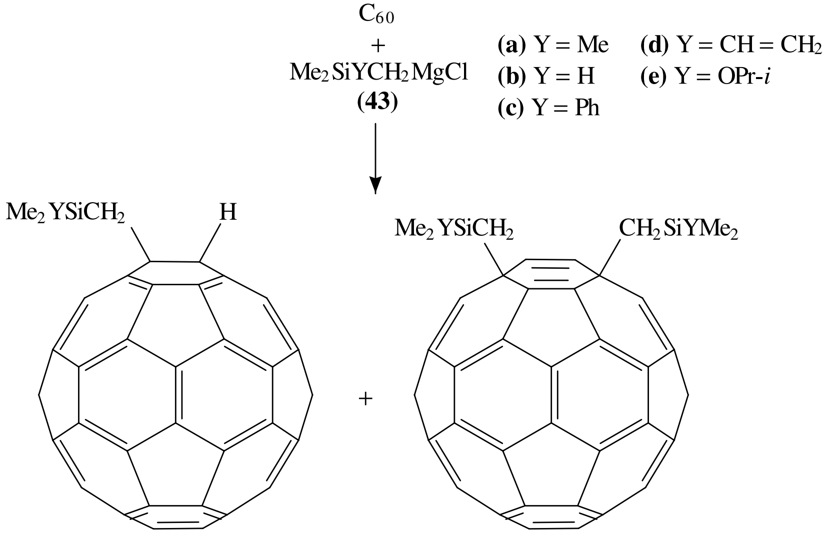

(44) **(45)**

(15)

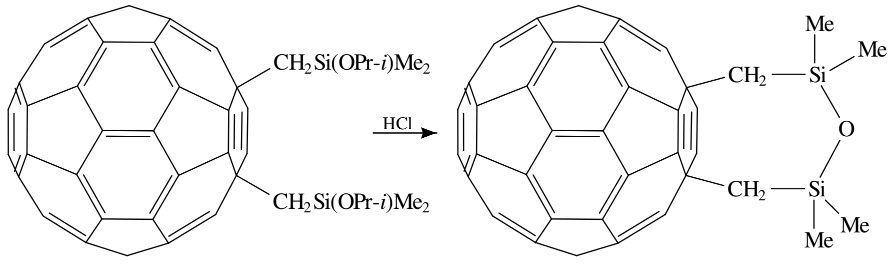

(45e) **(46)** (16)

Nagashima and coworkers prepared cyclic siloxane **46** in 76% yield by acidic hydrolysis of adduct **45e**[27]. This is the first well-characterized siloxane containing C_{60} (equation 16).

Treatment of **44e** with 3 equivalents of $AlCl_3$ gave chlorosilane **47**. Treatment of silica with **47** and pyridine in refluxing toluene gave modified silica **(48)** (equation 17). Its carbon content was 7.18%, suggesting that 0.21 molecule of C_{60} is present per 100 Å^2 of silica surface. A mixture of C_{60} and C_{70} was well separated by means of modified silica **(48)**. No separation occurred using unmodified silica as a stationary phase.

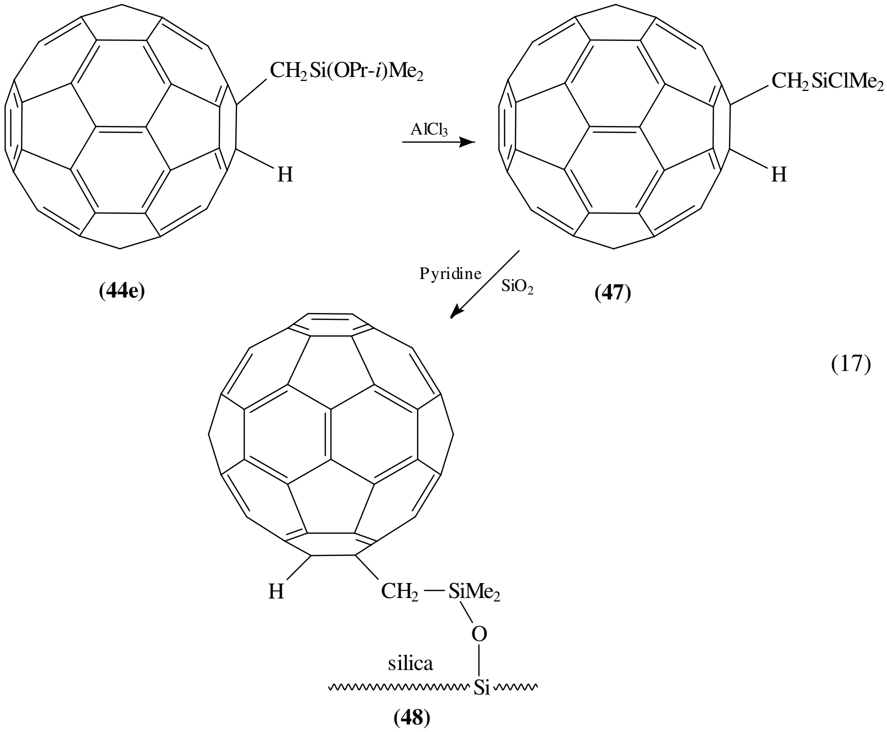

(17)

B. Reactions of Silyl-acetylene Nucleophiles

Nucleophilic addition of lithium trimethylsilylacetylide **(49)** to C_{60} to produce the adduct **50** (equation 18) was reported by Diederich and coworkers[28]. The structure of

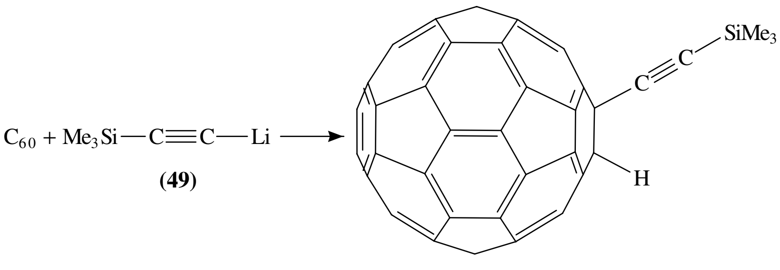

(18)

50 is evident from its spectral data. Its ^{1}H-NMR spectrum shows one singlet corresponding to the fullerene proton. The addition proceeds in a 1,2 fashion, as judged by the 32 fullerene resonances in the ^{13}C-NMR spectrum of **50**. At the same time, Komatsu and coworkers also reported the addition of **49** to the C_{60}[29].

VIII. REACTIONS OF SILYL DIAZONIUM COMPOUNDS

A broad variety of methano-bridged fullerenes are accessible by the reaction of C_{60} with different diazomethanes. This chemical transformation of C_{60} was discovered by Wudl and is based on the findings that C_{60} behaves as an 1,3-dipolarphile[3].

Reactions of the silyldiazonium compounds with C_{60} were examined[30]. To the toluene solution of C_{60} was slowly added the silyldiazonium compounds at room temperature and the products obtained were separated by gel permeation chromatography (equation 19). The yields of the mono-, bis- and tris-adducts are given in Table 7. The ^{1}H-NMR chemical shift of the methine proton and the $^{2,3}J_{C-H}$ coupling constants with the C_{60} carbon support the methanoannulene structure **(51)**.

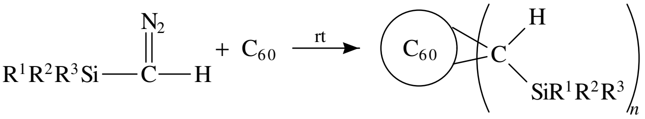

(19)

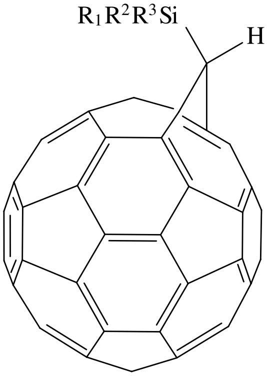

(51)

Under similar conditions, bis(silyl)diazonium compounds (**52**) do not react with C_{60} even under reflux (equation 20).

TABLE 7. Yields of methanoannulene products from reaction 19

	$n = 1$	$n = 2$	$n = 3$
$R^1 = R^2 = R^3 = Me$	34%	24%	22%
$R^1 = Ph, R^2 = R^3 = Me$	41%	29%	8%
$R^1 = 3,4\text{-}(MeO)_2C_6H_3, R^2 = R^3 = Me$	41%	29%	8%

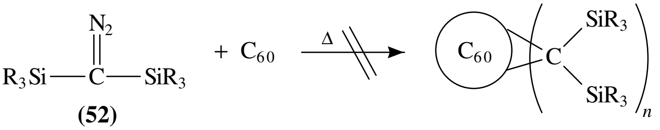

(20)

IX. REFERENCES

1. (a) H. W. Kroto, A. W. Allaf and S. P. Balm, *Chem. Rev.,* **91**, 1213 (1991).
   (b) H. W. Kroto, J. R. Heath, S. C. O'Brien, R. F. Curl and R. E. Smalley, *Nature*, **318**, 162 (1985).
   (c) W. Kräschmer, L. Lamb, K. Fostiropoulos and D. R. Huffman, *Nature*, **347**, 354 (1990).
   (d) W. Kräschmer, K. Fostiropoulos and D. R. Huffman, *Chem. Phys. Lett.*, **170**, 167 (1990).
2. See the issue of *Acc. Chem. Res.*, **25**, 98–175 (1992).
3. F. Diederich, L. Isaacs and D. Philip, *Chem. Soc. Rev.*, 243 (1994).
4. A. Hirsch, *Angew. Chem., Int. Ed. Engl.*, **32**, 1138 (1993).
5. G. Hammond and V. J. Kuck (Eds.), *Fullerenes: Synthesis, Properties, and Chemistry of Large Carbon Clusters*, ACS Symposium Series 481, American Chemical Society, Washington, DC, 1992.
6. R. West, In *The Chemistry of Organic Silicon Compounds* (Eds. S. Patai and Z. Rappoport), Chap. 19, Wiley, Chichester, 1989, pp. 1207–1240.
7. R. D. Miller and J. Michl, *Chem. Rev.*, **89**, 1359 (1989).
8. Y. Wang, R. West and C.-H. Yuan, *J. Am. Chem. Soc.*, **115**, 3844 (1993).
9. A. Watanabe and O. Ito, *J. Phys. Chem.*, **98**, 7736 (1994).
10. A. Watanabe, O. Ito and K. Mochida, *Organometallics*, **14**, 4281 (1995).
11. T. Akasaka, W. Ando, K. Kobayashi and S. Nagase, *J. Am. Chem. Soc.*, **115**, 1605 (1993).
12. T. Akasaka, E. Mitsuhida, W. Ando, K. Kobayashi and S. Nagase, *J. Chem. Soc., Chem. Commun.*, 1529 (1995).
13. T. Akasaka, W. Ando, K. Kobayashi and S. Nagase, *J. Am. Chem. Soc.*, **115**, 10366 (1993).
14. T. Akasaka, E. Mitsuhida, W. Ando, K. Kobayashi and S. Nagase, unpublished results.
15. T. Akasaka, T. Mizushima, W. Ando, K. Kobayashi and S. Nagase, unpublished results.
16. T. Akasaka, E. Mitsuhida, W. Ando, K. Kobayashi and S. Nagase, *J. Am. Chem. Soc.*, **116**, 2627 (1994).
17. T. Akasaka, T. Kato, K. Kobayashi, S. Nagase, K. Yamamoto, H. Funasaka and T. Takahashi, *Nature*, **374**, 600 (1995).
18. T. Akasaka, S. Nagase, K. Kobayashi, T. Suzuki, T. Kato, K. Yamamoto, H. Funasaka and T. Takahashi, *J. Chem. Soc., Chem. Commun.*, 1343 (1995).
19. T. Akasaka, S. Nagase, K. Kobayashi, T. Suzuki, T. Kato, K. Kikuchi, Y. Achiba, K. Yamamoto, H. Funasaka and T. Takahashi, *Angew. Chem., Int. Ed. Engl.*, **34**, 2139 (1995).
20. T. Kusukawa, A. Shike and W. Ando, *Tetrahedron*, **52**, 4995 (1996).
21. T. Kusukawa, Y. Kabe, T. Erata, B. Nestler and W. Ando, *Organometallics*, **13**, 4186 (1994).
22. T. Kusukawa, Y. Kabe and W. Ando, *Organometallics*, **14**, 2142 (1995).
23. T. Kusukawa, K. Ohkubo and W. Ando, *Organometallics*, in press.
24. T. Kusukawa and W. Ando, *Angew. Chem., Int. Ed. Engl.*, **35**, 1315 (1996).
25. T. Kusukawa and W. Ando, unpublished results.
26. H. Nagashima, H. Terasaki, E. Kimura, K. Nakajima and K. Itoh, *J. Org. Chem.*, **59**, 1246 (1994).
27. H. Nagashima, H. Terasaki, E. Kimura, K. Nakajima and K. Itoh, *J. Org. Chem.*, **60**, 4966 (1995).
28. H. L. Anderson, R. Faust, Y. Rubin and F. Diederich, *Angew. Chem., Int. Ed. Engl.*, **33**, 1366 (1994).
29. K. Komatsu, Y. Murata, N. Takimoto, S. Mori, N. Sugita and T. S. M. Wan, *J. Org. Chem.*, **59**, 6101 (1994).
30. Y. Kabe, K. Suzuki, Y. Yakushigawa and W. Ando, unpublished results.

CHAPTER **34**

Group 14 metalloles, ionic species and coordination compounds

JACQUES DUBAC

Hétérochimie Fondamentale et Appliquée (ESA-CNRS 5069), Université Paul-Sabatier, 118, Route de Narbonne, 31062 Toulouse Cedex, France
Fax: (33)5 61 55 82 04; e-mail: dubac@irit.ups-tlse.fr

CHRISTIAN GUÉRIN

Chimie Moléculaire et Organisation du Solide (UMR-CNRS 5637), Université Montpellier II, Place E. Bataillon, 34095 Montpellier Cedex 5, France
Fax: (33)4 67 14 38 88; e-mail: chguerin@crit.univ-montp2.fr

and

PHILIPPE MEUNIER

Synthèse et Electrosynthèse Organométalliques (UMR-CNRS 5632), Université de Bourgogne, 6 Boulevard Gabriel, 21004 Dijon Cedex, France
Fax: (33)3 80 39 61 00; e-mail: philippe.meunier@u.bourgogne.fr

---

I. INTRODUCTION

Five-membered heterocyclic dienes (**1**) are a very important class of organic heterocyclic compounds. Furan, thiophene and pyrrole derivatives are the best known, but numerous compounds have been described in which E is a main group or transition element.

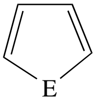

(**1**)

The rings are generally named heterocyclopentadienes, *heteroles* or *metalloles* according to the non-metallic or metallic character of E. The heterocycle can be 6 π aromatic ($E = O$, S, NR, PR), 4 π simple diene ($E = CR_2$, SiR_2) or 4 π antiaromatic ($E = BR$, AlR). Their stability obviously decreases in the same order, and boroles, which are particularly unstable, have been isolated only in the Diels–Alder dimer form[1]. However, in the case of a trivalent or tetravalent E atom, [1,5]-sigmatropic shifts can give rise to isomerization of **1** (1*H*-heterole) into tautomeric forms (2*H* or 3*H*-heterole), in particular for the phospholes[2].

With regard to group 14 metalloles, two reviews were published in 1990, the first on their synthesis and their properties[3], the second on their ionic species and their coordination compounds[4]. Here, we present a simplified review by concentrating particularly on the last five years' work.

II. SYNTHESIS

A. C-unsubstituted Metalloles

1. Siloles

Much sought-after by several laboratories, C-unsubstituted group 14 metalloles and parent metalloles, such as the silole **(2)**, have been the subject of one of the most interesting challenges in organometallic chemistry over more than three decades.

After a fairly large number of unfruitful attempts between 1960 and 1980[3], the synthesis of the first C-unsubstituted silole, 1-methylsilole **(3)**, was described by Barton and Burns[5] (equation 1).

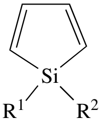

$R^1 = R^2 = H$ **(2)**

$R^1 = Me, R^2 = H$ **(3)**

$R^1 = R^2 = Me$ **(4)**

The flash vacuum pyrolysis (FVP) of 1-allyl-1-methyl-1-silacyclopent-3-ene gives rise to elimination of propene and formation of silole **3** identified as its dimer **5**, and by its Diels–Alder adducts with maleic anhydride and hexafluorobutyne. However, the silole **3** has been detected as a monomer by the MS-FVP technique[6].

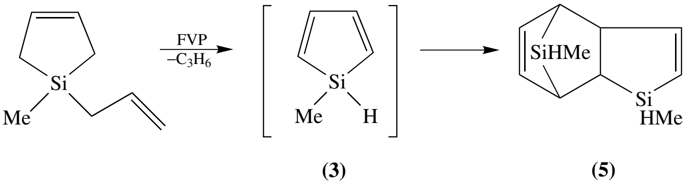

(1)

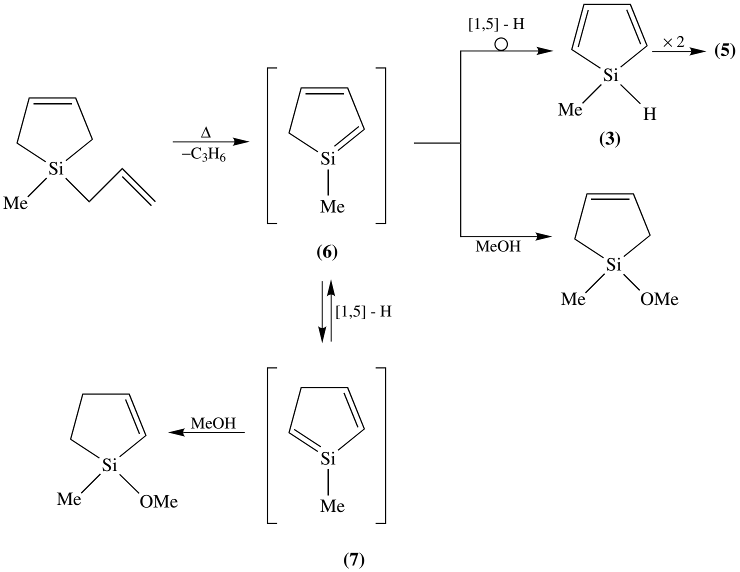

SCHEME 1

Thermolysis of allysilanes has been studied by several authors[7,8], but when carried out under low pressure (FVP), the main process is a retroene elimination of the corresponding alkene, for example propene[9]. In a kinetic study of the FVP of 1-allylsilacyclopent-3-enes, Davidson, Dubac and coworkers[6] have shown that the Arrhenius factor ($\log A = 11.0-11.6$) is the same as for acyclic allylsilanes, but the activation energy is significantly lower, $E_a = 179\,\mathrm{kJ\,mol^{-1}}$ instead of $230\,\mathrm{kJ\,mol^{-1}}$ (for allyltrimethylsilane). Consequently, the loss of propene involving the methyl group of 1-allyl-1-methylsilacyclopent-3-ene giving a Si=C exocyclic bond is insignificant compared with the endocyclic elimination process (Scheme 1). The latter involves the formation of a 2*H*-silole, 1-methyl-1-silacyclopenta-1,3-diene **(6)**, which is in equilibrium with its tautomers, 1-methyl-1-silacyclopenta-1,4-diene **(7)**, a 3*H*-silole, and 1-methyl-1-silacyclopenta-2,4-diene **(3)**. Indeed, the intermediate isosiloles **6** and **7** have been trapped by MeOH to give a 80 : 20 mixture of 1-methoxy-1-methylsilacyclopent-3-ene and 1-methoxy-1-methylsilacyclopent-2-ene (Scheme 1). Additionally, the exocyclic retroene process has also been excluded by means of MeOD trapping experiments.

The mechanistic study of this reaction has also shown that in the case of a substituted allyl group an exocyclic [1,3]-silatropic rearrangement is in competition ($E_a = 173-176\,\mathrm{kJ\,mol^{-1}}$) with the endocyclic retroene reaction[6]. Thus the yield of silole reaches at most about 40%. However, this method can be used for the synthesis of C-methylated siloles having a Si−H bond (see Section II.B.2.e).

The first C-unsusbstituted silole to be isolated, 1,1-dimethylsilole **(4)**, was reported simultaneously by Dubac and coworkers[10], and Burns and Barton[11] in 1981. This silole was prepared by dehydration of 1,1-dimethyl-1-silacyclopent-4-en-3-ol in the gas phase on alumina or thoria[10,12,13] (Scheme 2). In the presence of acidic reagents, the reaction results in β C−Si rather than β C−H bond cleavage, giving the dienic siloxane $(Me_2SiC_4H_5)_2O$. The Barton method consists of the flash vacuum pyrolysis of 3-(benzoyloxy)-1,1-dimethyl-1-silacyclopent-4-ene at 540 °C (equation 2).

The thermolysis of the corresponding *N*-phenylcarbamate takes place at a lower temperature (310 °C) (Scheme 2)[12,14].

The silole **4** can be identified in the monomeric state (NMR), but it dimerizes within a few minutes at RT. It can be trapped by a dienophile or in the form of a η^4-coordination complex (Scheme 2). Thus, the above methods[10–14] are successful because they take place in the gas phase, silole **4** being trapped at low temperature.

The decomposition of the *S*-methylxanthate ester of 1,1-dimethyl-1-silacyclopent-4-en-3-ol takes place in refluxing ether, but this ester cannot give the silole **4** which dimerizes *in situ* (61% yield), together with siloxane formation $(Me_2SiC_4H_5)_2O$ (31%) due to a β C−Si elimination[14].

However, in the case of a stable silole having hindered groups at silicon, this mild method allowed Nakadaira and coworkers to prepare 1,1-dimesitylsilole[15].

As regards the silole **2** itself, this has been the subject of several studies some of which could not be reproduced or have been refuted[3]. As we shall show, this was probable owing to the great instability of this compond, which has been identified only recently.

In 1974, Gaspar and coworkers suggested that **2** is formed in a gas-phase reaction of silicon atoms, resulting from the ^{31}P (n,p) ^{31}Si nuclear transformation, with 1,3-butadiene[16]. They proposed a mechanism in which the silylene **9**, 1-silacyclopent-3-ene-1,1-diyl, rearranges to silole **2**.

Other mechanisms have been proposed, and the formation of **2** was verified by high-temperature catalytic hydrogenation[17]. Although the identification of **2** in these experiments seems questionable[5,10], Gaspar and coworkers, in 1986, reported that gas-phase pyrolysis of 1,1,1,3,3,3-hexamethyltrisilane with butadiene gives the silole [2 + 4]

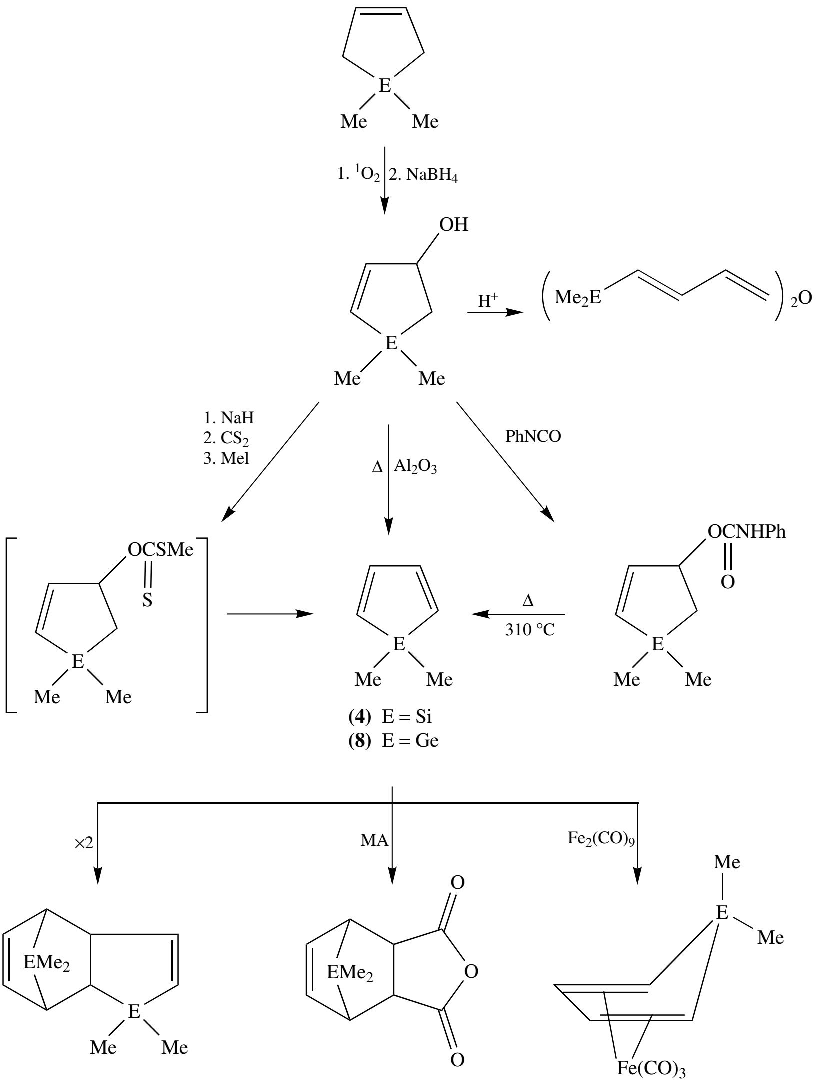

(4) E = Si
(8) E = Ge

SCHEME 2

dimer in low yield[18]. More recently, the same research group isolated and identified definitively this dimer **10**[19] (Scheme 3).

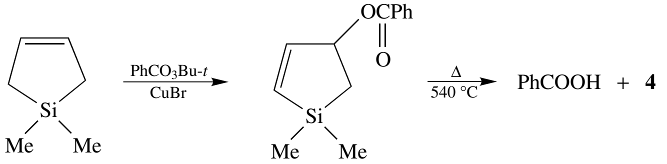

(2)

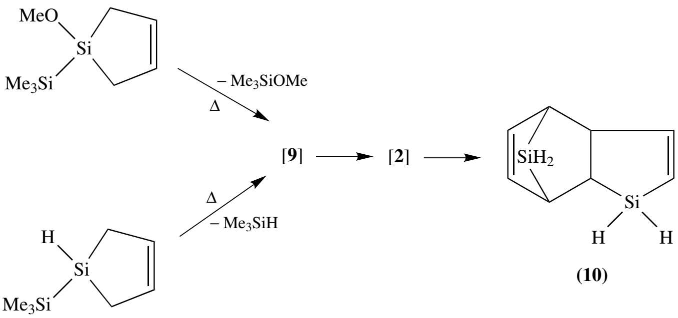

SCHEME 3

Attempts to isolate the silole monomer **2** or to trap it by reaction with maleic anhydride or perfluoro-2-butyne have failed. This is surprising given the successful trapping of 1-methylsilole[5] and 1,1-dimethylsilole[10]. The authors conclude that silole **2** is not very reactive in Diels–Alder cycloadditions, except toward self-reaction[19].

The mechanisms proposed by Gaspar and coworkers in their approach to the problem have a common point, the formation of the intermediate **9**. This silylene then undergoes two prototropic rearrangements: initial isomerization to a silene, the 2*H*-silole **(11)**, followed by a second to give the 1*H*-silole **(2)**[19] (equation 3).

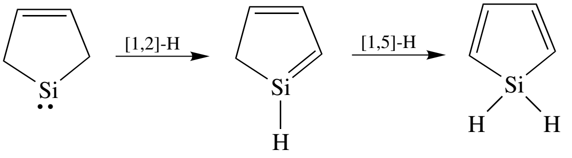

(9) **(11)** **(2)** (3)

This proposition is in agreement with the previous work of Davidson, Dubac and coworkers[6] (see above and Scheme 1).

Also in 1992, Michl, Nefedov and coworkers[20a,b] reported that vacuum pyrolysis (800 °C, 10^{-3}–10^{-4} Torr) of 5-silaspiro[4.4]nona-2,7-diene **(12)** resulted in the formation of silole **(2)**, that was isolated in an Ar matrix, and characterized by its IR and UV-visible spectra. Matrix photolysis and vacuum pyrolysis of 1,1-diazido-1-silacyclopent-3-ene **(13)** also produced the parent silole. After warming the pyrolysate to RT, the [2 + 4] dimer **10** of silole **2** was identified by GC-MS.

A very interesting photoreversible interconversion of **2** with **9, 11** and **14**, its three tautomeric forms, has been observed upon irradiation at selected wavelengths[20a,b]. Thus, Scheme 4 summarizes the mechanistic aspects of both the pyrolysis of **12**, and the pyrolysis or photolysis of **13** which proceed via common intermediates **9** and **11.** These results are in perfect agreement with the mechanistic study of the FVP of 1-allyl-1-methylsilacyclopent-3-ene[6] in which the silicon-methylated analogues of **11** and **14** have also been identified (Scheme 1). However, we think that **14** must be regarded as a possible intermediate not only in photolysis but also in pyrolysis reactions, because the methylated analogue **7** (Scheme 1) can be readily trapped.

A similar study, which supports previous claims involving the 3,4-dimethylsilole and its corresponding isomeric intermediates, has been also carried out on the 3,4-dimethyl derivatives of **12** and **13**[20a,b].

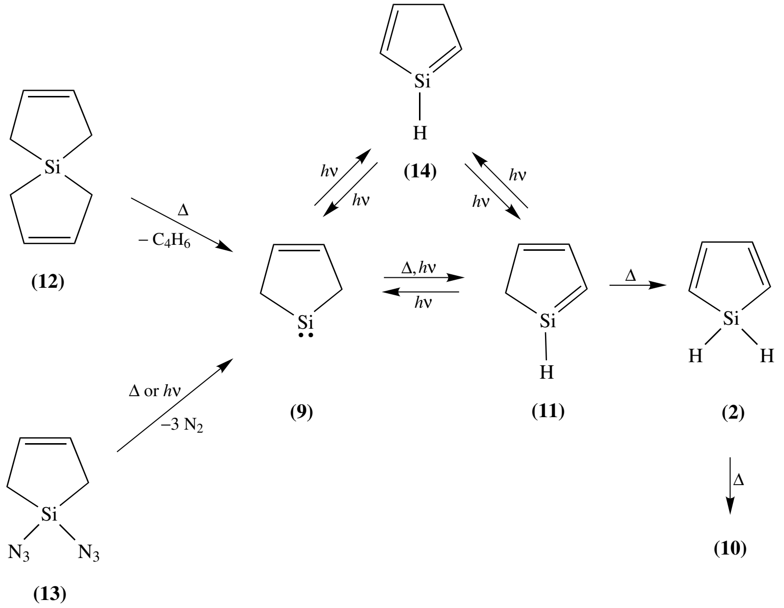

SCHEME 4

Vacuum pyrolysis of **12** has been recently studied by high-resolution mass spectrometry[20c]. The ionization potential (IP = 9.17±0.10 eV) for silole **2** was found to be in excellent agreement with the IP (9.26 eV) calculated by the semiempirical PM3 method. Thermodynamic calculations on possible decomposition mechanisms of **12** have shown that **2** is probably formed from the primary intermediate silylene **9** via two consecutive hydrogen shifts (equation 3).

2. Germoles

The first C-unsubstituted germole, 1,1-dimethylgermole **(8)**, was prepared in 1981 by Dubac and coworkers[21] by dehydration in the gas phase of 1,1-dimethyl-1-germacyclopent-4-en-3-ol (Scheme 2). At room temperature, as in the case of 1,1-dimethylsilole, the [2 + 4] dimer is formed. At low temperature, the monomer gives a Diels–Alder adduct with maleic anhydride, and forms a η^4-tricarbonyl iron complex[12,21]. The indirect dehydration of the same alcohol, via its *N*-phenylcarbamate, also produces the germole **8**[13,22] (Scheme 2).

Among synthetic methods of group 14 metalloles involving direct formation of the dienic ring[23a] are reactions of two alkyne molecules with a Σ_2E fragment[23b]. These reactions give C-substituted metalloles (see Section II.B.1.b). However, from ethyne, no C-unsubstituted derivative was obtained until Ando and coworkers described in 1990 the first Pd-catalysed reactions of germylenes with ethyne giving 1,1-dialkylmetalloles[24]. These reactions are not chemospecific. For example, in the presence of a catalytic amount of $Pd(PPh_3)_4$, hexamesitylcyclotrigermane and ethyne, at 80 °C in toluene, react to give two products, 1,1-dimesitylgermole **(15)** and 1,1,4,4-tetramesityl-1,4-digermacyclohexa-2,5-diene **(16)** (1.25 : 1) in 76% overall yield (equation 4).

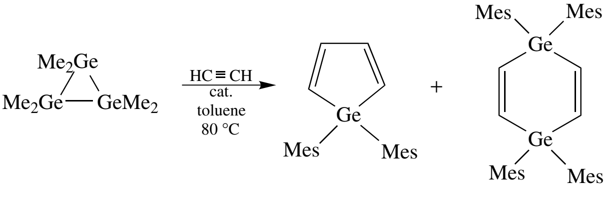

(4)

(15) **(16)**

In contrast to **8**, germole **15** is stable in the monomeric state, thanks to steric shielding by the bulky mesityl groups (see Section III.A.1). It reacts, nevertheless, with maleic anhydride and diiron nonacarbonyl.

The proposed mechanism for reaction 4 involves the thermal decomposition of cyclotrigermane into a germylene (Mes_2Ge:) and a digermene ($Mes_2Ge{=}GeMes_2$) which give products **15** and **16**, respectively[24] (see Section II.B.1.b and Scheme 11).

The germylene generated by thermal or photolytic cycloreversion from a 7-germanorbornadiene gives with alkynes many different products[25]. However, in the presence of a Pd-catalyst a germole can be obtained together with a digermacyclohexadiene[26]. From a 7-germanorbornadiene prepared from an easily accessible C-phenylated germole, the reaction with ethyne allows a C-unsubstituted germole **(17)** to be obtained specifically without formation of the corresponding digermacyclohexadiene[24a] (Scheme 5). In the absence of the Pd-catalyst the reaction

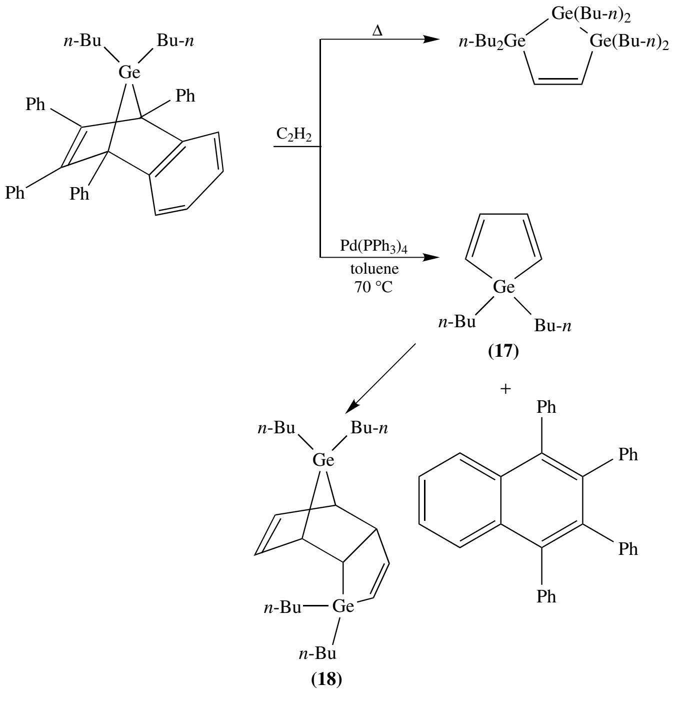

(17)

(18)

SCHEME 5

afforded a 1,2,3-trigermacyclopent-4-ene. The germole **17** dimerizes to **18**, but by distillation it can be isolated as the monomer.

Although FVP of 1-allyl-1-methyl-1-silacyclopent-3-ene affords 1-methylsilole (Section II.A.1), FVP of the germanium analogue did not give 1-methylgermole, but rather butadiene as the only volatile product, together with an amorphous solid containing germanium[27].

3. Stannoles

In 1988, Ashe and Mahmoud prepared the first C-unsubstituted stannole, 1,1-dibutylstannole **(19)**, by cyclization of 1,4-dilithio-1,3-butadiene with dibutyltin dichloride[28] (equation 5). This stannole, stable in the monomeric state, has been isolated by distillation (28% yield).

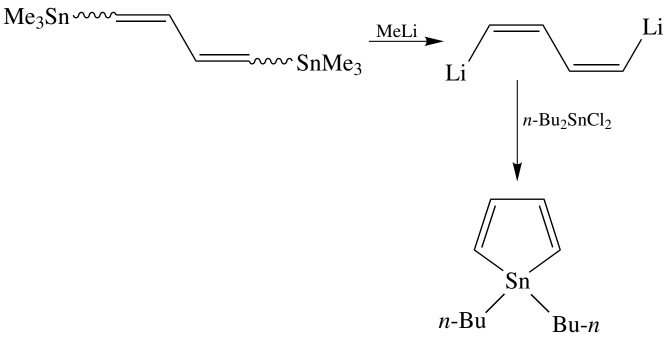

(19)

(5)

As with the germylene (see above), an alkyne can react with a stannylene to give a stannole. Here also, the result is dependent on experimental conditions[25]. With ethyne, SnR_2 [$R = CH(SiMe_3)_2$] reacts at room temperature to form a linear chain coupling product[29a], while metal-coordinated ethyne reacts differently[29b]. In particular, complexes **20** or **21** are converted by ethyne at room temperature into the Pd^0 ethyne complex **22** and the C-unsubstituted stannole $R_2Sn(C_4H_4)$ **(23)**[29b]. It must be pointed out that complexes **21** and **22** are analogues to the proposed intermediates for the Pd-catalysed reaction between a germylene and ethyne[24].

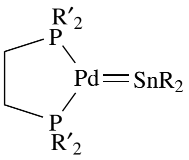

(20)

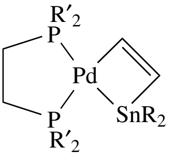

(21)

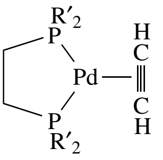

(22)

$R = CH(SiMe_3)_2$; R′ = *i*-Pr, *t*-Bu

The Pd-catalysed reaction is possible with a stannylene on condition that it is carried out at low temperature, in order to avoid the competing uncatalysed formation of a polymeric product, and in the presence of a labile complex as catalyst (equation 6). The stannole **23** was obtained in 87% yield.

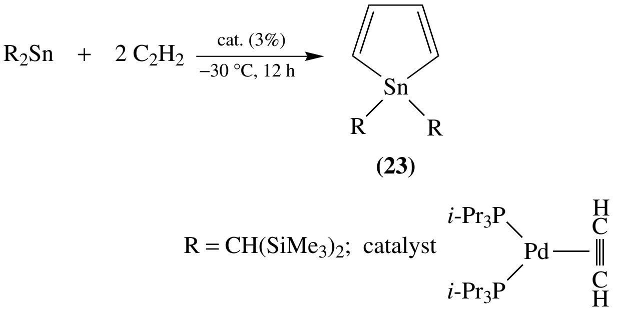

(23)

(6)

B. C-substituted Metalloles

These compounds form the largest class of group 14 metalloles known today[30]. We will review again the more outstanding results concerning the long-established synthetic methods for these heterocycles, as well as the more recent ones.

1. Synthetic methods involving direct formation of the dienic ring

a. Cyclization of 1,4-dilithio-1,3-butadienes by a polyfunctional compound R_nEX_{4-n} *(*$n = 0 - 2$*).* Leavitt, Manuel and Johnson[31] prepared the first group 14 metalloles containing germanium or tin, from 1,4-dilithio-1,2,3,4-tetraphenyl-1,3-butadiene (DTB) (equation 7). The silicon[32] and lead[33] analogues have been prepared in the same way.

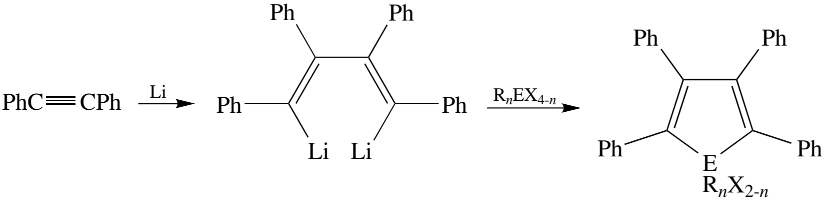

(7)

(24)

Since one or two E−X bonds (e.g. X = Cl) can survive the cyclization reaction, numerous derivatives bearing a variety of groups at the heteroatom can be prepared by substitution reactions[30]. Structures of the spirobimetallole type **(25)** are also known.

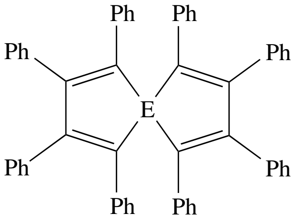

(25)

In 1967, an original synthesis of 1,4-dilithio-1,4 diphenyl-1,3-butadiene (DDB) from 1,1-dimethyl-2,5-diphenylsilole (see equation 17 below) was proposed by Gilman and coworkers[34]. This dilithium reagent reacts with polyhalides R_nEX_{4-n} to yield 2,5-diphenylmetalloles (**26**, E = Si[34,35], Ge[36], Sn[34]) (Scheme 6).

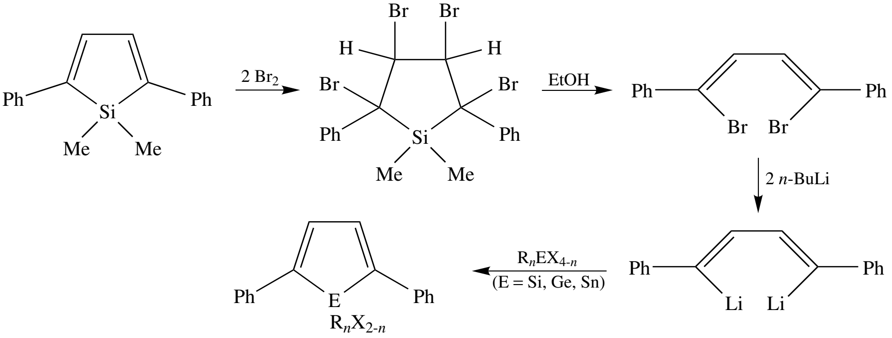

(26)

SCHEME 6

Corriu and coworkers[37] showed that alkoxysilanes $R_nSi(OR')_{4-n}$ [in particular $RSi(OMe)_3$] give better yields for the DDB cyclization than do chlorosilanes. The reaction of anionic pentacoordinated silicon complexes $[RSi(O_2C_6H_4\text{-}O)_2]^-$ Na^+ with DDB and subsequent $LiAlH_4$ reduction give 1-R-diphenylsiloles (R = Me, Ph)[38]. Bis(silacyclopentadien-1-yl)alkanes were formed from DDB and α, ω-bis(dihalomethylsilyl)alkanes[39].

In analogy to the preparation of DDB from a 2,5-diphenylated silole (Scheme 6), 1,4-dilithio-1,2,3,4-tetramethylbutadiene has been recently prepared from a C-methylated zirconacyclopentadiene. Thus, West and coworkers[40] were successful in preparing 1,1-dichloro-2,3,4,5-tetramethylsilole **(27)**, the first C-methylated silole having Si−Cl bonds, from bis(cyclopentadienyl)-2,3,4,5-tetramethylzirconacyclopenta-2,4-diene via (1*Z*, 3*Z*)-1,4-diiodo-1,2,3,4-tetramethylbuta-1,3-diene (equation 8).

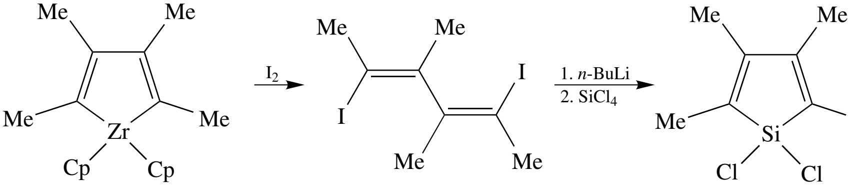

(8)

(27)

b. Cyclization of two acetylenic molecules with a Σ_2E fragment. This method can be carried out in two ways: the direct cyclization (Scheme 7, path a) of the two acetylenic molecules by a convenient reagent, e.g. Σ_2E: or Σ_2EX_2, or their cyclization through another element M (Scheme 7, path b), e.g. a transition element. This latter possibility will be developed below (see Section II.B.3).

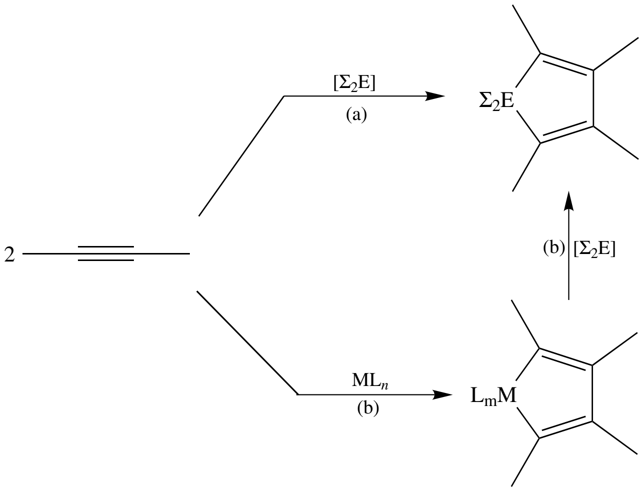

SCHEME 7

Many substrates have been used to prepare C-substituted group 14 metalloles by this method, in particular those which generate analogues of carbenes Σ_2E:[23b].

i. Reaction between an alkyne and a disilane, a silirene (1-silacyclopropene) or a cyclotrisilane.. The substrates generally used for the title reaction are disilanes[41-43] (or stannylsilanes[44]) and silirenes[45-50]. The reactions are usually catalytic.

Treatment of 1,1,2,2-tetramethyldisilane with an alkyne in the presence of a catalyst [$NiCl_2(PEt_3)_2$ or $PdCl_2(PEt_3)_2$] gives C-substituted siloles **28**[41,42] (equation 9).

$$HMe_2SiSiMe_2H + 2RC{\equiv}CR' \xrightarrow{\text{cat.}} Me_2SiH_2 +$$

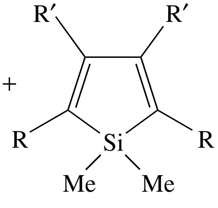

(9)

(R, R′ = alkyl, aryl or silyl groups)

(28)

Depending on the alkynes, the yields are variable, but they are very high in the case of disubstituted symmetrical alkynes (R = R′ = Me, Et, *n*-Bu). The reaction is sometimes not specific, giving also a 1,4-disilacyclohexa-2,5-diene. It was recently used by Ishikawa and coworkers to obtain a 3,4-diethynylsilole **(29)** (Scheme 8) which is a precursor of polymers containing silole rings[43] (see Section IV.C).

From (trialkylstannyl)dimethylsilane and terminal alkynes this method gives 3,4-disubstituted siloles (**28**, R = H, R′ = alkyl, aryl or alkoxy groups) in moderate to good yields[44]. Catalysis by Pd is better than by Ni or Rh. The proposed mechanism involves a palladium–silylene species **30** as an intermediate. This reacts with an alkyne giving successively a palladasilacyclobutene **(31)** and a palladacyclohexadiene **(32)**. In the final

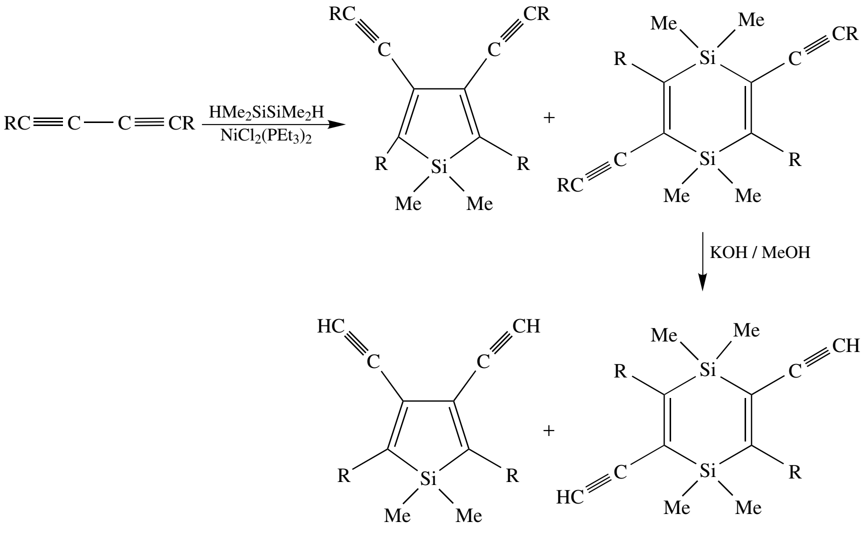

R = SiMe$_3$

(29) 27%   17%

SCHEME 8

step, reductive elimination of silole **28** regenerates the Pd^0-complex[44]. This mechanism is slightly different from that proposed for the reaction of a stannylene with ethyne[29b] (see Section II.A.3).

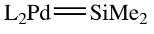

(30)

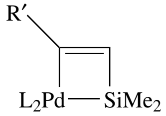

(31)

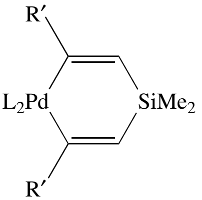

(32)

A silirene may also generate a silylene. In the absence of catalyst, thermolysis of a silirene can give various products resulting from its decomposition into a silylene and an alkyne[50]. Thus siloles are formed together with 1,2-disilacyclobutanes, 1,4-disilacyclohexadienes and other products. With silirenes bearing bulky substituents on the ring carbon atoms, siloles become the major products (Scheme 9).

The reaction of a silirene with an alkyne in the presence of a palladium catalyst allows cyclization of two molecules of the alkyne with the silylene, as in equation 9 above. For example, Seyferth and coworkers have prepared the silole **33** in 80% yield from 1,1-dimethyl-2,3-bis (trimethylsilyl) silirene and phenylacetylene (equation 10)[45]. Without catalyst, this reaction yielded the silole **34** and the ene-yne **35**, resulting respectively from ring expansion and cleavage by PhC≡CH of the silirene. Under UV irradiation, **35** alone was formed.

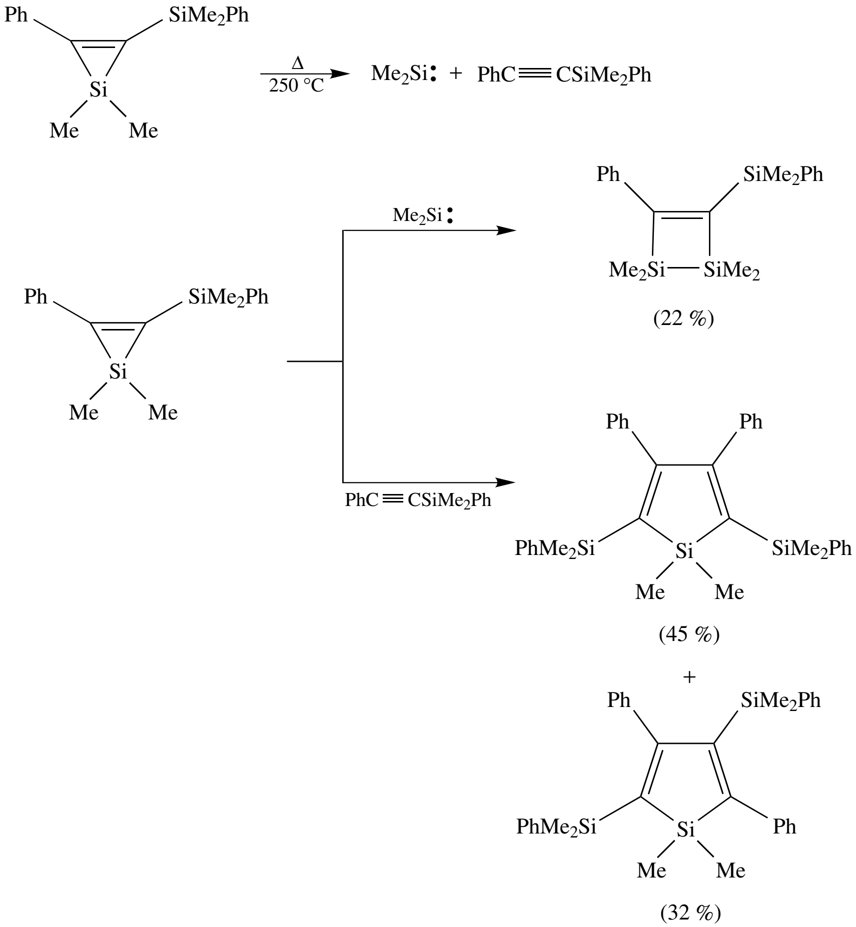

SCHEME 9

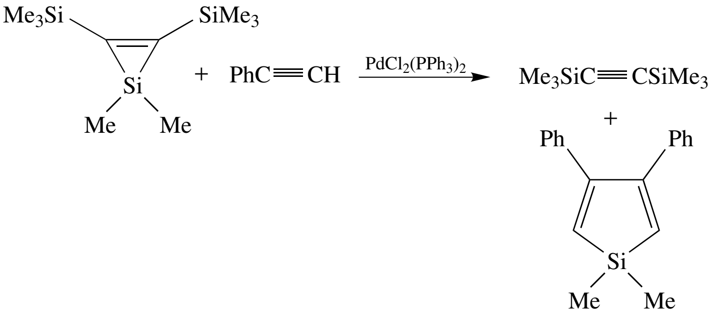

(10)

(33)

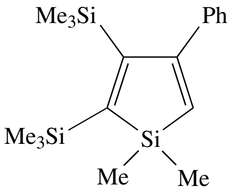

(34)

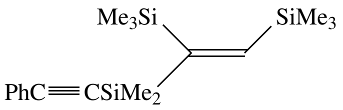

(35)

This method did not afford C-unsubstituted siloles, in particular in the case of the reaction of a silirene with ethyne[45d].

The catalysed cleavage of cyclotrisilanes (or trisiliranes) gives a disilene and a silylene. The latter can be trapped by various multiple-bonded compounds, in particular by 1-phenylacetylene leading to the silole **36** (equation 11)[51].

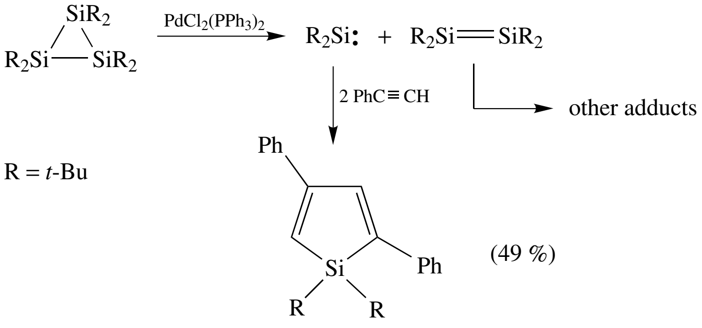

(36)

(11)

The same reaction between a cyclotrigermane and ethyne resulted in a C-unsubstituted germole (equation 4)[24].

ii. Reaction between an alkyne and a 7-metallanorbornadiene. In 1964, Gilman and coworkers[52] showed that a 7-silanorbornadiene thermally decomposes with formation of a silylene. Since then, many studies have developed the chemistry of group 14 metallanorbornadienes, demonstrating that their stability depends on both the metal and the substituents[53].

Since a 7-metallanorbornadiene is easily obtained in the C-phenylated metallole series, it appeared possible, by decomposition in the presence of an alkyne, to generate differently substituted metalloles (**37, 38**, Scheme 10). However, this reaction is only known for the germoles (Neumann and coworkers)[25,26], probably because decomposition temperature of germanorbornadiene is in the same range as that of the trapping of germylene. Nevertheless, the reaction can result in numerous products, and the selective formation of germoles, including that of regioisomer **37**, is limited to some alkynes in the presence of Pd-catalysts (e.g. $R^3/R^4 = n-\mathrm{Bu/H}$, 2-methylphenyl/H, CO_2Me/Me, CO_2Et/Ph, Ph/Ph)[26].

The Pd-catalysed reaction between ethyne and the germanorbornadiene derived from 1,1-dibutyl-2,3,4,5-tetraphenylgermole and benzyne gives a C-unsubstituted germole **(17)** (Scheme 5)[24a].

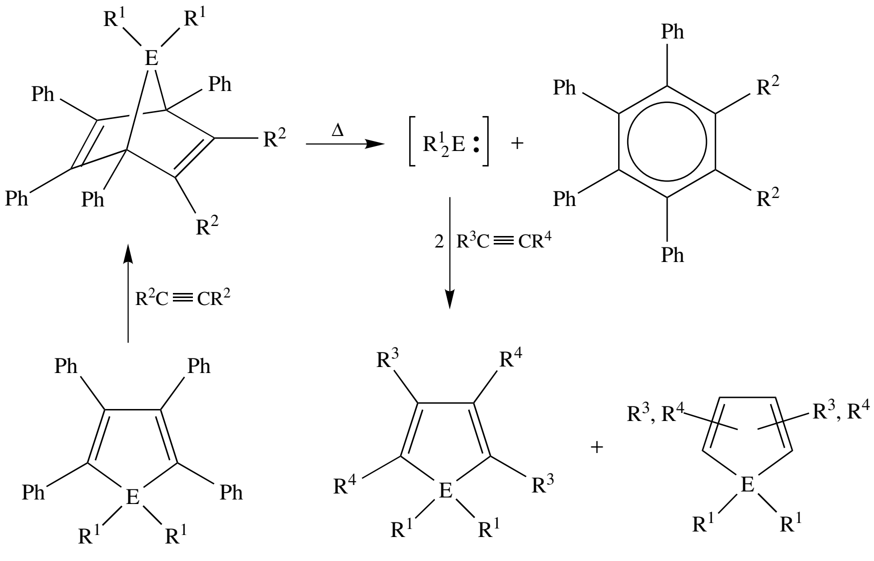

(37) **(38)**

SCHEME 10

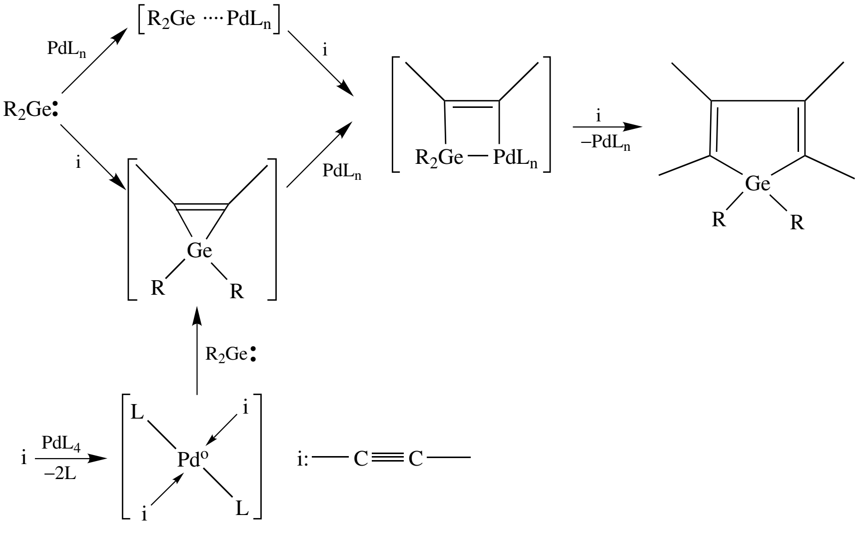

SCHEME 11

Mechanisms for the formation of germoles in these reactions have been discussed in terms of Scheme 11[24a,26].

iii. Reactions involving 1,n-diynes. If the two acetylenic groups are borne by the same carbon chain, cyclization on a Σ_2E fragment can give a bicyclic metallole as shown in equation 12^{54a}.

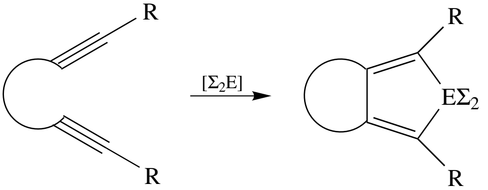

(12)

This is the intramolecular version of the previous reactions, and the precursors of the Σ_2E fragment are the same (e.g. disilanes)[54]. The reaction, however, has been applied only to 1,6-diynes bearing two aryl (or heteroaryl) groups in positions 1 and 7, in the presence of a Ni-catalyst.

Siloles **39** and **40** have been prepared in this way by Tamao and coworkers[54] in 64 and 40% yield, respectively, the 2,5-dithienylsilole **40** being a useful monomer unit for the synthesis of thiophene–silole copolymers (see Section IV.B).

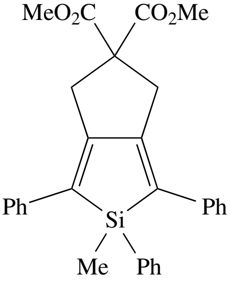

(39)

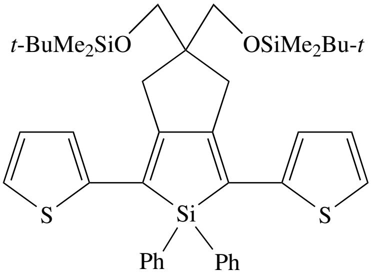

(40)

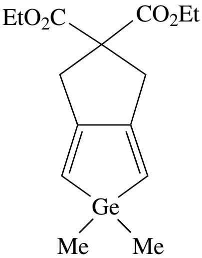

(41)

The reaction of diethyl dipropargylmalonate with cyanotrimethylgermane in refluxing toluene, with $PdCl_2$ as catalyst, gives the germole **41** in 77% yield[55].

c. Cyclization of two acetylenic groups bonded to a group 14 element. i. Reaction of trialkylboranes with dialkynyl derivatives of a group 14 element. The cyclization of two acetylenic groups bonded to a group 14 element to yield a metallole was achieved by

Wrackmeyer and coworkers using trialkylboranes[56–58] (equation 13).

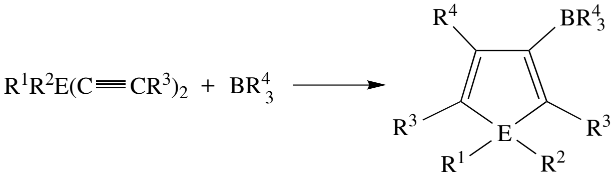

(42)

(13)

$E = Si^{56}, Ge^{56a,b}, Sn^{57}, Pb^{58}$

R^1, R^2 = Me, Et or *t*-BuN(CH_2)$_3$NBu-*t*; R^3 = alkyl, aryl, $SiMe_3$, $SnMe_3$, PPh_2 or organic group containing N, O, S; R^4 = Me, Et, *i*-Pr or *n*-Bu

Zwitterionic intermediates **43**, in which a tin centre is stabilized by intramolecular side-on coordination to the C≡C bond of an alkynylborate moiety, have been detected in solution by multinuclear NMR[57]. Moreover, the structures of some of these compounds **43** (E = Sn[57c,e,g], Pb[58b]) have been established by X-ray analysis.

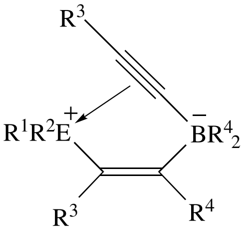

(43)

These reactions are not chemospecific, but the formation of other heterocycles can be avoided, and the yields of metallole are generally high. Some heteroatomic groups attached to the ring carbons can be substituted by hydrogen (e.g. in protodeborylation or protodestannylation reactions)[56c,d].

ii. Intramolecular reductive cyclization of diethynylsilanes. Diethynylsilanes undergo intramolecular reductive cyclization in an *endo-endo* mode upon treatment with lithium naphthalenide (NpLi) to form 2,5-dilithiosiloles **44** (equation 14)[59]. By treatment with electrophiles, these dilithium derivatives are converted into 2,5-difunctional siloles **(45)** which are precursors of oligosiloles (see Section IV.A).

Though this method is still limited to 3,4-diphenylsiloles, it represents a distinct advance in group 14 metallole synthesis.

d. Cyclization of a 1,3-diyne with a group 14 dihydride. An attractive and simple route to group 14 metalloles is the cyclization of a 1,3-diyne with a dihydride, e.g. R_2EH_2. However, only a single group 14 metallole, 1,1-dibutyl-2,5-dimethylstannole **(46)**, has been synthesized in this way in low yield (15%)[60] (equation 15).

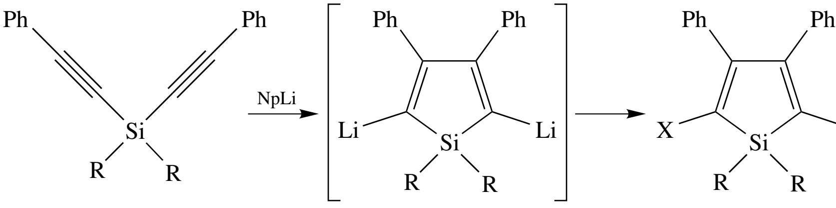

(14)

(44) **(45)**

X, Y = H, Br, $SiMe_3$, $SnMe_3$, SePh, C$\equiv$CPh, 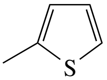

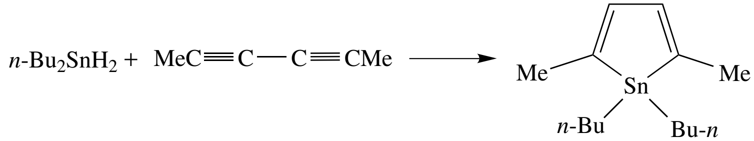

(15)

(46)

2. Synthetic methods involving a group 14 heterocycle as precursor

a. Dehydrogenation of metallacyclopentanes or metallacyclopentenes. Attempts to dehydrogenate C-unsubstituted metallacyclopentanes or -pentenes in order to obtain C-unsubstituted metalloles have failed[3]. The reaction is only successful for 2,5-diphenylated derivatives in the presence of DDQ (equation 16)[61].

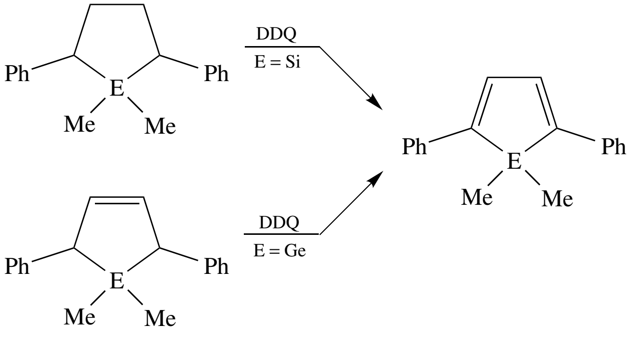

(16)

In the case of 3-methyl or 3,4-dimethylsiloles, the same reaction gives the transoid isomer of the corresponding silole[62].

b. Dehydrohalogenation of halogenometallacyclopentanes. One of the most noteworthy group 14 metallole syntheses is that of Gilman and coworkers[34], reported in 1967. This involves the synthesis of 1,1-dimethyl-2,5-diphenylsilole **(47)** by bromination/dehydrobromination of 1,1-dimethyl-2,5-diphenylsilacyclopentane which is easily accessible from styrene (equation 17).

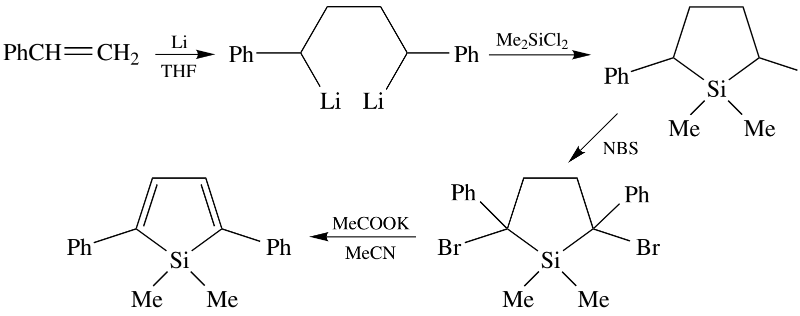

(47)

(17)

This method has been extended successfully to the germanium analogue[63], and to other 2,5-diphenylsiloles[39,64]. However, its main interest lies in the possibility of preparing 1,4-dilithio-1,4-diphenyl-1,3-butadiene (DDB) from **47** (see Scheme 6) giving access to other 2,5-diphenylmetalloles, especially those functionalized at the heteroatom[37].

Since the dehydrohalogenation method could not be extended to other group 14 metalloles and in particular to the simple metalloles[65], except for 1,1,3,4-tetramethylsilole[66], it seems clear today that Gilman's synthesis is specific to 2,5-diphenylsiloles owing to the benzylic positions involved.

c. Dehydration of 1-metallacyclopent-4-en-3-ols. The synthesis of sila- or germacyclopent-4-en-3-ols by photooxidation ($^1O_2$)/reduction of metallacyclopent-3-enes[10,21] (see Section II.A.1, Scheme 2) has been extended successfully to the C-methylated (equations 18 and 19)[12,67] and C-phenylated (equation 20)[68] derivatives.

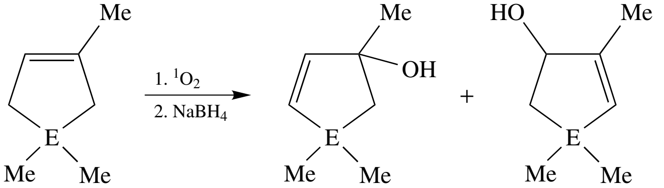

(18)

E = Si, Ge **(48)** **(49)**

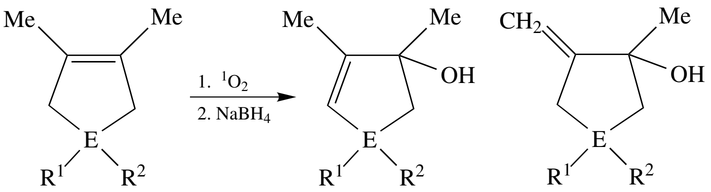

(19)

(50) **(51)**

E = Si, Ge

R^1, R^2 = alkyl, alkenyl or aryl groups

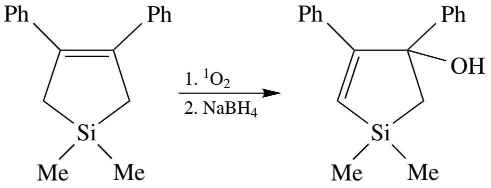

(52)

(20)

The method gives good yields in the case of a variety of substituents at silicon (or germanium), but it is not regiospecific for the C-methylated derivatives.

In the case of 3,4-dimethylated derivatives, the base-promoted rearrangement of the corresponding epoxides is a preferable method because it is regiospecific (equation 21)[69]. However, it does not take place in the case of derivatives having an alkenyl group at the heteroatom[12,67c].

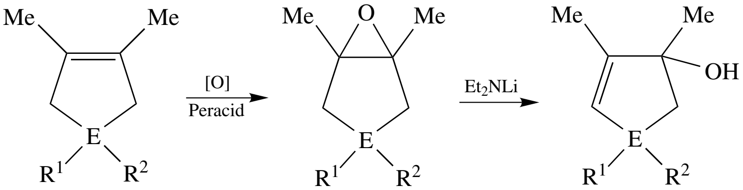

(50)

(21)

E = Si, Ge

R^1, R^2 = alkyl or aryl groups

The catalytic dehydration of metallacyclopentenols is not a convenient method for the synthesis of C-methylated metalloles since:

(a) catalysis by a protonic acid leads to a β C—E elimination, with formation of a dienic open siloxane (or germoxane) (Scheme 2);

(b) gas phase dehydration with alumina or thoria results in a mixture of C-methylated metalloles **53**, or **54**, and isomeric transoid dienes **55**, or **56**[67a,b,70]. The isomer ratio, in which the metallole is the minor product, is thermodynamically controlled.

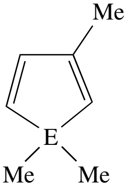

(53)

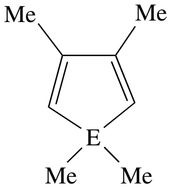

(54)

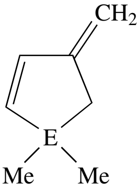

(55)

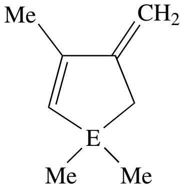

(56)

d. Thermolysis of esters of 1-metallacyclopent-4-en-3-ols. The synthesis of C-methylated metalloles **53** and **54** which avoids their isomerization requires milder conditions than those reported above. With this in mind, Dubac and coworkers investigated the thermolysis of esters of metallacyclopentenols, known to give elimination reactions at relatively low temperatures, such as carbamates or xanthates[12,14,22,67c,71].

In the case of 3,4-dimethylmetalloles **58**, which are stable in their monomeric form (see Section III.A.1), the method proposed was the thermolysis of *N*-phenylcarbamates **57**, the decomposition of which is regioselective (equation 22). Intracyclic β C−H elimination giving the metallole **58** is the main process (80–90%), and the transoid isomer **59** is always the minor product. Tertiary *N*-phenylcarbamates **57** decompose at about 70 °C in common solvents. In carbon tetrachloride, one can follow easily the progress of the reaction by NMR spectroscopy. An interesting one-pot synthesis is possible: with two equivalents of phenyl isocyanate, the side products are gaseous carbon dioxide and diphenylurea which precipitates (equation 23)[14,22,67c].

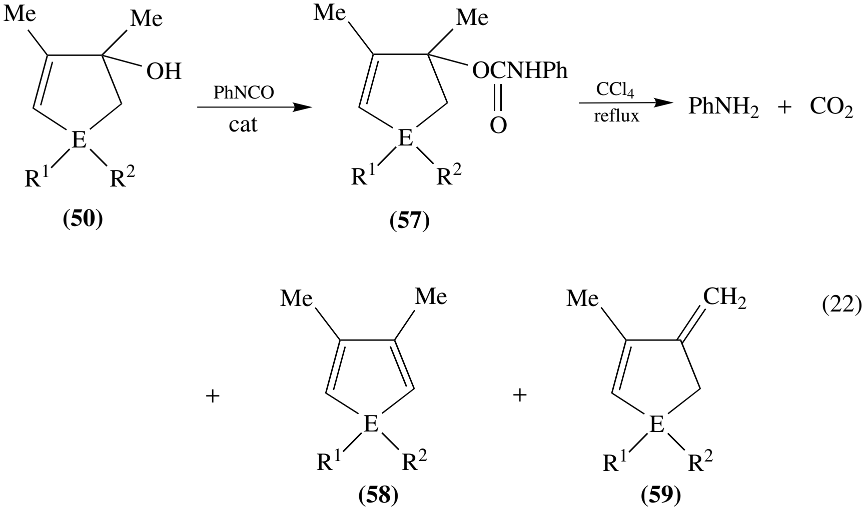

(22)

4:1 to 9:1

E = Si, Ge ; R^1, R^2 = alkenyl or aryl groups

Cat. = $[Me(CH_2)_6COO]_2$ Sn

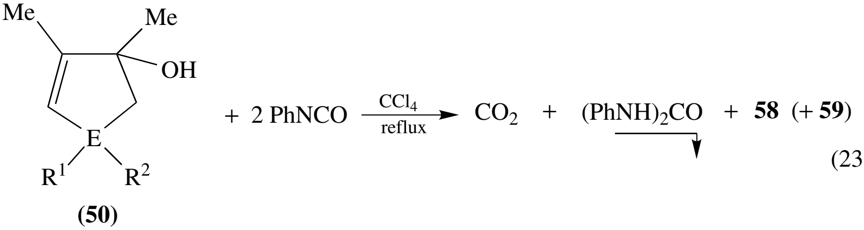

$$+ 2\,PhNCO \xrightarrow[reflux]{CCl_4} CO_2 + \underset{\downarrow}{(PhNH)_2CO} + \mathbf{58}\ (+\mathbf{59})$$

(23)

This route has allowed the synthesis of spirometalloles (**60**[72], **61**[73]) and of 1,1-dimethyl-3,4-diphenylsilole[68] in good yields.

S-Methylxanthates **62** derived from the same alcohols **50** are thermally less stable than the corresponding carbamates **57**. They decompose during their synthesis according to two competitive elimination pathways, β C−H and β C−Si (3/2) eliminations[14] (Scheme 12), giving rise to a lower metallole yield than from carbamates **57**.

The synthesis of 3-methylmetalloles is more difficult because they are unstable as monomers. Thermolysis of the tertiary carbamate corresponding to the alcohol **48** (under the experimental conditions of equations 22 or 23) gives the Diels–Alder dimer of

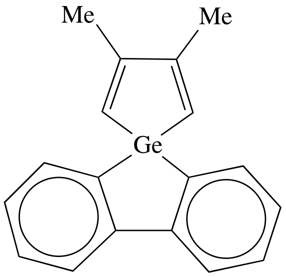

(60)

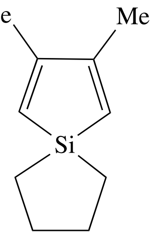

(61)

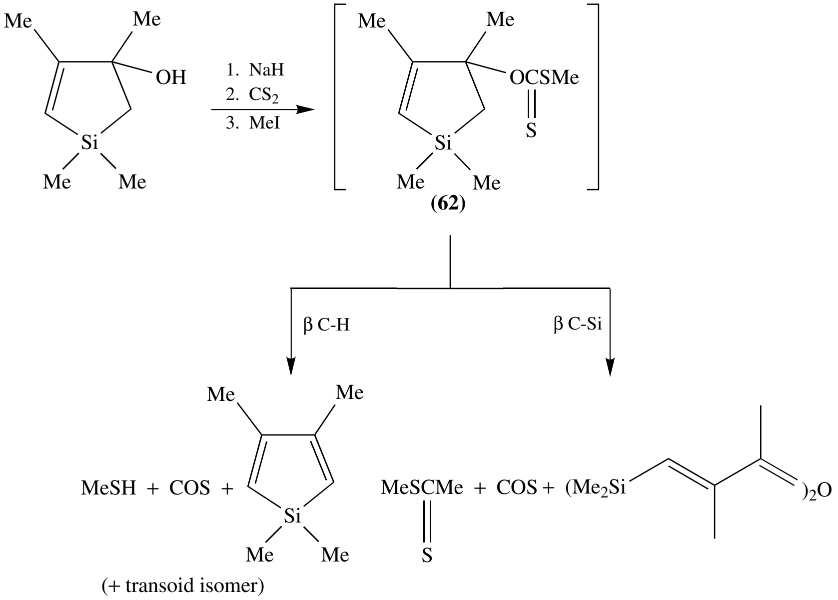

SCHEME 12

metallole **53**. Thermolysis at 310 °C of the secondary carbamate corresponding to the alcohol **49** affords 1,1,3-trimethylmetalloles **(53)** which can be trapped in monomeric state at low temperature[14,22].

e. Gas-phase pyrolysis of silacyclopent-3-enes. Flash vacuum pyrolysis of 1-allyl-1-methylsilacyclopent-3-ene gives 1-methylsilole **(3)** (equation 1), the first C-unsubstituted silole, which is unstable in the monomeric state[5]. 3,4-Dimethylsiloles having one or two silicon–hydrogen bonds **(63, 64**[6]**, 65**[74]**)**, which are stable in the monomeric state, were obtained in the same way. However, an exocyclic [1,3]-silyl shift in competition with the endocyclic retroene reaction[6] limits the silole yield which does not exceed 40%. Moreover, the transoid isomer of the silole is also formed.

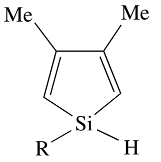

(63) R = Me
(64) R = Ph

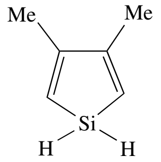

(65)

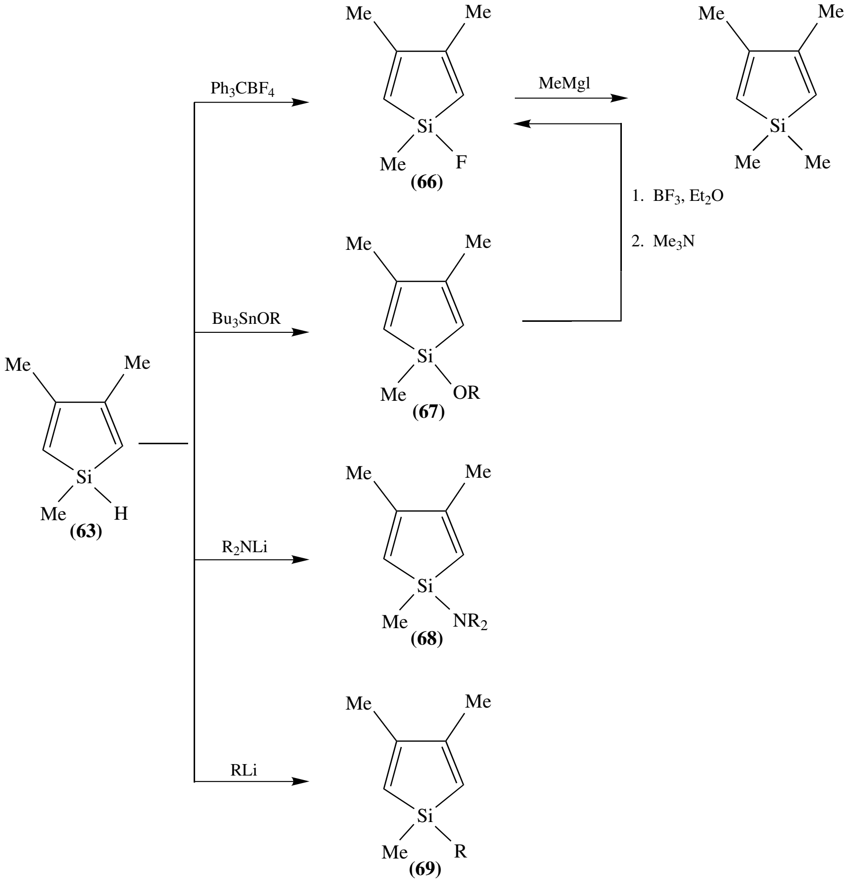

SCHEME 13

These three metalloles are the lower C-alkyl substituted Si–H bond-containing siloles which were isolated. The possible substitution of hydrogen bonded to silicon by another atom or a functional group appeared very attractive. Scheme 13 shows the functionalization reactions of 1,3,4-trimethylsilole **(63)** described by Dubac and coworkers[75]. 1-Fluoro-1,3,4-trimethylsilole **(66)** has been identified spectroscopically and chemically, but it is not stable enough to be isolated. Astonishingly, the chlorinated analogue was not obtained by chlorination of **63**; the chlorosilole seems to be very unstable (see Section III.A.4). This would appear to be unknown for a chlorosilane. In contrast, the alkoxylation and the amination of **63** proceed in excellent yield to give stable 1-alkoxy-1,3,4-trimethylsiloles (**67**, R = Me, *i*-Pr) and 1-diethylamino-1,3,4-trimethylsilole (**68**, R = Et). Reaction of **63** with lithium reagents gives the same siloles **69** as those obtained by the preceding method (equation 22).

Vacuum pyrolysis of the 2,3,7,8-tetramethyl derivative of spiro compound **12** gives the silole **65**, isolated in an Ar matrix[20]. A study of phototransformations of this silole showed isomeric forms analogous to those found for the parent silole (Scheme 4).

3. Exchange reactions (transmetallation) with other heterocyclopentadienes

Owing to the lability of the tin–carbon bond, stannoles were the first heterocyclopentadienes to be transformed into other heteroles: boroles[56a,76], arsoles or stiboles[60a,77] and auroles[78]. However, since their synthesis is presently less easy for the C-unsubstituted or alkyl substituted derivatives than in the case of the corresponding siloles or germoles, they are not useful reagents for preparing these heteroles.

More recently, Fagan and coworkers developed an interesting and general synthetic route to main group heterocycles by metallacycle transfer from zirconium[1,79]. The zirconacyclopentadienes **70**–**72** can be conveniently prepared by reduction of commercially available Cp_2ZrCl_2 ($Cp = \eta^5\text{-}C_5H_5$) with either Mg turnings or *n*-BuLi in the presence of 2-butyne, diphenylacetylene or deca-2,8-diyne[80], respectively.

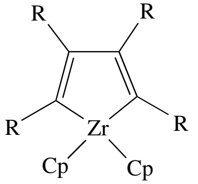

(70) R = Me
(71) R = Ph

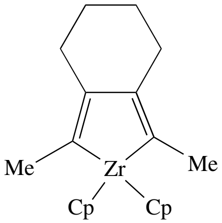

(72)

In THF solution the zirconacycles **70** and **72** reacted immediately at room temperature with main group electrophilic reagents affording main group heterocycles and zirconocene dihalide (equations 24 and 25) in about 80% yield. After removal of the solvent, the products can be easily extracted with hexane and isolated in the pure state by flash chromatography (alumina) with elution by hexane.

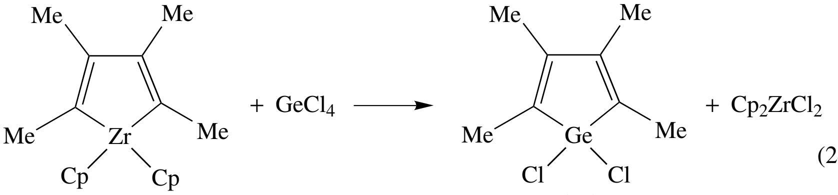

(70) **(73)**

(24)

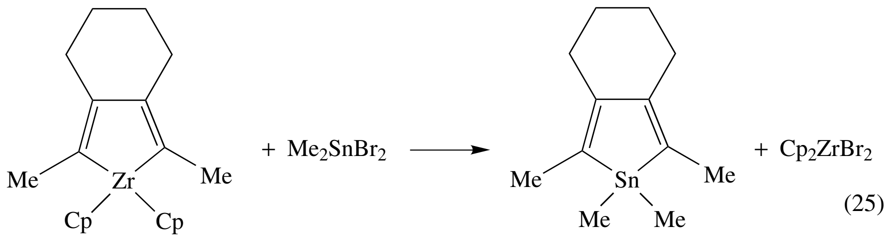

(72) **(74)**

(25)

By using the same method, many other group 13 (P, As, Sb, Bi) or 15 (S, Se) heterocycles can be readily obtained in good yields (50–85%).

Depending on the synthetic target, the zirconium metallacycle does not need to be isolated, and 'one pot' syntheses can be carried out. Addition of *n*-butyllithium to a THF slurry of Cp_2ZrCl_2 at −78 °C in the presence of the relevant alkyne, followed by warming to room temperature, generates zirconacycles. Dropwise addition of an hexane solution of a dichloride derivative of main group elements to this solution leads to a variety of heterocycles.

This methodology was extended by Dubac and coworkers[81] and Meier-Brocks and Weiss[82]. Titanacycles, zirconacycles and hafnacycles were treated with various halogenogermanes (equation 26).

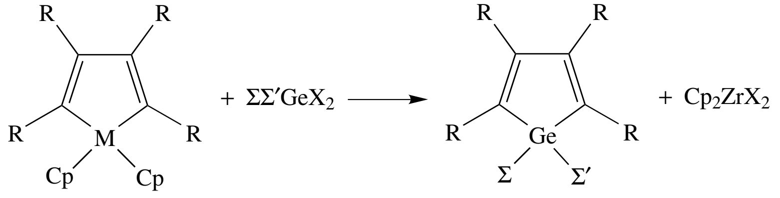

(26)

(70) M = Zr, R = Me $\Sigma = \Sigma' =$ Me, Ph, Cl X = Cl, Br
(71) M = Zr, R = Ph
(75) M = Ti, R = Ph
(76) M = Hf, R = Me

Starting from the titanium, zirconium or hafnium complex, germanium tetrachloride or tetrabromide undergoes transmetallation reactions under mild conditions (room temperature, THF or benzene solution) in good yields (70–90%). Dimethyldichlorogermane appeared less reactive than the tetrahalides in zirconium–germanium or hafnium–germanium exchange. Hafnium complexes are less efficient than the zirconium one. Methyltrichlorogermane readily reacts with zirconacycle **70** but the authors did not succeed in characterizing or isolating 1-chloropentamethylgermole, probably because it is unstable.

In the same way, the direct synthesis of 1-chloro-1-phenyltetramethylgermole **77** by Zr/Ge transmetallation starting from **70** and phenyltrichlorogermane was carried out in moderate yield owing to the low reactivity of $PhGeCl_3$. The desired chlorogermole **77** could be also obtained by chlorination of 1-phenyltetramethylgermole[81] (equation 27).

In the particular case of electrophilic silicon derivatives, the exchange reaction is very difficult to achieve. Transfer from Zr to Si is not possible in THF solution at room temperature and the zirconium complex could be recovered unchanged even after heating in neat $SiCl_4$. However, when the zirconacycle **70** was treated with neat $SiBr_4$ for 2 days at 150 °C, silole **78** was isolated as an impure liquid in 28% yield[1b] (equation 28).

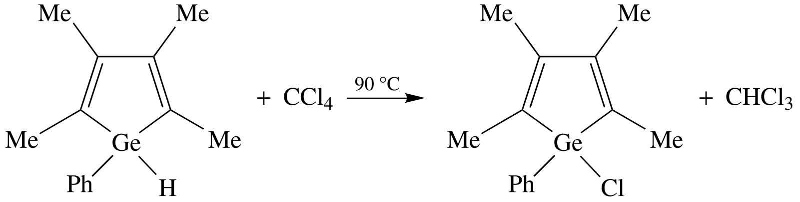

(77)

(27)

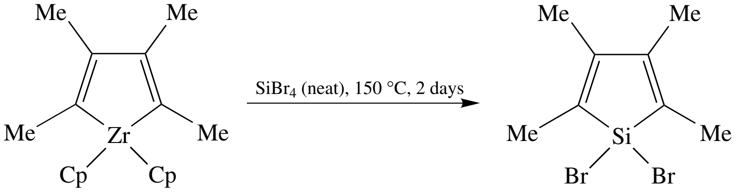

(70) **(78)**

(28)

The Zr-based route to main group heteroles is a convenient alternative to the method using 1,4-dilithio-2,3-butadienes (see Section II.B.1.a), the more so as these dilithium reagents are easily available from zirconacyclopentadienes. Thus, the synthesis of 1,1-dichloro-2,3,4,5-tetramethylsilole **(27)** was readily performed from **70** by use of the I_2/*n*-BuLi/$SiCl_4$ sequence of reagents[40] (see Section II.B.1, equation 8)

C. Dibenzometalloles or 9-Metallafluorenes

The main method for the synthesis of 9-metallafluorenes was first described by Gilman and coworkers[83]. A one-step reaction of 2,2′-dilithiobiphenyl with various organometallic halides provided a great number of sila-, germa-, stanna- and plumbafluorenes with various groups on the heteroatom (equation 29).

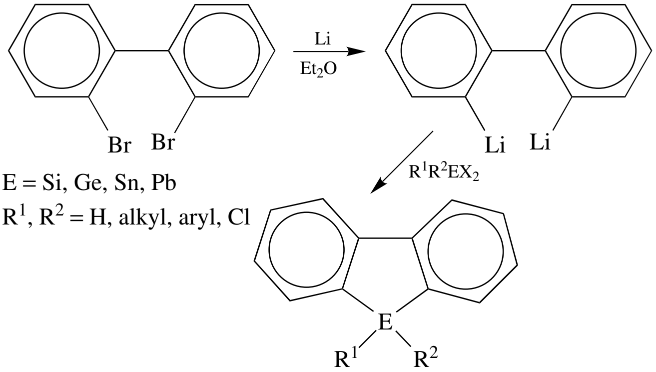

E = Si, Ge, Sn, Pb
R^1, R^2 = H, alkyl, aryl, Cl

(29)

2,2′-Dilithiobiphenyl also reacts with silicon, germanium or tin tetrahalides or hexachlorodisilane to give 5,5′-spirobi[dibenzometalloles] **(79)**[83b,d,84,85].

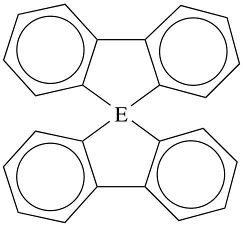

(79)

Reaction of 2-chloro-2′-bromobiphenyl with magnesium powder followed by addition of Me_2SiCl_2 gives in good yield (87%) 9,9-dimethyl-9-silafluorene **(80)**[86] (equation 30).

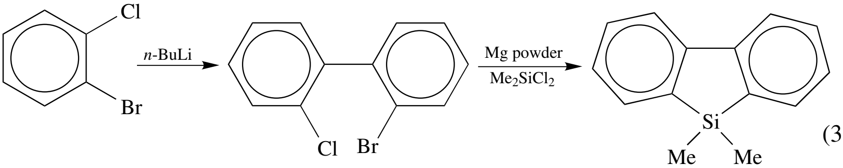

(30)

(80)

Metallaspirofluorenes **81**[87] and 9,9-dichloro-9-silafluorene **(82)**[88] were prepared by high temperature reactions of 2,2′-dihalogenobiphenyl with Ge or Sn powder or organochlorosilanes. The dichloride **82** was obtained in high yield by thermal reaction of (*o*-chlorophenyl)phenyldichlorosilane with various organochlorosilanes[89,90]. Substitution reactions on the metal also led to other functional metallafluorenes[91].

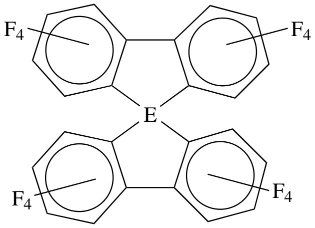

(81)

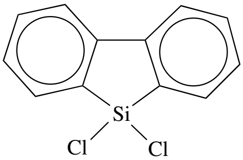

(82)

Irradiation of 1,1,2,2-tetramethyl-1,2-disila (or germa) dibenzocyclohexa-3,5-diene gave rise to 9,9-dimethyl-9-sila (or germa) fluorene **(83)** by a diradical process[92] (equation 31). This silafluorene could also be produced by pyrolysis of dimethyldiphenylsilane[93].

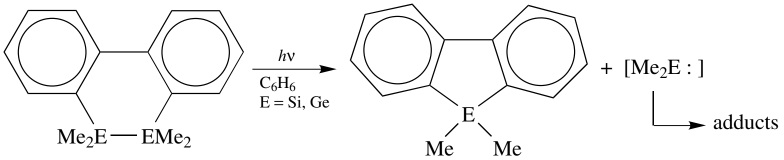

(31)

(83)

The photolytic cleavage of the Si−Si bond in 9-(trimethylsilyl)-9-silafluorenes in the presence of acetone afforded a Si−O(C) bond via a Si=C double bond[94]. The same reactions performed in neat alcohol (MeOH or EtOH) give rise to direct formation of a Si−H bond (Scheme 14).

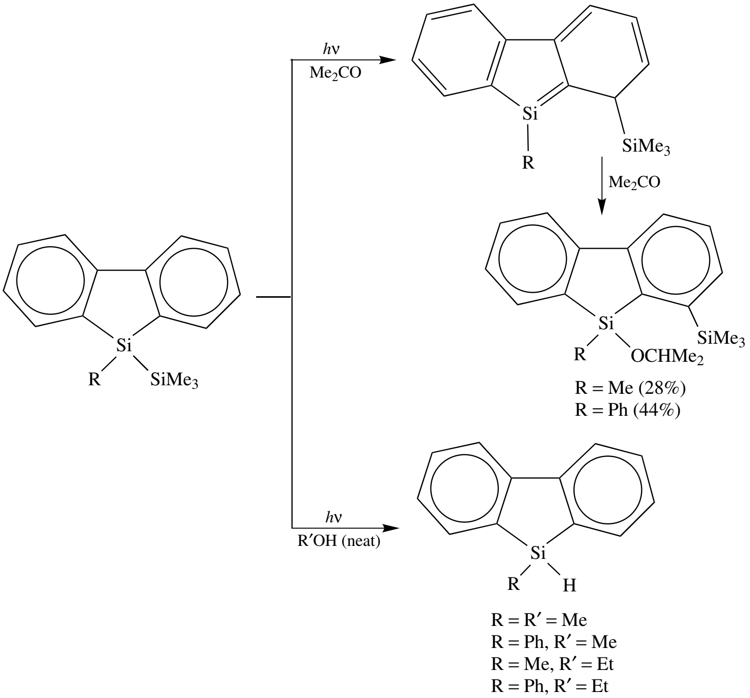

SCHEME 14

The reaction of MeLi and *n*-BuLi with various dibenzosiloles produces 1,1-dialkyldibenzosiloles in quantitative yields, while PhLi, and particularly *t*-BuLi, are less reactive[95] (equation 32).

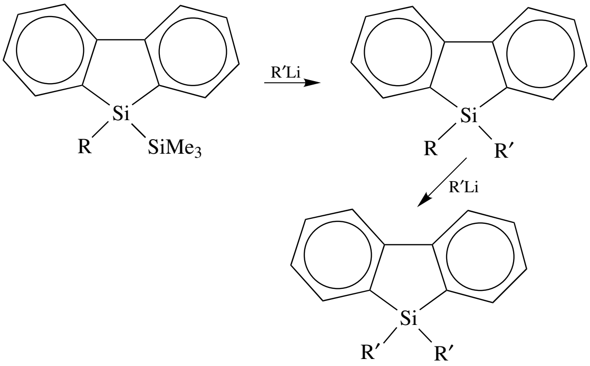

(32)

R = Me, Ph, $SiMe_3$; R′ = Me, *n*-Bu, *t*-Bu or Ph

D. Benzometalloles or 1-Metallaindenes

Several methods have been recently developed for synthesizing various metallaindenes.

1. Cyclization of 1-lithio-2-(2′-lithiophenyl)ethylene

Reaction of organometallic dihalides with the title dilithio reagent afforded silicon and tin metallaindenes (equation 33)[96].

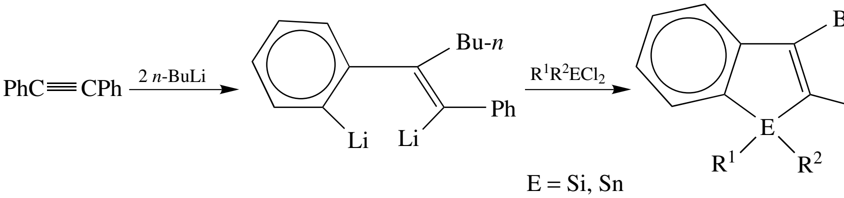

(33)

An extension of this method was developed by Kurita and coworkers[97]. 2-Trimethylsilyl-1-benzometalloles are prepared in four steps from phenylacetylene in about 60% yield. The advantage of the trimethylsilyl substituent is that it can be easily removed, leading to C-unsubstituted 1,1-dimethyl-1-benzometalloles **(84)** (Scheme 15)

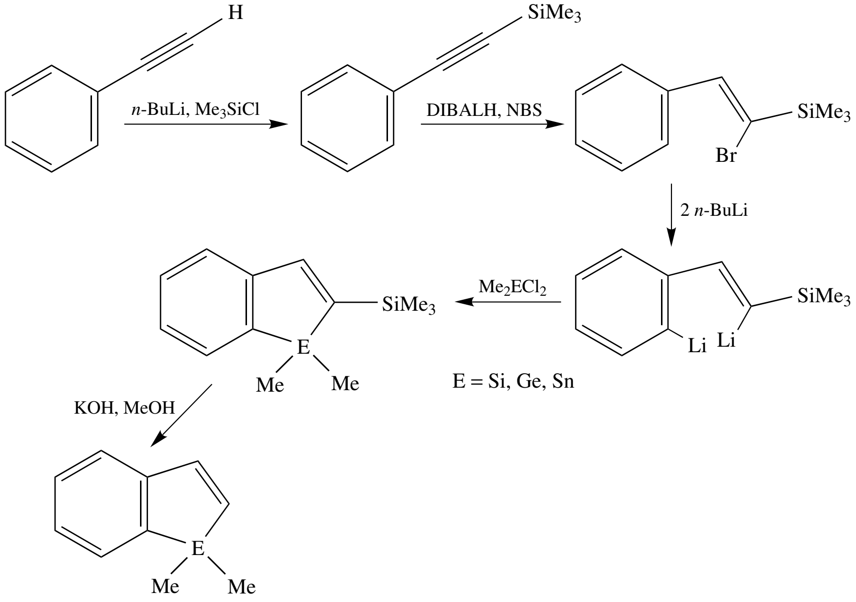

(84)

SCHEME 15

1,1-Dibutyl-1-benzostannole has been prepared in two steps from benzo[b]tellurophene by successive reactions of *n*-butyllithium and di-*n*-butyldichlorostannane **(85)** (equation 34)[98]. When Si, Ge and Sn tetrahalides are reacted with dilithio reagent **86**, spirometallaindenes **87–89** are obtained (equation 35)[96].

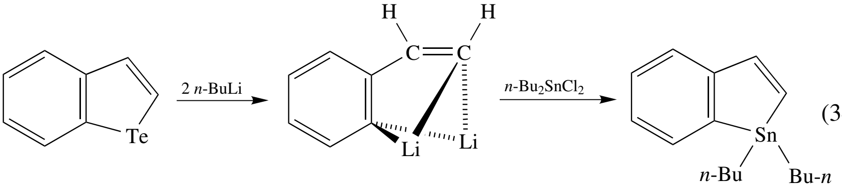

(85)

(34)

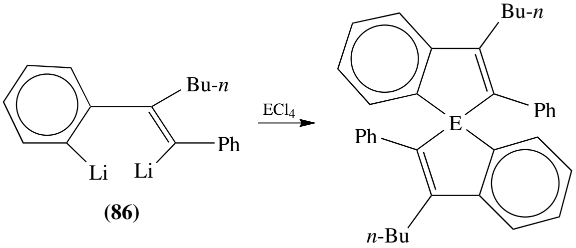

(86)

(35)

(87) E = Si (22%)
(88) E = Ge (28%)
(89) E = Sn (28%)

2. Transmetallation reactions

1-Zirconaindenes, which are easily obtained by insertion of various alkynes or an ynamine into the Zr−C bond of *in situ* generated[99,100] benzyne-zirconocene, are very good precursors of 1,1-dichloro-1-germaindenes **(90)** (Scheme 16)[101]. This method has been successfully extended to tin chemistry (Scheme 17)[102]. In this case, a convenient reaction was obtained even with alkyl or aryltrichlorostannane.

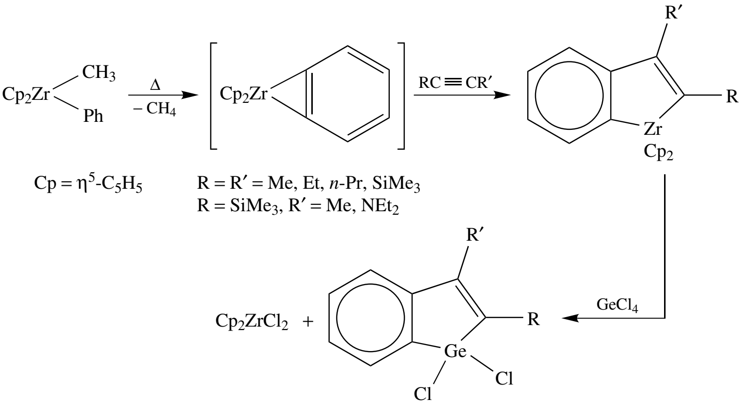

Cp = η^5-C$_5$H$_5$

R = R′ = Me, Et, n-Pr, SiMe$_3$
R = SiMe$_3$, R′ = Me, NEt$_2$

(90)

SCHEME 16

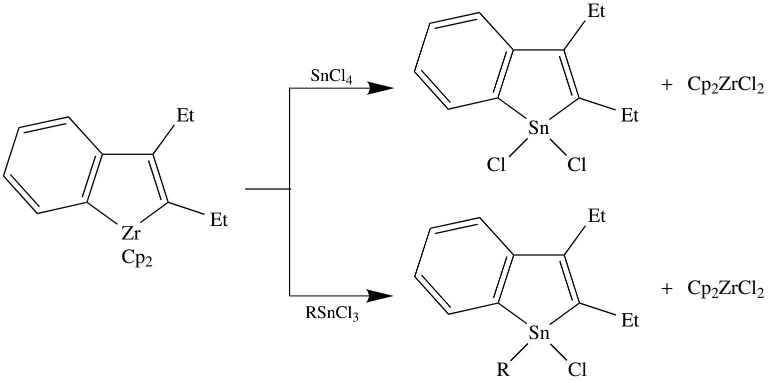

SCHEME 17

3. Nucleophilic substitution on the metal centre

Contrary to the tin series, transmetallation reaction with alkyl- or arylgermanium trichloride starting from zirconaindenes does not give monochloro 1-germaindene in good yield[103]. However, the required compounds were synthesized from 1,1-dichloro-1-germaindenes, by reaction of phenyl- or silyl-tris(trimethylsilyl)lithium (Scheme 18).

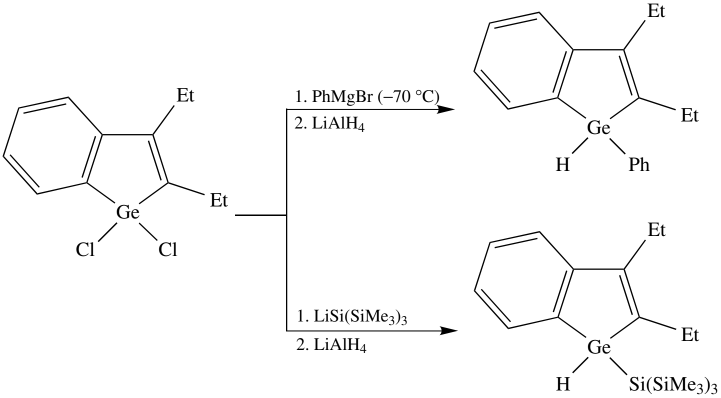

SCHEME 18

Sn−H bond-containing stannaindenes **(91)** are accessible by lithium aluminium hydride reduction of the monochloro derivative (equation 36)[103].

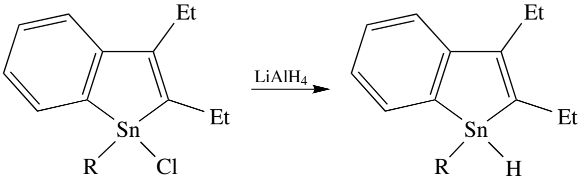

(36)

(91)

The Sn−H bond in these compounds has been characterized by ^{1}H NMR as a quartet in the range of 6–7 ppm ($^1J^{117}$ Sn−H = −1800 to −1900 Hz and $^1J^{119}$ Sn−H = −1880 to −1980 Hz). The ^{119}Sn NMR spectra exhibits a doublet near −150 ppm. Similarly, reduction of 1-chloro-1-phenylstannaindene **(92)** with $LiAlD_4$ leads to 1-deuterio-1-phenylstannaindene **(93)** after deuteriolysis under argon (equation 37).

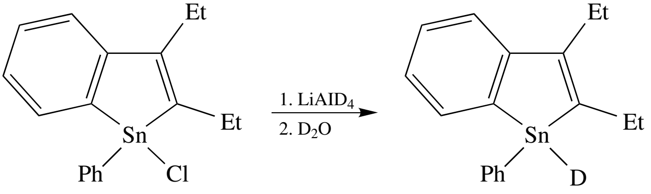

(92) **(93)**

(37)

In this case, the ^{119}Sn NMR spectrum showed a triplet at −153 ppm with a coupling constant $^1J^{119}$ Sn−D = −306 Hz.

It is well known[104] that organotin hydrides are very efficient reagents for organic halide reduction. Not surprisingly, therefore, 1-stannaindene **(94)** in $CDCl_3$ solution gives rise to 1-chloro-1-phenyl-1-stannaindene **(95)** (equation 38).

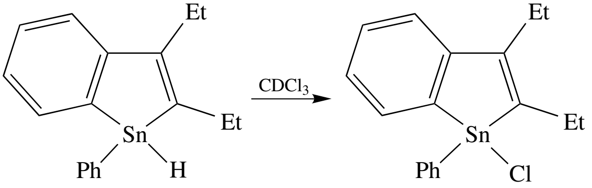

(94) **(95)**

(38)

4. Thermolytic reactions

1,1-Dichloro-1-silaindene **(96)** was obtained in moderate yield by reaction of dichlorosilylene (generated from hexachlorodisilane) and chlorinated phenylvinylchlorosilanes at 500 °C (equation 39)[89a]. Similarly, 1,1-dimethyl-1-silaindene **(97)** was generated in high yield by FVP of (*o*-dimethylsilylphenyl)acetylene at 800 °C (equation 40)[105a]. The same reaction, starting from (*o*-dimethylsilylphenyl)dimethylsilylacetylene, also affords the silaindene **97**[105a]. The formation of this product is likewise observed on addition of dimethylsilylene to cyclooctatetraene[105b].

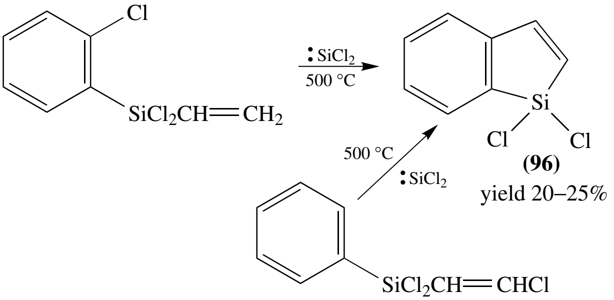

(96)
yield 20–25%

(39)

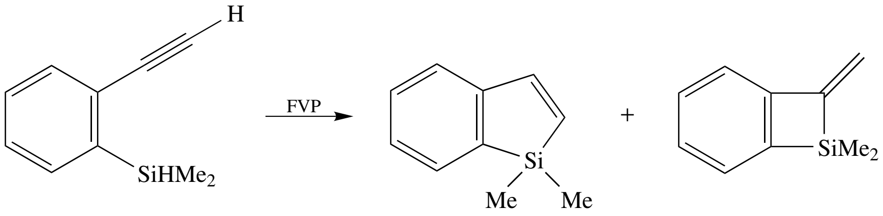

(40)

(97)

800 °C	84%	0%
650 °C	47%	34%

Barton and Burns[106] obtained 1-methyl-1*H*-1-silaindene **(98)** in moderate yield by FVP of 2-allyl-2-methyl-2-silaindane. The formation of this product was explained by the rearrangement of an initially formed 1*H*-2-silaindene via a retroene reaction (Scheme 19).

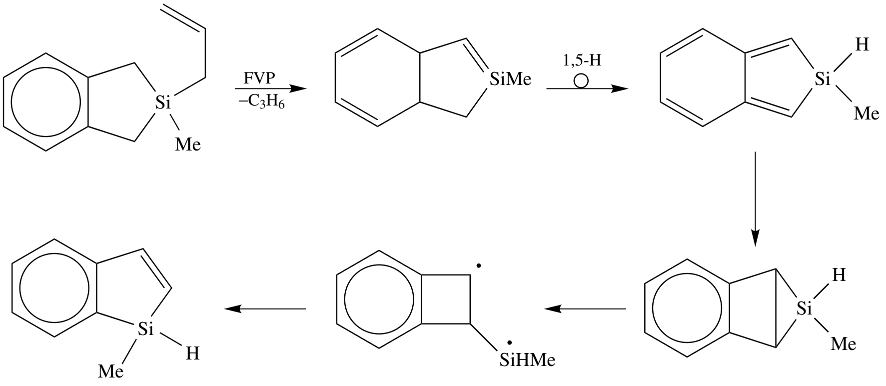

(98)

SCHEME 19

5. Other reaction

Seyferth and coworkers observed an interesting insertion reaction of a silirene into the C≡C bond of benzyne affording a 1,1-dimethyl-1-silaindene derivative **(99)** (equation 41)[45c].

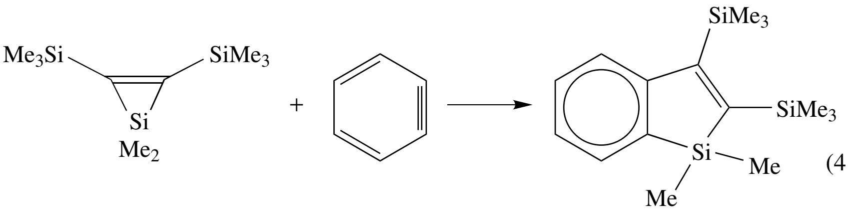

(41)

(99)

III. ORGANIC CHEMICAL PROPERTIES OF GROUP 14 METALLOLES

A. Stability and Isomerizations

1. Kinetic stability toward Diels–Alder dimerization

The kinetic stability of group 14 metalloles towards [4 + 2] dimerization is dependent on the nature of the heteroatom and on the substituents bonded to it and the ring carbons. Like cyclopentadiene, the silole **2** is unstable as a monomer. The silicon methylated derivatives (**3** and **4**) are also unstable, but two mesityl groups provide stabilization by steric hindrance of the [4 + 2] dimerization transition state[15]. The same effect has been observed for 1,1-dimesitylgermole[24].

Some observations seem to us interesting:

(a) 1,1-dimethylgermole **(18)** dimerizes more slowly than 1,1-dimethylsilole **(4)**[21];

(b) 1,1-di-*n*-butylstannole **(19)** is stable as a monomer[28], and 1,1-di-*n*-butylgermole **(17)**, which can be distilled, dimerizes only very slowly[24a];

(c) a kinetic stability comparison between 1,1-di-*n*-butylsilole and **17** [prepared by dehydration of the corresponding metallacyclopentenols (see Section II.A.1)] suggests that **17** dimerizes much slower than the silicon analogue[107].

Hence, kinetic stability towards [4+2] dimerization increases from siloles to stannoles. Intracyclic bond lengthening (Si−C < Ge−C < Sn−C) must give rise to a decrease in the ring angular strain and to HOMO stabilization. This inhibits dimerization by an increase in the frontier orbital (HOMO/LUMO) energy-level difference.

A similar effect brought about by electronic factors can also be obtained by polymethylation of the dienic ring, as with cyclopentadienes[108]. The 3,4-dimethylsiloles and -germoles are generally stable in the monomeric state, except for some functional derivatives[20,75]. The close analogy between the stability of C-unsubstituted and C-methylated siloles on the one hand and that of isoelectronic phospholium ions on the other has been emphasized[14].

Aromatic groups on the ring carbons stabilize strongly the C-phenylated group 14 metalloles, as in the case with phospholes[109], but the reactivity of the dienic system (i.e. Diels–Alder cycloadditions, formation of transition metal complexes) decreases[3,4].

2. Geometric isomerization into transoid dienes

C-alkylated metalloles, particularly C-methylated ones **(53, 55, 58, 60, 61, 63–69)**, isomerize readily into transoid dienes **(100)**, their thermodynamically more stable isomers.

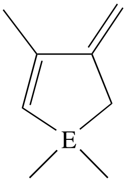

(100)

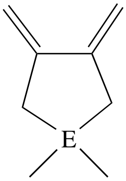

(101)

This disadvantage is overcome only with difficulty. Many catalysts or reagents induce this isomerization, e.g. alumina, thoria[67] and lithium reagents[110]. The best synthetic conditions which minimize production of the transoid diene are non-catalytic (see Section II.B.2.d.). In the pure state, the extent of isomerization is small at room temperature. However, storage at −20 °C or below is desirable. This isomerization under non-catalytic conditions implies a thermally allowed [1,3]-H antarafacial shift[111].

The presence of exocyclic cisoid isomers **101** has never been recorded. These derivatives have been prepared in other ways for silicon and germanium[112].

3. Tautomerism. 2H- and 3H-metalloles

The tautomerism phenomenon resulting from sigmatropic migrations of hydrogen atom or a substituent in cyclopentadiene and heterocyclopentadienes (pyrroles, phospholes) is well known[2*d*,113,114]. In pioneering work, Barton and coworkers[35c] observed during silole **102** thermolysis the formation of a [4 + 2] dimer **(104)** in which the 2*H*-tautomer **103** is the diene component and the 1*H*-silole **102** the dienophile (equation 42). **103** results from **102** by a [1,5]-Si shift. Other trapping products providing evidence for the formation of the reactive silole **103** were described (Scheme 20).

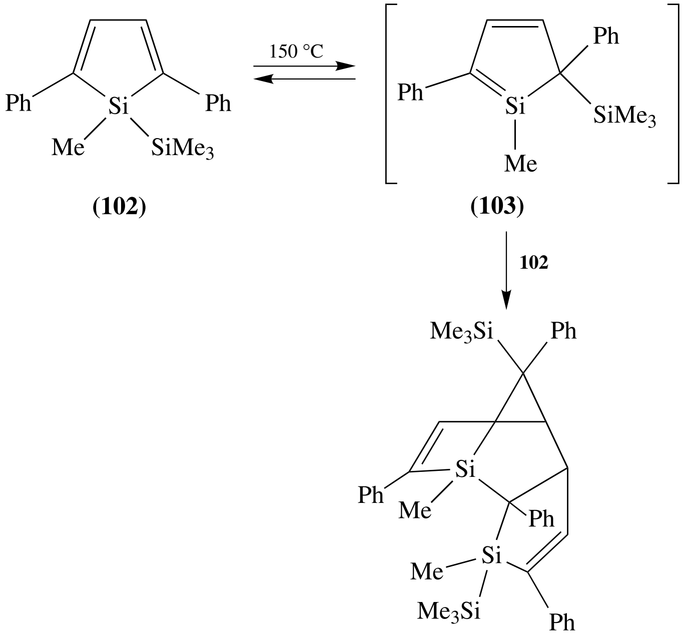

(102) **(103)**

(42)

(104)

2*H*-Siloles and 3*H*-siloles were suggested as reaction intermediates in the FVP of 1-allylsilacyclopentenes[5,6] (see Section II.A.1, Scheme 1), on the basis of trapping experiments. They were spectrometrically detected during vacuum pyrolysis of other silacyclopentenes[19,20] (see Section II.A.1, Scheme 4). A 2*H*-benzosilole has also been postulated in the case of FVP of a 2-allylsilaindane[106].

Comparing the [1,5]-sigmatropic hydrogen shifts in pyrrole and phosphole, at the MP2/6-31G* level, Bachrach has shown that the more stable tautomeric form is, respectively, 1*H*-pyrrole and 2*H*-phosphole[2d]. The activation enthalpies were computed to be 186 kJ mol^{-1} for 1*H*-pyrrole to 2*H*-pyrrole transformation and only 67 kJ mol^{-1}

for $1H$-phosphole to $2H$-phosphole rearrangement. However, in substituted phospholes, substitution is preferred at P rather than C[115]. Hence the $1H$-isomer is stabilized, probably for steric reasons[2d,115] and/or orbital overlap between the π-dienic system and the σ orbital of the P−R exocyclic bond[2a].

An extensive theoretical investigation does not exist for the siloles, but PM3 calculations of formation enthalpies of **2** and its tautomers have indicated that the $1H$-silole is the most thermodynamically stable species[20c]. The activation barrier for **11** → **2** isomerization was calculated to be 96 kJ mol^{-1}, comparable to that for cyclopentadiene[2d,116]. The $(1H + 1H)$ dimer **10**[19] is isolated rather than the $(2H + 1H)$ dimer as in the case of phosphole. This directly confirms the thermodynamic stability and the Diels–Alder kinetic instability of **2**. The marked difference in the stability of the parent silole and phosphole was explained[3] by the relative stabilities of the σ bonds in silanes and phosphines (Si > P) and of the π bonds in silenes and phosphenes (P > Si)[117].

No tautomeric forms of $1H$-germoles or stannoles are as yet known. In these metalloles, it is likely that the carbene analogue isomer (like **9**) should be more stable than the $2H$- or $3H$-forms.

4. Stability of functional and spiro derivatives

The instability of some halogenated group 14 metallole derivatives has been previously reported[118]. C-phenylated halometalloles are stable, but C-methylated derivatives are much less so. Although 1,1-dichloro- or 1,1-dibromo-2,3,4,5-tetramethylsilole[1b,40] and -germole[1,81] have been isolated, 1-halo-1,3,4-trimethylsiloles are unstable[75]: 1-fluoro-1,3,4-trimethylsilole has been observed but the chlorinated analogue could not be prepared. The latter has been isolated in complex form as (η^4-1-chloro-1,3,4-trimethylsilole) carbonyliron[119]. It has been also observed that 1-chloro-2,3,4,5-tetramethylphosphole[120], -stibole and -bismole[79] are thermally unstable. 1-Halo-3,4-dimethylphospholes have been stabilized as σ-tungsten pentacarbonyl complexes[121].

These observations, which prompted a theoretical investigation, have been explained[118] by an effect similar to *spiroconjugation* which is known to be responsible for modifications in the electronic spectra and chemical reactivity of halocyclopentadienes, cyclopentadiene ketals and 1,1-dioxothiophene[122]. This spiroconjugation phenomenon could be also involved in the destabilization of spirobisiloles with respect to spirobigermoles and spirobistannoles[118].

B. Cycloaddition Reactions

The cycloaddition reactions involving group 14 metalloles have been extensively reported in the previous review[123]. Here we summarize the main points, and give new results.

1. Diels–Alder [4 + 2] cycloadditions

a. With ethylenic dienophiles. Ethylenic dienophiles give relatively stable adducts (7-metallanorbornenes) with siloles and germoles[123] (equation 43). C-phenylated metalloles (R^3–R^6 = Ar) are less reactive. For example, with maleic anhydride (MA), C-unsubstituted[10,15] and C-methylated siloles[67a,c,74,110] react at room temperature while C-phenylated siloles react at higher temperatures[52,64,68,124,125]. Indeed, for the reaction between 1,1-dimethyl-2,3,4,5-tetraphenylsilole and MA, the activation energy is higher

(60.3 kJ mol^{-1}) than for 1,1-dimethyl-2,5 (or 3,4)-diphenylsilole (39.3 and 34.7 kJ mol^{-1}, respectively), and the large negative activation entropy values (−30 to −40 e.u.) are consistent with those previously found for Diels–Alder reactions.

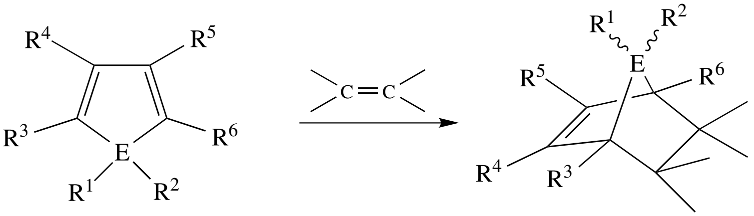

(43)

MA cycloaddition to metalloles seems to be always stereospecific and, according to Alder's rule, the *endo* configuration has been attributed to the adduct[125]. When two different groups R^1 and R^2 are present (equation 43), the major adduct results from the sterically more suitable transition state, i.e. the more bulky group is preferentially *syn* with respect to the C=C bond of the norbornene[6,67c].

Concerning the Diels–Alder dimers of unstable C-unsubstituted metalloles, only one ($1H + 1H$) dimer has been isolated, in a single configuration[10,12,19,21]. In the absence of crystallographic analysis of a solid dimer, an NMR study of hydrogen coupling constants was of help in determining the structure. The ^{1}H NMR of silole dimer **(10)**[19] did not allow measurement of the two hydrogen coupling constants which could give the required information. Dubac and coworkers[107] have calculated $J_{1,2}$ and $J_{6,7}$, which are related to H−C$_1$−C$_2$−H and H−C$_6$−C$_7$−H dihedral angles in the dimer of 1,1-dimethylsilole, from the ^{1}H NMR spectrum, decoupling experiments and the 2D COSY spectrum. The value obtained for these coupling constants (2 Hz) agrees with the corresponding dihedral angles of 60° and an *endo* configuration for the adduct.

The 7-silanorbornene-type adducts are relatively stable products, whose thermolysis or photolysis gives rise to the retro-Diels–Alder reaction or decomposition with extrusion of silylene[123]. With 7-stannanorbornenes this latter decomposition takes place at low temperatures[126]. Nucleophilic reagents provoke either silylene elimination[124] or cleavage of a single bridge Si−C bond[127].

From a $2H$-silole and benzophenone or stilbene, Diels–Alder adducts **105** and **106** are formed from the conjugated diene rather than the expected [2 + 2] adducts with the silicon–carbon double bond[35c] (Scheme 20).

The reaction between a disilene (*cis*- and *trans*-MePhSi=SiPhMe) and a silole (1,1-dimethyl-2,5-diphenylsilole) is a stereospecific Diels–Alder addition, as in the case of an ethylenic dienophile[128]. A digermene reacts in a similar way[129].

b. With acetylenic dienophiles. The [4 + 2] cycloaddition of an alkyne with a $1H$-metallole leads to a 7-metallanorbornadiene[123] (equation 44). These products are much less stable than 7-metallanorbornenes: they decompose by thermolysis or photolysis by elimination of the bridge [R^{1}R^{2}E:] and formation of a substituted aromatic compound. The instability increases from silicon to tin derivatives. This type of decomposition occurs when the substituents bonded to the norbornadiene are alkyl or aryl groups, including condensed rings. For example, 2,3-benzo-7,7-dimethyl-1,4,5,6-tetraphenyl-7-sila(or germa)norbornadiene decomposes at 300 °C^{52} (or 70 °C for the germanium derivative)[61b]

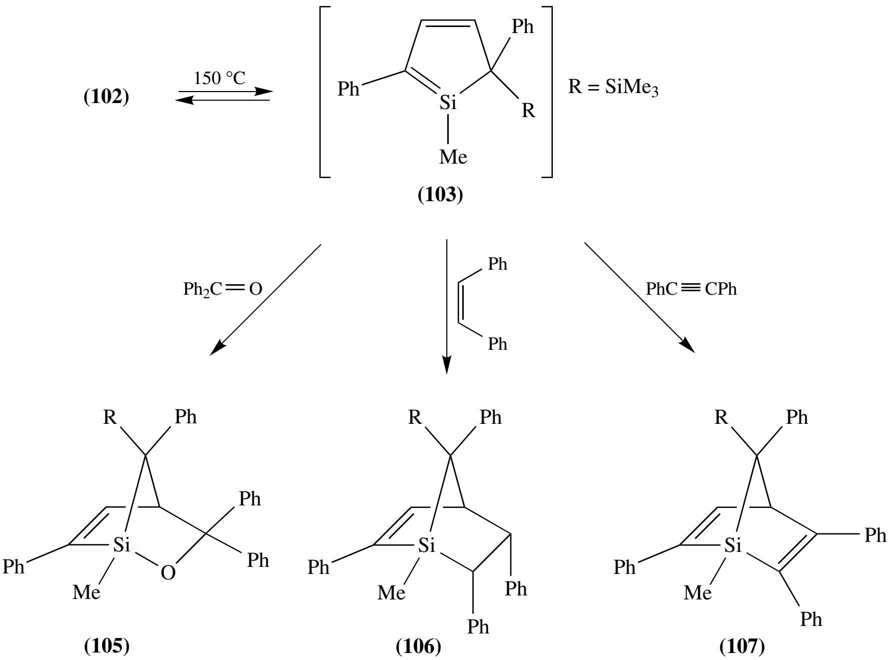

SCHEME 20

to give 1,2,3,4-tetraphenylnaphthalene and dimethylsilylene (or germylene) which can be trapped by reaction with diphenylacetylene (equation 45).

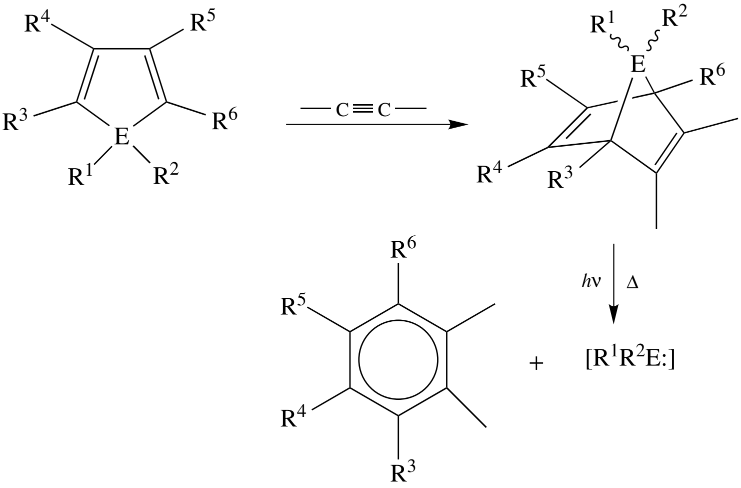

(44)

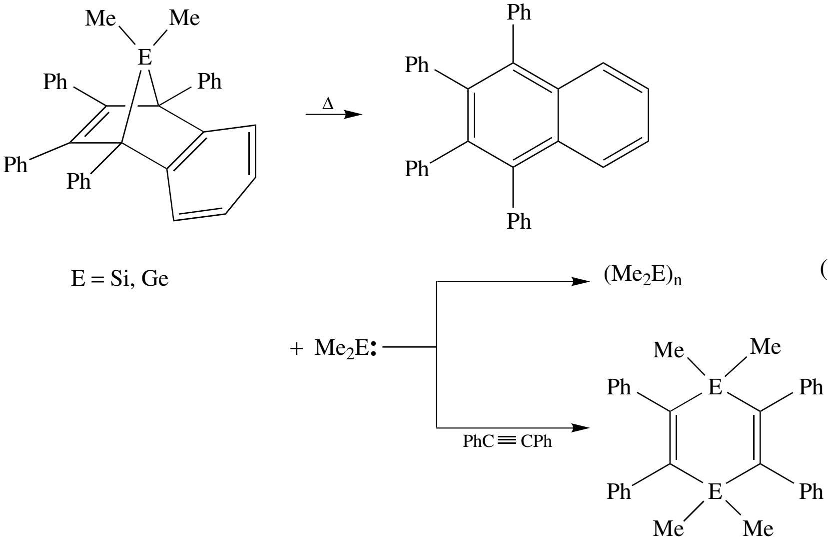

(45)

The main interest of this reaction is the possibility of generating silylenes, germylenes or other highly reactive group 14 species. One of the applications is the synthesis of germoles when the decomposition of germanorbornadiene is carried out in presence of an alkyne and a catalyst (see Section II.A.2, Scheme 5, and Section II.B.1.b.ii, Scheme 10). Other noteworthy applications are the generation of species with multiple bonding to silicon[7,123], for example disilenes[130] or a disilyne[131].

Another type of decomposition of metallanorbornadienes can arise in the case of derivatives incorporating certain substituents, in particular C=O or CF_3. They decompose by rearrangement with formation of stable Si−O or Si−F bonds[123]. These rearrangement reactions give several products depending on the solvent used.

Rearrangements of [4 + 2] adducts of siloles and dimethyl acetylenedicarboxylate have been extensively studied for C-phenylated siloles[52,64,124b,132,133] and, more recently, for C-methylated siloles[73]. However, the previously described decomposition pathway with silylene extrusion and formation of a substituted dimethyl phthalate is also observed[73,132]. An iron-substituted silylene [$Cp(CO)_2FeSiMe$] has been generated by using this method[134].

Only dimethyl acetylenedicarboxylate adducts with 2,3,4,5-tetraphenylsiloles are isolable but not those with 2,5-diphenyl- or 3,4-dimethylsiloles. The corresponding adducts with C-phenylated germoles[64,135] or a C-tetraphenylstannole[136] are not isolable either.

Reactions of 7-sila(or germa)norbornadienes with nucleophiles resulting in the cleavage of one or two endocyclic Si (or Ge)−C bonds have been described[137].

Ab initio SCF MO studies of the electronic structure of 7-sila(germa or stanna)norbornadienes[138] have shown that these molecules possess an inverted sequence of π levels [that is, the π_- (b_1) orbital lies energetically below the π_+ (a_1) orbital] in contrast to that found for the parent norbornadiene. The degree of level inversion increases along the series: Si(−0.17 eV) < Ge(−0.26 eV) < Sn(−0.87 eV). The main cause of this trend is probably the increase in the strength of through-bond interactions between the π-orbital and the bridge σ-molecular orbital. Replacement of C-7 in norbornadiene by the larger and more polarizable Si, Ge or Sn atom raises the energy of this σ-orbital, and also polarizes it. Moreover, the crystal structure determination of a 7-germanobornadiene showed a very small value (78.5°) for the endocyclic C−Ge−C angle[139]. All these data explain why these compounds, although stabilized by E or C-substitution, nevertheless remain fragile.

In contrast to the 7-silanorbornadienes, the less strained 1-silanorbornadiene ring system (derived from a 2*H*-silole) proved to be remarkably stable[35c].

c. Group 14 metalloles as dienophiles. At elevated temperatures, 1,1-dimethyl-2,5-diphenylsilole and dienes (2,3-dimethylbutadiene[140], tropone[141]) form [4+2] Diels-Alder adducts in which the silole behaves as the dienophile.

A 1*H*-silole can thermally isomerize to a 2*H*-silole leading to a dimer in which the 1*H*-silole is the dienophile fragment[35c] (equation 42).

2. [2 + 2] Cycloadditions

It has been reported that the low-energy irradiation of 1,1-dimethyl-2,5-diphenylsilole[142,143] and germole[142] yields [2 + 2] photodimers (equation 46).

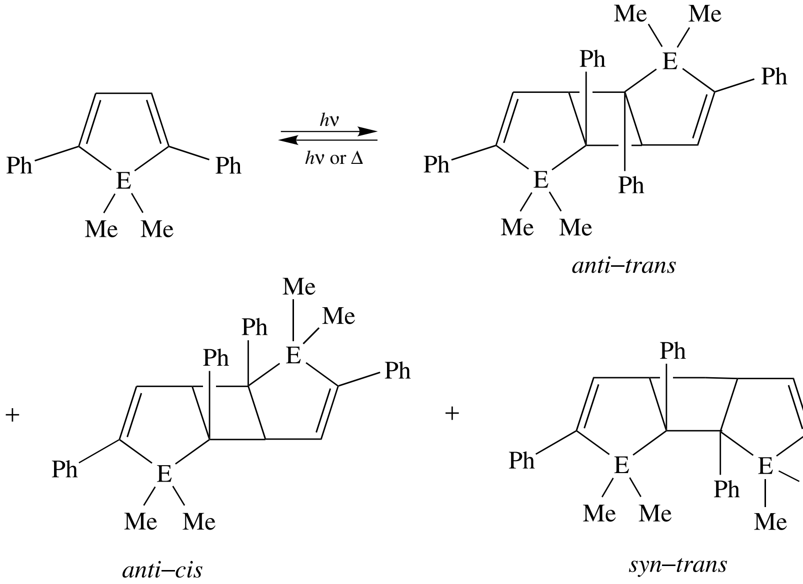

(46)

The major (almost exclusive) isomer formed is the *anti–trans* dimer, but two other dimers (*anti–cis* and *syn–trans*) are also obtained under a variety of conditions. The analogous intramolecular dimerization of α, ω-bis(1-methyl-2,5-diphenylsilacyclopentadienyl)alkanes has been also described[39].

A mechanistic study suggested that this photodimerization involves the excited single state of the silole[39]. It is thermally and photochemically reversible[39,143].

1,1-Dimethyl-2,3,4,5-tetraphenylsilole[144] is reported to be photochemically inactive whereas 1,1-dimethyl-2,5-diphenylstannole undergoes Sn−C cleavage leading to polymeric products[142].

The [2 + 2] photoadduct between 1,1-dimethyl-2,5-diphenylsilole and 1,1-dimethoxyethene was an intermediate in the synthesis of the first silacyclohepta-2,4,6-triene (silepin)[145]. Another, similar adduct is also formed when this silole reacts with *N*-chlorosulphonyl isocyanate[146].

C. Reactions with Halogens

Depending on the nature of both the halogen and the metal, the group 14 metalloles can react with halogens in three different ways: (i) addition of 1 or 2 equivalents of halogen to the diene system, with the cyclic structure preserved, (ii) cleavage of one or two endocyclic E-C bonds, with destruction of the cyclic structure, and (iii) substitution of one or two exocyclic substituents, with preservation of the metallole structure.

1. Silole series

Bromine follows reaction (i) with 1,1-dimethyl-2,5-diphenylsilole. If one equivalent of bromine is used, a mixture of dibromocyclopentenes in which the two halogen atoms are in the *trans* position is obtained (equation 47).

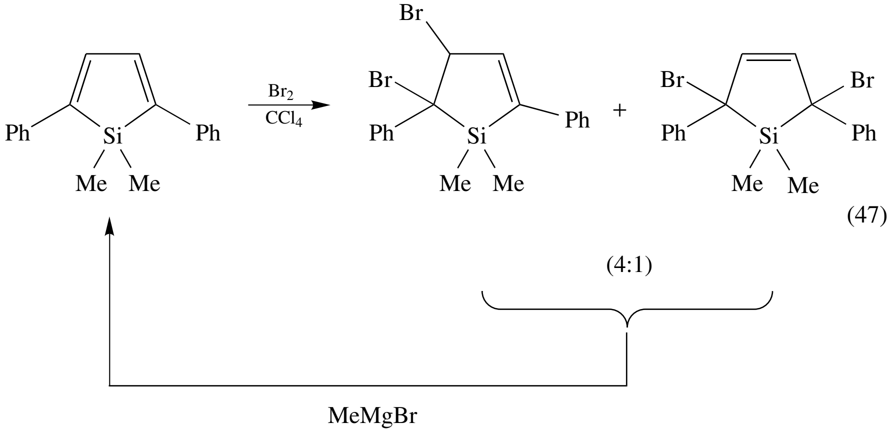

(47)

Treatment of the mixture with methylmagnesium bromide regenerates the starting silole[34]. Reaction of two equivalents of bromine with 1,1-dimethyl-2,5-diphenylsilole led to tetrabromosilacyclopentane from which a double β-elimination afforded (*E*,*E*)-1,4-dibromo-1,4-diphenylbutadiene (equation 48).

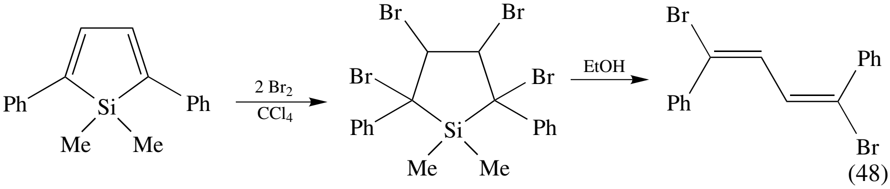

(48)

Iodine reacts differently with the C-methylated silole ring. Cleavage of the ring and formation of a complex mixture instead of the expected 1,4-diiodo-2,3-dimethylbutadiene is observed[12].

2. Germole and stannole series

Chlorine, bromine and iodine generally cleave germole and stannole rings[85c,147–150]. From 1,1-dimethyltetraphenylgermole or -stannole, [(*Z*,*Z*)-butadienyl]metal halides are formed in a quantitative yield (equation 49). The methyl–metal bonds remain intact. In the tin series, further chlorination or bromination gives rise to dimethyltin dihalide and dihalobutadiene (equation 50).

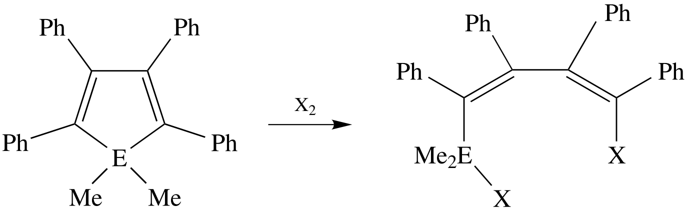

E = Ge, X = Cl
E = Sn, X = Br

(49)

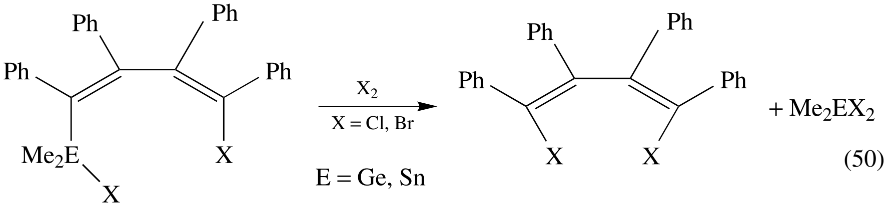

With the weaker electrophile iodine, mixed dihalobutadienes can be synthesized. Similarly, treatment with iodine monochloride converts the stannole into the same product (equation 51).

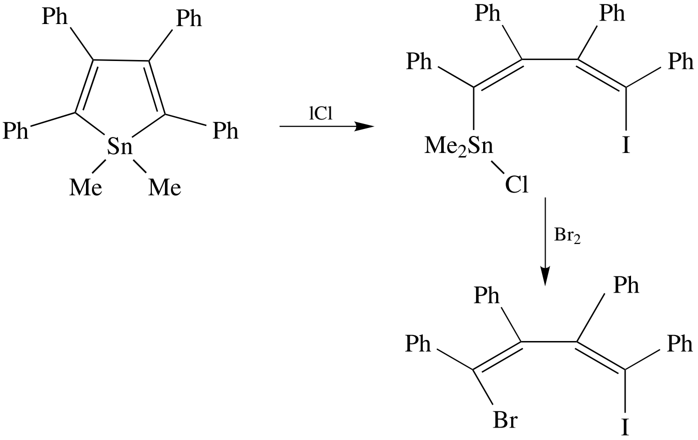

(51)

The reaction of iodine with 1,1-di-*n*-butyl-2,5-dimethylstannole leads to (*Z*,*Z*)-2,5-diiodohexa-2,4-diene, which is an interesting precursor for stibole and bismole synthesis[60b] (equation 52). By contrast, substitution of exocyclic substituents with conservation of the metallole structure has been discovered by Zuckerman and coworkers in the controlled bromination or iodination of hexaphenylstannole[151,152] (equation 53).

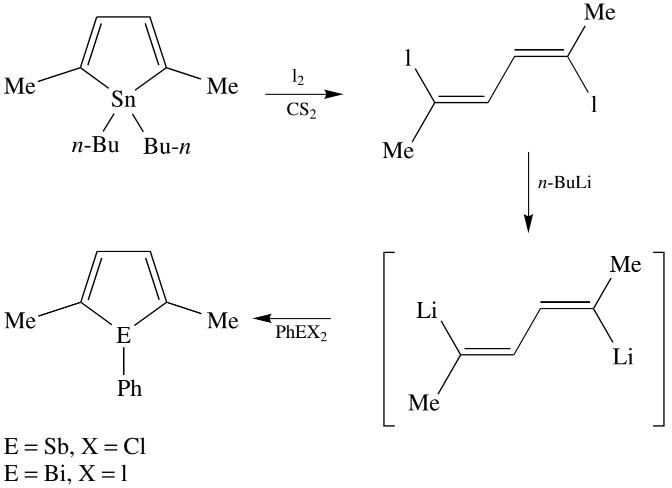

(52)

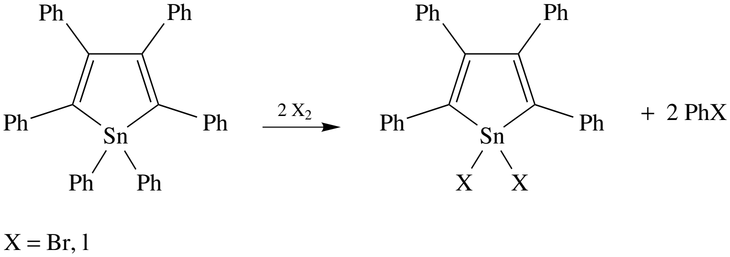

(53)

Dihalostannoles are very useful starting materials for the synthesis of many substituted stannoles[153]. They also give rise to the only known group 14 metalloles having a five- or six-coordinated heteroatom in the form of anionic or cationic species[152,153].

The particular reactivity of halogens toward stannoles was demonstrated by Sandel and coworkers[154]. Treatment of 1,1-dimethyltetraphenylstannole with iodine trichloride led to cleavage products and the Hückel aromatic 2,3,4,5-tetraphenyliodonium ion[154] (equation 54).

D. Reactions with Acids

The action of acids on siloles results in the cleavage of the two endocyclic Si−C bonds. Boiling concentrated hydrochloric acid, hydrogen bromide or glacial acetic acid promote the reaction, and the substituted butadienes, in which the geometry of the parent metallole is retained, are produced in high yield[34,155] (equation 55).

Stannoles are more easily cleaved by acids than are siloles. At room temperature, brief exposure of 1,1-dimethyltetraphenylstannole to a dilute solution of acetic acid in alcohol resulted in rapid cleavage of the two tin−carbon bonds, affording (*E*,*E*)-1,2,3,4-tetraphenylbutadiene.

The mechanism of the cleavage is probably the same for both silole and stannole, consisting of a two-step protodemetallation reaction (equation 56). The product of the first cleavage has been isolated in the case of stannole[156].

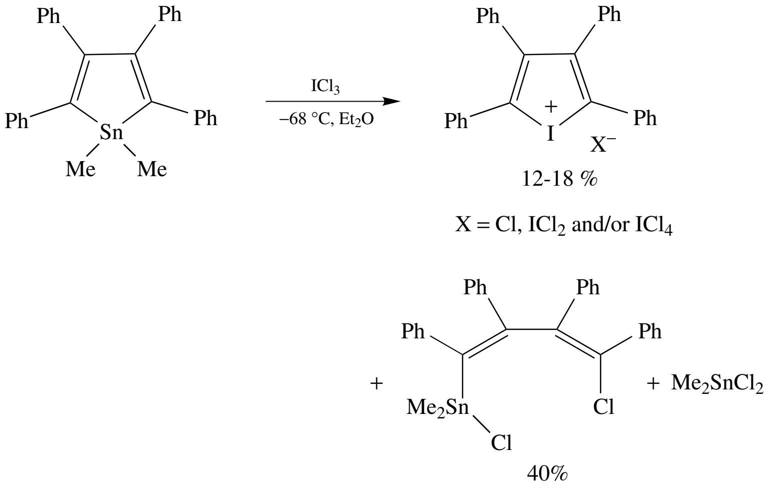

(54)

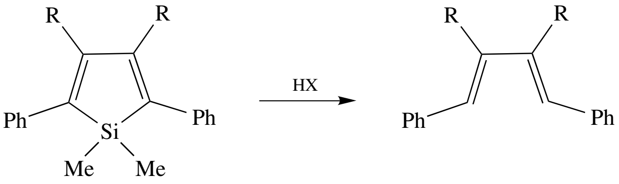

(55)

X = Cl, Br, OAc
R = H, Ph

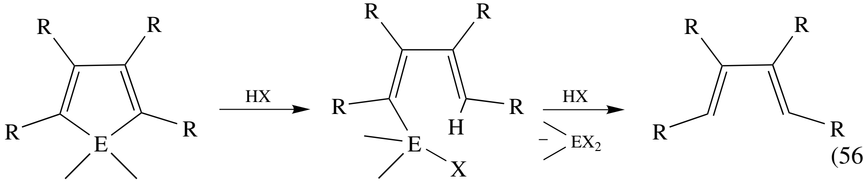

(56)

E = Sn, X = Br

E. Reactions with Bases

The alkaline cleavage of siloles (by ammonia[157] or sodium hydroxide[155,157]) leads to the same substituted butadiene as that obtained with the acid reaction (equation 57).

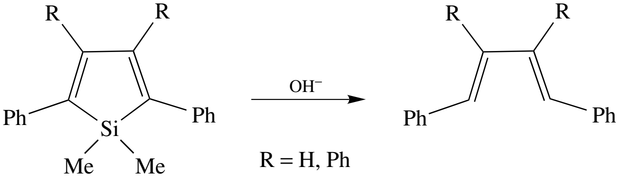

(57)

The reaction probably proceeds by nucleophilic attack of the hydroxide ion on silicon and subsequent ring opening with retention of the geometry of the starting silole[155]. In the case of 1,1,3,4-tetramethylsilole, the reaction stops after the first Si−C cleavage giving a dienyl siloxane[12]. Furthermore, the reaction of dilute NH_4OH with a methylene chloride solution of 1-chlorotetraphenylsilole or germole derivatives produces the corresponding 1-hydroxysilole and -germole[157] (equation 58).

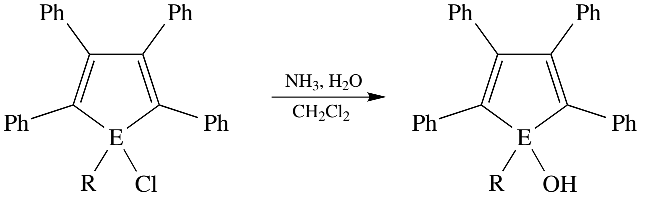

(58)

E = Si, R = Me
E = Ge, R = Ph

F. Reactions with Organometallic Reagents

These reagents are among the most important in group 14 chemistry for the promotion of substitution reactions (S_N2−M)[158] and metallacyclopentadienide anion generation (see Section V.A). Thus, 1,3,4-trimethylsilole **(63)** undergoes a classical S_N2−Si substitution[75,159] when treated with lithium reagents (Scheme 13). By contrast, in the case of pentaphenylsilole a secondary reaction occurs; a silacyclopentene ring is formed by 1,4-addition of the lithium hydride produced during the S_N2−Si reaction[160] (Scheme 21). This secondary reaction can be avoided by scavenging LiH *in situ* with Me_3SiCl[95a].

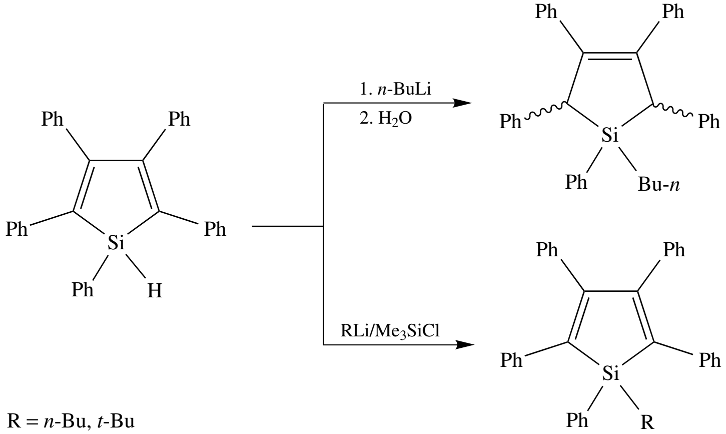

SCHEME 21

The hydrogermoles show different behaviour towards the lithium reagents. Metallation at the germanium atom is observed and germacyclopentadienide anions[157,161] are produced (see Section V.A).

The reactivity of lithium reagents with metalloles devoid of leaving groups on the heteroatom is very different. Methyllithium reacts with 1-silylsiloles by 1,4-addition to the π-system[160], leading essentially to the rearranged addition product together with a small amount of the 'normal' trimethylsilyl group substitution product[95a] (equation 59).

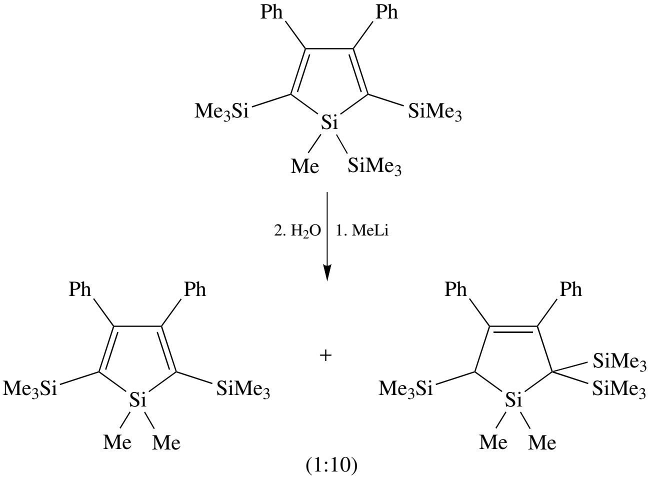

(59)

On the other hand, the reaction of RLi (R = n-Bu, Ph) at $-70\,^{\circ}$C in THF with 1,1,3,4-tetramethylsilole or -germole gives rise to a mono- or disubstitution reaction at the metal centre, depending on the proportion of the organolithium reagent[34,110] (Scheme 22). Phenyllithium is less reactive than n-butyllithium (9% and 70% yield, respectively, with tetramethylsilole) and the phenyl group is displaced in preference to the methyl group by

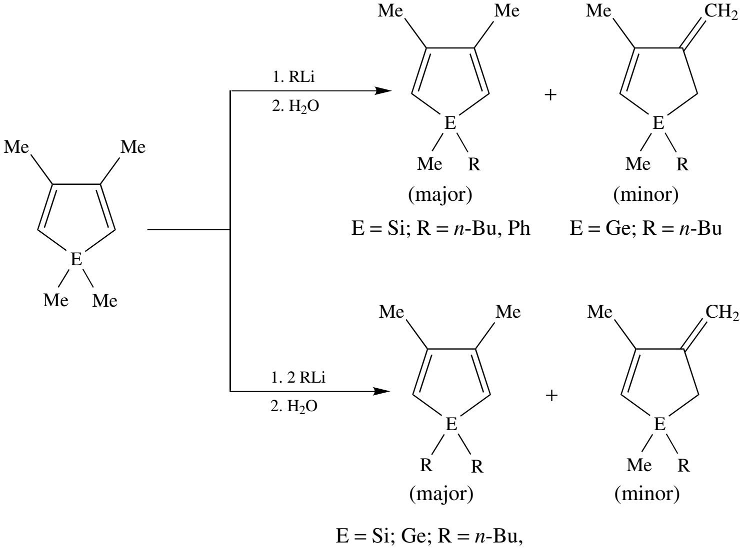

SCHEME 22

n-BuLi in 1-phenyl-1,3,4-trimethylsilole[34] (equation 60).

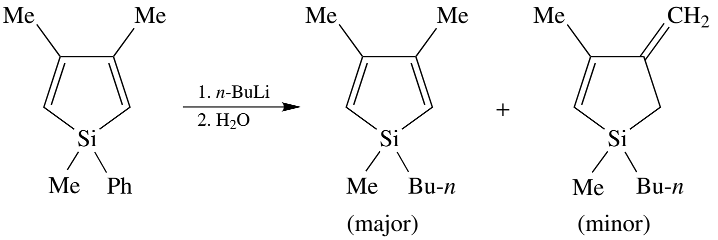

(60)

A predominant isomerization of metalloles to transoidal dienes occurs when *t*-BuLi is used[34]. This isomerization involves the formation of an allylic carbanion, which is protonated by water at the position α to Si (or Ge) and is silylated at the exocyclic carbon by Me_3SiCl[95a,110] (Scheme 23).

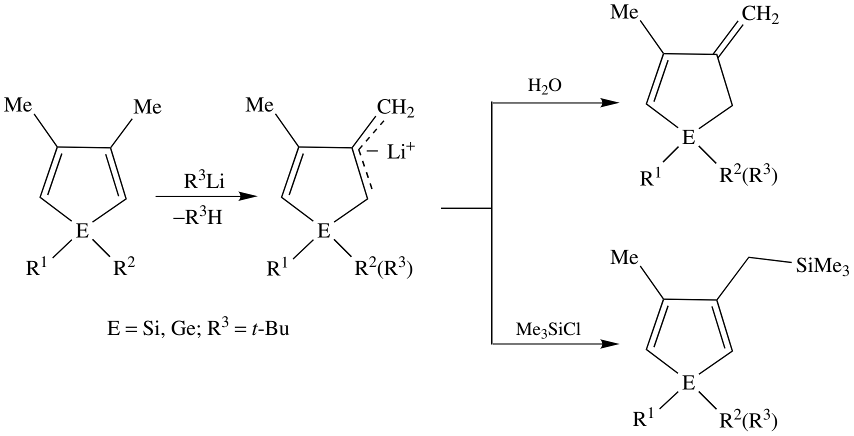

SCHEME 23

Substitution reactions[110] as well as certain rearrangements[95a] of exocyclic groups bonded to the heteroatom can occur via a five-coordinate anionic complex **(108)**.

In the stannole series, the reactions could be explained by the extraordinary reactivity of the exocyclic tin−carbon bonds with regard to lithium reagents. Thus, the reaction of 1,4-dilithio-1,2,3,4-tetraphenyl-1,3-butadiene with 1,1-dialkyl-2,3,4,5-tetraphenylstannole leads to alkyl−tin bond cleavage−cyclization by the dilithium reagent[33] (equation 61).

G. Oxidation

Photooxygenation of 1,1-dimethyl-2,3,4,5-tetraphenylsilole was studied by Sato and coworkers[144], and Sakurai and coworkers[162]. The intermediate endoperoxide was produced by 1,4-addition of singlet oxygen to the cyclic diene, leading to *cis*- and *trans*-dibenzoylstilbenes in addition to the major product (1 : 1.45), 3,3-dimethyl-1,5,6,7-tetraphenyl-2,4-dioxa-3-silabicyclo[3.2.0]heptene (Scheme 24). Under the same conditions, the photooxygenation of 1-methyl-1-vinyl-2,3,4,5-tetraphenylsilole leads to analogous products[163].

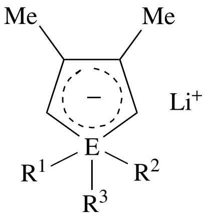

(108)

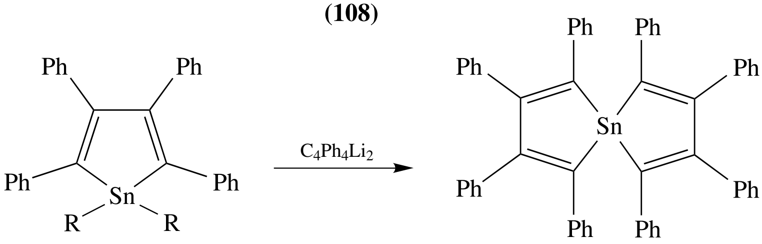

(61)

R = Alkyl

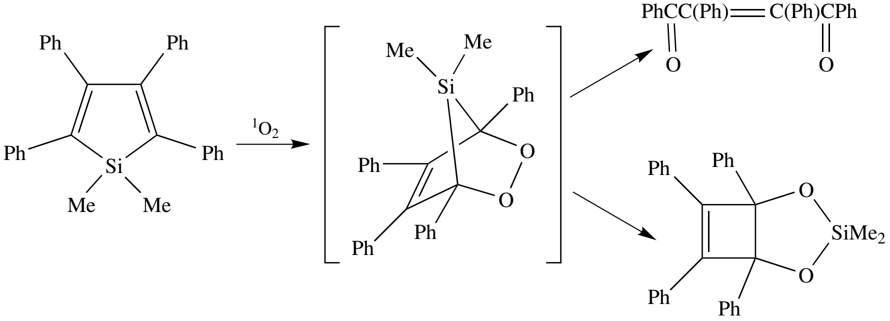

SCHEME 24

When treated with perbenzoic acid, 1-methyl-1,2,3,4,5-pentaphenylsilole yields a mixture of products, resulting from the oxidation of the diene system, various cleavages and rearrangements[163].

H. Reduction

1. Alkali metal reduction (see also Section V.A)

Formation of radical anions **109** and **110** from 1,1-dimethyl-2,5-diphenylsilole and 1,1-dimethyl-2,3,4,5-tetraphenylsilole[164], which are further reduced to the dianions **111** and **112**, respectively, has been shown by electron spin resonance and UV-visible spectrometry (equation 62).

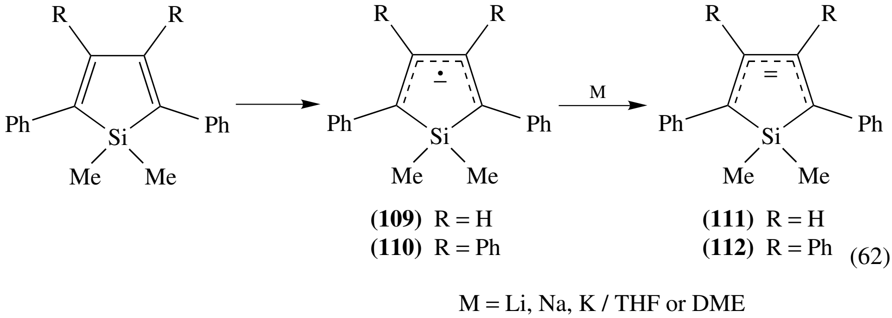

The presence of these dianions was also shown by aqueous quenching and the isolation of *cis*-dibenzylstilbene[155]. The dianions are remarkably stable even in the presence of alkali metal. Addition of metal to a solution of the dianion **112** (R = Ph) results in the formation of a new anionic species. ^{13}C NMR chemical shifts provide strong evidence that this is the tetraanion **113**.

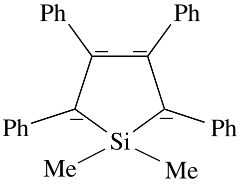

(**113**)

Reaction with an alkali metal gives substitution instead of reduction if the metallole possesses an exocyclic Si−Cl or Ge−Cl bond[160,161].

2. Electrode reactions

Two polarographic waves were observed in the electrochemical reduction of the same metalloles[165,166]. This means that they are reduced to a radical anion at the potential of the first wave and to a dianion at the potential of the second. The radical anions are stable enough to show ESR spectra.

3. Reaction with hydrides

$LiAlH_4$ is widely used for the synthesis of metalloles or benzometalloles with M−H bonds[167]. This hydride does not react by attacking the diene ring. Lithium hydride formed *in situ* may, however, give an addition reaction to the diene system[160].

Reaction of KH with C_4Ph_4SiMeH gives rise to a pentavalent silicate through simple addition of H^- to the silicon centre (see Section V.A.1).

I. Transmetallation Reactions

Stannoles differ significantly from other group 14 metalloles in their ability to undergo exchange reactions with boron, arsenic or antimony halides. Boroles[56a,76], arsoles and stiboles[60a,77] were obtained in good yields by this method (equations 63 and 64).

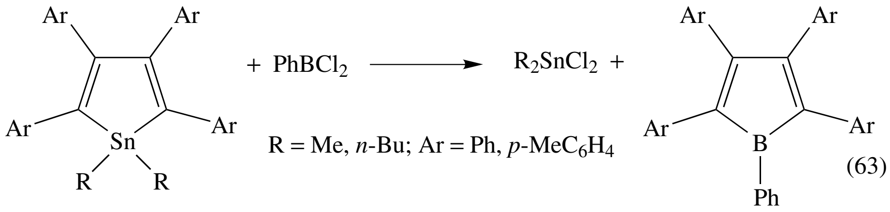

(63)

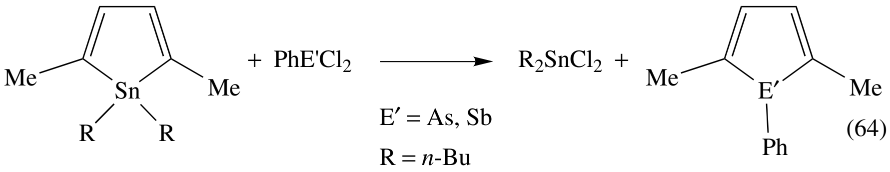

(64)

2,3,4,5-Tetraphenystannoles were also used in obtaining auroles by reaction with $AuCl_3$, THT[78] (equation 65).

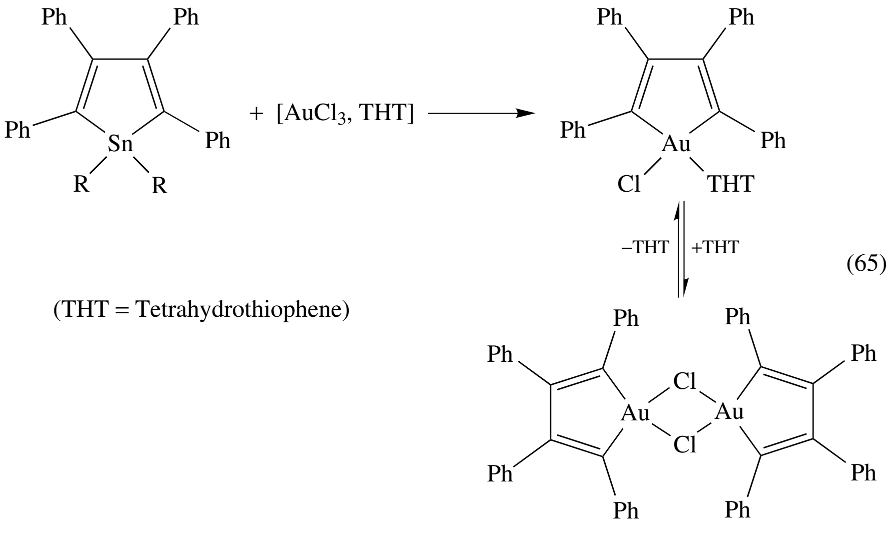

(65)

J. Ring Expansion

Ring expansion of a silacyclopentadienylcarbene generated from thermolysis or photolysis of (1-methyl-2,3,4,5-tetraphenylsilacyclopentadienyl)-diazomethane or -diazirine to silabenzene is known[168] (Scheme 25). With $AlCl_3$, 1-(chloromethyl)-1-methyl-2,3,4,5-tetraphenylsilole undergoes ring expansion leading to 1-chloro-1-methyl-2,3,4,5-tetraphenylsilacyclohexa-2,4-diene[169].

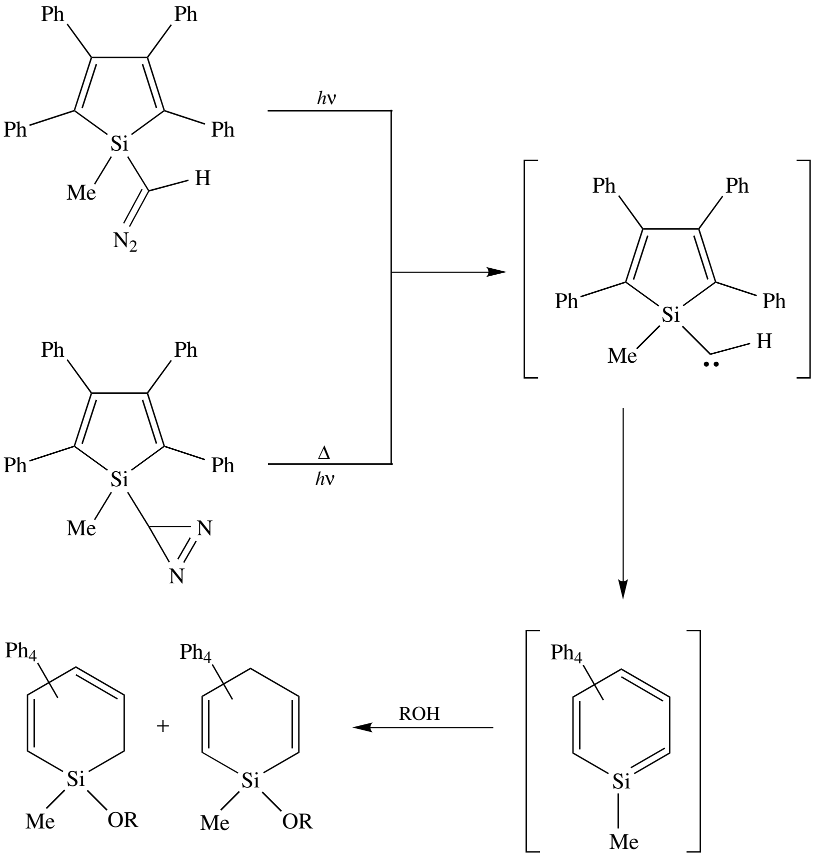

SCHEME 25

IV. POLYMERIC SILOLE-CONTAINING π-CONJUGATED SYSTEMS

π-Conjugated polymers containing silole rings have recently been highlighted as promising candidates for novel π-electronic materials, because of their potential properties such as conductivity, thermochromism and non-linear optical properties. Substituted siloles can behave as electron-accepting components in such polymeric derivatives[164]. Furthermore, *ab initio* molecular orbital calculations have demonstrated the unusual electronic structure of the silole ring which has relatively lower LUMO levels, compared with either cyclopentadiene or thiophene[170–172].

A. Synthesis, Structure and UV-Visible Absorption Data of Oligosiloles

Oligosiloles, from bisiloles to quatersiloles, have been prepared from functional siloles[59], the synthesis of which is discussed earlier (*vide supra*) (cf Section II.B.1.c).

Oxidative coupling of the 2,5-dilithiosilole **(44)** by use of an Fe(III) complex affords the 2,2′-bisilole **(114)** isolated as yellow crystals in only 9% yield, together with uncharacterizable polymeric materials (equation 66).

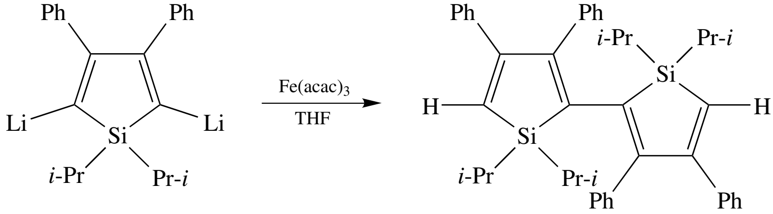

(66)

(**44**, R = *i*-Pr)

(114) 9%

Oxidative coupling via higher order cyanocuprates was shown to be most promising for the synthesis of higher oligosiloles and polysiloles, as illustrated in Scheme 26.

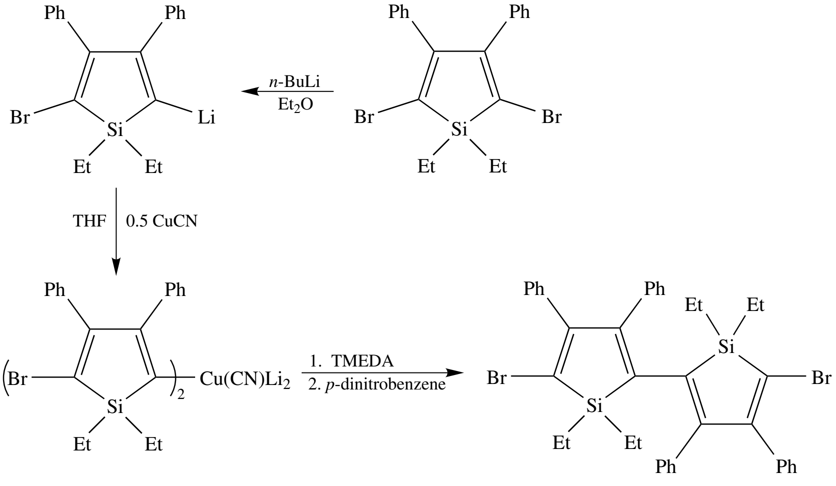

(115) 77%

SCHEME 26

Under essentially the same optimum conditions, dibromoquatersilole **(116)** was also obtained in 16% yield as an orange powder by coupling 5-bromo-5′-lithio-2,2′-bisilole, prepared *in situ* from **115** by monolithiation.

X-ray crystal structures of the bisiloles **114** and **115** show highly twisted arrangements between the two silole rings with torsion angles of 62–64°. ^{1}H NMR studies indicate a rapid equilibration between non-coplanar conformers in solution. In the UV-visible spectra, nevertheless, all of the oligosiloles have unusually long absorption maxima, i.e. λ_{max} 398 and 417 nm for **114** and **115**, respectively. Noticeably, there is a large bathochromic shift, more than 90 nm, upon changing from monosilole **117** to bisilole **115**, suggesting the development of a unique π-electronic structure by combination of two silole rings and a crucial role of the silicon atom therein. As pointed out by Tamao and coworkers[59a], the introduction of the bisilole component into a π-conjugated chain would be one of the promising routes to novel π-electronic materials.

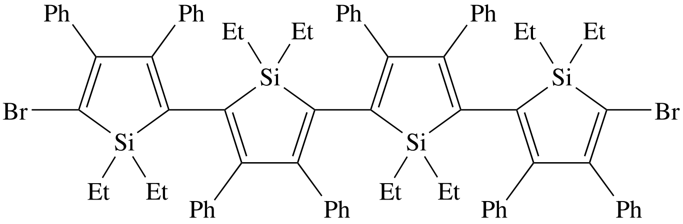

(116)

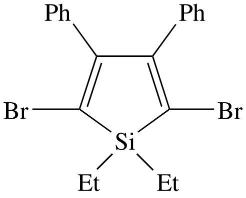

(117)

B. Silole–Thiophene and –Pyrrole Cooligomers and Copolymers

Air-stable silole–thiophene alternating 1 : 1 cooligomers (up to a seven-ring system) have been prepared by nickel(0)-promoted intramolecular cyclization of the corresponding thiophene–(1,6-heptadiyne) alternating cooligomers with hydrodisilanes[54b,173], as illustrated in Scheme 27.

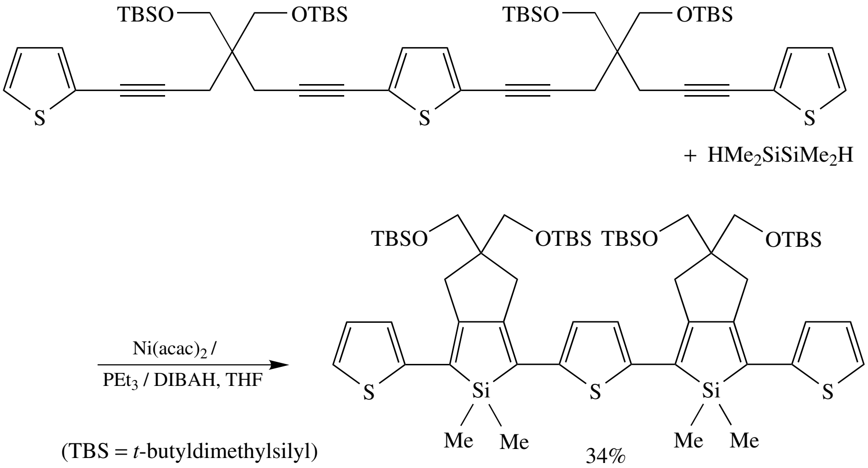

SCHEME 27

Silole–thiophene copolymers, with varying silole:thiophene ratios from 1 : 2 to 1 : 4, have been obtained by a palladium cross-coupling reaction[173], as outlined in Scheme 28.

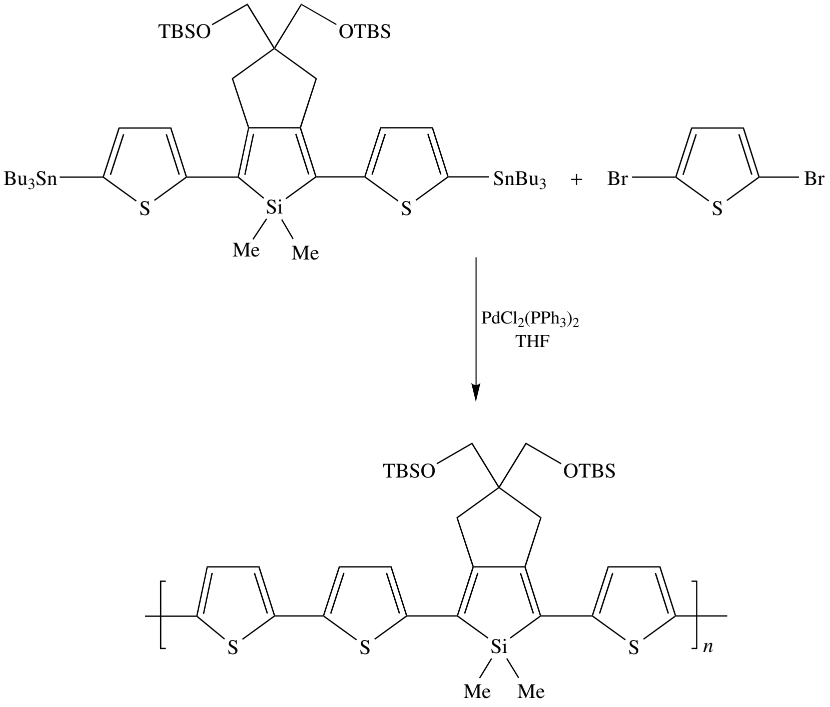

SCHEME 28

All of the series of the silole–thiophene copolymers are air-stable and soluble in common organic solvents such as THF, CH_2Cl_2 and $CHCl_3$. Molecular weight distributions were determined against polystyrene standards; the degrees of polymerization (DP) are in the range of about 20–40; the total number of rings in the main chain varies from *ca* 70 to 200.

The UV-visible absorption data in $CHCl_3$ of the silole–thiophene mixed systems show much longer absorptions in the visible region compared with thiophene homooligomers and homopolymers. Furthermore, significant bathochromic shifts accompany higher silole ratios. The results have been ascribed to the lowering of the LUMO level in the π-systems accompanied by an increase in the silole content, as demonstrated by *ab initio* calculation studies[173].

In contrast, the electrical conductivity tends to become higher with a lower silole content, reaching up to $2.4\ \mathrm{S\,cm^{-1}}$ upon doping with iodine. The bulky (*t*-butyldimethylsiloxy)methyl side groups in the silole unit are oriented out of the π-conjugated polymer plane and hence hinder the interaction between the polymer chains, which is known to be one of the key factors for high conductivity values[174].

C. σ–π Conjugated Polymers with an Alternating Arrangement of a Disilanylene Unit and 3,4-Diethynylene-Substituted Siloles

Polymers in which the regular alternating arrangement of a disilanyl moiety, $-SiR_2-SiR_2-$, and a π-electron system such as phenylene[175], ethynylene[176] and a butenyne group[177] is found in the backbone, are photoreactive and show conducting properties upon doping by exposure to SbF_5 vapour.

Treatment of 3,4-diethynylsilole **29** with 2 equivalents of lithium diisopropylamide, followed by the reaction of the resulting dilithio compound with 1,2-dichlorotetramethyl-, 1,2-dichlorotetraethyl- or 1,2-dibutyl-1,2-dichlorodimethyldisilane produces the cyclic silole derivatives **118**[43] (Scheme 29).

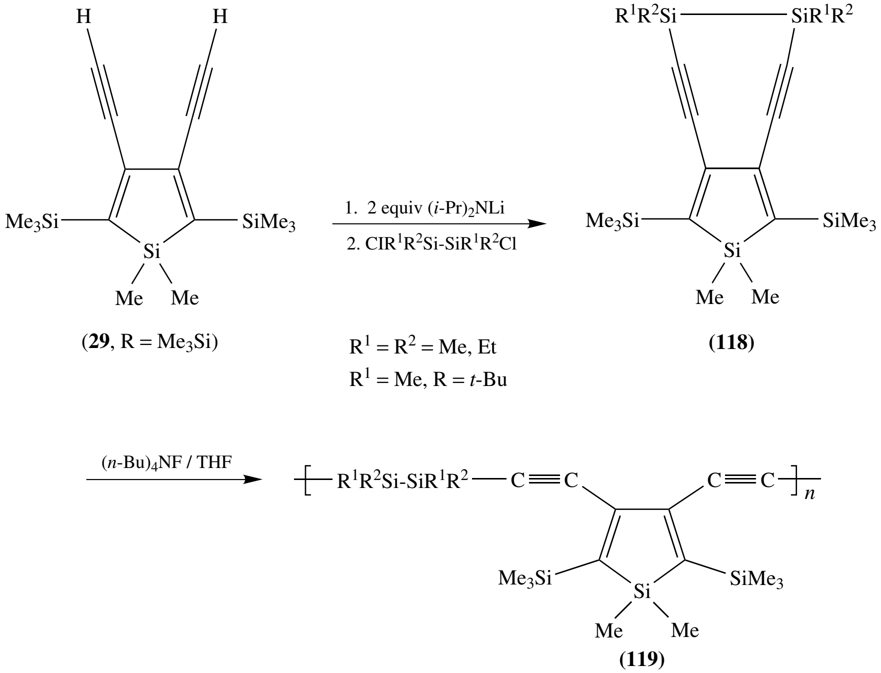

SCHEME 29

The anionic ring-opening polymerization of **118**[178] was carried out with the use of tetrabutylammonium fluoride (2 mol%) as catalyst in THF to give rise to the poly[(disilanylene)ethynylenes] **119** with high molecular weights.

D. Polymers Involving only the Silicon Atom of the Silole Ring in the Main Chain

The reaction of dilithiobutadiyne with 1-chloro-2,5-diphenylsilacyclopentadiene results in the cleavage of both exocyclic bonds, giving rise to the desired polymer[179] (equation 67).

In order to prepare polycarbosilanes containing organometallic fragments which could be precursors of transition-metal-containing ceramics[180], **120** was reacted with dicobalt octacarbonyl to give **121** with approximatively half of the triple bonds complexed with $Co_2(CO)_6$ moieties[181] (equation 68). η^4-Complexation of the silole ring was performed with $Fe_2(CO)_9$ and $Mo(CO)_4(COD)$[181].

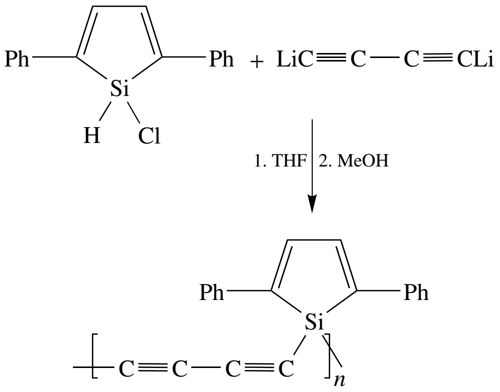

(67)

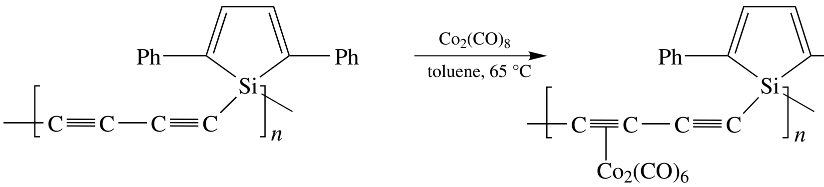

(68)

(120) **(121)**

Polycarbosilanes with the structure $[SiR_2-C\equiv C-Z-C\equiv C]_n$ (R_2Si: 2,3,4,5-tetraphenyl-1-sila-2,4-cyclopentadiene; *Z*: 1,4-benzene, 4,4′-biphenyl, 9,10-anthracene, 2,7-fluorene and 2,6-pyridine, 6,6′-bipyridine, 2,5-thiophene, 2,6-*p*-dimethylaminonitrobenzene, 2,6-*p*-nitroaniline, 2,6-*p*-nitrophenol and 2,7-fluoren-9-one) were prepared by the reaction of 1,1-diethynyl-2,3,4,5-tetraphenyl-1-sila-2,4-cyclopentadiene with the appropriate (hetero)aromatic dibromide or diiodide in the presence of $[(PPh_3)_2PdCl_2]$ and CuI[182] (equation 69).

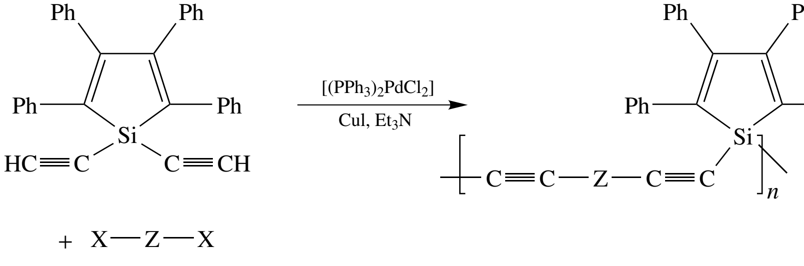

(69)

The oligomer where Z = p-C_6H_4 reacted with $Fe(CO)_5$ under UV irradiation to give an oligomer containing iron carbonyl units attached to *ca* 30% of the silole groups.

V. IONIC SPECIES AND COORDINATION COMPOUNDS

Recent years have seen renewed interest in the problem of chemical bonding in metalloles and metallole anions. After the initial report by Joo and coworkers[183] on the generation of the silole dianion $C_4Ph_4Si^{2-}$, a number of investigations concerned with characterizing the structural and chemical properties of π-electron heterole anionic systems, which may possess some degree of aromaticity, have been reported. η^5-Sila- or η^5-germacyclopentadienyl complexes have been vigorously pursued as potentially accessible sila-or germaaromatic derivatives, since transition metal fragments are known to stabilize many reactive species by coordination. Theoretical calculations support these views and provide some insight into the determination of the factors leading to aromaticity in these substances[184].

The earlier work, up to 1990, was the subject of a review by Corriu and coworkers[4]; the intent of this section is to focus upon the latest developments.

A. Group 14 Metallole Anionic Species

1. Silacyclopentadienide and silafluorenide anions

The reaction of 1-chlorosiloles with alkali metals leads to unstable species that react with methyl iodide, ethyl bromide or chlorotrimethylsilane in the manner expected for the 1-silacyclopentadienide anion. Interestingly, X-ray quality crystals were isolated from the reaction with Li in THF and the molecular structure was shown to be that of a [2 + 2] head-to-tail dimer, which is formed by the 1,5-rearrangement of the anion in the silole ring[185] (equation 70).

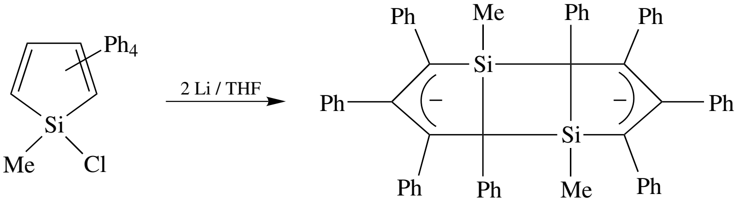

(70)

Recently, changing the methyl group bonded to silicon into the sterically demanding *t*-butyl substituent allowed Hong and Boudjouk to generate unambiguously the sodium and lithium derivatives of $[Ph_4C_4Si(Bu\text{-}t)]^-$ in THF via reductive cleavage of the Si−Si bond in $C_4Ph_4(Bu\text{-}t)Si{-}Si(t\text{-}Bu)C_4Ph_4$ with sodium or lithium, respectively[186] (equation 71).

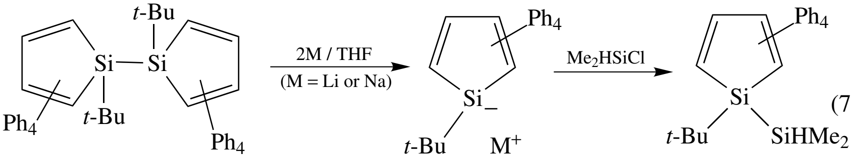

(71)

(122) **(123)**

Evidence for the formation of **123** was obtained by subsequent quenching with an excess of dimethylchlorosilane to produce the expected $C_4Ph_4Si(Bu\text{-}t)$ (SiHMe) in 74% yield. Analysis of the NMR parameters suggests some delocalization of the negative charge into the butadiene moiety. Consistent with sp^2 character of the ring silicon is the downfield shift of ^{29}Si NMR resonances on going from the starting disilane **122** (δ 3.62 ppm) to $[C_4Ph_4Si(Bu\text{-}t)]^-$ (δ 26.12 ppm; $\Delta\delta$ 22.50 ppm).

Nucleophilic cleavage of a Si−Si bond with benzylpotassium in the presence of 18-crown-6 provides an alternative approach[187]. This method works for the synthesis of 'free' silolyl anions **125** and **127** from **124** and **126**, respectively (equations 72 and 73).

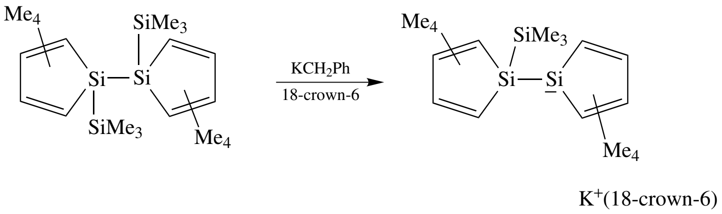

(124) **(125)** (72)

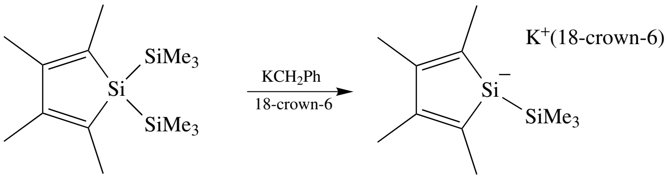

(126) **(127)** (73)

Interestingly, the ^{29}Si NMR resonances for **125** ($\delta = -53.43$ ppm) and **127** ($\delta = -41.52$ ppm) are shifted upfield relative to the corresponding resonances for the parent siloles (**124**: $\delta = -34.71$ ppm; **126**: $\delta = -34.26$ ppm). This trend is opposite to that reported by Hong and Boudjouk for M[$C_4Ph_4Si(Bu$-*t*)] (M = Li, Na)[186]; their ^{29}Si NMR resonances are shifted downfield relative to that of the starting material C_4Ph_4(Bu-*t*)Si−Si(*t*-Bu)C_4Ph_4. The difference between these two systems may be attributed to phenyl *vs* methyl substitution in the rings, and/or to different degrees of interaction between the alkali metal ion and the silolyl ring.

Solutions of 1-lithio-1-methyl-1-silafluorenide anion **(128)** were obtained by sonification of bis(1-methyl-1-silafluorenyl) and lithium in THF[188] (equation 74).

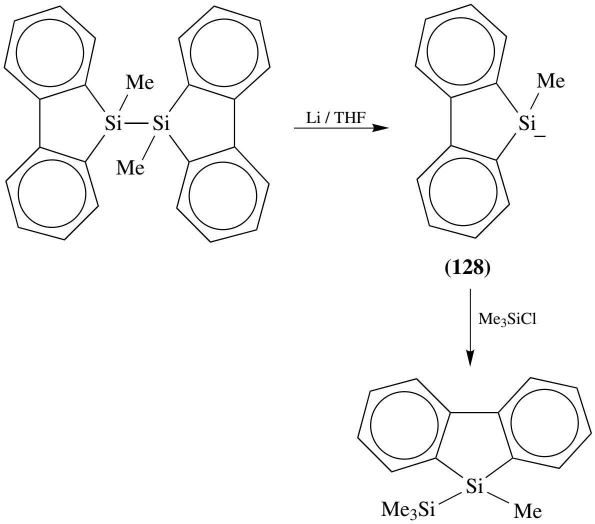

(128) (74)

The resulting dark green solution was converted into the expected 1-methyl-1-(trimethylsilyl)-1-silafluorene by reaction with an excess of Me_3SiCl. The ^{29}Si NMR chemical shift for **128** ($\delta = -22.09$ ppm) is in the range of aryl-substituted silyllithium compounds, e.g. $Ph_2MeSi^-Li^+$, which have no delocalization of the negative charge on silicon to the phenyl substituents. Downfield shifts of the ring carbons are also consistent with a localized silyl anion.

Treatment of hydrosilanes with potassium hydride is a known route to silyl anions and has been used to generate silacyclopentadienide anions. Reinvestigation of the reaction of KH with C_4Ph_4SiMeH has shown that the dominant pathway is simple addition of the hydride anion to the silicon centre to give the pentavalent silicate $[Ph_4C_4SiMeH_2]^-$ K^+ **(129)**[189] (equation 75). The Si−H coupling constants in **129** ($J_{Si-H} = 192.5$ and 179.6 Hz) are very close to $J_{Si-H} = 192$−225 Hz in $[HSi(OR)_4]^-$ K^+[190] and are consistent with a trigonal−bipyramidal structure in which one hydrogen and two carbons of the butadiene moiety occupy the equatorial positions.

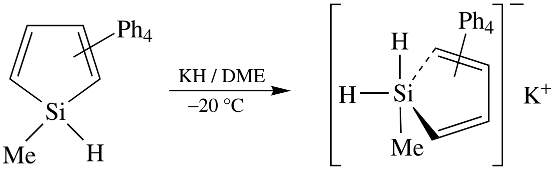

(75)

(129)

2. Germacyclopentadienide anions

The C-methylated germacyclopentadiene anion, $[C_4Me_4GePh]^-$, was reported in 1990 by Dubac and coworkers[191] (equation 76). ^{13}C NMR data were consistent with a substantial localization of negative charge on germanium.

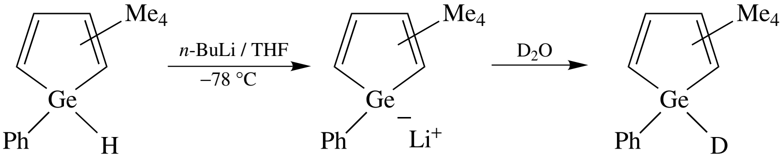

(76)

Tilley and coworkers have recently succeeded in the synthesis of isolated germacyclopentadienide derivatives, $[C_4Me_4GeSi(SiMe_3)_3]^-M^+$, as the alkaline metal salts (M = Li, K) *via* a deprotonation reaction[192], as outlined in equation 77.

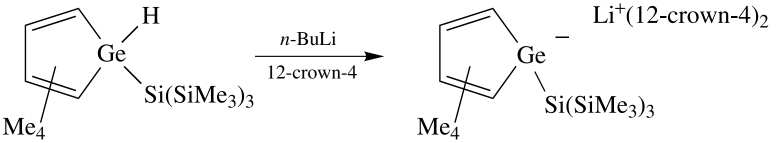

(77)

(130) **(131)**

Use of $KN(SiMe_3)_2$ in the presence of 18-crown-6 affords the corresponding potassium salt; the latter was also prepared from $C_4Me_4Ge[Si(SiMe_3)_3]_2$ by heterolytic cleavage of one Ge−Si bond with benzylpotassium.

The solid-state structure of [Li(12-crown-4)$_2$] [$C_4Me_4GeSi(SiMe_3)_3$] was determined by X-ray diffraction and shows well-separated cations and anions. A pyramidalization at the germanium centre is evidenced by the angle between the C_4Ge plane and the Ge−Si bond of only 100.1° versus 131.0° for **130**. The carbon portion of the ring contains inequivalent C−C distances that reflect isolated single [1.46(6) Å] and double [1.36(6), 1.35(5) Å] bonds and thus has a considerable diene character. The data clearly suggest that **131** gains very little stabilization by π-delocalization of the negative charge.

3. Germa- and stannaindenide anions

1-Lithio-1-metallaindenide anions are readily available from the parent hydrogermanes and stannane[193] (equation 78).

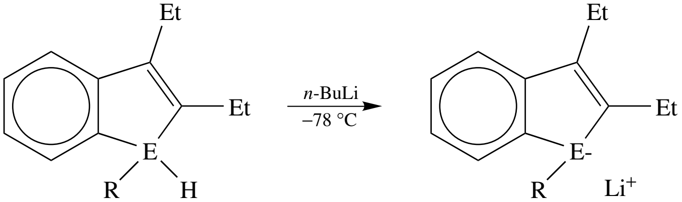

(78)

(132) E = Ge
(133) E = Sn

Chemical characterization of **132** and **133** was obtained by subsequent treatment with PhBr and CH_3I or deuteriolysis, respectively. As observed previously for $[C_4Me_4GePh]^-$ (*vide supra*), ^{13}C NMR data give no significant evidence of aromatic delocalization in both cases.

4. Silole dianions

In 1990, Joo and coworkers reported the conversion of 1,1-dichloro-2,3,4,5-tetraphenyl-1-silacyclopentadiene to the disodium salt by reaction with sodium metal[183].

The corresponding dilithium derivative was recently reported by Boudjouk and coworkers. Reduction of $C_4Ph_4SiCl_2$ with four equivalents of lithium in THF gives a dark red brown solution of dianion **134** as determined by subsequent quenching with Me_3SiCl[194] (equation 79).

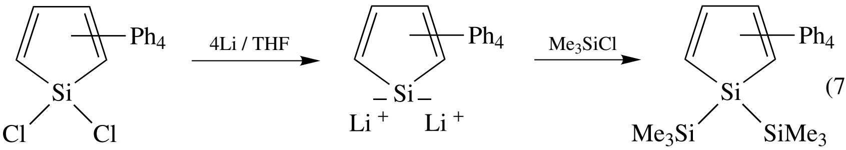

(79)

(134)

Interestingly, the ^{29}Si NMR resonance for this dianion ($\delta = 68.54$ ppm) is shifted downfield relative to the resonance for the parent $C_4Ph_4SiCl_2$ ($\Delta\delta = 61.74$ ppm). It is further downfield than the ^{29}Si shift of $[C_4Ph_4Si(Bu\text{-}t)]^-$ anion but in the range of the silenes ($\delta = 40-140$ ppm). In addition, Boudjouk and coworkers observed upfield shifts of the C_α and C_β atoms in the ring. These ^{13}C and ^{29}Si NMR observations were interpreted in terms of a silole dianion with considerable aromatic delocalization and strong participation of a resonance form with silylene character, **135**[194]. The latter is isolobal with the stable π-electron ring silylene **136**[195].

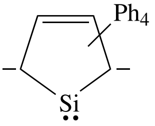

(135)

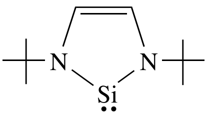

(136)

The dianion **134** was isolated in a crystalline form from THF[196]. The structure, **134a**, contains two different lithium atoms. One lithium is η^5-bonded to the silole ring and also coordinated to two THF molecules; the other is η^1-bonded to the silicon atom and coordinated to three THF molecules. The silole ring is almost planar; the C–C distances within the ring are nearly equal, ranging from 142.6 to 144.8 pm. The long Si–$Li_{(1)}$ distance suggests that the in-plane Si–Li interaction is predominantly ionic. The ^{13}C and ^{29}Si NMR spectra for solid **134a** are also consistent with the X-ray structure.

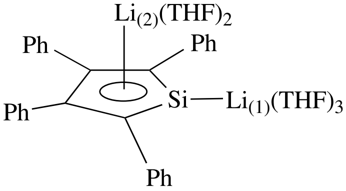

(134a)

When carrying out the sonication of $C_4Ph_4SiCl_2$ with lithium in a 1 : 3 ratio, the 1,1′-disila-2,2′,3,3′,4,4′,5,5′-octaphenylfulvalene dianion **137** is formed as the major product in addition to **134**[194]. Further reaction with lithium produces the silolyl dianion **134** exclusively (equation 80).

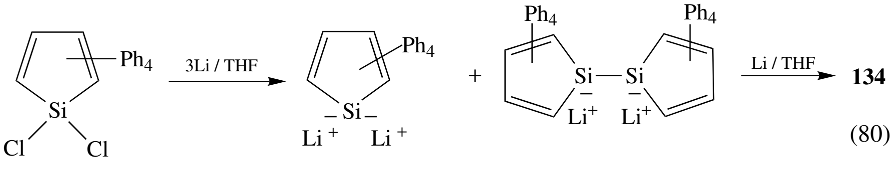

(134) **(137)**

(80)

Reaction of $C_4Me_4SiCl_2$ with four equivalents of lithium in THF gives rise to the analogous dianion[40]. As observed for **134**, ^1H, ^{13}C and ^{29}Si NMR shifts suggest delocalization of the negative charge into the silole ring.

The solid-state structure of the silolyl dianion is substantially affected by the nature of the substituents attached to the silole ring and of the metal alkali counterions. Stirring $C_4Me_4SiBr_2$ with four equivalents of potassium in the presence of 18-crown-6 gives complex **138** which was isolated in crystalline form[187] (equation 81).

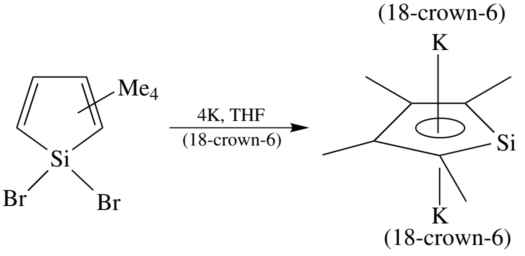

(138)

(81)

In the structure of **138**, the electrons within the five-membered ring are highly delocalized, which leads to nearly equal C−C bond lengths. Furthermore, **138** has a $\eta^5-\eta^5$ reverse-sandwich structure. The two potassium cations, each coordinated to a 18-crown-6 molecule, lie above and below the C_4Si ring within bonding distance of all five ring atoms.

5. Germole dianions

The germacyclopentadienide anions present structures consistent with substantial localization of the negative charge on germanium unlike silicon (*vide supra*); germole dianions would be reasonable candidates for stable aromatic germanium derivatives.

Tetraphenylgermole dianions have been studied by Hong and Boudjouk. Sonication of $C_4Ph_4GeCl_2$ with excess of lithium in THF gives $[C_4Ph_4Ge]^{2-}$ $(Li^+)_2$ **(139)** as the major product[197] (equation 82).

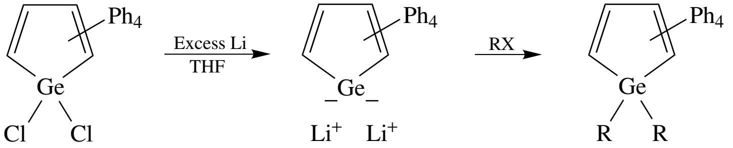

(139)

(82)

Derivatization of this salt with a series of organic halides, chlorodimethylsilane and chlorotrimethylsilane gives the 1,1-disubstituted-1-germacyclopentadienes in high yields. Furthermore, ^1H and ^{13}C NMR studies give evidence of a high degree of π-delocalization.

The X-ray structure of the dilithium salt of the tetraphenylgermole dianion **139** was recently reported[198]. **139** crystallizes from dioxane in two structurally distinct forms, **139a** and **139b**, depending upon the crystallization temperature.

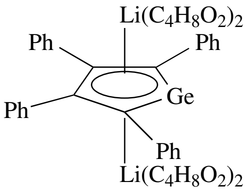

(139a)

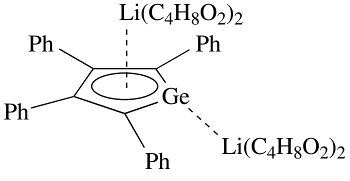

(139b)

The crystals obtained from dioxane at −20 °C, **139a**, have a reverse-sandwich structure with two η^5-coordinated lithium ions lying above and below the C_4Ge ring. Crystals of **139b** obtained at 25 °C show a η^1–η^5 dilithium structure; one lithium atom is η^1-coordinated to the germanium and the other is η^5-coordinated to the ring atoms. In both structures, the electrons are highly delocalized within the ring. Finally, the latter structure **139b** can be related to that published for $Li_2[C_4Ph_4Si]\cdot 5THF$ which also contains η^1- and η^5-coordinated lithium centres (*vide supra*). A significant difference between the structures is that in **134a** the arrangement at silicon is nearly planar, whereas in **139b** the η^1-coordinated lithium is shifted to the hemisphere *anti* to the η^5-coordinated lithium. The angle between the Li−Ge vector and the C−Ge−C plane is 42.9°.

In addition to the problem of the chemical bonding in metallole anions, these species may offer the promise of rich chemistry and lead to unusual structures. One example is provided by the synthesis and characterization of a novel trisgermole complex of lithium **140**[199] (equation 83).

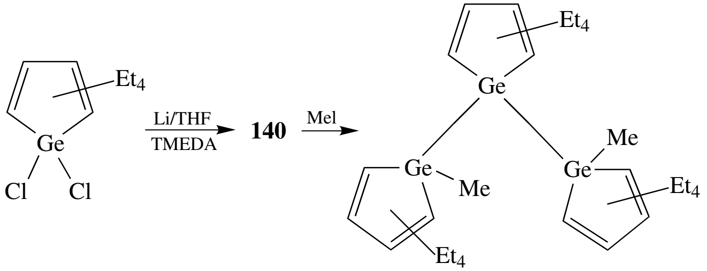

(83)

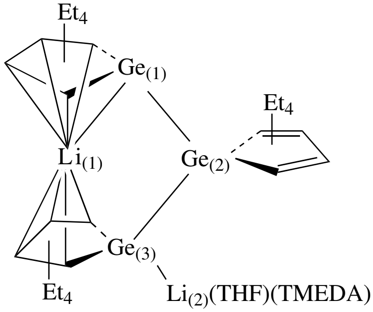

(140)

X-ray analysis of a single crystal of **140** reveals that this species has a sandwich structure in the solid state.

The essential structural features may be analyzed as follows: (1) two differently π-complexed rings, one with only π-bonding to the Li centre, the other ring with π-bonding to the $Li_{(1)}$ centre plus a σ $Ge_{(3)}$−$Li_{(2)}$ bond [$Ge_{(3)}$ is sp^3 hybridized]; (2) apparent η^5- and η^4-bonding to $Li_{(1)}$; (3) the least-squares planes for the two terminal rings form an angle of 10.7°; (4) $Li_{(1)}$ is positioned close to the centre of the two planes defined by $C_4Ge_{(1)}$ and $C_4Ge_{(3)}$, similar to the situation in lithocene or ferrocenophane derivatives.

In summary, the anions of group 14 metalloles (C_4E rings) have either localized nonaromatic or delocalized aromatic structures, depending of the metal E, Si vs Ge and Sn, and on the substituents, methyl vs phenyl group. As pointed out by West and coworkers[198], structural studies of metallole anions and dianions of this kind with different substituents will be of value. Additionally, it should be noted that experimentally observed structures in the solid state for silole and germole dianions are greatly influenced by the nature of the alkali metal counterion.

Recent theoretical calculations support these views and provide new insights into the determination factors leading to aromaticity in these species[184a,b]. For example, an approach based on structural, energetic and magnetic criteria demonstrates that lithium silolide, C_4H_4SiHLi, exhibits significant aromatic character and 80% of the stabilization energy of $Li^+C_5H_5^-$; in addition, Li^+ η^5-coordination in the ground state increases the aromaticity over that in free $[C_4H_4SiH]^-$ strongly. The high degree of aromatic character in the dianionic siloles $C_4H_4SiM_2$ (M = Li, Na, K) and $[C_4H_4SiLi]^-$ is also evident from structural, energetic and magnetic aspects. These criteria for aromaticity reveal that $[\eta^5\text{-CHSiLi}]^-$ is more aromatic than isoelectronic phosphole and thiophene systems and even approach the aromaticity of the cyclopentadiene anion. Furthermore, inverse sandwich structure with η^5-coordinated alkali metal ions would be preferred by $C_4H_4SiM_2$ species; such a structure is reported for $[K\ ([18]\ \text{crown-6})^+]_2\ [C_4Me_4Si^{2-}]$[187].

B. Stable η^5-Sila- and η^5-Germacyclopentadienyl Transition Metal Complexes

Numerous attempts to prepare η^5-sila- and η^5-germacyclopentadienyl transition metal complexes, usually from the corresponding η^4-silole or η^4-germole derivatives, have proven unsuccessful[4].

In 1993, Tilley and coworkers reported the first isolation and complete characterization of a stable η^5-germacyclopentadienyl ruthenium complex **(141)**[200], as indicated in equation 84.

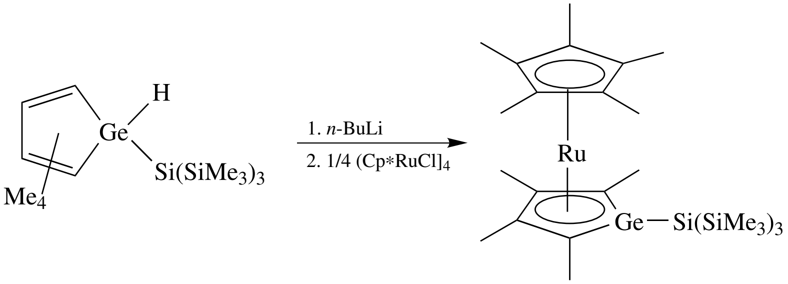

(84)

(141)

The molecular structure of **141** consists of two planar five-membered rings bound in a sandwich fashion to the ruthenium atom. The least-squares planes for the two five-membered rings form an angle of 8.6°, and the ruthenium atom is symmetrically positioned between the two planes. The germanium atom deviates by only 0.02 Å from the C_4Ge ring's least-squares plane; the summation of the angles about the Ge atom (358.1°) further reflects sp^2 hybridization. Thus, it appears that the $\eta^5\text{-}C_4Me_4GeSi(SiMe_3)_3$ and Cp* ligands are bonded similarly to Ru.

An irreversible oxidation wave was observed for **141** at $E_{1/2} = 0.250$ V (vs SCE) by cyclic voltametry. For comparison, decamethylruthenocene displays a reversible oxidation wave at 0.42 V (vs SCE)[201]. These data therefore suggest that the η^5-$C_4Me_4SiSi(SiMe_3)_3$ ligand is more electron-donating than η^5-C_5Me_5.

The preparation of the analogous transition metal η^5-silacyclopentadienyl complex requires a different synthetic approach[202], as shown in Scheme 30. The intermediate cationic species **143** has the general appearance of a protonated metallocene. The five-membered C_4Si ring of the silacyclopentadienyl ligand is planar; the summation of angles at the ring silicon atom (355.1°) reflect the considerable sp^2 character for that atom. An additional indication of electron delocalization in the silacyclopentadienyl ligand is the small difference between the C−C bond distances. The hydride ligand is nearer to the silacyclopentadienyl ring. The Ru−H−Si interaction is similar to Mn−H−Si arrangements in $Cp(CO)(L)Mn(\eta^2\text{-}HSiR)$ complexes[203]. The silyl group bends away from the ruthenium centre; the angle between the Si−Si bond and the C_4Si least-squares plane is 19°.

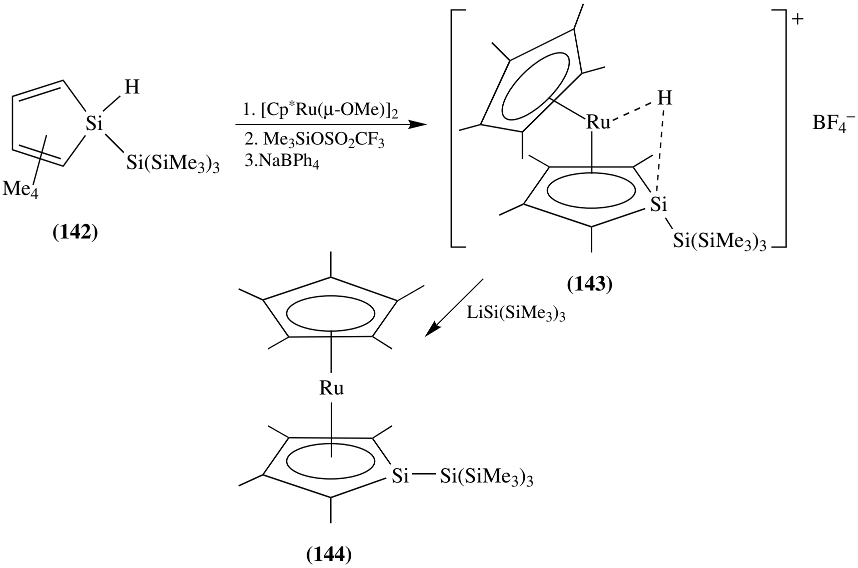

SCHEME 30

The deprotonation of **143** was only successful with $(THF)_3LiSi(SiMe_3)_3$ and gave rise to **144** in 50% yield. The ^1H and ^{13}C NMR spectra of **144** resemble those of **141**. Also consistent with increased sp^2 character for the ring silicon is the downfield progression of ^{29}Si NMR shifts on going from **142** ($\delta = -32.68$ ppm, $J_{Si-H} = 181$ Hz) to **143** ($\delta = -27.14$ ppm, $J_{Si-H} = 41$ Hz) to **144** ($\delta = -7.35$ ppm). The latter physical data suggest some delocalization of electron density in the SiC_4 ring of **143**, and considerably more for the related ring in **144**.

VI. ADDENDUM

Section II.A.2

Michl, Nefedov and coworkers[204] reported that UV irradiation of matrix-isolated 1,1-diazido-1-germacyclopent-3-ene (the germanium analog of **13**) produced 1*H*-germole and

1-germacyclopent-3-ene-1,1-diyl (the germanium analogs of **2** and **9**) as major products along with 2*H*-germole and 3*H*-germole (the germanium analogs of **11** and **14**) as minor products. As in the case of silicon species (Scheme 4), reversible photoconversion of these tautomeric germoles has been observed. Similar experiments were carried out on deuteriated analogs. IR and UV-VIS spectra of these germoles are interpreted and compared with those of silole isomers.

Section III.B.1.b

Stannoles bearing dialkylboryl groups in the 3-position **(145)** react with phosphaalkynes $R^4C\equiv P$ (R^4 = *t*-Bu, CH_2Bu-*t*) by [4 + 2] cycloaddition (isomeric adducts were not detected) and elimination of stannylene to give phosphabenzenes (**146** and **147**) in high yield[205].

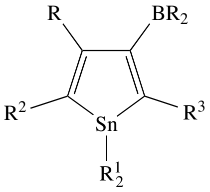

(145)

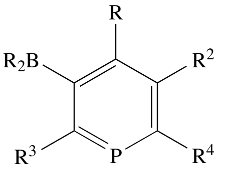

(146)

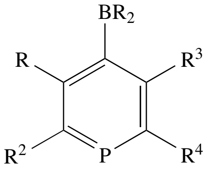

(147)

Section IV.A

A recent report from Yamaguchi and Tamao[206] describes semiempirical and *ab initio* calculations to elucidate the electronic structure of bisilole in comparison with that of bicyclopentadiene[207]. The silole ring, as well as the extended π-conjugated bisilole system, has an unusually low-lying LUMO level arising from $\sigma^*-\pi^*$ conjugation which is unexpectedly enhanced by molecular distortions in the case of bisilole. As a support of the calculation data, redox potentials of some silole derivatives and their carbon analogs have been determined by cyclic voltammetry. Siloles and polysiloles would thus have quite different electronic structures and properties from those of the conventional thiophene or pyrrole analogs. Noteworthy is the performance of the silole ring as a core component for efficient electron transporting materials[208].

Section IV.B

Silole–pyrrole cooligomers (containing up to nine rings) have been synthesized[209]. As expected, the combination of a π-electron-deficient silole[206] with a π-electron-rich pyrrole causes long UV-VIS absorption maxima in spite of twisted structures. As indicated by *ab initio* calculations, the LUMO of the parent pyrrole–silole–pyrrole is almost localized on the silole ring and lies at a much lower level than that of the parent terpyrrole; as a consequence, the HOMO–LUMO energy gap is about 1.3 eV smaller, strongly suggesting promising development in the area of novel low band π-conjugated polymers.

Section V.A.

A significant contribution by Tilley and coworkers, in addition to material cited earlier[187,192], describes the synthesis, structure and electronic properties of various silole and germole anions and dianions, in the $[C_4(alkyl)_4E\text{-}R]^-$ and $[C_4(alkyl)_4E]^{2-}$ series (E = Si, Ge; alkyl = Me, Et), respectively[210]. A brief discussion follows.

Alkali metal reduction of dihalide precursors is shown to be a valuable route to various silole and germole dianions in solution. Crystal structure determinations for $[K(18\text{-crown-}6)^+]_2(C_4Me_4Si^{2-}]$ and the dimer $[K_4(18\text{-crown-}6)_3][C_4Me_4Ge]_2$ are consistent with the presence of delocalized π-systems and with η^5-bonding modes for all of the potassium cations.

Deprotonation of hydrogermoles, reductive cleavage of the Ge−Ge bond or nucleophilic cleavage of a $E{-}SiMe_3$ bond (E = Si or Ge) can be employed for the generation of silolyl and germolyl anions. They exhibit ^{13}C and ^{29}Si NMR chemical shifts consistent with significant localization of the negative charge on the group 14 element and a non-aromatic structure; the countercation seems to have little effect on the electronic structure. Crystallographic studies reveal highly pyramidalized Ge and Si centres and pronounced double bond localization in the carbon portion of the ring. Nevertheless, the low barriers to inversion observed by variable-temperature ^{1}H NMR spectroscopy for $K[C_4Et_4E(SiMe_3)]$ and $[Li(12\text{-crown-}4)_2][C_4Et_4E(SiMe_3)]$ ion pairs (E = Si, Ge), i.e. approximatively 41.8 kJ mol^{-1} for germolyl anions and 29–33 kJ mol^{-1} for silolyl anions, suggest a stabilization of the transition state by delocalization of π-electron density in the ring. The difference in the barriers apparently reflects a slightly greater degree of delocalization in the silicon compounds; they also seem to be related to the nature of the countercation.

VII. CONCLUSION

Studies in the chemistry of group 14 metalloles over the past few years have been numerous. Mention should be made of the synthesis of the C-unsubstituted 1*H*-silole; the structures of the product itself, as well as of its tautomeric forms and dimer, have been established. Progress has also been made in developing new synthetic routes. By way of a transmetallation reaction from zirconacyclopentadiene, the synthesis of group 14 heterocyclopentadiene derivatives was considerably facilitated. On the other hand, though the method is limited to 3,4-diphenylsiloles, a further noticeable contribution was a general and versatile synthesis of the corresponding 2,5-difunctional derivatives.

Functional siloles have found applications in the elaboration of silole-containing π-conjugated systems. Because of its unique electronic properties, the introduction of a silole component or a silole cooligomer into an unsaturated chain should be a promising route to novel π-electronic materials and, in this connection, the preparation of new heterocyclopentadiene monomeric precursors remains a current challenge.

Stable group 14 heterole anionic or dianionic species are no longer curiosities. Recent work has focused on the structural behaviour, spectroscopic features and bonding patterns of heterole anionic or dianionic species so that we can use the data obtained so far as guidelines for further work. As far as the reactivity of the latter derivatives is concerned, much effort will be directed to the structure of the heterolyl salts and its dependence on the counterion.

Finally, heterocyclopentadienes or -dienides have been shown to be suitable as complex ligands. They can bind in a π-fashion to a metal complex fragment like the classical cyclopentadienyl ligand. The synthesis of **141** and **144** deserves particular attention in the light of vain attempts, until recently, to detect unambiguously a π-coordinated germa- and silacyclopentadienide in a complex. It is to be hoped that the remaining open questions pertaining to the chemical reactivity of such species will be answered by investigations in the near future.

VIII. ACKNOWLEDGEMENTS

We are grateful to Mrs S. Julia, Mrs M. Maris, Prof. M. A. Brook (McMaster University, Hamilton), Dr W. Douglas (Université de Montpellier) and Prof. B. Gautheron (Université de Bourgogne, Dijon) for their assistance in the production of the manuscript.

IX. REFERENCES

1. (a) P. J. Fagan, E. G. Burns and J. C. Calabrese, *J. Am. Chem. Soc.*, **110**, 2979 (1988).
   (b) P. J. Fagan, W. A. Nugent and J. C. Calabrese, *J. Am. Chem. Soc.*, **116**, 1880 (1994).
2. (a) F. Mathey, *Chem. Rev.*, **88**, 429 (1988).
   (b) F. Zurmühlen and M. Regitz, *J. Organomet. Chem.*, **332**, C1 (1987).
   (c) F. Laporte, F. Mercier, L. Ricard and F. Mathey, *Bull. Soc. Chim. Fr.*, **130**, 843 (1993).
   (d) S. M. Bachrach, *J. Org. Chem.*, **58**, 5414 (1993).
3. J. Dubac, A. Laporterie and G. Manuel, *Chem. Rev.*, **90**, 215 (1990).
4. E. Colomer, R. J. P. Corriu and M. Lheureux, *Chem. Rev.*, **90**, 265 (1990).
5. T. J. Barton and G. T. Burns, *J. Organomet. Chem.*, **179**, C17 (1979).
6. J. P. Béteille, M. P. Clarke, I. M. T. Davidson and J. Dubac, *Organometallics*, **8**, 1292 (1989).
7. G. Raabe and J. Michl, *Chem. Rev.*, **85**, 419 (1985).
8. J. Dubac and A. Laporterie, *Chem. Rev.*, **87**, 319 (1987).
9. (a) T. J. Barton, S. A. Burns, I. M. T. Davidson, S. Ijadi-Maghsoodi and I. T. Wood, *J. Am. Chem. Soc.*, **106**, 6367 (1984).
   (b) N. Auner, I. M. T. Davidson and S. Ijadi-Maghsoodi, *Organometallics*, **4**, 2210 (1985).
10. (a) A. Laporterie, P. Mazerolles, J. Dubac and H. Iloughmane, *J. Organomet. Chem.*, **206**, C25 (1981).
    (b) A. Laporterie, J. Dubac, P. Mazerolles and H. Iloughmane, *J. Organomet. Chem.*, **216**, 321 (1981).
11. G. T. Burns and T. J. Barton, *J. Organomet. Chem.*, **209**, C25 (1981).
12. H. Iloughmane, *Thesis*, Université Paul Sabatier, Toulouse, No. 1247 (1986).
13. A. Laporterie, H. Iloughmane and J. Dubac, *J. Organomet. Chem.*, **244**, C12 (1983).
14. J. Dubac, A. Laporterie and H. Iloughmane, *J. Organomet. Chem.*, **293**, 295 (1985).
15. M. Kako, S. Oba and Y. Nakadaira, *J. Organomet. Chem.*, **461**, 173 (1993).
16. (a) P. P. Gaspar, R.-J. Hwang and W. C. Eckelman, *J. Chem. Soc., Chem. Commun.*, 242 (1974).
    (b) R.-J. Hwang and P. P. Gaspar, *J. Am. Chem. Soc.*, **100**, 6626 (1978).
    (c) P. P. Gaspar, Y.-S. Chen, A. P. Helfer, S. Konieczny, E. C.-L. Ma and S.-H. Mo, *J. Am. Chem. Soc.*, **103**, 7344 (1981).
17. E. E. Siefert, K. L. Loh, R. A. Ferrieri and Y. N. Tang, *J. Am. Chem. Soc.*, **102**, 2285 (1980).
18. B. H. Boo and P. P. Gaspar, *Organometallics*, **5**, 698 (1986).
19. D. Lei, Y.-S. Chen, B. H. Boo, J. Frueh, D. L. Svoboda and P. P. Gaspar, *Organometallics*, **11**, 559 (1992).
20. (a) V. N. Khabashesku, V. Balaji, S. E. Boganov, S. A. Bashkirova, P. M. Matveichev, E. A. Chernyshev, O. M. Nefedov and J. Michl, *Mendeleev Commun.*, 38 (1992).
    (b) V. N. Khabashesku, V. Balaji, S. E. Boganov, O. M. Nefedov and J. Michl, *J. Am. Chem. Soc.*, **116**, 320 (1994).
    (c) V. N. Khabashesku, S. E. Boganov, V. I. Faustov, A. Gömöry, I. Besenyei, J. Tamas and O. M. Nefedov, *High Temp. Mater. Sci.*, **33**, 125 (1995).
21. A. Laporterie, G. Manuel, J. Dubac, P. Mazerolles and H. Iloughmane, *J. Organomet. Chem.*, **210**, C33 (1981).
22. C. Guimon, G. Pfister-Guillouzo, J. Dubac, A. Laporterie, G. Manuel and H. Iloughmane, *Organometallics*, **4**, 636 (1985).
23. (a) Reference 3, pp. 218–224 and references cited therein.
    (b) Reference 3, pp. 221–224 and references cited therein.
24. (a) T. Tsumuraya and W. Ando, *Organometallics*, **9**, 869 (1990).
    (b) T. Tsumuraya, Y. Kabe and W. Ando, *J. Organomet. Chem.*, **482**, 131 (1994).
25. W. P. Neumann, *Chem. Rev.*, **91**, 311 (1991).
26. (a) H. Brauer and W. P. Neumann, *Synlett*, 431 (1991).
    (b) G. Billeb, H. Brauer, W. P. Neumann and M. Weisbeck, *Organometallics*, **11**, 2069 (1992).
27. J. P. Béteille, A. Laporterie and J. Dubac, unpublished work.
28. A. J. Ashe III and S. Mahmoud, *Organometallics*, **7**, 1878 (1988).

29. (a) C. Pluta and K. R. Pörschke, *J. Organomet. Chem.*, **453**, C11 (1993).
    (b) J. Krause, C. Pluta, K. R. Pörschke and R. Goddard, *J. Chem. Soc., Chem. Commun.*, 1254 (1993).
30. Reference 3, pp. 218–231 and pp. 235–236 and references cited therein.
31. F. C. Leavitt, T. A. Manuel and F. Johnson, *J. Am. Chem. Soc.*, **81**, 3163 (1959).
32. K. W. Hübel and E. H. Braye, U. S. Patent 3 426 052 (1969); *Chem. Abstr.*, **70**, 106663 (1969).
33. J. G. Zavistoski and J. J. Zuckerman, *J. Org. Chem.*, **34**, 4197 (1969).
34. W. H. Atwell, D. R. Weyenberg and H. Gilman, *J. Org. Chem.*, **32**, 885 (1967).
35. (a) V. Hagen and K. Rühlman, *Z. Chem.*, **8**, 114 (1968).
    (b) R. Müller, *Z. Chem.*, **8**, 262 (1968).
    (c) T. J. Barton, W. D. Wulff, E. V. Arnold and J. Clardy, *J. Am. Chem. Soc.*, **101**, 2733 (1979).
36. T. J. Barton, A. J. Nelson and J. Clardy, *J. Org. Chem.*, **37**, 895 (1972).
37. (a) J. Y. Corey, C. Guérin, B. Henner, B. Kolani, W. W. C. Wong Chi Man and R. J. P. Corriu, *C. R. Séances Acad. Sci., Sér. 2*, **300**, 331 (1985).
    (b) F. Carré; E. Colomer, J. Y. Corey, R. J. P. Corriu, C. Guérin, B. J. L. Henner, B. Kolani and W. W. C. Wong Chi Man, *Organometallics*, **5**, 910 (1986).
38. A. Boudin, G. Cerveau, C. Chuit, R. J. P. Corriu and C. Reye, *Bull. Chem. Soc. Jpn.*, **61**, 101 (1988).
39. H. Sakurai, A. Nakamura and Y. Nakadaira, *Organometallics*, **2**, 1814 (1983).
40. U. Bankwitz, H. Sohn, D. R. Powell and R. West, *J. Organomet. Chem.*, **499**, C7 (1995).
41. (a) H. Okinoshima, K. Yamamoto and M. Kumada, *J. Am. Chem. Soc.*, **94**, 9263 (1972).
    (b) H. Okinoshima, K. Yamamoto and M. Kumada, *J. Organomet. Chem.*, **86**, C27 (1975).
42. M. Ishikawa, *Organomet. Synth.*, **4**, 527 (1988).
43. E. Toyoda, A. Kunai and M. Ishikawa, *Organometallics*, **14**, 1089 (1995).
44. K. Ikenaga, K. Hiramatsu, N. Nasaka and S. Matsumoto, *J. Org. Chem.*, **58**, 5045 (1993).
45. (a) D. Seyferth, D. P. Duncan and S. C. Vick, *J. Organomet. Chem.*, **125**, C5 (1977).
    (b) D. Seyferth, S. C. Vick, M. L. Shannon, T. F. O. Lim and D. P. Duncan, *J. Organomet. Chem.*, **135**, C37 (1977).
    (c) D. Seyferth, S. C. Vick and M. L. Shannon, *Organometallics*, **3**, 1897 (1984).
    (d) D. Seyferth, S. C. Vick and M. L. Shannon and T. F. O. Lim, *Organometallics*, **4**, 57 (1985).
46. H. Sakurai, Y. Kamiyama and Y. Nakadaira, *J. Am. Chem. Soc.*, **99**, 3879 (1977).
47. J. Belznerand and H. Ihmels, *Tetrahedron Lett.*, **34**, 6541 (1993).
48. (a) M. Ishikawa, H. Sugisawa, O. Harata and M. Kumada, *J. Organomet. Chem.*, **217**, 43 (1981).
    (b) M. Ishikawa, S. Matsuzawa, T. Higuchi, S. Kamitori and K. Hirotsu, *Organometallics*, **4**, 2040 (1985).
    (c) M. Ishikawa, S. Matsuzawa, T. Higuchi, S. Kamitori and K. Hirotsu, *Organometallics*, **3**, 1930 (1984).
49. M. Ishikawa, J. Ohshita, Y. Ito and J. Iyoda, *J. Am. Chem. Soc.*, **108**, 7417 (1986).
50. (a) M. Ishikawa, T. Fuchikami and M. Kumada, *J. Organomet. Chem.*, **142**, C45 (1977).
    (b) M. Ishikawa, H. Sugisawa, M. Kumada, H. Kawakami and T. Yamabe, *Organometallics*, **2**, 974 (1983).
51. A. Shäfer, M. Weidenbruch and S. Pohl, *J. Organomet. Chem.*, **282**, 305 (1985).
52. H. Gilman, S. G. Cottis and W. H. Atwell, *J. Am. Chem. Soc.*, **86**, 1596 and 5584 (1964).
53. Reference 3, pp. 240–245 and references cited therein.
54. (a) K. Tamao, K. Kobayashi and Y. Ito, *Synlett*, 539 (1992).
    (b) K. Tamao, S. Yamaguchi, M. Shiozaki, Y. Nakagawa and Y. Ito, *J. Am. Chem. Soc.* **114**, 5867 (1992).
55. N. Chatani, T. Morimoto, T. Muto and S. Murai, *J. Organomet. Chem.*, **473**, 335 (1974).
56. (a) B. Wrackmeyer, *J. Chem. Soc., Chem. Commun.*, 397 (1986).
    (b) B. Wrackmeyer, *J. Organomet. Chem.*, **310**, 151 (1986).
    (c) R. Köster, G. Seidel, J. Süb and B. Wrackmeyer, *Chem. Ber.*, **126**, 1107 (1993).
    (d) B. Wrackmeyer, G. Kehr and J. Süb, *Chem. Ber.*, **126**, 2221 (1993).
57. (a) L. Killian and B. Wrackmeyer, *J. Organomet. Chem.*, **132**, 213 (1977).
    (b) B. Wrackmeyer, G. Kehr and R. Boese, *Chem. Ber.*, **125**, 643 (1992).
    (c) B. Wrackmeyer, S. Kundler and R. Boese, *Chem. Ber.*, **126**, 1361 (1993).
    (d) B. Wrackmeyer, S. Kundler and A. Ariza-Castolo, *Phosporus, Sulfur and Silicon*, **91**, 229 (1994).
    (e) B. Wrackmeyer, S. Kundler, W. Milius and R. Boese, *Chem. Ber.*, **127**, 333 (1994).

(f) B. Wrackmeyer, G. Kehr and S. Ali, *Inorg. Chim. Acta*, **216**, 51 (1994).
(g) B. Wrackmeyer, G. Kehr and R. Boese, *Angew. Chem., Int. Ed. Engl.*, **30**, 1370 (1991) and references cited therein.
58. (a) B. Wrackmeyer and K. Horchler, *J. Organomet. Chem.*, **399**, 1 (1990).
(b) B. Wrackmeyer, K. Horchler and R. Boese, *Angew. Chem., Int. Ed. Engl.*, **28**, 1500 (1989).
59. (a) K. Tamao, S. Yamaguchi and M. Shiro, *J. Am. Chem. Soc.*, **116**, 11715 (1994).
(b) K. Tamao and S. Yamaguchi, *Jpn. Kokai Tokkyo Koho* JP 07,179,477 (1995); *Chem. Abstr.*, **124**, 56295 (1995).
60. (a) A. J. Ashe III and T. R. Diephouse, *J. Organomet. Chem.*, **202**, C95 (1980).
(b) A. J. Ashe III and F. J. Drone, *Organometallics*, **3**, 495 (1984).
61. (a) T. J. Barton and E. E. Gottsman, *Synth. React. Inorg. Met.-Org. Chem.*, **3**, 201 (1973).
(b) M. Schriewer and W. P. Neumann, *J. Am. Chem. Soc.*, **105**, 897 (1983).
62. (a) T. J. Barton, in *Comprehensive Organometallic Chemistry* (Eds. G. Wilkinson, F. G. A. Stone and E. W. Abel), Vol. 2, Pergamon Press, Oxford, 1982, p. 252.
(b) J. Dubac and A. Laporterie unpublished results.
63. A. Laporterie, *Thesis*, Université Paul Sabatier, Toulouse, n° 703 (1976).
64. J. C. Brunet and N. Demey, *Ann. Chim.*, **8**, 123 (1973).
65. Reference 3, pp. 217, 225.
66. W. C. Joo, H. S. Hwang and J. H. Hong, *Bull. Korean Chem. Soc.*, **6**, 348 (1985).
67. (a) A. Laporterie, G. Manuel, J. Dubac and P. Mazerolles, *Nouv. J. Chim.*, **6**, 67 (1982).
(b) A. Laporterie, G. Manuel, H. Iloughmane and J. Dubac, *Nouv. J. Chim.*, **8**, 437 (1984).
(c) J. Dubac, A. Laporterie, G. Manuel, H. Iloughmane, J. P. Béteille and P. Dufour, *Synth. React. Inorg. Met.-Org. Chem.*, **17**, 783 (1987).
68. G. K. Henry, R. Shinimoto, Q. Zhou and W. P. Weber, *J. Organomet. Chem.*, **350**, 3 (1988).
69. G. Manuel, G. Bertrand and F. El Anba, *Organometallics*, **2**, 391 (1983).
70. J. Dubac, A. Laporterie, G. Manuel and H. Iloughmane, *Phosphorus and Sulfur*, **27**, 191 (1986).
71. A. Laporterie, H. Iloughmane and J. Dubac, *Tetrahedron Lett.*, **24**, 3521 (1983).
72. J. D. Andriamisaka, C. Couret, J. Escudié, A. Laporterie, G. Manuel and M. Regitz, *J. Organomet. Chem.*, **419**, 57 (1991).
73. D. Terunuma, M. Hirose, Y. Motoyama and K. Kumano, *Bull. Chem. Soc. Jpn.*, **66**, 2682 (1993).
74. J. P. Béteille, A. Laporterie and J. Dubac, *J. Organomet. Chem.*, **426**, C1 (1992).
75. J. P. Béteille, A. Laporterie and J. Dubac, *Organometallics*, **8**, 1799 (1989).
76. (a) J. J. Eisch, N. K. Hota and S. Kozima, *J. Am. Chem. Soc.*, **91**, 4575 (1969).
(b) G. E. Herberich, B. Buller, B. Hessner and W. Oschmann, *J. Organomet. Chem.*, **195**, 253 (1980).
(c) L. Killian and B. Wrackmeyer, *J. Organomet. Chem.*, **148**, 137 (1978).
77. A. J. Ashe, III, W. M. Butler and T. R. Diephouse, *Organometallics*, **2**, 1005 (1983).
78. (a) R. Uson, J. Vicente and M. T. Chicote, *Inorg. Chim. Acta*, **35**, L 205 (1979).
(b) R. Uson, J. Vicente and M. T. Chicote, *J. Organomet. Chem.*, **209**, 271 (1981).
(c) R. Uson, J. Vicente, M. T. Chicote, P. G. Jones and G. M. Sheldrick, *J. Chem. Soc., Dalton Trans.*, 1131 (1983).
79. P. J. Fagan and W. A. Nugent, *J. Am. Chem. Soc.*, **110**, 2310 (1988).
80. (a) W. A. Nugent, D. L. Thorn and R. L. Harlow, *J. Am. Chem. Soc.*, **109**, 2788 (1987).
(b) A. Famili, M. F. Farona and S. Thanedar, *J. Chem. Soc., Chem. Commun.*, 435 (1983).
(c) E. Negishi, F. E. Cederbaum and T. Tamatsu, *Tetrahedron Lett.*, **27**, 2829 (1986).
81. P. Dufour, M. Dartiguenave, Y. Dartiguenave and J. Dubac, *J. Organomet. Chem.*, **384**, 61 (1990).
82. F. Meier-Brocks and E. Weiss, *J. Organomet. Chem.*, **453**, 33 (1993).
83. (a) H. Gilman and R. D. Gorsich, *J. Am. Chem. Soc.*, **77**, 6380 (1955).
(b) H. Gilman and R. D. Gorsich, *J. Am. Chem. Soc.*, **80**, 1883 (1958).
(c) D. Wittenberg and H. Gilman, *J. Am. Chem. Soc.*, **80**, 2677 (1958).
(d) H. Gilman and R. D. Gorsich, *J. Am. Chem. Soc.*, **80**, 3243 (1958).
84. R. Gelius, *Chem. Ber.*, **93**, 1759 (1960).
85. (a) S. C. Cohen and A. G. Massey, *J. Chem. Soc., Chem. Commun.*, 457 (1966).
(b) S. C. Cohen and A. G. Massey, *Tetrahedron Lett.*, 4393 (1966).
(c) S. C. Cohen and A. G. Massey, *J. Organomet. Chem.*, **10**, 471 (1967).
86. J. Y. Corey and L. S. Chang, *J. Organomet. Chem.*, **307**, 7 (1986).
87. S. C. Cohen, M. L. N. Reddy and A. G. Massey, *J. Chem. Soc., Chem. Commun.*, 451 (1967).

88. E. A. Chernyshev, S. A. Shehepinov, T. L. Krasnova, N. P. Filimonova and E. I. Petrova, *Izobret. Prom. Obraztsy, Tovarnye Znaki*, **45**, 21 (1968); *Chem. Abstr.*, **69**, 7250 (1968).
89. (a) E. A. Chernyshev, N. G. Komalenkova and S. A. Bashkirova, *J. Organomet. Chem.*, **271**, 129 (1984).
    (b) E. A. Chernyshev, N. G. Komalenkova, O. V. Elagina, V. L. Rogachevskii, S. A. Bashkirova and L. V. Dunaeva, *Zh. Obshch. Khim.*, **55**, 2314 (1985); *Chem. Abstr.*, **105**, 172554m (1986).
90. (a) E. A. Chernyshev, N. G. Komalenkova, L. N. Shamshin and S. A. Shchepinov, *Zh. Obshch. Khim.*, **41**, 843 (1971); *Chem. Abstr.*, **75**, 49195e (1971).
    (b) E. A. Chernyshev, N. G. Komalenkova and L. N. Shamshin, *Otkrytiya, Izobret., Prom. Obraztsy, Tovarnye Znaki*, **48**, 65 (1971); *Chem. Abstr.*, **75**, 390 (1971).
91. B. Becker, R. J. P. Corriu, B. J. L. Henner, W. Wojnowski, K. Peters and H. G. von Schnering, *J. Organomet. Chem.*, **312**, 305 (1986).
92. M. Kira, K. Sakamoto and H. Sakurai, *J. Am. Chem. Soc.*, **105**, 7469 (1983).
93. R. W. Coutant and A. Levy, *J. Organomet. Chem.*, **10**, 175 (1967).
94. M. Ishikawa, T. Tabohashi, M. Kumada and J. Iyoda, *J. Organomet. Chem.*, **264**, 79 (1984).
95. (a) M. Ishikawa, T. Tabohashi, H. Sugisawa, K. Nishimura and M. Kumada, *J. Organomet. Chem.*, **250**, 109 (1983).
    (b) M. Ishikawa, K. Nishimura, H. Sugisawa and M. Kumada, *J. Organomet. Chem.*, **218**, C21 (1981).
96. (a) M. D. Rausch and L. P. Klemann, *J. Am. Chem. Soc.*, **89**, 5732 (1967).
    (b) M. D. Rausch, L. P. Klemann and W. H. Boon, *Synth. React. Inorg. Met.-Org. Chem.*, **15**, 923 (1985).
97. J. Kurita, M. Ishuii, S. Yasuike and T. Tsuchiya, *J. Chem. Soc., Chem. Commun.*, 1309 (1993).
98. A. Maercker, H. Bodenstedt and L. Brandsma, *Angew. Chem., Int. Ed. Engl.*, **31**, 1339 (1992).
99. S. L. Buchwald, B. T. Watson and J. C. Huffman, *J. Am. Chem. Soc.*, **108**, 7411 (1986).
100. S. L. Buchwald and R. B. Nielsen, *Chem. Rev.*, **88**, 1047 (1988).
101. A. Kanj, P. Meunier, B. Gautheron, J. Dubac and J. C. Daran, *J. Organomet. Chem.*, **454**, 51 (1993).
102. A. Kanj, P. Meunier, B. Hanquet, B. Gautheron, J. Dubac and J. C. Daran, *Bull. Soc. Chim. Fr.*, **131**, 715 (1994).
103. A. Kanj, P. Meunier, C. Legrand, B. Gautheron, J. Dubac and P. Dufour, to appear.
104. M. Pereyre, J. P. Quintard and A. Rahm, *Tin in Organic Synthesis*, Butterworths, London, 1987.
105. (a) T. J. Barton and B. L. Groh, *Organometallics*, **4**, 575 (1985).
    (b) T. J. Barton and M. Juvet, *Tetrahedron Lett.*, 3893 (1975).
106. T. J. Barton and G. T. Burns, *Organometallics*, **1**, 1455 (1982).
107. J. Dubac, A. Laporterie and G. Manuel, unpublished work.
108. (a) O. A. Arefev, N. S. Vorob'era, V. I. Epishev and A. Petrov, *Neftekhimiya*, **12**, 171 (1972); *Chem. Abstr.*, **77**, 61348f (1977).
    (b) V. A. Mironov, A. P. Ivanov and A. A. Akhrem, *Izv. Akad. Nauk. SSSR, Ser. Khim.*, 363 (1973); *Chem. Abstr.*, **78**, 159013p (1973).
    (c) S. D. Mekhtiev, M. R. Musaev, M. A. Mardanov, S. M. Sharifova, G. T. Badirova and M. A. Aliev, *Dokl. Akad. Nauk SSSR*, **30**, 49 (1974); *Chem. Abstr.*, **82**, 15952d (1975).
    (d) S. Cradock, R. H. Findlay and M. H. Palmer, *J. Chem. Soc., Dalton Trans.*, 1650 (1974).
    (e) N. T. Anh, E. Canadell and O. Eisenstein, *Tetrahedron*, **34**, 2283 (1978).
109. F. Mathey, *Top. Phosphorus Chem.*, **10**, 1 (1980).
110. J. Dubac, H. Iloughmane, A. Laporterie and C. Roques, *Tetrahedron Lett.*, **26**, 1315 (1985).
111. I. Fleming, *Frontier Orbitals and Organic Chemical Reactions*, Wiley, New York, 1976.
112. (a) R. B. Bates, B. Gordon III, T. K. Highsmith and J. J. White, *J. Org. Chem.*, **49**, 2981 (1984).
    (b) P. Mazerolles and C. Laurent, *J. Organomet. Chem.*, **406**, 119 (1991).
    (c) C. Laurent and P. Mazerolles, *Synth. React. Inorg. Met.-Org. Chem.*, **22**, 1183 (1992).
113. (a) R. B. Woodward and R. Hoffmann, *Angew. Chem., Int. Ed. Engl.*, **8**, 781 (1969).
    (b) C. W. Spangler, *Chem. Rev.*, **76**, 187 (1976).
    (c) P. Jutzi, *Chem. Rev.*, **86**, 983 (1986).
114. (a) P. K. Chiu and M. P. Sammes, *Tetrahedron*, **46**, 3439 (1990).
    (b) F. Mathey, *Acc. Chem. Res.*, **25**, 90 (1992) and references cited therein.
115. S. M. Bachrach and L. Perriot, *J. Org. Chem.*, **59**, 3394 (1994).
116. W. R. Roth, *Tetrahedron Lett.*, 1009 (1964).

117. H. Sun, D. A. Hrovat and W. T. Borden, *J. Am. Chem. Soc.*, **109**, 5275 (1987).
118. Reference 3, p. 239
119. G. T. Burns, E. Colomer, R. J. P. Corriu, M. Lheureux, J. Dubac, A. Laporterie and H. Iloughmane, *Organometallics*, **6**, 1398 (1987).
120. T. Douglas and K. H. Theopold, *Angew. Chem., Int. Ed. Engl.*, **28**, 1367 (1989).
121. J. M. Alcaraz, J. Svara and F. Mathey, *Nouv. J. Chim.*, **10**, 321 (1986).
122. (a) H. E. Simmons and T. Fukunaga, *J. Am. Chem. Soc.*, **89**, 5208 (1967).
(b) R. Breslow, J. M. Hoffmann Jr. and C. Perchonock, *Tetrahedron Lett.*, 3723 (1973).
(c) E. W. Garbisch Jr. and R. F. Sprecher, *J. Am. Chem. Soc.*, **88**, 3433, 3434 (1966).
123. Reference 3, pp. 239–246 and referneces cited therein.
124. (a) B. Résibois, J. C. Brunet and J. Bertrand, *Bull. Soc. Chim. Fr.*, **2**, 681 (1968).
(b) B. Résibois and J. C. Brunet, *Ann. Chim.*, **5**, 199 (1970).
125. R. Balasubramanian and M. V. George, *Tetrahedron*, **29**, 2395 (1973).
126. C. Grugel, W. P. Neumann and M. Schriewer, *Angew. Chem., Int. Ed. Engl.*, **18**, 543 (1979).
127. D. Terunuma, K. Kumano and Y. Motoyama, *Bull. Chem. Soc. Jpn.*, **67**, 2763 (1994).
128. H. Sakurai, Y. Nakadaira and T. Kobayashi, *J. Am. Chem. Soc.*, **101**, 487 (1979).
129. H. Sakurai, Y. Nakadaira and H. Tobita, *Chem. Lett.*, 1855 (1982).
130. (a) Y. Nakadaira, T. Kobayashi, T. Otsuda and H. Sakurai, *J. Am. Chem. Soc.*, **101**, 486 (1979).
(b) H. Sakurai, H. Sakaba and Y. Nakadaira, *J. Am. Chem. Soc.*, **104**, 6156 (1982).
(c) H. Sakurai, Y. Nakadaira and H. Sabaka, *Organometallics*, **2**, 1484 (1983).
131. (a) A. Sekiguchi, S. S. Zigler, R. West and J. Michl, *J. Am. Chem. Soc.*, **108**, 4241 (1986).
(b) A. Sekiguchi, G. R. Gillette and R. West, *Organometallics*, **7**, 1226 (1988).
132. T. J. Barton, W. F. Goure, J. L. Witiak and W. D. Wulff, *J. Organomet. Chem.*, **225**, 87 (1982).
133. H. Appler, L. W. Gross, B. Mayer and W. P. Neumann, *J. Organomet. Chem.*, **291**, 9 (1985).
134. A. Marinetti-Mignani and R. West, *Organometallics*, **6**, 141 (1987).
135. N. K. Hota and C. J. Willis, *J. Organomet. Chem.*, **15**, 89 (1968).
136. K. Kunô, K. Kobayashi, M. Kawasini, S. Kosima and T. Hitomi, *J. Organomet. Chem.*, **137**, 349 (1977).
137. M. P. Egorov, A. M. Galminas, M. B. Ezhova, S. P. Kolesnikov and O. M. Nefedov, *Metalloorg. Khim.*, **6**, 15 (1993).
138. (a) M. N. Paddon-Row and K. D. Jordan, *J. Chem. Soc., Chem. Commun.*, 1508 (1988).
(b) M. N. Paddon-Row, S. S. Wong and K. D. Jordan, *J. Chem. Soc., Perkin Trans. 2*, 417 (1990).
139. M. P. Egorov, M. B. Ezhova, M. Yu. Antipin and Yu. T. Struchkov, *Main Group Met. Chem.*, **14**, 19 (1991).
140. R. Maruca, *J. Org. Chem.*, **36**, 1626 (1971).
141. Y. Fujise, Y. Chonan, H. Sakurai and S. Ito, *Tetrahedron Lett.*, 1585 (1974).
142. T. J. Barton and J. Nelson, *Tetrahedron Lett.*, 5037 (1969).
143. Y. Nakadaira and H. Sakurai, *Tetrahedron Lett.*, 1183 (1971).
144. T. Sato, N. Moritami and M. Matsuyama, *Tetrahedron Lett.*, 5113 (1969).
145. T. J. Barton, R. C. Kippenhan and A. J. Nelson, *J. Am. Chem. Soc.*, **96**, 2272 (1974).
146. T. J. Barton and R. J. Rogido, *J. Org. Chem.*, **40**, 582 (1975).
147. H. H. Freedman, US Patent 3090 797 (1963); *Chem. Abstr.*, **59**, 11560c (1963).
148. H. H. Freedman, *J. Org. Chem.*, **27**, 2298 (1962).
149. H. H. Freedman, *J. Am. Chem. Soc.*, **83**, 2194 (1961).
150. V. R. Sandel and H. H. Freedman, *J. Am. Chem. Soc.*, **90**, 2059 (1968).
151. W. Z. Rhee and J. J. Zuckerman, *J. Am. Chem. Soc.*, **97**, 2291 (1975).
152. W. A. Gustavson, L. M. Principe, W. Z. Rhee and J. J. Zuckerman, *J. Am. Chem. Soc.*, **103**, 4126 (1981).
153. W. A. Gustavson, L. M. Principe, W. Z. Rhee and J. J. Zuckerman, *Inorg. Chem.*, **20**, 3460 (1981).
154. V. R. Sandel, G. R. Buske, S. G. Maroldo, D. K. Bates, D. Whitman and G. Sypniewski, *J. Org. Chem.*, **46**, 4069 (1981).
155. R. Balasubramanian and M. V. George, *J. Organomet. Chem.*, **85**, 311 (1975).
156. J. J. Eisch, J. E. Galle and S. Kozima, *J. Am. Chem. Soc.*, **108**, 379 (1986).
157. M. D. Curtis, *J. Am. Chem. Soc.*, **91**, 6011 (1969).
158. (a) Si chemistry: R. J. P. Corriu, C. Guérin and J. J. E. Moreau, *Top. Stereochem.*, **15**, 158 (1984).
(b) Ge chemistry: J. Dubac, J. Cavezzan, A. Laporterie and P. Mazerolles, *J. Organomet. Chem.*, **209**, 25 (1981) and references cited therein.

159. J. P. Béteille, *Thesis*, Université Paul Sabatier, Toulouse, n° 335 (1988).
160. P. Jutzi and A. Karl, *J. Organomet. Chem.*, **214**, 289 (1981).
161. P. Jutzi and A. Karl, *J. Organomet. Chem.*, **215**, 19 (1981).
162. Y. Nakadaira, T. Nomura, S. Kanouchi, R. Sato, C. Kabuto and H. Sakurai, *Chem. Lett.*, 209 (1983).
163. M. P. Mahayan, R. Balasubramanian and M. V. George, *Tetrahedron*, **32**, 1549 (1976).
164. E. G. Janzen, J. B. Pickett and W. H. Atwell, *J. Organomet. Chem.*, **10**, P6 (1967).
165. R. E. Dessy and R. L. Pohl, *J. Am. Chem. Soc.*, **90**, 1995 (1968).
166. N. Tamaka, T. Ogata, Y. Uratani, Y. Nakadaira and H. Sakurai, *Inorg. Nucl. Chem. Lett.*, **8**, 1041 (1972).
167. Reference 3, pp. 235, 236 and references cited therein.
168. (a) W. Ando, H. Tanikawa and A. Sekiguchi, *Tetrahedron Lett.*, **24**, 4245 (1983).
    (b) A. Sekiguchi, H. Tanikawa and W. Ando, *Organometallics*, **4**, 584 (1985).
169. V. Hagen and K. Rühlmann, *Z. Chem.*, **9**, 309 (1969).
170. K. Tamao and S. Yamaguchi, *Pure Appl. Chem.*, **68**, 139 (1996).
171. Y. Yamaguchi and J. Shioya, *Mol. Eng.*, **2**, 339 (1993).
172. (a) V. N. Khabashesku, V. Balaji, S. E. Boganov, O. M. Nefedov and J. Michl, *J. Am. Chem. Soc.*, **116**, 320 (1994).
    (b) B. Goldfuss and P. v. R. Schleyer, *Organometallics*, **14**, 1553 (1995) and references cited therein.
173. K. Tamao, S. Yamaguchi, Y. Ito, Y. Matsuzaki, T. Yamabe, M. Fukushima and S. Mori, *Macromolecules*, **28**, 8668 (1995).
174. M. G. Hill, K. R. Mann, L. L. Miller and J.-F. Penneau, *J. Am. Chem. Soc.*, **114**, 2728 (1992).
175. (a) M. Ishikawa and K. Nate, in *Inorganic and Organometallic Polymers* (Eds. M. Zeldin, K. J. Wynne and H. R. Allcock), ACS Symposium Series 360, Chap 16, American Chemical Society, Washington DC, 1988.
    (b) J. Ohshita, D. Kanaya and T. Yamanaka, *J. Organomet. Chem.*, **369**, C18 (1989).
    (c) T. Imori, H-G. Woo, J. F. Walzer and T. D. Tilley, *Chem. Mater.*, **5**, 1487 (1993).
    (d) A. Kunai, E. Toyoda, K. Horata and M. Ishikawa, *Organometallics*, **14**, 714 (1995).
176. (a) S. Ijadi-Maghsoodi and T. J. Barton, *Macromolecules*, **24**, 1257 (1991).
    (b) T. Iwahara, S. Hayase and R. West, *Macromolecules*, **23**, 4485 (1990).
    (c) See also Reference 179.
177. (a) J. Ohshita, K. Furumori, M. Ishikawa and T. Yamanaka, *Organometallics*, **8**, 2084 (1989).
    (b) M. Ishikawa, *Pure Appl. Chem.*, **63**, 851 (1991).
    (c) J. Ohshita, A. Matsuguchi, K. Furumori, R.-F. Hong, M. Ishikawa, T. Yamanaka, T. Koike and J. Shioya, *Macromolecules*, **25**, 2134 (1992).
178. M. Ishikawa, T. Hatano, Y. Hasegawa, T. Horio, A. Kunai, A. Miyai, T. Ishida, T. Tsukihara, T. Yamanaka, T. Koike and J. Shioya, *Organometallics*, **11**, 1604 (1992) and references cited therein.
179. J. L. Brefort, R. Corriu, P. Gerbier, C. Guerin, B. Henner, A. Jean, T. Kuhlmann, F. Garnier and A. Yassar, *Organometallics*, **11**, 2500 (1992).
180. R. Corriu, N. Devylder, C. Guérin, B. Henner and A. Jean, *J. Organomet. Chem.*, **509**, 249 (1996).
181. R. Corriu, N. Devylder, C. Guérin, B. Henner and A. Jean, *Organometallics*, **13**, 3194 (1994).
182. R. Corriu, W. Douglas and Z.-X. Yang, *J. Organomet. Chem.*, **456**, 35 (1993).
183. W.-C. Joo, J.-H. Hong, S.-B. Choi and H.-E. Son, *J. Organomet. Chem.*, **391**, 27 (1990).
184. (a) H. Grützmacher, *Angew. Chem., Int. Ed. Engl.*, **34**, 295 (1995).
    (b) B. Goldfuss and P. v. R. Schleyer, *Organometallics*, **14**, 1553 (1995).
    (c) B. Goldfuss, P. v. R. Schleyer and F. Hampel, *Organometallics*, **15**, 1755 (1996).
185. W.-C. Joo, J.-H. Hong, H.-E. Son and J.-H. Kim, *Proceedings of the 9th International Symposium on Organosilicon Chemistry*, University of Edinburgh, UK, July 16–20, 1990, B 8.
186. J.-H. Hong and P. Boudjouk, *J. Am. Chem. Soc.*, **115**, 5883 (1993).
187. W. P. Freeman, T. D. Tilley, G. P. A. Yap and A. L. Rheingold, *Angew. Chem., Int. Ed. Engl.*, **35**, 882 (1996).
188. J.-H. Hong, P. Boudjouk and I. Stoenescu, *Organometallics*, **15**, 2179 (1996).
189. J.-H. Hong and P. Boudjouk, *Organometallics*, **14**, 574 (1995).
190. R. Corriu, C. Guérin, B. Henner and Q. Wang, *Organometallics*, **10**, 2297 (1991).
191. P. Dufour, J. Dubac, M. Dartiguenave and Y. Dartiguenave, *Organometallics*, **9**, 3001 (1990).

192. W. P. Freeman, T. D. Tilley, F. P. Arnold, A. L. Rheingold and P. K. Gantzel, *Angew. Chem., Int. Ed. Engl.*, **34**, 1887 (1995).
193. P. Meunier and J. Dubac, to appear.
194. J.-H. Hong, P. Boudjouk and S. Castellino, *Organometallics*, **13**, 3387 (1994).
195. M. Denk, R. Lennon, R. Hayashi, R. West, A. V. Belyakov, H. R. Verne, M. Wagner and N. Metzler, *J. Am. Chem. Soc.*, **116**, 2691 (1994).
196. R. West, H. Sohn, V. Bankwitz, J. Calabrese, Y. Apeloig and T. Mueller, *J. Am. Chem. Soc.*, **117**, 11608 (1995).
197. J.-H. Hong and P. Boudjouk, *Bull. Soc. Chim. Fr.*, **132**, 495 (1995).
198. R. West, H. Sohn, D. R. Powelll, T. Mueller and Y. Apeloig, *Angew. Chem., Int. Ed. Engl.*, **35**, 1002 (1996).
199. J.-H. Hong, Y. Pan and P. Boudjouk, *Angew. Chem., Int. Ed. Engl.*, **35**, 186 (1996) and references cited therein.
200. W. P. Freeman, T. D. Tilley, A. L. Rheingold and R. L. Ostrander, *Angew. Chem., Int. Ed. Engl.*, **32**, 1744 (1993).
201. P. G. Gassman and C. H. Winter, *J. Am. Chem. Soc.*, **110**, 6130 (1988).
202. W. P. Freeman, T. D. Tilley and A. L. Rheingold, *J. Am. Chem. Soc.*, **116**, 8428 (1994).
203. U. Schubert, G. Scholz, J. Müller, K. Ackermann, B. Wörle and R. F. D. Stansfield, *J. Organomet. Chem.*, **306**, 303 (1986).
204. V. N. Khabashesku, S. E. Boganov, D. Antic, O. M. Nefedov and J. Michl, *Organometallics*, **15**, 4714 (1996).
205. B. Wrackmeyer and U. Klaus, *J. Organomet. Chem.*, **520**, 211 (1996).
206. S. Yamaguchi and K. Tamao, *Bull. Chem. Soc. Jpn.*, **69**, 2327 (1996).
207. S. Yamaguchi and K. Tamao, *Tetrahedron Lett.*, **37**, 2983 (1996).
208. K. Tamao, M. Uchida, T. Izumizawa, K. Furukawa and S. Yamaguchi, *J. Am. Chem. Soc.*, in press.
209. K. Tamao, S. Ohno and S. Yamaguchi, *J. Chem. Soc., Chem. Commun.*, 1873 (1996).
210. W. P. Freeman, T. D. Tilley, L. M. Liable-Sands and A. L. Rheingold, *J. Am. Chem. Soc.*, **118**, 10457 (1996).

CHAPTER 35

Transition-metal silyl complexes

MORIS S. EISEN

Department of Chemistry, Technion — Israel Institute of Technology, Kiryat Hatechnion, Haifa 32000, Israel

I. ABBREVIATIONS

acac	acetylacetonate	dppb	bis(1,4-diphenylphosphino) butane
Ad	adamantyl	dppe	bis(1,2-diphenylphosphino) ethane
Cbb	cyclobuta-η^6-benzene	dppm	bis(diphenylphosphino) methane
cod	cyclooctadiene	HMPA	hexamethylphosphoric triamide
coe	cyclooctene	Mes	mesityl (2,4,6-$Me_3C_6H_2$)
cot	cyclooctatetraene	Np	neopentyl
Cp	η^5-C_5H_5	OTf	triflate
Cp*	η^5-$C_5(CH_3)_5$	Ph_2Pyr	2-(diphenylphosphino) pyridine
Cy	cyclohexyl	Pyr	pyridine
dcpe	bis(1,2-dicyclohexylphosphino) ethane	TFB	tetrafluorobenzobarrelene
dmpe	bis(1,2-dimethylphosphino) ethane	Trityl	triphenylmethyl
dmpm	bis(dimethylphosphino) methane	vdpp	vinylidenebis(diphenylphosphine)
dmpp	bis(1,3-dimethylphosphino) propane		

II. INTRODUCTION

Transition-metal chemistry is currently one of the most rapidly developing research areas. From Hein's discovery in 1941 of the first metal–silicon complex, followed by Wilkinson's $Cp(CO)_2FeSiMe_3$ complex synthesis in 1956 and Speier's catalytic hydrosilylation discovery in 1977, a new area of organometallic chemistry was entered in 1987 with the discovery of complexes with silicon multiply bonded to transition metals. In the last decade, coordination complexes of silylenes, silylynes, silenes, disilenes, silanimines, silaallenes and metallasilaallenes have been prepared with some of the compounds being the key intermediates in important technological processes. Numerous developments in this field in the last few years have provided evidence of the interest in the stoichiometric and catalytic chemistry of metal–silicon bonds. This chapter is an update of an earlier chapter[1] giving information on some of the newer developments, covering the literature from 1992 to approximately the middle of 1996. This review is organized according to the order of the groups in the Periodic Table and at the end of each group a compilation of metal–silicon bond distances and ^{29}Si NMR chemical shifts of the aforementioned complexes are given. Lanthanide and actinide silyl complexes are reviewed after group 3 and group 4, respectively, due to their isolobal relationship.

III. GROUP-3 SILYL COMPLEXES

Early-transition-metal complexes containing silicon ligands are becoming increasingly important in organometallic chemistry[1]. The first group-3 silyl complex

$Cp_2Sc[Si(SiMe_3)_3](THF)$ was prepared by Tilley and coworkers in 1990 by reacting the dimeric scandocene chloride $[Cp_2ScCl]_2$ with $(Me_3Si)_3SiLi{\cdot}3THF$. The complex obtained undergoes insertion with carbon monoxide or xylyl isocyanides yielding CO−CO coupling and ketene-derived products or the monoinsertion η^2-iminosilaacyl complex, respectively, whereas the analogous complex $Cp_2Sc(SiPh_2Bu\text{-}t)(THF)$ insert CO_2 yielding the dimeric silane carboxylate complex $[Cp_2Sc(\mu\text{-}O_2{-}CSiR_3)]_2$[1]. Recently, increasing the small number of group-3 silyl derivatives, Tilley and coworkers prepared a series of scandium complexes via the addition of the appropriate lithium silyl reagent to the dimeric scandocene chloride (equation 1).

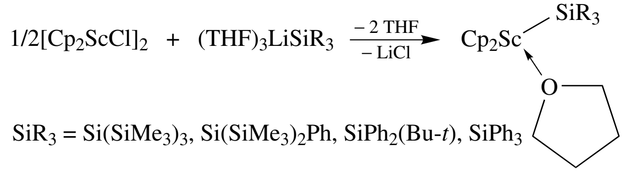

(1)

Solid state studies on the complex $Cp_2Sc[Si(SiMe_3)_3](THF)$ reveal a tetrahedral environment for the metal with a Sc−Si distance of 2.863(2) Å. This bond length is shorter than the isolobal Sm−Si bond [3.052(8) Å] (*vide infra*) found in the dimeric complex $[Cp_2{}^*SmH(SiMe_3)_2]_2$ by a distance of 0.19 Å, reflecting the difference in the anionic radii between Sc^{3+} and Sm^{3+}[2].

These unusually reactive d^0 silyl complexes have been found to catalyze the polymerization of ethylene to polyethylene with polydispersity ranges from 3.6 to 5.5 and with molecular weights from 27,000 to 410,000. It is noteworthy that the reaction of $Cp_2Sc[Si(SiMe_3)_3](THF)$ with propene yielded the organic compound $HSi(SiMe_3)_3$; however the allylic activation complex, $Cp_2Sc(\eta^3\text{-}C_3H_5)$, was not formed. Presumably, the formation of the $HSi(SiMe_3)_3$ is through a vinylic activation as found for lanthanides[3]. In addition, no reactivity was found for the silyl complex $Cp_2Sc[Si(SiMe_3)_3](THF)$ with butadiene or cyclohexene. However, addition of $PhC{\equiv}CH$ yielded $HSi(SiMe_3)_3$ and the expected dimeric complex $[Cp_2Sc(\mu\text{-}C{\equiv}CPh)]_2$[2].

IV. LANTHANIDE SILYL DERIVATIVES

Organolanthanide complexes have been found to be active catalysts for the dehydrogenative coupling of silanes, arguing that a lanthanide−silicon bond should be involved in such a process (*vide infra*). The reactivity of lanthanide silyl complexes is based on the σ-bond metathesis reaction, which appears to be highly sensitive to steric effects. For example, the isolobal group III yttrium complex $Cp_2{}^*YMe(THF)$ converts $PhSiH_3$ to $PhMeSiH_2$, indicating that the primary σ-bond metathesis process involves a four-center transition state that transfers the silyl group to the carbon rather than to the yttrium atom. Recently, based on this mechanism, Molander and Nichols have shown the use of $Cp_2{}^*YMe(THF)$ for the cyclization/silylation of 1,5- and 1,6-dienes[4]. In addition, Marks and coworkers have shown that silanes can be used as terminating chain transfer agents with a similar mechanism in the lanthanide-mediated ethylene polymerization with $(Cp_2{}^*SmH)_2$ and $PhSiH_3$[5].

The more hindered lanthanide alkyl complexes, as in $Cp_2{}^*LnCH(SiMe_3)_2$ (Ln = Nd, Sm), were found not to react with bulky silanes such as t- Bu_2SiH_2 or Ph_2MeSiH, but to react with unhindered silanes to produce $CH_2(SiMe_3)_2$, the corresponding dimeric hydride $(Cp_2{}^*LnH)_2$ complex, and a disilane resulting from the dehydrocoupling reaction (*vide infra*)[6]. Until 1992, the only lanthanide silyl derivatives reported were those corresponding

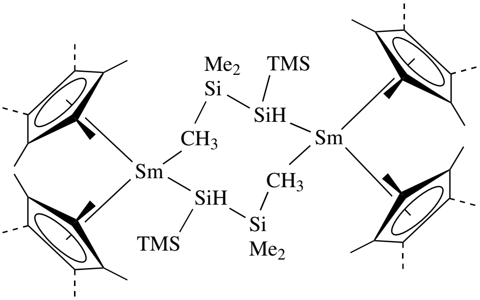

FIGURE 1. Dimeric structure of complex **1**

to the salt of type $[Li(DME)_3]^+[Cp_2Ln(SiMe_3)_2]^-$ (DME = dimethoxyethane)[7]. The first neutral lanthanide silyl complexes $Cp_2{}^*LnSiH(SiMe_3)_2$ [Ln = Sm (**1**), Nd] were obtained via a σ-bond metathesis of an excess of $SiH_2(SiMe_3)_2$ with $Cp_2{}^*LnCH(SiMe_3)_2$ or $Cp''_2LnCH(SiMe_3)_2$ (Ln = Nd, Sm; $Cp'' = \eta^5$-C_5Me_4Et)[8,9].

In the solid state, these lanthanide silyl compounds are dimeric (Figure 1) formed via intermolecular Sm•••CH_3−Si interactions ensuring a Sm−C(Me) distance of 2.97(2) Å. The Sm−Si bond length of 3.052(8) Å in **1** is longer than the Lu−Si bond of 2.888(2) Å in the anionic $[Cp_2Lu(SiMe_3)_2]^-$ complex (Table 1)[7]. This difference of 0.16 Å is somewhat larger than the one attributed to the lanthanide contraction (*ca* 0.10 Å). These new silyl complexes are monomeric in solution, displaying in the ^1H NMR chemical shifts a Curie−Weiss behavior up to −80 °C (Table 2). The Cp* resonances for the Nd compound coalesce into two singlets at 10 °C, which corresponds to an activation barrier for rotation about the Nd−Si bonds of 13.3 ± 1.0 kcal mol^{-1}[9].

Interestingly, Marks and coworkers have shown that lanthanide complexes of the type $Cp_2{}^*LnR$ [Ln = La, Nd, Sm, Y, Lu; R = H, $CH(TMS)_2$] in hydrocarbon solvents react with $R'SiH_3$ by eliminating H_2 (R = H) or $CH_2(TMS)_2$ [R = $CH(TMS)_2$], respectively, forming the corresponding lanthanocene silyl derivatives and the subsequent formation of the dimeric hydrides $[Cp_2{}^*LnH]_2$ and polysilanes. This result argues that the difference in reactivity found for the similar lanthanide complexes may be 'tuned' by either the silane group (R′), the presence of an olefin, as in the cyclization/silylation of dienes (*vide supra*), or specifically in the yttrium complex, by the solvent (*vide infra*). The relative rates of the dehydrogenative coupling of silanes for the different lanthanide complexes were found to follow the trend Lu > Y > Sm > Nd > La. This trend reveals no parallel with lanthanide III/II redox characteristics but correlates well with the metal ionic radius[10]. Lately, Marks and coworkers have proposed, based on kinetic measurements, mechanistic pathways for the dehydrogenative coupling of silanes (Scheme 1) and the hydrosilylation of olefins (Scheme 2) catalyzed by organolanthanides[5].

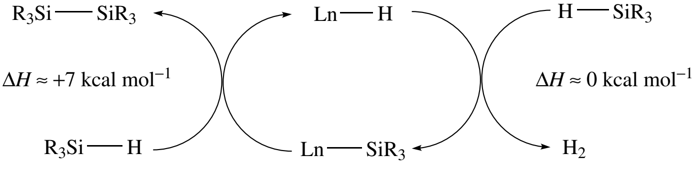

SCHEME 1

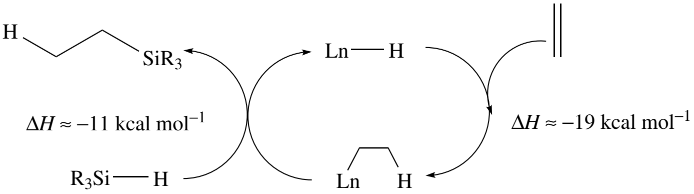

SCHEME 2

A close look at the hydrogenolysis reaction of the $Cp_2{}^*SmCH(TMS)_2$ complex with $H_2Si(SiMe_3)_2$ shows that the two compounds *do not react directly*. The kinetic profile shows an S-shape form with an induction time. This shape is consistent with a second-order autocatalytic mechanism in which the reaction is catalyzed by a product or an intermediate. Indeed, the induction period was completely eliminated by addition of catalytic amounts of H_2, $[Cp_2{}^*SmH]_2$, or of the complex $[Cp_2{}^*Sm\ (\mu\text{-}H)\ (\mu\text{-}CH_2C_5Me_4)SmCp^*]$, which is a decomposition product of the $[Cp_2{}^*SmH]_2$. Thus, two possible mechanistic pathways (Schemes 3 and 4) have been proposed to explain the hydrogenolysis reaction.

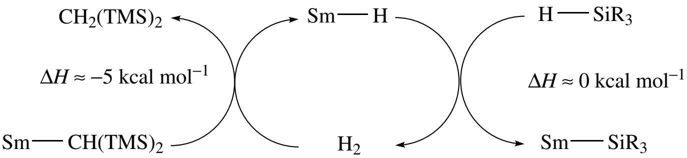

SCHEME 3

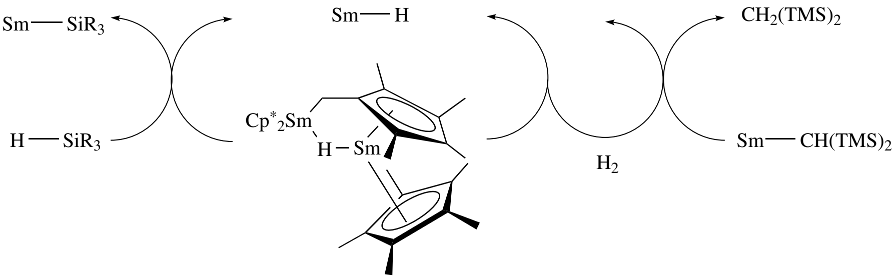

SCHEME 4

Kinetic studies by Radu and Tilley have shown that both Schemes 3 and 4 are observed, with a large preference for Scheme 3[11]. A similar S-shaped reaction profile has been observed recently for chiral $Cp_2{}^*SmR$ complexes in the presence of $PhSiH_3$[5].

The first neutral lanthanide(II) silyl complex $(Ph_3Si)_2Yb(THF)_4$ was synthesized by the reaction of Ph_3SiCl with metallic ytterbium in THF. The solid complex has a centrosymmetrical octahedral structure with a Yb atom bonded to four oxygen atoms of the THF molecules in the equatorial positions and to two Si atoms of the $SiPh_3$ fragment in the axial positions. The Yb−Si distance of 3.158(2) Å is 0.1 Å larger than the Sm−Si distance in $Cp_2{}^*SmSiH(SiMe_3)_2$ which is in agreement with the difference in ionic radius between Ln(II) and Ln(III) complexes[12].

V. GROUP-4 SILYL COMPLEXES

Pioneering studies by Tilley, Harrod and others have demonstrated that group-4 metal–silicon bonds are quite reactive, undergoing insertion reactions and participating in silane polymerizations and σ-bond metathesis reactions[1,13]. Zirconocene and hafnocene silyl hydride of the type $Cp_2M(SiPh_3)(PMe_3)(H)$ (M = Zr, Hf) complexes, which are believed to be active species participating in the catalytic hydrosilylation and dehydrogenative coupling of silanes, were synthesized by the addition of $HSiPh_3$ to solutions of the corresponding $Cp_2M(olefin)(PMe_3)$ (M = group-4). For Hf, intermediate **2** was observed, arguing in favor of an addition–elimination pathway instead of an oxidative addition mechanism as being responsible for the silyl hydride formation (equation 2). Additional evidence supporting the proposed mechanism was provided by deuterium labeling and the observation of complex **4** resulting from the reversible elimination of $HSiPh_3$ or $DSiPh_3$ from the proposed intermediate complex **3** (equation 3).

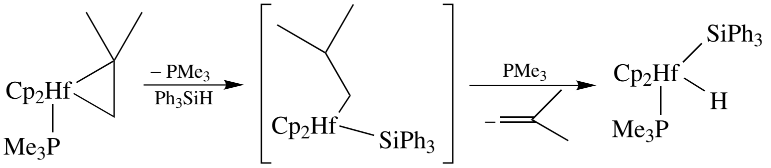

(2)

(2)

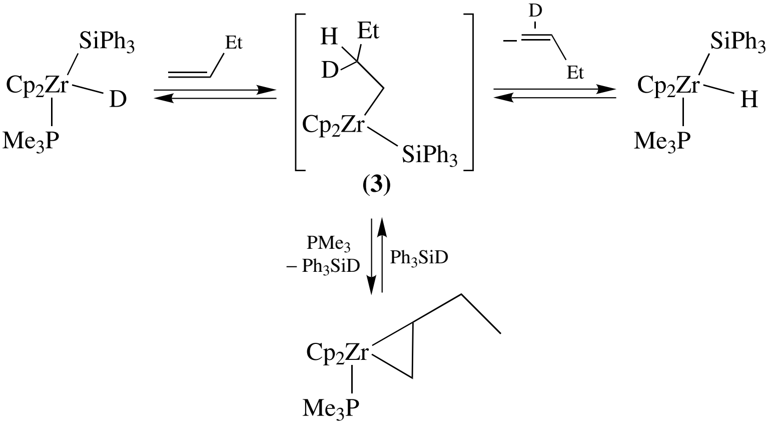

(4)

(3)

The hydride zirconium compound $Cp_2Zr(H)(SiPh_3)(PMe_3)$ reacts with *t*-BuNC, *t*-BuCN and acetone via insertion into the Zr–H bond, and undergoes σ-bond metathesis with Ph_2SiH_2 producing $HSiPh_3$ and two isomers of $Cp_2Zr(H)(SiHPh_2)(PMe_3)$. In addition, the reaction of $Cp_2Zr(H)(SiPh_3)(PMe_3)$ with the internal alkyne $CH_3C{\equiv}CCH_3$ produces the metallacycle complex **5** by elimination of the silane $HSiPh_3$ with the concomitant formation of the alkyne complex followed by two subsequent oxidative couplings (equation 4).

The X-ray crystal structure of the silyl-hydrido zirconium derivative $Cp_2Zr(H)(SiPh_3)(PMe_3)$ showed that the silyl and phosphine ligands are in the outward position in the CpZr wedge, with the hydride ligand in between[14].

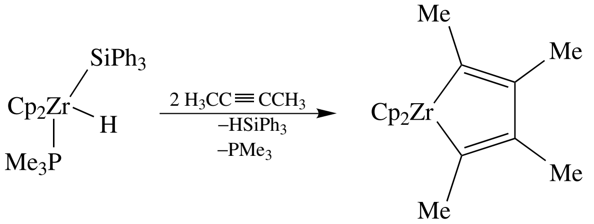

(5)

(4)

Similar silyl-hydrido metallocene derivatives, $Cp_2Zr(H)(SiHPh_2)(PR_2Me)$ (R = Me, Ph), have been found to be efficient catalysts for the high regioselective hydrosilylation of olefins. These complexes are obtained by trapping the organometallic hydride intermediate $Cp_2Zr(H)(SiHPh_2)$ with phosphines. In the absence of phosphine, the hydride dimerizes producing the surprisingly stable complex $[(\mu\text{-}H)Cp_2Zr(SiHPh_2)]_2$ **(6)**, which is inactive in the hydrosilylation of olefins. This dimer was also found to be inert to acetone, PMe_3 or 3N HCl. X-ray analysis of the trapped $Cp_2Zr(H)(SiHPh_2)(PMe_3)$ complex shows similar geometry features to those of the complex $Cp_2Zr(H)(SiPh_3)(PMe_3)$, although the Zr−Si bond is shorter by 0.014 Å[15].

For titanium silyl complexes of the type $Cp_2Ti(SiHRPh)(PMe_3)$ (R = H, Me) the X-ray analysis shows similar geometries with close bond lengths of 2.652(1) Å (R = H) and 2.646(2) Å (R = Me), respectively[16]. Titanium complexes of the type $Cp_2M(SiHRR')L$ [L = NH_3, M = Ti(III); L = H, M = Ti(IV); R = aryl or alkyl; R′ = H, $RSiH_2$ or $(RSiH)_n$] have been found to induce the dehydrocoupling of ammonia and silanes as shown in Scheme 5[17].

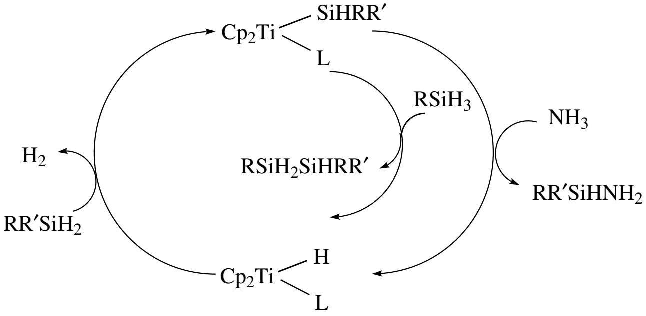

For Ti(IV), L = H; For Ti (III), L = NH_3, R = aryl, R′ = H, $RSiH_2$, $(RSiH)_n$

SCHEME 5

Although transition-metal silyl hydrides have been proposed as intermediates in the catalytic hydrosilylation of olefins and the polymerization of organosilanes, the complexes have been described classically as having η^1 or η^2 σ-bonds. The oxidative addition of Ph_2SiH_2 to $Cp_2Ti(PMe_3)_2$ produces the unstable complex $Cp_2Ti(Ph_2SiH_2)(PMe_3)$ **(7)** with an agostic hydrogen atom bridging the silyl−metal σ-bond. The complex decomposes to the binuclear species $[(\mu\text{-}(\eta^1:\eta^5\text{-}C_5H_4))(Cp)Ti(PMe_3)]_2$ and Ph_2SiH_2. The silane moiety in complex **7** is weakly bound and is readily displaced by nitrogen according to equation 5, leading to formation of the dinitrogen complex **8**. X-ray analysis of complex **7** shows a Ti−Si bond length of 2.597(2) Å, which is normal as compared to other titanocenes

(Table 1), although it displays a very interesting distorted trigonal bipyramid geometry at the silicon atom. The two hydrogens occupy the apical positions while the Ti and *ipso* carbons define the equatorial plane.

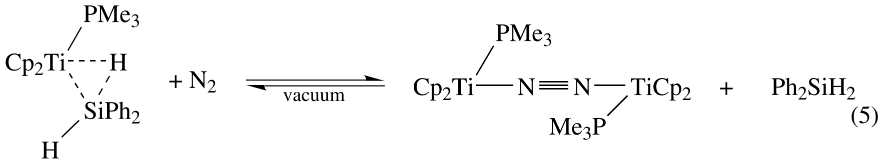

(5)

(7) **(8)**

^{29}Si NMR of **7** is consistent with a bridging hydrogen showing a doublet of doublets, indicating a coupling of two different hydrogens ($J_{\mathrm{SiH}_1} = 28$ Hz, $J_{\mathrm{SiH}_2} = 161$ Hz). The smaller value is slightly larger than the typical values observed for silyl-hydride complexes in which there is no interaction between Si and H[18].

Non-π-bound titanium amido silyl complex $(Me_2N)_3TiSi(SiMe_3)_3$ (Figure 2) was prepared from the titanium chloride complex $(Me_2N)_3TiCl$ with the corresponding lithium salt $(Me_3Si)_3SiLi{\bullet}3THF$. X-ray analysis shows a normal Ti−Si bond length of 2.635(2) Å[19].

The unsymmetrical silyl-hydrido zirconium dimer, $Cp_2Zr(SiPhMeH)(\mu\text{-}H)_2(SiPhMe_2)ZrCp_2$, similar to the above-mentioned complex **6**, was isolated from the dehydrogenative coupling reaction of phenylmethylsilane with dimethylzirconocene. The X-ray analysis of the dimer shows a disorder which is produced by the ordered superposition of two

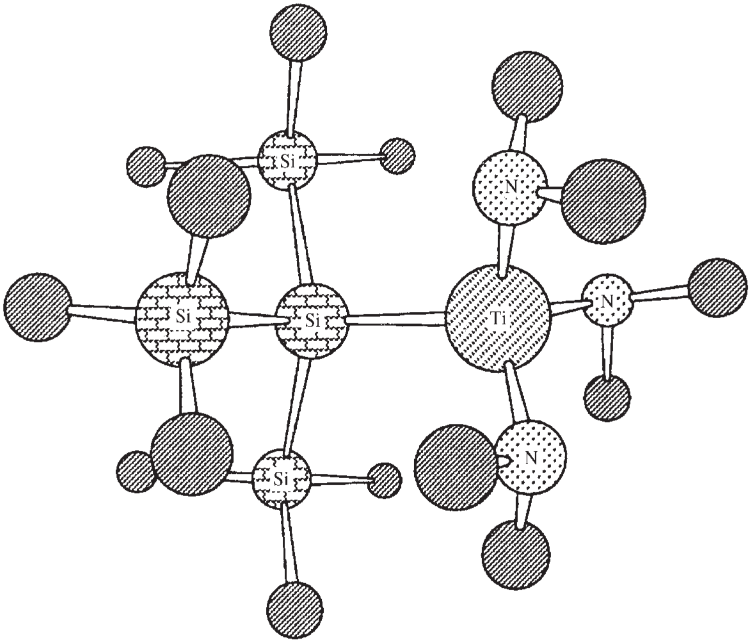

FIGURE 2. Structure view of $(Me_2N)_3TiSi(SiMe_3)_3$

enantiomers as shown in equation 6[13].

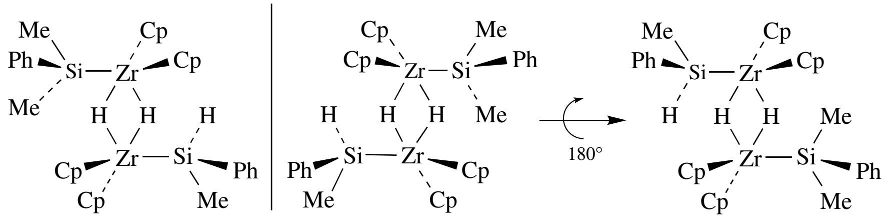

(6)

Group-4 monosilyl complexes of the types CpCp*M(SiPh$_3$)Cl and Cp$_2$*M(SiPh$_3$)Cl (M = Zr, Hf) were synthesized by the reaction of the corresponding metallocenes with Ph$_3$SiLi•3THF. These silyl complexes decompose slowly with a concomitant elimination of HSiPh$_3$. The decompositions in solution are accelerated in the light according to the following trends: CpCp*M(SiPh$_3$)Cl > Cp$_2$*M(SiPh$_3$)Cl; Hf > Zr. The reaction of complexes Cp$_2$*M(SiPh$_3$)Cl (M = Zr, Hf) with MeMgBr affords the corresponding methyl derivatives Cp$_2$*M(SiPh$_3$)Me (M = Zr, Hf) and hydrogenolysis of the triphenyl silyl complexes rapidly yield the corresponding hydrides with the elimination of HSiPh$_3$. Reaction of the mixed cyclopentadienyl complex CpCp*Hf(SiPh$_3$)Cl with one equivalent of PhSiH$_3$ under ambient fluorescent light afforded the σ-bond metathesis product CpCp*Hf(SiH$_2$Ph)Cl and the same reaction under ambient laboratory conditions produced the corresponding hydride and silane dehydrocoupling products. The reaction of a bis-cyclopentadienyl silyl complexes of Zr with CO and of a mixed cyclopentadienyl Hf complex with nitriles is shown in equations 7 and 8, respectively.

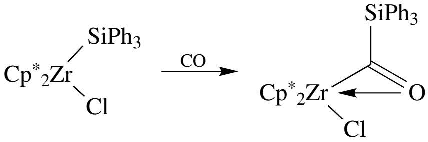

(7)

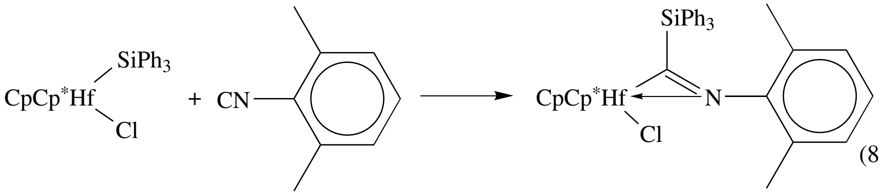

(8)

Interestingly, the Zr and Hf complexes, Cp$_2$*M(SiPh$_3$)Cl and CpCp*M(SiPh$_3$)Cl, were found not to react with acetylenes, ethylene, CS or phenyl isocyante[20]. σ-Bond metathesis reactions of Cp$_2$M(SiR$_3$)Cl (M = Zr, Hf; R = Me, SiMe$_3$) with PhSiH$_3$ yield the exchange products R$_3$SiH and Cp$_2$M(SiH$_2$Ph)Cl (M = Zr, Hf). The zirconium complexes rapidly combine with PhSiH$_3$ producing the polymeric hydride zirconium [CpZrHCl]$_n$, PhH$_2$Si−SiH$_2$Ph and PhH$_2$Si−SiHPh−SiH$_2$Ph. In contrast, similar reactions of the mixed cyclopentadienyl hafnium complex CpCp*Hf(Si(SiMe$_3$)$_3$)Cl (**9**) with hydrosilanes RR′SiH$_2$ under fluorescent room lighting cleanly gave the corresponding silyl derivatives CpCp*Hf(SiHRR′)Cl [SiHRR′ = SiH$_2$Ph, SiH$_2$(C$_6$H$_4$Me-*p*), SiH$_2$(C$_6$H$_4$OMe-*p*), SiH$_2$(C$_6$H$_4$F-*p*), SiH$_2$Mes, SiH$_2$CH$_2$Ph, SiH$_2$CH$_2$Cy, SiHPh$_2$, SiHPhMe and SiHPhSiH$_2$Ph]. The last two complexes are obtained as a 7:5 and 1:1

mixture of diastereomers, respectively. Reaction of complex **9** with 0.5 equivalent of the 1,4-bis(silyl)benzene affords the bimetallic silyl complex **10** through the monohafnium intermediate (equation 9).

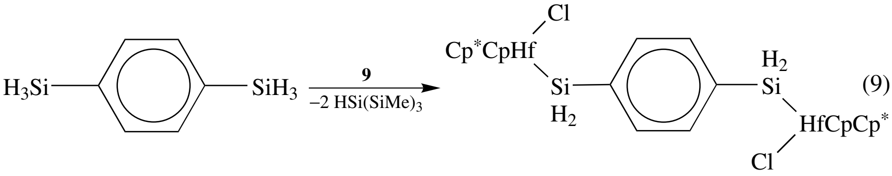

(10)

Following the course of equation 9, a bimetallic thiophene complex 2,5-$[CpCp^*Hf(SiH_2)Cl]_2C_4H_2S$ can be similarly obtained. The Hf−Cl bonds in the bimetallic complex are *trans* to one another, producing one set of diastereomeric SiH_2 protons as observed in the ^1H NMR spectrum (Table 2).

In the dark, the mixed cyclopentadienyl complex $CpCp^*Hf(SiH_2Ph)Cl$ reacts with another mixed complex, $CpCp^*Hf(SiH_2(C_6H_4Me\text{-}p))Br$, yielding an equilibrating mixture of the exchanged halide complexes. Similarly, the σ-bond metathesis of $CpCp^*Hf(SiH_2Ph)Cl$ with hydrosilanes leads to an equilibrium mixture of the silyl-exchanged complexes. The reactions in the dark are slower although well behaved. The σ-bond metathesis reaction of **9** with $PhSiH_3$ follows a second-order rate law (rate $= k[\mathbf{9}][PhSiH_3]$), showing a kinetic isotope effect $\{k(PhSiH_3)/k(PhSiD_3)\}$ of 2.5, arguing in favor of a four-center transition state. Under fluorescent room lighting, the reactions are very sensitive to the bulk of the silane and to low concentration of Lewis acids, indicating that in these photochemical σ-bond metathesis reactions, a reactive coordinatively unsaturated intermediate is involved. Reactions of complex **9** with alkoxyhydrosilanes $HSi(OMe)_2R''$ provides a route to the new complex $CpCp^*Hf(SiH_2Me)Cl$ when $R'' =$ Me and $CpCp^*Hf(SiH_3)Cl$ when $R'' =$ OMe. This reaction proceeds through initial metal-catalyzed redistribution of the alkoxyhydrosilanes, $3HSi(OMe)_2R'' \rightleftharpoons R''SiH_3 + 2R''Si(OMe)_3$, followed by trapping of the new hydrosilane by complex **9**[21].

X-ray analysis of complex **9** shows two independent molecules in the unit cell. The Hf−Si bonds of 2.881(4) Å and 2.888(4) Å are longer than those found in other d^0 Zr−Si derivatives (Table 1), reflecting the steric hindrance in **9.** The crystal structure of the mixed cyclopentadienyl complex $CpCp^*Hf(SiH_2Ph)Cl$ reveals a Hf−Si bond length of 2.729(3) Å, which is shorter than in **9**, presumably due to a lower steric interaction between the silyl ligand and the bulky Cp*[21]. In a very elegant way, Tilley and coworkers have shown by kinetic studies and the structure of the derived polymers that polysilyl and hydride complexes of early-transition metals are intermediates in the dehydrogenative coupling of silanes by the σ-bond metathesis mechanism. Thus, $CpCp^*Hf[Si(SiMe_3)_3]Me$, which is prepared by the reaction of $CpCp^*Hf[Si(SiMe_3)_3]Cl$ with MeMgBr, reacts with silanes to yield the corresponding hydride complexes and the dehydrogenative coupling product of silanes as shown in equation 10[22]. The σ-bond metathesis mechanism proposed by Tilley is shown in Scheme 6[23].

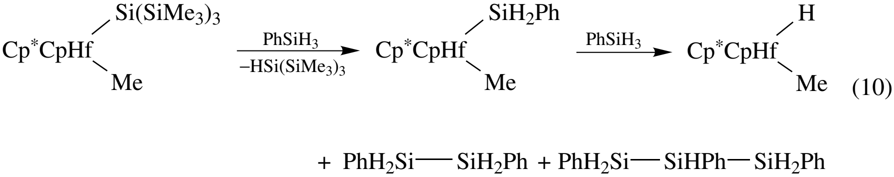

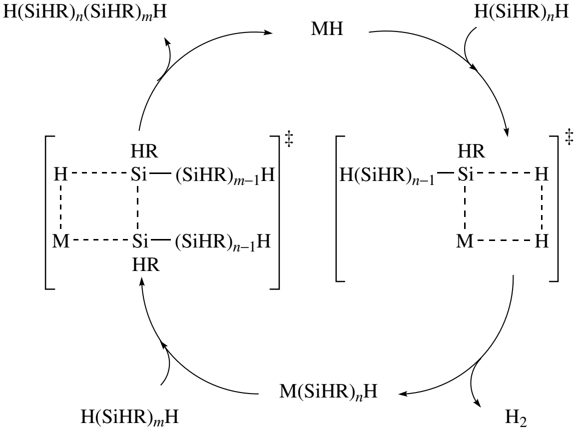

SCHEME 6

Interestingly, the complexes CpCp*Hf(SiHPhSiHPhSiH$_2$Ph)Cl and CpCp*Hf(SiHPh SiH$_2$Ph)Cl are observed to form concurrently with the small polysilanes. It seems that these complexes are not necessarily the intermediates in the dehydrogenative process as suggested in Scheme 6, but perhaps only side products formed via non-productive σ-bond metathesis reactions (equation 11)[22].

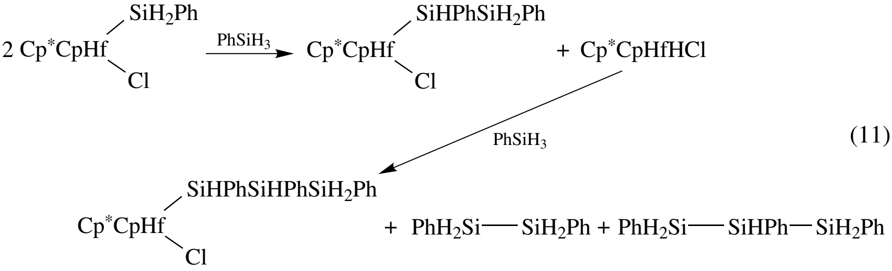

(11)

Cationic silicenium complexes of zirconium, **11** and **12**, have also been observed as intermediates in the high molecular weight dehydrogenative coupling of phenylsilanes. The cation-like structure is formed by the reaction of the corresponding zirconocene dichloride complexes with BuLi, $(C_6F_5)_3B$ and PhSiH$_3$. The incorporation of $(C_6F_5)_3B$ into the catalytic system reduces the overall activity of the catalyst, and strongly suppresses the ring formation. Special features of the complexes **11** and **12** are the silicenium-like ligand (^{29}Si $\delta = 106-108$ ppm) and the diastereotopic hydride presence in **12** suggesting that silicon is chiral[24].

Besides the σ-bond metathesis mechanism proposed by Tilley[23] for the dehydrogenative coupling of silanes, a Zr(II) pathway[25] and a silylene mechanism[26] have been proposed based on the nature of the products. The dehydrogenative polymerization of 1,2,3-trimethyltrisilane or of a mixture of diastereomers of 1,2,3,4-tetramethyltetrasilane showed evidence that, besides Tilley's mechanism, a further mechanism is present. The product formation can be explained by a silylene mechanism where the silylenes are formed by α-elimination from the silyl complexes by a new type of β-elimination which involves Si−Si bond cleavage (β^*-bond elimination) as described in Scheme 7[27].

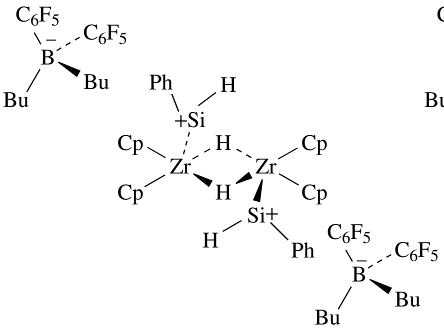

(11)

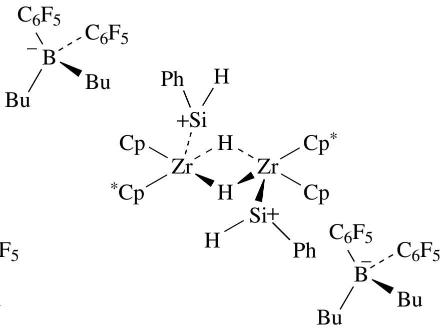

(12)

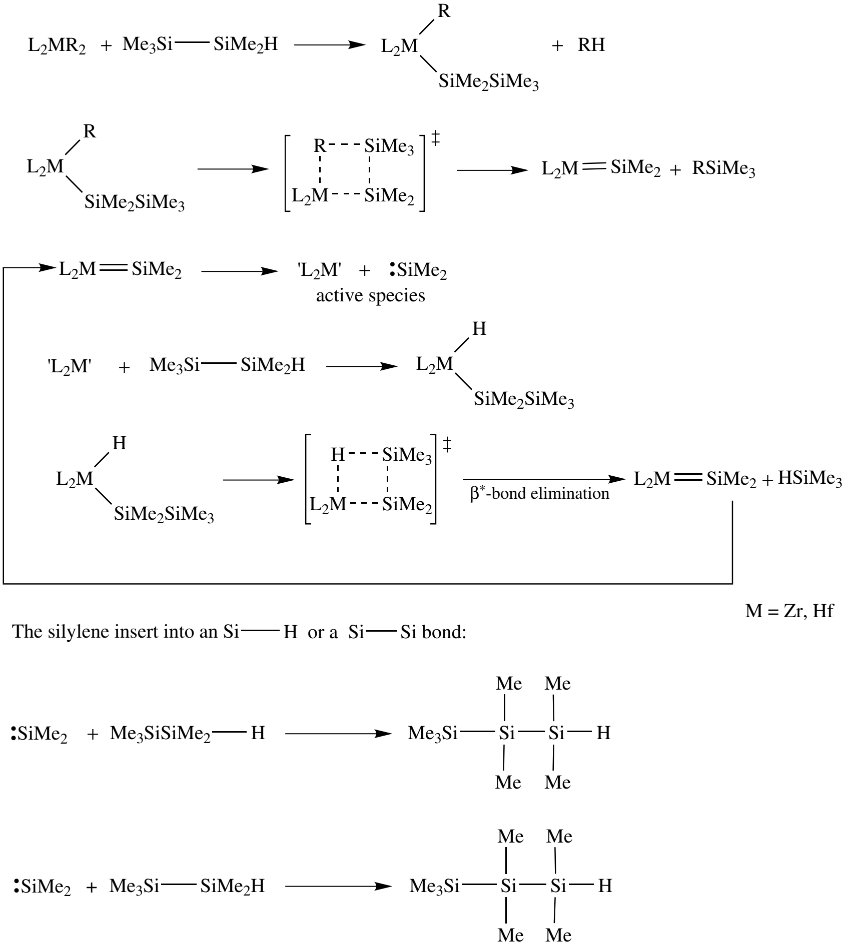

The silylene insert into an Si—H or a Si—Si bond:

SCHEME 7

The silyl chloride complex (η^5-$C_5H_4SiMe_3)_2Zr[Si(SiMe_3)_3]Cl$ and the silyl–tin chloride complexes $Cp_2M[Si(SnMe_3)_3]Cl$ (M = Ti, Zr, Hf) were prepared from the corresponding metallocene dichlorides with the corresponding silyl lithium reagent. Concomitant methylation to the methyl complexes is obtained by use of the methyl Grignard reagent. The molecular structure for the two Zr chloride complexes shows Zr−Si distances of 2.833(3) Å and an average of 2.768(4) Å for the $Zr-Si(SnMe_3)_3$ derivatives, respectively. The shorter Zr−Si in the latter compound presumably reflects a lower steric crowding. The complex (η^5 - $C_5H_4SiMe_3)_2$ $Zr[Si(SiMe_3)_3]Cl$ has been found to be an effective catalyst for the dehydropolymerization of $PhSiH_3$ and n-Bu_2SnH_2 to low molecular weight polymers. In as much as the complexes $Cp_2M[Si(SnMe_3)_3]Cl$ (M = Zr, Hf) do not react with CO, the Ti analog complex undergoes a CO-induced reductive elimination to $Cp_2Ti(CO)_2$ and $ClSi(SnMe_3)_3$[28]. Interestingly, theoretical studies on these Schrock-type silylidene complexes shows that, if formed, these complexes consist of contributions of the σ- and π-covalent, dative and back-bonding resonance structures based on the corresponding metal[29].

η^2-Silanimine complex $Cp_2Zr(\eta^2$-$Me_2Si{=}NBu$-$t)(PMe_3)$ (**13**) was obtained by addition of $LiCH_2SiMe_3$ to $Cp_2Zr(N(Bu$-$t)SiMe_2H)I$ in the presence of PMe_3. The η^2-bond ligation results from the intermolecular elimination of $SiMe_4$ from $Cp_2Zr(CH_2SiMe_3)(N(Bu$-$t)SiMe_2H)$. The structure of $Cp_2Zr(\eta^2$-$Me_2Si{=}NBu$-$t)(PMe_3)$ reveals short Zr−Si [2.654(1) Å] and long Si−N [1.687(3) Å] distances, suggesting the importance of the metallacyclic, Zr(IV) resonance form[30]. The preparation of complex **13** and its reaction with carbon monoxide, hydrogen, ethylene and ketene are shown in Scheme 8[31–33]. Reaction of η^2-silanimine complexes $Cp_2Zr(\eta^2$-$Me_2Si{=}NBu$-$t)(L)$ (L = CO, PMe_3) with CO_2 leads to a net oxygen insertion into the Zr−Si bond. The products are CO, and the dimeric oxazirconacycle [*cyclo*-$Cp_2Zr(OSiMe_2NBu$-$t)]_2$. Low-temperature ^1H and ^{13}C {H} NMR studies *in situ* allowed the observation of the *cyclo*-$Cp_2Zr[OC(=O)SiMe_2NBu$-$t]$ as the initial intermediate formed by the insertion of one of the C=O double bonds into the Zr−Si bond of $Cp_2Zr(\eta^2$-$Me_2Si{=}NBu$-$t)(L)$. Concomitant decarboxylation of the *cyclo*-$Cp_2Zr[OC(=O)SiMe_2NBu$-$t]$ at room temperature and dimerization leads to the oxazirconacycle complex [*cyclo*-$Cp_2Zr(OSiMe_2NBu$-$t)]_2$. Carbon disulfide was found to react with **13**, yielding the monomeric four-membered metallacycle complex *cyclo*-$Cp_2Zr(SSiMe_2NBu$-$t)$. Interestingly, the analog carbonyl monosulfide leads to a mixture of the oxygen and sulfur atom insertion products, as shown in equation 12[32].

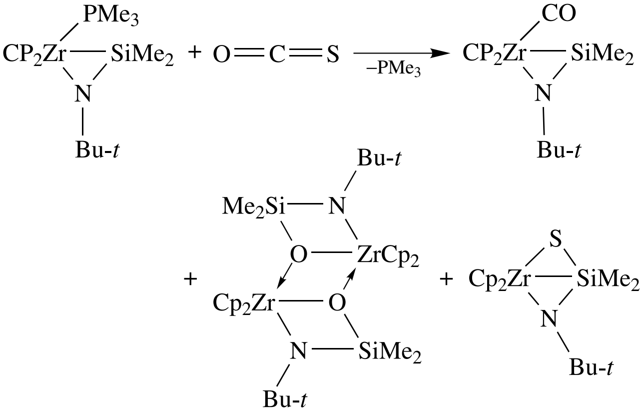

(12)

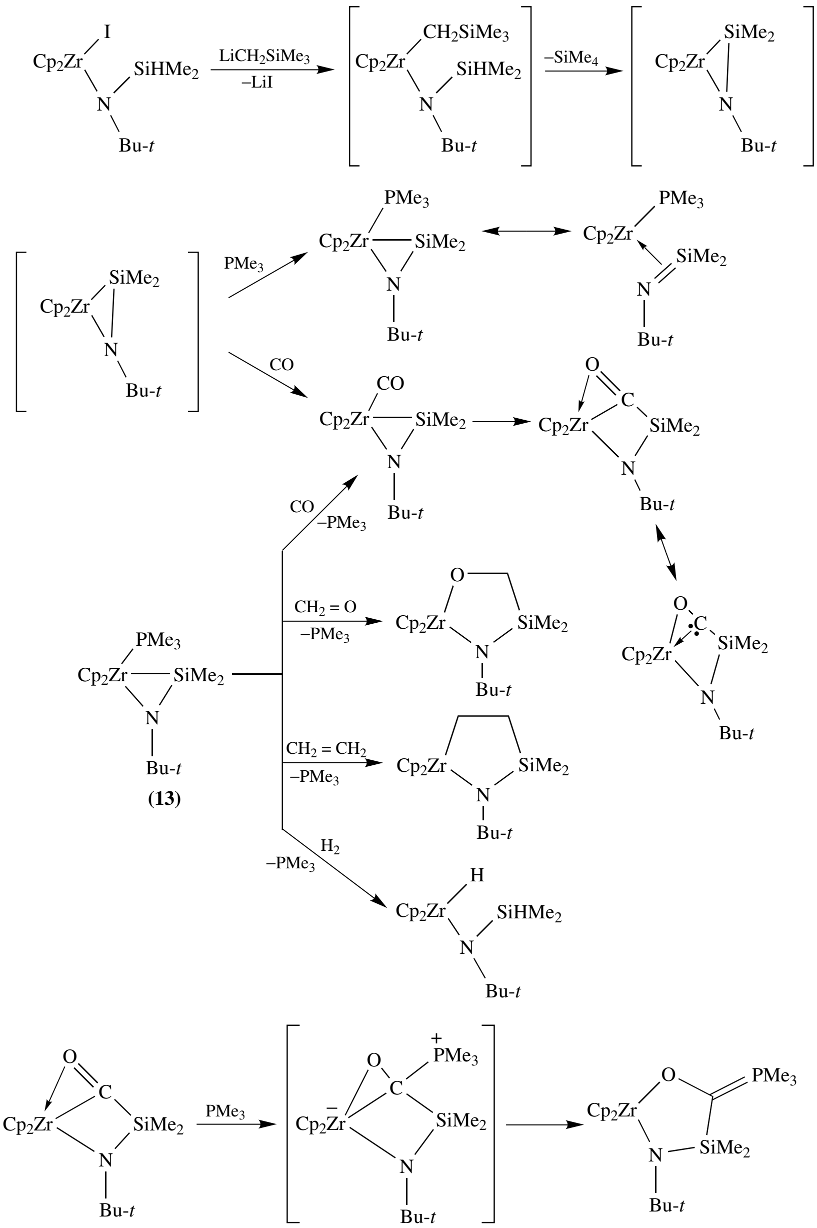

SCHEME 8

Reaction of $Cp_2Ti(\eta^2\text{-}Me_3SiC{\equiv}CSiMe_3)$ with $t\text{-}BuC{\equiv}CSiMe_2H$ in hexane leads to the alkyne substitution. The titanocene complex shows a temperature-dependent Si−H−Ti interaction as demonstrated by IR spectroscopy. This agostic interaction is ascertained by the ^{29}Si NMR (193 K) spectrum showing a signal at $\delta = 17.6$ ppm ($\delta = -0.5$ ppm at 303 K) with a coupling constant J_{SiH} of 93 Hz ($J_{\text{SiH}} = 123$ Hz at 303 K) compared with the J_{SiH} of 199 Hz of the free alkyne, indicating that the Ti−H bond formation is not complete and that the Si−H bond is not fully broken. The solid structure of the titanium complex reveals normal distances for the Ti−H [1.82(5) Å], Si−H [1.42(6) Å] and Ti−Si [2.655(2) Å] bonds. The symmetrical $Cp_2Ti(\eta^2\text{-}HMe_2SiC{\equiv}CSiMe_2H)$ which was obtained in a similar way carries two Si−H functions, exhibiting a dynamical behavior showing a 'flip-flop' coordination[34].

Free of anionic π-ligands, the bulky monomeric silyl complex $Np_3ZrSi(SiMe_3)_3$ (Np = neopentyl) has been prepared by the metathesis of Np_3SiCl with $(Me_3Si)_3SiLi{\cdot}3THF$. Interestingly, ^{29}Si {H} NMR of the complex exhibits a large upfield shift of the Zr−Si signal to −7.64 ppm (Table 2)[35].

TABLE 1. Selected M−Si distances in group-4 transition-metal silyl complexes

Compound	d^n Configuration	M−Si (Å)	Reference
$Cp_2Zr(H)(SiPh_3)(PMe_3)$	d^0	2.721(2)	14
$Cp_2Zr(H)(SiHPh_2)(PMe_3)$	d^0	2.707(5)	15
$[Cp_2Zr(\mu\text{-}H)(SiHPh_2)]_2$	d^0	2.759(8)	15
$Cp_2Zr(SiPhMeH)(\mu\text{-}H)_2(SiPhMe_2)ZrCp_2$	d^0	2.806(4)	13
$CpCp^*Hf[Si(SiMe_3)_3]Cl$	d^0	2.881(4), 2.888(4)	21
$CpCp^*Hf(SiH_2Ph)Cl$	d^0	2.729(3)	21
$Cp_2Ti(SiH_2Ph)PMe_3$	d^1	2.650(1)	16
$Cp_2Ti(SiHMePh)PMe_3$	d^1	2.646(2)	16
$[\eta_5\text{-}C_5H_4SiMe_3)_2Zr[Si(SiMe_3)_3Cl]$	d^0	2.833(4)	28
$Cp_2Zr[Si(SnMe_3)_3Cl]$	d^0	2.772(4), 2.765(4)	28
$Cp_2Ti(SiH_2Ph)PMe_3$	d^1	2.597(2)	18
$(Me_2N)_3TiSi(SiMe_3)_3$	d^0	2.635(2)	19
$Cp_2Zr(\eta^2\text{-}Me_2Si{=}NBu\text{-}t)(PMe_3)$	d^0	2.654(1)	31
$Cp_2Zr(\eta^2\text{-}Me_2Si{=}NBu\text{-}t)(CO)$	d^0	2.706(1)	30
$Cp_2Ti(\eta^2\text{-}(t\text{-}Bu)C{\equiv}CSiMe_2H)$	d^0	2.655(2)	34

TABLE 2. Selected ^{29}Si NMR chemical shifts for group-4 transition-metal silyl complexes[a]

Compound	^{29}Si NMR shift (ppm)	Reference
$Cp_2Zr(H)(SiPh_3)(PMe_3)$	39.48 ($^2J_{\text{SiP}} = 15$ Hz)	14
$Cp_2Zr(H)(SiHPh_2)(PMe_3)$	50.46	14
$CpCp^*Zr(SiPh_3)Cl$	42.42	20
$CpCp^*Hf(SiPh_3)Cl$	39.96	20
$Cp_2^*Zr(SiPh_3)Cl$	47.34	20
$Cp_2^*Hf(SiPh_3)Cl$	42.86	20
$CpCp^*Zr[Si_a(Si_bMe_3)_3]Cl$	−87.30 (Si_a); −6.03 (Si_b)	21
$CpCp^*Hf[Si_a(Si_bMe_3)_3]Cl$	−77.87 (Si_a); −4.85 (Si_b)	21
$CpCp^*Zr(SiH_2Ph)Cl$	−14.33 ($^1J_{\text{SiH}} = 144$ Hz)	21

(*continued overleaf*)

TABLE 2. (*continued*)

Compound	^{29}Si NMR shift (ppm)	Reference
$\mathrm{CpCp^*Hf(SiH_2Ph)Cl}$	$1.49\ (^1J_{\mathrm{SiH}} = 155\ \mathrm{Hz})$	21
$\mathrm{CpCp^*Hf[SiH_2(Tol\text{-}}p\mathrm{)]Cl}$	$1.46\ (^1J_{\mathrm{SiH}} = 157\ \mathrm{Hz})$	21
$\mathrm{CpCp^*Hf[SiH_2(Tol\text{-}}p\mathrm{)]Br}$	$7.74\ (^1J_{\mathrm{SiH}} = 153\ \mathrm{Hz})$	21
$\mathrm{CpCp^*Hf[SiH_2(C_6H_4OMe\text{-}}p\mathrm{)]Cl}$	$1.56\ (^1J_{\mathrm{SiH}} = 169\ \mathrm{Hz})$	21
$\mathrm{CpCp^*Hf[SiH_2(C_6H_4F\text{-}}p\mathrm{)]Cl}$	$1.17\ (^1J_{\mathrm{SiH}} = 160\ \mathrm{Hz})$	21
$\mathrm{CpCp^*Hf[SiH_2(Mes)]Cl}$	$1.50\ (^1J_{\mathrm{SiH}} = 157\ \mathrm{Hz})$	21
$\mathrm{CpCp^*Hf(SiH_2CH_2Ph)Cl}$	$9.69\ (^1J_{\mathrm{SiH}} = 153\ \mathrm{Hz})$	21
$\mathrm{CpCp^*Hf(SiH_2Cy)Cl}$	$14.83\ (^1J_{\mathrm{SiH}} = 145\ \mathrm{Hz})$	21
$\mathrm{Cp_2Hf(SiH_2Cy)Cl}$	$11.07\ (^1J_{\mathrm{SiH}} = 149\ \mathrm{Hz})$	21
$\mathrm{CpCp^*Hf(SiHPh_2)Cl}$	$32.25\ (^1J_{\mathrm{SiH}} = 158\ \mathrm{Hz})$	21
$\mathrm{Cp_2Hf(SiHPh_2)Cl}$	$31.88\ (^1J_{\mathrm{SiH}} = 148\ \mathrm{Hz})$	21
$\mathrm{CpCp^*Zr(SiPh_3)Cl}$	42.42	21
$\mathrm{CpCp^*Hf(SiPh_3)Cl}$	39.96	21
$\mathrm{CpCp^*Hf(SiHPhMe)Cl}$	$21.75\ (^1J_{\mathrm{SiH}} = 153\ \mathrm{Hz})$	21
(diastereomers)	$25.10\ (^1J_{\mathrm{SiH}} = 153\ \mathrm{Hz})$	
$\mathrm{CpCp^*Hf(Si_aHPhSi_bH_2Ph)Cl}$	$-9.05\ (\mathrm{Si_a};\ ^1J_{\mathrm{SiH}} = 152\ \mathrm{Hz})$	21
(diastereomers)	$-9.86\ (\mathrm{Si_a};\ ^1J_{\mathrm{SiH}} = 152\ \mathrm{Hz})$	
	$-43.91\ (\mathrm{Si_b};\ ^1J_{\mathrm{SiH}} = 183\ \mathrm{Hz})$	
	$-50.43\ (\mathrm{Si_b};\ ^1J_{\mathrm{SiH}} = 183\ \mathrm{Hz})$	
$\mathrm{CpCp^*Hf\ (SiH_2C_6H_4SiH_3\text{-}}p\mathrm{)Cl}$	$1.16\ (\mathrm{Si_a};\ ^1J_{\mathrm{SiH}} = 162\ \mathrm{Hz})$	21
	$-63.10\ (\mathrm{Si_b};\ ^1J_{\mathrm{SiH}} = 199\ \mathrm{Hz})$	
$\mathrm{2,5\text{-}[CpCp^*Hf\ (Cl)\ SiH_2]_2\ C_4H_2S}$	$-14.09\ (^1J_{\mathrm{SiH}} = 158\ \mathrm{Hz})$	21
$\mathrm{CpCp^*Hf\ (SiH_2CH_3)Cl}$	$-7.36\ (^1J_{\mathrm{SiH}} = 149\ \mathrm{Hz})$	21
$\mathrm{CpCp^*Hf\ (SiH_3)Cl}$	$-46.52\ (^1J_{\mathrm{SiH}} = 156\ \mathrm{Hz})$	21
$\mathrm{Cp_2Hf\ [Si(SnMe_3)_3Cl]}$	$7.61\ (^1J_{\mathrm{SiSn}} = 130.7\ \mathrm{Hz})$	28
$\mathrm{Cp_2Zr[Si(SnMe_3)_3Cl]}$	$1.88\ (^1J_{\mathrm{SiSn}} = 119.6\ \mathrm{Hz})$	28
$\mathrm{Cp_2Ti(SiH_2Ph)PMe_3}$	$49.90\ (^1J_{\mathrm{SiH}} = 161; 28\ \mathrm{Hz})$	18
$\mathrm{[Cp_2Zr(SiHPh)(\mu\text{-}H)]_2{}^{2+}\ [Bu_2(C_6F_5)_2B]_2{}^{2-}}$	108.04	24
$\mathrm{[CpCp^*Zr(SiHPh)(\mu\text{-}H)]_2{}^{2+}\ [Bu_2(C_6F_5)_2B]_2{}^{2-}}$	106.0	24
$\mathrm{Cp_2Zr(}\eta^2\mathrm{\text{-}Me_2Si{=}NBu\text{-}}t\mathrm{)(CO)}$	$69.9\ (^1J_{\mathrm{SiC}} = 24\ \mathrm{Hz})$	30
$\mathrm{Cp_2Ti(}\eta^2\mathrm{\text{-}(}t\mathrm{\text{-}Bu)C{\equiv}CSiMe_2H)}$	$-0.5\ (^1J_{\mathrm{SiH}} = 123\ \mathrm{Hz\ at\ 303\ K})$	34
	$17.6\ (^1J_{\mathrm{SiH}} = 93\ \mathrm{Hz\ at\ 193\ K})$	
$\mathrm{Cp_2Ti(}\eta^2\mathrm{\text{-}HMe_2SiC{\equiv}CSiMe_2H)}$	$0.46\ (^1J_{\mathrm{SiH}} = 147\ \mathrm{Hz\ at\ 303\ K})$	34
$\mathrm{Np_3ZrSi_a(Si_bMe_3)_3}$[b]	$-7.64\ (\mathrm{Si_a});\ -85.77\ (\mathrm{Si_b})$	35

[a] Reporting ^{29}Si NMR data for transition-metal silyl complexes is now a routine. Although some trends have emerged, it is sometimes difficult to interpret satisfactorily the meaning of chemical shift data. However, ^{29}Si NMR spectroscopy can be very useful in cases where coupling constants can be obtained, or where comparison among closely related systems is possible.

[b] Np = neopentyl.

VI. ACTINIDE SILYL COMPLEXES

For reasons that are currently unclear, actinide silyl complexes have proven very difficult to isolate, with the first reported success being Cp_3USiPh_3[36]. Similarly, $Cp_3USi(TMS)_3$ has been prepared by the metathesis reaction of $(Me_3Si)_3SiLi{\bullet}3THF$ with the corresponding Cp_3UCl. The uranium–silicon bond dissociation enthalpies have been measured to be as low as *ca* 37 ± 3 $kcal\,mol^{-1}$, arguing presumably for the high reactivity of the actinide–silyl bonds[37]. Recently, use of the benzamidinate ancillary ligands, which are regarded as cyclopentadienyl equivalents, allows the preparation of thorium and uranium silyl complexes as described in equation 13. These benzamidinate complexes were found to be active for the dehydrogenative coupling of $PhSiH_3$[38].

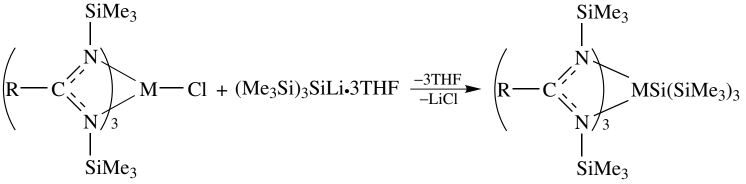

(13)

R = 4-MeC_6H_4
R = Ph
M = Th, U

Recently, double insertion of CO into the reactive thorium–silicon bond of $Cp_2{}^*ThSiR_3(Cl)$ allowed the isolation of the first metalloxy ketene complex **14**. Reactivity studies of complex **14** are described in Scheme 9[39].

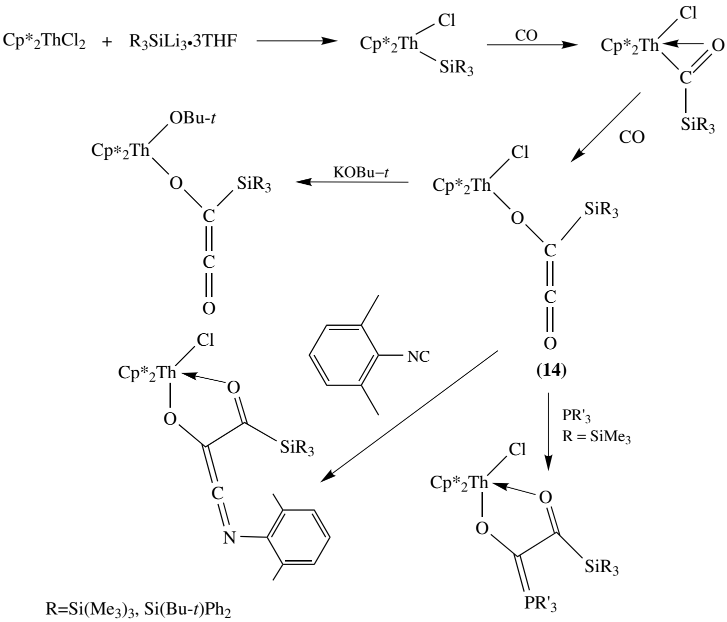

R=$Si(Me_3)_3$, Si(Bu-*t*)Ph_2
PR'_3=PMe_3, $PMePh_2$

SCHEME 9

VII. GROUP-5 SILYL COMPLEXES

Organosilicon complexes of group-5 metals are among the most recently explored in the transition-metal series. The first vanadium silyl compound was reported in 1976[40], whereas the first niobium and tantalum silyl complexes were reported only in 1985[41]. The two most common methods for preparing metal–silicon bonds are: (1) Salt elimination reactions, starting either from halosilanes and an anionic metal complex or from a metal halide and the corresponding anionic silyl derivative. (2) Oxidative addition of hydrosilanes to coordinatively unsaturated transition-metal complexes. The latter route has been widely applied for the synthesis of late-transition-metal silyl complexes and was recently developed to prepare group-5 silyl complexes by the direct reaction of hydrosilanes with tantalum complexes. Thus, thermolysis (>100 °C) of Cp_2TaH_3 or photolysis (350 nm) of $Cp_2Ta(L)H$ ($L = CO$, PMe_3, ethylene) in the presence of hydrosilanes ($HSiR_3$) affords the corresponding tantalum silyl dihydrides $Cp_2Ta(H)_2(SiR_3)$ [$SiR_3 = SiH_3$, $SiMeH_2$, $SiMe_2H$, $SiMe_3$, $SiMe_2Cl$ and $Si(OMe)_3$]. The proposed mechanism for the formation of these tantalum complexes involves, at the first step, the formation of the coordinatively unsaturated hydride which undergoes the oxidative addition as shown in equation 14.

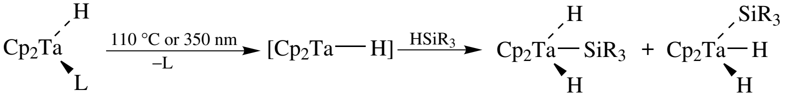

(14)

^1H NMR spectroscopy shows that both isomers interconvert in solution with an isomerization rate for SiR_3 which follows the trend $SiH_3 \approx SiMe_2Cl < Si(OMe)_3 \approx SiMeH_2 < SiMe_2H < SiMe_3$[42]. Bis(silyl) complexes of Ta(V) $Cp_2Ta(H)(SiR_3)_2$ [$SiR_3 = SiMeH_2$, $SiMe_2H$, $SiMe_3$, $SiMe_2Cl$ and $Si(OMe)_3$] were prepared by the reaction of the Ta(III) complex $Cp_2Ta(L)(CH_3)$ ($L = PMe_3$, ethylene) with an excess of the corresponding hydrosilane $HSiR_3$ under photolytic or thermolytic conditions. The predominant isomer observed is the symmetrical one with the two silyl groups occupying the two equivalent lateral positions. The mechanism for the bis(silyl) complex formation can be explained in terms of simple oxidative addition and reductive elimination steps as described in Scheme 10. A thermal or photolytic activation of the ligand L from $Cp_2Ta(L)Me$ to the 16-electron intermediate **15**, followed by oxidative addition of $HSiR_3$ to **16**, could give the two rapidly interconverting isomers **16** and **17**. Reductive elimination of methane from **17** and subsequent oxidative addition of a second $HSiR_3$ molecule would yield the bis(silyl) product.

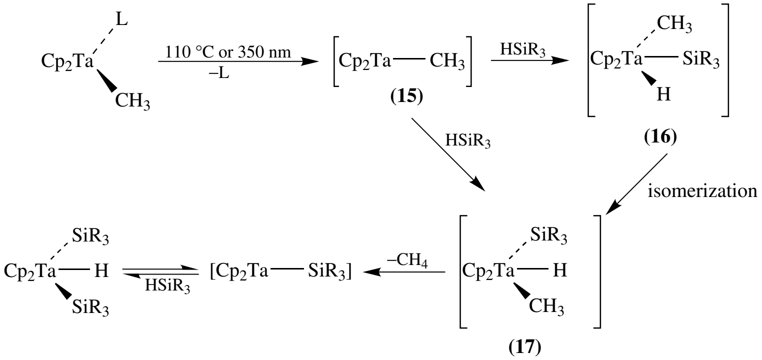

SCHEME 10

Tantalum(III) silyl complexes of the type $Cp_2Ta(PMe_3)(SiR_3)$ [$SiR_3 = SiMeH_2$, $SiMe_3$, $SiMe_2Cl$ and $Si(OMe)_3$] have been prepared from the corresponding bis(silyl) compounds by thermolysis in the presence of a phosphine (equation 15). In addition, the $Cp_2Ta(PMe_3)$ [$SiH(Bu\text{-}t)_2$] complex has been prepared in a one-pot synthesis from $Cp_2Ta(PMe_3)Me$ and large excess of $H_2Si(Bu\text{-}t)_2$ under 350-nm radiation. The reaction should be performed in non-aromatic solvents since the silyl complex induces a C−H activation of arenes[42].

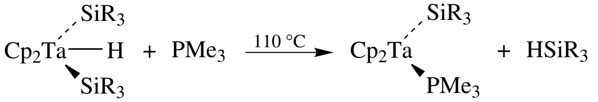

$$\mathrm{Cp_2Ta(SiR_3)_2H} + \mathrm{PMe_3} \xrightarrow{110\,^{\circ}\mathrm{C}} \mathrm{Cp_2Ta(SiR_3)(PMe_3)} + \mathrm{HSiR_3} \qquad (15)$$

Interestingly, thermodynamic studies on the bond dissociation energies of $Cp_2Ta(PMe_3)(SiH(Bu\text{-}t)_2)$ and $Cp_2Ta(PMe_3)(SiMe_3)$ which react in neat arenes (ArH) to produce the C−H activation complex $Cp_2Ta(PMe_3)Ar$ have shown that the Ta−Si bonds in these two complexes are respectively 5.4 and 7.9 $\mathrm{kcal\,mol^{-1}}$ weaker than the Ta−Ph bond in $Cp_2Ta(PMe_3)Ph$. However, metal−phenyl bonds are generally much stronger than metal−alkyl bonds and the Ta−Si bond dissociation energies (BDE) are probably similar to or greater than those of the tantalum−alkyl bonds. For the tantalum−silyl complexes, the bulkier silyl exhibits the lower Ta−Si BDE, but surprisingly the lower stability of $Cp_2Ta(PMe_3)(SiH(Bu\text{-}t)_2)$ with respect to the phenyl complex $Cp_2Ta(PMe_3)Ph$ is primarily due to a large and favorable entropy change (34 ± 3 eu) resulting from the reduction of steric congestion upon converting the silyl into the phenyl complex[43]. The phosphine ligand in the Ta(III) complexes $Cp_2Ta(PMe_3)(SiR_3)$ [$SiR_3 = SiMe_3$, $SiH(Bu\text{-}t)_2$] can be replaced by CO, either by thermolysis or by photolytic cleavage, yielding the corresponding $Cp_2Ta(CO)(SiR_3)$ [$SiR_3 = SiMe_3$, $SiH(Bu\text{-}t)_2$] complexes.

Solid state structures of $Cp_2TaH(SiMe_2H)_2$ and $Cp_2Ta(PMe_3)SiMe_3$ show normal Ta−Si bond lengths of 2.633(2) Å and 2.624(2) Å for the former complex and 2.639(4) Å for the latter complex (Table 3)[42]. In addition, for the carbon monoxide analog, $Cp_2Ta(CO)(SiMe_3)$, a similar bond length of 2.631(2) Å was found[32]. Regarding the structural similarities and ignoring the hydride, all the molecules exhibit tetrahedral geometries which are typical for bent metallocene complexes. Solid structures for the sterically hindered silyl tantalum complexes $Cp_2Ta(PMe_3)(SiH(Bu\text{-}t)_2)$ and $Cp_2Ta(Co)(SiH(Bu\text{-}t)_2)$ exhibit bond lengths of 2.740(1) Å and 2.684(1) Å, respectively. It is noteworthy that the Ta−Si bond lengths in the two di-*tert*-butyl silyl complexes are quite different and that the more electron-rich phosphine complex exhibits the longer distance whereas the ^{29}Si NMR chemical shifts of both complexes are similar (Table 4).

Monosilyl complexes of niobium of the type $Nb(\eta^5\text{-}C_5H_4SiMe_3)_2H_2(SiR_3)$ ($SiR_3 = SiMe_2Ph$, $SiMePh_2$, $SiPhH_2$, $SiPh_2H$, $SiPh_3$) have been obtained by the thermolytic reaction of $Nb(\eta^5\text{-}C_5H_4SiMe_3)_2H_3$ with the corresponding organosilicon hydride. In all cases only the isomer with the silyl group in the central equatorial position was obtained. The Nb−Si bond length of 2.616(3) Å in the molecular structure of $Nb(\eta^5\text{-}C_5H_4SiMe_3)_2)_2H_2$ $(SiPh_2H)$ is *ca* 0.016 Å shorter than in similar Ta(V) complexes (Table 3), and in agreement with the corresponding ionic radius[44].

Niobium bis(silyl) complexes of the type $Cp_2Nb(SiMe_2X)_2H$ (X = Cl, Ph) have been prepared by the oxidative addition of $HSiMe_2X$ to the corresponding monoalkylniobocene $Cp_2NbCH_2CH_2Ph$. The structures of the bis(silyl)niobocene complexes are isostructural and exhibit the typical trisubstituted geometry. In $Cp_2Nb(SiMe_2Cl)_2H$ the Nb−Si bond lengths are 2.584(5) Å and 2.611(5) Å. Those distances were found to be shorter than in the $Cp_2Nb(SiMe_2Ph)_2H$ derivative, with Nb−Si bond lengths of 2.646(5) Å and 2.665(5) Å, respectively. The short Nb−Si and the long Si−Cl distances found in the former complex have been explained as due to interaction of 5c–6e hypervalent ligand Cl•••Si•••H•••Si•••Cl[45].

Reaction of the tantalum(III) complex $Cp_2Ta(PMe_3)(Si(Bu\text{-}t)_2H)$ with 2 equivalents of an amine-borane adduct, $L{\bullet}BH_3$ ($L = Et_3N$, N-methylmorpholine), results in the formation of the silyl substituted η^2-borohydride complex $Cp_2Ta\{\eta^2\text{-}BH_3(Si(Bu\text{-}t)_2H)\}$ **(18)**. Complex **18** reacts with PMe_3 forming the $Cp_2Ta\{\eta^1\text{-}BH_3(Si(Bu\text{-}t)_2H)\}PMe_3$ (**19**) complex and with a large excess of the phosphine, yielding the silylborane adduct and the $Cp_2Ta(PMe_3)(H)$ complex, as shown in equation 16[46].

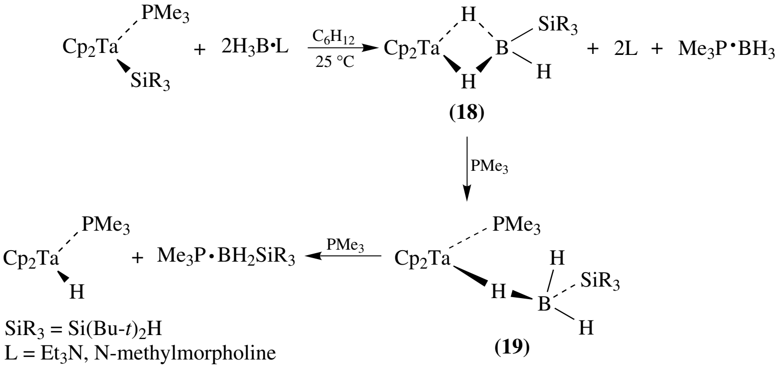

$SiR_3 = Si(Bu\text{-}t)_2H$
$L = Et_3N$, N-methylmorpholine

(16)

Berry and coworkers have observed the thermally labile silyl alkylidene complex $Cp_2Ta({=}CH_2)(Si(Bu\text{-}t)_2H)$ *in situ* at −70 °C in the photolysis of $Cp_2Ta(PMe_3)(Si(Bu\text{-}t)_2H)$ in the presence of $Me_3P{=}CH_2$[46]. In contrast, and besides the theoretical studies in Schrock-type metal silylidene complexes which predict a strong Nb=Si bond[47], the alkylidene silyl complex $Np_2Ta(Si(SiMe_3)_3)({=}CHBu\text{-}t)$ was obtained by the metathesis reaction of Np_3TaCl_2 with 2 equivalents of $(Me_3Si)_3SiLi{\bullet}3THF$ and the concomitant elimination of one equivalent of $HSi(SiMe_3)_3$. The molecular structure of $Cp_2Ta({=}CH_2)(Si(Bu\text{-}t)_2H)$ imposed a 3-fold rotation axis containing the Ta−Si bond, giving a disorder among the *t*-BuCH= moiety and the two neopentyl groups. The Ta−Si bond length of 2.680(15) Å is comparable to those in other Ta−silyl complexes (Table 3)[35].

TABLE 3. Selected M−Si distances in group-5 transition-metal silyl complexes

Compound	d^n Configuration	M−Si (Å)	Reference
$Cp_2Ta(PMe_3)(SiMe_3)$	d^2	2.639(4)	42
$Cp_2TaH(SiMe_2H)_2$	d^0	2.633(2), 2.624(2)	42
$Cp_2Ta(CO)(SiMe_3)$	d^2	2.631(2)	43
$Cp_2Ta(PMe_3)(Si(Bu\text{-}t)_2H)$	d^2	2.740(1)	43
$Cp_2Ta(CO)(Si(Bu\text{-}t)_2H)$	d^2	2.684(1)	43
$Np_2Ta(Si(SiMe_3)_3)({=}CHBu\text{-}t)$	d^0	2.680(15)	35
$Cp_2Nb(SiMe_2Cl)_2H$	d^0	2.584(5), 2.611(5)	45
$Cp_2Nb(SiMe_2Ph)_2H$	d^0	2.646(5), 2.665(5)	45
$Nb(\eta^5\text{-}C_5H_4SiMe_3)_2H_2(SiPh_2H)$	d^0	2.616(3)	44

TABLE 4. Selected ^{29}Si NMR chemical shifts for group-5 transition-metal silyl complexes

Compound	^{29}Si NMR shift (ppm)	Reference
$Cp_2TaH_2(SiH_3)$	−74.1 symmetrical isomer	42
$Cp_2TaH(SiH_3)H$	−40.1 unsymmetrical isomer	42
$Cp_2TaH_2(SiMeH_2)$	−33.5 symmetrical isomer	42
$Cp_2TaH(SiMeH_2)H$	−7.0 unsymmetrical isomer	42
$Cp_2TaH_2(SiMe_2H)_2$	−5.2 symmetrical isomer	42
$Cp_2TaH(SiMe_2H)H$	15.0 unsymmetrical isomer	42
$Cp_2TaH_2(SiMe_3)$	10.4 symmetrical isomer	42
$Cp_2TaH(SiMe_3)H$	27.3 unsymmetrical isomer	42
$Cp_2TaH_2(SiMe_2Cl)$	76.2 symmetrical isomer	42
$Cp_2TaH(SiMe_2Cl)H$	83.0 unsymmetrical isomer	42
$Cp_2TaH_2(Si(OMe)_3)$	40.9 symmetrical isomer	42
$Cp_2TaH(Si(OMe)_3)H$	40.7 unsymmetrical isomer	42
$Cp_2TaH(SiMeH_2)_2$	−11.7 symmetrical isomer	42
$Cp_2TaH(SiMeH_2)_2$	−5.9; −23.4 unsymmetrical isomer	42
$Cp_2TaH(SiMe_2H)_2$	11.5 symmetrical isomer	42
$Cp_2TaH(SiMe_3)_2$	24.5 symmetrical isomer	42
$Cp_2TaH(SiMe_2Cl)_2$	81.0 symmetrical isomer	42
$Cp_2TaH(Si(OMe)_3)_2$	36.6 symmetrical isomer	42
$Cp_2Ta(PMe_3)(SiMeH_2)$	−21.3 ($^2J_{PSi}$ = 15.1 Hz)	42
$Cp_2Ta(PMe_3)(SiMe_3)$	9.7 ($^2J_{PSi}$ = 11.5 Hz)	42
$Cp_2Ta(PMe_3)(SiMe_2Cl)$	89.7 ($^2J_{PSi}$ = 8.6 Hz)	42
$Cp_2Ta(PMe_3)(Si(OMe)_3)$	30.4 ($^2J_{PSi}$ = 22.9 Hz)	42
$Cp_2Ta(PMe_3)(Si(Bu\text{-}t)_2H)$	46.4 ($^2J_{PSi}$ = 8.9 Hz)	42
$Cp_2Ta(CO)SiMe_3$	7.5	42
$Cp_2Ta((CO)(Si(Bu\text{-}t)_2H)$	51.1	42
$Np_2Ta(Si(SiMe_3)_3)(=CHBu\text{-}t)$	−53.47 (*Si*SiMe$_3$), −5.3 (*Si*Me$_3$)	35
$Nb(\eta^5\text{-}C_5H_4SiMe_3)_2H_2(SiMePh_2)$	26.7 ($SiMePh_2$), −3.0 (*Si*C$_5$H$_4$)	44
$Nb(\eta^5\text{-}C_5H_4SiMe_3)_2H_2(SiPh_2H)$	23.8 ($^2J_{SiH}$ = 177 Hz, *Si*Ph$_2$H) −0.3 (*Si*C$_5$H$_4$)	44

VIII. GENERAL INTRODUCTION TO LATE-TRANSITION-METAL SILICON-CONTAINING COMPLEXES

Major advances in organometallic chemistry during the last years have been achieved in the area of silicon−metal multiple bonding and silicon with low coordination numbers. For late transition metals, new complexes have been synthesized such as silanediyl **(A)**, silene **(B)**, silaimine **(C)**, disilene **(D)**, silatrimethylenemethane **(E)**, silacarbynes **(F)**, cyclic silylenes **(G)**, silacyclopentadiene **(H)** and metalla-sila-allenes **(I)** (Figure 3).

The existence of such a diverse silaorganometallic chemistry made it clear that coordination compounds of subvalent silicon ligands are common species playing an important role in many reactions and having important applications in industrial processes. The links made by silaorganometallic chemistry among organic and inorganic chemistry and the exploration of this highly interdisciplinary field raise a challenge for the future[48−50].

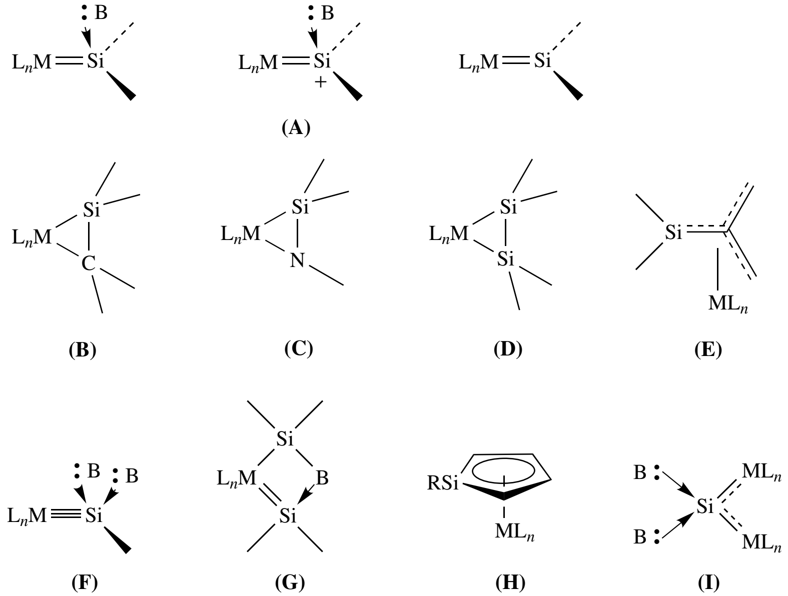

FIGURE 3. Some late-transition-metal silyl derivatives

IX. GROUP-6 SILYLENE COMPLEXES

The formation of a metal–silicon double bond is most effective by the 'salt elimination route'. It is accomplished in a one-step procedure reacting the supernucleophilic metallate dianions with dihalosilanes in polar solvents as HMPA, as shown for chromium in equation 17.

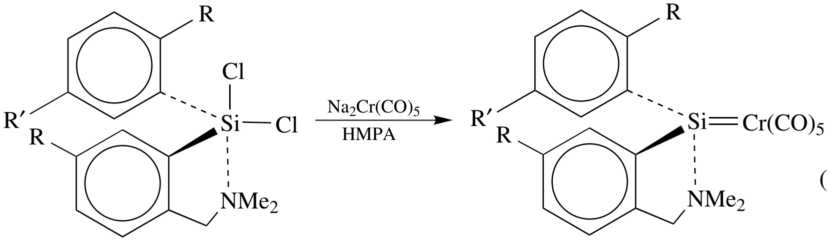

(17)

(20) $R = R' = H$

(21) $R = H, R' = CH_2NMe_2$

(22) $R = CH_2NMe_2, R' = t\text{-Bu}$

The chromium complexes are proved to be silanediyl complexes, as shown by the silicon–transition metal bond lengths (Table 5) and by the extreme low field shift of the ^{29}Si NMR signals (124.9 and 121.2) at 22 °C for $R = H$ and CH_2NMe_2, respectively (Table 6). The ^{29}Si NMR shifts of these complexes are temperature-dependent due to the hindered rotation of the phenyl ring and dynamic coordination of the nitrogens to the Si atom.

Thus in **21**, below 21 °C (coalescence barrier $\Delta G^{\ddagger} = 12.9 \pm 1$ kcal mol^{-1}) one nitrogen is attached to the Si atom, at 58 °C the two substituents on the Si atom are magnetically equivalent and above 58 °C the dynamic behavior disappears and no N−Si bonds are observed as shown by the ^{29}Si NMR signal at 138.8 ppm which is in line with a three-coordinative silicon atom. For **20**, the dimethylamino substituent is rigidly coordinated to the silicon atom and coalescence was obtained only at 95 °C ($\Delta G^{\ddagger} = 19.1 \pm 1$ kcal mol^{-1}). The solid structure of **21** shows the silanediyl ligand coordinated to the octahedral metal fragment with a short Cr−Si bond length of 2.408(1) Å[51,52]. Photochemical activation of CO in **21** or **22** results in a 1,2-shift of the amine donor-substituent from the silicon to the metal, yielding the complex $(2\text{-}Me_2NCH_2C_6H_4)(2\text{-}Me_2\overline{NCH_2C_6H_4)Si{=}C}r(CO)_4$. This shift causes a shortening in the Cr=Si bond to 2.3610(4) Å, reflecting the stronger Cr=Si bond obtained by the electron transfer from the amine to the metal atom. Similar tandem photolytic 1,2-shifts have been observed in the phosphane-stabilized silylene complex as depicted in Scheme 11. The starting phosphane exhibits, in analogy to what was presented above, the flip-flop coordination and has a Cr=Si bond length of 2.414(1) Å, which is comparable to other chromium silylene complexes (Table 5)[53]. A similar strategy has been used to prepare a large number of base-stabilized group 6 and 7 (*vide infra*) silylene complexes as shown in equation 18.

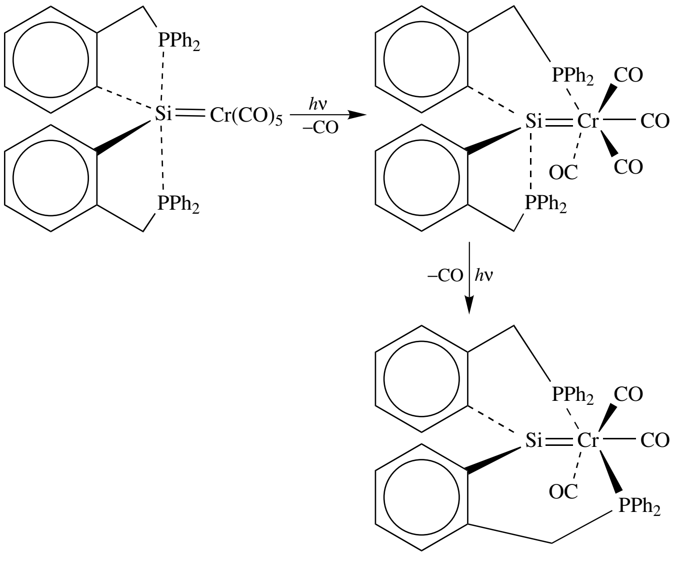

SCHEME 11

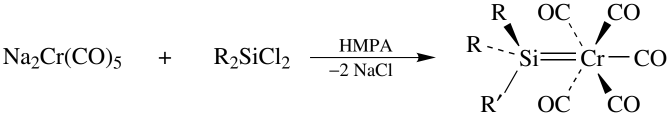

(18)

R = *t*–BuO, *t*–BuS, CH_3, Cl, 1-AdO, 2–AdO, NpO, Ph_3CO; R′ = HMPA

In addition, on reacting $Na_2Cr(CO)_5$ with *t*-$Bu_2Si(OTf)_2$ in THF, similarly to equation 18, the salt adduct $(CO)_5Cr{=}Si(Bu\text{-}t)_2{\cdot}Na(OTf){\cdot}2THF$ was obtained with an oxygen atom of the triflate anion coordinated to the subvalent silicon atom. The solid structure of the salt adduct complex exhibits a $Cr{=}Si$ bond length of 2.475(1) Å. The salt adduct is readily exchange by HMPA, yielding the respective $(CO)_5Cr{=}Si(Bu\text{-}t)_2(HMPA)$ complex[54]. For these chromium complexes, the ^{29}Si NMR chemical shift data cover a range of 100 ppm with no linear correlation with the electronegativity of the particular substituent at the silicon atom. Instead, a quadratic dependency between the overall electronegativity of the silicon substituents and the ^{29}Si NMR chemical shifts was observed. This result argues for a superposition of diamagnetic and paramagnetic shift influences on silicon. The observed trend on the ^{29}Si NMR shifts is analogous to that known for regular tetravalent silicon. The coupling constants P−Si for the HMPA complexes were found to be invariant with changes of temperature in the range of -90 to $+110\,^{\circ}C$, indicating the rigid coordination to the HMPA base.

Solid state structures of the silylene complexes $(CO)_5Cr{=}Si(HMPA)Me_2$, $(CO)_5Cr{=}Si(HMPA)Cl_2$, $(CO)_5Cr{=}Si(Bu\text{-}t)_2{\bullet}Na(OTf){\bullet}2THF$ and $(CO)_5Cr{=}Si(HMPA)(Bu\text{-}t)_2$ have been shown to be isostructural with the Si ligand in the apical position of the octahedral metal environment and to have bond lengths of 2.410(1) Å, 2.342(1) Å, 2.475(1) Å and 2.527(1) Å, respectively. The latter complex can be described better as a σ-donor $Si \rightarrow Cr$ complex[53,55]. Photolysis of the complex $(CO)_5Cr{=}Si(HMPA)(OBu\text{-}t)_2$ in the presence of triphenylphosphine yields the *trans* diphosphine complex $(CO)_5Cr(PPh_3)_2$ together with HMPA and a polysilane. When the reaction, as described in equation 18, is carried out in the presence of dimethyl carbonate, a sila-Wittig reaction (metathesis of $M{=}Si$ and $C{=}O$) takes place forming the (dimethoxycarbene)chromium pentacarbonyl complex $(CO)_5Cr{=}C(OMe)_2$ and hexamethyltrisiloxane[55].

An alternative synthetic pathway to silylene complexes can be achieved by the photolytic reaction of the 16-electron metal complex $Cr(CO)_6$ with the trihydrosilane $2\text{-}Me_2NCH_2C_6H_4SiH_3$, yielding complex **23** after elimination of H_2 and CO, as shown in equation 19[52,56]. Complex **23** eliminates two CO molecules in a tandem fashion under photolytic conditions in the presence of phosphine, phosphite or diphosphines. In the latter case the *cis* isomer is obtained. At room temperature, complex **23** was found to react with either Ph_3CBF_4, CH_3COBr, $Ph_3COSO_2CF_3$ or with CH_3COCl exchanging the hydrosilane hydrogen, forming respectively the F, Br, OSO_2CF_3 or Cl derivatives of complex **23**[57]. An unexpected reactivity was found for complex **23** and for its halide substituted complexes, when they reacted with alkyl lithium reagents. Instead of the expected nucleophilic attack at the CO ligand, the alkyl substituted complex is obtained as shown for the hydride complex **23** in equation 20. In general, the reactivity trend of **23** and analogous complexes was found to follow the order of $F > H \gg Br \geqslant Cl$[57].

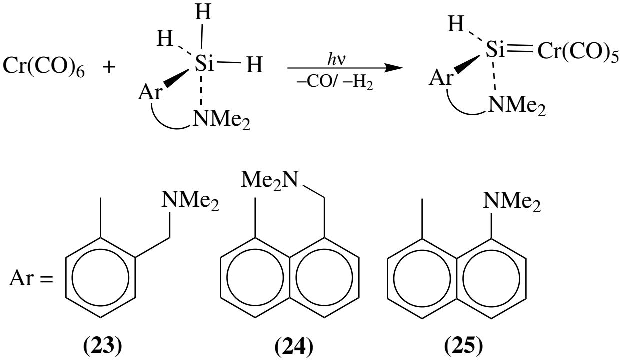

(19)

(23) **(24)** **(25)**

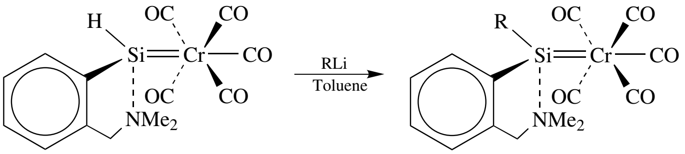

(20)

R = Ph, Me, *t*-Bu, $Me_3SiC{\equiv}C$, $PhC{\equiv}C$

X. GROUP-6 SILYL COMPLEXES

Reaction of the lithium or the tetramethylphosphonium metallates $M'[M(PMe_3)(CO)_2C_5R_5]$ ($M' = Li, Me_4P$; $M = Mo, W$; $R = H, Me$) with the trichlorosilanes $R'SiCl_3$ ($R' = H, SiCl_3$) leads to the formation of monosilyl complexes of the type $C_5R_5(CO)_2(Me_3P)M{-}SiCl_2R'$. These complexes react with $LiAlH_4$ replacing all the chlorine atoms, forming the corresponding hydrosilane complexes as shown in Scheme 12[58]. When $R' = SiCl_3$, the hydrido disilene complex can be reconverted back into the pentachloro(metallo) disilane by reacting it with tetrachloromethane[59].

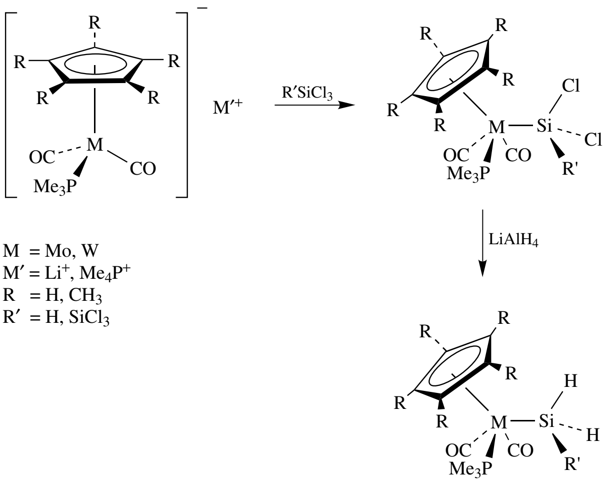

M = Mo, W
M′ = Li^+, Me_4P^+
R = H, CH_3
R′ = H, $SiCl_3$

SCHEME 12

In a similar fashion the monosilyl complexes $C_5Me_5(CO)_2(PMe_3)W{-}SiR_3$ ($SiR_3 = SiHMe_2$, $SiHClMe$ and $SiHCl_2$) are prepared from the lithium metallate $C_5Me_5(CO)_2(PMe_3)WLi$ with the corresponding chlorosilane. The latter two chlorine complexes have been reacted with $LiAlH_4$ yielding the hydrosilyl complexes $C_5Me_5(CO)_2(PMe_3)W{-}SiH_3$ and $C_5Me_5(CO)_2(PMe_3)W{-}SiH_2Me$, respectively. Crystal data for the complexes $C_5Me_5(CO)_2(PMe_3)W{-}SiCl_2SiCl_3$ and $C_5Me_5(CO)_2(PMe_3)W{-}SiH_2R$ ($R = H, Me$) reveal a pseudo-tetrahedral arrangement of the ligands around the metal with the cyclopentadienyl ligand in the axial position. The 2.469(2) Å W−Si bond length for the former is *ca* 0.1 Å shorter than the bond lengths of 2.533(3) Å and 2.559(2) Å for the latter two complexes, respectively, reflecting the difference in the inductive $-I$ effect. This effect can also be recognized in the slightly enhanced coupling constant $^1J_{SiW}$ of the last two complexes (Table 6)[60]. The monosilyl complexes $C_5Me_5(CO)_2(PMe_3)M{-}SiH_3$ ($M = Mo, W$) were found to react with dimethyloxirane, yielding the trihydroxy complexes, $C_5Me_5(CO)_2(PMe_3)M{-}Si(OH)_3$ (M = Mo, W). A concomitant reaction with $Me_2Si(H)Cl$ led to the trisiloxane complexes $C_5Me_5(CO)_2(PMe_3)MSi(OSiMe_2H)_3$ (M = Mo, W), respectively[61,62].

Photochemical reactions at 350 nm of group-6 metallocene dihydrides Cp_2MH_2 (M = Mo, W) with hydrosilanes, $HSiR_3$, produced in good yields the corresponding silyl hydride complexes, $Cp_2MH(SiR_3)$ [M = Mo; SiR_3 = $SiMe_2H$, $SiMe_2Cl$, $SiMe_3$, $Si(Bu\text{-}t)_2H$, $Si(Bu\text{-}t)_2Cl$; M = W; SiR_3 = $SiMe_2Cl$, $SiMe_3$]. The pentamethylcyclopentadienyl derivatives $Cp_2{}^*M(H)(SiR_3)$ [M = Mo; SiR_3 = $SiMe_3$, $Si(Bu\text{-}t)_2H$] were prepared in a similar fashion, whereas bis(silyl) complexes of the type $Cp_2W(SiMe_3)(SiR_3)$ were synthesized from the silene complex $Cp_2W(\eta^2\text{-}SiMe_2{=}CH_2)$ upon reaction with the corresponding hydrosilane as described, together with the proposed mechanism, in Scheme 13[63].

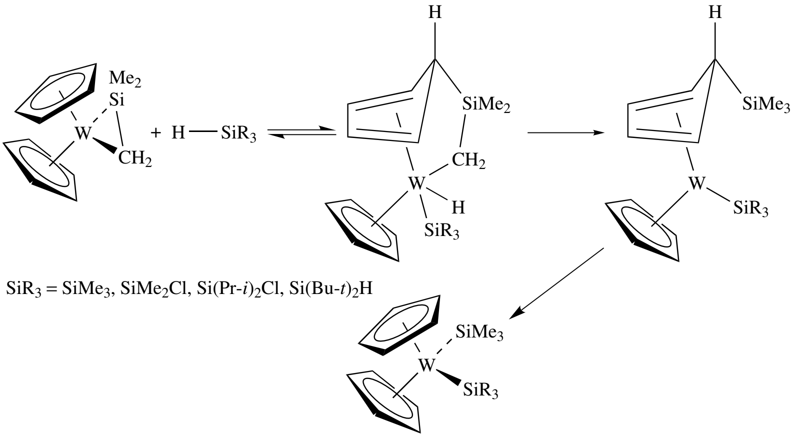

SCHEME 13

Crystal structures for some mono and bis(silyl) complexes of group 6 have been determined showing metal–silicon bond lengths which generally correlate with the steric congestion around the metal. Exceptions have been found for the chlorosilyl derivatives which exhibit short Group 6–Si and long Si–Cl distances (Table 5). This peculiar feature of the chlorosilyl complexes is ascribed to both inductive and π-backbonding effects from the metal to the Si–Cl σ^* orbital, inducing some degree of silylene character. This silylene character is evidenced by the ^{29}Si NMR ($^1J_{WSi}$) (Table 6) coupling constants[63]. The bis(silyl)tungsten complexes $Cp_2W(SiMe_3)(SiR_2X)$ (R = i-Pr, CH_3, CD_3; X = Cl, OTf) have been found to undergo thermal isomerization of the methyl groups through a silyl–silylene intermediate forming the mixed $Cp_2W(SiMe_2X)(SiR_2Me)$ complexes. The proposed mechanism is described in Scheme 14 in which an electrophilic cationic silyl(silylene) tungstenocene is formed by dissociation of X^-, followed by migration of a methyl group to the electrophilic silylene center, and reassociation of X^- to the second silicon to complete the process. As can be expected, the rates are strongly dependent on the nature of the R and X moieties, solvent polarity and the presence of strong Lewis acid catalysts, such as $B(C_6F_5)_3$[64].

Using the same strategy Berry and coworkers recently described the synthesis of mixed tungsten germyl silyl complexes $Cp_2W(SiMe_3)(GeR_3)$ [GeR_3 = $GeMe_3$, $GeMe_2H$, $Ge(Bu\text{-}t)_2H$, $GePh_2H$, $GeMe_2Cl$, $Ge(Bu\text{-}t)_2Cl$, $GePh_2Cl$, $GeMe_2OTf$, $Ge(Bu\text{-}t)_2Me$], which display the same methyl rearrangement described in Scheme 14 for the bis(silyl) complexes[65].

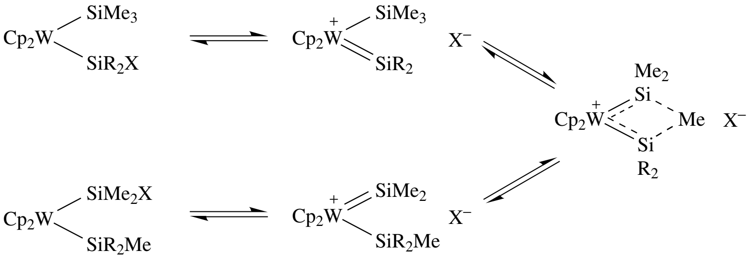

SCHEME 14

Arene complexes of the type (η^6-arene)Cr(CO)$_2$(H)(SiCl$_3$) (η^6-arene = C_6H_6, 1,3,5-$Me_3C_6H_3$, C_6Me_6, C_6H_5Me, Cbb) have been obtained by the photolytic CO activation of the corresponding chromium tricarbonyl complex after oxidative addition of the trichlorosilane. Further photolysis of the complexes causes the elimination of H_2 and formation of the (η^6-arene)Cr(CO)$_2$(SiCl$_3$)$_2$ complexes, respectively. During the last step, the arene ligand becomes labilized and can be exchanged with other arene ligands[66,67]. Recently, the intermediate complexes, (η^6-arene)Cr(CO)(H)$_2$(SiCl$_3$)$_2$ (η^6-arene = C_6H_5F, 1,3,5-$Me_3C_6H_3$), in the formation of (η^6-arene)Cr(CO)$_2$(SiCl$_3$)$_2$, were isolated and characterized. The former crystallized as a 1:1 cocrystallite with the product (η^6-arene)Cr(CO)$_2$(SiCl$_3$)$_2$. The structure is described as a distorted three-legged piano stool where two legs are trichlorosilyl ligands and the third leg is the carbonyl. The two hydrides bridge the Si−Cr bonds. In the latter molecule, a similar three-legged piano-stool structure is observed, except that one hydrogen is considerably further and almost equidistant from the two silicon atoms. Thus, the best formulation of these compounds is as the dihydrides of formally Cr(IV). Noteworthy is the fluxional behavior of the two hydrogen atoms in the intermediate complex, which exchange in solution according to the mechanism proposed in Scheme 15[68].

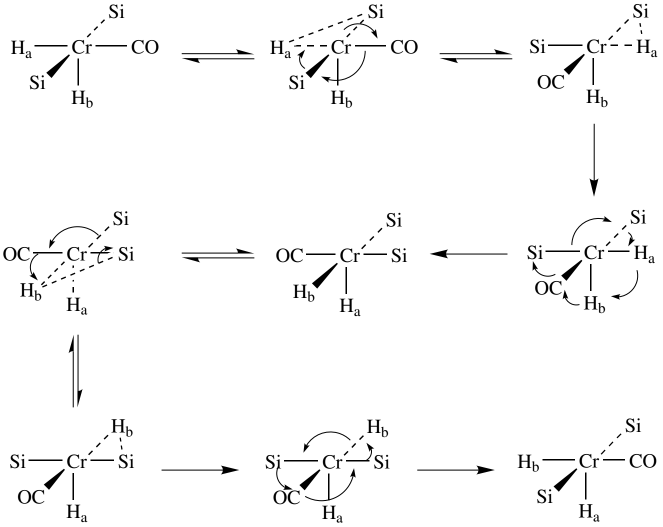

SCHEME 15

Chelate complexes of tungsten $(CO)_4\overline{W(PPh_2PCH_2CH_2SiHR_2)}$ (R = Me, Ph) containing three-center two-electron bonds were prepared photochemically from $W(CO)_6$ and $Ph_2PCH_2CH_2SiR_2H$. The non-chelated phosphino silyl tungsten complexes $(CO)_5W(PPh_2PCH_2CH_2SiR_2H)$ have been found to be the intermediates in this reaction. The NMR coupling constants $^1J_{SiWH}$ in the chelating complexes (98.1 and 95.2 Hz for R = Me and Ph, respectively) are lower than the coupling constant for the uncoordinated complex $(CO)_5W(PH_2PCH_2CH_2SiR_2H)$ ($^1J_{SiH} = 196.5$ Hz) indicating that, due to the chelation, an earlier stage of the oxidative addition of the silane bond is frozen in the corresponding non-chelated complexes. The stabilization obtained by the chelating ligand is slightly larger than the electronic effect caused by substituting another CO by a PR_3 ligand or by replacing SiR_3 (R = alkyl, aryl) by $SiCl_3$ in the non-chelating complexes[69,70].

The first monosilyl alkylidyne complex of tungsten without anionic π-bonding ligands $Np_2W(\equiv CBu\text{-}t)(Si(SiMe_3)_3)$ was prepared recently upon metathesis of a neopentyl tungstenyl chloride derivative with the salt $(Me_3Si)_3SiLi$ (equation 21)[35].

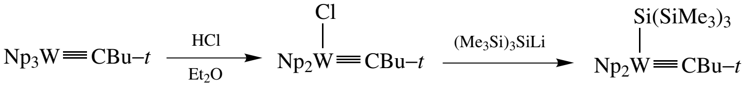

$$Np_3W{\equiv}CBu\text{-}t \xrightarrow[Et_2O]{HCl} Np_2W(Cl){\equiv}CBu\text{-}t \xrightarrow{(Me_3Si)_3SiLi} Np_2W(Si(SiMe_3)_3){\equiv}CBu\text{-}t \qquad (21)$$

Np = neopentyl

A. η^2-Silyl Complexes

Berry and coworkers have shown that $Cp_2Mo(\eta^2\text{-}Me_2Si{=}SiMe_2)$ reacts readily with elemental sulfur to yield the symmetrical insertion product *cyclo*-$Cp_2Mo(Me_2SiSSiMe_2)$[71]. Recently, Berry and coworkers have shown that the isolobal tungsten disilene complex $Cp_2W(\eta^2\text{-}Me_2Si{=}SiMe_2)$ (**26**) reacts with the heavier elemental chalcogens to yield the symmetrical insertion products *cyclo*-$Cp_2W(Me_2SiESiMe_2)$ (E = S, Se, Te)[72]. Although complex **26** does not react cleanly with oxygen, the insertion product *cyclo*-$Cp_2W(Me_2SiOSiMe_2)$ can be prepared by the reaction of **26** with trimethylamine N-oxide. The four-membered ring compounds *cyclo*-$Cp_2W(Me_2SiESiMe_2)$ (E = S, Se) can likewise be formed in the reaction of **26** with phosphine chalcogenides, although varying amounts of the unsymmetrical isomers *cyclo*-$Cp_2W(EMe_2SiSiMe_2)$ are produced as well. The ratio of unsymmetrical to symmetrical isomers formed have been found to be strongly dependent on the size of the phosphine chalcogenide. The proposed mechanism for the formation of both sulfur isomers (Scheme 16) involves an initial nucleophilic attack by the phosphine sulfide at either a silicon atom or at the tungsten atom. Cleavage of the silicon–silicon bond would generate a zwitterionic intermediate, **J**, consisting of silyl anion and phosphonium cation moieties. Intramolecular nucleophilic displacement would then lead to the symmetrical four-membered ring complex. In the second case, breaking the metal–silicon bond would form a different zwitterionic complex, **K**, and intramolecular nucleophilic displacement of the phosphine will generate the unsymmetrical complex. As the size of the phosphine sulfide is increased, the greater is the hindrance at the metal center, disfavoring the metal–silicon cleavage and hence the formation of the unsymmetrical isomer[72].

The structures of the oxygen and selenium metallacycle complexes *cyclo*-$Cp_2W(Me_2SiESiMe_2)$ (E = O, Se) were determined by single-crystal X-ray diffraction methods. When E = O, the metal lies on the crystallographic plane bisecting the two Cp rings and the planar WSi_2O ring. When E = S, two unique molecules are present in the unit cell with the only difference among them being the planarity of the WSi_2Se rings. The unique W–Si distance in the former complex [2.551(2) Å] is essentially identical

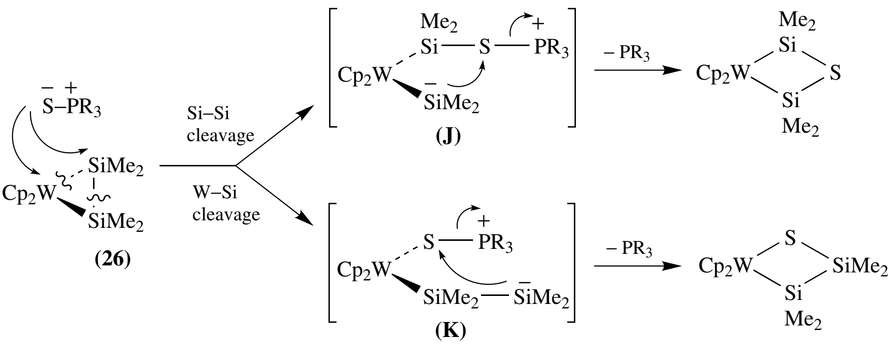

SCHEME 16

to the average (2.554 Å) of the four W−Si distances in the latter which range from 2.544(4) to 2.565(4) Å. The ^{29}Si NMR chemical shifts for the symmetrical complexes *cyclo*-$Cp_2W(Me_2SiESiMe_2)$ are 20.6 ($^1J_{WSi}$ = 85.9 Hz), −17.8 ($^1J_{WSi}$ = 96.4 Hz), −30.5 ($^1J_{WSi}$ = 99.2 Hz) and −68.1 ppm ($^1J_{WSi}$ = 103.1 Hz) for E = O, S, Se and Te, respectively. Hence, two trends are apparent from the ^{29}Si NMR data. The first is the upfield shift obtained by going down the series as found for the disilyl chalcogenides $(Me_3Si)_2E$, and has been ascribed to more effective shielding of silicon by the larger chalcogens. The second is the increase in the one-bond ^{29}Si−^{183}W coupling constant down the series indicating greater s-orbital character in the Si−W bonds of the heavier chalcogenide derivatives[72].

η^2-Silane complexes of molybdenum have been prepared by the reaction of the formally 16-electron complex $Mo(CO)(R_2PCH_2CH_2PR_2)_2$ with silanes (equation 22.)

$$Mo(CO)(R_2PCH_2CH_2PR_2)_2 \quad + \quad R''R'SiH_2 \longrightarrow \qquad (22)$$

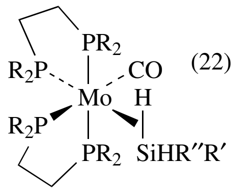

R = Et, R′ = R″ = Ph, *n*–C_6H_{13}
R = Et, R′ = H, R″ = Ph
R = CH_2Ph, R′ = H, R″ = Ph, *n*–C_6H_{13}
R = Ph, *i*-Bu, R′ = R″ = H

The η^2-silane coordination was established by the observation of the $^1J_{SiH}$ coupling constants for the bound η^2-Si−H bonds which are in the range of 20−70 Hz. Consequently, these complexes are better described as six-coordinate η^2-silane complexes than seven-coordinate hydride complex[73,74]. Remarkably, in solution the η^2-SiH_4 complex *cis*-$Mo(\eta^2\text{-}SiH_4)(CO)(Et_2PCH_2CH_2PEt_2)_2$ was found to be in equilibrium with its seven - coordinate hydrosilyl tautomer $Mo(CO)(H)(SiH_3)(Et_2PCH_2CH_2PEt_2)_2$. Crystal structures for the complexes *cis*-$Mo(\eta^2\text{-}SiH_2Ph{-}H)(CO)(Et_2PCH_2CH_2PEt_2)_2$ and *cis*-$Mo(\eta^2\text{-}SiH_3{-}H)(CO)(Et_2PCH_2CH_2PEt_2)_2$ evince an octahedral environment with the η^2-silane ligand *cis* to the CO, and similar Mo−Si bond lengths of 2.501(2) Å and 2.556(4) Å (Table 5), respectively[74].

TABLE 5. Selected M–Si distances in group-6 transition-metal silylene and silyl complexes

Compound	d^n Configuration	M–Si (Å)	Reference
Silylene Complexes			
$(CO)_5Cr{=}Si(o\text{-}Me_2NCH_2C_6H_4)_2$	d^6	2.408(1)	51
$(CO)_5Cr{=}Si(o\text{-}Me_2NCH_2C_6H_4)(C_6H_5)$	d^6	2.409(1)	52
$(CO)_5Cr{=}Si(HMPA)Me_2$	d^6	2.410(1)	55
$(CO)_5Cr{=}Si(HMPA)Cl_2$	d^6	2.342(1)	55
$[2\text{-}Me_2NCH_2C_6H_4][2\text{-}Me_2\overline{NCH_2C_6H_4]\ Si{=}C}r(CO)_4$	d^6	2.3610(4)	52
$(CO)_5Cr{=}Si(Bu\text{-}t)_2\bullet$ NaOTf•2THF	d^6	2.475(1)	53
$(CO)_5Cr{=}Si(Bu\text{-}t)_2(HMPA)$	d^6	2.527(1)	53
Silyl Complexes			
$(C_5Me_5)(CO)_2(Me_3P)W{-}SiH_3$	d^6	2.533(3)	60
$(C_5Me_5)(CO)_2(Me_3P)W{-}SiH_2Me$	d^6	2.559(2)	60
$(C_5Me_5)(CO)_2(Me_3P)W{-}SiCl_2SiCl_3$	d^6	2.469(2)	59
$(C_5H_5)_2Mo(H)SiMe_2H$	d^2	2.538(2), 2.541(2)	63
$(C_5H_5)_2Mo(H)SiMe_2Cl$	d^2	2.513(1)	63
$(C_5Me_5)_2Mo(H)SiMe_3$	d^2	2.560(1)	63
$(C_5H_5)_2Mo(H)Si(Bu\text{-}t)_2H$	d^2	2.604(1)	63
$(C_5H_5)_2W(H)SiMe_3$	d^2	2.560(1)	63
$(C_5H_5)_2W(SiMe_3)(Si(Pr\text{-}i)_2Cl)$	d^2	2.602(1)	63
$(C_5Me_5)_2W(SiMe_3)(Si(Bu\text{-}t)_2H)$	d^2	2.599(1)	63
$(C_5H_5)_2W(SiMe_3)(GeMe_2Cl)$	d^2	2.591(3)	65
$(\eta^6\text{-}C_6H_5F)Cr(CO)_2(SiCl_3)_2$	d^4	2.376(2) 2.377(2)	68
$(\eta^6\text{-}C_6H_5F)Cr(CO)(H)_2(SiCl_3)_2$	d^2	2.361(2) 2.368(2)	68
$(\eta^6\text{-}1,3,5\text{-}Me_3C_6H_3)Cr(CO)(H)_2(SiCl_3)_2$	d^4	2.365(1) 2.373(1)	68
$(\eta^6\text{-}1,3,5\text{-}Me_3C_6H_3)Cr(CO)_2(SiCl_3)_2$	d^4	2.383(3) 2.382(3)	66
cyclo-$Cp_2W(Me_2SiOSiMe_2)$	d^4	2.551(2)	72
cyclo-$Cp_2W(Me_2SiSeSiMe_2)$	d^4	2.547(4) 2.559(4) 2.544(4) 2.565(4)	72
cis-$Mo(\eta^2\text{-}SiH_2Ph\text{-}H)(CO)(Et_2PCH_2CH_2PEt_2)_2$	d^6	2.501(2)	73
cis-$Mo(\eta^2\text{-}SiH_3\text{-}H)(CO)(Et_2PCH_2CH_2PEt_2)_2$	d^6	2.556(4)	74

TABLE 6. Selected ^{29}Si NMR chemical shifts for group-6 transition-metal silylene and silyl complexes

Compound	^{29}Si NMR shift (ppm)	Reference
Silylene Complexes		
$(CO)_5Cr{=}Si(o\text{-}Me_2NCH_2C_6H_4)_2$	124.9 (58 °C)	51
$(CO)_5Cr{=}Si(o\text{-}Me_2NCH_2C_6H_4)(C_6H_5)$	121.2 (22 °C)	51
$(CO)_5Cr{=}Si(HMPA)(OBu\text{-}t)_2$	12.7 ($^2J_{PSi} = 37.2$ Hz)	55
$(CO)_5Cr{=}Si(HMPA)Me_2$	101.4 ($^2J_{PSi} = 31.3$ Hz)	55
$(CO)_5Cr{=}Si(HMPA)Cl_2$	55.0 ($^2J_{PSi} = 41.4$ Hz)	55
$(CO)_5Cr{=}Si(HMPA)(OAd\text{-}1)_2$	11.9 ($^2J_{PSi} = 30.1$ Hz)	55
$(CO)_5Cr{=}Si(HMPA)(OAd\text{-}2)_2$	11.7 ($^2J_{PSi} = 30.2$ Hz)	55
$(CO)_5Cr{=}Si(HMPA)(ONp)_2$	12.5 ($^2J_{PSi} = 31.1$ Hz)	55
$(CO)_5Cr{=}Si(HMPA)(OCPh_3)_2$	10.9 ($^2J_{PSi} = 32.0$ Hz)	55
$(CO)_5Cr{=}Si(HMPA)(SBu\text{-}t)_2$	83.2 ($^2J_{PSi} = 31.0$ Hz)	55
$[o\text{-}Me_2NCH_2C_6H_4]$ $\text{-}[o\text{-}Me_2\overline{NCH_2C_6H_4]Si{=}C}r(CO)_4$	143.2	52
$(CO)_5Cr{=}Si(HMPA)(Bu\text{-}t)_2$	133.1 ($^2J_{PSi} = 37.2$ Hz)	53
$(CO)_5Cr{=}Si(THF)(Bu\text{-}t)_2$	149.7	53
$(CO)_5Cr{=}Si(Bu\text{-}t)_2\bullet NaOTf\bullet 2THF$	150.7	53
$(CO)_5Cr{=}Si(H)(o\text{-}Me_2NCH_2C_6H_4)$	110.9 ($^1J_{HSi} = 162.3$ Hz)	56
$(CO)_5Cr{=}Si(H)[8\text{-}(Me_2NCH_2)C_{10}H_6]$	102.1 ($^1J_{HSi} = 165.3$ Hz)	57
$(CO)_5Cr{=}Si(H)[8\text{-}(Me_2N)C_{10}H_6]$	120.4 ($^1J_{HSi} = 164.9$ Hz)	57
$(CO)_5Cr{=}Si(F)(o\text{-}Me_2NCH_2C_6H_4)$	117.2 ($^1J_{FSi} = 398.5$ Hz)	57
$(CO)_5Cr{=}Si(Br)(o\text{-}Me_2NCH_2C_6H_4)$	119.4	57
$(CO)_5Cr{=}Si(OSO_2CF_3)$ $(o\text{-}Me_2NCH_2C_6H_4)$	123.5	57
$(CO)_5Cr{=}Si(Cl)(o\text{-}Me_2NCH_2C_6H_4)$	122.9	57
$(CO)_5Cr{=}Si(Ph)(o\text{-}Me_2NCH_2C_6H_4)$	122.0	57
$(CO)_5Cr{=}Si(Me)(o\text{-}Me_2NCH_2C_6H_4)$	126.1	57
$(CO)_5Cr{=}Si(Bu\text{-}t)(o\text{-}Me_2NCH_2C_6H_4)$	138.5	57
$(CO)_5Cr{=}Si(Me_3SiC{\equiv}C)$ $(o\text{-}Me_2NCH_2C_6H_4)$	92.3 ($SiC{\equiv}$), −18.1 ($SiMe_3$)	57
$(CO)_5Cr{=}Si(PhC{\equiv}C)$ $(o\text{-}Me_2NCH_2C_6H_4)$	92.2	57
Silyl Complexes		
$(C_5Me_5)(CO)_2(Me_3P)WSiH_3$	−43.2 ($^2J_{SiP} = 13.2$ Hz, $^1J_{SiW} = 49.8$ Hz)	60
$(C_5Me_5)(CO)_2(Me_3P)WSiH_2Me$	10.3 ($^2J_{SiP} = 12.5$ Hz, $^1J_{SiW} = 45.8$ Hz)	60
$(C_5Me_5)(CO)_2(Me_3P)WSiHMe_2$	7.4 ($^2J_{SiP} = 11.7$ Hz, $^1J_{SiW} = 41.8$ Hz)	60

(*continued overleaf*)

TABLE 6. (*continued*)

Compound	^{29}Si NMR shift (ppm)	Reference
$(C_5Me_5)(CO)_2(Me_3P)WSiH(Cl)Me$	58.3 ($^2J_{SiP} = 15.4$ Hz, $^1J_{SiW} = 64.1$ Hz)	60
$(C_5Me_5)(CO)_2(Me_3P)WSiHCl_2$	60.87 ($^2J_{SiP} = 14.7$ Hz)	60
$(C_5Me_5)(CO)_2(Me_3P)WSiCl_2SiCl_3$	52.87 (W–Si) ($^2J_{SiP} = 18.1$ Hz) 4.41 (Si–Si) ($^3J_{SiP} = 4.4$ Hz)	59
$(C_5H_5)(CO)_2(Me_3P)WSiCl_2SiCl_3$	52.91 (W–Si) ($^2J_{SiP} = 17.0$ Hz) 3.80 (Si–Si)	59
$(C_5Me_5)(CO)_2(Me_3P)WSiH_2SiH_3$	−61.2 ($^2J_{SiP} = 13.9$ Hz, $^1J_{Wsi} = 52.0$ Hz −94.4 (SiH_3) ($^3J_{PSi} = 1.5$ Hz)	59
$(C_5H_5)(CO)_2(Me_3P)WSiH_2SiH_3$	−76.84 ($^2J_{SiP} = 14.6$ Hz, $^1J_{WSi} = 45.4$ Hz) −96.5 (SiH_3)	59
$(C_5Me_5)(CO)_2(Me_3P)WSiH_3$	−56.87 ($^2J_{SiP} = 15.1$ Hz, $^1J_{WSi} = 44.0$ Hz)	58
$(C_5H_5)_2Mo(H)SiMe_2H$	19.9	63
$(C_5H_5)_2Mo(H)SiMe_2Cl$	86.4	63
$(C_5H_5)_2Mo(Cl)SiMe_2Cl$	70.6	63
$(C_5H_5)_2Mo(H)SiMe_3$	27.0	63
$(C_5Me_5)_2Mo(H)SiMe_3$	27.8	63
$(C_5H_5)_2Mo(H)Si(Bu\text{-}t)_2H$	66.8	63
$(C_5Me_5)_2Mo(H)Si(Bu\text{-}t)_2H$	68.2	63
$(C_5H_5)_2Mo(H)Si(Bu\text{-}t)_2Cl$	108.3	63
$(C_5H_5)_2W(H)SiMe_2Cl$	55.8 ($^1J_{WSi} = 118$ Hz)	63
$(C_5H_5)_2W(H)SiMe_3$	0.5 ($^1J_{WSi} = 84$ Hz)	63
$(C_5H_5)_2W(SiMe_3)_2$	0.3 ($^1J_{WSi} = 106$ Hz)	63
$(C_5H_5)_2W(SiMe_3)(SiMe_2Cl)$	70.0 ($SiMe_2Cl$), ($^1J_{WSi} = 141$ Hz) 4.5 ($SiMe_3$), ($^1J_{WSi} = 100$ Hz)	63
$(C_5H_5)_2W(SiMe_3)(Si(Pr\text{-}i)_2Cl)$	70.7 ($Si(Pr\text{-}i)_2Cl$), ($^1J_{WSi} = 144$ Hz), 2.7 ($SiMe_3$) ($^1J_{WSi} = 102$ Hz)	63
$(C_5Me_5)_2W(SiMe_3)(Si(Bu\text{-}t)_2H)$	38.8 ($Si(Bu\text{-}t)_2H$), ($^1J_{WSi} = 118$ Hz) −3.3 ($SiMe_3$), ($^1J_{WSi} = 111$ Hz)	63
$(C_5H_5)_2W(SiMe_3)(GeMe_3)$	2.1 ($^1J_{WSi} = 90$ Hz)	65
$(C_5H_5)_2W(SiMe_3)(GeMe_2H)$	1.3 ($^1J_{WSi} = 94$ Hz)	65
$(C_5H_5)_2W(SiMe_3)(Ge(Bu\text{-}t)_2H)$	−0.6 ($^1J_{WSi} = 107$ Hz)	65
$(C_5H_5)_2W(SiMe_3)(GePh_2H)$	1.6 ($^1J_{WSi} = 90$ Hz)	65
$(C_5H_5)_2W(SiMe_3)(GeMe_2Cl)$	2.7 ($^1J_{WSi} = 95$ Hz)	65
$(C_5H_5)_2W(SiMe_3)(Ge(Bu\text{-}t)_2Cl)$	−1.5 ($^1J_{WSi} = 103$ Hz)	65
$(C_5H_5)_2W(SiMe_3)(GePh_2Cl)$	3.5 ($^1J_{WSi} = 90$ Hz)	65

TABLE 6. (*continued*)

Compound	^{29}Si NMR shift (ppm)	Reference
$(C_5H_5)_2W(SiMe_3)(GeMe_2OTf)$	2.4 ($^1J_{WSi} = 88$ Hz)	65
$(C_5H_5)_2W(SiMe_3)(Ge(Bu\text{-}t)_2Me)$	113.6 ($^1J_{WSi} = 154$ Hz)	65
cyclo-$Cp_2W(Me_2SiOSiMe_2)$	20.6 ($^1J_{WSi} = 85.9$ Hz)	72
cyclo-$Cp_2W(Me_2SiSSiMe_2)$	−30.5 ($^1J_{WSi} = 96.4$ Hz)	72
cyclo-$Cp_2W(Me_2SiSeSiMe_2)$	−30.5 ($^1J_{WSi} = 99.2$ Hz)	72
cyclo-$Cp_2W(Me_2SiSeSiMe_2)$	−61.3 ($^1J_{WSi} = 103.1$ Hz)	72

XI. GROUP-7 SILYLENE COMPLEXES

The first donor-stabilized manganese bis(silylene) complex $(CO)_4\overline{MnSiMe_2(\mu\text{-}OMe)Si}Me_2$ has been prepared by the photolytic decarbonylation of $(CO)_5Mn(SiMe_2SiMe_2OMe)$ with a concomitant 1,2-shift of the silane, allowing cyclization/stabilization by the oxygen atom[75]. Analogous to complexes **23–25,** silylene complexes of manganese of the type $Ar(L)Si(H){=}Mn(CO)_2(C_5H_4R)$ ($L = H$, $R = H$, Me[57]; $L = Ar$, $R = H$, Me[76]) have been prepared following an analogous synthetic procedure to that of equation 19. Cationic base-free silylene rhenium complexes of the form $[CpRe(NO)(PPh_3)({=}SiMe_2)]^+X^-$ ($X = AlCl_4^-$, $Al_2Cl_7^-$) were found to be in equilibrium with the silyl-adduct derivative $CpRe(NO)(PPh_3)(SiMe_2Cl){-}AlCl_3$. Interestingly, other rhenium silyl and Lewis acid ECl_3 (E = B, Al) derivatives have shown the complexed $Re{-}ECl_3$ and $ReNO{-}ECl_3$ structures in different ratios[77]. Structural data for group VII–silylene complexes are given in Table 7 and the corresponding ^{29}Si NMR data are presented in Table 8.

XII. GROUP-7 SILYL DERIVATIVES

The reaction of $CpRe(NO)(PPh_3)(SiMe_2H)$ and the halomethane substrates $CHCl_3$, CBr_4 and CHI_3 gave the halosilyl complexes $CpRe(NO)(PPh_3)(SiMe_2X)$ (X = Cl, Br, I), respectively. $CpRe(NO)(PPh_3)(SiMe_2Cl)$ was found to react with Me_3SiOTf, yielding the corresponding triflate which reacts either with pyridine yielding the base stabilized $[CpRe(NO)(PPh_3)\{SiMe_2(NC_5H_5)\}]^+OTf^-$ complex or with $(Me_2N)_3S^+[SiMe_3F_2]^-$ to give the fluoro derivative $CpRe(NO)(PPh_3)(SiMe_2F)$. Solution of the complex $CpRe(NO)(PPh_3)(SiMe_2Cl)$ was found to form with BCl_3 the $CpRe(NOBCl_3)(PPh_3)(SiMe_2Cl)$ adduct which has been structurally characterized (Table 7)[77]. Bridging siloxy hydride rhenium complexes has been obtained as described in equation 23, with comparable Re−Si bond lengths in the range of 2.477(3) Å −2.499(3) Å for all the three silyloxy complexes (Table 7)[78].

Photolysis in hydrocarbon solutions of $CpMn(CO)(P_2)$ [P_2 = dmpe, dmpp, dmpm, $(PMe_3)_2$] with the silanes $SiPh_nH_{4-n}$ ($n = 1{-}3$) yielded the corresponding manganese silyl hydrides complexes $CpMn(CO)(P_2)(H)(SiPh_nH_{3-n})$ [P_2 = dmpe, $n = 1{-}3$; P_2 = dmpp, $n = 1{-}3$; P_2 = dmpm, $n = 2$; $P_2 = (PMe_3)_2$; $n = 2$]. The crystal structure of the monosilyl derivative $CpMn(CO)(dmpe)(H)(SiPh_2H)$ features a distorted three-legged piano-stool geometry with a vacant coordination site presumably occupied by the (non-observed) hydride ligand. The silyl and hydride ligands exchange positions through a pseudorotation of a seven-coordinate Mn center[79].

High-valent rhenium silyl hydrides $ReH_5(PPh(Pr\text{-}i)_2)_2(SiHPh_2)_2$ **(27)** and $ReH_5(PCy_3)_2(SiH_2Ph)_2$ have been characterized by neutron and X-ray diffraction, respectively. The complexes were prepared from the corresponding hydrides $ReH_7(PPh(Pr\text{-}i)_2)_2$ and

$ReH_7(PCy_3)_2$ with SiH_2Ph_2 and SiH_3Ph, respectively. The neutron diffraction study on **27** shows that the geometry coordination of the rhenium is better described as a monocapped twisted rhombic antiprism (Figure 4) with metal–silicon bond lengths of 2.510(9) Å and 2.501(2) Å for the $ReH_5(PPh(Pr\text{-}i)_2)_2(SiHPh_2)_2$ **(27)** and $ReH_5(PCy_3)_2(SiH_2Ph)_2$ complexes, respectively[80].

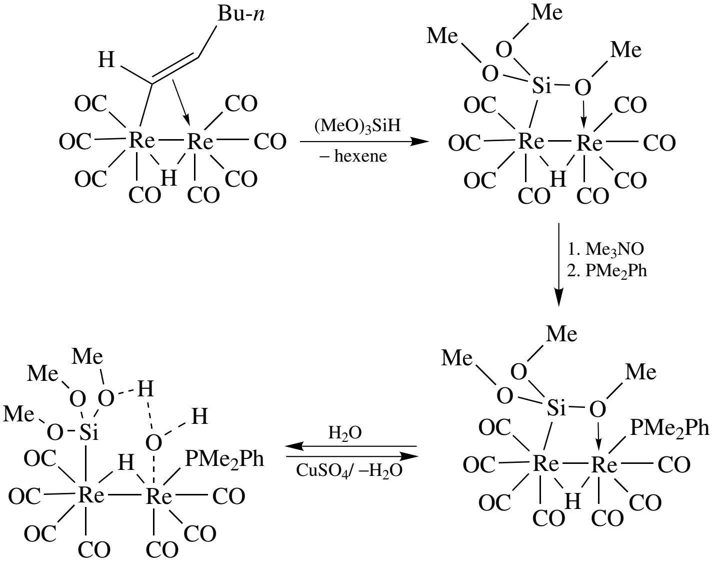

(23)

Similar rhenium complexes having a chelating disilyl ligand $ReH_5(\text{disilyl})(PPh_3)_2$ [disilyl = 1, 2-bis(dimethylsilyl)benzene **(28)** and 1,2-bis(dimethylsilyl)ethane] have been prepared by similar reaction of the disilyl derivatives with $ReH_7(PPh_3)_2$[81]. The structure of the aromatic silyl rhenium derivative is not the tricapped trigonal prism as found for other nine-coordinate rhenium polyhydrides or the monocapped twisted rhombic prism as in complex **27**, but rather a dodecahedral structure typical for eight-coordination is adopted. Thus, the compound is described as a $ReH_3(H_2)(\text{disilyl})(PPh_3)_2$ containing a stretched η^2-H_2 ligand (Figure 4). These complexes were found to be active catalysts for the dehydrogenation of *tert*-butylethylene although with low turnover frequencies[82].

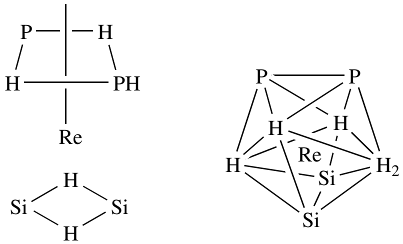

(27) **(28)**

FIGURE 4. Coordination geometries for $ReH_5(PPh(Pr\text{-}i)_2)_2(SiHPh_2)_2)$ (**27**, monocapped antiprism) and $ReH_5(\text{disilyl})(PPh_3)_2$ (**28**, eight-coordinate octahedron)

TABLE 7. Selected M−Si distances in group-7 transition-metal silylene and silyl complexes

Compound	d^n/configuration	M−Si (Å)	Reference
$(CO)_4\overline{MnSiMe_2(\mu\text{-}OMe)Si}Me_2$	d^4	2.336(2) 2.344(2)	75
$CpRe(NOBCl_3)(PPh_3)(SiMe_2Cl)$	d^6	2.476(3)	77
$CpMn(CO)(dmpe)(H)(SiPh_2H)$	d^3	2.319(4)	79
$Re_2(CO)_8[Si(\mu\text{-}\eta^2\text{-}OMe)(OMe)_2](\mu\text{-}H)$	d^6	2.477(3)	78
$Re_2(CO)_7(PMe_2Ph)[Si(\mu\text{-}\eta^2\text{-}OMe)(OMe)_2](\mu\text{-}H)$	d^6	2.477(4)	78
$Re_2(CO)_7(PMe_2Ph)[Si(OMe)_3](H_2O)(\mu\text{-}H)$	d^6	2.499(3)	78
$ReH_5(PPh(Pr\text{-}i)_2)_2((SiHPh_2)_2)$	d^0	2.510(9)	80
$ReH_5(PCy_3)_2((SiH_2Ph)_2)$	d^0	2.501(2)	80
$ReH_3(H_2)[o\text{-}C_6H_4(Me_2SiH)_2](PPh_3)_2$	d^0	2.495(2) 2.489(3)	82

TABLE 8. Selected ^{29}Si NMR chemical shifts for group-7 transition-metal silylene complexes

Compound	^{29}Si NMR shift (ppm)	Reference
$(CO)_4\overline{MnSiMe_2(\mu\text{-}OMe)Si}Me_2$	115.4	75
$Cp(CO)_2Mn{=}SiH(o\text{-}Me_2NCH_2C_6H_4)$	130.89 ($^1J_{HSi}$ = 156.8 Hz)	57
$MeCp(CO)_2Mn{=}SiH(o\text{-}Me_2NCH_2C_6H_4)$	131 ($^1J_{\text{HSi}}$ = 149 Hz)	57
$Cp(CO)_2Mn{=}SiH[8\text{-}(Me_2NCH_2)C_{10}H_6]$	119.82 ($^1J_{HSi}$ = 165.46 Hz)	57
$MeCp(CO)_2Mn{=}SiH[8\text{-}(Me_2NCH_2)C_{10}H_6]$	124.49 ($^1J_{\text{HSi}}$ = 165.96 Hz)	57
$MeCp(CO)_2Mn{=}SiH[8\text{-}(Me_2N)C_{10}H_6]$	141.85 ($^1J_{HSi}$ = 163.97 Hz)	57
$MeCp(CO)_2Mn{=}Si(Ph)(o\text{-}Me_2NCH_2C_6H_4)$	145.2	76
$MeCp(CO)_2Mn{=}Si(Ph)[8\text{-}(Me_2N)C_{10}H_6]$	124.3	76
$Cp(CO)_2Mn{=}Si(Ph)[8\text{-}(Me_2N)C_{10}H_6]$	125.2	76
$Cp(CO)_2Mn{=}Si(Np)[8\text{-}(Me_2N)C_{10}H_6]$	127.1	76
$Cp(CO)_2Mn{=}Si(o\text{-}Me_2NCH_2C_6H_4)_2$	147.4	76

XIII. GROUP-8 SILYL DERIVATIVES

During the last five years, a vast amount of research has been focused on the chemistry of group-8 silicon complexes. This section takes into account only those complexes containing well-characterized metal–silicon bonds but does not take into account intermediary compounds in stoichiometric or catalytic reactions in which such species may be formed.

A. Bimetallic Silyl Complexes

Phosphine substituted hydrido silyl complexes of the type *mer*-$FeH(SiR_3)(CO)_3L$ [R = OMe, L = dppm, $Ph_2PCH_2C(=O)Ph$, PPh_2H; R = OEt, L = dppm, R = Ph, L = dppb] in which only one phosphorous atom is bonded to the metal center, or the chelating complex *cis*-$FeH\{Si(OMe)_3\}(CO)_2L$ [L = vinylidene(diphenylphosphine) = vdpp] have been easily prepared by carbonyl substitution in the complex *cis*-$[FeH(SiR_3)(CO)_4]$ with the corresponding phosphine. The anionic potassium silyl complexes $K[Fe(SiR_3)(CO)_3L]$ [R = OMe, L = dppm, $Ph_2PCH_2C(=O)Ph$; R = OEt, L = dppm; R = Ph, L = dppb] or the sodium complexes $Na[Fe(CO)_3(PR'_3)(SiR_3)]$ (PR'_3 = PMe_3, SiR_3 = $SiMePh_2$, $SiMe_3$; PR'_3 = PBu_3, SiR_3 = $SiMePh_2$; PR'_3 = PPh_2H, SiR_3 = $SiMe_2Ph$, $SiMePh_2$)[83] were prepared from the corresponding hydrides in polar solvents with KH or NaH, respectively. These anionic silyl complexes have been used widely to prepare metal–metal heterobinuclear silicon-containing complexes[83]. Thus, for example, *mer*-$[(CO)_3(Ph_2MeSi)Fe{-}ML]$ (ML = $AgPPh_2CH_2C_6H_5$, $AuPPh_2CH_2C_6H_5$, HgBr)[83]; *mer*-$[LM(\mu\text{-dppm})FeSi(OMe)_3(CO)_3]$ (M = Cu, Ag, Au, L = PPh_3; M = Cu, L = MeCN, M = Ag, L = $AsPh_3$)[84] and (M = Pd, L = η^3-2-Me-allyl, η^3-allyl; M = Pt, L = η^3-allyl)[85] were prepared from their anionic silyl complexes with the corresponding counterpart in the form of the metal halide complexes. Enticingly the arsine ligand, $AsPh_3$, in the complex *mer*-$[Ph_3AsAg(\mu\text{-dppm})FeSi(OMe)_3(CO)_3]$ dissociates in solution forming the corresponding *mer*-$[Ag(\mu\text{-dppm})Fe\{(OMe)Si(OMe)_2\}(CO)_3$ with a η^2-μ_2-SiO bridge among the two metal centers[84]. A similar bridged complex with the η^2-μ_2-SiO moiety $Fe\{\mu\text{-}Si(OMe)_2(OMe)\}(CO)_3(\mu\text{-dppm})Pd(SnPh_3)$ was obtained by the replacement of the allylic moiety and elimination of hydrogen in $[\eta^3\text{-2-Me-allyl})Pd(\mu\text{-dppm})FeSi(OMe)_3(CO)_3]$ with an excess of $HSnPh_3^{85}$. The reaction of the anionic complex, $[Fe(SiR_3)(CO)_3PR'_3]^-$, with CdX_2 (X = Cl, Br) results in the formation of three different types of products, depending on the nature of the phosphine and X ligands. The PMe_3 substituted complexes $[Fe(SiR_3)(CO)_3(PMe_3)]^-$ (SiR_3 = $SiPh_3$, $SiMePh_2$) exclusively gave the 2:1 (Fe:Cd) ratio complexes [*fac*-$(Me_3P)(R_3Si)(CO)_3Fe]_2Cd$ (**29a**). The 2:1 ratio complexes $[\{(MeO)_3P\}(Ph_2MeSi)(CO)_3Fe]_2$ (**29b**) and $[\{(MeO)_3Si\}(CO)_3Fe(\mu\text{-}Ph_2PPyr)]_2Cd$ can be also obtained similarly; however, the arrangement of the CO ligands was found to be meridional.

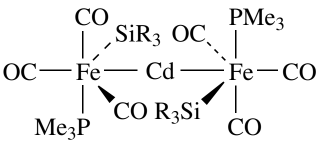

(29a)

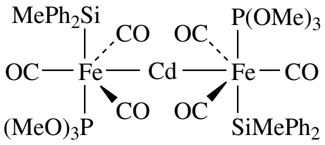

(29b)

In addition to the 2:1 metal ratio complexes, the 1:1 ratio compounds *mer*-$[(R'_3P)(R_3Si)(CO)_3FeCd(\mu\text{-}X)]_2$ were also obtained by the reaction of the ferrosilyl anion $[Fe\{Si(OMe)_3\}(CO)_3(Ph_2PPyr)]^-$ with $CdBr_2$, the reaction of $[Fe(SiPh_2Me)(CO)_3P(OMe)_3]^-$ with $CdCl_2$, and the reaction of $[Fe(SiR_3)(CO)_3PPh_2H]^-$ (SiR_3 = $SiPh_3$, $SiMePh_2$) with $CdCl_2$ and $CdBr_2$[86]. Similar bimetallic Fe–late transition metal complexes, main group elements and trimetallic systems have been studied comprehensively by Braunstein and coworkers. Structural Fe–Si data for the bimetallic and trimetallic complexes are collected in Table 9[87–95].

When the salt $[Bu_4N][AuX_2]$ (X = Cl, Br) was reacted with 2 equiv of the dppm-substituted iron silyl metallate $K[Fe\{Si(OMe)_3\}(CO)_3(dppm)]$, instead of the expected $[Fe-Au-Fe]^-$ silyl derivative anion chain, the complex $[AuFe\{Si(OMe)_3\}(CO)_3(\mu\text{-}dppm)]_2{\cdot}CH_2Cl_2$ **(30)** was obtained with a Au−Au and two Au−Fe bonds. It is interesting to point out that complex **30** forms a 10-membered-ring structure in which the Au−Au interaction is reminiscent of the transannular interactions that occur in organic cycles of middle size (8–12). The similar reaction with $HgCl_2$ yielded the expected Fe−Hg−Fe complex **(31)**[96].

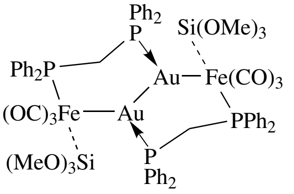

(30)

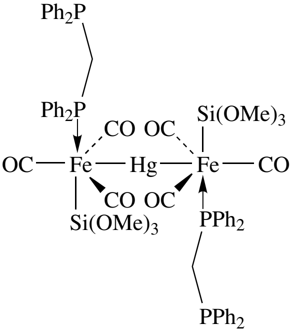

(31)

Photochemical decarbonylation reaction of $(CO)_2(dppe)Fe(H)(SiR_3)$ with $HSiR_3$ [SiR_3 = $Si(OMe)_3$, $Si(OEt)_3$, $SiMe_3$, $SiMe_2Ph$, $SiPh_3$] yields the trihydrido silyl complexes $(CO)(dppe)FeH_3(SiR_3)$. The analogous silyl triphosphine complexes $(PR'Ph_2)_3FeH_3(SiR_3)$ can also be prepared by the reaction of the H_2-complexes, $(PR'Ph_2)_3FeH_2(H_2)$, with the corresponding silanes $HSiR_3$. Additional silyl derivatives of the above-mentioned carbonyl and phosphine trihydrido complexes were obtained by simple silane exchange starting from the corresponding $(CO)(dppe)FeH_3(SiR_3)$ or $(PR'Ph_2)_3FeH_3(SiR_3)$, respectively. Interestingly, the mono and trihydrido silyl complexes $(CO)_2(dppe)Fe(H)(SiR_3)$ and $(PR'Ph_2)_3FeH_3(SiR_3)$ were found to show fluxional behavior in solutions with an exchange mechanism involving a η^2-$HSiR_3$ ligation[97]. The trihydrido silyl complexes $(PEtPh_2)_3FeH_3(SiPh_nMe_{3-n})(n = 1\text{–}3)$ were found to react selectively with HBF_4 to give the corresponding fluorinated complexes $(PEtPh_2)_3FeH_3(SiF_nMe_{3-n})$ by cleavage of the Si−Ph bonds[98]. Trihydrido silyl complexes of the type $Fe(CO)(dppe)H_3(Si(OEt)_3)$ were deprotonated in the presence of KH/18-crown-6 to the anionic silyl complex [K(18-crown-6)] $[Fe(CO)(dppe)H_2(Si(OEt)_3)]$. This complex can react with Me_3ECl (E = Sn, Pb) affording the capped octahedral complex $Fe(CO)(dppe)H_2(Si(OEt)_3(EMe_3)$ with the dppe, ER_3, and CO ligands in the plane, one hydride ligand in the axial position and the other hydride capping the triangular face[99].

Dinuclear silyl-substituted complexes of the type $(CO)_3(R_3Si)Fe(\mu\text{-}PR'R'')Pt(PPh_3)_2$ [$PHR'R''$ = $PHPh_2$, PH_2Ph, PH_2Cy; SiR_3 = $SiPh_3$, $SiPh_2Me$, $SiPhMe_2$, $Si(OMe)_3$] were prepared by an oxidative addition across the P−H and Fe−H bonds of the corresponding hydro-silyl phosphine complexes with the platinum (0) complex, $Pt(CH_2{=}CH_2)(PPh_3)_2$. For the bridged (μ-PPh_2) complexes, the PPh_3 ligand *trans* to the bridge can be replaced by CO (Scheme 17)[100] or by a number of phosphine and diphosphine ligands[101]. Braunstein and coworkers have found the unprecedented CO-promoted transfer of a silyl group from a metal to a metal in $(CO)_3(SiR_3)Fe(\mu\text{-}PPh_2)Pt(PPh_3)CO(Fe{-}Pt)$ as described in Scheme 17.

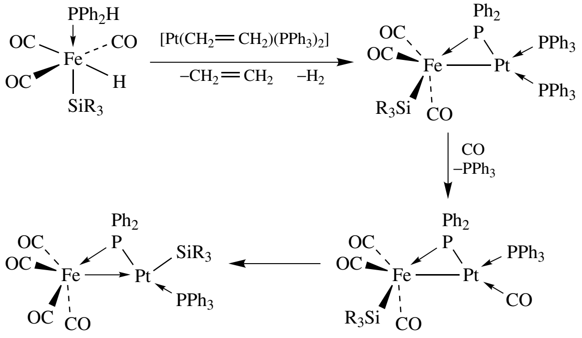

SiR_3 = $Si(OMe)_3$, $SiMe_2Ph$

SCHEME 17

The migration was found to be faster for the methoxide silyl derivative than for the dimethylphenyl silyl derivative and it could be prevented by using $SiPh_3$ or stronger σ-donor / π-acceptor ligands on Pt such as *t*-BuCN and dppm[102]. In related dppm-bridged Fe−Pt complexes containing a Pt−Alkyl bond *trans* with respect to the metal−metal bond, facile CO insertion has been found, affording the corresponding bimetallic acyl complexes of the type η^2-μ_2-SiO[$(CO)_3$Fe{μ-$Si(OMe)_2(OMe)$}(μ-dppm)Pt{C(=O)R}] (R = Me, Et, norbornyl) with the acyl group *trans* with respect to the metal−metal bond[103]. The addition of phosphine or phosphite ligands induced silyl migration from the iron to the acyl group leading to the μ-siloxycarbene complex[104]. Similar silyl migration and μ-siloxycarbene bridged formation has been observed for the complex [$(CO)_3$Fe{μ-$Si(OSiMe_3)_2(OSiMe_3)$}(μ-dppm)Pd(Me)] upon reaction with CO[105]. Likewise, μ_2-η^2-SiO−Fe−Pd and Fe−Pt silyloxy complexes undergo methoxy exchange with fluoro atoms by the reaction of the corresponding complexes with $BF_3 \bullet Et_2O$ forming μ_2-η^2-SiF−Fe−Pd and μ-SiF−Fe−Pt−H interactions as outlined in Scheme 18[87].

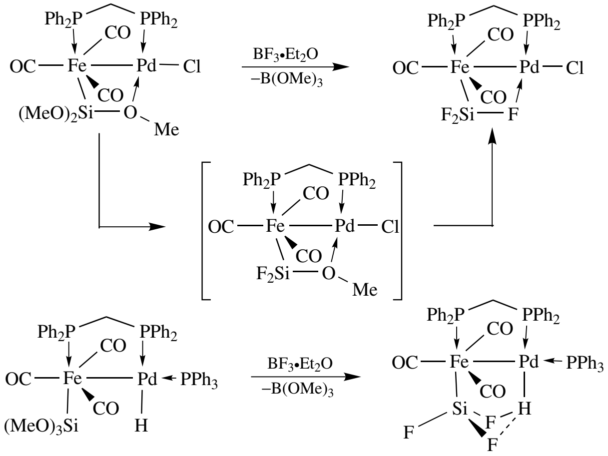

SCHEME 18

B. Clusters Containing Silyl Groups

The oxidative addition of $Os_3(CO)_{10}(NCMe)_2$ with $HSi(OEt)_3$ yielded the bridging hydride complex $Os_3(CO)_{10}(NCMe)[Si(OEt)_3](\mu\text{-H})$ **(32)**, which was transformed to the first $\mu_3\text{-}\eta^3$-SiO complex, $Os_3(CO)_9(NCMe)[\mu_3\text{-}\eta^3\text{-}Si(OEt)_3](\mu\text{-H})$ (**33**), by reflux in non-polar solvents (equation 24). The molecular structure of **33** consists of a triangular triosmium cluster with a η^3-$Si(OEt)_3$ ligand bridging one face of the cluster. Complex **33** was found to add 2 equivalents of CO forming the complex $Os_3(CO)_{11}[Si(OEt)_3](\mu\text{-H})$, which is believed to be geometrically similar to complex **32** with a CO ligand replacing the NCMe ligand^{106,107}.

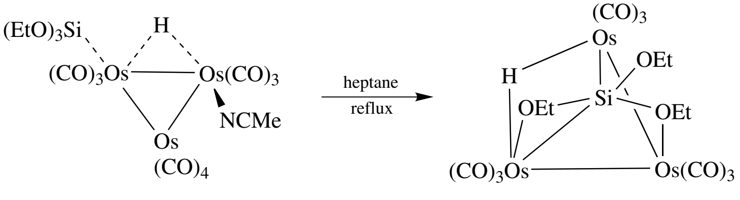

(24)

(32) **(33)**

The comparable methoxy hydride cluster $Os_3(CO)_{10}(NCMe)[Si(OMe)_3](\mu\text{-H})$ **(34)** was found to react with terminal alkynes (t-BuC≡CH) forming a *tert*-butylvinyl η^2-bridge among the metal centers by insertion of the hydride into the triple bond. Concomitant addition of CO produced the hydrosilylation silyl olefin product *trans*-t-BuCH=CHSi(OMe)$_3$^{107}. Reaction of complex **34** with the phosphine ligand, dppm, replaced the NCMe ligand affording the complex $Os_3(CO)_{10}(\eta^1\text{-dppm})[Si(OMe)_3](\mu\text{-H})$, and reaction of the latter with $Pt(COD)_2$ (COD $=$ 1,5-cyclooctadiene) yields the cluster $(\mu\text{-H})PtOs_3(CO)_{10}(\mu\text{-}\eta^2\text{-dppm})[Si(OMe)_3]$ **(35)**. The structure of **35** consist of a planar butterfly cluster of four metal atoms, with the platinum atom located in one of the 'hinge' sites. Irradiation of **35** produced the isomeric complex $PtOs_3(\mu\text{-H})(CO)_{10}(\mu\text{-}\eta^2\text{-dppm})[Si(OMe)_3]$ **(36)** which slowly converts back thermally to **35**. The transformation of **35** to **36** was proposed to occur via a tetrahedral-like cluster complex **37** through the formation of a bond between the wing tip metal atoms (Os) in **35** (equation 25)^{108}.

Bridging between two osmium centers has been observed through the oxidative addition of a sila-phosphine ligand and $Os_3(CO)_{10}(MeCN)_2$ as observed by the NMR coupling constants (Table 10)^{109}, whereas the oxidative addition reaction of an isolobal sila-amine (e.g. 2-$Me_2SiHC_5H_4N$) ligand with the cluster $[Os_3(CO)_{10}(\mu\text{-H})_2]_2$ produced the disilyl triosmium cluster $Os_3(CO)_{10}(\mu\text{-H})_2$ {2-$Me_2SiHC_5H_4N$}$_2$ with no bonding of the nitrogen to the metal center^{110}. Similar diaza-bridged Ru carbonyl clusters have been prepared by the oxidative addition of the silanes $HSiR_3$, with the succeeding series of $[Ru_3(\mu\text{-H})(\mu_3,\eta^2\text{-ampy})(PPh_3)(CO)_{9-n}]$ ($n = 0$–2; Hampy $=$ 2-amino-6-methylpyridine), $[Ru_3(\mu\text{-}C_4H_4N_2)(\mu\text{-CO})_3(CO)_7]$ ($C_4H_4N_2$ $=$ pyridazine) and $[Ru_3(\mu\text{-dmpz})(\mu\text{-CO})_3(CO)_7$ (Hdmpz $=$ 3,5-dimethylpyrazole) complexes$^{111-114}$. An interesting symmetric triruthenium dihydrido cluster bridged by 1,1-ferrocenediyl bis(dimethylsilylene) was obtained by the reaction of 1,1′-bis(dimethylsilyl)ferrocene with $Ru_3(CO)_{12}$^{115}.

C. Silyl Complexes

Girolami and coworkers have shown that the methylene/silyl complex $Cp^*Ru(\mu\text{-}CH_2)(\mu\text{-Cl})Cp^*Ru(SiMe_3)$ undergoes low-and high-energy dynamic processes in which the silyl group migrates between the two metal centers. The low-energy dynamic process has $\Delta H^{\ddagger} = 8.9 \pm 0.1$ kcal mol^{-1} which involves a migration through a symmetric Ru(μ- SiMe$_3$)Ru intermediate whereas the consecutive high-energy dynamic process has $\Delta H^{\ddagger} = 12.0 \pm 0.1$ kcal mol^{-1} involving a remarkable reversible C−Si bond cleavage (equation 26)[116,117]. Treatment of the silyl/methylene complex with acetylene gave the first unsubstituted metallabenzene complex [Ru$_2$(η^5-C$_5$Me$_5$)$_2$(η^2,η^5-C$_5$H$_5$)(SiMe$_3$)] (equation 27)[116].

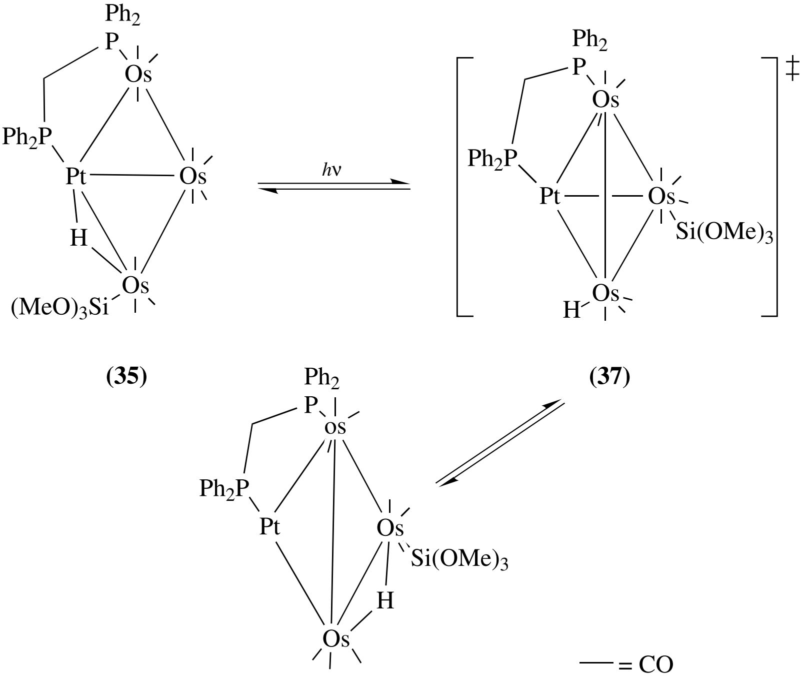

(35) **(37)** (25)

(36)

Oxidative addition of the penta-coordinative Os(CO)$_2$(PPh$_3$)$_3$ with the hydrosilanes HSiR$_3$ (SiR$_3$ = SiMe$_3$, SiEt$_3$, SiPh$_2$H) affords the corresponding octahedral monosilyl hydride complexes, OsH(SiR$_3$)(CO)$_2$(PPh$_3$)$_2$[118], whereas the reaction of the penta-coordinative phenyl complex Ru(Ph)(CO)Cl(PPh$_3$)$_2$ with the appropriate silanes HSiR$_3$ yields the corresponding five-coordinate silyl complexes Ru(SiR$_3$)Cl(CO)(PPh$_3$)$_2$ upon the reductive elimination of benzene. These complexes have been found to be effective catalysts for the hydrosilylation of alkynes to vinylsilanes[119].

Reaction of silyl−late transition metal complexes with amines normally induces the removal of the silicon ligand to obtain the Si−N bonded product. Interestingly, the reaction of Ru(CO)$_4$Si(Me$_2$Ph)I with benzylamine yields the octahedral complex, Ru(CO)$_2$(H$_2$NCH$_2$Ph)$_2$(SiMe$_2$Ph)I, with the carbonyl and the nitrogens of the benzylamine ligands in the *trans* position of the equatorial plane, and a short Ru−Si bond length compared with other Ru(II)−silyl complexes (Table 9)[120]. Monomeric and dimeric silanetriols of similar osmium complexes were obtained by the basic hydrolysis of the corresponding trichlorosilanes as outlined in equation 28[119].

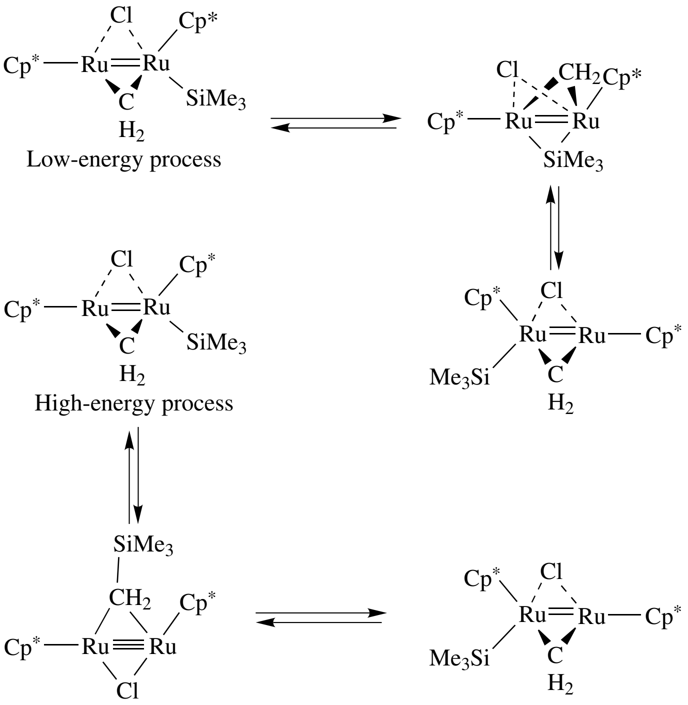
Low-energy process
High-energy process

(26)

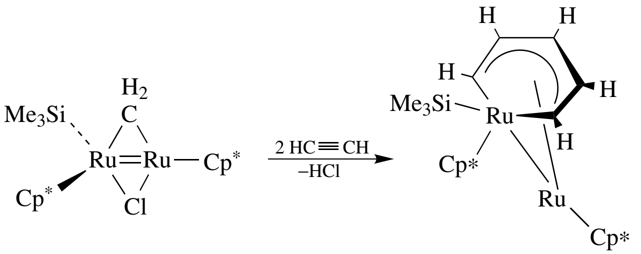
2 HC≡CH
−HCl

(27)

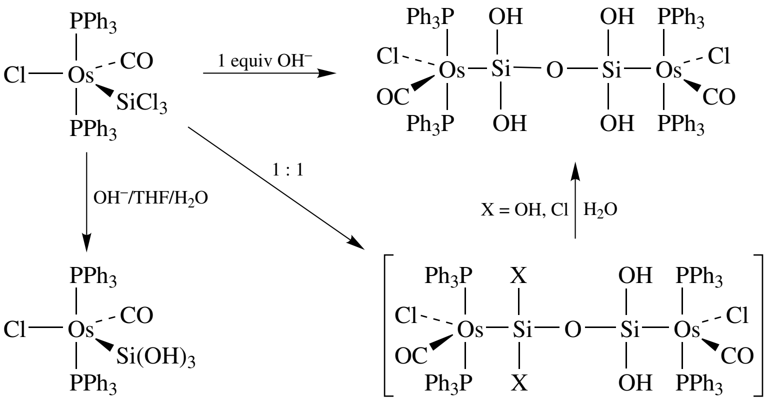
1 equiv OH⁻
1 : 1
OH⁻/THF/H2O
X = OH, Cl
H2O

(28)

Other Cp(CO)(L)Fe (L = CO, PPh_3) silaneols, silanediols and silanetriols have been prepared via hydrolysis of the corresponding metallochlorosilanes or via oxyfunctionalization of metallo-hydrosilanes with dimethyldioxirane as described above for the tungsten complexes *(vide supra)*. Bifunctional metallosilylamines have been synthesized from the metallohydridosilanes by H/Cl exchange and upon dehydrohalogenation with $Me_3P{=}CH_2$, giving access to the corresponding silanimine complexes. The latter complexes add amines, acetone and alcohols in a 1,2 fashion yielding the corresponding disubstituted metallasilanes (Scheme 19)[62]. Recently, the ferro- and ruthenio-trihydridosilanes $(C_5R_5)(CO)_2MSiH_3$ (R = H, Me; M = Fe, Ru) were prepared via reaction of the ferro- and ruthenio-dichlorosilanes $(C_5R_5)(CO)_2MSiCl_2H$ with $LiAlH_4$. Photo-induced substitution of the CO ligands with other ligands can be achieved for the iron complex with Me_3P or Ph_3P[121]. The ruthenio-hydridosilanes $(C_5Me_5)(CO)_2RuSiR_2H$ (R = Me, *o*-MeC_6H_4) were accessible from the reaction of the metallating salt $K[Ru(CO)_2C_5Me_5]$ and the corresponding chlorosilanes R_2SiHCl with a concomitant reduction by $LiAlH_4$. Oxofunctionalization with dimethyldioxirane afforded the corresponding ruthenio-silanol $(C_5Me_5)(CO)_2RuSiR_2OH$ (R = Me, *o*-MeC_6H_4) complexes[122].

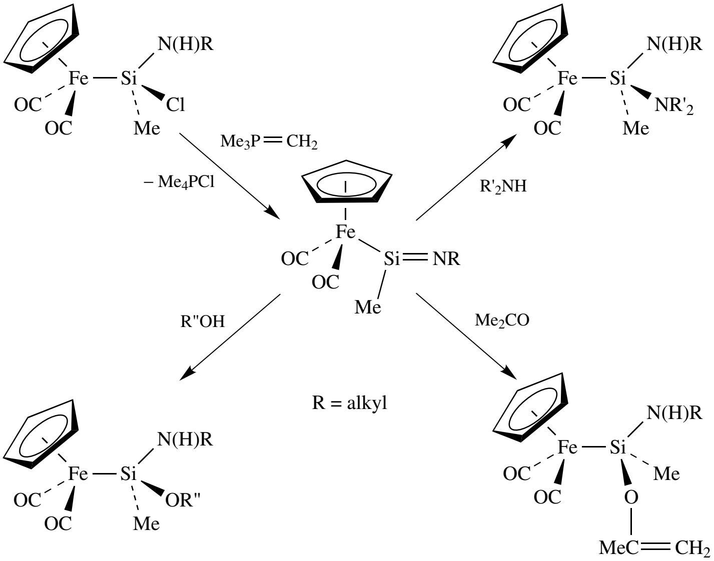

SCHEME 19

A series of ruthenium silyl complexes of the type $CpRu(PMe_3)_2(SiR_3)$ ($SiR_3 = SiHCl_2$, $SiCl_3$, $SiMeHCl$, $SiMeCl_2$, $SiMe_2Cl$) have been obtained by HCl elimination from the reaction of the $Cp(Me_3P)_2RuH$ with the corresponding chlorosilanes, presumably through a nucleophilic exchange mechanism involving a cationic ruthenium silyl hydride derivative exhibiting an agostic Ru−Si−H interaction. Interestingly, a trend of decreasing the $^2J_{SiP}$ coupling constants is observed when less electronegative substituents replaced the electronegative atoms at the silicon center, in line with Bent's rule (Table 10)[123]. The first reported example of a cationic metal silyl hydride was prepared by the protonation of $Cp(Me_3P)_2RuSiCl_3$ with the borane salt $[H(Et_2O)_2][B(C_6H_3(CF_3)_2\text{-}3,5)_4]$ as shown in equation 29. The small $^2J_{PH}$ value of 29 Hz suggests a weakened Ru−H interaction, arguing for an agostic interaction which is also consistent with the large $^{2}J_{SiH}$ value of 48 Hz[123].

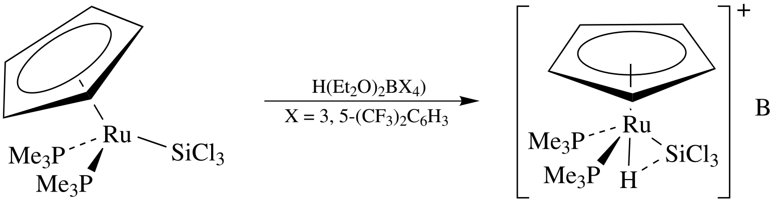

(29)

Recently, Lemke and coworkers prepared the Cp(PMe$_3$)$_2$RuSiCl$_2$(η^1-Cp*) complex by reacting Cp(PMe$_3$)$_2$RuCH$_2$SiMe$_3$ with (η^1-Cp*) SiHCl$_2$. The Cp* in the complex is σ-bound to the silicon and behaves as 'static' on the NMR time scale at room temperature. The η^1-Cp* configuration was confirmed by single-crystal X-ray diffraction showing a three-legged piano-stool geometry with a Ru−Si bond length of 2.335(1) Å, consistent with a single bond within the range of 2.27−2.51 Å (Table 9) as observed for other d^6 ruthenium silyl complexes[124]. Similar Ru−Si−H agostic interaction was obtained in the 1-sila-allene complex of Ru which was prepared using Tilley and coworkers'[125] synthesis for encumbered silenes as shown in equation 30. Here also, in contrast with similar systems prepared by Tilley and coworkers[125], the values $^{2}J_{SiH} = 66$ Hz and $^{2}J_{SiP} = 34.7$ Hz show that the hydrogen is not totally transferred to the metal center. This observation is verified by the hydrogen position at the silicon atom, which is disposed in the crystal structure almost symmetrically between the Ru and Si atoms [Ru−H = 1.58(5) Å and H−Si = 1.70(3) Å][126]. Caulton and coworkers have shown that no agostic Ru−H−Si interactions are observed in the similar systems Ru(CO)H(P(Bu-*t*)$_2$Me)$_2$SiHPh$_2$ and Cp*RuH(P(Pr-*i*)$_2$ Ph)HSiHPh$_2$ prepared by the reactions of Ru(CO)(P(Bu-*t*)$_2$Me)$_2$ and Cp*Ru(P(Pr-*i*)$_2$ Ph)(OCH$_2$CF$_3$); respectively, with H$_2$SiPh$_2$ (Table 10)[127,128].

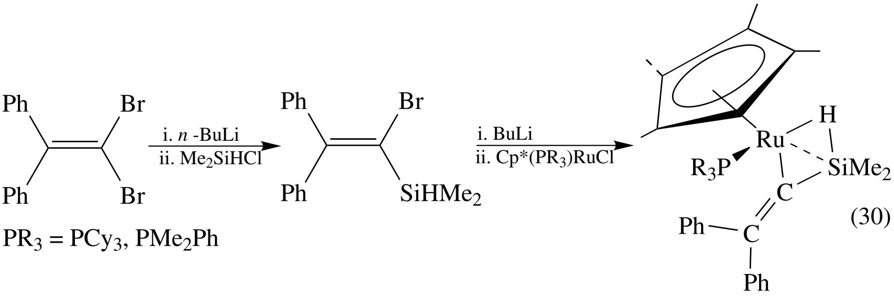

(30)

D. Bis(silyl) Complexes

Four-legged 'piano stool' bis(silyl) complexes of the arrangement (η^6-arene)RuH$_2$ (SiMe$_3$)$_2$ (arene = C$_6$Me$_6$, C$_6$H$_6$, *p*-cymene) have been prepared by the oxidative addition of an excess of Me$_3$SiH with the dimeric [(η^6-arene)Ru(Cl)$_2$]$_2$ complex. The solid structure of the complex (arene = C$_6$Me$_6$) revealed a transoid disposition of the silyl and hydride ligands. In general, these complexes show a remarkable reactivity when heated at 150 °C with deuteriated benzene which results in a complete H/D exchange in *all* the positions of the molecule, presumably through a η^2-Si=C intermediate, with concurrent arene exchange[129]. Similar (η^6-arene)Fe(H)$_2$(SiX$_3$)$_2$(X = Cl, F) complexes have been prepared from the arene solvated iron atoms in the presence of the trihalosilane and their solid state crystal structures have been determined[130–132].

Reaction of the bridged dinuclear tetrahydride complex [(C$_5$Me$_5$)Ru(μ-H)$_4$Ru(C$_5$Me$_5$)] with R$_2$SiH$_2$ yields the dinuclear μ-silyl complexes [{(C$_5$Me$_5$)Ru(μ-η^2-HSiR$_2$)}$_2$ (μ-H)(H)] (R = Et, Ph), having two three-center two-electron interactions. Pyrolysis of the latter complex in toluene at 150 °C afforded the dinuclear μ-silylene complex [(C$_5$Me$_5$)Ru(μ-SiPh$_2$)$_2$(μ-H)$_2$Ru(C$_5$Me$_5$)] which inserts acetylene, yielding the disilaruthenacyclopentene complex **38** (equation 31) or reacts with CO under high pressure to obtain the complex [(C$_5$Me$_5$)(CO)Ru(μ-SiPh$_2$)$_2$Ru(CO)(C$_5$Me$_5$)] with the two Cp* rings in the transoid position with respect to the Ru−Ru vector[133,134]. Starting from the coordinatively unsaturated dimer [Cp*Ru(μ-OMe)]$_2$ with the silane Ph$_2$SiH$_2$, the triple-bridged complex {[Cp*Ru]$_2$(μ-SiPhOMe)(μ-OMe)(μ-H)} was obtained[135]. Recently, similar complexes with one μ-silyl bridged group have been obtained in a similar manner, by the reaction of the bridged dinuclear tetrahydride complex [(C$_5$Me$_5$)Ru(μ-H)$_4$Ru(C$_5$Me$_5$)] with bulky t-Bu$_2$SiH$_2$. This complex can react with an excess of a less crowded silane to obtain mixed μ-silyl bridged derivatives (Table 10)[136].

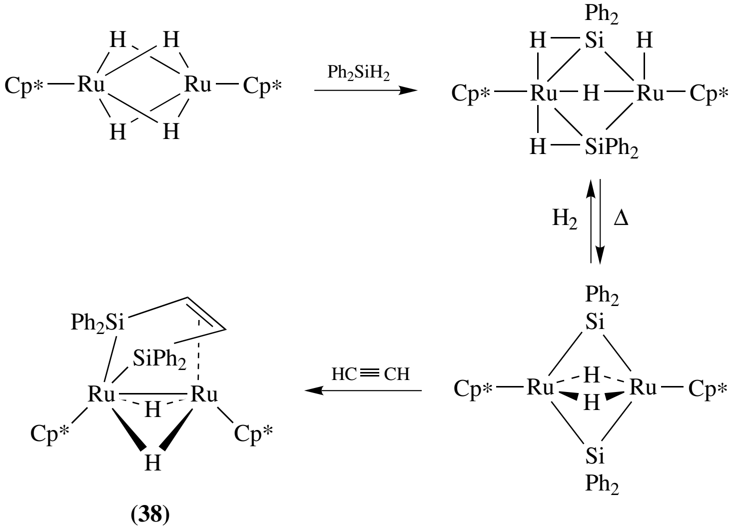

(38)

(31)

Akita and coworkers have shown the use of silanes as an H$_2$ equivalent for the reduction of organometallic ruthenium complexes. Thus, the reaction of the ruthenium carbonyl complex Cp$_2$Ru(CO)$_4$ with di- or trihydrosilanes at 150 °C resulted in the deoxygenative reduction of the carbonyl ligand, yielding a mixture of mono- and di-μ-methylene complexes. Further treatment of the mono-μ-methylene complex with monohydrosilanes produced methane (Scheme 20). The reaction mechanism, which involves an initial dissociation of CO, was investigated by using the labile μ-methylene acetonitrile complex which afforded instantaneously the hydrido-silyl-μ-CH$_2$ and disilyl-μ-CH$_2$ complexes, and by concomitant reaction with HSiR$_3$ yielded methane[137–141].

Reactions of the silene hydride complex [Cp*Ru(P(Pr-i)$_3$)(H)(η^2-CH$_2$=SiPh$_2$)] with hydrosilanes proceed via an initial migration of the hydride to the silene ligand, affording as the final products either the disilyl hydride or the mono silyl dihydrido ruthenium(IV) complexes as described in Scheme 21. Similar reductive elimination and

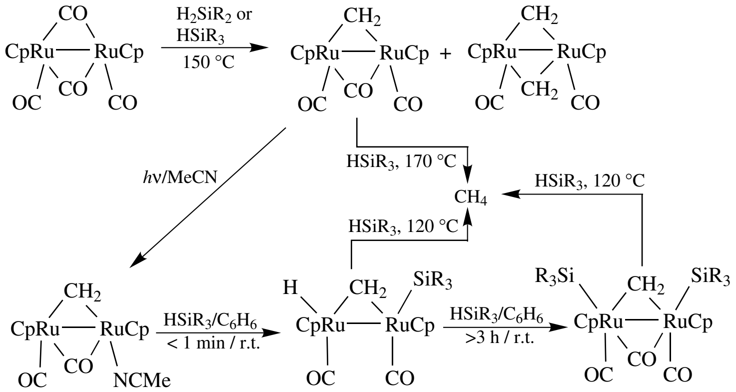

SCHEME 20

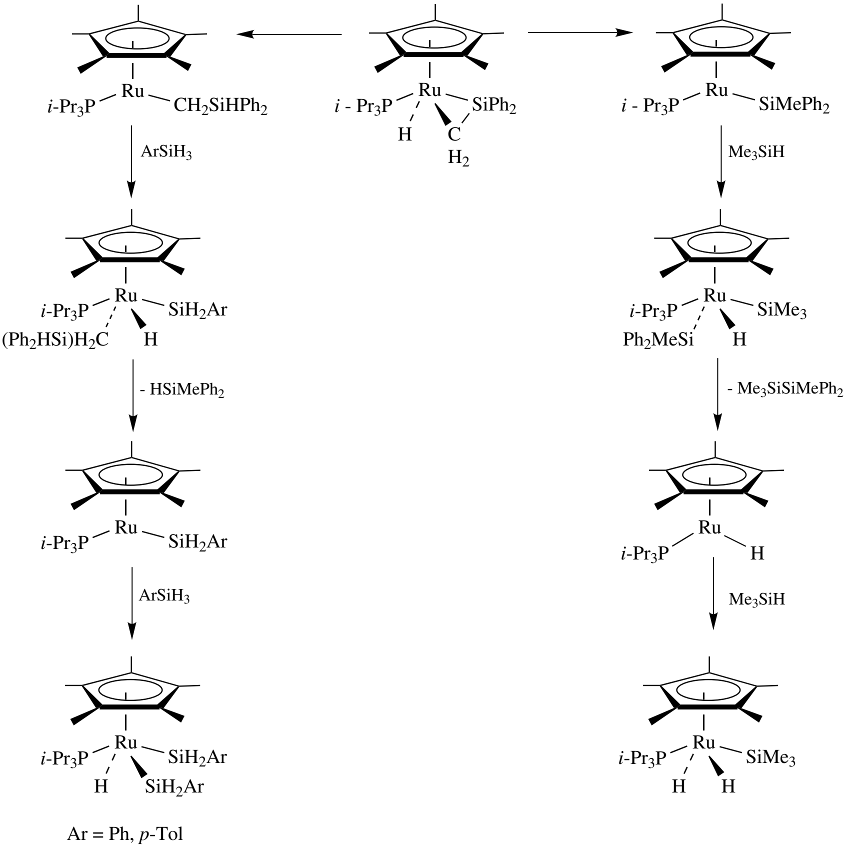

Ar = Ph, *p*-Tol

SCHEME 21

oxidative addition of a MesSi(Cl)H ligand was applied in the reaction of Cp*Ru(P(Pr-*i*)$_3$)Cl with MesSiH$_3$, producing the dihydrido monosilane complex Cp*Ru(P(Pr-*i*)$_3$)(H)$_2$(SiHClMes)[125,135,142].

E. Silacyclopentadienyl Complexes

The first silacyclopentadienyl ruthenium complex [Cp*Ru{η^5-Me$_4$C$_4$SiSi(SiMe$_3$)$_3$}] was prepared by Tilley and coworkers by the deprotonation of the corresponding tetraphenylborate salt, [Cp*Ru(H){η^5-Me$_4$C$_4$SiSi(SiMe$_3$)$_3$}] [BPh$_4$] **(40)**, with (Me$_3$Si)$_3$SiLi•3THF in 50% yield. The ruthenium salt was generated by the oxidative addition of the silole **39** to Cp*Ru$^+$, which was prepared *in situ* by reacting the dimer [Cp*Ru (μ-OMe)]$_2$ with Me$_3$SiOTf, after the addition of NaBH$_4$ (Scheme 22). The crystal structure of the complex salt shows the general protonated metallocene appearance with identical Ru–ring centroid distances within the experimental error (1.84 Å). The Ru–Si bond length of 2.441(3) Å is representative of a single bond (Table 9) and the $^1J_{\text{SiH}}$ coupling constant of 41 Hz is in the lower end for η^2-Si–H interactions[143].

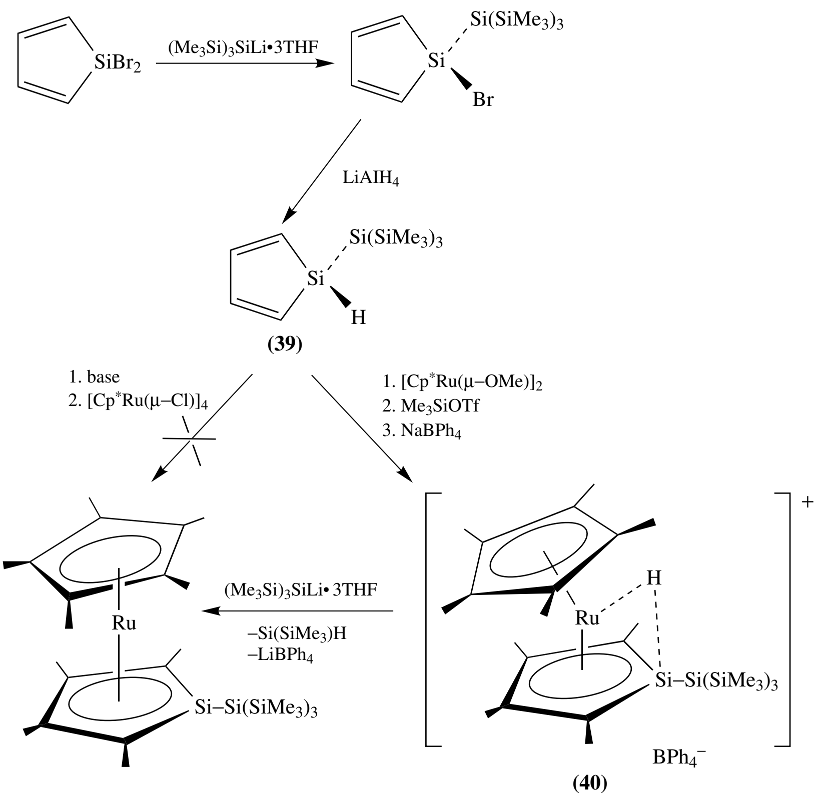

SCHEME 22

η^1-Tetraphenylsilacyclopentadienyl complexes of Fe and Ru have been prepared from the corresponding tetraphenylalkyl silyl chloride with NaMCp(CO)$_2$ (M = Ru, Fe). The complexes were found to react as dienes in spite of the presence of the electronegative phenyl substituents. Thus, the reaction of the substituted silacyclopentadiene complex with dimethyl acetylenedicarboxylate was found to yield the 7-silanorbornadiene complex with a Ru−Si bond length of 2.372(1) Å. The reaction of the latter with 2,3-dimethylbutadiene or 2,3-butanedione formed the corresponding 2,3-silacyclopentene complex and the dimethyl tetraphenylphthalate (Scheme 23)[144].

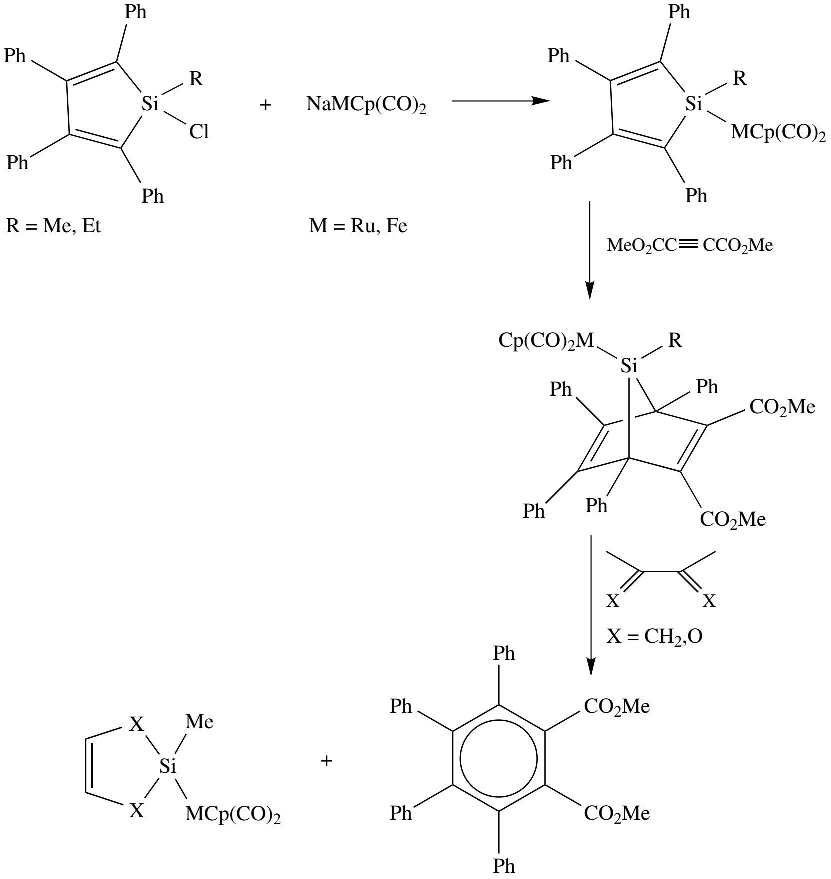

SCHEME 23

Many cyclic and linear transition metal−silicon compounds have been obtained by the elimination of alkali halides with the corresponding transition metal salts[145,146]. The synthesis and reactivity of the Fe−oligosilane systems have been studied in detail by Pannell[147−154] and this area has been recently reviewed[155].

F. Silene and Silylene Complexes

Lewis-base-stabilized iron−silylene complexes have been prepared by Corriu (equation 19) and Zybill (equation 17 and 18) in a similar fashion to that described for groups 6 and 7 silylene complexes (Tables 5–8)[55–57,76,156]. The reactivity of the Fe=Si bond with dienes, acetylenes and alcohols can be summarized for the silylene complex **41** as shown in Scheme 24.

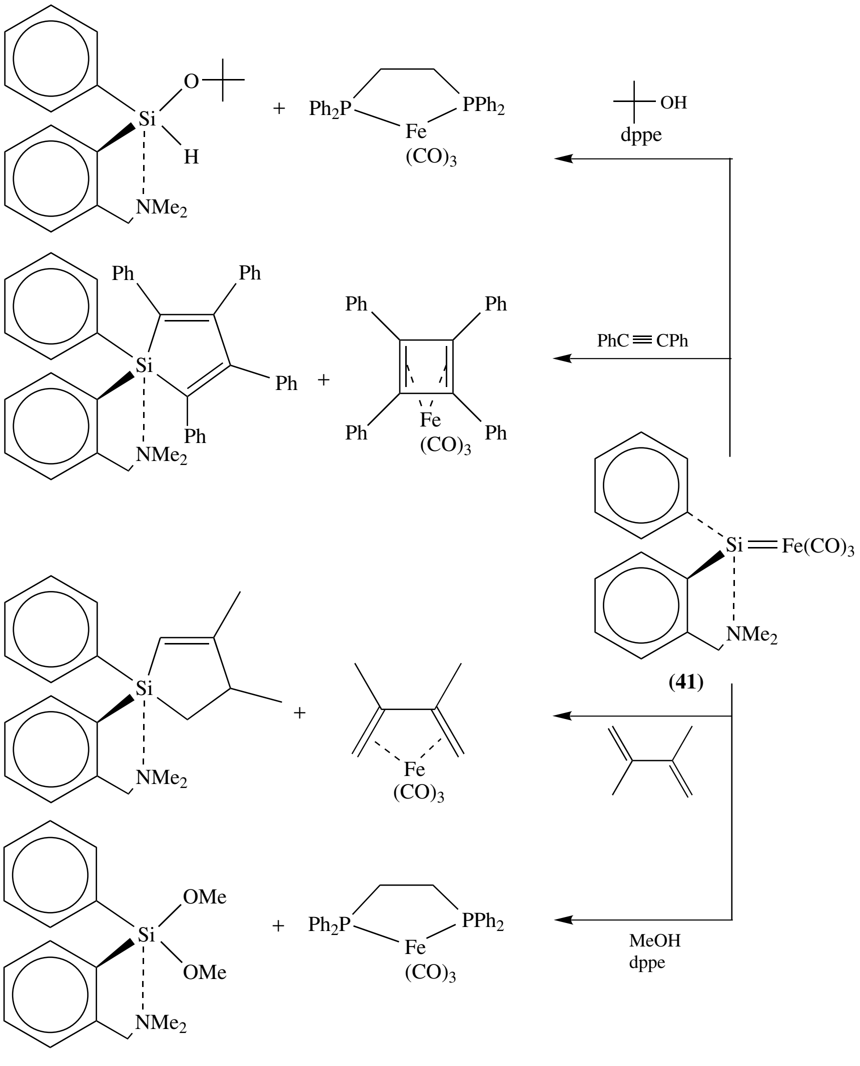

SCHEME 24

The photochemical reaction of $Fe(CO)_5$ with $HSi(NMe_2)_3$ yields the amine-stabilized silylene complex $(CO)_4Fe{=}Si(NMe_2)_2(NHMe_2)$ **(42)**. Reaction of complex **42** with $Pt(C_2H_4)(PR_3)_2$ (R = Ph, p-MeC_6H_4) resulted in the displacement of the dimethylamino and the ethylene ligands yielding the η^2-Pt–disilene complex **43**. The ^{29}Si NMR chemical shift of $\delta = 119$ found in complex **43** is consistent with a silylene complex and the $^2J_{SiPt} = 136.4$ Hz indicates that the $Pt(PR_3)_2$ fragment does not rotate freely. Similar photochemical reaction of the complex $Fe(CO)_4\{P(OEt)_3\}$ with $HSi(NMe_2)_3$ proceeds with an unprecedented ligand rearrangement to produce complex **44**. Two ethoxy groups of the phosphite ligand were exchanged with two NMe_2 substituents groups of the silicon atom forming a $HNMe_2$-stabilized diethoxysilylene complex having one of the shortest Fe−Si bond lengths [2.218(2) Å, 2.216(2) Å] (Table 9)[157].

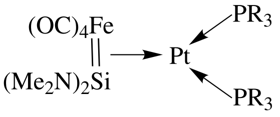

(43)

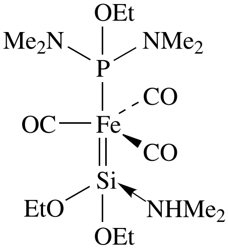

(44)

Recently, additional silacyclobutenes **45** and **46**[158] and isopropoxide[159] Fe=Si stabilized complexes were prepared from Collman's salt ($Na_2Fe(CO)_4$) with the corresponding dichlorosilane as described in equations 32 and 33, respectively. In complexes **45** and **46** a mixture of the *E/Z* diastereomers was obtained because of the possibility for the HMPA solvent to coordinate to the silicon center either *E* or *Z* relative to the neopentyl group. Thus, in the ^{29}Si NMR spectra of complexes **45** and **46**, the coordination to HMPA leads to a line splitting into doublets at 75.58 ($^2J_{SiP}$ = 36.4 Hz) for *E*-**45** and 77.90 ($^2J_{SiP}$ = 47.0 Hz) for *Z*-**45**, or at 72.03 ($^2J_{SiP}$ = 32.3 Hz) for *E*-**46** and 76.25 ($^2J_{SiP}$ = 29.4 Hz) for *Z*-**46**. The signals in **45** and **46** are shifted to higher fields (Table 10) due to the strong shielding at the silicon atom produced by the more electron-rich silacyclobutene rings. The two isopropoxy methyl groups are diastereotopic due to the pyramidal configuration of the silicon atom which is maintained even at high temperatures (100 °C). Similar base-stabilized ruthenium(0) silanediyl complexes have been prepared by Zybill following the approach described in equation 16 (Table 10)[160].

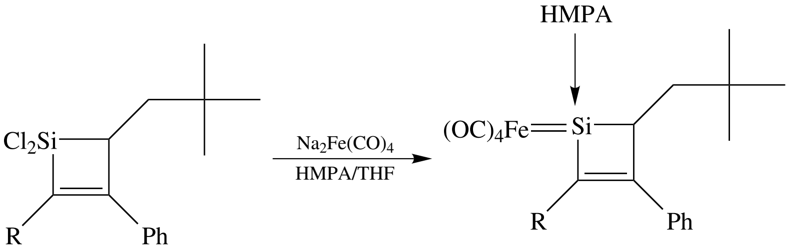

R = Me **(45)**
Ph **(46)**

(32)

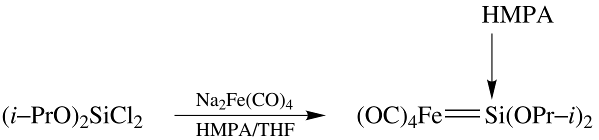

$$(i\text{–PrO})_2SiCl_2 \xrightarrow[\text{HMPA/THF}]{Na_2Fe(CO)_4} (OC)_4Fe{=}\overset{\overset{\text{HMPA}}{\downarrow}}{Si}(OPr\text{–}i)_2 \qquad (33)$$

Base-stabilized ruthenium silylyne complex [$Cp^*(PMe_3)_2Ru{\equiv}Si(SC_6H_4Me$-*p*)(phen)] [$(OTf)_2$] **(47)** has been prepared by Tilley and coworkers by the displacement of two triflate groups from $Cp^*(PMe_3)_2RuSi(SC_6H_4Me$-*p*)$(OTf)_2$ in the presence of 1,10-phenantroline (Phen) (Scheme 25). Reaction of the silylyne complex with sodium amalgam produced complex **48**, which resulted from a reductive coupling of **47** leading to a carbon−carbon bond formation. The Ru−Si bond length in **47** [2.269(5) Å] is quite short and the rather long Si−N distances [1.95(1) Å and 1.91(1) Å] reflect the coordinate dative bond distances[161].

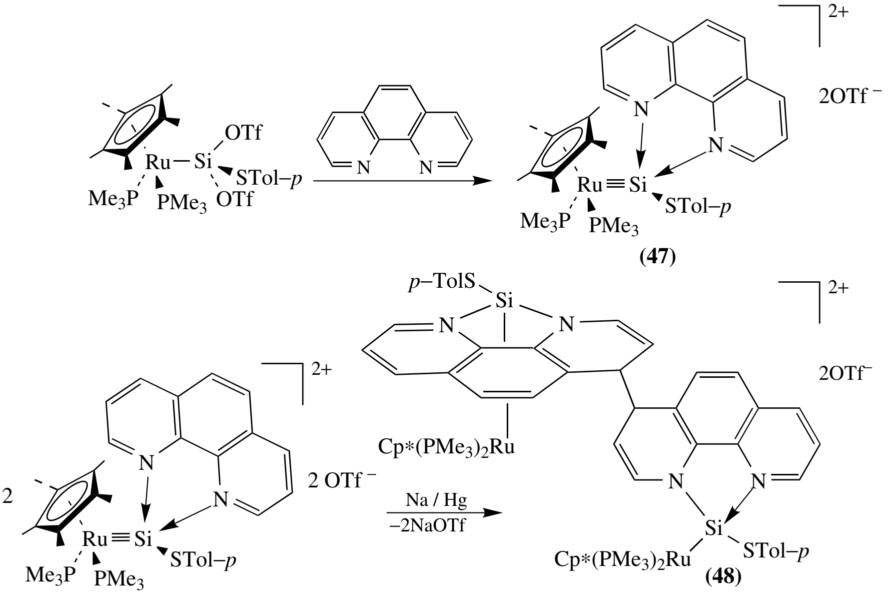

SCHEME 25

In a similar fashion, an organometallic stabilization of the silylene complex $(OC)_4OsSi(SC_6H_4Me$-*p*) [$Ru(Cp^*)(PMe_3)_2$] **(49)**, predicted by Aylett in 1980[162], has been obtained after displacement of the two triflates in $Cp^*(PMe_3)_2RuSi(SC_6H_4Me$-*p*)$(OTf)_2$ in the reaction with $Na_2Os(CO)_4$. The molecular structure of **49** reveals a planar silicon atom suggesting a π-bonding to one or more substituents with the possible resonance structures given in **L**, **M** and **N**.

The Os−Si distance of 2.419(2) Å is typical for a Os−Si single bond. The Si−S bond distance of 2.172(4) Å is rather shorter than the comparable distances in $Cp^*(PMe_3)_2RuSi(SC_6H_4Me$-*p*$)_3$ [2.223(1) Å, 2.195(1) Å and 2.196(1) Å[163]], implying some degree of Si−S π-bonding interactions, and the Ru-Si bond length of 2.286(2) Å is shorter than in $Cp^*(PMe_3)_2RuSi(SC_6H_4Me$-*p*$)_3$ [2.350(1) Å] (see Table 9 for similar complexes)[163]. Thus, it seems that the structure corresponding to a ruthenium silylene complex **(N)** is the most important hybrid describing the bonding in complex **49**.

The first base-free silylene ruthenium complexes without a π-donor stabilization were prepared by Tilley and coworkers by displacement of a triflate ion by a non-coordinating lithium perfluorotetraphenyl borate (equation 34). The base-free silylene

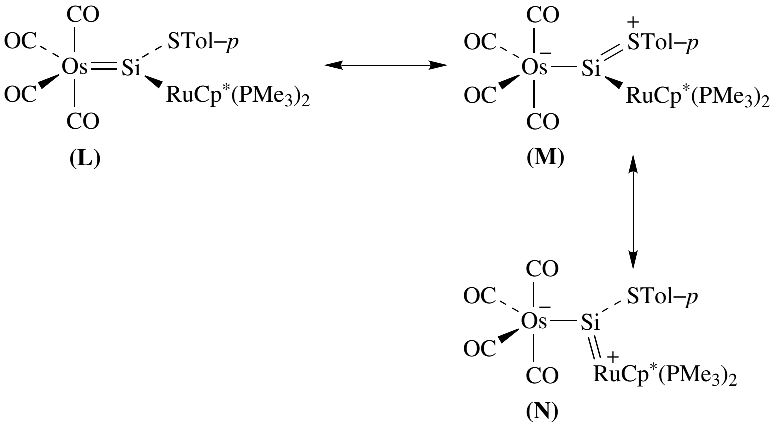

complexes were found to be unstable in solutions and decomposed with half-lives up to 7 hours. The structure of the silylene complex (R = Me) consists of a planar silicon with a Ru−Si bond length of 2.238(2) Å, which is the shortest yet reported distance for a ruthenium silylene complex (Table 9)[164]. A similar abstraction route to a cationic base-stabilized silylene complex $Cp(CO)_2\overline{Fe{=}SiMe(o\text{-}Me_2N}CH_2C_6H_4)^+PF_6^-$ has been recently developed by the reaction of $Cp(CO)_2FeSi\{HMe(o\text{-}Me_2NCH_2C_6H_4)\}$ with Ph_3CPF_6. The cationic silylene complex reacts with MeOH affording the methoxy silyl complex $FpSiMe(OMe)\{o\text{-}Me_2N(H)CH_2C_6H_4\}$ [Fp = $CpFe(CO)_2$] with a Fe−Si distance of 2.305(2) Å and a ^{29}Si NMR signal at $\delta = 7.40$ ppm. These values can be compared with a Fe−Si distance of 2.266(1) Å and $\delta = 118.3$ ppm for the parent cationic complex[165].

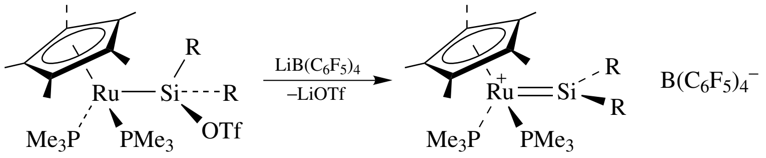

(34)

R = Me, Ph

Photolysis of the complex $FpSiMe_2SiMe_2$ [Fp = $CpFe(CO)_2$] has been studied extensively by Pannell and Sharma[150,155] and Ogino and coworkers[166]. At early stages of the photolysis a mixture of all the geometric isomers of $[CpFe(CO)]_2(\mu\text{-}CO)\{\mu\text{-}SiMe(SiMe_3)\}$ and small amounts of $[CpFe(CO)]_2(\mu\text{-}SiMe_2)_2$ were obtained. The isomer ratio is 44:29:27 for the *cis*-SiMe$_3$: *cis*-Me : *trans* isomers, respectively[167], whereas a prolonged photolysis gave only the *cis* and *trans* $[CpFe(CO)]_2(\mu\text{-}SiMe_2)_2$ complexes quantitatively[166]. Exchanging the iodine atom on the silanediyl bridge of the μ-silanediyl complex **50** by a strong Lewis base, *N*-methylimidazole (NMI) or 4-dimethylaminopyridine (DAMP), resulted in the formation of a donor-stabilized cationic silanetriyl diiron complex (equation 35). The Fe−Si bond lengths of 2.262(2) Å and 2.266(3) Å for the NMI and DAMP complexes respectively are shorter than those for other neutral silanediyl-bridged diiron complexes, although larger than those for the mononuclear iron silyl complexes (Table 9)[168].

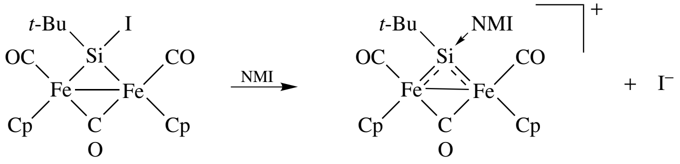

(50)

(35)

The cationic complexes can be easily reduced by $NaBH_4$ to the corresponding silane $[CpFe(CO)]_2(\mu\text{-}CO)(\mu\text{-}Si(Bu\text{-}t)H)$ **(51)** whereas the iodine complex **50** does not react under similar conditions[169]. μ-Halosilanes have been prepared from complex **51** with the corresponding di-, tri- and tetra-halomethane for the iodine, bromine and chlorine complexes, respectively[168]. Complex **51** has also been prepared by the photoreaction of $CpFe(CO)_2SiMe_3$ with $t\text{-}BuSiH_3$. Its X-ray crystal structure revealed that it adopts a geometry in which the two Cp rings and a Si−H bond are located on the same side with respect to the $SiFe_2C$ four-membered ring. The ^{29}Si NMR spectra of the complex shows a signal at a remarkably low field ($\delta = 254.4$) which is characteristic for silylene bridging complexes[170]. Thermal or photochemical isomerization processes were found to take place among the similar *cis* and *trans*-$Cp'_2Fe_2(CO)_3(\mu\text{-}SiHCH_2C_6H_5)$ complexes. However, the composition obtained by thermal equilibration ($cis\text{:}trans = 2\text{:}98$) differs considerably from the photostationary composition ($cis\text{:}trans = 70 : 30$)[170].

Upon irradiation of the alkoxy-substituted disilairon complexes $FpSiMe_2SiMe(OMe)_2$ [$Fp = Cp'Fe(CO)_2$, $Cp' = Cp$ or Cp^*] an interconverting mixture of bis(silylene) iron complexes with *syn* and *anti* configurations was obtained (equation 36)[171,172]. Both complexes have been observed as a mixture in the solid state crystal structure [*anti* isomer Fe−Si 2.222(3) Å and 2.207(3) Å], ^{29}Si NMR ($\delta = 121.1, 101.9$). Each exist as a combination of two resonance structures where the silylene group is base stabilized by the methoxy group[173]. Similarly, mixed silylene−germylene methoxy stabilized iron complexes or the amino-bridged bis(silylene) iron complexes were obtained starting from the corresponding complexes, $FpGeMe_2SiMe_2OMe$ or $FpSiMe_2SiMe_2NEt_2$, respectively[174−176].

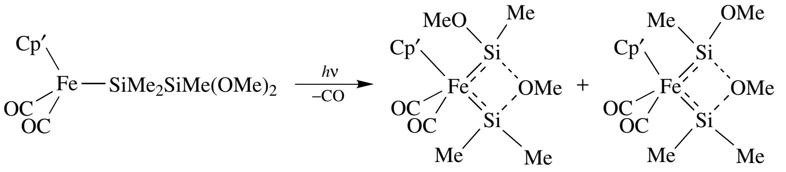

(36)

The first donor stabilized bis(silylene)ruthenium complex of the type $Cp(PPh_3)_2Ru(SiMe_2{-}O(Me){-}SiMe_2)$ was synthesized by the thermal reaction of $Cp(PPh_3)_2RuMe$ with $HSiMe_2SiMe_2OMe$. The X-ray crystal structure reveals a distorted piano-stool structure, containing a $RuSi_2O$ four-membered chelate ring with two equal short Ru−Si distances of 2.333(5) Å and two long Si−O bond distances [1.79(1) Å and 1.85(1) Å]. The ^{29}Si NMR chemical shift of 108.7 ppm ($^2J = 24$ Hz) is comparable to those for the isolobal alkoxy-bridged iron complexes (Table 10)[177]. In the gas phase, cationic iron silylene and silenes complexes have been generated by either an electron impact of $Fe(CO)_5$ which produces $FeCO^+$, or by $Fe(CH_2CH_2)^+$ produced by the reaction of Fe^+ formed by laser desorption with n-butane, with silanes Me_xSiH_{4-x}[178−180].

G. η^4-Silatrimethylenemethane Complexes

η^4-Silatrimethylenemethane complexes of iron and ruthenium have been obtained by the reaction of an alkylidenesilirane with the corresponding metal carbonyl as described in Scheme 26. Complexes (*Z*/*E*)-**52** and (*Z*/*E*)-**53** are obtained regioselectively from the corresponding *Z*/*E*-alkylidenesilirane. Of particular interest are the ^{29}Si chemical shifts of 43.5 (*Z*-**52**), 23.1 (*E*-**52**), 40.1 (*Z*-**53**) and 18.9 (*E*-**53**) and 19.1 ppm for **54**, respectively. These shifts are at considerably lower field than the shifts for other silene complexes (Table 10). The X-ray diffraction of these complexes exhibited an umbrella-shape ligation for the η^4-silatrimethylenemethane ligand with the three substituents at the central carbon bent away from the metal center and with Fe−Si bond lengths of 2.422(2) Å and 2.395(1) Å for complexes *Z*-**52** and **54**, respectively (Table 9). The formation of *Z*-**53** was accompanied by a competitive formation of an alkylidenesilirane containing triruthenium complex, thus reducing the yield of **53** to 17%[181,182].

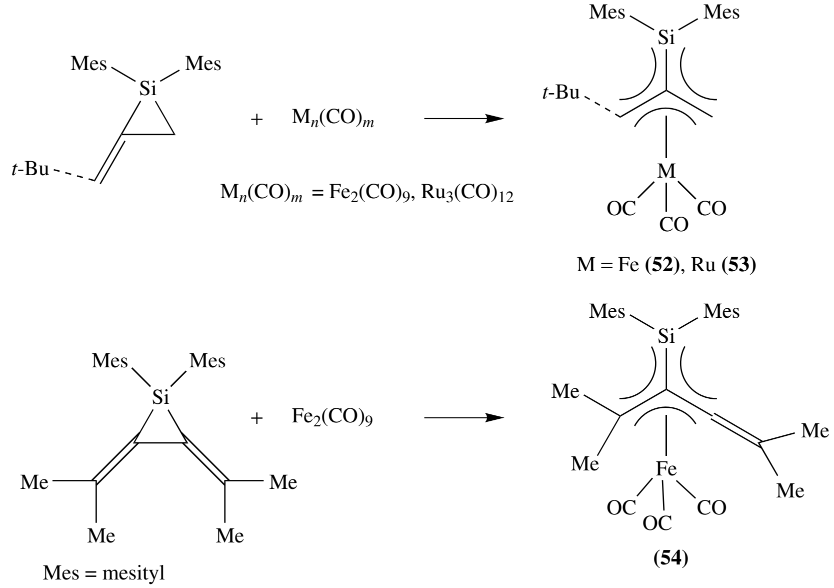

SCHEME 26

TABLE 9. Selected M−Si distances in group-8 transition-metal silicon-containing complexes

Compound	d^n Configuration	M−Si (Å)	Reference
Silylene Complexes			
$(CO)_4Fe{=}Si(C_6H_5)(o\text{-}Me_2NCH_2C_6H_4)$	d^8	2.259(1)	76
$[\{(Me_2N)_2OEt\}P(CO)_3Fe{=}Si\{NHMe_2\}(OEt)_2]$	d^8	2.218(2), 2.216(2)	157
$(CO)_4Fe{=}Si(HMPA)Me_2$	d^8	2.280(1), 2.294(1)	55
$(CO)_4Fe{=}Si(HMPA)Cl_2$	d^8	2.214(5), 2.221(1)	55

(*continued overleaf*)

TABLE 9. (*continued*)

Compound	d^n Configuration	M–Si (Å)	Reference
(CO)$_4$Fe=Si(HMPA)(SBu -*t*)$_2$	d^8	2.278(1)	156
(CO)$_4$Fe=Si(HMPA)(OPr-*i*)$_2$	d^8	2.261(2)	159
E-**45**	d^8	2.277(1)	158
E-**46**	d^8	2.272(1)	158
(CO)$_4$Ru=Si(HMPA)(OBu-*t*)$_2$	d^8	2.414(1)	160
[Cp*(PMe$_3$)$_2$Ru≡Si(STol-*p*)(phen)][(OTf)$_2$]^a	d^6	2.269(5)	161
48	d^6	2.281(5)	161
(CO)$_4$OsSi(STol-*p*)[Ru(Cp*)(PMe$_3$)$_2$]	d^6	2.419(2) (Os–Si) 2.286(2) (Ru–Si)	183
[(Cp*)(PMe$_3$)$_2$Ru=Si(Me)$_2$][B(C$_6$F$_5$)$_4$]	d^6	2.238(2)	164
Cp*(PMe$_3$)$_2$RuSi(STol-*p*)$_3$	d^6	2.350(1)	163
Cp*(PMe$_3$)$_2$RuSi (STol-*p*)$_2$OTf	d^6	2.306(2)	163
Cp*(PMe$_3$)$_2$RuSi(STol-*p*)(OTf)$_2$	d^6	2.269(3)	163
[(Cp*)(PMe$_3$)$_2$Ru=Si(STol-*p*)$_2$(NCMe)][BPh$_4$]	d^6	2.284(3)	163
[(Cp*)(PMe$_3$)$_2$Ru=SiMe$_2$(NCMe)][BPh$_4$]	d^6	2.258(4), 2.190(14)	163
[CpFe(CO)]$_2$(μ-CO){μ-SiMe(SiMe$_3$)}	d^8	2.294(1)	166
[{CpFe(CO)}$_2${μ-Si(Bu-*t*)(NMI)}]I^b	d^8	2.262(1)	169
[{CpFe(CO)}$_2${μ-Si(Bu-*t*)(DAMP)}]I^c	d^8	2.266(3)	168
Cp(CO)$_2$Fe=SiMe(*o*-Me$_2$NCH$_2$C$_6$H$_4$) PF$_6$	d^6	2.266(1)	165
Silyl Complexes			
[PPh$_3$Cu(μ-dppm)Fe{Si(OMe)$_3$}(CO)$_3$	d^8	2.271(4)	84
[(CO)$_3$(SiF$_3$)Fe(μ-dppm)Pt(H)(PPh$_3$)	d^8	2.249(3)	87
(η^3-2-Me-allyl)Pd(μ-dppm)Fe{Si(OMe)$_3$}(CO)$_3$	d^8	2.303(1)	85
Fe{μ-Si(OMe)$_2$(OMe)}(CO)$_3$(μ-dppm)Pd(SnPh$_3$)	d^8	2.258(1)	85
[(CO)$_3$Fe{μ-Si(OSiMe$_3$)$_2$(OSiMe$_3$)}(μ-dppm)Pd(Cl)]	d^8	2.277(3)	105
[(PPh$_3$)(CO)$_3$Fe{μ-Si(OMe)$_2$(OMe)}InCl$_2$–(O=PPh$_3$)]	d^8	2.311(2)	88
[{MeO)$_3$Si}(CO)$_3$Fe(μ-dppm)InCl{Mo(C$_5$H$_4$Me)(CO)$_3$}	d^8	2.307(1)	88
[(CO)$_3$Fe{μ-Si(OMe)$_2$(OMe)}(μ-dppm)Pt{C≡N-(xylyl-2,6)}][PF$_6$].	d^8	2.263(2)	91
[{[(MeO)$_3$Si](CO)$_3$Fe(μ-dppm)Cd(μ-Cl)}$_2$]•C$_6$H$_{14}$	d^8	2.286(5)	90
[(CO)$_3${Si(OMe)$_3$}Fe(μ-dppm)Hg(C$_6$Cl$_5$)]	d^8	2.311(3)	94
[(CO)$_3${Si(OMe)$_3$}Fe(μ-dppm)HgPt(C$_6$Cl$_5$)(*t*-BuNC)(PPh$_3$)]•CH$_2$Cl$_2$	d^8	2.316(13)	94

TABLE 9. (*continued*)

Compound	d^n Configuration	M–Si (Å)	Reference
[(CO)$_3$\{Si(OMe)$_3$\}Fe(μ-dppm)(μ-SnCl$_2$)PtCl(PEt$_3$)]•CH$_2$Cl$_2$	d^8	2.326(3)	94
Fe\{μ-Si(OMe)$_2$(OMe)\}(CO)$_3$(μ-dppm)Rh(CO	d^8	2.249(1)	89
[(CO)$_3$(Ph$_2$MeSi)Fe−AgPh$_2$CH$_2$C$_6$H$_5$]	d^8	2.327(3)	83
[(CO)$_3$(Ph$_2$MeSi)Fe−AuPh$_2$CH$_2$C$_6$H$_5$]	d^8	2.330(10)	83
[AuFe\{Si(OMe)$_3$\}(CO)$_3$(μ-dppm)]$_2$•CH$_2$Cl$_2$	d^8	2.268(8), 2.282(7)	96
Hg[Fe\{Si(OMe)$_3$\}(CO)$_3$(dppm)]$_2$	d^8	2.290(3), 2.285(3)	96
[(CO)$_3$(Ph$_2$MeSi)Fe−HgBr]	d^8	2.399(6)	83
mer-[\{(MeO)$_3$Si\}(CO)$_3$Fe(μ-Ph$_2$PPyr)]$_2$Cd	d^8	2.286(1)	86
mer-[(Ph$_2$HP)(Ph$_3$Si)(CO)$_3$FeCd(μ-Br)]$_2$	d^8	2.364(5)	86
(CO)(dppe)FeH$_3$(Si(OEt)$_3$)	d^6	2.250(4)	97
(CO)$_3$(R$_3$Si)Fe(μ-PR′R″)Pt(PPh$_3$)$_2$(Fe−Pt)	d^8	2.339(2)	100
(CO)$_4$Fe(μ-PPh$_2$)Pt\{Si(OMe)$_3$\}(PPh$_3$)(Fe−Pt)	d^8	2.288(1)	102
Os$_3$(CO)$_{10}$(NCMe)[Si(OEt)$_3$](μ-H)	d^6	2.39(1)	106
Os$_3$(CO)$_9$[μ$_3$-η^3-Si(OEt)$_3$](μ-H)	d^6	2.32(1)	106
Os$_3$(CO)$_{10}$[Si(OMe)$_3$][μ-CH=CHBu-*t*]	d^6	2.427(4)	107
Os$_3$(CO)$_{10}$(μ-H)$_2$\{*o*-Me$_2$SiHC$_5$H$_4$N\}$_2$	d^6	2.434(4), 2.431(4)	110
Os$_3$(CO)$_8$[μ-PMe$_2$(*o*-C$_6$H$_4$)][Si(OMe)$_3$](μ-H)$_2$	d^6	2.369(5)	184
Os$_3$(CO)$_{10}$(μ-H)(MeCN)\{*o*-BrC$_6$H$_4$SiH$_2$Me$_2$\}	d^6	2.452(5)	110
Os$_3$(CO)$_{10}$(μ-H)(PPh$_3$)\{*o*-BrC$_6$H$_4$SiH$_2$Me$_2$\}	d^6	2.463(9)	110
Os$_3$(CO)$_{10}$(μ-H)(*o*-Ph$_2$PC$_6$H$_4$CH$_2$SiMe$_2$)	d^6	2.444(4)	109
Os$_3$(CO)$_{10}$(μ-H)(*o*-Me$_2$SiC$_6$H$_4$CH$_2$PPh$_2$)	d^6	2.453(5)	109
Os$_3$(CO)$_{10}$(μ-H)(*o*-MeHSiC$_6$H$_4$CH$_2$PPh$_2$)	d^6	2.425(7)	109
Os$_3$(CO)$_8$(μ-H)$_3$(*o*-Me$_2$SiC$_6$H$_4$CH$_2$PPh$_2$)	d^6	2.432(6)	109
Ru$_3$(μ-H)$_2$(μ-SiMe$_2$C$_5$H$_4$FeC$_5$H$_4$SiMe$_2$)(CO)$_{10}$	d^6	2.459(4)	115
Ru$_3$(μ-H)$_2$(SiEt$_3$)$_2$(μ-C$_4$H$_4$N$_2$)(CO)$_8$[d]	d^6	2.455(5)	112
Ru$_3$(μ-H)$_2$(SiEt$_3$)(μ$_3$, η^2-ampy)(CO)$_8$[e]	d^6	2.435(4)	111
Os(SiEt$_3$)H(PPh$_3$)$_2$(CO)$_2$	d^6	2.493(2)	118
Ru(CO)$_2$(NH$_2$CH$_2$Ph)$_2$(SiMe$_2$Ph)I	d^6	2.412(2)	120
Cp$_2$*Ru$_2$(μ-CH$_2$)(μ-Cl)(SiMe$_3$)	d^4	2.387(2)	117
OsCl(CO)(PPh$_3$)$_2$(Si(OH)$_3$)	d^6	2.319(2)	119
[OsCl(CO)(PPh$_3$)$_2$Si(OH)$_2$]$_2$O	d^6	2.318(5), 2.337(5)	119
Cp(CO)$_2$Fe\{Si(Cl)(Tol-*o*)(NMes)\}	d^6	2.284(2)	62
(C$_5$Me$_5$)(CO)$_2$FeSiH$_3$	d^6	2.287(2)	121
(C$_5$Me$_5$)(CO)$_2$RuSi(Tol-*o*)$_2$OH	d^6	2.411(2)	122

(*continued overleaf*)

TABLE 9. (*continued*)

Compound	d^n Configuration	M–Si (Å)	Reference
$\mathrm{Cp^*(PCy_3)}\overline{\underline{\mathrm{Ru{-}C({=}CPh_2)S}}\mathrm{iMe_2H}}$	d^6	2.507(2)	126
$(\eta^6\text{-}C_6H_6)RuH_2(SiMe_3)_2$	d^4	2.396(1), 2.391(1)	129
$(\eta^6\text{-}C_6H_5Me)FeH_2(SiCl_3)_2$	d^4	2.222(2), 2.218(2)	130
$(\eta^6\text{-}p\text{-}Me_2C_6H_4)FeH_2(SiCl_3)_2$	d^4	2.226(2), 2.222(2)	132
$(\eta^6\text{-}C_6H_6)FeH_2(SiCl_3)_2$	d^4	2.210(3), 2.207(3)	132
$(\eta^6\text{-}C_6H_5Me)FeH_2(SiF_3)_2$	d^4	2.251(5), 2.261(5)	131
$\{Cp^*Ru(\mu\text{-}\eta^2\text{-}HSiEt_2)\}_2(\mu\text{-}H)H$	d^4	2.544(2), 2.551(2)	133
		2.338(1), 2.335(1)	
$[\{Cp^*Ru(\mu\text{-}SiPh_2)(\mu\text{-}H)\}_2]$	d^4	2.364(1), 2.360(1)	133
$\{Cp^*Ru(\mu\text{-}SiPh_2CH{=}CHSiPh_2)(\mu\text{-}H)_2RuCp^*\}$	d^4	2.410(2), 2.421(2)	134
$[Cp^*Ru(CO)_2]_2(\mu\text{-}\eta^2:\eta^2\text{-}H_2Si(Bu\text{-}t)_2)$	d^6	2.447(1), 2.457(1)	136
$[Cp^*Ru]_2(\mu\text{-}\eta^2\text{-}HSi(Bu\text{-}t)_2H)(\mu\text{-}\eta^2\text{-}HSiPhH)(\mu\text{-}H)H$	d^4	2.300(1), 2.375(1)	136
		2.438(1), 2.675(1)	
$[Cp^*Ru]_2(\mu\text{-}\eta^2\text{-}HSi(Bu\text{-}t)_2H)(\mu\text{-}\eta^2\text{-}HSiEtH)(\mu\text{-}H)H$	d^4	2.322(3), 2.365(3)	136
		2.414(4), 2.680(3)	
$Cp^*Ru(P(Pr\text{-}i)_3)H_2(SiHClMes)$	d^4	2.303(3)	135
$\{[Cp^*Ru]_2(\mu\text{-}SiPh(OMe))(\mu\text{-}OMe)(\mu\text{-}H)\}$	d^4	2.309(10), 2.288(11)	135
$[Cp^*Ru\{C_4Me_4Si(\mu\text{-}H)Si(SiMe_3)_3\}][BPh_4]$	d^6	2.441(3)	143
$Cp^*Ru(P(Pr\text{-}i)_3)H(\eta^2\text{-}CH_2{=}SiPh_2)$	d^6	2.382(4)	125
$FpSiMe(OMe)\{o\text{-}Me_2N(H)CH_2C_6H_4\}$	d^6	2.305(2)	165
$Z\text{-}Fe(CO)_3[\eta^4\text{-}Mes_2SiC(CH_2)CHBu\text{-}t)]$	d^6	2.422(2)	181
$Fe(CO)_3[\eta^4\text{-}Mes_2SiC(CMe_2)_2(C{=}CMe_2)]$	d^6	2.395(1)	182

[a] Phen = 1,10-phenanthroline.

[b] NMI = *N*-methylimidazole.

[c] DAMP = dimethylaminopyridine.

[d] $C_2H_4N_2$ = pyridazine.

[e] ampy = 2-amino-6-methylpyridinate.

TABLE 10. Selected ^{29}Si NMR chemical shifts for group-8 transition-metal silicon containing complexes

Compound	^{29}Si NMR shift (ppm)	Reference
$Cp(Me_3P)_2RuSiHCl_2$	66.79 ($^1J_{SiH}$ = 199.6 Hz, $^2J_{SiP}$ = 36.2 Hz)	123
$Cp(Me_3P)_2RuSiCl_3$	42.11 ($^2J_{SiP}$ = 43.6 Hz)	123
$Cp(Me_3P)_2RuSiHMeCl$	57.17 ($^1J_{SiH}$ = 163.6 Hz, $^2J_{SiP}$ = 30.5 Hz)	123
$Cp(Me_3P)_2RuSiCl_2Me$	92.16 ($^2J_{SiP}$ = 35.4 Hz)	123
$Cp(Me_3P)_2RuSiClMe_2$	87.29 ($^2J_{SiP}$ = 30.2 Hz)	123
$Cp(PMe_3)_2RuSiCl_2(\eta^1\text{-}Cp^*)$	82.71 ($^2J_{SiP}$ = 33.0 Hz)	124
$[Cp(Me_2P)_2RuHSiCl_3]$ $[B(3,5\text{-}(CF_3)_2C_6H_3)_4]$	30.60 ($^2J_{SiH}$ = 48.8 Hz)	123
$Ru(SiMe_3)Cl(CO)(PPh_3)_2$	55.74 (t, $^2J_{SiP}$ = 10.9 Hz)	185
$Ru(SiEt_3)Cl(CO)(PPh_3)_2$	71.70 (t, $^2J_{SiP}$ = 11.7 Hz)	185
$Ru(SiPh_3)Cl(CO)(PPh_3)_2$	40.3 (t, $^2J_{SiP}$ = 13.1 Hz)	185
$Cp^*(PCy_3)\underline{\overline{Ru-C{=}CPh_2)SiMe_2H}}$	−81.30 ($^1J_{SiH}$ = 66 Hz, $^2J_{SiP}$ = 34.7 Hz)	126
$Cp^*Ru(P(Pr\text{-}i)_2Ph)H_2Si(OMe)_3$	−55.2	127
$Cp^*Ru(P(Pr\text{-}i)_2Ph)H_2SiPh_3$	−8.5	127
$Cp^*Ru(P(Pr\text{-}i)_2Ph)H_2SiMe_3$	10.7 ($^2J_{SiP}$ = 8 Hz)	127
$Cp^*Ru(P(Pr\text{-}i)_2Ph)H_2(Si(H)Ph_2)$	5.86 ($^1J_{SiH}$ = 182 Hz)	127
$\{Cp^*Ru(\mu\text{-}SiPh_2CH{=}CHSiPh_2)(\mu\text{-}H)_2RuCp^*\}$	4.6 (broad)	134
$[Cp^*Ru(\mu\text{-}H)]_2(\mu\text{-}\eta^2:\eta^2\text{-}H_2Si(Bu\text{-}t)_2)$	75.5 (quintet, $^1J_{SiH}$ = 34.2 Hz)	136
$[Cp^*Ru(CO)_2]_2(\mu\text{-}\eta^2:\eta^2\text{-}H_2Si(Bu\text{-}t)_2)$	186.2 (t, $^1J_{SiH}$ = 22.4 Hz)	136
$[Cp^*Ru(CO)_2]_2$ $(\mu\text{-}\eta^2\text{-}H_2Si(Bu\text{-}t)_2)H$	168.7 (dd, $^1J_{SiH}$ = 31.6, 7.9 Hz)	136
$[Cp^*Ru\{C_4Me_4Si$ $(\mu\text{-}H)Si(SiMe_3)_3\}]$ $[BPh_4]$	−27.14 ($^1J_{SiH}$ = 41)	143
Cp^*Ru $\{C_4Me_4Si\text{-}Si(SiMe_3)_3\}$	7.35	143
$\{[Cp^*Ru]_2$ $(\mu\text{-}SiPh$ $(OMe))(\mu\text{-}OMe)(\mu\text{-}H)\}$	211.12	135
$Cp^*Ru(P(Pr\text{-}i)_3)(H)(\eta^2\text{-}CH_2{=}SiPh_2)$	6.14 (m, ^2J = 21 Hz)	125
$Cp^*(PMe_3)_2RuSi(STol\text{-}p)_3$	49.03 (t, $^2J_{SiP}$ = 34 Hz)	163
$Cp^*(PMe_3)_2RuSi(OTol\text{-}p)_3$	−1.22 (t, $^2J_{SiP}$ = 42 Hz)	163
$Cp^*(PMe_3)_2RuSiMe_2(STol\text{-}p)$	50.19 (t, $^2J_{SiP}$ = 42 Hz)	163
$Cp^*(PMe_3)_2RuSi(STol\text{-}p)_2OTf$	77.14 (t, $^2J_{SiP}$ = 36 Hz)	163
$Cp^*(PMe_3)_2RuSi(OTol\text{-}p)_2OTf$	−0.01 (t, $^2J_{SiP}$ = 45 Hz)	163
$Cp^*(PMe_3)_2RuSiMe_2OTf$	133.29 (t, $^2J_{SiP}$ = 33 Hz)	163
$Cp^*(PMe_3)_2RuSi(STol\text{-}p)(OTf)_2$	37.10 (t, $^2J_{SiP}$ = 39 Hz)	163
$FpSiMe(OMe)\{o\text{-}Me_2$ $N(H)CH_2C_6H_4\}$	7.40	165
$(CO)_4Fe{=}SiH(C_6H_5)\bullet DMI^a$	83.52 ($^1J_{HSi}$ = 199)	57
$(CO)_4Fe{=}SiH(1\text{-}C_{10}H_7)\bullet DMI^a$	81.51 ($^1J_{HSi}$ = 218.61)	57
$(CO)_4Fe{=}SiMe(o\text{-}Me_2NCH_2C_6H_4)$	123.6	76
$Cp(CO)_2Fe{=}SiMe(o\text{-}Me_2NCH_2C_6H_4)$	118.3	165

(*continued overleaf*)

TABLE 10. (*continued*)

Compound	^{29}Si NMR shift (ppm)	Reference
$(CO)_4Fe{=}SiPh(o\text{-}Me_2NCH_2C_6H_4)$	118.1	76
$(CO)_4Fe{=}SiPh(8\text{-}(Me_2NCH_2)C_{10}H_6)$	101.1	76
$(CO)_4Fe{=}SiPh(8\text{-}(Me_2N)C_{10}H_6)$	125.7	76
$(CO)_4Fe{=}Si(o\text{-}Me_2NCH_2C_6H_4)_2$	115	76
$(CO)_4Fe{=}Si(NMe_2)_2(NHMe_2)$	68.2	157
$[(Ph_3P)_2Pt(\eta^2\text{-}\{(CO)_4Fe{=}Si(NMe_2)_2\})]$	113.9 ($^2J_{SiPt}$ = 136.4 Hz)	157
$[\{(Me_2N)_2EtO\}P(CO)_3Fe{=}Si\{NHMe_2\}(OEt)_2]$	57.4 (d, $^2J_{SiP}$ = 34 Hz)	157
$(CO)_4Fe{=}Si(HMPA)(OBu\text{-}t)_2$	7.1 (d, $^2J_{SiP}$ = 26.4 Hz)	55
$(CO)_4Fe{=}Si(HMPA)(SBu\text{-}t)_2$	74.7 (d, $^2\mathrm{J}_{SiP}$ = 25.3 Hz)	156
$(CO)_4Fe{=}Si(HMPA)Me_2$	92.3 (d, $^2J_{SiP}$ = 17.5 Hz)	55
$(CO)_4Fe{=}Si(HMPA)Cl_2$	59.7 (d, $^2J_{SiP}$ = 31.2 Hz)	55
$(CO)_4Fe{=}Si(HMPA)(OPr\text{-}i)_2$	20.9 (d, $^2J_{SiP}$ = 25.6 Hz)	159
E-**45**	75.58 ($^2J_{SiP}$ = 36.4 Hz)	158
Z-**45**	77.90 ($^2J_{SiP}$ = 47.0 Hz)	158
E-**46**	72.03 ($^2J_{SiP}$ = 32.3 Hz)	158
Z-**46**	76.25 ($^2J_{SiP}$ = 29.4 Hz)	158
$(CO)_4Ru{=}Si(HMPA)Me_2$	79.0 ($^2J_{SiP}$ = 23 Hz)	160
$(CO)_4Ru{=}Si(HMPA)Cl_2$	33.2($^2J_{SiP}$ = 32.2 Hz)	160
$(CO)_4Ru{=}Si(HMPA)(OBu\text{-}t)_2$	−5.3 ($^2J_{SiP}$ = 25.7 Hz)	160
$(CO)_4Ru{=}Si(HMPA)(Ph)_2$	73.9 ($^2J_{SiP}$ = 21.1 Hz)	160
$(CO)_4OsSi(STol\text{-}p)[Ru(Cp^*)(PMe_3)_2]$	19.43 ($^2J_{SiP}$ = 23 Hz)	183
$[(Cp^*)(PMe_3)_2Ru{=}SiMe_2][B(C_6F_5)_4]$	311.4	164
$[(Cp^*)(PMe_3)_2Ru{=}SiPh_2][B(C_6F_5)_4]$	299 (t, $^2J_{SiP}$ = 32 Hz)	164
$[(Cp^*)(PMe_3)_2Ru{=}Si(STol\text{-}p)_2(NCMe)][BPh_4]$	58.30 (t, $^2J_{SiP}$ = 39 Hz)	163
$[(Cp^*)(PMe_3)_2Ru{=}Si(OTol\text{-}p)_2(NCMe)][BPh_4]$	14.33 (t, $^2J_{SiP}$ = 47 Hz)	163
$[(Cp^*)(PMe_3)_2Ru{=}SiMe_2(NCMe)][BPh_4]$	110.03 (t, $^2J_{SiP}$ = 30 Hz)	163
$[CpFe(CO)]_2(\mu\text{-}CO)\{\mu - SiMe(SiMe_3)\}$	232.1 (μ-Si), −3.7 ($SiMe_3$)	166
$[CpFe(CO)]_2(\mu\text{-}SiMe_2)_2$	243.8, 229.5	166
$[\{CpFe(CO)\}_2\{\mu\text{-}Si(Bu\text{-}t)(NMI)\}]I^b$	251.5	169
$[\{CpFe(CO)\}_2\{\mu\text{-}Si(Bu\text{-}t)(DMAP)\}]I^c$	264.6	168
$[\{CpFe(CO)\}_2(\mu\text{-}CO)(\mu\text{-}Si(Bu\text{-}t)H)]$	254.4	168
$[\{CpFe(CO)\}_2(\mu\text{-}CO)(\mu\text{-}Si(Bu\text{-}t)Cl)]$	276.3	168
$[\{CpFe(CO)\}_2(\mu\text{-}CO)(\mu\text{-}Si(Bu\text{-}t)Br)]$	284.8	168
$[\{CpFe(CO)\}_2(\mu\text{-}CO)(\mu\text{-}Si(Bu\text{-}t)I)]$	289.1	168
$[\{CpFe(CO)\}_2(\mu\text{-}CO)(\mu\text{-}Si(Bu\text{-}t)Me)]$	267.4	168
$(Z)\text{-}Fe(CO)_3[\eta^4\text{-}Mes_2SiC(CH_2)CHBu\text{-}t)]$	43.6	181
$(E)\text{-}Fe(CO)_3[\eta^4\text{-}Mes_2SiC(CH_2)CHBu\text{-}t)]$	23.1	182
$(Z)\text{-}Ru(CO)_3[\eta^4\text{-}Mes_2SiC(CH_2)CHBu\text{-}t)]$	40.1	181
$(E)\text{-}Ru(CO)_3[\eta^4\text{-}Mes_2SiC(CH_2)CHBu\text{-}t)]$	18.9	182
$Fe(CO)_3[\eta^4\text{-}Mes_2SiC(CMe_2)_2(C{=}CMe_2)]^d$	19.1	182

TABLE 10. (*continued*)

Compound	^{29}SiNMR shift (ppm)	Reference
$(C_5H_5)(CO)_2FeSiCl_2H$	71.7	121
$(C_5H_5)(CO)_2RuSiCl_2H$	52.6	121
$(C_5Me_5)(CO)_2FeSiCl_2H$	79.9	121
$(C_5H_5)(CO)_2FeSiH_3$	−42.2	121
$(C_5H_5)(CO)_2RuSiH_3$	−64.6	121
$(C_5Me_5)(CO)_2FeSiH_3$	−31.24	121
$(C_5Me_5)(CO)_2RuSiH_3$	−49.44	121
$(C_5H_5)(CO)(Ph_3P)FeSiH_3$	−35.68	121
$(C_5H_5)(Ph_3P)_2FeSiH_3$	−36.4	121
$(C_5Me_5)(CO)_2RuSiMe_2H$	13.70	122
$(C_5Me_5)(CO)_2RuSi(Tol\text{-}o)_2H$	10.18	122
$(C_5Me_5)(CO)_2RuSiMe_2OH$	52.41	122
$(C_5Me_5)(CO)_2RuSi(Tol\text{-}o)_2OH$	48.24	122

[a] DMI = 1,3-dimethyl-2-imidazolidinone.

[b] NMI = *N*-methylimidazole.

[c] DAMP = 4-dimethylaminopyridine.

[d] η^4-silatrimethylenemethane framework.

XIV. GROUP-9 SILICON-CONTAINING COMPLEXES

A. Silylene Complexes

Recently, the first base-stabilized iridium silylene complexes, $IrH_2\{Si(OTf)Ph_2\}(TFB)(PR_3)$ (TFB = tetrafluorobenzobarrelene), were prepared and characterized following the reaction sequence of Scheme 27. As expected, in the complex with $PR_3 = P(Pr\text{-}i)_3$, the Ir−Si distance of 2.337(2) Å is significantly shorter than those determined previously for the six-coordinate silyliridium(III) complexes (Table 11). The silylene character was also supported by the relatively long Si−O bond of 1.790(5) Å compared with the normal range of 1.63–1.66 Å[186].

B. Silyl and Bis(silyl) Complexes

The reaction of the complex $[Ir(\mu\text{-}OMe)(TFB)]_2$ with acetic acid in polar solvents leads to the formation of the dimeric carboxylate compound $(Ir(\mu, \eta^2\text{-}O_2\ CMe_3)(TFB)]_2$. This dimeric acetate complex reacted with monodentate phosphine ligands yielding the square-planar monomeric derivatives, Ir(OCOMe)(TFB)L [L = Pyr, PPh_3, PCy_3, $P(Pr\text{-}i)_3$], which upon reaction with trisubstituted silanes of the type $HSiEt_3$ or $HSiPh_3$ afforded the corresponding octahedral dihydride silyl complexes $IrH_2\ (SiR_3)(TFB)L$ (R = Et, Ph) and with the dihydrosilane, H_2SiPh_2, the complex $IrH_2(Ph_2SiOCOMe)(TFB)L$ [L = PPh_3, PCy_3, $P(Pr\text{-}i)_3$] was formed. $IrH_2(SiEt_3)(TFB)L$ [L = PPh_3, PCy_3, $P(Pr\text{-}i)_3$] were found to catalyze the hydrosilylation and the dehydrogenative silylation of phenylacetylene with triethylsilane, yielding in all cases a mixture of $PhCH{=}CH_2$, *cis*- and *trans*-$PhCH{=}CHSiEt_3$ and $PhC(SiEt_3){=}CH_2$. Interestingly, the reaction of these dihydrosilane complexes with CO causes the reductive elimination of the silane and the formation of Ir $(\eta^1:\eta^2\text{-}C_{12}F_4H_7)(CO)_2L$ (equation 37)[187].

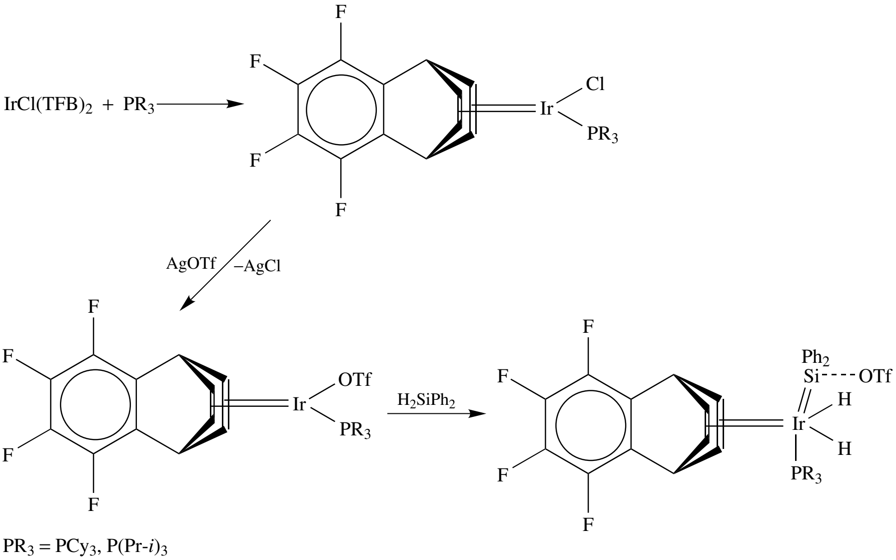

SCHEME 27

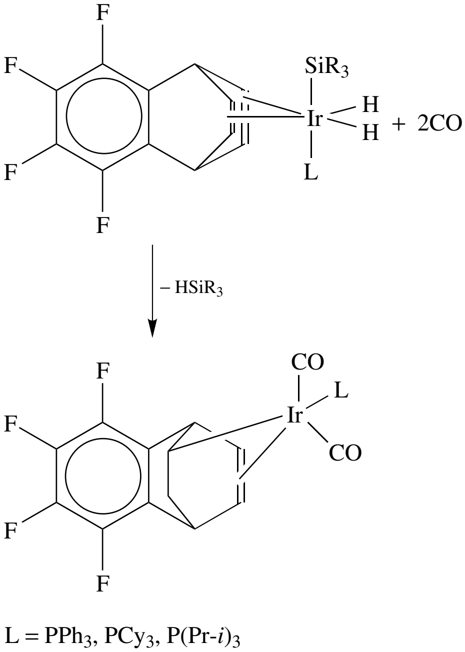

(37)

The complex Ir(OCOMe)(TFB)(PCy_3) was found to react with CO, yielding the *cis*-dicarbonyl compound Ir(η^1-OCOMe)$(CO)_2$(PCy_3) **(55)**. Treatment of **55** with 1 equivalent each of $HSiPh_3$ and CO in toluene led to the air-stable tricarbonyl complex $Ir(CO)_3(SiPh_3)$

(PCy_3) **(56)** exhibiting a P−Si coupling of 66 Hz, which suggests a *trans* disposition of the silane and phosphine ligands. Complex **56** reacts with molecular hydrogen to give the dihydrido compound **57**. Reaction of complex **55** with 3 equivalents of the $HSiR_3$ gives **57** or its triethylsilyl analogue (equation 38). The reaction of **55** with 1 equivalent of H_2SiPh_2 yields the analogous dihydride $IrH_2(Ph_2SiOCOMe)(CO)_2(PCy_3)$ and with 2 equivalents of $H_{x+1}SiPh_{3-x}$ affords the bis(silyl) derivatives **58** and **59** (equation 39). The bis(silyl) complex **58** reacts with acetic acid yielding $IrH_2(Ph_2SiOCOMe)(CO)_2(PCy_3)$. **58** and **59** react with alcohols, yielding the alkoxysilyl and dialkoxysilyl derivatives, respectively[188].

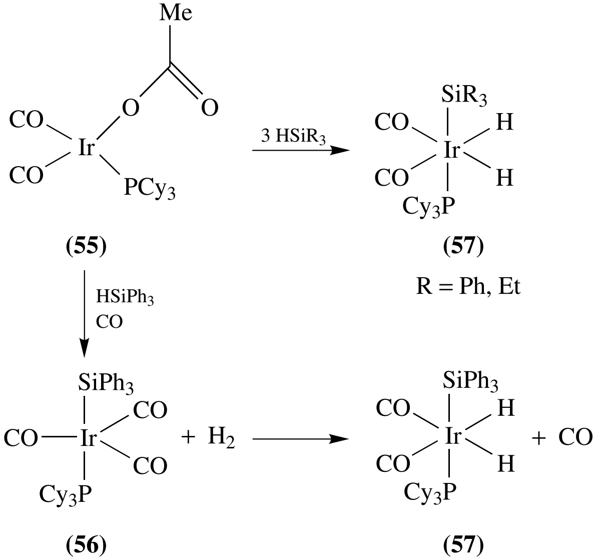

(55) **(57)** R = Ph, Et

(56) **(57)**

(38)

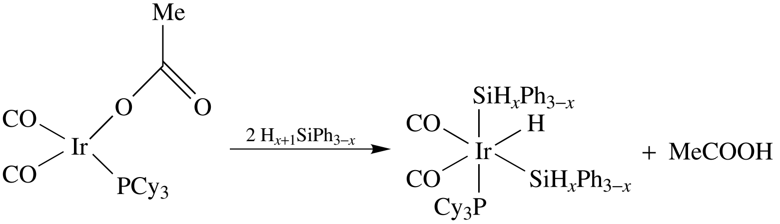

(55)

(58) $x = 1$
(59) $x = 2$

(39)

The square-planar *cis*-dicarbonyl acetylide complex $Ir(C{\equiv}CPh)(CO)_2(PCy_3)$ was found to react with $HSiR_3$ to give the corresponding alkynyl-hydridosilyl derivatives $HIr(C{\equiv}CPh)(CO)_2(SiR_3)$ ($SiR_3 = SiEt_3, SiPh_3, SiHPh_2, SiH_2Ph$). The oxidative addition of the silane to the metal center is generally viewed as a diastereoselective concerted *cis* addition process with a specific substrate orientation. The exclusive formation of the complex with *trans* P−Si orientation argues that the addition of the silane occurs along the OC−Ir−P axis with the silicon atom occupying a position above the carbonyl group. The reaction of the related $Ir(C{\equiv}CPh)(TFB)(PCy_3)$ complexes with $HSiR_3$ (R = Et, Ph) and H_2SiPh_2 is described in Scheme 28[189].

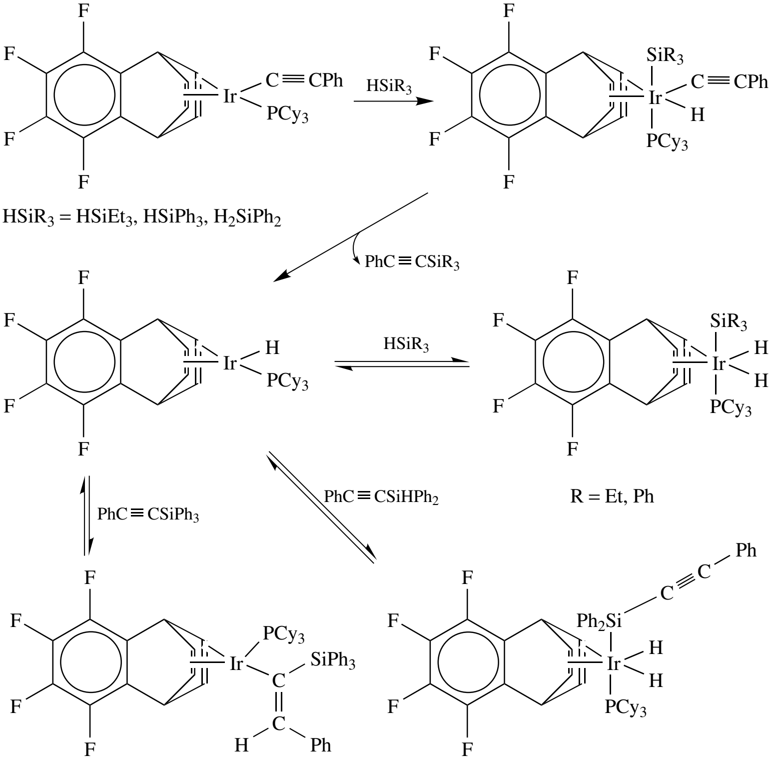

SCHEME 28

Complexes of the type Ir(acac)(coe)L [L = PCy_3 **(60)**, P(Pr-*i*)$_3$ **(61)**; coe = cyclooctene] reacted with dimethyl acetylenedicarboxylate to give the corresponding complexes Ir(acac)(η^2-$MeO_2C{-}C{\equiv}C{-}CO_2Me$)L [L = PCy_3 **(62)**, P(Pr-*i*)$_3$ **(63)**]. Consecutive reactions with H_2SiPh_2 afforded the silavinyl complexes **64** and **65** (Scheme 29)[190]. In addition, complex **60** reacts with silanes $HSiR_3$ (SiR_3 = $SiEt_3$, $SiPh_3$, $SiHPh_2$) yielding the square-pyramid five-coordinate hydridosilyl complexes Ir(acac)H (SiR_3)(PCy_3) **(65a)**. These complexes do not react with tricyclohexylphosphine, but the addition of 1 equivalent of the silane in the presence of the phosphine affords the six-coordinate hydridosilyl derivatives with the phosphine ligands in *trans* disposition (Scheme 29)[191]. The formation of complexes **64** and **65** can be regarded as a result of a net transformation involving addition of one Si−H bond across the C=O bond and an addition of an Ir−H across the alkyne triple bond. The X-ray diffraction of **65a** indicates that the bonding situation in the Ir−Si−O sequence can be described as an intermediate state between a metal silylene stabilized by an oxygen base and a tetrahedral silicon. The Ir−Si distance of 2.264(2) Å in **65a** (R = Et) is shorter than in Ir(acac)H($SiEt_3$)(PCy_3) [Ir−Si 2.307(1) Å] and other Ir(III) complexes (Table 11)[190,191].

The pentahydride complex $IrH_5(PPh_3)_2$ was found to react with chelating silanes with loss of hydrogen to form the classical seven-coordinate, distorted pentagonal bipyramidal silyl polyhydride complexes, IrH_3(disilyl)$(PPh_3)_2$ [disilyl = 1,2-dimethylsilylbenzene (dmsb) **(66)**, 1,1,3,3-tetraisopropyldisiloxane (tids)], and with monodentate silanes to give

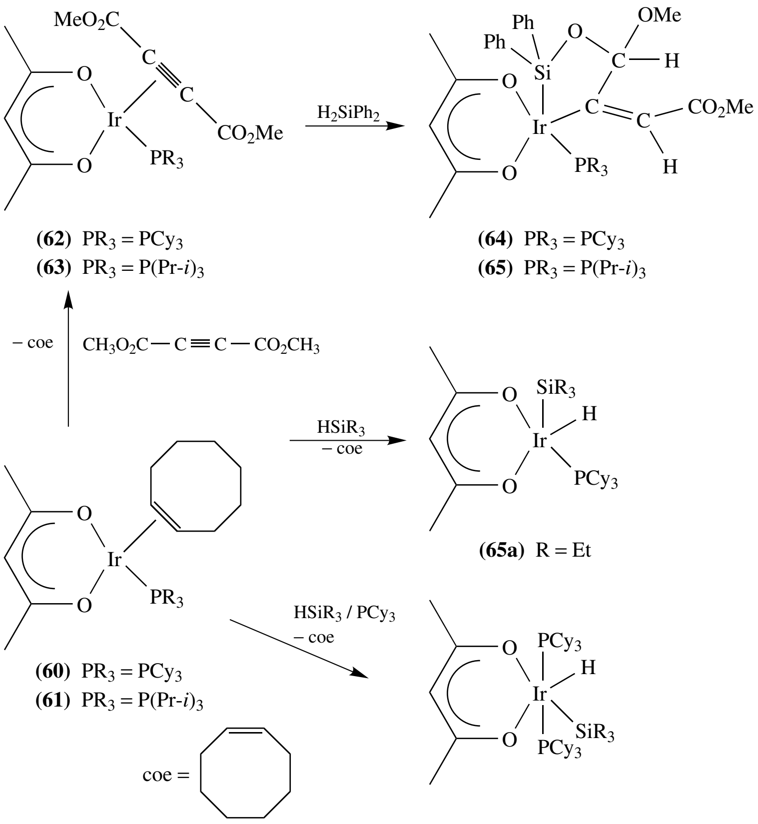

SCHEME 29

the complexes $IrH_4(SiR_3)(PPh_3)_2$ (R = Et, Ph). Complex **66** displays coalescence of the hydrides on Ir at 70 °C which implies a barrier of 13 kcal mol^{-1} for the fluxional exchange. The X-ray diffraction studies on this complex reveal Ir−Si bond lengths of 2.437(1) Å and 2.430(1) Å, which are comparable to other Ir(III) silyl complexes (Table 11). The structure of complex **66** is unusual since the phosphine ligands are in *cis* configuration, although other examples of *cis* complexes are known. Complex **66** reacts with CO to yield the complex $Ir(dmsb)H(CO)_2PPh_3$ which has not been isolated yet in a pure condition, and reacts with $P(OMe)_3$ yielding $Ir(dmsb)\{P(OMe)_3\}_2(H)PPh_3$ (equation 40)[192].

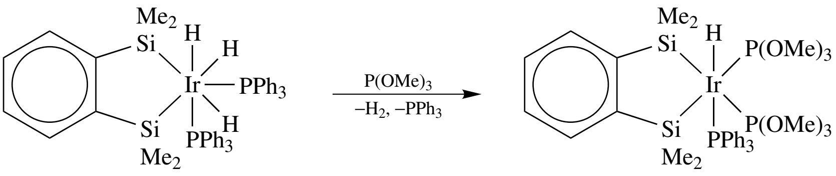

(66)

(40)

$IrH_3(CO)(dppe)$ reacts with primary, secondary and tertiary silanes yielding mono- and bis(silyl) hydride complexes, $IrH_2(SiRR'_2)(CO)(dppe)$ and $IrH(SiRR'_2)_2(CO)(dppe)$, respectively. In the mono(silyl) dihydride complexes, the hydrides are disposed in a *cis* configuration with one hydride being *trans* to CO and the other *trans* to the phosphine. The silyl ligand is *trans* to the second phosphine ligand. The structures for the bis(silyl) complexes show equivalent silyl groups disposed *trans* to the dppe ligand. The solid state structures of $IrH(SiClMe_2)_2(CO)(dppe)$ and $IrH(SiClMe_2)(SiHMe_2)(CO)(dppe)$ have been characterized. In the former the Ir−Si bond lengths are 2.396(2) Å and 2.397(2) Å whereas for the latter the Ir−Si bond lengths are 2.394(3) Å and 2.418(3) Å in the $Ir{-}SiClMe_2$ and $Ir{-}SiHMe_2$ moieties, respectively. This difference is attributed to the chloro substituent on the silyl group which makes the Ir−Si bond of the former slightly stronger. This view was corroborated by the Ir−P and Ir−CO bond distances [2.368(2) Å and 1.93(1) Å, respectively] which are slightly longer relative to those in closely related systems. Interestingly, the reaction of the bis(silyl) complex $IrH(SiH_2Et)_2(CO)(dppe)$ with $BF_3{\bullet}OEt_2$ afforded the bis(fluorosilyl) complex $IrH(SiF_2Et)_2(CO)(dppe)$ having similar Ir−Si distances [2.349(7) Å; 2.372(7) Å] to those in the bis(chlorosilyl) complex[193].

Wang and Eisenberg have studied the reaction between primary and secondary silanes with dppm-bridged dinuclear Rh dihydride complexes which gives bis μ-silylene bridged complexes for primary silanes ($R' = H$), and unusual P−Si bond containing products for secondary silanes. In both cases, the reaction proceeds through the intermediacy of the fluxional μ-SiRR′ dihydride **67** (equation 41). For the μ-SiRH derivatives of the fluxional complex **67**, the hydrogens at the Rh and Si atoms undergo exchange. The mechanism proposed for this process involves a reductive elimination/oxidative addition via the intermediacy of the unsaturated complex **68**[194]. Complex **67** has also been found to promote the reaction between silanes and simple amines leading to silazane oligomers with a similar dihydride complex, **69**, as an intermediate[195]. Exchange reactions between complex **67** and free alkyl silanes show that the complexes with μ-SiRR′ bridges with $R' = H$ are more stable than those with disubstituted bridges and that aryl substituents on the silicon increase the bridge stability. The relative reactivity of silanes with the dihydride complex $Rh_2H_2(CO)_2(dppm)_2$ was found to follow the order $PhSiH_3 > n\text{-}HexSiH_3 > MePhSiH_2 > Ph_2SiH_2 > Et_2SiH_2$. The primary silanes are more reactive than the secondary silanes, and the order or reactivity is correlated with the stability order[194].

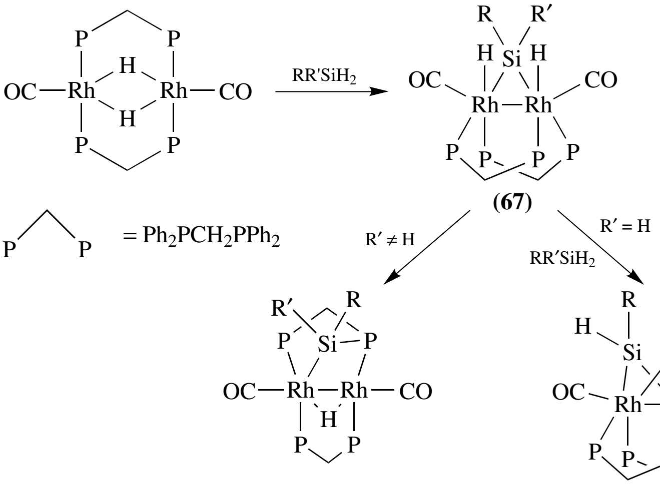

(41)

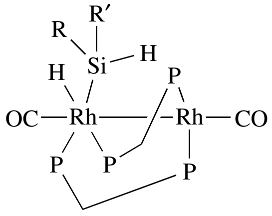

(68)

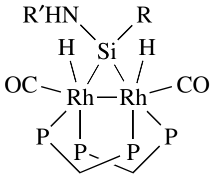

(69)

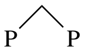 $= Ph_2PCH_2PPh_2$

R′ = Me, H
R = Et, Hex

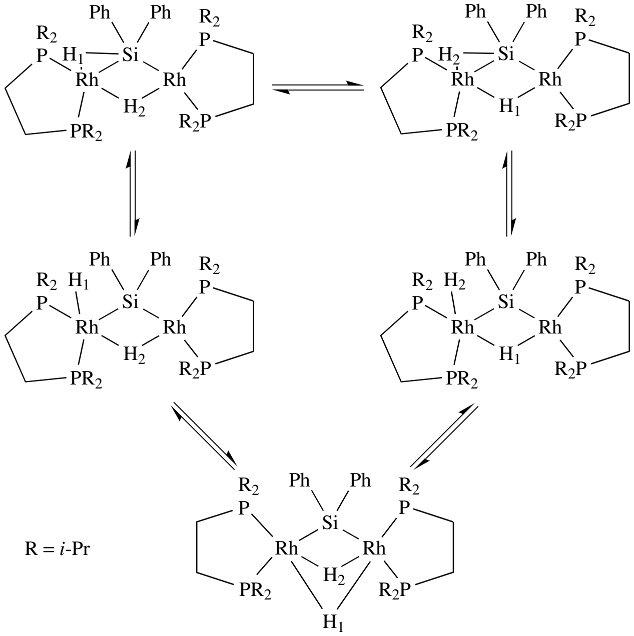

R = *i*-Pr

SCHEME 30

Stoichiometric reaction of Ph_2SiH_2 with $[(dippe)Rh]_2(\mu\text{-}H)_2$ [dippe = 1,2-di(isopropylphosphino)ethane] produced the fluxional complex $[(dippe)Rh]_2(\mu\text{-}\eta^2\text{-}HSiPh_2)(\mu\text{-}H)$ **(70)** which exchanges the silane hydride with the bridging hydride presumably through the mechanism described in Scheme 30[196]. The X-ray structure of **70** indicates the presence of a three-center, two-electron Rh−Si−H interaction similar to the interaction found for complex **67** with the bridging $\mu\text{-}SiPh_2$[194]. Addition of a second equivalent of H_2SiPh_2 to complex **70** gives an equilibrium reaction to the symmetric complex $[(dippe)Rh]_2(\mu\text{-}SiPh_2)_2$[196]. The reaction of the dinuclear rhodium complex $[(dippe)Rh]_2(\mu\text{-}H)_2$ with 2 equivalents of primary silanes afforded the dinuclear bis(μ-silylene) complexes $[(dippe)Rh]_2(\mu\text{-}SiR_2)_2$ (R = *n*-Bu, *p*-$CH_3C_6H_4$) which were reacted with hydrogen producing the corresponding $[(dippe)Rh]_2(\mu\text{-}\eta^2\text{-H-SiR}_2)_2$ complexes. Addition of a large excess of the primary silane to the rhodium hydride dimer $[(dippe)Rh]_2(\mu\text{-H})_2$ generates the dinuclear rhodium derivatives with three silicon-containing ligands $[(dippe)Rh]_2(\mu\text{-SiHR})(\mu\text{-}\eta^2\text{-H-SiHR})_2$[197].

The rhodium silyl complexes, $(Me_3P)_3RhSiR_2Ph$ (R = Me, Ph), have been shown to induce a catalytic and selective C−F activation of partially fluorinated and perfluorobenzenes, producing in the latter case the complex $(Me_3P)_3RhC_6F_5$ (Scheme 31). This complex adds silanes oxidatively and eliminates exclusively C_6F_5H, reforming the starting silyl complex. For $(EtO)_3SiH$, the octahedral intermediate in which perfluorobenzene and the silane are disposed *trans* to one another has been structurally characterized. This geometry is responsible for the selective C−H elimination of the C_6F_5H[198].

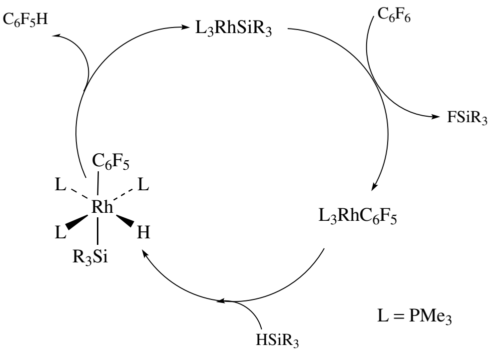

SCHEME 31

Similar octahedral facial silyl methyl hydride complexes of the type $IrL_3H(SiR_3)Me$ have been shown to induce competitive C−H/Si−C reductive elimination depending on the electronic properties of the silyl ligand, thus affording a novel example of a metallation of silyl ligands or the metallation of the sp^3C−H bond of the ethyl moiety when R = OEt. For the complex with R = Et, mixtures of different complexes are formed by the thermolysis with benzene (Scheme 32)[198,199].

Similar competitive reductive elimination of C−H and Si−H bonds have been observed for the complex $IrH(SiHPh_2)(Mes)(CO)(dppe)$ in benzene, leading to the iridium complexes Ir(Mes)(CO)(dppe) and $Ir(SiHPh_2)(CO)(dppe)$ following first-order kinetics for both eliminations[200].

Duckett and Perutz have shown the stoichiometric reaction of the $CpRh(C_2H_4)(SiR_3)H$ (R = Et, *i*-Pr) complexes (Scheme 33)[201]. These complexes have been found to act as precursors to the catalytically active species for the hydrosilylation of ethene with Et_3SiH but are not within the catalytic cycle. The mechanism proposed in Scheme 34 for the hydrosilylation of ethene was found to be equivalent to the Seitz–Wrighton hydrosilylation mechanism catalyzed by cobalt carbonyls complexes[202].

Silanes of the form $HSiR'_3$ (SiR'_3 = $SiMe_2Ph$, $SiMeEt_2$, $SiEt_3$, $SiPh_3$) have been found to cleave the cobalt acetyl complexes $CH_3C(O)Co(CO)_3(PR_3)$ (PR_3 = PPh_2Me, PPh_3) at room temperature to give cobalt silyl compounds $R'_3SiCo(CO)_3(PR_3)$ and ethoxysilanes. Interestingly, acetaldehyde or α-siloxyethyl complexes, $CH_3CH(OSiR'_3)Co(CO)_3(PR_3)$, were not produced. The presence of CO, phosphine or benzaldehyde inhibits the reaction whereas the presence of $RhCl(PPh_3)_3$ has no effect on the reaction rate or on the outcome other than in the hydrosilylation of acetaldehyde with $PhMe_2SiH$ to give $EtOSiMe_2Ph$[203].

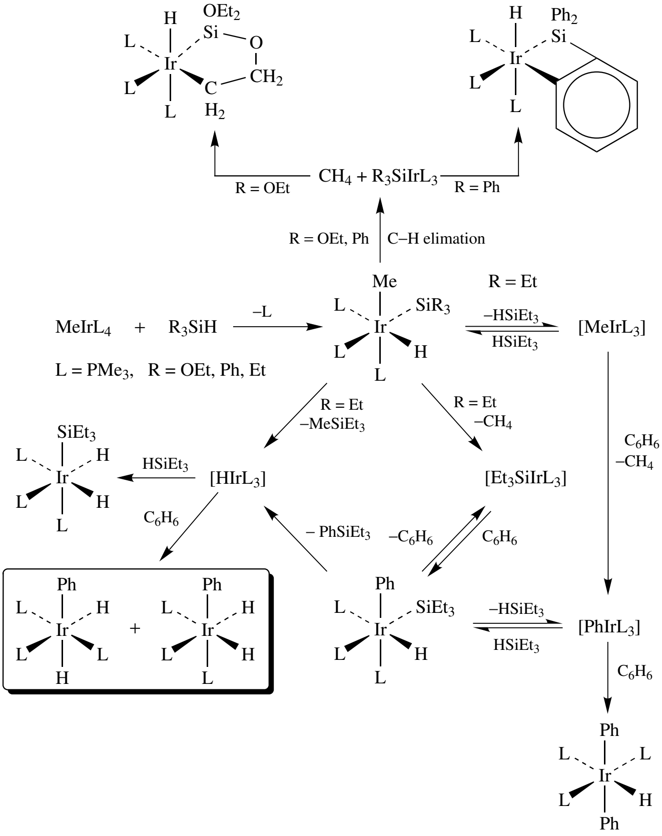

SCHEME 32

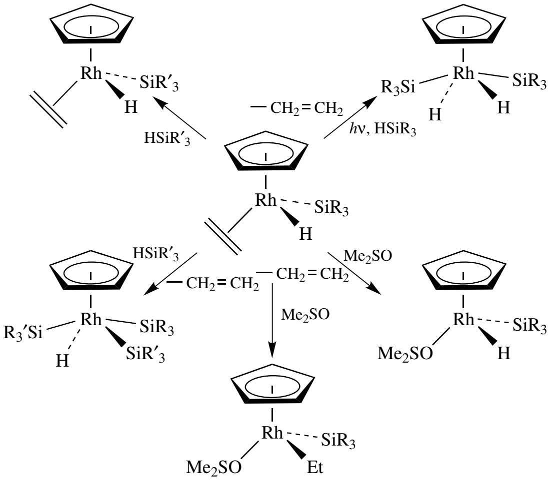

SCHEME 33

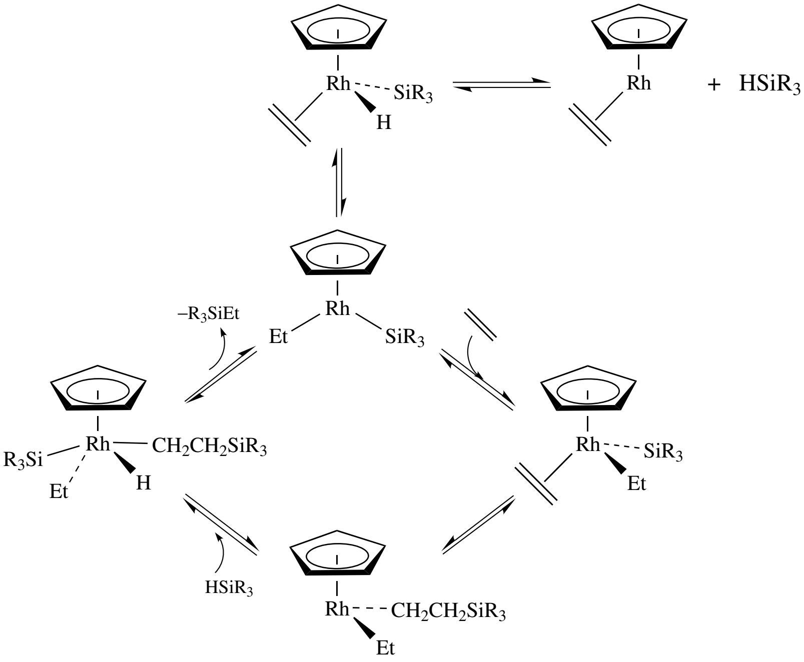

SCHEME 34

Using the metalloradical reactivity of the Rh(II)OEP (OEP = 2,3,7,8,12,13,17,18-octaethylphorphynato) dimer, the preparation of silyl rhodium complexes was achieved by the hydrogen elimination reaction with silanes $R_2R'SiH$ (R = R′ = Et, Ph; R = Me, R′ = Ph, OEt). The Rh−Si bond length of 2.32(1) Å, found when R = Et, is comparable to those in other Rh(III) complexes (Table 11). The crystal packing indicates that all the ethyl groups on the porphyrin periphery are directed toward the silyl group. Consequently, the aromatic part of one complex molecule is in contact with the aromatic part of the next molecule and the aliphatic part is in contact with the aliphatic part of the next molecule[204].

Complexes of the type $M(PPh_3)_3(CO)H$ (M = Rh, Ir) were reacted with an excess of dmsiqn-H [dmsiqn-H = (8-quinolyl)dimethylsilane] in toluene producing the tris N−Si chelating facial five-membered ring $M(dmsiqn)_3$ (equation 42). The fused aromatic quinoline ring system provides a low energy π acceptor orbital which, in conjunction with the silyl group and the easily oxidized metal center such as M(III), leads to complexes with low-energy metal-to-ligand charge transfer (MLCT) transitions.

$$\mathrm{M(PPh_3)_3(CO)H + 3dmsiqn\text{-}H \rightarrow M(dmsiqn)_3 + 3PPh_3 + 2H_2 + CO} \qquad (42)$$

For M = Rh, the Rh−Si bond lengths [2.28–2.31 (Å)] are shorter than in comparable complexes (Table 11). An unusual feature of these complexes is the packing of the molecules in the crystal lattice. The two different enantiomers of the complex segregate into columns which are aligned in adjacent rows, creating alternating sheets of Δ and Λ isomers. These sheets are also arranged in such a way that the 3-fold axes of the complexes are oriented in parallel to each other so that the molecular dipoles point in the same direction. The alignment of the molecules impart the crystal with a net polarization which leads to the observation of non-linear optical behavior[205].

Reaction of $(Me_3P)_3RhCl$ with the lithium salt, $(Me_3Si)_3SiLi{\bullet}3THF$, generated the thermally unstable complex $(Me_3P)_3RhSiMe_2SiMe(SiMe_3)_3$ presumably via a series of 1,2- and 1,3-migrations as shown for the Cp(CO)Fe fragment by Sharma and Pannell[155], by Ogino and coworkers[171–173] and by Berry and coworkers[64] for the Cp_2W moiety (*vide supra*). The analogous reaction of the iridium complex results in a similar rearrangement, yielding a mixture of diastereomers of the iridacycle complex $(Me_3P)_3(H)\overline{IrSiMe_2SiMe(SiMe_3)SiMe_2C}H_2$ (Scheme 35). The two isomers can be interconverted by catalytic amounts of hydrogen to their equilibrium mixture by reversing the processes cyclometallation, oxidative addition of hydrogen to the Ir(I) center, rotation and cyclometallation with elimination of hydrogen[206].

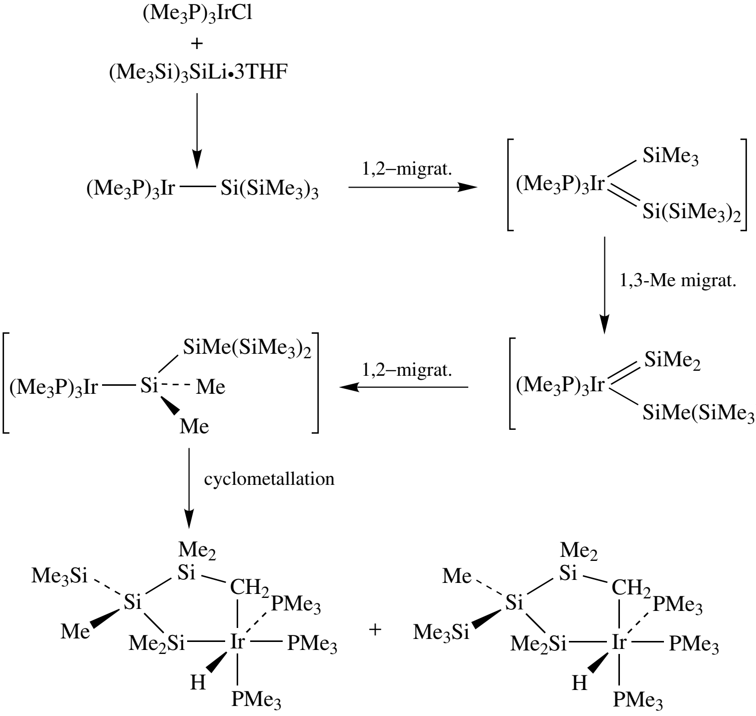

SCHEME 35

Fac-tris(trimethylphosphino)iridium(III) silane complexes of the form $IrHX(PMe_3)_3SiRR'_2$ (X = H, D; R = H, D, Cl, Ph; R′ = Ph, *t*-Bu) have been prepared by the oxidative addition of $SiXRR'_2$ to $IrH(PMe_3)_4$ with the loss of PMe_3. The exclusive formation of the facial isomers is attributed to a preferential *cis* addition of the $R_3Si{-}H$ moiety parallel to the P–Ir–P axis, yielding the *cis* hydride products in which the silicon is *trans* to a phosphine[207].

The methyl iridium triflate complex $Cp^*(Me_3P)IrMe(OTf)$ reacted efficiently with silanes leading to rearrangement products of the presumably initial Si–H products. Thus, trimethylsilane produced methane and, instead of the expected (trimethylsilyl)iridium complex, the methyliridium dimethylsilyl triflate $Cp^*(Me_3P)Ir(Me)(SiMe_2OTf)$ was obtained. Similarly, phenylsilane produced the analog $Cp^*(Me_3P)Ir(Ph)(SiPh_2OTf)$.

Phenyldimethylsilane and diphenylsilane gave the phenyl and the hydride migration products, Cp*$(Me_3P)Ir(Ph)(SiMe_2OTf)$ and Cp*$(Me_3P)IrH(SiPh_2OTf)$, respectively[208].

Direct alkyne insertion into a Rh−Si bond has been observed for the intermediate rhodium silyl complex (dtbpm) $Rh[Si(OEt)_3]$ (PMe_3) [dtbpm = di(*tert*-butyl)phosphino methane] in the hydrosilylation of 2-butyne with triethoxysilane catalyzed by the rhodium alkyl complex (dtbpm)$RhMe(PMe_3)$. The crystal structure of (dtbpm)$Rh[Si(OEt)_3]$ (PMe_3) shows that the coordination around the Rh metal is planar with a Rh−Si bond length [2.325(2) Å] similar to that found for the complex $(Me_3P)_3RhH(C_6F_5)\{Si(OEt)_3\}$ (Table 11)[209]. The proposed mechanism for the hydrosilylation reaction of 2-butyne with $HSi(OEt)_3$ yielding mainly the *E*-isomer of $MeCH{=}C(Me)Si(OEt)_3$ is outlined in Scheme 36.

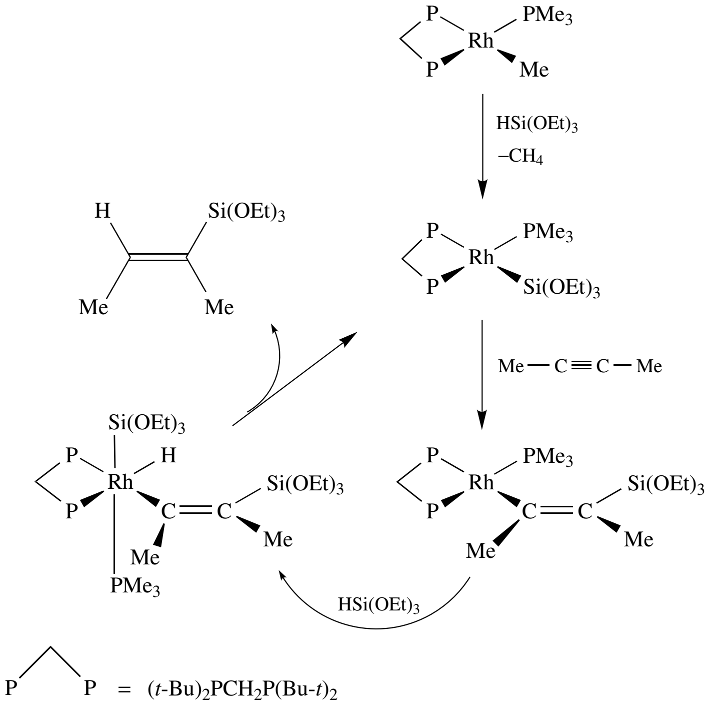

SCHEME 36

The behavior of the $SiMe_2H$-substituted alkyne in $Me_2HSiC{\equiv}CSiMe_2H$ toward $[RhCl(P(Pr\text{-}i)_3)_2]_n$ has been shown to be different from that of the analog $Me_3SiC{\equiv}CSiMe_3$. Instead of the expected mononuclear vinylidene complex *trans*-$[ClRh(C(SiMe_2H){=}CH(SiMe_2H))(P(Pr\text{-}i)_3)_2]$, the dinuclear symmetrical hydrido(silyl) complex was obtained by oxidative addition of both terminal Si−H bonds to two metal centers (equation 43)[210]. Interestingly, reaction of the *in situ* prepared phenylthio rhodium complex $Rh(SPh)(PMe_3)_3$ with two equivalents of the more flexible disilane, $HMe_2SiCH_2CH_2SiMe_2H$, afforded a mixture of the complexes *cis, mer*-$[RhH_2(SPh)(PMe_3)_3]$ and disilarhodacycle *fac*-$[\overline{Rh(SiMe_2CH_2CH_2Si}Me_2)H(PMe_3)_3]$ with a concomitant elimination of thiophenol. The Rh−Si distances [2.383(2) Å and

2.389(2) Å] observed for the latter complex are longer than for similar Rh complexes (Table 11)[211].

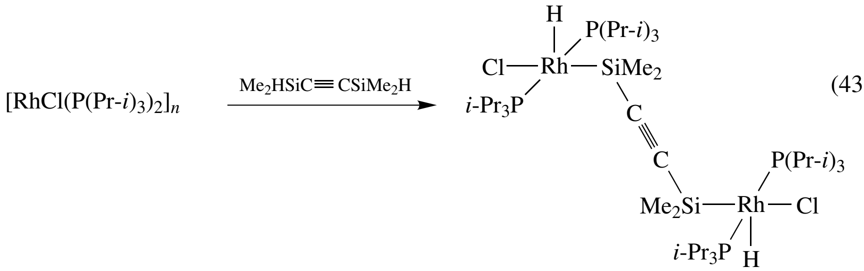

(43)

μ-Cyclopentadienyldiene dicobalt complexes **(71)** reacted with trimethylsilylacetylenes by eliminating ethene and forming the unusual binuclear complexes **(72)** with a cobaltabicyclic ring system as a ligand (equation 44). The crystal structure of complex **72** with $R^1{}_5$ = Me_4Et, R^2 = $SiMe_3$ exhibit similar Co−Si bond distance [2.281(2) Å][212] to those found in the silasesquioxane complex $Co(CO)_4(H_7Si_8O_{12})$ [2.285(1) Å][213]. A number of interesting multinuclear cobalt silicon clusters have been obtained by the reactions of Co_2CO_8 with chloro and alkyl silanes[214−218]. In addition, a monosubstituted cobalt silyl octanuclear silasesquioxane cage exhibiting a metal−silicon bond of 2.285(1) Å was recently obtained from the reaction of Co_2CO_8 with octahydrosilasesquioxane $H_8Si_8O_{12}$[213].

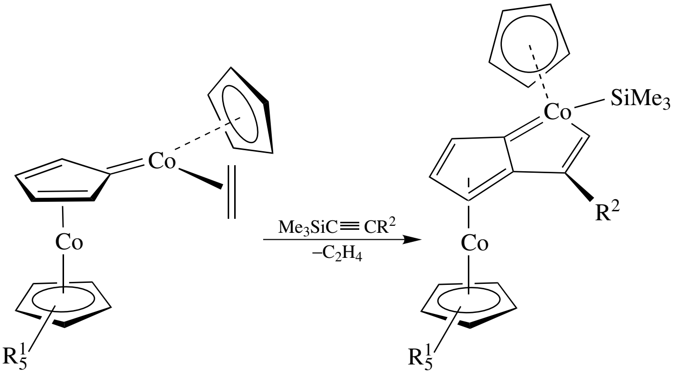

(44)

R^1_5 = H_5, Me_5, Me_4Et

R^2 = $SiMe_3$, $SiEt_3$, $SiMe_2Bu$-*t*

(71) **(72)**

C. Silanol Complexes

The iridium silanol complexes of the form $(Et_3P)_2IrH(Cl)(SiR_2OH)$ [R = *i*-Pr **(73)**, *t*-Bu] have been prepared from low-valent Ir(I) complexes and the corresponding dialkylsilanol. The 16-electron coordinatively unsaturated complex **73** with a short Ir−Si bond length [2.313(6) Å] adopts a trigonal bipyramidal arrangement rather than a square pyramidal configuration, due to the partial multiple bond present between the metal center and the π-donor chlorine atom. Reaction of **73** with a strong base (BuLi) selectively deprotonates the silanol, yielding a planar dihydride metallosilanolate **74** (equation 45)[219].

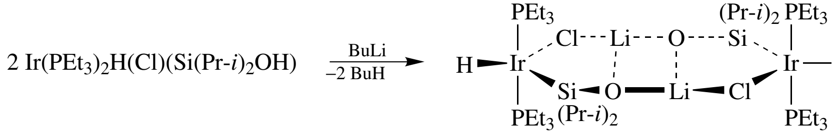

(73) **(74)** (45)

Analogous iridium silanethiol complexes $(PPh_3)_2(CO)IrH_2(Si(SEt)_3)$, *fac*-$(PMe_3)_3IrMeH(Si(SEt)_3)$ and *mer*-$(PMe_3)_3Ir(C_6F_5)H(Si(SEt)_3)$ were prepared by the oxidative addition of $HSi(SEt)_3$ to $HIr(CO)\ (PPh_3)_3$, $MeIr(PMe_3)_4$ and $C_6F_5Ir(PMe_3)_3$, respectively. Unlike the extremely easily hydrolyzable parent silane, the iridium complexes are stable in neutral and basic H_2O/THF solutions. This stabilization is attributed to the electron-donating capacity of the metal center which reduces efficiently the electrophilicity of the silicon. Interestingly, the rhodium analog *mer*-$(Me_3P)_3Rh\ (C_6F_5)H(Si(SEt)_3)$ reacts with 5 equivalents of H_2O, producing the thioethyl complex *mer*-$(Me_3P)_3Rh(C_6F_5)H(SEt)$ due to its high propensity to reductively eliminate the Si−H bond[220].

TABLE 11. Selected M−Si distances in group-9 transition-metal silicon-containing complexes

Compound	d^n Configuration	M−Si (Å)	Reference
$\overline{Ir(acac)\{C[CH(OCH_3)OSi}Ph_2]{=}CHCO_2CH_3\}PCy_3$	d^6	2.264(2)	190
$In(acac)H(SiEt_3)(PCy_3)$	d^6	2.307(1)	191
$Ir(dmsb)H_3(PPh_3)_2$[a]	d^4	2.437(1), 2.430(1)	192
$IrH(SiClMe_2)_2(CO)(dppe)$[b]	d^6	2.396(2), 2.397(2)	193
$IrH(SiClMe_2)(SIHMe_2)(CO)(dppe)$[b]	d^6	2.394(3), 2.418(3)	193
$IrH(SiF_2Et)_2(CO)(dppe)$[b]	d^6	2.349(7), 2.372(7)	193
$[(dippe)Rh]_2(\mu\text{-}H)(\mu - \eta^2\text{-}HSiPh_2)]$[c]	d^8	2.298(2), 2.487(2)	196
$[(dippe)Rh]_2(\mu\text{-}Si(Bu\text{-}n)_2]$[c]	d^6	2.334(1), 2.335(1)	197
$[(dippe)Rh]_2(\mu\text{-}SiHTol\text{-}p)(\mu\text{-}\eta^2\text{-}H\text{-}SiHTol\text{-}p)_2]$[c]	d^7	2.336(2), 2.349(2) 2.444(2), 2.477(2) 2.350(2), 2.356(2)	197
$(PMe_3)_3RhH(C_6F_5)\{Si(OEt)_3\}$	d^6	2.325(4)	198
fac-$(Me_3P)_3IrMeH(SiPh_3)$	d^6	2.381(3)	199
fac-$(Me_3P)_3IrMeH(SiEt_3)$	d^6	2.424(2)	199
$IrH_2\{Si(OTf)Ph_2\}(TFB)(P(Pr\text{-}i)_3)$[d]	d^6	2.337(2)	186
$(Me_3P)_3\overline{Ir\{SiPh_2(o\text{-}C}_6H_4)$	d^6	2.404(3)	198
$(Et_3P)_2IrH(Cl)(Si(Pr\text{-}i)_2OH)$	d^6	2.313(6)	219
$[(Et_3P)_2IrH(Cl)(Si(Pr\text{-}i)_2OLi)]_2$	d^6	2.344(2)	219
$(OEP)RhSiEt_3$[e]	d^6	2.32(1)	204
$Rh(dmsiqn)_3$[f]	d^6	2.278(1), 2.290(1) 2.301(1)	205

TABLE 11. (*continued)*)

Compound	d_n Configuration	M−Si (Å)	Reference
$(Me_3P)_3H\overline{IrSiMe_2SiMe(SiMe_3)SiMe_2C}H_2$	d^6	2.441(3)	206
$IrH_2(PMe_3)_3(SiHPPh_2)$	d^6	2.361(3), 2.369(3)	207
$IrH_2(PMe_3)_3(SiPPh_3)$	d^6	2.382(4)	207
$IrH_2(PMe_3)_3(Si(Bu\text{-}t)_2Cl$	d^6	2.392(3)	207
$(dtbpm)Rh[Si(OEt)_2](PMe_3)^g$	d^6	2.325(2)	209
fac-$[\overline{Rh(SiMe_2CH_2CH_2Si}Me_2)H(PMe_3)_3]$	d^6	2.383(2), 2.389(2)	211
72	d^6	2.281(2)	212
$Co(CO)_4(H_7Si_8O_{12})$	d^8	2.285(1)	213

[a] dmsb = 1,2-dimethylsilylbenzene.

[b] dppe = diphenylphosphinoethane.

[c] dippe = di(isopropyl)phosphinoethane.

[d] TFB = tetrafluorobenzobarrelene.

[e] OEP = 2,3,7,8,12,13,17,18-octaethylphorphynato.

[f] dmsiqn = (8 − quinoyl)dimethylsilane.

[g] dtbpm = di(*tert*-butyl)phosphinomethane.

TABLE 12. Selected ^{29}Si NMR chemical shifts for group-9 transition-metal silicon-containing complexes

Compound	^{29}Si NMR shift (ppm)	Reference
$[(dippe)Rh]_2(\mu\text{-}Si(Bu\text{-}n)H)(\mu\text{-}\eta^2\text{-}H\text{-}SiH(Bu\text{-}n))_2{}^a$	125.5 (br t, 2Si, $^1J_{Si-H}$ = 180 Hz)	197
$[(dippe)Rh]_2(\mu\text{-}SiHTol\text{-}p)(\mu\text{-}\eta^2\text{-}H\text{-}SiHTol\text{-}P)_2{}^a$	100−142 br	197
$CpRh(Si(Pr\text{-}i)_3)_2H_2$	52.2 (d, $^1J_{SiRh}$ = 18.3 Hz)	202
$PhMe_2SiCo(CO)_3(PPh_2Me)$	32.3 (d, $^2J_{SiP}$ = 28.9 Hz)	203
$EtMe_2SiCo(CO)_3(PPh_2Me)$	42.2 (d, $^2J_{SiP}$ = 26.0Hz)	203
$Et_3SiCo(CO)_3(PPh_2Me)$	51.8 (d, $^2J_{SiP}$ = 25.0 Hz)	203
$Ph_3SiCo(CO)_3(PPh_2Me)$	29.8 (d, $^2J_{SiP}$ = 33.0 Hz)	203
$PhMe_2SiCo(CO)_3(PPh_3)$	33.1 (d, $^2J_{SiP}$ = 29.4 Hz)	203
$Et_3SiCo(CO)_3(PPh_3)$	52.9 (d, $^2J_{SiP}$ = 25.4 Hz)	203
$(OEP)Rh(SiEt_3)^b$	51.98 (d, $^1J_{SiRh}$ = 29.3 Hz)	204
$(OEP)Rh(SiPh_3)^b$	11.56 (d, $^1J_{SiRh}$ = 35.7 Hz)	204
$(OEP)Rh(SiMe_2Ph)^b$	28.3 (d, $^1J_{SiRh}$ = 30.2 Hz)	204
$(OEP)Rh\{SiMe_2(OEt)\}^b$	37.24 (d, $^1J_{SiRh}$ = 30.5 Hz)	204
$Rh(dmsiqn)_3{}^c$	23.60 (d, $^1J_{SiRh}$ = 41.7 Hz)	205
$Ir(dmsiqn)_3{}^c$	−10.14	205
$IrH_2(PMe_3)_3(Si(Bu\text{-}t)_2H)$	23.70 (dt, $^1J_{SiH}$ = 126 Hz, $^3J_{SIH}$ = 9 Hz)	207
$IrH_2(PMe_3)_3(SiPPh_3)$	0.094 (dt, $^1J_{SiH}$ = 134 Hz, $^3J_{SiH}$ = 8 Hz)	207
$[Rh_2H_2Cl_2(P(Pr\text{-}i)_3)_4(\mu\text{-}Me_2SiC{\equiv}CSiMe_2)]$	14.52 (dt, $^1J_{SiRh}$ = 36.4 Hz, $^2J_{SiP}$ = 9.7 Hz)	210

[a] dippe = di(isopropyl)phosphinoethane.

[b] OEP = 2,3,7,8,12,13,17,18-octaethylphorphynato.

[c] dmsiqn = (8 − quinoyl)dimethylsilane.

XV. GROUP-10 SILICON-CONTAINING COMPLEXES

A. Silyl, Bis(silyl) and Silanol Complexes

Reaction of halotrimethylsilanes with electron-rich Pt(II) complexes resulted in a facile oxidative addition of the Si−X bond (X = Cl, Br, I) (equation 46). The crystal structure of the complex [$PtIMe_2(SiMe_3)$(2,2′-bipyridyl)] shows normal Pt−Si bond distance of 2.313(6) Å (Table 13) and exceptionally long Pt−I bond distance which arises from the strong *trans* influence of the trimethylsilyl group[221].

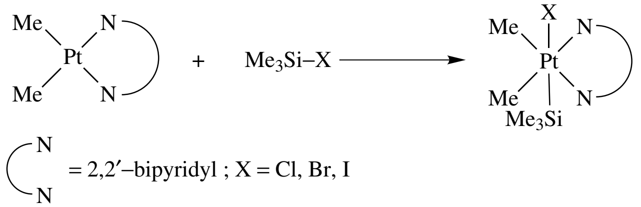

(46)

Cis- and *trans*-$PtMe(SiPh_3)(PMePh_2)_2$ have been prepared selectively by reacting for both cases the complex *trans*-$Pt(Cl)(SiPh_3)(PMePh_2)_2$ either with an excess amount of MeLi followed by methanolysis, or by Me_2Mg in THF, respectively. Thermolysis of both isomers in benzene solutions yields quantitatively $MeSiPh_3$ as the reducting elimination product. The thermolysis of the *cis* isomer was initiated by dissociation of the $PMePh_2$ ligand and has been accelerated by the addition of alkynes and olefins[222]. Oxidative addition of Me_3SiH to $Pt(C_2H_4)(PPh_3)_2$ afforded the distorted square-planar hydrido *cis*-$PtH(SiMe_3)(PPh_3)_2$ complex. The Pt−P bond *trans* to the silicon is significantly longer than that of the *cis* Pt−P bond to the silicon, in accord with the *trans* influence of the trimethylsilyl group[223].

Reaction of 1-silyl dienol silyl ethers **(75)** with Li_2PdCl_4 in the presence of Li_2CO_3 in MeOH gave the (η^3-1-(silylcarbonyl)allyl)palladium chloride complexes **(76)** (equation 47). These complexes undergo catalytic decarbonylation to give the corresponding (η^3-1-(silylallyl))palladium chloride complexes. The mechanism proposed proceeds through the formation of an η^1-allyl complex **(77)** as the first step, followed by β-elimination of the TMS group affording the vinyl ketene intermediate complex **(78)**. Subsequent addition of the silyl-palladium moiety to the ketene in the reverse regiochemistry yielded the acylpalladium complex **(79)** and its decarbonylation lead to the (η^1-allyl)palladium and (η^3-allyl)palladium species (Scheme 37)[224].

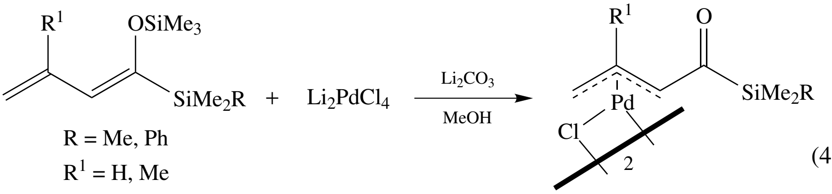

(75) **(76)**

(47)

Braunstein and coworkers have shown (*vide supra*) that in the bimetallic Fe−Pt complex $(CO)_3(SiR_3)\overline{Fe(\mu\text{-}PPh_2)Pt}(PPh_3)CO(Fe{-}Pt)$, a silyl migration occurred from the Fe to the Pt center (Scheme 17)[102]. Remarkably, the first example of a well-characterized insertion of a transition-metal fragment into a strained silicon−carbon bond of a silicon-bridged [1]ferrocenophane was recently reported by Sheridan, Lough and Manners. The

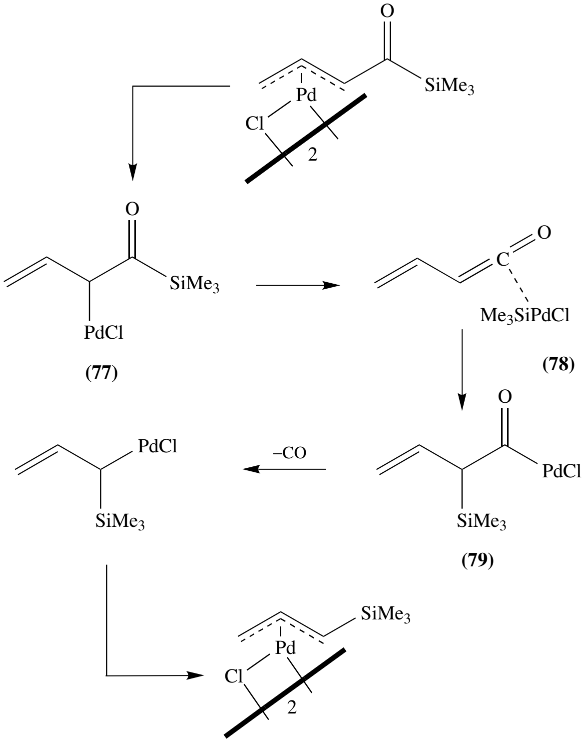

SCHEME 37

reaction of $Fe(\eta^5\text{-}C_5H_4)_2SiMe_2$ with $Pt(PEt_3)_3$ afforded the complex [2]platinasilaferrocenophane $Fe(\eta^5\text{-}C_5H_4)_2Pt(PEt_3)_2SiMe_2$ (equation 48). X-ray diffraction study of the complex reveals that the platinum metal is in a distorted square-planar environment with large P−Pt−P angles and compressed P−Pt−Cp and Cp−Pt−Si angles (Table 13)[225].

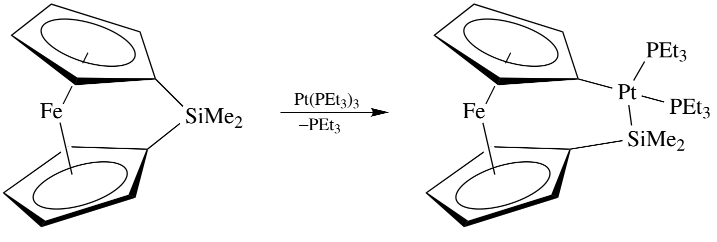

(48)

Thermolytic orthometallation of the polysilyl chloroplatinum complex **80** in a refluxing mixture of methanol in benzene (1:8) yielded the cyclometallated complex **81** which was cleaved by water to complex **82** having a platinum−phenyl bond and a silanol moiety on the polysilyl ligand. Interestingly, in the absence of methanol, under refluxing conditions, complex **80** undergoes an exchange reaction among the trimethylsilyl and chloride moieties across the platinum−silicon bond yielding complex **83**. Complex **83** reacted with methanol producing the bis(silyl) complex **84** (Scheme 38)[226].

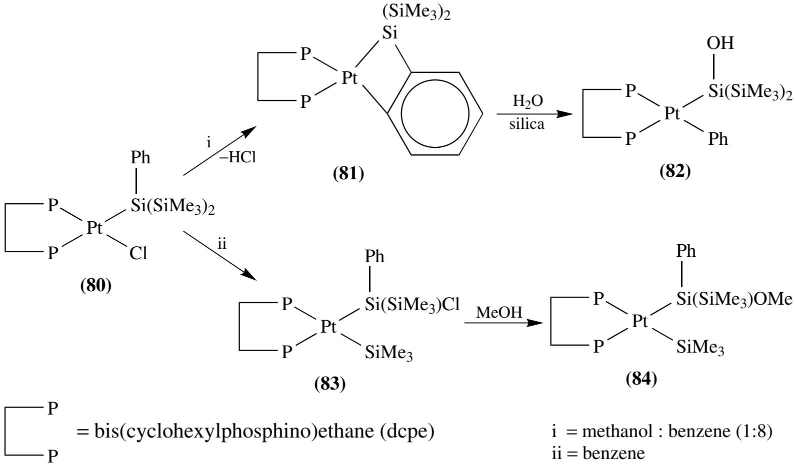

SCHEME 38

Similar bis(silyl) chelating platinum complexes have been obtained by the oxidative addition of disilanes H_3SiSiH_3 to the dihydride complex (dcpe)PtH_2. A rapid addition of the disilane to the hydride afforded selectively complex **85** whereas a slow addition afforded a mixture of complexes **85** and **87**, presumably through complex **86** via an α-silyl shift. X-ray determination indicates that the Pt_2Si_4 ring core adopts a chair conformation in **85** (Scheme 39)[227].

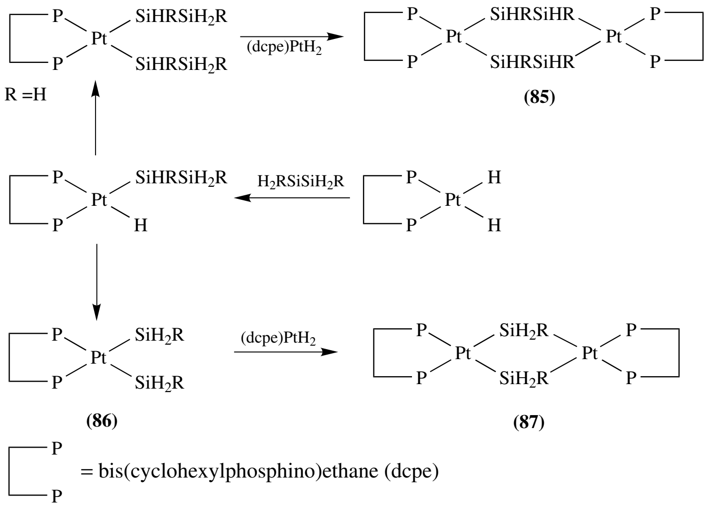

SCHEME 39

Similar reactivity has been found for the isolobal Pd hydrides upon reaction with either hydrosilanes or 1,2-dihydrodisilanes. Thus, the reaction of the dinuclear palladium hydride $[(dcpe)Pd]_2(\mu\text{-}H)_2$ with either H_2SiPhR (R = Ph, Me, H) or $HR'MeSiSiMeR'H$ ($R' = H$, Me) afforded the mononuclear (dcpe)$Pd(SiHRPh)_2$ and (dcpe)$Pd(SiHR'Me)_2$

complexes, respectively. The latter complex with R′ = Me has been characterized by X-ray diffraction. It exhibit Pd−Si bond lengths of 2.3563(9) Å and 2.359(1) Å, which are within the range for Pt−Si bond lengths in similar complexes (Table 13). The palladium bis(silyl) complex (dcpe)Pd$(SiHMe_2)_2$ was found to react with 2.5 equivalents of $MeO_2CC{\equiv}CCO_2Me$ affording stereospecifically the double hydrosilylation compound, dimethyl bis(dimethylsilyl)maleate, and the palladium π-complex of the corresponding alkyne (equation 49)[228].

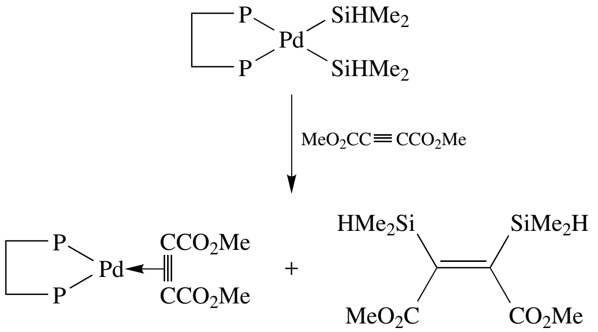

(49)

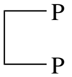

= bis(cyclohexylphosphino)ethane (dcpe)

Tilley and coworkers[229] have shown that the reactivity of Pt(0) complexes with arylsilanes is strongly dependent on the ratio of the reactants. The reaction of 1 equivalent of $ArSiH_3$ with 2 equivalents of $Pt(PEt_3)_3$ gave quantitatively the Tessier−Young dimers $(Et_3P)_2Pt(\eta^2,\eta^2\text{-ArHSiSiHAr})Pt(PEt_3)_2$ (Ar = Ph, p-MeC_6H_4, Mes). Performing the same reaction with a 3:1 ratio of silane to the platinum complex gave the corresponding *cis*-bis(silyl) complexes, *cis*-$(Et_3P)_2Pt(SiH_2Ar)_2$, which isomerized to *cis*/*trans* mixtures in solution. The *cis* isomers decompose in solution to the bridged disilane dimers (equation 50).

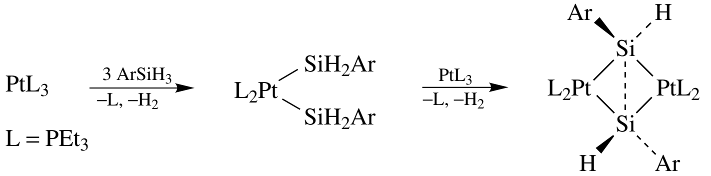

(50)

Reaction of the bis(silyl) complex $(Et_3P)_2Pt(SiH_2Mes)_2$ with the chelating phosphine dmpe afforded the expected ligand exchange producing the complex (dmpe)Pt$(SiH_2Mes)_2$. The reaction with less sterically demanding silyl ligands gave dimeric species [(dmpe)Pt$(SiH_2Ar)_2]_2(\mu$-dmpe) (Ar = Ph, p-$CH_3C_6H_4$), which were found to be in equilibrium with the corresponding monomers. The thermolysis of these dimeric complexes produced the unusual compounds (dmpe)HPt$(\mu^2\text{-SiHAr})_2[\mu\text{-}\eta^1,\eta^1\text{-ArHSiSiHAr}]$PtH(dmpe) (**88**) (Ar = Ph), which possess an η^1,η^1-disilene ligand and two bridging silylene ligands. Complex **88** was found to react with 4 equivalents of $PhSiH_3$ yielding the disilane PhH_2SiSiH_2Ph and the Pt(IV) silyl *fac*-(dmpe)PtH$(SiH_2Ph)_3$ (**89**), which thermally decomposes with loss of H_2 and $PhSiH_3$, regenerating complex

88 (equation 51)[229]. Similarly, Tanaka and coworkers have found that the reaction of an excess of the disilane $HMe_2SiSiMe_2H$ with $Pt(PEt_3)_3$ affords the complex *cis*-$(HMe_2Si)_2Pt(PEt_3)_2$ and oligosilanes of the type $H(SiMe_2)_nH$ ($n < 7$). The thermolysis of this platinum complex produced mainly Me_2SiH_2 while the reaction with 3 equivalents of phenylacetylene afforded the platinacycle complex **90** that, under heating, reductively eliminates 1,1-dimethyl-3,4-diphenyl-1-sila-2,4-cyclopentadiene **(91)** (equation 52)[230].

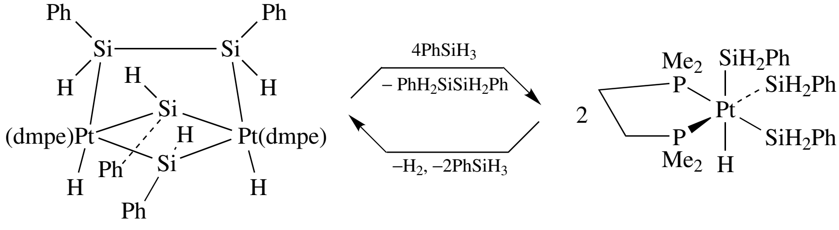

(88) **(89)**

(51)

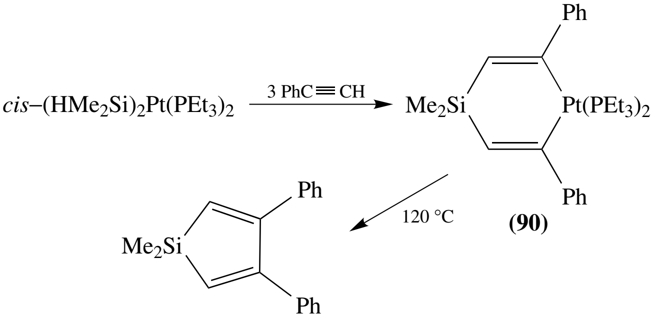

(90)

(91)

(52)

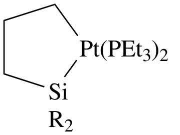

R = Ph, Cl, Me

(92)

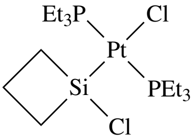

(93)

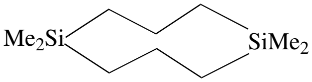

(94)

Oxidative addition of the Si−C bond of silacyclobutanes to $Pt(PEt_3)_3$ afforded selectively 1-platina-2 silacyclopentanes. Thus, complex **92** was obtained from 1,1-diphenyl-1-silacyclobutane. Complex **92** exhibits a slightly distorted square-planar coordination geometry, with a Pt−Si bond length of 2.354(1) Å. For the dichloro silacyclobutane compound, in addition to a complex analogous to complex **92**, 10% of the Si−Cl addition product *trans*-**93** was also observed, whereas from the dimethysilacyclobutane the reaction afforded, besides the analogous complex **92**, large amounts of its dimer **94**[231].

The reactivity of the Pt(0) complex, $Pt(PEt_3)_3$, with equivalent amounts of 1,2-disilanes at different temperatures afforded the first $Pt(IV)Si_4P_2$ **(95)** type complex which was characterized by X-ray diffraction and the dinuclear mixed valence $Pt(II)Pt(IV)Si_4P_4$ **(96)**

type complex (Scheme 40)[232]. Large excess of the disilanes allowed the formation of the well known cyclic Pt(II)Si_2P_2 complex reported in 1973 by Eaborn and coworkers[233].

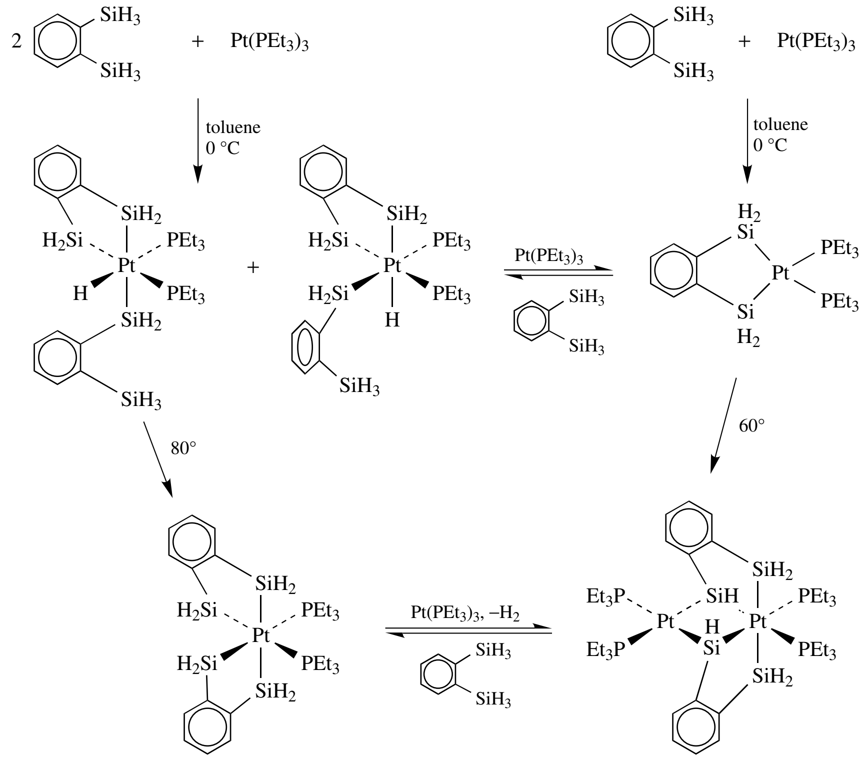

(95) **(96)**

SCHEME 40

Secondary silanes $RR'SiH_2$ ($R = R' =$ Me, Et, Ph; $R =$ Me, $R' =$ Ph) were found to react with the binuclear zero-valent platinum complex $[Pt_2(\mu\text{-}CO)(CO)_2(\mu\text{-}dppm)_2]$ to give the corresponding μ-SiRR′ complexes of the form $[Pt_2(\mu\text{-}SiRR')(CO)_2(\mu\text{-}dppm)_2]$. The $^{31}P\{H\}$ NMR data suggest that these compounds are better formulated as *W* frame complexes. When $R = R' =$ Ph, low-temperature NMR data showed that the reaction proceeds via the intermediate $[Pt_2H(SiHPh_2)(CO)(\mu\text{-}dppm)_2]$ which is the result of the Si−H addition to one Pt atom with concomitant loss of two CO molecules[234]. Enticingly, the reaction of $Cl(SiMe_2)_3Cl$ with $Pt(PEt_3)_3$ afforded the complex *cis*-$(ClMe_2Si)(Me_3SiClMeSi)Pt(PEt_3)_2$ **(97)**. Complex **97** can also be obtained by the reaction of $Pt(PEt_3)_3$ with $ClMe_2SiSiClMeSiMe_3$. Thermolysis of **97** produced the complex *cis*-$(ClMe_2Si)_2Pt(PEt_3)_2$ and the dimethylsilylene $[Me_2Si\mathbf{:}]$, presumably via a silylene−platinum intermediate. This reaction has been used to explain the unexpected formation of 1,4-disilacyclohexa-2,5-dienes in the palladium-catalyzed reaction of $Cl(SiMe_2)_3Cl$ with acetylenes[235].

The bis(silylation) of C−C triple bonds is a reaction in which two Si−C bonds are created in the same molecule. Palladium complexes are the most often used catalysts and the redox cycle of the palladium in the generally postulated mechanism consists of two major pathways: Oxidative addition of the Si−Si bond to the palladium(0), and transfer of the two organosilyl groups to the C−C triple bond regenerating the palladium(0) (Scheme 41).

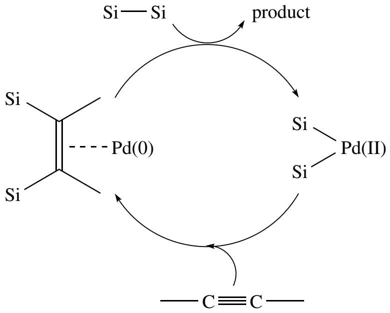

SCHEME 41

Recently Ito and coworkers have prepared, structurally determined and interconverted bis(silyl)alkane palladium(II) **(98)** and bis(silyl)palladium(0) **(99)** complexes, supporting the postulated mechanism for the bis(silylation) of triple bonds (equation 53)[236]. Similar supporting evidence has been recently obtained using mixed silyl−stannyl compounds[237], by the unsymmetrical substituted disilane Me_3SiSiF_2Ph[238], and by theoretical studies by Sakaki[239−241] Márquez[242,243] and others[244−247].

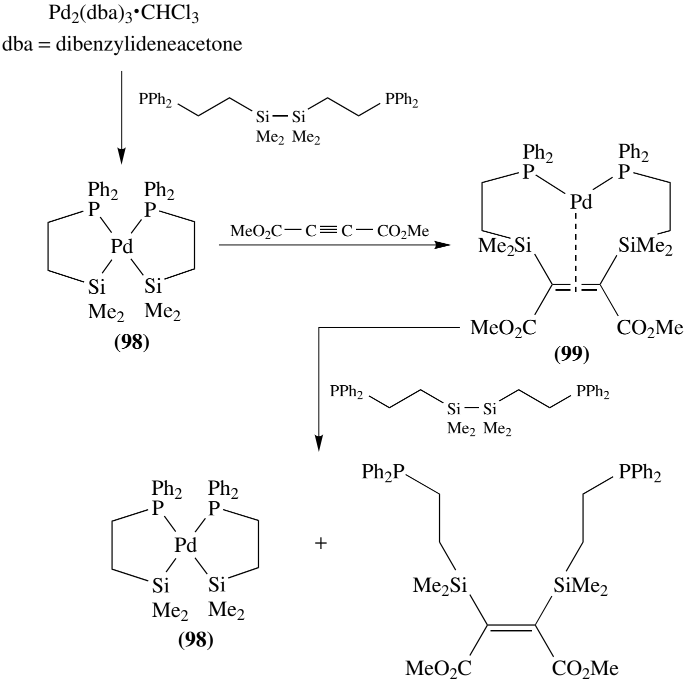

(53)

Activation of two Si–Si bonds in bis(disilanyl)alkanes with palladium(0) bis(*tert*-alkyl isocyanide) induced the formation of the cyclic bis(silyl)palladium(II) bis(*tert*-alkyl isocyanide) complexes **(100)** and disilanes described schematically in Scheme 42. These complexes were found to react with phenylacetylene, affording different amounts of five-membered cyclic products and acyclic products which are derived from the insertion of the alkyne into the general intermediate complex **101** (Scheme 42, equation 54). The bis(silanyl)dithiane palladium complex **(102)** was isolated and characterized in the solid state: the two silicon atoms, the two isocyano carbons and the palladium atom are nearly in a plane with a short cross-ring Si–Si distance of 2.613(2) Å, suggesting the possibility of covalently bonded two Si–Si atoms in the four-membered ring. Similar reaction with cyclic disilanes afforded oligomers, and cyclic 20-membered compounds have been prepared in the presence of nitriles[248,249].

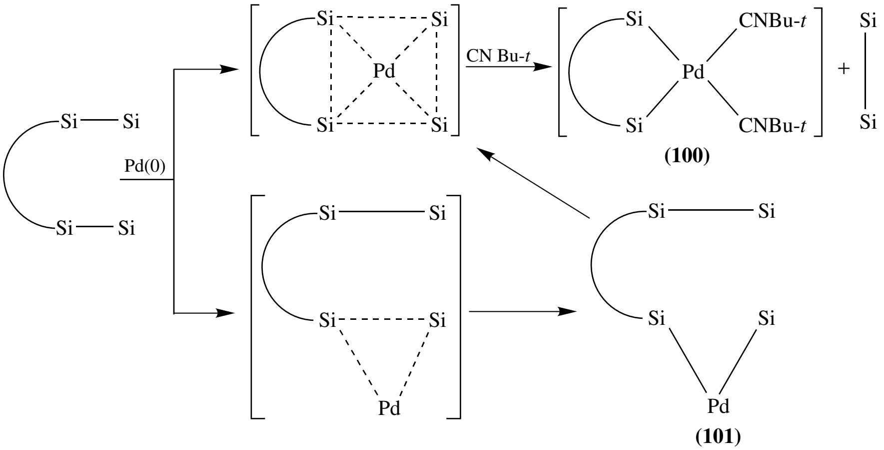

SCHEME 42

Synthetic application of group-10 complexes in catalytic and stoichiometric reactions with silanes has produced a large number of interesting compounds which have been recently reviewed elsewhere[231,250–253].

B. Silylene Complexes

Fischer-type cationic platinum silylene complexes of the type *cis*-$[(Cy_3P)_2HPt{=}Si(DMAP)(SEt)_2]\ BPh_4$ and *trans*-$[(Cy_3P)_2HPt{=}Si(SEt)_2]\ BPh_4$ were prepared by Tilley and coworkers. The former base-stabilized silylene complex was obtained by displacing a labile triflate group with the neutral two-electron donor (dimethylamino)pyridine (DMAP) from the complex *trans*-$(Cy_3P)_2HPt\{Si(SEt)_2OTf\}$. Isomerization to the *cis* complex took place upon recrystallization. The latter base-free silylene complex was formed in the reaction of *trans*-$(Cy_3P)_2HPt\{Si(SEt)_2OTf\}$ with $NaBPh_4$ (Scheme 43). The structure of the cationic $[(Cy_3P)_2HPt{=}Si(SEt)_2]^+$ reveals a square-planar geometry for the platinum with no interionic interactions. The silylene fragment is planar, reflecting the sp^2 hybridization. The plane of the silylene ligand is rotated 76° out of the least-squares plane of platinum donor atoms, implying that π-donation from the d_{xz} level contributes more to the molecular bonding. The Pt–Si bond length of 2.270(2) Å is short in comparison with related complexes (Table 13) and the large downfield ^{29}Si chemical shift of 308.65 ppm is in accord with other values for base-free silylene complexes (Table 14)[254].

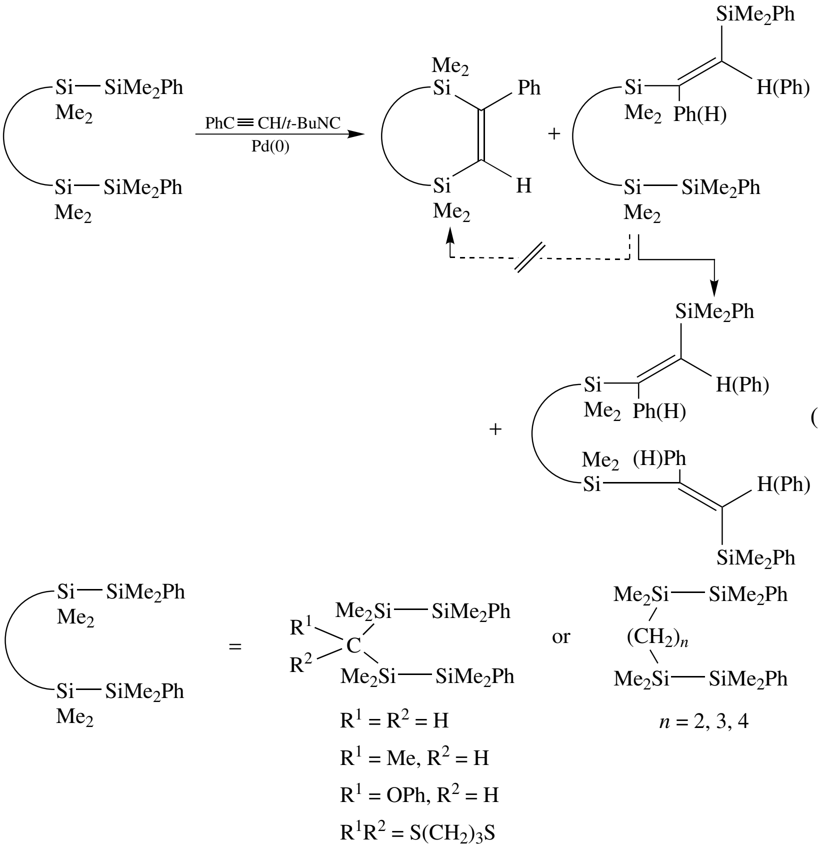

(54)

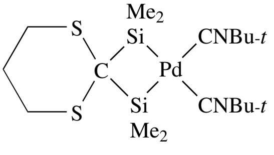

(102)

The first donor-free thermally stable (mp = 160 °C) bis(silylene)nickel complex **105** has been obtained from the reaction of the stable silylene 1,3-di-*tert*-butyl-2,3-dihydro-1*H*-1,3,2-diazasilol-2-ylidine **(103)** with nickel tetracarbonyl[255]. Remarkably, no monosubstitution complex **(104)** or comproportionation of complex **105** with $Ni(CO)_4$ was observed (equation 55). The structure of **105** shows a slightly distorted tetrahedral arrangement of two silylene and two carbonyl ligands around the metal. The small N−Si−N angle (90°) is close to that predicted for free silylenes and the Si−Ni bond lengths of 2.207(2) Å and 2.216(2) Å are close to the theoretical expectations[29]. Interestingly, the deshielding

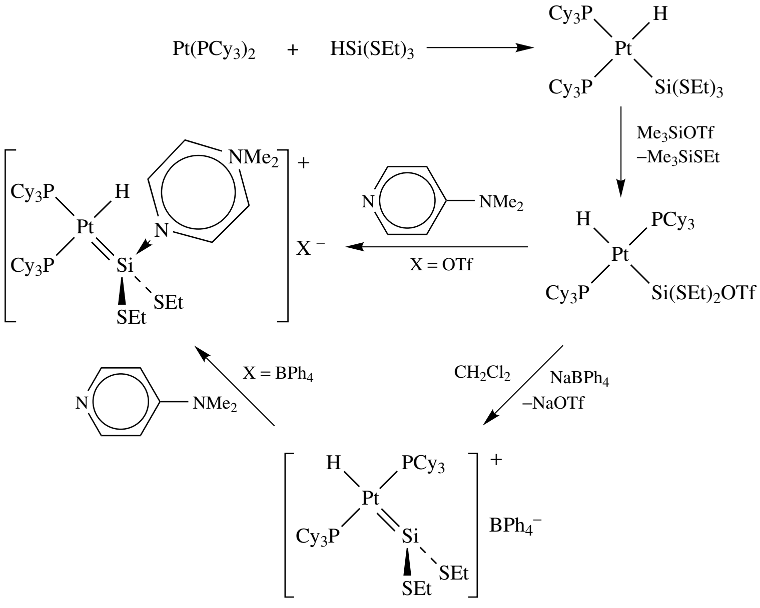

SCHEME 43

expected for this base-free silylene is only moderate in comparison with the starting silylene (^{29}Si $\delta_{\mathbf{103}} = 78.4$ ppm; $\delta_{\mathbf{105}} = 97.5$ ppm)[255].

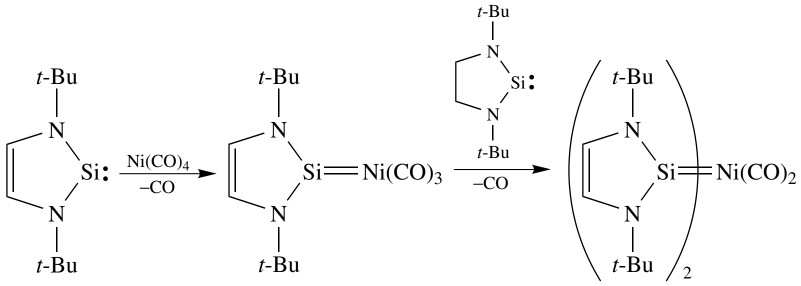

(55)

(103) **(104)** **(105)**

Recently, Tamao and coworkers have found that palladium catalyzed the skeletal rearrangement of alkoxy(oligosilanes) (equation 56), presumably via formation of a silyloxy base-stabilized silylene complex **(106)** (equation 57)[256].

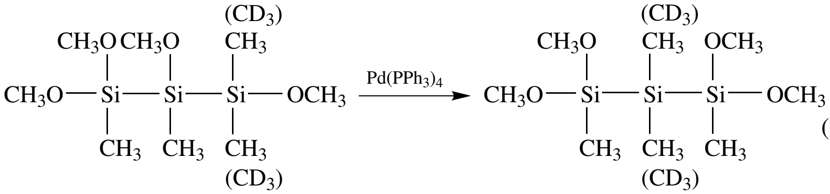

$$CH_3O-\underset{\substack{|\\ CH_3}}{\overset{\substack{CH_3O\\ |}}{Si}}-\underset{\substack{|\\ CH_3}}{\overset{\substack{CH_3O\\ |}}{Si}}-\underset{\substack{|\\ CH_3\\ (CD_3)}}{\overset{\substack{(CD_3)\\ CH_3\\ |}}{Si}}-OCH_3 \xrightarrow{Pd(PPh_3)_4} CH_3O-\underset{\substack{|\\ CH_3}}{\overset{\substack{CH_3O\\ |}}{Si}}-\underset{\substack{|\\ CH_3\\ (CD_3)}}{\overset{\substack{(CD_3)\\ CH_3\\ |}}{Si}}-\underset{\substack{|\\ CH_3}}{\overset{\substack{OCH_3\\ |}}{Si}}-OCH_3 \qquad (56)$$

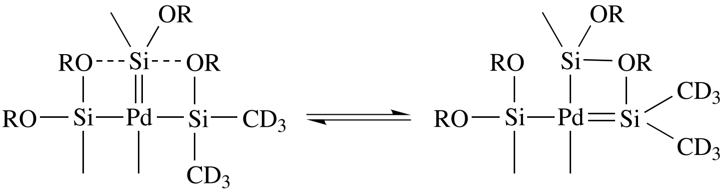
(57)

(106)

TABLE 13. Selected M–Si distances in group-10 transition-metal silicon-containing complexes

Compound	d^n Configuration	M–Si (Å)	Reference
$PtIMe_2(SiMe_3)(2,2'\text{-bipyridyl})$	d^6	2.313(6)	221
cis-$PtMe(SiPh_3)(PMePh_2)_2{\bullet}OEt_2$	d^8	2.381(2)	222
cis-$Pt(H)(SiMe_3)(PPh_3)_2{\bullet}1/2OEt_2$	d^8	2.357(3)	223
$(dcpe)Pt(Ph)\{Si(SiMe_3)_2OH\}^a$	d^8	2.360(2)	226
$Fe(\eta^5\text{-}C_5H_4)_2Pt(PEt_3)_2SiMe_2$	d^8	2.385(1)	225
$[(dcpe)Pt]_2(\mu_2\text{-}SiH_2SiH_2)_2{}^a$	d^8	2.378(1), 2.369(1)	227
$(dcpe)Pd(SiHMe_2)_2{}^a$	d^8	2.3563(9), 2.359(1)	228
$(dmpe)HPt(\mu\text{-}SiHPh)_2[\mu\text{-}\eta^1,\eta^1\text{-}ArHSiSiHPh]PtH(dmpe)^b$	d^6	2.382(4), 2.379(4) 2.426(4)	229
fac-$(dmpe)Pt(H)(SiH_2Ph)_3{}^b$	d^6	2.385(5), 2.406(5) 2.362(5)	229
$(Et_3P)_2\overline{Pt\{Si(Ph_2)CH_2CH_2C}H_2\}$	d^8	2.354(1)	231
$(Et_3P)_2Pt[1,2\text{-}(SiH_2)_2C_6H_4]_2$	d^6	2.428(2), 2.383(1) 2.430(2), 2.376(2)	232
96	d^8, d^6	2.415(9), 2.44(1) 2.40(1), 2.41(1) 2.39(1), 2.352(9)	232
$(\eta^2\text{-}SiMe_2CH_2CH_2PPh_2)_2Pd$	d^8	2.368(1), 2.367(1)	236
$(\eta^2\text{-}SiMe_2CH_2CH_2PPh_2)Pd(\eta^2\text{-}SnMe_2CH_2CH_2PPh_2)$	d^8	2.59(1), 2.43(1)	237
102	d^8	2.336(1), 2.356(1)	248
Silylene Complexes			
$[(Cy_3P)_2(H)Pt{=}Si(SEt)_2]$ BPh_4	d^8	2.270(2)	254
105	d^8	2.207(2), 2.216(2)	255

[a] dcpe = bis(1,2-dicyclohexylphosphino)ethane.

[b] dmpe = bis(1,2-dimethylphosphino)ethane.

TABLE 14. Selected ^{29}Si NMR chemical shifts for group-10 transition-metal silicon-containing complexes

Compound	^{29}Si NMR shift (ppm)	Reference
$Fe(\eta^5\text{-}C_5H_4)_2Pt(PEt_3)_2SiMe_2$	5.18 ($^1J_{PtSi}$ = 1312 Hz, $^2J_{PSi}$ = 181, 14.5 Hz)	225
$(dcpe)Pt(Ph)\{Si(SiMe_3)_2OH\}$[a]	30.88 ($^1J_{SiPt}$ = 1222 Hz, $^2J_{SiP}$ = 7, 179 Hz)	226
$(dcpe)\overline{Pt\{o\text{-}C_6H_4Si}(SiMe_3)_2\}$[a]	36.47 ($^1J_{SiPt}$ = 1246 Hz, $^2J_{SiP}$ = 5, 183 Hz)	226
$(Et_3P)_2\overline{Pt\{Si(Ph_2)CH_2CH_2C}H_2\}$	35.9 (dd, $^1J_{SiPt}$ = 1421 Hz, $^2J_{SiP}$ = 14.5, 172 Hz)	231
$(Et_3P)_2\overline{Pt\{Si(Cl_2)CH_2CH_2C}H_2\}$	79.4 (dd, $^1J_{SiPt}$ = 2061 Hz, $^2J_{SiP}$ = 19.3, 257 Hz)	231
$(Et_3P)_2\overline{Pt\{Si(Me_2)CH_2CH_2C}H_2\}$	34.6 (dd, $^1J_{SiPt}$ = 1281 Hz, $^2J_{SiP}$ = 14.0, 163 Hz)	231
trans-$(\overline{CH_2CH_2CH_2(Cl)Si})PtCl(PEt_3)_2$	34.4 (t, $^1J_{SiPt}$ = 1574 Hz, $^2J_{SiP}$ = 14.5 Hz)	231
$(Et_3P)_2Pt[1,2\text{-}(SiH_2)_2C_6H_4]_2$	−27.36 (t, $^1J_{SiPt}$ = 617 Hz, $^2J_{SiP}$ = 14.Hz)	232
	−12.89 (dd, $^1J_{SiPt}$ = 596 Hz, $^2J_{SiP}$ = 136, 21 Hz)	
96	−54.94 (ddd, $^1J_{SiPt}$ = 362, 771 Hz, $^2J_{SiP}$ = 99, 104, 8Hz)	232
	−26.86 (t, $^1J_{SiPt}$ = 733 Hz, $^2J_{SiP}$ = 17 Hz, $^3J_{PtSi}$ = 16 Hz)	
$(ClMe_2Si)(Me_3Si(Cl)(Me)Si)Pt(PEt_3)_2$	43.0 (t, $^1J_{Ptsi}$ = 1220 Hz, $^2J_{PSi}$ = 70 Hz)	235
	46.4 (t, $^1J_{PtSi}$ = 1361 Hz, $^2J_{PSi}$ = 76 Hz)	
Silylene Complexes		
$[(Cy_3P)_2(H)Pt{=}Si(SEt)_2]BPh_4$	308.65 ($^1J_{PtSi}$ = 1558)	254
105	97.5	255

[a] dcpe = bis(1,2-dicyclohexylphosphino)ethane.

XVI. COPPER AND MERCURY SILYL COMPLEXES

Copper silyl complexes of the type $(Ph_3P)_3CuSiR_3$ were synthesized by reacting the hexameric complex, $[Ph_3PCuH]_6$, with equivalent amounts of the corresponding silane R_3SiH (equation 58)[257].

$$1/6[Ph_3PCuH]_6 + HSiR_3 \xrightarrow[SiR_3\ =\ SiPh_3,\ SiPh_2Cl]{} (Ph_3P)_3Cu{-}SiR_3 + H_2 \qquad (58)$$

The first mercury(I) silyl complex $[(Me_3SiMe_2Si)_3Si]_2Hg_2$ was prepared by the reaction of an excess of $(Me_3SiMe_2Si)_3SiH$ with $(t\text{-}Bu)_2Hg$. The solid structure of the complex displays linear Si−Hg−Hg−Si fragment with regular metal−silicon bond lengths

[Hg–Si = 2.485(2) *Å*] and large metal–metal bond distances [2.656(1) Å]. Irradiation of the complex leads to the coupling silyl product and metallic mercury (Scheme 44)[258].

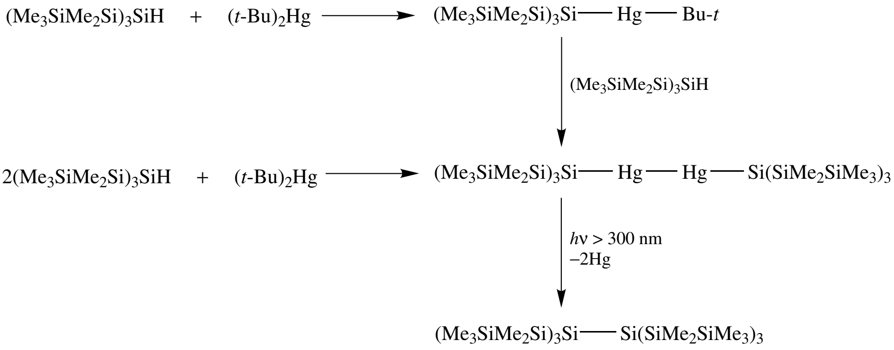

SCHEME 44

XVII. ACKNOWLEDGMENTS

The author thanks Profs. Y. Apeloig and M. Akita and Dr D. Bravo-Zhivotovskii who assisted in the preparation of this review by supplying manuscripts prior to publication.

XVIII. REFERENCES

1. (a) T. D. Tilley, in *The Silicon–Heteroatom Bond* (Eds. S. Patai and Z. Rappoport), Wiley, Chichester, 1991, pp. 245–359.
   (b) T. D. Tilley, in *The Chemistry of Organic Silicon Compounds* (Eds. S. Patai and Z. Rappoport), Chap. 24, Wiley, New York 1989.
2. B. K. Campion, R. H. Heyn and T. D. Tilley, *Organometallics*, **12**, 2584 (1993).
3. P. L. Watson and G. W. Parshall, *Acc. Chem. Res.*, **18**, 51 (1985).
4. G. A. Molander and P. J. Nichols, *J. Am. Chem. Soc.*, **117**, 4415 (1995).
5. F. Peng-Fei, L. Brard, L. Yanwu and T. J. Marks, *J. Am. Chem. Soc.*, **117**, 7157 (1995).
6. T. D. Tilley, in *Organosilicon Chemistry. From Molecules to Materials* (Eds. N. Auner and J. Weis), VCH, Weinheim, 1994, p. 225.
7. H. Schumann, A. Meese-Marktscheffel and F. E. Hahn, *J. Organomet. Chem.*, **390**, 301 (1990).
8. N. S. Radu, T. D. Tilley and A. L. Rheingold, *J. Organomet. Chem.*, **516**, 41 (1996).
9. N. S. Radu, T. D. Tilley and A. L. Rheingold, *J. Am. Chem. Soc.*, **114**, 8293 (1992).
10. C. M. Forsyth, S. P. Nolan and T. J. Marks, *Organometallics*, **10**, 2543 (1991).
11. N. S. Radu and T. D. Tilley, *J. Am. Chem. Soc.*, **117**, 5863 (1995).
12. L. N. Bochkarev, V. M. Makarov, Y. N. Hrzhanovskaya, L. N. Zakharov, G. K. Fukin, A. I. Yanovsky and Y. T. Struchkov, *J. Organometal. Chem.*, **467**, C3 (1994).
13. Y. Mu, C. Aitken, B. Cote, J. F. Harrod and E. Samuel, *Can. J. Chem.*, **69**, 264 (1991).
14. K. A. Kreutzer, R. A. Fisher, W. M. Davis, E. Spaltenstein and S. L. Buchwald, *Organometallics*, **10**, 4031 (1991).
15. T. Takahashi, M. Hasegawa, N. Suzuki, M. Saburi, C. J. Rousset, P. E. Fanwick and E. Negishi, *J. Am. Chem. Soc.*, **113**, 8564 (1991).
16. J. Britten, Y. Mu, J. F. Harrod, J. Polowin, M. C. Baird and E. Samuel, *Organometallics*, **12**, 2672 (1993).
17. H. Q. Liu and J. F. Harrod, *Organometallics*, **11**, 822 (1992).
18. E. Spaltenstein, P. Palma, K. A. Kreutzer, C. A. Willoughby, W. M. Davis and S. L. Buchwald, *J. Am. Chem. Soc.*, **116**, 10308 (1994).

19. Y. E. Ovechinikov, V. A. Igonin, T. V. Timofeeva, S. V. Lindeman, Y. T. Struchkov, M. V. Ustinov and D. A. Bravo-Zhivotovskii, *Metallorgan. Khim.*, **5**, 1155 (1992); *Chem. Abstr.*, **118**, 147614s (1992).
20. H. G. Woo, W. P. Freeman and T. D. Tilley, *Organometallics*, **11**, 2198 (1992).
21. H. G. Woo, R. H. Heyn and T. D. Tilley, *J. Am. Chem. Soc.*, **114**, 5698 (1992).
22. H. G. Woo, J. F. Walzer and T. D. Tilley, *J. Am. Chem. Soc.*, **114**, 7047 (1992).
23. T. D. Tilley, *Acc. Chem. Res.*, **26**, 22 (1993).
24. V. K. Dioumaev and J. F. Harrod, *Organometallics*, **13**, 1548 (1994).
25. J. Y. Corey, X. H. Zhu, T. C. Bedard and L.D. Lange, *Organometallics*, **10**, 924 (1991).
26. J. F. Harrod, C. T. Aitken and E. Samuel, *J. Am. Chem. Soc.*, **108**, 4059 (1986).
27. E. Hengge and M. Weinberger, *J. Organomet. Chem.*, **443**, 167 (1993).
28. T. Imori, R. H. Heyn, T. D. Tilley and A. L. Rheingold, *J. Organomet. Chem.*, **493**, 83 (1995).
29. T. R. Cundari and M. S. Gordon, *J. Phys. Chem.*, **96**, 631 (1992).
30. L. J. Procopio, P. J. Carroll and D. H. Berry, *Polyhedron*, **14**, 45 (1995).
31. L. J. Procopio, P. J. Caroll and D. H. Berry, *J. Am. Chem. Soc.*, **113**, 1870 (1991).
32. L. J. Procopio, P. J. Carroll and D. H. Berry, *Organometallics*, **12**, 3087 (1993).
33. L. J. Procopio, P. J. Carroll and D. H. Berry, *J. Am. Chem. Soc.*, **116**, 177 (1994).
34. A. Ohff, P. Kosse, W. Baumann, A. Tillack, R. Kempe, H. Görls, V. V. Burlakov and U. Rosenthal, *J. Am. Chem. Soc.*, **117**, 10399 (1995).
35. Z. Xue, L. Li, L. K. Hoyt, J. B. Diminnie and J. L. Pollitte, *J. Am. Chem. Soc.*, **116**, 2169 (1994).
36. M. Porchia, N. Brianse, U. Casellato, F. Ossola, G. Rossetto, P. Zanella and R. Graziani, *J. Chem. Soc., Dalton Trans.*, 677 (1989).
37. W. A. King and T. J. Marks, *Inorg. Chim. Acta*, **229**, 343 (1995).
38. A. Lisovski and M. S. Eisen, unpublished results.
39. N. S. Radu, M. P. Engeler, C. P. Gerlach, T. D. Tilley and A. L. Rheingold, *J. Am. Chem. Soc.*, **117**, 3261 (1995).
40. J. S. Allison, B. J. Aylett and H. M. Colquhoun, *J. Organomet. Chem.*, **112**, C7 (1976).
41. M. D. Curtis, L. G. Bell and W. M. Butler, *Organometallics*, **4**, 701 (1985).
42. Q. Jiang, P. J. Carroll and D. H. Berry, *Organometallics*, **10**, 3648 (1991).
43. Q. Jiang, D. C. Pestana, P. J. Carrol and D. H. Berry, *Organometallics*, **13**, 3679 (1994).
44. A. Antiñolo, F. Carrillo, M. Fajarado, A. Otero, M. Lanfranchi and M. A. Pellinghelli, *Organometallics*, **14**, 1518 (1995).
45. G. I. Nikonov, L. G. Kuzmina, D. A. Lemenovskii and V. V. Kotov, *J. Am. Chem. Soc.*, **117**, 10133 (1995).
46. Q. Jiang, P. J. Carroll and D. H. Berry, *Organometallics*, **12**, 177 (1993).
47. H. Nakatsuji, M. Hada and K. Kondo, *Chem. Phys. Lett.*, **196**, 404 (1992).
48. C. Zybill, H. Handwerker and H. Friedrich, *Adv. Organomet. Chem.*, **36**, 229 (1994).
49. C. E. Zybill and C. Liu, *Synlett*, **7**, 687 (1995).
50. P. Braunstein and M. Knorr, *J. Organomet. Chem.*, **500**, 21 (1995).
51. R. Probst, C. Leis, S. Gamper, E. Herdtweck, C. Zybill and N. Auner, *Angew. Chem., Int. Ed. Engl.*, **30**, 1132 (1991).
52. H. Handwerker, C. Leis, R. Probst, P. Bissinger, A. Grohmann, P. Kiprof, E. Herdtweck, J. Blümel, N. Auner and C. Zybill, *Organometallics*, **12**, 2162 (1993).
53. H. Handwerker, M. Paul, J. Blümel and C. Zybill, *Angew. Chem., Int. Ed. Engl.*, **32**, 1313 (1993).
54. H. Handwerker, M. Paul, J. Riede and C. Zybill, *J. Organomet. Chem.*, **459**, 151 (1993).
55. C. Leis, D. L. Wilkinson, H. Handwerker and C. Zybill, *Organometallics*, **11**, 514 (1992).
56. R. J. P. Corriu, G. F. Lanneau and B. P. S. Chauhan, *Organometallics*, **12**, 2001 (1993).
57. R. J. P. Corriu, B. P. S. Chauhan and G. F. Lanneau, *Organometallics*, **14**, 1646 (1995).
58. W. Malisch, R. Lankat, S. Schmitzer, R. Pikl, U. Posset and W. Kiefer, *Organometallics*, **14**, 5622 (1995).
59. W. Malisch, R. Lankat, W. Seelbach, J. Reising, M. Noltemeyer, R. Pikl, U. Posset and W. Kiefer, *Chem. Ber.*, **128**, 1109 (1995).
60. S. Schmitzer, U. Weis, H. Käb, W. Buchner, W. Malisch, T. Polzer, U. Posset and W. Kiefer, *Inorg. Chem.*, **32**, 303 (1993).
61. W. Malisch, R. Lankat, S. Schmitzer and J. Reising, *Inorg. Chem.*, **34**, 5701 (1995).
62. W. Malisch, S. Schmitzer, G. Kaupp, K. Hindahl, H. Käb and U. Wachtler, in *Organosilicon Chemistry. From Molecules to Materials* (Eds. N. Auner and J. Weis), VCH, Weinheim, 1994, p. 185.

63. T. S. Koloski, D. C. Pestana, P. J. Carrol and D. H. Berry, *Organometallics*, **13**, 489 (1994).
64. D. C. Pestana, T. S. Koloski and D. H. Berry, *Organometallics*, **13**, 4173 (1994).
65. L. K. Figge, P. J. Carroll and D. H. Berry, *Organometallics*, **15**, 209 (1996).
66. G. N. Glavee, B. R. Jagirdar, J. J. Schneider, K. J. Klabunde, L. J. Radonovich and K. Dodd, *Organometallics*, **11**, 1043 (1992).
67. B. R. Jagirdar and K. J. Klabunde, *J. Coord. Chem.*, **34**, 31 (1995).
68. B. R. Jagirdar, R. Palmer, K. J. Klabunde and L. J. Radonovich, *Inorg. Chem.*, **34**, 278 (1995).
69. U. Schubert and H. Gilges, *Organometallics*, **15**, 2373 (1996).
70. U. Schubert, *Progress in Organosilicon Chemistry*, Gordon and Breach, Basel, 1995.
71. D. H. Berry, J. C. Chey, H. S. Zipin and P. J. Carroll, *Polyhedron*, **10**, 1189 (1991).
72. P. Hong, N. H. Damrauer, P. J. Carrol and D. H. Berry, *Organometallics*, **12**, 3698 (1993).
73. X. -L. Lou, G. J. Kubas, J. C. Bryan, C. J. Burns and C. J. Unkefer, *J. Am. Chem. Soc.*, **116**, 10312 (1994).
74. X. Luo, G. J. Kubas, C. J. Burns, J. C. Bryan and C. J. Unkefer, *J. Am. Chem. Soc.*, **117**, 1159 (1995).
75. T. Takeuchi, H. Tobita and H. Ogino, *Organometallics*, **10**, 835 (1991).
76. B. P. S. Chauhan, R. J. P. Corriu, G. F. Lanneau, C. Priou, N. Auner, H. Handwerker and E. Herdtweck, *Organometallics*, **14**, 1657 (1995).
77. K. E. Lee, A. M. Arif and J. A. Gladysz, *Chem. Ber.*, **124**, 309 (1991).
78. R. D. Adams, J. E. Cortopassi and J. H. Yamamoto, *Organometallics*, **12**, 3036 (1993).
79. J. Sun, R. S. Lu, R. Bau and G. K. Yang, *Organometallics*, **13**, 1317 (1994).
80. J. A. K. Howard, P. A. Keller, T. Vogt, A. L. Taylor, N. D. Dix and J. L. Spencer, *Acta Crystallogr.*, **B48**, 438 (1992).
81. R. H. Crabtree, *Angew. Chem., Int. Ed. Engl.*, **32**, 789 (1993).
82. M. L. Loza, S. R. De Gala and R. H. Crabtree, *Inorg. Chem.*, **33**, 5073 (1994).
83. G. Reinhard, B. Hirle and U. Schubert, *J. Organomet. Chem.*, **427**, 173 (1992).
84. P. Braunstein, M. Knorr, U. Schubert, M. Lanfranchi and A. Tripicchio, *J. Chem. Soc., Dalton Trans.*, 1507 (1991).
85. P. Braunstein, M. Knorr, H. Piana and U. Schubert, *Organometallics*, **10**, 828 (1991).
86. G. Reinhard, B. Hirle, U. Schubert, M. Knorr, P. Braunstein, A. DeCian and J. Fischer, *Inorg. Chem.*, **32**, 1656 (1993).
87. P. Braunstein, E. Colomer, M. Knorr, A. Tiripicchio and M. Tiripicchio-Camellini, *J. Chem. Soc., Dalton Trans.*, 903 (1992).
88. P. Braunstein, M. Knorr, M. Strampfer, A. DeCian and J. Fischer, *J. Chem. Soc., Dalton Trans.*, 117 (1994).
89. P. Braunstein, M. Knorr, E. Villarroya, A. DeCian and J. Fischer, *Organometallics*, **10**, 3714 (1991).
90. P. Braunstein, L. Douce, M. Knorr, M. Strampfer, M. Lanfranchi and A. Tiripicchio, *J. Chem. Soc., Dalton Trans.*, 331 (1992).
91. P. Braunstein, T. Faure, M. Knorr, F. Balegroune and D. Grandjean, *J. Organomet. Chem.*, **462**, 271 (1993).
92. M. Strampfer, M. Knorr and P. Braunstein, in *Organosilicon Chemistry. From Molecules to Materials* (Eds. N. Auner and J. Weis), VCH, Weinheim, 1994, p. 199.
93. T. Faure, M. Knorr and P. Braunstein, in *Organosilicon Chemistry. From Molecules to Materials* (Eds. N. Auner and J. Weis), VCH, Weinheim, 1994, p. 201.
94. P. Braunstein, M. Knorr, M. Strampfer, A. Tiripicchio and F. Ugozzoli, *Organometallics*, **13**, 3038 (1994).
95. P. Braunstein, T. Faure, M. Knorr, T. Stährfeldt, A. DeCian and J. Fischer, *Gazz. Chim. Ital.*, **125**, 35 (1995).
96. P. Braunstein, M. Knorr, A. Tiripicchio and M. Tiripicchio-Camellini, *Inorg. Chem.*, **31**, 3685 (1992).
97. S. Gilbert, M. Knorr, S. Mock and U. Schubert, *J. Organomet. Chem.*, **480**, 241 (1994).
98. S. Gilbert and U. Schubert, *J. Organomet. Chem.*, **444**, C12 (1993).
99. U. Schubert, S. Gilbert and M. Knorr, *J. Organomet. Chem.*, **454**, 79 (1993).
100. G. Reinhard, M. Knorr, P. Braunstein, U. Schubert, S. Khan, C. E. Strouse, H. D. Kaesz and A. Zinn, *Chem. Ber.*, **126**, 17 (1993).
101. M. Knorr, T. Stährfeldt, P. Braunstein, G. Reinhard, P. Hauenstein, B. Mayer, U. Schubert, S. Khan and H. D. Kaesz, *Chem. Ber.*, **127**, 295 (1994).

102. P. Braunstein, M. Knorr, B. Hirle, G. Reinhard and U. Schubert, *Angew. Chem., Int. Ed. Engl.*, **31**, 1583 (1992).
103. P. Braunstein, M. Knorr and T. Stährfeldt, *J. Chem. Soc., Chem. Commun.*, 1913 (1994).
104. M. Knorr, P. Braunstein, A. DeCian and J. Fischer, *Organometallics*, **14**, 1302 (1995).
105. M. Knorr, P. Braunstein, A. Tiripicchio and F. Ugozzoli, *Organometallics*, **14**, 4910 (1995).
106. R. D. Adams, J. E. Cortopassi and M. P. Pompeo, *Inorg. Chem.*, **30**, 2960 (1991).
107. R. D. Adams, J. E. Cortopassi and M. P. Pompeo, *Organometallics*, **11**, 1 (1992).
108. R. D. Adams, J. E. Cortopassi, J. Aust and M. Myrick, *J. Am. Chem. Soc.*, **115**, 8877 (1993).
109. H. G. Ang, B. Chang and W. L. Kwik, *J. Chem. Soc., Dalton Trans.*, 2161 (1992).
110. H. G. Ang, B. Chang, W. L. Kwik and E. S. H. Sim, *J. Organomet. Chem.*, **474**, 153 (1994).
111. J. A. Cabeza, A. Llamazares, V. Riera, S. Triki and L. Ouahab, *Organometallics*, **11**, 3334 (1992).
112. J. A. Cabeza, R. J. Franco, A. Llamazares, V. Riera, C. Bois and Y. Jeannin, *Inorg. Chem.*, **32**, 4640 (1993).
113. J. A. Cabeza, S. García-Granda, A. Llamazares, V. Riera and J. F. Van der Maelen, *Organometallics*, **12**, 2973 (1993).
114. J. A. Cabeza, R. J. Franco, V. Riera, S. García-Granda and J. F. Van der Maelen, *Organometallics*, **14**, 3342 (1995).
115. S. Kotani, T. Tanizawa, T. Adaci, T. Yoshida and K. Sonogashira, *Chem. Lett.*, 1665 (1994).
116. W. Lin, S. R. Wilson and G. S. Girolami, *J. Chem. Soc., Chem. Commun.*, 284 (1993).
117. W. Lin, S. R. Wilson and G. S. Girolami, *Organometallics*, **13**, 2309 (1994).
118. G. R. Clark, K. R. Flower, C. E. F. Rickard, W. R. Roper, D. M. Salter and L. J. Wright, *J. Organomet. Chem.*, **462**, 331 (1993).
119. C. E. F. Rickard, W. R. Roper, D. M. Salter and L. J. Wright, *J. Am. Chem. Soc.*, **114**, 9682 (1992).
120. B. J. Rappoli, K. J. McGrath, C. F. George and J. C. Cooper, *J. Organomet. Chem.*, **450**, 85 (1993).
121. W. Malisch, S. Möller, O. Fey, H.-U. Wekel, R. Pikl, U. Posset and W. Kiefer, *J. Organomet. Chem.*, **507**, 117 (1996).
122. S. Möller, O. Fey, W. Malisch and W. Seelbach, *J. Organomet. Chem.*, **507**, 239 (1996).
123. F. R. Lemke, *J. Am. Chem. Soc.*, **116**, 11183 (1994).
124. F. R. Lemke, R. S. Simons and W. J. Youngs, *Organometallics*, **15**, 216 (1996).
125. B. K. Campion, R. H. Heyn, T. D. Tilley and A. L. Rheingold, *J. Am. Chem. Soc.*, **115**, 5527 (1993).
126. J. Yin, J. Klosin, K. A. Abboud and W. M. Jones, *J. Am. Chem. Soc.*, **117**, 3298 (1995).
127. T. J. Johnson, P. S. Coan and K. G. Caulton, *Inorg. Chem.*, **32**, 4594 (1993).
128. R. H. Heyn, J. C. Huffman and K. G. Caulton, *New. J. Chem.*, **17**, 797 (1993).
129. P. I. Djurovich, P. J. Carroll and D. H. Berry, *Organometallics*, **13**, 2551 (1994).
130. V. S. Asirvatham, Z. Yao and K. J. Klabunde, *J. Am. Chem. Soc.*, **116**, 5493 (1994).
131. Z. Yao and K. J. Klabunde, *Organometallics*, **14**, 5013 (1995).
132. Z. Yao, K. J. Klabunde and S. Asirvatham, *Inorg. Chem.*, **34**, 5289 (1995).
133. H. Suzuki, T. Takao, M. Tanaka and Y. Moro-oka, *J. Chem. Soc., Chem. Commun.*, 476 (1992).
134. T. Takao, H. Suzuki and M. Tanaka, *Organometallics*, **13**, 2554 (1994).
135. B. K. Campion, R. H. Heyn and T. D. Tilley, *J. Chem. Soc., Chem. Commun.*, 1201 (1992).
136. T. Takao, S. Yoshida, H. Suzuki and M. Tanaka, *Organometallics*, **14**, 3855 (1995).
137. M. Akita, R. Hua, T. Oku and Y. Moro-oka, *J. Chem. Soc., Chem. Commun.*, 1031 (1992).
138. M. Akita, R. Hua, T. Oku and Y. Moro-oka, *J. Chem. Soc., Chem. Commun.*, 1670 (1993).
139. M. Akita, R. Hua, T. Oku and Y. Moro-oka, *J. Chem. Soc., Chem. Commun.*, 541 (1996).
140. M. Akita, N. Kazumi, T. Yoshiaki and Y. Moro-oka, *Organometallics*, **14**, 5209 (1995).
141. M. Akita, personal communication.
142. T. D. Tilley, B. K. Campion, S. D. Grumbine, D. A. Straus and R. H. Heyn, *Transition-metal Complexes of Reactive Silicon Intermediates*, Royal Society of Chemistry, London, 1991.
143. W. P. Freeman, T. D. Tilley and A. L. Rheingold, *J. Am. Chem. Soc.*, **116**, 8428 (1994).
144. C. Paek, J. Ko, Y. Kong, C. H. Kim and M. E. Lee, *Bull. Korean Chem. Soc.*, **15**, 460 (1994).
145. B. Stadelmann, P. Lassacher, H. Stüger and E. Hengge, *J. Organomet. Chem.*, **482**, 201 (1994).
146. E. Hengge, M. Eibl, B. E. Stadelmann, A. Zechmann and H. Siegl, in *Organosilicon Chemistry. From Molecules to Materials* (Eds. N. Auner and J. Weis), VCH, Weinheim, 1994. p. 213.

147. S. Sharma, J. Cervantes, J. L. Mata-Mata, M. -C. Brun, F. Cervantes-Lee and K. H. Pannell, *Organometallics*, **14**, 4269 (1995).
148. K. H. Pannell, M. -C. Brun, H. Sharma, K. Jones and S. Sharma, *Organometallics*, **13**, 1075 (1994).
149. K. H. Pannell, T. Kobayashi and R. N. Kapoor, *Organometallics*, **11**, 2229 (1992).
150. K. H. Pannell and S. Sharma, *Organometallics*, **10**, 954 (1991).
151. K. L. Jones and K. H. Pannell, *J. Am. Chem. Soc.*, **115**, 11336 (1993).
152. C. Hernandez, H. K. Sharma and K. H. Pannell, *J. Organomet. Chem.*, **462**, 259 (1993).
153. H. Sharma and K. H. Pannell, *Organometallics*, **13**, 4946 (1994).
154. Z. Zhang, R. Sanchez and K. H. Pannell, *Organometallics*, **14**, 2605 (1995).
155. H. K. Sharma and K. H. Pannell, *Chem. Rev.*, **95**, 1351 (1995).
156. C. Leis, C. Zybill, J. Lachmann and G. Müller, *Polyhedron*, **10**, 163 (1991).
157. U. Bodensieck, P. Braunstein, W. Deck, T. Faure, M. Knorr and C. Stern, *Angew. Chem., Int. Ed. Engl.*, **33**, 2440 (1994).
158. N. Auner, C. Wagner, E. Herdtweck, M. Heckel and W. Hiller, *Bull. Soc. Chim. Fr.*, **132**, 599 (1995).
159. M. E. Lee, J. S. Han and C. H. Kim, *Bull. Korean Chem. Soc.*, **15**, 335 (1994).
160. H. Handwerker, C. Leis, S. Gamper and C. Zybill, *Inorg. Chim. Acta*, **198–200**, 763 (1992).
161. S. D. Grumbine, R. K. Chadha and T. D. Tilley, *J. Am. Chem. Soc.*, **114**, 1518 (1992).
162. B. J. Aylett, *J. Organomet. Chem.*, **327**, 9 (1980).
163. S. K. Grumbine, D. A. Straus, T. D. Tilley and A. L. Rheingold, *Polyhedron*, **14**, 127 (1995).
164. S. K. Grumbine, T. D. Tilley, F. P. Arnold and A. L. Rheingold, *J. Am. Chem. Soc.*, **116**, 5495 (1994).
165. H. Kobayashi, K. Ueno and H. Ogino, *Organometallics*, **14**, 5490 (1995).
166. K. Ueno, N. Hamashima, M. Shimoi and H. Ogino, *Organometallics*, **10**, 959 (1991).
167. K. Ueno, N. Hamashima and H. Ogino, *Organometallics*, **11**, 1435 (1992).
168. Y. Kawano, H. Tobita, M. Shimoi and H. Ogino, *J. Am. Chem. Soc.*, **116**, 8575 (1994).
169. Y. Kawano, H. Tobita and H. Ogino, *Angew. Chem., Int. Ed. Engl.*, **30**, 843 (1991).
170. Y. Kawano, H. Tobita and H. Ogino, *Organometallics*, **11**, 499 (1992).
171. K. Ueno and H. Ogino, *Bull. Chem. Soc. Jpn.*, **68**, 1955 (1995).
172. K. Ueno, S. Seki and H. Ogino, *Chem. Lett.*, 2159 (1993).
173. K. Ueno, H. Tobita and H. Ogino, *J. Organomet. Chem.*, **430**, 93 (1992).
174. J. R. Koe, H. Tobita and H. Ogino, *Organometallics*, **11**, 2479 (1992).
175. K. Ueno, S. Ito, K. -I. Endo, H. Tobita, S. Inomata and H. Ogino, *Organometallics*, **13**, 3309 (1994).
176. H. Tobita and H. Ogino, *J. Synth. Org. Chem. (Japan)*, **53**, 530 (1995).
177. H. Tobita, H. Wada, K. Ueno and H. Ogino, *Organometallics*, **13**, 2545 (1994).
178. R. Bakhtiar, C. M. Holzangel and D. B. Jacobson, *J. Am. Chem. Soc.*, **115**, 3038 (1993).
179. R. Bakhtiar and D. B. Jacobson, *Organometallics*, **12**, 2876 (1993).
180. D. B. Jacobson and R. Bakhtiar, *J. Am. Chem. Soc.*, **115**, 10830 (1993).
181. W. Ando, T. Yamamoto, H. Saso and Y. Kabe, *J. Am. Chem. Soc.*, **113**, 2791 (1991).
182. Y. Kabe, T. Yamamoto and W. Ando, *Organometallics*, **13**, 4606 (1994).
183. S. D. Grumbine, T. D. Tilley and A. L. Rheingold, *J. Am. Chem. Soc.*, **115**, 358 (1993).
184. R. D. Adams and J. E. Cortopassi, *J. Clus. Sci.*, **6**, 437 (1995).
185. S. M. Maddock, C. E. F. Rickard, W. R. Roper and L. J. Wright, *Organometallics*, **15**, 1793 (1996).
186. W. Chen, A. J. Edwards, M. A. Esteruelas, F. J. Lahoz, M. Oliván and L. A. Oro, *Organometallics*, **15**, 2185 (1996).
187. M. A. Esteruelas, O. Nürnberg, M. Oliván, L. A. Oro and H. Werner, *Organometallics*, **12**, 3264 (1993).
188. M. A. Esteruelas, F. J. Lahoz, M. Oliván, E. Oñate and L. A. Oro, *Organometallics*, **13**, 4246 (1994).
189. M. A. Esteruelas, M. Oliván and L. A. Oro, *Organometallics*, **15**, 814 (1996).
190. M. A. Esteruelas, F. J. Lahoz, E. Oñate, L. A. Oro and L. Rodríguez, *Organometallics*, **14**, 263 (1995).
191. M. A. Esteruelas, F. J. Lahoz, E. Oñate, L. A. Oro and L. Rodríguez, *Organometallics*, **15**, 823 (1996).
192. M. Loza, J. W. Faller and R. H. Crabtree, *Inorg. Chem.*, **34**, 2937 (1995).

193. M. K. Hays and R. Eisenberg, *Inorg. Chem.*, **30**, 2623 (1991).
194. W. -D. Wang and R. Eisenberg, *Organometallics*, **11**, 908 (1992).
195. W. -D. Wang and R. Eisenberg, *Organometallics*, **10**, 2222 (1991).
196. M. D. Fryzuk, L. Rosenberg and S. J. Rettig, *Organometallics*, **10**, 2537 (1991).
197. M. D. Fryzuk, L. Rosenberg and S. J. Rettig, *Inorg. Chim. Acta*, **222**, 345 (1994).
198. M. Aizenberg and D. Milstein, *Angew. Chem., Int. Ed. Engl.*, **33**, 317 (1994).
199. M. Aizenberg and D. Milstein, *J. Am. Chem. Soc.*, **117**, 6456 (1995).
200. B. P. Cleary, R. Mehta and R. Eisenberg, *Organometallics*, **14**, 2297 (1995).
201. S. B. Duckett and R. N. Perutz, *J. Chem. Soc., Chem. Commun.*, 28 (1991).
202. S. B. Duckett and R. N. Perutz, *Organometallics*, **11**, 90 (1992).
203. B. T. Gregg and A. R. Cutler, *Organometallics*, **11**, 4276 (1992).
204. T. Mizutani, T. Uesaka and H. Ogoshi, *Organometallics*, **14**, 341 (1995).
205. P. I. Djurovich, A. L. Safir, N. L. Keder and R. J. Watts, *Inorg. Chem.*, **31**, 3195 (1992).
206. G. P. Mitchell, T. D. Tilley, G. P. A. Yap and A. L. Rheingold, *Organometallics*, **14**, 5472 (1995).
207. E. A. Zarate, V. O. Kennedy, J. A. McCune, R. S. Simons and C. A. Tessier, *Organometallics*, **14**, 1802 (1995).
208. P. Burger and R. G. Bergman, *J. Am. Chem. Soc.*, **115**, 10462 (1993).
209. P. Hofmann, C. Meier, W. Hiller, M. Heckel, J. Riede and M. U. Schmidt, *J. Organomet. Chem.*, **490**, 51 (1995).
210. H. Werner, M. Baum, D. Schneider and B. Windmüller, *Organometallics*, **13**, 1089 (1994).
211. K. Osakada, K. Hataya, Y. Nakamura, M. Tanaka and T. Yamamoto, *J. Chem. Soc., Chem. Commun.*, 576 (1993).
212. H. Wadepohl, W. Galm, H. Pritzkow and A. Wolf, *Angew. Chem., Int. Ed. Engl.*, **31**, 1058 (1992).
213. G. Calzaferri, R. Inhof and K. W. Törnroos, *J. Chem. Soc., Dalton Trans.*, 3741 (1993).
214. J. Borgdorff, N. W. Duffy, B. H. Robinson and J. Simpson, *Inorg. Chim. Acta*, **224**, 73 (1994).
215. H. Lang, U. Lay and L. Zsolnai, *J. Organomet. Chem.*, **417**, 377 (1991).
216. M. Van Tiel, K. M. Mackay and B. K. Nicholson, *J. Organomet. Chem.*, **462**, 79 (1993).
217. S. G. Anema, S. K. Lee, K. M. Mackay and B. K. Nicholson, *J. Organomet. Chem.*, **444**, 211 (1993).
218. G. C. Barris, K. M. Mackay and B. K. Nicholson, *Acta Crystallogr.*, **C48**, 1204 (1992).
219. R. Goikhman, M. Aizenberg, H. B. Kraatz and D. Milstein, *J. Am. Chem. Soc.*, **117**, 5865 (1995).
220. M. Aizenberg, R. Goikhman and D. Milstein, *Organometallics*, **15**, 1075 (1996).
221. C. J. Levy, R. J. Puddephatt and J. J. Vittal, *Organometallics*, **13**, 1559 (1994).
222. F. Ozawa, T. Hikida and T. Hayashi, *J. Am. Chem. Soc.*, **116**, 2844 (1994).
223. L. Abdol Latif, C. Eaborn, A. P. Pidcock and N. S. Weng, *J. Organomet. Chem.*, **474**, 217 (1994).
224. S. Ogoshi, K. Ohe, N. Chatani, H. Kurosawa and S. Murai, *Organometallics*, **10**, 3813 (1991).
225. J. B. Sheridan, A. J. Lough and I. Manners, *Organometallics*, **15**, 2195 (1996).
226. L. S. Chang, M. P. Johnson and M. J. Fink, *Organometallics*, **10**, 1219 (1991).
227. M. J. Michalczyk, C. A. Recatto, J. C. Calabrese and M. J. Fink, *J. Am. Chem. Soc.*, **114**, 7955 (1992).
228. Y. Pan, J. T. Mague and M. J. Fink, *Organometallics*, **11**, 3495 (1992).
229. R. H. Heyn and T. D. Tilley, *J. Am. Chem. Soc.*, **114**, 1917 (1992).
230. H. Yamashita, M. Tanaka and M. Goto, *Organometallics*, **11**, 3227 (1992).
231. H. Yamashita and M. Tanaka, *Bull. Chem. Soc. Jpn.*, **68**, 403 (1995).
232. S. Shimada, M. Tanaka and A. Honda, *J. Am. Chem. Soc.*, **117**, 8289 (1995).
233. C. Eaborn, T. N. Metham and A. Pidcock, *J. Organomet. Chem.*, **63**, 107 (1973).
234. K. A. Brittingham, T. N. Gallaher and S. Schreiner, *Organometallics*, **14**, 1070 (1995).
235. Y. Tanaka, H. Yamashita and M. Tanaka, *Organometallics*, **14**, 530 (1995).
236. M. Murakami, T. Yoshida and Y. Ito, *Organometallics*, **13**, 2900 (1994).
237. M. Murakami, T. Yoshida, S. Kawanami and Y. Ito, *J. Am. Chem. Soc.*, **117**, 6408 (1995).
238. F. Ozawa, M. Sugawara and T. Hayashi, *Organometallics*, **13**, 3237 (1994).
239. S. Sakaki and M. Eiki, *Inorg. Chem.*, **30**, 4218 (1991).
240. S. Sakaki and M. Eiki, *J. Am. Chem. Soc.*, **115**, 2373 (1993).
241. S. Sakaki, M. Ogawa, Y. Musashi and T. Arai, *J. Am. Chem. Soc.*, **116**, 7258 (1994).
242. A. Márquez and J. F. Sanz, *J. Am. Chem. Soc.*, **114**, 2903 (1992).
243. A. Márquez and J. F. Sanz, *J. Am. Chem. Soc.*, **114**, 10019 (1992).
244. N. Koga and K. Morokuma, *J. Am. Chem. Soc.*, **115**, 6883 (1993).

245. D. G. Musaev, K. Morokuma and N. Koga, *J. Chem. Phys.*, **99**, 7859 (1993).
246. T. R. Cundari and M. S. Gordon, *J. Mol. Struct.*, **313**, 47 (1994).
247. H. Jacobsen and T. Ziegler, *Organometallics*, **14**, 224 (1995).
248. M. Sunginome, H. Oike and Y. Ito, *Organometallics*, **13**, 4148 (1994).
249. M. Sunginome, H. Oike and Y. Ito, *J. Am. Chem. Soc.*, **117**, 1665 (1995).
250. K. Horn, *Chem. Rev.*, **95**, 1317 (1995).
251. P. Hofmann, in *Organosilicon Chemistry. From Molecules to Materials* (Eds. N. Auner and J. Weis), VCH, Weinheim, 1994.
252. U. Schubert, *Angew. Chem., Int. Ed. Engl.*, **33**, 419 (1994).
253. C. J. Herzig, in *Organosilicon Chemistry. From Molecules to Materials* (Eds. N. Auner and J. Weis), VCH, Weinheim, 1994.
254. S. D. Grumbine, T. D. Tilley, F. P. Arnold and A. L. Rheingold, *J. Am. Chem. Soc.*, **115**, 7884 (1993).
255. M. Denk, R. K. Hayashi and R. West, *J. Chem Soc., Chem. Commun.*, 33 (1994).
256. K. Tamao, G. -R. Sun and A. Kawachi, *J. Am. Chem. Soc.*, **117**, 8043 (1995).
257. U. Schubert, B. Mayer and C. Rub, *Chem. Ber.*, **127**, 2189 (1994).
258. D. Bravo-Zhivotovskii, M. Yuzefovich, M. Bendikov, Y. Apeloig and K. Klinkhammer, personal communication.

CHAPTER 36

Cyclopentadienyl silicon compounds

PETER JUTZI

Faculty of Chemistry, University of Bielefeld, 33615 Bielefeld, Germany
Fax: +49 521 106 6026; e-mail: peter.jutzi@uni-bielefeld.de

I. INTRODUCTION

Cyclopentadienyl systems are the most common ligands in the molecular chemistry of s-, p-, d- and f-block elements. Their versatile application is based on the wide variety of possible bonding modes which allow for the most appropriate interaction with each acceptor. Furthermore, several kinds of substituents can be readily introduced to the C_5-perimeter, offering many variations in structure and chemistry. Finally, the potential of cyclopentadienyl ligands to behave as leaving groups gives them interesting utility in synthetic chemistry.

Not surprisingly, cyclopentadienyl ligands also play an important role in silicon chemistry,where novel bonding leads to fascinating variations in structure and properties. This account presents basic features of structure and bonding in the various classes of cyclopentadienyl silicon compounds and describes the chemistry with a special emphasis on organometallic aspects. Some directions of this chemistry have already been treated in earlier reports. A review by Abel and coworkers[1] gave the state-of-the-art in cyclopentadienyl silicon chemistry at the beginning of the 1970s. Discussion of structure, bonding and reactivity are spread over several chapters of part 1 and part 2 of this series[2] and in the series *Comprehensive Organometallic Chemistry*[3] and *Comprehensive Organic Chemistry*[4]. Finally, reviews dealing with the fluxionality in cyclopentadienyl compounds[5] and with the π-complex chemistry of main group elements[6] are also available.

II. COMPOUNDS CONTAINING CYCLOPENTADIENYL-SILICON σ-BONDS

A. Basic Features of Structure and Bonding

Compounds with a cyclopentadienyl-silicon σ-bond adopt a variety of bonding arrangements, which can be classified on the basis of the hybridization of the corresponding cyclopentadienyl carbon atom, as displayed in Scheme 1. In species of type **1**, the silicon atom is bound to an sp^3-hybridized carbon atom, i.e. to an allylic carbon within a cyclopentadiene unit. The silicon atom is bound to an sp^2-hybridized carbon atom in species of type **2–6**, including silylcyclopentadienyl radicals (**2**), ionic silylcyclopentadienide species (**3**), and silylcyclopentadienyl fragments bound in a η^5-fashion to a metal centre (**4**). Species **5** represents the ionic resonance structure of a silafulvene, and structure **6** stands for the vinylic isomers of a σ-cyclopentadienylsilane (type **1**), but these two types of compound are not examined in detail in this article.

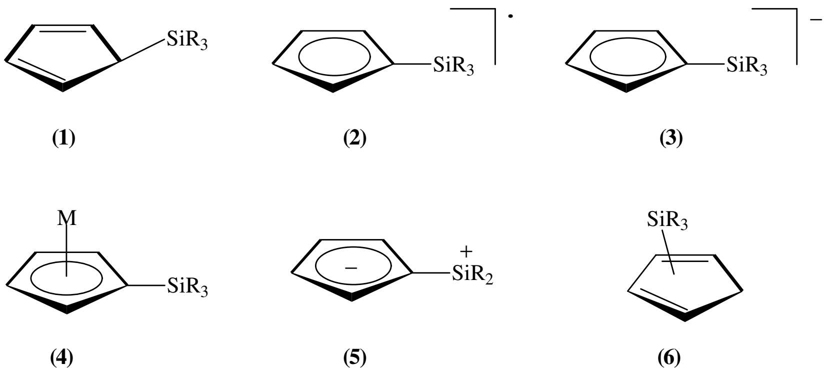

SCHEME 1. Classification of σ-cyclopentadienyl silicon compounds

TABLE 1. Structural parameters of **7** and **8** in Å and deg

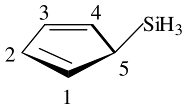

(7)

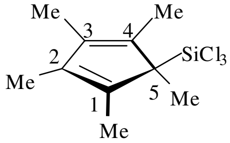

(8)

	7 (GED)	**8** (X-ray)
C(1)−C(2)	1.389 ± 0.013	1.34
C(2)−C(3)	1.436 ± fixed	1.46
C(3)−C(4)	1.389 ± 0.013	1.34
C(4)−C(5)	1.500 ± 0.013	1.51
C(5)−C(1)	1.500 ± 0.013	1.51
Si−C(5)	1.881 ± 0.010	1.87
C(4)C(5)C(1)	100.3 ± 1.5	103.2
C(5)C(1)C(2)	112.0 ± 1.0	108.7
C(1)C(2)C(3)	107.9 ± 0.6	109.6

1. Silicon bound to an sp^3-hybridized carbon atom

a. Structural data. The molecular structure of the parent cyclopentadienylsilane, $H_5C_5SiH_3$ **(7)**, in the gas phase was determined in the 1970s by a gas electron diffraction (GED) study[7]. The cyclopentadiene ring was found to be planar, consistent with theoretical predictions[8,9], and the carbon−carbon bond lengths and bond angles (Table 1) are close to those found in cyclopentadiene itself. The structure is typical of the whole class of cyclopentadienyl silicon compounds with the silicon atom in an allylic position.

The crystal structure parameters for pentamethylcyclopentadienyltrichlorosilane, $Me_5C_5SiCl_3$ **(8)**[10], obtained from X-ray data, are also presented in Table 1 for comparison. The C_5 ring is again essentially planar, and the Si−C bond length is typical despite the steric demand of the Me_5C_5 group, which is evident from the fact that the ClSiCl bond angles within the $SiCl_3$ moiety are 2−5° less than the tetrahedral angle. Even more pronounced steric effects are observed for silicon compounds with two pentamethylcyclopentadienyl ligands, e.g. for $(Me_5C_5)_2SiCl_2$[11] and for $(Me_5C_5)_2Si(OH)_2$[12].

b. Bonding and fluxionality. Experimental and theoretical studies together have led to an understanding of both the bonding and the dynamic behaviour of cyclopentadienylsilanes. *Ab initio* calculations[13] for cyclopentadiene derivatives with a silyl group in allylic position predict strong interactions between the σ-C−Si bond and the π-system. The drawings of the occupied π-molecular orbitals for a silylated cyclopentadiene in Scheme 2 show that silyl substitution will have a more pronounced effect on the $b_1(\pi_2)$-type orbital because of the nodal plane through the substitution centre in the $a_2(\pi_1)$-orbital.

This feature is illustrated experimentally by comparing the vertical π_1 and π_2 ionization energies of cyclopentadiene and some silyl derivatives, which have been obtained from the PE spectra[14,15], as shown in Table 2. Adjustments in the ionization energies due to silylation are more pronounced for the $b_1(\pi_2)$ MO than for the $a_2(\pi_1)$ MO. This is consistent with a more effective σ/π interaction in the b_1 MO made possible by the fixed orientation with the σC−Si bond collinear to the π-system. Generally, trialkylsilyl groups in a β-position to a π-system are powerful electron donors, which enormously

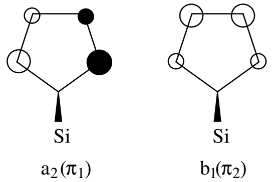

SCHEME 2. Representation of the π-MOs in a silylated cyclopentadiene

modify the properties of the parent π-system[15,16]. Thus, the data obtained for the silylated cyclopentadienes are typical for the introduction of silyl groups in a β-position to a π-system.

The fluxionality of η^1-cyclopentadienyl compounds of silicon and of Main Group elements in general is also well defined[5]. The 1,2 migration of silicon, germanium and tin was first discussed in 1965[17], and the important observation that competitive prototropic rearrangements might occur was presented soon after[18]. In cyclopentadienyl silicon compounds of the type $H_5C_5SiR_3$, degenerate silicon and non-degenerate hydrogen shifts take place, as illustrated in Figure 1. These dynamic processes are classified as symmetry-allowed, suprafacial 1,5-sigmatropic rearrangements[19]. Substituents at the migrating element have a surprisingly large influence on the rate of sigmatropic rearrangements, especially in boron and phosphorus chemistry. In silicon chemistry, these substituent effects are comparatively small due to restricted possibilities of influencing transition state energies[5].

TABLE 2. Vertical π-ionization energies (eV) of cyclopentadiene and some silyl derivatives

	IE (π_1)	IE(π_2)		IE(π_1)	IE (π_2)
H_6C_5	8.6	10.7	$H_5C_5SiMe_3$	8.3	9.1
$H_5C_5SiH_3$	8.7	10.2	$H_4C_5(SiMe_3)_2$	8.0	9.1

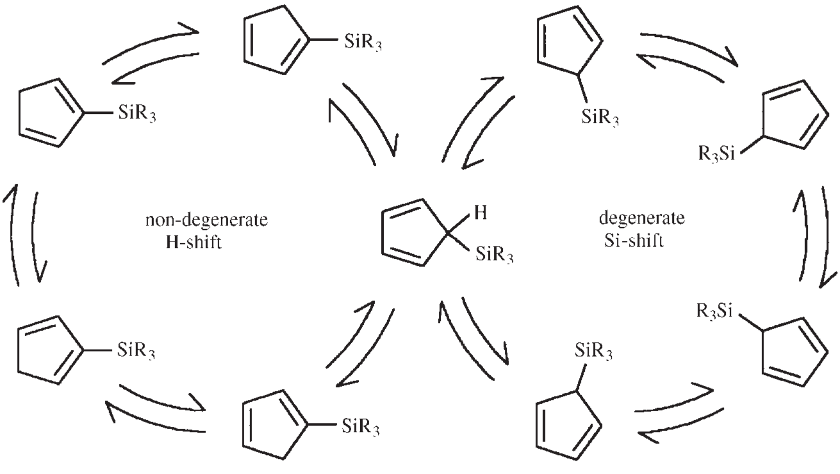

FIGURE 1. Sigmatropic rearrangements in $H_5C_5SiR_3$-type compounds

Activation energies for hydrogen shifts are higher than those for silicon shifts. As seen in Figure 1, hydrogen shifts allow the formation of isomers, in which the silicon group resides in a vinylic position of the cyclopentadiene system rather than allylic. This process may be desired or not desired depending on the synthetic target. The substitution of all hydrogen atoms is necessary to avoid hydrogen shifts. For this reason, several pentamethylcyclopentadienyl silicon compounds were synthesized and studied in more detail[5,11]. In the case of only partial hydrogen substitution, the silyl group prefers a ring position with a geminal hydrogen atom. For example, an overall 1,3 silicon shift caused by two successive 1,2 shifts is favoured in the rearrangement process of (1,2,4-trimethylcyclopentadienyl)trimethylsilane **(9)** to **9′**[20], as shown in equation 1. Also in 5,5-bis(trimethylsilyl)cyclopentadiene **(10)**, an overall 1,3 silicon shift to **12** takes place[21,22], as depicted in equation 2. Due to steric constraints of the trimethylsilyl group, the intermediate 1,5-bis(trimethylsilyl)cyclopentadiene **(11)** is of higher energy and cannot be observed by NMR techniques or trapped by chemical reactions. On the other hand, even more pronounced steric constraints can prevent the overall 1,3 shift and enforce isomer formation via a 1,2 silicon shift. This is demonstrated with two typical examples in equation 3 [a degenerate rearrangement (**13** $\rightleftharpoons$ **13′**)][23] and in equation 4 [a non-degenerate process (**14** $\rightleftharpoons$ **15**)[24]].

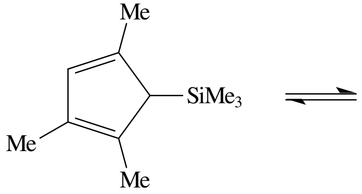

(9) **(9′)**

(1)

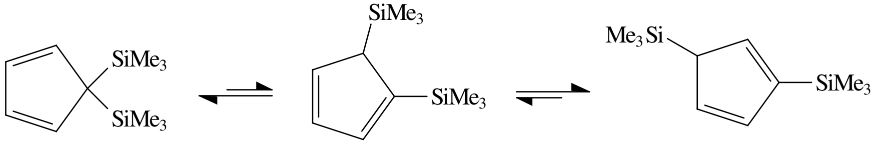

(10) **(11)** **(12)**

(2)

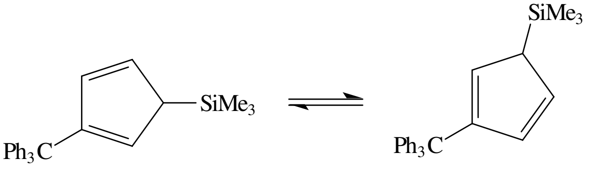

(13) **(13′)**

(3)

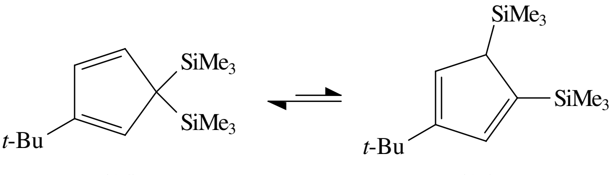

(14) **(15)**

(4)

Dynamic processes, such as those in equations 1–4, are of great importance in synthetic cyclopentadienylsilicon chemistry. They allow design of multiply substituted cyclopentadienyl compounds using the regioselectivity in silicon–carbon and also in carbon–carbon bond formation (see Sections II.D and II.E).

2. Silicon bound to an sp^2-hybridized carbon atom

In this chapter, compounds of type **2–4** are described in which the respective silyl group is directly bonded to a cyclopentadienyl π-system, raising more questions concerning the consequences of electronic interaction. Answers will be given on the basis of X-ray crystal structure investigations and of physico-chemical measurements (X-PES, CV, ESR) performed on typical silylcyclopentadienyl species.

a. X-ray crystal structure data. An η^0-substituted cyclopentadienide species of type **3** in Scheme 1 is present in the compound $[Li(12crown4)_2][1,2,4\text{-}(Me_3Si)_3C_5H_2]$ **(16)**[25] and is the most appropriate example to discuss the influence of trimethylsilyl groups on the structure of a cyclopentadienide anion. **16** is comprised of well-separated cations and anions, as depicted in Figure 2, and does not involve the cation contacts evident in compounds like $\{[\mu-\eta^5:\eta^5\text{-}C_5H_4(SiMe_3)]Li\}_n$[26] and $\{[\mu-\eta^5:\eta^5\text{-}C_5H_4(SiMe_3)]K\}_n$[27]. Selected bond distances and angles are presented in Table 3.

The average C–C bond length within the cyclopentadienide unit is 1.42 Å, which is significantly greater than in the free C_5H_5 ion (1.399 Å)[28] and the average C–C bond length within the η^5-H_5C_5 ring of (12crown4)Li(η^5-H_5C_5) (1.395 Å)[25]. Four of the C–C distances in **16** are remarkably similar [1.414(3) Å], whereas the C_1–C_2 bond, which involves the carbon atoms bearing adjacent Me_3Si substituents, is 1.446(3). The Si–C distances in **16** are in the range 1.835(2) Å to 1.842(2) Å, and the average Si–C bond length is 1.84 Å, slightly shorter than normally observed (Si–C_{sp^2} 1.85 Å[29]). The

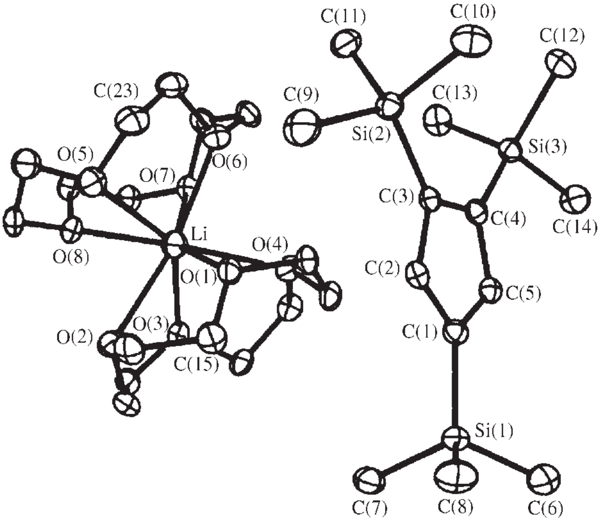

FIGURE 2. Solid-state structure of **16**. Reprinted with permission from Ref. 25. Copyright (1991) American Chemical Society

TABLE 3. Selected bond distances (Å) and angles (deg) for the anion of **(16)**

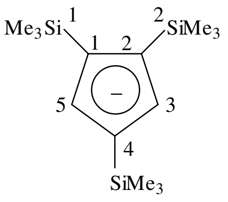	C(1)–C(2)	1.446(3)	C(1)–C(2)–C(3)	106.3(2)
	C(2)–C(3)	1.414(3)	C(2)–C(3)–C(4)	110.9(2)
	C(3)–C(4)	1.414(3)	C(3)–C(4)–C(5)	105.4(2)
	C(4)–C(5)	1.414(3)	C(4)–C(5)–C(1)	110.7(2)
	C(5)–C(1)	1.413(3)	C(5)–C(1)–C(2)	106.7(2)
	Si(1)–C(1)	1.836(2)	C(5)–C(4)–Si(3)	127.9(1)
	Si(2)–C(2)	1.842(2)	C(5)–C(1)–Si(1)	122.1(1)
(16$^-$)	Si(3)–C(4)	1.835(2)	C(1)–C(2)–Si(2)	132.3(2)

relatively long C–C distances as well as the slightly shortened Si–C distances in **16** are probably a result of the electronic effects of the Me$_3$Si substituents, whose ability to stabilize negatively charged species such as carbanions is well documented[2]. The three Me$_3$Si groups provide stabilization by lowering the negative charge density through delocalization by π-σ^* interaction.

In η^5-silylcyclopentadienyl metal complexes of type **4** in Scheme 1, the π-orbitals of the cyclopentadienyl fragment are intimately involved in bonding with low-lying metal valence orbitals. The ferrocene derivatives are representative of this class of compounds, and illustrate the influence of silylation on structural and electronic parameters. A single-crystal X-ray diffraction study of 1,1′,3,3′-tetrakis(trimethylsilyl)ferrocene, Fe[η^5-(1.3-SiMe$_3$)$_2$H$_3$C$_5$]$_2$ **(17)**[30], has revealed a conformation of C$_2$ symmetry in which the trimethylsilyl groups are arranged in a staggered fashion, with the five-membered rings nearly eclipsed, as portrayed in Figure 3. Selected bond distances and angles are presented in Table 4.

The average Fe–C(ring) bond length of 2.059(2) Å is comparable to that in ferrocene, as are the C–C bond distances [average 1.432(3) Å] within the five-membered ring. The trimethylsilyl groups are bent away from the metal centre (average 8°) probably for steric reasons. The average Si–C distance is 1.854(2) Å. It is informative to compare C–C and Si–C bond lengths within the silylated cyclopentadienyl fragments in the ionic

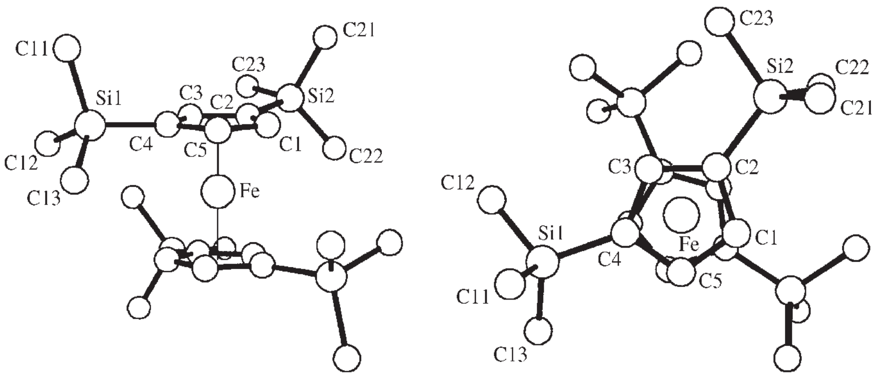

Side view top view

FIGURE 3. Molecular structure of **(17)**

TABLE 4. Selected bond distances (Å) and angles (deg) for **17** (for numbering scheme see Figure 3)

C(1)-C(2)	1.442(3)	C(1)-C(2)-C(3)	105.5(2)
C(2)-C(3)	1.424(3)	C(2)-C(3)-C(4)	112.0(2)
C(3)-C(4)	1.429(3)	C(3)-C(4)-C(5)	104.6(2)
C(4)-C(5)	1.441(3)	C(1)-C(5)-C(4)	109.5(2)
C(5)-C(1)	1.422(3)	C(2)-C(1)-C(5)	108.7(2)
Si(1)-C(4)	1.848(2)	Si(2)-C(2)-C(1)	126.0(2)
Si(2)-C(2)	1.861(2)	Si(2)-C(2)-C(3)	128.3(2)

cyclopentadienide species **(16)** with those in the covalent ferrocene derivative **(17)**, which exhibits significantly longer C−C and Si−C distances. This is likely due to the transfer of electron density from the cyclopentadienyl ligands to the metal centre, which weakens the C−C as well as the Si−C bonds to some extent.

b. Cyclic voltammetry data. It is well known that ferrocene and its derivatives exhibit reversible one-electron oxidations, and cyclic voltammetry is a useful tool to determine the effect of different kind of substituents on the redox properties of the corresponding compounds. The trimethylsilylated ferrocenes **17**–**21** have been studied by cyclic voltammetry[31]. Their redox potentials, $E_{1/2}$, which are internally referenced to ferrocene **(22)**, are presented in Table 5. For the sake of comparison, the $E_{1/2}$ values are also given for $(Me_5C_5)_2Fe$ **(23)**[33], $Me_5C_5(H_5C_5)Fe$ **(24)**[34] and $[1,3(t\text{-}Bu)_2H_3C_5]_2Fe$ **(25)**[31].

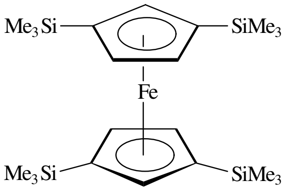

(17)

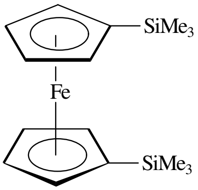

(18)

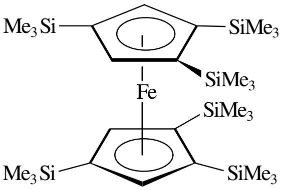

(19)

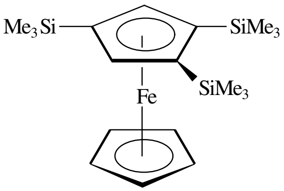

(20)

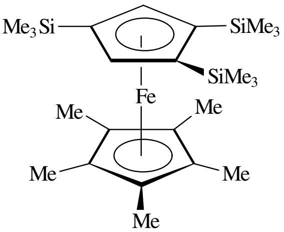

(21)

Table 5 shows that alkyl groups such as methyl or *t*-butyl at the ring periphery cathodically shift the oxidation potential of the substituted ferrocene by *ca* 50 mV per alkyl group relative to the parent compound. This reflects the steady increase of electron density at the iron centre by successive ring substitution with electron-donating groups[31]. On the other hand, anodic shifts of the oxidation potential are observed for the trimethylsilyl substituted ferrocenes **17**, **20** and **21** compared with those of the parent compounds **22**

TABLE 5. Redox potential data for ferrocene derivatives[31]

		$E_{1/2}$ (mV)[a]			$E_{1/2}$ (mV)[a]
$[1,3\text{-}(Me_3Si)_2H_3C_5]_2Fe$	**(17)**	+33[b]	$(H_5C_5)_2Fe$	**(22)**	0[b]
$[(Me_3Si)H_4C_5]_2Fe$	**(18)**	0[c,32]	$(Me_5C_5)_2Fe$	**(23)**	-550[c,33]
$[1,2,4\text{-}(Me_3Si)_3H_2C_5]_2Fe$	**(19)**	-104[b]	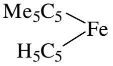	**(24)**	-270[b,34]
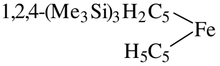	**(20)**	+17[b]	$[1,3\text{-}(Me_3C)_2H_3C_5]_2Fe$	**(25)**	-250[b]
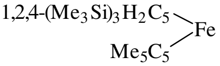	**(21)**	-359[b]			

[a] $E_{1/2} = 1/2\ (E_p{}^{ox} + E_p{}^{red})$.

[b] In CH_2Cl_2 solution; Ag/AgCl reference electrode; $Bu_4N^+PF_6{}^-$ as supporting electrolyte.

[c] In CH_3CN solution.

and **23**. This reflects the decrease of electron density at the respective iron centre by successive ring substitution with electron-accepting trimethylsilyl groups. These observations further support the concept of π-σ^* interaction. The unexpectedly low $E_{1/2}$ for the hexakis-substituted ferrocene derivative **19** must be due to steric factors[31].

c. X-PES data. The electronic effects of trimethylsilyl substituents in cyclopentadienyl π-complexes have also been probed by X-ray photoelectron spectroscopy for a series of ferrocenes and Group 14 metallocenes[35]. Table 6 lists the binding energies of inner-shell electrons for several compounds with trimethylsilyl substituents on the cyclopentadienyl ring and for appropriate reference compounds. For each metal, the binding energy decreases by about 0.1 eV per trimethylsilyl group, indicating that the trimethylsilyl group is unexpectedly weakly electron-donating according to this physical method.

d. ESR data. Electron spin-resonance (ESR) spectroscopy has provided detailed structural information on the paramagnetic silylated cyclopentadienyl species of type **2** in Scheme 1. The orbital degeneracy in the cyclopentadienyl radical is removed by substitution so that the form of the ESR spectra depends critically on the symmetry properties of the orbital in which the unpaired electron resides[36,37]. As an unpaired electron must

TABLE 6. Binding energies of inner-shell electrons for ferrocenes and Group IV metallocenes

Compound	Electron	Binding energy ±0.1 eV
$(H_5C_5)Fe$ **(22)**	$2p_{3/2}$	708.0
$[(Me_3Si)_3H_2C_5]_2Fe$ **(19)**	$2p_{3/2}$	707.3
$(Me_5C_5)_2Fe$ **(23)**	$2p_{3/2}$	707.1
$(H_5C_5)_2ZrCl_2$	$3d_{5/2}$	181.7
$[(Me_3Si)H_4C_5]_2ZrCl_2$	$3d_{5/2}$	181.5
$[(Me_3Si)_2H_3C_5]_2ZrCl_2$	$3d_{5/2}$	181.4
$[(Me_3Si)_3H_2C_2]_2ZrCl_2$	$3d_{5/2}$	181.2
$(Me_5C_5)_2ZrCl_2$	$3d_{5/2}$	181.0
$(H_5C_5)_2HfCl_2$	$4f_{7/2}$	17.1
$[(Me_3Si)_3H_2C_5]_2HfCl_2$	$4f_{7/2}$	16.5
$(Me_5C_5)_2HfCl_2$	$4f_{7/2}$	16.5

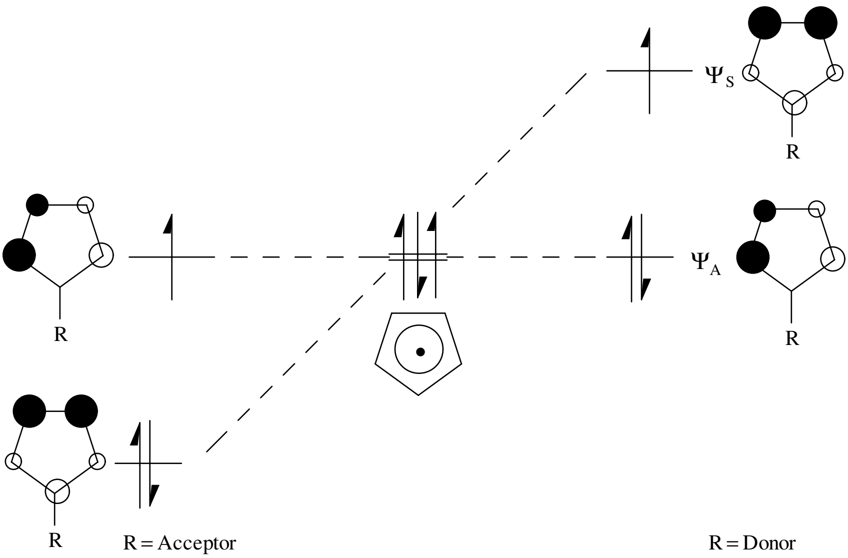

FIGURE 4. Breaking the degeneracy in the highest occupied molecular orbitals in a monosubstituted cyclopentadienyl radical[36,37]

occupy a bonding π-orbital, substituent effects are directly observed. Figure 4 is a simplified diagram illustrating the degeneracy of the highest occupied molecular orbitals in a cyclopentadienyl radical and how the degeneracy is split by electron-accepting or electron-donating substituents R. An electron-donating substituent raises the ψ_S level favouring the electronic configuration $\psi_A^2\psi_S^1$, while an electron-accepting substituent lowers the ψ_S level favouring the $\psi_S^2\psi_A^1$ configuration. Analyses of the temperature-dependent ESR spectra revealed a thermal equilibrium between radicals in the symmetric and antisymmetric orbitals.

Two experimental studies with silylated cyclopentadienyl radicals are reported in the literature which show how other substituents at the relevant silicon atom influence the donor/acceptor qualitites of a SiR_3 group. In one study the observed spin densities at the point of substituent attachment indicate that the Ph_2MeSi, $PhMe_2Si$, and Me_3Si fragments are electron-accepting and that the Me_5Si_2 and Me_7Si_3 fragments are electron-donating[36]. In the other study it was shown that the Me_3Si, Me_2HSi, Me_2ClSi, Me_2FSi, and Cl_3Si fragments are increasingly electron-accepting[37]. The electron attraction is due to π-σ^* conjugation, and the electron donation is due to π-σ conjugation.

From the different physical methods described in this chapter, the electronic effect of the most frequently used Me_3Si group can be summarized as weakly electron-accepting rather than weakly electron-donating.

B. Synthesis of Compounds with Silicon–Cyclopentadienyl Bonds

This section describes representative strategies for the synthesis of silylated cyclopentadienes of type **1**, and for silylcyclopentadienyl metal complexes of type **4**.

The basic synthetic principles (Schemes 3–9) will be illustrated by some typical examples. More comprehensive treatments can be found in standard textbooks for organic and organometallic synthesis[2–4] and recent review articles[6,38–40].

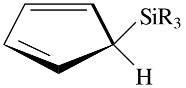

(1)

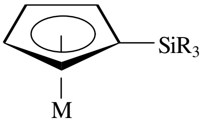

(4)

1. Silylated cyclopentadienes

The reaction of metal cyclopentadienyl compounds with organosilicon electrophiles has been the most widely applied method for the synthesis of silylated cyclopentadienes (see Scheme 3) since the beginning of cyclopentadienylsilicon chemistry[1].

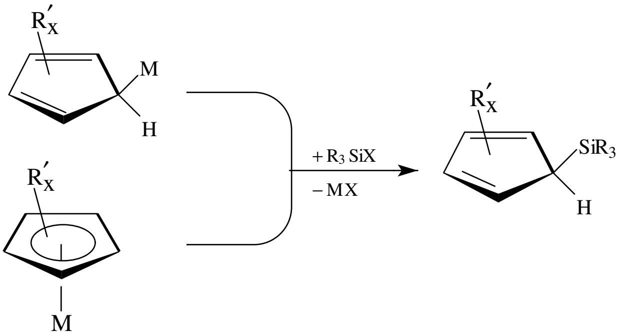

SCHEME 3

Cyclopentadienyl compounds of lithium, sodium, potassium, magnesium and thallium are most commonly used. The synthesis of these cyclopentadienyl-transfer agents is described in more detail in Section II.B.2. Organosilicon halides and alkoxides are the most convenient substrates. The synthesis of side-chain functionalized cyclopentadienyl silanes is described in equation 5[41,42] as a typical example of this strategy.

$$H_5C_5Li + Ph_2P(CH_2)_nSiMe_2Cl \longrightarrow H_5C_5SiMe_2(CH_2)_nPPh_2 \tag{5}$$

The reaction sequence shown in Scheme 4 is exceptional for the synthesis of a multisilylated cyclopentadiene involving six-fold silylation in the reaction of hexabromocyclopentadiene with dimethylchlorosilane and magnesium[43]. Grignard-type compounds are presumably the intermediates in this process. More simple is the formation of the Grignard compound pentamethylcyclopentadienylmagnesium bromide from the reaction of bromopentamethylcyclopentadiene with magnesium[44].

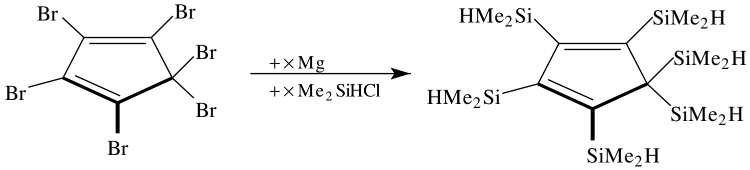

SCHEME 4

2. Silylcyclopentadienyl metal complexes

The most important synthetic methods for the preparation of silylcyclopentadienyl metal compounds are depicted in Schemes 5–9. Metallation of silylated cyclopentadienes, as depicted in Scheme 5, is a very often used and efficient strategy. Hydrogen abstraction and reduction can be easily performed with reactive metals like potassium (equation 6[45]), calcium, strontium or barium (equation 7[46]). An advantage of these reagents is their non-nucleophilic behaviour, which allows for the synthesis of compounds possessing functionalized silyl groups. Deprotonation takes place with butyllithium (equation 8[1]) and with dimethylmagnesium (equation 9[47]). Different kinds of metal amides can also be used, as shown for calcium amide (equation 10[48]) and for tetrakis(dimethylamino)zirconium (equation 11[49]). Under appropriate conditions metallation can be achieved with reagents possessing low nucleophilicity including thallium alkoxides (equation 12[50]) and cyclopentadienylindium (equation 13[51]). It can also be accomplished with transition-metal carbonyl complexes, as demonstrated in the reaction with pentacarbonyliron (equation 14[52]) and with octacarbonyldicobalt (equation 15[52]). In the corresponding reaction with decacarbonyldimanganese, competing silicon–carbon bond fission takes place[52].

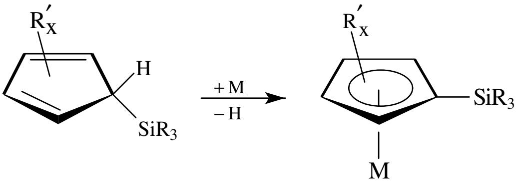

SCHEME 5

$$(Me_3Si)H_5C_5 + K \longrightarrow [(Me_3Si)H_4C_5]K + \tfrac{1}{2}H_2 \tag{6}$$

$$2[2,5\text{-}(Me_3Si)_2H_4C_5] + Ca(Sr,Ba) \longrightarrow [1,3\text{-}(Me_3Si)_2H_3C_5]_2Ca(Sr,Ba) + H_2 \tag{7}$$

$$(Me_3Si)H_5C_5 + LiBu \longrightarrow [(Me_3Si)H_4C_5]Li + BuH \tag{8}$$

$$2,4,5\text{-}(Me_3Si)_3H_3C_5 + MgMe_2 + TMEDA \longrightarrow [1,2,4\text{-}(Me_3Si)_3H_2C_5 \; MgMe{\bullet}TMEDA + MeH \tag{9}$$

$$2(Me_3Si)H_5C_5 + Ca(NH_2)_2 \longrightarrow [(Me_3Si)H_4C_5]_2Ca + 2NH_3 \tag{10}$$

$$2,4,5\text{-}(Me_3Si)_3H_3C_5 + Zr(NMe_2)_4 \longrightarrow [1,2,4\text{-}(Me_3Si)_3H_2C_5]Zr(NMe_2)_3 + Me_2NH \tag{11}$$

$$(Me_3Si)H_5C_5 + TlOEt \longrightarrow [(Me_3Si)H_4C_5]Tl + EtOH \tag{12}$$

$$(Me_3Si)H_5C_5 + InC_5H_5 \longrightarrow [(Me_3Si)H_4C_5]In + C_5H_6 \tag{13}$$

$$2(Me_3Si)H_5C_5 + 2Fe(CO)_5 \longrightarrow \{[Me_3Si)H_4C_5]Fe(CO)_2\}_2 + 6CO + H_2 \tag{14}$$

$$2(Me_3Si)H_5C_5 + Co_2(CO)_8 \longrightarrow 2[(Me_3Si)H_4C_5]Co(CO)_2 + 4CO + H_2 \tag{15}$$

Desilylation or destannylation of the corresponding cyclopentadiene derivatives can be easily performed in addition to deprotonation, as shown schematically in Scheme 6. The possibility for desilylation indicates the pronounced reactivity of the silicon–carbon bond, which is described in more detail in Section III. Nucleophiles as well as

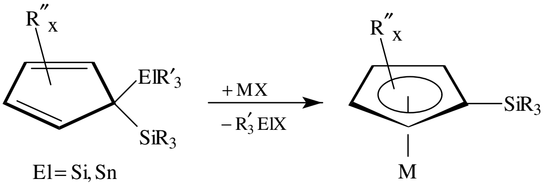

SCHEME 6

electrophiles can initiate the desilylation (destannylation) process as illustrated in the following examples. A regioselective Si−C bond cleavage takes place in the reaction of hexakis(dimethylsilyl)cyclopentadiene with butyllithium (equation 16[43]) and also in the reaction of multiply trimethylsilylated cyclopentadienes with titanium or zirconium tetrachloride (equations 17[53] and 18[54]). An allylic silicon−carbon bond is cleaved in both cases. The comparatively more reactive trimethylstannylated cyclopentadienes are required in the reaction with less electrophilic transition-metal halides in the process of silylcyclopentadienyl metal complex formation (equations 19[52] and 20[52]).

$$(\mathrm{Me_2SiH})_6\mathrm{C_5} + \mathrm{BuLi} \longrightarrow [(\mathrm{Me_2SiH})_5\mathrm{C_5}]\mathrm{Li} + \mathrm{Me_2Si(H)Bu} \tag{16}$$

$$1,3,5\text{-}(\mathrm{Me_3Si})_3\mathrm{H_3C_5} + \mathrm{TiCl_4} \longrightarrow [1,3\text{-}(\mathrm{Me_3Si})_2\mathrm{H_3C_5}]\mathrm{TiCl_3} + \mathrm{Me_3SiCl} \tag{17}$$

$$2[2,5\text{-}(\mathrm{Me_3Si})_2\mathrm{H_4C_5}] + \mathrm{ZrCl_4} \longrightarrow [(\mathrm{Me_3Si})\mathrm{H_4C_5}]_2\mathrm{ZrCl_2} + 2\mathrm{Me_3SiCl} \tag{18}$$

$$\begin{aligned}(\mathrm{Me_3Sn})(\mathrm{Me_3Si})\mathrm{H_4C_5} + (\mathrm{OC})_5\mathrm{MnBr} \longrightarrow\ & [(\mathrm{Me_3Si})\mathrm{H_4C_5}]\mathrm{Mn(CO)_3} \\ & + \mathrm{Me_3SnBr} + 2\mathrm{CO}\end{aligned} \tag{19}$$

$$\begin{aligned}2(\mathrm{Me_3Sn})(\mathrm{Me_3Si})\mathrm{H_4C_5} + [\mathrm{Rh(CO)_2Cl}]_2 \longrightarrow\ & 2[(\mathrm{Me_3Si})\mathrm{H_4C_5}]\mathrm{Rh(CO)_2} \\ & + 2\mathrm{Me_3SnCl}\end{aligned} \tag{20}$$

An alternative approach to silylcyclopentadienyl metal complexes employs the deprotonation/silylation process in cyclopentadienyl metal complexes, as shown in Scheme 7. Deprotonation with an organolithium compound and subsequent reaction with an electrophilic organosilicon compound is shown in equations 21[55] and 22[56]. Halogen−lithium exchange is another possibility to produce a lithiated cyclopentadienyl complex which further reacts with an organosilicon halide to form the final product (equation 23[57]). Interestingly, a fivefold silylation can be achieved after a series of halogen−lithium exchange reactions (equation 24[58]). Furthermore, Friedel−Crafts type conditions can be chosen to introduce an electrophilic organosilyl group into a cyclopentadienyl fragment (equation 25[59,60]). Alternatively, trimethylsilyl trifluormethylsulphonate can be used as the electrophilic reagent (equation 26[61]).

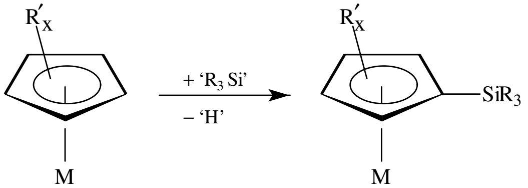

SCHEME 7

$$\mathrm{Fe(C_5H_5)_2} \xrightarrow[\text{2. Me}_3\text{SiCl}]{\text{1. LiBu}} \mathrm{Fe(C_5H_5)C_5H_4SiMe_3} \qquad (21)$$

$$\mathrm{Sn(C_5H_5)_2} \xrightarrow[\text{2. 2Me}_3\text{SiCl}]{\text{1. 2LiBu}} \mathrm{Sn(C_5H_4SiMe_3)_2} \qquad (22)$$

$$\mathrm{(OC)_3Mn(C_5Cl_4Br)} \xrightarrow[\text{2. Me}_3\text{SiCl}]{\text{1. LiBu}} \mathrm{(OC)_3Mn(C_5Cl_4SiMe_3)} \qquad (23)$$

$$\mathrm{(OC)_3Mn(C_5Br_5)} \xrightarrow[\text{2. 5 Me}_2\text{HSiCl}]{\text{1. 5 LiBu}} \mathrm{(OC)_3Mn[C_5(SiMe_2H)_5]} \qquad (24)$$

$$\mathrm{Fe(C_5H_5)_2} \xrightarrow[\text{AlCl}_3]{\text{Me}_3\text{SiCl}} \mathrm{Fe(C_5H_5)C_5H_4SiMe_3} \qquad (25)$$

$$\mathrm{(Me_3P)_2CoC_5H_5} \xrightarrow[\text{2. NH}_4{}^+\ \text{PF}_6{}^-]{\text{1. Me}_3\text{SiOSO}_2\text{CF}_3} \mathrm{(Me_3P)_2(H)CoC_5H_4SiMe_3{}^+PF_6{}^-}$$

$$\mathrm{(Me_3P)_2(H)CoC_5H_4SiMe_3{}^+PF_6{}^-} \xrightarrow[-\text{H}_2]{\text{NaH}} \mathrm{(Me_3P)_2CoC_5H_4SiMe_3} \qquad (26)$$

Silyl group migration from a transition-metal centre to a carbanionic cyclopentadienyl carbon atom[62-70] is indicated in Scheme 8. In the first step, a cyclopentadienyl C—H unit is deprotonated and the resulting carbanionic carbon centre induces a silyl group migration from the transition metal to the carbon atom. Subsequently, an electrophile attacks the negatively charged transition-metal centre to form a neutral compound. Crossover experiments show the reactions to be intramolecular; the silyl group migration occurs with retention of configuration at silicon. A concerted mechanism for the migration involving front-side nucleophilic attack at silicon has been suggested[65]. Examples for this synthetic strategy from iron[62-67], ruthenium[66,67], rhenium[68,69] and molybdenum[70] chemistry are collected in equations 27–31. In the reaction shown in equation 30, a cyclization with LiCl elimination gives the final disilametallacycle[69].

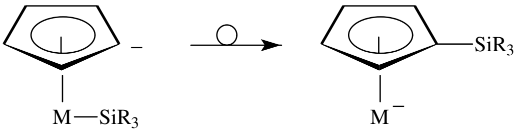

SCHEME 8

$$\begin{array}{l}\mathrm{H_5C_5Fe(CO)_2SiMe_2R}\\ \mathrm{R = Me,Pr,Ph,NMe_2; R' = Me}\end{array} \xrightarrow[\text{2. R}'\text{X}]{\text{1. LiBu or LiNMe}_2} \mathrm{(RMe_2Si)H_4C_5Fe(CO)_2R'} \qquad (27)$$

$$\begin{array}{l}\mathrm{H_5C_5M(CO)_2(SiMe_2)_nSiMe_3}\\ \mathrm{M = Fe,Ru}\end{array} \xrightarrow[\text{2. MeI}]{\text{1. LiNMe}_2} \mathrm{[Me_3Si(SiMe_2)_n]H_4C_5M(CO)_2Me} \qquad (28)$$

$$\begin{array}{c}\mathrm{H_5C_5Re(H)(CO)_2SiPh_3}\\ \mathrm{N_p} = \text{neopentyl}\end{array} \xrightarrow[\text{2. HX}]{\text{1. LiNp}} \mathrm{(Ph_3Si)H_4C_5Re(CO)_2(H)_2} \qquad (29)$$

$$\mathrm{H_5C_5Re(NO)(PPh_3)SiMe_2SiMe_2Cl} \xrightarrow{\mathrm{LiBu}} \mathrm{(Me_2SiSiMe_2)H_4C_5Re(NO)(PPh_3)} \quad (30)$$

$$\mathrm{H_5C_5Mo(H)SiMe_2Ph} \xrightarrow[\text{2. HX}]{\text{1. LiBu}} \mathrm{(PhMe_2Si)H_4C_5H_5C_5MoH_2} \quad (31)$$

‘ A similar process to that shown in Scheme 8 also involves formation of a carbanionic cyclopentadienyl carbon centre. But in this case, silicon–carbon bond formation stems from the migration of a silylmethyl group, which proceeds with rearrangement, as shown in Scheme 9. These surprising rearrangement processes are observed with iron and with tungsten compounds[71,72], as shown in equations 32 and 33.

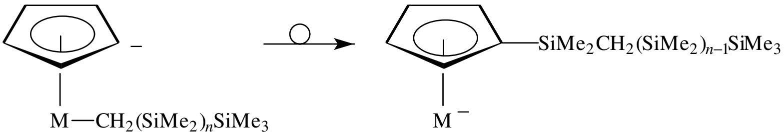

SCHEME 9

$$\mathrm{H_5C_5Fe(CO)_2CH_2(SiMe_2)_{\mathit{n}}\ SiMe_3} \xrightarrow[\text{2. MeI}]{\text{1. LiNMe}_2} \begin{matrix}\mathrm{[Me_3Si(SiMe_2)_{\mathit{n}-1}CH_2SiMe_2]} \\ \mathrm{H_4C_5Fe(CO)_2Me}\end{matrix} \quad (32)$$

$$\mathrm{H_5C_5W(CO)_3CH_2(SiMe_2)_{\mathit{n}}SiMe_3} \xrightarrow[\text{2. MeI}]{\text{1. LiNMe}_2} \begin{matrix}\mathrm{[Me_3Si(SiMe_2)_{\mathit{n}-1}CH_2SiMe_2]} \\ \mathrm{H_4C_5W(CO)_3Me}\end{matrix} \quad (33)$$

Presumably, a new kind of rearrangement process takes place in the reaction of dicyclopentadienyltungsten dichloride with tris(trimethylsilyl)silyllithium (equation 34[73]). Silyl complexes formed as intermediates spontaneously rearrange with formation of silylcyclopentadienyl complexes, but the mechanism of this process is not yet clear.

$$\mathrm{(H_5C_5)_2WCl_2 + 2LiSi(SiMe_3)_3} \longrightarrow \mathrm{\{[Me_3Si)_3Si]H_4C_5\}_2WH_2 + 2LiCl} \quad (34)$$

C. Methods of Silicon–Cyclopentadienyl Bond Cleavage

The silicon–carbon bond in cyclopentadienyl silicon compounds of type **1** (Scheme 1) is comparatively weak, and is susceptible to sigmatropic rearrangements. Si–C bond fission might be a disadvantage in certain synthetic strategies or in some practical applications; however, it has been successfully used in the design of new silicon compounds as illustrated in the following section. Scheme 10 shows a collection of different kinds of Si–C(Cp) cleavage reactions involving cyclopentadienyltrimethylsilane.

Halide-promoted cleavage of $\mathrm{C_{sp^3}}$–Si bonds is most extensively demonstrated with the fluoride ion, due to the high dissociation energy of the silicon–fluorine bond[74]. A novel chloride ion-induced desilylation process with trimethylsilylcyclopentadiene, bis(trimethylsilyl)cyclopentadiene or tris(trimethylsilyl)cyclopentadiene in alcoholic solvents has been described only recently[75]. Another nucleophilic substitution process with Si–C bond cleavage takes place in the reaction of trimethylsilylcyclopentadiene with secondary amines[76]. Electrophilic attack at the π-system is the basis for the cleavage reactions observed with several element halides, which clearly demonstrate that trimethylsilylcyclopentadiene is a mild and effective cyclopentadienyl transfer agent[52,77–81]. The reaction

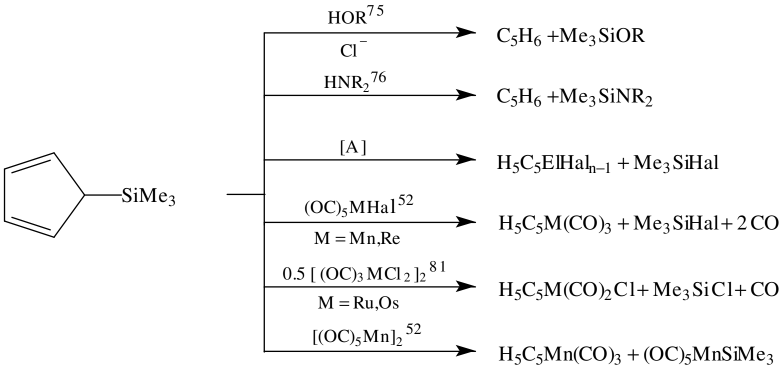

$[A] = BHal_3{}^{77}, AsHal_3{}^{78}, R_2AsHal^{78}, SbHal_3{}^{79}, TiHal_3{}^{80},$
$TiCl_4{}^{80}, ZrCl_4{}^{80}, HfCl_4{}^{80}, NbHal_5{}^{80}, TaHal_5{}^{80},$
$H_5C_5ZrCl_3{}^{55,80}, H_5C_5HfCl_3{}^{80}$

SCHEME 10. Si−C(Cp) bond cleavage in cyclopentadienyltrimethylsilane

of trimethylsilylcyclopentadiene with dimanganese decacarbonyl takes two paths[52]: One in which the silicon−ring bond remains intact, and the other in which silicon−ring fission takes place, as shown in Scheme 10.

Preparatively useful cleavage reactions with other cyclopentadienyl silicon substrates are shown in equations 35–40. A regioselective introduction of $BHal_2$ groups is possible according to the process in equation 35[77]. A novel chloride-catalysed cleavage reaction is the basis for the sequence shown in equation 36[82]. The transfer of $BR_2{}^-$, $ClMe_2Si$- and Me_3Si-substituted cyclopentadienyl fragments to Group IV transition metal centres is illustrated in equations 37–40[54,83–86].

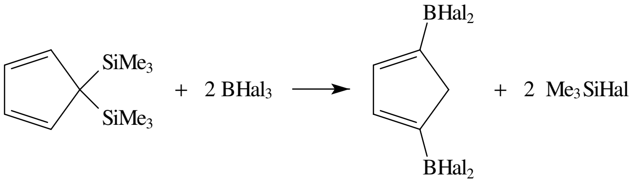

(35)[77]

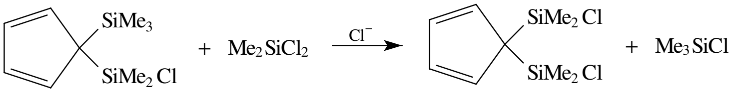

(36)[82]

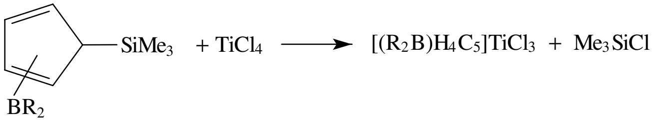

(37)[83]

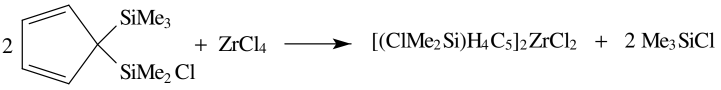

(38)[84]

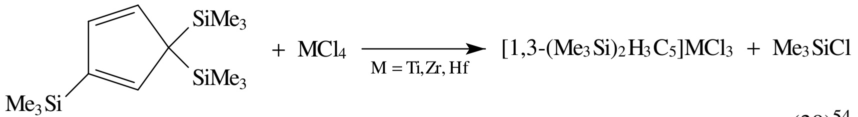

(39)[54,85]

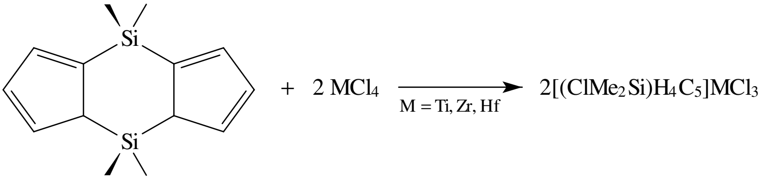

(40)[86]

Other examples of Si—C(Cp) bond cleavage reactions deal with pentamethylcyclopentadienyl (Cp*) substituted silicon compounds. Scheme 11 shows a collection of different kinds of reactions with (pentamethylcyclopentadienyl)trimethylsilane as the substrate. Nucleophilic as well as electrophilic attack is the basis for Si—C(Cp) bond fission[97]. Reactions with various element halides involved in pentamethylcyclopentadienyl transfer are very useful in synthetic chemistry[88–91] (see also Sections II.B and II.E).

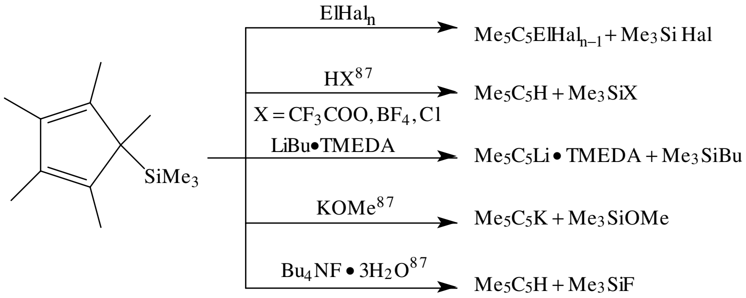

$ElHal_n = BHal_3$[88], $AlCl_3$[89], $TiHal_4$[90], $ZrCl_4$[90], $HfCl_4$[90], $NbCl_5$[91], $TaCl_5$[91]

SCHEME 11. Si—C(Cp*) bond cleavage in (pentamethylcyclopentadienyl)trimethylsilane.

It is possible to selectively cleave a Si—C(Cp*)bond even in the presence of silicon–transition metal bonds as shown in reactions with nucleophiles, electrophiles and chlorinated hydrocarbons (equations 41 and 42)[92,93].

The thermal decomposition of Cp* substituted silicon compounds with the elimination of pentamethylcyclopentadiene (Cp*H) turns out to be synthetically very useful. As shown in equations 43–45, extreme conditions are necessary to selectively cleave the respective Si—C(Cp*) bond[94–96]. In this context, it is important to mention the use of cyclopentadienyl silicon compounds in the metalorganic chemical vapour deposition (MOCVD) process or in related techniques[95,96].

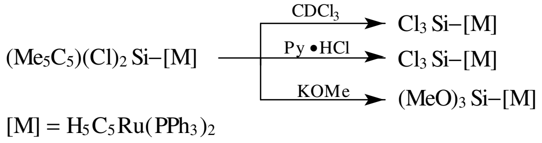

(41)[92]

$$Me_5C_5(H)(R)Si{-}Fe(H_5C_5)(CO)_2 \xrightarrow{CCl_4} Cl(H)(R)Si{-}Fe(H_5C_5)(CO)_2$$

(42)[93]

$R = Cl, Me$

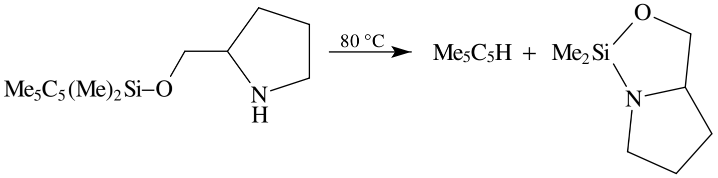

(43)[94]

$$Me_5C_5SiH_3 \xrightarrow[\text{Plasma-MOCVD}]{200\,^{\circ}C} Si + Me_5C_5H + H_2$$

(44)[95]

$$[Me_5C_5(PH_2)SiPH]_2 \xrightarrow{700\,^{\circ}C} 2SiP_2 + 2Me_5C_5H + 2H_2$$

(45)[96]

There are some reports in the literature concerning the cleavage of bonds between silicon and an sp^2-hybridized carbon in silylcyclopentadienyl compounds of type **4** (Section II.B). For example, equation 46[97] shows hydrolytic fission in the reaction of a tris(trimethylsilyl) substituted ferrocene derivative with aqueous tetrabutylammonium fluoride.

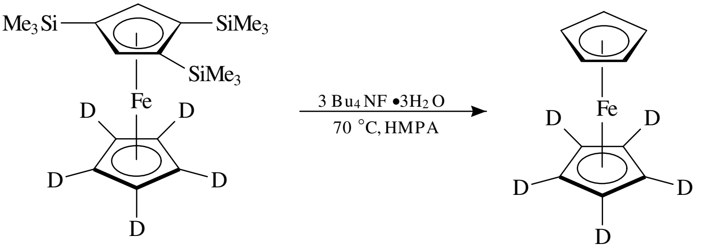

(46)

Another impressive example is the facile cleavage of Si–C(Cp) bonds in strained [1]-ferrocenophanes with bridging silicon. This behaviour is the basis for the synthesis of high-molecular-weight poly(ferrocenylsilanes) (equation 47) and will be described in more detail in Section II.E.1.

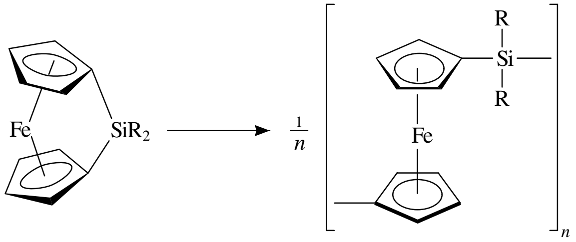

(47)

D. Multiple Silylation of Cyclopentadiene and Cyclopentadienyl Complexes

1. Effects of multisilylation

Multisilylation of cyclopentadienyl compounds can lead to drastic changes in structure and properties due to steric interaction. For example, 1,1′,2,2′,4,4′-hexakis(trimethylsilyl)ferrocene **(19)** exhibits hindered rotation of the cyclopentadienyl rings, comparatively long Fe−C (ring) distances and an unexpected redox behaviour[31,98]. Drastic changes in solubility are also observed due to lipophilic wrapping. For example, the base-free 1,2,4-tris(trimethylsilyl)cyclopentadienyllithium **(26)** is soluble even in hydrocarbon solvents[25], whilst the parent compound, cyclopentadienyllithium, is essentially insoluble in most solvents. The base adduct **(26)**•THF is a monomer in solution and in the solid state[25], whereas cyclopentadienyllithium is an amorphous, polymeric species.

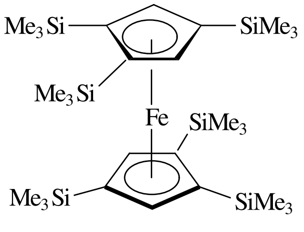

(19)

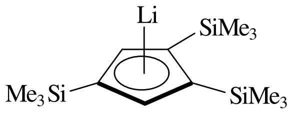

(26)

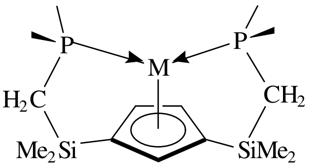

(27)

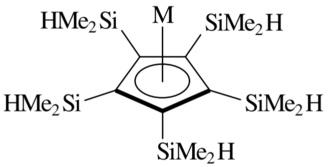

(28) **(29)**

M = Li•THF Mn(CO)$_3$

The introduction of functionalized silyl substituents into a cyclopentadienyl fragment allows for regioselective incorporation of side-chain functionalities and is therefore of high synthetic value. For example, two (di-isopropylphosphino)methyldimethylsilyl groups can be introduced in 1,3 position of a cyclopentadienyl system to create the potentially tridentate ligand, as shown in **27**[99]. Here, the chelate effect provides additional control of a reactive metal centre and generates a more stereochemically defined coordination sphere[100]. Finally, the five-fold dimethylsilylated cyclopentadienyl complexes of type **28**[43] (M = Li•THF) and **29**[58] [M = Mn(CO)$_3$] offer promising possibilities for functionalizations by hydrosilylation reactions.

2. Synthetic methods

Two strategies can be followed for the synthesis of polysilylated cyclopentadienyl compounds. One employs sigmatropic rearrangements of silylated cyclopentadienes, and the other is based on substitution reactions in cyclopentadiene and in cyclopentadienyl metal complexes. As already pointed out in Section I, the fluxionality of silyl substituted cyclopentadienes involves sila- and prototropic rearrangement processes, while the former have comparatively lower activation energies. Silatropic shifts generate isomers regiospecifically with a hydrogen atom in allylic position by a formal 1,3 silicon shift. These isomers are sometimes present in negligible amounts in equilibrium, but deprotonation with stoichiometric amounts of organolithiums allow for quantitative isomerization. The underlying reaction sequences are shown in Scheme 12. Is is worth mentioning that further silatropic shifts are not observed in the tetrasilyl-substituted cyclopentadiene. It is possible to synthesize cyclopentadienyl metal complexes with silyl groups of different kinds in 1,3- and in 1,2,4-position of the cyclopentadienyl ring.

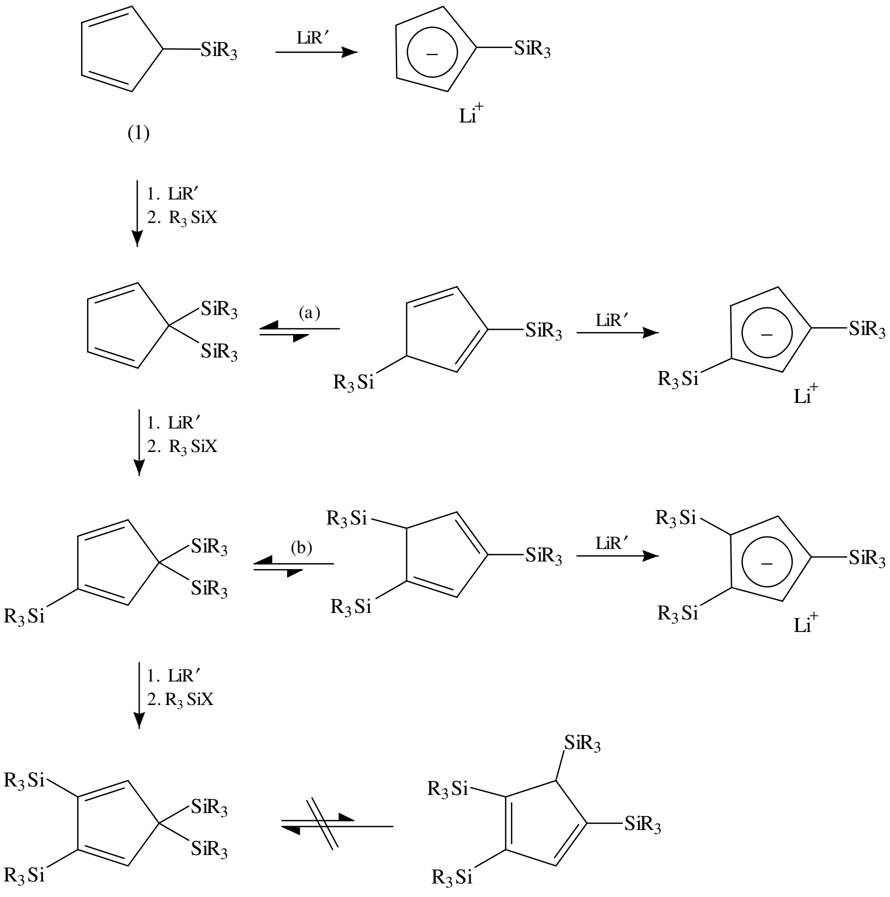

SiR_3: $SiMe_3$[22], Si_2Me_5[101]

SCHEME 12. Silatropic shifts and deprotonation/silylation reactions in silylated cyclopentadienes

As already illustrated in equations 3 and 4, steric interactions prevent the generally preferred 1,3-silicon shift in favour of a 1,2-shift allowing introduction of two silyl groups in neighbouring positions (equation 4). It should also be noted that the analogous 1,2-shift cannot be excluded in step (b) for the rearrangement processes shown in Scheme 12.

Other methods for the synthesis of polysilylated cyclopentadienyl compounds involve two different substitution reactions. Firstly, repeated halogen–metal exchange and subsequent reaction with dimethylchlorosilane allows the persilylation of a cyclopentadienyl metal complex and also of cyclopentadiene. (Pentabromocyclopentadienyl)tricarbonylmanganese can be converted to the corresponding pentasilylated complex by a series of halogen–lithium exchange reactions and silylations using dimethylchlorosilane[58] (equation 48). Similarly, a six-fold silylation takes place in the reaction of hexabromocyclopentadiene with dimethylchlorosilane and magnesium, as already pointed out in Section II, Scheme 4. Treatment of the reaction product with butyllithium in THF leads to the formation of the THF adduct of pentakis(dimethylsilyl)cyclopentadienyllithium **(28)**[43] (equation 49). Secondly, multifold silylation is possible by repeated deprotonation and silylation of cyclopentadienyl metal complexes. For example, the stepwise lithiation and trimethylsilylation of stannocene is shown in equation 50[56].

$$(OC)_3Mn(C_5Br_5) \xrightarrow[5\ Me_2SiHCl]{5\ LiBu} (OC)_3Mn[C_5(SiMe_2H)_5] \tag{48}$$

$$C_5(SiMe_2H)_6 \xrightarrow[THF]{LiBu} Li[C_5(SiMe_2H)_5]{\cdot}THF \tag{49}$$

$$Sn(C_5H_5)_2 \xrightarrow[2.\ 2\ Me_3SiCl]{1.\ 2\ LiBu} Sn[C_5H_4(SiMe_3)]_2 \xrightarrow[2.\ 2\ Me_3SiCl]{1.\ 2\ LiBu} Sn[C_5H_3(SiMe_3)_2\text{-}1,3]_2 \tag{50}$$

E. Silicon-bridged Cyclopentadienyl Complexes

In recent years, bridging of two or more cyclopentadienyl fragments by silicon-containing units has become a very important synthetic tool in the chemistry of s-, p-, d- and f-block elements. In mononuclear compounds, bridging limits the relative orientation of two cyclopentadienyl ligands enforcing conformations around the metal centre, which might lead to changes in structure and reactivity. In dinuclear compounds, bridging inherently retains the metal centres in close proximity, which might induce pronounced structural changes in comparison to the non-bridged species and might allow cooperative effects by direct metal–metal interaction or by propagation through the bridging silicon unit. Similar effects are expected in bridged polynuclear compounds. In view of the vast number of cyclopentadienyl compounds in organometallic chemistry and their huge synthetic potential, many applications for the strategy of bridging with silicon units can be envisaged.

The choice of silicon as the bridging atom results primarily from the ease with which these compounds can be prepared (*vide infra*). Nevertheless, certain silicon-containing bridging units have been chosen for electronic reasons; for example, it is well known that a disilanyl group qualitatively behaves like an ethylene unit.

Cyclopentadienyl systems bridged by a single silicon-containing unit are described in Section II.E.1. Cyclopentadienyl units which are held together by a double bridge are described in Section II.E.2. Section II.E.3. describes cooperative effects exerted by dimethylsilyl groups as bridging units, with special emphasis on polyferrocenyl compounds.

1. Single-bridged cyclopentadienyl systems

The most important single-bridged cyclopentadienyl systems described in the literature (**30**–**37**) are collected in Scheme 13. The silicon-containing bridging units range from the dimethylsilyl (type **30**) to a polysiloxane group (type **35**). Tetramethyldisilanyl groups can connect three (type **36**) or even four (type **37**) cyclopentadienyl fragments.

The strategies used to synthesize metal complexes with the cyclopentadienyl ligands portrayed in Scheme 13 are briefly described below. The most widely used procedure begins with the corresponding cyclopentadiene derivative, which can be transformed into a cyclopentadienyl metal complex by a variety of metallation methods as described in

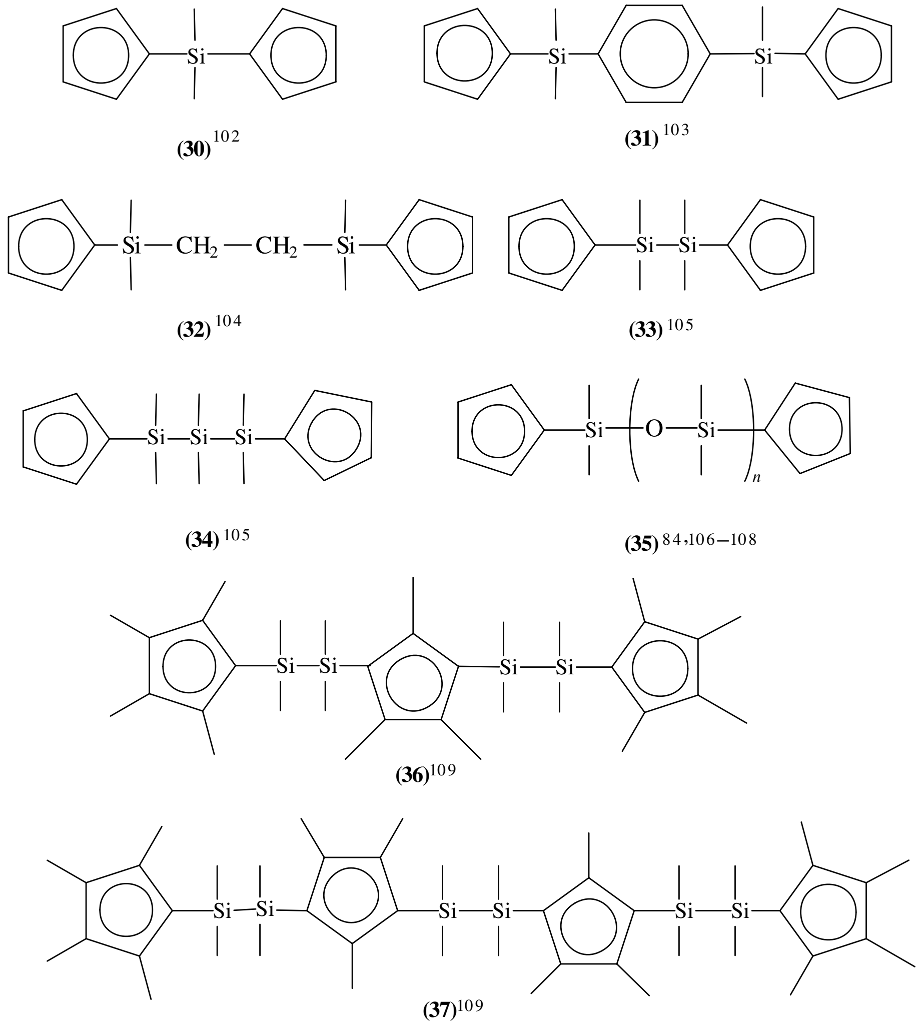

SCHEME 13. Single-bridged cyclopentadienyl systems

Section II. A regioselective introduction of disilanyl bridges is necessary in the process to synthesize complexes with ligands of types **36** or **37**[109], and this has been made possible by methylation of the cyclopentadienyl fragments. Due to prototropic rearrangements, the protonated derivatives of **36** and **37** exist as a complicated mixture of isomers. The synthesis of the thallium derivative of **37**[109] is shown in equation 51.

$$\begin{aligned}&\mathrm{Me_4HC_5(Si_2Me_4)Me_3HC_5(Si_2Me_4)Me_3HC_5(Si_2Me_4)C_5HMe_4}\\&\quad +4\mathrm{TlOEt} \longrightarrow \mathrm{Tl_4}(\mathbf{37}) + 4\mathrm{EtOH}\end{aligned} \qquad (51)$$

Another synthetic procedure is based on the reaction of dilithioferrocene with difunctional electrophilic silicon substrates, as shown in equation 52. For example, $\mathrm{Me_2Si}$[110],

Me_4Si_2[105], and Me_6Si_3[105] groups have been introduced by this classical procedure.

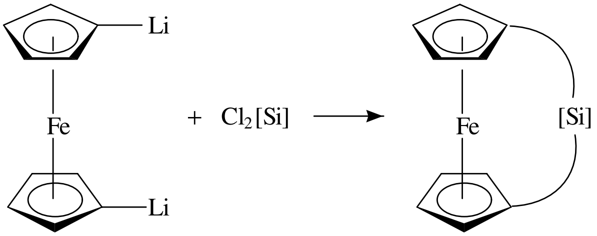

(52)

Bridges containing SiOSi units have been introduced by condensation reactions of dicyclopentadienyl complexes containing functionalized silyl groups (equation 53)[84,107] or by oxygen insertion into a preformed Si−Si bridge (equation 54)[108].

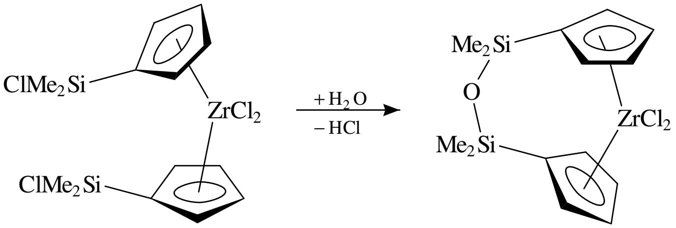

(53)

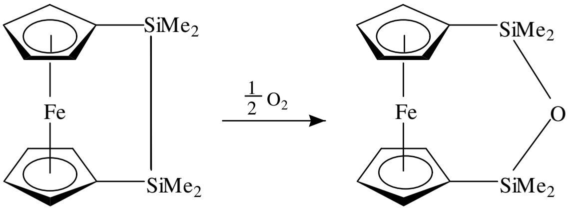

(54)

In the following section we will concentrate on the most important classes of compounds which have been studied with the dimethylsilyl-bis(cyclopentadienyl) ligand system **(30)**. In Scheme 14, five different types of complexes are portrayed, showing two principally different coordination modes of type **30**: connection of two metal centres in binuclear units (type **38**, **39** and **40**) and chelation of one metal centre in mononuclear complexes (type **41** and **42**).

Complexes of type **38** have been realized with several metal centres. Representative examples are collected in Figure 5. Most of these complexes have been synthesized with the aim of studying the interaction between the two metal centres since the silicon retains these centres in close proximity. Limited rotational freedom in this class of compounds leads to preferred conformations in the solid and presumably also in solution. As portrayed in Figure 6, three conformations are possible: *exo*/*exo*, *exo*/*endo* and *endo*/*endo*.

X-ray crystal structure studies show only the *exo*/*exo* [M = $Fe(CO)_2I$[114]] and the *exo/endo* [M = $Mn(CO)_3$[113], $TiCl_3$[111]] conformations with some deviations from ideal geometry. These orientations allow the metals to achieve maximum separation. The activation energies for conformational changes depend on the steric bulk of the [M] unit. Reactions which result in the formation of metal−metal links by either M−M bonds or M−X−M bridges must involve transformation into the *endo*/*endo* conformation[111,117,118].

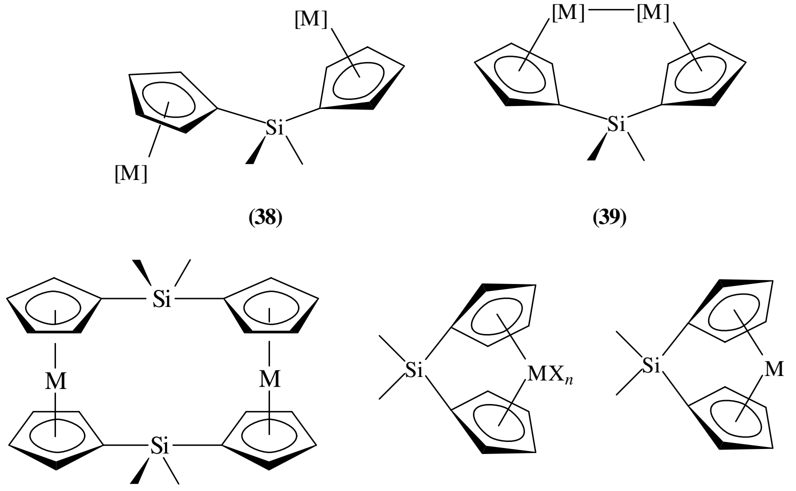

(38) **(39)**

(40) **(41)** **(42)**

SCHEME 14. Structure types of complexes with the ligand system **30**

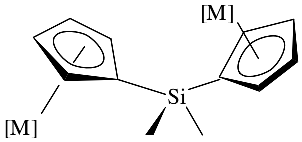

$[M] = Li^{102}, Tl^{111}, Co(CO)_2{}^{112}, Mn(CO)_3{}^{113}, Fe(CO)_2X^{114}, Mo(CO)_3X^{115}, TiCl_3{}^{111,116}, W(CO)_3X^{117}, ZrCl_3{}^{111}$

FIGURE 5. Metal complexes of type **38**

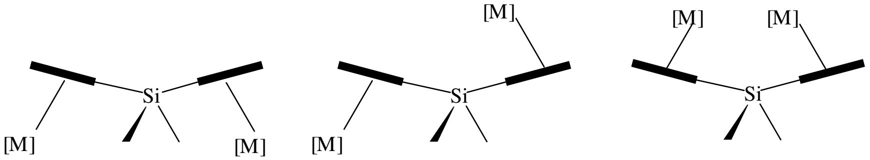

exo/exo *exo/endo* *endo/endo*

FIGURE 6. Conformations in complexes of type **38**

In general, the induced geometrical restrictions in compounds of type **38** modify the chemical behaviour to some extent in relation to the corresponding unbridged species.

Representative examples of dinuclear Me_2Si-bridged metal complexes belonging to type **39** in Scheme 14 are listed in Figure 7. The additional metal–metal bridge enforces the *endo/endo* orientation of the metal fragments and induces a pronounced stereochemical rigidity. As a consequence, noticeable changes in structure and reactivity compared with the unbridged species are observed[112,119,121]. Furthermore, cooperative interactions of the two neighbouring metal centres have to be considered[120–123], but it is still an open question whether the observed electronic effects are mediated by the bridging silicon atom.

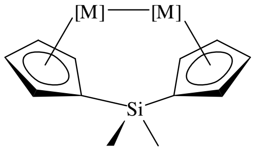

L = 2-electron donor

[M] − [M] = $Fe_2(CO)_2L_2$[112,119,123], $Cr_2(CO)_4L_2$[120], $Mo_2(CO)_4L_2$[121], $W_2(CO)_4L_2$[121,122]

FIGURE 7. Metal complexes of type **39**

Silicon-bridged [1,1]metallocenophanes of type **40** in Scheme 14 represent another class of dinuclear compounds with the ligand system **(30)**. The synthesis of the 1,1,12,12-tetramethyl [1,1] silaferrocenophane was reported by two groups only recently. In one procedure, the dilithium salt of dicyclopentadienyldimethylsilane was reacted with ferrous chloride to give a mixture of the metallocenophane with poly(ferrocenyldimethylsilane) (equation 55)[124]. In the other procedure, this compound was prepared in a multistep synthesis starting from dilithio ferrocene, as shown in equation 56[125]

$$Me_2Si(C_5H_4Li)_2 + FeCl_2 \longrightarrow [Me_2Si(H_4C_5)_2Fe]_2 + [Me_2Si(H_4C_5)_2Fe]_n \qquad (55)$$

$$(LiH_4C_5)_2Fe \xrightarrow{(a)} \{[(Et_2N)SiMe_2]H_4C_5\}_2Fe \xrightarrow{(b)} [(ClSiMe_2)H_4C_5]_2Fe$$

$$\xrightarrow{(c)} \{[(H_5C_5)SiMe_2]H_4C_5\}_2Fe \xrightarrow{(d)} [Me_2Si(H_4C_5)]_2Fe]_2 \qquad (56)$$

(a) $SiMe_2Cl(NEt_2)$;(b) MeCOCl; (c) LiC_5H_5; (d)1. BuLi; 2. $FeCl_2$

A single-crystal X-ray diffraction study revealed that the two ferrocene units are in *anti* conformation. Cyclic voltammetric results are in accord with a strong interaction between the iron centres. Electronic interactions through bonds are mediated by the bridging dimethylsilyl groups and this is discussed in more detail in Section II.E.3.

Bent metallocenes with bridging silicon of type **41** in Scheme 14 are known for many early d-block elements and also for many f-block elements (mainly actinides). Therefore, this class of compounds has been successfully utilized as catalysts or precatalysts in different types of reactions. The most prominent application is in the field of stereo- and enantio-selective polymerization of alkenes, which requires chiral catalysts. Chirality is introduced by a chiral auxiliary as cyclopentadienyl ring substituent, as bridging silicon substituent or by a chiral metal centre. The bridging silicon unit together with further substituents at the cyclopentadienyl rings introduces conformational constraints with respect to the coordination gap aperture angle and to the lateral coordination gap extension angle. Once again, the straightforward synthesis of silyl-substituted cyclopentadienyl compounds is the principal advantage. The interested reader is referred to recent original publications[126], review articles[41,127,128] and monographs[129].

There are very few examples of silicon-bridged bent-metallocenes of type **42** in Scheme 14 described in the literature. The class of silicon-bridged [1]-ferrocenophanes is most important due to the exceptional structure and reactivity, and representative examples **43–52** are listed in Scheme 15.

The first reported examples, $Fe(C_5H_4)_2SiPh_2$ **(47)** and the spiro compound $Si(H_4C_5FeC_5H_4)_2$ **(52)**[131], were synthesized by a classical procedure (see Section II) via the reaction of dilithioferrocene·TMEDA with diphenyldichlorosilane and tetrachlorosilane, respectively. The other members in this class were prepared analogously or via the reaction of ferrous chloride with the corresponding dilithiated bis(cyclopentadienyl)dimethylsilane[110,132–134].

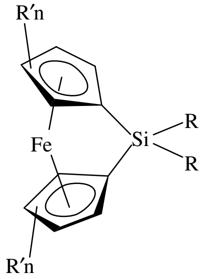

(43–51)

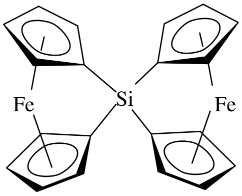

(52)[131]

Compound	**43**[130]	**44**[110]	**45**[110]	**46**[110]	**47**[131]	**48**[132]	**49**[133]	**50**[132]	**51**[134]
$\mathrm{Cp}^{R'_n}$	H_4C_5	H_3MeC_5	Me_4C_5	H_4C_5	H_4C_5	H_4C_5	H_4C_5	H_4C_5	H_4C_5
$\mathrm{Cp}^{R'_n}$	H_4C_5	H_3MeC_5	Me_4C_5	Me_4C_5	H_4C_5	H_4C_5	RH_3C_5	H_4C_5	H_4C_5
R	Me	Me	Me	Me	Ph	Ph	Cl	Cl	Me
R	Me	Me	Me	Me	Ph	Cl	Cl	Cl	Cl

R = $Me_2N(Me)HC$

SCHEME 15. Iron complexes of type **42**

X-ray diffraction studies of the compounds **43**–**45** and **47**–**49** revealed highly strained, ring-tilted structures. In Table 7, the strain is expressed by the tilt angle α between the cyclopentadienyl ring planes and by the averaged angle β between the cyclopentadienyl ring planes and the *ipso* (Cp)–Si bonds. With increasing ring methylation, the tilt angle α decreases and the corresponding angle β increases. A similar effect is observed when a methyl group at silicon is replaced by a phenyl group or a chlorine atom.

The strain in silicon-bridged [1]-ferrocenophanes has drastic consequences for the chemistry of such compounds, which is dominated by an easy silicon–(Cp)carbon bond cleavage. This bond fission is used for the thermal or transition-metal catalysed or the anionic ring-opening polymerization, which leads to the interesting class of poly(ferrocenylsilanes)[134], as shown in equation 57. Reaction of **43** with $Pt(PEt_3)_3$ yields a novel [2]-platinasilaferrocenophane (equation 58), representing the first example of the insertion of a transition metal into the strained Si–C bond[138]. The compound is of interest as a model of the proposed intermediate during the transition-metal catalysed polymerization process.

Derivatization of surfaces via the reaction of strained Si–C bonds also results in ring-opening reactions. Thus, the reaction of silaferrocenophanes like **49** with an electrode surface is a useful means of attaching a ferrocenyl group, as shown in equation 59[133]. In

TABLE 7. Distortions in ferrocenophanes defining the angles α and β

	Compound	**43**[137]	**44**[110]	**45**[110]	**47**[136]	**48**[132]	**49**[133]
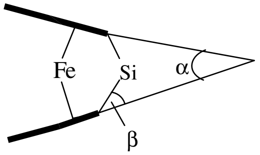	$\alpha(^\circ)$	20.8(5)	18.6(3)	16.1(3)	19.1(10)	19.0(2)	19.0(2)
	$\beta(^\circ)$	37.0(6)	39.1(2)	40.3(2)	40.0(9)	40.96(2)	40.96(2)

a similar procedure, compound **50** has been shown to derivatize n-type semiconducting silicon photoelectrodes, thus representing the first example of a photoelectroactive surface-attached species[132].

$$\mathbf{43} \xrightarrow[\substack{\text{(b) [M]}\\ \text{(c) LiR}}]{\text{(a) heat}} \left[\text{Me}_2\text{Si}(\text{H}_4\text{C}_5)\text{Fe}(\text{C}_5\text{H}_4)\right]_n \qquad (57)$$

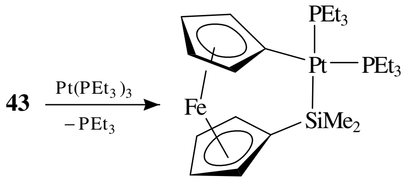

(58)

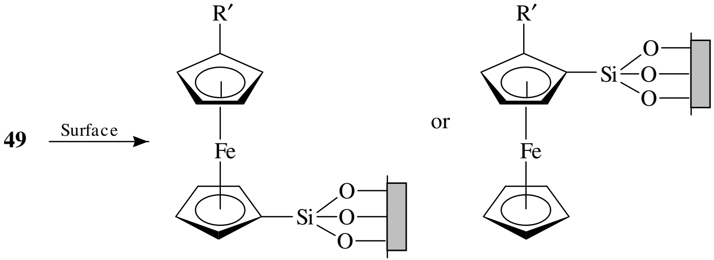

(59)

R′ = H, CHMeNMe$_2$

The easy silicon–(Cp)carbon bond cleavage in compounds of type **42** is also apparent from electrochemical studies, which have been performed with compound **43** and with ferrocenophanes having tetramethyldisilanyl and hexamethyltrisilanyl bridges. Cyclic voltammetric studies showed a marked dependency upon the oligosilyl bridge[135]. Complex **43** undergoes decomposition upon oxidation, while the complex with the disilanyl bridge exhibits partial reversibility. Finally, the complex with the trisilanyl bridge shows a completely reversible oxidation process. This trend reflects the differing capacity of the three bridges to incorporate the increase in Fe−Cp ring distance that is established to occur upon oxidation to ferrocenium ions.

2. Double-bridged cyclopentadienyl systems

Double-bridging of two cyclopentadienyl units inevitably reduces the conformational flexibility and allows the formation of rather rigid systems. These are excellently suited for assembling metal centres in a stereochemically well-defined manner, and therefore are attractive building blocks for many purposes. The most important ligand systems of this type, which contain the dimethylsilyl(dimethylsilandiyl), the tetramethyldisilanyl and the tetramethyldisiloxanyl bridges, are listed in Scheme 16.

All of these ligand systems have only recently been introduced in metal complex chemistry, and strategies for their synthesis are described below.

Two cyclopentadienyl units are bridged in 1,2 position by two dimethylsilyl groups in the ligand system **53**. The isomeric mixture of 4,4,8,8-tetramethyltetrahydro-4,8-disila-*s*-indacene[139−144] is the starting material for metal complexes of a different kind. Deprotonation of this compound and metallation with alkali metal compounds have been investigated in detail[142,143] (equation 60).

In the ligand system **54**, two cyclopentadienyl units are bridged asymmetrically in 1,2 positions by a dimethylsilyl and by a teramethyldisilanyl group, which imposes chirality

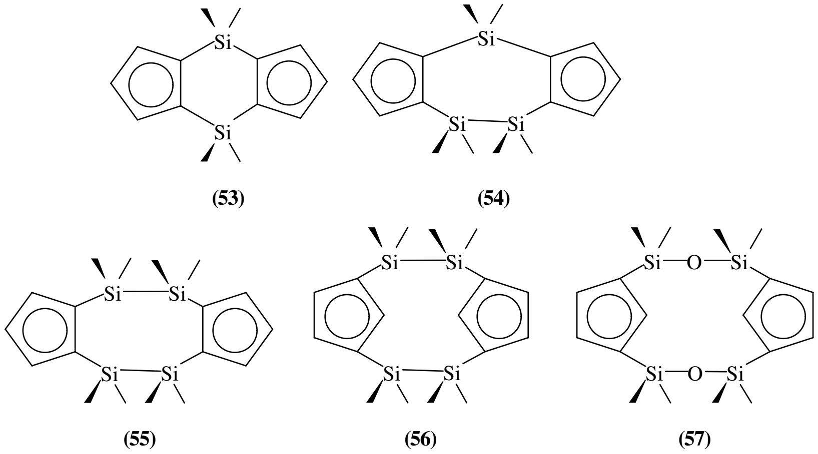

SCHEME 16. Double-bridged cyclopentadienyl systems

at the complexed metal centre[144]. As shown in equation 61, a silatropic shift in the protonated precursor is necessary to generate the desired ligand. Double-bridging with two tetramethyldisilanyl groups occurs in the ligand systems **55**, involving the 1,2 positions of the cyclopentadienyl fragments, and **56** involving the 1,3 positions. Interestingly, both ligand systems are generated from the same precursor molecule, as shown in equation 62[145]. Once more, silatropic shifts are necessary to create isomers which can be deprotonated. In the reaction with butyllithium, two different conformations of the ligand **55** can be generated; in the reaction with dicobalt octacarbonyl, the ligand **56** is formed[145]. Finally, a [3,3]-ferrocenophane containing the ligand system **57** in Scheme 16 is formed from a tetra(alkoxysilyl)ferrocene under hydrolytic conditions, as shown in equation 63[107].

In the following section, we will concentrate on the different kinds of metal complexes which can be derived from the ligand system **53**. The conformational freedom in **53** is restricted to a butterfly-like movement. Although the ligand is rather rigid, the fold angle between the two cyclopentadienyl planes may vary quite substantially, and therefore the ligand system can be adapted to the space-filling requirements of the respective metal fragments. Typical structures for complexes with ligand **53** are presented schematically in Scheme 17.

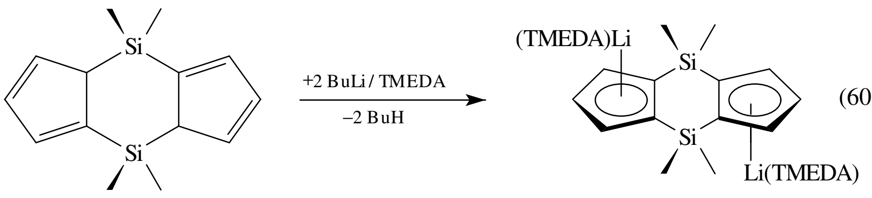

(60)

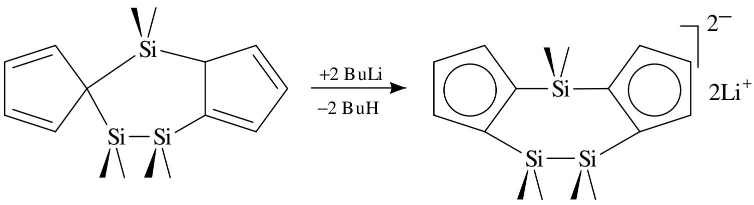

(61)

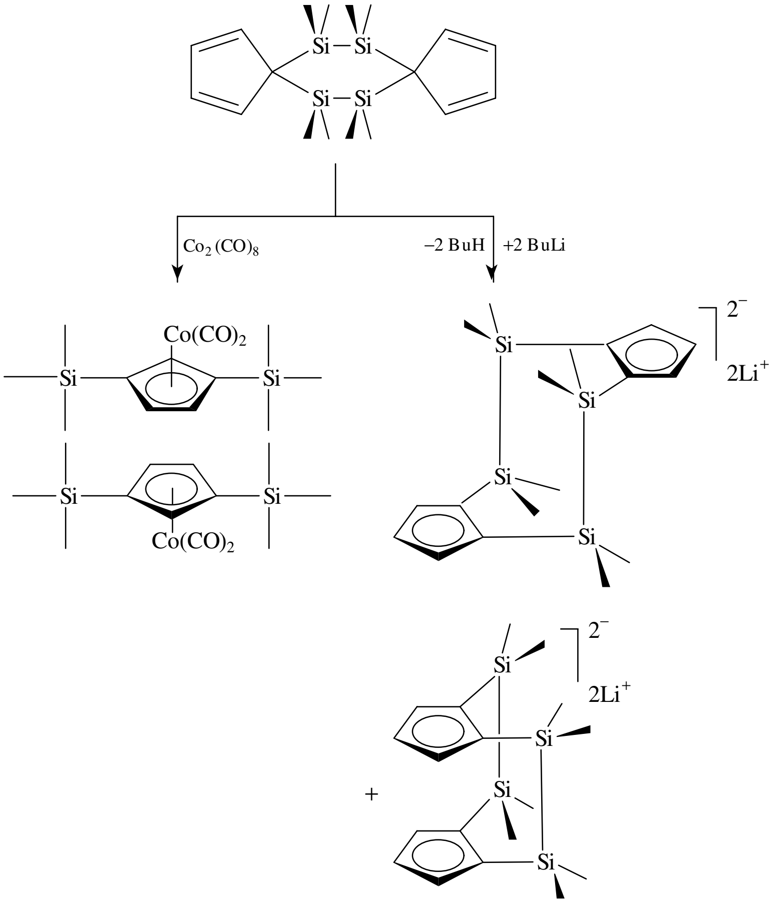

(62)

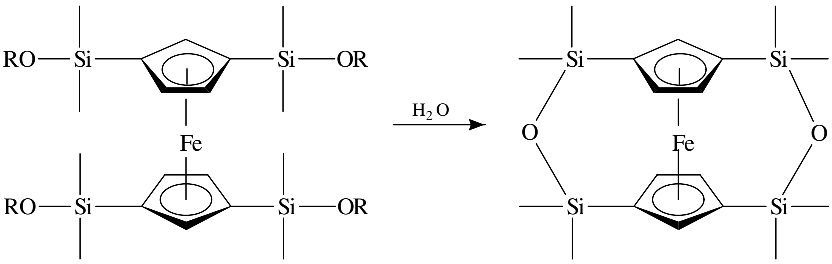

(63)

The comparatively smallest fold angles are found in the chelated bent-metallocenes of type **58**, which have been realized with the Group IV elements titanium[146], zirconium[146,147] and hafnium[146] as central atoms. In the X-ray crystal structure of $[H_3C_5(Me_2Si)_2C_5H_3]ZrCl_2$, the (Cp)C−Si−C(Cp) angles are nearly 92°, and the fold angle between the two cyclopentadienyl planes is 69.2°[147]. Comparable structural features

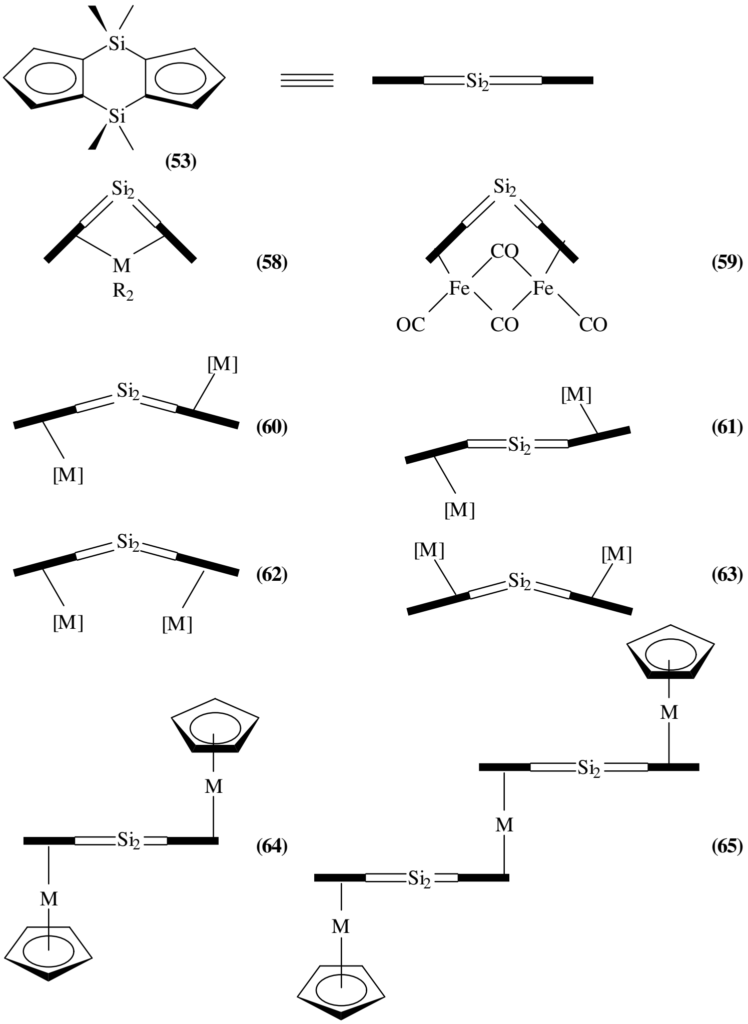

SCHEME 17. Structure types in complexes with ligand **53**

are found for the corresponding Cp-methylated species[148]. An even smaller fold angle of 64.4° is observed in the structure of $[H_3C_5(Me_2Si)_2C_5H_3]TiCl_2$[146]. Compounds of this class are interesting model substances in the catalytic olefin polymerization. In the dinuclear complex **59**[143], the steric constraints induced by the $Fe_2(CO)_4$ fragment are likely to impose a small fold angle, but X-ray crystal structure data for this compound are not available.

Several dinuclear metal complexes with the ligand system **53** as bridging unit are now known, where steric constraints are much less pronounced and where fold angles are much greater or nearly 180°. These complexes belong to the structure types **60**–**63**, where the metal fragments reside in *trans*-configuration, i.e. on different sides of the

π-ligand (types **60** and **61**), or in *cis*-configuration, i.e. on the same side of the ligand (types **62** and **63**). Differences in conformation are observed for the *trans*- as well as for the *cis*-configured compounds, at least in the solid state. In the *trans*-complexes, a conformation with a planar central Si_2C_4 ring (type **61**) is found beside the expected butterfly conformation (type **60**). In the *cis*-complexes, the metal fragments occupy either the convex (*exo/exo*; type **63**) or the concave surface (*endo/endo*; type **62**) of the bridging ligand. For steric grounds, the *endo/endo* fixation should be less favourable. Some homobimetallic complexes have been obtained as *cis* isomers, others as *trans* isomers, and others as *cis* and *trans* mixtures. The stereoselective formation of *cis* or *trans* complexes may depend on the synthetic route employed, as exemplified for the synthesis of the molybdenum complex $Cl(OC)_3MoC_5H_3(Me_2Si)_2H_3C_5Mo(CO)_3Cl$[149]: the *trans* complex belongs to (type **61**) with a planar central six-membered ring and a fold angle of 7.8° with the annelated cyclopentadienyl planes; the *cis*-complex belongs to type **62** with a fold angle of 21° (average value). In the titanium complex *trans*-$Cl_3TiC_5H_3(Me_2Si)_2H_3C_5TiCl_3$, the fold angle is 4(2)°[146] (type **61**), so that the bridging ligand is almost exactly planar. A similar disposition has been found for the complex *trans* -Li(tmeda)$C_5H_3(Me_2Si)_2H_3C_5$Li(tmeda)[142].

Detailed investigations have been performed with metallocene-type species **64** and **65** using the ligand **53** as a stereochemically well-defined building block. In compounds of class **64**, the following metal combinations have been realized: FeFe[143,150,151], RuRu[143], CrCr[152], NiNi[152], CoCo[152], VV[152] and FeNi[152]. In the compounds of class **65**, the following MM′M combinations are found: FeFeFe[151,153], FeVFe[154], FeCrFe[154], FeNiFe[154], CoCrCo[154], NiVNi[154], NiCrNi[154,155], NiCoNi[154] and NiFeNi[154]. Due to the special redox properties of metallocenes[32], interesting electronic properties are envisaged for such molecules. In polymetallocenes with diamagnetic and paramagnetic metal centres, appreciable spin density can be transferred. The role of silicon as a spacer and as a mediator for electronic effects is of special interest and will be discussed in more detail in Section II.E.3.

3. Cooperative effects in silicon-bridged ferrocenes

The bridging of two or more metallocene units is of great interest with regard to the potential for electronic interaction between the metal centres. Cooperative effects may be observed as the result of electronic transmission through the bridge or by direct metal–metal interaction[156]. New physical and chemical properties can be envisaged. In partially oxidized or reduced polymetallocenes, different kinds of mixed-valence behaviour are expected. The properties of such mixed-valence compounds will depend on the amount of delocalization, i.e. on the extent of interaction between the metallocene centres involved (class I,II or III according to Robin and Day[157]).

The special interest in silicon-bridged metallocene units stems from the observation that silicon atoms possess electronic transmission characteristics of unsaturated alkene or alkyne fragments[158–161].

In the class of metallocenes, ferrocene systems fulfill several prerequisites for the investigation of electronic effects[32,162]. Therefore, it is not surprising that ferrocenyl-substituted silicon compounds have been studied most extensively. We will concentrate on this class of compounds in the following discussion.

The development of processible high-molecular-weight polymers with skeletal transition metal atoms, as present in ferrocenes, represents a synthetic challenge, and a variety of materials with novel electrical, optical and magnetic properties can be expected[163]. In this context, polymers containing repeating ferrocenyl units are of great interest. Some representative examples are listed in Scheme 18.

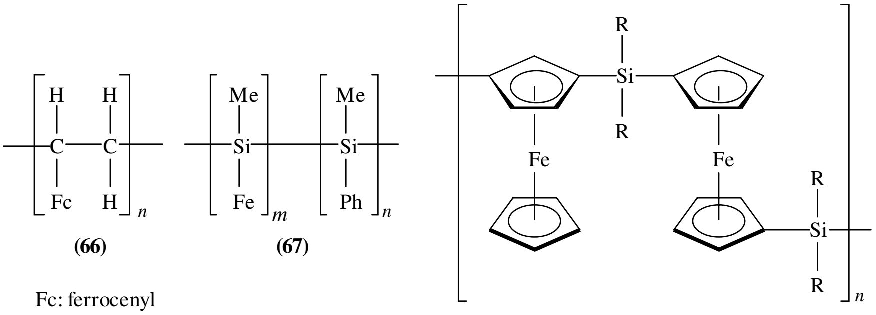

(66) **(67)** **(68)**

Fc: ferrocenyl

SCHEME 18. Polymers containing repeating ferrocenyl units

In polymers such as poly(vinylferrocene) **(66)**, the iron centres are essentially non-interacting, and a single reversible oxidation wave is detected by cyclic voltammetry. Similarly, the ferrocenyl(methyl)silane–phenyl(methyl)silane copolymers of type **67** exhibit reversible redox properties with no evidence for electronic interactions between the ferrocenyl units or between the pendant ferrocenyl groups and the polysilane chain segments[164,165]. In contrast, poly(ferrocenyl)silanes of type **68** show two reversible oxidation waves in their cyclic voltammograms; this phenomenon has been interpreted in terms of cooperative interactions between the iron centres[166–169]. The peak-to-peak separation $\Delta E_{1/2}$ [$\Delta E_{1/2} = E_{pa}(1) - E_{pa}(2)$] in the cyclovoltammograms, which gives an indication of the degree of interaction, has been found to vary with the side groups R at silicon, which indicates that the electronic effects are tunable[166].

The copolymers of type **67** exhibit the characteristic photochemical depolymerization noted for polysilanes, a source of their potential as photoresist materials. However, the presence of the ferrocenyl substituents results in a significant retardation of this depolymerization, presumably due to the ability of ferrocene to quench the triplet state responsible for the polysilane photochemistry[164]. Polymers of type **67** can be regarded as polysilanes with reversible redox behaviour.

In Scheme 19, a series of silicon-bridged diferrocenyl compounds is collected, together with the corresponding $\Delta E_{1/2}$ values. The $(SiMe_2)_n$ groups ($n = 1$–6) in the compounds **72–75** serve as single bridging units; in compound **71**, the $SiMe_2$-groups are double bridging (ligand system **53**). The diferrocenyl compounds **69** and **70** with directly C—C connected cyclopentadienyl fragments are presented for comparison.

Most of these compounds exhibit two discrete reversible oxidations. The greatest separation between the oxidation potentials, and thus presumably the most pronounced interaction, is observed for the directly linked ferrocenyl units in compounds **69**[169] and **70**[170], with the highest degree of cooperation in the rigid and coplanar dicyclopentadienyl system in **69**. The conformationally rather rigid double-bridged complex **71**[151] offers the best possibilities for electronic interaction within the silicon-bridged species, which becomes progressively smaller in the sequence **72** > **73** > **74**[171]. For compounds of type **75**, only a single oxidation process is observed, which excludes any electronic interaction[171]. In comparison with the analogous carbon-bridged diferrocenyl compounds, $Fc(CH_2)_nFe$ (Fc = ferrocenyl), the silicon-bridged species clearly turn out to be superior for the mediation of electronic effects[171,172].

A series of [*n*,*n*]-ferrocenophanes is listed in Scheme 20 together with their $\Delta E_{1/2}$ values. The introduction of a second bridge enforces the *cis*-configuration and a comparatively shorter Fe—Fe distance. Thus, the geometrical restrictions enhance the possibility

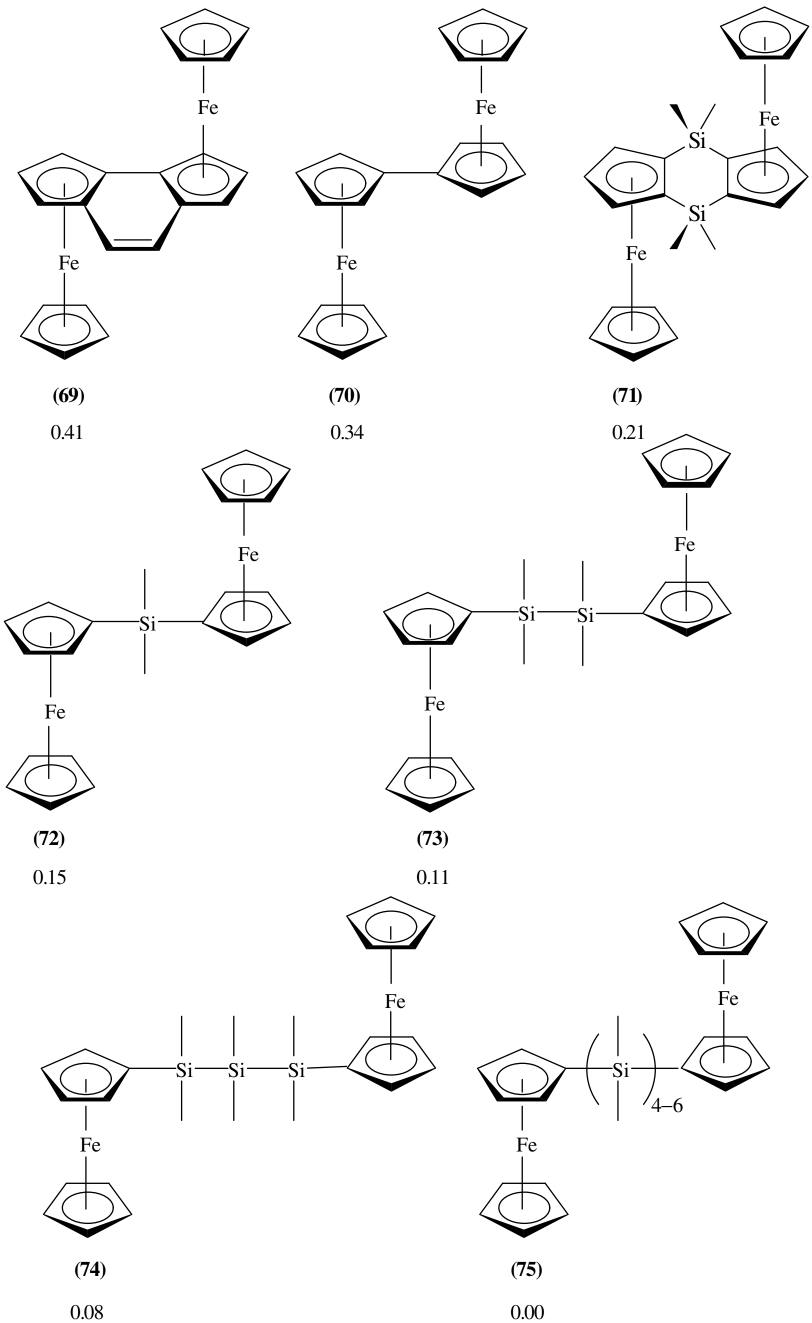

(69) 0.41

(70) 0.34

(71) 0.21

(72) 0.15

(73) 0.11

(74) 0.08

(75) 0.00

SCHEME 19. Representative bridged diferrocenyl compounds and their $\Delta E_{1/2}$ (V) values

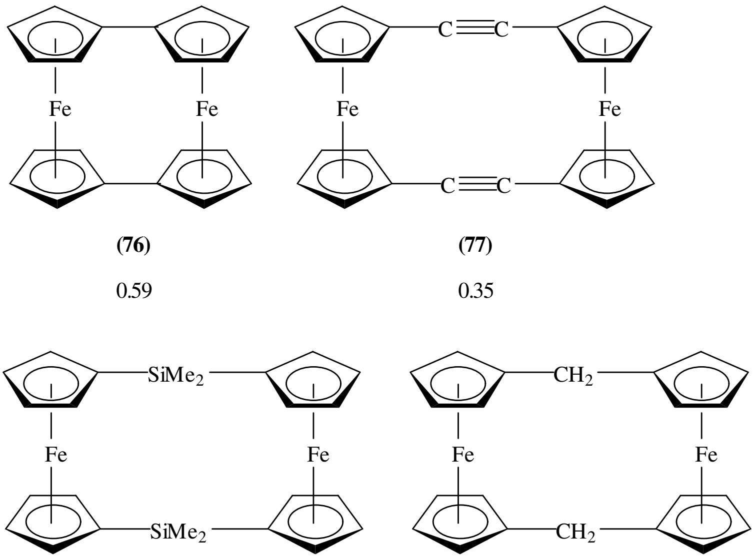

(76) 0.59

(77) 0.35

(78) 0.25

(79) 0.20

SCHEME 20. Representative $[n,n]$-ferrocenophanes and their $\Delta E_{1/2}$ (V)values

for cooperative effects by both through-bond and through-space interactions. It is interesting to compare the effect of different bridging situations on the extent of electronic interaction.

Very strong interactions have been observed for biferrocenylene (bisfulvalenediiron) **(76)** with directly linked cyclopentadienyl units and also for the bis(alkynyl)-bridged species **(77)**; the monocations of these compounds are fully delocalized on all spectroscopic time scales[172,173] (class III according to Robin and Day[157]). On the basis of the measured $\Delta E_{1/2}$ values, the two dimethylsilyl bridges in **78**[124,125] mediate electron delocalization better than the two methylene bridges in **79**[174].

Substantial differences in the electrochemical behaviour have been observed for triferrocenes bridged by methylene (compound **80**) and by dimethylsilyl (compound **81**) units (Scheme 21). Cyclic voltammetry experiments reveal that **80** exhibits three reversible redox processes[175], whereas for **81** only two redox events are observed[176]. The three reversible waves in the carbon-bridged ferrocene **(80)** are in the ratio 1 : 1 : 1 and can be assigned to successive redox events at each iron center, as described in Scheme 21. The two reversible waves in the silicon-bridged ferrocene **(81)** are in the ratio 2 : 1 and are consistent with oxidation of alternate ferrocene units, with subsequent oxidation of the intervening iron site (see Scheme 21).

Comparable effects have been described for silicon-bridged species with up to eight ferrocenyl units[176] and also for poly(ferrocenylsilanes) of type **68**[163]. The difference in the electrochemical behaviour of carbon and silicon substituted multiferrocenes may be explained by the different electron donating or withdrawing effects exerted by these substituents on a ferrocene unit. The phenomena described show that a proper choice of the bridges allows one to determine whether a molecule with three or more ferrocenyl units is first oxidized in the center or at the periphery[151].

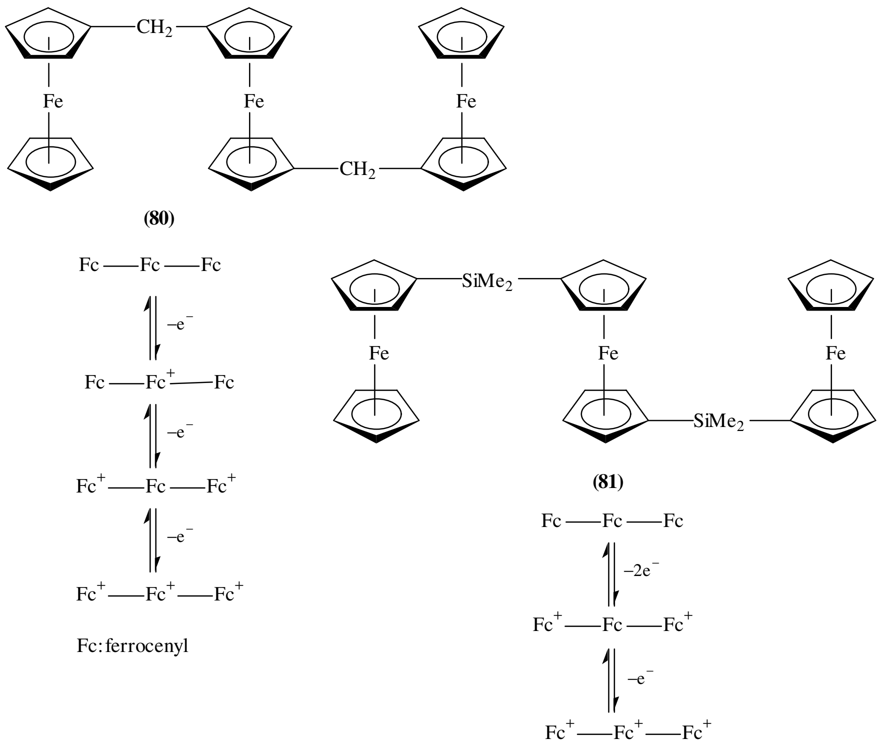

SCHEME 21. Carbon- or silicon-bridged triferrocenes and their redox behaviour

III. COMPOUNDS CONTAINING CYCLOPENTADIENYL–SILICON π-BONDS

A. Introduction

The area of metallocene chemistry started in 1952 with the successful synthesis of ferrocene[177], $Fe(C_5H_5)_2$, and with the description of a new type of bonding in this sandwich-like compound[178,179].

Only a short time after the discovery of ferrocene, plumbocene, $Pb(C_5H_5)_2$[180] was the first Group 14 sandwich compound to be synthesized. There are now many derivatives of Group 14 metallocenes reported[6], including decamethylsilicocene, $Si(C_5Me_5)_2$ **(82)**, the first stable π-complex with divalent silicon as central atom[181,182]. The characterization of this compound and of other less stable silicon species with π-bonded cyclopentadienyl ligands is described below.

B. Decamethylsilicocene

1. Synthesis, structure and bonding

Reaction of dichloro(pentamethylcyclopentadienyl)silane with lithium, sodium or potassium naphthalenide gives a mixture of elemental silicon, the corresponding alkali metal pentamethylcyclopentadienide and decamethylsilicocene **(82)** (equation 64)[181]. Compound **82** is formed as the only product in the reduction of dibromobis(pentamethylcyclopentadienyl)silane with potassium anthracenide (equation 65)[182].

The complex is stable in air for a short time, but is sensitive to hydrolysis; it melts at 171 °C without decomposition. From equations 64 and 65 it can be assumed that **82** is reduced by alkali metal naphthalenides, but not by potassium anthracenide, and this assumption was proved in separate experiments[182].

$$(Me_5C_5)_2SiCl_2 \xrightarrow[-MCl,\ -MC_5Me_5,\ -Si,\ -C_{10}H_8]{+MC_{10}H_8} \underset{\textbf{(82)}}{(Me_5C_5)_2Si} \qquad (64)$$

$$(Me_5C_5)_2SiBr_2 + 2KC_{14}H_{10} \longrightarrow \underset{\textbf{(82)}}{(Me_5C_5)_2Si} + 2KBr + 2C_{14}H_{10} \qquad (65)$$

The X-ray crystal structure analysis of **82** surprisingly revealed two conformers, one with a parallel **(82a)** and the other with a bent **(82b)** arrangement (interplane angle: 25°) of the pentamethylcyclopentadienyl rings (see Figure 8). Molecular models indicate that the interplane angle in **82b** is the largest possible value. Both exhibit rather long silicon–carbon bond distances (**82a**, 2.42 Å; **82b** 2.32–2.54 Å) (see also Scheme 22). The solid-state (CP-MAS) ^{29}Si NMR spectrum of **82** reflects the gross structural features determinded in the X-ray analysis[183]. The ^{29}Si nuclear shielding in **82a** is found to be 20.2 ppm higher than that of the bent structure in **82b**, which is close to that found for **82** in solution[182]. The high-field chemical shift for **82** (−398 ppm in solution) is exceptional for an organosilicon compound, but corresponds to the observed shift for decamethylstannocene and for decamethylplumbocene in the ^{119}Sn- and in the ^{207}Pb-NMR spectrum[182], respectively.

Extensive calculations have been performed for the parent silicocene, Si(C_5H_5)$_2$, some of them probably at insufficient levels of theory. At the SCF DZP level[184], silicocene is predicted to adopt a bent C_s structure. However, the difference in energy between the low-symmetry (C_s, C_2) and C_{2v} conformers is only 2.4 kcal mol^{-1}, with the D_{5d} conformer lying 8.8 kcal mol^{-1} higher in energy. The d-polarization function indicates that d-orbitals play no significant role in the π-bonding[184]. It is evident from all calculations that the silicocene potential energy surface is flat with respect to the interconversion between several conformers and there is a low-energy barrier for the rotation of the

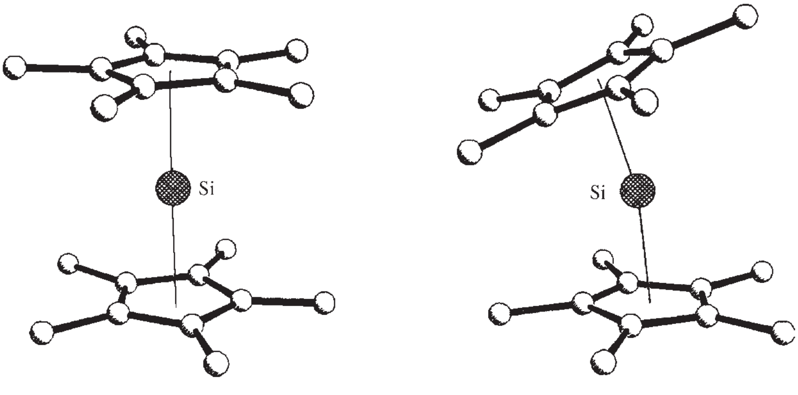

(82a) **(82b)**

FIGURE 8. Molecular structure of decamethylsilicocene (**82**), reproduced by permission of VCH Verlagsgesellschaft, Weinheim, from Ref. 181

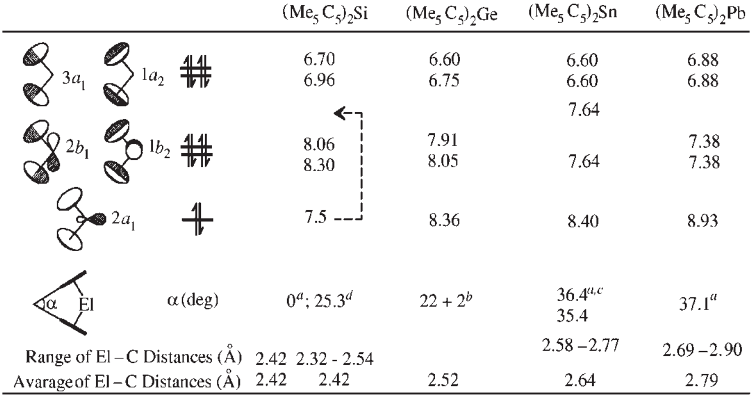

SCHEME 22. MO-Scheme[e]), PES data (eV), and structural parameters of the Group 14-decamethylmetallocenes [a]X-ray; [b]gED; [c]two independent molecules; [d]two conformers in the unit cell; [e]in orbital notation for C_{2v} symmetry

cyclopentadienyl rings. The total electron population of the silicon center is calculated to be 13.5, in agreement with weak π-interactions and explaining the rather long Si–C distances observed for **82**[16].

In Scheme 22, a qualitative molecular orbital scheme is presented for the highest occupied orbitals in the Group 14 (El) metallocenes, and the vertical ionization energies from the PE spectra of decamethylsilicocene[182], -germanocene[185], -stannocene[185], and -plumbocene[182] are presented and assigned in the context of Koopmans' theorem. In addition, some structural parameters of these metallocenes are given (interplane angle α, El–C distances)[6].

The following conclusions can be drawn from the MO scheme and the PE data:

(I) The HOMOs in all metallocenes are non-bonding with respect to cyclopentadienyl–metal interactions, as indicated by the first ionization energies which essentially remain constant.

(II) The $2b_1$ and $1b_2$ type orbitals provide the strongest contributions to cyclopentadienyl–metal bonding, and the respective ionization energies depend strongly on the metal involved.

(III) The orbital representing the 'lone-pair' at the Group 14 element is rather low in energy in the case of the germanium, tin and lead compound, but is higher in energy and in the region of the frontier orbitals in the case of the silicon compound. These differences in energy have implications concerning the chemistry of the Group 14 metallocenes.

(IV) The observed bathochromic shift in the electronic absorption spectra (**82**: colorless; Cp^*_2Ge: light yellow; Cp^*_2Sn: orange; Cp^*_2Pb: red) can be correlated with the lowering in energy of the respective LUMO, which can be described as the antibonding linear combination between the ligand π-MOs and the p orbitals at the relevant central atom[182].

Cyclovoltammetric data show that **82** cannot be reduced in the region available (up to −1.7 V versus SCE)[182], consistent with the chemical behaviour of **82** in reduction processes, as shown in equations 64 and 65. An irreversible oxidation process takes place at +0.4 V versus SCE. Presumably, the radical cation of **82** is unstable due to the easy loss of the pentamethylcyclopentadienyl radical[186,187]. The mass-spectrometric observations support this assumption: The molecular ion cannot be observed in EI as well as in CI studies, and the fragment with the highest mass corresponds to the $Me_5C_5Si^+$ ion. It is evident from these studies that the $(Me_5C_5)_2Si^+$ radical ion, which has its positive charge exclusively delocalized within the π-system of the pentamethylcyclopentadienyl ligands, is rather unstable in solution and in the gas phase, and easily loses a Me_5C_5 radical[182].

2. Chemistry of decamethylsilicocene

Decamethylsilicocene **(82)** can be regarded as an electron-rich silicon(II) compound containing a hypercoordinated silicon atom. The chemistry of **82** is determined by (a) the nucleophilicity of the silicon lone-pair (σ-donor function towards electrophiles, oxidative–addition processes) and (b) the weakness of the silicon–(cyclopentadienyl)carbon π-bond (η^5–η^1 rearrangement, Si–C bond cleavage). In the following section, the chemistry of **82** will be illustrated with some typical examples.

Reductive dehalogenation of substrates with geminal or vicinal halogen ligands can be performed under very mild conditions (equations 66–68[188]). Thus, organic dibromides with the halogen atoms in vicinal position are transferred to the corresponding alkene derivatives (equation 66), and the 1,2-bis(pentamethylcyclopenadienyl)-1,2-diiodo-diphosphane is converted to the corresponding diphosphene (equation 67). Finally, decamethylstannocene is formed from the tin(IV) compound bis(pentamethylcyclopentadienyl)dichlorostannane in the reaction with **82** (equation 68).

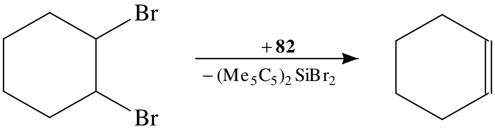

(66)

$$Me_5C_5(I)P{-}P(I)C_5Me_5 \xrightarrow[-(Me_5C_5)_2SiI_2]{+\mathbf{82}} Me_5C_5P{=}PC_5Me_5 \tag{67}$$

$$(Me_5C_5)_2SnCl_2 \xrightarrow[-(Me_5C_5)_2SiCl_2]{+\mathbf{82}} (Me_5C_5)_2Sn \tag{68}$$

As expected for a nucleophilic silicon(II) compound, **82** does not react with triethylsilane, but with the electrophilic trichlorosilane to form the corresponding unsymmetrical disilane (equation 69)[189]. Other polar and non-polar substrates react in a similar fashion to give the corresponding oxidative addition products (equations 69[188] and 70)[190].

$$\underset{\mathbf{(82)}}{(Me_5C_5)_2Si} + RX \longrightarrow (Me_5C_5)_2Si(R)X \tag{69}$$

$$RX = HSiCl_3, MeBr, MeI, Me_3SiCN, BrCN$$

$$\underset{\mathbf{(82)}}{(Me_5C_5)_2Si + X_2} \longrightarrow (Me_5C_5)_2SiX_2 \tag{70}$$

$$X_2 = Br_2, I_2, RSSR$$

The reaction of **82** with protic substrates HX can follow different pathways, as depicted in Scheme 23. In most of the cases studied so far, simple oxidative addition takes place leading to compounds of the type $(Me_5C_5)_2Si(H)X$[190]. The reaction of **82** with tetrafluoroboric acid leads to elimination of pentamethylcyclopentadiene and to the formation of a cyclotetrasilane derivative, via several intermediates with divalent silicon from which the dimeric pentamethylcyclopentadienyl(fluoro)silylene was proved by Si NMR spectroscopy[191,192]. In contrast, an HF-oxidation product is formed in the reaction of **82** with the pyridinium salt of HBF_4[189]. The influence of the acidity of the relevant protic substrates on the final reaction products is further demonstrated by the reaction of **82** with two equivalents of trifluoromethanesulfonic acid giving an ionic species containing the bis(pentamethylcyclopentadienyl)hydridosilicon cation[193] and with its pyridinium salt giving the oxidative addition product[189].

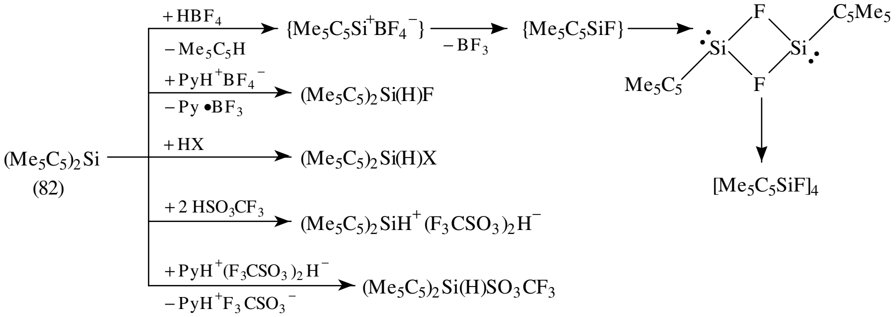

$HX = HF, HCl, HBr, EtCO_2H, F_3CCO_2H, F_3CSO_3H, C_6H_5OH, p\text{-}MeC_6H_4SH, R_2C{=}NOH$

SCHEME 23. Reaction of $(Me_5C_5)_2Si$ (**82**) with protic substrates

Differences in the reactivity of **82** and its heavier homologues towards protic substrates become evident also from the reaction with catechol: Whereas oxidation addition and subsequent H_2-elimination is observed with **82**, a substitution process takes place with decamethylstannocene (equations 71 and 72)[190]. **82** undergoes an oxidative addition with compounds formally delivering 6-electron species, giving intermediates of the type $(Me_5C_5)_2Si{=}X$ with a silicon element (p-p)π-bond. These species are highly reactive under the reaction conditions (equation 73). Substrates like trimethylamine oxide and carbon dioxide can be used as a source of oxygen[194,195], and elemental sulphur[194], organic isothiocyanates[195] and carbon oxosulphide[195] can function as a source of sulphur. Intermediates were not detected in the reaction with tri-*n*-butylphosphane telluride, and the final product is a tritelluradisilole derivative (equation 74)[194].

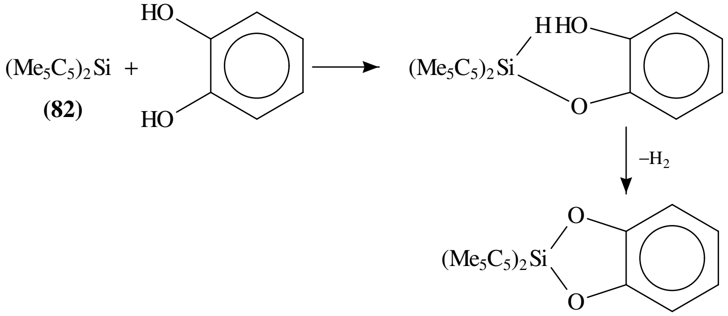

(71)

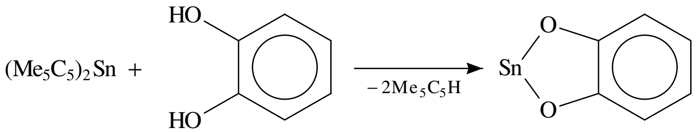

(72)

$$\underset{\textbf{(82)}}{(Me_5C_5)_2Si} + X \longrightarrow \{(Me_5C_5)_2Si = X\} \longrightarrow\longrightarrow \text{product} \qquad (73)$$

X : O from CO_2, Me_3NO; S from S_8, COS, RNCS; Se from n-$Bu_3P{=}Se$

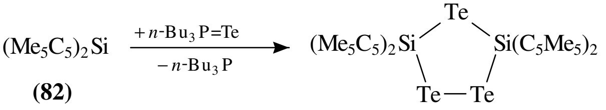

(74)

Several kinds of cycloaddition products have been observed in the reaction of **82** with various activated double and triple bond species. A simple 2:1 cycloaddition takes place in the reaction of **82** with alkynes possessing electron-withdrawing substituents (equation 75)[199]. In contrast, five-membered silaheterocycles are formed regio- and stereospecifically in multi-step reactions with certain organic carbonyl[196] (equation 76) and nitrile compounds (equation 77)[197]. The observed C−C bond formation, which generally takes place under mild reaction conditions, might be of synthetic value.

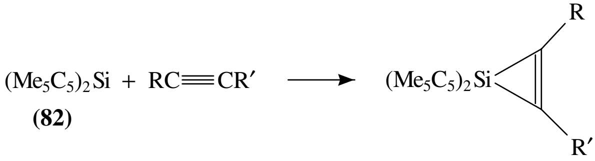

(75)

$RC{\equiv}CR'$: $MeO_2CC{\equiv}CCO_2Me$; $Me_3SiC{\equiv}CSO_2Ph$

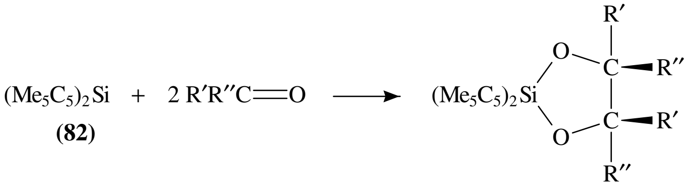

(76)

$R'R''CO$: $C_6H_5C(H)O$; $C_6H_5CH{=}CHC(H)O$; Me_2CO

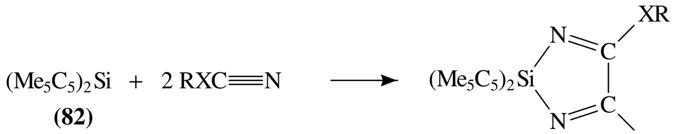

(77)

$RXC{\equiv}N$: ArOCN, MeSCN, Me_2NCN

The weakness of the Si−C(cyclopentadienyl) bond in **82** and its derivatives becomes apparent in several reactions. This phenomenon (see Section II.C) sometimes leads to complicated cyclopentadienyl migration processes as well as to the elimination of cyclopentadienyl fragments. For example, the formation of pentamethylcyclopentadiene has been observed in the stoichiometric reactions of **82** with tetrafluoroboric acid (see Scheme 23) and with pentacarbonyl(hydrido)manganese (equation 78)[189]. Dyotropic rearrangements are presumably the basis for the observed cyclopentadienyl group transfer from silicon to other elements. Thus, a multi-step reaction of **82** with boron trihalides leads to the final products with halogen substituents at silicon and a pentamethylcyclopentadienyl group at boron (equation 79)[188]. Reaction of **82** with carbon disulphide (equation 80)[195] involves a surprising reaction sequence including the exchange of two cyclopentadienyl and two sulphur ligands.

$$\underset{\textbf{(82)}}{(Me_5C_5)_2Si} + 2HMn(CO)_5 \longrightarrow Me_5C_5(H)Si[Mn(CO)_5]_2 + Me_5C_5H \qquad (78)$$

$$\underset{\textbf{(82)}}{(Me_5C_5)_2Si} + BHal_3 \longrightarrow Me_5C_5(Hal)_2Si - B(Hal)C_5Me_5 \qquad (79)$$

Hal : Cl, Br, I

$$\underset{\textbf{(82)}}{2(Me_5C_5)_2Si} + 2\,CS_2 \longrightarrow$$

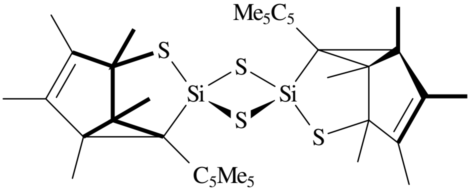

(80)

The formal oxidation state of silicon changes from +II to +IV in nearly all of the reactions with decamethylsilicocene **(82)** described so far, and the hapticity of the cyclopentadienyl ligand changes from η^5 to η^1. The latter phenomenon raises the question about the possibility of a haptotropic shift in the ground state molecule, which should lead to quite different silicon species in equilibrium, as shown in equation 81.

$$\underset{\textbf{(82)}}{(\eta5\text{-}Me_5C_5)_2Si} \rightleftharpoons \underset{\textbf{(83)}}{(\eta1\text{-}Me_5C_5)_2Si} \qquad (81)$$

Variable-temperature NMR studies give no evidence for such an equilibrium[189], but cannot exclude the presence of small quantities of the classical silylene (η^1-$Me_5C_5)_2Si$ **(83)**. Recent experiments performed with decamethylsilicocene in cryosolutions and accompanying theoretical studies indicate the presence of small quantities of isomer **83** in equilibrium. In liquid xenon (LXe), the formation of the monocarbonyl complex $(Me_5C_5)_2Si(CO)$ and of the mono(dinitrogen) complex $(Me_5C_5)_2Si(N_2)$ has been proven by IR spectroscopic studies (equations 82 and 83)[198]. The reactions were found to be incomplete under a few bar of CO or N_2 and reversible when the pressure was released. From the spectroscopic studies it was concluded that less than one percent of the complex is formed under the reaction conditions. *Ab initio* calculations[199] show that an equilibrium as shown in equation 81 is the first step before CO or N_2 form adducts.

$$\underset{\textbf{(82)}}{(Me_5C_5)_2Si} \xrightarrow[\text{1.5 bar CO}]{\text{LXe/253 K}} (Me_5C_5)_2Si(CO) \qquad (82)$$

$$\underset{\textbf{(82)}}{(Me_5C_5)_2Si} \xrightarrow[\text{20 bar } N_2]{\text{LXe/173 K}} (Me_5C_5)_2Si(N_2) \qquad (83)$$

C. Other π-Complexes

During the course of the investigation of the chemistry of decamethylsilicocene **(82)**, few experiments gave evidence for the formation of compounds in which the π-bonding between silicon and the cyclopentadienyl ligand remained intact. These compounds will be presented shortly. As already described (see Section III.B.2; Scheme 23), reaction of **82** with one equivalent of a protic substrate HX does not lead to $(Me_5C_5)_2SiH^+X^-$ containing a silyl cation, in which silicon is bonded to hydrogen and to two π-pentamethylcyclopentadienyl ligands. This cation was, however, unexpectedly formed as one component in the multi-step reaction of **82** with catechol and with catechol derivatives[200], and is most likely also generated by the reaction of **82** with two equivalents of trifluoromethanesulphonic acid[200] (Scheme 23). The structure was inferred from the ^{29}Si NMR spectrum, showing a shift at δ -12.1, which represents a deshielding of 386 ppm compared with that of **82**. The observed ^{29}Si−H coupling constant of 302 Hz is consistent with involvement of an sp^2-type orbital at silicon. The cation $(Me_5C_5)_2SiH^+$ was proposed to have a structure with η^2/η^3-bound cyclopentadienyl ligands, whereby the π-ligands undergo rapid haptotropic rearrangements.

The nucleophilic character of **82** has stimulated experiments to use this compound as a silylene-type ligand in transition-metal chemistry but with only one useful result[189], presumably due to the steric restrictions imposed by the bulky pentamethylcyclopentadienyl ligands. Reaction of **82** with carbonylgold(I) chloride led to the formation of [bis(pentamethylcyclopentadienyl)silanediyl]gold chloride, $(Me_5C_5)_2SiAuCl$. The structure was established by temperature-dependent ^{1}H NMR studies, which indicate that one of the Cp ligands is bound in a σ-fashion and the other is bound in a π-fashion, but the exact hapticity of the π-bonded ligand could not be determined[201].

Half-sandwich complexes of the type $Me_5C_5El^+X^-$ with El = Ge, Sn and Pb are stable under standard conditions and have been well characterized. However, the corresponding silicon derivatives have only been identified by mass spectrometry. An environment of very low basicity and nucleophilicity will be necessary in order to further stabilize compounds of this type.

In general, the extensive series of metallocene derivatives that are known for the heavier elements of Group 14 have not been readily extrapolated to silicon chemistry. It is intriguing that in spite of a huge effort in this area over many years, decamethylsilicocene remains the only derivative that has been comprehensively characterized, and the challenges with this chemistry are still numerous.

IV. ACKNOWLEDGEMENTS

The indispensable and stimulating contributions of the coworkers mentioned in the references are very gratefully acknowledged. The author wishes to thank Mrs.B. Neumann for preparing the drawings, Mrs. H. Niermann for typing the manuscript and Prof. N. Burford (Dalhousie University, Halifax, Canada) for helpful comments and for improving the English. Finally, financial support of our work by the Deutsche Forschungsgemeinschaft, the Fonds der Chemischen Industrie and the University of Bielefeld is gratefully acknowledged.

V. REFERENCES

1. E. W. Abel, M. O. Dunster and A. Waters, *J.Organomet. Chem.*, **49**, 287 (1973).
2. S. Patai and Z. Rappoport (Eds.), *The Chemistry of Organic Silicon Compounds*, Wiley, New York, 1989.
3. D. A. Armitage, *'Organosilanes'*, in *Comprehensive Organometallic Chemistry*, Vol. 2 (Eds. G. Wilkinson, F. G. A. Stone and E. W. Abel), Pergamon Press, Oxford−New York, 1982.
4. I. Fleming, *'Organic Silicon Chemistry'*, in *Comprehensive Organic Chemistry*, Vol. 3 (Eds. D. Barton and W. D. Ollis), Pergamon Press, Oxford−New York, 1979.
5. P. Jutzi, *Chem. Rev.*, **86**, 983 (1986).

6. P. Jutzi, *Adv. Organomet. Chem.*, **26**, 217 (1986).
7. J. E. Bentham and D. W. H. Rankin, *J. Organomet. Chem.*, **30**, C54 (1971).
8. G. A. Shchembelov and Yu. A. Ustynyuk, *Dokl. Akad. Nauk SSSR*, **173**, 847 (1967); *Engl. Transl.*, **173**, 847 (1967).
9. A. F. Cuthbertson and C. Glidewell, *J. Organomet. Chem.*, **221**, 19 (1981).
10. A. H. Cowley, E. A. V. Ebsworth, S. K. Mehrotra, D. W. H. Rankin and M. D. Walkinshaw, *J. Chem. Soc., Chem. Commun.*, 1099 (1982).
11. P. Jutzi, D. Kanne, M. B. Hursthouse and A. J. Haves, *Chem. Ber.*, **121**, 1299 (1988).
12. S. S. Al-Inaid, C. Eaborn, P. P. Hitchcock. P. Lickiss, A. Möhrke and P. Jutzi, *J. Organomet. Chem.*, **384**, 33 (1990).
13. S. Cradock, R. H. Findlay and M. H. Palmer, *J. Chem. Soc., Dalton Trans.*, 1650 (1974).
14. S. Cradock, E. A. V. Ebsworth, H. Moretto and D. W. H. Rankin, *J. Chem. Soc., Dalton Trans.*, 390 (1975).
15. H. Bock and W. Kaim, *J. Am. Chem. Soc.*, **102**, 4429 (1980).
16. H. Bock, *Angew. Chem.*, **101**, 1659 (1989); *Angew. Chem., Int. Ed. Engl.*, **28**, 1627 (1989).
17. H. P. Fritz and C. G. Kreiter, *J. Organomet. Chem.*, **4**, 313 (1965).
18. Y. A. Ustynyuk, A. V. Kisin and D. W. Oksinoid, *Zh. Obshch Khim.*, **38**, 391 (1968); *Chem Abstr.*, **69**, 76368w (1969).
19. A. Bonny, R. D. Holmes-Smith, G. Hunter and S. R. Stobart, *J. Am. Chem. Soc.*, **104**, 1855 (1982).
20. Yu. A. Ustynyuk, A. V. Kisin, J. M. Pribytkova, A. A. Zarkin and N. D. Antonova, *J. Organometal. Chem*, **42**, 47 (1972).
21. R. Krallmann, Ph. D. Thesis, University of Bielefeld, 1991.
22. P. Jutzi and J. Sauer, *J. Organomet. Chem.*, **50**, C29 (1973).
23. W. Kläui and H. Werner, *Helv. Chim. Acta*, **59**, 844 (1978).
24. J. Okuda, *Chem. Ber.*, **122**, 1075 (1989).
25. H. Chen. P. Jutzi, W. Leffers, M. M. Olmstead and P. P. Power, *Organometallics*, **10**, 1282 (1991).
26. W. J. Evans, T. J. Boyle and J. W. Ziller, *Organometallics*, **11**, 3903 (1992).
27. P. Jutzi, W. Leffers, B. Hampel, S. Pohl and W. Saak, *Angew. Chem.*, **99**, 563 (1987); *Angew. Chem., Int. Ed. Engl.*, **26**, 583 (1987).
28. C. P. Casey, J. M. O'Connor and K. J. Haller, *J. Am. Chem. Soc.*, **107**, 1241 (1985).
29. W. S. Sheldrick, 'Structural Chemistry of Organic Silicon Compounds', in *The Chemistry of Organic Silicon Compounds* (Eds. S. Patai and Z. Rappoport), Wiley, New York, 1989.
30. J. Okuda and E. Herdtweck, *J. Organomet. Chem.*, **373**, 99 (1989).
31. J. Okuda, R. W. Albach, E. Herdtweck and F. E. Wagner, *Polyhedron*, **10**, 1741 (1991).
32. D. Astruc, (Ed.) *Electron Transfer and Radical Processes in Transition-Metal Chemistry*, VCH Publ., Weinheim, 1995.
33. U. Koelle and F. Khouzami, *Angew. Chem.*, **92**, 658 (1980); *Angew. Chem., Int. Ed. Engl.*, **19**, 640 (1980); J. L. Robbins, N. Edelstein, B. Spencer and J. C. Smart, *J. Am. Chem. Soc.*, **104**, 1882 (1982).
34. P. G. Gassman, D. W. Macomber and D. W. Hershberger, *Organometallics*, **2**, 1471 (1983).
35. P. G. Gassman, P. A. Deck, C. H. Winter, D. A. Dobbs and D. H. Cao, *Organometallics*, **11**, 959 (1992).
36. M. Kira, M. Watanabe and H. Sakurai, *J. Am. Chem. Soc.*, **99**, 7780 (1977).
37. P. J. Parker, A. G. Davies, R. Henriquez and J.-Y. Nedalec, *J. Chem. Soc., Perkin Trans. 2*, 745 (1982).
38. J. Okuda, *Top. Curr. Chem.*, **160**, 97 (1991).
39. C. Janiak and H. Schumann. *Adv. Organomet. Chem.*, **33**, 291 (1991).
40. R. L. Haltermann, *Chem. Rev.*, **92**, 965 (1992).
41. N. E. Schore, *J. Am. Chem. Soc.*, **101**, 7410 (1979).
42. N. E. Schore and S. Sundar, *J. Organomet. Chem.*, **184**, C44 (1980).
43. A. Sekegudi, Y. Sagai, K. Ebata, C. Kabuto and H. Sakurai, *J. Am. Chem. Soc.*, **115**, 1144 (1993).
44. P. Jutzi and K.-H. Schwartzen, *Chem. Ber.*, **122**, 287 (1989).
45. P. Jutzi, W. Leffers, B. Hampel, S. Pohl and W. Saak, *Angew. Chem.*, **99**, 563 (1987); *Angew. Chem., Int. Ed. Engl.*, **26**, 583 (1987).
46. L. M. Engelhardt, P. C. Junk, C. L. Rastah and A. H. White, *J. Chem Soc., Chem. Commun.*, 1500 (1988).

47. C. P. Morley, P. Jutzi, C. Krüger and J. M. Wallis, *Organometallics*, **6**, 1084 (1987).
48. P. Jutzi, W. Leffers, G. Müller and B. Huber, *Chem. Ber.*, **122**, 879 (1989).
49. A. K. Hughes, A. Meetsma and J. H. Teuben, *Organometallics*, **12**, 1936 (1993).
50. S. Harvey, C. L. Raston, B. W. Shelton, A. H. White, M. F. Lappert and G. Soistiva, *J. Organomet. Chem.*, **328**, C1 (1987).
51. P. Jutzi, W. Leffers and G. Müller, *J. Organomet. Chem.*, **334**, C24 (1987).
52. E. W. Abel and S. Moorhouse, *J. Organomet. Chem.*, **28**, 211 (1971).
53. P. Jutzi and M. Kuhn, *J. Organomet. Chem.*, **173**, 221 (1979).
54. C. H. Winter, X.-X. Zhau, D. A. Dobbs and M. J. Heeg, *Organometallics*, **10**, 210 (1991).
55. M. D. Rausch, M. Vogel and H. Rosenberg, *J. Organomet. Chem.*, **22**, 900 (1957).
56. A. H. Cowley, P. Jutzi, F. X. Kohl, J. G. Lasch, N. C. Norman and E. Schlüter, *Angew. Chem.*, **96**, 603 (1984).
57. K. Sünkel and D. Motz, *Chem. Ber.*, **121**, 799 (1988).
58. K. Sünkel and J. Hofmann, *Organometallics*, **11**, 3923 (1992).
59. G. P. Sollot and W. R. Peterson Jr., *J. Am. Chem. Soc.*, **89**, 5054 (1967).
60. G. A. Olah, T. Bach and G. K. S. Prakash, *New. J. Chem.*, **15**, 57 (1991).
61. H. Werner and W. Hofman, *Chem. Ber.*, **114**, 2681 (1981).
62. S. R. Berryhill and B. Sharmow, *J. Organomet. Chem.*, **221**, 143 (1981).
63. G. Thum, W. Ries, D. Greisinger and W. Malisch, *J. Organomet. Chem.*, **252**, C61 (1983).
64. S. R. Berryhill, G. L. Clevenger and F. Y. Burdulu, *Organometallics*, **4**, 1509 (1985).
65. S. R. Berryhill and R. J. P. Corriu, *J. Organomet. Chem.*, **370**, C1 (1989).
66. K. H. Pannell, J. M. Rozell and W. M. Tsai, *Organometallics*, **6**, 2085 (1987).
67. K. H. Pannell, J. Castillo-Ramirez and L. Cervantes, *Organometallics*, **11**, 3139 (1992).
68. P. Pasman and J. J. Suel, *J. Organomet. Chem.*, **301**, 329 (1986).
69. G. L. Crocco, C. S. Young, K. E. Lee and J. A. Gladysz, *Organometallics*, **7**, 2158 (1988).
70. S. Seebald, B. Mayer and U. Schubert, *J. Organomet. Chem.*, **462**, 225 (1993).
71. K. H. Pannell, S. R. Vincenti and R. S. Scott III, *Organometallics*, **6**, 1593 (1987).
72. S. Sharma, R. N. Kapoor, F. Cervantes-Lee and K. H. Pannell, *Polyhedron*, **10**, 1177 (1991).
73. U. Schubert and A. Schenkel, *Chem. Ber.*, **121**, 939 (1988).
74. G. G. Furin, O. A. Vyazankina, B. A. Gostevsky and N. S. Vyazankin, *Tetrahedron*, **44**, 2675 (1988).
75. C. H. Winter, S. Pirzard, D. D. Graf, D. H. Cao and M. J. Heeg, *Inorg. Chem.*, **32**, 3654 (1993).
76. A. P. Hagen and P. J. Russo, *Inorg. Nucl. Chem.*, **6**, 507 (1970).
77. P. Jutzi and A. Seufert, *Angew. Chem.*, **88**, 333 (1976).
78. P. Jutzi and M. Kuhn, *Chem. Ber.*, **107**, 1228 (1974).
79. P. Jutzi, M. Kuhn and F. Herzog, *Chem. Ber.*, **108**, 2439 (1975).
80. A. M. Cardoso, R. J. H. Clark and S. Moorhouse, *J. Chem. Soc., Dalton Trans.*, 1156 (1980).
81. S. Dev and J. P. Selegue, *J. Organomet. Chem.*, **469**, 107 (1994).
82. J. M. Rozell, Jr. and R. R. Janes, *Organometallics*, **4**, 2206 (1985).
83. P. Jutzi and A. Seufert, *J. Organomet. Chem.*, **169**, 373 (1979).
84. S. Ciruelos, J. Cuenca, P. Goméz-Sal, A. Manzanero and P. Royo, *Organometallics*, **14**, 177 (1995).
85. P. Jutzi and M. Kuhn, *J. Organomet. Chem.*, **173**, 221 (1979).
86. A. V. Churakov, *Khim.*, **35**, 483 (1994); *Chem Abstr.*, **122**, 187720 (1994)
87. P. Jutzi and M. Schneider, unpublished results.
88. P. Jutzi, B. Krato, M. Hursthouse and A. J. Howes, *Chem. Ber.*, **120**, 585 (1987).
89. H. W. Roesky, S. Schulz, H. J. Koch, G. M. Sheldrick, D. Stalke and A. Kuhn, *Angew. Chem.*, **105**, 1828 (1993).
90. G. H. Mena, F. Palacios, P. Royo and R. Serrano, *J. Organomet. Chem.*, **340**, 37 (1988).
91. T. Okamato, H. Yasuda, A. Nakamura, Y. Kai, N. Kanehisa and N. Kasai, *J. Am. Chem. Soc.*, **110**, 5008 (1988).
92. F. R. Lembke, R. S. Simons and W. J. Youngs, *Organometallics*, **15**, 216 (1996).
93. W. Malisch, G. Thum, D. Wilson, P. Lorz, U. Wachter and W. Seelbach, in *Silicon Chemistry* (Eds. J. Y. Corey, E. R. Corey and P. P. Gaspar), Ellis Horwood, Chichester, 1988.
94. U. The and N. E. Purs, *Polyhedron*, **14**, 1 (1995).
95. J. Dahlhaus, P. Jutzi, H. J. Frenck and W. Kulisch, *Adv. Mat.*, **5**, 321 (1993).
96. M. Waltz, M. Nieger, D. Gudat and E. Niecke, *Z. Anorg, Allg. Chem.*, **621**, 1951 (1995); M. Waltz, M. Nieger and E. Niecke, *Organosilicon Chemistry II, From Molecules to Materials* (Eds. N. Auner and J. Weis), VCH Publ., Weinheim, 1996.

97. A. F. Cummingham, Jr., *Organometallics*, **13**, 2480 (1994).
98. J. Okuda and E. Herdtweck, *Chem. Ber.*, **121**, 1899 (1988).
99. M. D. Fryzuk, S. S. M. Mao, P. B. Duval and S. J. Rettig, *Polyhedron*, **14**, 11 (1995).
100. J. Okuda, *Comments Inorg. Chem.*, **16**, 185 (1994).
101. P. Jutzi, J. Kleimeier, R. Krallmann, H.-G. Stammler and B. Neumann, *J. Organomet. Chem.*, **462**, 57 (1993).
102. H. Köpf and W. Kahl, *J. Organomet. Chem.*, **64**, C37 (1974).
103. H. Plenio, *J. Organomet. Chem.*, **435**, 21 (1992)
104. K. D. Janda, W. W. McConnell, G. O. Nelson and M. E. Wright, *J. Organomet. Chem.*, **259**, 139 (1983).
105. M. Kumada, T. Kondo, K. Mimura, H. Ishikawa, K. Yamamoto, S. Ikeda and M. Kondo, *J. Organomet. Chem.*, **43**, 293 (1972).
106. M. D. Curtis, J. J. D'Enrico, D. N. Duffi, P. S. Epstein and L. G. Bell, *Organometallics*, **2**, 1808 (1983).
107. U. Siemeling, B. Neumann and H. G. Stammler, *Chem. Ber.*, **126**, 1311 (1993).
108. U. Siemeling, R. Krallmann, P. Jutzi, B. Neumann and H. G. Stammler, *Monatsh. Chem.*, **125**, 579 (1994).
109. P. Jutzi and J. Dahlhaus, *Phosphorous, Sulfur, and Silicon*, **87**, 73 (1994).
110. J. K. Pudelski, D. A. Foucher, C. H. Honeyman, A. J. Lough, I. Manners, S. Barlow and D. O'Hare, *Organometallics*, **14**, 2470 (1995).
111. S. Ciruelos, T. Cuenca, J. C. Flores, R. Goméz, P. Goméz-Sol and P. Royo, *Organometallics*, **12**, 944 (1993).
112. P. A. Wegner, V. A. Uski, R. P. Kiesler, S. Dabestani and V. W. Day, *J. Am. Chem. Soc.*, **99**, 4847 (1977).
113. A. W. Cordes. B. Durham and E. Askew, *Acta Crystallogr.*, **C46**, 896 (1990).
114. V. W. Day, H. R. Thompson, G. O. Nelson and M. E. Wright, *Organometallics*, **2**, 494 (1983).
115. P. Goméz-Sal, E. de Jesús, A. J. Pérez and P. Royo, *Organometallics*, **12**, 4633 (1993).
116. J. E. Nifant'ev, K. A. Butakov, Z. G. Aliev and J. F. Urazovskii, *Metallorg. Khim.*, **4**, 1265 (1991); *Chem. Abstr.*, **116**, 59554a (1992).
117. F. Amor, P. Goméz-Sal, E. de Jesús, A. Martin, A. J. Pérez, P. Royo and A. Vázquez de Migel, *Organometallics*, **15**, 2103 (1996).
118. H. Werner, F. Lippert and T. Boley, *Z. Anorg. Allg. Chem.*, **620**, 2053 (1994).
119. G. O. Nelson and M. E. Wright, *J. Organomet. Chem.*, **206**, C21 (1981).
120. J. Heck, K. A. Kriebisch and H. Mellinghoff, *Chem. Ber.*, **121**, 1753 (1988).
121. W. Abriel, G. Baum, J. Heck and K. A. Kriebisch, *Chem. Ber.*, **123**, 1767 (1990).
122. W. Abriel, G. Baum, H. Burdorf and J. Heck, *Z. Naturforsch.*, **46b**, 841 (1991).
123. W. van den Berg, C. E. Boot, J. G. M. van der Linden, W. P. Bosman, J. M. M. Smits, P. T. Beurskens and J. Heck, *Inorg. Chim. Acta*, **216**, 1 (1994).
124. J. Park, Y. Seo, S. Cho, D. Wuang, K. Kim and I. Chang, *J. Organomet. Chem.*, **489**, 23 (1995).
125. D. L. Zechel, D. A. Foucher, J. K. Pudelski, G. P. A. Yap, A. L. Rheingold and I. Manners, *J. Chem. Soc., Dalton Trans.*, 1893 (1995).
126. M. A. Giardello, V. P. Conticello, L. Brard, M. R. Gagne and T. J. Marks, *J. Am. Chem. Soc.*, **116**, 12041 (1994).
127. H. Schumann, J. A. Meese-Marktschaffel and L. Esser, *Chem. Rev.*, **95**, 865 (1995).
128. H. H. Brintzinger, D. Fischer, R. Mühlhaupt, B. Rieger and R. Waymouth, *Angew. Chem.*, **107**, 1255 (1995); *Angew. Chem., Int. Ed. Engl.*, **34**, 1134 (1995).
129. G. Fink, R. Mühlhaupt and H. H. Brintzinger (Eds.), *Ziegler Catalysts*, Springer-Verlag, Berlin–Heidelberg, 1995.
130. A. B. Fischer, J. B. Kinney, R. H. Staley and M. S. Wrighton, *J. Am. Chem. Soc.*, **101**, 6501 (1979).
131. A. G. Osborne and R. H. Whiteley, *J. Organomet. Chem.*, **101**, C27 (1975).
132. M. S. Wrighton, M. C. Palazotto, A. B. Bocarsly, J. M. Bolts, A. B. Fischer and L. Nadjo, *J. Am. Chem. Soc.*, **100**, 7264 (1978).
133. J. R. Butler, W. R. Cullen and S. J. Rettig, *Can. J. Chem.*, **65**, 1452 (1987).
134. D. L. Zechel, K. C. Hultsch, R. Rulkens, D. Balaishis, Y. Ni, J. K. Pudelski, A. J. Lough, I. Manners and D. A. Foucher, *Organometallics*, **15**, 1972 (1996).
135. V. V. Dement'ev, F. Cervantes-Lee, L. Parkanyi, H. Sharma, K. H. Pannell, M. T. Nguyen and A. Diaz, *Organometallics*, **12**, 1983 (1993).

136. H. Evans-Stoeckli, A. G. Osborne and R. H. Whiteley, *Helv. Chim. Acta*, **59**, 2402 (1976).
137. W. Finckh, B. Z. Tang, D. A. Foucher, D. B. Zamble, R. Ziembinski, A. Lough and I. Manners, *Organometallics*, **12**, 823 (1993).
138. J. B. Sheridan, A. J. Lough and I. Manners, *Organometallics*, **15**, 2195 (1996).
139. P. R. Jones, J. M. Rozell, Jr. and B. M. Campbell, *Organometallics*, **4**, 133 (1985).
140. T. J. Barton, G. T. Burns, E. V. Arnold and J. Clardy, *Tetrahedron Lett.*, **22**, 7 (1981).
141. V. K. Belsky, N. N. Zemlyansky, J. V. Borisova, N. D. Kolosova and J. P. Beletskaya, *Cryst. Struct. Commun.*, **11**, 497 (1982).
142. J. Hiermeier, F. H. Köhler and G. Müller, *Organometallics*, **10**, 1787 (1991).
143. U. Siemeling, P. Jutzi, B. Neumann, H.-G. Stammler and M. B. Hursthouse, *Organometallics*, **11**, 1328 (1992).
144. P. Jutzi, I. Mieling, B. Neumann and H.-G. Stammler, *J. Organomet. Chem.*, in press.
145. P. Jutzi, R. Krallmann, G. Wolf, B. Neumann and H. G. Stammler, *Chem. Ber.*, **124**, 2391 (1991).
146. A. Cano, T. Cuenca, P. Goméz-Sal, B. Royo and P. Royo, *Organometallics*, **13**, 1688 (1994).
147. I. Mieling, Ph. D. Thesis, University of Bielefeld, 1993.
148. W. Mengele, J. Diebold, C. Troll, W. Röll and H. H. Brintzinger, *Organometallics*, **12**, 1931 (1993).
149. F. Amor, P. Goméz-Sal, E. de Jesús, P. Royo and A. V. de Miguel, *Organometallics*, **13**, 4322 (1994).
150. U. Siemeling, P. Jutzi, E. Bill and A. V. Trautwein, *J. Organomet. Chem.*, **463**, 151 (1993).
151. H. Atzkern, J. Hiermeier, F. H. Köhler and A. Steck, *J. Organomet. Chem.*, **408**, 281 (1991).
152. H. Atzkern, B. Bergerat, M. Fritz, J. Hiermeier, P. Hudeszek, O. Kahn, B. Kanellakopulus, F. H. Köhler and M. Ruhs, *Chem. Ber.*, **127**, 277 (1994).
153. U. Siemeling and P. Jutzi, *Chem. Ber.*, **125**, 31 (1992).
154. H. Atzkern, P. Bergerat., H. Beruda, M. Fritz, J. Hiermeier, P. Hudeszek, O. Kahn, F. H. Köhler, M. Paul and B. Weber, *J. Am. Chem. Soc.*, **117**, 997 (1995).
155. P. Bergerat, J. Blümel, M. Fritz, J. Hiermeier, P. Hudeszek, O. Kahn and F. H. Köhler, *Angew. Chem.*, **104**, 1285 (1992).
156. D. O. Cowan, C. Le Vanda, J. Park and F. Kaufmann, *Acc. Chem. Res.*, **6**, 1 (1973).
157. M. V. Robin and P. Day, *Inorg. Chem. Radiochem.*, **10**, 247 (1967).
158. H. O. Findea and D. Hanshow, *J. Am. Chem. Soc.*, **114**, 3173 (1992).
159. C. Elschenbroich, A. Bretschneider-Hurley, J. Hurley, W. Massa, S. Wocadlo and J. Pebler, *Inorg. Chem.*, **32**, 5421 (1993).
160. H. Sakurai, S. Hoshi, A. Kamiga, A. Hosomi and C. Kabuto, *Chem. Lett.*, 1781 (1986).
161. J. Michl, ‘Polysilanes’, in *The Chemistry of Organic Silicon Compounds* (Eds. S. Patai and Z. Rappoport), Wiley, New York, 1989.
162. A. Togni and T. Hayashi, *Ferrocenes*, VCH Publ., Weinheim, 1995.
163. I. Manners, *Adv. Mater.*, **6**, 68 (1994).
164. A. F. Diaz, C. M- Seymour, K. H. Pannell and J. M. Rozell, *J. Electrochem. Soc.*, **137**, 503 (1990).
165. K. H. Pannell, J. M. Rozell and J. M. Ziegler, *Macromolecules*, **21**, 276 (1988).
166. D. A. Foucher, C. H. Honeyman, J. M. Nelson, B. Z. Tang and I. Manners, *Angew. Chem., Int. Ed. Engl.*, **32**, 1709 (1993).
167. I. Manners, *Adv. Organomet. Chem.*, **37**, 131 (1995).
168. M. T. Nguyen, A. F. Diaz, V. V. Dement’ev and K. H. Pannell, *Chem. Mat.*, **5**, 1389 (1993).
169. S. Iijima, J. Motoyama and H. Sano, *Bull. Chem. Soc. Jpn.*, **53**, 3180 (1980).
170. W. H. Morrison, S. Krogsrud and N. Hendrickson, *Inorg. Chem.*, **12**, 1998 (1973).
171. V. V. Dement’ev and K. H. Pannell, *Organometallics*, **12**, 1983 (1993).
172. C. Le Vanda, K. Bechgaard and D. O. Cowan, *J. Org. Chem.*, **41**, 2700 (1976).
173. C. Le Vanda, K. Bechgaard, D. O. Cowan, U. T. Mueller-Westerhoff, P. Eilbracht, G. A. Candela and R. L. Collins, *J. Am. Chem. Soc.*, **98**, 3181 (1976).
174. J. E. Gorton, H. L. Lentzner and W. E. Watts, *Tetrahedron*, **27**, 4353 (1971).
175. S. Barlow, V. J. Murphy, J. S. O. Evans and D. O’Hare, *Organometallics*, **14**, 3461 (1995).
176. R. Rulkens, A. J. Lough and I. Manners, *J. Am. Chem. Soc.*, **116**, 797 (1994).
177. T. J. Kealy and P. L. Pauson, *Nature (London)*, **168**, 1039 (1951).
178. E. O. Fischer and W. Pfab, *Z. Naturforsch.*, **B7**, 377 (1952).
179. G. Wilkinson, M. Rosenblum, M. C. Whiting and R. B. Woodward, *J. Am. Chem. Soc.*, **74**, 2125 (1952).

180. E. O. Fischer and H. Grubert, *Z. Anorg. Allg. Chem.*, **286**, 237 (1956).
181. P. Jutzi, D. Kanne and C. Krüger, *Angew. Chem.*, **98**, 163 (1986).
182. P. Jutzi, U. Holtmann, D. Kanne, C. Krüger, R. Blom, R. Gleiter and J. Hyla-Kryspin, *Chem. Ber.*, **122**, 1629 (1989).
183. B. Wrackmeyer, A. Sebald and L. H. Marwin, *Magn. Reson. Chem.*, **29**, 260 (1991).
184. T. J. Lee and J. E. Rice, *J. Am. Chem. Soc.*, **111**, 2011 (1989).
185. G. Bruno, E. Ciliberto, J. L. Fragala and P. Jutzi, *J. Organomet. Chem.*, **289**, 268 (1985).
186. A. G. Davies and J. Lusztyk, *J. Chem. Soc., Perkin Trans. 2*, 692 (1981).
187. P. Jutzi, *Comments Inorg. Chem.*, **6**, 123 (1987).
188. P. Jutzi, in *Frontiers of Organosilicon Chemistry* (Eds. A. R. Bassindale and P. P. Gaspar), The Royal Society of Chemistry, Cambridge, 1991.
189. P. Jutzi. U. Holtmann, A. Möhrke, E. A. Bunte and D. Eikenberg, unpublished results; P. Jutzi, in *Organosilicon Chemistry* (Eds. N. Auner and J. Weis), VCH-Publ., Weinheim, 1993.
190. P. Jutzi, E. A. Bunte, U. Holtmann, B. Neumann and H.-G. Stammler, *J. Organomet. Chem.*, **446**, 139 (1993).
191. P. Jutzi, U. Holtmann, H. Bögge and A. Müller, *J. Chem. Soc., Chem. Commun.*, 305 (1988).
192. J. Maxka and Y. Apeloig, *J. Chem. Soc., Chem. Commun.*, 737 (1990).
193. P. Jutzi and E. A. Bunte, *Angew. Chem.*, **104**, 1636 (1992); *Angew. Chem., Int. Ed. Engl.*, **31**, 1605 (1992).
194. P. Jutzi, A. Möhrke, A. Müller and H. Bögge, *Angew. Chem.*, **101**, 1527 (1989); *Angew. Chem., Int. Ed. Engl.*, **28**, 1518 (1989).
195. P. Jutzi, D. Eikenberg, A. Möhrke, B. Neumann and H. G. Stammler, *Organometallics*, **15**, 753 (1996).
196. P. Jutzi, D. Eikenberg, E. A. Bunte, A. Möhrke, B. Neumann and H.-G. Stammler, *Organometallics*, **15**, 1930 (1996).
197. P. Jutzi, D. Eikenberg, B. Neumann and H.-G. Stammler, *Organometallics*, **15**, 3659 (1996).
198. M. Tacke, C. Klein, D. J. Stufkens, A. Oskam, P. Jutzi and E. A. Bunte, *Z. Anorg. Allg. Chem.*, **619**, 865 (1993).
199. M. Tacke, in *Organosilicon Chemistry III* (Eds. N. Auner and J. Weis), VCH-Publ., Weinheim, in press.
200. P. Jutzi and E. A. Bunte, *Angew. Chem.*, **104**, 1636 (1992); *Angew. Chem., Int. Ed. Engl.*, **31**, 1605 (1992).
201. P. Jutzi and A. Möhrke, *Angew. Chem.*, **102**, 913 (1990); *Angew. Chem., Int. Ed. Engl.*, **29**, 893 (1990).

CHAPTER **37**

Recent advances in the chemistry of cyclopolysilanes

EDWIN HENGGE† and HARALD STÜGER

Institute of Inorganic Chemistry, Technical University, Graz, Austria
Fax: +43 316 873 8701; e-mail: stueger@anorg.tu-graz.ac.at

I. INTRODUCTION

Cyclopolysilanes have been known since the fundamental work of Kipping in 1921, who synthesized the four-, five- and six-membered perphenylcyclopolysilanes from diphenyldichlorosilane and sodium.[1] After a long period of no activity in this field, Burkhard published the synthesis of dodecamethylcyclohexasilane $(Me_2Si)_6$, the first peralkylated polysilane ring, in 1949.[2] Since then numerous cyclopolysilane derivatives bearing organic substituents have been prepared mainly in the groups of Gilman, West and Kumada[3a–c]. The first solely inorganic substituted cyclopolysilanes $(SiX_2)_n$ ($n = 4$, 5 and 6; X = Cl, Br and I), from which the parent cyclopolysilanes Si_5H_{10} and Si_6H_{12} are readily accessible simply by $LiAlH_4$ reduction, have been found by Hengge and coworkers[4a–d].

---

† Deceased February 1997

The parent cyclotetrasilane Si_4H_8 and all the perfluorinated cyclopolysilanes are so far still unknown. More recently, the efforts in cyclopolysilane chemistry are mainly directed towards polycyclic and cage-like compounds and towards partially functionalized derivatives, which may be used as synthons for larger polysilane frameworks.

The chemistry and properties of cyclopolysilanes have been summarized in various earlier reviews. The review published in 1995 by Hengge and Janoschek provides the most up-to-date summary of the field of cyclopolysilane chemistry and covers the literature up to 1994[5a–d]. In the current chapter, therefore, recent results gained since 1994 will be emphasized and only a short survey of older investigations will be given. The interested reader is referred to the reviews cited above for further details of previous work. Cyclopolysilanes containing endocyclic heteroatoms are also beyond the scope of this article.

II. GENERAL METHODS FOR CYCLOPOLYSILANE SYNTHESIS

Organocyclopolysilanes are usually made by the dehalogenative coupling of dialkyl- or diaryldichlorosilanes with alkali metals. The cyclopolysilane yield and the preferred ring size obtained depend strongly on the kind of alkali metal, the solvent and the reaction conditions. Therefore, optimized procedures have to be worked out for the high-yield synthesis of specific compounds in most cases. The perphenylcyclopolysilanes $(Ph_2Si)_4$, $(Ph_2Si)_5$ and $(Ph_2Si)_6$, for instance, are usually made from Ph_2SiCl_2 using lithium metal in refluxing THF (equation 1).

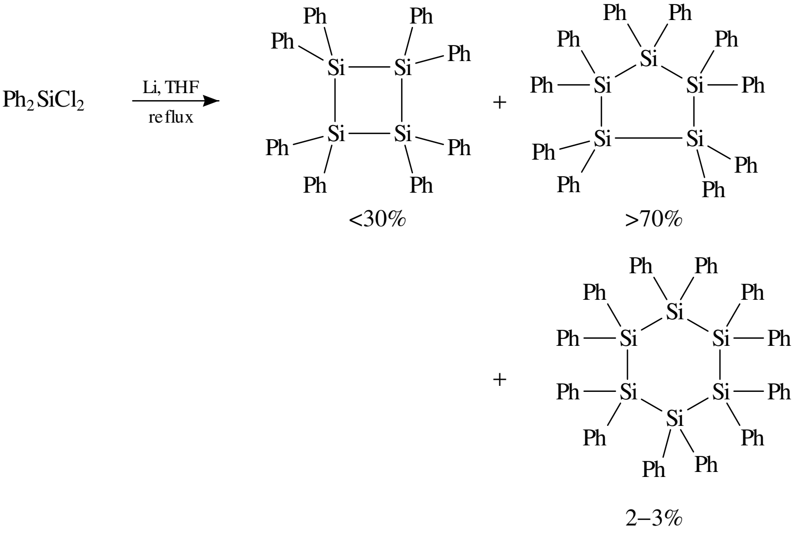

(1)

Carrying out the condensation reaction with 2.0 equivalents of lithium yields $(Ph_2Si)_4$ as the major product in yields up to 30% in a kinetically controlled reaction. Larger amounts of lithium and longer reaction times give rise to rearrangement reactions and lead finally to the thermodynamically most stable five-membered ring (optimum yield >70%). $(Ph_2Si)_6$ is only produced in yields of 2–3% as a by-product.

The six-membered permethylated analogue dodecamethylcyclohexasilane, however, can be prepared conveniently from Me_2SiCl_2 with sodium–potassium alloy in THF in the presence of an equilibrating catalyst, which causes depolymerization of the initially formed permethylpolysilane polymer[6,7] (equation 2).

$$Me_2SiCl_2 \xrightarrow[\text{naphthalene}]{\text{Na/K, THF}} \underset{> 80\%}{(Me_2Si)_6} + \underset{<10\%}{(Me_2Si)_5} + \underset{\text{traces}}{(Me_2Si)_7} \tag{2}$$

The preferred ring size in the equilibrium mixture obtained from diorganodichlorosilanes and alkali metals, therefore, is additionally governed by the bulk of the organic groups attached to silicon. For small substituents like methyl, the six-membered ring is favored, while five- and four-membered rings are preferentially obtained in case of larger groups like phenyl or *i*-propyl. Even larger substituents like mesityl or *t*-butyl give rise to the formation of three-membered rings.

In order to quantify the dependence of the preferred ring size obtained in cyclopolysilane synthesis on the bulk of the substituent groups on the silicon Cartledge postulated a set of parameters derived from the rates of acid catalyzed hydrolysis of appropriate hydrosilanes[8]. The model, however, was applied only with limited success[9].

The electrochemical formation of Si−Si bonds by cathodic reduction of dichlorosilanes provides an alternative access to cyclopolysilanes[10,11]. Electrolyses are carried out in single compartment cells with THF/Bu_4NBF_4 as solvent/electrolyte system at current intensities of about 1 $mA\,cm^{-2}$. The cathode material is stainless steel, the anode consists of a sacrificial metal, e.g. magnesium or aluminum. A modified hydrogen anode especially designed for this type of electrolysis[12] can also be used alternatively, and this may be advantageous for large-scale or industrial processes because it avoids the formation of huge amounts of metal halides. Presumably, the reaction is neither thermodynamically nor kinetically controlled in all cases, the determinant factor obviously being the steric conditions on the cathode surface. Perarylated silanes like Ph_2SiCl_2 always give cyclotetrasilanes as the sole cyclic reaction products and polymeric material is formed only in negligible amounts. When the aryl substituents on the silicon are replaced by methyl groups, ring formation is observed only at low dichlorosilane concentrations. Thus, electrolyses carried out with silane concentrations below 0.5 $mol\,l^{-1}$ yield $(Me_2Si)_6$ in case of Me_2SiCl_2 or $(MePhSi)_5$ in case of $MePhSiCl_2$, respectively, as the main cyclic reaction products. With increasing dichlorosilane concentration, intermolecular reaction favors the formation of linear polymers in both cases. Cyclic organohydropolysilanes $(RHSi)_n$ cannot be synthesized electrochemically at all. The electrolysis of organohydrodichlorosilane solutions under various conditions exclusively yields polymeric material[11]. In certain cases the electrochemical method can be used for the synthesis of cyclopolysilanes, which are not accessible by the usual Wurtz-type route. Bis(pentafluorophenyl)dichlorosilane, for instance, affords the corresponding four-membered ring only electrochemically but not under the influence of alkali metals. Further examples are given elsewhere[13,14].

Catalytic dehydrogenative coupling of organohydrosilanes, a common method for the formation of linear polysilanes, can also be applied to cyclopolysilane synthesis. Thus, benzylsilane reacts to give all-*trans*-hexabenzylcyclohexasilane in the presence of dimethyltitanocene (equation 3). However, extremely long reaction times are required and only moderate yields are obtained[15].

$$PhCH_2SiH_3 \xrightarrow[\text{6 weeks, r.t.}]{Cp_2TiMe_2\text{, toluene}} \underset{35\%}{[Si(H)CH_2Ph]_6} + \text{oligomers} \tag{3}$$

Cyclopolysilanes bearing several different substituents can be assembled in a step-by-step procedure from small appropriately substituted organosilane precursor molecules. An example originally presented by Uhlig[16] and modified later in order to obtain the reaction product free of polymers[17] is shown in Scheme 1, where

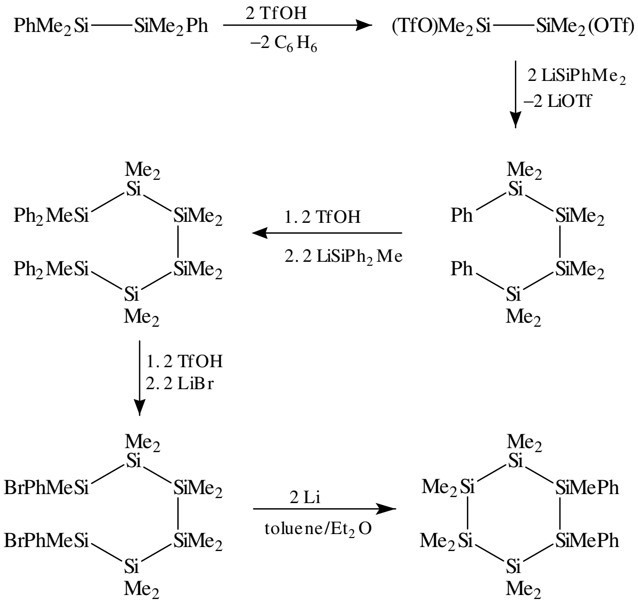

SCHEME 1

1,2-diphenyldecamethylcyclohexasilane is synthesized systematically starting from 1,2-diphenyltetramethyldisilane by several Si−Si bond formation and selective substituent exchange steps.

III. GENERAL PROPERTIES OF CYCLOPOLYSILANES

The chemical and thermal stability of cyclic polysilanes varies strongly with the ring size and the kind of substituents on silicon. Most of the peralkylated and perarylated cyclosilanes do not react with oxygen or atmospheric moisture and therefore can be handled and stored without any additional precautions. The perarylated cyclosilanes furthermore exhibit high melting points and are remarkably stable at elevated temperatures. With decreasing ring size or in the presence of reactive substituents, however, the reactivity of cyclopolysilanes is strongly enhanced. While $(SiPh_2)_6$, for instance, reacts with mild halogenating agents, hydrogen halides or lithium only under forcing conditions to give small fragments, $(SiPh_2)_4$ is easily cleaved to the corresponding 1,4-disubstituted products. The perhalo derivatives $(SiX_2)_n$ ($n = 4$, 5 and 6; X = Cl, Br and I) immediately react with traces of water due to the sensitivity of the Si−halogen bonds. $(SiCl_2)_4$, $(SiBr_2)_4$ and $(SiI_2)_4$, but also $(SiMe_2)_4$, additionally undergo thermal ring-opening polymerization even at ambient temperatures (compare Section IV.B). Cyclotrisilanes generally need to be stabilized by the presence of sterically demanding substituents because of their high ring strain. Hexakis(2,6-dimethylphenyl)cyclotrisilane, for instance, is totally stable against the atmosphere and melts above 200 °C without any decomposition, whereas cyclotrisilanes with smaller substituents only can be isolated in argon matrices at low temperatures.

Compared to hydrocarbon rings, cyclopolysilanes are much more flexible due to their rather flat potential energy surfaces. Five- and six-membered cyclopolysilanes usually adopt folded conformations. The energy differences between stable conformers, however, exhibit values of only 5–9.2 $kJ\,mol^{-1}$ in Si_5H_{10} and Si_6H_{12}. Additionally, the rotational barriers around the Si−Si bonds in cyclopolysilanes are low, and this generally facilitates the interconversion of different conformers[18,19]. The flexibility of the cyclopolysilane skeletons is also reflected by the variable structures of the four-membered rings. Depending on the substituents, dihedral angles between 39.39° in 1,1,2,2-tetraneopentyl-3,3,4,4-tetraisopropylcyclotetrasilane and 0° in $[(Me_3Si)_2Si]_4$ have been found. A compilation of the dihedral angles in cyclotetrasilanes measured so far can be found in Ref. 5d. $(Me_2Si)_4$ adopts a planar structure in the solid state according to X-ray crystallography[20]. Electron diffraction measurements, however, exhibit a puckered conformation with a folding angle of 29.4° for the same molecule in the gas phase[21]. An explanation for these marked differences in the structures of various cyclotetrasilane derivatives has not yet been given.

One of the most striking properties of cyclopolysilanes is their strong absorption of light in the near-UV/visible region; λ_{max} values for the lowest-energy UV absorption bands range from 250 up to nearly 420 nm, depending on the ring size and the substituents attached to the cyclopolysilane ring. Representative examples for low-energy UV absorption bands of cyclopolysilanes are summarized in Table 1.

In cyclic polysilanes, delocalization of σ-(Si−Si) electrons over the ring is regarded as responsible for the unusual electronic properties[22]. The UV absorption spectra of the cyclic compounds $(R_2Si)_n$ with $n = 3–8$ exhibit a bathochromic shift as the ring size decreases. Larger rings behave like linear polysilanes; the UV absorption maxima move to longer wavelengths with an increasing number of silicon atoms. Thus, the lowest electronic excitation energies are observed for cyclotri- and tetrasilanes, which at least can be partially explained by ring strain present in these small ring compounds causing an increase in the energy of the highest occupied molecular orbitals. The relative energies of the HOMOs in cyclopolysilanes can be easily derived from the UPS spectra[23]. As follows from comparison of the electronic excitation energies with the ionization potentials, the destabilization of the HOMOs cannot be responsible exclusively for the trends observed for the low-energy UV absorption bands of cyclopolysilanes. Progressive stabilization of the LUMOs with decreasing ring size also occurs and must be taken into account.

Substituent influences on UV excitation energies of cyclopolysilanes are also well pronounced. For cyclosilane derivatives $(SiX_2)_n$ of the same ring size, bathochromic shifts of the first absorption bands are observed in the order $X = H < alkyl < MeO \sim Cl < Br < I$[24] (Table 1). Extraordinarily low energy first UV absorption bands are shown by the perhalocyclopolysilanes, so that some of these compounds even exhibit colors. UPS measurements and theoretical calculations of the HOMO–LUMO energies suggest that intramolecular charge transfer might be responsible for the unusual low energy of the corresponding electronic transitions[25].

The cyclic polysilanes can be reduced to radical anions either electrolytically or by reaction with alkali metals quite similar to aromatic rings. Numerous substituted

TABLE 1. Low-energy UV absorption bands of selected cyclopolysilanes

X	Si_4X_8		Si_5X_{10}		Si_6X_{12}		References
	λ_{max} (nm)	ε	λ_{max} (nm)	ε	λ_{max} (nm)	ε	
H	—	—	215	3000	192	6000	31
Me	302	250	275sh	700	258sh	1100	24,32
Et	304	180	266	1400	259sh	1900	33
MeO	—	—	295sh	1000	316	1000	24
Cl	394	50	305sh	1000	322	300	24
Br	402	50	320sh	900	344	300	24
I	424	75	380sh	500	400sh	450	24

cyclopolysilane radical anions have been made; however, attempts to reduce the parent compound Si_5H_{10} failed. Detailed ESR[26,27] and ENDOR[28] investigations of cyclosilane radical anions exhibit complete delocalization of the odd electron over the cyclosilane ring, consistent with the assumption of σ-(Si—Si) delocalization in larger Si—Si bonded systems. Important information about the nature of the unfilled orbitals in cyclopolysilanes can also be obtained from ESR studies of their radical anions. The corresponding results have been reviewed recently[22]. Radical cations of cyclopolysilanes have also been observed by ESR[29] after treatment of the solutions of cyclopolysilanes in CH_2Cl_2 with $AlCl_3$. The oxidation of cyclopolysilanes, however, has so far not been studied so extensively.

The magnitude of the Si—Si vibrational force constants in cyclopolysilane rings also depends on the ring size and on the substituents attached to silicon. Compared with other silanes like disilanes, the force constants are generally weaker. Detailed results are summarized elsewhere[5d].

Semiempirical calculations (AM1), which are in good agreement with *ab initio* calculations and experimental data, showed for cyclic polysilanes that the first ionization energy is higher with increasing number of silicon atoms. This stands in contrast to linear chains, where the ionization energy decreases with the number of silicon atoms[30].

IV. MONOCYCLIC SILANES

A. Cyclotrisilanes

Hexakis(2,6-dimethylphenyl)cyclotrisilane, the first known stable three-membered cyclosilane, was prepared in 1982 by Masamune and coworkers from dichlorobis(2,6-dimethylphenyl)silane by the reductive dechlorination with lithium naphthalenide in low yield[34]. Other cyclotrisilanes bearing substituents of comparable steric bulk have been synthesized analogously. The chemistry of the cyclotrisilanes presently known has recently been reviewed[35].

For the preparation of derivatives with sterically less demanding side groups, alternative routes have to be used. Thus, for instance, $[(Et_2CH)_2Si)]_3$ and $[(i\text{-}Pr)_2Si)]_3$ are accessible only by the reductive dechlorination of the corresponding 1,3-dichlorotrisilanes applying highly specific experimental conditions[36] (equation 4).

$$Cl(SiR_2)_3Cl \xrightarrow[\text{THF/pentane}]{t\text{-BuLi/Li/}C_{10}H_8} [R_2Si]_3 \tag{4}$$

$$R = Me_2CH,\ Et_2CH$$

In case of exceptionally strained cyclotrisilanes like $[(t\text{-Bu})_2Si)]_3$, it turned out to be advantageous to start from the diorganodibromo- or the diorganodiiodosilane instead of the dichlorosilane. Due to the lower Si–halogen bond energy in these cases, the reduction proceeds much smoother and the desired reaction product is obtained in good yield[37] (equation 5).

$$\underset{X\,=\,Br,\ I}{(t\text{-Bu})_2SiX_2} \xrightarrow{Li/C_{10}H_8} [(t\text{-Bu})_2Si]_3 \tag{5}$$

The preparative application of photolytic ring contraction reactions of cyclotetrasilanes, which also lead to the formation of cyclotrisilanes, is largely impeded by the limited stability of the cyclotrisilane moiety. The photolysis of octaisopropylcyclotetrasilane, for instance, affords the corresponding cyclotrisilane only as an intermediate, which can be detected by UV spectroscopy. Further silylene extrusion gives rise to the formation of the unstable tetraisopropyldisilene and its successive decomposition products (equation 6)[38,39].

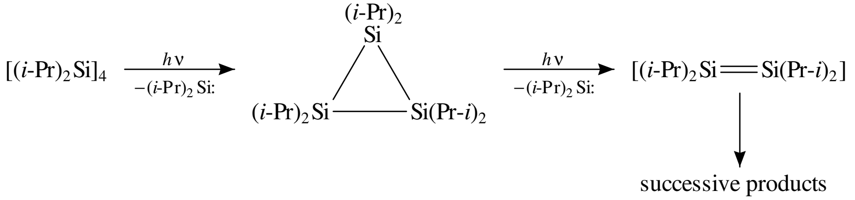

(6)

Functionalized cyclotrisilane derivatives bearing oxygen- or nitrogen-containing substituents are also known. The synthesis of the aryl-alkoxy cyclotrisilane trimesityltris(2,6-diisopropylphenoxy)cyclotrisilane can be easily accomplished by the photolysis of 2-mesityl-2-(2,6-diisopropylphenoxy)-1,1,1,3,3,3-hexamethyltrisilane via several silylene extrusion and addition steps (equation 7)[40].

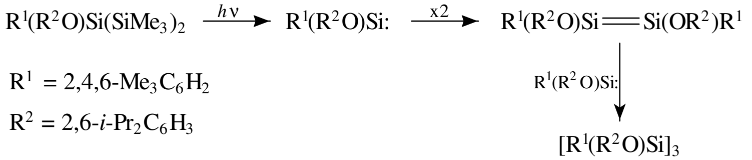

$$R^1(R^2O)Si(SiMe_3)_2 \xrightarrow{h\nu} R^1(R^2O)Si: \xrightarrow{x2} R^1(R^2O)Si{=}Si(OR^2)R^1 \xrightarrow{R^1(R^2O)Si:} [R^1(R^2O)Si]_3 \qquad (7)$$

$R^1 = 2,4,6\text{-}Me_3C_6H_2$

$R^2 = 2,6\text{-}i\text{-}Pr_2C_6H_3$

The aminofunctional cyclotrisilane derivative hexakis[2-(dimethylaminomethyl)phenyl] cyclotrisilane can be formed by the reductive dechlorination of the corresponding dichloride Ar_2SiCl_2 ($Ar = 2\text{-}Me_2NCH_2C_6H_4$) with magnesium[41].

Molecular structures and physical properties of cyclotrisilanes primarily reflect the inherent ring strain of the three-membered ring. The cyclotrisilanes typically show isosceles or equal-sided triangle structures. The Si—Si bond distances observed are generally longer compared with the normal value of about 234 pm. The longest Si—Si distance detected so far was found for $[(t\text{-Bu})_2Si)]_3$ with a bond length of 251.1 pm[37]. Despite the elongated Si—Si bonds, the ^{29}Si-NMR spectra of the cyclotrisilanes exhibit considerable shielding of the ^{29}Si nuclei. Typical ^{29}Si-chemical shift values for the alkyl and arylcyclotrisilanes, for instance, fall into the range between −4 and −82 ppm. A more comprehensive discussion of structural and physicochemical aspects of cyclotrisilanes can be found in several recent reviews[35,42,43].

The chemical reactions of the three-membered polysilane rings are initiated quite generally by Si—Si bond cleavage in order to relieve the high ring strain. Three fundamental pathways for the degradation of the cyclotrisilane ring are possible: (1) scission of one Si—Si bond yielding linear trisilanes, (2) scission of two Si—Si bonds leading to the formation of a disilene and a silylene and (3) scission of all Si—Si bonds giving monosilanes (Scheme 2).

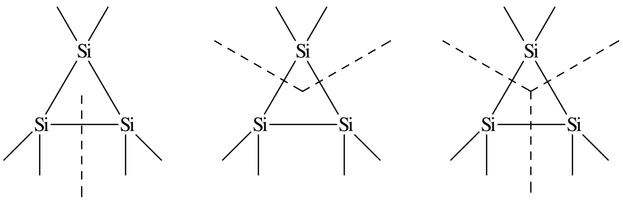

SCHEME 2

In the absence of light or a catalyst, cyclotrisilanes usually react to give acyclic trisilanes or products of ring expansion, depending on the reaction partner. Thus, $[(t\text{-Bu})_2Si)]_3$ and the heavier halogens, for instance, afford the corresponding hexa-t-butyl-1,3-dihalotrisilanes. With elemental oxygen or DMSO, however, the oxatrisiletane and the 1,3-dioxatrisilolane are formed (Scheme 3)[35].

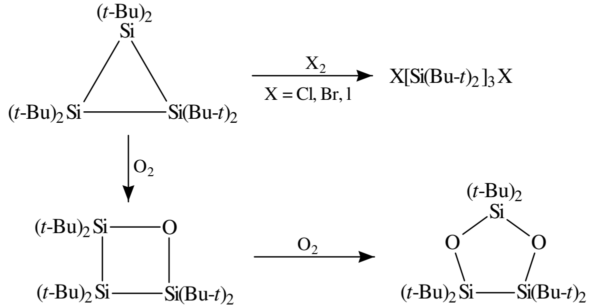

SCHEME 3

The photolysis of cyclotrisilanes bearing at least one aryl group on each silicon atom usually affords the corresponding disilene and a silylene, which dimerizes to give more disilene. Persilylated derivatives behave similarly; stable tetraalkyldisilenes, however, cannot be prepared using this route. Thus, when arylcyclotrisilanes are photolyzed in the presence of suitable trapping agents, disiliranes are produced selectively via [2 + 1]-cycloaddition reactions[35]. In the case of $[(t\text{-Bu})_2Si)]_3$, which also gives the corresponding disilene and a short-lived silylene upon UV irradiation, the formation of trapping products of both reactive intermediates can be observed, depending on the nature of the trapping reagent a–b (Scheme 4)[44].

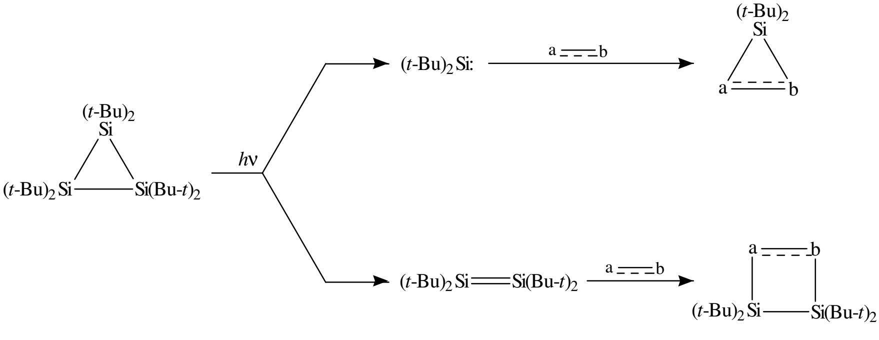

SCHEME 4

The photolysis and thermolysis of hexa-t-butylcyclotrisilane in the absence of trapping reagents was investigated recently[45]. Heating the compound in a sealed tube to 185 °C affords a 5-methylene-1,2,3,7,8,9-hexasilanonane derivative (Scheme 5).

When $[(t\text{-Bu})_2Si)]_3$ is photolyzed in the UV with wavelengths < 300 nm, a complex mixture of products containing t-Bu−Si and H−Si bonds is obtained. The only isolated product was hepta-t-butylcyclotetrasilane (compare equation 8).

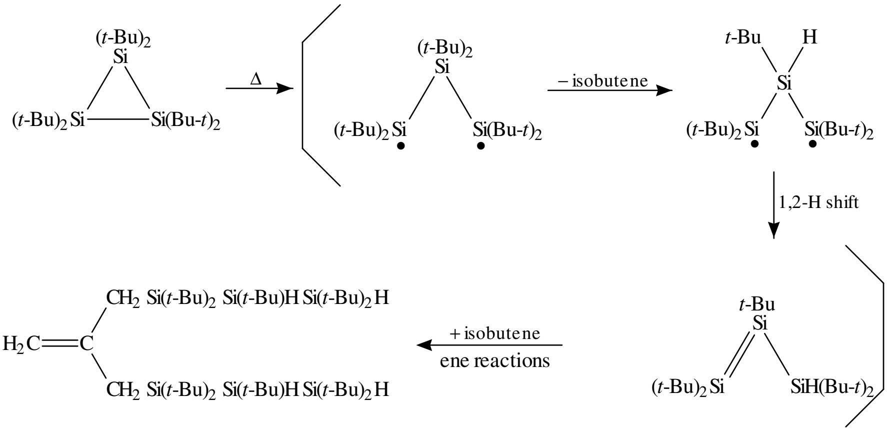

SCHEME 5

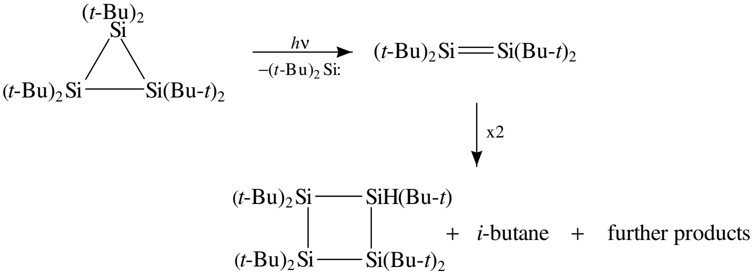

(8)

Further cycloaddition reactions of silylenes generated by the photolysis of cyclotrisilanes have been published since Weidenbruch and coworkers summarized these reactions in an excellent review. Different siliranes were prepared by [2+1]-cycloaddition of di-*t*-butylsilylene to various alkenes and dienes (Scheme 6)[46]. Quite interesting results are obtained from the photolysis of hexa-*t*-butylcyclotrisilane in the presence of unsaturated five-membered ring compounds[47] (Scheme 7). With cyclopentadiene and furane, [4 + 2]-cycloaddition of the photolytically generated disilene occurs only as a side reaction. Furthermore, [2 + 1]-cycloaddition of the intermediately formed silylene is highly favored and siliranes are primarily obtained. A totally different course is observed for the reaction in the presence of thiophene. The disilene abstracts the sulfur atom with the formation of the 1,2-disilathiirane as the major product with an extremely short Si−Si distance of 230.49 pm.

Addition of phenylacetylene or pent-1-yne to a solution of hexakis[2-(dimethylaminomethyl)phenyl]cyclotrisilane yields spectroscopically pure 1,2-disilacyclobutenes (equation 9)[41].

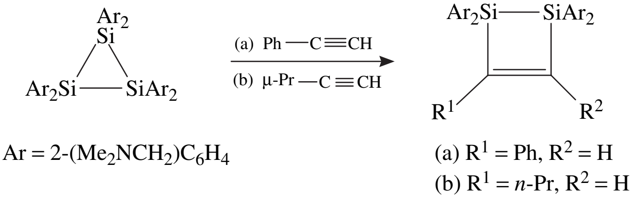

(9)

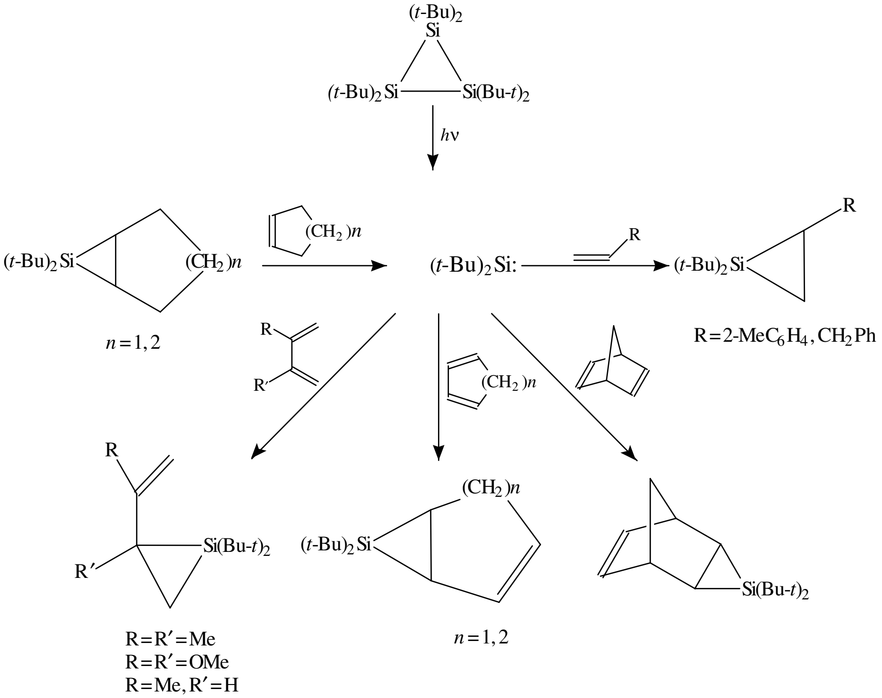

SCHEME 6

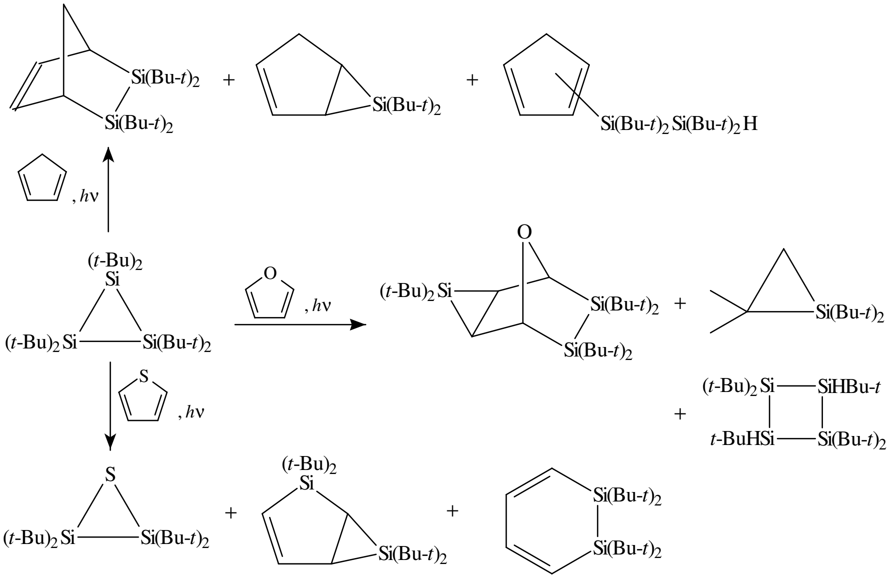

SCHEME 7

Monitoring the reaction by ^{1}H-NMR spectroscopy clearly indicates the formation of the 1,2-disilacyclobutenes by a two-step addition–insertion process. Primarily, the silylene generated by thermal decomposition of the cyclotrisilane adds to the C−C triple bond yielding the silacyclopropene. Further insertion of a second silylene into the Si−C bond of the silacyclopropene finally affords the corresponding 1,2-disilacyclobutene.

Siliranes are also formed by the reaction of the cyclotrisilane $[2\text{-}(Me_2NCH_2)C_6H_4]_6Si_3$ with terminal and strained internal olefins under mild thermal conditions. The products obtained from the thermolysis of the siliranes thus prepared suggest a thermal equilibrium of the silirane with the cyclotrisilane and the corresponding alkene. This observation provides evidence for an equilibrium between the silylene and the cyclotrisilane and, moreover, proves that free silylenes are involved in the silylene transfer reaction[48].

B. Cyclotetrasilanes

As has already been mentioned in Section III for $(SiPh_2)_4$ cyclotetrasilanes are cleaved selectively by various nucleophiles and electrophiles like the halogens, hydrogen halides, Li, RLi, alkoxides etc. to the corresponding linear 1,4-disubstituted tetrasilanes. The reaction can be accomplished by most reagents known to cleave Si−Si bonds (for details consult Ref. 5d). Matyjaszewski and coworkers published a series of papers about the ring-opening polymerization of cyclotetrasilanes yielding highly polymeric polysilanes with molecular weights up to M = 100.000[49−52]. Compared with larger polysilanes, the strained four-membered ring turned out to be best suited for ring-opening polymerization. As for any chemical reaction, a decrease in the free energy is necessary for successful ring-opening polymerization. Polymerization, however, is usually accompanied by loss of entropy, because each monomer molecule loses three degrees of translational freedom on conversion to a polymer segment. Thus, a sufficient gain of enthalpy has to be provided by the ring cleavage reaction, and this can only be realized using strained monomers.

Anionic ring-opening polymerization of 1,2,3,4-tetramethyl-1,2,3,4-tetraphenylcyclotetrasilane is quite effectively initiated by butyllithium or silyl potassium initiators. The process resembles the anionic polymerization of other monomers where solvent effects play an important role. In THF, the reaction takes place very rapidly but mainly cyclic five- and six-membered oligomers are formed. Polymerization is very slow in nonpolar media (toluene, benzene); however, reactions are accelerated by the addition of small amounts of THF or crown ethers. The stereochemical control leading to the formation of syndiotactic, heterotactic or isotactic polymers is poor in all cases. In order to improve the stereoselectivity of the polymerization reaction, more sluggish initiators like silyl cuprates are very effective. A possible reaction mechanism is discussed elsewhere[49,52].

Strained and polymerizable cyclotetrasilanes $Si_4Me_nPh_{8-n}$ (n = 3,4,5,6) are accessible by the partial dearylation of octaphenylcyclotetrasilane and subsequent displacement with MeMgBr[49]. 1,2,3,4-Tetramethyl-1,2,3,4-tetraphenylcyclotetrasilane, for instance, is formed by the reaction of $(SiPh_2)_4$ with 4 equivalents of triflic acid followed by treatment with 4 equivalents of methyl magnesium bromide. Three of the four possible isomers are obtained in a ratio of **1a** : **1b** : **1c** = 45 : 15 : 40, whereas the all-*cis*-isomer **1d** has not been observed (Scheme 8). Recrystallization from cold hexane yields isomer **1a** in 95% purity[53].

The introduction of the novel educt 1,2,3,4-tetraphenyl-1,2,3,4-tetra-*p*-tolylcyclotetrasilane enables the selective monofunctionalization of perarylated cyclotetrasilanes[54]. [Ph(*p*-Tol)Si$_4$] is easily prepared by the reaction of [Ph(*p*-Tol)SiCl$_2$ with lithium and shows significantly higher solubility and reactivity compared to $(SiPh_2)_4$. From [Ph(*p*-Tol)Si$_4$] the monofunctional cyclotetrasilane derivatives $Si_4Ph_4(p\text{-Tol})_3X$ with X = OSO_2CF_3, F, Cl, Br, I, H or *t*-Bu are accessible simply by dearylation with triflic acid and

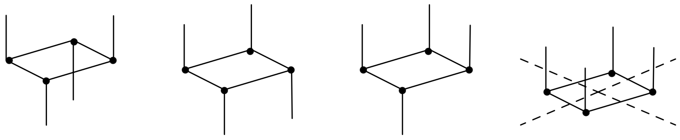

(1a) **(1b)** **(1c)** **(1d)**

• = SiPh

SCHEME 8

subsequent reaction with lithium or potassium halides, $NaBH_4$ or *t*-BuLi (equations 10 and 11).

$$\mathrm{Ph}(p\text{-Tol})\mathrm{SiCl_2} \xrightarrow[\mathrm{THF}]{\mathrm{Li}} [\mathrm{Ph}(p\text{-Tol})\mathrm{Si}]_4 \xrightarrow[\mathrm{TfOH\ =\ CF_3SO_3H}]{\mathrm{TfOH}}$$

$$\mathrm{Si_4Ph_4}(p\text{-Tol})_3\mathrm{OTf} \xrightarrow[\mathrm{X\ =\ F,Cl,Br,I}]{\mathrm{LiX}} \mathrm{Si_4Ph_4}(p\text{-Tol})_3\mathrm{X} \qquad (10)$$

$$\mathrm{Si_4Ph_4}(p\text{-Tol})_3\mathrm{H} \xleftarrow{\mathrm{NaBH_4}} \mathrm{Si_4Ph_4}(p\text{-Tol})_3\mathrm{Br} \xrightarrow{t\text{-}\mathrm{BuLi}} \mathrm{Si_4Ph_4}(p\text{-Tol})_3\mathrm{Bu}\text{-}t \qquad (11)$$

The reaction of $(t\text{-Bu})_2SiCl_2$ with lithium affords the highly hindered products hepta-*t*-butylcyclotetrasilane and *trans*-1,1,2,3,3,4-hexa-*t*-butylcyclotetrasilane[55] (equation 12).

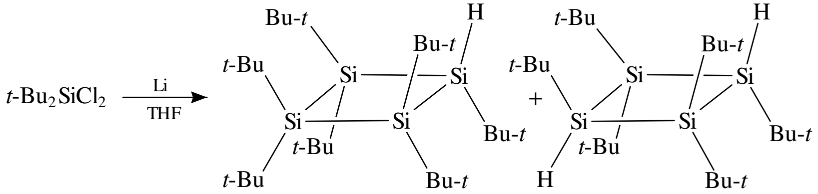

(12)

+ $\mathrm{H}(t\text{-Bu})_2\mathrm{SiSi}(\mathrm{Bu}\text{-}t)_2\mathrm{H}$

Quite interesting structural features are found for both compounds. The Si—Si bond distance in hepta-*t*-butylcyclotetrasilane with 254.2 pm is the longest reported so far in cyclotetrasilanes, while the dihedral angles near 16° are relatively small compared with those of other *t*-butyl-substituted cyclotetrasilanes. The hexa-*t*-butyl derivative, however, adopts a planar conformation with unexceptional Si—Si bond lengths of 238.7 pm. In the UV spectrum of hepta-*t*-butylcyclotetrasilane the longest-wavelength absorption maximum appears at 315 nm. This is the lowest electron transition energy of all alkyl-substituted cyclotetrasilanes reported so far.

C. Cyclopenta- and Cyclohexasilanes

The Si—C bonds in the five- and six-membered peralkyl- and perarylcyclopolysilanes exhibit considerable stability under various conditions. This results in Si—Si bond scission prior to substituent exchange in the course of many reactions employing cyclopolysilane substrates. The introduction of reactive side groups into polysilane rings, therefore, is much desirable in order to allow the performance of chemical reactions under preservation of the polysilane ring skeleton. As a consequence, recent research in cyclopenta- and cyclohexasilane chemistry mainly focused on substituent exchange reactions giving rise to the formation of mono- or polyfunctional cyclosilanes and further derivatives thereof.

Perphenylcyclopolysilanes are easily dephenylated by anhydrous hydrogen halides[56]. The reactivity decreases sharply in the order HI > HBr > HCl. In the presence of catalytic amounts of the corresponding aluminum halide or under forcing conditions (excess HX, high pressure), all phenyl groups are replaced by halogen and the perhalocyclopolysilanes $(SiX_2)_n$ with X = Cl, Br and I and $n = 4$, 5 and 6 are obtained. Partial dephenylation, however, is sometimes also possible under proper reaction conditions. Generally, the reaction follows an electrophilic substitution mechanism of the aromatic ring. Alkyl-substituted phenyl groups like *p*-tolyl or mesityl exhibit enhanced reactivity, which can sometimes be utilized for the synthesis of partially functionalized cyclopolysilanes[54].

Triflic acid also readily cleaves the Si−C bonds in arylcyclopolysilanes. The method, which has been studied by Uhlig in detail[57,58], has been recently applied to the synthesis of previously unknown cyclopentasilane derivatives Si_5Ph_9X with X = CF_3SO_3, F, Cl, Br, I, H, NMe_2, PPh_2, *i*-PrO, Me, $SiPh_3$ and $SnPh_3$[59,60]. Dearylation of Si_5Ph_{10} using one equivalent of triflic acid selectively yields Si_5Ph_9OTf, from which the other derivatives are easily accessible by nucleophilic substitution of the triflate group (Scheme 9).

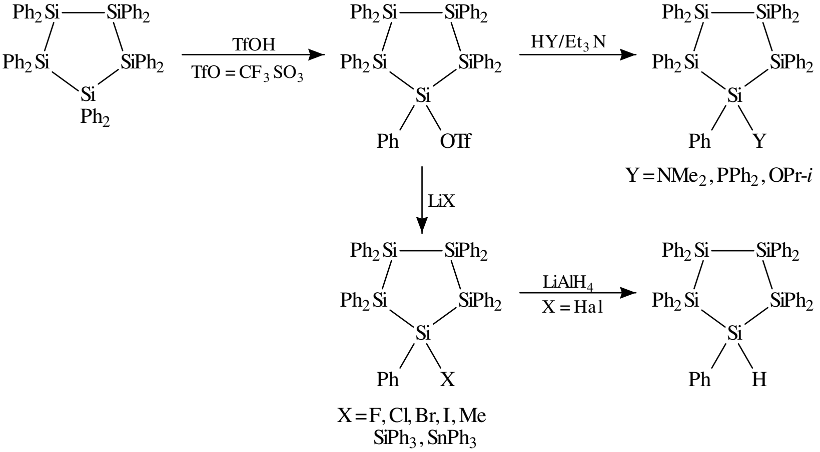

SCHEME 9

The scission of Si−aryl bonds with triflic acid takes place very easily under mild reaction conditions and shows high selectivity. Depending on the stoichiometric ratio, one or more phenyl groups can be removed step by step. When two phenyl groups are attached to the same silicon atom, the first one reacts much faster due to the high electronegativity of the triflate substituent[61]. Ditriflation of Si_5Ph_{10} by the addition of two equivalents of triflic acid, therefore, rather affords *trans*-1,3-$Si_5Ph_8(OTf)_2$ as the major product along with small amounts of the 1,2-isomers instead of the 1,1-disubstitution product[60] (Scheme 10).

The octa- and the nonahalocyclopentasilanes $H_2Si_5X_8$ and HSi_5X_9 with X = Cl, Br, I are accessible by dearylation of the corresponding phenylated cyclosilanes $H_2Si_5Ph_8$ and HSi_5Ph_9 with HX/AlX_3[62].

Methyl groups on cyclopolysilanes can also be substituted by halogens without destruction of the ring structure. With $SbCl_5$, for instance two or three methyl groups can be removed from $(Me_2Si)_6$ depending on the stoichiometric ratio of the reactants. In case of the dichlorodecamethylcyclohexasilanes, the 1,3- and 1,4-isomers are produced exclusively (Scheme 11). Formation of the 1,2 dichloride was never observed.

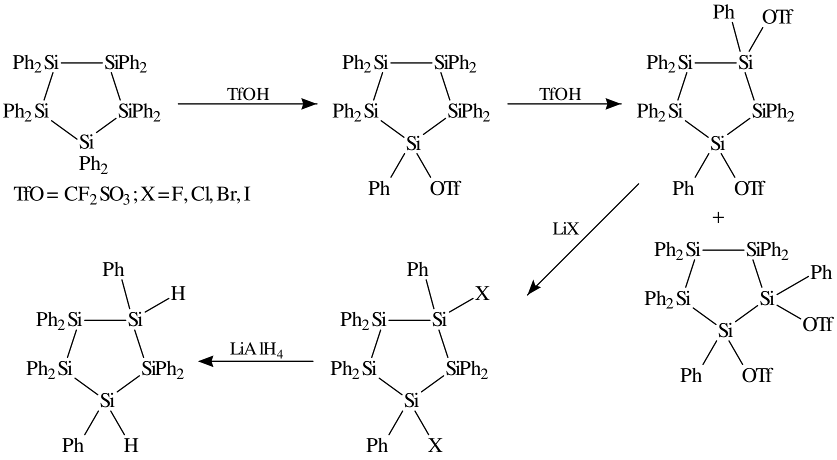

SCHEME 10

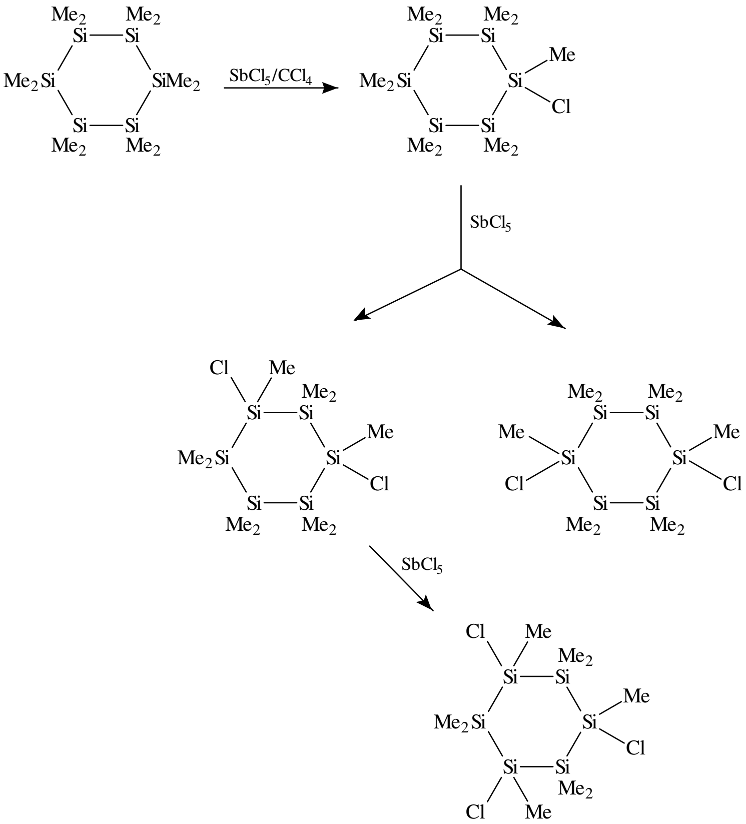

SCHEME 11

The course of the reaction is strongly influenced by solvent effects. Thus, a detailed study of the optimum reaction conditions has been performed using five-membered ring substrates. According to these investigations CCl_4 turned out to be the most suitable solvent[63].

Separation of 1,3- and 1,4-dichlorodecamethylcyclohexasilane can only be accomplished by derivatization. With $Na[(CO)_2CpFe]$, for instance, both regioisomers are converted into the bis(iron) derivatives which show different solubilities[64]. Simple hydrolysis of mixtures of 1,3- and 1,4- dichlorodecamethylcyclohexasilane affords the corresponding dihydroxy derivatives, which exhibit remarkably different stabilities with respect to intramolecular condensation to heterocyclic siloxanes. While the 1,3-isomer is stable, the 1,4-dihydroxy compound readily loses water on heating and the oxygen-bridged heterocycle decamethyl-7-oxa-1,2,3,4,5,6-hexasilanorbornane is formed. The crystal structure of the condensation product depicted in Figure 1 clearly shows the Si_6 ring in boat conformation and the bridging oxygen[65]. Both products have different boiling points and may be purified by distillation. On prolonged heating, however, considerable amounts of siloxane polymers are obtained by intermolecular condensation. The Si−O bonds in 1,3-dihydroxydecamethylcyclohexasilane and in decamethyl-7-oxa-1,2,3,4,5,6-hexasilanorbornane can finally be chlorinated with acetyl chloride to give pure 1,3- or 1,4-dichlorodecamethylcyclohexasilane, respectively (Scheme 12)[66].

The partially chlorinated cyclosilanes are valuable starting materials for the synthesis of other derivatives like di- and polycyclic polysilanes (see Section V.A). The dehalogenative coupling with alkali metals, however, only gives low yields and many side products are formed. Salt elimination of cyclosilanyl halides and cyclosilanyl alkali metal compounds

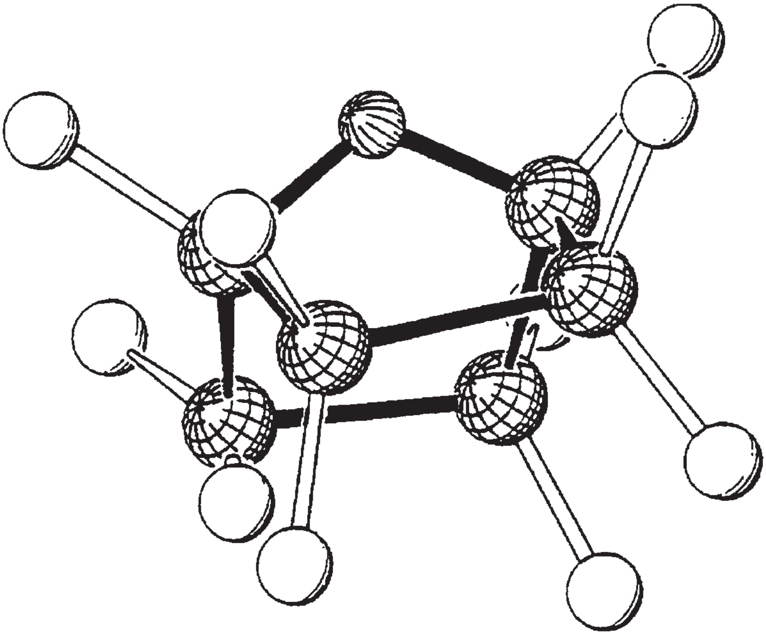

FIGURE 1. Crystal structure of decamethyl-7-oxahexasilanorbornane* (cocrystallized with 1,4-dihydroxydecamethylcyclohexasilane[66]. Reprinted from Hengge *et al.*, *J. Organomet. Chem.*, **499**, 241 (1995) with kind permission from Elsevier Science S.A., P.O. Box 564, 1001 Lausanne, Switzerland

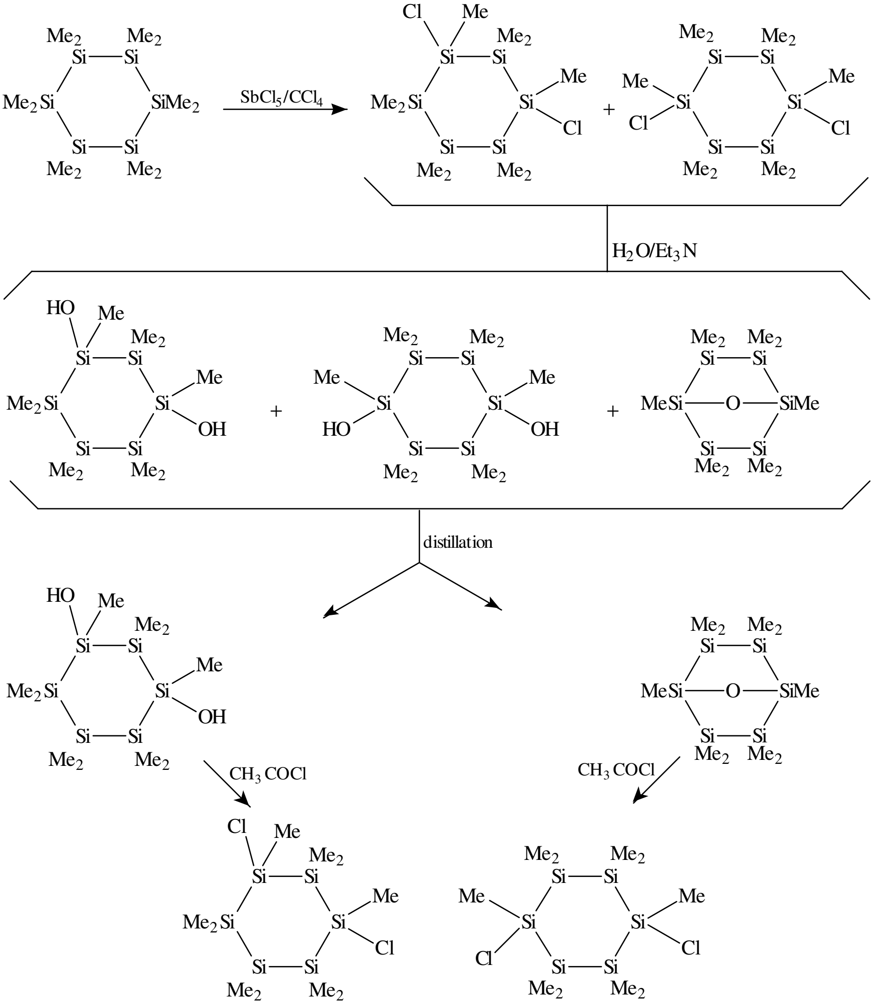

SCHEME 12

turned out to be much more effective, though alkali metal derivatives of cyclosilanes have only been available by a multistep synthesis via the corresponding mercury compounds until recently[67] (Scheme 13).

Lately, a more satisfactory synthesis was found[68]. When a diglyme solution of $(Me_2Si)_6$ with potassium *t*-butoxide is stirred at room temperature for 7–8 days, undecamethylcyclohexasilanylpotassium is obtained in 70% yield (equation 13).

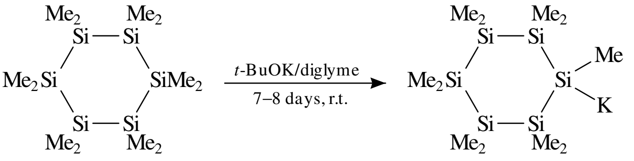

(13)

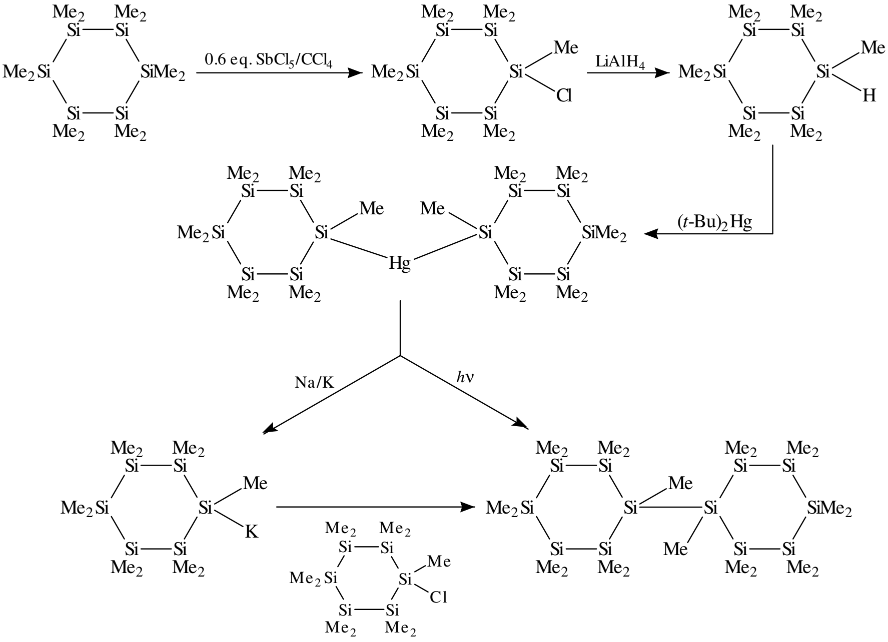

SCHEME 13

When the reaction is monitored by ^{29}Si-NMR, surprisingly, nonamethylcyclopentasilanylpotassium is found as an intermediate. This observation suggests the initial splitting of the six-membered ring by potassium *t*-butoxide followed by the formation of the kinetically preferred five-membered ring and trimethylsilyl *t*-butoxide, which can be isolated in the expected amounts. Subsequently, rearrangement to the thermodynamically stable six-membered ring may take place. Similar rearrangements have been described earlier[2,69–72].

Undecamethylcyclohexasilanylpotassium is a useful starting material for the synthesis of various cyclohexasilane derivatives, as shown in Scheme 14. Reactions affording bicyclic and polycyclic silanes are reviewed in Section V.A.

Treatment of 1-halo- or 1,4-dihalopermethylcyclohexasilane with alkali metal thiolates MSPh (M = Li, Na, K) yields the corresponding thiocyclohexasilanes which subsequently can be reacted with silanyl alkali metal compounds to give cyclohexasilanes containing exocyclic Si−Si bonds[73] (equations 14 and 15) without the formation of considerable amounts of by-products due to transmetallation reactions.

$$\mathrm{Si_6Me_{11}X + MSPh \longrightarrow Si_6Me_{11}SPh + MX} \tag{14}$$

$$\mathrm{X = Cl, Br; M = Li, Na, K}$$

$$\mathrm{Si_6Me_{11}SPh + MSiR_3 \longrightarrow Si_6Me_{11}SiR_3 + MSPh} \tag{15}$$

$$\mathrm{R = Me, Ph; M = Li, K}$$

Another route to cyclohexasilane rings with silanyl side chains begins with cyclosilanylpotassium and chlorosilanes $\mathrm{Ph}_n\mathrm{Me}_{3-n}\mathrm{SiCl}$ (Scheme 15). Dephenylation of the resulting silyl-substituted cyclohexasilanes with triflic acid and subsequent reduction

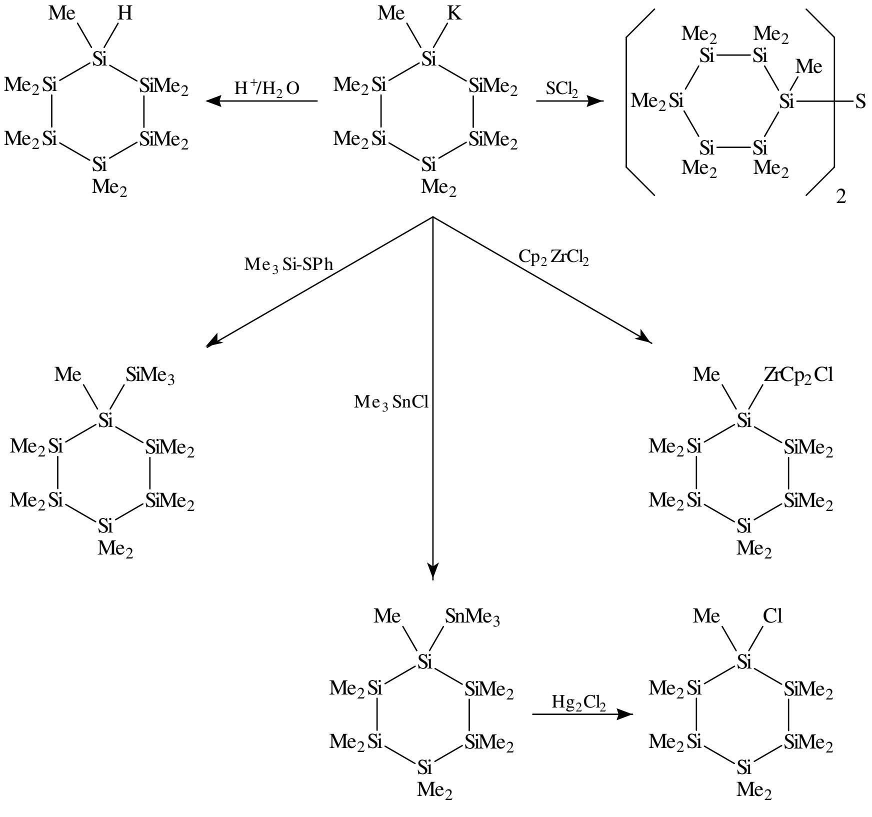

SCHEME 14

of the silyl triflates thus obtained affords cyclohexasilane derivatives with Si−H functional silanyl side chains[74], which can be used for the synthesis of new polycyclic silanes (see Section V.A).

A similar reaction sequence starting from 1,4-dichlorodecamethylcyclohexasilane and $Ph_nMe_{3-n}SiLi$ leads to 1,4-disilylcyclohexasilanes[74] (Scheme 16), which can also be converted to larger polycyclic frameworks (Section V.A).

Partially hydrogenated halocyclopolysilanes are not accessible by simple $LiAlH_4$ reduction of the corresponding perhalogenated precursor molecules. The reaction of Si_5Cl_{10}, for instance, with deficient amounts of $LiAlH_4$ only affords a mixture of Si_5Cl_{10} and Si_5H_{10}. With 5 equivalents of Me_3SnH or n-Bu_3SnH, which have been used successfully for the synthesis of hydrochlorodisilanes[75], one, two or three chlorine atoms in Si_5Cl_{10} are replaced by hydrogen and mixtures of partially hydrogenated cyclopentasilanes are obtained[76] (Scheme 17). Analogous reactions are possible using cyclohexasilane substrates.

Partially functionalized cyclopolysilanes recently attracted attention as model substances for siloxene and luminescent silicon. The yellow luminescent silicon is formed by the anodic oxidation of elemental silicon in HF-containing solutions and may be used for the development of silicon-based materials for light-emitting structures which could be integrated into optoelectronic devices[77]. Because the visible photoluminescence of

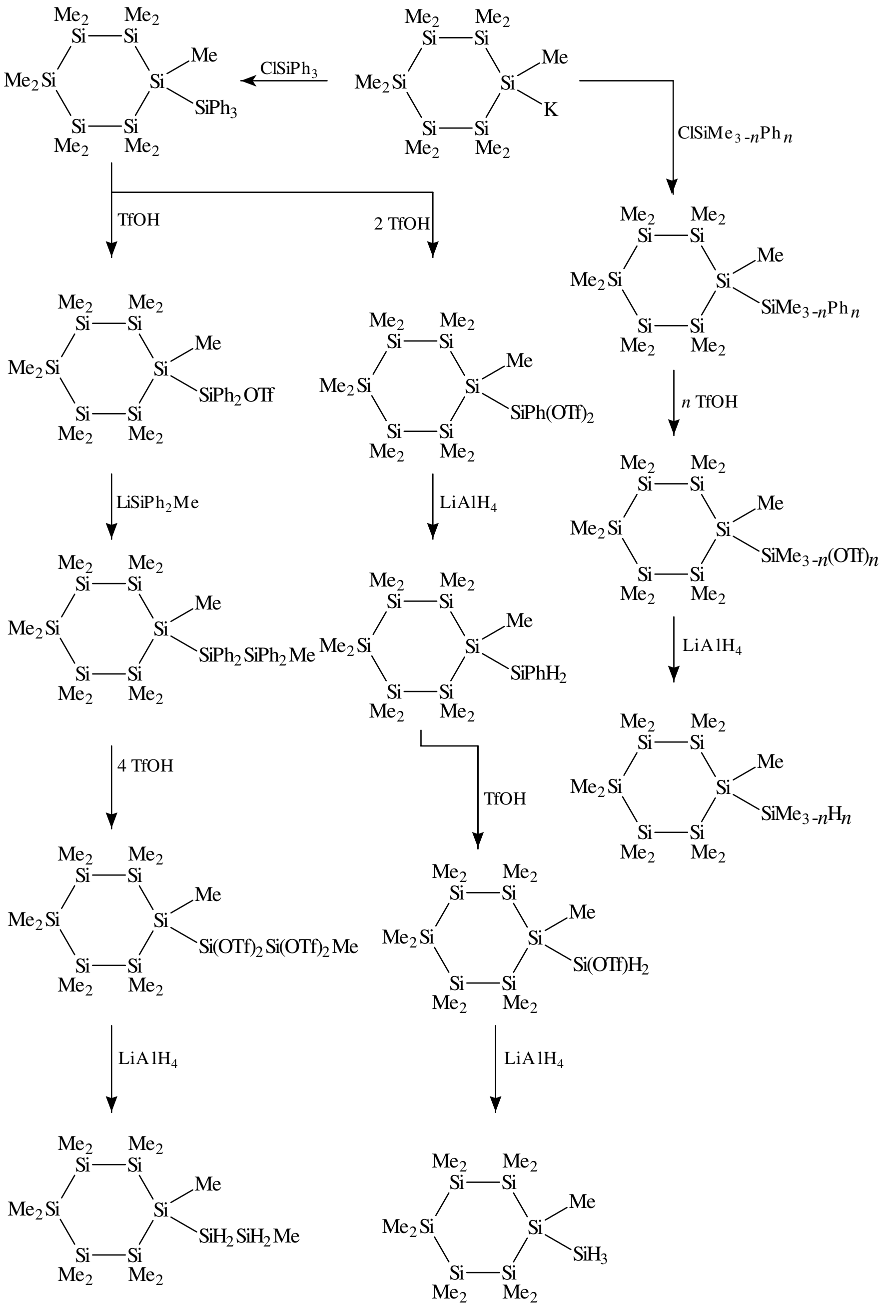
ClSiPh3
ClSiMe3-nPhn
TfOH
2 TfOH
n TfOH
LiSiPh2Me
LiAlH4
4 TfOH
TfOH
LiAlH4
LiAlH4
LiAlH4

SCHEME 15

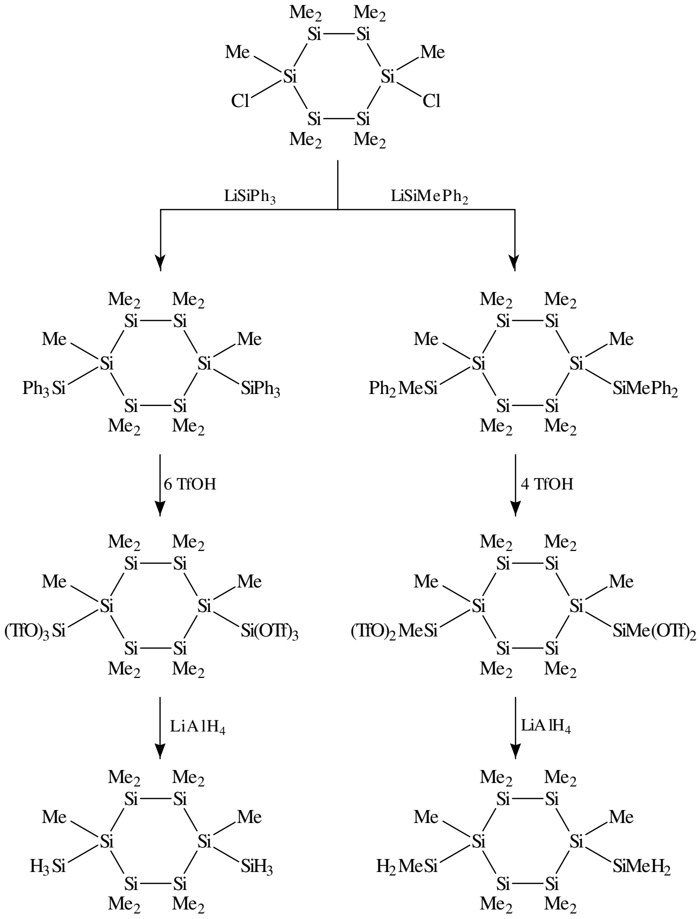

SCHEME 16

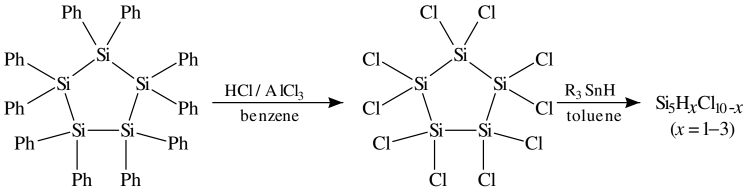

SCHEME 17

porous silicon is very similar to the photoluminescence of siloxene, some researchers have argued that layers of siloxene or siloxene-like structures are responsible for the optical properties of the material[78a]. Siloxene $(Si_6O_3H_6)_n$ was discovered by Wöhler as a product of the reaction of calcium disilicide with hydrochloric acid. The results of Wöhler were reinvestigated by Kautsky[78b] using milder reaction conditions resulting in a more

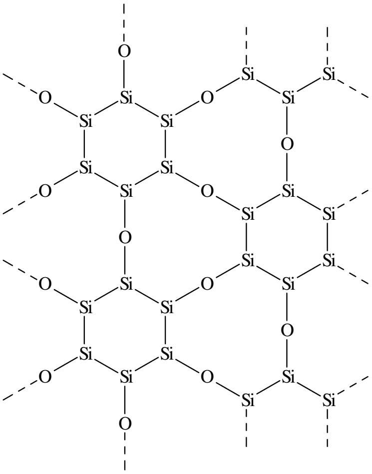

SCHEME 18

$ClMe_2SiSiMe_2Cl$
(1)

$ClMe_2SiSiMeClSiMe_2Cl$
(2)

$ClMe_2Si(SiMeCl)_2SiMe_2Cl$
(3)

$Cl_2MeSi(SiMeCl)_2SiMeCl_2$
(4)

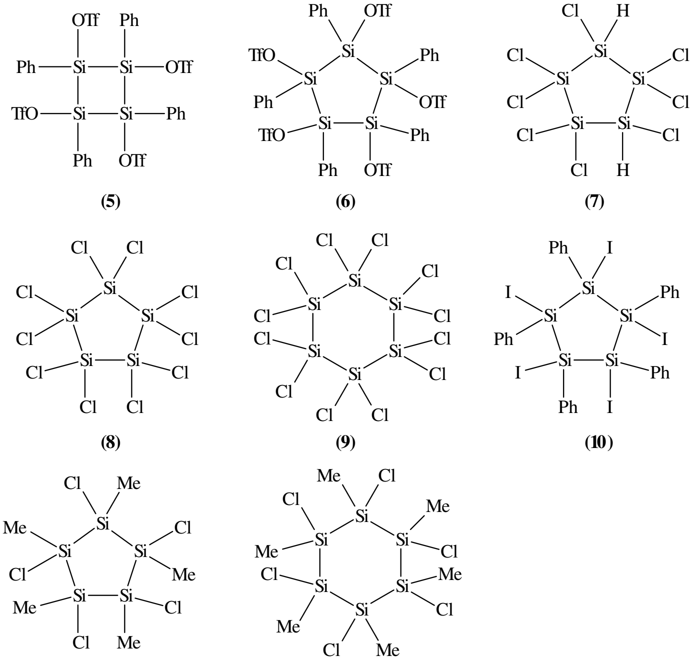

(5) **(6)** **(7)**

(8) **(9)** **(10)**

(11) **(12)**

SCHEME 19

TABLE 2. Fluorescence maxima and appearance of siloxene-like polymers derived from compounds **1–12**

Starting material		Product description	Fluorescence maximum (nm)
$Si_2Me_4Cl_2$	**1**	slightly yellowish, thin oil	none
$Si_3Me_5Cl_3$	**2**	opaque, thick oil	none
$Si_4Me_6Cl_4$	**3**	white solid	very weak (399)
$Si_4Me_4Cl_6$	**4**	white solid	weak (413)
$Si_4Ph_4(OTf)_4$	**5**	dark yellow solid	553
$Si_5Ph_5(OTf)_5$	**6**	dark yellow solid	522
1,3-$H_2Si_5Cl_8$	**7**	pale orange solid	486
Si_5Cl_{10}	**8**	white solid	400
Si_6Cl_{12}	**9**	white solid	432
$Si_5Ph_5I_5$	**10**	dark yellow-green solid	540
$Si_5Me_5Cl_5$	**11**	slightly yellow-green solid	505
$Si_6Me_6Cl_6$	**12**	slightly yellow-green solid	436

defined product. Kautsky proposed a structure for siloxene with cyclohexasilanyl rings in chair conformation connected by oxygen bridges to form a highly polymeric layer. The axial positions of the cyclohexasilane rings are occupied by hydrogen atoms (Scheme 18, hydrogens neglected).

The hydrogen atoms of siloxene can easily be replaced by stepwise bromination resulting in products of the general formula $(Si_6O_3)H_{6-n}Br_n$. The bromides can subsequently be converted to amines, hydroxides or alkoxy derivatives. All siloxene derivatives exhibit color and strong fluorescence. Detailed studies of the chemical and physicochemical properties, including substituent effects on the optical spectra of siloxene derivatives, have already been performed in the early days and have been thoroughly reviewed[79].

Although there is much evidence that the structure of siloxene fits the one depicted in Scheme 18, a clear proof is still missing. Recently, attempts were made to elucidate this question by rebuilding the proposed structure of siloxene starting from well-defined low molecular weight polysilanes[80] instead of $CaSi_2$. Therefore, several cyclic and linear polysilanes containing silicon–halogen or silicon–triflate functions (compounds **1–12** in Scheme 19) were hydrolyzed and thermally condensed to polymeric siloxanes. Depending on the starting materials, the fluorescence maxima of the products thus obtained range from 400 to 500 nm, as shown in Table 2.

Since only polymers obtained from the cyclic starting materials **5**, **6**, **7**, **10**, **11** and **12**, which are likely to have siloxene-like structures, exhibit color and fluorescence, the polysilane ring seems to be essential for the exceptional optical properties of siloxene. This is in agreement with the original idea of Kautsky, who assumed the cycle to be the chromophore.

V. POLYCYCLIC SILANES AND CAGES

A. Linearly Connected Cyclosilanes

In contrast to annelated polycyclic polysilanes, where two cyclopolysilane units share two common silicon atoms, in linearly connected polycyclosilanes mainly two or three polysilane rings are linked by exocyclic Si−Si bonds. Selected compounds, which recently have been described in the literature, are presented in Scheme 20. More details and bibliography can be found elsewhere[5d,22].

Linearly connected polycyclic silanes are usually made by salt elimination reactions, whenever the cyclosilanyl alkali metal compound involved is stable enough. Otherwise, the photochemical cleavage of bis(cyclosilanyl)mercury compounds may be employed. An example is shown in Scheme 13, where bi(undecamethylcyclohexasilanyl) is synthesized either from XSi_6Me_{11} (X = Cl, Br) and KSi_6Me_{11} or by photolysis of $(Si_6Me_{11})_2Hg$. Both methods can also be used to make polycyclic systems containing cyclopentasilanyl units. When $BrSi_6Me_{11}$ or 1,4-$Br_2Si_6Me_{10}$ are reacted with KSi_5Me_9, polycyclic polysilanes are formed containing both five- and six-membered rings[81].

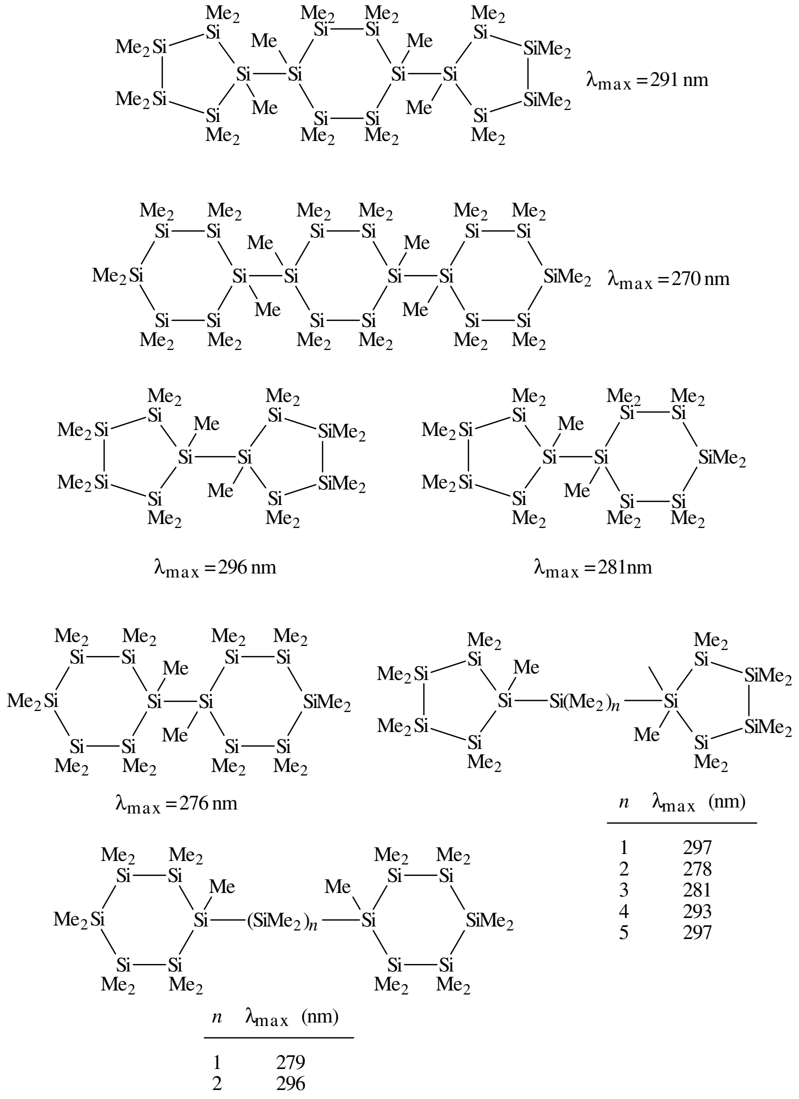

n	λ_{max} (nm)
1	297
2	278
3	281
4	293
5	297

n	λ_{max} (nm)
1	279
2	296

SCHEME 20

Interesting features are shown by the UV absorption spectra of the linearly connected polycyclic silanes (Scheme 20 also gives the longest-wavelength UV absorption maxima)[81]. A marked bathochromic shift of the first UV-maximum relative to the corresponding monocyclic compound results when two cyclosilanyl systems are bonded directly to each other, particularly in the case of two cyclopentasilane rings. When six-membered rings are involved, the effect becomes less pronounced; this strongly suggests the presence of distinct electronic interactions between two Si_5 moieties, which become less favorable with the six-membered analogs. Tricyclic systems behave similarly. Compounds with two cyclosilanyl rings linked by a $-(SiMe_2)_n-$ bridge exhibit a regular bathochromic shift of the first UV absorption maximum with an increasing length of the connecting $-(SiMe_2)_n-$ chain quite similar to linear polysilanes (compare Section III).

The partial dephenylation of diphenyldecamethylcyclohexasilanes with stoichiometric amounts of triflic acid provides an entry into the class of functional polycyclic silanes[82], which subsequently may be used as starting materials for further syntheses. Thus, 1,3- or 1,4-$Ph_2Si_6Me_{10}$, now easily available by the reaction of the pure isomers 1,3- or 1,4-$Cl_2Si_6Me_{10}$ (compare Section IV.C) with PhLi, react with one equivalent of CF_3SO_3H to give the corresponding monotriflates, from which 1,3- and 1,4-$XPhSi_6Me_{10}$ (X = Cl, Br) are accessible with LiX (Scheme 21).[†]

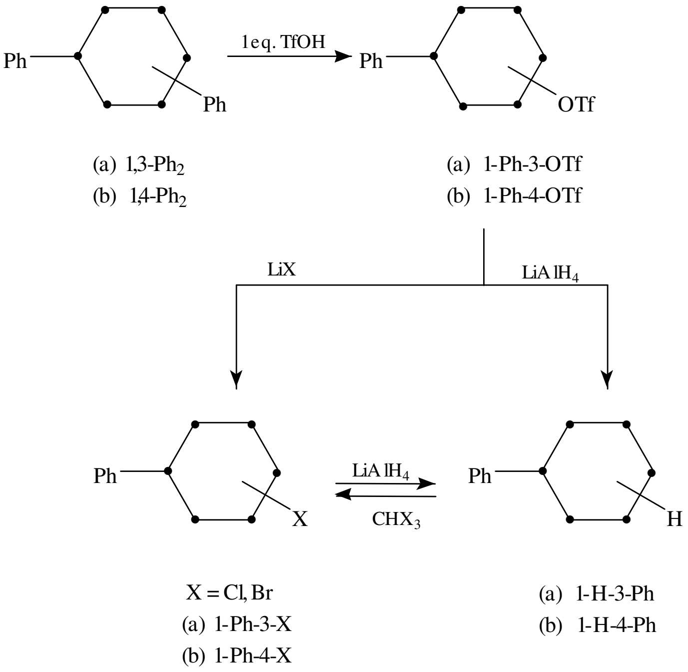

SCHEME 21

Further reaction of 1,3- or 1,4-$XPhSi_6Me_{10}$ with KSi_6Me_{11} affords the corresponding monophenylated permethylcyclohexasilanyl dimers, which again can be converted to the halo derivatives with CF_3SO_3H/LiX, as shown in equation 16.[†]

[†] In Scheme 21 and equation 16 a dot represents a silicon atom with methyl groups attached, sufficient to bring the total coordination number to four.

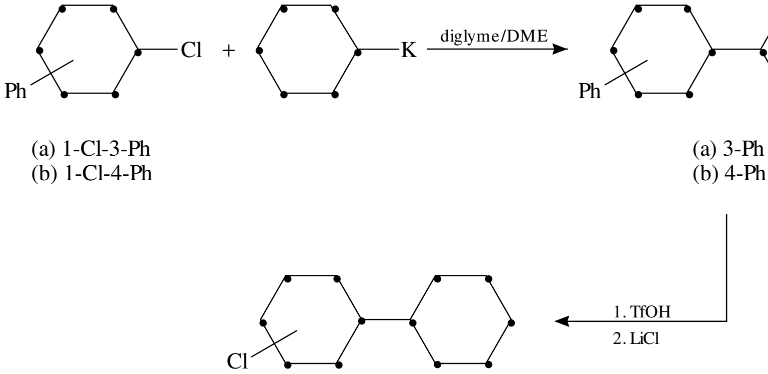

(a) 1-Cl-3-Ph
(b) 1-Cl-4-Ph

(a) 3-Ph
(b) 4-Ph

(16)

(a) 3-Cl
(b) 4-Cl

A system with two cyclohexasilanyl substituents on one phenyl ring is obtained from the phenyl-1,4-di-Grignard reagent and $ClSi_6Me_{11}$[83,84] (equation 17).

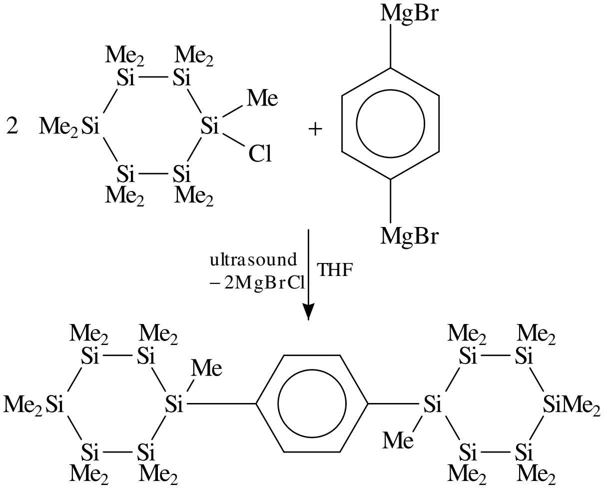

(17)

The X-ray structure of 1,4-bis(undecamethylcyclohexasilanyl)benzene (Figure 2) exhibits a triclinic unit cell with the benzene ring in axial positions of the two cyclohexasilanyl chairs, which both adopt *cis*-positions relative to the plane of the benzene ring.

Compounds containing two cyclohexasilanyl rings linked by a functional −SiMeX− group have also been synthesized[85]. Starting materials are monocyclic silanes with $SiPh_nMe_{3-n}$ ($n = 2, 3$) side chains. A typical reaction sequence is shown in equation 18. $Ph_2MeSi{-}Si_6Me_{11}$ affords the corresponding dihalomethylsilyl derivative after treatment with two equivalents of $CF_3SO_3H/LiCl$, which subsequently can be converted to the Cl or H functional bicyclosilanes with KSi_6Me_{11} and $LiAlH_4$. At this point it needs to be emphasized that a phenyl group bonded to the central Si atom cannot be removed by the

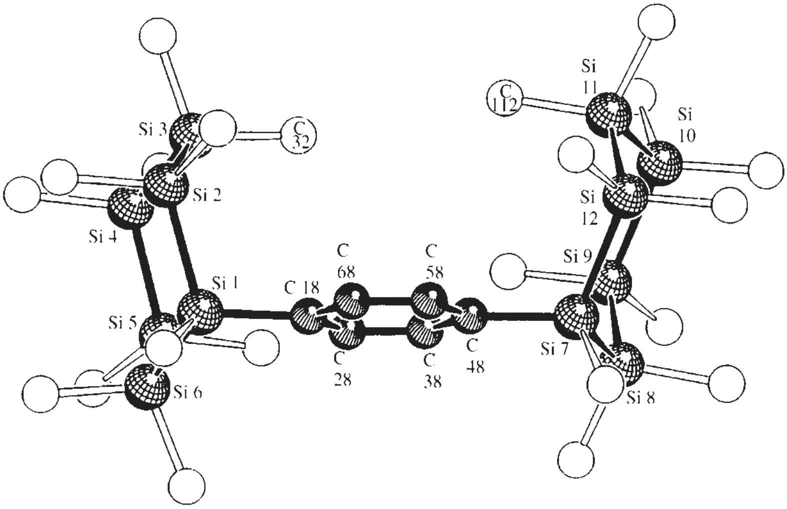

FIGURE 2. Crystal structure of 1,4-bis(undecamethylcyclohexasilanyl)benzene. Reprinted from Hengge *et al.*, *J. Organomet. Chem.*, **524**, 187, (1996) with kind permission from Elsevier Science S.A., P.O. Box. 564 1001 Lausanne, Switzerland

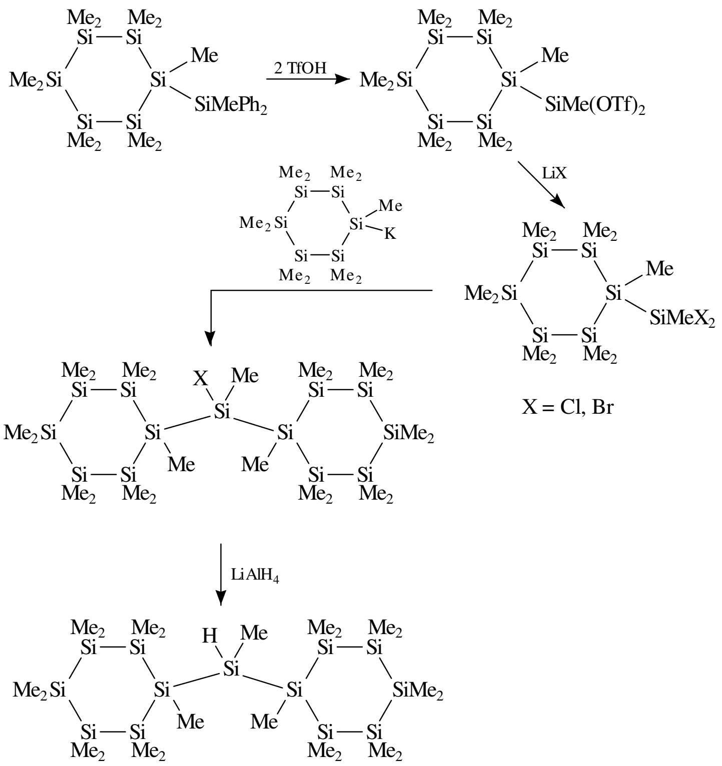

(18)

usual methods with triflic acid or with HX/AlX$_3$, very likely for steric reasons. Attempts to attach a third Si$_6$Me$_{11}$ group to the central Si atom also failed. Three cyclohexasilanyl groups, however, can easily be linked to a larger central Sn atom as has been shown recently by Uhlig and coworkers[86].

Catalytic dehydrogenative coupling of cyclosilanes bearing Si−H functional side groups has also been used for the synthesis of polycyclic polysilanes[74]. Thus, H$_3$SiSi$_6$Me$_{11}$ reacts in the presence of catalytic amounts of Cp$_2$ZrMe$_2$ or Cp$_2$TiMe$_2$ to give the dimeric product, whereas MeH$_2$SiH$_2$Si−Si$_6$Me$_{11}$ or 1,4- MeH$_2$Si−Si$_6$Me$_{10}$−SiH$_2$Me react to give oligomers containing 2 to 4 monomeric units. Under similar reaction conditions a soluble polymer, for which a linear structure is suggested by NMR investigations, is obtained from 1,4-H$_3$Si−Si$_6$Me$_{10}$−SiH$_3$ (equations 19–21). Gel permeation chromatography shows molecular weights of M$_w$ = 10500 (with Cp$_2$ZrMe$_2$) and M$_w$ = 4200 (with Cp$_2$TiMe$_2$), respectively, versus polystyrene.

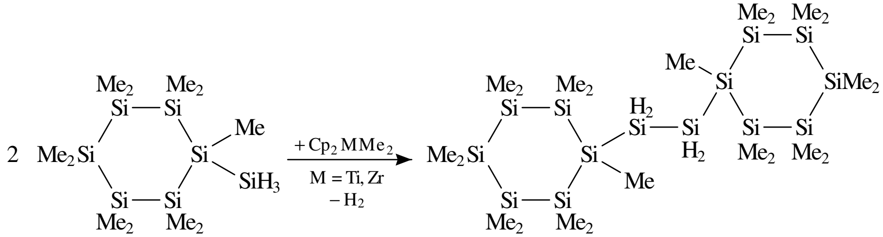

(19)

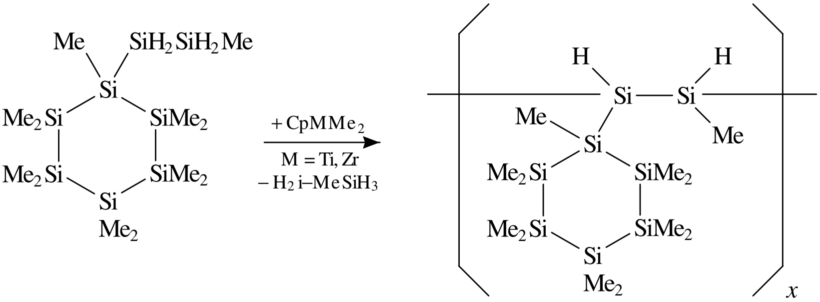

$x = 2, 3, 4$

(20)

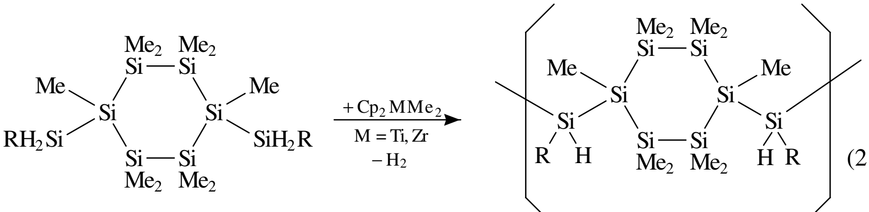

R = H, Me

R = Me: $x = 2, 3, 4$
R = H: x = polymer

(21)

Cyclosilanes with hydrogen atoms directly attached to the ring do not react to give oligomers in the presence of the usual catalysts like Cp$_2$ZrMe$_2$ or Cp$_2$TiMe$_2$.

Recently, a first example of a purely inorganic cyclopolysilane dimer has been described[87]. As shown in Scheme 22, Si_5Cl_9H[62] can easily be converted to bi(nonachlorocyclopentasilanyl) upon treatment with $(t\text{-Bu})_2Hg$. The reaction of Si_5Ph_9Br[60] with naphthyl lithium affords the phenyl derivative bi(nonaphenylcyclopentasilanyl). When the perhalogenated cyclopentasilanedimers are reacted with $LiAlH_4$, about 15% of Si_5H_{10} are obtained along with the expected product bi(cyclopentasilanyl), which demonstrates the remarkable sensitivity of the central Si−Si bond towards nucleophilic attack.

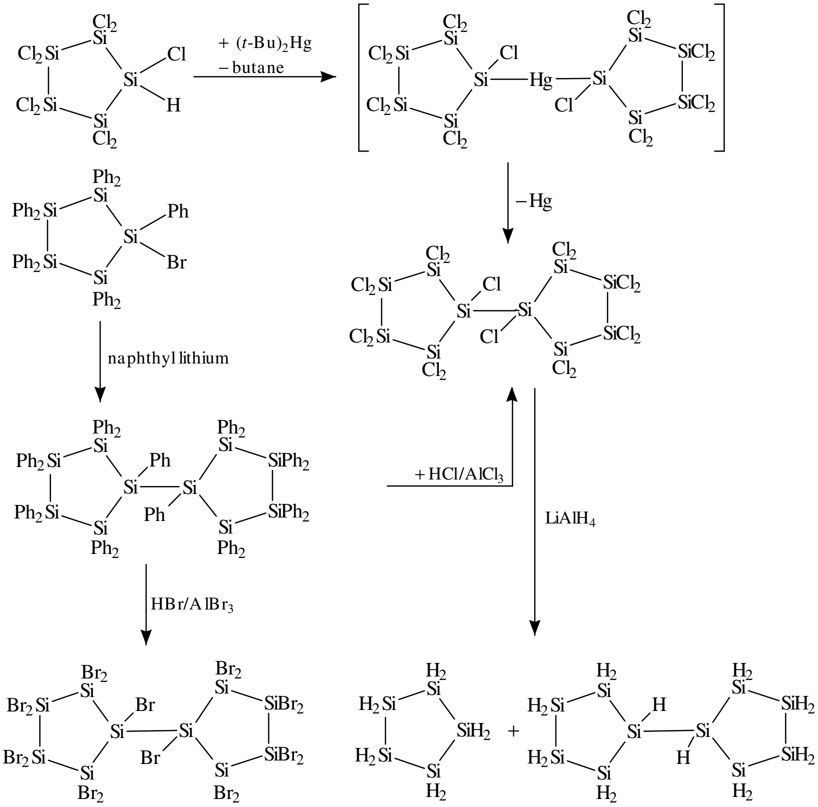

SCHEME 22

B. Annelated Cyclosilanes

Only a handful of annelated cyclosilanes are known. Nothing substantial has been published on the topic since the last review appeared[5d]. The best investigated compound is octadecamethylbicyclo[4.4.0]decasilane **13**. It is formed in the reaction of a mixture of Me_2SiCl_2 and $MeSiCl_3$ with Na/K alloy[88]. Recently, an improved synthesis has been published together with spectroscopic properties and an X-ray structure determination[89]. The radical anion of the compound, which can be generated by action of Na/K alloy at 130 K, is stable only at low temperatures. Further investigations will be necessary to understand the electronic structure of this bicyclic radical anion.

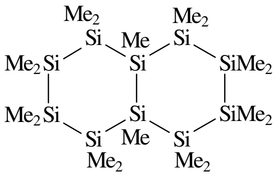

(13)

C. Polysilane Cages

Recently, some attention has been focused on the synthesis and on the properties of strained cage compounds made up exclusively of Si atoms. As a consequence a number of derivatives of tetrasilatetrahedrane, hexasilaprismane and octasilacubane have been synthesized. The current knowledge in the field up to 1994 has been summarized elsewhere[5d,22,43].

Polysilane cages are usually prepared by the reductive coupling of bulky organohalosilane precursors mainly with Li, Na or Mg metal as shown in equations 22 and 23 for octakis(2,6-diethylphenyl)octasilacubane or hexakis(2,6-diisopropylphenyl)hexasilaprismane[90,91].

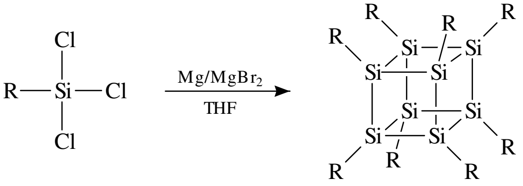

R = 2,6-$Et_2C_6H_3$

(22)

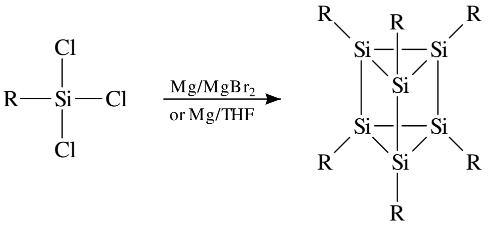

R = 2,6-*i*-$Pr_2C_6H_3$

(23)

The highly strained tetrasilatetrahedrane structure can only be stabilized using extremely bulky substituents like the tri-*t*-butylsilyl (= supersilyl) group. Thus the only tetrasilatetrahedrane derivative known so far has been synthesized by coupling (t-Bu)$_3$SiSiBr$_2$SiBr$_2$Si(Bu-t)$_3$ with two equivalents of (t-Bu)$_3$SiNa[92] (equation 24).

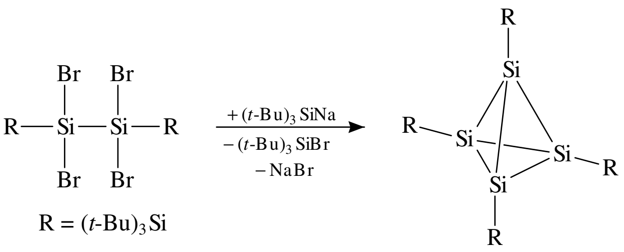

R = (*t*-Bu)$_3$Si

(24)

Remarkable photosensitivity is observed for the hexasilaprismane mentioned above[90]. Upon irradiation with light of wavelengths between 360–380 nm in solution at 223 K or in a glass matrix at 77 K, new absorption bands appear which are very likely due to the formation of hexasila-Dewar benzene containing highly reactive Si=Si double bonds. The hexasilaprismane is immediately regenerated thermally or by excitation of the new absorption bands with light of wavelengths longer than 460 nm (equation 25). The activation energy for the reverse reaction has been calculated to be only 57.4 kJ mol^{-1}. This small E_a value is consistent with the high reactivity of Si=Si double bonds.

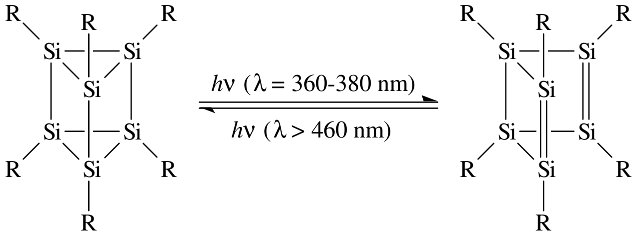

(25)

R = 2, 6-i-$Pr_2C_6H_3$

An unprecedented skeletal rearrangement leading to the formation of octakis(1,1,2-trimethylpropyl)octasilacubane has been recently reported[93] (Scheme 23). The octasilacubane derivative, which is usually made from (1,1,2-trimethylpropyl)trichlorosilane and sodium in 2.6% yield[94], is formed in 70% yield by the reductive dehalogenation of 4,8-dichloro-, 4,8-dibromo- and 4,8-diiodooctakis(1,1,2-trimethylpropyl)tetracyclo[3.3.0.0^{2,7}0^{3,6}]octasilanes with sodium in toluene at 110 °C along with a reduced product 4,8-dihydrooctakis(1,1,2-trimethylpropyl)tetracyclo[3.3.0.0^{2,7}0^{3,6}]-octasilane.

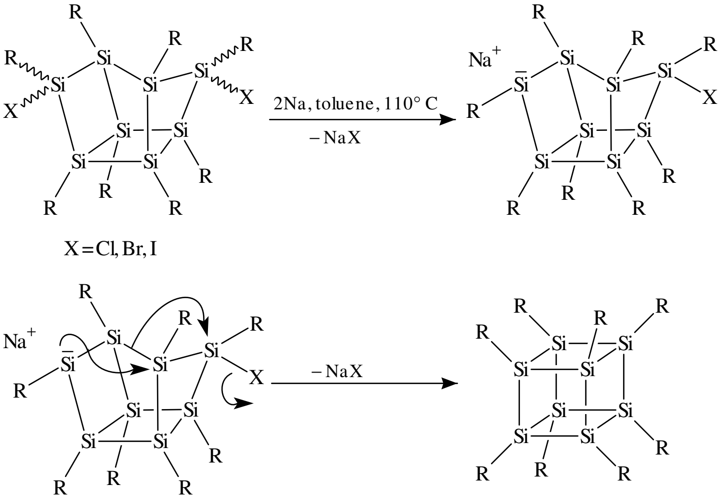

R = CMe_2CHMe_2

SCHEME 23

The formation of the octasilacubane skeleton in the reaction described above is quite remarkable in light of previous work by Masamune and coworkers, who found that treatment of 4,8-dichloroocta-*t*-butyl-tetracyclo[3.3.0.0^{2,7}0^{3,6}]octasilane with lithium naphthalenide in toluene had provided only the reduced product 4,8-dihydroocta-*t*-butyl-tetracyclo[3.3.0.0^{2,7}0^{3,6}]octasilane[95].

The 4,8-dihalotetracyclooctasilane starting materials were synthesized by treating the octasilacubane with PCl_5, Br_2 or I_2, respectively (equation 26). Thus, not really a new route to octasilacubanes has been discovered, but a new mechanism, which might be able to provide an entry into new synthetic strategies.

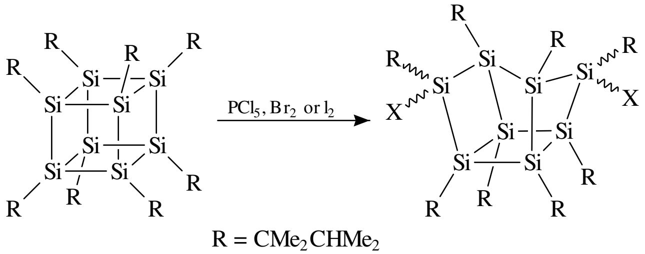

(26)

R = CMe_2CHMe_2
X = Cl, Br, I

The halogenation of octakis(1,1,2-trimethylpropyl)octasilacubane results in the formation of three possible stereoisomeric 4,8-dihalooctakis(1,1,2-trimethylpropyl)tetracyclo [3.3.0.0^{2,7}0^{3,6}] octasilanes (Scheme 24) which can be separated by preparative HPLC and characterized spectroscopically and by X-ray crystallography[93,96]. Compared to the structures of octasilacubanes, which are almost perfectly cubic, all three isomers adopt highly distorted conformations with folded cyclotetrasilane rings and Si−Si−Si bond angles varying from 81.2° to 93.9°. The Si−Si bond distances are considerably lengthened compared to the normal value of about 234 nm and vary from 235.1 to 247.1 pm. In agreement with the X-ray structures the ^{29}Si-NMR spectra of the *endo,exo* isomers show eight resonance lines, indicating that all silicon atoms are nonequivalent, whereas the other isomers only exhibit four signals because of their higher symmetry.

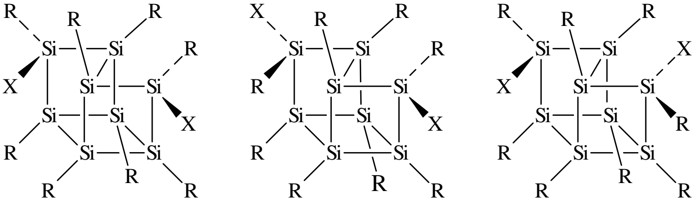

endo,exo *exo,exo* *endo,endo*

SCHEME 24

In the case of X = Cl or Br, the *endo,exo* isomer is generated preferentially in yields of 37 and 32%, respectively, whereas the *exo,exo* form of the diiodide is most abundant (39% yield). The *endo,endo* product is obtained in yields of about 10–15% in all cases.

A series of complex cage polysilanes has been synthesized starting from *t*-$BuCl_2SiSiCl_2Bu$-*t* by Masamune and coworkers[95]. When *t*-$BuCl_2SiSiCl_2Bu$-*t* is treated with lithium naphthalenide in DME, reductive oligomerization takes place and, somewhat surprisingly, tricyclo[2.2.0.0^{2,5}]hexasilane and tetracyclo[3.3.0.0^{2,7}.0^{3,6}]octasilane derivatives are obtained (Scheme 25). The unexpected structures of the products were established by double quantum coherence ^{29}Si-NMR spectroscopy[97] and X-ray crystallography.

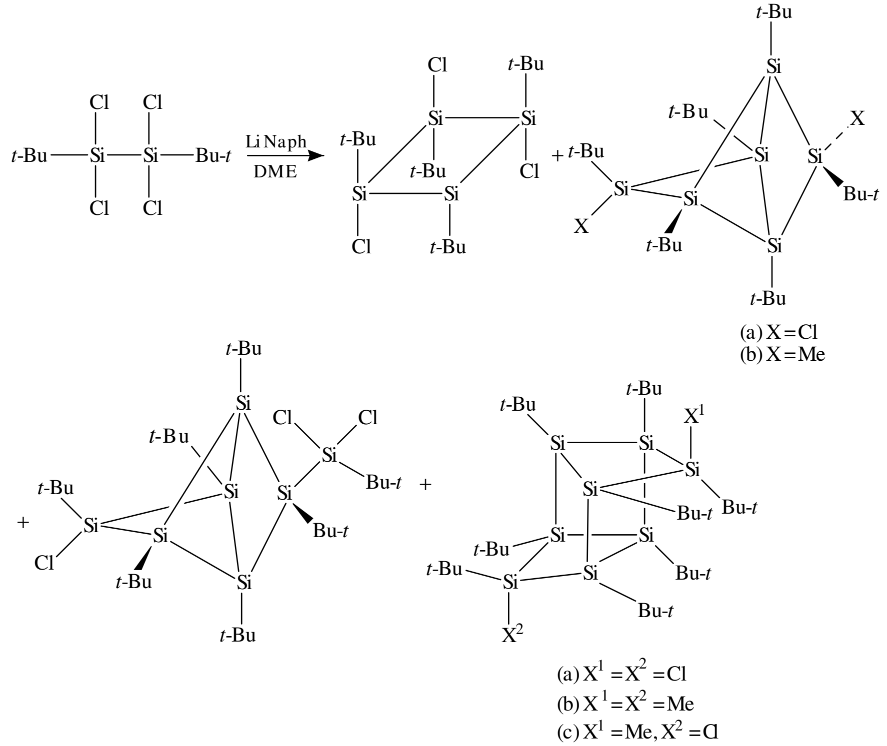

SCHEME 25

Another recent study[98] does not deal with the formation of homocyclic polysilane cages, but with the insertion of oxygen into a strained bicyclic ladder polysilane. The introduction of heteroatoms into ladder polysilane skeletons seems interesting because of possible perturbations of the σ-(Si−Si) conjugation system. The oxidation of decaisopropylbicyclo[2.2.0]hexasilane with a deficient amount of *m*-chloroperbenzoic acid (0.7 equivalents) affords the monooxidation products decaisopropyl-7-oxabicyclo[2.2.1]heptasilane in 32% yield and decaisopropyl-2-oxabicyclo[3.2.0]heptasilane in 18% yield (equation 27), which can be easily separated by HPLC.

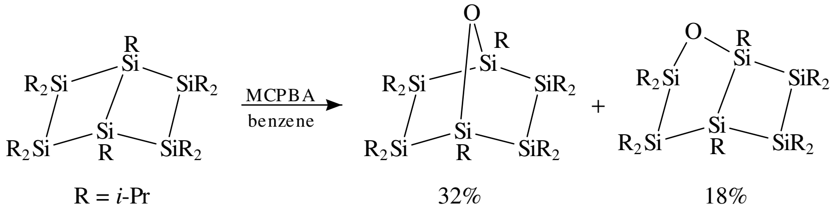

(27)

Decaisopropyl-7-oxabicyclo[2.2.1]heptasilane exhibits unique spectral properties. In the UV absorption spectrum two bands between 270–340 nm with a fairly large extinction coefficient of 5100 appear. The compound also shows considerably stronger fluorescence, with a maximum at 373 nm and a quantum yield of $\Phi = 0.014$, than the second oxidation product or the unoxidized ladder polysilane. *Ab initio* (STO-3G) calculations assign the unusual spectral properties of the compound to novel σ-n conjugation resulting from interaction of the oxygen lone pairs and the σ-(Si−Si) skeleton. An unusually small Si−O−Si bond angle of 120.2° and a long Si−O bond distance of 168.3 pm are also reported for decaisopropyl-7-oxabicyclo[2.2.1]heptasilane [compare $Me_3Si{-}O{-}SiMe_3$: $\angle(Si{-}O{-}Si) = 148.8°; d(Si{-}O) = 162.6$ pm].

VI. TRANSITION METAL CONTAINING CYCLOPOLYSILANES

Just a few reactions among the wide range of synthetic methods available for the formation of transition-metal silicon bonds turned out to be suitable for the synthesis of transition-metal derivatives of cyclopolysilanes. So far only some five- and six-membered polysilane rings bearing mostly iron or cobalt containing side groups have been made mainly by salt elimination reactions of cyclosilanyl halides and transition metal anions[5d]. Major problems associated with the cyclopolysilanyl substrates are ring cleavage and transmetallation reactions.

The first successful synthesis of a cyclosilanyl transition-metal compound was published by West and coworkers[99] in 1980, who prepared methylated cyclopentasilane derivatives containing one or two $[Fe(CO)_2Cp]$ ligands from the cyclopentasilanyl chlorides and $Na[Fe(CO)_2Cp]$ (equations 28 and 29).

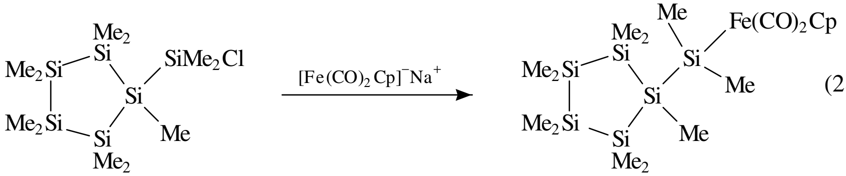

(28)

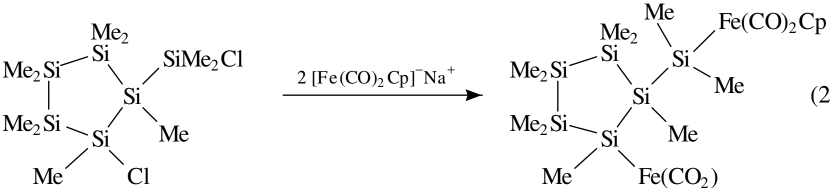

(29)

The cyclohexasilane derivatives $[(CO)_2CpFe]{-}Si_6Me_{11}$, $[(CO)_3PPh_3Co]{-}Si_6Me_{11}$, 1,3- or 1,4-$[(CO)_2CpFe]_2{-}Si_6Me_{10}$ and 1,4-$[(CO)_3PPh_3Co]_2{-}Si_6Me_{10}$ can be made quite similarly[100,101]. Manganese derivatives of cyclosilanes have also been prepared[102]. An 'inverse' salt elimination procedure, however, has to be applied in order to prevent extensive transmetallation reactions (equation 30).

$$Si_6Me_{11}K + [Mn(CO)_5]Br \longrightarrow Si_6Me_{11}[Mn(CO)_5] + KBr \qquad (30)$$

The synthesis of cobalt-substituted cyclosilanes is only possible in the presence of electron-donating ligands like PPh_3 at the transition metal center, increasing the nucleophilic character of the transition metal anion. Furthermore, use of cyclosilanyl triflates as the starting materials instead of the chloro derivatives turned out to be advantageous in order to minimize transmetallation reactions. Thus, a number of high-yield syntheses of cyclosilane derivatives containing $[Fe(CO)_2Cp]$, $[Co(CO)_3PPh_3]$, $[W(CO)_3Cp']$

(Cp′ = methylcyclopentadienyl) or [Mo(CO)$_3$Cp] fragments can only be performed starting from the corresponding cyclosilanyl triflates[100,103,104] (equations 31–33).

$$\mathrm{Me_9Si_5{-}OTf} \xrightarrow{\mathrm{Na[M]}} \mathrm{Me_9Si_5\text{-}[M]} \qquad (31)$$

(a) [M] = [Fe(CO)$_2$Cp]
(b) [M] = [Co(CO)$_3$PPh$_3$]

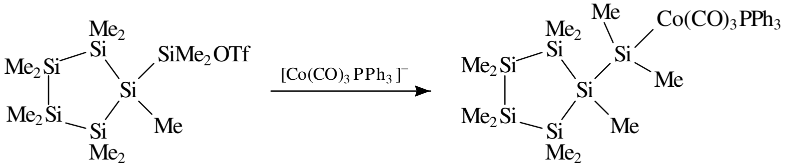

(32)

$$\mathrm{Me_{11}Si_6{-}OTf} \xrightarrow{\mathrm{K[M]}} \mathrm{Me_{11}Si_6\text{-}[M]} \qquad (33)$$

(a) [M] = [W(CO)$_3$Cp′]
(b) [M] = [Mo(CO)$_3$Cp]

At least in one example the phenylthio substituent has also been used as a leaving group in the reaction of transition metal anions and cyclopolysilanes[73]. Thus, $\mathrm{Si_6Me_{11}[Fe(CO)_2Cp]}$ is formed in excellent yields by the reaction of $\mathrm{Si_6Me_{11}SPh}$ with Na[Fe(CO)$_2$Cp] without any detectable side-products due to transmetallation reactions (equation 34). The method very likely will gain increasing importance in the future.

$$\mathrm{Si_6Me_{11}SPh + Na[Fe(CO)_2Cp] \longrightarrow Si_6Me_{11}[Fe(CO)_2Cp] + NaSPh} \qquad (34)$$

As shown in Scheme 26, cyclohexasilane derivatives bearing two different transition metal fragments are accessible from 1,4-$\mathrm{Br_2Si_6Me_{10}}$ by temporarily protecting one of the Si–Br valences with hydrogen[101].

The increased reactivity of triflate groups bonded to silicon relative to halogen substituents can also be utilized for the synthesis of multifunctional cyclopolysilane transition metal derivatives, as has recently been shown for 1,3-disubstituted cyclohexasilanes[104] (equation 35).

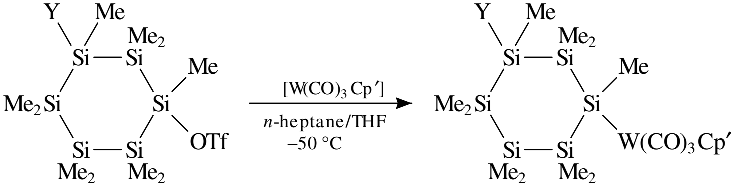

(35)

Y = Cl, Br
Cp′ = MeC$_5$H$_4$

The electron-rich late transition elements are best suited for the formation of stable bonds to silicon. Therefore, most of the cyclosilanyl transition metal compounds described in the literature so far contain transition metals belonging to the groups 7–10. A few examples with early transition elements, however, are also known[105]. $\mathrm{Cp_2ZrCl_2}$, for instance, reacts with $\mathrm{KSi_6Me_{11}}$ to give red crystals containing one cyclohexasilanyl and one chlorine substituent on the zirconium. The second chlorine atom can be easily replaced by treatment with MeLi. Addition of excess $\mathrm{KSi_6Me_{11}}$ to the monochloride, however, does not afford the dicyclosilanyl derivative (Scheme 27).

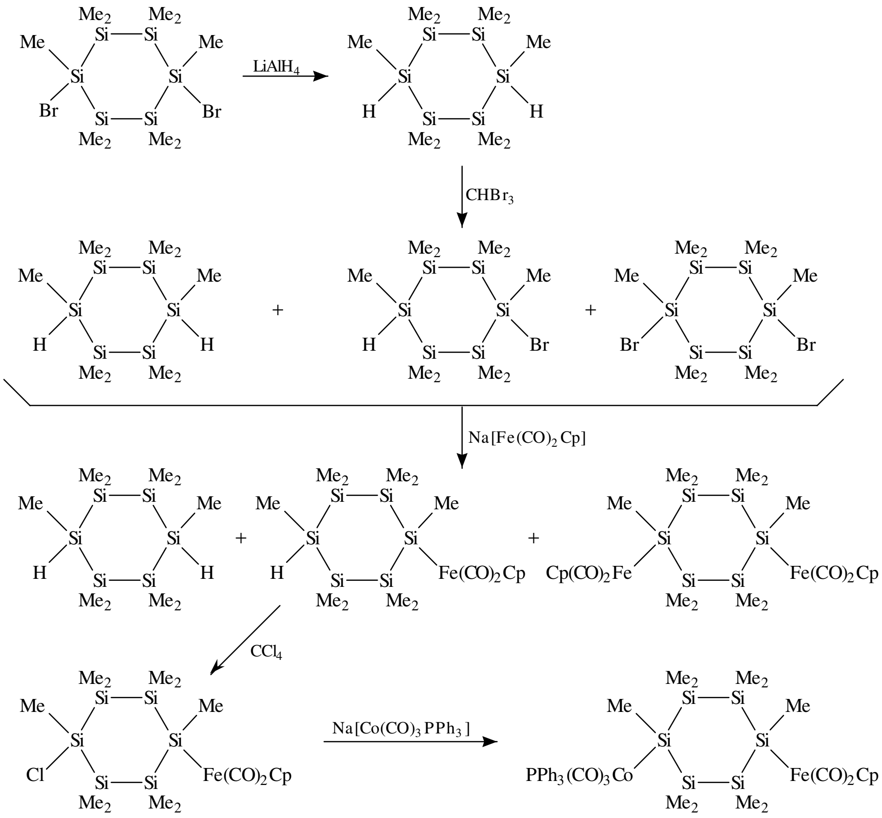

SCHEME 26

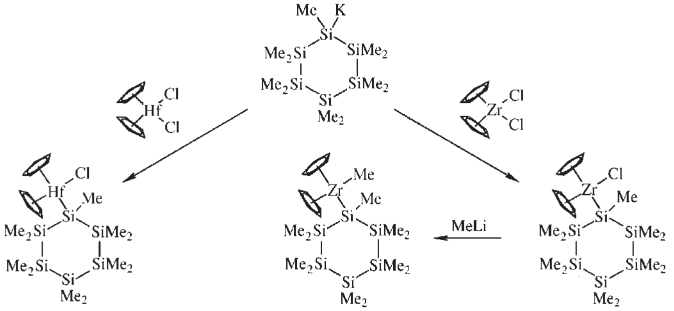

SCHEME 27

The corresponding hafnium compound behaves similarly. Attempts to make the titanium derivative using this method failed. Primarily titanium is reduced, as indicated by the color change of the solution from green to brown. Variation of the reaction conditions did not provide better results, in all cases only bi(undecamethylcyclohexasilanyl) could be identified among the reaction products.

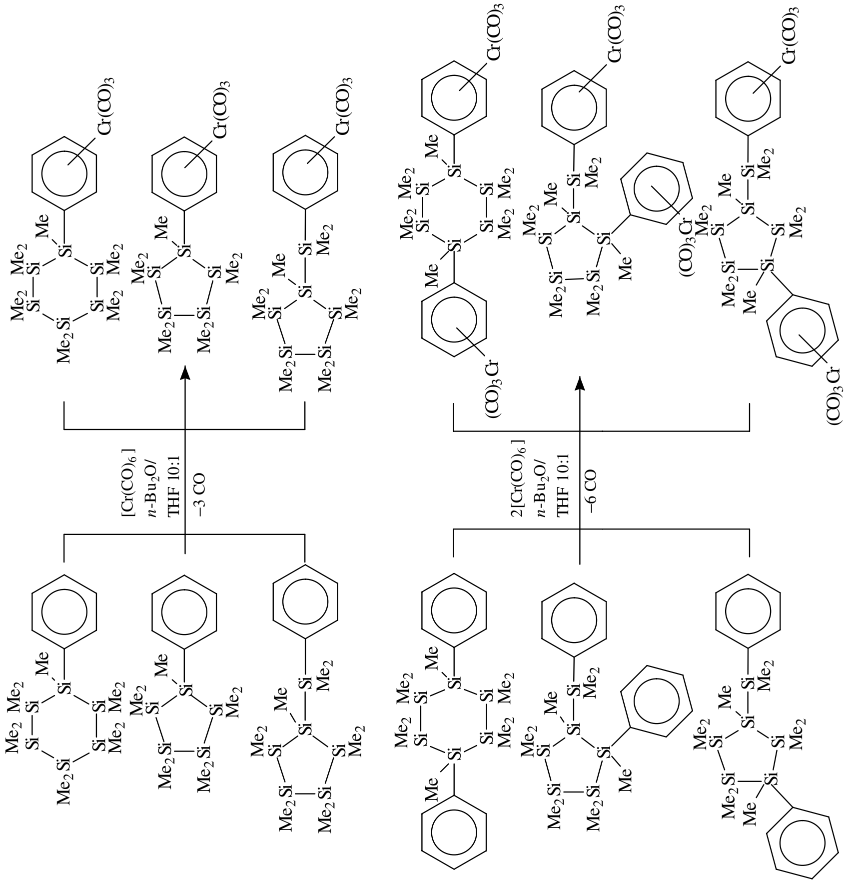

SCHEME 28

Compounds containing chromium directly linked to a cyclosilanyl ring are not known so far. From hexacarbonylchromium and mono- or diphenylcyclopenta- and hexasilanes, however, the corresponding tricarbonylchromium η^6-phenyl complexes have recently been synthesized[106] (Scheme 28).

The complexation of the phenyl groups causes a noticeable low-field shift of the ^{29}Si−NMR signal (*ca* 5 ppm) assigned to the silicon atom directly bonded to the aromatic ring, due to the presence of the electron-withdrawing tricarbonylchromium group. The different solubilities of the corresponding tricarbonylchromium complexes can be utilized for the isolation of pure 1-phenyl-2-(phenyldimethylsilyl)octamethylcyclopentasilane. This compound is usually obtained as a mixture with its 1,3-isomer, which cannot be separated by common techniques[107]. After separation of the isomeric chromium complexes by fractional crystallization the $Cr(CO)_3$ group can easily be removed by oxidation.

The chemical properties of cyclosilanyl transition metal compounds have hardly been investigated. The silicon transition metal bond is generally cleaved by acids, halogens or strong nucleophiles. However, it is remarkably stable against hydrogenation. Silicon−halogen bonds in linear oligosilanes, for instance, can be reduced with $LiAlH_4$ without any cleavage of adjacent Si−Fe bonds[108]; this also should be possible on cyclosilanyl substrates.

Some interesting rearrangement reactions of cyclosilanyl transition metal compounds were studied by Pannell and coworkers. Upon photolysis, $Si_6Me_{11}[Fe(CO)_2Cp]$ undergoes ring contraction to dicarbonyl(η^5-cyclopentadienyl)[octamethyl(trimethylsilyl)cyclopentasilanyl]iron[109] (equation 36).

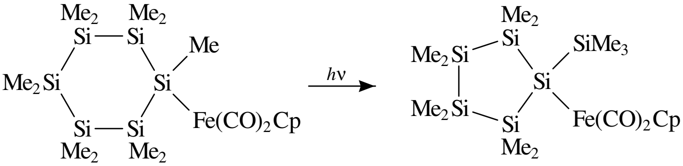

(36)

When dicarbonyl(η^5-indenyl)(undecamethylcyclohexasilanyl)iron is treated with (i-Pr)$_2$NLi and subsequently with MeI, migration of the cyclosilanyl group to the 2-position of the indenyl ligand takes place[110].

VII. ACKNOWLEDGMENTS

The authors would like to thank Dr Peter Gspaltl for drawing the formulae and his helpful comments, and Dr Christa Grogger for her assistance in the preparation of this manuscript.

VIII. REFERENCES

1. F. S. Kipping and J. E. Sands, *J. Chem. Soc.*, **119**, 830 (1921).
2. C. A. Burkhard, *J. Am. Chem. Soc.*, **71**, 963 (1949).
3. a) H. Gilman and G. L. Schwebke, *Adv. Organomet. Chem.*, **1**, 89 (1964). b) R. West and E. Carberry, *Science*, **184**, 179 (1975). c) M. Kumada and K. Tamao, *Adv. Organomet. Chem.*, **6**, 19 (1968).
4. a) E. Hengge and D. Kovar, *Angew. Chem.*, **93**, 698 (1981). b) E. Hengge and D. Kovar, *Z. Anorg. Allg. Chem.*, **458**, 163 (1979). c) E. Hengge and G. Bauer, *Monatsh. Chem.*, **106**, 503 (1975). d) E. Hengge and D. Kovar, *Angew. Chem.*, **89**, 417 (1977).
5. (a) R. West, in *Comprehensive Organometallic Chemistry*, Vol. 2 (Eds. G. Wilkinson, F. G. A. Stone and E. W. Abel), Chap. 9.4, Pergamon Press, Oxford, 1982, p. 365.
   (b) E. Hengge and K. Hassler, in *The Chemistry of Inorganic Homo- and Heterocycles* (Eds. I. Haiduc and D. B. Sowerby), Vol. 1, Academic Press, London, 1987, p. 191.

(c) R. West, *Pure Appl. Chem.*, **54**, 1041 (1982).
(d) E. Hengge and R. Janoschek, *Chem. Rev.*, **95**, 1495 (1995).

6. L. F. Brough and R. West, *J. Organomet. Chem.*, **145**, 139 (1980).
7. E. Carberry and R. West, *J. Am. Chem. Soc.*, **91**, 5440 (1969).
8. F. K. Cartledge, *Organometallics*, **2**, 425 (1983).
9. M. Weidenbruch, K.-L. Thom, S. Pohl and W. Saak, *J. Organomet. Chem.*, **329**, 151 (1987).
10. E. Hengge and G. Litscher, *Angew. Chem.*, **88**, 414 (1976).
11. S. Graschy, C. Grogger and E. Hengge, in *Organosilicon Chemistry III* (Eds. J. Weis and N. Auner), Verlag Chemie, Weinheim, 1997.
12. C. Jammegg, S. Graschy and E. Hengge, *Organometallics*, **13**, 2397 (1994).
13. E. Hengge and H. Firgo, *J. Organomet. Chem.*, **212**, 155 (1981).
14. E. Hengge and G. Litscher, *Monatsh. Chem.*, **109**, 1217 (1978).
15. H. Li, I. S. Butler and J. F. Harrod, *Organometallics*, **12**, 4553 (1993).
16. W. Uhlig, *J. Organomet. Chem.*, **452**, C6 (1993).
17. P. Gspaltl and E. Hengge, unpublished results.
18. Z. Smith, H. M. Seip, E. Hengge and G. Bauer, *Acta Chem. Scand.*, **A30**, 697 (1976).
19. Z. Smith, A. Almenningen, E. Hengge and D. Kovar, *J. Am. Chem. Soc.*, **104**, 4362 (1982).
20. C. Kratky, H. G. Schuster and E. Hengge, *J. Organomet. Chem.*, **247**, 253 (1983).
21. V. S. Mastryukov, S. A. Strelkov, L. V. Vilkov, M. Kolonits, B. Rozsondai, H. G. Schuster and E. Hengge, *J. Mol. Struct.*, **238**, 433 (1990).
22. R. West, in *Comprehensive Organometallic Chemistry II*, Vol. 2 (Eds. G. Wilkinson, F. G. A. Stone and E. W. Abel), Chap. 3.5, Pergamon Press, Oxford, 1995, p. 91–95 and references cited therein.
23. H. Bock and B. Solouki, in *The Chemistry of Organic Silicon Compounds* (Eds. S. Patai and Z. Rappoport), Wiley, Chichester, 1989, p. 203.
24. H. Stüger and E. Hengge, *Monatsh. Chem.*, **119**, 873 (1988).
25. H. Stüger and R. Janoschek, *Phosphorus, Sulfur, and Silicon*, **68**, 129 (1992).
26. C. L. Wadsworth and R. West, *Organometallics*, **4**, 1664 (1985).
27. C. L. Wadsworth, R. West, Y. Nagai, H. Watanabe and T. Muraoka, *Organometallics*, **4**, 1659 (1985).
28. B. Kirste, R. West and H. Kurreck, *J. Am. Chem. Soc.*, **107**, 3013 (1985).
29. H. Bock, W. Kaim, M. Kira and R. West, *J. Am. Chem. Soc.*, **101**, 7667 (1979).
30. Y. Apeloig and D. Danovich, *Organometallics*, **15**, 350 (1996).
31. H. Stüger, E. Hengge and R. Janoschek, *Phosphorus, Sulfur, and Silicon*, **48**, 189 (1990).
32. L. F. Brough and R. West, *J. Am. Chem. Soc.*, **103**, 3049 (1981).
33. C. W. Carlson and R. West, *Organometallics*, **2**, 1792 (1983).
34. S. Masamune, Y. Hanzawa, S. Murakami, T. Bally and J. F. Blount, *J. Am. Chem. Soc.*, **104**, 1150 (1982).
35. M. Weidenbruch, *Chem. Rev.*, **95**, 1479 (1995).
36. S. Masamune, H. Tobita and S. Murakami, *J. Am. Chem. Soc.*, **105**, 6524 (1983).
37. A. Schäfer, M. Weidenbruch, K. Peters and H. G. von Schnering, *Angew. Chem.*, **96**, 311 (1984).
38. H. Watanabe, Y. Kougo, M. Kato, H. Kuwabara, T. Okawa and Y. Nagai, *Bull. Chem. Soc. Jpn.*, **57**, 3019 (1984).
39. H. Watanabe, Y. Kougo and Y. Nagai, *J. Chem. Soc., Chem. Commun.*, 66 (1984).
40. G. Gillette, G. Nora and R. West, *Organometallics*, **9**, 2925 (1990).
41. J. Belzner, H. Ihmels, B. O. Kneisel and R. Herbst-Irmer, *J. Chem. Soc., Chem. Commun.*, 1989 (1994).
42. H. Watanabe, M. Kato, T. Okawa, Y. Kougo, Y. Nagai and M. Goto, *Appl. Organomet. Chem.*, **1**, 157 (1987).
43. T. Tsumuraya, S. A. Batcheller and S. Masamune, *Angew. Chem.*, **103**, 916 (1991).
44. M. Weidenbruch, *Front. Organosilicon Chem., [Proc. Int. Symp. Organosilicon Chem.]*, 9th, 122 (1990).
45. M. Weidenbruch, E. Kroke, S. Pohl, W. Saak and H. Marsmann, *J. Organomet. Chem.*, **499**, 229 (1995).
46. E. Kroke, S. Willms, M. Weidenbruch, W. Saak, S. Pohl and H. Marsmann, *Tetrahedron Lett.*, **37**, 3675 (1996).
47. E. Kroke, M. Weidenbruch, W. Saak, S. Pohl and H. Marsmann, *Organometallics*, **14**, 5695 (1995).

48. J. Belzner, H. Ihmels, B. O. Kneisel, R. O. Gould and R. Herbst-Irmer, *Organometallics*, **14**, 305 (1995).
49. E. Fossum, M. Mohan and K. Matyjaszewski, in: *Progress in Organosilicon Chemistry* (Eds. B. Marciniec, J. Chojnowski), Gordon and Breach, 1995, pp. 429–443.
50. E. Fossum and K. Matyjaszewski, *ACS Symp. Ser.*, **579**, 433 (1994).
51. K. Matyjaszewski, *Makromol. Chem., Macromol. Symp.*, **4243**, 269 (1991).
52. E. Fossum, J. Chrusciel and K. Matyjaszewski, *ACS Symp. Ser.*, **572**, 32 (1994).
53. E. Fossum, S. W. Gordon-Wylie and K. Matyjaszewski, *Organometallics*, **13**, 1695 (1994).
54. U. Pöschl and K. Hassler, *Organometallics*, **14**, 4948 (1995).
55. S. Kyushin, H. Sakurai and H. Matsumoto, *J. Organomet. Chem.*, **499**, 235 (1995).
56. Ref. 5d, pp. 195–203 and references therein.
57. W. Uhlig, *Organosilicon Chem.* (Eds. F. Weis and N. Auner), VCH, Weinheim, 1996, p. 21.
58. W. Uhlig, *Chem. Ber.*, **125**, 47 (1992).
59. W. Uhlig and C. Tretner, *J. Organomet. Chem.*, **436**, C1 (1992).
60. U. Pöschl, H. Siegl and K. Hassler, *J. Organomet. Chem.*, **506**, 93 (1996).
61. K. E. Ruehl and K. Matyjaszewski, *J. Organomet. Chem.*, **410**, 1 (1991).
62. U. Pöschl and K. Hassler, *Organometallics*, **15**, 3238 (1996).
63. E. Hengge and P. K. Jenkner, *Z. Anorg. Allg. Chem.*, **604**, 69 (1991).
64. E. Hengge and M. Eibl, *J. Organomet. Chem.*, **428**, 335 (1992).
65. A. Spielberger, P. Gspaltl and E. Hengge, *Phosphorus, Sulfur, and Silicon*, **93–94**, 355 (1994).
66. A. Spielberger, P. Gspaltl, H. Siegl, E. Hengge and K. Gruber, *J. Organomet. Chem.*, **499**, 241 (1995).
67. E. Hengge and F. K. Mitter, *Monatsh. Chem.*, **117**, 721 (1986).
68. F. Uhlig, P. Gspaltl, M. Trabi and E. Hengge, *J. Organomet. Chem.*, **493**, 33 (1995).
69. A. L. Allred, R. T. Smart and D. A. Van Beek Jr., *Organometallics*, **11**, 4225 (1992).
70. E. Carberry, R. West and G. E. Glass, *J. Am. Chem. Soc.*, **91**, 5446 (1969).
71. R. West and E. S. Kean, *J. Organomet. Chem.*, **96**, 323 (1975).
72. A. C. Buchanan III and R. West, *J. Organomet. Chem.*, **172**, 273 (1979).
73. F. Uhlig, B. Stadelmann, A. Zechmann, P. Lassacher, H. Stüger and E. Hengge, *Phosphorus, Sulfur, and Silicon*, **90**, 29 (1994).
74. E. Hengge P. Gspaltl and E. Pinter, *J. Organomet. Chem.*, **521**, 145 (1996).
75. U. Herzog, G. Roewer and U. Pätzold, *J. Organomet. Chem.*, **494**, 143 (1995).
76. E. Hengge and U. Pätzold, unpublished results.
77. M. Tischler, R. Collins, M. Thewalt and G. Abstreiter *Silicon-Based Optoelectronic Materials*, (Eds.), MRS Symposia Proceedings **290**, Materials Research Society, Pittsburg, 1993.
78. (a) M. S. Brandt, H. D. Fuchs, M. Stutzmann, J. Weber and M. Cardona, *Solid State Commun.*, **81**, 307 (1992); (b) H. Kautsky, *Z. Anorg. Allg. Chem.*, **117**, 209 (1921).
79. E. Hengge, *Fortschr. Chem. Forsch.*, **51**, 1 (1974).
80. A. Kleewein, U. Pätzold, E. Hengge, S. Tasch and G. Leising in *Organosilicon III* (Eds. J. Weis and N. Auner), VCH, Weinheim, 1997.
81. E. Hengge, P. Gspaltl and A. Spielberger, *J. Organomet. Chem.*, **479**, 165 (1994).
82. P. Gspaltl, A. Spielberger, A. Zechmann and E. Hengge, *J. Organomet. Chem.*, **503**, 129 (1995).
83. P. Gspaltl, A. Spielberger and E. Hengge, *Phosphorus, Sulfur, and Silicon*, **93–94**, 353 (1994).
84. P. Gspaltl, S. Graschy, H. Siegl, E. Hengge and K. Gruber *J. Organomet. Chem.*, **524**, 187 (1996).
85. E. Hengge, E. Pinter and F. Uhlig, to appear.
86. F. Uhlig, U. Hermann, K. Klinkhammer and E. Hengge, in *Organosilicon Chemistry III* (Eds. J. Weis and N. Auner), VCH, Weinheim, 1997.
87. H. Stüger, P. Lassacher and E. Hengge, *Z. Allg. Anorg. Chem.*, **621**, 1517 (1995).
88. R. West and A. Indriksons, *J. Am. Chem. Soc.*, **94**, 6110 (1972).
89. P. K. Jenkner, E. Hengge, R. Czaputa and C. Kratky, *J. Organomet. Chem.*, **446**, 83 (1993).
90. A. Sekiguchi, T. Yatabe, S. Do and H. Sakurai, *Phosphorus, Sulfur and Silicon*, **93–94**, 193 (1994).
91. A. Sekiguchi, T. Yatabe, H. Kamatani, C. Kabuto and H. Sakurai, *J. Am. Chem. Soc.*, **114**, 6260 (1992).
92. N. Wiberg, C. M. Finger and K. Polborn, *Angew. Chem.*, **105**, 1140 (1993).
93. M. Unno, H. Shioyama, M. Ida and H. Matsumoto, *Organometallics*, **14**, 4004 (1995).
94. H. Matsumoto, K. Higuchi, S. Kyushin and M. Goto, *Angew. Chem.*, **104**, 1410 (1992).

95. Y. Kabe, M. Kuroda, Y. Honda, O. Yamashita, T. Kawase and S. Masamune, *Angew. Chem.*, **100**, 1793 (1988).
96. M. Unno, K. Higuchi, M. Ida, H. Shioyama, S. Kyushin, H. Matsumoto and M. Goto, *Organometallics*, **13**, 4633 (1994).
97. M. Kuroda, Y. Kabe, M. Hashimoto and S. Masamune, *Angew. Chem.*, **100**, 1795 (1988).
98. S. Kyushin, H. Sakurai, H. Yamaguchi, M. Goto and H. Matsumoto, *Chem. Lett.* 815, (1995).
99. T. S. Drahnak, R. West and S. C. Calabrese, *J. Organomet. Chem.*, **198**, 55 (1980).
100. E. Hengge, M. Eibl and F. Schrank, *J. Organomet. Chem.*, **369**, C23 (1989).
101. E. Hengge, and M. Eibl, *Organometallics*, **10**, 3185 (1991).
102. E. Hengge, E. Pinter, M. Eibl and F. Uhlig, *Bull. Soc. Chim. France*, **132**, 509 (1995).
103. E. Hengge, H. Siegl and B. Stadelmann, *J. Organomet. Chem.*, **479**, 187 (1994).
104. E. Hengge and A. Zechmann, *J. Organomet. Chem.*, **508**, 227 (1996).
105. T. D. Tilley, *Acc. Chem. Res.*, **26**, 22 (1993).
106. B. Stadelmann, P. Gspaltl, A. Spielberger and E. Hengge, *Phosphorus, Sulfur and Silicon*, **93–94**, 357 (1994).
107. E. Hengge, P. K. Jenkner, A. Spielberger and P. Gspaltl, *Monatsh. Chem.*, **124**, 1005 (1993).
108. B. Stadelmann, P. Lassacher, H. Stüger and E. Hengge, *J. Organomet. Chem.*, **482**, 201 (1994).
109. K. H. Pannell, L. J. Wang and J. M. Rozell, *Organometallics*, **8**, 550 (1989).
110. K. Pannell, J. Castillo-Ramirez and F. Cervantes-Lee, *Organometallics*, **11**, 3139 (1992).

CHAPTER 38

Recent advances in the chemistry of siloxane polymers and copolymers

ROBERT DRAKE, IAIN MacKINNON and RICHARD TAYLOR

Dow Corning Ltd, Cardiff Road, Barry, South Glamorgan CF63 2YL, UK

I. THE POLYMERIZATION OF SILICONES

A. Introduction

Several reviews have appeared between 1991 and 1996 concerned with the polymerization and properties of silicones. Chojnowski[1] reviews the kinetically controlled ring opening of hexamethylcyclotrisiloxane (D_3). Both anionic and cationic initiation mechanisms are discussed in connection with their use in polymer synthesis. The focus of the review is on association phenomena at the initiating site and oligomer formation processes. He also reviews the behaviour of the silanol group in polycondensation reactions[2]. A review by Penezek and Duda[3] on the thermodynamics, kinetics and mechanism of anionic ring-opening polymerization discusses both organic and silicone monomers. Methods for the synthesis, characterization and properties of cyclic polymers including siloxanes are reviewed by Semlyen, Wood and Hodge[4]. Kopylov and coworkers review the mechanism of hydrolytic polycondensation of organochlorosilanes[5]. Data on the reaction kinetics and the effect of reaction conditions, reagent ratio and various additives on the course of the reaction are analysed. Hetero and metallasiloxanes derived from silanediols, disilanols, silanetriols and trisilanols are reviewed by Roesky and coworkers[6]. Additional reviews on methods of catalysis of ring-opening polymerization of cyclosiloxanes[7], macrokinetics of hydrolytic polycondensation of organochlorosilanes[8], the synthesis of silicone polymers[9] and synthesis of new silicon-based condensation polymers[10] have also appeared.

B. Polymerization of Cyclosiloxanes

1. Anionic polymerization of cyclosiloxanes

Boileau and coworkers[11] have used a novel trimethylsilylmethyl lithium initiator Me_3SiCH_2Li (**1**), in combination with a cryptand [211], for the ring-opening polymerization of cyclosiloxanes. Initiation of hexamethylcyclotrisiloxane (D_3) and octamethylcyclotetrasiloxane (D_4) polymerization has been followed by ^1H, ^7Li, ^{13}C and ^{29}Si NMR.

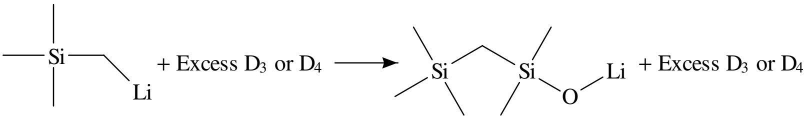

(1)

(1) **(2)**

The complex $Me_3SiCH_2SiMe_2OLi$ (**2**) (^7Li shift 0.74 ppm) is the only product identified in the reaction of **1** (^7Li shift 2.5 ppm) with D_3 or D_4 at 20 °C in toluene even in the presence of excess siloxane, as shown in equation 1. Addition of the cryptand [211] shifted the Li resonance to -0.93 ppm in agreement with other lithium cryptand [211] complexes. This lithium silanolate was then shown to initiate polymerization of D_3, D_4, D_6 and functional cyclics such as $(SiMe(HC{=}CH_2)O)_4$ and $(SiMe(CH_2CH_2CF_3)O)_3$. Kinetic measurements using this initiator show a reactivity order of $D_3 \gg D_4 > D_5 > D_6$ and the results are in good agreement with those previously reported for anionic polymerization under similar conditions. Co-polymerization reaction involving vinyl dimethyl cyclics have been shown by ^{29}Si NMR to give, under certain conditions, polymers with a microblock structure where little intramolecular redistribution takes place.

Other novel initiators include the use of an aluminium–tetraphenylporphyrin complex Et–Al(TPP)[12]. Only D_3 is polymerized at 25 °C over 6 days to give a monodispersed ($M_n/M_w = 1.12$, $M_n = 1550$) polymer. D_4 and D_5 do not react under similar conditions and linear equilibration is suppressed. In addition, they report that this initiator will oligomerize functional cyclics such as $(SiMeHO)_4$ and $(SiPh_2O)_3$.

A fast catalyst for the ring-opening polymerization of D_4 in solution or in the bulk has been reported by Molenberg and Moller[13]. They report the use of a phosphazene base in combination with methanol as the initiator, compound **3**.

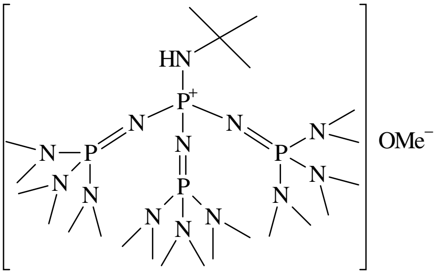

(3)

Very high polymerization and equilibration rates have been observed both in the bulk and in solution which are faster than those with KOH or CsOH. Some initial kinetic measurements have been reported. This catalyst system has recently been used by Van Dyke and Clarson[14] to initiate the ring-opening polymerization of tetraphenyltetramethyltetrasiloxane. Again very fast initiation is observed even at room temperature to give high molecular weight polymers within minutes. Using KOH under equivalent conditions gave no reaction.

Time-of-flight secondary ion mass spectroscopy (TOF-SIMS)[15] has been used for observing the initiating species in anionic ring-opening polymerizations of D_3. The PDMS mass spectrum shows peaks of varying intensity with local maxima every 3 silicon repeat units. This distribution is attributed to the relative concentrations of the three initiating species, I1, I2 and I3, shown in equation 2 which can be determined from the peak intensities.

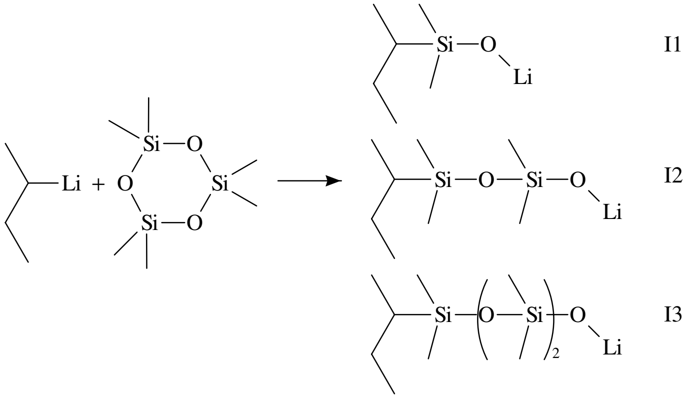

(2)

Hemery and coworkers[16] have investigated the polymerization of D_4 in aqueous emulsion. An emulsifying agent (benzyldimethyldodecylammonium hydroxide) was used as the initiator. Stable emulsions of α,ω-dihydroxypolydimethylsiloxanes with low polydispersities and controllable molecular weights up to 15,000 were obtained after polymerization. This method of polymerization was reported to give 70% conversion to polymer with only trace amounts of macrocycles, in contrast to bulk polymerizations which give large polydispersities and higher levels of macrocycles. Kinetic analysis and computer simulation were in good agreement with a mechanism involving a simultaneous polyaddition/polycondensation process. At high monomer conversion, polycondensation predominates leading to a broadening of the molecular weight distribution. Apparent rate constants for the initiation, propagation and polycondensation at different temperatures were determined. From the data activation parameters for these processes could be estimated.

There has been some interest in the preparation of monodispersed siloxanes which contain two different end groups on each polymer chain[17]. Typically, the process involves the ring opening of D_3 using a lithium reagent and then quenching the living polymer obtained with a chlorosilane. Two different groups can thus be incorporated, one from the lithium reagent used and one from the chlorosilane neutralizing agent. These materials can be used as macromonomers leading to siloxane/organic hybrid polymers.

2. Cationic polymerization of cyclosiloxanes

Cyclosiloxanes such as D_3 and D_4 have very different reactivities and generally do not give the same types of cyclic products when polymerization is initiated by cationic catalysts. Sigwalt and coworkers[18] have further examined the analogies and differences between these two monomers with respect to initiation by trifluoromethanesulphonic acid. The formation of water during these ring-opening reactions and the effect of water and other additives were examined. ^1H and ^{19}F NMR spectra were used to investigate the formation of triflate esters and hence the formation of water. Differences in the formation of water between D_3 and D_4 during the ring opening were not significant. The addition of water, however, has a large effect on the reactions. When water is premixed with the triflic acid prior to addition to the monomer, the ring opening initiation is effectively inhibited in both cases. If the water is added to the reactions *in situ*, then in the case of D_3 it acts as an effective cocatalyst whereas in the D_4 reaction it acts as an inhibitor. Extensions of this work[19] for D_3 ring opening initiated with triflic acid in CH_2Cl_2 have shown that the growth of linear high polymer as well as the formation of cyclics (mainly multiples of the monomer D_3, i.e. D_{3x}) involve a silyl triflate end group. These silyltriflic esters are inactive catalytic sites in the absence of triflic acid but are activated in the presence of the acid. The formation of small cyclics and macrocyclics is also discussed in depth. D_6 is mainly formed, sometimes in large amounts, which in some cases are greater than the amount of high polymer. The authors postulate that this occurs through a special type of back biting involving a transient tertiary oxonium ion PolyD-D_3^+ (**4**). This rearranges to form another oxonium ion polyD-D_6^+ (**5**) which leads to D_6 (Scheme 1). A smaller fraction of D_6 and the major fraction of D_9 are formed through cyclization of silanolesters HD_6OTf, HD_9OTf etc. resulting from addition of D_3 to the silanol ester HD_3OTf, as shown in Scheme 2. The acid reformed by this cyclization maintains a stationary concentration of silyl esters by reaction with D_3. The larger macrocyclics are also formed by cyclization of silanol esters.

The effect of ultrasound on the ring-opening polymerization of D_4 has been investigated by Price and coworkers[20]. Sonication increased the rate of polymerization over conventional stirring, giving polymers with higher molecular weights and lower polydispersities. This was explained in terms of more efficient mixing and dispersion of the acid catalyst by sonication.

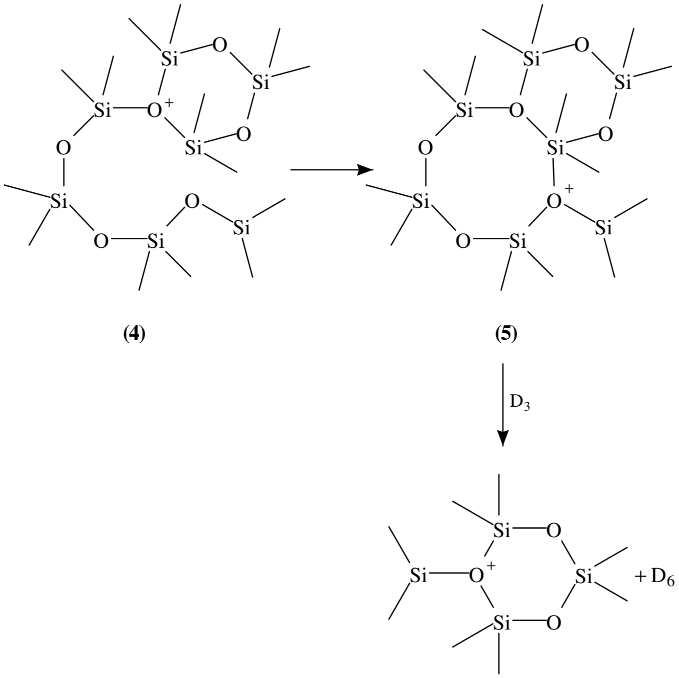

SCHEME 1

$$\begin{tikzcd}
HD_3OTf \arrow[r, "D_3"] & HD_6OTf \arrow[r, "D_3"] \arrow[d] & HD_9OTf \arrow[r, "D_3"] \arrow[d] & HD_{12}OTf \arrow[r, "?"] \arrow[d] & \text{High Polymer} \\
 & D_6 + TfOH & D_9 + TfOH & D_{12} + TfOH &
\end{tikzcd}$$

SCHEME 2

C. Condensation Polymerization of Linear Siloxanes

1. Cationic polycondensation of linear siloxanes

There has been an increased interest in this area of siloxane polymerization in recent years. Many publications have appeared on the kinetics of acid-catalysed condensation and disproportionation. Chojnowski, Rubinsztajn and Cypryk[21] report the kinetics and disproportionation behaviour of oligo(dimethylsilanols), $HO(SiMe_2O)_nH$, $n = 2$ or 5 and $Me(SiMe_2O)_nH$, $n = 2$ or 5, in the presence of protic acids in both acid–base inert solvents such as methylene chloride and in the basic solvent dioxane. The kinetics in the two systems were very different. In methylene chloride they found that two molecules of $HO(SiMe_2O)_5H$ participate in the transition state and that water did not participate in this reaction. Siloxane bond cleavage was shown to be strongly affected by other silanol groups in the siloxane diols, $HO(SiMe_2O)_nH$, by comparison with the kinetics for the monosiloxanols, $Me(SiMe_2O)_nH$. The intra- (cf. **6**) and inter-molecular assistance (cf. **7**) of a third silanol group plays an important role in siloxane bond cleavage, shown in

Scheme 3. This third group acts as a base receiving a proton from the silanol group attacking the acid complex.

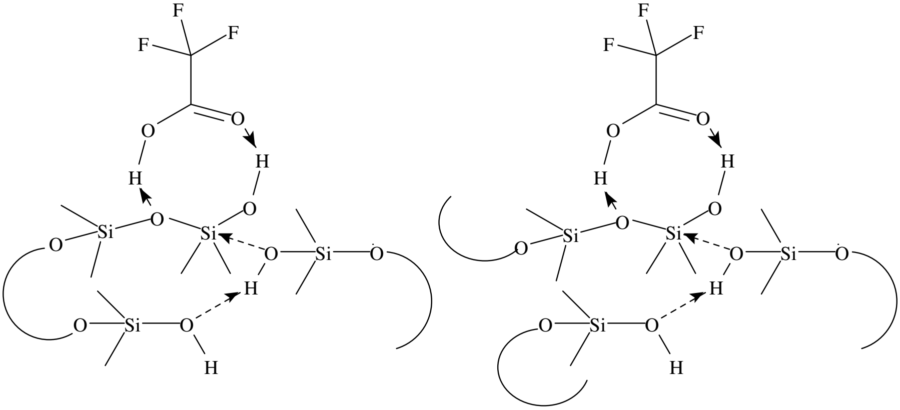

(6) **(7)**

SCHEME 3

The kinetics of these reactions are strongly affected by the conversion of the protic acid catalyst to a silyl ester as shown in equation 3.

$$X(SiMe_2O)_nH + HOSO_2CF_3 \rightleftharpoons X(SiMe_2O)_nSO_2CF_3 + H_2O \qquad (3)$$

Because the rates of this reaction are very rapid, normal sampling techniques were not satisfactory and an infrared technique was used. This esterification reaction was shown to be about 100 times faster than the disproportionation reaction and inter–intra-molecular assistance was also found to be important. This assistance seems to be a common pattern in acid-catalysed processes of oligosiloxanols in inert solvents. In dioxane solvent the redistribution kinetics can be interpreted in terms of an unzipping mechanism. The rate-determining step is terminal silanol cleavage by water forming dimethylsilanediol which rapidly reacts with other substrate silanols (Scheme 4).

$$\begin{tikzcd}
X(SiMe_2O)_nSiMe_2OH \arrow[r, "H_2O\,(H^+)"] & X(SiMe_2O)_nH + HOSiMe_2OH \arrow[d] \\
 & \text{Condensation Products}
\end{tikzcd}$$

SCHEME 4

Work by Sigwalt, Bischoff and Cypryk[22] have used this inter–and intramolecular catalysis to explain the condensation kinetics and cyclic formation processes in siloxane condensations. The kinetics show a very complex dependence on siloxane chain length, complicated by equilibria involving acid, silanol and water. They do indicate that the dominating reaction in the process is condensation and that chain disproportionation and chain scrambling are negligible! The kinetics of condensation are influenced by the involvement of triflic acid in several equilibria, i.e. the formation of triflate esters, shown in equation 3, the possible involvement of triflic acid in the reaction of these esters with silanol, shown in equation 4 and the hydration of the triflic acid itself, shown in equation 5.

$$\begin{aligned} &\mathrm{X(SiMe_2O)}_n\mathrm{SiMe_2OSO_2CF_3} + \mathrm{HOSiMe_2(OSiMe)}_n\mathrm{X} \rightleftharpoons \mathrm{HOSO_2CF_3} \\ &\quad + \mathrm{X(SiMe_2O)}_n\mathrm{SiMe_2OSiMe_2(SiMe_2O)}_n\mathrm{X} \end{aligned} \tag{4}$$

$$\mathrm{HOSO_2CF_3{\bullet}H_2O} \overset{\mathrm{H_2O}}{\rightleftharpoons} \mathrm{HOSO_2CF_3{\bullet}H_2O} \overset{n\mathrm{H_2O}}{\rightleftharpoons} \mathrm{HOSO_2CF_3.}(n+1)\mathrm{H_2O} \tag{5}$$

Alkoxysilane silanol condensation reactions play an important role in sol-gel technology, the manufacture of silicone resins, the vulcanization of silicones and in surface modification by alkoxysilanes. There have been recent investigations by Chojnowski and coworkers[23] into the kinetics of acid-catalysed heterofunctional condensation of model alkoxy and silanol functional siloxanes. The heterofunctional reaction involving SiOEt and SiOH competes with the homofunctional reaction of SiOH with SiOH. The rates of each process are similar, but are influenced by the medium and hence by the concentration of the reactants. Hydrolysis of the ethoxysiloxane as well as ethanolysis of the silanol groups leads to extensive interconversion of functional groups. These interconversion processes are two orders of magnitude faster than those of the condensation reactions.

Other publications have also appeared describing condensation kinetics with heterogeneous catalysts by a designed experimental approach to optimize reaction conditions[24], stannous octanoate condensation catalysis[25] and the role of bifunctional catalysis mechanisms[26]. A 'bifunctional transition state', shown for compound **8**, was postulated to explain the kinetics of heterofunctional condensation reactions catalysed by $\mathrm{Cl_3CCOOH}$, $\mathrm{Et_2NOH}$, MeEtC=NOH or $\mathrm{CH_3COOH}$ (equation 6).

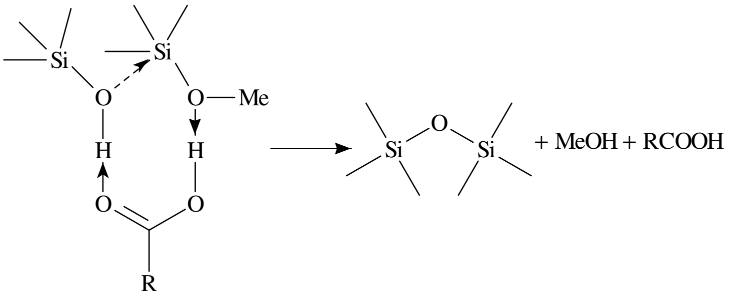

(8)

(6)

Most of the references cited in this section have been concerned with the kinetics and mechanism of the reactions. There have also been some relevant patents published on catalysts for silanol condensation. These catalysts are of the general family of chlorophosphazenes, $(-\mathrm{Cl_2P{=}N}-)_n$. Wacker Chemie[27] have had several patents on the use of oxygen-containing phosphazenes for the condensation of hydroxy terminated siloxanes. Hagger[28] and Weis have also published their findings in journals and at conferences. Nunchritz[29] and General Electric[30] have also filed patents in this area although the Wacker patents seem to have priority. Dow Corning[31] has also patented the use of chlorophosphazenes and processes for their use. There has also been some discussion of the kinetics and mechanism of condensation using these unusual catalysts[32].

A very unusual initiator which has been discussed recently is the hotly disputed silicenium ion. A patent by Schulz Lambert, and Kania[33] shows that an initiator of the type $\mathrm{R_3SiA}$, where A is a non-coordinating anion, can be used under anhydrous conditions to ring-open D_3 to give mixtures of cyclic and linear polymers. This initiator is also discussed by Olah and coworkers for the polymerization of organic and siloxane monomers[34].

2. Anionic polycondensation of linear siloxanes

An interesting approach to the synthesis of siloxanes has been patented by Kolaczkowski and Serbetcioglu[35]. Their process uses a K_3PO_4 heterogeneous catalyst dispersed on a monolithic ceramic support and can be used for condensation or ring-opening polymerizations. The advantages are that the catalyst is easily removed and high reaction rates and high throughput rates are obtained. Other anionic catalyst systems include the use of a quaternary ammonium borate, phosphate, carbonate or silicate by Westall[36].

The polymerization of silicones to give functional siloxane polymers has also been discussed. A commercially important class of polymers are the amine functional silicone fluids. McGrath and Spinu[37] discuss the use of D_4 and an aminofunctional cyclic siloxane in the presence of a tetramethylammonium silanolate catalyst. Sauvet and Helary[38] report condensation kinetic data for the condensation of an aminoalkylalkoxysilane ($H_2N(CH_2)_3SiMe(OMe)_2$) and a monosilanol ($PhMe_2SiOH$) as well as with oligosiloxanediols $HO(SiMe_2O)_nH$. This is a useful method for the synthesis of amine polymers of well-defined structure and proceeds without the need for a catalyst. Homofunctional condensation reactions and functional group exchange can be minimized by continuous removal of methanol and control of the reaction temperature. The reactivities of the two alkoxy groups in the silane are very different. The first reacts readily at room temperature, but higher temperatures are required to substitute the second. By using this large difference in reactivity of the two alkoxy groups, block copolymers of dimethyl and methylphenylsiloxanes were prepared. Polymers with arylamine functional groups have also been reported. Babu and coworkers[39] prepared a lithium complex of a protected aniline, $(Me_3Si)_2NC_6H_4Li$, to initiate the ring-opening polymerization of D_3 which was then terminated with a protected aniline functional chlorosilane, p-$(Me_3Si)_2NC_6H_4SiMe_2Cl$. The protected oligomer is then converted to the free amine with methanol.

An interesting variation of an ammonium silanolate catalyst was described by Hoffman and Leir[40]. They prepared tetramethylammonium 3-aminopropyldimethylsilanolate and used it to synthesize 3-aminopropyl terminated Polydimethylsiloxane (PDMS).

Another class of functional siloxane polymer that has received some attention are the fluorosiloxane materials, especially 3,3,3-trifluoropropylmethylsiloxanes. The use of conventional equilibration catalysts to produce these materials gives products which favour the cyclosiloxane in the bulk. Clarson and coworkers[41] report the use of specific condensation catalysts such as stannous octanoate, potassium carbonate and barium hydroxide to prepare hydroxy terminated fluorosilicone polymers.

Stannous octanoate has also been studied as a catalyst for the synthesis of polydimethyl- and poly(methylphenyl)siloxanes via polycondensation.

Other methods of polymerization that have appeared recently include plasma polymerization[42] and photopolymerization[43], but they give partially or highly crosslinked films.

II. ORGANOFUNCTIONAL SILOXANES

A. Synthesis of Organofunctional Siloxanes

As in previous years the major method used for attaching an organofunctional group to a siloxane backbone is hydrosilylation. Even in this much studied field there is still the potential for surprising and potentially very useful results. Thus, Crivello and Bi observed that the Rh-catalysed hydrosilylation of unsaturated epoxides with α,ω-SiH functional siloxanes proceeded in a discrete stepwise fashion[44]. Using $(Ph_3P)_3RhCl$, $(HMe_2Si)_2O$ added to the unsaturated epoxide, 3-vinyl-7-oxabicyclo[4.1.0]heptane, to yield almost exclusively the mono-adduct **9**. Rate studies attributed this to a large difference in the activation energies of the two SiH groups, $E_a = ca\ 109\ \text{kJ mol}^{-1}$ for the first site and *ca* $243\ \text{kJ mol}^{-1}$ for the second, so that with short reaction times and low temperatures, and even in the presence of excess unsaturated epoxide, the mono-adduct was formed in high yield. A further surprise was that under the same conditions, $HMe_2SiO(Me_2SiO)_2Me_2SiH$, with 6 bonds separating the two SiH groups, also formed the mono-adduct in *ca* 95% yield. This has already made possible the synthesis of a series of compounds with both SiH and epoxy functionality in the same molecule or of molecules with two dissimilar epoxy functional groups.

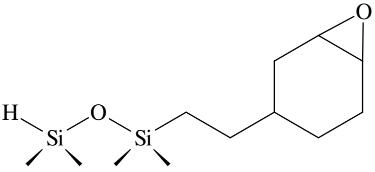

(9)

An alternative route to asymmetric α,ω-organofunctional siloxanes or to siloxanes bearing exclusively functionality at one end is by terminating living anionic polymerizations with appropriate functional-derivatives (see Section I.B.1)[45,46]. Alternatively, the asymmetric disiloxane, $H_2N(CH_2)_3Me_2SiOSiMe_2CH{=}CH_2$, was prepared by base-catalysed equilibration of the symmetrical disiloxanes, $[H_2N(CH_2)_3Me_2Si]_2O$ and $(CH_2{=}CHMe_2Si)_2O$, followed by fractional distillation of the statistical distribution of products. Although equilibration is probably not a route which is generally applicable for the preparation of pure higher homologues, a range of asymmetric α,ω-organofunctional siloxanes prepared by this method, $H_2N(CH_2)_3(Me_2SiO)_nMe_2SiCH{=}CH_2$, have been claimed as compatibilizers for polymer blends[47].

In some instances direct hydrosilylation of an olefin derivative of the intended functional group can lead to serious side-reactions, may proceed in poor yield or may simply call for unusual and difficult to prepare intermediates. Thus, Mitchell and coworkers were interested in preparing siloxanes bearing photoactive cinnamate moieties[48]. Hydrosilylation of a suitable substrate such as the allyl ester of 4-methoxycinnamic acid with poly(methylhydrogensiloxane) or poly(dimethyl-*co*-methylhydrogensiloxane) resulted in problems such as coloured material, crosslinking during work-up and reduction of some cinnamate double bonds. A far more successful method was to functionalize the siloxane backbone with allyl acetate, hydrolyse the acetate to the alcohol and then esterify with the acid chloride of the cinnamic acid derivative. Polymers so formed were nearly colourless, showed no signs of crosslinking during work-up and no reduction of the cinnamate double bond occurred. In a similar two-step route, workers at Wacker Chemie prepared anhydride functional siloxanes in good yield[49]. Hydrosilylation of an acetylenic alcohol gave a polysiloxane bearing alkenol groups, When heated in the presence of an acid catalyst these groups eliminate water to form a butadienyl-functional polysiloxane. When this dehydration is conducted in the presence of an unsaturated anhydride, e.g. maleic anhydride, the butadienyl-functional polysiloxane undergoes an immediate Diels–Alder reaction to form an anhydride functional polysiloxane (Scheme 5).

Some researchers continue to investigate alternatives to hydrosilylation or Grignard chemistry for the preparation of organofunctional siloxanes. One such example is the

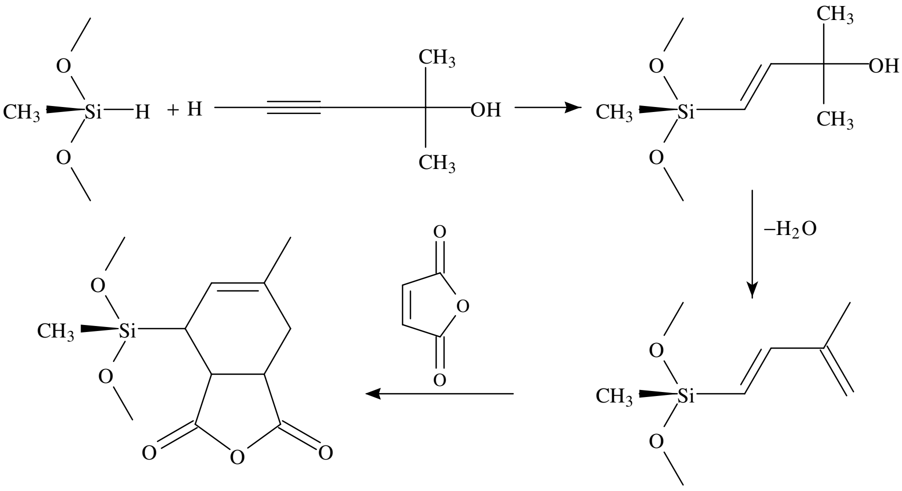

SCHEME 5

preparation by Bennetau, Dunoguès, Boileau and coworkers of precursors to highly fluorinated siloxanes, e.g. $(C_8F_{17}CH_2CH_2SiMeO)_4$[50]. Using ultrasound, with sodium dithionite as catalyst in a mixture of acetonitrile and water, the perfluoroalkyl iodide, $C_8F_{17}I$, added regioselectively to a vinylsiloxane to give an α-iodofunctional intermediate, $C_8F_{17}CH_2CH(I)Si{\equiv}$, which then underwent reductive cleavage with Bu_3SnH to give the desired product in 80–85% yield. Another interesting alternative strategy has been exploited by workers at Siemens AG who nitrated poly(methylphenyl)siloxane with a mixture of Ac_2O and concentrated HNO_3[51]. Other functionalities were introduced by reduction of the nitro group (preferably with Fe and AcOH in ethanol) to the corresponding amine which is then converted to, e.g., hydroxyl, halogen, cyano or maleimide.

B. Applications of Organofunctional Siloxanes

The crosslinking of siloxanes via UV-curable organofunctional groups is of ever increasing interest. Systems of this type generally have a low energy requirement (cf thermally cured systems) and produce no hazardous by-products (cf hydrolytic condensation). Several different approaches have been utilized. To date the most commonly studied method is the very rapid polymerization of (meth)acrylate-functional siloxanes and there remains a great deal of patent activity in this area[52]. Several research groups, most notably at GE, have also studied photopolymerization of epoxy-functional siloxanes[53] and another non-acrylate system has been much studied by workers at Loctite Corp. based on thiol-functional and norbornene-functional siloxanes (so-called thiol-ene polymerization)[54]. The thiol-ene systems were determined to have a higher photoresponse than comparable acrylate systems; this was partly ascribed to the low inhibition of the thiol-ene systems by ambient oxygen. Vinyl ethers and related cationically curable functionalities have also been the subject of much recent investigation[55]. Thus, Cazaux and Coqueret prepared telechelic vinyl ether-functional siloxanes by treating α,ω-SiH functional siloxanes with a twenty-fold excess of suitable commercial divinyl ethers, $CH_2{=}CHOROCH{=}CH_2$, R $=$ $CH_2(CH_2OCH_2)_2CH_2$ or $CH_2(c\text{-Hex})CH_2$ and a Pt catalyst[56]. The large excess of divinyl ether prevented appreciable polycondensation. An alternative method, in this case to the related propenyl ether-functional siloxanes, was devised by Crivello and coworkers[57]. They used chemoselective hydrosilylation of 1-allyloxy-4-(1-propenoxy)butane [i.e. $CH_3CH{=}CHO(CH_2)_4OCH_2CH{=}CH_2$]. Hydrosilylation of a terminal double bond is so rapid when compared with hydrosilylation of an internal double bond that the propenyl ether-functional siloxane is effectively the sole product. Rather than just having a photopolymerizable siloxane, Coqueret and Pouliquen have developed siloxanes which bear the photoinitiators, e.g. a benzophenone or thioxanthone group in combination with a tertiary amine function[58]. Such polymeric photoinitiators may be more compatible with the monomeric system and give rise to reduced levels of volatiles and extractables after curing.

Interest in siloxanes bearing various mesogens is still an area of growing interest and patent activity. These liquid crystal polymers may be used in a variety of electro-optical, opto-optical, magneto-optical, mechanical or thermo-optical devices, with or without the addition of other polymeric or low molar mass mesogenic materials[59]. There is little else which is particularly novel in the area of applications. There has been a continuing growth in the number and variety of uses of functional siloxanes for hair care. Although ‘traditional’ functionality such as amine[60] and glycol[61] graft copolymers are well represented, other functionalities include acrylic (to replace peroxide)[62], thioglycolamide (for conditioning with good curl and low odour)[63], poly-*N*-acyl alkeneimine (gloss, smoothness)[64] or even protein-siloxane copolymers[65]. For skin care, glycerol functional polysiloxane have been shown to be useful as humectants, being durable and skin substantive[66]. Where the glycerol unit is linked to the siloxane via a Si−OC link, in use the compounds will hydrolyse on the skin, delivering the humectant glycerol and a silanol functional organo-Si compound which itself acts as a durable water-repellent and softening agent[67]. In the textile industry, the major use of siloxanes is as fabric softeners and many applications are based on amino-functional siloxanes. One of the major concerns is still imparting softness but avoiding the yellowing often seen with amino-functional siloxanes[68]. This is generally achieved by modifying the chemical structure of the amino residue in some manner, e.g. alkylation or acylation. One novel use of a polysiloxane in the textile industry is the incorporation of polysiloxane units into a copolymer, e.g. polyethylene terephthalate and polydimethylsiloxane(PDMS). A monofilament of this composition has been prepared, and claimed uses include the making of dense precision fabrics for filters, screens and screen-printing screens without flaking or attrition[69]. Besides their uses in the textile and hair-care areas, amino-functional siloxanes are used in a variety of other applications, e.g. they may be reacted with epoxy resins to give materials with increased fracture toughness while retaining the good mechanical and hot-wet properties of the original untoughened resins[70]. Amino-functional siloxanes have also been proposed for the reduction of atmospheric pollution through their use in the removal of CO_2, SO_x and NO_x from gaseous mixtures[71].

III. DEGRADATION OF POLYSILOXANES

A. Introduction

The degradation of linear siloxanes under conditions ranging from dry Michigan soils to outer space continues to be a topic of great interest, both academically and industrially. The previous two reviews in this series[72] have comprehensively covered the mechanisms and kinetics of thermolysis of linear polysiloxanes and little new work, on this aspect of siloxane degradation, appears to have been reported. The pyrolysis of resinous polysiloxane materials to give silicon-containing ceramics[73] is, however, an area of current interest and study.

B. Linear Polydimethylsiloxanes

1. Acid-catalysed rearrangement

Chojnowski and coworkers have examined the acid-catalysed disproportionation of oligomeric dimethylsiloxanols in dioxane in the presence of water[21b]. The results are interpreted in terms of a rate-determining cleavage of the terminal siloxane unit by water, followed by condensation of the resultant dimethylsilanediol (**10**) with the remaining dimethylsiloxanols (equations 7 and 8).

$$\mathrm{H_2O + H[OSiMe_2]_{\mathit{n}}OH \xrightarrow{slow} H[OSiMe_2]_{\mathit{n}-1}OH + \underset{\textbf{(10)}}{Me_2Si(OH)_2}} \tag{7}$$

$$\mathrm{H[OSiMe_2]_{\mathit{n}}OH + \underset{\textbf{(10)}}{Me_2Si(OH)_2} \xrightarrow{fast} H[OSiMe_2]_{\mathit{n}+1}OH} \tag{8}$$

This disproportionation offers an insight into the mechanism of hydrolytic degradation of PDMS, especially in the presence of traces of acid. Thus, the siloxane chain may undergo a slow scission in the presence of water to give a silanol ended chain, which then depolymerizes by loss of dimethylsiloxanediol.

2. Thermal depolymerization of siloxanes

One of the major commercial uses of polydimethylsiloxanes is the preparation of elastomeric materials. To obtain suitable material properties inorganic oxides, notably silica[74], are added to high molecular weight polydimethylsiloxanes, which are then crosslinked. The addition of an inorganic oxide can increase or decrease the thermal stability of polydimethylsiloxane depending on the acidic or basic nature of the filler and the specific interactions between polymer and filler[75]. Sohoni and Mark[75] showed that use of pyrogenic silica as a filler marginally increased the thermal stability of a crosslinked polydimethylsiloxane network. A much larger effect was observed, however[75], for silicas that were prepared by *in situ* hydrolysis of tetraethylorthosilicate within the polymer network. For example, the temperature for onset of degradation could be raised from around 410 °C to around 450 °C by incorporation of as little as 6% precipitated silica prepared *in situ*. The mechanism of this stabilization was postulated to result from deactivation of terminal silanol groups on the polymer by interaction with the silica[75]. A pyrogenic silica and an alumino silicate have been treated with a range of silanes and silicones and the thermal stability studied[76]. The results are shown in Table 1. The siloxanes grafted onto silica are stated to be slightly more stable than the corresponding polysiloxane polymers, though comparative data are not given[76]. Grafting of hexamethylcyclotrisiloxane to an aluminosilicate surface[76] produces a coating which has a decomposition temperature approximately 40 °C higher than that of the corresponding coating on silica. The order of stability depends on the organic substituent on silicon and decreases with the presence of hydrogen or higher alkyl substituents according to the following series:

$$\mathrm{PhMeSiO > Me_2SiO > Me_3SiO_{1/2} > CF_3CH_2CH_2MeSiO > MeHSiO > EtHSiO}$$

Poly[oxybis(dimethylsilylene)][77] (**11**) starts to depolymerize at 250 °C predominatly by loss of octamethyl-1,4-dioxatetrasilacyclohexane (**12**).

The activation enthalpy for initiation of depolymerization was approximately 75 kJ mol^{-1}. This low value rules out spontaneous cleavage of Si−O or Si−Si bonds

TABLE 1. Thermal breakdown data in air for organosiloxanes grafted to silica[76]

Treating Agent	T_0 (°C)[a]	T_{max} (°C)[b]	E_a (kJ mol^{-1})
$(Me_3Si)_2NH$	390	440	164
$[Me_2SiO]_3$	420	490 ± 10	176
$[Me_2SiO]_4$	420	480 ± 10	174
$[MeHSiO]_4$	380		
$[EtHSiO]_4$	250	280	126
$[(H_2C{=}CH)MeSiO]_4$	230	280	126
$[CF_3CH_2CH_2MeSiO]_4$	390	430	162
$[PhMeSiO]_4$	430	560	193

[a] Temperature of onset of degradation, as indicated by IR spectroscopy.
[b] Temperature of maximum rate of weight loss from TGA.

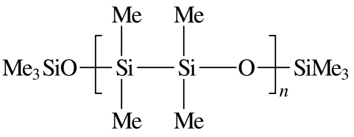

$Me_3SiO{+}SiMe_2{-}SiMe_2{-}O{+}_n SiMe_3$

(11)

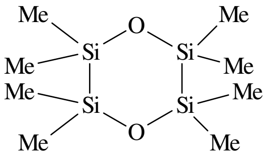

(12)

as the initiating reactions and suggests an ionic mechanism involving trace contaminants. Rearrangement of **11** to polysiloxane-b-polysilylene copolymers **(13)** (equation 9) was observed, as was ready oxidation of the polysilylene to polysiloxane[78].

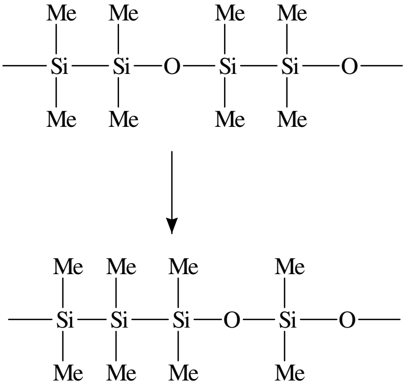

(9)

(13)

3. Degradation of polydimethylsiloxane in soil

The depolymerization of polydimethylsiloxane to dimethylsilanediol **(10)** on exposure to dry soil was reported in 1979 by Buch and Ingebridtson[79]. The presence of moisture markedly decreased the rate of depolymerization.

Several groups[80,81] have now further studied this depolymerization using a range of soils and conditions. Under moist soil conditions, very little depolymerization is observed with the majority of the polydimethylsiloxane remaining soluble in organic solvents[81a]. Once the soil moisture drops below about 4%, depolymerization of the siloxane occurs over a period of days to give siloxanol oligomers[80,81a] **(14)**, $n \leqslant 9$, which are water soluble. This was demonstrated (Figure 1) by using soil treated with ^{14}C-labelled polydimethylsiloxane (PDMS) and monitoring both the soil moisture level and the ^{14}C levels desorbed from the soil on water washing. As PDMS is insoluble in water, the presence of ^{14}C containing species was taken as being indicative of formation of siloxanol oligomers **(14)**.

$$\mathrm{HO(Me_2SiO)}_n\mathrm{H}(n = 2\text{–}9)$$

(**14**)

The mechanism of this depolymerization is unlikely to be biological but rather is thought to involve catalysis by clay minerals within the soil. At high water levels, access of the hydrophobic polydimethylsiloxane to the active sites on the clay may be limited, thus slowing the depolymerization. The dimethylsilanediol **(10)** is the major product species

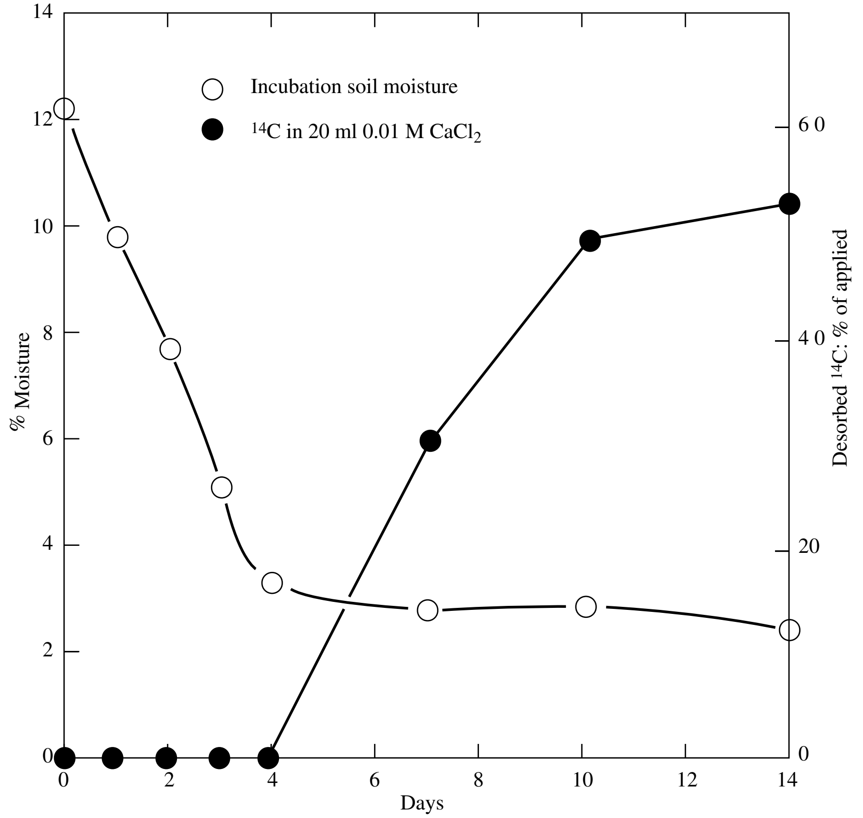

FIGURE 1. Breakdown of polydimethylsiloxane into water-soluble species in dry soil as evidenced by desorbable ^{14}C. Reproduced by permission of Pergamon Press from Reference 81a

found in all studies carried out to date. There is evidence[81b] that this species breaks down further with cleavage of the Si−C bond and release of CO_2. It is possible that this degradation may be due to microbes using **10** directly as a food source, but it is more likely that the known secretion of H_2O_2 and certain enzymes by some fungi results in a radical cleavage of the Si−C bond[81b]. Diemethylsilanediol **(10)** is a volatile substance and the major part of it is lost to the atmosphere by evaporation where it is thought to degrade by photo-oxidation to yield silica, carbon dioxide and water[81e].

4. Oxidation of polydimethylsiloxanes

A number of groups have looked at the photooxidation of siloxanes under irradiation at a range of wavelengths[82−86]. In all cases, loss of organic radicals from silicon as a range of oxidized species was observed with the residual material being silica. The rate of oxidation increases as the wavelength of UV light is decreased, as would be expected, due to the increasing energy of the photons. It is not clear, however, if the observed degradation is due to optically induced bond breaking or to local heating due to energy dissipation[84]. In the absence of oxygen no degradation is observed on irradiation at 193 nm[84] but loss of methane, ethane and phenyl groups was observed on irradiation at 147 nm and 123.6 nm[86]. Pelizzetti and coworkers[87] have shown that octaphenylcyclotetrasiloxane **(15)** and poly(methylphenylsiloxane) **(16)** can be photocatalytically degraded to CO_2 and inorganic silicates using TiO_2 and visible light. The mechanism of this degradation is postulated to involve an initial formation of radicals at the phenyl substituent either by hydrogen atom extraction or by •OH addition.

$$\underset{\textbf{(15)}}{[Ph_2SiO]_4} \qquad \underset{\textbf{(16)}}{[PhMeSiO]_n}$$

Atomic oxygen is a highly reactive species that can pose serious problems for spacecraft in low Earth orbit due to degradation of materials of construction. In the case of siloxane elastomers and coatings[88,89], it has been shown that surface oxidation occurs to give a silica layer which then protects the bulk material from further oxidation, with the result that little loss of physical properties occurs.

C. Thermal Degradation of Siloxane Resins

Corriu and coworkers have studied the thermal decomposition of hydrosilsesquioxane resins[90] **(17)** and have observed the evolution of silane **(18)** between 350 °C and 480 °C (equation 10). Above this temperature hydrogen is observed.

$$\underset{\textbf{(17)}}{4HSiO_{1.5}} \longrightarrow \underset{\textbf{(18)}}{SiH_4} + 3SiO_2 \tag{10}$$

The loss of silane is due to redistribution reactions between Si−H and Si−O bonds which may be catalysed by residual silanol groups acting as basic catalysts[90]. The preparative method for the gel was shown to greatly affect the percentage weight loss due to silane evolution, depending on the presence or absence of catalytic species. In the presence of air, oxidation of the hydrosilsesquioxane to silica was observed[90]. The same workers extended this study to a series of resins containing D (Me_2SiO), D^H (MeHSiO), T ($MeSiO_{1.5}$) and T^H ($HSiO_{1.5}$) units. Use of TG/MS and solid state NMR clearly demonstrated that redistribution reactions could take place between Si−C and Si−O bonds (equation 11), as well as between Si−H and Si−O bonds; Si−O exchange with Si−O also occurs[91].

$$2MeSiO_{1.5} \longrightarrow Me_2SiO + SiO_2 \tag{11}$$

Temperatures around 600 °C are required for exchange reactions involving silicon–carbon bonds whilst silicon–hydrogen bonds will redistribute at temperatures as low as 300 °C. The exchange of Si–C bonds has also been observed for mixed siloxane–titania gels derived from dimethyldiethoxysilane and titanium tetraisopropoxide[92]. At 600 °C, loss of methyl groups from silicon was observed with formation of Si–O bonds and Ti–C bonds, thus demonstrating an exchange of carbon between silicon and titanium.

Wachholz and coworkers[93] have used a combination of cryo-GC/FT-IR and GC/MS to study the siloxane pyrolysis products of a silicone resin prepared from a mixture of Me_3SiCl (0.34 mol), $MeHSiCl_2$ (0.56 mol), $Me(CH_2{=}CH)SiCl_2$ (0.56 mol) and $PhSiCl_3$ (1.56 mol). Heating at 500 °C gave an oil which contained over 30 compounds. FT-IR and MS analysis of three of the major signals allowed the identification of **19**, **20** and **21**. It is not clear if these species were present in the resin as made or if they result from siloxane bond redistribution during the pyrolysis.

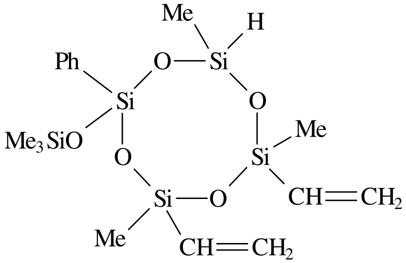

(19)

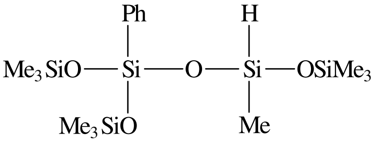

$$Me_3SiO{-}\overset{Ph}{\underset{Me_3SiO}{Si}}{-}O{-}\overset{H}{\underset{Me}{Si}}{-}OSiMe_3$$

(20)

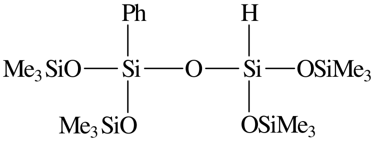

$$Me_3SiO{-}\overset{Ph}{\underset{Me_3SiO}{Si}}{-}O{-}\overset{H}{\underset{OSiMe_3}{Si}}{-}OSiMe_3$$

(21)

The pyrolysis of polyphenylsilsesquioxane above 500 °C proceeds with loss of benzene; some methane and hydrogen was observed above 600 °C. Approximately one-third of the phenyl rings were eliminated during pyrolysis[94] to give an amorphous silicon oxycarbide. Similar results were found for silsesquioxane copolymers containing mixtures of methyl and phenyl substituents on silicon[95]. Zank and coworkers have examined degradation pathways for a series of poly[methyl-*co*-phenylsilsesquioxane] resins containing vinyldimethylsiloxy units **(22)**[96].

$$(PhSiO_{1.5})_x(MeSiO_{1.5})_y[(H_2C{=}CH)Me_2SiO_{0.5}]_z$$

$$x = 0.25\text{–}0.75,\ y = 0.05\text{–}0.50,\ z = 0 \text{ or } 0.25$$

(22)

Benzene, ethylene and acetylene were the predominate observed volatiles at 550 °C whilst methane was evolved from 650 °C to 875 °C. An amorphous SiCO material was obtained at 1200 °C and bond redistribution and carbothermic reduction occurred up to 1800 °C to give a ceramic material composed of substantial amounts of crystalline β-silicon carbide. The preparation of bulk ceramic components from materials in the system

Si−Met−C−N−O (Met = Ti, Cr, V, Mo, Si, B, $CrSi_2$, $MoSi_2$ etc.) from organosilicon polymers has been well reviewed by Greil[73].

The thermolysis, under nitrogen, of polyhedral oligomeric cyclohexylsilsequioxane macromers and siloxane copolymers proceeds via a number of processes[97]. Fully condensed species such as c-$Hex_8Si_8O_{12}$ **(23)** undergo complete sublimation at around 380 °C with retention of the silicon−oxygen cages. For the partly condensed species **24**, silanol condensation between 390 °C and 450 °C prevents complete sublimation; loss of cyclohexane and cyclohexene occurs on further heating to 550 °C. The copolymer **25** exhibited loss of cyclic dimethylsiloxanes, D_3 and D_4 as well as loss of cyclohexane and cyclohexene between 400° and 500 °C.

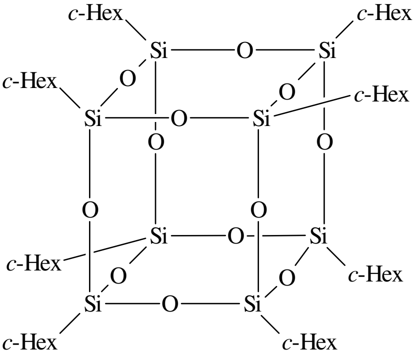

(23)

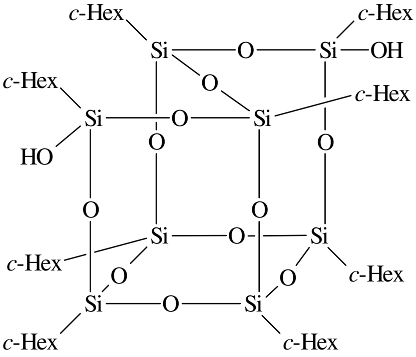

(24)

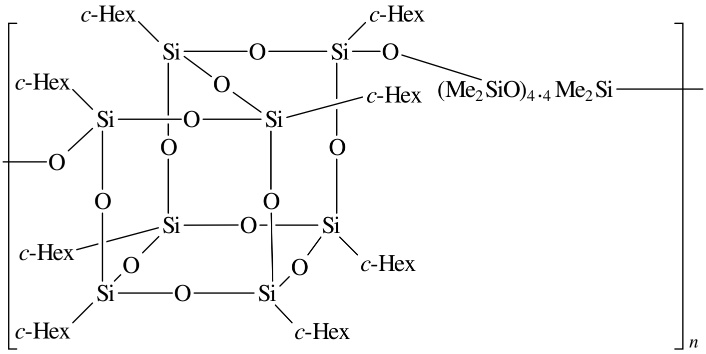

(25)

Silanes and silicones are extensively used as surface treating agents for silica, glass, aluminium and a range of other substrates[98] and the thermal stability of such coatings is an important factor in their performance. The polysiloxane resin coating obtaining on treating a glass fibre with an aqueous solution of 3-chloropropyltriethoxysilane[99] underwent an initial weight loss on heating to 130 °C due to loss of residual ethoxy groups and formation of siloxane bonds in the coating. Most of the organic functionality is lost at 360 °C, whilst the residue remaining after heating to 550 °C consists of SiO_2 with SiOH groups.

IV. THE SURFACE ACTIVITY OF LINEAR SILOXANE POLYMERS AND COPOLYMERS

A. Introduction

The novel surface properties of polydimethylsiloxanes (PDMS) derive from the combination of very surface active methyl groups attached to a very flexible and stable backbone, and they account for many of the industrial applications of PDMS. The surface chemistry and applications of polydimethylsiloxanes have recently been well reviewed by Owen[100] as have techniques for the surface analysis of silicones[101,102].

Many of the bulk properties of polymers are molecular weight dependent and can be expressed in the general form:

$$X = X_\infty - k_0/M_n$$

where X is the property of interest for a number-average molecular weight M_n and X_∞ is the same property at infinite molecular weight. This behaviour is attributed to the end groups of the polymer which may have differing properties from the repeat unit, thus as the molecular weight increases the influence of the end groups is diluted. The groups of Sauer[103] and Koberstein[104] have examined the dependence of surface tension on molecular weight and end-group type for PDMS and found a similar relationship when σ is the surface tension and σ_∞ is the surface tension at infinite dilution:

$$\sigma = \sigma_\infty - k_1/(M_n)^x$$

At high molecular weight x approaches unity, whilst at low molecular weight x approaches 2/3. The surface tension of the $-Me_2SiO-$ repeat unit was calculated to be 20.1 mN m^{-1} whilst the surface tensions of Me_3SiO-, $HOMe_2SiO-$ and $H_2N(CH_2)_3Me_2SiO-$ end groups were calculated to be 15.5, 26.9 and 32.8 mN m^{-1}, respectively[104a]. The surface of an amino terminated PDMS has been shown to be depleted in nitrogen as expected, given the high surface tension of this group[104b].

Whilst the migration of PDMS to liquid–air or liquid–liquid interfaces is well known and exploited commercially in silicone antifoams[100] and silicone surfactants[100,105], there is growing interest in the migration of siloxane copolymers to solid interfaces which will be the focus of this review.

B. Siloxane Copolymer Migration to Solid–Air Interfaces

The surface distribution of siloxane copolymers within polymer matrices has been studied by a range of techniques, most commonly X-ray Photoelectron Spectroscopy (XPS), combined with contact angle measurements and Attenuated Total Reflectance FTIR (ATR-FTIR) spectroscopy. By varying the incident angle of the X-ray beam with respect to the surface, the sampling depth can be varied and a profile of the various atomic constituents of the copolymers generated. There is good agreement in the literature that siloxanes copolymers can migrate to solid–air interfaces and that the nature of the resultant siloxane rich layer depends on a range of factors, including the length of the siloxane block and the architecture of the copolymer.

1. Block copolymers

Chen, Gardella and Kumler[106] have studied a series of polydimethylsiloxane-polystyrene block copolymers and examined the surface composition by ATR-FTIR and XPS. For AB-type PS-PDMS diblock copolymers **(26)** with siloxane block molecular weights of between 38,000 and 99,000, the surface was found to be exclusively polydimethylsiloxane down to a depth of 10 nm by XPS. ATR-FTIR, which samples

$$-(CH_2CHPh)_m-\ (Me_2SiO)_n-$$

(26)

at a depth of up to 2.4 μm[106], showed only PDMS in the case of a copolymer with a large siloxane block ($M_n = 99,000$), whereas in the case of a smaller siloxane block ($M_n = 38,000$) polystyrene was observed in the surface layer by ATR-FTIR but at a lower concentration than present in the bulk. Changing the copolymer morphology to an ABA-type PS-PDMS-PS triblock copolymer resulted in less efficient surface segregation of the siloxane. A siloxane segment with double the molecular weight of that used in the AB-type case was required to give a comparable siloxane surface layer. This result can be rationalized by assuming that the polystyrene segments are located within the bulk of the copolymer and that in the ABA-type copolymer case this will result in the siloxane segment being bent over, thus effectively halving its length (Figure 2). Annealing for the ABA-type copolymers was found to promote the surface segregation of the low-energy PDMS phase[106].

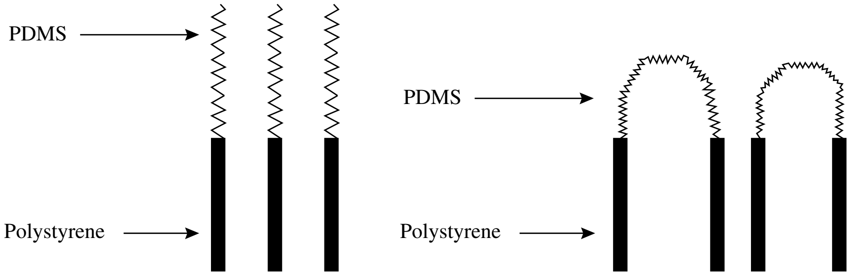

FIGURE 2. Schematic representations of a siloxane-polystyrene AB-type (left) and ABA-type (right) copolymer at a polystyrene surface

Jérôme and coworkers[107] have reported similar results with a PDMS-PS block copolymer in which the siloxane block was much smaller, $M_n = 3,300$. The copolymer was blended into polystyrene at up to 10% and films were prepared by either solvent casting from THF or by spin coating. Analysis by either XPS or Secondary Ion Mass Spectroscopy (SIMS) showed the air–polymer interface to be enriched in PDMS. However, polystyrene was also observable at even the shallowest sampling depths possible for either technique. Surface tension measurements showed that at above 0.5% added copolymer the surface properties of the blend closely match that of polydimethylsiloxane. With 10% of added copolymer no siloxane was observed beyond *ca* 27 nm depth. Interestingly, siloxane was also observed at the polymer–aluminium interface for spin cast films, but at only a quarter of the concentration observed at the air interface; on annealing the film this siloxane migrated to the air interface. A combination of Time of Flight Secondary Ion Mass Spectroscopy (TOF-SIMS) and XPS[108] has also shown surface layers with high polydimethylsiloxane character for blends of PDMS-PS block copolymers in polystyrene (2 wt% siloxane). Polydimethylsiloxane-urethane-ethylene oxide block copolymers of ABA **(27)** or BAB **(28)** architecture also showed differing efficiencies towards surface segregation, with the copolymers having siloxane as the terminal polymer **(27)** being the more efficient[109].

$$[H(OSiMe_2)_{21}CH_2OCH_2CH_2OC(O)\text{-}[1,2,4]\text{-}NHC_6H_3(CH_3)NHC(O)(OCH_2CH_2)_n]_2O$$

(27) $n = 4$ or 17

$[H(OCH_2CH_2)_mOC(O)\text{-}[1,2,4]\text{-}NHC_6H_3(CH_3)NHC(O)OCH_2CH_2OCH_2(SiMe_2O)_{10}]_2SiMe_2$

(28) $m = 8$ or 34

Interestingly, at very low additive levels both types of copolymer, **27** and **28**, behave similarly which, it was suggested, may be due to a change in surface alignment of the siloxane segment of the copolymer from perpendicular to the surface to parallel. Pertsin and coworkers[110] have shown that, for blends of siloxane-sulphone or siloxane-carbonate multiblock copolymers with various homopolymers or copolymers, the nature of the surface layer depends on the amount of copolymer present. At low additive levels of the copolymer, the surface layer was thin and the copolymers were oriented parallel to the surface; at higher additive levels the surface layer was thicker and the copolymer tended to orient perpendicular to the surface. Gardella and coworkers[111] have demonstrated that siloxane block length, bulk concentration of siloxane and annealing of the sample all determine the thickness of the siloxane layer observed for a polydimethylsiloxane-polycarbonate multiblock copolymer.

Careful XPS analysis of a series of poly(dimethylsiloxane-urea-urethane) multiblock copolymers demonstrated that, as well as a surface layer of siloxane, there was a layer enriched in the hard block immediately beneath this. The thickness of both these layers depended on the molecular weights of the soft and hard block segments, respectively[112]. Annealing of these copolymers increased the thickness of both layers. The same authors have also shown that the thickness of these layers of hard and soft blocks could be modified by use of solvent mixtures which selectively precipitate the polar hard block during film formation by solvent casting[113].

TOF-SIMS analysis of the surface of poly(methylphenylsiloxane)-polystyrene copolymers gave signals due to both poly(methylphenylsiloxane) and polystyrene[114]. The higher surface energy of poly(methylphenylsiloxane) compared to polydimethylsiloxane would be expected to reduce the thermodynamic driving force for surface segregation of the siloxane in this case. The siloxane block of these copolymers was trimethylsilyl terminated and the strong signal observed for this group by TOF-SIMS is evidence that the terminal trimethylsilyl group was at the air interface, as might be expected considering both the low surface energy of the Me_3Si group and free volume considerations[114].

2. Graft copolymers

Poly(methyl methacrylate)-g-poly(dimethylsiloxane) copolymers have been prepared by free radical copolymerizations of acrylate-functional siloxane macromonomers **(29)** with methyl methacrylate. Siloxane macromonomers **(29)** of between 1,000 and 20,000 molecular weight were utilized to give a range of copolymers with between 4 and 17 wt% silicone[115].

$$Bu(Me_2SiO)_nMe_2Si(CH_2)_3OC(O)CMe{=}CH_2$$

(29)

Contact angle measurements and XPS demonstrated that the surface layer was silicone rich, especially for copolymers with high molecular weight siloxane arms. A layer of pure polydimethylsiloxane was observed to a depth of 1.5 nm for a copolymer prepared from **29** of 20,000 molecular weight. The corresponding copolymer derived from **29** of 10,000 molecular weight had a thinner surface layer of siloxane and only contained 95 wt% polydimethylsiloxane when probed to a depth of 1.5 nm. The percentage of siloxane in the surface layer continued to decrease as the molecular weight of **29** decreased[115]. Copolymers of methyl methacrylate and glycidyl methacrylate with acrylate functional siloxane macromonomers **(29)** of 5,000 molecular weight have been incorporated into epoxy resins[116]. Surface enrichment of the siloxane was observed, though XPS analysis suggested that the siloxane layer was less than 3 nm thick even if 10 wt% of these copolymers was added. The addition of these siloxane copolymers was shown to very effectively reduce the force needed to peel an adhesive tape from the surface of the epoxy resin[116], thus demonstrating the siloxane-like nature of the surface.

Ober and coworkers[117] have grafted siloxanes onto a styrene-isoprene block copolymer via hydrosilylation of the pendant vinyl groups of the diene block with pentamethyldisiloxane **(30)** (equation 12).

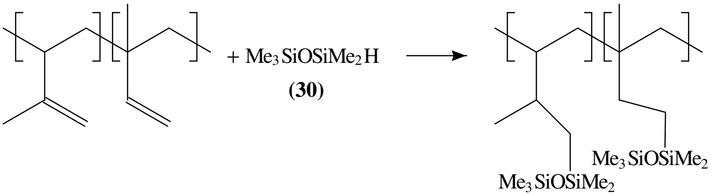

(12)

Blends of this copolymer with polystyrene were analysed by contact angle measurements and Rutherford backscattering (RBS) both of which showed that the surface was silicone rich.

Allcock and Smith[118] have prepared a series of poly(organophosphazenes) containing siloxane grafts and/or trifluoroethoxy side groups **(31–34)**. Polymers **31** and **32** had critical surface tensions of 16–17 mN m^{-1} and surface layers which were enriched in fluorine. In the case of **32**, silicone was not observed at the surface. Polymer **33** had a critical surface tension of 31 mN m^{-1}, which is higher than that for pure PDMS at 24 mN m^{-1}[119], and XPS analysis of this polymer showed that the surface was substantially enriched in siloxane. The surface modification of **34** via hydrosilylation of a swelled film was demonstrated with silicon being observed to a depth of 60 μm by energy-dispersive X-ray analysis of a cross section of the resultant film[118].

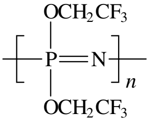

$$\left[\overset{OCH_2CF_3}{\underset{OCH_2CF_3}{P}} = N \right]_n$$

(31)

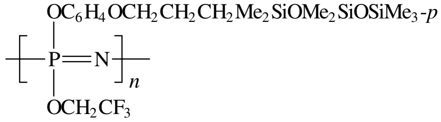

$$\left[\overset{OC_6H_4OCH_2CH_2CH_2Me_2SiOMe_2SiOSiMe_3\text{-}p}{\underset{OCH_2CF_3}{P}} = N \right]_n$$

(32)

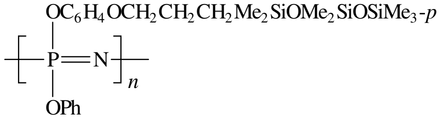

$$\left[\overset{OC_6H_4OCH_2CH_2CH_2Me_2SiOMe_2SiOSiMe_3\text{-}p}{\underset{OPh}{P}} = N \right]_n$$

(33)

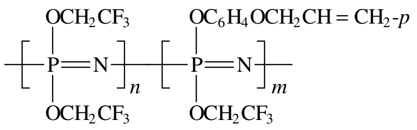

$$\left[\overset{OCH_2CF_3}{\underset{OCH_2CF_3}{P}} = N \right]_n \left[\overset{OC_6H_4OCH_2CH=CH_2\text{-}p}{\underset{OCH_2CF_3}{P}} = N \right]_m$$

(34)

The combination of XPS with cryogenic sample-handling techniques has allowed the study of hydrated polymer surfaces and surface rearrangements on dehydration[120]. A polydimethylsiloxane grafted with poly(hydroxyethyl methacrylate) (HEMA) was found to contain 95 atomic% HEMA at the surface in the hydrated state, but on vaccum drying the surface became 90 atomic% PDMS. Unfortunately, equipment limitations prevented study of the kinetics of this rearrangement. Similar changes in surface composition for hydrated and dehydrated states were observed for a polyurethane containing a polydimethylsiloxane soft block[120].

C. Blend Compatibilization

The properties of immiscible polymers blends are strongly dependent on the morphology of the blend, with optimal mechanical properties only being obtained at a critical particle size for the dispersed phase. As the size of the dispersed phase is directly proportional to the interfacial tension between the components of the blend, there is much interest in interfacial tension modification. Copolymers, either preformed or formed *in situ*, can localize at the interface and effectively modify the interfacial tension of polymer blends. The incorporation of PDMS phases is desirable as a method to improve properties such as impact resistance, toughness, tensile strength, elongation at break, thermal stability and lubrication.

1. Pre-formed copolymers

Koberstein and coworkers[121] have examined the effects of a polydimethylsiloxane-polystyrene (PDMS-PS) block copolymer on the interfacial tensions of blends of PDMS and polystyrene. As little as 0.002 wt% of the copolymer, added to the siloxane phase, was sufficient to lower the interfacial tension by 82% in the case of a blend of polystyrene ($M_n = 4{,}000$) and PDMS ($M_n = 4{,}500$). No further reduction in interfacial tension was observed at higher copolymer levels due to micelle formation. Riess[122] has polymerized styrene in the presence of a silicon oil and a polydimethylsiloxane-polystyrene block copolymer to obtain a polystyrene in which 0.1–1 μm droplets of silicone oil are dispersed. This material displayed a lowered coefficient of kinetic friction on steel compared to pure polystyrene.

Addition of a polydimethylsiloxane-graft-polyethylene oxide copolymer to a blend of PDMS and polyethylene oxide (PEO) resulted in time-dependent changes in the interfacial tension over a period of hours[123]. The interfacial tension initially decreased to a minimum and then increased to a final equilibrium value. It is believed[123] that this represents adsorption of the copolymer at the interface followed by an ordering of the copolymer phase at the interface. The addition of triblock polydimethylsiloxane-polyethylene oxide copolymers, P(DMS$_n$-EO$_m$-DMS$_n$) (**35**) to blends of PDMS and polyethylene oxide demonstrated a dependence of the interfacial tension on the size of the siloxane segment and reached a minimum for **35** with $n \geqslant 16$[124]. Increasing the length of the ethylene oxide segment slightly increased the interfacial tension. Reversing the order of the polymer blocks to give a P(EO$_m$-DMS$_n$-EO$_m$) was found to give similar results to those obtained with **35** of comparable PDMS and PEO block lengths.

Branched copolymers of PDMS and poly(caprolactone) have been prepared as shown in equation 13. They were incorporated into epoxy resin via reaction at the terminal hydroxy groups and acted as toughening agents, with a three-fold increase in impact strength being observed with 5 wt% of **36** present. The siloxane phases were in the range of 10–20 nm, resulting in an optically clear material[125].

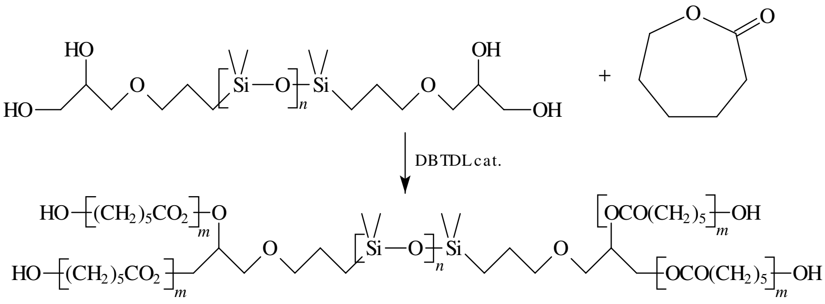

(13)

(36)

The end groups of a PDMS polymer have been shown to affect the interfacial tension of blends with poly(butadiene)[126]. Thus, substitution of an amine-terminated PDMS for a trimethylsilyl-terminated PDMS can reduce the interfacial tension by up to 30%. This effect is postulated to arise due to the amine end group having a surface energy closer to that of butadiene than does the trimethylsilyl group and thus being present at the interface.

2. Reactive blending

As an alternative to addition of pre-formed block copolymers to polymer blends, the copolymer compatibilizers can be formed *in situ* during processing; such reactive blending may have economic advantages. Nando and coworkers[127,128] have shown that a vinyl functional dimethylsiloxane **(37)** will react with an ethylene–methyl acrylate copolymer (EMA) **(38)** at temperatures over 150 °C. The mechanism of this reaction involves a homolytic cleavage of the hydrogen atom from the α-carbon adjacent to the ester group of **38**, followed by addition of the carbon radical to the double bond of **37** followed by hydrogen abstraction (Scheme 6).

$-(Me_2SiO)_n-((H_2C{=}CH)MeSiO)_m-$ **(37)**

$-(CH_2CH_2)_x-(CH_2CH(CO_2Me))_y-$ **(38)**

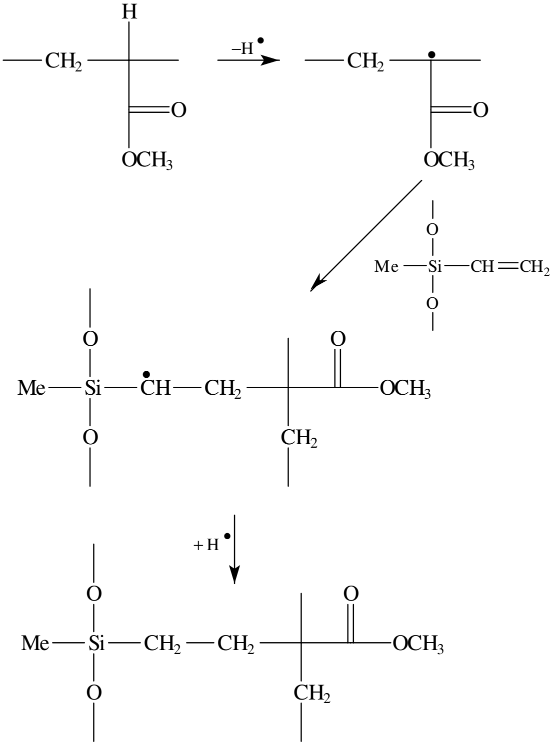

(39)

SCHEME 6. Mechanism of radical addition of EMA to vinyl functional PDMS

The resulting ethylene methyl acrylate-graft-polydimethylsiloxane **(39)** exhibited a single glass transition temperature, which was composition dependent, demonstrating polymer miscibility[127]. This reaction (Scheme 6) was carried out *in situ* during the blending of a 1:1 mixture of PDMS and polyethylene to give **39**, which acted as a blend compatibilizer. It was found that the presence of **39** improved adhesion between the blend components, reduced the dispersed domain size of PDMS in polyethylene and increased the degree of crystallinity within the blend[129]. **39** was also found to compatibilize blends of PDMS and an ethylene-propylene-diene rubber[130] and blends of PDMS and polyurethane[131], with improvements in tensile strength, elongation at break and thermal stability being observed. An alternative to reactive blending has been demonstrated[132] by addition of a carboxy-terminated polybutadiene and a difunctional amino-terminated PDMS to the respective homopolymers in blends of polybutadiene and PDMS. An ammonium carboxylate salt forms at the interface and this behaves like a block copolymer with reductions of up to 70% in the interfacial tension being observed.

It is clear that siloxane copolymers can migrate within solids and beneficially modify interface properties. The efficiency of this migration depends on a wide range of factors including the block lengths of the copolymer, the morphology of the copolymer and the method of sample preparation, and is an area of ongoing study.

V. REFERENCES

1. J. Chojnowski, *J. Inorg. Organomet. Polym.*, **1**, 299 (1991).
2. J. Chojnowski, *Spec. Publ. R. Soc. Chem.*, **166**, 59 (1995).
3. S. Penezek and A. Duda, *Makromol. Chem., Macromol. Symp.*, **67**, 15 (1993).
4. J. A. Semlyen, B. R. Wood and P. Hodge, *Polym. Adv. Technol.*, **5**, 473 (1994).
5. V. M. Kopylov, L. M. Khananashvili, O. V. Shkol'nik and A. G. Ivanov, *Vysokomol. Soedin., Ser. A,* **37**, 395 (1995); *Chem. Abstr.*, **123**, 170322 (1995).
6. R. Murugavel, A. Voight, M. G. Walawalker and H. W. Roesky, *Chem. Rev.*, **96**, 2205 (1996).
7. T. A. Kolomiets, N. N. Laskovenko and S. I. Omel'chaiko, *Kompoz. Polim. Mater.*, **50**, 9 (1991); *Chem. Abstr.*, **119**, 73139 (1991).
8. P. V. Ivanov, *Vysokomol. Soedin., Ser. A*, **37**, 417 (1995); *Chem. Abstr.*, **123**, 144672 (1995).
9. H. Inoue, *Nipon Gomu Kyokaishi*, **66**, 660 (1993); *Chem. Abstr.*, **120**, 325489 (1993).
10. Y. Imai, *J. Macromol. Sci. Chem., A*, **28**, 1115 (1991).
11. (a) L. Lestel and S. Boileau, *Makromol. Chem., Macromol. Symp.*, **47**, 293 (1991).
    (b) S. Boileau, *Makromol. Chem., Macromol. Symp.*, **73**, 177 (1993).
    (c) J. Ming Yu, D. Teyssie, R. B. Khalifa and S. Boileau, *Polym. Bull.*, **32**, 35 (1994).
    (d) T. Zundel, J. Ming Yu, L. Lestel, D. Teyssie and S. Boileau, *Makromol. Symp.*, **88**, 177 (1994).
12. M. K. Yoshinaga and Y. Iida, *Chem. Lett.*, 1057 (1991).
13. (a) A. Molenberg and M. Moller, *Macromol. Rapid Commun.*, **16**, 449 (1995).
    (b) A. Molenberg and M. Moller, *Macromol. Symp.*, **107**, 331 (1996).
14. M. E. Van Dyke and S. Clarson, *Poly. Prepr., Am. Chem. Soc.*, **37**, 668 (1996).
15. (a) M. O. Hunt, A. M. Belu, R. W. Linton and J. M. DeSimon, *Polym. Prepr., Am. Chem. Soc.*, **34**, 530 (1993).
    (b) M. O. Hunt, A. M. Belu, R. W. Linton and J. M. DeSimon, *Polym. Prepr., Am. Chem. Soc.*, **34**, 445 (1993).
    (c) M. O. Hunt, A. M. Belu, R. W. Linton and J. M. DeSimon, *Polym. Prepr., Am. Chem. Soc.*, **34**, 883 (1993).
16. A. DeGunzbourg, J-C. Favier and P. Hemery, *Polym. Int.*, **35**, 179 (1994).
17. (a) T. Okawa, Dow Corning Toray Silicone Co. Ltd., EP 679674, Nov. 1995.
    (b) I. Jansen, S. Kupfer and K. Ruehlmann, Huels Silicone GmbH, DE 4436076, Nov. 1996.
18. P. Sigwalt, P. Gobin, M. Moreau and M. Masure, *Makromol. Chem., Macromol. Symp.*, **42/43**, 229 (1991).
19. (a) G. Toskas, G. Besztercey, M. Moreau, M. Masure and P. Sigwalt, *Macromol. Chem. Phys.* **196**, 2715 (1995).

(b) P. Nicol, M. Masure and P. Sigwalt, *Macromol. Chem. Phys.*, **195**, 2327 (1994).
(c) P. Sigwalt, M. Masure, M. Moreau and R. Bischoff, *Makromol. Chem., Macromol. Symp.*, **73**, 147 (1993).

20. G. J. Price, M. P. Hearn, E. N. K. Wallace and A. M. Patel, *Polymer*, **37**, 2303 (1996).
21. (a) M. Cypryk, S. Rubinsztajn and J. Chojnowski, *Macromolecules*, **26**, 5389 (1993).
    (b) M. Cypryk, S. Rubinsztajn and J. Chojnowski, *J. Organomet. Chem.*, **446**, 91 (1993).
    (c) M. Cypryk, *Polymery (Warsaw)*, **40**, 421 (1995).
22. (a) M. Cypryk and P, Sigwalt *Macromolecules*, **27**, 6245 (1994).
    (b) R. Bischoff and P. Sigwalt, *Polym. Prepr., Am. Chem. Soc., Div. Polym. Chem.*, **37**, 349 (1996).
23. K. Kazmirski, J. Chojnowski and J. McVie, *Eur. Polym. J.*, **30**, 515 (1994).
24. M. Marcus, M. Simionescu, M. Cazacu and S. Lazarescu, *Iran. J. Polym. Sci. Technol.*, **3**, 95 (1994).
25. X. W. He and J. E. Herz, *Eur. Polym. J.*, **27**, 449 (1991).
26. H. K. Chu, R. P. Cross and D. I. Crossen, *J. Organomet. Chem.*, **425**, 9 (1992).
27. (a) R. Hagger and J. Weis, Wacker Chemie, EP0626414 May 1994.
    (b) R. Hagger and J. Weis, Wacker Chemie, EP0626415 May 1994.
    (c) R. Hagger R. Braun, O. Schneider and B. Deubzer, Wacker Chemie, DE 4422813, June 1996.
28. R. Hagger and J. Weis, *Z. Naturforsch., B: Chem. Sci.*, **49**, 1774 (1994).
29. (a) H. Schickmann, R. Lehnert, H-D. Wendt, H-G. Serbny and H. Rautschek, Chemiewerk Nunchritz GmbH, DE 4344664, Dec. 1993.
    (b) H. Schickmann, R. Lehnert, H-D. Wendt, H-G. Serbny and H. Rautschek, Chemiewerk Nunchritz GmbH, DE 4323188, July 1993.
    (c) H. Schickmann, R. Lehnert and H-D. Wendt, Chemiewerk Nunchritz GmbH, DE 4323185, July 1993.
    (d) R. Lehnert, H-D. Wendt and H. Schickmann, Huels Silicone GmbH, DE 4446515, May 1996.
30. (a) S. Rubinsztajn, General Electric Company, GB 2279945, Jan 1995.
    (b) J. S. Razzano, D. P. Thompson, P. P. Anderson and S. Rubinsztajn, General Electric Company, GB 2279959, January 1995.
31. (a) Dow Corning Ltd., EP 0522776, July 1991.
    (b) Dow Corning Ltd., EP 0503825, March 1991.
    (c) Dow Corning Ltd., GB 2252975, February 1991.
32. (a) J. Chojnowski, R. Taylor, J. Habimana, M. Cypryk, W. Fortuniak and K. Kazmierski, *J. Organomet. Chem.*, in press (1996).
    (b) J. Chojnowski, R. Taylor, M. Cypryk, W. Fortuniak and K. Kazmierski, *J. Organomet. Chem.*, in press (1996).
33. W. Schulz, J. Lambert and L. Kania, Dow Corning Corp., US 5196559, March 1993.
34. G. A. Olah, O. Wang, G. Rasol, G. K. S. Prakash, H. Zhang and T. E. Hogen-Esch, *Polym. Prepr., Am. Chem. Soc.*, **37**, 805 (1996).
35. (a) S. T. Kolaczkowski and S. Serbetcioglu, Dow Corning Ltd., EP 605143, July 1994.
    (b) S. Serbetcioglu, PhD Thesis, University of Bath, 1995.
36. S. Westall, Dow Corning Ltd., EP 587343 A2, March 1994.
37. J. E. McGrath and M. Spinu, *J. Polym. Sci., Part A, Polym. Chem.*, **29**, 657 (1991).
38. G. Sauvet and G. Helary, *Eur. Polym. J.*, **28**, 37 (1992).
39. R. Babu, G. Sinai-Zingde and J. S. Riffle *J. Polym. Sci., Part A, Polym. Chem.*, **31**, 1645 (1993).
40. J. J. Hoffman and C. M. Leir, *Polym. Int.*, **24**, 131 (1991).
41. (a) L. E. Drechsler, A. van der Helm, C. M. Kuo and S. J. Clarson., *Polym. Prepr., Am. Chem. Soc.*, **33**, 986 (1992).
    (b) C. M. Kuo and S. J. Clarson., *Polym. Prepr., Am. Chem. Soc.*, **32**, 183 (1991).
    (c) S. J. Clarson and A. M. S. Al-Ghamdi., *Polym. Commun.*, **31**, 322 (1990).
42. (a) S. Cai, J. Fang and X. Yu, *J. Appl. Polym. Sci.*, **44**, 135 (1992).
    (b) G. Akovali, Z. M. O. Rzaev and D. H. Mamedov, *Polym. Int.*, **37**, 119 (1995).
43. D. B. Yang, *J. Polym. Sci., Part A, Polym. Chem.*, **31**, 199 (1993).
44. J. V. Crivello and D. Bi, *J. Polym. Sci., Part A*, **31**, 2563, 2729, 3109, 3121 (1993); J. V. Crivello, D. Bi and Mingxin Fang, *J. Macromol. Sci., Pure Appl. Chem.*, **A31**, 1001 (1994).
45. T. Suzuki, S. Yamada and T. Okawa, *Polym. J. (Tokyo)*, **25**, 411 (1993).
46. M. A. Peters, A. M. Belu, R. W. Linton, L. Dupray, T. J. Meyer and J. M. DeSimone, *J. Am. Chem. Soc.*, **117**, 3380 (1995).

47. D. A. Williams, P. R. Willey and B. J. Ward, US 4992512, February 1991.
48. S. H. Barley, A. Gilbert and G. R. Mitchell, *Makromol. Chem.*, **192**, 2801 (1991).
49. C. Herzig and J. Esterbauer, US 5015700, May 1991.
50. E. Beyou, P. Babin, B. Bennetau, J. Dunoguès, D. Teyssié and S. Boileau, *Tetrahedron Lett.*, **36**, 1843 (1995).
51. H. Hacker, J. Huber, G. Kolodziej, G. Piecha and D. Wilhelm, DE 4014882, November 1991.
52. S. Aoki, Y. Hara, and T. Ohba, US 5190988, February 1992; W. V. Gentzkow, W. Rogler, F. Zapf and G. Zeidler, DE 4110654, October 1992; T. Saruyama and M. Yoshitake, EP 0656386, November 1995; T. E. Hohenwarter, RadTech 92 North Am. UV/EB Conf. Expo., Conference Proceedings, Vol. 1, RadTech Int. North Am., Northbrook, IL, 1992, pp. 108–111.
53. R. P. Eckberg, US 4987158, January 1991; R. F. Agars and R. P. Eckberg, EP 0599615, June 1994; R. P. Eckberg and R. Griswold, US 5397813, March 1995.
54. A. F. Jacobine, D. M. Glaser, S. T. Nakos, M. Masterson, P. J. Grabek, M. A. Rakas, D. Mancini and J. G. Woods, *Spec. Publ. R. Soc. Chem.*, **89** (Radiat. Curing Polym. 2), 342 (1991); M. A. Rakas and A. F. Jacobine, RadTech 92 North Am. UV/EB Conf. Expo., Conference Proceedings, Vol. 1, RadTech Int. North Am., Northbrook, IL, 1992, pp. 462–473; M. A. Rakas and A. F. Jacobine, *J. Adhes.*, **36**, 247 (1992).
55. S. V. Pertz and S. O. Glover, EP 0625533, May 1994; G. R. Homan and S. O. Glover, EP 0625534, May 1994.
56. F. Cazaux and X. Coqueret, *Eur. Polym. J.*, **31**, 521 (1995).
57. J. V. Crivello, Bo Yang and W. G. Kim, *J. Polym. Sci., Part A*, **33**, 2415 (1995).
58. X. Coqueret and L. Pouliquen, *Macromol. Symp.*, **87**, 17 (1994).
59. H. J. Coles, J. P. Hannington and D. R. Thomas, GB 2274649, August 1994; H. J. Coles, J. P. Hannington and D. R. Thomas, GB 2274652, August 1994.
60. S. A. Daunheimer and D. J. Halloran, EP 0574156, December 1993; D. J. Halloran and J. M. Vincent, US 5326483, July 1994.
61. G. S. Kohl, P. A. Giwa-Agbomeirele and J. M. Vincent, US 5063044, November 1991.
62. D. J. Halloran, EP 0437075, July 1991.
63. D. J. Halloran, EP 0437099, July 1991.
64. Y. Ito, EP 0524612, January 1993.
65. M. Humphries, *Cosmet. News*, **16**, 313 (1993).
66. A. M. Vincent, A. A. Wilson and A. Zombeck, US 5262155, March 1993.
67. A. J. Disapio, S. F. Rentsch and A. H. Ward, US 5208360, May 1993.
68. H. J. Lautenschlager, J. Bindl and K. G. Huhn, *Text. Chem. Color.*, **27**, 27 (1995).
69. H. Baris and E. Fleury, WO 9504847, February 1995.
70. G. T. Decker, K. Tobukuro and G. A. Gornowicz, EP 0475611, March 1992.
71. W. A. Starke and M. J. Ziemelis, EP 0674936, October 1995.
72. T. C. Kendrick, B. Parbhoo and J. W. White, in *The Silicon-Heteroatom Bond* (Eds S. Patai and Z. Rappoport), Chap. 3 and 4, Wiley, Chichester, 1991.
73. P. Greil, *J. Am. Ceram. Soc.*, **78**, 835 (1995).
74. E. L. Warrick, O. R. Pierce, K. E. Polmanteer and J. C. Saam, *Rubber Chem. Techol.*, **52**, 437 (1979).
75. G. B. Sohoni and J. E. Mark, *J. Appl. Polym. Sci.*, **45**, 1763 (1992).
76. G. Ya. Guba, V. I. Bogillo, M. I. Terets and A. A. Chuiko, *Ukr. Khim. Zh.*, **60**, 380 (1994); *Ukr. Chem. J.*, **60**, 4 (1994).
77. J. Chojnowski, J. Kurjata, S. Rubinsztajn, M. Scibiorek and M. Zeldin, *J. Inorg. Organomet. Polym.*, **2**, 387 (1992).
78. J. Chojnowski, J. Kurjata, S. Rubinsztajn and M. Scibiorek, in *Frontiers of Organosilicon Chemistry* (Eds. A. R. Bassindale and P. P. Gaspar), Royal Society of Chemistry, Cambridge, 1991, p. 70.
79. R. R. Buch and D. N. Ingebrigtson, *Environ. Sci. Technol.*, **13**, 676 (1979).
80. J. C. Carpenter, J. A. Cella and S. B. Dorn, *Environ. Sci. Technol.*, **29**, 864 (1995).
81. (a) R. G. Lehmann, S. Varaprath and C. L. Frye, *Environ. Toxicol. Chem.*, **13**, 1061 (1994).
    (b) R. G. Lehmann, S. Varaprath and C. L. Frye, *Environ. Toxicol. Chem.*, **13**, 1753 (1994).
    (c) R. G. Lehmann, S. Varaprath, R. B. Annelin and J. L. Arndt, *Environ. Toxicol. Chem.*, **14**, 1299 (1995).
    (d) R. G. Lehmann and T. R. Miller, *Environ. Toxicol. Chem.*, **15**, 1455 (1996).
    (e) R. Sommerlade, H. Parlar, D. Wrobel and P. Kocks, *Environ. Sci. Technol.*, **27**, 2435 (1993).

82. Y. Israëli, J. Cavezzan and J. Lacoste, *Polym. Degrad. Stab.*, **37**, 201 (1992).
83. T. Imakoma, Y. Suzuki, O. Fujii and I. Nakajima, *Proc. Int. Conf. Prop. Appl. Dielectr. Mater.*, **1**, 306 (1994).
84. O. Joubert, G. Hollinger, C. Fiori, R. A. B. Devine, P. Paniez and R. Pantel, *J. Appl. Phys.*, **69**, 6647 (1991).
85. V. N. Vasilets, A. V. Kovalchuk and A. N. Ponomarev, *J. Photopolym. Sci. Technol.*, **7**, 165 (1994).
86. V. E. Skurat and Y. I. Dorofeev, *Angew. Makromol. Chem.*, **216**, 205 (1994).
87. C. Minero, V. Maurino and E. Pelizzetti, *Langmuir*, **11**, 4440 (1995).
88. A. F. Whitaker and B. Z. Jang, *SAMPE J.*, **30**, 30 (1994).
89. J. W. Connell, J. V. Crivello and D. Bi, *J. Appl. Polym. Sci.*, **57**, 1251 (1995).
90. (a) V. Belot, R. J. P. Corriu, A. M. Flank, D. Leclercq, P. H. Mutin and A. Vioux, *Eur. Mater. Res. Soc. Monogr. (Eurogel '91).*, 77 (1992).
    (b) V. Belot, R. J. P. Corriu, D. Leclercq, P. H. Mutin and A. Vioux, *Chem. Mater.*, **3**, 127 (1991).
91. V. Belot, R. J. P. Corriu, D. Leclercq, P. H. Mutin and A. Vioux, *J. Polym. Sci., Part A, Polym. Chem.*, **30**, 613 (1992).
92. S. Diré and F. Babonneau, *J. Sol-Gel Sci. Technol.*, **2**, 139 (1994).
93. S. Wachholz, U. Just. F. Keider, H. Geißler and K. Käppler, *Fresenius Z. Anal. Chem.*, **352**, 515 (1995).
94. A. M. Wilson, J. N. Riemers, E. W. Fuller and J. R. Dahn, *Solid State Ionics*, **74**, 249 (1994).
95. F. I. Hurwitz, P. Heimann, S. C. Farmer and D. M. Hembree Jr., *J. Mater. Sci.*, **28**, 6622 (1993).
96. G. T. Burns, R. B. Taylor, Y. Xu, A. Zangvil and G. A. Zank, *Chem. Mater.*, **4**, 1313 (1992).
97. J. D. Lichtenhan, R. A. Mantz, P. A. Jones, J. W. Gilman, K. P. Chaffe, I. M. K. Ismial and M. J. Burmiester, *Polym. Prepr., Am. Chem. Soc., Div. Polym. Chem.*, **36**, 334 (1995).
98. E. P. Pluddemann, *Silane Coupling Agents*, Plenum, New York, 1991
99. A. Lorena, M. C. Matias and J. Martinez Urreaga, *Spectrosc. Lett.*, **25**, 1121 (1992).
100. M. J. Owen, in *Siloxane Polymers* (Eds. S. J. Clarson and J. A. Semlyen), PTR Prentice Hall, New Jersey, 1993, pp. 309–372.
101. M. J. Owen in *The Analytical Chemistry of Silicones* Chap. V (Ed. A. L. Smith), Wiley, New York, 1991.
102. M. J. Owen, '*New Directions in Organosilicon Surface Science' in Front. Polym. Adv. Mater., Proc. Int. Conf.*, Vol. 9 (Ed. P.N. Prasad), Plenum press New York, 1993, p. 677.
103. (a) B. B. Sauer and G. T. Dee, *Macromolecules*, **24**, 2124 (1991).
     (b) B. B. Sauer and G. T. Dee, *Mater. Res. Soc. Symp. Proc.*, **248**, 441 (1992).
     (c) G. T. Dee and B. B. Sauer, *Macromolecules*, **26**, 2771 (1993).
     (d) B. B. Sauer and G. T. Dee, *J. Colloid Interface Sci.*, **162**, 25 (1994).
     (e) G. T. Dee and B. B. Sauer, *Polymer*, **36**, 1673 (1995).
104. (a) C. Jalbert, J. T. Koberstein, I. Yilgor, P. Gallagher and V. Krukonis, *Macromolecules*, **26**, 3069 (1993).
     (b) C. Jalbert, J. T. Koberstein, R. Balaji, Q. Bhatia, L. Salvati and I. Yilgor, *Macromolecules*, **27**, 2409 (1994).
     (c) T. J. Lenk, D. H. T. Lee and J. T. Koberstein, *Langmuir*, **10**, 1857 (1994).
105. (a) M. He, R. M. Hill, H. A. Doumaux, F. S. Bates, H. T. Davis, D. F. Evans and L. E. Scriven, *ACS Symp. Ser.*, **578**, 192 (1994).
     (b) M. J. Owen and H. Kobayashi, *Surf. Coat. Int.*, **78**, 52 (1995).
106. X. Chen. J. A. Gardella and P. L. Kumler, *Macromolecules*, **25**, 6621 (1992).
107. S. Petitjean, G. Ghitti, R. Jérôme, Ph. Teyssié, J. Marzien, J. Riga and J. Verbist, *Macromolecules*, **27**, 4127 (1994).
108. C. E. Selby, J. O. Stuart, S. J. Clarson, S. D. Smith, A. Sabata, W. J. Van Ooij and N. G. Cave, *J. Inorg. Organomet. Polym.*, **4**, 85 (1994).
109. M. M. Gorelova, A. J. Pertsin, I. O. Volkov, L. V. Filimonova, L. I. Makarova and A. A. Zhdanov, *J. Appl. Polym. Sci.*, **57**, 227 (1995).
110. (a) A. J. Pertsin, M. M. Gorelova, V. Yu. Levin and L. I. Makarova, *J. Appl. Polym. Sci.*, **45**, 1195 (1992).
     (b) A. J. Pertsin, M. M. Gorelova, V. Yu. Levin and L. I. Makarova, *Makromol. Chem., Macromol. Symp.*, **44**, 317 (1991).
111. X. Chen, H. F. Lee and J. A. Gardella Jr., *Macromolecules*, **26**, 4601 (1993).

112. X. Chen, J. A. Gardella Jr., T. Ho and K. J. Wynne, *Macromolecules*, **28**, 1635 (1995).
113. J. A. Gardella Jr., T. Ho, K. J. Wynne and H.-Z. Zhong, *J. Colloid Interface Sci.*, **176**, 277 (1995).
114. S. J. Clarson, J. O. Stuart, C. E. Selby, A. Sabata, S. D. Smith and A. Ashraf, *Macromolecules*, **28**, 674 (1995).
115. S. D. Smith, J. M. Desimone, H. Huang, G. York, D. W. Dwight, G. L. Wilkes and J. E. McGrath, *Macromolecules*, **25**, 2575 (1992).
116. T. Kasemura, C. Komatu, H. Nishihara, S. Takahashi, Y. Oshibe, H. Onmura and T. Yamamoto, *J. Adhes.*, **47**, 17 (1994).
117. S. S. Hwang, C. K. Ober, S. Perutz, D. R. Iyengar, L. A. Schneggenburger and E. J. Kramer, *Polymer*, **36**, 1321 (1995).
118. H. A. Allcock and D. E. Smith, *Chem. Mater.*, **7**, 1469 (1995).
119. E. G. Shafrin in *Polymer Handbook*, 2nd ed. (Eds. J. Brandrup and E. H. Immurgut), Wiley, New York, 1975, pp. 221–228.
120. K. B. Lewis and B. D. Ratner, *J. Colloid Interface Sci.*, **159**, 77 (1993).
121. W. Hu, J. T. Koberstein, J. P. Lingelser and Y. Gallot, *Macromolecules*, **28**, 5209 (1995).
122. G. Riess, *Makromol. Chem., Macromol. Symp.*, **69**, 125 (1993).
123. G. Schreyeck and P. Marie, *C. R. Acad. Sci., Ser. II: Mec., Phys., Chim., Astron.*, **320**, 653 (1995); *Chem. Abstr.*, **123**, 113536 (1995).
124. M. Wagner and B. A. Wolf, *Polymer*, **34**, 1460 (1993).
125. R. Mülhaupt, U. Buchholz, J. Rösch and N. Steinhauser, *Angew. Makromol. Chem.*, **223**, 47 (1994).
126. C. A. Fleischer, J. T. Koberstein, V. Krukonis and P. A. Wetmore, *Macromolecules*, **26**, 4172 (1993).
127. R. A. Santra, S. Roy, A. K. Bhowmick and G. B. Nando, *Polym. Eng. Sci.*, **33**, 1352 (1993).
128. R. A. Santra, S. Roy and G. B. Nando, *Polym.-Plast. Technol. Eng.*, **33**, 23 (1994).
129. R. A. Santra, B. K. Samantaray, A. K. Bhowmick and G. B. Nando, *J. Polym. Sci.*, **49**, 1145 (1993).
130. S. Kole, R. Santra and A. K. Bhowmick, *Rubber Chem. Technol.*, **67**, 119 (1994).
131. R. A. Santra, S. Roy, V. K. Tikku and G. B. Nando, *Adv. Polym. Technol.*, **14**, 59 (1995).
132. C. A. Fleischer, A. R. Morales and J. T. Koberstein, *Macromolecules*, **27**, 379 (1994).

CHAPTER 39

Si-containing ceramic precursors

R. M. LAINE

Departments of Materials Science and Engineering and Chemistry, University of Michigan, Ann Arbor, MI 48109-2136, USA
Fax: (313)764-6203; e-mail: talsdad@umich.edu

and

A. SELLINGER

Sandia National Laboratory, Advanced Materials Laboratory, 1001 University Blvd. S.E., University of New Mexico, Albuquerque, NM 87106, USA

I. INTRODUCTION

The purpose of this chapter is to provide an overview of how Si-containing compounds or polymers are used to form glass and ceramic shapes. In ceramics terminology, the fabrication of glass or ceramic materials using chemical compounds is called 'chemical processing'[1−7]. Chemical processing methods range in sophistication from simple precipitation of fine crystallites of common inorganic compounds, e.g. alum [$NH_4Al(SO_4)_2$, an alumina powder precursor], to spinning preceramic polymer fibers that will survive pyrolytic conversion to ceramic fibers. Chemical processing approaches can generally be divided into hydrolytic (sol-gel) and nonhydrolytic (precursor) methods. Sol-gel processing is a diverse area that has an immense literature, has been reviewed many times, is the subject of a well-written book[1a], is reviewed in this book[1b], and has its own journal[2]. Consequently, sol-gel processing will not be discussed here except as it relates to precursor processing methods.

Precursor processing can be subdivided into gas (e.g. chemical vapor deposition, CVD) and condensed phase methods. Gas phase methods, especially CVD (also plasma assisted CVD, etc.), because of microelectronics applications has spawned an entire field with an extensive literature that cannot be properly addressed here. Our focus will be on the use of silicon-containing organometallic and metalloorganic precursors as condensed phase sources of glass and ceramic materials. The term, organometallic, refers to compounds containing silicon−carbon bonds, e.g. polycarbosilanes, whereas the term metalloorganic refers to silicon compounds where Si−C bonds are absent, e.g. $Si(OR)_4$.

Although sol-gel processing is often used to generate materials for optical and electronic applications, with few exceptions, Si-containing precursors are used to produce glasses and/or ceramic materials of value because of their mechanical properties. Hence, most of the discussion that follows will be concerned with how the design, synthesis and processing of precursors can be used to realize better (optimal) mechanical properties. Despite these provisos, the literature available on precursor chemistry and precursor derived materials is still considerable. Consequently, even though we limit discussion to silicon-containing precursors to materials with structural applications, it is still not possible to cite all of the relevant literature. Because of the rapidity with which new precursor articles appear, and the extent of overlap of current publications (e.g. in SiC precursors), it was necessary to choose selected, exemplary articles in specific areas rather than attempt to review every publication.

We begin by providing a general definition of a precursor. We then discuss criteria that define 'useful' precursors in terms of processing shapes and then identify general types of materials properties and microstructures that are sought in the production of glass or ceramic materials. A combination of these criteria and desired materials properties/microstructures are used to identify precursors and precursor chemistries for both oxide and nonoxide glass and ceramic materials. Our overall goal is to delineate general principles that guide choices of chemistries, processing methods and materials properties, thereby permitting desired shapes with appropriate properties to be produced in a time and cost effective manner.

A precursor is any chemical compound that transforms, when decomposed in an energetic environment, to a glass or ceramic material. Thus alum [$NH_4Al(SO_4)_2$], which can be recrystallized to a purity of 99.995%, transforms on heating to high purity Al_2O_3 powder[8]. This type of chemical processing represents the simplest and most mature aspect of the field. The most exciting, newest and least mature aspect is the development of rheologically useful precursors that can be shaped[9]. This aspect represents the primary subject of this chapter.

To properly explore the subject area we begin by defining the concept 'useful'. Because processing ceramic fibers is the most demanding in terms of precursor properties, the criteria developed below emphasize 'useful' in terms of fiber precursors. To be 'useful' for fiber forming, a precursor must offer: (1) controllable rheology, (2) latent reactivity[6b], (3) controllable pyrolytic degradation, (4) high ceramic yield, (5) high selectivity to desired ceramic product and (6) controllable densification and microstructural development. The following paragraphs briefly define the specifics in each category.

II. CRITERIA THAT DEFINE A USEFUL PRECURSOR

A. Rheology

The type of fiber-forming procedure used (extrusion from solution or melt, with or without drawing) places some constraints on what is considered useful polymer rheology. In general, the precursor should exhibit thixotropic or non-newtonian viscoelastic behavior such that, during extrusion, it will flow readily without necking. The viscosity should be sufficiently high at zero shear so that the formed fiber retains its new shape and is self-supporting. Non-newtonian viscoelasticity normally arises in linear polymers with minimum molecular weights of 10–20 k Da as a result of chain entanglement. However, with a few notable exceptions (see below), all spinnable preceramics developed to date are low molecular weight, highly branched oligomers that exhibit non-newtonian behavior because the branches chain entangle. The correlation between rheology and 'spinnability' has been discussed in the literature[10,11].

B. Latent Reactivity

Not only must precursor fibers be self-supporting as extruded, they must also remain intact (e.g. not melt or creep) during pyrolytic transformation to ceramic fibers. Thus, precursor fibers (especially melt spun fibers) must retain some chemical reactivity so that the fibers can be rendered infusible before or during pyrolysis. Infusibility is commonly obtained through reactions that provide extensive crosslinking. These include free radical, condensation, oxidatively or thermally induced molecular rearrangements.

C. Pyrolytic Degradation

Most precursors contain extraneous organic ligands that are added to aid processability or provide latent reactivity. During pyrolysis these extraneous ligands must be eliminated as gaseous products. The rates and mechanisms of decomposition to gases require close monitoring to ensure conversion to the correct ceramic material, to prevent retention of impurities or creation of gas-generated flaws (e.g. pores). The processes involved can be likened to binder burnout in ceramic powder compacts[12,13]. In principle, this criterion is best satisfied if hydrogen is the only extraneous ligand required for stability and/or processability. Indeed, there is often a trade-off between precursor stability or processability and ceramic product purity that mandates processing with a less stable precursor to obtain higher quality ceramic products. In this instance, quality is equated with purity as detailed below. For example, Nicalon fibers derived from polycarbosilane, $-[\mathrm{MeSiCH_2}]_n-$, are not stoichiometric SiC because the original precursor is only processable with a 2 : 1 C : Si ratio (see below). More recently, polymethylsilane (PMS), $-[\mathrm{MeSiH}]_n-$, was found to provide access to phase and chemically pure SiC fibers. Unfortunately, in some forms this polymer is highly susceptible to air oxidation.

D. High Ceramic Yield

This criterion, which is product rather than precursor-property driven, is critical to the design and synthesis of new precursors. The need for high ceramic yields arises because of the excessive volume changes associated with pyrolytic conversion to ceramic materials. Scheme 1 illustrates these changes for a SiC precursor with an 80% ceramic yield of phase pure SiC ($3.2\ \mathrm{g\,ml^{-1}}$). Most precursors densities are close to $1\ \mathrm{g\,ml^{-1}}$, whereas most Si ceramic densities range from 2.5 to $3.5\ \mathrm{g\,ml^{-1}}$.

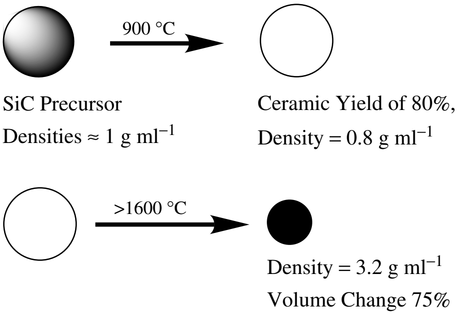

SCHEME 1. Volume changes during densification of an SiC precursor to phase pure SiC

If we have a ceramic yield of 100% (nothing is volatilized) and complete densification occurs, the total volume change will still be *ca* 70%. A 100% ceramic yield is unrealistic. Even PMS, which in principle only needs to lose $2\mathrm{H_2}$ molecules per monomer unit to form SiC, has a theoretical ceramic yield of 91 wt%. Thus, a precursor with a ceramic yield of *ca* 50 wt% (e.g. polycarbosilane)[7] will undergo volume changes of 85%. The possibility of achieving near net shape in the final ceramic product becomes very difficult. The result can be shape distortion. Furthermore, the 50 wt% that leaves as gases can cause pores, uneven densification and leave entrapped impurities. Only in processing thin films or fibers can a 50% ceramic yield still be viable because mass transport and shrinkage are minimal in at least one dimension (in fibers, the diametrical dimension) and shape integrity can be retained[7,9]. Because diffusion distances for mass transport are very short (in fibers, the diametrical direction), gaseous byproducts can leave easily, permitting ready densification at higher temperatures. Finally, gaseous byproducts represent potential pollution problems that must be dealt with in commercial processes.

Hence, for most applications, high ceramic yield precursors are essential. Consequently, it is important to formulate a preceramic polymer that contains minimal amounts of extraneous ligands that allow it to meet the processability criterion and yet provide high weight percent conversions to ceramic product. Thus, in many of the precursors discussed in this chapter, hydrogen and methyl are the ligands of choice. A good ceramic yield typically ranges 80–85 wt%, because most precursor syntheses produce some quantity of low molecular weight species that evaporate rather than decompose during pyrolysis.

Still another concern arises in reading or reporting ceramic yields. It is common to indicate ceramic yields at 1000 °C. For oxide ceramics, this temperature is usually acceptable. However, nonoxide ceramic precursors, especially SiC and Si_3N_4 systems, often retain 1–2 wt% hydrogen at temperatures up to 1400 °C. In 100 g of material this corresponds to one mole of H_2 per 2.5 moles of SiC, if the end product is phase pure SiC. A 1000 °C product with 2 wt% hydrogen can be thought of as a solid solution of SiC and hydrogen. These materials will not exhibit the properties of phase pure SiC, because the hydrogen, which is most likely present at grain boundaries, does not permit normal microstructural development to occur until it is eliminated. Furthermore, unanticipated outgassing at higher temperatures can cause cracking, compositional changes or pores in ceramic shapes. Thus, care must be taken in reading and reporting ceramic yields.

These last two points concern how precursor design and synthesis are influenced by the precursor-to-ceramic conversion process. The next set of criteria identify materials properties that drive precursor design and synthesis including product selectivity.

E. Selectivity to Phase and Chemically Pure Glasses or Ceramics

Chemical and phase purity are critical issues that drive precursor design because optimal mechanical properties are achieved only with high purity. For example, ceramics grade Nicalon fibers, with a chemical composition of *ca* $SiC_{1.45}O_{0.36}$ and densities of 2.3–2.5 $g\,ml^{-1}$[7,9], offer tensile strengths of 2.0–2.5 GPa and elastic moduli of *ca* 200 GPa. In the last five years, new precursors have been developed that provide sufficient chemical purity, following pyrolysis, to generate pure SiC. Stoichiometric SiC fibers were recently produced from these precursors, as discussed below. These fibers have densities $>3.1\ g\,ml^{-1}$, tensile strengths of 3.0–3.5 GPa and elastic moduli of 400–470 GPa[7,9]. These values are equivalent to literature values for dense, pure SiC produced via standard ceramic processing methods.

Note: It is sometimes possible to achieve the same end product from off stoichiometry precursors or pyrolysis products by further processing steps after precursor pyrolysis. Thus, as will be discussed below, stoichiometrically correct precursors are not always the answer.

Chemical purity is sometimes insufficient to realize optimal strength properties. Phase purity is also quite important, although this issue is often ignored in precursor studies. Thus, it is relatively easy to obtain mullite ($2SiO_2{\bullet}3Al_2O_3$) composition gels using sol-gel processing[14–17]. However, these gels are amorphous and, despite much literature which suggests they crystallize to mullite at 1000 °C, they actually convert to phase pure, orthorhombic mullite only on heating to *ca* 1300 °C. Presumably true mullite properties are only realized at this temperature.

Chemical and phase purity are not always desirable. For example, H- and N-doped silicon carbide films behave as high temperature semiconductors, while silicon carbonitride glasses offer properties akin to glassy carbon with room temperature conductivities of 10^3 $\Omega\ cm^{-1}$[18]. Additional reasons for targeting materials that are not chemically or phase pure stem from the desire to control microstructural properties.

F. Control of Microstructure and Densification

As noted above, densified products provide optimal mechanical properties. Unfortunately, heating a precursor to high temperatures to convert it to phase pure materials frequently does not lead to dense materials. For example, precursor-derived phase pure SiC will crystallize and undergo grain growth on heating to 1800 °C; however, grain growth occurs without coincidental sintering (densification) leading to porous materials[19]. This problem can be solved by adding small amounts of boron (0.3–0.5 wt%) which promotes densification without much grain growth. Thus, boron must be incorporated in the precursor synthesis or processing strategies to achieve the correct microstructure. In this instance, the desired microstructure drives precursor design.

In some instances, subtle changes in the precursor architecture can change the composition and microstructure of the final pyrolysis product. For example, pyrolysis of $-[\mathrm{MeHSiNH}]_x-$ leads to amorphous, silicon carbide nitride (SiCN) solid solutions at $>1000\,^\circ\mathrm{C}$ (see SiCN section). At *ca* 1500 °C, these material transform to Si_3N_4/SiC nanocomposites, of interest because they undergo superplastic deformation[20]. In contrast, chemically identical but isostructural $-[\mathrm{H_2SiNMe}]_x-$ transforms to Si_3N_4/carbon nanocomposites on heating, as discussed in more detail below[21].

Essentially all nonoxide and many oxide ceramic fibers currently produced commercially are amorphous or combinations of nanocrystallites in an amorphous phase. Indeed, until recently the general consensus in the ceramics community was that crystalline fibers would fail more readily than glassy fibers because of flaws at grain boundaries[6,22,23]. Thus, many studies discussed below are directed toward the development of high temperature, glassy fibers with good mechanical and thermal properties. As noted above, recent studies show that phase pure, microcrystalline SiC fibers provide properties and high temperature stability superior to current commercial fibers[7,9]. Thus, nano- or microcrystalline fibers may be better in some or many applications, especially where creep is a problem.

As a final comment on criteria for the design, synthesis and processing of precursors, if the precursor targeted is for coatings applications only, where the substrate provides most of the mechanical properties, a few additional criteria must be considered. First, the precursor must wet the substrate effectively to form uniform, adherent coatings. Some reaction with the substrate may or may not be desirable as a means of achieving either chemical or/and mechanical adhesion. Additionally, to process flaw (pore and crack) free ceramic coatings using dip, spin on or spray coating processes, it is generally necessary to limit coating thicknesses to $<2\ \mu\mathrm{m}$ and more commonly to $<1\ \mu\mathrm{m}$. This is because mismatches in coefficients of thermal expansion and the overall densification process lead to compressive stresses in the films. These stresses can provide improved coating adhesion and abrasion resistance; however, at higher thicknesses the compressive stresses cause coatings to crack, unless a ceramic powder is used as a filler to offset dimensional changes.

These general criteria serve as a basis for the selection of candidate precursors potentially of use for processing both oxide and nonoxide ceramics. For specific materials, additional criteria can also play a role including ease of synthesis, purification and stability toward air and moisture. One final and critical criterion is cost. Costly syntheses can reduce the general utility of a given precursor. However, in ceramic fiber processing, the pyrolytic conversion and post-processing heat treatments designed to provide optimal fiber mechanical properties are often much more costly than the chemistry.

The above criteria provide guidelines for the design and synthesis of new precursors, and as a means of evaluating materials currently extant. The following sections attempt to provide an overview of recent work in nonoxide and oxide materials. We begin by examining precursors to Si−N containing materials beginning with phase pure Si_3N_4 and then moving to more complex Si−N−E (E = element) systems. We next focus on selected SiC precursors and follow with examples of Si−C−B and Si−C−O systems. We then move to precursors to Si−O, Si−Al−O precursors and end with transition metal silicate precursors.

III. PRECURSORS CONTAINING Si AND N

Precursors that fall in this category are generically called polysilazanes or polysilsesquiazanes. Synthetic routes to these materials have been reviewed[6a,24]; thus, we provide an overview of typical methods. The most common route to polysilazanes is via ammonolysis/aminolysis of chlorosilanes[25–27].

$$\mathrm{MeHSiCl_2 + 3NH_3 \xrightarrow{Et_2O/-78\,^\circ C} 2NH_4Cl + -[MeHSiNH]_{\mathit{x}}-} \quad (1)$$

$$\mathrm{H_2SiCl_2 + 3MeNH_2 \xrightarrow{THF/-78\,^\circ C} 2MeNH_3Cl + -[H_2SiNMe]_{\mathit{x}}-} \quad (2)$$

$$\mathrm{MeSiCl_3 + 4.5NH_3 \xrightarrow{THF/-78\,^\circ C} 3NH_4Cl + -[MeSi(NH)_{0.5}]_{\mathit{x}}-} \quad (3)$$

The products resulting from reactions 1 and 2 are short-chain oligomers mixed with 6- and 8-member cyclics, with M_n values ranging from 600–2000 Da. These molecular weights are generally too low to offer good rheological properties or ceramic yields unless modified (see below). Another drawback to these reactions is that two moles of ammonium chloride are produced per mole of polymer and it is difficult to separate the two products cleanly.

Silsesquiazanes such as formed in reaction 3 are often crosslinked and intractable, although they can afford good ceramic yields.

Polysilazanes can also be synthesized by catalytic dehydrocoupling (equation 4)[28,29]. The reaction works best with monosubstituted silanes ($MeSiH_3$ is flammable); however, as with the ammonolysis reactions, molecular weights are normally less than 2000 Da. Hence, as-formed oligomers are not useful precursors. However, combinations of ammonolysis followed by catalytic dehydrocoupling provide access to useful precursors as discussed in the SiCN section.

$$\mathrm{RSiH_3 + R'NH_2 \xrightarrow{catalyst} H_2 + H-[RHSiNR']_{\mathit{x}}-H} \quad (4)$$

Recent work by Soum and coworkers provides a novel route to the first high molecular weight polysilazanes ever formed[30]. Although ring-opening polymerization (ROP) of cyclic silazanes has been attempted previously[24], Soum and coworkers report the first successful ionic ROP of cyclodisilazanes to form high molecular weight polysilazanes (equation 5). Molecular weights up to $M_n = 100$ kDa were observed. The key is to use low temperatures (−40 °C) to inhibit depolymerization reactions. If vinyl groups are used instead of methyl groups, curing the resulting polymers with AIBN gives moderate to high ceramic yields of SiCN (exact ceramic yields were not provided). Without the latent reactivity offered by the vinyl groups, heating tends to depolymerize these linear polymers to form volatile cyclic species.

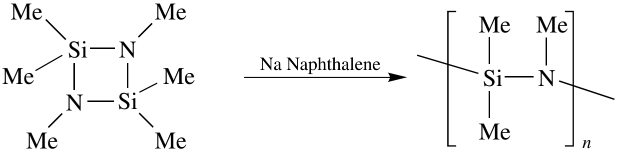

(5)

Although related SiN precursor systems have been developed, the above sets of reactions provide launch points for synthesizing the majority of SiN-containing precursors studied to date. Various groups have learned to manipulate oligomers prepared as above to develop 'useful' precursors. We begin by discussing those that provide phase pure silicon nitride.

A. Precursors to Si_3N_4

Access to phase pure silicon nitride materials via processable precursors is limited to just three approaches. The first, shown in reaction 6, provides one of the first oligomers exploited as a preceramic polymer[24,25a]. This simple polysilazane, containing only Si, N and H, is known to be relatively unstable and will crosslink on its own to give intractable gels. Furthermore, it does not offer the 3Si : 4N stoichiometry required for Si_3N_4. Nonetheless, it is useful as a binder and for fiber-reinforced ceramic matrix composites (CMCs)[31].

$$H_2SiCl_2 + 3NH_3 \xrightarrow{Et_2O/-78\,^\circ C} 2NH_4Cl + -[H_2SiNH]_x- \tag{6}$$

Because H_2SiCl_2 is a flammable gas that is difficult to work with, researchers at Tonen devised a novel approach to ammonolysis wherein the silyl halide is modified by complexation to pyridine (py) prior to ammonolysis and subsequent heat treatment of the isolated oligomer[23,32]:

$$H_2SiCl_2 + 2py \xrightarrow{0\,^\circ C} H_2SiCl_2{\bullet}2py \tag{7}$$

$$H_2SiCl_2{\bullet}2py + \text{excess } NH_3 \longrightarrow NH_4Cl(\text{or } py{\bullet}HCl) + -[H_2SiNH]_x- \tag{8}$$

$$-[H_2SiNH]_x- \xrightarrow{120\,^\circ C/py/4\ h/NH_3} -[H_2SiNH]_x-(\text{white solid following solvent removal}) \tag{9}$$

The oligosilazanes formed via this approach give higher molecular weights than obtainable by direct ammonolysis. The product (M_n *ca* 1600 Da) is polydisperse and highly branched. This oligomer is also not stable and crosslinks to form an intractable product in a short time in the absence of solvent. Pyrolysis gives an 80% ceramic yield of silicon nitride mixed with 20 wt% Si as expected based on the 1 : 1 Si : N precursor stoichiometry. Silicon is found even when pyrolysis is conducted under an NH_3 atmosphere. A tentative structure for the oligomer can be proposed:

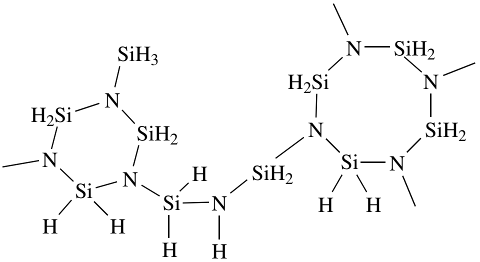

Characterization by IR and NMR indicates oligosilazane chains capped with SiH_3 groups. Analysis of the gases given off during synthesis reveals the presence of SiH_4 as a minor product. Both SiH_4 and the SiH_3 endcaps arise as a consequence of pyridine or ammonia catalyzed redistribution processes. The endcaps probably limit the degree to which higher molecular weight polymer can form.

In using the perhydropolysilazanes to process either composites or thin (10 µm diameter) fibers, heating to temperatures of 1100 °C, even in N_2, leads to crystallization of quantities of Si[31,32]. Blanchard and Schwab[31] indicate that up to 20 wt% Si appears at temperatures of 1200 to 1400 °C whether the processing atmosphere is N_2 or NH_3. This Si eventually reacts with the processing atmosphere, converting slowly to Si_3N_4 at higher temperatures. Conversion to Si_3N_4 is complete at *ca* 1700 °C in N_2 and 1580 °C in NH_3.

Work at Tonen indicates that fiber properties decrease with the appearance of Si metal, as it promotes Si_3N_4 crystallization. For example, the fiber tensile strengths, which are reported to be 2.5 GPa ($E = 250$ GPa) at room temperature, diminish by 10% after heating at 1200 °C for 10 h. On heating to 1300 °C for 10 h, the tensile strengths drop by 40%. Based on the observation that crystallization of Si_3N_4 is promoted by free Si and that crystallization leads to a loss in fiber strength, the fibers are processed to minimize Si content and up to 3 wt% oxygen is incorporated to aid in maintaining a glassy or amorphous nature.

As noted in the introduction, inexact stoichiometries and poor ceramic properties can be ameliorated during processing rather than by precursor design. The first example of this approach is the conversion of SiCN and SiC/C containing ceramics directly to Si_3N_4 by treating the precursor before, during or after initial pyrolysis processing with NH_3 at temperatures high enough to cleave N−H bonds (typically >500 °C).

Thus, a number of researchers have chosen ammonolysis as a route to phase and chemically pure Si_3N_4[33−37]. This process involves removal of excess free C and displacement of carbon in Si−C bonds with Si−N bonds. The process is assumed to involve free radical reactions. There is no apparent relationship between precursor structure or functionality and the extent of carbon removal[33]. *During the ammonolysis process, the carbon leaves as toxic HCN, thus care should be used in this approach*[38].

Schaible and coworkers find that ammonolysis of cyclotetra(dimethylsilazane) at 900 °C results in the formation of crystalline silicon diimide, Si_2N_2NH[37]. On further heating α-Si_3N_4 then crystallizes. It is important to recognize the potential for generating novel intermediate phases, as noted above, because these phases may be the key to developing the final microstructure.

The above studies indicate that phase pure Si_3N_4 can be obtained by careful choice of precursor, processing conditions or a combination of both. Several groups note that optimal mechanical properties for fibers are only obtained when the product is amorphous and often nonstoichiometric, because crystallization leads to grain grown and flaws at grain boundaries[6,22,23,32,36]. This then provides one motivation for the development of amorphous SiN-based ceramic systems. An additional driver is the fact that Si_3N_4 is not stable at >1700 °C, decomposing to Si and N_2. Thus, efforts to stabilize the system to nitrogen loss, while minimizing crystallization, have targeted modified SiN systems. These are discussed in the following sections. In closing, it is important to recognize that phase pure Si_3N_4 is still quite desirable for monolithic applications that do not involve fibers. In addition, pure Si_3N_4 remains a very valuable material in electronic applications.

B. Precursors to SiCN

Although there is considerable reason for developing modified SiN systems as just noted, most SiCN precursor systems were developed with the goal of processing Si_3N_4 fibers. In the early stages of this development, researchers explored methods that emphasized spinnability rather than product properties. However, the importance of minimizing C content was recognized, resulting in precursors with monomer units containing only −H and $-CH_3$ groups as shown below[21,24−28,39−48].

As noted above, for the most part, the first synthetic step resulted in oligomers with low ceramic yields, poor rheological properties and/or limited latent reactivity. As such, numerous approaches were explored with the idea of introducing latent reactivity and better viscoelastic properties. In the following, we discuss several of these synthetic approaches, some of the materials that result and a few applications.

Verbeek and coworkers[39] described the first processable SiCN precursors in the early 1970s. The approach, explored further recently[6,40], was to polymerize $MeSi(NHMe)_3$

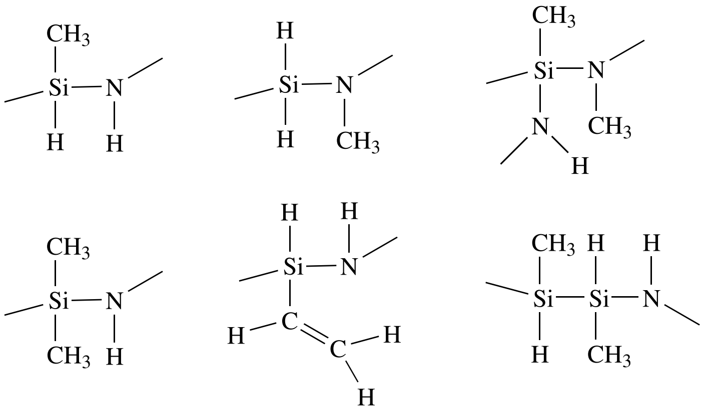

by self-condensation (equation 10) to obtain a polysilazane with $M_w \approx 4000$ Da. This polysilazane could be hand drawn to form 10–20 μm precursor fibers. In this instance, the precursor fibers were rendered infusible by exposure to humid air. Pyrolysis converts the crosslinked precursor fibers to ceramic fibers with ceramic yields of *ca* 55%. The ceramic products are mainly amorphous SiCN with some SiO_2 (a consequence of H_2O vapor used to crosslink the spun fibers)[6,40].

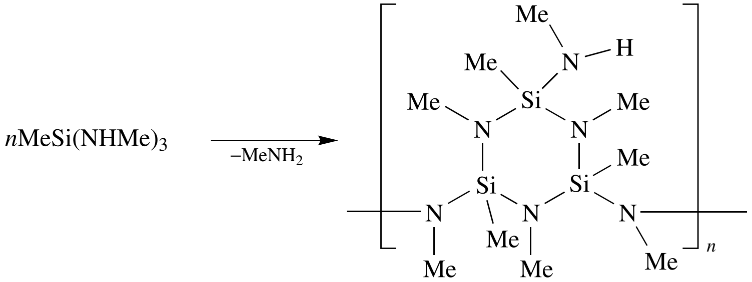

(10)

Interrante and coworkers have explored the related condensation polymerization of $Si(NHEt)_4$. Unfortunately, polymerization leads to an insoluble, rather than a processable, polymer with a 60 wt% (1000 °C/Ar) ceramic yield. Based on solid state NMR data, the polymer structure given in equation 11 was proposed[41].

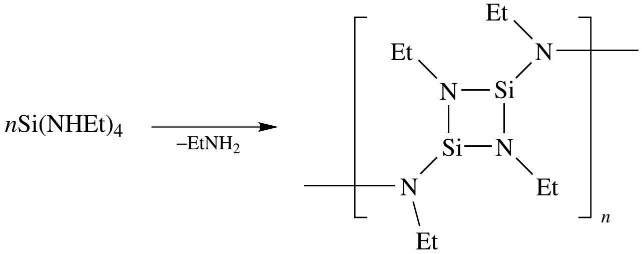

(11)

^{29}Si NMRs taken of samples during the pyrolysis process indicate that the polymer first converts to a material in which all of the Si−N bonds are retained, and some Et groups are retained as free C. The conclusion is that amorphous Si_3N_4 forms coincident with free C. *Because the precursor does not contain Si−C bonds, SiCN is not formed as an intermediate product.* On heating to temperatures of 1500–1600 °C, the material transforms to either Si_3N_4/SiC (pyrolyzed in N_2) or SiC (pyrolyzed in Ar). Si_3N_4 begins to decompose at $\geqslant$1500 °C (as noted above) and will react with free C to form SiC. A similar result is observed in pyrolysis studies of $-[H_2SiNMe]_x-$ (*N*-methylpolysilazane), see below[21,28].

A novel method of improving the processability of the cyclic $-[MeHSiNH]_x-$ oligosilazanes (from reaction 1) by reaction with urea was recently described by Seyferth and coworkers (equation 12)[42].

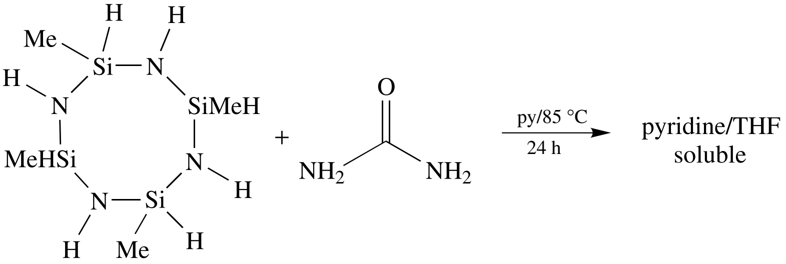

(12)

The original precursor materials give ceramic yields in the 15–20 wt% range, whereas the materials recovered from reaction 12 give ceramic yields (950 °C) of 80 + wt%. A typical sample gave a composition of $SiN_{1.06}C_{0.60}$. No precursor structure was offered; however, the presence of N−CO−N moieties was inferred from the gases evolved during pyrolysis and NMR data. Although some oxygen may be retained in the polymer, NMR studies do not indicate the presence of species with Si−O bonds in the final ceramic product. Because of the sensitivity of the polymer to hydrolysis, no molecular weight measurements were made. The processability of this polymer has not been described to date.

The above work follows earlier and more comprehensive efforts by the Seyferth group[25] on the use of base catalyzed crosslinking of cyclotetrasilazane, $-[MeHSiNH]_4-$, to increase its ceramic yield and processability. The currently proposed mechanism is suggested to involve silaimine formation followed by an addition reaction across the reactive double bond, as illustrated in equation 13[25,26].

The final oligomer has a M_n of 800–2000 Da depending on the reaction conditions and consists of two monomer types, $-[MeHSiNH]_x-$ and $-[MeSiN]_y-$. It is THF soluble and has ceramic yields of 80–85 wt% (1000 °C/N_2). A typical 1000 °C ceramic composition is $SiC_{0.50}N_{0.88}O_{0.04}$. Originally it was thought that this composition indicated an intimate mixture of SiC and Si_3N_4; however, recent solid state ^{29}Si NMR results suggest otherwise[21,43]. On heating to $\leqslant$1400 °C, the material remains amorphous and shows the presence of numerous species of the type SiN_xC_{4-x}. Only on heating to $\geqslant$1500 °C does the material transform to a true Si_3N_4/SiC mixture.

Transition-metal-catalyzed dehydrocoupling is an alternate catalytic method of turning lower molecular weight oligosilazanes into processable polysilazanes[21,28,44]. This process begins with the oligomers formed in reactions 1, 2 or 6. These oligomers usually contain internal Si−H bonds and $-NH_2$ or −MeNH endcaps. These endcaps are more reactive toward dehydrocoupling with Si−H bonds (reaction 4) than internal N−H bonds. Consequently, it is possible to form highly branched, polydisperse, viscoelastic precursors (equation 14)[28,44]. The GPC trace of a polydisperse polymer prepared via reaction 14 is shown in Figure 1.

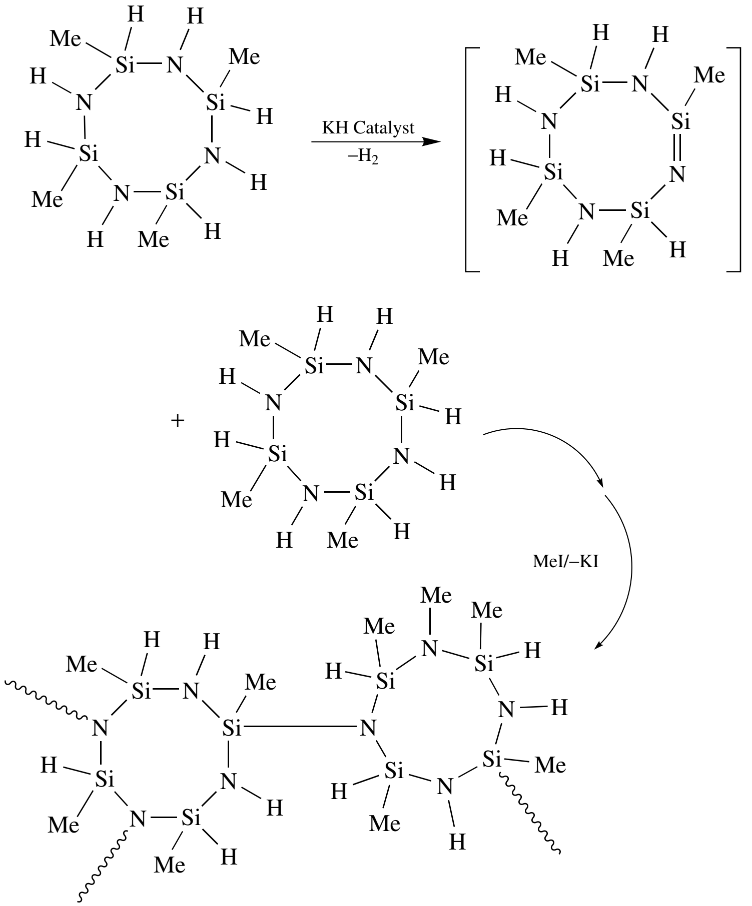

(13)

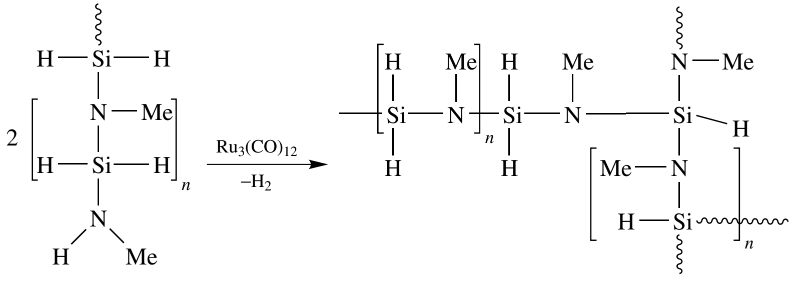

(14)

If $-[\mathrm{MeHSiNH}]_x-$ is used in place of $-[\mathrm{H_2SiNMe}]_x-$ in reaction 14, the resulting precursor is similar to the product of reaction 13. The solid state ^{29}Si NMR of this polymer heated to selected temperatures is shown in Figure 2[21]. The broad envelope of Si magnetic environments results from the series of $\mathrm{SiN}_x\mathrm{C}_{4-x}$ structures, as seen previously[43].

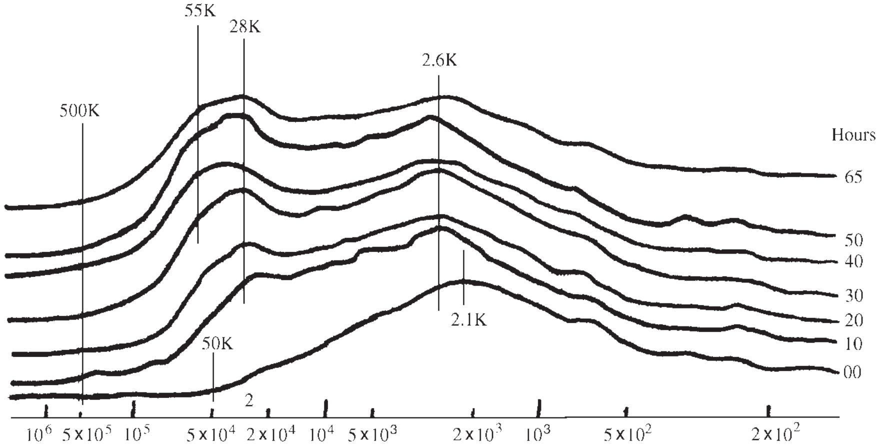

FIGURE 1. Gel permeation chromatogram of Ru-catalyzed chain extension of $HMeN{-}[SiH_2NMe]_x{-}H$

N-Methylpolysilazane is chemically identical to $-[MeHSiNH]_x-$ (Si-methylpolysilazane), studied by many researchers[25,42], but isostructural. Following catalytic modification as in reaction 14, the chemical evolution of *N*-methylpolysilazane on pyrolysis was followed by ^{29}Si (Figure 3). A detailed analysis has already been published[21]. The pertinent points are that by 600 °C, the major portion of the Si centers experience a magnetic environment centered around −46 ppm, which shifts to −49 ppm on heating to 800 °C and then 1000 °C. Similar results are obtained for samples heated to 1400 °C. The 1000 °C ^{29}Si NMR spectrum can be simulated with a single line centered at −49 ppm with a 1110 Hz linewidth. This is typical of values (1600 Hz) reported previously for amorphous Si_3N_4[21]. Despite the fact that up to 25 wt% free carbon is present, it in no way influences the chemistry at Si, up to 1400 °C. Note that the 800 °C spectrum is similar to that seen for the $Si(NHEt)_4$ derived materials[41].

One further finding with the $-[H_2NMe]_x-$ pyrolysis studies comes from Raman studies of the ceramic product. The NMR data show no traces of Si−C bonds, nor does the Raman spectrum. However, the Raman spectrum does show the presence of C−N bonds up to 1200 °C (the highest temperature studied). This suggests that the silicon nitride nanoparticles interact with the carbon matrix through C−N bonds. One might speculate that the interface looks somewhat like C_3N_4.

Thus, by shifting a methyl group from Si to N, the mechanism of transformation has been changed entirely. The products from pyrolysis of $-[H_2NMe]_x-$ and $-[MeHSiNH]_x-$ are quite different as clearly seen in Figure 4, which compares the ^{29}Si NMR spectra for both materials pyrolyzed to 1000 °C. This is proof that polymer architecture can strongly influence the type of ceramic material produced on pyrolysis.

Riedel and coworkers have also uncovered some extremely novel chemistry based on the use of carbodiimide chemistry, including a case where precursor architecture influences phase and compositional development[49]. The process begins with the very simple synthesis of silylcarbodiimides (equations 15 and 16). In the case where R = Me, the compound is a 16-atom heterocycle ($x = 4$). For R = H, a polymer is obtained that gives a 65 wt% ceramic yield at 1500 °C and a $SiC_{1.8}N_{1.3}$ (1000 °C) composition.

$$2Me_3SiCl + H_2NCN + 2py \longrightarrow Me_3SiN{=}C{=}NSiMe_3 + 2py{\bullet}HCl \qquad (15)$$

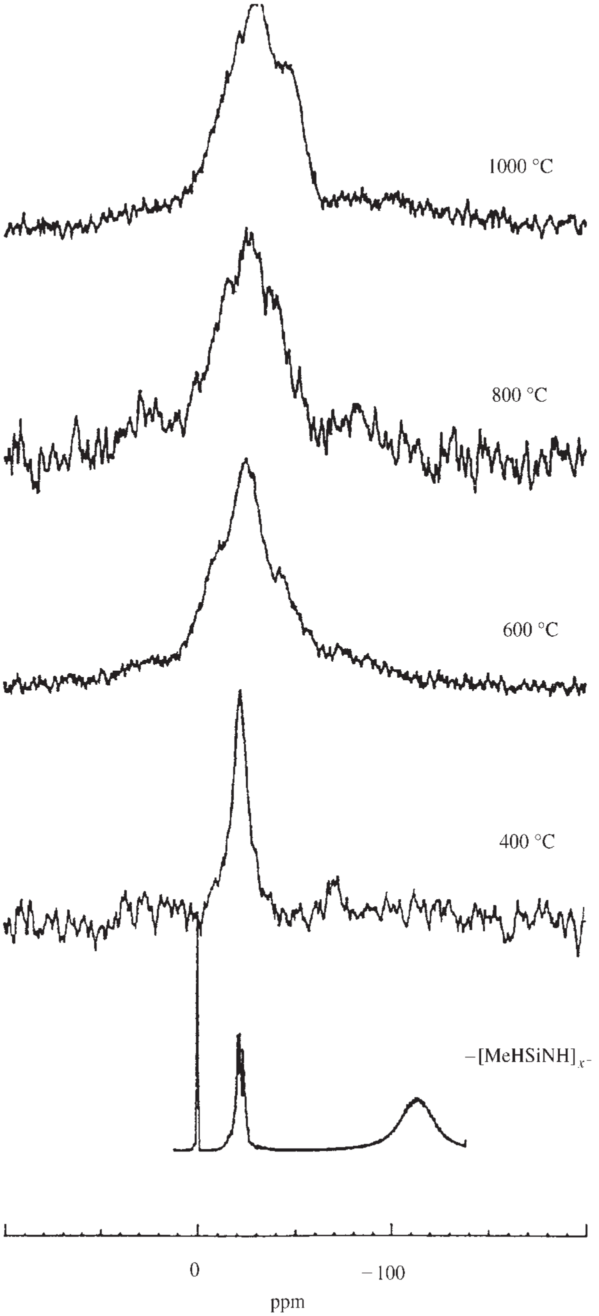

FIGURE 2. Solid state ^{29}Si MAS NMR of chain extended (65 h reaction time) $-[\text{MeHSiNH}_2]_x-$ heat treated (2 h/N_2) to selected temperatures. Note how the ^{29}Si peak broadens with the formation of various $\text{SiN}_x\text{C}_{4-x}$ species

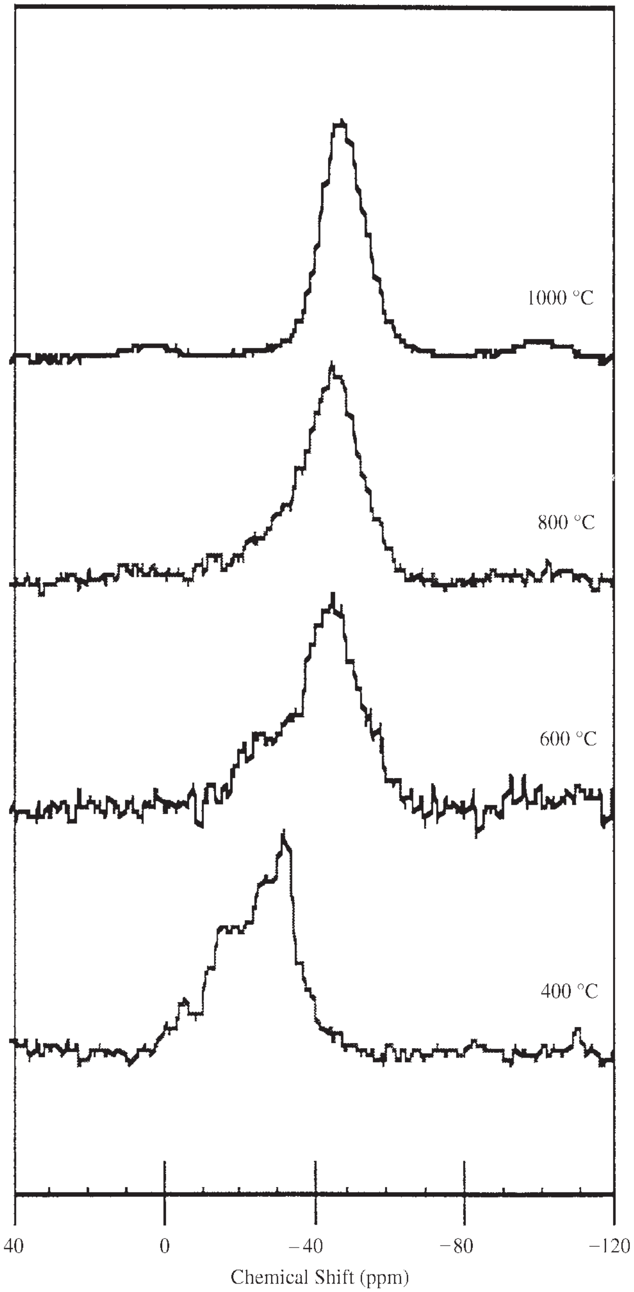

FIGURE 3. Solid state ^{29}Si MAS NMR of 65 h $-[H_2SiNMe]_x-$ heat treated (2 h/N_2) to selected temperatures. Note how the ^{29}Si peak becomes sharper at increasing temperatures with the formation of amorphous Si_3N_4

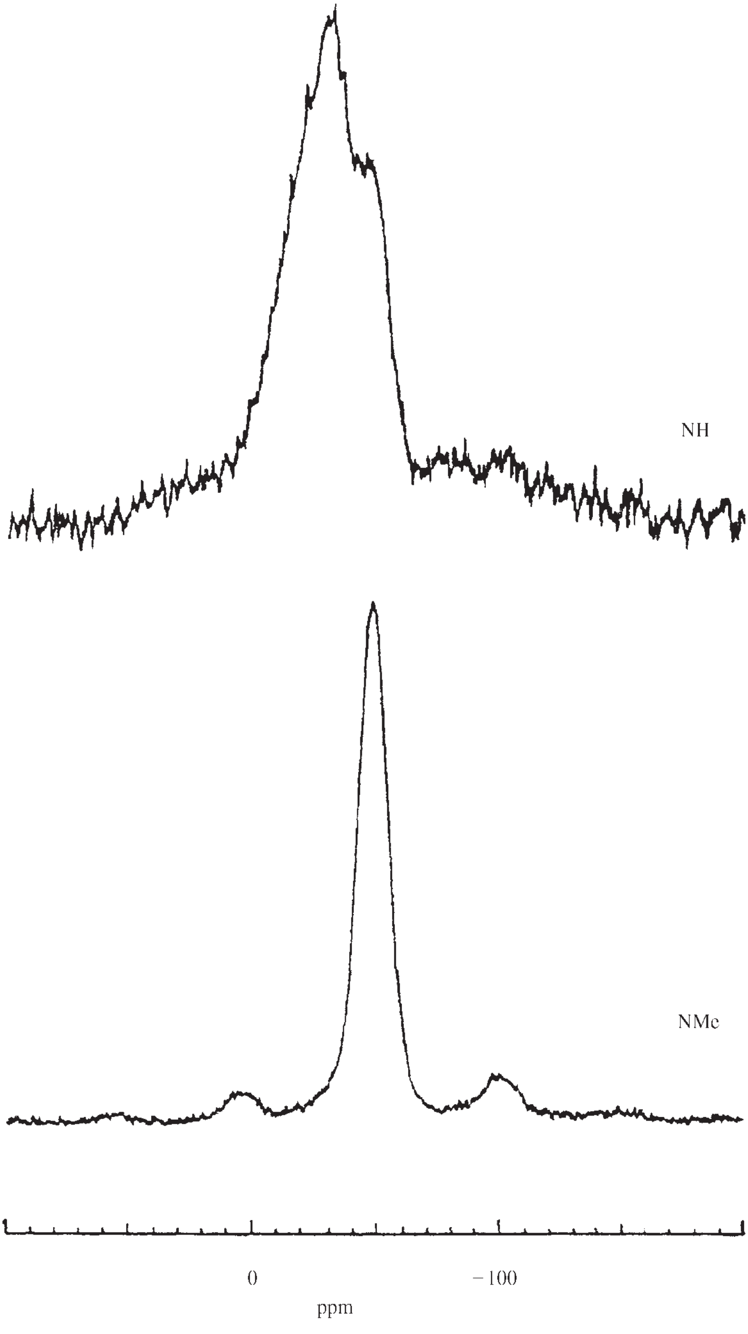

FIGURE 4. Comparison of $-[\mathrm{MeHSiNH_2}]_x-$ and $-[\mathrm{H_2SiNMe}]_x-$ heat treated at 1000 °C (2 h/N_2)

Another facet of the $Me_3SiN{=}C{=}NSiMe_3$ chemistry is that it can be reacted with chlorosilanes to obtain transparent gels (equation 17).

$$x\mathrm{MeRSiCl_2} + x\mathrm{H_2NCN} + 2x\mathrm{py} \longrightarrow -[\mathrm{MeRSiN{=}C{=}N}]_x- + 2x\mathrm{py{\cdot}HCl} \qquad (16)$$

$$\mathrm{py} = \mathrm{pyridine}$$

$$2\mathrm{Me_3SiN{=}C{=}NSiMe_3} + \mathrm{SiCl_4} \xrightarrow{\text{py catalyst}} [\mathrm{Si(N{=}C{=}N)_2}]_n + 4\mathrm{Me_3SiCl}\uparrow \qquad (17)$$

These gels are precursors to SiCN materials and offer opportunities for processing porous materials. However, perhaps the most important finding is the apparent discovery of a new phase in the Si−C−N ternary system. On heating the product from reaction 17 to 600 °C, an air-sensitive product is obtained that analyzes for SiC_2N_4. This product is crystalline by XRD (crystallizes at 400 °C), has a single ^{29}Si peak at −103 ppm and a single ^{13}C peak at 120 ppm in the MAS NMR spectra. Above 920 °C it decomposes with loss of cyanogen (C_2N_2) to form a colorless, air-stable material that analyzes for Si_2CN_2. This material contains a carbodiimide unit as indicated by the IR spectrum (νN=C=N = 2170 cm^{-1}) and the single ^{13}C peak at 116 ppm, with a ^{29}Si peak at −67 ppm in the MAS NMR spectra. The compound's crystal structure is similar to Si_2ON_2. On heating above 1000 °C, amorphous SiCN obtains, and then a mixture of SiC/Si_3N_4 at >1500 °C. This represents one of the clearest examples of how precursor design can provide access to totally new materials not available by standard ceramics processing methods.

To date, SiCN materials have been used to make coatings[44,50,51], monolithic and extruded shapes[52−55], for binder applications[44,56], fibers[45,57−61] and composite processing[44,52,55]. Recently, photopolymerizable precursors have been considered for rapid prototyping applications[62].

In general, the pyrolysis of polysilazanes with carbon groups on silicon leads to initial formation (400–1400 °C) of amorphous materials wherein silicon is present in a number of bonding environments of the general formula $Si_xN_yC_z$ ($x + y + z = 4$) (Si−H bonds not considered). Heating to higher temperatures in N_2 (1500–1700 °C), especially with sintering aids, causes crystallization of Si_3N_4/SiC nanocomposites[20,63−65]. Heating to the same temperatures in Ar drives the reaction toward the formation of SiC. In contrast, heating polysilazanes that contain only Si−N bonds can provide either Si_3N_4/Si or Si_3N_4/C nanocomposites depending on the polysilazane. At higher temperatures, in the absence of N_2, the Si_3N_4/C composites transform to SiC as Si_3N_4 decomposes. Surprisingly, heating shaped SiCN composites in air at temperatures of 1600 °C for periods of up to 60 h results in incorporation of only small amounts of oxygen (0.4 wt%) that passivate surfaces against further oxidation[54c].

C. Precursors to Silicon Oxynitride (Si_2ON_2)

Silicon oxynitride exhibits better resistance to thermal downshock and oxidation than silicon nitride, although it decomposes under similar conditions with loss of N_2[66]. Thus, it represents a practical target for precursor synthetic methods. Unfortunately, it is difficult to achieve the exact 2Si : O : 2N stoichiometry in a processable precursor and retain this ratio during pyrolysis. Hence, very little work has been directed toward developing Si_2ON_2 precursors[67−70]. Furthermore, the approaches used to date rely on processing with NH_3 to achieve the correct stoichiometry.

The earliest work in this area was that of Yu and Mah[67], and Seyferth and coworkers[68]. An approach related to reaction 13 is used, wherein $-[\mathrm{MeHSiO}]_x-$ oligomers are grafted on before MeI is added. Alternately, the two oligomers are copolymerized. Based on reaction 13, a plausible copolymerization process is described in equation 18. Molecular weights (M_n) ranged from about 800 to 2700 Da with the graft-cooligomers giving somewhat higher average molecular weights.

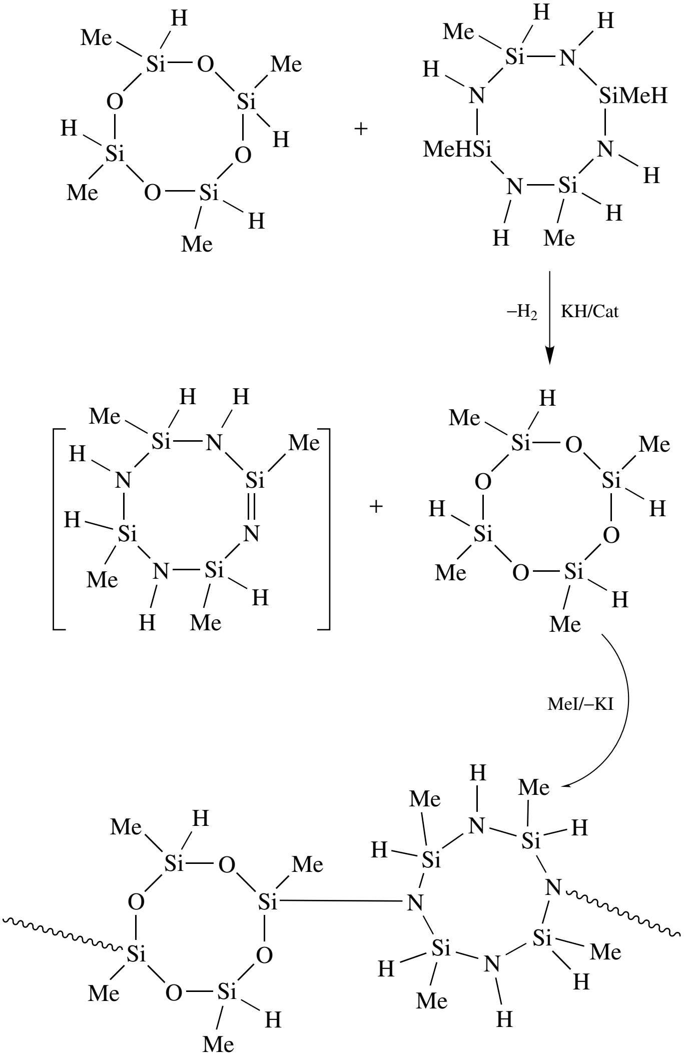

(18)

Recent work by Yu and coworkers suggests that Si–Si linkages may also form in reaction 18 as indicated by the presence of a ^{29}Si NMR signal at 0.3 ppm[71]. Furthermore, Yu and coworkers report that the hydridosiloxane reacts at a much slower rate than the silazane, leading to formation of block copolymer-like structures. It appears that most of the cyclosilazanes react to form oligomeric materials and then cyclosiloxanes react afterward. The end result would appear to be the same as the grafting reaction. However, Yu and Mah report that the grafted polymers behave somewhat differently from the cooligomers.

On heating the grafted and copolymerized oligomers to temperatures of 800 °C in NH_3, ceramic yields range from 78–86 wt%. At 800 °C the products are amorphous, but transform to crystalline Si_2ON_2 on heating to $> 1300\,°C$. The 1 : 1 copolymerized oligomers gave essentially pure Si_2ON_2, whereas the graft 1 : 1 oligomers gave a material that was mostly Si_2ON_2 with some Si_3N_4. A 5 : 1 siloxane/silazane copolymer gave a material that contained both Si_2ON_2 and SiO_2.

Si_2ON_2 precursors have also been made via catalytic dehydrocoupling[69]. Linear polysiloxazanes prepared via reaction 19 gave materials with $M_n = 5–7$ KDa; however, the ceramic yields were poor.

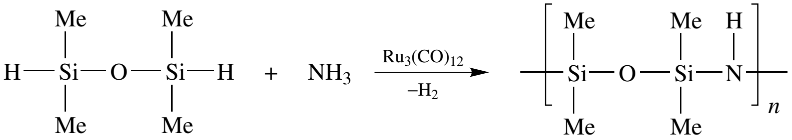

$$\mathrm{H{-}\underset{Me}{\overset{Me}{Si}}{-}O{-}\underset{Me}{\overset{Me}{Si}}{-}H} + \mathrm{NH_3} \xrightarrow[-\mathrm{H_2}]{\mathrm{Ru_3(CO)_{12}}} \left[\mathrm{\underset{Me}{\overset{Me}{Si}}{-}O{-}\underset{Me}{\overset{Me}{Si}}{-}\overset{H}{N}}\right]_n \qquad (19)$$

By switching to a cyclic tetrameric hydridomethylsiloxane a processable, partially crosslinked liquid precursor could be obtained with $M_n = 1.2–1.5$ KDa (equation 20).

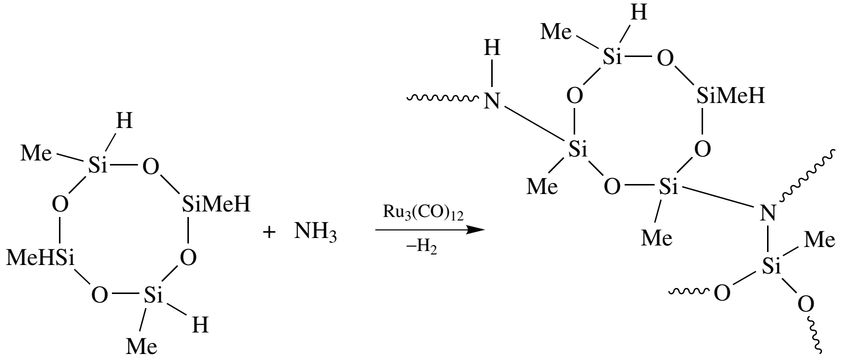

(20)

Pyrolysis of this type of polymer to 800 °C in N_2 provides ceramic yields of *ca* 75 wt%. In NH_3, the same material gave an 88 wt% ceramic yield at 800 °C. On heating to 1600 °C the ceramic yields drop to 64 wt% in N_2 and 78 wt% in NH_3. XRD studies of the 1600 °C materials heated in both atmospheres indicate that the primary crystalline phase is Si_2ON_2. This is despite the presence of some 12 wt% carbon for the sample heated in N_2. No carbon is detected for the sample heated in NH_3. This sample appears to be essentially phase pure Si_2ON_2.

Finally, Okamura and coworkers[70] have described the preparation of SiO_xN_y fibers from precursors. These 10–13 μm diameter fibers were prepared by pyrolysis of oxygen-cured polycarbosilane (see below) in an NH_3 atmosphere. These fibers, with densities of 2.3 $g\,ml^{-1}$, offer tensile strength of *ca* 1.8 GPa with elastic moduli of 200–220 GPa. Because the theoretical density of Si_2ON_2 is close to 2.8 $g\,ml^{-1}$, these values are not those expected of fully dense Si_2ON_2 fibers.

Because it is possible to convert amorphous SiO_2 directly to Si_2ON_2 using NH_3 at 900–1100 °C without recourse to precursors[66,72], the impetus for pursuing precursor routes to Si_2ON_2 is not high, except perhaps for processing thin films or fibers. However, the above studies are important as they provide the basis for processing more complex multicomponent oxynitrides, wherein Si_2ON_2 may be one of the pyrolysis products. The primary rationale for exploring the utility of multicomponent precursors is that mentioned above, wherein preventing high temperature crystallization allows fiber strength properties to be maintained. The following sections look at three- and four-component SiN-based materials.

D. Precursors to Si−Al−O−N Materials

Silicon−aluminum oxynitrides (SiAlONs) have been studied in great detail because they are: (1) easily made, high melting, glasses; (2) stable to reasonably high temperatures; (3) good sintering aids for silicon nitride and they (4) offer high hardness and (5) provide good-to-excellent mechanical properties[73−76]. Despite the importance of SiAlONs to the ceramics industry, very few groups have developed precursor routes to these materials[77−79].

Thus, Schmidt and coworkers[77] briefly described the synthesis of a Si−Al−O−N precursor by reacting a cyclovinyl silazane with an alkoxyaluminane (equation 21). The ratio of Si : Al was varied between 3 and 0.33. In all instances, the resulting products ranged from clear viscous liquids to slightly yellow solids. Fibers could be hand-drawn from the intermediate materials. Pyrolysis in NH_3 gave ceramic yields (1000 °C) ranging from 30 to 50 wt%. The resulting materials were reported to be SiAlON-like based on ^{27}Al solid state NMR. No other characterization was reported.

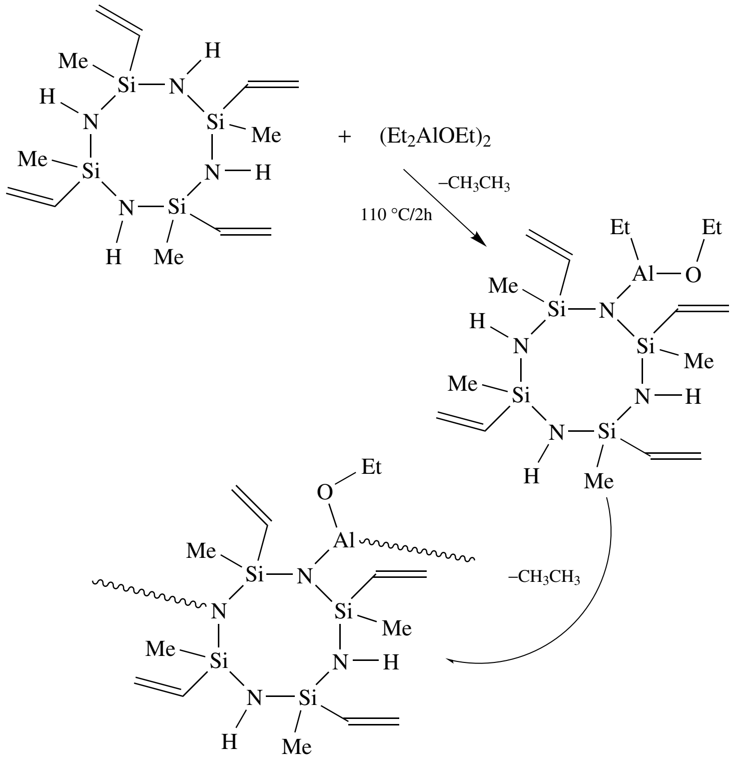

(21)

The earliest successful efforts to produce SiAlON were those of Soraru and coworkers[78,79]. The approach was simply to react a commercial polycarbosilane, $-[MeHSiCH_2]_x[Me_2Si]_y-$, with Al(OBu-$t$)$_3$ in refluxing xylene for 1 h to obtain a clear solution. Removal of solvent gave a clear liquid that, on heating slowly to 300 °C, gave a 'polyaluminocarbosilane' which was then heated in flowing NH_3 at temperatures up to 1000 °C to form SiAlON. A typical chemical analysis for the precursor prior to nitridation in ammonia was $SiAl_{0.17}C_{2.37}O_{0.53}H_{5.84}$. Following nitridation at 1000 °C and then heating to 1500 °C, a typical chemical analysis was $SiAl_{0.16}O_{0.6}N_{1.48}$.

NMR characterization of the resulting clear liquid indicates that it is a blend rather than a copolymer. That is, no reaction appears to occur between $Al(OBu\text{-}t)_3$ and the polycarbosilane. However, the resulting blend provides materials with high enough viscosities to permit fibers to be spun and nitrided ($\geqslant$500 °C) to SiAlON-like materials. Ceramic fibers of 12–30 μm diameter could be processed. The highest tensile strengths (1–1.8 GPa) were found for fibers with diameters of 10–15 μm after heating to 1000–1200 °C. Above 1200 °C, the fiber strengths drop as the material crystallizes, exhibiting a powder pattern in between that of β-Si_3N_4 and the crystalline oxynitride, β-SiAlON, with an average chemical composition of $Si_{2.5}Al_{0.5}O_{0.5}N_{3.5}$.

To delay crystallization, an additional element can be added, e.g. yttrium or magnesium[76]. Thus, Laine and coworkers[80] have shown that ammonolysis of a cordierite ($2MgO{\bullet}2Al_2O_3{\bullet}5SiO_2$) precursor system provides access to MgSiAlON materials. The development of a cordierite precursor is described below in the sections on silicate precursors.

E. Precursors to Si—N—B—X Materials

The first report on SiNBC materials was published in the patent literature by Takamizawa and coworkers[81]. Based on this early work and arguments presented above, several research groups have sought to develop new materials wherein crystallization is inhibited, for high temperature fiber applications. These efforts have been primarily empirical in nature; however, most of them have targeted modifications of SiC or Si_3N_4, in part because precursors to SiC and Si_3N_4 have already been developed and in part because SiC and Si_3N_4 already offer good-to-excellent high temperature properties. Again, as noted above, there are three strategies for preparing these materials: one is through synthesis, another is through processing and a third is a combination of the first two approaches.

In the area of direct synthesis, only the Tonen group has explored the preparation of precursors to Si—B—N materials free from other elements[82]. They find that perhydropolysilazane (see above) will react with a variety of boron-containing compounds to produce SiNB precursors. Thus, reaction of perhydrosilazane with BH_3 leads to oligomers (equation 22). Pyrolysis under N_2 to 900 °C gives black ceramic materials in >95 wt% yield. On heating to 1700 °C, a typical chemical composition was found to be $SiB_{0.33}N_{1.52}C_{0.06}O_{0.06}$. XRD studies indicate that the 1700 °C material is amorphous; thus boron addition retards crystallization of Si_3N_4. Fibers (10 μm diameter) were spun from related systems; however, no details about the properties were provided. Su and coworkers[83] find that a Dow Corning HPZ[45,84] polymer with a $(HSi)_{0.33}(Me_3Si)_{0.17}(NH)_{0.33}N_{0.17}$ [$SiN_{1.04}C_{1.16}H_{4.69}$] composition will react with borazine according to the generic reaction shown in equation 23.

The above general structure is supported by both NMR and FTIR studies. No evidence was found for the formation of borazine oligomers via dehydrocoupling. Depending on the ratio of borazine to HPZ, the compositions and molecular weights of the resulting polymers varied. Thus, polymer compositions ranged from $SiB_{0.08}N_{0.84}C_{1.08}H_{4.58}$ to $SiB_{1.68}N_{2.59}C_{1.04}H_{6.25}$. The molecular weights of these polymers were M_n = 23K Da and 5.5K Da with polydispersities of 5 and 10, respectively. They are soluble in most common organic solvents. The first polymer exhibited a 70 wt% ceramic yield (1400 °C/Ar) and a corresponding composition of $Si_{2.25}B_{0.2}N_{2.42}C$ whereas the second one gave a 76%

ceramic yield and a composition of $Si_{1.94}B_{2.57}N_{4.77}C$. Both pyrolysis products appeared nanocrystalline/amorphous by XRD. On heating to 1800 °C, the ceramic yield of the first polymer dropped to 51 wt% and the composition changed to $Si_{1.72}B_{0.18}N_{0.80}C$. At this temperature α- and β-Si_3N_4 and SiC crystallize. However, no crystallization is seen below this temperature. Thus, boron addition retards crystallization by some 300 °C. Furthermore, it inhibits decomposition of Si_3N_4.

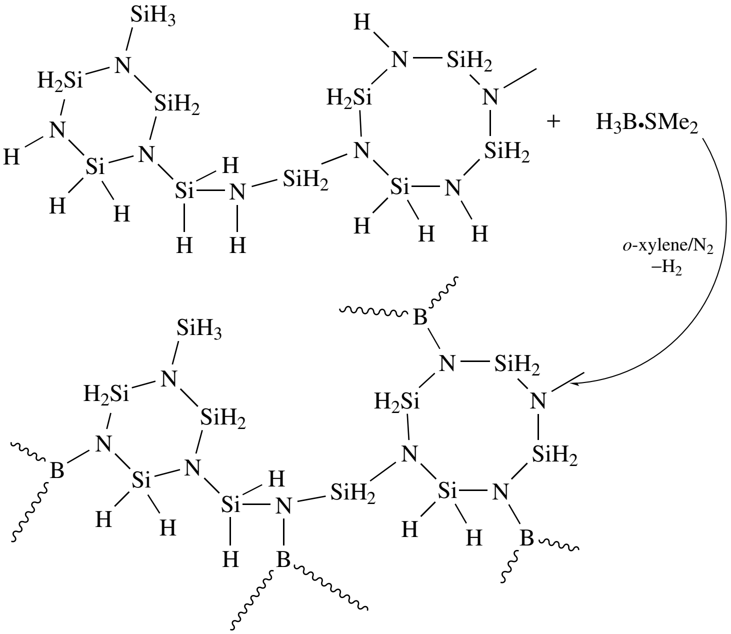

(22)

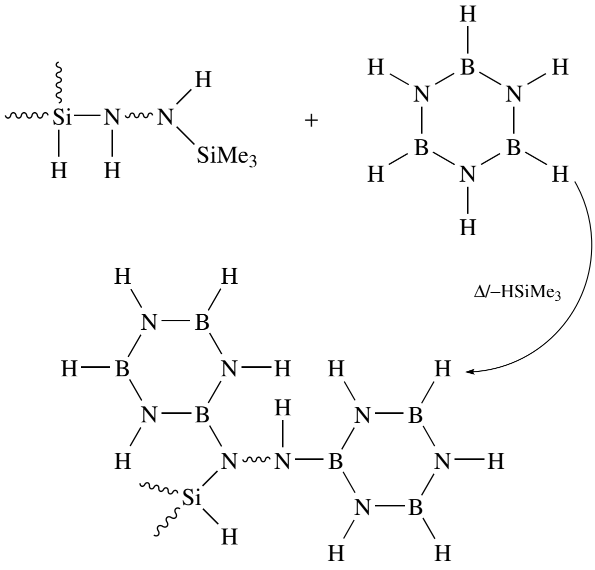

(23)

Riedel and coworkers have synthesized a series of Si−N−B−C precursors via reactions 24 and 25, as well as by hydroboration of the carbodiimide produced in reaction 17. The chemical composition of a typical reaction 24 product was found to be $Si_{2.84}BC_{9.05}N_{2.84}O_{0.64}H_{24.46}$. The polymer is soluble in common solvents and melts at 180 °C[49,85]. This polymer provides a TGA (1000 °C/He) ceramic yield of *ca* 70 wt% and an apparent stoichiometry of $Si_3BC_4N_2$. A typical chemical composition for the reaction 25 product is $Si_{2.02}BC_{6.63}N_{2.76}O_{0.09}H_{19.84}$. This polymer is also soluble in common solvents and gives an amorphous material (*ca* 55 wt% ceramic yield, 1000 °C/He) on heating, with an approximate composition of Si_2BCN. Both materials remain amorphous on heating to higher temperatures. Furthermore, both materials are much more stable than related SiCN and Si_3N_4 materials, as illustrated in the high temperature TGA studies shown below. The 2–3% mass loss above 2000 °C for both compounds results from volatilization of oxygenate impurities introduced during polymer processing/handling.

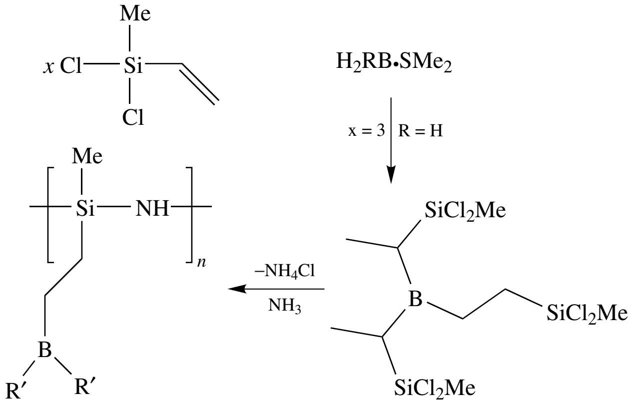

(24)

R′ = —CH(Me)Si(Me)NH—

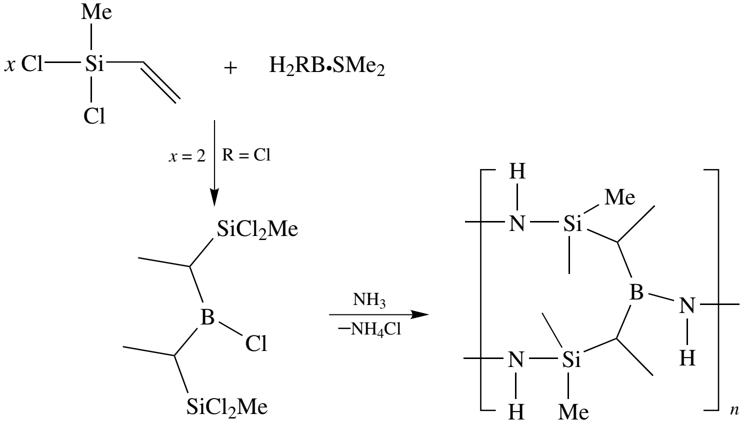

(25)

The stability of these two amorphous materials compared with Si_3N_4 and SiCN at high temperatures (see Figure 5) suggests that in fiber form they would offer superior properties. Preliminary studies suggest that Si−B−N−C fibers with diameters of 10–12 μm offer

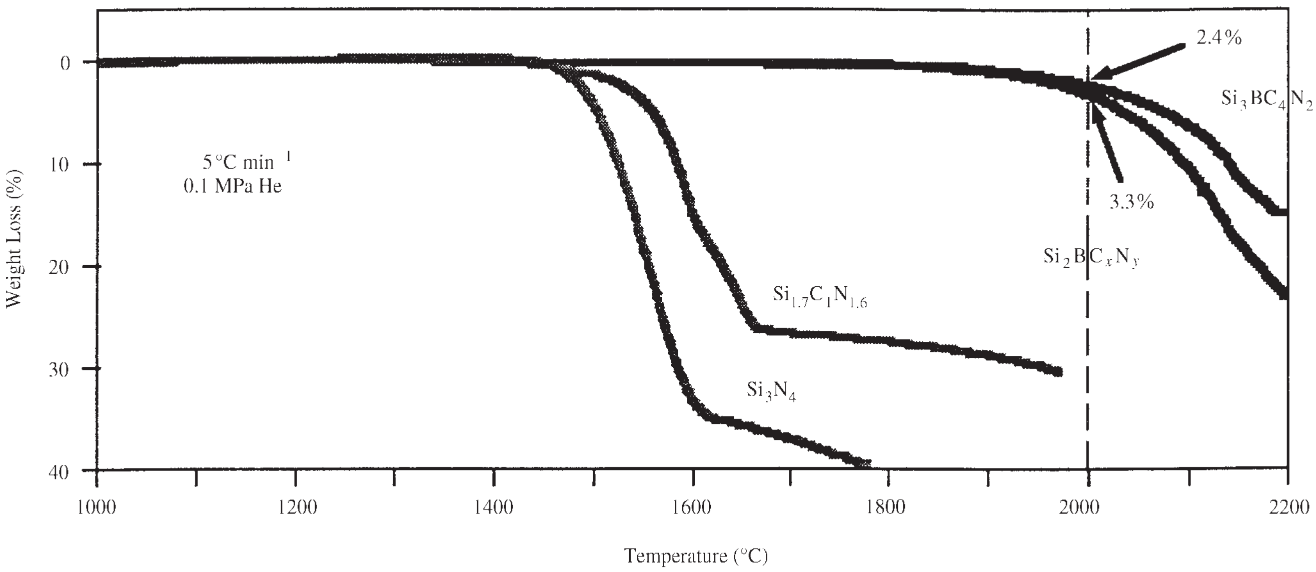

FIGURE 5. Comparison of the temperature stability (Ar) of various Si–N–C–B materials

tensile strengths of 3–4 GPa and elastic moduli of 200–210 GPa[6e]. Thus their mechanical properties are comparable with those of the known Tonen's silicon nitride fibers and Nicalon fibers, which degrade above 1400 °C[7,9].

Although Si−N−B−O materials containing trace amounts of nitrogen (2–3 wt%) have been prepared solely via a processing approach (ammonolysis of a borosilicate gel), complete conversion to Si−N−B was not achieved[86]. However, there are several literature examples of routes to Si−N−B materials that couple synthesis with a specific processing approach. These include early work on Si−N−B precursors by Seyferth and Plenio, who reacted the now ubiquitous $-[\text{MeHSiNH}]_x-$ polysilazane with $H_3B{\cdot}SMe_2$[87] as shown in equation 26.

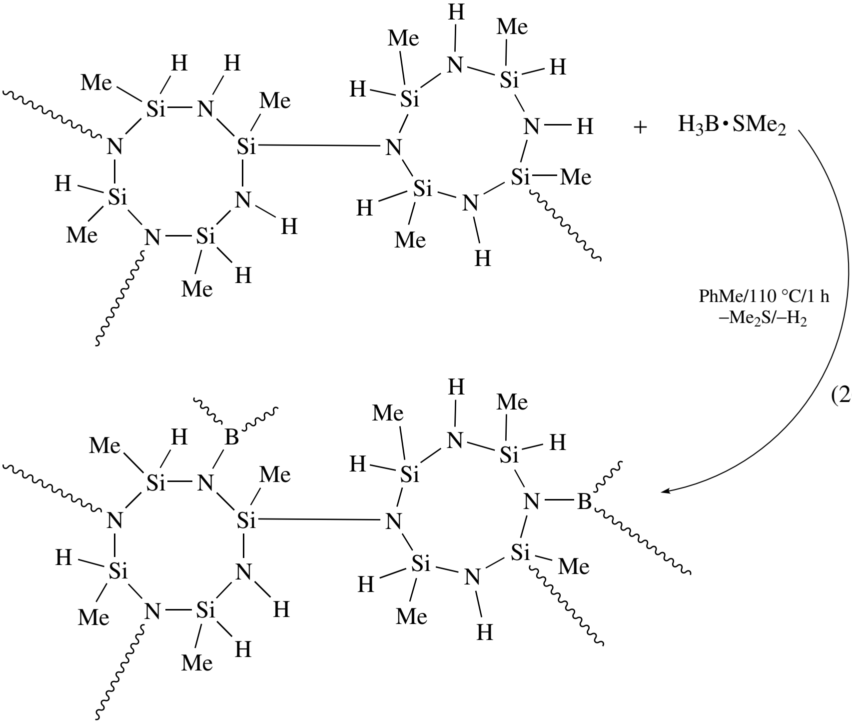

(26)

An oligomer made with a 4 : 1 ratio of silazane to borane had an M_n *ca* 800 Da and a chemical composition of $SiN_{1.02}B_{0.24}C_{0.98}H_{3.65}$. This oligomer was soluble in common solvents and gave a 76 wt% ceramic yield at 1000 °C. Pyrolysis in NH_3 at 1000 °C gave a material with a composition of $SiN_{1.89}B_{0.31}$. By changing the ratio of the initial reactants, the Si:B:N ratio in the final ceramic product could be changed over a relatively wide range. Fibers could be hand-drawn from toluene solutions and pyrolyzed in ammonia to generate the corresponding ceramic fibers. No details of the phases formed at higher temperatures were presented, nor were efforts made to explore the direct conversion of these precursors to Si−N−B−C materials, which is unfortunate given the results of Riedel above, and Jansen and coworkers below.

Jansen and coworkers[88] described the synthesis of Si−N−B−C materials (equation 27). The ratio of the two reactants can be varied from 10 : 1 to 1 : 10 with a concomitant change in the composition of the ceramic product. For a typical reaction with a 1 : 1

ratio of reactants, the composition of the isolated polymer, following curing in NH_3/1 h/RT, was found to be $SiN_{4.37}BC_{3.68}H_{13.47}$. The TGA ceramic yield (1000 °C/He) was *ca* 65 wt%. Carbon can be removed by pyrolysis in NH_3 at 1000 °C/10–20 h. The resulting product is a pure Si–N–B material that does not crystallize on heating at 1500 °C for up to 72 h in N_2. The composition was close to that calculated for $Si_3B_3N_7$ or Si_3N_4•3BN. Ceramics produced in the Si–N–B system resist crystallization (1500 °C) even with B contents as low as 2 wt%.

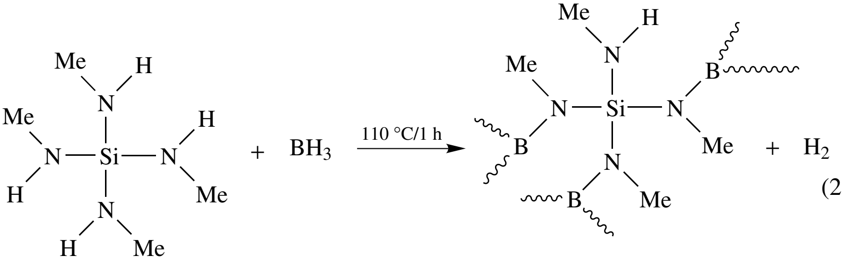

(27)

The same article describes the substitution of Al for B in reaction 27. For a reaction with a 1 : 2 Al:Si ratio, the resulting precursor's chemical composition was $SiAl_{0.59}BC_{3.03}H_{10.89}N_{2.85}$. Following ammonolysis and heat treatment under identical conditions, the resulting ceramic composition was close to that calculated for $Si_3Al_2N_6$ or Si_3N_4•2AlN. Although it was not considered, this precursor might be a candidate for processing AlN/SiC composite materials as discussed below.

Most recently, Jansen described[88] the simple synthesis of a spinnable precursor via the set of reactions given in equations 28–31. It appears that $(Me_3Si)_2NH$ reacts only once with $SiCl_4$ under mild reaction conditions to give the liquid chlorosilylsilazane of reaction 28. By heating this material under more forcing conditions, the second Me_3Si–N bond can be cleaved to form the chloroborosilazane in reaction 29. The product in reaction 30 is a proposed intermediate but is not isolated as the polymerization shown in reaction 31 proceeds coincidentally. This material can be reacted directly with NH_3 to form Si–N–B materials. However, the use of NH_3 does not provide a tractable precursor. Thus, $MeNH_2$ is used to prepare the polymethylaminoborosilazane, which is a distillable liquid and can be used for CVD studies. Alternately, by heating, deamination reactions akin to those shown in equation 10 are proposed to occur such that by controlled heating a processable oligomer is obtained that can be spun. If spinning is conducted with heating, the polymer is reported to self-crosslink and can be cured and pyrolyzed to temperatures of 2000 °C without decomposition and without crystallization. The resulting 10–20 μm diameter Si–N–B–C fibers are reported[88] to offer densities of *ca* 1.8 g ml^{-1} with tensile strengths of 4 GPa and elastic moduli of 400 GPa. Furthermore, the fibers are reported to be stable to 1500 °C in air for hundreds of hours. If these preliminary results prove correct, then these fibers represent a truly significant advance.

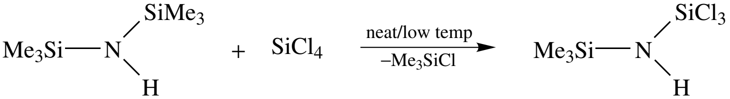
$$Me_3Si{-}N(SiMe_3)H + SiCl_4 \xrightarrow[-Me_3SiCl]{\text{neat/low temp}} Me_3Si{-}N(SiCl_3)H \quad (28)$$

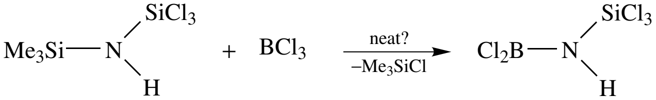
$$Me_3Si{-}N(SiCl_3)H + BCl_3 \xrightarrow[-Me_3SiCl]{\text{neat?}} Cl_2B{-}N(SiCl_3)H \quad (29)$$

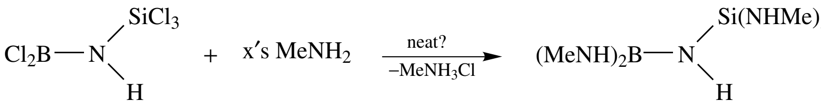

(30)

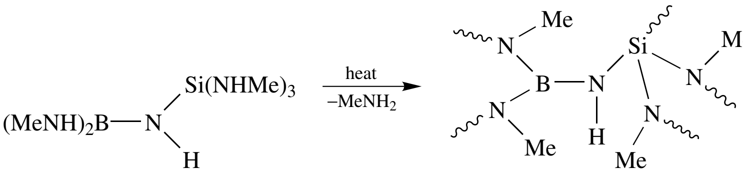

(31)

The Tonen group has also described a combined synthesis and processing approach to Si−N−B ceramics, but with considerable amounts of oxygen. Their work is based on the reaction of perhydridopolysilazane with trimethylborate [$B(OMe)_3$][89]. Thus, a pyridine solution of perhydrosilazane was mixed with 0.33 equivalents of $B(OMe)_3$ and heated at 120 °C in an autoclave for 3 h. Addition of dry *o*-xylene followed by distillative removal of solvent gave a white polymeric powder with M_n *ca* 2400 Da. A typical chemical analysis ($SiB_{0.36}N_{0.99}O_{0.42}C_{0.40}H_{4.86}$) shows the expected Si:B 3 : 1 ratio based on the reactant ratios. The given TGA ceramic yields were only for samples pyrolyzed in NH_3, which were $\leqslant$ 80 wt% at 1000 °C. A polymer sample heated in NH_3 (1200 °C/10 °C min^{-1}/10 min hold) provided an amorphous material with the following chemical analysis: $SiB_{0.38}N_{1.21}O_{0.38}C_{0.03}H_{0.68}$. Given that the oxygen content remains relatively constant from the polymer to the ceramic, and the observation by Riedel and coworkers that the weight losses observed in their Si−N−B−C ceramics occur because of oxygen impurities, it is likely that the Tonen ceramic product has a much lower use temperature. No information was provided about the processability of this material.

One other Si−N−B−X precursor type, where X = Ti, has been made by several groups[85,90,91]. The approach used has been to react $Ti(NMe_2)_4$ with a polysilazane as illustrated in equation 32. Note that the initial reaction with $Ti(NMe_2)_4$ can be exothermic and even violent if Si−H bonds are present. However, processable polymers are

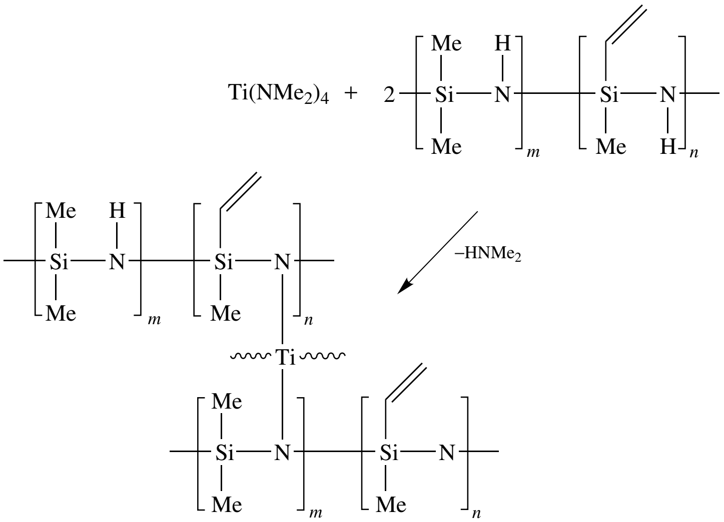

(32)

only obtained on heating to *ca* 115 °C for several hours depending on whether the vinyl group or some other substituent (e.g. H) is used. Molecular weights were not reported. Only the precursors made with vinyl and hydrogen substituents gave reasonable ceramic yields (60–70 wt% at 800 °C) when the initial Si:Ti ratio was approximately 5 : 1. Thus, a composition for the 5 : 1 hydridopolysilazane/$Ti(NMe_2)_4$ reaction product was $Si_{4.55}TiN_{6.39}C_{11.48}H_{38.2}$. The composition of the ceramic product obtained at 1000 °C was $Si_{4.54}TiN_{5.84}C_{3.52}H_{0.21}O_{0.18}$. This material appears to be carbon rich and may be susceptible to oxidation, although the amounts of Ti incorporated can be adjusted by adjusting the initial ratios. Some work was done to demonstrate that these precursors could be used to infiltrate fiber preforms to make composite structures wherein the matrix was precursor derived. No information about high temperature phase formation was provided.

IV. PRECURSORS CONTAINING Si AND C

A. Precursors to SiC

Historically, one of the first routes to a processable SiC precursor was that reported by Yajima and coworkers[92–94] in 1975, wherein polydimethylsilane was processed (see Scheme 2) to produce SiC-containing ceramic fibers. This approach is still used to produce the only SiC precursor and SiC-containing fibers currently available commercially: Nicalon™ fibers (Nippon Carbon, $SiC_{1.45}O_{0.36}H_{0.03}$)[7,92–94], Tyranno™ fibers (Ube Industries, $SiC_{1.43}O_{0.46}T_{0.13}$)[95–97] and Mark I PCS (Shin-Etsu Co.) precursor polymer[6a]. As indicated by their respective compositional formulas, both Nicalon™ and Tyranno™ fibers are not phase pure SiC. Thus, their properties are inferior to those of phase pure SiC as shown in Table 1.

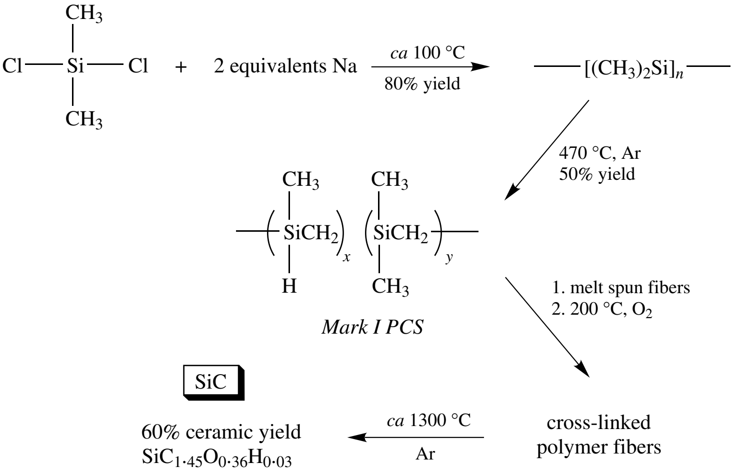

SCHEME 2. Original Yajima process for producing $SiC_{1.45}O_{0.36}H_{0.03}$ fibers

In addition to not offering properties expected for phase pure SiC, the original Yajima process suffers from other drawbacks that include a multistep precursor synthesis and the inability to self-cure. Finally, the presence of oxygen limits the upper use temperature for both Nicalon and Tyranno fibers to *ca* 1200 °C because above this temperature CO and SiO gases evolve, generating defects (large crystallites, pores and voids) that contribute to substantial decreases in mechanical properties.

TABLE 1. Comparison of properties of SiC-containing materials[7]

Type	Tensile strength (GPa)	Elastic moduli (GPa)
Nicalon^{TM}	2.0–2.5	<300
Tyranno^{TM}	3.0	>170
SiC whisker (single crystal)	8.0	580
Bulk SiC (hot pressed)	N/A	450

As a result of these disadvantages, tremendous efforts over the past 20 years have focused on developing chemistries/processes to improve or replace the Yajima process. At this point, as discussed below, several precursors can be synthesized and/or processed to produce phase pure SiC shapes with controlled microstructures that offer the exceptional properties expected of SiC. Thus, this area of precursor chemistry can now be considered to be mature. Consequently, only engineering and/or cost considerations now dictate which precursor systems are useful for a given application. Furthermore, because the general area of SiC precursors has been reviewed in detail[6,7], we focus here only on those precursors and processing methods that provide phase pure SiC.

To date, two precursor types have been identified that transform to nearly phase pure SiC. These are polymethylsilane (PMS, $-CH_3HSi-$) and polysilaethylene (equation 33), which are related by the fact that heating PMS >300 °C transforms it via the Kumada rearrangement[7] to polysilaethylene.

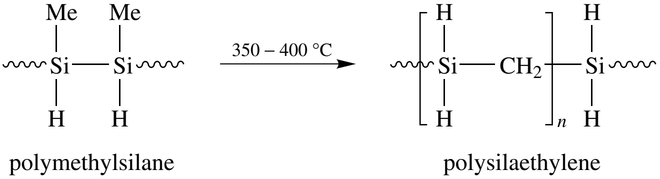

(33)

Both PMS and polysilaethylene or polyperhydridocarbosilane have a 1 : 1 Si:C ratio and in principle are designed to generate phase pure SiC. In practice this is often not the case for a variety of reasons, as discussed below. Several related precursor systems and processing methods that provide essentially phase pure SiC are also discussed below to provide perspective.

Two general routes are used to synthesize PMS: Wurtz dehalocoupling of CH_3HSiCl_2 and transition-metal-catalyzed dehydrocoupling of methylsilane.

1. PMS via dehalocoupling[98,99]

Seyferth and coworkers[99] described dehalocoupling of CH_3HSiCl_2 with Na (Wurtz coupling), to synthesize PMS (equation 34). CH_3HSiCl_2 is added slowly to a mixture of Na sand in 7 : 1 hexane: THF with reflux under Ar for 20 h. The polymer product can be isolated in 60–70% yield as a viscous, hydrocarbon-soluble liquid that gives a negative Beilstein test for Cl.

^{1}H NMR characterization suggests a composition consistent with that shown, i.e. 20 mol% of the original Si–H bonds are consumed by Na and/or reactive silyl intermediates (silyl radicals) resulting in Si atoms bonded to three other Si atoms. ^{29}Si NMR data reveal the presence of $-SiH_2$ moieties in addition to the $-Si$ and $-SiH$ species suggested by ^{1}H NMR. The $-SiH_2$ groups are suggested to form by reaction of CH_3HSiCl_2

or $-CH_3HSiCl$ end groups with NaH (formed from Na and SiH) or by silyl radical processes.

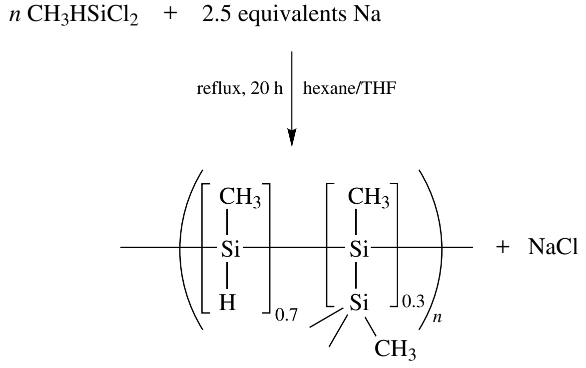

(34)

A molecular weight of 660 Da was determined cryoscopically (benzene); however, polydispersities were not reported. Pyrolysis of PMS (10 °C min^{-1}/950 °C) provides ceramic yields of 12–27%, with a $Si_{1.42}C_{1.00}H_{0.14}$ composition. Low MW oligomers present in PMS volatilize prior to pyrolysis, contributing to the low ceramic yields. The high Si contents are thought to arise from high temperature reactions (>350 °C) of Si–H with $SiCH_3$ to form CH_4 (identified by TGA/FTIR studies) and Si–Si bonds.

To increase ceramic yields and carbon content during transformation of PMS to SiC, Seyferth and coworkers explored hydrosilylative crosslinking of PMS with $[CH_3(CH_2{=}CH)SiNH]_3$ using catalytic amounts of AIBN. For example, reactions using $SiH{:}SiCH{=}CH_2$ ratios $\geqslant 6$ in refluxing benzene provide quantitative yields of soluble precursor with a 68–77 wt% ceramic yield (1000 °C). Presumably, hydrosilylation ties the volatile, low MW oligomers (MW values not given) to the larger oligomeric chains leading to higher ceramic yields. The pyrolyzed material exhibits a $(SiC)_{1.00}(Si_3N_4)_{0.033}C_{0.040}$ composition at 1000 °C, but at 1500 °C only SiC was observed (XRD) to crystallize. Given the above work on SiCN, we presume that the 1000 °C material is actually an SiCN composite (see work of Toreki and coworkers below).

These workers also explored transition-metal-promoted crosslinking of PMS as an approach to increase ceramic yields and SiC purity. Because transition metals, e.g. $Ru_3(CO)_{12}$, are known to catalyze redistribution reactions between Si–H and Si–Si bonds[100], efforts were made to modify PMS via a chain-extension process to generate higher M_n values. Thus, a set of metal carbonyls were used (1–2 mol%) to effect redistribution reactions that might lead to improved ceramic yields[99c]. For example, 1–2 wt% $Ru_3(CO)_{12}$ added to PMS followed by irradiation for 4 h (140 watts at *ca* 300 nm) provided a polymer with a 55% ceramic yield of a Si-rich material (amount of excess Si not reported). To increase carbon content Mark I $[(-MeSiHCH_2-)_n]$ was combined with PMS in a 1 : 2 wt ratio and subjected to the $Ru_3(CO)_{12}$ catalyzed crosslinking. NMR analysis of the resultant polymer showed depletion of Si–H bonds, suggesting Si–Si bond redistribution reactions at the expense of the Si–H bonds. Molecular weights and polydispersities for the crosslinked PMS were not given. Pyrolysis of this polymer gave a 68% ceramic yield of high purity SiC, $Si_{0.99}C_{1.00}$. Although the polymer was reported to be moderately soluble in organic solvents, its processability was not discussed (Scheme 3).

Based on the extensive work of Harrod and coworkers[101], Seyferth and coworkers also examined metallocene (i.e. Cp_2ZrH_2) catalyzed dehydrogenative crosslinking of PMS as another method of increasing ceramic yields and carbon content during transformation

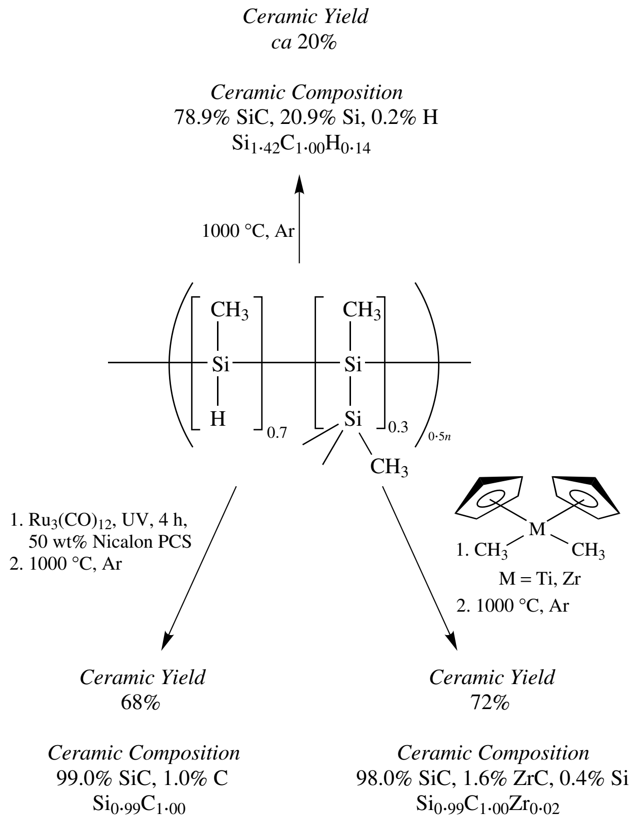

SCHEME 3. Modifying PMS to increase ceramic yields and SiC purity

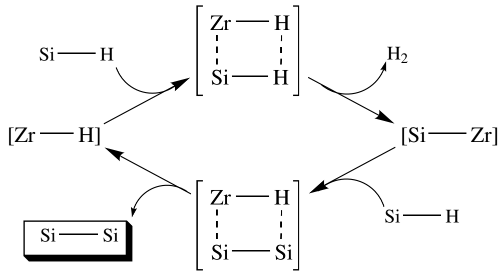

SCHEME 4. Dehydrocoupling mechanism to produce Si−Si bonds[102]

of PMS to SiC[99] (Scheme 4). The addition of 0.6 mol% Cp_2ZrH_2 to a hexane solution of PMS followed by reflux for 2 h resulted in loss of Si−H bonds, as determined by NMR, especially the SiH_2 groups as expected. Pyrolysis to 1500 °C gave ceramic yields of 70−80% with SiC purity as high as 98% (ZrC and Si were the primary side products in 1.6 and 0.4 wt%, respectively, $Si_{0.99}C_{1.00}Zr_{0.02}$). Unfortunately, fibers drawn from this

PMS required UV curing for 1.5 h prior to pyrolysis in order to retain the fiber shape. Additionally, the use of metallocene catalysts renders PMS highly oxygen-sensitive and pyrophoric.

In conclusion, Seyferth's work showed that PMS can be transformed from a poor (ceramic yields *ca* 20%, >20% excess Si) to an effective precursor (ceramic yields 60–80%, *ca* 1% excess Si or C) using relatively simple chemistry. The routes chosen provide the following advantages over the Yajima process: (1) a Wurtz coupling synthesis that provides a polymer with an inherent 1 : 1 Si:C ratio, (2) high ceramic yields, (3) some processability as fibers can be drawn and (4) essentially phase pure SiC following chemical modification. Drawbacks to this work include: (1) precursors that are not self-curing, (2) the use of pyrophoric catalysts (Cp_2ZrH_2) leading to pyrophoric PMS or (3) the use of Ru catalysts, which may be too expensive for scale-up processes.

2. *PMS by catalytic dehydrocoupling of MeSiH*$_3$

PMS can also be synthesized by catalytic dehydrocoupling of methylsilane ($MeSiH_3$) using Cp_2MMe_2 (M = Ti, Zr) catalysts, as described by Harrod and coworkers, and Laine and coworkers[101,103,104] (equation 35). The reaction is run in a toluene/cyclohexene solvent system at 25–60 °C under *ca* 10 atm $MeSiH_3$ for 1–9 days using 0.2 mol% catalyst. The H_2 byproduct is consumed simultaneously by metal-catalyzed hydrogenation of cyclohexene to cyclohexane, to minimize pressure build-up and depolymerization. PMS can be obtained in >90% yield. The ^1H NMR spectrum suggests a partially branched structure based on the integration of the $C\underline{H}_3Si$:SiH ratio of 4 : 1. SEC indicates M_n of *ca* 1200–1300 Da (DP *ca* 30) with a PDI of *ca* 5–10. The M_n and PDI values were quite high relative to analogous dehydropolymerization of phenylsilane, which converts to both linear (DP *ca* 10) and cyclic structures (P = 5, 6), with no evidence of branching[105]. The higher M_n and PDI values for methylsilane polymerization were attributed to a lack of steric hindrance (methyl vs phenyl), resulting in a greater degree of branching, due to reaction with all three Si–H sites. Pyrolysis (1000 °C/1 h/10 °C min^{-1}/Ar) provides a *ca* 77 wt% ceramic yield of a material with a composition of $Si_{1.0}C_{0.9}H_{<0.2}O_{0.1}$ (6.0, 0.5 and 4.0 wt% excess Si, H and O respectively)[103,104]. The oxygen appears to arise from handling.

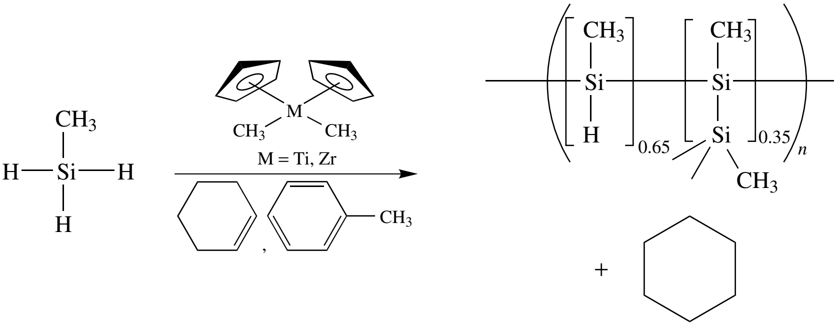

(35)

Figure 6 provides a series of ^{29}Si MAS NMRs taken of PMS samples heated to selected temperatures. The Kumada rearrangement occurs at 400 °C and essentially phase pure SiC (2–4 nm crystallites by TEM) crystallizes at 1000 °C. Holding the polymer for periods of 5–10 h at 800 or 900 °C also results in crystallization. Additional MAS^{29}Si NMR studies on samples pyrolyzed to 1400 °C showed no changes in peak position (from −15.7 ppm), suggesting the formation of well-defined β-SiC crystalline phases at 1000 °C.

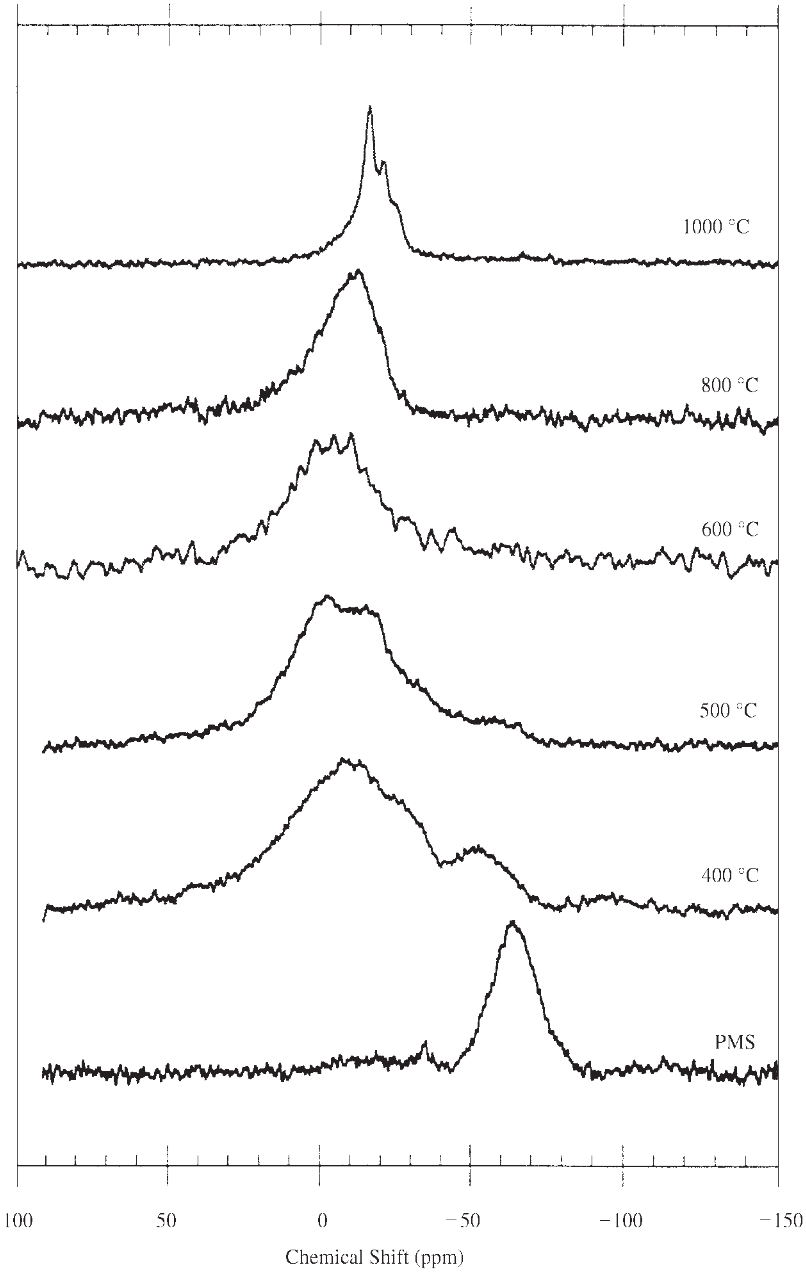

FIGURE 6. ^{29}Si MAS NMR spectra recording the pyrolytic transformation of polymethylsilane, $-[\mathrm{MeSiH}]_n-$, heated to selected temperatures for 1 h. Note the Kumada rearrangement to polycarbosilane, $-[\mathrm{H_2SiCH_2}]_x-$, that occurs at 400 °C. Crystalline β-SiC forms at 1000 °C

Fibers spun from a hyperbranched version of PMS (mPMS) and doped with 0.2 wt% boron are self-curing and can be pyrolyzed directly at rates of 20 °C min^{-1} to 1800 °C to give essentially phase pure, fully dense (>3.1 g ml^{-1} SiC fibers with controlled microstructures (crystallite sizes range from 2 nm at 1200 °C to 500 nm at 1800 °C)[104,106]. When subjected to bend stress analyses, these fibers exhibit bend strengths that average 3 GPa. The estimated elastic modulus for these fibers is >400 GPa. Furthermore, mPMS with M_n of *ca* 2000 Da and MW of *ca* 7000 Da can also be used (1) for joining ceramic parts, (2) for polymer infiltration and pyrolysis processing of ceramic powder and ceramic fiber reinforced matrices and (3) for coating other inorganic materials, e.g. carbon fibers.

The disadvantages of the PMS precursor are: (1) $MeSiH_3$ is costly and pyrophoric, forming potentially explosive mixtures with ambient air, (2) the Ti/Zr dehydropolymerization catalysts are also pyrophoric, leading to pyrophoric PMS and (3) metallocene-derived PMS is also highly pyrophoric. For example, a 20 wt% increase was observed after exposure of PMS samples to dry air for 5 h at RT. In contrast, the mPMS derivative mentioned above exhibits only a 3 wt% increase in air over a 5 h period.

Tanaka and coworkers[107] also describe $MeSiH_3$ dehydropolymerization to PMS in 68% yield, using $Cp_2NdCH(SiMe_3)_2$ as catalyst. The reaction, run under pressure (glass-lined autoclave, 8 kg cm^{-2}/benzene/>90 °C/2 d), gives solid PMS with H_2 and CH_4 as byproducts. The evolution of H_2 was expected whereas the appearance of CH_4 was not. A mechanism for Si$-$$CH_3$ bond scission leading to CH_4 formation was proposed (Scheme 5) wherein a methylneodymium complex forms. Both the $[Nd]CH_3$ and silylene species are proposed to react with Si$-$H to give CH_4, Nd$-$Si (active polymerization species) and branch sites within the growing chain. ^{1}H NMR analysis showed a $SiC\underline{H}_3 : Si\underline{H}$ ratio of *ca* 3 : 1, suggesting a linear polymer with no branching. Because *β*-methyl abstraction should result in loss of both $Si-\underline{H}$ and $Si\underline{CH}_3$ simultaneously, a heavily branched polymer may still form even though the $SiC\underline{H}_3:Si\underline{H}$ ratio remains 3 : 1.

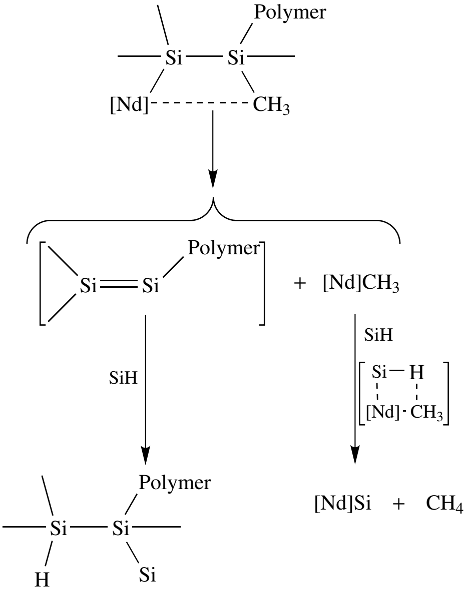

SCHEME 5. *β*-Methyl elimination during dehydropolymerization of $MeSiH_3$ using $Cp_2NdCH(SiMe_3)_2$

SEC analysis gave $M_n = 1470$ Da with a PDI = 5.00, very similar to the Ti and Zr values reported by Harrod. Pyrolysis to 900 °C in Ar provided ceramic yields of *ca* 74% with excess Si metal (amount not reported). To balance the excess Si, polyphenylsilane (MW = 1600 Da, 22 wt%) was blended with PMS to give phase pure β-SiC in 58% ceramic yield.

The disadvantages of this process, in addition to those described above for $MeSiH_3$, include (1) the availability of Nd catalysts for large-scale reactions and (2) the low (58%) ceramic yields.

3. PMS by dehydrocoupling of $CH_3SiH_2SiH_2CH_3$

Hengge and coworkers[108] studied Cp_2MMe_2 (M = Ti, Zr) catalyzed dehydrocoupling of $CH_3SiH_2SiH_2CH_3$. They report that Cp_2ZrMe_2 catalytically dehydropolymerizes neat, liquid $CH_3SiH_2SiH_2CH_3$ at room temperature in minutes to give an insoluble material with a general composition of $H{-}[MeSiH)_{0.58}(MeSi)_{0.42}]_n{-}H$ (equation 36).

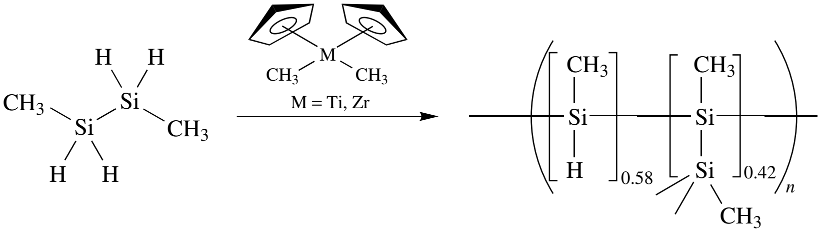

(36)

During reaction, the liquid initially turns yellow, then orange as H_2 evolves vigorously and then gels are formed. The resultant crosslinked polymer is insoluble in common solvents, decomposes before melting and is pyrophoric. GC analysis of similar disilane systems reveals odd-numbered oligosilanes, suggesting Si−Si bond cleavage. A mechanism, termed β^*-bond elimination (Scheme 6), was proposed for this process.

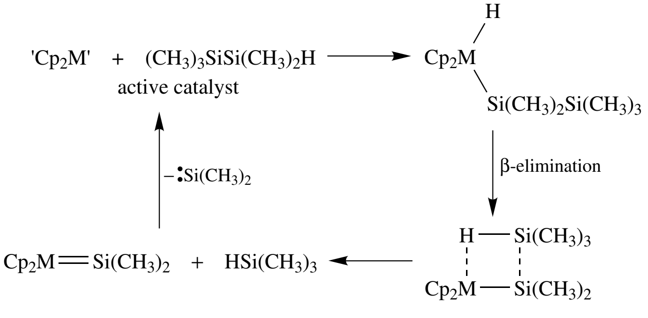

SCHEME 6. β^*-Bond elimination mechanism for the coupling of disilanes[109]

The authors suggest that polymeric products are derived from simultaneous dehydrocoupling and β^*-bond elimination mechanisms[110]. Presumably, the silylene species lost in the final step in the Scheme 6 cycle inserts into either Si−H or Si−Si bonds, creating odd-numbered oligosilanes. NMR studies of PMS reveal depletion of the Si−H bonds, suggesting crosslinking through Si−H sites, as found by Harrod and coworkers[101]. Pyrolysis provides *ca* 88% ceramic yields (1500 °C/Ar) of SiC.

The Hengge process appears attractive because the starting dimer (1) offers a 1 : 1 Si:C ratio, (2) is a liquid, rather than gaseous CH_3SiH, (3) polymerizes rapidly and because (4) the ceramic product appears to be phase pure SiC. The drawbacks are: (1) dimer requires $LiAlH_4$ reduction of $CH_3SiCl_2SiCl_2CH_3$ (from the direct process, Hengge obtained $CH_3SiH_2SiH_2CH_3$ from Wacker Chemie), (2) polymers without rheological utility and (3) pyrophoric polymers. It is likely that if a solvent were used, a soluble, processable precursor might be obtained. Unfortunately, it is very difficult to obtain $CH_3SiCl_2SiCl_2CH_3$ free from $(CH_3)_2SiClSiCl_2CH_3$ as the two compounds are difficult to separate.

$CH_3SiH_2SiH_2CH_3/(CH_3)_2SiHSiH_2CH_3$ mixtures can be copolymerized using Cp_2ZrMe_2 as shown above for $MeSiH_3$[111]. However, the resultant polymer gives low ceramic yields (50–60 wt% at 1000 °C) and is difficult to process. The Me_2SiH moiety appears to lead to early chain termination, resulting in low molecular weight products that volatilize on pyrolysis. Studies in this area are thwarted by the lack of a reliable source of pure $CH_3SiCl_2SiCl_2CH_3$ or its perhydrido analog.

4. PMS from the Bu_4PCl-catalyzed redistribution of chlorosilanes

Researchers at Dow Corning report synthesizing highly branched PMS by catalytic redistribution (1 wt% Bu_4PCl) of chlorodisilanes[112] (Scheme 7).

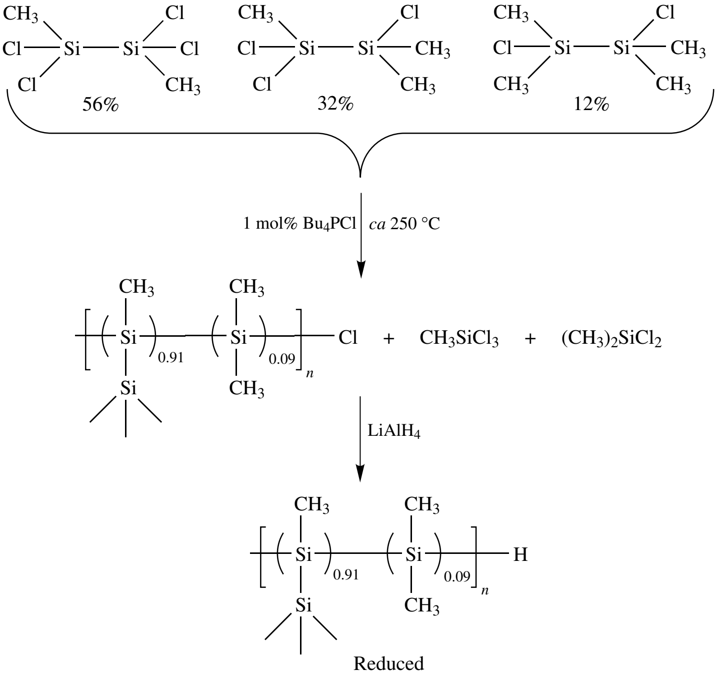

SCHEME 7. Catalytic redistribution of chlorodisilanes to give highly branched PMS[112]

This process has advantages in that the reaction is homogeneous and avoids the heterogeneous Na Wurtz coupling procedure, commonly used to polymerize chlorosilanes.

Furthermore, the disilanes used are byproducts of the 'direct process' used industrially to make methylchlorosilanes. The disilane monomer composition used was: 56.0% $CH_3SiCl_2SiCl_2CH_3$, 31.9% $(CH_3)_2SiClSiCl_2CH_3$, 12.5% $(CH_3)_2SiClSiCl(CH_3)_2$. Bu_4PCl (1 wt%) added to the mixture catalyzes redistribution of the disilanes. If the reaction mixture is heated slowly to 250 °C, a pyrophoric yellow glassy solid that is toluene-soluble forms in 15–20% yields. The remaining 80–85% of distillate consists of CH_3SiCl_3, $(CH_3)_2SiCl_2$ and $[(CH_3)_4Cl_2Si]_2$ (does not undergo redistribution), and small amounts of Si−H-containing species formed via a Kumada rearrangement (Scheme 8).

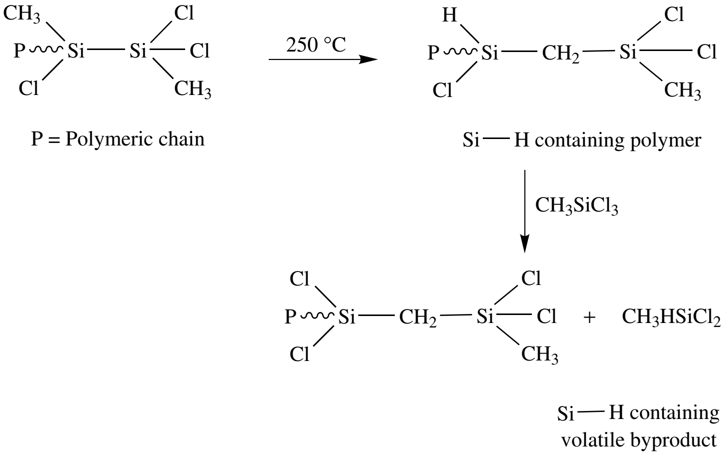

SCHEME 8. Kumada rearrangement of chlorosilanes[113]

$LiAlH_4$ reduction of the redistribution product gives a polymer with a composition of $-(MeSi)_{0.91}(Me_2Si)_{0.09}(H)_{0.4}-$. No NMR characterization was provided, although a M_n of *ca* 1130 Da was found by ebulliometry. Pyrolysis to 1560 °C gave 90% ceramic yields of 'essentially pure SiC', although no quantitative analyses were given. However, given the above polymer composition, the theoretical yield to SiC would be 88.4%, suggesting the presence of some excess carbon.

The advantages offered by this process are (1) a one-step synthesis to poly(methylchlorosilanes), (2) low cost dimers and (3) fiber processing that leads to phase pure SiC fibers. The primary drawbacks to the Dow-Corning process are (1) a low polymer yield (15–20%), (2) a multistep process and (3) the high cost of $LiAlH_4$ reduction of the chlorinated polymer.

5. Polycarbosilanes as precursors to SiC

Pillot and coworkers[113] reported the Wurtz polymerization of 2,4-dichloro-2,4-disilapentane (DCDP, **3**, to give a precursor to SiC (Scheme 9). DCDP was synthesized via Mg/Zn coupling of dichloromethane **1** with excess methyldichlorosilane **2** in *ca* 35% yield. DCDP was polymerized via Wurtz coupling, followed by $LiAlH_4$ reduction of residual Si−Cl, to poly(disilapentane), **4**, in 61% yield with $M_n = 1400$ Da and PDI = 3.1. No polymer yields were given for **4**.

^1H NMR spectra of **4** show depletion of Si−H bonds, as determined from an integration ratio $(C\underline{H}_3+C\underline{H}_2)/Si-\underline{H}$ of 5.5, higher than the expected value of 4.0. ^{29}Si NMR revealed three signals at −40, −36 and −6 assigned to $\underline{Si}Si_2C_2$, $-CH_2\underline{Si}(CH_3)H-Si$ and $\underline{Si}HC_3$

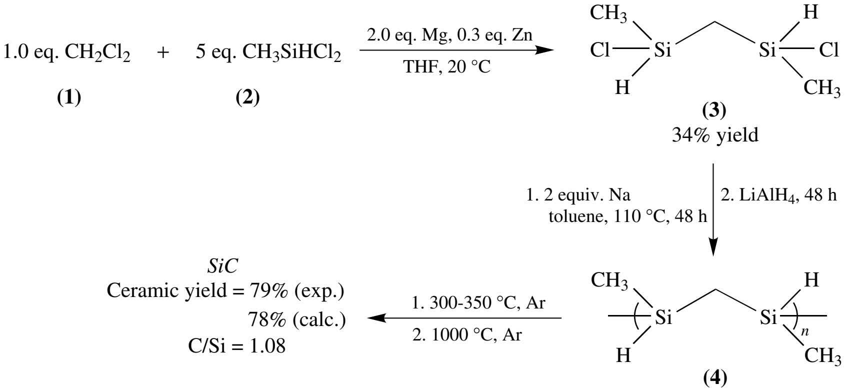

SCHEME 9. Synthesis of the SiC precursor, poly(2,4-disilapentane)

respectively. On heating to 300–350 °C, **4** converts to the corresponding polycarbosilane (MW = 7650 Da, PDI = 3.0, softening point *ca* 245 °C). Pyrolysis of this polycarbosilane gave ceramic yields of 79% (vs 78% theoretical) with a 1.08 C:Si ratio and 1.1 mol% O. The source of oxygen was not discussed, but it is assumed to incorporate during handling. Direct pyrolysis of polymer **4** without prior heat treatments gave <10 wt% ceramic yields.

Relatively phase pure, high ceramic yield SiC was obtained by this method; however, some disadvantages include (a) a multistep, low yield synthesis, (b) heat treatments to *ca* 350 °C prior to pyrolysis and (c) the high cost of $LiAlH_4$.

A related poly(disilapentane) precursor was developed by Corriu and coworkers[114] via metallocene catalyzed dehydropolymerization of 1,4-disilapentane (DSP) as depicted in Scheme 10. DSP was synthesized in 85% yield in two steps from the Pt catalyzed hydrosilylation of trichloro(vinyl)silane with $MeSiHCl_2$ followed by $LiAlH_4$ reduction. Reacting DSP with 0.5 mol% Cp_2TiMe_2 at room temperature for 48 h gave a polymer with $M_n = 990$ Da and PDI = 1.05. ^1H, ^{13}C and ^{29}Si NMR analyses indicate formation of a linear polymer with no reaction at the resulting SiH_2 sites. Reactions run for 72 h showed partial depletion of the SiH_2 groups giving branched, highly viscous liquids with $M_n = 3260$ Da and PDI = 10.1. At 50 °C, crosslinking occurred rapidly to give an insoluble material within 30 min.

Both low ($M_n = 990$ Da) and high ($M_n = 3260$ Da) molecular weight products, as described above, gave high ceramic yields (>73 wt% yield vs 78 wt% theoretical) of nearly phase-pure SiC ($Si_{1.01}C_{1.00}$) after pyrolysis. Conversion to crystalline β-SiC commenced at 1100 °C and was complete by 1400 °C, as determined by XRD. Ti was necessary during the pyrolytic transformation to SiC, as samples of poly(2,4-disilapentane) pyrolyzed without Ti gave 30% ceramic yields. Ti appears to catalyze crosslinking of volatile lower molecular weight species, which would otherwise volatilize on heating, into a more thermally stable crosslinked network, accounting for the high ceramic yields.

This method provides an attractive homogeneous route to SiC. The monomer can be synthesized in high yield from inexpensive starting materials and subsequent polymerizations were easily tuned by the reaction conditions. Thus, depending on the application, the resultant viscosity may easily be adjusted (i.e. fiber spinning). Drawbacks include (a) the use of $LiAlH_4$ (high cost and multistep) in the monomer synthesis, (b) use of pyrophoric Ti catalysts leading to pyrophoric poly(2,4-disilapentane) and (c) 2 : 3 Si:C ratio in the precursor polymer, contributing to lower ceramic yields.

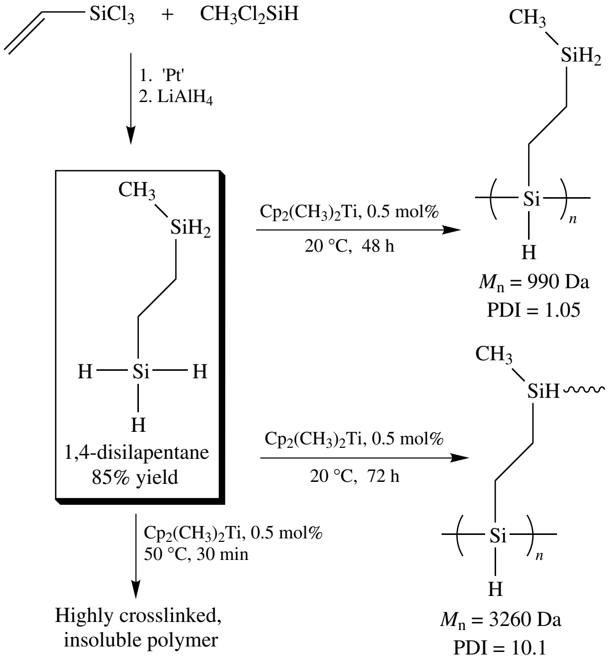

SCHEME 10. Ti-catalyzed dehydropolymerization of 2,4-disilapentane

6. Polysilaethylene (PSE) precursors

A brief patent by Smith[115] reports the Pt-catalyzed ring-opening polymerization of 1,3-disilacyclobutane in heptane or toluene to produce a linear PSE structure which, when pyrolyzed to 900 °C, gave SiC in 85% ceramic yield. The patent claims that the PSE can be processed and then pyrolyzed to give SiC fibers, films and molded shapes. However, neither the syntheses of 1,3-disilacyclobutane (from 1,1,3,3-tetrachloro-1,3-disilacyclobutane, Scheme 11) or PSE, nor ceramic product characterization (beyond brief IR claims) are provided.

Interrante and coworkers developed two polysilaethylene precursor systems, which upon pyrolysis gave nearly phase-pure SiC (95–99% SiC) in high ceramic yield (75–90%) (Scheme 11)[116]. The first procedure begins with a multistep synthesis of 1,1,3,3-tetrachloro-1,3-disilacyclobutane (monomer), **5**. Alternately, gas phase pyrolysis will convert **6** to **5**.

Pt-catalyzed ring-opening polymerization of monomer **5** gives poly(1,1-dichloro-1-silaethylene), **7**, which is reduced *in situ* with $LiAlH_4$. PSE, **8** is nearly linear with trace quantities of —SiHMe— branches (*ca* 1 per 200 chain Si atoms by NMR), which result from residual $Cl_2Si(CH_3)_2$ in the Cl_3SiMe starting material[116]. PSE molecular weights from SEC and NMR end group analysis gave $M_n = 24$ kDa and 11 kDa, respectively. The authors prefer NMR end group analysis rather than SEC (hydrodynamic volume relative to polystyrene) to estimate molecular weights.

As in traditional chain polymerization, the molecular weights are controlled by the catalyst concentration. Thus the more catalyst used, the lower the molecular weights. SEC indicates quite high MW (>130 kDa), that likely contributes to good rheological properties. PSE heated in the TGA under Ar to 1000 °C, undergoes smooth mass loss

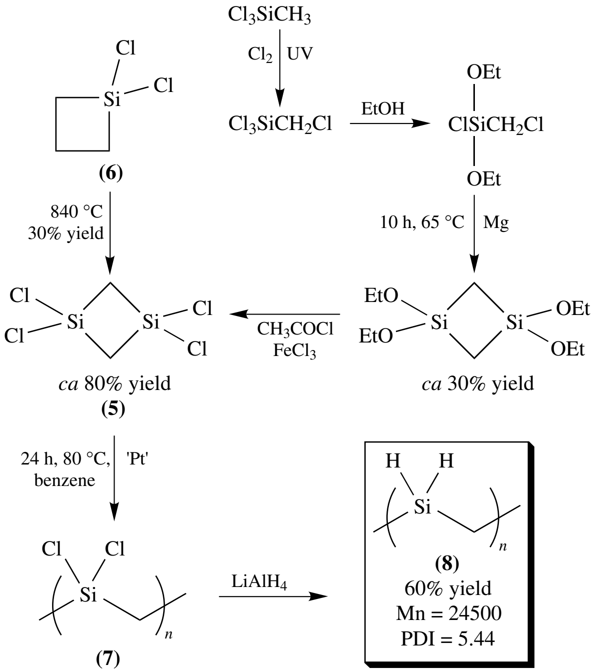

SCHEME 11. Synthesis of poly(silaethylene)[116]

between 100 and 600 °C, providing excellent ceramic yields of 87% (90.9% theoretical). The high ceramic yields are thought to result from the formation of silylene intermediates (=Si**:**) during pyrolysis, which crosslink the polymer prior to volatilization (self-curing). Samples heated to 1000 °C crystallized to β-SiC (by XRD) with average crystallite sizes of 2.5 nm.

Although their results were encouraging, the multistep, low yield monomer synthesis makes this route unlikely for the large-scale production of SiC. As a result, the Interrante group changed their synthetic tack. They recently reported the synthesis of a highly branched poly(silaethylene) **8** derived from Grignard-based polymerization of $ClCH_2SiCl_3$, followed by $LiAlH_4$ reduction[116] (Scheme 12).

The reaction, performed in refluxing diethyl ether (4 d), provides chlorinated polycarbosilane **7** in 50–60% yields with a typical composition of *ca* $SiCl_{1.70}(OEt)_{0.15}Et_{0.15}CH_2$, suggesting side reactions with the solvent. This highly branched intermediate was generally not isolated but was reduced *in situ* with $LiAlH_4$ to give $SiH_{1.85}Et_{0.15}CH_2$. The traces of the ethyl substituents appear to have minimal effect on the ceramic composition after pyrolysis (see below).

The product is an ether/hydrocarbon soluble, air stable (by TGA) yellow liquid at RT. Additionally, no changes in the NMR or IR spectra occur in samples exposed to air for days. IR and NMR data are consistent with a highly branched structure, as anticipated for tetra-functional $ClCH_2SiCl_3$. For example, ^{29}Si NMR indicates the presence of $(CH_2)_4Si$ (1–7 ppm), $(CH_2)_3SiH$ (−5 to −19 ppm), $(CH_2)_2SiH_2$ (−25 to −40 ppm) and CH_2SiH_3 (−50 to −75 ppm) moieties. SEC indicates $M_n = 745$ Da with a PDI of *ca* 7, also consistent with a highly branched structure.

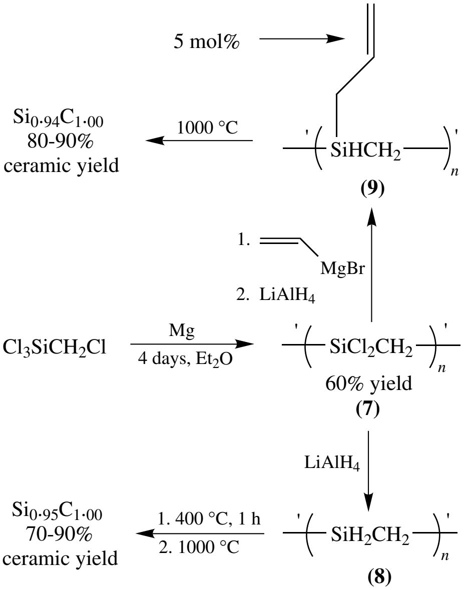

SCHEME 12. The synthesis of highly branched poly(silaethylene)

Pyrolysis of **8** in Ar to 1000 °C gave ceramic yields of only *ca* 50% vs 90.9% theoretical. The low ceramic yield results from vaporization of low MW fractions between 100 and 250 °C. However, ceramic yields of *ca* 80 wt% of nearly stoichiometric SiC (0.9, 0.7 and 3.5 wt% excess C, H and O, respectively) were obtained for partially crosslinked polymers, for example, on heating the polymer for 4 h in Ar between 200–400 °C, or on heating the polymer in the presence of a dehydrocoupling catalyst [$Cp_2M(CH_3)_2$, M = Zr, Ti] (as above) at 100 °C. Samples are amorphous after pyrolysis to 1000 °C and crystallize (crystallite size *ca* 30 nm) to β-SiC at 1600 °C with an additional weight loss of 10–15%. This weight loss was suggested to arise from loss of CO and SiO as the residual oxygen within the material is eliminated.

The addition of 4 mol% allyl or vinyl groups to **8** followed by $LiAlH_4$ reduction provided **9**, which crosslinks at 150 °C to give 80–90% amorphous SiC (5% wt excess C) on pyrolysis to 1000 °C.

This polymer precursor (1) requires relatively inexpensive starting materials, (2) is quite stable in air, (3) offers good processability for polymer infiltration processing of composites, (4) provides excellent SiC ceramic yields and (5) high purity with controllable microstructures. However, one important drawback is the use of costly $LiAlH_4$. This polymer is now available commercially (Starfire Inc., NY).

7. Phase pure SiC via processing

Many modifications to the existing Yajima polycarbosilanes (PCS) precursors have been reported in efforts to improve ceramic yields, phase purity and the mechanical properties[6,7]. Only a few of these actually provide phase pure SiC through processing efforts alone. For example, Dow Corning work reports that thermally stable, substantially dense polycrystalline SiC fibers (>2.9 g ml^{-1} vs 3.2 g ml^{-1} theoretical) can be processed from polydimethylsilane-derived PCS by adding boron during the processing step[117].

PCS was first melt spun into fibers at *ca* 300 °C and sequentially exposed to NO/diborane, or ammonia/BCl_3 or NO_2/BCl_3 gases (rather than O_2) at temperatures between 25–200 °C for periods of 4–24 h to render the fibers infusible. The residual N, O and excess carbon are eliminated during sintering as gaseous byproducts (e.g. SiO and CO) at 1400 °C resulting in pores and voids, that weakened the fiber. However, continued heating with B to >1600 °C results in smooth densification (decreasing porosity), and overall strengthening of the fiber. B aids sintering and promotes densification at high temperatures (>1400 °C) and is necessary to retain fiber integrity.

The final, near stoichiometric β-SiC fibers have oxygen contents of <0.1 wt%, when heated >1600 °C. They exhibit average tensile strengths of 2.6 GPa and elastic moduli >420 GPa. Nicalon fibers do not survive similar heat treatments. The advantages of these fibers are that they rely on an existing process and provide properties expected of fully dense, phase pure SiC. Dow Corning has announced that they will make these fibers available commercially in the near future. Although the properties found for these fibers are essentially those of bulk SiC, there are some drawbacks: (1) the precursor synthesis process is multistep, (2) the ceramic yields are low and (3) the spun fibers required multiple heat treatments at 100–300 °C for 4–24 h with BCl_3 or diborane.

As an aside, Jacobson and DeJonghe have reported that simply heating Nicalon or Tyranno fibers at temperatures of *ca* 1600 °C with sources of boron (e.g. boron metal, TiB_2 etc.) leads to sufficient incorporation of boron into the fibers such that they densify and stable, nearly phase pure, SiC fibers are obtained. No data are provided about fiber composition[118].

Toreki and coworkers have described processing SiC fibers (UF fibers) from a novel PCS with low oxygen content and better high-temperature stability than Nicalon fibers[119]. The PCS was synthesized by pressure pyrolysis of polydimethylsilane in an autoclave. Control of the molecular weight (MW) is the key to successfully producing PCS fibers by solution processing. For example, fibers derived from PCS with Mn <5000 Da melted before curing, while those derived from PCS >10000 Da were not soluble, thus not suitable for spinning fibers.

Thus, in the presence of spinning aids (polysilazane and polyisobutylene), PCS of Mn 5000–10000 Da can be dry spun and then pyrolyzed in N_2 to form SiC-containing fibers. The polymer is self-curing. The resultant fibers have 80% ceramic yields (950 °C, 20 °C per min), low oxygen contents (1.1–2.6 wt%) and mechanical properties similar to Nicalon (tensile strength of *ca* 3.0 GPa, ambient). The pyrolyzed fibers have excess carbon, and thus perform below expectations for phase pure SiC. However, Sacks and coworkers have recently[120] described near stoichiometric SiC fibers ($\leqslant$0.1 wt% O) with high tensile strength (*ca* 2.8 GPa), fine grain sizes (*ca* 0.05–0.2 μm), high densities (*ca* 3.1–3.2 $\mathrm{g\,ml^{-1}}$) with small residual pore sizes ($\leqslant$0.1 μm). The synthesis of the polymer precursor for this process was not reported; however, it was stated that dopant additions were made. The fibers (designated UF-HM fibers) retained *ca* 92% of their initial strength (2.70 GPa) after heat treatments to 1800 °C, suggesting the dopants contained B or other sintering agents to prevent grain growth. Electron microprobe analysis (EMA) showed an average fiber composition of 68.5% Si, 31.5% C, $\leqslant$ 0.1% O ($Si_{0.93}C_{1.00}$).

Few fibers have the excellent mechanical properties reported for the UF-HM fibers; however, if the synthesis parallels the original one (see above), the expected drawbacks for the process include: (1) the use of an autoclave, not desirable for large-scale production and (2) low ceramic yields of SiC, given that the fiber is derived from a polymer precursor containing a 1 : 2 Si:C ratio.

As mentioned above, there are now several polymer systems that provide access to phase pure, fully dense SiC with the properties expected based on SiC materials made by traditional methods. This does not mean that no further development need take place in this area. There are still cost issues that limit the utility of many of these precursors.

Furthermore, not all applications will need or benefit from the availability of phase pure SiC. For example, in polymer infiltration and pyrolysis processing of composites, the reinforcing material frequently is oxidized at the surface. Thus, an SiC precursor that produces excess carbon may be required to ensure that the oxide surface layer is reduced off during processing so that good interfaces are obtained.

One continuing and unresolved issue is whether or not a crystalline fiber is more desirable than an amorphous fiber. Thus, efforts to make amorphous, SiC-based ceramics are still an area of interest as suggested by the following section.

B. Precursors to Si—C—B Materials

In work directed toward the development of phase and chemically pure SiC with controlled microstructures, boron was added to control oxygen content and improve sintering behavior. Unrelated efforts sought routes to Si—C—B materials because of their potential to provide lightweight, high-strength ceramic/amorphous materials. The earliest efforts in this area are those of Riccitiello and coworkers[121]. The objective of these studies was to make a material that would exhibit exceptional stability at high temperatures in oxidizing environments. It was proposed that Si—C—B materials would oxidize slowly at high temperatures to generate borosilicate glass coatings on the oxidizing surface, that would act as barriers to further oxidation.

Efforts to prepare Si—C—B materials focused on dehalocoupling mixtures of boron halides and Me_2SiCl_2 (equations 37 and 38).

$$BCl_3 + 1.5Me_2SiCl_2 + 6Na \xrightarrow{120\,^\circ C/2-3\ d} \underset{50-60\%}{-[B(Me_2Si)_3]_n-} + NaCl \tag{37}$$

$$MeBBr_2 + Me_2SiCl_2 + 6Na \xrightarrow{120\,^\circ C/4-8\ h} \underset{50-60\%}{-[MeB(Me_2Si)_2]_n-} + NaCl/NaBr \tag{38}$$

The stoichiometry used to synthesize the first polymer can in principle lead to a completely crosslinked and insoluble polymer; however, when xylenes were used as solvent, a 60% yield of soluble precursors were obtained. When octane was used as solvent, the soluble fraction was only 40–50%. The second polymer type, which in principle should give only linear materials, also gave 50–60% yields of soluble precursor.

A number of other polymers were made wherein the ratios of the two principle ingredients in both of the above reactions were varied. The resulting polymers differ very little. Efforts to incorporate vinyl groups attached to Si centers led to further crosslinking as the vinyl groups reacted under the dehalocoupling conditions.

FTIR analyses of the polymers revealed no surprises, i.e. the presence of Si—H and B—H bonds were minimal. The presence of possible Si—B bonds was inferred by the presence of three absorptions in the 620–690 cm^{-1} region of the polymer spectra. Theoretical calculations suggest that the Si—B band should appear at *ca* 650 cm^{-1}. An additional absorption at 1315 cm^{-1} was assigned to a B—C stretching vibration. UV absorption spectra contain no peaks in the 300–350 nm region that can be associated with long polysilane blocks, suggesting that the polymers consist of, at most, short Si—Si segments linked to boron. All of the polymers are air- and moisture-sensitive, oxidizing rapidly in air.

The chemical composition of the soluble fraction of the first polymer was $SiC_{1.96}B_{0.54}H_{5.14}$ and that of the second polymer was $SiC_{3.26}B_{0.93}H_{7.03}$. Oxygen contents were 3–4 wt%. Some of the xylene solvent appears to be incorporated in the polymers as evidenced by the presence of aromatic peaks in the proton NMRs. TGA of the first polymer shows a 65–70 wt% ceramic yield (1000 °C/N$_2$). The second polymer's ceramic yield was just slightly lower. Most of the polymers made had an $M_n = 700$–1500 Da range with the majority being at the low end of this molecular weight range. The polymers had softening points in the range of 50–180 °C, depending on boron content. Typically, polymers with less boron (lower crosslink density) softened and or melted at lower temperatures.

Pyrolysis of the first polymer (1100 °C per 1 h/Ar) gave a material with a $Si_{1.92}C_{2.53}B_{0.71}H_{0.08}$ composition. XRD analysis suggested the presence of crystalline SiC (polytype not specified) following further heating to 1300 °C (1 h/Ar). Solid state ^{13}C, ^{29}Si, and ^{11}B NMR of the 1000 and 1300 °C samples indicates that the carbon is present mostly as SiC with little if any B_4C. On heating in air (TGA), these high-temperature samples appear to exhibit excellent oxidation resistance with gains of only 1–2 wt% at 1000 °C, which the authors suggest indicates little free carbon. Note that phase pure SiC oxidizes to SiO_2 with a weight gain of 50%. Hence a combination of SiC and free carbon could also lead to weight gains of 1–2 wt%, thus care must be taken to ensure spectroscopically that following air oxidation the material remains substantially the same.

These same polymers, sometimes made with small amounts of isopropyl or phenylsilyl chlorides, can be melt-spun in air to produce green fibers with 10–17 μm diameters. UV/air curing for 18–24 h gave infusible fibers that could be converted to ceramic fibers by passing through (90 cm min^{-1}) a furnace held at 1100–1300 °C (30 cm hot zone). An alternate, low-oxygen cured green fiber was obtained by sealing green fibers in a quartz tube, introducing hydrazine vapor and irradiating *in situ* for the same times as above.

The tensile strengths of the oxygen-cured fibers heated to 1000–1300 °C averaged 1 GPa, with an elastic modulus of *ca* 150 GPa. The tensile strengths of the hydrazine-cured fibers were slightly higher at 1.2–1.6 GPa and modestly higher elastic moduli of up to 180 GPa. The oxygen contents of both fibers were still quite high (several percent) because they were spun in air.

Another approach to Si–C–B materials was explored by Riedel and coworkers wherein polymethylvinylsilanes were hydroborated (BH_3). Thus, polymethylvinylsilane was prepared by equation 39[122].

$$\begin{array}{c} 0.77\mathrm{Me(CH_2{=\!=}CH)SiCl_2} \quad + \quad 0.44\mathrm{Me_2SiCl_2} \quad + \quad 0.39\mathrm{Me_3SiCl} \quad + \quad 3\mathrm{Na} \\ \Big\downarrow \text{THF/toluene/100 °C} \\ \mathrm{NaCl} \quad + \quad -\!\!-[\mathrm{Me(CH_2{=\!=}CH)1Si}]_{0{\cdot}77}(\mathrm{Me_2Si})_{0{\cdot}44}(\mathrm{Me_3Si})_{0{\cdot}39}]_n -\!\!- \end{array} \tag{39}$$

This product is then treated with a borane derivative (equation 40).

$$\begin{array}{c} -\!\!-[(\mathrm{Me(CH_2{=\!=}CH)1Si})_{0{\cdot}77}(\mathrm{Me_2Si})_{0{\cdot}44}(\mathrm{Me_3Si})_{0{\cdot}39}]_n -\!\!- \quad + \quad \mathrm{H_3B{\bullet}SMe_2} \\ \Big\downarrow \text{toluene/RT to 110 °C} \\ \mathrm{Me_2S} \quad + \quad -\!\!-[\mathrm{Me({=\!=}BCH_2CH_2)Si})_{0{\cdot}77}(\mathrm{Me_2Si})_{0{\cdot}44}(\mathrm{Me_3Si})_{0{\cdot}39}]_n -\!\!- \end{array} \tag{40}$$

Hydroboration reaction can also be performed (*ca* 65% yield) with $H_3B{\bullet}THF$. The M_n for the vinylsilane is *ca* 800 Da and goes up to *ca* 1220 Da on hydroboration. A typical chemical composition for the 1220 Da polymer is $SiC_{2.90}B_{0.29}H_{7.43}O_{0.06}$. FTIR analysis of the polymer shows a ν_{B-H} band at 2530 cm^{-1}, indicating that hydroboration is incomplete. A band at 2100 cm^{-1}, typical of ν_{Si-H}, suggests that some Si−Cl/B−H exchange occurs along with hydroboration. It also indicates that not all of the Si−Cl bonds are consumed during dehalocoupling. The ^1H NMR spectrum indicates a 1 : 6.5 vinyl-to-methyl ratio in the starting oligomer. Based on the initial stoichiometry, this should be closer to 1 : 3, thus some of the vinyl groups are probably consumed during dehalocoupling as seen by Riccitiello and coworkers.

In both cases, on heating to 200 °C for 1 h in argon, a yellow polymer powder is obtained. On further pyrolysis to 1000 °C (Ar) the polymers convert to amorphous Si−C−B materials. A typical found composition is $Si_{1.7}C_{3.20}B_{0.6}$. If this material is heated to higher temperatures, the composition changes slightly. Thus, heating at 2200 °C (1 h/Ar) leads to a composition of $Si_{1.8}C_{3.4}B_{0.5}$. Samples heated $\geqslant$1500 °C start to crystallize as broad β-SiC peaks (25 nm average grain size) appear first. At temperatures $\geqslant$1700 °C, SiC, graphitic carbon and B_4C powder patterns are discernible, with average grain sizes reaching *ca* 250 nm at *ca* 2000 °C. At this temperature, β-SiC converts to α-SiC. Thus, SiC/graphite/B_4C composite materials are produced as a consequence of phase segregation as the precursor-derived material is heated to higher temperatures. This work actually serves as the basis for the Si−N−B−C work from the Riedel group discussed above.

C. Precursors to Si−C−O Materials

Because it is possible to generate SiC from silsesquioxanes, $-[RO_{1.5}]_n-$, considerable early work on SiC syntheses focused on transforming siloxane and silsesquioxane precursors to SiC[123−126]. Unfortunately, the transformation process requires temperatures of >1300 °C to effect carbothermal reduction of the intermediate SiC_xO_{4-x} phase to generate CO and SiC[125,126]. Thus, interest in the use of silsesquioxanes as SiC precursors waned. However, these initial studies demonstrated that properly developed silsesquioxanes were very easy to process into a wide variety of shapes and the pyrolysis product, SiC_xO_{4-x} or black glass, offers reasonable mechanical properties[127−135]. Consequently, more recent work has targeted processing black glass. Much of the work in this area relies on sol-gel synthesis of processable silsesquioxanes and is therefore outside the objectives of this review; however, several pertinent references are provided.

Several chemical synthesis routes to black glass precursors have also been developed, as will be discussed below. In general, the properties of the materials produced by both methods are much the same. For example, Agaskar described the use of several novel polyhedral silsesquioxanes as precursors to microporous 'organolithic materials'. His approach was to synthesize functionalized polyhedral silsesquioxanes (equations 41 and 42)[136].

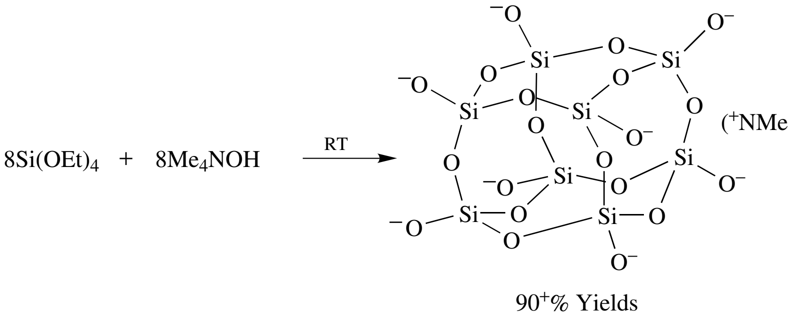

(41)

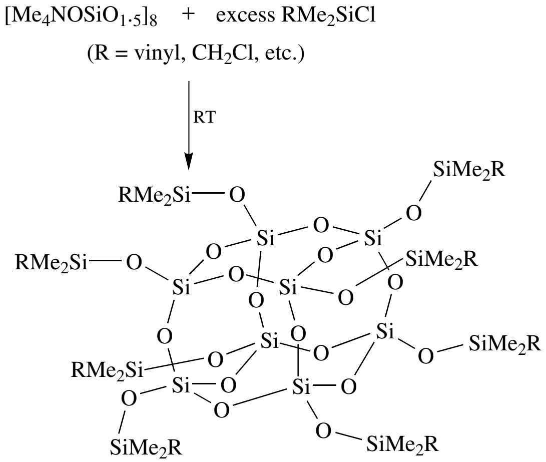

(42)

The vinyl substituted cube readily hydrosilylates on reaction with $(p\text{-HSiMe}_2\text{C}_6\text{H}_4)_2\text{O}$ in the presence of platinum catalysts in THF. Pyrolysis in nitrogen to 800 °C (75 wt% ceramic yield) forms a black glass whose solid state ^{29}Si MAS NMR exhibits a variety of species consistent with the formation of $\text{SiC}_x\text{O}_{4-x}$. The NMR results are very similar to those discussed just below. Agaskar finds that if this material is leached with HF (48%/30 h), *ca* 40% of the mass is lost as a significant portion of the SiO_2 (actually Q_4) species are selectively removed with little change in the oxycarbide phase. The resulting material is microporous and exhibits a specific surface area of nearly 600 $\text{m}^2\,\text{g}^{-1}$ and a pore volume of *ca* 0.2 $\text{ml}\,\text{g}^{-1}$. Microporous materials are of considerable interest for a variety of applications, as briefly discussed below.

An alternate, but less elegant route than that to polysilsesquioxane black glass precursors takes advantage of early work reported by Harrod and coworkers[137] on a novel disproportionation reaction (equation 43). When the same catalyst is applied to redistribute a polymethylhydridosiloxane, the result is a processable silsesquioxane polymer (equation 44)[138].

$$3\text{MeHSi(OEt)}_2 \xrightarrow{0.05\ \text{mol\%}\ \text{Cp}_2\text{TiMe}_2/20\,^\circ\text{C}} \text{MeSiH}_3 + 2\text{MeSi(OEt)}_3 \qquad (43)$$

$$-[\text{MeHSiO}]_x- \xrightarrow{0.05\ \text{mol\%}\ \text{Cp}_2\text{TiMe}_2/72\ \text{h}/20\ ^\circ\text{C}} 0.33x\text{MeSiH}_3 + -[\text{MeHSiO}]_{0.3}[\text{MeSiO}_{1.5}]_{0.7}- \qquad (44)$$

The copolymer $-[\text{MeHSiO}]_{0.3}[\text{MeSiO}_{1.5}]_{0.7}-$ forms as a gel if neat methylhydridooligosiloxane, $\text{Me}_3\text{Si}-[\text{MeHSiO}]_x-\text{H}$ (M_n *ca* 2 kDa), is reacted with the catalyst. Gelation can be avoided if polymerization is conducted in toluene with a greater than 5 : 1 toluene to $-[\text{MeHSiO}]_x-$ volume ratio. The resulting polymer solution can be used to coat a variety of materials, including fibers[139].

Although the 5 : 1 volume ratio solutions can be used for coating applications, the gel-like material that results on solvent removal limits the copolymer's utility. Fortunately, the reactive Si−H bonds that remain in the copolymer can be used to further modify polymer properties. The presence of the catalyst in the final reaction solution provides a simple means of further modifying the original copolymer. Thus, after 72 h of reaction, the original royal blue toluene solutions of reaction 44 turn yellow-orange on addition of alcohols as the catalyst promotes alcoholysis of the remaining Si−H bonds (equation 45).

$$\begin{array}{c}
-[\mathrm{MeHSiO}]_{0\cdot3}[\mathrm{MeSiO}_{1\cdot5}]_{0\cdot7}- \quad + \quad \mathrm{ROH} \\
\Big\downarrow \mathrm{Cp_2TiMe_2/20\ ^\circ C} \\
-[\mathrm{Me(RO)SiO}]_{0\cdot3}[\mathrm{MeSiO}_{1\cdot5}]_{0\cdot7}- \quad + \quad \mathrm{H_2}
\end{array} \qquad (45)$$

The blue color corresponds to a Ti(III) species, produced during reaction, which may or may not be the true catalyst. The yellow-orange color is typical of a Ti(IV) species. Alcoholysis creates more $[\mathrm{MeSiO}_{1.5}]$ groups, masked as alkoxy derivatives, [Me(RO)SiO]. If R is a long-chain alkyl group, more flexibility obtains and much of the gel character can be eliminated.

With MeOH, the reaction is rapid and vigorous H_2 evolution results. This polymer does not show much improvement in processability. However, the *n*-Bu derivative is completely tractable following solvent removal; however, it is expedient to redissolve the polymer in *n*-BuOH as gelation can still occur with time (days to weeks).

The original $-[\mathrm{MeHSiO}]_{0.3}[\mathrm{MeSiO}_{1.5}]_{0.7}-$ and $-[\mathrm{Me(RO)SiO}]_{0.3}[\mathrm{MeSiO}_{1.5}]_{0.7}-$ copolymers were characterized by ^{1}H, ^{13}C and by ^{29}Si NMR[138]. The starting oligomer, $-[\mathrm{MeHSiO}]_n-$, is capped by $\mathrm{Me_3SiO}$ (M) and OH (DOH) groups. Thus, the actual composition of the 'Ti' catalyzed redistribution product is $[\mathrm{MeSiO}_{1.5}]_{0.65}$ $[\mathrm{MeHSiO}]_{0.28}[\mathrm{MeSi(OH)O}]_{0.04}[\mathrm{Me_3SiO}]_{0.03}$. The MeHSiO (D) ^{29}Si peak appears at −34.6 ppm. The ^{1}H MAS NMR spectrum also reveals the presence of Si−H groups at 4.5 ppm. The ^{13}C MAS spectrum shows two peaks at 1.1 and −2.9 ppm that can be assigned to the MeHSiO and $\mathrm{MeSiO}_{1.5}$ (T) units, respectively. The ^{29}Si NMR spectrum also shows several peaks at −33 to −36 ppm and two peaks at −57.2 and −65.5 ppm, which are typical of cubic silsesquioxanes. These results, when coupled with the reproducible 30 : 70 [MeHSiO] : $[\mathrm{MeSiO}_{1.5}]$ ratio, suggest a polymer structure that consists of open cubes of T groups ($\mathrm{MeSiO}_{1.5}$) bridged by one or two −MeHSiO− groups. The peak at −57.2 ppm is much smaller than the peak at −65.5 ppm. Thus, we assign this peak to the silicon vertices on the open edge of the cube and the −65.5 ppm peak to the remaining T group silicons in the cube. In the alkoxy derivatives, the −34.6 peak is replaced by a peak at *ca* −64 ppm. Note that silsesquioxane polymers are frequently described in the literature as ladder polymers when in fact they are best represented as discussed above. Frye and Klosowski addressed this misapprehension some 25 years ago[140].

Although the alkoxy derivatives are easier to process than $-[\mathrm{MeHSiO}]_{0.3}$ $[\mathrm{MeSiO}_{1.5}]_{0.7}-$, the pyrolysis behavior of both types of materials is much the same. Thus we will briefly look at the transformation processes that occur as $-[\mathrm{MeHSiO}]_{0.3}$ $[\mathrm{MeSiO}_{1.5}]_{0.7}-$ decomposes to black glass. Pyrolysis of $-[\mathrm{MeHSiO}]_{0.3}[\mathrm{MeSiO}_{1.5}]_{0.7}-$ in air leads to formation of pure silica (80–85% ceramic yield) at temperatures of 800–900 °C. In nitrogen, the ceramic yield is 70–75 wt% at 900 °C.

The simplest way to follow the polymer-to-ceramic transformation process is by solid state MAS ^{29}Si NMR spectroscopy. Thus, Figure 7 shows the MAS ^{29}Si NMR spectra of samples of copolymer heated to selected temperatures in N_2. Figure 8 provides an integration of the various species and how the relative amounts of each change on pyrolysis.

Heating the copolymer to 200 °C appears to have little effect on the polymer composition as seen in Figures 7 and 8. One might expect any Si−OH groups present to cocondense, react with $\mathrm{Me_3SiO}$− or Si−H groups to form Si−O−Si bonds and release H_2O, $\mathrm{Me_3Si{-}OH}$ or H_2. However, the concentrations of these species and their diffusivities are too low for significant reaction to occur.

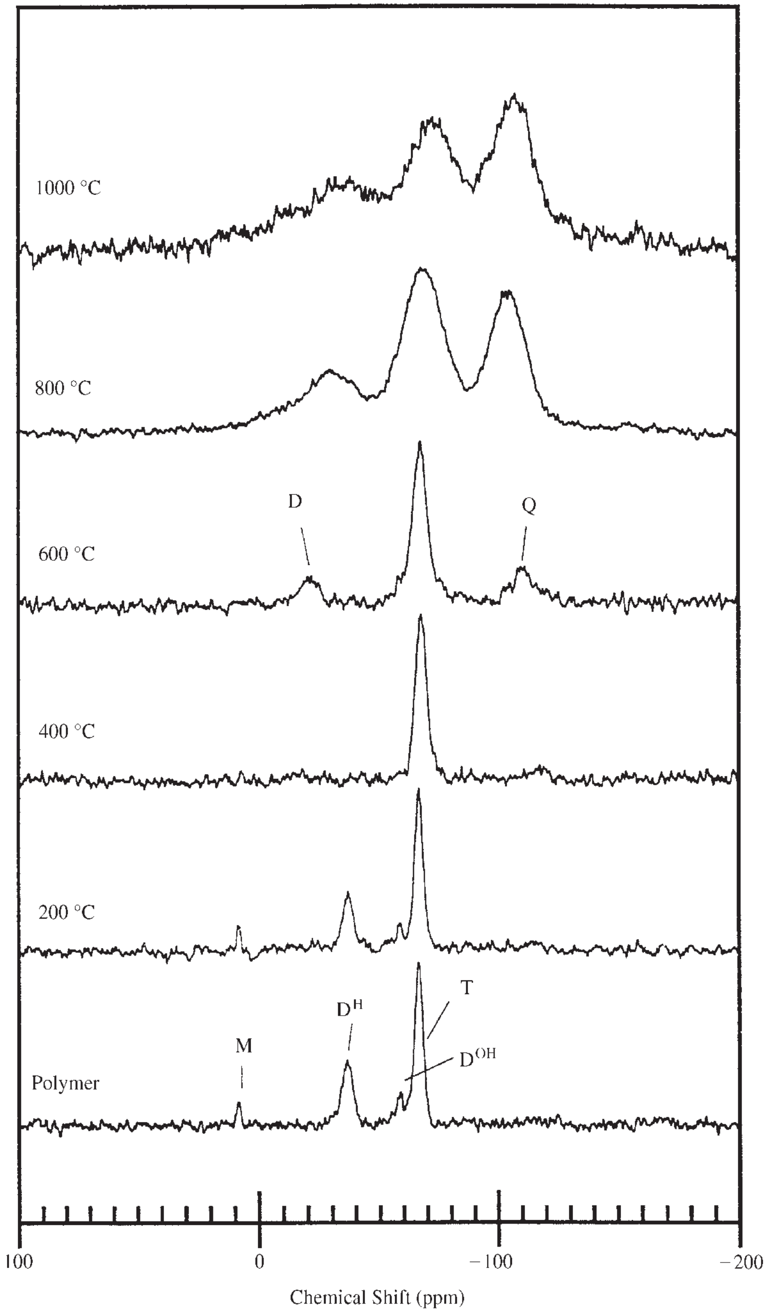

FIGURE 7. ^{29}Si MAS NMR spectra of samples of $-[MeHSiO]_{0.3}[MeSiO_{1.5}]_{0.7}-$ copolymer heated to selected temperatures in N_2. For definitions of abbreviations, see Figure 8

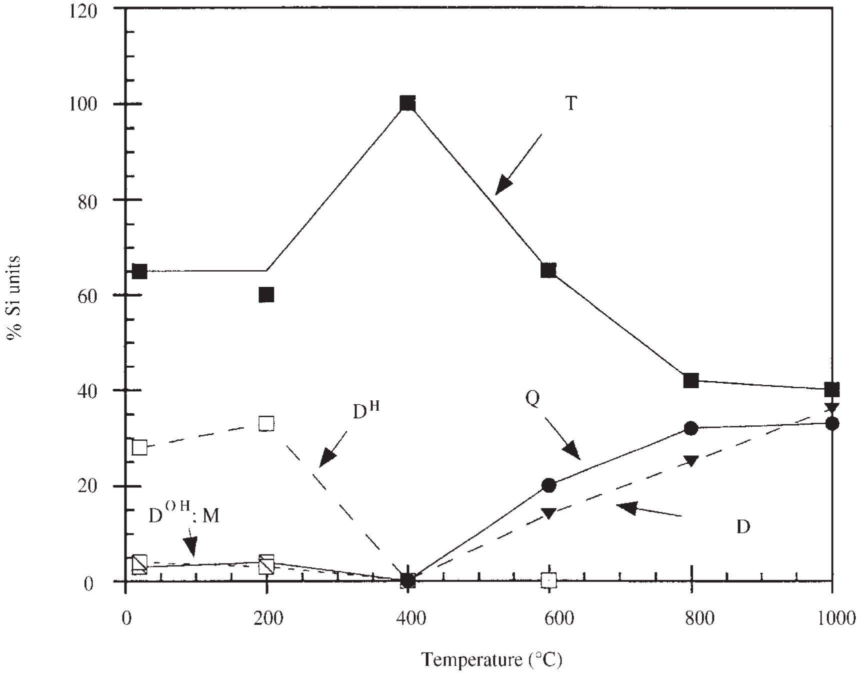

FIGURE 8. Integration of the various species on pyrolysis of $-[\mathrm{MeHSiO}]_{0.3}[\mathrm{MeSiO}_{1.5}]_{0.7}-$ to selected temperatures. M = $\mathrm{Me_3SiO}-$, D = $\mathrm{Me_2Si(O-)_2}$, $\mathrm{D^H}$ = $\mathrm{MeHSi(O-)_2}$, D^{OH} = $\mathrm{Me(OH)Si(O-)_2}$, T = $\mathrm{MeSi(O-)_3}$, Q = $\mathrm{Si(O-)_4}$

At 400 °C, the TGA (not shown) indicates a 20% mass loss which appears to result from depolymerization and redistribution of $-[\mathrm{MeHSiO}]_x-$ segments. The ^{29}Si MAS and ^{1}H NMR spectra suggest that the 400 °C sample is now composed solely of $-[\mathrm{MeSi(O)}_{1.5}]_x-$. However, the cross polarization NMR spectrum (not shown) reveals the presence of remnants of the $-[\mathrm{MeHSiO}]_x-$ and $[\mathrm{MeSi(OH)O}]-$ groups. The ^{13}C spectrum changes somewhat as the 1.1 ppm peak is reduced to a shoulder on the major peak which shifts from −2.9 to −3.5 ppm.

At 600 °C, a number of chemical changes occur in the polymer structure. For example, the number of T units decrease from *ca* 100% to 65% coincident with the appearance of D-type $[\mathrm{MeSi(CH}_x\mathrm{)O}]$ units (14%) and Q ($\mathrm{SiO_4}$, 20%) units (Figure 8). The relative amounts of each are close, suggesting that these species arise by direct redistribution of the T groups. ^{13}C NMR shows some changes as the peak attributable to $\mathrm{Si-CH}_x$ species broadens and shifts to −4.2 ppm, in keeping with the formation of new D-type units. Groups containing Si−H or SiO−H functionality are no longer present.

On heating to 800 °C, all resemblance to a polymer structure disappears. All of the ^{29}Si peaks broaden greatly. The presence of Q units becomes significant as the number of T units continues to decrease (42%). The most important observation is the reappearance of DH units in the ^{29}Si spectrum and in the ^{1}H NMR spectrum (Si−H) as confirmed by FTIR studies[138]. These DH units result from carbothermal reduction by reaction of Si−O linkages with neighboring methyl groups. The 800 °C spectrum in Figure 7 is very similar to the ^{29}Si spectrum obtained by Agaskar on heating the polyhedral silsesquioxane above in nitrogen to 800 °C.

The ^{29}Si MAS NMR spectrum indicates that the 800 °C material is composed of SiO_4 (35%), SiO_3C (42%), SiO_2C_2 (<10%) and SiO_2CH (<20%) units. However, chemical analysis indicates that the Si:C ratio does not change during the heating process. Consequently, some free carbon appears to form. Thus, in principle, segregation occurs at temperatures $\geqslant$800 °C which has implications on the properties of black glass at these temperatures. For example, segregation could lead to a higher susceptibility to oxidation as the segregated carbon is no longer part of the oxycarbide network. Alternately, it might provide the opportunity to make microporous materials if the carbon can be removed selectively and uniformly. It is important to reiterate that the behavior of these precursors on pyrolysis is much the same as that of sol-gel derived materials[141,142]. Thus, the above described polymers may in principle provide the advantage of shelf-life not possible with the sol-gel derived materials.

Although silsesquioxane precursors do not provide the high-temperature properties of SiC, they still remain particularly useful for low-temperature applications, e.g. for providing oxidation and scratch-resistant coatings. Thus, adhesion and wettability are important issues as noted above. Therefore, efforts to improve the reactivity of these precursors with substrates can provide access to more uniform and adherent coatings. The $-[MeHSiO]_{0.3}[MeSi(O)_{1.5}]_{0.7}-$ copolymer could also be modified with acids (equation 46), to provide pendant SiO_2R groups (e.g. R = Pr) that appear to be more susceptible to hydrolysis than the OR groups. It was anticipated that surface hydroxyls would react faster with RCO_2Si groups to provide good adhesion, which proved to be the case[139].

$$-[MeHSiO]_{0.3}[MeSi(O)_{1.5}]_{0.7}- + RCO_2H \xrightarrow{\text{'Ti'/20 °C}} H_2 + -[Me(RCO_2)SiO]_{0.3}[MeSiO_{1.5}]_{0.7}- \qquad (46)$$

V. PRECURSORS TO Si−O CONTAINING MATERIALS

The development of processable organometallic and metalloorganic precursors to oxide materials that contain silicon has been very slow by comparison with development of precursors to nonoxide materials. This is chiefly a consequence of the exceptional success of sol-gel processing as a route to silicon containing ceramics[1,2,91]. However, sol-gel processing suffers some disadvantages that are difficult to overcome, especially in processing multimetallic materials. First, sol-gel processing relies on hydrolysis and condensation most commonly of $Si(OEt)_4$, TEOS. (Note that the methoxy derivative is poisonous.) However, when other metals are added, their hydrolysis and condensation rates are often orders of magnitude faster than that of TEOS. The end result is that atomic mixing, a primary motivation for using chemical processing, is lost. Alternately, the processing times required to retain atomic mixing become inordinately long. For example, the synthesis of atomically-mixed gel precursors to mullite ($2SiO_2{\cdot}3Al_2O_3$) requires hydrolysis/condensation times as long as one month[14−17]. Another problem is that processable (spinnable, coatable etc.) gel intermediates often have limited shelf life, because continued condensation eventually results in a three-dimensional, highly-crosslinked covalent network. While this is often desirable (see latent reactivity above), it means that new gels must be made up each time they are used.

In precursor processing, shelf life is rarely a problem as noncovalent bonding interactions between molecules and solvent content define processability. Furthermore, atomic mixing and multimetallic compounds are readily accessible as will be amply demonstrated below. Thus, there is recent interest in developing oxide precursors for processing multimetallic oxides. Our discussion begins with a few simple SiO_2 precursors, but the more important precursors are the multimetallic precursors covered afterward.

A. SiO_2 Precursors

Although a number of SiO_2 precursors are used industrially, most are used for CVD of silica insulating layers in electronic device manufacture[1]. As such, they will not be discussed here. Many of the silicon oxycarbide precursors discussed above can be oxidized to SiO_2 and thus can be considered precursors. However, this is simply a processing approach. The chemistry remains the same as described above. Thus, further discussion is not warranted.

The generation of controlled porosity materials for membrane applications, catalysis, controlled release, filtration and insulation (both thermal and electronic) represents an area of intense interest wherein chemical processing is essential. Precursors to pure SiO_2 are receiving particular attention in these areas[1]. Perhaps the most recent and important use of silica precursors (on a cost basis) is spin-on silica films for electronics applications[143–147]. There are two objectives in this area: One is to develop spin-on coatings not based on sol-gel because of shelf life issues as above, and the second is to develop lower dielectric insulators for ultrahigh density integrated circuits[143,145,146]. We begin by addressing the second application.

As the distance between features in electronic circuitry becomes smaller (0.35 μm is the next target), even low dielectric insulating materials such as silica start to offer sufficiently strong capacitance that crosstalk can occur between features. Current, insulating silica (gap fill and interlevel) dielectrics are produced by spinning on sol-gel solutions made from $Si(OEt)_4$ followed by exposure to an oxygen plasma or through the use of methylsilsesquioxane precursors (see above). The resulting materials have dielectric constants in the range $k = 2.9–3.1$[143,145,146]. However, if one could use silsesquioxanes of the type **10** and **11**, then the open structure (pore size *ca* 3.3 Å) will give a material that is mechanically strong but with a lower dielectric constant. A number of groups have now studied the utility of preparing silica dielectrics with one or other of these materials and report dielectric constants as low as $k = 2.2$ after curing in an oxygen plasma at temperatures <400 °C[145]. If dielectric constants can be lowered to 2.2–2.4 without a sacrifice in mechanical properties, then these types of material will facilitate the production of the next generation of ultra-high, large scale integrated circuits.

Both $H_8Si_8O_{12}$ and the related polymer (resin) are made by hydrolysis of $HSiCl_3$ under water-starved conditions. One method that gives high yields of the polyhedral

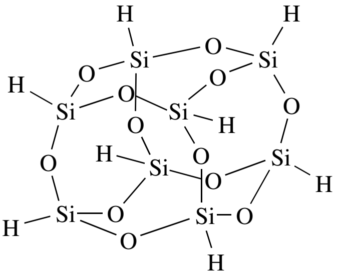

(10) T_8H_8

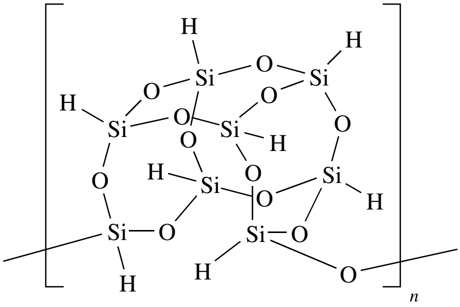

(11) Ring-opened polymer of T_8H_8

silsesquioxanes, developed by Agaskar, is shown in equation 47[148].

$$\begin{array}{lccc} HSiCl_3 + (FeCl_3{\cdot}H_2O) \longrightarrow & H_{10}Si_{10}O_{15} + & H_8Si_8O_{12} & + \text{resin} \\ & 5\% \text{ yield} & 20\% \text{ yield} & \textit{ca } 75\% \text{ yield} \end{array} \qquad (47)$$

All of the products dissolve in most organic solvents, although if the resin still retains Si−OH groups it can be expected to be less soluble. The resin is used for spin coating either as a toluene or heptane solution. Note that solvent volatility and ability to wet the coating substrate are important issues in determining whether or not a solvent and a precursor are useful. Another issue is the volatility of $H_8Si_8O_{12}$, which sublimes easily but has been used for both spin-on and CVD applications[149]. In air, $H_8Si_8O_{12}$ begins to decompose at *ca* 250 °C and converts to phase pure SiO_2 at approximately 400 °C, depending on the processing conditions[143]. One paper mentions a glass transition temperature at *ca* 250 °C, probably for the resin[145], which appears to be the basis of the Dow-Corning Flowable Oxide™ spin-on silica coating method[147]. At temperatures of 300 °C, following decomposition in oxygen, ^{29}Si MAS NMR spectroscopy suggests that the cubic structure (−83 ppm) of the starting material is retained in the resulting ceramic product. However, heating to 350 °C (0.5 h) converts the material to amorphous silica (−109 ppm). Thus, processing conditions are likely to be critical in achieving the desired drop in dielectric behavior.

Still another approach to developing spin-on silica precursors has been explored by Berry and Figge[146] and is based on unique *β*-haloethylsilsesquioxane resins. The key objective was to develop a processable silsesquioxane for spin-on glass applications that could be readily converted to pure silica at low-to-moderate temperatures. A critical step was to develop a 'mask' that provides processability but is easily removed without generating difficult-to-remove impurities. Hence, the mask must form an easily eliminated, volatile product on thermal or photochemical activation.

Based on these criteria, *β*-chloro- or *β*-bromoethyltrichlorosilanes are potentially attractive starting materials for this approach. First, because they are easily synthesized by equation 48 and then easily converted to the methoxy derivatives via equation 49. Finally, simple hydrolysis in methanol with a catalytic amount of HCl leads to a THF soluble gel (equation 50).

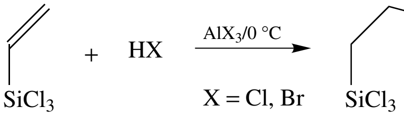

(48)

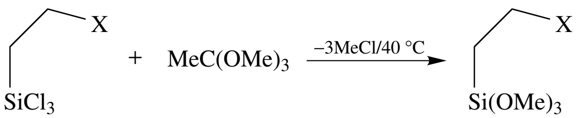

(49)

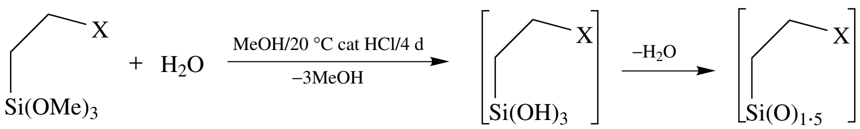

(50)

The resulting THF-soluble material is actually a low molecular weight oligomeric material that still retains some Si−OH groups. Molecular weight measurements indicate that the as-formed material consists of dimers, trimers and some high MW species; however, with time, continued condensation leads to materials with M_n *ca* 4k Da (after 70 d) that remain completely THF soluble.

The behavior of the β-chloro- and β-bromoethylsilsesquioxane on heating was studied by TGA. In a typical profile (10 °C per min/air/H_2O) mass loss onset for the β-chloro derivative occurs at 150 °C and coincides with detection of HCl and ethylene by mass spectrometry. The final ceramic yield was 52.5 wt% at 600 °C. A similar run in Ar gave a 63 wt% ceramic yield. The β-bromoethylsilsesquioxane exhibits, on heating, a nearly identical onset temperature with an 800 °C final ceramic yield of 38.5 wt% that reflects the higher mass of bromine. The primary decomposition process is thought to be as shown in equation 51. A second contributing mechanism is suggested to be that shown in equation 52.

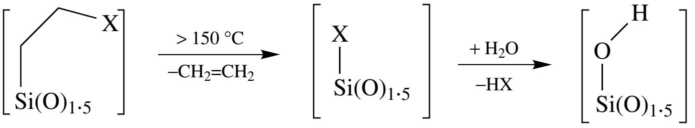

(51)

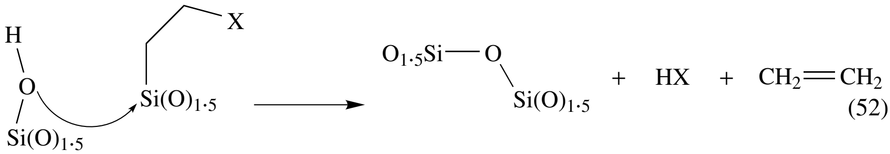

(52)

On heating bulk samples of the β-chloro derivative to 1000 °C (1 h/air/H_2O), the resulting material is a black glass with a $C_{0.45}SiO_{1.95}$ composition. Thus, the original goal of producing phase pure, spun-on SiO_2 was not met. However, when thin spun-on glass films (100s nm) were photochemically decomposed with a 193-nm UV laser (in air or Ar), 200−300 nm films with negligible carbon contents (below detection limit) could be produced, albeit with exposure times of up to 8 h. In contrast, similar films heated to 450 °C for *ca* 8 h still contain as much as 8 wt% carbon. Of notable interest is the fact that chlorine or bromine contamination was rarely evident. The key problem was a partitioning of the decomposition reaction between loss of HCl and ethylene and formation of Si−carbon−Si bridges by other mechanisms. Some of these mechanisms are common to alkyl silsesquioxane decomposition processes as seen in the preparation of SiO_xC_y materials, as discussed above.

Thus, high quality (high purity, uniform thickness, pore and defect-free) SiO_2 films for electronic applications remain a precursor and processing chemistry challenge. This challenge can be met, but the current solutions remain costly. Inexpensive precursors and processing methods remain viable targets for the materials chemist. One low-cost route to a processable SiO_2 precursor that may find use in some applications is discussed in the following paragraph.

A simple SiO_2 precursor can be made by direct reaction of SiO_2 with triethanolamine (equation 53)[72]. The resulting product, a silatrane glycol, **12**, forms quantitatively and can be recrystallized from hot ethylene glycol (EG) to give a high purity water-soluble precursor. **12** is an intermediate of considerable utility in the synthesis of aluminosilicate precursors (see below) but can also be used as a silica precursor. Thus, pyrolysis of a highly concentrated solution of **12** in ethylene glycol in a furnace preheated to 400−550 °C provides access to a carbon-contaminated porous material. Following oxidative removal of carbon at 450 °C, microporous silica can be made with specific surface areas (SSAs) as high as 570 m^2 g^{-1}[72]. These silicas are readily nitrided (NH_3) at low temperatures (700–800 °C) to produce SiON materials, as mentioned above.

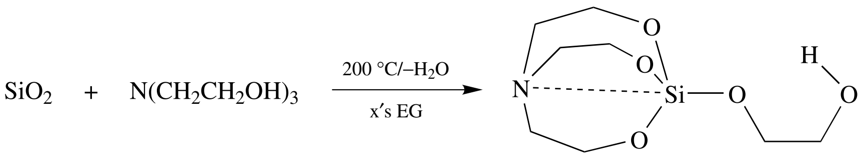

(**12**) (53)

One further comment on silatrane precursors. Frye and coworkers[149] report that several silatrane complexes, such as **12**, are soluble and quite stable in water. Thus, in principle, water-soluble silatranes can be used to minimize processing with organics and represent a 'green' or environmentally benign precursor (triethanolamine is used in cosmetics!).

B. Group I and II Silicate Precursors

Because group I and II silicates are readily available from commercial inorganic, high temperature reactions, there is no obvious need for precursors to these materials. Nonetheless, several precursors have been synthesized and their reactivity explored. A whole series of group I silicate precursors can be made via the general reaction shown in equation 54[150].

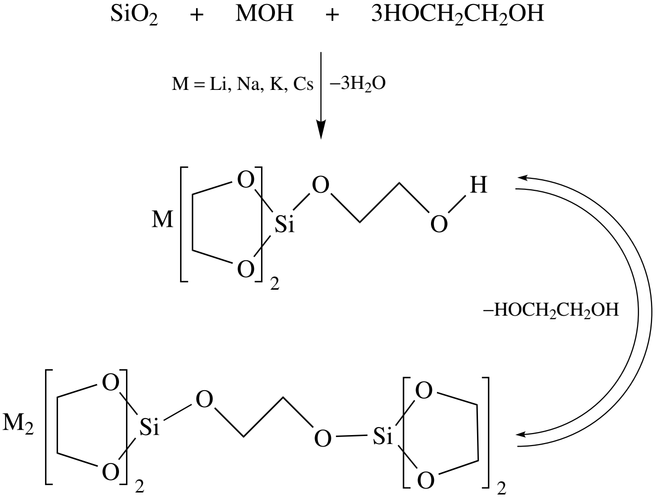

(54)

The yields of these compounds are nearly quantitative. Pyrolysis in air to 1000 °C gives the corresponding silicates quantitatively and usually phase pure[151]. Figure 9 shows the TGA of the monomeric lithium compound, $LiSi(OCH_2CH_2O)_2OCH_2CH_2OH$, on heating in air to 1000 °C. The ceramic yield is essentially that calculated for formation of phase pure $Li_2O{\bullet}2SiO_2$, although trace amounts of the $Li_2O{\bullet}SiO_2$ product are occasionally seen. BaO, CaO and (with difficulty) MgO can be made to work in reaction 55; however, if not done correctly, the reaction product is an unusual hexacoordinate complex[152].

These crystalline compounds are precursors to $MO{\bullet}2SiO_2$ if the pentacoordinate precursor is made and to $MO{\bullet}SiO_2$ if the hexacoordinated material is made[152]. On heating

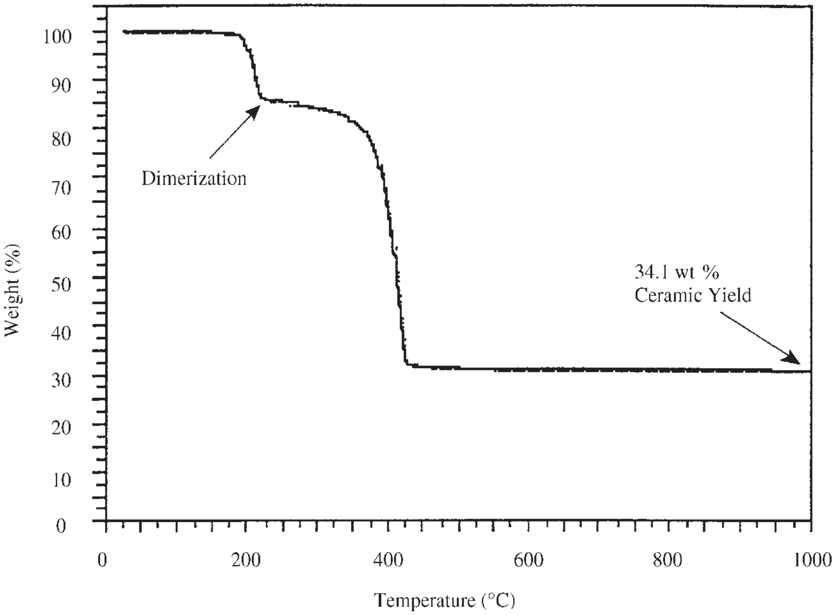

FIGURE 9. TGA of LiSi $(OCH_2CH_2O)_2OCH_2CH_2OH$ on heating in air to 1000 °C

in air these materials transform with the coincident formation of the amorphous metal carbonates, MCO_3, even if oxygen is used instead of air. Thus, processing temperatures close to the melting or decomposition temperature of the carbonates are required to produce the phase pure material.

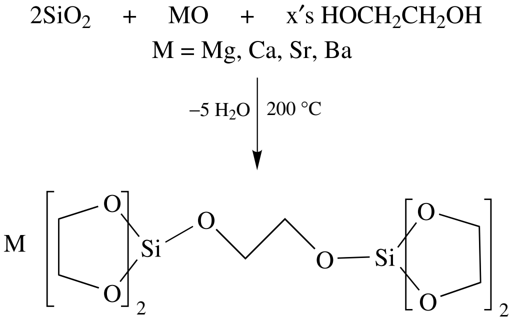

(55)

Because these compounds are crystalline, they offer no useful rheological properties. However, exchange with high diols (1,4-diols or longer) leads to formation of polymeric materials that are soluble in alcoholic solvents and offer the potential for coatings and membrane applications[153]. These precursors can be used to produce aluminosilicates, as discussed in the following sections. Although it has not been attempted, it is conceivable that by exchange with transition metals, these materials may provide access to transition metal silicate precursors (equation 56).

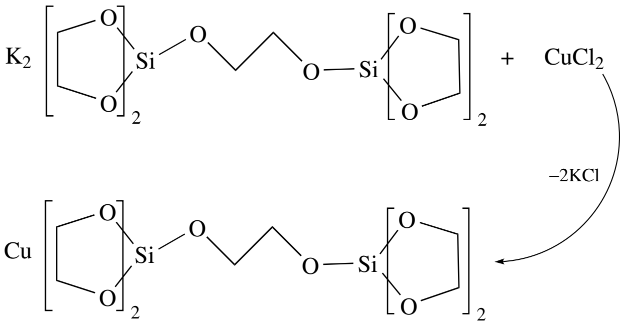

(56)

C. Precursors to Aluminosilicates

Although aluminosilicate double alkoxides have been available commercially for many years, their utility as direct precursors (via pyrolysis) to aluminosilicates has been poorly explored for the reasons stated above. One of the earliest studies in this area, from Tilley and coworkers, examined the use of compounds formed via equations 57 and 58[154].

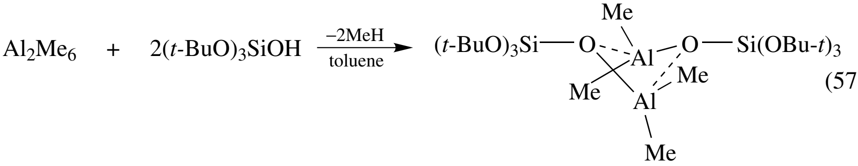

(57)

$$Al_2Si_2[O(t\text{-Bu})O]_2Me_4 + t\text{-BuOH} \xrightarrow[\text{toluene}]{-2\text{MeH}} MeAl[OSi(OBu\text{-}t)_3](OBu\text{-}t) \qquad (58)$$

These air- and moisture-sensitive compounds are soluble in most nonprotic organic solvents (presumably protic solvents will react). TGA studies on the first compound (O_2) show a rapid mass loss at 100–150 °C to give a ceramic yield of 30.9 wt% (at 1066 °C) vs an expected ceramic yield of 34.6 wt% for $Al_2O_3\text{•}2SiO_2$. Note that this is not a stoichiometry known for aluminosilicate line compounds. On heating to 1000 °C, partial crystallization of mullite ($3Al_2O_3\text{•}2SiO_2$) occurs, presumably with formation of amorphous silica. This dimer can also be thermally decomposed in refluxing toluene to generate materials with specific surface areas (SSAs) of 210 $m^2\,g^{-1}$ but containing 4 wt% carbon. Heating to 800 °C/O_2 actually causes an increase in SSA to 280 $m^2\,g^{-1}$ with a concomitant reduction in C content to 0.4 wt%.

TGA (O_2) of the second compound, MeAl[OSi(OBu-*t*)$_3$](OBu-*t*), gives a very similar decomposition profile with a ceramic yield (1017 °C) of 29.5 wt% vs a theoretical value of 29.3 wt% for $Al_2O_3\text{•}2SiO_2$. The decomposition process for both compounds is believed to occur by elimination of isobutene, methane and some water as discussed below for the Zr and Hf analogs.

A sample of MeAl[OSi(OBu-*t*)$_3$](OBu-*t*) heated to 200 °C for 1 h was found to exhibit SSAs of 270 $m^2\,g^{-1}$. Further heating to 800 °C for 1 h gave an SSA of 160 $m^2\,g^{-1}$ as some sintering of the original nanocrystalline product occurred. At temperatures $>$1000 °C, mullite starts to crystallize. The carbon content of these materials was $<$0.1 wt%.

Most recently, Roesky and coworkers described several elegant molecules of the type shown in equations 59 that offer potential as aluminosilicate precursors[155].

$$\mathrm{Me_4Al_2[OSi(OBu\text{-}\mathit{t})_2]_2} + 2\mathit{t}\text{-}\mathrm{BuOH} \xrightarrow[\mathrm{THF}]{-2\mathit{i}\text{-}\mathrm{BuH/H_2}} \mathrm{Me_2Al_2[OSi(OBu\text{-}\mathit{t})_2]_2(OBu\text{-}\mathit{t})_2} \tag{59}$$

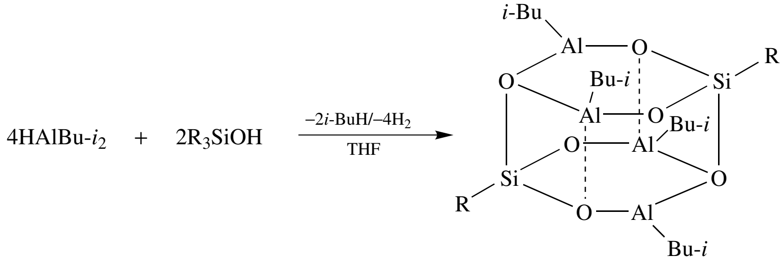

(60)

In principle these compounds offer access to materials with $Al_2O_3{\bullet}SiO_2$ and $Al_2O_3{\bullet}2SiO_2$ stoichiometries. The latter stoichiometry is equivalent to the Al[OSi(OBu-*t*)$_3$(OBu-*t*)] precursor. The major drawbacks with these materials are their air and moisture sensitivity, and the cost of the starting materials. Although the idealized stoichiometries of the above ceramics products are not those of crystalline aluminosilicates, amorphous aluminosilicate glasses are often important in optical applications or in scratch-resistant coatings. Furthermore, they may offer potential for CVD-type applications. There still remains considerable need for simple precursors to crystalline aluminosilicates, especially for structural applications. Dense, phase pure crystalline ceramic materials are desired for optimal mechanical properties, e.g. ceramic fibers for composite manufacture.

We recently described a general, low cost route to aluminosilicate precursors that permits control of precursor stoichiometry and processability[156–159]. This 'oxide one pot synthesis' (OOPS) approach basically evolved from several earlier studies, some of which are mentioned above. Thus, one can react any mixture of silica, $Al(OH)_3$ and a group I hydroxide, or group II oxide, in ethylene glycol with one equivalent of triethanolamine $[N(CH_2CH_2OH)_3]$ per metal. If this mixture is heated to the boiling point of ethylene glycol (*ca* 200 °C) such that byproduct water is removed by distillation, one forms a viscous, rheologically useful precursor to a ceramic with the stoichiometry of the initial ratio of oxides and hydroxides. To date, we have made precursors to mullite ($3Al_2O_3{\bullet}2SiO_2$), cordierite ($2MgO{\bullet}2Al_2O_3{\bullet}5SiO_2$), spinel ($MgO{\bullet}Al_2O_3$), group I aluminosilicates including ($M_2O{\bullet}Al_2O_3{\bullet}2SiO_2$) where M = Li, Na and K, and the group II aluminosilicates ($MO{\bullet}Al_2O_3{\bullet}2SiO_2$) where M = Mg, Sr and Ba. In some instances, molecular complexes form as found for the spinel precursor **14**, as per equation 61.

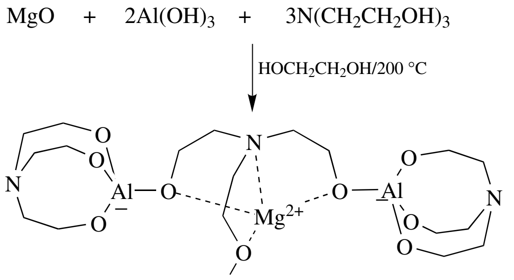

(61)

(14)

In the case of the alkali aluminosilicate complexes, NMR, mass spectrometry TGA ceramic yield and ceramic product purity analyses support the formation of simple trimetallic precursors of the type **15**.

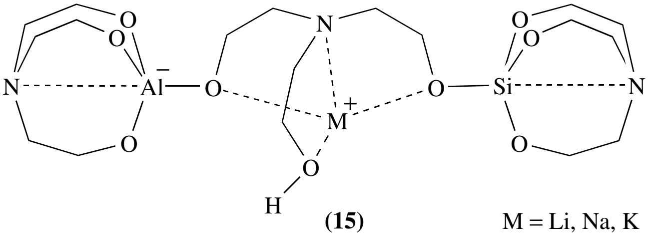

(15)

A related structure may form during the synthesis of group II analogs, as shown for the Ba complex **16**.

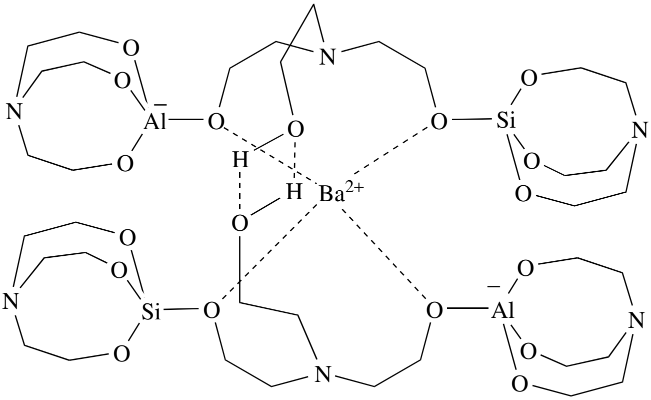

(16)

For other precursors, the polymer-like products appear to be simple, homogeneous mixtures of materials. Thus, the mullite precursor **17** likely consists of a 6 Al to 2 Si ratio.

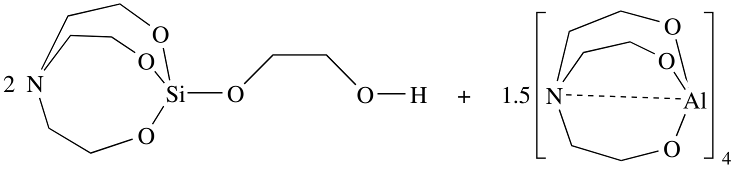

(17)

Note that reaction of $Al(OH)_3$ with triethanolamine produces a tetrameric alumatrane[159]. Despite the fact that this material is likely to be only a homogeneous mixture, it behaves as if it is atomically mixed. The following sections provide an example of how this mixture pyrolytically transforms to phase pure mullite. The purpose is to provide an example of how one establishes a processing window for conversion of a precursor to a desirable ceramic product. It also provides an example where instrumental analytical tools may fail to truly define what the actual ceramic products are. Thus, Figure 10 shows the TGA of the OOPS derived mullite precursor. The shown ceramic yield of only 23 wt% (vs *ca* 29 wt% theory) reflects the presence of residual ethylene glycol, which is difficult to remove even by vacuum drying, but its presence aids in providing desirable rheological properties.

Figure 11 shows the DTA of the precursor as it is heated in air (10 °C per min). Based on the TGA, most of the mass is actually lost before the first exotherm, maximum at *ca* 380 °C. Because this mass is associated with the decomposition of organic ligands, the first exotherm is only partly associated with oxidation of ligands as they decompose. This exotherm also appears to result partially from initial formation of an oxide network from the individual oxide fragments derived from the decomposition process. Indeed, a small exotherm is also seen in nitrogen which supports the contention that it is not indicative of oxidation. The second major exotherm centered at 610 °C arises as a result of char oxidation. Char forms as part of the ligand decomposition process (in air or nitrogen), which partitions between forming volatile fragments and crosslinked species. Although only a few wt% char material forms, it is actually the only serious drawback to using OOPS derived precursors. The final, very sharp exotherm at 990 °C is typical of crystallization of mullite and is often used as a primary indicator of mullite formation in atomically-mixed precursor systems.

The formation of mullite at *ca* 1000 °C is supported by the XRD data shown in Figure 12. Thus, based on DTA, TGA and XRD, one might decide that phase pure mullite without carbon contamination is produced by pyrolysis of precursor to 1000 °C. This then would represent a processing goal for making mullite materials. Also, it appears to be similar to the SiC precursor results, where nanocrystalline, phase pure SiC is obtained

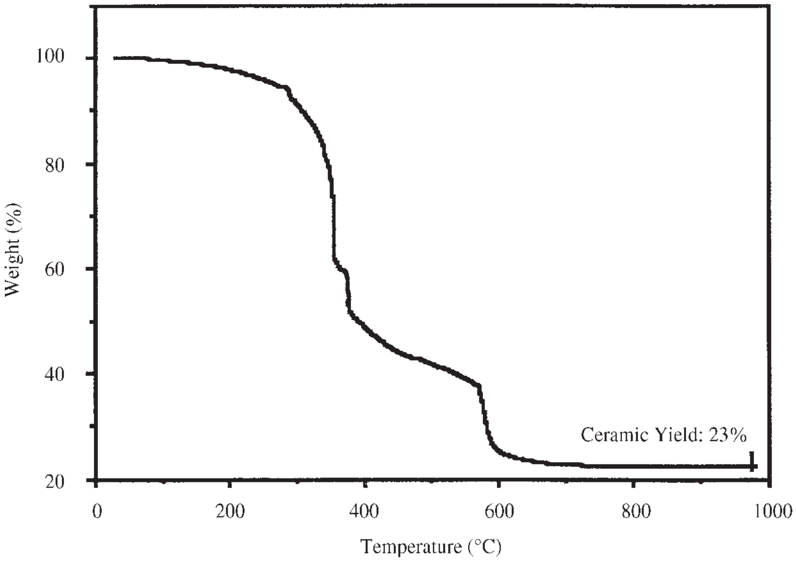

FIGURE 10. TGA of OOPS derived mullite precursor. The shown ceramic yield is only 23 wt% (vs. *ca* 29 wt% theory) owing to traces of excess ethylene glycol and triethanolamine retained in the sample to provide processability

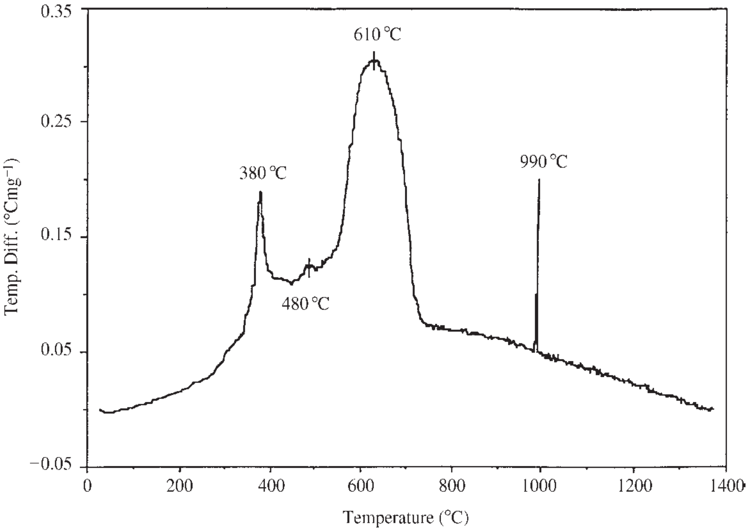

FIGURE 11. DTA (air/10 °C/min) of OOPS derived mullite precursor

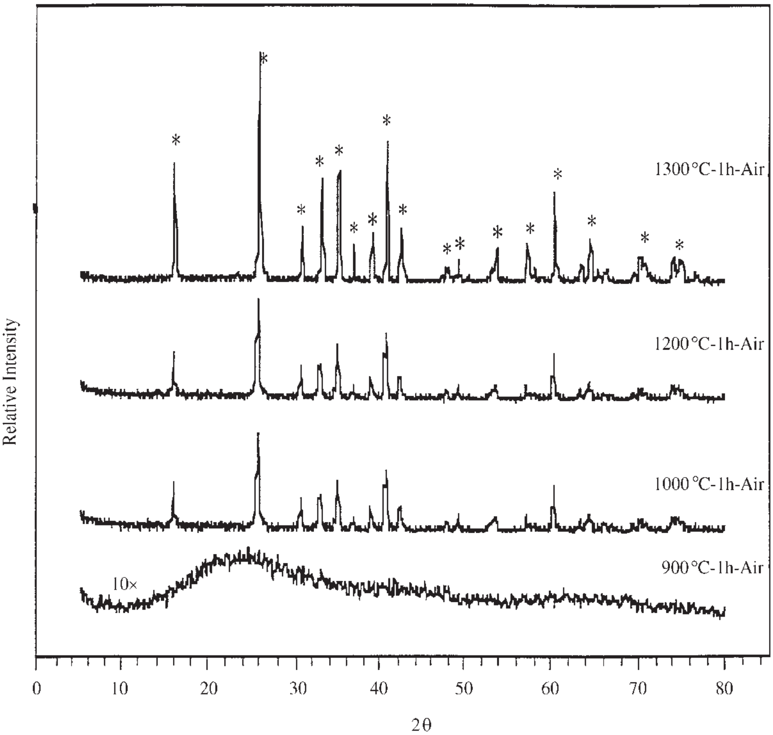

FIGURE 12. XRD of OOPS mullite precursor heated to selected temperatures (air/10 °C/min/1 h dwell)

at 1000–1200 °C. However, the diffuse reflectance IR (DRIFT) spectroscopy data tell another story as seen in Figure 13.

The DRIFT spectra show the typical broad peaks of an amorphous material up to approximately 1200 °C. Indeed, even at 1400 °C the sharp peaks indicative of a highly ordered, crystalline material are not really evident. These data suggest that the material is not particularly crystalline, possibly even up to 1400 °C. The solid state ^{29}Si MAS NMR data suggest the same thing as shown in Figure 14.

The spectra show an envelope of peaks resulting from nearly atomic mixing at the lowest temperatures. This envelope results from a statistical distribution of Al—O—Si linkages around tetrahedral silicon atoms, $Si(OAl)_{4-x}(OSi)_x$. Given that the Al : Si ratio is 3 : 1, then on average, each silicon will be surrounded by about 3 O—Al linkages — this is the maximum in intensity at temperatures below 950 °C. On moving above 950 °C, an unusual segregation occurs that leads to the formation of a poorly characterized, alumina rich, tetragonal mullite and nanoscale regions of pure silica. These react at higher temperatures to produce normal, orthorhombic mullite which is highly crystalline only at 1400 °C, as indicated by the sharp peaks finally seen in the NMR spectrum at this temperature. Thus, precursor processing may approach the correct material, but the final steps may require high temperature, post-pyrolysis heat treatments. The above material is presented in more detail elsewhere[157].

Only one paper that we are aware of explores a combined synthesis and processing route to aluminosilicates. Kemmitt and Milestone use precursors made by reaction of sodium hydroxide, boehmite $[Al(O)OH]_x$ and silica in ethylene glycol in a 4 : 3 : 1 ratio[160]. The precursor structures are related to those shown above. On removal of solvent (ethylene glycol) a glycolate precursor is obtained that contains a pentacoordinated

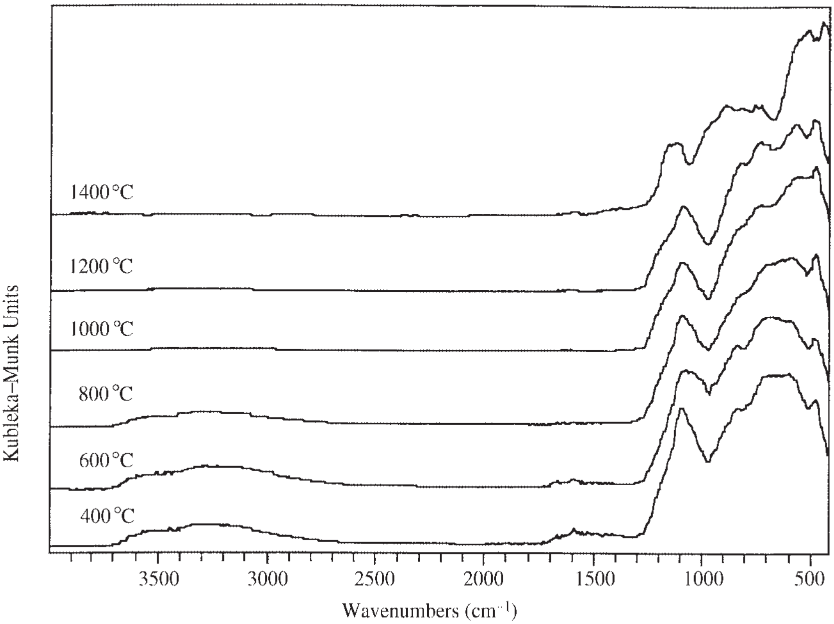

FIGURE 13. Diffuse reflectance infrared Fourier transform spectra of OOPS mullite precursor heated to selected temperatures (air/10 °C/min/1 h dwell)

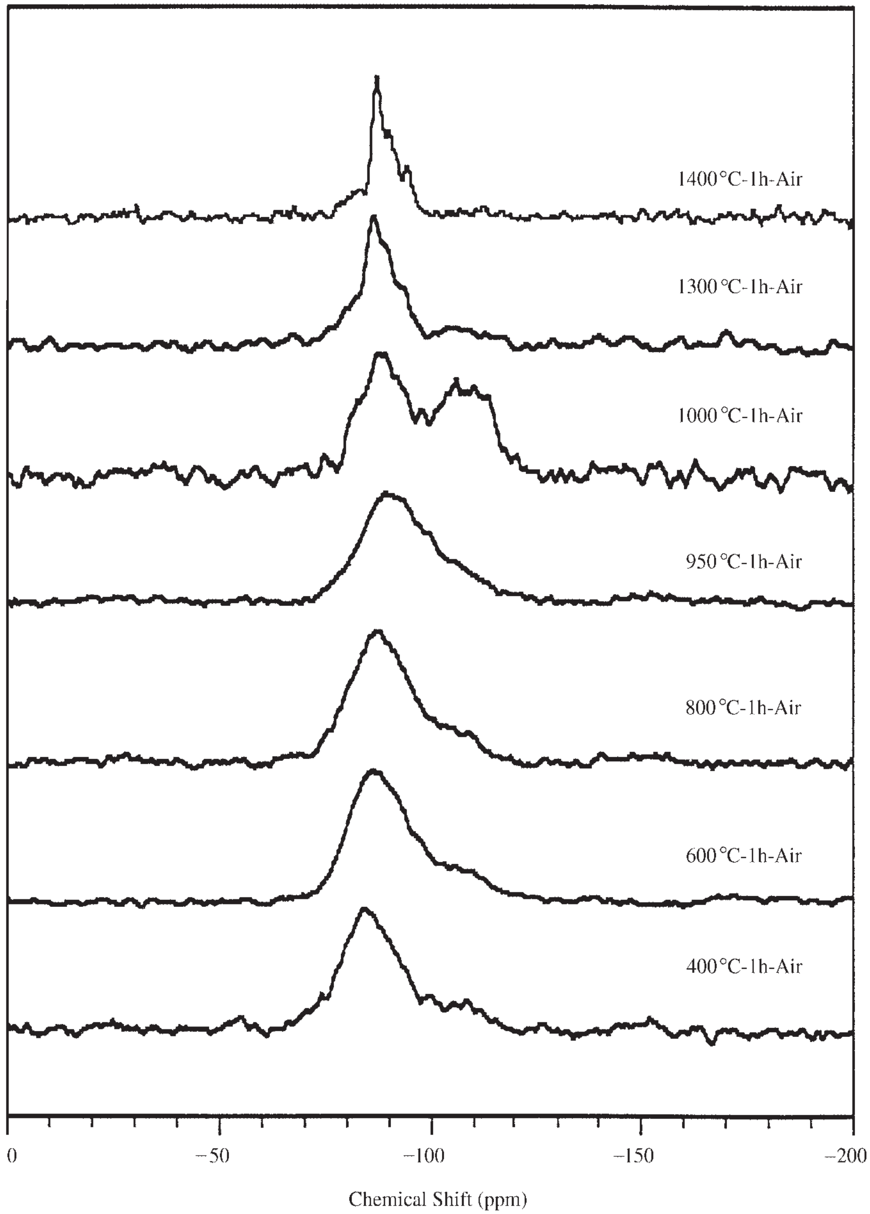

FIGURE 14. Solid state ^{29}Si MAS NMR spectra of OOPS mullite precursor heated to selected temperatures (air/10 °C/min/1 h dwell). Note the segregation that occurs at 1000 °C and the final appearance of crystalline mullite only at 1400 °C

silicon as determined by solid state MAS NMR spectroscopy (−103.8 ppm for ^{29}Si), and octahedral and tetrahedral Al (4.3 and 53 ppm for ^{27}Al) with the tetrahedral species being approximately three times as abundant. On pyrolysis of this precursor at 400, 500 or 950 °C the material transforms first to a mostly amorphous material at 400 °C, and then to a crystalline material with a composition $4Na_2O{\cdot}3Al_2O_3{\cdot}2SiO_2$.

The unusual step occurs when the authors treat the 400 °C material with SO_2 for 4 h which converts all of the Na present to Na_2SO_4. The Na_2SO_4 is simply washed away with water and the resulting amorphous material then has the $3Al_2O_3{\cdot}2SiO_2$ composition which is that of mullite. Heating the amorphous material to 1200 °C for 16 h produces the desired mullite.

Finally, it is worth noting that the mullite precursors shown above can be made at the kilogram scale in a matter of hours, whereas sol-gel derived materials can require up to one month to obtain atomically mixed gels. To date, no attempts have been made to form transition metal precursors via the OOPS or the Kemmitt and Milestone processes. However, the following section suggests that there are good reasons to explore this approach.

D. Precursors to Transition Metal Silicates

The earliest work in the development of simple molecular precursors to transition metal silicates is that of Hrncir and Skiles[161]. These workers report that the reaction of silanols with metal alkyls provides a low temperature, clean, quantitative route to pure Zr and Hf metallasiloxanes:

$$M(CH_2SiMe_3)_4 + 4R_3SiOH \xrightarrow{0-25\,^{\circ}C} 4SiMe_4 + M(OSiR_3)_4 \qquad (62)$$
$$M = Hf, Zr$$

The resulting moisture-sensitive compounds, $M(OSiR_3)_4$, are liquids when R = Et, and solids when the R groups are Me/*t*-Bu, Me/Ph or Ph. Those compounds with some R = Me groups are soluble in aromatic solvents, whereas those where R = Ph are insoluble.

On heating to 700 °C, all of the compounds decompose to white, insoluble products. The decomposition process was followed by IR and appears to begin with partial decomposition at 160 °C that retains most of the spectrum seen in the as-prepared product, with the exception of an additional Zr−O−Si stretching band at 970 cm^{-1}. At 350 °C, all resemblance to a molecular material is lost and broad, featureless spectra are observed which remain unchanged to 700 °C.

TGA analysis of the decomposition process for the Hf (R = Ph) compound suggests the stoichiometric conversion shown in equation 63.

$$Hf(OSiPh_3)_4 \xrightarrow{600\,^{\circ}C/air/1\ h} HfSi_4O_{10} \qquad (63)$$

ESCA indicates that only 2% carbon remains following pyrolysis; it also reveals a Si (2p) binding energy of 104.2 eV, which is higher than that found for silica (103.5 eV). This change in binding energy may be attributable to the influence of Hf−O−Si linkages. Unfortunately, substantiation via XRD was not possible as the material was X-ray amorphous.

Recent work by Terry and Tilley describes the preparation and pyrolytic behavior of the related $M[OSi(OBu\text{-}t)_3]_4$ (M = Ti, Zr, Hf) precursors. The $M[OSi(OBu\text{-}t)_3]_4$ compounds were prepared by reaction of the silanol with a metal amide[162,163] (equations 64 and 65).

$$Ti(NMe_2)_4 + 4(t\text{-}BuO)_3SiOH \xrightarrow{110\,^{\circ}C/PhMe} 4HNMe_2 + Ti[OSi(OBu\text{-}t)_3]_4 \qquad (64)$$

$$\mathrm{M(NEt_2)_4} + 4t\text{-}\mathrm{BuO_3SiOH} \xrightarrow{0-20\,^\circ\mathrm{C/pentane}} 4\mathrm{HNEt_2} + \mathrm{M[OSi(OBu}\text{-}t)_3]_4 \quad (\mathrm{M} = \mathrm{Zr, Hf}) \tag{65}$$

The Ti and Hf compounds are monomers, whereas the Zr complex was dimeric. As found by Hrncir and Skiles, the series of $\mathrm{M[OSi(OBu}\text{-}t)_3]_4$ compounds are all moisture-sensitive. TGA studies indicate that the Ti complex decomposes cleanly at temperatures >240 °C and gives a ceramic yield of 25 wt% whereas the theoretical ceramic yield for $\mathrm{TiSiO_4}$ should be 29.07 wt%. The primary gaseous thermolysis products were identified by mass spectroscopy to be isobutene and water. A likely pathway for decomposition appears to involve β-hydrogen elimination followed by condensation of the resulting Si—OH groups to generate isobutene, water and an oxide network as shown in equations 66 and 67.

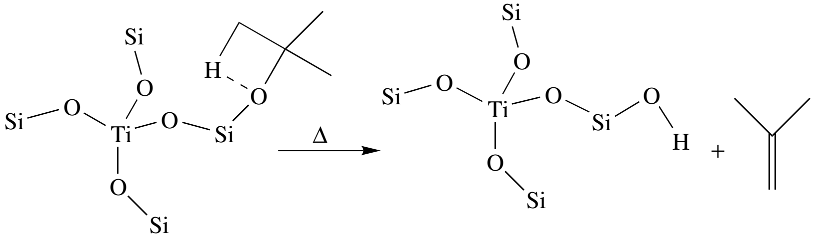

(66)

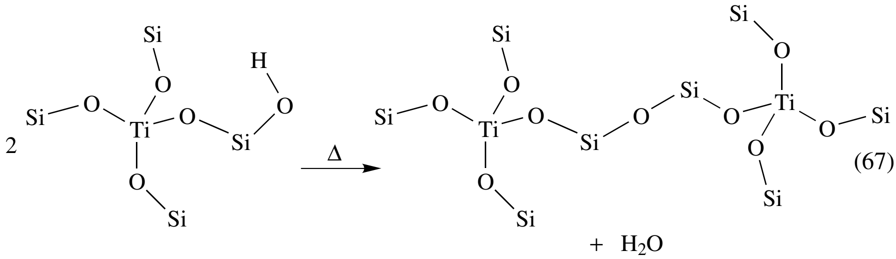

(67)

On heating to higher temperatures, no crystalline phases are observed until anatase crystallizes at 1000 °C. At 1400 °C, anatase, rutile and crystobalite are the only products. No single-phase material is obtained. The lack of correspondence between the TGA ceramic yield and the theoretical ceramic yield calculated for $\mathrm{TiSiO_4}$ presages this problem. The exact reasons for the formation of a mixed-oxide phase are unknown at the moment, but they clearly contrast with the behavior of the Zr and Hf analogs.

The Zr and Hf compounds decompose cleanly at much lower temperatures (*ca* 140 °C) and give ceramic yields that are expected assuming $\mathrm{MSiO_4}$ is the product. Heating to 400 °C generates amorphous, $\mathrm{MSiO}_x\mathrm{(OH)}_y$ materials with surface areas of 500 $\mathrm{m^2\,g^{-1}}$. These materials are potentially interesting as catalysts or catalyst supports.

On heating to 1500 °C/6 h/Ar, the Zr material crystallizes to a mixture of monoclinic and tetragonal zirconia and crystobalite with loss of considerable original surface area (36 $\mathrm{m^2\,g^{-1}}$). The Hf material behaves similarly, although it partially crystallizes at 1000 °C to produce cubic or tetragonal hafnia. Cristobalite is only observed in materials heated to 1400 °C. Finally, thin films of the Zr and Hf derivatives could be cast from hydrocarbon solutions on quartz and then converted to thin films of the corresponding amorphous or ceramic materials.

A related study explores the use of $\mathrm{OSi(OBu}\text{-}t)_3$ chemistry, to prepare manganese-doped zinc orthosilicates, e.g. $\mathrm{Zn_2SiO_4}$ (willemite) which are used in electroluminescent devices. Two types of precursors were prepared, two molecular compounds and a set of oligomers (equations 68–70).

$$2\mathrm{Me_2Zn} + 2\mathrm{HOSi(OBu\text{-}\mathit{t})_3} \xrightarrow{-78\,^{\circ}\mathrm{C/toluene}} 2\mathrm{MeH} + [\mathrm{MeZnOSi(OBu\text{-}\mathit{t})_3}]_2 \qquad (68)$$

$$\mathrm{Me_2Zn} + 2\mathrm{HOSi(OBu\text{-}\mathit{t})_3} \xrightarrow{-78\,^{\circ}\mathrm{C/toluene}} 2\mathrm{MeH} + \mathrm{Zn[OSi(OBu\text{-}\mathit{t})_3]_2} \qquad (69)$$

$$\mathrm{Me_2Zn} + \mathrm{(HO)_2Si(OBu\text{-}\mathit{t})_2} \xrightarrow{-40\,^{\circ}\mathrm{C/toluene}} 2\mathrm{MeH} + [\mathrm{ZnOSi(OBu\text{-}\mathit{t})_2O}]_n \qquad (70)$$

At set of toluene soluble oligomers of the type shown in equation 70 were made with various metal to silane diol ratios in order to achieve the appropriate Zn_2SiO_4 stoichiometry. The oligomer molecular weights varied from $M_n = ca$ 1.8 kDa to 11 kDa, as determined by NMR end group analysis.

Based on work done with the precursors synthesized in equations 57 and 58, these precursors were all assumed (and found) to decompose in a similar manner. The air- and moisture-sensitive dimer decomposes readily in the 100–250 °C range with a found ceramic yield of 22 wt%, which is close to the 24 wt% calculated for $Zn_2SiO_4{\bullet}SiO_2$ by equation 71. Pyrolysis to 1100 °C for 1 h generated willemite (by XRD). No crystalline SiO_2 compound was observed coincidentally.

$$[\mathrm{MeZnOSi(OBu\text{-}\mathit{t})_3}]_2 \xrightarrow{>100\,^{\circ}\mathrm{C}} \mathrm{Zn_2SiO_4{\bullet}SiO_2} + 2\mathrm{HOSi(OBu\text{-}\mathit{t})_3} + \mathrm{CH_2{=}CMe_2} + \mathrm{H_2O} + \mathit{t}\text{-}\mathrm{BuOH} \qquad (71)$$

As with the dimeric compound, the oligomers decompose in the 100–250 °C temperature range. However, unlike the dimer, $HOSi(OBu\text{-}t)_3$ is not observed as a pyrolysis product. One oligomer, with a chemical composition close to $C_8H_{18}O_4SiZn$, gave a 230 °C ceramic yield of 52.1 wt%, which is in good agreement with the 52.2 wt% calculated ceramic yield for $Zn_2SiO_4{\bullet}SiO_2$. However, mass loss continues with further heating. Thus, the 1110 °C/Ar ceramic yield is 48 wt% and at 1350 °C it is 42.5 wt%. The 1100 °C ceramic product composition was $(Zn_2SiO_4)_{0.37}(SiO_2)_{0.41}$ suggesting that some Zn is lost. This material contains <0.2 wt% carbon and <0.1 wt% H, thus the source of the *ca* 6 wt% change between 1100 and 1350 °C is not clear.

XRD analysis of the polymer pyrolysis products reveals formation of partially crystalline Zn_2SiO_4 on heating to $\geqslant$ 850 °C/2 h/Ar as expected based on an 800 °C exotherm seen in the DTA profile. SEMs of materials heated to 1350 °C indicate formation of a glassy material, although no XRD data are provided[162,163]. The authors point out that the melting points for cristobalite and α-Zn_2SiO_4 are 1713 °C and 1512 °C, respectively. Thus, there appears to be no explanation for the formation of the glassy phase. However, the almost 6 wt% mass change that occurs on heating to 1350 °C might result from loss of Zn metal (reduced by residual C/H) or loss of volatile SiO. More work needs to be done to understand this process.

Finally, polymer blends were prepared by mixing $[ZnOSi(OBu\text{-}t)_2O]_n$ with $Mn(CH_2SiMe_3)_2$ in diethyl ether in 1–15 wt% amounts in order to develop an electroluminescent precursor. Pyrolysis of these blends at 1000 °C/Ar produced materials which showed no evidence of segregated Mn containing phases at <3 wt% Mn. At higher concentrations ω-MnO_2 was observed to form. The resulting materials offer the desired photoluminescent properties, although more emission lines were observed than anticipated.

The absence of ZnO in any of the materials produced via these types of precursors suggests that, at least initially, atomic mixing is achieved. At higher temperatures, where segregation is seen, thermodynamics may play a role in driving phase segregation. The fact that exact stoichiometry precursors were not prepared may also strongly influence the final products and microstructures observed. Further precursor design studies are likely to sort out these problems.

VI. REFERENCES

1. (a) C. J. Brinker and G. Scherer, *Sol-Gel Science: The Physics and Chemistry of Sol-Gel Processing*, Academic Press, Boston, 1990.
   (b) D. Avnir, L. C. Klein, D. Levy, U. Schubert and A. B. Wojork, Chapter 40 of this book
2. *Journal of Sol-Gel Science and Technology*, Elsevier.
3. C. K. Narula, *Ceramic Precursor Technology and Its Applications*, M. Dekker, New York, 1995.
4. (a) K. Wynne, M. Zeldin and H. Allcock (Eds.), *Inorganic and Organometallic Polymers*, Am. Chem. Soc. Symp. Ser. Vol. 360, Am. Chem. Soc., Washington D.C., 1988.
   (b) K. Wynne, P. W. Nielson and H. Allock (Eds) *Inorganic and Organometallic Polymers II*, Am. Chem. Soc. Symp. Ser., Vol. 572, Am. Chem. Soc., Washington D.C. 1994.
5. (a) R. M. Laine (Ed.), *Transformation of Organometallics into Common and Exotic Materials: Design and Activation*, NATO ASI Ser. E: Appl. Sci.-No., Vol. 141, Kluwer Publ., Dordrecht, 1988.
   (b) R. M. Laine (Ed.), *Inorganic and Organometallic Polymers with Special Properties*, NATO ASI Ser. E: Appl. Sci.-No., Vol. 206, Kluwer Publ., Dordrecht, 1991.
   (c) J. F. Harrod and R. M. Laine (Eds.), *Applications of Organometallic Chemistry in the Preparation and Processing of Advanced Materials*, NATO ASI Ser. E: Appl. Sci.-No., Vol. 297, Kluwer Publ., Dordrecht, 1995.
6. (a) M. Birot, J-P. Pillot and J. Dunogues, *Chem. Rev.*, **95**, 1443 (1995).
   (b) K. J. Wynne and R. W. Rice, *Annu. Rev. Mater. Sci.*, **14**, 297 (1984).
   (c) R. R. Wills, R. A. Markle and S. P. Mukherjee, *Ceram. Bull.*, **62**, 904 (1983).
   (d) R. H. Baney and G. Chandra, in *Encyclopedia of Polymer Science and Engineering*, Vol 13, Wiley, New York, 1988, pp. 312–344.
   (e) J. Bill and F. Aldinger, *Adv. Mater.*, **7**, 775 (1995).
   (f) W. Toreki, *Polym. News*, **16**, 6 (1991).
   (g) G. Pouskouleli, *Ceram. Int.*, **15**, 213 (1989).
7. R. M. Laine and F. Babonneau, *Chem. Mater.*, **5**, 260 (1993).
8. J. A. Reed, *Principles of Ceramic Processing*, Second ed., Wiley Interscience, New York, 1995, p.57.
9. R. M. Laine, Z.-F. Zhang, K. W. Chew, M. Kannisto and C. Scotto, in *Ceramic Processing Science and Technology* (Eds. H. Hausner, G. Messing and S. Hirano), Am. Ceram. Soc., Westerville, OH, 1995, pp. 179–186.
10. C. D. Han, *Rheology in Polymer Processing*, Academic Press, New York, 1976.
11. A. Ziabicki, *Fundamentals of Fiber Formation*, Wiley, New York, 1976.
12. P. Calvert and M. J. Cima, *J. Am. Ceram. Soc.*, **73**, 575 (1990).
13. M. J. Cima, J. A. Lewis and A. D. Devoe, *J. Am. Ceram. Soc.*, **72**, 1192 (1989).
14. C. Gerardin, S. Sundaresan, J. Benziger and A. Navrotsky, *Chem. Mater.*, **6**, 160 (1994).
15. D. X. Li and W. J. Thomson, *J. Mater. Res.*, **6**, 819 (1991).
16. (a) J. C. Huling and G. Messing, *J. Non-Cryst. Solids*, **147**, 213 (1992).
    (b) J. C. Huling and G. L. Messing, *J. Am. Ceram. Soc.*, **72**, 1725 (1989).
17. P. Kansal, R. M. Laine and F. Babonneau, *J. Am. Ceram. Soc.*, **80**, 2597 (1997).
18. M. Scarlete, J. He, J. F. Harrod, and I. S. Butler, in *Applications of Organometallic Chemistry in the Preparation and Processing of Advanced Materials*, NATO ASI Ser. E: Appl. Sci.-Vol. 297 (Eds. J. F. Harrod and R. M. Laine), Kluwer Publ., Dordrecht, 1995, pp. 125–140 and references cited therein.
19. Z-F. Zhang, S. Scotto and R. M. Laine, *Ceram. Eng. Sci. Proc.*, **15**, 152 (1994).
20. F. Wakai, Y. Kodama, S. Sakaguchi, N. Murayama, K. Izaki and K. Niihara, *Nature* **344**, 421 (1990).
21. R. M. Laine, F. Babonneau, K. Y. Blohowiak, R. A. Kennish, J. A. Rahn, K. F. Waldner and G. J. Exarhos, *J. Am. Ceram. Soc.*, **78**, 137 (1995).
22. K. Su, E. E. Remsen, G. A. Zank and L. G. Sneddon, *Chem. Mater.*, **5**, 547 (1993).
23. (a) O. Funayama, M. Arai, Y. Tashiro, H. Aoki, T. Suzuki, K. Tamura, H. Kaya, H. Nishii and T. Isoda, *Nippon Seram. Kyokai, Gaku. Ron.*, **98** 104 (1990); *Chem. Abstr.* **111**, 218411s (1990).
    (b) H. Aoki, T. Suzuki, T. Katahata, M. Haino, G. Nishimura, H. Kaya, T. Isoda, Y. Tashiro, O. Funayama and M. Arai, European patent application 89302178.2; date of filing 03/03/89. Publication No. 0 332 357.
24. R. M. Laine, Y. Blum, D. Tse and R. Glaser, in *Inorganic and Organometallic Polymers*, Am. Chem. Soc. Symp. Ser. Vol. 360 (Eds. K. Wynne, M. Zeldin and H. Allcock), 1988, pp. 124–142.

25. (a) D. Seyferth, G. H. Wiseman and C. C. Prud'homme, *J. Am. Ceram. Soc.*, **66**, C-13 (1983).
(b) D. Seyferth and G. H. Wiseman, in *Ultrastructure Processing of Ceramics and Composites* (Eds. L. L. Hench and D. R. Ulrich), Wiley, New York, 1984, p. 265.
(c) D. Seyferth and G. H. Wiseman, in *Ultrastructure Processing of Ceramics and Composites II* (Eds. J. D. Mackenzie and D. R. Ulrich), Chap. 38, Wiley, New York, 1987.
(d) D. Seyferth, in *Transformation of Organometallics into Common and Exotic Materials: Design and Activation*, NATO ASI Ser. E: Appl. Sci.-No. Vol. 141 (Ed. R. M. Laine), Kluwer Publ., Dordrecht, 1988, pp. 133–154 and references cited therein.
(e) D. Seyferth, H. Plenio, W. S. Rees and K. Büchner. *Frontiers of Organosilicon Chemistry* (Eds. A. R. Bassindale and P. P. Gaspar), Royal Society of Chemistry, London, 1991, pp. 15–27.
26. N.S.C. K. Yive, R. Corriu, D. Leclercq, P. H. Mutin and A. Voiux, *New J. Chem.*, **15**, 85 (1991).
27. (a) G. T. Burns, T. P. Angelotti, L. F. Hanneman, G. Chandra and J. A. Moore, *J. Mater. Sci.*, **22**, 2609 (1987).
(b) Y. Abe, T. Ozai, Y. Kumo, Y. Nagao and T. Misono, *J. Inorg. Organomet. Polym.*, **2**, 143 (1992).
28. (a) R. M. Laine, *Platinum Met. Rev.*, **32**, 64 (1988).
(b) Y. D. Blum, K. B. Schwartz and R. M. Laine, *J. Mater. Sci.*, **24**, 1707 (1989).
(c) K. A. Youngdahl, R. M. Laine, R. A. Kennish, T. R. Cronin and G. A. Balavoine, in *Better Ceramics Through Chemistry III.* Mat. Res. Symp. Proc. Vol. 121 (Eds. C. J. Brinker, D. E. Clark and D.R. Ulrich), 1988 pp. 489–495.
(d) Y. D. Blum and R. M. Laine, *Organometallics*, **5**, 2801 (1986).
29. (a) H. Q. Liu and J. F. Harrod, *Organometallics*, **11**, 822 (1992).
(b) J. He, H. Q. Liu, J. F. Harrod and R. Hynes, *Organometallics*, **13**, 336 (1994).
30. (a) E. Duguet, M. Schappacher and A. Soum, *Macromolecules*, **25**, 4835 (1992).
(b) E. Duguet, M. Schappacher and A. Soum, WO 92/17527, PCT/FR92/0300 Oct. 15, 1992.
31. (a) C. R. Blanchard and S. T. Schwab, *J. Am. Ceram. Soc.*, **77**, 1729 (1994).
(b) S. T. Schwab, R. C. Graef, Y. M. Pan and D. L. Davidson, NASA Conf. Publ., CP-3175 [Part 2], 721 (1992).
(c) S. T. Schwab, C. R. Blanchard and R. C. Graef, *J. Mater. Sci.*, in press.
32. (a) T. Isoda, H. Kaya, H. Nishii, O. Funayama, T. Suzuki and Y. Tashiro, *J. Inorg. Organomet. Polym.*, **2**, 151 (1992).
(b) M. Arai and T. Isoda, Japan Patent JP. 145903 (1985) *Chem. Abstr.*, **104**, 36340r (1985).
(c) M. Arai, S. Sakurada, T. Isoda and T. Tomizawa, *Am. Chem. Soc., Polym. Div., Polym. Prepr.*, **27**, 407 (1987).
(d) T. Isoda, in *Silicon Nitride Ceramics 2* (Eds. M. Mitomo and S. Somiya) U. Rokakuho 45 (1990).
(e) Tonen technical data sheets, 9104 series.
33. G. T. Burns and G. Chandra, *J. Am. Ceram. Soc.*, **72**, 333 (1989).
34. T. Taki, M. Inui, K. Okamura and M. Sato, *J. Mater. Sci. Lett.*, **8**, 1119 (1989).
35. W. R. Schmidt, P. S. Marchetti, L. V. Interrante, W. J. Hurley, R. H. Lewis, R. H. Doremus and G. E. Maciel, *Chem. Mater.*, **4**, 937 (1992).
36. M. Peukert, T. Vaahs and M. Brück, *Adv. Mater.*, **2**, 398 (1990).
37. (a) S. Schaible, R. Riedel, E. Werner and U. Klingebiel, *Appl. Orgnaomet. Chem.*, **7**, 53 (1993).
(b) R. Riedel and M. Seher, *J. Eur. Ceram. Soc.*, **7**, 21 (1991).
38. L. Maya, D. R. Cole and E. W. Hagaman, *J. Am. Ceram. Soc.*, **74**, 1686 (1991) and references cited therein.
39. (a) W. Verbeek, U. S. Patent No. 3, 853, 567 (Dec. 1974).
(b) G. Winter, W. Verbeek and M. Mansmann, U. S. Patent No. 3,892,583 (July 1975).
40. (a) B. G. Penn, F. E. Ledbetter III and J. M. Clemons, *Ind. Eng. Chem., Process Des. Dev.*, **23**, 217 (1984).
(b) B. G. Penn, J. G. Daniels, F. E. Ledbetter and J. M. Clemons, *Polym. Eng. Sci.*, **26**, 1191 (1986).
(c) B. G. Penn, F. E. Ledbetter III, J. M. Clemons and J. G. Daniels, *J. Appl. Polym. Sci.*, **27**, 3751 (1982).
41. D. M. Narsavage, L. V. Interrante, P. S. Marchetti and G. E. Maciel, *Chem. Mater.*, **3**, 721 (1991).
42. D. Seyferth, C. Strohmann, N. R. Dando and A. J. Perrotta, *Chem. Mater.*, **7**, 2058 (1995).
43. N. R. Dando, A. J. Perrotta, C. Strohmann, R. M. Stewart and D. Seyferth, *Chem. Mater.*, **5**, 1624 (1993).

44. (a) Y. D. Blum, K. B. Schwartz, E. J. Crawford and R. D. Hamlin, in *Better Ceramics Through Chemistry III*, MRS Symp. Proc. Vol. 121 (Eds. C. J. Brinker, D. E. Clark and D. R. Ulrich), Mater. Res. Soc., Pittsburgh, 1988, pp. 565–570.
    (b) Y. D. Blum, S. M. Johnston and G. A. McDermott, in *Science, Technology, and Commercialization of Powder Synthesis and Shape Forming Processes* (Eds. J. J. Kingsley, C. H. Schilling and J. H. Adair), *Ceramic Trans.*, **62**, 67 (1996).
    (c) J. T. McGinn, Y. Blum, S. M. Johnson, M. I. Gusman and G. A. McDermott, in *Better Ceramics Through Chemistry VI*, MRS Symp. Proc. Vol. 346 (Eds. A. K. Cheetham, C. J. Brinker, M. L. Mecartney and C. Sanchez), Mater. Res. Soc., Pittsburgh, 1994, pp. 409–414.
45. (a) G. E. Legrow, T. F. Lim, J. Lipowitz and R. S. Reaoch, *Am. Ceram. Soc. Bull.*, **66**, 363 (1987).
    (b) J. Lipowitz, H. A. Freeman, R. T. Chen and E. R. Prack, *Adv. Ceram. Mater.*, **2**, 121 (1987).
    (c) G. E. Legrow, T. F. Lim, J. Lipowitz and R. S. Reaoch, *Am. Ceram. Soc. Bull.*, **66**, 363 (1987).
    (d) G. E. Legrow, T. F. Lim and J. Lipowitz, *J. Chim. Phys.*, **83**, 869 (1986).
46. F. Siriex, P. Goursat, A. Lecomte and A. Dauger, *Compos. Sci. Tech.*, **37**, 7 (1990).
47. (a) N. S. C. K. Yive, R. J. P. Corriu, D. Leclercq, P. H. Mutin and A. Voiux, *Chem. Mater.*, **4**, 141 (1992).
    (b) N. S. C. K. Yive, R. J. P. Corriu, D. Leclercq, P. H. Mutin and A. Vioux, *Chem. Mater.*, **4**, 1263 (1992).
48. T. Vaahs, Hoechst High Chem, Polysilazane ET 70, VT 50 Facts Sheets, AFE 23 25e, 1990.
49. (a) R. Riedel, A. Kienzle and M. Fuess, in *Applications of Organometalic Chemistry in the Preparation and Processing of Advanced Materials*, NATO ASI Ser. E: Appl. Sci.-Vol. 297 (Eds. J. F. Harrod and R. M. Laine) Kluwer Publ., Dordrecht, 1995, pp. 155–171 and references cited therein.
    (b) A. O. Gabriel and R. Riedel, poster PB107 at the XI International Symp. on Organosilicon Chemistry.
    (c) R. Riedel, A. Greiner, G. Miehe, W. Dressler, H. Fuss and J. Bill, submitted for publication.
50. S. J. Lenhart, Y. D. Blum and R. M. Laine, *J. Corrosion*, **45**, 503 (1989).
51. T. Sugama and N. Carciello, *Mater. Lett.*, **14**, 322 (1992).
52. J. M. Schwark and A. Lukacs, in *Inorganic and Organometallic Polymers II*, Am. Chem. Soc. Symp. Ser. Vol. 572, (Eds. K. Wynne, P. W. Nielson and H. Allcock), *Am. Chem. Soc.*, 1994, pp. 43–54.
53. B. C. Mutsuddy, in *High Tech Ceramics* (Ed. P. Vincenzini), Elsevier Sci. Publ., Amsterdam, 1987, pp. 571–589.
54. (a) R. Riedel, G. Passing, H. Schönfelder and R. J. Brook, *Nature*, **355**, 714 (1992).
    (b) R. Riedel, M. Seher and G. Becker, *J. Eur. Ceram. Soc.*, **5**, 113 (1989).
    (c) R. Riedel, H-J. Kleebe, H. Schönfelder and F. Aldinger, *Nature*, **374**, 526 (1995).
55. G. T. Burns, C. K. Saha, G. A. Zank and H. A. Freeman, *J. Mater. Sci.*, **27**, 2131 (1992).
56. M. F. Gonon, G. Fantozzi, M. Murat and J. P. Disson, *J. Eur. Ceram. Soc.*, **15**, 591 (1995).
57. V. S. R. Murthy and M. H. Lewis, *Curr. Sci.*, **62**, 744 (1992).
58. Y. Nakaido, Y. Otani, N. Kozakai and S. Otani, *Chem. Lett.*, 706 (1987).
59. H. Porte and J-J. Lebrun, European Pat. Application 0 202 176 A1 (Nov. 20, 1986).
60. D. Mocaer, R. Pailler, R. Naslain, C. Richard, J. P. Pillot, J. Dunogues, C. Darnez, M. Chambon and M. Lahaye, *J. Mater. Sci.*, **28**, 3049 (1993).
61. T. Vaahs, M. Brück and W. D. G. Böcker, *Adv. Mater.*, **4**, 224 (1992).
62. C. K. Saha, G. Zank and A. Ghosh, in *Manufacture of Ceramic Components, Ceramic Trans.*, **49**, 155 (1995).
63. A. Greiner, P. Kroll, R. Riedel and J. Bill, in *Adv. Ceram.-Matrix-Composites II, Ceramic Trans.*, **46**, 497 (1994).
64. N. Brodie, J-P. Majoral and J-P. Disson, *Inorg. Chem.*, **32**, 4646 (1993).
65. M. G. Salvetti, M. Pijolat, M. Soustelle and E. Chassagneux, *Sol. State Ion.*, **63–5**, 332 (1993).
66. R. van Weeren, E. A. Leone, S. Curran, L. C. Klein and S. C. Danforth, *J. Am. Ceram. Soc.*, **77**, 2699 (1994) and references cited therein.
67. (a) Y.-F. Yu and T.-I. Mah, in *Better Ceramics Through Chemistry II*, Mater. Res. Soc. Symp. Proc. Vol. 73 (Eds. C. J. Brinker, D. E. Clark and D. R. Ulrich), 1986, pp. 559–565.
    (b) Y.-F. Yu and T.-I. Mah, in *Ultrastructure Processing of Advanced Ceramics* (Eds. J. D. Mackenzie and D. R. Ulrich), Wiley, New York, 1988, pp. 773–781.

68. D. Seyferth, Y.-F. Yu and T. S. Targos, U. S. Patent 4,705,837 (Nov. 1987).
69. R. M. Laine, Y. D. Blum, R. D. Hamlin and A. Chow, in *Ultrastructure Processing of Advanced Ceramics* (Eds. D. D. Mackenzie and D. R. Ulrich), Wiley, New York, 1986, pp. 761–769.
70. K. Okamura, *Composites*, 107 (1988).
71. G-E. Yu, J. Parrick, M. Edirisinghe, D. Finch and B. Ralph, *J. Mater. Sci.*, **29**, 5569 (1994) and references cited therein.
72. C. R. Bickmore and R. M. Laine, *J. Am. Ceram. Soc.*, **79**, 2865 (1996) and references cited therein.
73. F. L. Riley (Ed.), *Progress in Nitrogen Ceramics*, NATO ASI Series E: Applied Sci. Vol. 65, 1983.
74. K. H. Jack, *J. Mater. Sci.*, **11**, 1135 (1976).
75. I-W. Chen, P. F. Becher, M. Mitomo, G. Petzow and T-S. Yen (Eds.), *Silicon Nitride Ceramics*, Mater. Res. Soc. Symp. Proc. Vol. 287, Pittsburgh, 1993.
76. D. R. Messier and R. P. Gleisner, U. S. Army Materials Technology Laboratory Publication MTL TR 92-6.
77. W. R. Schmidt, W. J. Hurley, R. H. Doremus, L. V. Interrante and P. S. Marchetti, in *Advanced Composite Materials, Ceram. Trans.*, **19**, 19 (1991).
78. G. D. Soraru, A. Ravagni, R. Campostrini and F. Babonneau, *J. Am. Ceram. Soc.*, **74**, 2220 (1991).
79. G. D. Soraru, M. Mercadini, R. D. Maschio, F. Taulelle and F. Babonneau, *J. Am. Ceram. Soc.*, **76**, 2595 (1993).
80. R. M. Laine, C. R. Bickmore, K. F. Waldner, B. L. Mueller and H. W. Estry, in *Silicon Nitride Ceramics* (Eds. I.-W. Chen. P. F. Becher, M. Mitomo, G. Petzow and T.-S. Yen), Mater. Res. Soc. Symp. Proc. Vol. 287, Mater. Res. Soc., Pittsburgh, 1993, pp. 251–256.
81. (a) M. Takamizawa, T. Kobayashi, A. Hayashida and Y. Takeda, U.S. Patent 4,550,151 (1985).
    (b) M. Takamizawa, T. Kobayashi, A. Hayashida and Y. Takeda, U.S. Patent 4,604, 367 (1986).
82. (a) O. Funayama, H. Nakhara, M. Okoda, M. Okumura and T. Isoda, *J. Mater. Sci.*, **30**, 410 (1995).
    (b) O. Funayama, Y. Tashiro, T. Kato and T. Isoda, Int. Symp. Organosilicon Chem. Directed Towards Mater. Sci., Sendai, Japan, Abstracts, 1990, pp. 95–96.
83. (a) K. Su, E. E. Remsen, G. A. Zank and L. G. Sneddon, *Chem. Mater.*, **5**, 547 (1993).
    (b) T. Wideman, K.Su, E. E. Remsen, G. A. Zank and L. G. Sneddon, *Chem. Mater.*, **7**, 2203 (1995).
    (c) T. Wideman, K. Su, E. E. Remsen, G. A. Zank and L. G. Sneddon, in *Mater. Res. Soc. Symp. Proc.* Vol. 410, Mater. Res. Soc., Pittsburgh, 1996, pp. 185–189.
84. (a) J. Lipowitz, *Am. Ceram. Soc. Ceram. Bull.*, **70**, 1888 (1991).
    (b) J. Lipowitz, *J. Inorg. Organomet. Polym.*, **1**, 277 (1991).
85. (a) R. Riedel and W. Dressler, *Ceram. Int.*, **22**, 233 (1996).
    (b) R. Riedel, A. Kienzle, W. Dressler, L. M. Ruwisch, J. Bill and F. Aldinger, *Nature*, **693**, 796 (1996).
86. Reference 1, pp. 655–662.
87. D. Seyferth and H. Plenio, *J. Am. Ceram. Soc.*, **73**, 2131 (1990).
88. (a) J. Löffelholz and M. Jansen, *Adv. Mater.*, **7**, 289 (1995).
    (b) H.-P. Baldus, O. Wagner and M. Jansen in *Better Ceramics Through Chemistry VI*, (Eds. A. K. Cheetham, C. J. Brinker, M. L. McCartney and C. Sanchez) Mater. Res. Soc. Symp. Proc. Vol. 271, Pittsburgh, 1994, pp. 821–826.
    (c) H.-P. Baldus and G. Passing in *Mater. Res. Soc. Symp. Proc.* Vol. 346, Mater. Res. Soc., Pittsburgh, 1994 pp. 617–622.
    (d) M. Jansen, H.-P. Baldus and O. Wagner, Pat. Application DE 41 07 A1, disclosed Oct. 1992.
    (e) H.-P. Baldus, M. Jansen and O. Wagner, *Key Engineering Materials*, **89–91**, 75 (1994).
    (f) R. Riedel, A. Kienzle, G. Petzow M. Brück and T. Vaahs, Pat. Application DE 43 20 784 A1, disclosed May 1994.
89. O. Funayama, H. Nakahara, M. Okoda, M. Okumura and T. Isoda, *J. Mater. Sci.*, **30**, 410 (1995).
90. J. Bill, M. Friess, F. Aldinger and R. Riedel, in *Better Ceramics Through Chemistry VI*, (Eds. A. K. Cheetham, C. J. Brinker, M. L. McCartney and C. Sanchez) Mater. Res. Soc. Symp. Proc. Vol. 271, Pittsburgh, 1994, p. 839.
91. J. Hapke and G. Ziegler, *Adv. Mater.*, **7**, 380 (1995).

92. (a) S. Yajima, K. Okamura and J. Hayashi, *Chem. Lett.*, 1209 (1975).
    (b) S. Yajima, M. Omori, J. Hayashi, K. Okamura, T. Matsuzawa and C.-F. Liaw, *Chem. Lett.*, 551 (1976).
    (c) S. Yajima, H. Kayano, K. Okamura, M. Omori, J. Hayashi, T. Matsuzawa and K. Akutsu, *J. Am. Ceram. Soc.*, **55**, 1065 (1976).
93. (a) S. Yajima, K. Okamura, J. Hayashi and M. Omori, *J. Am. Ceram. Soc.*, **59**, 324 (1976).
    (b) S. Yajima, J. Hayashi, M. Omori and K. Okamura, *Nature*, **261**, 683 (1976).
    (c) S. Yajima, T. Shishido and H. Kayano, *Nature*, **273**, 525 (1978).
94. (a) S. Yajima, Y. Hasegawa, J. Hayashi and M. Iimura, *J. Mater. Sci.*, **13**, 2569 (1978).
    (b) Y. Hasegawa, M. Iimura and S. Yajima, *J. Mater. Sci.*, **15**, 720 (1980).
    (c) Y. Hasegawa and K. Okamura, *J. Mater. Sci.*, **18**, 3633 (1980).
95. T. Yamamura, T. Ishikawa, M. Shibuya and T. Hisayuki, *J. Mater. Sci.*, **23**, 2589 (1988).
96. Y. C. Song, Y. Hasegawa, S.-J. Yang and M. Sato, *J. Mater. Sci.*, **23**, 1911 (1988).
97. T. Yammura, *Am. Chem. Soc., Polym. Div., Polym. Prepr.*, **25**, 8 (1984).
98. K. A. Brown-Wensley and R. A. Sinclair, U. S. Patent 4,537,942 (1985).
99. (a) D. Seyferth, T. G. Wood, H. J. Tracy and J. L. Robison, *J. Am. Ceram. Soc.*, **75**, 1300 (1992).
    (b) D. Seyferth, H. J. Tracy and J. L. Robison, U. S. Patent No. 5,204,380 (1993).
    (c) D. Seyferth, C. A. Sobon and J. Borm, *New J. Chem.*, **14**, 545 (1990).
100. (a) F. Höfler, *Top. Curr. Chem.*, **50**, 129 (1974).
    (b) M. D. Curtis and P. S. Epstein. *Adv. Organomet. Chem.*, **19**, 213 (1981).
101. (a) Y. Mu and J. F. Harrod, in *Inorganic and Organometallic Oligomers and Polymers*, IUPAC 33rd Symp. on Macromol. (Eds. J. F. Harrod and R. M. Laine), Kluwer Publ., Dordrecht, 1991, p. 23.
    (b) J. F. Harrod, in *Inorganic and Organometallic Polymers with Special Properties* (Ed. R. M. Laine), NATO ASI Ser. E, Vol. 206, Kluwer Publ., Dordrecht, 1991, p. 87.
102. (a) T. D. Tilley, *Acc. Chem. Res.*, **26**, 22 (1993).
    (b) T. D. Tilley, H. G. Woo in *Inorganic and Organometallic Oligomers and Polymers*, IUPAC 33rd Symp. on Macromol. (Eds. J. F. Harrod and R. M. Laine), Kluwer Publ., Dordrecht, 1991, p. 3.
103. Z.-F. Zhang, F. Babonneau, R. M. Laine, Y. Mu, J. F. Harrod and J. A. Rahn, *J. Am. Ceram. Soc.*, **74**, 670 (1991).
104. (a) Z.-F. Zhang, S. Scotto and R. M. Laine, in *Covalent Ceramics II: Non-oxides*, Mater. Res. Soc. Symp. Proc. Vol. 327 (Ed. R. Gottschalk), Mater. Res. Soc., Pittsburgh, 1994, pp. 207–213.
    (b) Z.-F. Zhang, S. Scotto and R. M. Laine, in *Ceram. Eng. Sci. Proc.*, **15**, 152 (1994).
    (c) R. M. Laine, Z.-F. Zhang, K. W. Chew, M. Kannisto and C. Scotto, in *Ceramic Processing Science and Technology* (Eds. H. Hausner, G. Messing and S. Hirano), Am. Ceram. Soc., Wester ville, OH, 1995, pp. 79–186.
105. J. P. Banovetz, R. M. Stein and R. M. Waymouth, *Organometallics*, **10**, 3430 (1991).
106. Z.-F. Zhang, Ph.D. Thesis, University of Michigan, 1996.
107. T. Kobayashi, T. Sakakura, T. Hayashi, M. Yumura and M. Tanaka, *Chem. Lett.*, 1157 (1992).
108. E. Hengge, M. Weinberger and C. Jammegg, *J. Organomet. Chem.*, **410**, Cl (1991).
109. E. Hengge, *Organosilicon Chem. II*, **2**, 275 (1996).
110. E. Hengge and M. Weinberger, *J. Organometallic Chem.*, **433**, 21 (1992).
111. R. M. Laine and M. Kannisto, unpublished results.
112. (a) R. H. Baney, J. H. Gaul Jr and T. K. Hilty, *Organometallics*, **2**, 859 (1983).
    (b) R. H. Baney, U.S. Patent No. 4,310,482 (1982).
113. A. Tazi Hemida, J.-P. Pillot, M. Birot, J. Dunogues and R. Pailler, *J. Chem. Soc., Chem. Commun.*, 2337 (1994).
114. R. J. P. Corriu, M. Enders, S. Huille and J. J. E. Moreau, *Chem. Mater.*, **6**, 15 (1994).
115. T. L. Smith, U.S. Patent No. 4,631,179 (1986).
116. (a) L. V. Interrante and Q. H. Shen, *Macromolecules*, **29**, 5788 (1996).
    (b) L. V. Interrante, C. W. Whitmarsh, C.-Y. Yang and W. Sherwood, in *Silicon-Based Structural Ceramics*, Mat. Res. Soc. Symp. Proc. Vol. 365, Mater. Res. Soc., Pittsburgh, 1995, pp. 139–147.
117. (a) D. C. Deleeuw, J. Lipowitz and P. P. Lu, U.S. Patent No. 5,071,600 (1991).
    (b) J. Lipowitz, J. A. Rabe and G. A. Zank, *Ceram. Eng. Sci. Proc.*, **12**, 1819 (1991).
    (c) J. Lipowitz, T. Barnard, J. Bujalski, J. A. Rabe, G. A. Zank, A. Zangvil and Y. Xu, *Comp. Sci. Tech.*, **51**, 167 (1994).

118. C. P. Jacobson and L. C. DeJonghe, PCT WO 94/02430 (March, 1994).
119. W. Toreki, C. D. Batich, M. D. Sacks, M. Saleem, G. Choi and A. A. Morrone, *Comp. Sci. Tech.*, **51**, 145 (1994).
120. M. D. Sacks, G. W. Scheiffele, M. Saleem, G. A. Staab, A. A. Morrone and T. J. Williams in Mater. Res. Soc. Symp. Proc. Vol. **365**, 3 (1995).
121. (a) M.-T. S. Hsu, T. S. Chen and S. R. Riccitiello *J. Appl. Polym. Sci.*, **42**, 851 (1991).
    (b) S. R. Riccitiello, M. S. Hsu and T. S. Chen, *SAMPE Quarterly*, April, 1993, pp. 9–14.
122. R. Riedel, A. Kienzle, V. Szabo and J. Mayer, *J. Mater. Sci.*, **28**, 3931 (1993).
123. R. H. Baney, M. Itoh, A. Sakaibara and T. Suzuki, *Chem. Rev.*, **95**, 1409 (1995).
124. J. R. January, U. S. Pat. 4,472,510 (Sept. 1984).
125. D. A. White, S. M. Oleff, R. D. Boyer, P. A. Budinger and J. R. Fox, *Adv. Ceram. Mater.*, **2**, 45 (1987).
126. D. A. White, S. M. Oleff and J. R. Fox, *Adv. Ceram. Mater.*, **2**, 53 (1987).
127. F. I. Hurwitz, L. Hyatt, J. Gorecki and L. D'Amore, *Ceram. Eng. Sci. Proc.*, **8**, 732 (1987).
128. F. Babonneau, K. Thorne and J. D. Mackenzie, *Chem. Mater.*, **1**, 554 (1989).
129. K. Kamiya, T. Yoko, K. Tanaka and M. Takeuchi, *J. Non-Cryst. Solids*, **121**, 182 (1990).
130. H. Ishida, R. Shick and F. Hurwitz, *Macromolecules*, **23**, 5279 (1990).
131. H. Ishida, R. Shick and F. Hurwitz, *J. Polym. Sci.: Part B: Polymer Physics*, **29**, 1095 (1991).
132. F. I. Hurwitz, S. C. Farmer, F. M. Terepka and T. A. Leonhardt, *J. Mater. Sci.*, **26**, 1247 (1991).
133. H. Zhang and C. G. Pantano, *J. Am. Ceram. Soc.*, **73**, 958 (1990).
134. R. M. Renlund, S. Prochazka and R. H. Doremus, *J. Mater. Res.*, **6**, 2716, 2723 (1991).
135. F. I. Hurwitz, 24th International SAMPE Technical Conference, Oct. 20, 1992, pp. T950–961.
136. (a) P. A. Agaskar, *J. Am. Chem. Soc.*, **111**, 6859 (1989).
    (b) P. A. Agaskar, *J. Chem. Soc., Chem. Commun.*, 1024 (1992).
    (c) P. A. Agaskar, *Colloids and Surfaces*, **63**, 131 (1992).
137. X. Xin, C. Aitken, J. F. Harrod and Y. Mu, *Can. J. Chem.*, **68**, 471 (1990).
138. (a) R. M. Laine, K. A. Youngdahl, F. Babonneau, J. F. Harrod, M. L. Hoppe and J. A. Rahn., *Chem. Mater.*, **2**, 464 (1990).
    (b) R. M. Laine, F. Babonneau, J. A. Rahn, Z.-F. Zhang and K. A. Youngdahl, in *Thirty-Seventh Sagamore Army Materials Research Conference Proceedings* (Ed.), D. J. Viechnicki), Publ. Dept. of the Army, 1991, pp. 159–169.
    (c) R. M. Laine, J. A. Rahn, K. A. Youngdahl and J. F. Harrod, in *Adv. Chem. Series; New Science in Transition Metal Catalyzed Reactions*, Vol. 230 (Eds. D. Slocum and W. R. Moser), 1992, pp. 553–565.
139. (a) M. Harris, T. Choudhary, D. Treadwell, R. M. Laine and L. Drzal, *Mater. Sci. Eng. A*, **A195**, 223 (1995).
    (b) T. M. Choudhary, H. Ho, D. Treadwell, M. Harris, R. M. Laine and L. Drzal, *Mater. Sci. Eng. A*, **A195**, 237 (1995).
140. C. L. Frye and J. M. Klosowski *J. Am. Chem. Soc.*, **93**, 4599 (1971).
141. V. Belot, R. J. P. Corriu, D. Leclercq, P. H. Mutin and A. Vioux, *J. Non-Cryst. Solids*, **148**, 52 (1992).
142. L. Bois, J. Maquet, F. Babonneau, H. Mutin and D. Bahloul, *Chem. Mater.* **6**, 796 (1994).
143. M. D. Nyman, S. B. Desu and C. H. Peng *Chem. Mater.* **5**, 1636 (1993).
144. L. A. Haluska, K. W. Michael and L. Tarhay, U. S. Patent 4,756,977 (July, 1988).
145. S.-P. Jeng, K. Taylor, T. Seha, M.-C. Chang J. Fattaruso and R. H. Havemann, *Symp. on VLSI Tech.*, Digest of Tech. papers, Jap. Soc. Appl. Phys., Tokyo, Japan, 1995, pp. 61–62.
146. (a) L. K. Figge, Ph.D. dissertation, Univ. of Pennsylvania (Oct. 1996).
    (b) D. H. Berry and L. K. Figge, submitted.
147. See Dow Corning, Inc. fact sheets on Flowable Oxide^{TM}.
148. P. A. Agaskar, *Inorg. Chem.*, **30**, 2708 (1991).
149. C. L. Frye, G. A. Vincent and W. A. Finzel, *J. Am. Chem. Soc.*, **93**, 6805 (1971).
150. (a) R. M. Laine, K. Y. Blohowiak, T. R. Robinson, M. L. Hoppe, P. Nardi, J. Kampf and J. Uhm, *Nature*, **353**, 642 (1991).
    (b) K. Y. Blohowiak, D. R. Treadwell, B. L. Mueller, M. L. Hoppe, S. Jouppi, P. Kansal, K. W. Chew, C. L. S. Scotto, F. Babonneau, J. Kampf and R. M. Laine, *Chem. Mater.*, **6**, 2177 (1994).
151. P. Kansal and R. M. Laine, *J. Am. Ceram. Soc.*, **77**, 875 (1994).

152. (a) M. L. Hoppe, R. M. Laine, J. Kampf, M. S. Gordon and L. W. Burggraf, *Angew. Chem., Int. Ed. Engl*, **32**, 287 (1993).
(b) P. Kansal and R. M. Laine, *J. Am. Ceram. Soc.*, **78**, 529 (1995).
153. R. M. Laine, in *Applications of Organometallic Chemistry in the Preparation and Processing of Advanced Materials*, NATO ASI Ser. E: Appl. Sci.-Vol. 297 (Eds. J. F. Harrod and R. M. Laine), Kluwer Publ., Dordrecht, 1995, pp. 69–78.
154. K. W. Terry, P. K. Ganzel and T. D. Tilley, *Chem. Mater.*, **4**, 1290 (1992).
155. M. L. Montero, I. Uson and H. W. Roesky, *Angew. Chem. Int. Ed. Engl.*, **33**, 2103 (1994).
156. R. Baranwal and R. M. Laine, *J. Am. Ceram. Soc.*, **80**, 1436 (1997).
157. R. M. Laine, D. R. Treadwell, B. L. Mueller, C. R. Bickmore, K. F. Waldner and T. Hinklin, *J. Chem. Mater.*, **6**, 1441 (1996).
158. R. Baranwal, A. Zika, B. L. Mueller and R. M. Laine, in *Electrorheological Fluids* (Eds. F. Filisko and K. Havelka), Plenum Press, New York, 1995, pp. 157–169.
159. K. Waldner, R. Laine, C. Bickmore, S. Dumrongvaraporn and S. Tayaniphan, *Chem. Mater.* **8**, 2850 (1996).
160. T. Kemmitt and N. B. Milestone, in *Silicon Containing Polymers* (Ed. R. G. Jones), Royal Soc. Chem., Cambridge, England, 1995, pp. 107–112.
161. D. C. Hrncir and G. D. Skiles, *J. Mater. Res.*, **3**, 410 (1988).
162. K. W. Terry and T. D. Tilley, *Chem. Mater.*, **3**, 1001 (1991).
163. K. Su, T. D. Tilley and M. J. Sailor, *J. Am. Chem. Soc.*, **118**, 3459 (1996).

CHAPTER 40

Organo-silica sol–gel materials

DAVID AVNIR

Institute of Chemistry, The Hebrew University of Jerusalem, Jerusalem 91904, Israel

LISA C. KLEIN

Ceramics Department, Rutgers— The State University of New Jersey, Piscataway, NJ 08855-0909, USA

DAVID LEVY

Instituto de Ciencia de Materiales de Madrid, C.S.I.C., Cantoblanco, 28049 Madrid, Spain

ULRICH SCHUBERT

Institute for Inorganic Chemistry, the Technical University of Vienna, A-1060 Vienna, Austria

and

ANNA B. WOJCIK

Ceramics Department, Rutgers— The State University of New Jersey, Piscataway, NJ 08855-0909, USA

I. INTRODUCTION

This chapter describes a recent revolution in the chemistry and physics of materials. It has been founded on the interdisciplinary merging of organic chemistry and the world of ceramic materials, which traditionally have had little overlap between them. We hope that once the reader is exposed to the immense diversity of applications and unique properties of this novel family of materials, the justification of the word ‘revolution’ will become evident.

When one considers the unique properties of ceramics on the one hand, and the vastness of organic chemistry on the other, it seems almost inevitable that merging these domains of chemical research should lead to novel materials and to novel reaction configurations. We summarize in this chapter some representative research activities towards this goal, mainly since the early 80’s which marked the emerging of this field from obscurity into a self-contained domain, with research activities in many academic and industrial laboratories[1–6]. The inherent difficulty in combining organic chemistry with glass and ceramic chemistry is the temperature parameter: organic compounds rarely survive temperatures higher than 200 °C (and biomolecules much less) but typical manipulation temperatures of ceramics and glasses can be well above 1000 °C. It is for this reason that over the millennia of the history of ceramics and glass production[7] one finds additives (e.g. colorants), only such that could withstand the high temperatures, namely inorganic salts and other oxides.

It has been known for quite some time[8] that inorganic oxides, with chemical compositions identical to glasses and ceramics, can be prepared at room temperatures, by polycondensation, precipitation and coagulation procedures of metal and semi-metal hydroxides or of their organic ethers (alkoxides) or esters[9]. Compared with the voluminous activity in the field of organic polymers, the study of formation of inorganic oxides by polycondensation remained for many years relatively low-key. The late 70's and early 80's witnessed a dramatic change: The recognition that better ceramic materials can be obtained through the detailed tailoring of the chemical aspects of the polycondensation[10] led to a world-wide burst of activity and to the birth of what became known as 'Sol–Gel Science'[9,10e,11]. Although sol–gel transitions are, of course, well documented in many polymerization and precipitation phenomena, the terms 'sol–gel materials', 'sol–gel process' etc. are used today in the connotation of the synthesis of inorganic materials from suitable monomers, passing indeed through sol, gel and xerogel (dry gel) stages.

It became clear that the sol–gel process is a promising candidate for closing the ceramics–organic gap, by virtue of the ambient temperatures employed up to the xerogel stage. This gap closure has three principle aspects, summarized in this chapter: the direct physical doping of ceramic materials with organic and bioorganic molecules; the functional modification of the ceramic matrix by copolymerization with organo-metal-alkoxides; and the formation of organo-ceramic composites by copolymerizations. As we shall see below, the applications of these novel materials cross chemistry from coast to coast, bridging in many instances traditional domains of chemistry, namely inorganic chemistry, organic chemistry, biochemistry, polymer chemistry, environmental chemistry, photochemistry, electrochemistry, optics, catalysis and more.

The main message of this chapter is that the chemistry and physics of organic molecules are carryable within ceramic matrices, allowing a plethora of novel and classical applications, and providing new insight on properties of both the organic component and of the matrix itself.

II. THE SILICA SOL–GEL PROCESS AND SILICA SOL–GEL MATERIALS

Most of the inorganic oxides, MO_n (where M is a metal or semi-metal, and n is not necessarily an integer), as well as many mixed oxides, have been prepared by the sol–gel process[9–11]. Many studies concentrated on SiO_2, the topic of this chapter, although for most applications described below, this need not be the optimal matrix, and one may also consider oxides such as TiO_2, ZrO_2, Al_2O_3 as well as their composites with silica such as SiO_2/ZrO_2.

The formation of a sol–gel porous material is through a hydrolysis–polycondensation reaction. An example is given in equation 1 with the methoxide of silicon (tetramethylorthosilicate, TMOS), but many other alkoxides, aryl oxides and acyl oxides can be used, as well as Si−N and Si−Cl compounds.

$$\mathrm{Si(OCH_3)_4 + H_2O \xrightarrow{H^+ \text{ or } OH^-} (SiO}_m\mathrm{H}_n)_p + \mathrm{CH_3OH} \qquad \text{(unbalanced)} \qquad (1)$$

The hydrolysis introduces all of the oxygen into the silicon oxide matrix, i.e. all of the oxygen comes from the water molecules. The underlying details of the chemistry are extremely complex[12–14] and the detailed description of mechanistic studies is beyond the scope of the topic of this chapter, except for mechanistic studies which involve organic molecules and polymers — these are given in the various sections below. Here, some general aspects are summarized.

The values of m, n and p in the general silica equation are dictated by a host of parameters. These include water/silane ratio ($= r$), concentration of H^+ or OH^-, co-solvent, temperature, method and rate of drying, the existence of dopants and other additives, the size and shape of the product (thin film, monolith, powder) and even the chemical nature of the surface of the reaction container or thin film support. Typically, $(SiO_mH_n)_p$ are highly porous materials with pore size distributions which are centered around several tens of Angstroms, with surface areas usually in the range of several hundreds of $m^2 g^{-1}$, although surface areas as low as a few $m^2 g^{-1}$ have been recorded as well[13]. As for the values of m and n, the theoretical minimal composition is m close to 2 and n close to zero, for completely nonporous SiO_2. However, the surface of the porous product is densely coated with various types of silanols [$-SiOH$, $-Si(OH)_2$] moieties, so that the other hypothetical extreme (all Si is at the surface) is about SiO_3H_2. Adsorbed water molecules, which are always there, affect the n/m ratio as well. It is the fact that the silica has actually the SiO_mH_n composition (and not the commonly cited SiO_2) that is crucial for many of the special properties listed below. The value of p in the general formula can also be very high: since the monomer has four arms, the resulting polymer is extremely branched and a monolithic sol–gel block can in principle be one huge molecule with p approaching Avogradro's number.

The complexity of the polycondensation process has two levels. The first one is the competition between the hydrolysis rate of the Si−OR groups, forming Si−OH + ROH, and the rate of the polycondensation steps. The second one is that in the growing oligomers, each of the Si−OH and Si−OR groups has a distinctly different electronic and steric environment resulting in distinct hydrolysis and condensation rates for each of these groups. It is not surprising therefore that the control of the physical properties of porous sol–gel materials is still a matter of experimental exploration (for some typical mechanistic studies, see elsewhere[14]). It should be noted however, that the very ability to control it is an important advantageous property of this class of materials.

III. DIRECT ENTRAPMENT OF ORGANIC AND BIOORGANIC MOLECULES IN SOL–GEL MATRICES

A. General Aspects

The doping procedure is simple and straightforward: the host molecule is added to the polymerizing mixture. When the polycondensation is completed, the dopant molecules are entangled in the inorganic polymeric network (Figure 1).

Intensive studies[15] of the entrapment of organic molecules in sol–gel matrices evolved over the years into the following generalizations:

1. Most molecules can be entrapped in sol–gel matrices.
2. The entrapped molecule retains much of its characteristic physical properties.
3. The entrapped molecule retains much of its chemical properties.
4. The entrapped molecules are accessible to external reagents through the pore network: chemical reactions and interactions are possible.
5. Sol–gel materials such as monolithic silicas or silica films are transparent well into the UV: optical applications are possible.

Other properties which have contributed to the attractiveness and versatility of the sol–gel doping approach are the chemical, photochemical and electrochemical inertness as well as the thermal stability of the matrix; the ability to induce electrical conductivity[16]; the richness of ways to modify chemically the matrix and its surface as well as the above-mentioned controllability of matrix structural properties; the enhanced stability of the entrapped molecule[1,17]; the ability of employing the chromatographic properties of the matrix for enhanced selectivity and sensitivity of reactions with the dopant[4]; the simplicity of the entrapment procedure; the ability to obtain the doped sol–gel material in any desired shape (powders, monoliths, films, fibers); and the ability to miniaturize it[18,19].

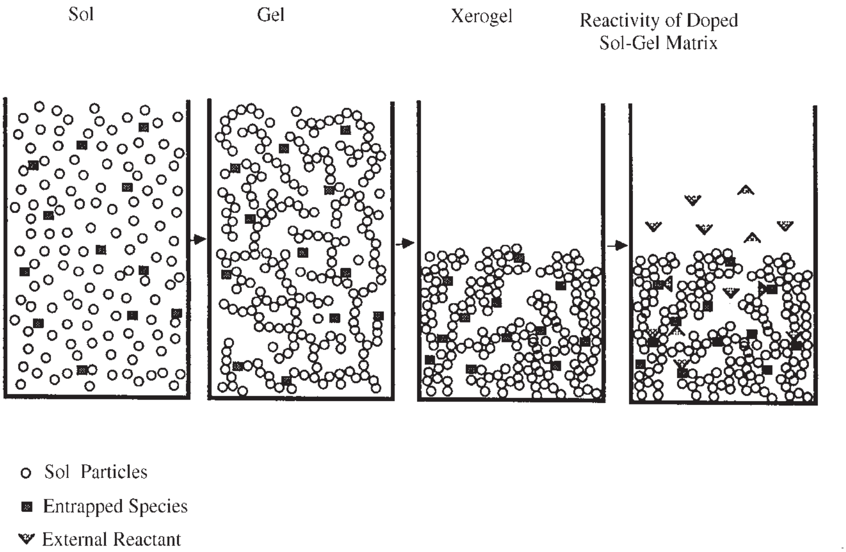

FIGURE 1. The sol–gel polymerization and entrapment process. (a) A sol of silica or other inorganic oxide particles (○) is prepared by polymerization of metal alkoxides in the presence of the desired dopant molecules, or of other monomers or polymers (■). (b) The sol turns into a gel within which the dopant molecules are entangled. Reactive monomers will form covalent bonds with the growing oxide network. It then dries and shrinks, forming a porous xerogel, (c), within which the dopant molecules are physically entrapped, or covalently attached. The pores are sufficiently narrow to render the matrix transparent, allowing optical applications. (d) The pore network allows external molecules (▲) to diffuse into the matrix and react with the trapped dopant (■). Sensing, catalysis, photochemistry and biocatalysis have been demonstrated

In the next sections we survey some of the applications of *reactive* organically doped sol–gel silicas. We return to optics and photophysical applications in Section VI, although historically, the first investigations were concentrated on optics[1,20] and it became evident only several years later that the entrapped molecule can also be involved in chemical reactions.

B. Applications in Analytical Chemistry: Sol–Gel Sensors

Our first family of applications of reactive doped sol–gel materials is the one that attracted most attention, namely in analytical chemistry[21]. Actually, the widest array of chemical reactions which has been carried out within sol–gel matrices was revealed while developing the doped sol–gel methodology for chemical sensing purposes[21–24]. They include proton-transfer reactions (such as pH indicators), redox reactions, complexations, ligand exchanges, enzymatic reactions and more. Common to these reactions is their ability to sense chemical changes in the environment of the entrapped molecule, revealing it through color-developing reactions between the entrapped reagent and an external diffusable chemical species or through emission of light. The chemical inertness and the optical transparency of SiO_2 sol–gel matrices have made the doping methodology quite attractive for sensor developments. Sensing reactions that have been demonstrated successfully with the sol–gel methodology include, for instance, many toxic metal cations, anions and various pollutants[21–24]. Another attractive feature for sensing purposes is that sol–gel materials can be made in various forms, as the analytical or optical method requires. Thus, one can prepare the sensing materials as a monolithic block[25], as a microscopic grain[18,19], as a thin film on a flat support[26], as an optical fiber coating[27,28] and in chromatographic capillary tubes[29].

High sensitivities are achievable with sol–gel sensors. An example is the sensing of Fe^{2+}[22], detected through its red-colored complex with three molecules of *o*-phenanthroline. This color evolution is far from being obvious: *three* entrapped phenanthroline molecules must complex with the penetrating Fe^{2+}, in order to form a color which is identical to the one formed in aqueous solution, as indeed is the case[23,30] (we return to this point below). The response curve of an e-*ortho*-phenanthroline (0.025%) SiO_2 porous glass to various concentrations of Fe^{2+} revealed an exceedingly high sensitivity with a detection limit of about 100 ppt (about two magnitudes of order better than conventional solution absorption spectroscopy)[23,30]. This very high sensitivity is due to a unique feature of the sol–gel matrix: being actually a high-surface area adsorbent, it *concentrates* by adsorption the impurity and then detects it. Facile detection of Fe^{+2} was also demonstrated by Lev and coworkers who developed the use of doped sol–gel particles as sensing chromatographic materials, packed within capillaries[29]. The idea is simple and convenient: the capillary is immersed in a given volume of solution containing the analyte; the solution is driven up by capillary forces, leaving behind a stain, the length of which is proportional to the concentration of the analyte. Besides Fe^{+2}, this approach was demonstrated for other analytes[29].

The development of sol–gel pH sensors attracted several laboratories, employing various indicators and various techniques based on both light absorption[29] and fluorescence emission[28,31]. Techniques included, as mentioned above, simple monolithic discs embedded with various routine indicators[22,25], thin films[27], various fluorescent fiber optics configurations[27,28], the capillaries[29,32] as well as prototype pH-meters constructed with some of these techniques[25,28]. For continuous, long-term, reversible applications leaching must be eliminated, and so covalent anchoring of trialkoxysilyl derivatives as described in Section IV below, of the pH indicators, may become desirable. A representative example is methyl-red, which was derivatized through its carboxylate moiety with trimethoxysilylpropylamine[19], shifting the pK_i from 5.2 to 3.0. Performance shifts in the case of copolymerization is a cost one should bear in mind. Another convenient method for eliminating leading is the co-entrapment of surfactants[25].

An important future aspect for the development of Useful applications of doped sol–gel sensors is miniaturization. One step towards that goal was undertaken[18] with the fluorescent pH-probe pyranine[33]. A pH-meter based on a 10-micron piece of doped sol–gel was constructed by incorporating it in a near-field optical microscopy configuration, which consists of metal-coated micropipette tips: a good, reversible titration curve was obtained. Further miniaturizing to *ca* 1 micron was achieved as well, with subsecond response time[18].

C. Catalysis with Entrapped Organometallic Ion-pairs and Complexes

The sol–gel approach has been used in catalysis in four main directions: preparation of inorganic oxide catalysts[34]; entrapment of metal microcrystallites[35]; polymerization of trialkoxysilyl derivatives of metal ligands[36,37]; and by direct, straightforward entrapment of organometallic catalysts in sol–gel matrices[38–40]. In this Section we concentrate on the latter and compare it with covalent attachment of trialkoxy derivatives, which is fully described in Section IV. As a representative example we consider the case of ion-pair catalysts[41,42] and, in particular, $RhCl_3$/Aliquat 336® and $RhCl_3/[Me_3N(CH_2)_3$

TABLE 1. Hydrogenation of several unsaturated compounds by the sol–gel entrapped ion-pair catalysts **1** and **2**[a]

Substrate	Catalyst	Products (yield in 1st run, %)
Styrene	**1**	ethylbenzene (100)
Styrene	**2**	ethylbenzene (48)
trans-Stilbene	**1**	bibenzyl (35)
trans-Stilbene	**2**	bibenzyl (64)
Benzalacetone	**1**	4-phenylbutan-2-one (62)
Benzalacetone	**2**	4-phenylbutan-2-one (72)
Phenylacetylene	**1**	styrene (72), ethylbenzene (20)
Phenylacetylene	**2**	styrene (18), ethylbenzene (3)
Benzene	**1**	cyclohexane (100)
Benzene	**2**	cyclohexane (68)
Acenaphthylene	**1**	acenaphthene (85)
Acenaphthylene	**2**	acenaphthene (54)
Naphthalene	**1**	tetralin (33), *cis*-decalin (66)
Naphthalene	**2**	tetralin (32), *cis*-decalin (66)
1-Naphthol	**1**	5-hydroxytetralin (24)
1-Naphthol	**1**	*cis*-decalin (12), *trans*-1-hydroxydecalin (37), *trans*-1-decalone (51)
1-Naphthol	**2**	1-hydroxytetralin (13), 5-hydroxytetralin (56)
1-Naphthol	**2**	*cis*-1-hydroxydecalin (52), *cis*-1-decalone (47)
Benzyl bromide	**1**	toluene (53)
Benzyl bromide	**2**	toluene (60)
(3-Bromopropyl) benzene	**2**	(3-bromopropyl)cyclohexane (50)
Nitrobenzene	**1**	aniline (34)
Nitrobenzene	**2**	aniline (50), aminocyclohexane (50)
Benzonitrile	**1**	benzylamine (98)
Benzonitrile	**2**	benzylamine (88)

[a] Typical procedure[39,40]: Entrapment of the catalysts was carried out by adding $RhCl_3$ and an equimolar amount of the appropriate quaternary ammonium salt to a water–methanol–tetramethoxysilane mixture in two steps. After drying and washing, the catalyst and the substrate were heated to 104 °C for 40 minutes. Upon reaction completion, the catalyst is simply filtered out and washed for re-use.

TABLE 2. Hydroformylation of some olefins by the sol–gel entrapped ion-pair catalysts **1** and **2**[a]

Substrate	Catalyst	Products (yield in 1st run, %)
Cyclopentene	**1**	c-C_5H_9CHO (95)
Cyclopentene	**2**	c-C_5H_9CHO (50)
Cyclohexene	**1**	c-$C_6H_{11}CHO$ (94)
Cyclohexene	**2**	c-$C_6H_{11}CHO$ (8)
1-Decene	**2**	$Me(CH_2)_9CHO$ (41), $Me(CH_2)_7CH(CHO)Me$ (41), $Me(CH_2)_6CH(CHO)Et$ (8), $Me(CH_2)_5CH(CHO)Pr$ (8)
Styrene	**1**	$Ph(CH_2)_2CHO$ (68), $PhCH(CHO)Me$ (31)
Styrene	**2**	$Ph(CH_2)_2CHO$ (59), $PhCH(CHO)Me$ (27)
1-Methylstyrene	**1**	$PhCH(Me)CH_2CHO$ (12)
1-Methylstyrene	**2**	$PhCH(Me)CH_2CHO$ (85)

[a] Reaction conditions: see footnote *a* to Table 1.

$Si(OMe)_3]Cl$, both entrapped in SiO_2 sol–gel matrices[39,40a]. While the former represents direct physical entrapment (catalyst **1**), the latter forms a covalent bond within the cage (catalyst **2**). These catalysts were used in numerous hydrogenation, hydroformylation and disproportionation reactions, and proved to be stable, leach-proof and recyclable. Occasionally, the catalytic efficiency dropped upon recycling, owing to pore blockage, but the activity could be restored by treatment with boiling water. The performances of the sol–gel-entrapped ion-pairs were compared with those of the homogeneous $RhCl_3$/Aliquat 336 catalyst and, in most cases, the immobilized catalysts proved superior to their homogeneous version. The results for many successful hydrogenation and hydroformylation reactions are collected in Tables 1 and 2. These immobilized ion-pair catalysts also proved to be stable, leach-proof and recyclable catalysts for disproportionation reactions of 1,3-cyclohexadiene and several other *vic*-dihydroarenes (Scheme 1 and Table 3). In these reactions, equimolar quantities of the respective tetrahydro and fully aromatic compounds were obtained. The entrapped catalysts, in most cases, proved to be more efficient and more selective than their homogeneous analogs. The reaction rates and conversions were shown to depend strongly on steric effects of substituents and on the bulkiness of the substrate skeleton. The recorded first-order kinetics in the substrates suggested that the mechanism involves stepwise addition of two molecules of the dihydroarenes to the rhodium nucleus, and that the addition of the first substrate molecule is rate-limiting.

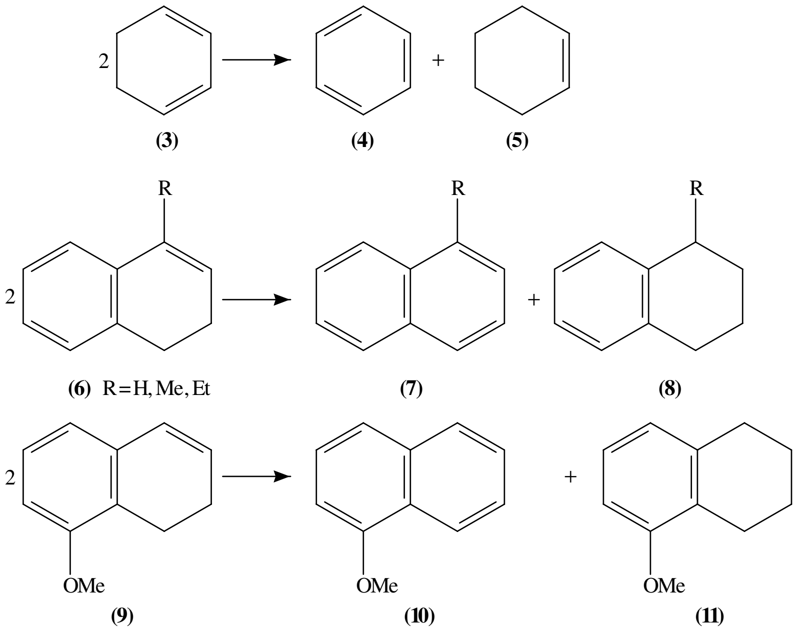

SCHEME 1

Finally, we mention the successful direct entrapment of the phosphinated complexes $RuCl_2(PPh_3)_3$, $RhCl(PPh_3)_3$, $IrCl(CO)(PPh_3)_2$ (see also Section IV), their water-soluble sulfonated analogs $RuCl_2[Ph_2P(3\text{-}C_6H_4SO_3Na)]_2{\cdot}4H_2O$, $RhCl[Ph_2P(3\text{-}C_6H_4SO_3Na)]_3{\cdot}4H_2O$, $IrCl(CO)[Ph_2P(3\text{-}C_6H_4SO_3Na)]_2$, and the dirhodium compounds *trans*-$[Rh(CO)(PPh_3)(\mu\text{-}1\text{-pyrazole})]_2$ and *trans*-$[Rh(CO)\ (PPh_3)(\mu\text{-}Cl)]_2$, in silica sol–gel matrices. The catalysts proved to be active and efficient towards allylbenzene

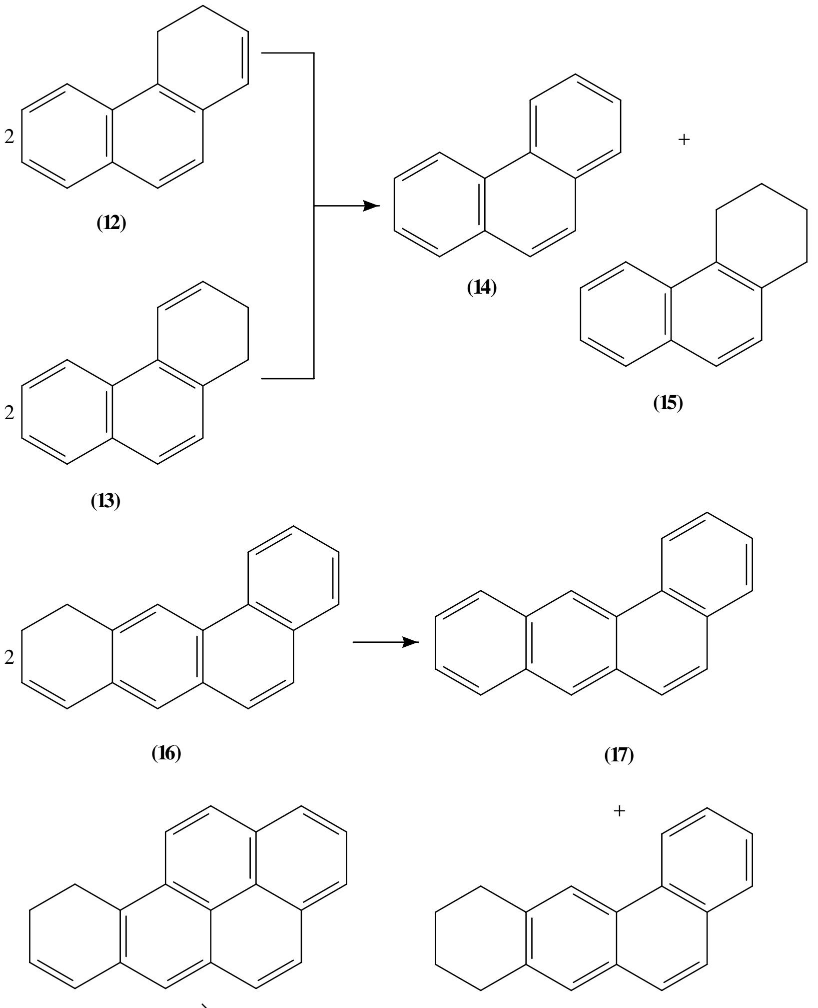

SCHEME 1. (*continued*)

isomerization[40b] (equation 2).

$$\mathrm{PhCH_2CH{=}CH_2} \xrightarrow{\text{e-(RuCl}_2\text{)(PPh}_3\text{)}_3} \textit{cis}\text{- and } \textit{trans}\text{-}\mathrm{Ph{-}CH{=}CHCH_3} \qquad (2)$$

D. Biochemistry Within Sol–Gel Matrices: The Entrapment of Enzymes and Antibodies

A priori there was no reason to believe that sol–gel encapsulation of enzymes will keep them alive. When one considers the ability of the alkoxide to react with the enzyme

TABLE 3. Disproportionation of some *vic*-dihydroarenes by catalysts **1** and **2**[a]

Substrate[b]	Products[b]	Yields after 40 min (%)	
		catalyst **1**	catalyst **2**
3	**4**, **5**	97	96
6, R = H	**7**, R = H; **8**, R = H	83	99
6, R = Me	**7**, R = Me; **8**, R = Me	58	41
6, R = Et	**7**, R = Et; **8**, R = Et	16	17
9	**10**, **11**	52	87
12	**14**, **15**	28	73
13	**14**, **15**	20	50
16	**17**, **18**	8	23
19	no products	—	—

[a] See Reference 40a for experimental details; see Table 1.

[b] See Scheme 1 for substrates, reactions and products.

surface and active site, the pressure build-up on the protein as the matrix shrinks, the release of toxic alcohol during hydrolysis and the need to have the active site of the entrapped protein exposed to the pore-network, one appreciates the nontriviality of this remarkable aspect of doped sol–gel chemistry. The ability to merge the world of sol–gel ceramics with biochemistry[43], has motivated intensive activity[44,45d,e]. Some highlights are summarized next.

An intensively studied entrapped enzyme has been glucose oxidase[45a,b,46,47], which catalyzes the oxidation of D-glucose. That reaction is of appreciable diagnostic value, and this application is routinely carried out by utilizing the released H_2O_2 (a reaction product if oxygen is used as an oxidant) by forming a secondary colored product via a peroxidase catalyzed oxidation of aromatic aza compounds. Performing this procedure in a sol–gel matrix demonstrated the ability to carry out a multiple-enzyme network of reactions. Actually, enzymes that are hostile to each other and destructive in solution can be brought together in a harmless way when entrapped in the sol–gel matrix. For instance, trypsin autodigests itself completely in solution; by contrast, SiO_2-entrapped trypsin retained its full activity for several months, when incubated at pH 7.5[46]. Returning to glucose oxidase, a reversible optical glucose sensor was constructed by Shtelzer and Braun[48] employing the decoloration of the isoalloxazine moiety in the enzyme upon reductive complexation with glucose. Electrochemical detection of glucose with sol–gel enzymatic electrodes was carried out by several research groups (see also Section III.E)[49].

Some of the entrapped enzymes show remarkable enhancement in stability[43,50]. Thus, acid phosphatase, which in solution at 70 °C and pH 5.6 lived less than 0.1 min, had a two orders of magnitude jump in its half-life to 12 min in the entrapped form[50]. Since denaturation of enzymes involves folding–unfolding of the peptide chain, one may attribute the enhanced stability to the rigidity of the SiO_2 cage, which apparently restricts such motions. It has been demonstrated in a number of experiments that the geometric accessibility of the entrapped enzyme to incoming substrate molecules is perhaps the most important parameter which dictates its activity[43,50]. For instance, the efficiency of trypsin inhibitors, a set of benzoyl-arginine derivatives, was found to be linked to their size[46].

Many enzymes have been entrapped successfully in sol–gel matrices[44,45d–h]. The entrapment of parathion hydrolase[44,51], which is capable of detoxifying and detecting the pesticide Parathion, demonstrates the potential of the sol–gel methodology in environmental applications.

Of special interest are the entrapments of antibodies. Although still in its infancy, a number of promising recent reports point to the great potential of this direction. An example is that of monoclonal anti-atrazine mouse antibody which was entrapped successfully in SiO_2 sol–gel matrices, prepared from tetramethoxysilane by several methods, retaining its ability to bind free antigen from an aqueous solution[52]. Atrazine was selected as a model compound for that study, within the framework of the development of immunochemical-based methods for monitoring of pesticide residues and other organo-synthetic environmental contaminants. Nanogram quantities of atrazine were applied on SiO_2–sol–gel columns doped with this antibody, and the amount of eluted antigen was determined using an Enzyme Linked ImmunoSorbent Assay (ELISA). The results showed that under appropriate sol–gel-forming conditions, the amounts of atrazine that were bound to the sol–gels were high, ranging between 60% to 91% of the amount applied to the column. The combination of the properties of the sol–gel matrix (e.g. stability, inertness, high porosity, high surface area and optical clarity) together with the selectivity and sensitivity of the antibodies bear a potential for further development of novel immunosensors which can be used for purification, concentration and monitoring of a variety of residues from different sources.

Indeed, more recent studies have shown the feasibility of this approach to yet another important group of pollutants, namely the nitroaromatics[58]. The nitroaromatic derivatives which are found most frequently as environmental contaminants are 2,4-dinitrotoluene and 2,6-dinitrotoluene used in plastics, dye and munitions manufacture, nitrophenols which are used as pesticides and 2,4,6-trinitrotoluene or 1,3,5-trinitrobenzene which are products of the munitions industry[53]. Large quantities of nitroaromatic compounds are currently manufactured all over the world, and their toxicity, mutagenicity and carcinogenicity are well established[53]. Accordingly, the need for extensive monitoring of nitroaromatic compounds in the environment (production effluents, toxic waste disposal sites, working places etc.) clearly exists. Nitroaromatic derivatives are also used in agriculture as insecticides, [e.g. parathion, (4,6-dinitro-*o*-cresol)], as herbicides (e.g. Ethalfluralin) and as fungicides (e.g. Quintozene). These compounds and their metabolites are often found as contaminants of food, soil and water. Towards this goal, the successful encapsulation of purified polyclonal IgG binding free antigen in aqueous solutions was reported[53]. The study was performed using a rabbit *anti*-2,4-dinitrobenzene (DNB) polyclonal antiserum and a 2,4-dinitrophenylhydrazine (DNPH) antigen which exhibits a high degree of cross-reactivity with the antiserum[54].

Additional reports include the covalent bonding of antibodies to functionalized sol–gel films[55], the entrapment of polyclonal fluorescein[56], the development of a sol–gel enzyme-linked immunosorbent assay (ELISA) test for antigenic parasitic protozoa[57] and an immunoassay for the detection of 1-nitropyrene[58].

To conclude this section we finally mention that various nonenzymatic proteins, whole cell extracts and whole intact cells were also entrapped successfully in silica sol–gel matrices[59], and these are reviewed elsewhere[44].

E. Electrochemistry with Organically Doped Sol–Gel Electrodes

The versatility of the doped sol–gel matrices was revealed also in the construction of electrochemical sensors. Tatsu and coworkers[60] constructed the first sol–gel glucose flow injection analyzer using an electrochemical sensor. The sensor was comprised of a silica sol–gel glucose oxidase powder which was attached to an oxygen electrode by a Nylon net and a cellulose membrane. Oxygen depletion was used for quantification of the converted glucose. The sol–gel methodology was also used employing redox-mediated electrodes. These sensors utilize an immobilized redox compound (e.g. ferrocene or hexacyanoferrate) which serves as an electron acceptor and affords oxygen-independent signal. The reduced mediator is regenerated by the anode and the exchanged Faradaic current is proportional to the amount of converted glucose. Audebert, Demaille and Sanchez constructed a ferrocene-mediated sol–gel biosensor by two successful methods[49a]: a two-stage silica sol–gel preparation procedure, and three gels prepared from commercial colloidal silica of various particle sizes. When this gel was kept in wet conditions, it maintained excellent activity and permitted good mobility of the analyte and the chemical mediator. The authors show that more than 80% of the glucose oxidase remained active in the gel, and that the Faradaic response of the electrode agrees well with theoretical calculations based on this activity.

Motivated by the need to produce stable bioactive silica films on conducting supports Lev and coworkers used two alternative approaches for the production of sol–gel derived amperometric biosensors[49b,61]. Thin films of glucose oxidase doped vanadium pentoxide (V_2O_5) were prepared from colloidal suspension. V_2O_5 doped with V^{4+} exhibits good electrical conductivity and adheres well to platinum and other conductive supports. This, and the ability to intercalate organic molecules[49b] made it suitable as a supporting matrix for active proteins. Sensing in this case is via the produced hydrogen peroxide which is electrooxidized on the metal support. A similar procedure was also used to prepare hydrogen peroxidase vanadium pentoxide biosensor[61].

Composite Carbon-silicate Electrodes (CCEs) were developed by Lev and coworkers[16,62–73]. The basic ingredients of the electrochemical sensors are graphite or carbon black powders dispersed in methyl-silicate sol–gel network. The carbon or graphite powder provides electric conductivity by an electron percolation mechanism and the porous silicate matrix contributes rigid and brittle construction. The hydrophobicity of the methyl modifiers prevents penetration of water to the electrode and thus only the outermost section of the electrode remains in contact with the electrolyte. These electrodes showed up to three orders improved Faradaic signal/background (capacitive) noise as compared to glassy carbon electrodes[63]. The electrode can be molded in diverse configurations including supported or unsupported thick films, rods, disks and even in the form of microelectrodes (approx. 20 micron in diameter)[62,63].

Incorporation of hydrophilic additives, such as polyethylene glycol or tetramethoxysilane in the sol–gel starting solution, endows a degree of hydrophilicity and a controlled section of the electrode can be wetted by the electrolyte. The wetted section is very stable and remains constant even after several weeks immersion in an electrolyte[65]. Graphite exhibits poor electrocatalytic activity but addition of trace metal or organometallic catalysts improves its electrocatalytic activity. CCEs containing organometallic catalysts such as cobalt phthalocyanine and cobalt porphyrin showed pronounced electrocatalytic activity toward the reduction of dioxygen[65,66]. Incorporation of the catalysts can be done by impregnation of the carbon powder with the organometallic catalysts prior to mixing with the sol–gel precursors or by adding the catalyst to the sol–gel precursors–carbon mixture. Inert metal ions (e.g. Pd, Pt) can also be added in ionic form to the sol–gel precursors and after electrode molding they can be reduced *in situ* by a flow of hydrogen gas through the porous electrodes[67,68]. Since the electrodes are porous, the inert metal and organometallic modified CCEs can act as gas electrodes such as oxygen, carbon monoxide and sulfur dioxide[67,68].

Since CCEs are molded at room temperature it is possible to incorporate enzymes into it as well[69–74]. The simplest form is comprised of glucose oxidase/methyl silicate (or silica)/graphite composite[16,69]. Dissolved oxygen served as electron acceptor and the resulting hydrogen peroxide is electrooxidized on the electrode. In order to lower the over-voltage that is required for hydrogen peroxide oxidation, palladium catalyst is added to the above construction. Electrodes for lactate (with lactate oxidase) and aminoacids (aminoacid oxidase) were prepared in a similar manner[64]. Another method to reduce the signal dependence on the level of oxygen was to incorporate a mediator into the sol–gel starting solution: Tetrathiafulvalene and glucose oxidase doped CCE was indeed found to show oxygen-independent response[69,70]. In another modification[71] ferrocenyl groups were covalently bonded to the glucose oxidase, which was encapsulated in the sol–gel matrix. Finally, a new type of porous, hybrid organic–inorganic material was synthesized and used for direct wiring of active enzymes[72,73]. The material was comprised of a dispersion of graphite powder and glucose oxidase incorporated in multifunctional, ferrocene-, amine- and methyl-modified silicate sol–gel backbone. Each component in this integrated construction accomplishes a specialized task: The graphite provides conductivity by percolation; the silicate provides highly crosslinked and rigid backbone, which is used to cage the redox enzyme; ferrocene is responsible for the signal transduction from the active center of the enzyme to the electron conductive surface; amine groups were incorporated for their high affinity to excess negative charges on the surface of glucose oxidase; and finally, the combination of methyl and amine groups allows control of the wetted electroactive section of the electrode. Recently, Wang and coworkers[74] showed that CCEs can be produced by thick film, ink jet technology. This technology enables highly reproducible mass production of biosensors.

IV. COVALENT ENTRAPMENT OF ORGANIC FUNCTIONAL GROUPS

A. Trialkoxysilanes as Precursors for Functionalization

The development of hybrid materials with covalent bonds between the organic and inorganic entities is based on molecular precursors of the general type $RSiY_3$, where R is an organic group bonded to the silicon atom via a Si−C bond. Compounds of the type R_2SiY_2 would serve the same purpose, but are hardly used for the development of sol–gel materials. We restrict ourselves to alkoxysilanes, $Y = OR'$, which are nearly exclusively employed in sol–gel chemistry. Hydrolysis and condensation of $RSi(OR')_3$ results in the formation of silsesquioxanes $RSiO_{3/2}$[75] in which the organic groups R are covalently bonded to the polysiloxane network. The materials can be inorganically 'diluted' by co-hydrolysis of $RSi(OR')_3$ (or mixtures of silanes with different organic groups R) with $Si(OR')_4$ in any ratio. The higher the amount of $Si(OR')_4$ in the starting mixture, the lower is the concentration of the organic groups in the final material and the more 'inorganic' are its properties. This blending of materials properties by using mixtures of different precursors is the basic idea behind the development of inorganic–organic hybrid materials. The sol–gel processing of mixtures of different alkoxides requires careful elaboration of the reaction conditions to avoid uncontrolled phase separations or to obtain a defined distribution of the different building blocks.

The group R can be almost any organic group if it is hydrolytically stable. It may serve several purposes, such as modifying the network structure, introducing organic functionalities into the inorganic network or providing reactive groups for organic crosslinking reactions.

When $Si(OR')_4$ is successively replaced by $RSi(OR')_3$, condensation sites are blocked and the average degree of crosslinking per silicon atom drops from 4 to 3. In reality the degree of crosslinking is somewhat smaller, due to residual Si−OR′ and Si−OH groups in the final materials. Lowering the degree of crosslinking results in a modification of the microstructure and the physical properties associated with that (mechanical properties, for example). If this is the only goal of the system modification, simple organic groups, such as alkyl or phenyl groups, can be used as the substituents R. It should be kept in mind, however, that lowering the degree of crosslinking is an inevitable side-effect when organic groups are introduced for other purposes. For some applications it may therefore be necessary to balance the $RSi(OR')_3/Si(OR')_4$ ratio carefully.

The introduction of organo*functional* groups, i.e. the use of alkoxysilanes of the type $(R'O)_3Si{-}X{-}A$, where A is a functional organic group and X is a chemically inert spacer permanently linking Si and A, results in a more extensive chemical modification of the materials[76]. The properties of the organic functions A supplement the properties of the polysiloxane matrix formed by hydrolysis and condensation of the $Si(OR')_3$ and $Si(OR')_4$ units.

A variety of precursors of the type $(R'O)_3Si{-}X{-}A$ is commercially available or can easily be prepared. The spacer X is a $(CH_2)_n$ ($n = 2, 3$) chain in most cases. The preparation of such compounds has been reviewed elsewhere[77,78]. Therefore we restrict ourselves to demonstrating the more general routes by selected examples:

(i) *Hydrosilylation of alkenes or alkynes*, i.e. the rhenium catalyzed addition of Si−H bonds to double or triple bonds, e.g. equation 3[79].

(ii) *Substitution of organic groups*, e.g. equation 4[80].

(iii) *Addition to organic groups*, e.g. equations 5 and 6[81−84].

(iv) *Substitution of $(R'O)_3SiCl$ by Grignard or organolithium reagents*, e.g. equation 7[85].

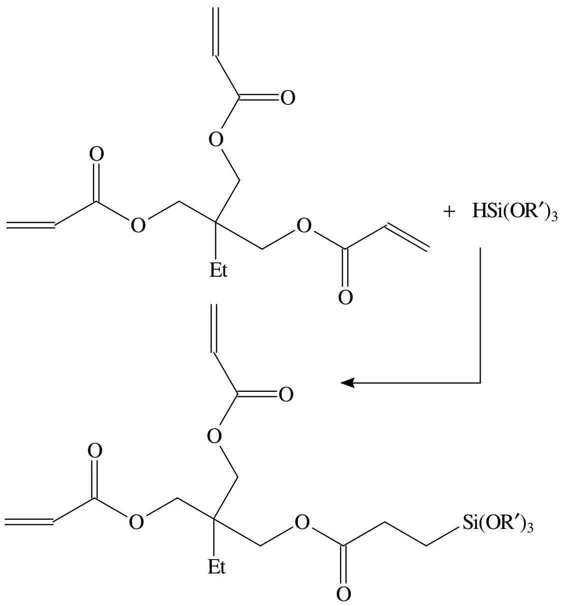

(3)

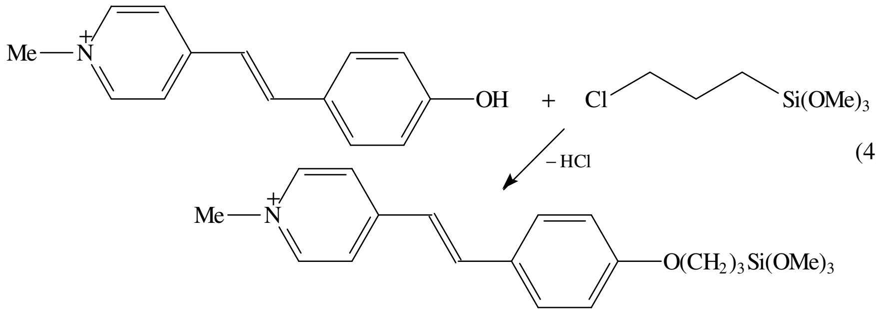

(4)

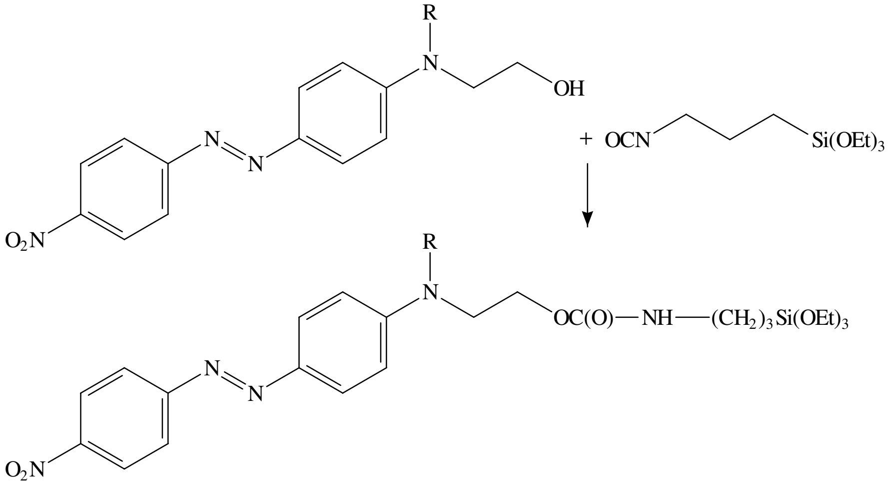

(5)

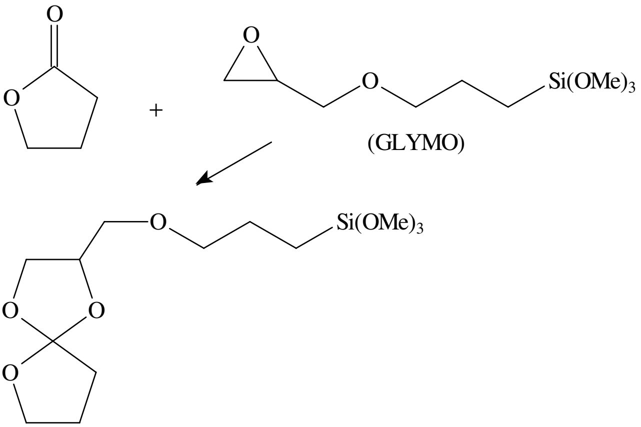

(6)

$$\mathrm{LiC{\equiv}C{-}C{\equiv}CLi + 2ClSi(OMe)_3 \longrightarrow (MeO)_3SiC{\equiv}C{-}C{\equiv}CSi(OMe)_3 + 2LiCl} \qquad (7)$$

B. Alkyl- and Aryl-substituted Materials

Methyl- or phenyl-substituted silsesquioxanes obtained by hydrolysis and condensation of $RSi(OR')_3$ or $RSiCl_3$ (R = Me, Ph) were studied extensively by several groups[75]. MeSi– and PhSi– units are the classical components of silicones. The molecular weight and structure of methyl- or phenyl-substituted silsesquioxane polymers, and thus their physical properties (solubility, mechanical properties, etc.), depend very much on the reaction conditions. Since silicones are not the topic of this article, the interested reader is referred to the relevant literature.

In the context of sol–gel processing, $RSi(OR')_3/Si(OR')_4$ mixtures (R = simple aryl or alkyl groups) are interesting for several reasons:

(i) These groups allow an easy modification of the inorganic network (reduction of the average degree of crosslinking per silicon atom) without introducing too bulky or reactive organic groups.

(ii) Alkyl or aryl groups provide hydrophobicity to the resulting materials.

(iii) These mixtures are model systems for studying the sol–gel chemistry of $RSi(OR')_3/Si(OR')_4$ mixtures with less simple organic groups R.

Although alkyl groups already make sol–gel materials more hydrophobic than unmodified silica gels, fluorinated groups are even better for this purpose. The surface tension of 3,3,4,4,5,5,6,6,6-nonafluorohexylsilsesquioxane was found to be only one third of that of methylsilsesquioxane[86]. Addition of fluorinated alkoxysilanes of the type $(R'O)_3Si(CH_2)_n(CF_2)_mCF_3$ to a mixture of other precursors resulted in low energy coatings with antisoiling properties[87] or functional coatings on glass with increased hydrophobicity[88].

Considering the steric and electronic influence of different organic groups R on the hydrolysis and condensation rates of $RSi(OR')_3$ (relative to that of $Si(OR)'_4$), it is obvious that in multicomponent precursor systems a statistical distribution of the molecular building blocks in the final materials is rather unlikely. This was, for example, demonstrated by ^{29}Si NMR spectra of gels obtained by cohydrolysis of $Me_2Si(OEt)_2$ and $Si(OEt)_4$ in a neutral or acidic medium[89,90]. Signals typical for hydrolyzed $Me_2Si(OEt)_2$ and for hydrolyzed $Si(OEt)_4$ were found, but also new signals assigned to links between both building blocks. Based on the NMR results structural models were proposed, depending on the $Me_2Si(OEt)_2/Si(OEt)_4$ ratio, x. For an excess of $Me_2Si(OEt)_2$ ($x \geqslant 2$), the tetrafunctional units derived from $Si(OEt)_4$ are rather isolated and serve to crosslink the polydimethylsiloxane chains derived from $Me_2Si(OEt)_2$. For $x < 2$, the spectra are characteristic for an interconnected network of $Si(-O-)_4$ and $MeSi(-O-)_3$ units. In any case, the $(Me_2SiO)_n$ chains appear to be rather long. $Ti(OR)_4$ and $Zr(OR)_4$ instead of $Si(OR)_4$ do not only act as crosslinking agents between the difunctional units, but also catalyze their condensation reaction[90].

The various reaction rates of different alkoxides are not just an obstacle on the way to homogeneous materials. They can be exploited for the deliberate engineering of some nanoheterogeneity (i.e. of the micro- and nanostructure) and thus provide additional possibilities for materials developments. A recent example to illustrate this point is the development of inorganic–organic hybrid aerogels from $RSi(OMe)_3/Si(OMe)_4$ mixtures (R = terminal alkyl and aryl, or certain functional organic groups)[91,92]. It is known that under basic conditions hydrolysis and condensation of $Si(OR')_4$ is faster than that of $RSi(OR')_3$. Therefore, the build-up of the gel network from $RSi(OMe)_3/Si(OMe)_4$ mixtures under these conditions is basically a two-step process. In the first stage, $SiO_x(OH)_y(OMe)_z$ clusters are formed by hydrolysis and condensation of $Si(OMe)_4$, while $RSi(OMe)_3$ basically is a co-solvent. The $RSi\equiv$ units condense at the surface of the primary clusters in the later stage of the reaction. Self-condensation of the $RSi-$ units does not play an important role under these conditions and with the proper $RSi(OMe)_3/Si(OMe)_4$ ratio. The latter depends on the nature of R and on the density of the gel. As a rule of thumb, 10–30 mol% $RSi(OMe)_3$ are sufficient to cover the inner surface of the aerogels, but do not affect their nanostructure from which the unique physical properties originate. The fate of the individual alkoxides was monitored by Raman spectroscopy, which provided clear evidence for the two-step process[92].

Since the $RSi\equiv$ units cap the $SiO_x(OH)_y(OMe)_z$ clusters formed during sol–gel processing of $Si(OMe)_4$, a hydrophobic inner surface is created, and the resulting aerogels are permanently stable against moisture (unmodified silica aerogels are immediately destroyed on contact with water). The uniform coverage of the inner aerogel surface by the organic groups also allows one to generate nanosized carbon structures by controlled pyrolysis of the organic groups. They partly cover the silica nanospheres from which the aerogel skeleton is composed, and result in an efficient infrared opacification necessary to improve the heat insulation properties of aerogels at high temperatures[93].

C. Materials Substituted by Polymerizable Organic Groups

Alkoxysilanes $(R'O)_3Si{-}X{-}A$, in which the group A can undergo organic polymerization reactions, are extremely interesting because they allow the preparation of inorganic–organic hybrid polymers. Polymerization (or any other crosslinking reaction) of the organic groups after sol–gel processing results in a dual network structure, where the inorganic and organic substructures are covalently linked to each other. Such polymers are mostly applied for coatings for different purposes, but recently also as bulk materials. They constitute the technically most advanced applications for inorganic–organic hybrid polymers.

The methacrylate substituted silane $(MeO)_3Si(CH_2)_3OC(O)C(CH_3){=}CH_2$ (MEMO), vinyltrimethoxysilane $(MeO)_3SiCH{=}CH_2$ (VTMS) or the epoxy-substituted silane $(MeO)_3Si(CH_2)_3OCH_2(\overline{CHCH_2O})$, all being commercially available, are frequently used as precursors for this purpose.

Alkoxysilanes $(R'O)_3Si{-}X{-}A$ with different spacer groups X between the unsaturated organic group and the $Si(OR')_3$ moiety (different lengths and/or different chemical constitution) and/or with multiply unsaturated groups (to achieve a higher degree of organic crosslinking) allow the development of copolymers with tailored mechanical and optical properties. Such precursors were synthesized by using *one* double bond of a multiply unsaturated organic monomer to anchor the $Si(OR')_3$ group and retain the other double bond(s) for later polymerization reactions. An example is given in equation 3; many other multiply unsaturated organic compounds are available. Other coupling reactions can be utilized, such as SH addition of $(R'O)_3Si(CH_2)_3SH$ to $C{=}C$ bonds or coupling of $(EtO)_3Si(CH_2)_3NCO$ with OH-terminated bis(acrylates)[79,94,95]. Other reactive groups suitable for organic crosslinking by polymerization reactions can, of course, be linked analogously to $Si(OR')_3$ groups. For example, the spiro orthoester moiety shown in equation 6 is capable of ring-opening polymerization with only a very low shrinkage[84].

The influence of the steric and electronic properties of the group R on the hydrolysis and condensation kinetics of organically substituted alkoxysilanes $RSi(OR')_3$ was recently discussed in a review article[96]. It can be implied that functional and nonfunctional groups R of comparable size and electronic properties have the same influence if the organic function A in $(R'O)_3Si{-}X{-}A$ does not interact with the silicon atom or does not catalyze the reaction. Since polymerizable groups usually do not have basic or acidic properties, a catalytic effect on the sol–gel reactions cannot be expected. Only their steric bulk could influence the build-up and properties of the gel network. However, there are two other issues which are very important for the later polymerization of the organic groups: (i) are the functional groups retained during sol–gel processing? and (ii) where are the organic groups located in the primary hydrolysis products (which constitute the inorganic building blocks)? This is a particularly important question if mixtures of two or more different precursors are used, which is the case for most applications.

The hydrolysis and condensation reactions, and the development of the molar mass distribution of VTMS[97], GLYMO (equation 6)[98,99] and MEMO[98,100–103] was investigated by GPC (gas permeation chromatography), ^{29}Si NMR and FTIR. The uncatalyzed hydrolysis of both GLYMO and MEMO resulted in the slow formation of rather small oligomers[98,104]. The degree of oligomerization was influenced by the silane : water ratio.

Both basic and acidic catalysts accelerate the reaction rates and the growth of the oligomers, as expected. The influence of the kind of catalyst on the growth of oligomers from MEMO was studied by GPC[98]. With 1-methylimidazole, methacrylic acid or $Zr(OPr\text{-}n)_2(OMe)_2$ as catalysts, condensation essentially stopped at the stage of medium-sized oligomers ($M_p < 10^4$). Only with the strongly basic dimethylaminoethanol or with HF as the catalysts larger polymers were formed. In the dimethylaminoethanol catalyzed reaction, the polymer growth was not finished after 3 months[98,101]. The HCl-catalyzed hydrolysis of VTMS, MEMO or GLYMO also gave only medium-sized oligomers ($M_w = 1.0\text{–}1.5 \times 10^3$)[99,105].

The results of these studies can be summarized as follows. The growth mechanism of the siloxane oligomers is probably the same as proposed by Brown for the condensation of cyclohexyl- or phenylsilanetriol via cyclic tetramers and cubic octamers[106]. Condensation of the functionalized silanes stops at the stage of rather small oligomers unless *very* active catalysts are used. Even then, hydrolysis and condensation is not complete (residual Si−OH and Si−OR′ groups) over rather long periods. This is probably due to steric effects of the rather bulky organic groups. Both the configuration and the molar mass distribution of the polymers depend on the solution pH.

Although random or ladder structures (Figure 2) have been proposed in some cases, the molecular weight distributions for the GLYMO and MEMO hydrolysates[98] indicate that octameric species play an important role in the formation of the polymers. Silsesquioxanes $(RSiO_{3/2})_8$ (Figure 2) with various groups R have been synthesized[107] and can be considered model compounds for the hydrolysis intermediates.

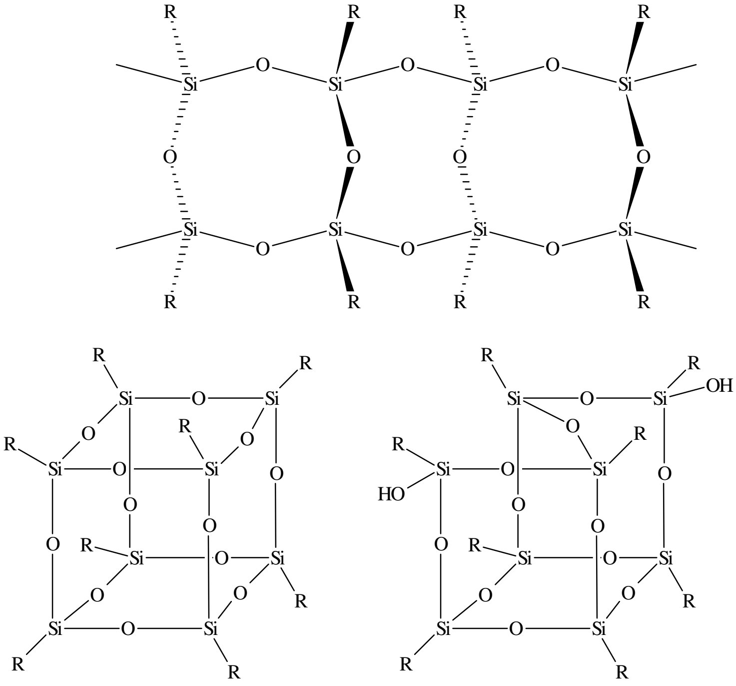

FIGURE 2. Structures of silsesquioxanes. Left: ladder structure; middle: 'double four-ring' (= cubic octamer); right: partial cage structure

In a mixture of two alkoxide precursors a mutual influence on the hydrolysis and condensation processes can be expected. How the molar mass develops in $Si(OR')_4/(R'O)_3Si{-}X{-}A$ mixtures is a question which was hardly investigated. For the MEMO/$Si(OEt)_4$ system this was studied by measuring the gel times (t_G)[108]. The addition of MEMO to an acidic mixture of $Si(OEt)_4$, ethanol and water resulted in a considerable increase of t_G. Under basic conditions the increase of t_G was less dramatic. The influence of MEMO is probably due to steric hindrance by the methacrylate group during formation of the gel network and the decrease of the average degree of crosslinking [partial replacement of $Si({-}O{-})_4$ by $RSi({-}O{-})_3$].

A major concern is the fate of the functional organic group A during sol–gel processing, particularly if it is not totally inert towards water. For example, hydrolytic ring opening of the epoxy group in GLYMO to give diol units is catalyzed by many basic or acidic compounds[109]. Since a catalyst has to be used for sol–gel processing to get real polymers (see above), its influence on the epoxy group is crucial. However, under neutral or slightly basic conditions the rate of the epoxide hydrolysis reaction is slow compared with the siloxane polycondensation reaction. The different reaction rates allow the preparation of hybrid materials by a two-step process, in which formation of the $Si{-}O{-}Si$ network is carried out first and later the epoxy polymerization is induced[104,110]. For example, a highly flexible, nevertheless abrasion-resistant coating for polyethyleneterephthalate or polycarbonate was obtained from GLYMO, with 1-methylimidazole as the catalyst. 1-Methylimidazole acts as a sol–gel catalyst at room temperature, and in the second step of the materials synthesis as an initiator for the epoxide polymerization at a higher temperature[104,110]. Sol–gel processing of GLYMO can, of course, also be run in a way to deliberately produce diol units. Contact lenses[111] and antifogging coatings on glass[87] were developed by this approach. The preparation of hybrid polymers from the bifunctional molecular precursors $(R'O)_3Si{-}X{-}A$ is usually performed in the two-stage process described for GLYMO. The precursors are first reacted with water to form the inorganic structure to which the polymerizable organic groups A are attached. While gelation occurs, the materials can be molded or applied as coatings with conventional coating techniques (spray, dip, spin-on coating etc.). The organic groups are then polymerized or crosslinked to form the organic network. This results in a permanent hardening of the materials. Both reaction steps may occur more or less simultaneously, but the reaction in most cases is initiated by the addition of water and the catalyst, i.e. by starting the sol–gel process.

Another recent example also shows very elegantly this stepwise build-up of the inorganic and organic substructures. Transparent gels containing bridging 1,3-butadiyne units were obtained by sol–gel processing of $(MeO)_3SiC{\equiv}C{-}C{\equiv}CSi(OMe)_3$ (see equation 7). When the dried gels were heated in the solid state to about 200 °C, the highly reactive diyne units polymerized to give a more crosslinked inorganic–organic hybrid polymer[112].

There are several options by which the composition, structure and properties of the hybrid polymers can be varied:

(i) Cocondensation with other alkoxides: either with $Si(OR')_4$ or binary alkoxides of other elements [$E(OR')_n$] and/or with other organically or organofunctionally substituted alkoxides.

(ii) Organic copolymerization with organic monomers, macromolecules or reactive substituents of other organofunctional alkoxides.

(iii) Choice of thermal or photochemical polymerization. Whether thermal or photochemical curing is more suitable depends on the chemical system and the kind of application. Photochemical curing is preferred for coatings of polymers with low thermal stability or for applications in which very rapid curing is essential.

With these options, there are many possibilities to modify organic–inorganic hybrid polymers chemically and thus to tailor their macroscopic properties. Not only the kind and connectivity of both the organic and inorganic building blocks can be varied (including combinations of different groupings in both parts), but also their ratio. Although sometimes difficult to control, multicomponent systems allow to some extent the fine-tuning of macroscopic materials properties, due to the specific functions and properties of each component.

1. Cocondensation with $E(OR')_n$

'Dilution' of an organofunctional alkoxysilane $(R'O)_3Si{-}X{-}A$ with an unsubstituted metal or semi-metal alkoxide $E(OR')_n$ results in materials with properties between those of the silsesquioxane $O_{3/2}Si{-}X{-}A$ and the oxide $EO_{n/2}$. A steady change of materials properties between the two extremes is in principle possible by varying the ratio of the two alkoxides. Employing another alkoxide than $Si(OR')_4$ additionally allows some variation of the chemical nature of the inorganic building blocks and of the materials properties originating from them.

The first commercial application of inorganic–organic hybrid polymers may illustrate this point. A scratch-resistant, transparent coating for optical polycarbonate lenses was developed from mixtures of GLYMO, $Si(OMe)_4$ and $E(OR)_n$ [$E(OR)_n = Ti(OEt)_4$, $Zr(OPr)_4$ or $Al(OR)_3$, respectively][113]. The binary alkoxides have two functions: they build up the inorganic substructure of the final material, and the nonsilicon alkoxides $E(OR)_n$ already at room temperature catalyze the polymerization of the epoxide groups[109]. Since the rates for the reaction of the different alkoxides with water are very different, the way how the water (and the catalyst) is added to the precursor mixture is very crucial in obtaining homogeneous and transparent materials. The ratio of GLYMO, $Si(OMe)_4$ and $E(OR)_m$ is another parameter that influences both the rate of the polymerization reaction (and thus the viscosity increase and the processability) and the macroscopic properties of the coatings[113,114].

For the development of a scratch- and abrasion-resistant, corrosion-preventing coating system for brass, the system had to be modified. A better adhesion to the inorganic surface and also a reduction of the brittleness of the coating was achieved by sol–gel processing of a mixture of GLYMO, $PrSi(OMe)_3$ and $Al(OBu\text{-}s)_3$. Adhesion to the metal surface was very good even after weathering, due to the covalent bonding between the metal surface and the coating[115].

2. Cocondensation of different organically modified alkoxides.

The use of more than one organofunctional alkoxide precursor can serve different purposes:

(i) to enable organic crosslinking by addition reactions without polymerization,

(ii) to modulate the organic substructure, or

(iii) to link different inorganic building blocks.

In the first example two different silanes were used, which allow different ways of organic crosslinking. A coating system for the mechanical protection of plastics, particularly polymethylmethacrylate, was obtained from $(MeO)_3SiCH{=}CH_2$ (VTMS) and $(MeO)_3Si(CH_2)_3SH$ (MPTMS). Two crosslinking modes of the organic groups are possible upon UV irradiation: the vinyl groups may polymerize to yield polymethylene links between silicon atoms, or the $-SH$ function may add to a vinyl group to give $-(CH_2)_2{-}S{-}(CH_2)_3-$ links. When VTMS and MPTMS were employed in a 9:1 molar ratio, vinyl polymerization prevailed, whereas with a 1:1 ratio the thiol addition reaction was dominating. In the latter case, the coatings were then cured in about half the time because this reaction is faster than vinyl polymerization. Owing to the different chain lengths of the alternative links, the flexibility of the coating can be varied by the ratio of the starting compounds[110].

Very versatile hybrid materials for applications in microsystem technologies were prepared from a mixture of MEMO, GLYMO, $Si(OEt)_4$, VTMS or diphenylsilanediol[116]. These materials were used, *inter alia*, for passivation and encapsulation of electrical components, as protective coatings for thin film capacitors[117] or as patternable coatings. The photolithographic structuring procedure illustrates the functions of the different precursors. The inorganic network is formed during sol–gel processing. The thus-obtained coating lacquer was applied to the substrates by standard techniques. The methacrylate groups of MEMO were photochemically polymerized by structuring UV irradiation (masks or laser writing). The nonexposed parts of the coating was then dissolved by a developer solution. Finally, the structured coating was thermally cured by polymerization of the epoxy groups of GLYMO[116].

Another example shows that two different inorganic building blocks, i.e. silicate and zirconate structures, can also be linked by organic polymer units. A scratch-resistant coating material for polycarbonate (for instance, compact disks)[101,110] for optical and microoptical applications[103] and transparent monoliths[118] was developed by copolymerizing the methacrylate units of $(n\text{-PrO})_3Zr(\text{methacrylate})$ or $(n\text{-PrO})_2Zr(\text{methacrylate})_2$ and MEMO after sol–gel processing of the precursor mixture.

3. Copolymerization with organic monomers

When hybrid polymers are prepared from only $(R'O)_3Si{-}X{-}A$, the crosslinking of all available organic groups is often difficult, probably for steric reasons.

The dimension of the organic structures and the degree of organic crosslinking in inorganic–organic hybrid polymers can be increased by copolymerizing the reactive groups of the organofunctional alkoxide $(R'O)_3Si{-}X{-}A$ with organic monomers or small oligomers. For example, photochemical polymerization of an aged gel, obtained from a 1:1 mixture of MEMO and $Si(OEt)_4$, left about 20% of the initial double bonds unreacted. However, when two equivalents of methylmethacrylate (MMA) were added, UV irradiation resulted in the complete polymerization of the methacrylate groups from both sources (MEMO and MMA)[102]. A mixture of MEMO, $MeSi(OEt)_3$ and $CF_3CH_2CH_2Si(OMe)_3$ was also copolymerized with fluorinated acrylic monomers and oligomers[119]. Other simple examples of this very useful approach include the copolymerization of hydrolyzed *N*-(3-trimethoxysilylpropyl)pyrrole with pyrrole[120] or GLYMO with cycloaliphatic diepoxide monomers[121].

The latter reaction provided a new type of Li^+ conducting polymer. MEMO and GLYMO were hydrolyzed and then ethylene glycol diglycidyl ether was added. Methylimidazole was used both as a catalyst for the sol–gel step and the copolymerization of the epoxide groups of GLYMO and the diglycidyl ether. Due to the presence of polyethylene oxide units, $LiClO_4$ is easily dissolved in the hybrid polymer. The obtained material is amorphous after curing and can be applied as coatings or in bulk[122].

A modification of the approach to facilitate crosslinking by adding organic monomers is to use pre-formed silicate clusters capped by reactive organic groups and to crosslink them by organic entities. Hybrid polymers with very defined structures are thus obtained[123]. As discussed above, spherosilicates $(ROSiO_{3/2})_8$ or silsesquioxanes $(RSiO_{3/2})_8$ (Figure 2) with various groups OR or R can be prepared. Examples for this approach include the coupling between $(HMe_2Si{-}O{-}SiO_{3/2})_8$ and vinyl-substituted siloxanes or, *vice versa*, between $(CH_2{=}CHSiMe_2{-}O{-}SiO_{3/2})_8$ and hydrogenosiloxanes by hydrosilylation[123,124]. Recently, heterocoupling between $(HMe_2Si{-}O{-}SiO_{3/2})_8$ and allyl acetoacetate-modified aluminum and zirconium alkoxides was also reported[123].

The copolymerization of unsaturated organofunctional alkoxysilanes with organic monomers or the use of different organofunctional alkoxysilanes allows the tailoring of materials properties by variation of the organic polymer structures. In order to avoid the potential problems associated with precursor mixtures, but still to use this option, one was led to the development of the above-mentioned precursors by coupling multiply unsaturated organic monomers with $Si(OR')_3$-containing compounds

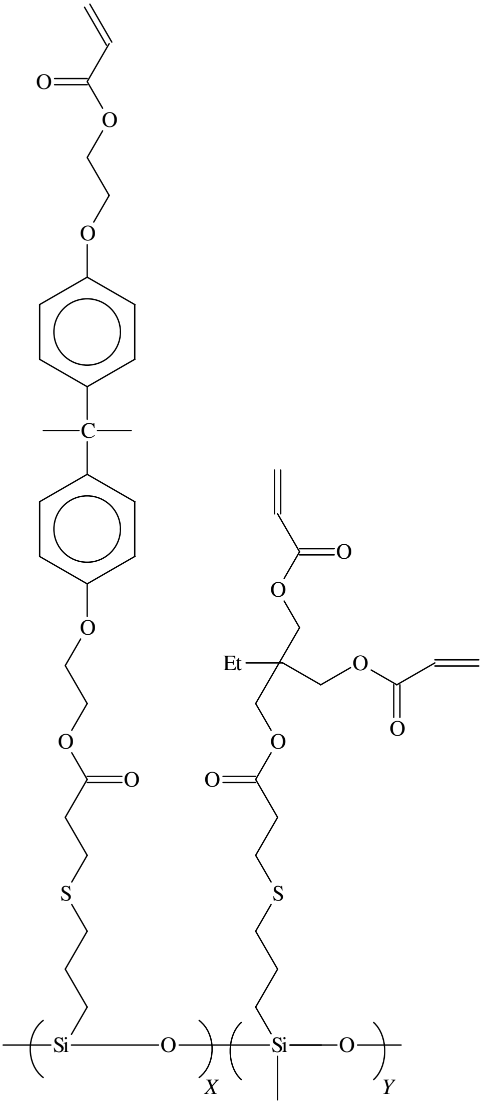

FIGURE 3. A schematic sketch of the polysiloxane used for rapidly curing coatings of optical glass fibers

(e.g. equation 3). Although they are single precursors, the structure of the organic spacer between the unsaturated group(s) and the $(R'O)_3Si$ group, as well as the number of unsaturated groups available for polymerization (i.e. the degree of organic crosslinking) is easily modulated[79,94,95]. It was shown that the Young's modulus of the photochemical crosslinked materials and the thermal expansion coefficient can be varied in a very wide range just by varying the organic structures[95]. Some other advantages of hybrid polymers prepared from these precursors, such as low shrinkage, high flexural strength and the low water adsorption, led to their application as dental filling materials (combined with some inorganic fillers) and for the production of optical lenses[95]. Lenses made from such precursors had comparable optical properties and densities to those made from purely organic polymers. However, their abrasion resistance was distinctly better[94].

Combination of different silanes allowed the development of fast curing primary and secondary coatings for optical glass fibers. UV curing is possible in less than 0.1 s, even on a technical scale, due to the high density of unsaturated organic groups (as shown schematically in Figure 3). The different modulus of elasticity and scratch resistance required for primary or secondary coatings was adjusted by the ratio of the two silanes ($x : y$ in Figure 3)[94].

D. Materials Substituted by Aminoalkyl or Phosphinoalkyl Groups

The most often used amino-substituted alkoxysilanes are $(R'O)_3Si(CH_2)_3NH_2$ (and the corresponding NMe_2 and NEt_2 derivatives) and the ethylene diamine derivative $(R'O)_3Si(CH_2)_3NH(CH_2)_2NH_2$ (DIAMO), which are commercially available. The phosphinoalkyl derivative $(R'O)_3Si(CH_2)_2PPh_2$ is easily prepared by addition of $HPPh_2$ to the vinylic double bond of VTMS.

Contrary to the above-discussed alkoxysilanes with unsaturated organic groups it can no longer be assumed that the organic functionalities will not interfere with the sol–gel chemistry of the $Si(OR')_3$ group during sol–gel processing. Both internal coordination of the basic amino group to the weakly Lewis-acidic silicon atom and strong hydrogen bonds between the Si–OH groups and the NH_2 group were debated for hydrolyzed aminopropyltrialkoxysilanes[125]. Due to these interactions, the rates of the uncatalyzed hydrolysis and condensation reactions of aminopropyltrialkoxysilanes are similar to those of alkyltrialkoxysilanes in the presence of a base catalyst[126,127].

Upon addition of water to $(EtO)_3Si(CH_2)_3NEt_2$, octameric species $[Et_2N(CH_2)_3SiO_{3/2}]_8$ were predominantly formed in methanolic solution according to gel permeation chromatographic studies[127]. A structure in which organofunctional groups are located at the outside of the polysiloxane building blocks was also postulated from a ^{29}Si and ^{31}P solid-state NMR study of a gel obtained from $(MeO)_3Si(CH_2)_6P(Ph)(CH_2)_2OMe$ and $Si(OEt)_4$ (1:2)[128].

There are four major functions of amino groups attached to organically modified silica gels:

(i) Amino groups provide hydrophilicity to the materials, due to their basic properties. For example, coatings with good long-term adhesion to glass, scratch and abrasion resistance, and stability against weathering and corrosive deamination were prepared from $PhSi(OEt)_3$, $Al(OBu\text{-}s)_3$ and MEMO (for photochemical curing) or GLYMO (for thermal curing). The polarity of the surface was varied by addition of tridecafluorooctyltrimethoxysilane (increased hydrophobicity) or DIAMO (increased hydrophilicity), respectively[88].

For the preparation of proton-conducting polymers, aminoalkyl-substituted siloxanes made by sol–gel processing of $(MeO)_3Si(CH_2)_3NR_2$ [for example, $NR_2 = NH_2$, $NH(CH_2)_2NH_2$, $NH(CH_2)_2NH(CH_2)_2NH_2$] were doped with CF_3SO_3H[129].

(ii) Amino groups may act as coupling sites for organic crosslinking reactions. For example, hydrolyzed GLYMO and $(EtO)_3Si(CH_2)_3NH_2$ react by formation of β-amino alcohol links[130]. Similarly, the reaction of $(EtO)_3Si(CH_2)_3NH_2$ with phthalic anhydride or pyromellitic dianhydride provided the hydrophilic function in a polymer with potential application for ultrafiltration and reverse osmosis membranes[131].

A sensor with a nonleachable pH indicator was prepared from a $(MeO)_3Si$-substituted derivative of methyl red $[(p\text{-}Me_2N)C_6H_4N{=}N(C_6H_4COOH\text{-}o)]$ obtained by coupling of the COOH groups with $(MeO)_3Si(CH_2)_3NH_2$[132]. For the development of an optical immunosensor, a sol prepared from $(EtO)_3Si(CH_2)_3A$ (A = NHMe, NH_2 or SH) was coated on gold-coated glass surfaces. After activation of the organofunctional hybrid polymer films in aqueous buffers by bifunctional coupling agents, immunoglobulin was covalently anchored to the transducer surface with an optimal stability and biological activity[55].

(iii) Amino groups form weak adducts with SO_2 or CO_2. The incorporation of aminoalkyl groups into sol–gel materials can therefore be utilized for the development of gas sensors. For example, the sensitive layers of SO_2 gas sensor systems were synthesized from 7:3 mixtures of $(EtO)_3Si(CH_2)_3NR_2$ (R = Me, Et) and n-$PrSi(OEt)_3$[114,133,134]. Two gas-sensitive layers for different SO_2 concentration ranges were developed in another work: for low concentration (*ca* 2 ppm) based on $(EtO)_3Si(CH_2)_3NMe_2$, and for concentrations up to 6000 ppm based on $(EtO)_3Si(CH_2)_3NEt_2$[135]. Replacement of the NR_2 group in the starting alkoxysilane by NH_2 resulted in a material suitable for the detection of CO_2[134].

(iv) Amino groups, particularly the ethylenediamine entity, are capable of binding metal ions. Sol–gel processing of metal alkoxides in the presence of metal ions mostly does not result in a stable incorporation of the metal ions. They are leached from the resulting oxide materials by water or alcohols. This is prevented when amino-substituted alkoxides are employed. The ethylenediamine derivative $(EtO)_3Si(CH_2)_3NHCH_2CH_2NH_2$ proved to be very effective for anchoring Cd^{2+}, Co^{2+}, Cu^{2+}, Ni^{2+}, Pd^{2+} or Pt^{2+}, while Ag^+ was better coordinated by $(EtO)_3Si(CH_2)_3NH_2$ or $(EtO)_3Si(CH_2)_3CN$[136]. The substituted thiourea $(EtO)_3Si(CH_2)_3NHC(S)NHPh$ was prepared by reaction of $(EtO)_3Si(CH_2)_3NH_2$ with PhNCS and was used to coordinate Pd^{2+} ions[137]. When the organofunctional silane and a metal salt are mixed, metal (M) complexes of the type $[(R'O)_3Si(CH_2)_3A]_mM^{n+}$ are formed *in situ*. Coordination of the metal ions is retained during sol–gel processing[136].

The high dispersion of metal ions achieved by their coordination with $(EtO)_3Si(CH_2)_3A$ and by tethering the resulting metal complexes to the silicate matrix during sol–gel processing was used to develop a method of preparing nanosized metal or alloy particles in SiO_2 matrices. In the second step of the preparation procedure, metal oxide particles are formed by oxidation of the metal complex containing gels in air under carefully controlled conditions. Because of the high dispersion of the metal precursor, very small metal oxide particles with a very narrow size distribution are formed, which are then reduced to give the metal particles[136].

In a related approach, amino-substituted organofunctional alkoxysilanes were used to stabilize small CdS or metal clusters in sol–gel matrices[138].

The sol–gel method is also an attractive possibility to tether metal *complexes* to silica-type materials, mainly for the heterogenization of homogeneous metal complex catalysts. Work in this area was reviewed in other articles, where also a list of selected sol–gel heterogenized metal complexes is given[78,139]. For the tethering of catalytically active complexes, nearly any ligating group known from coordination chemistry can be used. In most examples, however, phosphanyl- or amino-substituted groups were employed. A typical approach for the preparation of the $Si(OR)_3$-containing complexes is shown in equation 8[140].

The $(EtO)_3Si(CH_2)_2PPh_2$-substituted complex is prepared as the corresponding complex $(Ph_3P)_2Rh(CO)Cl$, a very well-known homogeneous catalyst, i.e. PPh_3 is just replaced by another phosphine. The complexes $[(R'O)_3Si{-}X{-}A]_nML_m$ (where ML_m is a metal complex moiety) can be used in sol–gel chemistry as any other precursor with some functional group. In the known examples, the structures of the complexes are only insignificantly altered by the modification of the ligand and by sol–gel processing compared with the corresponding complexes with unmodified ligands. This means that the (porous) silica gel matrix surrounding the metal complexes does not interact significantly with the metal centers.

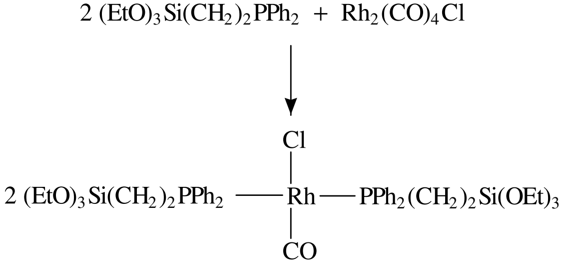

$$\begin{array}{c} 2\,(\mathrm{EtO})_3\mathrm{Si}(\mathrm{CH_2})_2\mathrm{PPh_2} + \mathrm{Rh_2(CO)_4Cl} \\ \downarrow \\ 2\,(\mathrm{EtO})_3\mathrm{Si}(\mathrm{CH_2})_2\mathrm{PPh_2} - \overset{\mathrm{Cl}}{\underset{\mathrm{CO}}{\mathrm{Rh}}} - \mathrm{PPh_2}(\mathrm{CH_2})_2\mathrm{Si}(\mathrm{OEt})_3 \end{array} \qquad (8)$$

The chemistry of the complexes $[(R'O)_3Si{-}X{-}A]_nML_m$ was mainly developed with regard to grafting catalytically active metal complexes on silica as a solid support[141]. The sol–gel approach for the heterogenization of such complexes has several advantages. Compared with other methods, a much higher metal loading can be achieved. The important difference is that in the sol–gel derived materials the catalytically active metal moieties are homogeneously distributed throughout the whole material. This has very beneficial effects on the catalyst stability. Since the structure (porosity, surface area, etc.) of the support can be tailored to some extent, the catalytically active centers are still accessible to the reactants. Therefore, the catalytic activity of the sol–gel catalysts is not inhibited, provided that the matrix structure is appropriate. This was shown, for example, by a comparison of the catalytic activity of sol–gel derived $[O_{3/2}Si(CH_2)_2PPh_2]_2Rh(CO)Cl{\cdot}SiO_2$ with that of dissolved $(Ph_3P)_2Rh(CO)Cl$[142].

E. Materials Substituted by Miscellaneous Groups

In principle, $(R'O)_3Si$-containing groups can be anchored to almost any organic entity by one of the discussed methods. A selection of silanes is shown in Figure 4.

While considerable progress has been made in the preparation of ceramic membranes by sol–gel processing, the development of membranes from hybrid polymers is in its infancy (see also Section V). This is, nevertheless, a very promising area of development, because the possibility of forming mechanically stable membranes by inorganic polycondensation is implemented by the possibility to incorporate organic functions.

Membranes for gas filtration or nanofiltration were prepared from $[(EtO)_2R'Si(CH_2)_3NHC(O)]_2C_6H_4$-*p* ($R' =$ Me or OEt) (Figure 4, bottom) by casting the gels obtained from these precursors on alumina supports[143]. Facilitated transport membranes were prepared by co-hydrolysis with the $Si(OR')_3$-substituted crown ether (Figure 4, top). The transport selectivity of K^+ over Li^+ was about 4 and only due to the presence of the crown ether moieties. Since the selectivity is in good agreement with the properties of benzo-15-crown-5, the character of the carrier was not changed by incorporation into the membrane[143].

The *N*,*N*-dioctadecylsuccinate-substituted silane (Figure 4, middle) was used for immobilized amphiphilic monolayers on glass plates. A covalently bonded monolayer of the silane amphiphile was immobilized on a porous glass plate by the Langmuir–Blodgett

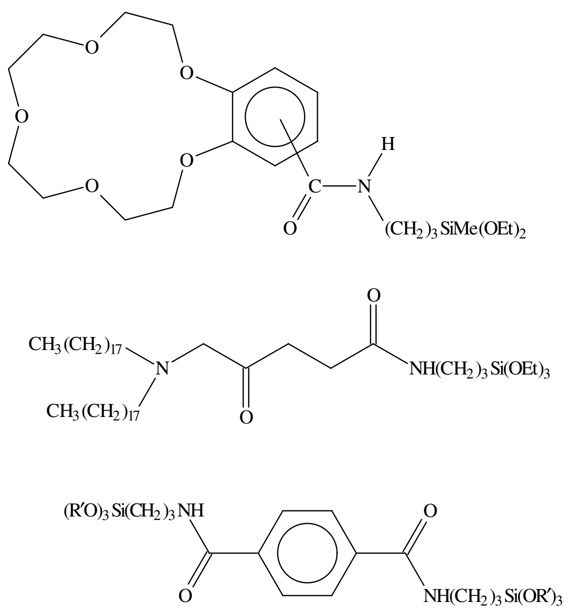

FIGURE 4. Di- and trialkoxysilyl derivatives with various functional organic groups

technique. The lipid monolayer acted as a gate membrane for permeation of ions and water-soluble fluorescent probes[144].

V. ORGANIC/INORGANIC SOL–GEL COPOLYMERIZATIONS

In a sol–gel process carried out with a precursor containing direct organic/inorganic links, it is possible to form homogeneous materials where all bonds are covalent bonds, C–C, Si–C and Si–O. This class of hybrid gels constitutes organic/inorganic polymers. Undoubtedly, the largest class of inorganic/organic gels is made up of hybrids linked via Si–C bonds that are stable and do not undergo hydrolysis under the sol–gel processing conditions[145].

As already described above, in the last decade sol–gel technology has become a popular way to create organic/inorganic hybrid materials[146]. Hybrid is a good generic term for an organic/inorganic material. Another name commonly applied to organic/inorganic gels is nanocomposite, to emphasize the nanometer level of mixing[147]. Nanocomposite usually refers to hybrids where organic and inorganic constituents are not covalently bonded. The forces acting between the constituents vary from weak to relatively strong. Sanchez and Ribot[148] divide hybrid gels into two classes: Class I corresponds to hybrids where organic molecules are blended into the inorganic network, whereas Class II includes hybrids, where inorganic and organic constituents are linked together via covalent or iono-covalent bonds. According to this definition, this Section deals with Class I hybrids, although some Class II hybrids are described at its end.

A. Physical Hybrids (Class I[149])

Physical hybrids containing silica and polymer are typically interpenetrating networks (IPNs). They can be subdivided into simultaneous or sequential IPNs. The terminology of

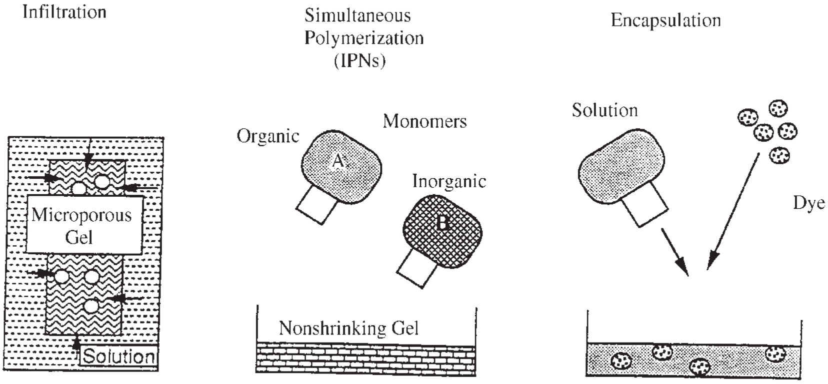

FIGURE 5. Schematics of a rigid porous silica xerogel infiltrated with monomer

interpenetrating polymer networks is borrowed from organic polymer technology[149]. In some cases, semisequential is used to reflect the linear structure of the organic polymer in which the silica gel forms.

Some of the earliest sol–gel hybrids were achieved by monomer infiltration into previously formed silica gel. Starting with a dried silica gel (xerogel), the porous shape is filled with monomer. The monomer is polymerized *in situ*. This is shown schematically in Figure 5. Interpenetration is achieved when the impregnating monomer polymerizes in the open pores of the rigid silica matrix.

In the polymer impregnated gels, some porosity typically remains. Although some copolymers of methyl methacrylate, butadiene and styrene have been used to impregnate silica, the best known system is still silica impregnated with polymethyl methacrylate (PMMA)[150–153]. While this type of hybrid was important at first, it has been surpassed by other methods of hybrid synthesis that are simpler, with fewer steps and shorter times.

B. Sequential Organic/Inorganic Interpenetrating Networks

Silica precursors, tetraethoxysilane and tetramethoxysilane (TEOS and TMOS) are able to solvate some organic polymers. This enables the silica precursor to polymerize in the environment of an organic polymer solution. The number of polymers that form solutions with sol–gel formulations is, however, limited. Some initially soluble polymers tend to precipitate during gelation when a change in solvent composition leads to phase separation.

For select polymers that are soluble, the method is very simple. The polymerization of the silica precursor occurs around the preformed polymer chains or domains. When the organic polymer is formed before the inorganic polymer, the result is a sequential organic/inorganic interpenetrating polymer network.

Generally, it is found that polymerization of TEOS in the presence of preformed polymers under acidic conditions generates small, well dispersed silica particles. Depending on the choice of polymer, highly transparent, lightweight materials can be obtained. Among the polymers used to form sequential IPNs, there are several capable of forming hydrogen bonds with hydroxylated SiO_2 particles[154]. Strong interactions between silanols, having the character of Bronsted acids, and specific groups on the polymer that are hydrogen acceptors are responsible for the high degree of two-phase mixing. Linear polymers with hydrogen acceptor groups, amide, carbonyl and carbinol have been used in semisequential organic/inorganic IPNs. These polymers are poly(*N*,*N*-dimethacrylamide), poly(2-methyl 2-oxazoline), poly(methyl methacrylate) (PMMA), poly(vinyl pyrrolidone) (PVP), poly(acrylic acid) (PAA) and its copolymers, poly(vinyl acetate) (PVAc) and poly(vinyl alcohol) (PVA)[154–158].

In detail, the properties of the hybrids are functions of the relative fractions of the polymer and TEOS in the sol–gel formulation, along with the chemistry and length of the polymer chain. When TEOS is polymerized in the presence of the polymer, the glass transition (T_g) of the polymer increases or becomes undetectable. The density of the hybrid does not follow a mixing rule for the inorganic and organic components, but is suppressed even with high inorganic contents.

C. Simultaneous Organic/Inorganic Interpenetrating Networks

While only a few organic polymers are soluble in sol–gel formulations, many organic monomers are soluble in TEOS. These monomers can be introduced directly into sol–gel formulations. Both ring-opening polymerizations and free-radical polymerizations can be carried out simultaneously with the hydrolysis–condensation of TEOS. The resulting hybrids have no covalent linkages between the organic and inorganic components. This simultaneous route captures insoluble organic polymers within a sol–gel inorganic network.

In the preparation of simultaneous networks, it is important to control both polymerizations rates. Systems with inorganic condensation rates much faster than the organic polymerization rates turn into brittle hybrids that shrink. The polymer content is low due to evaporation of unreacted monomer. Systems with fast organic polymerization rates usually show uncontrolled polymer precipitation leading to heterogeneous composites. In practice, the kinetics of polymerization are difficult to control, so the success of the simultaneous approach rests on the careful selection of the monomers and their composition.

The idea of simultaneous interpenetrating networks has been advanced by Novak and coworkers[159–162]. Several monomers of acrylate type (free-radical polymerization) or cyclic alkenes (ring-opening metathesis) have been used. They include acrylamide/*N*,*N*′-bisacrylamide monomer system, 2-hydroxyethyl or hydroxymethyl acrylate, and 7-oxanorbornene and its derivatives. In order to get nonshrinking hybrids, tetraacryloxyethoxysilane was used instead of TEOS. The acrylate monomer liberated due to hydrolysis acted as a cosolvent to solvate the polymerizing silica network. The result was transparent hybrids with no shrinkage. Ellsworth and Novak[159,160] also used soluble oligomers of silicic acid instead of TEOS in a condensation with (meth)acryl trialkoxysilane. This route involves a direct Si−C covalent bond to increase the silica content of the organic/inorganic hybrids and further reduce shrinkage, meaning the product is no longer simply a physical hybrid[163].

Wojcik and Klein[164] have studied the incorporation of silica with di- and triacrylate monomers, hexanediol diacrylate (HDDA) and glyceryl propoxy triacrylate (GPTA). These simultaneous IPNs are transparent hybrids with good mechanical strength. A drawback in these systems is the fact that the gelation times under acidic conditions are quite long, as long as weeks. The reason for the long gelation times may be the low concentration of alkoxysilyl groups and steric hindrance from organics in the system. However, the process can be accelerated by photocuring with UV or using a tri-monomer system. Related to the HDDA and GPTA/TEOS systems, Wojcik and Klein[164] tried the tri-monomer system TEOS-vinyltriethoxysilane (VTES)-hydroxyethyl methacrylate (HEMA). By introducing VTES, Si−C links result, meaning that this system, like the silicic acid/(meth)acryl trialkoxysilane system, is not strictly a physical hybrid[159,165].

Another example of a physical hybrid with a functionalized silica is the work of Hoebbel and coworkers[166], who used tetramethylammonium silicate ($[N(CH_3)_4]_8Si_8O_{20}\cdot 69H_2O$)

converted by an ion-exchange process into double-four ring (D4R) oligomers of silicic acid ($H_8Si_8O_{20}$). This oligomer was stabilized by reaction with functional siloxanes containing polymerizable groups like vinyl, allyl, hydrido- or chloromethyl. The functionalized derivative can be polymerized while preserving silicic acid cages in the structure.

Cellular structures are observed in poly(dimethylsiloxane) (PDMS)/silica gels when the sol–gel parameters (H_2O, HCl concentration and temperature) are adjusted to accelerate the gelation process[167]. PDMS, which contains direct Si−C bonds along its Si−O backbone, can co-condense with TEOS, as shown in equation 9.

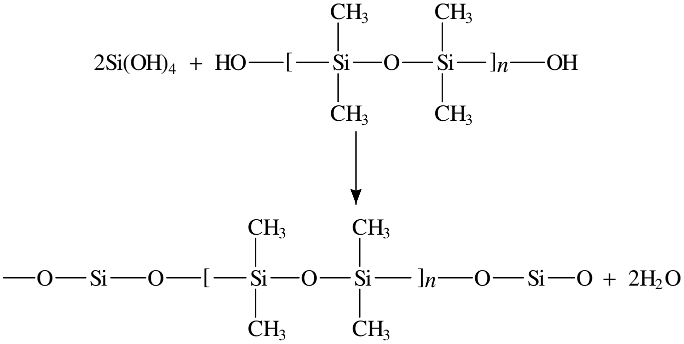

$$2\mathrm{Si(OH)_4} + \mathrm{HO}{-}[{-}\mathrm{Si(CH_3)_2}{-}\mathrm{O}{-}\mathrm{Si(CH_3)_2}{-}]_n{-}\mathrm{OH} \longrightarrow {-}\mathrm{O}{-}\mathrm{Si}{-}\mathrm{O}{-}[{-}\mathrm{Si(CH_3)_2}{-}\mathrm{O}{-}\mathrm{Si(CH_3)_2}{-}]_n{-}\mathrm{O}{-}\mathrm{Si}{-}\mathrm{O} + 2\mathrm{H_2O} \qquad (9)$$

Since this system contains covalent bonding, it represents a hybrid that is not strictly a Class I hybrid[167] although the co-condensation involves only silanol groups. Porosity remains for small concentrations of organic polymer in these PDMS/silica hybrids, although most hybrids are designed ideally to have low porosity. With high concentrations of the organic component, hybrids have low densities, indicating high free volumes characteristic of the organic polymers.

In a way similar to PDMS and TEOS, other organic polymers have been functionalized with alkoxysilyl groups and covalently bonded to silica. Polymers that have been coupled with silica are PTMO-based polyurethane oligomers[168,169], polyoxazolines[170], polyimide[168], poly(arylene ether ketone)[171], poly(arylene ether sulfone)[172], polystyrene[173], polyoxopropylene (PPO)[174], polyacrylonitrile[175], copolymers of methyl methacrylate and allyl methacrylate[176] and cyclophosphazenes[177].

Generally, it is claimed that PDMS/silica-type hybrids combine the flexibility and mechanical properties of the organic polymer chains with the hardness and stiffness of silica. In detail, the properties of the hybrids are governed by the chemistry, presence of side chains or pendant groups and length of polymeric chains. Especially important are the concentration and distribution of alkoxysilyl groups attached to the polymeric chain, as they directly affect the rigidity or flexibility of the system.

D. Silsesquioxane-containing Hybrids (Class II[148])

It is difficult to deal exclusively with Class I hybrids, because many of them fall into both categories to some degree. One type of Class II hybrid is discussed here. Organically modified silicas (Ormosils)[146], which have been treated more fully in Section IV, are formed from $R'Si(OR)_3$-type organosilanes where radical R has a network modifying effect and is used to introduce new functionalities into the inorganic network. Polymerization of $R'Si(OR)_3$ alone leads to formation of silsesquioxanes of general formula $(RSiO)_{1.5}$, i.e. a silicate framework where each Si is linked covalently to an organic radical R.

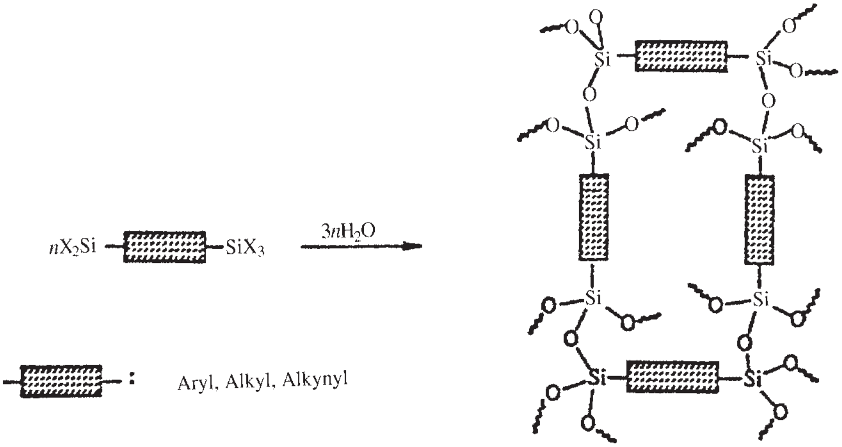

FIGURE 6. Schematics of polymerization of a monomer with an organic spacer between two silicon atoms (after Shea and coworkers[180])

Bifunctional silanes of formula $R'R''Si(OR)_2$ can also be used to prepare Ormosils. Upon polymerization, these organoalkoxysilanes form cyclic species or linear chains and are therefore not able to crosslink and form networks themselves. They can be used with tetrafunctional silanes (TEOS) to incorporate desirable functionality into the hybrid network. For example, hydrophobicity can be achieved by introducing a methyl, phenyl or fluoroalkyl chain as R[178,179]. There are also Ormosils where radical R forms a bridge between two Si atoms. A good example of this is arylene or alkylene-bridged polysilsesquioxanes synthesized from bis(triethoxysilyl) or bis(trichlorosilyl) aryl or alkyl monomers[180–182]. Various aliphatic or aromatic molecules have been used as the organic spacer between two silicon atoms and this is shown schematically in Figure 6.

In concluding this Section we note that, while attempts have been made to classify physical hybrids or interpenetrating networks, it is not always straightforward. A simple classification reflects the timing of polymerization — whether the silica and organic polymers react simultaneously or sequentially. Thermodynamic factors relating to solubility and miscibility and the kinetics of phase separation influence the outcome of the processing. The scale of mixing leads to the subdivision of the microstructure or the distribution of the components. The microstructure, in turn, influences a variety of physical, chemical and optical properties.

VI. PHOTOCHEMISTRY, PHOTOPHYSICS AND OPTICS OF DOPED SOL–GEL MATERIALS

A. Photoprobes for the Sol to Gel to Xerogel Transitions and for the Study of the Properties of the Sol–Gel Cage

Various spectroscopies were used for studying cage properties and their evolution in time along the monomer → oligomer → sol → gel → xerogel transition. The main tools have been UV-visible absorption and emission spectroscopies, and to a lesser extent other spectroscopies such as EPR[183]. The evolution of the sol–gel process and the evolution of various cage properties, was first followed with pyrene[184,185] (Py) because of its relatively long singlet life-time (*ca* 100 ns), its distinct vibronic peaks in the fluorescence spectrum, its ability to form an excited state dimer, i.e. the excimer, Py^*_2, and because of the sensitivity of these parameters to changes in environmental conditions. With this probe, the changing polarity and the changing structure around the probe, from adsorption onto the surface of the growing SiO_2 particles up to the complete isolation in microporous cages, were detected and monitored[185]. Many sol–gel studies have utilized that useful probe[186].

Some other photophysical probes which were used for following the sol–gel transitions include 7-azaindole[187], 1- and 2-naphthols[188], pyrene-3-carboxaldehyde[189], $ReCl(CO_3)$bipyridine (as a probe for cage rigidity)[190], thymol blue[191] and Rhodamine B[17b]. Photochromic compounds were also used for the investigation of the sol–gel xerogel transition in $Si(OCH_3)_4$[184,192,193] and the substituent's effects on the point of the change from normal to reversed photochromism were analyzed in terms of the Hammett relationship[192].

A pyrene derivative, 8-hydroxy-1,3,6-pyrenesulfonic acid (pyranine), was successfully used[33] for the detection of water during the early stages of the polycondensation of $Si(OCH_3)_4$. The idea of using this probe molecule is based on the fact that its excited state is a short-lived strong acid, capable of efficient proton transfer to neighboring water molecules, leaving behind the anion of pyranine in its excited state. Pyranine was also used by Pouxviel and coworkers for studying aluminosilicate sol–gels: here too, that probe proved to be a highly sensitive probe to changes in water content[194].

In addition to the spectroscopic follow-up of the sol–gel process, much research was devoted to the analysis of the cage properties at the final xerogel stage. Early detailed spectroscopic analysis of absorption and emission spectra of rhodamine 6G (R6G), a laser dye, in SiO_2 sol–gel[1] indicated that the polarity of the immediate environment of the dopant is high and due to hydroxyls, although less polar than water (as obtained also with Py as a probe). The ability of the matrix to isolate efficiently one molecule from the other, even at high concentration, first observed for that dopant[1], lead to an intensive study of doped sol–gel materials for a variety of optical uses, notably as dye laser components[195]. We know today, however, that this is not universal and that high concentrations may lead eventually to some aggregation. This was found for proteins[44] and for $Ru(bpy)_3{}^{+2}$[196]. Dopant aggregation may also be the way in which three doped *o*-phenanthroline ligands find their way to complex a single Fe^{2+} ion[23].

An indication as to the homogeneity of the entrapment comes from the analysis of the decay profile of the excited state in the final xerogel. First-order decays point to homogeneity of distribution, and were found, for instance, in $Ru(bpy)_3{}^{2+}/SiO_2-TiO_2$ films[20,196] and in biphenylcarboxylic acid/SiO_2[197]. The protective nature of the sol–gel cage has been clearly evident in these two cases and later on in many other studies. For instance, in the case of $Ru(bpy)_3{}^{2+}$, the observed life-time in solution at a concentration of 1×10^{-3} M is 0.3 μs, but at the same concentration in a sol–gel matrix, there is a sixfold increase to 1.9 μs[196]. Photostability to prolonged irradiation is another indication for the protective nature of the cage[1,17b]. For instance, the degradation half-life of 4-oxazine increased fourfold by entrapment, compared to solution[196]. One of the most striking manifestations of the special protective properties of the sol–gel caging has been the ability to obtain room-temperature phosphorescence (RTP), under regular atmospheric conditions, from a very wide range of organic molecules[197], many of which reveal that emission only at cryogenic temperatures and in vacuum. Examples include polycyclic hydrocarbons[184,197], dyes like eosin-y, bases like quinine and acids such as 4-biphenylcarboxylic acid.

The question of rigidity of the sol–gel cage[183,190] accompanied the research in this class of materials from its very beginning. Both the rigidity and polarity of the cage can be altered by changing the monomer, by the incorporation of suitable additives and by copolymerization. A nice example is the encapsulation of photochromic spiropyranes mentioned above[184,192,193]. When entrapped in pure SiO_2, the photochromism is observable only up to the wet-gel stage[192]. Beyond it, the cage becomes so rigid that the isomerization between the closed colorless spiro form and the open merocyanine colored zwitterion stops at the final dried xerogel stage. A straightforward method to relax the rigidity is to use a three-dentate monomer, rather than the normal tetraalkoxy monomer, thus reducing the degree of crosslinking. Indeed, entrapment of the spiropyranes in a sol–gel matrix prepared from ethyltriethoxysilane provided the needed flexibility for lasting photochromism. A marked effect of an additive on cage properties was observed in the case of entrapped pH-indicators[25]: addition of a surface active agent, such as cetyltrimethylammonium bromide, shifted the pK_i by 2 units to a more acidic range.

For practical applications, a delicate balance should be found between good isolation and protection on the one hand, and sufficient accessibility of the entrapped molecule to external reactants on the other. Evidence is accumulating that high acidity and low water/silane ratio do the trick, at least in some cases (for example in the entrapment of pyranine[18,19] as a fluorescent pH sensor and in the entrapment of Py[19,198] as a fluorescent sensor for oxygen). However, these need not be necessary conditions: the entrapped quaternary ammonium metal catalysts mentioned above do not leach out even though prepared under neutral conditions[38], and enzymes and antibodies do not leach out because of their sheer size[44].

The last cage property we would like to comment on is its symmetry. This property was studied by entrapment of Eu^{3+} (as its chloride, obtained *in situ* from Eu_2O_3/HCl) in SiO_2 sol–gel[199], and although it is an inorganic dopant, we are describing it here because that report led to many studies of Eu^{3+} doped sol–gel matrices, including both organic and inorganic ligands[200], as well as to many studies of doping with other transition-metal cations[201]. Symmetry in the chemical sciences is a rather complex issue[202], and the cage symmetry of sol–gel materials is no exception, especially since it involves a population of cages with varying degrees of symmetries (for the concept of degree of symmetry, see elsewhere[202]). Yet Eu^{3+}, which is known to be an excellent indicator for site-symmetry[200], allows at least an average picture of that property. The basis of this symmetry probe is that the lowering of local symmetry enhances radiative transitions in that cation, and particularly sensitive is the $^5D_0 \rightarrow {}^7F_2$ emission at 615 nm. In general, it was found that the symmetry around Eu^{3+} resembles the solvation shell found in a polar solvent, up to the nonheated, mature wet-gel stage. Upon heating to 100 °C, solvent leaves the gel and the fluorescence spectrum reveals this change by an overall increase in intensity and by a relative increase in the $^5D_0 \rightarrow {}^7F_2$ transition intensity. Thus, as the amount of O–H groups is reduced, the symmetry around the cation decreases.

B. Organic Photochemistry within Sol–Gel Matrices

The first family of reactions studied in detail were, as mentioned above, the photochromic isomerizations of Aberchrome 670[184] and of various spiropyranes[192,193]. The motivation was to develop novel materials for information processing and for other optics applications, and it serves as a good illustration of what the organically doped sol–gel methodology can offer: traditionally, photochromic glass preparations have been limited to a few dopants that can withstand the high temperatures of glass melting; by contrast, organic photochromism offers several tens of thousands of molecules with which one can tailor the shade of color change, the direction of the photochromism, the rate of change in color intensity, reversibility (optical gates) or unidirectionality (information recording). We return to it in the next section.

The ability to separate reactive species that otherwise annihilate each other is another feature which the sol–gel methodology allows by virtue of the entrapment–isolation. This was best demonstrated in a study aimed at storage of light energy in the form of a photogenerated ionic radical pair[203]. A notorious problem in this field of research has been the dissipation of the absorbed energy through fast back-reaction of the radical pair. An exceedingly long-lived — several hours! — charge-separated pair was obtained in SiO_2 sol–gel between the photogenerated pyrene cation (Py^+) and methyl-viologen cation (MV^+) (equation 10):

$$Py^* + MV^{+2} \rightleftharpoons Py^+ + MV^+ \tag{10}$$

This is a very reactive pair which, under free diffusing conditions, would immediately quench each other with the back-reaction. The back-reaction was inhibited by entrapment of both Py and MV^{+2} while allowing them to communicate chemically with a mobile charge carrier, *N*,*N*′-tetramethylene-2,2′-bipyridinium, which diffused freely in the aqueous solution within the porous network.

Photoinduced charge separations of this type can be used for subsequent useful reactions[204–206]. An example is the series of reactions in which H_3O^+ was reduced to H_2: A donor, $Ru(bpy)_3{}^{2+}$ [Ru(II)], and an acceptor, $Ir(bpy)_2\ (C,{}^3N')bpy)^{+3}$ [Ir(III)], were co-entrapped in an SiO_2 sol–gel matrix, and dimethoxybenzene (DMB) was used as the redox shuttler between the Ir and Ru (equations 11–13):

$$Ir(III)^* + DMB \longrightarrow Ir(II) + DMB^+ \tag{11}$$

$$DMB^+ + Ru(II) \longrightarrow Ru(III) + DMB \tag{12}$$

$$2H^+ + Ir(II) \longrightarrow Ir(IV) + H_2 \tag{13}$$

C. Sol–Gel Optics

1. Photochromic sol–gel glasses

In Section VI.B we have seen the use of photochromic materials for following the sol–gel process, and described the first successful preparation of organically doped photochromic materials. Here we comment further on this topic, from the point of view of the needs of optical materials. In addition to the entrapment in silica sol–gels, it is relevant in this context to mention also that aluminosilicate gels were reported as good host matrices for photochromic molecules[207–209]. These authors pointed out that thermal reversibility of the photochromism in silica gels was the main problem to become a thermally stable photochromic material. Improvements in the photochromic properties of the silica-doped gels have been performed both by modifications in the host matrix as well as by the use of different photochromic compounds. Modifications in the silica matrix by the use of trifunctional silane precursors[210,211] or by the impregnation of the porous material with an organic polymer[212] improved the photochromic response as well as the fading rate. Low levels of photofatigue[207] and a high color stability were thus achieved[210,211]. Improvements in this sense were also performed by the incorporation of new photochromic compounds such as diarylethene derivatives, which do not show thermal conversion below 140 °C. Other photochromic compounds which showed good thermal stability were reported[207,210,211], such as the spironaphtho-oxazines, both in pure silica matrix as in hybrid silica matrix. Thermal isomerization of azobenzenes in sol–gel glasses was described as dependent on the amount of water on the silica surface[212], which is in concordance with previous results found by other authors, where hybrid matrices improve the photochromic properties of the material[192,193,210,211,213,214].

The matrix itself must be photochemically stable, offering at the same time a favorable environment to the photochromic dye. Efforts to improve the photochromic properties of the material were conducted through the incorporation of several additives to the silica matrix. Materials with high photochromic intensity and low photofatigue were found using perfluoroalkoxysilane derivatives or an imidazole derivative[207]. Other types of photochromic materials are being studied and preliminary results are very promising[211].

In another application of doped sol–gel materials, it has been demonstrated that photochromic-doped sol–gel materials can be attached to optical fibers[215–217], although the properties of the light throughput may be modified. Simple fiberoptic/photochromic devices made of two optical fibers placed in a V-groove removable connector have been prepared. Once cured, these devices behave as optically addressed variable delay generators. The same devices can be used for preparing simple optical switches and routing systems. Silica gel-glasses obtained by the sol–gel process are chemically and optically very similar to the optical fiber itself. Therefore the Fresnel losses are drastically reduced, allowing the possibility of using doped sol–gel glasses for modifying the properties of the fiber light throughput. With these materials it is possible not only to make low-loss interconnections from fiber to bulk devices, but to build smart waveguides for applications traditionally associated with integrated optics (modulators, switches, wavelength filters) where the light can be optically processed.

The use of covalently bound photochromics via the use of trialkoxysilane derivatives of spiropyranes is mentioned below in Section VI.C.3.

2. Optical and photophysical properties of entrapped organic molecules

The development of novel optical devices requires suitable materials which have the required chemical and photochemical stability, with appropriate optical features, which can also be made into usable forms such as thin films and bulk pieces. Since the sol–gel process[9,10,218,219] offers a very attractive possibility with the ability to incorporate organic materials in inorganic matrices at low temperatures in the form of monolithic glasses or thin films, it has opened the way to many possible applications in optics[1,6c,190,192,193,196,220–222] and electrooptics[2,223,224].

From the point of view of optics applications, luminescent dyes (fluorescent and phosphorescent) were the organic compounds most frequently used for the preparation of doped sol–gel materials. The characteristics of these materials were studied extensively, from properties at the steady state (emission–excitation)[188] to properties of the dynamic state (lifetimes)[225], and to properties derived from anisotropy[226] and/or energy transfer[227]. Knowledge of the effects that the surface may have on the organic molecule is an important factor in understanding the spectroscopic properties of the entrapped molecule in its inorganic/organic environment.

Pure silica gels[228,229] or mixed titania-silica, alumina-silica, zirconia-silica gels[194,196,230,231] have been used as inorganic host for organic dopants. The use of mixtures is of interest because of the high Lewis acid character of the pure oxides of Ti, Al and Zr which may degrade the organic dye[232]. For this reason, the preparation of hybrid matrices has been intensively developed in recent years. Doped hybrid matrices[230] may be prepared by the impregnation of organic polymers or monomers which are polymerized inside the matrix[222–235], yielding matrices with a highly organic character, thus increasing the chemical compatibility between dye and surface. Other ways to prepare these hybrid materials consist of the use of the trifunctional silane precursors, yielding a silica matrix with nonfunctional ligand bonded to the silica surface[236,237] (see the next section). The presence of such ligands opens the possibility to bind covalently the organic dye which is incorporated to the silica matrix. Such systems may show enhancement in the stability of the organic dye[238].

Numerous lasing dyes have been incorporated within sol–gel, such as rhodamines[1,239], coumarins[240–242], oxazines[232,243] and cyanines[194,232]. A general feature of these dopants in the inorganic matrices is the high concentration which can be reached without self-quenching and/or self-absorption processes. Often observed is an increase in the fluorescence intensity of the dopant, ascribed to the greater rigidity and isolation of the dye in the silica host compared to solution. Laser dye doped sol–gel glasses for fabrication of narrow and broad band antireflective coatings, multilayered dielectric mirrors and polarizing thin films have been developed for the proposed[244] French megajoule neodymium-glass laser.

Lebeau and coworkers[232] have first reported on the optical properties of near-infrared (NIR) organic dyes (700–1000 nm)[245] when incorporated in silica-based gel. NIR dyes have led to applications well beyond optical recording technology: high-density optical data storage, thermal writing displays, laser printer and laser filter, infrared photography, medical applications and persistent (non) photochemical hole burning[246] as multiwavelength optical memory[247] are some examples. The dye employed for these purposes is the polymethine dye 1,1′,3,3,3′,3′-hexamethylindotricarbocyanine iodide (HITC) using 4-dimethylaminopyridine (DMAP) as a catalyst.

Recently, del Monte and Levy[248] reported on the spectral behavior and chemical stability of 1-oxazine and HITC doped gel-glasses. The fluorescence properties of HITC gel-glasses, which vary widely depending on conditions during gel formation, may be controlled with the chemical composition of the starting mixture. The entrapment of HITC in gel-glasses required dye protection from chemical degradation. This was achieved by using tetramethoxysilane (TMOS) in order to produce high-density matrices. Alternative strategies to protect HITC inside gel-glasses were achieved by using a modification of the techniques proposed by Pope and Mackenzie[222] and by Reisfeld and coworkers[249] in which the sol–gel matrix is blocked with organic polymers [by mixing dissolved polymethyl methacrylate (PMMA) in the starting solution]. This procedure results in transparent materials of excellent optical and mechanical quality. Chemical stabilization of HITC involves the detachment of the dopant from the surface silanols, which are the primary cause of the HITC degradation in gel-glasses. This isolation is apparently achieved by the use of the PMMA. The fluorescence of the resulting composite gel-glass showed no signal loss over 10 months[248].

The combination of organic dopants with oriented assemblies of organic compounds with high-order nonlinear polarization or organic substances of large third-order susceptibility, $\chi^{(3)}$[250,251], with inorganic sol–gel matrices, offers a greatly expanded capability for applications in nonlinear optics. These materials are essential for photonics in the coming 21st century and are thought to be applicable to optical switches, optical memories[252] and optical branches[253]. Semiconductor particles in a dielectric matrix have attracted much interest for nonlinear optics applications[254,255], and consequently, silica sol–gel materials were proposed as possible hosts due to their excellent physical performance[222].

Reisfeld[256] showed that nonlinear sol–gel glasses, and especially sol–gel thin films, form an interesting class of optoelectronic devices, and investigated the origin of strong nonlinearities on a millisecond to nanosecond scale of glasses doped with fluorescein, acridine and methyl orange.

Another unique aspect of the sol–gel process in this context is the synthesis of Ormocers (organically modified ceramics)[111]. Different organic–inorganic sol–gel precursors have been used for this purpose for the development of new glasses with second-order nonlinearities[257–261]. In these materials, organic chromophores are chemically bonded to the oxide backbone via the use of functionalized silicon alkoxide precursors (see also the next section). Chaput and coworkers[81] have reported the preparation of an organic–inorganic composite material in which the organic active molecule is covalently bound into the silica network, and demonstrated the ability of orientation of organic molecules via the photoisomerization of active azo molecules. For instance, azobenzenes are very useful molecules in the preparation of NLO (nonlinear optics) materials[262] when bonded to the silica surface. When this type of molecule is covalently attached to the surface by both ends, their thermal relaxation is decreased and a long-term stability of the nonlinear properties is obtained[263–265]. The covalent bond to the silicon atom must be introduced in order to avoid its rupture during the acid hydrolysis of the sol–gel process[81,266], which may cause a loss in the NLO properties[267].

Other types of organic molecules used as sol–gel dopants to form NLO materials are phthalocyanines, porphyrins and fullerenes. For the phthalocyanines entrapped in hybrid matrices prepared from trifunctional silane precursors[268,269], a very good stability was observed. Porphyrins doped in aluminosilicate gels showed a concentration-dependent nonlinear absorption behavior[270]. Fullerenes have recently incorporated into silica matrices of high porosity (aerogels)[271], also showing a concentration effect.

For electrooptics applications, the sol–gel process has been recently used[223,224,272] for the trapping of microdroplets of nematogenic organic compounds (i.e. liquid crystals, LCs) in a thin film of a silica-gel based matrix (GDLC, Gel-glass Dispersed Liquid Crystal). The compounds [a commercial nematic mixture (E7 from BDH Ltd)], composed of several *n*-alkyl cyanobiphenyl homologues and a cholesteric liquid-crystal dopant or two nematic liquid crystals, 4-pentyl-4,4′-biphenylcarbonitrile (K15, Aldrich) and ZLI-1221 (Merck, a well known commercial LC mixture for twisted nematic displays), were dissolved in the starting mixture; further hydrolysis and polycondensation reactions lead to a phase separation that results in the formation of pores which are filled with the organic

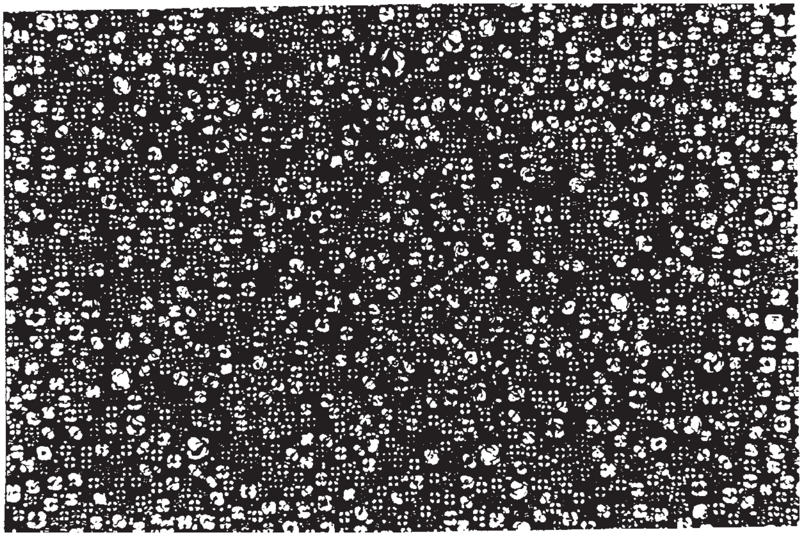

FIGURE 7. Optical microscope picture with crossed polarizers of the microdroplets showing a liquid-crystal state filling the pores of a GDLC thin film. The orientations in microdroplets can be observed as the result of the specific sol–gel processing (parallel polarizers gave Maltese crosses of LC microdroplets and a black image of the silica-gel substrate)

compound. If adequate processing of the preparation of the microdroplets is achieved, the organic compound recovers its nematic liquid-crystal state, its molecules being oriented in microdomains according to the pore inner-surface anchoring (organic group on the walls of the pores, e.g. $-CH_3$, $-C_2H_3$, $-C_6H_5$, etc.) and orienting properties (Figure 7). Introducing a two-functional aminosilane, 3-[diethoxymethylsilyl]propylamine, in the composition of matrix raw materials resulted in better matrix flexibility, higher conductivity and greater capacity for trapping LC[273]. Once the phase separation in GDLC formation takes place, the LC microdroplet dispersion becomes related to the number and density of microdroplets within the silica-gel matrix. In this manner, the resulting properties of the LC microdroplets may allow the use of GDLC films as electrooptical devices. GDLC films scatter visible light according to the number of droplets and the relative refractive indices of the LC and the silica matrix[274]. Color may be included in the sol-gel matrix or in the liquid crystal itself. A comparative study of different dyes for GDLC color displays demonstrated that dyes may be either embedded in the sol-gel matrix or dissolved in the liquid-crystal microdroplets. In the first case, the liquid crystal scatters out the backlight when no voltage is applied, whereas a transparent colored pixel is obtained upon switching. In the second case, the dye is oriented by the liquid crystal, its absorption being modified by the liquid-crystal reorientation. This affects the display contrast, brightness and viewing angle[275,276].

3. Materials substituted by chromophores

The possibility to tailor the chemical and physical properties of sol–gel materials, their excellent optical quality, their low preparation temperatures and their easy deposition as coatings makes them ideally suited for optical applications. Mainly SiO_2 [prepared from $Si(OR')_4$], but also inorganic–organic hybrid polymers were used as a host for dyes. For example, the above-mentioned hybrid polymer obtained from the GLYMO and $Al(OBu\text{-}s)_3$ was shown to be a very interesting host for laser dyes. By doping with $YbCl_3$ and dihydroxyanthraquinone (DAQ) or Oxazine 170 (9-ethylamino-5-ethylimino-10-methyl-5*H*-benzo(*a*)phenoxazonium perchlorate), materials for optical data storage in the frequency domain were obtained[277].

Physical trapping dye molecules in sol–gel materials are reviewed elsewhere in this chapter. A comparatively recent approach is to have the dye molecules chemically *bonded* to the oxide matrix. This approach requires the chemical modification of the dye molecules by $Si(OR')_3$-containing groups, i.e. the preparation of compounds $(R'O)_3Si-X-A$, in which A is a chromophore, by the methods shown in equations 3–7. This is mostly not a trivial task, since the chromophore has to remain undisturbed.

Therefore, the chemical linking of the dye molecules is only worthwhile if it results in a substantially better performance of the resulting materials. For the reasons discussed below, this is mainly expected for nonlinear optics (NLO) dyes. However, other dye-containing materials were also prepared by this approach. For example, new transparent photochromic hybrid materials were prepared by sol–gel processing of $Si(OEt)_4$, silanol-terminated dimethylsiloxane oligomers and triethoxysilylpropyl-substituted spirobenzopyranes[278], and fluorescent glasses and films from pyrene derivatives covalently tethered to $RSiO_{3/2}$ (R = alkyl, phenyl)[279].

There are several potential benefits from chemically linking the dye molecules to the matrix compared to just trapping them:

(i) The dye concentration in the final material can be considerably increased. It was demonstrated for several types of $(R'O)_3Si$-functionalized NLO dyes that the chemical bonding to the oxide network allowed high dye concentrations without any crystallization occurring[81,82,250,257–260,280,281]. Coloration of glass by anthraquinone or naphthoquinone doped sols was not possible, because of their low solubility. This was not a problem when $(EtO)_3$ Si-substituted phenoxazinium and phenazinium dyes were used[282].

(ii) Leaching of the dye is prevented by its covalent bonding to the sol–gel matrix. For example, when Rhodamine 110 was only embedded in a sol–gel derived silica matrix, leaching was a severe problem. When the dye was covalently bonded to the matrix, no leaching was observed[283].

(iii) Glass-like sol–gel matrices appear to be more suitable hosts for NLO dyes than organic polymers, because they provide for better stability of the nonlinearity after alignment. Tethering the dye molecules to the matrix results in higher stabilities than physical doping.

The effect of binding the dye to the oxide network was studied in several cases[80,81,250,257–260,280–282] by preparing poled and cured films either by chemical binding of the $Si(OR')_3$-substituted dye to the sol–gel polymer or by incorporating the unmodified dye in the same matrix without chemical bonding. The former systems had a much better stability. This was, *inter alia*, attributed to restriction of the molecular motion of the segments, due to the bonding between the chromophore and the polysiloxane[260,280]. The relaxation behavior of NLO chromophores depends strongly on the rigidity of the matrix, which is influenced by the processing conditions and their composition[284,285]. Particularly the degree of crosslinking of the matrix appears to be critical. Preliminary attempts to get a higher degree of crosslinking (and thus a better optical response or stability) by using inorganic–organic hybrid polymers (organic *and* inorganic crosslinking) did not result in a real improvement[286]. It was also shown that the isomerization kinetics of azo dyes is different in sol–gel films and bulk materials, which was attributed to the larger free volume in the bulk material due to larger pores[287].

The presence of only one $Si(OR')_3$ unit per chromophore makes the formation of a highly crosslinked sol–gel network very difficult. The high mobility of the NLO dye in the free volume of the host network causes relaxation of the poling-induced order. Presently, the most promising approach to improve the stability of the second-order optical nonlinearity is therefore the use of multiple-substituted dyes, such as **20**[83].

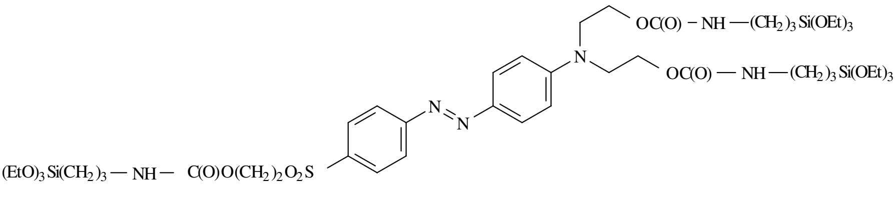

(20)

VII. CONCLUDING REMARK

It is our hope that this chapter on a new family of materials, at the crossroads of organic and inorganic chemistry, will stimulate researchers and students to consider this new frontier of silicon materials chemistry for solving problems of their own scientific endeavors, for embarking on further basic science explorations and as a potential solution for the design of useful devices.

VIII. ACKNOWLEDGMENTS

D. A. thanks his collaborators R. Reisfeld, M. Altstein, J. Blum, S. Braun, D. Huppert, V. R. Kaufman, O. Lev, M. Ottolenghi, Y. Polevaya, A. Rosenfeld, C. Rotmann, J. Samuel, H. Sertchook, H. Schumann, A. Slama-Schwok and R. Zusman. D. A. also thanks the Volkswagen Foundation and the Israel Ministry for Science and Arts, for currently supporting the sol–gel research. L. C. K. thanks her collaborators, C. Beaudry, L. Laby and S. Yamazaki, for helpful discussions and greatly appreciates the support of the NJ Commission on Science and Technology. D. A. and L. C. K. acknowledge gratefully the joint support of the US–Israel Binational Science Foundation. D. L. thanks the CICYT for research grant MAT95-0040-C02-01 and his colleagues, C. J. Serna, J. M. Otón, M. Ocaña and M. L. Amo, A. Serrano, F. del Monte, E. Moreno, T. Prieto, G. Fiksman, I. R. Matías and P. Datta, and C. Alonso for his helpful technical assistance. U. S. acknowledges the assistance of N. Hüsing and A. Lorenz in preparing the chapter, and the Fonds zur Förderung der Wissenschaftlischen Forschung for current support of sol–gel research. D. A. is a member of the F. Haber Research Center for Molecular Dynamics and of the Farkas Center for Light Energy Conversion.

IX. REFERENCES

1. D. Avnir, D. Levy and R. Reisfeld, *J. Phys. Chem.*, **88**, 5956 (1984).
2. D. Levy, *J. Non-Cryst. Solids*, **147 & 148**, 621 (1992).
3. L. C. Klein, T. Bloxom and R. Woodman, *Coll. Surf.*, **63**, 173 (1992).
4. E.g., U. Schubert, *J. Chem. Soc. Dalton*, 3343 (1996).
5. J. I. Zink and B. Dunn, *J. Ceram. Soc. Jpn.*, **10**, 878 (1991).
6. (a) S. Sakka, *J. Sol–Gel Sci. Technol.*, **3**, 69 (1994).
   (b) L. L. Hench and J. K. West, *Chem. Rev.*, **90**, 33 (1990).
   (c) R. Reisfeld and C. K. Jorgensen, Editors, 'Chemistry, Spectroscopy and Applications of Sol–Gel Glasses', *Structure and Bonding*, **85**, (1996), Springer, Berlin, the whole volume.
7. A. Engle, *Reading in Glass History*, No. 23, Phoenix Publications, Jerusalem, 1991.
8. (a) T. Graham, *J. Chem. Soc.*, 618 (1864).
   (b) E. Hatschek (Ed.), *The Foundations of Colloid Chemistry*, Ernest Benn, London, 1925.
9. C. J. Brinker and G. W. Scherer, *Sol–Gel Science*, Academic Press, New York, 1990.
10. (a) J. Livage, M. Henry and C. Sanchez, *Prog. Solid State Chem.*, **18**, 259 (1988).
    (b) L. L. Hench and J. K. West, *Chem. Rev.*, **90**, 33 (1990).
    (c) H. Dislich, *J. Non-Cryst. Solids*, **73**, 599 (1985).
    (d) J. Zarzycki, *Heterogen. Chem. Rev.*, **1**, 243 (1994).
    (e) C. Sanchez, M. L. Mecartney, C. J. Brinker and A. Cheetham, (Eds.), *Better Ceramics Through Chemistry, VI*, *Mater. Res. Soc. Symp. Proc.*, **346** (1994); and other volumes in this series.
11. See current issues of the journal, *J. Sol–Gel Sci. Technol.*
12. (a) A. M. Buckley and M. Greenblatt, *J. Chem. Educ.*, **71**, 599 (1994).
    (b) V. R. Kaufman and D. Avnir, in *Better Ceramics Through Chemistry, II* (Eds. C. J. Brinker, D. E. Clarck and D. R. Ulrich), *Mater. Res. Soc. Symp. Proc.*, **73**, 145 (1986).
    (c) D. Avnir and V. R. Kaufman, *J. Non-Cryst. Solids*, **192**, 181 (1987).
13. Y. Polevaya, J. Samuel, M. Ottolenghi and D. Avnir, *J. Sol–Gel Sci. Technol.*, **5**, 65 (1995).
14. L. V. Ng and A. V. McCormick, *J. Phys. Chem.*, **100**, 12517 (1996).
15. D. Avnir, *Acc. Chem Res.*, **28**, 328 (1995).
16. M. Tsionsky, G. Gun, V. Glezer and O. Lev, *Anal. Chem.*, **66**, 1747 (1994).
17. (a) T. Fujii, A. Ishii and M. Anpo, *J. Photochem. Photobiol.*, **54A**, 231 (1990).
    (b) N. Negishi, M. Fujino, H. Yamashita, M. A. Fox and M. Anpo, *Langmuir*, **10**, 1772 (1994).
18. J. Samuel, A. Strinkovski, S. Shalom, K. Lieberman, M. Ottolenghi, D. Avnir and A. Lewis, *Mater. Lett.*, **21**, 431 (1994).
19. N. Aharonson, M. Altstein, G. Avidan, D. Avnir, A. Bronshtein, A. Lewis, K. Lieberman, M. Ottolenghi, Y. Polevaya, C. Rottman, J. Samuel, S. Shalom, A. Strinkovski and A. Turiansky, in *Better Ceramics Through Chemistry, VI* (Eds. C. Sanchez, M. L. Mecartney, C. J. Brinker and A. Cheetham), *Mater. Res. Soc. Symp. Proc.* **346**, 519 (1994).
20. T. Tani, A. Namikawa, K. Arai and A. Makishima, *J. Appl. Phys.*, **58,** 3559 (1985).
21. O. Lev, *Analusis*, **20**, 543 (1990).
22. R. Zusman, C. Rottman, M. Ottolenghi and D. Avnir, *J. Non-Cryst. Solids*, **122**, 107 (1990).
23. (a) B. Iosefzon-Kuyavskaya, I. Gigozin, M. Ottolenghi, D. Avnir and O. Lev, *J. Non-Cryst. Solids*, **147 & 148**, 808 (1992).

(b) O. Lev, B. Kuyavskaya, Y. Sacharov, C. Rottmann, A. Kuselman, D. Avnir, and M. Ottolenghi, in *Environmental Monitoring* (Ed. T. Vo-Dinh), *SPIE Proc. Ser.*, **1716**, 357 (1993).

24. Reviews: (a) O. S. Wolfbeis, R. Reisfeld and I. Oehme, *Structure and Bonding*, **85**, 52, (1996).
    (b) O. Lev, M. Tsionski, L. Rabinovich, V. Glezer, S. Sampath, I. Pankratov and J. Gun, *Anal. Chem.*, **67**, 22A, (1995).
25. C. Rottman, M. Ottolenghi, R. Zusman, O. Lev, M. Smith, G. Gong, M. L. Kagan and D. Avnir, *Mater. Lett.*, **13**, 293 (1992).
26. P. Kiernan, C. McDonagh, B. D. MacCraith and K. Mongey *J. Sol–Gel Sci. Technol.* **2**, 513 (1994).
27. M. Kubeckova, M. Pospisilova and V. Matejec, *J. Sol–Gel Sci. Technol.*, **2**, 591 (1994).
28. K. T. V. Grattan, G. E. Badini, A. W. Palmer and A. C. C. Tseung, *Sens. Actuators A*, **25–27**, 483 (1991).
29. I. Kuselman, B. I. Kuyavskaya and O. Lev, *Anal. Chim. Acta*, **256**, 65 (1992).
30. O. Lev, B. Iosefson-Kuyavskaya, I. Gigozin, M. Ottolenghi and D. Avnir, *Fresenius J. Anal. Chem.*, **343**, 370 (1992).
31. V. Chernyak, R. Reisfeld, R. Gviski and D. Venezky, *Sens. Mater.*, **2**, 117 (1990).
32. M. Tsyonsky and O. Lev, *Analyst*, **118**, 557 (1993).
33. V. R. Kaufman, D. Avnir, P. Pines-Rojanski and D. Huppert, *J. Non-Cryst. Solids*, **99**, 379 (1988).
34. D. Bianchi, M. Lacross, J. M. Pajonk and J. Teichner, *J. Catal.*, **68**, 411 (1981).
35. T. Lopez, M. Villa and R. Gomez, *J. Phys. Chem.*, **95**, 1690 (1991).
36. J. R. Hardee, S. E. Tunney, J. Frye and J. K. Stille, *J. Polym. Sci.*, **28A**, 3669 (1991).
37. K. V. Parish, D. Habibi and V. Mohammadi, *J. Organomet. Chem.*, **369**, 17 (1989).
38. A. Rosenfeld, D. Avnir and J. Blum, *J. Chem. Soc., Chem. Commun.*, 583 (1993).
39. J. Blum, A. Rosenfeld, N. Polak, O. Israelson, H. Schumann and D. Avnir, *J. Mol. Catal.*, **107**, 217 (1996).
40. (a) A. Rosenfeld, J. Blum and D. Avnir, *J. Catal.*, **164**, 363 (1996).
    (b) H. Sertchook, D. Avnir, J. Blum, F. Joo, A. Katho, H. Schumann, R. Weinmann and S. Wernik, *J. Mol. Catal. A*, **108**, 153 (1996).
41. I. Amer, V. Orshav and J. Blum, *J. Mol. Catal.*, **45**, 207 (1988).
42. J. Blum, H. Huminer and H. Alper, *J. Mol. Catal.*, **75**, 153 (1992).
43. S. Braun, S. Rappoport, R. Zusman, D. Avnir and M. Ottolenghi, *Mater. Lett.*, **10**, 1 (1990).
44. (a) *Biochemical Aspects of Sol–Gel Science and Technology*, D. Avnir, and S. Braun, Editors, Kluwer Academic Publishers, Boston, 1996.
    (b) D. Avnir, S. Braun, O. Lev and M. Ottolenghi, *Chem. Mater.*, **6**, 1605 (1994).
45. (a) S. Shtelzer and S. Braun, *Biotechnol. Appl. Biochem.*, **19**, 293 (1994).
    (b) S. A. Yamanaka, F. Nishida, L. M. Ellerby, C. R. Nishida, B. Dunn, J. S. Valentine and J. I. Zink, *Chem. Mater.*, **4**, 495 (1992).
    (c) Y. P. Tatsu, K. Yamashita, M. Yamaguchi, S. Yamamura, H. Yamamoto and S. Yoshikawa, *Chem. Lett.*, 1615 (1992).
    (d) B. C. Dave, B. Dunn, J. S. Valentine and J. I. Zink, *Anal. Chem.*, **66**, 1120A (1994).
    (e) J. Livage, *C.R. Acad. Sci. Paris, II*, **322**, 417 (1996).
    (f) M. T. Reetz, A. Zonta and A. Simpelkamp, *J. Biotechnol. Bioeng.*, **49**, 527 (1996).
    (g) C. Dosoretz, R. Armon, J. Starosvetzky, and N. Rothschild, *J. Sol–Gel Sci. Tech.*, **7**, 7 (1996).
    (h) J. Zuhlke, D. Knopp and R. Niessner, *Fresenius J. Anal. Chem.*, **352**, 654 (1995).
46. (a) S. Shtelzer, S. Rappoport, D. Avnir, M. Ottolenghi and S. Braun, *Biotechnol. Appl. Biochem.*, **15**, 227 (1992).
    (b) S. Braun, S. Shtelzer, S. Rappoport, D. Avnir and M. Ottolenghi, *J. Non-Cryst. Solids*, **147 & 148**, 739 (1992).
47. U. Narang, P. N. Prasad, F. V. Bright, K. N. Ramanathan, K. Deepak, B. D. Malhotra, M. N. Kalamansan and S. Chandra, *Anal. Chem.*, **66**, 3139 (1994).
48. S. Shtelzer and S. Braun, *Biotechnol. Appl. Biochem.*, **19**, 293 (1994).
49. (a) P. Audebert, C. Demaille and C. Sanchez, *Chem. Mater.*, **5**, 911 (1993).
    (b) V. Glezer and O. Lev, *J. Am. Chem. Soc.*, **115**, 2533 (1993).
50. S. Braun, S. Rappoport, S. Shtelzer, R. Zusman, S. Druckman, D. Avnir and M. Ottolenghi, in *Biotechnology: Bridging Research and Applications* (Eds. D. Kamely, A. M. Chakrabary and S. E. Kornguth), Kluwer, Boston, 1991, pp. 205–218.
51. C. Dozorets, R. Armon and N. Rothchild, *J. Sol–Gel Sci. Technol.*, **4**, 7 (1996).

52. A. Turniansky, D. Avnir, A. Bronshtein, N. Aharonson and M. Altstein, *J. Sol–Gel Sci. Technol.*, **7**, 135 (1996).
53. M. Sun, *Science*, **233**, 1143 (1986).
54. D. R. Nair and J. L. Schnoor, *Environ. Sci. Technol.*, **26**, 2298 (1992).
55. R. Collino, J. Therasse, P. Binder, F. Chaput, B.-P. Boilot and Y. Levy, *J. Sol–Gel Sci. Technol.*, **2**, 823 (1994).
56. R. Wang, U. Narang, P. N. Prasad and F. V. Bright, *Anal. Chem.*, **65**, 2671 (1993).
57. J. Livage, C. Roux and J. M. Da Cost, *J. Sol–Gel Sci. Technol.*, **4**, 45 (1996).
58. J. Zuhlke, D. Knopp and R. Niessner, *Fresenius J. Anal. Chem.*, **352**, 654 (1995).
59. P. L. Edmiston, C. L. Wambolt, M. K. Smith and S. S. Saavedra, *J. Colloid Interface Sci.*, **163**, 395 (1994).
60. Y. Tatsu, K. Yamashita, M. Yamaguchi, S. Yamamura, H. Yamamoto and S. Yoshikawa, *Chem. Lett.*, 1615 (1992).
61. V. Glezer, G. Gun, M. Tsionsky and O. Lev, *Abstracts of the 44th Int. Soc. Electrochem. Meeting*, Berlin, Germany, September 14, 1993.
62. G. Gun, M. Tsionsky and O. Lev, *Anal. Chim. Acta*, **294**, 261 (1994).
63. G. Gun, M. Tsionsky and O. Lev, in *Better Ceramics Through Chemistry, VI*, (Eds. C. Sanchez, M. L. Mecartney, C. J. Brinker and A. Cheetham), *Mater. Res. Soc. Symp. Proc.*, **346**, 1011 (1994).
64. S. Sampath and O. Lev, *Anal. Chem.*, **68**, 2015 (1996).
65. M. Tsionsky and O. Lev, *J. Electrochem. Soc.*, **142**, 2154 (1995).
66. M. Tsionsky and O. Lev, *Anal. Chem.*, **67**, 2409 (1995).
67. J. Gun, M. Tsionsky, L. Rabinovich, Y. Golan, I. Rubinstein and O. Lev, *J. Electroanal. Chem.*, **395**, 57 (1995).
68. L. Rabinovich, M. Tsionsky, V. Glezer, J. Gun and O. Lev, *J. Sol–Gel Sci. Technol.*, in press (1997).
69. I. Pankratov and O. Lev, *J. Electroanal. Chem.*, **393**, 35 (1995).
70. S. Sampath, I. Pankratov, J. Gun and O. Lev, *J. Sol–Gel Sci. Technol.*, **7**, 123 (1996).
71. S. Sampath and O. Lev, *Electroanalysis,* **8**, 1112 (1996).
72. J. Gun and O. Lev, *Anal. Lett.*, **29**, 1933 (1996).
73. J. Gun and O. Lev *Anal. Chim. Acta*, **330**, 95 (1996).
74. J. Wang, P. V. A. Pamidi and D. S. Park, *Anal. Chem.*, **68**, 2705 (1996).
75. Review: R. H. Baney, M. Itoh, A. Sakakibara and T. Suzuki, *Chem. Rev.*, **95**, 1409 (1995).
76. Review: U. Schubert, N. Hüsing and A. Lorenz, *Chem. Mater.*, **7**, 2010 (1995).
77. W. Noll, *Chemie und Technologie der Silicone*, Verlag Chemie, Weinheim, 1968.
78. U. Deschler, P. Kleinschmit and P. Panster, *Angew. Chem.*, **98,** 237 (1986); *Angew. Chem., Int. Ed. Engl.,* **25**, 236 (1986).
79. H. Wolter, W. Glaubitt and K. Rose, *Mater. Res. Soc. Proc.*, **271**, 719 (1992).
80. Y. Nosaka, N. Tohriiwa, T. Kobayashi and N. Fujii, *Chem. Mater.*, **5**, 930 (1993).
81. F. Chaput, D. Riehl, Y. Levy and J. P. Boilot, *Chem. Mater.*, **5**, 589 (1993); F. Chaput, J. P. Boilot, D. Riehl and Y. Levy, *J. Sol–Gel Sci. Technol.*, **2**, 779 (1994).
82. B. Lebeau, C. Guermeur and C. Sanchez, *Mater. Res. Soc. Symp. Proc.*, **346**, 315 (1994).
83. M. Ueda, H.-B. Kim, T. Ikeda and K. Ichimura, *J. Non-Cryst. Solids*, **163**, 125 (1993); Z. Yang, C. Xu, B. Wu, L. R. Dalton, S. Kalluri, W. H. Steier, Y. Shi and J. H. Bechtel, *Chem. Mater.*, **6**, 1899 (1994).
84. H. Wolter and W. Storch, *J. Sol–Gel Sci. Technol.*, **2**, 93 (1994).
85. J. L. Brefort, R. J. P. Corriu, P. Gerbier, C. Guerin, B. J. L. Henner, A. Jean, T. Kuhlmann, F. Garnier and A. Yassar, *Organometallics*, **11**, 2500 (1992).
86. H. Kobayashi, *Makromol. Chem.*, **194**, 2569 (1993).
87. R. Kasemann and H. Schmidt, *New J. Chem.*, **18**, 1117 (1994).
88. J. Kron, S. Amberg-Schwab and G. Schottner, *J. Sol–Gel Sci. Technol.*, **2**, 189 (1994).
89. F. Babonneau, K. Thorne and J. D. Mackenzie, *Chem. Mater.*, **1**, 554 (1989).
90. F. Babonneau, *Polyhedron*, **13**, 1123 (1994).
91. F. Schwertfeger, W. Glaubitt and U. Schubert, *J. Non-Cryst. Solids*, **145**, 85 (1992); F. Schwertfeger, N. Hüsing and U. Schubert, *J. Sol–Gel Sci. Technol.*, **2**, 103 (1994); F. Schwertfeger, A. Emmerling, J. Gross, U. Schubert and J. Fricke, in *Sol–Gel Processing and Applications* (Ed. Y. A. Attia), Plenum Press, New York, 1994, p. 351; U. Schubert, F. Schwertfeger, N. Hüsing and E. Seyfried, *Mater. Res. Soc. Symp. Proc.,* **346**, 151 (1994); N. Hüsing, F. Schwertfeger,

W. Tappert and U. Schubert, *J. Non-Cryst. Solids,* **186**, 37 (1995); N. Hüsing and U. Schubert, *J. Sol–Gel Sci. Technol.,* **8**, 807 (1997).

92. N. Hüsing, U. Schubert, B. Riegel and W. Kiefer, *Mater. Res. Soc. Symp. Proc.*, **435**, 339 (1996).
93. F. Schwertfeger and U. Schubert, *Chem. Mater.*, **7**, 1909 (1995).
94. K. Rose, H. Wolter and W. Glaubitt, *Mater. Res. Soc. Proc.*, **271**, 731 (1992).
95. H. Wolter, W. Storch and H. Ott, *Mater. Res. Soc. Proc.*, **346**, 143 (1994).
96. F. D. Osterholtz and E. R. Pohl, *J. Adhesion Sci. Technol.*, **6**, 127 (1992).
97. Y. Abe, K. Taguchi, H. Hatano, G. Takahiro, Y. Nagao and T. Misono, *J. Sol–Gel Sci. Technol.*, **2**, 131 (1994); F. Devreux, J. P. Boilot, F. Chaput and A. Lecomte, *Mater. Res. Soc. Symp. Proc.*, **180**, 211 (1990).
98. K. Piana and U. Schubert, *Chem. Mater.*, **6**, 1504 (1994).
99. J. P. Grey, *Adhesion (London)*, **12**, 106 (1988).
100. J. D. Miller, K.-P. Hoh and H. Ishida, *Polymer Compos.*, **5**, 18 (1984).
101. K. Greiwe, W. Glaubitt, S. Amberg-Schwab and K. Piana, *Mater. Res. Soc. Symp. Proc.*, **271**, 725 (1992).
102. L. Delattre, C. Dupuy and F. Babonneau, *J. Sol–Gel Sci. Technol.*, **2**, 185 (1994).
103. H. Krug and H. Schmidt, *New J. Chem.*, **18**, 1125 (1994).
104. R. Nass, E. Arpac, W. Glaubitt and H. Schmidt, *J. Non-Cryst. Solids*, **121**, 370 (1990).
105. N. Yamazaki, S. Nakahama, J. Goto, T. Nagawa and A. Hirao, *Contemp. Top. Polym. Sci.*, **4**, 105 (1984); Y. Abe, T. Namiki, K. Tsuchida, Y. Nagao and T. Misono, *J. Non-Cryst. Solids*, **147 & 148**, 47 (1992).
106. J. F. Brown and L. H. Vogt, *J. Am. Chem. Soc.*, **87**, 4313 (1965); J. F. Brown, *J. Am. Chem. Soc.*, **87**, 4317 (1965).
107. G. M. Voronkov and V. I. Lavrent'yev, *Top. Curr. Chem.*, **102**, 199 (1982); U. Dittmar, B. J. Hendan, U. Flörke and H. C. Marsmann, *J. Organomet. Chem.*, **489**, 185 (1995).
108. M. J. van Bommel, P. M. C. Ten Wolde and T. N. N. Bernards, *J. Sol–Gel Sci. Technol.*, **2**, 167 (1994).
109. G. Philipp and H. Schmidt, *J. Non-Cryst. Solids*, **82**, 31 (1986).
110. S. Amberg-Schwab, E. Arpac, W. Glaubitt, K. Rose, G. Schottner and U. Schubert, in *High Performance Films and Coatings* (Ed. P. Vincenzini), Elsevier, Amsterdam, 1991, p. 203.
111. H. Schmidt and G. Philipp, *J. Non-Cryst. Solids*, **63**, 283 (1984); H. Schmidt and G. Philipp, in *Glass: Current Issues* (Eds. A. F. Wright and J. Dupuy), Martinus Nijhoff Publ., Dordrecht, 1985, p. 580.
112. R. J. P. Corriu, J. J. E. Moreau, P. Thepot and M. Wong Chi Man, *Chem. Mater.*, **8**, 100 (1996).
113. H. Schmidt, B. Seiferling, G. Philipp and K. Deichmann, in *Ultrastructure Processing of Advanced Ceramics* (Eds. J. D. Mackenzie and D. R. Ulrich), Wiley, New York, 1988, p. 651.
114. H. Schmidt and B. Seiferling, *Mater. Res. Soc. Symp. Proc.*, **73**, 739 (1986).
115. K. Greiwe, *Farbe und lack*, **11**, 968 (1991).
116. M. Popall, J. Kappel, M. Pilz and J. Schulz, *Mater. Res. Soc. Symp. Proc.*, **264**, 353 (1992); M. Popall, J. Kappel and J. Schulz, in *Micro System Technologies '94* (Eds. H. Reichl and A. Heuberger), VDE-Verlag, Berlin, 1995.
117. M. Popall, J. Kappel, M. Pilz, J. Schulz and G. Feyder, *J. Sol–Gel Sci. Technol.*, **2**, 157 (1994).
118. R. Nass, H. Schmidt and E. Arpac, *SPIE, Sol–Gel Optics*, **1328**, 258 (1990).
119. N. Kaneko, Jap. Patent Kokai-H-5-586193 (1993); *Chem. Abstr.*, **119**, 73383 (1993).
120. C. Sanchez, B. Alonso, F. Chapusot, F. Ribot and P. Audebert, *J. Sol–Gel Sci. Technol.*, **2**, 161 (1994).
121. G. A. Sigel, R. C. Domszy and W. C. Welch, *Mates. Res. Soc. Symp. Proc.*, **346**, 135 (1994).
122. M. Popall and H. Durand, *Electrochim. Acta*, **37**, 1593 (1992).
123. D. Hoebbel, K. Endres, T. Reinert and H. Schmidt, *Mater. Res. Soc. Symp. Proc.*, **346**, 863 (1994).
124. P. A. Agaskar, *J. Am. Chem. Soc.*, **111**, 6858 (1989); D. Hoebbel, I. Pitsch, D. Heidemann, H. Jancke and W. Hiller, *Z. Anorg. Allg. Chem.*, **583**, 133 (1990); D. Hoebbel, I. Pitsch and D. Heidemann, *Z. Anorg. Allg. Chem.*, **592**, 207 (1991); D. Hoebbel, K. Endres, T. Reinert and I. Pitsch, *J. Non-Cryst. Solids*, **176**, 179 (1994).
125. E. P. Plueddemann, in *Silylated Surfaces* (Eds. D. E. Leyden and W. T. Collins), Gordon & Breach, New York, 1980, p. 31; H. Ishida, C. Chiang and J. L. Koenig, *Polymer*, **23**, 251 (1982); H. Ishida, S. Naviroj, S. K. Tripathy, J. J. Fitzgerald and J. L. Koenig, *J. Polym. Sci.*, **20**, 701 (1982); K. C. Vrancken, P. van der Voort, I. Gillis-D'Hamers and E. F. Vansant, *J. Chem. Soc., Faraday Trans.*, **88**, 3197 (1992).

126. V. de Zea Bermudez, M. Armand, C. Poinsignon, L. Abello and J.-Y. Sanchez, *Electrochim. Acta*, **37**, 1603 (1992); W. Cao and A. J. Hunt, *Mater. Res. Soc. Symp. Proc.*, **346**, 631 (1994).
127. K. Piana and U. Schubert, *Chem. Mater.*, **7**, 1932 (1995).
128. E. Lindner, A. Bader and H. A. Mayer, *Inorg. Chem.*, **30**, 3783 (1991).
129. Y. Charbouillot, D. Ravaine, M. Armand and C. Poinsignon, *J. Non-Cryst. Solids*, **103**, 325 (1988); H. Schmidt, M. Popall, F. Rousseau, C. Poinsignon, M. Armand and J. Y. Sanchez, in *Proc. 2nd Int. Symp. on Polymer Electrolytes* (Ed. B. Scrosati), Elsevier, London, 1990, p. 325.
130. U. Posset, M. Lankers, W. Kiefer, H. Steins and G. Schottner, *Appl. Spectrosc.*, **47**, 1600 (1993).
131. M. P. Beslard, N. Hovnanian, A. Larbot, L. Cot, J. Sanz, I. Sobrados and M. Gregorkiewitz, *J. Am. Chem. Soc.*, **113**, 1982 (1991).
132. N. Aharonson, M. Altstein, G. Avidan, D. Avnir, A. Bronshtein, A. Lewis, K. Liberman, M. Ottolenghi, Y. Polevaya, C. Rottman, J. Samuel, S. Shalom, A. Strinkovski and A. Turniansky, *Mater. Res. Soc. Symp. Proc.*, **346**, 519 (1994).
133. H.-E. Endres, L. D. Mickle, C. Kösslinger, S. Drost and F. Hutter, *Sensors and Actuators B*, **6**, 285 (1992).
134. A. Brandenburg and R. Edelhäuser, *Sensors and Actuators B*, **11**, 361 (1993).
135. J. Lin, S. Möller and E. Obermeier, *Sensors and Actuators B*, **5**, 219 (1991).
136. B. Breitscheidel, J. Zieder and U. Schubert, *Chem. Mater.*, **3**, 559 (1991); U. Schubert, B. Breitscheidel, H. Buhler, C. Egger and W. Urbaniak, *Mater. Res. Soc. Symp. Proc.*, **271**, 621 (1992); U. Schubert, C. Görsmann, S. Tewinkel, A. Kaiser and T. Heinrich, *Mater. Res. Soc. Symp. Proc.*, **351**, 141 (1994); A. Kaiser, C. Görsmann and U. Schubert, *J. Sol–Gel Sci. Technol.*, **8**, 795 (1997); C. Görsmann and U. Schubert, *Mater. Res. Soc. Symp. Proc.*, **435**, 625 (1996).
137. C. Ferrari, G. Predieri and A. Tiripicchio, *Chem. Mater.*, **4**, 243 (1992).
138. L. Spanhel, E. Arpac and H. Schmidt, *J. Non-Cryst. Solids*, **147 & 148**, 657 (1992); T. Burkhart, M. Mennig, H. Schmidt and A. Licciulli, *Mater. Res. Soc. Symp. Proc.*, **346**, 779 (1994).
139. U. Schubert, *New. J. Chem.*, **18**, 1049 (1994).
140. K. G. Allum, R. D. Hancock, I. V. Horwell, S. McKenzie, R. C. Pikethly and P. J. Robinson, *J. Organomet. Chem.*, **107**, 393 (1976).
141. Leading references: F. R. Hartley, *Supported Metal Complexes*, Reidel, Dordrecht, 1985; Yu. I. Yermakov, B. N. Kuznetsov and V. A. Zakharov, *Catalysis by Supported Complexes*, Elsevier, Amsterdam, 1981.
142. U. Schubert, C. Egger, K. Rose and C. Alt, *J. Mol. Catal.*, **55**, 330 (1989).
143. C. Guizard and P. Lacan, *New J. Chem.*, **18**, 1097 (1994).
144. K. Arija and Y. Okahata, *J. Am. Chem. Soc.*, **111**, 5618 (1989).
145. J. E. Mark, *Heterog. Chem. Rev.*, **3**, 307 (1996).
146. H. Schmidt, in *Sol–Gel Optics* (Ed. L.C. Klein), Kluwer Academic Publ., Boston, 1994, pp. 451–481.
147. R. A. Roy and R. Roy, *Mater. Res. Bull.*, **19**, 169 (1984).
148. C. Sanchez and F. Ribot, *New J. Chem.*, **18**, 1007 (1994).
149. L. H. Sperling, *Interpenetrating Polymer Networks and Related Materials*, Plenum Press, New York, 1981.
150. E. J. A. Pope, M. Asami and J. D. Mackenzie, *J. Mater. Res.*, **4**, 1018 (1989).
151. L. C. Klein, in *Sol–Gel Optics* (Ed. L.C. Klein), Kluwer Academic Publ., Boston, 1994, p. 215.
152. B. Abramoff and L. C. Klein, in *Chemical Processing of Advanced Materials* (Eds. L. L. Hench and J. K. West), Wiley, New York, 1992, pp. 815–821.
153. B. Abramoff and L. C. Klein, *SPIE*, **1328**, 241 (1990).
154. C. J. T. Landry, B. K. Coltrain, J. A. Wesson, N. Zumbuluyadis and J. C. Lippart, *Polymer*, **33**, 1496 (1992).
155. C. J. T. Landry, B.K. Coltrain and B. K. Brady, *Polymer*, **33**, 1486 (1992).
156. A. B. Wojcik and L. C. Klein, *SPIE*, **2018**, 160 (1993).
157. C. L. Beaudry, L. C. Klein and R. A. McCauley, *J. Therm. Anal.*, **46**, 55 (1996).
158. C. L. Beaudry and L. C. Klein, in *Nanotechnology of Molecularly Designed Materials* (Eds. G.-M. Chow and K. E. Gonsalves), *Am. Chem. Soc. Symp.*, **622**, 1996, p. 382.
159. M. W. Ellsworth and B. M. Novak, *Polym. Prepr.*, **33**, 1088 (1992).
160. M. W. Ellsworth and B. M. Novak, *J. Am. Chem. Soc.*, **113**, 2756 (1991).
161. B. M. Novak, *Adv. Mater.*, **5**, 422 (1993).
162. B. M. Novak and C. Davies, *Macromolecules*, **24**, 5481 (1991).
163. A. B. Wojcik and L. C. Klein, *J. Sol–Gel Sci. Technol.*, **2**, 115 (1994).

164. A. B. Wojcik and L. C. Klein, *J. Sol–Gel Sci. Technol.*, **4**, 57 (1995).
165. A. B. Wojcik and L. C. Klein, *J. Sol–Gel Sci. Technol.*, **5**, 77 (1995).
166. D. Hoebbel and W. Wieker, *Z. Anorg. Allg. Chem.*, **384**, 43 (1991).
167. Y. Hu and J. D. Mackenzie, *MRS. Symp. Proc.*, **271**, 681 (1992); J. D. Mackenzie, Y. J. Chung and Y. Hu, *J. Non-Cryst. Solids*, **147 & 148**, 271 (1992); Y. Hoshino and J. D. Mackenzie, *J. Sol–Gel Sci. Technol.*, **5**, 83 (1995).
168. B. Wang, G. L. Wilkes, J. C. Hedrick, S. C. Liptak and J. E. McGrath, *Macromolecules*, **24**, 3449 (1991).
169. H. H. Huang, G. L. Wilkes and J. G. Carlson, *Polymer*, **30**, 2001 (1989).
170. Y. Chujo, E. Ihara, H. Ihara and T. Saegusa, *Macromolecules*, **22**, 2040 (1989).
171. J. Thompson, H. H. Fox, I. Gorodisher, G. Teowee, D. Calvert and D. R. Uhlmann, *MRS Symp. Proc.*, **180**, 987 (1990).
172. D. Xu, S. H. Wang and J. E. Mark, *MRS Symp. Proc.*, **180**, 445 (1990).
173. T. H. Mouray, S. M. Miller, J. A. Wesson, T. E. Long and L. W. Kelt, *Macromolecules*, **25**, 45 (1992).
174. S. Kohjiya, K. Ochial and S. Yamashita, *J. Non-Cryst. Solids*, **119**, 132 (1990).
175. Y. Wei, D. Yang and L. Tang, *Macromol. Chem., Rapid. Commun.*, **14**, 273 (1993).
176. Y. Wei, R. Bakthavatachalam and C. K. Whitecar, *Chem. Mater.*, **2**, 337 (1990).
177. M. Guglielmi, P. Colombo, G. Brusetin, G. Facchin and M. Gleria, *J. Sol–Gel Sci. Technol.*, **2**, 109 (1994).
178. H. Schmidt and M. Popall, *SPIE*, **1328**, 249 (1990).
179. H. Schmidt, H. Scholze and G. Tunker, *J. Non-Cryst. Solids*, **80**, 557 (1986).
180. K. J. Shea, D. A. Loy and O. W. Webster, *Chem. Mater.*, **1**, 572 (1989).
181. D. A. Loy, R. J. Buss, R. A. Assink, K. J. Shea and H. Oviatt, *Mater. Res. Soc. Symp. Ser.*, **346**, 825 (1994).
182. (a) K. M. Choi and K. J. Shea, *J. Sol–Gel Sci. Technol.*, **5**, 143 (1995).
     (b) D. A. Loy and K. J. Shea, *Chem. Rev.*, **95,** 143 (1995).
183. (a) S. Ikoma, S. Takano, E. Nomoto and H. Yokoi, *J. Non-Cryst. Solids*, **113**, 130 (1989).
     (b) A. Shames, O. Lev and B. Iosefson-Kuyavskaya *J. Non-Cryst. Solids*, **175**, 14 (1994).
184. V. R. Kaufman, D. Levy and D. Avnir, *J. Non-Cryst. Solids*, **82**, 103 (1986).
185. V. R. Kaufman and D. Avnir, *Langmuir*, **2**, 717 (1986).
186. (a) For a review, see, M. Anpo, T. Fujii and N. Negishi, *Heterogen. Chem. Rev.*, **1**, 231 (1994); some other examples:
     (b) K. Matsui, M. Tominaga, Y. Arai, H. Satoh and M. Kyoto, *J. Non-Cryst. Solids*, **169**, 295 (1994).
     (c) C. J. Brinker, A. J. Hurd, P. R. Schank, G. C. Frye and C. S. Ashley, *J. Non-Cryst. Solids*, **147&148**, 424 (1992).
     (d) N. Negishi, T. Fujii and M. Anpo, *Langmuir*, **9**, 3320 (1993).
187. K. Matsui, T. Matsuzuka and H. Fujita, *J. Chem. Phys.*, **93**, 4991 (1989).
188. T. Fujii, T. Mabuchi and I. Mitsui, *Chem. Phys. Lett.*, **68**, 5 (1990).
189. K. Matsui and T. Nakazawa, *Bull. Chem. Soc. Jpn.*, **63**, 11 (1990).
190. J. McKiernan, J. C. Pouxviel, B. Dunn and J. I. Zink, *J. Phys. Chem.*, **93**, 2129 (1989).
191. T. Fujii and K. Toriumi, *J. Chem. Soc., Faraday Trans.*, **89**, 3437 (1993).
192. D. Levy and D. Avnir, *J. Phys. Chem.*, **92,** 4734 (1988).
193. D. Levy, S. Einhorn and D. Avnir, *J. Non-Cryst. Solids*, **113**, 137 (1989).
194. J. C. Pouxviel, B. Dunn and J. I. Zink, *J. Phys. Chem.*, **93**, 2134 (1989).
195. (a) *SPIE Proc. Series* on Sol–Gel Optics, (Ed. J. D. Mackenzie), every two years since 1990.
     (b) L. C. Klein (Ed.), *Sol-Gel Optics*, Kluwer, Boston, 1994.
196. D. Avnir, V. R. Kaufman and R. Reisfeld, *J. Non-Cryst. Solids*, **74**, 395 (1985).
197. D. Levy and D. Avnir, *J. Photochem. Photobiol. A: Chem.*, **57**, 41 (1991).
198. J. Samuel, Y. Polevaya, M. Ottolenghi and D. Avnir, *Chem. Mater.*, **6**, 1457 (1994).
199. D. Levy, R. Reisfeld and D. Avnir, *Chem. Phys. Lett.*, **109**, 593 (1984).
200. L. R. Matthews and E. T. Knobbe, *Chem. Mater.*, **5**, 1697 (1993) and references cited therein.
201. E.g.: S. S. Ostapenko, A. J. Neuhalfen and B. W. Wessels, *Mater. Sci. Forum*, **143–147**, 743 (1994).
202. (a) H. Zabrodsky, S. Peleg and D. Avnir, *J. Am. Chem. Soc.*, **114**, 7843 (1992).
     (b) H. Zabrodsky, S. Peleg and D. Avnir, *J. Am. Chem. Soc.*, **115**, 8278 (1993).
     (c) H. Zabrodsky and D. Avnir, *J. Am. Chem. Soc.,* **117**, 462 (1995).

203. A. Slama-Schwok, M. Ottolenghi and D. Avnir, *Nature*, **355**, 240(1992).
204. A. Slama-Schwok, D. Avnir and M. Ottolenghi, *J. Phys. Chem.*, **93**, 7544 (1989).
205. (a) A. Slama-Schwok, D. Avnir and M. Ottolenghi, *J. Am. Chem. Soc.*, **113**, 3984 (1991).
(b) A. Slama-Schwok, D. Avnir and M. Ottolenghi, *Photochem. Photobiol.*, **54**, 525 (1991).
206. C.f. also: F. N. Castellano, T. A. Heimer, T. M. Tandhasetti and G. J. Meyer, *Chem. Mater.*, **6**, 1041 (1994).
207. M. Nogami and Y. Abe, *J. Mater. Sci.*, **30**, 5789 (1995).
208. D. Preston, J. Pouxviel, T. Novinson, W. C. Kaska, B. Dunn and J. I. Zink, *Phys. Chem.*, **94**, 4167 (1990).
209. M. Nogami and T. Sugiura, *J. Mater. Sci. Lett.*, **12**, 1544 (1993).
210. (a) M. Ueda, H.-B. Kim, T. Ikeda and K. Ichimura, *J. Non-Cryst. Solids*, **163**, 125 (1993).
(b) M. Ueda, H.-B. Kim, T. Ikeda and K. Ichimura, *Chem. Mater.*, **4**, 1229 (1992).
211. L. Hou, M. Mennig and H. Schmidt, *SPIE Sol–Gel Optics III*, **2288**, 328 (1994).
212. E. J. A. Pope, *SPIE Sol–Gel Optics III*, **2288**, 410 (1994).
213. H. Nakazumi, R. Nagashiro, S. Matsumoto and K. Isagawa, *SPIE Sol–Gel Optics III*, **2288**, 402 (1994).
214. H. Nakazumi, K. Makita and R. Nagashiro, *J. Sol–Gel Sci. Technol.*, **8**, 901 (1997).
215. D. Levy, M. López-Amo, J. M. Otón, F. del Monte, P. Datta and I. Matías, in *Advanced Networks and Services, SPIE Proc.* (Ed. T. Russel Hsing), SPIE, Bellingham Washington 1995, p. 2449.
216. D. Yuan-Chieh, PhD Thesis, Rutgers, The State University of New-Jersey, 1993.
217. D. Levy, F. del Monte, J. M. Otón, I. Matias, P. Datta and M. Lopez-Amo, *J. Sol–Gel Sci. Technol.*, **8**, 931, (1997).
218. D. R. Ulrich, *J. Non-Cryst. Solids*, **100**, 174 (1988).
219. M. Yamane, S. Aso and T. Sakaino, *J. Mater. Sci.*, **13**, 865 (1978).
220. B. Dunn, E. Knobbe, J. M. MacKiernan, J. C. Pouxviel and J. I. Zink, *Mater. Res. Soc. Symp. Proc.*, **121**, 331 (1988).
221. T. Fujii, A. Ishii, H. Nagai, M. Niwano, N. Negishi and M. Anpo, *Chem. Express*, **4**, 1 (1989).
222. E. J. A. Pope and J. D. Mackenzie, *MRS Bulletin*, p. 29, March 17, 1987.
223. D. Levy, C. J. Serna and J. M. Otón, *Mater. Lett.*, **10**, 470 (1991).
224. J. M. Otón, A. Serrano, C. J. Serna and D. Levy, *Liq. Cryst.*, **10**, 733 (1991).
225. D. Levy, M. Ocaña and C. J. Serna, *Langmuir*, **10**, 2683 (1994).
226. U. P. Narang, R. Wang, P. N. Prasad and F. V. Bright, *J. Phys. Chem.*, **98**, 17 (1994).
227. S. C. Laperrière, J. W. Mullens, D. L'Espérance and E. L. Chronister, *Chem. Phys. Lett.*, **243**, 114 (1995).
228. Y. Kobayashi, Y. Imai and Y. Kurokawa, *J. Mater. Sci. Lett.*, **7**, 1148 (1988).
229. W. Nei, B. Dunn, C. Sanchez and P. Griesmar, *Mater. Res. Soc. Proc.*, **271**, 639 (1992).
230. Y. Haruvy, A. Heller and S. E. Webber, *Am. Chem. Soc. Symp. Ser.*, **499**, 405 (1992).
231. D. L'Esperance and E. L. Chronister, *Chem. Phys. Lett.*, **195**, 387 (1995).
232. B. Lebeau, N. Herlet, J. Livage and C. Sanchez, *Chem. Phys. Lett.*, **206**, 15 (1993).
233. M. D. Ranh and T. A. King, *SPIE Sol–Gel Optics III*, **2288**, 364 (1994).
234. R. Reisfeld, D. Brusilovsky, M. Eyal, E. Miron, Z. Burshtein and J. Ivri, *Chem. Phys. Lett.*, **160**, 43 (1989).
235. A. B. Wojcik and L. C. Klein, *SPIE Sol–Gel Optics III*, **2288**, 392 (1994).
236. M. Canva, A. Dubois, P. Georges, A. Brun, F. Chaput, A. Ranger and J. P. Boilot, *SPIE Sol–Gel Optics III*, **2288**, 298 (1994).
237. T. Surtwala, Z. Gardlund, J. M. Boulton, D. R. Uhlmann, J. Watson and N. Peyghambarian, *SPIE Sol–Gel Optics III*, **2288**, 310 (1994).
238. H. Nakazumi, S. Amano and K. Sakai, *SPIE Sol–Gel Optics III*, **2288**, 356 (1994).
239. T. Fujii and A. Ishii, *J. Photochem. Photobiol., A: Chem.*, **54**, 231 (1990).
240. B. Dunn and J. I. Zink, *J. Mater. Chem.*, **1**, 903 (1991).
241. E. Knobbe, B. Dunn, P. Fuqua and F. Nishida, *Appl. Opt.*, **29**, 2729 (1990).
242. L. A. M. K. Shun, L. O. Dennis and W. Kin Hung, *Appl. Opt.*, **34**, 3380 (1995).
243. R. Gvishi and R. Reisfeld, *J. Non-Cryst. Solids*, **128**, 69 (1991).
244. H. G. Floch, P. F. Belleville, J. J. Priotton, P. M. Pegon, C. S. Dijonneau and J. Guerain, *Am. Ceram. Soc., Bull.*, **74**, 60 (1995).
245. J. Fabian, H. Nakazumi and M. Matsuoka, *Chem. Rev.*, **92**, 1197 (1992).
246. H. Nakatsuka, K. Inouye, S. Uemura and R. Yano, *Chem. Phys. Lett.*, **171**, 245 (1990).

247. F. M. Schellenberg, W. Lenth and G. C. Bjorklund, *Appl. Opt.*, **25**, 3207 (1986).
248. F. del Monte and D. Levy, *Chem. Mater.*, **7**, 292 (1995).
249. R. Reisfeld, D. Brusilovsky, M. Eyal, E. Miron, Z. Burshtein and J. Ivri, *Chem. Phys. Lett.*, **160**, 43 (1989).
250. E. Toussaere, J. Zyss, P. Griesmar and C. Sanchez, *Nonlinear Optics*, **1**, 349 (1991).
251. M. Nakamura, H. Naso and K. Kamiya, *J. Non-Cryst. Solids*, **135**, 1 (1991).
252. M. Canva, G. Le Saux, P. Georges, A. Brun, F. Chaput and J. P. Boilot, *Opt. Lett.*, **17**, 218 (1992).
253. K. Kubodera and T. Kaino, in *Nonlinear Optics of Organic and Semiconductors* (Ed. T. Kobayashi), Springer, Berlin, 1989, p. 163.
254. R. K. Jain and R. C. Lind, *J. Opt. Soc. Am.*, **73**, 647 (1983).
255. S. S. Yao, C. Karaguleff, A. Gabel, R. Fortenberry, C. T. Seaton and G. I. Stegeman, *Appl. Phys. Lett.*, **46**, 801 (1985).
256. R. Reisfeld, *SPIE Sol–Gel Optics II*, **1758**, 546 (1992).
257. G. Pucetti, E. Toussaere, I. Ledoux, J. Zyss, P. Griesmar and C. Sanchez, *Am. Chem. Soc., Div. Polym. Chem.*, **32**, 61 (1991).
258. P. Griesmar, C. Sanchez, G. Pucetti, I. Ledoux and J. Zyss, *Mol. Eng.*, **1**, 205 (1991).
259. J. Kim, J. L. Plawsky, R. La Peruta and G. M. Korenowski, *Chem. Mater*, **4**, 249 (1992).
260. R. J. Jeng, Y. V. Chen, A. K. Jain, J. Kumar and S. K. Tripathy, *Chem. Mater.*, **4**, 972 (1992).
261. J. Livage, C. Schmutz, P. Griesmar, P. Barboux and C. Sanchez, *SPIE Sol–Gel Optics II*, **1758**, 274 (1992).
262. G. S. He, J. D. Bhawalkar, C. F. Zhao and P. N. Prasad, *Appl. Phys. Lett.*, **67**, 2433 (1995).
263. Z. Yang, C. Xu, B. Wu, L. R. Dalton, S. Kalluri, W. Steier, Y. Shi and J. H. Bechtel, *Chem. Mater.*, **6**, 1899 (1994).
264. B. Lebeau, C. Sanchez, S. Brasselet, J. Zyss, G. Froc and M. Dumont *New J. Chem.*, **20**, 13 (1996).
265. S. Kalluri, Y. Shi, W. Steier, Z. Yang, C. Xu, B. Wu and L. R. Dalton, *Appl. Phys. Lett.*, **65**, 2651 (1994).
266. D. Riehl, F. Chaput, A. Roustamian, Y. Lévy and J. P. Boilot, *Nonlinear Optics*, **8**, 141 (1994).
267. D. Riehl, F. Chaput, Y. Lévy, J. P. Boilot, F. Kajzar and P. A. Chollet, *Chem. Phys. Lett.*, **245**, 36 (1995).
268. C. A. Capozzi and A. B. Seddon, *SPIE Sol–Gel Optics III*, **2288**, 340 (1994).
269. G. J. Gall, T. A. King, S. N. Oliver, C. A. Capozzi, A. B. Seddon, C. A. S. Hill and A. E. Underhill, *SPIE Sol–Gel Optics III*, **2288**, 372 (1994).
270. X. Wang, L. M. Yates III and E. T. Knobe, *SPIE Sol–Gel Optics III*, **2288**, 264 (1994).
271. L. Zhu, Y. Li, J. Wang and J. Shen, *Chem. Phys. Lett.,* **239**, 393 (1995).
272. D. Levy, J. M. S. Pena and C. J. Serna, *J. Non-Cryst. Solids*, **147 & 148,** 646 (1992).
273. W.-P. Chang, W.-T. Whang and J.-C. Wong, *Jpn. J. Appl. Phys.*, **34**, 1888 (1995).
274. D. Levy, A. Serrano and J. M. Otón, *J. Sol–Gel Sci. Technol.*, **2**, 803 (1994).
275. D. Levy, X. Quintana, C. Rodrigo and J. M. Otón, *SPIE Sol–Gel Optics III*, **2288**, 60 (1994).
276. J. M. Otón, J. M. S. Pena, A. Serrano and D. Levy, *Appl. Phys. Lett.*, **66**, 2804 (1995).
277. G. Schottner, W. Grond, L. Kümmerl and D. Haarer, *J. Sol–Gel Sci. Technol.*, **2**, 657 (1994).
278. R. Nakao, N. Ueda, Y. Abe, T. Horii and H. Inoue, *Polym. Adv. Technol.*, **5**, 240 (1994).
279. R. C. Chambers, Y. Haruvy and M. A. Fox, *Chem. Mater.*, **6**, 1351 (1994).
280. S. K. Tripathy, J. Kumar, J. T. Chen, S. Marturunkalkul, R. J. Jung, L. Li and X. L. Jiang, *Mater, Res. Soc. Symp. Proc.*, **346**, 351 (1994).
281. C. Sanchez, P. Griesmar, E. Toussaere, G. Puccetti, I. Ledoux and J. Zyss, *Nonlinear Optics*, **2**, 245 (1992).
282. H. Nakazumi and S. Amano, *J. Chem. Soc., Chem. Commun.*, 1079 (1992).
283. I. J. M. Snijkers-Hendrickx, M. W. J. L. Oomen, N. Wittouck and F. De Schryver, *Proc. 1st Europ. Workshop on Hybrid Organic–Inorganic Materials* (Eds. C. Sanchez and F. Ribot), Paris, 1993, p. 237.
284. C. Sanchez and B. Lebeau, *Pure Appl. Opt.*, **5**, 689 (1996).
285. B. Lebeau, J. Maquet, C. Sanchez, E. Toussaere, R. Hierle and J. Zyss, *J. Chem. Mater.*, **4**, 1855 (1994).
286. L. Kador, R. Fischer, D. Haarer, R. Kasemann, S. Brück, H. Schmidt and H. Dürr, *Adv. Mater.*, **5**, 270 (1993).
287. M. Ueda, H.-B. Kim and K. Ichimura, *Chem. Mater.*, **6**, 1771 (1994).

CHAPTER 41

Chirality in bioorganosilicon chemistry

REINHOLD TACKE and STEPHAN A. WAGNER

Institut für Anorganische Chemie, Universität Würzburg, Am Hubland, D-97074 Würzburg, Germany

I. INTRODUCTION

Bioorganosilicon chemistry represents a fascinating, rapidly expanding branch of organosilicon chemistry[1–9]. This area has been dominated by basic research for a long time; however, in recent years practical aspects are becoming of increasing importance. The development of new organosilicon drugs and agrochemicals and the application of biocatalysis in synthetic organosilicon chemistry are examples of this.

This short review deals with the topical subject 'chirality in bioorganosilicon chemistry'. Two different aspects will be discussed: (i) 'biological recognition of enantiomeric organosilicon drugs' and (ii) 'biocatalysis as a method for the preparation of optically active organosilicon compounds'. Most of the experimental material described in this article (which does not lay claim to completeness) comes from our own laboratory.

II. BIOLOGICAL RECOGNITION OF ENANTIOMERIC ORGANOSILICON DRUGS

During the past two decades, a variety of highly potent and receptor-selective silicon-based muscarinic antagonists have been developed[10–36]. The silanols sila-pridinol **(1)**, sila-difenidol **(2)**, sila-procyclidine **(3)**, sila-trihexyphenidyl **(4)**, hexahydro-sila-difenidol **(5)** and *p*-fluoro-hexahydro-sila-difenidol **(6)** are examples of this particular type of compound. The racemic mixtures of the silanols **5** (HHSiD) and **6** (*p*-F-HHSiD) are the most prominent drugs in this series of muscarinic antagonists. Both compounds are commercially available and are used worldwide as selective tools for the classification of muscarinic receptor subtypes. In the last few years, numerous biological data for HHSiD and *p*-F-HHSiD have been reported by many laboratories in more than 400 publications.

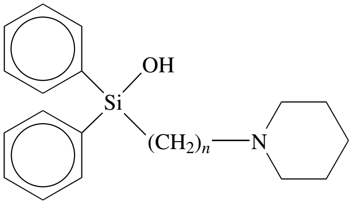

(1) $n = 2$
(2) $n = 3$

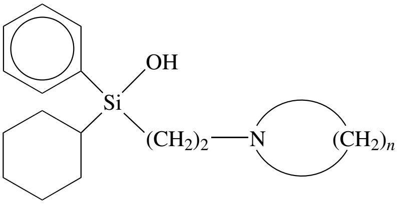

(3) $n = 4$
(4) $n = 5$

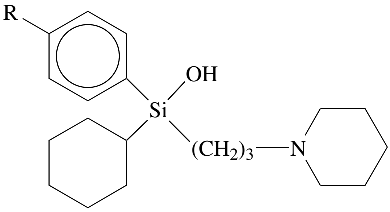

(5) R = H
(6) R = F

As can be seen from the formulas of **3**–**6**, these silanols are chiral compounds containing the silicon atom as the center of chirality. In order to study their stereoselectivity of antimuscarinic action, the enantiomers of sila-procyclidine **(3)** and of its methiodide sila-tricyclamol iodide **(7)** were prepared (Scheme 1)[20]. The optically active silanols (*R*)-**3** and (*S*)-**3** were obtained from the racemate *rac*-**3** (for syntheses of this compound[15,19], see Schemes 2 and 3) by a classical racemate resolution using (*L*)-(+)-tartaric acid and (*D*)-(−)-tartaric acid, respectively, as resolving agents (partial resolution by crystallization of diastereomeric salts and subsequent fractional crystallizations of the corresponding optically active free amine bases). The enantiomers (*R*)-**3** and (*S*)-**3** were isolated as crystalline solids with enantiomeric purities of >97% ee (NMR) and 99.7% ee (differential scanning calorimetry), respectively (in this context, see also Reference 32). The almost enantiomerically pure amines (*R*)-**3** and (*S*)-**3** were then transformed into the corresponding methiodides (*R*)-**7** and (*S*)-**7** by reaction with methyl iodide. The absolute configuration of the silanols (*R*)-**3**, (*S*)-**3**, (*R*)-**7** and (*S*)-**7** was established on the basis of a single-crystal X-ray diffraction analysis of (*R*)-sila-procyclidine [(*R*)-**3**][17]. The structure of the silanol (*R*)-**3** in the crystal is depicted in Figure 1.

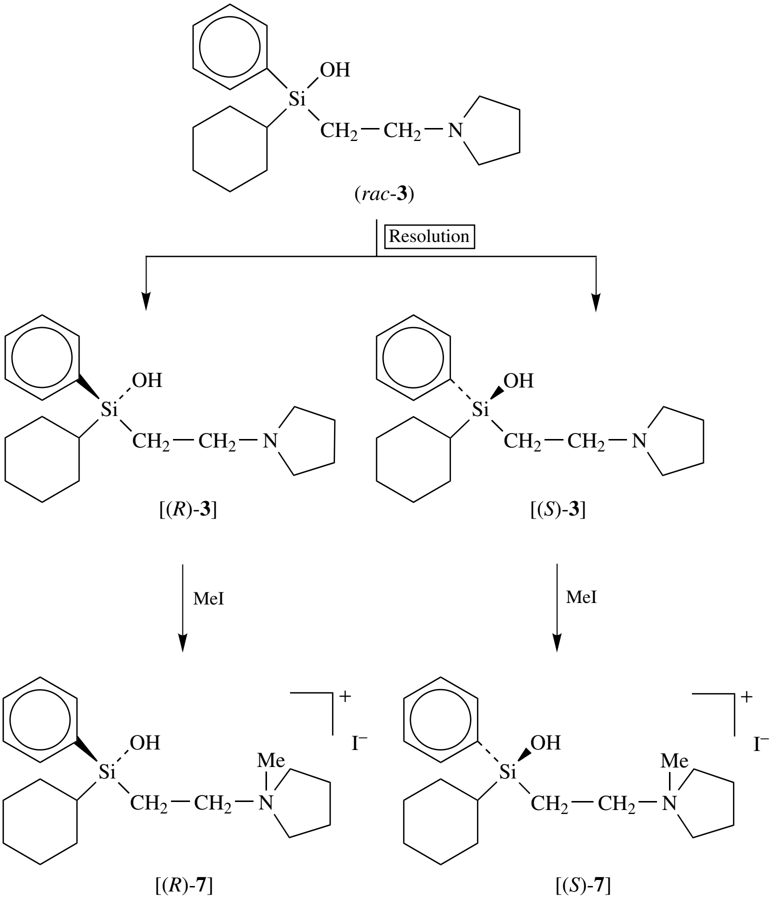

SCHEME 1

Compounds (*R*)-**3**, (*S*)-**3**, (*R*)-**7** and (*S*)-**7** are the first optically active silanols which were isolated as almost pure enantiomers. All compounds were found to be configurationally stable in the crystalline state and in inert organic solvents; however, in aqueous solution the optically active silanols racemize (**7** faster than **3**)[20]. This racemization can be described in terms of a nucleophilic attack of water (or OH^-) at the silicon atom which leads to substitution of the OH group bound to the silicon atom by the entering OH group.

The pure enantiomers of sila-procyclidine (**3**) and sila-tricyclamol iodide (**7**) were studied for their affinities for muscarinic M2 (guinea-pig atria) and M3 receptors (guinea-pig ileum) using carbachol as the agonist[20]. As the optically active silanols undergo a racemization under physiological conditions, a special experimental protocol was used for these studies (temperature, 32 °C; pH value, 7.4; equilibration time, 10 min). All compounds were found to exhibit an apparently competitive antagonism at muscarinic M2 and M3 receptors in these functional pharmacological experiments. The receptor affinities [pA_2

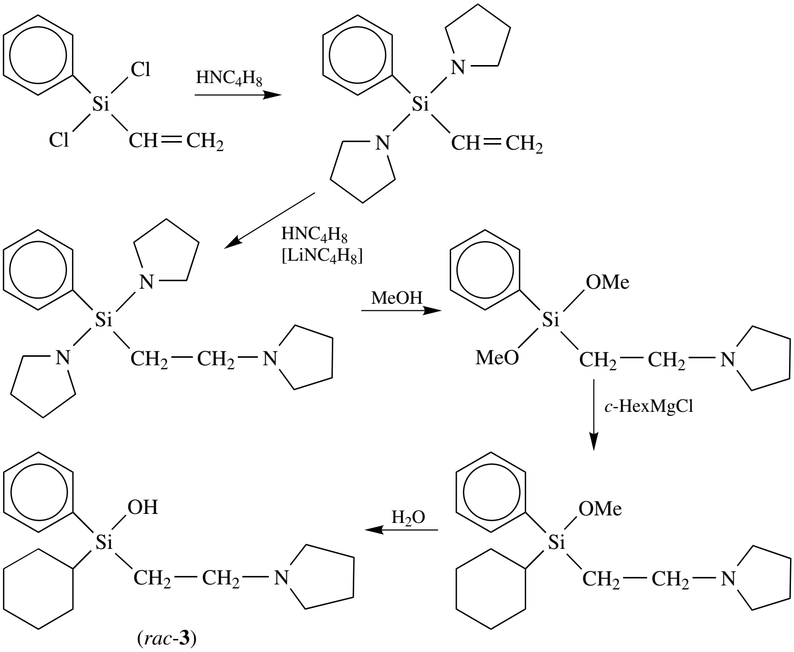

SCHEME 2

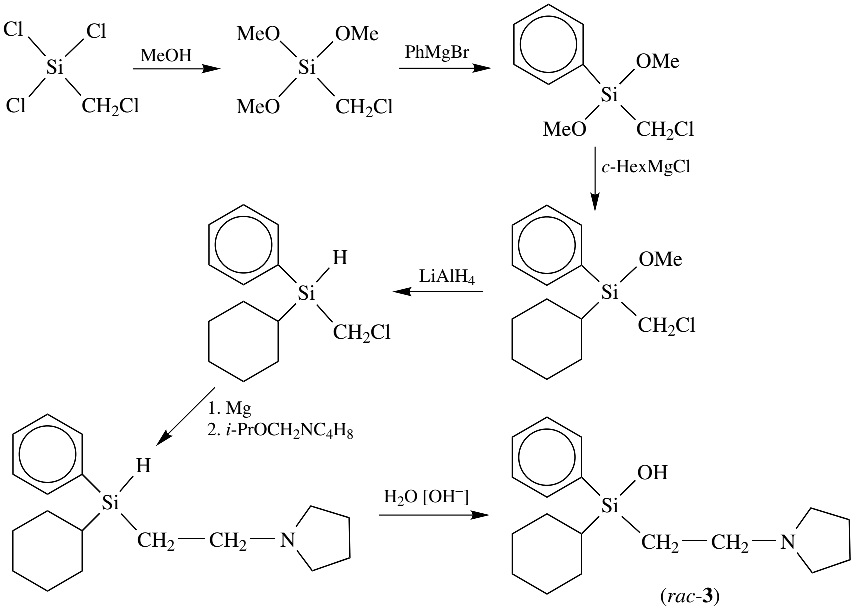

SCHEME 3

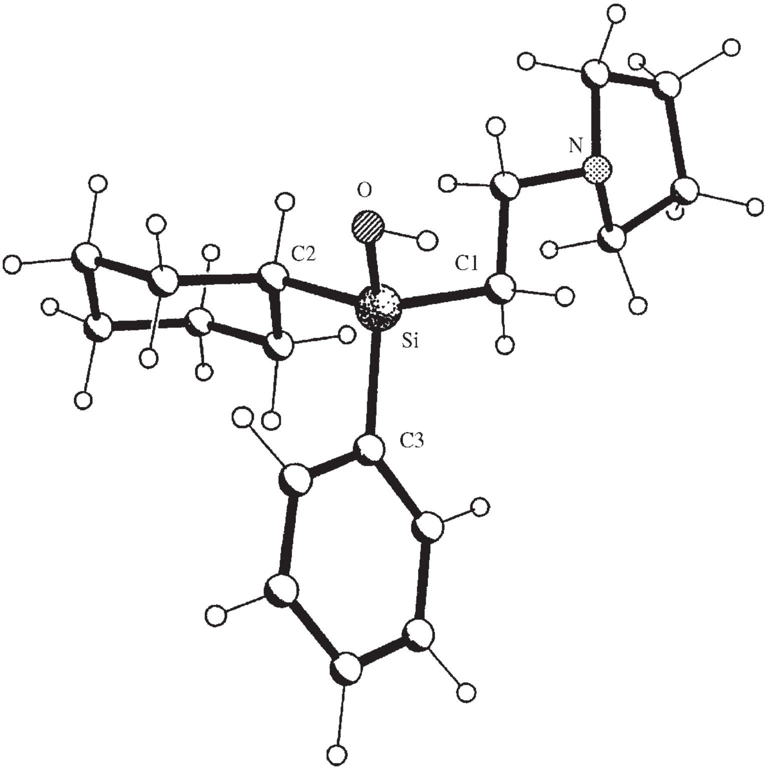

FIGURE 1. Structure of the silanol (*R*)-**3** in the crystal. Selected bond distances (pm) and angles (deg): Si−C(1), 186.8(4); Si−C(2), 187.8(3); Si−C(3), 188.2(3); Si−O, 163.5(3); C(1)−Si−C(2), 109.9(2); C(1)−Si−C(3), 109.4(2); C(1)−Si−O, 111.3(1); C(2)−Si−C(3), 109.8(2); C(2)−Si−O, 107.1(1); C(3)−Si−O, 109.2(1). The molecules are connected by intermolecular O−H···N hydrogen bonds [O···N, 2.792(5) pm] to form infinite chains parallel to the *c* axis

values; $pA_2 = -\log K_D$ (K_D = dissociation constant of the drug−receptor complex)] obtained in these studies are given in Table 1 and Figure 2. From the kinetics of the racemization of the silanols, a maximum error of the pA_2 values by a factor of 2 can be estimated. The racemization kinetics were established by functional pharmacological experiments at muscarinic M3 receptors[20].

As can be seen from Figure 2, the (*R*)-enantiomers (eutomers) of the silanols **3** and **7** show a significantly higher affinity for muscarinic M2 and M3 receptors than the corresponding (*S*)-antipodes (distomers). To the best of our knowledge, this is the first example of a biological discrimination between enantiomeric silicon compounds, with the silicon atom as the center of chirality. The stereoselectivity indices *SI* [$SI = K_D(S)/K_D(R)$] for sila-procyclidine (**3**) are 1.8 (M2) and 4.1 (M3), respectively. For sila-tricyclamol iodide (**7**), *SI* values of 21 (M2) and 23 (M3) were found. Qualitatively analogous stereoselectivities were observed for the enantiomers of the related carbon analogues procyclidine (**8**) and tricyclamol iodide (**9**) which are configurationally stable under physiological conditions[37]. The silanols (*R*)-**3**, (*S*)-**3**, (*R*)-**7** and (*S*)-**7** exhibit a higher antimuscarinic

TABLE 1. Affinities (pA_2 values) of the (*R*)- and (*S*)-enantiomers of **3, 7** and **10–13** for muscarinic M1 (rabbit vas deferens), M2 (guinea-pig atria) and M3 receptors (guinea-pig ileum)

Compound	pA_2 value		
	M1	M2	M3
(*R*)-**3**	n.d.[a]	7.15 ± 0.04	8.26 ± 0.03
(*S*)-**3**	n.d.[a]	6.90 ± 0.05	7.65 ± 0.03
(*R*)-**7**	n.d.[a]	8.37 ± 0.05	8.72 ± 0.04
(*S*)-**7**	n.d.[a]	7.04 ± 0.04	7.36 ± 0.04
(*R*)-**10**	7.39 ± 0.05	6.76 ± 0.04	7.32 ± 0.03
(*S*)-**10**	6.53 ± 0.04	6.26 ± 0.03	6.15 ± 0.02
(*R*)-**11**	7.16 ± 0.06	6.24 ± 0.05	7.27 ± 0.06
(*S*)-**11**	6.23 ± 0.08	5.43 ± 0.05	6.25 ± 0.08
(*R*)-**12**	9.09 ± 0.06	8.21 ± 0.01	8.65 ± 0.05
(*S*)-**12**	7.74 ± 0.04	7.56 ± 0.04	7.36 ± 0.03
(*R*)-**13**	7.74 ± 0.03	7.15 ± 0.05	7.19 ± 0.04
(*S*)-**13**	7.15 ± 0.06	6.85 ± 0.03	6.54 ± 0.04

[a] Not determined.

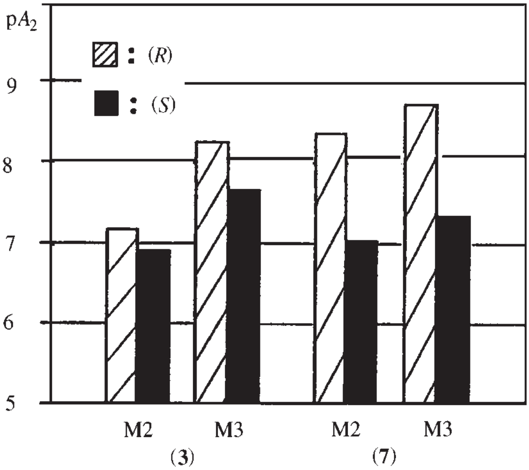

FIGURE 2. Affinities (pA_2 values) of the (*R*)- and (*S*)-enantiomers of **3** and **7** for muscarinic M2 (guinea-pig atria) and M3 receptors (guinea-pig ileum)

potency than the corresponding carbon analogues (*R*)-**8**, (*S*)-**8**, (*R*)-**9** and (*S*)-**9**; however, the stereoselectivity at the muscarinic receptors is more pronounced for the carbon compounds.

In order to overcome the experimental problems connected with the racemization of (*R*)-**3**, (*S*)-**3**, (*R*)-**7** and (*S*)-**7**, pharmacological stereoselectivity studies with the pure enantiomers of the related (hydroxymethyl)silanes **10–13** were carried out[34,38–40]. In

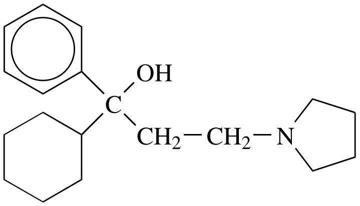

(8)

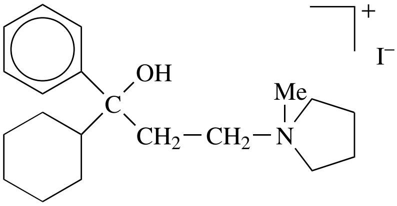

(9)

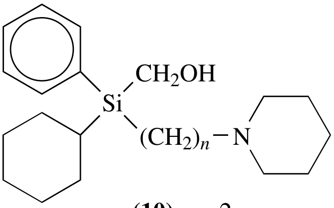

(10) $n = 2$
(11) $n = 3$

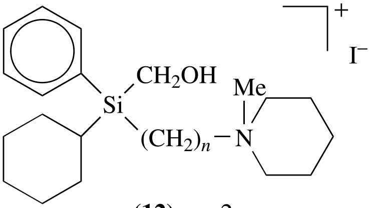

(12) $n = 2$
(13) $n = 3$

contrast to the silanols **3** and **7**, the (hydroxymethyl)silanes **10**–**13** are configurationally stable under physiological conditions.

The enantiomers of the silanes **10**[34] and **11**[39] were obtained from the corresponding racemic mixtures *rac*-**10** (for its synthesis see Scheme 4)[34] and *rac*-**11** (for its synthesis see Scheme 5)[39] by a classical racemate resolution using the enantiomers of *O*,*O*′-di-*p*-toluoyltartaric acid and 1,1′-binaphthyl-2,2′-diyl hydrogen phosphate, respectively, as resolving agents (for resolution by fractional crystallization of diastereomeric salts see Scheme 6)[34,39]. The silanes (*R*)-**10**, (*S*)-**10**, (*R*)-**11** and (*S*)-**11** were isolated as almost enantiomerically pure crystalline solids; their enantiomeric purities were determined by NMR experiments using chiral shift reagents[34,39]. Furthermore, the enantiomeric purities of (*R*)-**10** and (*S*)-**10** were established by liquid chromatography (HPLC) using chemically modified amylose as the chiral stationary phase[32]. The enantiomers of the ammonium salts **12** and **13** were obtained by reaction of the corresponding amines (*R*)-**10**, (*S*)-**10**, (*R*)-**11** and (*S*)-**11** with methyl iodide (Scheme 6). The absolute configurations of the silanes (*R*)-**10**, (*S*)-**10**, (*R*)-**12** and (*S*)-**12** were established on the basis of a single-crystal X-ray diffraction analysis of (*R*)-**12**[34]. The absolute configurations of the (*R*)- and (*S*)-enantiomers of the silanes **11** and **13** were determined by a crystal structure analysis of (*R*)-**11**·(*S*)-BNP·Me_2CO (BNP = 1,1′-binaphthyl-2,2′-diyl hydrogen phosphate)[39]. The

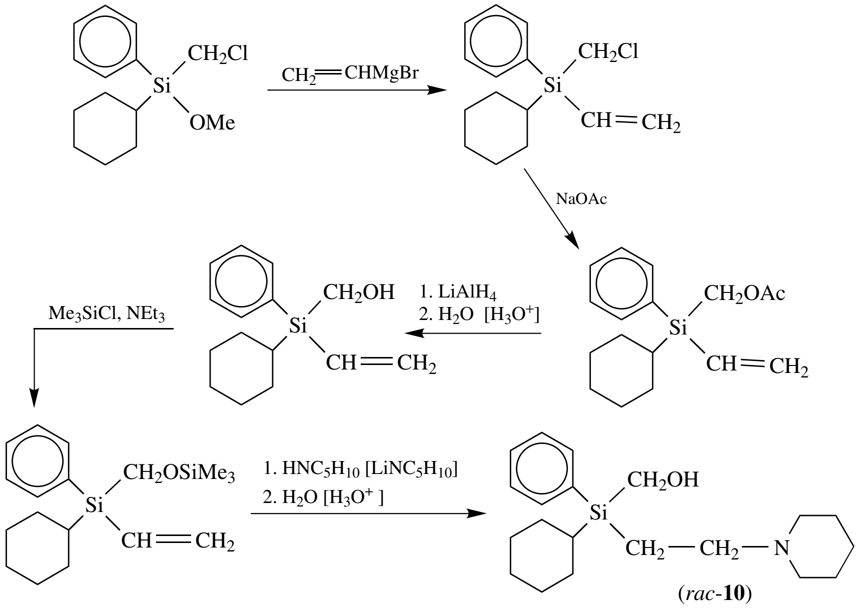

SCHEME 4

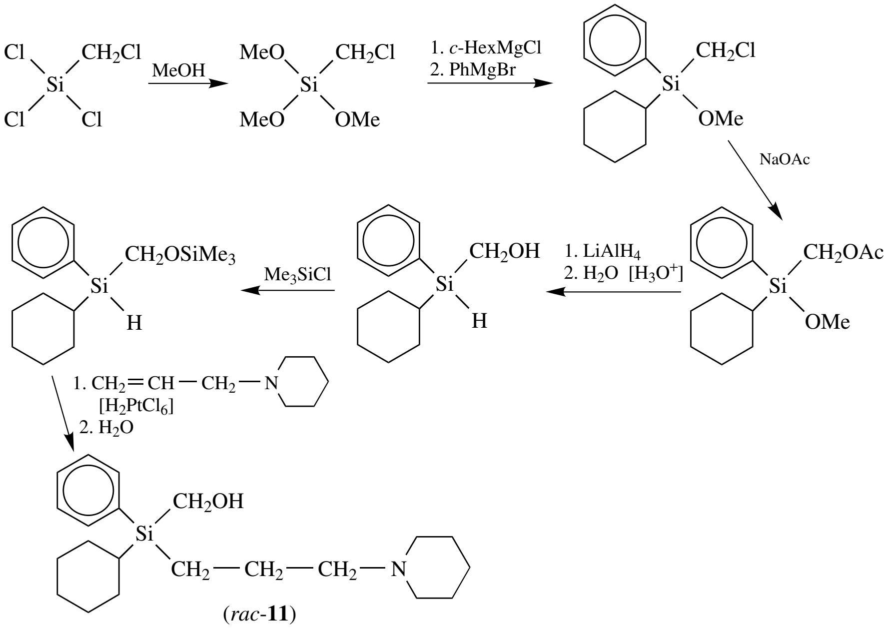

SCHEME 5

structures of the respective cations in the crystal of (*R*)-**12** and (*R*)-**11**·(*S*)-BNP·Me_2CO are depicted in Figures 3 and 4, respectively.

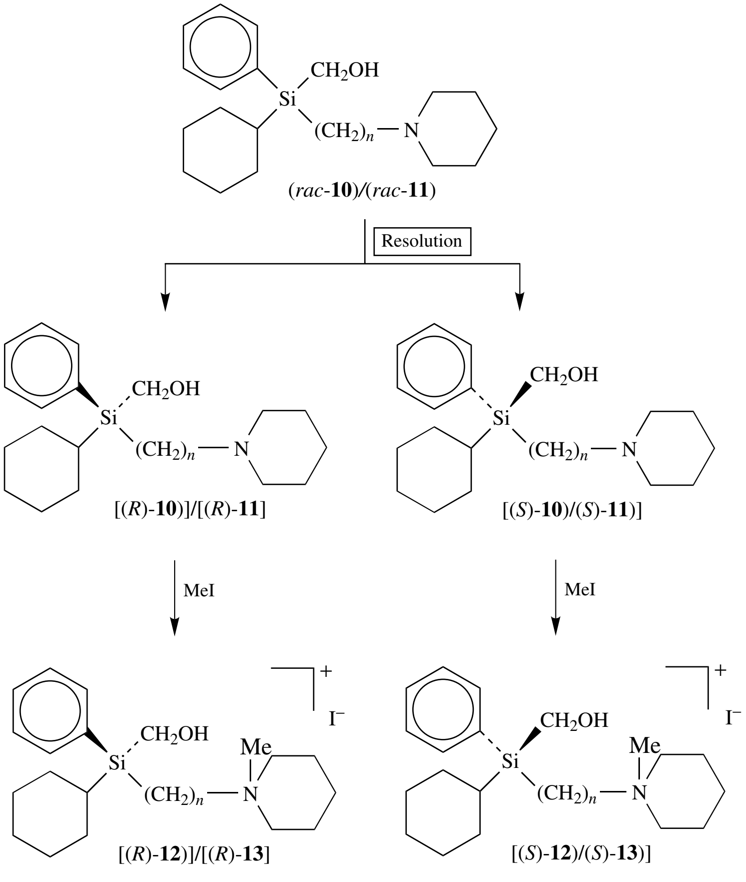
(*rac*-**10**)/(*rac*-**11**)

[(*R*)-**10**)]/[(*R*)-**11**]

[(*S*)-**10**)/(*S*)-**11**)]

[(*R*)-**12**)]/[(*R*)-**13**]

[(*S*)-**12**)/(*S*)-**13**)]

	10	**11**	**12**	**13**
n	2	3	2	3

SCHEME 6

The pure (*R*)- and (*S*)-enantiomers of the silanes **10–13** were studied for their affinities for muscarinic M1 (rabbit vas deferens), M2 (guinea-pig atria) and M3 receptors (guinea-pig ileum) in functional pharmacological experiments using 4-F-PyMcN$^+$ (= 1-[4-[[(4-fluorophenyl)carbamoyl]oxy]-2-butyn-1-yl]-1-methylpyrrolidinium tosylate) (M1) and arecaidine propargyl ester (M2, M3) as the agonist[34,38,40]. In addition, the affinities of these compounds for muscarinic M1 (human NB-OK 1 cells), M2 (rat heart), M3 (rat pancreas) and M4 receptors (rat striatum) were determined in radioligand binding studies using [^{3}H]-*N*-methylscopolamine as the radioligand[34,38,40]. All compounds investigated exhibited an apparently competitive antagonism at M1–M3 receptors in functional studies

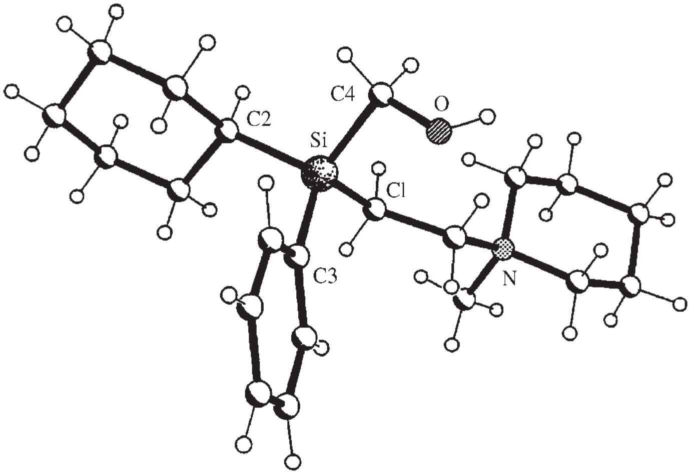

FIGURE 3. Structure of the cation of (*R*)-**12** in the crystal. Selected bond distances (pm) and angles (deg): Si–C(1), 188.8(2); Si–C(2), 188.5(2); Si–C(3), 187.7(2); Si–C(4), 188.2(2); C(1)–Si–C(2), 107.40(10); C(1)–Si–C(3), 111.47(10); C(1)–Si–C(4), 109.30(10); C(2)–Si–C(3), 110.57(9); C(2)–Si–C(4), 111.13(10); C(3)–Si–C(4), 106.99(11). The cation and anion of (*R*)-**12** are connected by an O–H···I hydrogen bond [O···I, 345.0(2) pm]

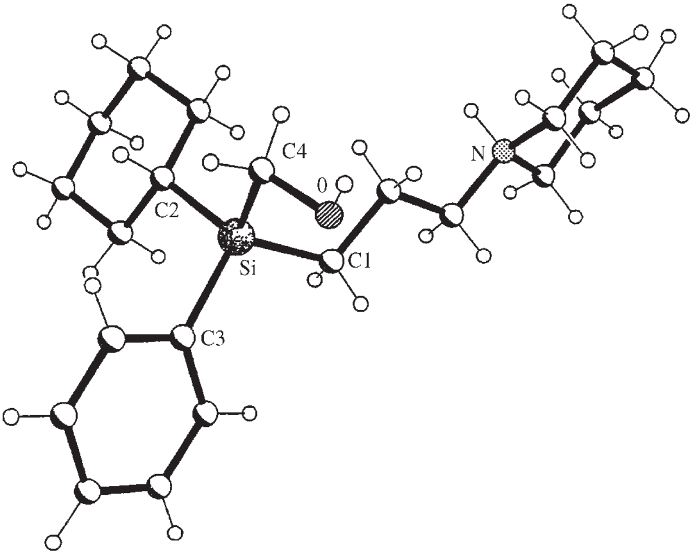

FIGURE 4. Structure of the cation of (*R*)-**11**·(*S*)-BNP·Me_2CO in the crystal. Selected bond distances (pm) and angles (deg): Si–C(1), 189(1); Si–C(2), 190.2(9); Si–C(3), 189(1); Si–C(4), 190(1); C(1)–Si–C(2), 112.7(5); C(1)–Si–C(3), 109.5(5); C(1)–Si–C(4), 112.7(5); C(2)–Si–C(3), 106.4(4); C(2)–Si–C(4), 108.6(5); C(3)–Si–C(4), 109.2(5)

and at M1–M4 receptors in binding experiments. The antimuscarinic potencies (pA_2 values) obtained in the functional studies are given in Table 1 as well as in Figure 5 (enantiomers of **10** and **12**) and Figure 6 (enantiomers of **11** and **13**). The corresponding binding affinities determined in the radioligand competition experiments correspond reasonably to these data.

As can be seen from Figures 5 and 6, the (*R*)-enantiomers (eutomers) of the silanes **10**–**13** show higher affinities for muscarinic M1–M3 receptors than their corresponding (*S*)-antipodes (distomers). Analogous results were obtained in the radioligand binding studies at M1–M4 receptors. These results again demonstrate that biological systems can

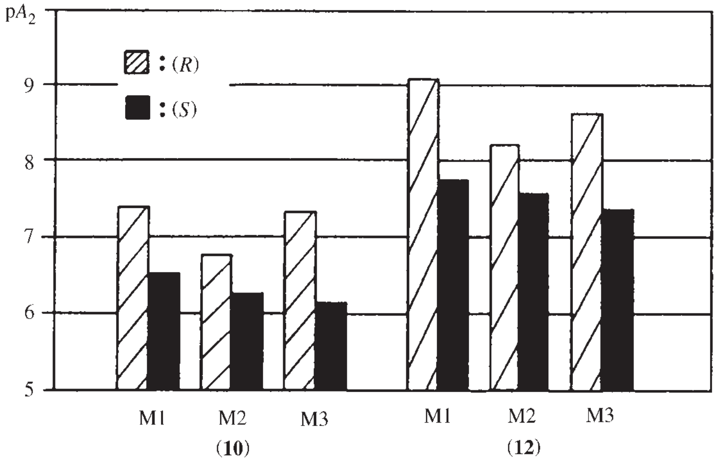

FIGURE 5. Affinities (pA_2 values) of the (*R*)- and (*S*)-enantiomers of **10** and **12** for muscarinic M1 (rabbit vas deferens), M2 (guinea-pig atria) and M3 receptors (guinea-pig ileum)

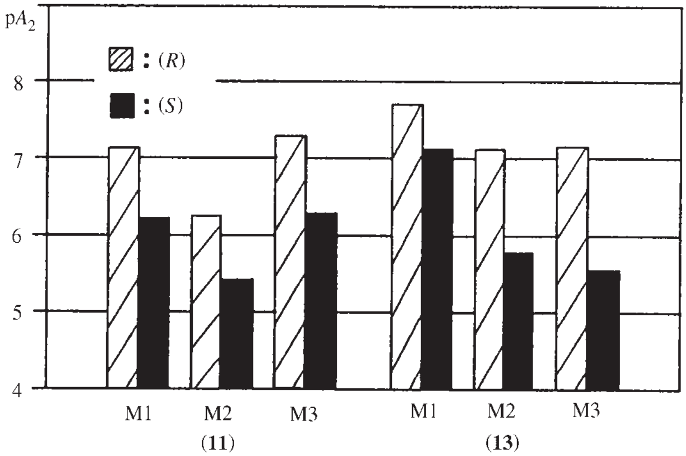

FIGURE 6. Affinities (pA_2 values) of the (*R*)- and (*S*)-enantiomers of **11** and **13** for muscarinic M1 (rabbit vas deferens), M2 (guinea-pig atria) and M3 receptors (guinea-pig ileum)

discriminate between the antipodes of chiral silicon compounds, with the silicon atom as the center of chirality. The highest stereoselectivity indices (functional studies) were observed for the silane **12** [*SI* = 22 (M1), 4.4 (M2), 20 (M3)].

Compounds **14–17** are derivatives of the corresponding silanes **10** and **12**. Functional pharmacological studies (M1–M3 receptors) and radioligand binding experiments (M1–M4 receptors) with the pure (*R*)- and (*S*)-enantiomers of these compounds revealed very similar pA_2 values as observed for the antipodes of the related analogues **10** and **12**[34]. The highest stereoselectivity indices (functional studies) were determined for **17** [*SI* = 44 (M1), 7.6 (M2), 20 (M3)].

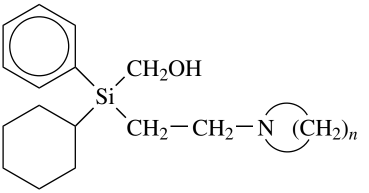

(14) *n* = 4
(15) *n* = 6

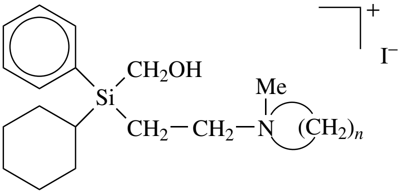

(16) *n* = 4
(17) *n* = 6

The germanium analogues of the (*R*)- and (*S*)-enantiomers of the silicon compounds **10** and **12** [(*R*)-**18**, (*S*)-**18**, (*R*)-**19**, (*S*)-**19**] were also studied for their antimuscarinic properties (studies on Si/Ge bioisosterism)[36]. By analogy with the parent silicon compounds, these germanes were also found to be configurationally stable under physiological conditions. The enantiomerically pure antipodes of **18** and **19** revealed similar pA_2 values and stereoselectivities as determined for their corresponding silicon analogues indicating a strongly pronounced Si/Ge bioisosterism.

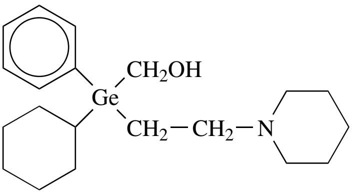

(18)

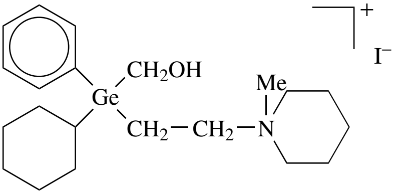

(19)

As shown in Figure 7 for sila-procyclidine **(3)** as an example, the stereoselective interaction of muscarinic receptors with the antipodes of **3** and **7–19** can be described in terms of a four-binding site model. According to this concept, these muscarinic antagonists might be recognized by the receptors with subsites for the ammonium group (protonated amino group in the case of **3**, **8**, **10**, **11**, **14**, **15** and **18**), the hydroxyl moiety and the phenyl and cyclohexyl group. Stereoselective interaction of the two enantiomers of these antagonists with muscarinic receptors is based on opposite binding of the phenyl and cyclohexyl ring to *site 1* and *site 2* as well as on identical binding of the hydroxyl and ammonium group to *site 3* and *site 4*, respectively. Thus, the stereoselectivities of receptor binding observed for these compounds are best explained by weaker binding of the phenyl and cyclohexyl group of the less potent enantiomers (distomers). This suggestion is strongly supported by the results obtained in pharmacological studies with the related achiral compounds **20–35**[36,38–40] (in this context, see also References 41–43).

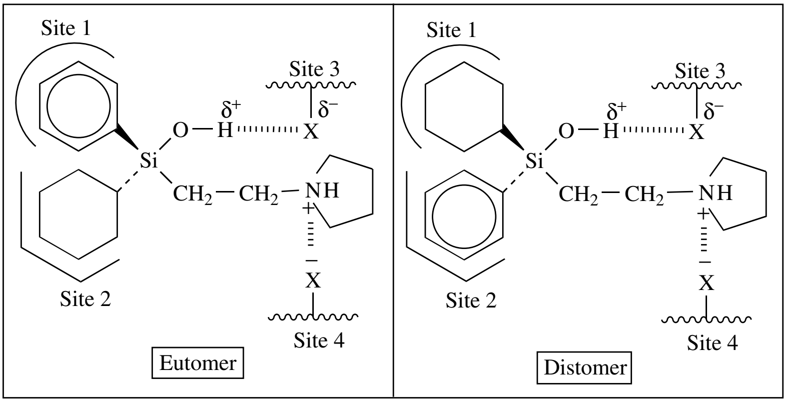

FIGURE 7. Four-binding-sites model for the stereoselective interaction of the (*R*)- and (*S*)-enantiomer of protonated sila-procyclidine **(3)** with four subsites of muscarinic receptors: *site 1* = phenyl-preferring hydrophobic subsite; *site 2* = cyclohexyl-preferring subsite; *site 3* = subsite for the hydroxyl group, probably forming a hydrogen bond (O—H···X); *site 4* = negatively charged subsite for the ammonium group (under physiological conditions, the pyrrolidino group of **3** is protonated). This model can also be used to describe the analogous stereoselective interaction of the antipodes of **7–19** with muscarinic receptors

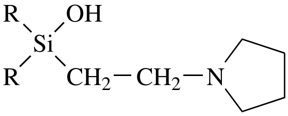

(20) R = Ph
(21) R = *c*-Hex

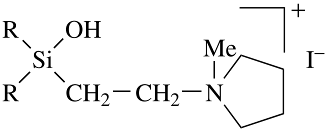

(22) R = Ph
(23) R = *c*-Hex

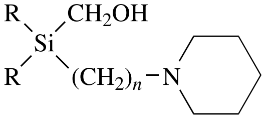

(24) R = Ph, *n* = 2
(25) R = *c*-Hex, *n* = 2
(26) R = Ph, *n* = 3
(27) R = *c*-Hex, *n* = 3

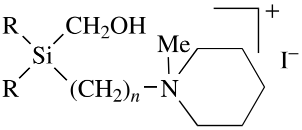

(28) R = Ph, *n* = 2
(29) R = *c*-Hex, *n* = 2
(30) R = Ph, *n* = 3
(31) R = *c*-Hex, *n* = 3

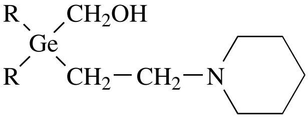

(32) R = Ph
(33) R = *c*-Hex

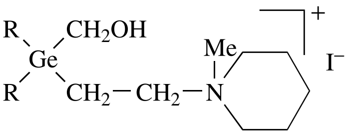

(34) R = Ph
(35) R = *c*-Hex

III. BIOCATALYSIS AS A METHOD FOR THE PREPARATION OF OPTICALLY ACTIVE ORGANOSILICON COMPOUNDS

A. Introductory Remarks

The results described in Section II clearly demonstrate that enantiomeric silanols and silanes may generally differ in their biological properties. Since biologically active organosilicon compounds have a great potential of application as agrochemicals, drugs and diagnostics, the development of appropriate preparative methods for the synthesis of enantiomerically pure silicon compounds, with the silicon atom as the center of chirality, is necessary (for reviews on optically active silicon compounds, see References 44 and 45). In most cases (see, for example, Section II) optically active silicon compounds have been obtained by (i) classical resolution of the respective racemic mixtures via fractional crystallization of appropriate diastereomeric derivatives and (ii) stereoselective chemical transformation of the resolved enantiomers. Asymmetric chemical syntheses[46] and chromatographic racemate resolutions[32], in principle, are alternative methods for the preparation of enantiomeric silicon compounds. As will be demonstrated in this section, stereoselective biotransformations represent a further challenge for the synthesis of optically active silicon compounds, with the silicon atom as the center of chirality.

B. Reductions

Since there are many examples of strongly pronounced bioisosteric relationships between analogous carbon and silicon compounds (in this context, see Reference 8), attempts have been made to apply well-known biotransformations of organic compounds to sila-analogous substrates. The first example of this is the enantioselective microbial reduction of the organosilicon compounds **36** and **38** with growing cells of the yeast *Kloeckera corticis* (ATCC 20109)[47]. By analogy with their corresponding carbon analogues (Si/C exchange), the prochiral silicon compounds **36** and **38** could be transformed into the optically active products (*S*)-**37** and (*S*)-**39**, respectively (Scheme 7). The enantiomeric purities of the isolated biotransformation products were moderate [(*S*)-**37**, 80% ee; (*S*)-**39**, 65% ee)].

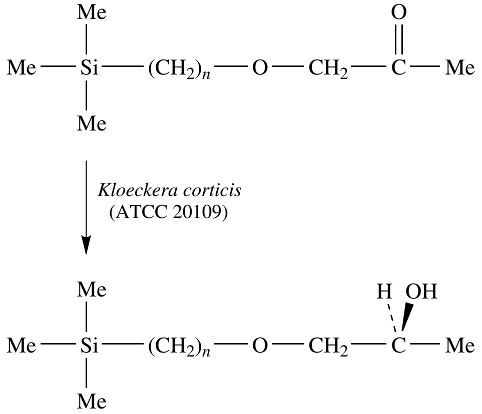

$\mathrm{Me_3Si(CH_2)_nOCH_2C(=O)Me}$

(36) $n = 1$
(38) $n = 2$

$\mathrm{Me_3Si(CH_2)_nOCH_2CH(OH)Me}$

[(*S*)-**(37)**] $n = 1$
[(*S*)-**(39)**] $n = 2$

SCHEME 7

In the prochiral organosilicon substrates **36** and **38**, the carbonyl groups are relatively far away from the silicon atoms present in these molecules. However, by analogy with many organic ketones of the general formula type $R_3C{-}CO{-}CR_3$, the silaketones (acylsilanes) **40** and **42** (belonging to the formula type $R_3Si{-}CO{-}CR_3$) were also found to be accepted as substrates by ketone-reducing microorganisms and to be converted into the optically active biotransformation products (*R*)-**41** and (*R*)-**43**, respectively (Scheme 8).

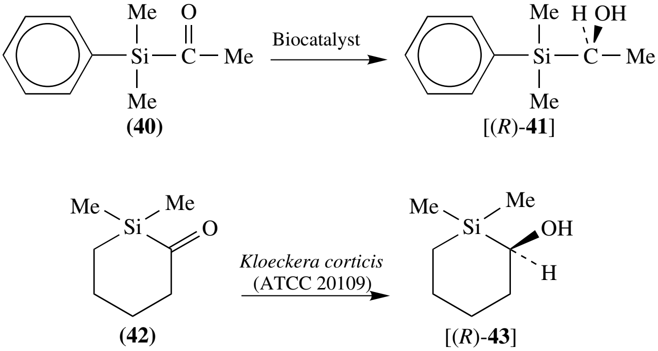

SCHEME 8

Thirty strains of microorganisms (bacteria, yeasts, fungi and green algae) were tested as resting free cells for their ability to transform the prochiral acetylsilane **40** into the corresponding (1-hydroxyethyl)silane (*R*)-**41**[48]. In these studies, some of these microorganisms were found to be good (or even excellent) biocatalysts for this conversion (Table 2). The biotransformation product (*R*)-**41** was obtained with enantiomeric purities of up to >95% ee. Immobilized cells (immobilization with calcium alginate) of the yeast *Trigonopsis variabilis* (DSM 70714), of the cyanobacterium *Synechococcus leopoliensis* (SAG 1402-1) and of the green alga *Chlorella fusca* (SAG 211/8b) can also be used for this particular type of bioconversion[49].

Studies with resting free cells of *Trigonopsis variabilis* (DSM 70714) demonstrated that the enantiomeric purity of (*R*)-**41** depends significantly on the substrate concentration

TABLE 2. Enantioselective microbial reduction of the acetylsilane **40** into the (1-hydroxyethyl)silane (*R*)-**41**

Microorganism	ee Value[a]
Acinetobacter calcoaceticus (ATCC 31012)	>95
Arthrobacter paraffinius (ATCC 15591)	85
Brevibacterium species (ATCC 21860)	90
Corynebacterium dioxydans (ATCC 21766)	>95
Candida albicans (ATCC 10231)	86
Candida humicola (DSM 70067)	90
Candida utilis (DSM 2361)	81
Kloeckera corticis (ATCC 20108)	80
Trigonopsis variabilis (DSM 70714)	86
Cunninghamella elegans (ATCC 26269)	94
Synechococcus leopoliensis (SAG 1402-1)	94
Chlamydomas reinhardii (Y-1)	85
Chlorella fusca (SAG 211/8b)	75

[a] Enantiomeric purity (% ee) of (*R*)-**41** as determined by HPLC using cellulose triacetate as a chiral stationary phase.

used[50]. At a concentration of 0.25 g of **40** per liter culture broth, the silane (*R*)-**41** was obtained on a preparative scale with an enantiomeric purity of 86% ee (yield *ca* 70%). An even enantiomerically pure (>99% ee) product could be prepared with resting cells of the yeast *Saccharomyces cerevisiae* (DHW S-3)[51]. This biotransformation was also performed on a preparative scale (yield 40%). Even plant cell suspension cultures of *Symphytum officinale* L. or *Ruta graveolens* L. were used for the enantioselective conversion of **40** into (*R*)-**41** on a preparative scale [enantiomeric purities: 81% ee (*Symphytum*), 60% ee (*Ruta*); yields: 15% (*Symphytum*), 9% (*Ruta*); reaction conditions not optimized][52].

Preliminary studies with the ketone **44** (carbon analogue of **40**) and with the germaketone **46** (germanium analogue of **40**) have shown that these compounds are also accepted as substrates by *Trigonopsis variabilis* (DSM 70714) to give the corresponding reduction products (*S*)-**45** and (*R*)-**47**, respectively[50]. Interestingly, the acetylsilane **40** was found to be reduced about 20 times faster than its carbon analogue **44** and about two times faster than its germanium analogue **46**.

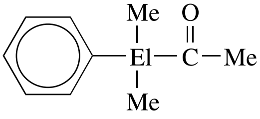

(**44**) El = C
(**46**) El = Ge

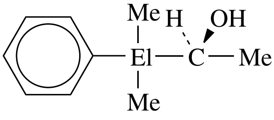

[(*S*)-**45**] El = C
[(*R*)-**47**] El = Ge

Enantioselective reduction of the prochiral cyclic acylsilane **42** with growing cells of the yeast *Kloeckera corticis* (ATCC 20109) yielded the optically active reduction product (*R*)-**43** (Scheme 8)[53]. On a preparative scale, the 1-silacyclohexan-2-ol (*R*)-**43** was isolated in 60% yield with an enantiomeric purity of 92% ee. Repeated recrystallization of the biotransformation product from *n*-hexane raised the enantiomeric purity to 99% ee.

Based on the results obtained with the enantioselective microbial reduction of the achiral acylsilanes **40** and **42**, attempts were made to use this particular type of bioconversion for the synthesis of optically active silanes with the silicon atom as the center of chirality. The high preparative potential of this method was first demonstrated for the (*R*)-selective microbial reduction of racemic acetyl(*t*-butyl)methyl(phenyl)silane (*rac*-**48**; for the synthesis[54] of this compound, see Scheme 9) with resting free cells of the yeast *Trigonopsis variabilis* (DSM 70714) or with the bacterium *Corynebacterium dioxydans* (ATCC 21766)[55,56]. As shown in Scheme 10, these bioconversions yielded the diastereomeric optically active (1-hydroxyethyl)silanes (Si*R*,C*R*)-**49** and (Si*S*,C*R*)-**50** which were separated by column chromatography on silica gel. Under preparative conditions (10 g scale), compounds (Si*R*,C*R*)-**49** and (Si*S*,C*R*)-**50** were obtained with high enantiomeric purities [*Trigonopsis variabilis*: (Si*R*,C*R*)-**49**, 97% ee; (Si*S*,C*R*)-**50**, 96% ee. *Corynebacterium dioxydans*: (Si*R*,C*R*)-**49**, ⩾99% ee; (Si*S*,C*R*)-**50**, ⩾99% ee]. The products produced by *Trigonopsis variabilis* (DSM 70714) were obtained in good yields [(Si*R*,C*R*)-**49**, 74%; (Si*S*,C*R*)-**50**, 78%; yields relative to (*R*)-**48** and (*S*)-**48**, respectively, in the racemic substrate]. In the case of *Corynebacterium dioxydans* (ATCC 21766), the yields were significantly lower [(Si*R*,C*R*)-**49**, 20%; (Si*S*,C*R*)-**50**, 20%; reaction conditions not optimized]. Subsequent chemical oxidation (DMSO, DCC, pyridinium trifluoroacetate) of the diastereomeric (1-hydroxyethyl)silanes (Si*R*,C*R*)-**49** and (Si*S*,C*R*)-**50** gave the almost enantiomerically pure acetylsilanes (*R*)-**48** and (*S*)-**48**, respectively (Scheme 10). These examples clearly demonstrate that stereoselective biotransformations, as key steps in a

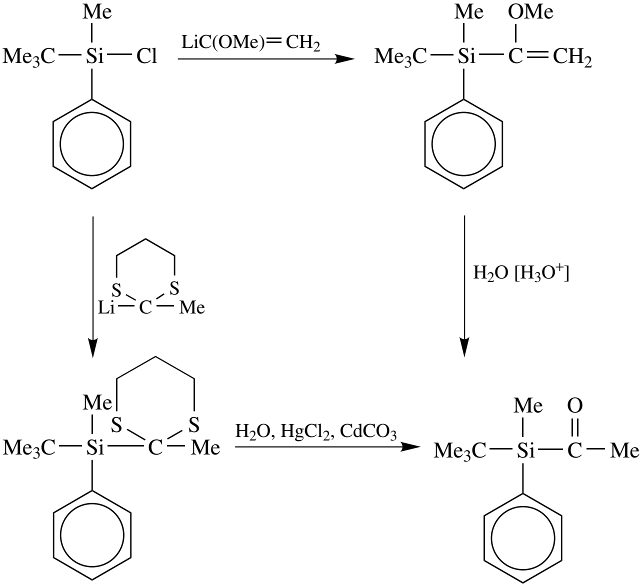

(*rac*-**48**)

SCHEME 9

reaction sequence, can be used for the preparation of optically active silanes with the silicon atom as the center of chirality.

Recently, it has been demonstrated that the yeast *Saccharomyces cerevisiae* (DHW S-3) can also be used for the (*R*)-selective reduction of the acetylsilane *rac*-**48**. By analogy with the bioconversions illustrated in Scheme 10, incubation of *rac*-**48** with resting free cells of this microorganism yielded a 1:1 mixture of the corresponding diastereomeric (1-hydroxyethyl)silanes (Si*R*,C*R*)-**49** and (Si*S*,C*R*)-**50**[57]. Under preparative conditions, the biotransformation products were isolated in 43% yield (relative to *rac*-**48**). The enantiomeric purities of the silanes (Si*R*,C*R*)-**49** and (Si*S*,C*R*)-**50** were $\geqslant$98% ee.

Very similar results were obtained with the germanium analogue of the acetylsilane *rac*-**48**, the acetylgermane *rac*-**51**; its microbial reduction with *Saccharomyces cerevisiae* (DHW S-3) yielded a 1:1 mixture of the corresponding diastereomeric (1-hydroxyethyl)germanes (Ge*R*,C*R*)-**52** and (Ge*S*,C*R*)-**53** (yield 60%; enantiomeric purity of both diastereomers $\geqslant$98% ee)[57] which could also be separated by column chromatography on silica gel. Analogous (*R*)-selective microbial reductions (preparative scale) of the related acetylsilanes *rac*-**54** and *rac*-**57** with the yeast *Trigonopsis variabilis* (DSM 70714) have also been reported[7,58]. The bioconversion of the acetylsilane *rac*-**54** (resting free cells) yielded a 1:1 mixture of the (1-hydroxyethyl)silanes (Si*R*,C*R*)-**55** and (Si*S*,C*R*)-**56** (yield 72%; enantiomeric purity of both diastereomers *ca* 94% ee)[7]. The analogous biotransformation of the acetylsilane *rac*-**57** (immobilized resting cells; calcium alginate matrix) gave a 1:1 mixture of the (1-hydroxyethyl)silanes (Si*R*,C*R*)-**58** and (Si*S*,C*R*)-**59** (yield 99%; enantiomeric purity of both diastereomers >96% ee)[58].

By analogy with the stereoselective microbial reduction of the acetylsilane *rac*-**48** (Scheme 10) and its derivatives *rac*-**51**, *rac*-**54** and *rac*-**57**, the related acetyldisilane *rac*-**60** was also found to be reduced (*R*)-selectively with resting free cells of *Trigonopsis variabilis* (DSM 70714) to give a 1:1 mixture of the corresponding diastereomeric

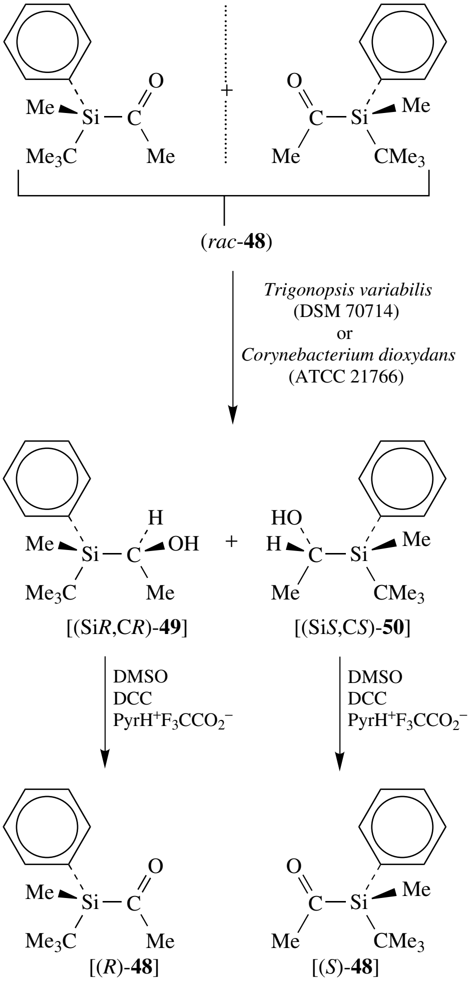

SCHEME 10

(1-hydroxyethyl)disilanes (Si*R*,C*R*)-**61** and (Si*S*,C*R*)-**62** (yield 75%; enantiomeric purity of both diastereomers ⩾98% ee) (Scheme 11)[7,59]. Similar results were obtained with resting free cells of the yeast *Saccharomyces cerevisiae* (DHW S-3)[57]. These microbial transformations are especially remarkable since they could be realized without a noticeable degree of hydrolytic cleavage of the Si−Si bond. Compounds (Si*R*,C*R*)-**61** and (Si*S*,C*R*)-**62** are the first optically active disilanes obtained by stereoselective biotransformations.

Interestingly, the related acetyldigermane *rac*-**63** could be converted analogously into a 1:1 mixture of the diastereomeric (1-hydroxyethyl)digermanes (Ge*R*,C*R*)-**64** and (Ge*S*,C*R*)-**65** (yield 62%; enantiomeric purity of both diastereomers ⩾98% ee)[57]. Obviously, the Ge−Ge bonds of the substrate and products are rather stable against hydrolytic cleavage under the bioconversion conditions used.

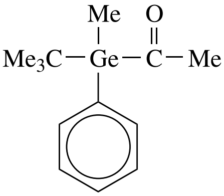

(51)

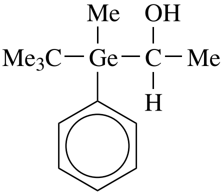

(52/53)

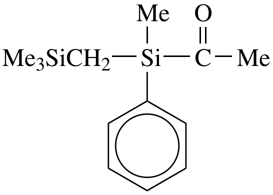

(54)

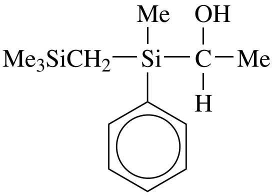

(55/56)

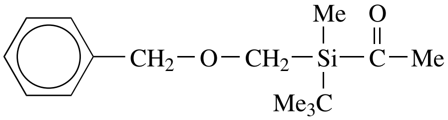

(57)

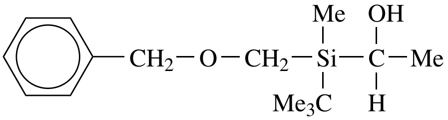

(58/59)

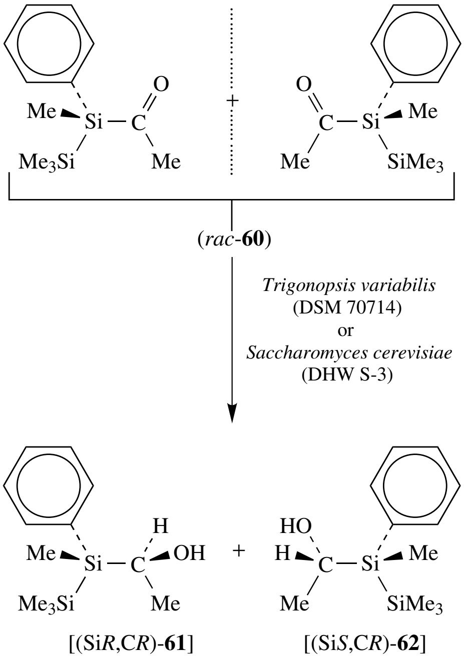

SCHEME 11

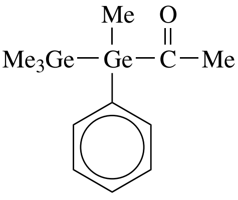

(63)

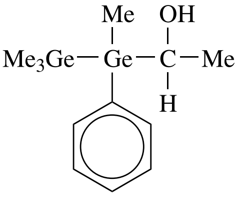

(64/65)

A quite different result was obtained when incubating the related acetyl(silyl)germane *rac*-**66** with resting free cells of *Saccharomyces cerevisiae* (DHW S-3). When using the same conditions as applied for the microbial reduction of the acetyldisilane *rac*-**60** and the acetyldigermane *rac*-**63**, cleavage of the Si—Ge bond was observed. As shown in Scheme 12, compound *rac*-**66** was converted into a 1:1 mixture of the diastereomeric (1-hydroxyethyl)hydridogermanes (Ge*S*,C*R*)-**67** and (Ge*R*,C*R*)-**68** (yield 50%; enantiomeric purity of both diastereomers ⩾98% ee). The Si—Ge bond cleavage is probably a nonenzymatic reaction.

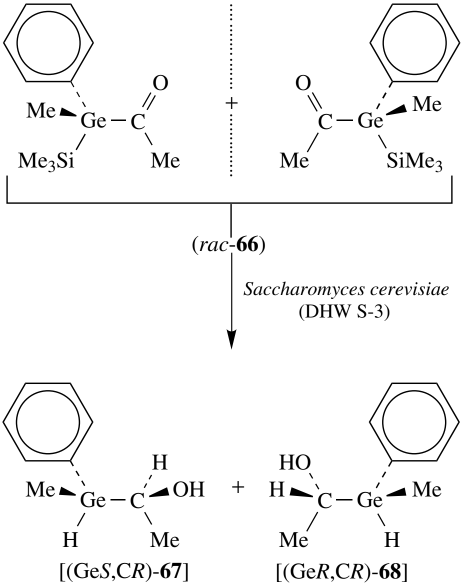

SCHEME 12

The microbial reductions of the acetylsilanes *rac*-**48**, *rac*-**54** and *rac*-**57**, of the acetylgermanes *rac*-**51** and *rac*-**66**, of the acetyldisilane *rac*-**60** and of the acetyldigermane *rac*-**63** represent (*R*)-selective bioconversions yielding 1:1 mixtures of the corresponding optically active diastereomeric reduction products. In contrast, incubation of the cyclic acylsilane *rac*-**69** with growing cells of the yeast *Kloeckera corticis* (ATCC 20109) gave a 1:1 mixture of the enantiomeric products (Si*S*,C*R*)-**70** and (Si*R*,C*S*)-**70** (yield *ca* 95%) (Scheme 13) [59,60]. Only small amounts of the corresponding diastereomers with the (Si*R*,C*R*)- and (Si*S*,C*S*)-configuration could be detected. Thus, this particular type of bioconversion can be regarded as a diastereoselective reduction (diastereomeric purity *ca* 90% de).

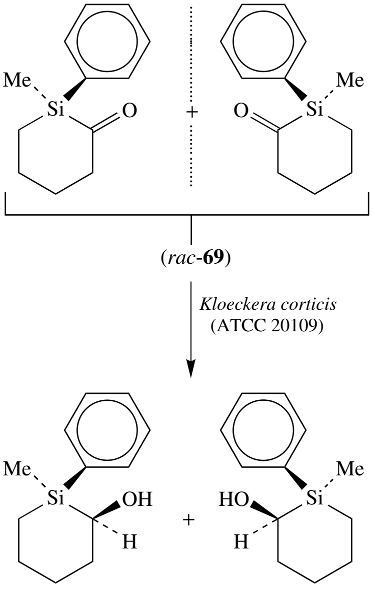

[(Si*S*,C*R*)-**70**] [(Si*R*,C*S*)-**70**]

SCHEME 13

As the last example of stereoselective reductions of acylsilanes, the enantioselective microbial reduction of the benzoylsilane **71** shall be discussed. Nine from thirteen strains of yeasts or bacteria were found to convert the prochiral compound **71** enantioselectively into the corresponding optically active (1-hydroxybenzyl)silane (*S*)-**72**; the other microorganisms produced the corresponding antipode (*R*)-**72** (Scheme 14)[61]. The yeasts and bacteria used in these studies and the stereochemical results obtained are summarized in Table 3. Analogous investigations were carried out with the carbon **(73)** and germanium analogue **(75)** of the silane **71**. These compounds were also found to be reduced enantioselectively to yield the (*R*)- or (*S*)-enantiomers of the corresponding reduction products **74** and **76**, respectively (Table 3). Comparison of the conversion rates for the microbial transformations **71**→**72**, **73**→**74** and **75**→**76** demonstrated that the silicon compound **71** is most readily reduced, followed by its germanium analogue **75**. The lowest reaction rate was found for the carbon compound **73**. Analogous kinetics have already been reported for the microbial reduction of the acetylsilane **40** and its carbon **(44)** and germanium analogue **(46)**[50].

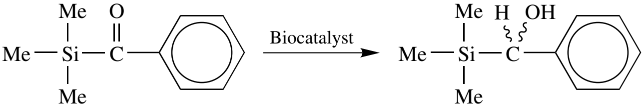

(71) **(72)**

SCHEME 14

TABLE 3. Enantioselective microbial reduction of the benzoylsilane **71** and of its carbon **(73)** and germanium analogue **(75)** (formation of **72**, **74** and **76**)

Microorganism	Enantiomeric purity (% ee) and absolute configuration (in parentheses)		
	72	**74**	**76**
Saccharomyces cerevisiae	78 (*S*)	60 (*S*)	86 (*S*)
Torulopsis magnoliae (IFO 661)	94 (*S*)	75 (*S*)	96 (*S*)
Candida tropicalis (IFO 199)	98 (*S*)	93 (*S*)	99 (*S*)
Pichia miso (FERM P-404)	24 (*S*)	92 (*R*)	62 (*S*)
Saccharomyces rosei (IFO 428)	80 (*S*)	7 (*R*)	85 (*S*)
Saccharomyces (sp. H-1)	65 (*S*)	70 (*S*)	61 (*S*)
Rhodotorula rubra (IFO 889)	93 (*S*)	65 (*S*)	94 (*S*)
Nocardia erythropolis (IAM 12122)	25 (*R*)	50 (*R*)	19 (*S*)
Corynebacterium equi (IFO 3730)	65 (*R*)	88 (*R*)	57 (*R*)
Xanthomonas campestris (NIAS 1076)	17 (*S*)	57 (*R*)	56 (*S*)
Micrococcus luteus (M2-7)	12 (*R*)	80 (*R*)	31 (*S*)
Bacillus brevis (M4-5)	46 (*R*)	65 (*R*)	31 (*R*)
Baker's yeast	30 (*S*)	4 (*S*)	90 (*S*)

As can be seen from Table 3, there are also some significant stereochemical differences observed for the microbial reductions of the Si/C/Ge analogues **71**, **73** and **75**. In general, a gradual change from (*R*)-selectivity to (*S*)-selectivity was observed when going from the carbon compound **73** to its silicon **(71)** and germanium analogue **(75)**. In some cases, this change even led to opposite absolute configurations of the analogous reduction products **72**, **74** and **76**. This interesting result can be probably explained by the different covalent radii of carbon, silicon and germanium.

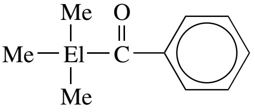

(73) El = C
(75) El = Ge

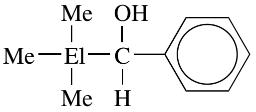

(74) El = C
(76) El = Ge

C. Hydrolyses

Stereoselective enzymatic hydrolyses of esters represent a further type of biotransformation that has been used for the synthesis of optically active organosilicon compounds. The first example of this particular type of bioconversion is illustrated in Scheme 15. Starting from the racemic (1-acetoxyethyl)silane *rac*-**77**, the optically active (1-hydroxyethyl)silane (*S*)-**41** was obtained by a kinetic racemate resolution using porcine liver esterase (*PLE*; E.C. 3.1.1.1) as the biocatalyst[7]. The silane (*S*)-**41** (isolated with an enantiomeric purity of 60% ee; bioconversion not optimized) is the antipode of compound (*R*)-**41** which was obtained by an enantioselective microbial reduction of the acetylsilane **40** (see Scheme 8).

The enantioselective hydrolysis of the racemic 2-acetoxy-1-silacyclohexane *rac*-**78** represents a further example of an enzymatic kinetic racemate resolution (Scheme 15). Hydrolysis of this compound in the presence of porcine liver esterase (*PLE*; E.C. 3.1.1.1) yielded the optically active 1-silacyclohexan-2-ol (*S*)-**43** which was isolated with an enantiomeric purity of 93% ee[7]. Similar results were obtained when using a crude lipase preparation from *Candida cylindracea* (*CCL*; E.C. 3.1.1.3) as the biocatalyst

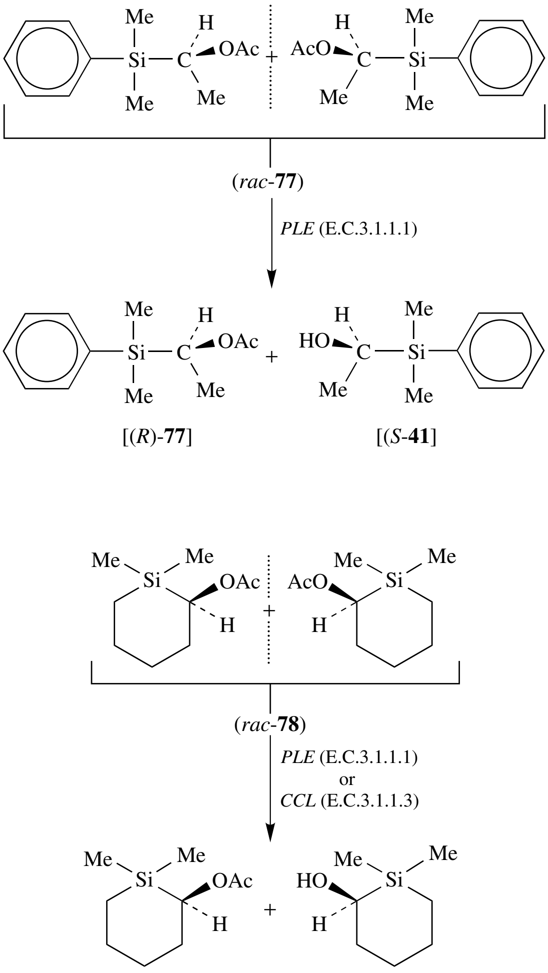

SCHEME 15

(Scheme 15)[62]. After terminating the reaction at a conversion of 38% (relative to total amount of substrate *rac*-**78**), the product (*S*)-**43** was separated from the nonreacted substrate by column chromatography on silica gel and isolated on a preparative scale in 71% yield (relative to total amount of converted *rac*-**78**) with an enantiomeric purity of 95% ee. Recrystallization led to an improvement of the enantiomeric purity by up to >98% ee. The biotransformation product (*S*)-**43** is the antipode of compound (*R*)-**43** which was obtained by enantioselective microbial reduction of the acylsilane **42** (see Scheme 8)[53]. The nonreacted substrate (*R*)-**78** was isolated in 81% yield (relative to total amount of nonconverted *rac*-**78**) with an enantiomeric purity of 57% ee. For further enantioselective enzymatic hydrolyses of racemic organosilicon esters, with the carbon atom as the center of chirality, see References 63 and 64.

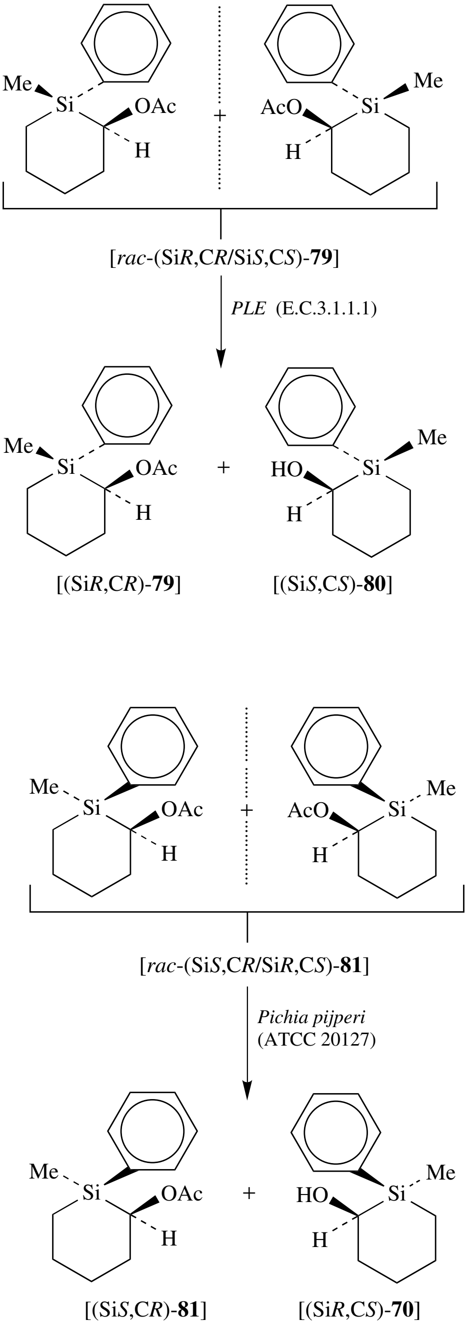

[*rac*-(Si*R*,C*R*/Si*S*,C*S*)-**79**]

[(Si*R*,C*R*)-**79**] [(Si*S*,C*S*)-**80**]

[*rac*-(Si*S*,C*R*/Si*R*,C*S*)-**81**]

[(Si*S*,C*R*)-**81**] [(Si*R*,C*S*)-**70**]

SCHEME 16

Enantioselective enzymatic ester hydrolyses have also been used for the preparation of optically active silicon compounds with the silicon atom as the center of chirality. An example of this is the kinetic resolution of the racemic 2-acetoxy-1-silacyclohexane *rac*-(Si*R*,C*R*/Si*S*,C*S*)-**79** with porcine liver esterase (*PLE*; E.C. 3.1.1.1) (Scheme 16)[65]. Under preparative conditions, the optically active 1-silacyclohexan-2-ol (Si*S*,C*S*)-**80** was obtained as an almost enantiomerically pure product (enantiomeric purity $\geqslant$96% ee) in *ca* 60% yield [relative to (Si*S*,C*S*)-**79** in the racemic substrate]. The biotransformation product could be easily separated from the nonhydrolyzed substrate by column chromatography on silica gel.

Intact microbial cells have also been used as biocatalyst for this particular type of bioconversion. Incubation of the racemic 2-acetoxy-1-silacyclohexane *rac*-(Si*S*,C*R*/Si*R*,C*S*)-**81** with growing cells of the yeast *Pichia pijperi* (ATCC 20127) yielded the optically active 1-silacyclohexan-2-ol (Si*R*,C*S*)-**70** (Scheme 16)[66,67]. Under preparative conditions, this biotransformation product was isolated as an almost enantiomerically pure compound (enantiomeric purity >96% ee) in *ca* 80% yield [relative to (Si*R*,C*S*)-**81** in the racemic substrate].

Enantioselective enzymatic ester hydrolyses of prochiral trimethylsilyl-substituted diesters of the malonate type have been applied for the synthesis of the related optically active monoesters[68]. As an example of this particular type of biotransformation, the enantioselective conversion of the diester **82** is illustrated in Scheme 17. Hydrolysis of compound **82** in phosphate buffer, catalyzed by porcine liver esterase (*PLE*; E.C. 3.1.1.1) or horse liver acetonic powder (*HLAP*), gave the optically active monoester **83** (absolute configuration not reported) in 86% and 49% yield, respectively. The enantiomeric purities

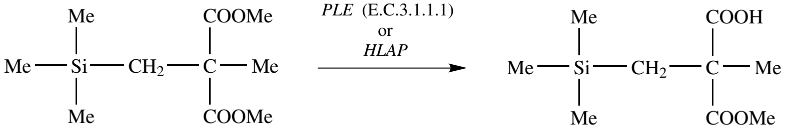

$$\mathrm{Me_3Si{-}CH_2{-}C(Me)(COOMe)_2} \xrightarrow[HLAP]{PLE\ (E.C.3.1.1.1)\ \text{or}} \mathrm{Me_3Si{-}CH_2{-}C(Me)(COOH)(COOMe)}$$

(82) **(83)**

SCHEME 17

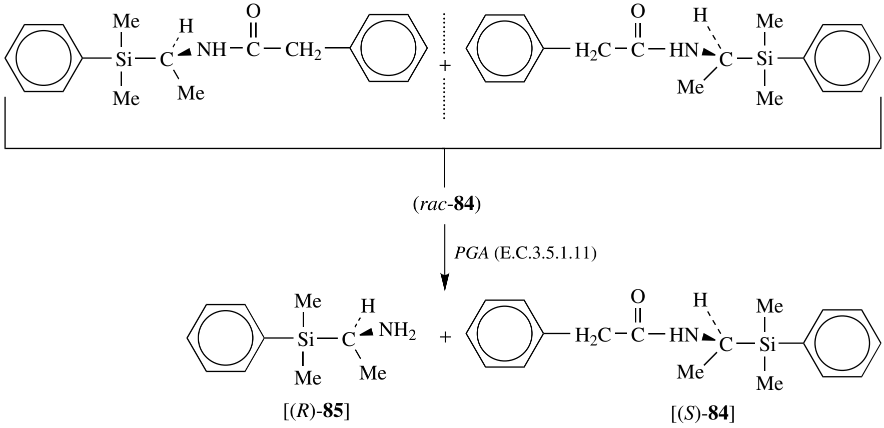

(*rac*-**84**)

[(*R*)-**85**] [(*S*)-**84**]

SCHEME 18

of the products were 88% ee (*PLE*) and 81% ee (*HLAP*). In the case of the *PLE*-catalyzed hydrolysis, addition of 50% DMSO to the reaction mixture led to an improvement of the yield (95%) and of the enantiomeric purity (98% ee). This particular type of biotransformation has not yet been applied for the synthesis of optically active silanes with the silicon atom as the center of chirality.

Enantioselective enzymatic amide hydrolyses can also be applied for the preparation of optically active organosilicon compounds. The first example of this is the kinetic resolution of the racemic [1-(phenylacetamido)ethyl]silane *rac*-**84** using immobilized penicillin G acylase (*PGA*; E.C. 3.5.1.11) from *Escherichia coli* as the biocatalyst (Scheme 18)[69]. (*R*)-selective hydrolysis of *rac*-**84** yielded the corresponding (1-aminoethyl)silane (*R*)-**85** which was obtained on a preparative scale in 40% yield (relative to *rac*-**84**). The enantiomeric purity of the biotransformation product was 92% ee. This method has not yet been used for the synthesis of optically active silicon compounds with the silicon atom as the center of chirality.

D. Transesterifications

Enantioselective enzymatic transesterifications have been used as a complementary method to enantioselective enzymatic ester hydrolyses. The first example of this particular type of biotransformation is the synthesis of the optically active 2-acetoxy-1-silacyclohexane (*S*)-**78** (Scheme 19). This compound was obtained by an enantioselective transesterification of the racemic 1-silacyclohexan-2-ol *rac*-**43** with triacetin (acetate source) in isooctane, catalyzed by a crude lipase preparation from *Candida cylindracea* (*CCL*; E.C. 3.1.1.3)[62]. After terminating the reaction at 52% conversion (relative to total amount of substrate *rac*-**43**), the product (*S*)-**78** was separated from the nonreacted substrate by column chromatography on silica gel and isolated in 92% yield (relative to total amount of converted *rac*-**43**) with an enantiomeric purity of 95% ee. The remaining 1-silacyclohexan-2-ol (*R*)-**43** was obtained in 76% yield (relative to total amount of nonconverted *rac*-**43**) with an enantiomeric purity of 96% ee. Repeated recrystallization of (*R*)-**43** led to an improvement of enantiomeric purity by up to >98% ee. Compound (*R*)-**43** has already earlier been prepared by an enantioselective microbial reduction of the 1-silacyclohexan-2-one **42** (see Scheme 8)[53]. The 1-silacyclohexan-2-ol (*R*)-**43** is the antipode of compound (*S*)-**43** which was obtained by a kinetic enzymatic resolution of the racemic 2-acetoxy-1-silacyclohexane *rac*-**78** (see Scheme 15)[62]. For further enantioselective enzymatic transesterifications of racemic organosilicon substrates, with a carbon atom as the center of chirality, see References 64 and 70–72.

Enantioselective enzymatic transesterifications have been successfully used for the synthesis of optically active silanes with the silicon atom as the center of chirality. As shown in Scheme 20, the prochiral bis(hydroxymethyl)silanes **86** and **88** were transformed into the corresponding chiral dextrorotatory isobutyrates (+)-**87** and (+)-**89**, respectively, using *Candida cylindracea* lipase (*CCL*; E.C. 3.1.1.3) as the biocatalyst[73]. For these bioconversions, methyl isobutyrate was used as solvent and acylation agent. When using acetoxime isobutyrate as the acylation agent and *Chromobacterium viscosum* lipase (*CVL*; E.C. 3.1.1.3) as the biocatalyst, the prochiral silanes **86** and **88** were transformed into the levorotatory isobutyrates (−)-**87** and (−)-**89**, respectively (Scheme 20)[73]. The latter conversions were carried out in diisopropyl ether (with **86**) and tetrahydrofuran (with **88**) as solvent. The yields and enantiomeric purities obtained with the transesterifications of **86** and **88** with *CCL* and *CVL* are summarized in Table 4. The absolute configurations of the biotransformation products are unknown.

A similar enantioselective enzymatic transesterification of the prochiral bis(hydroxymethyl)germane **90** (a germanium analogue of the silane **86**) has also been reported[74]. Transesterification of the germane **90** with vinyl acetate (serving as the acetate source and

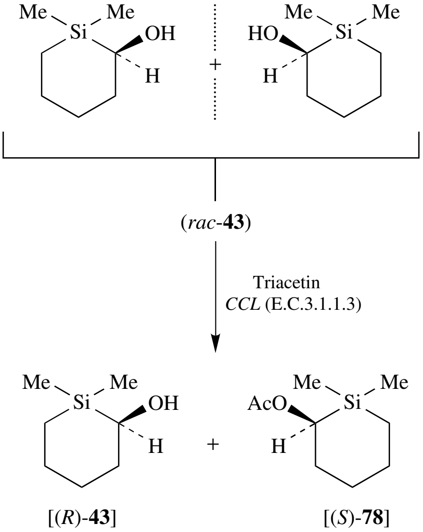

SCHEME 19

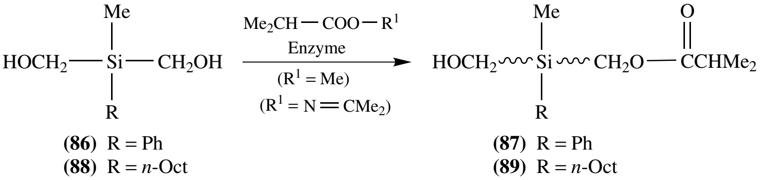

SCHEME 20

solvent), catalyzed by Eupergit-immobilized porcine liver esterase (*PLE*; E.C. 3.1.1.1), yielded the levorotatory germane (−)-**91** (absolute configuration unknown). Both the yield (57%) and the enantiomeric purity (50% ee) of the product were moderate.

Enantioselective enzymatic transesterification has also been used for a kinetic racemate resolution[75]. Starting from the racemic (hydroxymethyl)silane *rac*-**92** (analytical scale), transesterification with vinyl acetate in water-saturated 2,2,4-trimethylpentane, catalyzed by a commercial crude papain preparation (E.C. 3.4.22.2), yielded the corresponding optically active (acetoxymethyl)silane **93** (sign of optical rotation and absolute configuration not reported) (Scheme 21). The enantiomeric purity of the remaining dextrorotatory (hydroxymethyl)silane (+)-**92** was moderate (49% ee).

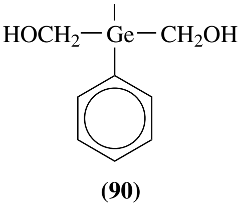

(90)

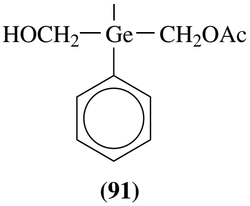

(91)

TABLE 4. Enantioselective transesterifications of the bis(hydroxymethyl)silanes **86** and **88** (formation of **87** and **89**)

Substrate	Enzyme	Acylation agent	Product	Yield (%)	ee Value (%)
86	*CCL*	$Me_2CHCOOMe$	(+)-**87**	80	70
88	*CCL*	$Me_2CHCOOMe$	(+)-**89**	63	75
86	*CVL*	$Me_2CHCOON{=}CMe_2$	(−)-**87**	50	70
88	*CVL*	$Me_2CHCOON{=}CMe_2$	(−)-**89**	70	76

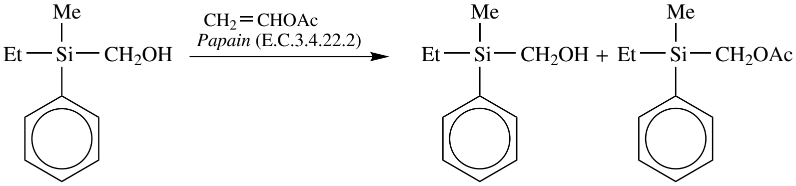

(*rac*-**92**) [(+)-**92**] **(93)**

SCHEME 21

E. Esterifications

Enantioselective enzymatic esterifications represent a further type of biotransformation that has been used for the synthesis of optically active organosilicon compounds. The first example of this particular type of bioconversion (kinetic racemate resolution) is illustrated in Scheme 22. Starting from the racemic 1-silacyclohexan-2-ol *rac*-**43**, the optically active 5-phenylpentanoate (*S*)-**94** was prepared by enantioselective esterification with 5-phenylpentanoic acid using 2-methylheptane as solvent and crude *Candida cylindracea* lipase (*CCL*; E.C. 3.1.1.3) as biocatalyst[7]. The enantiomeric purity of (*S*)-**94** was *ca* 65% ee (bioconversion not optimized).

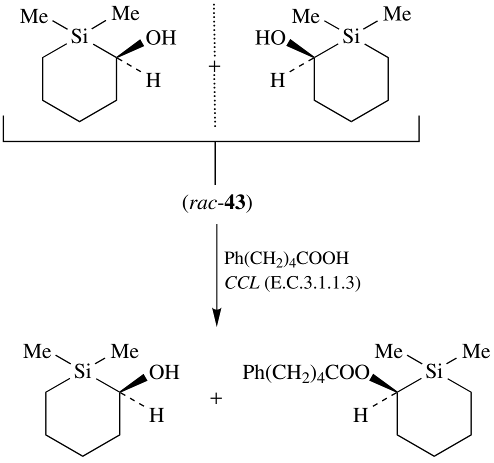

[(*R*)-**43**] [(*S*)-**94**]

SCHEME 22

Enantioselective enzymatic esterifications of trimethylsilyl-substituted alcohols with racemic 2-(4-chlorophenoxy)propanoic acid in water-saturated benzene, catalyzed by the *Candida cylindracea* lipase OF 360 (*CCL* OF 360; E.C. 3.1.1.3) have been used to prepare (−)-2-(4-chlorophenoxy)propanoic acid[76,77]. As shown in Scheme 23, the (trimethylsilyl)alkanols **95**, **97** and **99** were converted enantioselectively into the corresponding (trimethylsilyl)alkyl (+)-2-(4-chlorophenoxy)propanoates **96**, **98** and **100**. The enantiomeric purity of the remaining (−)-2-(4-chlorophenoxy)propanoic acid was 95.8% ee **(95)**, 76.1% ee **(97)** and 77.5% ee **(99)**.

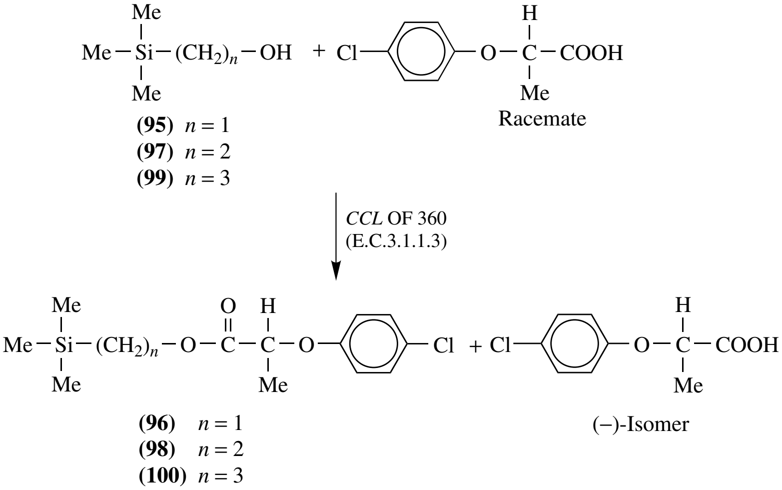

SCHEME 23

Analogous results were obtained for the enantioselective enzymatic esterifications of the related *t*-butyl-substituted alcohols **101** and **103** (carbon analogues of the silanes **95** and **97**, respectively). Reaction with racemic 2-(4-chlorophenoxy)propanoic acid in water-saturated benzene yielded the corresponding *t*-butylalkyl (+)-2-(4-chlorophenoxy)propanoates **102** and **104**, respectively[76,77]. The enantiomeric purity of the remaining (−)-2-(4-chlorophenoxy)propanoic acid was somewhat lower than that observed for the esterification of the analogous silicon compounds [91.1% ee **(101)**, 71.6% ee **(103)**]. No esterification was observed for the Si/C analogues trimethylsilanol (Me_3SiOH) and *t*-butanol (Me_3COH).

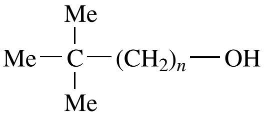

$$\mathrm{Me-\underset{Me}{\overset{Me}{C}}-(CH_2)_n-OH}$$

(101) $n = 1$
(103) $n = 2$

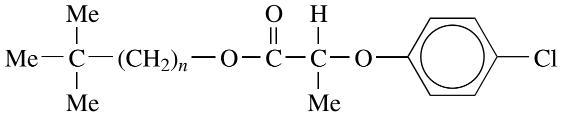

(102) $n = 1$
(104) $n = 2$

Interestingly, for the Si/C analogues **97** and **103** very similar reaction rates were observed, whereas the enzymatic esterifications of the Si/C analogues **95** and **101** are characterized by striking differences. The rate observed for the bioconversion of the silicon compound **95** was about ten times higher than that for the esterification of its carbon analogue **101**, indicating that *Candida cylindracea* lipase OF 360 (E.C. 3.1.1.3) clearly differentiates between silicon and carbon in this particular system. Analogous results were also obtained for lipases from other sources[76,77]. Both the different covalent radii and the different electronic properties of silicon and carbon may be responsible for this. Obviously, these differences do not affect the reaction rates for the Si/C analogues **97** and **103**; in these compounds, the longer ethylene group (instead of methylene) between the OH group and the silicon and carbon atom, respectively, prevents a significant enzymatic discrimination between silicon and carbon.

Enantioselective enzymatic esterifications of the racemic trimethylsilyl-substituted alcohols *rac*-**105**, *rac*-**107** and *rac*-**109** with 5-phenylpentanoic acid in water-saturated 2,2,4-trimethylpentane have been applied for efficient kinetic resolution of these compounds[78]. In systematic studies with five different Celite-adsorbed hydrolases, a particular enzyme was chosen for the bioconversion of each of the three isomers of (trimethylsilyl)propanol (Scheme 24). For the esterification of *rac*-**105**, cholesterol esterase (Type A from *Pseudomonas* sp.; E.C. 3.1.1.13) was used, yielding the alcohol (*S*)-**105** (93% ee) and the ester (*R*)-**106**. Esterification of *rac*-**107** with lipoprotein lipase (Typ A from *Pseudomonas* sp.; E.C. 3.1.1.34) gave the alcohol (*R*)-**107** (96% ee) and the ester (*S*)-**108**. Thus, the stereochemical course of these two conversions is analogous. For the esterification of *rac*-**109**, lipase Salken 100 (from *Rhizopus japonicus*; E.C. 3.1.1.3) was applied to give the alcohol (−)-**109** (95% ee; absolute configuration not reported) and the optically active ester **110** (sign of optical rotation and absolute configuration not reported). As can be seen from these data, the three isomers of (trimethylsilyl)propanol were found to undergo highly enantioselective esterifications. The conversions of the (2-hydroxyalkyl)silanes *rac*-**105** and *rac*-**109** are especially remarkable, since (2-hydroxyalkyl)silanes are known to undergo an Si−C bond cleavage (β-elimination) under the conditions of nonenzymatic acid- and base-catalyzed esterifications.

The carbon analogues (Si/C exchange) of the three (hydroxyalkyl)silanes *rac*-**105**, *rac*-**107** and *rac*-**109** (compounds *rac*-**111**, *rac*-**113** and *rac*-**115**) were also studied for an enzymatic kinetic resolution with hydrolases[78]. These experiments were performed under the same conditions as reported for the parent silicon compounds. By analogy with the (2-hydroxyalkyl)silanes *rac*-**105** and *rac*-**109**, the corresponding carbon analogues *rac*-**111** and *rac*-**115** were also found to undergo an enantioselective esterification with 5-phenylpentanoic acid. When using cholesterol esterase (Type A from *Pseudomonas* sp.; E.C. 3.1.1.13) (*rac*-**111**) and lipase Salken 100 (from *Rhizopus japonicus*; E.C. 3.1.1.3) (*rac*-**115**), the optically active esters (*S*)-**112** and (−)-**116** (absolute configuration not reported) were obtained with an enantiomeric purity of 88% ee and 45% ee, respectively. Thus, the enantioselectivies observed for the esterifications of the carbon compounds are lower than those for the kinetic resolutions of the corresponding silicon analogues. When using *Candida cylindracea* lipase OF 360 (E.C. 3.1.1.3) as the biocatalyst, the Si/C analogues *rac*-**105** and *rac*-**111** were esterified with inverse stereoselectivities, the remaining alcohols being (*R*)-**105** (8% ee) and (*S*)-**111** (15% ee), respectively. Interestingly, the carbon analogue of the (1-hydroxyalkyl)silane *rac*-**107** (compound *rac*-**113**) was found to be hardly esterified by all hydrolases studied (almost no formation of **114**)[78]. These results again demonstrate that enzymes can clearly differentiate between analogous silicon and carbon compounds.

Enzymatic kinetic resolutions via enantioselective esterifications have been successfully used for the preparation of optically active (hydroxymethyl)silanes, with the silicon atom

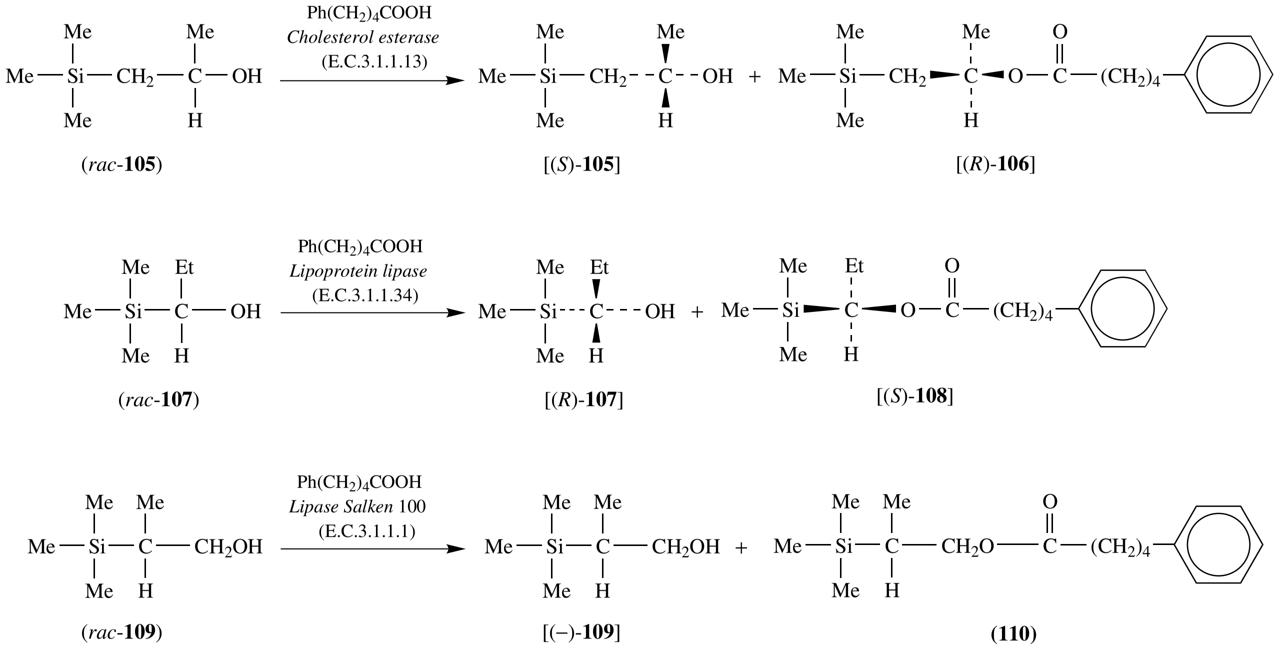
Ph(CH$_2$)$_4$COOH
Cholesterol esterase
(E.C.3.1.1.13)
(rac-105)
[(S)-105]
[(R)-106]
Ph(CH$_2$)$_4$COOH
Lipoprotein lipase
(E.C.3.1.1.34)
(rac-107)
[(R)-107]
[(S)-108]
Ph(CH$_2$)$_4$COOH
Lipase Salken 100
(E.C.3.1.1.1)
(rac-109)
[(−)-109]
(110)

SCHEME 24

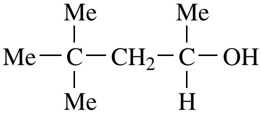

$\mathrm{Me-\overset{Me}{\underset{Me}{C}}-CH_2-\overset{Me}{\underset{H}{C}}-OH}$

(111)

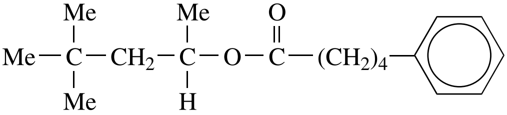

(112)

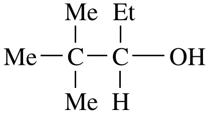

$\mathrm{Me-\overset{Me}{\underset{Me}{C}}-\overset{Et}{\underset{H}{C}}-OH}$

(113)

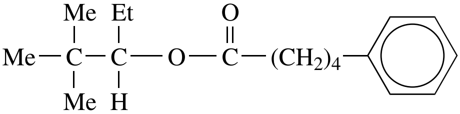

(114)

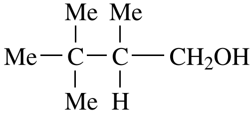

$\mathrm{Me-\overset{Me}{\underset{Me}{C}}-\overset{Me}{\underset{H}{C}}-CH_2OH}$

(115)

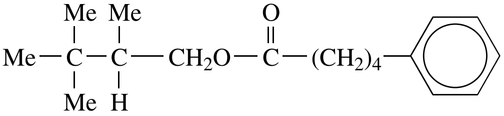

(116)

as the center of chirality[75]. As a result of screening experiments with twenty kinds of commercially available hydrolases, a crude papain preparation (E.C. 3.4.22.2) was chosen as the most suitable biocatalyst for this particular synthetic purpose. As shown in Scheme 25, the racemic (hydroxymethyl)silanes *rac*-**92**, *rac*-**118**, *rac*-**120** and *rac*-**122** were converted into the corresponding levorotatory esters (−)-**117** (67% ee), (−)-**119** (64% ee), (−)-**121** (68% ee) and (−)-**123** (70% ee). The esterifications were carried out on a preparative scale in water-saturated 2,2,4-trimethylpentane using 5-phenylpentanoic acid as the acyl donor and Celite-adsorbed papain as the biocatalyst. In the sense of a kinetic racemate resolution, the remaining dextrorotatory (hydroxymethyl)silanes (+)-**92** (92% ee), (+)-**118** (93% ee), (+)-**120** (97% ee) and (+)-**122** (99% ee) were obtained with high enantiomeric purity. The optically active esters formed and the remaining (hydroxymethyl)silanes were isolated by column chromatography on silica gel. Data on the absolute configurations of these compounds have not been reported. The enzymatic resolutions of *rac*-**92**, *rac*-**118**, *rac*-**120** and *rac*-**122** are characterized by remarkably high enantioselectivities, demonstrating again the high synthetic potential of biocatalyzed reactions for the preparation of almost enantiomerically pure silanes, with the silicon atom as the center of chirality.

F. Oxidations

In order to assess the synthetic potential of enzymatic oxidations for organosilicon chemistry, the (hydroxyalkyl)silanes **95**, **97** and **99** have been studied for their oxidation (dehydrogenation) with horse liver alcohol dehydrogenase (*HLADH*; E.C. 1.1.1.1)[79]. For this purpose, these compounds were incubated with *HLADH* in a TRIS-HCl buffer/THF system in the presence of NAD^+. As monitored spectrophotometrically (increase of absorbance of the NADH formed), the (2-hydroxyethyl)silane **97** and the (3-hydroxypropyl)silane **99** were better substrates for *HLADH* than ethanol, whereas the related (hydroxymethyl)silane **95** was not a substrate under the experimental conditions used. Interestingly, the corresponding carbon analogue **101** was found to be accepted by *HLADH*. On the other hand, the (2-hydroxyethyl)silane **97** was found to be a better

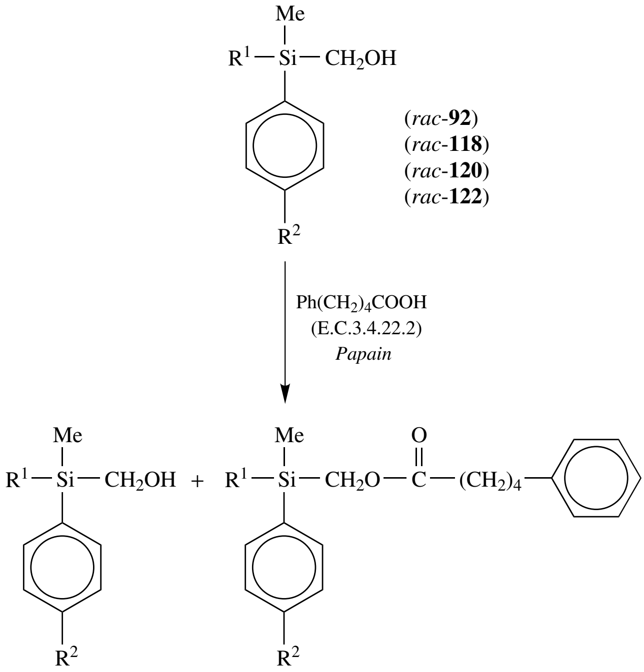

(*rac*-**92**)
(*rac*-**118**)
(*rac*-**120**)
(*rac*-**122**)

[(+)-**92**]
[(+)-**118**]
[(+)-**120**]
[(+)-**122**]

[(−)-**117**]
[(−)-**119**]
[(−)-**121**]
[(−)-**123**]

	R^1	R^2
92, 117	Et	H
118, 119	*n*-Pr	H
120, 121	Et	Me
122, 123	Et	F

SCHEME 25

substrate than its carbon analogue **103**. As demonstrated by kinetic studies at different temperatures (20–30 °C), replacement of the silicon atom in **97** by a carbon atom (cf **103**) leads to an increase of both the activation energy and the frequency factor. The different effects observed for the Si/C pairs **95/101** and **97/103** have been discussed in terms of the different electronic properties and covalent radii of silicon and carbon.

Another study on the enzymatic oxidation of the (hydroxyalkyl)silanes **95**, **97** and **99** [and related (hydroxyalkyl)silanes] with *HLADH* also demonstrated that these compounds (including **95**) are oxidized by this enzyme under the experimental conditions used[80]. Although the (hydroxymethyl)silane **95** was claimed to be not a substrate for *HLADH* in Reference 79, the order of activity of *HLADH* on the Si/C pairs **95/101** and **97/103** reported in References 79 and 80 is the same.

Based on these results, attempts have been made to apply enantioselective dehydrogenations with horse liver alcohol dehydrogenase (*HLADH*; E.C. 1.1.1.1), in the presence of NAD$^+$, for kinetic resolution of the isomeric (hydroxyalkyl)silanes *rac*-**105**, *rac*-**107**

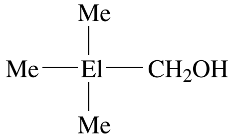

$\mathrm{Me_3El{-}CH_2OH}$

(95) El = Si
(101) El = C

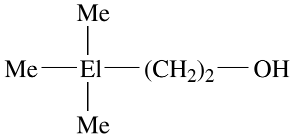

$\mathrm{Me_3El{-}(CH_2)_2{-}OH}$

(97) El = Si
(103) El = C

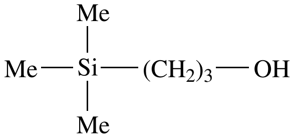

$\mathrm{Me_3Si{-}(CH_2)_3{-}OH}$

(99)

and *rac*-**109**[81]. The corresponding carbon analogues *rac*-**111**, *rac*-**113** and *rac*-**115** were included in these studies. The reactions were carried out in a water−*n*-hexane two-layer system with coenzyme regeneration (oxidation of NADH to NAD^+ coupled with *L*-glutamate dehydrogenase-catalyzed reductive amination of 2-oxoglutarate to *L*-glutamate). With the (2-hydroxyalkyl)silane *rac*-**105**, the dehydrogenation proceeded quickly and stopped at 50% conversion, whereas the carbon analogue *rac*-**111** reacted significantly slower and the conversion reached over 50%. The Si/C analogues *rac*-**109** and *rac*-**115** were found to undergo dehydrogenation at high rates (the silicon compound reacting faster than its carbon analogue) and the conversions continued above 50% conversion. In contrast, the dehydrogenation of the (1-hydroxyalkyl)silane *rac*-**107** and of its carbon analogue *rac*-**113** was negligible under the reaction conditions used. Stereochemical studies (analysis of the remaining alcohols) demonstrated the enantioselective course of the dehydrogenations of *rac*-**105**, *rac*-**109**, *rac*-**111** and *rac*-**115**. In the case of the Si/C analogues *rac*-**105** and *rac*-**111**, the enzymatic kinetic resolution yielded the remaining alcohols (*R*)-**105** and (*R*)-**111** with enantiomeric purities of >99% ee and 85% ee, respectively (degree of conversion 50%). In the case of the Si/C analogues *rac*-**109** and *rac*-**115**, the remaining levorotatory alcohols (−)-**109** and (−)-**115** (absolute configurations not reported) were obtained with enantiomeric purities of 70% ee and 59% ee, respectively (degree of conversion 70%). Thus, both the reaction rates and the stereoselectivities of the dehydrogenations of the silicon compounds were higher than those observed for their corresponding carbon analogues. In the two-layer system used for these biotransformations, accumulation of the oxidation products of the carbon compounds *rac*-**111** and *rac*-**115** was observed, while those obtained by oxidation of the silicon analogues *rac*-**105** and *rac*-**109** were not accumulated. This can be easily explained by hydrolytic Si−C bond cleavage of the resulting (1-acylalkyl)silanes yielding trimethylsilanol and the corresponding ketone and aldehyde, respectively. Absence of product inhibition derived from this hydrolytic decomposition may be one of the reasons for the higher reaction rates observed for the silicon compounds.

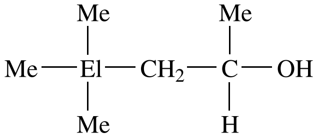

$\mathrm{Me_3El{-}CH_2{-}CH(Me){-}OH}$

(105) El = Si
(111) El = C

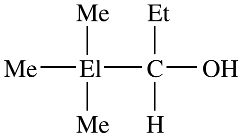

$\mathrm{Me_3El{-}CH(Et){-}OH}$

(107) El = Si
(113) El = C

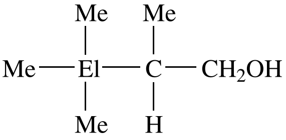

$\mathrm{Me_3El{-}CH(Me){-}CH_2OH}$

(109) El = Si
(115) El = C

Due to the hydrolytic decomposition of (1-acylalkyl)silanes, enzymatic kinetic resolution of racemic (2-hydroxyalkyl)silanes, catalyzed by *HLADH*, can only be used for the preparation of one of the two enantiomers. In contrast, resolution of related carbon compounds (including subsequent chemical oxidation of the dehydrogenated bioconversion product), in principle, can yield both enantiomers.

IV. CONCLUDING REMARKS

Chirality has become an important subject in bioorganosilicon chemistry. As demonstrated by pharmacological studies with enantiomerically pure chiral silanols and silanes, with the silicon atom as the center of chirality, biological systems can discriminate between the two enantiomers of organosilicon drugs. In these investigations, significant differences in both pharmacological potency and pharmacological selectivity have been observed. Thus, for future developments of new chiral silicon-based agrochemicals, drugs and diagnostics, biological studies with the pure enantiomers of such compounds are necessary. For this reason, the availability of sufficient preparative methods for the synthesis of enantiomerically pure silicon compounds is of great importance.

On the other hand, it has been demonstrated that the synthetic potential of biological systems represent a challenge for the preparation of enantiomerically pure silicon compounds, with the silicon atom as the center of chirality. Stereoselective biotransformations with whole microbial cells or isolated enzymes have been demonstrated to be very useful for the synthesis of such compounds. Free microbial cells or enzymes and immobilized biocatalysts as well have been used for synthetic purposes. Preliminary studies have shown that plant cell suspension cultures may also be interesting biocatalysts. In general, the favorable characteristics of biotransformations (mild reaction conditions, chemoselectivity, regioselectivity, diastereoselectivity, enantioselectivity) offer a variety of synthetic applications in organosilicon chemistry. By taking advantage of the stereoselective course of enzyme-catalyzed reactions, the synthesis of new types of optically active silicon compounds, with the silicon atom as the center of chirality, is possible. As chemical reactions at the stereogenic silicon center of chiral silicon compounds often proceed with high stereoselectivity, optically active biotransformation products may serve as starting materials for the preparation of further, chemically modified optically active derivatives.

So far, only biocatalyzed reductions, oxidations, ester and amide hydrolyses, esterifications and transesterifications have been used for synthetic purposes in silicon chemistry. However, the application of many other reaction types also appears possible. Although the utilization of biocatalysis in organosilicon chemistry is generally restricted by the hydrolytic sensitivity of certain silicon-element bonds, this particular problem might by overcome, at least in part, (i) by optimizing the bioconversion conditions in aqueous solution (pH and temperature control) and (ii) by using biotransformations in organic media. Lipase-catalyzed conversions in organic solvents appear to be particularly promising in this respect.

Using the powerful methods of modern biotechnology, a scale-up of stereoselective biotransformations and thus the production of larger amounts of optically active organosilicon compounds, in principle, is possible. Development of organosilicon biotechnology, as the basis for large-scale applications of optically active organosilicon compounds in science and technology, represents a big challenge.

V. ACKNOWLEDGMENTS

R.T. wishes to express his sincere thanks to his coworkers and colleagues without whose contributions this article could not have been written; their names are cited in the references. In addition, financial support of our work by the Deutsche Forschungsgemeinschaft, the Volkswagenstiftung, the Fonds der Chemischen Industrie, the

Doktor Robert Pfleger-Stiftung and the Bayer AG (Leverkusen and Wuppertal-Elberfeld) is gratefully acknowledged.

VI. REFERENCES

1. R. J. Fessenden and J. S. Fessenden, *Adv. Drug Res.*, **4**, 95 (1967).
2. R. Tacke and U. Wannagat, *Top. Curr. Chem.*, **84**, 1 (1979).
3. M. G. Voronkov, *Top. Curr. Chem.*, **84**, 77 (1979).
4. R. J. Fessenden and J. S. Fessenden, *Adv. Organomet. Chem.*, **18**, 275 (1980).
5. R. Tacke and H. Zilch, *Endeavour, New Series*, **10**, 191 (1986).
6. R. Tacke and B. Becker, *Main Group Met. Chem.*, **10**, 169 (1987).
7. C. Syldatk, A. Stoffregen, A. Brans, K. Fritsche, H. Andree, F. Wagner, H. Hengelsberg, A. Tafel, F. Wuttke, H. Zilch and R. Tacke, in *Enzyme Engineering 9* (Eds. H. W. Blanch and A. M. Klibanov), *Ann. N. Y. Acad. Sci.*, Vol. 542, The New York Academy of Sciences, New York, 1988, pp. 330–338.
8. R. Tacke and H. Linoh, in *The Chemistry of Organic Silicon Compounds, Part 2* (Eds. S. Patai and Z. Rappoport), Wiley, Chichester, 1989, pp. 1143–1206, and references cited therein.
9. R. Tacke, S. Brakmann, M. Kropfgans, C. Strohmann, F. Wuttke, G. Lambrecht, E. Mutschler, P. Proksch, H.-M. Schiebel and L. Witte, in *Frontiers of Organosilicon Chemistry* (Eds. A. R. Bassindale and P. P. Gaspar), The Royal Society of Chemistry, Cambridge, 1991, pp. 218–228.
10. R. Tacke, M. Strecker, W. S. Sheldrick, E. Heeg, B. Berndt and K. M. Knapstein, *Z. Naturforsch.*, **34b**, 1279 (1979).
11. L. Steiling, R. Tacke and U. Wannagat, *Liebigs Ann. Chem.*, 1554 (1979).
12. R. Tacke, M. Strecker, W. S. Sheldrick, L. Ernst, E. Heeg, B. Berndt, C.-M. Knapstein and R. Niedner, *Chem. Ber.*, **113**, 1962 (1980).
13. R. Tacke, E. Zimonyi-Hegedüs, M. Strecker, E. Heeg, B. Berndt and R. Langner, *Arch. Pharm. (Weinheim)*, **313**, 515 (1980).
14. R. Tacke, H. Lange, W. S. Sheldrick, G. Lambrecht, U. Moser and E. Mutschler, *Z. Naturforsch.*, **38b**, 738 (1983).
15. R. Tacke, M. Strecker, G. Lambrecht, U. Moser and E. Mutschler, *Liebigs Ann. Chem.*, 922 (1983).
16. R. Tacke, M. Strecker, G. Lambrecht, U. Moser and E. Mutschler, *Arch. Pharm. (Weinheim)*, **317**, 207 (1984)
17. W. S. Sheldrick, H. Linoh, R. Tacke, G. Lambrecht, U. Moser and E. Mutschler, *J. Chem. Soc. Dalton Trans.*, 1743 (1985).
18. R. Tacke, H. Linoh, H. Zilch, J. Wess, U. Moser, E. Mutschler and G. Lambrecht, *Liebigs Ann. Chem.*, 2223 (1985).
19. R. Tacke, J. Pikies, H. Linoh, R. Rohr-Aehle and S. Gönne, *Liebigs Ann. Chem.*, 51 (1987).
20. R. Tacke, H. Linoh, L. Ernst, U. Moser, E. Mutschler, S. Sarge, H. K. Cammenga and G. Lambrecht, *Chem. Ber.*, **120**, 1229 (1987).
21. M. Waelbroeck, M. Tastenoy, J. Camus, J. Christophe, C. Strohmann, H. Linoh, H. Zilch, R. Tacke, E. Mutschler and G. Lambrecht, *Br. J. Pharmacol.*, **98**, 197 (1989).
22. G. Lambrecht, R. Feifel, M. Wagner-Röder, C. Strohmann, H. Zilch, R. Tacke, M. Waelbroeck, J. Christophe, H. Boddeke and E. Mutschler, *Eur. J. Pharmacol.*, **168**, 71 (1989).
23. R. Tacke, H. Linoh, K. Rafeiner, G. Lambrecht and E. Mutschler, *J. Organomet. Chem.*, **359**, 159 (1989).
24. G. Lambrecht, R. Feifel, U. Moser, M. Wagner-Röder, L. K. Choo, J. Camus, M. Tastenoy, M. Waelbroeck, C. Strohmann, R. Tacke, J. F. Rodrigues de Miranda, J. Christophe and E. Mutschler, *Trends Pharmacol. Sci. Suppl.*, **10**, 60 (1989).
25. M. Waelbroeck, J. Camus, M. Tastenoy, E. Mutschler, C. Strohmann, R. Tacke, G. Lambrecht and J. Christophe, *Eur. J. Pharmacol., Mol. Pharmacol. Sect.*, **206**, 95 (1991).
26. R. Tacke, K. Mahner, C. Strohmann, B. Forth, E. Mutschler, T. Friebe and G. Lambrecht, *J. Organomet. Chem.*, **417**, 339 (1991).
27. M. Waelbroeck, J. Camus, M. Tastenoy, G. Lambrecht, E. Mutschler, M. Kropfgans, J. Sperlich, F. Wiesenberger, R. Tacke and J. Christophe, *Br. J. Pharmacol.*, **109**, 360 (1993).
28. R. Tacke, J. Pikies, F. Wiesenberger, L. Ernst, D. Schomburg, M. Waelbroeck, J. Christophe, G. Lambrecht, J. Gross and E. Mutschler, *J. Organomet. Chem.*, **466**, 15 (1994).

29. M. Waelbroeck, J. Camus, M. Tastenoy, R. Feifel, E. Mutschler, R. Tacke, C. Strohmann, K. Rafeiner, J. F. Rodrigues de Miranda and G. Lambrecht, *Br. J. Pharmacol.*, **112**, 505 (1994).
30. R. Tacke, M. Kropfgans, A. Tafel, F. Wiesenberger, W. S. Sheldrick, E. Mutschler, H. Egerer, N. Rettenmayr, J. Gross, M. Waelbroeck and G. Lambrecht, *Z. Naturforsch.*, **49b**, 898 (1994).
31. R. Tacke, D. Terunuma, A. Tafel, M. Mühleisen, B. Forth, M. Waelbroeck, J. Gross, E. Mutschler, T. Friebe and G. Lambrecht, *J. Organomet. Chem.*, **501**, 145 (1995).
32. R. Tacke, D. Reichel, K. Günther and S. Merget, *Z. Naturforsch.*, **50b**, 568 (1995).
33. R. Tacke, B. Forth, M. Waelbroeck, J. Gross, E. Mutschler and G. Lambrecht, *J. Organomet. Chem.*, **505**, 73 (1995).
34. R. Tacke, D. Reichel, M. Kropfgans, P. G. Jones, E. Mutschler, J. Gross, X. Hou, M. Waelbroeck and G. Lambrecht, *Organometallics*, **14**, 251 (1995).
35. D. Reichel, R. Tacke, P. G. Jones, G. Lambrecht, J. Gross, E. Mutschler and M. Waelbroeck, in *Organosilicon Chemistry II—From Molecules to Materials* (Eds. N. Auner and J. Weis), VCH, Weinheim, 1996, pp. 231–236.
36. R. Tacke, D. Reichel, P. G. Jones, X. Hou, M. Waelbroeck, J. Gross, E. Mutschler and G. Lambrecht, *J. Organomet. Chem.*, **521**, 305 (1996).
37. R. Tacke, H. Linoh, D. Schomburg, L. Ernst, U. Moser, E. Mutschler and G. Lambrecht, *Liebigs Ann. Chem.*, 242 (1986).
38. E. Mutschler, H. A. Ensinger, J. Gross, A. Leis, K. Mendla, U. Moser, O. Pfaff, D. Reichel, K. Rühlmann, R. Tacke, M. Waelbroeck, J. Wehrle and G. Lambrecht, in *Perspectives in Receptor Research* (Eds. D. Giardinà, A. Piergentili and M. Migini), Elsevier Science Publishers B. V., Amsterdam, 1996, pp. 51–65.
39. M. Kropfgans, *Dissertation*, University of Karlsruhe, 1992; R. Tacke, M. Kropfgans, G. Mattern, J. Sperlich, G. Lambrecht, E. Mutschler and M. Waelbroeck, unpublished results.
40. H.-J. Egerer, *Dissertation*, University of Frankfurt, 1993; G. Lambrecht, E. Mutschler, H.-J. Egerer, R. Tacke and M. Waelbroeck, unpublished results.
41. M. Waelbroeck, J. Camus, M. Tastenoy, G. Lambrecht, E. Mutschler, R. Tacke and J. Christophe, *Eur. J. Pharmacol., Mol. Pharmacol. Sect.*, **189**, 135 (1990).
42. M. Waelbroeck, J. Camus, M. Tastenoy, E. Mutschler, C. Strohmann, R. Tacke, G. Lambrecht and J. Christophe, *Chirality*, **3**, 118 (1991).
43. M. Waelbroeck, J. Camus, M. Tastenoy, E. Mutschler, C. Strohmann, R. Tacke, L. Schjelderup, A. Aasen, G. Lambrecht and J. Christophe, *Eur. J. Pharmacol., Mol. Pharmacol. Sect.*, **227**, 33 (1992).
44. R. J. P. Corriu and C. Guérin, *Adv. Organomet. Chem.*, **20**, 265 (1982).
45. R. J. P. Corriu, C. Guérin and J. J. E. Moreau, *Top. Stereochem.*, **15**, 43 (1984).
46. T. Ohta, M. Ito, A. Tsuneto and H. Takaya, *J. Chem. Soc., Chem. Commun.*, 2525 (1994).
47. R. Tacke, H. Linoh, B. Stumpf, W.-R. Abraham, K. Kieslich and L. Ernst, *Z. Naturforsch.*, **38b**, 616 (1983).
48. C. Syldatk, A. Stoffregen, F. Wuttke and R. Tacke, *Biotechnol. Lett.*, **10**, 731 (1988).
49. C. Syldatk, J. Fooladi, A. Stoffregen, R. Tacke, F. Wagner and M. Wettern, in *Physiology of Immobilized Cells* (Eds. J. A. M. de Bont, J. Visser, B. Mattiasson and J. Tramper), Elsevier Science Publishers B. V., Amsterdam, 1990, pp. 377–385.
50. C. Syldatk, H. Andree, A. Stoffregen, F. Wagner, B. Stumpf, L. Ernst, H. Zilch and R. Tacke, *Appl. Microbiol. Biotechnol.*, **27**, 152 (1987).
51. L. Fischer, S. A. Wagner and R. Tacke, *Appl. Microbiol. Biotechnol.*, **42**, 671 (1995).
52. R. Tacke, S. A. Wagner, S. Brakmann, F. Wuttke, U. Eilert, L. Fischer and C. Syldatk, *J. Organomet. Chem.*, **458**, 13 (1993).
53. R. Tacke, H. Hengelsberg, H. Zilch and B. Stumpf, *J. Organomet. Chem.*, **379**, 211 (1989).
54. R. Tacke, K. Fritsche, A. Tafel and F. Wuttke, *J. Organomet. Chem.*, **388**, 47 (1990).
55. R. Tacke, S. Brakmann, F. Wuttke, J. Fooladi, C. Syldatk and D. Schomburg, *J. Organomet. Chem.*, **403**, 29 (1991).
56. R. Tacke, F. Wuttke and H. Henke, *J. Organomet. Chem.*, **424**, 273 (1992).
57. S. A. Wagner, S. Brakmann and R. Tacke, in *Organosilicon Chemistry II—From Molecules to Materials* (Eds. N. Auner and J. Weis), VCH, Weinheim, 1996, pp. 237–242.
58. F. Huber, S. Bratovanov, S. Bienz, C. Syldatk and M. Pietzsch, *Tetrahedron Asymmetry*, **7**, 69 (1996).
59. H. Hengelsberg, *Dissertation*, Technical University of Braunschweig, 1989; R. Tacke and H. Hengelsberg, unpublished results.

60. H. Zilch, *Dissertation*, Technical University of Braunschweig, 1986; R. Tacke, H. Zilch, B. Stumpf, L. Ernst and D. Schomburg, unpublished results.
61. Y. Yamazaki and H. Kobayashi, *Chemistry Express*, **8**, 97 (1993).
62. K. Fritsche, C. Syldatk, F. Wagner, H. Hengelsberg and R. Tacke, *Appl. Microbiol. Biotechnol.*, **31**, 107 (1989).
63. M. Shimizu, H. Kawanami and T. Fujisawa, *Chem. Lett.*, 107 (1992).
64. N. Belair, H. Deleuze, B. De Jeso and B. Maillard, *Main Group Met. Chem.*, **15**, 187 (1992).
65. R. Tacke, K. Fritsche, H. Hengelsberg, A. Tafel, F. Wuttke, H. Zilch, C. Syldatk, H. Andree, A. Stoffregen and F. Wagner, *VIIIth International Symposium on Organosilicon Chemistry, Abstracts*, St. Louis, 1987, p. 51.
66. R. Tacke, in *Organosilicon and Bioorganosilicon Chemistry: Structure, Bonding, Reactivity and Synthetic Application* (Ed. H. Sakurai), Ellis Horwood, Chichester, 1985, pp. 251–262.
67. C. Syldatk, H. Andree, F. Wagner, F. Wuttke, H. Zilch and R. Tacke, *4. DECHEMA Jahrestagung der Biotechnologen, Abstracts*, Frankfurt/Main, 1986, pp. 171–172.
68. B. De Jeso, N. Belair, H. Deleuze, M.-C. Rascle and B. Maillard, *Tetrahedron Lett.*, **31**, 653 (1990).
69. H. Hengelsberg, R. Tacke, K. Fritsche, C. Syldatk and F. Wagner, *J. Organomet. Chem.*, **415**, 39 (1991).
70. M. A. Sparks and J. S. Panek, *Tetrahedron Lett.*, **32**, 4085 (1991).
71. P. Grisenti, P. Ferraboschi, A. Manzocchi and E. Santaniello, *Tetrahedron*, **48**, 3827 (1992).
72. V. Fiandanese, O. Hassan, F. Naso and A. Scilimati, *Synlett*, 491 (1993).
73. A.-H. Djerourou and L. Blanco, *Tetrahedron Lett.*, **32**, 6325 (1991).
74. R. Tacke, S. A. Wagner and J. Sperlich, *Chem. Ber.*, **127**, 639 (1994).
75. T. Fukui, T. Kawamoto and A. Tanaka, *Tetrahedron Asymmetry*, **5**, 73 (1994).
76. A. Tanaka, T. Kawamoto and K. Sonomoto, in *Enzyme Engineering 10* (Eds. H. Okada, A. Tanaka and H. W. Blanch), *Ann. N. Y. Acad. Sci.*, Vol. 613, The New York Academy of Sciences, New York, 1990, pp. 702–706.
77. T. Kawamoto, K. Sonomoto and A. Tanaka, *J. Biotechnol.*, **18**, 85 (1992).
78. A. Uejima, T. Fukui, E. Fukusaki, T. Omata, T. Kawamoto, K. Sonomoto and A. Tanaka, *Appl. Microbiol. Biotechnol.*, **38**, 482 (1993).
79. M.-H. Zong, T. Fukui, T. Kawamoto and A. Tanaka, *Appl. Microbiol. Biotechnol.*, **36**, 40 (1991).
80. K. Sonomoto, H. Oiki and Y. Kato, *Enzyme Microbiol. Technol.*, **14**, 640 (1992).
81. T. Fukui, M.-H. Zong, T. Kawamoto and A. Tanaka, *Appl. Microbiol. Biotechnol.*, **37**, 209 (1992).

CHAPTER **42**

Highly reactive small-ring monosilacycles and medium-ring oligosilacycles

WATARU ANDO and YOSHIO KABE

Department of Chemistry, University of Tsukuba, Tsukuba, Ibaraki 305, Japan

I. INTRODUCTION

Our research interest gravitated to organosilicon chemistry when the formation of a silicon carbon double bond (silene) intermediate was found in the decomposition of silyl diazo compounds in 1973 (Section II.A, B and D). This process involves a 1,2-alkyl migration of a silyl carbene from a silicon to a carbene center which corresponds to a general process in carbene chemistry, i.e. 1,2-alkyl rearrangement of carbene to form alkenes. Although the first stable silene and disilene with bulky substituents were isolated by Brook and West, respectively, in 1979 and 1981, our reactive silene has proved to be a convenient source to a variety of functionalized silenes which are otherwise accessed with difficulty, such as silabenzene, silafulvene (Section II.F), silaacrylate, siladienone (Section I.C), 1,4-disilabutadiene and 1,5-disilapentadiene (Section I.E), respectively. Another aspect of this chemistry involves a ready assembly of new silicon ring systems, such as silaoxetane, silaoxetene (Section II.C), trisilabicyclo[1.1.1]pentane, trisilabicyclo[2.1.0]pentane, tetrasilabicyclo[3.1.0]hexane and tetrasilabicyclo[2.2.0]hexane (Section II.E) from the reactive silenes.

A silyl carbene can also undergo an intramolecular carbene insertion into the α-CH bond to form a silacyclopropane (silirane). The elusiveness of siliranes has long attracted our interest to small-ring compounds containing silicon atoms. At that time we suggested silirane as the intermediate in the decomposition of silyl diazo compounds. After isolation of the first stable silirane by Seyferth and of its unsaturated analogue (silirene) by Gaspar, Kumada and Sakurai, we started our study of silylene addition to ketones and thioketones. This research has not only culminated in the first isolation of oxa(thia)silirane but has also yielded a rich ylide chemistry (Section III.A). The silylene addition strategy to alkenes and cummulenes provided a variety of silicon ring systems such as silirane, alkylidenesilirane and bisalkylidenesilirane (Section III.B). In the latter case, the alkylidene moiety increased the reactivity of the silirane ring toward a variety of electrophiles and nucleophiles. Especially, transition metals promoted the Si$-$C bond cleavage to give silatrimethylenemethane complexes, i.e. silene complexes of trimethylenemethane analogue.

Meanwhile, the addition reaction of disilene has been reported by West's and Masamune's groups, respectively, to give a variety of three- and four-membered ring compounds containing Si$-$Si bonds. The structural analysis of disilacyclopropanes (disiliranes) indicates relatively short bonds and an almost planar geometry about each silicon atom, which is interpreted in terms of a π-complex of a disilene. This observation supported the conclusion that Si$-$Si σ-bonds in the small-ring systems have some analogous character and reactivity to C$-$C π-bonds. Similar structural and reactivity features of digermiranes were delineated by our group. In addition to digermiranes, the ring expansion reaction of disiliranes, disiletene and bisalkylidenedisiletane was found to be a successful tool for derivatization of silicon ring systems. Especially, this study was culminated in finding the transition metal promoted ring expansion of bisalkylidenesiletenes, which can be prepared by both intramolecular Wurtz and Diyne coupling reactions (Section IV.B).

Kumada's group developed the photochemical silylene extrusion and ring contraction reactions of cyclohexasilane in 1969 and this process has become very popular in organosilicon chemistry, e.g. in West's and Masamune's disilene syntheses of linear- and cyclotrisilanes. This process was adopted as another tool for ring contraction and derivatization of oligosilabridged cyclosilanes containing C$-$C unsaturated bonds (Section V.A). Fortunately, in the course of these studies, the presence of long Si$-$Si bonds was found to enable the direct preparation of strained ring systems by Kipping reaction (Section V.B). Our research along these lines culminated in the synthesis of *trans*-trisilacycloheptene, the first stable seven-membered cyclic *trans*-olefin, [7]pentasilacyclophane (Section IV.A), [3.1.1]trisilapropellane (Section V.A), oligosilabridged and doubly bridged allenes and bisallenes (Section V.C) and tetrasilacyclohexynes (Section V.B), the first stable six-membered cyclic acetylenes. West's and Masamune's disilenes which are discussed above are highly protected by bulky substituents and more functionalized disilenes constructed into an aromatic system have not been explored up to this point. In this context, it was found that silyl dianions such as 1,2-disilaacenaphthene and 9,10-disilaanthracene prepared by Gilman reaction act as synthetic equivalents of disilaaromatics in the presence of oxidizing reagents and in the reaction with α,ω-dichlorooligosilanes (Section V.D).

Hence this chapter provides analogy between silylene and carbene chemistry as a useful approach for construction of small-ring monosilacycles. Furthermore, intramolecular Wurtz, Diyne coupling, Kipping and Gilman reactions have been shown to be useful tools for construction of medium-ring oligosilacycles.

II. SILYL CARBENE-TO-SILENE REARRANGEMENT AND RING FORMATION

A. Decomposition of Monosilanyl Diazo Compounds

When ethyl trimethylsilyldiazoacetate **(1a)** is photolyzed with a high-pressure mercury lamp in alcohols, four products (**2**–**5**) are obtained. Products **2** and **3** may be rationalized in terms of insertion reaction of trimethylsilyl carboethoxycarbene and product **4** has been explained by a Wolf rearrangement.

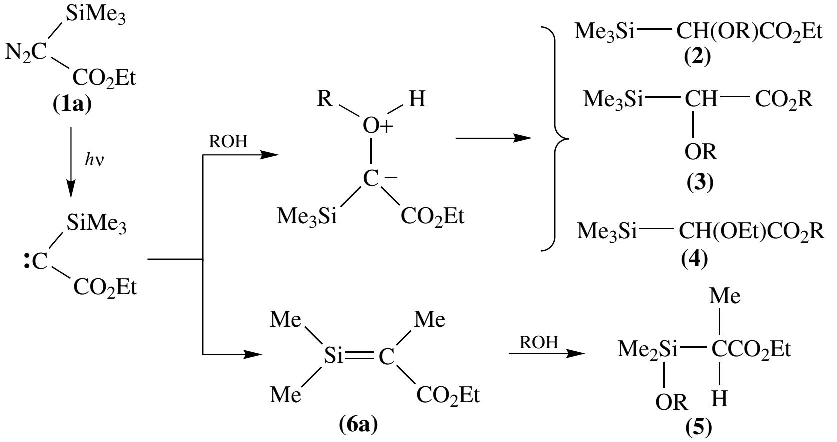

(1)

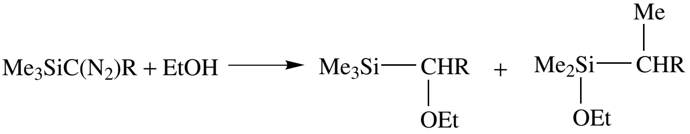

$$\mathrm{Me_3SiC(N_2)R + EtOH \longrightarrow Me_3Si{-}\underset{\displaystyle OEt}{CHR} + \underset{\displaystyle OEt}{Me_2Si}{-}\overset{\displaystyle Me}{CHR}} \qquad (2)$$

R = CO_2Et	**1a**	85%	15%
R = Ph	**7**	100	0
R = H	**8**	0	100

The formation of **5**, which involves a methyl migration, is interesting from a mechanistic point of view. It was rationalized by invoking the intermediacy of the silicon–carbon double bond species (silene) **(6a)** (equation 1)[1]. The extent of this silylcarbene-to-silene rearrangement is highly dependent on substituents. For example, phenyl trimethylsilyldiazomethane **(7)** gave only O–H insertion products, while trimethylsilyldiazomethane **(8)** afforded only methyl migration product (equation 2)[2]. The gas-phase pyrolysis of **1b** and **7** gave controversial results. When methyl trimethylsilyldiazoacetate **(1b)** was evaporated through a Pyrex tube maintained at 360 °C and the products were then treated with methanol, the Wolf rearrangement product **(9)** and methyl migration product **(10)** were obtained[3]. To our surprise the trapping of the pyrolysate in alcohols showed that both alkoxy groups in **10** are derived from the added alcohol. This observation led us to isolate ketene **11a** (R = Me) as the suspected intermediate. A major question that remained was the source of **11a** which could be formed by a dytropic rearrangement of ketene **12**, or by a rapid isomerization of **6b** (equation 3)[4].

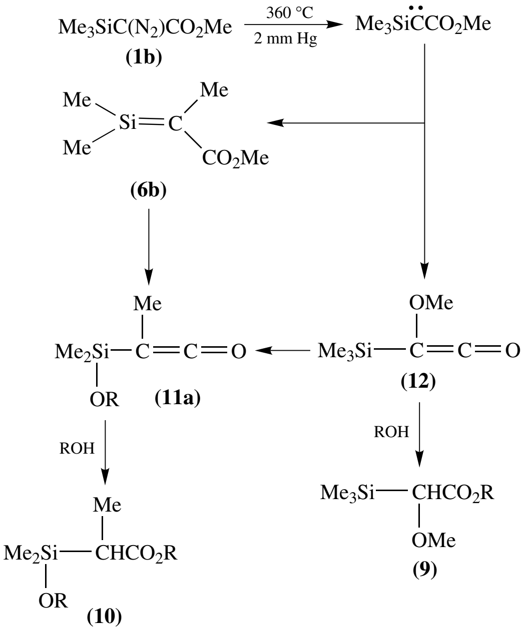

(3)

Pyrolysis of **7** gave four products (equation 4)[5]. Product **15** is easily rationalized as the dimerization product of the silyl carbene. Product **14** involves an abstraction of hydrogen by the silylcarbene and is a typical minor product of carbene reactions. A ^{13}C labeling experiment[6] was consistent with the proposal that **13** is formed as a result of a carbene–carbene rearrangement and also ruled out an earlier suggestion that a silirane was involved[7]. However, a silene is also formed in the reaction because, in the presence of an alcohol, a ketone and 2,3-dimethylbutadiene, alcohol insertion, Wittig type and Diels–Alder adducts were also isolated along with **13** and **14**[7,8]. The styrene is formed either by decomposition of the product of carbon–hydrogen insertion, 1,1-dimethyl-2-phenylsilirane or by dissociation of the silene to dimethylsilylene and methylphenylcarbene, which subsequently yield styrene.

B. Decomposition of Oligosilanyl Diazo Compounds

During the 1970s Brook's group had been studying the photochemistry of acylsilanes[9], which resulted in a 1,2-shift of the silyl group from carbon to oxygen forming a siloxycarbene. On replacing the silyl groups by disilanyl groups, it was found that the products formed included not only the 1,2-silyl shifted disiloxycarbene, but also a silene formed by a 1,3-shift of silyl group from silicon to oxygen[9]. Ultimately the use of a tris(trimethylsilyl)silyl group led to an exclusive 1,3-shift to afford the first stable silenes[10–12]. The good migrating ability of a silyl group induced us to pursue a project aimed at obtaining oligosilanyl silenes. An exclusive migration of a trimethylsilyl group to a carbene center was observed in both thermal and photochemical decomposition of oligosilylated diazomethanes (**16a,b** and **18**) (equation 5)[13]. The formation of the transient silenes **17** and **19** was deduced from trapping with alcohol and ketones. Photolysis of disilanyl diazoacetate **(1c)** in THF cleanly produced ketene **21** in quantitative yield (equation 6)[14]. Another interesting ketene **11b** was also obtained when **21** was treated with methanol. Support for the intermediacy of the silene **(6c)** in the reaction of **1c** was obtained by a reaction in methanol **(20)** and in cyclohexanone **(22)**[15]. It is now clear that silaacrylate **(6c)** isomerizes to alkoxyketene **(21)** by a spontaneous migration of the alkoxy group to silicon (see Section II.A).

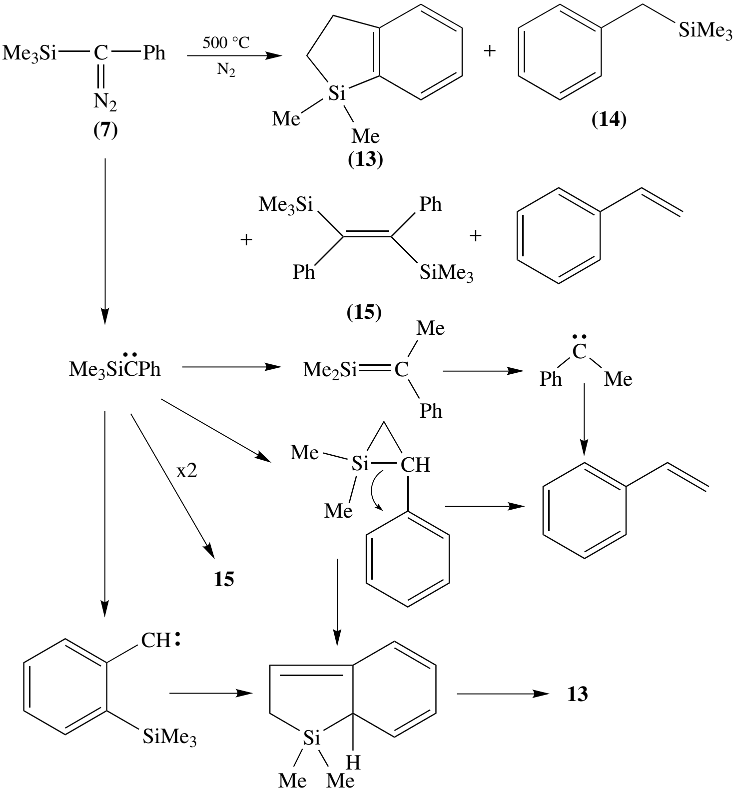

(4)

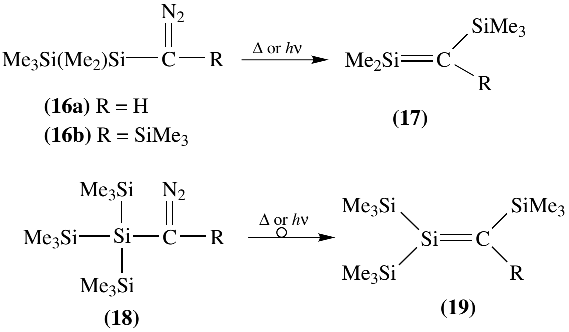

(5)

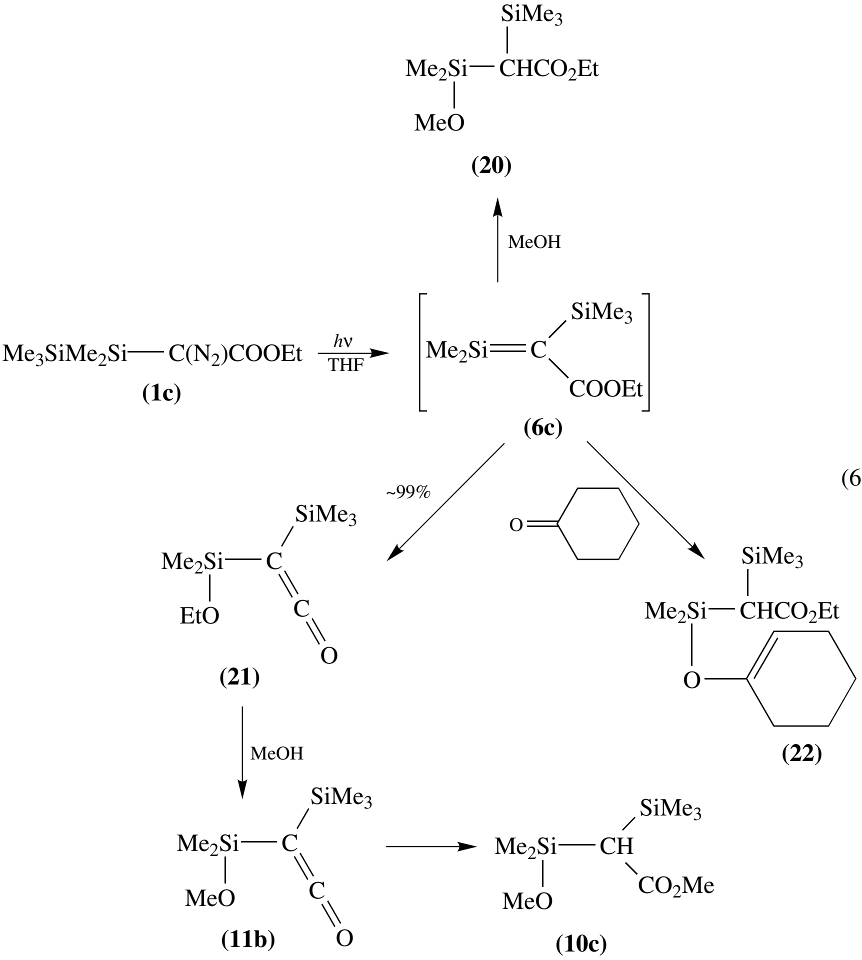

(6)

C. Oxasiletane and Oxasiletene

Pyrolysis of siletane had been the most reliable method for the generation of transient silene, and Gusel'nikov and coworkers confirmed the existence of such silenes by kinetic and chemical trapping experiments[16]. Barton[17] and Sommer[18] and their coworkers have found that co-pyrolysis of siletane with an aldehyde or ketone yielded a cyclic siloxane and an olefin. It is generally agreed that this reaction proceeds through cycloaddition of the silene to the carbonyl group to produce an unstable oxasiletane, which thermally decomposes to the olefin and a silanone, which then thermally undergo a cyclic oligomerization. In the hope of obtaining an oxasiletane, silene formation under mild conditions in the presence of carbonyl compounds was employed. In fact, thermal generation (180 °C) of silene **6c** from pentamethyldislanyl diazoacetate **(1c)** in 7-norbornanone yields an isolable product for which the oxasiletane structure **23** was proposed[19]. Soon after, Barton and coworkers convincingly reinterpreted the structure as ketene acetal **24**[20]. If Barton is correct, the reaction should be classified as [4 + 2] cycloaddition of the silaacrylate **6c** (equation 7). Märkl, Wiberg and Brook demonstrated that stable silenes with ketones having aromatic rings undergo both [2 + 2] and [2 + 4] cycloadditions[21–23].

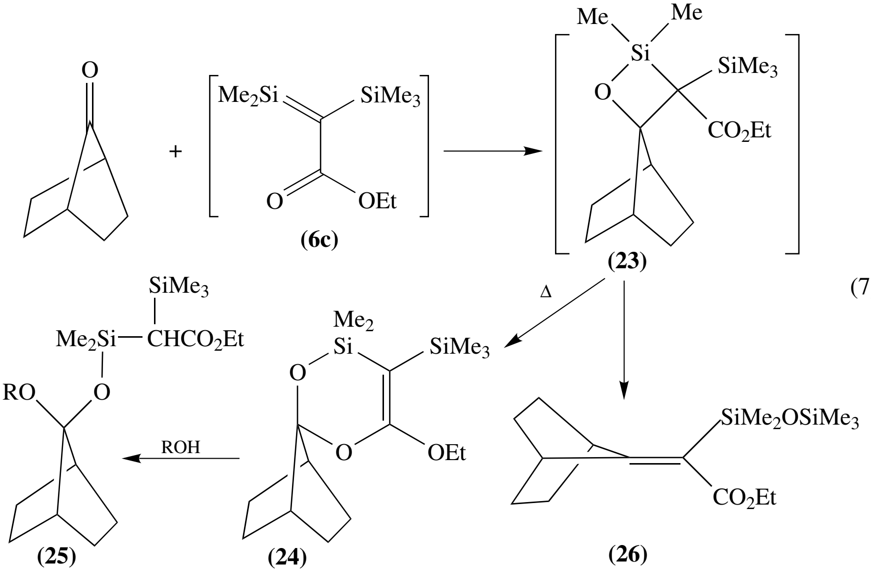

(7)

The formation of methanolysis product **25** (R = Me) was easily understood in terms of ketene acetal structure **24**. However, the isolated thermal product **26** is not directly derived from the ketene acetal **24**. It is not unreasonable to suggest that thermal transformation of the [2 + 4] adduct **24** into the [2 + 2] adduct **23** takes place, followed by intramolecular migration of the trimethylsilyl group to afford vinylsiloxane **26** (equation 7). The behavior of these stable oxasiletanes suggests that fragmentation to silanone and olefin is not a facile process. The formation of free silanones in reactions of this type has recently been questioned on the basis of calculations, which suggested that fragmentation of oxasiletane is too endothermic to occur at a significant rate under the pyrolytic conditions. Instead, Bachrach and Streitwieser proposed a bimolecular mechanism for the reactions[24].

Oxasiletene, the unsaturated analogue of oxasiletane, was first postulated by Seyferth and coworkers as a reactive intermediate in the reaction of 1,1-dimethyl-2,3-bis(trimethylsilyl)-1-silirene with dimethyl sulfoxide[25]. The photochemical generation of siladienone intermediate **28** from (pentamethyldisilanyl)diazomethyl 1-adamantyl ketone **27** led to an intramolecular [2 + 2] cyclization to yield the oxasiletene **29**, quantitatively (equation 8)[26]. Thermally, **29** is a very labile molecule. It is readily converted to **30** along with dimethylsilanone and the latter was trapped by using hexamethylcyclotrisiloxane as well as dimethyldimethoxysilane. More recently, we have studied the photochemical decomposition of a series of disilanyl diazomethyl ketones (**27**)[27,28]. We found that the products are highly dependent on the bulk of the substituents: oxasiletene (**29**) is formed when 1-adamantyl and *tert*-butyl groups are the substituents R, and head-to-tail cyclodimers **31** are formed when R is isopropyl or methyl. When R = Me, ketone **32** and bis(trimethyl) ketene are formed (equation 8).

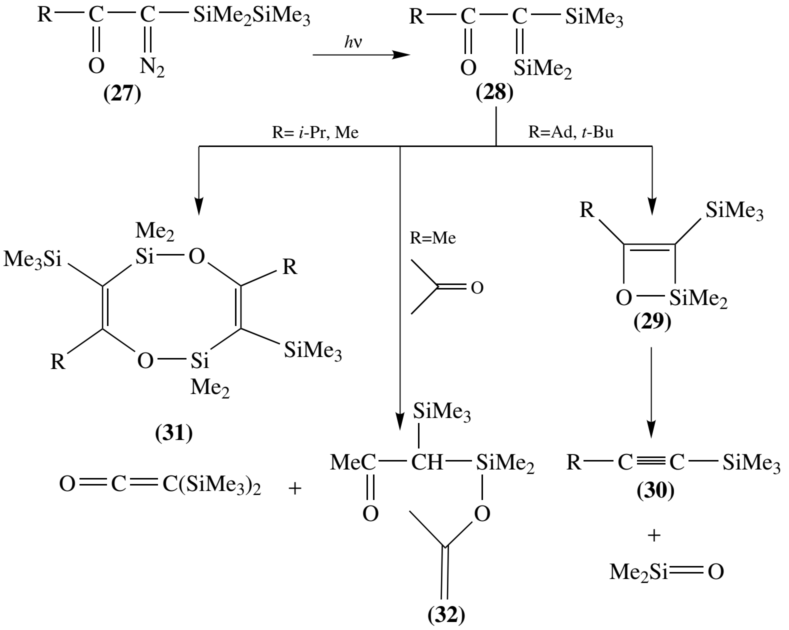

(8)

D. Spectroscopic Studies of Silenes

For comparative study, various silenes were isolated in 3-methylpentane matrix at 77 K by photolysis of the corresponding silyldiazo compounds and their ultraviolet spectra are measured. The results are summarized in Table 1. The introduction of trimethylsilyl group on carbon results in slight red shift compared with the parent silene ($H_2Si{=}CH_2$, 258 nm). As one might expect, considerable bathochromic shifts have been observed for conjugated silenes such as **6c, 6d** and **28**[29,30].

E. Decomposition of Bis(silyldiazomethyl)oligosilanes

Photolysis of **36a** with a high pressure mercury lamp in *tert*-butyl alcohol gave the adduct **37a** that incorporates two molecules of *tert*-butyl alcohol to give

TABLE 1. UV-absorption maxima of silenes

Silenes	λ_{max} (nm)	Precursor
$Me_2Si{=}CHMe$ **(33)**	255	Me_3SiCHN_2 **(8)**
$Me_2Si{=}CHSiMe_3$ **(17a)**	265	$Me_3SiMe_2SiCHN_2$ **(16a)**
$Me_2Si{=}C(Me)SiMe_3$ **(35)**	274	$(Me_3Si)_2CN_2$ **(34)**
$Me_2Si{=}C(SiMe_3)_2$ **(17b)**	278	$Me_3SiMe_2SiC(N_2)SiMe_3$ **(16b)**
$Me_2Si{=}C(Ph)CO_2Me$ **(6d)**	280	$PhMe_2SiC(N_2)CO_2Me$ **(1d)**
$Me_2Si{=}C(SiMe_3)COAd\text{-}1$ **(28)**	284	$Me_3SiMe_2SiC(N_2)COAd\text{-}1$ **(27)**
$Me_2Si{=}C(SiMe_3)CO_2Et$ **(6c)**	293	$Me_3SiMe_2SiC(N_2)CO_2Et$ **(1c)**

38a[31]. The photolysis of **36a** without a trapping reagent gave the interesting trisilabicyclo[1.1.1]pentane **40a** in low yields. Photolysis of **36b** in cyclohexane gave **40b** whose structure was confirmed by X-ray analysis (Figure 1a) and also **43b**, which is derived from the oxygenation of trisilabicyclo[2.1.0]pentane **39b** (equations 9 and 10). Photolysis of **36b** in cyclohexane-d_{12} revealed the existence of **39b**, which is easily polymerized at room temperature but was trapped by *tert*-butyl alcohol to give **44b**. On the other hand, pyrolyses of **36a** and **36b** gave only **40a** and **40b** as almost a sole volatile product. 1,5-Disilapentadiene **(37a,b)** is thought to be a common intermediate of both **39b** and **40a,b**. Although transient silene is known to dimerize in a head-to-tail fashion, **39b** was rationalized to be also derived from a head-to-head [2 + 2] cycloaddition of **37b**. In another alternative, the formation of **39b** implies the bicycloazo compound **(42b)** as an intermediate formed via an intramolecular [2 + 3] cycloaddition of the diazosilene **(41b)**. To corroborate this mechanism, a new bis(silyldiazomethyl)tetrasilane **(36c)** was employed in the photochemical reactions[32].

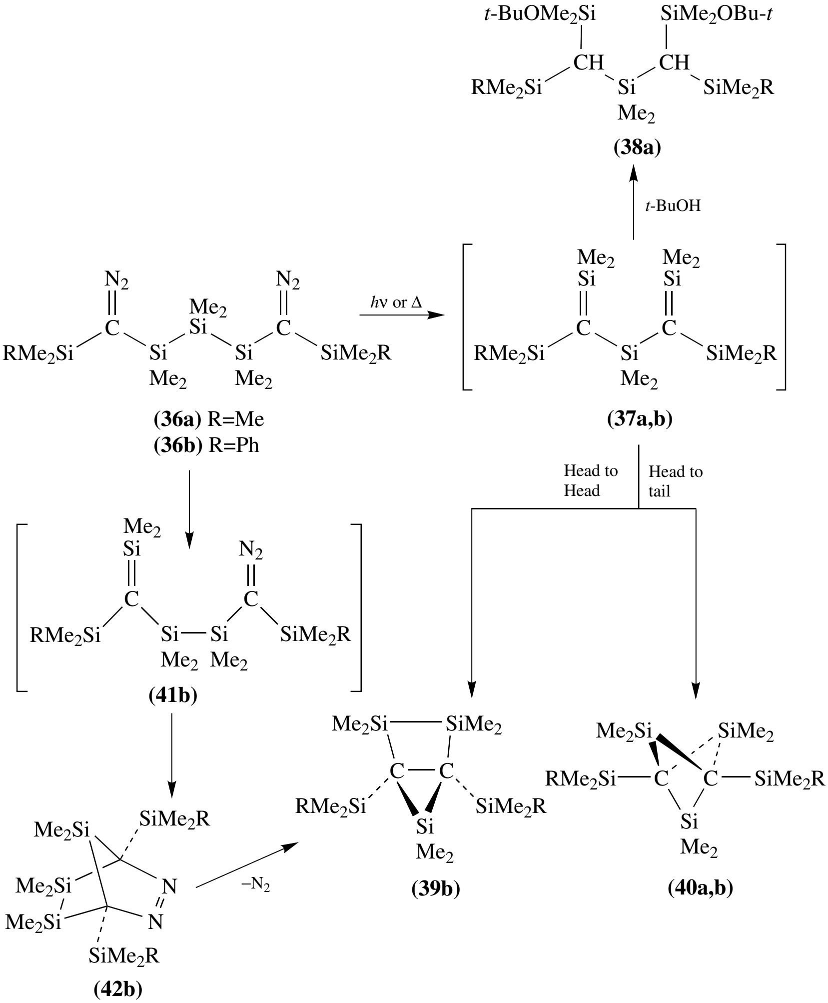

(9)

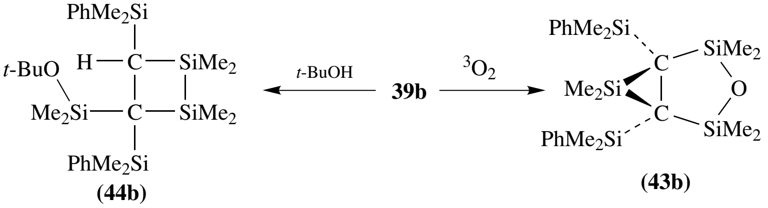

(10)

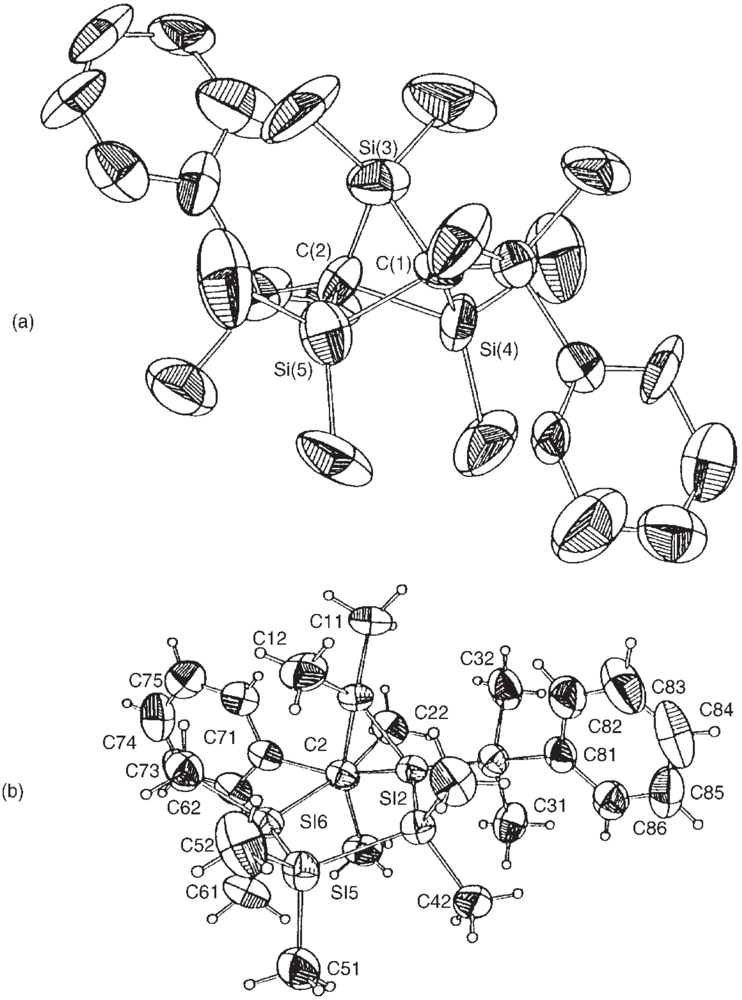

FIGURE 1. ORTEP drawings of (a) **40b** (reprinted with permission from Reference 31. Copyright 1991 American Chemical Society), and (b) **45** (reproduced by permission of Elsevier Science from Reference 32)

As long as the two silyldiazomethyl groups were linked with 1,1,2,2,3,3-hexamethyltrisilanylene unit (cf **36a,b**), the formation of product **39b** could be interpreted by both modes of reaction. However, if the number of dimethylsilanylene units was increased to four in **36c**, the two modes of reaction are expected to produce completely different ring frameworks. Actually, photolysis of **36c** under the same conditions and separation of the products by preparative TLC gave rise to tetrasilabicyclo[3.1.0]hexane **(45)** in 25% yield (equation 11)[32]. The three possible ring frameworks of tetrasilabicyclo[2.1.1]hexane **(40c)**, tetrasilabicyclo[2.2.0]hexane **(39c)** and tetrasilabicyclo[3.1.0]hexane **(45)** require, respectively, four (4 : 4 : 2 : 2), three (4 : 4 : 4) and eight (2 : 2 : 2 : 2 : 1 : 1 : 1 : 1) resonances of SiMe groups in the ^{1}H-NMR spectra, based on their molecular symmetry. Indeed, compound **45** showed eight resonances of SiMe groups in the ^{1}H-NMR spectrum with four resonances in the ^{29}Si-NMR spectrum in which the most upfield shift at -54.1 ppm is characteristic of the silirane ring silicon. An X-ray analysis confirmed the structure of **45** (Figure 1b). Interestingly, compound **45** can be regarded as one of the most stable siliranes bearing methyl substituents on the silicon atom. Thus compound **45** is derived by nitrogen extrusion from the bicyclic azo compound **(42c)** and there is no need to invoke head-to-head [2 + 2] cycloaddition of 1,2,3,4-tetrasila-1,5-hexadiene **(37c)** to give tetrasila[2.2.0]hexane **(39c)**, at least in the photochemical reaction (equation 11). Furthermore, flow pyrolysis of dilute solution of **36c** at 500 °C gave 9% of a compound **40c**, whose ^{1}H-NMR spectrum contains four resonances of SiMe group, which is consistent with tetrasila[2.1.1]hexane **(40c)**. There was no indication that tetrasila[2.2.0]hexane **(39c)** was present among the pyrolytic products.

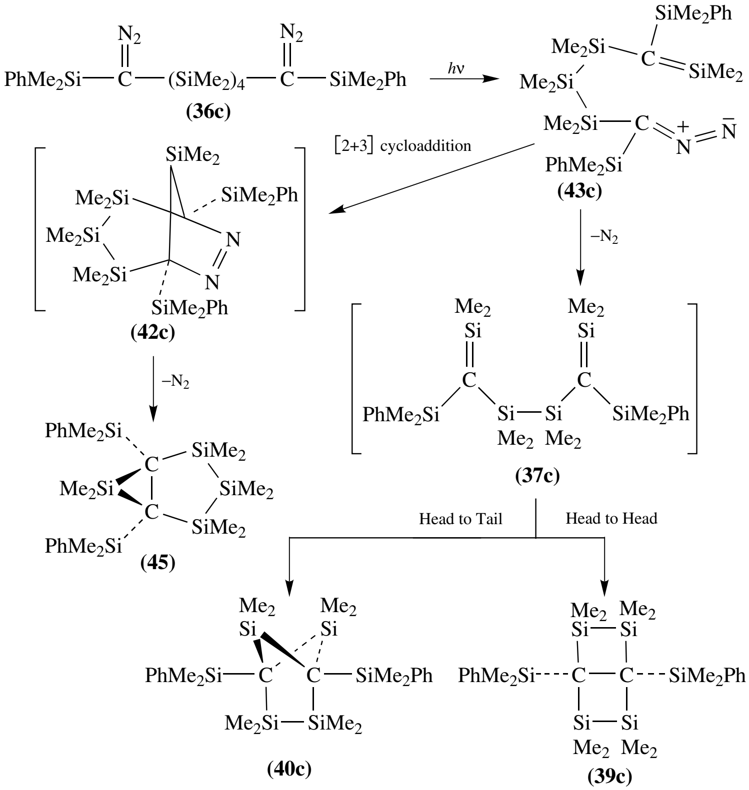

(11)

In conclusion, it is clear that the photochemical decomposition of bis(silyldiazomethyl) oligosilanes produces one silene moiety **(43c)** in the molecule, followed by a [2 + 3] silene–diazo cycloaddition, while thermal decomposition gives two silene moieties **(37c)** at the same molecule which undergo a [2+2] silene–silene cycloaddition in a head-to-tail (not head-to-head) fashion.

F. Silabenzene and 6-Silafulvenes

Both silabenzene **(46)** and 6-silafulvene **(47)** are attractive molecules in silicon chemistry. Thermally induced retro ene reactions to silabenzene and 6-silafulvene were explored by the groups of Barton and Sakurai[33–35]. One might expect that 2-silacyclohexadienylidene **(48)** or silacyclopentadienylcarbene **(49)** would give silabenzene **(46)** or 6-silafulvene **(47)** by a 1,2-migration of the substituent (equation 12). When a benzene solution of 1-diazo-2,2-dimethyl-3,4,5,6-tetraphenyl-2-silacyclohexane-3,5-diene **(50)** containing an excess of *tert*-butyl alcohol was refluxed in a sealed Pyrex tube at 100 °C, an adduct of *tert*-butyl alcohol **(51)** was formed in high yield (equation 13)[36]. The formation of **51** provides strong evidence for 6-silafulvene **(47a)** formed by migration of the dienyl group to the carbene center of **46a**. It seems reasonable that the dipolar form of the silafulvene would have enhanced importance due to the stability of the cyclopentadienyl anion. The evidence for the presence of silafulvene **(47a)** was further substantiated by a reaction with methanol and benzophenone to give adduct **52** which resembles **51**, and a Wittig type product **54**, (formed via **53**), respectively[37].

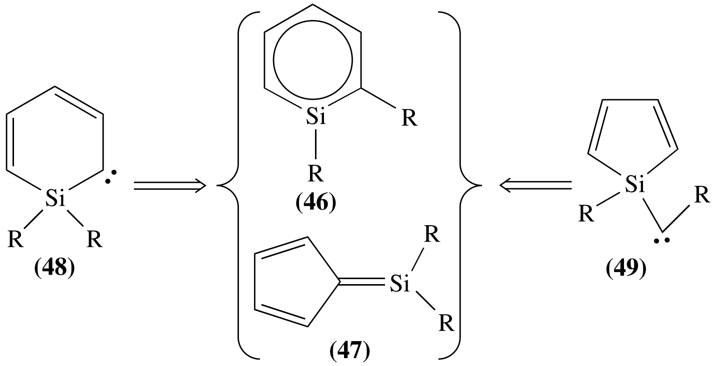

(12)

Photolysis of 1-methyl-2,3,4,5-tetraphenylsilacyclopentadienyldiazomethane **(55)** with an excess of methanol gave the diazirine **56** and the methanol adducts **59, 60** and **61** (equation 14)[38]. Products **59** and **60** appear to be derived from the methanolysis of silabenzene **(46b)**, which could arise by a ring expansion of silacyclopentadienylmethylcarbene **(49b)**. On the other hand, compound **61** is the evident product of methanolysis of 5-silafulvene **(57)** formed by a methyl shift in **49b**. Diazirine **56** was also found to produce silylcarbene under photochemical and thermal conditions and led to the same products **59,60** and **61**.

Further evidence for the generation of silabenzene **(46b)** and 5-silafulvene **(57)** as intermediates comes from their reaction with 2,3-dimethylbutadiene and benzophenone, which gave **58** and 1,1-diphenylpropene, respectively[37]. In an extension of this strategy Märkel and Schlosser succeeded later to stabilize silabenzene in solution at $-100\,^{\circ}\mathrm{C}$[39].

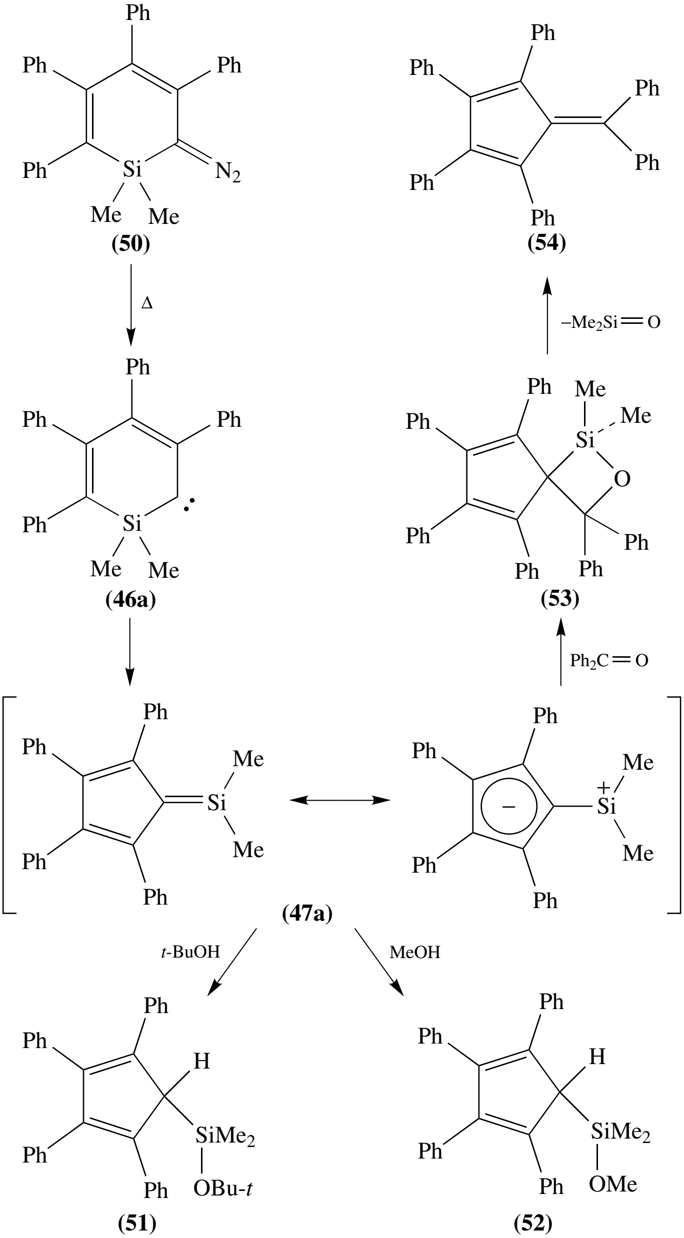

(13)

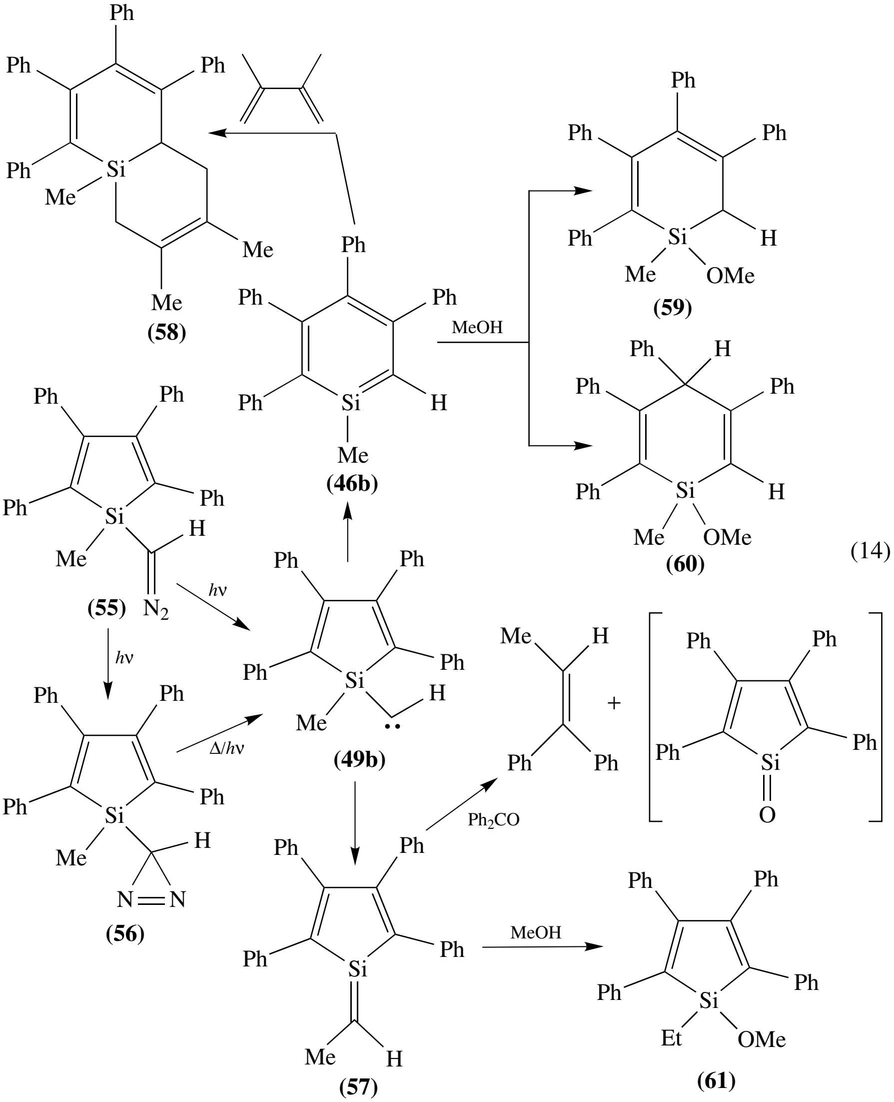

III. YLIDE AND SMALL-RING FORMATIONS BY SILYLENE REACTIONS WITH HETEROATOMS AND CUMULENES

A. Oxa(thia)siliranes and Sila(thio)carbonyl Ylides

Thermal generation of dimethylsilylene in the presence of carbonyl compounds leads to the addition of the silylene to the C=O bond with the formation of oxasilirane (e.g. **62** and **65**), followed by rearrangement[40]. Formation of tetraphenylethylene from benzophenone was attributed to carbenic fragmentation of the oxasilirane **(62)**, whereas aliphatic ketones afford enol ether product **66** derived from oxasilirane intermediates **(65)**. The formation of tetraphenylethylene by this mechanism is certainly not uniquely demanded by the data. Since the initial formation of ylide **63** leads to the same product (equation 15), oxasilirane **62** could thermally cleave the silicon–carbon bond to give 1,3-diradical followed by addition to benzene ring to give product **64**. Under milder conditions more direct evidence was found for the intermediacy of oxasiliranes. When 2-adamantanone **(67a)** and 7-norbornenone **(67b)** were allowed to react with photochemically generated dimethylsilylene, the major products could be formulated as dimers **(69)** and insertion products **(70)** of oxasiliranes **(68)** (equation 16)[41]. Indeed **68** could be trapped with ethanol to give **71**. Dimethylsilylene reacts with α-diketones to yield 1,3-dioxa-2-silacyclopentane-4-ene derivatives (**72** and **73**) (equation 17)[42].

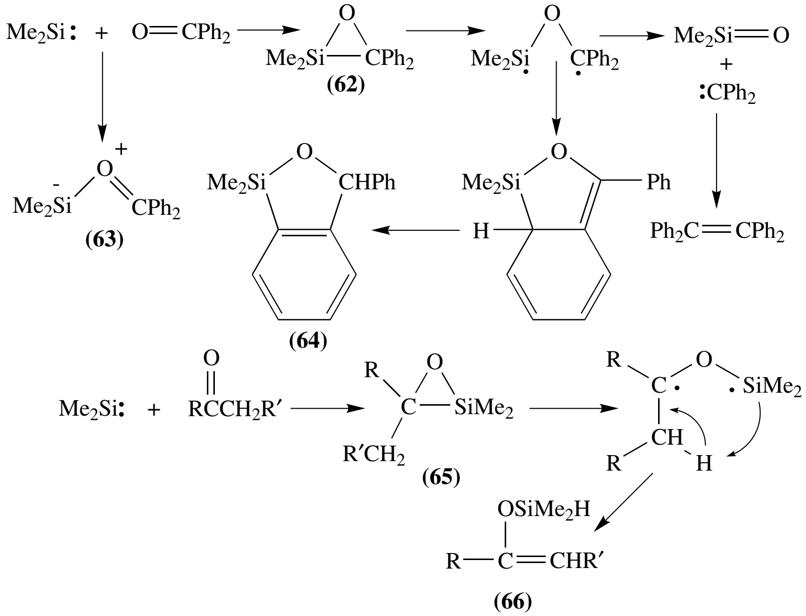

(15)

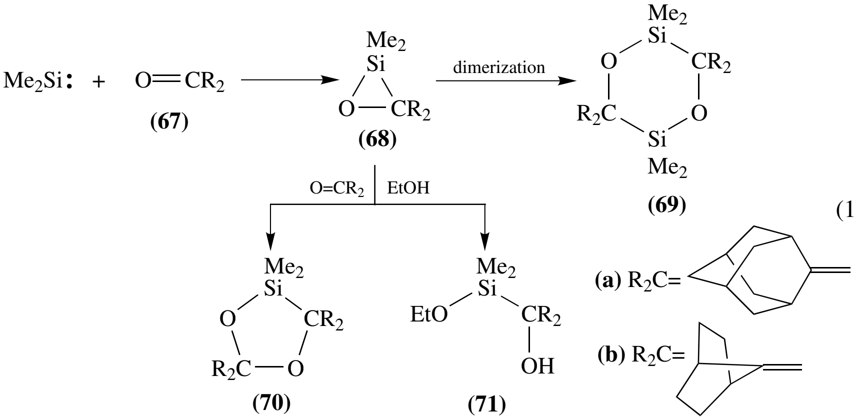

(16)

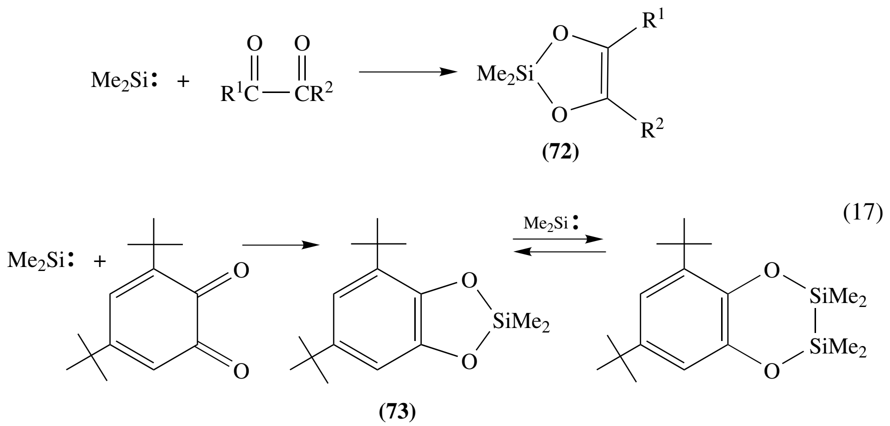

(17)

In 1980, Kumada and coworkers showed that when a bulky substituent, a mesityl group, was introduced onto the ring silicon atom of a silirene, atmospheric oxygen, moisture or alcohol surprisingly had no effect on the silirane at room temperature[43]. In the next year West and coworkers demonstrated that the dimesitylsilylene, isolated in matrix, dimerizes to a stable tetramesityldisilene at room temperature[44], while Masamune and coworkers reported that the employment of a bulky 2,6-dimethylphenyl group as substituents on silicon leads to the isolation of cyclotrisilane derivatives, the first of their kind[45]. From these studies, the simple concept of steric protection with bulky substituents provided significant progress in the small-ring chemistry of silicon. Guore and Barton[46], Tzeng and Weber[47] and Tortorelli and Jones[48] proposed the intermediacy of a sila-ylide in the reaction of dimethylsilylene with epoxides, which then produced silanone or rearranged. We observed that dimesitylsilylene generated by the photolysis of 2,2-dimesitylhexamethyltrisilane reacted with epoxides to give dimesitylsilanone-epoxide adducts **(74)** (equation 18)[49]. It seems that oxasilirane could be stabilized by the protection of a long silicon bond and by bulky substituents. Stable oxasilirane **(75a)** was isolated by the reaction of photochemically generated dimesitylsilylene with 1,1,3,3-tetramethyl-2-indanone **(76a)**[50]. The sulfur analogue, thiasilirane **(75b)**, was also isolated from the reaction of dimesitylsilylene with 1,1,3,3-tetramethyl-2-indanethione **(76b)**. Whereas adamantanone **(67a)** yielded with dimesitylsilylene 2 : 1 adduct **(70a)** instead of oxasilirane, adamantanethione **(67c)** gave a stable thiasilirane **(75c)** (equation 19)[51]. Oxasilirane **(75a)** and thiasiliranes (**75b** and **75c**) were inert to oxygen and moisture and their structures were finally confirmed by X-ray crystal analyses (Figure 2). Belzner and coworkers succeeded later in isolating oxasilirane in the reaction with diarylsilylene, which is generated by thermolysis of cyclotrisilanes with adamantanone **(67a)**[52].

Using matrix isolation techniques, we obtained the first spectroscopic evidence for the intermediacy of the hitherto unknown silacarbonyl and silathiocarbonyl ylides in a low temperature matrix[53]. Irradiation of the oxasilirane **(75a)** in an isopentane/3-methylpentane (Ip/3-Mp) matrix at 77 K with a low-pressure mercury lamp led to the appearance of a new band at 610 nm in the UV-vis spectrum and the matrix became interestingly blue in color. This absorption band was stable at 77 K on prolonged standing. However, it immediately disappeared on brief irradiation with a Xenon lamp (λ >460 nm) or when the matrix was allowed to melt. This colored species was independently generated by the reaction of dimesitylsilylene with 1,1,3,3-tetramethyl-2-indanone **(76a)**. Furthermore, irradiation of 2,2-dimesitylhexamethyltrisilane in the presence of **76a** in IP/3-MP at 77 K with a low-pressure mercury lamp produced a colored species with a λ_{max} at 573 nm due to dimesitylsilylene[53]. The absorption bands at 610 and 420 nm increased in intensity in the dark at almost the same rate as the decrease of the band at 573 nm, showing that dimesitylsilylene reacts with **76a** or dimerizes to tetramesitylsilene (420 nm) in the matrix at 77 K. Irradiation of the red solution of the 610 nm species, with a wavelength of light greater than 460 nm or melting the matrix, resulted in the production of the oxasilirane **(75a)**. On the basis of these results, it is quite reasonable to assume that the colored intermediate is the silacarbonyl ylide **(77a)**. Similar spectroscopic evidence was gathered for the formation of silathiocarbonyl ylide **(77b)** (485 nm) from **75b** and **76b** (equation 20).

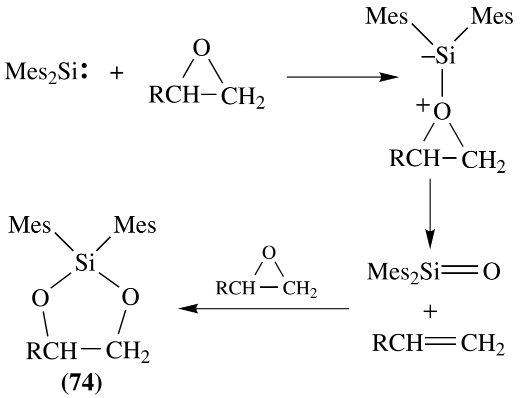

(18)

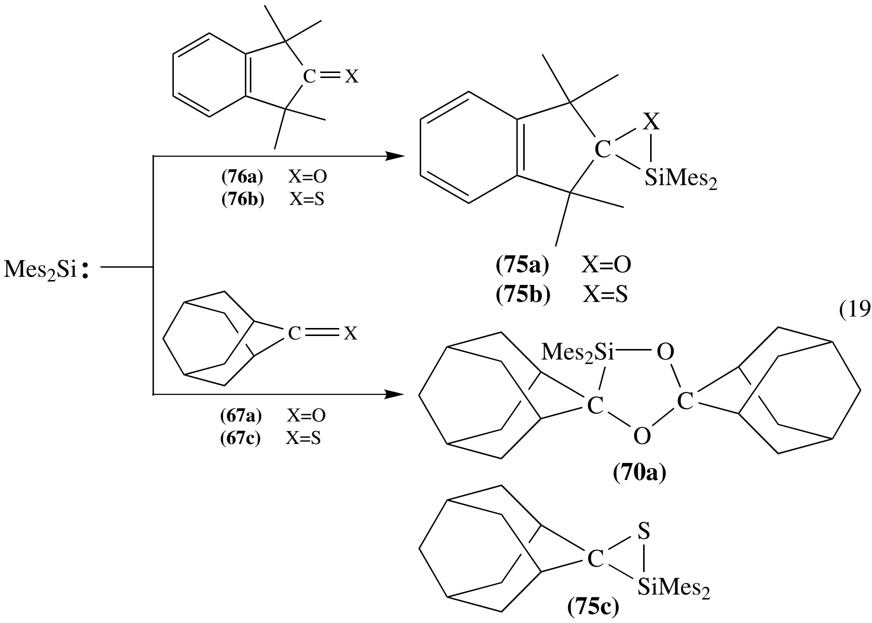

(19)

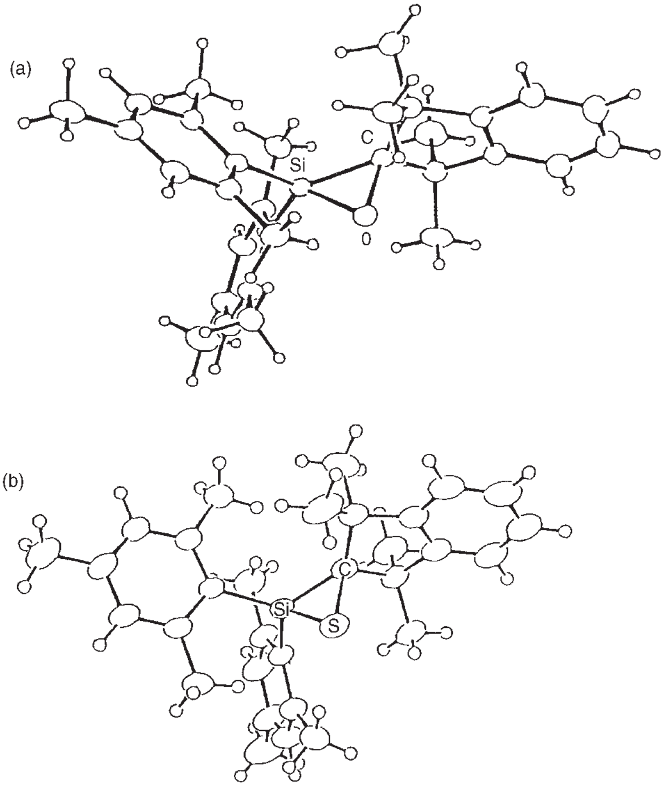

FIGURE 2. ORTEP drawings of (a) **75a** and (b) **75b** (reproduced by permission of Pergamon Press from References 50 and 51)

B. Siliranes and Alkylidenesiliranes

While the reactions of silylenes with olefins have been studied quite extensively, there have been few reports on the stereochemistry of silylene addition. The scarcity and ambiguity of the stereochemical information are due to the extreme instability of siliranes which are readily attacked by nucleophiles to give ring-opened products. Photolysis of 2,2-dimesityl or 2,2-bis(2,4,6-triisopropylphenyl)-1,1,1,3,3,3-hexamethyltrisilanes and a large excess of (*Z*)-2-butene in hexane at −5 °C was carried out by a low-pressure mercury lamp to give (*Z*)-silirane (**Z-78a** and **Z-78b**) as the major product and 1–7% of (*E*)-isomer (**E-78a** and **E-78b**) (equation 21)[54]. Siliranes **Z-78a,b** and **E-78a,b** are extremely stable and the structures of the (*Z*)-siliranes are easily distinguished by ^{1}H and ^{13}C NMR since **Z-78a** and **Z-78b** have nonequivalent aryl groups. The structure of products **Z-78b** was confirmed by X-ray crystal analysis (Figure 3a). Surprisingly, the photolysis of trisilanes in (*E*)-2-butene gave a considerable amount of the (*Z*)-isomer in addition to (*E*)-silirane. The most marked change occurred at −95 °C when the nonstereospecific adduct becomes the dominant product. In analogy with the reactivity of triplet carbene, triplet silylenes may add to the olefin to produce a diradical in which rotation around carbon–carbon single bond competes with spin inversion and ring closure. On the other hand, if rotation prevailed sufficiently over closure, one would expect that a stepwise addition of singlet silylene might occur.

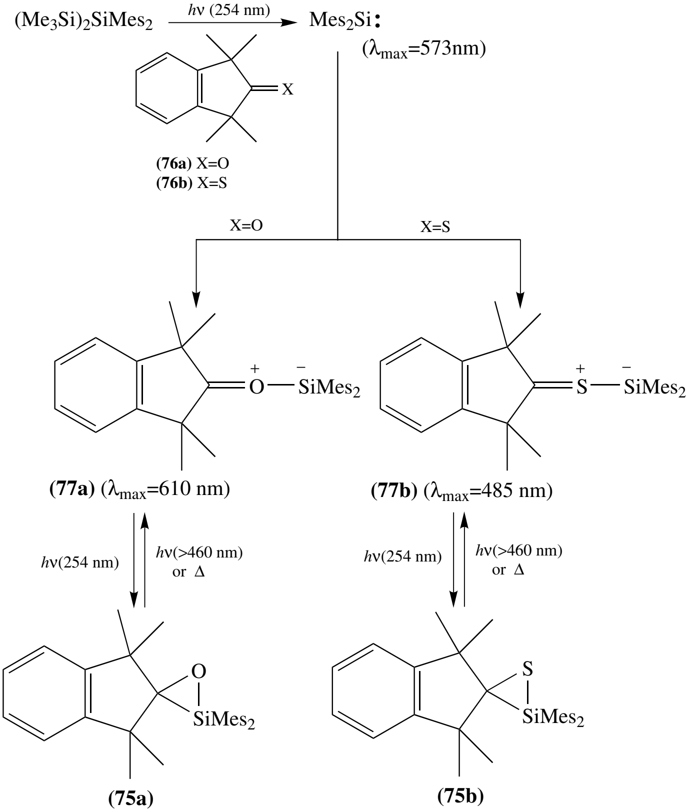

(20)

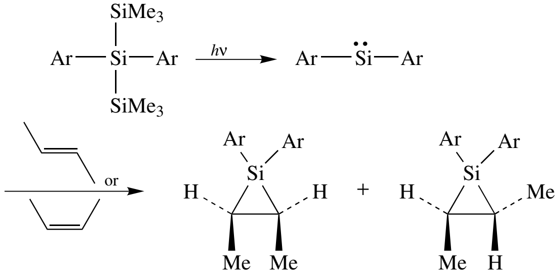

(Z-78) **(E-78)**

(21)

(a) Ar = Mes	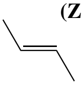	30%	70%
	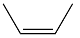	99	1
(b) Ar = 2,4,6-*i*-$Pr_3C_6H_2$	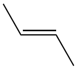	41	59
	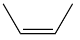	93	7

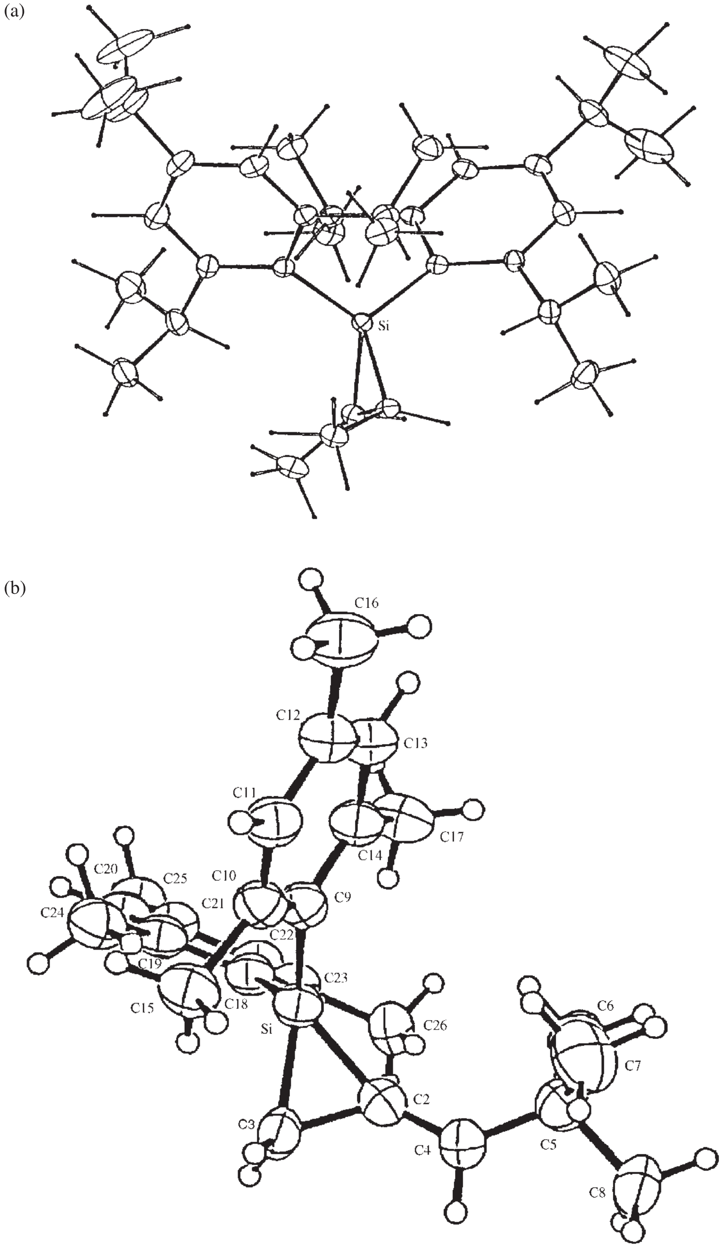

FIGURE 3. ORTEP drawings of (a) **Z-78b** (reprinted with permission from Reference 54. Copyright 1988. American Chemical Society), (b) **Z-79** (reproduced by permission of Pergamon Press from Reference 64) and (c) **91** (reprinted with permission from Reference 70. Copyright 1993 American Chemical Society)

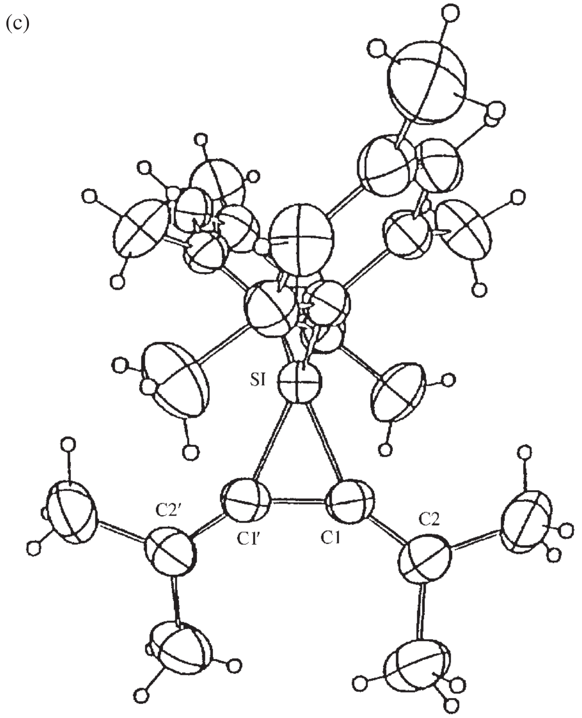

FIGURE 3. *(continued)*

In contrast, Conlin and coworkers reinvestigated our experiments and demonstrated that photogenerated dimesitylsilylene adds stereospecifically to other olefins with more than 98% retention[55,56]. They reinterpreted our nonstereospecific addition to (*E*)-2-butene on the basis that the (*E*)-2-butene used by us may have contained small amounts ($< 5\%$) of the (*Z*)-isomer. Because (*Z*)-2-butene is significantly more reactive than the (*E*)-isomer, (*E*)-2-butene containing 2.3% (*Z*)-isomer actually gave 40% (*Z*)- to 60% (*E*)-isomer of the silirane adduct. More recently, Boudjouk and coworkers[57], and Gaspar and coworkers[58] reported that stereospecific addition by bulky silylenes also took place.

Methylenecyclopropane is known to have an extra strain of 11 kcal mol^{-1} (theory)[59] and 13 kcal mol^{-1} (experiment) over cyclopropane[60]. Alkylidenesiliranes (**E/Z-79** and **80**) were prepared by photolysis of 2,2-dimesitylhexamethyltrisilane in the presence of *tert*-butyl allenes[61–64]. Whereas these alkylidenesiliranes were stable in air at temperatures below 80 °C for at least one day, under photochemical conditions they rapidly decomposed. The photolysis of (isolated) **81** gave (*E*/*Z*)-3-silyl-1,3-hexadienes **(82)** which can be understood in terms of the intermediacy of a silatrimethylenemethane **(83)** (equation 22). The structure of **Z-79** was verified by X-ray crystal analysis (Figure 3b). Seyferth and coworkers found that aldehydes, ketones and olefins reacted with hexamethylsilirane and silirene with a two-atom insertion into the SiC rings to give silacyclopentanes and silacyclopentene[65–67]. The (*E*/*Z*)-alkylidenesilirane (**E/Z-**

79) showed high reactivity toward benzaldehyde in solvents other than methanol (equation 23). These reactions were initiated by nucleophilic attack on silicon atom, followed by Si−C bond cleavage. The selectivity in the direction of bond cleavage might depend on the (*Z*) and (*E*) regiochemistry of **79** and the nature of the nucleophile. The Si−vinyl bond cleavage for the formation of **84** and **88** is quite surprising since opening of alkylidenecyclopropane and its hetero analogue were found to proceed with the cleavage of C−C or C−hetero bond which is not bonded to the sp^2 center. A Si−C(sp^3) bond cleavage of **E-79** with simultaneous π-bond migration seems to afford **87**. Reaction with methanol gave **85** and **86**. The reaction of **Z-79** with oxygen-transfer reagents gave attractive 1,2-oxasiletane products **89** and **90** (equation 24)[62]. The different synthetic routes for 1,2-oxasiletane were mentioned in Section II.C. It is especially noteworthy that the formation of 1,2-oxasiletanes is regiospecific depending on the oxidants. Both the 1,2-oxasiletane products were thermally stable but were found to undergo thermal [2 + 2] cycloreversion reactions to produce silanone and allene (equation 24). More recently, Boudjouk and coworkers succeeded in showing that the reaction of di-*tert*-butylsilirane with elemental sulfur results in the formation of a stable thiasiletane via a single-atom insertion reaction[68,69].

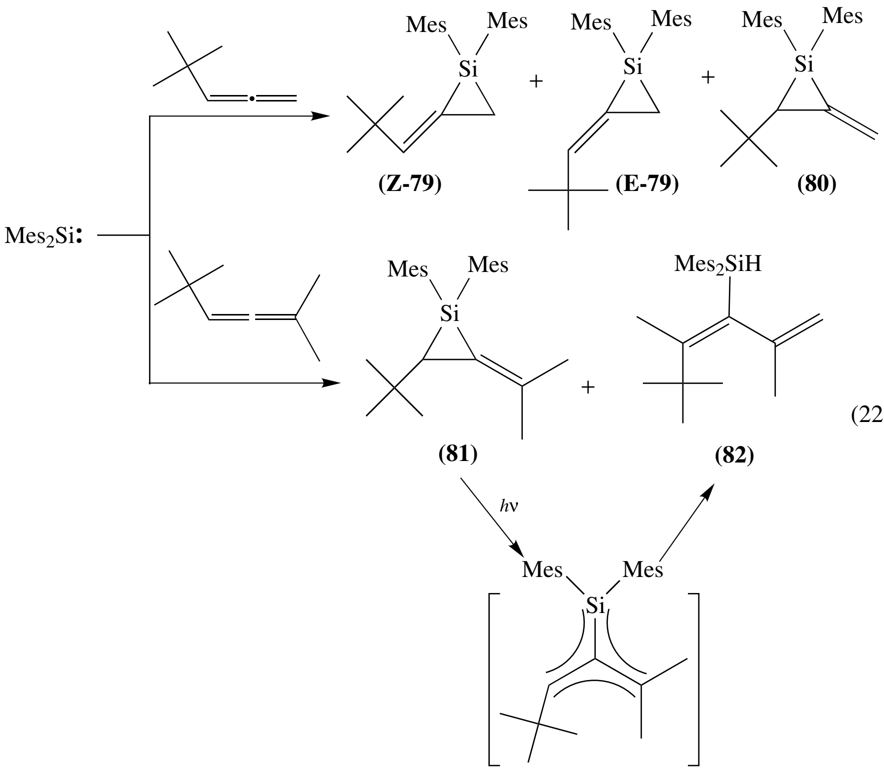

(Z-79) **(E-79)** **(80)**

(81) **(82)**

(22)

(83)

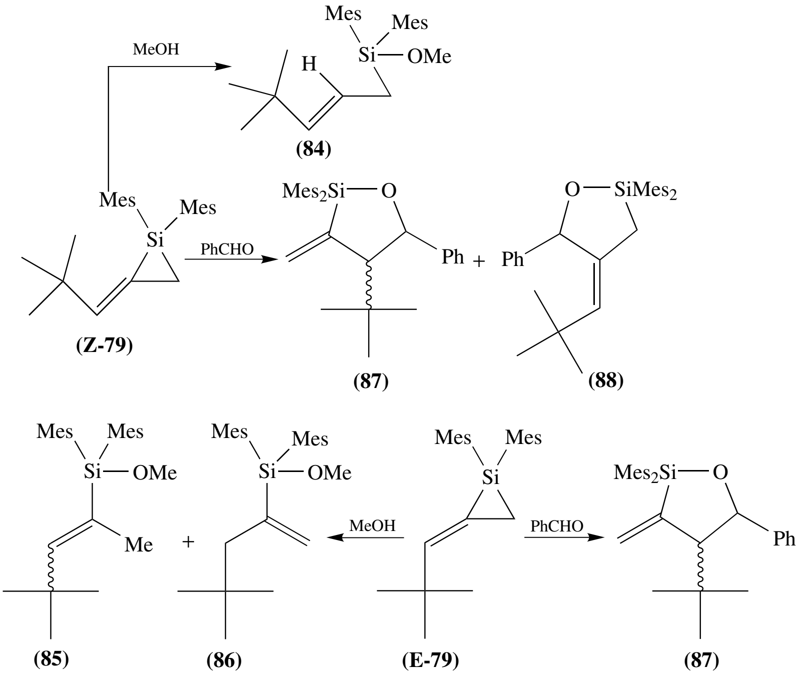

(23)

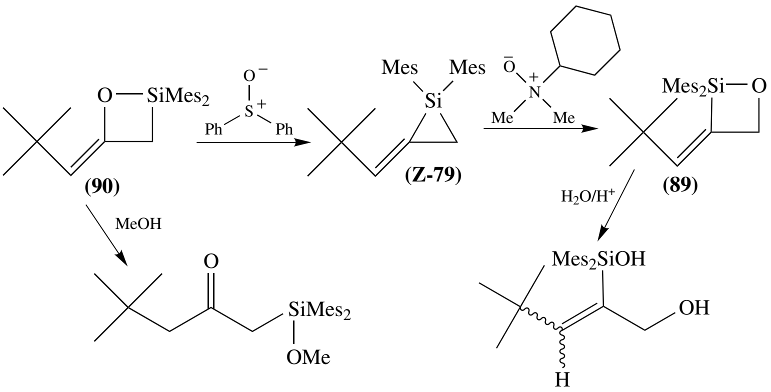

(24)

As a logical corollary, we have tried the reaction of dimesitylsilylene with 1,2,3-butatrienes, in the hope of an efficient route to the bisalkylidenesiliranes. In fact, the photolysis of 2,2-dimesitylhexamethyltrisilane and an excess of tetramethylbutatriene followed by methanolysis produced **94** together with trace amounts of **95** and **96** (equation 25)[70]. The structures **94** and **95** are consistent with the intermediacy of bisalkylidenesiliranes **91** and the allenic silirane **92**. Actually, in the absence of methanol, **91** can be isolated as a fairly stable compound, while low yields and hygroscopic instability precluded the isolation of **92**. In the photolysis of **91**, silatrimethylenemethane **(93)** is assumed to be initially formed. It then undergoes a 1,4-hydrogen shift to produce **96**.

The structure of **91**, a new bisalkylidenesilirane (sila[3]radialene) system, was confirmed by X-ray structure analysis (Figure 3c). Because of the high kinetic stability of **91** due to steric protection, aldehydes such as benzaldehyde as well as ketones did not react. However, [2 + 4] cycloaddition chemistry of **91** with 4-methyl-1,2,4-triazoline-3,5-dione resulted in the formation of a new ring-fused silirene **(97)** (equation 26).

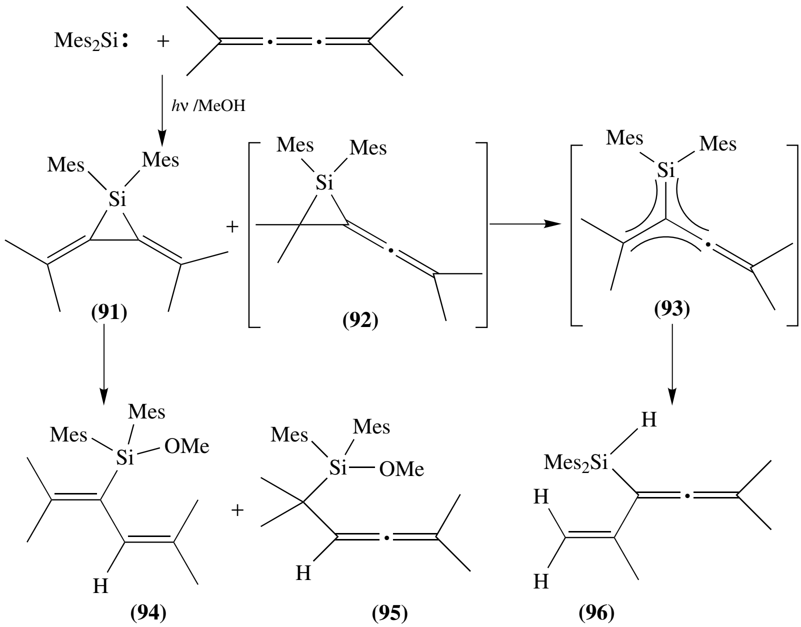

(25)

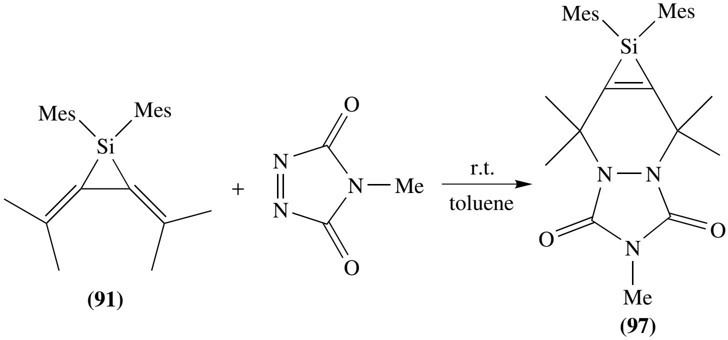

(26)

The reaction of methylenecyclopropanes with transition metal complexes is well known to promote a catalytic σ–π cycloaddition reaction with unsaturated compounds, in which a trimethylenemethane complex might exist[71–76]. Recently, much interest has been focused on the interaction of strained silicon–carbon bonds with transition metal complexes. In particular, the reaction of siliranes with acetylene in the presence of transition metal catalysts was extensively investigated by Seyferth's and Ishikawa's groups[77–79]. In the course of our studies on alkylidenesilirane, we found that palladium catalyzed reaction of **Z-79** and **E-79** with unsaturated compounds displayed ring expansion reaction modes that depend on the (*Z*) and (*E*) regiochemistry of **79** as well as the nature of the unsaturated compounds[63]. In the reactions of **79** with electron-deficient olefins such as alkyl acetylenedicarboxylate and methyl methacrylate, insertion into Si−C bonds to form **98, 99** and **102** as well as silole formation **(101)** but no cyclization to **100** took place (equation 27). When electron-rich olefins or diphenylacetylene were used as reagent, no adduct with **Z-79** was formed; instead **103** and **104** were formed via elimination and subsequent addition of *tert*-butylallene (equation 28). In these reactions, no evidence for the existence of silatrimethylenemethane complex was obtained. Nevertheless, the formation of a hydrosilane (**82** and **96**) in the photolysis of alkylidenesiliranes does suggest the intermediacy of silatrimethylenemethane. In order to clarify this situation we tried the stoichiometric reaction of alkylidenesiliranes (**79** and **91**) with $Fe_2(CO)_9$. Silatrimethylenemethane (**E/Z-105** and **106**) was found to be attached to metal ligands in a η^4 manner[80,81]. The structures were confirmed by X-ray analysis (Figure 4). The alkylidenesiliranes retain their structural integrity in the complexation. The silatrimethylenemethane ligand is bound in a η^4-fashion, pyramidalized and staggered to the three carbonyl ligands in an analogous manner to that observed in the structurally characterized trimethylenemethane and η^4-heterotrimethylenemethane complexes[82−84]. The bond distances C(1)−Si, C(1)−C(2) and C(1)−C(3) are 1.840(8), 1.42(1), and 1.46(1) Å, respectively, values which are between C−Si or C−C single and double bonds. Especially notable is that the C(1)−Si distance is somewhat longer than the values found in the other silene complexes[85−87]: $Cp^*RuHPCy_3(\eta^2\text{-}CH_2{=}SiMe_2)$, 1.78−1.79 Å; $Cp^*IrPMe_3(\eta^2\text{-}CH_2{=}SiPh_2)$, 1.810 Å; $Cp_2W(\eta^2\text{-}CH_2{=}SiMe_2)$, 1.800 Å. The cross-conjugative interaction with the C−C double bond may be responsible for the slightly longer values of the C(1)−Si bond. When $Ru_3(CO)_{12}$ was used as the metal carbonyl, ruthenium analogues of (**E/Z-108**) were obtained along with an unexpected trinuclear ruthenium cluster **(107)**, which demanded a unique metal bound CO-insertion into the silirane ring (equation 29)[81].

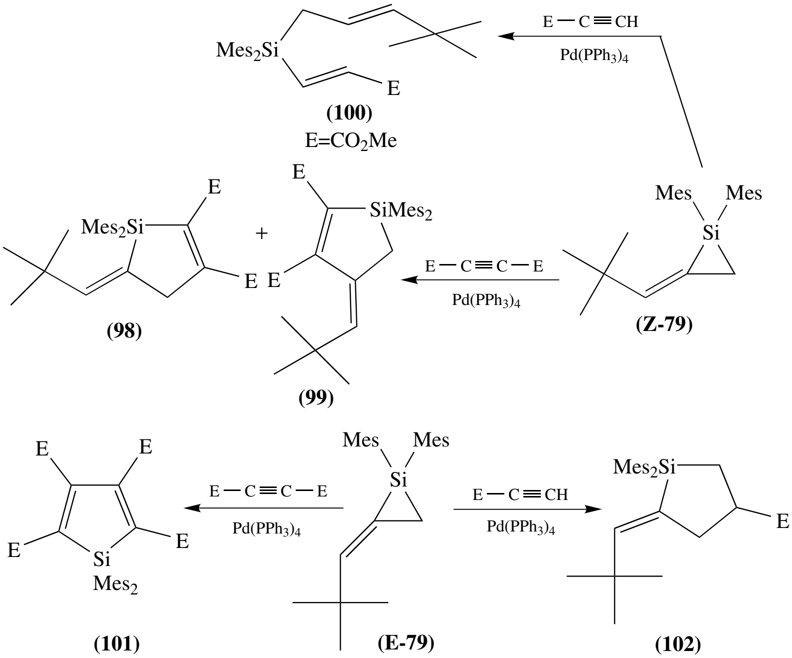

(27)

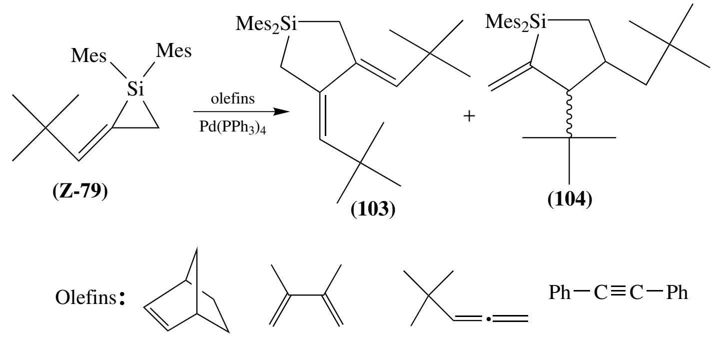

(Z-79) (103) (104)

(28)

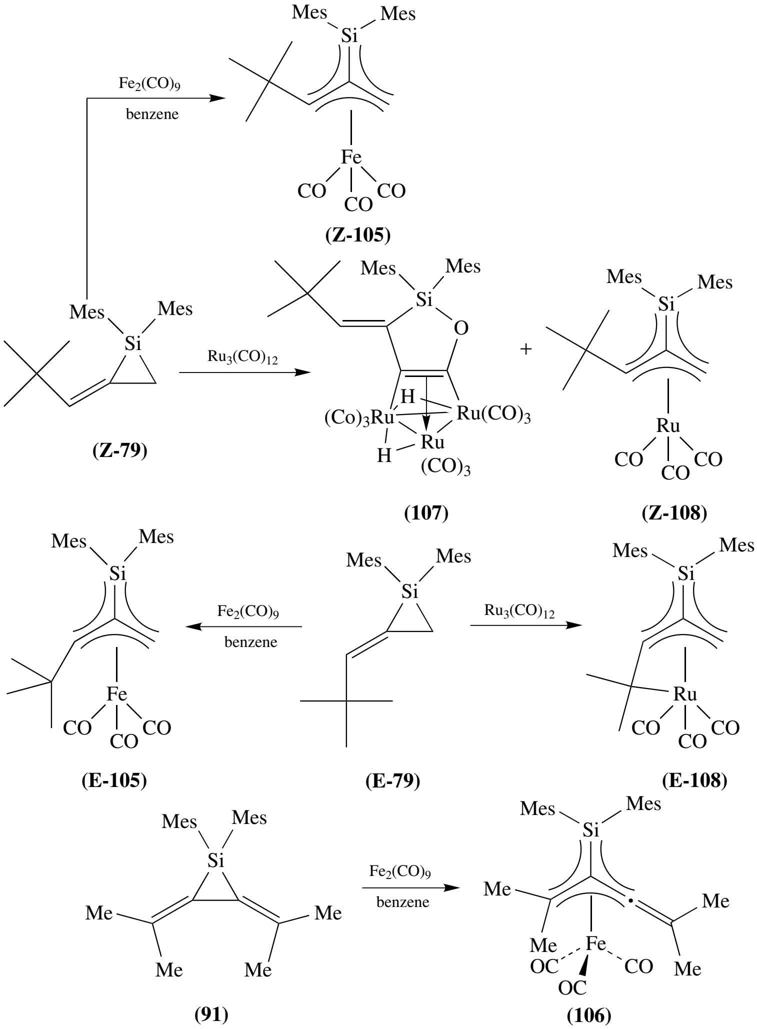

(Z-105)

(Z-79) (107) (Z-108)

(29)

(E-105) (E-79) (E-108)

(91) (106)

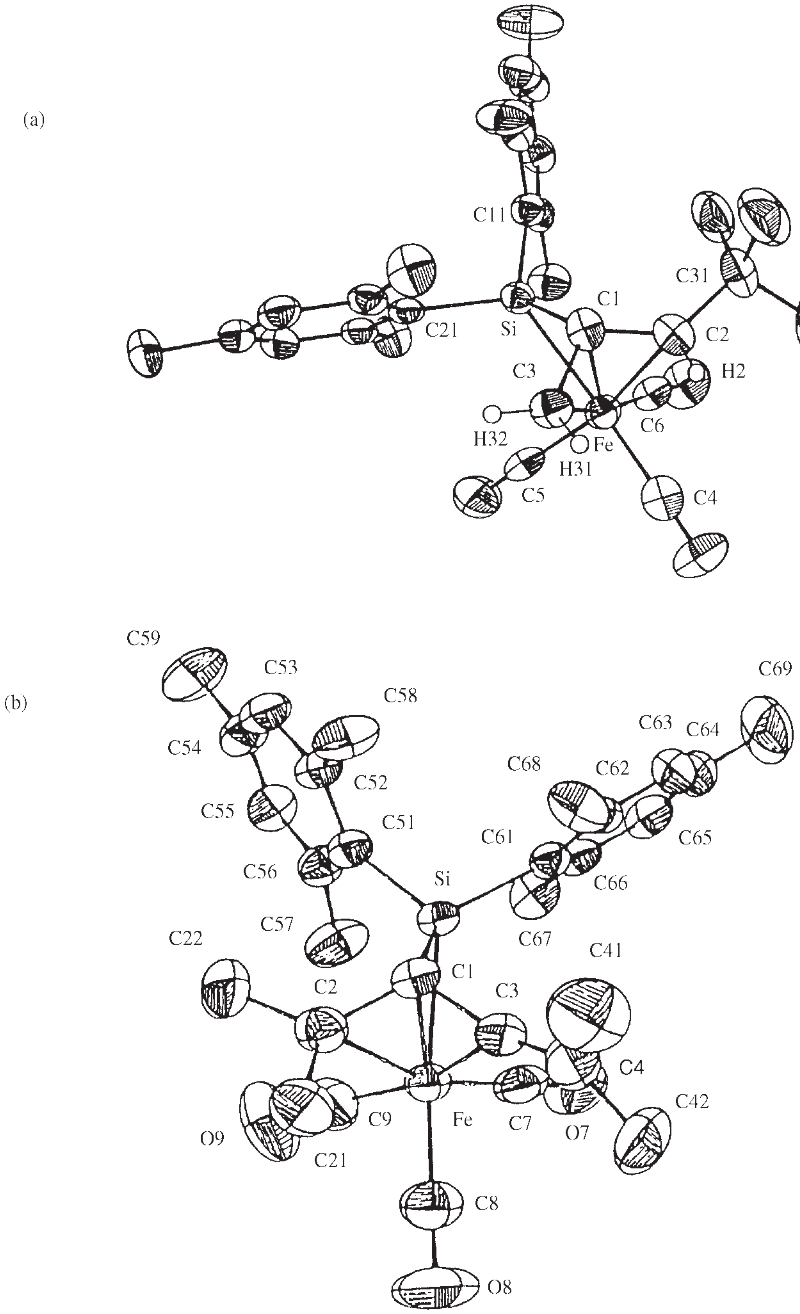

FIGURE 4. ORTEP drawings of (a) **Z-105** and (b) **106** (reprinted with permission from Reference 81. Copyright 1994 American Chemical Society)

IV. RING FORMATION BY WURTZ AND DIYNE COUPLING REACTIONS

A. Heptasila[7]paracyclophane

[*n*]Paracyclophanes have unique properties resulting from bending of the benzene ring. The smallest [*n*]paracyclophane so far isolated is the [6]isomer, first prepared by Jones and coworkers[88]. Recently Bickelhaupt, Tobe and coworkers succeeded in spectroscopic characterization of [5]paracyclophane[89], which is stable at low temperature in solution, but not isolable; more recently, a [4]paracyclophane system has been proposed as a reactive intermediate[90]. After many attempts, the Wurtz coupling of 1-chloro-6-*para*-chlorodimethylsilylphenyl-1,1,2,2,3,3,4,4,5,5,6,6-dodecamethylhexasilane **(109)** (prepared by equation 30) with sodium in refluxing toluene in the presence of [18]crown-6 produced heptasila[7]paracyclophane **(110)** in 1.6% yield, as colorless crystalline compound which is stable under atmospheric oxygen and moisture even when heated to its melting point (equation 31)[91].

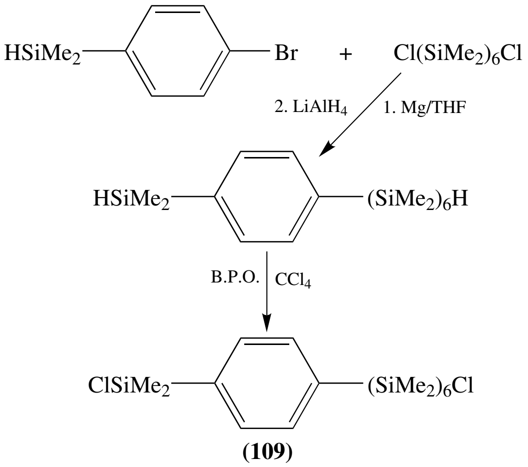

(30)

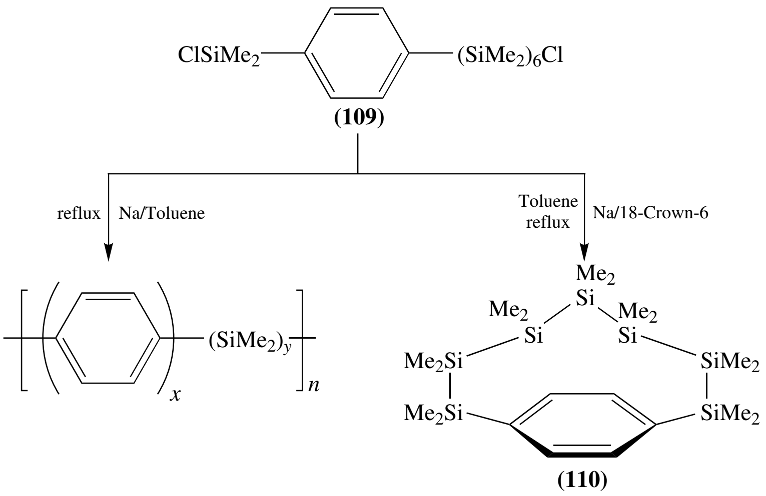

(31)

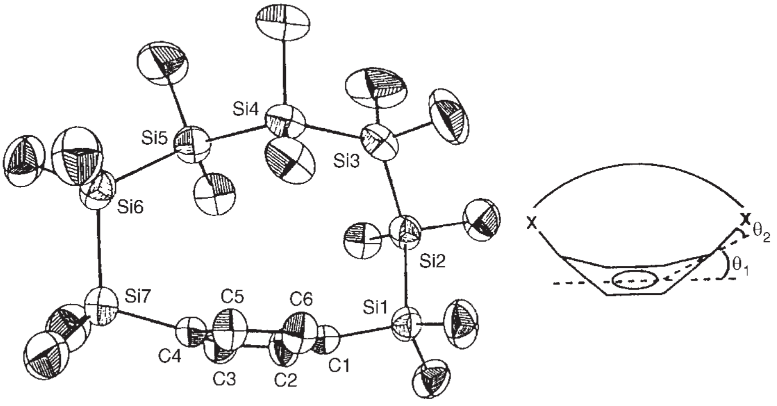

FIGURE 5. ORTEP drawing of **110** (reproduced by permission of VCH from Reference 91)

The presence of [18]crown-6 is essential for the formation of **110** and only polymeric substances were obtained in the absence of [18]crown-6 (equation 31). X-ray structural determination established unequivocally the molecular structure of **110** (Figure 5). Although the Si−Si bond lengths are normal and ranged between 2.338(5)–2.371(4) Å, there is an interesting alternation in the bond angles around the polysilane chain; the bond angles of C1−Si1−Si2 (105.5(3)°) and C4−Si7−Si6 (107.4(3)°) are contracted while those of Si1−Si2−Si3 (117.7(2)°), Si2−Si3−Si4 (126.5(2)°), Si3−Si4−Si5 (116.2(2)°), Si4−Si5−Si6 (115.6(2)°) and Si5−Si6−Si7 (113.7(2)°) are considerably expanded from the normal bond angles. The most interesting point in the structure of **110** is the deformation of the benzene ring from planarity, which is represented by the deviation angles θ_1 and θ_2. The deformation angles θ_1 of **110** are 6.6° and 4.5° and θ_2 are 6.5° and 9.0°, which are comparable with those observed for octamethyltetrasila[2,2]paracyclophane ($\theta_1 = 4.3°$, $\theta_2 = 15.0°$)[92] and its chromium complex ($\theta_1 = 2.5$, $2.2°$, $\theta_2 = 10.0$, $10.9°$)[93]. These θ values are smaller than those of [7]paracyclophane derivatives ($\theta_1 = 17°$, $\theta_2 = 23.5°$)[94] and those of [8]paracyclophane derivatives ($\theta_1 = 9°$, $\theta_2 = 15°$)[95]. These observations are best explained by the higher flexibility of the conformation in a polysilane chain compared with a methylene chain, involving an expansion of Si−Si−Si angles. Unfortunately, the low yield of **110** prevented further photochemical contraction to lower homologous [*n*]paracyclophanes (see Section V.B).

B. Bisalkylidenesiletanes

1,2-Dialkylidenecyclobutane possesses a large strain energy compared with cyclobutane (26.5 kcal mol^{-1})[96]. Tetramethyleneethane, or 2,2′-bis(allyl) diradical, has been postulated to be an intermediate in the thermal dimerization of allenes to form 1,2-dialkylidenecyclobutane. A small-ring system involving a silicon−silicon bond is interesting because of its expected high strain energy. Only a few examples concerning the formation of 1,2-disilacyclobutanes[97–100], 1,2-disilacyclobutenes[101–105], bisalkylidene-1,2-disilacyclobutane[106,107] and benzo-1,2-disilacyclobutene[108] have been reported.

Treatment of dilithiated tetramethylbutatriene with appropriate halosilane gave bissilanes that were chlorinated with $PdCl_2/CCl_4$. Wurtz coupling of the resulting bis(chlorosilane)s with sodium in toluene afforded the novel 3,4-dialkylidene-1,2-disilacyclobutanes **(111)**, as oxygen- and moisture-sensitive liquids (equation 32). While **111a** is readily polymerized and must be stored as a dilute solution in order to avoid polymerization **111b** is stable at room temperature for several months, even in the neat form[109,110].

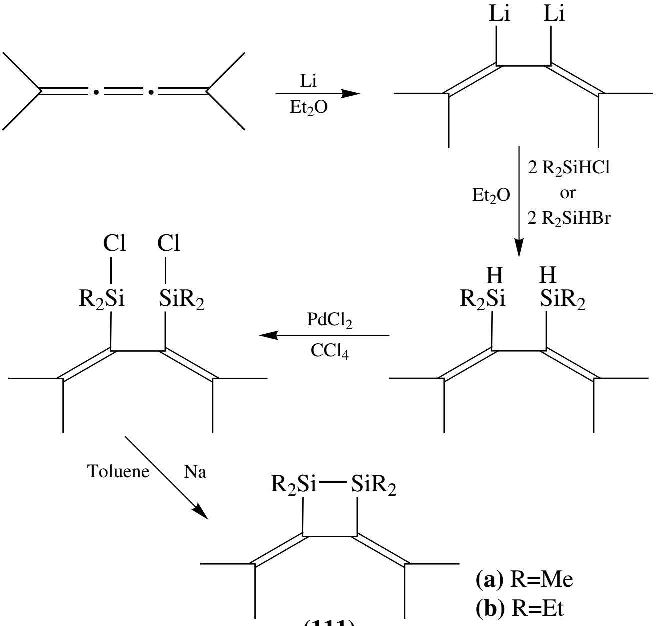

(111)

(32)

Transition metal catalyzed double silylation of C−C multiple bonds with disilanes is one of the most remarkable developments of organosilicon chemistry and numerous reports have dealt with this topic. Nevertheless, very little is known about the related disilane metathesis reaction in which, formally, a Si−Si bond is double silylated[111−117]. Diisopropylidenedisilacyclobutanes **111a** in the presence of a catalytic amount of Pd(PPh$_3$)$_4$ was cleanly converted into **112** in 93% yield (equation 33). When an equimolar mixture of **111a** and benzo derivatives **113** was treated with catalytic amounts of Pd(PPh$_3$)$_4$, the corresponding cross-metathesis products **115** were obtained, respectively, with high selectivity, in addition to minor amounts of homo-metathesis products **114**[110]. A favored formation of the cross metathesis product **116** was also observed in the conversion of a mixture of **113a** and **113b**, though with a lower degree of selectivity (equation 34). The structure of homo and cross metathesis products were confirmed by X-ray (Figure 6). Double silylation product **(117)** was obtained in the reaction of **111a** and excess alkynes in the presence of a catalytic amount of Pd(PPh$_3$)$_4$. In the case of diphenylacetylene, disilane metathesis and double silylation products were observed in the reaction, which showed moderate selectivity. The yield of **117** increased, if the ligands in catalyst were changed from the triphenylphosphines to benzonitrile ligands. The product distribution of disilane metathesis **(112)** and acetylene insertion **(117)** depends on the electrophilicity of the acetylenes, since in the case of dimethyl acetylenedicarboxylate mono-adduct **117** and a di-adduct **118** are obtained, and in the case of phenylacetylene only a mono-adduct **117** is obtained (equation 35).

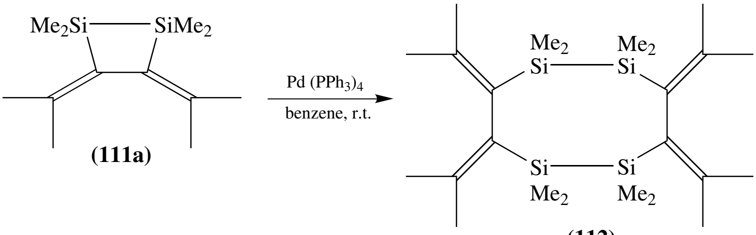

(111a) **(112)**

(33)

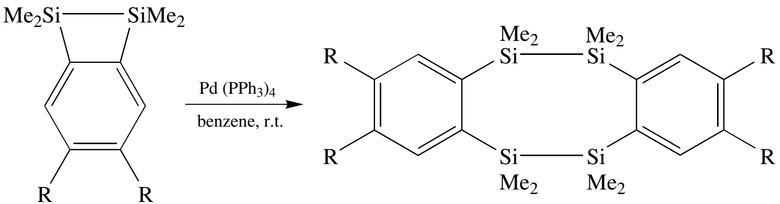

(113) **(114)**

(a) R = H
(b) R = Me

(34)

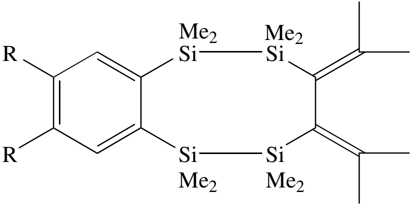

(115)

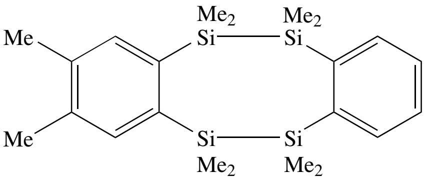

(116)

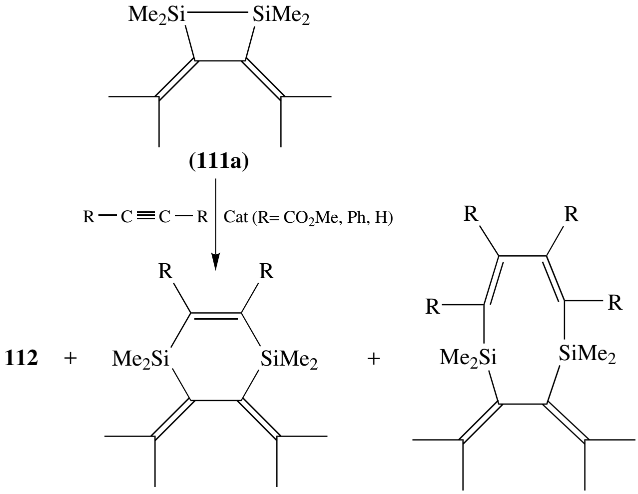

(117) **(118)**

(35)

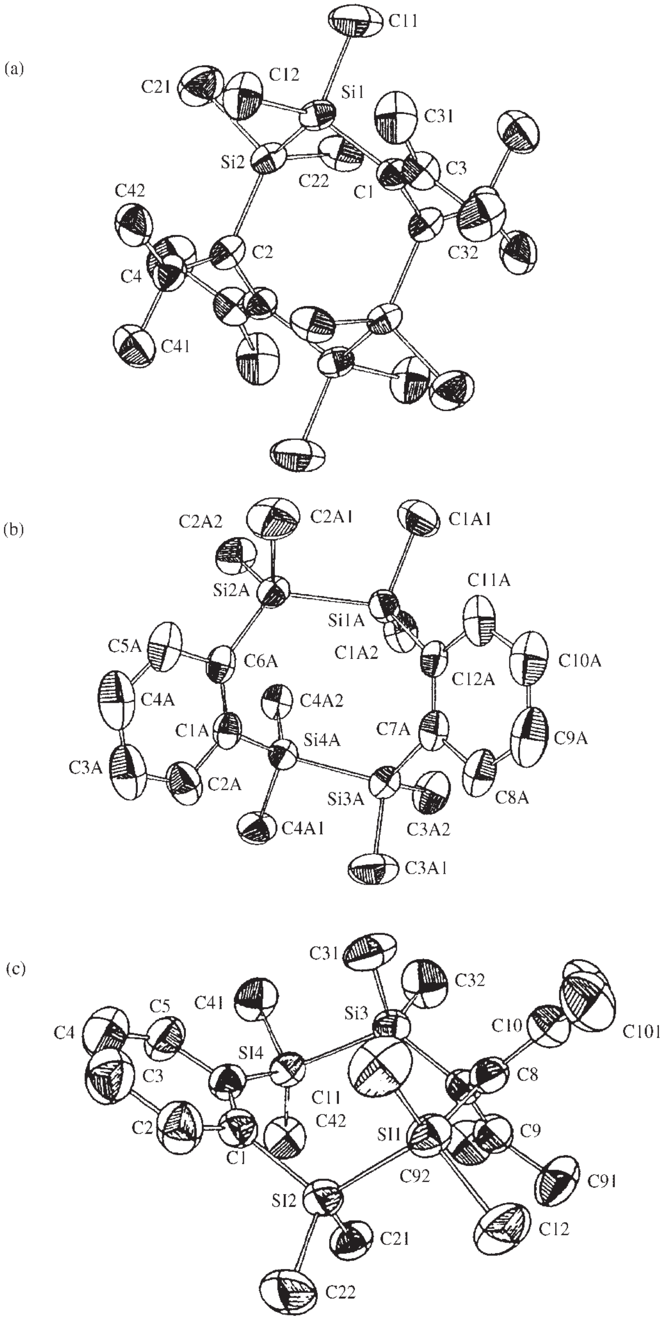

FIGURE 6. ORTEP drawings of (a) **112**, (b) **114a** and (c) **115a** (reprinted with permission from Reference 110. Copyright 1995 American Chemical Society)

2,3-Dimethyl-1,3-butadiene and benzaldehyde were unsuccessful in competing with a disilane metathesis reaction even if 5 equivalents of the unsaturated compound were employed in the presence of $Pd(PPh_3)_4$ catalyst at room temperature for 30 min, since only **112** was formed from **111a** in 74 and 80% yields, respectively. In contrast, $Pt(CH_2{=}CH_2)(PPh_3)_2$ catalyst (80 °C, 3 h) promoted a double silylation of **111a** to give **119** (41%), **120** (10%) and **121** (60%). Of special interest, 2,5-dimethyl-2,3,4-hexatriene moderately inhibited a disilane metathesis reaction to give **112** (15%) and 2,3,5,6-tetraisopropylidene-1,1,4,4-tetramethyl-1,4-disilacyclohexane **(122)** (68%) in the presence of $Pd(PPh_3)_4$. The latter was obtained as a 3 : 1 mixture of two conformational isomers, which do not interconvert at room temperature. *tert*-Butylallene also inhibited disilane metathesis to give 85% of **123** in the presence of $Pd(PPh_3)_4$. It is evident that the reaction involves a common intermediate with a double silylation reaction, i.e. bis(silyl)palladium(II) **(124)** (equation 36)[118,119]. Such an intermediate is followed by an insertion of unsaturated compounds. The selectivity of these pathways depends on the reactivity of the unsaturated compounds.

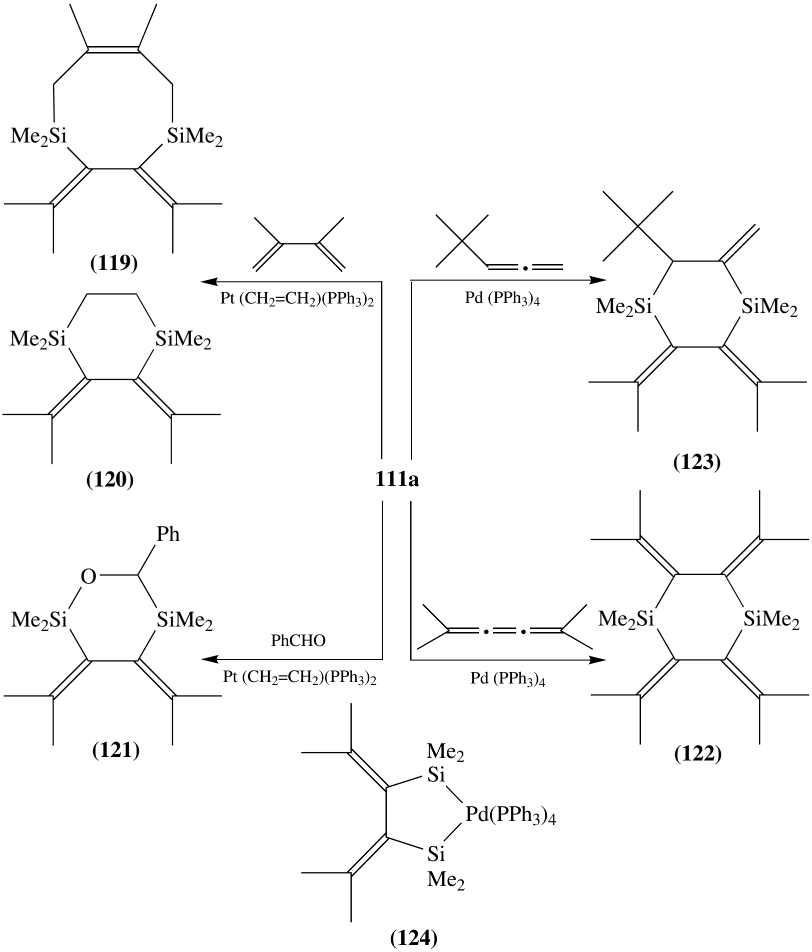

(36)

The group 4 metallocenes Cp_2M (M = Ti, Zr) induced bicyclization of terminally substituted α,ω-diyne is a powerful ring-forming method[120,121]. During the course of our study on bisalkylidene-1,2-disilacyclobutane, we have succeeded in the zirconocene-mediated synthesis of 1,2-disilacyclobutanes from 1,2-bis(ethoxyethynyl)disilane. Summarizing our attempts, we described a zirconocene-mediated small-ring formation which is dependent on the terminal substituents of the diyne. The small silacycles obtained in this route undergo unique spontaneous ring-opening polymerization (ROP).

Generation of a zirconocene transfer reagent $[Cp_2Zr(Bu\text{-}n)_2]$ (by addition of 2 equivalents of n-BuLi to Cp_2ZrCl_2 at −78 °C; Negishi's method) in the presence of 1,2-bis(1-propynyl)disilane **(125a)** resulted in the quantitative formation of a black air-sensitive polymer **126** (equation 37). Spectroscopic data of polymer **126** closely correspond to those for the model complex 2,5-bis(pentamethyldisilanyl)-3,4-dimethyl zirconacyclopentadiene **(127)**. Hydrolysis of **126** with CF_3CO_2H gave colorless polymer of high molecular weight (MW = 5780, MW/Mn = 1.8). These results are consistent with a regiospecific intermolecular coupling to afford 2,5-zirconacyclopentadiene rings in the polymer-backbone (equation 37). Once the polymer **126** was heated in THF, depolymerization followed by 1,2-migration of a silyl group took place to give a zirconabicyclo-containing 1,2-disilacyclopentene **(128a)** in moderate yield. A similar depolymerization has been applied recently to synthesize macrocyclic-containing zirconacyclopentadienes[122,123], while the same 1,2-silyl migration finds a recent precedent in the intramolecular zirconocene coupling of bis(phenylethynyl)dimethylmonosilane[124]. For trimethylsilyl and

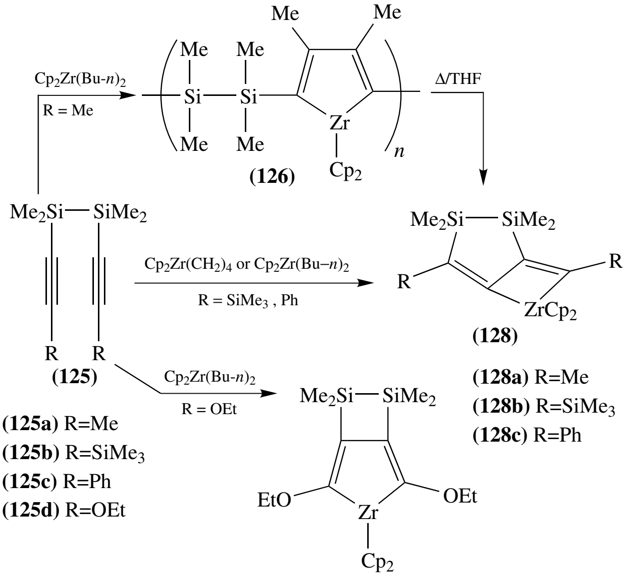

(37)

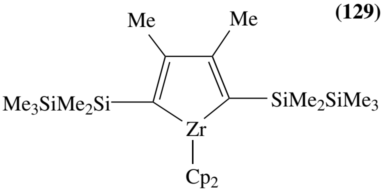

(127)

phenyl-substituted bisalkynyldisilane **(125b,c)**, the reaction with $Cp_2Zr(CH_2)_4$ at 40 °C and with $Cp_2Zr(Bu\text{-}n)_2$ at room temperature underwent direct intramolecular coupling to give 1,2-disilacyclopentene **(128b,c)** quantitatively (equation 37). When ethoxy groups which are strongly ligating to zirconium metal were employed as terminal substituents, the 1,2-migration was completely inhibited and the zirconabicycle **129**, which has a symmetrical 1,2-tetramethyldisilacyclobutane framework according to ^{1}H, ^{13}C and ^{29}Si NMR spectra, was obtained[125].

Further structural proof for **129** was demonstrated by the chemical derivatization illustrated in equation 38. First, hydrolysis of **129** with AcOH gave 3,4-bisalkylidene-1,2-disilacyclobutane **130** as an air-sensitive colorless oil in 78% yield. It is noteworthy that **130** showed a strong tendency to undergo a spontaneous ROP reaction and removal of the solvent is sufficient to initiate polymerization and to get a high molecular weight polymer (**131**; $Mw = 1.8 \times 10^5$, $Mw/Mn = 2.1$). The relatively narrow line widths observed in both ^{1}H and ^{13}C NMR spectra of **131** strongly suggest that the polymer backbone of this material has a regular structure. As compound **130** also possesses 1,4-diethoxydiene moiety, Diels–Alder additions to activated dienophiles of **130** proceeded smoothly at room

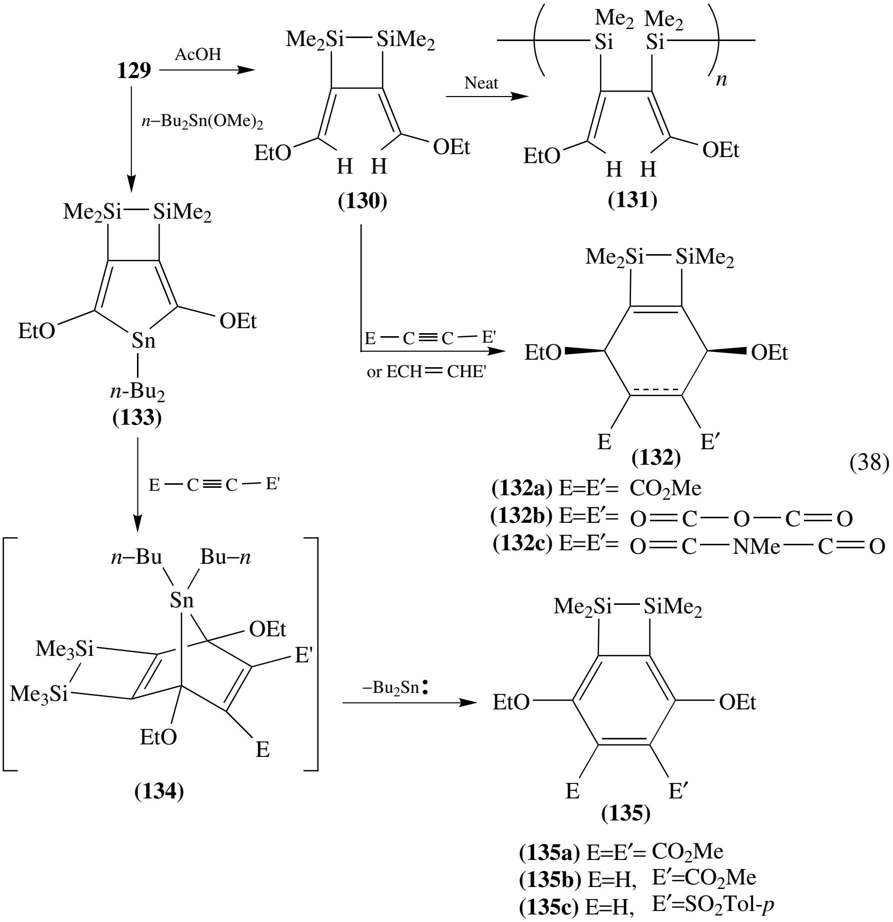

temperature to give adducts **132a, 132b** and **132c** in 32, 57 and 56% yields, respectively. Second, the conversion of readily prepared zirconacyclopentadienes into the corresponding main-group heterocycles by the Fagan–Nugent method has been shown to be extremely versatile[126]. Among various types of main-group electrophiles, treatment of **129** with one equivalent of dibutyltin dimethoxide[127] afforded quantitatively the expected stannole **(133)** based on ^{1}H and ^{13}C NMR spectra. Without isolation, stannole **133** was brought into contact with activated dienophiles. A Diels–Alder reaction readily occurred in moderate yields at room temperature due to activation by the strongly electron-donating ethoxy groups. Although the intermediate, 7-stannanorbornadiene adducts **(134)** could not be detected[128,129], the products obtained were 3,4-benzo-1,2-tetramethyldisilacyclobutanes **(135a-c)**, which can be regarded as the dibutyl stannylene extrusion product from the intermediates **(134)**. Compound **135a** was characterized by X-ray diffraction (Figure 7). This is important since the first 3,4-benzo-tetramethyldisilacyclobutane was synthesized in 1986[108], and so far no structural details could be obtained because of its polymerizability by a ROP reaction. The four-membered Si_2C_2 ring of compound **135a** is almost planar. The Si(1)–Si(2)–C(2) and Si(2)–Si(1)–C(1) angles have fairly acute values, such as 75.5° and 75.6°. Very similar values are observed for isolated 3,4-bisalkylidene-1,2-tetraphenyldisilacyclobutane (75.6° and 74.5°)[106] and 1,2-tetraaryldisilacyclobutene (75.4° and 74.7°)[104,105], respectively. Thus, the angle strain is responsible for the polymerizability of 1,2-tetramethyldisilacyclobutanes. Further inspection reveals that the conformational mobility of the two *ortho*-ethoxy groups of **135** could inhibit a new bond formation at the four-membered Si_2C_2 ring in a lateral direction. Actually **135a–c** were inert toward ROP reaction even at 180 °C. However, vertical insertion into the Si–Si bond could be accommodated, and indeed **135a-c** were still sensitive toward air oxidation.

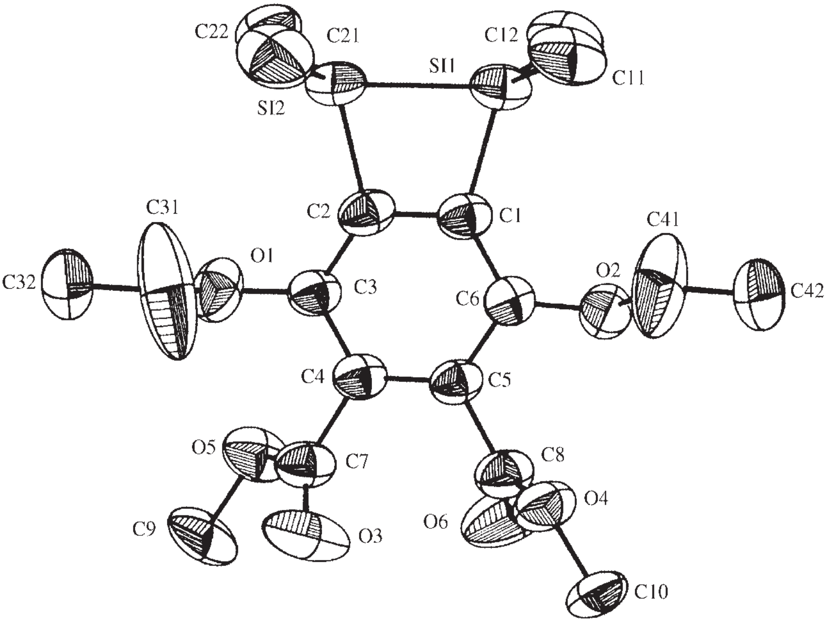

FIGURE 7. ORTEP drawing of **135a**

V. RING FORMATION BY KIPPING AND GILMAN REACTIONS

A. *trans*-Trisilacycloheptene and [3.1.1]Trisilapropellane

The first target molecules in these studies were considered to be the medium-ring *trans*-silacycloalkenes, which are a subject of considerable interest. *trans*-Cyclooctene is well known as the smallest *trans*-cycloalkene that is stable at room temperature. *trans*-Cycloheptene has been generated at room temperature and its existence was confirmed by chemical trapping with isobenzofuran or acidic methanol and also by ^{1}H NMR spectroscopy[130–133]. Even *trans*-cyclohexane has been generated[134]. However, isolation of *trans*-cycloheptenes has been unsuccessful, except for homoadamant-3-ene which is stabilized by a bulky substituent[135], because of the low thermal stability caused by the strained structure. *Cis*-1,2-diphenyl-4,4,5,5,6,6-hexamethyl-4,5,6-trisilacycloheptene (*cis*-**136**) was prepared by the reaction of 2,3-diphenyl-1,3-butadiene with $Cl(SiMe_2)_3Cl$ in the presence of Mg in 23% yield (equation 39). When the benzene-d_6 solution of *cis*-**136** was irradiated with a low-pressure mercury lamp through a quartz NMR tube, ^{1}H NMR measurements showed that the resonance for *cis*-**136** decreased in intensity and new resonances (three singlets at −0.29, 0.37 and 0.39 ppm and an AB quartet at 1.76 and 3.22 ppm, $J = 14.0$ Hz) had appeared. After purification and crystallization this new compound, *trans*-**136**, was obtained in 13% yield[136]. The molecular structure of *trans*-**136** was determined by X-ray crystal diffraction (Figure 8). The most interesting structural feature is the twisting around the C=C double bond. The torsion angle was found to be 32.7°. Photoisomerization reaction of *trans*-**136** gave *cis*-**136**. In this isomerization, a photoequilibrium exists and the photostationary *trans/cis* ratio is 0.99. This value is higher than that obtained in the photosensitized isomerization of *trans*-cycloheptene.

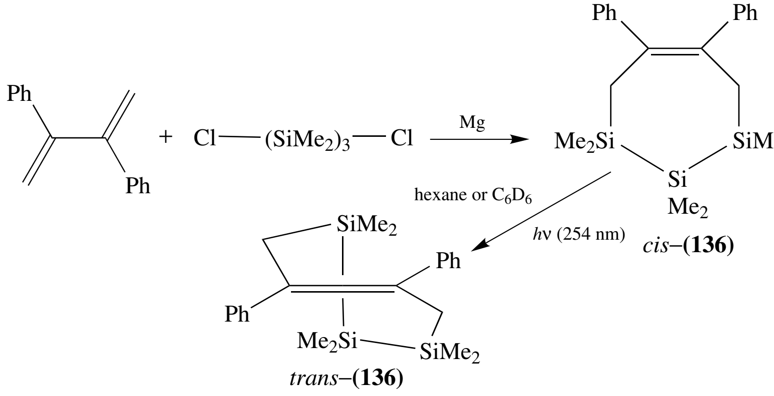

(39)

The next target molecule was a small-ring propellane such as [*n*.1.1]propellane, which have been of considerable interest because of the extremely high reactivity attributed to 'inverted tetrahedral' geometry at the bridgehead carbons[137,138]. The first [3.1.1]trisilapropellane **(138)** was prepared in 23% yield by the treatment of dilithium compound **137** with $Cl(SiMe_2)_3Cl$[139,140]. The air-sensitive compound **138** was also labile to acidic contamination such as silica gel in chromatography or HCl present in $CHCl_3$ and quantitatively rearranged to **140**. It is likely that the intermediate leading to **140** is the cation **139**, which is doubly stabilized by cyclopropyl and silyl substitution (equation 40). Cation **139** is probably attacked by chloride ion with concomitant rearrangement to the homoallyl skeleton of **140**. The ease of this reaction seems to be responsible for the liability of **138** toward acids.

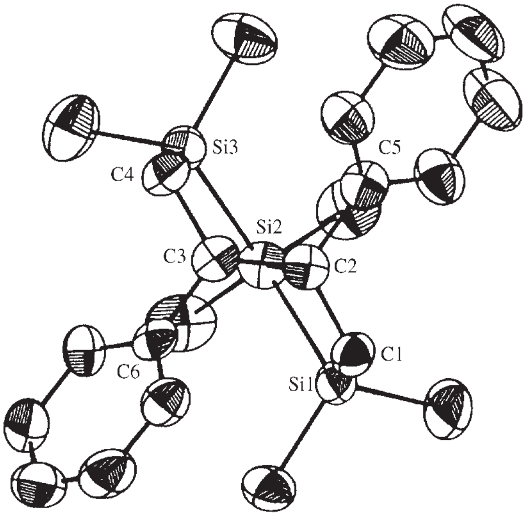

FIGURE 8. ORTEP drawing of *trans*-**136** (reprinted with permission from Reference 136. Copyright 1991 American Chemical Society)

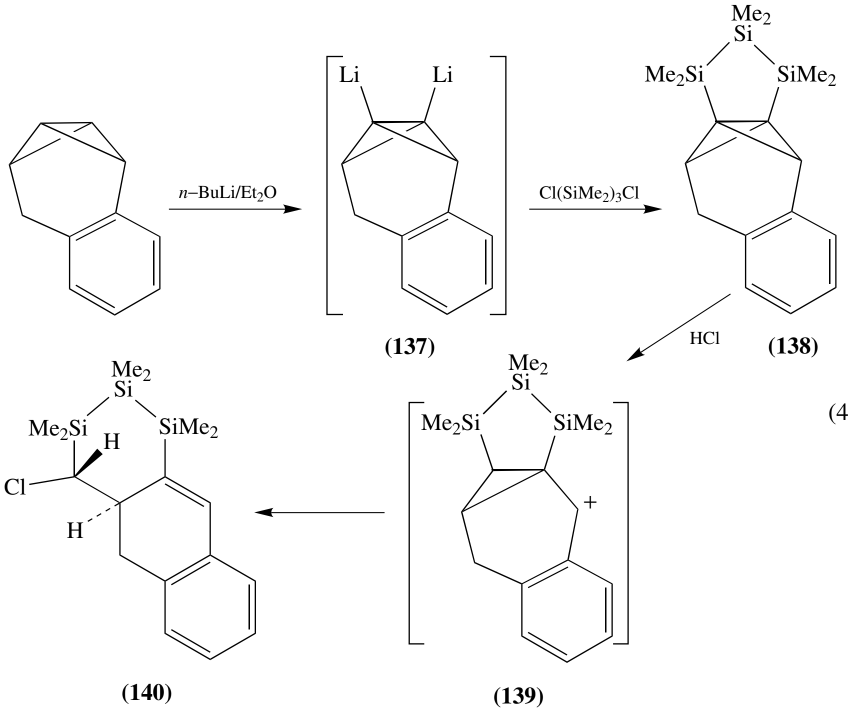

(137) **(138)** **(139)** **(140)**

(40)

B. Oligosilabridged Cyclic Acetylenes

The last target molecule was the small silacycloalkyne ring, which is a subject of considerable interest because of bond-angle strain at the sp carbons[141]. In this series, various examples of silicon-containing cycloalkynes have been reported so far[142–148]. Cycloheptynes with their seven carbons are generally unstable at room temperature[149,150]. However, cycloheptynes which contain one sulfur or silicon atom in the skeleton are thermally stable[151–153]. This difference in the stability of medium-ring acetylenes is due to the longer C−S or C−Si bond lengths compared with the C−C bond. Generation of some six-membered cyclic acetylenes has been achieved either by matrix isolation studies or by trapping and oligomerization experiments. However, no example of isolation of a cyclohexyne has been reported. Treatment of $Cl(SiMe_2)_6Cl$ with acetylene di-Grignard reagent under dilute conditions gave **141** as a stable colorless liquid in 46% yield. The photolysis of an hexane solution of **141** with a low-pressure mercury lamp in the presence of triethylsilane gave the lower homologous pentasilacycloheptyne **(142)** in 22% yield as colorless crystals (equation 41). This compound is stable to atmospheric oxygen and moisture[154]. The cycloheptyne **(142)** could also be obtained in 18% yield by thermolysis of **141**. The molecular structure of **142** could be established by X-ray diffraction (Figure 9). The Si−Si, Si−C single and C≡C triple bond lengths are normal, ranging between 2.34–2.35, 1.80–1.84 and 1.22 Å, respectively. However, there is an interesting alternation in the bond angle around the polysilane chain: the bond angles C(2)−Si(1)−Si(2) (100.4°) and C(1)−Si(5)−Si(4) (101.7°) are contracted, angles Si(1)−Si(2)−Si(3) (108.7°) and Si(3)−Si(4)−Si(5) (109.9°) are normal while the angle Si(2)−Si(3)−Si(4) (117.4°) is considerably expanded compared with the normal bond angles. The most interesting point in the structure of **142** is of course the bending of the acetylene bond from a linear geometry, as represented by the deviation angles θ_1 and θ_2. The bending angles θ_1 and θ_2 of **142** are 20.4 and 17.8°, respectively, values which are comparable with those observed in the nonsubstituted cyclooctyne ($\theta = 21.5°$) and cyclononyne (19.8°). Apparently, the structure of **142** reveals that the magnitude of the bending in acetylene decreases, but that the increase in the deformation of the polysilane chain is definitely noticeable. These observations are explained by the high flexibility of the conformation in the polysilane chain.

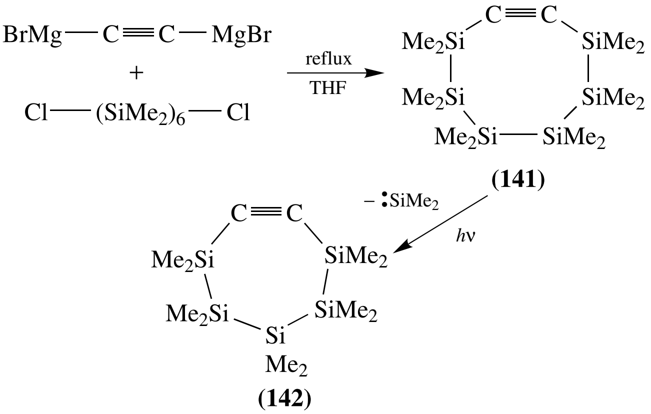

(41)

The photoirradiation of **141** in the presence of six equivalents of triethylsilane provided the ring-contracted pentasilacycloheptyne **142** in 22% yield, together with a small amount of bicyclic compounds **143** and **144** in yields of 0.8 and 0.6%, respectively

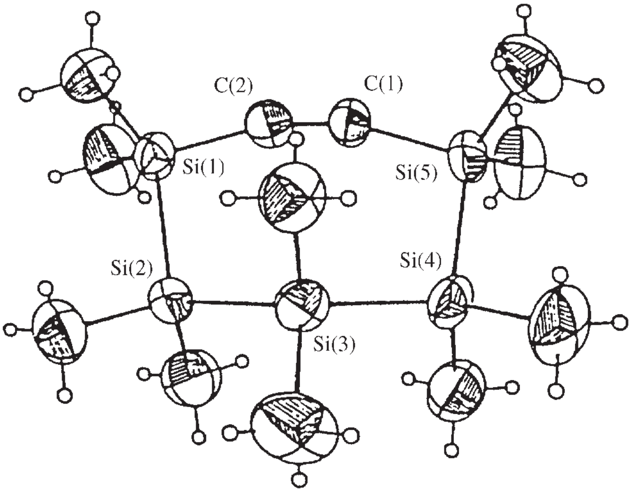

FIGURE 9. ORTEP drawing of **142** (reproduced by permission of Pergamon Press from Reference 154)

(equation 42)[155]. The structure of **144** was determined by X-ray crystallographic analysis. The bicyclic olefin **143** is considered to be formed by the oxidation of **145** after the addition of dimethylsilylene to **147**, which is generated in turn by the 1,2-silyl migration of **141**. The bicyclic olefin **144** is also considered to be formed by the oxidation of **146**, which is generated by the addition of dimethylsilylene to **148** after a 1,2-silyl migration of **142** (equation 43). When an acetone solution of **141** was irradiated with a low-pressure mercury lamp, bicyclic acetone adducts **149** and **150** were obtained in 4.4 and 1.8% yields, respectively, together with ring-reduced cycloheptyne **142** (21%) (equation 42). The formation of acetone adducts **149** and **150** can be explained by the acetone trapping process of the fused silacyclopropenes **147** and **148**. This photochemical behavior seems to indicate that the ring contraction of polysilacycloalkynes occurs via polysilabicyclo[*n*.1.0]alk-1($n + 2$)-ene derivatives. A plausible reaction mechanism is shown in equation 43. However, the photolysis of 3,3,8,8-tetraphenyloctamethylhexasilacyclooctyne **151a** leads to formation of two types of ring-contracted cycloheptynes **153a** and **153b** in yields of 16 and 14%, respectively (equation 44)[156]. These results indicate that the ring contraction of polysilacycloalkynes proceeds via two different routes. One is a direct desilylation and another is a process involving silacyclopropene intermediate **152**.

Finally, irradiation of a hexane solution of hexasilacyclooctyne **151b** with a low-pressure mercury lamp through a quartz tube gave three ring-contracted products, dediethylsilylated **154a**, dedimethylsilylated **154b** and dediphenylsilylated **154c** (formed via the rearranged **155**) in yields of 10, 10 and 9%, respectively (equation 45). These yields of pentasilacycloheptynes **154a, 154b** and **154c** are reasonable compared to those of pentasilacycloheptynes **153a** and **153b** formed by photoirradiation of hexasilacyclooctyne **151a**[156].

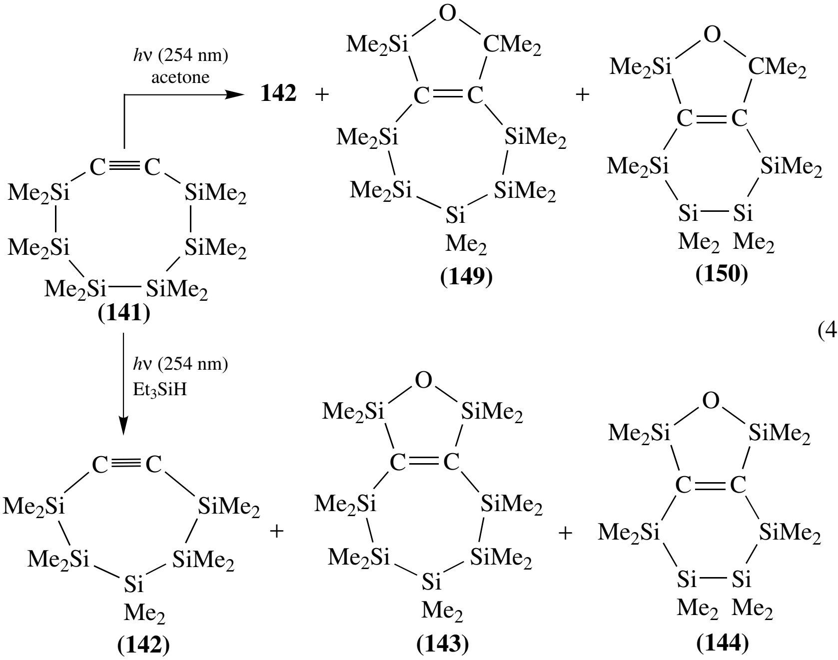
hν (254 nm)
acetone
142
(149)
(150)
(141)
hν (254 nm)
Et₃SiH
(142)
(143)
(144)

(42)

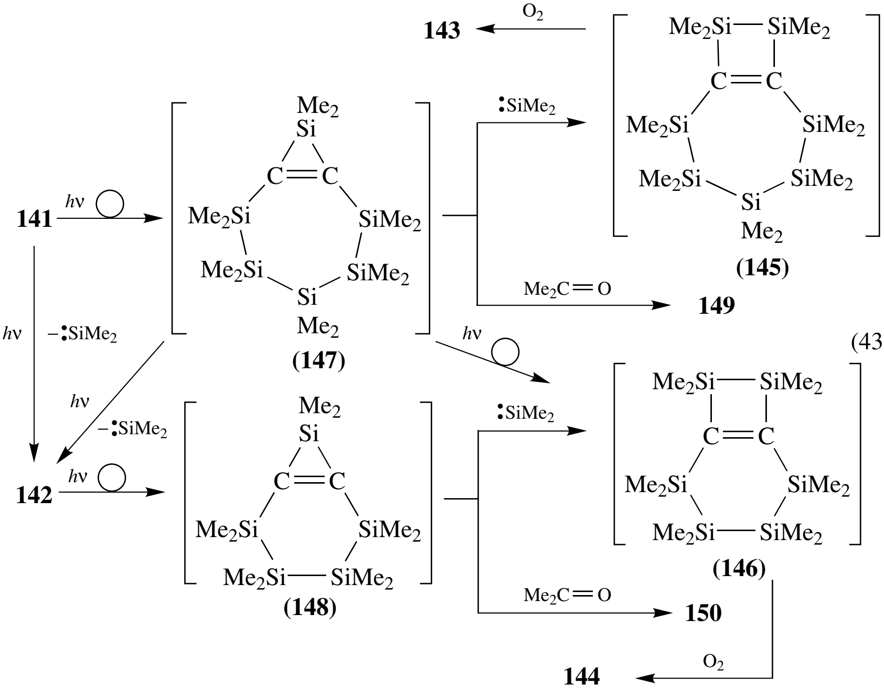
143
O₂
(145)
141
hν
:SiMe₂
Me₂C=O
149
(147)
hν
−:SiMe₂
142
(148)
(146)
150
144
O₂

(43)

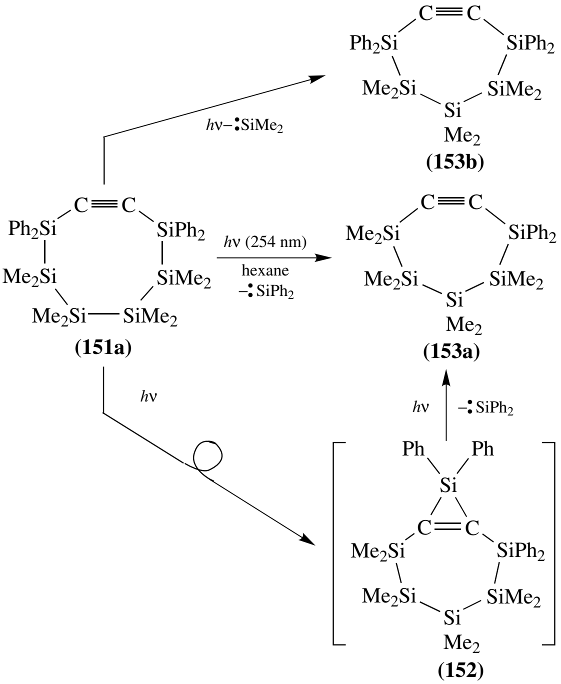

(44)

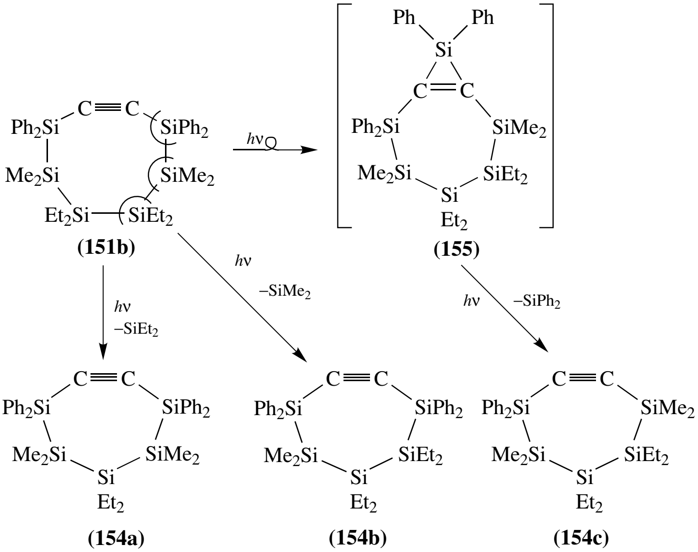

(45)

Generation of some small-ring cyclic acetylenes has been achieved either by matrix isolation studies or by trapping and oligomerization experiments[157–160]. However, no example of the isolation of cyclohexyne has been reported. While the six-membered cyclic acetylene **156a** was prepared for the first time by the ring-contracted photochemical reaction of pentasilacycloheptyne **142** in 20% yield, a later direct synthesis involved the reaction between the corresponding 1,4-dichlorotetrasilane with acetylene.

A di-Grignard reagent was also applied for the preparation of **156a** and **156b** in yields of 52% and 55%, respectively (equation 46)[155,161]. The spectroscopic analysis of **156a** indicates the strain at the sp carbons. Particularly, the ^{13}C-NMR signal of the acetylenic sp carbons of **156a** appears at 135.6 ppm, which is at a lower field than that observed in **141** and **142**. The UV absorption of **142** shows a maximum at 229 nm, which is at a shorter wavelength than that found for **141** (235 nm) because of the shortening of the silicon chain. However, the UV absorption maxima for **156a** appears at 237 nm, which is a bathochromic shift as compared with **142**. The X-ray crystallographic analysis of octaisopropyltetrasilacyclohexyne by Barton and coworkers shows the average bending angles of the sp carbons to be 31.4°[162].

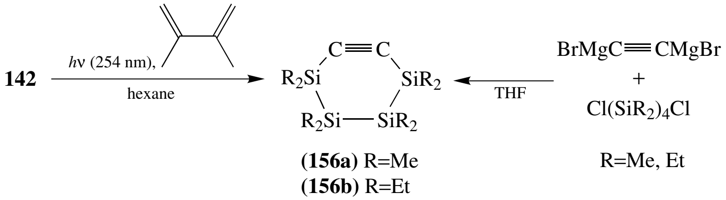

(46)

Tetrasilacyclohexyne **156a** was found to be thermally stable even in boiling hexane, but it slowly decomposed in boiling decane (174 °C; $t_{1/2} = 8$ h) to give a bicyclic compound **144**. However, tetrasilacyclohexynes **156a** and **156b** are unstable toward atmospheric moisture and give a complex mixture of products. Diels–Alder reaction of **156a** with 2,3-dimethyl-1,3-butadiene proceeds easily at room temperature to give the cycloadduct **157**. However, 1,3-diphenylisobenzofuran did not react with the tetrasilacyclohexyne **156a** because of a steric repulsion between the methyl groups of the latter with the phenyl groups of the former. Tetrasilacyclohexyne **156a** also reacted with phenyl azide and with diphenyldiazomethane to give the corresponding cycloadduct **158** and its rearranged product **159**, respectively (equation 47). Hexasilacyclooctyne **141** and pentasilacyclooctyne **142** did not react under the same conditions. The structure of **159** was also confirmed by X-ray diffraction.

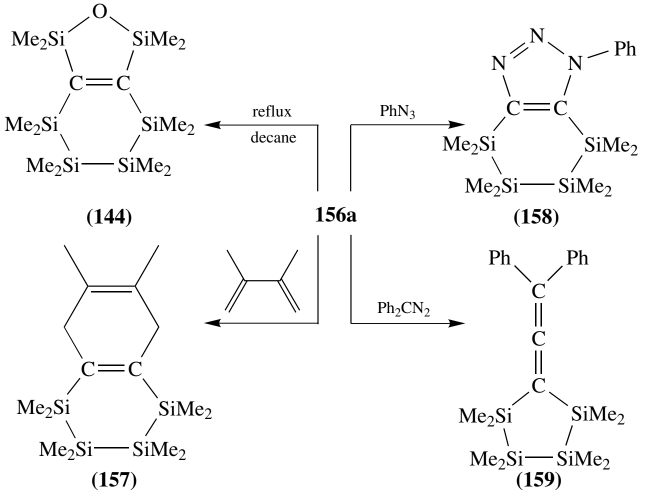

(47)

The reaction of hexasilacyclooctyne **141** with dimesitylsilylene generated from the photolysis of 2,2-dimesitylhexamethyltrisilane gave heptasilabicyclo[6.1.0]non-1(8)-ene **160** in 36% yield. The reaction of pentasilacycloheptyne **142** and tetrasilacyclohexyne **156a** give similarly the corresponding bicyclic compounds **161** and **162** in 37 and 15% yields, respectively (equation 48)[155]. The bicycic compounds **160** and **161** were purified by chromatography on silica gel. However, bicyclo[4.1.0]heptene **162** could not be isolated by silica gel chromatography because of its instability. Purification of **162** was achieved by gas chromatography. The structures of **160, 161** and **162** were determined by spectroscopic analysis and the structure of **162** was further confirmed by X-ray diffraction (Figure 10).

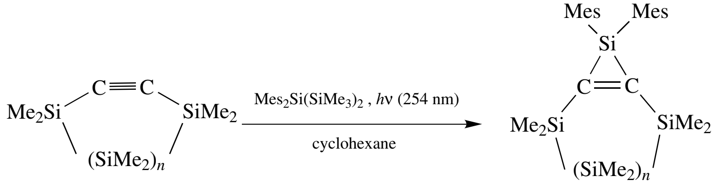

(48)

(141) $n = 4$
(142) $n = 3$
(156a) $n = 2$

(160) $n = 4$
(161) $n = 3$
(162) $n = 2$

Photochemical reactions of polysilabicyclo[n.1.0]alkenes **160** and **162** were examined. Irradiation of **160** in hexane with a high-pressure mercury lamp gave polysilacycloalkynes **141, 163** and **164** in 23, 58 and 11% yields, respectively. Similarly, the polysilacycloalkynes **156a** and **165** were also formed by photoirradiation of **162** in 18 and 71% yields, respectively (equation 49). In these reactions, the formation of cyclooctynes **141** and **156a** can be explained by direct or stepwise elimination of dimesitylsilylene. The 1,2-silyl shift of the silacyclopropenes is probably an important step for ring enlargement. The

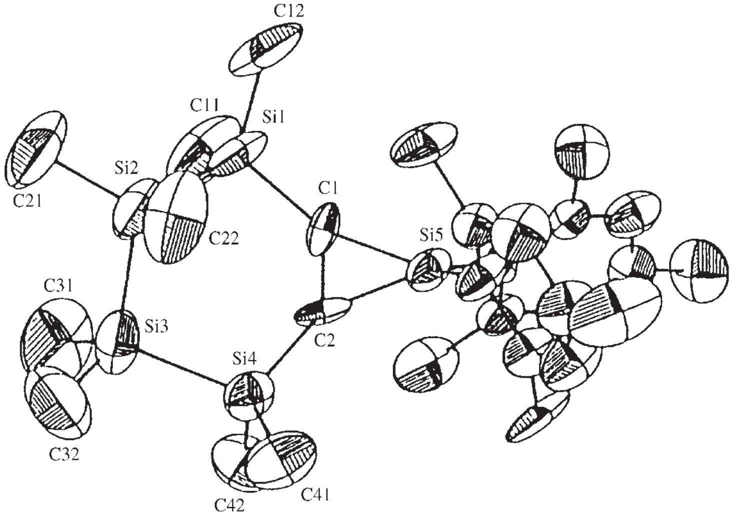

FIGURE 10. ORTEP drawing of **162** (reprinted with permission from Reference 155. Copyright 1993 American Chemical Society)

asymmetric cycloalkynes **163** and **165** can be considered to be formed by a 1,2-silyl migration of silacyclopropenes via 1,3-biradicals **(166)**. The formation of **164** may involve the elimination of dimethylsilylene before or after 1,2-silyl migration via the 1,3-biradical **166**.

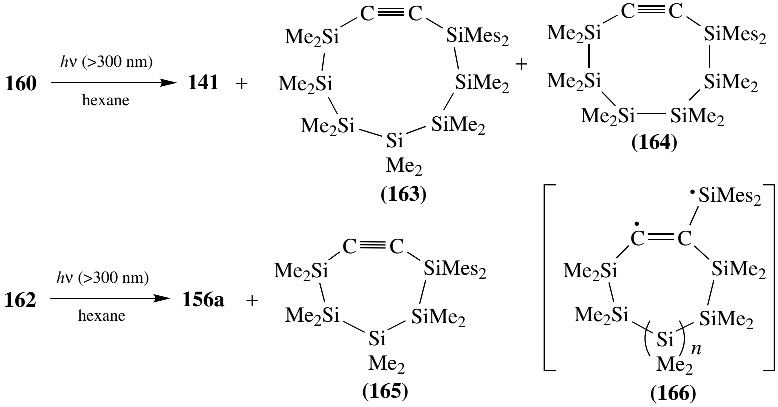

(163) **(164)** **(165)** **(166)**

(49)

The rearrangement of alkynes into vinylidenes in the coordination sphere of a transition metal has been intensively investigated in recent years[163]. The 1,2-silyl migration of disilylacetylene to a vinylidene complex proceeds analogously to the 1,2-hydrogen shift. The corresponding manganese[164] and rhodium[165] vinylidene complexes are isolated. Vollhardt and coworkers reported that in the reaction of neat bis(trimethylsilyl)acetylene with $CpCo(CO)_2$, a tetrakis(trimethylsilyl)triene was formed in a low yield via a 1,2-silyl shift[166]. The reaction of the pentasilacycloheptyne **142** with $CpCo(CO)_2$ in boiling *n*-decane gave the metallapentene derivative **168** in 82% yield. The yellow crystals of **168** are unstable toward oxygen. The structure of the compound **168** was determined by spectroscopic methods and X-ray crystallographic diffraction (equation 50)[167].

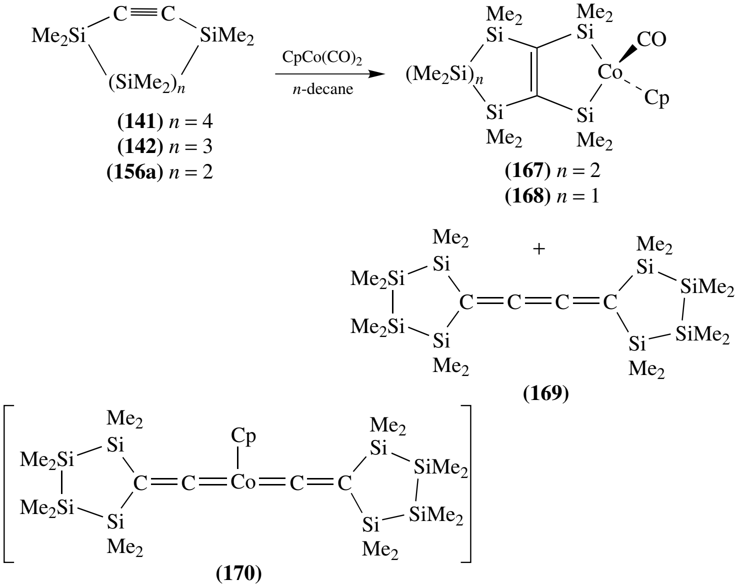

(141) $n = 4$
(142) $n = 3$
(156a) $n = 2$

(167) $n = 2$
(168) $n = 1$

(169)

(170)

(50)

The $CpCo(CO)_2$ also reacted readily with hexasilacyclooctyne **141** to give yellow stable crystals of metallapentene derivative **167** in 52% yield. The reaction of the acyclic acetylene with $CpCo(CO)_2$ under similar conditions did not give the metallapentene derivative and only an unidentified complex mixture was obtained. These results suggest that a ring structure is the requisite condition for the formation of a metallapentene derivative. Although the tetrasilacyclohexyne **156a** reacted with $CpCo(CO)_2$ in boiling hexane to give the triene derivative **169** in 52% yield, no metallapentene derivative was observed (equation 50). The triene derivative **169** is considered to be formed via the bisvinylidene complex **170**, similarly to Vollhardt's studies[166].

The reaction of the tetrasilacyclohexyne **156a** with $CpMn(CO)_3$ under photochemical conditions provided the vinylidene complex **172** and the triene derivative **169** in 46 and 11% yields, respectively, together with a small amount of trimer **173** (equation 51). When the hexasilacyclooctyne **141** reacted with $CpMn(CO)_3$ under similar conditions, the vinylidene complex **171** was formed in 36% yield; however, no triene and trimer derivatives were observed. The vinylidene complexes **171** and **172** regenerated the polysilacyclic acetylenes **156a** and **141**, respectively. The triene derivative **169** is considered to be formed by the reaction of the vinylidene complex **172** and the tetrasilacyclohexyne **156a**. The photochemical reaction of the vinylidene complex **172** or the tetrasilacyclohexyne **156a** gave the triene derivative **169** and the bisallene **173** in 30 and 18% yields, respectively. The structure was determined by spectroscopic and X-ray crystallographic analysis.

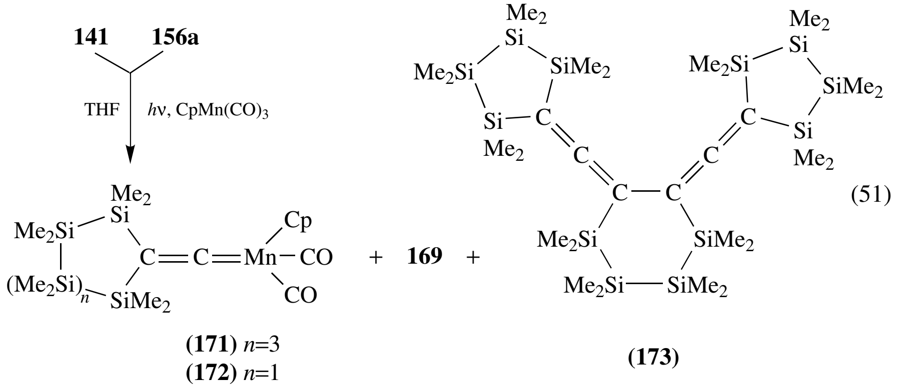

These results indicate that only when the tetrasilacyclohexyne **156a** reacts with vinylidene complexes, triene and bisallene derivatives formed. The reaction mechanism is shown in equation 52. A dissociation of carbonyl ligand from the vinylidene complex **172** generates an alkyne(vinylidene) complex **174**, which would be expected to form the metallacyclobutene **175**. The triene **169** is formed by reductive elimination reaction of **175** along with a 1,2-silyl shift. Insertion of a second molecule of the tetrasilacyclohexyne **156a** forms metallacyclohexadiene **176**. A reductive elimination reaction of **176** along with a 1,2-silyl shift results in the formation of the bisallene **173**.

C. Oligosilabridged and Doubly Bridged Allenes and Bisallenes

Cyclic allenes are the subject of considerable interest as strained unsaturated cyclic compounds[168–170]. *tert*-Butyl-substituted cycloocta-1,2-diene is known as the smallest isolable cyclic allene[170,171]. Seven- and six-membered cyclic allenes are also well known as important intermediates in organic synthesis, and many synthetic methods have been documented.

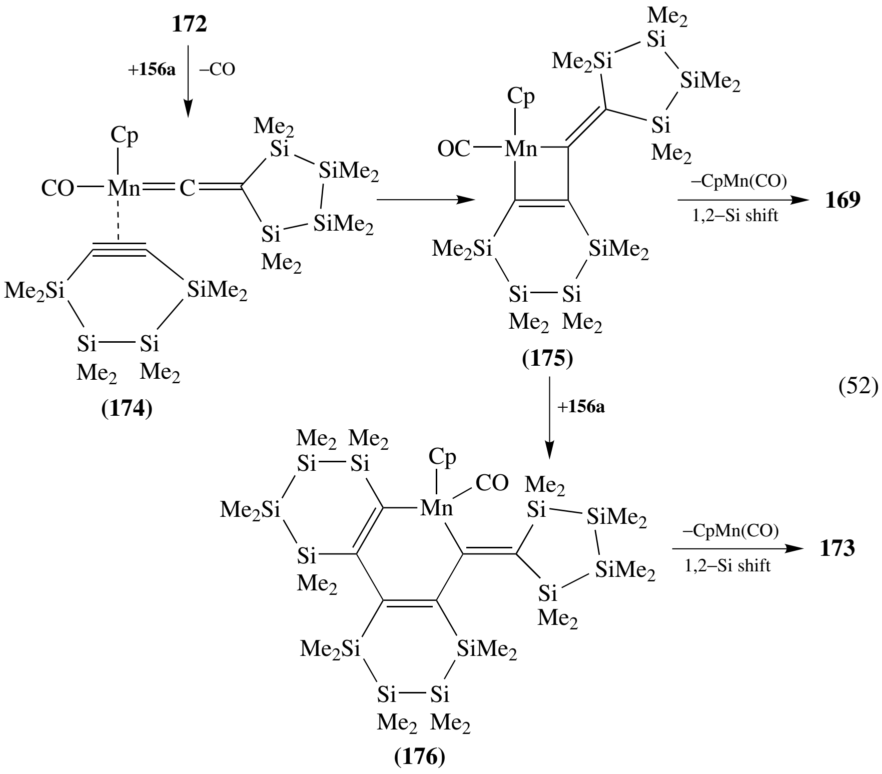

(52)

Ph_2C_3 dianion, prepared from 1,3-diphenylpropyne and 2 equivalents of butyllithium, reacted with 1,4-dicholorohexasilane and 1,6-dichlorotetrasilane in THF/hexane to give tetrasilacyclohepta-1,2-diene **177** and hexasilacyclonona-1,2-diene **178** in 24 and 72% yields, respectively[172]. A reaction of Ph_2C_3 dianion with 1,3-dichlorohexamethyltrisilane gave mainly polymeric products and no 1 : 1 cycloadduct could be detected. The six-membered cyclic allene **179** was obtained in 11% yield from the reaction of 1,3-dichloro-2,2-diphenyltetramethyltrisilane with the Ph_2C_3 dianion (equation 53). The difference in the reactivities of the two types of dichlorotrisilanes might be attributed to the steric effects of two phenyl groups on a central silicon atom, which prevent an intermolecular reaction. This is the first example of isolated six- and seven-membered cyclic allenes[172]. The X-ray crystallographic analyses of **177** and **179** (Figure 11) showed that the slightly longer bond lengths of the skeletal C−Si and Si−Si bonds of **179** (1.94 and 2.38 Å on average, respectively) compared with those of **177** (1.91 and 2.34 Å) result in a greater release of strain caused by the allenic moiety. The most interesting point concerning the structures of **177** and **179** is the geometry of the allenic moiety. The bond angle C1−C2−C3 at the sp carbons of **179** was found to be highly strained (19°) from a linear geometry, while that of **177** is almost strain-free (6°). The dihedral angles around the allenic moieties of **177** and **179** are also influenced by the ring strain. The dihedral angle Si1−C1−C3−Si3 of **179** is strongly contracted (52.2°) from the normal vertical geometry, while that of **177** is nearly perpendicular (85.3°).

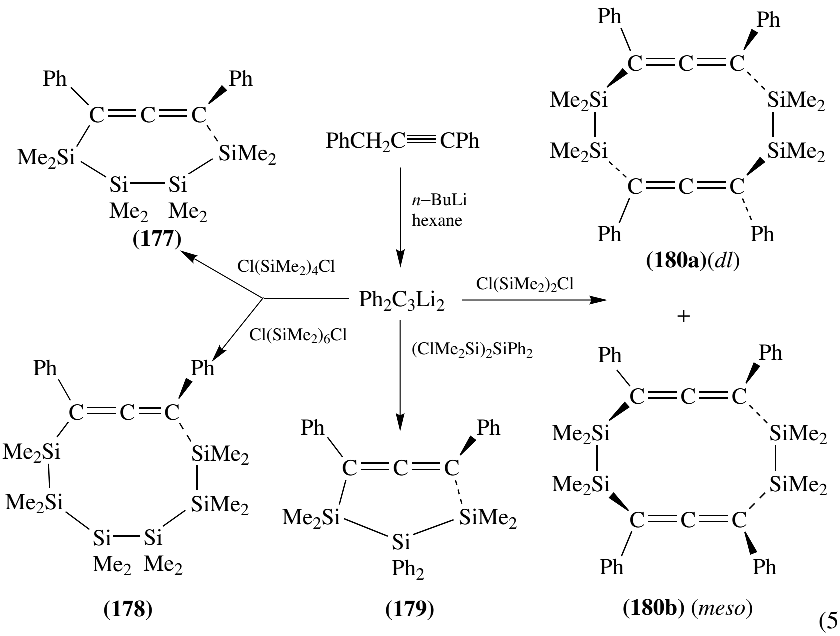

(53)

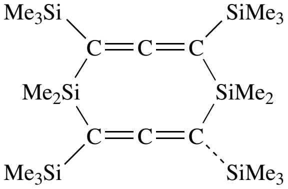

(181)

There have been attempts to synthesize dimeric allenes as well as cyclic bisallenes[173–178]. A ten-membered cyclic tetraene was synthesized by Skättebol for the first time as the smallest bisallene[173]. However, only the *meso* structure has been characterized, although the *dl* isomer does not appear to be seriously strained. The Ph_2C_3 dianion reacts readily with 1,2-dichlorotetramethyldisilane to give the two isomers of 1,2,6,7-tetrasilacyclodeca-3,4,8,9-tetraenes **180a** and **180b** (equation 53)[179]. The X-ray analysis of **180a** and **180b** shows that the average bent angle around the sp carbons C2 and C7 is 4° (Figure 12). The allene unit is slightly enlarged to 99–102° from the normal vertical geometry of allene. The eight-membered bisallene **181** was synthesized by the reaction of 1,3-dilithio-1,3-bis(trimethylsilyl)allene with dimethyldichlorosilane by Barton and coworkers[180]. Its X-ray diffraction shows that the allene unit is bent to 4.8° and twisted to 78.1°; the distance between the allenic central carbons is 2.859 Å.

There are few known examples of the bicyclic, doubly-bridged allenes as betweenallenes. The strained symmetrical betweenallenes can gain no strain relief by bending, since what is gained in one ring is lost in the other. Therefore, only twisting, as defined by a reduction in the normal allene dihedral angle of 90°, is available for strain relief. Nakazaki and coworkers synthesized [8.10]betweenallene, consisting of fused 11- and 13-membered rings, as the first example of a betweenallene[181].

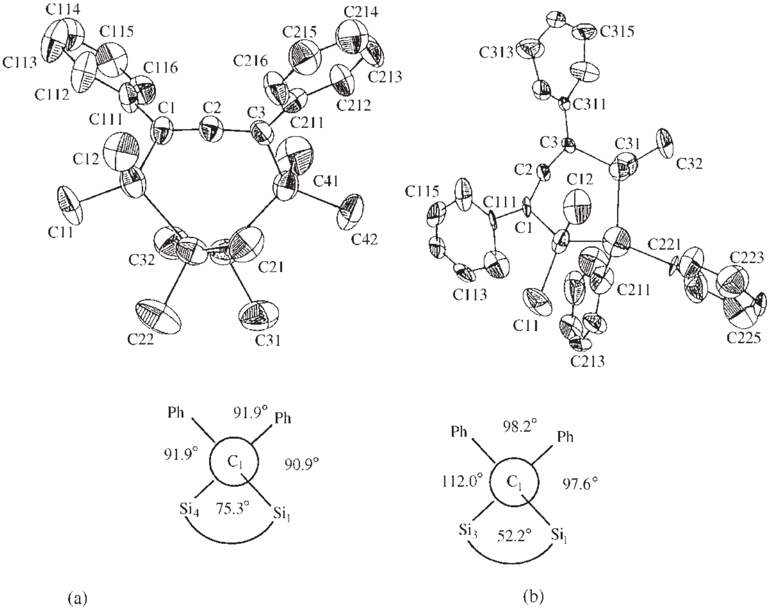

FIGURE 11. ORTEP drawings of (a) **177** and (b) **179** (reprinted with permission from Reference 172. Copyright 1993 American Chemical Society)

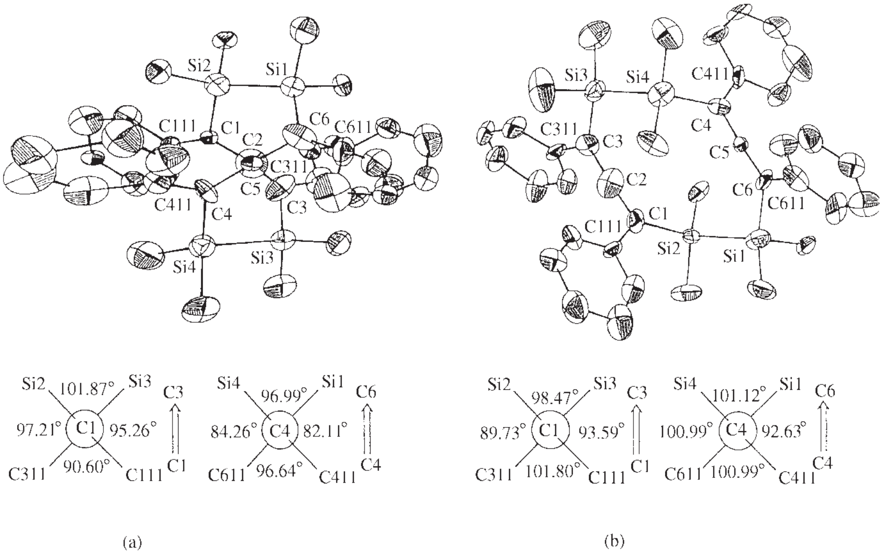

FIGURE 12. ORTEP drawings of (a)**180a** (*dl*) and (b) **180b** (*meso*) (reproduced by permission of The Chemical Society of Japan from Reference 179)

Octasila[4.4]betweenallene **182** was prepared by the reaction of hexachloropropene with 1,4-dichlorooctamethyltetrasilane in the presence of magnesium in 34% yield; the other expected isomer, i.e. **183**, could not be obtained[172]. The corresponding [3.3]betweenallene could not be isolated, and an unexpected 2 : 2 adduct **184** was isolated in 16% yield as a volatile product by the reaction of hexachloropropene with 1,3-dichlorohexamethyltrisilane (equation 54). The X-ray crystallographic analysis of **182** (Figure 13) showed a symmetrical conformation and almost normal bond lengths and angles. The torsional angles, Si1−C1−C3−Si4 and Si5−C1−C3−Si8, are 72.0° and 73.3°, respectively. This deformation of the allene from the vertical geometry is increased compared with that of **177**, which has the same-membered monocyclic system. The allenic sp carbon of **182** is almost linear, although in the case of **177** it is slightly bent. Therefore, the strain, as indicated by the dihedral angles of **181**, can be explained on the basis of the linear geometry of the allenic sp carbon. Barton and coworkers also reported on the synthesis of **182** (equation 54)[182,183].

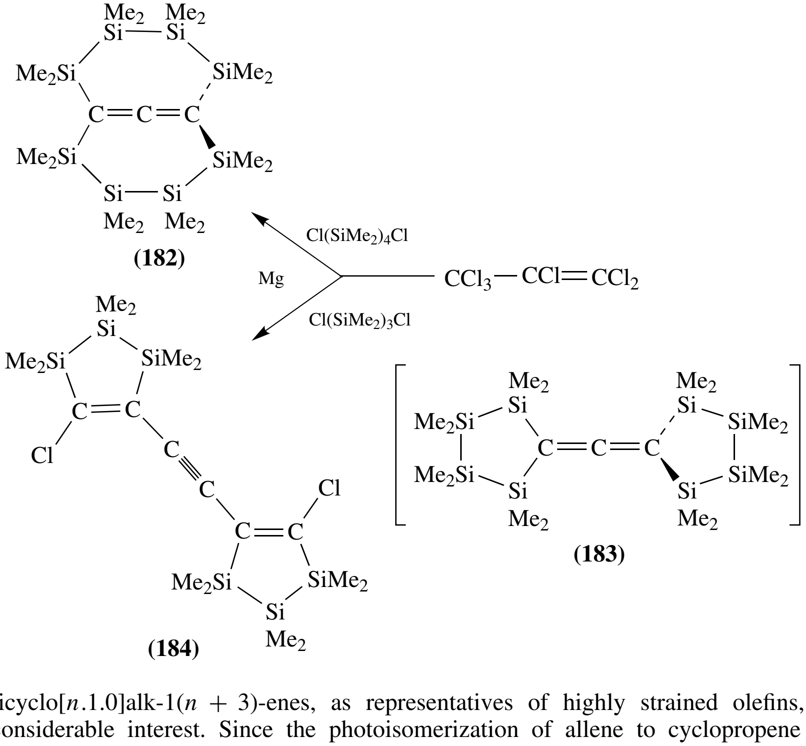

(182) **(183)** **(184)**

(54)

Bicyclo[n.1.0]alk-1(n + 3)-enes, as representatives of highly strained olefins, are of considerable interest. Since the photoisomerization of allene to cyclopropene and propyne was first reported by Chapman, allene photochemistry has received much attention[184]. Stierman and Johnson reported several photorearrangements of carbocyclic allenes giving the bicyclo[n.1.0] systems[185−189]. In a photochemical irradiation of hexasilacyclonona-1,2-diene **178** with a low-pressure mercury lamp, the corresponding hexasilabicyclo[6.1.0]non-1(9)-ene **185** was isolated in 59% yield; additionally, the ring-contracted allene **186** and pentasilabicyclo[5.1.0]oct-1(8)-ene **187** were obtained in 14% and 23% yields[190]. Irradiation of 5,7-diphenyl-1,2,3,4-tetrasilacyclohepta-5,6-diene **177** gave the tetrasilabicyclo[4.1.0]hept-1(7)-ene **188** and 2,3,4,7-tetrasilabicyclo[4.1.0]hept-5-ene **189** in 45% and 20% yields, respectively, probably via the vinylcarbene intermediate

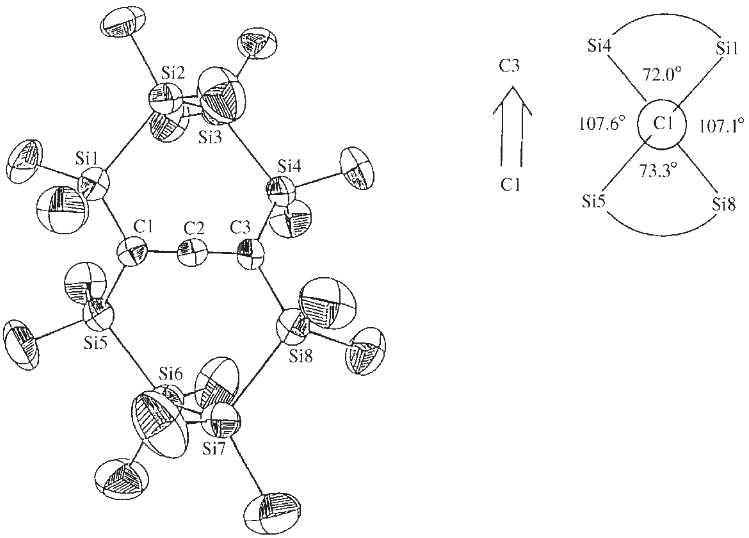

FIGURE 13. ORTEP drawing of **182** (reprinted with permission from Reference 172. Copyright 1993 American Chemical Society)

or via a concerted process (equations 55 and 56). The photolysis of a methanol solution

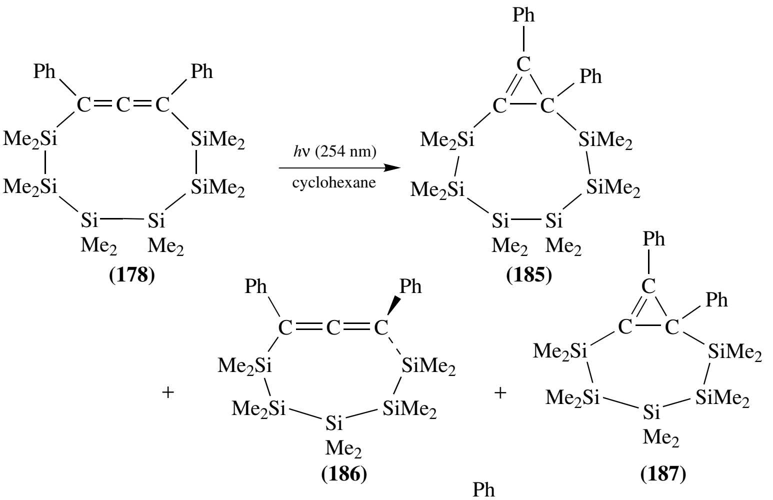

(55)

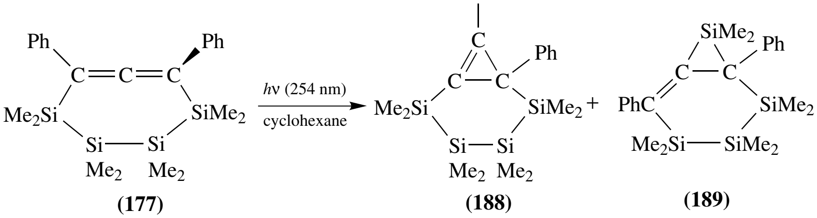

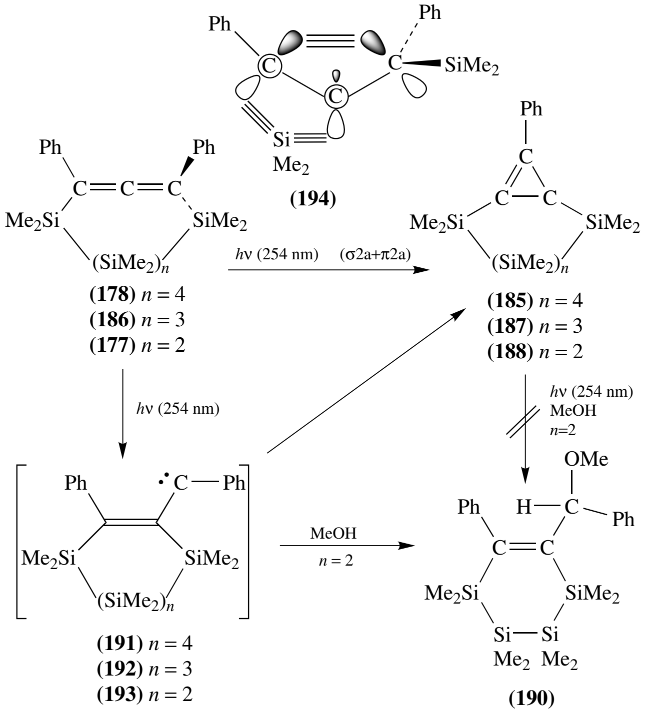

(56)

of tetrasilacyclohexa-1,2-diene **177** gave a methanol-incorporated product **190** in 54% yield, together with the bicyclo[4.1.0]heptene derivative **188** (8%). The formation of **190** can be explained by a methanol reaction of a vinylcarbene intermediate **193** generated by a 1,2-silyl shift. However, the photolysis of the bicyclo[4.1.0]heptene derivative **188** in methanol did not give a methanol-incorporated product **190**. No methanol-incorporated products **185, 187** and **188** were obtained in the photolysis of a methanol solution of 1,2,3,4,5,6-hexasilacyclonona-7,8-diene **178**. It is likely that there are two reasons for the inability to observe the vinylcarbene intermediate. One is that the mechanism might be concerted through **194**; another may be the very short lifetime of the corresponding vinylcarbene intermediates **191** and **192**.

D. 1,2-Disilaacenaphthene and 9,10-Disilaanthracene Silyl Dianions

There has been a remarkable interest in the reactivity, structure and bonding of organolithium compounds in recent years. However, so far there is no report concerning the reduction of a silicon–silicon double bond to afford a 1,2-dilithiodisilane. One of the best candidates for the generation of a 1,2-dilithiodisilane might be 1,2-dichloro-1,2-diisopropyl-1,2-disilaacenaphthene **(195)**. The particular advantage of **195** is that the two silicon atoms are in fixed positions and are separated by a single bond distance, and hence obviating the possibility of a double bond formation between them. We succeeded in the synthesis and characterization of the first 1,2-dilithiodisilane **(196)** derived by dilithiation of **195**. **195** and an excess lithium in THF were sonicated at room temperature under argon to afford a dark-blue solution (Gilman reaction)[191,192]. After removal of the unreacted lithium, addition of an excess of CH_3I to this solution afforded 1,2-dimethyl-1,2-diisopropyl-1,2-disilaacenaphthene in high yield. On treatment of this solution with CH_3OD, quantitative formation of 1,2-dideuterio-1,2-diisopropyl-1,2-disilaacenaphthene was observed. The formation of these products clearly reveals that the dichlorodisilane **195** is readily reduced by lithium to afford dilithium 1,2-disilaacenaphthendiide **(196)** (equation 57). The half-life of disappearance of **196** in THF is 13.5 h at 30 °C. The NMR measurement of the lithiated solution, however, showed the existence of a single product. Detailed NMR measurements (^{1}H, ^{13}C, H–H NOESY, H–C COSY, H–C COLOC and ^{13}C INVGATE NMR measurements) were carried out. The chemical shifts of the aromatic protons in **196** are shifted upfield in comparison with those of the corresponding disilanes. Upfield shifts of the ^{13}C NMR signals for the C-3-C-8 atoms in **196** are also observed. The most important factor affecting the upfield chemical shifts of protons and carbons in **196** is thought to be the presence of a negative charge on the silicon atom. The ^{29}Si NMR chemical shift for **196** was observed at -1.24 ppm, a large downfield shift compared with other silyl anions. Interestingly, the ^{29}Si resonance for **196**, however, is upfield shifted from 1-*tert*-butyl-2,3,4,5-tetraphenyl-1-silacyclopentadienide lithium. Based on the ^{1}H and ^{13}C NMR chemical shifts, the electronic structure of **196** is described in terms of the negative charge on the silicon atoms. In order to obtain further information on the structure of **196**, a low-temperature ^{29}Si NMR measurement was carried out in order to observe a scalar ^{29}Si–^{7}Li coupling. In the ^{29}Si NMR spectrum of **196**, a well-resolved quartet at low temperature was observed, indicative of the fact that **196** has at least a partial covalency at low temperature. In the presence of oxidizing reagents such as O_2 and Cd(II), the dilithium 1,2-disilaacenaphtendiide **(196)** further reacts with 2,3-dimethylbutadiene and 9,10-dimethylanthracene to afford cycloadducts **197** and **198** respectively. Consequently, **196** is synthetically equivalent to 1,2-disilaacenaphthene **(199)** (equation 57).

The chemistry of 9,10-dihydroanthracenes with silicon in position 9 and/or 10 has been considerably developed for some time by Jutzi[193,194] and Bickelhaupt and coworkers[195–197] and modified by Corey and coworkers[198,199].

A Wurtz coupling reaction of 9,10-dichloro-9,10-dimethyl-9,10-disilaanthracene **(200)** with sodium in toluene affords a bridged dimer **(202)** in 7% yield. The X-ray structure is given in Figure 14a. The reaction of a *cis/trans* mixture of 9,10-dihydro-9,10-dimethyl-9,10-disilaanthracene **(201)** with lithium in THF containing *N*,*N*,*N*′,*N*′-tetramethylethylenediamine (TMEDA) also produced **202** in 61% yield, probably via the silicon-centered 9,10-disilaanthracene biradical or its equivalent intermediate (equation 58). A silicon–silicon bond cleavage of the dimer **202** by excess lithium or potassium produced 9,10-disilaanthracene dianion **203a**, or **203b** (Gilman reaction)[200,201]. The ^{29}Si NMR chemical shifts in THF-d_8 were observed at -45.4 and -42.8 ppm, respectively, a large upfield shift compared to that of other silyl anions [Ph_3SiM: -9.0 ppm ($M = Li$), -7.5 ppm ($M = K$); Ph_2MeSiM: -20.6 ppm ($M = Li$), -18.5 ppm ($M = K$)][202,203].

NMR studies have been most informative of the structure in solution, and particularly important evidence has recently been obtained from a low-temperature measurement of ^{29}Si–^{7}Li scalar coupling. In the ^{29}Si NMR spectrum for the dilithium compound **(203a)** at 168 K in THF-d_8, a quartet with ^1J [^{29}Si–^{7}Li] $= 34$ Hz was observed. This implies that the two silicon atoms in the molecule are magnetically equivalent and one lithium atom binds to the silicon atom at low temperature. The ^{7}Li NMR signal appears at 3.7 ppm as a singlet at 298 K. Dramatic change was observed for the low temperature NMR measurements which yielded two different singlets at 2.8 and 5.2 ppm; unfortunately, no satellite signals due to the ^{29}Si scalar coupling were observed. However, it is clear from the ^{29}Si NMR spectrum that **203a** has a partial covalent bond between ^{29}Si and ^{7}Li at low temperature. The result of ^{7}Li NMR studies would be compatible with different environments for the two lithium atoms in the molecule at low temperature. Thus, the observed NMR data are compatible with a structure that contains jointly bridged silicons by one lithium.

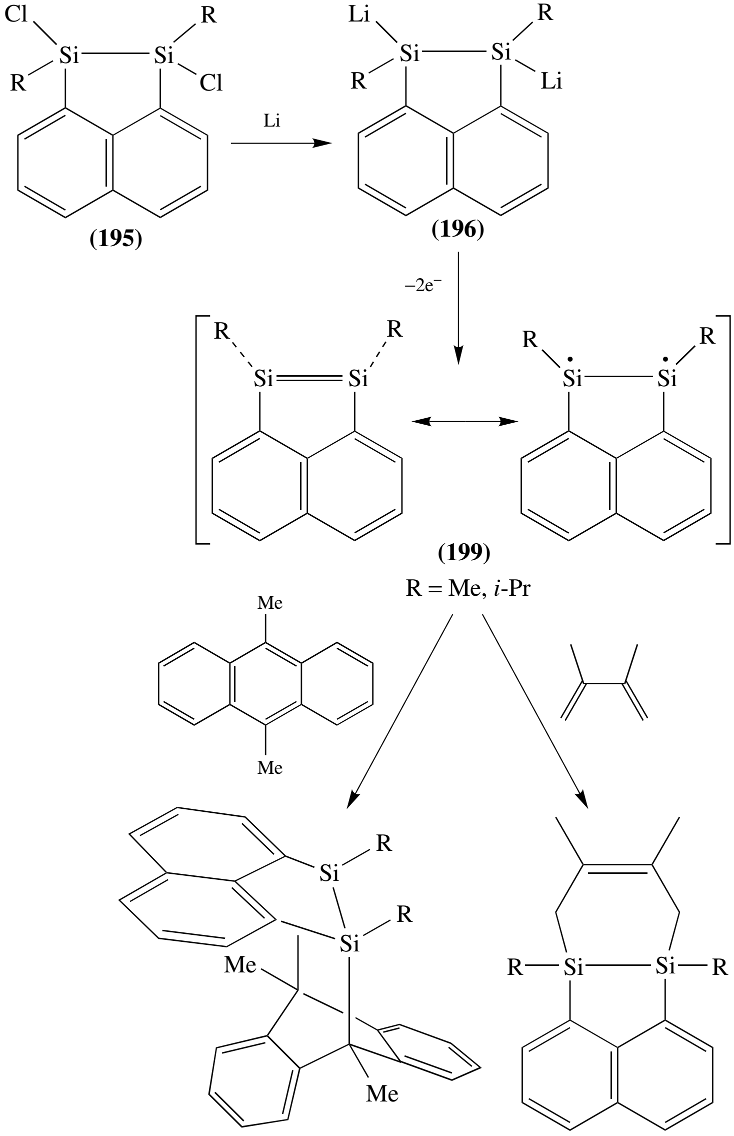

(195) **(196)** **(199)**

R = Me, *i*-Pr (57)

(198) **(197)**

During reactions of **202** with an equivalent amount of lithium or potassium, the reaction mixture became a yellow suspension which, when reacted with trimethylchlorosilane, gave

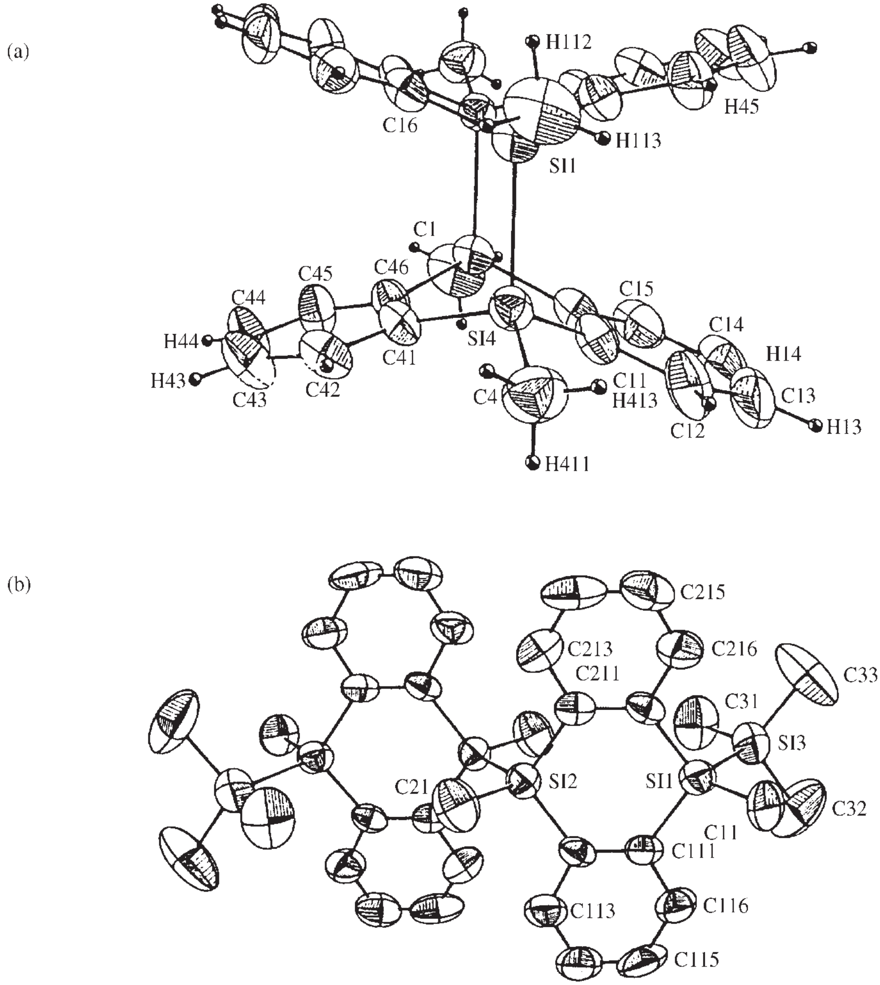

FIGURE 14. ORTEP drawings of (a) **202** and (b) **205** (reprinted with permission from Reference 200. Copyright 1995 American Chemical Society)

the opened dimer (**205**) via an intermediate **204** in 67% yield (equation 58). Since two methyl groups on the disilaanthracene unit of **205** were in a *cis* configuration (cf the X-ray structure in Figure 14b) the silicon–silicon bond cleavage of **202** with alkali metal proceeded with retention of the configuration around the silicon atom. The reactions of the dipotassium 9,10-dimethyl-9,10-disilaanthracene (**203b**) with trimethylchlorosilane gave the expected adduct (**206**) in 73% yield as one isomer. Compound **203b** reacts with dichlorodimethylsilane to give the expected dimethylsilyl adduct (**207**) bonded to the 9 and 10 positions of the disilaanthracene and its dimeric compound (**208**). Adducts **209** and **210** were obtained in good yields when the dipotassium salt **203b** reacted with 1,2-dichlorotetramethyldisilane and 1,3-dichlorohexamethyltrisilane, respectively, without forming dimeric products (equation 59). **203b** can be a valuable intermediate for the synthesis of a great variety of *cis*-9,10-disilaanthracene derivatives.

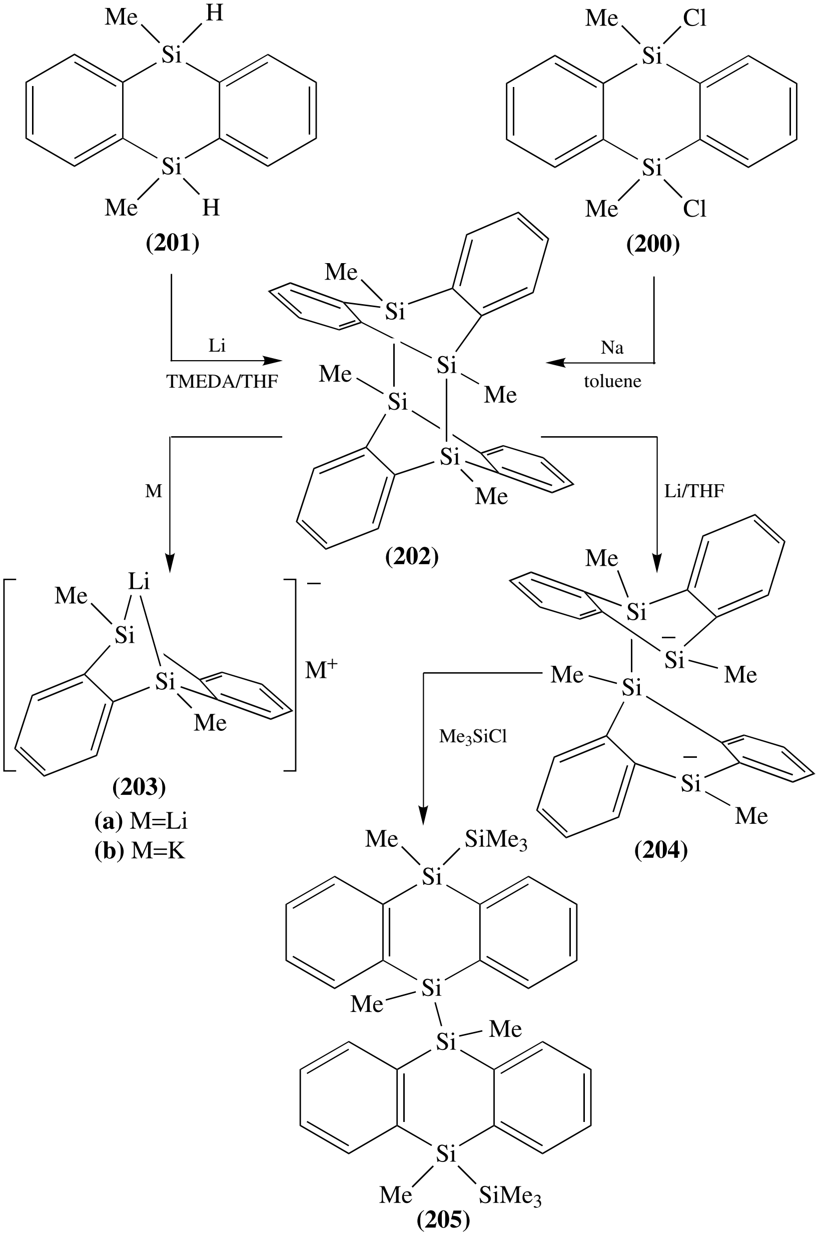

(58)

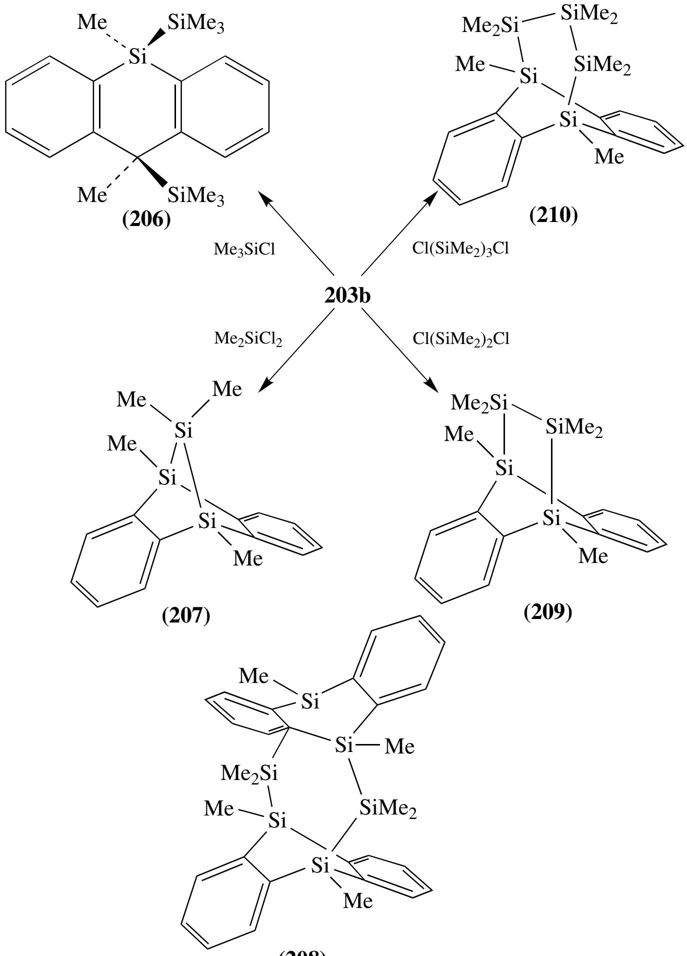

(59)

VI. REFERENCES

1. W. Ando, T. Hagiwara and T. Migita, *J. Am. Chem. Soc.*, **95**, 7518 (1973).
2. W. Ando, A. Sekiguchi and T. Migita, *Chem. Lett.*, 779 (1976).
3. W. Ando, A. Sekiguchi, T. Migita, S. Kammula, M. Green and M. Jones, Jr., *J. Am. Chem. Soc.*, **97**, 3818 (1975).
4. W. Ando, A. Sekiguchi, T. Hagiwara, T. Migita, V. Chowdhry, F. H. Westheimer, S. L. Kammula, M. Green and M. Jones, Jr., *J. Am. Chem. Soc.*, **101**, 6393 (1979).
5. W. Ando, A. Sekiguchi, T. Hagiwara and T. Migita, *J. Chem. Soc., Chem. Commun.*, 372 (1974).
6. T. J. Barton, J. A. Kilgour, R. R. Gallucci, A. J. Rothschild, J. Slutsky, A. D. Wolf and M. Jones, Jr., *J. Am. Chem. Soc.*, **97**, 657 (1975).
7. W. Ando, A. Sekiguchi, A. J. Rothschild, R. R. Gallucci, M. Jones, Jr., T. J. Barton and J. A. Kilgour, *J. Am. Chem. Soc.*, **99**, 6995 (1977).
8. W. Ando, A. Sekiguchi, J. Ogiwara and T. Migita, *J. Chem. Soc., Chem. Commun.*, 145 (1975).
9. A. G. Brook, J. W. Harris, J. Lennon and M. E. Sheikh, *J. Am. Chem. Soc.*, **101**, 83 (1979).

10. A. G. Brook, S. C. Nyburg, W. F. Reynolds, Y. C. Poon, Y.-M. Chang and J.-S. Lee, *J. Am. Chem. Soc.*, **101**, 6750 (1979).
11. A. G. Brook, F. Abdesaken, B. Gutekunst, G. Gutekunst and R. K. Kallury, *J. Chem. Soc., Chem. Commun.*, 191 (1981).
12. A. G. Brook, S. C. Nyburg, F. Abdesaken, B. Gutekunst, G. Gutekunst, R. Krishna, M. R. Kallury, Y. C. Poon, Y.-M. Chang and W. Wong-Ng, *J. Am. Chem. Soc.*, **104**, 5667 (1982).
13. A. Sekiguchi and W. Ando, *Organometallics*, **6**, 1857 (1987).
14. W. Ando, A. Sekiguchi and T. Sato, *J. Am. Chem. Soc.*, **103**, 5573 (1981).
15. A. Sekiguchi, T. Sato and W. Ando, *Organometallics*, **6**, 2337 (1987).
16. L. E. Gusel'nikov, N. S. Nametkin and V. M. Vdovin, *Acc. Chem. Res.*, **8**, 18 (1975).
17. T. J. Barton, G. Marquardt and J. A. Kilgour, *J. Organomet. Chem.*, **85**, 317 (1975).
18. C. M. Golino, R. D. Bush, P. On and L. H. Sommer, *J. Am. Chem. Soc.*, **97**, 1957 (1975).
19. A. Sekiguchi W. Ando and T. Sato, *J. Am. Chem. Soc.*, **104**, 6830 (1982).
20. T. J. Barton and G. P. Hussmann, *Organometallics*, **2**, 692 (1983).
21. G. Märkl and M. Horn, *Tetrahedron Lett.*, **24**, 1477 (1983).
22. N. Wiberg, *J. Organomet. Chem.*, **273**, 141 (1984).
23. A. G. Brook. W. J. Chatterton, J. F. Sawyer, D. W. Hughes and K. Vorspohl, *Organometallics*, **6**, 1246 (1987).
24. S. M. Bachrach and A. Streitwieser, Jr., *J. Am. Chem. Soc.*, **107**, 1186 (1985).
25. D. Seyferth, T. F. O. Lim and D. P. Duncan, *J. Am. Chem. Soc.*, **100**, 1626 (1978).
26. A. Sekiguchi and W. Ando, *J. Am. Chem. Soc.*, **106**, 1486 (1984).
27. G. Mass, K. Schneider and W. Ando, *J. Chem. Soc., Chem. Commun.*, 72 (1988).
28. K. Schneider, B. Daucher, A. Fronda and G. Mass, *Chem. Ber.*, **123**, 589 (1990).
29. A. Sekiguchi, W. Ando and K. Honda, *Tetrahedron Lett.*, **26**, 2337 (1985).
30. A. Sekiguchi and W. Ando, *Chem. Lett.*, 2025 (1986).
31. W. Ando, H. Yoshida, K. Kurishima and M. Sugiyama, *J. Am. Chem. Soc.*, **113**, 7790 (1991).
32. W. Ando, M. Sugiyama, T. Suzuki, C. Kato, Y. Arakawa and Y. Kabe, *J. Organomet. Chem.*, **499**, 99 (1995).
33. T. J. Barton and G. T. Burns, *J. Am. Chem. Soc.*, **100**, 5246 (1978).
34. T. J. Barton, G. T. Burns, E. V. Arnold and J. Clardy, *Tetrahedron Lett.*, **22**, 7 (1981).
35. Y. Nakadaira, H. Sakaba and H. Sakurai, *Chem. Lett.*, 1071 (1980).
36. A. Sekiguchi and W. Ando, *J. Am. Chem. Soc.*, **103**, 3579 (1981).
37. A. Sekiguchi, H. Tanikawa and W. Ando, *Organometallics*, **3**, 584 (1985).
38. W. Ando, H. Tanikawa and A. Sekiguchi, *Tetrahedron Lett.*, **24**, 4245 (1983).
39. G. Märkl and W. Schlosser, *Angew. Chem., Int. Ed. Engl.*, **27**, 963 (1988).
40. W. Ando, M. Ikeno and A. Sekiguchi, *J. Am. Chem. Soc.*, **99**, 6447 (1977).
41. W. Ando, M. Ikeno and A. Sekiguchi, *J. Am. Chem. Soc.*, **100**, 3613 (1978).
42. W. Ando and M. Ikeno *J. Chem. Soc., Chem. Commun.*, 655 (1979).
43. M. Ishikawa, K. Nishimura, H. Sugisawa and M. Kumada, *J. Organomet. Chem.*, **194**, 147 (1980).
44. R. West, M. J. Fink and J. Michl, *Science*, **214**, 1343 (1981).
45. T. Tsumuraya, S. A. Batcheller and S. Masamune, *Angew. Chem., Int. Ed. Engl.*, **30**, 902 (1991).
46. W. F. Guore and T. J. Barton, *J. Organomet. Chem.*, **199**, 33 (1980).
47. D. Tzeng and W. P. Weber, *J. Am. Chem. Soc.*, **102**, 1451 (1980).
48. V. J. Tortorelli and M. Jones, Jr, *J. Chem. Soc., Chem. Commun.*, 785 (1980).
49. W. Ando, M. Ikeno and Y. Hamada, *J. Chem. Soc., Chem. Commun.*, 621 (1981).
50. W. Ando, Y. Hamada, A. Sekiguchi and K. Ueno, *Tetrahedron Lett.*, **23**, 5323 (1982).
51. W. Ando, Y. Hamada, A. Sekiguchi and K. Ueno, *Tetrahedron Lett.*, **24**, 4033 (1983).
52. J. Belzner, H. Ihmels, L. Pauletto and M. Noltemeyer, *J. Org. Chem.*, **61**, 3315 (1996).
53. W. Ando, K. Hagiwara and A. Sekiguchi, *Organometallics*, **6**, 2270 (1987).
54. W. Ando, M. Fujita, H. Yoshida and A. Sekiguchi, *J. Am. Chem. Soc.*, **110**, 3310 (1988).
55. S. Zhang, P. E. Wagenseller and R. T. Conlin, *J. Am. Chem. Soc.*, **113**, 4278 (1991).
56. S. Zhang and R. T. Conlin, *J. Am. Chem. Soc.*, **113**, 4272 (1991).
57. P. Boudjouk, E. Blark and R. Kumarathasan, *Organometallics*, **10**, 2095 (1991).
58. D.-H. Pae, M. Xiao, M. Y. Chiang and P. P. Gaspar, *J. Am. Chem. Soc.*, **113**, 1281 (1991).
59. N. C. Baird and M. J. S. Dewar, *J. Am. Chem. Soc.*, **89**, 3966 (1967).
60. K. B. Wiberg and R. A. Fenoglio, *J. Am. Chem. Soc.*, **90**, 3395 (1968).
61. W. Ando and H. Saso, *Tetrahedron Lett.*, **27**, 5625 (1986).

62. H. Saso, H. Yoshida and W. Ando, *Tetrahedron Lett.*, **29**, 4747 (1988).
63. H. Saso and W. Ando, *Chem. Lett.*, 1567 (1988).
64. H. Saso, W. Ando and K. Ueno, *Tetrahedron*, **45**, 1929 (1989).
65. D. Seyferth, D. P. Duncan, M. L. Shannon and E. W. Goldman, *Organometallics*, **3**, 574 (1984).
66. D. Seyferth, D. P. Duncan and M. L. Shannon, *Organometallics*, **3**, 579 (1984).
67. D. Seyferth, S. C. Vick and M. L. Shannon, *Organometallics*, **3**, 1897 (1984).
68. P. Boudjouk and U. Samaraweera, *Organometallics*, **9**, 2205 (1990).
69. P. Boudjouk, E. Black, R. Kumarathasan, U. Samaraweera, S. Castellino, J. P. Oliver and J. W. Kampf, *Organometallics*, **13**, 3715 (1994).
70. T. Yamamoto, Y. Kabe and W. Ando, *Organometallics*, **12**, 1996 (1993).
71. R. Noyori, T. Nishimura and H. Takaya, *J. Chem. Soc., Chem. Commun.*, 89 (1969).
72. R. Noyori, T. Odagi and H. Takaya, *J. Am. Chem. Soc.*, **92**, 5780 (1970).
73. R. Noyori, Y. Kumagai, I. Umeda and H. Takaya, *J. Am. Chem. Soc.*, **94**, 4018 (1972).
74. R. Noyori, M. Yamakawa and H. Takaya, *Tetrahedron Lett.*, 4823 (1978).
75. P. Binger and U. Schuchardt, *Angew. Chem., Int. Ed. Engl.*, **16**, 249 (1977).
76. P. Binger, Q.-H. Liü and P. Wedemann, *Angew. Chem., Int. Ed. Engl.*, **24**, 316 (1985).
77. D. Seyferth, M. L. Shannon, S. C. Vick and T. F. O. Lim, *Organometallics*, **4**, 57 (1985).
78. M. Ishikawa, J. Oshita, Y. Ito and J. Iyoda, *J. Am. Chem. Soc.*, **108**, 7417 (1986).
79. J. Oshita, Y. Isomura and M. Ishikawa, *Organometallics*, **8**, 2050 (1989).
80. W. Ando, T. Yamamoto, H. Saso and Y. Kabe, *J. Am. Chem. Soc.*, **113**, 2791 (1991).
81. Y. Kabe, T. Yamamoto and W. Ando, *Organometallics*, **13**, 4606 (1994).
82. N. Choi, Y. Kabe and W. Ando, *Organometallics*, **11**, 1506 (1992).
83. J. F. Hartwig, R. A. Anderson and R. G. Bergman, *J. Am. Chem. Soc.*, **112**, 5670 (1990).
84. J. F. Hartwig, R. G. Bergman and R. A. Anderson, *Organometallics*, **10**, 3326 (1991).
85. B. K. Campion, R. H. Heyn and T. D. Tilley, *J. Am. Chem. Soc.*, **110**, 7558 (1988).
86. B. K. Campion, R. H. Heyn and T. D. Tilley, *J. Am. Chem. Soc.*, **112**, 4079 (1990).
87. T. S. Koloski, P. J. Carroll and D. H. Berry, *J. Am. Chem. Soc.*, **112**, 6405 (1990).
88. V. V. Kane, A. D. Wolf and and M. Jones Jr., *J. Am. Chem. Soc.*, **96**, 2643 (1974).
89. L. W. Jenneskens, F. J. J. de Kanter, P. A. Kraakman, L. A. M. Turkenburg, W. E. Koolhaas, W. H. de Wolf, F. Bickelhaupt, Y. Tobe, K. Kakiuchi and Y. Odaira, *J. Am. Chem. Soc.*, **107**, 3716 (1985).
90. T. Tsuji and S. Nishida, *J. Chem. Soc., Chem. Commun.*, 1189 (1987).
91. W. Ando, T. Tsumuraya and Y. Kabe, *Angew. Chem., Int. Ed. Engl.*, **29**, 778 (1990).
92. H. Sakurai, S. Hoshi, A. Kamiya, A. Hosomi and C. Kabuto, *Chem. Lett.*, 1781 (1986).
93. C. Elschenbroich, J. Hurley, W. Massa and G. Baum, *Angew. Chem., Int. Ed. Engl.*, **27**, 684 (1988).
94. N. L. Allinger, T. J. Walter and M. G. Newton, *J. Am. Chem. Soc.*, **96**, 4588 (1974).
95. M. G. Newton, T. J. Walter and N. L. Allinger, *J. Am. Chem. Soc.*, **95**, 5652 (1973).
96. P. Hemmersbach, M. Klessinger and P. Bruckmann, *J. Am. Chem. Soc.*, **100**, 6344 (1978).
97. D. Seyferth, E. W. Goldman and J. Escudie, *J. Organomet. Chem.*, **271**, 337 (1984).
98. L. E. Gusel'nikov and Y. P. Polyakov, in *Frontiers of Organosilicon Chemistry* (Eds. A. A. Bassindale and P. P. Gaspar), The Royal Society of Chemistry, 1991, pp. 50–61.
99. J. Ohshita, Y. Masaoka and M. Ishikawa, *Organometallics*, **10**, 3775 (1991).
100. D. Bravo-Zhivotovskii, V. Braude, A. Stanger, M. Kapon and Y. Apeloig, *Organometallics*, **11**, 2326 (1992).
101. W. H. Atwell and J. G. Uhlmann, *J. Organomet. Chem.*, **52**, C21 (1973).
102. H. Sakurai, T. Kobayashi and Y. Nakadaira, *J. Organomet. Chem.*, **162**, C43 (1978).
103. D. Seyferth, D. C. Annarelli and S. C. Vick, *J. Organomet. Chem.*, **272**, 123 (1984).
104. J. Belzner, H. Ihmels, B. O. Kneisel and R. Herbst-Irmer, *J. Chem. Soc., Chem. Commun.*, 1989 (1994).
105. K. Tamao, K. Nagata, M. Asahara, A. Kawachi, Y. Ito and M. Shiro, *J. Am. Chem. Soc.*, **117**, 11592 (1995).
106. M. Ishikawa, T. Fuchikami, M. Kumada, T. Higuchi and S. Miyamoto, *J. Am. Chem. Soc.*, **101**, 1348 (1979).
107. M. Ishikawa, K. Nishimura, H. Ochiai and M. Kumada, *J. Organomet. Chem.*, **236**, 7 (1982).
108. K. Shiina, *J. Organomet. Chem.*, **310**, C57 (1986).
109. T. Kusukawa, Y. Kabe and W. Ando, *Chem. Lett.*, 985 (1993).
110. T. Kusukawa, Y. Kabe, B. Nestler and W. Ando, *Organometallics*, **14**, 2556 (1995)

111. K. Tamao, T. Hayashi and M. Kumada, *J. Organomet. Chem.*, **114**, C19 (1976).
112. H. Sakurai, Y. Kamiyama and Y. Nakadaira, *J. Organomet. Chem.*, **131**, 147 (1977).
113. M. Suginome, H. Oike and Y. Ito, *Organometallics*, **13**, 4148 (1994).
114. M. Suginome, H. Oike and Y. Ito, *J. Am. Chem. Soc.*, **117**, 1665 (1995).
115. M. Suginome, H. Oike, P. H. Shuff and Y. Ito, *Organometallics*, **15**, 2170 (1996).
116. M. Suginome, H. Oike, S.-S. Park and Y. Ito, *Bull. Chem. Soc. Jpn.*, **69**, 289 (1996).
117. Y. Uchimaru, Y. Tanaka and M. Tanaka, *Chem. Lett.*, 164 (1995).
118. Y. Pan, J. T. Mauge and M. J. Fink, *Organometallics*, **11**, 3495 (1992).
119. M. Murakami, T. Yoshida and Y. Ito, *Organometallics*, **13**, 2900 (1994).
120. W. A. Nugent, D. L. Thorn and R. L. Harlow, *J. Am. Chem. Soc.*, **109**, 2788 (1987).
121. E. Negishi, J. S. Holmes, J. M. Tour, J. A. Miller, F. E. Cederbaum, D. R. Swanson and T. Takahashi, *J. Am. Chem. Soc.*, **111**, 3336 (1989).
122. S. S. H. Mao and T. D. Tilley, *J. Am. Chem. Soc.*, **117**, 5365 (1995).
123. S. S. H. Mao and T. D. Tilley, *J. Am. Chem. Soc.*, **117**, 7031 (1995).
124. T. Takahashi, Z. Xi, Y. Obora and N. Suzuki, *J. Am. Chem. Soc.*, **117**, 2665 (1995).
125. Y. Kabe, S. Kadoi, A. Sato and W. Ando, unpublished results.
126. P. J. Fagan, W. A. Nugent and J. C. Calabrese, *J. Am. Chem. Soc.*, **116**, 1880 (1994).
127. S. Kim and K. H. Kim, *Tetrahedron Lett.*, **36**, 3725 (1995).
128. C. Grugel, W. P. Neumann and M. Schriewer, *Angew. Chem., Int. Ed. Engl.*, **18**, 543 (1979).
129. K. Kuno, K. Kobayashi, M. Kawanishi, S. Kozima and T. Hitomi, *J. Organomet. Chem.*, **137**, 349 (1977).
130. E. J. Corey, F. A. Carey and R. A. Winter, *J. Am. Chem. Soc.*, **87**, 934 (1965).
131. P. J. Kroop, *J. Am. Chem. Soc.*, **91**, 5783 (1969).
132. Y. Inoue, S. Takamura and H. Sakurai, *J. Chem. Soc., Perkin Trans. 2*, 1635 (1977).
133. M. Squillacote, A. Bergman and J. D. Felippis, *Tetrahedron Lett.*, **30**, 6805 (1989).
134. J. L. Goodman, K. S. Peters, H. Misawa and R. A. Caldwell, *J. Am. Chem. Soc.*, **108**, 6803 (1986).
135. S. F. Sellers, T. C. Klebach, F. Hollowood and M. Jones, Jr., *J. Am. Chem. Soc.*, **104**, 5492 (1982).
136. T. Shimizu, K. Shimizu and W. Ando, *J. Am. Chem. Soc.*, **113**, 354 (1991).
137. K. B. Wiberg, *Chem. Rev.*, **89**, 975 (1989).
138. G. Szeimies, in *Strain and Its Implications in Organic Chemistry* (Eds. A. De Meijere and S. Blechert), Kluwer Academic, Dordrecht, 1989 p. 361.
139. W. Ando, Y. Igarashi, Y. Kabe and N. Tokitoh, *Tetrahedron Lett.*, **31**, 4185 (1990).
140. Y. Igarashi, Y. Kabe, T. Hagiwara and W. Ando, *Tetrahedron*, **48**, 89 (1992).
141. A. Krebs and J. Wilke, *Top. Curr. Chem.*, **109**, 189 (1983).
142. H. Sakurai, Y. Nakadaira, A. Hosomi, Y. Eriyama and C. Kabuto, *J. Am. Chem. Soc.*, **105**, 3359 (1983).
143. H. Sakurai, Y. Eriyama, A. Hosomi, Y. Nakadaira and C. Kabuto, *Chem. Lett.*, 595 (1984).
144. R. Bortolin, B. Parbhoo and S. S. D. Brown, *J. Chem. Soc., Chem. Commun.*, 1079 (1988).
145. M. Voronkov, O. Yarosh, G. Turkina, V. Vitkovskii and A. Albanov, *J. Organomet. Chem.*, **389**, 1 (1990).
146. T. Iwahara and R. West, *Chem. Lett.*, 545 (1991).
147. K. Sakamoto, M. Tumura and H. Sakurai, *Chem. Lett.*, 549 (1991).
148. M. Ishikawa, T. Hatano, Y. Hasegawa, T. Horio, A. Kunai, A. Miyai, T. Ishida, T. Tsukihara, T. Yamanaka, T. Koike and J. Shioya, *Organometallics*, **11**, 1604 (1992).
149. G. Wittig and J. Meske-Schüller, *Justus Liebigs Ann. Chem.*, **711**, 65 (1968).
150. A. Krebs and H. Kimling, *Angew. Chem., Int. Ed. Engl.*, **10**, 509 (1971).
151. S. F. Karaev and A. Krebs, *Tetrahedron Lett.*, 2853 (1973).
152. A. Krebs and H. Kimling, *Justus Liebigs Ann. Chem.*, 2074 (1974).
153. A. Krebs and G. Burgdöfer, *Tetrahedron Lett.*, 2063 (1973).
154. W. Ando, N. Nakayama, Y. Kabe and T. Shimizu, *Tetrahedron Lett.*, **31**, 3597 (1990).
155. F. Hojo, S. Sekigawa, N. Nakayama, T. Shimizu and W. Ando, *Organometallics*, **12**, 803 (1993).
156. S. Sekigawa, T. Shimizu and W. Ando, *Tetrahedron*, **49**, 6359 (1993).
157. P. Saxe and H. F. Schafer III, *J. Am. Chem. Soc.*, **102**, 3239 (1980).
158. G. Fitzgerald, P. Saxe and H. F. Schafer III, *J. Am. Chem. Soc.*, **105**, 690 (1983).
159. S. Olivella, M. A. Pericas, A. Riera and A. Sole, *J. Am. Chem. Soc.*, **108**, 6884 (1986).
160. S. Olivella, M. A. Pericas, A. Riera, F. Serratosa and A. Sole, *J. Am. Chem. Soc.*, **109**, 5600 (1987).

161. W. Ando, F. Hojo, S. Sekigawa, N. Nakayama and T. Shimizu, *Organometallics*, **11**, 1009 (1992).
162. Y. Pang, A. Schneider, T. J. Barton, M. S. Gordon and M. T. Carroll, *J. Am. Chem. Soc.*, **114**, 4920 (1992).
163. M. I. Bruce, *Chem. Rev.*, **91**, 197 (1991).
164. H. Sakurai, T. Fuji and K. Sakamoto, *Chem. Lett.*, 339 (1992).
165. D. Schnider and H. Werner, *Angew. Chem., Int. Ed. Engl.*, **30**, 700 (1991).
166. J. R. Fritch, K. P. C. Vollhardt, M. R. Thompson and V. W. Day, *J. Am. Chem. Soc.*, **101**, 2768 (1979).
167. F. Hojo, K. Fujiki and W. Ando, *Organometallics*, **15**, 3606 (1996).
168. W. Smadja, *Chem. Rev.*, **83**, 263 (1983).
169. D. J. Pasto, *Tetrahedron*, **40**, 2805 (1984).
170. R. P. Johnson, *Chem. Rev.*, **89**, 1111 (1989).
171. J. D. Price and R. P. Johnson, *Tetrahedron Lett.*, **27**, 4679 (1986).
172. T. Shimizu, F. Hojo and W. Ando, *J. Am. Chem. Soc.*, **115**, 3111 (1993).
173. L. Skättebol, *Tetrahedron Lett.*, 1967 (1961).
174. L. Skättebol and S. Solomon, *Org. Synth.*, **49**, 35 (1969).
175. P. J. Garratt, K. C. Nicolau and F. Sondheimer, *J. Am. Chem. Soc.*, **95**, 4582 (1973).
176. H. Irngartinger and H-U. Jäger, *Tetrahedron Lett.*, 3595 (1976).
177. W. R. Moore and H. R. Ward, *J. Org. Chem.*, **27**, 4179 (1962).
178. M. S. Baird and C. B. Reese, *Tetrahedron*, **32**, 2153 (1976).
179. F. Hojo, T. Shimizu and W. Ando, *Chem. Lett.*, 1171 (1993).
180. J. Lin, Y. Pang, V. G. Young, Jr. and T. J. Barton, *J. Am. Chem. Soc.*, **115**, 3794 (1993)
181. M. Nakazaki, K. Yamamoto, M. Maeda, O. Sato and T. Tsutsui, *J. Org. Chem.*, **47**, 1435 (1982).
182. S. A. Petrich, Y. Pang, V. G. Young, Jr. and T. J. Barton, *J. Am. Chem. Soc.*, **115**, 1591 (1993).
183. Y. Pang, S. A. Petrich, V. G. Young, Jr., M. S. Gordon and T. J. Barton, *J. Am. Chem. Soc.*, **115**, 2534 (1993).
184. O. L. Chapman, *Pure Appl. Chem.*, **40**, 511 (1974).
185. T. J. Stierman and R. P. Johnson, *J. Am. Chem. Soc.*, **105**, 2492 (1983).
186. T. J. Stierman and R. P. Johnson, *J. Am. Chem. Soc.*, **107**, 3971 (1985).
187. J. D. Price and R. P. Johnson, *J. Am. Chem. Soc.*, **107**, 2187 (1985).
188. T. J. Stierman, W. C. Shakespeare and R. P. Johnson, *J. Org. Chem.*, **55**, 1043 (1990).
189. J. P. Price and R. P. Johnson, *J. Org. Chem.*, **56**, 6372 (1991).
190. F. Hojo, T. Shimizu and W. Ando, *Organometallics*, **13**, 3402 (1994).
191. W. Ando, T. Wakahara, T. Akasaka and S. Nagase, *Organometallics*, **13**, 4683 (1994).
192. T. Wakahara, R. Kodama, T. Akasaka and W. Ando, *Bull. Chem. Soc. Jpn.*, **70**, 665 (1997).
193. P. Jutzi, *Chem. Ber.*, **104**, 1455 (1971).
194. P. Jutzi, *Angew. Chem., Int. Ed. Engl.*, **14**, 232 (1975).
195. Y. van den Winkel, B. L. M. van Baar, F. Bickelhaupt, W. Kulik, C. Sierakowski and G. Maier, *Chem. Ber.*, **124**, 185 (1991).
196. Y. van den Winkel, B. L. M. van Baar H., M. M. Bastiaans, F. Bickelhaupt, M. Schenkel and H. B. Stegmann *Tetrahedron*, **46**, 1009 (1990).
197. F. Bickelhaupt and G. L. van Mourik, *J. Organomet. Chem.*, **67**, 389 (1974).
198. W. Z. McCarthy, J. Y. Corey and E. R. Corey, *Organometallics*, **3**, 255 (1984).
199. J. Y. Corey and W. Z. McCarthy, *J. Organomet. Chem.*, **271**, 319 (1984).
200. W. Ando, K. Hatano and R. Urisaka, *Organometallics*, **14**, 3625 (1995).
201. K. Hatano, K. Morihashi, O. Kikuchi and W. Ando, *Chem. Lett.*, 293 (1997).
202. G. A. Olah and R. J. Hunadi, *J. Am. Chem. Soc.*, **102**, 6989 (1980).
203. U. Edlund and E. Buncel, *Prog. Phys. Org. Chem.*, **19**, 254 (1993).

CHAPTER 43

Silylenes

PETER P. GASPAR

Department of Chemistry, Washington University, St. Louis, Missouri 63130-4899, USA
Fax: 314-935-4481; e-mail: gaspar@wuchem.wustl.edu

and

ROBERT WEST

Department of Chemistry, University of Wisconsin at Madison, Wisconsin 53706, USA
Fax: 608-262-0381; e-mail: west@chem.wisc.edu

I. INTRODUCTION

It is now over a decade since the last attempts to survey all of silylene chemistry$^{1-5}$. While new work continues to be published at a brisk pace, it is fair to state that the field has reached a stage of maturity in which silylenes are tools for answering questions as much as ends in themselves. That implies a belief that the broad outlines of silylene chemistry are known and can be applied. This is not to say that there are no surprises, and indeed there is considerable healthy controversy, extending even to what one means by ‘silylene’.

The chapter table of contents contains subjects that were either unknown or merely distant hopes a decade ago, such as persistent silylenes, the dissociation of disilenes to silylenes and terminal silylene–transition metal complexes. The kinetics and spectroscopy of silylenes and theoretical treatments of silylene structure and reactivity have made such gigantic strides in the intervening years that they represent new vistas in our understanding.

Theoretical calculations of ‘chemical accuracy’ can now predict reaction pathways as well as structures and energies.

In what follows, emphasis will be placed on developments of the past decade, with sufficient (but brief) summaries of previous work and references to earlier reviews and seminal papers to allow this chapter to function as a stand-alone unit. We attempt to place silylene chemistry in a broader context and to interpret as well as describe important discoveries.

Reviews have been presented of inorganic silylenes[6], silylene chemistry in the gas phase[7] and sterically encumbered silylenes[8].

II. GENERATION OF SILYLENES

A. Thermolysis of Polysilanes

The pyrolysis of polysilanes played an important role in the discovery of silylene reactions[1–3,5] and is still widely used for the generation of silylenes in the gas phase. Many such reactions are concerted silylene extrusions in which a substituent migrates from the incipient divalent silicon atom during Si−Si bond cleavage (equation 1).

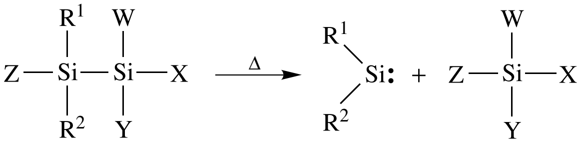

$$\text{Z—Si}(R^1)(R^2)\text{—Si}(W)(Y)\text{—X} \xrightarrow{\Delta} R^1R^2\text{Si:} + \text{Z—Si}(W)(Y)\text{—X} \qquad (1)$$

The migrating group Z can be hydrogen, halogen or alkoxy. It is not an overstatement that the 1966 discovery by Atwell and Weyenberg that the 1,2-shift of methoxy groups in disilanes takes place under relatively mild conditions ushered in the use of silylenes as synthetic reagents[9]. The ease of elimination, alkoxy > hydrogen > chlorine, has been measured quantitatively[10]. First-order rate constants for extrusion of Me_2Si at 350 °C from $Me_3SiSiMe_2X$ ($X = OMe$, H, Cl) were found to be 1.2×10^{-3}, 1.9×10^{-4} and 1.3×10^{-6} s^{-1}, respectively. The other groups can be virtually any substituent that migrates more slowly than Z[2]. The symmetrical precursors shown in equations 2 and 3 have seen wide use in the generation of Me_2Si and H_2Si, respectively.

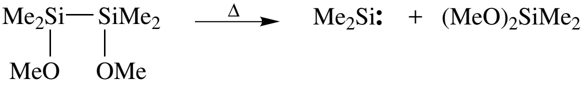

$$Me_2Si(OMe)\text{—}SiMe_2(OMe) \xrightarrow{\Delta} Me_2Si\text{:} + (MeO)_2SiMe_2 \qquad (2)$$

$$H_3Si\text{—}SiH_3 \xrightarrow{\Delta} H_2Si\text{:} + SiH_4 \qquad (3)$$

Trisilanes capable of the sequential pairwise loss of all four substituents from the central silicon can function as silicon atom synthons (see equation 4)[11]. Where comparison with reactions of atomic silicon has been possible, the product yield from the synthon has been higher.

The kinetics of the pyrolysis of disilane and substituted disilanes has received considerable attention in connection with the estimation of the heats of formation of silylenes. Martin, Ring and O’Neal reexamined the pyrolysis of Si_2H_6 (equation 3) in a static reactor and found both the high-pressure A-factor ($10^{15.6}$ to $10^{16.0}$ s^{-1}) and E_a (51.2 kcal mol^{-1}) to be higher than previously determined[12]. Walsh argued in 1988 that the A-factors for the disilanes $Me_nH_{3-n}SiSiH_3$ were all higher than the previous experimentally based estimates (with the exception of $Me_2HSiSiH_3$)[13]. Walsh's higher suggested activation parameters for MeH_2SiSiH_3 were very close to those subsequently found ($\log A = 15.6$ suggested versus 15.53 ± 0.28 found, $E_a = 51.7$ kcal mol^{-1} suggested versus 51.53 ± 0.65 kcal mol^{-1})[14]. Ring, O'Neal and coworkers found that eliminations of hydrogenated silylenes SiH_2 or H_3SiSiH proceed through 'looser' transition states with higher A-factors than do eliminations of alkylated silylenes such as MeHSi, Me_2Si, or $Me_2HSiSiH$[15]. Reexamination of the pyrolysis of $Me_3SiSiHMe_2$ and $Me_3SiSiMe_2SiHMe_2$ by Davidson and coworkers did, however, support earlier, lower values of the activation parameters[16].

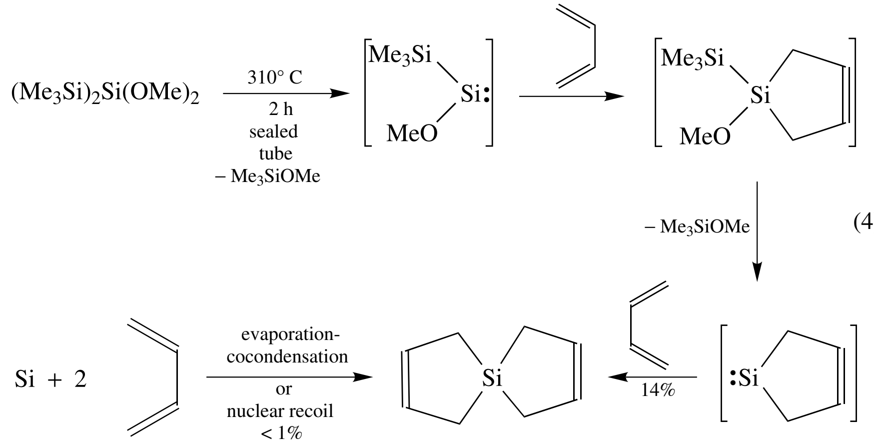

(4)

Ab initio molecular orbital calculations have been carried out by Ignacio and Schlegel on the thermal decomposition of disilane and the fluorinated disilanes $Si_2H_nF_{6-n}$[17]. Both 1,1-elimination of H_2 or HF and silylene extrusion by migration of H and F atoms concerted with Si−Si bond cleavage were considered. The transition states for the extrusion reactions all involved movement of the migrating atom toward the empty p-orbital of the extruded silylene in the insertion which is the retro-extrusion (equation 5).

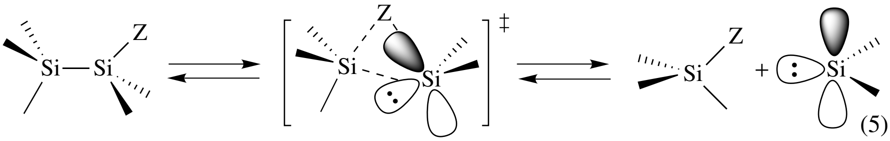

(5)

For all the fluorodisilanes considered, the barriers for the elimination of HF and the homolytic cleavage of an Si−Si bond were considerably higher than those for elimination of H_2 or the extrusion of a silylene.

Corriu and coworkers have suggested that pyrolysis of poly(silylethylene) $\left(SiH_2CH_2CH_2\right)_n$ can lead to silylenes by two processes: (1) Loss of H_2 without chain cleavage; (2) extrusion of a silylene $(SiH_2CH_2CH_2)_nSiH$ with cleavage of an Si−C bond and migration of an H-atom forming $CH_3CH_2(SiH_2CH_2CH_2)_n$[18]. The first process leads to crosslinking via silylene insertion into Si−H bonds, while the second accounts for fragmentation of the polymer with the formation of $EtSiH_2$ chain ends.

Recently, flow thermolysis of disilanes has been used by Heinicke and coworkers to obtain the silylenes Me(Cl)Si, Me(MeO)Si and Me(Me_2N)Si, which were trapped with dienes to give silacyclopentenes[19]. The results with Me(Cl)Si are outlined in equation 6. With 1,3-butadiene and isoprene small amounts of the silacyclopent-2-ene were obtained along with the major product, the silacyclopent-3-ene isomer.

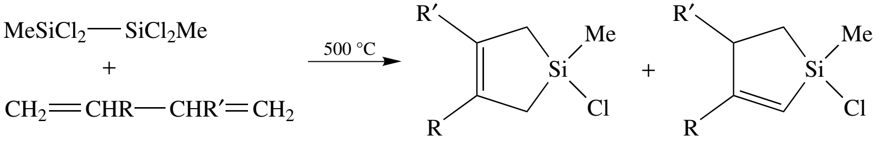

(6)

$R = R' = H$	88	:	12
$R = Me, R' = H$	85	:	15
$R = R' = Me$	100	:	0

Similar results were obtained with Me(MeO)Si and $Me(Me_2N)Si$, consistent with a stepwise mechanism in which initial (2+1)cycloaddition is followed by rearrangement, as proposed earlier by Lei and coworkers[20]. Under the experimental conditions, the temperatures required for silylene generation were 400 °C for $[MeSi(OMe)_2]_2$, 420 °C for $[MeSi(NMe_2)_2]_2$ and 500 °C for $[MeSiCl_2]_2$[20].

The silylenes were also generated in the presence of heterodienes, including unsaturated aldehydes and ketones, diimines, diketones and iminoketones, to yield a variety of five-ring heterocycles containing Si−N and/or Si−O bonds[21]. Two examples are given in equations 7 and 8. With the α,β-unsaturated ketone in equation 7, the major product is the 3-ene isomer, but with the unsaturated imine in equation 8, both the 2-ene and 3-ene isomers are formed. Both reactions probably proceed through initial cycloaddition of the silylene to the C−heteroatom bond, as shown. Formation of the 2-ene isomer certainly suggests a three-membered ring intermediate.

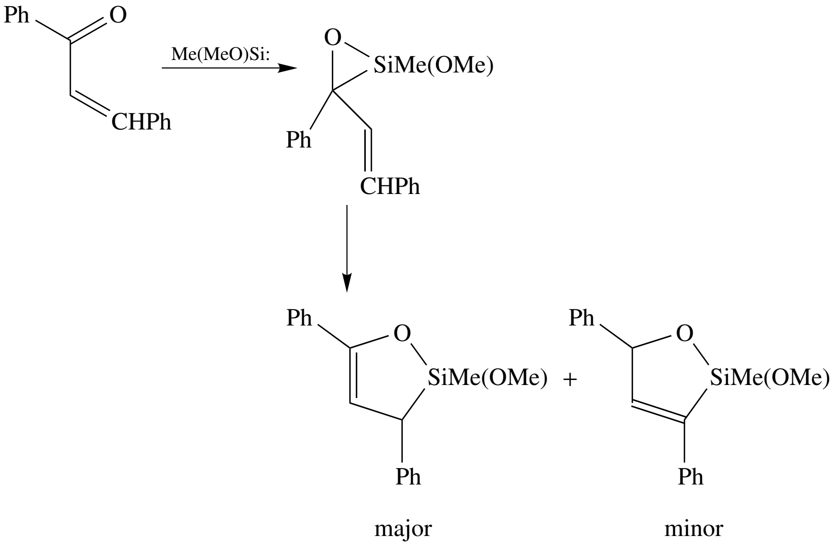

(7)

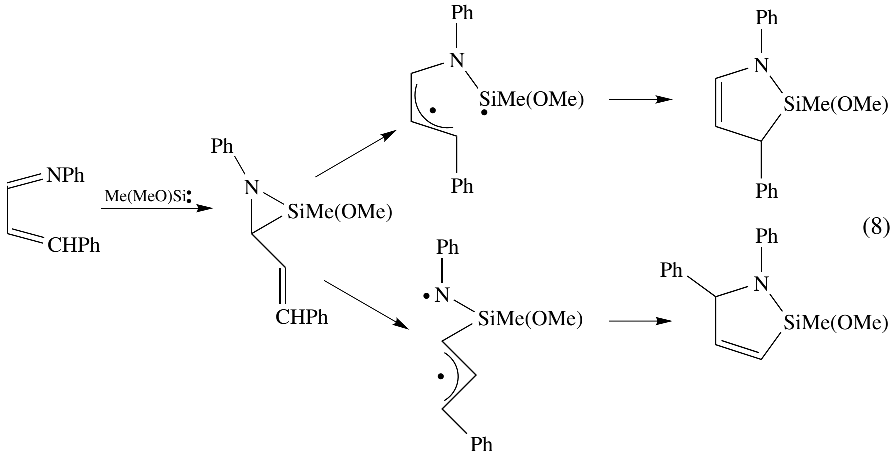

(8)

Intermolecular base-assisted disproportionation of disilanes also takes place, as was shown some years ago for Si_2Cl_6 and $MeSi_2Cl_5$[22]. These yielded branched oligosilanes upon treatment with Me_3N. Recently, the base-catalyzed disproportionation of the disilanes $MeSiCl_2SiCl_2Me$, $MeSiCl_2SiClMe_2$ and $Me_2SiClSiClMe_2$ has been investigated[23]. Catalysts employed were 1-methylimidazole, for homogeneous reactions, and a solid catalyst with $PO(NMe_2)_2$ groups attached to a silicate carrier for heterogeneous catalysis. A variety of branched oligomeric polysilanes was obtained. The reaction is thought to proceed via initial Lewis acid–Lewis base adduct formation, followed by a 1,2-chlorine shift to give a base-stabilized silylene which inserts into Si−Cl bonds to give the products. The preference for branched chains reflects the preference for insertion of the silylene into a central rather than a terminal Si−Cl bond. For example, see Scheme 1.

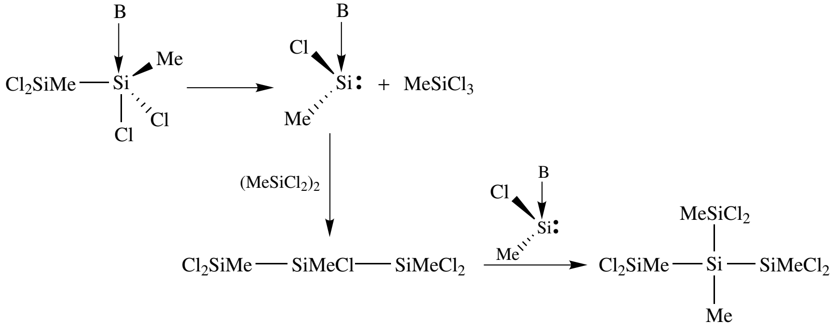

SCHEME 1

Fragmentation of pentacoordinate di- or polysilanes, assisted by intramolecular coordination by chelating nitrogen atoms, can occur at very modest temperatures (see Section VIII.D).

B. Silicon Atom Reactions

Insertion, addition and abstraction reactions of free silicon atoms can lead to the formation of silylenes (equation 9)[1–5]. Silylene formation for reaction, spectroscopic and mechanistic studies has been initiated by high-temperature evaporation of bulk silicon and cocondensation of the resulting vapor (consisting largely of free silicon atoms) with substrates. Silicon atom insertion into H_2 delivered matrix-isolated $H_2Si\colon$ for spectroscopic study[24]. Among the first mechanistic studies of silylenes were experiments employing free silicon atoms from the nuclear transformation $^{31}P(n,p)^{31}Si$[25–27].

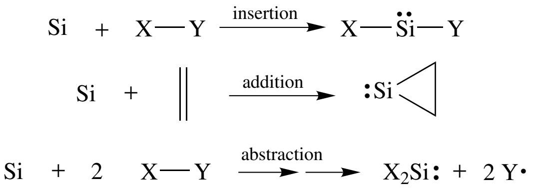

(9)

When a gaseous phosphorus-containing compound is irradiated with fast neutrons, high-energy silicon ions recoiling from this nuclear transformation break loose from the atoms to which their mother atoms were attached. Valence electrons are left behind as well, but neutralization and loss of energy occur before bond formation can occur. Thus the nuclear recoil method produces epithermal neutral silicon atoms that are radioactive ($t_{1/2} = 2.62$ h) and so carry a convenient label. It has been demonstrated that $^{31}SiH_2$ formed in recoil experiments is in its ground singlet state and at ambient temperature when it undergoes reaction[28].

C. Photolysis of Silanes

1. Photolysis of polysilanes

The generation of silylenes by extrusion from a chain or ring containing at least three adjacent Si atoms has long been known[2,3]. Polysilane high polymers undergo photolysis by two main processes, homolytic Si−Si bond cleavage to silyl radicals and silylene elimination[29]. Photolysis of poly(di-*n*-butylsilylene) and poly(di-*n*-hexlsilylene) with light of various wavelengths showed that silylenes are produced only with short-wavelength UV radiation ($\lambda < 300$ nm); only silyl radicals are formed at longer wavelengths[30] (equation 10).

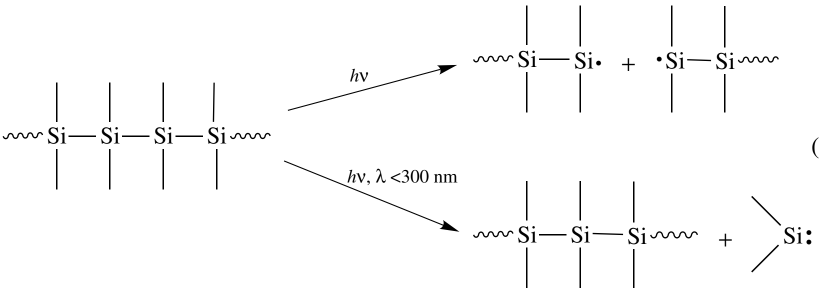

(10)

A recent flash photolytic study confirmed this unusual wavelength dependence for poly(phenylmethylsilylene). For this polymer also, irradiation at longer wavelengths (>300 nm) produced only silyl radicals. Light of higher energy yielded $PhMeSi\colon$[31], with $\lambda_{max} = 460$ nm, identified by trapping with triethylsilane. Similar results were obtained in the photolysis of network and branched polysilanes, $(Ph_2Si)_n(PhSi)_m$[32].

The photolysis of trisilanes, $RR'Si(SiMe_3)_2$, or of cyclosilanes $(RR'Si)_n$, is a well-established method for silylene generation[2,3]. Here we will describe only selected examples, concentrating especially on findings which bear on the mechanism of silylene elimination.

Photolysis of diphenylbis(trimethylsilyl)silane (**1**) produces diphenylsilylene, along with a significant amount of byproducts resulting from a 1,2-silyl shift to give a silatriene (Scheme 2). In an important study by Kira and coworkers[33] it was found that **1** undergoes nonresonant two-photon (NRTP) absorption upon laser irradiation at 532 nm, even though **1** shows no UV absorption beyond 300 nm. Thus **1** must belong to the class of molecules which have low-lying excited states to which NRTP is allowed, although single-photon absorption is forbidden. The most remarkable finding in this study was that the ratio of ethanol-trapped products, **2**:(**3A** + **3B**), depended on the absorption process. Irradiation of **1** at 266 nm gave yields of **2** and **3A** + **3B** of 53% and 30%, but NRTP at 532 nm produced these products in 80% and 13% yield, respectively. This unexpected selectivity provides an apparent exception to Kasha's rule[34], which states that rapid internal conversion to the lowest excited state takes place, so that photoproducts do not depend on the excitation mode. Such internal conversion must not happen for the NRTP excited state. It will be interesting to see if NRTP processes will provide product selectivity in other silane photolyses.

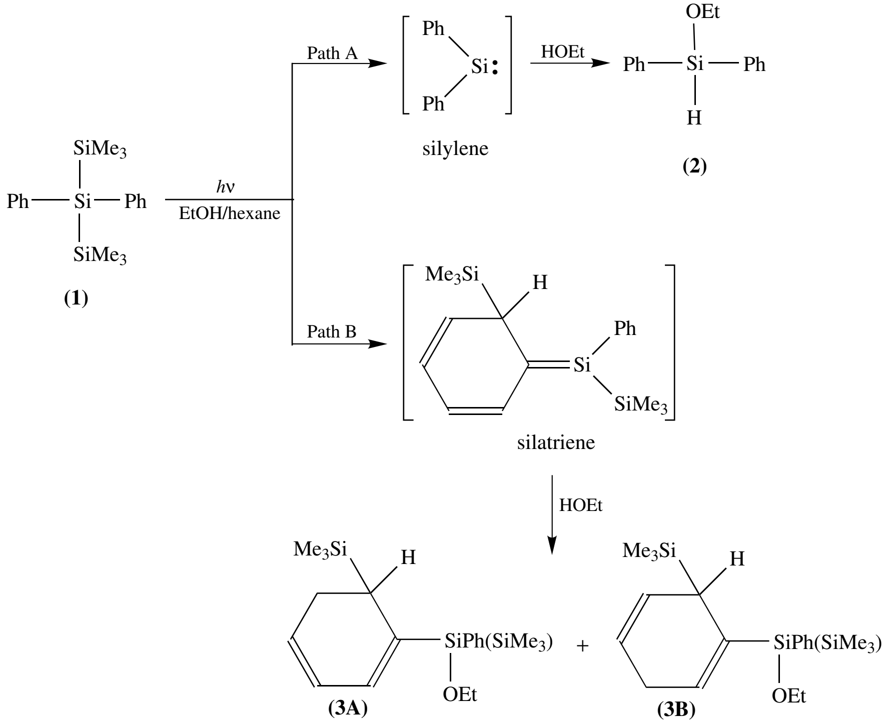

SCHEME 2

The photolysis of phenyltris(trimethylsilyl)silane in the presence of excess ethanol gave, as the first product, $PhSi(H)OEt{-}SiMe_3$. The amount of this product went through a maximum and then declined, being replaced by Me_3SiH and $PhSi(H)(OEt)_2$[35]. These results are best rationalized by sequential formation of two silylenes, as shown in equation 11.

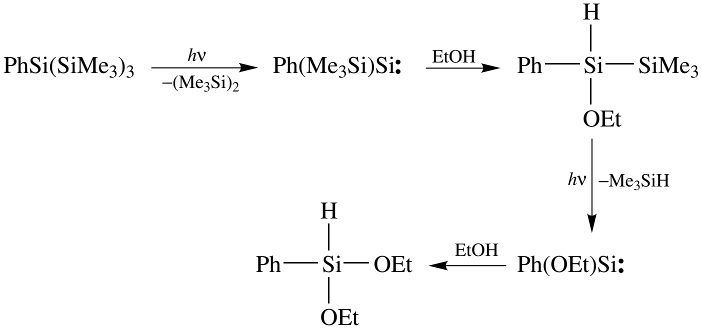

$$PhSi(SiMe_3)_3 \xrightarrow[-(Me_3Si)_2]{h\nu} Ph(Me_3Si)Si\colon \xrightarrow{EtOH} PhSi(H)(OEt)SiMe_3 \xrightarrow[-Me_3SiH]{h\nu} Ph(OEt)Si\colon \xrightarrow{EtOH} PhSi(H)(OEt)_2 \tag{11}$$

Photolysis of several polysilanes in a molecular beam has been investigated[36]. For $PhMeSi(SiMe_3)_2$ and $PhSi(SiMe_3)_3$, a single photon resulted in loss of only one $SiMe_3$ group; capture of a second photon was necessary for cleavage of a second Si−Si bond and formation of the silylene. For the cyclic silane $(Me_2Si)_6$, on the other hand, a single photon sufficed to bring about elimination of $Me_2Si\colon$ and formation of $(Me_2Si)_5$. The implication is that the mechanism of the photolysis is quite different for these compounds. The result for $(Me_2Si)_6$ is consistent with, but does not require, a concerted mechanism for silylene extrusion. In any case, if the result is general for cyclosilanes, it may open up a new method for gas-phase generation of silylenes.

Several papers have appeared in which aryltris(trimethylsilyl)silanes have been employed as photoprecursors to trimethylsilyl-substituted silylenes, $Ar(Me_3Si)Si\colon$[37,38]. In addition, Conlin and coworkers have photolyzed vinyltris(trimethylsilyl)silane at 254 nm, and shown by trapping experiments with 2-trimethylsiloxybutadiene that both silylene (**4**) and silene (**5**) are formed (equation 12)[39].

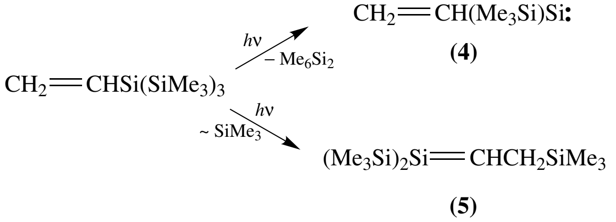

$$CH_2{=}CHSi(SiMe_3)_3 \xrightarrow[-Me_6Si_2]{h\nu} CH_2{=}CH(Me_3Si)Si\colon\ \textbf{(4)} \qquad CH_2{=}CHSi(SiMe_3)_3 \xrightarrow[\sim SiMe_3]{h\nu} (Me_3Si)_2Si{=}CHCH_2SiMe_3\ \textbf{(5)} \tag{12}$$

Photolysis of cyclic polysilanes to give silylenes was first pioneered in the 1970s by Kumada and Ishikawa[40]. The classic example is dodecamethylcyclohexasilane, $(Me_2Si)_6$, which yields $Me_2Si\colon$ and the ring-contracted product, $(Me_2Si)_5$[41,42]. UV light of $\lambda = 254$ nm from a mercury lamp is commonly used. Photolysis of polysilanes continues to be an important method for generation of silylenes; the readily-available five- and six-membered rings are most often employed. An example is the photolysis of the rotane **6** to cyclic silylene **7** (equation 13)[43].

Photolysis of cyclosilane rings containing heteroatoms also leads to silylenes, and sometimes this is the preferred route. An example is shown in equation 14[44]. Likewise, hexaneopentyl trisilaoxetane undergoes photolysis to give the silylene and a disilaoxirane

(equation 15)[45].

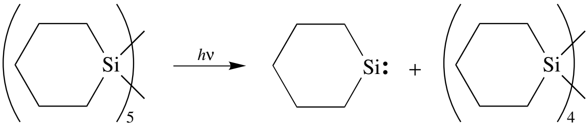

(6) **(7)**

(13)

$$(t\text{-BuMeSi})_4\text{O} \xrightarrow{h\nu} t\text{-BuMeSi}\colon + (t\text{-BuMeSi})_3\text{O} \tag{14}$$

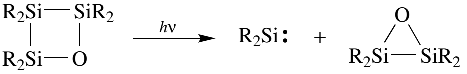

(15)

R = neopentyl

Shizuka and coworkers have shown that the photolysis of four-membered cyclosilanes depends on the ring conformation. Folded rings, such as $(i\text{-Pr}_2\text{Si})_4$ and $[\text{Me}(t\text{-Bu})\text{Si}]_4$, eliminate silylenes upon photolysis, but planar rings, $[(\text{Me}_3\text{Si})_2\text{Si}]_4$ and $[(\text{EtMe}_2\text{Si})_2]_4$, photolyze to two molecules of disilene, $\text{R}_2\text{Si}{=}\text{SiR}_2$[46].

In 1985[47], Weidenbruch and Pohl made the important discovery that hexa-*t*-butylcyclotrisilane photolyzes to yield both silylene and disilene (equation 16).

$$(t\text{-Bu}_2\text{Si})_3 \xrightarrow{h\nu} t\text{-Bu}_2\text{Si}\colon + t\text{-Bu}_2\text{Si}{=}\text{Si}(t\text{-Bu})_2 \tag{16}$$

This reaction, providing two highly reactive intermediates, has led to a remarkably rich and diverse reaction chemistry, too extensive for a complete treatment in this chapter. Readers are referred to Weidenbruch's comprehensive 1994 review of this area[8]; here we will describe only some developments stemming from this reaction since 1994.

Although the reaction of $t\text{-Bu}_2\text{Si}\colon$ with nitriles, isocyanides, carbonyl compounds and heterodienes had been studied earlier, the interaction with alkenes and dienes is new. Siliranes are obtained with alkenes, as predicted (equation 17)[48].

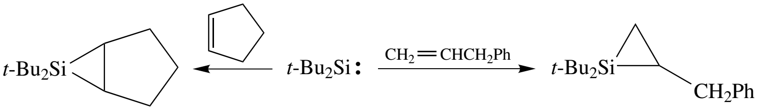

(17)

Silylene and disilene adducts are obtained with dienes (equation 18). With thiophene, desulfurization takes place and the products are more complicated, as shown in equation 19[49].

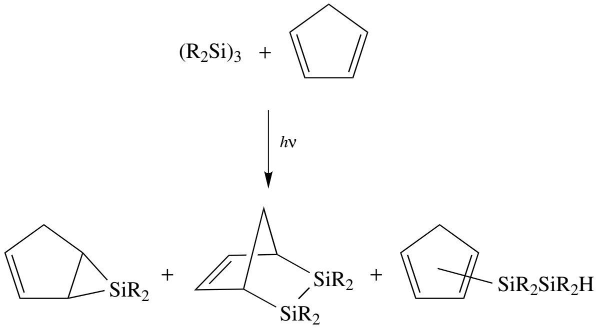

(18)

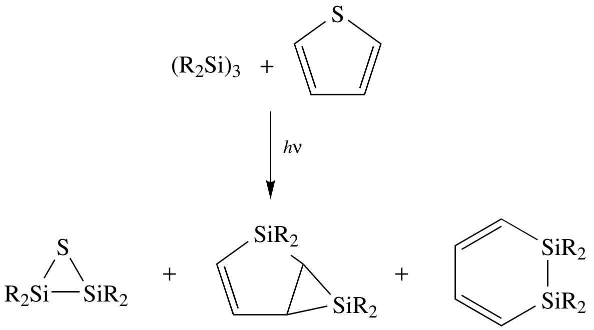

(19)

Complex products were also obtained from electron-poor dienes[50]. Photolysis of (t-$Bu_2Si)_3$ with tetrazine **8** gave a complex mixture of products, from which **9** and **10** could be isolated (equation 20). In **10**, one of the CF_3 groups has been completely degraded, with simultaneous rearrangement of the ring skeleton. The reaction with oxadiazole **11** also took an unexpected course (equation 21).

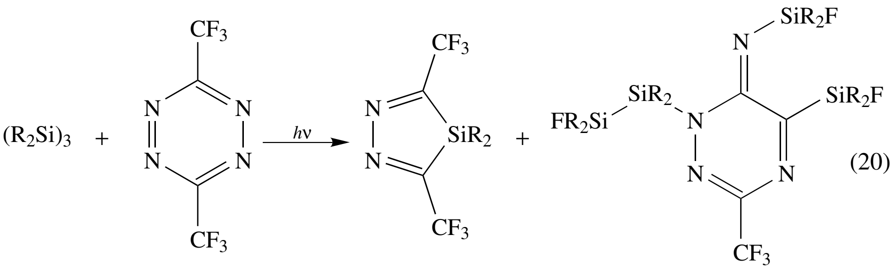

(20)

(8) **(9)** **(10)**

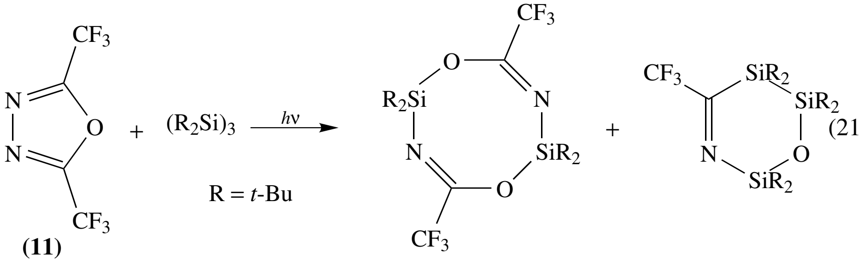

(21)

(11)

2. Other photolyses generating silylenes

Photochemical fragmentation of 7-silanorbornadienes is a convienent and frequently-used method for generation of silylenes. Nefedov and coworkers have studied this reaction for **12** using ^{1}H CIDNP to detect intermediate radicals[51]. The results indicate that the reaction proceeds through the reversible formation of a single biradical (**13**), which undergoes internal conversion to the triplet biradical. The latter eliminates dimethylsilylene irreversibly (Scheme 3). Similar conclusions were drawn for the germanium analog of **12**, which eliminates Me_2Ge: upon photolysis.

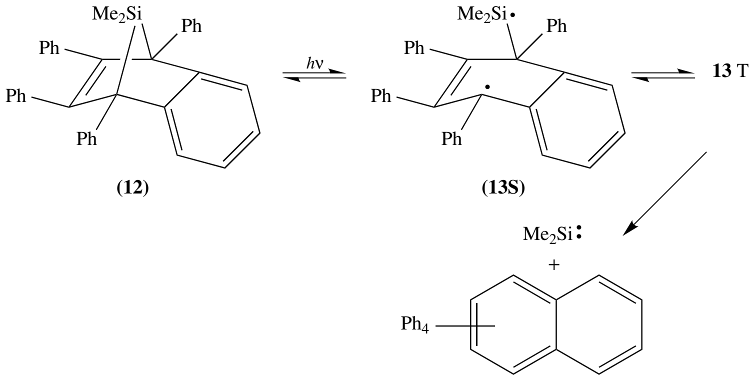

SCHEME 3

There is a difficulty with the mechanism of Scheme 3 in that the fragmentation of a triplet diradical should conserve spin, yet neither triplet Me_2Si: nor triplet tetraphenylnaphthalene have been detected. The diradical pathway for the photofragmentation of silanorbornadienes confirms an earlier proposal by Barton and coworkers[52]. There is always the possibility that diradical intermediates such as the singlet and triplet **13** S and **13** T could function as silylenoids. Thus, the assumption that products from pyrolysis of 7-silanorbornadienes are formed from free silylenes must be treated with caution.

A less-frequently employed route to silylenes is the photochemical cleavage of diazidosilanes, $RR'Si(N_3)_2$, first used for the matrix isolation of Me_2Si:[41]. Photolysis of $t\text{-}Bu_2Si(N_3)_2$ was studied in argon and 3-MP matrices, and found to give di-*t*-butylsilylene (**15**) through an intermediate assigned as diazosilane **14** (equation 22)[53]. Silylene **15** has an electronic absorption band at 480 nm; irradiation at 500 nm led to a hydrogen shift and formation of a silirane.

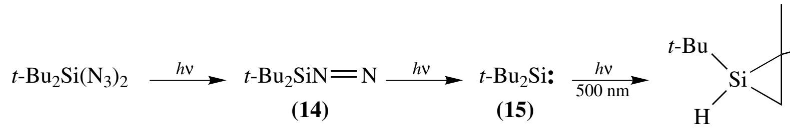

(22)

Other recent applications of the diazide photolysis route include the matrix isolation of some interesting cyclic silylenes (equations 23 and 24)[54,55]. Solution photolysis of diazides can give other reactive species in addition to silylenes.

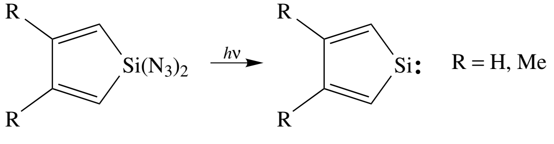

(23)

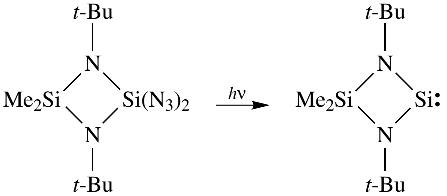

(24)

The use of siliranes as thermal sources of silylenes has long been known. At least in some cases, they can also yield silylenes photochemically. This has been demonstrated for di-*t*-butylsilylene[56] and di-1-adamantylsilylene (**16**)[57] as shown in equations 25 and 26.

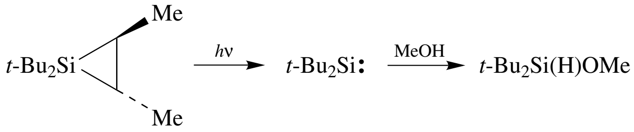

(25)

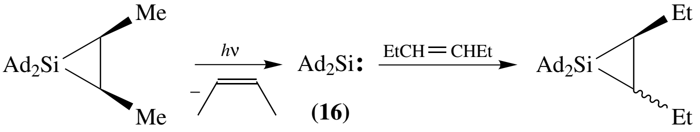

(16)

(26)

Most studies of silane photolysis have been conducted with radiation of wavelength 254 nm (high pressure mercury lamp) or lower energy. At higher energy, additional kinds of organosilanes may serve as silylene precursors. An initial foray in this direction has been reported by Steinmetz and Yu, who photolyzed silacyclopentene **17** with 214 nm radiation in methanol[58]. The predominant photoprocess was fragmentation to 1,3-butadiene and Me_2Si**:**. The silylene is partly trapped by methanol and partly reacts with the butadiene to give the vinylsilirane (**18**), which then undergoes stereoselective 1,4-addition of methanol (equation 27).

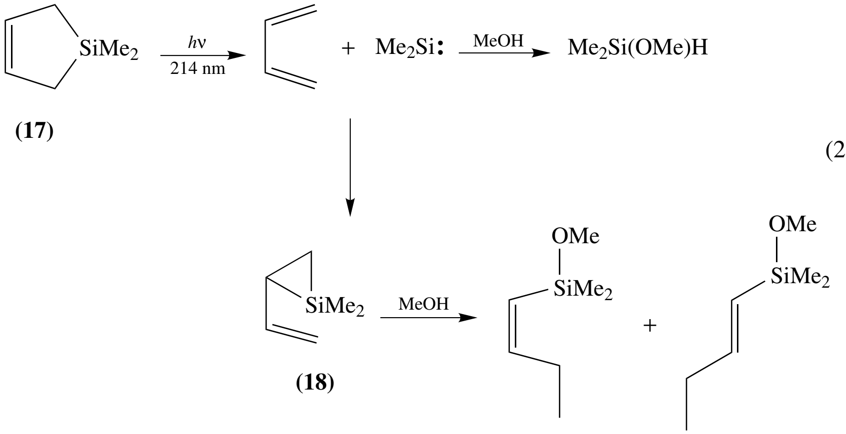

(17)

(18)

(27)

What is the effect of extremely high energies on silylene precursors? The fragmentation of polysilanes by gamma rays has been investigated by Nakao and coworkers[59,60]. Irradiation of $(Me_2Si)_6$ in a mixture of benzene and ethanol produced the silylene trapping product, $Me_2Si(H)OEt$, in yields up to 65%. Similarly, $PhMeSi(SiMe_3)_2$ was exposed to gamma rays in benzene-methanol, yielding PhMeSi(H)OMe as the major product. The reactions are thought to proceed through excitation of the benzene by the gamma rays, followed by collisional activation of the polysilane and loss of silylene.

D. Pyrolysis of Monosilanes

The simplest silylene SiH_2 can be formed by the homogeneous gas-phase elimination of H_2 from silane at temperatures above 380 °C (equation 28)[1–3]. This reaction has a long, controversial history and is of technological importance because of its contribution to the chemical vapor deposition of amorphous silicon from silane (*vide infra*). Pyrolysis of SiH_4 has seen little use in the study of silylene reactions, since it requires higher temperatures than the extrusion of SiH_2 from Si_2H_6 discussed in Section II.A (equation 3). The mechanism of silane pyrolysis has, however, been the subject of mechanistic studies for 60 years.

$$SiH_4 \xrightarrow{\Delta} H_2Si\mathbf{:} + H_2 \tag{28}$$

Ring, O'Neal and coworkers have contributed much to the understanding of silane decomposition. In 1985 they reexamined the kinetics of silane loss and its inhibition in the presence of excess H_2 which is common under CVD conditions[61]. They proposed an explanation for the transition from the initial stage (<1% conversion) of SiH_4 pyrolysis in which the reaction is 3/2 order to the middle stage (3 to 30% conversion) in which the reaction is first order and more rapid. It was suggested that, in the middle stage, elimination of H_2 from SiH_4 occurs as both a wall reaction and a gas-phase process, the onset of surface initiation being promoted by the deposition of oligomeric decomposition products. It was suggested that disilane and trisilane concentrations reach steady state due to their reversible formation by SiH_2 insertion reactions, and the reversible extrusion of SiH_4 from trisilane (equations 29–31).

$$H_2Si\mathbf{:} + SiH_4 \rightleftharpoons SiH_3SiH_3 \tag{29}$$

$$H_2Si\mathbf{:} + SiH_3SiH_3 \rightleftharpoons SiH_3SiH_2SiH_3 \tag{30}$$

$$SiH_3SiH_2SiH_3 \rightleftharpoons SiH_3SiH\mathbf{:} + SiH_4 \tag{31}$$

The dominant sink reaction for the removal of SiH_2 was believed to be 1,2-H_2-elimination from H_3SiSiH_3 forming $H_2Si{=}SiH_2$, which could undergo wall polymerization. In the final stage of silane pyrolysis (>30% conversion) reversal of H_2-elimination from SiH_4 could compete with other SiH_2 removal mechanisms, slowing the loss of SiH_4.

In 1991 Moffat, Jensen and Carr employed RRKM theory in the form of a non-linear regression analysis of experimental data to estimate the high-pressure Arrhenius parameters for elimination of H_2 from SiH_4 as $\log A = 15.79 \pm 0.5\ \mathrm{s}^{-1}$, $E_a = 59.99 \pm 2.0\ \mathrm{kcal\,mol^{-1}}$ and $\Delta H_f^\circ(SiH_2) = 65.5 \pm 1.0\ \mathrm{kcal\,mol^{-1}}$[62].

In 1992 Ring and O'Neal once more analyzed the thermal decomposition of SiH_4[63]. That the rates of SiH_2 insertion reactions and H_3SiSiH to $H_2Si{=}SiH_2$ rearrangement were much faster than previously believed, necessitated revisions in the reactions postulated to act as silylene 'sinks'. In a revised view of the elimination of H_2 from SiH_3SiH_3, the exclusive pathway was 1,1-elimination forming $H_3Si\ddot{S}iH$. Adsorption and subsequent decomposition on the walls of higher silanes such as tri- and tetrasilanes were believed to be the major processes responsible for removal of the gaseous species. The modeling of silane thermal decomposition also indicated that all silylene Si−H insertion reactions have negative activation energies (see Section VI).

Also in 1992 Becerra and Walsh suggested that the increase in the rate of silane loss in the 3 to 30% conversion middle stage of silane pyrolysis is due to the chain process (equation 32) in which the chemically activated silylene insertion product gives rise to a silylsilylene that can consume another silane molecule[64].

$$SiH_4 \xrightarrow[-H_2]{\Delta} H_2Si\mathbf{:} \xrightarrow{SiH_4} SiH_3SiH_3^* \xrightarrow[-H_2]{\Delta} SiH_3SiH\mathbf{:} \xrightarrow{SiH_4} SiH_3SiH_2SiH_3 \tag{32}$$

Silylene SiH_2 was directly detected during the pyrolytic decomposition of silane (and ethylsilane $EtSiH_3$) for the first time by intracavity laser spectroscopy in 1988[65]. The high detection sensitivity of this experiment allowed the pyrolysis mechanism to be examined under conditions that optimized film growth rather than spectroscopic conditions.

The decomposition of methylsilane was studied in 1987 via high level *ab initio* molecular orbital calculations with correlation corrections to the MP4 level of perturbation theory[66]. 1,1-Elimination of H_2 forming $CH_3SiH\colon$ was found to have the lowest activation energy, followed by elimination of methane forming $H_2Si\colon$. 1,2-H_2-elimination forming $CH_2{=}SiH_2$ was disfavored, as were homolytic bond cleavages.

Kinetic measurements in a shock tube on the pyrolysis of CH_3SiH_3[67,68], $EtSiH_3$[69], $CH_2{=}CHSiH_3$[70] and *n*-$PrSiH_3$[71] led to very similar activation parameters ($\log A$ *ca* 15, E_a 63–65 kcal mol^{-1}), and the primary dissociation processes were believed to be H_2-elimination, the 1,1-process being more important than the 1,2-process. In secondary decomposition processes $EtSiH\colon$ and higher alkylsilylenes can decompose to form alkenes and $H_2Si\colon$. Study of the pyrolytic formation and decomposition of *n*-$BuSiH\colon$ in a shock tube[72] and $EtSiH\colon$ in a static system[73] to elucidate the mechanisms for secondary silylene decomposition led to the conclusion that intramolecular C–H insertions forming silacycles mediate the formation of $H_2Si\colon$, as shown in equation 33 for $EtSiH\colon$. It should be noted that 1,2-H_2-elimination is no longer believed to contribute to the primary pyrolysis.

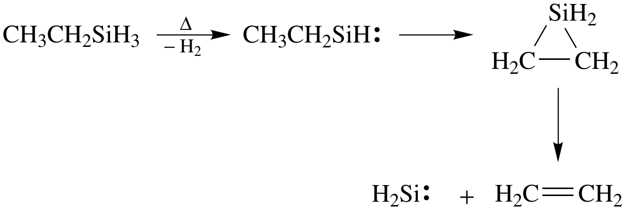
(33)

1,1-Elimination of H_2 has also been suggested as the primary step in the pyrolysis of Me_2SiH_2, but complex reaction mixtures are formed, and a number of secondary processes have been considered to account for them[74,75].

Pyrolysis of silacyclobutane leads to the formation of two silylenes ($H_2Si\colon$ and $MeHSi\colon$) and a silene ($H_2Si{=}CH_2$)[5]. Labeling studies by Barton and Tillman revealed that $H_2Si\colon$ was formed via a series of intramolecular rearrangements interconverting isomeric propylsilylenes via isomeric methylsiliranes that ultimately fragmented to silylene and propylene (equation 34)[76].

From studies of the reaction kinetics of butyl- and pentylsilylenes formed by ring opening of siliranes produced by addition of H_2Si to butenes and pentenes, generic high-pressure Arrhenius parameters could be deduced for silirane ring closure by intramolecular H–C insertion ($\log A = 12.3$, $E_a = 10.4$ kcal mol^{-1}), ring opening to a silylene ($\log A = 14.0$, $E_a = 64.3$ kcal mol^{-1}–silirane ring strain) and silylene extrusion ($\log A = 16.9$, $E_a = 75.7$ kcal mol^{-1}–silirane ring strain)[77].

Silirane pyrolysis has been employed as a mild route to silylenes since the pioneering work in the 1970s of Seyferth's group on hexamethylsilirane[2]. An important step forward was made by Boudjouk and coworkers when they found that bulky substituents (such as *t*-butyl) on silicon increased the stability of the silirane without preventing its thermolysis (equation 35)[56].

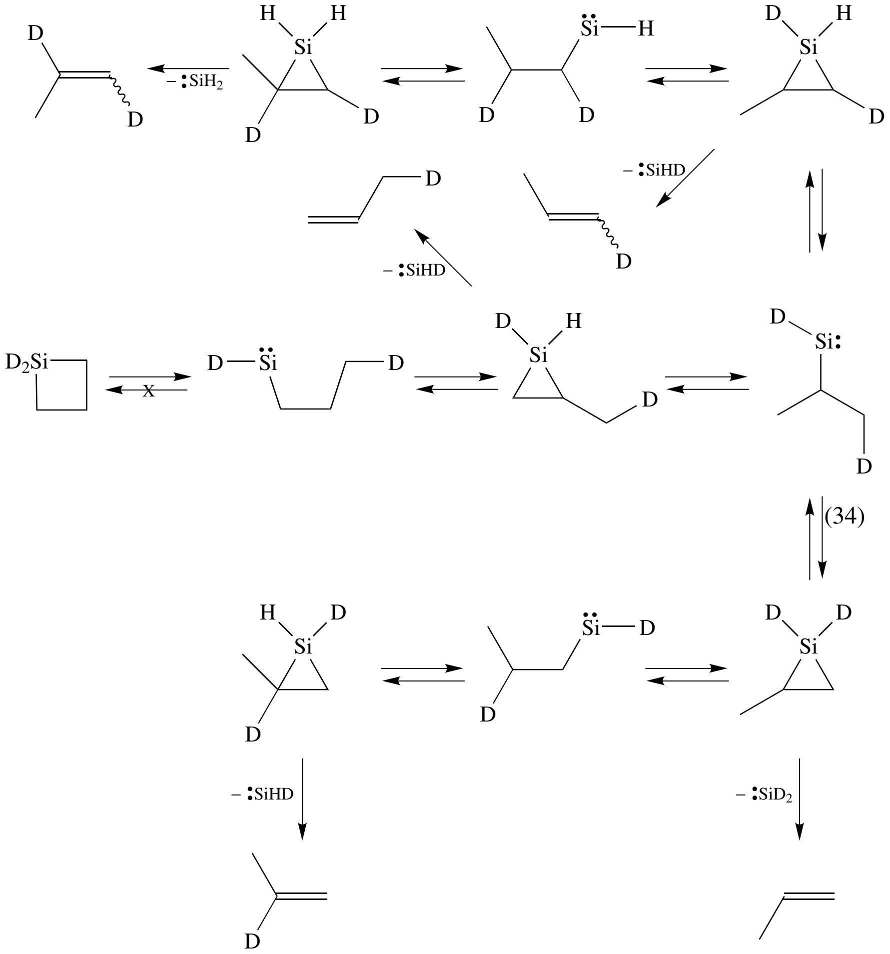
− :SiH$_2$
− :SiHD
− :SiHD
X
− :SiHD
− :SiD$_2$

(34)

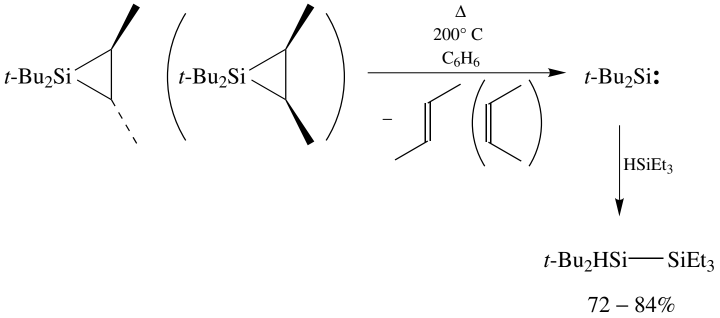
t-Bu$_2$Si
t-Bu$_2$Si
Δ
200° C
C$_6$H$_6$
t-Bu$_2$Si:
HSiEt$_3$
t-Bu$_2$HSi—SiEt$_3$
72 – 84%

(35)

To explain the formation of the expected product of insertion into the H−Si bond of $HSiEt_3$ in similar yields from different precursors, it was suggested that $t\text{-}Bu_2Si\colon$ also arises by ultrasound-promoted lithio-dehalogenation of $t\text{-}Bu_2SiX_2$ (X = Cl, Br, I); see also Section II.E. This would represent the first example of a metal-promoted α-elimination of dihalosilanes. In a related study of the chemistry of diadamantylsilylene $Ad_2Si\colon$ the reactive species formed from Ad_2SiI_2 upon treatment with lithium under ultrasonic irradiation was compared with that formed upon pyrolysis of a silirane, as shown in equations 36 and 37[57].

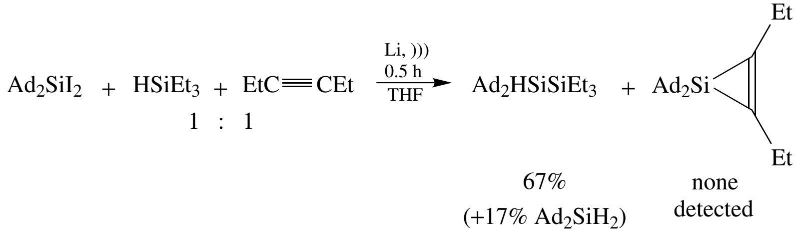

(36)

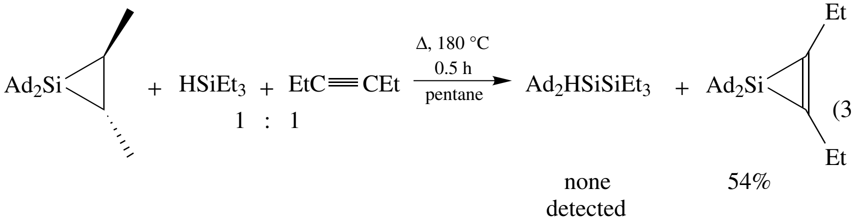

(37)

The inversion in selectivity between the insertion into an H−Si bond favored by the intermediate in the dehalogenation and the addition to a triple bond favored by the intermediate formed upon silirane pyrolysis suggests that different reactive intermediates are formed. Since free silylene is implicated in the silirane pyrolysis, the lithium-induced deiodination probably involves a silylenoid such as a complex of the silylene with LiI or with THF. For a further discussion of this possibility, see Section II.E.

The thermodynamic stability of unsubstituted silacyclopropane to fragmentation has been studied by *ab initio* quantum mechanical methods and the enthalpy of decomposition to $H_2Si\colon + CH_2{=}CH_2$ was predicted to be 44.8[78] and 43.2[79] kcal mol^{-1}. There is indirect experimental support for these theoretical estimates. When these values were employed in RRKM calculations on silirane decomposition, the pressure dependence of the bimolecular rate constant for addition of $H_2Si\colon$ to ethylene could be accurately modeled[80].

Calculations indicate that silacyclopropenes might also be employed as silylene precursors in thermolysis reactions. The enthalpy of dissociation of unsubstituted 1-silacycloprop-2-ene is predicted to be 50.4 kcal mol^{-1}, only *ca* 7 kcal mol^{-1} greater than for silirane[81].

Extrusion of a silylene from a silirane or silirene is of course the inverse of silylene addition to alkenes or alkynes, respectively. The reversibility of most silylene reactions allows the inverse of addition to 1,3-dienes to also be employed as a silylene source. The first such reaction was reported by Chernyshev and coworkers, who found that transfer of $SiCl_2$ units from 1,1-dichlorosilacyclopent-3-enes was a unimolecular process and hence was likely to consist of silylene extrusion and readdition (equation 38)[82]. Dimethylsilylene extrusion has been found in the pyrolysis of silacyclopentenes and other products of

Me_2Si: addition[83,84].

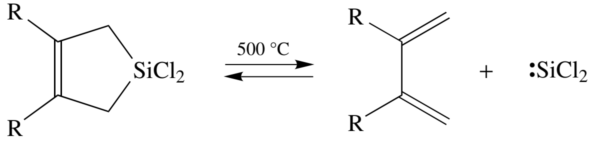

(38)

Product **19** in equation 39 is formed by trapping extruded Me_2Si:, but **20**, **21** and **22** are rearrangement products of silacyclopent-3-ene **23**. Their formation is in accord with stepwise retroaddition with silylene extrusion from a vinylsilirane that is an intermediate in a reversible addition mechanism. As expected from such a mechanism, **20**, **21** and **22** are coproducts with **23** in the addition of Me_2Si: to the piperylenes[20].

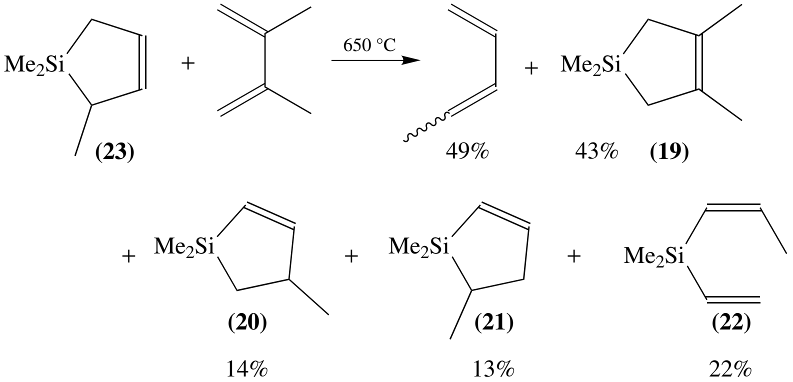

(39)

That product **22** in equation 39 is due to a retrohomo-ene reaction of a vinylsilirane intermediate was demonstrated by employing a vinyl(1-alkenyl)silirane as a starting material for silylene extrusion, as shown in equation 40[85]. As shown in equation 41, the first step in the extrusion of Me_2Si: from **23** is a homo-ene reaction forming a vinylsilirane that undergoes competing rearrangements to products **24** and **25** and extrusion of Me_2Si:. The silylene is trapped (reversibly) by isoprene as **26** that can rearrange to **27**.

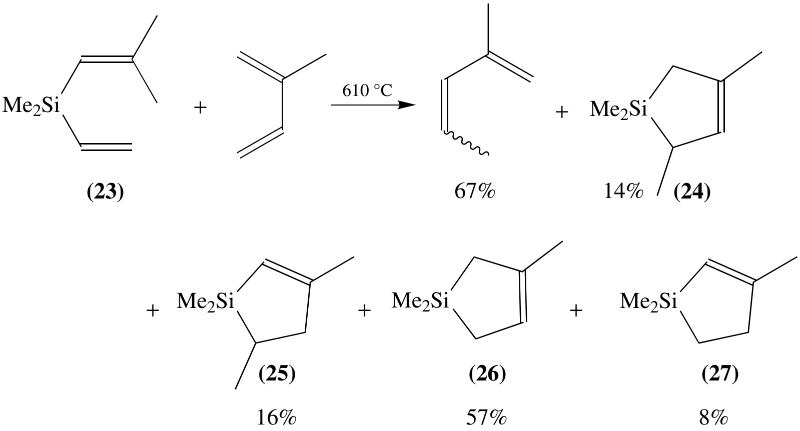

(40)

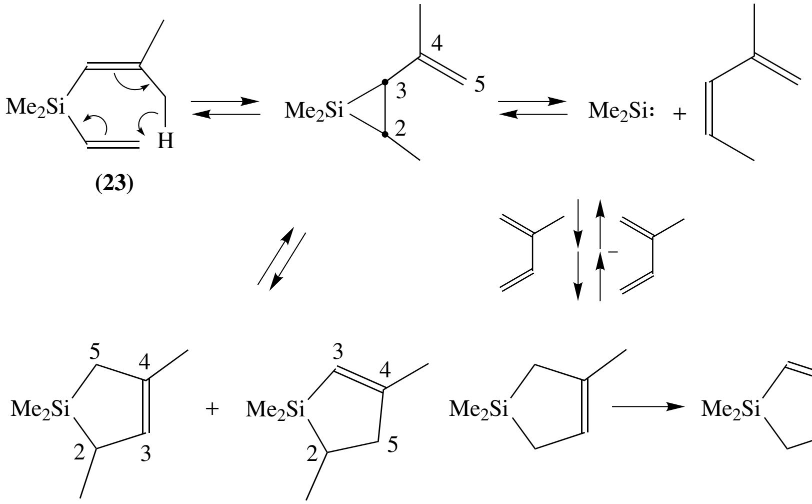

(23)

(41)

(24) (25) (26) (27)

E. Silylenes from Metal-Induced α-Eliminations

Some of the earliest evidence for organosilylenes arose from the gas-phase reactions of Me_2SiCl_2 with Na/K vapor, yielding Me_2Si:[86]. Beginning long before this, as early as the researches of Kipping, metal-induced elimination of halide from R_2SiX_2 in solution has been used to deliver R_2Si moieities in syntheses. Reductions with alkali metals are commonly employed for the synthesis of cyclic or linear polymeric polysilanes, for instance[87,88]. But these reactions do not necessarily involve free silylenes; they could equally well proceed through the intermediacy of *silylenoids*, R_2SiMX[89].

Carbenoids, α-heteroatom-substituted organometallic compounds which behave as masked carbenes, have been intensively investigated for more than thirty years, and have found important use as intermediates in organic synthesis[90]. A good example is CCl_3Li, which can give reactions like those of Cl_2C:. The silicon counterparts to the carbenoids, silylenoids, have often been suggested as reaction intermediates, especially in the synthesis of polysilanes from dichlorosilanes. Evidence for the existence of silylenoids was, however, lacking until the recent appearance of publications by the Kyoto University group of Tamao[91–93].

Earlier, these workers had found that electronegative atoms attached to silicon greatly stabilize silyl anions[94]. Thus the aminosilyllithium compounds $(Et_2N)Ph_2SiLi$, $(Et_2N)_2PhSiLi$ and $(Et_2N)PhMeSiLi$ can all be made from the corresponding chlorosilanes with lithium metal in THF at 0 °C, and are stable in solution at this temperature. These compounds behave simply as silyl anions, rather than silylenoids (they show no electrophilic behavior). The same is true for $(t\text{-}BuO)_2PhSiLi$. *Mono*alkoxysilyllithium compounds, however, show both electrophilic and nucleophilic properties, and so can be accurately viewed as silylenoids.

These silylenoid species have been made by lithium–tin exchange from a Si–Sn precursor[96], or by reduction of chlorosilanes with lithium 1-(dimethylamino)naphthalenide (LDMAN) at −78 °C (equations 42 and 43)[97]. The resulting silyllithium species react as nucleophiles with Me_3SiCl to give the corresponding disilanes (equation 44). An important reaction showing electrophilic, hence silylenoid, behavior is that with *n*-BuLi, which displaces the alkoxy group as shown in equation 44. No free silylene is formed from the silylenoids, however, since no silylene trapping reactions were observed with Et_2MeSiH, diphenylacetylene or dimethylbutadiene. Also, when 12-crown-4-ether was added to (t-BuO)Ph_2SiLi to separate the lithium cation from the silicon, the molecule lost silylenoid character and behaved simply as a silyl anion.

$$(t\text{-BuO})\text{Ph}_2\text{Si}{-}\text{SnMe}_3 + n\text{-BuLi} \xrightarrow[-78\,^{\circ}\text{C}]{\text{THF}} n\text{-BuSnMe}_3 + (t\text{-BuO})\text{Ph}_2\text{SiLi} \tag{42}$$

$$(\text{RO})\text{Ph}_2\text{SiCl} \xrightarrow[\text{THF, }-78\,^{\circ}\text{C}]{\text{LDMAN}} (\text{RO})\text{Ph}_2\text{SiLi} \tag{43}$$

$$\begin{tikzcd}
(\text{RO})\text{Ph}_2\text{Si-SiMe}_3 & (\text{RO})\text{Ph}_2\text{SiLi} \arrow[l, "\text{Me}_3\text{SiCl}", "\text{THF, }-78\,^{\circ}\text{C}"'] \arrow[r, "n\text{-BuLi}", "\text{THF, }-78\,^{\circ}\text{C}"'] \arrow[d, "\text{THF, }0\,^{\circ}\text{C}"] & n\text{-BuPh}_2\text{SiLi} \arrow[d, "\text{Me}_3\text{SiCl}"] \\
 & (\text{RO})\text{Ph}_2\text{Si}{-}\text{SiPh}_2\text{Li} & n\text{-BuPh}_2\text{Si}{-}\text{SiMe}_3
\end{tikzcd} \tag{44}$$

R = t-Bu, i-Pr, Me

A significant finding in these studies was that at 0 °C in THF, the silylenoids undergo bimolecular condensation to the dimeric intermediates $ROPh_2Si{-}SiPh_2Li$, which can then be trapped by Me_3SiCl (equation 44). Dimerized species of this sort are quite likely to be intermediates in the coupling of dihalosilanes to cyclic and linear polysilanes.

As mentioned in Section II.D, an important publication bearing on the question of dichlorosilane–metal reactions appeared in 1988[56]. Boudjouk and coworkers treated t-Bu_2SiX_2, X = Cl, Br and I, with lithium and ultrasound activation in the presence of Et_3SiH. Good yields (*ca* 60%) of $Et_3Si{-}SiH(Bu\text{-}t)_2$ were obtained in all three cases. This is rather persuasive evidence in favor of silylene formation, since Si–H bond insertion is characteristic for silylenes and it is difficult to see how the disilane could arise from the reaction of Et_3SiH with a silylenoid[95].

When the same dehalogenations were carried out in the absence of a trapping agent, however, the products depended on the nature of the halogen. With t-Bu_2SiBr_2 and t-Bu_2SiI_2 the cyclotrisilane was obtained, but with t-Bu_2SiCl_2 a disilane and a cyclotetrasilane were produced (equations 45 and 46). It follows that all three of these reactions cannot have proceeded through the free silylene and, in fact, none may have.

$$t\text{-Bu}_2\text{SiX}_2 \xrightarrow[\text{ultrasound}]{\text{Li}} (t\text{-Bu}_2\text{Si})_3 \tag{45}$$

$$\text{X} = \text{Br, I}$$

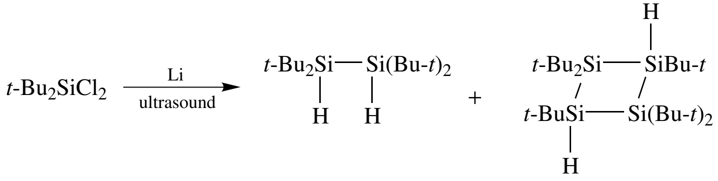

$$t\text{-Bu}_2\text{SiCl}_2 \xrightarrow[\text{ultrasound}]{\text{Li}} \underset{\text{H}}{\underset{|}{t\text{-Bu}_2\text{Si}}}{-}\underset{\text{H}}{\underset{|}{\text{Si(Bu-}t)_2}} + \begin{array}{ccc} & & \text{H} \\ & & | \\ t\text{-Bu}_2\text{Si} & - & \text{SiBu-}t \\ / & & / \\ t\text{-BuSi} & - & \text{Si(Bu-}t)_2 \\ | & & \\ \text{H} & & \end{array} \tag{46}$$

We will make a tentative suggestion as to how the results of Boudjouk's experiment might be explained. Possibly the halogen-containing silylenoids are in equilibrium with a very small amount of free silylene (equation 47).

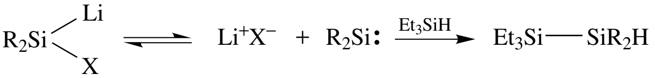

$$R_2Si\begin{matrix}Li\\X\end{matrix} \rightleftharpoons Li^+X^- + R_2Si\colon \xrightarrow{Et_3SiH} Et_3Si{-}SiR_2H \qquad (47)$$

If Et_3SiH is an efficient trapping agent for the silylene but does not react with the silylenoid, the reaction will proceed toward the right to give the disilane product. Other trapping agents may react instead with the silylenoid. When no trapping agent is present, silylenoid molecules would self-react, and the products might well depend on the nature of the halogen.

Another conceivable, but probably less likely, explanation of these experimental results[56] is that the triethylsilane somehow catalyzes the decomposition of silylenoid into free silylene, which can then insert into the Si–H bond. In any case, the intermediacy of silylenes in α-dehalogenations remains an open question, worthy of further study.

Different silylenoids may vary in their reactivity. When diiododiadamantylsilane was dehalogenated with lithium under ultrasonic activation in the presence of a mixture of Et_3SiH and 3-hexyne in THF, the silylenoid gave exclusively H–Si insertion product in high (67%) yield (equation 36)[57] Free $Ad_2Si\colon$ formed by silirane photolysis (*vide supra* equation 26) gave products of both H–Si insertion and π-addition, addition being the favored reaction.

The formation of silacyclopentenes from dichlorosilanes, alkali metals and 1,3-dienes is sometimes taken as evidence for silylene formation. Lithium and ultrasound were used in one such study, in which R_2Si moieties were intercepted by 2,3-dimethylbutadiene (equation 48) albeit in low yield; the result was interpreted in terms of a silylene intermediate[96].

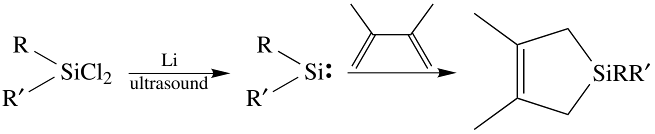

(48)

A report by the Corriu group, however, shows that this is not necessarily the case (equation 49)[97]. When difluorosilane was treated with lithium metal in the presence of dimethylbutadiene, the silacyclopentene was obtained in good yield; but no silylene was intercepted if Et_3SiH was present as the trapping agent. The product silacyclopentene could result either from reaction of the diene with a silylenoid, or from reaction of the diene with lithium and trapping of the lithium compound by the difluorosilane. In earlier studies of the alkali metal induced reactions of dihalosilanes with 1,3-dienes, it was found that the diene, rather than the dihalosilane, reacts initially with the metal[2].

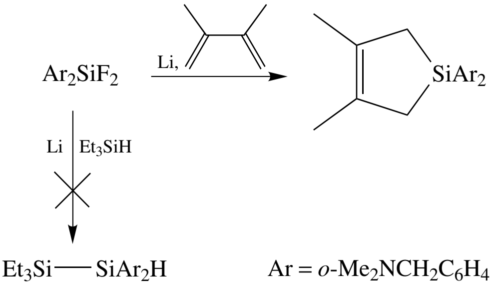

(49)

Ar = o-$Me_2NCH_2C_6H_4$

On the other hand, there is no doubt whatsoever that stable, nitrogen-stabilized silylenes are produced from dihalosilanes and alkali metals[98]. The chemistry of these silylenes is treated in Section VIII.C.

F. Silylenes from Rearrangements

Rearrangements of siliranes to alkylsilylenes by ring-opening α-elimination from silicon were discussed in Section II.D (see equation 34). Similar mechanisms have been written for rearrangements of silirenes to alkenylsilylenes[5].

The rearrangements of silenes to silylenes via migration of an H-atom[5] remains controversial. Conlin has found that the temperature dependence of the product ratio and of the rate of decomposition of 1-methylsilacyclobutane in the gas phase is in accord with a mechanism in which 1-methylsilene $\mathrm{MeHSi{=}CH_2}$ is formed as a trappable intermediate that rearranges to dimethylsilylene $\mathrm{Me_2Si}$**:** (equation 50)[99], Experimental evidence has been presented for the equilibration of $\mathrm{CH_3HSi{=}CH_2}$ and $\mathrm{(CH_3)_2Si}$**:** at the high temperatures at which they are generated in such experiments[100]. It has been pointed out that large differences in the rates of their addition reactions must be taken into account in the interpretation of trapping experiments[101].

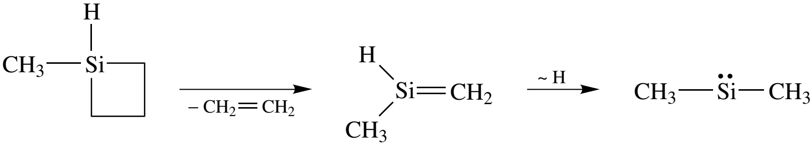

(50)

There seems to be agreement that the interconversion of $\mathrm{MeHSi{=}CH_2}$ and $\mathrm{Me_2Si}$**:** is nearly thermoneutral, with a barrier of *ca* 40 kcal mol^{-1},[102]. $\mathrm{MeHSi{=}CH_2}$ was found in higher concentration under conditions such that the two species could isomerize in a flowing-afterglow experiment[103].

Rearrangement of a silene to a silylene via migration of a $\mathrm{Me_3Si}$ group has been suggested as a step in the gas-phase silylene-to-silylene rearrangement $\mathrm{Me_3Si{-}\ddot{S}i{-}Me} \rightarrow \mathrm{H{-}\ddot{S}i{-}CH_2SiMe_3}$[104], Labeling experiments, however, have indicated that an alternative mechanism operates (equation 51)[105].

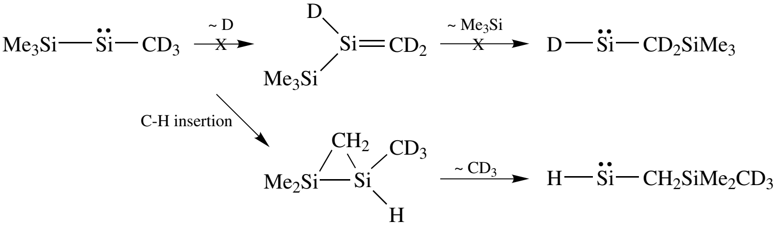

(51)

Rearrangements of disilenes to α-silylsilylenes are, however, well established (equation 52)[5] and are involved in the exchange of substituents between a silylene center and an adjacent silicon, a process that has been called a transposition (equation 53)[106].

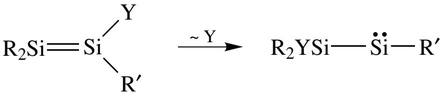

(52)

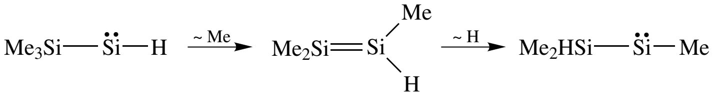

$$Me_3Si{-}\ddot{S}i{-}H \xrightarrow{\sim Me} Me_2Si{=}Si\begin{smallmatrix}Me\\ \\ H\end{smallmatrix} \xrightarrow{\sim H} Me_2HSi{-}\ddot{S}i{-}Me \qquad (53)$$

Puranik and Fink found that the low-temperature photoinduced rearrangement of a silylene to a silacyclobutadiene is reversible in a thermal reaction at 160 K (equation 54)[107]. The silylene persists in fluid solution at 200 K!

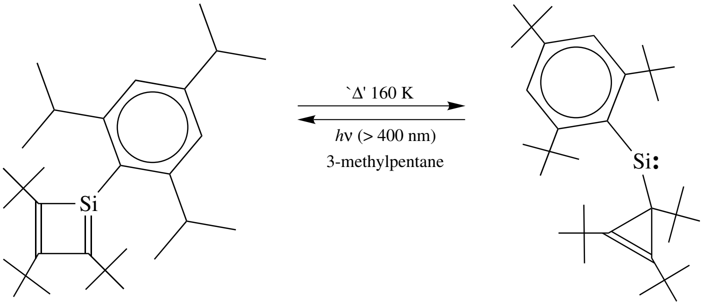

(54)

III. REACTIONS OF SILYLENES

A. Insertion

The first silylene reaction to be recognized, a half-century ago, was insertion of SiH_2 into silicon–hydrogen bonds[1]. The mechanism was found to be direct insertion[2]. Insertions of silylenes into a number of other bonds have been observed, including O–Si[1,2], N–Si[2], halogen–Si[2], strained O–C[2], Si–Si[3], H–O[3], H–N[3] and H–C (intramolecular only)[3]. There is both experimental and theoretical support for stepwise insertion of silylenes into O–Si, strained O–C and H–O bonds, initiated by the formation of silaylides by donation of a pair of electrons from an oxygen atom to form a bond to a divalent silicon atom (equation 55)[3,5]. Silylene insertion into a Cl–Si bond can follow a similar mechanism, or can result from halogen abstraction by the silylene followed by geminate recombination of the resulting radical pair[3,5].

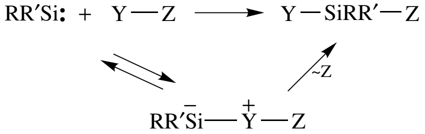

$$\begin{tikzcd} RR'Si\colon + Y{-}Z \arrow[r] \arrow[dr, shift left] & Y{-}SiRR'{-}Z \\ & RR'\overset{-}{Si}{-}\overset{+}{Y}{-}Z \arrow[u, "\sim Z"'] \arrow[ul, shift left] \end{tikzcd} \qquad (55)$$

Insertion of SiH_2 into H–H and H–C bonds, respectively, has been *assumed* in reports of rate constants from laser flash photolysis experiments for reactions of SiH_2 with H_2[108,109], D_2[109] and CH_4[108]. Since the rate of silylene insertion into the H–H bond was more rapid than previous estimates, interest was reawakened in the activation barrier[112–114]. The barrier for insertion of SiH_2 into H_2 was revised downward to *ca* 1 kcal mol^{-1}.

A number of Lewis base adducts of diorganosilylenes have been observed by electronic spectroscopy in frozen matrices (see Section V.A)[115]. The silylene-donor adducts of ethers, tertiary alcohols, tertiary amines and sulfides were found to revert to silylenes upon warming, but primary and secondary alcohol adducts underwent rearrangement to the H–O formal insertion products (equation 55).

The silaylides formed from coordination of silylenes to chlorocarbons are believed to undergo competitive rearrangement (to the formal Cl−C insertion product) and fragmentation (to the product of formal HCl abstraction by the silylene)[5]. In addition, these silaylides are believed to undergo dissociation into the radical pairs that would result from direct chlorine atom abstraction by the silylene[111].

A more complex reaction sequence may be responsible for the formation of the products of formal insertion of silylenes into the H−C bonds of carbaldimines[110,116]. As shown in equation 56, an initial Lewis base or π-bond adduct can undergo rearrangement to both of the products observed from reactions of diarylsilylenes and pyridine-2-carbaldimines. A common intermediate is suggested by the thermal isomerization of the insertion product to the cycloadduct which can be the exclusive product from addition of a silylene to a 2,2′-bipyridyl (see Section III.B)[117].

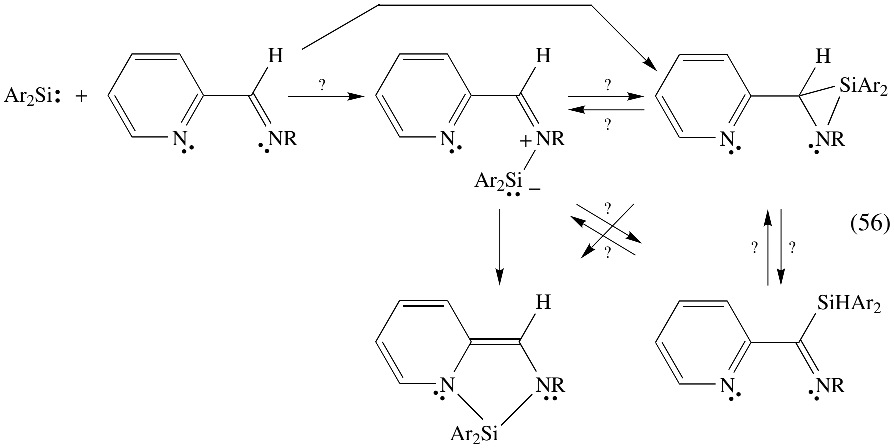

(56)

Insertion of bis(dialkylamino)silylenes into aromatic and benzylic H−C bonds has been suggested to explain the products formed from dehalogenation of the corresponding bis(dialkylamino)dihalosilanes by Na/K in solution[118,119]. Caution is advised regarding this mechanism, since previous investigations of the reductive dehalogenation of dihalosilanes in solution did *not* find evidence for the formation of free silylenes[2].

New insertion reactions of silylenes continue to be discovered. SiH_2 has been found to insert into an H−Ge bond of GeH_4[120]. Insertion of $SiMe_2$ into H−Ta bonds of $Cp_2TaH(PMe_3)$ and Cp_2TaH_3 has been reported, the latter reaction via a $Me_2Si(PMe_3)$ silylene−Lewis base adduct[121]. $SiMe_2$ has also been found to insert into the H−S bonds of trialkoxysilanethiols[122]. Apparent intermolecular H−C insertion by furyl(phenyl)silylene was observed to compete with addition to 2,3-dimethylbutadiene[123]. Formal insertion of two silylenes into a S=C double bond is believed to occur via rearrangement of a spiro di-adduct intermediate, as shown in equation 57[124].

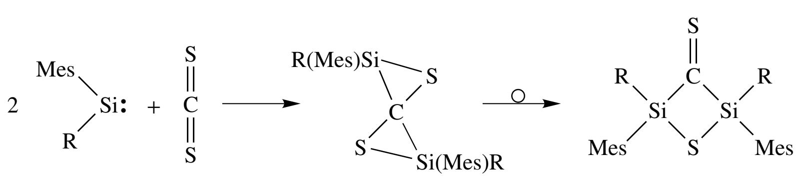

(57)

A bizarre silylene insertion into the I—I bond has been suggested as the initial step in the mechanism for the low-temperature (−90 °C) reaction of dihalosilylenes (SiF_2, $SiCl_2$, $SiBr_2$) with solutions of iodine in toluene, as shown in equation 58[125]. These reactions can be considered to involve electrophilic attack on an arene by SiX_2I^+[126].

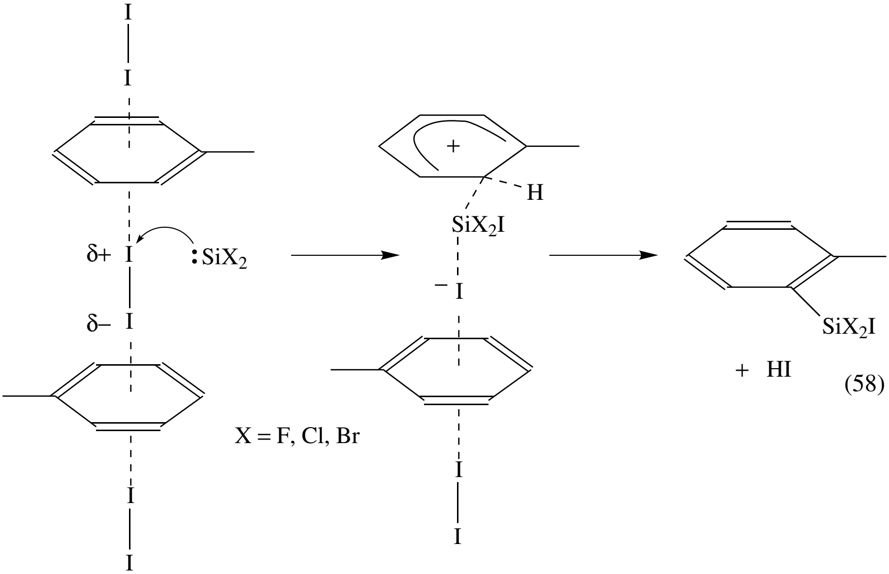

(58)

B. Addition

1. Mechanistic studies

Addition of silylenes to carbon–carbon π-bonds forming silirane and silirene intermediates had been inferred by the early 1960s, and by the middle 1970s such silylene addition products had been isolated (equation 59)[2]. The belief that addition of silylenes to olefins is a concerted process is based on the observation that additions to *cis*- and *trans*-olefins are stereospecific[3,5]. Since all reliably characterized silylenes have singlet ground electronic states, stereospecific addition is expected on the basis of the 'Skell rule' of carbene chemistry[127]. This pragmatically useful but theoretically shaky generalization can be stated as follows: since singlet carbenes (silylenes) *can* add to olefins in a single step, they will do so, and *E*,*Z*-stereochemistry of the olefin will be retained in the addition product; a triplet carbene(silylene) will add in a stepwise process including a triplet diradical intermediate in which stereochemistry can be scrambled by rotation about single bonds that competes with intersystem crossing and ring closure. A theoretical study of the reaction of SiH_2 with acetylene found that most observations can be accounted for by a model in which concerted formation of chemically activated silirene is followed by competition between dissociation, deactivation and rearrangement channels[128]. Experimental determinations of product yields from SiH_2 and ethylene were successfully modeled with a similar mechanism involving the formation of chemically activated silirane as the concerted primary step[129].

A singlet ground state was deduced for diadamantylsilylene when it was found to undergo stereospecific addition to *cis*- and *trans*-2-butene[57]. Stereospecific addition of cyclopropyl(phenyl)silylene has also been reported[130].

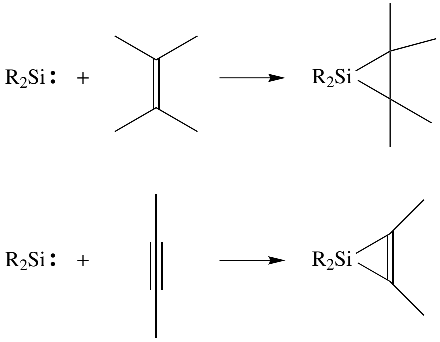

(59)

When nonstereospecific addition of dimesityl- and bis(2,4,6-triisopropylphenyl)silylene to *trans*-2-butene, and to a lesser extent to *cis*-2-butene, was reported, a stepwise addition mechanism was suspected[131]. However, the apparent nonstereospecificity was caused by a *cis*-butene impurity in the *trans*-butene and by photoisomerization of the *cis*- and *trans*-siliranes[132].

Recently, stereospecific addition of bis(triisopropylsilyl)silylene ($(i\text{-}Pr_3Si)_2Si$) to *cis*-2-butene has been observed[133]. Since a triplet ground state has been predicted on the basis of density functional calculations[134], stereospecific addition could be due to a violation of the Skell rule. Alternatively, the Skell rule could be obeyed if the triplet ground state is siphoned off via more rapid reactions of the low-lying excited singlet (which, according to the calculations, lies only 1.7 kcal mol^{-1} above the triplet[134]) that may be in equilibrium with the triplet.

The observation of ^{1}H CIDNP signals during the addition of Me_2Si (and Me_2Ge) to a strained alkyne (equation 60), has been interpreted as indicating stepwise addition of excited triplet states of the divalent species to the triple bond[135]. One wonders, however, if there are not other viable explanations for the CIDNP signals, such as silylene(germylene) transfer from a diradical formed by homolysis of one of the bridging Si−C(Ge−C) bonds in the precursor (Scheme 3, Section II.C.2). There is evidence that silylene extrusion from 7-silanorbornadienes may be a stepwise process[2], and thus 'silylene products' may in some cases be formed via silylenoid intermediates rather than free silylenes.

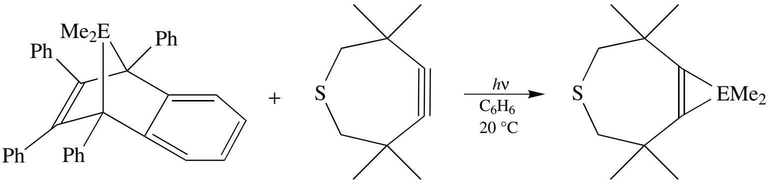

(60)

E = Si, Ge

In the past decade there has been considerable mechanistic study of the addition of silylenes to 1,3-dienes. From the first report of the formation of 1-silacyclopent-3-enes as major products thirty years ago, a stepwise mechanism including vinylsilirane intermediates was proposed, but concerted 1,4-addition was also considered[1−5]. Vinylsilirane intermediates were clearly identified in trapping experiments by 1975[2], but questions have remained about the concertedness of both the primary addition and rearrangement steps of equation 61.

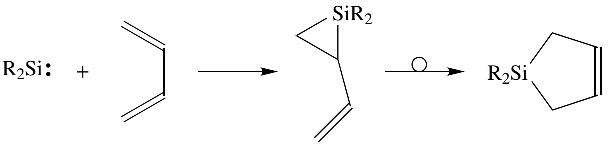

(61)

The current view of the mechanism of addition of silylenes to 1,3-dienes is based on the following experimental observations:

(a) The dramatic differences (shown in Table 1) in the distribution of the products of addition of Me$_2$Si to the three stereoisomers of 2,4-hexadiene can be explained by formation of alkenylsilirane intermediates by concerted addition[20,136]. It can be seen that with substituents on the 1- and 4-positions of 1,3-butadiene, the 1-silacyclopent-3-enes that are formal 1,4-addition products are formed in low yield. The major product from the *cis, cis*-diene results from a retro-homo-ene reaction already depicted in the forward direction in Section II.D (equation 41). The 1,1,2,3-tetramethyl-1-silacyclopent-4-enes that are the major products from the *cis,trans*- and *trans,trans*-2,4-hexadienes are also rearrangement products of vinylsilirane intermediates, requiring the migration of C−C bonds, as shown in equation 41. The formation of both *cis*- and *trans*-stereoisomers of the silacyclopentenes suggested that the ring expansions of the alkenylsilirane intermediates were stepwise processes[11]. With phenyl substituents at the 1- and 4-positions of butadiene, facile C−C bond cleavage of the vinylsilirane intermediates leads to silacyclopent-4-enes as the exclusive addition products[137].

TABLE 1. Product yields (%, based on moles of Me$_2$Si generated) from addition of Me$_2$Si: to 2,4-hexadienes

	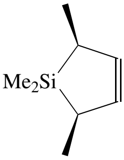 Me$_2$Si	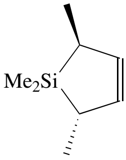 Me$_2$Si	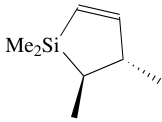 Me$_2$Si	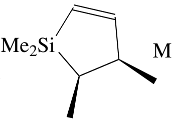 Me$_2$Si	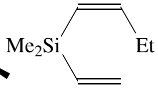 Me$_2$Si Et
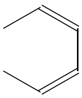	1.2	1.3	12.7	8.3	50.5
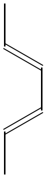	7.5	1.8	27.3	18.4	20.4
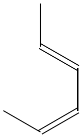	2.3	2.3	24.6	21.4	35.1

(b) Use of 1,4-dideutero-1,3-butadiene allowed the demonstration that at least one-third of the addition of Me_2Si to 'unsubstituted' butadiene occurs via a vinylsilirane intermediate[138]. The labeling pattern in the absence of stereochemical information does not preclude a contribution from direct, concerted 1,4-addition (see equation 62).

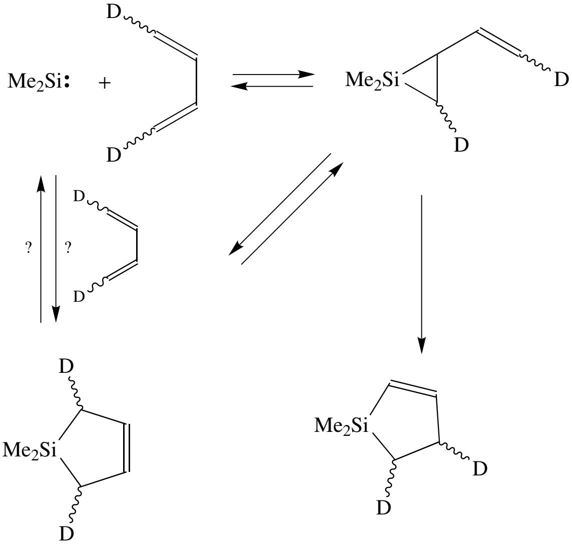

(62)

(c) Stereospecific 1,2-addition of the sterically shielded dimesitylsilylene to the stereoisomeric 2,4-hexadienes at room temperature in solution led to vinylsiliranes that were stable for months[139]. Longer irradiation led to the stereospecific conversion of the vinylsilirane formed from the *trans,trans*-isomer to the *cis*-2,3-dimethylsilirane that preserves the stereochemistry of the starting diene (equation 63). These important observations by Zhang and Conlin can be explained by concerted rearrangements of vinylsiliranes to 1-silacyclopent-3-enes, or by concerted photoreversion of vinylsiliranes to the silylene and diene from which they were formed, followed by concerted 1,4-addition of the silylene to the diene. Both possibilities were considered by Conlin[139].

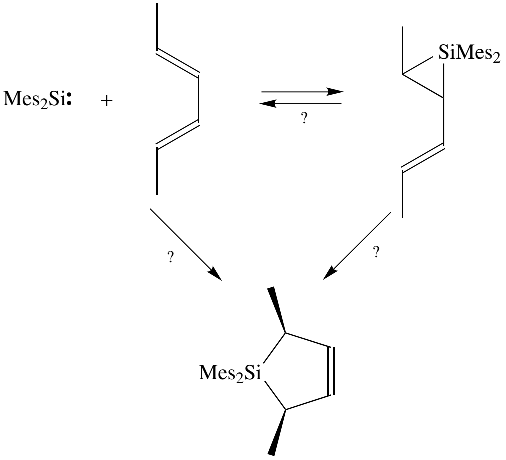

(63)

(d) The formation of 3,4-divinylsilacyclopentanes as 1 : 2-adducts from silylenes and unsubstituted butadiene not only provides examples of vinylsiliranes undergoing intermolecular reactions, but also lends support to the occurrence of direct 1,4-addition[140,141]. When silylenes (Ph_2Si:, PhMeSi:) are generated in solution in the presence of both butadiene and acetone, the products include vinylsiloxolanes incorporating a unit each of silylene, butadiene and acetone (equation 64).

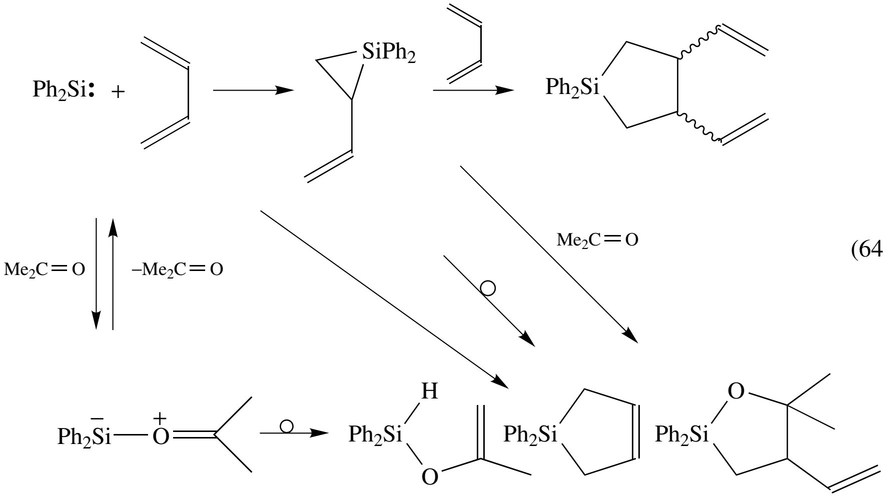

(64)

Steady-state kinetic analysis of a competition experiment led to the conclusion that the siloxolane is formed by reaction of a vinylsilirane intermediate with acetone, and that the vinylsilirane arises from addition of the free silylene to butadiene. Since silylenes are known to react more rapidly with acetone than with butadiene, the kinetic analysis further suggested that the carbonyl sila-ylide dissociates more rapidly than it rearranges to the silyl enol ether shown in equation 64[140].

Evidence for direct, 1,4-addition of Ph_2Si to butadiene comes from the observation that, at very low acetone concentrations, no divinylsilacyclopentane is formed, but the silacyclopent-3-ene is found. Since at the high (10 M) butadiene concentration employed in these experiments, reaction of the vinylsilirane with butadiene to form the divinylsilacyclopentane is more rapid than rearrangement to the silacyclopentene, there must be another route to the silacyclopentene, such as direct 1,4-addition[141].

2. Recently discovered addition reactions

a. Addition to n-donor bases. The first spectroscopic detection of silylene–ether complexes was achieved by annealing 3-methylpentane matrices doped with 2-methyltetrahydrofuran in which silylenes were photochemically generated at 77 K[142]. Trapping of the silylenes by the ether was shown to compete with silylene dimerization, and the silylene–ether complexes displayed a different reactivity from the free silylenes. Spectra of silylene complexes with N, O, P and S *n*-donor bases pyrrolidine, *N*-methylpyrrolidine, piperidine, tetrahydrofuran, tetrahydrothiophene, and Bu_3P have also been reported (see Section V.A.2)[113,143].

Sila-ylides from complexation of silylenes by carbonyl and thiocarbonyl compounds have been observed; their chemistry is discussed in Section V.A[144]. The first stable silylene–Lewis base complex was obtained in solution from an extremely hindered diarylsilylene and several isocyanides with bulky substituents as shown in equation 65[145]. Since the source of the silylene is the thermal dissociation of its highly congested disilene dimer, the possibility remains that the silylene complex was formed by addition of the isocyanide to the disilene rather than the free silylene. The free silylene route is quite plausible, since dimers of silaketenimines have been obtained from reactions of less crowded silylenes and isocyanides[146]. The spectroscopic properties of these silylene–isocyanide complexes are further discussed in Section III.C.2.

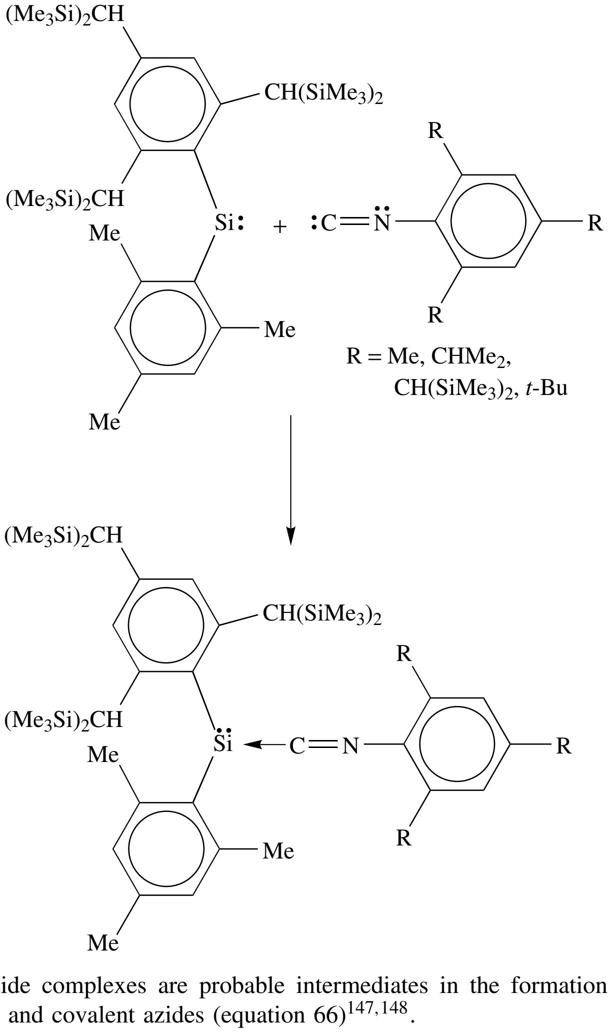

(65)

Silylene–azide complexes are probable intermediates in the formation of silaimines from silylenes and covalent azides (equation 66)[147,148].

$$R_2Si\colon + N_3SiR'_3 \xrightarrow[-N_2]{} R_2Si{=}NSiR'_3 \qquad (66)$$

Addition of a ‘persistent silylene’ (see Section V.III.C) to nickel carbonyl resulted in the first bis-silylene transition metal complex without Lewis base stabilization (equation 67)[149]. Other metal complexes of this 'stable silylene' are described in Section V.III.C.

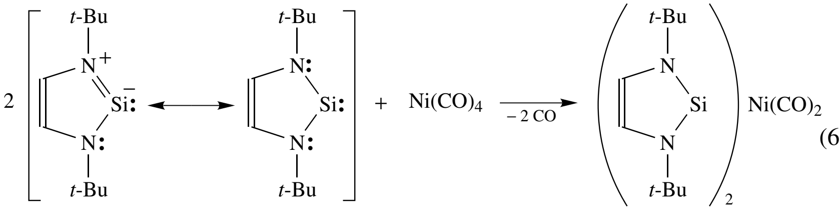

(67)

b. Addition to diatomic molecules. In a very difficult competition experiment it was found that SiH_2, formed by infrared multiphoton dissociation of SiH_4, reacts with nitric oxide NO with a rate constant similar to that for reaction of SiH_2 with SiH_4[150]. The products and the mechanism could not be determined.

Reaction of dimesitylsilylene with O_2 in an oxygen matrix at 16 K led to the formation of a silanone *O*-oxide $Mes_2Si{=}O{-}O$ as deduced from the infrared spectra of isotopomers with the help of theoretical calculations[151,152]. However, isotopic labeling led to the assignment of dioxasilirane structures to the photoproducts from SiF_2 and $SiCl_2$ respectively with O_2 in an argon matrix at 10 K[153]. That the thermal reactions of SiF_2 with O_2 and H_2 are very slow ($k_2 < 2 \times 10^{-17}$ cm^3 $molecule^{-1}$ s^{-1}) had been found earlier[154].

From the reactions of carbon monoxide in frozen matrices with Me_2Si[155] and several arylsilylenes Mes(R)Si (R = Mes, 2,6-diisopropylphenoxy, *t*-Bu)[156], adducts were formed (see Section V.A.2). Theoretical calculations led to consideration of both a linear silaketene and a pyramidal *n*-donor base complex structure for the $Me_2Si(CO)$ adduct[249]. The observation that warming the carbon monoxide adducts of the arylsilylenes led to the formation of disilenes was interpreted as indicating the formation of a nonplanar complex that could dissociate as do other silylene–*n*-donor base complexes[156].

c. Addition to π-bonds. The repertoire of silylene π-bond additions, previously limited to the formation of siliranes and silirenes from alkenes and alkynes, respectively[2–5], has been vastly expanded in the past decade. The contributions of the Ando laboratory to the study of silylene additions to various olefins have been reviewed[157]. Addition of dimesitylsilylene to 1-*t*-butyl-3,3-dimethylallene led to the first stable alkylidenesilirane (equation 68). The first bis(alkylidene)silirane was obtained from addition of Mes_2Si to tetramethylbutatriene[158]. Azasilirenes from addition of silylenes to the C−N triple bond of nitriles undergo rapid dimerization[159,160], but isolable phosphasilirenes have been obtained from *t*-Bu_2Si**:** and phosphalkynes, and these were the first three-membered rings containing phosphorus–carbon double bonds (equation 69)[161].

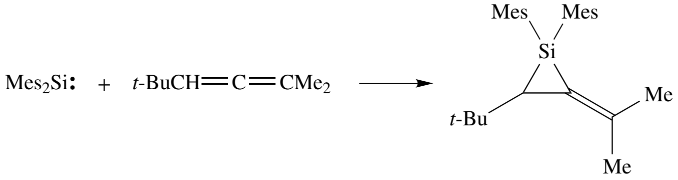

(68)

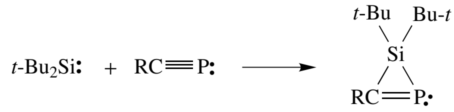

(69)

Addition of several sterically congested diarylsilylenes to carbon disulfide was presented in Section III.A. A diazasilirane was obtained from addition of Mes_2Si**:** to azobenzene, but the same product also resulted from nonsilylene pathways[162]. The sterically shielded and hence stable iminoboranes *t*-Bu$-$B=N$-$Bu-*t* and *i*-$Pr_2N-B=N-$Bu-*t* yielded stable three-membered rings upon addition of dimesitylsilylene Mes_2Si, but, with the less crowded dimethylsilylene Me_2Si, four- and six-membered rings were obtained[163].

There is a dramatic kinetic stabilization by bulky substituents of the three-membered ring products from silylene addition to π-bonds. Addition of *t*-Bu_2Si to ethylene led to the first silirane with no substituents on its ring carbon atoms as a distillable liquid![164]. Interestingly, 1,1-di(*tert*-butyl)silirane does *not* undergo photochemical or thermal silylene extrusion, but instead polymerizes. A distillable silirane was also reported from addition of *t*-Bu_2Si to 2-methylstyrene[165].

The first addition of a silylene to benzene and naphthalene has been reported (equation 70)[166]. Product **28** can be rationalized by intramolecular insertion of the silylene into a nearby activated H$-$C bond. While products **29** and **30** may indeed be the result of stepwise addition of two silylenes to aromatic rings, one wonders whether direct additions of the disilene starting material, or a diradical formed from the disilene by homolysis of the π-bond, might have occurred. It is curious that no adducts containing a single silylene unit were found. Less congested silylenes have *not* been found to undergo addition to aromatic rings.

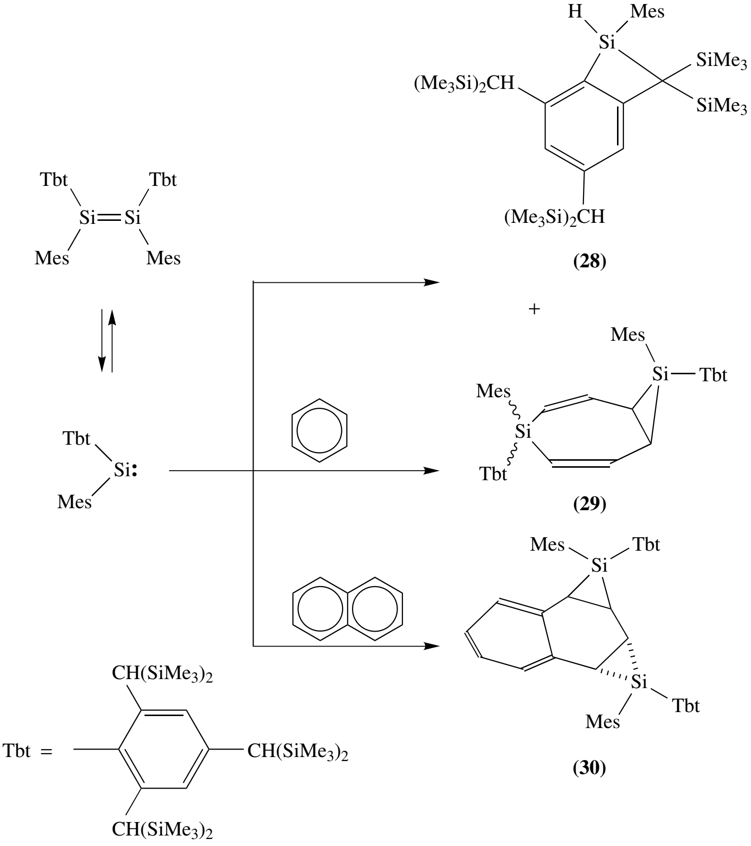

(28)

(29)

(30)

(70)

Silylene addition to 9,10-dimethylanthracene had previously been found to compete effectively with silylene dimerization (equation 71)[167]. Control experiments established that the silylene adduct did *not* undergo ring expansion to the disilene adduct.

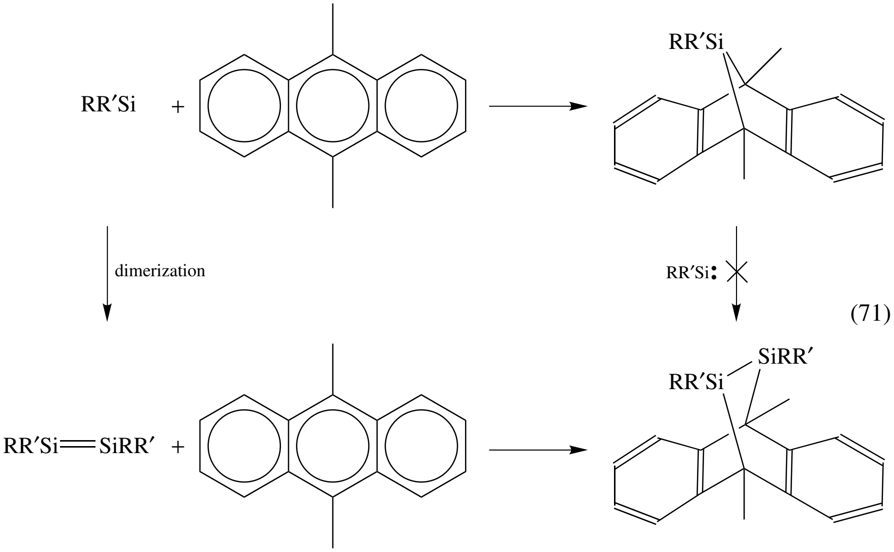

(71)

R = R′ = Me; R = R′ = Ph
R = Me, R′ = Ph

d. Addition to dienes and heterodienes. Dimethoxysilylene, while unreactive toward mono-olefins, has been found to undergo addition to 2,3-dimethylbutadiene with formation of the formal 1,4-adduct, 1,1-dimethoxy-3,4-dimethylsilacyclopent-3-ene[168]. As mentioned in Section II.A, a series of thermally generated silylenes $\mathrm{Me\ddot{S}iCl}$, $\mathrm{Me\ddot{S}iOMe}$ and $\mathrm{Me\ddot{S}iNMe_2}$ has been reacted with butadiene, isoprene and 2,3-dimethylbutadiene to yield mixtures of silacyclopent-2- and 3-enes[19]. Competition experiments indicated that the heterodienes (and heterotriene) shown in equation 72 react more rapidly than the simple dienes studied, and the structures of the heterocyclic products suggested that initial attack of the silylene was on the heteroatom or the hetero−olefinic bond[21,169].

The addition of t-$\mathrm{Bu_2Si}$ to 1,4-diaza-1,3-butadienes competes with dimerization of the silylene only when the concentration of t-$\mathrm{Bu_2Si}$ is low[170]. Subtle steric effects must also be responsible for the addition of t-$\mathrm{Bu_2Si}$ to the N-cyclohexyl mono-imine of benzil, while only the silylene dimer undergoes addition under similar conditions in the presence of the N-methyl mono-imine[171]. It may be that t-$\mathrm{Bu_2Si}$ and its dimer t-$\mathrm{Bu_2Si{=}SiBu}$-t_2, both formed simultaneously upon photolysis of cyclo (t-$\mathrm{Bu_2Si})_3$, are in equilibrium, and the steric effect is upon the (2+4) cycloaddition of the disilene.

Complex product mixtures have been obtained from addition of silylenes to 3,6-bis(trifluoromethyl)-1,2,4,5-tetrazine and 2,5-bis(trifluoromethyl)-1,3,4-oxadiazole[172].

Formal 1,4-addition of silylenes to 2,2′-bipyridyls leads to the formation of deep violet, highly air-sensitive adducts (equation 73)[173,174].

It is noteworthy that silylenes have been employed in the derivatization of fullerenes. Bis(2,6-diisopropylphenyl)silylene adds regiospecifically to a π-bond localized at a 6-ring, 6-ring juncture of C_{60} to give a single silirane derivative of C_{2v} symmetry[175]. The same silylene adds regioselectively to C_{70} to give two silirane adducts[176].

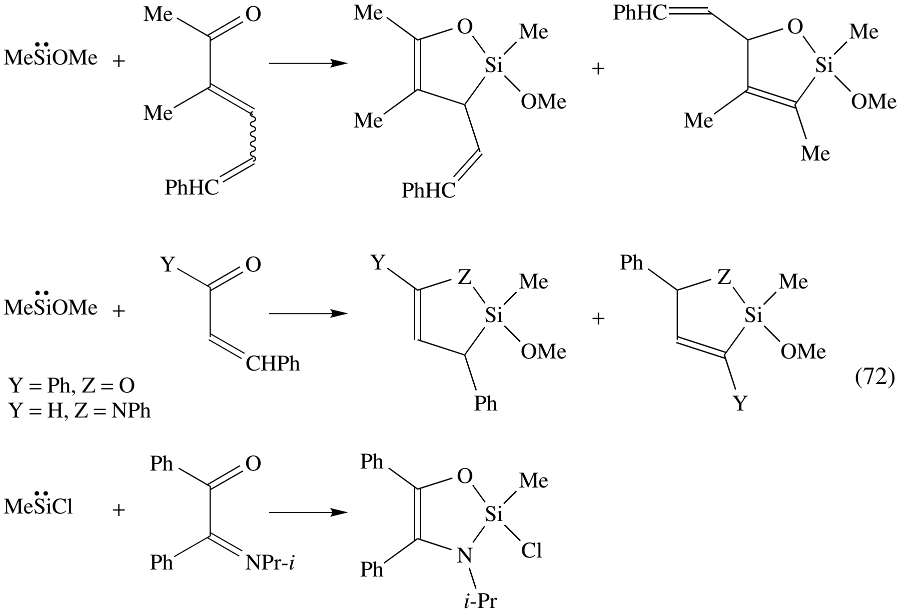

(72)

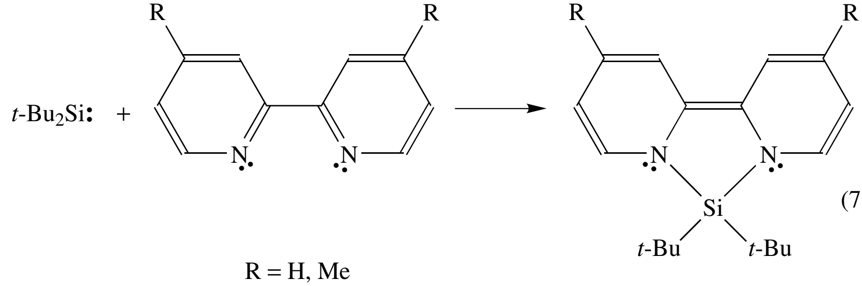

(73)

C. Silylene Dimerization and Disilene Dissociation

1. Silylene dimerization

The intermolecular reaction of two silylene molecules to form a disilene was first proposed for gas-phase reactions[177]. The flow pyrolysis of $MeOSiMe_2{-}SiMe_2OMe$ at 600 °C, which produces Me_2Si, yielded 1,3-disilacyclobutanes as major products; these compounds are known rearrangement products of $Me_2Si{=}SiMe_2$, implying that the disilene was an intermediate. In a study by Sakurai and coworkers[178], silylenes generated from thermolysis of either silanorbornadienes or methoxydisilanes were trapped with anthracene yielding disilane-bridged products, as shown in Scheme 4. Anthracene is known to trap disilenes to give bridged products, so the results again suggest that dimerization of the silylenes has taken place.

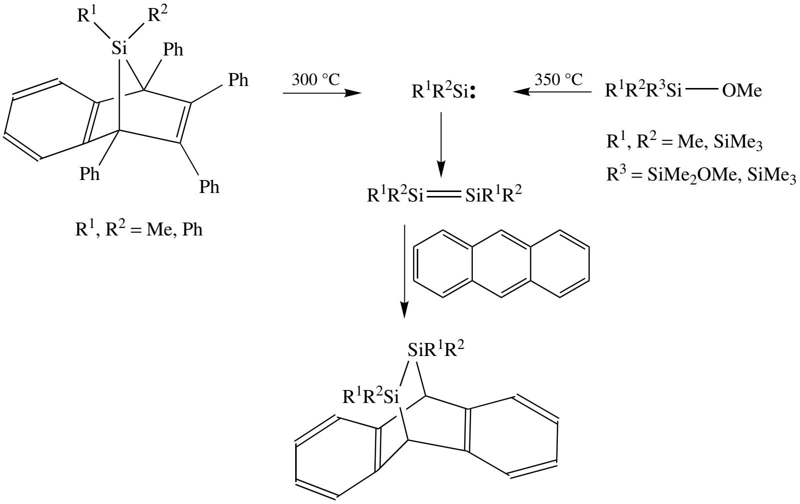

SCHEME 4

Direct evidence for dimerization of silylenes followed upon the isolation of silylenes in matrices, and it now appears that dimerization to the disilene is the usual route of deactivation for silylenes in solution if no trapping agent is present[179]. If the substituent groups are large enough, the resulting disilenes are thermally stable and can be isolated. Dimerization of silylenes, obtained by photolysis of trisilanes, led to the first isolation of a disilene[180] (equation 74) and is now the most general method for disilene synthesis. The 26 different stable disilenes which have been made by this route are listed in a review[181]. Although usually symmetrical disilenes, $R'RSi{=}SiR'R$, are obtained, cross-dimerization between two different silylenes has been employed to synthesize unsymmetrical disilenes (equation 75)[182].

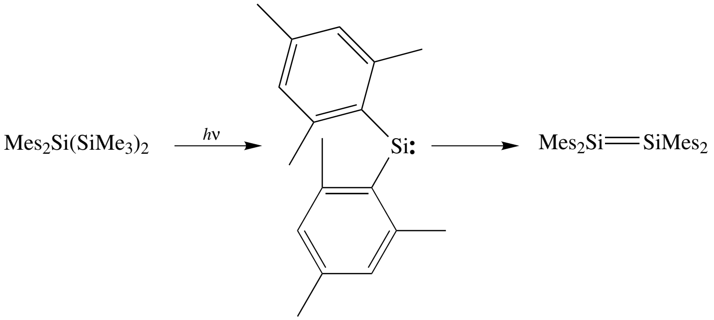

(74)

$$\begin{array}{c}Mes_2Si(SiMe_3)_2\\ +\\ Xyl_2Si(SiMe_3)_2\end{array} \xrightarrow{h\nu} \begin{array}{c}Mes_2Si{:}\\ +\\ Xyl_2Si{:}\end{array} \longrightarrow \begin{array}{c}Mes_2Si{=}SiMes_2\\ +\\ Xyl_2Si{=}SiXyl_2\\ +\\ Mes_2Si{=}SiXyl_2\end{array} \qquad (75)$$

$Xyl = 2,6\text{-}Me_2C_6H_3\text{–}$

Another route to stable disilenes is photolysis of hindered cyclotriarylsilanes (equation 76)[185]. In this reaction one disilene molecule is formed directly, and a second one is produced by eventual silylene dimerization.

$$(\mathrm{Ar_2Si})_3 \xrightarrow{h\nu} \mathrm{Ar_2Si{=\!=}SiAr_2} + \mathrm{Ar_2Si}\mathbf{:} \qquad (76)$$

When smaller substituent groups are present, the disilenes formed from silylene dimerization are themselves unstable. They may undergo a second dimerization to a four-membered ring, or polymerize, or decompose by other pathways. An intermediate case is provided by $\mathrm{Mes(Me_3CCH_2)Si}\mathbf{:}$, which can be generated in 3-MP matrix by photolysis of the trisilane precursor, $\mathrm{Mes(Me_3CCH_2)Si(SiMe_3)_2}$, at low temperatures[179]. This disilene persists in dilute solution up to 0 °C, but at 25 °C it disappears with a half-time of a few minutes (Figure 1).

Dimerization of silylenes has also been studied by flash photolysis. Dimethylsilylene, prepared by flash photolysis of $(\mathrm{Me_2Si})_6$ in cyclohexane, dimerizes to $\mathrm{Me_2Si{=}SiMe_2}$ following second-order kinetics at the diffusion-controlled rate[183]. Disappearance of $\mathrm{Mes_2Si}\mathbf{:}$ generated by flash photolysis also takes place at the diffusion-controlled limit[184], showing that steric shielding by mesityl groups does not impede dimerization.

2. Silylenes from disilenes

We have seen that silylenes normally undergo a dimerization to disilenes. The question then arises whether or not the reverse reaction takes place; that is, whether disilenes can separate at the Si=Si bond to produce silylenes.

There is fragmentary evidence for photolytic cleavage of disilenes to silylenes. For example, disilene **31** does not react with methanol, but under photolysis the methoxymonosilane product **32** is produced in good yield (equation 77)[185a]. A similar trapping reaction was reported earlier for $\mathrm{Xyl_2Si{=}SiXyl_2}$ (Xyl = 2, 6-$\mathrm{Me_2C_6H_3}$)[59]. These results suggest cleavage of the disilenes to silylenes, but of course other mechanisms could account for the products. In similar cases, photolytic cleavage of disilenes to

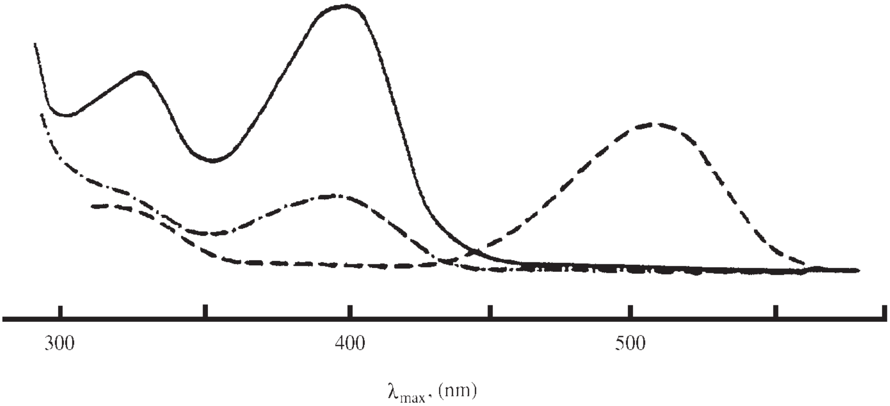

FIGURE 1. Mesityl(neopentyl)silylene and its dimerization: – – – – denotes electronic spectrum of $\mathrm{Mes(Me_3CCH_2Si}\mathbf{:}$ in 3-MP glass at 77 K, ——— denotes spectrum after annealing at 120 K; the silylene has dimerized to the disilene, —· — · — · denotes spectrum at 298 K, showing gradual disappearance of the disilene. Reproduced by permission from Reference 179

silylenes was not observed. For example, cophotolysis of a solution containing the two disilenes, $Xyl_2Si{=}SiXyl_2$ and $Mes_2Si{=}SiMes_2$, produced none of the mixed disilene, $Xyl_2Si{=}SiMes_2$[182].

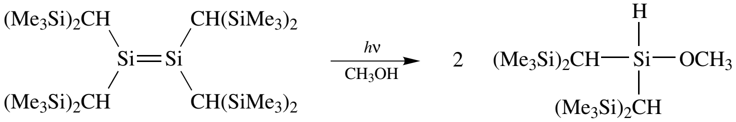

(31) **(32)** (77)

Apeloig and coworkers have trapped $(Me_3Si)_2Si$: from the photoinduced [2 + 2] cycloreversion to $(Me_3Si)_2Si{=}Si(SiMe_3)_2$ and 2,2′-biadamantylidene of the corresponding 1,2-disilacyclobutane[186]. Since laser flash photolysis experiments indicated that the disilene was the sole primary photoproduct, the silylene was believed to be formed by photodissociation of the disilene.

Until recently there was no evidence for thermally induced fragmentation of disilenes to silylenes. Early experiments with $Mes_2Si{=}SiMes_2$ showed that it did not react with the silylene trapping agent Et_3SiH on long heating at 80 °C. With Et_3SiH in toluene at 110 °C, the disilene slowly rearranged without cleaving to the disilene. Recent studies by Okazaki and coworkers have, however, suggested that thermal dissociation does take place for both the *cis* and *trans* isomer of the extremely hindered disilene **33**, under very mild conditions (70 °C)[166,187]. The resulting silylene **34**, was intercepted by the usual silylene trapping reagents, methanol, Et_3SiH and 2,3-dimethylbutadiene, to give the expected products (Scheme 5). Three-membered rings were obtained from **34** and unsaturated hydrocarbons, and trapping of **34** with sulfur and selenium led to interesting cyclic products. The most surprising reactions of **34** are those with naphthalene and benzene, illustrated in equation 70, Section III.B.2.C.

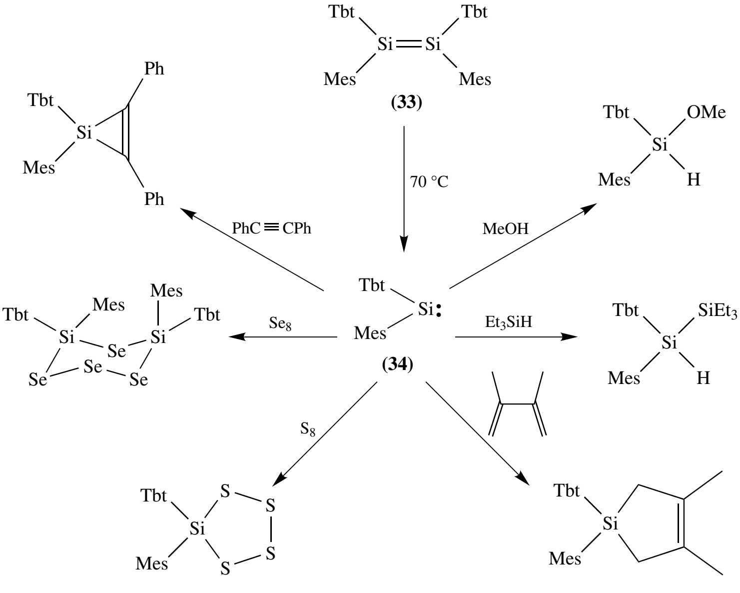

SCHEME 5

In a very recent report, Okazaki and coworkers describe the reaction of **34** with hindered isocyanides **35a–c**, leading to the first examples of stable silylene–Lewis base complexes **36a–c** (equation 78)[145]. The latter were isolated as blue-green to blue solids, stable up to 60 °C. Data for these complexes are listed in Table 2. The high-field ^{29}Si NMR resonances, and the very low values for the ^{29}Si–^{13}C coupling constants, are consistent with the acid–base complex formulation **36**, but incompatible with the alternative cumulene structure **37**. Crystal structures were not available, but quantum-mechanical calculations of the model complex $Ph_2Si \leftarrow C{=}NPh$ suggested a strongly bent structure, as proposed for other silylene–Lewis base complexes (see Section V.A.1).

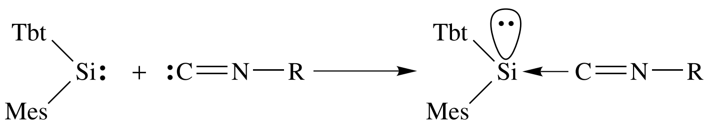

(34) **(35)** **(36)**

(78)

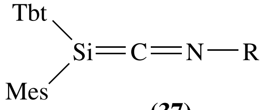

(37)

(a) R = Tip, 2,4,6-(i-Pr)$_3$C$_6$H$_2$
(b) R = Tbt
(c) R = 2,4,6-(t-Bu)$_3$C$_6$H$_2$

Trapping reactions were carried out for **36a–c**, leading in most cases to silylene trapping products with liberation of the isocyanide. Thus, for instance, reaction with Et$_3$SiH yielded the disilane, along with **35a–c** (Scheme 6). Reaction of **36a–c** with methanol also led mainly to the silylene trapping product, but in one case the complex itself (**36a**) was trapped in small yield, producing the imine.

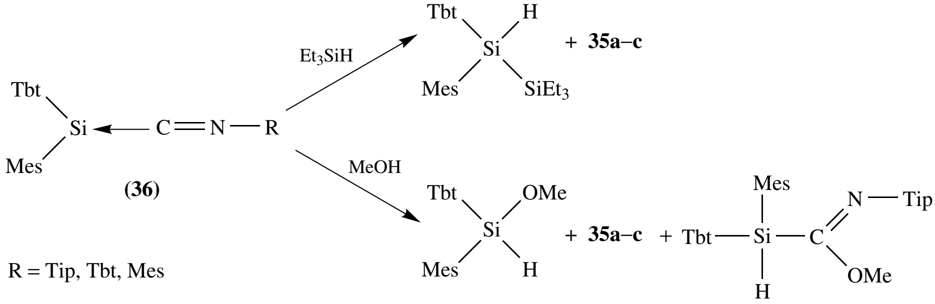

SCHEME 6

TABLE 2. Spectroscopic properties of silylene–isocycanide complexes

Compound	$\delta^{29}Si$–CN	δ Si–^{13}CN	$^1J_{\text{Si–CN}}$
36a	−53.6	209.2	38.6
36b	−57.4	196.6	22.1
36c	−48.6	178.5	1.0

Studies of the kinetics of *cis–trans* interconversion in disilene **33** indicate that it takes place by dissociation to the silylene and recombination, rather than by Si=Si bond rotation as is the case for other disilenes[187]. This isomerization occurs even at 50 °C.

A second example of thermal silylene cleavage has now been observed for the tetraalkyldisilene, $[(Me_3Si)_2CH]_2Si{=}Si[CH(SiMe_3)_2]_2$. No reaction occurs between this disilene and Et_3SiH at 80 °C, but at 120 °C the Si−H insertion product is formed (equation 79)[188]. These two examples suggest that the thermal fragmentation of disilenes into silylenes may be general for disilenes which do not undergo competing thermolytic reactions at lower temperatures.

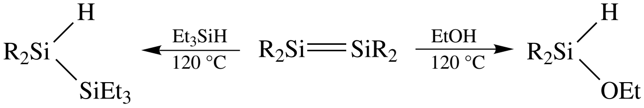

(79)

$R = (Me_3Si)_2CH$

D. Rearrangements and Other Reorganizations of Silylenes

The pioneering studies by the Barton laboratory on the reactions of $Me_3Si\ddot{Si}Me$ revealed the richness of the intramolecular transformations of substituted silylenes[3,5]. In a 1978 paper that profoundly influenced the development of modern organosilicon chemistry, Wulff, Goure and Barton suggested that α-silylsilylenes can rearrange to β-silylsilylenes via unprecedented intramolecular H−C insertion by silylenes and alkyl as well as hydrogen shifts in the course of intramolecular silylene extrusions[189]. These steps are included in equation 80, which also contains Barton's finding that tetramethyldisilene $Me_2Si{=}SiMe_2$ can rearrange to $Me_3Si\ddot{Si}Me$ via a methyl shift. This is the inverse of the well-known rearrangement of carbenes to olefins. The lower stability of disilenes compared with olefins and of carbenes relative to silylenes inverts the thermodynamics of the silicon and carbon systems.

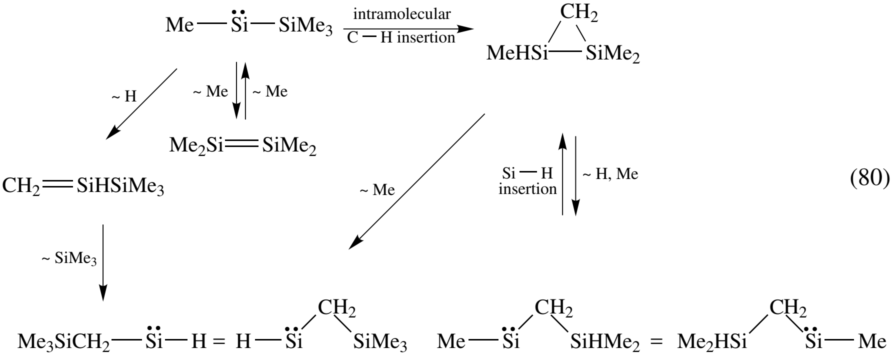

(80)

The rearrangements of silylenes, like those of carbenes, can involve H shifts and the shifts of C−C bonds (intramolecular insertion and ring expansion) or cyclization by intramolecular addition to C=C π-bonds[5]. The mechanism discovered by Barton for silylene-to-silylene rearrangements, silirane formation by H$-$C insertion, followed by ring cleavage via α-elimination, illustrates a major *difference* between silylenes and carbenes: silylene reactions are nearly always *reversible*, in contrast to carbene reactions.

Several questions about this reaction scheme did, however, remain unanswered until recently:

(a) Is the methyl shift that converts disilene $Me_2Si{=}SiMe_2$ to $Me_3Si\ddot{S}iMe$ reversible? Interconversions of silylenes and disilenes via silyl group shifts had been established[5,190], and a methyl shift was found to mediate the transposition of α- and β-substituents shown in equation 53[5,106]. The transposition deduced from trapping experiments (equation 53) and rendered nondegenerate and observable by use of a labeled silylene $CD_3\ddot{S}iSiMe_3$ (equation 81) finally established that the answer to this question is yes[105].

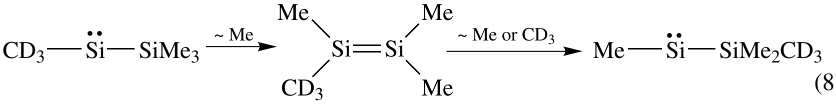

(81)

(b) Is ring opening of the disilirane in equation 80 with a concomitant methyl shift the major pathway leading to $H\ddot{S}iCH_2SiMe_3$? The alternative route shown in equation 80 from $Me\ddot{S}iSiMe_3$ to this β-silylsilylene via a hydrogen shift to a silene intermediate and a Me_3Si shift had been seriously considered[3,104]. Experiments with a labeled silylene $CD_3\ddot{S}iSiMe_3$ revealed that the silyl shift mechanism plays at most a minor role ($<5\%$)[105]. Discrepancies between quantum-mechanical calculations of this reaction and experiment have been resolved[191].

Ring opening of 2-ethylsilirane formed from addition of $H_2Si\colon$ to 1-butene led to the formation of *n*-butyl- and *sec*-butylsilylene[192]. It was deduced that *sec*-butylsilylene undergoes ring closure to 2,3-dimethylsilirane by intramolecular H$-$C insertion with an activation energy of 11.6 ± 2.6 kcal mol^{-1}. From this work a silylene-mediated polymerization of olefins can be envisioned (equation 82).

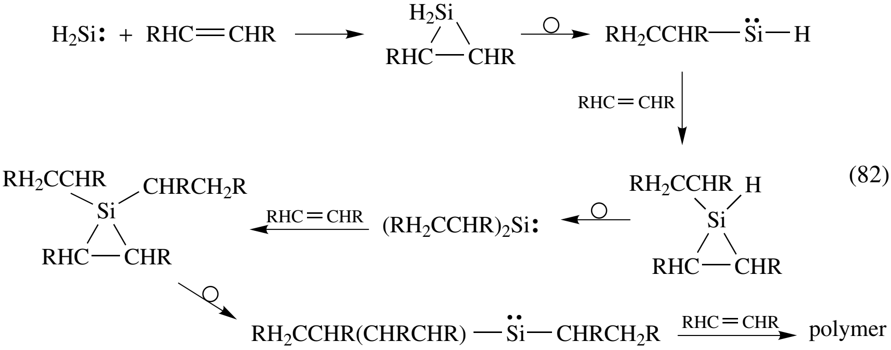

(82)

The Barton laboratory has found many other rearrangments of silylenes[3,5] including strong evidence for the thermal isomerization of silylenes to silanones (equation 83)[193]. Results were also found that were consistent with silanone-to-silylene[194] and silylene-to-silanone-to-silylene[143] rearrangements, but alternative mechanisms could be written, e.g.

equation 84.

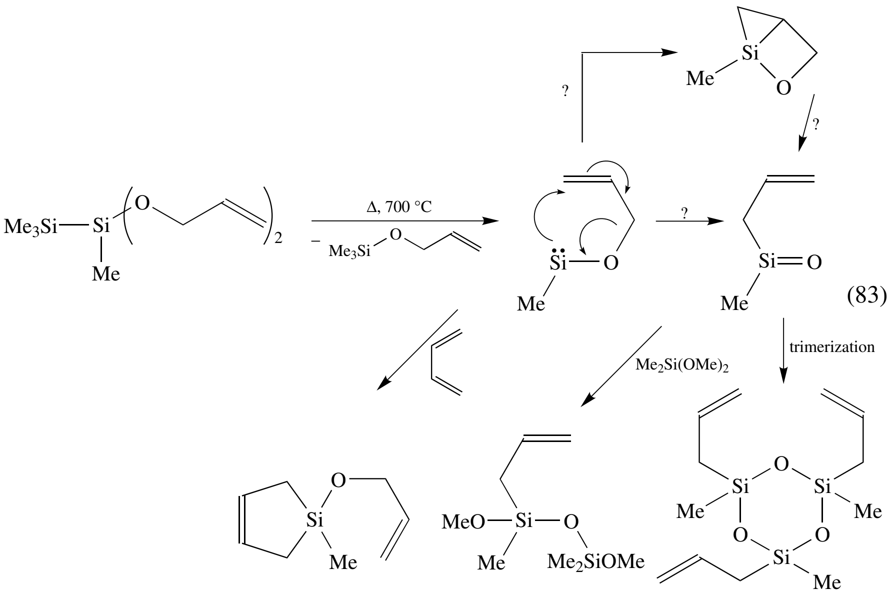

(83)

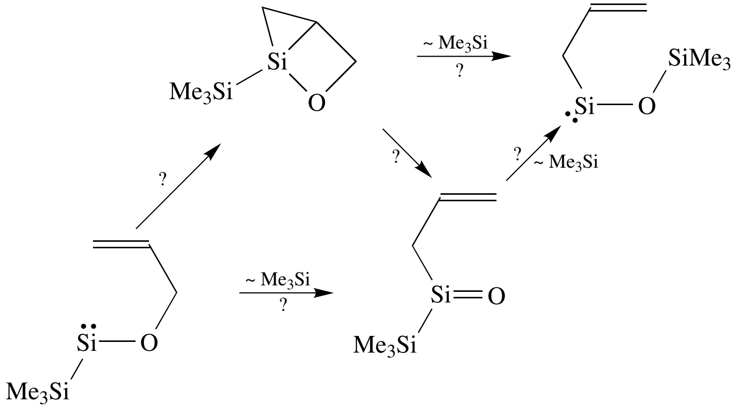

(84)

It should be noted that equation 84 is another example of a transposition in which α- and β-substituents on a silylene are exchanged.

The discovery by Fink, Puranik and Johnson of the rearrangement of a cyclopropenylsilylene to a silacyclobutadiene[195], an epic achievement, has been presented in the reverse direction in Section II.F (equation 54).

The rearrangement of 1-silacyclopent-3-en-1-ylidene to unsubstituted silole, first suggested in 1981[5], has been confirmed by the characterization of the silole dimer[196] and by the recording of UV-visible and IR spectra of the silylene, silole and 1-silacyclopenta-1,3-diene in matrix isolation experiments in which the isomeric silacyclopentadienes were interconverted photochemically (equation 85)[54,197].

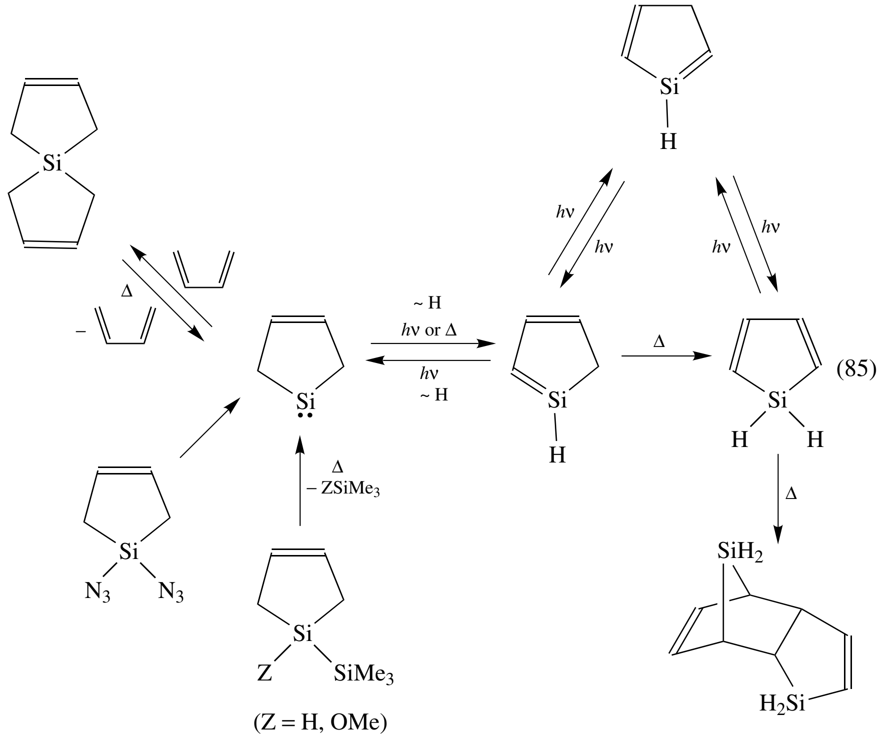

E. Miscellaneous Reactions of Silylenes

In a flowing afterglow experiment the reactions of pyrolytically generated $Me_2Si\colon$ with the anions F^- and $NH_2{}^-$ could be examined[103]. Addition (equation 86a) and deprotonation (equation 86b) were observed.

$$Me_2Si\colon + F^- \longrightarrow Me_2\ddot{S}iF^- \tag{86a}$$

$$Me_2Si\colon + NH_2{}^- \longrightarrow MeSiCH_2{}^- + NH_3 \tag{86b}$$

Dissociation of silylene into $^1D_2$ excited-state silicon atoms and H_2 was observed by excitation with a dye laser of $^1A_1$ ground-state $H_2Si\colon$ to high bending vibrational levels of its $^1B_1$ singlet state[198]. From the vibrational level at which the dissociation channel opened, a heat of formation was established: $\Delta H_f{}^\circ$ $(H_2Si) = 65.4 \pm 1.6\ \text{kcal mol}^{-1}$. Ground-state ^3P silicon atoms have also been observed upon laser excitation of $H_2Si\colon$ from its $^1A_1$ state to $^1B_1$[199]. Extensive mixing of the $^1B_1$ state of H_2Si with other low-lying electronic states, including several triplet states, was believed to lead to predissociation to ^3P silicon atoms[199].

IV. THEORETICAL CALCULATIONS

The accessibility of ever larger and faster computers and the resulting increase in the experience of theorists and confidence in their results has led to a considerable number of calculations on silylenes, including their reaction paths. Reviews of these efforts have appeared[200,201]. In 1989 Apeloig identified the areas of silylene chemistry that had received most attention as: (a) the energy difference between the lowest triplet and singlet electronic states and the effects of substituents on ΔE_{ST}; (b) the electronic (UV-visible) spectra of silylenes; (c) pathways and transition states for insertion and addition reactions of silylenes; (d) energy differences between silylenes and their π-bonded isomers. A very useful interpretation of substituent effects on silylene structures and energetics in terms of the second-order Jahn–Teller effect has been given[202]. Papers published since 1988 are included here.

A. Singlet–Triplet Energy Gaps

One of the important differences between silylenes and carbenes is the contrast between the occurrence of both triplet and singlet ground states for carbenes and the universality of singlet ground states for silylenes. Conversion from the σ^2-configuration of the lowest singlet to the σ, π-configuration of the lowest triplet involves a one-electron energy increase due to the promotion of an unshared electron from an s-weighted orbital (for all nonlinear silylenes) to a pure p-orbital (equation 87). There is also a two-electron energy decrease as the repulsion between the lone pair electrons is relieved by their separation upon going from singlet to triplet. Kutzelnigg has pointed out that formation of triplet carbenes and their analogs ZR_2 (Z = C, Si, Ge, Sn) requires the promotion of an electron from the s^2p^2 configuration of the ground electronic state of the free atom to the sp^3 valence configuration that is associated with hybridization, while formation of singlet ZR_2 does not require this promotion[203]. Hence there should be an increase in the Z–R bond strength in going from singlet to triplet ZR_2. Kutzelnigg associates the occurrence of carbenes with triplet ground states with the gain in bond energy (for CR_2 but not SiR_2, GeR_2 or SnR_2) compensating for the promotion energy[203].

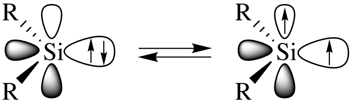

(87)

Configuration interaction (CI) calculations based on generalized valence bond wave functions, called dissociation consistent CI(DCCI), were applied to the calculation of ΔE_{ST} for SiH_2, SiHF and SiF_2[204]. For SiH_2 and SiF_2 the theoretical values agreed well with (experiment): 21.5 (20.7) and 76.6 (76.2) kcal mol^{-1}, respectively. For SiHF the prediction was 41.3 kcal mol^{-1}. Stabilization by fluorine of the singlet state relative to the triplet state was ascribed to donation of fluorine pπ-electrons to the silicon p-orbital and an increase in the s-character of the nonbonding σ-orbital of silicon holding the lone pair due to the electronegativity of the fluorine substituent[204].

Similar calculations on SiHCl and $SiCl_2$ yielded ΔE_{ST} of 35.8 and 55.2 kcal mol^{-1}, respectively[205]. An interesting result was the difference in the contribution of the silicon p-orbital to the Si–Z bonds in the singlet and triplet states: for SiHCl, 73.6% p in Si–H and 62.3% p in Si–Cl of the singlet but 38.5% p in Si–H and 44.8% p in Si–Cl of the triplet. For $SiCl_2$ the silicon p-character of Si–Cl was predicted to be 61.1% in the singlet and 39.6% in the triplet. There is, of course, a corresponding opposite effect on the p-character of the σ-nonbonding orbital[205].

Apeloig has pointed out that the electronegativity of substituents at the divalent silicon atom of a silylene has opposite effects on singlet and triplet states, triplets being stabilized by less electronegative substituents while singlets are stabilized by more electronegative substituents[201]. It has been known since 1985 that extremely electropositive substituents like Li could lead to ground-state triplet silylenes[201], but these molecules are difficult to prepare.

Grev and coworkers have suggested that the effects of electronegativity can be combined with those of bulky groups to design a silylene whose ground state is a triplet[206]. The larger the bond angle at the divalent silicon atom, the greater is the p-character of the σ-nonbonding orbital, and thus the smaller is the one-electron promotion energy required to convert the σ^2-configuration that dominates the lowest singlet state to the σ,π-configuration that dominates the lowest triplet. The singlet state has both unshared electrons in the σ-orbital that increases in p-character, and hence energy, with an increase in bond angle. Therefore the σ^2 singlet state increases in energy more rapidly with an increase in bond angle than does the σ,π triplet, one of whose unshared electrons occupies a pure p-orbital whose energy does not vary with bond angle. The singlet and triplet potential curves cross[206].

Thus, while Me_2Si has a lowest singlet state with $\angle C{-}Si{-}C = 98.8^\circ$, 25.1 kcal mol^{-1} below the triplet with $\angle C{-}Si{-}C = 117.9^\circ$, for bond angles $>140^\circ$, the triplet becomes the ground state. The implication is that for alkyl substituents with electronic effects similar to Me, it would be necessary to increase the bond angle by more than 40° in order to achieve a triplet ground state. This bond angle would be very difficult to achieve with even the bulkiest of substituents. However, for the less electronegative substituent SiH_3, there is a dramatic decrease in the predicted crossover angle beyond which the triplet is the ground state: 120° for $(H_3Si)_2Si\colon$ versus 140° for $(H_3C)_2Si\colon$[206].

It has thus become an accepted strategy for the design of a ground-state triplet silylene to employ electropositive substituents like silyl groups SiR_3 that are sufficiently bulky that the $\angle Si{-}Si{-}Si$ at which the singlet state has minimum energy is sufficiently large ($>120^\circ$) that the triplet will be the ground state. The first of these 'designer silylenes' $(i\text{-}Pr_3Si)_2Si\colon$ has been prepared, and preliminary results suggest that it has a triplet ground state[207] as predicted theoretically by Apeloig[134].

Calculations on a series of silylenes by Kalcher and Sax predicted that, relative to H, CH_3 is an electronegative substituent while SiH_3 and Li are electropositive[208]. The electron affinity of a silylene as well as its ΔE_{ST} were predicted to change with the electronegativity of the substituents. A decrease in ΔE_{ST} with decreasing electronegativity had been found previously, with $LiHSi\colon$ and Li_2Si possessing triplet ground states. Unexpected and unexplained was the prediction that the electron affinities (EAs) of silylenes dramatically *increase* with silyl or Li substituents — to the point that not only the ground states but also the first-excited states of the substituted silylene anions are bound states. In the case of silyl substituents the stabilization may be the result of charge-induced dipole interactions due to the polarizability of the substituent, but the effect of Li substituents was attributed to delocalization[208].

Kalcher and Sax also examined the lowest singlet and triplet states of *cyclo*-$(H_2Si)_2Si\colon$, a three-membered cyclic silylene. The Si−Si−Si angles at the divalent silicon are constrained to be much smaller than those in the open-chain $(H_3Si)_2Si$ for both the singlet (56.2° versus 95.9°) and the triplet (62.8° versus 125.4°) states. It is surprising that ΔE_{ST} is nearly the same in the cyclic (8.8 kcal mol^{-1}) and open-chain (8.3 kcal mol^{-1}) silylenes[208].

An interesting comparison has been made by Cremer and coworkers of calculations on the structures and energies of $^1A_1$ and $^3B_1$ H_2Si by two different high level computational methods, full valence active space SCF with multi-reference CI (CASSCF-MRCI), and density functional theory[209]. Both calculations predicted a ΔE_{ST} within 2 $\mathrm{kcal\,mol^{-1}}$ of the experimental estimate, but the CASSCF-MRCI calculations required several orders of magnitude more time than the density functional calculations (7,379 versus 50 s for $^1A_1$ and 13,873 versus 52 s for $^3B_1$ on a Cray supercomputer)! This large efficiency factor points to the growing importance of density functional calculations in dealing with the larger molecules of chemical interest. To predict ΔE_{ST} for $(i\text{-}Pr_3Si)_2Si$ (-1.7 $\mathrm{kcal\,mol^{-1}}$) required 170 *hours* of supercomputer time using density functional methods[210]! Apeloig and coworkers have calculated that $(t\text{-}Bu_3Si)_2Si$ is also a ground-state triplet, with ΔE_{ST} of -7.1 $\mathrm{kcal\,mol^{-1}}$ at the BLYP/DZVP (ECP) level[210]. Such calculations would not be feasible by methods (such as CASSCF-MRCI) requiring several orders of magnitude more time.

B. Thermochemical Calculations

Whether methylsilylene $CH_3\ddot{S}iH$ is more stable than its isomer silaethylene $H_2C{=}SiH_2$ has remained a subject of controversy and theoretical activity for two decades. Beauchamp, Goddard and coworkers summarized calculational results from 1978 to 1987 that predicted values for $\Delta E(CH_3\ddot{S}iH{-}H_2C{=}SiH_2)$ ranging from 11.6 to -6.8 $\mathrm{kcal\,mol^{-1}}$[211]. The Beauchamp, Goddard value ($+11.6$ $\mathrm{kcal\,mol^{-1}}$) obtained using a correlation consistent configuration interaction method based on generalized valence bond wavefunctions, which is in harmony with their experimental determination (see Section III.D), was immediately challenged by Grev, Schaefer, Gordon and coworkers[212]. Using much larger basis sets and higher level correlation treatments, these workers obtained $\Delta E(CH_3\ddot{S}iH{-}H_2C{=}SiH_2) = 3.6$ $\mathrm{kcal\,mol^{-1}}$. In 1990, Boatz and Gordon made a similar prediction (4.1 $\mathrm{kcal\,mol^{-1}}$) using large basis sets and quadratically convergent configuration interaction[213]. The predicted ΔH_f for $CH_3\ddot{S}iH$, 50.6 $\mathrm{kcal\,mol^{-1}}$, was similar to that predicted by Beauchamp, Goddard and coworkers (53 ± 4 $\mathrm{kcal\,mol^{-1}}$). Boatz and Gordon had previously estimated $\Delta H_f(CH_3\ddot{S}iH) = 49.2$ $\mathrm{kcal\,mol^{-1}}$ [and $\Delta H_f(Me_2\ddot{S}i) = 32{-}33$ $\mathrm{kcal\,mol^{-1}}$] from isodesmic reactions[214]. Silylsilylene $H_3Si\ddot{S}iH$ (calculated $\Delta H_f = 72.8$ $\mathrm{kcal\,mol^{-1}}$) was predicted to be 7.9 $\mathrm{kcal\,mol^{-1}}$ less stable than disilene $H_2Si{=}SiH_2$ ($\Delta H_f = 64.9$ $\mathrm{kcal\,mol^{-1}}$. Trinquier predicted $\Delta E(H_3Si\ddot{S}iH{-}H_2Si{=}SiH_2) = 9.8$ $\mathrm{kcal\,mol^{-1}}$[215].

Relativistic effects on the structure and energy of the heavier group 14 dihydrides have been studied[216]. For H_2Si, inclusion of relativistic effects caused little change in the predicted values: $<0.05°$ in $\angle$ H−Si−H, <0.0005 Å in r(Si−H), <0.02 D in the dipole moment and <0.6 $\mathrm{kcal\,mol^{-1}}$ in energy.

Ho and Melius have employed Hartree–Fock SCF calculations with modest basis sets (6-31G*) with MP4(SDTQ)/6-31G** perturbation theory correlation corrections at the HF/6-31G* geometries and bond additivity corrections to predict revised ΔH_f(298 K) values ($\mathrm{kcal\,mol^{-1}}$) for SiF_2 (-149.86 ± 4.00) and SiHF (-35.70 ± 2.85)[217]. Dissociation enthalpies for the formation of silylenes from SiF_4, SiF_3, $SiHF_3$, SiH_2F_2, SiH_3F, $SiHF_2$, SiH_2F and Si_2F_6 were also predicted[217].

Comparison of cyclic compounds **38** and **39** shown in equation 88 via correlated MP2/6-31G*//HF/6-31G* calculations indicated that the cyclic trisilylene **38** is more stable than the trisila-*s*-triazine structure **39** by 30 $\mathrm{kcal\,mol^{-1}}$ at the CCSD/6-31G*//MP2/ 6-31G* level of theory[218]. Similar calculations on 2-silapyridine-2-ylidene **40** and its silaimine isomer **41** (R = H) suggested that **40** might be a good candidate for a stable silylene, inert to dimerization[219]. **40** is calculated to be 8.8 kcal mol^{-1} more stable than **41**. Methyl substitution reverses the calculated order of energies, making **41** (R = Me) more stable than **40** (R = Me) by 4.7 kcal mol^{-1}.

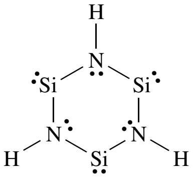
(38)

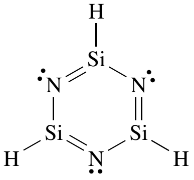
(39)

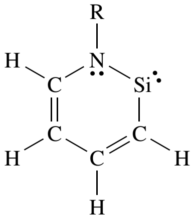
(40)

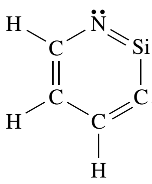
(41)

(88)

Despite the apparent difference in electron distribution suggested by the valence structures **38** and **39**, examination of homodesmic reactions leads to the prediction that both structures benefit from aromatic stabilization, the triazine more than the trisilylene. The greater strength of an N−H compared to a Si−H bond tips the scale in favor of the trisilylene structure[218].

Density functional calculations on the isomers of R_2Si_2 revealed that for R = H, Me, SiH_3, SiF_3, $SiMe_3$, $SiPh_3$ and $Si(SiH_3)_3$, the disilenylidene structure $R_2Si{=}Si\colon$ is lower in energy than a *trans*-bent disilyne $RSi{\equiv}SiR$ structure[220]. For R = H, the most stable structure is a doubly bridged 'butterfly'. Only for very bulky groups $(t\text{-}Bu)_3Si$ and $(2,6\text{-}Et_2C_6H_3)_3Si$ is the *trans*-bent $RSi{\equiv}SiR$ more stable than $R_2Si{=}Si\colon$. For a discussion of vinylidenesilylenes and other double-bonded $Z{=}Si\colon$ silylenes, see Section VIII.F.

C. Theoretical Predictions of Silylene Spectra

A diatomic silylene of astrophysical interest, silicon sulfide $S{=}Si\colon$, was treated by a three-stage calculation[221]. MOs from an HF-SCF treatment were employed in a complete active space SCF calculation whose optimized MOs were in turn used for a CI calculation that included as many as three million configurations! Comparison of various spectroscopic constants with those from experiment revealed fair agreement[221].

A coupled electron pair approach gave highly correlated wave functions for ground state $^1A_1$ and for first excited triplet $^3B_1$ SiH_2 from which theoretical rotational-vibrational spectra were calculated[222]. Calculated vibrational band origins agreed within 10−40 cm^{-1} with experimental values. Molecular geometries and vibrational frequencies, as well as force fields and mean-square amplitudes for SiF_2, $SiCl_2$ and $SiBr_2$ were calculated at the MP2/3-21G//HF/3-21G level in reasonable agreement with experiment[223].

Several calculations have aimed at interpreting the spectra of what has been called the first stable silylene (see Section VIII.C) shown in equation 89 as **42** (R = *t*-Bu). MP4/6-31G*//HF/6-31G* on **42** (R = H) suggested that the lowest energy peak in the photoelectron spectrum of **42** (R = *t*-Bu) corresponds to loss of an electron from a π-MO resulting from mixing of the Si 3p-orbital that would be the LUMO of a normal silylene with π_3 of a 1,4-diazabutadiene fragment[224]. This implies aromatic stabilization of **42** by N−Si π-bonding, also indicated by calculations on **43** and **44**. Density functional calculations led to similar assignments of the PES peaks, but the spherical distribution of electron density around the silicon atom of **42** (R = *t*-Bu) led to a description of the molecule as a silicon atom chelated to a diazabutadiene[225].

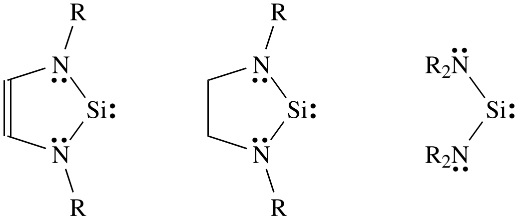

(42) **(43)** **(44)**

(89)

Calculations by Apeloig and coworkers on the electronic spectra of ethynyl- and vinylsilylenes have resolved earlier differences between theory and experiment and posed new questions[226]. The replacement of a methyl group of Me_2Si by a vinyl, ethynyl or aryl group causes a decrease in the transition energy, a red shift (see Section V.A.1). This is explained as due to excited-state stabilization by interaction of the singly occupied Si 3p-orbital with a π^* orbital of the substituent[226].

D. Benchmark Calculations on Silylenes

New advances in theoretical methodology have been tested by calculations on silylenes. The spin-coupled valence-bond theory is an *ab initio* technique that includes effects of electron correlation from the outset. Using small basis sets for Si (12s9p) and H (5s), accommodating the ($1s^22s^22p^6$) core electrons in MOs from RHF calculations and expanding the spin-coupled valence orbitals in a basis of 30 MOs, compact wave functions were employed to calculate the lowest singlet and triplet states of SiH_2[227]. The $\Delta E_{ST} = 17.1\ \text{kcal mol}^{-1}$ value is in good agreement with the results of more extensive CI calculations with much larger basis sets, suggesting that modern valence-bond descriptions treat singlets and triplets even-handedly. The spin-coupled valence orbitals resembled the sp^2 and pure 3p orbitals employed in qualitative descriptions.

As a first application of a new analytical gradient method employing UHF reference functions, seven different methods for inclusion of correlation effects were employed to optimize the geometry and calculate the harmonic vibrational frequencies and dipole moments of the lowest open-shell states for three simple hydrides including $^3B_1$ SiH_2[228]. As the degree of correlation correction increased, results approached those from the best multiconfiguration SCF calculation.

When a new population analysis method for the calculation of atomic charges, the generalized atomic polar tensor (GAPT) approach, was applied to singlet SiH_2, the results were not changed by a correlation correction[229]. The insensitivity to the basis sets used (deduced from other examples), and the fact that the GAPT charges are obtained as a byproduct of the construction of the Hessian matrix in many electronic structure calculations, suggested that the GAPT analysis might replace the classical Mulliken population analysis.

Inclusion of connected triple excitations in the equation-of-motion coupled-cluster method for calculating excitation energies was also tested on SiH_2[230]. Excitation energies predicted for the lowest triplet state and the two lowest excited singlet states $^1B_1$ and 2 $^1A_1$ were within a kcal mol^{-1} of the predictions of the full CI calculation when triple excitations were included, but only for the 2 $^1A_1$ state was there marked improvement over the inclusion of only single and double excitations.

SiH_2 and SiF_2 were among several species used as 'guinea pigs' for new pseudospectral algorithms for electronic structure calculations[231,232]. Absolute energies agreed to within 0.25 $kcal\,mol^{-1}$ with those from conventional basis sets, and relative energies were within 0.1 $kcal\,mol^{-1}$, with enhanced computation speeds. The pseudospectral numerical method is an alternative to all-integral methods for the calculation of Hartree–Fock molecular wave functions.

A perturbation-trajectory method for determining the dynamics of gas-surface collision processes was tested on the collision and subsequent surface reactions of SiH_2 on a Si(111) surface[233]. The predictions of an exact classical trajectory calculation[234] were confirmed: the sticking probabilities were unity at all temperatures, and it was found that surface SiH_2 can decompose by direct elimination of H_2 or by successive dissociation of Si−H bonds.

An efficient implementation of microcanonical classical variational transition state theory was applied to Si−H bond fission in SiH_2 and compared with trajectory calculations on the same potential surface[235].

E. Theoretical Treatments of Silylene Chemistry

Bond-order changes upon photoexcitation obtained from Sandorfy SCF-CI calculations have been employed to predict the ease of photoextrusion of a silylene from polysilane chains or rings[236]. Smaller bond-order changes with longer polysilane chains suggested that they are less efficient silylene sources. Similar conclusions were reached for branched and cyclic polysilanes. This approach focuses on σ to σ^* excitation without participation by Si 4s orbitals in descriptions of excited states[237].

Ab initio calculations suggested a bridged structure for the silver atom–SiO adduct[238]. The predicted structure was in better agreement with ESR observations than a previously proposed linear structure.

By theoretical prediction of its IR spectrum via *ab initio* SCF calculation, a structure of C_s symmetry with Si as the central atom was deduced for the photoproduct HClSi=S from Si=S and HCl in an argon matrix[239].

HF calculations have predicted two different transition states for the three-center concerted extrusion of SiH_2 from $EtSiH_3$[240]. The two transition states differ in energy by *ca* 10 $kcal\,mol^{-1}$ and in their structure by the orientation of the SiH_2 group. It was suggested that contributions from concerted extrusion may account for the formation of some C_2H_6 and the wide range of rotational states for SiH_2 observed in IR multiphoton dissociation experiments. The reverse reaction, insertion of SiH_2 into a C−H bond of ethane (which, in principle, should have the same two transition states as the corresponding extrusion reaction) was examined by the same group with inclusion of electron correlation at the MP2/6-31G*//HF/6-31G* level[241]. The energy difference between the two transition states shrank to 7.8 $kcal\,mol^{-1}$, with a sizeable (22.3 $kcal\,mol^{-1}$) barrier for the favored transition state. By comparison with insertion reactions of several carbenes, it was concluded that barrier heights for insertion correlate with ΔE_{ST} rather than with frontier orbital interactions or steric effects. In such a model, the insertion barrier is due to an avoided crossing between a surface on which the singlet carbene (or silylene) is converted to an excited state of the insertion product and the surface on which the ground state of the insertion product lies. The higher the energy of the singlet silylene(carbene), the lower the relative energy (energy barrier) of the avoided crossing[241].

Calculations by Francisco examined decomposition reactions of ethylsilylene EtSiH[242]. Elimination to form SiH_2 and ethylene is computed to be the lowest energy pathway, with no barrier in the reverse direction. Rearrangement to $CH_3CH{=}SiH_2$ is predicted to have a 32 kcal mol^{-1} energy barrier, 4 kcal mol^{-1} higher than that for elimination of SiH_2. Elimination of an Si atom from $\text{Et}\overset{\bullet\bullet}{\text{Si}}\text{H}$ is predicted to have a barrier of 72 kcal mol^{-1}.

Transition states and their energies for insertion of SiH_2 into C−C, C−Si, Si−Si, C−H and Si−H bonds have been obtained at the MP4/6-31G(d)//HF/3-21G* level[243]. Since the barriers decreased in the order C−C>C−Si>Si−Si, steric interactions appeared to be a major factor in determining barrier heights. The barrier for insertion of SiH_2 into a C−C bond of cyclopropane (20 kcal mol^{-1}) was *ca* 40 kcal mol^{-1} less than that for ethane. Despite its low calculated barrier of <5 kcal mol^{-1}, insertion of SiH_2 into an unstrained Si−Si bond is unknown. The insertions into C−Si and C−C bonds have higher barriers[243] and are likewise unknown.

An important theoretical result has been the finding [at MP2/6-3111G(d,p)] of a complex between SiH_2 and SiH_4 along the pathway for insertion into an H−Si bond[244]. This complex is 12.3 kcal mol^{-1} lower in energy than the separated reactants, but there is only a 1.6 kcal mol^{-1} barrier between the complex and the H_3SiSiH_3 insertion product. The experimentally observed negative activation energies for silylene insertion reactions (see Section VI) have been attributed to the intermediacy of such complexes, although other explanations are possible.

Ab initio study of the insertion of SiH_2 into the C−O and O−H bonds of methanol revealed that a complex is formed in which SiH_2 is coordinated to O[245]. Formation of the complex was found to be exothermic by 19.9 kcal mol^{-1} at MP2/6-31G*//HF/6-31G* with barriers for rearrangements to the O−H and C−O insertion products of 0.6 and 20.5 kcal mol^{-1}, respectively.

Insertion of SiH_2 into F_2 has been examined with a 6-31G* basis set and full geometry optimization at the MP2, CCD, CISD and QCISD levels[246]. Two transition states were found, differing by whether one of the F atoms approaches *syn* or *anti* to the Si lone pair. For *anti* approach there was no barrier found, while for *syn* approach a complex was found, whose energy is 2.5 kcal mol^{-1} below the reactants while a barrier of 0.5 kcal mol^{-1} separates the complex from the products.

Potential energy surfaces for the addition of SiH_2 to acetylene have been calculated at a very high *ab initio* level [QCISD/6-311G++(2df,2p)//MP2/6-31G(d,p), with corrections to the QCISD energies for triple excitations], and rate constants were calculated in the framework of the quantum-statistical RRK theory[128]. Negative activation energies for the formation of the silirene adduct were predicted, in accord with experimental observations, due to competition between stabilization and dissociation of vibrationally excited adduct. Rearrangement of silirene to $HC{\equiv}CSiH_3$ was predicted to occur via a 41.2 kcal mol^{-1} barrier, while a lower barrier of 36.8 kcal mol^{-1} was predicted for concerted rearrangement of silirene to vinylsilylene $H_2C{=}CHSiH$. The reverse rearrangement, ring closure of $H_2C{=}CH\overset{\bullet\bullet}{\text{Si}}H$ to silirene, was calculated to have a 30.2 kcal mol^{-1} barrier[128].

Dimerization of silylenes XHSi, where X = NH_2, OH and F, has been studied theoretically by Apeloig and coworkers[247]. Alternative pathways for the dimerization of XHSi to the corresponding disilenes or bridged structures are shown in equation 90. For the three XHSi silylenes, dimeric bridged structures were found to be minima on the potential energy surface. According to MP4/6-311G**//6-31G** calculations, the bridged structure is less stable than the classical disilene structure by 10.0 and 3.2 kcal mol^{-1} for X = F and OH, respectively, but for X = NH_2 the bridged structure is more stable by 10 kcal mol^{-1}[247a,b].

Insertion of SiH_2 into H−C and H−Si bonds of CH_4 and SiH_4, respectively, and H-abstraction are among the model reactions for silicon carbide formation that were examined at the HF/6-31G* level[248].

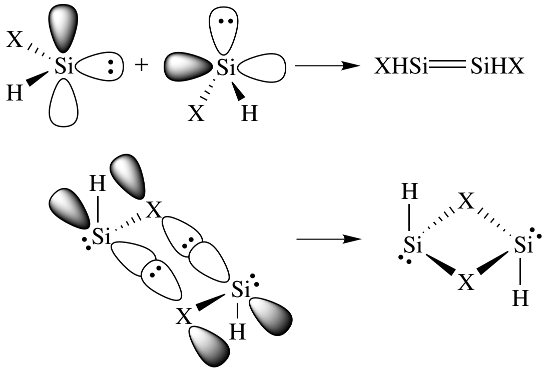

(90)

X = NH_2, OH, F

Theoretical investigation of the reaction between SiH_2 and CO found a weakly bound structure, pyramidal at Si, with a nonlinear array of the heavy atoms that corresponds to lone pair donation from the carbon and very little backbonding[249]. The addition is predicted to be exothermic by only 16 kcal mol^{-1}. Similar results have been reported, comparing the energies of planar and nonplanar adducts in which CO was coordinated to H_2Si at C and O, respectively[250].

The nature of the transition metal–silicon double bond has been examined by full optimized reaction space multiconfiguration SCF (FORS-MCSCF) calculations on $MSiH_2{}^+$ (M = Sc, Ti, V, Cr, Mn, Fe, Co and Ni) complexes[251]. It was found that the $MSiH_2{}^+$ complexes have significantly weaker bonds, as judged by the magnitude of the M−Si calculated force constants, than their $MCH_2{}^+$ counterparts. For the series $Cr{-}EH_2{}^+$ (E = C, Si, Ge and Sn) the silylene complex has a larger calculated force constant than the germylene and stannylene and thus was judged to represent a synthetically attainable target. At the SCF level the M−Si σ-bond was better described than the π-bond, the latter thus requiring a multiconfiguration wave function to include correlation effects for an accurate description of the bond. A qualitative description of the early transition metal complexes, e.g. $ScSiH_2{}^+$, is dominated by the double-bonded (M = E) and σ-ylide ($M \rightarrow E$) resonance structures with the σ-dative/π-backbond ($M \rightleftharpoons E$) structure making a small contribution, while late transition metal silylenes, e.g. $NiSiH_2{}^+$, are dominated by ($M \rightleftharpoons E$) and to a lesser extent by ($M \leftleftarrows E$) resonance structures[251].

Potential energy surfaces for dissociation of SiH_2 to SiH + H and Si + H_2, from various states up to 8 eV excitation energy, have been calculated by multiconfiguration SCF + multireference CI calculations[252].

V. SPECTROSCOPIC CHARACTERIZATION OF SILYLENES

A. Electronic Spectra

1. Free silylenes

The ultraviolet spectra of some inorganic silylenes, $SiCl_2$, SiF_2, SiH_2 and others, were measured in gas-phase experiments some years ago and are summarized in a 1992 review[253]. Studies of the electronic spectra of organosilylenes have appeared in recent years, following the discovery that photochemically generated silylenes could be isolated in argon matrices at temperatures near 10 K, or in hydrocarbon glasses at liquid nitrogen temperature[41]. Cyclosilanes or linear trisilanes are the most usual precursors, but other photochemical routes can also be used. The best studied of all silylenes in matrix conditions, dimethylsilylene, has been generated from no less than eight different precursors[254]. These are shown in Scheme 7, which illustrates the possible routes to silylenes in matrix.

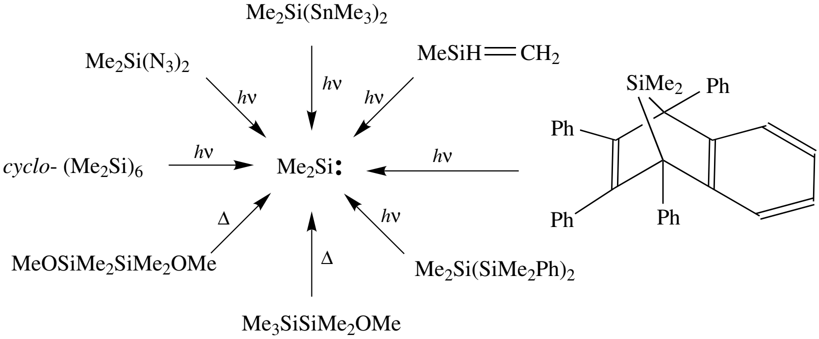

SCHEME 7

At liquid nitrogen temperature, 77 K, matrix isolation in hydrocarbons is successful for many silylenes because they are singlet species and so do not abstract hydrogen from C−H bonds, as would be expected for triplet molecules. The usual hydrocarbon is 3-methylpentane (3-MP) which forms a rigid glass at 77 K, but sometimes mixtures of hydrocarbons are used which are softer at this temperature, to allow some mobility of the silylene in the matrix. In a few cases, silylenes have also been identified from transient spectra obtained in flash photolysis experiments.

The electronic absorption of silylenes can be represented as a transition between the $^1A'$ singlet, S^0, with both electrons in a (mainly) 3s orbital on Si, to the $^1A''$ excited singlet, S^1, which has one electron in a 3p orbital perpendicular to the molecular plane (Figure 2). The energy of this transition usually places it in the visible region. Thus $Me_2Si\colon$ has $\lambda_{max} = 453$ nm in 3-MP, with a fluorescence at 645 nm[254]. The large Stokes shift indicates a substantial difference in geometry in the ground and excited states. This is consistent with calculations on silylene $H_2Si\colon$, which predict the H−Si−H angle to be much larger in the S^1 excited state (120°) than in the S^0 ground state (93.2°)[255,256].

Table 3 presents a fairly complete list of electronic absorption maxima for the $S^0 \rightarrow S^1$ transition of silylenes isolated in matrices; data are also included for some silylenes identified in flash photolysis experiments[184,257–260]. The absorptions span a wide range, from 221 to *ca* 770 nm.

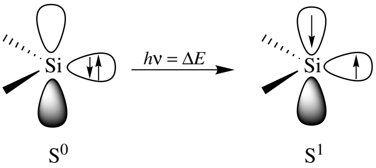

FIGURE 2. Electron distribution in ground and excited states of silylenes

TABLE 3. UV/vis absorption maxima for silylenes, RR′Si:

R	R′	λ_{max}	Reference
(A) In argon matrix, *ca* 10 K			
HC≡C	H	500	269
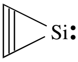		400–500	269
CH_3	C_6H_5	495	270,271
H	H	487	255,256
CH_3	H	480	270,271
CH_3	CH_3	460	254,270,271
CH_3	Cl	407	270,271
CH_3	OCH_3	355	168
H	NH_2	342	272
H	OCH_3	340	168
Cl	Cl	317	273
$H_2C{=}C{=}Si\colon$		310,325,340	269
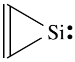		286	269
OPr-*i*	OPr-*i*	247	168
OCH_3	OCH_3	243	168
F	F	221 (gas phase)	274
(B) In 3-Methylpentane (3-MP), 77 K			
Me_3Si	Mes	760,776	37,275
Me_3Ge	Mes	730	37
Me_3Si	*p*-Tol	672	275
Me_3Si	*o*-Tol	662	275
Me_3Si	$C{\equiv}CSiMe_3$	660	37
Me_3Si	Ph	660	37,275
Me_3Ge	Ph	625	37
Me_3Si	$CH{=}CH_2$	619	275
Mes	Mes	577	172
Me_3Si	DEP[a]	578	37
Me_3Si	Tip[b]	568,570	37,275
Mes	C≡CPh	550	226
Mes	$C{\equiv}CSiMe_3$	545	226
Mes	Ph	530	179
Mes	1-Ad	526	142
Mes	C≡CH	524	226
Mes	*t*-Bu	505	142
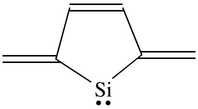		505	265

TABLE 3. (*continued*)

R	R′	λ_{max}	Reference
Me_3Si	$C{\equiv}CSiMe_3$	500	37
Mes	Me_3CCH_2	500	226
Mes	*i*-Pr	500	179
Mes	CH_3	496	179
Ph	Ph	495	179
Ph	CH_3	490	179
Mes	Cl	487	179
t-Bu	*t*-Bu	480	53
Me_3Si	*o*-$Me_2NCH_2C_6H_4$	480	275
	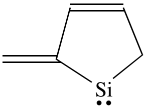	480	265
	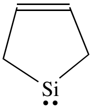	475	54,197
CH_3	$C{\equiv}CSiMe_3$	473	226
CH_3	*t*-Bu	470	276
CH_3	Et	459	179
CH_3	CH_3	453	254
CH_3	*p*-$CH_3OC_6H_4$	450	179
Mes	TTBCP[c]	450	277
	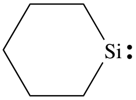	449	179
	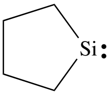	430	179
Mes	Tip[b]	430	275
Mes	OMes	425	278
Mes	NMe_2	405	179
Mes	$N(SiMe_3)_2$	404	179
Mes	OPh	400	278
Mes	OMe	390	278
(C) In cyclohexane solution (flash photolysis)			
Mes	Mes	580	150
	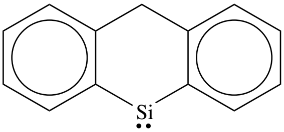	490	259

(*continued overleaf*)

TABLE 3. (*continued*)

R	R′	$\lambda_{\max}$	Reference
	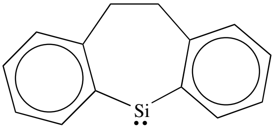	485	259
	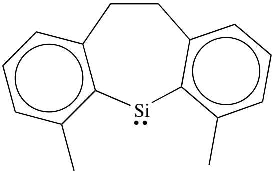	485	259
Me	Me	465–470	257,258
Ph	Me	440	259
t-Bu	*t*-Bu	440	259

[a] DEP = 2,6-diethylphenyl,
[b] Tip = 2,4,6-triisopropylphenyl.
[c] TTBCP = tris(*t*-butyl)cyclopropyl.

Substituent effects on the electronic transition are now rather well understood, mainly due to theoretical calculations by Apeloig and coworkers[226,247,261]. π-Donor substituents, NR_2, OR or Cl, can donate electrons into the empty silicon 3p orbital in the ground state (Figure 3). The effect is to shift the p-orbital upward in energy, increasing the n–3p energy gap and causing a blue shift. Compare Mes(Me)Si:, 496 nm; Mes(Cl)Si:, 487 nm; Mes(MeO)Si:, 425 nm; $\mathrm{Mes(Me_2N)Si}$:, 405 nm.

Electropositive, σ-donor substituents behave in opposite fashion. They donate electron density into the singly-occupied s-type orbital in the S^1 excited state, stabilizing it much more than the ground state, decreasing the energy gap and leading to a substantial red shift. Note the large effect on going from PhMeSi: (490 nm) to $\mathrm{Me_3Ge(Ph)Si}$: (625 nm) and $\mathrm{Me_3Si(Ph)Si}$: (660 nm). Finally, σ-acceptor substituents (F, CF_3) should withdraw electron density from the in-plane 3s-type orbital, stabilizing the ground state more than the excited state and producing a blue shift.

Aryl, vinyl and ethynyl substituents cause moderate bathochromic shifts compared with $\mathrm{(CH_3)_2Si}$:. Calculations[226] suggest that this effect is best explained by excited-state stabilization resulting from mixing of the singly-occupied 3p orbital on silicon with the π^* orbitals of these sustituents, as originally suggested for aryl substituents (Figure 4)[179].

Steric effects on the excitation energy are also quite marked. As the R–Si–R angle increases with the introduction of bulky substituents, the S^0 state becomes more like the S^1 state geometrically, and the excitation energy is expected to decrease. Evidence for this is seen from the $\lambda_{\max}$ for $\mathrm{Me_2Si}$: (453 nm), $\mathrm{Et_2Si}$: (469 nm), and $t\text{-}\mathrm{Bu_2Si}$: (480 nm). Decreasing the R–Si–R angle has the opposite effect, as seen in the series $\mathrm{Et_2Si}$: (469 nm), *cyclo*-$\mathrm{(CH_2)_5Si}$: (449 nm), *cyclo*-$\mathrm{(CH_2)_4Si}$: (436 nm). Combination of aryl substitution with steric hindrance leads to large bathochromic shifts. For example, although PhMeSi:, MesMeSi: and $\mathrm{Ph_2Si}$: all absorb near 490 nm, $\mathrm{Mes_2Si}$: has $\lambda_{\max} = 577$ nm.

Orientation of the substituent orbitals relative to the silicon 3p orbital is also significant. An example of this kind of conformational dependence has recently been reported by Kira

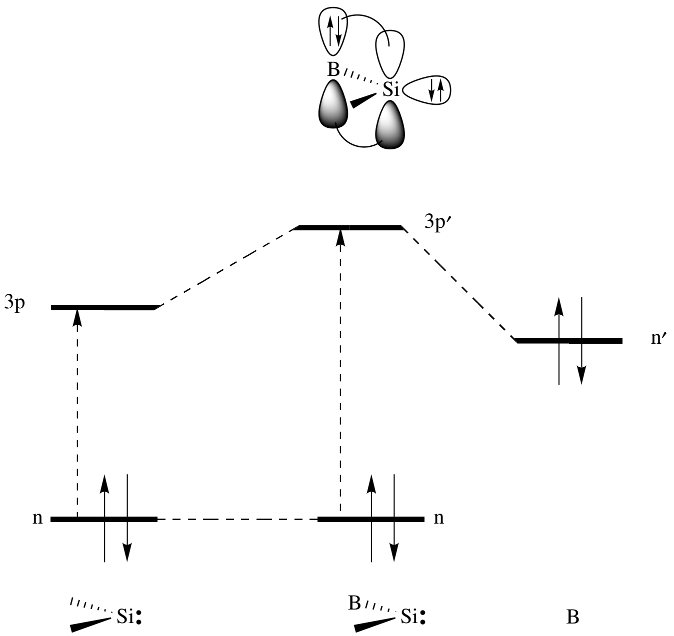

FIGURE 3. Qualitative orbital diagram for a silylene with a π-donor substituent

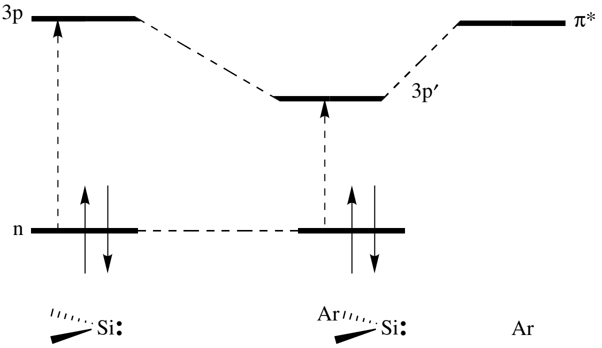

FIGURE 4. Orbital diagram for a silylene with a π-acceptor substituent

and coworkers[37]. In a series of aryl trimethylsilylsilylenes with increasing steric hindrance, λ_{max} (nm) increases from Ph(Me$_3$Si)Si: (660) to Mes(Me$_3$Si)Si: (790) but then decreases to 690 for 2,6-(C$_2$H$_5$)$_2$C$_6$H$_3$(Me$_3$Si)Si: and 2,4,6-(*i*-Pr)$_3$C$_6$H$_2$(Me$_3$Si)Si:. The decrease for the latter two silylenes was explained by rotation of the plane of the aromatic ring out of the plane containing the Si 3p orbital, reducing the conjugation.

Another example of an orientation effect was observed for the aryloxysilylenes Mes(OAr)Si:, where Ar = mesityl or 2,6-diisopropylphenyl, made by photolysis of the corresponding trisilanes at 77 K. These silylenes showed λ_{max} *ca* 430 nm in 3-MP glass but absorbed near 400 nm in a softer matrix, 3-MP/isopentane[142]. The difference was ascribed to a conformational change. In 3-MP the silylenes are believed to take a conformation similar to that of their precursors, in which the p lone pair on oxygen is twisted away from the vacant p-orbital on silicon, so that π-donation is limited. In the softer matrix the silylenes can relax into an equilibrium conformation with the p-orbitals on O and Si parallel, increasing conjugation and giving a further blue shift. Other silylenes with similar structure, Mes(OPh)Si**:** and Mes(OAlkyl)Si**:**, absorb near 400 nm in both matrices. For these less hindered silylenes, freezing-in of a nonequilibrium conformation does not take place.

The substituent and geometric effects on the electronic spectra of silylenes are well modeled by *ab initio* MO calculations, in all essential respects[226,247a,261]. For some substituents such as vinyl and ethynyl groups, the MO calculations are inaccurate because of contamination of the UHF states by higher-lying triplet states. Removal of this contamination by the method of spin projection gave results in good agreement with experimental trends[261].

2. Silylene–Lewis acid complexes

Since they have both a vacant low-energy orbital and a lone pair, silylenes might behave either as electron pair donors or acceptors. There is scant evidence for silylenes reacting as Lewis bases, but complexes of silylenes acting as Lewis acids are now well-established; these complexes can also be described as silaylides, $R_2Si^{-}{-}B^{+}$[262]. Trinquier has calculated that even SiH_4 should form a weak complex with H_2Si**:**, in which a silane hydrogen binds to the p-orbital of the silylene[263].

Indirect evidence for such complexing was put forward in 1980, based on the observation that the selectivity of $(CH_3)_2Si$**:** for reaction with pairs of alcohols was increased when the solvent was changed from hydrocarbon to diethyl ether to THF[264].

The first direct observation of silylene complexes was reported in 1987[142]. Four hindered silylenes, Mes(R)Si**:** where R = Mes, *t*-Bu, 1-adamantyl and 2,6-diisopropylphenyl, were generated by photoylsis of the corresponding trisilanes $Mes(R)Si(SiMe_3)_2$, in 3-MP and 2-methyltetrahydrofuran matrices. The long-wavelength band, falling from 577 to 425 nm for these silylenes in 3-MP, was replaced by an absorption near 350 nm for all four silylenes in 2-MeTHF, due to the formation of silylene complexes with the ether. In general, formation of silylene complexes with Lewis bases is signaled by a strong blue shift of the n–p absorption band. The base, by donating electrons into the 3p silicon orbital, greatly increases the energy of the S^1 excited state (equation 91). Large blue shifts upon formation of 2-MeTHF complexes were also observed by Kira, for vinylsilylenes[265].

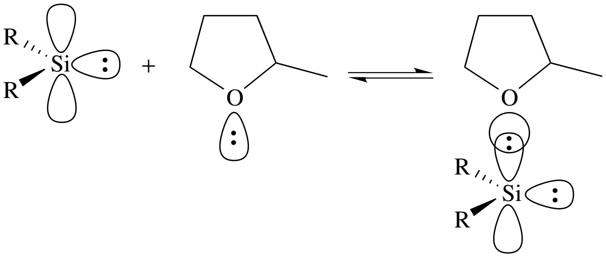

(91)

Later experiments were undertaken in mixed matrices containing 95% 3-MP and 5% Lewis base[113,143]. Irradiation of the trisilane precursors at 77 K gave initially the silylenes,

Mes_2Si**:**, Mes(*t*-Bu)Si**:**, Mes(Dip)Si**:** (Dip = 2,6-diisopropylphenyl) and Me_2Si**:**. When the matrix was annealed to allow some molecular motion, the absorption band for free silylene diminished and was replaced by a band at higher energy, assigned to the silylene complex. Representative data for absorption maxima of three silylenes with several bases are given in Table 4. The frequency shift upon complexation depends on the nature of both the base and the silylene and should be a measure of the strength of the interaction[113,143]. For the comparison of bases, the data for Me_2Si are most appropriate, since the silylene is unhindered. The frequency shifts increase in the order: phosphines < CO < sulfides < ethers < amines. This can be compared with the stability order for base–silylene complexes predicted from theoretical calculations: $HCl < H_2S < H_2O < PH_3 < NH_3$[266,267]. Agreement is satisfactory except for the phosphines, which are apparently much weaker bases than predicted according to frequency shifts.

Comparing different silylenes, it is interesting to note that the frequency shifts for the aryloxysilylene, Mes(ODip)Si**:**, are much smaller than for Me_2Si**:** or Mes_2Si**:**. This can be understood to result from π-donation by the aryloxy oxygen into the silicon 3p orbital, weakening the Lewis acidity[142].

In a similar study, dimesitylsilylene was generated photochemically from $Mes_2Si(SiMe_3)_2$ in a soft matrix, 4 : 1 isopentane:3-MP, in the presence of bases, at 77 K. The absorption frequencies in nm for the complexed silylene with various bases were: *N*-methylpyrrolidine, 324; pyrrolidine, 334; piperidine, 328; quinuclidine, 330; *n*-Bu_3P, 338; THF, 320; thiophene, 315. Agreement with the values in Table 4 is rather good[143].

Complexation of Me_2Si**:** by bases has also been observed in flash photolytic studies[257]. Photolysis of $(Me_2Si)_6$ in cyclohexane gave an absorption band at 465 nm assigned to Me_2Si**:**. This band shifted to 340 nm in CH_3CN, 310 nm in THF and 270 nm in Et_3N. Quenching experiments with various reactants showed that complexing reduced the reactivity of silylenes. Uncomplexed Me_2Si**:** reacted with alcohols, *n*-Pr_3SiH, THF and C=C and C≡C bonds essentially at the diffusion-controlled rate[257a], but reaction rates for silylene complexes were distinctly slower. Decreased reactivity of a complexed silylene has also been observed in solution. In 3-MP, Mes(1-Ad)Si**:** dimerizes immediately upon melting of the matrix, but in 2-MeTHF as solvent it gives a complex with 2-Me-THF which is stable up to *ca* −135 °C[142].

TABLE 4. Absorption bands (nm) for silylene complexes in 3MP[278]

Base	Me_2Si**:**	Mes_2Si**:**	Mes(ArO)Si**:**[a]
none	453	577	395
n-Bu_3N	287	325	346
Et_3N	287	350	348
2-Me-THF	294	326	330
Et_2O	299	320	332
i-PrOH		322	321
t-Bu_2S	322	316	350
CO	345	354	328
n-Bu_3P	390	345	358
Et_3P		336	349

[a] Ar = 2,6-diisopropylphenyl.

Alcohols are also bases toward silylenes. Complexes of alcohols with Mes_2Si**:** and other hindered silylenes are observed spectroscopically when a 3-MP matrix containing the silylene and 5% of 2-propanol or 2-butanol is annealed[113]. Melting of the matrix results in rapid reaction of the complex to give the O−H insertion product (equation 92). These results imply that formation of an acid−base complex is the probable first step in the reaction of silylenes with alcohols and perhaps with many other reagents[259].

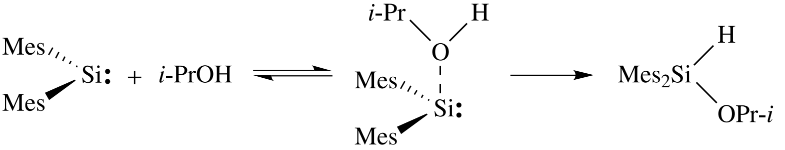

(92)

As described in Section III.B.2.b, carbon monoxide forms complexes with silylenes which are relatively weak, losing CO easily to give the disilene[155,156]. Therefore, it is likely that they have the acid−base complex structure **45**, in accord with theoretical prediction[249], rather than the alternative silaketene structure **46**. However, in addition to the absorption bands near 350 nm (Table 4), a weak absorption near 600 nm was observed for matrices containing silylenes and CO. These long-wavelength bands may possibly be due to the silaketene isomers.

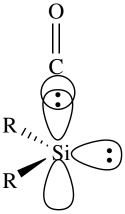

(45)

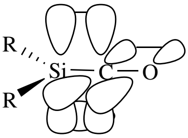

(46)

Carbonyl and thiocarbonyl complexes of Mes_2Si have been observed in a remarkable series of experiments by Ando and coworkers[144]. Photolysis of $Mes_2Si(SiMe_3)_2$ was carried out at 77 K in a 'soft' (3-MP/isopentane) matrix in the presence of tetramethyl-2-indanone or its sulfur analog. The free silylene was formed initially but it slowly reacted with the carbonyl (or thiocarbonyl) compound to give the complex, which can be formulated as a silacarbonyl ylide (Scheme 8). Further photolysis converted these ylide complexes to the silaoxirane or silathiirane, reversibly.

Another interesting compound which could be regarded as a silylene complex is the dioxygen adduct of dimesitylsilylene (mentioned in Section III.B.2.b) obtained by photogeneration of Mes_2Si in an oxygen matrix[151]. The infrared spectrum of the product showed a new band at 1084 cm^{-1}, assigned to Si−O stretching. Isotopic labeling with dioxygen was used to establish that the complex has an open structure, $Mes_2Si{-}O{-}O$ (equation 93). The Si−O bonding is probably strong, so the product can perhaps equally well be described as a silanone-O-oxide, $Mes_2Si{=}O^+{-}O^-$. Dimethylsilylene appears to form a similar open-chain oxygen complex when photogenerated in an oxygen matrix[268]. Cl_2Si**:** and F_2Si**:**, however, behave quite differently, forming dioxasiliranes (equation 94); see Section III.B.2.b[153].

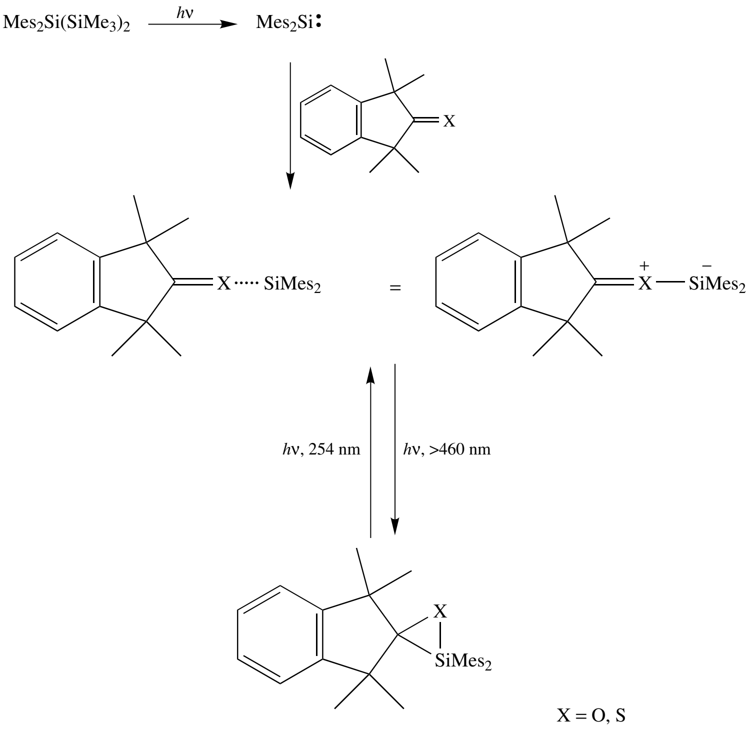

SCHEME 8

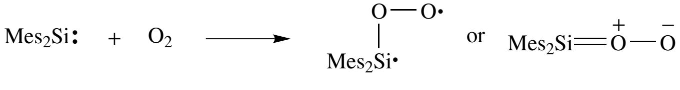

$$\mathrm{Mes_2Si\colon} + \mathrm{O_2} \longrightarrow \begin{array}{l}\mathrm{O{-}O^{\bullet}} \\ | \\ \mathrm{Mes_2Si^{\bullet}}\end{array} \quad \text{or} \quad \mathrm{Mes_2Si{=}\overset{+}{O}{-}\overset{-}{O}} \qquad (93)$$

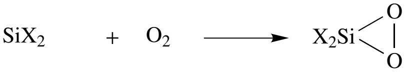

(94)

B. Other Spectroscopic Measurements

1. Silylene SiH_2

The importance of SiH_2 as an intermediate in the chemical vapor deposition (CVD) of silicon films from silanes (see Section VIII.D) has led to considerable effort in the development of sensitive spectroscopic methods for its detection *in situ*. The $^1B_1$ electronically excited state of SiH_2 reached by absorption is predissociated in higher vibrational levels, and thus laser-induced fluorescence (LIF) is difficult. The use of laser-spectroscopic techniques, including modified LIF and intracavity laser absorption spectroscopy (ILAS), has been reviewed[279,280]. ILAS has been used to detect SiH_2 in a parallel-plate RF-discharge system used in CVD of hydrogenated amorphous silicon[281]. A ring dye laser tuned to a single vibrational transition at *ca* 579 nm allowed the detection of SiH_2 during thermal decomposition of Si_2H_6[282].

SiH_2 was first detected using LIF by Inoue and Suzuki in 1984[283]. In 1986, SiH_2 was reported by LIF detection in the infrared multiphoton dissociation (IRMPD) of $EtSiH_3$[284]. The wide variations in the fluorescence lifetimes of individual rovibronic levels in the $^1B_1$ state of SiH_2 found by Thoman and coworkers was attributed to coupling of the $^1B_1$ (S_1), $^1A_1$ (S_0) and $^3B_1$ (T_1) states, manifested by predissociation of $^1B_1$ SiH_2 to $Si(^3P) + H_2$[285]. Dissociation of the $^1B_1$ SiH_2 formed in IRMPD of SiH_4 to singlet $(^1D_2)$ as well as triplet silicon atoms was found by state-selective two-photon LIF from the Si atoms formed[286]. A potential barrier of 4.4 to 6.2 kcal mol^{-1} for the dissociation of $^3B_1$ (T_1) SiH_2 to $Si(^3P) + H_2$ was inferred from LIF in a supersonic jet experiment[287]. Rotational analysis of emission from SiD_2 in a similar experiment also suggested predissociation to $Si(^3P) + D_2$[288]. LIF experiments also led to an estimate of the energy distributions of the fragments from the photolysis of $PhSiH_3$ at 193 and 248 nm[289]. It was concluded that SiH_2 is formed from highly vibrationally excited ground-state $PhSiH_3$, produced via internal conversion from higher singlet states reached by photoexcitation. Photodissociation of $PhSiH_3$ to SiH_2 in a supersonic jet has also been monitored by LIF[290].

SiH_2 has been detected by LIF in RF plasmas in mixtures of SiH_4 and Ar, He, Xe and H_2, allowing the optimization of working parameters to maximize the silylene concentration[291,292].

The time dependence of the Si atom concentration determined by atomic resonance absorption spectroscopy during shock-wave-induced thermal decomposition of SiH_4 was in accord with a stepwise dissociation via SiH_2 intermediates[293].

LIF excitation spectra allowed a detailed vibrational analysis of the SiH_2 $^1A_1$ ground state yielding exact accurate vibrational frequencies and anharmonic constants[294]. A similar analysis was carried out on the $^1B_1$ (S_1) excited state[295].

Infrared diode laser absorption spectroscopy has been employed to detect ground-state SiH_2 and allowed the first observation of its high-resolution IR spectrum by Yamada and coworkers in 1989[296]. State-selective multiphoton IR excitation of SiH_2 has been examined computationally[297]. The resonance-enhanced multiphoton ionization (REMPI) spectrum of SiH_2 was observed for the first time by Robertson and Rossi and was employed to measure the SiH_2 sticking coefficient on a silicon surface[298].

Photoionization mass spectrometric studies, by Berkowitz and coworkers, of SiH_2 formed by successive abstraction of H atoms from SiH_4 by F atoms allowed determination of the ionization potentials of the two lowest states: $^1A_1(S_0) = 9.15 \pm 0.02$ or 9.02 ± 0.02 eV and $^3B_1(T_1) = 8.24_4 \pm 0.02_5$ eV[299]. This important series of experiments[300] yielded a singlet–triplet separation for SiH_2 of either 0.78 ± 0.03 or 0.91 ± 0.03 eV.

Synchrotron radiation of 115 to 170 nm has been used to dissociate SiH_4 in a pulsed supersonic free jet, and the abundance of SiH_2 was measured by quadrupole mass spectrometry using 11 V sub-ionization threshold electron-impact energy[301]. The possible detection of SiH_2 in the outer envelope of a stellar object has been reported[302].

An SiH_2–HF complex was detected by infrared spectroscopy following matrix isolation of the reaction products from SiH_4 and F_2[303].

2. *Other silylenes*

a. HSiF. HSiF was detected by LIF in 1983 by Lee and deNeufville[304]. Suzuki and coworkers were able to assign 1300 rotational transitions of HSiF by LIF using a dye laser tuned to the frequency of excitation (410–430 nm) from the zeroth vibrational energy level of the ground singlet state to that of the first excited singlet state[305]. The structure derived from the rotational constants agreed well with predictions of *ab initio* calculations. From a different LIF experiment it was concluded that ∠H−Si−F increases from 98° to 115° upon electronic excitation from S_0 to S_1[306]. Via an intermodulated fluorescence technique, magnetic interactions in HSiF were studied[307]. No hyperfine structure was observed, but rotational *g*-factors could be derived from the Zeeman effect. An IR spectrum of an HSiF−HF complex has been reported in a matrix isolation experiment[303].

b. SiF_2. The laser excitation spectrum of SiF_2 from pyrolysis of Si_2F_6 was reported by Stanton *et al.* in 1985, and the concentration of SiF_2 was monitored by LIF following excitation at 221.6 nm with a dye laser[308]. SiF_2 produced by reaction of F_2 and NF_3 with solid Si was detected by 320.25 to 321.50 nm multiphoton ionization and mass spectrometric detection[274]. SiF_2 has been detected by REMPI mass spectrometry, following reaction of $SiHF_3$ with F atoms and of heated silicon crystals with F_2 under single gas-surface reaction conditions[309].

c. $SiCl_2$. $SiCl_2$ was detected by LIF in the 310 to 410 nm region for the first time in 1986[310]. Fluorescence from $SiCl_2$ in this region had been observed previously upon IR multiphoton excitation of SiH_2Cl_2 and vacuum UV photolysis of SiH_2Cl_2 and of $SiHCl_3$[311,312]. High resolution LIF spectra of $SiCl_2$ have been observed in a molecular beam[313]. Analysis of the spectra revealed that ∠Cl−Si−Cl opens up by 22° upon excitation from the $^1A_1$ to the $^1B_1$ state (from 101° to 123°). LIF detection of $SiCl_2$ in a pyrolysis jet showed that pyrolysis of $SiHCl_3$ is a good source of $SiCl_2$ for spectroscopic studies[314].

The microwave spectrum of $SiCl_2$ formed by conproportionation of $SiCl_4$ and solid Si has been recorded[315]. The large asymmetry of the Cl nuclear quadrupole coupling tensor was accounted for by large π-electron back-donation from Cl to Si. Emission from the products of reaction of excited $^3P_{2,0}$ Ar atoms with $SiCl_4$ and with SiH_2Cl_2 in a DC discharge flow system has been attributed to phosphorescence from $^3B_1$ $SiCl_2$ on the basis of the vibrational spacings[316].

d. $SiBr_2$, SiI_2. The He(I) photoelectron spectra of $SiBr_2$ and SiI_2 have been presented and analyzed by Bock and coworkers and compared with those of SiF_2 and $SiCl_2$[317]. Relativistic effects must be included for $SiBr_2$.

e. $SiMe_2$. The IR spectrum of matrix-isolated $SiMe_2$ from photolysis of $Me_2Si(N_3)_2$ was recorded, and six IR transitions were assigned as in-plane or out-of-plane polarized[318].

f. $SiMes_2$. The IR spectrum of a complex between dimesitylsilylene $SiMes_2$ and O_2 (see Section III. B.2.b) was reported following reaction of $SiMes_2$ and O_2 in an oxygen matrix at 16 K[151]. Comparison of the experimental spectrum (and oxygen isotope shifts) with model calculations ruled out siladioxirane, silanone and dimeric structures and were in accord with a nonlinear silanone *O*-oxide structure $Mes_2Si{=}O{-}O$.

g. Si=O. $^{29}Si{=}O$ has been observed by absorption at 85.76 GHz in Sagittarius B2, the most massive and complex giant molecular cloud in the galaxy[319]. The observation was by interferometry employing a radio telescope. Earlier, $^{29}Si{=}O$ had been observed in a radio telescope by maser emission from various stellar sources[320]. In the laboratory, the K-shell absorption spectrum of Si in Si=O vapor has been measured in the 1830 to 1875 eV region by X-ray spectrometry[321]. The fine structure at the K-absorption edge resembled that of the PO molecule.

VI. KINETICS OF SILYLENE REACTIONS

Despite the short lifetimes of most silylenes, improvements in flash photolysis techniques for their generation and time-resolved spectroscopic detection methods in the past decade have made possible direct kinetic measurements on the reactions of silylenes. The purpose of these kinetic studies has been to elucidate the mechanisms of silylene reactions. While considerable work remains to be done, transition state structures and activation barriers are emerging from these experiments, and aspects of silylene insertion and addition mechanisms have been revealed that were not uncovered by product studies and were, indeed, unexpected.

There have been excellent reviews by some of the groups most active in this area, and only their most important conclusions are summarized here. Gas-phase kinetic studies on SiH_2 are discussed by Jasinski, Becerra and Walsh[322]. Since SiH_2 turns out to be one of the most reactive species known, laser flash photolysis of such precursors as $PhSiH_3$ and Si_2H_6 are employed to generate it for kinetic studies, with most kinetic measurements using laser resonance absorption on the nanosecond and microsecond time scales to detect it. Laser-induced fluorescence has also been employed for the detection of SiH_2. An immediate result of these kinetic studies was to dispel the belief based on relative rate measurements that the insertion of SiH_2 into H_2 has a positive activation energy variously estimated to be as high as 10 kcal mol^{-1}.

Becerra and Walsh have presented a clear exposition of the mechanistic problems addressed by kinetic studies on silylenes and the conclusions that have been drawn to date[323]. Absolute rate studies have begun to throw light on the questions: How do the structures and energies of silylenes affect their reactivity? What are the transition state structures? What is the balance between the electrophilic and nucleophilic character of the attacking silylene in the transition state? What roles do steric and electronic effects play in silylene reactions?

The small negative activation energy for reaction of $SiH_2 + D_2$ (-0.49 kcal mol^{-1}), its pressure dependence and the observed isotope effects, all suggested a transition state in which an electrophilic interaction of the H−H bonding electrons with the empty 3p orbital of singlet SiH_2 takes place. A similar electrophilically led reaction with a weakly bound complex formed between the attacking silylene and its reaction substrate was suggested by the observation of small negative activation energies for insertion of SiH_2 into an H−Si bond of SiH_4 and addition to ethylene and acetylene (see equations 95 and 96).

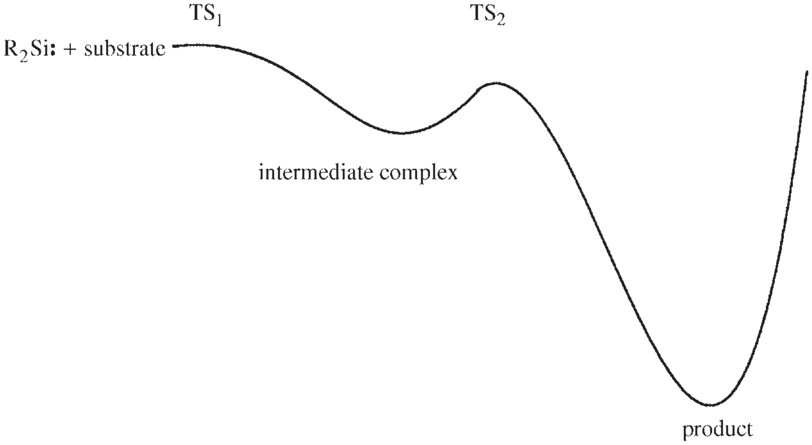

(95)

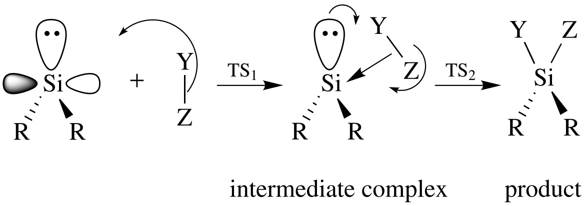

(96)

In this model the reaction rate decreases with increasing temperature because dissociation of the intermediate complex to the reactants has a higher barrier (i.e. via TS_1), than does the rearrangement of the complex (i.e. via TS_2) to the product of the silylene reaction. Thus, as the temperature increases, product formation is disfavored relative to regeneration of the silylene from the intermediate complex.

An alternative explanation for the occurrence of negative activation energies without an intermediate complex has been presented for carbenes by Houk and coworkers[324]. It requires that the free energy of activation be dominated by the $T\Delta S^{\ddagger}$ term, and allows ΔH to decrease between the reactants and the transition state. This model is not discussed by Becerra and Walsh.

The Walsh group found that replacement of H by Me on the silylene lowers the rate of reaction with the H−Si bond of $SiH_{4-n}Me_n$ ($n = 0, 1, 2, 3$). While SiH_2 reacts at nearly the collision rate, $SiMe_2$ reacts more slowly by more than two orders of magnitude. Substitution of Me for H on the silane substrate *increases* the reaction rate on a per H−Si bond basis. These substituent effects are explained by Becerra and Walsh as arising from the stepwise nature of the insertion reaction (equation 95). They propose that the methyl groups do not affect the electrophilic stage, i.e. the formation of a complex through donation of the electrons of the H−Si bond to the silylene LUMO (step 1 in equation 96). Becerra and Walsh argue that methyl groups influence the nucleophilic stage of the reaction, i.e. the transformation of the complex to the insertion product. Methyl groups being more electronegative than hydrogen atoms, substitution of a hydrogen on the silylene by a methyl increases the barrier for electron donation by the silylene. Substitution of a hydrogen on the substrate by a more electronegative methyl group lowers the barrier for electron donation from the silylene in the conversion of the intermediate complex to insertion product.

Astonishingly, SiH_2 is about twice as reactive toward carbon−carbon π-bonds as singlet methylene CH_2, long held to be the most reactive molecule in all of organic chemistry. Becerra and Walsh point out that the greater reactivity of SiH_2 is in accord with an electrophilic reaction in which the initial interaction is dominated by the size of the acceptor orbital, 3p for SiH_2 and 2p for CH_2. Silylene reactions are much less exothermic than carbene reactions, and thus the secondary reactions of silylene adducts are rather different from those of carbenes.

An important result of the recent kinetic experiments, when combined with theoretical calculations, has been to provide a refined estimate of the heat of formation of SiH_2 $\Delta H_f = 65.3 \pm 0.5\ \mathrm{kcal\,mol^{-1}}$[325]. Walsh has reviewed the problems associated with assigning heats of formation to methylsilylenes[326].

Reactions of silylenes with lone-pair donors such as alcohols and ethers are also quite rapid (*ca* 10% as fast as addition to π-bonds). For such reactions, the silylene-donor complexes have been spectroscopically detected (Section V.A). Even when rearrangement to stable products is facile, as in the case of alcohols, the second, nucleophilic, step is believed to have a higher barrier than the electrophilic complex-forming step.

Nevertheless, the temperature dependence of the rate constant for the reaction of $SiMe_2$ with MeOH yielded a negative activation energy of -3.75 kcal mol^{-1}[323]. The silylene complexes act as silylenoids, and their reactions are slower by one to three orders of magnitude than those of the corresponding free silylenes.

Kinetic measurements on the gas-phase reactions of the halosilylenes SiF_2, SiHCl, $SiCl_2$ and $SiBr_2$ have been reviewed by Strausz and coworkers[327]. Donation of lone-pair electrons from halogen substituents to the divalent silicon atom would be expected to decrease reactivity, and indeed SiF_2 does not react at an appreciable rate with H_2 even at 1400 K, nor with molecular oxygen whose rates of reaction with $SiCl_2$ and $SiBr_2$ could be measured. Only with oxygen atoms has SiF_2 been found to react at near the collision rate, while reactions with F_2 and Cl_2 are two orders of magnitude slower. SiHCl reacts at appreciable rates with both SiH_4 and SiH_2Cl_2, presumably by H−Si insertion.

All the kinetic experiments discussed thus far have been in the gas phase, whose advantages include the possibility of studying the effects of energy release through pressure-dependence studies, and the absence of complications due to solvents, such as the rapid complexation of silylenes.

Kinetic studies on silylene reactions have also been carried out in solution. Shizuka, Ishikawa and coworkers generated $SiMe_2$ in methylcyclohexane solution by irradiation of *cyclo*-$(SiMe_2)_6$ and obtained rate constants for reaction with MeOH and Et_3SiH in good accord with gas-phase experiments[258]. Similar experiments in cyclohexane by Levin and coworkers gave similar rate constants for H−O and H−Si insertion reactions in the range 10^9 M^{-1} s^{-1} and rapid complexation of $SiMe_2$ with THF[257a]. These rate constants were 10 to 100 times those found by Gaspar and coworkers in experiments employing $(PhMe_2Si)_2SiMe_2$ as the precursor for $SiMe_2$ despite the observation of a similar transient absorption spectrum[260]. There was also close agreement in the Gaspar lab between isotope effects and some (but not all) reactivity ratios in static photolysis competition experiments with rate constant ratios in laser flash photolysis experiments[260].

In the same paper from the Gaspar lab the rates of reaction with a number of substrates were reported for the $\lambda_{max} = 440$ nm transient from the cyclohexane solution-phase 266 nm laser flash photolysis of $(Me_3Si)_2SiMePh$. The transient was believed, on the basis of chemical trapping experiments and a comparison of rate constant ratios, with static photolysis product ratios, to be the silylene SiMePh, despite the observed shift to the blue of the λ_{max} by *ca* 40 nm from the value attributed to SiMePh in a matrix isolation photolysis experiment with the same precursor[180]. While the work of Ishikawa and Kumada on the photolysis of $(Me_3Si)_2SiMePh$ had shown that a silene is formed by a 1,3-Me_3Si shift to the phenyl ring in competition with silylene extrusion[328], the reactivity profile of the 440 nm transient in the laser flash experiments was inconsistent with a silene, an excited state of the precursor, or a silyl radical. Although the laser photolysis rate constant ratio for reaction of the 440 nm transient with EtOH and Et_3SiH was 10^3, the relative reactivity deduced from static photolysis product ratios was only 3. This was rationalized by pointing out that the reversible formation of a complex would consume a silylene upon reaction with alcohol, but the product yield would depend on the relative rates of dissociation and rearrangement of the complex. Hence the rate constant ratios and the product ratios might depend on different processes. A similar low ratio of reactivity toward EtOH and Et_3SiH for SiMePh had been found by Hawari *et al.* in product studies employing a different precursor[329].

Nevertheless, the rate constants for bimolecular decay of the 440 nm transient found for addition ($k_2 = ca\ 10^5\text{–}10^6$ M^{-1} s^{-1}) and H−Si insertion ($k_2 = 10^4\text{–}10^5$ M^{-1} s^{-1}) now seem too low to have been due to a silylene. Conlin and coworkers have found that dimesitylsilylene adds to π-bonds with $k_2 = 10^6$–10^7 M^{-1} s^{-1} and inserts into an H–Si bond of Et_3SiH with $k_2 = 8 \times 10^7$ M^{-1} s^{-1}[184]. It must therefore be advised with some regret that the rate constants for disappearance of other silylene precursors reported by Gaspar and coworkers[260] should be treated with suspicion until they are independently confirmed.

A number of rate constants for individual silylene reactions and the references to their original reports can be found in the major reviews cited here[322,323,327]. One must echo Becerra and Walsh[323] in stating that there remains much to be done in silylene kinetic studies. They have suggested intermediate complexes as a likely explanation for the activation parameters observed, but definite proof of the occurrence of these complexes along the reaction coordinates of most insertion and addition reactions remains to be accomplished. If electrophilic and nucleophilic stages of silylene reactions are indeed separated by energy barriers, then their individual kinetic characterization will be a formidable task. It would be marvelous if reaction kinetics could be developed into reaction dynamics by the study of state- and orientation-selected reactants in beam studies. Becerra and Walsh argue that silylenes, because of their lone-pair acceptor and donor properties, offer a rare example of experimentally accessible acid–base chemistry in the gas phase whose insights can be extended to other types of reactants. Since most silylene reactions occur in solution, more reliable ways to identify the transients produced in solution experiments, such as time-resolved laser-Raman spectroscopy, need to be employed.

VII. SILYLENE–TRANSITION METAL COMPLEXES

The past ten years have seen extensive development of the chemistry of silylene–transition metal complexes. Since this topic has been thoroughly treated in several recent reviews by Zybill and coworkers[330–332] and by Tilley[333,334], who have carried out much of the fundamental work, this active area will only be summarized here.

The most general method for synthesis of silylene–metal complexes is the reaction of a transition metal dianion with a dichlorosilane, in the presence of a donor molecule D to stabilize the resulting silylene complex (equation 97).

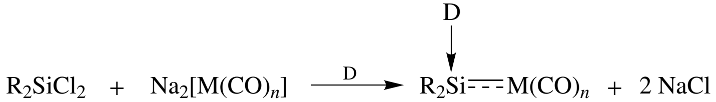

$$R_2SiCl_2 + Na_2[M(CO)_n] \xrightarrow{D} \overset{\overset{D}{\downarrow}}{R_2Si}\!\!=\!\!=\!\!=M(CO)_n + 2\,NaCl \tag{97}$$

The metal, M, can be Fe, Ru, Os (with $n = 4$) or Cr ($n = 5$). Substituents on silicon can vary widely, including aryl, alkyl, alkoxy and Et_2N groups. With a slight modification, the same reaction is useful for silylene–tungsten complexes (equation 98).

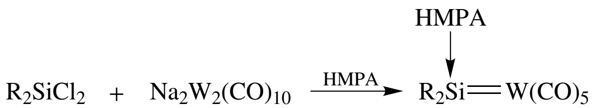

$$R_2SiCl_2 + Na_2W_2(CO)_{10} \xrightarrow{HMPA} \overset{\overset{HMPA}{\downarrow}}{R_2Si}{=}W(CO)_5 \tag{98}$$

When the silicon can be intramolecularly coordinated by a nitrogen or phosphorus atom, no added base is necessary. An example is shown in equation 99.

Silylene complexes with two intramolecular coordinating 'arms' can participate in dynamic behavior, involving a 'flip-flop' alternating coordination, illustrated in equation 100[335,336].

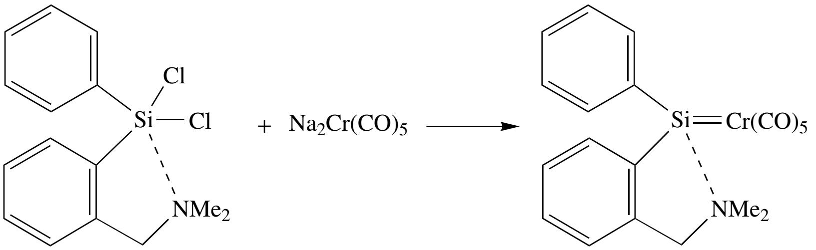

(99)

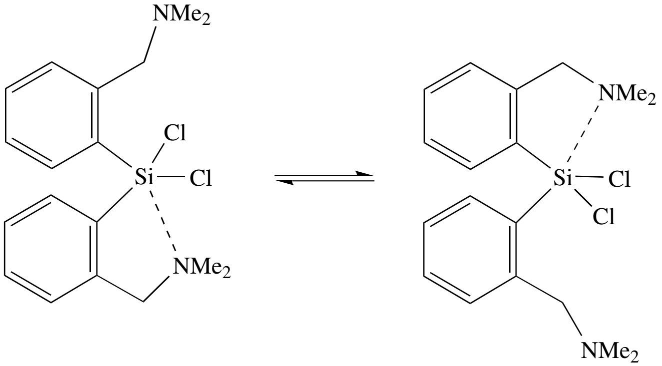

(100)

In some cases, insertion of coordinately unsaturated metals into Si–H bonds has been used for the synthesis of silylene complexes, as in the reaction of equation 101.

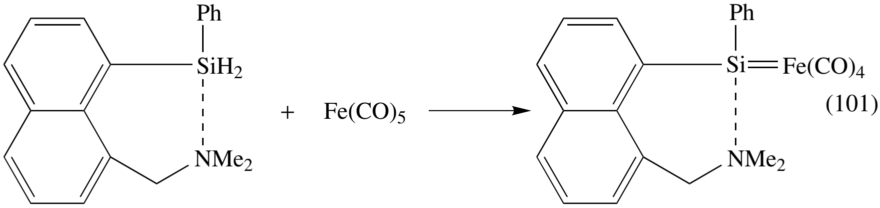

(101)

The displacement of triflate ion from silicon is important as a route to cationic silylene complexes, like the one shown in equation 102.

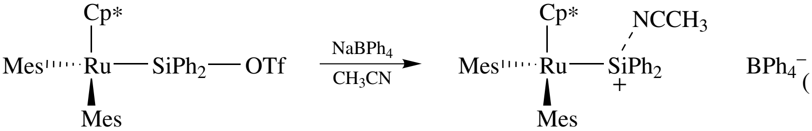

$$\mathrm{Mes}\cdots\underset{\mathrm{Mes}}{\overset{\mathrm{Cp^*}}{\mathrm{Ru}}}-\mathrm{SiPh_2}-\mathrm{OTf}\xrightarrow[\mathrm{CH_3CN}]{\mathrm{NaBPh_4}}\mathrm{Mes}\cdots\underset{\mathrm{Mes}}{\overset{\mathrm{Cp^*}}{\mathrm{Ru}}}-\underset{+}{\overset{\mathrm{NCCH_3}}{\mathrm{SiPh_2}}}\quad \mathrm{BPh_4}^-$$

(102)

Silylene–metal complexes, with tricoordinate silicon, free of coordinating donors, have been difficult to synthesize. Only a few examples were known until recently; one example is the osmium complex $Cp^*(Me_3P)_2RuSi{=}Os(CO)_4$ synthesized by Tilley and coworkers[337]. Now, with the availability of stable silylenes, tricoordinate silylene complexes are becoming much more easily available. These compounds are discussed in Section VIII.C.

The nature of the bonding in silylene–metal complexes, as compared with the better known metal–carbene complexes, is a question of considerable interest. MO calculations on $H_2Si{=}Mo(CO)_5$ indicate that the Si–Mo bond consists of a σ-donor and π-backbond component, like the carbon–metal complexes. The π-component is, however, weaker than for metal carbenes[251]. Infrared C=O frequencies for the base-free silylene metal complexes support this model. Theoretical considerations of the bonding in silylene–metal complexes are treated more fully in Section IV.E.

Bridged silylene complexes are the subject of a recent comprehensive review by Ogino and Tobita[338]. These complexes can be classified into three types: A, B and C (Scheme 9). In type A complexes there is no metal–metal bonding, the silicon is essentially tetravalent, and the bonding is similar to that in mononuclear metal–silyl complexes. In type C complexes, the bonding is best described as η^2-coordination of the Si–H bond to the metal, or alternatively as a metal–hydrogen–silicon 3-center 2-electron bond.

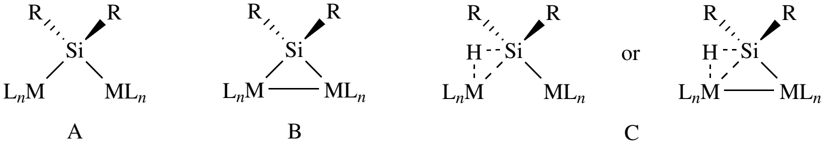

SCHEME 9

It is only in type B complexes that the silicon exhibits silylene character. In these molecules the M–Si–M angle is usually very acute, from 58° to 77°, and the silicon atoms show large downfield shifts in the ^{29}Si NMR. The bonding is best described in terms of a model originally suggested by Triplett and Curtis for germanium complexes[339], in which interaction takes place between a lone pair on the silylene fragment and the metal–metal bond. The silylene lone-pair orbital overlaps in σ-fashion with a symmetry-adapted combination of metal orbitals, and the vacant silylene p-orbital takes part in π-overlap with another such combination (Scheme 10). This orbital interaction is similar to, but slightly different from, that suggested for alkylidene-bridged metal complexes[340].

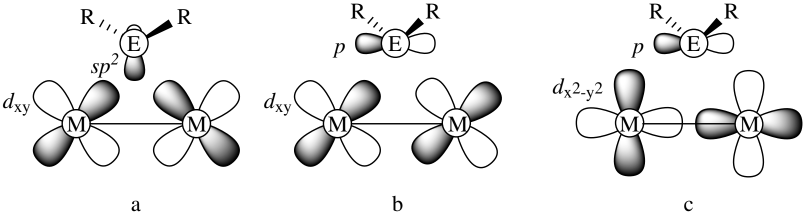

SCHEME 10

Many of the bridged silylene complexes show complex fluxional behavior or slow isomerization between different isomeric forms. An example is the iron–silylene complex shown in Scheme 11, in which the proposed mechanism is illustrated. A full discussion appears in Ogino and Tobita's review[338].

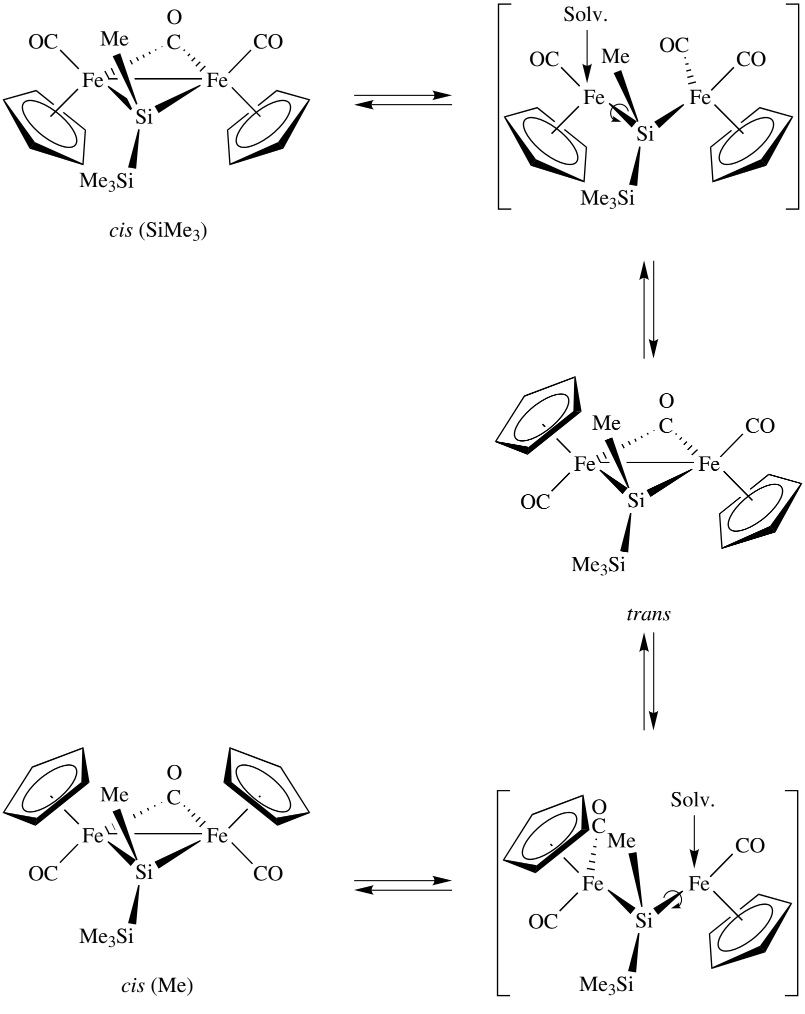

SCHEME 11

VIII. SPECIAL TOPICS

A. Silylene Centers on Activated Silicon

When finely divided silica is treated with methanol and then pyrolyzed, it becomes activated toward chemisorption of various gases[341–343]. Recent careful spectroscopic studies by Radzig and coworkers[344–347] and by Razskazovskii *et al.*[348,349] establish beyond reasonable doubt that the principal reactive sites are divalent silicons, $(\equiv Si{-}O)_2Si\textbf{:}$, 'silylene centers'[350], which participate in a rich chemistry.

A typical procedure for the preparation of reactive silica involves annealing of the sample in oxygen at 1220 K, then treatment with methanol vapor at 720 K followed by pyrolysis at 1220 K with pumping. Reactive silica may also be prepared by thorough grinding of SiO_2[351]. Like other silylenes, the silylene centers on silica are ground state singlets. They have a strong absorption based at 240 nm ($S_0 \rightarrow S_1$), a fluorescent emission at 290 nm ($S_1 \rightarrow S_0$, lifetime 5.6 ns) and a phosphorescence at 460 nm ($T_1 \rightarrow S_0$, lifetime 10.2 ns)[344,345]. The excitation spectrum is identical to the absorption spectrum. These properties are similar to those of gaseous $F_2Si:$.

Some of the silylene-like reactions which take place at the silylene centers are displayed in Scheme 12. The divalent silicon inserts into the H−H bond of dihydrogen, the S−H and O−H bonds of H_2S and H_2O, and the C−S bond of Me_2S[348].

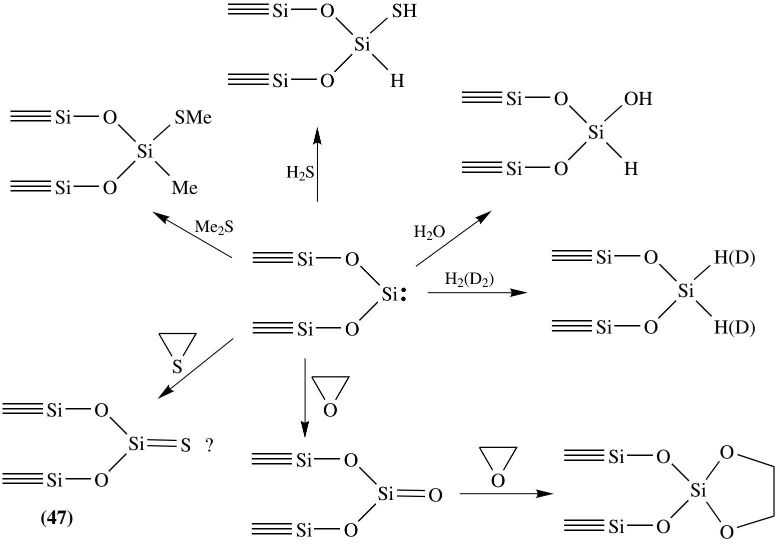

(47) **(48)** **(49)**

SCHEME 12

Reaction with ethylene sulfide yields ethylene and, possibly, a silanethione (**47**). With ethylene oxide, the first step is abstraction of an oxygen atom to yield the silanone (**48**), which adds to a second ethylene oxide molecule to give the siladioxolane (**49**). The products were identified mainly by infrared spectroscopy; in several cases the reaction kinetics were studied and activation energies determined[348].

Reaction of the silylene centers with dioxygen, or with N_2O at high temperature, produces the siladioxirane (**50**) (Scheme 13). The silylene center itself does not bind carbon monoxide, but the siladioxirane reacts with CO to yield the cyclic carbonate **51**. At 650 K, **51** loses CO_2 reversibly to give the silanone **48**[346]. The latter reacts reversibly with N_2O at 300−450 K to give **52**, but at higher temperature an irreversible reaction takes place to regenerate siladioxirane **50**.

The silylene center does not react with ethylene. In this respect it is similar to $Cl_2Si:$, which reacts with ethylene at a significant rate only at high temperatures (793 K). Ethylene, however, quenches the silylene fluorescence, as does CO[348]. In both cases a charge-transfer complex may be involved. (CO forms weak complexes with matrix-isolated silylenes; see Section V.A.2)

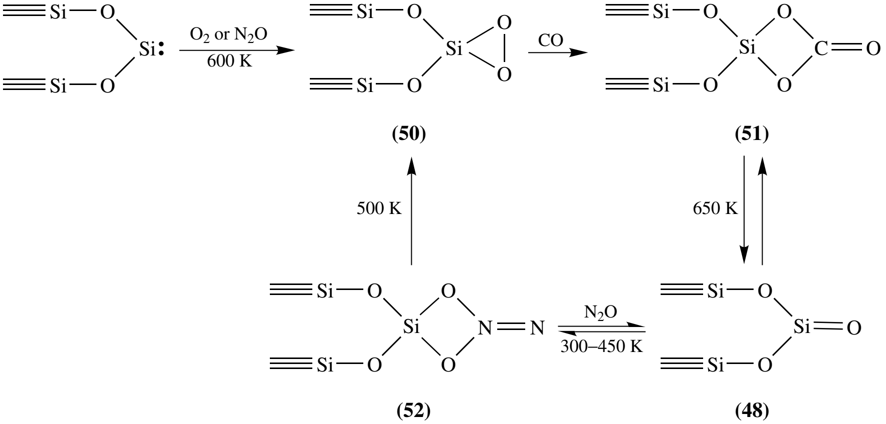

SCHEME 13

The reaction of silylene centers with dihydrogen has been studied in some detail[346]. It appears to proceed by a free-radical chain mechanism, initiated by radical sites on the silica surface which abstract hydrogen from H_2. The H atoms react with the silylene center to give a free radical, and a reaction chain can then ensue (equations 103–105). The hydrogen addition to silylene centers is reversible; the hydrogen is completely removed at temperatures near 1000 K.

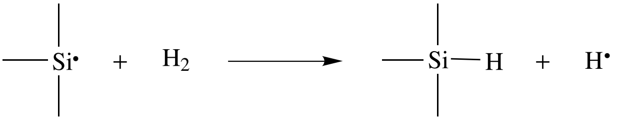
(103)

$$\equiv\!Si^{\bullet} + H_2 \longrightarrow \equiv\!Si{-}H + H^{\bullet} \qquad (103)$$

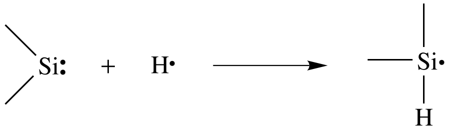
(104)

$$>\!Si\!: + H^{\bullet} \longrightarrow {-}\overset{|}{\underset{H}{Si^{\bullet}}} \qquad (104)$$

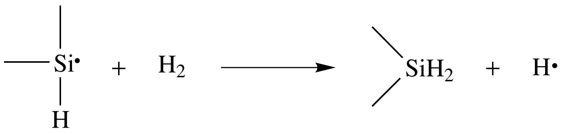
(105)

$$\overset{|}{\underset{H}{{-}Si^{\bullet}}} + H_2 \longrightarrow\ >\!SiH_2 + H^{\bullet} \qquad (105)$$

Quite recently, the reaction of photoexcited (singlet or triplet) silylene centers with dihydrogen has also been studied[346]. These excited states abstract hydrogen atoms from H_2 directly. For the excited singlet state, the process takes place with no discernable barrier.

The remarkable progress which has been made in the study of silylene centers on silica reflects the recent advances in surface spectroscopy. The silylene centers, $(\equiv Si{-}O)_2Si\!:$, represent a strongly stabilized form of divalent silicon. The reactions which they undergo may have important implications for the reactivity of silylenes generally.

B. Silylenes in the Direct Synthesis of Organosilicon Compounds

The ‘direct reaction’ of methyl chloride with silicon metal is the foundation stone of the worldwide silicone industry[352]. In corporate laboratories over the years, the reaction has been carefully engineered to provide the maximum amount of the desired product, dimethyldichlorosilane. Despite the industrial importance of the direct reaction, and the great amount of research devoted to it, its mechanism is still obscure[353]. Recently, however, a model has been suggested in which silicon in silylene form provides the crucial intermediate.

A careful study of the direct reaction was carried out by Clarke and Davidson[354], who interpreted their results in terms of surface-bound ‘silylenoid’ species, MeClSi: (surf) and Cl_2Si**:** (surf), which were thought to react with methyl chloride to give the principal products, Me_2SiCl_2 and $MeSiCl_3$. Consistent with this model, addition of butadiene to the gas stream led to formation of silacyclopent-3-enes (equation 106). Small amounts of gaseous MeClSi**:** and Cl_2Si**:** were also believed to be present, but were probably not the key intermediates in the direct process.

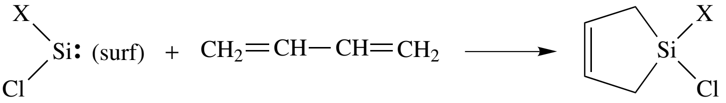

X = Me, Cl

(106)

Copper is an essential catalyst in the direct reaction, usually added in the form of Cu_3Si. Lewis and coworkers, in a review of the direct reaction[355], have suggested that a divalent silicon atom, perhaps attached to two copper atoms, reacts with methyl chloride to insert into the C−Cl bond, a typical silylene reaction (equation 107). The resulting intermediate (**53**) could then react with a second methyl chloride molecule by insertion into the C−Cl bond to yield Me_2SiCl_2. The other major products of the direct reaction, namely $MeSiCl_3$, $MeSiHCl_2$, $HSiCl_3$ and Me_3SiCl, can be accounted for by assuming the intermediacy of similar silylene-like species. In another book chapter, Ono and coworkers have presented kinetic evidence consistent with the silylene mechanism for the direct reaction[356]. At this point the evidence for silylene intermediates in the methyl chloride−silicon reaction is suggestive but not truly compelling.

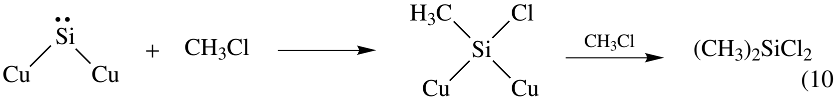

(107)

(53)

Silylene intermediates have also been proposed for the reaction of alcohols with silicon[357]. When phenol is reacted with silicon in the presence of CuCl as a catalyst, the major product $(PhO)_3SiH$ is obtained in 94% selectivity. This result is explained by insertion of a silylene **:**$Si(OPh)_2$ into the O−H bond of phenol. Addition of ethylene to the reaction produces 5.8% of $EtSi(H)(OPh)_2$, which can be accounted for by the reactions of Scheme 14[358].

Similarly, reaction of silicon, methanol and ethylene in an autoclave at 433 K produces ethylmethoxysilanes, $EtSi(H)(OMe)_2$ and $EtSi(OMe)_3$, as well as $HSi(OMe)_3$ and $Si(OMe)_4$. And, although 2-propanol does not react with silicon, a mixture of methanol and 2-propanol reacted with silicon to yield *i*-$PrOSi(H)(OMe)_2$[359]. Taken together, these results strongly suggest the intermediacy of silylene-like species in these reactions.

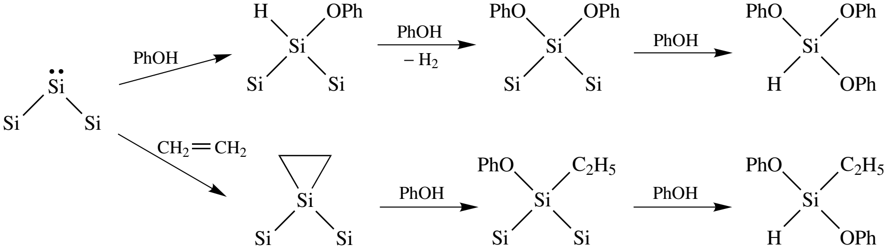

SCHEME 14

C. Stable Dicoordinate Silylenes

1. History

A major advance in silylene chemistry over the past five years has been the synthesis of persistent dicoordinate silicon compounds: 'stable silylenes'.

Thermally stable dicoordinate silicon compounds have been known since 1986, when Jutzi and coworkers reported the remarkable π-complex, $(Me_5C_5)_2Si$[360]. The chemistry of this compound, developed over the past decade, makes a fascinating story[361]. Other compounds of dicoordinate silicon include the four-coordinate phosphorous compound, $Si[(Me_2P)_2C(SiMe_3)]_2$[362]. These compounds, with coordination numbers at silicon greater than 2, behave rather differently from silylenes in their reactions and will not be covered here.

Dicoordinate lead and tin compounds have been known since the early days of chemistry. The study of dicoordinate germylenes began with Lappert's and Harris's pioneering work on the synthesis and reactions of the dinitrogen-substituted germylene, $[(Me_3Si)_2N]_2Ge$ (**54**)[363]. The chemistry of this and analogous germylenes has been well explored[364]. Compound **54** is a monomer both in solution and as a solid, but the isostructural carbon-substituted germylene, $[(Me_3Si)_2CH]_2Ge$ (**55**), although monomeric in solution, dimerizes to the digermene in the solid state[365]. The difference probably reflects stabilization of monomeric **54** by electron donation from nitrogen. Steric shielding by the bulky $(Me_3Si)_2N$ and $(Me_3Si)_2CH$ substituents, however, is undoubtedly important in stabilizing both **54** and **55**.

Can silylenes be stabilized in monomeric form simply by steric shielding? No final answer can be given, but the results so far are not very promising. The design of a group sufficiently bulky to discourage intermolecular reactions and sufficiently inert to prevent loss through intramolecular processes is a formidable problem. The silicon counterpart to **55** exists in the dimeric disilene form $[(Me_3Si)_2CH]_2Si{=}Si[CH(SiMe_3)_2]_2$ (**56**), although, as mentioned in Section. III.C.2, it gives silylene trapping products at 120 °C, suggesting that partial dissociation to silylene takes place at this temperature. The silicon analog to **54** is unknown, but a silylene bearing a $(Me_3Si)_2N$ and a mesityl substituent has been prepared in 3-MP at 77 K. Upon melting of the matrix, immediate dimerization of the silylene took place to give the disilene, $(Me_3Si)_2N(Mes)Si{=}Si(Mes)N(SiMe_3)_2$[179]. Perhaps the best example to date of stabilization by steric hindrance is the silylene **57a** of Puranik and Fink[107]. This species has a limited stability in solution, at least up to 200 K, but could not be isolated at room temperature.

A related silylene, the four-membered ring **57b** prepared by photolysis of the corresponding diazide, was reported by Veith and coworkers to decompose at very low temperatures[55].

A carbene, fully stable at room temperature, **58a**, was isolated in 1991 by Arduengo and coworkers, and since that time several other carbenes have been prepared, all having similar structure **(58a–f)**[366]. The synthesis of these carbenes left silicon as the last element with no dicoordinate, divalent compound stable at ordinary temperature. The stability of carbenes **58a–f** suggested that silicon-containing rings with similar structure might be good candidates for isolation at room temperature.

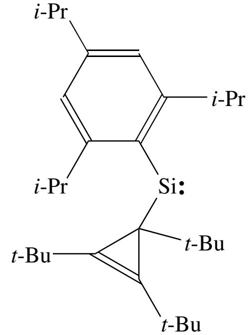

(57a)

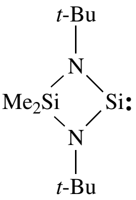

(57b)

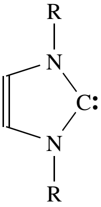

(58a) R = 1-adamantyl
(58b) R = *t*-butyl
(58c) R = *p*-tolyl
(58d) R = *p*-chlorophenyl
(58e) R = mesityl

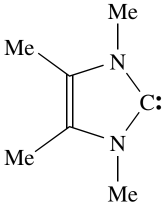

(58f)

The field of stable silylenes commenced with the synthesis of compound **59**, isostructural with carbene **58b**, in 1994[367]. This development was promptly followed by reports of four additional examples: **60**[98], the saturated analog to **59**; and the benzene-[368] and pyridine-[369] fused bicyclic silylenes **61**, **62** and **63**.

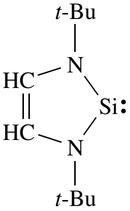

(59)

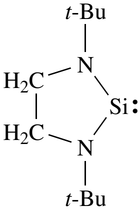

(60)

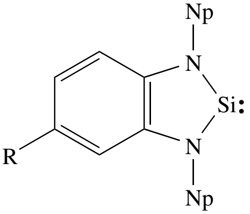

(61) R = H
(62) R = Me

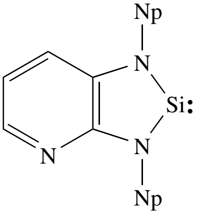

(63)

Np = neopentyl

2. Synthesis and characterization

Silylene **59** was obtained starting from glyoxal and *t*-butylamine, according to Scheme 15[367]. The final step, dehalogenation of the dichloride, was carried out using molten potassium metal in refluxing THF, and these rather vigorous conditions have become standard for the synthesis of stable silylenes of this type.

Silylenes **59** and **60** are colorless solids, while the benzannelated compounds **61** and **62** are yellow. Compound **59** possesses truly surprising thermal stability. It was purified by distillation at 90 °C (0.1 torr) and survived unchanged after heating in toluene at 150 °C for

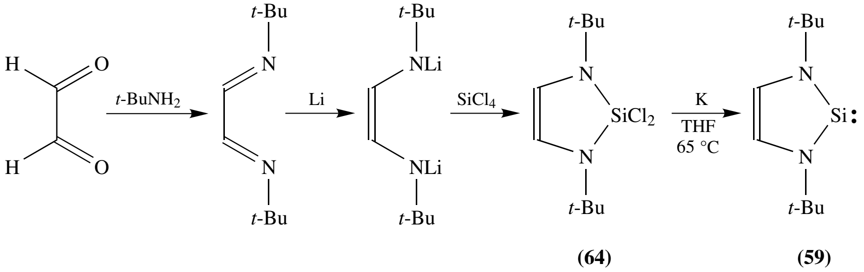

SCHEME 15

4 months. Solid **59** decomposes only at its melting point, *ca* 220 °C. Compounds **61** and **62** also appear to be quite stable to heating; for example, **62** was sublimed from a 155 °C bath during purification[368]. The saturated-ring compound **60**, on the other hand, is much less stable toward heating and there are indications that it slowly dimerizes. Apeloig and Müller[247b] predicted on the basis of *ab initio* calculations that **60** dimerizes to a μ^2-, nitrogen bridged compound as shown in equation 90, and not to the corresponding disilene.

In their ^{29}Si NMR spectra, the silylenes all show rather deshielded silicon atoms, consistent with theoretical calculations. Values recorded, in ppm, are **59**, 78.3; **60**, 119; **61**, 96.92; **62**, 97.22; **63**, 95.1.

X-ray crystal structures have been reported for **60** and **61**, and the structure of **59** was obtained from a gas-phase electron diffraction study. Structures for **59** and **60** are shown in Figures 5 and 6. The five-membered ring in **59** is nearly planar, but in **60** it is puckered as shown in the figure. Significant bond lengths and angles are given in Table 5.

As expected, the intraring C−C distances increase from **59** to **61** to **60**, as the C−C bond order is reduced from 2 to 1. Also predictable is the larger N−C distance in **60**, where the nitrogen is bonded to a tetrahedral carbon atom, than in **59** and **61**, where the bonding is N−C sp^2. The N−Si bond distances are slightly longer than for normal single bonds from nitrogen to silicon, which average near 170 pm. However, bonds to *divalent* silicon are expected to be longer, by about 8 pm. The N−Si distances in **59**−**61** are therefore consistent with partial double bonding in these molecules. Particularly interesting is the small but significant decrease in the N−Si distance, going from **59** and **61** to **60**. The possible bonding implications will be discussed in the following section.

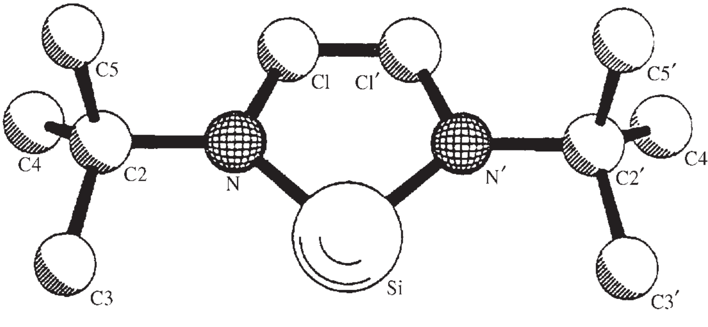

FIGURE 5. Structure of unsaturated silylene **59** from electron diffraction. Reprinted with permission from Reference 367. Copyright (1994) American Chemical Society

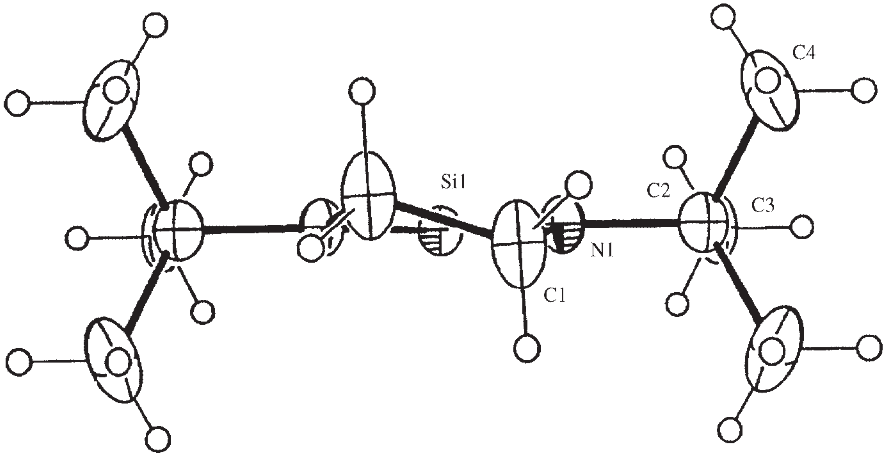

FIGURE 6. Structure of saturated silylene **60** from X-ray diffraction. Permission of The Royal Society of Chemistry from Reference 224.

TABLE 5. Selected intraring bond lengths (pm) and angles (deg) for silylenes

Silylene	Si–N	N–C	C–C	N–Si–N	Reference
59	175	140	135	90.5	367
60	171	150	152	92.0	224
61	175	138	142	88.2	370

3. Bonding and 'aromaticity'

The properties of the stable silylenes raise interesting questions of chemical bonding, many of which apply also to the carbenes, **58a–f**. First, why are these compounds so stable compared to ordinary silylenes (carbenes)? Steric hindrance may be a factor, but it is unlikely to be a major one; silylenes far more hindered than **59–63** dimerize at low temperatures, as was described in Section III.C[181].

Electron donation from nitrogen to silicon is undoubtedly important in stabilizing all of these molecules. Partial double-bonding between N and Si will tend to occupy the vacant p-orbital on silicon, which is the usual site of electrophilic reactivity of silylenes. This stabilization is shown in resonance drawings in Scheme 16. Greater π-donation from N to Si would be expected for **60** than for **59** or **61**, since in **60** the nitrogens are more basic. The Si–N bond lengths are consistent with this model, as mentioned above.

Structures **B** and **C** in Scheme 16 are ylidic, and objection is sometimes raised to the description of **59–63** as silylenes and **58a–f** as carbenes, on the grounds that they are really ylides. Indeed, it is likely that all these compounds have significant ylidic character (although a contrary view has been put forward for stable carbenes, see below). But this is really a question of degree, since stabilization of the vacant p-orbital on silicon, by π-electron donation or hyperconjugation, probably takes place to some extent for all silylenes except SiH_2. π-Donation to silicon probably explains the relatively low reactivity of SiF_2, for example. The nitrogen atoms in **59–63** serve as particularly good π-donors, and electrophilic reactivity is therefore reduced more strongly to the point where these compounds can be isolated.

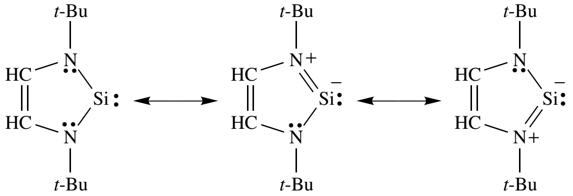

(A) **(B)** **(C)**

SCHEME 16

The greater stability of **59** compared to **60** also requires explanation. The ring is more nearly planar in **59** than in **60**, which may marginally increase steric shielding of the silicon atom, but this seems an insufficient rationalization. Instead, it has been suggested that **59** is stabilized by aromatic resonance, since it forms a 6 π-electron cyclic system, **59a**[98,367].

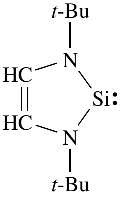

(59)

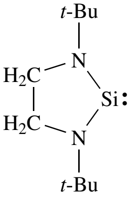

(60)

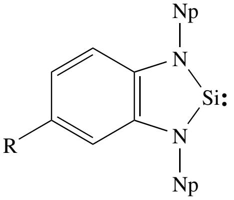

(61) R = H
(62) R = Me

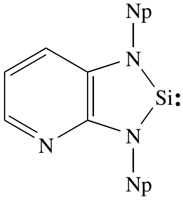

(63)

Np = neopentyl

Possible evidence for aromatic delocalization in **59** could come from proton NMR data. The chemical shifts of the vinyl protons in the model compounds **64** and **65** lie at 5.73 and 6.00 ppm. In **59** the vinyl proton resonance is shifted downfield to 6.75 ppm, consistent with deshielding due to an aromatic ring current.

To explore this possibility further, quantum chemical calculations were carried out for the isodesmic reactions of the model compounds **66** and **67** with dihydrogen to give the corresponding dihydrides (Scheme 17). These calculations showed that the reaction of **66** with H_2 is about 14 kcal mol^{-1} less exothermic than that of **67**. This difference may reflect aromatic resonance energy in the unsaturated molecule **66**, reducing the enthalpy of the hydrogenation reaction.

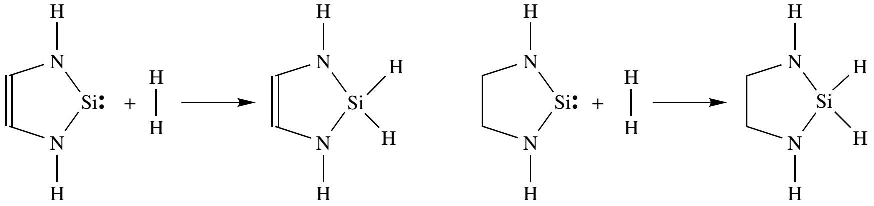

(66) **(67)**

SCHEME 17

The He(I) and He(II) photoelectron spectra have been determined for **59** and **60** and for the unsaturated dihydride **65**; in both **59** and **65**, the lowest energy ionization was assigned to an orbital of the π system (C−C bonding, C−N antibonding)[224], In **65**, this first ionization was observed at 6.56 eV, but for **59** it was significantly higher, 7.13 eV. Evidently the Si 3p orbital participates in the HOMO, stabilizing this ring π-orbital, just as expected if aromatic resonance is present. The ionization energies of the lone pair electrons in **59** and **60** were not very different, 8.21 and 8.11 eV, indicating that hydrogenation of the C=C bond in **59** does not greatly change the nature of the lone pair. A very similar study of photoelectron spectra has recently been reported for **61** and its dihydride, **68**[370]. The highest-lying molecular orbital was stabilized by 0.41 eV in **61** compared with **68**, again indicating mixing of the out-of-plane 3p orbital on silicon with the ring π-orbital, as expected for aromatic resonance. Calculations of isodesmic reactions carried out on model compounds for **61** were also consistent with aromatic stabilization in the silylene, although this is believed to be reduced by considerable ring strain.

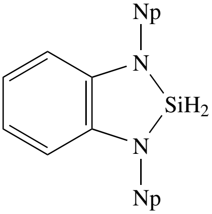

(68)

All these indications are consistent with some degree of aromatic delocalization in the unsaturated silylenes, **59** and **61**−**63**. This conclusion is supported by two recent theoretical papers, one based on calculations of hydrogenation enthalpies, magnetic anisotropy and a careful analysis of the electron density[371], and another quite complete treatment of energetics, structure, ionization energies and magnetic properties[372]. Both conclude that aromatic delocalization is present in silylenes like **59**, although it is less pronounced than in the isostructural carbenes. A distinctly different model, also based on photoelectron spectroscopy and theoretical considerations, has, however, been suggested by Arduengo *et al.*[225,373]. In this treatment the bonding in **59** is viewed in terms of σ-donation from a diimine to a neutral silicon atom **59b**, and the theoretical and experimental evidence is interpreted as showing that aromatic delocalization is not significant in carbenes, **58a**−**f**. The question of aromatic stabilization in these silylenes and carbenes is not fully closed; further studies are needed.

4. Chemical reactions

To date, chemical properties have been reported mainly for **59** and **61**. Occupancy of the silicon 3p orbital by electrons from nitrogen greatly reduces the electrophilicity of these silylenes. This, together with probable aromatic stabilization, significantly mutes the behavior of **59** and **61** as silylenes. For example, **59** does not insert into Si−H bonds, or react with alkynes such as PhC≡CPh[367], Moreover, **59** shows no Lewis acidic behavior, even toward bases as strong as pyridine.

The stable silylenes react, however, with water and alcohols, by straightforward insertion into O−H bonds. Silylenes **59**, **61** and **62** all react with methyl iodide, inserting into the C−I bond. Examples of these reactions are shown for **59** in Scheme 18. Compounds **59** and **61** also react with elemental chalcogens. For **61** with S_8, Se_8 or Te [370], and for **59** with

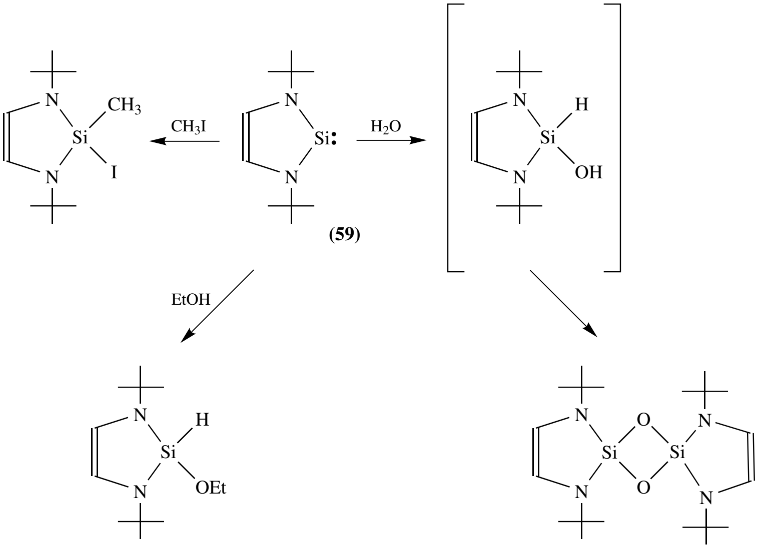

SCHEME 18

Se [374], the products are four-membered rings, as illustrated for **61** in equation 108. These products may arise from dimerization of a silicon–chalcogen doubly bonded intermediate.

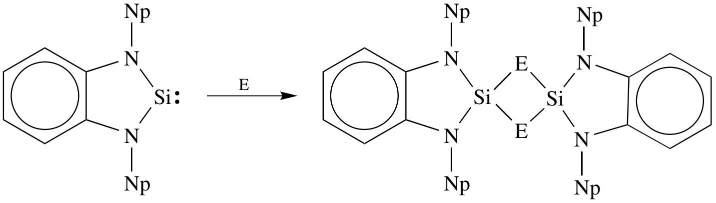

(108)

(61)

Np = neopentyl E = S, Se, Te

The reaction of **59** with sulfur is somewhat more complicated (Scheme 19). At low temperatures, an intermediate is observed with a ^{29}Si NMR chemical shift of +122.6 ppm; this deshielded value is consistent with the silanethione, **69**. Warming of the solution produces the 4-ring dimer, **70**. But when the reaction is carried out at room temperature this intermediate is not observed, and the major product is the trisilicon compound **71** in which a molecule of diimine has been lost from the central silicon[374]. The structure of **71** is somewhat similar to that of solid silicon disulfide.

In a number of ways the reactions of stable silylenes resemble those of phosphines, R_3P, to which they are isolobal analogs. Examples are provided by the reactions of **59** with covalent azides. Phosphines are known to react with azides to give phosphineimines, $Ph_3P{=}NR$. In similar fashion, **59** reacted with triphenylmethyl azide in THF to give the silanimine **72** as its THF complex (equation 109)[148]. This reaction provides a new method for synthesizing compounds containing Si=N double bonds, which have previously been made by salt elimination reactions[375].

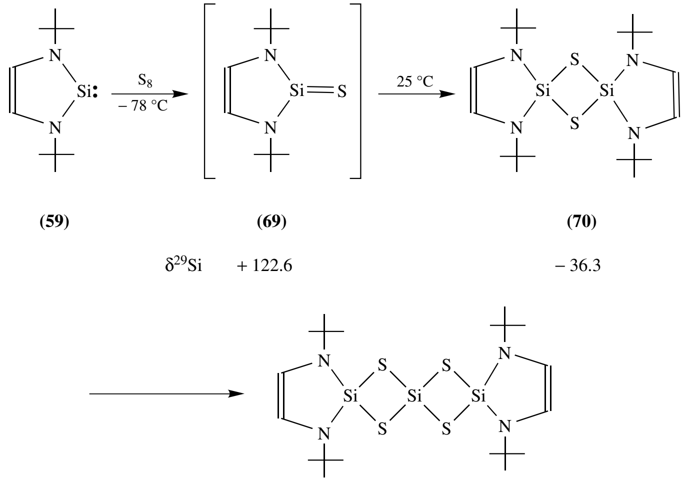

(59) **(69)** **(70)**

δ^{29}Si + 122.6 − 36.3

(71)

− 38.1, −44.3

SCHEME 19

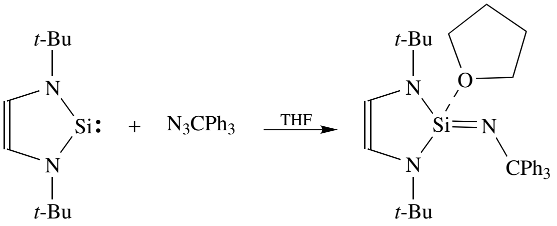

(109)

(72)

Reactions of **59** with less hindered azides can be more complex. With trimethylsilyl azide, the isolated product was the azidosilane **73**. The formation of **73** can be rationalized, however, as proceeding through the initial formation of a silanimine, followed by addition of Me_3Si-N_3 across the Si=N double bond, as shown in equation 110. When **59** was treated with 1-adamantyl azide, the product was the silatetrazoline **74**. Once again this product may have resulted from initial formation of a silanimine, followed in this case by $2 + 3$ cycloaddition of the azide to the Si=N double bond (equation 111)[98,148].

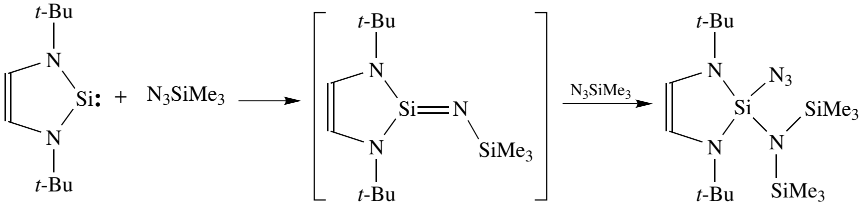

(110)

(59) **(73)**

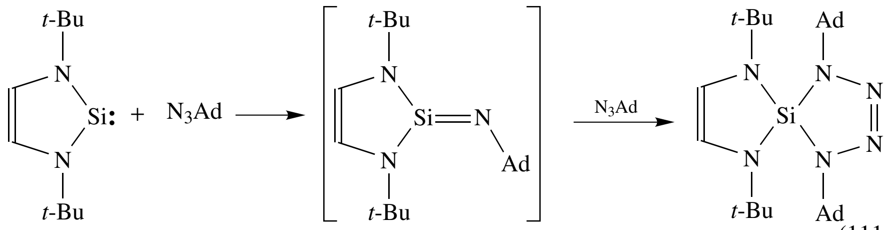

(59) **(74)** (111)

Silylene **59** also behaves somewhat like a phosphine in its interactions with metal carbonyls[98,149,376]. Typical reactions involve substitution of silylene for CO, to give a silylene–metal complex. Three examples are shown in Scheme 20, and the structure of the nickel complex **75** is displayed in Figure 7[149]. This complex is both the first silylene–nickel complex, and the first example of a bis-silylene–metal complex free of stabilization by Lewis base donors.

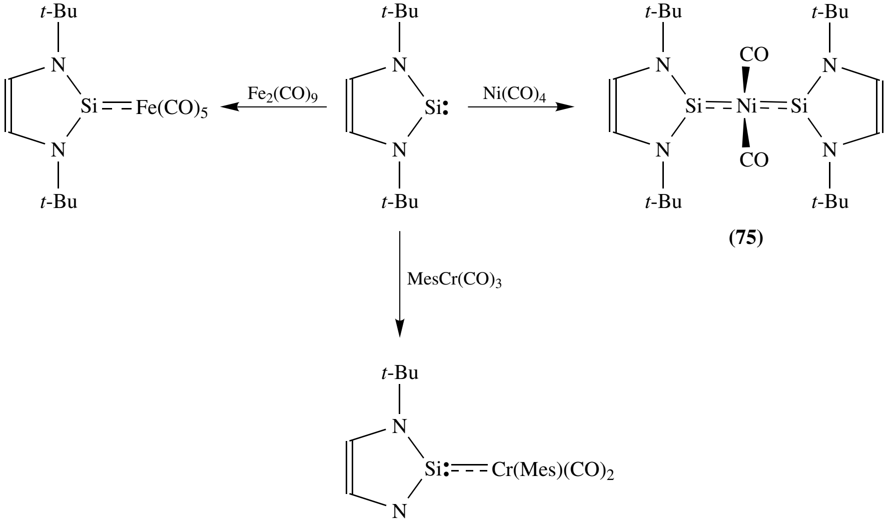

SCHEME 20

In all three complexes the Si–metal bond is short (Si–Fe = 219, Si–Ni = 221, Si–Cr = 228 pm). These distances are about 10 pm less than for typical Si–metal single bonds, consistent with partial back-bonding from the metal d-orbitals to the p-orbital on silicon. Reactions of **59** to form silylene–metal complexes appear to be general, and many more examples are likely to be prepared in the future, for this and other stable silylenes.

Silylene **59** also reacts with some dienes to give 1 + 4 cycloaddition products. With *trans,trans*-1,4-diphenylbutadiene, stereospecific addition takes place to give the *cis*-product, as expected for a singlet silylene (equation 112). A second example is the reaction

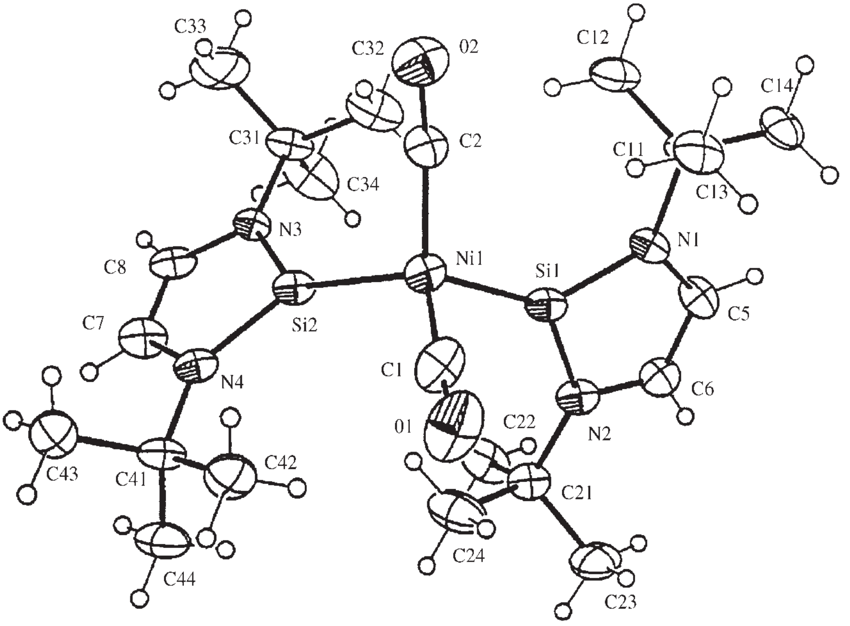

FIGURE 7. Structure of silylene–nickel carbonyl complex, **75**. Reproduced by permission of The Royal Society of Chemistry from Reference 149.

of **59** with the diimine used in its synthesis, illustrated in equation 113; the product is the spiro compound **76**[98,376].

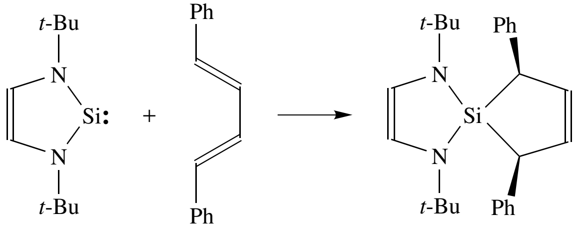

(112)

(59)

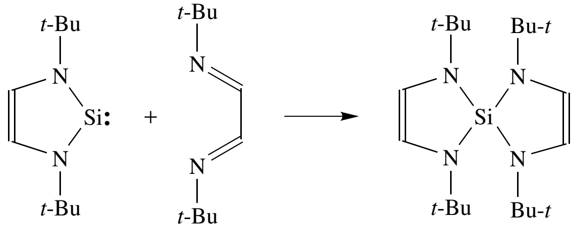

(113)

(59) **(76)**

Recently, a number of interesting products have been obtained from the reaction of **61** with various compounds containing C−O or C−N multiple bonds[377]. Several such reactions are illustrated in Scheme 21. The behavior of **59** as a Lewis base has been demonstrated in a reaction with $(C_6F_5)_3B$ to give the acid−base adduct, which slowly transfers a C_6F_5 group to silicon as shown in Scheme 22[378].

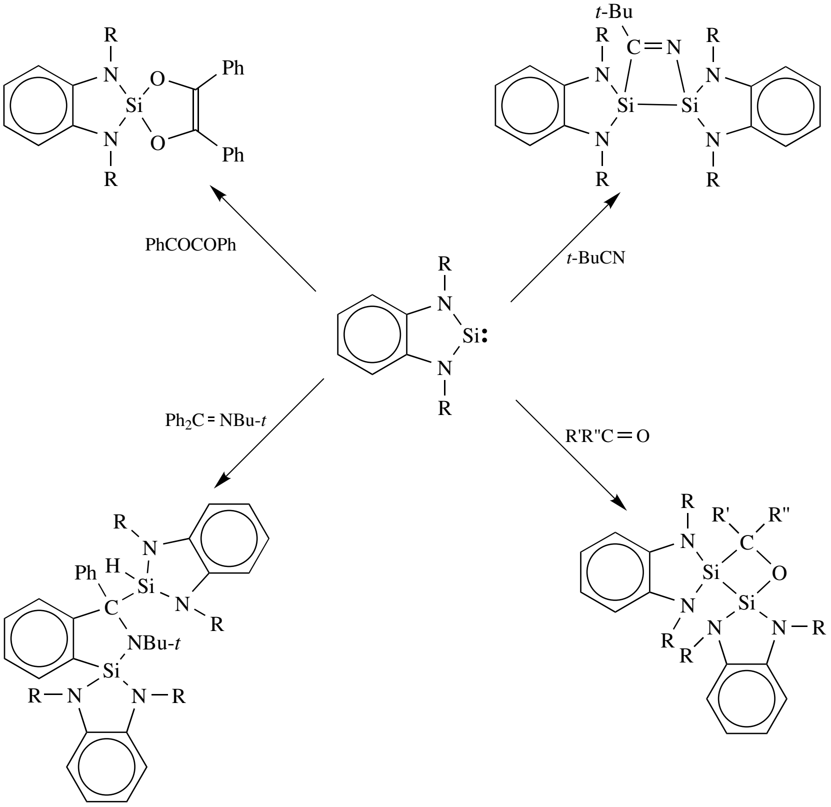

SCHEME 21

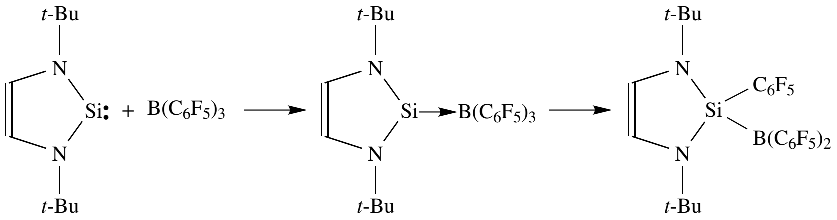

R = $CH_2C(CH_3)_3$

SCHEME 22

We see that although the stable silylenes lack some reaction pathways common for transient silylenes, they participate in many reactions previously unknown for silylenes. A number of these lead to products with structures of considerable interest. Further developments in the chemistry of stable silylenes are to be expected.

D. Silylene Intermediates in Chemical Vapor Deposition

The formation of thin solid films of silicon by the decomposition of a gaseous precursor such as SiH_4 plays a vital role in many areas of modern technology, including the manufacture of microelectronic devices and solar energy collectors. Depending on the conditions of temperature, pressure and on the precursor, the product film can range from amorphous hydrogenated Si to single-crystal epitaxial Si. Jasinski and Gates have provided a succinct introduction to the mechanisms of film formation from silicon hydrides[379]. The decomposition of silane (equation 114) is exothermic by 8.2 kcal mol^{-1}, but energy to overcome significant kinetic barriers must be provided by heat, light or plasma excitation to achieve useful rates of film growth.

$$SiH_4(g) \longrightarrow Si(s) + 2H_2(g) \tag{114}$$

$$SiH_4 \longrightarrow H_2Si\colon + H_2 \tag{115}$$

When SiH_4 is decomposed at pressures >0.1 torr and temperatures >900 K, the formation of SiH_2 in the gas phase is the dominant primary process (equation 115), and SiH_2 has been detected by laser absorption spectroscopy during silane pyrolysis[380]. SiH_2 has also been detected by laser-induced fluorescence at 0.2 torr in a silane plasma similar to those employed in plasma-enhanced CVD (PECVD) of amorphous hydrogenated silicon for solar cells[381]. Initially formed SiH_2 can undergo reversible insertion into an Si−H bond of SiH_4 and the resulting Si_2H_6 can form other reactive species that can lead to higher silane oligomers. The higher silanes react much more efficiently at surfaces than does parent SiH_4. Various species formed in the gas phase, such as SiH_2 and $H_3SiSiH\colon$, can react at surfaces if they are not consumed in gas-phase reactions, but only $H_3Si^\bullet$ is sufficiently unreactive toward saturated silanes to have a good chance of reaching the surface where film growth occurs. Even in low pressure CVD (LPCVD) at 0.1 to 1 torr, it has been estimated that SiH_2 reaching the surface can make a contribution to film growth only *ca* 5% that of SiH_4[382].

It has been suggested that when phosphorus-doped polycrystalline silicon is produced by LPCVD of SiH_4−PH_3 mixtures, gaseous SiH_2 that reaches the surface becomes the dominant contributor to film formation[383]. It seems, however, that the quality of the films deposited by LPCVD from SiH_4 increases if gas-phase decomposition, and hence SiH_2 formation, *decreases*[384].

PECVD can be carried out at temperatures sufficiently low (<500 K) that surface decomposition of SiH_4 plays a minor role. In the plasma, high-energy electrons are formed whose impact on silanes dissociates them into fragments, including SiH_2 and SiH_3. Orlicki and coworkers have carried out an extensive modeling study of a glow-discharge reactor operated at *ca* 1 torr and 475–525 K[385]. It was predicted that for film growth at the cathode (where the growth rate is higher) the contribution from SiH_2 reaching the surface can be slightly higher than that of SiH_3, or be significantly less, depending on the electron energy distribution function and on the branching ratio for formation of SiH_2 and SiH_3 from SiH_4 under electron impact. It has been suggested that, under PECVD conditions, reactions of silylenes with their silane precursors lead to the formation of higher silanes that are converted into gas-phase silicon clusters, which are deterimental to the growth of high quality films[386]. Recent modeling studies have revised sharply downward the ratio of SiH_2 to SiH_3 (from 5 : 1 to 1 : 10) produced upon electron impact on SiH_4 in PECVD reactors[387].

SiH_2 is also believed to contribute to film growth when vacuum ultraviolet radiation is employed to decompose silane, thus avoiding both high temperatures and plasma damage[388]. These conditions produce SiH, SiH_2 and H atoms as primary dissociation products in unknown ratios[388].

There is a range of mechanisms that can lead to Si film growth from SiH_4[379]. The competition between gas-phase chemistry and surface chemistry depends on the pressures and temperatures employed. At very low pressures (10^{-5}–10^{-2} torr) gas-phase collisions are rare, and unimolecular decomposition is slower than dissociative adsorption on the growing Si surface. Decomposition of surface SiH_3 and SiH_2 groups forms surface H atoms whose desorption in the form of H_2 can be the rate-controlling process in film growth, since desorption frees unsaturated surface sites ('dangling bonds') for further adsorption of SiH_4 from the gas phase. It has been argued from theoretical studies that desorption of H_2 occurs predominantly from a surface SiH_2 group[389]. Surface SiH is more robust, but also dissociates into another surface H and a surface Si atom that is incorporated into the lattice of the growing film[379].

It has been suggested that the difference between the lower temperatures required for PECVD (300–400 °C) and those required for thermal CVD from SiH_4 (500–700 °C) is due to the formation of surface unsaturation by silylene rearrangements $-Si-SiH_2- \rightarrow -SiH{=}SiH-$ in adsorbed polysilane chains[390]. The Si=Si double bonds thus formed are able to capture SiH_3 radicals formed in the plasma, but are unreactive toward saturated silanes. In thermal CVD processes SiH_3 radicals are not important, and in this model saturated silanes are captured by surface silylene H−Si insertions that can occur only at temperatures high enough to produce neighboring silylene sites without nearby hydrogens that can participate in rearrangements.

Surface SiH_3, SiH_2 and SiH have all been detected by infrared reflection absorption spectroscopy under conditions of plasma-enhanced CVD using a glow discharge in SiH_4 at 0.02 torr at 250 °C[391]. As the surface temperature is increased, there is a shift from surface SiH_3 to SiH_2 to SiH, also found with SiD_4 as the precursor[392]. A new Fourier-transform IR attenuated total reflectance technique has revealed the dominance of adsorbed SiH_2 in the early stages of plasma CVD from SiH_4[393].

There has been considerable controversy regarding the nature of the gas-phase reactive species that contribute to film growth formed in plasma-assisted CVD from SiH_4. Strong arguments have been presented in favor of SiH_2 formed by electron-impact induced fragmentation of SiH_4[394]. Insertion reactions of SiH_2 convert SiH_4 to Si_2H_6 and Si_2H_6 to Si_3H_8. The resulting higher silanes have much higher sticking coefficients to growing surfaces and thus contribute significantly to the formation of the hydrogenated amorphous Si films that are the desired products under these conditions.

If SiH_2 survives to reach a growing film surface, insertion into surface Si−H bonds can act as a primary step for film formation. It has been reported that the sticking coefficient for vibrationally excited SiH_2 formed by multiphoton IR laser dissociation (IRMPD) of n-$BuSiH_3$ is significantly higher (0.5 *vs* 0.1) than for cold SiH_2[395,396]. Use of resonance-enhanced multiphoton ionization to detect SiH_2 allowed hot and cold species to be distinguished.

Use of IRMPD to dissociate precursor silanes can initiate rather complex processes. The mechanism presented in equation 116 can explain the formation of both ground-state singlet SiH_2 and excited-state singlet ^1D Si atoms[396]. This mechanism is analogous to the phenylcarbene rearrangement[397] and has *not* been found for vibrationally unexcited phenylsilylenes formed in simple pyrolysis or photolysis experiments.

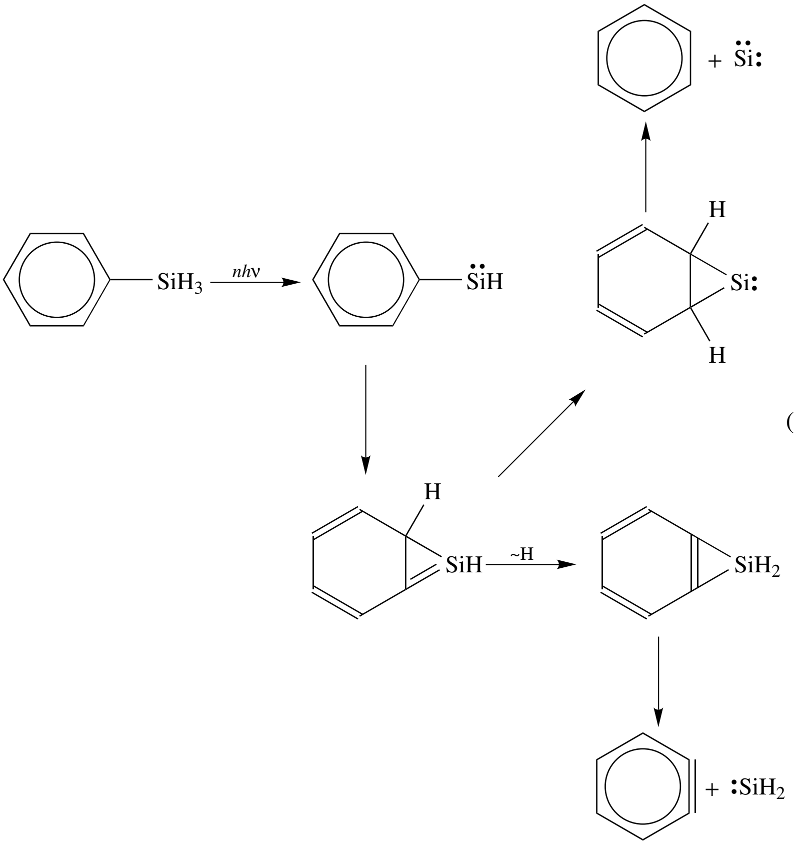

(116)

Differences have been suggested between the silylene chemistry that occurs under various film-forming conditions. Dietrich *et al.* have proposed, based on the monitoring of SiH_2 under CVD conditions and correlations with film growth rate, that IRMPD of SiH_4 and Si_2H_6 leads to SiH_2 as the primary species, and it is immediately consumed by insertion into an Si−H bond of a precursor molecule[398]. The vibrationally excited insertion products can revert to their precursors, regenerating SiH_2 or undergoing unimolecular decomposition. The reaction scheme shown in equation 117 accounts for the low efficiency of the film deposition process with IRMPD of SiH_4 and for a monotonic increase with SiH_4 concentration, a higher efficiency with a maximum with variation of precursor concentration upon IRMPD of Si_2H_6, and a yet higher efficiency but a monotonic decrease with concentration upon 193-nm laser photolysis of Si_2H_6.

In this mechanism the silylenes $H_2Si\colon$ and $H_3Si\ddot{S}iH$ are consumed before they reach the growing film surface. Disilene $H_2Si{=}SiH_2$ is postulated to be the species that can reach the growing surface and stick. The direct formation of silylsilylene $H_3Si\ddot{S}iH$ that can rearrange to $H_2Si{=}SiH_2$ by UV photolysis of Si_2H_6 leads to film formation with a high efficiency that diminishes due to the siphoning off of $H_3Si\ddot{S}iH$ at increasing precursor concentrations.

$$\begin{aligned}
&\mathrm{SiH_4} \xrightarrow[10.6\ \mu\mathrm{m}]{nh\nu} \mathbf{:}\mathrm{SiH_2} + \mathrm{H_2}\\
&\mathrm{Si_2H_6} \xrightarrow[10.6\ \mu\mathrm{m}]{nh\nu} \mathbf{:}\mathrm{SiH_2} + \mathrm{SiH_4}\\
&\mathrm{Si_2H_6} \xrightarrow[193\ \mathrm{nm}]{h\nu} \mathrm{H_3Si{-}\overset{\bullet\bullet}{Si}H} + \mathrm{H_2}\\
&\mathbf{:}\mathrm{SiH_2} + \mathrm{SiH_4} \rightleftharpoons \mathrm{Si_2H_6}^{*} \longrightarrow \mathrm{H_3Si{-}\overset{\bullet\bullet}{Si}H} + \mathrm{H_2}\\
&\mathbf{:}\mathrm{SiH_2} + \mathrm{Si_2H_6} \rightleftharpoons \mathrm{Si_3H_8}^{*} \longrightarrow \mathrm{H_3Si{-}\overset{\bullet\bullet}{Si}H} + \mathrm{SiH_4}\\
&\mathrm{H_3Si{-}\overset{\bullet\bullet}{Si}H} \longrightarrow \mathrm{H_2Si{=}SiH_2}\\
&\mathrm{H_3Si{-}\overset{\bullet\bullet}{Si}H} + \mathrm{SiH_4} \longrightarrow \mathrm{Si_3H_8}\\
&\mathrm{H_3Si{-}\overset{\bullet\bullet}{Si}H} + \mathrm{Si_2H_6} \longrightarrow \mathrm{Si_4H_{10}}
\end{aligned}\tag{117}$$

The tetrasilane insertion product from $\mathrm{H_3Si\overset{\bullet\bullet}{Si}H}$ and $\mathrm{Si_2H_6}$ is less effectively incorporated into the growing film than is $\mathrm{H_2Si{=}SiH_2}$. IRMPD of both $\mathrm{SiH_4}$ and $\mathrm{Si_2H_6}$ produce $\mathrm{SiH_2}$. The higher efficiency of film formation from IRMPD of $\mathrm{Si_2H_6}$ over $\mathrm{SiH_4}$ is believed to be due to the greater ease of formation of $\mathrm{SiH_3\overset{\bullet\bullet}{Si}H}$ (and hence $\mathrm{H_2Si{=}SiH_2}$) by unimolecular decomposition of $\mathrm{Si_3H_8}$ (formed from $\mathrm{SiH_2}$ and $\mathrm{Si_2H_6}$) than from unimolecular decomposition of $\mathrm{Si_2H_6}$ (formed from $\mathrm{SiH_2}$ and $\mathrm{SiH_4}$).

Detailed models continue to be devised for CVD reactors for the deposition of silicon from $\mathrm{SiH_4}$. Recently $\mathrm{SiH_2}$, $\mathrm{Si_2H_6}$, $\mathrm{H_3Si\overset{\bullet\bullet}{Si}H}$, $\mathrm{H_2Si{=}SiH_2}$ have all been included as potential participants in film formation in a LPCVD reactor model, with $\mathrm{SiH_2}$ and $\mathrm{Si_2H_6}$ estimated as contributing up to 20%[399]. A significant problem of many such models is that these mathematical models include large numbers of rate constants and their temperature dependences that have been estimated or measured by indirect means. The test of such a model is often a comparison of predicted and measured growth rates, but, like a reaction mechanism, such models can be disproved but never proved. One must therefore retain a certain degree of skepticism while appreciating the effort and ingenuity that has gone into developing them.

The deposition of silicon films from disilane $\mathrm{Si_2H_6}$ occurs at lower temperatures than from $\mathrm{SiH_4}$, thus permitting the use of a wider range of substrates. Since the formation of $\mathrm{SiH_2}$ from $\mathrm{Si_2H_6}$ (equation 118) occurs at lower temperatures than from $\mathrm{SiH_4}$ (equation 115), it has been suggested that $\mathrm{SiH_2}$ makes a greater contribution to film growth from $\mathrm{Si_2H_6}$[400].

$$\begin{aligned}
\mathrm{H_3Si{-}SiH_3} &\xrightarrow{\Delta} \mathrm{H_2Si}\mathbf{:} + \mathrm{SiH_4} \qquad \text{(major)}\\
&\xrightarrow{\Delta} \mathrm{H_3Si{-}\overset{\bullet\bullet}{Si}H} + \mathrm{H_2} \qquad \text{(minor)}
\end{aligned}\tag{118}$$

Since the reactive sticking coefficient of $\mathrm{Si_2H_6}$ is known to be much higher than that for $\mathrm{SiH_4}$[379], the differences between $\mathrm{Si_2H_6}$ and $\mathrm{SiH_4}$ as CVD precursors may extend beyond differences in ease of $\mathrm{SiH_2}$ formation. Success has been claimed for models for film growth from $\mathrm{Si_2H_6}$ in which both $\mathrm{SiH_2}$ and higher silanes from $\mathrm{SiH_2}$ gas-phase insertions reach the growing surface and react[401].

An attempt has been reported to detect reactive intermediates in the gas-phase chemistry in thermal CVD from $\mathrm{Si_2H_6}$, from 300 to 1000 K and 1 to 10 torr[402]. The reaction mixture was continuously sampled in the form of a supersonic molecular beam analyzed by multiphoton ionization MPI or resonance enhanced MPI (REMPI) and mass spectrometry. Species of mass 2, 28, 32 and 60 were detected, with maximum intensities at *ca* 700 K (a commonly employed CVD temperature) corresponding to H_2, Si, SiH_4 and Si_2H_4. The last of these could be due to $H_3Si\ddot{\mathrm{Si}}H$, a minor product of disilane pyrolysis (equation 118), or its rearrangement product $H_2Si{=}SiH_2$. SiH_4 is a major product of Si_2H_6, together with SiH_2, whose expected detection was unsuccessful. SiH and SiH_3 were also not detected. The mass of 28 was believed to be due to Si atoms formed by secondary decomposition of $H_3Si\ddot{\mathrm{Si}}H$ (major source) and SiH_2 (minor source).

Even lower temperatures can be employed in photochemical CVD from Si_2H_6, employing vacuum ultraviolet radiation to decompose the precursor. An elaborate and convincing model has been proposed for 147 and 185 nm radiation[403]. At 147 nm, much higher quality films can be grown from Si_2H_6 than from SiH_4. While SiH_2 is believed to be the major primary reactive species from both precursors (83% from SiH_4 and 61% from Si_2H_6), photoinduced homolysis of both precursors to silyl radicals and H atoms also occurs at these low wavelengths. Since the insertion of SiH_2 into H−Si bonds of Si_2H_6 is believed to be an order of magnitude more rapid than the insertion into SiH_4, the gas-phase concentration of SiH_2 is much lower in Si_2H_6. Due to their lower reactivity, the concentration of SiH_3 and Si_2H_5 radicals (formed mostly in secondary reactions) is much higher than that of SiH_2 despite their comparable or lower initial production rates (equation 119). In this model it is the SiH_3 and Si_2H_5 radicals that make the major contribution to the formation of high quality films.

$$\begin{array}{rlr}
SiH_4 & \xrightarrow{h\nu,\ 147\ \mathrm{nm}} H_2Si\colon + 2H^{\bullet} & 83\% \\
 & \xrightarrow{\qquad\quad} H_3Si^{\bullet} + H^{\bullet} & 17\% \\
H_3Si{-}SiH_3 & \xrightarrow{h\nu,\ 147\ \mathrm{nm}} H_2Si\colon + H_3Si^{\bullet} + H^{\bullet} & 61\% \\
 & \xrightarrow{\qquad\quad} Si_2H_4 + 2H^{\bullet} & 21\% \\
 & \xrightarrow{\qquad\quad} H_3Si{-}SiH_2^{\bullet} + H^{\bullet} & 18\%
\end{array} \tag{119}$$

It is believed that the smaller contribution to film formation from SiH_2 under the conditions of photo-CVD with Si_2H_6 precursor leads to better quality films, because interconnections of surface sites created from SiH_2 are slower than the interconnection of surface sites created from mono-radicals.

SiH_2 is believed to play an important role in the deposition of semi-insulating silicon films that are nonstoichiometric sub-oxides of silicon. When large ratios of N_2O and Si_2H_6 are subjected to LPCVD conditions, it has been suggested that Si and SiO are codeposited, with SiH_2 contributing to Si deposition[404]. It has been suggested that the species believed to be responsible for SiO deposition, the elusive parent silanone $H_2Si{=}O$, is formed from SiH_2 (equation 120)[405].

$$H_2Si\colon + N_2O \longrightarrow H_2Si{=}O + N_2 \tag{120}$$

SiH_2 is believed to play a role in the silicon doping of Ga−As films grown under MOCVD conditions. The efficiency of Si incorporation is much higher with Si_2H_6 as the silicon source than with SiH_4[406]. In a model for the doping process it was assumed that SiH_2 is formed by gas-phase pyrolysis of Si_2H_6 and inserts into an As−H bond of AsH_3 to form H_3SiAsH_2, which reacts at the growing film surface.

Known addition reactions of SiH_2 with ethylene and acetylene are believed to contribute to the carbon deposition process in the growth of SiC films from mixtures of Si_2H_6 and C_2H_4 or C_2H_2 at 873 to 1273 K under LPCVD conditions[407]. It is believed that SiF_2 can act as both the source of Si and as a halogen scavenger in the growth of titanium silicide films by CVD from gaseous mixtures of SiF_2 and $TiCl_4$[408].

E. Silylenes Stabilized by Intramolecular Coordination

In 1992 Belzner prepared the cyclotrisilane **77** by magnesium coupling of the pentacoordinate dichlorosilane **78** (equation 121). **77** reacted with silylene trapping agents under truly mild conditions, at 50 °C, to give three equivalents of trapping products[409]. The reactions with benzil and diphenylacetylene[410] are shown as examples in equations 122 and 123.

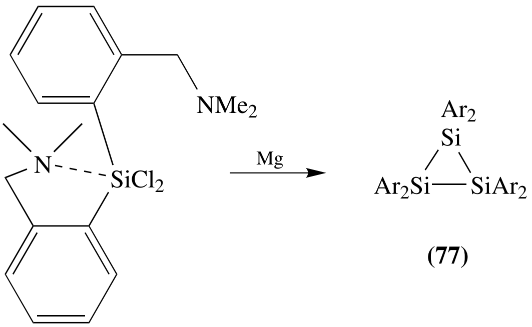

(121)

(77)

(78) Ar = o-$Me_2NCH_2C_6H_4$

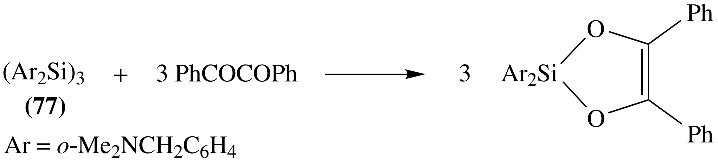

(122)

(77)

Ar = o-$Me_2NCH_2C_6H_4$

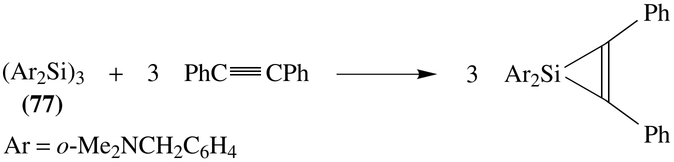

(123)

(77)

Ar = o-$Me_2NCH_2C_6H_4$

Many further reactions of **77** have been investigated, leading to a rather extensive chemistry of the base-stabilized silylene, **79**. In Scheme 23 the structure of **79** is shown as tetracoordinated, but could also be tricoordinate. Intramolecularly base-stabilized silylenes can also be depicted as silaylides, for instance **79a**.

In an especially significant paper Belzner reports the reaction of **77** with the terminal olefins 1-pentene and 1-hexene[411]. The products, siliranes **80a,b**, were found to be in

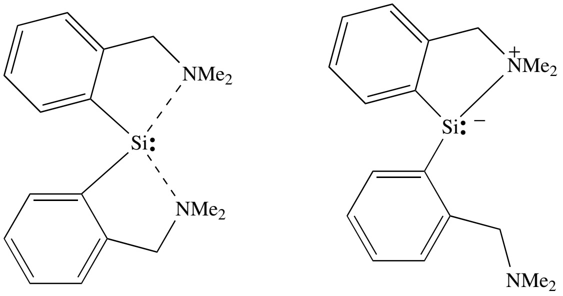

(79) **(79a)**

SCHEME 23

thermal equilibrium with the cyclotrisilane and the starting olefin (equation 124).

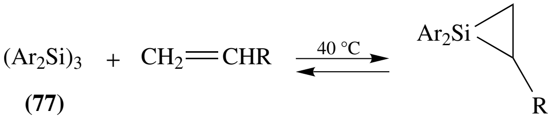

(77)

(80a) $R = n\text{-}C_3H_7$
(80b) $R = n\text{-}C_4H_9$ (124)

The first step of the retro-reaction involves loss of silylene **79**, which could be trapped with 1-pentyne to give the known silirene **81** (equation 125). In the absence of a trapping agent, **79** recondenses to **77**, probably by first dimerizing to the disilene $Ar_2Si{=}SiAr_2$ followed by 2+1 cycloaddition to give **77** (equation 126). From the principle of microscopic reversibility, the fact that silylene is formed in the retro-reaction leads to the conclusion that **79** must also be an intermediate in the cycloaddition reaction.

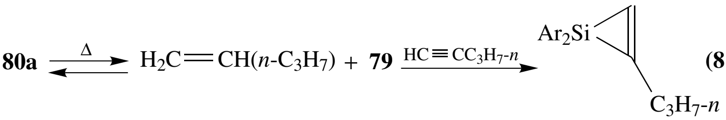

(81) (125)

$$\underset{(\mathbf{79})}{3Ar_2Si\mathbf{:}} \rightleftharpoons Ar_2Si\mathbf{:} + Ar_2Si{=}SiAr_2 \rightleftharpoons \underset{(\mathbf{77})}{(Ar_2Si)_3} \qquad (126)$$

$$Ar = o\text{-}Me_2NCH_2C_6H_4$$

This is the first time that an equilibrium between a silylene, a disilene and a cyclotrisilane has been demonstrated, but a similar photoequilibrium may exist for $(t\text{-}Bu_2Si)_3$, as shown by Weidenbruch[8].

Cyclotrisilane **77** reacts with *strained* (but not unstrained) internal olefins to give stable siliranes; an example is the reaction with norbornene (equation 127).

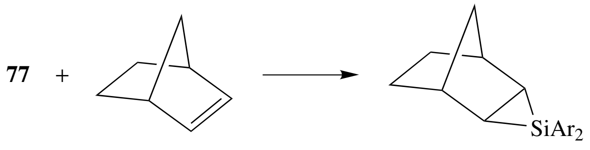

(127)

$$Ar = o\text{-}Me_2NCH_2C_6H_4$$

Other interesting and useful reactions of **77** are shown in equations 128–131. With pivalonitrile, a four-membered ring is formed, presumably through intermediate formation of the azasilacyclopropene **82** (equation 128)[412].

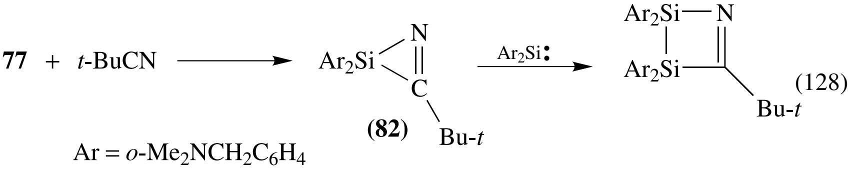

(128)

The silylene **79** abstracts oxygen or sulfur from isocyanates and isothiocyanates[413]. Cyclic siloxanes are the products with isocyanates (equation 129); these probably arise by polymerization of the silanone, $Ar_2Si{=}O$ (**83**).

$$\mathbf{77} + \mathrm{RNCO} \xrightarrow{70\,^{\circ}\mathrm{C}} \underset{(\mathbf{83})}{[\mathrm{Ar_2Si{=}O}]} \longrightarrow \underset{n\,=\,2,\,3}{(\mathrm{Ar_2SiO})_n}$$

$$\mathrm{Ar} = o\text{-}\mathrm{Me_2NCH_2C_6H_4} \qquad (129)$$

When $(Me_2SiO)_3$ (D_3) was present, the diarylsilanone (**83**) was intercepted as the cyclotetrasiloxane (equation 130); this is a known reaction for silanone capture.

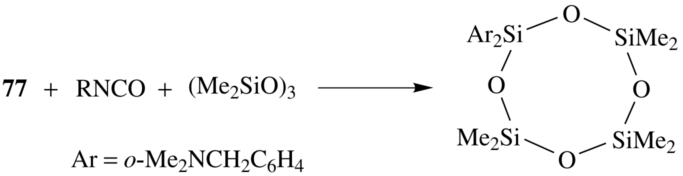

(130)

With isothiocyanates, the ‘silanethione’ (**84**) is obtained, without oligomerization. The ^{29}Si NMR of **84**, at −21.0 ppm, shows that the silicon atom is highly shielded, consistent with a pentacoordinate structure as shown in equation 131. The chemical shift can be compared with that for singly N-coordinated silanethiones, +22 to +41 ppm, and with that for a true tricoordinate silanethione, +166.6 ppm.

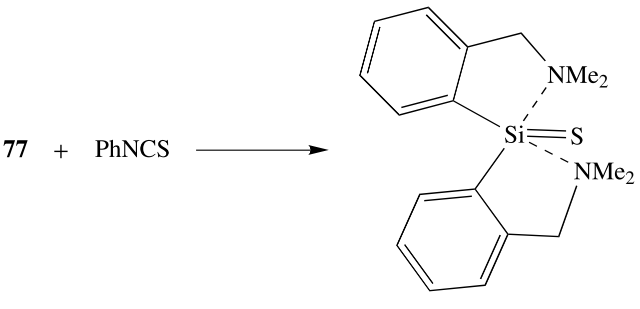

(131)

(84)

Various complex products were obtained in reactions of **77** with ketones[414]. With benzophenone, for example, the rearranged compound **85** was obtained, while fluorenone reacted in 2 : 1 ratio to give **86**, both shown in Scheme 24[415]. Reaction pathways leading to both products were suggested. For additional examples, the original papers should be consulted.

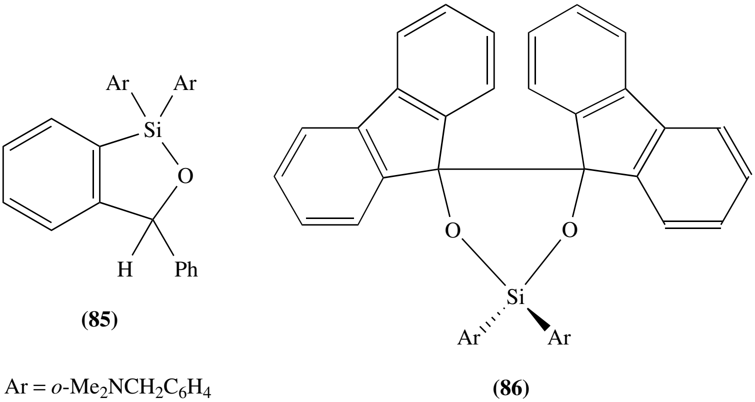

(85)

(86)

Ar = o-Me$_2$NCH$_2$C$_6$H$_4$

SCHEME 24

The same hypercoordinate silylene (**79**) was generated by the Corriu group in dehalogenation reactions; the best results were with the difluoride Ar$_2$SiF$_2$ (Ar = o-Me$_2$NCH$_2$Ph) and lithium metal or lithium naphthalene[97]. The silylene was trapped by 1,4-addition to 2,3-dimethylbutadiene. Similar defluorination reactions were used to obtain silylenes **87–89** shown in Scheme 25, all trapped with dimethylbutadiene.

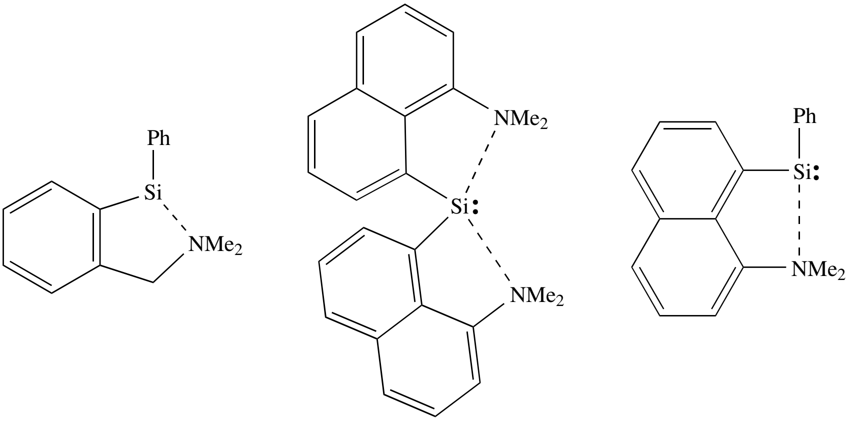

(87) **(88)** **(89)**

SCHEME 25

Also in this publication, the 3-MP matrix isolation of silylenes **90** and **91** was reported, from photolysis of the corresponding trisilanes (equation 132). The λ_{max} at 662 nm for

91 shifted to 478 nm in **90**, consistent with strong N→Si electron donation in the latter.

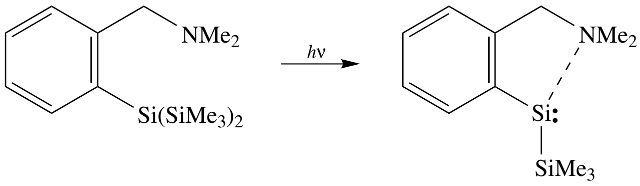

(90)

(132)

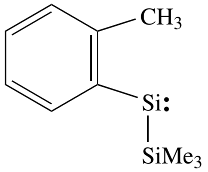

(91)

Remarkably facile thermal generation of a silylene has recently been demonstrated for the pentacoordinate alkoxydisilane **92**[416]. Intramolecular N→Si coordination in **92** was shown by X-ray crystallography. This disilane underwent thermolysis at 110 °C in toluene, or 90 °C in DMF, producing the silylene **93**, which was trapped with 2,3-dimethylbutadiene and diphenylacetylene (Scheme 26). The 2 : 1 adduct with diphenylacetylene was shown to have *one* nitrogen intramolecularly coordinated to silicon, even though the silicon atom lacks any electronegative substituents.

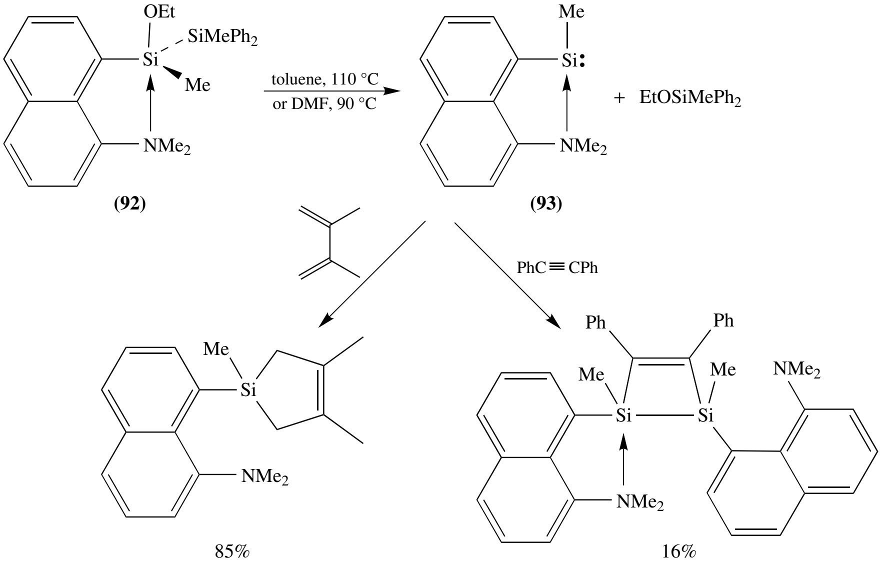

SCHEME 26

In a related investigation, the pseudo-pentacoordinated naphthylsilane (**94**), in the presence of a nickel catalyst, was found to react with diphenylacetylene to give the silole

95[417]. Presumably, this reaction proceeds through intermediate formation of the silylene **96**, stabilized by intramolecular coordination from nitrogen (equation 133).

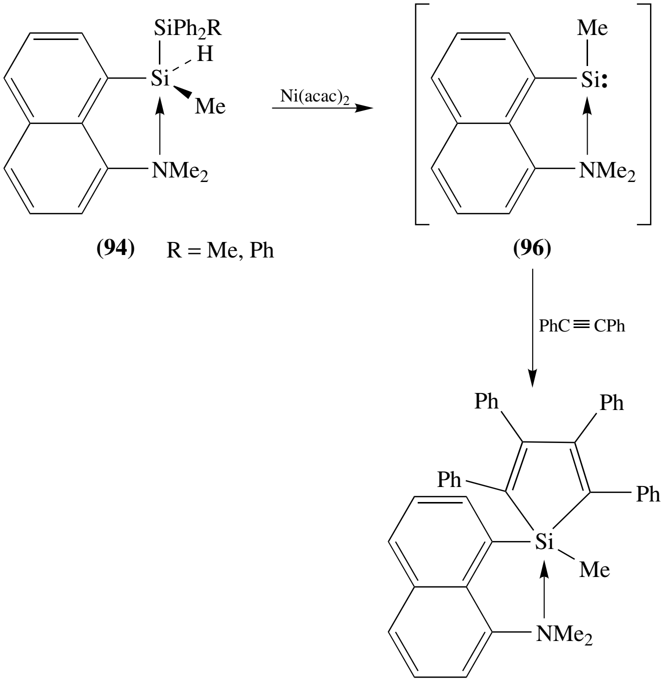

(94) R = Me, Ph

(96)

(95)

(133)

The research on silylenes with intramolecular coordination shows beyond doubt that such electron donation from nitrogen greatly stabilizes the silylenes. A persistent silylene stabilized in this manner has not yet appeared, but it seems possible that one might be made if just the right substituents are employed.

F. Vinylidenesilylene and other Double-bonded Silylenes Z=Si:

Silylenes with double bonds to silicon Z=Si: have long interested theorists (see Section IV.B for density functional calculations on disilenylidenes $R_2Si{=}Si$:) but experimental data concerning them are scarce. Theoretical calculations up to 1989 have been reviewed by Apeloig[201], himself an active investigator in the field.

In 1995 Apeloig and Albrecht carried out high level *ab initio* calculations on the effects of substituents on the energy barriers separating silanitriles RSi≡N: and silaisocyanides R−N=Si:[418]. For most substituents, i.e. R = H, Li, BeH, BH_2, CH_3, SiH_3, PH_2 and SH, the isocyanide was predicted to be more stable than the silanitrile by 22 to 76 kcal mol^{-1}, and the effects of substituents correlated well with R−Si *vs* R−N bond strengths. Only for R = F and OH was RSi≡N predicted to be more stable than RN=Si:. At the QCISD(T)/6-311G(2df,p)//QCISD/6-31G* level the calculated energy differences and barriers (kcal mol^{-1}) between RN=Si: and RSi≡N: were: R = H (65.2, 11.4), OH (−6.5, 35.8), F (−26.6, 49.3).

In 1997 Apeloig and Karni published similar computational studies on the effects of substituents on the potential energy surface for RHSiC (R = H, CH_3, SiH_3, F, OH)[419], In all cases except R = F, the energy calculated for the vinylidenesilylene $RHC{=}Si\colon$ was lower than that for the silacetylene $RSi{\equiv}CH$. At MP4SDTQ/6-31G(d,p)//MP2/6-31G(d,p) the energy differences and the barriers ($kcal\,mol^{-1}$) were: R = H (36.1, 9.0), CH_3 (25.8, 17.5), SiH_3 (33.0, 3.2), OH (4.3, 25.0), F(−6.4, 22.5). Thus, both silaisocyanides $R{-}N{=}Si\colon$[418] and silaacetylenes $RHC{=}Si\colon$[419] appear to be viable targets for synthesis.

Experimental information is limited to $H_2C{=}Si\colon$, whose electronic absorption spectrum was observed by Leclercq and Dubois in 1979 as a well resolved band system between 3400 and 3100 Å following a flash discharge through CH_3SiH_3[420]. For the $^1B_2$ excited state, an HCH bending frequency of 1110 cm^{-1} and a Si−C stretching frequency of 700 cm^{-1} were deduced from the vibrational analysis. The rotational analysis was in accord with C_{2v} symmetry for the molecule and a $^1A_1$ singlet ground state.

In 1988, Damrauer and cowerkers found the gas-phase acidity of $H_2C{=}Si\colon$ to lie between that of CH_3SH and acetophenone, making $H_2C{=}Si\colon$ a stronger acid than acetylene[421]. It was necessary for these workers to assume the $HCSi^-$ structure for the ion that they studied in tandem flowing afterglow selected ion flow tube proton-transfer experiments, as well as the $H_2C{=}Si\colon$ structure for the product.

In neutralization–reionization mass spectrometric experiments on $CH_2Si^{+\bullet}$ formed by electron-impact dissociative ionization of $ClCH_2SiH_3$, Srinivas, Sülzle and Schwarz found evidence for the formation of a viable neutral molecule whose fragmentation pattern and collisional activation mass spectrum were in accord with a $H_2C{=}Si\colon$ structure[422]. These authors suggested that their experiments supported electron-capture by $CH_2Si^{+\bullet}$ as a mechanism for the formation of $H_2C{=}Si\colon$ in interstellar space. Various models have predicted that $H_2C{=}Si\colon$ is one of the most abundant forms of silicon in dense interstellar clouds[423].

In 1995, Sherrill and Schaefer published new quantum mechanical calculations beginning at the restricted Hartree–Fock level with basis sets as large as TZ2pf and employing the coupled clusters method to the CCSD(T) level for correlation corrections[424]. Their work was stimulated by still unpublished photoelectron spectroscopic studies of H_2CSi^- and D_2CSi^- by Bengali and Leopold[425]. The equilibrium geometry predicted by Sherrill and Schaefer for the ground state of $H_2C{=}Si\colon$ was similar to those of earlier calculations, but the geometrical parameters, particularly the Si−C bond distance, were found to vary noticeably with basis set and correlation method. At the highest level of treatment $r(C{-}Si) = 1.720$ Å, $r(C{-}H) = 1.089$ Å and $\angle H{-}C{-}H = 113.4^{\circ}$[425].

There have been several other recent theoretical studies. In 1995, Nguyen, Sengupta and Vanquickenborne carried out high level calculations on the H_2CSi potential surface to study the effects of tunneling on the rearrangement of *trans*-$HC{\equiv}SiH$ to $H_2C{=}Si\colon$[426]. With a 6-3111++G(3df,3pd) basis set and geometry optimization including configuration interaction to the QCISD(T) level, the geometry predicted for $H_2C{=}Si\colon$ was $r(C{-}Si) = 1.726$ Å, $r(C{-}H) = 1.095$ Å and $\angle H{-}C{-}H = 118.4^{\circ}$. The calculated heats of formation were $\Delta H_f{}^o(H_2C{=}Si\colon) = 84.5 \pm 2\ kcal\,mol^{-1}$ and $\Delta H_f{}^o(HC{\equiv}SiH) = 118.3 \pm 2\ kcal\,mol^{-1}$[426]. The 1996 calculations on H_2CSi isomers by Stegmann and Frenking also employed correlated wave functions in geometry optimizations[427]. At CCSD(T)/TZ2P, the predicted structure of $H_2C{=}Si$ was $r(C{-}Si) = 1.721$ Å, $r(C{-}H) = 1.087$ Å and $\angle H{-}C{-}H = 118.4^{\circ}$. The energy difference between $H_2C{=}Si\colon$ and *trans*-$HC{\equiv}SiH$ predicted by Stegmann and Frenking, 34.1 $kcal\,mol^{-1}$, is almost exactly that calculated by Nguyen and coworkers[426]. In 1994, with a smaller 6-31G(d,p) basis set, Schoeller and Strutwolf had calculated $r(\mathrm{C-Si}) = 1.701$ Å, $r(\mathrm{C-H}) = 1.082$ Å and $\angle\mathrm{H-C-H} = 120.7°$ as geometrical parameters for $H_2C{=}Si$**:**[428].

The equilibrium rotational constants and the theoretical harmonic frequencies calculated by Sherrill and Schaefer[424] were in good agreement with the experimental ground-state rotational constants obtained by Leclercq and Dubois[420] and in reasonable accord with the experimental fundamental vibrational frequencies obtained by Bengali and Leopold[425].

In 1996, Izuha, Yamamoto and Saito observed the microwave spectrum of $H_2C{=}Si$**:** produced via a glow-discharge plasma in a gaseous mixture of SiH_4 and CO[429]. The rotational constants deduced were very close to those of Leclercq and Dubois[420]. The vibrational frequency of the CH_2 rocking mode was estimated to be 331 ± 5 cm^{-1}[429], rather close to the 305 cm^{-1} predicted by Sherrill and Schaefer[424] but higher than the *ca* 265 cm^{-1} found by Bengali and Leopold[425].

In 1997, Clouthier *et al.* presented laser-induced fluorescence spectra of $H_2C{=}Si$**:** produced by an electric discharge through dilute $Me_4Si{-}Ar$ mixtures[430]. The rotational analysis yielded geometric parameters in good agreement with theoretical predictions (given in brackets) employing TZ(2df,2pd) basis sets and correlation corrections at the CISD level: $r(\mathrm{C-Si}) = 1.706(5)$ [1.704] Å, $r(\mathrm{C-H}) = 1.099(3)$ [1.083] Å and $\angle\mathrm{H-C-H} = 114.4(2)$ [113.4]°[430]. The emission spectrum observed by Clouthier *et al.* agreed with the absorption spectrum reported by Leclercq and Dubois[420].

Thus, experiment and theory agree that $H_2C{=}Si$**:** is a planar C_{2v} molecule with C−H single and C=Si double bonds, and that it is the global minimum on the H_2SiC ground-state potential surface. Its chemistry, other than C−H ionization, is totally unexplored, but we predict that clean routes to its generation as well as that of substituted vinylidenesilylenes RR′C=Si will be developed in the near future that will allow the potentially useful and surely interesting chemistry of these molecules to be explored.

IX. SPECULATIONS ON THE FUTURE OF SILYLENE CHEMISTRY

In writing this chapter, the authors have been much impressed by the tremendous strides made since the silylenes were last comprehensively reviewed, more than a decade ago. Here we shall attempt to look ahead, and predict some of the discoveries concerning silylenes which may take place during the next ten years, foolhardy as this exercise of imagination may seem. We ask then: where is silylene chemistry likely to advance in the future?

An area obviously ready for expansion is the chemistry of persistent or ‘stable’ silylenes. Only four such compounds are now known, and their status as ‘true’ silylenes in the sense of containing a divalent silicon atom remains a subject of discussion, but dozens can readily be imagined. The persistent silylenes known today are stabilized by electron donation from a pair of nitrogen atoms. It seems likely that ways will be found to prepare persistent silylenes stabilized by other electron donors, oxygen, sulfur or phosphorus. The nitrogen atoms in known stable silylenes are directly attached to silicon, but this may not be necessary; persistent silylenes stabilized by intramolecular chelation may be synthesized. Moreover, the chemistry of stable silylenes is just beginning to be explored, and appears to be sufficiently different from that of transient silylenes. Especially, we look for an entire new series of base-free transition metal complexes of the stable silylenes stretching across the periodic table. The quest for silylenes stabilized solely by steric hindrance to attack at the silylene center has not been abandoned and may succeed in the near future. To find groups of sufficient size is no problem; the difficulty has been to make them sufficiently inert to avoid consuming the divalent silicon atom in an intramolecular reaction. It is confidently predicted that the challenge of generating ground-state triplet silylenes and studying their chemistry will finally be met in the immediate future.

Methods for the synthesis of transient silylenes are now well-developed, so that it is risky to predict the discovery of entirely new methods for the generation of silylenes, as desirable as these might be. But many questions remain about the details of silylene-generating reactions, and these may yield to mechanistic investigations in the coming years. For instance, the precise pathways for silylene extrusion reactions, both thermal and photochemical, are still obscure. Here, it seems likely that theoretical calculations, as much as experiment, will aid our understanding of these phenomena. This is not only a matter of intellectual curiosity. Silylene-generating reactions are often accompanied by undesired side-reactions, and thus deeper understanding is desired to enhance our control of silylene generation and thus increase its efficiency. The lack of silylene precursors as versatile and generally useful as diazo compounds are, for carbene generation, has materially limited the applications of silylene chemistry in organic and main-group synthesis.

The reactions of transient silylenes are so rapid that most of the limited mechanistic information that has been obtained over the past quarter-century has been through indirect means. Direct measurements of silylene reaction rates by kinetic spectroscopy in the past decade have yielded important new insights. One can predict with some confidence an explosion of mechanistic studies of silylenes employing fast spectroscopies capable of providing more structural information than traditional electronic absorption and emission techniques. The nearly universal reversibility of silylene reactions remains to be fully exploited through kinetic studies of retro-reactions. The mechanisms of most silylene reactions remain to be fully elucidated, and this task will increase in urgency as silylenes see more use in synthesis.

After more than fifty years of industrial use, the ‘direct reaction’ of methyl chloride with silicon, which underlies the entire silicone industry, is not understood. Promising recent experiments on this process are likely to be continued, and should at least settle the question of the nature of the intermediates. Are silylenes important in the process, either in the gas phase or at the silicon surface?

Also obscure is the nature of the reaction of dihalosilanes with active metals. Further experiments should show under what circumstances, if any, such dehalogenation reactions lead to silylenes, or to silylenoids, another area of likely future activity. In a related area, isolable silylenoids are quite new, and further development of their chemistry can be anticipated.

In the past few years, theoretical calculations have become increasingly important in guiding our understanding of silylenes, and indeed of organosilicon chemistry generally. The partnership between theory and experiment is likely to become even stronger and more important in the years ahead. The development of new computational techniques such as density functional theory, and the availability of larger and ever-faster computers have made chemically accurate calculations on large molecules and the mapping of potential surfaces for complex reactions an everyday reality. The computational experiment is an important component in the study of silylenes.

Last of all the authors continue to expect the unexpected. That is one of the reasons silylene chemistry is still such fun.

X. REFERENCES

1. P. P. Gaspar and B. Jerosch Herold, in *Carbene Chemistry*, 2nd ed. (Ed. W. Kirmse), Academic Press, New York, 1971, pp. 504–550.
2. P. P. Gaspar, in *Reactive Intermediates*, Vol. 1 (Eds. M. Jones, Jr. and R. A. Moss), Wiley, New York, 1978, pp. 229–277.

3. P. P. Gaspar, in *Reactive Intermediates*, Vol. 2 (Eds. M. Jones, Jr. and R. A. Moss), Wiley, New York, 1981, pp. 335–385.
4. Y.-N. Tang, in *Reactive Intermediates*, Vol. 2 (Ed. R. A. Abramovitch), Plenum Press, New York, 1982, pp. 297–366.
5. P. P. Gaspar, in *Reactive Intermediates*, Vol. 3 (Eds. M Jones, Jr. and R. A. Moss), Wiley, New York, 1985, pp. 333–427.
6. C.-S. Liu and T.-H. Hwang, *Adv. Inorg. Chem. Radiochem.*, **29**, 1 (1985).
7. E. A. Chernyshev and N. G. Komalenkova, *Russ. Chem. Rev.*, **59**, 531 (1990).
8. M. Weidenbruch, *Coord. Chem. Rev.*, **130**, 275 (1994).
9. W. H. Atwell and D. R. Weyenberg, *J. Organometal. Chem.*, **5**, 594 (1966); *Angew. Chem., Int. Ed. Engl.*, **8**, 469 (1969).
10. I. M. T. Davidson, K. J. Hughes and S. Ijadi-Maghsoodi, *Organometallics*, **6**, 639 (1986).
11. T. J. Barton, S. A. Burns, P. P. Gaspar and Y.-S. Chen, *Synth. React. Inorg. Met.-Org. Chem.*, **13**, 881 (1983).
12. J. G. Martin, M. A. Ring and H. E. O'Neal, *Int. J. Chem. Kinet.*, **19**, 715 (1987).
13. R. Walsh, *Organometallics*, **7**, 75 (1988).
14. M. E. Harris, M. A. Ring and H. E. O'Neal, *Organometallics*, **11**, 983 (1992).
15. K. E. Nares, M. E. Harris, M. A. Ring and H. E. O'Neal, *Organometallics*, **8**, 1964 (1989).
16. M. P. Clarke, I. M. T. Davidson and M. P. Dillon, *J. Chem. Soc., Chem. Commun.*, 1251 (1988).
17. E. W. Ignacio and H. B. Schlegel, *J. Phys. Chem.*, **96**, 1758 (1992).
18. R. J. P. Corriu, D. Leclercq, P. H. Mutin, J.-M. Planeix and A. Vioux, *Organometallics*, **12**, 454 (1993).
19. J. Heinicke, B. Gerhus and S. Meinel, *J. Organometal. Chem.*, **474**, 71 (1994).
20. D. Lei, R.-J. Hwang and P. P. Gaspar, *J. Organometal. Chem.*, **271**, 1 (1984).
21. J. Heinicke and B. Gerhus, *J. Organometal. Chem.*, **423**, 13 (1993).
22. A. Kaczmarczyk and G. Urry, *J. Am. Chem. Soc.*, **82**, 751 (1960); R. F. Trandell and G. Urry, *J. Inorg. Nucl. Chem.*, **40**, 1305 (1978).
23. U. Herzog, R. Richter, E. Brendler and G. Roewer, *J. Organometal. Chem.*, **507**, 221 (1996).
24. L. Fredin, R. H. Hauge, Z. H. Kafafi and J. L. Margrave, *J. Chem. Phys.*, **82**, 3542 (1985).
25. P. P. Gaspar, in *Organosilicon and Bioorganosilicon Chemistry* (Ed. H. Sakurai), Horwood, Chichester, 1985, pp. 87–98.
26. P. P. Gaspar, *Radiochim. Acta*, **43**, 89 (1988).
27. P. P. Gaspar, in *Handbook of Hot Atom Chemistry* (Eds. J.-P. Adloff, P. P. Gaspar, M. Imamura, A. G. Maddock, T. Matsuura, H. Sano and K. Yoshihara), Kodansha, Tokyo and VCH, Weinheim, 1992, pp. 85–104.
28. P. P. Gaspar, S. Konieczny and S. H. Mo, *J. Am. Chem. Soc.*, **106**, 424 (1984).
29. P. Trefonas, R. D. Miller and R. West, *J. Am. Chem. Soc.*, **107**, 2737 (1985).
30. T. Karatsu, R. D. Miller, R. Sooriyakumaran and J. Michl, *J. Am. Chem. Soc.*, **111**, 1140 (1989).
31. A. Watanabe and M. Matsuda, *Macromolecules*, **25**, 484 (1992).
32. A. Watanabe, H. Miike, Y. Tsutsumi and M. Matsuda, *Macromolecules*, **26**, 2111 (1993).
33. M. Kira, T. Miyazawa, S. Koshihara, Y. Segawa and H. Sakurai, *Chem. Lett.*, 3 (1995).
34. M. Kasha, *Discuss. Faraday Soc.*, **9**, 14 (1950).
35. K. Oka and R. Nakao, *Res. Chem. Intermed.*, **13**, 143 (1990).
36. Y. Huang, M. Sulkes and M. J. Fink, *J. Organomet. Chem.*, **499**, 1 (1995).
37. M. Kira, T. Maruyama and H. Sakurai, *Chem. Lett.*, 1345 (1993).
38. G. Bott, P. Marshall, P. E. Wagensteller, Y. Wang and R. T. Conlin, *J. Organomet. Chem.*, **489**, 11 (1995).
39. S. Zhang, M. B. Ezhova and R. T. Conlin, *Organometallics*, **14**, 1471 (1995).
40. M. Ishikawa and M. Kumada, *Adv. Organomet. Chem.*, **19**, 51 (1981).
41. T. J. Drahnak, R. West and J. Michl, *J. Am. Chem. Soc.*, **101**, 5427 (1979).
42. H. Vancik, G. Raabe, M. J. Michalczyk, R. West and J. Michl, *J. Am. Chem. Soc.*, **107**, 4097 (1985).
43. C. W. Carlson, K. J. Haller, X.-H. Zhang and R. West, *J. Am. Chem. Soc.*, **106**, 5521 (1989).
44. B. J. Helmer and R. West, *Organometallics*, **1**, 1458 (1982).
45. H. Watanabe, E. Tabei, M. Goto and Y. Nagai, *J. Chem. Soc., Chem. Commun.*, 522 (1987).
46. H. Shizuka, K. Murata, Y. Arai, K. Tonokura, H. Tanaka, H. Matsumoto, Y. Nagai, G. Gillette and R. West, *J. Chem. Soc., Faraday Trans.*, **85**, 2369 (1989).
47. M. Weidenbruch and S. Pohl, *J. Organomet. Chem.*, **282**, 305 (1985).

48. E. Kroke, S. Willms, M. Weidenbruch, S. Pohl and H. Marsmann, *Tetrahedron Lett.*, **37**, 3675 (1996).
49. E. Kroke, M. Weidenbruch, W. Saak, S. Pohl and H. Marsmann, *Organometallics*, **14**, 5695 (1995).
50. M. Weidenbruch, P. Will, K. Peters, H. G. von Schnering and H. Marsmann, *J. Organomet. Chem.*, **521**, 355 (1996).
51. S. P. Kolesnikov, M. D. Egorov, A. M. Galminas, M. B. Ezhova, O. M. Nefedov, T. V. Leshina, M. B. Taraban, A. I. Kruppa and V. I. Maryasova, *J. Organomet. Chem.*, **391**, C1 (1990).
52. T. J. Barton, W. F. Goure, J. L. Witiak and W. D. Wulff, *J. Organomet. Chem.*, **225**, 87 (1982).
53. K. M. Welsh, J. Michl and R. West, *J. Am. Chem. Soc.*, **110**, 6689 (1988).
54. V. N. Khabashesku, V. Balaji, S. E. Boganov, O. M. Nefedov and J. Michl, *J. Am. Chem. Soc.*, **116**, 320 (1994).
55. M. Veith, E. Werle, R. Lisowsky, R. Koppe and H. Schnoeckel, *Chem. Ber.*, **125**, 1375 (1992).
56. P. Boudjouk, V. Samaraweera, R. Sooriyakumaran, J. Chrusciel and K. R. Anderson, *Angew. Chem., Int. Ed. Engl.*, **27**, 1355 (1988).
57. D. H. Pae, M. Xiao, M. Y. Chiang and P. P. Gaspar, *J. Am. Chem. Soc.*, **113**, 1281 (1991).
58. M. G. Steinmetz and C. Yu, *Organometallics*, **11**, 2686 (1992).
59. (a) K. Oka, T. Dohmaru, Y. Nagai and R. Nakao, *J. Chem. Soc., Chem. Commun.*, 552 (1987). (b) K. Oka, R. Nakao, Y. Nagata and T. Dohmaru, *J. Chem. Soc., Perkin Trans. 2*, 337 (1987).
60. R. Nakao, K. Oka, S. Irie, T. Dohmaru, Y. Abe and T. Horii, *J. Chem. Soc., Perkin Trans. 2*, 755 (1991).
61. R. T. White, R. L. Espino-Rios, D. S. Rogers, M. A. Ring and H. E. O'Neal, *Int. J. Chem. Kinet.*, **17**, 1029 (1985).
62. H. K. Moffat, K. F. Jensen and R. W. Carr, *J. Phys. Chem.*, **95**, 145 (1991).
63. M. A. Ring and H. E. O'Neal, *J. Phys. Chem.*, **96**, 10848 (1992).
64. R. Becerra and R. Walsh, *J. Phys. Chem.*, **96**, 10856 (1992).
65. J. J. O'Brien and G. H. Atkinson, *J. Phys. Chem.*, **92**, 5782 (1988).
66. M. S. Gordon and T. N. Truong, *Chem. Phys. Lett.*, **142**, 110 (1987).
67. I. M. T. Davidson and M. A. Ring, *J. Chem. Soc., Faraday Trans. 1*, **76**, 1520 (1980).
68. B. A. Sawrey, H. E. O'Neal, M. A. Ring and D. Coffey, *Int. J. Chem. Kinet.*, **16**, 31 (1984).
69. S. F. Rickborn, M. A. Ring and H. E. O'Neal, *Int. J. Chem. Kinet.*, **16**, 1371 (1984).
70. S. F. Rickborn, M. A. Ring, H. E. O'Neal and D. Coffey, *Int. J. Chem. Kinet.*, **16**, 289 (1984).
71. B. A. Sawrey, H. E. O'Neal, M. A. Ring and D. Coffey, *Int. J. Chem. Kinet.*, **16**, 801 (1984).
72. B. A. Sawrey, H. E. O'Neal and M. A. Ring, *Organometallics*, **6**, 720 (1987).
73. R. E. Jardine, H. E. O'Neal, M. A. Ring and M. E. Beatie, *J. Phys. Chem.*, **99**, 12507 (1995).
74. S. F. Rickborn, D. S. Rogers, M. A. Ring and H. E. O'Neal, *J. Phys. Chem.*, **90**, 408 (1986).
75. H. E. O'Neal and M. A. Ring, *Organometallics*, **7**, 1017 (1988).
76. T. J. Barton and N. Tillman, *J. Am. Chem. Soc.*, **109**, 6711 (1987).
77. A. P. Dickinson, H. E. O'Neal and M. A. Ring, *Organometallics*, **10**, 3513 (1991).
78. J. A. Boatz and M. S. Gordon, *J. Phys. Chem.*, **93**, 3025 (1989).
79. D. A. Horner, R. S. Grev and H. F. Schaefer III, *J. Am. Chem. Soc.*, **114**, 2093 (1992).
80. N. Al-Rubaiey, H. M. Frey, B. P. Mason, C. McMahon and R. Walsh, *Chem. Phys. Lett.*, **204**, 301 (1993).
81. J. A. Boatz, M. S. Gordon and L. R. Sita, *J. Phys. Chem.*, **94**, 5488 (1990).
82. E. A. Chernyshev, N. G. Komalenkova and S. A. Bashkirova, *J. Organometal. Chem.*, **271**, 129 (1984) and references cited therein.
83. D. Lei and P. P. Gaspar, *Organometallics*, **4**, 1471 (1985).
84. P. P. Gaspar and D. Lei, *Organometallics*, **5**, 1276 (1986).
85. D. Lei, *A Mechanistic Study of the Addition of Silylenes to 1,3-Dienes in Both the Forward and Reverse Directions*, Doctoral Dissertation, Washington University, St. Louis, August 1988.
86. P. J. Skell and E. J. Goldstein, *J. Am. Chem. Soc.*, **86**, 1442 (1964).
87. R. West, in *The Chemistry of Organic Silicon Compounds* (Eds. S. Patai and Z. Rappoport), Chap. 19, Wiley, Chichester, 1989.
88. R. West, in *Comprehensive Organometallic Chemistry II* (Eds. E. W. Abel, F. G. A. Stone and G. Wilkinson), Vol. 2, Chap. 3, Pergamon Press, Oxford, 1995.
89. The familiar Wurtz synthesis of polysilanes from dichlorosilanes and alkali metal evidently does not involve free silylenes. See R. G. Jones, R. E. Benfield, R. H. Cragg, A. C. Swain and S. J. Webb, *Macromolecules*, **26**, 4878 (1993).

90. Reviews: G. Köbrich, *Angew. Chem., Int. Ed. Engl.*, **11**, 473 (1972); A. Maercker, *Angew. Chem., Int. Ed. Engl.*, **32**, 1023 (1993).
91. K. Tamao and A. Kawachi, *Angew. Chem., Int. Ed. Engl.*, **34**, 818 (1995).
92. K. Tamao and A. Kawachi, *Organometallics*, **14**, 3108 (1995).
93. A. Kawachi and K. Tamao, *Organometallics*, **15**, 4653 (1996).
94. Review: K. Tamao and A. Kawachi, *Adv. Organomet. Chem.*, **38**, 1 (1995).
95. Recently, similar experiments have been carried out with Mes_2SiCl_2, t-$BuMesSiCl_2$ and t-$BuPhSiCl_2$. The Si−H insertion product was obtained in all of these cases, although the yields reported were smaller than with t-Bu_2SiCl_2. E. P. Black, Ph.D. Thesis, North Dakota State University, 1995.
96. J. Grobe and T. Scherholt, in *Organosilicon Chemistry II* (Eds. N. Auner and J. Weis), VCH, Weinheim, 1996, pp. 317–319.
97. R. Corriu, G. Lanneau, C. Priou, F. Soulairol, N. Auner, R. Probst, R. Conlin and C. Tan, *J. Organomet. Chem.*, **466**, 55 (1994).
98. R. West and M. Denk, *Pure Appl. Chem.*, **68**, 785 (1996).
99. R. T. Conlin and Y.-W. Kwak, *J. Am. Chem. Soc.*, **108**, 834 (1986).
100. I. M. T. Davidson, S. Ijadi-Maghsoodi, T. J. Barton and N. Tillman, *J. Chem. Soc., Chem. Commun.*, 478 (1984).
101. R. Walsh, *J. Chem. Soc., Chem. Commun.*, 1415 (1982).
102. H. F. Schaefer III, *Acc. Chem. Res.*, **15**, 283 (1982).
103. R. Damrauer, C. H. DePuy, I. M. T. Davidson and K. J. Hughes, *Organometallics*, **5**, 2054 (1986).
104. I. M. T. Davidson and R. J. Scampton, *J. Organometal. Chem.*, **271**, 249 (1984).
105. M. E. Lee, M. A. North and P. P. Gaspar, *Phosphorus, Sulfur, and Silicon*, **56**, 203 (1991).
106. B.-H. Boo and P. P. Gaspar, *Organometallics*, **5**, 698 (1986).
107. D. B. Puranik and M. J. Fink, *J. Am. Chem. Soc.*, **111**, 5951 (1989).
108. G. Inoue and M. Suzuki, *Chem. Phys. Lett.*, **122**, 361 (1985).
109. J. M. Jasinski, *J. Phys. Chem.*, **90**, 555 (1986).
110. M. Weidenbruch, H. Piel, A. Lesch, K. Peters and H. G. von Schnering, *J. Organometal. Chem.*, **454**, 35 (1993).
111. K. Oka and R. Nakao, *J. Organometal. Chem.*, **390**, 7 (1990).
112. L. M. Raff, I. Noorbatcha and D. L. Thompson, *J. Chem. Phys.*, **85**, 3623 (1986).
113. J. M. Jasinski, *J. Chem. Phys.*, **86**, 3057 (1986).
114. L. M. Raff and D. L. Thompson, *J. Chem. Phys.*, **86**, 3059 (1986).
115. G. R. Gillette, G. H. Noren and R. West, *Organometallics*, **8**, 487 (1989).
116. M. Weidenbruch, H. Piel, K. Peters and H. G. von Schnering, *Organometallics*, **13**, 3990 (1994).
117. M. Weidenbruch, H. Piel, K. Peters and H. G. von Schnering, *Organometallics*, **12**, 2881 (1993).
118. F. Huppmann, W. Maringgele, T. Kottke and A. Meller, *J. Organometal. Chem.*, **434**, 35 (1992).
119. F. Huppmann, M. Noltemeyer and A. Meller, *J. Organometal. Chem.*, **483**, 217 (1994).
120. P. Zhu, M. Piserchio and F. W. Lampe, *J. Phys. Chem.*, **89**, 5344 (1985).
121. D. H. Berry and Q. Jiang, *J. Am. Chem. Soc.*, **109**, 6210 (1987).
122. S. Konieczny, K. Wrzesich and W. Wojnowski, *J. Organometal. Chem.*, **446**, 73 (1994).
123. S. Wu, G. Wu, F. Tao and Z. Lin, *Kexue Tongbao*, **31**, 1365 (1986).
124. N. Tokitoh, H. Suzuki and R. Okazaki, *J. Chem. Soc., Chem. Commun.*, 125 (1996).
125. P. L. Timms, *Chem. Soc. Rev.*, **25**, 93 (1996).
126. S. B. Church, C. G. Davies, R. Lümen, P. A. Mounier, G. Saint and P. L. Timms, *J. Chem. Soc., Dalton Trans.*, 227 (1996).
127. P. P. Gaspar and G. S. Hammond, in *Carbenes*, Vol. II (Eds. R. A. Moss and M. Jones, Jr.), Wiley, New York, 1975, pp. 207–362.
128. M. T. Nguyen, D. Sengupta and L. G. Vanquickenborne, *Chem. Phys. Lett.*, **240**, 513 (1995).
129. D. S. Rogers, K. L. Walker, M. A. Ring and H. E. O'Neal, *Organometallics*, **6**, 2313 (1987).
130. S.-H. Wu, F. Xiao and Y. Li, *Sci. China (Ser B)*, **33**, 129 (1990).
131. W. Ando, M. Fujita, H. Yoshida and A. Sekiguchi, *J. Am. Chem. Soc.*, **110**, 3310 (1988).
132. S. Zhang, P. E. Wagenseller and R. T. Conlin, *J. Am. Chem. Soc.*, **113**, 4278 (1991).
133. W. R. Winchester and P. P. Gaspar, unpublished results presented at the 30th Symposium on Organosilicon Chemistry, London, Ontario, May 30–31, 1997, Abstract A-16.
134. Y. Apeloig, unpublished results presented at the 30th Symposium on Organosilicon Chemistry, London, Ontario, May 30–31, 1997, Abstract C-4.

135. M. P. Egorov, M. B. Ezhova, S. P. Kolesnikov, O. M. Nefedov, M. B. Taraban, A. I. Kruppa and T. V. Leshina, *Mendeleev Commun.*, **4**, 143 (1991).
136. D. Lei and P. P. Gaspar, *J. Chem. Soc., Chem. Commun.*, 1149 (1985).
137. (a) H. Sakurai, Y. Kobayashi and Y. Nakadaira, *Chem. Lett.*, 1197 (1983).
     (b) H. Appler and W. P. Neumann, *J. Organometal. Chem.*, **314**, 261 (1986).
138. D. Lei and P. P. Gaspar, *Res. Chem. Intermed.*, **12**, 103 (1989).
139. S. Zhang and R. T. Conlin, *J. Am. Chem. Soc.*, **113**, 4272 (1991).
140. K. L. Bobbitt and P. P. Gaspar, *J. Organometal. Chem.*, **499**, 17 (1995).
141. K. L. Bobbitt, *Photochemical Generation of Germylenes and Silylenes: Mechanism of Germylene and Silylene Addition to 1,3-Dienes*, Doctoral Dissertation, Washington University, St. Louis, December 1990.
142. G. R. Gillette, G. H. Noren and R. West, *Organometallics*, **6**, 2617 (1987).
143. W. Ando, A. Sekiguchi, K. Hagiwara, A. Sakakibara and H. Yoshida, *Organometallics*, **7**, 558 (1988).
144. W. Ando, K. Hagiwara and A. Sekiguchi, *Organometallics*, **6**, 2270 (1987).
145. N. Takeda, H. Suzuki, N. Tokitoh, R. Okazaki and S. Nagase, *J. Am. Chem. Soc.*, **119**, 1456 (1997).
146. M. Weidenbruch, B. Brandt-Roth, S. Pohl and W. Saak, *Angew. Chem., Int. Ed. Engl.*, **29**, 90 (1990); *Polyhedron*, **10**, 1147 (1991).
147. M. Weidenbruch, B. Brand-Roth, S. Pohl and W. Saak, *J. Organometal. Chem.*, **379**, 217 (1989).
148. M. Denk, R. K. Hayashi and R. West, *J. Am. Chem. Soc.*, **116**, 10813 (1994).
149. M. Denk, R. K. Hayashi and R. West, *J. Chem. Soc., Chem. Commun.*, 33 (1994).
150. T. Dohmaru and F. W. Lampe, *J. Photochem. Photobiol., A*, **41**, 275 (1988).
151. T. Akasaka, S. Nagase, A. Yabe and W. Ando, *J. Am. Chem. Soc.*, **110**, 6270 (1988).
152. S. Nagase, T. Kudo, T. Akasaka and W. Ando, *Chem. Phys. Lett.*, **163**, 23 (1989).
153. A. Patyk, W. Sander, J. Gauss and D. Cremer, *Chem. Ber.*, **123**, 89 (1990).
154. A. C. Stanton, A. Freedman, J. Wormhoudt and P. P. Gaspar, *Chem. Phys. Lett.*, **122**, 190 (1985).
155. C. A. Arrington, J. T. Petty, S. E. Payne and W. C. K. Haskins, *J. Am. Chem. Soc.*, **110**, 6240 (1988).
156. M.-A. Pearsall and R. West, *J. Am. Chem. Soc.*, **110**, 7228 (1988).
157. W. Ando, *Pure Appl. Chem.*, **67**, 805 (1995).
158. T. Yamamoto, Y. Kabe and W. Ando, *Organometallics*, **12**, 1996 (1993).
159. M. Weidenbruch, A. Schäfer, K. Peters and H. G. von Schnering, *J. Organometal. Chem.*, **314**, 25 (1986).
160. M. Weidenbruch, B. Flintjer, S. Pohl and W. Saak, *Angew. Chem., Int. Ed., Engl.*, **28**, 95 (1989).
161. A. Schäfer, M. Weidenbruch, W. Saak and S. Pohl, *Angew. Chem., Int. Ed., Engl.*, **26**, 776 (1987).
162. A. Sakakibara, Y. Kabe, T. Shimizu and W. Ando, *J. Chem. Soc., Chem. Commun.*, 43 (1991).
163. P. Paetzold, D. Hahnfeld, U. Englert, W. Wojnowski, B. Dreczewski, Z. Pawelec and L. Walz, *Chem. Ber.*, **125**, 1073 (1992).
164. P. Boudjouk, E. Black and R. Kumarathasan, *Organometallics*, **10**, 2095 (1991).
165. M. Weidenbruch, E. Kroke, H. Marsmann, S. Pohl and W. Saak, *J. Chem. Soc., Chem. Commun.*, 1233 (1994).
166. H. Suzuki, N. Tokitoh and R. Okazaki, *J. Am. Chem. Soc.*, **116**, 11572 (1994).
167. A. Sekiguchi and R. West, *Organometallics*, **5**, 1911 (1986).
168. G. Maier, H. P. Reisenauer, K. Schöttler and U. Wessolek-Kraus, *J. Organometal. Chem.*, **366**, 25 (1989).
169. J. Heinicke and B. Gerhus, *Heteroatom Chem.*, **6**, 461 (1995).
170. M. Weidenbruch, A. Lesch and K. Peters, *J. Organometal. Chem.*, **407**, 31 (1991).
171. K. Peters, E. M. Peters, H. G. von Schnering, H. Piel and M. Weidenbruch, *Z. Kristallogr.*, **209**, 611 (1994).
172. M. Weidenbruch, P. Will, K. Peters, H. G. von Schnering and H. Marsmann, *J. Organometal. Chem.*, **521**, 355 (1996).
173. M. Weidenbruch, A. Schäfer and H. Marsmann, *J. Organometal. Chem.*, **354**, C12 (1988).
174. M. Weidenbruch, A. Lesch and H. Marsmann, *J. Organometal. Chem.*, **385**, C47 (1990).
175. T. Akasaka and W. Ando, *J. Am. Chem. Soc.*, **115**, 1605 (1993).
176. T. Akasaka, E. Mitsuhida, W. Ando, K. Kobayashi and S. Nagase, *J. Chem. Soc., Chem. Commun.*, 1529 (1995).
177. R. T. Conlin and P. P. Gaspar, *J. Am. Chem. Soc.*, **98**, 868 (1976).

178. Y. Nakadaira, T. Kobayashi, T. Otsuka and H. Sakurai, *J. Am. Chem. Soc.*, **101**, 486 (1979).
179. M. J. Michalczyk, M. J. Fink, D. J. DeYoung, C. W. Carlson, K. M. Welsh and R. West, *Silicon, Germanium, Tin and Lead Compounds*, **9**, 75 (1986).
180. R. West, M. J. Fink and J. Michl, *Science (Washington, D.C.)*, **214**, 1343 (1981).
181. R. Okazaki and R. West, *Adv. Organomet. Chem.*, **39**, 231 (1996).
182. H. B. Yokelson, D. A. Siegel, A. J. Millevolte, J. Maxka and R. West, *Organometallics*, **9**, 1005 (1990).
183. M. Yamaji, K. Hamanishi, T. Takahashi and H. Shizuka, *J. Photochem. Photobiol., A*, **81**, 1 (1994).
184. R. T. Conlin, J. C. Netto-Ferreira, S. Zhang and J. C. Scaiano, *Organometallics*, **9**, 1332 (1990).
185. (a) S. Masamune, Y. Eriyama and T. Kawase, *Angew. Chem., Int. Ed. Engl.*, **26**, 584 (1989).
(b) S. Masamune, S. Murakami, H. Tobita and D. J. Williams, *J. Am. Chem. Soc.*, **105**, 7776 (1983).
186. Y. Apeloig, D. Bravo-Zhivotovskii, I. Zharov, V. Panov, W. J. Leigh and G. W. Sluggett, *J. Am. Chem. Soc.*, **120**, 1398 (1998).
187. H. Suzuki, N. Tokitoh and R. Okazaki, *Bull. Chem. Soc. Jpn.*, **68**, 2471 (1995).
188. H. Spitzner and R. West, unpublished results.
189. W. D. Wulff, W. F. Goure and T. J. Barton, *J. Am. Chem. Soc.*, **100**, 6236 (1978).
190. H. Sakurai, Y. Nakadaira and H. Sakaba, *Organometallics*, **2**, 1484 (1983).
191. I. M. T. Davidson and G. H. Morgan, *Organometallics*, **12**, 289 (1993).
192. A. P. Dickenson, K. E. Nares, M. A. Ring and H. E. O'Neal, *Organometallics*, **6**, 2596 (1987).
193. L. Linder, A. Revis and T. J. Barton, *J. Am. Chem. Soc.*, **108**, 2742 (1986).
194. T. J. Barton and G. P. Hussmann, *J. Am. Chem. Soc.*, **107**, 7581 (1985).
195. M. J. Fink, D. B. Puranik and P. Johnson, *J. Am. Chem. Soc.*, **110**, 1315 (1988).
196. D. Lei, Y.-S. Chen, B. H. Boo, J. Frueh, D. L. Svoboda and P. P. Gaspar, *Organometallics*, **11**, 559 (1992).
197. V. N. Khabashesku, V. Balaji, S. E. Boganov, S. A. Bashkirova, P. M. Matveichev, E. A. Chernyshev, O. M. Nefedov and J. Michl, *Mendeleev Commun.*, 38 (1992).
198. C. M. Van Zoeren, J. W. Thoman, Jr., J. I. Steinfeld and M. W. Rainbird, *J. Phys. Chem.*, **92**, 9 (1988).
199. R. I. McKay, I. S. Uichanco, A. J. Bradley, J. R. Holdsworth, J. S. Francisco, J. I. Steinfeld and A. E. W. Knight, *J. Chem. Phys.*, **95**, 1688 (1991).
200. K. K. Baldridge, J. A. Boatz, S. Koseki and M. S. Gordon, *Annu. Rev. Phys. Chem.*, **38**, 211 (1987).
201. Y. Apeloig, in *The Chemistry of Organic Silicon Compounds*, Vol. 1 (Eds. S. Patai and Z. Rappoport), Wiley, New York, 1989, p. 57.
202. R. S. Grev, *Adv. Organometal. Chem.*, **33**, 125 (1991).
203. W. Kutzelnigg, *Angew. Chem., Int. Ed. Engl.*, **23**, 272 (1984).
204. S. K. Shin, W. A. Goddard III and J. L. Beauchamp, *J. Chem. Phys.*, **93**, 4986 (1990).
205. S. K. Shin, W. A. Goddard III and J. L. Beauchamp, *J. Phys. Chem.*, **94**, 6963 (1990).
206. R. S. Grev, H. F. Schaefer III and P. P. Gaspar, *J. Am. Chem. Soc.*, **113**, 5638 (1991).
207. P. P. Gaspar, A. M. Beatty, T. Chen, T. Haile, W. T. Klooster, T. F. Koetzle, D. Lei, T. S. Lin and W. R. Winchester, unpublished results presented at the 30th Symposium on Organosilicon Chemistry, London, Ontario, May 30–31, 1997, Abstract A-16.
208. J. Kalcher and A. F. Sax, *J. Mol. Struct. (Theochem)*, **253**, 287 (1992).
209. C. J. Cremer, F. J. Dulles, J. W. Storer and S. E. Worthington, *Chem. Phys. Lett.*, **218**, 387 (1994).
210. Y. Apeloig, Private communication.
211. S. K. Shin, K. K. Irikura, J. L. Beauchamp and W. A. Goddard, III, *J. Am. Chem. Soc.*, **110**, 24 (1988).
212. R. S. Grev, G. E. Scuseria, A. C. Scheiner, H. F. Schaefer, III and M. S. Gordon, *J. Am. Chem. Soc.*, **110**, 7337 (1988).
213. J. A. Boatz and M. S. Gordon, *J. Phys. Chem.*, **94**, 7331 (1990).
214. M. S. Gordon and J. A. Boatz, *Organometallics*, **8**, 1978 (1989).
215. G. Trinquier, *J. Am. Chem. Soc.*, **112**, 2130 (1990).
216. K. G. Dyall, *J. Chem. Phys.*, **96**, 1210 (1992).
217. P. Ho and C. F. Melius, *J. Phys. Chem.*, **94**, 5120 (1990).
218. L. Nyulászi, T. Kárpáti and T. Veszprémi, *J. Am. Chem. Soc.*, **116**, 7239 (1994).

219. T. Veszprémi, L. Nyulászi and T. Kárpáti, *J. Phys. Chem.*, **100**, 6262 (1996).
220. K. Kobayashi and S. Nagase, *Organometallics*, **16**, 2489 (1997).
221. S.-z. Li, D. Moncrieff, J.-g Zhao and F. B. Brown, *Chem. Phys. Lett.*, **151**, 403 (1988).
222. W. Gabriel, P. Rosmus, K. Yamashita and K. Morokuma, *Chem. Phys.*, **174**, 45 (1993).
223. M. Spoliti, F. Ramondo, L. Bencivenni, P. Kolandaivel and R. Kumaresann, *J. Mol. Struct. (Theochem)*, **283**, 73 (1993).
224. M. Denk, J. C. Green, N. Metzler and M. Wagner, *J. Chem. Soc., Dalton Trans.*, 2405 (1994).
225. A. J. Arduengo, III, H. Bock, H. Chen, M. Denk, D. A. Dixon, J. C. Green, W. A. Herrmann, N. L. Jones, M. Wagner and R. West, *J. Am. Chem. Soc.*, **116**, 6641 (1994).
226. Y. Apeloig, M. Karni, R. West and K. Welsh, *J. Am. Chem. Soc.*, **116**, 9719 (1994).
227. S. C. Wright, D. L. Cooper, M. Sironi, M. Raimondi and J. Garratt, *J. Chem. Soc., Perkin Trans. 2*, 369 (1990).
228. J. D. Watts, G. W. Trucks and R. J. Bartlett, *Chem. Phys. Lett.*, **164**, 502 (1989).
229. J. Cioslowski, T. Hamilton, G. Scuseria, B. A. Hess, Jr., J. Hu, L. J. Schaad and M. Dupuis, *J. Am. Chem. Soc.*, **112**, 4183 (1990).
230. J. D. Watts and R. J. Bartlett, *J. Chem. Phys.*, **101**, 3073 (1994).
231. J.-M. Langlois, R. P. Muller, T. R. Coley, W. A. Goddard III, M. N. Ringnalda, Y. Won and R. A. Friesner, *J. Chem. Phys.*, **92**, 7488 (1990).
232. B. H. Greeley, T. V. Russo, D. T. Mainz, J.-M Langlois, W. A. Goddard III, R. E. Donnelly, Jr. and M. N. Ringnalda, *J. Chem. Phys.*, **101**, 4028 (1994).
233. M. Jezercak, P. M. Agrawal, D. L. Thompson and L. M. Raff, *J. Chem. Phys.*, **90**, 3363 (1989).
234. P. M. Agrawal, D. L. Thompson and L. M. Raff, *Surf. Sci.*, **195**, 283 (1988).
235. H. W. Schranz, L. M. Raff and D. L. Thompson, *J. Chem. Phys.*, **94**, 4219 (1991).
236. S. Błoński, A. Herman and S. Konieczny, *Spectrochim. Acta*, **45A**, 747 (1989).
237. A. Herman, *Chem. Phys.*, **122**, 53 (1988).
238. J. S. Tse, *J. Chem. Soc., Chem. Commun.*, 1179 (1990).
239. R. Köppe and H. Schnöckel, *Z. Anorg. Allg. Chem.*, **607**, 41 (1992).
240. C. Gonzales, H. B. Schlegel and J. S. Francisco, *Mol. Phys.*, **66**, 859 (1989).
241. R. D. Bach, M.-D. Su, E. Aldebagh, J. L. Andrés and H. B. Schlegel, *J. Am. Chem. Soc.*, **115**, 10237 (1993).
242. J. S. Francisco, *Mol. Phys.*, **73**, 235 (1991).
243. D. R. Gano, M. S. Gordon and J. A. Boatz, *J. Am. Chem. Soc.*, **113**, 6711 (1991).
244. R. Becerra, H. M. Frey, B. P. Mason, R. Walsh and M. S. Gordon, *J. Am. Chem. Soc.*, **114**, 2751 (1992).
245. S. Y. Lee and B. H. Boo, *J. Mol. Struct.*, 79 (1996).
246. P. Y. Ayala and H. B. Schlegel, *Chem. Phys. Lett.*, **225**, 410 (1994).
247. For a review see:
    (a) Y. Apeloig, M. Karni and T. Müller, in *Organosilicon Chemsitry II. From Molecules to Materials*, (Eds. N. Auner and J. Weis), VCH, Weinheim, 1996, pp. 263–288).
    (b) Y. Apeloig and T. Müller, *J. Am. Chem. Soc.*, **117**, 5363 (1995).
    (c) Y. Apeloig, in *Heteroatom Chemistry: ICHAC-2*. (Ed. E. Block), VCH, New York, 1990, pp. 27–46.
    (d) Maxka and Y. Apeloig, *J. Chem. Soc., Chem. Commun.*, 737 (1990).
248. A. Tachibana, Y. Kurosaki, K. Yamaguchi and T. Yamabe, *J. Phys. Chem.*, **95**, 6849 (1991).
249. T. P. Hamilton and H. F. Schaefer III, *J. Chem. Phys.*, **90**, 1031 (1989).
250. I. I. Zhakharov and G. M. Zhidomirov, *React. Kinet. Catal. Lett.*, **41**, 59 (1990).
251. T. R. Cundari and M. S. Gordon, *J. Phys. Chem.*, **96**, 631 (1992).
252. C. Winter and P. Millie, *Chem. Phys.*, **174**, 177 (1993).
253. For a review see O. M. Nefedov, M. P. Egorov, A. I. Ioffe, C. G. Menchikov, P. S. Zuev, V. L. Minikin, B. V. Simkin and M. N. Glukhovtsev, *Pure Appl. Chem.*, **64**, 265 (1992).
254. H. Vancik, G. Raabe, M. J. Michalczyk, R. West and J. Michl, *J. Am. Chem. Soc.*, **107**, 4097 (1985).
255. I. Dubois, *Can. J. Phys.*, **46**, 2485 (1968).
256. D. E. Milligan and M. E. Jacox, *J. Chem. Phys.*, **52**, 2594 (1970).
257. (a) G. Levin, P. K. Das, C. Bilgren and C. L. Lee, *Organometallics*, **8**, 1206 (1989).
    (b) G. Levin, P. K. Das and C. L. Lee, *Organometallics*, **7**, 1231 (1988).
258. H. Shizuka, H. Tanaka, K. Tonokura, K. Murata, H. Hiratsuka, J. Ohshita and M. Ishikawa, *Chem. Phys. Lett.*, **143**, 225 (1988).

259. M. Yamaji, K. Hamanishi, T. Takahashi and H. Shizuka, *J. Photochem. Photobiol., A*, **81**, 1 (1994).
260. P. P. Gaspar, D. Holten, S. Konieczny and J. Y. Corey, *Acc. Chem. Res.*, **20**, 329 (1987).
261. Y. Apeloig and M. Karni, *J. Chem. Soc., Chem. Commun.*, 1048 (1985).
262. An early inorganic example of a silylene complex is HSiOH−OH_2, obtained by the reaction of silicon atoms with water. See Z. K. Ismail, R. M. Hauge, L. Fredin, J. W. Kauffman and J. L. Margrave, *J. Chem. Phys.*, **77**, 1617 (1982).
263. G. Trinquier, *J. Chem. Soc., Faraday Trans.*, **89**, 775 (1993).
264. K. P. Steele and W. P. Weber, *J. Am. Chem. Soc.*, **102**, 6095 (1980).
265. M. Kira, T. Maruyama and H. Sakurai, *Tetrahedron Lett.*, **33**, 243 (1992).
266. K. Raghavachari, J. Chandrashekar, M. S. Gordon and K. J. Dykema, *J. Am. Chem. Soc.*, **106**, 5853 (1984).
267. For a theoretical study of amine–silylene donor–acceptor bonding, see R. T. Conlin, D. Laasko and P. Marshall, *Organometallics*, **13**, 838 (1994).
268. T. Akasaka, W. Ando, S. Nagase and A. Yabe, *Nippon Kagaku Kaishi*, 1440 (1989).
269. G. Maier, H. D. Reisenauer and H. Pacl, *Angew. Chem., Int. Ed. Engl.*, **33**, 1248 (1994).
270. H. P. Reisenauer, G. Mihm and G. Maier, *Angew. Chem., Int. Ed. Engl.*, **21**, 854 (1982).
271. G. Maier, G. Mihm, H. P. Reisenauer and D. L. Littman, *Chem. Ber.*, **117**, 2369 (1984).
272. G. Maier, S. Glatthaar and H. P. Reisenauer, *Chem. Ber.*, **122**, 2403 (1989).
273. B. D. Ruzsicska, A. Jodhan, I. Safarik, O. P. Strausz and T. N. Bell, *Chem. Phys. Lett.*, **113**, 67 (1985).
274. J. A. Dagata, D. W. Squire, C. S. Dulcey, D. S. Y. Hsu and M. C. Lin, *Chem. Phys. Lett.*, **134**, 151 (1987).
275. S. G. Bott, P. Marshall, P. E. Wagenseller, Y. Wang and R. T. Conlin, *J. Organometal. Chem.*, **499**, 11 (1995).
276. B. D. Helmer and R. West, *Organometallics*, **1**, 1463 (1982).
277. M. J. Fink and D. B. Puranik, *Organometallics*, **6**, 1809 (1987).
278. G. R. Gillette, G. Noren and R. West, *Organometallics*, **9**, 2925 (1990).
279. T. Goto, *Mater. Res. Soc. Symp. Proc.*, **297**, 3 (1993).
280. G. H. Atkinson and J. J. O'Brien, *Prepr. Pap., Am. Chem. Soc., Div. Fuel Chem.*, **34**, 483 (1989).
281. K. Tachibana, T. Shirafuji and Y. Matsui, *Jpn. J. Appl. Phys.*, **31**, 2588 (1992).
282. M. W. Markus and P. Roth, *J. Quantum. Spectrosc. Radiat. Transfer*, **52**, 783 (1994).
283. G. Inoue and M. Suzuki, *Chem. Phys. Lett.*, **105**, 641 (1984).
284. D. M. Rayner, R. P. Steer, P. A. Hackett, C. L. Wilson and P. John, *Chem. Phys. Lett.*, **123**, 449 (1986).
285. J. W. Thoman, Jr., J. I. Steinfeld, R. I. McKay and A. E. W. Knight, *J. Chem. Phys.*, **86**, 5909 (1987).
286. E. Borsella and R. Pantoni, *Chem. Phys. Lett.*, **150**, 544 (1988).
287. M. Fukushima, S. Mayama and K. Obi, *J. Chem. Phys.*, **96**, 44 (1992).
288. M. Fukushima and K. Obi, *J. Chem. Phys.*, **100**, 6221 (1994).
289. H. Ishikawa and O. Kajimoto, *J. Phys. Chem.*, **98**, 122 (1994).
290. K. Obi, M. Fukushima and K. Saito, *Appl. Surf. Sci.*, **79/80**, 465 (1994).
291. A. Kono, N. Koike, K. Okuda and T. Goto, *Jpn. J. Appl. Phys.*, **32**, L543 (1993).
292. A. Kono, N. Koike, H. Nomura and T. Goto, *Jpn. J. Appl. Phys.*, **34**, 307 (1995).
293. H. J. Mick, Y. N. Smirnov and P. Roth, *Ber. Bunsenges. Phys. Chem.*, **97**, 793 (1993).
294. H. Ishikawa and O. Kajimoto, *J. Mol. Spectrosc.*, **150**, 610 (1991).
295. H. Ishikawa and O. Kajimoto, *J. Mol. Spectrosc.*, **160**, 1 (1993).
296. C. Yamada, H. Kanamori, E. Hirota, N. Nishiwaki, N. Itabashi, K. Kato and T. Goto, *J. Chem. Phys.*, **91**, 4582 (1989).
297. W. Gabriel and P. Rosmus, *J. Phys. Chem.*, **97**, 12644 (1993).
298. R. M. Robertson and M. J. Rossi, *J. Chem. Phys.*, **91**, 5037 (1989).
299. J. Berkowitz, J. P. Greene, H. Cho and B. Ruscic, *J. Chem. Phys.*, **86**, 1235 (1987).
300. J. Berkowitz, *Acc. Chem. Res.*, **22**, 413 (1989).
301. P. Fons, T. Motooka, K. Awazu and H. Onuki, *Appl. Surf. Sci.*, **79**, 476 (1994).
302. B. E. Turner, *Astrochemistry of Cosmic Phenomena* (Ed. P. D. Singh), I. A. U., Amsterdam, 1992, pp. 181–186.
303. T. C. McInnis and L. Andrews, *J. Phys. Chem.*, **96**, 5276 (1992).
304. H. U. Lee and J. P. deNeufville, *Chem. Phys. Lett.*, **99**, 394 (1983).

305. T. Suzuki, K. Hakuta, S. Saito and E. Hirota, *J. Chem. Phys.*, **82**, 3580 (1985).
306. R. N. Dixon and N. G. Wright, *Chem. Phys. Lett.*, **117**, 280 (1985).
307. T. Suzuki and E. Hirota, *J. Chem. Phys.*, **85**, 5541 (1986).
308. A. C. Stanton, A. Freedman, J. Wormhoudt and P. P. Gaspar, *Chem. Phys. Lett.*, **122**, 190 (1985).
309. J. S. Horwitz, C. S. Dulcey and M. C. Lin, *Chem. Phys. Lett.*, **150**, 165 (1988).
310. M. Suzuki, N. Washida and G. Inoue, *Chem. Phys. Lett.*, **131**, 24 (1986).
311. R. C. Sausa and A. M. Ronn, *Chem. Phys.*, **96**, 183 (1985).
312. N. Washida, Y. Matsumi, T. Hayashi, T. Ibuki, A. Hiraya and K. Shobatake, *J. Chem. Phys.*, **83**, 2769 (1985).
313. J. T. Hougen, *J. Mol. Spectrosc.*, **138**, 251 (1989).
314. J. Carolczak and D. J. Clouthier, *Chem. Phys. Lett.*, **201**, 409 (1993).
315. M. Tanimoto, H. Takeo, C. Matsumura, M. Fujitake and E. Hirota, *J. Chem. Phys.*, **91**, 2102 (1989).
316. H. Sekiya, Y. Nishimura and M. Tsuji, *Chem. Phys. Lett.*, **176**, 477 (1991).
317. H. Bock, M. Kremer, M. Dolg and H.-W. Preuss, *Angew. Chem., Int. Ed. Engl.*, **30**, 1186 (1991).
318. G. Raabe, H. Vancik, R. West and J. Michl, *J. Am. Chem. Soc.*, **108**, 671 (1986).
319. Y. Peng, S. N. Vogel and J. E. Carlstrom, *Astrophys. J.*, **455**, 223 (1995).
320. J. Chernicharo, V. Bujarrabul and R. Lucas, *Astron. Astrophys.*, **249**, L27 (1991).
321. E. Bouisset, J. M. Esteva, R. C. Karnatak, J. P. Connersde, A. M. Flank and P. Lagarde, *J. Phys. B*, **34**, 1609 (1991).
322. J. M. Jasinski, R. Becerra and R. Walsh, *Chem. Rev.*, **95**, 1203 (1995).
323. R. Becerra and R. Walsh, in *Research in Chemical Kinetics* (Eds. R. G. Compton and G. Hancock), Vol. 3, Elsevier Science, Amsterdam, 1995, p. 263.
324. K. N. Houk, N. G. Rondan and J. Mareda, *Tetrahedron*, **41**, 1555 (1985).
325. R. Becerra, H. M. Frey, B. P. Mason, R. Walsh and M. S. Gordon, *J. Chem. Soc., Faraday Trans.*, **91**, 2723 (1995).
326. R. Walsh, *Organometallics*, **8**, 1973 (1989).
327. I. Safarik, V. Sandhu, E. M. Lown, O. P. Strausz and T. N. Bell, *Res. Chem. Intermed.*, **14**, 105 (1990).
328. M. Ishikawa, K.-L. Nakagawa, R. Enokida and M. Kumada, *J. Organometal. Chem.*, **201**, 151 (1980).
329. J. A. Hawari, M. Lesage, D. Griller and W. P. Weber., *Organometallics*, **6**, 880 (1987).
330. C. Zybill, H. Handwerker and H. Friedrich, *Adv. Organometal. Chem.*, **36**, 229 (1994).
331. C. Zybill and C. Liu, *Synlett.*, 687 (1995).
332. C. Zybill, *Top. Curr. Chem.*, 160 (1991).
333. T. D. Tilley, in *The Silicon–Heteroatom Bond* (Eds. S. Patai and Z. Rappoport), Wiley, New York, 1991, p. 309.
334. T. D. Tilley, in *The Chemistry of Organic Silicon Compounds* (Eds. S. Patai and Z. Rappoport), Chap. 24, Wiley, Chichester, 1989, p. 1415.
335. T. Carré, G. Cerrau, C. Chuit, R. J. P. Corriu and C. Réyé, *Angew. Chem., Int. Ed. Engl.*, **28**, 489 (1989).
336. H. Handwerker, C. Leis, R. Probsty, P. Bissinger, A. Grohmann, P. Kiprof, E. Herdtweck, J. Bümel, N. Auner and C. Zybill, *Organometallics*, **12**, 2162 (1993).
337. S. O. Grumbine, T. D. Tilley and A. L. Rheingold, *J. Am. Chem. Soc.*, **115**, 358 (1993).
338. N. Ogino and H. Tobita, *Adv. Organometal. Chem.*, **42**, 223 (1998).
339. K. Triplett and M. D. Curtis, *J. Am. Chem. Soc.*, **97**, 5747 (1975).
340. W. A. Herrmann, *Adv. Organomet. Chem.*, **20**, 159 (1982).
341. C. Morterra and M. J. D. Low, *J. Phys. Chem.* **73**, 321, 327 (1989).
342. C. Morterra and M. J. D. Low, *Ann. N. Y. Acad. Sci.*, **220**, 173 (1973).
343. M. J. D. Low, Y. E. Rhodes and P. O. Orphanos, *J. Catal.*, **40**, 236 (1975).
344. V. A. Radzig, *Colloid Surf: A: Physicochem. Eng. Aspects*, **74**, 91 (1993).
345. V. A. Radzig, E. G. Baskis and V. A. Karobeu, *Kinet. Catal.*, **36**, 142, 568 (1995).
346. V. A. Radzig, *Kinet. Catal.*, **37**, 310, 418 (1996).
347. A. A. Bobyshev and V. A. Radzig, *Khim. Fiz.*, **7**, 950 (1988).
348. Yu. V. Razskazovskii, M. V. Roginskaya and M. Ya. Mel'nikov, *J. Organometal. Chem.*, **486**, 249 (1995).
349. M. V. Roginskaya, Yu. V. Razskazovskii and M. Ya. Mel'nikov, *Kinet. Catal.*, **33**, 521 (1992).
350. Free-radical sites are also formed by breaking of Si–O bonds, but evidently these are far less abundant than silylene centers.

351. V. A. Radzig and A. V. Bystrikov, *Kinet. Catal.*, **19**, 713 (1978).
352. E. G. Rochow, *Silicon and Silicones*, Springer, Berlin, 1987.
353. M. P. Clarke, *J. Organomet. Chem.*, **376**, 165 (1989).
354. M. P. Clarke and I. M. T. Davidson, *J. Organomet. Chem.*, **408**, 149 (1991).
355. K. M. Lewis, D. McLeod, B. Kanner, J. L. Falconer and T. Frank, in *Studies in Organic Chemistry 49. Catalyzed Direct Reactions at Silicon* (Eds. K. M. Lewis and D. S. Rethwisch), Elsevier, Amsterdam, 1993, pp. 333–340.
356. Y. Ono, M. Okano, N. Watanabe and E. Suzuki, in *Silicon for the Chemical Industry II* (Eds. H. A. Oye, H. M. Rong, L. Nygard, G. Schuessler and J. K. Tuset), Tapir Forlag, Trøndheim, Norway, 1994, pp. 185–186.
357. M. Okamoto, E. Suzuki and Y. Ono, *J. Catal.*, **145**, 537 (1994).
358. M. Okamoto, N. Watanabe, E. Suzuki and Y. Ono, *J. Organometal. Chem.*, **515**, 51 (1996).
359. M. Okamoto, N. Watanabe, E. Suzuki and Y. Ono, *J. Organometal. Chem.*, **489**, C12 (1995).
360. (a) P. Jutzi, D. Kanne and C. Krüger, *Angew. Chem., Int. Ed. Engl.*, **25**, 164 (1986).
     (b) P. Jutzi, U. Holtmann, D. Kanne, C. Krüger, R. Blom, R. Gleiter and I. Hyla-Krispin, *Chem. Ber.*, **122**, 1629 (1989).
361. (a) P. Jutzi, in *Organosilicon Chemistry: From Molecules to Materials* (Eds. N. Auner and J. Weis), VCH, Weinheim, 1994, pp. 87–92.
     (b) P. Jutzi, D. Eikenberg, B. Neumann and H. G. Stammler, *Organometallics*, **15**, 3659 (1998) and references cited therein.
     (c) M. Tacke, C. H. Klein, D. J. Stafkens, A. Oskam, P. Jutzi and E. A. Bunte, *Z. Anorg. Allg. Chem.*, **619**, 865 (1993).
362. H. M. Karsch, U. Keller, S. Gamper and G. Müller, *Angew. Chem., Int. Ed. Engl.*, **29**, 295 (1990).
363. D. H. Harris and M. F. Lappert, *J. Chem. Soc., Chem. Commun.*, 895 (1974).
364. M. S. J. Gyname, D. H. Harris, M. E. Lappert, P. P. Power, P. Riviere and M. Riviere-Baudet, *J. Chem. Soc., Dalton Trans.*, 2004 (1977).
365. D. H. Harris, M. F. Lappert, J. B. Pedley and G. J. Sharp, *J. Chem. Soc., Dalton Trans.*, 945 (1976).
366. A. J. Arduengo III, H. V. Rasika Dias, R. L. Harlow and M. Kline, *J. Am. Chem. Soc.*, **114**, 5330 (1992).
367. M. Denk, R. Lennon, R. Hayashi, R. West, A. V. Belyakov, H. P. Verne, A. Haaland, M. Wagner and N. Metzler, *J. Am. Chem. Soc.*, **116**, 2691 (1994).
368. B. Gerhus, M. F. Lappert, J. Heinicke, R. Boese and D. Blaser, *J. Chem. Soc., Chem. Commun.*, 11931 (1996).
369. J. Heinicke and A. Oprea, Abstracts of Papers, 11th International Symposium on Organosilicon Chemistry, Montpellier, France, Sept. 1–6, 1996, p. PA 28.
370. B. Gerhus, P. B. Hitchcock, M. F. Lappert, J. Heinicke, R. Boese and D. Bläser, *J. Organomet. Chem.*, **521**, 211 (1996).
371. C. Heinemann, T. Müller, Y. Apeloig and H. Schwartz, *J. Am. Chem. Soc.*, **118**, 2023 (1996).
372. (a) C. Boehme and G. Frenking, *J. Am. Chem. Soc.*, **118**, 2039 (1996).
     (b) C. Heinemann, W. A. Hermann and W. Thiel, *J. Organomet. Chem.*, **475**, 73 (1994).
373. (a) A. J. Arduengo, D. A. Dixon, R. L. Harlow, K. K. Kumashiro, C. Lee, W. P. Power and K. Zilm, *J. Am. Chem. Soc.*, **116**, 6361 (1994).
     (b) A. J. Arduengo, H. V. Rasika Dias, D. A. Dixon, R. L. Harlow, W. T. Klooster and T. F. Koetzle, *J. Am. Chem. Soc.*, **116**, 6812 (1994).
374. M. Haaf and R. West, unpublished investigation.
375. I. Hemme and U. Klingebiel, *Adv. Organomet. Chem.*, **39**, 159 (1996).
376. M. Denk and R. West, unpublished investigations.
377. B. Gerhus, P. B. Hitchcock and M. E. Lappert, Abstracts of Papers, 11th International Symposium on Organosilicon Chemistry, Montpellier, France, Sept. 1–6, 1996, p. OB 2.
378. N. Metzler and M. Denk, *J. Chem. Soc., Chem. Commun.*, 2657 (1996).
379. J. M. Jasinski and S. M. Gates, *Acc. Chem. Res.*, **24**, 9 (1991).
380. G. H. Atkinson and J. J. O'Brien, *J. Phys. Chem.*, **92**, 5782 (1988).
381. M. Heintze and G. H. Bauer, *J. Phys. D*, **28**, 2470 (1995).
382. S. Bismo, P. Duverneuil, L. Pibouleau, S. Domenech and J. P. Couderc, *Chem. Eng. Sci.*, **47**, 2921 (1992).
383. C. Azzaro, P. Duverneuil and J.-P. Couderc, *J. Electrochem. Soc.*, **139**, 305. (1992).
384. C. Cobianu, P. Cosimin, R. Plugaru, D. Descalu and J. Holloman, *Electrochem. Soc. Proc.*, **96**, 300 (1996).

385. D. Orlicki, V. Hlavacek and H. J. Viljoen, *J. Mater. Res.*, **7**, 2160 (1992).
386. S. Veprek, K. Schopper, O. Ambocher, W. Rieger and M. G. J. Veprek-Heijman, *J. Electrochem. Soc.*, **140**, 1935 (1993).
387. L. Layeillon, P. Duverneuil, J. P. Couderc and B. Despax, *Plasma Sources Sci. Technol.*, **3**, 61 (1994); L. Layeillon, A. Dollet, J. P. Couderc and B. Despax, *Plasma Sources Sci. Technol.*, **3**, 72 (1994).
388. Y. Sawado, T. Akiyama, T. Ueno, K. Kamisako, K. Kuroiwa and Y. Tarui, *Jpn. J. Appl. Phys.*, **33**, 950 (1994).
389. C. J. Wu, I. V. Ionova and E. A. Carter, *Surf. Sci.*, **295**, 64 (1993).
390. S. Oikawa, S. Ohtsuka and M. Tsuda, *Appl. Surf. Sci.*, **60/61**, 29 (1992).
391. Y. Toyoshima, K. Arai, A. Matsuda and K. Tanaka, *Appl. Phys. Lett.*, **56**, 1540 (1990); **57**, 1028 (1990).
392. Y. Toyoshima, A. Matsuda and K. Arai, *J. Noncrystal. Solids*, **164–166**, 103 (1993).
393. S. Miyazaki, H. Shin, Y. Miyoshi and M. Hirose, *Jpn. J. Appl. Phys.*, **34**, 787 (1995).
394. S. Veprek and M. G. J. Veprek-Heijman, *Appl. Phys. Lett.*, **56**, 1766 (1990).
395. R. M. Robertson and M. J. Rossi, *Appl. Phys. Lett.*, **54**, 185 (1989).
396. J. I. Steinfeld, *Spectrochim. Acta*, **46A**, 589 (1990).
397. P. P. Gaspar, J.-P. Hsu, S. Chari and M. Jones, Jr., *Tetrahedron*, **41**, 1479 (1985).
398. T. R. Dietrich, S. Chiussi, M. Marek, A. Roth and F. J. Comes, *J. Phys. Chem.*, **95**, 9302 (1991).
399. W. L. M. Weerts, M. H. J. M. de Croon and G. B. Marin, *Chem. Eng. Sci.*, **51**, 2109 (1996).
400. E. Scheid, J. J. Pedroviejo, P. Duverneuil, M. Gueye, J. Samitier, A. El Hassani and D. Bielle-Daspet, *Mater. Sci. Eng.*, **B17**, 72 (1993).
401. R. J. Bogaert, T. W. F. Russell, M. T. Klein, R. E. Rocheleau and R. N. Baron, *J. Electrochem. Soc.*, **136**, 2960 (1989).
402. J. E. Johannes and J. G. Ekerdt, *J. Electrochem. Soc.*, **141**, 2135 (1994).
403. T. Shirafuji, S. Nakajima, Y. F. Wang, T. Genji and K. Tachibana, *Jpn. J. Appl. Phys.*, **32**, 1546 (1993).
404. E. Dehan, J. J. Pedroviejo, E. Scheid and J. R. Morante, *Jpn. J. Appl. Phys.*, **34**, 4666 (1995).
405. J. D. Chapple-Sokol, C. J. Goiunta and R. G. Gordon, *J. Electrochem. Soc.*, **136**, 2993 (1989).
406. H. K. Moffat, T. F. Kuech, K. F. Jensen and P.-J. Wang, *J. Crystal Growth*, **93**, 594 (1988).
407. S. Tanaka, *J. Am. Ceram. Soc.*, **73**, 3046 (1990).
408. C. C. Chen, J. L. Yu, C. Y. Lee, C. S. Liu and H. T. Chiu, *J. Mater. Chem.*, **2**, 983 (1992).
409. J. Belzner, *J. Organomet. Chem.*, **430**, C51 (1992).
410. J. Belzner and H. Ihmels, *Tetrahedron Lett.*, 6541 (1993).
411. J. Belzner, H. Ihmels, B. O. Kneisel, R. O. Gould and R. Herbst-Irmer, *Organometallics*, **14**, 305 (1995).
412. J. Belzner, H. Ihmels and M. Noltemeyer, *Tetrahedron Lett.*, **36**, 8187 (1995).
413. J. Belzner, H. Ihmels, B. O. Knebel and R. Herbst-Irmer, *Chem. Ber.*, **129**, 125 (1996).
414. J. Belzner, H. Ihmels, L. Pauletto and M. Noltemeyer, *J. Org. Chem.*, **61**, 3315 (1995).
415. J. Belzner, D. Schaer, B. O. Kneisel and R. Herbst-Irmer, *Organometallics*, **14**, 1840 (1995).
416. K. Tamao, K. Nagata, M. Asahara, A. Kawachi, Y. Ito and M. Shiro, *J. Am. Chem. Soc.*, **117**, 11592 (1995).
417. K. Tamao, M. Asahara and A. Kawachi, *J. Organomet. Chem.*, **521**, 325 (1996).
418. Y. Apeloig and K. Albrecht, *J. Am. Chem. Soc.*, **117**, 7263 (1995).
419. Y. Apeloig and M. Karni, *Organometallics*, **16**, 310 (1997).
420. H. Leclercq and I. Dubois, *J. Mol. Spectr. Sc.*, **76**, 39 (1979).
421. R. Damrauer, C. H. DePuy, S. E. Barlow and S. Gronert, *J. Am. Chem. Soc.*, **110**, 2005 (1988).
422. R. Srinivas, D. Sülzle and H. Schwarz, *J. Am. Chem. Soc.*, **113**, 52 (1993).
423. E. Herbst, T. J. Millar, S. Wlodek and D. K. Bohme, *Astron. Astrophys.*, **222**, 205 (1989).
424. C. D. Sherrill and H. F. Schaefer III, *J. Phys. Chem.*, **99**, 1949 (1995).
425. A. A. Bengali and D. G. Leopold, to appear; A. A. Bengali, PhD Thesis, University of Minnesota, 1992.
426. M. T. Nguyen, D. Sengupta and L. G. Vanquickenborne, *Chem. Phys. Lett.*, **244**, 83 (1985).
427. R. Stegmann and G. Frenking, *J. Comput. Chem.*, **17**, 781 (1996).
428. W. W. Schoeller and J. Strutwolf, *J. Mol. Struct.*, **305**, 127 (1994).
429. M. Izuha, S. Yamamoto and S. Saito, *J. Chem. Phys.*, **105**, 4923 (1996).
430. W. W. Harper, E. A. Ferrall, R. K. Hilliard, S. M. Stogner, R. S. Grev and D. J. Clouthier, *J. Am. Chem. Soc.*, **119**, 8361 (1997).

Author index

This author index is designed to enable the reader to locate an author's name and work with the aid of the reference numbers appearing in the text. The page numbers are printed in normal type in ascending numerical order, followed by the reference numbers in parentheses. The numbers in *italics* refer to the pages on which the references are actually listed.

Index compiled by K. Raven

Subject index

Index compiled by P. Raven